BULLETIN OF THE CHEMICAL SOCIETY OF JAPAN VOL. 42 1—4 (1969)

Study on Fragmentation Process of Thymidine by Mattauch-Herzog Geometry High Resolution Mass Spectrograph

Sukenari TSUNAKAWA*1

Department of Chemistry, Massachusetts Institute of Technology, Cambridge, Massachusetts, U.S.A.

(Received November 27, 1967)

High resolution mass spectra of thymidine were studied by Mattauch-Herzog geometry mass spectrograph. The element map of it was presented and the fragmentation processes were shown by solid or dotted lines on the map. The spectra were measured with higher accelerating voltages (about 0.1 %) in order to obtain many metastable peaks on the photographic plate. By a single focusing mass spectrometer ten metastable peaks were measured and "intentionally defocused" high resolution spectra gave twenty five diffused peaks with slight shifts to the high mass region though no metastable peaks were observed under normal operating conditions.

Recently many remarkable improvements have been made on organic chemical applications of high resolution mass spectrometry.[1,2] It is also a well-developed technique at the present time to use metastable peaks as keys to the determination of the fragmentation process. Various reports have been published on their measurements and assignments.[3-8] In this paper, the author studied on slightly "defocused" high resolution mass spectrum of thymidine with Mattauch-Herzog geometry mass spectrograph so that the "metastable peaks" could be observed on the photographic plate at the same time with the "normal peaks." Barber and his coworkers[8] proposed a method to observe metastable transitions which occur in the field free region between the source and the electrostatic analyser by increasing the accelerating voltage, V, so that the daughter ions are permitted to pass through the analyser. In the studies of thymidine described here, the increment of V was restricted to only about 0.1%. This low increment permits all of the normal ions to be still in focus on the photographic plate together with metastable peaks.

Experimental

Reagent grade thymidine, $C_{10}H_{14}N_2O_5$, was used without further purification. Measurements were carried out with Hitachi RMU-6D 90° magnetic sector type single focusing mass spectrometer and CEC 110 Mattauch-Herzog geometry double focusing mass spectrograph. Sample introduction were made through direct inlet systems. The single focusing type was used in order to compare the results with those obtained double focusing. Ion source temperature was set at 230°C and ionization voltage at 70 eV in both cases.

By the single focusing measurement, a mass spectrum from 1 to 250 *m/e* was recorded within 1 min using an electron multiplier and a Honeywell visicorder.

In double focusing measurement, about 50 μg sample was introduced with the marker (PFK) according to the normal operating condition (accelerating voltage 8 kV), another two exposures were made successively on the same photographic plate with slight increases of accelerating voltage, +9.6 V (condition I), and +16.8 V (condition II) respectively. Accurate masses were determined by Datex comparator connected to the densitometer, and the center of the diffused peak was measured on the paper recorded spectra. Whole results were presented in Biemann's element map system.[9-11]

*1 Present address: The Central Research Laboratory of Mitsubishi Chemical Industries Ltd., Kawasaki-shi, Kanagawa.

1) K. Biemann, "Mass Spectrometry with Organic Chemical Applications," McGraw-Hill, New York (1962).

2) H. Budzikiewicz, C. Djerassi and D. H. Williams, "Interpretation of Mass Spectra of Organic Compounds" (1964), "Structure Elucidation of Natural Products by Mass Spectrometry," Vol. 1 and Vol. 2, Holden Day, San Francisco (1964).

3) M. Barber and R. M. Elliot, 12th Annual Conference on Mass Spectrometry and Allied Topics, Montreal, 1964.

4) J. H. Futrell, K. R. Ryan and L. W. Sieck, *J. Chem. Phys.*, **43**, 1832 (1965).

5) R. I. Reed and M. T. Robert-Lopes, 14th Annual Conference on Mass Spectrometry and Allied Topics, Dallas, 1966.

6) R. E. Rhodes, M. Barber and R. L. Anderson, *Anal. Chem.*, **38**, 48 (1966).

7) N. R. Mancuso, S. Tsunakawa and K. Biemann, *ibid.*, **38**, 1775 (1966).

8) M. Barber, W. A. Wolsterholme and K. R. Jennings, *Nature*, 214 (May 13), 664 (1967).

9) D. Desiderio and K. Biemann, 12th Annual Conference on Mass Spectrometry and Allied Topics, 1964, Montreal.

10) K. Biemann, P. Bommer and D. Desiderio, *Tetrahedron Letters*, **1964**, 1725.

11) D. Desiderio, Ph. D. Thesis, Massachusetts Institute of Technology, Cambridge (1965).

TABLE 1. METASTABLE PEAKS AND THEIR ORIGINS

CEC	Hitachi		Corresponding fissions		
	Obsd	Cald			
24.3		24.1	$C_3H_5O_2^+$	$\xrightarrow{}$	$C_2H_2O^+$
25.3		25.1	$C_2H_5^+$	$\xrightarrow{-H_2}$	$C_2H_3^+$
26.3*	26.1	26.0	C_4H_7O	$\xrightarrow{-CO}$	C_3H_7
27.3		27.0	$C_2H_5^+$	$\xrightarrow{-H}$	$C_2H_4^+$
28.1*	27.8	27.7	$C_3H_5O_2^+$	$\xrightarrow{-CO}$	$C_2H_5O^+$
	32.9	32.8	$C_5H_7O_2^+$	$\xrightarrow{-C_2H_2O}$	$C_3H_5O^+$
34.3		34.0	$C_5H_7O_2^+$	$\xrightarrow{-C_2HO}$	$C_3H_6O^+$
35.4		25.1	$C_4H_5NO^+$	$\xrightarrow{-CHO}$	$C_3H_4N^+$
36.3		36.0	$C_5H_7N^+$	$\xrightarrow{-C_2H_3}$	$C_3H_4N^+$
36.7*	36.5	36.5	$C_4H_5NO^+$	$\xrightarrow{-CO}$	$C_3H_5N^+$
37.4		37.4	$C_4H_6NO^+$	$\xrightarrow{-CO}$	$C_3H_6N^+$
38.4		38.0	$C_3H_4^+$	$\xrightarrow{-H}$	$C_3H_3^+$
39.4		39.1	$C_3H_7^+$	$\xrightarrow{-H_2}$	$C_3H_5^+$
40.4		40.0	$C_3H_6^+$	$\xrightarrow{-H}$	$C_3H_5^+$
41 1		41 1	$C_2H_5O^+$	$\xrightarrow{-H_2}$	$C_2H_3O^+$
42.4		42.1	C_2H_4O	$\xrightarrow{-H}$	$C_2H_3O^+$
	45.5	45.6	$C_5H_9O_3^+$	$\xrightarrow{C_2H_4O}$	$C_3H_5O_2^+$
48.4*	48.2	48.2	$C_5H_7O_2^+$	$\xrightarrow{-CH_2O}$	$C_4H_5O^+$
49.4		49.1	$C_5H_5O_2^+$	$\xrightarrow{-CO}$	$C_4H_5O^+$
50.4		50.0	$C_5H_6O_2$	$\xrightarrow{-CO}$	$C_4H_6O^+$
51.4*	51.0	50.9	$C_5H_7O_2^+$	$\xrightarrow{-CO}$	$C_4H_7O^+$
53.4		53.4	$C_5H_6N_2O_2^+$	$\xrightarrow{-CH_2NO}$	$C_4H_4NO^+$
54.4		53.8	$C_5H_7O_2^+$	$\xrightarrow{-C_2H_2}$	$C_3H_5O_2^+$
	54.8	54.6	$C_5H_6N_2O_2^+$	$\xrightarrow{-HNCO}$	$C_4H_5NO^+$
56.5		56.3	$C_4H_7O_2^+$	$\xrightarrow{-OH}$	$C_4H_6O^+$
	66.3	66.3	$C_5H_7O_2^+$	$\xrightarrow{-H_2O}$	$C_5H_5O^+$
79.5		79.1	$C_7H_9N_2O_2^+$	$\xrightarrow{-HNCO}$	$C_6H_8NO^+$
84.6*	83.8	83.9	$C_5H_9O_3^+$	$\xrightarrow{-H_2O}$	$C_5H_7O_2^+$
96.6		96.0	$C_5H_6O_2^+$	$\xrightarrow{-H}$	$C_5H_5O_2^+$

Results and Discussion

Low Resolution Spectra. Ten metastable peaks were obtained and completely assigned by use of N. Mancuso's computer program by considerations of the products of the intensities of the parent and daughter peaks and their elemental compostions.[7] Fragmentation processes are shown in Table 1 and also in Fig. 1 by solid lines. Assuming that neutral fragments are expelled as one piece, the daughter ions are derived easily without any drastic rearrangement from the thymidine structure, so the investigation of a metastable peak gives very important informations on the structure

12) J. A. McClosky, Ph. D. Thesis, Massachusetts Institute of Technology, Cambridge (1963).

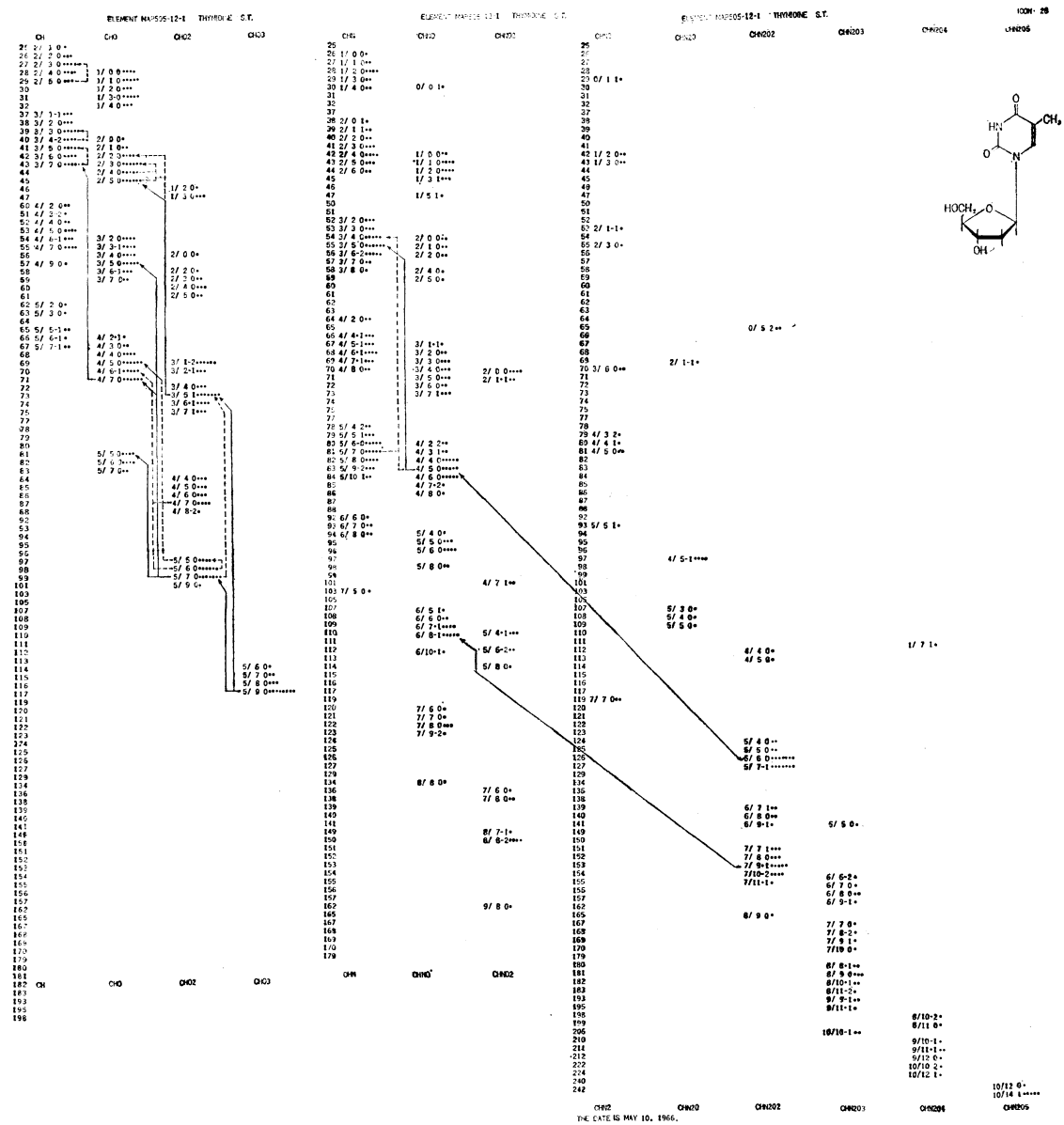

Fig. 1. Element map of thymidine.

of the sample.

Some of these fragmentation processes, for example, from $C_5H_6N_2O_2^+$ to $C_4H_5NO^+$, are well agreed with the previous reports[12,13] on some thymidine type compounds and make it clear that thymidine decomposes in the same manner as thymine.

Mattauch-Herzog Geometry High Resolution Spectra. No metastable peaks were observed under normal measuring conditions, indicating that the thymidine fragmentation is in a sense different from 1-*n*-butylthymine which shows many metastable peaks under usual operation.[7] In the case of thymidine no decomposition occurs in the field free region between electric and magnetic sector. If the fissions are supposed to proceed near the ion source, the daughter ions should be able to reach the detector by increasing the accelerating voltage to $V=m_1 \cdot V_0/m_2$,[4,5] where m_1 and m_2 are the masses of the parent and daughter ions respectively and V_0 is the usual accelerating voltage. Many diffused peaks were observed by "intentionally defocused" measurements (condition I and II). In the case of thymidine some fissions are thought to occur not only in the ionization chamber but also in the electric sector, probably

13) J. M. Rice, G. O. Dudek and M. Barber, *J. Am. Chem. Soc.*, **87**, 4569 (1965).

near the exit slit, because the increase of accelerating voltage, 9.6 or 16.8 V, is too small to carry the daughter ions through the electric sector to the detector. In Table 1, fissions of thymidine are listed in terms of the metastable peaks under condition I with corresponding reaction formulas. Under condition II, normal ion path is deflected more than under condition I, and then relative intensities of metastable peaks increase, accompanied with larger shifts to the high mass direction. It has been known that the diffused peaks of some hydrocarbons shift to the high mass region when the accelerating voltage is increased.[14,15] Then

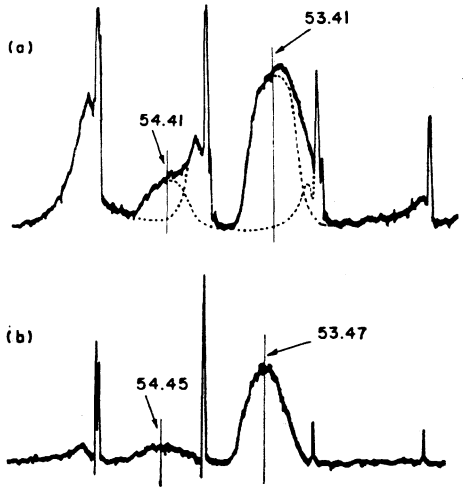

Fig. 2. Metastable peaks in the intentionally defocused thymidine spectra; (a) condition I, 8 kV 9.6 V. (b) condition II, 8 kV 16.8 V. The peaks in (a) show "tailing" on the high mas sides by the "defocusing."

14) Unpublished results by N. Mancuso and the author.

15) Private communications from JEOL mass spectroscopy reaserch group.

it follows that the relative positions of the metastable peaks on the photographic plate must depend upon the regions where the fissions occur. The amount of the displacement of the m^* position differs from peak to peak. This is reasonable bacause it is considered that the shift depends upon the position where the decomposition occurs, the energy loss at the moment of the fission and also upon the mass to charge ratios of the parent and daughter ion. Portions of the spectra measured under condition I and II are shown in Fig. 2 (a) and (b) respectively.

Under the considerations of these facts, the metastable peak assignment was carried out assuming that the theoretical value must have smaller mass to charge ratio, and the limit of the range is 0.7 mass unit in high and 0.4 mass unit in low mass region. The metastable peaks marked with * are those which are measured by single focusing instrument. Among ten reactions measured by single focusing, six are observed also by double focusing. It is worth to notice there are many metastable transitions which are observed only under these "intentionally defocused" conditions and not by the single focusing instrument. Besides the structural data, this method would supply valuable informations on chemical kinetics.

Element Map of Thymidine and Its Fragmentation Process. Figure 1 shows the element map of thymidine. A solid line shows the fission determined by the metastable peak measurement with Hitachi instrument and a dotted line that by intensionally defocused Mattauch-Herzog experiment under condition I.

The encouragement and support of Professor K. Biemann during this work carried out in M. I. T. are gratefully acknowledged. The author also express his thanks to Dr. N. Mancuso for his continuing interest and for giving the computer aided data.

BULLETIN OF THE CHEMICAL SOCIETY OF JAPAN VOL. 42 5—9 (1969)

Ultrasonic Relaxation of Water-Dioxane System

Kiyoshi ARAKAWA and Nobuo TAKENAKA

Research Institute of Applied Electricity, Hokkaido University, Sapporo

(Received January 31, 1968)

Ultrasonic investigations of the water-dioxane system were made by means of an ultrasonic pulse technique. The ultrasonic velocity and absorption of the solutions were measured in the frequency range from 5 to 45 Mc/sec. The temperature was varied from 20 to 60°C. It was observed in the velocity *vs.* concentration curves obtained at various temperatures that all curves converged at 0.03—0.04 mol fraction of dioxane. The ultrasonic absorption of pure dioxane was found to increase with the rise of temperature, which might be ascribed to the vibrational relaxation. From the ultrasonic absorption data obtained for the solutions of the water-dioxane system in various compositions and temperatures it was observed that at 0.3—0.4 mol fraction of dioxane an absorption peak was present in the absorption *vs.* concentration curve, and also that there was no shift of the concentration at the peak with the variation of temperature. Some discussion on the structure of the water-dioxane system was given from the ultrasonic data obtained.

Dioxane is completely miscible with water. The water-dioxane system is of considerable interest, since the dielectric constant of the system varies from the magnitude of about 80 for pure water to the magnitude of about 2 for pure dioxane with the variation of its composition. Also, the strong interactions, which are supposed to consist mainly of hydrogen bonding, are present between dioxane and water molecules, though dioxane molecules have no ability to form hydrogen bonding between themselves.

The physical properties of water and dioxane are similar in several respects. For example, the difference between their boiling points is within 15°C, and that between their freezing points is within 12°C, *etc.* The size and shape of molecules are however, fairly different.

From the view-points described above, the water-dioxane system has long been the object of thermodynamical,[1-5] viscometric,[6] dielectric,[7-9] NMR,[10] spectroscopic,[11] and ultrasonic studies.[12] However, no decisive conclusion has been obtained at present. We have measured the ultrasonic velocity and absorption of the water-dioxane system by means of an ultrasonic pulse technique, and discussed the structure of the solutions.

Experimental

Apparatus and Procedures for Measurements. The ultrasonic velocity and the absorption were measured according to the pulse method developed by Pinkerton[13] and others. The apparatus and the procedures for the measurements were described in the preceding paper.[14] The sound velocity was measured at a fixed frequency of 5 Mc/sec. The absorption was measured over the frequency range of 15—45 Mc/sec. All measurements in this experiment were made in the range of temperature from 20°C to 60°C with 10°C intervals, and the temperature was controlled to within ±0.1°C.

Materials. For the measurements of dioxane-water mixtures, the reagent-grade dioxane, obtained from Wako Pure Chemicals, was mixed with freshly distilled water. In the case of the measurements of pure dioxane the dioxane sample was further purified according to the following procedure:[15] after being treated with hydrochloric acid and thereafter with potassium hydroxide, the dioxane sample was refluxed with metallic

1) G. N. Malcolm and J. S. Rowlinson, *Trans. Faraday Soc.*, **53**, 921 (1953).
2) A-L. Vierk, *Z. anorg. Chem.*, **261**, 283 (1950).
3) A. L. Bacarella, A. Finch and E. Grunwald, *J. Phys. Chem.*, **60**, 573 (1956).
4) J. R. Goates and R. J. Sullivan, *ibid.*, **62**, 188 (1958).
5) F. Hovorka, R. A. Shaefer and D. Dreisbach, *J. Am. Chem. Soc.*, **58**, 2264 (1936).
6) J. A. Geddes, *ibid.*, **55**, 4832 (1933).
7) C. J. Clemett, E. Forest and C. P. Smyth, *J. Chem. Phys.*, **40**, 2123 (1964).
8) S. K. Garg and C. P. Smyth, *ibid.*, **43**, 2959 (1965).
9) A. R. Tourky, H. A. Rezk and Y. M. Girgis, *J. Phys. Chem.*, **65**, 40 (1961).
10) A. Fratiello and D. C. Douglass, *J. Mol. Spect.*, **11**, 465 (1963).
11) E. Greinacher, W. Lüttke and R. Mecke, *Zeit. für Elektrochem.*, **59**, 23 (1955).
12) C. J. Burton, *J. Acoust. Soc. Am.*, **20**, 186 (1948).
13) J. M. M. Pinkerton, *Proc. Phys. Soc.*, **B62**, 86, 129, 286 (1949).
14) K. Arakawa and N. Takenaka, This Bulletin, **40**, 2063 (1967).
15) A. Weissberger and E. S. Proskauer, "Organic Solvents," Interscience Pub., New York (1955), p. 372.

sodium and was fractionally distilled. The fraction in boiling range of 101.3—101.7°C was used for the measurement.

Results

Sound Velocity. The ultrasonic velocity at 5 Mc/sec obtained for the water-dioxane system of various compositions is plotted against temperature in Fig. 1. The accuracy of the data obtained is within 2 m/sec. As is seen in Fig. 1, the sound velocity of water-dioxane mixtures and also that of pure dioxane decrease linearly with the increase in temperature, being in sharp contrast with the increasing trend in the velocity *vs.* temperature curve for pure water which is given for comparison.

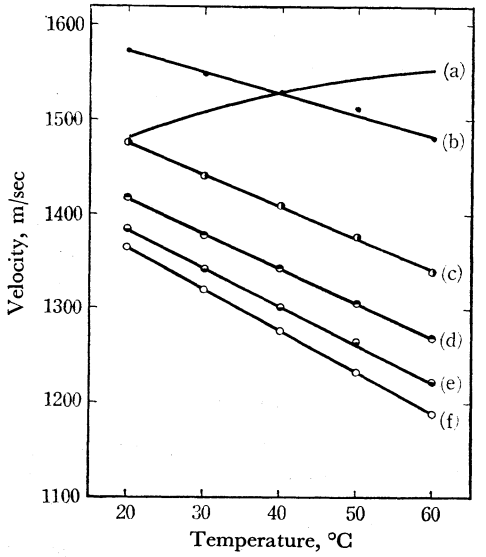

Fig. 1. Temperature dependence of ultrasonic velocity for the dioxane-water system.
dioxane mol%: (a) pure water, (b) 17.5 mol%, (c) 40 mol%, (d) 60 mol%, (e) 80 mol%, (f) pure dioxane

In order to investigate the concentration dependence of ultrasonic velocity, the velocity is plotted against dioxane concentration by mole % for each temperature in Fig. 2. It is seen that at about 3—4 mol% of dioxane (about 15 vol% of dioxane) all curves converge, and that the trend of the temperature dependence of sound velocity is reversed after passing through that concentration.

It is well known that the increasing trend of sound velocity in pure water with the increase of temperature in this temperature range is ascribed to the presence of the "open structure" in liquid water.[16-18] The disappearance of that trend after

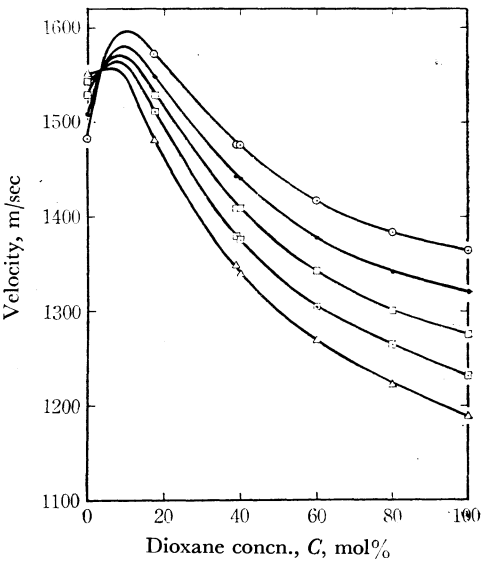

Fig. 2. Concentration dependence of ultrasonic velocity.
⊙ 20°C, ● 30°C, □ 40°C, ⊡ 50°C, △ 60°C

the addition of about 3—4 mol% of dioxane to water is supposed to occur from the strong interaction of dioxane molecules to the structure in water, where dioxane molecules behave as the hydrogen bonding acceptor and water molecules as the hydrogen bonding donor.

Ultrasonic Absorption of Dioxane. The absorption coefficient, α, was measured for the sample of pure dioxane over the frequency range from 15 to 45 Mc/sec. The data obtained are given in Fig. 3, which are plotted against frequency in a logarithmic scale. The accuracy of α obtained is within ±2%. As is clearly seen in Fig. 3, no characteristic relaxation frequency is observed in this frequency range. The magnitude of the absorption is found to increase with the increase of temperature. From these observations the

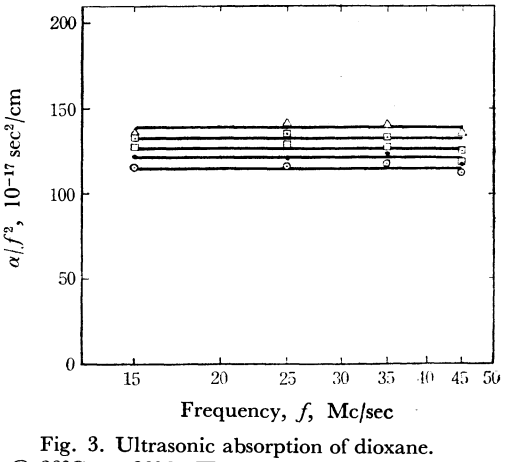

Fig. 3. Ultrasonic absorption of dioxane.
⊙ 20°C, ● 30°C, □ 40°C, ⊡ 50°C, △ 60°C

16) L. Hall, *Phys. Rev.*, **73**, 775 (1948).
17) G. Nénethy and H. A. Scheraga, *J. Chem. Phys.*, **36**, 3382 (1962).
18) K. Arakawa and N. Takenaka, This Bulletin, **40**, 2739 (1967).

source of the ultrasonic absorption in dioxane in this frequency range might be ascribed to the vibrational relaxation. The temperature dependence of α is also shown in Fig. 4. The value reported by Heasell and Lamb[19] is also given which is slightly smaller than our data in spite of the fairly large difference in the frequency used. We might say that no characteristic relaxation frequency should be present in the frequency range including the measurement of Heasell *et al.*

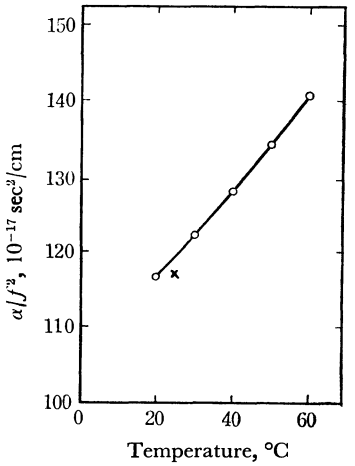

Fig. 4. Temperature dependence of ultrasonic absorption for dioxane.
× Heasell anb Lamb's data[19] at 24.6°C and 104 Mc/sec

Ultrasonic Absorption of Water-Dioxane System. The data of the ultrasonic absorption of the water-dioxane sytem are given in the form of α/f^2 *vs.* $\log f$ relation, where f is frequency, in

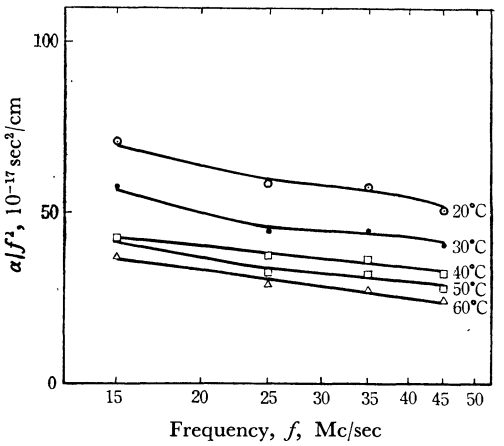

Fig. 5(a). Ultrassonic absorption of the water-dioxane system (17.5 mol% of dioxane).

19) E. L. Heasell and J. Lamb, *Proc. Phys. Soc.*, **B69**, 869 (1956).

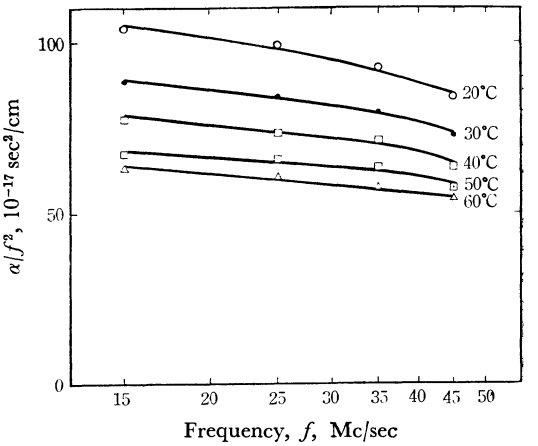

Fig. 5(b). Ultrasonic absorption of the water-dioxane system (40 mol% of dioxane).

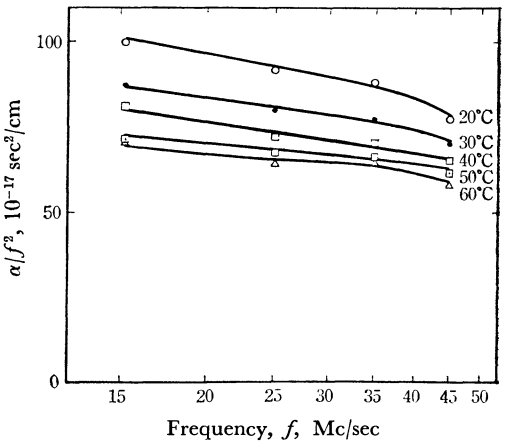

Fig. 5(c). Ultrasonic absorption of the water-dioxane system (60 mol% of dioxane).

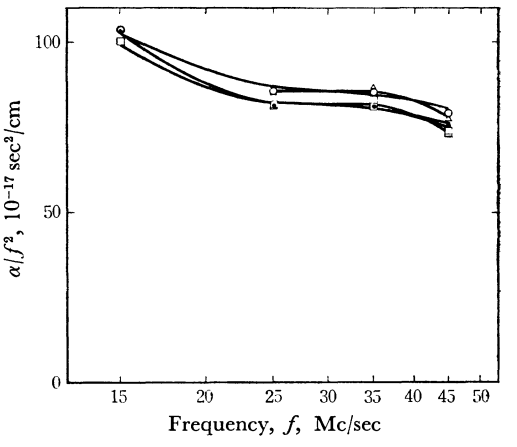

Fig. 5(d). Ultrasonic absorpption of the water-dioxane system (80 mol% of dioxane).
⊙ 20°C, ● 30°C, □ 40°C, ⊡ 50°C, △ 60°C

Fig. 5(a)—(d). The molar concentration of dioxane is 17.5, 40, 60, and 80 mol% respectively. As for the ultrasonic absorption of the water-dioxane system, the data obtained by means of an optical diffraction method was reported previously by Burton.[12] However, Burton's values are much larger than ours.

The concentration dependence of α/f^2 is shown in Fig. 6, where the absorption data for pure water reported by Pinkerton[13] and also our data for the solutions of 75 vol% (38.9 mol%) dioxane are added. A maximum of α/f^2 is seen in Fig. 6 at about 0.4 mol fraction of dioxane at lower temperatures. At higher temperature the maximum is found to deform into a shoulder, but the mole fraction at the shoulder is seen to be constant. The characteristic in the α/f^2 *vs.* mole fraction curve is found to be more discriminate, after the value of α/f^2 obtained according to the proportional calculation to the mole fraction of two components, $(\alpha/f^2)_{lin}$, has been subtracted from the observed value of $(\alpha/f^2)_{obs}$.

The value of the excess absorption,

$$\Delta = (\alpha/f^2)_{obs} - (\alpha/f^2)_{lin}$$

is plotted against the mol% of dioxane in Fig. 7.

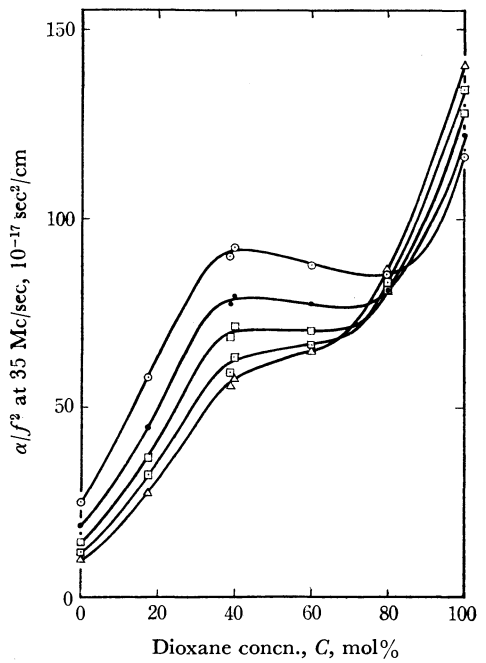

Fig. 6. Concentration dependence of ultrasonic absorption.
⊙ 20°C, ● 30°C, □ 40°C, ⊡ 50°C, △ 60°C

From Fig. 7 it is observed that a maximum of Δ is present always at about 0.35 mol fraction of dioxane irrespective of the variation of temperature though the magnitude of Δ becomes smaller with the increase in temperature.

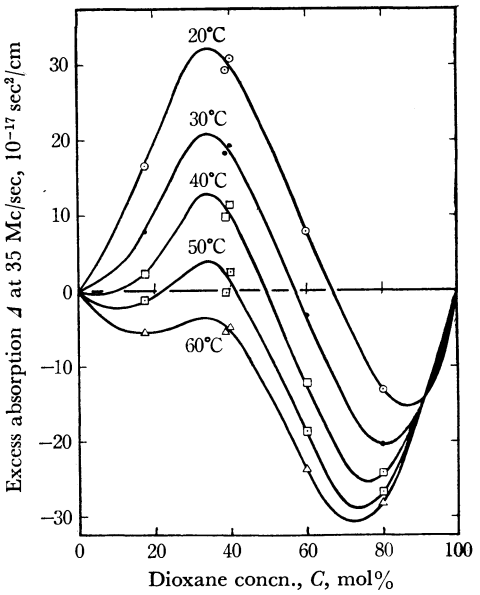

Fig. 7. Concentration dependence of excess absorption.

The temperature dependence of α/f^2 in each solution is shown in Fig. 8. As is clearly seen, the α/f^2 *vs.* temperature curves go downwards with the increase in temperature up to the 60 mol% solutions. In the solution of 80 mol% dioxane

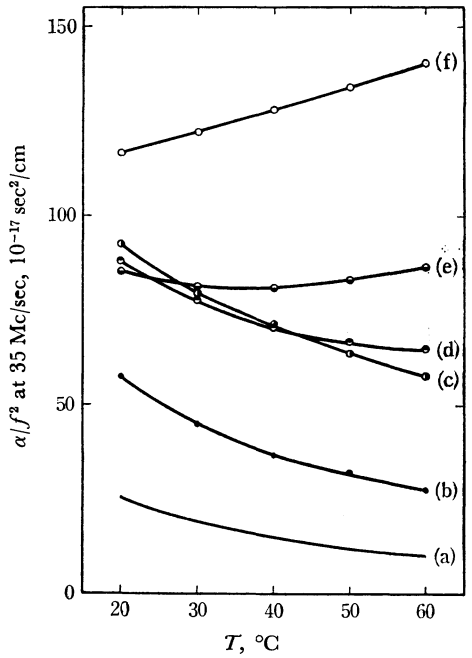

Fig. 8. Temperature dependence of ultrasonic absorption.
Dioxane mol%: (a) pure water, (b) 17.5 mol%, (c) 40 mol%, (d) 60 mol%, (e) 80 mol%, (f) pure dioxane

the cruve has a shallow minimum and is nearly flat.

Discussion

Vibrational Relaxation in Dioxane. As stated from the result given in Fig. 3, the source of ultrasonic absorption in dioxane is ascribed to the vibrational relaxation, which occurs from the time lag of energy transfer from the translational motion to the vibrational motion in dioxane molecules. When water is added to dioxane till the mole ratio of water to dioxane, 1 : 4 (the vol% of water in this composition is as small as about 5% since the dimension of dioxane molecule is larger than that of water molecule), this behavior practically disappears, as is seen in Fig. 8.

In the latter case some structure, which behaves as an energy bridge for the energy transfer from the external degree of freedom to the internal, may be formed in the solution as a result of the strong interaction, perhaps hydrogen bonding, between dioxane and water molecules.

Structure of Water-Dioxane System. It is observed in Fig. 6 and Fig. 7 that at 0.3—0.4 mol fraction of dioxane an absorption peak appears, and that the composition at the maximum absorption remains constant when the temperature is varied. The mole fraction at the maximum or shoulder corresponds to the composition of dioxane dihydrate. From the facts stated above the presence of dioxane dihydrate, which is proposed by Garg and Smyth on the basis of their dielectric measurements,[8] might be suggested.

The excess entropy of mixing, ΔS_E, reported by Vierk,[2] which was obtained from the data of the vapor pressure and the heat of mixing measured on the system, was found to have its maximum in the absolute magnitude at 0.35 mol fraction of dioxane at 20°C. Goates *et al.*[4] also reported from their calorimetric data that $|\Delta S_E|$ was maximum at about 0.3 mol fraction of dioxane at 25°C. According to the dilatometric data of Hovorka *et al.*,[5] the excess volume of mixing, ΔV_E at 25°C also was found to have its maximum value at 0.3—0.4 mol fraction of dioxane in its absolute magnitude at 20—50°C.

This thermodynamic data suggests the presence of some structure between water and dioxane molecules at the 0.3—0.4 mol fraction of dioxane, the composition of which approximately corresponds to dioxane dihydrate.

According to the dielectric relaxation measurements on the water-dioxane mixture reported recently by Garg and Smyth,[8] two relaxation times, τ_1 and τ_2, are present and the longer one, τ_1, which is of the order of 10^{-11} sec has its maximum value at 0.3—0.5 mol fraction of dioxane in the range of temperature, 10—55°C, where the mole fraction at its maximum is found to increase with the rise of temperature. Garg and Smyth have proposed the presence of dioxane dihydrate from their results according to the suggestion of Bak and Hynne.[8]

Geddes[6] proposed the presence of $C_4H_8O_2 \cdot 5H_2O$ from his viscometric results. According to Goates *et al.*[4] a dip in the mixing enthalpy was found at 0.15 mol fraction of dioxane and also in the case of the freezing point curve a sharp dip was found at the same mole fraction, which corresponded to the composition of $C_4H_8O_2 \cdot 6H_2O$. However in our ultrasonic relaxation data no feature is seen in that range of compsotion, and we can not state decisively the presence of hexahydrate or pentahydrate.

Summary and Conclusion

Ultrasonic investigations of the water-dioxane system have been made by the pulse method over the frequency range of 5—45 Mc/sec. The source of the ultrasonic absorption in this frequency range for pure dioxane has been ascribed to the vibrational relaxation. The ultrasonic absorption for the water-dioxane system has been found to have its maximum or shoulder at 0.3—0.4 mol fraction of dioxane and it has also been found that the mole fraction of maximum absorption is maintained to be nearly constant with the variation of temperature. The structure of the water-dioxane system has been discussed concerning the presence of dioxane dihydrate.

The authors wish to thank Miss Yuko Endo for her cooperation in carrying out this study.

BULLETIN OF THE CHEMICAL SOCIETY OF JAPAN VOL. 42 10—15 (1969)

The $n\rightarrow\pi^*$ Bands of Phenyl Carbonyl Compounds, α-Diketones, and Quinones at Low Temperatures

Akira KUBOYAMA, Ryuichi YAMAZAKI,[*1] Sanae YABE and Yoshio UEHARA[*2]

Government Chemical Industrial Research Institute, Tokyo, Shibuya-ku, Tokyo

(Received February 20, 1968)

The positions and intensities of the $n\rightarrow\pi^*$ absorption bands in solutions at 77°K (in the rigid glass state) and at 201°K (in the liquid state) have been studied in comparison with those at room temperature. At 201°K the positions and intensities are similar to those at room temperature. At 77°K some distinct facts have been found in EP (ether-isopentane (1:1) mixture) which are different from those which hold in the liquid state: 1) In desoxybenzoin the absorption is remarkably weak in intensity. 2) In some α-diketones and β-naphthoquinone, the $n\rightarrow\pi^*$ bands shift greatly to the blue. 3) In β-naphthoquinone the absorption is remarkably strong in intensity. Discussions of the obtained results have been presented.

Heretofore, the electronic spectra of organic compounds at low temperatures have not been very extensively studied. It is expected that, in some cases, low-temperature electronic spectra may show valuable information about the structural and analytical chemistry because of their sharp vibrational structures and strong solvent effects.

The positions and intensities of $n\rightarrow\pi^*$ absorption bands are, in general, structure- and solvent-sensitive. The $n\rightarrow\pi^*$ bands of phenyl carbonyl compounds, α-diketones, and quinones in solutions at room temperature have been studied by many authors. In this work, the positions and intensities of these $n\rightarrow\pi^*$ bands in solutions at low temperatures have been studied in comparison with those at room temperature.

Experimental

Measurements. The electronic spectra were measured with a Cary recording spectrophotometer, 14 M. The partly-silvered quartz vacuum-flasks and quartz cells used in this work are shown in Fig. 1. A cylindrical cell had a long tube through which a sample solution was introduced into the cell. The cell was immersed in a cooling medium except for a part of the tube. The shaded portions in Fig. 1 were flanges which were attached to the inner windows of the vacuum flask and used in order to support the cell and make bubbles deviate from the optical path. The distance between a window of the cell and an inner window of the vacuum flask was *ca.* 1 mm. Vacuum flasks with cells 1 and 5 cm in optical path were made. The solvents used in this work have shown no absorption in the wave-region studied at 201°K and 77°K, using those at room temperature as references. Therefore, usual cylindrical quartz cells with the same path length as those of the sample cells were used as references in this work. With this apparatus measurements at low temperatures were made easily and precisely. The solvents used in the measurements were an ethyl ether-isopentane (1 : 1) mixture (EP), an methanol-ethanol (1 : 4) mixture (ME), an ethyl ether - isopentane - ethanol (5 : 5 : 2) mixture (EPA), and methylcyclohexane (MCH). The measurements were carried out at the temperature of liquid nitrogen (77°K), at the temperature of dry ice - ethanol (201°K), and at room temperature. At 77°K all the solutions used were transparent in the rigid glass state, while at 201°K they were transparent in the liquid state.

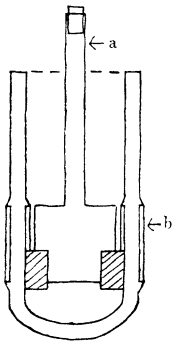

Fig. 1. Vaccuum flask and cell.
a cell b window

Materials. The reagents used in this work were all of the purest grade commercially available except for the β-naphthoquinone and the *N*-acetylisatin. The acetophenone, isobutyrophenone, and diacetyl of the G. R. grade of the Tokyo Kasei Kogyo Co., and the 1-phenyl-1,2-propanedione of the Eastman grade of

*1 Present address: Kanagawa Prefectural Industrial Research Institute, Tomioka-machi, Kanazawa-ku, Yokohama.

*2 Present address: Bokusui Sangyo Co., 2-1, Uchisaiwaicho, Chiyoda-ku, Tokyo.

Distillation Products Ind. were used without further purification. The benzophenone, desoxybenzoin, and benzil were purified by recrystallization. The *p*-benzoquinone was purified by sublimation. The 2-methylanthraquinone and camphorquinone were purified by vacuum sublimation. The α-naphthoquinone was purified according to Fieser's method.[1] The β-naphthoquinone was prepared and purified according to Fieser's method.[1] The *N*-acetylisatin was prepared by the *N*-acetylation of isatin and was purified by recrystallization. The *n*-heptane, ethyl ether, and isopentane were purified according to the methods described in our previous papers.[2,3] The methylcyclohexane, methanol, and ethanol were of the same quality as those described in a previous paper.[3]

Results

In order to compare the absorption intensities of the $n\rightarrow\pi^*$ bands at low temperatures with that at room temperature, a ratio of the integrated absorption intensity was obtained. The shift in the wave number of the positions of the $n\rightarrow\pi^*$ bands, ($\Delta\bar{\nu}$), and the ratio of the integrated absorption intensity of the $n\rightarrow\pi^*$ bands, (R.I.), between a low temperature and room temperature, are shown in Tables 1—3. In Tables 1—3, I—XIII are acetophenone, isobutyrophenone, desoxybenzoin, benzophenone, diacetyl, camphorquinone, 1-phenyl-1,2-propanedione, benzil, *N*-acetylisatin, *p*-benzoquinone, α-naphthoquinone, 2-methylanthraquinone, and β-naphthoquinone respectively. As for the $\Delta\bar{\nu}$ and R.I. in these tables, for example, if $\Delta\bar{\nu}$ is positive, the $n\rightarrow\pi^*$ band at a low temperature shifts to the blue relative to that at room temperature, and, for example, if R.I. is larger than one, the integrated absorption intensity of the $n\rightarrow\pi^*$ band at a low temperature is larger than that at room temperature. In order to correct for the volume contraction at a low temperature, the measured absorption intensities at low temperatures were multiplied by factors (0.9 for 201°K and 0.8 for 77°K) chosen in view of the reported data.[4] The results obtained at 77°K for α-naphthoquinone in EPA and desoxybenzoin in EP with 1 cm and 5 cm path cells were the same.

The $n\rightarrow\pi^*$ bands, obtained mainly in EP, are shown in Figs. 2—14. In these figures all the spectra have been corrected for the volume contraction at low temperatures. In quinones there are uncertainties in the R.I. values due to a large overlapping of $\pi\rightarrow\pi^*$ and $n\rightarrow\pi^*$ bands, as may be seen in Figs. 12—14.

Discussion

As is shown in Tables 1—3 and in Figs. 4, 6, and 14, the positions and absorption intensities at 201°K

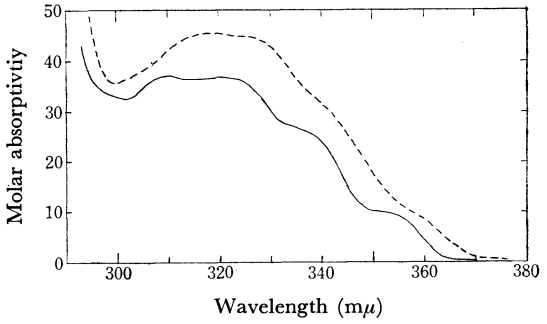

Fig. 2. Acetophenone, solvent EP.
------ Room temperature, —— 77°K

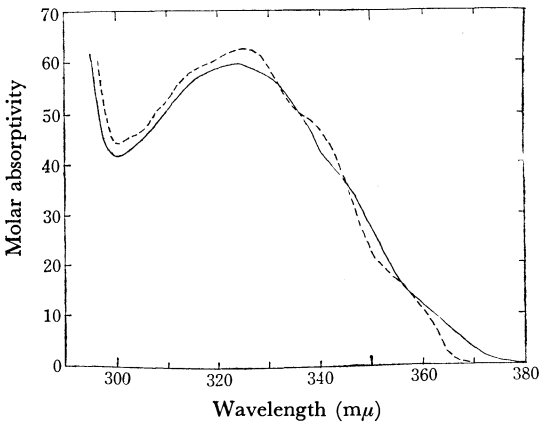

Fig. 3. Isobutyrophenone, solvent EP.
------ Room temperature, —— 77°K

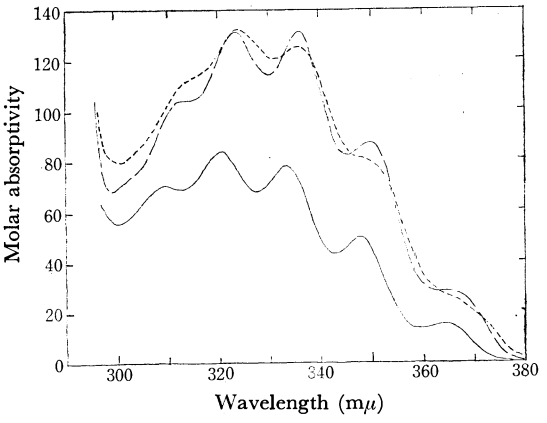

Fig. 4. Desoxybenzoin, solvent EP.
------ Room temperature, —— 201°K, —— 77°K

1) L. F. Fieser, "Experiment in Organic Chemistry," D. C. Heath and Co., Boston (1941), pp. 230, 232 and 233.
2) A. Kuboyama, This Bulletin, **33**, 1027 (1960).
3) A. Kuboyama and S. Yabe, *ibid.*, **40**, 2475 (1967).
4) KJ. Rosengren, *Acta Chem. Scand.*, **16**, 1421 (1962); R. Passerini and I. G. Ross, *J. Sci. Instr.*, **30**, 276 (1953).

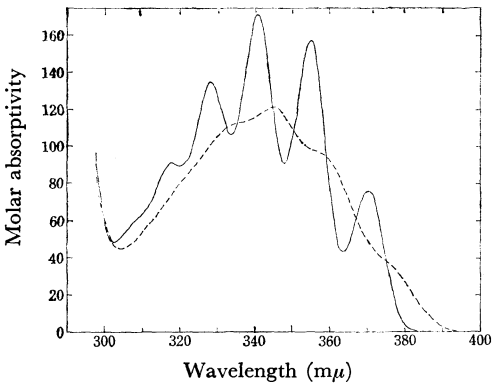

Fig. 5. Benzophenone, solvent EP.
------ Room temperature, —— 77°K

are in all cases similar to those at room temperature. This fact is thought to be mainly due to the fact that solutions at 201°K are in the liquid state the same as it is at room temperature.

As for the phenyl carbonyl compounds in Table 1, the $n\rightarrow\pi^*$ bands at 77°K shift to the blue relative to those in the liquid state except for that of isobutyrophenone, the shift of which at 77°K relative to that at room temperature is not clear. This blue-shift in EP may be mainly due to a charge transfer (CT) interaction of the n–π type,[5] to be mentioned later, between an oxygen atom in ethyl ether and phenyl carbonyl compounds, while the blue-shift in EPA may be due to hydrogen-bond formation between carbonyl groups and alcohols, both probably stronger than those in the liquid state.

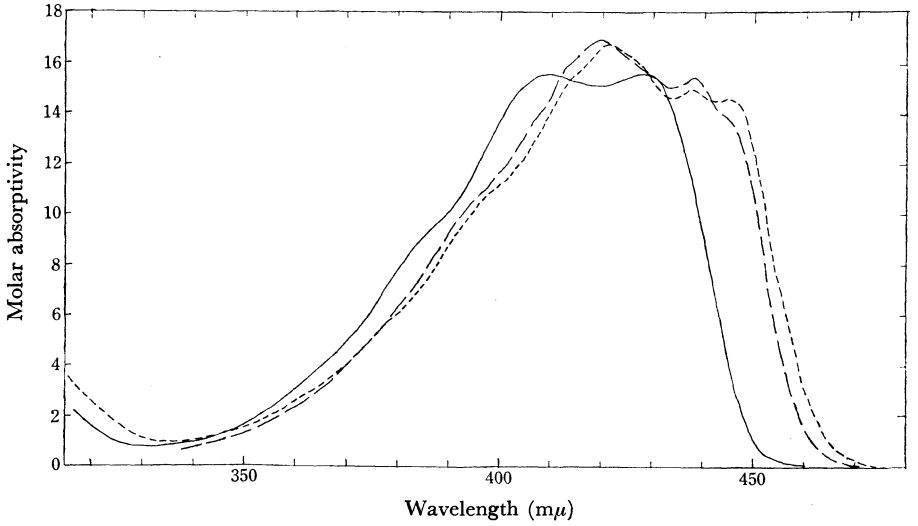

Fig. 6. Diacetyl, solvent EP.
------ Room temperature, —— 201°K, —— 77°K

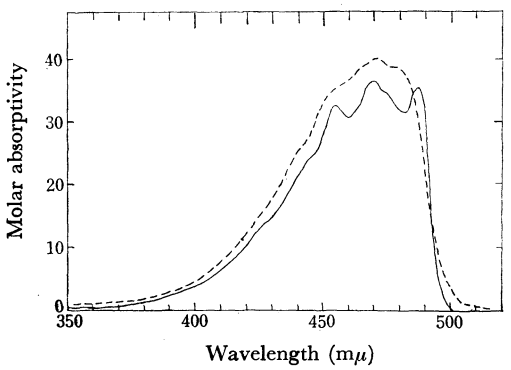

Fig. 7. Camphorquinone, solvent EP.
------ Room temperature, —— 77°K

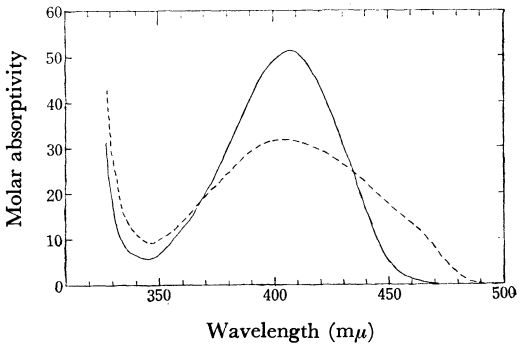

Fig. 8. 1-Phenyl-1,2-propanedione, solvent EP.
------ Room temperature, —— 77°K

5) R. S. Mulliken, *J. Phys. Chem.*, **56**, 801 (1952).

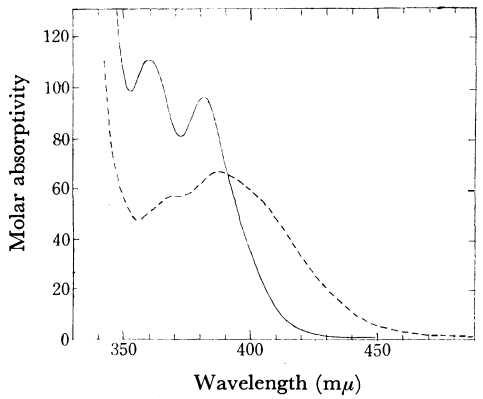

Fig. 9. Benzil, solvent EP.
----- Room temperature, —— 77°K

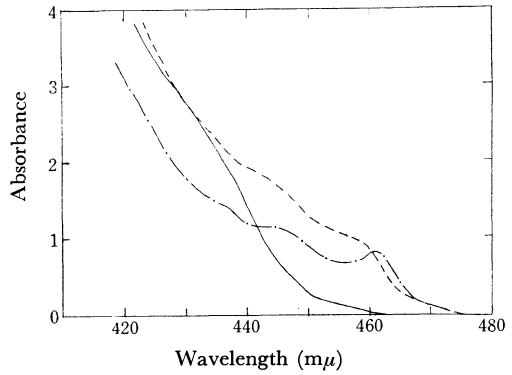

Fig. 10. *N*-Acetylisatin.
—·— *n*-Heptane (Room temperature),
------- EP (Room temperature),
—— EP (77°K),
(The scale of the ordinate is arbitrary.)

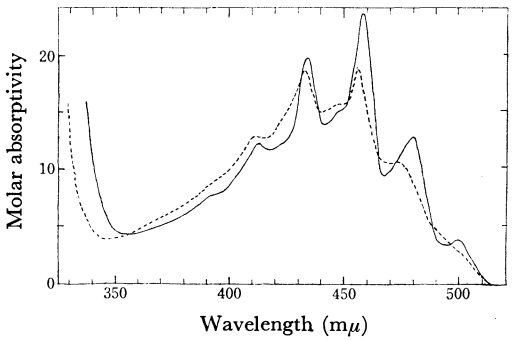

Fig. 11. *p*-Benzoquinone, solvent EP.
----- Room temperature, —— 77°K

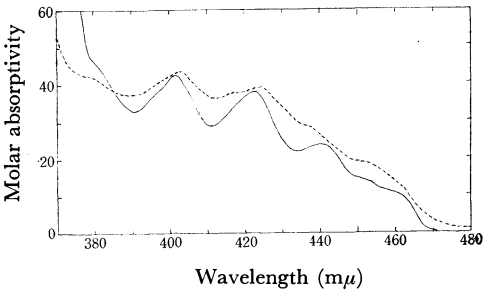

Fig. 12. *α*-Naphthoquinone, solvent EP.
----- Room temperature, —— 77°K

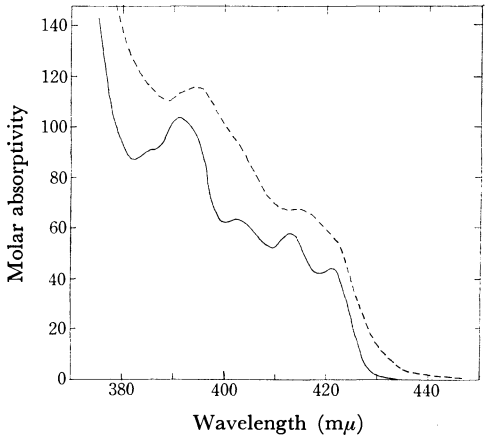

Fig. 13. 2-Methyl-anthraquinone, solvent EP.
----- Room temperature, —— 77°K

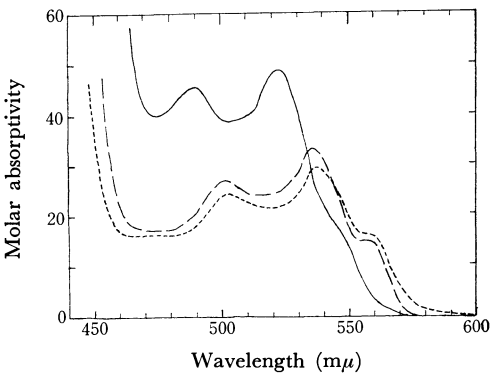

Fig. 14. *β*-Naphthoquinone, solvent EP.
----- Room temperature, —·— 201°K,
—— 77°K

As for the R.I. values in Table 1, a remarkable decrease in the absorption intensity of desoxybenzoin is found in EP and EPA at 77°K, especially in the former, relative to those in the liquid state, as may also be seen in Fig. 4. The strong intensity of the $n \rightarrow \pi^*$ band of benzophenone may be attributed to the mixing of the (n, π^*) state with (π, π^*) states due to the overlapping of the n-orbital of a carbonyl oxygen atom and the π-orbitals of two phenyl groups, because of the non-coplanarity of the benzophenone molecule resulting from steric hindrance between the two phenyl groups. On the other hand, the strong intensity of the $n \rightarrow \pi^*$ band of desoxybenzoin in the liquid state may

TABLE 1. PHENYL CARBONYL COMPOUNDS

		Solvent	$\Delta\bar{\nu}$ (cm^{-1})	IR	Temp. (°K)
(I)	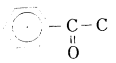	EP	~350	0.80	77
(II)	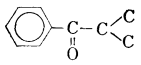	EP	~ 0	1.00	77
		MCH	0	0.98	201
		EP	0	0.95	201
(III)	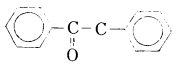	EP	300	0.59	77
		EPA	320	0.70	77
		ME	~480	~0.85	77
		MCH	80	1.10	201
(IV)	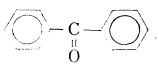	EP	320	1.13	77
		ME	~240	~0.9	77

TABLE 2. α-DIKETONES

		Solvent	$\Delta\bar{\nu}$ (cm^{-1})	IR	Temp. (°K)
(V)	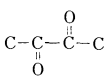	MCH	0	1.02	201
		EP	0	1.00	201
		EP	890	0.89	77
(VI)		EP	− 50		77
		EPA	−100	0.9	77
		ME	−200		77
(VII)	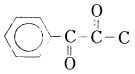	EP	−180	1.11	77
(VIII)	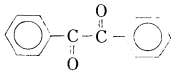	EP	~500	~1.0	77
(IX)	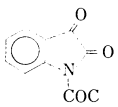	EP	~800		77

TABLE 3. QUINONES

		Solvent	$\Delta\bar{\nu}$ (cm^{-1})	IR	Temp. (°K)
(X)	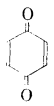	EP	− 50	1.00	201
		EP	− 90	1.0	77
(XI)	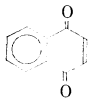	EP	110	0.8	77
		EPA	40	0.8	77
(XII)	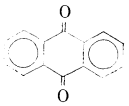	EPA	~120	0.8	77
(XIII)	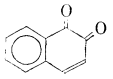	EP	50	1.05	201
		EP	550	~1.5	77

be assumed to be mainly attributable to the mixing of the (n, π^*) state with (π, π^*) states of the non-conjugated phenyl group, due to the overlapping of the n-orbital of the carbonyl oxygen atom and the π-orbitals of the non-conjugated phenyl group; this assumption is based on the facts about α-phenylcarbonyl compounds presented by Kumler *et al.*[6] Therfore, the above-mentioned fact about desoxybenzoin at 77°K may be attributed to the decrease in the overlapping of the oxygen n-orbital and the π-orbitals of the non-conjugated phenyl group in the rigid glass state relative to those in the liquid state.

As for the α-diketones in Table 2, it is noticeable that the $n\rightarrow\pi^*$ bands of diacetyl and *N*-acetylisatin in EP at 77°K shift greatly to the blue relative to those in the liquid state, while the $n\rightarrow\pi^*$ bands of camphorquinone and 1-phenyl-1,2-propanedione shift a little to the red, as may also be seen in Figs. 6, 7, 8, and 10. Such a large blue shift is also found in β-naphthoquinone, as may be seen in Table 3 and Fig. 14. In all the three α-diketones in Table 2 except 1-phenyl-1,2-propanedione and benzil, the two carbonyl groups are assumed to be nearly coplanar. This large blue shift is assumed to be due to a strong CT interaction of the n-π type between ethyl ether in EP on one hand, and α-diketones and β-naphthoquinone on the other hand, in the rigid glass state. In a previous work[2] we found that the $n\rightarrow\pi^*$ bands of *o*-quinones in dioxane at room temperature shift greatly to the blue relative to those in *n*-heptane, while those in ethyl ether shift only a little to the blue. In that work this large blue shift in *o*-quinones in dioxane was attributed to the strong CT interaction of the n-π type between dioxane and *o*-quinones, while the small blue shift in ethyl ether was attributed to a weakening of the CT interaction of the n-π type due to steric hindrance caused by the chains of ethyl ether.

It may be concluded from the theoretical considerations that an oxygen atom in dioxane coordinates itself to some point between two adjacent carbonyl carbon atoms in *o*-quinones in the CT interaction of the n-π type. This conclusion is supported by the results obtained by the X-ray crystal analyses of parabanic acid and chloranil.[7] It may be assumed on the basis of these results that the large blue shift in the α-diketones and β-naphthoquinone in EP mentioned above is due to a strong CT interaction of the n-π type between ethyl ether on the one hand, and α-diketones and β-naphthoquinone on the other hand, at 77°K, an interaction similar to that between dioxane and *o*-quinones at room temperature. This strong CT interaction of the n-π type between ethyl ether and α-diketones and β-naphthoquinone at 77°K is assumed to be ascribable to a weakening of the above-mentioned steric hindrance due to a weakening of thermal motion of the chains of ethyl ether, relative to that in the liquid state.

In camphorquinone a similar strong CT interaction cannot be expected, since the close approach of an oxygen atom in ethyl ether to the carbonyl carbon atoms in camphorquinone is prevented by steric hindrance. Therefore, the small red shift in camphorquinone in EP shown in Table 2 may be due to a reinforced van der Waals interaction between camphorquinone and EP at 77°K relative to that at room temperature. In EPA and ME, a hydrogen bond between camphorquinone and alcohols is assumed to be formed at 77°K as well as in the liquid state. Therefore, the effect of the hydrogen-bond formation on the shift of the $n\rightarrow\pi^*$ band at 77°K in camphorquinone is contrary to that in the phenyl carbonyl compounds shown in Table 1 and may be characteristic of camphorquinone.

As for 1-phenyl-1,2-propanedione and benzil, the molecules are assumed to be greatly twisted about the (O=)C–C(=O) bond due to the strong steric hindrance.[8] Therefore, any CT interaction of the n-π type between EP and 1-phenyl-1,2-propanedione and benzil may be weak. The twisting angles in these molecules in the rigid glass state may be somewhat different from those in the liquid state. At this stage further discussions about their $n\rightarrow\pi^*$ bands cannot be undertaken.

As for the quinones in Table 3, the blue shift at 77°K in α-naphthoquinone and 2-methylanthraquinone may be interpreted in the same manner as that in Table 1, while the red shift at 77°K in *p*-benzoquinone is rather puzzling. In the $n\rightarrow\pi^*$ band of β-naphthoquinone, a large blue shift and a large enhancement of its absorption intensity at 77°K relative to those in the liquid state are found, as is shown in Table 3 and Fig. 14. The former fact has already been discussed together with the situation in α-diketones. The latter fact may be due to the increased mixing of the (n, π^*) state with the low-energy (π, π^*) state at 77°K, where the both states are energetically closer to each other relative to those in the liquid state, as is shown in Fig. 14, because of the large blue shift of the $n\rightarrow\pi^*$ band mentioned before and the red shift of the $\pi\rightarrow\pi^*$ band at the longer wavelengths (the tail of which band may be seen in the figure) at 77°K relative to those in the liquid state.

6) W. D. Kumler, L. A. Strait and E. L. Alpen, *J. Am. Chem. Soc.*, **72**, 1463 (1950).

7) D. R. Davies, J. J. Blum, *Acta Cryst.*, **8**, 129 (1955); S. S. C. Chu, G. A. Jeffrey and T. Sakurai, *ibid.*, **15**, 661(1962).

8) I. Bernal, *Nature*, **200**, 1318 (1963); P. H. Cureton, C. G. Le Fèvre and R. J. W. Le Fèvre, *J. Chem. Soc.*, **1961**, 4447; H. Hirokawa and T. Ashida, *Acta Cryst.*, **14**, 77 (1961).

BULLETIN OF THE CHEMICAL SOCIETY OF JAPAN VOL. 42 16—19 (1969)

Transition Energy Diagram for Solvated Electrons and Its Application to the Interpretation of Their Absorption Spectra

Syozi NODA, Kenji FUEKI and Zen-ichiro KURI

Department of Synthetic Chemistry, Faculty of Engineering, Nagoya University, Chikusa-ku, Nagoya

(Received February 29, 1968)

The energy levels of solvated electrons have been calculated as a function of the static dielectric constant and of the cavity radius on the basis of a continuous dielectric model with an adiabatic approximation, and a contour diagram has been drawn up for the transition energy of solvated electrons. Using this diagram and the observed absorption spectra, the quantities on solvated electrons in alcohols have been estimated. The cavity radius, R, ranges from 0.9 to 1.6 Å, the charge distribution for the ground state, from 2.4 to 3.2 Å, and the variation in cavity radius, from 0.50 to 0.60 Å, at room temperature. From the calculations of the temperature dependence, $d(h\nu)/dt$, of the transition energy, it can be said that, for solvated electrons in alcohols, the contribution to $d(h\nu)/dt$ of the change in R with the temperature is rather more dominant than the change in the static dielectric constant with the temperature. It has also been found that there exists a correlation between the dR/dt value and the ratio of the number of the OH bond to the total number of bonds involved in each alcohol.

The formation of the solvated electron by the action of ionizing radiations on some polar media has been well established in recent years. The electronic absorption spectra of solvated electrons in alcohols and the effect of the temperature on their absorption spectra have been observed by the pulse radiolysis technique.[1,2] The experimental results suggest a simple relationship between the optical transition energy of solvated electrons and the dielectric constant of the medium within a series of alcohols.

On the other hand, the theory of solvated electrons has been developed on the basis of the continuous dielectric model[3] and applied with considerable success to the interpretation of the optical properties of solvated electrons in metal-ammonia solutions,[4] hydrated electrons,[5] and trapped electrons in an organic glass.[6,7]

For the present paper, we have calculated the energy levels of solvated electrons as a function of the static dielectric constant of solvents and of the radius of a cavity in which an electron is located on the basis of a continuous dielectric model with an adiabatic approximation, we have then drawn up a contour diagram for the transition energy of solvated electrons.

Using this diagram and the observed absorption spectra, we have estimated the charge distribution, the cavity radius, and the range of the cavity radii of solvated electrons in alcohols. We have also examined the factors which may be responsible for the temperature dependence of their absorption spectra.

Method of Calculation

Transition Energy of a Solvated Electron. The solvated electron interacts with the polarization filed of the dielectric medium, and the interaction energy is determined by the long-range interaction. The potential function, $V(r)$, in which an electron is bound, is expressed as follows:

$$\left.\begin{aligned} V(r) &= -\beta e^2/r \quad \text{for } r > R, \\ V(r) &= -\beta e^2/R \quad \text{for } r < R, \end{aligned}\right\} \qquad (1)$$

where $\beta = (1/D_{op}) - (1/D_s)$, D_s and D_{op} are the static and optical dielectric constants, and where R is the cavity radius. The reference state is that of a non-polarizing electron located in the medium at an infinite distance from the cavity.

The calculations were carried out using the variation method. The one-parameter wave function used for the ground state was of this form:

$$\psi_{1s} = (\mu^3/\pi)^{1/2} \exp(-\mu r) \qquad (2)$$

The energy of the ground state can be presented by:

1) M. C. Sauer, Jr., S. Arai and L. M. Dorfman, *J. Chem. Phys.*, **42**, 708 (1965).
2) S. Arai and M. C. Sauer, Jr., *J. Chem. Phys.*, **44**, 2297 (1966).
3) J. Jortner, *Mol. Phys.*, **5**, 257 (1962).
4) J. Jortner, *J. Chem. Phys.*, **30**, 859 (1959).
5) J. Jortner, *Radiation Res., Suppl.*, **4**, 24 (1964).
6) K. Fueki, *J. Chem. Phys.*, **44**, 3140 (1966).
7) M. J. Blandamer, L. Shields and M. C. R. Symons, *J. Chem. Soc.*, **1965**, 1127.

$$W_{1s} = \int_v \psi_{1s}[-\hbar^2/8\pi^2 m\nabla^2 + V(r)]\psi_{1s}dv, \quad (3)$$

where ∇^2 is the Laplacian operator.

For a given value of R and β, W_{1s} is obtained as a function of μ. The best value of μ is given by the condition $\partial W_{1s}/\partial\mu=0$. The substitution of this value of μ into (2) and (3) yields the wave function and the energy for the 1s state respectively. The mean radius for the 1s state is given by $r_{1s}=3/2\mu$. The 2p state can be treated in a manner similar to that used for the ground state.

According to the Franck-Condon principle, the value for R and the form of the potential selected for the 2p state are the same as those for the ground state. The energy of the 2p state was calculated using the one-parameter wave function:

$$\psi_{2p} = (\alpha^5/\pi)^{1/2} r\cos\theta\exp(-\alpha r) \quad (4)$$

The mean radius for the 2p state can be presented by $r_{2p}=5/2\alpha$. The electronic polarization energies for the 1s and 2p states are approximately given by:

$$\left.\begin{aligned} S_{1s} &= -(e^2\mu/3)(1-1/D_{op}),\\ S_{2p} &= -(e^2\alpha/5)(1-1/D_{op}). \end{aligned}\right\} \quad (5)$$

Thus, the total energy is obtained as:

and:

$$\left.\begin{aligned} E_{1s} &= W_{1s} + S_{1s},\\ E_{2p} &= W_{2p} + S_{2p}. \end{aligned}\right\} \quad (6)$$

The energy for the 1s→2p transition is given by:

$$h\nu = E_{2p} - E_{1s}, \quad (7)$$

which corresponds to the excitation energy at the absorption maximum.

Temperature Dependence of the Transition Energy. The energy shift presents the difference between the change in the energy of the ground and excited states:

$$d(h\nu)/dt = dE_{2p}/dt - dE_{1s}/dt, \quad (8)$$

where t is the temperature.

The temperature coefficient of the 1s state is obtained in the form:

$$\frac{dE_{1s}}{dt} = \left[\frac{\partial E_{1s}}{\partial\beta} - \left(\frac{\partial S_{1s}}{\partial\mu}\right)\left(\frac{\partial^2 W_{1s}/\partial\beta\partial\mu}{\partial^2 W_{1s}/\partial\mu^2}\right)\right]\left(\frac{d\beta}{dt}\right) + \left[\frac{\partial E_{1s}}{\partial R} - \left(\frac{\partial S_{1s}}{\partial\mu}\right)\left(\frac{\partial^2 W_{1s}/\partial R\partial\mu}{\partial^2 W_{1s}/\partial\mu^2}\right)\right]\left(\frac{dR}{dt}\right) \quad (9)$$

The temperature coefficient for the 2p state is given by Eq. (9) with E_{2p} substituted for E_{1s}, S_{2p} substituted for S_{1s}, and α substituted for μ. For a given value of R and β, dE_{1s}/dt and dE_{2p}/dt are presented by:

$$dE_{1s}/dt = a_1(d\beta/dt) + b_1(dR/dt), \quad (10)$$

and:

$$dE_{2p}/dt = a_2(d\beta/dt) + b_2(dR/dt), \quad (11)$$

where E is expressed in eV, where R is expressed in Å, and where a_1, b_1 and a_2, b_2 are defined by Eq. (9) and the corresponding equation for the 2p state respectively. From Eq. (8) we obtained:

$$d(h\nu)/dt = a(d\beta/dt) - b(dR/dt), \quad (12)$$

where $a=a_2-a_1$ and where $b=b_2-b_1$.

The temperature dependence of the energy levels and of the transition energy may thus be attributed to the temperature dependence of the properties of the dielectric medium which are roughly expressed by the temperature dependence of D_s and D_{op}, and to the temperature dependence of the mean cavity radius.

Results and Discussion

Transition Energy Diagram. The transition energy, $h\nu$, of a solvated electron is dependent on β and R. Since the optical dielectric constant, D_{op}, of any substance is not different from 2, we use a constant value, 2, for D_{op} in the calculation of $h\nu$, so that we may deal with the problem in a systematic way. Thus, we can construct a transition energy diagram by calculating $h\nu$ as a function of D_s and R.

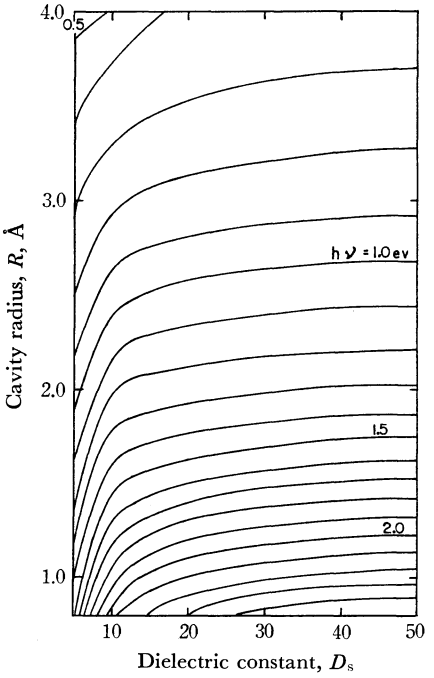

Fig. 1. Transition energy diagram for solvated electrons.

Figure 1 shows the calculated transition energy diagram, in which the contour lines for $h\nu$ are drawn every 0.1 eV, and where D_s the values range from 5 to 50 and the R values, from 0.8 to 4 Å. The results for high D_s values and the very small R values are not included in the diagram because the adiabatic approximation is less satisfactory for these cases. The adiabatic approximation is more

satisfactory for low D_s values and large R values because the binding energy of a solvated electron is small in such cases.

Solvated Electrons in Alcohols. From the transition energy diagram and the observed absorption spectra, the quantities of solvated electrons in alcohols at room temperature are obtained; they are given in Table 1.

Table 1. Charge distribution, the mean cavity radius, and the range of cavity radius of solvated electrons in alcohols at room temperature

Substance	$D_s^{25°C}$	$h\nu_{max}$ [1,2] (eV) (obs.)	$\bar{r}_{1s}$ (Å)	$\bar{r}_{2p}$ (Å)	R (Å)	$\pm\Delta R$ (Å)
Methanol	32.6	1.97	2.65	5.75	1.15	0.53
Ethanol	24.4	1.77	2.88	5.95	1.32	0.60
n-Propanol	20.8*	1.67	3.00	6.02	1.40	0.54
Iso-propanol	17.7	1.51	3.19	6.25	1.60	0.50
n-Butanol	17.1	1.80	2.83	6.10	1.20	0.60
Ethylene glycol	38.7*	2.14	2.54	5.68	1.03	0.50
Glycerol	42.5	2.35	2.40	5.62	0.90	0.50

* 20°C

In Table 1, $\bar{r}_{1s}$ and $\bar{r}_{2p}$ are the mean radii for the 1s and 2p states respectively, R is the mean cavity radius, and ΔR is the range of the cavity radius, which will be discussed below.

Transition Energy and Cavity Radius. It can be seen from Table 1 that the mean cavity radius for solvated electrons in alcohols is 0.9—1.6 Å*1 and that the mean radius of the solvated electron orbitals for the ground state is 2.4—3.2 Å.

The mean cavity radius is plotted against the transition energy in Fig. 2. It may be seen that there is a correlation between the cavity radius and the transition energy. The transition energy increases with a decrease in the cavity radius. The cavity radius decreases with an increase in the static dielectric constant for all these alcohols except *n*-butanol (Fig. 3).

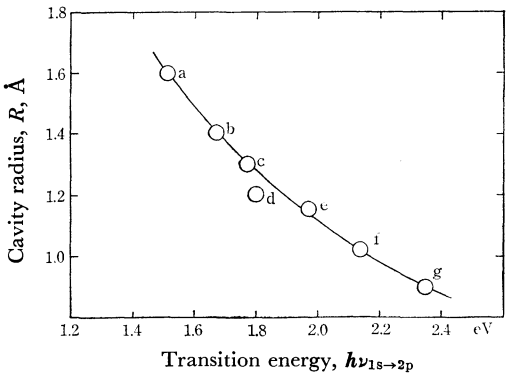

Fig. 2. Relation between the cavity radius and the transition energy for solvated electrons in alcohols.
a: isopropanol, b: *n*-propanol, c: ethanol, d: *n*-butanol, e: methanol, f: ethylene glycol, g: glycerol.

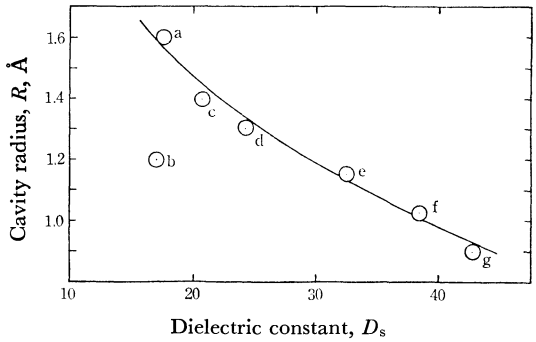

Fig. 3. Relation between the activity radius and the static dielectric constant for solvated electrons in alcohols.
a: isopropanol, b: *n*-butanol, c: *n*-propanol, d: ethanol, e: methanol, f: ethylene glycol, g: glycerol.

Absorption-band Width and the Range of the Cavity Radius. It is well known that the solvated electron exhibits a braod absorption spectrum. The high-energy side of the absorption band may be interpreted in terms of the transition of the solvated electron to higher excited states and an energy continuum as well as in terms of the broadening of the band due to variations in cavity size. On the other hand, the side with an energy lower than the band maximum is explicable only in terms of the broadening of the band due to various cavity sizes as long as the band maximum is interpreted as arising from the 1s→2p transition.

Table 2. Absorption band width and the range of cavity radius of solvated electrons at different temperatures

Temp.	Substance	$h\nu_{max}$ [1,2,7] (eV) (obs.)	$\Delta(h\nu)$ [1,2,7] (eV) (obs.)	R (Å)	$\pm\Delta R$ (Å)
25°C	Methanol	1.97	0.45	1.15	0.53
	Ethanol	1.77	0.45	1.32	0.60
	n-Butanol	1.80	0.44	1.20	0.60
− 78°C	Methanol	2.17	0.41	1.07	0.38
	Ethanol	2.18	0.50	1.05	0.47
	n-Butanol	2.28	0.53	0.90	0.50
−196°C	Methanol	2.41	0.27	0.89	0.23
	Ethanol	2.41	0.35	0.88	0.35
	n-Butanol	2.47	0.48	0.83	0.48

*1 It should be noted that, since the optical dielectric constants of methanol and ethanol are lower than 2 by about 10% the cavity radii for these alcohols will be found to be larger by about the same degree than those in Table 1 if the exact optical dielectric constants are used in these calculations.

TABLE 3. TEMPERATURE EFFECT ON THE TRANSITION ENERGY OF SOLVATED ELECTRONS IN ALCOHOLS

Substance	$d(h\nu)/dt$ (eV/deg) (obsd)[2]	$[d(h\nu)/dt]_I$ (eV/deg) (calcd)	$[d(h\nu)/dt]_{II}$* (eV/deg) (calcd)	dR/dt (Å/deg)	$\frac{[d(h\nu)/dt]_I}{d(h\nu)/dt}$
Methanol	-2.2×10^{-3}	-0.44×10^{-3}	-1.76×10^{-3}	1.5×10^{-3}	0.20
Ethanol	-3.4×10^{-3}	-0.41×10^{-3}	-2.99×10^{-3}	2.9×10^{-3}	0.12
Isopropanol	-3.5×10^{-3}	-0.60×10^{-3}	-2.90×10^{-3}	3.3×10^{-3}	0.18
n-Butanol	-4.5×10^{-3}	-0.77×10^{-3}	-3.73×10^{-3}	3.4×10^{-3}	0.17

* $[d(h\nu)/dt]_{II} = d(h\nu)/dt - [d(h\nu)/dt]_I$

Thus, the absorption-band width can be related to the cavity radius, which may be represented by the half-height width, ΔR, measured towards the low-energy side.

The values of ΔR for solvated electrons in alcohols at room temperature are given in Table 1. The effect of the temperature on ΔR is shown in Table 2. It can be seen from Table 2 that the range of the cavity radius decreases with a decrease in the temperature. It can also be seen that ΔR increases as the alkyl group in alcohols becomes bulky; this tendency is most clearly manifested at -196°C.*2

If the broadening of the absorption band towards the low-energy side is ascribed to the transition of solvated electrons in larger cavities, the photobleaching of these electrons by light with a selected energy limit will result in the blue shift of the absorption spectrum. Further experimental studies along this line are needed to substantiate such an interpretation.

Effect of Temperature on the Transition Energy. The calculated temperature dependence of the transition energies of solvated electrons in alcohols is given in Table 3, together with the observed one.

In these calculations the temperature dependence of β is presented approximately by $d\beta/dt = (1/D_s)\, d(\ln D_s)/dt$, since the temperature dependence of D_{op} is much smaller than that of D_s. The temperature coefficient of D_s is taken from the experimental data.

*2 Since there are no available data on D_s at -196°C, we have used the values of D_s at -78°C in the calculations at -196°C. This approximation is possible because the transition energy is relatively insensitive to the value of D_s for high D_s values (see Fig. 1) and because D_s is high enough to satisfy this requirement for alcohols at -78°C.

In Table 3, $[d(h\nu)/dt]_I$ and $[d(h\nu)/dt]_{II}$ represent the contribution to $d(h\nu)/dt$ of the changes in D_s and in the mean cavity radius with the temperature respectively. The contribution of the former to $d(h\nu)/dt$ is 20% at most, as is shown in the last column of the table. The calculated dR/dt is also given in Table 3. In Fig. 4 the value of dR/dt is plotted against the ratio of the number of the OH bond to the total number of bonds involved in each alcohol. There is a correlation

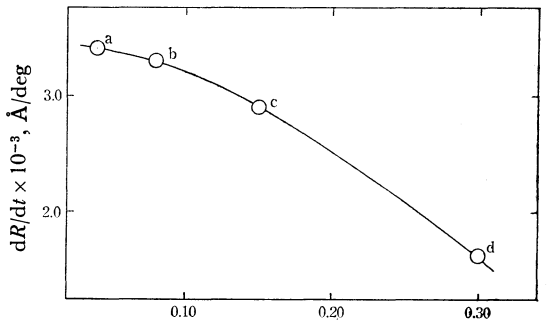

Fig. 4. Dependence of dR/dt on the ratio of the number of the OH bond to the number of bonds involved in each alcohol.
a: *n*-butanol, b: isopropanol, c: ethanol, d: methanol.

between these quantities, probably indicating a relation between the expansion of a cavity and the strength of such intermolecular interactions as hydrogen bonding.

It may be concluded that the temperature dependence of the transition energy of solvated electrons in alcohols is mainly attributable to the change in the cavity size with the temperature.

BULLETIN OF THE CHEMICAL SOCIETY OF JAPAN VOL. 42 20—24 (1969)

Studies of the Precipitation of Humic Acid by Cationic Polyelectrolytes

Hiroshi KUMANOMIDO

Resources Research Institute, Kotobuki-cho, Kawaguchi-shi, Saitama

(Received March 13, 1968)

In order to elucidate the mechanism of the precipitation of humic acid by two cationic polyelectrolytes, the *n*-butylamine-epichlorohydrin condensation polymer (BECP) and the cyclohexylamine-epichlorohydrin condensation polymer (CECP), electrophoresis and conductometric titration were made in conjunction with precipitation experiments in various concentrations of humic acid with an optimum dosage of cationic polyelectrolyte. The results of these experiments indicated that a cationic polyelectrolyte precipitates the humic acid by combining stoichiometrically with the negatively-charged groups of the humic acid. A possible mechanism for the precipitation was proposed schematically on the basis of the experimental results obtained.

Many previous studies[1-7] of the interaction between surface active agents and proteins have shown that precipitation takes place when they are oppositely charged. Thus, the electrostatic force between their opposite charges is considered to be responsible for the precipitation. However, only a few studies[8,9] have been reported on the interaction between polyelectrolytes with opposite charges.

Previously the present author[10] studied the precipitation of humic acid by cationic polyelectrolytes and found that some cationic polyelectrolytes are excellent precipitants for humic acid, and that the characteristics for the precipitation of humic acid with these cationic polyelectrolytes quite differ from those observed with inorganic salts($BaCl_2$, $Al_2(SO_4)_3$, *etc.*) or with a low-molecular-weight organic cation (*e. g.*, *p*-toluidine hydrochloride).

The present study intends to clarify the mechanism of the precipitation of humic acid with two cationic polyelectrolytes, the *n*-butylamine-epichlorohydrin condensation polymer (BECP) and the cyclohexylamine-epichlorohydrin condensation polymer (CECP).

The relationship between the humic acid concentration and the cationic polyelectrolyte dosage in the precipitation region is investigated in terms of conductometric titration and electrophoresis as well as the transmittance of the test solution.

Experimental

Humic Acid. To 500 g of −149 μ-size Nakayama-lignite, containing 7.92% ash and 10.09% moisture, 1*l* of a 5% aqueous solution of hydrogen peroxide was added; the mixture was then allowed to stand at room temperature (about 20°C). After 24 hr, the lignite was filtered, washed with distilled water, and dried at 107°C for 5 hr. Humic acids prepared by the oxidation of lignite were extracted by the digestion of the oxidized lignite with 5% ammonia water. The aqueous alkali extracts were filtered and boiled in a water bath in order to remove the excess ammonia, and then purified by the use of electrodialysis. The humic acid thus purified was filtered, dried, and dissolved in a sodium hydroxide solution. The aqueous solution of sodium humate of 2 g/*l* in a concentration of pH 7 was prepared as a stock solution and was used throughout the present studies.

The relationship between the concentration and the transmittance of the aqueous solution of sodium humate at pH 7 is illustrated in Fig. 1. The transmittance was measured using a photoelectric colorimeter (Model 7A of the Tokyo Photo-Electric Co., Ltd.) with an 18-mm light path and a 420-mμ filter.

The analyses of purified humic acid are shown in Table 1. The COOH equivalent and the phenolic-OH equivalent of humic acid were determined according to the methods of Higuchi and Shibutani.[11]

Cationic Polymers. As cationic polymers, BECP and CECP were synthesized. The reactions between amines and epichlorohydrin have been studied exten-

1) F. W. Putnum and H. Neurath, *J. Am. Chem. Soc.*, **66**, 692 (1944).
2) I. M. Klotz, *ibid.*, **68**, 2299 (1946).
3) C. F. Hiskey and T. A. Downey, *J. Phys. Chem.*, **58**, 835 (1954).
4) T. Kondo and K. Meguro, *Kagaku no Ryoiki* (*J. Japanese Chemistry*), **12**, 878 (1958).
5) K. Aoki, *J. Am. Chem. Soc.*, **80**, 4904 (1958).
6) K. Aoki and J. Hori, *ibid.*, **81**, 1885 (1959).
7) T. Isemura, F. Tokiwa and S. Ikeda, This Bulletin, **35**, 240 (1962).
8) R. Senzyu, *ibid.*, **25**, 131 (1952).
9) M. E. Wadsworth and I. B. Cutler, *Mining Engr.*, **8**, 830 (1956).
10) H. Kumanomido, *Kogyo Yosui*, No. 104, 20 (1967); No. 105, 58, 62 (1967); No. 106, 9 (1967); No. 108, 14 (1967); No. 110, 37 (1967).
11) K. Higuchi and H. Shibutani, *Nenryo-Kyokai-shi* (*J. Fuel Soc. Japan*), **33**, 366 (1954).

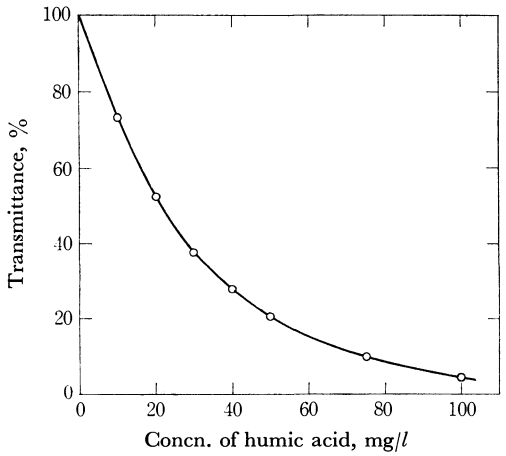

Fig. 1. Relationship between the concentration and the transmittance of the aqueous solution of humic acid.

TABLE 1. ANALYSES OF HUMIC ACID

C %	H %	N %	COOH equiv. g/equiv.	Phenolic-OH eqiuv. g/equiv.	Ash %	Moisture %
58.09	3.05	5.04	288	543	0.93	3.30

sively,[12-18] and it is widely recognized that the structure of monoamine-epichlorohydrin condensation polymers can be represented as follows:

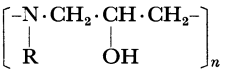

R: butyl or cyclohexyl radical

One mole of epichlorohydrin was poured slowly, with vigorous stirring, into a 200-m*l* flask containing 1 mol of *n*-butylamine or cyclohexylamine and 25 g of water. The mixture was then heated under reflux in a boiling-water bath. After 5 hr of heating, 1 mol of an aqueous solution of sodium hydroxide was added to the mixture, after which heating was continued for an additional 5 hr. The condensation polymer isolated from the reaction mixture by adding sodium hydroxide was washed with hot water, dissolved in benzene, and then washed with water until free from chloride ions; finally, the benzene was evaporated off.

The two condensation polymers obtained were dissolved in a stoichiometric hydrochloric acid solution to a concentration of 50 g/*l*.

12) W. Davies and W. E. Savige, *J. Chem. Soc.*, **1950**, 890.
13) R. F. Homer, *ibid.*, **1950**, 3690.
14) M. Sugihara, *Kagaku to Kogyo* (*Sci. and Ind.*), **28**, 44 (1954).
15) R. Wegler, *Angew. Chem.*, **67**, 582 (1955).
16) L. Shechter and J. Wynstra, *Ind. Eng. Chem.*, **48**, 94 (1956).
17) F. J. Allen and W. M. Hunter, *J. Appl. Chem.*, **7**, 86 (1957).
18) D. L. Heywood and B. Phillips, *J. Am. Chem. Soc.*, **80**, 1257 (1958).

The molecular weights of the polymers, determined by means of the cryoscopic method using a benzene solution, were 3080 for BECP and 1720 for CECP.

Nonionic and Anionic Polymers. The following nonionic and anionic polymers were used:

Nonionic polymers: Polyacrylamide, Polyvinylpyrrolidone, Polyvinyl alcohol, Polyethyleneglycol.

Anionic polymers: Polyacrylic acid, Urea-formaldehyde condensation polymer.

The analytical grades of these samples were satisfactory for use as delivered.

Precipitation Procedure. A calculated amount of an aqueous polymer solution was poured into an aqueous solution (20 m*l*) of sodium humate placed in a test tube. Immediately after the addition, the test tube was turned upside-down twenty times at equal time intervals. After it had then been left to stand for 30 min, the solution was filtered through No. 5C filter paper; then the transmittance of the filtrate was measured by the photoelectric colorimeter described above.

The transmittance of the filtrate was utilized as a convenient measure for representing the precipitation of humic acid, because the precipitate, which increases the transmittance of the filtrate, could be removed by filtration.

The dispersing power of cationic polymers for the humic acid precipitated was studied as follows:
An appropriate amount of an aqueous solution of the cationic polymer was added to the humic acid precipitate obtained with an optimum dosage of the cationic polymer. The mixture in a test tube was violently shaken, left to stand for 30 min, and filtered, and the transmittance of the filtrate was measured.

Conductometric Titration. The change in the electric conductivity of the aqueous solution (100 m*l*) of 1 g/*l* sodium humate upon the drop-by-drop addition of a cationic polymer solution (50 g/*l* in concentration) was measured with a conductometric titrator (Model CT-2 of the Shimadzu Seisakusho, Ltd.); at the same time, the precipitation curve of the humic acid - cationic polymer system was determined in a way previously described.

Electrophoresis. A calculated amount of an aqueous polymer solution was poured into an aqueous solution (100 m*l*) of 0.5 g/*l* sodium humate placed in a measuring cylinder. Immediately after the addition, the cylinder was turned upside-down thirty times and then left to stand for 30 min. The electrophoresis of the humic acid in the mixture was qualitatively observed using a U-tube. At the same time, a part of the mixture was filtered, and the transmittance of the filtrate was measured by means of the photoelectric colorimeter described above.

Results and Discussion

The Precipitation of Humic Acid with Water-soluble Polymers. It was found that the precipitation of humic acid occurs only by means of cationic polymers, not by means of nonionic or anionic polymers. The results obtained with two cationic polymers, BECP and CECP, are illustrated in Fig. 2. It is seen that the precipitation of humic acid occurs only within a particular range of concentration of cationic polymers; that

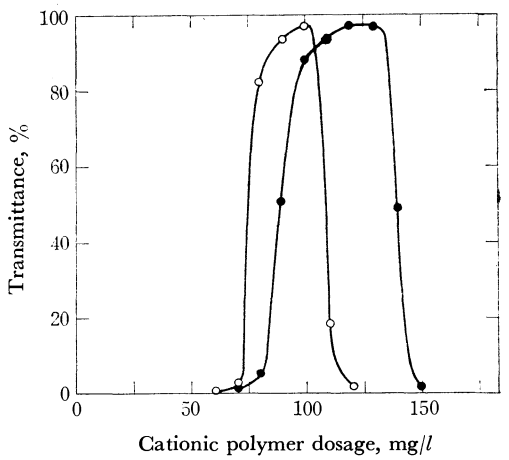

Fig. 2. The precipitation of humic acid by cationic polymers.
Concn. of humic acid: 200 mg/*l*
—○— BECP, —●— CECP

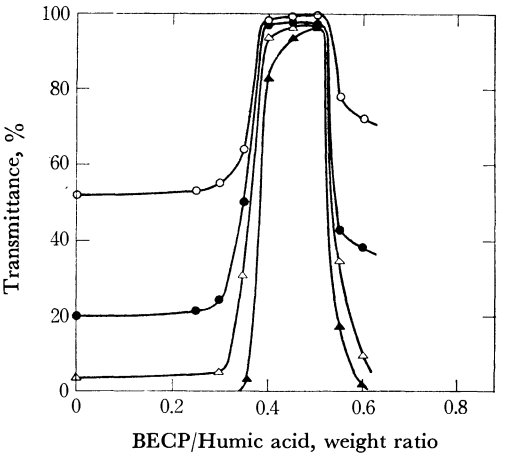

Fig. 3. The precipitation of humic acid by BECP at various concn. of humic acid.
Concn. of humic acid: —○— 20 mg/*l*, —●— 50 mg/*l*, —△— 100 mg/*l*, —▲— 200 mg/*l*

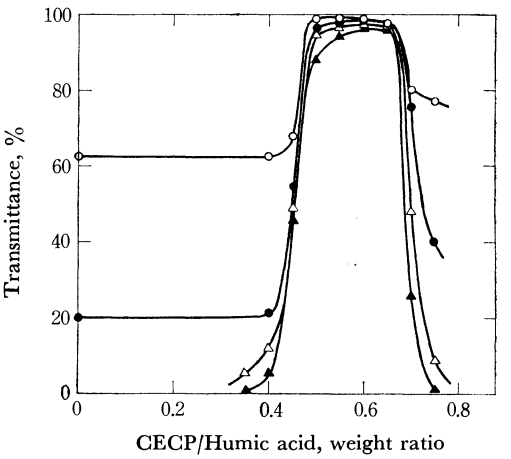

Fig. 4. The precipitation of humic acid by CECP at various concn. of humic acid.
Concn. of humic acid: —○— 20 mg/*l*, —●— 50 mg/*l*, —△— 100 mg/*l*, —▲— 200 mg/*l*

is, a sharp decrease in precipitating efficiency is observed with excess dosages of cationic polymers. The humic acids once precipitated with cationic polymers were not dispersed by an excess of cationic polymers.

The characteristics of precipitation in the system of humic acid-water soluble polymers are similar to those observed in the system of proteins-surface active agents, except that the proteins precipitated with surface active agents are dispersed by the addition of more of those surface active agents. Also, we know various systems of colloid-water-soluble polymers in which coagulation takes place in a way similar to that observed in the present experiment.

It may be suggested that the precipitation of humic acid with cationic polymers is caused, as in the other examples of colloidal coagulation, by electrostatic interaction between anionic sites of humic acid and cationic sites of cationic polymers. The following experimental results give further support to this idea.

Relation between Initial Humic Acid Concentration and Optimum Cationic Polymer Dosage. The effect of a variation in the cationic polymer dose on the precipitation of a given amount of humic acid was studied at four different humic-acid concentrations (20, 50, 100, and 200 mg/*l*) at room temperature.

The results obtained are illustrated in Figs. 3 and 4. The abscissa in Figs. 3 and 4 represent the weight-mixing ratio of the cationic polymer to humic acid. The following characteristics may be observed in these figures (Figs. 3 and 4).

(1) Precipitation occurs only over a narrow weight-ratio range of humic acid and cationic polymers, and the range seems to be independent of the initial concentration of humic acid studied; that is, the precipitation of humic acid with a cationic polymer is stoichiometric.

(2) The precipitation of humic acid by BECP occurs in the range of the weight-mixing ratio between 0.35 and 0.55, as is shown in Fig. 3. Since the ratio of the cationic group equivalent (g/equiv.) of BECP to the carboxyl group equivalent (g/equiv.) of humic acid is 0.45, we may infer that the midpoint of the precipitation range corresponds to the point where the number of the cationic group is equal to that of the carboxylic group in the solution. Similar results are observed with CECP. These facts imply that cationic polymers act to precipitate humic acid by combining stoichiometrically with the negatively-charged carboxyl groups of humic acid.

Conductometric Titration. The results obtained with BECP and with CECP are illustrated in Figs. 5 and 6 respectively. It may be noted in Figs. 5 and 6 that there is a break point in the titration curves, the composition of which nearly coincides with that of the optimum precipitation.

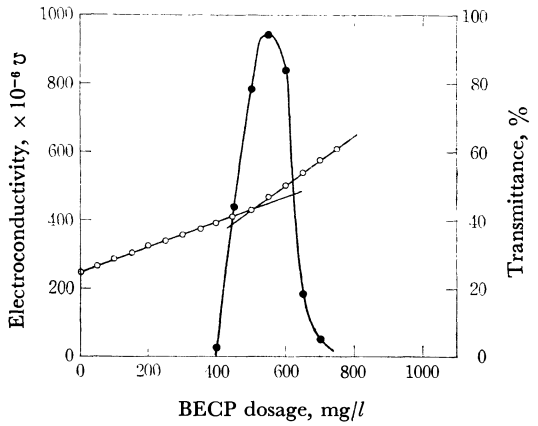

Fig. 5. Relationship between electroconductivity and precipitation in the system humic acid-BECP.
Concn. of humic acid: 1 g/l
—○— electroconductivity
—●— transmittance

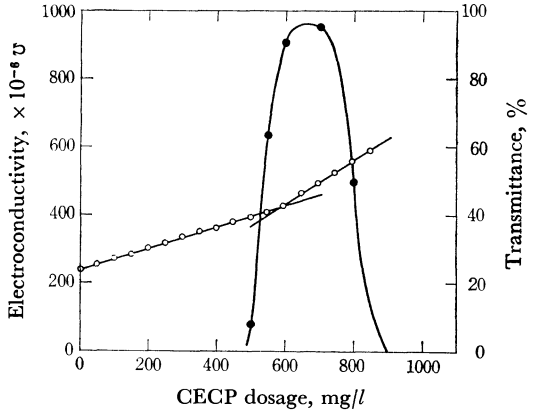

Fig. 6. Relationship between electroconductivity and precipitation in the system humic acid-CECP.
Concn. of humic acid: 1 g/l
—○— electroconductivity
—●— transmittance

The results suggest that the precipitation of humic acid occurs as a result of the neutralization of carboxyl groups with a cationic polymer, with a consequent loss of the charge of binding sites.

Electrophoresis. The results obtained with BECP and CECP are summarized in Tables 2 and 3. It is apparent from these tables that the humic acid is negatively charged in the absence of a cationic polymer, that a reversal of charge occurs when the latter reaches a certain concentration, and that optimum precipitation occurs in the narrow range in which the charge of humic acid changes from negative to positive. The decrease in the precipitating efficiency for excess dosages of cationic polymers is caused by a reversal of the charge of humic acid, leading to an increase in the hydrophilic property of humic acid (humic acid-cationic polymer complexes). The phenomena described above in the humic acid-cationic polymer system may be the same as the flocculation-dispersion phenomena in the colloid-polyelectrolyte system, which has opposite charges.

Table 2. Electrophoresis of humic acid-BECP mixtures

BECP added (mg/l)	Precipitation of humic acid	Transmittance of filtrate	Charge on humic acid
0			−
5			−
10			−
15		1.0	−
17.5		3.0	
20	precipitation	41.4	
22.5	precipitation	84.2	
25	precipitation	96.2	
27.5		67.0	
30		5.0	+
32.5		1.0	+
35			+

Table 3. Electrophoresis of humic acid-CECP mixtures

CECP added (mg/l)	Precipitation of humic acid	Transmittance of filtrate	Charge on humic acid
0			−
5			−
10			−
15			−
20		2.9	−
22.5		18.3	
25	precipitation	67.3	
27.5	precipitation	90.0	
30	precipitation	95.3	
32.5	precipitation	96.4	
35		80.0	
37.5		11.2	+
40		3.1	+
45			+

The Mechanism of Precipitation

Humic acids and cationic polymers possess a number of ionized sites on the molecule; for example, the number of cationic groups per molecule

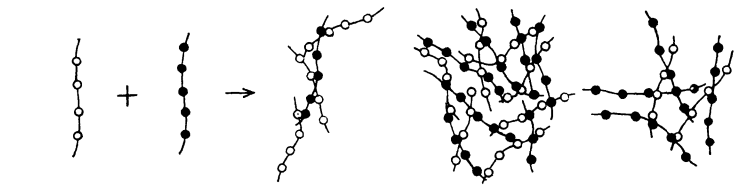

Fig. 7. The precipitation of humic acid by cationic polyelectrolyte.

of BECP is about 24 when the molecular weight is 3080, and that of CECP is about 11 when the molecular weight is 1720. Therefore, it appears to be general true that humic acids may be bridged together by cationic polymers as a result of electrostatic interaction between the carboxyl groups of a humic acid and the cationic groups of a cationic polymer; that is, precipitation is caused by the formation of hydrophobic complexes by a bridging mechanism similar to the polymer-bridging mechanism[19-21] for the flocculation of colloidal suspensions.

Consideration of all of the results obtained in this study leads to the conclusion that the precipitation of humic acid by a cationic polymer is caused by electrostatic and stoichiometric interaction between the anionic sites of humic acid and the cationic sites of the cationic polymer, leading to the formation of salt-like complexes by means of a bridging mechanism. Thus, the precipitation of humic acid by a cationic polymer may be represented schematically as is shown in Fig. 7.

The author wishes to express his gratitude to Professor Tsunetaka Sasaki of Tokyo Metropolitan University and Professor Rhohei Matsuura of Kyushu University for their many valuable discussions. The author also wishes to thank Dr. Michihiro Noda of this Institute for his many valuable discussions and for the help given during the course of this study.

19) A. S. Michaels, *Ind. Eng. Chem.*, **46**, 1485 (1951).
20) M. F. McCarty and R. S. Olson, *Mining Engr.*, **11**, 61 (1959).
21) M. Noda, *Nippon Kagaku Zasshi* (*J. Chem. Soc. Japan, Pure Chem. Sect.*), **82**, 1611 (1961).

BULLETIN OF THE CHEMICAL SOCIETY OF JAPAN VOL. 42 25—35 (1969)

Studies of the Transient Intermediates of a Thiopyronine Aqueous Solution under Flash Excitation

Masaharu MORITA*1 and Shunji KATO

Institute of Chemistry, College of General Education, Osaka University, Toyonaka, Osaka

(Received March 18, 1968)

Flash photolytic studies of the transient intermediates produced in the flash excitation of an aqueous buffered solution of the photosensitizing dye "thiopyronine" were undertaken in order to obtain direct insight into the reaction mechanism of the photosensitizing action of the dye. As had been expected from the structural similarity to a well-known photosensitizer, methylene blue, previously reported on, the flash excitation of thiopyronine, in a deaerated buffered solution at pH 7.4 without any substrate, produced three transient intermediates: a triplet-state (D^t), a half-oxidized form (Oxd), and a half-reduced form or semiquinone (Red) of the dye. Red and Oxd were generated simultaneously through electron tansfer reactions, *i. e.*, $D^t + D^t \rightarrow Red + Oxd$ and $D^t + D \rightarrow Red + Oxd$, where D is the dye in the ground state. Thiopyronine solutions containing some reducing and oxidizing agents were studied in order to identify the intermediates. The absorption spectra of these intermediates were identified, and their reaction mechanism studied. The rate constants of some elementary processes obtained are:

$$\begin{aligned}
D^t &\longrightarrow k_1 = 2.3_6 \times 10^3\ sec^{-1} \\
D^t + D^t &\longrightarrow k' = 7.6_9 \times 10^8\ M^{-1}sec^{-1} \\
D^t + D &\longrightarrow k'' = 7.6_9 \times 10^8\ M^{-1}sec^{-1} \\
Red + Red &\longrightarrow k_6 = (1—2) \times 10^9\ M^{-1}sec^{-1} \\
Oxd &\longrightarrow k_7 = (1—3) \times 10^3\ sec^{-1} \\
D^t + EDTA &\longrightarrow k_8 = 1.6 \times 10^7\ M^{-1}sec^{-1} \\
D^t + ATU &\longrightarrow k_9 \approx \text{small} \\
Oxd + ATU &\longrightarrow k_{10} = (2—5) \times 10^6\ M^{-1}sec^{-1}.
\end{aligned}$$

The high efficiency of thiopyronine in its photodynamic effect was discussed in connection with the high quantum yield of triplet-state production and the high reversibility of the photochemical redox reaction of the dye.

Thiopyronine (I) is an efficient photosensitizing dye; it has a structure similar to that of the well-known photosensitizer, methylene blue (II).

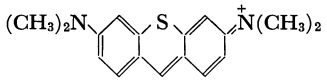

(I)

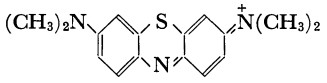

(II)

Recently, investigations of the photodynamic effect of thiopyronine, as a photosensitizer, on various systems, such as bacterium, virus, nucleic acids, and their base components, have been reported by several authors, and the reaction mechanisms have been discussed.[1] However, all these investigations have been performed by steady-light illumination and were concerned only with the product analysis of the reaction or with physicochemical changes in the irradiated systems.

A more direct investigation of the intermediates is now necessary in order to elucidate the reaction mechanism.

Flash photolytic studies of the transient intermediates in the photoreduction of methylene blue

*1 Present address: Department of Chemistry, Faculty of Science, Nagoya University, Chikusa, Nagoya.

1) K. Herzberg, K. Reuss and R. Dahn, *Naturwissenschaften*, **10**, 376 (1963); A. Wacker, G. Türck and A. Gerstenberger, *ibid.*, **10**, 377 (1963); A. Wacker, H. Dellweg, L. Träger, A. Kornhauser, E. Lodeman, G. Türck, R. Selzer, P. Chandra and M. Ishimoto, *Photochem. Photobiol.*, **3**, 369 (1964); J. S. Bellin and L. I. Grossman, *ibid.*, **4**, 45 (1965); H. Dellweg and W. Oprée, *Biophysik*, **3**, 241 (1966); E.-R. Lochmann, *ibid.*, **3**, 300 (1967); E.-R. Lochmann, *Z. Naturforschg.*, **22b**, 196 (1967).

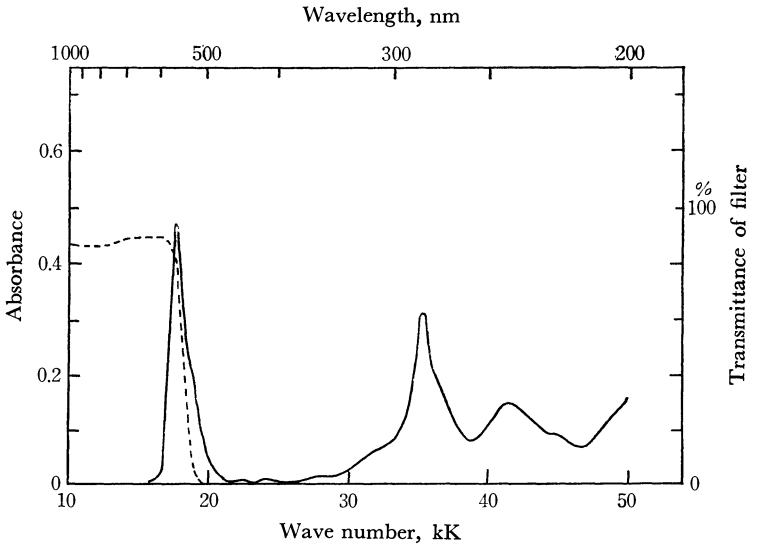

Fig. 1. Absorption spectrum of thiopyronine in buffered solution at pH 7.4; Dye concn. 6.4 μM. Optical path 1.0 cm. Broken line: Transmittance of the orange glass filter (Hoya Crystal Co., 0-54) used.

and thionine have been reported previously by the present authors.[2] That paper reported that the triplet-state of methylene blue produced by flash excitation interacts with the ground-state dye, producing semiquinone and a half-oxidized form.

This is an essential process in the photoreduction of methylene blue in a deaerated phosphate buffered solution in the absence of any reducing agent. A similar result obtained for thionine shows that the photochemical self redox reactions of these dyes take place readily.[3]

The photosensitizing efficiency of dyes has been discussed in connection with their photochemical redox reversibility.[4]

It will be interesting to investigate the correlation between the photosensitizing ability and the photochemical redox properties of these dyes from the point of view described above.

Also, it is expected that thiopyronine has a photochemical redox property similar to that of methylene blue, for the molecular structures are similar, and both have high photosensitizing powers. Thus, the flash photolytic investigation of thiopyronine was undertaken in order to clarify the reaction mechanism of the dye-sensitized photochemistry.

Some results have already been reported in a short form.[5] The aim of the present paper is to report in detail the spectroscopic and kinetic behavior of the transient intermediates of thiopyronine in an aqueous solution with or without substrate.

Experimental

Chemicals. The thiopyronine was synthesized in the way described by Biehringer and Topaloff.[6]

The results of an elementary analysis of the synthesized dye as a zinc double salt were in good agreement with the calculated values. (Found: C, 51.02; H, 4.97; N, 7.00%. Calcd for $C_{17}H_{19}N_2S \cdot \frac{1}{2}ZnCl_2$: C, 52.70; H, 4.95; N, 7.24%.)

After the zinc had been removed by adding ammonia, the dye was recrystallized, in the form of golden-green needles, from concentrated hydrochloric acid as the dichloride ($C_{17}H_{19}N_2SCl \cdot HCl$) which was then recrystallized three times from concentrated hydrochloric acid and desiccated over calcium oxide and concentrated sulfuric acid. The purity was checked by paper chromatography. The solvent used was a mixture of butanol (4), acetic acid (1), and water (4). The chromatogram showed only one distinct single R_f value, 0.61_4. The absorption spectrum of thiopyronine in a buffered solution at pH 7.4 is shown in Fig. 1. The molar extinction coefficient is $7.4 \times 10^4 M^{-1} cm^{-1}$ at 564 nm.

The *p*-benzoquinone (Wako Junyaku Co., G.R.-grade reagent) was recrystallized from ethanol. The hydroquinone (Wako Junyaku Co., G.R.-grade reagent),

2) S. Kato, M. Morita and M. Koizumi, This Bulletin, **37**, 117 (1964).

3) M. Morita and S. Kato, The 18th Annual Meeting of Chem. Soc. Japan, Osaka (1965).

4) L. Lindqvist, *Arkiu Kemi*, **16**, 79 (1960); V. Kasche and L. Lindqvist, *Photochem. Photobiol.*, **4**, 923 (1965); L. Lindqvist, *Acta Chem. Scand.*, **20**, 2067 (1966).

5) M. Morita and S. Kato, *Z. Naturforschg.*, **Ser. b,** in press.

6) J. Biehringer and W. Topaloff, *J. Prakt. Chem.*, **65/66**, 499 (1902).

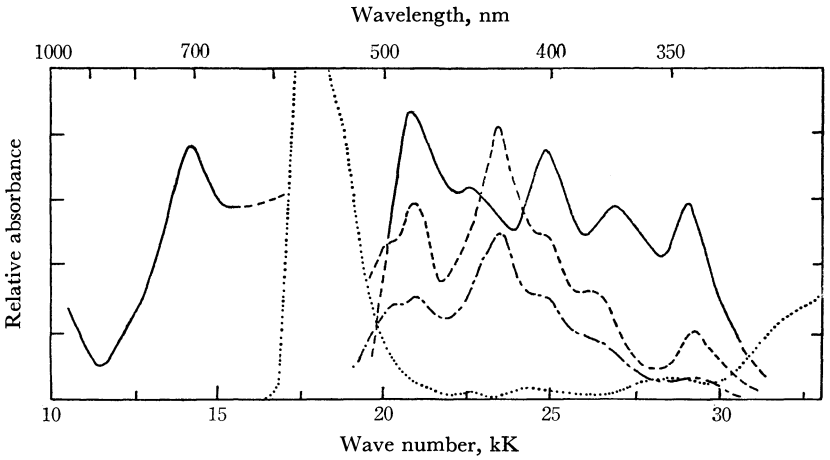

Fig. 2. Transient absorption spectra of thiopyronine in phosphate buffered solution at pH 7.4; Dye concn. 6.5 μM.
—— 22 μsec; – – – 130 μsec; —·— 200 μsec after flashing. The absorption spectrum in near-infrared region was constructed by an extrapolation of the decay curves measured at a series of wavelengths to zero time flashing. The absorption spectrum of thiopyronine is shown for the sake of comparison ·····.

allylthiourea (ATU) (Tokyo Kasei Co., G.R.-grade), and potassium dihydrogen phosphate (Wako Junyaku Co., G.R.-grade) were recrystallized three times from redistilled water. The sodium hydroxide solutions were prepared from a saturated solution of Wako Junyaku Co., G.R.-grade reagent. The disodium ethylene diamine tetraacetate (EDTA) and potassium persulfate, both Wako Junyaku Co., G.R.-grade reagent, were used without further treatment.

Preparation of Sample Solutions. The sample solutions were prepared from a stock thiopyronine solution of 5×10^{-4} M; the pH values were controlled with a 1/25 M KH_2PO_4-NaOH buffered solution and measured with a Hitachi-Horiba M-5 pH meter.

The solution was deaerated by more than five cycles of freezing-pumping-thawing. The absorption spectra before and after flashing were measured by means of a Shimadzu QB50 spectrophotometer or a Shimadzu multipurpose, auto-recording spectrophotometer (MPS-50).

Every measurement of flash photolysis was made with a fresh sample, even when the permanent change resulted from a single flash was negligibly small.

Apparatus. For photolysis, two quartz flash lamps filled with xenon (Ushio Electric Co., UF-693) were powered by a 4-μF capacitor charged up to 10 kV, if not otherwise mentioned. The duration time of photolysis lamps was 15 μsec.

A capillary flash lamp filled with argon was employed as a light source for the spectrophotography; it was worked at 3 kV with a 10-μF capacitor. The transient spectra were taken on Fuji Neopan plates, Fuji Neopan SS films, or Sakura Infrared 750 films by means of a Nalumi RM-23 grating spectrograph, which could also be used as a monochromator by turning a reflecting mirror. A triggering circuit controlled the time interval between the photolysis and the spectro flash from 10 μsec to 800 msec. Some measurements of the transient spectra were photographed by a double-beam flash apparatus described elswhere.[7]

The decays of the transient absorption spectra were measured with a xenon short-arc lamp (Ushio Electric Co., UXL-150D), photomultipliers (RCA 1P28 for the UV and visible region and 7102, Hamamatsu TV Co., for the red to near-infrared region), the monochromator described above, and a Hitachi V-116 synchroscope working through a cathode follower. The photolysis cells were glass tubes 10 cm long and 8 mm in inner diameter, to both ends of which were cemented quartz plane plates.

Hoya 0-54 orange glass cut-off filters were inserted between the photolysis flash lamps and the photolysis cell so as to exclude any light shorter than 540 nm, as is shown in Fig. 1, where the absorption spectrum of the dye is also depicted.

Results and Discussion

A. Transient Intermediates in the System Without Any Substrate. A deaerated, plain, aqueous solution and a buffered solution of the dye were almost completely decolorized transiently just after irradiation by a 200 J flash. The permanent bleaching by a single flash was, however, less than 2%.

The transient absorption spectrum has rather complex feature, as is shown in Fig. 2. It has many peaks which behave in different ways.

The absorption around 350 nm and those in the near-infrared region decay rapidly, while the peak at 425 nm increases after flashing and the

7) S. Kato, "Zikken Kagaku Koza, Zoku 11, Denshisupekutoru (Handbook of Experimental Chemistry, Continued Vol. 11)," ed. by S. Nagakura, Maruzen Inc., Tokyo (1965).

peak at 475—500 nm decays slowly.

From this kinetical difference, it is clear that the overall spectrum consists of several bands of different natures, overlapping with each other.

The absorption decays measured at 340 and 690 nm were analyzed according to the first-order rate formura, as is shown in Fig. 3; the same rate constant was obtained for both wavelengths.

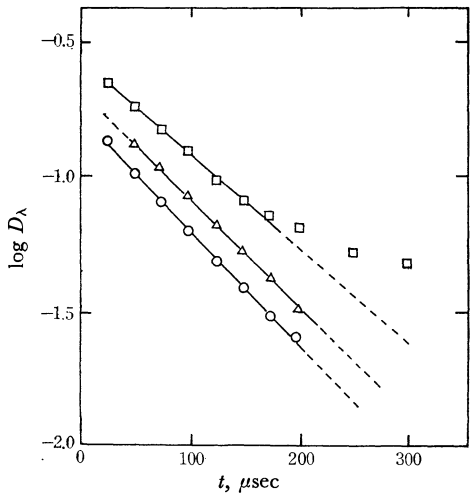

Fig. 3. First-order decay of the triplet state of the dye.
Dye concn. 8.8 μM. pH 7.4.
Wavelengths: ○ 340 nm, □ 375 nm, △ 690 nm

The plot for the first order at 375 nm is also nearly parallel, in the first part, to the other lines.

The coincidence of the rate constants make it possible to attribute these peaks to a single species, which may be assigned to the triplet-state of the dye. This assignment is strongly supported by the good correlation of the peaks with the energies for the triplet-triplet transition caluculated by means of the LCAO-MO-SCF method based on a variable *beta* approximation.[8)]

Every single run for the decay at 340 or 690 nm can be well described as a first-order process, but the observed rate constant increases linearly with the initial dye concentration, as is shown in Fig. 4, which gives the following relation:

$$k_{obs} = k_1 + k(D).$$

On the other hand, the rate constant are quite independent of the flash intensity, whether it is high enough to make a complete transient decoloralization or is so low as to make a 20% conversion (see Fig. 5).

These results can be explained only by a postulating that the triplet-state and the ground-state of the dye make the same contribution to the decay

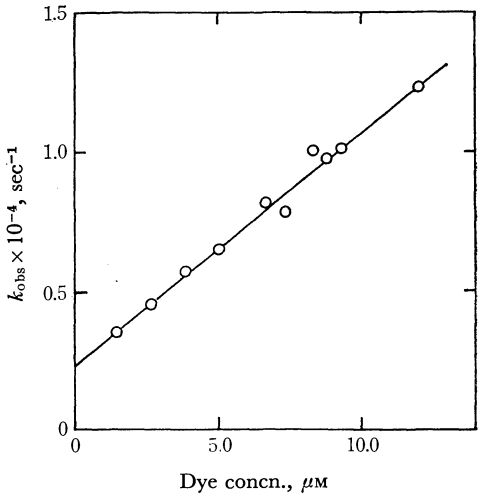

Fig. 4. Concentration dependence of the decay rate of the thiopyronine triplet in a phosphate buffered soultion at pH 7.4 measured at 340 nm.

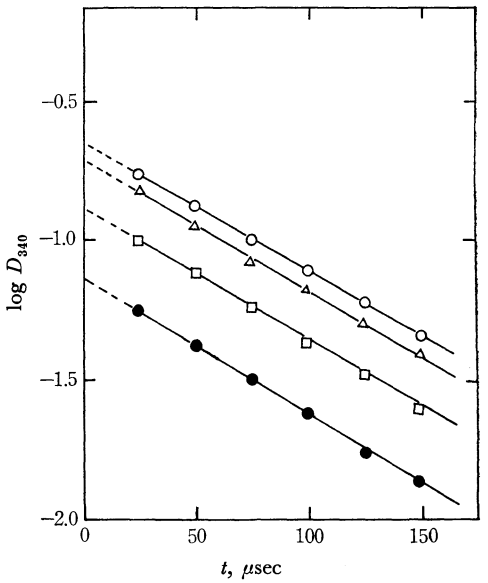

Fig. 5. The effect of the flash-light intensity (as a function of the input electric energy) on the decay rate of the triplet state measured at 340 nm.
Dye concn. 8.4 mμ. pH 7.4.
○ 200J, △ 180J, □ 72J, ● 32J

of the triplet-state:

$$D^t \longrightarrow k_1$$
$$D^t + D^t \longrightarrow k'$$
$$D^t + D \longrightarrow k''.$$

The peaks at 425 and 475—500 nm have distinctly longer lives than the triplet state, but the kinetical behavior is rather too complex for quantitative analysis. This means that at least two species have absorption bands, greatly overlapping, in

8) M. Morita, S. Kato, K. Nishimoto and L. S. Forster, to be published.

this spectral region. Qualitatively speaking, there exist at least two species, one of which decays in the first-order with a lifetime of less than 100 μsec, and while the other decays in the second order.

From the experimental evidence presented above, and also analogously with the results for methylene blue,[2] it is conceivable to attribute these long-living peaks to the half-oxidized form (475—500 nm) and the half-reduced form or semiquinone (425 nm) of the dye. This assignment was confirmed by the experiments to be described later.

The following reaction mechanism may, then, be proposed for the primary processes of thiopyronine in a buffered solution (pH 7.4) without any substrate:

$$\begin{aligned}
D + h\nu &\longrightarrow D^* \\
D^* &\longrightarrow D^t \\
D^t &\longrightarrow D & k_1 \quad (1)\\
D^t + D &\longrightarrow 2D & k_2 \quad (2)\\
D^t + D^t &\longrightarrow D^t + D & k_3 \quad (3)\\
D^t + D &\longrightarrow \text{Red} + \text{Oxd} & k_4 \quad (4)\\
D^t + D^t &\longrightarrow \text{Red} + \text{Oxd} & k_5 \quad (5)
\end{aligned}$$

where D, D*, D^t, Red, and Oxd are the ground state, the first excited singlet state, the triplet-state, the half-reduced form, and the half-oxidized form of the dye respectively.

The decay of the triplet-state can now be represented as:

$$-d(D^t)/dt = k_1(D^t) + k_2(D^t)(D) + k_3(D^t)^2 + k_4(D^t)(D) + 2k_5(D^t)^2.$$

When (k_2+k_4) is assumed to be equal to (k_3+2k_5), the above equation turns into the following:

$$-d(D^t)/dt = k_1(D^t) + (k_3 + 2k_5)(D_0)(D^t),$$

where $(D_0) = (D^t) + (D)$,

and where (D_0) is the initial dye concentration. The integration of the simplified equation yields:

$$-d\ln(D^t)/dt = k_{obs} = k_1 + (k_3 + 2k_5)(D_0).$$

This also holds in the case of eosine.[9]

Using the values obtained from Fig. 4, one obtains:

$$k_1 = 2.3_6 \times 10^3 \text{ sec}^{-1}$$
$$k_3 + 2k_5 = 7.6_9 \times 10^8 \text{ M}^{-1}\text{sec}^{-1}$$
$$k_2 + k_4 = 7.6_9 \times 10^8 \text{ M}^{-1}\text{sec}^{-1}.$$

B. Transient Intermediates in the Systems Containing Oxidants. *Potassium Persulfate* ($K_2S_2O_8$). In the presence of $K_2S_2O_8$ added as an oxidant, a partial fading of the dye gradually took place in a deaerated solution, even in the dark. When the solution containing 5×10^{-4} M $K_2S_2O_8$ at pH 6.9 was flashed, there appeared only one absorption band, between 450 and 510 nm, as is shown in Fig. 6, and a permanent bleaching of the dye was observed.

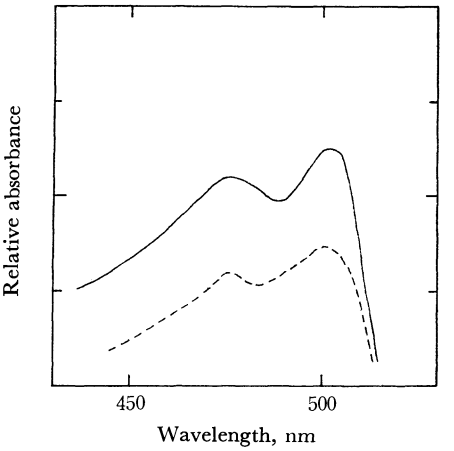

Fig. 6. Absorption spectra of transient species in a buffered solution at pH 6.9 containing 5×10^{-4} M $K_2S_2O_8$.
Dye concn. 3 μM
—— 40 μsec; – – – 105 μsec after flashing.

The absorption spectrum of the product has no distinct band, except for some rise in the shorter wavelength region.

p-Benzoquinone. In the case of the addition of *p*-benzoquinone as an oxidizing agent, two different transient absorption spectra were observed by flash excitation. Figure 7 shows the transient absorption spectra in this system.

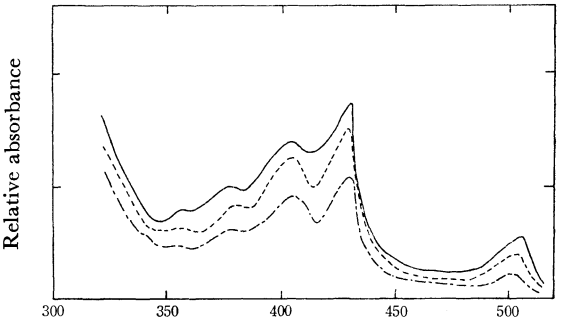

Fig. 7. Transient absorption spectra of thiopyronine phosphate buffered solution containing 5×10^{-4} M *p*-benzoquinone at pH 7.4.
Dye concn. 8 μM
—— 85 μsec; – – – 200 μsec; —·— 440 μsec after flashing.

One has four peaks, at 355, 375, 405, and 432 nm, and the other has one peak, at 500—505 nm. The former agrees with the absorption spectrum of the *p*-benzosemiquinone ion reported by several authors.[10]

9) T. Ohno, S. Kato and M. Koizumi, This Bulletin, **39**, 232 (1966).

10) H. Diebler, M. Eigen and P. Matthies, *Z. Elektrochem.*, **65**, 634 (1961); G. E. Adams and B. D. Michael, *Trans. Faraday Soc.*, **63**, 1171 (1967).

Also, some kinetic studies undertaken at 430 and 370 nm show that these transient species decay according to the second-order rate formula, as is shown in Fig. 8; the slopes of the decay curves give the rate constant of $1.7_3\times10^8$ M^{-1} sec^{-1} at 430 nm and of $1.8_2\times10^8$ M^{-1} sec^{-1} at 370 nm, using $\varepsilon_{430}=7.3\times10^3$ M^{-1} cm^{-1} and $\varepsilon_{370}=4.6\times10^3$ M^{-1}·cm^{-1} as the extinction coefficients of the *p*-benzosemiquinone ion at 430 and 370 nm respectively.

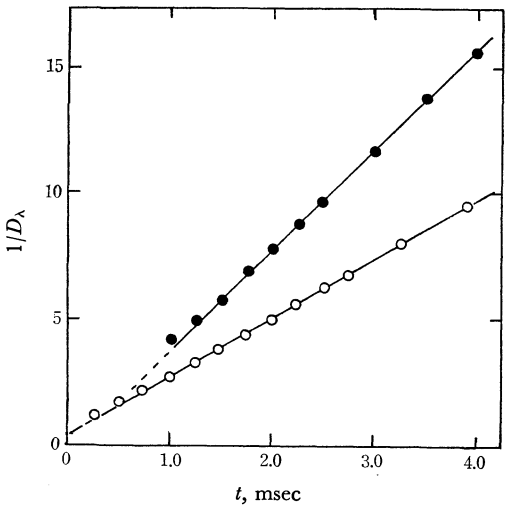

Fig. 8. Second-order decay of the *p*-benzosemiquinone ion.
Dye concn. 8.0 μM. *p*-Benzoquinone concn. 5×10^{-4}M. pH 7.4. Wavelengths: ● 370 nm, ○ 430 mn

These rate constants agree with the value for the dismutation process of the *p*-benzosemiquinone ion previously reported by Diebler, Eigen, and Matthies if one takes into account the temperature difference in the measurements.[10]

Thus, it is very likely that the *p*-benzosemiquinone ion decays through its own dismutation process, without interaction with a dye or any other intermediates.

The transient species, the absorption spectrum of which appeared in the region from 480 to 510 nm, with the peak at 500—505 nm may be identified as the half-oxidized form of the dye on the basis of a comparison with the case of $K_2S_2O_8$. There is no doubt that this intermediate is produced by the following reaction:

$$D^t + Q \longrightarrow Oxd + Q^-$$

where Q and Q^- indicate *p*-benzoquinone and its semiquinone ion respectively. The transient decay kinetics at 490 nm gave the first-order decay rate constant of 1×10^3 sec^{-1}. This evidence confirms conclusively that the transient species with an absorption around 500 nm is not due to the semiquinnoe ion of *p*-benzoquinone, but to the half-oxidized form of the dye.

Aerated Buffered Solution. When an aerated solution of the dye was subjected to flash excitation, only a weak transient absorption spectrum appeared during irradiation; it was in the region from 450 to 510 nm, with two peaks, at 475 and 505 nm. The other transient absorption had completely vanished.

This shows that the transient intermediates which appear in a deaerated solution are due to oxygen sensitive species, *i. e.*, the triplet-state of the dye and the intermediates with longer lifetimes produced from the triplet state. This finding confirms the assignment presented above.

The intermediate with the weak absorption around 450—510 nm may be produced by the reaction between the triplet state of the dye and oxygen. However, a large portion of the triplet state of the dye is likely to be quenched physically with oxygen, thus regenerating the ground-state dye. It seems that only a small portion of the triplet-state dye reacts to give the transient species *via* the following process:

$$D^t + O_2 \longrightarrow Oxd + O_2^-.$$

Thus, the transient intermediate with an absorption around 450—510 nm may be assigned to the half-oxidized form of the dye.

C. Transient Intermediates in the Systems Containing Reductants. *Hydroquinone.* In the presence of 5×10^{-4} M hydroquinone added as a reducing agent, upon flash excitation, there appeared a very intense transient absorption spectrum, with 343, 370, 405, and 428 nm peaks as is shown in Fig. 9.

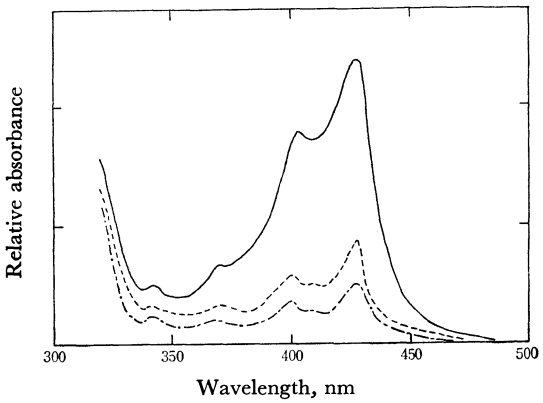

Fig. 9. Transient absorption spectra of a thiopyronine phosphate buffered solution at pH 7.4 containing 5×10^{-4} M benzohydroquinone.
Dye concn. 7.2 μM
—— 55 μsec; - - - 250 μsec; —·— 550 μsec after flashing.

The spectra obtained at 250 μsec and at 550 μsec have almost the same structure as that shown in Fig. 7 in the region from 350 to 450 nm. There is no doubt that these spectra are due to the *p*-

benzosemiquinone ion. On the other hand, the spectrum at 55 μsec is similar to the others in its peak positions, but different in the relative intensities. These results lead to the conclusion that an absorption band of another transient species is superposed in this spectral region; this species is certainly a semiquinone of the dye and has a shorter lifetime. In the case of methylene blue, the superposition of the transient absorptions due to the corresponding semiquinone in this wavelength region has been reported previously.[11] It may be noted that the transient absorption band from 470 to 510 nm which appeared in the dye-*p*-benzoquinone system completely vanishes in this system. Thus, there is scarcely any doubt that the electron transfer or hydrogen transfer occurs from the hydroquinone to the triplet state of the dye. Decay kinetics were undertaken at 430 and 370 nm. As is shown in Fig. 10, decay curves plotted on the second-order rate formula give the rate constants of $1.8_7\times10^8$ M^{-1} sec^{-1} at 430 nm and of $1.6_2\times10^8$ M^{-1} sec^{-1} at 370 nm, using the values of extinction coefficient for each wavelength presented above.

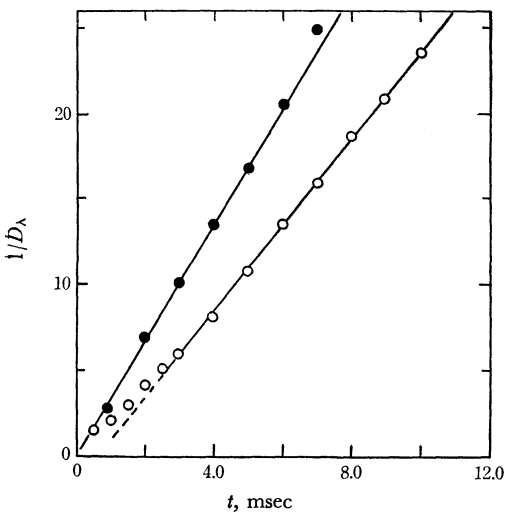

Fig. 10. Second-order decay of the *p*-benzosemiquinone ion.
Dye concn. 7.2 μM
Hydroquinone concn. 5×10^{-4} M. pH 7.4.
Wavelengths: ● 370 nm, ○ 430 nm

These values are in very good agreement with that of the dismutation rate constant of the *p*-benzoquinone ion obtained in the dye-*p*-benzoquinone system. This finding leads to the conclusion that the *p*-benzosemiquinone ion mainly disappears through its own dismutation process in any system examined. Meanwhile, the dye-hydroquinone solution became almost completely transparent at 205 nm, which is within the absorption region of the original dye, immediately after flashing, and then it turned back to become perfectly opaque in 200 μsec. The ground-state dye recovers according to the first-order rate formula. As regards the recovery process of the ground-state dye, such reactions as follows may be supposed:

$$\text{Red} + \text{Red} \longrightarrow \text{D} + \text{Leuco}$$

or:

$$\text{Red} + \text{Q}^- \longrightarrow \text{D} + \text{QH}_2$$

where Q^- and QH_2 are the *p*-benzosemiquinone ion and hydroquinone. If such is the case, the recovery of the ground-state dye should be analyzed according to the second-order rate formula. Thus, this rapid recovery of the ground-state dye is likely to take place directly from an intermediate with a shorter lifetime, an intermediate which is certainly the triplet-state.

Disodium Ethylene Diamine Tetraacetate (EDTA). EDTA has been used as a reducing agent for the photochemical reduction of various classes of dyes.[12] When a deaerated thiopyronine solution containing 5×10^{-3} M EDTA was flashed, more than 50% of the dye was permanently bleached by a single flash.

The completely photobleached solution has a rather diffuse absorption spectrum in the UV region, as is shown in Fig. 11, in contrast to those of methylene blue and thionine.[13]

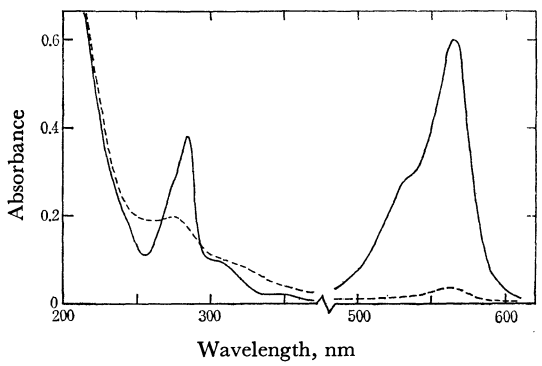

Fig. 11. Absorption spectrum of the photoproduct of thiopyronine containing 5×10^{-3} M EDTA as a reductant.
Dye concn. 8.1 μM
—— before flashing; - - - after flashing (photoproduct)

With the help of light, the photobleached solutions recover their color up to 60% or more of the original

11) S. Matsumoto, This Bulletin, **37**, 491 (1964).

12) W. J. Nickerson and J. R. Merkel, *Biochem. Biophys. Acta*, **14**, 303 (1954); G. Oster and N. Wotherspoon, *J. Am. Chem. Soc.*, **79**, 4836 (1957); B. Holmström, *Photochem. Photobiol.*, **3**, 97 (1964).

13) Y. Usui, H. Obata and M. Koizumi, This Bulletin, **34**, 1049 (1961); H. Obata, This Bulletin, **34**, 1057 (1961).

color upon the introduction of air. This shows that the major part of the photoproduct is the leuco dye. However, color recovery does not take place in dark, unlike the case of methylene blue and thionine.[14] When a buffered solution of thiopyronine at pH 7.4 containing 5×10^{-3} M EDTA was flashed, the absorption of the dye disappeared and a transient absorption spectrum with a peak at 426 nm appeared, as is shown in Fig. 12.

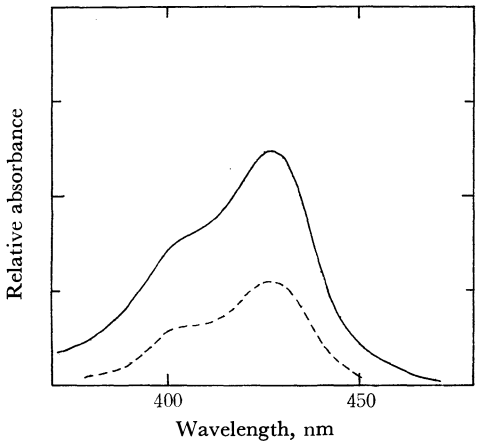

Fig. 12. Transient absorption spectrum of thiopyronine containing 5×10^{-3} M EDTA. pH 7.4.
Dye concn. 8.2 μM
—— 60 μsec; - - - 260 μsec after flashing.

On the other hand, at lower concentrations of EDTA, transient spectra similar to those in the case of the plain aqueous solution and a buffered solution appeared at the initial stage, and then the 426 nm peak increased and the other peaks simultaneously decreased. At 200 μsec after flashing, the 426 nm peak alone survived. The general features of the photobleaching described above and the following kinetic investigations strongly suggest that this intermediate is due to the half-reduced form or the semiquinone of the dye.

The decay of the triplet state of the dye was accelerated by the addition of EDTA, as has been stated above. From the dependence of the decay-rate constant on the EDTA concentration, one can obtain the bimolecular rate constants for the following processes:

$$D^t + EDTA \longrightarrow Red + EDTA_{oxd} \quad k_r$$
$$\searrow D + EDTA \quad k_d.$$

From the slope of the plot of the decay rate constant *vs.* the concentration of EDTA, the quenching constant k_q was obtained:

$$k_q = k_r + k_d = 1.6\times10^7\ M^{-1}sec^{-1}.$$

This value is comparable with that of methylene blue-EDTA, $k_r = k_d = 1.2\times10^7\ M^{-1}\ sec^{-1}$.[15]

14) Y. Usui, This Bulletin, **38**, 206 (1965) and Ref. 13.
15) N. Kosui, K. Uchida and M. Koizumi, *ibid.*, **38**, 1958 (1965).

The decay of the semiquinone, measured at 430 nm, is second order, as is shown in Fig. 13.

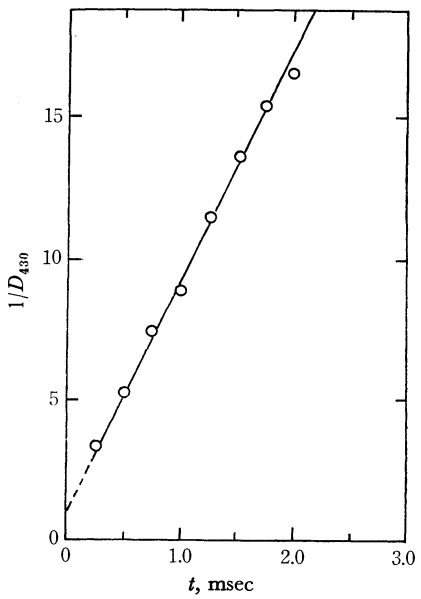

Fig. 13. Second-order decay of the semiquinone of thiopyronine.
Dye concn. 8.0 μM. EDTA concn. 5×10^{-3} M.
pH 7.4
Monitored wavelengths: 430 nm

The slope of the line gives $k/\varepsilon_{430}d$, where k, ε_{430}, and d are the second-order rate constant, the extinction coefficient of the semiquinone at 430 nm, and the optical depth of the reaction cell respectively. It is not easy to determine the absolute value of k since ε_{430} is not certain. However, if it is assumed that the permanent photobleaching, or the production of leuco dye, takes place only through the dismutation process of the semiquinone:

$$Red + Red \longrightarrow D + Leuco,$$

and if no other absorption band overlaps at this wavelength, (this is a reasonable assumption at a high EDTA concentration because it may effectively

TABLE 1. THE SECOND-ORDER RATE CONSTANT OF THE SEMIQUINONE OF THIOPYRONINE
Dye concn. 5.0μM. pH 7.4.

EDTA concn. M	k $M^{-1}sec^{-1}$
1.0×10^{-4}	$0.9_8\times10^9$
2.0×10^{-4}	$0.9_5\times10^9$
4.0×10^{-4}	$1.1_6\times10^9$
5.0×10^{-4}	$1.0_0\times10^9$
8.0×10^{-4}	$1.1_3\times10^9$
5.0×10^{-3}	$0.8_0\times10^9$
Average	$1.0_0\times10^9$

consume the triplet-state, a state of which otherwise interferes with the measurement at this wavelength), ε_{430} can be estimated to be 1.0×10^4 M^{-1}cm^{-1} from the amount of the permanent bleaching and the transient increase in the absorbance at 430 nm.

The rate constants for the similar processes of rhodamine B, thionine, and methylene blue are illustrated in Table 2 for the sake of comparison, though the experimental conditions are not alike. The values for thiopyronine and methylene blue are as large as can be expected for a diffusion-controlled process.

TABLE 2. THE SECOND-ORDER RATE CONSTANTS FOR THE DECAY OF SEMIQUINONES OF CATIONIC DYES

Dyes	Conditions	k M^{-1}sec^{-1}	Ref.
Rhodamine B	EtOH/H_2O	6.8×10^6	16)
	i-PrOH/H_2O (pH 6.2)	2.3×10^6	16)
Thionine	0.1N H_2SO_4	2.4×10^9	17)
Methylene blue	0.1N H_2SO_4	1.5×10^9	18)

Allylthiourea (ATU). ATU has also been used as a reducing agent for the photoreductions of several dyes;[19] however, it is milder in reducing power than EDTA.

Thiopyronine solutions containing ATU were photobleached by steady-light irradiation as well as by flash excitation, but the rate of the bleaching is slower than for EDTA by the factor of ten. For a thiopyronine solution containing 5×10^{-3} M ATU, only about 5% of the original dye was photobleached by a single flash. The absorption spectrum of the photoproduct has no distinct band, as in the case of the EDTA system. After almost complete bleaching with steady illumination, the introduction of air into the reaction cell and the irradiation of UV light recovered about 20% of the original dye, without any shift of the absorption peak at 564 nm. This definite recovery of the original dye confirms that a considerable fraction of the photoproduct is leuco dye.

The transient spectrum of this system, as is shown in Fig. 14, consists of all the characteristic bands of the triplet state (340, 370, and 400 nm), the half-oxidized form (475 nm), and the semiquinone (430 nm) of the dye, which appeared in the plain aqueous solution and the buffered solution.

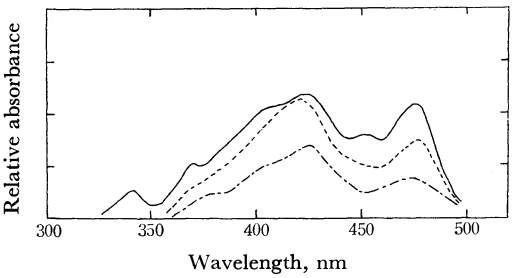

Fig. 14. Transient absorption spectrum of a thiopyronine buffered solution containing 5.0×10^{-3} M ATU. pH 7.6.
Dye concn. 10 μM
—— 45 μsec; - - - 110 μsec; —·— 255 μsec after flashing.

Kinetic investigations were undertaken at 430 nm for Red and at 480—500 nm for Oxd. Red decays according to the second-order rate formula, as is shown in Fig. 15.

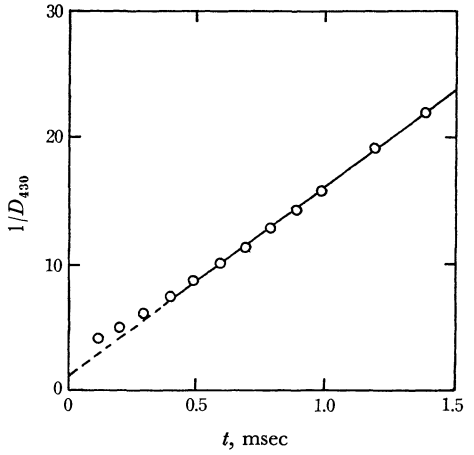

Fig. 15. Second-order decay of semiquinone of the thiopyronine.
Dye concn. 7.2 μM. ATU concn. 5×10^{-3} M.
pH 7.6.
Monitored wavelength: 430 nm

The slope of this line gives 1.5×10^9 M^{-1}sec^{-1} for the second-order rate constant, using the value, $\varepsilon_{430}=1.0\times10^4$ M^{-1}cm^{-1}, estimated above. This rate constant is independent of the concentration of ATU added to the solution.

On the other hand, the half-oxidized form of the dye follows a pseudo first-order decay kinetics, the rate constant of which depends linearly on the concentration of the added ATU. From this relation, one obtains the rate constant for the following reaction:

$$\text{Oxd} + \text{ATU} \longrightarrow$$

to be $(2—5)\times10^6$ M^{-1}sec^{-1}.

Photochemically, ATU is not such a strong reducing agent as EDTA to the triplet-state of the

16) B. Stevens, R. P. Sharpe and W. S. W. Bingham, *Photochem. Photobiol.*, **6**, 83 (1967).
17) C. G. Hatchard and C. A. Parker, *Trans. Faraday Soc.*, **57**, 1093 (1961).
18) C. A. Parker, *J. Phys. Chem.*, **63**, 26 (1959).
19) M. Pestemer, *Z. Elektrochem.*, **58**, 121 (1954); G. Oster and A. H. Adelman, *J. Am. Chem. Soc.*, **78**, 913 (1956); F. Millich and G. Oster, *ibid.*, **81**, 1357 (1959); K. Kikuchi and M. Koizumi, This Bulletin, **40**, 736 (1967).

dye. Because of this characteristics, the electron transfer between a dye molecule in the triplet-state and another in the ground-state or in the triplet-state predominates over the reaction between a dye molecule in the triplet-state and ATU.

Thus, the formation of the semiquinone and the half-oxidized form of the dye through dye-dye interaction is much more important than the direct attack of ATU on the triplet-state. Accordingly, ATU acts as a reductant mainly in the reaction with the half-oxidized form of the dye:

$$\text{Oxd} + \text{ATU} \longrightarrow \text{D} + \text{ATU}_{\text{oxd}}$$

where ATU_{oxd} is a one electron-oxidized form of ATU. This process takes place in the photoreduction of thiazine dyes, methylene blue and thionine. Koizumi and his co-workers have discussed this mechanism.[20]

If the photoreduction proceeds through this mechanism, the rate formula of the photoreduction by steady-illumination can be expected to be analyzed approximately by the second order with regard to the dye, as Koizumi *et al.* suggested. From this point of view, the steady-light photoreduction of thiopyronine was studied in our laboratory; this relation was confirmed in the case of ATU.

In general, two kinds of reaction

$$\text{D}^t + \text{D or D}^t \longrightarrow$$

and

$$\text{D}^t + \text{Reductant or Oxidant} \longrightarrow$$

compete with each other; the fraction of each path depends both on the reactivity of the added reagent and on its concentration relative to that of the dye.

This has been clearly demonstrated in the steady-light photoreduction of methylene blue reported by Kosui, Uchida, and Koizumi.[15]

The general features of the photochemical reactions of thiopyronine are very much like those of thiazine dyes.

To summarizing the results obtained in the present investigation, the elementary reactions of thiopyronine are as follows:

$$\text{D} + h\nu \longrightarrow \text{D}^*$$

$$\text{D}^* \longrightarrow \text{D} + h\nu_f$$

$$\text{D}^* \longrightarrow \text{D} + \text{heat}$$

$$\text{D}^* \longrightarrow \text{D}^t$$

$$\text{D}^t \longrightarrow \text{D} \qquad k_1 = 2.3_6 \times 10^3\ \text{sec}^{-1} \qquad (1)$$

$$\text{D}^t + \text{D} \longrightarrow 2\text{D} \qquad k_2 \qquad (2)$$

$$\text{D}^t + \text{D}^t \longrightarrow \text{D}^t + \text{D} \quad k_3 \qquad (3)$$

$$\searrow \quad 2\text{D}$$

$$\text{D}^t + \text{D} \longrightarrow \text{Red} + \text{Oxd} \quad k_4 \qquad (4)$$

$$\text{D}^t + \text{D}^t \longrightarrow \text{Red} + \text{Oxd} \quad k_5 \qquad (5)$$

$$k' = k_3 + 2k_5 = 7.6_9 \times 10^8\ \text{M}^{-1}\text{sec}^{-1}$$

$$k'' = k_2 + k_4 = 7.6_9 \times 10^8\ \text{M}^{-1}\text{sec}^{-1}$$

$$\text{Red} + \text{Red} \longrightarrow \text{D} + \text{Leuco} \qquad (6)$$

$$k_6 = (1-2) \times 10^9\ \text{M}^{-1}\text{sec}^{-1}$$

$$\text{Oxd} \longrightarrow \text{X} \qquad (7)$$

$$k_7 = (1-3) \times 10^3\ \text{sec}^{-1}$$

$$\text{D}^t + \text{EDTA} \longrightarrow k_8 = 1.6 \times 10^7\ \text{M}^{-1}\text{sec}^{-1} \qquad (8)$$

$$\text{D}^t + \text{ATU} \longrightarrow k_9 \approx \text{small} \qquad (9)$$

$$\text{Oxd} + \text{ATU} \longrightarrow k_{10} = (2-5) \times 10^6\ \text{M}^{-1}\text{sec}^{-1}. \qquad (10)$$

Lindqvist gave weight to the reversible photochemical redox property of dye in the photosensitizing activity in his extensive investigations of the flash photolysis of xanthene dyes.[4] The efficient photosensitizing power of thiopyronine as well as of methylene blue can be well understood in the light of this photochemical redox reversibility.

By the way, pyronine G, with a structure similar to that of thiopyronine, was studied by the flash method, but no transient absorption appeared under our experimental conditions.

In order to examine the concentration change in the dye in the ground-state, further studies were undertaken by the fluorescence method, which makes it possible to evaluate the amount of the transient bleaching of the dye by measuring the change in fluorescence intensity during flash excitation.[21]

These results showed that the transient bleaching did not take place in the phosphate buffered solution of pyronine G at pH 7.4.

On the other hand, in the case of thiopyronine, it was found that 90% or more of the ground state of the dye was converted to the triplet-state or to intermediate species with long lives during 200 J flash excitation. In the case of rhodamine B, with a structure similar to that of pyronine G, it has been reported that no transient absorption was observed in an aqueous solution.[16]

At any rate, these results are in good agreement with the fact that pyronine G has little photodynamic effect.

The failure to find any intermediates for pyronine G might be due either to their short lifetimes under our experimental conditions, or to the low extinction coefficient of the transient species in the spectral region available. However, this latter seems not to be the case, because our theoretical studies of these photosensitizing dyes predict that they will have very similar electronic structures.[8] Therefore, thiopyronine and pyronine G may be expected to exhibit similar spectroscopic behavior.

An alternative interpretation of this different situation between thiopyronine and pyronine G may be made in terms of the heteroatom effect.

20) M. Koizumi, H. Obata and S. Hayashi, This Bulletin, **37**, 108 (1964).

21) A. Kira and S. Kato, *Sci. Rep. Tohoku Univ., Ser. 1*, **158**, 142 (1965).

It is well known that the introduction of a heteroatom into an aromatic system facilitates intersystem crossing.[22]

Nurmukhametov and Gobov have studied the phosphorescence of a series of compounds, *i. e.*, fluorenone, diphenylene oxide, diphenylene sulfide, and carbazole.[23]

They have found that the presence of a nitrogen atom or, more especially, a sulfur atom in an aromatic system appreciably increases the probability of the S*–T intersystem crossing. This was observed as an increase of the phosphorescence yield.

Since the intersystem crossing competes successfully with fluorescence, a decreased fluorescence quantum yield should result. This was confirmed experimentally in the series of compounds mentioned above.[24]

As to pyronine G, there seem no such experimental results. However, comparing the fluorescence quantum yield of pyronine G with that of rhodamine B, a high quantum yield of fluorescence of pyronine G may be anticipated from the structural similarity of these dyes.[25]

On the other hand, the fluorescence quantum yield, Φ_f, and the quantum yield of the triplet-state production, Φ_{S^*-T}, of thiopyronine were determined experimentally in our laboratory to be $\Phi_f = 0.20$ and $\Phi_{S^*-T} = 0.67$.[26]

Thus, the difference in photochemical properties between thiopyronine and pyronine G can be well understood in terms of the difference in the quantum yield of the triplet-state production of the dyes.

Conclusion

The flash excitation of a deaerated buffered solution of thiopyronine without any substrate leads to three transient intermediates: the triplet-state (D^t), the half-oxidized form (Oxd), and the half-reduced or the semiquinone (Red) of the dye.

Red and Oxd were generated simultaneously through the electron-transfer reactions between D^t and D^t and between D^t and D.

It has been established that the high efficiency of thiopyronine in the photodynamic effect is due to the high quantum yield of the triplet-state production and to the high photochemical redox reversibility of the dye.

Thanks are due to Professor H. Tsubomura of the Faculty of Engineering Science, Osaka University, for his permission to use the microphotodensitometer. The authors wish also to thank the Ministry of Education for its Scientific Research Grant-in-Aid.

22) M. Kasha and S. P. McGlynn, *Ann. Rev. Phys. Chem.*, **7**, 403 (1956).

23) R. N. Nurmukhametov and G. V. Gobov, *Optics and Spectry.*, **18**, 126 (1965) (*Optika i Spektroskopiya*, **18**, 227 (1965)).

24) D. W. Ellis and B. S. Solomon, *J. Chem. Phys.*, **46**, 3497 (1967).

25) W. H. Melhuish, *J. Opt. Soc. Am.*, **52**, 1256 (1962); H. V. Prushel, A. L. Sommers and R. C. Cox, *Anal. Chem.*, **35**, 2166 (1963).

26) Unpublished results obtained in our laboratory.

BULLETIN OF THE CHEMICAL SOCIETY OF JAPAN VOL. 42 35—40 (1969)

Heat of Mixing for Binary Mixtures: Pyridine Derivatives+Benzene, and +Cyclohexane Systems

Takeshi MURAKAMI, Sachio MURAKAMI and Ryoichi FUJISHIRO

Department of Chemistry, Faculty of Science, Osaka City University, Sumiyoshi-ku, Osaka

(Received March 19, 1968)

The heat of mixing was measured for binary mixtures of pyridine derivatives (α-picoline, β-picoline, γ-picoline, and 2,6-lutidine) with benzene or cyclohexane at 25.0±0.01°C, and for a binary mixture of pyridine with benzene, or cyclohexane, at 30.0±0.01°C. The small values of the heat of mixing for pyridine derivatives-a benzene system were interpreted as an indication of strong specific interactions between pyridine derivatives and benzene. By treating the results in the manner described in a previous paper (*Bull. Chem. Soc. Japan*, **39**, 720 (1966)), the specific interaction energies of pyridine derivatives with benzene were estimated. The strengths of the molecular interaction energy were in the order: γ-picoline>pyridine>β-picoline>α-picoline> 2,6-lutidine; the order was discussed in terms of the molecular complexes.

Recently extensive studies of the formation of molecular compounds have been made by various techiques, but only a little information has been obtained by direct calorimetry measurements, which

seem to give the most reliable data on molecular interaction energy. In a previous paper,[1] we measured the heat of mixing for binary solutions and estimated the interaction energies of donor-accepter type complexes. Morcom *et al.* have measured the heat of mixing of pyridine derivatives+the carbon tetrachloride system and have discussed the specific interaction in terms of a possible donor-accepter interaction. In our experiment, we measured the heat of mixing for binary solutions of pyridine derivatives [pyridine (py), α-picoline (α-pi), β-picoline (β-pi), γ-picoline (γ-pi), and 2,6-lutidine (2,6-lut)]with benzene or cyclohexane. The small values of the heat of mixing for pyridine derivatives with benzene indicate the estimate of a specific interaction similar to that between pyridine derivatives and carbon tetrachloride. We will estimate the specific molecular energy between pyridine derivatives and benzene in a cyclohexane solution by using the enthalpy cycle, and will discuss the molecular interaction in terms of various types of molecular complexes.

Experimental

The calorimeter for measuring the heat of mixing was described in the previous paper,[1] but we made an improvement in the mixing cell. The mixing cell was made of glass instead of stainless steel, and its shape was similar to that used by Larkin and McGlashan[2] and by Amaya[3]. The experimental procedure was the same as before.

The technique of thermal compensation[1] was used for almost all the experiments. The pyridine was purified by a method described in the literature.[4] The methyl pyridines were supplied by the Tanabe Pharmaceutical Co., Ltd. All these samples except β-picoline were fractionally distilled over P_2O_5 and then under reduced pressure in a nitrogen atmosphere before use. The β-picoline was used without further purification, since no impurity was detected by gas chromatography.

The cyclohexane was treated with a concentrated sulfuric-nitric acid mixture, and then shaken with a

TABLE 1-1. HEAT OF MIXING FOR PYRIDINE + BENZENE AT 30.0°C

x_1	n_1 $\times 10^2$·mol	n_2 $\times 10^2$·mol	Q J	ΔH^M_{x2} J·mix^{-1}	ΔH_{x1} J·mol^{-1}
0.0665	0.1862	2.5091	0.41	15	219
0.1228	0.2567	1.8083	0.36	17	144
0.2862	0.5007	1.2482	0.30	17	59
0.4954	0.5838	0.5947	0.09	8	16
0.7705	1.3504	0.4022	0.20	12	15

1: pyridine 2: benznene

TABLE 1-2. HEAT OF MIXING FOR α-PICOLINE + BENZENE AT 25.0°C

x_1	n_1 $\times 10^2$·mol	n_2 $\times 10^2$·mol	Q J	ΔH^M_{x1} J·mix^{-1}	ΔH_{x1} J·mol^{-1}
0.1800	0.1330	0.6059	0.69	9.3	52.2
0.2293	0.2319	0.7774	0.16	15.4	67.2
0.3004	0.4050	0.9429	0.20	14.8	43.6
0.3830	0.2884	0.4647	0.17	22.6	59.0
0.5493	0.7463	0.3364	0.20	27.3	27.2
0.7412	0.4838	0.1689	0.16	23.9	32.2
0.7419	0.6647	0.2312	0.15	13.3	22.4
0.7999	0.8950	0.2238	0.15	13.3	16.7

1: α-picolihe 2: benzene

TABLE 1-3. HEAT OF MIXING FOR β-PICOLINE + BENZENE AT 25.0°C

x_1	n_1 $\times 10^2$·mol	n_2 $\times 10^2$·mol	Q J	ΔH^M_{x1} J·mix^{-1}	ΔH_{x1} J·mol^{-1}
0.1836	0.1863	0.8284	−0.14	−14.2	−77.7
0.2982	0.2474	0.2557	−0.13	−15.5	−52.0
0.5548	0.4482	0.3596	−0.04	−4.5	−8.2
0.6675	0.6033	0.3004	0.04	4.7	7.1
0.7182	0.6540	0.2557	0.10	11.4	15.8
0.8118	0.7249	0.1681	0.05	69.5	5.6

1: β-picoline 2: benzene

TABLE 1-4. HEAT OF MIXING FOR γ-PICOLINE + BENZENE AT 25.0°C

x_1	n_1 $\times 10^2$·mol	n_2 $\times 10^2$·mol	Q J	ΔH^M_{x1} J·mix^{-1}	ΔH_{x1} J·mol^{-1}
0.1184	0.1105	0.8212	0.09	10	77
0.2342	0.2246	0.7341	0.12	12	53
0.4831	0.4475	0.4788	0.15	16	34

1: γ-picoline 2: benzene

TABLE 1-5. HEAT OF MIXING FOR 2,6-LUTIDINE + BENZENE AT 25.0°C

x_1	n_1 $\times 10^2$·mol	n_2 $\times 10^2$·mol	Q J	ΔH^M_{x1} $\times 10^{-2}$· J·mix^{-1}	ΔH_{x1} $\times 10^{-2}$· J·mol^{-1}
0.1061	0.0917	0.7732	0.22	0.26	0.24
0.1402	0.1273	0.7806	0.30	0.33	0.23
0.1505	0.1823	0.9538	0.40	0.35	0.22
0.2915	0.3300	0.8023	0.53	0.47	0.16
0.3289	0.3531	0.7204	0.61	0.56	0.19
0.3951	0.3232	0.4949	0.50	0.58	0.15
0.4637	0.4247	0.4912	0.55	0.60	0.13
0.6713	0.6858	0.3357	0.44	0.43	0.06

1: 2,6-lutidine 2: benzene

1) S. Murakami and R. Fujishiro, This Bulletin, **39**, 720 (1966); M. Takami, S. Murakami and R. Fujishiro, *ibid.*, **38**, 291 (1965).

2) J. A. Larkin and M. L. McGlashan, *J. Chem. Soc.*, **1961**, 3425.

3) K. Amaya, This Bulletin, **34**, 1287 (1961).

4) D. G. Leis and B. C. Currans, *J. Am. Chem. Soc.*, **67**, 79 (1945).

Table 1-6. Heat of mixing for pyridine + cyclohexane at 30.0°C

x_1	n_1 $\times 10^2$·mol	n_2 $\times 10^2$·mol	Q J	ΔH^M_{x1} $\times 10^{-3}$. J·mix^{-1}	ΔH_{x1} $\times 10^{-3}$. J·mol^{-1}
*0.0491	0.1880	3.6444	14.98	0.39	7.97
*0.0689	0.2128	2.8772	15.55	0.50	7.30
*0.0812	0.2392	2.7084	17.33	0.59	7.24
0.0852	0.2190	2.3503	14.34	0.56	6.55
0.1067	0.2030	1.6990	12.32	0.65	6.07
*0.1474	0.1880	1.0874	11.05	0.87	5.88
*0.2434	0.2905	0.9027	15.15	1.27	5.21
*0.2374	0.2852	0.9161	14.01	1.17	4.91
0.3065	0.4284	0.9692	17.43	1.25	4.07
0.3233	0.5064	1.0598	20.82	1.33	4.11
0.4786	0.6116	0.6663	18.51	1.45	3.03
0.5942	0.6597	0.4505	14.70	1.32	2.22
0.6627	1.0823	0.5509	20.18	1.24	1.86
0.8011	1.4351	0.3563	15.40	0.86	1.07

* measured at 35.0°C
1: pyridine 2: cyclohexane

Table 1-7. Heat of mixing for α-picoline + cyclohexane at 25.0°C

x_1	n_1 $\times 10^2$·mol	n_2 $\times 10^2$·mol	Q J	ΔH^M_{x1} $\times 10^{-3}$. J·mix^{-1}	ΔH_{x1} $\times 10^{-3}$. J·mol^{-1}
*0.0658	0.0452	0.6168	2.78	0.41	6.16
*0.0848	0.0571	0.4867	3.47	0.52	6.08
*0.1163	0.1112	0.8445	4.73	0.63	5.39
0.1754	0.1600	0.7523	7.55	0.83	4.72
0.2380	0.2088	0.6686	9.08	1.03	4.35
0.2671	0.2226	0.6106	9.20	1.10	4.14
0.3902	0.3735	0.5835	11.97	1.25	3.21
0.5312	0.4978	0.4386	11.50	1.23	2.31
0.6734	0.5520	0.2676	12.55	1.03	1.53
0.7693	0.6079	0.1822	6.38	0.81	1.05

* calculated from heat of dilution
1: α-picoline 2: cyclohexane

Table 1-8. Heat of mixing for β-picoline + cyclohexane at 25.0°C

x_1	n_1 $\times 10^2$·mol	n_2 $\times 10^2$·mol	Q J	ΔH^M_{x1} $\times 10^{-3}$. J·mix^{-1}	ΔH_{x1} $\times 10^{-3}$. J·mol^{-1}
*0.0444	0.0282	0.5629	2.11	0.31	6.98
0.1081	0.0733	0.6774	4.44	0.66	6.06
0.1983	0.1865	0.9407	9.22	0.98	4.94
0.2841	0.2262	0.5699	9.35	1.17	4.13
0.3873	0.3953	0.6252	13.57	1.32	3.43
0.4340	0.3821	0.4982	11.78	1.33	3.08
0.5125	0.3985	0.3790	10.14	1.30	2.54
0.7326	0.4193	0.5723	5.51	0.96	1.31
0.7878	0.6579	0.1772	6.79	0.81	1.03

* calculated from heat of dilution
1: β-picoline 2: cyclohexane

Table 1-9. Heat of mixing for γ-picoline + cyclohexane at 25.0°C

x_1	n_1 $\times 10^2$·mol	n_2 $\times 10^2$·mol	Q J	ΔH^M_{x1} $\times 10^{-3}$. J·mix^{-1}	ΔH_{x1} $\times 10^{-3}$. J·mol^{-1}
0.1420	0.1556	0.9403	8.92	0.81	5.73
0.1550	0.1407	0.7570	8.12	0.89	5.77
0.2419	0.2202	0.6273	10.39	1.23	4.72
0.4777	0.5413	0.5917	15.74	1.39	2.91

1: γ-picoline 2: cyclohexane

Table 1 -10. Heat of mixing for 2,6-lutidine + cyclohexane at 25.0°C

x_1	n_1 $\times 10^2$·mol	n_2 $\times 10^2$·mol	Q J	ΔH^M_{x1} $\times 10^{-3}$. J·mix^{-1}	ΔH_{x1} $\times 10^{-3}$. J·mol^{-1}
0.0843	0.0846	0.9186	4.19	0.42	4.94
0.1062	0.0880	0.7404	4.79	0.54	5.04
0.1651	0.1555	0.7869	6.12	0.65	3.93
0.2041	0.1624	0.6334	5.71	0.72	3.51
0.2930	0.2348	0.7666	6.54	0.82	2.78
0.3941	0.5892	0.3570	6.01	1.02	2.59
0.4043	0.4786	0.7053	12.49	1.06	2.61
0.4721	0.3406	0.3808	7.36	1.02	2.16
0.7307	0.4076	0.1502	3.84	0.69	0.94
0.8104	0.6832	0.1598	4.50	0.53	0.66

1: 2,6-lutidine 2: cyclohexane

Table 1-11. Heat of mixing for benzene + cyclohexane at 30°C

x_1	n_1 $\times 10^2$·mol	n_2 $\times 10^2$·mol	Q J	ΔH^M_{x1} $\times 10^{-3}$. J·mix^{-1}	ΔH_{x1} $\times 10^{-3}$. J·mol^{-1}
0.0614	0.1633	2.4968	4.73	0.18	2.90
0.1472	0.2367	1.3710	5.93	0.37	2.51
0.3878	0.5861	0.9250	10.34	0.68	1.76

1: benzene, 2: cyclohexane

sodium hydroxide aqueous solution and with distilled water. Then it was twice passed through about 1 m silica gel column. The benzene was shaken with concentrated sulfuric acid, a sodium hydroxide aqeuous solution, and distilled water. The cyclohexane and benzene were shaken with mercury and distilled over metal sodium respectively. Gas-chromatographic analysis showed only a single peak for each sample.

Results and Discussion

The results obtained for eleven systems are given in Tables 1-1—1-11, where x_i and n_i ($i=1$ or 2) are the mole fraction and the number of the mole of the i component, respectively. Q is the quantity of heat produced during the mixing process, while ΔH_{x_i} and $\Delta H^M_{x_i}$ are the heats of mixing per mole of the 1 component and per mole of the mixture

respectively. For the mixtures with lower mole fractions, the heat of mixing was measured by diluting a solution, the heat of mixing of which was known from a previous run, with the other component. In eleven systems, for pyridine+cyclohexane or +benzene, and benzene+cyclohexane systems, the heat of mixing was measured at 30.0°C, while for the other systems it was measured at 25.0°C. The heat of mixing for benzene with cyclohexane agrees with that of the literature.[5] Our results for the pyridine+benzene system were endothermic over the whole concentration range, though they were almost zero; Amaya[3,6] found that this system at 25.0°C changed from endothermic to exothermic in the neighborhood of an equimolar composition, though the absolute values will be very small. The heat of mixing at 30°C, $\Delta H^{M}_{x_i}(30°C)$, is related to that at 25°C, $\Delta H^{M}_{x_i}(25°C)$, as follows: $\Delta H^{M}_{x_i}(30°C) = \Delta H^{M}_{x_i}(25°C) + (30-25)C^{E}_{p}$, where C^{E}_{p} is the excess heat capacity. According to Morcom and Travers,[7] C^{E}_{p} for the pyridine-benzene system is positive. Therefore, our data seem to be consistent with those obtained by Amaya.

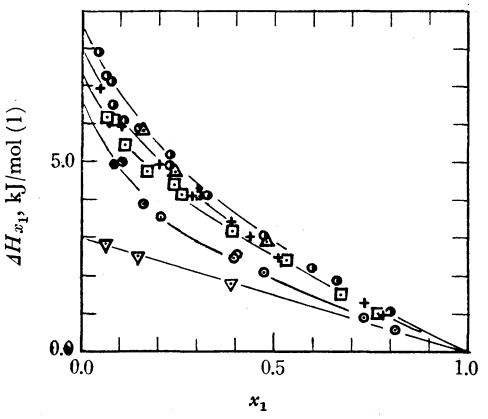

Fig. 1. Heat of mixing for pyridine derivative with cyclohexane.
◐ pyridine, ⊡ α-picoline, + β-picoline, △ γ-picoline, ⊙ 2,6-lutidine, and ▽ benzene with cyclohexane

The experimental data for ΔH_{x_i} have been plotted against the mole fraction in Figs. 1 and 2. By smoothing and extrapolating the curves to an infinite dilution for each system, we can obtain the heat of mixing per mole of the pyridine derivatives at an infinite dilution ($\lim_{x_i \to 0} \Delta H_{x_i}$). These values are given in Table 2.

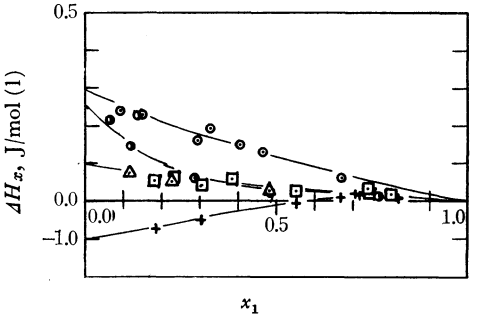

Fig. 2. Heat of mixing for pyrine derivative with benzene.
◐ pyridine, ⊡ α-picoline, + β-picoline, △ γ-picoline, and ⊙ 2,6-lutidine with benzene

TABLE 2. HEAT OF MIXING AT INFINITE DILUTION

	in benzene: ΔH_c kJ·mol^{-1}	in cyclohexane: ΔH_a kJ·mol^{-1}
Pyridine	0.3	8.5
α-Picoline	0.1	7.3
β-Picoline	−0.1	7.9
γ-Picoline	0.1	8.5
2,6-Lutidine	0.3	6.5
Benzene		3.0 (: ΔH_b)

The values of $\lim_{x_i \to 0} \Delta H_{x_i}$ correspond to the energy changes from the pure pyridine derivatives state to that in which each pyridine derivative molecule is surrounded by a large amount of the solvent medium. As may be seen in Table 2, the values of $\lim_{x_i \to 0} \Delta H_{x_i}$ in benzene are cosiderably smaller than the corresponding values in cyclohexane. This may suggest that a pyridine derivative molecule exists more stably in a benzene solution, by making a specific interaction or by forming a complex with a benzene molecule, than in a cyclohexane solution. The possibility of such a complex formation is supported by the NMR[8] measurements for the pyridine-benzene system. Further, according to Ott *et al.*,[9] the positive excess heat capacity in the binary mixture shows the existence of a specific interaction, or the formation of a complex between the solvent and solute molecules, and the pyridine-benzene solution is a system in which the excess heat capacity is positive.

In order to estimate the interaction energy between a pyridine derivative and benzene molecules, we carried out a treatment described in the

5) A. E. P. Watson, I. A. McLure, J. E. Bennet and G. C. Benson, *J. Phys. Chem.*, **69**, 2753 (1965).
6) H. Loiseleur, J. C. Merlin and R. A. Paris, *J. Chim. Phys.*, **62**, 1380 (1965).
7) K. W. Morcom and D. N. Travers, *Trans. Faraday Soc.*, **62**, 2063 (1966).
8) J. N. Murrel and V. M. S. Gill, *ibid.*, **61**, 402 (1965).
9) J. R. Goates, R. J. Sullivan and J. Bevan. Ott, *J. Phys. Chem.*, **63**, 589 (1959); L. R. McKinnon and A. G. Williamson, *Aust. J. Chem.*, **17**, 1374 (1964).

previous paper.[1] In the enthalpy cycle shown in Fig. 3, ΔH_a is the energy of breaking up all the interaction between pure pyridine deriatives by adding a large quantity of cyclohexane; ΔH_b is equal to the value of $\lim_{x_i \to 0} \Delta H_{x_i}$ for the benzene-cyclohexane system, and ΔH_c is the energy change produced by the dilution of pure pyridine derivative with x mol of benzene, where $x \gg 1$: these enthalpy changes were also measured in the present work. ΔH_d consists of two parts; one is equal to $(x+1) \cdot \Delta H_b$, while the other is due to the enthalpy change from the state in which pyridine-benzene associated complexes are surrounded by benzene to that in which they are surrounded by cyclohexane. The latter part of ΔH_d may be put at zero, or even neglected because the two media have almost equal dielectric constants and the dipole stabilization energies of a complex in the two media are considered to be nearly equal.[10]

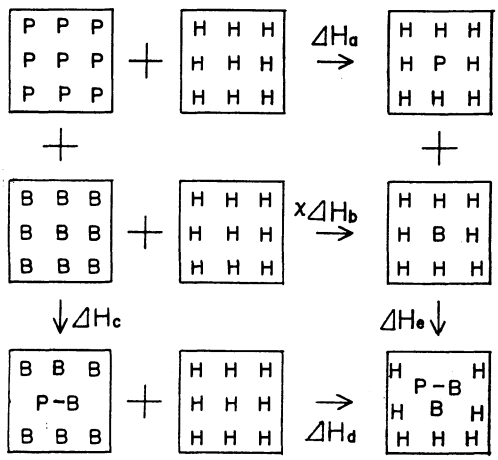

Fig. 3. Enthalpy cycle.[1]

The energies of the specific interaction between a pyridine derivative and benzene in the cyclohexane solution thus obtained from the enthalpy cycle:

$$\Delta H_e = \Delta H_c + \Delta H_d - \Delta H_a - \Delta H_b$$

are tablated in Table 3. Morcom *et al.*[7] measured the heats of mixing for the binary mixtures of carbon tetrachloride with pyridine derivatives; they found that there exists a specific interaction between carbon tetrahcloride and a pyridine derivative. Using their data,[7,11] and following the method of treatment described above, we calculated the specific interaction energies between pyridine derivatives and cabon tetrachloride; they are listed in Table 3. The strength of the specific interaction between

Table 3. The strength of the specific interaction for pyridine derivative with benzene, or carbon tetrachloride

	Benzene kJ·mol^{-1}	CCl_4 [7,11] kJ·mol^{-1}
Pyridine	−5.2	−7.4
α-Picoline	−4.2	−7.5
β-Picoline	−5.1	
γ-Picoline	−5.4	−8.3
2,6-Lutidine	−3.2	−7.2

pyridine derivatives and benzene in cyclohexane is in the order of; γ-pi>py>β-pi>α-pi>2,6-lut, while the specific interactions between pyridine derivatives and carbon tetrachloride in cyclohexane solutions are in the order: γ-pi>α-pi≃py≃2,6-lut.

A pyridine molecule has nonbonding lone pair electrons and π-electrons; these n- and π-electrons may be expected to play an important role in complex formation with other molecules. Therefore, the complex formation between pyridine derivatives and benzene may be considered to take place between n- or π-electrons in pyridine derivatives and between π-electrons in benzene. First, we will take up the n–π complex formation. The strength of the complex formation depends upon the ease with which n-electron can be released, and is measured by the pK_a value.[12] According to the pK_a value in Table 4, the strengths of the complexes

Table 4. The values of pK_a[12] and heat of reaction[13] for pyridine derivative with BF_3, ½ B_2H_6, and CH_3SO_3H

	pK_a	BF_3 kcal·mol^{-1}	½B_2H_6 kcal·mol^{-1}	CH_3SO_3H kcal·mol^{-1}
Pyridine	6.75	−17.5	−16.3	−19.5
γ-Picoline	6.02			
β-Picoline	5.68			
α-Picoline	5.97	−23.0	−17.2	−18.3
2,6-Lutidine	5.14	−25.0	−17.9	−17.1

will be in the following order: 2,6-lut>α-pi>γ-pi>β-pi>py. In fact, the measurement[13] of the heats of reaction of pyridine derivatives with CH_3SO_3H shows that the absolute values of the heat of reaction increase with the pK_a value of pyridines, in accordance with the order mentioned above. However, our data obtained for the specific interaction of pyridine derivatives with benzene result in the opposite order except for γ-picoline. This inversion is not particularly surprising, however, since it has been known that

10) H. Fröhlich, "The Theory of Dielectrics," Clarendon Press, Oxford (1949), p. 49.
11) J. S. Rowlinson, "Liquid and Liquid Mxiture," Butterworths, London (1959), p. 153.
12) L. Sacconi, P. Paoletti and M. Ciampolinl, *J. Am. Chem. Soc.*, **82**, 3828 (1960).
13) C. T. Mortimer, "Reaction Heat and Bond Strength," Pergamon Press, London (1963), p. 111.

because of the steric hindrance of the methyl group of 2,6-lutidine or α-picoline, the heat of the reaction[10] of the pyridine derivative with BF_3, or $(1/2)B_2H_6$ is in the order of: py$>\alpha$-pi$>$2,6-lut.

Thus, it seems that the methyl group of 2,6-lutidine or α-picoline offers steric hindrance to the approach of the benzene molecule; this results in a corresponding decrease in the strength of the molecular interaction. We can qualitatively explain our result in terms of the n–π interaction. On the other hand, in the pyridine derivative-carbon tetrachloride systems we can find only a small change in the strength of the molecular interaction, as shown in Table 3. This may be illustrated as follows. Provided that the carbon tetrachloride molecule interacts with the nitrogen of the pyridine derivative, we know that the carbon tetrachloride molecule is not sterically interfered with so much as the benzene molecule by the methyl group of the pyridine derivative. The strengths of the interaction of pyridine, α-picoline, and 2,6-lutidine with carbon tetrachloride are nearly equal to each other as a result of the cancellation of the inductive effect of the electron-releasing by the methyl group and the effect of the steric hindrance.

On the other hand, the molecular interaction of the π-electrons of the pyridine derivative with the π-electron of the benzene molecule can be shown to be highly plausible. Comparing the ionization potential, or the electron affinity of the pyridine derivatives with that of benzene, it seems reasonable to regard the benzene molecule as a donor. In this case, it seems that the strengths of the interaction are in the order of: py$>\beta$-pi$>$ α-pi$>\gamma$-pi$>$2,6-lut. Our results show the same trend except for γ-pi.

Then, it seems reasonable to explain the specific interaction of pyridine derivatives with benzene in terms of a n–π interaction. On the basis of a thermochemical study alone, however, it can not be decided whether the specific interaction of pyridine derivatives with benzene is an n–π or π–π interaction.

BULLETIN OF THE CHEMICAL SOCIETY OF JAPAN VOL. 42 40—46 (1969)

Anomalous Magnetic Properties of Stable Crystalline Phenoxyl Radicals

Kazuo MUKAI*1

Department of Chemistry, Faculty of Science, Kyoto University, Sakyo-ku, Kyoto

(Received April 13, 1968)

The results of static magnetic susceptibility measurements in the 1.8—300°K temperature range are reported on powder samples of the stable aromatic free radicals: 2,6-di-*t*-butyl-4(3,5-di-*t*-butyl-4-oxocyclohexa-2,5-dienylidene methyl) phenoxyl (Galvinoxyl) and 2,6-di-*t*-butyl-4(3,5-di-*t*-butyl-4-oxocyclohexa-2,5-dienylidene amino) phenoxyl (BIP) radicals. The susceptibility of Galvinoxyl follows the Curie-Weiss law above $T_c=81\pm1$°K, depending on the sample, with a Weiss constant of 11 ± 3°K. However, at $T_c=81$°K, χ_p rapidly decreases, and below 66°K the susceptibility again increases, with different spin concentrations for independently-prepared samples as the temperature is lowered. A maximum at 81°K was also found by the EPR measurements; the anomaly of the susceptibility at this temperature is probably due to a first-order phase transition induced magnetically, accompanying the pairing of magnetic spins, judging from the results of differential thermal analysis and the magnetic susceptibility measurements. On the other hand, the magnetic susceptibility of the BIP radical exhibits a broad maximum at 54 ± 2°K. This susceptibility can be explained approximately using a model which consists of a singlet ground state and a triplet state lying slightly above the ground state.

2,6-Di-*t*-butyl-4-R-substituted-phenols produce the corresponding phenoxyl radicals upon oxidation with lead peroxide or, preferably, with an alkaline solution of potassium ferricyanide in various organic solvents. The magnetic properties of these phenoxyls in solution have been studied by a number of investigators with the aid of the electron paramagnetic resonance (EPR) spectra.[1-3]

Solvent-free solids of the phenoxyls produced with such oxidations were studied by Müller *et al.*

*1 Present address: Department of Chemistry, Faculty of Science, Ehime University, Matsuyama.

1) A. L. Buchachenko, Stable Radicals Chapter III (Consultants Bureau, New York, 1965).

2) K. H. Hausser, H. Brunner and J. C. Jochims, *Mol. Phys.*, **10**, 253 (1966).

3) K. Mukai, H. Nishiguchi, K. Ishizu, Y. Deguchi and H. Takaki, This Bulletin, **40**, 2731 (1967).

at room temperature[4,5] and, in some cases, at the temperature of liquid nitrogen[6]; they ascertained the absolute paramagnetic contribution to the susceptibility by using Pascal's constants to estimate the diamagnetic correction, χ_d, thus estimating the concentration of the radicals. However, it has not been clear whether or not the observed susceptibility generally follows the Curie-Weiss law.

In a previous paper[7] we have reported an anomaly in the magnetic susceptibility of the Galvinoxyl radical at 82.5°K from the results of the susceptibility measurements between 63°K and 289°K, and have suggested that this radical may have similarities with the well-known anomaly in the magnetic susceptibility of Wurster's blue perchlorate (WB) at 186°K,[8-11] which is explained by the orthorhombic-monoclinic phase transition in which Wurster's blue cations pair up to form dimers with ground singlet states and excited triplet states.[12] Recently, another explanation has been proposed by G. T. Pott *et al.* for the mechanism of the above transition.[13]

In the present paper, first, in order to obtain further information about the transition of Galvinoxyl and the general nature of these neutral radical solids, we have measured the temperature dependence of the magnetic susceptibilities of the solid radicals of a similar molecular structure, including 2,6-di-*t*-butyl-4(3,5-di-*t*-butyl-4-oxocyclohexa-2,5-dienylidene methyl) phenoxyl (Galvinoxyl) and 2,6-di-*t*-butyl-4(3,5-di-*t*-butyl-4-oxocyclohexa-2,5-dienylidene amino) phenoxyl (Bisindophenoxyl; BIP) radical, between 1.8°K and 300°K; these radicals are known to be thermally stable and to be inert to oxygen. Secondly, the measurements of the electron paramagnetic resonance of Galvinoxyl and the differential thermal analyses of the phenoxyl radical and the corresponding phenol were undertaken in order to investigate the properties of the transition.

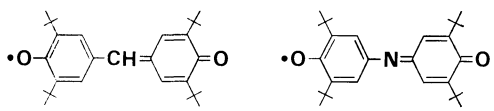

Galvinoxyl BIP

† : tBu

Extensive work, has been performed on other free radical solids,[14-17] especially tetracyanoquinodimethane (TCNQ) salts, in which the electrons interact to form singlet-triplet pairs. The present evidence indicates that such pairing is also present in the BIP radical hindered by tertiary butyl groups, but in the case of Galvinoxyl the susceptibility below the transition point can not be explained by the hypothesis of a simple pairing such as was observed in Wurster's blue perchlorate.

Experimental

Preparation of Specimens. Galvinoxyl, mp 151.5—153.0°C, was prepared from 2,6-di-*t*-butylphenol according to the method of Kharash and Joshi[18] or Coppinger.[19] After condensation with formaldehyde, the product was oxidized with lead peroxide in ether. A very dark blue crystalline compound was isolated from the ethereal solution.

The BIP radical, mp 155°C, was synthesized following the method of Coppinger[20] and then recrystallized from isooctane under nitrogen gas in a freezer. This melting point is higher than that (132—133°C) of the corresponding phenol. The samples were stored in the dark at a cool ambient temperature under a vacuum.

Measurements. The susceptibility measurements were carried out in the continuous temperature range between 1.8°K and 300°K using a magnetic torsion balance on powder samples of about 100 mg in a heterogeneous magnetic field up to about 10 koe. The details of the apparatus were described previously.[21] After loading the samples in an open quartz bucket into the apparatus, the sample chamber was evacuated to about 10^{-5} mmHg and a small amount of helium was admitted to the apparatus to act as a heat-transfer gas. The temperature of the sample was determined by a AuCo-Chromel thermocouple for the higher temperatures and by a carbon resistance thermometer for the low temperatures, with a supplement of Mn-tutton salt.

The data have been corrected for diamagnetism using the Pascal's constants.[22] The diamagnetic contribution to Galvinoxyl was calculated to be $-276\times$

4) E. Müller and K. Ley, *Chem. Ber.*, **87**, 922 (1954).
5) E. Müller, A. Schick and K. Scheffler, *ibid.*, **92**, 474 (1959).
6) E. Müller, K. Ley and W. Schmidhuber, *ibid.*, **89**, 1738 (1956).
7) K. Mukai, H. Nishiguchi and Y. Deguchi, *J. Phys. Soc. Japan*, **23**, 125 (1967).
8) N. Elliot and M. Wolfsberg, *Phys. Rev.*, **91**, 435 (1953).
9) K. H. Hausser and H. Kainer, *Chem. Ber.*, **86**, 1563 (1953).
10) W. Duffy, Jr., *J. Chem. Phys.*, **36**, 490 (1962).
11) K. Okumura, *J. Phys. Soc. Japan*, **18**, 69 (1963).
12) D. D. Thomas, H. Keller and H. M. McConnell, *J. Chem. Phys.*, **39**, 2321 (1963). Other references are therein.
13) G. T. Pott and J. Kommandeur, *ibid.*, **47**, 395 (1967).
14) D. B. Chesnut and W. D. Phillips, *ibid.*, **35**, 1002 (1961).
15) R. G. Kepler, *ibid.*, **39**, 3528 (1963).
16) W. Duffy, Jr., and D. L. Strandburg, *ibid.*, **46**, 456 (1967).
17) H. Nishiguchi, This Bulletin, **40**, 1587 (1967).
18) M. S. Kharasch and B. S. Joshi, *J. Org. Chem.*, **22**, 1435 (1957).
19) G. M. Coppinger, *J. Am. Chem. Soc.*, **79**, 501 (1957).
20) G. M. Coppinger, *Tetrahedron*, **18**, 61 (1962).
21) M. Mekata, *J. Phys. Soc. Japan*, **17**, 796 (1962).
22) P. W. Selwood, "Magnetochemistry," 2nd Ed., Interscience Publisher, New York (1956).

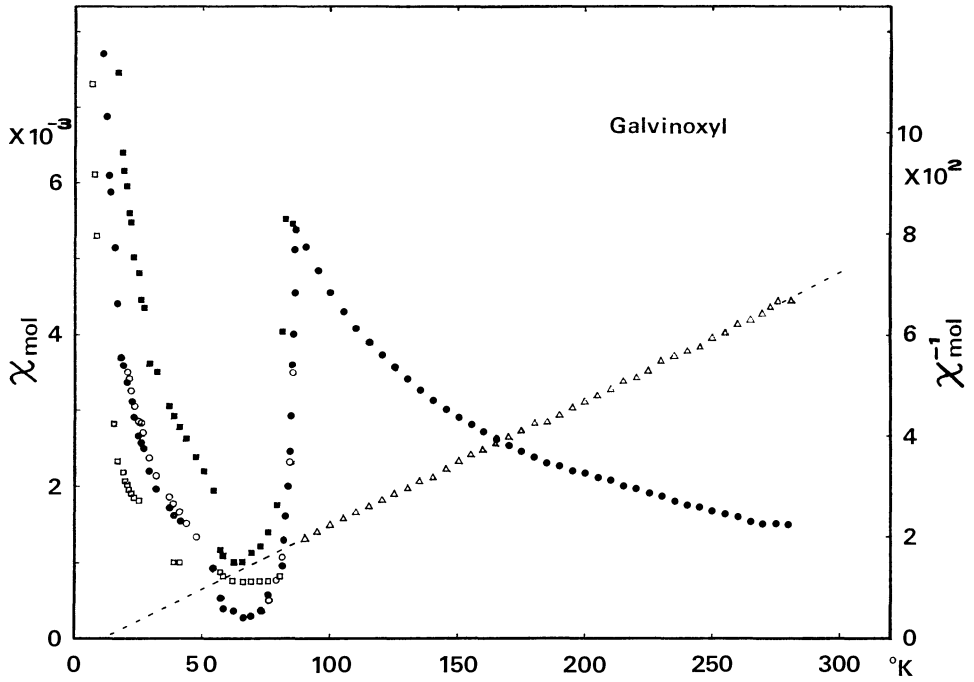

Fig. 1. (a) Molar susceptibilities of the Galvinoxyl radicals *versus* temperature (1.8—300°K). Sample numbers 1, 2, 3 and 3′ are denoted in the figure as ■, □, ● and ○, respectively. (b) Inverse molar susceptibility of the Galvinoxyl in the high-temperature region (82—300°K) (open triangle, △).

10^{-6} emu/mol, a value which agrees well with the measured value of -265×10^{-6} emu/mol for the corresponding phenol. The diamagnetic correction for BIP was also obtained from the Pascal's constants and/or from the measured values for the corresponding phenol. The absolute susceptibilities were determined using Mn-tutton salt or Mohr's salt as standards. The relative data were estimated to be reliable to within about ±3% over the entire temperature range, while the absolute susceptibilities were estimated to be correct to within ±5%.

All the EPR measurements were taken with a JEOL 3BX spectrometer, with a 100-kc-field modulation and equipped with a field dial and a variable temperature-control unit. Highly-diluted crystals such as Mn^{2+} in CdS were used as standards. The first derivative of the absorption was observed, and the relative magnetic susceptibility was taken as proportional to the product of the height times the square of the peak-to-peak linewidth of the first derivative.

Results and Discussion

Galvinoxyl. The magnetic susceptibilities obtained for three independently-prepared Galvinoxyl radicals (denoted as Sample Nos. 1, 2 and 3) are shown in Fig. 1 as a function of the temperature. These have been corrected for the diamagnetic contribution of $\chi_{dia}=-276\times10^{-6}$ emu/mol calculated by the Pascal's method. This value agrees well with the measured value of $\chi_{dia}=-265\times10^{-6}$ emu/mol for the corresponding phenol. When the temperature of the radical sample is lowered from room temperature, χ_p increases following the Curie-Weiss law, $\chi_p=C/(T-\theta)$, with the same C_H and θ_H values within the range of experimental errors, reaching a maximum at about $T_c=81$°K, depending on the sample. After passing through the maximum, within about three degrees χ_p decreases rapidly by about 80 percent of its maximum value, and afterward falls off gradually till 66°K. However, below 66°K the susceptibilities increase again as the temperature is lowered. The radical spins in the low-temperature region (5—50°K) obey only the Curie-Weiss law, as is apparent from the $1/\chi_p$-T curve shown in Fig. 2. On the other hand, the spin concentrations differ individually for each sample. The different values of C_L and θ_L obtained for three samples are listed in Table 1, where the subscripts, L and H, refer to the low- and high-temperature regions respectively. These values of C_L are from about three to ten times smaller than that in the high-temperature section (83—300°K). At still lower temperatures (1.8—5°K) the susceptibility again deviates from the Curie-Weiss law. Further, two independent runs about the sample 3 were examined, resulting in a considerable accordance (denotd as 3′ in Fig. 2).

EPR measurements were done with a polycrystalline Galvinoxyl radical in the temperature range between room temperature and the temperature of liquid nitrogen, using a microwave

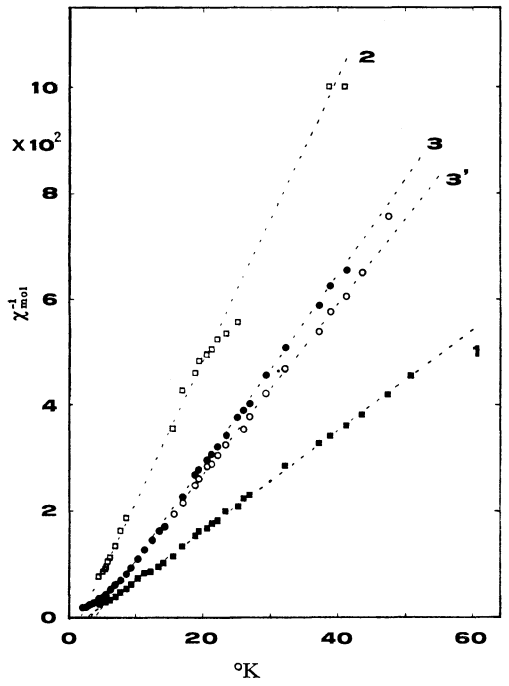

Fig. 2. Inverse molar susceptibilities of the Galvinoxyl radicals *versus* temperature (1.8—50°K). Sample numbers 1, 2, 3 and 3′ are denoted in the figure as ■, □, ● and ○, respectively.

frequency of about 9300 Mc/sec, in order to ascertain the anomaly in the magnetic susceptibility. The paramagnetic absorption spectrum of the Galvinoxyl exhibits one asymmetric line, with a line width of about 5 gauss; this can usually be attributed to the presence of an anisotropic g-value. The line-width is temperature-independent within the range of experimental error from 77°K to room temperature. Since a transition has been found by measuring the static magnetic susceptibility, the absorption was carefully examined above and below $T_c=81$°K. However, no appreciable change in the position and shape of the absorption line could be found in this temperature range. Since the line-width of the magnetic-resonance absorption curve of this radical is approximately constant, the height of the derivative is proportional to the susceptibility. This relative magnetic susceptibility. I_{EPR}, of Galvinoxyl as a function of the temperature is shown in Fig. 3; the maximum of the static susceptibility at 81°K was also found by measuring the electron paramagnetic resonance. The value of the Curie-Weiss constant obtained from the $1/I_{EPR}$-T curve, shown in Fig. 3, $\theta=1\pm5$°K, shows a qualitative agreement with the value, $\theta=11\pm3$°K, obtained from the static magnetic measurements.

If the sudden decrease in magnetic susceptibility is due to the first-order phase transition, the maximum should be found by differential thermal analysis (DTA). In fact, the DTA curve of powdered Galvinoxyl shows a peak around 82°K. On the other hand, the DTA for the corresponding phenol does not show any anomaly at the transition

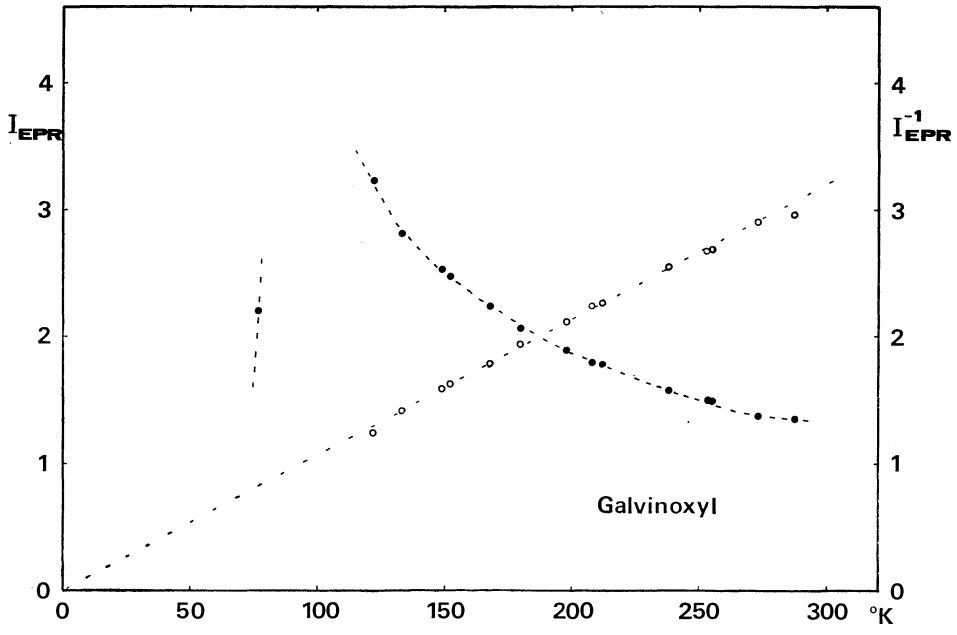

Fig. 3. (a) Relative intensity (full circle, ●) and (b) relative inverse intensity(open circle, ○) of the EPR absorption of the Galvinoxyl radical.

Table 1. Values of T_C, C_H, θ_H, C_H/C_T, C_L, θ_L, C_L/C_T, and C_L/C_H

Sample	T_C (°K)	C_H (emu °K/mol)	θ_H (°K)	C_H/C_T (%)	C_L (emu °K/mol)	θ_L (°K)	C_L/C_T (%)	C_L/C_H (%)
1	81	0.400	11	106	0.105	2.8	27.7	26.2
2	84.5	0.419	8	111	0.037	1.8	10.0	9.0
3	86	0.401	11	106	0.056	3.9	14.7	13.9
3′	86	0.401	11	106	0.058	3.2	15.3	14.4

temperature.[23] The high-temperature structure of the Galvinoxyl radical can be understood simply as a molecular crystal composed of unpaired neutral radicals, showing a spin concentration of about 106% as $S=1/2$, following the Curie-Weiss law. Therefore, it is highly probable that the transition found by measuring magnetic susceptibility and the electron paramagnetic resonance absorption for Galvinoxyl is due to the first-order phase transition induced magnetically, accompanied by a pairing of the magnetic spins. This magnetically-induced phase transition of Galvinoxyl differs from that of WB, which can be explained remarkably well in terms of an elementary theory of non-interacting triplet excitons, judging from the results of the pressure dependence of the exchange-narrowed magnetic resonance.[24]

The anomalies in magnetic susceptibility and DTA observed for the Galvinoxyl radical may be characteristic of the hindered phenoxyl radical solids. For example, the rotation of the tertiary butyl group or the intermolecular bonding between oxygen atoms may be responsible for the anomaly. Thus, we have measured the magnetic susceptibility of the BIP radical between 1.8°K and 300°K, for this radical has a molecular structure similar to that of the Galvinoxyl radical. The magnetic susceptibility of the BIP radical, the –CH= group situated at the center of the Galvinoxyl replaced with the –N= group, shows a broad maximum around 54°K, as will be described below. This experimental fact shows that the transition in Galvinoxyl is presumably related to the –CH= group.

Since the anomaly in Galvinoxyl is thought to be the transition accompanied by a pairing of the magnetic spins at the position of the –CH= group, and since the magnetic susceptibilities in the low-temperature region (5—50°K) obey the Curie-Weiss law, with different spin concentrations for the three samples, the low-temperature susceptibilities are probably due to the residual unpaired Galvinoxyl radicals with a spin of 1/2, radicals which will be randomly located in the lattice. Their concentrations, which can be calculated from the C_L values in Table 1, have been found to vary from about 10 to 30 mol%. This explanation can be supported by assuming that the magnetic spins are mostly clustered in groups of two in the crystals and that the exchange interactions between radical spins are large.

Another possible explanation is that the increase in susceptibility at low temperatures may be caused by the linear Ising rings, consisting of odd numbers of the radical molecules. When the phase transition induced by a coupling of magnetic spins leaves an odd number of coupled electrons in a segment, one electron spin will remain unpaired as the spins couple antiferromagnetically at a low temperature.

On the other hand, the values of θ in Table 1 are positive in both the high- and low-temperature regions of Galvinoxyl. This is unlike the negative values of θ obtained from most other organic radical solids, including several phenoxyl radicals.[25] This fact shows a possibility of weak ferromagnetism. The question about the observed ferromagnetic Weiss constants will be discussed elsewhere.

Bisindophenoxyl. The results of the susceptibility measurements on BIP are presented in Fig. 4, where the data have been corrected for a calculated diamagnetism of -268×10^{-6} emu/mol. This diamagnetism value also accords well with the measured value of $\chi_{dia}=-258\times10^{-6}$ emu/mol for the corresponding phenol.

The data were corrected for the presence of paramagnetic impurities by using the low-temperature measurements to determine their concentrations. In the region from 1.8—10.1°K, the Curie-Weiss law was observed corresponding to a spin concentration of 3.6% and a Weiss constant of -1.6 ± 0.1°K. When this low-temperature impurity curve is extrapolated to higher temperatures and subtracted from the experimental curve observed there, the corrected curve shown in Fig. 5 is obtained. The experimental curve has a general appearance very similar to that observed for such crystalline organic radicals as TCNQ salts,[15] picryl amino carbazyl (PAC),[16] and biphenyl-potassium salts.[17] In the case of the BIP radical. the unpaired electrons on the

23) Motivated with these findings, we now proceed to measure the low temperature heat capacities of Galvinoxyl and the phenol from 13 to 300°K. There is a sharp rise in the heat capacity of Galvinoxyl at 81.5°K. Details will be published in this Bulletin by S. Seki, H. Suga, A. Kosaki, Y. Deguchi and the author.

24) R. C. Hughes, A. W. Merkl and H. M. McConnell, *J. Chem. Phys.*, **44**, 1720 (1966).

25) Private communication.

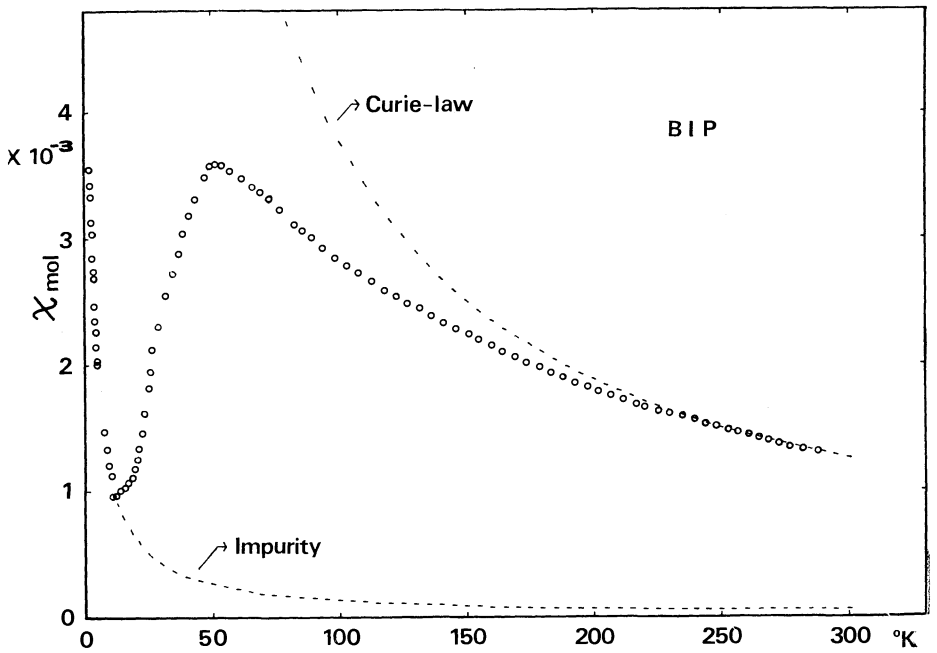

Fig. 4. Molar susceptibility of the BIP radical *versus* temperature (1.8—300°K). The "impurity curve" is an extrapolation of the low-temperature Curie-Weiss data.

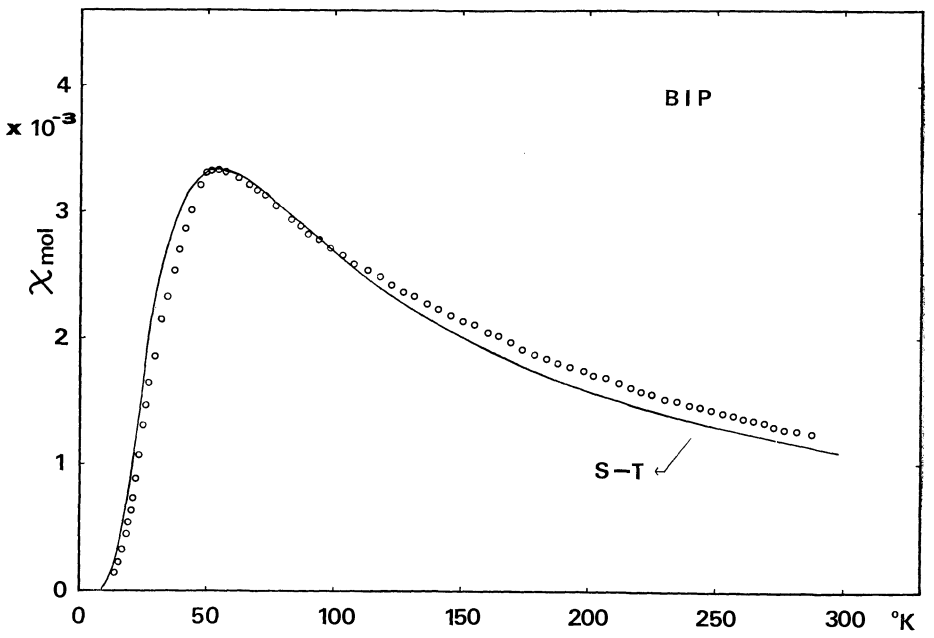

Fig. 5. Subtracted molar susceptibility of the BIP radical *versus* temperature (1.8—300°K). The solid curve is theoretical fits as explained in the text.

BIP molecules also appear to be paired up by an exchange interaction in quasimolecular states. The paramagnetic contribution to the susceptibility of BIP can be fitted approximately to the expression:

$$\chi_p = \frac{2Ng^2\beta^2}{kT} \cdot \frac{1}{3+e^{\delta/kT}} \qquad (1)$$

which corresponds to an assembly of N quasi-molecules with a singlet ground state and a triplet state lying by an energy, δ, above the ground state. If the temperature at which the susceptibility shows a maximum is defined as T_{max}, one can determine the singlet-triplet separation (δ) by using the relation $\delta = 1.61kT_{max}$. The theoreti-

cal curves require multiplication by a constant p to match the experimental data. Thus, with $\delta/k=87$ and $p=0.964$, the theoretical curves can be fitted to the experimental data, assuming that N is equal to one half of the number of BIP radicals and that $g=2.00$. The agreement between theory and experiment in the case of BIP is enough to conclude that the BIP radical forms radical dimers. The singlet-triplet separation can be estimated to be $\delta=60.5\ cm^{-1}$, using the value for $T_{max}(54\pm2°K)$ determined from the experiment.

In order to obtain further information about the magnetic property of the above radical, EPR measurements were made. The EPR spectrum of BIP shows one sharp, asymmetric line, with a line width of 3 gauss, which is temperature-independent between 77°K and room temperature. The expected zero-field splittings for the BIP entities in the triplet states are not observed over the accessible temperature range, although the magnetic susceptibility of BIP follows Eq. (1). This is probably because the zero-field splittings for BIP are collapsed into a single sharp line by the exchange-narrowing effect arising from the high concentration of triplet-state entities in this temperature range.

The crystalline organic free radicals, such as Wurster's blue perchlorate (WB),[12] TCNQ salts,[14,15] and PAC,[16] in which the electrons interact to form singlet-triplet pairs, are thought to be plate-like molecules and to be stacked face-to-face to form alternating chains. In the case of BIP, each phenyl ring (π-ring) being masked by the tertiary butyl groups, the oxygen atoms in BIP may play an important role in the above pairing. However, we could not observe any broad maxima for the other hindered phenoxyl radical solids.[25] Thus, the present evidence indicates that no such pairing is present in hinderd phenoxyl radicals.

EPR measurements of the photodissociation-products of tetraphenyl-hydrazine in a rigid solution at 77°K have indicated that the principal product of this dissociation is the dimer of the diphenyl amino (DPA) radical; this has been established by observing the half-field signal and the computer simulation of the EPR spectra.[26] It was proposed that, in the DPA radical dimer, a configuration of minimal repulsion, that is, with the planes each containing two nitrogens and the axes of the phenyl rings at right angles to each other, might be favored, particularly at low temperatures. The BIP radical dimer may have a configuration similar to that of the diphenyl amino radical dimer. However, until the crystal structure analyses are worked out in sufficient detail to give the exact relative positions of the magnetic molecules, they are of dubious value for our understanding of the exchange interactions in these compounds.

On the other hand, the theoretical value of the susceptibility at T_{max} exhibits a good agreement with the experimental value, as is shown in Fig. 5. However, the experimental susceptibility for BIP was observed to fall a little more rapidly than the theoretical susceptibility at temperatures below T_{max}, while above T_{max} the reverse is preferably true. It is well known that the exchange interaction, J, is strongly dependent on the intermolecular distance, and that the physical systems of interest are those in which the molecular entities are really supermolecules, that is, aggregates of weakly-bound molecules. Therefore, the exchange interaction between the BIP radicals, $|J|$ $(=\delta/2)$, may show temperature-dependence. In fact, the values for $|J|$ calculated from the magnitude of the susceptibility at 20, 30, 40, 54, 72.6, 98.5, 127, 160, 202, 240, and 288°K were 33.2, 32.2, 31.9, 30.2, 30.4, 30.0, 25.4, 18.0, 11.1, 4.1, and 1.0 cm^{-1} respectively.

Such deviations from normal behavior have also been found by, for example, magnetic susceptibility measurements[15] or the anomalous exchange-narrowing results in the EPR spectra[27] of some TCNQ salts. Chesnut[28] has suggested that the presence of an attractive interaction between the excitons may be responsible for the experimentally-observed decreases in J with the temperature. However, a self consistent-field treatment by Soos[29] of a linear antiferromagnetic lattice of any degree of alternation also predicts a decrease in the energy gap, δ, with an increase in the temperature. In addition, other explanations,[30,31] opposite to the model of interacting triplet excitons, have been proposed. Consequently, better theoretical and experimental studies will be required before the temperature dependence of the exchange interaction on the BIP radical can be fully interpreted.

This study was largely carried out under the guidance of Professor Hideo Takaki and Professor Yasuo Deguchi. The author is also indebted to Drs. Mamoru Mekata and Hiroaki Nishiguchi for their helpful discussions. Moreover, he is greatly indebted to Professor Syuzo Seki, Professor Hiroshi Suga, and Mr. Akio Kosaki of Osaka University for the differential thermal analyses.

26) D. A. Wiersma and J. Kommandeur, *Mol. Phys.*, **13**, 241 (1967).

27) M. T. Jones and D. B. Chesnut, *J. Chem. Phys.*, **38**, 1311 (1963).

28) D. B. Chesnut, *ibid.*, **40**, 405 (1964).

29) Z. G. Soos, *ibid.*, **43**, 1121 (1965).

30) H. M. McConnell and Z. G. Soos, *ibid.*, **40**, 586 (1964).

31) A. W. Merkl, R. C. Hughes, L. J. Berliner and H. M. McConnell, *ibid.*, **43**, 953 (1965).

BULLETIN OF THE CHEMICAL SOCIETY OF JAPAN VOL. 42 47—52 (1969)

Molecular Orbital Treatment of Nitric Oxide Radicals. I. Electronic Structure and Spectrum of the H_2NO Radical

Osamu KIKUCHI

Department of Chemistry, Tokyo Kyoiku University, Otsuka, Tokyo

(Received April 16, 1968)

A theoretical treatment of the H_2NO radical is presented. In the calculation, the approximate SCF method of Longuet-Higgins and Pople for open-shell molecules is applied to the valence electron system, the CNDO/2 approximation is adopted, and the molecular excited states are approximated by linear combinations of some doublet Slater determinants constructed by means of the SCF MO for the ground state. The results thus obtained for the electronic structure of the H_2NO radical are discussed. The calculated spectrum for the H_2NO radical shows that the longest wavelength band has the $n\rightarrow\pi^*$ character, and the $\pi\rightarrow\pi^*$ transition energy is smaller than that for the $n\rightarrow\sigma^*$ transition. The $\pi\rightarrow\pi^*$ transition energy, 5.77 eV, calculated by the method in which only the π-electrons were explicitly considered, indicated that the $\pi\rightarrow\pi^*$ band falls into the area near 240 mμ. From the calculated results for the H_2NO radical and the solvent effect on the absorption bands of aliphatic nitric oxide radicals, two bands, at 450 mμ, and 240 mμ, characteristic of the latter radicals have been assigned to the $n\rightarrow\pi^*$ and $\pi\rightarrow\pi^*$ transitions respectively.

Nitric oxide radicals are among the most typical organic radicals and have been widely investigated by maens of the ESR method.[1,2] Briere, Lemaire, and Rassat have studied the electronic structures of various stable nitric oxide radicals by the IR, UV, and ESR methods.[2] They have synthesized some aliphatic nitric oxide radicals and measured their electronic absorption spectra and ESR spectra; they found that two electronic absorption bands appear, at 450 mμ and 240 mμ, and that the nitrogen hyperfine splitting constant and the g value are 15—16 gauss and 2.0055 respectively. Since, in these nitric oxide radicals, an odd electron is almost completely localized on the $2p\pi$ orbitals of nitrogen and oxygen, the above characteristic properties can be expected to be understood on the basis of the electronic structure of the N-O group.

In theoretical treatment attempting to determine the electronic structure of open-shell systems such as aliphatic nitric oxide radicals, it is necessary to treat not only π-electrons, but also σ-electrons at the same time. An approximate method to obtain the LCAO-SCF-MO for the π-electron system of open-shell molecules was proposed by Longuet-Higgins and Pople[3] and was later applied to a theoretical treatment of the π-electronic structures of organic radicals.[4] An approximate method for obtaining SCF molecular orbitals for all valence electrons in closed-shell molecules was presented by Pople, Santry, and Segal.[5] They found that completely neglecting the differential overlap (CNDO) approximation in electron-repulsion integrals leads to results which are invariant to simple transformations of the atomic orbital basis set when these integrals satisfy a further restrictive relationship. This approximate method with CNDO was later modified in some ways; the new method was denoted the "CNDO/2 approximation".[5] They used this CNDO/2 method to calculate molecular orbitals for the valence electrons of some closed-shell molecules and have obtained reasonable theoretical results for some electronic properties of molecules.[5]

As the first step of the molecular orbital treatment of nitric oxide radicals, the present investigation intends to obtain information about the electronic

1) Y. Deguchi, This Bulletin, **34**, 910 (1961); J. Pannell, *Mol. Phys.*, **7**, 317 (1964); J. Yamauchi, H. Nishiguchi, K. Mukai, Y. Deguchi and H. Takaki, This Bulletin, **40**, 2512 (1967); A. L. Buchachenko, *Akad. Nauk S. S. S. R.*, **6**, 1120 (1963); G. Chapelet-Letourneux, H. Lemaire, A. Rassat and J. P. Ravet, *Bull. Soc. Chim. France*, **1965**, 1975; O. Kikuchi and K. Someno, This Bulletin, **40**, 2549 (1967); A. K. Hoffman and A. T. Henderson, *J. Am. Chem. Soc.*, **83**, 4671 (1961); N. B. Neiman, E. G. Rozanzev and Yu. G. Mamedova, *Nature*, **196**, 476 (1963).

2) R. Briere, H. Lemaire and A. Rassat, *Bull. Soc. Chim. France*, **1965**, 3273.

3) H. C. Longuet-Higgins and J. A. Pople, *Proc. Phys. Soc.*, **68**, 591 (1955).

4) A. Ishitani and S. Nagakura, *Theoret. Chim. Acta (Berl.)*, **4**, 236 (1966).

5) J. A. Pople, D. P. Santry and G. A. Segal, *J. Chem. Phys.*, **43**, S129 (1965); J. A. Pople and G. A. Segal, *ibid.*, **44**, 3289 (1966); J. A. Pople and G. A. Segal, *ibid.*, **43**, S136 (1965).

structure of aliphatic nitric oxide radicals and to assign the two characteristic absorption bands at 450 mμ and 240 mμ. For this purpose, we will use the H_2NO radical, which is the simplest nitric oxide radical and the ESR spectrum of which has been obtained.[6] The approximate SCF method of Longuet-Higgins and Pople will be applied to the valence electron system with the CNDO/2 approximation, and the electronic structure and spectrum of the H_2NO radical will be discussed.

Theoretical

The Hamiltonian operator, $\mathcal{H}$, is expressed in the form:

$$\mathcal{H} = \sum_i H_{\text{core}}(i) + \sum_{i>j} e^2/r_{ij} \tag{1}$$

where $H_{core}(i)$ is the sum of the kinetic energy operator for the valence electron, i (the 1s electron for hydrogen and the 2s and 2p electrons for carbon, nitrogen, and oxygen atoms), and the potential energy operator in the core field (nucleus and inner electrons).

The ground configuration of the free radical is doublet, and its antisymmetrized wave function is described by:

$$\Psi_g = |\, \phi_1\bar{\phi}_1 \cdots \phi_{m-1}\bar{\phi}_{m-1}\phi_m \,| \tag{2}$$

where the number of valence electrons is $2m-1$. The excited doublet configurations considered are of the following four types:

$$\left.\begin{aligned}
\Psi_{m\to k} &= |\, \phi_1\bar{\phi}_1 \cdots \phi_{m-1}\bar{\phi}_{m-1}\phi_k \,| \\
\Psi_{i\to m} &= |\, \phi_1\bar{\phi}_1 \cdots \phi_i\bar{\phi}_m \cdots \phi_{m-1}\bar{\phi}_{m-1}\phi_m \,| \\
\Psi_{i\to k}(\mathrm{I}) &= \frac{1}{\sqrt{2}}\{|\, \phi_1\bar{\phi}_1 \cdots \phi_i\bar{\phi}_k \cdots \phi_{m-1}\bar{\phi}_{m-1}\phi_m \,| \\
&\quad + |\, \phi_1\bar{\phi}_1 \cdots \phi_k\bar{\phi}_i \cdots \phi_{m-1}\bar{\phi}_{m-1}\phi_m \,|\} \\
\Psi_{i\to k}(\mathrm{II}) &= \frac{1}{\sqrt{6}}\{|\, \phi_1\bar{\phi}_1 \cdots \phi_i\bar{\phi}_k \cdots \phi_{m-1}\bar{\phi}_{m-1}\phi_m \,| \\
&\quad - |\, \phi_1\bar{\phi}_1 \cdots \phi_k\bar{\phi}_i \cdots \phi_{m-1}\bar{\phi}_{m-1}\phi_m| \,\} \\
&\quad - 2|\, \phi_1\bar{\phi}_1 \cdots \phi_i\phi_k \cdots \phi_{m-1}\bar{\phi}_{m-1}\bar{\phi}_m \,|
\end{aligned}\right\} \tag{3}$$

where i and k are labeled as the doubly-occupied and the unoccupied orbitals respectively in the ground configuration. In the present treatment, the electronic wave functions for ground and excited doublet states are approximated by linear combinations of the above configurations:

$$\Phi = \sum_i A_i\Psi_i \tag{4}$$

For the open-shell molecules, an approximate method for obtaining self-consistent molecular orbitals for π-electrons was proposed by Longuet-Higgins and Pople.[3] We applied their method to the valence electron system using the CNDO/2 approximation. The valence electrons are assigned to LCAO molecular orbitals:

$$\phi_i = \sum_r C_{ri}\chi_r \tag{5}$$

where χ_r are valence atomic orbitals. The molecular orbital energies and LCAO coefficients are obtained by:

$$\sum_s (F_{rs} - \delta_{rs}\varepsilon)C_{si} = 0 \tag{6}$$

and the matrix elements are given by:

$$\left.\begin{aligned}
F_{rr} &= U_{rr} + \left(P_{AA} - \frac{1}{2}P_{rr}\right)\gamma_{AA} + \sum_{B(\neq A)}(P_{BB} - \zeta_B)\gamma_{AB} \\
F_{rs} &= \frac{1}{2}(\beta_A + \beta_B)S_{rs} - \frac{1}{2}P_{rs}\gamma_{AB} \quad (r \neq s)
\end{aligned}\right\} \tag{7}$$

where the electron-density and bond-order matrix, P_{rs}, is given by:

$$P_{rs} = \sum_{i=1}^{m-1} 2C_{ri}C_{si} + C_{rm}C_{sm} \tag{8}$$

and where the other notations are the same as those given by Pople *et al.*[5] The choice of all the parameters except the bonding parameters are entirely based on them; the bonding parameters, β_A, are determined by the method to be described in the next section.

An initial calculation of the molecular orbital coefficients is carried out by a Hückel-type calculation; iterations are then performed until self-consistency is achieved on all orbital energies with a tolerance of 0.00005 eV. All the present calculations were carried out with the HIPAC 103 computer of Tokyo Kyoiku University.

Results and Discussion

At first the values of bonding parameters, β_A, were reexamined. Pople *et al.* have determined the values of bonding parameters empirically so that the CNDO calculations give the best over-all fit with the accurate LCAO-SCF calculations on diatomic molecules.[5] For the orbital energy intervals, the bonding parameters listed in their article reproduce almost well those obtained by the full LCAO-SCF calculations. However their results also show that the orbital energy intervals $(\varepsilon_j - \varepsilon_i)$ are not satisfactory for π-orbitals; the discrepancy from the results obtained by the full LCAO-SCF calculations is about 3.5 eV for some diatomic molecules. Therefore, their values will not be the best ones to discuss all the kinds of electronic transitions, such as $n\to\pi^*$, $n\to\sigma^*$, and $\pi\to\pi^*$, at the same time. To obtain bonding parameters appropriate to the present calculations, the formaldehyde molecule was chosen as an example; for it the $n\to\pi^*$, $n\to\sigma^*$, and $\pi\to\pi^*$

6) C. J. W. Gutch and W. A. Waters, *J. Chem. Soc.*, **1965**, 751; J. Q. Adams, S. W. Nicksic and J. R. Thomas, *J. Chem. Phys.*, **45**, 654 (1966).

TABLE 1. LCAO SCF MO'S OF FORMALDEHYDE*1

MO	Orbital energy (eV)	Symmetry	Coefficients									
			1s(H_1)	1s(H_2)	2s(C)	2p_x(C)	2p_y(C)	2p_z(C)	2s(O)	2p_x(O)	2p_y(O)	2p_z(O)
ϕ_1	−39.96	a_1	0.1258	0.1258	0.4357	0.0000	0.2643	0.0000	0.8352	0.0000	−0.1055	0.0000
ϕ_2	−26.67	a_1	0.3782	0.3782	0.6222	0.0000	−0.2666	0.0000	−0.3941	0.0000	−0.3167	0.0000
ϕ_3	−22.46	b_2	0.3403	−0.3403	0.0000	0.5828	0.0000	0.0000	0.0000	0.6548	0.0000	0.0000
ϕ_4	−18.48	a_1	0.2334	0.2334	−0.0248	0.0000	−0.5692	0.0000	0.2140	0.0000	0.7216	0.0000
ϕ_5	−16.97	b_1	0.0000	0.0000	0.0000	0.0000	0.0000	0.6284	0.0000	0.0000	0.0000	0.7779
ϕ_6	−14.52	b_2	0.4127	−0.4127	0.0000	0.3442	0.0000	0.0000	0.0000	−0.7354	0.0000	0.0000
ϕ_7	2.99	b_1	0.0000	0.0000	0.0000	0.0000	0.0000	0.7779	0.0000	0.0000	0.0000	−0.6284
ϕ_8	3.15	a_1	0.5154	0.5154	−0.6127	0.0000	0.1903	0.0000	0.0755	0.0000	−0.2267	0.0000
ϕ_9	6.34	b_2	0.4626	−0.4626	0.0000	−0.7361	0.0000	0.0000	0.0000	0.1746	0.0000	0.0000
ϕ_{10}	9.10	a_1	0.1449	0.1449	0.2169	0.0000	0.7063	0.0000	−0.3093	0.0000	0.5625	0.0000

*1 C-O axis taken as y axis; z axis perpendicular to molecular plane.

TABLE 2. CALCULATED LOWER EXCITED STATE OF FORMALDEHYDE

Exp.*1	Excited state	Energy (eV)	Symmetry	Nature of the excited state*2	Configurations mainly contributing to each state	
4.26	Φ_1	3.50	A_2	$n\rightarrow\pi^*$	$\Psi_{6\rightarrow7}$ (94.8%)	$\Psi_{3\rightarrow7}$ (5.2%)
	Φ_2	6.75	B_1	$\sigma\rightarrow\pi^*$	$\Psi_{4\rightarrow7}$ (98.4%)	
7.1	Φ_3	7.31	B_2	$n\rightarrow\sigma^*$	$\Psi_{6\rightarrow8}$ (61.4%)	$\Psi_{6\rightarrow10}$ (33.2%)
8.0	Φ_4	7.76	A_1	$\pi\rightarrow\pi^*$	$\Psi_{5\rightarrow7}$ (64.7%)	$\Psi_{4\rightarrow10}$ (17.7%)
	Φ_5	8.25	B_1	$\pi\rightarrow\sigma^*$	$\Psi_{5\rightarrow8}$ (81.5%)	$\Psi_{5\rightarrow10}$ (18.5%)

*1 Reference 7.

*2 A symbol "$n\rightarrow\pi^*$" is used when the excited state wave function is mainly consist of the configurations in which one electron in the ground configuration is excited from n(non-bonding)-orbital to π^*(π-anti-bonding)-orbital, and the transition from the ground state to this state is $n\rightarrow\pi^*$ transition.

absorptions are confirmed experimentally.[7] In the calculation of the H_2CO molecule, the C–H and C–O bond lengths were assumed to be 1.09 Å and 1.21 Å respectively,[8] and all the bond angles, to be 120°. We also assumed a planar structure with a C_{2v} symmetry for the ground and excited states. The SCF equations for closed-shell molecules derived by Pople *et al.* were used, and after the usual configurational interaction calculation for excited singlet states, the electronic transition energies for the H_2CO molecule were obtained. The values of β_H, β_C, and β_O were determined to be −8, −14, and −25 eV respectively. These values well reproduce the experimental $n\rightarrow\sigma^*$ and $\pi\rightarrow\pi^*$ transition energies, while for the $n\rightarrow\pi^*$ transition, the calculated energy was somewhat lower than the experimental one. The calculated SCF molecular orbitals are shown in Table 1, and the results of the configulation interaction treatment are shown in Table 2. By a number of calculations for the H_2CO molecule, the following results were also obtained: (1) the bonding parameter for the hydrogen atom does not change the calculated excitation energies so much as those of the carbon and oxygen atoms, (2) the parameters obtained, $\beta_H=-8$ eV, $\beta_C=-14$ eV, and $\beta_O=-25$ eV, almost completely reproduce the bond-order and electron-density matrix calculated by the parameters listed by Pople *et al.* but give a better agreement with the experimental transition energies than their parameters.

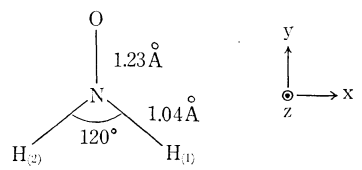

Fig. 1. Assumed structure of the H_2NO radical.[9]

The electronic structure of the H_2NO radical has been calculated assuming the planar configuration shown in Fig. 1. The bonding parameters obtained by calibration from the formaldehyde was used; for the bonding parameter of the nitrongen

7) H. Sponer and E. Teller, *Rev. Modern Phys.*, **13**, 75 (1941).

8) D. P. Stevensen, J. E. LuValle and V. Schomaker, *J. Am. Chem. Soc.*, **61**, 2508 (1939).

9) A. W. Hanson, *Acta Cryst.*, **6**, 32 (1953).

TABLE 3. LCAO SCF MO'S OF H_2NO RADICAL

MO	Orbital energy (eV)	Symmetry	Coefficients									
			1s(H_1)	1s(H_2)	2s(N)	2p_x(N)	2p_y(N)	2p_z(N)	2s(O)	2p_x(O)	2p_y(O)	2p_z(O)
ϕ_1	−41.24	a_1	0.1865	0.1865	0.5937	0.0000	0.2107	0.0000	0.7130	0.0000	−0.1590	0.0000
ϕ_2	−29.80	a_1	0.3180	0.3180	0.5577	0.0000	−0.3326	0.0000	−0.5781	0.0000	−0.2045	0.0000
ϕ_3	−22.90	b_2	0.3815	−0.3815	0.0000	0.6449	0.0000	0.0000	0.0000	0.5414	0.0000	0.0000
ϕ_4	−19.20	a_1	0.2194	0.2194	−0.0861	0.0000	−0.6240	0.0000	0.2867	0.0000	0.6518	0.0000
ϕ_5	−18.53	b_1	0.0000	0.0000	0.0000	0.0000	0.0000	0.7694	0.0000	0.0000	0.0000	0.6387
ϕ_6	−14.75	b_2	0.3335	−0.3335	0.0000	0.3012	0.0000	0.0000	0.0000	−0.8288	0.0000	0.0000
ϕ_7	−4.96	b_1	0.0000	0.0000	0.0000	0.0000	0.0000	0.6387	0.0000	0.0000	0.0000	−0.7694
ϕ_8	3.40	a_1	0.5403	0.5403	−0.5476	0.0000	0.1904	0.0000	0.0551	0.0000	−0.2779	0.0000
ϕ_9	6.99	b_2	0.4932	−0.4932	0.0000	−0.7024	0.0000	0.0000	0.0000	0.1471	0.0000	0.0000
ϕ_{10}	10.34	a_1	0.1552	0.1552	0.1713	0.0000	0.6476	0.0000	−0.2688	0.0000	0.6564	0.0000

TABLE 4. ELECTRON-DENSITY AND BOND-ORDER MATRIX OF H_2NO RADICAL

	1s(H_1)	1s(H_2)	2s(N)	2p_x(N)	2p_y(N)	2p_z(N)	2s(O)	2p_x(O)	2p_y(O)	2p_z(O)
1s(H_1)	0.8815	−0.1454	0.5384	0.6929	−0.4067	0.0000	0.0239	−0.1397	0.0966	0.0000
1s(H_2)		0.8815	0.5384	−0.6929	−0.4067	0.0000	0.0239	0.1397	0.0966	0.0000
2s(N)			1.3419	0.0000	−0.0134	0.0000	0.1524	0.0000	−0.5291	0.0000
2p_x(N)				1.0132	0.0000	0.0000	0.0000	0.1990	0.0000	0.0000
2p_y(N)					1.0886	0.0000	0.3272	0.0000	−0.7444	0.0000
2p_z(N)						1.5920	0.0000	0.0000	0.0000	0.4915
2s(O)							1.8494	0.0000	0.3835	0.0000
2p_x(O)								1.9599	0.0000	0.0000
2p_y(O)									0.9839	0.0000
2p_z(O)										1.4080

atom, β_N, the value of −20 eV was used for no particular reason. This value is between those for carbon and oxygen atoms; the effect of the variation in β_N on the results will be examined below. The orbital energies and LCAO coefficients obtained are listed in Table 3, and the bond-order and electron-density matrix, in Table 4. These tables show the following features of the electronic structure of the H_2NO radical:

(1) The ground-state electron configuration is:

$$(1a_1)^2(2a_1)^2(1b_2)^2(3a_1)^2(1b_1)^2(2b_2)^2(2b_1)^1$$

where the orbitals, $3a_1$, $1b_1$, $2b_2$, and $2b_1$, are understood to be the N-O σ-bonding orbital (by the $2p_y$ atomic orbitals of the nitrogen and oxygen atoms), the π-bonding orbital (by the $2p_z$ orbitals of the nitrogen and oxygen atoms), the non-bonding orbital of the oxygen atom, and the π-anti-bonding orbital respectively. This electron configuration show that the odd electron occupies the anti-bonding π-orbital, that the non-bonding orbital ($2p_x$(O)) is the highest doubly-occupied orbital, and that this makes the nitric oxide radical have a large g_{yy} tensor in the ESR spectra.[10]

(2) The spin density on the oxygen atom is larger than that on the nitrogen atom. When only the π-system of the N-O group is considered, however, this difference is very small (Table 6).

(3) The coefficients for $2p_x$(O) show that the lone-pair orbital on the oxygen atom partially distributes on the hydrogen atoms through the pseudo-π-orbital constructed by two 1s orbitals of the hydrogen atoms and the $2p_x$ orbitals of the nitrogen and oxygen atoms.

In the configurational interaction treatment for the H_2NO radical, all singly-excited configurations of the form in Eq. (3) were considered. The energy levels and the configurations contributing to each state are tabulated in Table 5. The ground state has a B_1 symmetry, and the excited states are of 4 types, A_1, A_2, B_1, and B_2. The intensities are expected to be small for the transitions to A_1 and B_2 states because the basis set of the π-orbital is different from that of the non-bonding orbital or the σ-orbitals.*1 The $B_1 \rightarrow A_2$ ($n \rightarrow \sigma^*$) and the $B_1 \rightarrow B_1$ ($\pi \rightarrow \pi^*$) transitions will have strong intensities, but for the $n \rightarrow \sigma^*$ transitons it must be noted that the electronic oscillator strength is

10) O. H. Griffith, D. W. Cornell and H. M. McConnell, *J. Chem. Phys.*, **43**, 2909 (1965).

*1 The predicted intensity of the $B_1 \rightarrow B_2$ transition will be zero for the electric-dipole radiation, and for the $B_1 \rightarrow A_1$ transition the transition moment will be finite as a result of the 2s atomic orbitals in the LCAO σ-orbital, but the intensity will not be strong.

Table 5. Calculated lower states of H_2NO radical

Exp.*1	State	Energy (eV)	Symmetry	Nature of the states*2	Configurations mainly contributing to each state			
	Φ_G	0.000	B_1	ground state	Ψ_g	(98.3%)		
2.76	Φ_{E1}	1.68	B_2	$n\rightarrow\pi^*$	$\Psi_{6\rightarrow7}$	(93.4%)	$\Psi_{3\rightarrow7}$	(6.6%)
	Φ_{E2}	2.96	A_1	$\pi\rightarrow\sigma^*$	$\Psi_{7\rightarrow8}$	(87.9%)	$\Psi_{5\rightarrow8}$(II)	(6.1%)
	Φ_{E3}	5.81	A_2	$n\rightarrow\sigma^*$	$\Psi_{6\rightarrow8}$(II)	(80.5%)	$\Psi_{6\rightarrow10}$(II)	(14.2%)
	Φ_{E4}	5.89	B_2	$\pi\rightarrow\sigma^*$	$\Psi_{7\rightarrow9}$	(85.3%)	$\Psi_{5\rightarrow9}$(II)	(11.0%)
5.17	Φ_{E5}	6.00	B_1	$\pi\rightarrow\pi^*$	$\Psi_{5\rightarrow7}$	(83.7%)	$\Psi_{4\rightarrow10}$(I)	(8.5%)
	Φ_{E6}	6.58	A_1	$\sigma\rightarrow\pi^*$	$\Psi_{4\rightarrow7}$	(97.9%)		
	Φ_{E7}	6.77	A_1	$\pi\rightarrow\sigma^*$	$\Psi_{5\rightarrow8}$(I)	(71.6%)	$\Psi_{5\rightarrow8}$(II)	(23.9%)
	Φ_{E8}	6.78	A_2	$n\rightarrow\sigma^*$	$\Psi_{6\rightarrow8}$(I)	(57.4%)	$\Psi_{6\rightarrow10}$(I)	(37.9%)

*1 Reference 2
*2 See the footnote of Table 2.

small for the $\Phi_G\rightarrow\Phi_{E3}$ transition because of the porperties of the two electronic wave functions, Φ_G and Φ_{E3}.*2 The calculated results indicate that the longest wavelength band corresponds to the $n\rightarrow\pi^*$ transition and that the two transitions at 6.00 eV and at 6.78 eV have strong intensities. As has been described before, Briere *et al.*[2] have reported the characteristic bands for aliphatic nitric oxide radicals, 2.76 eV (450 mμ, $\varepsilon=10$) and 5.17 eV (240 mμ, $\varepsilon=3000$). They assigned the band at 450 mμ to the $n\rightarrow\pi^*$ transition on the basis of its weak intensity and the facts that this band is sensitive to the polarity of the solvent and shifts to the shorter wavelength region in the polar solvent. The calculated energy for the $n\rightarrow\pi^*$ transition is lower than the experimental value by about 1 eV; this tendency also appeared in the calculation of the formaldehyde by the present calculation method. For the band at 240 mμ, from its intensity, they supposed it to be a $\pi\rightarrow\pi^*$ or $n\rightarrow\sigma^*$ transition. Their experimental results have also shown that this band is not sensitive to the polarity of the solvent and may be assigned to the $\pi\rightarrow\pi^*$ transition. The present calculated energy for the $\pi\rightarrow\pi^*$ is lower than that for the $n\rightarrow\sigma^*$ transition ($\Phi_G\rightarrow\Phi_{E8}$); this indicates that the band at 240 mμ corresponds to the $\pi\rightarrow\pi^*$ transition. A number of calculations for the H_2NO radical have shown that the above results for the H_2NO radical were consistent even with variations in the bonding parameter for the nitrogen atom (-15 —— -23 eV) and in the N-O bond length (1.20—1.30 Å). Namely, the longest wavelength band has the $n\rightarrow\pi^*$ character, the transition energy for the $\pi\rightarrow\pi^*$ is always lower than that for $n\rightarrow\sigma^*$ ($\Phi_G\rightarrow\Phi_{E8}$ in Table 5), and some weak band exist in the ultraviolet and visible regions.

The $\pi\rightarrow\pi^*$ transition energy for the H_2NO radical, calculated by the method in which only the π-electrons were explicitly considered, is shown in Table 6. The calculation method and semi-empirical parameters used were the same as those reported elsewhere.[11] This result supports the assignment that the band at 240 mμ is the $\pi\rightarrow\pi^*$ transition.

Table 6. Energy levels and wave-functions of H_2NO radical*1

Energy (eV)	Wave-function*2
0.00	$\Phi_G = 0.999\lvert\phi_1\bar{\phi}_1\phi_2\rvert + 0.035\lvert\phi_1\bar{\phi}_2\phi_2\rvert$
5.77	$\Phi_E = 0.035\lvert\phi_1\bar{\phi}_1\phi_2\rvert - 0.999\lvert\phi_1\bar{\phi}_2\phi_2\rvert$

*1 π-electrons only were explicitly considered. The calculation method were same as that in Ref. 11.
*2 LCAO MO's are
$\phi_1 = 0.706$: $2p_z(N) + 0.708$: $2p_z(O)$
$\phi_2 = 0.708$: $2p_z(N) - 0.706$: $2p_z(O)$

The results for the $(CH_3)_2NO$ radical are added. The experimental values used in this paper are those for aliphatic nitric oxide radicals, and so the present calculations of the H_2NO radical do not strictly correspond to them. Therefore, the substituent effect on the results obtained above was examined. The results were parallel to those for the H_2NO radical; the calculated transition energies for the $(CH_3)_2NO$ radical corresponding to the $n\rightarrow\pi^*$, $\pi\rightarrow\pi^*$, and $n\rightarrow\sigma^*$ transitions of the H_2NO radical are 2.00, 6.77, and 8.33 eV respectively.

Some unsatisfactory points remain in this study: (1) In spite of the trial calculation for the H_2CO molecule, it is uncertain whether the method with CNDO approximation gives the proper results for the electronic transition energy of free radicals; (2) The molecular structure in the excited state was assumed to be the same as that of the ground state. In this study, the effect of these defects on the calculated results was not estimated and so some uncertainty may remain as to the assignment of

*2 $\langle\Psi_g\lvert\sum_n er_u\rvert\Psi_{i\rightarrow k}(\mathrm{II})\rangle = 0$ (See Table 5).

11) O. Kikuchi and K. Someno, This Bulletin, **40**, 2972 (1967).

the band at 240 mμ because the calculated $\pi \rightarrow \pi^*$ transition energy is near that of the $n \rightarrow \sigma^*$ transition.

The author wishes to express his thanks to Professor Keizo Suzuki, Tokyo Kyoiku University, and to Dr. Kazuo Someno, Government Chemical Industrial Research Institute, Tokyo, for their helpful suggestions.

BULLETIN OF THE CHEMICAL SOCIETY OF JAPAN VOL. 42 52—57 (1969)

Photochemistry of Acetanilide. II. The Primary Processes in the Photochemical Reaction

Haruo SHIZUKA[1)]

Laboratory of Physical Chemistry, Tokyo Institute of Technology, Ookayama, Meguro-ku, Tokyo

(Received May 10, 1968)

The photochemical primary processes of acetanilide have been discussed on the basis of the quantum yields in various solvents, the dependences of the quantum yields on the excitation wavelength, and the emission spectra. The quantum yields of the products (*o*-aminoacetophenone and *p*-aminoacetophenone) at 2537 Å decreased greatly in polar solvents. A non-linear relationship between the quantum yield and the fraction of hydrogen-bonded acetanilide in the cyclohexane-ethanol solution was obtained. No variation in the quantum yield was observed upon the change of the excitation from 2537 to 2740 Å. These results indicate the occurrence of a radiationless internal conversion, $S_1(\pi\pi^*) \leftarrow S_2(\pi\pi^*)$. The relative fluorescence intensity in a polar solvent was larger than that in a nonpolar solvent. On the basis of these studies, it can reasonably be considered that the primary process in the photochemical reaction of acetanilide involves predissociation.

In a previous paper[2)] on the photochemical reaction of acetanilide, it has been shown that the quantum yields under various conditions and the kinetic data of benzene photosensitization indicate a mechanism *via* the lowest excited singlet state, $S_1(\pi\pi^*)$, not the triplet state, $T_1(\pi\pi^*)$.

The excitation of acetanilide at 2537 Å occurs from the ground state, S_0, to the secondary excited singlet state, $S_2(\pi\pi^*)$. The occurrence of a non-radiative internal conversion, $S_1(\pi\pi^*) \leftarrow S_2(\pi\pi^*)$, is to be expected. Since acetanilide has a carbonyl group involving non-bonding electrons, it is also interesting to consider the role of $S_1(n\pi^*)$ or $T_1(n\pi^*)$ in the photochemical primary processes. Measurements of fluorescence and phosphorescence spectra are useful for obtaining knowledge of electronic excited states in acetanilide. The purpose of the present work is to clarify the mechanism of photochemical primary processes in acetanilide.

This paper will report on the measurements of quantum yields in various solvents, the relationship between the quantum yield and the fraction of hydrogen-bonded acetanilide, the effect of the excitation wavelength of the quantum yield, measurements of emission spectra, and a theoretical estimation of the n-π^* energy level relative to the π-π^* energy levels by means of the intramolecular charge transfer theory.[3)] It will also include a discussion of the primary processes in this photochemical reaction.

Experimental

The experimental procedure and reagents were similar to those previously described.[2)] A low-pressure mercury lamp was used as the 2537 Å radiation source with a Vycor glass filter, while a high-pressure mercury lamp was used in the 2740 Å range with an interference filter UV-D-25. The fluorescence and phosphorescence spectra were observed by means of a Hitachi MPF-2 Spectrophotofluorometer and an Aminco Bowman Spectrophotofluorometer respectively. In these measurements, the concentrations of the solutions were adjusted so that the values of optical density were 0.600 at 2537 Å. The methylcyclohexane, ether, and ethanol were Tokyo Kasei Co. G. R.-grade products, while the methylcyclohexane was purified by passing it through silica-gel and by distillation.

1) Present address: Department of Chemistry, Faculty of Engineering, Gunma University, Tenjincho, Kiryu, Gunma.

2) H. Shizuka and I. Tanaka, This Bulletin, **41**, 2343 (1968).

3) S. Nagakura and J. Tanaka, *J. Chem. Phys.*, **22**, 236 (1954); S. Nagakura and S. Kuboyama, *J. Am. Chem. Soc.*, **76**, 1003 (1954); S. Nagakura, *J. Chem. Phys.*, **23**, 1441 (1955).

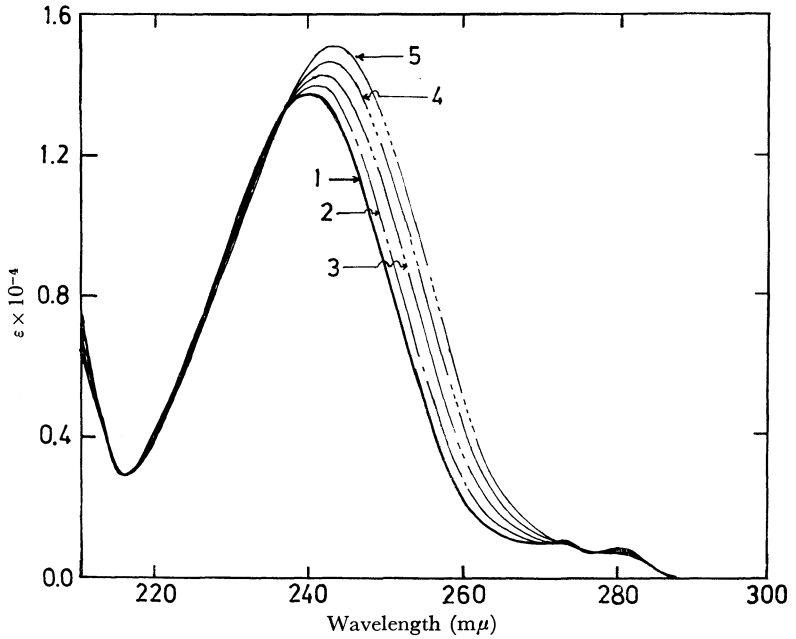

Fig. 1. Spectra of acetanilide in ethanol-cyclohexane mixture at room temperature. Ethanol concentrations are: 1, 0; 2, 0.041; 3, 0.082; 4, 0.205; and 5, 0.410 mol/*l*.

Experimental Results

1) Effect of Solvent. The quantum yields in various solvents were measured in a manner similar to that described in a preceding paper.[2] The results are shown in Table 1.

Table 1. Quantum yields of the products in various solvents at 2537 Å

Solvent	Quantum yield (Φ)	
	Φ_o	Φ_p
Cyclohexane[2]	7×10^{-2}	6×10^{-2}
Ether	4.3×10^{-2}	3.7×10^{-2}
Ethanol	1.7×10^{-2}	1.4×10^{-2}
H_2O	4.8×10^{-3}	1.8×10^{-3}

Φ_o: Φ of *o*-aminoacetophenone
Φ_p: Φ of *p*-aminoacetophenone

Polar solvents decreased the quantum yields. The dependence of quantum yields on the solvents was examined by means of the method reported by Shinzawa and Tanaka.[4] The ultraviolet spectra of acetanilide in an ethanol - cyclohexane solution varied with the composition of the solvents, as is shown in Fig. 1. The concentrations of ethanol were about 100 times greater than those of acetanilide.

Acetanilide has been revealed, by means of a study of its ultraviolet spectra, to form hydrogen bonds with dioxane and cyclohexanone as proton acceptors.[5] Assuming a hydrogen bond between

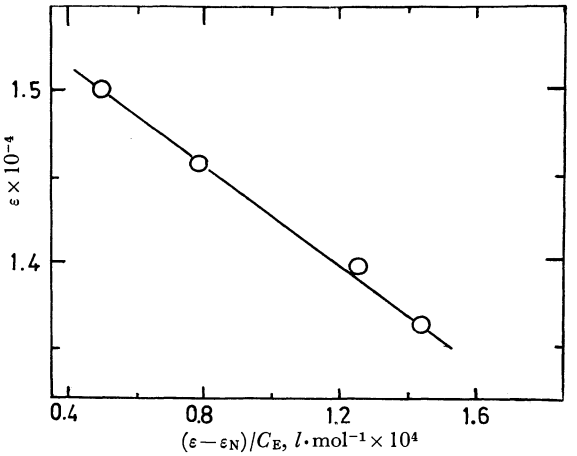

Fig. 2. Plot of ε against $(\varepsilon-\varepsilon_N)/C_E$ to obtain the equilibrium constant K of the bond formation using the relation.
$\varepsilon=-(\varepsilon-\varepsilon_N)/C_EK+\varepsilon_H$; slope of the curve indicates reciprocal value of K observed for 243 mμ at room temperature; ε, molar extinction of acetanilide in ethanol-cyclohexane solution; ε_N, molar extinction of acetanilide in cyclohexane; ε_H, molar extinction of hydrogen-bonded acetanilide; and C_E, concentration of ethanol.
$K=6.5\,l\cdot mol^{-1}$ for 243 mμ

4) K. Shinzawa and I. Tanaka, *J. Phys. Chem.*, **68**, 1205 (1964).

5) S. Suzuki and H. Baba, *Nippon Kagaku Zasshi* (*J. Chem. Soc. Japan, Pure Chem. Sect.*), **81**, 366 (1960).

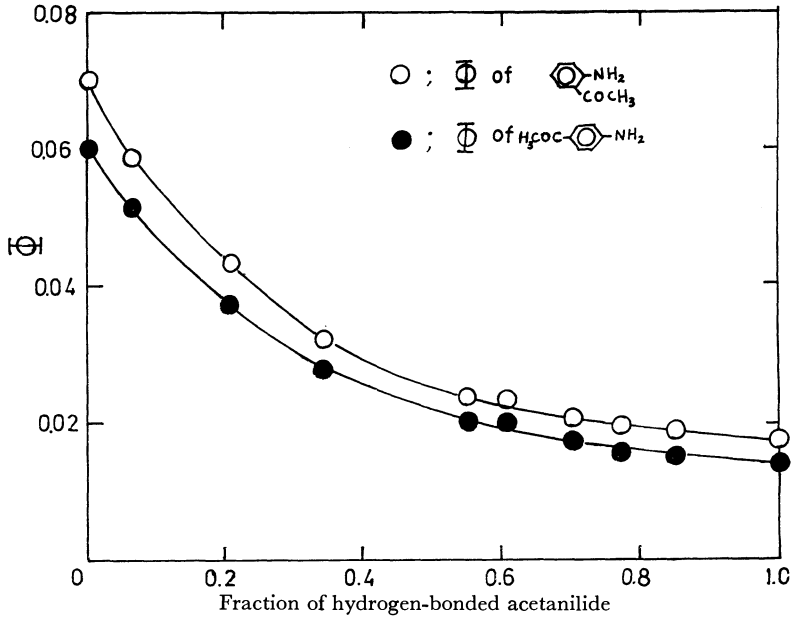

Fig. 3. Plot of quantum yield against fraction of hydrogen-bonded acetanilide molecules.

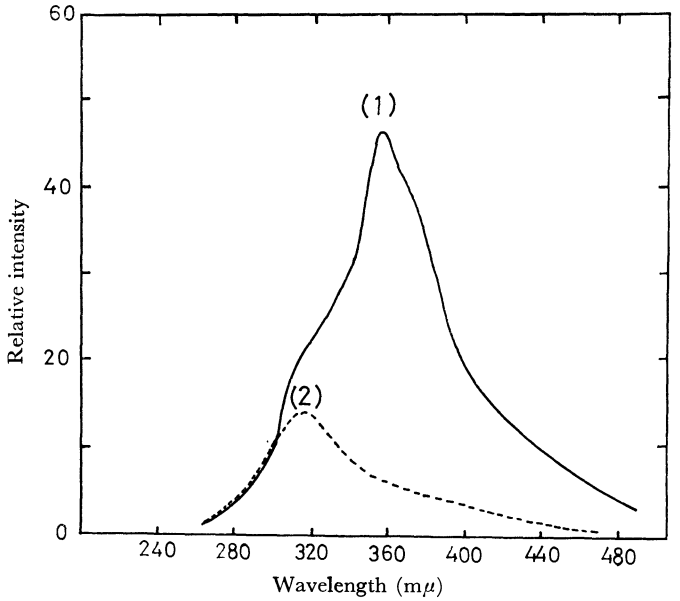

Fig. 4. Fluorescence spectra of acetanilide by the excitation at 2537 Å at room temperature.
(1): In ethanol (2): In cyclohexane

acetanilide and ethanol in the present study, the equilibrium constant, K, of the bond formation was calculated by the method obtained by Baba and Nagakura.[6] The value of K obtained from Fig. 2 was ~6.5 l/mol.

In order to ascertain the relation between the quantum yield and hydrogen-bond formation, the quantum yields are plotted in Fig. 3 against the fractions of the hydrogen-bonded molecules calculated from the K value.

A non-linear relationship was obtained, as is shown in Fig. 3.

2) Effect of Excitation Wavelength. A high-pressure mercury lamp was used for the 2740 Å

6) H. Baba and S. Nagakura, *Nippon Kagaku Zasshi* (*J. Chem. Soc. Japan, Pure Chem. Sect.*) **72**, 3 (1951); S. Nagakura and H. Baba, *J. Am. Chem. Soc.*, **74**, 5693 (1952).

range, which corresponds to the lowest excited singlet state, $S_1(\pi\pi^*)$,[7] with an interference filter, UV-D-25. The quantum yields of *o*-aminoacetophenone and *p*-aminoacetophenone by irradiation with a 2740 Å range light were 0.07 and 0.06 respectively in a cyclohexane solution. No effect of excitation wavelength on the quantum yields was observed from 2537 to 2740 Å.

3) Emission Spectra. In order to study the behavior of acetanilide in electronically-excited states, the emission spectra were measured. Figure 4 shows the fluorescence spectra of acetanilide in ethanol and cyclohexane solutions.

These data are summarized in Table 2.

Table 2. Fluorescence and phosphorescence spectra of acetanilide at 2537 Å.

Solvent	Fluorescence at room temperature		Phosphorescence at 77°K	
	λ_{max} (mμ)	I^F_{rel}	λ_{max} (mμ)	I^P_{rel}
Cyclohexane	317	13		
Methylcyclohexane			373	1
Ethanol	356	47	388	30

The concentrations were adjusted so that the optical densities at 2537 Å were 0.600.

I^F_{rel} and I^P_{rel} are the relative intensities of the fluorescence and phosphorescence maxima respectively.

In view of its red shift in a polar solvent, it is reasonable to assume that the fluorescence was the emission from $S_1(\pi\pi^*)$ to S_0. The phosphorescence can be assigned to the emission from the triplet state, $T_1(\pi\pi^*)$, to S_0, since the lifetime of the phosphorescence was a few seconds at 77°K. The natural radiative lifetime, τ_0, was calculated from Eq. (1):

$$\tau_0 = \frac{3.47\times10^8}{(\bar{\nu}_{max})^2\int\varepsilon(\bar{\nu})d\bar{\nu}} = 1.12\times10^{-7}\text{sec} \quad (1)$$

where $\bar{\nu}_{max}$ is the wave number of Absorption Band I,[7] which corresponds to $S_1(\pi\pi^*)$, $3.65\times10^4\text{cm}^{-1}$, and where $\int\varepsilon(\bar{\nu})d\bar{\nu}$ is the experimental extinction coefficient integrated over the width of Band I, 2.32×10^6 cm/mmol. The fluorescence lifetime is given by:

$$\tau_F = \tau_0\cdot Q_F = \sim10^{-10}\text{sec} \quad (2)$$

where Q_F is the fluorescence quantum yield of acetanilide in a cyclohexane solution, and where the order of magnitude is $\sim10^{-3}$, a value which was obtained by comparison with the relative fluorescence intensity of carbazole, whose fluorescence quantum yield is 0.35.[8]

Discussion

It has been reported that, in the nitrone→oxazirane photoisomerization, the lifetime of the excited nitrone molecule should be shorter than the relaxation time ($\sim10^{-11}$ sec)[9] of the arrangement between solute and solvent, since the linear relationship between the decrease in the quantum yield of the nitrone in anet hanol-cyclohexane solution and the fraction of hydrogen-bonded nitron molecules indicates that no rearrangement of solvent surrounding the excited nitrone molecule occurs before the photochemical reaction of the nitrone takes place.[4] In constrat to this, a non-linear relationship between the decrease in the quantum yield of acetanilide in an ethanol-cyclohexane solution and the fraction of hydrogen-bonded acetanilide was obtained, as is shown in Fig. 3. It is a possible explanation that the lifetime of an excited acetanilide molecule is longer than the relaxation time ($\sim10^{-11}$ sec)[9] of the arrangement of solute and solvent, and that therefore the radiationless internal conversion, $S_1(\pi\pi^*)\leftarrow S_2(\pi\pi^*)$, may occur.

In addition to this, no variation in the quantum yield was observed upon the change of excitation wavelength from 2537 to 2740 Å. This finding supports the occurrence of an internal conversion, $S_1(\pi\pi^*)\leftarrow S_2(\pi\pi^*)$, and of a Boltzmann distribution in $S_1(\pi\pi^*)$.

The n–π^* absorption band in acetanilide could not be observed, even at high concentrations ($\sim3\times10^{-3}$ mol/*l*). It is known that n–π^* transition in the molecules with a carbonyl group adjacent to the electron-donating group result in a large blue shift.[10] These phenomena have been theoretically explained by Nagakura *et al.*[3] and by Baba.[10] A theoretical estimation of the n–π^* energy level relative to π–π^* levels was carried out by means of the intramolecular charge transfer theory.[3]

The highest occupied (H_B, H_S) and the lowest vacant levels (V_B, V_S) were determined by means

7) H. Baba and S. Suzuki, *J. Chem. Phys.*, **32**, 1706 (1960).

8) D. W. Ellis and B. S. Solomon, *ibid.*, **46**, 3497 (1967).

9) E. Lippert, *Z. Naturforsch.*, **10a**, 541 (1955); *Z. Elektrochem.*, **61**, 962 (1957).

10) H. Baba, *Nippon Kagaku Zasshi* (*J. Chem. Soc. Japan, Pure Chem. Sect.*), **72**, 74, 341 (1951).

	$n\pi^*$ absorption band (Å)
HCHO	2940
CH_3COCH_3	2790
CH_3COCl	2345
CH_3COOH	2040
CH_3CONH_2	2050

of aniline and acetone, using experimental knowledge of their ionization potentials[11] and their near-UV absorption spectra. The highest occupied orbital of aniline (H_B) interacts with the lowest vacant orbital (V_B) of the substituent group (carbonyl group). Consequently, two new levels, W_n and W_e, result, as is shown in Fig. 5.

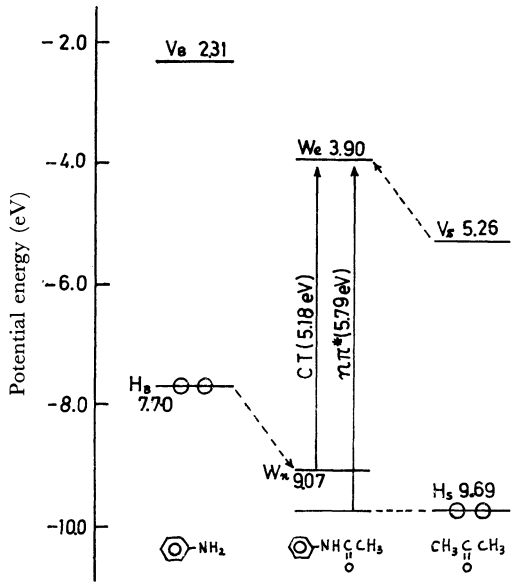

Fig. 5. Estimation of n–π^* transition in acetanilide

Their wave functions, Ψ, and energy levels, W_n and W_e can be represented as follows:

$$\Psi = a\varphi_B + b\varphi_S \quad (3)$$

$$W_n = \frac{1}{2}[H_B + V_S - \{(H_B - V_S)^2 + 4\beta^2\}^{1/2}] \quad (4)$$

$$W_e = \frac{1}{2}[H_B + V_S + \{(H_B - V_S)^2 + 4\beta^2\}^{1/2}] \quad (5)$$

where φ_B and φ_S are the wave functions for the H_B and V_S levels respectively and where β is the exchange integral.

Baba and Suzuki have reported that the lower excited singlet states in acetanilide consist of $S_1(\pi\pi^*)$ ($^1B_2$, 4.532 eV) and $S_2(\pi\pi^*)$ ($^1A_1$, 5.183 eV).[7] The $W_e \leftarrow W_n$ excitation corresponds to the $^1A_1 \leftarrow {}^1A_1$ transition and has a polarization of the transition dipole along the long axis.[7] Therefore, this transition is assigned to $S_2(\pi\pi^*) \leftarrow S_0$. The $S_1(n\pi^*)$ transition energy in acetanilide can then be estimated as 5.79 eV, as is shown in Fig. 5. The n–π^* transition energy is larger than that of $S_2(\pi\pi^*)$. Considering the energy levels as shown in Fig. 5, the photochemical reaction of acetanilide can not occur through the n–π^* state.

It has also been shown that $S_1(\pi\pi^*)$ in acetanilide is the lowest excited singlet state from the fluorescence spectra. The energy difference, ΔE, between $h\nu$ and $h\nu'$ can be calculated from the experimental data of absorption[12] and the emission spectra:

$$\left.\begin{aligned}(\Delta E)_{CH} &= 4900\ \text{cm}^{-1}\\ (\Delta E)_{EtOH} &= 8500\ \text{cm}^{-1}\end{aligned}\right\} \quad (6)$$

ΔE was larger in the polar solvent than in the nonpolar solvent. This indicates that the potential curve of the lowest excited singlet state, $S_1(\pi\pi^*)$, in the polar solvent lines below that in the nonpolar solvent. The repulsive potential curve of $^3\sigma_0$(N–C) may be approximately the same in polar and nonpolar solvents, since, in general, the triplet energy level is scarcely affected at all by a poar solvent. As has been described above, excited acetanilide molecules in $S_1(\pi\pi^*)$ are distributed according to the Boltzmann law. Therefore, the potential barrier which corresponds to the energy difference between their crossing point and the zero point energy level in $S_1(\pi\pi^*)$ may be larger in polar solvents. The effect of polar solvents on the quantum yield was very large, and the quantum yield decreased significantly in polar solvents, as is shown in Table 1. Moreover, the fluorescence intensity in a polar solvent was larger than that in a nonpolar solvent, as Table 2 shows.

It is reasonable to assume the intersystem crossing

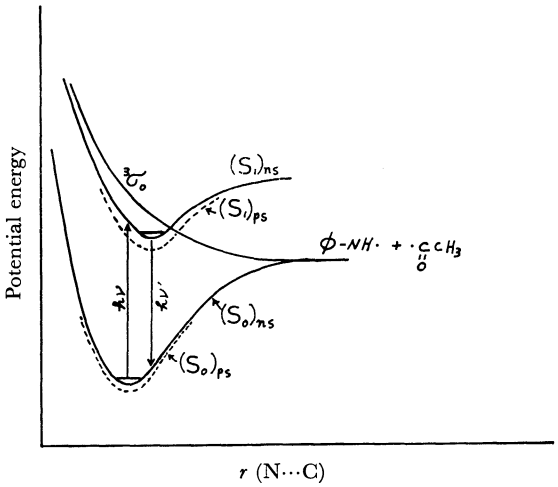

Fig. 6. A schematic potential energy diagram for ϕ–H···$\overset{\overset{O}{\|}}{N}$–$CCH_3$ system.
ns: nonpolar solvent ps: polar solvent

11) Ionization potential data are obtained from following references.
Aniline: K. Watanabe, *J. Chem. Phys.*, **26**, 542 (1957); R. Bralsfold, P. V. Harris and W. C. Price, *Proc. Roy. Soc.*, **A258**, 459 (1960).
Acetone: K. Watanabe, *J. Chem. Phys.*, **22**, 1895 (1954).

between $S_1(\pi\pi^*)$ and $^3\sigma_0$(N–C) repulsive state. Figure 6 shows a schematic potential energy diagram.

It has also been found that the quantum yield for the predissociation is dependent on the temperature and that this temperature dependency is affected by the polarity of a solvent.[13] Thus, the deactivation processes ($k_S+k_F+k_C$; see below) become more important than the nonpolar solvents. The primary processes in the photochemical reaction at 2537 Å can be represented by the following equations:

$$S_0 \xrightarrow{h\nu} S_2(\pi\pi^*) \quad (8)$$

$$S_2(\pi\pi^*) \xrightarrow{k_{ic}} S_1(\pi\pi^*) \quad (9)$$

$$S_1(\pi\pi^*) \xrightarrow{k_S} S_0 \quad (10)$$

$$S_1(\pi\pi^*) \xrightarrow{k_F} S_0 + h\nu' \quad (11)$$

$$S_1(\pi\pi^*) \xrightarrow{k_c} T_1(\pi\pi^*) \quad (12)$$

$$S_1(\pi\pi^*) \xrightarrow{k_{dis}} \phi\text{-NH}\cdot + \cdot\text{COCH}_3 \quad (13)$$

$$T_1(\pi\pi^*) \xrightarrow{k_T} S_0 \quad (14)$$

$$T_1(\pi\pi^*) \xrightarrow{k_p} S_0 + h\nu'' \quad (15)$$

Although this singlet-triplet transition, $^3\sigma_0$(N–C)$\leftarrow S_1(\pi\pi^*)$, is spin-forbidden, it must have a high transition probability to compete with the other deactivation processes for the lowest excited singlet state, $S_1(\pi\pi^*)$, in acetanilide. The probability of the $^3\sigma_0$(N–C)$\leftarrow S_1(\pi\pi^*)$ transition may result from the vibronic coupling between $S_1(\pi\pi^*)$ and $T_1(n\pi^*)$.

In conclusion, the photochemical reaction of acetanilide occurred from the lowest excited singelt state, $S_1(\pi\pi^*)$. The $S_1(\pi\pi^*)$ state might cross over to the $^3\sigma_0$(N–C) repulsive state, resulting in the fission of the N–C bond and the liberation of the ϕ-NH and $COCH_3$ radicals in their doublet ground states. It is reasonable to consider that the primary processes in this photochemical reaction involve the predissociation of the N–C bond.

The author is greatly indebted to Professor Ikuzo Tanaka and Associate Professor Yuji Miro of the Tokyo Institute of Technology for their generous and very helpful discussions of this paper.

12) Absorption band I: 274 mμ in cyclohexane, 273 mμ in ethanol,

13) H. Shizuka, This Bulletin, **42**, 57 (1969).

BULLETIN OF THE CHEMICAL SOCIETY OF JAPAN VOL. 42 57—65 (1969)

Photochemistry of Acetanilide. III. The Secondary Processes in the Photochemical Reaction

Haruo SHIZUKA[1)]

Laboratory of Physical Chemistry, Tokyo Institute of Technology, Ookayama, Meguro-ku, Tokyo

(Received June 18, 1968)

The photochemical secondary processes of acetanilide have been studied. The photochemical reaction of *p*-methylacetanilide at 2537 Å did not produce the *p*-rearrangement product, but the *o*-rearrangement one. The quantum yields of the *o*-rearrangement and of the disappearance of *p*-methylacetanilide were 0.09_2 and 0.12 respectively. Comparing the quantum yields of acetanilide with those of *p*-methylacetanilide, the values of the quantum yields for the predissociation of the N-C bond, the back reaction, and the recombination ratio were estimated to be 0.25, 0.10, and 0.9 respectively. These results indicate that the recombination reaction between the pair radicals formed by the predissociation of the N–C bond occur efficiently in a solvent cage. The rate constants of the back reaction, the *o*-rearrangement, and the *p*-rearrangement were proportional to the odd π electron densities of the anilino radical. No intermediate was observed by the flash photolysis. The small dependence of the quantum yields of acetanilide on the temperature supports the predissociation mechanism previously described.[2)] On the basis of these studies, the mechanism of the photochemical reaction of acetanilide in the liquid phase has been proposed.

In the second paper of this series,[2)] it has been shown that the photochemical primary process of acetanilide involves the predissociation caused by intersystem crossing, ${}^3\sigma_0(\mathrm{N\text{–}C}) \leftarrow s_1(\pi\pi^*)$. It is expected that, in the liquid phase, the recombination between the pair radicals formed by the predisso-

1) Present address: Department of Chemistry, Faculty of Engineering, Gunma University, Tenjin-cho, Kiryu, Gunma.

2) H. Shizuka, This Bulletin, **42**, 52 (1969).

ciation will occur with a high probability; this is the so-called "cage effect".[3] Many investigations of the cage effect have been reported by Noyes and by others.[4–10]

In order to determine the photochemical secondary processes of acetanilide, it is necessary to obtain the values of the quantum yields for the predissociation of the N–C bond, Φ_{dis}, the back reaction, Φ_B, and the recombination ratio, β. Considering their UV absorption spectra, the electronically-excited states in acetanilide and *p*-methylacetanilide are the same in a first approximation. Therefore, the photochemical primary process of *p*-methylacetanilide would be the same as that of acetanilide. However, the photochemical reaction of *p*-methylacetanilide at 2537 Å did not produce the *p*-rearrangement product but, rather, the *o*-rearrangement product, because its *p*-position is blocked by the methyl group.

The values of Φ_{dis} and Φ_B may be estimated by comparing the quantum yields of acetanilide with those of *p*-methylacetanilide.

On the other hand, flash photolysis is useful in detecting some intermediates, and the effect of the temperature on the quantum yield is also useful in discussing the mechanism of the photochemical reaction of acetanilide. This paper will report on the photochemical reactions of *p*-substituted acetanilide at 2537 Å, the dependence of the quantum yield on the temperature, the data of flash photolysis, and the estimations of Φ_{dis}, Φ_B, and β, it will also include a discussion of the photochemical secondary processes of acetanilide.

Experimental

The experimental technique was similar to that previously described.[2,11] The flash apparatus was an ordinary one. The excitation flash lamp with 150 mmHg of xenon gas, was made of quartz. The condenser for the excitation flash lamp with a capacity of 25μF was charged to 4 kV; the energy corresponded to 200 J. The pulse had a half-value width of about 50μsec. The flash lamp for spectroscopy, with 150 mmHg of xenon, was made of quartz. The condenser for the spectral flash lamp with a capacity of 8μF was charged to 4 kV; the energy corresponded to 64 J. The pulse had a half-value width of about 20μsec.

p-Methyl-, *p*-chloro-, *p*-bromo-, *p*-iodo-, and *p*-nitroacetanilides were prepared by treating reagent-grade products of *p*-substituted anilines with glacial anhydride and were purified by repeated recrystallizations from water. *p*-Amino- and *p*-hydroxyacetanilides were Tokyo Kasei Co. reagent-grade products and were purified by recrystallization from water.

Results and Discussion

1) Irradiation of *p*-Substituted Acetanilides at 2537 Å. The absorption spectra of the solutions of *p*-substituted acetanilides were similar to that of acetanilide, except in the case of *p*-nitroacetanilide.[12] The spectra of all the solutions of *p*-substituted acetanilides except *p*-nitroacetanilide changed markedly by upon irradiation with a 2537 Å light. The photochemical reactions of *p*-substituted acetanilides may be classified into the following four types.

a) Photochemical Reactions of p-Methyl- and p-Chloroacetanilides. Figure 1(a) shows the spectral change in a cyclohexane solution of *p*-methylacetanilide at 2537 Å. The absorption Band II (243 mμ) decreased and new bands appeared with maxima of 228 and 363 mμ as the irradiation time increased; there were three isosbestic points at 213, 235, and 260 mμ. The product which had absorption peaks at 228. and 363 mμ was assigned to 2-amino-5-methylacetophenone (*o*-rearrangement product) by gas chromatography. A similar spectral change was observed in the case of *p*-chloroacetanilide, as is shown in Fig. 1(b).
The quantum yields were obtained spectrophotometrically in cyclohexane.*1 The disappearance quantum yields of *p*-methyl- and *p*-chloroacetanilides were 0.12 and 0.13 respectively at 20°C. The quantum yields of 2-amino-5-methyl- and 2-amino-5-chloroacetophenones were 0.09_2 and 0.09_7 respectively. These photochemical reactions are analogous to those reported by Kobsa for *p-t*-butylphenylacetate derivatives,[13] as is shown in Eqs. (1) and (2):

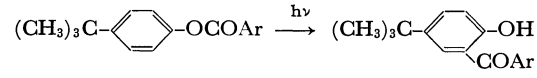

(1)

3) J. Franck and E. Rabinowitch, *Trans. Faraday Soc.*, **30**, 120 (1934).
4) F. W. Lampe and R. M. Noyes, *J. Am. Chem. Soc.*, **76**, 2140 (1954).
5) R. M. Noyes, *J. Chem. Phys.*, **22**, 1349 (1954).
6) R. M. Noyes, *J. Am. Chem. Soc.*, **77**, 2042 (1955); *ibid.*, **78**, 5486 (1956).
7) R. M. Noyes, *J. Phys. Chem.*, **65**, 763 (1961).
8) J. C. Roy, R. R. Williams, Jr., and W. H. Hamill, *J. Am. Chem. Soc.*, **76**, 3274 (1954).
9) L. Monchick, *J. Chem. Phys.*, **24**, 381 (1956).
10) H. P. Waits and G. S. Hammond, *J. Am. Chem. Soc.*, **86**, 1911 (1964); G. S. Hammond and J. R. Fox, *ibid.*, **86**, 1918 (1964).
11) H. Shizuka and I. Tanaka, This Bulletin, **41**, 2343 (1968).
12) H. E. Ungnade, *J. Am. Chem. Soc.*, **76**, 5133 (1954).

*1 The molar extinction coefficients, ε:
p-methylacetanilide Band II 243 mμ 13800
2-amino-5-methylacetophenone 363 mμ 3600
p-chloroacetanilide Band II 246 mμ 14300
2-amino-5-chloroacetophenone 365 mμ 3000

13) H. Kobsa, *J. Org. Chem.*, **27**, 2293 (1962).

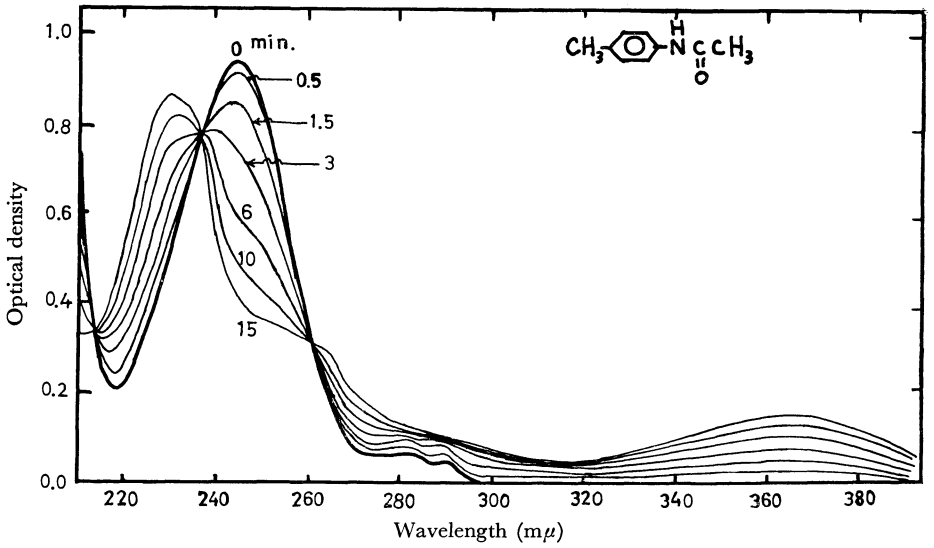

Fig. 1 (a).

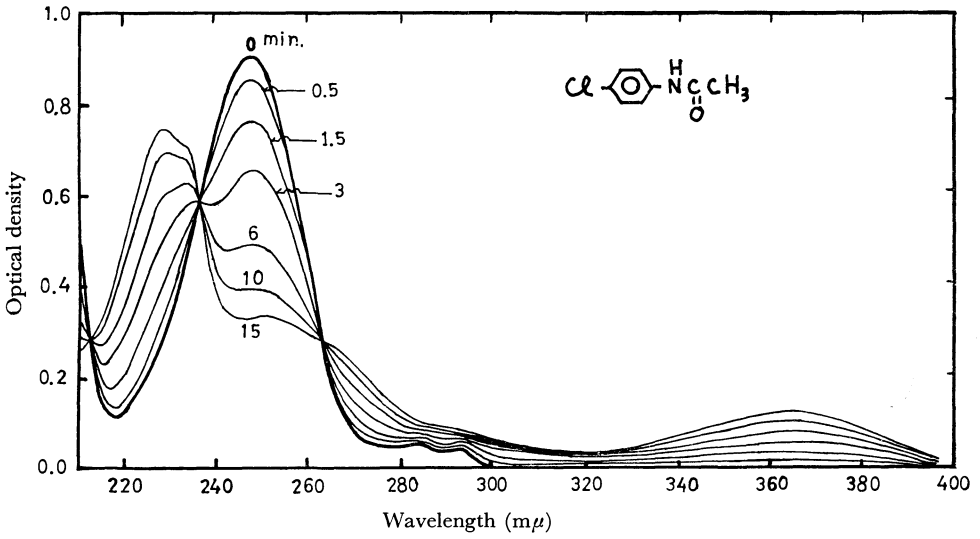

Fig. 1(b).

Fig. 1. Spectral changes of cyclohexane solutions of *p*-methylacetanilide (a) and of *p*-chloroacetanilide (b) with lapse of irradiation time at 2537 Å.

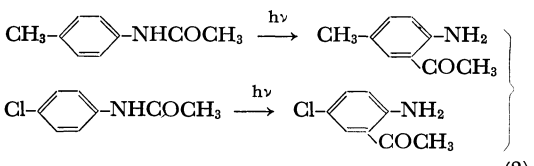

(2)

where Ar represents a phenyl substituent.

b) Photochemical Reactions of p-Bromo- and p-Iodo-Acetanilides. Figure 2(a) shows the spectral change in the solution of *p*-bromoacetanilide. The Absorption Band II (250 mμ) decreased and new bands with the maxima of 225, 290, and 365 mμ appeared, but with no clear isosbestic point such as those in the cases of *p*-methyl- and *p*-chloroacetanilides. The appearance of the 290 mμ peak probably indicates that *p*-aminoacetophenone was also produced by the irradiation with 2537 Å.[11] A similar spectral change was observed in the case of *p*-iodoacetanilide, as is shown in Fig. 2(b). In the photochemical reactions of *p*-bromo- and *p*-iodoacetanilides, it is reasonable to assume that the predissociation at the C–Br or at the C–I bond was caused by irradiation, resulting in acetanilide. Therefore, the *p*-rearrangement at 2537 Å might occur as well as the *o*-rearrangement.

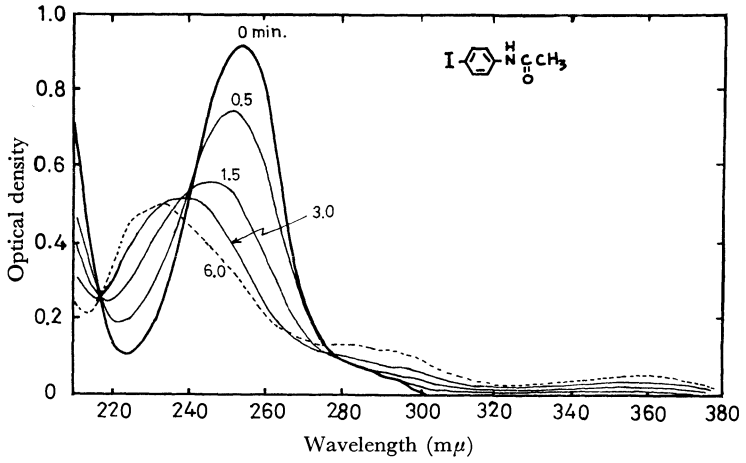

Fig. 2(a).

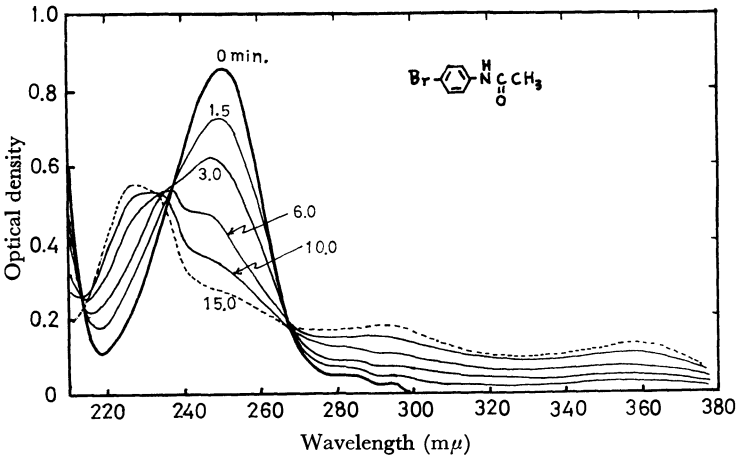

Fig. 2(b).

Fig. 2. Spectral changes of cyclohexane solutions of *p*-bromoacetanilide (a) and of *p*-iodoacetanilide (b) at 2537 Å.

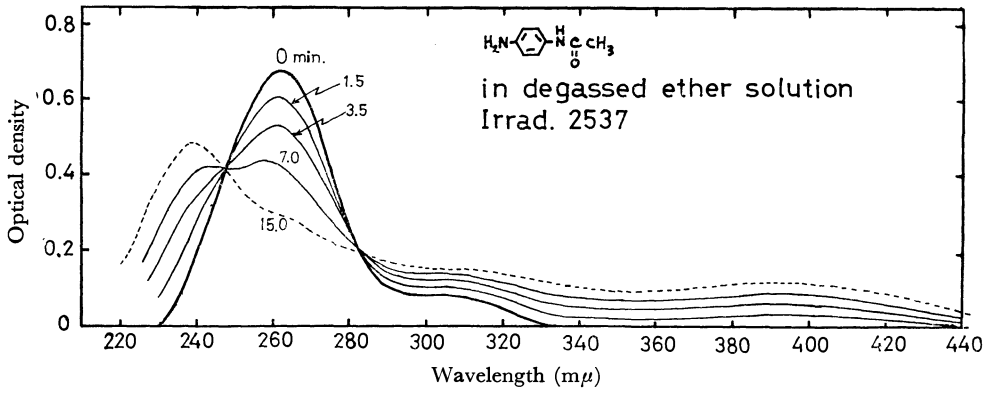

Fig. 3(a).

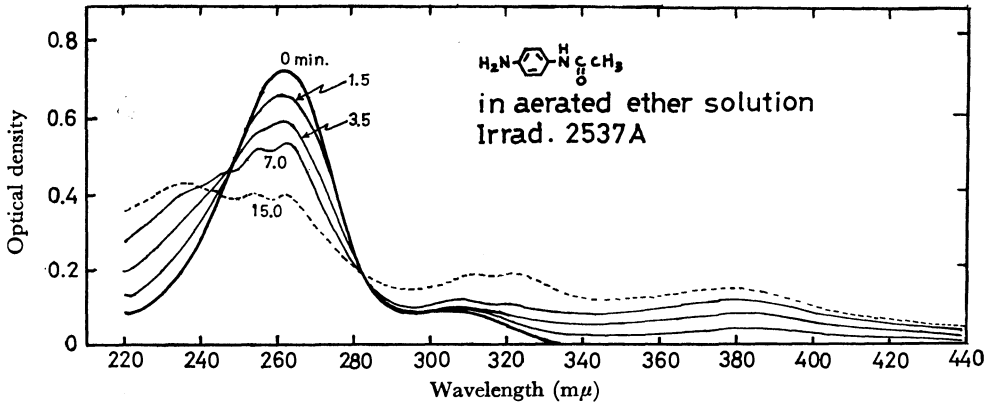

Fig. 3(b).

Fig. 3. Spectral changes of ether solutions of *p*-aminoacetanilide at 2537 Å.
(a) degassed (b) aerated

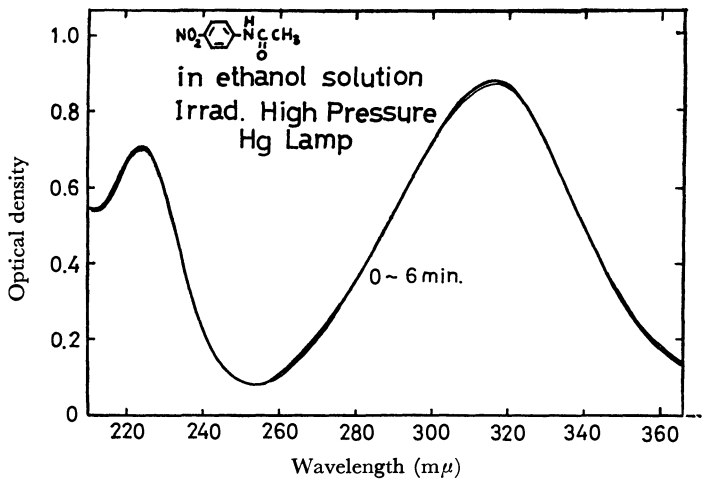

Fig. 4. The spectral change of ethanol solution of *p*-nitroacetanilide by irradiation with a high pressure mercury lamp.

c) *Photochemical Reactions of p-Amino- and p-Hydroxyacetanilides.* *p*-Amino- and *p*-hydroxyacetanilides had very poor solubilities in cyclohexane at room temperature. Therefore, ether was used as the solvent. Figure 3(a) shows the spectral change in a degassed ether solution of *p*-aminoacetanilide at 2537 Å. The Absorption Band II (262 mμ) decreased and new bands with the maxima of 237 and 395 mμ appeared, as well as those of *p*-methyl- and *p*-chloroacetanilides. However, in an aerated ether solution, the spectral change was different from that in a degassed solution, as is shown in Fig. 3(b).

In the case of an aerated ether solution, the Absorption Band II (262 mμ) decreased and new peaks appeared at 237, 243, 254, 263, 322, and 378 mμ. The increase in the 237 mμ peak corresponds to the *o*-rearrangement. The appearance of peaks at 243, 254, and 263 mμ in an aerated solution of *p*-aminoacetanilide was similar to that in an aerated solution of *p*-phenylenediamine at 2537 Å found by Hinohara.[14] Similar results were observed in the cases of degassed and aerated ether solutions of *p*-hydroxyacetanilide at 2537 Å.

It may be considered that, in the presence of dissolved oxygen, 2,5-diaminoacetophenone (the *o*-rearrangement product) was oxidised to the corresponding imine.

d) *Phntochemical Reaction of p-Nitroacetanilide.* Scarcely no spectral change was observed in an aerated ethanol solution of *p*-nitroacetanilide upon irradiation with a high-pressure mercury lamp, as is shown in Fig. 4.

The quenching mechanism by the substitution of

14) T. Hinohara, Presented at the 20th Annual Meeting of the Chemical Society of Japan, Tokyo, April, 1967.

the nitro group has been explained by Tanaka *et al.*[15]; internal quenching is caused by the atomic rearrangement of the nitro group (especially the oxygen atom) in the excited Franck-Condon state. Kokubun and Kobayashi supported this quenching mechanism on the basis of their investigation of the fluorescence quantum yield and the lifetime of *m*-nitrodimethylaniline.[16]

2) Estimation of Dissociation and Back-reaction Quantum Yields. The quantum yields for *p*-X substituted acetanilides at 2537 Å are summarized in Table 1. By *p*-methyl or *p*-chloro substitution, the disappearance quantum yields decreased, the quantum yields of the *o*-rearrangement increased, and the *p*-rearrangement did not occur.

TABLE 1. QUANTUM YIELDS FOR *p*-X SUBSTITUTED ACETANILIDE AT 2537 Å

X	Quantum yield (Φ)					
	Observed			Calculated		
	Φ_o	Φ_p	Φ_{dec}	Φ_N	Φ_B	Φ_{dis}
H[a]	0.07	0.06	0.15	0.02	0.10	0.25
CH_3	0.09_2	0	0.12	0.02_8	0.13	0.25
Cl	0.09_7	0	0.13	0.03_3	0.14	0.27

a) See Footnote 11.

Φ_o and Φ_p are the quantum yields of *o*- and *p*-rearrangements respectively; Φ_{dec}, the decrease quantum yield of acetanilide; Φ_N, the quantum yield of *p*-X substituted aniline; Φ_B, the quantum yield of the back reaction, and Φ_{dis}, the dissociation quantum yield for the N–C bond.

In the present work, aniline could not be observed by the spectrophotometric method.[11] Elad reported the formation of aniline as well as of *o*- and *p*-aminoacetophenones in the photochemical reaction of acetanilide.[17] Therefore, the quantum yields of *p*-X aniline (Φ_N) may be evaluated approximately by Eq. (3):

$$\Phi_N \approx \Phi_{dec} - (\Phi_o + \Phi_p) \tag{3}$$

The electronically excited states in acetanilide and *p*-methylacetanilide are the same in a first approximation, since the shapes of their UV absorption spectra are about the same. Therefore, it is reasonable to assume that these photochemical reactions can occur through the same primary processes; the dissociation quantum yields for the N–C bond have the same value, as is shown in Eq. (4):

$$\Phi^{H}_{dis} \approx \Phi^{CH_3}_{dis} \tag{4}$$

On the other hand, the observed quantum yields, Φ_o, Φ_p, and Φ_{dec}, of *p*-methylacetanilide differ from those of acetanilide, as is shown in Table 1. These differences can be explained as follows. In the photochemical primary process, anilino and acetyl radicals are produced by the intersystem crossing, ${}^3\sigma_0(\text{N–C}) \leftarrow S_1(\pi\pi^*)$.[2] The *p*-position being blocked in the anilino radical by the methyl group, the acetyl radical can not move to the *p*-position. Therefore, the acetyl radical which is expected to rearrange at the *p*-position follows this course:

1) recombination with the anilino radical at the *o*-position, which causes an increase in the Φ_o.

2) recombination with the anilino radical at the nitrogen dot; this is the back reaction, which decreases the Φ_{dec} and increases the Φ_B.

3) abstraction reaction, resulting in *p*-X-aniline formation, which in turn increases the Φ_N.

In order to estimate the dissociation and back-reaction quantum yields, the ratio of Φ_B to 1/2 Φ_o was obtained as follows:

$$\Delta\Phi_o = \Phi^{CH_3}_o - \Phi^{H}_o = 0.022 \tag{5}$$

$$\Delta\Phi_B = \Phi^{CH_3}_B - \Phi^{H}_B = \Phi^{H}_{dec} - \Phi^{CH_3}_{dec} = 0.03 \tag{6}$$

where:

$$\Phi^{H}_{dis} = \Phi^{H}_B + \Phi^{H}_{dec}, \quad \Phi^{CH_3}_{dis} = \Phi^{CH_3}_B + \Phi^{CH_3}_{dec}$$

and $$\Phi^{H}_{dis} = \Phi^{CH_3}_{dis}$$

$$\frac{\Delta\Phi_B}{\frac{1}{2}\Delta\Phi_o} = 2.9 \tag{7}$$

$$\frac{\Phi_B}{\frac{1}{2}\Phi_o} \approx \frac{\Delta\Phi_B}{\frac{1}{2}\Delta\Phi_o} = 2.9 \tag{7'}$$

The rate of the back reaction was 2.9 times that of the *o*-rearrangement. Thus, the values of $\Phi^{CH_3}_B$, Φ^{H}_B, $\Phi^{CH_3}_{dis}$, and Φ^{H}_{dis} are given by:

$$\Phi^{CH_3}_B = \frac{1}{2}\Phi^{CH_3}_o \times 2.9 = 0.13 \tag{8}$$

$$\Phi^{CH_3}_{dis} = \Phi^{CH_3}_B + \Phi^{CH_3}_{dec} = 0.25 \tag{9}$$

$$\Phi^{H}_B = \frac{1}{2}\Phi^{H}_o \times 2.9 = 0.10 \tag{10}$$

$$\Phi^{H}_{dis} = \Phi^{H}_B + \Phi^{H}_{dec} = 0.25 \tag{11}$$

The values of Φ^{Cl}_B and Φ^{Cl}_{dis} were also estimated:

$$\Phi^{Cl}_B = \frac{1}{2}\Phi^{Cl}_o \times 2.9 = 0.14 \tag{12}$$

$$\Phi^{Cl}_{dis} = \Phi^{Cl}_B + \Phi^{Cl}_{dec} = 0.27 \tag{13}$$

As has previously been described,[2] the fluorescence lifetime, τ_F, is of the order of magnitude of $\sim 10^{-10}$ sec. The dissociation rate constant, k_{dis}, can be evaluated as follows:

15) I. Tanaka, Y. Mori *et al.*, Presented at the Symposium on Electronic state, Osaka, Oct., 1966.

16) H. Kokubun and M. Kobayashi, Presented at the 20th Annual Meeting of the Chemical Society of Japan, Tokyo, April, 1967.

17) D. Elad, *Tetrahedron Letters*, **1963**, 873. D. Elad, D. V. Rao and V. I. Stenberg, *J. Org. Chem.*, **30**, 3252 (1965).

$$\left.\begin{aligned} S_1(\pi\pi^*) &\xrightarrow{k_s} S_0 \\ S_1(\pi\pi^*) &\xrightarrow{k_F} S_0 + h\nu' \\ S_1(\pi\pi^*) &\xrightarrow{k_c} T_1(\pi\pi^*) \\ S_1(\pi\pi^*) &\xrightarrow{k_{dis}} \phi\text{-NH} + \text{CCH}_3 \\ & \qquad\qquad\quad \| \\ & \qquad\qquad\quad \text{O} \end{aligned}\right\} \quad (14)^{b)}$$

b) See Footnote 2.

$$\Phi^{H}_{dis} = \frac{k_{dis}}{k_s + k_F + k_c + k_{dis}} = 0.25 \quad (15)$$

$$k_{dis} = \frac{0.25}{\tau_F} = \sim 10^9\ \text{sec}^{-1} \quad (16)$$

3) Secondary Processes. The photochemical rearrangement of acetanilide was an intramolecular reaction, since no effect of the quantum yield on the concentration has been observed.[11] It is interesting to note that the value of the high recombination ratio (β) between anilino and acetyl radicals in the liquid phase is quite high, as is shown in Eq. (17):

$$\left.\begin{aligned} \beta_H &= \frac{\Phi^H_o + \Phi^H_p + \Phi^H_B}{\Phi^H_{dis}} = 0.92 \\ \beta_{CH_3} &= \frac{\Phi^{CH_3}_o + \Phi^{CH_3}_B}{\Phi^{CH_3}_{dis}} = 0.89 \\ \beta_{Cl} &= \frac{\Phi^{Cl}_o + \Phi^{Cl}_B}{\Phi^{Cl}_{dis}} = 0.88 \end{aligned}\right\} \quad (17)$$

These results indicate that the recombination reaction between pair radicals occurs efficiently in a solvent cage. The little hydrogen-atom abstraction from the solvent may be caused by the anilino or the acetyl radical. Figure 5 shows the reaction model in a solvent cage.

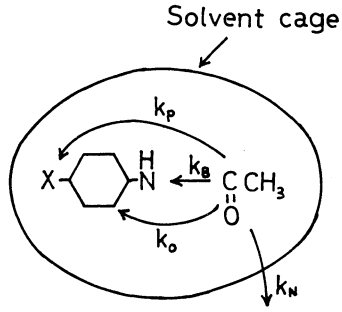

Fig. 5. Reaction model in a solvent cage.

The photochemical secondary processes of acetanilide can be represented as in the following equations:

Recombination Reactions.

a) Back reaction:

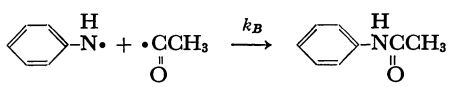

(18)

b) *o*-Rearrangement:

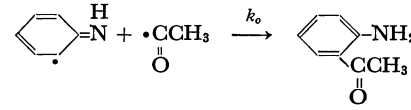

(19)

c) *p*-Rearrangement:

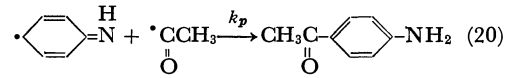

(20)

where k_B, k_o, and k_p are the rate constants of the back reaction, the *o*-rearrangement, and the *p*-rearrangement respectively. In the recombination reaction between the pair radicals, the correlation between the rate constants (k_B, k_o, and k_p) and the odd π electron densities (ρ_7, ρ_2, and ρ_4) was obtained as follows. To the first approximation,the odd π electron densities of the anilino radical were obtained from a semiempirical ASMO-CI calculation on aniline,[18] as is shown in Fig. 6.

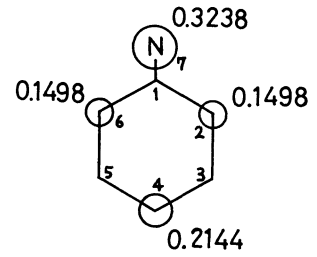

Fig. 6. Odd π electron densities of anilino radical.[18]

$$k_B : k_o : k_p = \Phi_B : \frac{1}{2}\Phi_o : \Phi_p = 1 : 0.35 : 0.6 \quad (21)$$

$$\rho_7 : \rho_2 : \rho_4 = 1 : 0.46 : 0.66 \quad (22)$$

$$k_B : k_o : k_p \approx \rho_7 : \rho_2 : \rho_4 \quad (23)$$

The rate constants, k_B, k_o, and k_p, were proportional to the odd π electron desities, ρ_7, ρ_2, and ρ_4 respectively. These results lend some support to the radical mechanism for the photochemical secondary processes in acetanilide. The recombination between the pair radicals in a solvent cage may occur within several collisions, since k_B, k_o, and k_p are all larger than k_N. It is assumed that these recombination rate constants are of the order of magnitude of 10^{11}—10^{12} sec^{-1}, considering the number of collisions between solute and solvent to be about 10^{13} sec^{-1}.[19]

No intermediate could be observed by the flash

18) H. Baba, This Bulletin, **34**, 76 (1961); N. Mataga, *ibid.*, **36**, 1607 (1963). The highest occupied molecular orbital of aniline ϕ_4:

$$\phi_4 = 0.356\chi_1 + 0.387(\chi_2 + \chi_6) - 0.133(\chi_3 + \chi_5) - 0.463\chi_4 - 0.569\chi_7$$

Odd electron densities were obtained from the square of the coefficient of atomic orbital χ_i in ϕ_4

19) *E. g.*, M. Tamura, "Kokagaku," Shibundo, Tokyo (1947), p. 160; M. Koizumi, "Kokagaku-gairon," Asakurashoten, Tokyo (1963), p. 78.

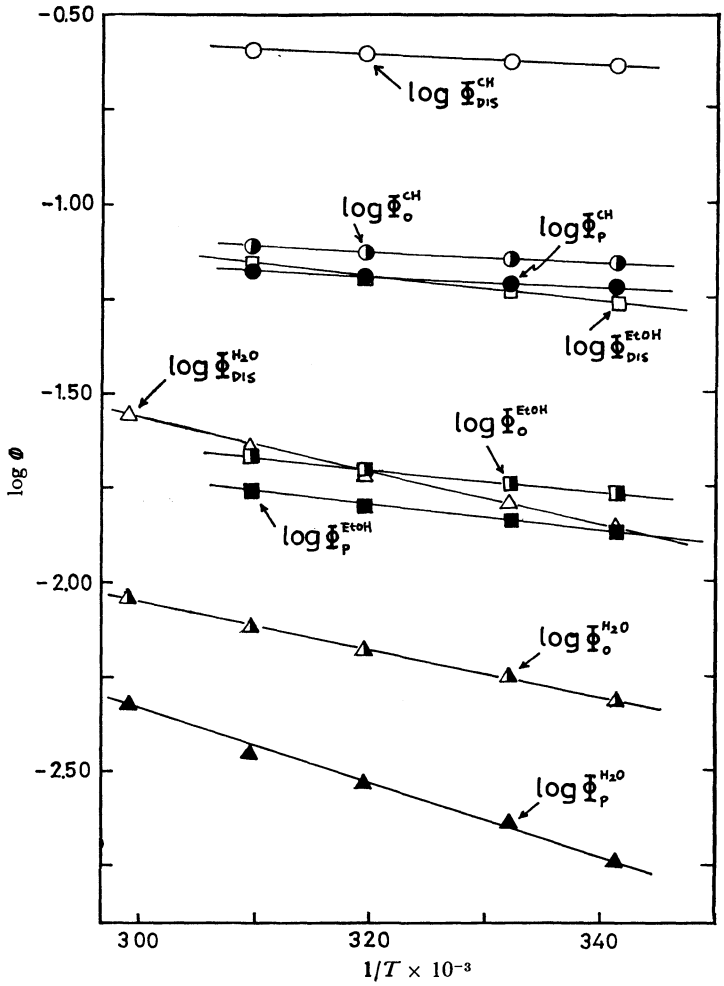

Fig. 7. Plots of logarithm of quantum yields against reciprocal of temperature.

technique. The absorption of the products appeared within the shortest delay time (20 μsec) observed.

4) Dependence of the Quantum Yield on the Temperature. The quantum yields (Φ) in various solvents were measured while varying the temperature in the range from 20 to 70°C. The quantum yields depended on the temperature; plots of log Φ against $1/T$ fell on a straight line, as is shown in Fig. 7. Moreover, a linear relationship was obtained between log Φ_{dis}*2 and $1/T$.
The activation energies in the photochemical rearrangement of acetanilide were calculated to be as shown in Table 2.

The values of the activation energies in polar solvents were larger than those in nonpolar solvents. However, even these values were very low in comparison with those of the hydrogen-atom abstraction reaction by radicals.[20] These results also suggest that hydrogen-atom abstraction reactions are not involved in the *o*- and *p*-rearrangements:

Table 2. Activation energies in the photochemical reaction of acetanilide

Solvent	Activation energy, kcal/mol		
	E_o	E_p	E_{dis}
Cyclohexane	0.6_0	0.6_1	0.6
Ethanol	1.4_5	1.6_0	1.5
Water	2.8_2	4.1_5	3.0

E_o, E_p, and E_{dis} are the activation energies of the *o*-rearrangement, the *p*-rearrangement, and the dissociation for the N-C bond respectively.

*2 The Φ_{dis} values were estimated as follows:

$$\Phi_{dis} \approx \Phi_B + \Phi_o + \Phi_p \approx 2.43\,\Phi_o + \Phi_p$$

20) *E. g.*, M. H. J. Wijnen, *J. Am. Chem. Soc.*, **80**, 2394 (1958).

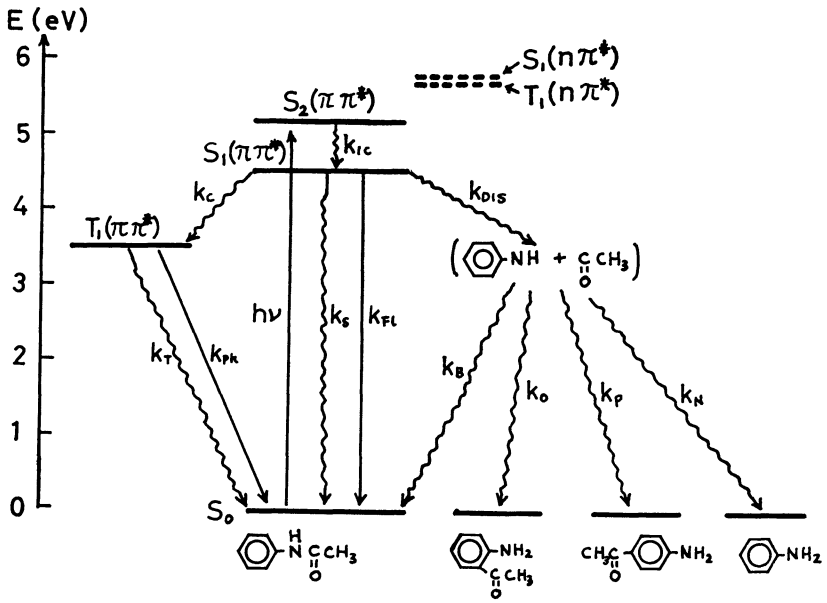

Fig. 8. Energy state diagram for acetanilide.

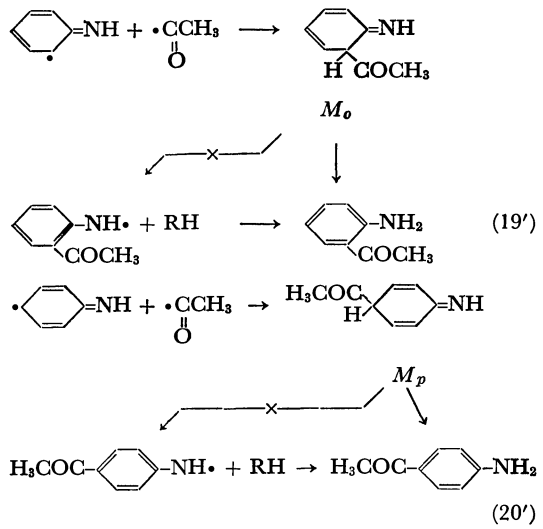

Since the M_o and M_p intermediates might have highly vibrational and rotational energies when a pair of radicals recombine, the values of their lifetimes would be very short; probably one may assume an order of magnitude of $\sim 10^{-12}$ sec. In fact, no intermediate could be observed by means of the flash technique, as has been mentioned above. It is more reasonable to consider that the rearrangements occurred immeadiately, as is shown in Eqs. (19) and (20).

The results regarding the activation energies for the dissociation quantum yields E_{dis}, lend some support to a photochemical primary process[2] which involves the predissociation of the N-C bond in acetanilide.

Conclusion

From these studies, the reaction scheme of acetanilide at 2537 Å can be written as is shown in Fig. 8.

The mechanism of the photochemical reaction of acetanilide involves the lowest excited singlet state, $S_1(\pi\pi^*)$; the predissociation by intersystem crossing, ${}^3\sigma_0(\text{N-C}) \leftarrow S_1(\pi\pi^*)$, and the recombination reaction between the pair radicals in a solvent cage.

The author is greatly indebted to Professor Ikuzo Tanaka and Associate Professor Yuji Mori of the Tokyo Institute of Technology for their generous and very helpful discussion of this paper.

BULLETIN OF THE CHEMICAL SOCIETY OF JAPAN VOL. 42 66—70 (1969)

Mechanism of a Stereospecific, Photosensitized, Cyclization Reaction of 3-Methylene-1,5-heptadiene

Sin-ichiro KITA*1 and Ken-ichi FUKUI

Department of Hydrocarbon Chemistry, Faculty of Engineering, Kyoto University, Yoshida, Sakyo-ku, Kyoto

(Received May 30, 1968)

In order to understand the mechanism of the photosensitized, stereospecific cyclization of 3-methylene-1,5-heptadiene, we calculated the electronic state of two intermediates (13 imaginary conformations) by the extended Hückel molecular orbital method and discussed its rotation angle dependency. We obtained the following conclusions. 1) In the two intermediates, the second model (we suppose this to be more like a real intermediate) has lower energy than the first model (we suppose this to be an initial intermediate) both in the ground state and the excited state. 2) If it is necessary for this cyclization that an overlap stabilization exists between two carbon atoms to be bonded and the intermediate has lower energy in that state, the intermediate seems to cyclize after the transition to the ground state singlet. 3) The overlap stabilization between two carbon atoms mentioned above is mainly defined by the interaction between 2p electrons in the highest occupied orbital. This fact coincides with the consequence of the frontier electron theory. 4) The existence of the overlap stabilization between 2p electrons mentioend above corresponds to the fact that the special valence atomic orbital of that two carbon atoms has the same symmetry. This fact is in line with the Woodward-Hoffmann rule on "electrocyclic reactions."

The photosensitized bicyclization reaction of 3-methylene-1,5-hexadiene derivatives (I) has been reported by Charton *et al.*[1], Liu,[2] and Liu *et al.*[3]

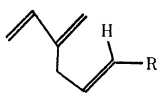

(I)

In their reports,[2,3] Liu has shown that either *trans* or *cis* 3-methylene-1,5-heptadiene (IIa or IIb) gave an identical product mixture of two products (III and IV) in a ratio of 5.8 to 1 (in this point this reaction is stereospecific) and regardless of the initial composition of the triene mixture the relative amounts of the two products remained unchanged throughout the reaction and at the same time the relative amounts of the starting materials were found unchanged.

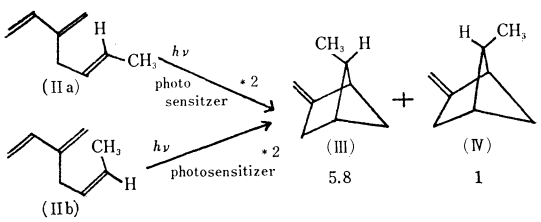

From the fact mentioned above and other facts, he has considered the presence of long lived intermediate (V)*3 in these reactions.

In this report, we calculated the electronic state of an intermediate (V) by Hoffmann's extended

*1 Present address: Ohe Work, Sumitomo Chemical Industry Co. Ltd., Ohe, Niihama, Ehime, Japan.

1) J. L. Charlton, P. de Mayo and L. Skattebol, *Tetrahedron Letters*, **1965**, 4679.

2) R. S. H. Liu, *ibid.*, **1966**, 2159.

3) R. S. H. Liu and G. S. Hammond, *J. Am. Chem. Soc.*, **89**, 4936 (1967).

*2 β-Acetonaphthone, triphenylene, benzophenone or fluorenone.

*3 As intermediates, one can also consider the followings.

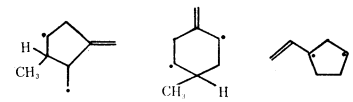

(VI) (VII) (VIII)

Liu has considered that VI is an unlikely intermediate in these reaction on the grounds of energy considerations.[2] As regards VII and VIII, we found that the following experimental rule exists in these reactions. "In the cyclization of an excited triplet state, intermediates which contain two unpaired electrons in one ring structure, such as VII and VIII, can not exist, while in the cyclization of an excited singlet state the restriction mentioned above does not exist." This rule was justified in the case of the photocyclization of 1,5-hexadiene,[4] 1,6-heptadiene,[5] myrcene,[6] 1,5-cyclooctadiene[7] and neryl acetate.[8]

4) R. Srinivasan, *J. Phys. Chem.*, **67**, 1367 (1963).

5) R. Srinivasan and K. A. Hill, *J. Am. Chem. Soc.*, **87**, 4988 (1965).

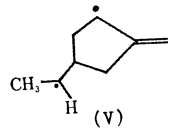

(V)

Hückel molecular orbital (MO) method[9] and discussed the mechanism of its stereospecific cyclization.

The Parameters used and the Coordinates

The MO's to describe this system are represented by a linear combination of valence atomic orbitals (AO); that is, the 1s orbital of the hydrogen atom and the 2s, 2px, 2py, 2pz orbitals of the carbon atom. The Coulomb integrals of these AO's, H_{pp}, are given as follows.

$$H_{pp}\ (1s, H) = -13.60\ eV$$
$$H_{pp}\ (2s, C) = -21.43\ eV$$
$$H_{pp}\ (2p, C) = -11.42\ eV$$

The resonance integral between ith and jth AO's, H_{pq}, is calculated by the equation

$$H_{pq} = 0.875(H_{pp} + H_{qq})S_{pq}$$

where S_{pq} is the overlap integral.[9] The effective nuclear charges for these atoms are $\mathcal{Z}_H = 1.00$, $\mathcal{Z}_C = 3.25$.

The bond distances, the bond angles and the coordinates of models used in this paper are presented in Table 1 and Fig. 1.

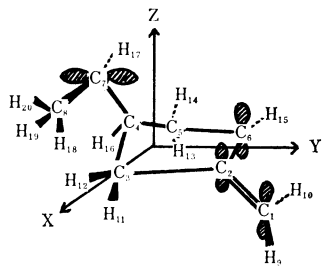

Fig. 1. Coordinates of the model.
(θ: the angle between the C_8, C_7, C_4-plane and the C_7, C_4, H_{16}-plane)

Total energy

$$2\sum_{i}^{occ}\varepsilon_i = 2\sum_{i}^{occ}\sum_{p}(C_{pi})^2H_{pp} + 4\sum_{i}^{occ}\sum_{\substack{p\\(p\neq q)}}\sum_{q}C_{pi}C_{qi}H_{pq}$$

Table 1. The bond distances and the bond angles used

C–C distance

sp^3–sp^3	1.54 Å
sp^3–sp^2	1.52 Å
sp^2–sp^2	1.40 Å
(allylic resonanced)	

C–H distance

sp^3	1.09 Å
sp^2	1.06 Å

bond angle (except otherwise indicated)

sp^3	109°28′
sp^2	120°

1) first model*4 (C_1, C_2, C_3, C_4, C_5, C_6 are on the same plane)

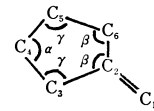

α: 108°
β: 111°03′
γ: 104°57′

2) second model (C_1, C_2, C_3, C_5, C_6 are on the same plane and C_4–C_7 axis is perpendicular to that plane)

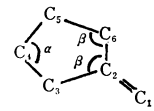

α: 108°
β: 111°03′

Atomic bond population[11] (A.B.P.) in atom pair X–Y

$$4\sum_{p}^{on X}\sum_{q}^{on Y}\sum_{i}^{occ}C_{pi}C_{qi}S_{pq}$$

AO bond population[11] (A.O.B.P.) in AO pair p–q

$$4\sum_{i}^{occ}C_{pi}C_{qi}S_{pq}$$

Partial AO bond population[11] in AO pair p–q in the highest occupied orbital (HO orbital)

$$4\,C_{p\cdot HO}C_{q\cdot HO}S_{pq}$$

Results and Discussion

In cyclopentane, the ring is nearly planar[10] and the intermediate (V) is considered as a long lived one.[2,3] Therefore, it is supposed that the 5-membered ring of the intermediate (V) is planar. The first model refers to this case. Next, if the intermediate (V) cyclizes to III or IV, C_6 and C_7 which are to become bonded in this reaction must approach nearer than in the case of the first model. The second model refers to one of these cases.

6) a) K. J. Crowly, *Acta. Cient. Venezolana Supl.*, No 1, 194 (1959—1963); *Proc. Chem. Soc.*, **245**, 334 (1962); *Tetrahedron*, **21**, 1001 (1965). b) W. G. Dauben and W. T. Wipke, *Pure Appl. Chem.*, **9**, 539 (1964). c) R. S. H. Liu and G. S. Hammond, *J. Am. Chem. Soc.*, **86**, 1892 (1964).

7) R. Srinivasan, *J. Am. Chem. Soc.*, **85**, 819 (1963); *ibid.*, **86**, 3318 (1964).

8) R. C. Cookson, *Pure Appl. Chem.*, **9**, 575 (1964).

9) R. Hoffmann, *J. Chem. Phys.*, **39**, 1397 (1963); *ibid.*, **40**, 2474 (1964).

*4 In cyclopentane, the ring is nearly planar.[10]

10) G. W. Wheland, "Resonance in Organic Chemistry" John Wiley and Sons, Inc., New York (1955), p. 739.

11) R. S. Mulliken, *J. Chem. Phys.*, **23**, 1833, 1841, 2338, 2343 (1955).

Figure 2 shows the θ dependence of the total energy in the first model and in the second model. θ is the angle between the C_8, C_7, C_4-plane and the C_7, C_4, H_{16}-plane and is measured from the C_2, C_3, C_5, C_6-plane side of the former plane to the direction of a C_2–C_1 double bond. From Fig. 2, it can be seen that the second model has lower energy than the first model both in the ground state and the excited state. Therefore, it can be supposed that the cyclization of intermediate (V) proceeds *via* the route from the first model to the second model.

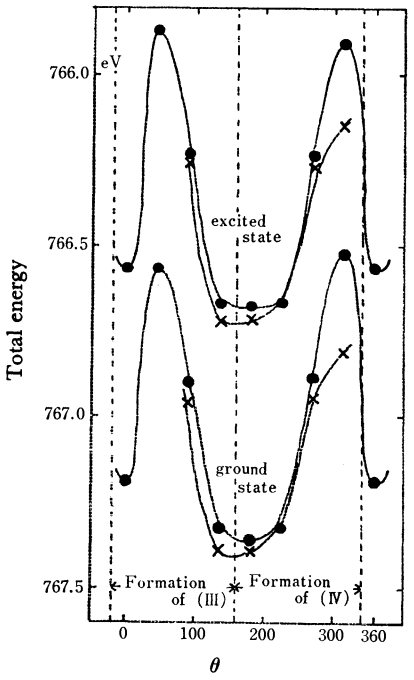

Fig. 2. θ dependence of total energy.
● first model × second model

In the following discussion, we discuss mainly using the first model only for the convenience of calculations and qualitatively one can obtain the same conclusion even if one uses the second model.

Here we suppose that it is necessary for this cyclization that an overlap stabilization[12] exists between C_6 and C_7. Figure 3 shows the θ dependence of the bond energy*5 between C_6 and C_7. In the case of the ground state of the first model, C_6 and C_7 are "bonding" in two θ ranges, the one corresponding to the formation of III, and the other to the formation of IV. If one considers the total energy of these two "bonding" θ ranges, it is apparent that the energy of the fomrer range

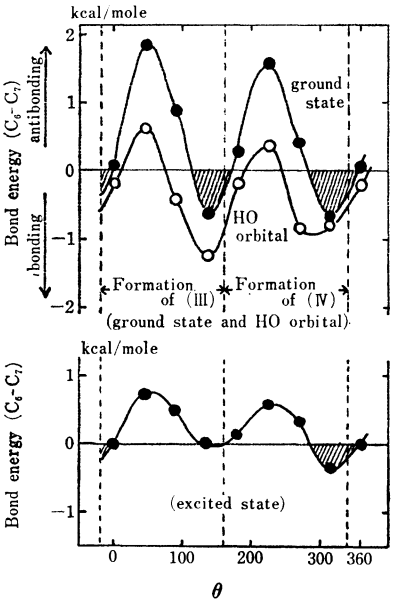

Fig. 3. θ dependence of bond energy (first model).

is lower than that of the latter range. This relation holds also in the second model. In the case of the excited state, C_6 and C_7 are "bonding" in one θ range only, which corresponds to the formation of IV. From the experimental data,[2,3] it is seen that III occurs more than IV. Therefore, the intermediate (V) (excited triplet) seems to cyclize after the transition to the ground state singlet.

Furthermore, let us consider the reason why C_6 and C_7 is "bonding" in the special θ ranges only. Figure 3 also shows the bond energy between C_6 and C_7 in the HO orbital. From Fig. 3, it is apparent that the "bonding" in the ground state corresponds to that in the HO orbital. This fact is interesting, because it coincides with the theoretical consequence of the frontier electron theory.[13] From Table 3, it can be seen that the interaction of 2p electrons contributes mainly to this "bonding." Figure 4 shows the atomic bond population and the AO bond population of the ground state and the HO orbital. From Fig. 4, it is apparent that the main reason of the "bonding" is the interaction between $6\,C_{2pz}$ and $7\,C_{2py}$ and this interaction corresponds to that in the HO orbital. Therefore, the phenomenon that C_6 and C_7 is "bonding" is mainly defined by the fact that $6\,C_{2pz}$ and $7\,C_{2py}$ is "bonding."

Next, let us consider the reason why the AO bond population between $6C_{2pz}$ and $7C_{2py}$ in the HO orbital has positive values in the special θ ranges. Figure 5 shows the θ dependence of the coefficients of $6C_{2pz}$ and $7C_{2py}$ in the HO orbital.

12) K. Fukui, This Bulletin, **39**, 498 (1966); *Tetrahedron Letters*, **1965**, 2009.

*5 $4\sum_{i}^{occ}\sum_{\substack{p\\(p\neq q)}}\sum_{q} C_{pi}C_{qi}H_{pq}$

13) K. Fukui *et al.*, *J. Chem. Phys.*, **20**, 722 (1952); *ibid.*, **22**, 1433 (1954).

TABLE 2. TOTAL ENERGY (eV UNIT) AND ATOMIC BOND POPULATION (first model)

		θ			
		0°	45°	90°	135°
Total energy	Ground state	−767.1967	−766.5647	−766.9025	−767.3217
Total energy	Excited state	−766.5689	−765.8679	−766.2259	−766.6647
A.B.P. (C_6–C_7)	Ground state	−0.000234	−0.003932	−0.001862	0.001290

		θ			
		180°	225°	270°	315°
Total energy	Ground state	−767.3632	−767.3259	−766.8888	−766.5244
Total energy	Excited state	−766.6721	−766.6645	−766.2327	−765.9044
A.B.P. (C_6–C_7)	Ground state	−0.000556	−0.003304	−0.000864	0.001350

(second model)

		θ			
		0°	45°	90°	135°
Total energy	Ground state			−766.9572	−767.3972
Total energy	Excited state			−766.2594	−766.7183

		θ			
		180°	225°	270°	315°
Total energy	Ground state	−767.3843		−766.9453	−766.8124
Total energy	Excited state	−766.7130		−766.2694	−766.1502

TABLE 3. BOND ENERGY BETWEEN C_6 AND C_7 (kcal/mol) (first model)

		θ							
		0°	45°	90°	135°	180°	225°	270°	315°
Ground state	2s–2s	0.04	0.03	−0.01	−0.01	0.04	0.04	0.01	0.00
	2s–2p	−0.13	0.14	0.13	−0.11	−0.09	0.11	0.07	−0.16
	2p–2p	0.18	1.69	0.77	−0.51	0.30	1.42	0.34	−0.51
	Total	0.09	1.86	0.89	−0.63	0.25	1.57	0.42	−0.67
HO orbital	2s–2s	0.00	0.00	0.00	−0.00	0.00	0.00	−0.00	−0.00
	2s–2p	−0.20	−0.20	−0.26	−0.28	−0.20	−0.20	−0.24	−0.24
	2p–2p	−0.00	0.82	−0.20	−0.96	0.02	0.56	−0.60	−0.58
	Total	−0.20	0.62	−0.46	−1.22	−0.18	0.36	−0.84	−0.82
Excited state	2s–2s	0.04	0.03	−0.01	−0.01	0.04	0.04	0.01	0.00
	2s–2p	−0.04	0.09	0.06	−0.03	−0.00	0.08	−0.00	−0.11
	2p–2p	−0.04	0.60	0.43	0.03	0.07	0.45	0.33	−0.25
	Total	−0.04	0.72	0.48	−0.01	0.11	0.57	0.34	−0.36

TABLE 4. ATOMIC ORBITAL BOND POPULATION BETWEEN $6C_{2p_z}$ AND $7C_{2p_y}$ (first model)

	θ							
	0°	45°	90°	135°	180°	225°	270°	315°
Ground state	0.000034	−0.001766	−0.000408	0.001226	0.000066	−0.001300	0.000346	0.000778
HO orbital	0.000700	−0.001412	0.000292	0.002364	0.000760	−0.000884	0.001268	0.001532

TABLE 5. COEFFICIENTS OF $6C_{2pz}$ AND $7C_{2py}$ IN THE HO ORBITAL (first model)

	θ							
	0°	45°	90°	135°	180°	225°	270°	315°
$6C_{2pz}$	0.719081	0.719920	0.722513	0.721535	0.720406	0.719852	0.719092	0.711559
$7C_{2py}$	0.030310	−0.061174	0.012585	0.102371	0.032881	−0.038349	0.055131	0.067280

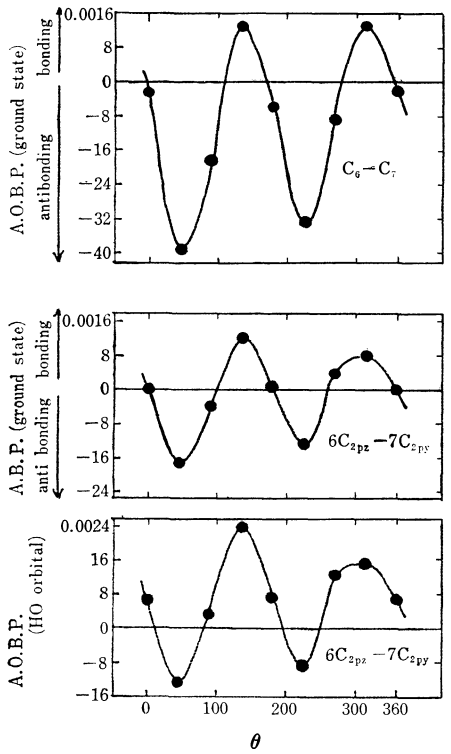

Fig. 4. θ dependence of atomic bond population and atomic orbital bond population.

From Fig. 5, it is apparent that the phenomenon mentioned above is due to the fact that the coefficients of $6C_{2pz}$ and $7C_{2py}$ have the same sign, in other words, the valence AO of $6C_{2pz}$ and $7C_{2py}$ have the same symmetry in the θ range

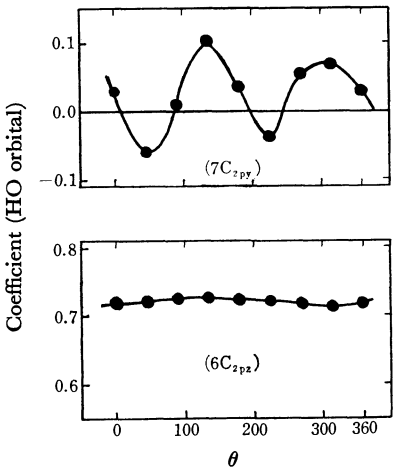

Fig. 5. θ dependence of the coefficients of $6C_{2pz}$ and $7C_{2py}$ in the HO orbital.

mentioned above. This fact is interesting, because it is in line with the Woodward-Hoffmann rule on electrocyclic reactions.[14]

The calculations have been carried out on an HITAC 5020 computer at Tokyo University. One of the authors (S.K.) is grateful to Mr. R. Kuroda, Dr. O. Saheki and Dr. T. Irie for their interest in this work. He also wishes to thank the Sumitomo Chemical Industry Co. Ltd. for permission to publish this paper.

14) R. B. Woodward and R. Hoffmann, *J. Am. Chem. Soc.*, **87**, 395 (1965).

BULLETIN OF THE CHEMICAL SOCIETY OF JAPAN VOL. 42 71—75 (1969)

Electronic Spectra of Crystalline TCNQ Anion Radical Salts. I. Simple Salts*1

Yôichi IIDA

Department of Chemistry, Faculty of Science, Hokkaido University, Sapporo

(Received May 31, 1968)

The present paper deals with crystalline TCNQ anion radical "simple" salts of M^+ $TCNQ^-$, where M^+ represents a diamagnetic counter cation. Their crystalline electronic spectra were measured in the range between 4.0 and 30.8 kK by means of diffuse reflectance. The crystalline spectra thus obtained were quite different from that of the TCNQ radical anion monomer and exhibited a broad and intense low-energy band around 9 kK in the low-conductivity compounds and at 4.3 kK in the high-conductivity compound. These bands were ascribed to inter-radical charge-transfer in the solid state. The crystalline spectra were found to be closely correlated to their unusual electrical and magnetic properties. It was concluded that these physical properties were based on a unique TCNQ molecular arrangement in groups of several or an infinite number of face-to-face molecular systems.

In a previous paper,[1] it has been shown that Würster's salts exhibit characteristic electronic and magnetic properties in the solid state. These properties result from charge-transfer interaction between the cation radicals. Unusual low-energy bands in the diffuse reflectance spectra have been identified as inter-radical charge-transfer bands. In connection with them, the magnetic properties of the salts have been speculated on on the basis of antiferromagnetic interaction between ion radicals. Charge-transfer interaction might make a significant contribution to the stabilization of the antiferromagnetic interaction.

However, these interesting physical properties may not be restricted to Würster's salts, but may be regarded as of the nature of ion (cation and anion) radical salts. In ion radical salts, the unpaired electrons play a predominant role in causing these properties. Along this line, measurements of the magnetic susceptibility and ESR have been powerful tools for clarifying the solid-state interactions among unpaired electrons.[2-8] However, the study of the crystalline electronic spectra may still provide us with useful information concerning these interaction mechanisms. With this hope, we will deal with the anion radical salts of 7,7,8,8-tetracyanoquinodimethane (TCNQ).[9] TCNQ is a well-known strong electron acceptor which forms stable crystalline anion radical "simple" salts of the M^+ $TCNQ^-$ type and new classes of "complex" salts of $(M^+)_2(TCNQ)_3^{--}$ and $M^+(TCNQ)_2^-$, which contain the formally neutral TCNQ and the anion radical $TCNQ^-$. The advantage in dealing with TCNQ salts is that their salts are easily obtained as stable single crystals and that, consequently, their electrical and magnetic properties have been extensively studied.[5-11] Thus, their crystalline electronic spectra can be studied in connection with these properties. The purpose of the present paper is to clarify the crystalline electronic spectra of TCNQ anion radical simple salts by means of diffuse reflectance and to discuss the solid-state interactions among unpaired electrons.

Experimental

Materials. The ten TCNQ simple salts under investigation are Li^+TCNQ^-, Na^+TCNQ^-, K^+TCNQ^-, NH_4^+ $TCNQ^-$, Triethylammonium$^+$ $TCNQ^-$, Methyltriphenylphosphonium$^+TCNQ^-$, Methyltriphenylarsonium$^+TCNQ^-$, Morpholinium$^+TCNQ^-$, *N*-Methylquinolinium$^+TCNQ^-$, and *N*-Methylphenazinium$^+TCNQ^-$.

Li^+TCNQ^-, Na^+TCNQ^-, K^+TCNQ^-, NH_4^+ $TCNQ^-$, and Morpholinium$^+TCNQ^-$ were prepared

*1 Presented in part at the 20th Annual Meeting of the Chemical Society of Japan, Tokyo, April, 1967, and at the Symposium on Molecular Structure, Sapporo, October, 1967.

1) Y. Iida and Y. Matsunaga, This Bulletin, **41**, 2615 (1968).
2) W. Duffy, Jr., *J. Chem. Phys.*, **36**, 490 (1962).
3) K. Okumura, *J. Phys. Soc. Japan*, **18**, 69 (1963).
4) D. D. Thomas, H. Keller and H. M. McConnell, *J. Chem. Phys.*, **39**, 2321 (1963).
5) D. B. Chesnut and W. D. Phillips, *ibid.*, **35**, 1002 (1961).
6) D. B. Chesnut and P. Arthur, Jr., *ibid.*, **36**, 2969 (1962).
7) M. T. Jones and D. B. Chesnut, *ibid.*, **38**, 1311 (1963).
8) R. G. Kepler, *ibid.*, **39**, 3528 (1963).

by a direct reaction between TCNQ and the iodides in acetonitrile.[9] The other compounds were prepared by the metatheses of the corresponding cation sources with Li^+TCNQ^-.[9,11]

Measurements. The electronic absorption spectra in acetonitrile were measured in concentrations of the order of 10^{-5} mol/*l* at room temperature, using a Beckman DK-2A spectrometer.

The crystalline electronic spectra were measured in the range between 4.0 and 30.8 kK by means of diffuse reflectance at room temperature. The electronic absorption spectra were reproduced employing the Kubelka-Munk function $f(R)=(1-R)^2/2R$, where R is the reflectance. The experimental details are the same as those described in a previous paper.[1] Potassium bromide, sodium chloride, and naphthalene were used as solid diluents and also as references.

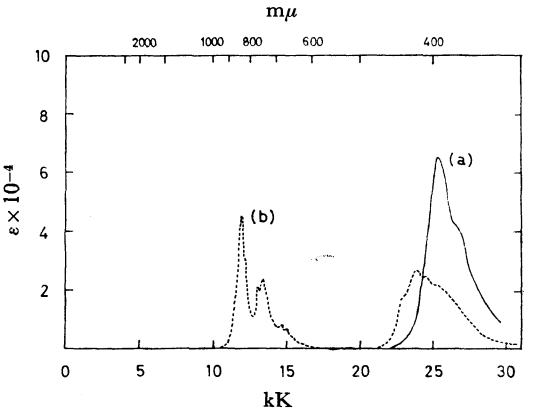

Fig. 1. Absorption spectra of TCNQ (Curve a) and K^+TCNQ^- (Curve b) in acetonitrile solution.

Results and Discussion

The absorption spectra of neutral TCNQ and anion radical $TCNQ^-$ in acetonitrile are illustrated in Fig. 1, Curve a and Curve b respectively. The absorption spectrum of TCNQ has a peak at 25.3 kK with a molar extinction coefficient (ε) of 65000, while that of $TCNQ^-$ shows $\varepsilon=21500$ at 25.3 kK and $\varepsilon=45000$ at 11.9 kK. The natures of these absorption bands have been investigated by Lowitz by the molecular orbital method.[12] The reversible dimerization of $TCNQ^-$ in an aqueous solution has been noted by Boyd and Phillips.[13] According to them, the dimer spectrum exhibits new absorption peaks around 15.6 and 27.0 kK.

In discussing the experimental results, the crystalline $TCNQ^-$ simple salts can be divided into two classes: those with low electrical conductivity and those with high conductivity.[10] These two classes are not well-defined, but this classification facilitates the presentation of the results and the discussion.

Low-conductivity Compounds. All of the simple salts except the *N*-methylphenazinium salt belong to this group. These compounds have conductivities of 10^{-4} $\Omega^{-1}cm^{-1}$ or less and activation energies as high as 0.3 eV.[9,10] As for the magnetic properties, they are diamagnetic at low temperatures, and at higher temperatures are still diamagnetic or exhibit a small paramagnetic contribution to the susceptibility, which increases with an increase in the temperature. This phenomenon has been tentatively interpreted in terms of a ground singlet and an excited triplet equilibrium with a relatively high energy separation.[8] If this is the case, the weak paramagnetic contribution is due to the population in the thermally-accessible triplet state. The paramagnetic contribution (χ) to the susceptibility is written as:

$$\chi = \frac{2\mathcal{N}g^2\beta^2}{kT[3+\exp(J/kT)]} \qquad (1)$$

where $\mathcal{N}$ is the number of spin-coupled pairs and J, the singlet-triplet energy separation.

In the following paragraphs, the results of experiments on sample low-conductivity compounds will be presented and discussed.

K^+TCNQ^-. According to Anderson and Fritchie,[14] this salt crystallizes in a monoclinic system. The crystal structure consists of columns of $TCNQ^-$ with face-to-face stacking parallel to the *a* axis; the molecular axes normal to the molecular plane nearly coincide with the column axis. It is not clear whether or not there is an alternation in the inter-radical spacings within the column. Unless one assumes such an alternation, the inter-radical spacing is 3.4—3.5 Å.

The absorption spectrum in acetonitrile has already been illustrated in Fig. 1, Curve b. The crystalline spectrum (Fig. 2, Curve a) shows a similarity to that of the $TCNQ^-$ dimer in an aqueous solution.[13] The crystalline spectrum has peaks at 8.5, 16.4, and 27.8 kK. The latter two peaks almost agree with the 15.6 and 27.0 kK peaks respectively in the dimer spectrum. The nature of these bands in the solid state is not clear, but the bands should be assigned to the shifted bands of the $TCNQ^-$ monomer. The low-energy band at 8.5 kK observed in the solid state should correspond to the charge-transfer transition between the anion radicals. If this is the case, its electronic transiton will be allowed with the polarization out

9) L. R. Melby, R. J. Harder, W. R. Hertler, W. Mahler, R. E. Benson and W. E. Mochel, *J. Am. Chem. Soc.*, **84**, 3374 (1962).
10) W. J. Siemons, P. E. Bierstedt, and R. G. Kepler, *J. Chem. Phys.*, **39**, 3523 (1963).
11) L. R. Melby, *Canad. J. Chem.*, **43**, 1448 (1965).
12) D. A. Lowitz, *J. Chem. Phys.*, **46**, 4698 (1967).
13) R. H. Boyd and W. D. Phillips, *ibid.*, **43**, 2927 (1965).
14) G. R. Anderson and C. J. Fritchie, Jr., Second National Meeting, Society for Applied Spectroscopy, San Diego, Paper 111 (1963).

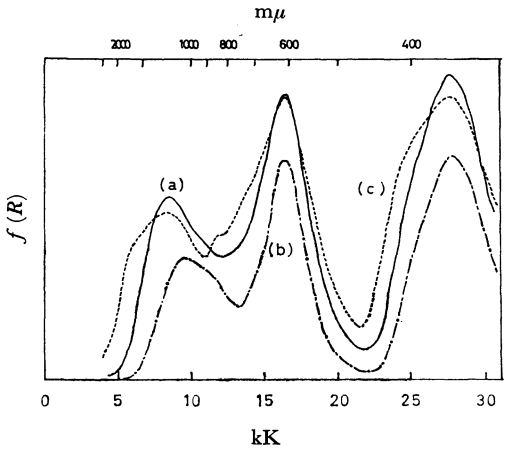

Fig. 2. Crystalline electronic spectra of K^+ $TCNQ^-$ (Curve a), Morpholinium$^+$ $TCNQ^-$ (Curve b) and Li^+ $TCNQ^-$ (Curve c).

of the molecular plane (*i. e.*, along the *a* crystal axis). Anderson and Fritchie have confirmed this prediction experimentally using a near-normal incident reflection.[14] The corresponding charge-transfer band of the dimer in the solution has not yet been obtained, presumably because of the absorption of the solvent. The present question is whether the system of the linear chain column of $TCNQ^-$ with molecular spacing as relatively long, as 3.4—3.5 Å should exhibit a spectral resemblance to the dimer. The electronic state of the isolated ion radical dimer has been examined by Hausser and Murrell.[15] If the spacings are strongly alternate in such a solid, the electronic state might appear to be similar to that in the dimer. However, even if we accept the assumption, the charge-transfer energy in such an ionic crystal should be appreciably different from that in an isolated dimer. Accordingly, the charge-transfer band observed at 8.5 kK is regarded as "crystalline." Nevertheless, because of the experimental similarity of the crystalline spectrum to that of the dimer in the region of high-energy bands, it must be emphasized that all the crystalline electronic state except for the charge-transfer process may be described approximately in terms of the dimer. The approximation might become probable by assuming one of the two possibilities, namely, that ion radicals are equally spaced and weakly coupled with two neighbors each or that ion radicals are alternatingly spaced and rather strongly coupled with one neighbor each. That the molecular spacing, 3.4—3.5 Å, in the case of equally-spaced ion radicals is regarded as relatively long compared with that of a high-conductivity compound (see below) affords evidence for the "weakly-coupled" nature in the former case. The finding that this salt has a low electrical conductivity and a high activation energy[10] supports both possibilities. On the other hand, its almost diamagnetic susceptibility (-1.3×10^{-4} emu/mol at 300°K)[16] has been tentatively described by Eq. (1) with $J\sim0.2$ eV.[8] This description may imply a strong alternation in $TCNQ^-$ stacking, which will support the latter assumption. Under these circumstances, further, detailed study of the crystal structure analysis is necessary to distinguish these two possibilities. At any rate, at the present time, its magnetic property is regarded as based on a non-alternating or alternating linear-chain Heisenberg antiferromagnet, which should produce its almost diamagnetic susceptibility, as is almost the case with certain Würster's salts.[1] Again in TCNQ salts, the contribution of the charge-transfer interaction to the antiferromagnetic interaction is important.

Morpholinium$^+$ TCNQ$^-$. According to Maréchal and McConnell,[17] this substance crystallizes with triclinic symmetry. Its absorption spectrum in acetonitrile is the same as that of the potassium salt. The crystalline spectrum (Fig. 2, Curve b) also exhibits a similarity to that of the dimer. The band peaks are located at 9.5, 16.3, and 27.7 kK. The band at 9.5 kK corresponds to the charge-transfer transition. The latter two bands should be identified as shifted bands of the $TCNQ^-$ monomer.

Here, in this salt, the magnetic property has been well described by Eq. (1) with $J=0.41$ eV.[5] The triplet-state spin-Hamiltonian is written as:

$$\mathcal{H} = \beta \boldsymbol{H}\cdot g\cdot \boldsymbol{S} + DS_z^2 + E(S_x^2 - S_y^2) \qquad (2)$$

where D and E are zero-field splitting parameters. It has been found by ESR study[17] that the z and x axes of the fine-structure Hamiltonian are approximately coincident with the (111) and ($1\bar{1}0$) axes respectively. Here, one assumes a $TCNQ^-$ dimer with a D_{2h} symmetry of face-to-face stacking, where the z and x axes are normal to and along the short axis of the molecules respectively. Theoretical values of D and E can be calculated approximately in terms of magnetic dipole-dipole interaction between unpaired electrons in the dimer. If one uses the spin densities of free $TCNQ^-$ given by Rieger and Fraenkel[18] and the molecular structure given by Hanson,[19] the D and E *versus* inter-planar spacing (z) of the dimer shown in Fig. 3 can be obtained.*2 In order to coincide with the experimental results of $|D|_{obs}=450.2\pm0.4$ and $|E|_{obs}=$

15) K. H. Hausser and J. N. Murrell, *J. Chem. Phys.*, **27**, 500 (1957).

16) R. G. Kepler, P. E. Bierstedt and R. E. Merrifield, *Phys. Rev. Letters*, **5**, 503 (1960).

17) M-A. Maréchal and H. M. McConnell, *J. Chem. Phys.*, **43**, 497 (1965).

18) P. H. Rieger and G. K. Fraenkel, *ibid.*, **37**, 2795 (1962).

19) A. W. Hanson, *Acta Cryst.*, **19**, 610 (1965).

*2 The calculations were carried out on the NEAC 2203G in the Computer Center, Hokkaido University.

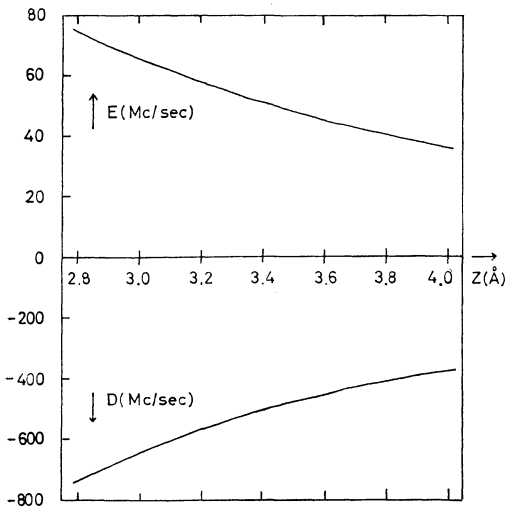

Fig. 3. Calculated zero-field splitting parameters (D and E) in the triplet state of $TCNQ^-$ dimer in Eq. (2) *versus* intermolecular spacing (z).

53.82±0.12 Mc/sec by Marechal and McConnell,[17] z should be 3.4—3.5 Å. Although the crystal structure is not yet available in detail, the estimated value of z is quite reasonable compared to the 3.4—3.5 Å in the potassium salt. Therefore, it may be concluded that $TCNQ^-$ molecules in the morpholinium salt pair up to produce a dimer with an almost D_{2h} symmetry. Its crystalline spectrum supports this conclusion.

Although there exists a rough resemblance of the crystalline spectra and even an exact agreement in high-energy bands between the potassium and the morpholinium salts, their low-energy charge-transfer band peaks show a shift of 1.0 kK; this shift is considered to be due to the difference in the modes of $TCNQ^-$ stacking and/or to that in the sizes of the cations between these two salts. In addition, the finding of a remarkable difference in their electrical conductivities at 23°C between the potassium salt (1×10^{-4} $\Omega^{-1}cm^{-1}$)[10] and the morpholinium salt (1×10^{-9} $\Omega^{-1}cm^{-1}$)[10] may also indicate the importance of the difference in $TCNQ^-$ stacking modes between them.

In connection with the calculations of D and E, it should be mentioned that the lowest triplet wave-function cannot be mixed theoretically with the charge-transfer configuration conceived, because the charge-transfer configuration is a singlet and mixing is forbidden by the spin multiplicity. Thus, the triplet state is probably repulsive.[15] This concept implies that the spin densities in the triplet state of the dimer may be approximately described in terms of the individual doublet spin densities. This speculation is strongly supported by the finding that the observed D and E values in the triplet state are well represented by the magnetic dipole-dipole interaction between a pair of anion radicals with doublet spin densities.

The Other Compounds. All of the other compounds with low conductivity exhibit, more or less, a spectral resemblance to the spectra of the potassium or the morpholinium salt. The three band peaks of their crystalline spectra listed in Table 1 are designated as CT-, α-, and β-bands in the order of increasing energy. Apparently, the locations of the corresponding bands, especially the low-energy charge-transfer (CT) bands, in these compounds depend on the kind of cation. The main reason for the band shifts is also the difference in the modes of $TCNQ^-$ stacking in the crystal and/or that in the sizes of the cations. Nonetheless, all of them have relatively weak interactions among unpaired electrons, producing the rough resemblance of the spectra to that of the dimer.

Table 1. The data for three band peaks in the crystalline electronic spectra of the low-conductivity compounds

Compound	CT-Band (kK)	α-Band (kK)	β-Band (kK)
Li^+TCNQ^-	8.2	16.2	27.5
Na^+TCNQ^-	9.3	16.3	27.5
K^+TCNQ^-	8.5	16.4	27.8
$NH_4^+TCNQ^-$	8.9	16.3	27.8
Triethylammonium$^+$ $TCNQ^-$	8.7	16.4	27.6
Methyltriphenyl-phosphonium$^+TCNQ^-$	10.3	15.3	26.7
Methyltriphenyl-arsonium$^+TCNQ^-$	10.3	15.2	26.3
Morpholinium$^+TCNQ^-$	9.5	16.3	27.7
N-Methylquinolinium$^+$ $TCNQ^-$	9.4	16.1	27.0

In Li^+TCNQ^- the slight but distinct peak at 11.9 kK in the crystalline spectrum (Fig. 2, Curve c) must be noted. It probably arises from the $TCNQ^-$ monomer in some kinds of defects, because in this salt an appreciable ionic conduction, presumably due to the defect, has been found to contribute to its electrical conductivity.[20]

High-conductivity Compound. *N*-Methylphenazinium$^+$ $TCNQ^-$ is the only example exhibiting an electrical conductivity as high as $1.4\times10^2\Omega^{-1}cm^{-1}$. According to Fritchie,[21] it crystallizes as blue-black needles with triclinic symmetry. $TCNQ^-$ molecules form a charge-transfer-bonded, regular, linear chain column parallel to the a crystal axis, with interplanar spacing of 3.26 Å and without any interplanar distance alternation. It is noteworthy that this interplanar spacing is relatively short compared with the 3.4—3.5 Å in the low-conductivity compounds.

20) Y. Iida, M. Kinoshita, M. Sano and H. Akamatu, This Bulletin, **37**, 428 (1964).
21) C. J. Fritchie, Jr., *Acta Cryst.*, **20**, 892 (1966).

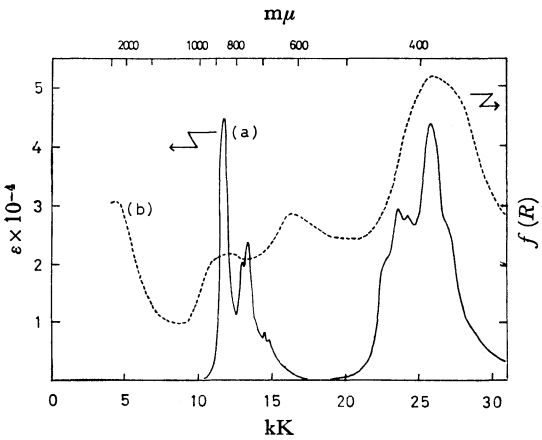

Fig. 4. Absorption spectrum in acetonitrile solution (Curve a) and crystalline electronic spectrum (Curve b) of *N*-Methylphenazinium$^+$ TCNQ$^-$.

The absorption spectrum of the *N*-methylphenazinium salt in acetonitrile, shown in Fig. 4, Curve a, is essentially the same as that of the potassium salt, with the addition of the cation spectrum peak at 25.8 kK. The crystalline spectrum, shown in Fig. 4, Curve b, has peaks at 4.3, 11.8, 16.4, and 25.8 kK. In the previous section the low-conductivity compounds have been found to exhibit approximately the dimer spectrum, whereas the spectrum of the *N*-methylphenazinium salt bears no resemblance to those of the low-conductivity compounds. This must be due to the difference in the manners of TCNQ$^-$ intermolecular interactions in the solid state. It has been demonstrated that some Würster's salts with more-than-pairwise and strong intermolecular interaction exhibit spectra different from either the monomer or dimer spectrum and extending to the lower-energy region.[1] Furthermore, Würster's red bromide has two charge-transfer bands in the low-energy region.[1] Being similar to these salts, the *N*-methylphenazinium salt is characterized by a "strongly-coupled" linear chain system, in which the lowest-energy band observed, at 4.3 kK, may be regarded as an inter-radical charge-transfer absorption. There is a possibility that the band at 11.8 kK is due to the second charge-transfer band or to the shifted band of the TCNQ$^-$ monomer; this point, not yet clear, may be distinguished by means of the polarized spectrum. Although the natures of the bands at 16.4 and 25.8 kK may be similar to those of the α- and β-bands in the low-conductivity compounds respectively, the band at 25.8 kK should comprise that of the cation spectrum, too. However, it must be noted that the elctronic absorption bands in the *N*-methylphenazinium salt are appreciably diffused and continuously overlap with each other. In addition, the facts that the *N*-methylphenazinium salt is the most highly electrically conductive organic compound[11] and that the ions are arranged as a "strongly-coupled" linear chain[21] would imply the delocalization of the unpaired electrons, probably leading to the establishment of a band model for the electrical conduction. It is likely that the lowest-energy band, at 4.3 kK, identified as an inter-radical charge-transfer band, may be associated with the transition from the valence band to the conduction band.[22] Although further work is necessary to explain the relation fully, this speculation is supported by the finding that highly conductive "complex" salts of TCNQ also show a strong low-energy band with an absorption peak around 2—3 kK (see Ref. 23).

Summary

We have divided TCNQ$^-$ simple salts into low- and high-conductivity compounds.

Although the mode of TCNQ$^-$ stacking in the low-conductivity compounds is the dimer (*e. g.*, the morpholinium salt) or the infinite linear chain with equally-spaced ion radicals (*e g.*, one with the assumed model for the potassium salt), the molecular spacings are regarded as being as large as 3.4—3.5 Å in these systems. This gives rise to a relatively small overlap integral of unpaired-electron molecular orbitals between the nearest-neighbor ion radicals. Their crystalline spectra resemble that of the dimer in an aqueous solution, exhibiting the charge-transfer band around 9 kK. Charge-transfer interaction should contribute significantly to the stabilization of antiferromagnetic interaction, resulting in their almost diamagnetic susceptibilities and, in some cases, a singlet-triplet equilibrium for the dimer. The relatively small overlap integral still produces their low electrical conductivities and high activation energies. The relations between the overlap integral and these physical properties remain to be elucidated.

The mode of TCNQ$^-$ stacking in the *N*-methylphenazinium salt is an infinite linear chain column with molecular spacing as little as 3.26 Å. Therefore, the overlap integral of unpaired-electron molecular orbitals is regarded as large. The crystalline spectrum bears no resemblance to those of the low-conductivity compounds and has a low-energy charge-transfer band at 4.3 kK; the reason for this is probably related to its unusually high electrical conductivity.

The author would like to express his appreciation to Professor Yoshio Matsunaga for his generous support to this work and to Mr. Nobuhiko Miyajima for his technical assistance.

22) T. Kondow, K. Siratori and H. Inokuchi, *J. Phys. Soc. Japan*, **21**, 824 (1966); **23**, 98 (1967).
23) Y. Iida, to be published.

BULLETIN OF THE CHEMICAL SOCIETY OF JAPAN VOL. 42 76—83 (1969)

Electronic Structure of Lone Pairs. I. Azine Compounds and Quinones*1

Teijiro YONEZAWA, Hiroko YAMABE and Hiroshi KATO

Faculty of Engineering, Kyoto University, Sakyo-ku, Kyoto

(Received June 6, 1968)

Molecular orbital investigations of the electronic structures of lone pairs of some azine compounds and quinones are carried out by the Hückel method and the extended Hückel method for σ and π electron systems. The delocalization and the s–p mixing of lone pairs are investigated. Qualitative discussions of the splitting of the lone-pair levels and the calculated n–π^* transitions of these compounds are made. It is revealed that the Hückel method, which does not include direct interactions, gives an incorrect prediction for the symmetry of the energy levels of pyridazine. After comparative discussions, it is concluded that the lone paris couple with each other directly "through-space" as well as "through-bond."

Many theoretical investigations[1] of the electronic structures of such azine compounds as pyridine, diazines and triazine have been carried out in order to discuss the n–π^* transitions in these compounds.

Since the theoretical procedure for treating the lone pair has never been settled, there exist few theoretical approaches to the problems of the delocalization of the lone pair, its hybridization, and the mode of interaction between two lone pairs in a molecule.

Recently, however, Hoffmann[2] proposed an extended Hückel calculation in which all the valence electrons were taken into account and established the delocalization of the lone pair whose 2s character is less than 10%.

These conclusions were further confirmed by Lipscomb[3] and his co-workers on the basis of a more rigorous SCF MO treatment. They concluded that an accurate quantitative work should take into account the appreciable amount of delocalization and the smaller 2s participation of the nitrogen lone pair than one would predict on the basis of an sp^2 hybridization.

In the present paper, we make use mainly of two alternative MO methods in order to investigate the problems stated above in azine compounds and some quinones. The first method is the Hückel treatment for σ electronic systems proposed by Sandorfy and Yosizumi[4] and developed by some of the present authors.[5] This will be abbreviated hereafter to as the H method. Since the resonance integrals between non-adjacent AO's are neglected, this method may be considered to treat the delocalized lone pair with the through-bond interaction.*2 The second method is the extended Hückel method, to be referred to as the E-H method. This method is suitable for discussing the electronic structure of two lone-pair couplings, "through-bond" as well as "through-space."*2

By comparative discussions, the following conclusions are obtained. The delocalization of lone-pair electrons and the appropriate mutual interaction between them must be taken into account in arriving at a better interpretation of the n–π^* transitions.

The electron distribution and the splitting of the lone-pair levels due to mutual interaction as calculated by the Hückel method for σ electron systems seems to be adequate. However, as the direct interaction (through-space interaction) of the lone pair is not taken into account in this method, it gives an incorrect prediction for the symmetry of the energy levels, as in the case of pyridazine. Therefore, for a more accurate discussion of, for instance, the 2s participation in the lone pair and the interaction of two separate lone pairs, it seems better to use the extended Hückel method.

*1 Presented at the 20th Annual Meeting of The Chemical Society of Japan, April, 1967.

1) T. Anno, *J. Chem. Phys.*, **29**, 1161, 1170 (1958); *ibid.*, **32**, 619, 867 (1960); L. Goodman, *J. Mol. Spectry.*, **6**, 109 (1961).

2) R. Hoffmann, *J. Chem. Phys.*, **39**, 1397 (1963); *ibid.*, **40**, 2745 (1964).

3) F. P. Boer, M. D. Newton and W. N. Lipscomb, *J. Am. Chem. Soc.*, **88**, 2361 (1966).

4) C. Sandorfy, *Can. J. Chem.*, **33**, 1337 (1955); H. Yoshizumi, *Trans. Farad. Soc.*, **53**, 125 (1957).

5) K. Fukui, H. Kato and T. Yonezawa, This Bulletin, **34**, 442, 1111 (1962); K. Fukui, H. Kato, T. Yonezawa, K. Morokuma, A. Imamura and C. Nagata, *ibid.*, **35**, 38 (1962).

*2 On the through-bond and through-space couplings, see the paper by R. Hoffmann, A. Imamura and W. J. Hehre (*J. Am. Chem. Soc.*, **90**, 1499 (1968)).

Theoretical

The parameters used in the Hückel method for σ electron systems are tabulated in Table 1.

Table 1. Parameters in Hückel calculation for σ electron systems

Coulomb integrals for σ system		Resonance integrals for σ systems	
C (sp^2)	α	C–C	β
N (sp^2)	$\alpha+0.2\beta$	C (sp^2)	0.38β*
H	$\alpha-0.2\beta$	C–N	β
O	$\alpha+0.3\beta$	N–N	β
		N (sp^2)	0.4β*
		C–H	0.94β
		C–O	1.2β
		O	0.3β*

* Resonance integrals between two σ orbitals belonging to the same atom.

The resonance integrals between non adjacent AO's are ignored, as is usual with the Hückel method.[5] In the extended Hückel calculations, the resonance integral, H_{rs}, is evaluated by $H_{rs}=\frac{K}{2}S_{rs}(H_{rr}+H_{ss})$, putting $K=1.75$, where S_{rs} is the overlap integral between the atomic orbitals, χ_r and χ_s. The Coulomb integral, H_{rr}, for which the valence state ionization potential is usually used, is modified to improve the overestimated electron distribution in this calculation and to obtain a more reasonable energy for the lone-pair orbital. For this purpose, we refer to the results of the application of the ω_A-technique[6] in the extended Hückel method. These H_{rr} values are listed in Table 2. The bond lengths and angles employed are shown in Fig. 1. These values are

Table 2. The values of H_{rr}'s in extended Hückel calculations (eV)

	s	p_x	p_y	p_z
H	−14.9			
C	−21.5	−12.0	−12.0	−11.9
N	−24.2	−11.2	−11.2	−11.9
O	−28.6	−11.7	−11.7	−12.9

adopted with reference to the Table of Interatomic Distances edited by Sutton and the experimental results of Wheatley.[7]

Results and Discussion

Delocalization of Lone Pair. Since the Hückel calculation needs the values of the hybridization of constituent atoms in order to estimate the Coulomb and resonance integrals of a lone-pair AO, an sp^2 hybridization for the nitrogen atom in azine compounds is assumed.

It may be noted that, in the Hückel calculation, the highest occupied σ orbitals in azine compounds are, without exception, remarkably localized on the lone-pair AO of the nitrogen atom. These MO's will be referred as lone-pair MO's hereafter in the present paper.

The electron distributions of these lone-pair MO's as obtained by the Hückel calculation are given in Fig. 2. For the diazines, the distribution is obtained by summing two lone-pair MO's, the highest occupied MO and the next highest occupied MO. For triazine and tetrazine, three and four lone-pair MO's are summed respectively. In view of the partial electron density at the lone-pair AO, about 80%—90% of the lone-pair electrons are localized on that orbital and the electron density increases with a decrease in the distance between nitrogen atoms in diazine compounds. It can also be seen that these partial electron densities run parallel with the observed pK values[8] and also with the blue shifts of the n–π* bands,[8] accompanied by the change in solvent from cyclohexane to an aqueous solution except in the case of pyridine.

Figure 3 lists the total σ electron densities obtained by the Hückel calculation in these compounds. These electron distributions may also indicate the extent of lone-pair delocalization. Namely, the total electron density at the lone-pair AO is always less than 2, and about a 20%—30% delocalization of lone-pair electrons is observed. The total electron densities of the lone-pair AO in four heteroaromatic compounds decrease in the order:

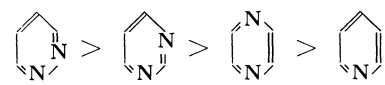

This order is parallel with the order obtained by the partial electron densities of the lone-pair MO.

Next, for the sake of comparison, let us discuss the electron distribution of the azine compounds obtained by the extended Hückel calculation. The atomic population and the atomic orbital population of lone-pair MO's at the nitrogen atom are shown in Table 3, together with the values obtained by the Hückel calculation.

There exists a definite parallelism between the π-electron densities of the nitrogen atom obtained by the Hückel calculation and the atomic orbital populations of the p_z orbital of the nitrogen atoms in azine compounds. Namely, they decrease in the order:

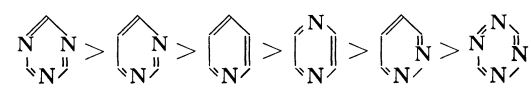

6) H. Konishi, H. Kato and T. Yonezawa, Symposium on the electronic structure of molecules, Osaka, October, 1966.

7) P. J. Wheatly, *Acta. Cryst.*, **13**, 80 (1960).

8) S. F. Mason, *J. Chem. Soc.*, **1959**, 1240.

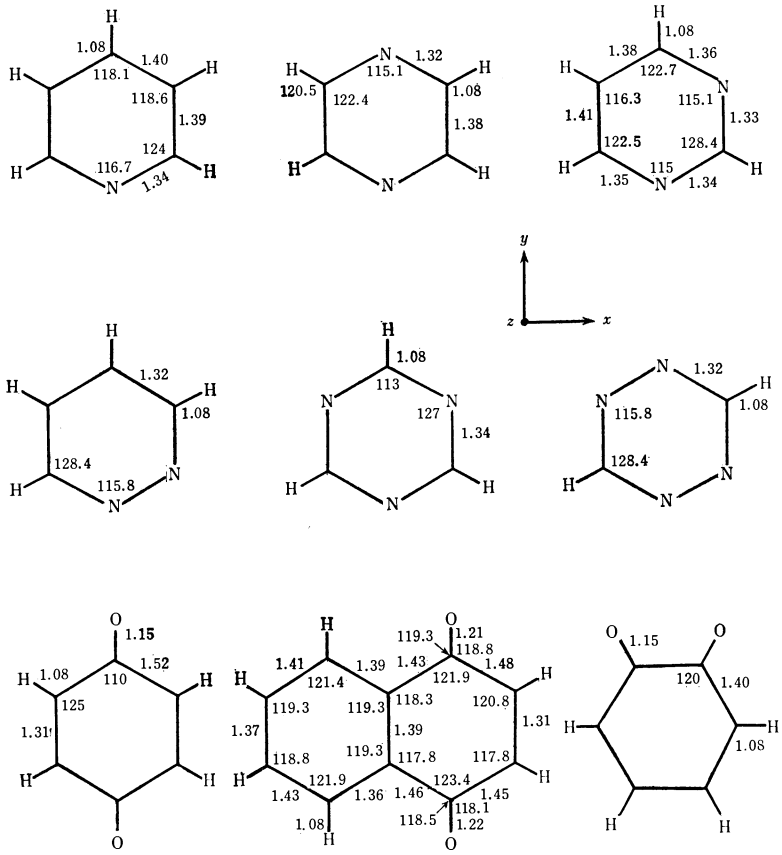

Fig. 1. Bond angles (in degree), bond lengths (in Å) and coordinate axis.

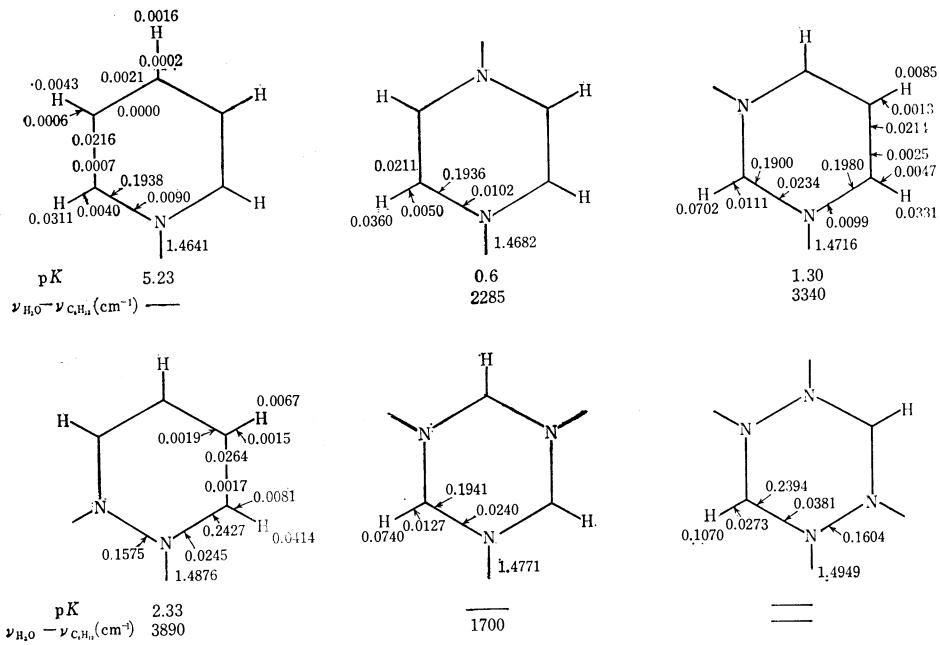

Fig. 2. The electron distribution in the lone-pair MO's of azine compounds.

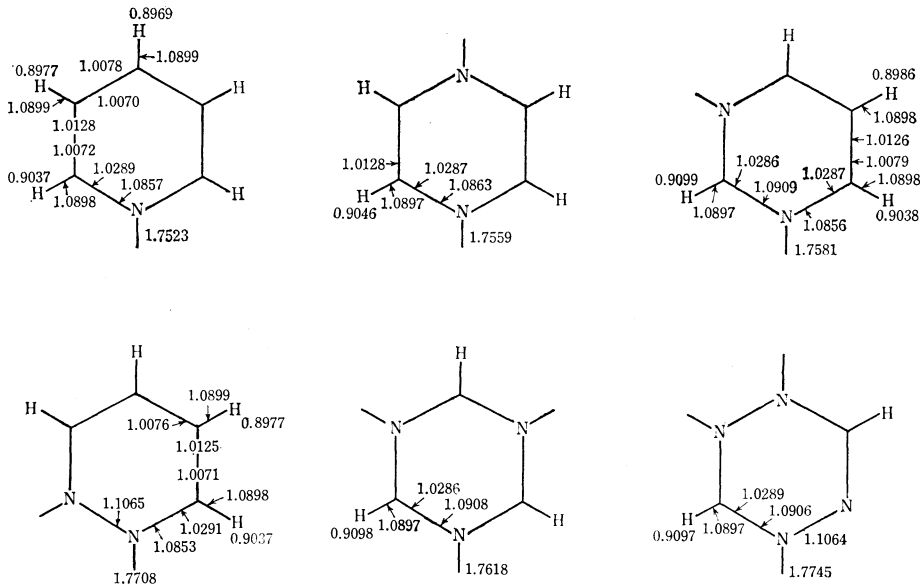

Fig. 3. Total σ electron density of azine compounds.

TABLE 3. AO POPULATIONS AND ATOM POPULATIONS OF THE NITROGEN ATOM OF AZINE COMPOUNDS

Compound	E-H: Atomic orbital population s	p_x	p_y	p_z	E-H: Atom population	H*: $\sum_r^{\text{on N}} q_r$	H*: $\sum_r^{\text{on N}} q_r^{\sigma}$	H*: q_N^{π}
Pyridine	1.4212	0.9974	1.7820	1.0060	5.2066	5.2935	3.9238	1.3697
Pyrazine	1.4175	1.0083	1.7838	0.9736	5.1832	5.2172	3.9285	1.2887
Pyrimidine	1.4256	1.0168	1.7623	1.0203	5.2250	5.3085	3.9347	1.3738
Pyridazine	1.4742	0.9241	1.7499	0.9065	5.0547	5.2260	3.9626	1.2634
s-Triazine	1.4239	1.0413	1.7439	1.0333	5.2425	5.3224	3.9434	1.3790
s-Tetrazine	1.4729	0.9315	1.7401	0.8773	5.0218	5.1158	3.9715	1.1443

* q^{π}; Total π electron density of the nitrogen atom N.

$\sum_r^{\text{on N}} q_r^{\sigma}$; Summation of the σ electron density of AO's belonging to the nitrogen atom

$$\sum_r^{\text{on N}} q_r = q_r^{\pi} + q_r^{\sigma}$$

An agreement is also observed between the atom population and the total density obtained by summing all the σ electron densities and the π electron density around the nitrogen atom in the Hückel calculation.

However, it should be noted that the parallelism between the sum of the AO populations of s, p_x, and p_y and the summed σ electron density around the nitrogen atom, $\sum_r^{\text{on N}} q_r^{\sigma}$, obtained by the H-method does not hold.

Electron Distribution of Some Quinones. The lone-pair electron densities of *p*- and *o*-benzoquinones, 1,4-naphthoquinone, and 9,10-anthraquinone have been calculated by the H method and E-H method. In the H calculation a lone pair of the 2p type is assumed on the oxygen atom.[*3] The highest occupied and the next highest occupied σ orbitals obtained are considerably localized on the lone-pair AO of the oxygen atom of these quinones.

The total and partial lone-pair electron densities on the oxygen atoms of quinones are shown in Fig. 4. The partial electron densities in the lone-pair MO's are shown by the parentheses. About 98% of the lone-pair electrons are localized on the lone-pair AO of the oxygen atom; this magnitude is larger than that of the nitrogen atom of azines.

Both the total and partial electron densities at

*3 This assumption is made with reference to the conclusion on the s nature of the lone-pair orbital at the oxygen atom to be presented below.

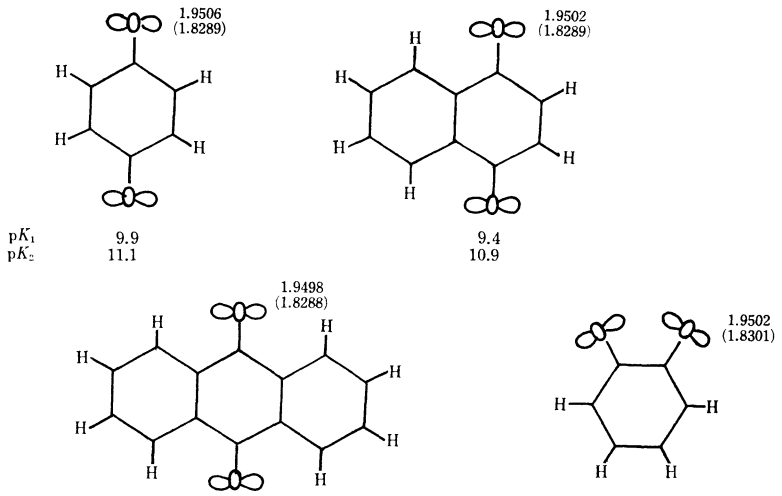

Fig. 4. Total and partial lone-pair electron densities of some quinones.

TABLE 4. AO POPULATIONS AND ATOM POPULATIONS OF THE OXYGEN ATOM OF SOME QUINONES

Compound	E-H					H		
	Atomic orbital population				Atom population	$\sum_{r}^{\text{on O}} q_r$	$\sum_{r}^{\text{on O}} q_r^{\sigma}$ *	q_0^{π} **
	s	p_x	p_y	p_z				
p-Benzoquinone	1.6391	1.9401	1.6770	1.2686	6.5248	6.5811	5.0811	1.500
1,4-Naphthoquinone	1.6873	1.9701	1.6492	1.3638	6.6704	6.6221	5.0801	1.542
9,10-Anthraquinone	—	—	—	—	—	6.6461	5.0791	1.567
o-Benzoquinone	1.6473	1.2005	1.6313	1.7224	6.2016	6.5428	5.0798	1.463

* The value 2 is added as the contribution of two 2s electrons.
** A. Kuboyama, This Bulletin, **31**, 752 (1958); *ibid.*, **32**, 1226 (1959).

TABLE 5. MOLECULAR OTBITAL COEFFICIENT OF THE LONE-PAIR MO'S OF PYRAZINE AND *p*-BENZOQUINONE

Compound	Atom	HO* next HO (eV)	The coefficient of the AO's in the lone-pair MO's			
			s	p_x	p_y	p_z
Pyrazine	N	−10.53	0.162	0.000	0.639	0.000
		−11.91	0.164	0.000	0.659	0.000
p-Benzoquinone	O	−10.94	0.000	0.644	0.000	0.000
		−11.25	0.000	0.676	0.000	0.000

* HO; Highest occupied MO.

TABLE 6. OSCILLATOR STRENGTHS OF n–π^* TRANSITIONS IN AZINE COMPOUNDS

Compound	Transition (allowed)	Transition energy obs. (cm^{-1})[8]	Oscillator strength			
			obs.[8]	H	E-H	Localized model
Pyridine	$n_{a_1} \rightarrow \pi_{b_1}$	37000	0.0030	0.0062	0.0032	0.0100
Pyrazine	$n_{a_{1g}} \rightarrow \pi_{b_{3u}}$	30515	0.0104	0.0042	0.0025	0.0169
Pyrimidine	$n_{b_2} \rightarrow \pi_{a_2}$	33500	0.0069	0.0029	0.0011	0.0102
Pyridazine	$n_{b_2} \rightarrow \pi_{a_2}$	29410	0.0058	0.0075	0.0033	0.0176

the lone-pair AO of the oxygen atom decrease in the order:

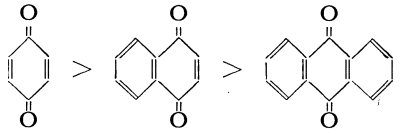

Moreover, the electron density at the lone-pair AO runs parallel with the observed pK values[9] cited in Fig. 4 for *p*-benzoquinone and 1,4-naphthoquinone.

The electron distributions of these compounds as obtained by the H and E-H calculations are given in Table 4 In the E-H calculation, the highest and next highest occupied σ orbitals of the quinones are lone-pair MO's, as in the H calculation. The atomic orbital populations of p_x and $s+p_x$ of the oxygen atom, which would correspond to the population of the lone-pair AO, increase in an order reverse to that of the H calculation.

However, a parallelism is observed between the π-electron densities of the oxygen atom of quinones obtained by the H calculation for π electron systems and the AO population of p_z of the oxygen atom obtained by the E-H calculation. Furthermore, in the 6th and 7th columns, there is a parallelism between the atom population obtained by the E-H calculation and the total density obtained by summing all the σ and π electron densities around the oxygen atom in the H calculation.

2s Participation in the Lone-pair MO. Since the hybridizations of the atoms are assumed *a priori*, the Hückel calculation is not applicable to a discussion of the s contribution of the nitrogen atom to the lone-pair orbital. Hence, the extended Hückel treatment is adopted for investigating the hybridizations of the nitrogen and oxygen atoms. The molecular orbital coefficients of the lone-pair MO's of pyrazine and *p*-benzoquinone are listed in Table 5.

In pyrazine, the lone-pair MO's consist of only 2s and $2p_y$ AO's of the nitrogen atom. This indicates that the nitrogen atom has a sp^n-type hybridization. On the other hand, in the lone-pair MO's of *p*-benzoquinone, only the $2p_x$ orbital of the oxygen atom is involved in the highest and the next highest occupied MO's. Therefore, the lone pairs of the diazine and *p*-benzoquinone may be referred to as a hybridized-type and a *p*-type lone pair respectively. Hence, it can be pointed out that the lone pairs of azine compounds, ammonia, and hydrogen cyanide belong to the former type, while those of aldehydes, quinones, and alcoholes belong to the latter type.

To estimate the s character of these compounds, the oscillator strength of n-π^* transition, which depends mainly on the s character of the lone pair is calculated.

9) M. E. Peover, *J. Chem. Soc.*, **1962**, 4540.

Some of the oscillator strengths calculated by the three different methods are listed in Table 6. In the table, the values in the last column are the results obtained by combining the ordinary Hückel procedure for π electrons with the Hückel treatment based upon a completely-localized sp^2 hybridized lone-pair model. The results are in a poor agreement with the experimental results, so further improvement is required to make a quantitative discussion. However, it may be generally remarked that the results calculated by three methods decrease in the order:

$$\text{HD method} > \text{H method} > \text{E-H method}$$

This order is parallel with the decrease in the s contribution of the lone pair in the three methods and also with the increase in the delocalization of lone-pair electrons.

In these circumstances, it can easily be understood that, since the magnitude of the oscillator strength depends on the 2s contribution, the n-π^* transitions due to the pure p-type lone pair has an approximately zero or a very small oscillator strength, in accordance with the experimental results.*4

Interaction between Lone Pairs. In the molecules in which more than two lone-pair AO's are involved, the interaction between these lone-pair AO's should be taken into account. The mode of the interaction between two lone-pair AO's has, however, never been studied comprehensively. In the present paper this problem is studied by the three different methods described above.

The characteristics of the three methods are illustrated in Fig. 5. In the HD method, only the direct interaction of the lone pair is considered, as it is based upon the localized model. In the Hückel approach, only the through-bond interaction is taken into account. In the extended Hückel method, however, both interactions, through bond and through space (direct), are considered.

An energy-level diagram of the lone pair as determined by the H calculation is shown in Fig. 6. In the figure, the orbital symmetries, the observed n-π^* transition energies[8] (in cm^{-1}), the splitting of the lone-pair levels as estimated by Mason[8] (written in parentheses in cm^{-1}), and the observed ionization potentials[10] are cited. The Hückel approximation does not include electronic interactions explicity; therefore, only a qualitative discussion is possible. For diazines a rough linear

*4 Nagakura (*Nippon Kagaku Zasshi* (*J. Chem. Soc. Japan, Pure Chem. Sect.*), **74**, 499 (1953)) and Sidman (*J. Am. Chem. Soc.*, **78**, 2363, 4567 (1956)) reported values of 10—100 for the molar extinction coefficient of the n-π^* transitions of *o*- and *p*-benzoquinones, 1,4- and 1,2-naphthoquinones, and 9,10-anthraquinone.

10) I. Omura, H. Baba, K. Higasi and Y. Kanaoka, This Bulletin, **30**, 633 (1957).

Method of calculation		HD	H	E-H
Mode of interaction		Direct	Through-bond	Direct and Through-bond
		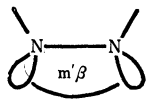	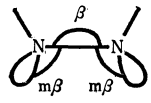	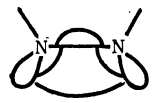
Symmetry of lone-pair MO		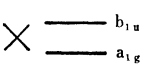		
				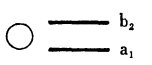
			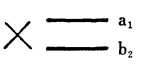	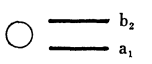

Fig. 5. Interaction between lone-pairs.

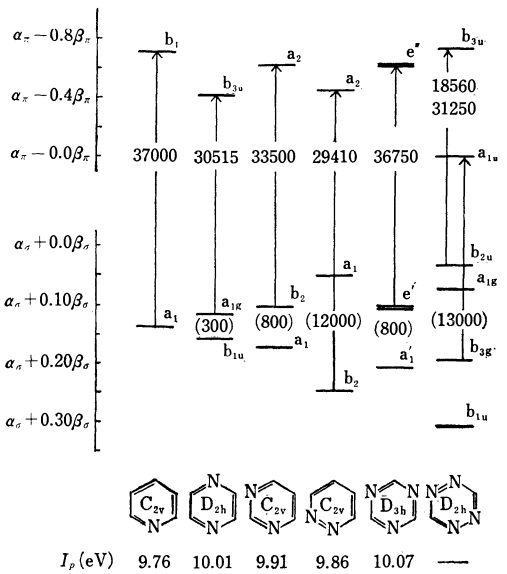

Fig. 6. Lone-pair MO's and lowest vacant orbitals of azine compounds.

relation is obtained between the highest occupied level and the ionization potential. From Fig. 6, it can be seen that the splitting of lone-pair levels becomes larger with a decrease in the mutual distance of two nitrogen atoms; this is in accordance with Mason's estimation.[8] These results suggest an interpretation of the long-wavelength n–π^* band. In the case of pyridazine, however, the symmetry of the two lone-pair orbitals is inverse to the experimental suggestion[8] that the highest occupied must be B_2, and the next one, A_1. This is probably because the allowed transition of pyridazine is $n(B_2) \rightarrow \pi^*(A_2)$ and because its absorption band is at the longest wavelength among these azines. This discrepancy seems to be a defect of the method, in which the direct interaction of the adjacent lone pairs of the nitrogen atom, which may have sizable overlaps,*5 is not taken into account. These circumstances are shown in Fig. 5. "Circle" denotes the agreement of the level sequence obtained by the experiment and by calculation, while "Cross" denotes their disagreement. In the E-H method the higher one is B_2, and the lower one is A_1, they agree with the experimental suggestions, in contrast to the results of H calculation. However, the trend of the splitting expected from the experiment, that is a small splitting for pyrazine, a large one for pyridazine, and an intermediate one for pyrimidine, can not be interpreted. The splittings calculated by the E-H method are pyrazine (1.38 eV), pyrimidine (0.63 eV), and pyridazine (0.66 eV). In the localized model, as is shown in Fig. 5, the higher one is B, the antibonding orbital of two lone pairs, and the lower one is A, the bonding orbital, for all the azines; these results contradict the experimental suggestions regarding pyrazine.*6

Summarizing these discussions, it may be concluded that the lone-pairs interact directly through space as well as through bond. When two lone pairs lie in close proximity to each other, as in pyridazine, the through-space interaction should not be neglected. On the other hand, when two lone pairs are separated by several bonds,

*5 It is estimated as 0.08β by the use of tables (R. S. Mulliken and C. A. Rieke, D. Orloff and H. Orloff, *J. Chem. Phys.*, **17**, 1248 (1949)) for the sp^2-type lone-pair orbitals of pyridazine.

*6 Mason mentioned (Ref. 8) in his localized model, in which the through-bond interaction is not considered, that the higher-energy lone-pair molecular orbital of pyrazine is b_{1u} in D_{2h} and that the lower one is a_g.

as in pyrazine, the through-bond interaction should not be neglected.

The Direct Interaction. In the preceding section we mentioned that the H method, which does not include direct interactions among lone-pair orbitals, gives incorrect level sequences for the symmetry of pyridazine. In order to test the effect of the direct interaction, we modified the H calculation by including that of the neighboring lone pairs of pyridazine. Though interactions among all the non-bonding orbitals should be taken into account, we picked up only one interaction, that between lone-pairs, as the most important direct interaction that affects the lone-pair levels. The calculated lone-pair levels of two methods are illustrated in Fig. 7. In method I, the direct interaction is not considered. In the method II, a direct interaction of 0.2β is assumed. It may be noted that the lower level of method I becomes the upper one of method II and coincides with the orbital sequence obtained by the E-H method, as had been anticipated. On the other hand, the sequence of the other occupied levels is not changed.

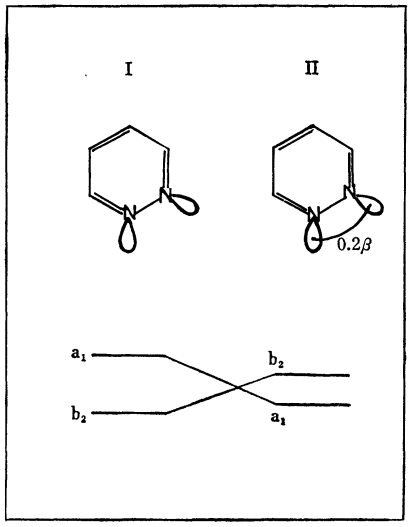

Fig. 7. Direct interaction of lone-pairs of pyridazine.

The electron distribution of method II is shown in Fig. 8. When it is compared with the electron distribution of method I in Fig. 3, it is noted that the value, 1.7910, of the lone-pair electron density in Fig. 8. deviates conspicuously from the value in the series of diazines shown in Fig. 3. When the direct interaction of lone pairs is included, the Coulomb and resonance integrals should be evaluated newly, taking into account the main direct interactions among orbitals other than lone pairs.

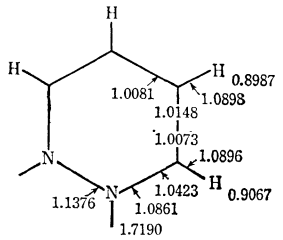

Fig. 8. Total σ electron density of pyridazine in including the direct interaction of 0.2β.

The calculations have been carried out on an IBM 7090 computer at the Japan IBM CO., with the permission of the UNICON committee, and on an HITAC 5020 computer at the Computation Center of the University of Tokyo.

BULLETIN OF THE CHEMICAL SOCIETY OF JAPAN VOL. 42 84—91 (1969)

Thermodynamic Properties of Neopentane from 4°K to the Melting Point and Comparison with Spectroscopic Data*1

Hisae ENOKIDO,*2 Takako SHINODA and Yo-ichiro MASHIKO

Government Chemical Industrial Research Institute, Tokyo, Shibuya-ku, Tokyo

(Received June 4, 1968)

Heat capacities, latent heats and vapor pressures of solid and liquid neopentane were measured and the following values were obtained; heat of transition = 628.7±0.3 cal/mol, T(trans. pt.) = 140.498±0.05°K, heat of fusion = 740.0±0.3 cal/mol, T(triple pt.) = 256.750°K, and P(triple pt.) = 268.47±0.13 Torr. The amount of impurity in the sample after purification was estimated from a plot of the equilibrium temperature against the reciprocal of the fraction melted. From the result the impurity present was found to be 0.003_2 mol%. Despite of high purity, C_p value in the region below the melting point increases unexpectedly with temperature. This is interpreted as an effect of formation of vacancies in the crystals. The enthalpy required to form vacancies was estimated to be 3240±220 cal/mol from the analysis of the heat capacity curve in the region below the melting point. The molal entropy of the ideal gas at the boiling point, calculated from the calorimetric data, was 71.24±0.3 *e. u.* To bring this value into agreement with the value calculated from the infrared and Raman frequencies and the moments of inertia, requires the assumption of three equal potential energy maxima of 4.4 kcal/mol for hindered internal rotation of the methyl groups.

Non-polar tetrahedral molecules are grouped into two classes: one which undergoes phase transition in the solid state, and the other which does not.[1] Probably, this can be mainly accounted for by interaction between molecular octupoles. We have treated neopentane first in a series of structural thermodynamic studies of tetrahedral molecular crystals.

Neopentane crystal is known to have a transition below its melting point, which was confirmed from the measurement of heat capacity by Aston *et al.*[2] Also X-ray structural study of neopentane crystal[3] shows that its unit cell is face-centered cubic with four molecules at −50±5°C, and tetragonal at −150±5°C. But no information about the orientations of the molecular axes in the unit cell is given yet. Aston *et al.* measured heat capacity of neopentane from 13.22°K to the boiling point, the amount of impurity in their specimen used being 0.727 mol%. And the premelting phenomenon observed was ascribed to the impurities involved in the specimen.

The present paper will describe some results of the measurement of the thermodynamic properties of highly purified neopentane from 4 to 260°K.

The heat capacity curve in the region below the melting point was analyzed so as to study the premelting phenomenon of neopentane crystal. And a comparison of the entropy calculated from spectroscopic data with calorimetric data was made based on the third law of thermodynamics.

Experimental

Material. A chemically pure-grade reagent neopentane obtained from Philips Co., Ltd. (purity; 99.52 mol%[4]) was further purified by means of the "Spinning band fractional distillation column" SB618 (effective height of column is 3 m and the number of theoretical plates is 180) developed by Tokyo Kagaku Seiki Co., Ltd. and a Molecular Sieve 5A adsorption column. The resulting material was twice distilled, at dry ice temperature, through pyrex glass fractionating bulb A (Fig. 1), in which fractionation could be carried out in the absence of air in a vacuum system. The middle fraction was collected in the sample bulb B with a cock connected to the vacuum line by a pyrex glass joint. This sample was cooled to liquid nitrogen temperature and pumped out to less than 5×10^{-4} Torr, melted, cooled again and repumped to remove the trace of air from the sample. The cock attached to the sample bulb was closed and the weight of the sample together with the bulb was measured. For introduction of the sample into the calorimeter, the sample bulb

*1 Presented before the 21st Annual Meeting of the Chemical Society of Japan, Osaka, April, 1968.

*2 Present address: Tokyo Kasei Kogyo Co., Ltd., 6-Chome, Toshima, Kita-ku, Tokyo, Japan.

1) I. Nitta, *Z. Krist.*, **112**, 234 (1959).

2) J. G. Aston and G. H. Messerly, *J. Am. Chem. Soc.*, **58**, 2354 (1936).

3) A. H. Mones and B. Post, *J. Chem. Phys.*, **20**, 755 (1952).

4) T. Shinoda, H. Enokido and Y. Mashiko, *Japan Analysst*, **17**, 1358 (1968).

weighed was attached again to the filling line which was evacuated to less than 10^{-5} Torr. After condensing the neopentane into the calorimeter vessel, the neopentane left in the vacuum line was collected in the sample bulb cooled to liquid nitrogen temperature and weighed together with the bulb. The weight of the actual specimen was estimated by subtracting the leavings from the weight measured first. A schematic diagram of the calorimeter filling system which attaches to the vapor pressure measurement and purification apparatus is shown in Fig. 1. As grease of cock a particular 'Phynal' which is soluble in water was employed instead of silicone grease, since the latter is

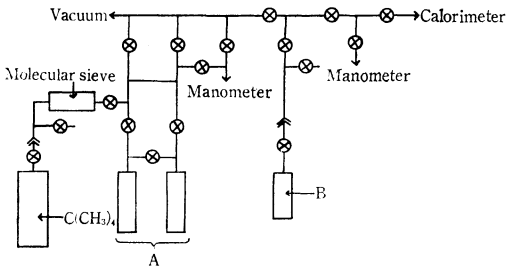

Fig. 1. Schematic diagram of the calorimeter filling system which attaches to the vapor pressure measurement and purification apparatus.

dissolved by hydrocarbon liquid and vapor.

The amount of impurity in the specimen was determined from measurements of the melting point range.

Apparatus. The cryostat and the calorimeter vessel were the same as described previously.[5] The heat input and the resistances of the thermometers were recorded on a Hitachi recorder and a Rubicon six-dial double microvolt potentiometer as a function of time, respectively. The monitoring and control of the adiabatic conditions were automatically made. For this purpose, the highly sensitive *d. c.* amplifier which was possible to detect $\pm 2 \times 10^{-9}$ V was designed and constructed. When the thermocouple signaled, the current in the heater circuit was regulated so as to be proportional to the temperature difference between the calorimeter and the adiabatic shield. All adjusting operations of the intercept and slope of the proportion were carried out according to the conditions of measurement. These adiabatic controls were separately adjusted in three parts of the shield. The controlling operations for measurement below 15°K were carried out manually, since the temperature difference thermocouple tended to lose its sensitivity rapidly at low temperatures.

The working thermometer for $T<13.5$°K was a germanium resistor (Minneapolis-Honeywell Reg. Co.) calibrated by thermodynamic temperature scale. We shall describe below the procedure by which the temperature scales were fixed.

Measurement for the calibration was reported previously.[5] Recently Plumb *et al.*[6] attempted to fit the resistance-temperature data for germanium resistors to a polynomial of the form

$$\log_{10} R = \sum_{n=0}^{m} A_n (\log_{10} T)^n \qquad (1)$$

where the upper limit of m is varied from 3 to 8 depending on individual resistor. Owing to the difficulty of computation we attempted to find four formulas which would fit separately to the regions; 12.00—15.00°, 9.75—12.00°, 6.36—9.75° and 1.50—6.36°. The formulas are given in the following:

$$\log_{10} R = (-K)/(\log_{10} R) + A + (B/T'),$$
$$T - T' = a(T-b)(T-c)(T-d)(T-e) + f. \qquad (2)$$

Coefficients determined are given in Table 1. The deviations of the observed values from the calculated curve, by using the formulas Eq. (2) are within ±0.01° as shown in Fig. 2.

Table 1. Coefficients determined by fitting Eq. (1) to the calibration data of Ge-resistor

T (°K)	1.50—6.36	6.36—9.75	9.75—12.00	12.00—15.00
A	4.676183	3.352358	2.124168	2.191166
B	1.355019	3.542044	7.257872	6.589340
K	5.943370	3.352985	1.505155	1.528695
a	0.00357	0.0129	0.0193	0.00756
b	1.560	6.249	9.364	12.107
c	3.980	7.651	11.031	13.440
d	6.104	9.164	12.367	15.011
e	1.268	$(T-e)=1$	$(T-e)=1$	$(T-e)=1$
f	−0.001	0.0	0.002	0.0

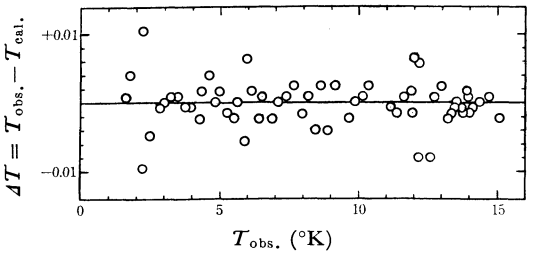

Fig. 2. Deviation of observed temperature of a germanium thermometer from the calculated temperature by using Eq. (2).

Results and Discussion

Heat Capacity of $C(CH_3)_4$. The calorimeter contained 7.4675 g (=0.10350 mol) in measurement series I and 14.4073 g (=0.19968 mol) in measurement series II. Series I and II were taken from separate filling from the same sample. The measured values of the heat capacity in the region of 4 to 260°K are listed in Table 2. The second virial coefficient of gaseous neopentane has not been determined experimentally below 300°K. Therefore its value at low temperatures was estimated by extrapolation of high temperature results using

5) T. Shinoda, T. Atake, H. Chihara, Y. Mashiko and S. Seki, *Kogyo Kagaku Zasshi* (*J. Chem. Soc. Japan, Ind. Chem. Sect.*), **69**, 1619 (1966).

6) G. Cataland and H. Plumb, *J. Rev. NBS*, **70A**, 243 (1966).

Table 2. Heat capacity of neopentane
(Molecular weight 72.151; 1 cal = 4.1840 absolute joules; 0°C = 273.15°K)

T (°K)	C_p (cal/deg mol)	T (°K)	C_p (cal/deg mol)	T (°K)	C_p (cal/deg mol)	T (°K)	C_p (cal/deg mol)
4.141	0.03662	75.473	13.44	139.335	27.01	206.082	28.42
4.535	0.05003	77.485	13.74	140.498	'Transition'	208.108	28.55
4.927	0.06307	79.462	14.08	141.715	34.58	210.210	28.72
5.304	0.08185	81.405	14.38	142.424	26.28	211.885	28.78
5.825	0.1197	83.319	14.70	142.552	25.74	212.496	28.88
6.409	0.1688	85.303	15.00	143.338	24.32	214.667	29.04
6.985	0.2348	87.359	15.29	144.082	24.38	216.187	29.17
7.593	0.3095	89.391	15.60	144.887	24.39	216.827	29.26
8.241	0.4117	91.394	15.84	146.085	24.47	218.274	29.40
8.857	0.5189	92.956	16.03	146.887	24.52	218.963	29.46
9.444	0.6313	94.911	16.30	148.882	24.65	220.360	29.55
10.043	0.7766	96.936	16.61	150.849	24.85	221.268	29.61
10.661	0.9432	99.127	17.02	152.884	25.05	222.443	29.75
11.290	1.101	101.293	17.43	155.007	25.23	223.646	29.88
11.872	1.263	103.333	17.81	157.116	25.41	224.605	29.95
12.497	1.415	105.355	18.19	159.221	25.56	226.844	30.18
13.004	1.576	107.352	18.56	161.296	25.77	229.081	30.38
13.309	1.665	109.325	18.94	163.379	25.97	231.275	30.51
14.176	1.956	111.277	19.34	165.450	26.12	235.589	30.93
14.951	2.223	113.113	19.69	167.509	26.25	237.738	31.07
14.972	2.219	115.027	20.20	169.554	26.37	239.880	31.21
15.739	2.508	116.922	20.51	170.175	26.42	242.013	31.39
15.939	2.565	118.883	20.96	172.219	26.54	243.634	31.50
17.167	2.995	120.903	21.44	174.228	26.64	245.738	31.68
18.587	3.467	122.985	21.91	176.240	26.75	247.842	31.87
20.164	4.010	125.124	22.40	178.287	26.82	249.939	32.07
61.576	11.56	126.395	22.67	180.398	26.95	252.009	32.33
63.489	11.76	128.571	23.19	182.043	27.07	254.044	32.86
65.161	11.97	130.720	23.72	184.272	27.17	255.166	34.04
65.642	12.03	132.764	24.26	186.461	27.29	255.446	34.81
67.148	12.24	134.780	24.93	188.292	27.39	255.807	37.11
67.549	12.31	136.216	25.43	195.516	27.77	256.750	'Fusion'
69.202	12.53	136.775	25.65	197.662	27.91	258.051	36.21
69.417	12.55	137.887	26.10	199.788	28.01	258.132	36.43
71.330	12.81	138.290	26.23	201.904	28.14	259.929	36.59
73.424	13.12	139.014	26.60	204.011	28.31		

the (7, 28) Lennard-Jones potential.[7] The heat capacity of gaseous neopentane used was those estimated from experimental equation obtained by Spencer *et al.*[8] The density taken for the liquid was given by Whitmore *et al.*,[9] and that for the solid was ascertained by the reference data of X-ray analysis.[3] The value of heat of vaporization was that obtained by Aston *et al.*[2] Corrections were made for curvature where necessary.

The results of measurements of the heat capacity are plotted in Fig. 3 along with those given by Aston *et al.*[2] Their results deviate considerably from ours, particularly in the ranges of melting point and transition point. This is probably due to the fact that the higher amount of impurity was involved in the specimen employed by them.

The time required for the calorimeter system to reach equilibrium after heating was a few seconds at $4<T<6$°K, a few minutes at $10<T<20$°K and about ten minutes at $T>60$°K. But in the middle point of the transition and the melting duration, the time for equilibration after heating became about an hour and 20—30 min, respectively.

The transition, the maximum of which is at 140.498 ± 0.05°K, should in principle be second-

7) S. D. Hamann and J. A. Lawbert, *Australian J. Chem.*, **7**, 1 (1954); S. D. Hamann, J. A. Lambert and R. B. Thomas, *ibid.*, **8**, 149 (1955).

8) H. M. Spencer and G. N. Flannagan, *J. Am. Chem. Soc.*, **64**, 2511 (1942).

9) F. C. Whitmore and G. H. Fleming, *ibid.*, **55**, 3803 (1933).

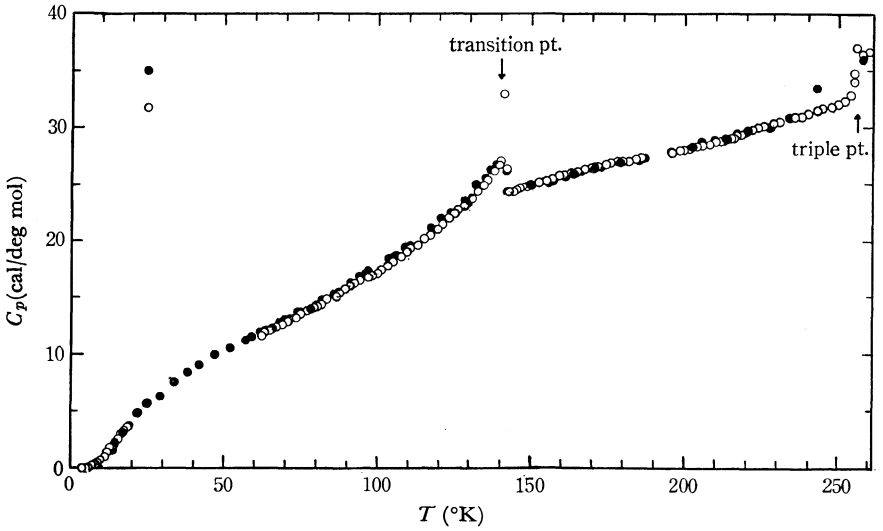

Fig. 3. Heat capacity curve of neopentane.
●: Aston *et al.* ○: Present research

TABLE 3. THE TRIPLE POINT OF NEOPENTANE

Fraction melted	T (°K)		P (Torr)
0.20214	256.7284		268.40
0.27607	256.7341		268.43
0.36610	256.7401		268.45
0.55641	256.7454		268.60
0.81611	256.7493		268.49
		average	268.47±0.13
T_{tr} (pure neopentane)	256.756		
Lwow[9] (1871)	253		
Whitmore and Fleming[9] (1933)	253.7		
Aston and Messerly[2] (1936)	256.53±0.10		

TABLE 4. HEATS OF FUSION AND TRANSITION OF NEOPENTANE

	Temperature interval (°K)	Corrected heat input (cal/mol)	$\int C_p dT$ (cal/mol)	Premelting (cal/mol)	ΔH (cal/mol)
	"Fusion"				
	(mol wt 72.151; (i) 0.10350 mol, (ii) 0.19968 mol)				
(i)	256.119—257.202	779.1	38.9	—	740.2
(ii)	256.455—258.901	828.0	88.3	—	739.7
				average	740.0±0.3
	Aston and Messerly (1936) (mol wt 72.09; 0.25778 mol)				
	240.407—259.847	1609.9	854.1	23.5	779.3
	240.913—261.442	1662.7	910.7	25.0	777.0
				average	778.2±3.5
	"Transition" (140—142°K)				
	139.374—143.046	728.8	100.4		628.4
	139.562—143.358	759.5	130.5		629.0
				average	628.7±0.3

order as was shown in Fig. 3, but actually nearly first-order. We observed no dependence of the heat capacity anomaly of the sample on its thermal history.

The Triple Point and Purity Determination. The equilibrium temperature and pressure of the system were observed during the fusion. The results are given in Table 3. The triple point of pure neopentane, given as 256.756°K, was estimated from a plot of the equilibrium temperature against the reciprocal of the fraction melted. The amount of impurity present in the specimen was also found to be 0.003_2 mol% from the plot.

The present result for the triple point temperature of neopentane deviates considerably from the other results except from that of Aston *et al.* as shown in Table 3. This is also interpreted as an effect induced by impurities.

The Heats of Fusion and of Transition. Two measurements of the heat of fusion are summarized in Table 4, and the average result is compared with that obtained by Aston *et al.* In spite of their correction for premelting, their average result deviates remarkably from the present result.

Aston *et al.* treated the abnormal rise in the heat capacity curve at about 140°K as an isothermal transition. However, we obtained that the transition may be in principle second-order type, with very high heat capacity (*i. e.* 34.58 cal/mol at 141.715°K) over a narrow temperature range. As to the heat of transition, two determinations of the heat supplied to the specimen in the region between 140 and 142°K were made, and the results are also given in Table 4. This average value is to be compared with the heat of transition of 615.9±0.6 cal/mol reported by Aston *et al.*

Heat Capacities in the Premelting Range. Using highly purified neopentane we reexamined the existence of premelting effect found by Aston *et al.* The measurements of the heat capacity in the vicinity of the melting point were made several times with various temperature rise (0.5—1°C) to determine the detailed shape of the heat capacity curve in this region. The result is plotted in Fig. 4, and analysed by ascribing to it several causes.

In the region far below the melting point the data of C_p (normal) can be expressed with sufficient accuracy in the form $A+BT$. Thus, we first attempted to find a formula which would fit to the observed values of heat capacity in the region from 195 to 215°K. The formula obtained is the following:

$$C_p(\text{normal}) = 14.369 + (0.068327)T, \qquad (3)$$

and the plots of C_p(normal) *versus* T as determined from the formula (3) in the region below the melting point are shown with small open circles connected with solid line in Fig. 4.

We, then, estimated[10] the effect on the heat capacity induced by impurities that we determined in the previous section, and the results are shown by the dashed curve in Fig. 4, which is still below the observed values.

We assumed finally, that the excess heat capacity

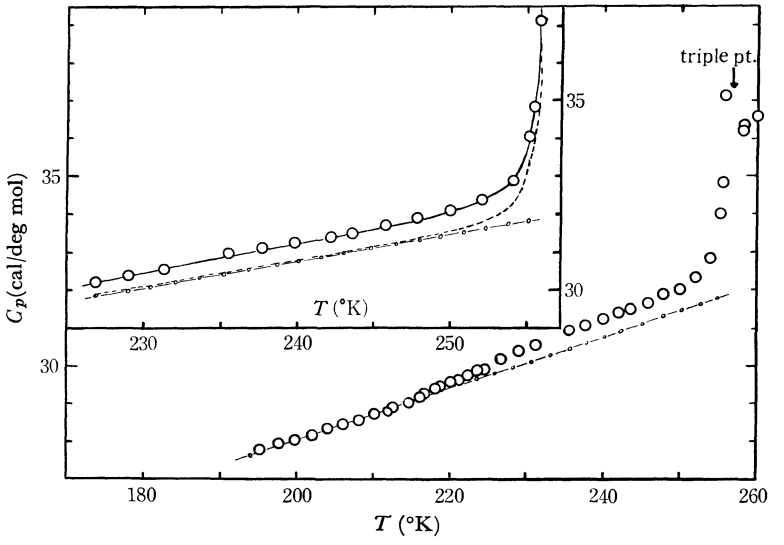

Fig. 4. Heat capacity in the premelting range.
○ : C_p(obs.)
———: C_p(normal) + C_p(impurity) + C_p(vac.)
—o—o—: C_p(normal) = 14.369 + 0.068327T
– – – –: C_p(normal) + C_p(impurity)

10) Y. Mashiko, *Japan Analyst*, **15**, 1151 (1966).

remained in subtracting C_p(normal) and C_p (impurity) from the total is caused by the thermal creation of imperfections, asssuming such as the Schottky-type vacancies. The assumption may be supported by the facts that neopentane crystal transforms to a plastic crystal phase below its melting point, and self-diffusion was observed by the experiment of proton T_1(spin lattice relaxation time) in this phase.[11]

The enthalpy to form the vacancies was calculated from the theory of Schottky vacancy. $\log_{10}(\Delta C_p \times T^2)$ was plotted against $1/T$, where $\Delta C_p = C_p$ (obs.) $- C_p$(normal) $- C_p$(impurity), and a straight line was obtained as shown in Fig. 5. By using the information contained in the intercept and slope of its line, we obtained the following expression:

$$n/N = 4 \times \exp\left[\frac{-3240(\pm 220)}{RT}\right], \qquad (4)$$

where n is the number of vacancies, and N Avogadro's number. The value of 3240 ± 220 cal/mol is the enthalpy of formation of vacancies obtained from the plot. Using the Eq. (4) it is calculated the vacancies of $(n/N)_{T.P.} = 0.69\%$ are to be formed in the crystal at the tiple point.

If the excess heat capacity due to vacancy formation is denoted by C_p(vac.), the plots of C_p (normal) $+ C_p$(impurity) $+ C_p$(vac.) *versus* T are shown by the solid cruve in Fig. 4. The observed values (open circles) of heat capacity for $C(CH_3)_4$

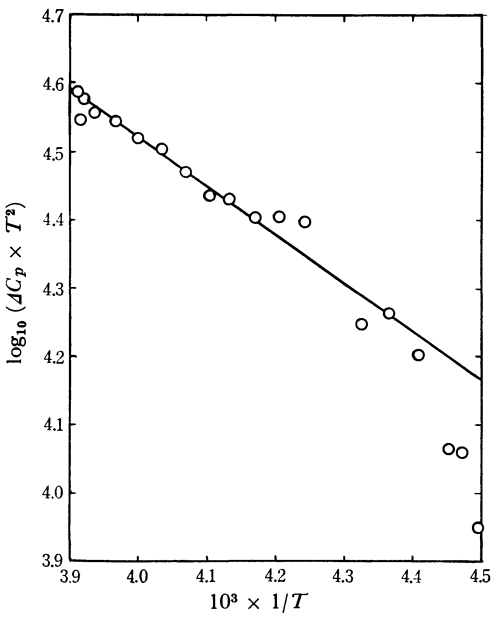

Fig. 5. Plot of $\log_{10}(\Delta C_p \times T^2)$ against $1/T$ for neopentane.

Table 5. Vapor pressure of solid and liquid neopentane

T (°K)	P (Torr)	$P - P$ (Eqs. (5) and (6)) (Torr)
Solid		
194.448	3.71	−0.12
196.585	4.73	+0.09
198.726	5.67	+0.07
200.848	6.66	−0.07
202.960	8.13	+0.08
205.065	9.60	+0.02
207.097	11.32	+0.03
209.120	13.38	+0.12
211.303	15.67	−0.03
213.589	18.61	−0.07
217.898	25.57	−0.07
220.039	29.77	−0.09
223.493	37.93	+0.01
224.801	41.43	−0.01
225.734	44.07	−0.05
227.971	51.13	0.00
230.182	58.97	−0.02
232.364	67.72	−0.02
234.495	77.38	+0.07
236.664	88.30	+0.07
238.812	100.32	+0.06
240.952	113.75	+0.06
243.075	128.43	0.00
244.694	140.75	0.00
246.800	158.27	+0.04
248.896	177.63	+0.03
250.979	198.99	+0.62
253.038	221.97	+0.88
254.959	245.36	+1.14
255.064	246.73	+1.25
255.925	257.57	+0.97
256.116	260.38	+1.29
256.537	265.70	+1.01
Liquid		
257.126	273.21	−0.19
257.108	273.93	+0.75
257.205	274.03	−0.34
258.994	297.06	−0.18
259.058	297.67	−0.38
260.875	323.17	+0.31

may be found to be in excellent agreement with the calculated values. Although there is no example of the creation of vacancies in molecular crystals except for inert gas crystals investigated by Morrison *et al.*,[12] the consideration of lattice vacancies seems to be important in treating premelting phenomenon as shown in this experiment.

11) E. O. Stejskal, D. E. Woessner, T. C. Farrar and H. S. Gutowsky, *J. Chem. Phys.*, **31**, 55 (1959).

12) R. H. Beaumont, H. Chihara and J. A. Morrison, *Proc. Phys. Soc.* (*London*) **A74**, 1462 (1961).

The Vapor Pressure Measurements. The measurements were made in the region of 194 to 260°K as already described,[5] and the results are listed in Table 5.

An attempt was made to find coefficients which would fit the equation based on the theory of ideal gas, liquid and crystal to the observed values. The final equations are given in the following:

i) 194°K$<T<$triple point

$$\log_{10} P + 2(\log_{10} T) + \exp(-g_s/RT) = -1672.65/T + 13.76190, \quad (5)$$

where the third term on the left hand side is the contribution due to the creation of vacancies described in the previous section, and g_s is the Gibbs energy of formation of the vacancies.

ii) $T>$triple point

$$\log_{10} P + 2(\log_{10} T) = -(1517.19)/T + 13.15766. \quad (6)$$

The deviations of the calculated values (horizontal line), using Eqs. (5) and (6), from the observed one are shown by the open circles in Fig. 6. Also in Fig. 6 are illustrated the deviations between the pressures observed by Whitmore *et al.*[9] and by Aston *et al.* and those calculated. The other results show strong deviation from the present results, and this may arise from the facts that the sample used in the measurements by Aston *et al.* was stated to be 99.273 mol% pure, but the amount of impurity in the sample used by Whitmore *et al.* was not reported.

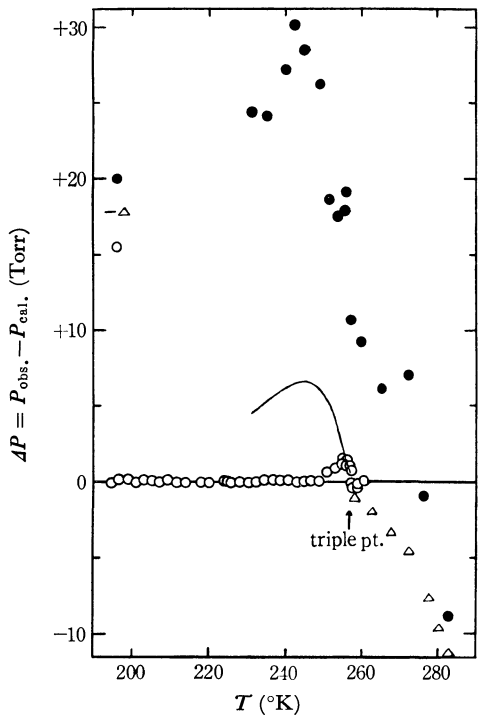

Fig. 6. Deviation of observed vapor pressure of neopentane from the calculated one by using Eqs. (5) and (6).
●: Whitmore *et al.* −△: Aston *et al.*
○: Present research

The Entropy. The calculation of the entropy of neopentane gas at the boiling point from the calorimetric data was made, and the result is summarized and compared with the result obtained by Aston *et al.* in Table 6. The entropy below

TABLE 6. THE ENTROPY OF NEOPENTANE GAS AT THE BOILING POINT

'Calorimetric'

Aston *et al.*	e.u.	Present research	e.u.
0—13.14°K	0.56	0—13.14°K	0.55
13.14—140.02°K	24.13	13.14—140.00°K	23.81
Transition	4.39	Transition (140.00—142.00°K)	4.47
140.02—256.53°K	16.55	142.00—256.75°K	16.47
Fusion	3.03	Fusion	2.88
265.53—282.61°K	3.63	256.75—282.61°K	3.64±0.05
Vaporization	19.24	Vaporization	19.24±0.20
Ideal gas correction	0.18	Ideal gas correction	0.18
	71.71±0.3		71.24±0.3

'Spectroscopic'

	Aston *et al.*	Present research
Translational and Rotational	73.34	73.09
Vibrational (carbon skelton)	5.38	5.34
Vibrational (other modes)	0.17	0.25
Total	78.89	78.68
Calorimetric	71.71	71.24
$(S_f - S) \times 4$ (difference from the value for free rotation)	7.18	7.44

4°K was estimated by using the values of Debye characteristic temperature obtained from the extrapolation of plots of Debye temperature *versus* T. The entropy from 260°K to the boiling point was estimated by using the thermal data observed by Aston *et al.*

The spectroscopic entropy of neopentane gas at the boiling point calculated from its infrared and Raman spectra[13] and the moment of inertia ($I=186.2\times10^{-40}$ g·cm^2), are given in Table 6 along with that obtained by Aston *et al.* The difference of the vibrational entropy between the present result and their one is due to the difference of the spectroscopic data used in the calculations; in their calculation earlier data by Rank *et al.*[14] were employed.

To bring the calorimetric value into agreement with the spectroscopic, requires the assumption of three equal potential energy maxima of 4.4 kcal/mol for hindered internal rotation of the methyl groups (moment of inertia $I_{Me}=5.14\times10^{-40}$ g·cm^2). This value of hindering potential is reasonable in comparison with the observed value of 5.2 kcal/mol, for solid neopentane obtained by cold neutron scattering.[15]

13) D. H. Rank, B. D. Saksaena and E. R. Shull, *Discussions Faraday Soc.*, **9**, 187 (1950).

14) D. H. Rank and E. R. Bordner, *J. Chem. Phys.*, **3**, 248 (1935).

15) J. J. Rush, *ibid.*, **46**, 2285 (1967).

BULLETIN OF THE CHEMICAL SOCIETY OF JAPAN VOL. 42 91—101 (1969)

The Crystal Structure of Two Crystalline Polymorphs of *N*-(*p*-Methoxyphenyl-3-propyl)-*p*-bromobenzamide

Noritake YASUOKA, Nobutami KASAI and Masao KAKUDO

Department of Applied Chemistry, Faculty of Engineering, Osaka University, Yamada-kami, Suita, Osaka

(Received June 6, 1968)

The crystal structure analysis of *N*-(*p*-methoxyphenyl-3-propyl)-*p*-bromobenzamide was carried out by means of X-rays. This compound crystallizes in two crystalline polymorphs, both belonging to the monoclinic system.

α-form: $a = 14.59_2$, $b = 9.57_2$, $c = 11.24_2$ Å, $\beta = 94.2_6°$; $Z = 4$; space group $P2_1/c$.

β-form: $a = 11.94_0$, $b = 10.01_9$, $c = 6.57_7$ Å, $\beta = 90.5_6°$; $Z = 2$; space group $P2_1$.

A little difference in structure is observed between the molecules in the two polymorphs, while the conformations of the carbon-carbon bonds in the 3-aminopropyl group are of the *trans* form. In both forms, belts of molecules parallel to the *b* axis are formed by hydrogen bonds between the amide groups of the molecules related by the twofold screw axis. These belts are packed anti-parallel in the α-form, but parallel in the β-form.

The first step in the interpretation of an X-ray fiber diagram is, generally, to build up a plausible model which accounts for the observed fiber period.

In the X-ray structure analysis of a series of polyamides prepared by the condensation of 1,2-bis-[*p*-(3-aminopropyl)phenoxy]ethane and adipic acid or its homologues,[1] the fiber periods of all these polyamides have been observed to be shorter by 3—4 Å than the calculated values, assuming the ordinary bond lengths and bond angles in the calculation, and the *trans* conformations for all the single bonds in the polymer chains. This "shortening" of the observed fiber periods suggests the presence of conformations other than *trans*, or of bond lengths or angles different from the normal ones.

These polyamides, $[NHCH_2CH_2CH_2C_6H_4O(CH_2)_nOC_6H_4CH_2CH_2CH_2NHCO(CH_2)_mCO]_p$ ($n=1,2,3,4,5,6$ $m=4,8$), have very complicated repeating units. In addition, these polyamides are poorly crystalline and the diffraction data available from these fibers are not sufficient to build up a model of a molecular skeleton which accounts for the "shortening" of the observed fiber periods. In these cases it is effective to carry out the complete crystal structure analysis of some simple compounds containing the important parts of the polymer chain and to deduce the chain structure of the polymer on the basis of the determined conformations of the parts along the chain.

1) T. Ando, N. Yasuoka and S. Kuribayashi, *Nippon Kagaku Zasshi* (*J. Chem. Soc. Japan, Pure Chem. Sect.*), **87**, 536 (1966).

From these considerations, we undertook crystal structure analyses of a series of compounds with the formula of $XC_6H_4O(CH_2)_nOC_6H_4X$ ($n=2,3$ or 4, X=H, Cl or Br) to determine the conformation of methylene groups between phenoxy groups. The structures of *p,p'*-dichlorodiphenoxy-1,2-ethane ($n=2$ and X=Cl) and 1,2-diphenoxyethane ($n=2$ and X=H) have already been determined and reported,[2,3] and it has been found that the OCH_2-CH_2O groups are of the *gauche* form.

Next, the crystal structure analysis of *N*-(*p*-methoxyphenyl-3-propyl)-*p*-bromobenzamide was carried out in order to determine what the detailed structure of the $-C_6H_4CH_2CH_2CH_2NH-$ group is in the crystalline state. In addition, the finding of the polymorphism of this substance prompted us to make a complete crystal structure analysis and to ascertain what the difference is between two polymorphic forms.

Experimental

The two crystalline polymorphs of *N*-(*p*-methoxyphenyl-3-aminopropyl)-*p*-bromobenzamide were found to be stable at room temperature. Preliminary X-ray work revealed that both forms belong to the monoclinic system, but to different space groups: one is $P2_1/c$ and the other $P2_1$. The crystal of the $P2_1/c$ space group is named the *α*-form, and that of the $P2_1$ space group, the *β*-form. The crystal data of both polymorphs are summarized in Table 1.

TABLE 1. CRYSTAL DATA OF *N*-(*p*-METHOXYPHENYL-3-PROPYL)-*p*-BROMOBENZAMIDE

Br–C$_6$H$_4$–CO–NH–CH$_2$–CH$_2$–CH$_2$–C$_6$H$_4$–O–CH$_3$

	α-form	*β*-form
a =	14.592 ± 0.007	11.940 ± 0.007 Å
b =	9.572 ± 0.005	10.019 ± 0.006 Å
c =	11.242 ± 0.006	6.557 ± 0.004 Å
β =	94.26 ± 0.03	90.56 ± 0.03°
V =	1565.9	784.4 Å^3
Z =	4	2
D_x =	1.476	1.474 g cm^{-3}
	$P2_1/c$	$P2_1$

Crystals of the *α*-form were obtained by slowly evaporating an ethanol solution saturated with this substance. After the *α*-form crystals had been picked up, the mother liquor was left to vaporize. When it was dried up, crystals of a different behavior from those of the *α*-form were obtained, these were later found to be the *β*-form.

The unit cell dimensions and reflection intensities were measured with a General Electric XRD-5 goniostat using zirconium-filtered Mo*Kα* radiation within a range of $\sin\theta/\lambda$ less than 0.59 ($2\theta=50°$). Each independenet reflection intensity was measured by the stationary-crystal stationary-counter technique at a counting time of 20 sec. 2743 reflections were collected in the case of the *α*-form and 1474 in the case of the *β*-form. The crystals used had the dimensions of $0.10\times0.15\times0.15$ mm^3 and $0.10\times0.15\times0.20$ mm^3 for the *α*- and *β*-forms respectively. No correction was made for the absorption, while the corrections for Lorentz and polarization factors were made in the usual way.

The infrared absorption spectra were measured in a KBr disk with a Hitachi EPI-1 spectrometer.

Structure Determination

α-Form. The three-dimensional Patterson function was synthesized, and the position of the bromine atom was easily obtained from it. Then the structure was solved by the minimum function method by superposing four sets of three-dimensional Patterson maps with coordinates of the bromine atoms at the four equivalent positions of the $P2_1/c$ space group. Significant peaks appeared on the minimum function map, and the coordinates of all the atoms except hydrogen could be read off. The structure factors were calculated with these atoms, and the three-dimensional electron density distribution was computed. The peak height of each atom was reasonable considering the chemical constitution of this compound.

Then the structure was subjected to least-squares refinement using the block-diagonal matrix approximation. After six cycles the discrepancy index decreased from 0.313 to 0.136. In the refinement, 2743 measured reflections were used. At this stage, the difference Fourier function was synthesized. Several residual peaks with heights of from 0.4 to 0.8 e.Å^{-3} appeared, most of them were found at sites where hydrogen atoms were expected to be present. All the hydrogen atoms with isotropic temperature factors were included in the refinement thereafter. The final discrepancy index is 0.124 for 2421 non-zero reflections, and 0.143 for all reflections.

The atomic scattering factors used in the calculations were taken from those of Hanson and his co-workers.[4] In the least-squares refinement the weight assigned for each reflections was 1.00 for most of them, but 0.25 for the few weakest ones. The computations throughout this work were done on a NEAC 2200 computer in this University and on a HITAC 5020 computer in the University of Tokyo, using programs written by Dr. Tamaichi Ashida of the Institute for Protein Research of this University.

The final atomic and thermal parameters are listed in Table 2. Tables of the observed and

2) N. Yasuoka, T. Ando and S. Kuribayashi, This Bulletin, **40**, 256 (1967).

3) N. Yasuoka, T. Ando and S. Kuribayashi, *ibid.*, **40**, 270 (1967).

4) H. P. Hanson, F. Herman, J. D. Lea and S. Skillamn, *Acta Cryst.* **17**, 1040 (1964).

calculated structure factors are preserved by the Chemical Society of Japan.*1 The three-dimensional electron density map is shown in Fig. 1.

β-Form. From the Patterson projection on (101), the x and z coordinates of the bromine atom were obtained. Since the y coordinate of one atom could be chosen arbitrarily in the $P2_1$ space group, that of the bromine atom was chosen as 0.0. The

TABLE 2. ATOMIC PARAMETERS OF α-FORM

(a) Atomic coordinates (in fraction of cell edges) and their standard deviations (in 10^{-3} Å)

Atom	x	$\sigma(x)$	y	$\sigma(y)$	z	$\sigma(z)$
Br	1.2890	1	0.2829	1	0.6991	1
O(1)	1.0572	6	0.6293	6	0.2386	7
O(2)	0.4558	7	0.1207	7	−0.1152	7
N	0.9701	7	0.4362	7	0.2306	8
C(1)	1.2114	10	0.3523	9	0.5670	8
C(2)	1.1197	10	0.3098	9	0.5572	9
C(3)	1.0657	9	0.3594	9	0.4600	10
C(4)	1.0990	8	0.4510	8	0.3801	9
C(5)	1.1911	10	0.4898	9	0.3914	10
C(6)	1.2487	9	0.4363	10	0.4852	10
C(7)	1.0419	9	0.5133	9	0.2764	10
C(8)	0.9099	9	0.4965	10	0.1343	11
C(9)	0.8289	9	0.3968	10	0.1017	10
C(10)	0.7697	11	0.4594	10	−0.0048	10
C(11)	0.6884	9	0.3684	9	−0.0365	9
C(12)	0.6052	10	0.3861	10	0.0150	9
C(13)	0.5306	10	0.3042	10	−0.0098	10
C(14)	0.5358	8	0.1977	9	−0.0953	9
C(15)	0.6154	10	0.1782	10	−0.1516	9
C(16)	0.6897	9	0.2630	9	−0.1226	9
C(17)	0.4591	10	0.0042	11	−0.1966	11

(b) Temperature factors in form of $\exp(-(\beta_{11}h^2+\beta_{22}k^2+\beta_{33}l^2+\beta_{12}hk+\beta_{13}hl+\beta_{23}kl))$

Atom	β_{11}	β_{22}	β_{33}	β_{12}	β_{13}	β_{23}
Br	0.0081	0.0153	0.0115	0.0002	−0.0047	0.0027
O(1)	0.0062	0.0099	0.0155	−0.0004	−0.0049	0.0004
O(2)	0.0065	0.0169	0.0128	−0.0022	−0.0004	−0.0027
N	0.0049	0.0090	0.0151	−0.0020	−0.0033	0.0003
C(1)	0.0080	0.0080	0.0075	0.0040	−0.0016	−0.0004
C(2)	0.0071	0.0121	0.0096	−0.0047	0.0040	0.0028
C(3)	0.0061	0.0108	0.0108	0.0008	0.0019	0.0010
C(4)	0.0040	0.0090	0.0103	−0.0003	0.0012	−0.0036
C(5)	0.0061	0.0083	0.0124	−0.0012	−0.0001	0.0018
C(6)	0.0051	0.0130	0.0120	0.0026	−0.0008	0.0038
C(7)	0.0059	0.0074	0.0121	0.0024	0.0013	0.0001
C(8)	0.0044	0.0130	0.0147	−0.0013	−0.0030	0.0066
C(9)	0.0049	0.0118	0.0128	0.0009	−0.0025	0.0035
C(10)	0.0078	0.0121	0.0117	−0.0021	−0.0060	0.0035
C(11)	0.0062	0.0095	0.0091	0.0020	−0.0028	0.0058
C(12)	0.0068	0.0132	0.0084	−0.0005	−0.0013	−0.0002
C(13)	0.0072	0.0126	0.0110	−0.0014	0.0022	−0.0016
C(14)	0.0052	0.0107	0.0105	−0.0023	−0.0047	0.0029
C(15)	0.0061	0.0146	0.0093	0.0007	−0.0007	−0.0012
C(16)	0.0063	0.0120	0.0093	0.0006	0.0001	0.0010
C(17)	0.0066	0.0155	0.0142	−0.0072	−0.0025	−0.0076

*1 The complete data of the F_o-F_c table are kept as Document No. 6901 at the office of the Bulletin of the Chemical Society of Japan. A copy may be secured by citing the document number and by remitting, in advance, ¥300 for photoprints. Pay by check or money order, payable to: The Chemical Society of Japan.

(c) Atomic coordinates and isotropic temperature factors for the hydrogen atoms

Atom	x	y	z	B
H(1)	1.081	0.246	0.614	3.6
H(2)	0.994	0.331	0.463	3.7
H(3)	1.221	0.565	0.338	3.3
H(4)	1.319	0.451	0.496	3.6
H(5)	0.958	0.350	0.259	3.6
H(6)	0.947	0.508	0.059	2.9
H(7)	0.886	0.583	0.162	5.4
H(8)	0.779	0.396	0.177	3.4
H(9)	0.858	0.315	0.061	4.4
H(10)	0.809	0.489	−0.074	4.7
H(11)	0.752	0.572	0.011	3.5
H(12)	0.599	0.470	0.081	2.0
H(13)	0.464	0.277	0.051	3.5
H(14)	0.618	0.120	−0.239	4.8
H(15)	0.747	0.259	−0.161	4.5
H(16)	0.512	0.045	−0.258	6.0
H(17)	0.499	−0.046	−0.145	5.9
H(18)	0.405	−0.040	−0.193	2.4

three-dimensional electron density distribution was then computed using all the observed reflections, with phases assigned by the bromine atom only. Atoms of the benzene ring to which the bromine atom attached and those of the amide group could be found easily, but it did not seem possible to assign those of the *p*-methoxyphenylpropyl group without error. The second Fourier synthesis was carried out on the basis of phases assigned by the Br, C(1) to C(7), N, and O(1) atoms. The coordinates of other non-hydrogen atoms could thus be obtained.

The atomic parameters were then refined by the least-squares method. The refinement was carried out with all the measured reflections. After 7 cycles the discrepancy factor was reduced from 0.233 to 0.081. The difference Fourier function was synthesized. Several peaks were found at sites where hydrogen atoms were expected to be present. All the hydrogen atoms with isotropic temperature factors were then included in the refinement. After two cycles, some hydrogen atoms were shifted in such a way that the bond distances to the attached atoms were rather long. The parameters of these shifted atoms were, therefore, restored to their original positions, after which two cycles of refinements were carried out with hydrogen atoms fixed in their original positions. The final discrepancy index is 0.070 for 1332 non-zero reflections, and 0.089 for all reflections.

The final atomic and thermal parameters are listed in Table 3. Tables of the observed and calculated structure factors are preserved by the Chemical Society of Japan. The three-dimensional electron density map is shown in Fig. 2.

Discussion

The bond lengths and bond angles in the molecules of the α- and β-form calculated from the final atomic coordinates are shown in Figs. 3 and 4 respectively. The estimated standard deviations of the bond lengths are from 0.010 to 0.015 Å in the α-form and from 0.012 to 0.030 Å in the β-form. Those of the bond angles are from 0.73 to 0.82°

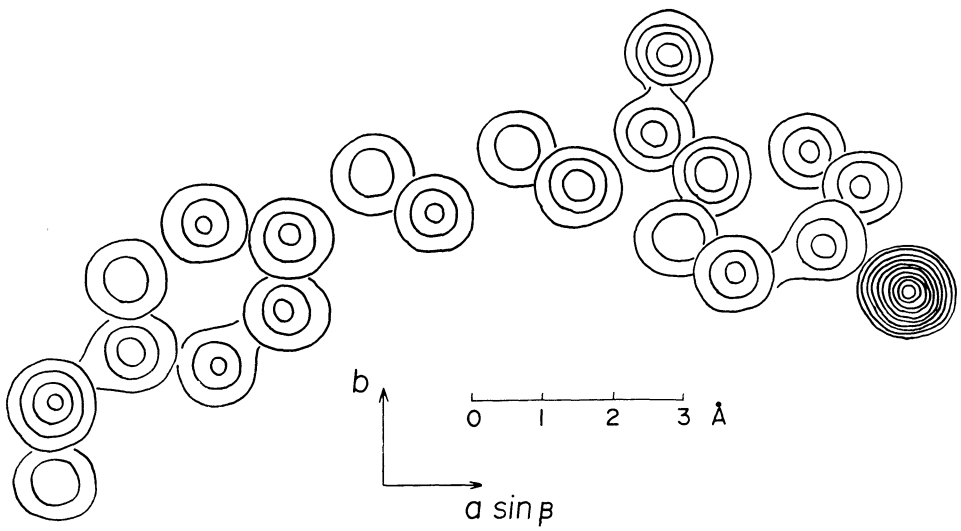

Fig. 1. The final electron density distribution of α-form. Composite diagram of sections parallel to (001) plane. Contours are at intervals of 2 e.Å^{-3}, beginning with the 2 e.Å^{-3} contour. For Br, contours are at intervals of 5 e.Å^{-3} beginning with 10 e.Å^{-3}.

TABLE 3. ATOMIC PARAMETERS OF β-FORM

(a) Atomic coordinates (in fraction of cell edges) and their standard deviations (in 10^{-3} Å)

Atom	x	$\sigma(x)$	y	$\sigma(y)$	z	$\sigma(z)$
Br	0.2332	1	0.0000	4	1.3365	1
O(1)	0.4526	10	0.3483	11	0.5382	9
O(2)	1.0444	11	−0.1778	12	−0.3723	11
N	0.5315	12	0.1497	12	0.4633	12
C(1)	0.3035	15	0.0676	15	1.1025	12
C(2)	0.3959	11	−0.0042	26	1.0269	11
C(3)	0.4489	12	0.0495	14	0.8514	12
C(4)	0.4079	13	0.1649	14	0.7586	12
C(5)	0.3139	16	0.2285	16	0.8374	14
C(6)	0.2560	14	0.1764	17	1.0052	14
C(7)	0.4660	14	0.2306	15	0.5804	13
C(8)	0.5923	14	0.2082	16	0.2959	13
C(9)	0.6762	14	0.1079	16	0.2107	13
C(10)	0.7443	14	0.1701	15	0.0347	13
C(11)	0.8177	13	0.0737	15	−0.0743	13
C(12)	0.9242	15	0.0523	16	−0.0019	14
C(13)	0.9986	14	−0.0327	16	−0.1028	14
C(14)	0.9629	15	−0.0967	15	−0.2797	13
C(15)	0.8535	14	−0.0796	17	−0.3510	13
C(16)	0.7839	11	0.0054	27	−0.2457	11
C(17)	1.0129	24	−0.2468	22	−0.5475	16

(b) Temperature factors in form of $\exp(-(\beta_{11}h^2+\beta_{22}k^2+\beta_{33}l^2+\beta_{12}hk+\beta_{13}hl+\beta_{23}kl))$

Atom	β_{11}	β_{22}	β_{33}	β_{12}	β_{13}	β_{23}
Br	0.0090	0.0177	0.0207	−0.0045	0.0098	0.0032
O(1)	0.0109	0.0116	0.0237	0.0034	0.0137	0.0023
O(2)	0.0102	0.0141	0.0324	0.0058	0.0147	0.0024
N	0.0093	0.0070	0.0309	−0.0020	0.0149	−0.0008
C(1)	0.0098	0.0104	0.0159	−0.0074	0.0054	−0.0064
C(2)	0.0066	0.0109	0.0229	−0.0022	0.0002	−0.0097
C(3)	0.0063	0.0106	0.0162	−0.0006	0.0030	0.0001
C(4)	0.0069	0.0076	0.0171	−0.0002	0.0047	−0.0038
C(5)	0.0099	0.0093	0.0258	0.0007	0.0109	−0.0001
C(6)	0.0076	0.0125	0.0260	0.0012	0.0112	−0.0014
C(7)	0.0071	0.0100	0.0219	−0.0004	0.0081	0.0004
C(8)	0.0073	0.0112	0.0188	0.0013	0.0079	0.0053
C(9)	0.0086	0.0115	0.0212	0.0030	0.0163	0.0059
C(10)	0.0080	0.0099	0.0201	0.0005	0.0087	0.0033
C(11)	0.0072	0.0106	0.0235	0.0002	0.0136	0.0027
C(12)	0.0090	0.0117	0.0248	−0.0021	0.0031	−0.0049
C(13)	0.0084	0.0118	0.0283	0.0038	−0.0054	−0.0049
C(14)	0.0090	0.0091	0.0188	−0.0012	0.0096	−0.0013
C(15)	0.0077	0.0140	0.0206	0.0020	0.0064	−0.0023
C(16)	0.0060	0.0139	0.0205	−0.0043	0.0078	0.0006
C(17)	0.0167	0.0116	0.0259	0.0061	0.0169	−0.0114

(c) Atomic coordinates and isotropic temperature factors for the hydrogen atoms

Atom	x	y	z	B	Atom	x	y	z	B
H(1)	0.427	−0.093	1.104	3.5	H(5)	0.527	0.045	0.477	4.3
H(2)	0.523	0.002	0.787	3.6	H(6)	0.616	0.318	0.346	4.3
H(3)	0.269	0.325	0.798	4.5	H(7)	0.535	0.239	0.177	4.0
H(4)	0.168	0.213	1.042	4.6	H(8)	0.641	0.007	0.189	4.3

H(9)	0.732	0.074	0.331	3.6	H(14)	0.804	−0.153	−0.447	3.7
H(10)	0.789	0.254	0.084	4.0	H(15)	0.703	0.004	−0.303	5.3
H(11)	0.688	0.216	−0.073	4.0	H(16)	0.975	−0.188	−0.667	4.0
H(12)	0.951	0.103	0.139	4.0	H(17)	0.925	−0.274	−0.532	4.0
H(13)	1.083	−0.050	−0.038	4.0	H(18)	1.090	−0.280	−0.633	4.0

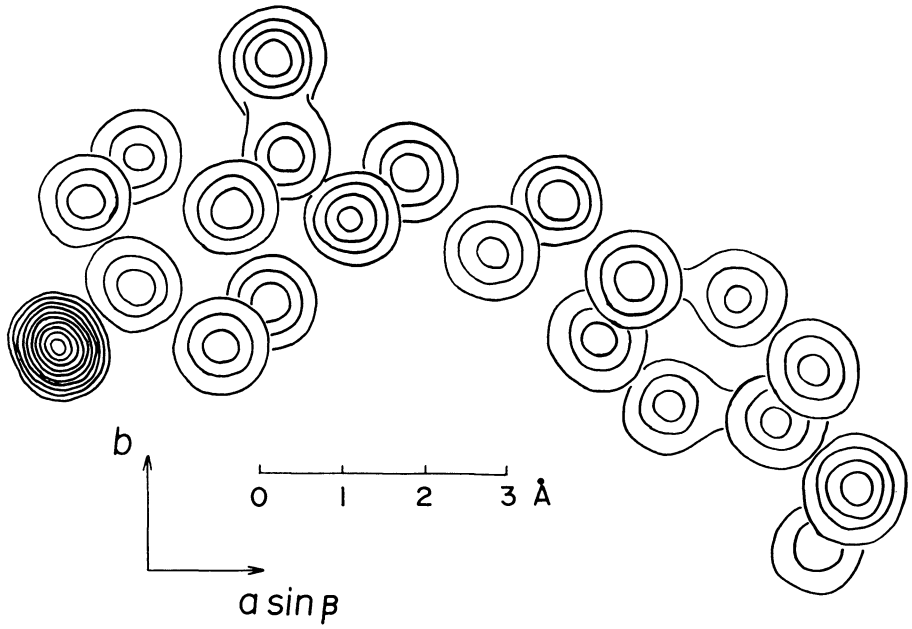

Fig. 2. The final electron density distribution of β-form.

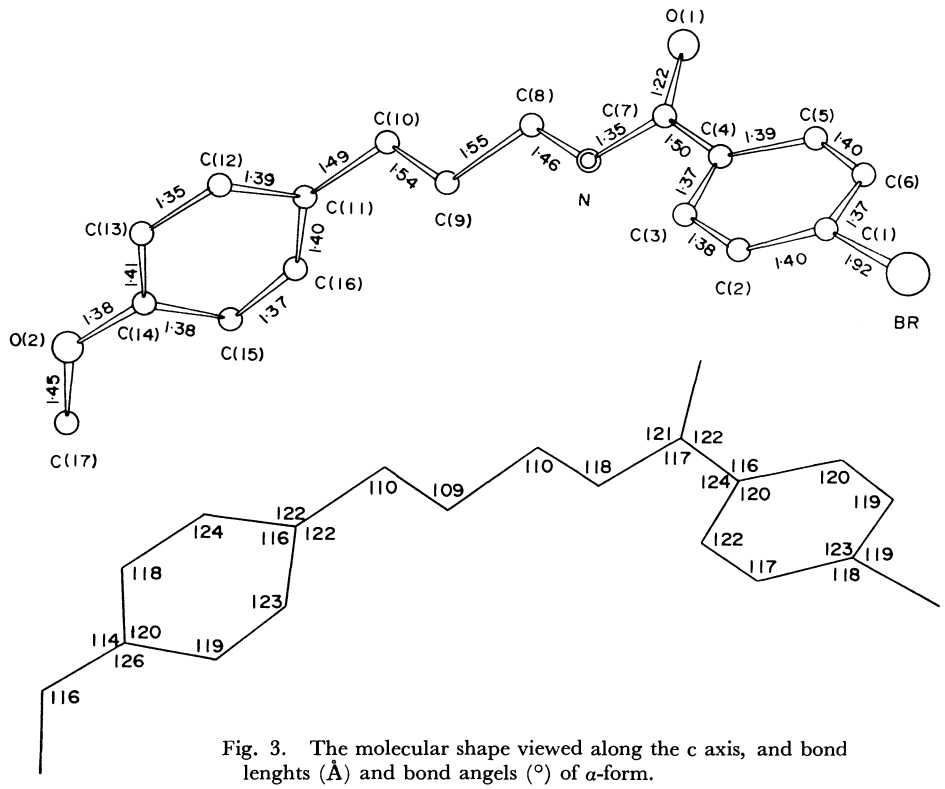

Fig. 3. The molecular shape viewed along the c axis, and bond lenghts (Å) and bond angels (°) of α-form.

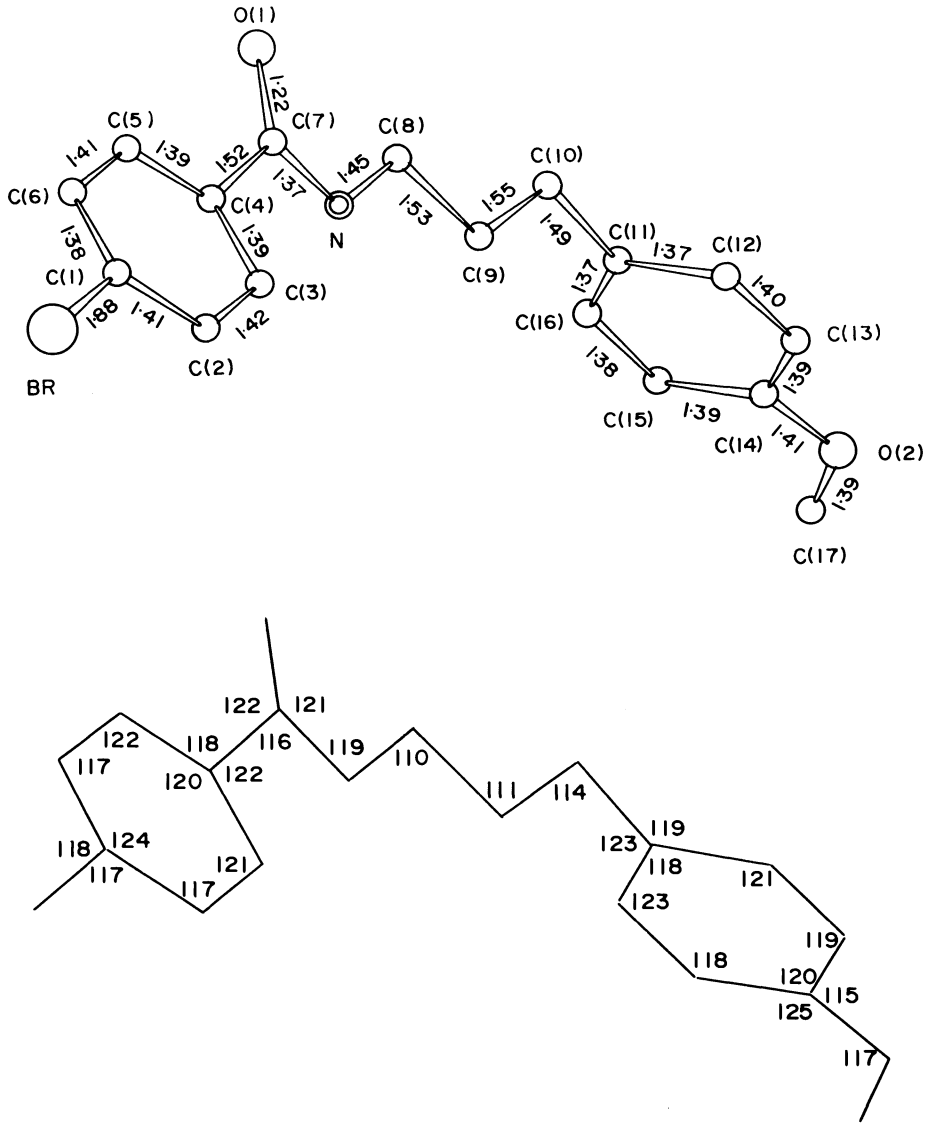

Fig. 4. The molecular shape viewed along the c axis, and bond lengths (Å) and bond angels (°) of β-form.

and from 1.01 to 1.81° in the α- and β-forms respectively. The smaller values of the estimated standard deviations in the α-form than in the β-form are considered to be due to the greater quantity of reflection data (2743 to 1474).

The atomic distances of the corrresponding bonds in the molecules of the two forms give very similar values. The differences of 0.05 Å in C(12)–C(13) and of 0.06 Å in C(17)–O(2) are not significant.

Concerning the 3-aminipropyl group, however, the internal rotation angles are slightly different from each other. Figure 5 illustrates a part of the molecule of each form projected on the best plane of the amide group. The values of the internal rotation angles are listed in Table 4. In

Table 4. Internal rotation angles

	C(4)—C(7)—N	C(7)—N—C(8)	N—C(8)—C(9)	C(8)—C(9)—C(10)	C(9)—C(10)—C(11)
α-form	29.4	−3.4	− 4.2	−3.2	−2.0	89.6
β-form	21.3	2.3	−10.6	1.4	7.4	88.0

Table 4, the internal rotation angles for a bond are defined as follows: looking from the right atom to the left, the clockwise rotation is taken as + and exact *trans* conformation, as 0°. The conformations of the propyl group in two forms are all *trans* in principle, but they show slight differences. First, the internal rotation angles about the C(4)–C(7) bond show a difference of 8.1°, the different inclination angle of the benzene ring to the amide plane

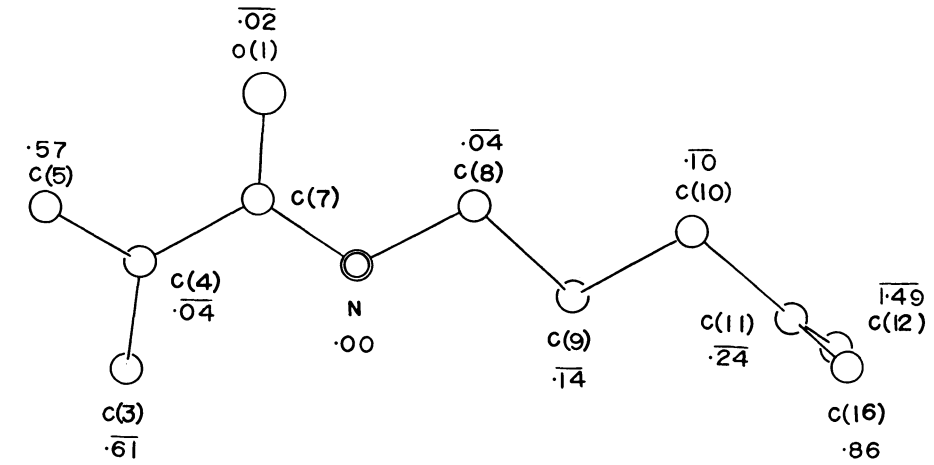

(a)

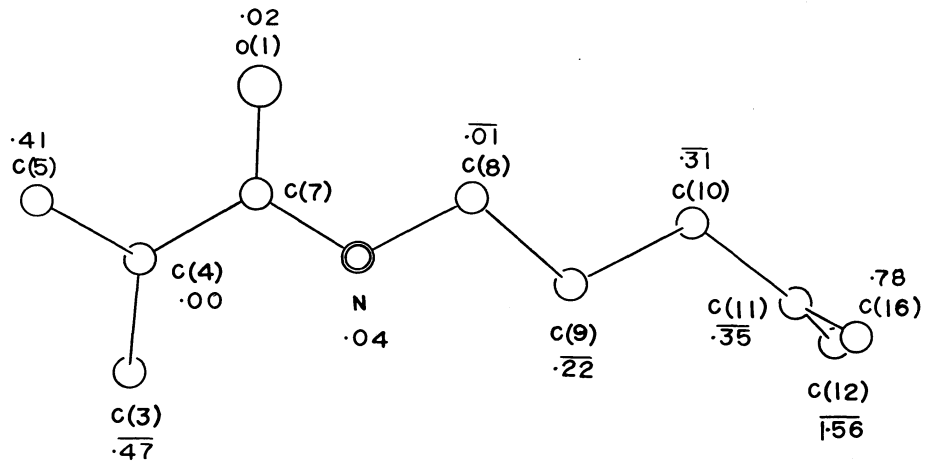

(b)

Fig. 5. The parts of the molecule projected on the best plane of the amide group.
(a) α-form; (b) β-form.
The figures on the names of atoms show the deviations from the plane.

results from this. Secondly, those about the N–C(8) and C(8)–C(9) bonds are different by some degrees. Therefore, the deviation of C(10) from the amide plane is different, as may be seen in Fig. 5. The angle about the C(9)–C(10) bond is different by 9.4° and somewhat releases the difference in the deviation of C(11) from the amide plane. Such a difference in the conformations of the two forms is considered to be due to interactions between adjacent molecules in the crystal.

The crystal structures of both forms projected along the *b* and *c* axes are shown in Figs. 6 and 7 respectively. In both forms the amide group of a molecule forms the hydrogen bond with that of the molecule related by the twofold screw axis parallel to the *b* axis. Thus, the belts of the molecules are formed by the hydrogen bonds. In the β-form the belts are packed together parallel to the *b* axis, but in the α-form the belts are packed antiparallel in the *b* direction. This difference is

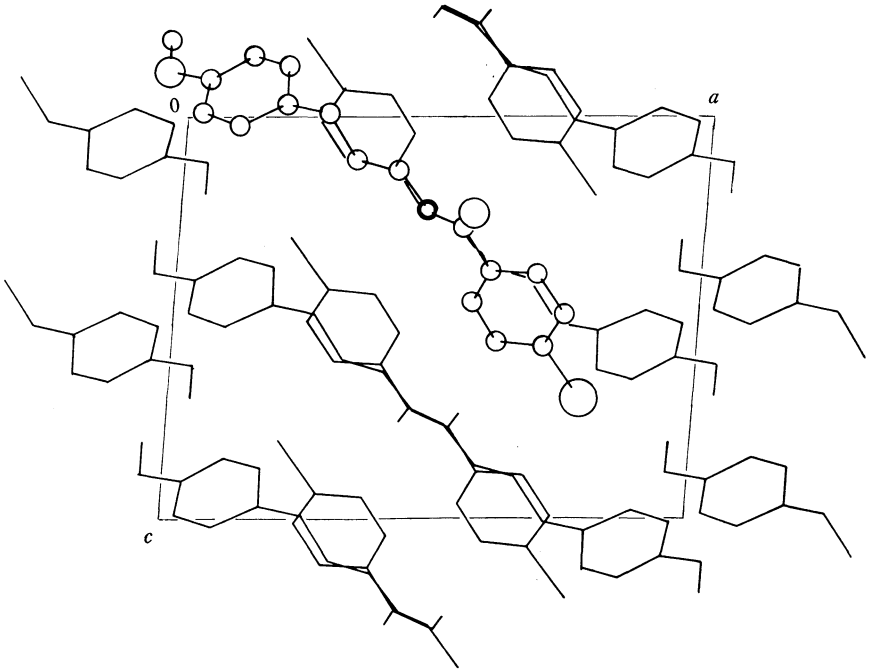

(a) *α*-form

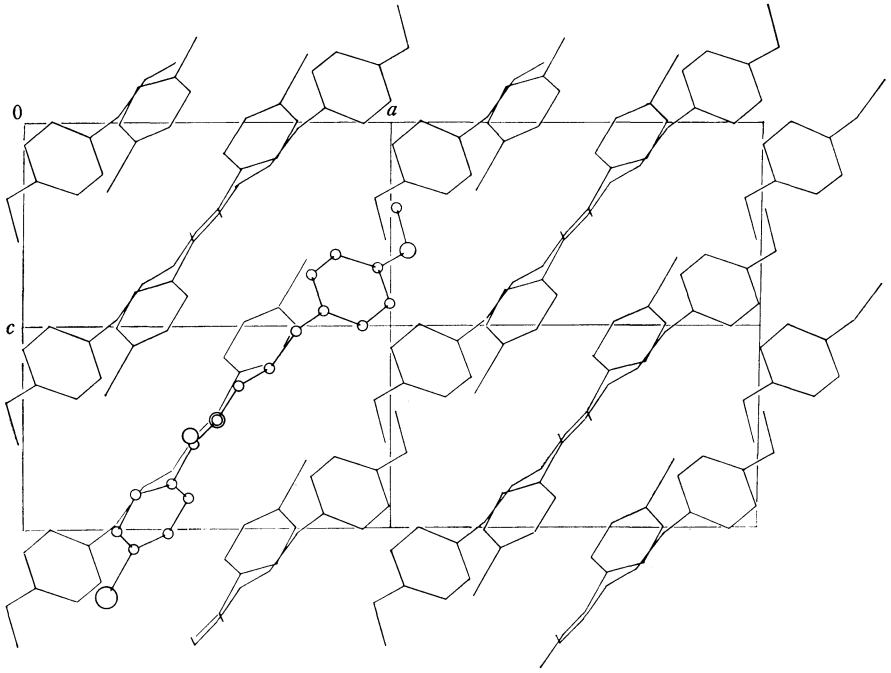

(b) *β*-form

Fig. 6. Arrangement of the molecules viewed along the *b* axis.

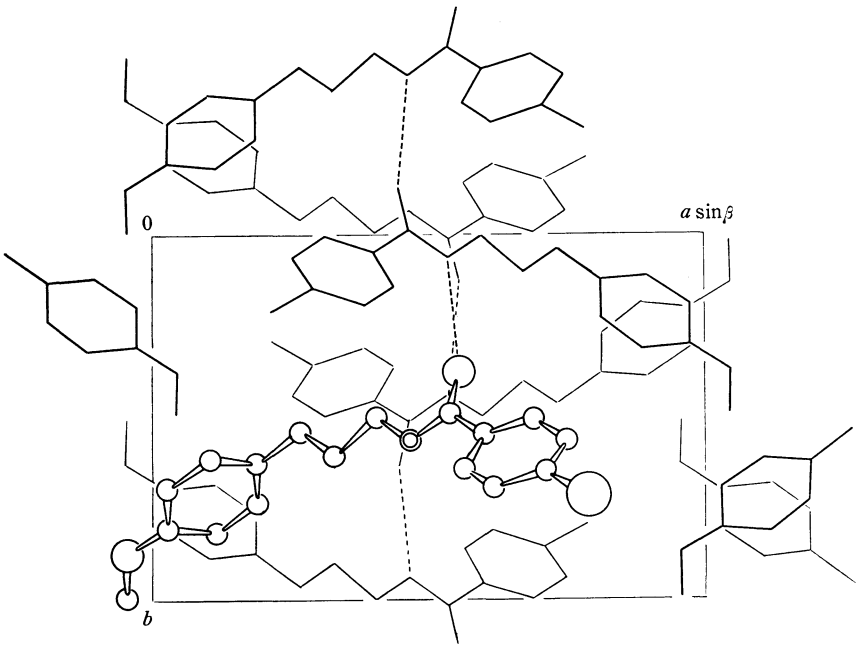

(a) α-form

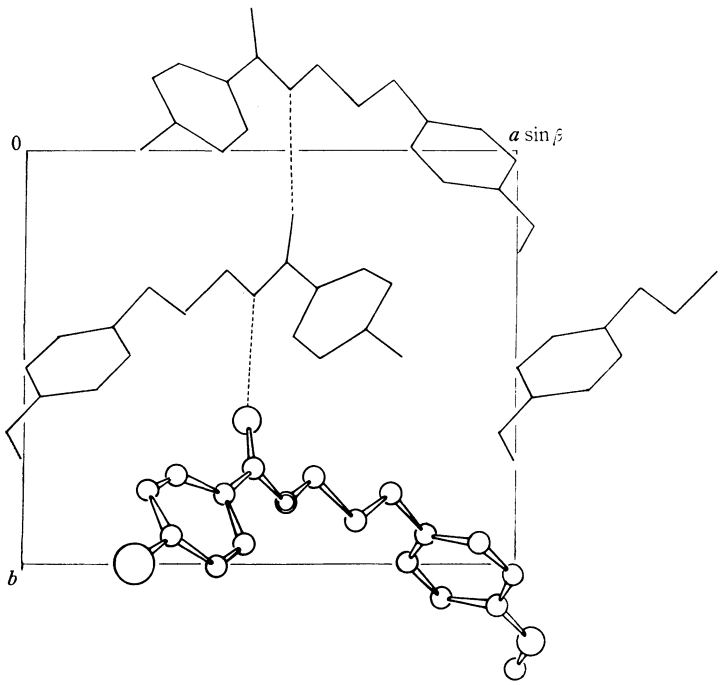

(b) β-form

Fig. 7. Arrangement of the molecules viewed along the *c* axis.

TABLE 5. CLOSE CONTACTS OF ATOMS IN NEIGHBORING MOLECULES (Å)

α-form		β-form	
	Equiv. 2		
O(1)–N	2.99	O(1)–N	3.03
O(1)–C(3)	3.53	O(1)–C(3)	3.47
O(1)–C(7)	3.95	O(1)–C(7)	4.03
O(1)–C(8)	3.81	O(1)–C(8)	3.81
O(1)–C(9)	3.48	O(1)–C(9)	3.45
C(5)–C(9)	3.91	C(5)–C(9)	3.82
C(5)–C(16)	3.99	C(5)–C(16)	4.04
C(6)–C(14)	4.14	C(6)–C(14)	3.92
C(6)–C(15)	3.50	C(6)–C(15)	3.59
C(6)–C(16)	3.57	C(6)–C(16)	3.69
C(8)–C(2)	3.70	C(8)–C(2)	3.58
C(8)–C(3)	3.66	C(8)–C(3)	3.59
C(10)–Br	3.85	C(10)–Br	4.12
C(10)–C(1)	3.84	C(10)–C(1)	4.12
	Equiv. 3		
C(11)–C(17)	3.79	C(11)–C(17)	3.68
C(12)–C(17)	3.80	C(12)–C(17)	3.66
C(13)–C(17)	3.83	C(13)–C(17)	3.67
C(14)–C(17)	3.76	C(14)–C(17)	3.70
C(15)–C(17)	3.68	C(15)–C(17)	3.76
C(16)–C(17)	3.68	C(16)–C(17)	3.74
	Equiv. 4		
O(1)–C(3)	3.95	Br–N	3.95
N–C(2)	3.71	Br–C(4)	3.83
C(2)–C(7)	3.55	Br–C(7)	3.94
C(2)–C(8)	3.99	N–C(16)	3.83
C(3)–O(1)	3.95	C(1)–N	3.68
C(3)–C(3)	3.46	C(1)–C(8)	3.92
C(3)–C(4)	3.60	C(2)–N	3.62
C(3)–C(7)	3.66	C(2)–C(8)	3.61
		C(2)–C(9)	3.72
		C(3)–C(8)	3.72
		C(3)–C(9)	3.62
		C(3)–C(10)	3.91
	Equiv. 5		
C(12)–C(12)	3.76	C(10)–O(2)	3.67
C(12)–C(13)	3.56	C(12)–O(2)	3.67
C(13)–C(13)	3.86		
	Equiv. 6		
O(1)–C(2)	3.63	O(1)–C(2)	3.67
	Equiv. 7		
Br–C(5)	3.74		
Br–C(6)	3.92		
C(2)–N	3.84		
C(12)–C(15)	3.79		
	Equiv. 8		
Br–O(2)	3.46		
Br–C(17)	3.77		

Designation of equivalent positions

	α-form	β-from
Equiv. 2	$2-x, 1/2+y, 1/2-z$	$1-x, 1/2+y, 1-z$
Equiv. 3	$1-x, 1/2+y, -1/2-z$	$2-x, 1/2+y, -1-z$
Equiv. 4	$2-x, 1-y, 1-z$	$x, y, 1+z$
Equiv. 5	$1-x, 1-y, -z$	$2-x, 1/2+y, -z$
Equiv. 6	$2-x, -y, 1-z$	$1-x, 1/2+y, 2-z$
Equiv. 7	$x, 1/2-y, 1/2+z$	
Equiv. 8	$1+x, y, 1+z$	

due to the absence or presence of the glide plane normal to the *b* axis in the β-form or α-form crystal respectively. The intermolecular approaches less than 4 Å are summarized in Table 5. These values are shown as the distances from the original molecule (x, y, z) to the equivalent molecule (*e. g.*, $\bar{x}, \bar{y}, \bar{z}$) related by the space group symmetry. The intermolecular contacts shown as Equiv. 2 in Table 5 are those between molecules related by the twofold screw axis (Fig. 7). The corresponding distances are all shown. Very similar contact distances are seen in two polymorphic forms.

The hydrogen bond distances are listed in Table 6 with estimated standard deviations and also

TABLE 6. NH STRETCHING FREQUENCY AND HYDROGEN BOND DISTANCE

	ν(NH)	N···O distance
α-form	3323 cm^{-1}	2.988 ± 0.011 Å
β-form	3345 cm^{-1}	3.026 ± 0.014 Å

with infrared absorption frequencies of the NH stretching band. It is well established that the stretching frequencies are lowered by the presence of hydrogen bonds and that the frequency shift is monotonic and approximately a linear function of the hydrogen bond distance. Though the difference between the two hydrogen bond distance is not fully significant, the lower frequency of the α-form corresponds to the shorter hydrogen bond distance, and *vice versa* in the β-form. This is in good agreement with Nakamoto's results.[5]

On the basis of the conformations of the 3-aminopropyl group determined above, and of those of the $-OCH_2CH_2O-$ group already reported,[2,3] a possible chain structure of the polyamide obtained by the condensation of 1,2-bis-[*p*-(3-aminipropyl)-phenoxy]ethane and adipic acid has been proposed.[6] The fiber period per repeating unit of this structure model is 26.4 Å, a value which agrees well with the observed value of 26.3 Å.

The authors wish to express their deep thanks to Dr. Tadanao Ando for supplying the samples. They are also grateful to Dr. Tamaichi Ashida and Dr. Tatzuo Ueki, who supplied their computer programs.

5) K. Nakamoto, M. Margoshes and R. E. Rundle, *J. Am. Chem. Soc.*, **77**, 6480 (1955).

6) N. Yasuoka, N. Kasai, M. Kakudo, T. Ando and S. Kuribayashi, *Repts. Prog. Polymer Phys. Japan*, **11**, 149 (1968).

BULLETIN OF THE CHEMICAL SOCIETY OF JAPAN VOL. 42 102—107 (1969)

Infrared Spectra of a Few Transfer Ribonucleic Acids

Masamichi Tsuboi,* Katsuichi Shuto,** Shosuke Takemura** and Susumu Nishimura***

* *Faculty of Pharmaceutical Sciences, The University of Tokyo, Bunkyo-ku, Tokyo*
** *Institute of Molecular Biology, Faculty of Science, Nagoya University, Chikusa-ku, Nagoya*
*** *Virology Division, National Cancer Center Research Institute, Chuo-ku, Tokyo*

(Received June 6, 1968)

Infrared absorptions have been observed in the 1800—700 cm^{-1} region of four purified amino-acid transfer ribonucleic acids (tRNA's): alanine tRNA and valine-I tRNA from *Torulopsis utilis* (torula yeast) and methionine tRNA and tyrosine tRNA from *Escherichia coli* in their deuterated film. Spectral features in the 1550—1750 cm^{-1} region of the valine, methionine, and tyrosine tRNA's indicate that each of these tRNA's has an amount of base-pairs, which is in accord with the "clover leaf" structure previously proposed. The relative amounts of the paired and unpaired cytosine residues are estimated on the assumption that the intensity ratio of the 1523 and 1500 cm^{-1} bands is 0.18 for the paired cytosine residue and 0.84 for the unpaired cytosine residue. The results are also compatible with the "clover leaf" structure.

This is a preliminary report of our infrared absorption measurements of four purified amino-acid transfer ribonucleic acids (tRNA's). Our aim of such measurements is to obtain an information of the secondary structure of a tRNA and of its change caused by a change of the environment. Here we describe only the results obtained of the deuterated films of these tRNA's, from which a piece of the desired information has been obtained.

Abbreviations used in this paper are AMP=adenosine-5′-monophosphate, UMP=uridine-5′-monophosphate, GMP=guanosine-5′-monophosphate, CMP=cytidine-5′-monophosphate, A=unpaired adenosine, U=unpaired uridine, G=unpaired guanosine, C=unpaired cytidine, AU=adenine-uracil base pair, and GC=guanine-cytosine base pair, Ψ=pseudouridine, DiHU=5,6-dihydrouridine.

Experimental

Four tRNA samples were used: (1) alanine-specific tRNA from *Torulopsis utilis* (torula yeast), (2) one of the two valine-specific tRNA's (named "valine-I tRNA") from *T. utilis*, (3) methionine-specific tRNA from *Escherichia coli*, and (4) tyrosine-specific tRNA from *E. coli*. The former two were prepared as has been described by Takemura *et al.*[1,2] and the latter two as has been described by Nishimura *et al.*[3] The first two samples were precipitated by ethanol, washed by ether, and dried in vacuum. Each of the last two samples (about 1 mg) was brought into a concentrated aqueous solution. This was dialysed against a 0.01 M $MgCl_2$ solution to remove polyatomic anions and then lyophilized. A film of each sample was prepared on a AgCl plate. The control of the humidity of the air over the sample film and deuteration of the sample were made by the method described by Sutherland and Tsuboi.[4]

Results and Interpretation

1) General Feature. In Fig. 1, whole the spectrum of the 700—1750 cm^{-1} region observed of alanine tRNA is illustrated. Here, the recorded transmission-wavenumber curve is converted into an absorbance-wave number curve, because one of our aims is to conduct a quantitative analysis (as to the amounts of nucleotide residues located at different intramolecular environments).

In many respects, the spectral features of the four tRNA's are similar to one another, to that of double-helical RNA from rice dwarf virus,[5] and to that of ribosomal RNA from rat liver.[6] All of the four tRNA's (deuterated) give strong absorptions in the 1070—1100 cm^{-1} region, 1220—1260 cm^{-1} region, and 1640—1700 cm^{-1} region. These are attributable respectively to the PO_2^- symmetric

1) S. Takemura, M. Miyazaki, M. Kawata, T. Mizutani, S. Hashimoto and M. Murakami, 7th Intern. Congr. Biochem., Symp. I-5, 1967, Tokyo.

2) M. Kawata, M. Miyazaki and S. Takemura, *J. Biochemistry (Tokyo)*, **62**, 287 (1967).

3) S. Nishimura, F. Harada, U. Narusima and T. Seno, *Biochim. Biophys. Acta*, **142**, 133 (1967).

4) G. B. B. M. Sutherland and M. Tsuboi, *Proc. Roy. Soc. (London)*, **A239**, 446 (1957).

5) T. Sato, Y. Kyogoku, S. Higuchi, Y. Mitsui, Y. Iitaka, M. Tsuboi and K. Miura, *J. Mol. Biol.*, **16**, 180 (1966).

6) Y. Kyogoku, Doctor Thesis, p. 28, the University of Tokyo, 1963.

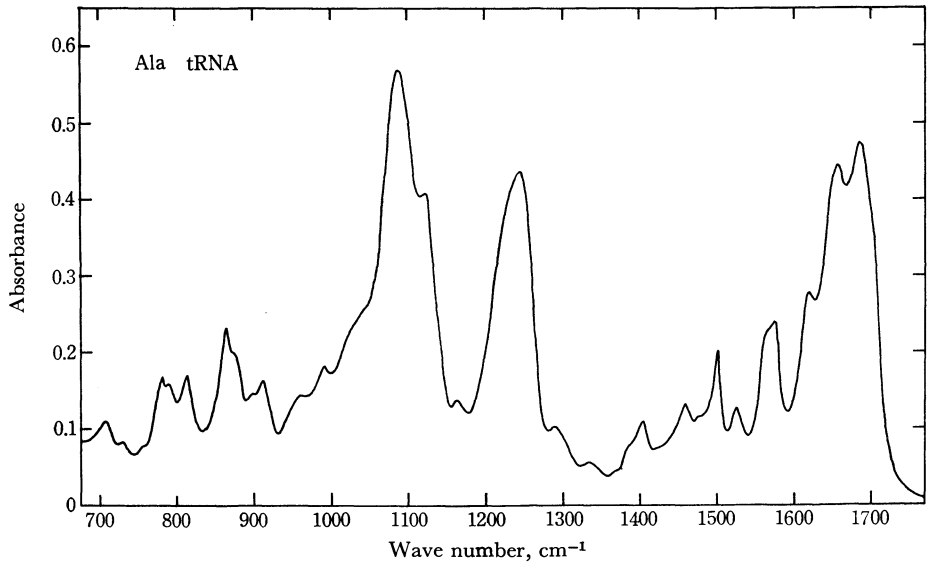

Fig. 1. Infrared absorption curve (in the 700—1750 cm^{-1} region) of a deuterated film of alanine tRNA from *Torulopsis utilis* placed in the atmosphere of 92% relative humidity (D_2O vapor).

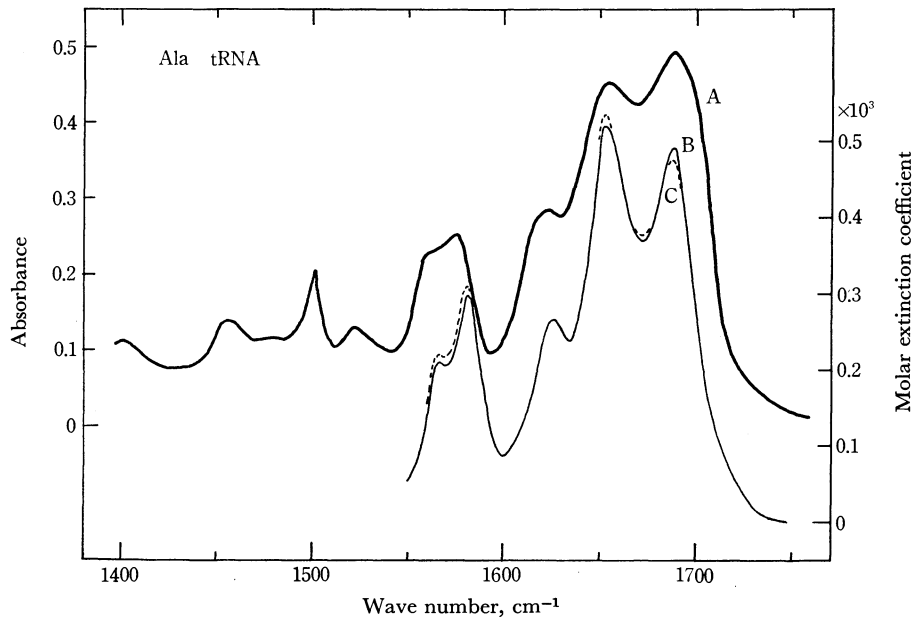

Fig. 2. A: Infrared absorption curve observed (in the 1400—1750 cm^{-1} region) of a deuterated film of alanine tRNA from *Torulopsis utilis* placed in the atmosphere of 92% relative humidity (D_2O vapor).

B: Calculated curve (1550—1750 cm^{-1}) for 0.060 AU + 0.508 GC + 0.090 AMP + 0.134 UMP + 0.119 GMP + 0.089 CMP (corresponding to 2 AU + 17 GC + 6A + 9U + 8G + 6C).

C: Calculated curve (1550—1750 cm^{-1}) for 0.060 AU + 0.478 GC + 0.090 AMP + 0.134 UMP + 0.134 GMP + 0.104 CMP (Corresponding to 2AU + 16GC + 6A + 9U + 9G + 7C).

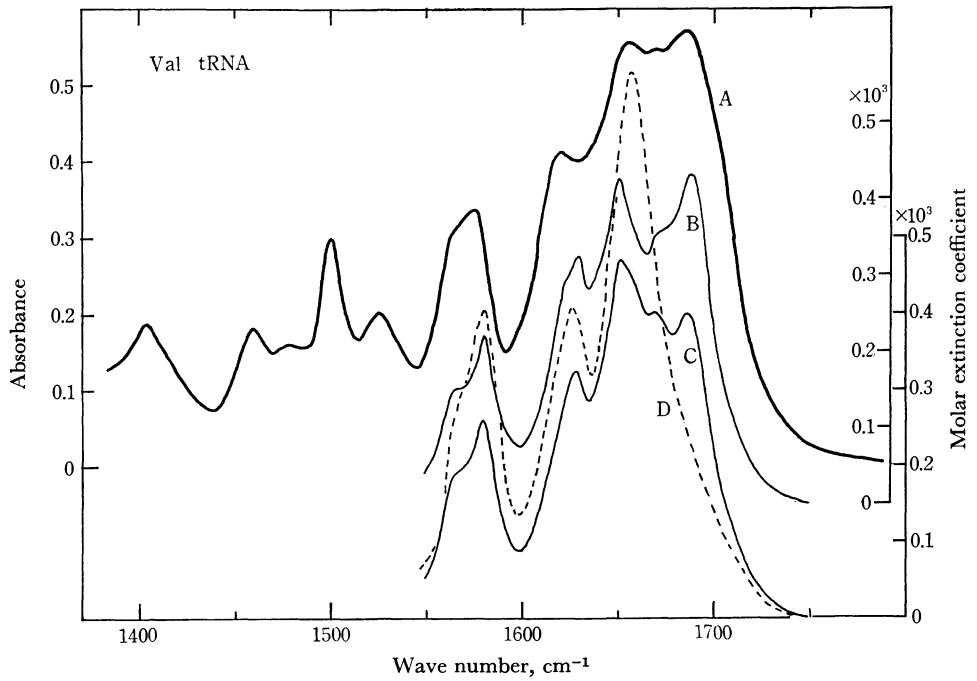

Fig. 3. A: Infrared absorption curve observed (in the 1400—1750 cm^{-1} region) of a deuterated film of valine-I tRNA from *Torulopsis utilis* placed in the atmosphere of 92% relative humidity (D_2O vapor). B: Calculated curve (1550—1750 cm^{-1}) for 0.219 AU + 0.406 GC + 0.125 AMP + 0.063 UMP + 0.063 GMP + 0.125 CMP (corresponding to 7 AU + 13 GC + 8A + 4U + 4G + 8C). C: Calculated curve (1550—1750 cm^{-1}) for 0.187 AU + 0.312 GC + 0.125 AMP + 0.094 UMP + 0.125 GMP + 0.156 CMP (corresponding to 6AU + 10 GC + 8A + 6U + 8G + 10C). D: Calculated curve (1550—1750 cm^{-1}) for 0.222 AMP + 0.175 UMP + 0.286 GMP + 0.318 CMP (corresponding to 14A + 11U + 18G + 20C).

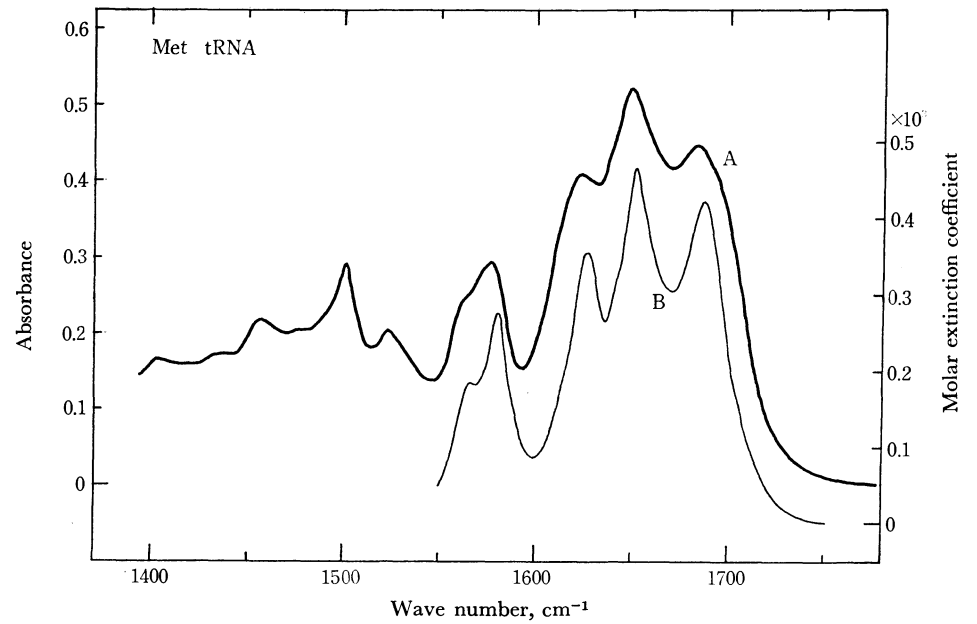

Fig. 4. A: Infrared absorption curve (in the 1400—1750 cm^{-1} region) of a deuterated film of methionine tRNA placed in the atmosphere of 75% relative humidity (D_2O vapor). B: Calculated curve (1550—1750 cm^{-1}) for 0.057 AU + 0.486 GC + 0.186 AMP + 0.071 UMP + 0.086 GMP + 0.114 CMP (corresponding to 2 AU + 17 GC + 13A + 5U + 6G + 8C).

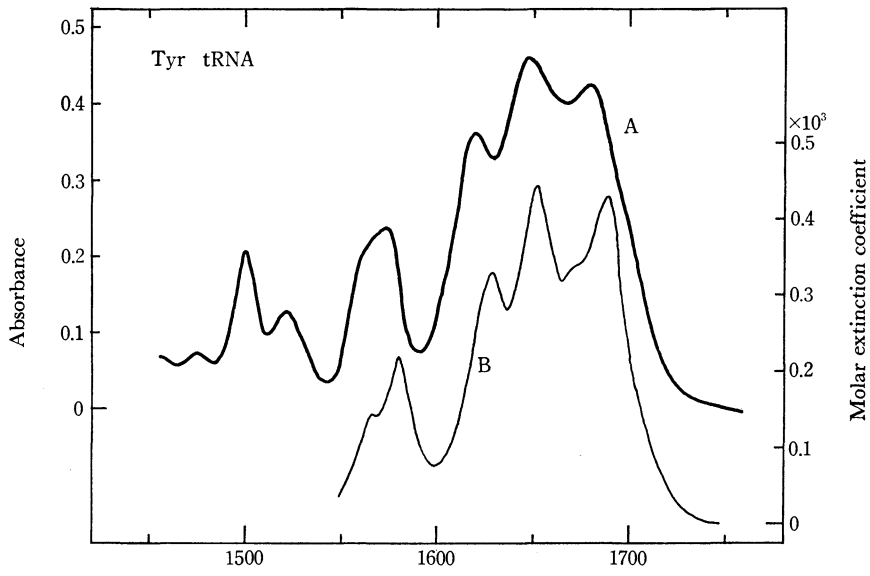

Fig. 5. A: Infrared absorption curve (in the 1450—1750 cm^{-1} region) of a deuterated film of methionine tRNA placed in the atmosphere of 75% relative humidity (D_2O vapor).

B: Calculated curve (1550—1750 cm^{-1}) for 0.177 AU + 0.430 GC + 0.139 AMP + 0.076 UMP + 0.051 GMP + 0.126 CMP (corresponding to 7AU + 17GC + 11A + 6U + 4G + 10C).

stretching, PO_2^- antisymmetric stretching + D_2O deformation, and in-plane stretching vibrations of the base residues.[4] There are moderately strong absorption bands at 1575 and 1500 cm^{-1} assignable respectively to the guanine and cytosine residues.[7,7a] The absorption bands at 1125 and 810 cm^{-1} are characteristic of RNA and are assigned to $\begin{matrix}C\\C\end{matrix}\rangle$C-O degenerate and symmetric stretching vibrations around the 2'C in the ribose residue.[8]

The details of the spectrum in the 1400—1750 cm^{-1} and 760—840 cm^{-1} regions, on the other hand, are somewhat different for different RNA's. The absorption curves of the four tRNA's in these spectral regions are shown in Figs. 2—6.

2) The 1550—1750 cm^{-1} Region. Recently, Thomas[9] described a method for evaluating of the fractions of AU and GC base pairs contributing to the secondary structure of a given RNA from its infrared absorption spectrum in the 1550—1750 cm^{-1} region. For such an evaluation, he presented a catalog of infrared absorption spectra

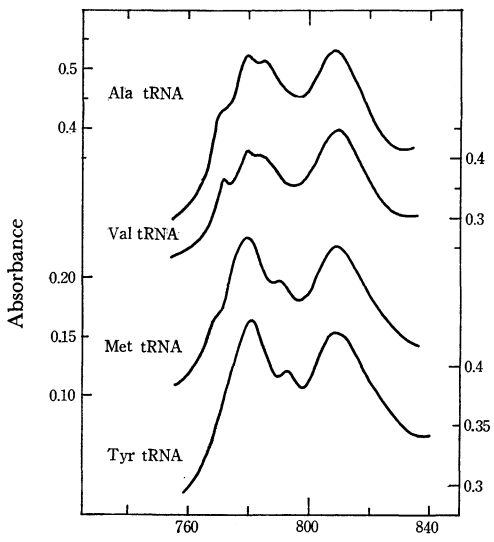

Fig. 6. Infrared absorption curves (760—840 cm^{-1} region) of deuterated films of alanine tRNA, valine-I tRNA, methionine tRNA, and tyrosine tRNA.

of poly(A+U), poly(G+C), AMP, UMP, GMP, and CMP in their D_2O solutions. We have been attempting similar base analyses, and what we observed of poly(A+U) and poly(G+C) in D_2O

7) M. Tsuboi, K. Shuto and S. Higuchi, This Bulletin, **41**, 1821 (1968).

7a) H. Fritzsche, *Biopolymers,* **5**, 863 (1967).

8) M. Tsuboi, K. Matsuo, T. Shimanouchi and Y. Kyogoku, *Spectrochim. Acta,* **19**, 1617 (1963).

9) G. J. Thomas, Jr., *Biopolymers,* in press. We thank Dr. Thomas for kindly showing his results before publication.

are found to be in accord with what Thomas independently observed. We have not yet determined, however, the molar extinction coefficient for each point in the absorption curve, as Thomas did. In addition, we have been using the absorption curves of adenosine, uridine, guanosine, and cytidine in D_2O[10] which may be slightly less suitable than the curves of AMP, UMP, GMP, and CMP as the standard curves for evaluating the amounts of unpaired bases. Let us use, therefore, the standard curves presented by Thomas in our present infrared analyses.

The infrared base-analyses of tRNA's have an additional difficulty: we have no standard spectra of minor bases in tRNA. In the present preliminary analyses, we neglect their contribution. It is true that the total amount of the minor bases in each tRNA is not small at all. For example, valine-I tRNA molecule has altogether 12 minor base residues in the total 75 base residues. They consist, however, of smaller numbers of several different minor bases, and the contribution of each base is different from another and is rather small.

The observed absorption curve of our alanine tRNA (Fig. 2,A) indicates that some of the base residues in it are hydrogen-bonded (paired) and others are unpaired; the absorption peak at 1690 cm^{-1} is caused mainly by the AU and GC base pairs, whereas absorptions at 1655 and 1625 cm^{-1} are mainly attributable to the unpaired bases.[9,11] The determination of the chemical structure of alanine tRNA from torula yeast is not yet completed. For alanine tRNA from baker's yeast, however, the nucleotide sequence was determined by Holley *et al.*[12] On the basis of this sequence, Holley[13] suggested a "clover leaf" model,[13a] which contains 2 AU pairs, 17 GC pairs, and 6A, 9U, 8G, and 6C unpaired. On the basis of this base-pair composition, a synthetic spectrum in the 1550—1750 cm^{-1} region was calculated by the use of Thomas' standard curves. The result is given in Fig. 2, B. As another trial, a calculated curve (Fig. 2, C) was obtained for a "clover-leaf" model in which the so-called "DiHU arm.[14] has only three GC pairs instead of four (most of other "clover-leaf" models so far presented have only three base pairs in the "DiHU arm"). A comparison of the curves A, B, and C in Fig. 2 indicates that the structure of alanine tRNA of torula yeast is somewhat different from what was proposed of baker's yeast. It is suggested that the former has more base pairs or less unpaired bases than the latter, because the relative intensity of the 1690 cm^{-1} peak is found to be greater in the observed spectrum than that in the calculated spectra. In some respects, however, the alanine tRNA in question seems to be similar to the "clover-leaf" model of alanine tRNA of baker's yeast. For example, the relative intensity of the 1623 cm^{-1} peak is lower in the alanine tRNA in question than in the other three tRNA's examined (Figs. 3—5). This fact indicates that the number of unpaired A is relatively small in this tRNA. This is the case also in the "clover-leaf" model of alanine tRNA of baker's yeasts; there are only 6 A's, whereas in most of the "clover-leaf" models of other tRNA, there are more than 10 A's.

Valine-I tRNA should have 5AU, 12GC, 1AΨ, and 2GU base pairs and 8A, 4U, 4G, and 8C unpaired, if the "clover-leaf" model is adopted.[15] Because we do not yet know the standard curves for AΨ and GU pairs, let us assume for trial that there are 7AU and 13GC in obtaining the synthetic spectrum. The result is given in Fig. 3, B. Figure 3, C is a calculated spectrum for a structure which is obtained from the "clover-leaf" model by breaking the three base pairs (two GC and one GU) in the "DiHU arm"[14] and one GU pair in the "amino-acid arm."[14] (This may be the structure obtained in the first stage of the melting process of the "clover-structure). Figure 3, D is a calculated spectrum which is expected for the completely denatured form. Among these three calculated spectra (B, C, and D), spectrum B is in the best agreement with the observed spectrum (Fig. 3, A). Therefore, it may be concluded that valine-I tRNA now in question has base pairing contents which are almost equal to those in its "clover-leaf" model.

Similar examinations were made also for methionine and tyrosine tRNA's from *E. coli*. In each case, the calculated spectrum on the basis of the "clover-leaf" model[16,17] is in a good agreement with the observed spectrum (see Figs. 4 and 5). Both of these two tRNA's show relatively strong

10) M. Tsuboi, Y. Kyogoku and T. Shimanouchi, *Biochim. Biophys. Acta*, **55**, 1 (1962).

11) Y. Kyogoku, M. Tsuboi, T. Shimanouchi and I. Watanabe, *Nature*, **189**, 120 (1961).

12) R. W. Holley, J. Apgar, G. A. Everett, J. T. Madison, M. Marquisee, S. H. Merrill, J. R. Penswick and A. Zamir, *Science*, **147**, 1462 (1965).

13) R. W. Holley, *Scientific American*, **214**, Feb. 30 (1966).

13 a) The "clover leaf" model is what was proposed by Holley[13] as one of possible models of the secondary structure of alanine-tRNA from baker's yeast. It has four arms named[14] "amino-acid arm," "T, Ψ arm," "anticodon arm," and "DiHU arm," which have seven, five, five and four base-pairs respectively. Nucleotide sequences determined later for a number of amino-acid specific tRNA molecules indicated that a similar model is reached when each tRNA molecule is folded so that the number of intramolecular Watson-Crick base-pairs is a maximum.

14) W. Fuller and A. Hodgson, *Nature*, **215**, 817 (1967).

15) S. Takemura, T. Mizutani and M. Miyazaki, *J. Biochemistry (Tokyo)*, in press.

16) S. K. Dube, K. A. Marcker, B. F. C. Clark and S. Cory, *Nature*, **218**, 232 (1968).

17) H. M. Goodman, J. Abelson, A. Landy, S. Brenner and J. D. Smith, *ibid*, **217**, 1019 (1968).

1650 and 1623 cm^{-1} peaks. This fact indicates that the relative amounts of the GC pair and unpaired A are great in these tRNA. These amounts are certainly great if their "clover-leaf" models are valid: 17GC and 13A in methionine tRNA and 17GC and 11A in tyrosine tRNA.

3) The 1400—1550 cm^{-1} Region. The moderately strong band at 1500 cm^{-1} is assigned to the cytosine residue.[7,7a] This band seems to appear irrespective of whether the cytosine residue is hydrogen-bonded or not. Another band attributable to the cytosine residue at 1523 cm^{-1}, on the other hand, is strong only when the residue is unpaired. The intensity ratio of the 1523 to 1500 cm^{-1} bands, $I(1523\ cm^{-1})/I(1500\ cm^{-1})$ is about 0.84 in completely heat denatured DNA in D_2O solution.[18] It has about the same value in cytidine and in CMP in D_2O solutions. While, the $I(1523\ cm^{-1})/I(1500\ cm^{-1})$ value is 0.18 in native double-helical DNA in D_2O. It has almost the same value for double-helical RNA.[5] Fortunately, there are almost no disturbing bands of other base residues in this spectral region, and therefore these two bands are useful in estimating the relative amounts of paired and unpaired cytosine residues. It is assumed that the mole ratio r of the paired cytosine *versus* total cytosine residues is given by

$$r = 1.27 - 1.52\ I(1523\ cm^{-1})/I(1500\ cm^{-1}) \quad (1)$$

so that $r=0$ when $I(1523\ cm^{-1})/I(1500\ cm^{-1}) = 0.84$, and $r=1$ when $I(1523\ cm^{-1})/I(1500\ cm^{-1}) = 0.18$. $I(1523\ cm^{-1})/I(1500\ cm^{-1})$ is found to be 0.30, 0.43, 0.39, and 0.45 respectively for alanine, valine-I, methionine, and tyrosine tRNA's. By the use of Eq. (1), r is calculated to be 0.79, 0.62, 0.68, and 0.59. The paired C/total C values determined from the infrared data for valine-I, methionine, and tyrosine tRNA's (0.62, 0.68, and 0.59, respectively) are in accord with what are expected on the "clover-leaf" models (0.60, 0.68, and 0.63, respectively) within the experimental error which would be about ± 0.05. The paired C/total C values determined from the infrared data of alanine tRNA of torula yeast (0.79) is not greatly different from what is expected on the "clover-leaf" model of alanine tRNA of baker's yeast (0.74).

In the spectral region of 1450—1480 cm^{-1}, poly(G+C) gives no absorptions, while polyAU- (copolymer with adenylic acid and uridylic acid in the alternating sequence) gives two bands here: a weaker band at 1480 cm^{-1} and a stronger band at 1460 cm^{-1}.[18] Therefore, from the spectral features of tRNA's in this spectral region an information on the content of the AU pair may be drawn. This is, however, yet to be done.

4) The 760—840 cm^{-1} Region. The absorptions in the 770 − 790 cm^{-1} region are assignable to out-of-plane vibrations of the base residues.[7] Poly (G+C) gives a strong band at 780 cm^{-1}, whose absorption intensity is more than three times of that of the 810 cm^{-1} band (skeletal stretching vibration around the 2'COH group of the ribose residue).[18] While, polyAU gives much weaker bands at 790 and 770 cm^{-1}.[18] The spectral features of the four tRNA's examined are somewhat different from one another (see Fig. 6). Thus, the spectrosopy in this region is also considered to be useful for an base analysis of tRNA's. This again is yet to be done.

This work was supported by a grant from the Ministry of Education of Japan and by a grant from the United States Public Health Service GM 10024-04.

18) M. Tsuboi, Y. Kyogoku and S. Higuchi, to be published.

BULLETIN OF THE CHEMICAL SOCIETY OF JAPAN VOL. 42 108—116 (1969)

Deuteron Magnetic Resonance Study in $Co(ND_3)_6Cl_3$

Takeshi Ito

Department of Chemistry, Faculty of Science, Tokyo Institute of Technology, Ookayama, Meguro-ku, Tokyo

and Takehiko Chiba

Department of Chemistry, Nihon University, Sakurajosui, Setagaya-ku, Tokyo

(Received June 10, 1968)

Deuteron quadrupole coupling tensors in $Co(ND_3)_6Cl_3$ were determined at various temperatures. The observed quadrupole coupling shows that $Co(ND_3)_6^{3+}$ ions execute a rapid isotropic reorientation at high temperatures (above 320°K for one of the sites (the 4f sites) and above 190°K for another (the 2e sites)), while at low temperatures (below 190°K for the 4f sites, and 170°K for the 2e sites), only a C_3 axis reorientation of the ligand ND_3 groups is present. The deuteron resonance spectra clearly show that $Co(ND_3)_6^{3+}$ ions in the 4f sites begin to reorient about one of the three C_4 axes at intermediate temperatures (about 240°K). On the basis of the orientation of quadrupole tensors, probable orientations of $Co(ND_3)_6^{3+}$ ions in the 4f sites in the crystal are proposed. Additional measurements of the proton resonance on a single crystal of $Co(NH_3)_6Cl_3$ support the results obtained from the deuteron resonance. To obtain the reorientation rates and the activation energies of these reorientational motions, the deuteron resonance line width at the 4f sites is measured at various temperatures and at various crystal orientations. From the temperature dependence of the line width, the presence of two cations with slightly different rates at the 4f sites is suggested. However, because of the limits set by the various experimental conditions, reliable values of the reorientation rates and activation energies could not be obtained.

Structure and molecular motions in the hexamminecobalt(III) chloride crystal have been studied by several authors by measurements of the line shape and of the second moment of the proton magnetic resonance. Murray and Waugh[1] investigated the $Co(NH_3)_6X_3$-type compounds and found that the protons of the NH_3 ligand reorient about its C_3 axis at the temperature of liquid nitrogen. They also found that these complex salts show unusual and very broad line-width transitions in the cases of X=Cl, Br, I, and NO_3. They explained these phenomena in terms of over-all reorientations of complex cations occupying two nonequivalent crystal sites. Dharmatti, Saraswati, and Vijayaraghavan[2] confirmed the existence of two kinds of crystal sites in cobalt atoms by observing the ^{59}Co NMR line, which splits into two components at a static magnetic field of 3 k gauss. Kim[3] measured the proton second moment of $Co(NH_3)_6Cl_3$ at very low temperatures and showed that the reorientation of ammonia molecules about their C_3 axes does not freeze, even at the temperature of liquid helium. In order to obtain detailed information about the structure and motions in this crystal, we measured the deuteron magnetic resonance on single crystals of deuterated hexamminecobalt(III) chloride.

In a nucleus with a nuclear spin greater than 1/2, the NMR spectrum exhibits quadrupole splitting, which is often strongly affected by nuclear motions. It is well known that if two nuclei at different sites exchange positions at a rate much greater than the separation between the lines of the two sites, the field gradient at the nucleus is averaged and the absorption line is observed at the averaged position of the two lines.[4]

In the present case, the field gradient of the deuteron is averaged by the C_3 axis reorientation of ND_3 in a $Co(ND_3)_6^{3+}$ ion because this motion is sufficiently rapid. Assuming an axially symmetric field gradient in the direction of the N–D bond, the direction of the maximum principal component of the averaged field gradient, q_{zz}, can be assumed to be parallel to the Co–N bond direction. Since the $Co(ND_3)_6^{3+}$ ion possesses an approximate O_h symmetry, three types of over-all reorientational motions may be considered——the reorientations about three C_4 axes, those about four C_3 axes, and those about six C_2 axes. If the reorientation about one of the C_4 or C_2 axes is sufficiently rapid, two

1) G. R. Murray, Jr., and J. S. Waugh, *J. Chem. Phys.*, **29**, 207(1958).

2) S. S. Dharmatti, V. Saraswati and R. Vijayaraghavan, *Proc. Colloque Ampere,* **13**, 133 (1960).

3) P. H. Kim, *J. Phys. Soc. Japan,* **15**, 445 (1960).

4) A. Abragam, "The Principles of Nuclear Magnetism," Oxford Clarendon Press, Oxford (1961), Ch. 10.

of the three axially-symmetric q-tensors in the three N-Co-N directions average to a new axially-symmetric q-tensor, one which has $-(1/2)$ the original value and which is parallel to the third. On the other hand, if the reorientation about any one of the C_3 axes is rapid, the field gradient becomes nearly zero. If the reorientations about various axes occur simultaneously (isotropic reorientation), so that all the six ligand molecules can exchange their positions, the field gradient also becomes nearly zero. Therefore, by deuteron resonance study, we can expect to find out what type of motion is present in the crystal.

Experimental

The sample was prepared by the usual method.[5] Deuteration was easily performed by the successive isotope exchange of $Co(NH_3)_6Cl_3$ with D_2O. A single crystal was obtained by slowly cooling a saturated heavy-water solution. The over-all dimensions of a typical sample used in the present experiment are about $10\times 7\times 7$ mm^3. The measurements were carried out at 10 Mc/sec using a Robinson-type detector. The output signal of the spectrometer was amplified by a narrow-band 'lock-in' amplifier, and the derivative of the absorption line was recorded. Temperature control was accomplished by using an electric heater wound outside the probe or by passing through cooled nitrogen gas obtained by boiling liquid nitrogen. Temperature control within ± 1°C was attained by this method. For the deuteron, the nuclear spin $I=1$; therefore, the quadrupole interaction gives a pair of lines ($m=1\leftrightarrow 0$ and $0\leftrightarrow -1$). In order to eliminate the second-order effect of quadrupole interaction and the error due to field drift, the frequency separation between the pair of lines ($2\Delta\nu$) was measured instead of the separation of each sideband from the Larmor frequency. The angular dependence of the quadrupole splitting is given by:

$$2\Delta\mu = \frac{3}{4h}e^2Q\left\{-q_{zz}+(q_{xx}-q_{yy})\cos 2\theta_z + 2q_{xy}\sin 2\theta_z\right\} \quad (1)$$

where q_{ij} is the ij element of the field gradient tensor, where x, y, and z are the coordinates fixed to the probe head, z being along the axis of rotation, and where θ_z is the angle of rotation of H_0 measured from the x axis. From the measurements of rotation patterns about three mutually orthogonal axes, all the components of the p-tensor can be determined.[6] Since the crystal structure of $Co(NH_3)_6Cl_3$ is monoclinic ($\beta=91°19'$),[7] we measured the rotation patterns about the b axis, c axis, and the a* axis (perpendicular to the b and c axes).

Results

The observed spectra are strongly dependent on the temperature. At 320°K, a single broad line at the Larmor frequency (denoted by line 1) and a pair of sharp lines with a separation of several gauss (lines 2) are observed. The intensity of line 1 decreases as the temperature is lowered,

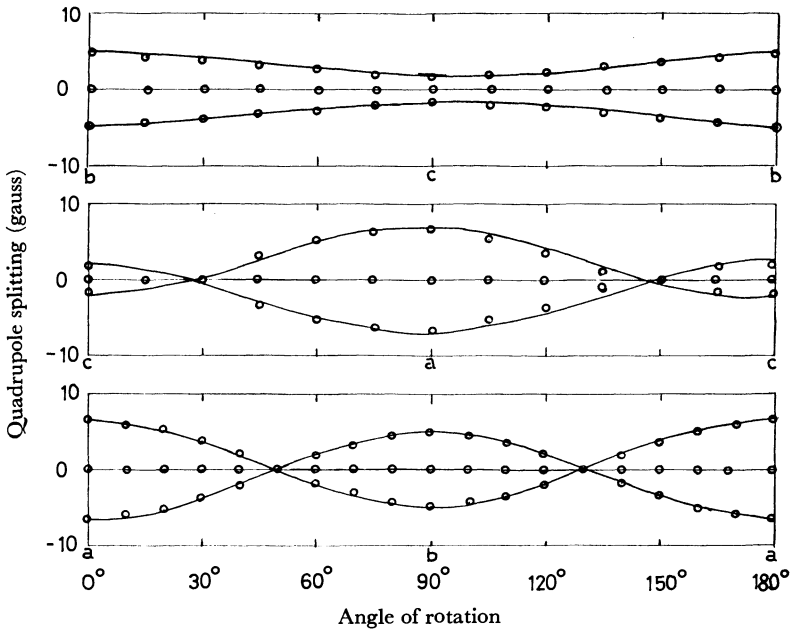

Fig. 1. Rotation pattern of deuteron resonance in $Co(ND_3)_6Cl_3$ at 320°K.

5) K. Yamasaki, "Zikken Kagaku Koza," Vol. 11, Maruzen, Tokyo (1958), p. 18.
6) G. M. Volkoff, H. D. Petch and D. W. Smellie, *Can. J. Phys.*, **30**, 270 (1952).
7) P. Groth, "Chemische Kristallographie," Teil 1, Engelman, Leipzig (1906).

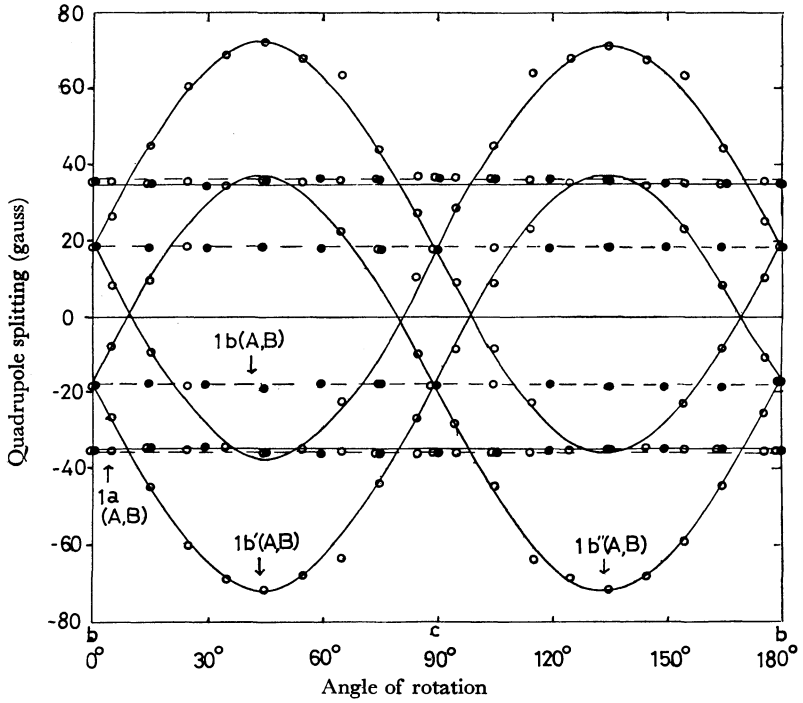

Fig. 2. a*Axis rotation pattern of deuteron resonance in $Co(ND_3)_6Cl_3$.
● at 240°K. ○ at 190°K.
In this pattern the lines due to the ions A and B defined in Fig. 6 overlap each other.

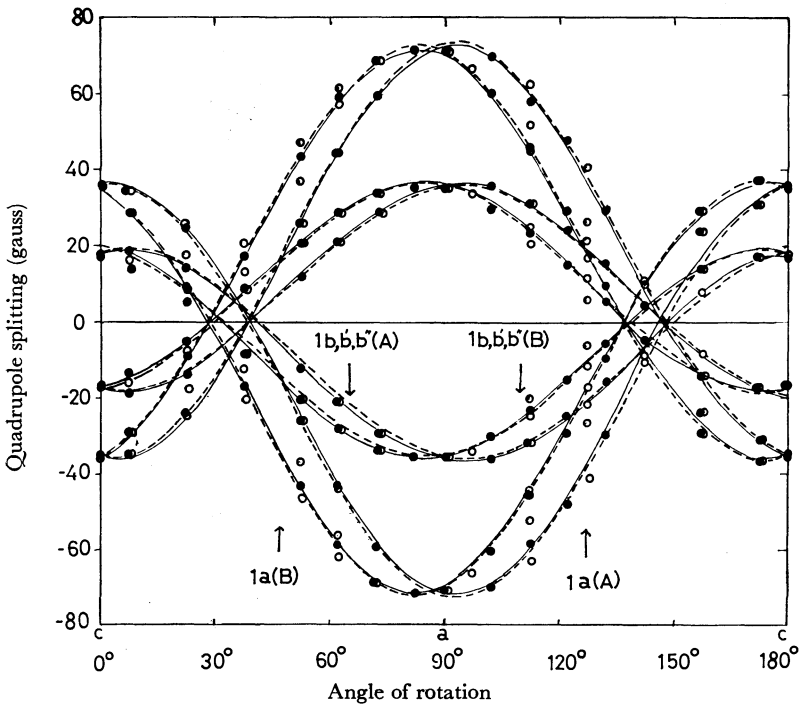

Fig. 3. b Axis rotation pattern of deuteron resoance in $Co(ND_3)_6Cl_3$
● at 240°K, ○ at 190°K.
In this pattern, the lines due to the ions A and B defined in Fig. 6 are separately observed, but the lines 1b′ and 1b′′ overlap each other.

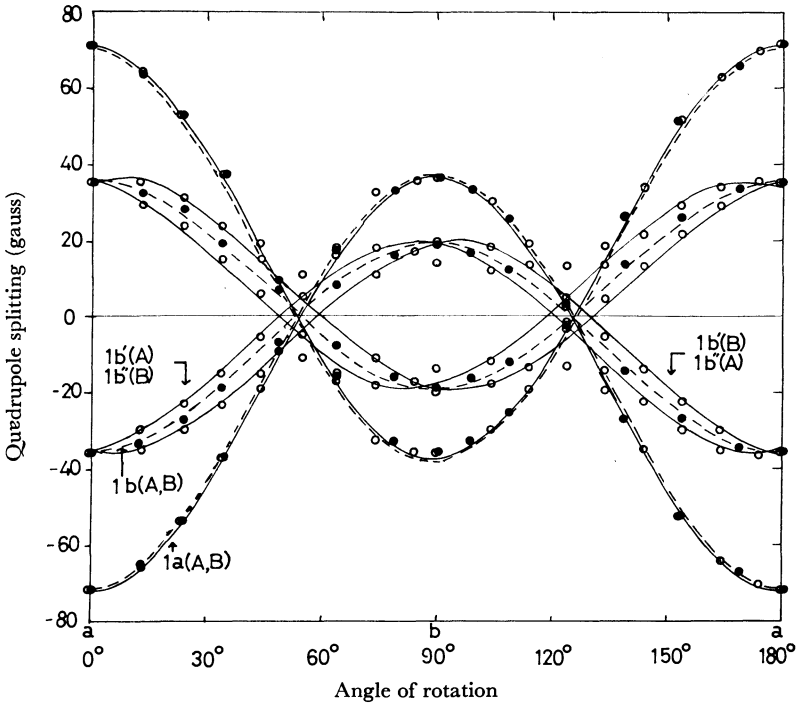

Fig. 4. c Axis rotation pattern of deuteron resonance in $Co(ND_3)_6Cl_3$.
● at 240°K, ○ at 190°K.
In this pattern, the lines 1b′ (A) and 1b″ (B) or 1b″ (A) and 1b′ (B) overlap each other.

until it almost fades out at 305°K. New weak lines begin to appear at this temperature. These lines are clearly distinguished as pairs of lines (1a and 1b) at 240°K. At 190°K, the line 1b further splits into two lines (1b′ and 1b″). The lines 2 become weak as the temperature is lowered and almost fade out at 170°K. Eight or nine pairs of lines are observed at the temperature of liquid nitrogen.

a) Lines 1 and 2. The spectrum at 320°K consists of lines 1 and 2. The rotation patterns are shown in Fig. 1. Line 1 has no angular dependence, but at a particular angle a small splitting is observed when the modulation width is decreased. The analysis of the two rotation patterns, 1 and 2 gives $e^2qQ/h \fallingdotseq 0$ for line 1 and $e^2qQ/h = 5.6 \pm 0.5$ kc/sec, $\eta = 0.45$ for line 2. The principal axes, z, y, and x, of the field gradient tensor of the deuteron for line 2 are nearly parallel to the a, b, and c axes respectively. The spectrum at room temperature consists of lines 2 and lines 1a and 1b. Lines 1a and 1b are broad and weak. The lines 2 at room temperature are identical to that at 320°K within the limits of experimental error.

b) Lines 1a, 1b, 1b′, and 1b″. At 240°K, the lines 1a and 1b are observed in addition to the lines 2. In the b axis rotation pattern, the lines 1a and 1b consist of four pairs of lines (1a(A), 1a(B), 1b(A), and 1b(B)), while in the c axis and the a* axis rotation patterns these lines consist of two pairs ([1a(A), 1a(B)] and [1b(A), 1b(B)]).*1 The rotation patterns at 240°K are shown in Figs. 2, 3, and 4 by solid circles.

At 190°K, the lines 1b split into 1b′ and 1b″ but 1a remains unchanged. In the a* axis rotation pattern, the spectra consist of three pairs of lines ([1a(A), 1a(B)], [1b′(A), 1b′(B)], and [1b″(A), 1b″(B)]). In the b axis rotation pattern, the spectra consist of four pairs (1a(A), 1a(B), [1b′(A), 1b″(A)], and [1b′(B), 1b″(B)]). In the c axis rotation pattern, the spectra consist of three pairs ([1a(A), 1a(B)], [1b′(A), 1b″(B)], and [1b″(A), 1b′(B)]). The rotation patterns at this temperature are shown in Figs. 2, 3, and 4 by open circles. In Figs. 2, 3, and 4, the lines 2 are omitted because they are almost identical to those at 320°K. The field gradient tensors derived from the analysis of the rotation patterns at 240°K and 190°K are shown in Table 1. The quadrupole coupling constants corresponding to the lines 1a(A), 1a(B), 1b′(A), 1b′(B), 1b″(A), and 1b″(B) are the same (about 63 kc/sec) within the limits of experimental error. Similarly, the coupling constants corresponding to the lines 1b(A) and 1b(B) are nearly the same

*1 [1a(A), 1a(B)] signifies that lines 1a(A) and 1a(B) are observed as a single line because they approximately overlap.

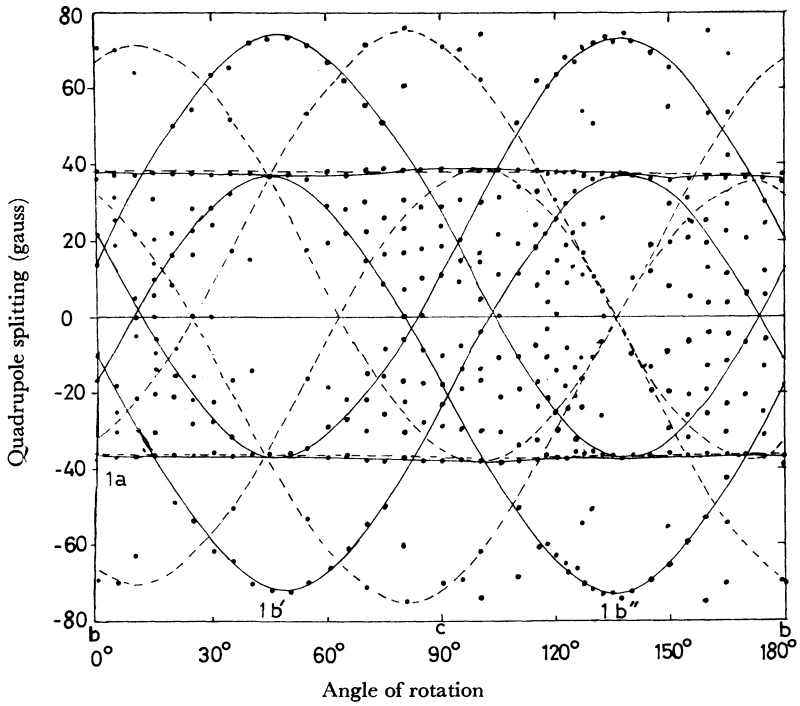

Fig. 5. a* Axis rotation pattern of deuteron resonance in $Co(ND_3)_6Cl_3$ at 77°K.

Table 1. Observed deuteron quadrupole interactions in $Co(ND_3)_6Cl_3$

Temperature		240°K			
Absorption line		1a A	1a B	1b A	1b B
e^2qQ/h (±1 kc)		62.7	63.6	32.2	32.6
η (±0.05)		0.02	0.01	0.02	0.02
Direction of q_{zz} axis* (±3°)	θ	3°	7°	3°	7°
	φ	180°	0°	180°	0°

Temperature		190°K					
Absorption line		1a A	1a B	1b' A	1b' B	1b'' A	1b'' B
e^2qQ/h (±1 kc)		62.7	63.0	64.0	63.8	63.5	63.5
η (±0.05)		0.04	0.00	0.02	0.03	0.00	0.05
Direction of q_{zz} axis* (±3°)	θ	3°	4°	86°	93°	94°	86°
	φ	180°	0°	45°	45°	−45°	−45°

* θ is the polar angle with respect to the a* axis.
ϕ is the azimuthal angle measured from the b axis.

(about 32 kc/sec). The latter value is approximately one half the former value. The asymmetry parameter, η, is nearly zero in all cases.

c) Spectra at the Temperature of Liquid Nitrogen. The spectra at the temperature of liquid nitrogen are very complicated. Although the lines 1a, 1b', and 1b'' are still recognizable, many other lines appear over the range of about 150 gauss. Therefore, it is almost impossible to get each curve of the rotation pattern separately. The a* axis rotation pattern is shown in Fig. 5 as an example.

Discussion

Waugh and Murray[1] reported that the crystal structure of the hexamminecobalt(III) chloride is monoclinic, containing three cobalt atoms in a unit cell, and that these three atoms are at two different crystallographic sites in a relative abundance of 2 : 1. However, Giménez-Hugget[8] recently reported that the space group for this compound is $P2_1/m$ and that a unit cell contains twelve cobalt atoms at two 4f sites and two 2e sites. He also concluded that the nitrogen atoms of four NH_3 groups lie on a (010) plane and that of the other two NH_3 groups, one lies above and one below this plane. The integrated intensity ratio of lines 1 and 2 at 320°K at the angle of maximum separation is approximately 2 : 1. Therefore, the lines 1 and 2 are assigned to the signals from the ions at the 4f and 2e sites respectively. The temperatures at which these lines disappear (260—320°K for the lines 1, and 170—190°K for the lines 2) are in good agreement with the proton line-width transition temperatures, 260—330°K and 150—230°K respectively.[1] Since the quadrupole splittings of the lines 1 and 2 are both very small, it is confirmed that a rapid isotropic reorientation

8) M. Giménez-Hugnet, *Dissertation Abstr.*, **22**, 2209 (1962), Thesis, Purdue Univ. (1961).

occurs in the complex cations at both sites above room temperature. The small quadrupole coupling may be due to the distortion of a $Co(ND_3)_6^{3+}$ ion from the O_h symmetry and the effect of the external crystal field, a situation similar to that in the case of the rapidly reorienting ND_4^+ ion in some ammonium salts.

Lines 1a, 1b, 1b′, and 1b″ seem to originate from the complex cations belonging to the 4f sites, because on cooling they appear after line 1 has faded out. On the basis of knowledge obtained from proton resonance studies, NH_3 ligands can be said to reorient rapidly about their C_3 axes throughout the temperature range of our experiment. Therefore, at 190°K, the maximum principal axis of the field gradient tensor of the deuteron is found to be approximately parallel to the Co–N bond direction by motional averaging. If the D–N–D angles of a coordinated ammonia molecule are tetrahedral, the motionally-averaged deuteron quadrupole coupling constant will be one-third that of the rigid molecule, assuming an axially symmetric field gradient in the direction of the N–D bond. From the known deuteron quadrupole coupling constants for the rigid ND_4^+ ion[9,10] (179.9 kc/sec, 180.0 kc/sec, and 174 kc/sec in ND_4Cl, ND_4Br, and $(ND_4)_2SO_4$ respectively), the quadrupole coupling averaged by the C_3 axis reorientation of ND_3 can be estimated to be about 60 kc/sec. This is in good agreement with the observed quadrupole coupling constants in $Co(ND_3)_6Cl_3$ at 190°K, about 63 kc/sec. Therefore, the lines 1a, 1b′, and 1b″ at 190°K are assigned to signals from ND_3 groups of the three different Co–N bond directions of a $Co(ND_3)_6^{3+}$ ion. The fact that absorption lines due to ND_3 groups corresponding to three Co–N bond directions are separately observed indicates that the complex cations at 4f sites are stationary at 190°K. From the directions of the field gradient tensors, the following conclusions concerning the orientations of $Co(ND_3)_6^{3+}$ ions at the 4f sites can be reached: (1) $Co(ND_3)_6^{3+}$ ions at the 4f sites have two different orientations, shown as A and B in Fig. 6 (A and B each seem to correspond to one of the two 4f sites). (2) One of the Co–N bond directions in a $Co(ND_3)_6^{3+}$ ion (1–2 in Fig. 6) is about 5° away from the a* axis on the a*c plane, while the other two Co–N bond directions (3–4 and 5–6) make angles of about 45° with the b axis, where deuterons at 1 and 2 give lines 1a, deuterons at 3 and 4 give lines 1b′, and deuterons at 5 and 6 give lines 1b″. These conclusions are not in accord with Giménez-Hugget's findings that four NH_3 are here placed in a (010) plane and that all $Co(NH_3)_6^{3+}$ ions have the same orientation. However, since the deuteron resonance spectra clearly show more than one orientation of $Co(ND_3)_6^{3+}$ ions, his conclusion concerning the nitrogen positions does not seem to be correct.

At 240°K, the lines 1b appear at the averaged positions of the lines 1b′ and 1b″, which have already faded out by this temperature, while the lines 1a remain the same as those at 190°K. This can be explained by a uniaxial reorientation of the $Co(ND_3)_6^{3+}$ ion about the axis 1—2 of Fig. 6, one of its C_4 axes. Since this motion gives rise to an exchange between the 3 and 4, and 5 and 6, positions of Fig. 6, the lines 1b′ and 1b″ are averaged. The reorientation about the C_2 axis perpendicular to the 1—2 direction will also have the same effect. However, in this case, all the ligands must change their positions, so the potential barrier to this motion may be much higher than that to the reorientation about the C_4 axis. Therefore, the reorientation about the C_2 axes is unlikely. Although we have assumed in the above discussion that the motion at a high temperature is an isotropic one, there remains an alternative possibility that this motion is a uniaxial reorientation about any one of the four C_3 axes, because the averaged field

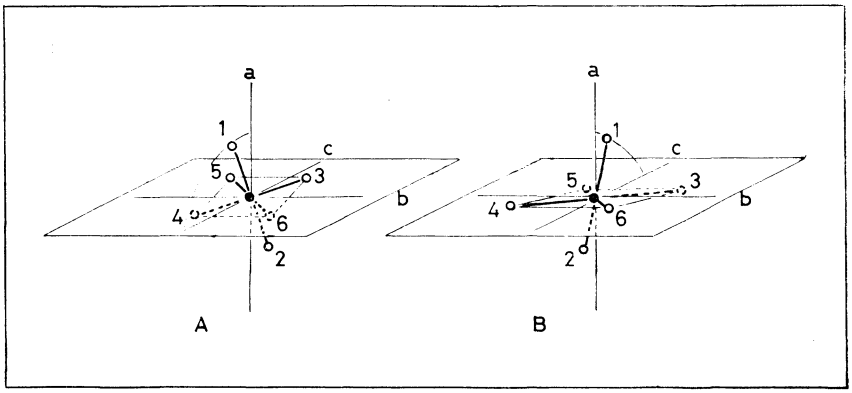

Fig. 6. Two possible orientations of $Co(ND_3)_6^{3+}$ ions at 4f sites.

9) P. Pyykkö and J.-L. Calais, *Kondens. Materie*, **5**, 1 (1966).

10) D. E. O'Reilly and T. Tsang, *J. Chem. Phys.*, **46**, 1291 (1967).

gradient by such a motion is nearly zero. However, since the reorientation about the C_4 axis has already been excited at lower temperatures, it is unlikely that the motion at a high temperature is an over-all reorientation about the C_3 axis only.

At about 190°K, the lines 2 are sharp lines with a small separation, indicating an isotropic reorientation of the complex cations at the 2e sites down to this temperature. At the temperature of liquid nitrogen the over-all motions of all the complex cations must be frozen, for the absorption lines are split into many components. The spectra are so complicated that the orientation of $Co(ND_3)_6^{3+}$ ions at the 2e sites could not be determined. For the same reason the possibility of a uniaxial motion of this ion at the intermediate temperatures could not be ascertained. However, because the maximum splitting is observed when H_0 is nearly parallel to the a*, b, or c axis in the rotation patterns at the temperature of liquid nitrogen, the three Co–N bond directions in a $Co(ND_3)_6^{3+}$ ion in the 2e sites are probably nearly parallel to the a*, b, and c axes.

The proton resonance on a single crystal of $Co(NH_3)_6Cl_3$ was also measured. The resonance line exhibits a structure characteristic of a rotating three-spin system.[11] When the reorientation axis is perpendicular to the plane of the spin triangle, the spectrum is a triplet line with a peak separation of $C(3\cos^2\theta-1)$, where C is a constant determined from the proton-proton distance, and θ is the angle between H_0 and the reorientation axis. When H_0 is applied parallel to the a* axis, the spectrum at 200°K consists of two pairs of peaks with a strong center line. When H_0 is applied parallel to the b axis, only a single line with unresolved shoulders appears.

These spectra can be interpreted as follows. In the case of the H_0//a* axis, one of the reorientation axes of NH_3 is parallel to $H_0(\theta=0)$ and the other two are perpendicular to it ($\theta=\pi/2$), so that the spectral lines consist of a triplet line with a peak separation of $2C$ and that with a peak separation of $-C$. Thus, the spectrum will be a central line with two pairs of peaks. The observed peak separation, $2C$, is about 20 gauss. Assuming the H–H distance of NH_3 to be 1.67 Å,[1] the theoretical value for the rotating three-spin system is 18.4 gauss, which is in reasonable agreement with the observed value. In the case of the H_0//b axis, one of the reorientation axes is perpendicular to H_0 and the other two make an angle of 45° with H_0, so that the spectrum consists of triplet lines with a peak separation of $-C$ and those with a peak separation of $(1/2)C$. Since the total spread of the line is small, the spectrum may be seen as a broad line with unresolved shoulders. When H_0 is applied in the direction 45° from the b axis in the bc plane, the line with two pairs of peaks was observed at 200°K, while the line with unresolved shoulders was observed at 240°K. In this case, one of the reorientation axes of NH_3 (3–4 in Fig. 6) is parallel to H_0, and the other two (5–6 and 1–2) are perpendicular to it. Since the uniaxial motion about the axis 1–2 gives rise to exchange between the 3 and 4, and 5 and 6, positions, the spectrum at 240°K consists of triplet lines, one with a separation of $-C$ (a line that originates from 1 and 2), one with a separation of $(1/2)C$ which is produced by averaging the triplet lines, one with separation of $2C$ (a line originating from 3 and 4), and one with a separation of $-C$ (a line originating from 5 and 6). Although the effect of uniaxial motion on the second moment of a powdered sample is not clear,[1] single crystal spectra show the occurrence of this motion in $Co(NH_3)_6Cl_3$. At 77°K, the proton line is a single broad line exhibiting no structure. If there are several orientations for $Co(NH_3)_6^{3+}$ ions, as suggested by the deuteron resonance, this can be understood as a single broad line resulting from the superposition of several triplet lines with various separations.

The rate of the motion can be estimated from the width of spectral lines. In the present case, the line widths at the limits of slow and rapid exchange rates can be derived from the general formula[4] as follows:

(I) Uniaxial motion

slow exchange limit ($\Omega \ll \delta$):

$$\Delta\nu_{motion} = \Omega/2\pi \tag{2}$$

rapid exchange limit ($\Omega \gg \delta$):

$$\Delta\nu_{motion} = \pi\delta^2/\Omega \tag{3}$$

(II) Isotropic motion

slow exchange limit ($\Omega \ll \delta$)

parallel to rotation axis:

$$\Delta\nu_{motion} = \Omega/\pi \tag{4}$$

perpendicular to rotation axis:

$$\Delta\nu_{motion} = \Omega/2\pi \tag{5}$$

rapid exchange limit ($\Omega \gg \delta$):

$$\Delta\nu_{motion} = \left(\frac{16}{27}\right)\pi\delta^2/\Omega \tag{6}$$

$\Delta\nu_{motion}$ is the line width due to the motion, Ω is the rate of the motion, and 2δ is the frequency separation of the two sites. The rate of the motion can be calculated from the observed line width due to the motion. However, in solid samples it is difficult to estimate $\Delta\nu_{motion}$ because the signal-to-noise ratio for the broadened lines is generally poor and the absorption lines possess a dipolar width. For the $Co(ND_3)_6^{3+}$ ions at the 4f sites for which the stationary orientation has been well determined, the $\Delta\nu_{motion}$ is estimated from the observed line

11) E. R. Andrew and R. Bersohn, *J. Chem Phys.*, **18**, 159 (1950).

width by an approximate procedure,[12] from which Ω is derived using Eqs. (2)—(6). The results are shown in Fig. 7. One can immediately

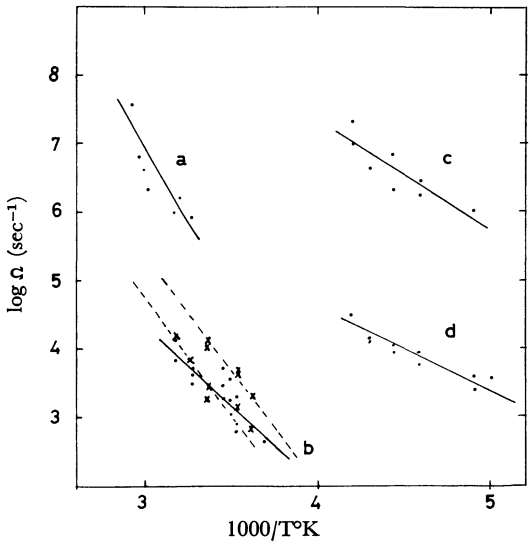

Fig. 7. Temperature dependence of reorientation rates of a $Co(ND_3)_6^{3+}$ ion.

a) Isotropic motion (rapid limit)
b) Isotropic motion (slow limit)
c) Uniaxial motion (rapid limit)
d) Uniaxial motion (slow limit)

notice that there is a vast disagreement between the line connecting points of Ω from the rapid exchange limit and the line connecting points of Ω from the slow exchange limit. As will be described below, this discrepancy originates from the presence of two crystallographically-nonequivalent 4f sites for $Co(NH_3)_6^{3+}$ ions, ions which have approximately the same orientation but which are subject to a slightly different barrier hindering reorientation.

As can clearly be seen in the typical example of line broadening given in Fig. 8, the lines corresponding to the stationary ions (slow-limit spectrum) and their motionally-averaged lines (rapid-limit spectrum) are simultaneously observed at some temperatures. The theory of motional averaging predicts no such spectra (the coexistence of a spectrum of a slow exchange limit and that of a fast exchange limit) in the intermediate temperature range. In tracing the motional broadening of deuteron resonance lines, there is commonly a range of temperature where the spectrum is completely washed out and unobservable between the two limiting ranges. The rather peculiar phenomenon in the present experiment can be explained by assuming that the complex cations at the two 4f sites (A and B in Fig. 6) have slightly different

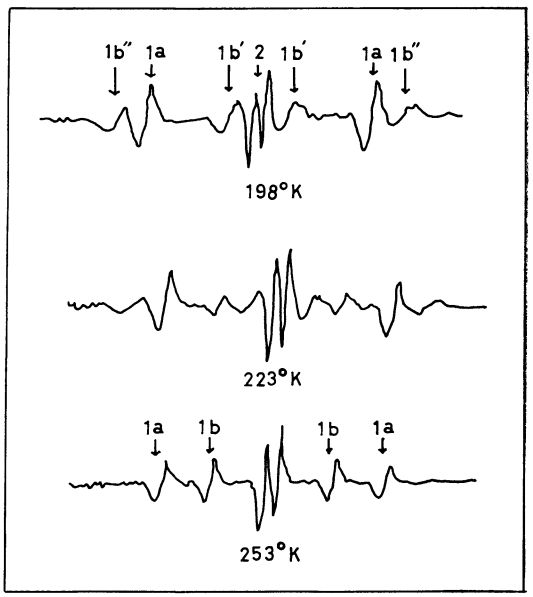

Fig. 8. Shapes of spectral lines. $H_0//15°$ from c axis in the bc plane.

Upper: At low temperature range (198°K), the lines 1a, 1b′ and 1b″ corresponding to the stationary ion are observed.
Lower: At high temperature range (253°K), the lines 1a and 1b corresponding to rapid reorienting ion are observed.
Middle: At intermediate temperature range (223° K), the lines 1b are observed together with the lines 1a, 1b′ and 1b″.

environments, and that, as a consequence, the cations at the two different 4f sites begin to reorient at different temperatures. The broadening process of the lines for the A and B of 4f sites cannot be observed separately except for the slow-exchange limit of the isotropic motion, because they overlap with each other in most of the crystal orientations. The presence of two 4f sites with different rates is verified by the b axis rotation spectrum, where the lines corresponding to the A and B of the 4f sites can be observed separately. The line broadening, in fact, takes place at different temperatures for the A and B sites: the lines 1a(A) and 1b(A) fade out at a lower temperature than do the lines 1a(B) and 1b(B). The rates obtained individually from these observations are also shown in Fig. 7 (by × marks). The apparent reorientation rates obtained here from the broadening of the spectrum such as that shown in Fig. 8 may, therefore, be considered to be subject to the effect of motions at the two sites, A and B. In the spectrum at 223°K of Fig. 8, the slow-limit lines (1b′ and 1b″) originate from the site with the slower exchange rate (site B),*2 while the central rapid-limit line originates from the site with the faster exchange

12) T. Chiba and Y. Kakiuchi, This Bulletin, **41**, 828 (1968).

rate (site A).*2 Therefore, the rate derived from the slow limit may be predominantly of the site B, and the rate derived from the rapid limit may be predominantly of the site A. This is in qualitative agreement with the results shown in Fig. 7.

Limited as they are by various experimental conditions, the exchange rates derived in this experiment are not sufficient for the determination of potential barriers hindering the reorientations. However, we believe that the qualitative features of the motions in this crystal are rather well defined.

One of the authors (T. I.) would like to thank Professor Hiroshi Kobayashi for his encouragement throughout this work.

*2 The site with the larger exchange rate for the isotropic motion is A. Although the rate for the uniaxial reorientation has not been determined for each site separately, it may be reasonable to assume that for this motion the ions at the site A have also a greater exchange rate than those at the site B.

BULLETIN OF THE CHEMICAL SOCIETY OF JAPAN VOL. 42 116—118 (1969)

Effect of Additives in the Radiolysis of Gaseous Ammonia at High Densities

Masaru NISHIKAWA, Kazufumi KURODA and Niro MATSUURA

Department of Pure and Applied Sciences, The University of Tokyo, Komaba, Meguro-ku, Tokyo

(Received June 17, 1968)

The effect of additives and density on the radiolysis of ammonia at 140°C was studied over the density range 0.07 to 0.13 g/cc. The observation of a sharp decrease of G values in the radiolysis of pure ammonia at $d\sim0.1$ g/cc confirmed the result reported by Toi *et al.* (*Radiation Res.*, **17**, 399 (1962)). The yield of hydrogen in the presence of ~1.5 mol% C_3H_6 was practically independent of density at $G=0.65$ over the density range studied. $G(H_2)$ in the presence of C_3H_8, estimated by extrapolation to zero propane concentration, was also constant at $G\simeq5.7$ at $d\simeq0.07$ and 0.13 g/cc. These observations were discussed in relation to the mechanism for depression of G values in the radiolysis of pure ammonia at higher densities.

The radiolysis of gaseous ammonia at high densities above the critical temperature has been investigated by Toi *et al.*[1] They observed a sharp depression in $G(H_2)$ and $G(N_2)$ at a density near 0.1 g/cc and concluded that such a decrease is consistent with the formation of ion clusters. Cluster formation in the irradiated ammonia has in fact observed in the high-pressure mass spectrometer,[2] apparently in support of their conclusion. However, the fact that observed ionic species are only clusters of $NH_4^+\cdot(NH_3)_n$ type, with n as large as 20 at 200 Torr, implies that, if the ion clustering is to be invoked as the process responsible for the decrease, neutralization of charge in such a density region involves ion-ion recombination, since the neutralization of NH_4^+ whether clustered or unclustered is bound to end up in hydrogen formation as long as it occurs by way of ion-electron recombination. One such possibility as the mechanism at high densities has been proposed in a previous publication in terms of the neutralization between NH_4^+ and NH_2^-.[3] In an attempt to provide further informations as to the processes occuring at a high density, the effect of additives such as propylene and propane, which act as hydrogen atom scavengers, was investigated over the density range of 0.065 to 0.13 g/cc at 140±1°C.

Experimental

Purification of materials was described.[3] Gas chromatographic analysis of propane indicated that no organic impurities were present at levels exceeding 10^{-3} mol%.

Irradiations were carried out in glass cells of about 2 m*l* made of a glass tubing of 7 mm in outer diameter and 5 mm in inner diameter without a break-seal placed in a stainless steel autoclave in which a known volume of ammonia was introduced in order to balance the pressure in- and outside of glass cells. During irradiation in a source of approximately 1000 Ci of ^{60}Co, temperature was kept constant at 140±1°C by a heater with thermostat.

The absorbed dose in ammonia (E_a) was calculated from that determined by Fricke dosimetry on the basis

1) Y. Toi, D. B. Peterson and M. Burton, *Radiation Res.*, **17**, 399 (1962).

2) A. M. Hogg and P. Kebarle, *J. Chem. Phys.*, **43**, 449 (1965).

3) M. Nishikawa and N. Shinohara, *Radiation Res.*, **33**, 194 (1968).

of electron density ratios. It was previously shown by Toi *et al.*[1] that the calculation is permissible in the density range $d \gtrsim 0.07$ g/cc. The dose absorbed in propane (E_p) was calculated from E_a using the ratio of stopping powers obtained by Meisels.[4] The dose rate in ammonia at $d=0.10$ g/cc was 2.34×10^{13} eV/ml/sec.

The products non-condensable at 77°K were analyzed by combustion over cupric oxide in a furnace heated at $\gtrsim$350°C.

Results and Discussion

Figure 1 shows the dependence on density of the yield of hydrogen from pure ammonia, ammonia mixed with propylene, and with propane. The concentration of propylene (~1.5 mol%) was

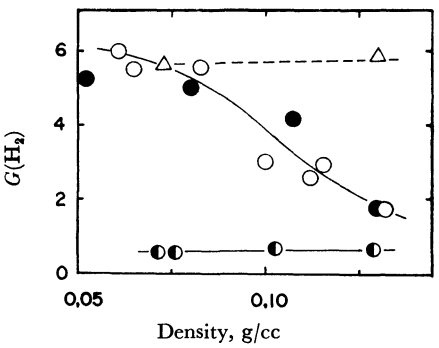

Fig. 1. Effect of density on $G(H_2)$ in the radiolysis of ammonia at 140°C.
○, from pure ammonia (this work); ●, (Toi *et al.*[1]); △, with propane (the intercept of Fig. 2); ◐, with propylene.

indicated to be sufficient as the H atom scavenger by a previous study.[3] The yield of hydrogen in the presence of propylene is demonstrated to be practically independent of density at $G(H_2)=$ 0.61—0.69, which is in agreement with $G_{H_2}=0.74$ determined previously at 50 cmHg and 22°C,[3] and also with $G(H_2)=0.70$ cited as a lower limit for G_{H_2} in liquid ammonia at 20°C.[5],*1 The dependence of $G(H_2)$ on the propane concentration is essentially the same as that observed at the ammonia pressure ~50 cmHg and 22°C. Since hydrogen is one of the main products of propane radiolysis, correction is necessary for determining the yield of hydrogen from the ammonia fraction *via* the reaction

$$H + C_3H_8 \rightarrow H_2 + C_3H_7 \qquad (1)$$

and *via* the processes leading to molecular hydrogen.

The estimate of the contribution of propane fraction to hydrogen production was made by plotting G-values of the total hydrogen ($G(H_2)_t$) calculated for the total energy absorbed by the mixture ($E_t = E_a + E_p$) against the fraction of energy absorbed by propane ($f_p = E_p/E_t$). The plot is based on the equation which is applicable only in the region where energy transfer between the components of the mixture is negligible;

$$G(H_2)_t = G(H_2)^\circ_a \cdot f_a + G(H_2)^\circ_p \cdot f_p$$

where G°_a and G°_p are those due to energy deposited in ammonia and in propane, respectively, and f_a and f_p are the fraction of energy deposited, *i. e.*, $f_a + f_p = 1$. Figure 2 shows that $G(H_2)_t$ at high densities lies, within the experimental error, on the same straight line obtained at ~50 cmHg

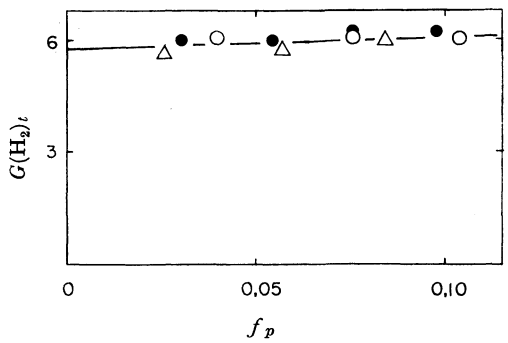

Fig. 2. Dependence of $G(H_2)_t$ from $NH_3 + C_3H_8$ mixtures at 140°C on the fraction of energy absorbed by C_3H_8 ($f_p = E_p/E_t$).
○, $d \cong 0.13$ g/cc; △, $d \cong 0.07$ g/cc;
●, $d \cong 0.0005$g/cc (~50 cmHg) at 22°C

and 22°C. Extrapolation to $f_p=0$, by the least square method over the points including those for ~50 cmHg, yields $G(H_2)^\circ_a = 5.74 \pm 0.13$, which should be a measure of $G_H + G_{H_2}$ of ammonia radiolysis. $G_H=5.1$ thus determined is significantly lower than the values hitherto reported.[7,8] The disagreement in the value of G_H will be discussed elsewhere.[6]

The observed yield of hydrogen in the presence of propylene and of propane appears to indicate that G_H and G_{H_2} are independent of temperature and density. "Molecular" hydrogen seems less likely to be associated with the observed depression in the yield at $d \cong 0.1$ g/cc as it is relatively unimportant at the lower density region. It is, therefore, the behavior of G_H that is playing the major role in the observed phenomenon. The finding that G_H is apparently constant at $d \cong 0.07$ and at 0.13 g/cc

4) G. G. Meisels, *J. Chem. Phys.*, **41**, 51 (1964).
5) F. S. Dainton, T. Skwarski, D. Smithies and E. Wezranowski, *Trans. Faraday Soc.*, **60**, 1068 (1964).
*1 The value is also in agreement with $G(H_2)=0.81$ at $d=0.15$ g/cc and 17°C determined using 1.5 mol% C_2D_4. (M. Nishikawa, D. B. Peterson and M. Burton, unpublished.)
6) To be published separately.
7) F. T. Jones and T. J. Sworski, *Trans. Faraday Soc.*, **63**, 2411 (1967).
8) G. R. A. Johnson and M. Simic, *Nature*, **216**, 479 (1967).

may be interpreted at least in two ways in this regard. First the yield of hydrogen atoms is really independent of density; it follows that the processes responsible for the depression must be those in which hydrogen atoms disappear with the precursor for nitrogen. Secondly the apparent constancy of G_H is due to alterations in the reaction paths caused by the addition of propane, and that in pure ammonia G_H itself is influenced by the density change. For the former case, one of the most probable processes is the geminate recombination of radical pairs

$$H + NH_2 \xrightarrow{M} NH_3 \qquad (2)$$

whose specific rate is estimated to be 1.2×10^{10} M^{-1}·sec^{-1} at 1 atm.[9] This reaction appears to be favored by higher density because of the track effect leading to relatively high local concentration of radicals. However, Toi *et al.* noted that the track effect is not sufficiently sensitive to density to account for the sudden decrease in the yield. Furthermore, the specific rate for the reaction

$$H + NH_3 \longrightarrow NH_2 + H_2 \qquad (3)$$

is of the order of 10^4 M^{-1}·sec^{-1} at 140°C,[10] so that it is expected to compete successfully with (2) in the bulk ammonia. The extent of "cage" effect $d \sim 0.1$ g/cc and 140°C would not be large enough for reaction (2) to be efficient. Then, the latter seems to be more likely.

$G(N_2)$ in the presence of 1—3 mol% propane is 0.6 at $d=0.07$ and 0.13 g/cc, which is markedly lower than $G(N_2)=1.7$ in the pure ammonia at $d=0.07$ g/cc, but about equal at $d=0.13$ g/cc. The depression of $G(N_2)$ by propane suggests the occurrence of the reaction

$$NH_2 + C_3H_8 \longrightarrow NH_3 + C_3H_7 \qquad (4)$$

If reaction (4) proceeds faster at 140°C than the reaction

$$NH_2 + e^- \longrightarrow NH_2^- \qquad (5)$$

which was included in the mechanism proposed to explain the depression of G values in pure ammonia at $d \sim 0.1$ g/cc, the apparent independence of $G(H_2)$ on density observed in the $NH_3+C_3H_8$ mixtures is compatible with the mechanism; namely, in pure ammonia at high densities, the presence of large clusters lowers the electrostatic field of NH_4^+ to such an extent that reaction (5) can compete for electrons, and the neutralization NH_4^+(clustered)$+NH_2^-$(clustered)$\rightarrow 2NH_3$ reduces both $G(H_2)$ and $G(N_2)$, while in the presence of propane the neutralization $NH_4^+ + e^- \rightarrow H + NH_3$ takes place, which followed by reaction (1) keeps the yield of hydrogen constant. The difference in $G(H_2)$ of pure ammonia at $d=0.07$ and at 0.13 g/cc, $\Delta G(H_2) \simeq 4.5$, is somewhat larger than the value of $100/W$ ($W=26.5$ eV[4]), which is expected if it is to be related to the change in the neutralization process. This apparently excessive decrease might also be explained by the depletion of NH_2 *via* reaction (5) which inhibits processes leading to additional hydrogen formation from precursors other than H atoms. The observation that at 1 atm $G(H_2)$ from pure ammonia at $\gtrsim$100°C is significantly larger than $G(H_2)$ in the presence of propane at the same temperature[8] suggests the occurrence of such processes as a mode of hydrogen formation at a higher temperature, since all the H atoms are expected to be converted into H_2 by reaction (1) in the presence of propane, and by reaction (3) in pure ammonia. This mechanism has the desired sensitivity to density, since it is based on the presence of large clusters. The observation that N_2O has little effect on $G(H_2)$ in liquid ammonia[5] appears to support the mechanism in which it suggests the neutralization in the liquid phase is occurring mostly by $NH_4^+ + NH_2^-$. It is desirable to test the effect of electron scavengers in this density range to see if there is change in the importance of ionic processes. However, most of the compounds used for such a purpose act as hydrogen atom scavenger as well at 140°C, and since the addition of propane has the possibility of changing the reaction paths, neither the use of electron scavengers together with propane can be expected to yield useful informations in this regard. At this stage,the present study could not confirm the proposed mechanism, but appears, at least, to be consistent with it.

We should like to thank Professor M. Takahashi of this department and Dr. K. Fueki of Nagoya University for valuable discussions.

9) M. H. Hanes and E. J. Blair, *J. Chem. Phys.*, **38**, 672 (1963).

10) M. Schiavello and G. G. Volpi, *ibid.*, **37**, 1510 (1962).

BULLETIN OF THE CHEMICAL SOCIETY OF JAPAN VOL. 42 119—126 (1969)

The Optical Resolution and Circular Dichroism of Cobalt(III) Complexes of the $[Co(O-O)_2(O-N)]^{2-}$ Type

Kiyoshi YAMASAKI, Jinsai HIDAKA and Yoichi SHIMURA

Department of Chemistry, Faculty of Science, Osaka University, Toyonaka, Osaka

(Received January 31, 1968)

Four cobalt(III) complexes of the tris-chelate type containing two dicarboxylate anions and one aminocarboxylate anion have been newly prepared and separated into their optical isomers by a chemical resolution method: they are bismalonatoglycinato-, bismalonato(L-alaninato)-, bisoxalato(L-alaninato)- and bisoxalato(β-alaninato)-cobalt(III) complexes. The diastereomeric isomers of bisoxalato(L-alaninato)cobalt(III) complex have also been separated by the solubility difference between their barium salts. The absorption spectra, circular dichroism spectra and rotatory dispersion of these complexes have been measured and discussed in relation to the splitting of the d-d transition bands. The absolute configurations of the complexes have been inferred from their circular dichroism spectra. The additivity of configurational and vicinal contributions to the optical activity has been substantiated for the bisoxalato- and bismalonato-(L-alaninato)-cobalt(III) complexes, and some considerations concerning the less stereospecific formation of the L-alaninato diastereomeric isomers have been made in relation to the additivity.

The splitting of the d-d transition bands has been studied for many types of complexes on the basis of their CD (circular dichroism) spectra and their RD (rotatory dispersion) curves.[1-6] It seems, however, that the splitting trend of the first absorption band for a bis(dicarboxylato)mono(aminocarboxylato)cobalt(III) type complex is not completely clear at the present time, because the bisoxalatoglycinatocobalt(III) complex is the only known example.[4]

Bürer pointed out that cobalt(III) complexes containing three six-membered chelate rings differ from those with three five-membered chelate rings in CD behavior of the first absorption band.[7] However, this type of problem has still not been solved. Thus it was thought desirable to study the CD spectra of complexes containing six- and five-membered chelate rings mixed.

In the present paper, the preparations and optical resolutions of four new tris-chelate complexes of the $[Co(O-O)_2(O-N)]^{2-}$ type*1 will be reported. The CD spectra of the complexes will be compared with one another, and their absolute configurations inferred from their CD spectra. The additivity of configurational and vicinal contributions to the optical activity will be substantiated for the two L-alaninato complexes, and considered in relation to the formation ratio of the diastereomeric isomers. The solubility difference between the diastereomers containing these cobalt(III) complex ions will be briefly considered.

Experimental

Preparations of Malonato Complexes. The malonato complexes were prepared using a dark-green solution containing $[Co(mal)_3]^{3-}$.

1) $Ba[Co(mal)_2(gly)]\cdot 1.5H_2O$: To a solution containing 7.9 g of malonic acid and 11.1 g of sodium malonate in 30 m*l* of water were added 12.0 g of cobalt(II) acetate tetrahydrate, 6 m*l* of 50% acetic acid and 10 g of lead dioxide. The resulting mixture was cooled in an ice bath and mechanically stirred for about one hour. After the color of solution had changed from dark-red to dark-green, 3.7 g of glycine was added. The color of the solution gradually changed to dark-

1) B. E. Douglas, R. A. Haines and J. C. Brushmiller, *Inorg. Chem.*, **2**, 1195 (1963).
2) C. T. Liu and B. E. Douglas, *ibid.*, **3**, 1356 (1964).
3) A. J. McCaffery and S. F. Mason, *Mol. Phys.*, **6**, 359 (1963); A. J. McCaffery, S. F. Mason and R. E. Ballard, *J. Chem. Soc.*, **1965**, 2883; A. J. McCaffery, S. F. Mason and B. J. Norman, *ibid.*, **1965**, 5094; B. J. Norman, *Inorg. Chim. Acta*, **1**, 177 (1967).
4) F. P. Dwyer, I. K. Reid and A. M. Sargeson, *Aust. J. Chem.*, **18**, 1919 (1965).
5) J. Hidaka, Y. Shimura and R. Tsuchida, This Bulletin, **35**, 567 (1962); T. Yasui, J. Hidaka and Y. Shimura, *J. Am. Chem. Soc.*, **87**, 2762 (1965); K. Ohkawa, J. Hidaka and Y. Shimura, This Bulletin, **39**, 1715 (1966); T. Yasui, J. Hidaka and Y. Shimura, *ibid.*, **39**, 2417 (1966); T. Komorita, J. Hidaka and Y. Shimura, to be published.
6) J. Hidaka and Y. Shimura, This Bulletin, **40**, 2312 (1967).
7) Th. Bürer, *Helv. Chim. Acta*, **46**, 2388 (1963).

*1 The abbreviation (O-O) denotes a malonate(mal) or oxalate (ox) ion, and (O-N) a glycinate (gly), L-alaninate (L-ala) or β-alaninate (β-ala) ion.

blue when the resulting mixture was stirred at about 60°C for about 40 min. The dark-blue solution was placed in an ice bath for an hour, and then most insoluble material filtered off. To the filtrate, 4 m*l* of 30% aqueous solution of barium perchlorate was added, and the barium malonate deposited removed by filtration. The blue complex desired began to crystallize out when an additional 50 m*l* of barium perchlorate solution was added to the filtrate. After the solution had been cooled in an ice bath for an hour, the crude complex was filtered and washed with water, then methanol, and dried in air. 11 g.

The purification of this complex was performed as follows. Seven grams of the crude complex was added to a solution of 2.4 g of anhydrous sodium sulfate in 50 m*l* of water, and then the barium sulfate which precipitated out was filtered off. To the filtrate was added a solution of 8 g of barium perchlorate in 10 m*l* of water. After a small amount of the barium malonate deposited had been filtered off, the filtrate was kept in a refrigerator overnight. The complex which separated out was filtered and washed with an appropriate amount of water, then methanol, and dried in a vacuum desiccator over phosphorus pentoxide.

Found: C, 19.34; H, 2.21; N, 2.75%. Calcd for $Ba[Co(C_3H_2O_4)_2(C_2H_4NO_2)]\cdot 1.5H_2O$: C, 19.14; H, 2.20; N, 2.80%.

2) Ba[Co(mal)$_2$(L-ala)]: This complex was obtained by a procedure similar to that in 1) using L-alanine instead of glycine. The dark-green solution, containing 4.4 g of L-alanine, was kept at 60°C on a water bath with stirring for 40 min. After the mixture had been cooled to room temperature, most insoluble material was removed by filtration. Twenty grams of barium perchlorate was dissolved in the filtrate, and then the barium malonate which precipitated out was filtered off. An additional precipitate, which deposited upon adding 50 m*l* of methanol to the filtrate, was removed by filtration. The desired complex was precipitated out by adding 100 m*l* of a methanol-ethanol mixture (1 : 1) to the filtrate, and was filtered, washed with methanol and dried in a vacuum desiccator. 10 g.

The crude complex was dissolved in 40 m*l* of water, and to this solution was added 40 m*l* of methanol. After a small amount of the resulting insoluble material had been removed, 5 g of barium perchlorate was dissolved in the filtrate and 60 m*l* of methanol added to it with stirring. The fine bluish-violet crystals which deposited were filtered off, washed with methanol and dried in a vacuum desiccator over phosphorus pentoxide.

Found: C, 22.14; H, 2.16; N, 2.71%. Calcd for $Ba[Co(C_3H_2O_4)_2(C_3H_6NO_2)]$: C, 22.13; H, 2.07; N, 2.87%. $[M]_{546}=-400°$, $[M]_{589}=+50°$.

Preparations of Oxalato Complexes. The oxalato complexes were prepared in the following two ways. In the first one, the binuclear complex, $Na_4[(ox)_2Co(OH)_2Co(ox)_2]\cdot 5H_2O$,[8] was used as starting material. In another one, a solution containing cobalt(II) chloride, potassium oxalate and amino acid (1 : 2 : 1) was oxidized with lead dioxide.

1) Ba[Co(ox)$_2$(gly)]·0.5H$_2$O: The preparation of this complex was reported by Dwyer *et al.*[4] In the present work, however, two different methods were attempted.

1-a). To a solution of 7.0 g of $Na_4[Co_2(ox)_4(OH)_2]\cdot 5H_2O$ and 1.5 g of glycine in 20 m*l* of water were added 3 g of lead dioxide and 6 m*l* of 25% acetic acid. The resulting mixture was kept on a water bath at 65°C with stirring for 20 min. After the color of solution had changed from dark-green to dark-blue, the mixture was cooled to room temperature and then lead dioxide removed by filtration. One gram of barium perchlorate was added to the filtrate, and then a small amount of the insoluble material which appeared filtered off. A further 8 g of barium perchlorate was dissolved in the filtrate and the solution cooled in an ice bath for an hour. The blue complex desired precipitated out and was filtered and dried in air. 3.4 g. The crude complex was purified as described in 1) of Preparation of Malonato Complexes.

Found: C, 15.82; H, 1.19; N, 3.00%. Calcd for $Ba[Co(C_2O_4)_2(C_2H_4NO_2)]\cdot 0.5H_2O$: C, 15.79; H, 1.11; N, 3.07%.

1-b). Twenty grams of potassium oxalate monohydrate and 4.3 g of glycine were dissolved in 40 m*l* of hot water. To the solution was added a solution containing 12.0 g of cobalt(II) chloride hexahydrate in 15 m*l* of hot water. The mixture was kept at 70°C on a water bath and 20 g of lead dioxide added, little by little. The color of solution gradually changed to dark bluish-violet within one hour. After the mixture had been cooled to room temperature, a large amount of the insoluble material which precipitated out was filtered off. The filtrate was kept in a refrigerator overnight. Additional insoluble material which deposited was filtered off, and a small amount of ethanol added to the filtrate. The blue precipitate was removed, and then the potassium salt of the desired blue complex was obtained by adding a large amount of ethanol to the filtrate. The crude product was recrystallized from water by the addition of ethanol. The crystals were filtered, washed with ethanol and ether and dried in a vacuum desiccator over phosphorus pentoxide.

Found: C, 18.87; H, 1.10; N, 3.72%. Calcd for $K_2[Co(C_2O_4)_2(C_2H_4NO_2)]\cdot 3H_2O$: C, 18.61; H, 1.04; N, 3.61%.

The potassium salt can be easily changed to the barium salt with barium acetate monohydrate.

2) K$_2$[Co(ox)$_2$(L-ala)]: In the preparation of this complex, the same procedure as described in 1-a) was employed, but with 1.7 g of L-alanine instead of 1.5 g of glycine. After the lead dioxide had been removed, 4 g of potassium acetate was dissolved in the filtrate. To the solution was added 70 m*l* of methanol, and the slurry precipitate removed by filtration. The blue complex desired was obtained by adding a further 100 m*l* of methanol to the filtrate. Recrystallization was carried out from water by the addition of methanol. The crystals deposited were filtered, washed with methanol and acetone and dried in a vacuum desiccator over phosphorus pentoxide.

Found: C, 21.18; H, 1.81; N, 3.54%. Calcd for $K_2[Co(C_2O_4)_2(C_3H_6NO_2)]$: C, 20.94; H, 1.50; N, 3.48%. $[M]_{546}=-80°$, $[M]_{589}=+440°$.

3) Ba[Co(ox)$_2$(β-ala)]: The β-alaninato complex was prepared using 1.7 g of β-alanine instead of 1.5 g of glycine as in 1-a). After the lead dioxide had been removed, 8 g of barium perchlorate was dissolved in the filtrate and the solution cooled in an ice bath. A small

8) H. F. Holtzclaw, Jr., "Inorganic Syntheses," Vol. VIII, p. 204 (1966).

amount of the colorless insoluble material which precipitated out was filtered off, and then 10 m*l* of methanol added to the filtrate. After a small amount of the slurry precipitate which resulted had been removed, a further 30 m*l* of methanol was added to the filtrate with stirring. The barium salt of the desired blue complex which precipitated out was filtered off, washed with a water-methanol mixture(1 : 1), acetone and then ether, and dried in a desiccator. 4.7 g.

The crude complex was recrystallized two times from water by adding methanol. The crystals obtained were dried in a vacuum desiccator over phosphorus pentoxide.

Found: C, 18.14; H, 1.70; N, 3.02%. Calcd for $Ba[Co(C_2O_4)_2(C_3H_6NO_2)]$: C, 18.28; H, 1.31; N, 3.04%.

Optical Resolutions. The five complexes described above were resolved using strychnium sulfate and $(+)_{546}$- or $(-)_{546}$-$[Co(ox)(en)_2]I$ as resolving agents. The optical isomers of $[Co(ox)_2(L\text{-ala})]^{2-}$ were also separated without resolving agent.

i) Bismalonatoglycinatocobalt(III) Complex: *i-a) With Strychnium Sulfate.* Seven grams of strychnium sulfate pentahydrate was suspended in 40 m*l* of water and 4.0 g of $Ba[Co(mal)_2(gly)]\cdot 1.5H_2O$ added. The mixture was vigorously shaken and barium sulfate which precipitated out was removed. When the filtrate was cooled in an ice bath and the vessle scrubbed with a glass rod, a pale blue diastereomer began to crystallize out. After the solution had been cooled in an ice bath for a while, the less soluble diastereomer which precipitated out was filtered off and washed with a little ice water. The diastereomer was dissolved in 5 m*l* of water and an excess of sodium perchlorate added to the solution. Then the strychnium perchlorate which precipitated out was removed. When an excess of barium perchlorate was dissolved in the filtrate and 5 m*l* of methanol added to it, the optically active barium salt of the complex crystallized out. The complex was filtered, washed with a little ice water, methanol and then acetone, and dried in a vacuum desiccator over phosphorus pentoxide.

Found: C, 18.54; H, 2.32; N, 2.66%. Calcd for $Ba[Co(C_3H_2O_4)_2(C_2H_4NO_2)]\cdot 2.5H_2O$: C, 18.50; H,2.51; N, 2.70%. $[M]_{546}=-2400°$, $[M]_{589}=-4600°$.

i-b) By $(-)_{546}$-[Co(ox)(en)$_2$]I. To a solution containing 1.2 g of anhydrous sodium sulfate in 15 m*l* of hot water was added 4.0 g of $Ba[Co(mal)_2(gly)]\cdot 1.5H_2O$. Then the barium sulfate which deposited was filtered off and washed with 5 m*l* of water. The washing was combined with the filtrate (solution "a"). Silver acetate (1.3 g) and $(-)_{546}$-$[Co(ox)(en)_2]I$ (3.6 g) were shaken well in 15 m*l* of water, and the silver iodide which precipitated out was filtered off and washed with 5 m*l* of water. The washing was combined with the filtrate (solution "b"). To solution "a" was added solution "b", and the resultant solution concentrated in a vacuum desiccator over phosphorus pentoxide until the red-brown diastereomer appeared. The diastereomer was filtered off, washed with a water-methanol mixture (2 : 1) and then acetone, and dried in a vacuum desiccator over phosphorus pentoxide. The less soluble diastereomer, $(-)_{546}$-$[Co(ox)(en)_2]_2\cdot(-)_{546}$-$[Co(mal)_2$-$(gly)]\cdot 2H_2O$, was recrystallized from water by the addition of a methanol-ethanol mixture(1 : 1).

Found: C, 26.12; H, 4.63; N, 13.89%. Calcd for $[Co(C_2O_4)(C_2H_8N_2)_2]_2\cdot[Co(C_3H_2O_4)_2(C_2H_4NO_2)]\cdot 2H_2O$: C, 26.48; H, 4.89; N, 13.90%. $[M]_{546}=-10270°$, $[M]_{589}=-10390°$.

The diastereomer was suspended in a small amount of water, and a slight excess of sodium iodide added to the suspension. After the mixture had been stirred well, $(-)_{546}$-$[Co(ox)(en)_2]I$ which precipitated out was filtered off and an excess of barium perchlorate dissolved in the filtrate. The barium salt of the optically active complex was obtained by adding methanol to the solution and cooling it in an ice bath. This was filtered, washed with a water-methanol mixture (1 : 1), methanol and then acetone, and dried in a vacuum desiccator over phosphorus pentoxide. $[M]_{546}=-2550°$, $[M]_{589}=-4700°$.

ii) Bismalonato(L-alaninato)cobalt(III) Complex: *ii-a) With Strychnium Sulfate.* A small excess of strychnium sulfate pentahydrate (4.5 g) was added to a solution containing 2.5 g of unresolved $Ba[Co(mal)_2(L\text{-ala})]$ in 15 m*l* of water. The diastereomer obtained by a procedure similar to that of i-a) was filtered off and washed with a methanol-ether mixture (1 : 1). Recrystallization was carried out from methanol by the addition of ether. When the recrystallized diastereomer was dissolved in a small amount of water and treated with an excess of barium perchlorate, strychnium perchlorate deposited out. After it had been removed, the configurationally optically active barium salt of the complex was obtained by the addition of methanol and ether to the filtrate. The complex was filtered, washed with a methanol-ether mixture (1 : 1) and dried in a vacuum desiccator over phosphorus pentoxide.

Found: C, 22.26; H, 2.32; N, 2.87%. Calcd for $Ba[Co(C_3H_2O_4)_2(C_3H_6NO_2)]$: C, 22.13; H, 2.07; N, 2.87%. $[M]_{546}=+1300°$, $[M]_{589}=+3200°$.

ii-b) By $(+)_{546}$- or $(-)_{546}$-[Co(ox)(en)$_2$]I. Solution "a", containing the sodium salt of the complex (obtained from 4.9 g of unresolved $Ba[Co(mal)_2(L\text{-ala})]$, 1.4 g of anhydrous sodium sulfate and 15 m*l* of water), and solution "b", containing the acetate of $(+)_{546}$-$[Co(ox)$-$(en)_2]^+$ (obtained from 7.9 g of $(+)_{546}$-$[Co(ox)(en)_2]I$, 3.3 g of silver acetate and 20 m*l* of water), were mixed together. When the mixed solution was cooled in an ice bath, the less soluble diastereomer, $(+)_{546}$-$[Co(ox)$-$(en)_2]_2\cdot(-)_{546}$-$[Co(mal)_2(L\text{-ala})]\cdot H_2O$, crystallized out. The diastereomer was recrystallized from water by the addition of methanol. The crystals were filtered, washed with methanol and then acetone, and dried in a vacuum desiccator over phosphorus pentoxide.

Found: C, 27.90; H, 5.05; N, 13.37%. Calcd for $[Co(C_2O_4)(C_2H_8N_2)_2]_2\cdot[Co(C_3H_2O_4)_2(C_3H_6NO_2)]\cdot H_2O$: C, 27.93; H, 4.91; N, 13.96%. $[M]_{546}=+5450°$, $[M]_{589}=+1460°$.

The configurationally optically active barium salt was obtained by the same method as in i-b). It was recrystallized from water by adding a methanol-ethanol mixture (1 : 1). The fine crystals obtained were filtered, washed with methanol and then acetone, and dried in a vacuum desiccator over phosphorus pentoxide.

Found: C, 22.56; H, 1.93; N, 2.83%. Calcd for $Ba[Co(C_3H_2O_4)_2(C_3H_6NO_2)]$: C, 22.13; H, 2.07; N, 2.87%. $[M]_{546}=-2800°$, $[M]_{589}=-4400°$.

When $(-)_{546}$-$[Co(ox)(en)_2]I$ was used instead of $(+)_{546}$-$[Co(ox)(en)_2]I$ in the above procedure, the less soluble diastereomer obtained was $(-)_{546}$-$[Co(ox)$-$(en)_2]_2\cdot(-)_{546}$-$[Co(mal)_2(L\text{-ala})]\cdot 1.5H_2O$.

Found: C, 27.74; H, 4.86; N, 13.54%. Calcd

for $[Co(C_2O_4)(C_2H_8N_2)_2]_2\cdot[Co(C_3H_2O_4)_2(C_3H_6NO_2)]\cdot 1.5H_2O$: C, 27.65; H, 4.97; N, 13.82%. $[M]_{546}=-9100°$, $[M]_{589}=-7140°$.

iii) Bisoxalatoglycinatocobalt(III) Complex: This complex has been resolved by Dwyer *et al.*[4] A slightly modified method was employed in the present study. Namely, a solution containing the sodium salt of the complex (obtained from $Ba[Co(ox)_2(gly)]\cdot 0.5H_2O$, sodium sulfate and water in the same way as in i-b)) was used instead of $Na_2[Co(ox)_2(gly)]\cdot 1.5H_2O$ as in the reported procedure. The barium salt of the $(-)_{546}$-isomer, which was obtained from the less soluble diastereomer with $(+)_{546}$-$[Co(ox)(en)_2]^+$, was dried in a vacuum desiccator over phosphorus pentoxide.

Found: C, 14.87; H, 1.77; N, 2.99%. Calcd for $Ba[Co(C_2O_4)_2(C_2H_4NO_2)]\cdot 2H_2O$: C, 14.94; H, 1.66; N, 2.90%. $[M]_{546}=-8100°$, $[M]_{589}=-1300°$.

iv) Bisoxalato(L-alaninato)cobalt(III) Complex: *iv-a) Without Resolving Agent.* Eight grams of barium perchlorate was dissolved in a solution containing the sodium salt of the complex as described in 2) of Preparation of Oxalato Complexes, and the less soluble diastereomer of the barium salt, $(+)_{546}$-$Ba[Co(ox)_2(L\text{-}ala)]\cdot 0.5H_2O$, crystallized out. After the mixture had been cooled in an ice bath for one hour, the barium salt was filtered, washed with water, methanol and then acetone, and dried in a vacuum desiccator over phosphorus pentoxide.

Found: C, 18.05; H, 1.53; N, 2.98%. Calcd for $Ba[Co(C_2O_4)_2(C_3H_6NO_2)]\cdot 0.5H_2O$: C, 17.93; H, 1.50; N, 2.99%. $[M]_{546}=+7100°$, $[M]_{589}=+1300°$.

iv-b) By $(+)_{546}$- or $(-)_{546}$-[Co(ox)(en)$_2$]I. This method is almost the same as i-b). A solution of 4.0 g of $K_2[Co(ox)_2(L\text{-}ala)]$ in 25 m*l* of water was used instead of solution "a" containing $Na_2[Co(mal)_2(gly)]$ in i-b). The less soluble diastereomer formed by using $(+)_{546}$-$[Co(ox)(en)_2]I$ was $(+)_{546}$-$[Co(ox)(en)_2]_2\cdot(-)_{546}$-$[Co(ox)_2(L\text{-}ala)]\cdot H_2O$.

Found: C, 26.03; H, 4.64; N, 14.40%. Calcd for $[Co(C_2O_4)(C_2H_8N_2)_2]_2\cdot[Co(C_2O_4)_2(C_3H_6NO_2)]\cdot H_2O$: C, 26.06; H, 4.57; N, 14.40%. $[M]_{546}=0°$, $[M]_{589}=+5100°$.

By the same method as in i-b), the barium salt of the $(-)_{546}$-isomer was obtained from the diastereomer.

Found: C, 17.54; H, 1.40; N, 2.68%. Calcd for $Ba[Co(C_2O_4)_2(C_3H_6NO_2)]\cdot H_2O$: C, 17.57; H, 1.67; N, 2.93%. $[M]_{546}=-7050°$, $[M]_{589}=-500°$.

When $(-)_{546}$-$[Co(ox)(en)_2]I$ was used as a resolving agent, the less soluble diastereomer obtained was $(-)_{546}$-$[Co(ox)(en)_2]_2\cdot(+)_{546}$-$[Co(ox)_2(L\text{-}ala)]\cdot 0.5H_2O$.

Found: C, 26.44; H, 4.83; N, 14.12%. Calcd for $[Co(C_2O_4)(C_2H_8N_2)_2]_2\cdot[Co(C_2O_4)_2(C_3H_6NO_2)]\cdot 0.5H_2O$: C, 26.35; H, 4.54; N, 14.56%. $[M]_{546}=-6560°$, $[M]_{589}=-5280°$.

The barium salt of the $(+)_{546}$-isomer was obtained from the diastereomer. $[M]_{546}=+7100°$, $[M]_{589}=+1300°$.

v) Bisoxalato(β-alaninato)cobalt(III) Complex: Similar to the method of i-b), a mixed solution containing the sodium salt of the complex and the acetate of $(-)_{546}$-$[Co(ox)(en)_2]^+$ was cooled in an ice bath for one hour. The less soluble diastereomer deposited, $(-)_{546}$-$[Co(ox)(en)_2]_2\cdot(-)_{546}$-$[Co(ox)_2(\beta\text{-ala})]$, was filtered, washed with a little ice water and dried in air. Recrystallization was carried out from hot water by adding methanol and cooling in an ice bath. The crystals deposited were filtered, washed with a small amount of water, methanol and then acetone, and dried in a vacuum desiccator over phosphorus pentoxide.

Found: C, 26.76; H, 4.72; N, 14.35%. Calcd for $[Co(C_2O_4)(C_2H_8N_2)_2]_2\cdot[Co(C_2O_4)_2(C_3H_6NO_2)]$: C, 26.60; H, 4.43; N, 14.40%. $[M]_{546}=-1200°$, $[M]_{589}=-9700°$.

The optically active barium salt of the complex was obtained from the diastereomer by the same method as in i-b).

Found: C, 18.86; H, 1.32; N, 3.18%. Calcd for $Ba[Co(C_2O_4)_2(C_3H_6NO_2)]$: C, 18.28; H, 1.32; N, 3.04%. $[M]_{546}=-4900°$, $[M]_{589}=-3300°$.

Measurements. Electronic absorption spectra were measured with a Beckman DU spectrophotomer. CD spectra were recorded with a Roussel-Jouan Dichrographe and RD curves with a Yanagimoto recording spectropolarimeter, Model-185. All measurements were made in aqueous solutions at room temperature.

Results and Discussion

The d–d Transition Bands. The absorption, CD and RD curves of $(-)_{546}$-$[Co(ox)_2(gly)]^{2-}$, $(-)_{546}$-$[Co(ox)_2(\beta\text{-ala})]^{2-}$ and $(-)_{546}$-$[Co(mal)_2(gly)]^{2-}$ are shown in Figs. 1 and 2, and those of the unresolved L-alaninato complexes, $K_2[Co(ox)_2(L\text{-ala})]$ and $Ba[Co(mal)_2(L\text{-ala})]$, in Fig. 3. The

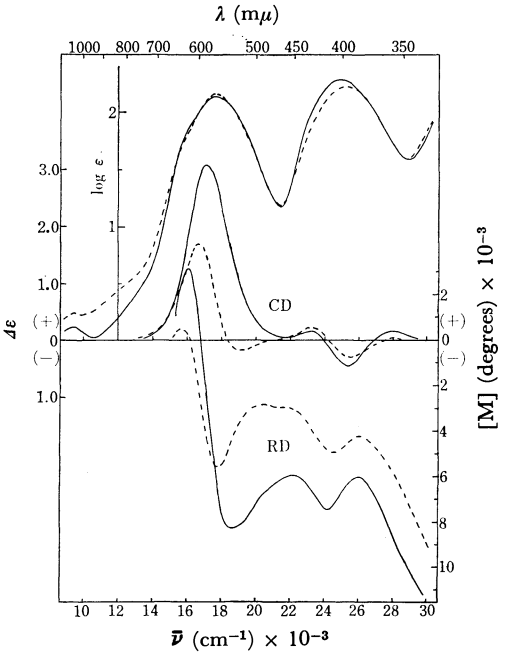

Fig. 1. Absorption, CD, and RD curves of $(-)_{546}$-$Ba[Co(ox)_2(gly)]\cdot 2H_2O$ (——) and $(-)_{546}$-$Ba[Co(ox)_2(\beta\text{-ala})]$ (------).

first absorption bands of the complexes show a vague shoulder (at about 640 mμ) at the lower energy side of the main peak. This absorption behavior coincides with the result expected from

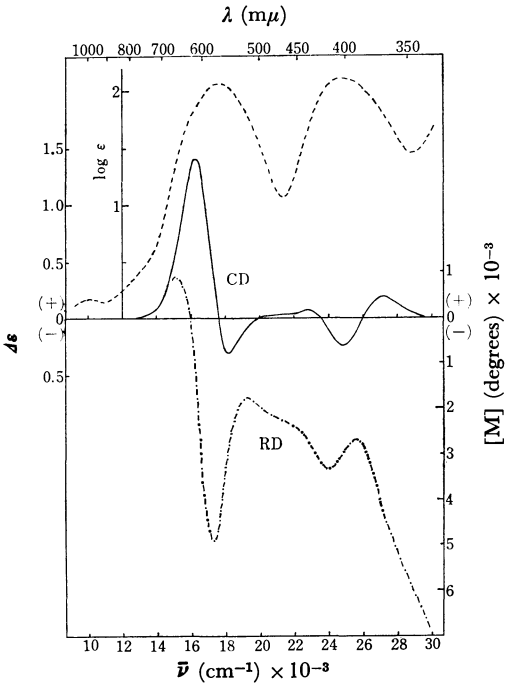

Fig. 2. Absorption (------), CD (——), and RD (—·—·—) curves of $(-)_{546}$-$Ba[Co(mal)_2(gly)]\cdot 2.5H_2O$.

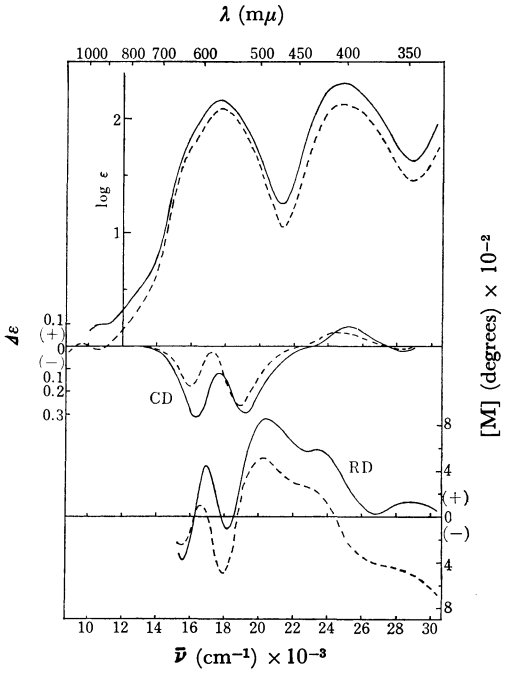

Fig. 3. Absorption, CD, and RD curves of unresolved $K_2[Co(ox)_2$(L-ala)] (——) and $Ba[Co(mal)_2$(L-ala)] (------).

a theory based on the approximation that the effective symmetry of the complexes is C_{4v}.[9] In the corresponding region, the CD cruve of $(-)_{546}$-$[Co(ox)_2(gly)]^{2-}$ shows a positive band, while the CD curves of $(-)_{546}$-$[Co(ox)_2(\beta\text{-ala})]^{2-}$ and $(-)_{546}$-$[Co(mal)_2(gly)]^{2-}$ show two bands (+ and −, listing from the lower energy side), as is seen in Figs. 1 and 2. It is noted, however, that the shape of the CD band of $(-)_{546}$-$[Co(ox)_2(gly)]^{2-}$ is not symmetrical. This trend may indicate that another weak CD band located on the higher energy side is overlapped by the main CD band at 584 mμ. This suggestion is supported by a comparison of the CD behavior with that of $(-)_{546}$-$[Co(ox)_2(\beta\text{-ala})]^{2-}$ or $(-)_{546}$-$[Co(mal)_2(gly)]^{2-}$. Moreover, the unresolved L-alaninato complexes also show two CD bands (− and −) in the corresponding region, as shown in Fig. 3. A similar consideration of the relationship between the CD and the first absorption band has been reported for aminocarboxylatobisethylenediaminecobalt(III) complexes,[2] which also belong to the same symmetry, C_1, as the present complexes. From these facts, it is indicated that all complexes treated in the present paper have at least two CD bands in the first absorption band region.

The second absorption bands of the complexes do not appear to have any splitting. However, the CD spectra of the $(-)_{546}$-isomers have three CD bands (+, − and +) in the corresponding region, though their intensities are somewhat different from one another, as seen in Figs. 1 and 2 and Table 1. From this fact, it might be thought that these three CD bands correspond to three A components under C_1 symmetry, because the true symmetry of the present complexes is C_1.

The absolute configuration Δ (left-handed screw along the pseudo-C_3 axis) has been assigned for $(-)_{546}$-$[Co(ox)_2(gly)]^{2-}$ by Dwyer *et al.*, on the basis of the CD behavior in the first absorption band region.[4] From a comparison of the net sign[10] of the CD bands in the first absorption band region with that of the CD bands of Δ-$(+)_{589}$-$[Co(en)_3]^{3+}$, the Δ configuration can be assigned to all the $(-)_{546}$-isomers in this paper, including those of the two L-alaninato complexes, and the Λ configuration to the $(+)_{546}$-isomers. The absolute configurations of the optical isomers, which formed the less soluble diastereomers with strychnium cation or optically active $[Co(ox)(en)_2]^+$, are summarized in Table 2. It is not surprising that the $(-)_{546}$-isomer of $[Co(mal)_2$(L-ala)$]^{2-}$ forms the less soluble diastereomer with both $(-)_{546}$- and $(+)_{546}$-$[Co(ox)(en)_2]^+$, because $(+)_{546}$- and $(-)_{546}$-$[Co(mal)_2$(L-ala)$]^{2-}$ are not antipodal with each other.

9) N. Matsuoka, J. Hidaka and Y. Shimura, This Bulletin, **40**, 1868 (1967).

10) J. I. Legg and B. E. Douglas, *J. Am. Chem. Soc.*, **88**, 2697 (1966); C. J. Hawkins and E. Larsen, *Acta Chem. Scand.*, **19**, 185 (1965).

TABLE 1. ABSORPTION AND CIRCULAR DICHROISM DATA OF $[Co(O-O)_2(O-N)]^{2-}$ TYPE COMPLEXES

Complex ion	Absorption bands $\bar{\nu}_{max}$ (log ε)	CD bands $\bar{\nu}_{ext}$ ($\Delta\varepsilon$)
$(-)_{546}$-$[Co(mal)_2(gly)]^{2-}$	17.7 (2.06)	16.3 (+1.40) 18.2 (−0.31)
	24.7 (2.12)	22.8 (+0.06) 24.9 (−0.24) 27.2 (+0.19)
$[Co(mal)_2$(L-ala)$]^{2-}$ (unresolved)	17.8 (2.09)	16.0 (−0.18) 18.9 (−0.27)
	24.9 (2.13)	24.5 (+0.06) 28.3 (−0.01)
$(-)_{546}$-$[Co(mal)_2$(L-ala)$]^{2-}$	17.8 (2.09)	16.3 (+1.20) 18.3 (−0.44)
	24.9 (2.13)	22.9 (+0.06) 24.9 (−0.15) 27.3 (+0.26)
$(+)_{546}$-$[Co(mal)_2$(L-ala)$]^{2-}$	17.8 (2.09)	16.3 (−1.32) 17.9 (+0.03) 19.2 (−0.32)
	24.9 (2.13)	24.9 (+0.30) 27.5 (−0.18)
$(-)_{546}$-$[Co(ox)_2(gly)]^{2-}$	17.7 (2.14)	17.2 (+3.08)
	24.9 (2.28)	23.1 (+0.16) 25.4 (−0.44) 27.9 (+0.15)
$[Co(ox)_2$(L-ala)$]^{2-}$ (unresolved)	17.7 (2.16)	16.3 (−0.32) 19.2 (−0.30)
	24.9 (2.31)	25.3 (+0.09) 28.2 (−0.02)
$(-)_{546}$-$[Co(ox)_2$(L-ala)$]^{2-}$	17.7 (2.16)	17.4 (+2.65)
	24.9 (2.31)	23.1 (+0.13) 25.3 (−0.34) 28.1 (+0.13)
$(+)_{546}$-$[Co(ox)_2$(L-ala)$]^{2-}$	17.7 (2.16)	17.3 (−3.03)
	24.9 (2.31)	23.1 (−0.15) 25.3 (+0.52) 28.1 (−0.16)
$(-)_{546}$-$[Co(ox)_2(\beta$-ala)$]^{2-}$	17.7 (2.15)	16.7 (+1.69) 19.1 (−0.18)
	25.3 (2.23)	23.2 (+0.22) 25.5 (−0.30) 27.9 (+0.03)

The frequencies are given in 10^3 cm^{-1}.

TABLE 2. OPTICAL ISOMER FORMING THE LESS SOLUBLE DIASTEREOMER WITH CATION OF RESOLVING AGENT

Complex anion	Cation of the resolving agent		
	$(-)_{546}$-$[Co(ox)(en)_2]^+$	$(+)_{546}$-$[Co(ox)(en)_2]^+$	Strychnium cation
$[Co(ox)_2(gly)]^{2-}$	Λ-$(+)_{546}$	Δ-$(-)_{546}$	#
$[Co(ox)_2$(L-ala)$]^{2-}$*	Λ-$(+)_{546}$	Δ-$(-)_{546}$	#
$[Co(ox)_2(\beta$-ala)$]^{2-}$	Δ-$(-)_{546}$	Λ-$(+)_{546}$	#
$[Co(mal)_2(gly)]^{2-}$	Δ-$(-)_{546}$	Λ-$(+)_{546}$	Δ-$(-)_{546}$
$[Co(mal)_2$(L-ala)$]^{2-}$	Δ-$(-)_{546}$	Δ-$(-)_{546}$	Λ-$(+)_{546}$

* The isomer of this complex forming the less soluble barium salt is the Λ-$(+)_{546}$-isomer.
\# The resolution has not been tried.

The configurationally optically active isomers, Δ- and Λ-$[Co-(OO)_2(L\text{-ala})]^{2-}$, are not antipodal, but diastereomeric to each other, as mentioned above. It is expected, therefore, that separation of the isomers due to the solubility difference between them is possible as in the case of *trans(N)*-oxalatobis(L-alaninato)cobalt(III) complex[6] or tris-(L-alaninato)cobalt(III) complexes.[11,12] In fact, the diastereomeric barium salts, Δ- and Λ-$Ba[Co(ox)_2(L\text{-ala})]$, were completely separated only by crystallization, as described in the Experimental section, though it was unsuccessful in the case of the potassium salts. From this fact, it is pointed out that even only one asymmetric carbon atom of a ligand is effective for separation of the diastereomers, and that the possibility of separation depends merely on the solubilities of the salts employed.

Additivity of Configurational and Vicinal Effects. The CD and RD curves of Δ-$(-)_{546}$- and Λ-$(+)_{546}$-$[Co(ox)_2(L\text{-ala})]^{2-}$ are shown in Fig. 4. The two isomers are not antipodal, but

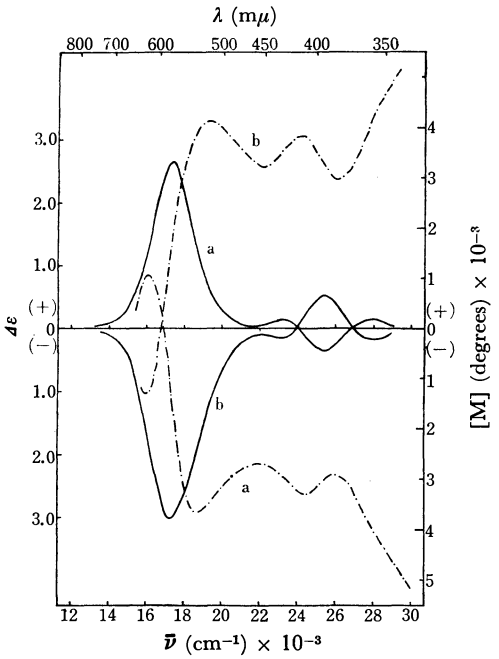

Fig. 4. CD (——) and RD (—·—) curves of Δ-$(-)_{546}$-$Ba[Co(ox)_2(L\text{-ala})]\cdot H_2O$ (a) and Λ-$(-)_{546}$-$Ba[Co(ox)_2(L\text{-ala})]\cdot 0.5H_2O$ (b).

diastereomeric to each other. It was reported for some cobalt(III) complexes that the configurational and vicinal contributions to CD are almost separable and additive.[2,12,13] If this is also true for $[Co(ox)_2(L\text{-ala})]^{2-}$, the following relationships will hold

$$\Delta\varepsilon(L) = \frac{1}{2}\left\{\Delta\varepsilon(\Delta_L) + \Delta\varepsilon(\Lambda_L)\right\} \quad (1)$$

$$\Delta\varepsilon(\Delta) = \frac{1}{2}\left\{\Delta\varepsilon(\Delta_L) - \Delta\varepsilon(\Lambda_L)\right\} \quad (2)$$

$$\Delta\varepsilon(\Delta) + \Delta\varepsilon(\Lambda) = 0 \quad (3)$$

The vicinal CD due to the coordinated L-alaninate, $\Delta\varepsilon(L)$, and the configurational CD, $\Delta\varepsilon(\Delta)$ or $\Delta\varepsilon(\Lambda)$, can be calculated by applying the relationships (1)—(3) to the observed CD cruves for Δ-$[Co(ox)_2(L\text{-ala})]^{2-}$ and Λ-$[Co(ox)_2(L\text{-ala})]^{2-}$, namely $\Delta\varepsilon(\Delta_L)$ and $\Delta\varepsilon(\Lambda_L)$. The calculated cruves are shown with the observed cruves of Δ-$[Co(ox)_2(gly)]^{2-}$ (configurational effect without vicinal) and the unresolved $[Co(ox)_2(L\text{-ala})]^{2-}$(vicinal effect without configurational) in Fig. 5. The good agreement

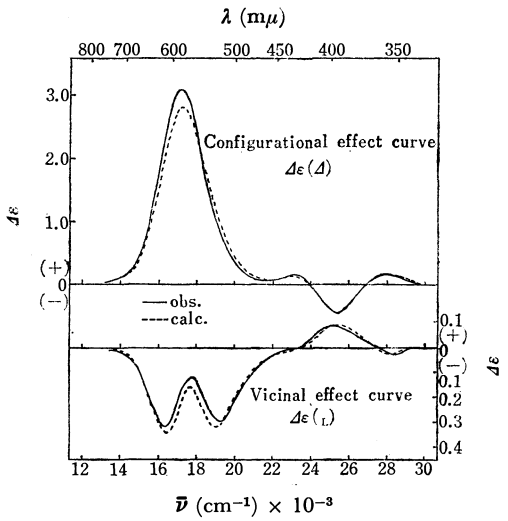

Fig. 5. Upper: The observed CD curve of Δ-$(-)_{546}$-$Ba[Co(ox)_2(gly)]\cdot 2H_2O$ and the configurational effect curve for $[Co(ox)_2(L\text{-ala})]^{2-}$ calculated from the cuves in Fig. 4.
Lower: The observed CD curve of unresolved $K_2[Co(ox)_2(L\text{-ala})]$ and the vicinal effect curve calculated from the curves in Fig. 4.

between the calculated curves and the observed ones substantiate the additivity, and indicate that the unresolved complex is the (1 : 1) mixture of Δ_L- and Λ_L-isomers. Furthermore, the observed CD curve of the reacted solution of $[Co_2(ox)_4(OH)_2]^{4-}$ with L-alanine coincides with that of the unresolved complex which was isolated from the solution. It is concluded, therefore, that this reaction is not stereospecific; in other words, equal amounts of the two diastereomers were produced in this reaction.

The CD and RD curves of Δ- and Λ-$[Co(mal)_2(L\text{-ala})]^{2-}$ are shown in Fig. 6. They are also a couple of diastereomeric isomers. The curves concerning the additivity are shown in Fig. 7. In this case, however, the calculated cruves of Δ- and Λ-$[Co(mal)_2(L\text{-ala})]^{2-}$ were derived from

11) J. Lifschitz, *Z. phys. Chem.*, **114**, 485 (1925).
12) B. E. Douglas and S. Yamada, *Inorg. Chem.*, **4**, 1561 (1965).
13) J. I. Legg, D. W. Cooke and B. E. Douglas, *ibid.*, **6**, 700 (1967).

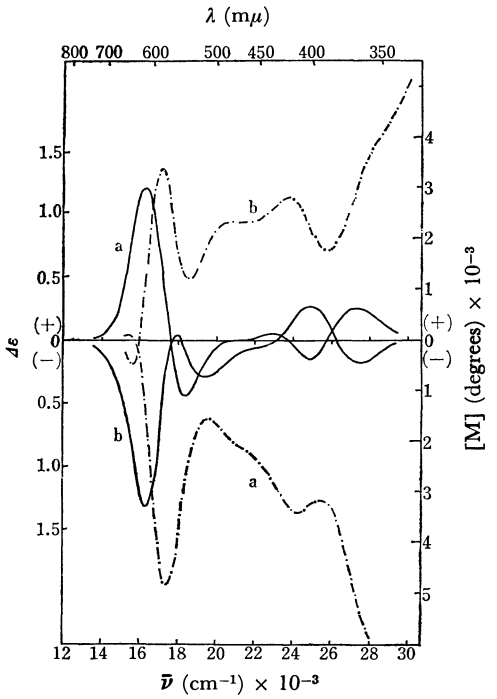

Fig. 6. CD (——) and RD (— · —) curves of Δ-(−)$_{546}$-Ba[Co(mal)$_2$(L-ala)] (a) and Λ-(+)$_{546}$-Ba-[Co(mal)$_2$(L-ala)] (b).

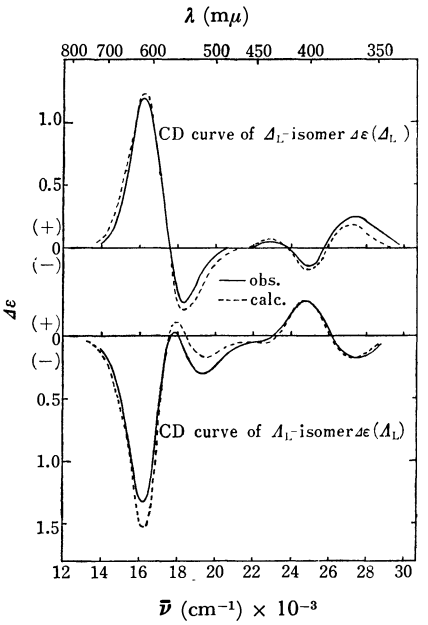

Fig. 7. Upper: The observed CD cruve of Δ-(−)$_{546}$-Ba[Co(mal)$_2$(L-ala)] and the calculated one from the curves of unresolved Ba[Co(mal)$_2$-(L-ala)] and Δ-(−)$_{546}$-Ba[Co(mal)$_2$(gly)]·2.5H$_2$O. Lower: The observed CD curve of Λ-(+)$_{546}$-Ba-[Co(mal)$_2$(L-ala)] and the calculated one.

the curves of Δ-[Co(mal)$_2$(gly)]$^{2-}$ (configurational effect without vicinal) and the unresolved [Co(mal)$_2$-(L-ala)]$^{2-}$ (vicinal effect without configurational). The result was achieved by applying the relationships (3), (4) and (5).

$$\Delta\varepsilon(\Delta_L) = \Delta\varepsilon(\Delta) + \Delta\varepsilon(L) \quad (4)$$

$$\Delta\varepsilon(\Lambda_L) = \Delta\varepsilon(\Lambda) + \Delta\varepsilon(L) \quad (5)$$

The calculated cruves agree quite well with the observed ones of Δ- and Λ-[Co(mal)$_2$(L-ala)]$^{2-}$. From this result and the experimental fact that the CD curve of the reacted solution of [Co(mal)$_3$]$^{3-}$ with L-alanine coincided well with that of the unresolved complex isolated as crystals, it is pointed out that in this reaction Δ- and Λ-[Co(mal)$_2$(L-ala)]$^{2-}$ were produced in almost equal amounts, as in the case of [Co(ox)$_2$(L-ala)]$^{2-}$.

From these facts, it may be concluded that in the oxalato and malonato complexes, the coordinated L-alaninate does not have a notable stereospecific effect. This conclusion can be easily understood for the oxalato complexes, because the oxalate chelate rings are planar. This consideration is supported by the fact that almost equal amounts of Δ- and Λ-[Co(ox)$_2${(−)-pn}]$^-$ ions occur in equilibrium.[14] In the malonate system, the chelate ring of the dicarboxylate is not planar. It is expected, however, that the L-alaninate chelate ring is near-planar and hence the interaction of the CH_3 group with the two malonates in the one configuration is not so different from that in the other configuration. As a result, it is reasonable to consider that the energy difference between the Δ- and Λ-isomers is very small, as in the case of [Co(ox)$_2$(L-ala)]$^{2-}$. A similar result has recently been reported for the [Co(en)$_2$(L-ala)]$^{2+}$ system,[15] in which two gauche ethylenediamines are coordinated to cobalt(III) instead of the two non-planar malonates of the present complexes.

14) F. P. Dwyer, T. E. MacDermott and A. M. Sargeson, *J. Am. Chem. Soc.*, **85**, 661 (1963).

15) D. A. Buckingham, L. G. Marzilli and A. M. Sargeson, *ibid.*, **89**, 5133 (1967).

BULLETIN OF THE CHEMICAL SOCIETY OF JAPAN VOL. 42 127—131 (1969)

On the Presence of Tetrafluoroborate Ions in Natural Waters[1)]

Tomio ONISHI

The College of Liberal Arts, Kagoshima University, Kamoike-cho, Kagoshima

(Received February 27, 1968)

Tetrafluoroborate ions (BF_4^-) can be formed only in a strongly acid solution. Certain acid thermal waters and volcanic gases in the active volcanic zone can be expected to be the media of BF_4^- formation. When BF_4^- is supplied to natural waters, its rate of hydrolysis is relatively low, suggesting the possibility of the occurrence of BF_4^- in natural waters. The contents of BF_4^- have been determined in various thermal water samples from a volcano in Satsuma Iwo-jima, and the presence of BF_4^- confirmed. The BF_4^- content in the condensed water of volcanic gas from a fumarole with the high temperature of 745°C is 304 mg/*l*, which is 26% of the total F, and 79% of the total B content. The BF_4^- content in a sample of water from Kitabira Spa (pH 1.1) is 8.0 mg/*l*, which is about 50% of the total F or B. However, the presence of BF_4^- can not be confirmed in ordinary natural waters such as land and sea waters.

Ducret[2)] reported a colorimetric method of analysis for B which consisted of the addition of a solution consisting of HF and NH_4F to a sample of water containing B, turning B into BF_4^-, and extracting the complex thus formed by the addition of methylene blue (MB) with 1,2-dichloroethane (DCE). Pasztor[3)] and Utsumi *et al.*[4,5)] have reported improved versions of this method. A series of these analytical methods aimed at determining the quantity of B by utilizing BF_4^- formation. Hosokawa and Morinaga,[6)] and Muto,[7)] taking the advantage of this method, attempted to make the complex of BF_4^- with MB directly, and to extract the BF_4^--MB complex with DCE. Hosokawa and Morinaga, and also Muto, then announced the presence of BF_4^- in sea and river waters and in hot spring water respectively.

On the other hand, in a preliminary study of natural water, a considerable quantity of material forming complexes with MB was extracted by the present author.[8)] However, these complexes might consist of materials other than BF_4^-, such as alkylbenzenesulfonate ions (ABS^-) in river water and Cl^- in sea water. For this reason, the presence of BF_4^- in ordinary natural water is strongly suspected.

BF_4^- can be formed only in a strongly acid solution containing an amount of F larger than that of B.[1,2,4)] If BF_4^- existed in ordinary natural waters, it could not have been formed in the present sea water, nor in land water. Certain acid thermal waters and volcanic gases in the active volcanic zone may be expected to have been the media of BF_4^- formation.

Actually, the formation of Avogadrite (K,Rb)BF_4 had been reported shortly after the eruption of Vesuvius in 1906.[9)] Even if BF_4^- originatin in such volcanoes could exist in a stable state in natural waters, the presence of BF_4^- would be confirmed only in special areas. For the purpose of examining the survival of BF_4^-, KBF_4 was added to various kinds of natural waters, and its rate of hydrolysis was measured. It was found that BF_4^- was relatively stable in an aqueous solution. If there is any source of BF_4^-, BF_4^- may be expected to exist in natural waters under favorable conditions.

Volcanic gases from the volcano in Satsuma Iwo-jima contain a large quantity of the F compound. Large amounts of the H_3BO_3 sublimate were found around some fumaroles,[10,11)] satisfying the requirements for the formation medium of

1) I. Iwasaki, M. Kamada, T. Onishi and H. Sakamoto, *Nippon Kagaku Zasshi* (*J. Chem. Soc. Japan, Pure Chem. Sect.*), **89**, 324 (1968), Short communication.

2) L. Ducret, *Anal. Chim. Acta*, **17**, 213 (1957).

3) L. Pasztor and J. D. Bode, *Anal. Chem.*, **32**, 277 (1960).

4) S. Utsumi, S. Ito and A. Isozaki, *Nippon Kagaku Zasshi* (*J. Chem. Soc. Japan, Pure Chem. Sect.*), **86**, 921 (1965).

5) S. Utsumi and A. Isozaki, *ibid.*, **88**, 545 (1967).

6) I. Hosokawa and T. Morinaga, Preprints for the Annual Meeting of The Geochemical Society of Japan, Tokyo (October, 1965), p. 153.

7) K. Muto, *ibid.*, Kanazawa (October, 1966), p. 193.

8) I. Iwasaki, T. Onishi, H. Sakamoto and M. Kamada, *ibid*, p. 195.

9) V. M. Goldschmidt, "Geochemistry," ed. by A. Muir, Oxford University Press, Oxford (1954), p. 573.

10) M. Yoshida, T. Ozawa and J. Ossaka, *Ganseki Koobutsu Kosho Gatsukaishi* (*J. Japan Assoc. Min. Petrog. Econ. Geol.*), **55**, 201, 262 (1966).

11) M. Kamada, *Chinetsu* (*Geothermy*), **3**, 1 (1964).

BF_4^-. The BF_4^- contents have been determined in various samples from this volcano, and the presence of BF_4^- has been confirmed in all of these samples.

Experimental

Analysis of BF_4^-. When the MB complex method was directly applied to natural water in the presence of many interfering materials, the effects of those materials, particularly Cl^-, Br^-, I^-, and ABS^-, posed a problem. Utsumi *et al.*[5] removed the ABS^- in advance with DCE, and also removed the Cl^- by washing with a Ag_2SO_4 solution when the colorimetric method was adopted for the determination of the B in the water. The present author aimed at the direct determination of BF_4^-, but since considerable quantities of ABS^- and Cl^- were considered to exist in river and in sea waters respectively, the quantity of BF_4^- was determined by first extracting ABS^- with DCE only, adding MB to the sample water after removing the ABS^-, extracting the complexes with DCE, and backwashing the complex of F^- extracted with water, backwashing it again with a Ag_2SO_4 solution, and separating the halogen ions other than F^-. Further, it was found that BO_3^{3-} did not interfere because it did not form a complex with MB.

Procedure. A sample solution (20 m*l*) was taken in a polyethylene separating funnel, to which 10 m*l* of DCE was added, after the funnel had been shaken for 1 min, the organic phase was separated. Five milliliters of 0.001 M MB and 10 m*l* of DCE were then added to the water phase, and the mixture was shaken for 1 min. After it had then been left for 10 min, the organic phase was separated, washed with 5 m*l* of water and again with 5 m*l* of 0.01 M Ag_2SO_4, and then transferred into a glass-stoppered test tube. Then about 0.2 g of anhydrous Na_2SO_4 was added to the organic phase, and the mixture was shaken in order to remove the water completely. The optical absorbance of the organic phase was measured at the wavelength of 660 mμ using a blank test solution as a reference. The calibration curve is shown in Fig. 1.

Sensitivity of BF_4^- in the Method of Analyzing F. Various methods of analyzing F which have been widely used do not pay any attention to the presence of BF_4^--type F. However, if BF_4^--type F exists in natural waters, attention should be paid to the behavior

Table 1. Recovery test of F in various states

Sample	Given (μg as F)	Found (μg as F)	Recovery (%)
F^-	500	495	99.0
BF_4^-	500	495	99.0
$F^- + BF_4^-$	1000	988	98.8
$BF_4^- + H_3BO_3$†	500	486	97.2
$F^- + Al_2(SO_4)_3$†	500	486	97.2
$BF_4^- + H_3BO_3$†	500	490	98.0
$BF_4^- + Al_2(SO_4)_3$†	500	480	96.0
$BF_4^- + SiO_2$†	500	490	98.0

† With respect to the amounts of $Al_2(SO_4)_3$, H_3BO_3 and SiO_2, 1000 mg as Al, B and Si were added.

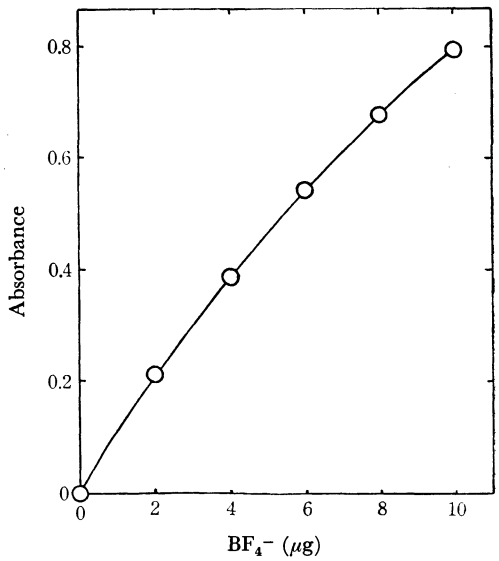

Fig. 1. Optical absorbance of BF_4^--MB complex at 660 mμ.

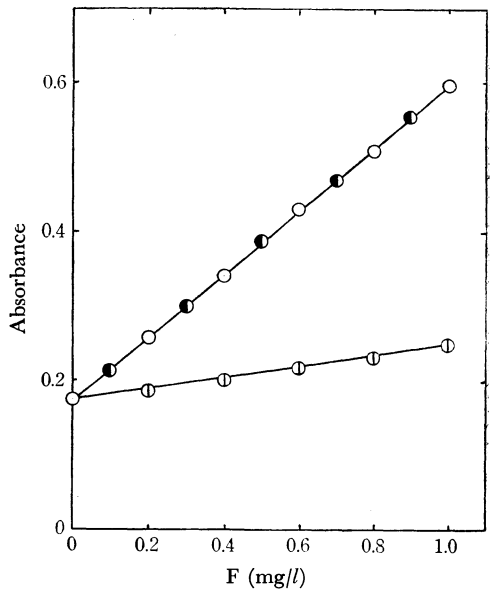

Fig. 2. Plot of F concentration *versus* optical absorbance of F-bearing ions.
○ F^- ◐ SiF_6^{2-} ⓘ BF_4^-

of F in any analytical procedure. Curves of the concentration *versus* the optical absorbances of F^-, SiF_6^{2-}, and BF_4^-, obtained by a method using "Azo-dye,"[12,13] are shown in Fig. 2.

From Fig. 2, it is evident that the sensitivity with

12) M. Kamada and T. Onishi, *Nippon Kagaku Zasshi* (*J. Chem. Soc. Japan, Pure Chem. Sect.*), **80**, 275 (1959).
13) M. Kamada, T. Onishi and M. Ota, This Bulletin, **28**, 149 (1955).

Table 2. Necessary information on sample waters

Sample water	Sampling date	pH	F (mg/l)	B (mg/l)	Locality
Rain	May 16 '64	6.2	0.100	0.06	Kagoshima city
River	Aug. 2 '65	6.7	0.060	0.05	Kotsuki-gawa
Well	Aug. 4 '65	7.0	0.101	0.13	Kagoshima city
Sea	July 29 '55	8.2	1.42	4.7	Okinoerabu Is.

respect to the optical absorbance of BF_4^- is only 15% of those of F^- and SiF_6^{2-}. Therefore, if BF_4^--type F exists in rain or river water, the conventional colorimetric method for F will give only a part of the F content.

On the other hand, in the case of samples containing much co-existing material, F is usually subjected to distillation in a strongly acid solution prior to the colorimetric determination to separate it from interfering materials. However, if BF_4^- is present in the water sample, or if B is also present, there is a question as to whether the complete recovery of F can be secured by means of distillation. To answer this question, the recovery test of F was conducted by distillation in the presence of interfering materials. The results are given in Table 1. As is shown in Table 1, BF_4^--type F could be sufficiently recovered and did not interfere with the analysis of F at all.

Stability of BF_4^-. The precious reports on hydrolysis have mentioned only its susceptibility to the decomposition of BF_4^-.[7,14] Thus, the experiment was conducted by adding freshly-prepared KBF_4 in pure water and various kinds of natural waters, immediately after the addition, the solutions in a polyethylene bottle were left in a bath with a constant temperature of 20°C. The rate of the decomposition of BF_4^- was traced by both the MB method and the indirect method using F formed through the decomposition of BF_4^-.

The necessary information on the water sample for the stability test of BF_4^- is given in Table 2, while the test results are shown in Fig. 3.

The results shown in Fig. 3 may be summarized as follows:

A. BF_4^- was relatively stable when left in an aqueous solution for one year at room temperature. Twenty percent of it remained in pure water, 25% in river water, and 30% in sea water. With respect the natural water, the higher the salt concentration, the more stable BF_4^- is.

B. As the concentration of BF_4^- increased, the stability also increased. An increase in the temperature of the solution from 5°C to 50°C caused a great increase in the rate of decomposition.

C. When BF_4^- was added to a solution of NaOH with the pH of 12, it was almost completely decomposed in 20 hr. Therefore, generally speaking, as the pH increased, the rate of decomposition increased.

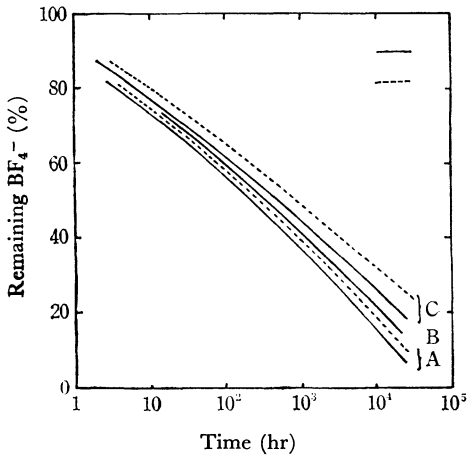

Fig. 3. Stability of BF_4^- in various natural waters.
A Pure water
B River and well waters
C Sea water
F as BF_4^- (1 mg/l) ——
F as BF_4^- (10 mg/l) ------

14) C. A. Wamser, *J. Am. Chem. Soc.*, **73**, 409 (1951).

Results and Discussion

Confirmation of the Presence of BF_4^- in the Active Volcano Zone. The volcanic gases of Satsuma Iwo-jima contain a large amount of F compound, sometimes as much as 16.5% HF in vol% of gas excluding water vapor. Also, sublimates of B were found around the crater of the volcano. Thus, the BF_4^- contents were determined in various water samples from a volcano on Iwo-jima. The results are given in Table 3.

Condensed water from volcanic gas (No. 1) was collected on July 26, 1961, because of its high temperature (745°C), it was collected by means of quartz tubing instead of Teflon tubing. The cooling parts and sampling apparatus used were made of glass. There is a possibility of the contamination of B as well as of the reaction of BF_4^- with SiO_2 in galss, and also the possibility of a change in the state of the chemical species in the gas. To eliminate these defects, quartz tubing was inserted in a fumarole in the sampling of No. 2, and the gas was conducted through quartz tubing into chilled water in a polyethylene bottle. Here again, the reaction of BF_4^- with SiO_2 is possible. The No. 3 sample was obtained by using Teflon tubing since

Table 3. Contents of BF_4^- in samples from Iwo-zima

No.	Sample	F mg/l	B mg/l	B as BF_4^- mg/l	F as BF_4^- mg/l	(B as $BF_4^-/\Sigma B$) × 100 %	(F as $BF_4^-/\Sigma F$) × 100 %
1	Condensed water from a fumarole (Kamanokuchi)	1015	48.0	38.0	266	79	26
2	Condensed water from a fumarole (Kamanokuchi)	10.5	0.38	0.29	2.03	77	19
3	Condensed water from a fumarole (Kuromoe)	18.5	0.63	0.57	3.99	90	22
4	Hot spring water (Kitabira)	15	1.9	1.0	7.0	53	47
5	Hot spring water (Higashi)	16	1.7	0.4	2.8	24	18
6	Sea water (near Higashi hot spring)	1.6	5.1	0.005	0.035	0.1	2.2
7	Silica sublimate (Kamanokuchi)	11.6%	66 ppm	66 ppm	462 ppm	100	0.4

Table 4. Contents of BF_4^- in natural waters

No.	Sample	F mg/l	B mg/l	B as BF_4^- mg/l	F as BF_4^- mg/l
1	Rain water Oct. 30 '66 Kagoshima city	0.10	0.06	0.00	0.00
2	Rain water Aug. 25 '67 Kagoshima city	0.054	0.03	0.00	0.00
3	Lake water Sept. 23 '65 Okutama-ko	0.080	0.11	0.00	0.00
4	Lake water Oct. 3 '66 Ikeda-ko	0.085	0.04	0.00	0.00
5	River water May 1 '66 Kotsuki-gawa	0.08	0.045	0.00	0.00
6	Ground water Oct. 8 '65 Nishihodaka	0.022	0.017	0.00	0.00
7	Sea water Nov. 15 '66 Kagoshima bay	1.36	4.7	0.00	0.00
8	Sea water Aug. 16 '67 Okinoerabu Is.	1.40	4.38	0.00	0.00

the temperature of the fumarole was below 250°C; we thus avoided mixing the B compound in the solid form and conducting the gas into water.

In very case, BF_4^- was detected; the ratio of the BF_4^--type B against the total B was 77—90%, while that of the BF_4^--type F against the total F was 19—26%. In the subsurface part of fumaroles, no liquid phase is expected to exist. Therefore, the presence of BF_4^- in the condensed water indicates that most of the B is present in the form of BF_3 in the gas phase. The $BF_3(aq.)+F^- \rightarrow BF_4^-$ reaction may be responsible for the formation of BF_4^- in

the liquid phase. The K_p (4×10^{11}, at 25°C) of this reaction indicates that this is highly probable.

A "unique sublimate"*1 (No. 7) was obtained beneath the Kamanokuchi fumarole area. Yoshida *et al.*[10] reported that this material contained a strongly acid aqueous solution consisting mostly of halogen compounds inside, and that its total F content reached 11.6%. If trace amounts of B are embodied in such a sublimate, the most suitable environment for the formation of BF_4^- is realized. The test results indicated that all of the B was present in the BF_4^- form.

BF_4^- was confirmed to exist also in some acid thermal waters near the volcano, such as Kitabira hot spring water (No. 4), with a pH of 1.1, and Higashi hot spring water (No. 5), with pH of 1.6. The change in the BF_4^- content during the storage of hot spring water in a bottle at room temperature for 1 year was pursued. There was no change at all for the No. 4 sample, but No. 5 indicated a 70% decrease in the BF_4^- content over a 10-day period. This may be attributed to the difference in stability caused by the difference in pH.

Sea water (No. 6) was a special sample, a mixture of hot spring water (No. 5) with coastal sea water; its pH was 4.0. There was formed a white suspension composed of amorphous $Al_2O_3\cdot xH_2O$ and $SiO_2\cdot xH_2O$ produced by hydrolysis. The filtrate was analyzed after the precipitates separated, and the presence of BF_4^-, though only a trace, was confirmed. However, sea water like this is extraordinary.

Presence of BF_4^- in Normal Natural Waters. For the purpose of ascertaining the presence of BF_4^-, normal natural water was also analyzed. The results are given in Table 4.

The presence of BF_4^- was not confirmed within the 0.00 mg/*l* detection limits of sea, river, and rain water. Although considerable quantities of F and B exist in sea water, these cannot be expected in the formation of BF_4^- because of the higher pH values of the water sample.*2

The author wishes to thank Dr. M. Kamada of Kagoshima University, Dr. I. Iwasaki, Dr. T. Ozawa and Dr. M. Yoshida of the Tokyo Institute of Technology, Dr. S. Utsumi of Nihon University, and Dr. T. Koh of Tokai University, for their many helpful discussions and suggestions during this work. Thanks are also due Mr. H. Sakamoto for his assistance in the experimental work.

*1 Yoshida *et al.*[10] have reported on the general chemical properties and formation mechanism of this sublimate.

*2 Utsumi and Isozaki[5] suspected the presence of BF_4^- while using the indirect method in analyzing the B in sea water.

BULLETIN OF THE CHEMICAL SOCIETY OF JAPAN VOL. 42 131—136 (1969)

Nickel(II) and Copper(II) Complexes of *C,N*-Disubstituted Salicylideneimines with Steric Hindrance

Shoichiro YAMADA, Akira TAKEUCHI, Kuniko YAMANOUCHI and Katsumoto IWASAKI

Institute of Chemistry, College of General Education, Osaka University, Toyonaka, Osaka

(Received May 21, 1968)

Many new nickel(II) and copper(II) complexes (abbreviated as $M(X\text{-sal.}R)_2$) of Schiff bases were obtained from *C*-substituted salicylaldehydes and 2,6-dimethyl- and 2,6-diethyl-aniline, where X denotes 5-Br, 5-Cl, 5,6-benzo, 5-NO_2 and 3-CH_3O. For X = 5-Cl, the corresponding nickel(II) complex with R = 2,6-dichlorophenyl was also synthesized. All these nickel(II) complexes consist of square-planar molecules in the solid state and in non-donor solvents. The nickel(II) complexes, when dissolved in pyridine, either take up two pyridine molecules to form six-coordinated complexes or retain the original planar configuration. The configuration in pyridine depends upon the nature of X, demonstrating that the effect of X on the electronic state of the ligand may also be important, besides the steric factor, in determining the configuration of the nickel(II) complexes. The corresponding copper(II) complexes, which are square-planar in the solid state and in non-donor solvents, combine with one or two pyridine molecules, when dissolved in pyridine.

Numerous papers have been published about nickel(II) and copper(II) complexes of Schiff bases obtained from *C*-substituted salicylaldehydes (Fig. 1).*1 It is expected, however, that a com-

*1 These metal complexes are abbreviated as $M(X\text{-sal.}R)_2$ in this paper.

plication may occur with these complexes, when steric hindrance is considerable. For R=2,6-$(CH_3)_2$Ph and 2,6-$(C_2H_5)_2$Ph,*2 for example, where steric hindrance is large, complexes of the

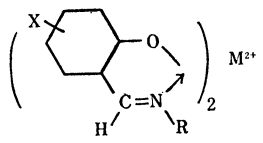

Fig. 1. M(X-sal.R)$_2$.

Ni(X-sal.R)$_2$ type are known to behave differently from the complexes of a similar type with R= phenyl or monosubstituted phenyl showing little or no steric hindrance.[1-3] The behavior of these complexes may also depend upon the nature of X, since the electronic state of the oxygen and the nitrogen atom of these ligands, X-sal.R, may be expected to change in a delicate way on changing X. In order to see the possible effect of the substituent X on the stereochemistry of the metal complexes and to explore a possibility of finding 5-coordinated complexes, the nickel(II) complexes of the Ni(X-sal.R)$_2$ type have been synthesized in the present work with 2,6-$(CH_3)_2$Ph and 2,6-$(C_2H_5)_2$Ph for R. A similar study has also been carried out about the corresponding copper(II) complexes for comparison with the nickel(II) complexes.

Experimental

Materials. Bis(*N*-aryl-*C*-substituted salicylideneiminato)nickel(II) complexes were prepared by a method similar to that previously reported either by reaction of a bis(*C*-substituted salicylaldehydato)nickel(II) with an amine or by reaction of nickel(II) acetate with a mixture of a *C*-substituted salicylaldehyde and an amine.[1,4] Pure crystals of the compounds were obtained by recrystallization of crude product using suitable organic solvents like ethanol, acetone and ethyl ether. Elemental analyses of the new nickel(II) compounds are given in Table 1. They are all green.

Bis(*N*-aryl-*C*-substituted salicylideneiminato)copper-(II) complexes were also prepared by a method similar to that previously reported.[1,2,4] Purification of the complexes was carried out by recrystallization of crude product from suitable organic solvents like ethanol, chloroform and ethyl ether. Elemental analyses of the new copper(II) complexes are given in Table 2.

Measurements. The electronic absorption spectra of the metal complexes in solution and reflection spectra of the solid were determined with a Shimadzu QR-50 spectrophotometer and a Shimadzu MPS-50L spectrophotometer. Pyridine for a solvent was purified, whenever necessary, by distillation after having been dried with potassium carbonate.

The magnetic measurements were carried out by the Gouy method at room temperature using $CoHg(SCN)_4$ as a standard.

Results and Discussion

The Nickel(II) Complexes of *N*-Aryl-*C*-Substituted Salicylideneimines. Many new nickel(II) complexes of the Ni(X-sal.R)$_2$ type have been prepared in the present work (Table 1). The result that all these nickel(II) complexes are diamagnetic in the solid state indicates the planar configuration of these complexes. They afford examples of the green nickel(II) complexes which are diamagnetic and planar.

TABLE 1. ANALYTICAL DATA OF NICKEL(II) COMPLEXES OF THE Ni(X-sal.R)$_2$ TYPE

X	R*	Calcd, %			Found, %		
		C	H	N	C	H	N
5-Cl	$(CH_3)_2$Ph	62.54	4.55	4.86	62.49	4.79	4.87
	$(C_2H_5)_2$Ph	64.59	5.42	4.43	64.25	5.52	4.56
	Cl_2Ph	47.47	2.14	4.26	47.75	1.81	4.30
5-Br	$(CH_3)_2$Ph	54.18	3.94	4.21	54.47	3.80	4.25
	$(C_2H_5)_2$Ph	56.61	4.75	3.88	56.77	4.51	3.80
5,6-Benzo	$(CH_3)_2$Ph	74.89	5.62	4.60	75.57	5.21	4.67
	$(C_2H_5)_2$Ph	75.79	6.36	4.21	75.93	6.02	4.24
3-CH_3O	$(CH_3)_2$Ph	67.75	5.68	4.94	67.50	5.56	4.86
	$(C_2H_5)Ph_2$	69.36	6.47	4.49	69.10	6.43	4.55
5-NO_2	$(CH_3)_2$Ph	60.33	4.39	9.38	60.19	4.11	9.71
	$(C_2H_5)_2$Ph	62.50	5.25	8.58	61.43	5.07	8.98

* 2,6-disubstituted phenyl groups

*2 The notation Ph denotes a benzene nucleus.

1) S. Yamada, *Coordin. Chem. Reviews*, **1**, 415 (1966).
2) S. Yamada, H. Nishikawa and E. Yoshida, This Bulletin, **39**, 994 (1966).
3) S. Yamada, E. Ohno, Y. Kuge, A. Takeuchi, K. Yamanouchi and K. Iwasaki, *Coordin. Chem. Reviews*, **3**, 247 (1968).
4) R. H. Holm, G. W. Everett, Jr., and A. Chakravorty, "Progress in Inorganic Chemistry," Vol. VII, ed. by F. A. Cotton, Interscience Publishers, New York, N. Y. (1966), p. 83.

TABLE 2. ANALYTICAL DATA OF COPPER(II) COMPLEXES OF THE $Cu(X\text{-sal.}R)_2$ TYPE

X	R*	Calcd, %			Found, %		
		C	H	N	C	H	N
5-Cl	$(CH_3)_2Ph$	62.02	4.51	4.82	61.99	4.36	4.93
	$(C_2H_5)_2Ph$	64.09	5.38	4.40	63.65	5.28	4.44
5,6-Benzo	$(CH_3)_2Ph$	74.55	5.27	4.58	73.68	5.00	4.52
	$(CH_3)_2Ph$**				74.20	5.12	4.63
	$(C_2H_5)_2Ph$	75.48	6.03	4.19	75.27	6.11	4.20
3-CH_3O	$(CH_3)_2Ph$	67.18	5.64	4.90	67.09	5.71	5.02
	$(CH_3)_2Ph$**				67.25	5.72	5.14
	$(C_2H_5)_2Ph$	68.82	6.42	4.46	68.54	6.52	4.28
5-NO_2	$(CH_3)_2Ph$	59.84	4.35	9.31	59.90	4.72	8.96
	$(C_2H_5)_2Ph$	62.04	5.21	8.51	60.99	4.99	8.38

* 2,6-disubstituted phenyl groups, unless otherwise indicated.
** 2,5-disubstituted phenyl groups.

It is well known that the electronic spectrum of a nickel(II) complex varies remarkably according as the nickel(II) complex is square-planar, tetrahedral, five-coordinated, or octahedral.[1-3] The present work shows that the electronic spectra of Ni(X-sal.2,6-$(CH_3)_2Ph)_2$ and Ni(X-sal.2,6-)$C_2H_5)_2$-$Ph)_2$ in non-donor solvents are typical of the square-planar nickel(II) complex (Fig. 2 and Table 3), and similar to the spectra of Ni(H-sal.2,6-$(CH_3)_2Ph)_2$ and Ni(H-sal.2,6-$(C_2H_5)_2Ph)_2$, which were previously concluded to be square-planar.[2] These complexes show no absorption band at about 900—1000 mμ, where the tetrahedral or the octahedral nickel(II) complexes are expected to absorb. Hence, both the presence of the monomeric, tetrahedral species and the association of the square-planar complexes may be excluded near room temperature. It is known[6,7] that bis(*N*-monosubstituted phenylsalicylideneiminato)nickel-(II) complexes in non-donor solvents consist of the square-planar monomer, the associated polymer with the six-coordinated nickel(II), and the tetrahedral monomer, the former two being in equilibrium with each other near room temperature. The difference in this respect between the *N*-monosubstituted phenyl- and the *N*-2,6-disub-

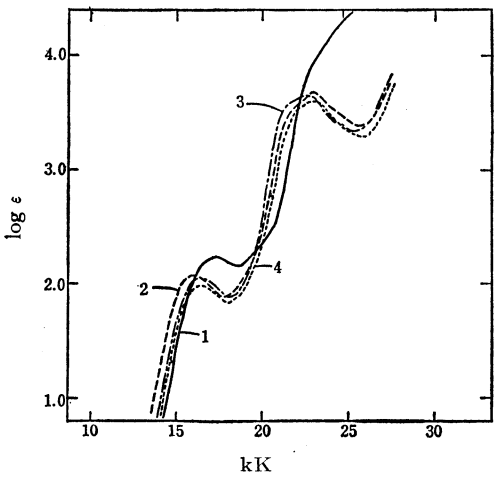

Fig. 2. Electronic absorption spectra of (NiX-sal.-2,6-$Y_2Ph)_2$ in chloroform.
1, X=5-NO_2, Y=CH_3; 2, X=3-CH_3O, Y=CH_3; 3, X=5-Cl, Y=C_2H_5; 4, X=H, Y=C_2H_5

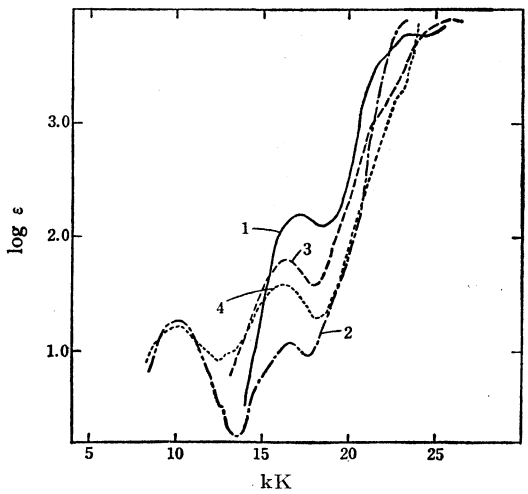

Fig. 3. Electronic absorption spectra of Ni(X-sal.-2,6-$Y_2Ph)_2$ in pyridine.
1, X=5,6-benzo, Y=CH_3; 2, X=5-Cl, Y=CH_3; 3, X=5-Br, Y=CH_3; 4, X=5-NO_2, Y=CH_3

5) S. Yamada and H. Nishikawa, This Bulletin, **36**, 755 (1963).
6) L. Sacconi, "Essays in Coordination Chemistry," ed. by W. Schneider, G. Anderegg and R. Gut, Birkhäuser Verlag, Basel (1964), p. 148.
7) R. H. Holm and K. Swaminathan, *Inorg. Chem.*, **1**, 599 (1962).

stituted phenyl-salicylideneiminato-nickel(II) complexes was ascribed mainly to the steric condition.[2] The same explanation applies to Ni(X-sal.2,6-$(CH_3)_2$Ph)$_2$ and Ni(X-sal.2,6-$(C_2H_5)_2$Ph)$_2$, which have been concluded to be square-planar in the solid state and in non-donor solvents.

The configuration of these nickel(II) complexes in pyridine, however, remarkably depends upon the substituent X. Electronic absorption spectra (Fig. 3 and Table 3) clearly show that, for X=5,6-benzo and 5-Br and R=2,6-$(CH_3)_2$Ph and 2,6-$(C_2H_5)_2$Ph, the complexes of the Ni(X-sal.R)$_2$ type bind no additional pyridine molecule, the original square-planar configuration being retained in pyridine. This result, which is the same as that for X=H, is considered to be due mainly to the steric hindrance arising from the two alkyl groups.

TABLE 3. ABSORPTION MAXIMA OF NICKEL(II) COMPLEXES OF THE Ni(X-sal.R)$_2$ TYPE*

X	Y	Solvent	ν**	log ε
5-Br	CH_3	$CHCl_3$	16.6	2.07
		Pyridine	16.3	1.80
	C_2H_5	CH_2Cl_2	16.4	2.04
		Pyridine	16.7	1.84
5-Cl	CH_3	CH_2Cl_2	16.1	2.08
		Pyridine	10.1	1.26
			16.6	1.08
	C_2H_5	$CHCl_3$	16.3	2.05
		Pyridine	16.2	1.84
	Cl	$CHCl_3$	16.0	2.04
		Pyridine	10.0	1.00
			16.2	1.55
5,6-Benzo	CH_3	$CHCl_3$	16.9	2.26
		Pyridine	17.1	2.20
	C_2H_5	$CHCl_3$	16.9	2.21
		Pyridine	17.1	2.22
5-NO_2	CH_3	$CHCl_3$	17.2	2.23
		Pyridine	10.1	1.13
			16.2	1.50
	C_2H_5	$CHCl_3$	17.1	2.25
		Pyridine	9.9	1.20
			16.1	1.58
3-CH_3O	CH_3	$CHCl_3$	16.0	2.07
		Pyridine	9.4	1.10
			15.9	1.40
	C_2H_5	$CHCl_3$	16.0	2.03
		Pyridine	9.5	1.06
			15.9	1.38

* R=2,6-Y_2Ph ** ν, 10^3 cm^{-1}

It is found from the spectra (Fig. 3 and Table 3) that for X=5-NO_2 and 3-CH_3O, the complexes of the Ni(X-sal.2,6-$(CH_3)_2$Ph)$_2$ and Ni(X-sal.2,6-$(C_2H_5)_2$Ph)$_2$ type, when dissolved in pyridine, exist as the six-coordinated pyridine solvates of the Ni(X-sal.2,6-Y_2Ph)$_2$(py)$_2$ type,*3 which show electronic spectra typical of octahedral, six-coordinated nickel(II) complexes. The absorption maxima of these pyridine solvates at about 10 and 16 kK may be assigned as $^3T_{2g} \leftarrow {}^3A_{2g}$ and $^3T_{1g}(F) \leftarrow {}^3A_{2g}$ in the scheme of the O_h ligand field symmetry.

Since Beer's law was obeyed, no equilibrium between the octahedral complex and another species may be likely. This difference between the two types of the substituent for X, which is not considered to be due to the steric factor, indicates that, although steric hindrance in these nickel(II) complexes seems to be more or less effective, it does not absolutely exclude the coordination number exceeding four. This result may be interpreted in terms of the difference in the electronic factor due to various X groups.

For X=5-Cl, anomalous behavior was observed. For example, the Ni(X-sal.2,6-$(CH_3)_2$Ph)$_2$ in pyridine exists as a six-coordinated complex, Ni(X-sal.R)$_2$(py)$_2$, as clearly seen from the electronic spectrum (Fig. 3 and Table 3). On the contrary, Ni(5-Cl.sal.2,6-$(C_2H_5)_2$Ph)$_2$ in pyridine retains the planar configuration. The difference between the complexes with X=5-Cl and with X=5-Br on one hand and between the complexes with R=2,6-$(CH_3)_2$Ph and with R=2,6-$(C_2H_5)_2$Ph for X=5-Cl on the other may also be due to the electronic factor. This fact seems to be in agreement with the fact that the band maximum and consequently the ligand field strength for X=5-Cl and R=2,6-$(CH_3)_2$Ph is slightly lower than the maximum for X=5-Cl and R=2,6-$(C_2H_5)_2$Ph.

It is significant that there is a remarkable difference between the two types of substituents for X. One includes 5-Br and 5,6-benzo, in addition to X=H, and the other 5-NO_2 and 3-CH_3O. The

TABLE 4. CONFIGURATION OF NICKEL(II) COMPLEXES OF THE Ni(X-sal.2,6-Y_2Ph)$_2$ TYPE IN PYRIDINE

X	Y	Config. in pyridine
H	CH_3	four-coordinated (original)
	C_2H_5	four-coordinated (original)
5-Br	CH_3	four-coordinated (original)
	C_2H_5	four-coordinated (original)
5-Cl	CH_3	six-coordinated solvate
	C_2H_5	four-coordinated (original)
	Cl	six-coordinated solvate
5,6-Benzo	CH_3	four-coordinated (original)
	C_2H_5	four-coordinated (original)
5-NO_2	CH_3	six-coordinated solvate
	C_2H_5	six-coordinated solvate
3-CH_3O	CH_3	six-coordinated solvate
	C_2H_5	six-coordinated solvate

*3 The notation py denotes a pyridine molecule.

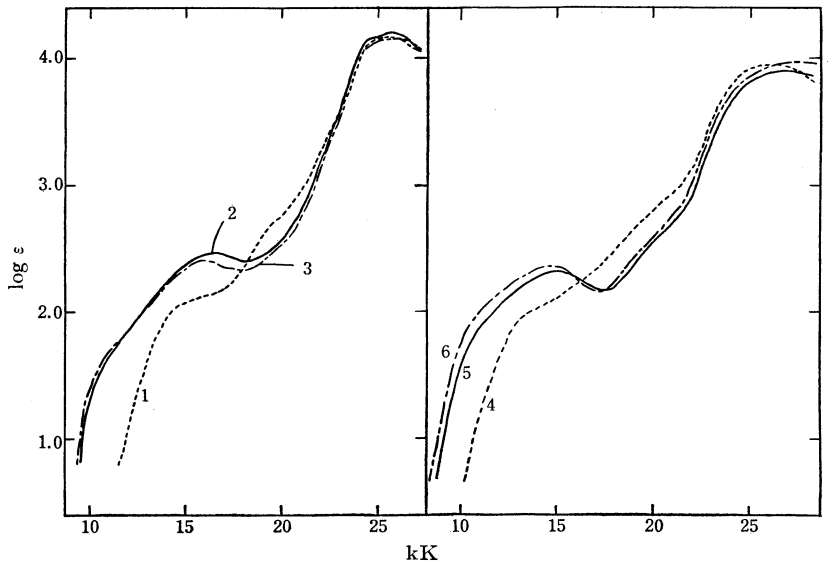

Fig. 4. Electronic absorption spectra of Cu(X-sal.2,6-Y_2Ph)$_2$ in solution.
1, X=5,6-benzo, Y=CH_3, in chloroform; 2, X=5,6-benzo, Y=CH_3, in pyridine;
3, X=5,6-benzo, Y=C_2H_5, in pyridine; 4, X=3-CH_3O, Y=CH_3, in chloroform;
5, X=3-CH_3O, Y=CH_3, in pyridine; 6, X=3-CH_3O, Y=C_2H_5, in pyridine

result of the examination in this work about the configuration of these nickel(II) complexes in pyridine is summarized in Table 4.

In the case of the corresponding cobalt(II) complexes, five-coordinated pyridine solvates of the Co(X-sal.2,6-Y_2Ph)$_2$(py) type were often formed.[8,9] Comparison of the results in the present work with that of the cobalt(II) complexes shows that the stability of the five-coordinated species *vis-a-vis* the four- and the six-coordinated ones is lower for the nickel(II) complexes than for the cobalt(II) complexes.

The Copper(II) Complexes of *N*-Aryl-*C*-substitutued Salicylideneimines. Many new copper(II) complexes of the *C*-substituted salicylideneimines, which are shown in Table 2, have been prepared in the present work. The planar configuration is most likely for these copper(II) complexes, since the tendency of the copper(II) complexes to take the square-planar configuration is known to be very high for the ligands of this series. The square-planar configuration may also be most likely even for 2,6-disubstituted phenyl derivatives in spite of the steric condition, since the corresponding nickel(II) complexes as well as the corresponding copper(II) complexes of salicylideneimines[2] have also been found to be square-planar. This presumption is supported by the present finding that the complexes of the Cu(X-sal.2,6-Y_2Ph)$_2$ type show ligand field bands at frequencies nearly identical with those of Cu(X-sal.YPh)$_2$, which were previously concluded to be planar.[2] It was also concluded previously that the ligand field band was shifted toward a considerably lower frequency when the copper(II) complex was distorted appreciably from the square-planar configuration.[4,6]

The spectral change in the ligand field band region of these copper(II) complexes on going from a non-donor solvent to pyridine (Figs. 4 and 5) is similar to the change observed previously when the four-coordinated complex of copper(II) takes up one or two additional ligands to form a five- or a six-coordinated complex.[2,10] It may be concluded, therefore, that all the copper(II) complexes examined in the present work combine with one or two pyridine molecules in the pyridine solution. This result is the same as the previous conclusion[2] with Cu(H-sal.2,6-Y_2Ph)$_2$, Y_2 being $(CH_3)_2$ and $(C_2H_5)_2$. It is, however, difficult at the moment to determine from the spectrum alone whether the pyridine solvate is five- or six-coordinated.

It is interesting to point out that the behaviour of Cu(X-sal.2,6-Y_2Ph)$_2$ in pyridine is different

8) S. Yamada and H. Nishikawa, This Bulletin, **38**, 683 (1965).

9) S. Yamada and E. Yoshida, *ibid.*, **40**, 1298, 1854 (1967); Proceedings Tenth International Conference on Coordination Chemistry (X. ICCC) (Tokyo, 1967), p. 275.

10) M. Honda and G. Schwarzenbach, *Helv. Chim. Acta*, **40**, 27 (1957); R. L. Belford and T. S. Piper, *Mol. Phys.*, **5**, 251 (1962).

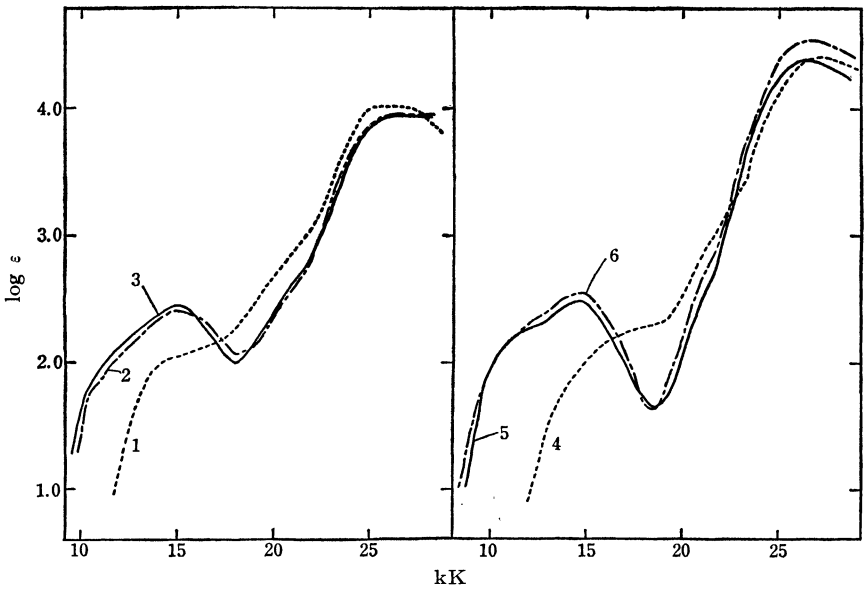

Fig. 5. Electronic absorption spectra of Cu(X-sal.2,6-Y_2Ph)$_2$ in solution.
1, X=5-Cl, Y=CH_3, in chloroform; 2, X=5-Cl, Y=CH_3, in pyridine; 3, X=5-Cl, Y=C_2H_5, in pyridine; 4, X=5-NO_2, Y=CH_3, in chloroform; 5, X=5-NO_2, Y=CH_3, in pyridine; 6, X=5-NO_2, Y=C_2H_5 in pyridine

from that of the corresponding nickel(II) complexes when X denotes H, 5-Cl, 5-Br and 5,6-benzo. This may also be considered to be an example showing that the coordination number larger than four in copper(II) complexes occurs at a slightly weaker ligand field than in the corresponding nickel(II) complexes.[2,11] This difference between the nickel(II) and the copper(II) complexes may be discussed in terms of the bonding nature of the metal ions and the steric condition arising from the two alkyl groups.[2]

Support of this work by the Ministry of Education is gratefully acknowledged.

11) S. Yamada, H. Nishikawa, Y. Kuge and K. Yamanouchi, *Sci. Reports Coll.Gen. Educ., Osaka Univ.*, **16**, 11 (1967).

BULLETIN OF THE CHEMICAL SOCIETY OF JAPAN VOL. 42 136—140 (1969)

Trimethylenediamine Complexes. I. Some Trimethylenediamine Complexes Derived from *trans*-[$CoCl_2tn_2$]Cl in Methanol

Hiroshi KAWAGUCHI, Naomichi YANO and Shinichi KAWAGUCHI

Department of Chemistry, Faculty of Science, Osaka City University, Sumiyoshi-ku, Osaka

(Received May 24, 1968)

Several diacidobis(trimethylenediamine)cobalt(III) complexes including nitrate, nitrite and thiocyanate ions as ligands have been prepared by ligand substitution reactions of *trans*-dichlorobis(trimethylenediamine)cobalt(III) chloride in methanol. All these compounds were assumed to have the trans configuration according to the Baldwin's criterion based on the CH_2 rocking vibration. Isomeric pairs of chloronitro and chloronitrito complexes were also characterized by means of infrared data.

The metal complexes of ethylenediamine have been extensively studied in various aspects, but the investigations on the corresponding trimethylenediamine complexes have been quite limited. The X-ray analysis of *trans*-[$CoCl_2tn_2$]Cl·HCl·$2H_2O$ has been performed by Matsumoto, Ooi and

Kuroya. It was reported[1] that the six-membered chelate ring has a chair form and the bond angles around cobalt and nitrogen atoms are all larger than those in the corresponding ethylenediamine complex. The difference in stabilities of five- and six-membered chelate rings may be reflected in the labilities of ethylenediamine and trimethylenediamine complexes.

The preliminary data by Pearson, Boston and Basolo[2] show that *trans*-$CoCl_2tn_2^+$ hydrolyzes rapidly although the rate of hydrolysis of the mixed complex *trans*-$CoCl_2entn^+$ is only ten times as large as that of *trans*-$CoCl_2en_2^+$. However the rate of carbonate exchange of $CoCO_3tn_2^+$ was reported to be much smaller than that of $CoCO_3en_2^+$ ion.[3] Thus it seems quite necessary to compare the chemistry of trimethylenediamine complexes with that of the corresponding ethylenediamine complexes in more detailed fashion. This paper reports several compounds derived from *trans*-dichlorobis(trimethylenediamine)cobalt(III) chloride by the ligand substitution reactions in methanol.

Experimental

The starting material *trans*-[$CoCl_2tn_2$]Cl was synthesized according to the methods by Bailar and Work,[4] and Werner.[5] The latter method *via* [$Co(NO_2)_2tn_2$]NO_2 is preferable.

Found: C, 23.11; H, 6.59; N, 17.42; Cl, 34.44; Co, 18.97%. Calcd for $C_6H_{20}N_4Cl_3Co$=[$CoCl_2tn_2$]Cl: C, 23.00; H, 6.38; N, 17.87; Cl, 33.94; Co, 18.83%.

1) Nitrato Complexes. A methanol solution of silver nitrate (0.65 g, 3.8 mmol) in 15 m*l* was added to a methanol solution of *trans*-[$CoCl_2tn_2$]Cl (1.2 g, 3.8 mmol) in 120 m*l*. Silver chloride produced was warmed and filtered off during hot. The filtrate was evaporated up to about 50 m*l* and kept standing overnight at room temperature. Bright green leaflet crystals deposited, which were filtered, washed with methanol and dried in air. Yield: 1.1 g. The same compound was also produced by the reaction between *trans*-[$CoCl_2tn_2$]Cl and potassium nitrate in hot methanol.

Found: C, 21.45; H, 6.02; N, 21.14%. Calcd for $C_6H_{20}N_5O_3Cl_2Co$=[$CoCl_2tn_2$]NO_3: C, 21.19; H, 5.93; N, 20.59%.

When 1.3 g (7.6 mmol) or more than 2.0 g (11.8 mmol) of silver nitrate was employed in the above reaction, dark green crystals of [$CoCl(NO_3)tn_2$]NO_3 or russety plates of [$Co(NO_3)_2tn_2$]NO_3 were obtained, respectively.

Found: C, 19.87; H, 5.75; N, 22.68%. Calcd for $C_6H_{20}N_6O_6ClCo$=[$CoCl(NO_3)tn_2$]NO_3: C, 19.66; H, 5.50; N, 22.92%.

Found: C, 18.70; H, 5.11; N, 25.14; Co, 14.96%. Calcd for $C_6H_{20}N_7O_9Co$=[$Co(NO_3)_2tn_2$]NO_3: C, 18.33; H, 5.13; N, 24.94; Co, 14.99%.

2) Isothiocyanato Complexes. A methanol solution of potassium thiocyanate (1.5 g, 15.4 mmol) in 50 m*l* was added gradually into a methanol solution of *trans*-[$CoCl_2tn_2$]Cl (1.0 g) in 140 m*l*. The mixture was cooled with ice and salt for several hours. Deposited green needles were separated, washed with methanol and dried in air. Yield: 0.9 g.

Found: C, 25.28; H, 6.65; N, 20.15%. Calcd for $C_7H_{20}N_5SCl_2Co$=[$CoCl_2tn_2$]SCN: C, 25.16; H, 6.03; N, 20.95%.

To a hot solution of *trans*-[$CoCl_2tn_2$]Cl (1.0 g, 3.1 mmol) in 200 m*l* of methanol was added 0.3 g (3.1 mmol) of solid potassium thiocyanate. The solution was heated for about 5 min and then kept standing overnight at room temperature. Purple crystals of [CoCl(NCS)tn_2]Cl were obtained. Yield: 0.8 g. The same compound was also produced when 1.0 g of *trans*-[$CoCl_2tn_2$]SCN was dissolved in about 200 m*l* of hot methanol, and the solution was heated for about 5 min, concentrated to about 50 m*l* under reduced pressure and cooled in ice overnight. Yield: 0.6 g. In this experiment a prolonged heating should be avoided since a disproportionation to dichloro- and dithiocyanato-complexes occurs.

Found: C, 25.03; H, 6.26; N, 20.36%.

When twice as many moles or large excess of potassium thiocyanate was employed against the starting dichloro-complex in the above experiment, purple crystals of [$Co(NCS)_2tn_2$]Cl (yield 0.85 g) or dark purple crystals of [$Co(NCS)_2tn_2$]SCN (yield 0.7 g) were obtained, respectively.

Found: C, 27.17; H, 5.79; N, 23.30%. Calcd for $C_8H_{20}N_6S_2ClCo$=[$Co(NCS)_2tn_2$]Cl: C, 26.78; H, 5.62; N, 23.42%.

Found: C, 28.50; H, 5.42; N, 25.66%. Calcd for $C_9H_{20}N_7S_3Co$=[$Co(NCS)_2tn_2$]SCN: C, 28.34; H, 5.28; N, 25.71%.

If solid potassium thiocyanate is added in excess to a methanol solution of [CoCl(NCS)tn_2]Cl or [$Co(NCS)_2$-tn_2]Cl, and the solution is cooled, the respective thiocyanate is obtained, [CoCl(NCS)tn_2]SCN appearing as grayish blue needles.

Found: C, 27.43; H, 6.04; N, 22.68%.

3) Nitro Complexes. A cold methanol solution of sodium nitrite (0.30 g, 4.37 mmol) was added gradually to a cold solution of *trans*-[$CoCl_2tn_2$]Cl (1.37 g, 4.37 mmol) in 200 m*l* methanol under vigorous agitation. The solution was evaporated up to about 150 m*l* under reduced pressure at room temperature and then cooled for a few hours with ice and salt. Orange red powder was obtained. Yield: 0.35 g.

Found: C, 22.27; H, 6.29; N, 20.20%. Calcd for $C_6H_{20}N_5O_2Cl_2Co$=[$CoCl(NO_2)tn_2$]Cl: C, 22.23; H, 6.22; N, 21.61%.

If the above reaction mixture is heated for a while, evaporated on a hot water bath, and then cooled in ice, brown crystals were obtained. Yield: 0.97 g. Results of the elemental analysis are quite the same with the above compound.

Found: C, 21.90; H, 6.28; N, 19.85%.

1) K. Matsumoto, S. Ooi and H. Kuroya, Preprints for the 17th Annual Meeting of the Chemical Society of Japan (1964), 31W08.

2) R. G. Pearson, C. R. Boston and F. Basolo, *J. Am. Chem. Soc.*, **75**, 3089 (1953).

3) J. E. Boyle and G. M. Harris, *ibid.*, **80**, 782 (1958).

4) J. C. Bailar, Jr., and J. B. Work, *ibid.*, **88**, 232 (1946).

5) A. Werner, *Ann.*, **386**, 265 (1912).

Solid sodium nitrite (1.5 g, 21.7 mmol) was added to a hot solution of *trans*-[$CoCl_2tn_2$]Cl (1.0 g) in about 100 ml of methanol, and heated for a while. The solution changed from green to yellow, and was kept standing overnight at room temperature. Lustrous yellow crystals were separated. The filtrate was evaporated to about half the volume, and further quantity of crystals were obtained. All crystals were joined, washed with methanol and dried in air.

Found: C, 20.33; H, 5.91; N, 27.22%. Calcd for $C_6H_{20}N_7O_6Co$=[$Co(NO_2)_2tn_2$]NO_2: C, 20.88; H, 5.84; N, 28.40%.

Results and Discussion

The infrared absorption spectrum of dinitrobis(trimethylenediamine)cobalt (III) nitrite derived from *trans*-[$CoCl_2tn_2$]Cl in methanol completely coincides with that of *trans*-[$Cc(NO_2)_2tn_2$]NO_2 which was synthesized by the reaction between potassium hexanitrocobaltate(III) and trimethylenediamine in water according to the Werner's direction.[5] The other compounds now obtained are all new compounds and their structures are very interesting.

Several attempts have been made to distinguish between geometrical isomers of cobalt (III) bis(ethylenediamine) complexes by means of the infrared absorption data.[6] Baldwin[7] suggested that the most consistent variation between the spectra of cis and trans isomers is found in the CH_2 rocking region (900—870 cm^{-1}), cis isomers showing two peaks while trans isomers only one, and that these bands are insensitive to natures of A, B and X in complexes of the type [$CoABen_2$]X.

TABLE 1. THE CH_2 ROCKING FREQUENCIES OF [$CoABtn_2$]X COMPLEXES DERIVED FROM *trans*-[$CoCl_2tn_2$]Cl IN METHANOL

Compound	Frequency, cm^{-1}
trans-[$CoCl_2tn_2$]Cl*	889
[$CoCl_2tn_2$]NO_3	887
[$CoCl(NO_3)tn_2$]NO_3	891
[$Co(NO_3)_2tn_2$]NO_3	895
[$CoCl_2tn_2$]SCN	886
[$CoCl(NCS)tn_2$]Cl	885
[$CoCl(NCS)tn_2$]SCN	885
[$Co(NCS)_2tn_2$]Cl	889, 895
[$Co(NCS)_2tn_2$]SCN	890
[$CoCl(NO_2)tn_2$]Cl (red)	896
[$CoCl(NO_2)tn_2$]Cl (brown)	895
trans-[$Co(NO_2)_2tn_2$]NO_2	899

* Starting material

As shown in Table 1 these diacidobis(trimethylenediamine)cobalt(III) complexes, except [$Co(NCS)_2tn_2$]Cl, show a single peak respectively in the CH_2 rocking region. If Baldwin's empirical rule can be applied to these trimethylenediamine complexes, all these compounds are considered to be trans isomers. Diisothiocyanatobis(trimethylenediamine)cobalt(III) chloride shows two distinct peaks at 889 and 895 cm^{-1}. Therefore it should be assigned the cis configuration according to this criterion. It is not conceivable, however, that only this compound is a cis isomer while the corresponding thiocyanate [$Co(NCS)_2tn_2$]SCN assumes the trans configuration. Baldwin's rule must be concluded not to hold in this case. The X-ray analysis of [$Co(NO_3)_2tn_2$]NO_3 is now being performed by Komiyama and his coworkers. According to their preliminary report[8] crystals are monoclinic and the cobalt atom lies at the center of symmetry, certifying the trans configuration of this complex ion.

It is well known that methanol is much more favorable than water for the trans form of dichlorobis(ethylenediamine)cobalt(III) complex.[9] Such a solvent effect is considered to be due to the lesser power than water of stabilizing the cis form by solvation, and will also apply to the diacidobis(trimethylenediamine)cobalt(III) complexes. On the contrary water will be suitable in synthesizing the corresponding cis compounds.

Two compounds, orange red and brown crystals, were obtained whose analytical data both correspond to the formula [$CoCl(NO_2)tn_2$]Cl, suggesting that they are isomeric. The red form is unstable and easily transformed by heat to the brown form. The frequencies of CH_2 rocking vibration of these compounds indicate that both of them have the trans configuration. The other possibility to be considered is the linkage isomerism. It has been reported[10] that nitropentaamminecobalt(III) shows the NO_2 symmetric stretching peak at 1310 cm^{-1} but nitritopentaamminecobalt(III) at 1065 cm^{-1}. In the present case the less stable red form of this compound shows a very strong peak at 1170 cm^{-1}, but the brown form does not have such a peak. Thus the red isomer can safely be concluded to be a nitrito complex, [$CoCl(ONO)tn_2$]Cl.

Formation of nitritopentaamminecobalt(III) complex by the reaction between aquopentaamminecobalt(III) and nitrous acid in water is believed to

6) M. N. Hughes and W. R. McWhinnie, *J. Inorg. Nucl. Chem.*, **28**, 1659 (1966).

7) M. E. Baldwin, *J. Chem. Soc.*, **1960**, 4369.

8) H. Yazaki, I. Onishi and Y. Komiyama, Reported at the 17th Symposium on the Chemistry of Metal Coordination Compounds of the Chemical Society of Japan, Hiroshima, December, 1967.

9) D. D. Brown and R. S. Nyholm, *J. Chem. Soc.*, **1953**, 2696; W. R. Fitzgerald and D. W. Watts, *J. Am. Chem. Soc.*, **89**, 821 (1967).

10) R. B. Penland, T. J. Lane and J. V. Quagliano, *J. Am. Chem. Soc.*, **78**, 887 (1956); K. Nakamoto, "Infrared Spectra of Inorganic and Coordination Compounds," Wiley, New York, N. Y. (1963), p. 155.

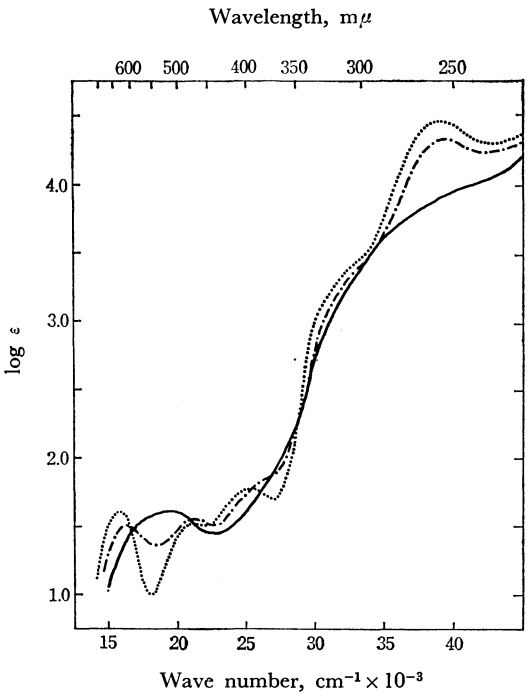

Fig. 1. Absorption spectra in methanol.
—— *trans*-[$Co(NO_3)_2tn_2$]NO_3
—·— *trans*-[$CoCl(NO_3)tn_2$]NO_3
····· *trans*-[$CoCl_2tn_2$]NO_3

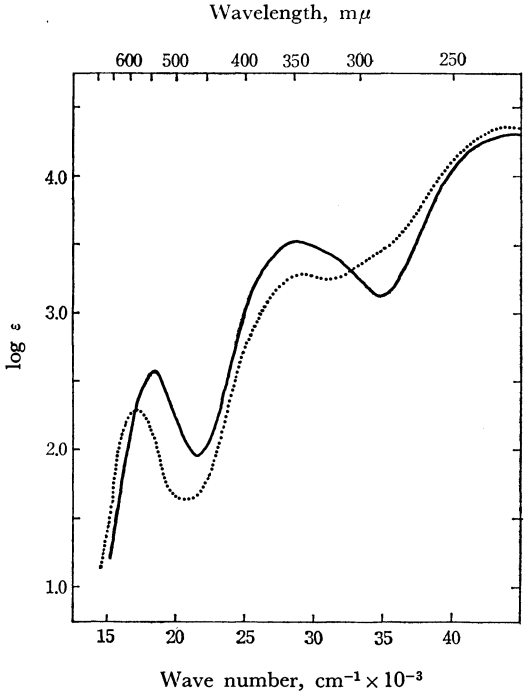

Fig. 2. Absorption spectra in methanol.
—— *trans*-[$Co(NCS)_2tn_2$]SCN
····· *trans*-[$CoCl(NCS)tn_2$]Cl

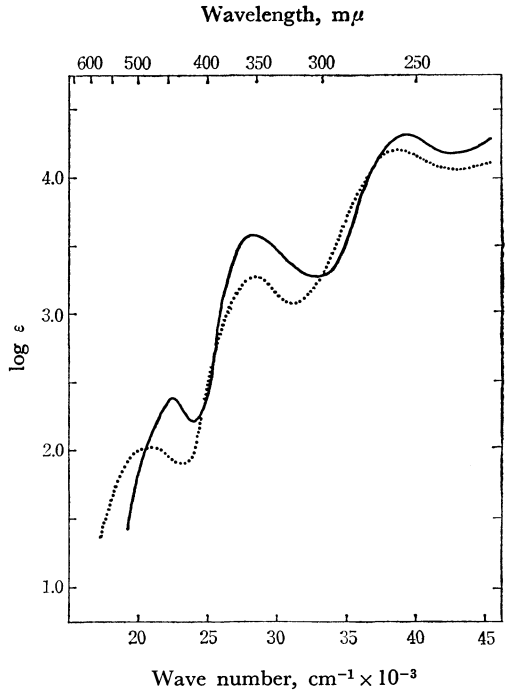

Fig. 3. Absorption spectra in methanol.
—— *trans*-[$Co(NO_2)_2tn_2$]NO_2
····· *trans*-[$CoCl(NO_2)tn_2$]Cl

proceed as a nitrosation reaction keeping the Co–O bond intact.[11] In the present case, however, the chloronitrito complex was obtained by the reaction between the dichloro complex and sodium nitrite in methanol. It is not certain whether the overall reaction proceeds *via* the solvolysis process or not, but some novel reaction pathway might be passed through. Kinetic and tracer studies will soon be undertaken to clarify the reaction mechanism.

Absorption spectra of several trimethylenediamine complexes are shown in Figs. 1—3. The first band of $CoClXtn_2^+$ shifts to the shorter wavelength side progressively as the acido group X is substituted from Cl^- to NO_3^-, NCS^- and NO_2^- in accordance with the widely accepted order in the spectrochemical series.[12] Comparison of absorption data of these *trans*-diacidobis(trimethylenediamine)cobalt(III) complexes with corresponding bis(ethylenediamine) complexes as shown in Table 2 clearly indicates that trimethylenediamine is a weaker field ligand than ethylenediamine.

Aquation reactions were examined preliminarily. Dichloro complexes hydrolyze quickly, and the

11) F. Basolo and R. G. Pearson, "Mechanisms of Inorganic Reactions," Wiley, New York, N. Y. (1967), p. 230.

12) T. M. Dunn, "Modern Coordination Chemistry," ed. by J. Lewis and R. G. Wilkins, Interscience Publishers, New York, N. Y. (1960), p. 266.

TABLE 2. ABSORPTION BANDS OF SOME *trans*-DIACIDOBIS(DIAMINE)COBALT (III) COMPLEXES

Compound	Solvent	λ_{max}, mμ (ε)			
$[CoCl_2tn_2]Cl$	MeOH	650 (38.3)	475 (29.0)	398 (54.8)	259 (21330)
$[CoCl_2en_2]Cl$*	MeOH-Water	625 (34.7)	450 (25.2)	385 (43.7)	252 (20500)
$[CoCl(NO_3)tn_2]NO_3$	MeOH	610 (32.0)	470 (36.4)	380sh (69.4)	255 (21200)
$[Co(NO_3)_2tn_2]NO_3$	MeOH	510 (40.5)	310sh	250—260sh	
$[Co(NO_3)_2en_2]NO_3$**	60% $HClO_4$ aq	517 (63)	455 (40)	353 (80)	
$[CoCl(NCS)tn_2]Cl$	MeOH	580 (203)	350 (1796)	227 (22300)	
$[CoCl(NCS)en_2]SCN$*	MeOH-Water	520 (175)	335 (2500)		
$[Co(NCS)_2tn_2]SCN$	MeOH	550 (331)	348 (3292)	223 (20000)	
$[Co(NCS)_2en_2]SCN$*	MeOH-Water	515 (365)	335 (3250)		
$[CoCl(NO_2)tn_2]Cl$	MeOH	500 (87)	353 (1475)	259 (21900)	
$[CoCl(NO_2)en_2]NO_3$*	MeOH-Water	466 (81)	340 (1380)	245 (15500)	
$[Co(NO_2)_2tn_2]NO_2$	MeOH	450 (222)	358 (3900)	255 (21500)	
$[Co(NO_2)_2en_2]NO_2$*	MeOH-Water	433 (220)	347 (4200)	250 (12400)	

* F. Basolo, *J. Am. Chem. Soc.*, **72**, 4393 (1950).

** Y. Shimura, R. Tsuchida, *Nippon Kagaku Zassi* (*J. Chem. Soc. Japan, Pure Chem. Sect.*), **77**, 734 (1956).

half time of about 6 min was observed at 0°C in either case. Chloronitrato and dinitrato complexes react more rapidly and the half time was about 1 min. On the other hand diisothiocyanato and dinitro complexes are quite inert, whose absorption spectra in aqueous solutions do not change even after 24 hr at room temperature. Detailed features of these reactions must await further investigations.

The authors are indebted to Mr. Jun-ichi Gohda and Mrs. Hiromi Aotani for the organic elemental analyses and infrared measuerments.

BULLETIN OF THE CHEMICAL SOCIETY OF JAPAN VOL. 42 140—145 (1969)

Polarographic Studies of Dissolved Oxygen in DMSO-Water Mixtures

Taitiro FUJINAGA, Kosuke IZUTSU and Takeo ADACHI

Department of Chemistry, Faculty of Science, Kyoto University, Sakyo-ku, Kyoto

(Received May 29, 1968)

The solubility and polarographic behavior of dissolved oxygen have been investigated in air-saturated DMSO-water mixtures at 25°C and 45°C. The first oxygen wave, which corresponds to one-electron reduction to superoxide ions in water-poor DMSO solutions of 0.1 M Et_4NClO_4, changes to a two-electron process in the range of water content between 10 and 30% because of the protonation reaction due to water. The rate of protonation is potential-dependent. The rate also depends on the species and the concentrations of the supporting electrolytes. The temperature effect is small. Using the solubility and polarographic data obtained, the polarographic diffusion coefficients of oxygen in the mixed solvent have been calculated.

The polarographic reduction of dissolved oxygen has been studied by a number of authors using different electrodes and solvents (for a survey, see Ref. 1). At tha dropping mercury electrode, dissolved oxygen in an aqueous solution usually gives two waves, each corresponding to a two-electron reduction. Recently, however, several authors have found that the reduction of oxygen in dipolar aprotic solvents occurs in two steps, and that the first wave is a one-electron process involving

1) K. J. Vetter, "Elektrochemische Kinetik," Springer Verlag, Berlin (1961), p. 518; R. Takahashi, *Talanta*, **12**, 1211 (1965).

the formation of superoxide anion radicals.[2-7] The effects of acids[2,3,5] and metal cations[4,7] on oxygen waves in aprotic solvents have been studied, but a detailed investigation of the effect of water on the polarographic behavior of dissolved oxygen does not seem to have been undertaken yet. In the present work, we studied the behavior of oxygen in the mixed solvent of DMSO and water.

Apparatus and Reagents

Dc and ac polarograms were recorded with a Yanagimoto Polarograph, PA-102. The constant current source for chronopotentiometry was constructed from a high dc voltage source (225V) with large resistors. Potential-time curves were measured using a Shimadzu pH meter as a high input-impedance preamplifier and a Varicorder VR-100G as a voltage recorder. An H-type cell with a fine porosity sintered glass disk between the two compartments was used, except in the determination of the solubility of dissolved oxygen. In measurement, a sample solution was put in both compartments of the cell and aqueous SCE with a tip of fine porosity sintered glass disk was inserted in the reference compartment. Contamination from the aqueous SCE into the sample compartment of the H-type cell was negligible during measurement. The characteristics of the DME were $m=0.73$ mg/sec and $t=4.0$ sec at -0.4 V *vs.* SCE in a 0.1 M Et_4NClO_4 aqueous solution at 25°C. For the chronopotentiometric measurement, a glassy carbon disk electrode 3 mm in diameter was used. A mercury-coated rotating disk electrode with a diameter of 0.5 mm was prepared by plating gold on the surface of the platinum disk electrode and by amalgamating it. The electrode was rotated at 800 rpm in measuring the current-potential curves. The viscosity of the mixed solvent was measured with a Ostwald viscometer. Experiments were carried out at 25 ± 0.1°C or at 45 ± 0.1°C.

Dimethyl sulfoxide (DMSO) obtained from the Katayama Chemicals Co. was vacuum distilled twice. The water content just after distillation was less than 0.05%, as determined through a Karl Fischer titration. *n*-Bu_4NClO_4 was prepared from an aqueous solution of *n*-Bu_4NBr by adding an equivalent amount of concentrated perchloric acid, and was purified by recrystallization from ethanol solutions. *n*-Bu_4NBr was prepared by refluxing acetonitrile solutions of tri-*n*-butylamine and *n*-butyl bromide for 36 hr.[8] After evaporation of acetonitrile, *n*-Bu_4NBr was recrystallized several times from ethyl acetate. *n*-Pr_4NClO_4 was prepared by neutralizing 10% solutions of *n*-Pr_4NOH, obtained from the Wako Pure Chemicals Industries, Ltd., with perchloric acid and was purified by recrystallization from ethanol. Et_4NClO_4 was prepared by adding an equivalent amount of perchloric acid to Et_4NI in water and was recrystallized from water. Anhydrous $KClO_4$ was of analytical reagent grade and was used without further purification.

Results and Discussion

Solubility of Oxygen in DMSO-Water Mixtures. The concentration of dissolved oxygen in air-saturated DMSO-water mixtures was determined polarographically, because the application of the Winkler method was difficult for systems containing 0.1 M Et_4NClO_4. The dissolved oxygen in the air-saturated 0.1 M Et_4NClO_4 solution of $(100-x)$% DMSO - x%water mixture was determined as follows: In a 100 m*l* tall beaker, thermostated at 25°C or 45°C, 40.0 m*l* of 0.1 N NaOH, 5.0 m*l* of x% DMSO - $(100-x)$% water mixture and a magnetic stirrer were taken. The beaker was closed with a silicon rubber stopper with holes through which DME and aqueous SCE were passed, and with inlets and outlets for nitrogen and an inlet for the sample solution. After the solution was deaerated with nitrogen, the residual current was recorded between -0.3 and -0.5 V *vs.* SCE. Then, while the solution in the beaker was being stirred with a magnetic stirrer and nitrogen gas passed over the solution, 5.00 m*l* of the sample solution of 0.1 M Et_4NClO_4 in a $(100-x)$% DMSO - x% water mixture, which has been saturated with air in a thermostat controlled at 25°C or 45°C, was put with a pipette into the bottom of the beaker. After the solution has been sufficiently mixed, stirring was stopped and the current recorded between -0.3 and -0.5 V *vs.* SCE. By comparing the

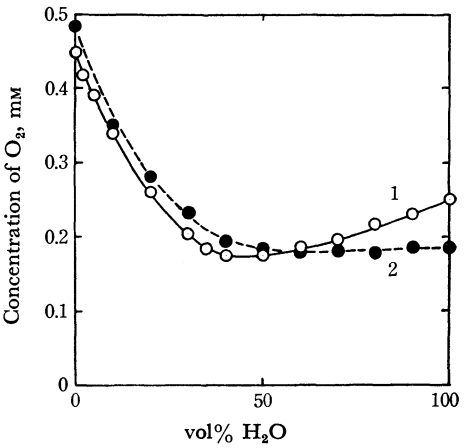

Fig. 1. Solubility of oxygen in air-saturated DMSO-water mixtures containing 0.1M Et_4NClO_4. Curve 1 is at 25°C and curve 2 at 45°C.

2) M. E. Peover and B. S. White, *Electrochim. Acta*, **11**, 1061 (1966); *Chem. Commun.*, **10**, 183 (1965).
3) D. L. Maricle and W. G. Hodgson, *Anal. Chem.*, **37**, 1562 (1965).
4) L. Johnson, K. H. Pool and R. E. Hamm, *ibid.*, **38**, 183 (1966).
5) D. T. Sawyer and J. L. Roberts, Jr., *J. Electroanal. Chem.*, **12**, 106 (1966).
6) M. E. Peover and J. S. Powell, *J. Polarog., Soc.*, **12**, 106 (1966).
7) L. Johnson, K. H. Pool and R. E. Hamm, *Anal. Chem.*, **39**, 888 (1967).
8) R. U. Lemieux and J. Hayami, *Can. J. Chem.*, **43**, 2162 (1965).

diffusion currents obtained for sample solutions of various values of x, the relative solubilities of oxygen in the air-saturated DMSO-water mixtures could be determined. The absolute solubilities could be calculated by measuring the diffusion current for a sample of air-saturated pure water and by assuming the solubilities of oxygen in the air-saturated pure water to be 0.254 mM at 25°C and 0.193 mM at 45°C, respectively.[9] The results are shown in Fig. 1 and Table 1. The reproducibility of the results was within ±2%. The solubility of oxygen at 25°C became minimum in the range 40 to 50% water. In a water-free, 0.1 M Et_4NClO_4 DMSO solution, the solubility was 0.44 mM, which is in agreement with the result of Sawyer and Roberts.[5] At 45°C, the solubility of oxygen was approximately constant over a water content of 50 to 100%. With a smaller water content, the solubility increased rapidly, as in the case at 25°C.

Table 1. Solubility and diffusion coefficient of oxygen in air-saturated DMSO-water mixtures containing 0.1M Et_4NClO_4

vol% H_2O	Solubility of O_2, mM	Viscosity η, cp	$D\times10^5$ cm²/sec	$D\eta\times10^5$ cp·cm²/sec
		at 25°C		
0	0.44_6	1.95	(2.7_6)	(5.3_8)
10	0.34_0	2.55	1.7_2	4.3_8
20	0.26_0	3.25	1.3_5	4.3_9
30	0.20_5	3.65	1.1_9	4.3_5
40	0.17_5	3.42	1.0_9	3.7_3
50	0.17_5	2.95	1.1_5	3.3_9
60	0.18_2	2.26	1.3_9	3.1_4
70	0.19_5	1.81	1.4_9	2.7_0
80	0.21_8	1.42	1.5_5	2.2_0
90	0.23_0	1.05	1.7_8	1.8_7
100	0.25_1	0.85	1.9_9	1.6_9
		at 45°C		
0	0.49_2	1.39	(3.3_5)	(4.6_6)
10	0.35_2	1.72	2.4_7	4.2_5
20	0.28_1	1.97	2.1_6	4.2_6
30	0.32_3	2.18	1.8_6	4.0_5
40	0.19_3	2.07	1.9_1	3.9_5
50	0.18_6	1.83	1.9_2	3.5_1
60	0.18_0	1.44	2.0_4	2.9_4
70	0.18_2	1.14	2.3_0	2.6_2
80	0.17_9	0.93	2.5_6	2.3_8
90	0.18_4	0.72	2.7_4	1.9_7
100	0.18_5	0.60	2.9_0	1.7_4

D and $D\eta$ in water-free DMSO solution were determined from the height of the first wave.

The viscosities of DMSO-water mixtures containing 0.1 M Et_4NClO_4 were measured with an Ostwald viscometer at 25°C and 45°C. The results were almost in agreement with those of Cowie and Toporowski[10] determined for Et_4NClO_4-free mixed solvents.

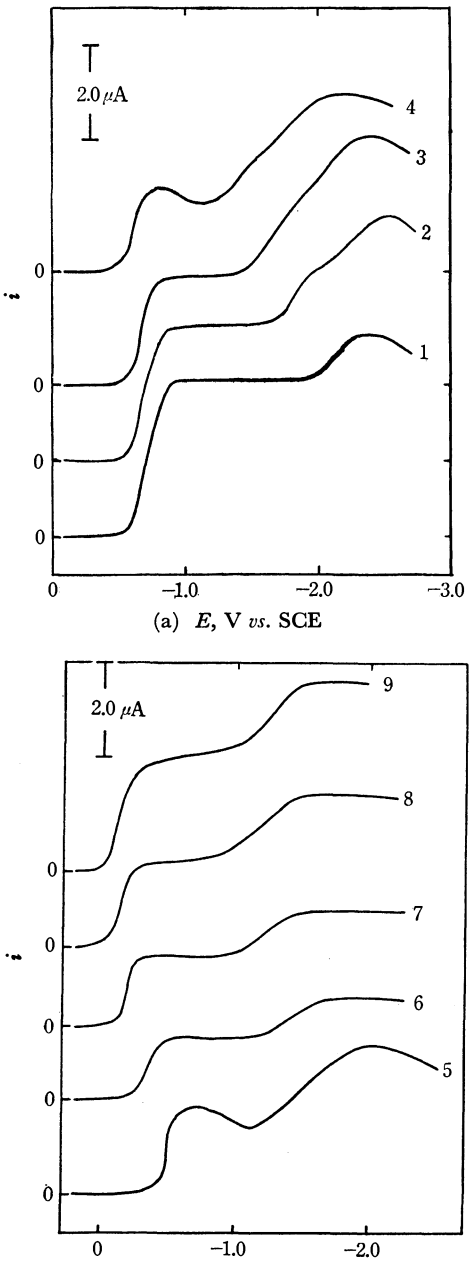

Fig. 2. Oxygen waves in air-saturated DMSO-water mixtures containing 0.1M Et_4NClO_4 at 25°C.
Water contents are:
1, water-free; 2, 1%; 3, 6%; 4, 15%, 5, 25%; 6, 40%; 7, 60%; 8, 80%; and 9, 100%.

9) "Mizu no Bunseki (Analysis of Water)," ed. by Hokkaido Div. of Japan Soc. for Analytical Chemistry, Kagakudojin, Kyoto (1966), p. 181.

10) J. M. G. Cowie and P. M. Toporowski, *Can. J. Chem.*, **39**, 2280 (1961).

Polarographic Behavior of Oxygen in Mixed Solvents. The curves in Fig. 2 are polarograms of dissolved oxygen in air-saturated 0.1 M Et_4NClO_4 solutions in DMSO-water mixtures. In a water-free solution, two waves were obtained at -0.77 and -2.2 V, respectively. The first wave corresponded to a one-electron reduction to superoxide anion radicals and the second wave to the formation of peroxide anions.[2-7] As reported in the literature,[4] the height of the second wave is smaller than that of the first, even after correction for change in drop-time. The second wave was very sensitive to a small amount of water and, in the presence of more than 0.1% water, the wave shifted to more positive potentials and the wave height was much increased. Increase in the second wave height occurred because peroxide ions were further reduced to hydroxyl ions. The effects of water on the half-wave potential of the first wave and on the potential at which the second wave began to occur are given in Fig. 3. When the water content was 6%, the

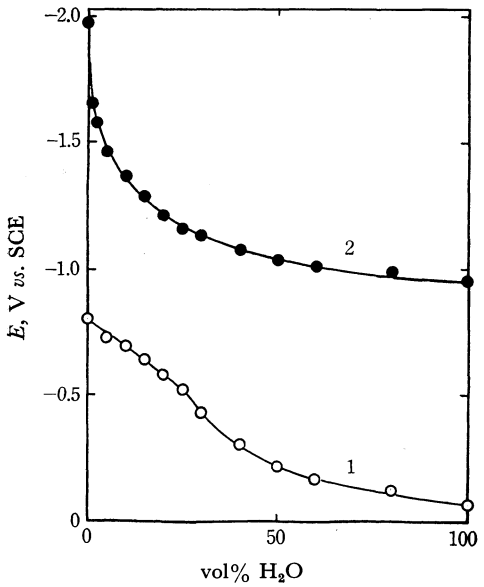

Fig. 3. Half-wave potential of the first wave (curve 1) and the potential at the beginning of the second wave (curve 2) of oxygen in air-saturated DMSO-water mixtures containing 0.1M Et_4NClO_4 at 25°C.

first wave still corresponded to a one-electron reduction, but the total wave approximately to a four-electron reduction (formation of hydroxyl ions). If the water content became greater than 10%, the current at the beginning of the plateau of the first wave increased because some superoxide ions became protonated by water and were further reduced to peroxide ions. Thus, between a water content of 15 and 30%, a distinct minimum was obtained just before the second wave. When the water content was greater than 35%, the minimum disappeared and the first and the second waves became approximately equal in height, both corresponding to two-electron reductions. A similar minimum to that obtained in a 0.1M Et_4NClO_4 solution containing water between 15 and 30% was observed even in solutions containing other supporting electrolytes, such as 0.1M n-Bu_4NClO_4, 0.1M n-Pr_4NClO_4 and 0.1M $KClO_4$. The addition of surface active substances, halide ions and hydroxyl ions did not influence the shape of the oxygen wave. Moreover, such a minimum was obtained even at a mercury-coated disk electrode rotating at 800 rpm. This is probably due to the fact that the rate of the protonation reaction of superoxide ions is potential dependent, and the reaction is faster at more positive potentials. This potential dependence of the protonation reaction may be caused by a change in the surface concentration of superoxide anions with electrode potential: when the potential becomes more negative, negatively charged superoxide ions will be repelled more strongly from the electrode and the surface concentration will become smaller.

The ratio of the total wave height $(i_d)_t$ to that of the first wave $(i_d)_1$ was calculated after correction for change in drop time. A simple Ilkovic equation was assumed for this correction. The results are shown in Fig. 4. Curve 1 was obtained by measuring the height of the first wave at the potential at which the current became maximum, and curve 2 at the potential at which the current became minimum. From these curves, it is apparent that the total wave, which is approximately a two-

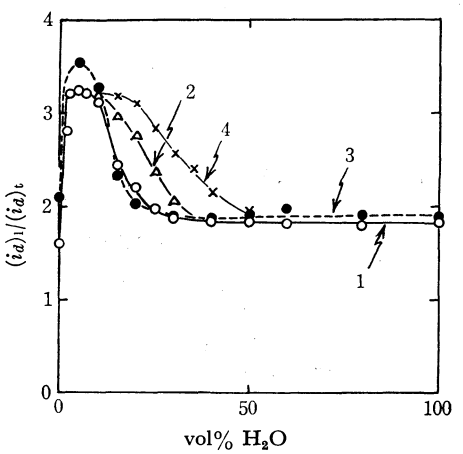

Fig. 4. Ratio of the total wave height to that of the first wave of dissolved oxygen in air-saturated 0.1M (curves 1, 2 and 3) and 0.01M (curve 4) Et_4NClO_4 solutions. Curves 1, 2 and 4 are at 25°C and curve 3 at 45°C. Curves 1 and 3 were obtained by measuring the maximum current of the first wave and curves 2 and 4 the minimum current.

electron reduction in water-free DMSO solution, approaches a four-electron reduction by the addition of several percents of water. The ratio does not become four and is much smaller, probably due to the fact that the drop time at the second wave is so small compared to that at the first wave that the diffusion current may significantly deviate from that given by the Ilkovic equation. The first wave, on the other hand, changed from a one- to a two-electron process between a water content of about 10 and 30%, both at 25°C (curves 1 and 2) and at 45°C (curve 3). The temperature effect was not large. The water content necessary to convert the first wave from a one-electron reduction to a two-electron reduction changed considerably with species and concentrations of supporting electrolytes. When the concentration of the supporting electrolyte decreased, the necessary water content increased, as in curve 4, Fig. 4. The necessary water content also increased with the species of supproting electrolyte in the following order (Fig. 5):

$$KClO_4 < Et_4NClO_4 < n\text{-}Pr_4NClO_4 < n\text{-}Bu_4NClO_4$$

The larger the ionic radius of the cation of the supporting electrolyte, the more water was necessary for the first wave to change from a one-electron process to a two-electron one.

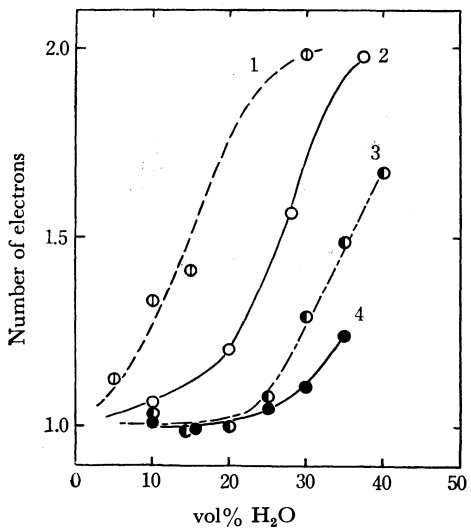

Fig. 5. Number of electrons taking part in the first wave of oxygen in various supporting electrolytes at 25°C.
Supporting electrolytes are: 1, 0.1M $KClO_4$; 2, 0.1M Et_4NClO_4; 3, 0.1M n-Pr_4NClO_4; and 4, 0.1M n-Bu_4NClO_4. Estimated from the current at the minimum of the first wave.

The addition of Et_4NOH to the solution containing water between 15 and 30% did not influence the behavior of the oxygen wave, though a big increase in pH was expected due to hydroxyl ions. From this result, the protonation reaction seems to occur as a reaction between a superoxide anion and a water molecule, and not through a reaction between a superoxide anion and a proton produced by the dissociation of water.

The first wave of oxygen in water-free dipolar aprotic solvents has been reported to be very reversible ac polarographically.[2,6] In an aqueous, unbuffered neutral solution, on the other hand, only a small ac wave can be obtained.[11] In this report, ac polarograms were measured in DMSO-water mixtures and the values of $i_{ac}/i_{dc}\cdot t^{1/2}$ were calculated as a measure of the reversibility of the first oxygen wave. The results are shown in Fig. 6.

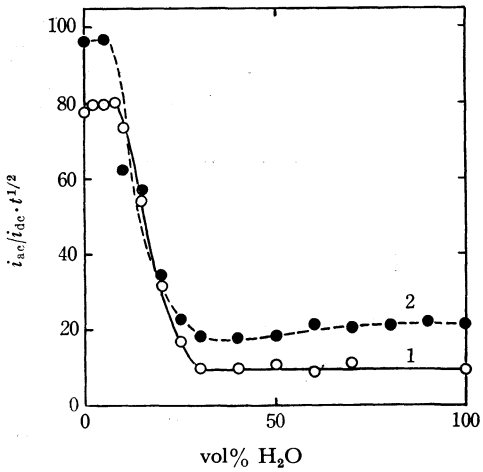

Fig. 6. $i_{ac}/i_{dc}\cdot t^{1/2}$ values for the first wave of oxygen in 0.1M Et_4NClO_4 solutions at 25°C (curve 1) and at 45°C (curve 2).

In solutions at 25°C with a water concentration below 8%, fairly high ac waves with values of $i_{ac}/i_{dc}\cdot t^{1/2}$ of about 80 were obtained. In the range of water concentration between 10 and 30%, in which the first dc wave changed from a one-electron to a two-electron process, the value of $i_{ac}/i_{dc}\cdot t^{1/2}$ decreased gradually, showing a decrease in the reversibility of the electrode reaction. At a water content above 30%, it was almost constant at 10. The ac polarographic behavior at 45°C was approximately similar to that at 25°C.

Reverse chronopotentiometry at the glassy carbon electrode seems to provide, though qualitatively, knowledge concerning the lifetime of superoxide anion radicals. In oxygen-saturated DMSO-water mixtures, potential-time curves for the reduction of oxygen at constant current were measured. Before the transition time of the first wave was attained, the direction of the current was reversed and the potential-time curves for the re-oxidation of the superoxide ions were recorded. From the chronopotentiograms obtained, the time intervals

11) S. Hacobian, *Australian. J. Chem.*, **6**, 211 (1953).

for the reduction (τ_{red}) and the transition time for the re-oxidation (τ_{ox}) were measured. In Fig. 7,

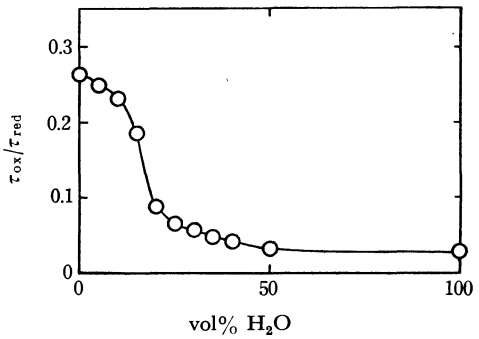

Fig. 7. Ratio of τ_{ox}/τ_{red} obtained by reverse chronopotentiometry at the glassy carbon electrode in oxygen-saturated 0.1M Et_4NClO_4 solutions. τ_{red} = 30 sec.

the values τ_{ox}/τ_{red} are plotted for the case in which $\tau_{red}=30$ sec. Because the mechanisms of further reductions of superoxide anion radicals at the glassy carbon electrode are still unestablished and are probably somewhat different from those at the dropping mercury electrode, the results cannot be analysed theoretically to determine the lifetime of the radical anions. The value of τ_{ox}/τ_{red} for a water concentration below 10%, however, seems to show that the superoxide anions are fairly stable chronopotentiometrically. The rapid decrease of the ratio between 10 and 30% water indicates that superoxide ions disappear rapidly in water-rich solutions in agreement with the results of dc and ac polarography at the dropping mercury electrode.

Polarographic Diffusion Coefficients of Dissolved Oxygen in Mixed Solvents. From the oxygen waves in DMSO-water mixtures, the polarographic diffusion coefficients was calculated using the modified Ilkovic equation:

$$i_d = 607nD^{1/2}Cm^{2/3}t^{1/6}(1 + AD^{1/2}m^{-1/3}t^{1/6}),$$

where the value of A was assumed to be 25. The limiting currents used in the calculation of these diffusion coefficients were confirmed to be diffusion-controlled by the linear proportionality of the currents to the oxygen concentration, and also to the square root of the height of the mercury reservoir. The results are shown in Fig. 8 and Table 1. Curves 1, 2 and 3 are the results at 25°C, and curve 1′ at 45°C. Curves 1 and 1′ were calculated using the total wave heights (assuming four-electron reduction), whereas curves 2 and 3 were calculated from the heights of the first wave. Here, the first wave was supposed to be a one-electron process at a water content below 5% (curve 2) and to be a two-electron process at a water content above

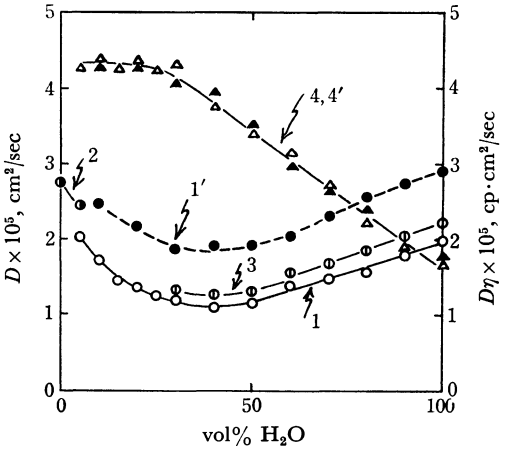

Fig. 8. Diffusion coefficient, D, of oxygen (curves 1, 2, 3 and 1′) and the product, $D\eta$, of the diffusion coefficient and the viscosity (curves 4 and 4′) of the solution containing 0.1M Et_4NClO_4. Curves 1, 2, 3 nd 4 are at 25°C and curves 1′ and 4′ at 45°C. Curves 1 and 1′ were obtained from the total wave heights, curves 2 and 3 from the first wave heights and curves 4 and 4′ were calculated using the values of curves 1 and 1′.

30% (curve 3). In these curves, the diffusion coefficients obtained by measuring the first wave are always larger than the values calculated from the total wave heights. This may be due to several reasons, such as the incompleteness of the diffusion current equation used, the occurrence of the reduction of a small amount of hydrogen peroxide at the potential at which the first wave height was measured, and the depletion effect of the depolarizer which is more pronounced at the potential of the total wave height because of the absence of appropriate maximum suppressors.[12] Moreover, when the water content is small (5% to 15%), the accuracy of the diffusion coefficients obtained from the total wave heights may decrease to some extent because the drop time is very small. Though the polarographic diffusion coefficients suffer from these limitations, they provide sufficient knowledge concerning their variation with composition of mixed solvent. From Fig. 8, the diffusion coefficient becomes a minimum at a water concentration between 30 and 50%, both at 25°C and 45°C. Curves 4 and 4′ are the products $D\eta$ of the diffusion coefficient and the viscosity of the solvent. Both at 25°C and 45°C, when the water content is greater than 30%, the value of $D\eta$ is not constant and increases almost linearly with decrease in water content, but below 30%, it is approximately constant.

12) I. M. Kolthoff and K. Izutsu, *J. Am. Chem. Soc.*, **86**, 1275 (1964).

BULLETIN OF THE CHEMICAL SOCIETY OF JAPAN VOL. 42 146—152 (1969)

Spectroscopic Studies of Polynuclear Complexes. I. Preparations and Circular Dichroisms of Tetrakis(*l*-propylenediamine)-dicobalt(III) Complexes Containing μ-Amido Group

Yoichi SASAKI, Junnosuke FUJITA and Kazuo SAITO

Department of Chemistry, Faculty of Science, Tohoku University, Katahira-cho, Sendai

(Received June 5, 1968)

New binuclear cobalt(III) complexes, $(-)_D$-$[(l\text{-pn})_2Co(\mu\text{-}NH_2,O_2)Co(l\text{-pn})_2](NO_3)_4\cdot 3H_2O$, $(+)_D$-$[(l\text{-pn})_2Co(\mu\text{-}NH_2,O_2)Co(l\text{-pn})_2]I_3\cdot 6H_2O$, $(+)_D$-$[(l\text{-pn})_2Co(\mu\text{-}NH_2,NO_2)Co(l\text{-pn})_2]Br_4\cdot 6H_2O$, $(+)_D$-$[(l\text{-pn})_2Co(\mu\text{-}NH_2,OH)Co(l\text{-pn})_2](NO_3)_4\cdot 2H_2O$ and $(-)_D$-$[(l\text{-pn})_2Co(\mu\text{-}NH_2,SO_4)Co(l\text{-pn})_2](NO_3)_3$ were prepared and their absolute configurations determined to be $\Lambda\Lambda$ on the consideration of the stereospecific coordination of *l*-propylenediamine (*l*-pn) to the metal ion. On the basis of these identifications, absolute configurations of the corresponding ethylenediamine-(en) complex ions were assigned. The nature of the d–d bands of these polynuclear complexes seems to be very similar to those of uninuclear cobalt(III) complexes. One of the two central cobalt(III) ions is regarded as a member of an asymmetric chelate ligand to the other cobalt ion, and the CD corresponding to the d–d bands appears to depend mainly on the strength of vicinal effect due to such a chelate ring.

Since the resolution of several binuclear complexes of the type, $[(en)_2Co(\mu\text{-}NH_2,a)Co(en)_2]^{n+}$,[1] and two quadrinuclear hexol complexes, $[Co\{(\mu\text{-}OH,OH)Co(NH_3)_4\}_3]^{6+}$ and $[Co\{(\mu\text{-}OH,OH)Co(en)_2\}_3]^{6+}$ [2] by Werner, there has been little work reported[3–6] on the preparation and optical properties of polynuclear cobalt(III) complexes. In 1938, Mathieu[3] measured the circular dichroism (CD) spectra of some of Werner's binuclear complexes, and concluded that the absolute configuration of the polynuclear complexes could not be assigned from their CD behavior.

As a first step of studying the structure and optical properties of such complexes, we have attempted to prepare new binuclear complexes, of which the absolute configuration can be assigned by a consideration of the stereospecific coordination of an optically active ligand to the metal ion. In this paper we report the preparation and the absolute configuration of new optically active binuclear complexes of the type, $[(l\text{-pn})_2Co(\mu\text{-}NH_2,a)Co(l\text{-pn})_2]^{n+}$ *1 (a = O_2^-, O_2^{2-}, NO_2^-, OH^-, and "SO_4^{2-}"*2) and compare their optical properties with those of corresponding Werner's ethylenediamine complexes.

Experimental

Preparations of the Complexes. *(1) Octaammine-μ-amido-μ-superoxo-dicobalt(III)**3 *Nitrate.* $[(NH_3)_4Co(\mu\text{-}NH_2,O_2)Co(NH_3)_4](NO_3)_4$ was prepared and purified by Mori, Weil and Ishiguro's new method[7] with concentrated nitric acid at 20—30°C as oxidizing agent instead of diammonium hexanitratocerate(IV). From 50 g of cobalt nitrate hexahydrate, 10 g of the complex was obtained.

*(2) $(+)_D$*4*-Tetrakis(ethylenediamine)μ-amido-μ-hydroxo-dicobalt(III) Nitrate.* $(+)_D$-$[(en)_2Co(\mu\text{-}NH_2,OH)Co(en)_2](NO_3)_4$was prepared by a new method from "$(+)_D$-$[(en)_2Co(\mu\text{-}NH_2,SO_4)Co(en)_2](NO_3)_3\cdot 2H_2O$". The starting complex (500 mg) was dissolved in 0.1 N sodium hydroxide (10 ml), set aside for 1 day at room tempera-

1) A. Werner, *Ber.*, **46**, 3674 (1913); **47**, 1959 (1914).
2) A. Werner, *ibid.*, **47**, 1977, 3087 (1914).
3) J. P. Mathieu, *Bull. soc. chim.*, [5], **5**, 103 (1938).
4) S. F. Mason and J. W. Wood, *Chem. Commun.*, **1967**, 209.
5) R. D. Kern and R. A. D. Wentworth, *Inorg. Chem.*, **6**, 1018 (1967).
6) G. R. Bulbaker and B. E. Douglas, *ibid.*, **6**, 1562 (1967).

*1 In this paper most of the binuclear complexes have double bridging structure: *e.g.* $[(l\text{-pn})_2Co\langle{}^{NH_2}_{a}\rangle Co(l\text{-pn})_2]^{n+}$. Such a structure is expressed by the formula $[(l\text{-pn})_2Co(\mu\text{-}NH_2,a)Co(l\text{-pn})_2]^{n+}$.

*2 Concerning the structure of the "sulfato bridge," nothing decisive can be stated at the present stage. (see p. 151).

*3 The name "μ-superoxo" was used for paramagnetic μ-O_2^- complexes, according to the proposal of U. Thewalt and R. Marsh. (*J. Am. Chem. Soc.*, **89**, 6364 (1967)).

7) M. Mori, J. A. Weil and M. Ishiguro, *J. Am. Chem. Soc.*, **90**, 615 (1968).

*4 $(+)_D$ and $(-)_D$ refer to the signs of the optical rotation at sodium D-line (589 mμ).

ture, and cooled in an ice bath. The red crystals were filtered off, dissolved in a little water and a small quantity of barium nitrate was added. The barium sulfate was removed and the filtrate concentrated till the crystals appeared and cooled to 0°C. The orangered crystals were recrystallized from hot water. Yield 200 mg.

Found: C, 15.27; H, 6.03; N, 28.43%. Calcd for $C_8H_{35}N_{13}O_{13}Co_2$: C, 15.03; H, 5.52; N, 28.48%.

(3) (−)D-Tetrakis(l-propylenediamine) μ-amido-μ-superoxo-dicobalt(III) Nitrate Trihydrate, (−)D-[(l-pn)$_2$Co(μ-NH_2,O_2)Co(l-pn)$_2$]$(NO_3)_4\cdot 3H_2O$. [$(NH_3)_4$Co(μ-NH_2,O_2)Co$(NH_3)_4$]$(NO_3)_4$ (20 g) in 5% aqueous l-propylenediamine (300 ml) was warmed at about 55°C on a water bath for about 5 hr, then cooled to room temperature, the brown solution treated with concentrated nitric acid until the color changed to green, and then with a large volume of ethanol. Green hygroscopic precipitate was filtered. When the filtrate was green, ethanol was added to obtain further aliquot. The product was recrystallized from 0.1 N nitric acid. The circular dichroism curve of the green fine needles remained unchanged on further recrystallization. Yield 5–7 g. The product seems to consist of only one of the optical isomers.

Found: C, 18.80; H, 6.28; N, 23.64%. Calcd for $C_{12}H_{48}N_{13}O_{17}Co_2$: C, 18.85; H, 6.33; N, 23.83%.

(4) (+)D-Tetrakis(l-propylenediamine) μ-amido-μ-peroxo-dicobalt(III) Iodide Hexahydrate, (+)D-[(l-pn)$_2$Co(μ-NH_2,O_2)Co(l-pn)$_2$]$I_3\cdot 6H_2O$. (−)D-[(l-pn)$_2$Co(μ-NH_2,O_2)Co(l-pn)$_2$]$(NO_3)_4\cdot 3H_2O$ (500 mg) was dissolved in 28% aqueous ammonia (3 ml). To this solution an excess of ammonium iodide was added. The brown precipitate was recrystallized from 15% aqueous ammonia by adding excessive ammonium iodide. Brown powder, yield 100 mg.

Found: C, 15.07; H, 5.40; N, 13.16%. Calcd for $C_{12}H_{54}N_9O_8I_3Co_2$: C, 15.15; H, 5.72; N, 13.25%.

(5) (+)D-Tetrakis(l-propylenediamine) μ-amido-μ-nitrito-dicobalt(III) Bromide Hexahydrate, (+)D-[(l-pn)$_2$Co(μ-NH_2,NO_2)Co(l-pn)$_2$]$Br_4\cdot 6H_2O$. (−)D-[(l-pn)$_2$Co(μ-NH_2,O_2)-Co(l-pn)$_2$]$(NO_3)_4\cdot 3H_2O$ (1 g) was dissolved in 5 ml of water, and treated with sodium nitrate (1 g). The color of the solution gradually changed from green to dark brown. The solution was kept at room temperature for 1 hr, then cooled in an ice bath and treated with concentrated hydrobromic acid (3 ml) slowly and carefully with stirring. The reddish orange crystals were filtered off and recrystallized from water. Yield 300 mg.

Found: C, 15.89; H, 5.49; N, 15.39%. Calcd for $C_{12}H_{54}N_{10}O_8Br_4Co_2$: C, 15.94; H, 5.80; N, 15.49%.

(6) (−)D-Tetrakis(l-propylendiamine) μ-amido-μ-"sulfato"-dicobalt(III) Nitrate, (−)L-[(l-pn)$_2$Co(μ-NH_2,SO_4)-Co(l-pn)$_2$]$(NO_3)_3$·(−)D-[(l-pn)$_2$Co(μ-NH_2,O_2)Co(l-pn)$_2$]$(NO_3)_4\cdot 3H_2O$ (1 g) was suspended in water (2 ml) saturated with sulfur dioxide, warmed on a water bath (60—70°C) for a few minutes and kept in an ice bath. The dark red crystals were filtered off, treated with water (2 ml) saturated with sulfur dioxide, and finally recrystallized from hot water. Reddish violet crystals, yield 400 mg.

Found: C, 20.57; H, 6.01; N, 23.60%. Calcd for $C_{12}H_{42}N_{12}O_{13}S_1Co_2$: C, 20.23; H, 5.94; N, 23.59%. The structure will be discussed in the following section.

(7) (+)D-Tetrakis(l-propylenediamine) μ-amido-μ-hydoxo-dicobalt(III) Nitrate Dihydrate. (+)D-[(l-pn)$_2$Co(μ-NH_2,OH)Co(l-pn$_2$](NO$_3$)$_4\cdot 2H_2O$ was prepared from "(−)D-[(l-pn)$_2$Co(μ-NH_2,SO_4)Co(l-pn)$_2$]$(NO_3)_3$" by a similar method to that for (+)D-[(en)$_2$Co(μ-NH_2,OH)Co(en)$_2$]-$(NO_3)_4$. From 500 mg of the starting material, 200 mg of the complex was obtained. Found: C, 19.58; H, 6.86; N, 24.79%. Calcd for $C_{12}H_{47}N_{13}O_{15}Co_2$: C, 19.71; H, 6.48; N, 24.89%.

Resolution of Tetrakis(ethylenediamine)-μ-amido-μ-superoxo-dicobalt(III) Ion. This was resolved by Werner's method[1] with silver d-bromcamphorsulfonate. Yield, 2 g of nitrate of (−)D form and 3 g of (+)D form from 35 g of [(en)$_2$Co(μ-NH_2,O_2)Co(en)$_2$]Br_4.

Measurements. Absorption and circular dichroism spectra were measured with Hitachi 124 Spectrophotometer and JASCO Model ORD/UV-5 recorder with CD attachment respectively in water at room temperature. All the complexes were stable in water.

Results and Discussion

Stereospecificity of l-Propylenediamine for Binuclear Complexes. It is known that the stable conformation of the chelated l-(D)-propylenediamine will be a λ-form with equatorial methyl group.[8] In tris complexes of l-propylenediamine, the two diastereoisomers, *Δ* and *Λ*[*5] have the "ob" and the "lel" structure, respectively. The lel isomer is estimated to be more stable than the ob isomer.[8] In fact, the products obtained on the reaction between cobalt and l-propylenediamine always consist mostly of *Λ*-[Co(l-pn)$_3$]$^{3+}$ with the lel structure.[9]

The energy difference between the ob and the lel isomer is said to be small for *cis*-bis-(l-propylenediamine) complexes. As stated before, however, the reaction of [$(NH_3)_4$Co(μ-NH_2,O_2)Co$(NH_3)_4$]$^{4+}$ and l-propylenediamine in an aqueous solution seemed to yield only one of the three possible optical isomers of [(l-pn)$_2$Co(μ-NH_2,O_2)Co(l-pn)$_2$]$^{4+}$. We ignore the geometrical isomers depending on the position of the methyl groups, since they would have structurally similar stabilization energies with one another, and could not be separated by usual chemical methods. The pure crystalline isomer exhibits a strong CD, indicating that it is one of the two diastereoisomers *ΔΔ* and *ΛΛ*, and not *ΔΛ* (so-called "meso" form). The isomer, (−)D-[(l-pn)$_2$Co(μ-NH_2,O_2)Co(l-pn)$_2$]$^{4+}$, could be assigned reasonably to the *ΛΛ* configuration, when the stereospecific coordination of l-propylenediamine mentioned above is considered.

No indication of the formation of the other isomers was observed from the CD measurements of many samples obtained at different stages of recrystallization. Studies with molecular models

8) E. J. Corey and J. C. Bailar, Jr., *J. Am. Chem. Soc.*, **81**, 2620 (1959).

*5 The symbols *Δ* and *Λ* designate the absolute configuration around the central metal ion, suggested by the Commission on the Nomenclature of Inorganic Compounds of IUPAC (1966).

9) E. P. Dwyer and F. L. Garvan, *J. Am. Chem. Soc.*, **81**, 2955 (1959).

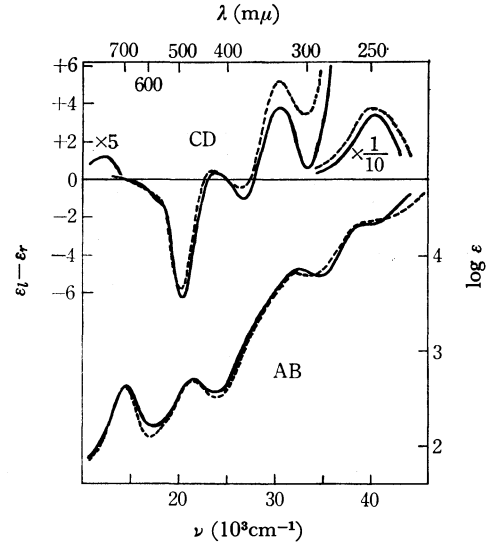

Fig. 1. The absorption (AB) and CD spectra of $(-)_D$-$[(en)_2Co(\mu\text{-}NH_2,O_2)Co(en)_2](NO_3)_4$ (——) and $(-)_D$-$[(l\text{-}pn)_2Co(\mu\text{-}NH_2,O_2)Co(l\text{-}pn)_2](NO_3)_4$ (------) in water.

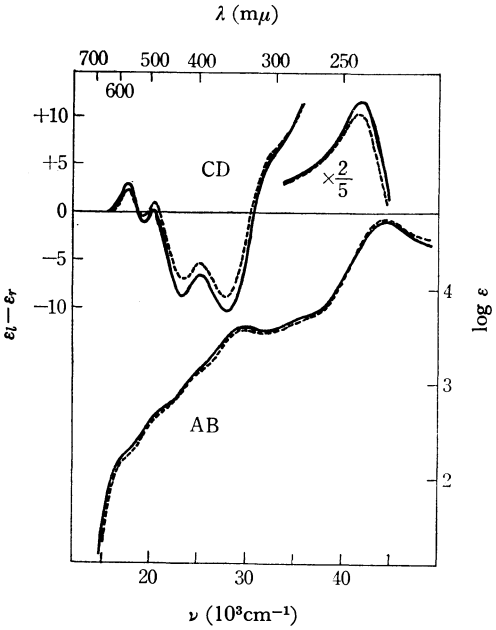

Fig. 2. The absorption (AB) and CD spectra of $(+)_D$-$[(en)_2Co(\mu\text{-}NH_2,O_2)Co(en)_2]I_3$ (——) and $(+)_D$-$[(l\text{-}pn)_2Co(\mu\text{-}NH_2,O_2)Co(l\text{-}pn)_2]I_3$ (------) in water.

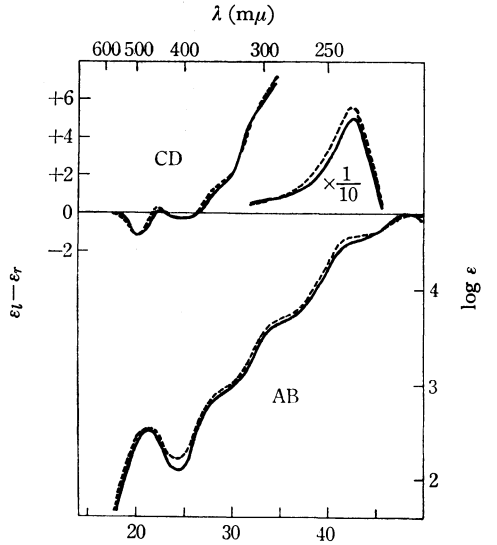

Fig. 3. The absorption (AB) and CD spectra of $(+)_D$-$[(en)_2Co(\mu\text{-}NH_2,NO_2)Co(en)_2](NO_3)_4$(——) and $(+)_D$-$[(l\text{-}pn)_2Co(\mu\text{-}NH_2,NO_2)Co(l\text{-}pn)_2]Br_4$ (------) in water.

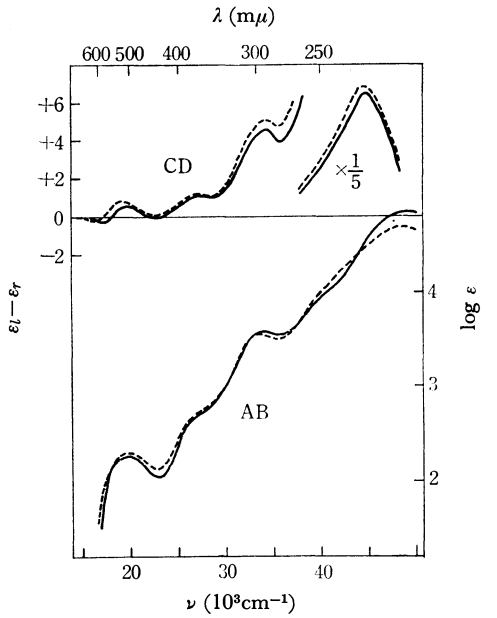

Fig. 4. The absorption (AB) and CD spectra of $(+)_D$-$[(en)_2Co(\mu\text{-}NH_2,OH)Co(en)_2](NO_3)_4$ (——) and $(+)_D$-$[(l\text{-}pn)_2Co(\mu\text{-}NH_2,OH)Co(l\text{-}pn)_2]$-$(NO_3)_4$ (------) in water.

of the isomers show that the repulsion between the amino groups of *l*-propylenediamines around the bridging region seems to be less in the *ΔΔ* and the *ΛΛ* form than in the *ΔΛ* form.

Four complexes, $(+)_D$-$[(l\text{-}pn)_2Co(\mu\text{-}NH_2,O_2)Co(l\text{-}pn)_2]^{3+}$, $(+)_D$-$[(l\text{-}pn)_2Co(\mu\text{-}NH_2,NO_2)Co(l\text{-}pn)_2]^{4+}$, $(-)_D$-$[(l\text{-}pn)_2Co(\mu\text{-}NH_2,SO_4)Co(l\text{-}pn)_2]^{3+}$ and $(+)_D$-$[(l\text{-}pn)_2Co(\mu\text{-}NH_2,OH)Co(l\text{-}pn)_2]^{4+}$, which were derived from the *ΛΛ*-$[(l\text{-}pn)_2Co(\mu\text{-}NH_2,O_2)$-$Co(l\text{-}pn)_2]^{4+}$, would be concluded to have the same *ΛΛ* configuration too, from their CD measurement, as discussed later. Complete inversion to the *ΔΔ* form during their syntheses from the *ΛΛ* isomers seems to be very improbable for these

binuclear complexes.

With these *l*-propylenediamine complexes as standard, the absolute configurations of the corresponding ethylenediamine complexes could be assigned safely from their CD spectra. As Fig. 1 shows, the CD spectra of the two $(-)_D$-μ-amido-μ-superoxo-dicobalt complexes of ethylenediamine and *l*-propylenediamine are very similar to each other. Therefore, we conclude that the isomer, $(-)_D$-$[(en)_2Co(\mu\text{-}NH_2,O_2)Co(en)_2]^{4+}$ has the $\Lambda\Lambda$ configuration. The following complex ions prepared from this isomer would be assigned to the $\Lambda\Lambda$ configuration; $(-)_D$-$[(en)_2Co(\mu\text{-}NH_2,O_2)Co(en)_2]^{3+}$, $(+)_D$-$[(en)_2Co(\mu\text{-}NH_2,NO_2)Co(en)_2]^{4+}$, $(+)_D$-$[(en)_2Co(\mu\text{-}NH_2,SO_4)Co(en)_2]^{3+}$ and $(+)_D$-$[(en)_2Co(\mu\text{-}NH_2,OH)Co(en)_2]^{4+}$.

The assignment for the ethylenediamine complexes coincides with that by Garbett and Gillard.[10] They obtained the uninuclear complexes of the known absolute configuration Λ by decomposing $(+)_D$-$[(en)_2NH_3Co(\mu\text{-}NH_2)CoNH_3(en)_2]^{5+}$, derived from $(-)_D$-$[(en)_2Co(\mu\text{-}NH_2,O_2)Co(en)_2]^{4+}$, which was assigned to have $\Lambda\Lambda$ configuration as stated above.

Absorption and Circular Dichroism Spectra. Absorption spectra of the present binuclear complexes exhibit a similar pattern in essential to that of uninuclear complexes, indicating that no strong metal-metal interaction will exist in them. Fairly strong absorptions at *ca.* 30000 to 35000 cm^{-1} known as "the polynuclear band" seem probably to owe to charge transfer transitions between the metal ions and the bridging ligand groups, although the origin is still uncertain.[11]

Medium intensity bands in the visible region seem to be the so called "first" band, corresponding approximately to the d–d transitions ($^1A_1$–$^1T_1$),

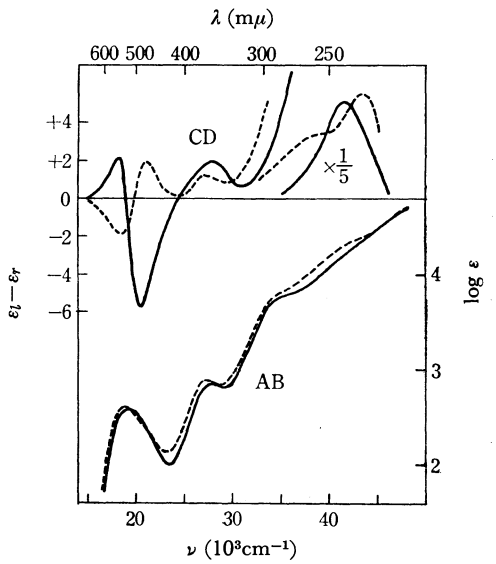

Fig. 5. The absorption (AB) and CD spectra of "$(+)_D$-$[(en)_2(\mu\text{-}NH_2,SO_4)Co(en)_2](NO_3)_3$" (——) and "$(-)_D$-$[(l\text{-}pn)_2Co(\mu\text{-}NH_2,SO_4)Co(l\text{-}pn)_2](NO_3)_3$" (------) in water.

of uninuclear complexes. Table 1 shows that the shifts of these bands can be interpreted by the spectrochemical series,[12] although the field strength of a ligand seems to increase somewhat upon bridging coordination. A similar observation was made by Brubaker and Douglas[6] in their new trinuclear complexes.

Ammine complexes with the superoxo bridge have a characteristic absorption band at *ca.* 14500 cm^{-1} with a medium intensity. Linhard and Weigel[13] assigned such a band in the complex, $[(NH_3)_5Co(O_2)Co(NH_3)_5]^{5+}$ to a split component

Table 1. Numerical data of absorption in water

	ν_{max}*(logε)	ν_{max}*(logε)	ν_{max}*(logε)	ν_{max}*(logε)	ν_{max}*(logε)
$[(NH_3)_5Co(\mu\text{-}O_2)Co(NH_3)_5]Cl_5$	14.9(2.92)	20.8(2.43)		33.6(4.35)	
$[(NH_3)_4Co(\mu\text{-}NH_2,O_2)Co(NH_3)_4]Cl_4$	14.3(2.45)	20.8(2.50)		33.0(3.61)	41.3(4.21)
$\Lambda\Lambda$-$[(en)_2Co(\mu\text{-}NH_2,O_2)Co(en)_2](NO_3)_4$	14.6(2.64)	21.4(2.72)		32.5(3.87)	39.5(4.3)**
$\Lambda\Lambda$-$[(l\text{-}pn)_2Co(\mu\text{-}NH_2,O_2)Co(l\text{-}pn)_2](NO_3)_4$	14.4(2.61)	21.3(2.72)		32.4(3.82)	39.5(4.3)**
$\Lambda\Lambda$-$[(en)_2Co(\mu\text{-}NH_2,O_2)Co(en)_2]I_3$	17 (2.2)**	20 (2.6)**	24 (3.0)**	29.8(3.59)	44.5(4.74)
$\Lambda\Lambda$-$[(l\text{-}pn)_2Co(\mu\text{-}NH_2,O_2)Co(l\text{-}pn)_2]I_3$	17 (2.2)**	20 (2.6)**	24 (3.0)**	29.7(3.52)	44.3(4.74)
$\Lambda\Lambda$-$[(en)_2Co(\mu\text{-}NH_2,NO_2)Co(en)_2](NO_3)_4$		21.1(2.51)	29 (2.9)**	35 (3.7)**	48.5(4.76)
$\Lambda\Lambda$-$[(l\text{-}pn)_2Co(\mu\text{-}NH_2,NO_2)Co(l\text{-}pn)_2]Br_4$		21.1(2.54)	29 (2.9)**	35 (3.7)**	46.5(4.63)
$\Lambda\Lambda$-$[(en)_2Co(\mu\text{-}NH_2,OH)Co(en)_2](NO_3)_4$		19.7(2.27)	27 (2.7)**	33.9(3.59)	48.5(4.8)**
$\Lambda\Lambda$-$[(l\text{-}pn)_2Co(\mu\text{-}NH_2,OH)Co(l\text{-}pn)_2](NO_3)_4$		20.0(2.28)	27 (2.7)**	33.9(3.53)	48.3(4.63)
$\Lambda\Lambda$-$[(en)_2Co(\mu\text{-}NH_2,SO_4)Co(en)_2](NO_3)_3$		19.1(2.57)	27.8(2.84)	35 (3.8)**	48.5(4.69)
$\Lambda\Lambda$-$[(l\text{-}pn)_2Co(\mu\text{-}NH_2,SO_4)Co(l\text{-}pn)_2](NO_3)_3$		18.9(2.60)	27.6(2.90)	35 (3.8)**	48 (4.7)**

* The frequencies are given in 10^3cm^{-1}. ** shoulder

10) K. Garbett and R. D. Gillard, *Chem. Commun.*, **1966**, 99.

11) Y. Inamura and Y. Kondo, *Nippon Kagaku Zassi* (*J. Chem. Soc. Japan, Pure Chem. Sect.*), **74**, 627 (1953); A. W. Chester and C. H. Brubaker, Jr., *J. Inorg. Nucl. Chem.*, **30**, 213 (1968).

12) Y. Shimura and R. Tsuchida., This Bulletin, **29**, 311 (1956).

13) M. Linhard and M. Weigel., *Z. anorg. Chem.*, **308**, 254 (1961).

Table 2. Numerical data of circular dichroisms in water

	ν_{max}*($\Delta\varepsilon$)	ν_{max}*($\Delta\varepsilon$)	ν_{max}*($\Delta\varepsilon$)	ν_{max}*($\Delta\varepsilon$)
$\Lambda\Lambda$-$[(en)_2Co(\mu\text{-}NH_2,O_2)(Co(en)_2](NO_3)_4$	20.4(−6.20)	26.7(−1.05)	30.3(+ 3.82)	*ca.* 40(ca.+34)
	23.8(+0.48)			
$\Lambda\Lambda$-$[(l\text{-pn})_2Co(\mu\text{-}NH_2,O_2)Co(l\text{-pn})_2](NO_3)_4$	20.2(−5.90)	26.5(−0.45)	30.3(+ 5.52)	*ca.* 40(*ca.*+35)
	23.3(+0.50)			
$\Lambda\Lambda$-$[(en)_2Co(\mu\text{-}NH_2,O_2)Co(en)_2]I_3$	17.5(+3.06)	23.3(−8.76)	27.8(−10.33)	*ca.* 42(*ca.*+30)
	19.4(−1.16)			
	20.4(+0.33)			
$\Lambda\Lambda$-$[(l\text{-pn})_2Co(\mu\text{-}NH_2,O_2)Co(l\text{-pn})_2]I_3$	17.3(+2.49)	23.4(−7.07)	27.8(− 8.61)	*ca.* 42(*ca.*+25)
	19.3(−0.77)			
	20.5(+0.71)			
$\Lambda\Lambda$-$[(en)_2Co(\mu\text{-}NH_2,NO_2)Co(en)_2](NO_3)_4$	20.3(−1.28)	*ca.*25.5(−0.30)**		*ca.* 42(*ca.*+50)
	22.3(+0.09)			
$\Lambda\Lambda$-$[(l\text{-pn})_2Co(\mu\text{-}NH_2,NO_2)Co(l\text{-pn})_2]Br_4$	20.2(−1.16)	*ca.*25.0(−0.25)**		*ca.* 42(*ca.*+50)
	22.1(+0.25)			
$\Lambda\Lambda$-$[(en)_2Co(\mu\text{-}NH_2,OH)Co(en)_2](NO_3)_4$	17.2(−0.35)	26.9(+1.05)	34.0(+ 4.6)	*ca.* 44(*ca.*+30)
	19.9(+0.57)			
	22.7(−0.07)			
$\Lambda\Lambda$-$[(l\text{-pn})_2Co(\mu\text{-}NH_2,OH)Co(l\text{-pn})_2](NO_3)_4$	16.7(−0.23)	26.7(+1.05)	34.0(+ 4.5)	*ca.* 44(*ca.*+30)
	18.9(+0.78)			
$\Lambda\Lambda$-$[(en)_2Co(\mu\text{-}NH_2,SO_4)Co(en)_2](NO_3)_3$	17.7(+2.24)	27.8(+2.04)		*ca.* 42(*ca.*+25)
	20.4(−5.66)			
$\Lambda\Lambda$-$[(l\text{-pn})_2Co(\mu\text{-}NH_2,SO_4)Co(l\text{-pn})_2](NO_3)_3$	18.5(−2.55)	27.4(+1.28)		*ca.* 42(*ca.*+25)
	21.0(+1.91)			

* The frequencies are given in 10^3 cm^{-1} ** shoulder.

of the first band (I_a). However, this band would be more appropriately assinged to a spin-forbidden d–d transition or to a charge transfer between the superoxo group and the metal ion, since the present μ-amido-μ-superoxo complexes do not show distinct CD in this band region. Split components of the magnetically allowed first band should be optically active. Ohkawa *et al.*[14] detected no CD band in the region of the strong spin-forbidden band of the $(-)_{546}$-*cis*-$[Co(I)(CN)(en)_2]^+$ ion.

The CD spectra corresponding to the d–d transitions ($^1A_1$–$^1T_1$) of the $\Lambda\Lambda$-$[(diamine)_2Co(\mu\text{-}NH_2,a)Co(diamine)_2]^{n+}$ exhibit various appearances depending on the kinds of substituent a, as pointed out by Mathieu.[3] Such a variety could be interpreted by considering "a kind of vicinal effect" of the chelate ring involving an optically active cobalt ion. For example, when we designate the cobalt(III) ions in the binuclear complex as $Co^{(1)}$ and $Co^{(2)}$, the $Co^{(1)}$ is considered to be coordinated with two diamines and a chelate ligand involving an asymmetric $Co^{(2)}$ ion (Fig. 6a). Such an optically active chelate ligand might give a significant vicinal effect more or less to the bands due to $Co^{(1)}$ ion.

The CD of the $(-)_D$-$[Co^{(a)}\{(\mu\text{-}OH,OH)Co^{(b)}(NH_3)_4\}_3]^{6+}$ in the d–d transition ($^1A_1$–$^1T_1$)

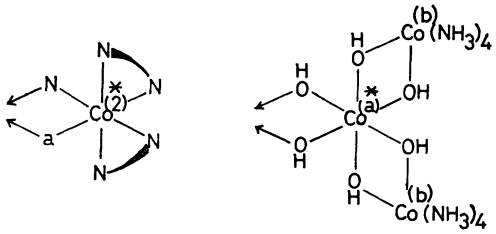

(a) (b)

Fig. 6. Bidentate ligands involving asymmetric cobalt ion(s).

region[4] would be interpreted by considering this vicinal effect (Fig. 7). The two absorption peaks at *ca.* 16000 and 20000 cm^{-1} of this complex may correspond approximately to the $^1A_1$–$^1T_1$ transition of the $Co^{(a)}$ and the $Co^{(b)}$ ion, respectively. The higher energy band exhibits a distinct CD, although the terminal $Co^{(b)}$ ions have no asymmetry around themselves. The optical activity of this band will be considered to be introduced by the vicinal effect of the chelate ring involving the optically active $Co^{(a)}$ ion (Fig. 6b). Mason and Wood[4] assigned the $(-)_D$-isomer of this complex to the Δ configuration, since the main CD component corresponding to the band at *ca.* 16000 cm^{-1} (d–d transition of $Co^{(a)}$) has a plus sign. These results suggest that in polynuclear complexes, the vicinal effect of asymmetric cobalt ion with a Δ configura-

14) K. Ohkawa, J. Hidaka and Y. Shimura, This Bulletin, **40**, 2830 (1967).

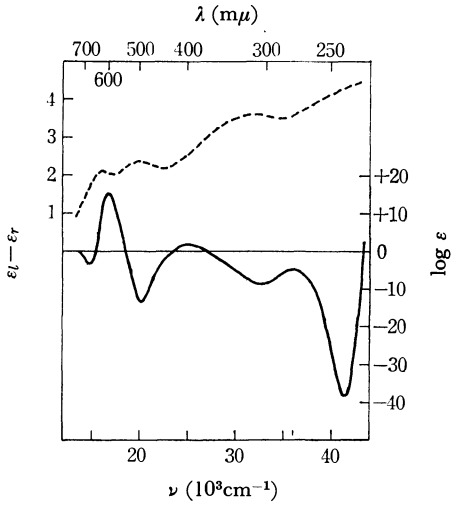

Fig. 7. The absorption (------) and CD spectra (——) of (−)-[Co{(μ-OH,OH)Co(NH$_3$)$_4$}$_3$]$^{6+}$ ion in water. (Ref. 4)

tion gives a negative CD sign for the d–d band ($^1A_1$–$^1T_1$) of the other cobalt ions.

The present binuclear complexes, *ΔΔ*-[(diamine)$_2$Co(μ-NH$_2$,a)Co(diamine)$_2$]$^{n+}$, should show strong negative CD bands in their first band region, if such a vicinal effect were very weak. This will be the case for the μ-superoxo complexes, as is seen in Fig. 1. The other μ-NO$_2$ and μ-hydroxo complexes, on the other hand, exhibit very weak CD bands in this region. Strong negative CD components corresponding to each *Δ*-cobalt ion would be compensated by the positive CD bands resulting from the vicinal effect of each of other asymmetric cobalt ion with the same configuration.

Such an interpretation would be supported by examining the vicinal effect curve of *l*-propylenediamine. In general, the vicinal effect curve of *l*-propylenediamine in cobalt(III) complexes shows one medium strong positive and one small negative peak from longer to shorter wavelength in the region of the first band.[15] The vicinal effect curve of the *l*-propylenediamine for the binuclear complexes could be obtained by subtracting the CD curve of the ethylenediamine complex from that of the corresponding *l*-propylenediamine complex. Both contributions from the configurational and the vicinal effect of the asymmetric cobalt ions would be eliminated from these curves so far as these effects are additive. As Fig. 8 shows, the curves thus obtained show similar appearances to those of uninuclear complexes of *l*-propylenediamine. These results seem to indicate the following conclusions; the nature of the d–d bands of polynuclear cobalt(III) complexes are very similar to those of uninuclear cobalt(III) complexes, and therefore, the CD behavior corresponding to these bands depends mainly on the strength of the vicinal effect of asymmetric cobalt(III) ion.

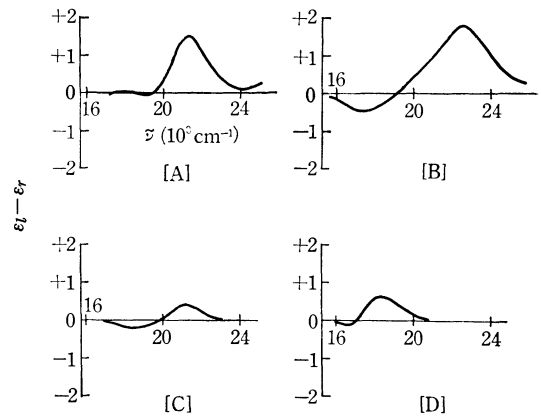

Fig. 8. The vicinal effect curves of four chelated *l*-propylenediamine in the complexes, [(*l*-pn)$_2$Co(μ-NH$_2$,a)Co(*l*-pn)$_2$]$^{n+}$.
(A) a=O$_2^-$ (B) a=O$_2^{2-}$ (C) a=NO$_2^-$ (D) a=OH$^-$
(obtained by subtracting the CD of *ΔΔ*-[(en)$_2$Co(μ-NH$_2$,a)Co(en)$_2$]$^{n+}$ from that of *ΔΔ*-[(*l*-pn)$_2$Co(μ-NH$_2$,a)Co(*l*-pn)$_2$]$^{n+}$.)

Weak CD bands were observed in the region of the other d–d band ($^1A_1$–$^1T_2$), but their behavior has not been made clear.

Corresponding to the so-called polynuclear band at *ca.* 30000 to 35000 cm^{-1} region, the *ΔΔ* complexes exhibit fairly strong CD bands with a positive sign. Although the origin of these bands is uncertain, the fact that the CD sign is always positive as that of the CD for strong charge transfer bands at *ca.* 40000 cm^{-1} indicates that these bands would have also a charge transfer character.

Concerning the CD of charge transfer bands in tris-diamine[16] and tris-aminoalcohol[17] cobalt(III) complexes, it has been suggested that their sign depends mainly on the absolute configuration around the metal ion, and that it will be positive for a *Δ*-type complex and negative for a *Λ*-type complex. Although a positive CD component due to the vicinal effect of the chelated diamines with *λ*-form[16] may be involved in these CD bands, their positive sign seems to support the previous conclusion that all the complexes have the *ΔΔ* configuration.

"μ-Sulfato" Complexes. All the *l*-propylenediamine complexes except for the "μ-amido-μ-sulfato" complex give very similar absorption and CD curves to those of the corresponding ethyl-

15) C. J. Hawkins, E. Larsen and I. Olsen, *Acta Chem. Scand.*, **19**, 1915 (1965).

16) K. Ogino, K. Murano and J. Fujita, *J. Inorg. Nucl. Chem. Letters*, **4**, 351 (1968).

17) K. Ohashi, J. Fujita, B. Shimoyama and K. Saito, This Bulletin, **41**, 2422 (1968).

enediamine complexes. However, the CD curves of the two "μ-sulfato" complexes appear almost enantiomeric with each other in the d–d transition band region. Such a difference might be originated in a difference between the bonding structure of the bridging sulfato ligands in these two complexes, since both the complexes would have the same $\Lambda\Lambda$ configuration. The aqueous solutions of these complexes decompose gradually to give the $\Lambda\Lambda$-μ-amido-μ-hydroxo complexes.[3,18] Furthermore, addition of barium ions to these solutions results in only a slow precipitation of barium sulfate upon warming, to indicate that the sulfate ions coordinate to the metal ions, and are not the outer sphere ions. Detailed studies about these problems are now in progress, and will be published later.

We express our sincere thanks to the Ministry of Education for Grant-in-Aid.

18) A. G. Sykes and R. D. Mast, *J. Chem. Soc.*, (*A*), **1967**, 784.

BULLETIN OF THE CHEMICAL SOCIETY OF JAPAN VOL. 42 152—156 (1969)

The Oxovanadium(IV) Complexes of Schiff Bases Obtained from Substituted Salicylaldehydes and Alkyl Amines*1

Shoichiro YAMADA and Yoshio KUGE*2

Institute of Chemistry, College of General Education, Osaka University, Toyonaka, Osaka

(Received June 5, 1968)

Many new oxovanadium(IV) complexes (abbreviated as $VO(X\text{-sal.R})_2$) of Schiff bases obtained from substituted salicylaldehydes and alkylamines have been synthesized as crystals, where X=H and 3-CH_3O and R=CH_3, C_2H_5, *n*-C_3H_7, *n*-C_4H_9, *iso*-C_3H_7, $CH(CH_3)(C_2H_5)$, $CH_2CH(CH_3)_2$ and cyclohexyl. Since all these complexes show similar electronic spectra, it is considered that they take an essentially similar configuration, that is, a square-pyramidal one in the solid state and in chloroform, even for $R=\alpha$-branched alkyls. This result is different from that of the copper (II) complexes. It is also concluded that these oxovanadium(IV) complexes, when dissolved in pyridine, take up one pyridine molecule to form a six-coordinated species. The configuration of the pyridine solvate depends upon R.

In previous papers from this laboratory,[1-3] Schiff base complexes of various transition metal ions were described and their stereochemistry was discussed. As an extension of these studies, the oxovanadium(IV) complexes of these Schiff bases have been studied in the present work. The oxovanadium(IV) ion has an electronic configuration d^1, so that its complexes are expected to be somewhat similar to the complexes of copper(II) having a configuration d^9.

Some of the oxovanadium(IV) complexes of this series were previously reported,[4,5] but a systematic study seems to be insufficient. The present paper describes the results of the investigations about the oxovanadium(IV) complexes of the Schiff bases obtained from substituted salicylaldehydes and alkyl amines (Fig. 1).*3

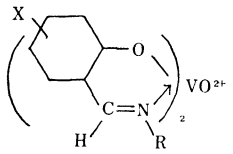

Fig. 1. $VO(X\text{-sal.R})_2$

Experimental

Materials. The complexes of the $VO(X\text{-sal.R})_2$

*1 Presented at the 21st Annual Meeting of the Chemical Society of Japan, Osaka, Apirl, 1968.

*2 Present address: Osaka Public Health Institute, Morimachi, Higashi-ku, Osaka.

1) S. Yamada, *Coordin. Chem. Revs.*, **1**, 415 (1966).

2) S. Yamada, H. Nishikawa, Y. Kuge and K. Yamanouchi, *Sci. Rep., Coll. Gen. Educ. Osaka Univ.*, **16**, 11 (1967).

3) S. Yamada, E. Ohno, Y. Kuge, A. Takeuchi, K. Yamanouchi and K. Iwasaki, *Coordin. Chem. Revs.*, **3**, 247 (1968).

4) J. Selbin, *ibid.*, **1**, 293 (1966).

5) L. Sacconi and U. Campigli, *Inorg. Chem.*, **5**, 606 (1966).

*3 The complexes of this type are abbreviated in this paper as $VO(X\text{-sal.R})_2$.

type, where X=H and 3-CH_3O, were synthesized by a method similar to that previously reported for complexes of other metal ions.[1] One of the typical examples of the syntheses is given below for VO(3-CH_3O-sal.CH_3)$_2$. To a solution of oxovanadium (IV) chloride (0.01 mol) in ethanol were added 3-methoxysalicylaldehyde (0.02 mol), a 40% aqueous solution of methyl amine (0.02 mol) and sodium acetate (0.02 mol). The solution was heated with stirring on a water-bath at about 60°C for about three hours. The solution was allowed to stand overnight, and the precipitate was collected by filtration. Recrystallization from ethanol yielded green crystals of VO(3-CH_3O-sal.CH_3)$_2$.

All the complexes were purified by recrystallization of the crude product from ethanol. Ethanol containing a small amount of pyridine was occasionally used for the recrystallization of the less soluble compounds like VO(H-sal.C_2H_5)$_2$.

The salicylideneiminato-complexes are grey-brownish green, and the 3-methoxysalicylideneiminato-complexes are green. They are soluble in chloroform and dichloromethane, but less soluble in methanol, ethanol and benzene. The complexes of the VO(H-sal.R)$_2$ type are less soluble in common organic solvents than the complexes of the VO(3-CH_3O-sal.R)$_2$ type. Analytical data of the complexes are given in Tables 1 and 2.

Table 1. Analytical data of oxovanadium(IV) complexes of the VO(H-sal.R)$_2$ type

R	Calcd %			Found %		
	C	H	N	C	H	N
C_2H_5	60.05	5.66	7.09	59.58	5.55	7.71
n-C_3H_7	61.38	6.18	7.16	61.21	6.11	8.04
i-C_3H_7				61.91	6.08	6.88
n-C_4H_9	63.00	6.73	6.67	62.96	6.82	6.68
$CH(CH_3)(C_2H_5)$				62.58	6.75	6.16
$CH_2CH(CH_3)_2$				62.81	6.89	6.28
Cyclohexyl	66.52	6.44	5.29	65.59	6.72	6.20

Table 2. Analytical data of oxovanadium(IV) complexes of the VO(3-CH_3O-sal.R)$_2$ type

R	Calcd %			Found %		
	C	H	N	C	H	N
CH_3	54.69	5.09	7.09	54.72	5.07	7.48
C_2H_5	55.90	5.76	7.05	56.74	5.71	6.62
n-C_3H_7	58.54	6.25	6.21	58.53	6.40	6.37
i-C_3H_7				58.21	6.10	6.15
n-C_4H_9	60.12	6.73	5.86	59.93	6.89	6.04
$CH(CH_3)(C_2H_5)$				59.72	6.70	5.94
$CH_2CH(CH_3)_2$				59.39	6.70	6.13
Cyclohexyl	63.51	6.47	5.29	62.59	6.71	5.44

Cu(H-sal.*iso*-C_3H_7)$_2$ was prepared as previously reported.[6]

Measurements. The electronic absorption spectra of the compounds in solution and the reflection spectra of the solid were determined with a Shimadzu QR-50 spectrophotometer and a Shimadzu MPS-50L spectrophotometer.

Results and Discussion

The Oxovanadium(IV) Complexes of *N*-*n*-Alkyl-substituted Schiff Bases. Numerous new oxovanadium(IV) complexes of the Schiff bases have been synthesized in the present work. All these complexes are considered to consist of penta-coordinated molecules.[4,5] When R denotes an *n*-alkyl group, there is no or very little steric hindrance, so that the complexes of the VO(X-sal.R)$_2$ type are expected to be square-pyramidal, with the two groups of X-sal.R most probably taking a nearly trans-planar configuration.[5]

Electronic spectra of these complexes in non-donor solvents are essentially similar to the spectra of the same complexes in the solid state (Figs. 2 and 3, and Tables 3 and 4).*4 It is, therefore, most likely that their configuration in such a non-donor solvent as chloroform is similar to that in the solid state, the solvent molecule not being bound with the vanadium(IV) ion. It is also concluded that all these complexes take a similar configuration, that is, a square-pyramidal one, regardless of the substituent, R, since they show similar spectra. The main features of the spectra of these complexes are in agreement with those for the related complexes.[5]

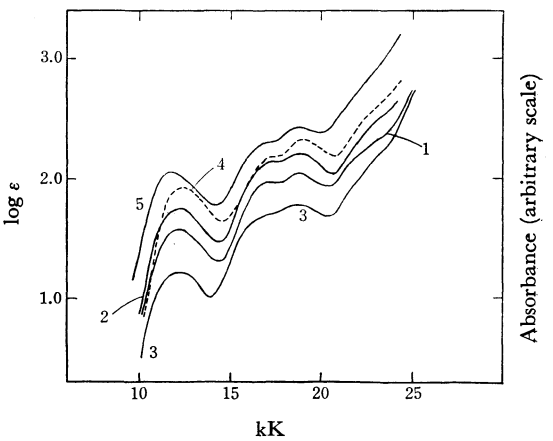

Fig. 2. Electronic absorption spectra of VO(H-sal.R)$_2$: 1, R=C_2H_5, solid; 2, R=*n*-C_4H_9, solid; 3, R=$CH_2CH(CH_3)_2$, in chloroform; 4, R=CH_2-$CH(CH_3)_2$, solid; 5, R=$CH(CH_3)(C_2H_5)$, solid.

6) S. Yamada and H. Nishikawa, This Bulletin, **36**, 755 (1963).

*4 Solubility of these complexes is rather low in common organic solvents other than chloroform and dichloromethane. In this work, the spectra were measured mostly using chloroform as a solvent. Measurements were also carried out with some of the complexes in dichloromethane, but the spectra were found to be essentially similar to the spectra of the chloroform solution.

TABLE 3. ABSORPTION MAXIMA OF OXOVANADIUM(IV) COMPLEXES OF THE VO(H-sal.R)$_2$ TYPE

R	State	ν(logε)	ν(logε)	ν(logε)
C_2H_5	Solid	12.1	16.9sh	18.9
	Pyridine	14.0*(1.40)	17.0sh(1.46)	19.3(1.72)
n-C_3H_7	Soild	12.2	17.0sh	18.8
	Pyridine	14.0*(1.28)	17.0sh(1.45)	19.3(1.70)
i-C_3H_7	Solid	12.1	16.8sh	18.9
	Pyridine	12.2*(1.51)	17.0sh(1.52)	19.5(1.78)
n-C_4H_9	Solid	12.1	16.8sh	18.8
	Pyridine	14.0*(1.31)	17.0sh(1.35)	19.3(1.68)
$CH_2CH(CH_3)_2$	Solid	12.5	17.0sh	19.0
	$CHCl_3$	12.3 (1.22)	16.7sh(1.60)	18.8(1.75)
	Pyridine	14.1*(1.40)	17.0sh(1.35)	19.1(1.64)
$CH(CH_3)(C_2H_5)$	Solid	11.8	16.8sh	18.9
	Pyridine	12.2*(1.76)	flat	flat
Cyclohexyl	Solid	11.9	16.7sh	18.3
	Pyridine	12.9*(1.37)	17.0sh(1.52)	19.5(1.80)

* With a shoulder on the lower frequency side. ν: cm^{-1} sh: shoulder. The values of ν and ε for the shoulders are intended to be only approximate.

TABLE 4. ABSORPTION MAXIMA OF OXOVANADIUM(IV) COMPLEXES OF THE VO(3-CH_3O-sal.R)$_2$ TYPE

R	State	ν(logε)	ν(logε)	ν(logε)
CH_3	Solid	12.2	17sh	18.9
	$CHCl_3$	12.1 (1.10)	16.7sh(1.56)	18.7(1.78)
	Pyridine	13.8*(1.27)	16.9sh(1.52)	19.0(1.75)
C_2H_5	Solid	12.1	16.3sh	18.4sh
	$CHCl_3$	12.1 (1.05)	16.7sh(1.55)	18.8(1.83)
	Pyridine	13.0*(1.30)	16.6sh(1.55)	18.7(1.70)
n-C_3H_7	Solid	12.2	16.0sh	18.4sh
	$CHCl_3$	12.3 (1.19)	16.7sh(1.60)	18.7(1.78)
	Pyridine	13.9*(1.25)	16.7sh(1.53)	18.8(1.71)
i-C_3H_7	Solid	11.8	16.2sh	18.7
	$CHCl_3$	12.2 (1.32)	16.6sh(1.66)	18.8(1.85)
	Pyridine	12.8*(1.29)	16.4sh(1.46)	18.4(1.71)
n-C_4H_9	Solid	12.2	16.7sh	18.6
	$CHCl_3$	12.2 (1.20)	16.7sh(1.60)	18.7(1.77)
	CH_2Cl_2	12.3 (1.27)	16.6sh(1.62)	18.8(1.81)
	Pyridine	13.8*(1.27)	16.5sh(1.55)	18.7(1.70)
$CH_2CH(CH_3)_2$	Solid	12.4	16.7sh	18.7
	$CHCl_3$	12.2 (1.16)	16.5sh(1.58)	18.9(1.76)
	Pyridine	14.0*(1.25)	16.5sh(1.55)	18.8(1.68)
$CH(CH_3)(C_2H_5)$	Solid	12.0	16.3sh	18.7
	CH_2Cl_2	12.4 (1.51)	16.6sh(1.76)	19.1(1.98)
	Pyridine	12.7*(1.42)	16.6sh(1.50)	19.0(1.75)
Cyclohexyl	Solid	12.2	16.3sh	18.3sh
	$CHCl_3$	12.1 (1.42)	16.6sh(1.75)	18.8(1.90)
	Pyridine	13.4*(1.20)	17.1sh(1.50)	19.3(1.71)

* With a shoulder on the lower frequency side. ν: cm^{-1} sh: shoulder. The values of ν and ε for the shoulders are intended to be only approximate.

It is interesting to note that three band maxima are observed in the region of *d–d* bands for these complexes. About an unambiguous assignment of the *d–d* absorption bands of the oxovanadium(IV) complexes there still seems to remain some dipute.[4,7] The three bands at about 12 kK,

7) J. Selbin, *Chem. Revs.*, **65**, 153 (1965).

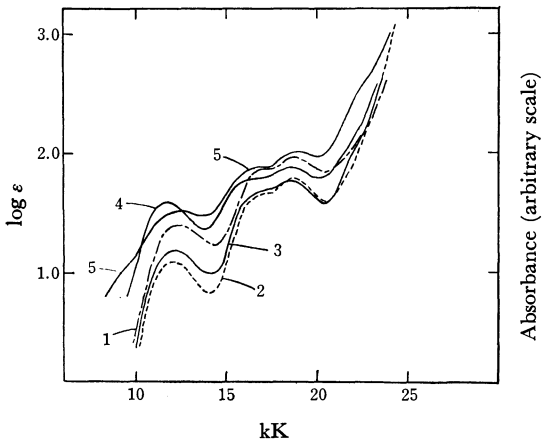

Fig. 3. Electronic absorption spectra of VO-(3-CH_3O-sal.R)$_2$: 1, R=CH_3, solid; 2, R=CH_3, in chloroform; 3, R=n-C_4H_9, in chloroform; 4, R=iso-C_3H_7, solid; 5, R=$CH(CH_3)(C_2H_5)$, in dichloromethane.

16—17 kK and 18.5—19 kK may tentatively be assinged as transitions $d(xz)$, $d(yz)\leftarrow d(xy)$, $d(x^2-y^2)\leftarrow d(xy)$ and $d(z^2)\leftarrow d(xy)$, respectively, on the basis of the "clustered levels" scheme.[5,7]

These complexes in pyridine show electronic spectra, which are different from the spectra of the same complexes in the solid state and in chloroform (Figs. 4 and 5, and Tables 3 and 4). The change in the spectrum on going from a non-donor solvent to pyridine is not very large, but quite characteristic. This fact seems to indicate that the oxovanadium(IV) complexes, when dissolved in pyridine, combine with one molecule of pyridine to form six-coordinated solvates. It is to be noted that for the pyridine solution there appears a shoulder at about 12 kK, in addition to the peak at about 13—14 kK and two other peaks. The two peaks at the lower frequencies may tentatively be assigned as the transitions $d(xz)\leftarrow d(xy)$ and $d(yz)\leftarrow d(xy)$.

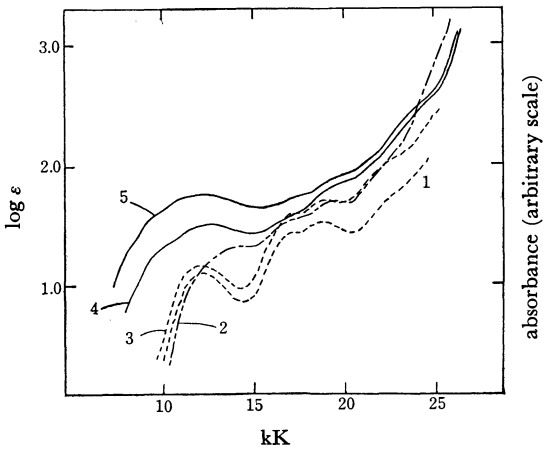

Fig. 4. Electronic absorption spectra of VO(H-sal.R)$_2$: 1, R=n-C_3H_7, solid; 2, R=n-C_3H_7, in pyridine; 3, R=iso-C_3H_7, solid; 4, R=iso-C_3H_7, in pyridine; 5, R=$CH(CH_3)(C_2H_5)$, in pyridine.

The Oxovanadium(IV) Complexes of *N*-α-Branched Alkyl-substituted Schiff Bases. For

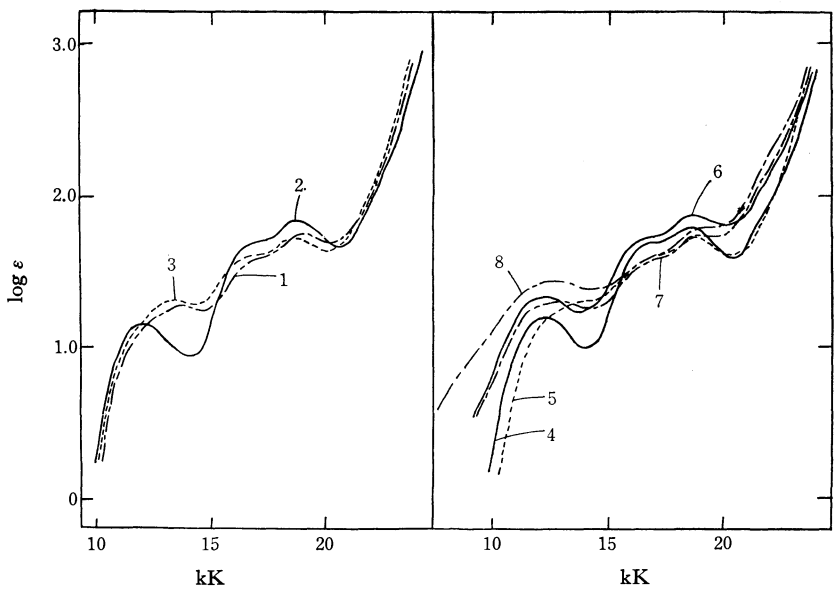

Fig. 5. Electronic absorption spectra of VO(3-CH_3O-sal.R)$_2$: 1, R=CH_3, in pyridine; 2, R=C_2H_5, in chloroform; 3, R=C_2H_5, in pyridine; 4, R=n-C_3H_7, in chloroform; 5, R=n-C_3H_7, in pyridine; 6, R=iso-C_3H_7, in chloroform; 7, R=iso-C_3H_7, in pyridine; 8, R=$CH(CH_3)(C_2H_5)$, in pyridine.

R=2-methylpropyl, there is no serious steric hindrance to the planar coordination of the two ligands around the vanadium(IV) ion. For R= isopropyl, 1-methylpropyl and cyclohexyl, however, there may be more or less remarkable steric hindrance to the planar coordination, since the corresponding copper(II) complexes of the Cu(X-sal.R)$_2$ type were found to be planar or distorted from the planar configuration, depending upon the nature of X.[6,8] On the contrary, the complexes of the VO(X-sal.R)$_2$ type for R=α-branched alkyls in chloroform and in the solid state show electronic absorption spectra quite similar to the corresponding complexes with R=*n*-alkyl groups. It is, therefore, most likely that for all these oxovanadium(IV) complexes the coordination of the two ligand groups may be nearly planar. This difference between the oxovanadium(IV) complexes and the corresponding copper(II) complexes indicates that the configuration distorted from the planar one is destabilized to a more or lesser extent for the oxovanadium(IV) ion, as compared with the copper(II) ion. This may be due, at least partly, to the steric effect of the oxygen atom bound to the vanadium(IV) ion, in addition to the difference in the bonding nature of the metal ions. It is, however, to be noted that the intensity of the *d–d* bands, particularly that of the band at the lowest frequency, becomes higher on going from R=*n*-alkyl to R=α-branched alkyl or cyclohexyl for X=3-CH_3O, as shown in Fig. 5 and Table 4. The change is not quite large but definite, and it is most likely that the coordination of the two Schiff bases to the vanadium(IV) ion may be distorted from the planar one to an only small extent.

For R=α-branched alkyl groups, the electronic spectra of VO(3-CH_3O-sal.R)$_2$ in pyridine are clearly different from the spectra of the same complexes in the solid state and in chloroform, as shown in Fig. 5 and Table 4. This fact indicates that the oxovanadium(IV) complexes of this series, when dissolved in pyridine, take up a pyridine molecule. Since, for R=α-branched alkyl groups as well as 2-methylpropyl, the change in the spectra of VO(3-CH_3O-sal.R)$_2$ on going from a non-donor solvent to pyridine is essentially similar to that of VO(3-CH_3O-sal.*n*-alkyl)$_2$, the configuration of the pyridine solvates for these substituents, R, may be similar to the corresponding solvates for R=*n*-alkyl groups.

On the contrary, for R=α-branched alkyl groups or cyclohexyl, the electronic spectra of VO(H-sal.R)$_2$ in pyridine are quite different from the spectra of the same complexes in chloroform and in the solid state (Fig. 4 and Table 3). The *d–d* bands at the lowest frequencies of these complexes are found to become much broader, extending into a considerably lower frequency region on going from chloroform to pyridine. This result is different from that for VO(H-sal.*n*-alkyl)$_2$ and VO(3-CH_3O-sal.alkyl)$_2$. It is most likely that this anomalous change of spectra in VO(H-sal.α-branched alkyl)$_2$ may be due to the steric hindrance leading to a distorted configuration for the pyridine solvates.

For R=α-branched alkyl groups, it is thus found that the behavior of VO(H-sal. R)$_2$ is different from that of VO(3-CH_3O-sal.R)$_2$. This difference provides one of the examples showing that a small difference in the electronic factor due to the substituent X may cause a drastic change in the stereochemistry of the Schiff base metal complexes.

It is also interesting to compare VO(H-sal.*iso*-C_3H_7)$_2$, for example, with the corresponding copper(II) complexes, Cu(H-sal.*iso*-C_3H_7)$_2$. This copper(II) complex, which takes a distorted tetrahedral configuration in non-donor solvents,[6,8] retains the same configuration in pyridine, since its electronic spectrum in pyridine is essentially similar to the spectrum in non-donor solvents. This is another example showing that the distorted tetrahedral configuration is more stable in the copper(II) complex than in the oxovanadium(IV) complex.

Support of this work by the Ministry of Education is gratefully acknowledged.

8) L. Sacconi, "Essays in Coordination Chemistry," ed. by W. Schneider, G. Anderegg and R.Gut, Birkhäuser Verlag, Basel (1964), p. 148.

BULLETIN OF THE CHEMICAL SOCIETY OF JAPAN VOL. 42 157—162 (1969)

Reactions of Nickel(II), Copper(II) and Palladium(II) Complexes of Bis(acetylacetone)ethylenediimine with Nitric Oxide

Isao MASUDA, Motonori TAMAKI and Koichiro SHINRA

Department of Applied Chemistry, Faculty of Engineering, Osaka University, Yamada, Suita, Osaka

(Received June 6, 1968)

Through reaction with nitric oxide, divalent Ni, Cu, and Pd complexes of bis(acetylacetone)-ethylenediimine have been shown to yield fine crystalline compounds of the general formula $M(C_{12}H_{17}N_3O_3)$, where M=Ni or Cu, and of $M(C_{12}H_{16}N_4O_4)$ where M=Ni, Cu or Pd, depending on experimental conditions. They are insoluble in water. The former compounds are rather soluble in common organic solvents, but the latter are sparingly soluble, except in pyridine. On the basis of analytical data and IR-spectral analyses, they are thought not to be nitrosyl metal-complexes but oxime type complexes.

It is well known that the γ-H of metal acetylacetonates can be replaced by halogens or nitro groups.[1] However, the reactivity of chelate complexes, such as acetylacetonate, towards nitric oxide is not yet clarified. In this connection, only a few examples are found in the following studies. Djordjenič *et al.*[2] reported that through reaction with nitrosyl chloride in benzene, platinum(II) acetylacetonate yields a γ-chlorosubstituted compelx, whereas nickel(II) complex yields a compound which is thought to be either an oxime or a nitroso compound. By reaction with nitrite ions in the presence of ammonia, nickel(II) and palladium(II) complexes of acetylacetone yield a compound thought to be a γ-nitroso substituted complex, as shown in Fig. 1. On the other hand, it was shown by Nast *et al.*[3] that cobalt(II) acetylacetonate reacts with nitric oxide to yield a nitrosyl complex, CoA_2*1(NO), in which nitric oxide is bonded to the central metal.

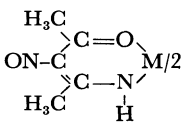

Fig. 1. M=Ni(II); Pd(II)

In the present work, nickel(II), copper(II) and palladium(II) complexes of bis(acetylacetone)ethylenediimine, which have metal-chelate rings analogous to that of acetylacetonate are reported to react with nitric oxide in organic solvents to form new complexes which are thought to have the structures shown in Figs. 2 and 3.

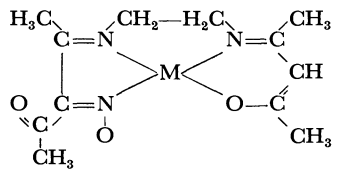

Fig. 2. Complex I; M=Ni(II)
Complex III; M=Cu(II)

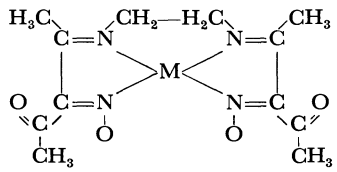

Fig. 3. Complex II; M=Ni(II)
Complex IV; M=Cu(II)
Complex V; M=Pd(II)

Experimental

Materials. Metal complexes of bis(acetylacetone)-ethylenediimine used in the reactions with nitric oxide were prepared according to McCarthy *et al.*[4] NiAE*2 was purified by recrystallization from an 80% aqueous acetone solution, then dried at 100°C, obtaining reddish brown crystals. CuAE, recrystallized from acetone, was dried at 100°C, yielding dark violet crystals. PdAE, recrystallized from benzene, was dried at 100°C, yielding yellow crystals.

Nitric oxide was generated by the reaction of copper with aqueous nitric acid, and purified by passage through aqueous sodium hydroxide and a tower containing pellets of sodium hydroxide.

1) J. P. Collman, "Reactions of Coordinated Ligands," Am. Chem. Soc., New York (1960), p. 78.

2) C. Djordjevič, J. Lewis and R. S. Nyholm, *J. Chem. Soc.*, **1962**, 4778.

3) R. Nast and H. Bier, *Ber.*, **92**, 1858 (1959).

*1 A represents acetylacetonato.

4) P. J. McCarthy, R. J. Hovey, K. Ueno and A. E. Martell, *J. Am. Chem. Soc.*, **77**, 5820 (1950).

*2 AE represents bis(acetylacetone)ethylenediiminato.

TABLE 1. ELEMENTAL ANALYSES OF THE COMPLEXES

Formula	Complex	Cacld %				Found %			
		Metal	C	H	N	Metal	C	H	N
$NiC_{12}H_{17}N_3O_3$	I	18.9	46.35	5.83	13.50	18.7	46.35	5.53	14.06
$NiC_{12}H_{16}N_4O_4$	II		42.52	4.76	16.53		42.59	5.01	16.79
$CuC_{12}H_{17}N_3O_3$	III		45.40	5.71	13.24		45.54	5.52	13.88
$CuC_{12}H_{16}N_4O_4$	IV		41.92	4.69	16.29		41.99	4.69	16.22
$PdC_{12}H_{16}N_4O_4$	V	27.5	37.30	4.17	14.45	28.4	37.18	4.59	14.20

Reactions with Nitric Oxide. NiAE: 2.0 g of NiAE was dissolved in 100 m*l* of chloroform, and nitric oxide bubbled through the ice-cooled solution for about fifty minutes until the reddish-brown color of the solution turned to red. Then, the nitric oxide in the solution was driven off by bubbling nitrogen gas through the solution. The orange precipitate was filtered off, and the filtrate evaporated *in vacuo* to leave a red solid. The precipitate was recrystallized from methanol or toluene to give fine red crystals (complex I). The results of elementary analysis, given in Table 1, correspond to the formula shown in Fig. 2. The molecular weight determined with an ebulliometer in toluene for a 0.02 M solution was 298, showing the complex to be monomeric.

Using dichloromethane as a solvent, and bubbling nitric oxide through the solution for 30—40 min, an orange complex precipitated. The precipitate was recrystallized by dissolving it in a large volume of boiling dichloromethane and then cooling the solution. Fine orange crystals (complex II) were obtained. The results of elementary analysis, given in Table 1, correspond to the formula shown in Fig. 3. The orange complex differed from the red complex that was obtained through reaction in chloroform and was only slightly soluble in most organic solvents. It is stable in pyridine, and the complex that was obtained from pyridine solution after the solution was boiled for three hours gave the same infrared spectrum as that of the original orange complex.

CuAE: Two grams of CuAE were dissolved in 100 m*l* of chloroform, and air expelled from the solution and reaction flask by bubbling in nitrogen. Then the ice-cooled solution was saturated with nitric oxide by passing the gas through it for about 20 min. Stirring the solution in air for 20—30 min changed its color from violet to dark red-violet. The solution was evaporated *in vacuo*, leaving a precipitate, which was washed with ether to remove unreacted CuAE. It was recrystallized by dissolution in 50 m*l* of hot methanol and then cooling. Dark red-violet crystals (complex III) were obtained. The analytical results given in Table 1 indicate the formula shown in Fig. 2.

When nitrogen oxide was bubbled through the chloroform solution of CuAE in a similar way as mentioned above, for about two hours, a brown colored complex precipitated. The precipitate was filtered off, washed with chloroform and air-dried. It was recrystallized from methanol to give yellowish-brown crystals (complex IV). The complex was less soluble in most organic solvents than the red complex; analysis indicates the formula shown in Fig. 3.

PdAE: 0.2 g of PdAE dissolved in 50 m*l* of benzene was reacted with nitrogen oxide in the same way as above. After bubbling in nitric oxide for 30—50 min, the solution changed in color from yellow to orange, and an orange complex precipitated. The precipitate was filtered off and washed with benzene and then ether. Recrystallization from dichlorobenzene or pyridine gave fine orange crystals (complex V). Elementary analysis indicated the formula shown in Fig. 3.

Infrared Spectra. Infrared spectra were measured in KBr using a Shimadzu IR-27C spectrometer in the 650—4000 cm^{-1} region. Spectra in the 250—700 cm^{-1} region were obtained in KBr with an Hitachi EPI-L spectrometer.

Results and Discussion

Elementary analyses show that complexes II, IV and V have compositions which correspond to compounds with metal-AE : NO molecular ratios of 1 : 2. As for complexes I and III, analysis indicates a metal-AE: NO molecular ratio of 1 : 1. The solubilities of the complexes, their being insoluble in water and soluble in common organic solvents, suggest that they are non-ionic.

In order to formulate the complexes, their infrared spectra were examined. As is seen in Figs. 6—8, complexes II, IV and V display quite similar spectra, indicating similar structures.

It is well known that metal complexes of AE[5] or β-ketoamine,[6] which have unsaturated, six-membered metal chelate rings, such as shown in Fig. 4, are characterized by two or three absorption

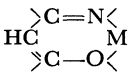

Fig. 4

bands with strong intensities in the 1500—1600 cm^{-1} region, and the band due to π_{C-H} at about 760 cm^{-1}. Compared with this, the spectra of complexes II, IV and V are conspicuous by the absence of strong bands in the 1500—1600 cm^{-1} region and the band due to π_{C-H} (Figs. 6—8). However, the complexes exhibit strong bands in

5) K. Ueno and A. E. Martell, *J. Am. Chem. Soc.*, **59**, 998 (1955).

6) H. F. Holtzclaw, J. P. Collman and R. M. Alire, *ibid.*, **80**, 1100 (1958); R. D. Archer, *Inorg. Chem.*, **2**, 292 (1963).

a higher wave number region, 1660—1689 cm^{-1}. The new bands are attributed to the stretching frequencies of N=O, C=O or C=N from general considerations of their positions and intensities. But in the case of these complexes, the absence of the strong bands in the 1500—1600 cm^{-1} region is thought to eliminate a formula where an N=O group is bound to the γ-C (Fig. 4) on the chelate rings of the original metal-AE, though the π_{C-H} band apparently disappeared. Since in the spectra of metal acetylacetonates, bands analogous to those of metal-AE in the 1500—1600 cm^{-1} region are known not to vanish by substitution on γ-C of an unsaturated group such as nitro-, phenyl- or formyl-groups.[7] A nitrosyl type of structure is also discarded for the following reason. Nitrosyls of nickel, copper and cobalt complexes with AE, where the NO group is bound to the central metal,

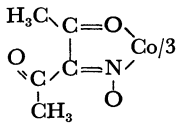

Fig. 5

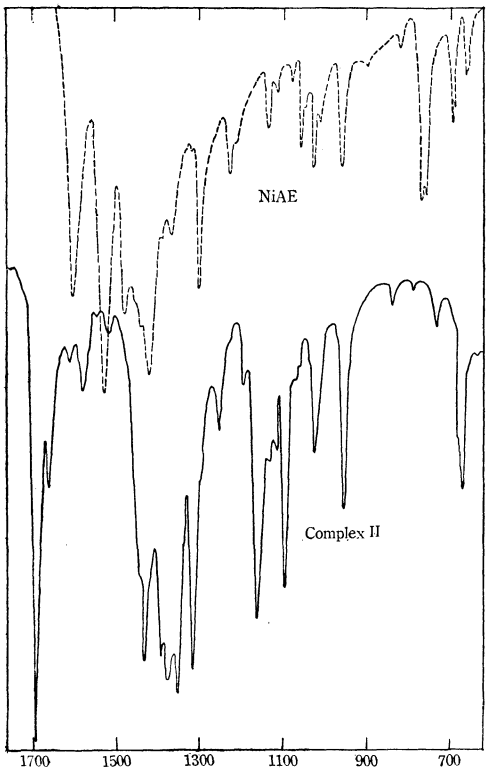

Wave number, cm^{-1}

Fig. 6. IR spectra of NiAE and complex II.

were synthesized by another method.[8] Their spectra show strong bands at about 1680 cm^{-1}, which resemble in position the bands at 1660—1689 cm^{-1} obtained for complexes II, IV and V. However, in the case of these nitrosyls, they still retain the strong 1500—1600 cm^{-1} bands that are diagnostic of the parent metal-AE, and also retain the π_{C-H} band at about 760 cm^{-1}.

Thus, the evidences described above reject the most probable structures containing NO groups in the complexes. A considerably different skeleton for the structures of the complexes from that of the original metal-AE is then proposed. The spectrum of tris(isonitrosoacetylacetonato)Co(III) was inspected and compared with that of the complexes. $Co(INA)_3$*3 has been formulated as shown in Fig. 5,[9] and its spectrum given in Fig. 9 has no strong band in the 1500—1600 cm^{-1} region except

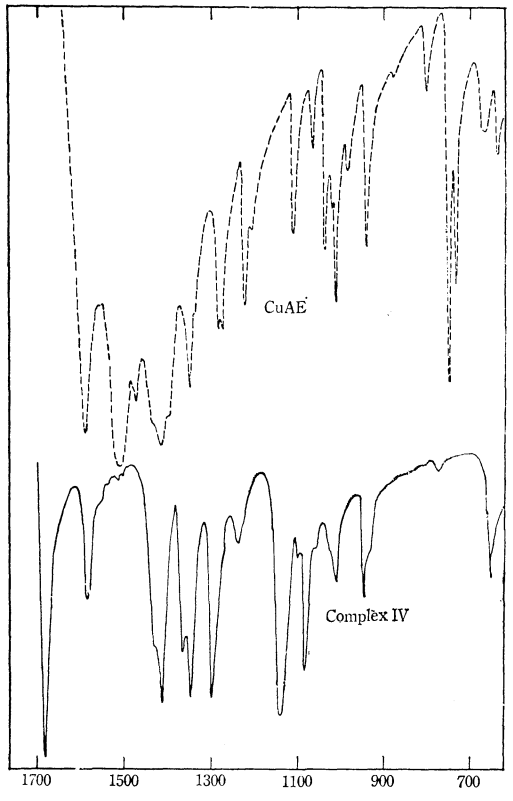

Wave number, cm^{-1}

Fig. 7. IR spectra of CuAE and complex IV.

7) J. P. Collman, R. L. Marshall, W. L. Young and S. D. Goldby, *Inorg. Chem.*, **1**, 704 (1962); H. F. Holtzclaw and J. P. Collman, *J. Am. Chem. Soc.*, **79**, 3318 (1957).

8) M. Tamaki, Y. Nigo, I. Masuda and K. Shinra, Presented at the 21th Annual Meeting of the Chemical Society of Japan, Osaka, April, 1968.

*3 Tris(isonitrosoacetylacetonato)Co(III) is abbreviated $Co(INA)_3$.

9) C. Matsumoto and K. Shinra, *Nippon Kagaku Zasshi* (*J. Chem. Soc. Japan, Pure Chem. Sect.*), **88**, 340 (1967).

for a band at 1520 cm^{-1}. This band can be assigned to the stretching frequency of C=O that is coordinated to the cobalt atom; the corresponding bands are not observed for complexes II, IV and V (Figs. 6—8). The stretching frequency of non-coordianted C=O to the metal in $Co(IAN)_3$ appeared at 1660 cm^{-1}.

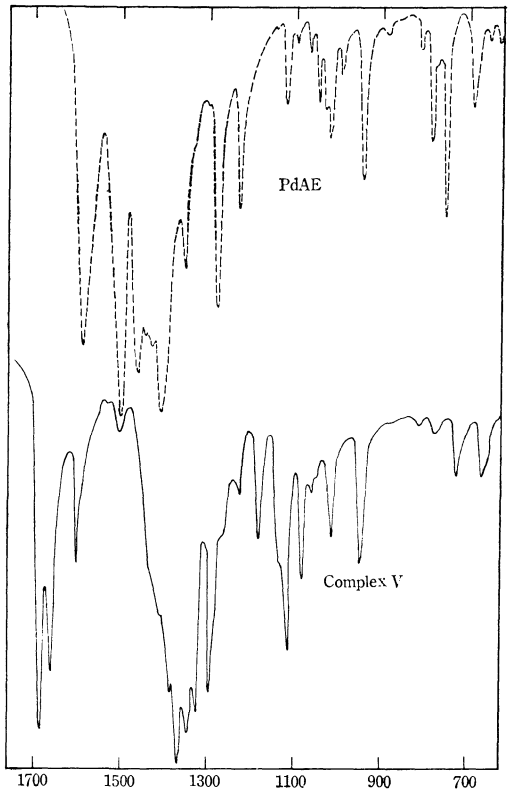

Fig. 8. IR spectra of PdAE and complex V.

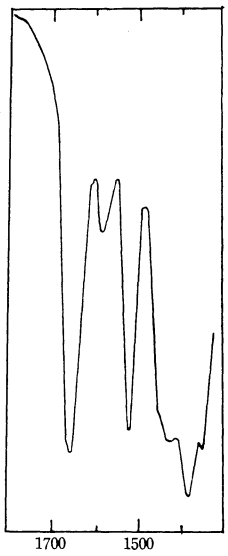

Fig. 9. IR spectra of $Co(INA)_3$.

On the basis of the spectrum of $Co(INA)_3$, the spectra of complexes II, IV and V may be reasonably explained by proposing the structures shown in Fig. 3. Assignments are listed in Table 2. The band at 1682—1689 cm^{-1} has been assinged to the stretching frequency of C=O that is not bound to the central metal atom. As for the subsidiary peak at a lower wave number (1660—1662), it is discussed later and is ascribed to the freqnency of the imine type C=N stretching in the porposed structure (Fig. 3).

Complex I shows interesting spectral features in that it possesses essentially the same frequencies of both complex II and the original NiAE. For example, as shown in Fig. 10 and Table 2, it exhibits bands at 1685 and 1652 cm^{-1}, corresponding to

TABLE 2. CHARACTERISTIC IR ABSORPTIONS OF THE COMPLEXES

Complex	Predominant modes					
	C=O str.	C=N str.[a]		C=O str.[b]		π_{C-H}
NiAE*[2]				1598 s	1522 s	765 m, 755 m
I	1685 s	1652 s		1605 s	1520 s	778 m
II	1689 vs	1660 m	1568 w			
CuAE				1588 s	1510 s	745 s, 730 m
III	1679 s			1598 s	1510 s	762 m
IV	1682 s		1587 m			
PdAE				1596 s	1502 s	758 m
V	1683 s	1662 s	1600 m			
$Co(INA)_3$*[3]	1660 s		1590 w		1520 s	

a) imine type C=N in chelate, b) C=O in chelate.

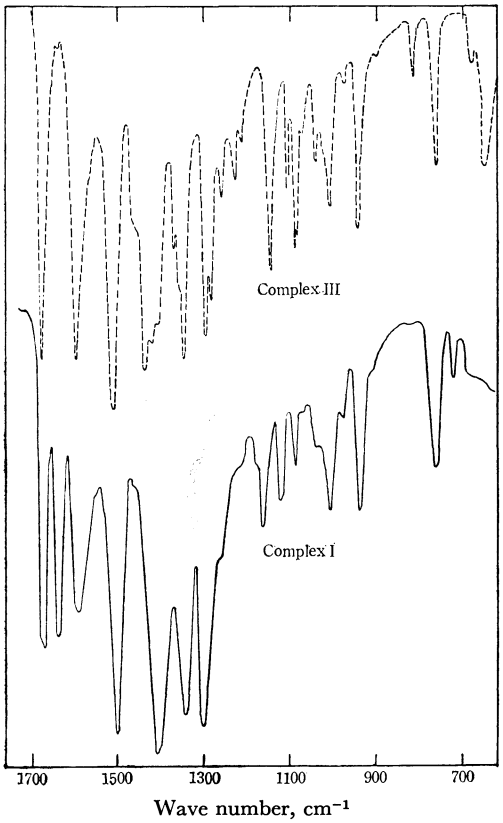

Fig. 10. IR spectra of complex I and complex III.

those at 1689 and 1660 cm^{-1} for complex II, and frequencies at 1605 and 1520 cm^{-1} corresponding to those at 1598 and 1522 cm^{-1} for NiAE. This peculiar feature of the spectrum is found over the 1700—300 cm^{-1} region (Figs. 10 and 11). In addition, complex I still shows the π_{C-H} band at 778 cm^{-1}. Cu complex III also has a rather similar spectrum to complex I (Figs. 10 and 12), indicating similar structures.

This fact may make one suspect complex I to be a mixed crystal of NiAE and complex II. However, from a chloroform solution of NiAE and complex II in a 1 : 1 molar ratio, a red crystal of complex I was not successfully crystallized. Complex I is shown to be monomeric in toluene by a molecular weight measurement. Thus, without presuming a structure such as shown in Fig. 2, the spectral features of complex I, described above, could hardly be understood.

Presuming this structure (Fig. 2), the bands at 1685 and 1520 cm^{-1} for complex I can be assigned to the stretching vibrations of the non-coordinated and coordinated C=O groups, respectively. The band at 1652 cm^{-1} is likely to be due to the stretching vibration of the imine type C=N groups in the complex (Fig. 2).

A chloroform solution of complex I has two peaks at 1685 and 1652 cm^{-1}, as in KBr. These two peaks do not change in intensity ratio with concentration of the complex. This fact indicates that the band at 1652 cm^{-1} can not be attributed to the associated C=O group, although the association of C=O is known to gives rise to a subsidiary peak at a lower wave number than the main peak of the unassociated C=O, as is seen in the case of a 1,2-diketonemonoxime such as diacetylmonoxime.[10] The value, 1652 cm^{-1}, is thought to be considerably higher than that of the C=N stretching frequency of the oxime group in a complex. Usually the frequency of the oxime type C=N stretching in a conjugate system is observed[10] at about 1630 cm^{-1}, and it can be expected to absorb below 1600 cm^{-1} in an unsaturated metal chelate such as shown in Fig. 2, judging from infrared evidence on metal - dimethylglyoximato complexes.[11] The band at 1652 cm^{-1} for complex

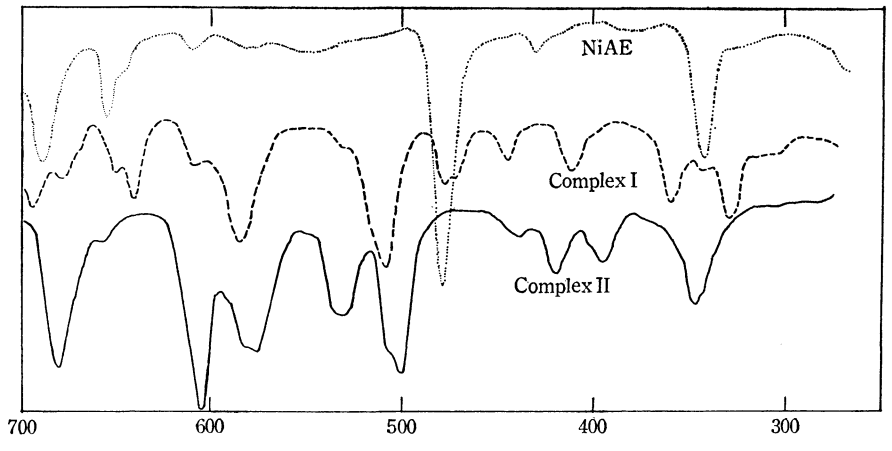

Fig. 11. IR spectra of NiAE, complex I and complex II.

10) M. Kimura, Y. Kuroda and H. Takagi, This Bulletin, **33**, 1086 (1960).

11) K. Burger, I. Ruff and F. Ruff, *J. Inorg. Nucl. Chem.*, **27**, 179 (1965).

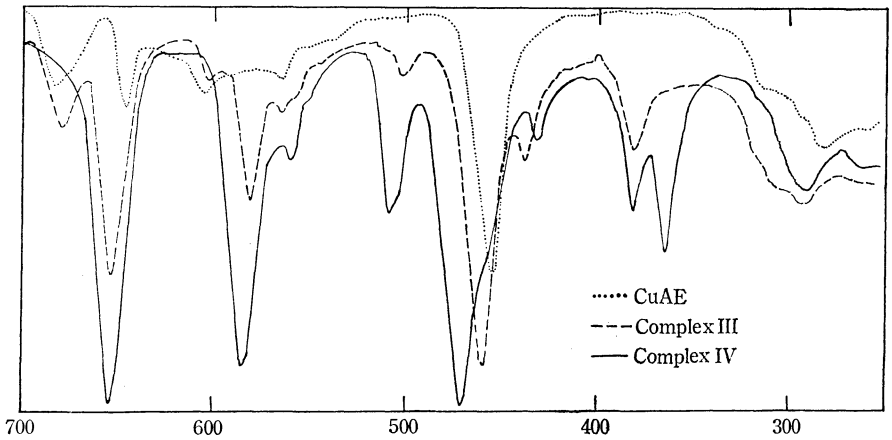

Fig. 12. IR spectra of CuAE, complex III and complex IV.

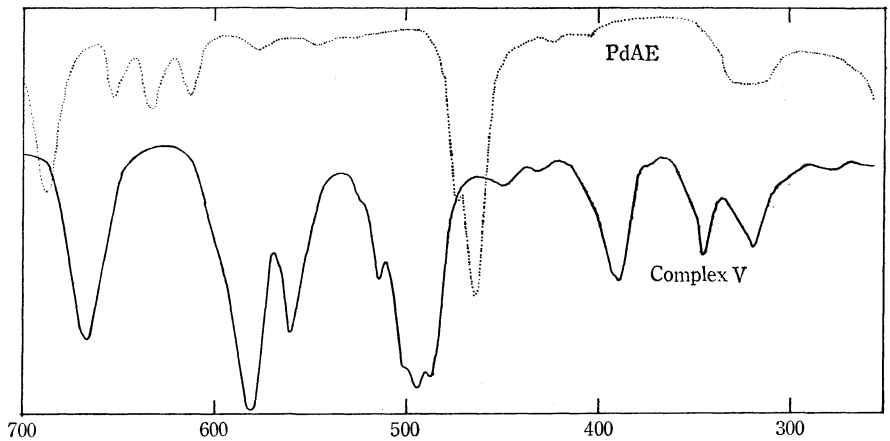

Fig. 13. IR spectra of PdAE and complex V.

I has therefore been ascribed to the stretching of the imine type C=N in the five-membered metal-chelate ring (Fig. 2).

In the spectra of Cu complexes III and IV (Figs. 7 and 10, and Table 2), the band due to the imine type C=N is not observed in the corresponding wave number region. In these cases, the absorption of C=O probably obscures the C=N absorption, whose frequency would be shifted toward higher wave numbers than for the other complexes.

BULLETIN OF THE CHEMICAL SOCIETY OF JAPAN VOL. 42 163—168 (1969)

Kinetics of Multidentate Ligand Substitution Reactions. IV. Substitution Reactions of BT with Cobalt(II) and Nickel(II) Chelates of 1,2-Diaminocyclohexanetetraacetic Acid and Diethylenetriaminepentaacetic Acid

Mutsuo KODAMA, Chifumi SASAKI and Katsumi MIYAMOTO

Department of Chemistry, Ibaraki University, Mito, Ibaraki

(Received June 8, 1968)

The substitution reactions of Eriochrom Black T (BT) with cobalt(II) and nickel(II) chelates of 1,2-diaminocyclohexanetetraacetic acid (CyDTA) and of diethylenetriaminepentaacetic acid (DTPA) were studied spectrophotometrically. The reactions of BT with CyDTA and DTPA chelates of these metal(II) ions were found to have the same reaction mechanism as the reactions with EDTA chelates did, but to be considerably slower than the latter reactions. On the basis of a comparison of the observed rate constants with those calculated on the basis of the proposed reaction mechanism (glycinate intermediate), the steric effect due to the cyclohexane ring in the CyDTA or $-CH_2-CH_2-N(CH_2-COO^-)-CH_2-CH_2-N(CH_2-COO^-)_2$ group in DTPA on the reaction rate was discussed in a quantitative manner. The effect due to the former group was estimated to be smaller than that due to the latter group.

We have studied a series of substitution reactions of Eriochrom Black T (BT) with cobalt(II)- and nickel(II)-polyaminocarboxylate chelates.[1-3] The reactions were invariably first-order in BT and first-order in the metal(II)-polyaminocarboxylate chelate.

In the present paper, the kinetics of the substitution reactions of BT with cobalt(II) and nickel(II) chelates of 1,2-diaminocyclohexanetetraacetic acid (CyDTA) and of diethylenetriaminepentaacetic acid (DTPA) are dealt with spectrophotometrically. On the basis of a comparison of the rate constants of the substitution reactions of CyDTA and DTPA chelates with those of EDTA chelates, the steric effect of the cyclohexane ring in the CyDTA or $-CH_2-CH_2-N(CH_2-COO^-)-CH_2-CH_2-N(CH_2-COO^-)_2$ group in DTPA on the rate of the substitution reaction is discussed.

Experimental

Reagents. The preparation and the standardization of solutions of cobalt(II) and nickel(II) perchlorates have been described in previous papers.[1,2] Reagent-grade CyDTA and DTPA recrystallized from water were used. The concentration of the CyDTA solution was standardized against the standard lead(II) solution by a volumetric titration, using BT as an indicator.[4] The concentration of DTPA was determined by the same procedure as has been proposed for the EDTA titration of copper(II).[5] The other reagents were of a guaranteed reagent grade and were used without further purification.

Apparatus and Procedure. The apparatus and the experimental procedure were the same as have been described in a previous paper.[1] In this study, all the measurements were conducted on solutions with an ionic strength of 0.30 ($NaClO_4$), and no buffer reagent was used, because free CyDTA and DTPA have enough buffer capacity to maintain the pH values of solutions constant in the pH range from 9.50 to 10.50 in which the present study was conducted.

Results and Discussion

All the exchange reactions were studied in solutions with pH values from 9.50 to 10.50 containing large excesses of complexed and uncomplexed CyDTA or DTPA. Therefore, the exchange reactions can be treated as pseudo first-odrer reactions. In the cases of the reactions of BT with cobalt(II) and nickel(II) chelates of EDTA,[1,2] EDTA-OH[3] and GEDTA,[3] the apparent rate constants of the pseudo first-order reactions could be determined from the slope of the linear relation

1) M. Kodama, This Bulletin, **40**, 2575 (1967).
2) M. Kodama, C. Sasaki and M. Murata, *ibid.*, **41**, 1333 (1968).
3) M. Kodama, C. Sasaki and T. Noda, *ibid.*, **41**, 2033 (1968).
4) C. A. Goetz and F. J. Debbrecht, *Anal. Chem.*, **27**, 1972 (1955).
5) H. Flaschka, *Microchemie ver. Microchim. Acta*, **39**, 38 (1952).

between $\log(A_D/(A-A_{MD}))$ and time, t. Here, A_D, A, and A_{MD} have the same meanings as were used previously.[2,3] However, in the reactions of BT with CyDTA and DTPA chelates of these metal(II) ions, the concentration of uncomplexed BT at equilibrium, $[BT]_e$, can not be neglected as compared with that at t, $[BT]_f$, and the initial concentration of BT, $[BT]_0$, because the stability constants of cobalt(II) and nickel(II) chelates of CyDTA and DTPA are comparable to those of corresponding BT chelates. Therefore, in the present substitution reactions, the apparent rate constants should be estimated from the slope of the linear relation between $\log([A_D-A_e]/[A-A_e])$ and t. Here A_e denotes the absorbance at equilibrium and $[A_D-A_e]/[A-A_e]$ can be equated with $([BT]_0-[BT]_e)/([BT]_f-[BT]_e)$ in the Eq. (7) in Ref. (1). Hence, the slope of the linear relation of $\log([A_D-A_e]/[A-A_e])$ and t can be exactly expressed as:

$$\text{slope} = k^+\left(1+\frac{[MZ^{2-m}]}{K_h[Z]_f}\right)\cdot\frac{1}{2.303} \qquad (1)$$

where k^+ corresponds to the apparent rate constant of the pseudo first-order reaction (2),[1-3] where $[MZ^{2-m}]$ and $[Z]_f$ are the concentrations of complexed and uncomplexed CyDTA or DTPA, and where $K_h=K_{MD}\cdot(\alpha_H)_Z/K_{MZ}\cdot(\alpha_H)_{BT}=k^+\cdot(Z)_f/k^-\cdot[MZ^{2-m}]$.

$$\begin{cases} HD^{2-} \\ \uparrow\downarrow \\ D^{3-} \end{cases} \overset{k^+}{\underset{k^-}{\rightleftarrows}} MD^- \qquad (2)$$

The other notation definitions used here are as follows. HD^{2-} and D^{3-} mean doubly- and completely-deprotonated BT anions respectively, and MD^-, the metal(II)-BT chelate. K_{MD} and K_{MZ} are stability constants of the metal(II)-BT chelate and the -CyDTA or -DTPA chelate respectively. $(\alpha_H)_Z$ and $(\alpha_H)_{BT}$ have the same meanings as previously.[3]

k^+ in Eq. (1) can also be determined from the apparent initial rate of the reaction, $(-\Delta[BT]/\Delta t)_0$, with the aid of Eq. (3):

$$\left(-\frac{\Delta[BT]}{\Delta t}\right)_0 = k^+\left(1+\frac{[MZ^{2-m}]}{K_h[Z]_f}\right)[BT]_0 \qquad (3)$$

where $(-\Delta[BT]/\Delta t)_0$ and $[BT]_0$ can be equated with $(-\Delta A/\Delta t\cdot\varepsilon_{BT})_0$ and A_D/ε_{BT},[2] respectively.

In the case of the reactions of BT with nickel(II) chelates of CyDTA and DTPA, the absorbance decreases almost linearly with the time. Therefore, the apparent rate constant was determined from the initial slope of the absorbance *versus* time curve. On the other hand, in the case of the reactions of BT with cobalt(II) chelates, the apparent rate constant, k^+, was calculated from the slope of the linear relation between $\log[(A_D-A_e)/(A-A_e)]$ and t. The A_e*1 value used in the log-

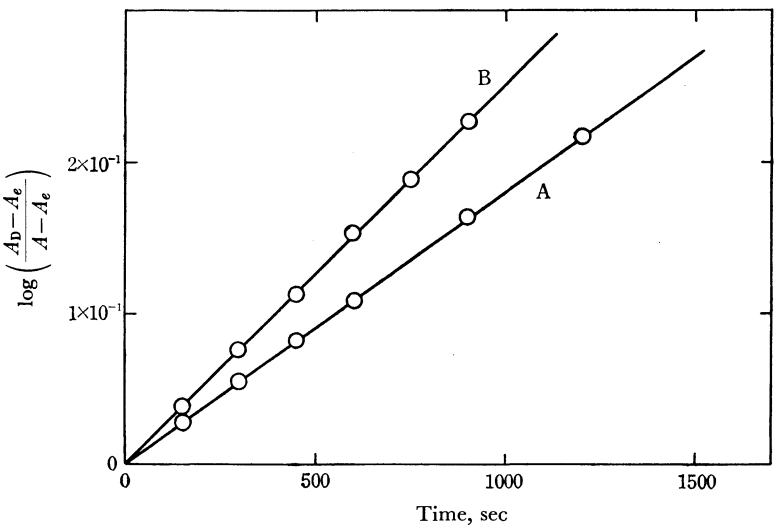

Fig. 1. The plot of $\log[(A_D-A_e)/(A-A_e)]$ against t.
$\mu = 0.30$, $\lambda = 630$ mμ
Initial concentration of BT = 2.5×10^{-5} M
A: Concentration of cobalt(II)-CyDTA chelate = 10.0 mM
Concentration of uncomplexes CyDTA = 10.0 mM
pH = 9.95
B: Concentration of cobalt(II)-DTPA chelate = 7.13 mM
Concetration of uncomplexed DTPA = 10.0 mM
pH = 10.40

*1 The calculated A_e value agreed well with the observed value.

plot examination was calculated by using K_{MD} and K_{MZ} values. Typical linear relations between $\log[(A_D-A_e)/(A-A_e)]$ and t are shown in Fig. 1.

In all the substitution reactions of BT studied in this paper, we found the following experimental facts with regard to the apparent rate constant, k^+:

i) In solutions of a given pH, a given concentration of the metal(II) chelate of CyDTA or DTPA, and a given initial concentration of BT, k^+ is independent of the concentration of the uncomplexed chelating agent (CyDTA or DTPA) (Table 1).

Table 1. Dependence of k^+ on the concentration of uncomplexed chelating agent
$\mu = 0.30$, $\lambda = 630$ mμ

i) Cobalt(II)-CyDTA system		
Concentration of CyDTA, mM	k^+ M^{-1} sec^{-1}	
5.0	1.79×10^{-4}	pH = 9.95
10.0	1.78×10^{-4}	$[BT]_0 = 2.5\times10^{-5}$ M
15.0	1.78×10^{-4}	$[CoZ^{2-}] = 10.0$ mM
ii) Nickel(II)-CyDTA system		
Concentration of CyDTA, mM	k^+ M^{-1} sec^{-1}	
5.0	7.12×10^{-5}	pH = 10.00
10.0	7.13×10^{-5}	$[BT]_0 = 2.5\times10^{-5}$ M
30.0	7.14×10^{-5}	$[NiZ^{2-}] = 8.25_5$ mM
iii) Cobalt(II)-DTPA system		
Concentration of DTPA, mM	k^+ M^{-1} sec^{-1}	
5.0	2.00×10^{-4}	pH = 10.30
10.0	2.00×10^{-4}	$[BT]_0 = 2.5\times10^{-5}$ M
20.0	2.02×10^{-4}	$[CoZ^{3-}] = 7.13$ mM
iv) Nickel(II)-DTPA system		
Concentration of DTPA, mM	k^+ M^{-1} sec^{-1}	
5.0	1.27×10^{-5}	pH = 10.12
10.0	1.30×10^{-5}	$[BT]_0 = 2.0\times10^{-5}$ M
20.0	1.29×10^{-5}	$[NiZ^{3-}] = 10.45$ mM

ii) In solutions of a given pH and given concentrations of uncomplexed and complexed chelating agents CyDTA or DTPA, k^+ is independent of the initial concentration of BT, $[BT]_0$ (Table 2).

iii) In solutions of a given pH, a given concentration of a chelating agent (CyDTA or DTPA), and a given initial concentration of BT, k^+ is exactly proportional to the concentration of the metal(II) chelate of CyDTA or DTPA (Table 3).

iv) As is shown by the curves in Fig. 2, in solutions of a given initial concentration of BT and given concentrations of a free chelating agent (CyDTA or DTPA) and its metal(II) chelate, k^+ is a linear function of the reciprocal of the concentration of hydrogen ions and is given by:

Table 2. Dependence of k^+ on the initial concentration of BT
$\mu = 0.30$, $\lambda = 630$ mμ

i) Cobalt(II)-CyDTA system		
Concentration of BT, M	k^+ M^{-1} sec^{-1}	
1.0×10^{-5}	1.76×10^{-4}	pH = 9.95
2.5×10^{-5}	1.78×10^{-4}	$[CoZ^{2-}] = 10.0$ mM
3.5×10^{-5}	1.77×10^{-4}	$[Z]_f = 10.0$ mM
ii) Nickel(II)-CyDTA system		
Concentration of BT, M	k^+ M^{-1} sec^{-1}	
1.25×10^{-5}	7.14×10^{-5}	pH = 10.00
2.50×10^{-5}	7.13×10^{-5}	$[NiZ^{2-}] = 8.25_5$ mM
3.75×10^{-5}	7.15×10^{-5}	$[Z]_f = 10.0$ mM
iii) Cobalt(II)-DTPA system		
Concentration of BT, M	k^+ M^{-1} sec^{-1}	
2.5×10^{-5}	2.36×10^{-4}	pH = 10.39
3.5×10^{-5}	2.32×10^{-4}	$[CoZ^{3-}] = 7.13$ mM
5.0×10^{-5}	2.40×10^{-4}	$[Z]_f = 10.0$ mM
iv) Nickel(II)-DTPA system		
Concentration of BT, M	k^+ M^{-1} sec^{-1}	
2.0×10^{-5}	1.32×10^{-5}	pH = 10.12
4.0×10^{-5}	1.30×10^{-5}	$[NiZ^{3-}] = 10.45$ mM
6.0×10^{-5}	1.33×10^{-5}	$[Z]_f = 10.0$ mM

$$k^+ = k_\alpha + k_\beta/[H^+] \quad (4)$$

As in the case of the exchange reactions of BT with cobalt(II) and nickel(II) chelates of EDTA,[1,2] these facts clearly indicate that the present reactions also proceed through the following two simultaneous reaction paths:

$$\text{i)}\quad HD^{2-} + MZ^{2-m} \underset{k_1^-}{\overset{k_1^+}{\rightleftarrows}} MD^- + HZ^{1-m}$$

$$\text{ii)}\quad HD^{2-} \overset{\text{rapid}}{\rightleftarrows} H^+ + D^{3-}$$

$$D^{3-} + MZ^{2-m} \underset{k_2^-}{\overset{k_2^+}{\rightleftarrows}} MD^- + Z^{m-}$$

rate-determining step

where HZ^{1-m} and Z^{m-} mean incompletely- and completely-deprotonated CyDTA or DTPA anions, and MZ^{2-m} the metal(II) chelate of CyDTA or DTPA.

Consequently, k^+ should be given by:

$$k^+ = (k_1^+ + k_2^+ \cdot k_2/[H^+])[MZ^{2-m}] \quad (5)$$

where k_2 refers to the dissociation constant of the second phenolic group of BT.[6]

From the slopes of the linear relation between $k^+/[MZ^{2-m}]$ and $1/[H^+]$ and the intercepts, the k_1^+ and k_2^+ values were estimated. These values

6) G. Schwarzenbach and W. Biedermann, *Helv. Chim. Acta*, **31**, 678 (1948).

TABLE 3. DEPENDENCE OF k^+ ON THE CONCENTRATION OF METAL(II) CHELATE
$\mu = 0.30$, $\lambda = 630$ mμ

i) Cobalt(II)-CyDTA system

Concentration of Co(II)-CyDTA mM	k^+ M^{-1} sec^{-1}	Ratio Calcd	Ratio Obsd	
5.0	8.82×10^{-5}	1.00	1.00	pH = 9.95
10.0	1.78×10^{-4}	2.00	2.02	$[BT]_0 = 2.5\times10^{-5}$ M
15.0	2.73×10^{-4}	3.00	3.10	$[Z]_f = 10.0$ mM

ii) Nickel(II)-CyDTA system

Concentration of Ni(II)-CyDTA mM	k^+ M^{-1} sec^{-1}	Ratio Calcd	Ratio Obsd	
4.13	3.56×10^{-5}	1.00	1.00	pH = 10.00
8.25_5	7.13×10^{-5}	2.00	2.01	$[BT]_0 = 2.5\times10^{-5}$ M
16.51	1.42×10^{-4}	4.00	3.99	$[Z]_f = 10.0$ mM

iii) Cobalt(II)-DTPA system

Concentration of Co(II)-DTPA mM	k^+ M^{-1} sec^{-1}	Ratio Calcd	Ratio Obsd	
5.10	8.14×10^{-5}	1.00	1.00	pH = 10.00
7.13	1.18×10^{-4}	1.40	1.45	$[BT]_0 = 2.5\times10^{-5}$ M
10.20	1.70×10^{-4}	2.00	2.09	$[Z]_f = 10.0$ mM

iv) Nickel(II)-DTPA system

Concentration of Ni(II)-DTPA, mM	k^+ M^{-1} sec^{-1}	Ratio Calcd	Ratio Obsd	
5.0	8.70×10^{-6}	1.00	1.00	pH = 10.12
10.0	1.69×10^{-5}	2.00	1.94	$[BT]_0 = 4\times10^{-5}$ M
15.0	2.55×10^{-5}	3.00	2.93	$[Z]_f = 10.0$ mM

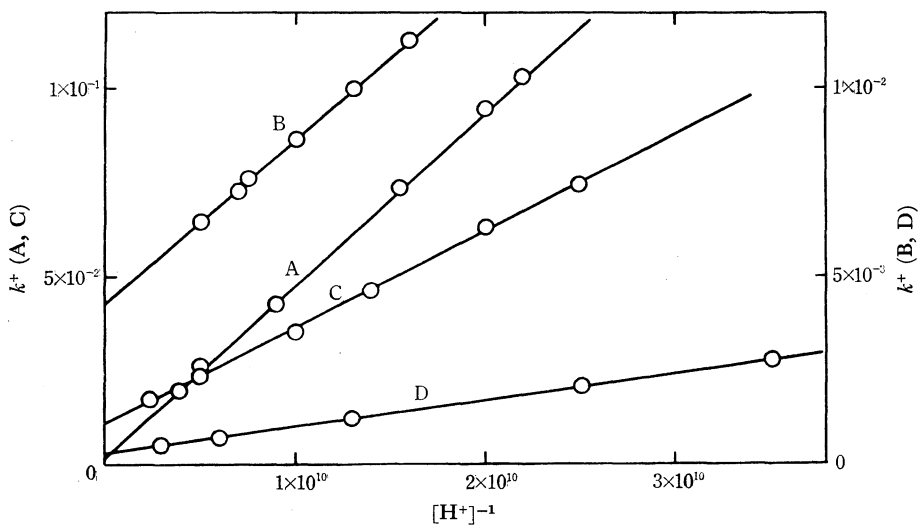

Fig. 2. The relation between $k^+/[MZ^{2-m}]$ and the concentration of hydrogen ion.
$\mu = 0.30$, $\lambda = 630$ mμ
Initial concentration of BT = 2.5×10^{-5} M
A : Co(II)-CyDTA system
B : Ni(II)-CyDTA system
C : Co(II)-DTPA system
D : Ni(II)-DTPA system

are given in Table 4, together with those for the reactions of EDTA chelates reported previously.[1,2] Margerum *et al.* have mentioned in their report[7] that, in the substitution reactions of polyamines

7) J. D. Carr, R. A. Libby and D. W. Margerum, *Inorg. Chem.*, **6**, 1083 (1967).

TABLE 4. k^+ VALUES

i) Cobalt(II) system (20°C)

System	k_1^+* M^{-1} sec^{-1}	k_2^+ M^{-1} sec^{-1}
EDTA[1]	—	6.76×10^{2}
CyDTA	1.7×10^{-3}	9.26×10^{-1}
DTPA	1.1×10^{-2}	5.25×10^{-1}

ii) Nickel(II) system (15°C)

System	k_1^+* M^{-1} sec^{-1}	k_2^+ M^{-1} sec^{-1}
EDTA[2]	—	1.24
CyDTA	4.25×10^{-3}	8.90×10^{-2}
DTPA	2.9×10^{-4}	1.48×10^{-2}

* These values are less accurate.

with a copper(II)-CyDTA chelate, the cyclohexane ring in CyDTA does not change the general reaction mechanism (glycinate intermediate mechanism), but does affect the exchange rate considerably. Generally, if two exchange reactions involving metal chelate have the same reaction mechanism, the reaction with the stable chelate will be slower than that with a less stable chelate, because the stable reactant, as compared with the less stable one, often corresponds to the less stable transition state, and hence, to the diminished reactivity.

In the exchange reactions of BT with cobalt(II) and nickel(II) chelates of CyDTA have the same reaction mechanism as those with EDTA chelates (glycinate mechanism), we can estimate the relative rate constants as was done previously.[3] Hence, from a comparison of the observed rate constant with the theoretically-calculated one, we can probably estimate the steric effect of the cyclohexane ring on the exchange reaction of BT in a quantitative manner. Relative rate constants calculated with the aid of Eq. (5) of Ref. 3 by using the numerical values listed in Table 5 are given in

TABLE 5. STABILITY CONSTANTS*

1) EDTA chelates
$K_{CoY} = 10^{15.71}$[10], $K_{NiY} = 10^{18.02}$[10]
$K_{CuY} = 10^{18.70}$[15]**
2) CyDTA chelates
$K_{CoZ} = 10^{18.32}$[10], $K_{NiZ} = 10^{18.80}$[11]
$K_{CuZ} = 10^{21.96}$[16]**
3) DTPA chelates[12]
$K_{CoZ} = 10^{18.17}$, $K_{NiZ} = 10^{19.38}$
4) α-Amino-α-methylpropionate[13]
$K_{CoX} = 10^{3.51}$, $K_{NiX} = 10^{4.56}$
$K_{CuX} = 10^{8.26}$**
5) 1-Aminocyclohexanecarboxylate[14]
$K_{CoX} = 10^{3.87}$, $K_{NiX} = 10^{4.90}$
$K_{CuX} = 10^{8.59}$**

* These values are calculated from the relevant stability constants in solutions of ionic strength 0.10 and the activity constants of the ions calculated by means of Davies equation.[17]
** Values at $\mu = 0.10$.

Table 6, together with the observed values.*2 Here, the calculation was carried out by choosing both α-amino-α-methylpropionate and 1-aminocyclohexanecarboxylate as models; the statistical factor and the stabilization due to the electrostatic attraction[8] were also taken into consideration. The results clearly show that in the reactions of BT with both cobalt(II) and nickel(II) chelates of CyDTA, the steric effect due to the cyclohexane ring is surprisingly small. A small steric effect of the cyclohexane ring on the oxidation reaction of the iron(II)-CyDTA chelate by dissolved oxygen was also mentioned by Kurimura *et al.*[9] The

TABLE 6. k^+ RATIO

	EDTA			CyDTA					DTPA		
	Calcd	Obsd	R*	Calcd$_1$**	Calcd$_2$***	Obsd	R_1*	R_2*	Calcd	Obsd	R*
Co(II)	1.00	1.00	1.00	5.61×10^{-3}	2.45×10^{-3}	1.37×10^{-3}	4.1	1.8	4.35×10^{-3}	7.76×10^{-4}	5.6
Ni(II)	1.00	1.00	1.00	3.62×10^{-1}	1.66×10^{-1}	8.90×10^{-2}	4.1	1.9	7.90×10^{-2}	1.19×10^{-2}	6.6

* Ratio between k^+ calculated and that observed.
** 1-Aminocyclohexanecarboxylate was chosen as a model.
*** α-Amino-α-methylpropionate was chosen as a model.

8) T. J. Bydalek and D. W. Margerum, *Inorg. Chem.*, **2**, 678 (1963).
9) Y. Kurimura, R. Ochiai and N. Matsuura, This Bulletin, **41**, 2234 (1968).
*2 Here, the k_2^+ values were compared with the calculated ones, because the k_1^+ values are less accurate.
10) G. Schwarzenbach, R. Gut and G. Anderegg, *Helv. Chim. Acta*, **37**, 937 (1954).
11) J. H. Holloway and C. N. Reilley, *Anal. Chem.*, **32**, 249 (1960).
12) E. J. Durham and D. P. Ryskiewick, *J. Am. Chem. Soc.*, **80**, 4813 (1958).
13) H. Irving and L. D. Pittit, *J. Chem. Soc.*, **1963**, 1946.
14) H. Irving and L. D. Pittit, *ibid.*, **1963**, 1546.
15) B. D. Sarma and P. Ray, *J. Indian Chem. Soc.*, **33**, 841 (1956).
16) G. Anderegg, *Helv. Chim. Acta*, **46**, 1833 (1963).
17) J. N. Butler, "Ionic Equilibrium," Addison-Wesley Publishing Co., Reading, Massachusetts (1964), p. 437.

above explanation, that the diminished activity of CyDTA chelates observed can be ascribed to the steric hindrance due to the cyclohexane ring, is also supported by the fact that ratio between the k^+ ratio calculated and that observed, R, was almost constant, irrespective of the metal(II) ion (Table 6).

In the case of the reaction of copper(II) chelates with polyamine, the ratio between the observed rate constant and the one theoretically predicted on the basis of the glycinate intermediate was calculated to be about 1 : 50. The smaller steric effect of the cyclohexane ring on the reaction of BT can probably ascribed to the planar configuration of the BT anion in the mixed ligand intermediate.

In a similar way, by using the numerical values in Table 5, the relative rate constants for the reactions of BT with DTPA chelates were calculated on the basis of the glycinate mechanism; they are compared with the observed values in Table 6. The results may indicate that the $-CH_2-CH_2-N(CH_2-COO^-)-CH_2-CH_2-N(CH_2-COO^-)_2$ group of DTPA has a larger steric effect on the exchange reactions of BT than does the cyclohexane ring in CyDTA.

BULLETIN OF THE CHEMICAL SOCIETY OF JAPAN VOL. 42 168—177 (1969)

Metal Complexes with Amino Acid Amides. II. Preparations and Circular Dichroism Behavior of the Copper(II) Complexes

Takashi KOMORITA, Jinsai HIDAKA and Yoichi SHIMURA

Department of Chemistry, Faculty of Science, Osaka University, Toyonaka, Osaka

(Received June 10, 1968)

Planar bis-type complexes of copper(II) with L-leucine-, L-valine-, L-phenylalanine- and L-proline-amidate ligands have been newly synthesized and characterized mainly spectroscopically together with the known complexes with glycine- and L-alanine-amidates. The geometrical structures of these $[Cu(N)_4]$-type complexes have been tentatively determined. The blue colored complexes, $Cu(glycine\text{-}amide)_2SO_4$ and its L-alanine amide analogue, have been isolated, too. The circular dichroism spectra of the complexes containing optically active ligands have been measured in various solvents and discussed in comparison with the available data for square planar d^8-complexes or for amino acidato complexes. A number of interesting relations were observed among the circular dichroism spectra of the copper(II) and the square planar d^8 complexes with optically active bidentate ligands.

It has been well known that most of copper(II) complexes have tetragonally distorted octahedral structures.[1] Since the degree of the distortion, which has been called tetragonality, seems to vary continuously up to the limit of a square planar structure,[2] there are some difficulties in studying the structures of copper(II) complexes in solution. Jørgensen has marked out the tetragonalities of various copper(II) complexes in solution by comparing their electronic spectra with those of the corresponding nickel(II) complexes which have essentially octahedral symmetry.[2] This method, however, cannot be applied to a group of the copper(II) complexes, to which diamagnetic square planar, not octahedral, nickel(II) complexes correspond.

Yasui *et al.*[3] have ascertained experimentally the possibility to resolve the ligand field bands of copper(II) complexes in solution into their split components by means of the circular dichroism (CD), and Wellman *et al.*[4] have suggested a relationship between the signs (and the magnitudes also) of the Cotton effects and the chelate ring conformations of the amino acidato copper(II) complexes. This suggestion has been somewhat modified by Martin *et al.*[5] In these circumstances, it is thought to be desirable to apply a CD study to the copper(II) complexes to which diamagnetic planar nickel(II) complexes correspond.

1) L. E. Orgel and J. D. Dunitz, *Nature*, **179**, 462 (1957).

2) C. K. Jørgensen, *Acta Chem. Scand.*, **9**, 1362 (1955).

3) T. Yasui, J. Hidaka and Y. Shimura, *J. Am. Chem. Soc.*, **87**, 2762 (1965); T. Yasui, This Bulletin, **38**, 1746 (1965).

4) K. M. Wellman, T. G. Mecca, W. Mungall and C. R. Hare, *J. Am. Chem. Soc.*, **89**, 3646, 3647 (1967); **90**, 805 (1968); *Chem. Eng. News*, **48**, (Oct. 2, 1967).

5) R. B. Martin, J. M. Tsangaris and J. W. Chang, *J. Am. Chem. Soc.*, **90**, 821 (1968).

In the first paper of this series,[6] the two types of nickel(II) complexes, Ni(α-amino-acid-amide)$_2$-$SO_4 \cdot xH_2O$ and Ni(α-amino-acid-amidate)$_2 \cdot xH_2O$, have been reported. The copper(II) complexes (R-type)[7] corresponding to the latter type of nickel(II) complexes with glycine-, L-alanine- or D,L-leucine-amidate have been already prepared,[8] but none of them has been studied concerning their electronic spectra.

In the present paper, we report the preparations of some new complexes of R-type with L-leucine-, L-valine-, L-phenylalanine- or L-proline-amidate and of another new type (B-type)[7] of the copper-(II) complexes, $Cu(glyaH)_2SO_4$ and Cu(L-alaaH)$_2$-$SO_4 \cdot H_2O$,[9] which corresponds to the former type of nickel(II) complexes cited above. The electronic absorption and CD spectral data of all these complexes obtained are discussed in relation to their structures.

Experimental

Preparation. *1) Amino Acid Amides.*[9] The following six amino acid amides used as ligands were derived from the corresponding amino acids by the similar method as described in literature.[10]

glyaH (from chloroform); mp 67.5—68.5°C.

L-alaaH (from chloroform); mp 83—84°C; $[\alpha]_{589} = +11.1°$.

L-leuaH (from benzene); mp 103—104°C; $[\alpha]_{589} = +7.3°$.

Found: N, 21.60%. Calcd for $C_6H_{14}N_2O$: N, 21.52%.

L-valaH (from benzene); mp 87—89°C; $[\alpha]_{589} = +12.2°$.

Found: N, 24.27%. Calcd for $C_5H_{12}N_2O$: N, 24.33%.

L-phalaaH (from benzene); mp 95—96°C; $[\alpha]_{589} = +17.8°$.

Found: N, 17.14%. Calcd for $C_9H_{12}N_2O$: N, 17.06%.

L-proaH (from benzene); mp 106.5—107.5°C; $[\alpha]_{589} = -79.3°$.

Found: N, 24.56%. Calcd for $C_5H_{10}N_2O$: N, 24.54%.

The measurements of the specific rotations were made for the aqueous solutions ($c = 10$) at room temperature (19—21°C). All the melting points were uncorrected.

2) Bis(amino-acid-amidato)copper(II) Complexes. The general preparation procedure of these complexes are as follows. Eleven milliformoles (mF) of amino acid amide was dissolved in 5—30 m*l* of water and the solution was added to the solution containing 1.0 g (5 mF) of copper(II) acetate monohydrate in 15 m*l* of water. Then 5—10 m*l* of the aqueous solution containing 0.40 g (10 mF) of sodium hydroxide was added dropwise to the bluish violet solution with mechanical stirring. The desired complex was crystallized out from the resulted reddish violet solution[11] (filtered if necessary) by an appropriate procedure of the followings, namely, vacuum concentration below 35°C, addition of ethanol (or methanol) and then of ether, or the combined procedure.

Freshly prepared copper(II) hydroxide was also good starting material, which could be used in place of copper(II) acetate monohydrate and sodium hydroxide in the above procedure. All the complexes in this category were obtained in good yields, and only one kind of crystals[12] could be isolated for each of the ligands. Recrystallization was made by one of the following procedures: (I) ethanol and then ether were added to the concentrated aqueous solution, (II) ether was added to the concentrated methanolic solution, (III) the aqueous solution was concentrated *in vacuo*, or (IV) the methanolic solution was concentrated by evaporating in air.

Bis(glycine-amidato)copper(II) Monohydrate: $Cu(glya)_2 \cdot H_2O$. Recrystallized by I.

Found: C, 21.31; H, 5.44; N, 24.65%. Calcd for $C_4H_{12}N_4O_3Cu$: C, 21.08; H, 5.31; N, 24.61%.

Bis(L-alanine-amidato)copper(II): Cu(L-alaa)$_2$. Recrystallized by I.

Found: C, 30.22; H, 5.37; N, 23.63%. Calcd for $C_6H_{14}N_4O_2Cu$: C, 30.31; H, 5.94; N, 23.57%.

Bis(L-leucine-amidato)copper(II): Cu(L-leua)$_2$. Recrystallized by IV and dried over calcium chloride; pink needles; soluble in methanol and moderately soluble in water and ethanol. The raw product was the mixture of the two forms of crystals, the needle and the plate: infrared spectra in NaCl region, however, showed no difference between them.

Found: C, 44.40; H, 8.07; N, 17.19%. Calcd for $C_{12}H_{26}N_4O_2Cu$: C, 44.78; H, 8.14; N, 17.40%.

Bis(L-valine-amidato)copper(II) Dihydrate: Cu(L-vala)$_2 \cdot 2H_2O$. Recrystallized by (IV) and dried in air; violet plates; soluble in water, methanol and ethanol to give reddish violet solutions.

Found: C, 36.48; H, 7.58; N, 16.79%. Calcd for $C_{10}H_{26}N_4O_4Cu$: C, 36.41; H, 7.94; N, 16.98%.

Bis(L-phenylalanine-amidato)copper(II) Dihydrate and Anhydrate: Cu(L-phalaa)$_2 \cdot 2H_2O$ and Cu(L-phalaa)$_2$.

Dihydrate: recrystallized by (III) and dried in air; reddish violet plates; soluble in water, methanol and ethanol.

Found: C, 50.69; H, 6.12; N, 13.13%. Calcd for $C_{18}H_{26}N_4O_4Cu$: C, 50.75; H, 6.15; N, 13.15%.

Anhydrate: derived from the dihydrate by drying *in vacuo* over phosphorus pentoxide overnight; pink solid.

Found: C, 55.15; H, 5.74; N, 14.26%. Calcd for

6) T. Komorita, J. Hidaka and Y. Shimura, This Bulletin, **41**, 854 (1968).

7) R-type: red colored Cu(II) complex, B-type: blue colored Cu(II) complex.

8) P. Bergell and T. Brugsch, *Z. physiol. Chem.*, **67**, 97 (1910); M. M. Rising and P. S. Yang, *J. Biol. Chem.*, **99**, 755 (1933).

9) The following abbreviations are used for ligands: glyaH=glycine amide, alaaH=alanine amide, leuaH=leucine amide, valaH=valine amide, phalaaH=phenylalanine amide, proaH=proline amide, glyH=glycine, alaH=alanine, leuH=leucine, valH=valine, proH=proline, hyproH=hydroxyproline, piaH=α-picoline amide, $biuH_2$=biuret and $glyglyH_2$=glycylglycine.

10) P. S. Yang and M. M. Rising, *J. Am. Chem. Soc.*, **53**, 3183 (1931); G. Hillmann, *Z. Naturforsch.*, **1**, 682 (1946).

11) When L-leuaH or L-phalaaH was used as the ligand, the desired crystals separated out at this stage.

12) As for the L-leucine amidato complex, see below.

$C_{18}H_{22}N_4O_2Cu$: C, 55.44; H, 5.69; N, 14.37%.

Bis(L-proline-amidato)copper(II) Dihydrate: Cu(L-proa)$_2$·2H$_2$O. Recrystallized by (II) and dried *in vacuo* over calcium chloride; pink needles; soluble in water, methanol, ethanol and *N*,*N*-dimethylformamide, and slightly soluble in pyridine.

Found: C, 36.85; H, 6.83; N, 17.10%. Calcd for $C_{10}H_{22}N_4O_4Cu$: C, 36.86; H, 6.81; N, 17.19%.

3) Bis(amino-acid-amide)copper(II) Sulfates. Bis(glycine-amide)copper(II) Sulfate: Cu(glyaH)$_2$SO$_4$. Copper(II) sulfate pentahydrate (0.84 g) and 0.50 g of glycine amide were dissolved in 5 m*l* of water. After stirring the solution for several min, the blue crystals were obtained by adding a small amount of methanol to the blue solution. This complex was recrystallized from the aqueous solution by adding a small amount of methanol, washed with methanol and then with ether, and dried *in vacuo* over phosphorus pentoxide overnight; very soluble in water but insoluble in methanol and ethanol.

Found: C, 15.34; H, 4.00; N, 17.51%. Calcd for $C_4H_{12}N_4O_6SCu$: C, 15.61; H, 3.93; N, 18.21%.

Bis(L-alanine-amide)copper(II) Sulfate Monohydrate: Cu(L-alaaH)$_2$SO$_4$·H$_2$O. Preparation and purification of this complex was carried out in the same way as given for the corresponding complex with glycine amide. The yield was almost quantitative. Shiny blue plates; very soluble in water but insoluble in methanol and ethanol.

Found: C, 20.70; H, 4.77; N, 15.11; H$_2$O, 4.94%. Calcd for $C_6H_{18}N_4O_7SCu$: C, 20.37; H, 5.13; N, 15.83; H$_2$O, 5.09%.

The water of crystallization was analyzed by the weight loss under aspirator pressure at 60°C.

4) Glycinato(glycine-amidato)copper(II) Monohydrate: Cu(gly)(glya)·H$_2$O. Bis(glycine-amidato)copper(II) in aqueous solution undergoes stepwise hydrolysis of the ligands during several weeks at room temperature and finally changes into bis(glycinato)copper(II). Glycinato-(glycine-amidato)copper(II) monohydrate, an intermediate of the hydrolysis, separated out when a concentrated aqueous solution of Cu(glya)$_2$·H$_2$O was allowed to stand on a warm water bath for several hours. This intermediate complex was also obtained easily by concentrating rapidly the aqueous solution containing Cu(gly)$_2$·H$_2$O and Cu(glya)$_2$·H$_2$O (1 : 1). Recrystallization was made by adding methanol to the aqueous solution of the complex. Shiny violet plates; soluble in water, slightly soluble in methanol and insoluble in ethanol.

Found: C, 21.16; H, 4.90; N, 18.34%. Calcd for $C_4H_{11}N_3O_4Cu$: C, 21.01; H, 4.85; N, 18.37%.

5) *Bis(amino-acid-amide)copper(II) Sulfate Solutions.* The five and ten milliformoles per liter aqueous solutions of bis(amino-acid-amide)copper(II) sulfate were prepared for the absorption and CD spectral measurements, respectively: one (or two) milliliter(s) of the 100 mF $CuSO_4$ and 0.2 mF (or 0.4 mF) of the ligand (L-leuaH, L-valaH, L-phalaaH or L-proaH) were dissolved in water, and the total volume was adjusted to 20 m*l*. Copper (II) sulfate pentahydrate used was a Special Grade reagent produced by Wako Pure Chemical Industries, Ltd.

Measurements. The absorption, diffuse reflectance and CD measurements were made by a Beckman DU spectrophotometer, a Hitachi EPU-2A spectrophotometer and a Roussel-Jouan dichrographe, respectively, at room temperature. Ethanol and methanol used for these measurements as the solvents were dehydrated by refluxing with corresponding magnesium alkoxide and distilled. The solvent *N*,*N*-dimethylformamide was a commercial Spectro Grade one produced by Dojindo & Co., Ltd. No significant change of the spectra was found during every measurement.

Results and Discussion

1) N–O and N–N Coordination of the α-

Table 1. Absorption and reflectance spectral data of the B-type complexes

Complex[a)]	Solvent or condition[b)]	Maximum[c)] ν_{max} (log ε)	Band-width[c,d)] δ	Concentration[e)]
$Cu(glyaH)_2SO_4$	(S)	14.9	4.9	—
	(W)	15.2 (1.53)	5.7	6.5
$Cu(L\text{-}alaaH)_2SO_4\cdot H_2O$	(S)	15.3	4.9	—
	(W)	15.6 (1.49)	5.8	5.5
$Cu(L\text{-}leuaH)_2SO_4$	(W)[f)]	15.7 (1.59)	6.0	5.0
$Cu(L\text{-}valaH)_2SO_4$	(W)[f)]	15.7 (1.57)	6.4	5.0
$Cu(L\text{-}phalaaH)_2SO_4$	(W)[f)]	15.6 (1.56)	6.1	5.0
$Cu(L\text{-}proaH)_2SO_4$	(W)[f)]	16.0 (1.65)	6.0	5.0
trans-$Cu(gly)_2\cdot H_2O$	(S)[g)]	16.3	4.8	—
cis-$Cu(gly)_2\cdot H_2O$	(S)[g)]	15.7	4.0	—
	(W)[g)]	15.9 (1.65)	4.7	5.0
$[Cu(piaH)_2(OH_2)_2]Cl_2$	(W)[h)]	14.5 (1.47)	5.0	7.15

a) Abbreviations: footnote 9.
b) Abbreviations: S=solid, W=water.
c) Wave number's are given in 10^3 cm^{-1} unit.
d) Apparent band-width at half extinction.
e) 10^{-3} F unit.
f) These solutions were prepared as described in the Experimental section 5).
g) Ref. 13; either the trans or the cis complex gives the same spectrum in aqueous solution.
h) Ref. 14 and M. Sekizaki, private communication.

Amino Acid Amides. In Table 1, the electronic absorption data of the B-type complexes are summarized with some referable data. It has been concluded in the former paper[6] that α-amino acid amide chelates through an amide oxygen and an amino nitrogen to a central metal ion in the bis-(amino-acid-amide)nickel(II) complexes. The N-O coordination is also inferred for the corresponding B-type copper(II) complexes, $Cu(glyaH)_2SO_4$ and $Cu(L\text{-}alaaH)_2SO_4\cdot H_2O$, in the solutions and in the solid states from their electronic spectra. Another support for the common type of coordination between the bis(amino-acid-amide)-copper(II) and -nickel(II) complexes is furnished from the infrared (IR) spectra. The IR spectra of all these complexes show two very strong bands, which are very specific to this type of complexes, in each of their 6μ regions.[15] It may be possible to suggest that the $[Cu(L\text{-amino-acid-amide})_2(OH_2)_2]^{2+}$ ion is only the probable species in the solution.[16]

The electronic absorption and reflectance data of the R-type complexes are summarized with some references in Table 2. The $K_2[Cu(biu)_2]\cdot 4H_2O$[18] and $K_2Cu(glygly)_2\cdot 6H_2O$[20] have been known to have planar $Cu(N)_4$ structure. From the comparison with the electronic spectral data in the solutions and in the solid states and the referable data, it may be concluded that the amino acid amidato ligands in the R-type complexes have the N-N coordination through an amino nitrogen and an amidato nitrogen. The same conclusion has been previously applied for the corresponding nickel(II) and palladium(II) complexes.[6]

2) Solvation and Geometrical Isomerism. The following factors may be inferred to influence considerably the ligand field bands of both the B- and R-type complexes: (a) interaction between copper(II) ion and solvent molecules along with the normal of the coordination square, (b) geometrical isomerism of the complexes, and (c) electronic and structural characteristics of the ligands.

With respect to the five R-type complexes with the L-amino acid amidato ligands, the absorption maxima (ν_{max}) are distributed within the ranges 19000—19500 in water and 19900—20100 cm^{-1} in ethanol respectively, as shown in Table 2. This fact reveals that the effect of the factor (c) is relatively small among the five L-amino acid amidates. The solvent dependence of ν_{max}, derived from the factor (a), is clearly larger than the effect (c). For instance, the difference of ν_{max}'s between the aqueous and the dimethylformamide solutions of $Cu(L\text{-}proa)_2$ is 1200 cm^{-1} and the one between the aqueous and the chloroform solutions of $Cu(pia)_2$, 1800 cm^{-1} (Table 2). The difference of ν_{max}'s between *trans*- and *cis*-$Cu(gly)_2\cdot H_2O$, derived from the factor (b), is only 600 cm^{-1} (Table 1). However, the factor (b) may probably be intensified in the R-type complexes because of the increased covalency in the coordination square.

Now, the ν_{max}'s of the ligand field bands of the R-type complexes shift to lower wave number's and the apparent band widths (δ) decrease in the following order of solvents (or condition): solid→dimethylformamide→ethanol→methanol→water, except for $Cu(L\text{-}vala)_2\cdot 2H_2O$ and $Cu(L\text{-}phalaa)_2\cdot 2H_2O$ in the solid states (Table 2). This spectral behavior including the case of $Cu(L\text{-}phalaa)_2\cdot 2H_2O$ may be understood on the basis of the donor properties of the solvent molecules, that is, of the factor (a). The ν_{max} value of $Cu(L\text{-}vala)_2\cdot 2H_2O$ in only the solid state exceedingly deviates from the above sequence and, in fact, is lower by as much as 1000 cm^{-1} than the value in the aqueous solution (Table 2). This cannot be explained by the coordination of water, that is, factor (a), and the factor (b) should be taken into account. Judging from the facts that most of the copper(II) bis-chelated complexes, the structures of which have been known, have trans ones[16] and that the ν_{max} of *cis*-$Cu(gly)_2\cdot H_2O$ is lower than that of the corresponding trans complex (Table 1), the geometrical structure of $Cu(L\text{-}vala)_2\cdot 2H_2O$ may be tentatively assigned to cis in the solid state and, on the contrary, to trans in the aqueous and the alcoholic solutions. Another support to the trans structure in solution may be furnished by the following observation: when a methanolic solution containing the crystals was rapidly concentrated *in vacuo*, a small amount of red crystals, which may presumably be trans, was found mixed together with the ordinary violet crystals. The other five complexes of R-type may be tentatively considered to have trans structures

13) T. Yasui and Y. Shimura, This Bulletin, **39**, 604 (1966) and T. Yasui, private communication.

14) M. Sekizaki and K. Yamasaki, *Nippon Kagaku Zasshi* (*J. Chem. Soc. Japan, Pure Chem. Sect.*), **87**, 1053 (1966).

15) T. Komorita, J. Hidaka and Y. Shimura, unpublished.

16) H. C. Freeman, "The Biochemistry of Copper," ed. by Peisach, P. Aisen and W. E. Blumberg, Academic Press, New York, N. Y. (1966), p. 77; according to a number of the X-ray analytical data, it may be reasonable to consider relatively strongly bounded $Cu(N)_2(O)_2$ square planar moieties in these complexes. See also the Discussion section 2) of the present paper.

17) Y. Nakao, K. Sakurai and A. Nakahara, This Bulletin, **39**, 1608(1966) and Y. Nakao, private communication.

18) H. C. Freeman, J. E. W. L. Smith and J. C. Taylor, *Acta Cryst.*, **14**, 407 (1961).

19) M. Kato, Y. Komuro and K. Sone, *Nippon Kagaku Zasshi* (*J. Chem. Soc. Japan, Pure Chem. Sect.*), **78**, 896 (1957).

20) A. Sugihara, T. Ashida, Y. Sasada and M. Kakudo, *Acta Cryst.*, **B24**, 203 (1968); in this complex, two water molecules are linked to the copper(II) along with the normal of the $Cu(N)_4$ plane with the Cu-O distance, 2.77 Å.

TABLE 2. ABSORPTION AND REFLECTANCE SPECTRAL DATA OF THE R-TYPE COMPLEXES

Complex[a]	Solvent or condition[b]	Maxima[c,f] ν_{max} (log ε)	Band-width[c,d] δ	Concentration[e]
$Cu(glya)_2 \cdot H_2O$	(S)	19.2	6.1	—
	(W)	18.7 (1.67)	5.6	7.1
	(Me)	18.9 (1.71), ~29 sh	5.8	4.0
$Cu(L\text{-}alaa)_2$	(S)	20.7	6.2	—
	(W)	19.1 (1.74)	5.4	2.8
	(Me)	19.6 (1.77), ~29 sh	5.9	2.7
	(Et)	20.0 (1.78), ~29 sh	5.9	2.8
$Cu(L\text{-}leua)_2$	(S)	21.2	6.4	—
	(W)	19.4 (1.76)	5.5	5.4
	(Me)	19.8 (1.79), ~29 sh	5.8	3.1
	(Et)	20.0 (1.82), ~28.5 sh	6.0	1.3
$Cu(L\text{-}vala)_2 \cdot 2H_2O$	(S)	18.5	6.5	—
	(W)	19.5 (1.74)	5.5	5.0
	(Et)	20.1 (1.78), ~28 sh	5.8	5.0
$Cu(L\text{-}phalaa)_2 \cdot 2H_2O$	(S)	19.6	6.4	—
$Cu(L\text{-}phalaa)_2$	(S)	20.7	6.7	—
	(W)	19.2 (1.73)	5.4	5.0
	(Et)	19.9 (1.78), ~28.5 sh	5.6	5.0
$Cu(L\text{-}proa)_2 \cdot 2H_2O$	(S)	~13 sh, 20.9	5.9	—
	(W)	19.5 (1.90)	5.5	5.0
	(Et)	20.1 (1.93)	5.8	5.0
	(DMF)	20.7 (1.96)	5.9	5.0
$[Cu(pia)_2] \cdot 5H_2O$	(W)[g]	17.1 (1.68)	5.8	0.98
	($CHCl_3$)[g]	18.9 (1.86)	5.2	0.38
$K_2[Cu(glygly)_2] \cdot 6H_2O$	(W)[h]	18.0 (1.72)	6.2	10
$K_2[Cu(biu)_2] \cdot 4H_2O$	(S)[i]	19.8		—
$[Cu(biu)_2]^{2-}$	(W)[j]	19.8 (1.65)		

a) Abbreviations: footnote 9.
b) Abbreviations: S=solid, W=water, Me=methanol, Et=ethanol and DMF=*N*,*N*-dimethylformamide.
c), d) and e) See Table 1.
f) shoulder.
g) See Table 1.
h) In aqueous solution (1 F glyglyH$_2$ and 2 F KOH); Ref. 17.
i) Ref. 18.
j) Ref. 19.

both in the solid states and in the solutions from the above discussion.

The ν_{max}'s of $Cu(glya)_2 \cdot H_2O$ both in the solid state and in the solutions considerably shift to lower wave number's than those in the corresponding conditions of the other R-type complexes, which are considered to be trans (Table 2). Similar shift is also observed for $Cu(glyaH)_2SO_4$ compared with the other B-type complexes (Table 1). These behavior should be attributed to the combined effect of the factors (a) and (c).

More quantitative informations about the factor (a) in these complexes may be supplied by comparing their ν_{max}'s with those of the corresponding nickel(II) complexes.[6,15] As far as the B-type is concerned, the tetragonality ratios can be obtained by Jørgensen's definition[2] as shown in Table 3; these values are very close to the value, 1.60, for bis(glycinato)copper(II). Now, concerning the R-type, the corresponding nickel(II) complexes are diamagnetic square planar ones. Neverthless we applied the ratio, ν_{Cu}/ν_{Ni}, also to these complexes, using the ligand field ν_{max}'s of the planar nickel(II) complexes (Table 3). Bis(biuretato)-cuprate(II) and -nickolate(II) may be regarded as "true" square planar complexes, since each the complex reveals the same ν_{max} value between in the aqueous solution and in the solid state. Therefore, the value, 0.91, may be considered to suggest that the nickel(II) complex has larger tetragonality than the copper(II) complex. (This value could be expected to be larger than 1 for a certain tetragonality, or for a certain octahedral field splitting (Δ), after taking the interelectronic repulsion of d^8-configuration into account.) This consideration is compatible with the theory that one electron

TABLE 3. ν_{Cu}/ν_{Ni} VALUES

B-type complex[a]	Solvent or condition	ν_{Cu}	ν_{Ni}[b]	ν_{Cu}/ν_{Ni}
$(glyaH)_2(OH_2)_2$	(W)	15.2	9.7[f]	1.57
$(L\text{-}alaaH)_2(OH_2)_2$	(W)	15.6	9.7[f]	1.61
$(piaH)_2(OH_2)_2$	(W)[c]	14.5	9.8	1.48
R-type complex				
$(glya)_2$	(S)[d]	19.2	22.9[f]	0.84
	(W)	18.7	23.1[g]	0.81
$(L\text{-}alaa)_2$	(S)	20.7	23.7[f]	0.87
	(W)	19.1	23.2[g]	0.82
	(Me)	19.6	23.4[f]	0.84
$(L\text{-}leua)_2$	(Me)	19.8	23.4[f]	0.85
$(L\text{-}vala)_2$	(Et)	20.1	23.3[g]	0.86
$(L\text{-}phalaa)_2$	(Et)	19.9	23.1[g]	0.86
$(L\text{-}proa)_2$	(W)	19.5	23.0[g]	0.85
	(Et)	20.1	23.1[g]	0.87
	(DMF)	20.7	23.4[g]	0.88
$(pia)_2$	$(CHCl_3)$[c]	18.9	23.1	0.82
$(biu)_2$	(S, W)[e]	19.8	21.7	0.91

a) Abbreviations: footnote 9.
b) Ref. 2 for B-type and see text for R-type.
c) Ref. 14.
d) Monohydrate.
e) Refs. 18 and 19.
f) Ref. 6.
g) Footnote 15.

TABLE 4. CD EXTREMA OF THE B- AND THE R-TYPE COMPLEXES

Complex[a]	Solvent	Extrema[b]	Concentration[c]
$Cu(L\text{-}alaaH)_2SO_4\cdot H_2O$	(W)	15.7 (−0.12)	40
$Cu(L\text{-}leuaH)_2SO_4$	(W)[d]	16.5 (−0.14)	10
$Cu(L\text{-}valaH)_2SO_4$	(W)[d]	17.2 (−0.22)	10
$Cu(L\text{-}phalaaH)_2SO_4$	(W)[d]	16.5 (−0.28)	10
$Cu(L\text{-}proaH)_2SO_4$	(W)[d]	14.8 (+0.13), 18.7 (−0.07)	10
$Cu(L\text{-}alaa)_2$	(W)	18.5 (−0.34)	20
	(Et)	18.5 (−0.33), 22.8 (+0.02)	20
$Cu(L\text{-}leua)_2$	(W)	18.3 (−0.43)	5
	(Me)	18.5 (−0.38)	15
	(Et)	18.4 (−0.38)	1
$Cu(L\text{-}vala)_2\cdot 2H_2O$	(W)	13.9 (+0.005), 18.7 (−0.45)	20, 10[e]
	(Et)	13.6 (+0.004), 18.5 (−0.50), 22.8 (+0.03)	20, 10[e]
$Cu(L\text{-}phalaa)_2$	(W)	13.6 (+0.004), 17.9 (−0.28), ~20 sh (−)	20, 10[e]
	(Et)	17.3 (−0.31), ~20 sh (−)	20, 10[e]
$Cu(L\text{-}proa)_2\cdot 2H_2O$	(W)	13.9 (+0.007), 17.6 (−0.30), 21.3 (−0.42)	20, 10[e]
	(Et)	17.2 (−0.44), 21.9 (−0.52)	20, 10[e]
	(DMF)	16.7 (−0.25), 19.1 (+0.20), 22.1 (−0.58)	8.5, 5[e]

a) Abbreviations: footnote 9.
b) Wave number's are given in 10^3 cm^{-1} unit and the intensities, $\varepsilon_l - \varepsilon_d$ in parentheses; sh=shoulder.
c) 10^{-3} F unit.
d) See f) of Table 1.
e) The more concentrated solution of these two was used to detect weak extrema at lower wave number's.

and none, respectively, is accommodated in the σ-antibonding (x^2-y^2)-orbital in the ground state of the copper(II) and nickel(II) complexes. The R-type copper(II) complexes seem to be more extensively influenced by the factor (a) than the corresponding nickel(II) complexes. However, it may be reasonable to regard the R-type complexes, including even the glycine amidato one, as "square planar" complexes since their ν_{Cu}/ν_{Ni} values distribute continuously in a rather narrow range, 0.81—0.88, and the minimum is comparable with 0.82 for the bis(picoline-amidato) complexes in "chloroform." It may be worthwhile to note that the ν_{max}'s of the B-type complexes shift to

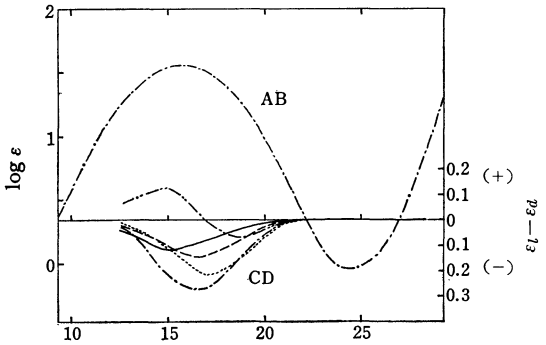

Fig. 1. Absorption and CD spectra of Cu(L-amino-acid-amide)$_2$SO$_4$ in water.
——— alaaH-; — — — leuaH-; ····· valaH-; —·—·— phalaaH-; and —··—··— proaH-complexes.

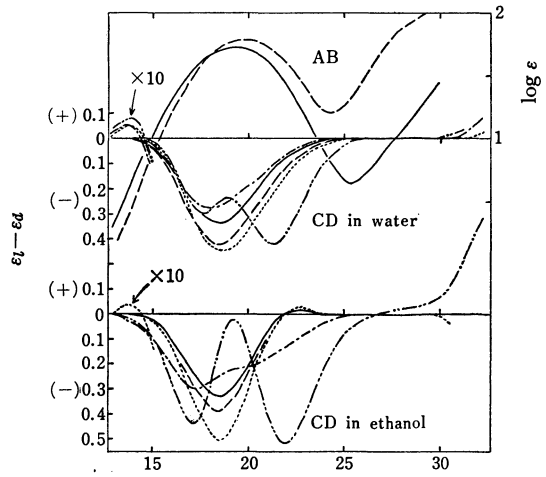

Fig. 2. Absorption and CD spectra of Cu(L-amino-acid-amidate)$_2$.
Absorption curves of Cu(L-phalaa)$_2$; —— in water; and — — — in ethanol.
CD crucves in water and in ethanol: —— alaa-; — — — leua-; ····· vala-; —·—·— phalaa-; and —··—··— proa-complexes.

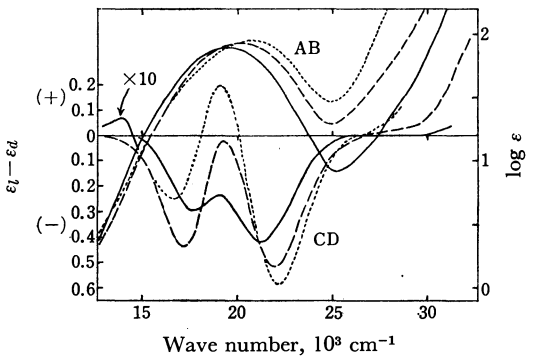

Fig. 3. Absorption and CD curves of Cu(L-proa)$_2$.
——— in water; — — — in ethanol; and ····· in DMF.

higher wave number's and the δ's increase with changing the condition from the solid states to the aqueous solutions, in contrast with those of the R-type.

3) CD of the Complexes. In general, the negative CD components are dominant in the ligand field band region of the B- and the R-type complexes with the L-optically active ligands (Table 4 and Figs. 1—3); the CD behavior of Cu(L-proaH)$_2$SO$_4$ in the aqueous solution is only the exception. It has been reported[3] that bis(L-α-amino-acidato)copper(II) complexes also exhibit ligand field CD bands, the negative components of which are dominant, too, except for those of the L-prolinato and the L-hydroxyprolinato complexes. Wellman *et al.*[4] have explained the negative Cotton effect in this region on the assumption of the puckered conformation of amino acidato chelate ring as of ethylenediamine one (Fig. 4c).

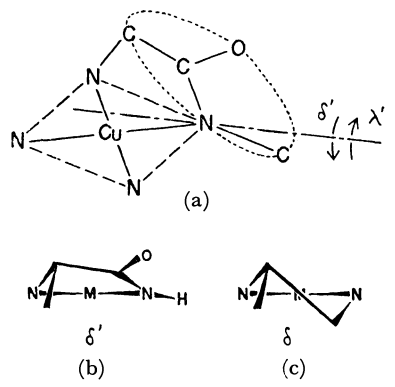

Fig. 4. Conformations of chelate rings of (a) glygly$^-$ in $K_2Cu(glygly)_2\cdot 6H_2O$ (Arrows: the C–CO–N–C plane is inclined), (b) L-amino acid amidate and (c) (+)-propylenediamine.

Informations about the conformation of α-amino acidato or α-amino acid amidato ligand will be obtained from the X-ray analytical data for *cis*-

$Cu(gly)_2 \cdot H_2O$[21] or $K_2Cu(glygly)_2 \cdot 6H_2O$.[20] In the latter complex, both the $Cu(N)_4$ square and the C–CO–N–C moiety of the ligand have good planarity respectively, but these two planes are inclined to each other, intersecting along the axis which passes through the amidato nitrogen and nearly bisects the Cu–N(amino) bond as shown in Fig. 4a. The conformation of the glycinato chelate ring in *cis*-$Cu(gly)_2 \cdot H_2O$ seems to be very similar to that of the glycylglycinato chelate ring mentioned above, and is considerably different, especially around the coordinated oxygen, from that assumed by Wellman *et al.* as shown in Figs. 4b and 4c. Now, two oppositely twisted forms are denoted by δ' and λ' as shown in Fig. 4a. Of course, it is not necessary for the explanation of the optical activity of complexes with optically active ligands to take into account any puckering of chelate rings.[22] However, dissymmetric electron distributions around the coordinated atoms, if present, could be the main origins of ligand field Cotton effects as in the treatment of the simple molecular orbital theory.[23] Since the equatorial conformations of the C_α-substituents are considered to be the preferred forms from the observations in propylenediamine chelate rings (Fig. 4c), δ'-conformation may be assigned to the predominant form in both the chelate rings of L-α-amino acid-amide and -amidate in the complexes in solution as shown in Fig. 4b.

The ligand field CD bands of the bis(L-α-amino-acid-amidato) complexes of copper(II), nickel(II) and palladium(II) have predominantly negative sign over-all.[6,15] Such a CD spectral correspondence between d^8 spin paired and d^9 complexes of bis-chelated square planar structure may be also inferred from Liehr's theory.[23] However, a possibility of direct interactions between the C_α-substituents and the metal chromophores as a source of the Cotton effects cannot be ruled out. Recently, it has been reported[24] that the mono- and bis-type complexes of palladium(II), platinum(II) and gold(III) with (−)-propylenediamine and (−)-cyclohexanediamine reveal predominantly positive CD components in the ligand field band regions, where the ligands coordinate in λ-conformations. Thus, L-α-amino acidate, L-α-amino acid-amide and -amidate and (+)-propylenediamine as bidentate ligands seem to generally give the same sign to the Cotton effects caused by a particular d–d transition.

Now, whether (α) the puckerings of chelate rings or (β) the dispositions of C_α-substituents are the main origins of the Cotton effects? As shown in Figs. 5a and 5b, Wellman *et al.*[4] and Martin

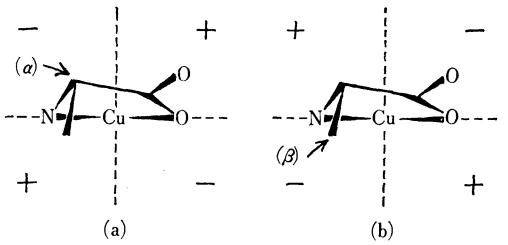

Fig. 5. (a) Wellman's and (b) Martin's spaces applied to the proposed model of L-amino acidato complex.
The signs are given to the front octants or sectors which contain the ligand. (α) and (β) indicate the supposed origins for the negative Cotton effects.

et al.[5] have applied oppositely signed spaces to L-α-amino acidato copper(II) complexes and explained their Cotton effects. This contradiction is resulted from the fact that they have simply regarded the different origin, (α) or (β), as the main source of the Cotton effects. Both explanations could revive even when each of the two spaces is applied to the models of the complexes with δ'- or λ'-conformations. It is to be noted, however, that the visible absorption band of any of these copper(II) complexes would possibly be the overlap of four components, that different origins would possibly be effective to different CD components, and consequently that such an alternately (+)- and (−)-signed space as the octant one for the n–π^* transition of ketones should be determined for a particular transition rather than for a particular geometry of the molecules. Indeed, it is in question whether the main positive CD components of the copper(II) complexes with L-prolinate, L-proline-amide and -amidate, and L-histidine amide[15] and the main negative ones of the corresponding copper-(II) complexes with the other simple L-α-amino acid derivatives (like L-alanine derivatives) might be assigned to the same d–d transition or not. More investigations seem to be necessary to answer these questions.

The CD spectra of the R-type complexes are considerably influenced by changing the solvent. However, a general pattern of the curve for each the complex is well retained as may be seen in Figs. 2 and 3. This fact may point out that the change of solvent gives rise to little changes in the equilibria between the chelate ring conformations (inclined to δ') and between the geometrical isomers (presumably inclined to trans).

21) H. C. Freeman, M. R. Snow, I. Nitta and K. Tomita, *ibid.*, **17**, 1463 (1964).

22) The puckering found in the glycinato or the glycylglycinato chelate ring is somewhat smaller in size, and might be more flexible, than that of ethylenediamine chelate ring. CD data for the copper(II) complexes with some tetradentate ligands seem to reveal such a somewhat ambiguous nature of the conformations of the ligands; Ref. 5, and M. Parris and A. E. Hodges, *J. Am. Chem. Soc.*, **90**, 1909 (1968).

23) A. D. Liehr, *J. Phys. Chem.*, **68**, 3629 (1964).

24) H. Ito, J. Fujita and K. Saito, This Bulletin, **40**, 2584 (1967).

It is interesting to examine the relative order of the dissymmetric field strengths of the bidentate ligands in the complexes. The following orders are easily derived from the CD or the rotatory dispersion data:

L-alaaH$<$L-leuaH$<$L-valaH

for the B-type,

L-alaa$^-<$L-leua$^-<$L-vala$^-$

for the R-type, and

L-ala$^-<$L-leu$^-<$L-val$^-$

for the amino acidato copper(II) complexes.[3,4] From these orders, the relative dissymmetric field strengths seem to be determined by the mother amino acids. In addition the relative order, L-amino acidate$\sim$L-amino acid amide$<$L-amino acid amidate, is apparently observed for a series of the bis-type copper(II) complexes[3,4] with the ligands derived from a particular amino acid, and considered to originate from the different covalency in the coordination squares or from the different degree of the puckerings of the chelate rings.

4) CD Behavior of the Complexes with L-Proline-Amide, -Amidate and L-Prolinate. As shown in Fig. 1, the CD spectrum of Cu(L-proaH)$_2$SO$_4$ in the aqueous solution is markedly different from those of the corresponding species with the other four L-amino acid amides. It has been known[3] that Cu(L-pro)$_2$ and Cu(L-hypro)$_2$ reveal more distinct ligand field CD bands than those of the corresponding species with the other simple L-amino acidates. The CD spectrum of Cu(L-proaH)$_2$SO$_4$ is very similar to that of Cu(L-pro)$_2$ in aqueous solution. Cu(L-proa)$_2$ also reveals a very specific CD behavior, although its negative CD components are dominant as those of the other R-type complexes (Figs. 2 and 3). Similar behavior has been observed in Ni(L-proa)$_2$, too.[15] A common nature in the CD behavior among Cu(L-proa)$_2$, Cu(L-proaH)$_2^{2+}$ and Cu(L-pro)$_2$ could be derived from the fact that a positive component of the former complex in the dimethylformamide solution is so conspicuous as those of the latter two in the aqueous solutions (Fig. 3).

From these considerations, it may be possible to say that the dissymmetric fields produced near the Cu(N)$_4$ chromophores are specified by the coordinated L-proline-amide, -amidate and L-prolinate.[25] The specificity might potentially be derived from the following origins: i) asymmetry of the pyrrolidine nitrogen;[3] ii) direct interaction between the chromophore and one of the two hydrogen atoms attached to the fifth carbon atom of the pyrrolidine ring, which projects over the coordination square as shown in Fig. 6; and iii)

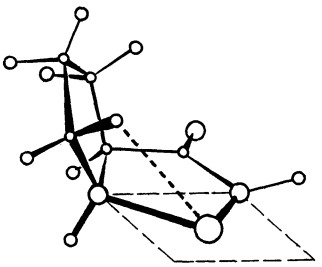

Fig. 6

fixed form of the chelate ring, which might be forced by the pyrrolidine ring together with the C–CO–O, C–CN–O or C–CO–N moiety. It may be said that the data for bis(*N*-methyl-L-prolinato)copper(II) show the effectiveness of i) or ii).[5] On the other hand, the CD behavior of Cu(L-proa)$_2$, which is considerably different from that of Cu(L-pro)$_2$ or Cu(L-proaH)$_2^{2+}$, may be considered to show the effectiveness of iii). As a consequence of iii), asymmetry of the electron distribution near the amidato nitrogen (or the coordinated carboxyl oxygen) should be noted. This effect cannot be simply ruled out, since the charge transfer band of Cu(L-proa)$_2$ (presumably, metal-amidate in nature), for example, occurs at rather lower wave number's (Fig. 3).

5) The Near-Ultraviolet Absorption Band of R-type Complex. All the R-type complexes

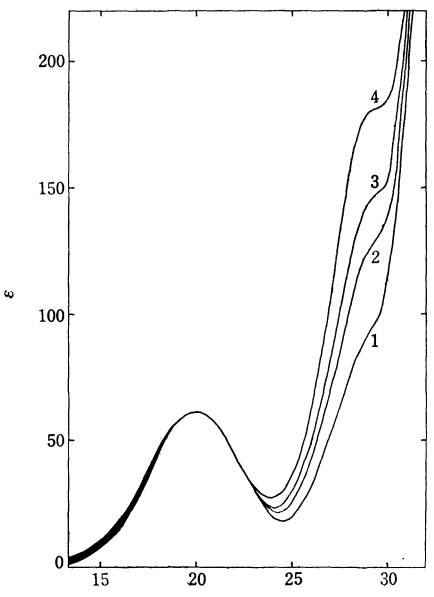

Fig. 7. Absorption spectrum of Cu(L-alaa)$_2$ in ethanol.
1: 8.4 mF 2: 2.8 mF 3: 1.4 mF 4: 0.7 mF

25) On the basis of this specification and the presumed trans structure of Cu(L-proa)$_2$, it seems to be rather unreasonable to assign cis structure to Cu(L-pro)$_2$ in water; R. D. Gillard, *Inorg. Chim. Acta Rev.*, **1967**, 69.

exhibit another kind of absorption bands (Band II) at about 29000 cm^{-1} in the alcoholic solutions (Table 2 and Figs. 2 and 7). (Band II seems to be almost embedded in the charge transfer band in the spectrum of the L-proline amidato complex.) These bands disappear in aqueous solution or in solid state, though the disappearance is not perfect in aqueous solution. As may be seen in Fig. 7, the Band II of Cu(L-alaa)$_2$ in the ethanolic solution is accompanied with the increase of intensity when the solution is diluted. Similar concentration dependence of Band II was observed for every R-type complex in the methanolic and aqueous solutions. The Band II cannot be, therefore, considered to originate in any association among the complexes. Cotton effects of the R-type complexes are negligible at about 29000 cm^{-1} as shown in Figs. 2 and 3. As a consequence, if Band II might be assigned to one of d–d transitions, it should be to $(z^2)\rightarrow(x^2-y^2)$ transition from a theoretical consideration.[6] Band II of Cu(L-alaa)$_2$ was, however, inclined to shift to lower wave number's when the solvent was changed from water to methanol, and to ethanol.[15] This behavior of the Band II cannot be consistently interpreted on the basis of the band assignment. It may be concluded, therefore, that Band II cannot be assigned to any d–d transition.

The authors wish to thank Mr. Masao Sekizaki of Nagoya University, Mr. Yasuo Nakao and Dr. Takaji Yasui of Osaka University for supplying their absorption data, which were very useful in the inspections of our data. The authors also wish to thank Mr. Norio Koine of Ehime University, whose suggestions were very helpful in preparing some of the ligands, and Dr. Seiko Komorita of Osaka University for valuable comments.

BULLETIN OF THE CHEMICAL SOCIETY OF JAPAN VOL. 42 177—180 (1969)

The Alkaline Hydrolysis of Halophenols*1

Shigeru OAE, Naomichi FURUKAWA and Takashi ASARI

Department of Applied Chemistry, Faculty of Engineering, Osaka City University, Sugimoto-cho, Sumiyoshi-ku, Osaka

(Received April 12, 1968)

The mechanism of both the alkaline fusion and the alkaline hydrolysis of halophenols has been investigated. In case of alkaline fusion, the product identified is resorcinol, the formation of which has been found to proceed through the benzyne intermediate. While the alkaline hydrolysis of halophenols gives different ratio of dihydroxyphenol and phenol by changing the mole ratio of halophenol to alkali, by utilizing ^{14}C tracer experiment and substituted halophenol, the mechanism of the formation of both products has been revealed to proceed by way of the direct substitution of halide with hydroxide. Copper compounds are found to be effective in this reaction.

The aqueous alkaline hydrolysis of halobenzenes has been shown to proceed by way of benzyne mechanism, though it gives somewhat different results depending upon the reaction temperatures, halogen species and the concentration of alkali applied.[1] Whereas, the alkaline hydrolysis of halobenzenes activated with nitro or sulfone group, has been demonstrated to proceed through an S_N2 type substitution on carbon atom bearing halogen atom.[2] Although the alkaline hydrolysis of halophenols apparently gives several unusual products, for example, phenol which cannot possibly be obtained through either the benzyne process or the concerted S_N2 route alone, this process is patented as one of promising methods of preparing dihydroxyphenols, such as catechol.[3] However, the mechanism of this reaction has been completely unkown. Apparently the reaction carried out with molten alkali at high temperature proceeds through a different route from that performed in aqueous alkali at a moderately low temperature. Usually, the treatment of molten alkali on halophenols gives rearranged dihydroxy-benzene, for

*1 Phenol and Phenolic Esters. XVII.

1) A. T. Bottini and J. D. Roberts, *J. Am. Chem. Soc.*, **79**, 1458 (1957); A. Lüttringhaus and D. Ambros, *Chem. Ber.*, **89**, 463 (1956).

2) S. Oae and Y. H. Khim, This Bulletin, **40**, 1716 (1967).

3) German Pat. 1040563 (*Chem. Abstr.*, **55**, 10391g (1961)); Brit. Pat. 834254 (*Chem. Abstr.*, **54**, 20986d (1960)).

example, resorcinol from *o*-chlorophenol, suggesting that the reaction proceeds through the route involving benzyne formation. While, the aqueous alkali gives unrearranged products, catechol from *o*-chlorophenol and the reaction can be interpreted as an aromatic S_N2 types subtitution, no clear cut mechanism has yet been suggested. The remarkable feature of this aqueous alkaline hydrolysis of the halophenol is that the reaction is catalyzed by heavy metals or metal ions such as copper. This paper will describe the preliminary results of our investigation and the implication on the mechanism of these reactions.

Results and Discussion

The Alkaline Fusion of Halophenols. The reactions of halophenols with molten alkali have been known to give phenol, dihydroxybenzene and unidentified products.[4] Usually, the yield of dihydroxybenzene by alkaline fusion is not as good as that of the aqueous alkaline hydrolysis of halophenols; usually yielding the product in less than 20%. Meoreover dihydroxybenzene obtained by this alkaline fusion is rearranged products; for example, the only isolable product in the alkaline fusion of both *o*- and *p*-chlorophenols is resorcinol.

One possibility is that resorcinol may be formed by way of the incipient formation of benzyne as an intermediate (Eq. (1)). Another conceivable mechanism may be the route involving the prior formation of phenol, followed by the oxidation of it to resorcinol (Eq. (2)), since it has been known that resorcinol can be prepared from the reaction of phenol with molten alkali.[5] The mechanisms may be illustrated as shown below.

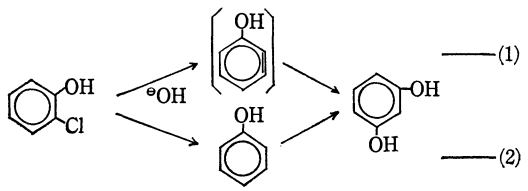

Fig. 1. Mechanism of the formation of resorcinol.

The choice between these two possible mechanisms can be readily made by means of ^{14}C tracer experiment using ^{14}C labeled phenol. Providing that the reaction would proceed through "benzyne route," resorcinol obtained would not have any ^{14}C activity, whereas if phenol would be the initial intermediate the original ^{14}C activity should be found in resorcinol. Accordingly *o*- or *p*-chlorophenol was mixed with the ^{14}C labeled phenol and the mixture was reacted with molten alkali for several hours and the resulting resorcinol was converted to its tribromide. From the activity measurement of the tribromoresorcinol obtained from the reaction was found to contain no ^{14}C activity. The ^{14}C tracer experiment reveals very clearly that "benzyne route" is considered to be the only plausible pathway for the alkaline fusion of halophenols.[2]

The Aqueous Alkaline Hydrolysis of Halophenols. The reaction is usually carried out in a copper tube which is placed in an autoclave kept at a temperature between 160—200°C for 4—6 hr. The reaction can also be carried out in a glass sealed tube containing a catalytic amount of a copper compound. After the reaction, the products were isolated as usual and identified by comparing their bp, mp, infrared spectra and gas-chromatographic behaviors with those of the authentic samples. The reaction has following few characteristic features. a) The main products are phenol and catechol but the product ratio changes by the change of the mole ratio of alkali to halophenol. The products and their yields are shown in Table 1. b) The relative ease of the halide - displacement in the halophenols appears to be in the following sequence $o \rangle p \gg m$. Although there is no detailed kinetic study available, *o*-chlorophenol appears to undergo the most facile reaction to afford the products under the reaction conditions. Under the same conditions, however, only a small amount of phenol can be detected through gas chromatography from the reaction of *p*-chlorophenol. *m*-Chlorophenol apparently do not react and can be recovered almost quantitatively. c) The reaction has been known to be facilitated by copper catalysts. Moreover, under the reaction condition of hydrolysis in which the formation of phenol is favorable, the reaction is catalyzed only by copper and no other metal exhibit any effective catalytic activity. Among the following metal compounds tested for catalyst only copper compounds showed noticeable activities;

Table 1. The yields of phenol and catechol

NaOH / Cl, OH — Mole ratio	Products		
	Phenol (%)	Catechol (%)	Residue (%)
1	56	trace	44
1.5	25	15	50
2	trace	58	42

Cu^0(Cu-tube), Cu^{1+}(Cu_2O), Cu^{2+}(CuO, $CuSO_4$); Ag^{+1}($AgNO_3$); Hg^{2+}($Hg(CN)_2$, $HgCl_2$); Fe^{2+} ($FeCl_2$), Fe^{3+}($FeCl_3$); Ni^{2+}($Ni(NO_3)_2$). Based on these observations one can construct the mechanisms of the hydrolysis reactions, especially of the formations of the two major products, *i.e.*,

4) H. E. Fierz-David and G. Stamm, *Helv. Chim. Acta*, **25**, 256 (1942).

5) J. F. Bunnett and R. E. Zahler, *Chem. Revs.*, **46**, 304 (1950).

phenol and catechol.

Mechanism of the Formation of Phenol. The yield of phenol was found to reach the maximum value when the reaction was carried out with 1:1 mole ratio of alkali to *o*-halophenol. The probable mechanism can be illustrated in Fig. 2.

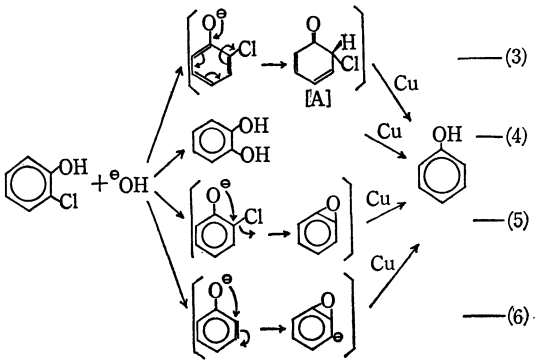

Fig. 2. Mechanism of the formation of phenol.

The Eq. (3), tentatively called as direct chlorine substitution, involves the initial formation of phenoxy anion followed by prototropy to form an intermediate (A) from which chlorine is abstracted by copper metal to produce phenol. Equation (4) demands that phenol is formed by way of the initial formation of catechol. This mechanism is also possible because catechol is always formed even when the concentration of alkali is relatively low. Equations (5) and (6) involve the incipient formation of the intermediate epoxy compound from which phenol is to be formed. The choice between the mechanisms, namely Eq. (3) and those (5) or (6) can be achieved by using a suitably substituted halophenol such as 2-bromo-4-methylphenol. Equation (3) will require cresol obtained from 2-bromo-4-methyl phenol to be *p*-cresol alone, whereas according to Eq. (5) or (6) both *m*- and *p*-cresols should be formed. When 2-bromo-4-methylphenol was actually subjected to the hydrolysis with an equal mole of alkali, phenolic products obtained in 35% yield contained phenol (5%) and *p*-cresol (30%), but no *m*-cresol. Since *m*- and *p*-cresols have characteristically different IR absorption spectra, their absence is readily confirmed. Consequently Eqs. (5) and (6), *i. e.*, the oxygen migration mechanism, can now be ruled out. Since no phenol formation was observed when catechol was treated under the same condition that applied to the hydrolysis, Eq. (4) can also be eliminated. Thus the phenol formation is considered to follow Eq. (3).

Now a question arises why *o*-halophenol is especially so reactive, since a similar mechainsm can be applied to *p*-halophenol which does not produce phenol so readily. The reason is probably illustrated by a complex formation between copper and *o*-halophenol at the transition state especially with *o*-hydroxyl group and halogen as shown below and the formation of such a complex may decrease the activation energy of the reaction. Moreover, the change of product ratio by changing the amount of alkali to *o*-halophenol can be explained by such a complex formation. Namely, when an excess amount of alkali to halophenol is used, hydroxide anion attacks preferentially the *o*-carbon atom bearing halogen atom, since carbon-halogen bond is probably loosen by such a complex formation, thus catechol is produced as a main product. While, in case of an equimolar amount of alkali, only halogen is abstracted by copper giving rise to phenol.

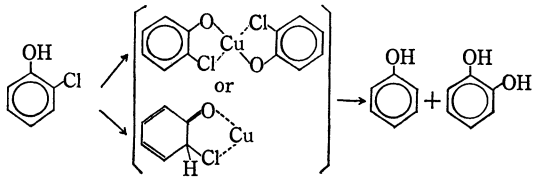

Fig. 3. Complex formation.

The Mechanism of the Formation of Catechol. The formation of catechol is also interesting in connection with the phenol formation, because copper catalyst is also necessary in this reaction.

Among several mechanisms conceivable, the one involving the initial benzyne formation followed by the epoxy intermediate formation can be ruled out from the afore-mentioned experiment using 2-bromo-4-methylphenol. While it is considered that the formation of catechol may be achieved by the direct nucleophilic substitution of chlorine by hydroxy group, there is another possibility, namely, the process involving the initial formation of phenol which is then oxidized to catechol in the presence of copper catalyst. The two mechanisms are depicted as shown below.

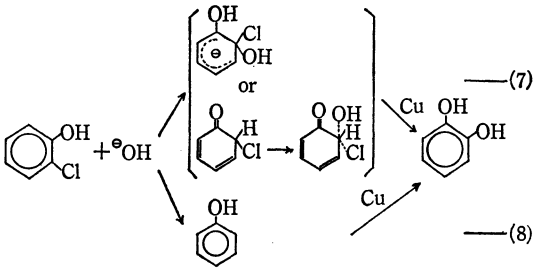

Fig. 4. The mechanism of the formation of catechol.

In order to make a choice between the two mechanisms, we have carried out a ^{14}C-tracer experiment using a small amount of ^{14}C-labeled phenol mixed with *o*-chlorophenol. If the reaction proceeds according to Eq. (8), the catechol obtained should have ^{14}C activity, whereas according to the

Eq. (7), catechol should have no ^{14}C activity. Our result revealed that less than 2% of the original ^{14}C activity was found in catechol. Moreover, from this experiment we have found that more than 95% of phenol was recovered unchanged. Therefore Eq. (8) can be eliminated. Thus the formation of resorcinol is considered to proceed through the direct nucleophilic substitution of chlorine by hydroxide, probably assisted by copper ion which acts as a Lewis acid.

Experimental

The Alkaline Fusion of *p*-Chlorophenol Mixed with ^{14}C Labeled Phenol. The experimental condition was same as that Fierz-David described. A mixture of sodium *p*-chlorophenolate (3 g) and sodium phenolate-^{14}C (0.5 g) was reacted in a nickel muffle heated in a silicone oil bath, the temperature of which was kept at 300°C for 5 hr. After the reaction, the vessel was cooled and the products were dissolved into a large amount of water To this aqueous solution was added bromine water. Solid precipitates were collected and dried. The yellow colored solid was extracted with *n*-hexane. The hexane solution was cooled with ice-bath. Crystalline precipitates were collected, recrystallized from *n*-hexane and then sublimed. Colorless needles were obtained, mp 104—106°C, and ^{14}C activities were measured by a liquid scintillation counter. The specific activities were: phenol, 9.2×10^4 dpm/mmol (as tribromide); resorcinol, 2.2×10^3 dpm/mmol (as tribromide).

The Aqueous Alkaline Hydrolysis of *o*-Halophenols. A typical example of the experiments are the following. *o*-Chlorophenol (commercially available, 1 g) was dissolved in 3 m*l* of water containing 0.4 g of sodium hydroxide and the whole mixture was placed in an ampoule. To this solution was added 1% of cuprous oxide. The ampoule was sealed and heated in an autoclave at a temperature between 180—200°C for 4 hr. After cooling the ampoule was broken and the mixture was filtered to remove polymeric substance and the catalyst. The filtrate was acidified with concentrated hydrochloric acid and extracted with ether. The ether extract was dried over magnesium sulfate. After ether was removed, the residue was distilled and product (0.4 g, bp 160—180°C) was obtained. Among the products identified were phenol and a small amount of recovered *o*-chlorophenol. The yield of phenol was 56%.

Similar experiments were carried out by changing catalyst, alkali concentration and halophenols. The results are summarized in Table 1.

2-Bromo-4-methylphenol. The titled phenol was prepared from *p*-cresol and bromine in carbon tetrachloride solution in 66% yield. The alkaline hydrolysis of 2-bromo-4-methylphenol (3 g) gave 1.1 g of liquid products (bp 160—200°C) among which were isolated *ca.* 1.5% of phenol and *p*-cresol (33%). The identification of these phenols was made by IR and gas chromatography.

The Reaction of Catechol with Alkali. A mixture of 1.0 g and 10 m*l* of 10% aqueous sodium hydroxide was sealed into a glass ampoule and was heated in an autoclave for 3 hr at 200°C. The isolation of products were performed similarly. Catechol was recovered in 50% yield but no phenol was isolated.

The Alkaline Hydrolysis of *o*-Chlorophenol and Phenol-1-^{14}C. *o*-Chlorophenol (2.62 g) and phenol-1-^{14}C (0.5 g) prepared from aniline-1-^{14}C was treated as similarly. After the reaction, catechol obtained was purified by sublimation, yield 58%, mp 104—106°C. ^{14}C activity was measured by a liquid scintillation counter. Sp. activity: Phenol-1-^{14}C (as tribromide), 1.12×10^5 dpm/mmol. Catechol, 1.36×10^3 dpm/mmol. Thus, 1.2% of the original ^{14}C activity was incorporated in catechol.

Recovery Test of Phenol-1-^{14}C. Phenol-1-^{14}C (0.41 g) was dissolved into 1 m*l* of 20% aqueous sodium hydroxide solution containing Cu_2O. The mixture was heated for 4 hr at 170—180°C. After the reaction was added 430 mg of the authentic phenol. The phenol recovered was converted to the tribromide and ^{14}C activities of the initial and the recovered tribromophenol were measured by a liquid scintillation counter. The ^{14}C activities are 4.19×10^4 dpm/mmol for the initial phenol and 2.02×10^4 dpm/mmol for the recovered phenol.

Thus, by means of the isotope dilution method, 95% of phenol was found to be recovered under the alkaline hydrolysis.

BULLETIN OF THE CHEMICAL SOCIETY OF JAPAN VOL. 42 181—185 (1969)

Studies of Acenaphthene Derivatives. XVI.[1] The Wittig Reaction with Acenaphthenequinone*1

Otohiko TSUGE, Masashi TASHIRO and Ichiro SHINKAI

Research Institute of Industrial Science, Kyushu University, Hakozaki, Fukuoka

(Received April 25, 1968)

The reactions of acenaphthenequinone (III) with several Wittig reagents have been studied. When III was reacted with equimolar amounts of benzylidenetriphenylphosphoranes (IV) at room temperature, the corresponding benzylideneacenaphthenones (V) were obtained in fairly good yields, but the reactions of benzil and phenanthrenequinone with IV did not take place under similar conditions. The reaction of III with two equivalents of IV under severe conditions afforded only V, and no dibenzylidene compounds were obtained. The reaction of III with resonance-stabilized phosphoranes, such as acetonylidene-, phenacylidene- and *p*-chlorophenacylidenephosphoranes, afforded the expected α,β-unsaturated ketones. In the reaction with ethoxycarbonylmethylenephosphorane, two stereo-isomeric ethoxycarbonylmethyleneacenaphthenones, which were also obtained from the reaction with diethyl ethoxycarbonylmethylphosphonate, were formed. The structures of the isomers were confirmed on the basis of NMR, UV, and mass spectral studies. Methylenephosphorane reacted with III to give methyleneacenaphthenone in a poor yield. On the contrary, the reaction with ethylidenephosphorane gave bis-2,2′-methyleneacenaphthenone, which was also formed by the reaction of acenaphthenone with glyoxal, in a good yield.

It has been shown that the 1,2-bismethylene derivative was obtained in an 85% yield by the Wittig reaction of benzocyclobutenedione with two equivalents of ethoxycarbonylmethylenetriphenylphosphorane at room temperature.[2] On the other hand, Parrick[3] has reported that some α-diketones, such as benzil (I) and phenanthrenequinone (II), will not react with two equivalents of a phosphorane. In both cases, the corresponding monobenzylidene compounds were obtained in low yields from the reaction with benzylidenetriphenylphosphorane at only one carbonyl group.

In earlier papers[4–7] in this series we have found that acenaphthenequinone (III) behaved differently from I and II in some reactions, and it was deduced that one carbonyl group in III is more reactive than that in I or II.

We have little information about the Wittig reaction with III. Accordingly, it will be interesting to investigate whether or not III will be able to react with two equivalents of a phosphorane, and to compare the reactivities of I, II, and III against the phosphorane.

When III was treated with benzylidenetriphenylphosphoranes (IV) in ethanol at room temperature, the corresponding benzylideneacenaphthenones (V) were obtained in fairly good yields. Under similar conditions, however, the reactions of I and II with IV did not take place. Even when two equivalents of IV were used under severe reaction conditions,

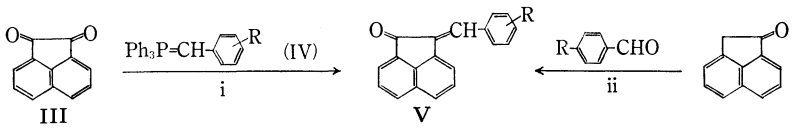

III V

a: R = H, b: R = *p*-CH_3, c: R = *p*-OCH_3 d: R = *p*-Cl,
e: R = *p*-NO_2, f: R = 3,4-Cl_2

1) Part XV: O. Tsuge and M. Tashiro, *Reports of the Research Institute of Industrial Science, Kyushu University*, No. 46, 19 (1967).

*1 Presented at the 20th Annual Meeting of the Chemical Society of Japan, Tokyo, April, 1967.

2) M. P. Cava and R. J. Pohl, *J. Am. Chem. Soc.*, **82**, 5242 (1960).

3) J. Parrick, *Can. J. Chem.*, **42**, 190 (1964).

4) O. Tsuge and M. Tashiro, This Bulletin, **36**, 970 (1963).

5) O. Tsuge and M. Tashiro, *ibid.*, **38**, 399 (1965).

6) O. Tsuge and M. Tashiro, *ibid.*, **39**, 2477 (1966).

7) O. Tsuge, M. Tashiro and H. Yamashita, *Reports of the Research Institute of Industrial Science, Kyushu University*, No. 46, 11 (1967).

Table 1. Benzylideneacenaphthenones (V)

V	R	Yield, % i	Yield, % ii	Mp,°C (From solvent)	Appearance	IR (C=O) cm^{-1}	Microanalyses, % Found C	Found H	Found N	Calcd C	Calcd H	Calcd N
a	H	90	84	120 (MeOH)	yellow needles	1700	89.33	4.80	—	89.04	4.72	—
b	*p*-Me	58	68	116 (EtOH)	yellow needles	1705	88.84	5.13	—	88.86	5.22	—
c	*p*-OMe	61	48	114 (EtOH)	yellow needles	1710	83.91	4.89	—	83.90	4.93	—
d	*p*-Cl	91	92	175 (benzene)	pale yellow needles	1710	78.74	3.85	—	78.62	3.79	—
e	*p*-NO_2	81	90	239 (acetone)	brilliant yellow needles	1710	75.89	3.68	4.35	75.74	3.68	4.65
f	3,4-Cl_2	82	—	142 (EtOH)	yellow needles	1700	70.38	3.12	—	70.15	3.08	—

a) UV λ_{max}^{EtOH} mμ (ε): Va 233.6 (49000), 313 (27000); Vd 232.5 (49000), 324 (22000).
b) NMR in $CDCl_3$ (τ): 6.8 (singlet, OCH_3), 2.5 (multiplet, 10H aromatic protons), 2.2 (singlet, =CH–).
c) Reported mp 113°C (J. W. Ager, F. A. Fastwood and R. Robinson, *Tetrahedron, Suppl.* **7**, 277 (1966)).

Table 2. Carbonylmethylene acenaphthenones (VII)

VII	R	Reaction time (min)	Yield (%)	Mp, °C (solvent)	Appearance	IR, cm^{-1}	Microanalyses, % Found C	Found H	Calcd C	Calcd H
a	Me	30	45	117—119 (CH*)	yellow needles	1710, 1675 (C=O) 1620 (C=C)	81.41	4.30	81.06	4.54
b	Ph	30	91	109—110 (EtOH)	yellow needles	1710, 1650 (C=O) 1620 (C=C)	84.43	4.20	84.49	4.25
c	*p*-ClC_6H_4	60	49	186—187 (EtOH)	yellow needles	1710, 1650 (C=O) 1620 (C=C)	75.43	3.31	75.47	3.46
d	OEt	120	48	102 (MeOH)	yellow needles	1720, 1700 (C=O) 1640 (C=C)	76.52	4.57	76.18	4.80
d′	OEt		8	97 (MeOH)	white prisms	1720, 1700 (C=O) 1640 (C=C)	76.45	4.43	76.18	4.80

* CH: cyclohexane

IV reacted with only one carbonyl group in III to form V, and no 1,2-dibenzylideneacenaphthenes were obtained.

The yields in the reaction of III with equimolar amounts of IV at room temperature for 15 min (method i), and the physical properties and elemental analyses of V are summarized in Table 1.

The compounds V were proved, by admixed melting points and by a study of their infrared spectra as well as by elemental analyses, to be identical with the authentic samples prepared by the reaction of acenaphthenone with the respective benzaldehydes in the presence of sodium hydroxide (method ii). The yields in the method ii are also shown in Table 1.

In general, it is accepted that the reactivity of the phosphorane IV decreases with an increase in the electron-withdrawing power of the substituent. The data in Table 1 show that the phosphoranes with electron-withdrawing substituents, such as the *p*-chloro (IVd), *p*-nitro (IVe), and 3,4-dichloro compounds (IVf), are more reactive than *p*-methyl- (IVb) and *p*-methoxybenzylidene-phosphorane (IVc).

On the basis of the above observations and other data,[4-7] it may be expected that one carbonyl group in III will be able to react with a resonance-stabilized phosphorane.

The reaction of III with acetonylidene- (VIa), phenacylidene- (VIb), *p*-chlorophenacylidene- (VIc), and ethoxycarbonylmethylenetriphenyl-

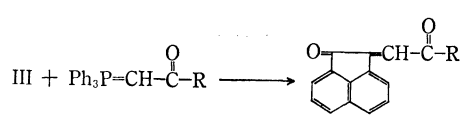

VI VII

a: R = CH_3, b: R = C_6H_5, c: R = *p*-ClC_6H_4, d: R = OC_2H_5

phosphorane (VId) at room temperature in ethanol gave the corresponding α,β-unsaturated ketones (VII).

The yields, physical properties, and results of the elemental analyses of VII are listed in Table 2.

In the reaction of III with VId, two compounds, VIId and VIId′, were obtained. The reaction of III with diethyl ethoxycarbonylmethylphosphonate in dioxane in the presence of sodium hydride also gave VIId and VIId′ in 60 and 4% yields respectively.

On the basis of the NMR, mass spectra, and elemental analyses, it is deduced that compounds VIId and VIId′ are cis-trans isomers of ethoxycarbonylmethyleneacenaphthenone. The NMR spectra of VIId and VIId′ are illustrated in Fig. 1.

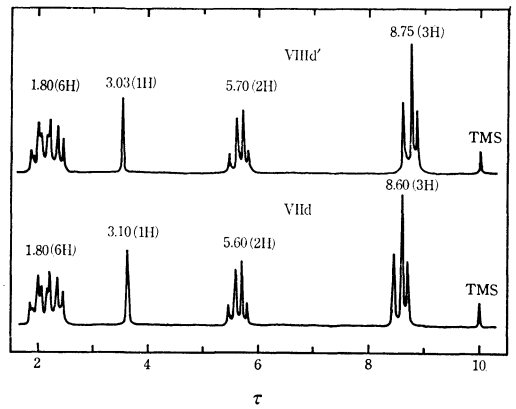

Fig. 1. NMR spectra of VIId and VIId′ in $CDCl_3$.

The vinyl-proton signal of VIId and the methylene-protons signal of VIId′ appeared at a field higher than those of VIId′ and VIId respectively. The differences can be understood in terms of the deshielding effect of the carbonyl group in the ethoxycarbonyl moiety and in terms of the shielding effect of the acenaphthene ring in the respective case.

The ultraviolet spectrum of VIId exhibited an absorption compatible with conjugation, but that of VIId′ indicated the presumable absence of conjugation. In addition, the fragmentation of VIId on electron impact was almost the same as that of VIId′. The mass spectrum of VIId is shown in Fig. 2.

The above observations can be explained by the structures for VIId and VIId′ which are shown in Fig. 3. The moiety, O=C–C=CHCOEt, in VIId is in a coplanar conformation, while that in VIId′ is not.

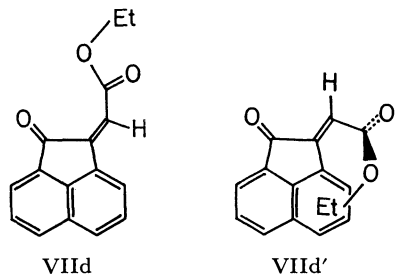

Fig. 3

The reaction of III with alkylidenetriphenylphosphoranes (VIII) was also investigated.

When III was allowed to react with methylenephosphorane (VIIIa) at room temperature, the expected methyleneacenaphthenone (IX) was obtained in a poor yield, accompanied by a larger amount of resinous material.

The reaction with ethylidenephosphorane (VIIIb) gave yellow needles (X), whose infrared spectrum was similar to that of 2,2′-diacenaphthylidene-

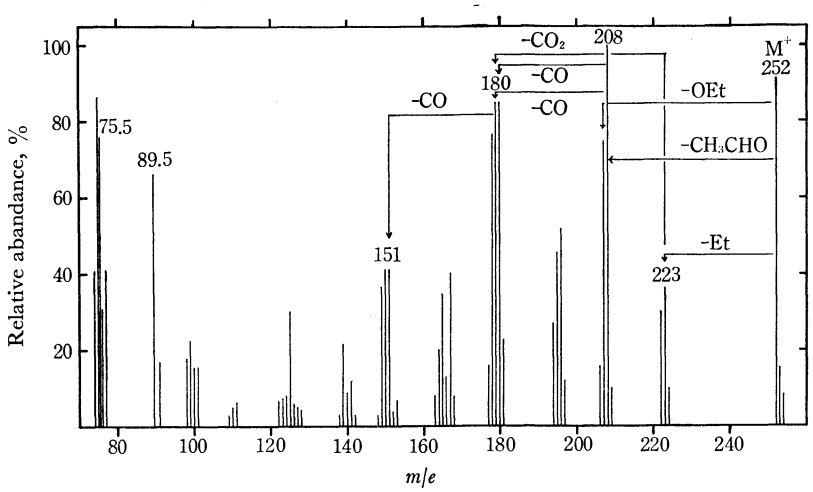

Fig. 2. Mass spectrum of VIId.

1,1′-dione,[8] in an 86% yield. The compound X was proved, by an admixed-melting-point determination and by a study of its infrared spectrum as well as by elemental analysis, to be identical with bis-2,2′-methyleneacenaphthenone prepared by the reaction of acenaphthenone with glyoxal in the presence of sodium hydroxide.

It may be considered that the compound X is formed by the condensation of the expected ethylideneacenaphthenone with a second quinone molecule.

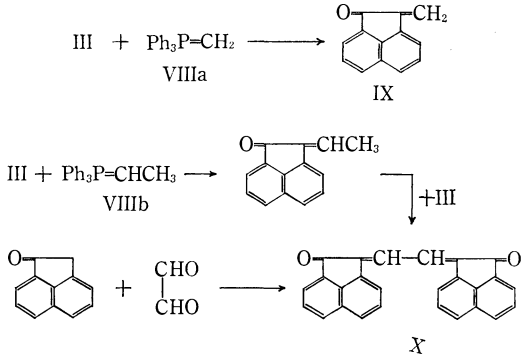

On the other hand, the reaction with propylidenephosphorane (VIIIc) gave a resinous material exclusively under various conditions.

Experimental

All the melting points are uncorrected. The infrared spectra were measured in KBr disks, and the NMR spectra were determined at 60 Mc with a Japan Electron Optics JNM-3H-60 NMR spectrometer, using TMS as the internal reference. The mass spectra were obtained on a Hitachi RMU-6D instrument using a heated inlet, an ionization energy of 70 eV, an inlet temperature of 200—250°C, and a source temperature of 250°C. The elemental analyses were done by Mr. Eiji Shiozaki in our laboratory.

General Method for the Reaction of Acenaphthenequinone (III) with the Benzylidenetriphenylphosphorane (IV). A solution of 0.005 mol of the benzyltriphenylphosphonium bromide in 25 m*l* of absolute ethanol was treated with 5.5 m*l* of a 0.001 M solution of sodium ethoxide in ethanol with continuous stirring under an atmosphere of nitrogen; the orange color of the phosphorane (IV) appeared immediately.

After the solution had been stirred for 10 min, 0.9 g (0.005 mol) of III[9] was added, and then the mixture was stirred at room temperature for 15 min. During this time the mixture turned into a clear solution, except in the reactions with IVd and IVe. The reaction mixture was quenched with 20—30 m*l* of water and then heated on a steam-bath, affording yellow crystals. The crystals were collected by filtration; recrystallization gave the benzylideneacenaphthenone (V).

The yields, physical properties, and results of the elemental analyses of V are listed in Table 1.

General Method for the Reaction of Acenaphthenone with the Benzaldehyde. To a solution of 1.68 g (0.01 mol) of acenaphthenone[10] and 0.012 mol of the benzaldehyde, in 25 m*l* of ethanol, 3 m*l* of a 1 N aqueous solution of sodium hydroxide was added, drop by drop, at room temperature. The mixture was stirred at room temperature for 20 min and then refluxed for another 5 min.

After 5 m*l* of 1 N hydrochloric acid had been added to the reaction mixture, yellow crystals were collected, washed with water, and dried. Recrystallization gave V; the yields are shown in Table 1.

The Reaction with Ethoxycarbonylmethylenetriphenylphosphorane (VId). To a solution of the phosphorane (VId) in 30 m*l* of ethanol which had been prepared by the treatment of ethoxycarbonylmethyltriphenylphosphonium bromide (2.1 g) with sodium ethoxide, 0.9 g of III was added. After the mixture had been stirred at room temperature for 2 hr, filtration gave 0.6 g of a mixture of yellow and white crystals. Fractional recrystallizations from ethanol gave 0.48 g of yellow needles (VIId), mp 102°C, and 0.1 g of white prisms (VIId′), mp 97°C.

VIId: IR (KBr) 1720 (sh, C=O), 1700 cm^{-1} (vs, C=O); UV λ_{max}^{EtOH} mμ (logε) 225 (4.73), 232 (4.83), 274 (4.22), 312.8 (4.0).

VIId′: IR (KBr) 1720 (vs, C=O), 1700 cm^{-1} (sh, C=O); UV λ_{max}^{EtOH} mμ (logε) 220 (4.46), 260 (3.90).

Similar reactions with other phosphoranes (VIa–VIc) gave the expected α,β-unsaturated ketones (VIIa–VIIc). The yields, physical properties, and results of the elemental analyses of VII are summarized in Table 2.

The Reaction with the Ethoxycarbonylmethylphosphonate Anion. To a suspension of 0.9 g of III and 1.1 g of diethyl ethoxycarbonylmethylphosphonate in 15 m*l* of dioxane, 60 mg of sodium hydride in 50% mineral oil was added, drop by drop, with stirring at room temperature. The mixture was stirred at room temperature for 20 min and then heated at 60—70°C for 5 min. During this time the reaction mixture turned from violet to yellow.

After the reaction mixture had been quenched with 10 m*l* of water, the crystals were collected by filtration. The crystals were then extracted with petroleum benzine (bp 45—60°C), leaving 0.02 g of a solid. After the extract had been concentrated *in vacuo*, the fractional recrystallization of the residue from methanol gave 1.5 g of yellow needles, mp 102°C, and 0.1 g of white prisms, mp 97°C. These compounds were, respectively, identical with the two ethoxycarbonylmethyleneacenaphthenones, VIId and VIId′, which were obtained from the reaction of III with VId.

The Reaction with Methylenetriphenylphosphorane (VIIIa). Into a suspension of 0.9 g of methyltriphenylphosphonium bromide and 0.46 g of III in 20 m*l* of dioxane, 60 mg of sodium hydride in 50% mineral oil was added, drop by drop, with stirring. The reaction mixture was stirred at room temperature

8) O. Tsuge and M. Tashiro, *Reports of the Research Institute of Industrial Science, Kyushu University,* No. 36, 1 (1963).

9) C. F. H. Allen and J. A. VanAllan, "Organic Syntheses," Coll. Vol. III. p. 1 (1955).

10) L. F. Fieser and J. Cason, *J. Am. Chem. Soc.*, **62**, 432 (1942).

for 10 hr and then heated at 55—60°C for 1 hr.

The reaction mixture was then quenched with 10 m*l* of water, and the resultant mixture was extracted with 30 m*l* of ether. The extract was washed with 10 m*l* of 50% aqueous ethanol and dried over sodium sulfate. The ether solution was chromatographed on alumina, affording a large amount of resinous materials and 23 mg (5%) of methyleneacenaphthenone (IX) as yellow needles, mp 148°C (decomp.).

Found: C, 86.43; H, 4.35%. Calcd for $C_{13}H_8O$: C, 86.65; H, 4.48%. IR (KBr): 1720 cm^{-1} (C=O).

The reaction with VIIIa, which had been prepared from the phosphonium bromide and sodium ethoxide in ethanol, at room temperature for 30 min gave IX in a 10% yield.

The Reaction with Ethylidenetriphenylphosphorane (VIIIb). To a solution of the phosphorane VIIIb in 30 m*l* of absolute ethanol, which had been prepared from 2.6 g of ethyltriphenylphosphonium bromide and sodium ethoxide, 1.8 g of III was added. After the reaction mixture had then been stirred at room temperature for 10 hr, filtration gave crystals; these crystals were then washed with ethanol and dried, giving 0.48 g (86%) of orange yellow crystals, mp 240—244°C. Recrystallization from dimethylformamide afforded bis-2,2′-methyleneacenaphthenone (X) as orange yellow needles, mp 245°C.

Found: C, 87.41; H, 3.92%. Calcd for $C_{26}H_{14}O_2$: C, 87.10; H, 3.91%. IR (KBr): 1700 cm^{-1} (C=O).

The Reaction of Acenaphthenone with Glyoxal. To a solution of 0.16 g of acenaphthenone and 0.06 g of glyoxal in 10 m*l* of ethanol, 0.5 m*l* of 1 N sodium hydroxide was added, drop by drop, at room temperature; crystals appeared immediately. Filtration gave 0.17 g (96%) of orange yellow crystals which, on recrystallization from dimethylformamide, gave X, mp 245°C. This compound was identical with the product obtained from the reaction of III with VIIIb.

BULLETIN OF THE CHEMICAL SOCIETY OF JAPAN VOL. 42 185—190 (1969)

Studies of Acenaphthene Derivatives. XVII.[1] The Reaction of Benzylideneacenaphthenone with Hydrazines*1

Otohiko TSUGE, Ichiro SHINKAI and Masashi TASHIRO

Research Institute of Industrial Science, Kyushu University, Hakozaki, Fukuoka

(Received May 6, 1968)

The reactions of benzylideneacenaphthenones with hydrazines are reported. The reaction of benzylideneacenaphthenone with hydrazine hydrate in methanol at 40°C gave 1-hydroxy-2-hydrazinobenzylacenaphthylene, which was then cyclized to the 1-acetylpyrazoline by treating it with acetic anhydride. The hydrazino compound reacted with phenyl isocyanate to give the 1:2-adduct, which, when then treated with hydrochloric acid, suffered ring closure to the pyrazoline compound. Under severe conditions with hydrazine hydrate, however, the reductive cleavage reaction took place, giving the hydrazones of both acenaphthenone and benzaldehyde. Similar phenomena were also observed in the reaction with *p*-substituted benzylideneacenaphthenones. On the other hand, the reaction with phenylhydrazines in ethanol containing sulfuric acid afforded directly the expected pyrazolines, from which pyrazoles were then prepared by treating them with lead tetraacetate. Furthermore, the corresponding pyridazine was formed in the reaction of phenacylideneacenaphthenone with hydrazine hydrate, while the reaction with 2,4-dinitrophenylhydrazine gave the pyrazoline compound.

Although it is well known that the most general synthetic method for pyrazolines, which are of interest as intermediates in the preparation of cyclopropanes, is the reaction of α,β-unsaturated carbonyl compounds with hydrazines,[2] little has been reported relating to the reaction of benzylideneacenaphthenones (I)[1] with hydrazines.

In the course of preparing the pyrazolines starting with I, we have found that the reaction of I with hydrazine hydrate (II) revealed unusal phenomena, while the reaction with phenylhydrazines (III) in ethanol containing a little sulfuric acid gave the expected pyrazolines in excellent yields; these results will be described in this paper.

This paper will also deal with the reaction of phenacylideneacenaphthenone (IV)[1] with hydrazines.

1) Part XVI: O. Tsuge, M. Tashiro and I. Shinkai, This Bulletin, **42**, 181 (1969).

*1 Presented at the 20th Annual Meeting of the Chemical Society of Japan, Tokyo, April, 1967.

2) R. C. Elderfield, "Heterocyclic Compounds," Vol. V, John Wiley & Sons, New York, N. Y. (1957), p. 45.

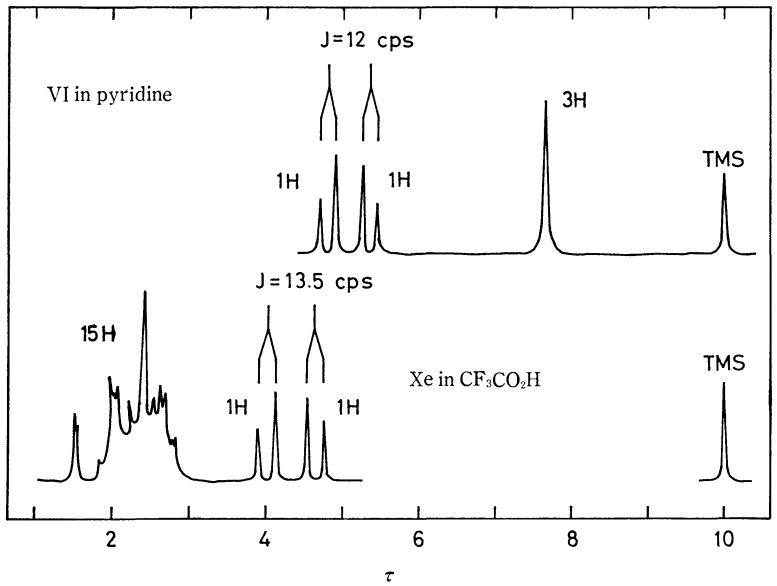

Fig. 1. The NMR spectra of VI and Xe.

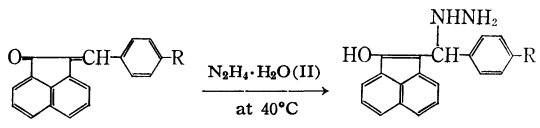

I V

a: R=H, b: R=Me, c: R=OMe, d: R=Cl, e: R=NO_2

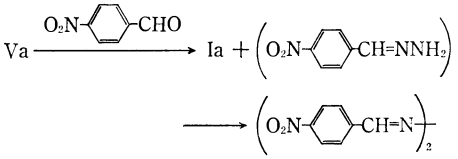

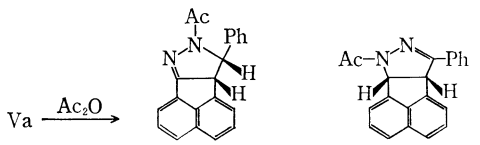

VI VI'

When benzylideneacenaphthenone (Ia) was treated with II in a 1 : 3 molar ratio in methanol at 40°C for 20 min, white needles (Va), $C_{19}H_{16}ON_2$, were obtained in a 96% yield, instead of the expected hydrazone, azine or pyrazoline compound. The infrared spectrum of Va exhibited characteristic bands due to the hydroxyl group at 3400 cm^{-1} and to the NH group at 3280 and 3220 cm^{-1}, but it did not reveal any bands for the carbonyl group. The NMR spectrum in DMSO-d_6 exhibited peaks at τ 7.5 (1H, methine-proton, singlet), 5.2–6.2 (4H, hydroxyl- and NH-protons, broad peak), and 2.2 (11H, aromatic protons, multiplet).

The above observations can be explained on the assumption that Va is 1-hydroxy-2-(hydrazinobenzyl)acenaphthylene. This structure was also confirmed by the following results.

The treatment of Va with *p*-nitrobenzaldehyde in ether at room temperature afforded Ia and *p*-nitrobenzaldazine; the latter was formed by the condensation of the hydrazone and aldehyde.

When Va was allowed to react with acetic anhydride at room temperature for 2 hr, the *N*-acetylpyrazoline compound (VI) was obtained in a 53% yield. Its structure was confirmed by the results of elemental analysis and by the infrared and NMR spectra. The infrared spectrum of VI showed absorptions at 1670 and 1620 cm^{-1}, while the NMR spectrum in pyridine exhibited peaks at τ 7.6 (3H, acetyl-protons, singlet), 5.3 (1H, methine-proton, doublet), and 4.8 (1H, methine-proton, doublet) (J=12 cps), as is shown in Fig. 1.

It has been reported by Hassner and Michelson[3] that *cis*-pyrazolines exhibit higher coupling constants (10—14 cps) than those (3–10 cps) of the corresponding *trans* isomers. On the other hand, in our study of the NMR spectra of acenaphtho[1,2-*d*]oxazolidines, in which 1- and 2-hydrogen are located in the *cis*-manner, the protons appeared as doublets at τ 4.0 and 4.3 (J=6 cps) respectively.[4]

Although two pyrazoline structures for VI are possible, the above observations support the structure of 4,5-*cis*-1-acetyl-5-phenylpyrazoline com-

3) A. Hassner and M. J. Michelson, *J. Org. Chem.*, **27**, 3974 (1962).

4) O. Tsuge, M. Tashiro and K. Oe, The 20th Annual Meeting of the Chemical Society of Japan, Tokyo, April, 1967.

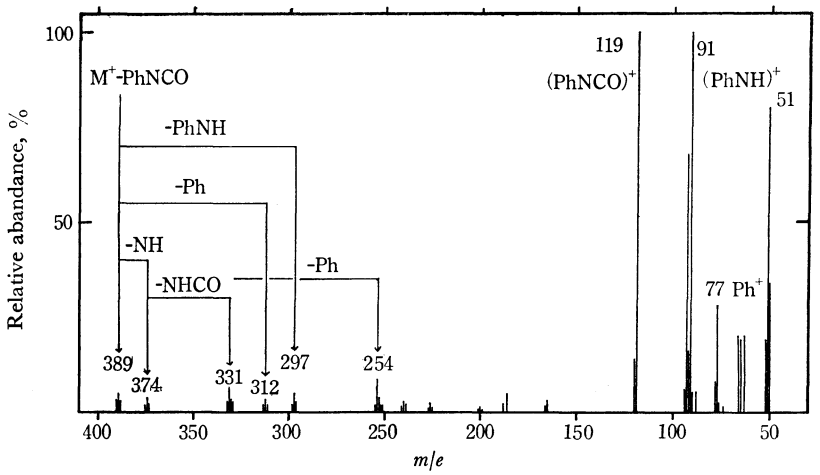

Fig. 2. The mass spectrum of VIII.

pound (VI) rather than the isomeric 4,5-*cis*-1-acetyl-3-phenylpyrazoline (VI').

Furthermore, the treatment of Va with two equivalents of phenyl isocyanate afforded the 1:2-adduct (VII) ($C_{33}H_{26}O_3N_3$) in a 96% yield. Its infrared spectrum showed bands to be ascribed to the NH group at 3300 cm^{-1} and to the carbonyl groups at 1700, 1690, and 1670 cm^{-1}. Also, VII hydrolyzed with 15% hydrochloric acid, giving *N*,*N*'-bisphenylcarbamoylhydrazine and orange yellow grains (VIII) in 34 and 44% yields respectively.

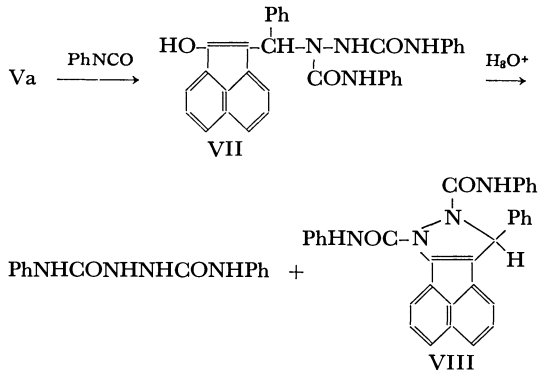

Compound VIII was assumed, on the basis of elemental analysis and a study of its infrared and mass spectra, to be 1,2-bisphenylcarbamoyl-3-phenylacenaphtho[1,2-*c*]pyrazoline. Its infrared spectrum exhibited characteristic bands due to carbonyl groups at 1720, 1680, and 1650 cm^{-1}, but it did not reveal any bands for the hydroxyl and NH groups.

The fragmentation on electron impact supported the proposed structure for VIII. As is shown in Fig. 2, the mass spectrum shows the *m/e* 389 peak, which is derived from the molecular ion upon the loss of a phenyl isocyanate moiety.

Similar reactions of *p*-methoxy- (Ic) and *p*-chlorobenzylideneacenaphthenone (Id) with II afforded the corresponding 1-hydroxy-2-hydrazinobenzyl compounds, Vc and Vd, in quantitative yields.

When an ethanol solution of Ia and II was refluxed for 10 min, the hydrazones of both acenaphthenone (IX) and benzaldehyde were obtained in excellent yields. In the reaction of Ib (R=Me), Id, and Ie ($R=NO_2$) under similar conditions, IX and the respective benzaldehyde hydrazone were obtained.

Similar phenomena were observed by Musante[5]: ω-nitrostyrene was cleft with II to give the azine and nitromethane.

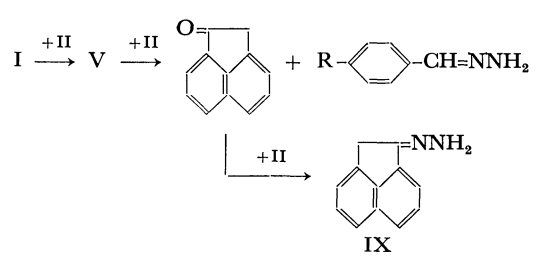

It may be inferred that both the hydrazones are formed by the reductive cleavage of the carbon-carbon bond in V with II.

Raiford and Manley[6] have reported that phenyl hydrazones, which rearrange to isomeric pyrazolines on refluxing, can be isolated in the reaction of chalcones with phenylhydrazine (IIIa) in acetic acid at room temperature, and that pyrazolines forms directly when methanol containing a little acetic acid is used as the reaction medium.

When I was allowed to react with III in acetic

5) C. Musante, *Gazz. Chim. Ital.*, **67**, 579 (1937).
6) L. C. Raiford and R. H. Manley, *J. Org. Chem.*, **5**, 590 (1940).

acid at room temperature, the expected phenylhydrazones were not obtained; instead, a resinous material was exclusively formed.

In a methanol solution containing a little acetic acid, Id and Ie reacted with IIIa and IIIb (R′=NO_2, R″=H) to give the corresponding pyrazolines in moderate yields (60—75%). In the reactions of Ia, Ib, and Ic, however, a resinous material was formed exclusively. When Id and Ie were treated with IIIc (R′=R″=NO_2) under similar conditions, the expected pyrazoline was not obtained, but predominantly a resinous material was formed.

On the other hand, it has been found that I reacted smoothly with III in ethanol containing a little sulfuric acid, giving the corresponding pyrazolines (X) in quantitative yields.

The structures for X were confirmed on the basis

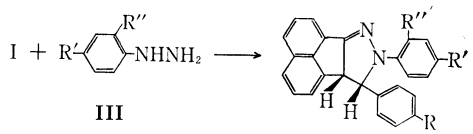

III

a : R′=R″=H
b : R′=NO_2, R″=H
c : R′=R″=NO_2

X

of elemental analyses, and on the basis of a study of the infrared and NMR spectra. The infrared spectra of all X structures exhibited the band ascribed to the C=N bond at about 1600 cm^{-1}, but there were no bands for the carbonyl, hydroxyl, and NH groups.

As is shown in Fig. 1, the NMR spectrum of Xe (R=Cl, R′=R″=H) in trifluoroacetic acid reveals peaks at τ 4.64, 4.04 (each 1H, methine-proton,

Table 1. 4,5-*cis*-1,5-Diarylacenaphtho[1,2-*c*]pyrazolines (X)

	X			Mp, °C (From solvent)	IR (C=N) cm^{-1}	Appearance	Microanalyses, % Found			Calcd		
	R	R′	R″				C	H	N	C	H	N
a	H	NO_2	H	231 (pyridine)	1600	red needles	76.69	3.94	10.67	76.07	4.34	10.73
b	H	NO_2	NO_2	266 (dioxane)	1610	brown needles	68.99	3.17	12.26	68.70	3.66	12.83
c	CH_3	NO_2	H	233 (dioxane-MeOH)	1600	brown needles	77.11	4.26	9.94	77.10	4.69	10.35
d	CH_3	NO_2	NO_2	261 (dioxane)	1610	brown needles	69.01	3.81	11.97	69.30	4.00	12.42
e	Cl	H	H	172 (benzene-EtOH)	1600	reddish yellow needles	79.29	4.10	7.41	79.00	4.47	7.36
f	Cl	NO_2	H	238 (benzene-EtOH)	1595	reddish yellow needles	71.16	3.27	9.70	70.70	3.76	9.89
g	Cl	NO_2	NO_2	278 (pyridine)	1610	brown needles	63.94	2.97	11.88	63.80	3.19	11.90
h	NO_2	H	H	192 (pyridine)	1600	brown needles	76.68	3.93	10.41	76.70	4.35	10.75
i	NO_2	NO_2	H	281 (pyridine-dioxane)	1595	red needles	69.02	3.24	12.43	68.80	3.67	12.83
j	NO_2	NO_2	NO_2	291 (pyridine)	1610	yellow needles	62.63	2.93	13.99	62.40	3.12	14.55

Table 2. 1,5-Diarylacenaphtho[1,2-*c*]pyrazoles (XI)

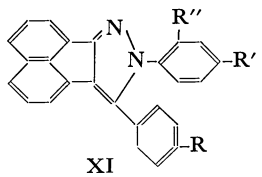

XI

	XI			Yield %	Mp, °C (From solvent)	IR (C=N) cm^{-1}	Appearance	Microanalyses, % Found			Calcd		
	R	R′	R″					C	H	N	C	H	N
a	CH_3	NO_2	NO_2	53	242 (benzene-EtOH)	1610	brown needles	69.57	3.43	12.27	69.50	3.56	12.49
b	Cl	NO_2	H	48	142 (EtOH)	1610	brown needles	71.04	3.41	9.86	71.10	3.32	9.95
c	Cl	NO_2	NO_2	60	270 (EtOH)	1615	yellow needles	63.87	2.53	11.74	63.96	2.77	11.92

doublet, $J=13.5$ cps), and 2.4 (15H, aromatic protons, multiplet). For reasons pointed out in the discussion of VI, the above observations indicate that Xe is the 4,5-*cis*-1-phenyl-5-*p*-chlorophenyl-pyrazoline compound.

The physical properties and elemental analyses are summarized in Table 1.

It has been reported by Gladstone and Norman[7] that lead tetraacetate is an effective reagent for oxidizing pyrazolines to pyrazoles.

When X was oxidized with lead tetraacetate in dichloromethane, the corresponding pyrazole (XI), whose infrared spectrum was very similar to that of the pyrazoline, was obtained in a fairly good yield.

The yields, physical properties, and results of the elemental analyses of XI are listed in Table 2.

On the other hand, an ethanol solution of phenacylideneacenaphthenone (IV) and II was refluxed for 30 min, giving yellow needles (XII), mp 147°C, in a 33% yield. The molecular formula of XII agreed with $C_{20}H_{12}N_2$, and its infrared spectrum exhibited the band ascribed to the C=N bond at 1610 cm^{-1}, but it did not reveal any bands for the carbonyl group. On the basis of the above observations, the compound XII was assumed to be the pyridazine compound which was formed through the hydrazone intermediate (XI).

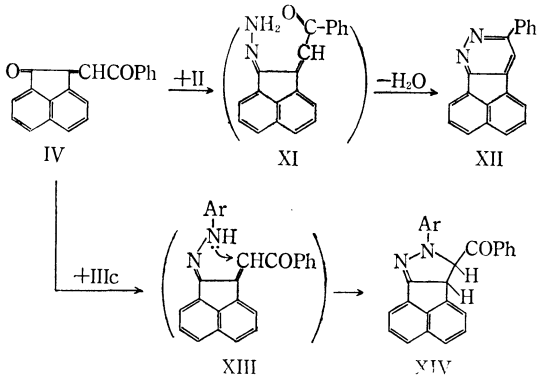

Ar=2,4-dinitrophenyl

While II exclusively attacked the carbon atom of benzylidene moiety in I, the reaction with IV proceeded through the formation of hydrazone.

When IV was treated with IIIc in ethanol containing a little sulfuric acid, reddish brown needles (XIV), mp 253°C, were obtained in a 75% yield. The compound XIV agreed with the formula, $C_{26}H_{16}O_5N_4$, and its infrared spectrum exhibited characteristic bands due to the carbonyl and C=N groups at 1650 and 1610 cm^{-1} respectively.

Considering the above observations, it may be deduced that the compound XIV is the pyrazoline compound formed through the hydrazone (XIII).

Experimental

All melting points are uncorrected. The infrared spectra were measured in KBr disks, and the NMR spectra were determined at 60 Mc with a Japan Electron Optics JNM-3H-60 NMR spectrometer, using TMS as the internal reference. The mass spectrum was obtained on a Hitachi RMU-6D instrument using a heated inlet, an ionization energy of 70 eV, an inlet temperature of 250°C, and a source temperature of 250°C. The elemental analyses were done by Mr. Eiji Shiozaki in our laboratory.

Benzylidene- (I) and phenacylideneacenaphthenone (IV) were prepared by a previously-reported method.[1]

General Method for the Reaction of the Benzylideneacenaphthenone (I) with Hydrazine Hydrate (II). i) After a solution of I (1.5 mmol) and II (4.5 mmol) in methanol (20 m*l*) had been heated at 40°C for 20 min, the reaction mixture was evaporated *in vacuo* to give white crystals. Recrystallization from methanol gave the corresponding 1-hydroxy-2-(hydrazinobenzyl)acenaphthylene (V).

Va (R=H), yield, 96%. Mp 74—75°C (decomp.), white needles. Found: C, 78.95; H, 5.59; N, 9.27%. Calcd for $C_{19}H_{16}ON_2$: C, 79.10; H, 5.56; N, 9.71%.

Vc (R=OCH_3), quantitative yield. Mp 96°C (decomp), white needles. Found: C, 75.13; H, 5.45; N, 9.25%. Calcd for $C_{20}H_{18}O_2N_2$: C, 75.45; H, 5.70; N, 8.80%.

Vd (R=Cl), quantitative yield. Mp 62°C (decomp.), white needles. Found: C, 70.04; H, 4.20; N, 8.55%. Calcd for $C_{19}H_{15}ON_2Cl$: C, 70.60; H, 4.64; N, 8.67%.

ii) After a solution of I (3 mmol) and II (9 mmol) in ethanol (20 m*l*) had been refluxed for 10 min, ethanol was distilled off *in vacuo* to leave an oily material. A solution of the oily material in petroleum benzine (bp 45—60°C) was then allowed to stand overnight, giving white crystals. Filtration afforded acenaphthenone hydrazone (IX), mp 107°C (decomp.), as white needles, in an excellent yield.

This compound was identical with the authentic sample prepared from acenaphthenone and II.

Found: C, 79.32; H, 5.27; N, 15.30%. Calcd for $C_{12}H_{10}N_2$: C, 79.12; H, 5.49; N, 15.39%.

A petroleum benzine solution was concentrated, leaving the benzaldehyde hydrazone as a colorless liquid. The corresponding benzaldazine was obtained by the treatment of the hydrazone with acetic acid.

The Reaction of Va with *p*-Nitrobenzaldehyde. A solution of Va (280 mg) and *p*-nitrobenzaldehyde (150 mg) in ether (10 m*l*) was stirred at room temperature for 2 hr: during this time yellow crystals appeared. Filtration gave *p*-nitrobenzaldazine (mp 293—295°C (decomp.)) in a quantitative yield. The ether filtrate was concentrated to give Ia.

The Reaction of Va with Acetic Anhydride. After acetic anhydride (430 mg) had been added to a solution of Va (1.2 g) in ether (30 m*l*), the reaction mixture was stirred at room temperature for 2 hr; during this time white crystals appeared. The crystals were collected by filtration, washed with ether, and dried. Yield, 645 mg (53%). Recrystallization from

7) W. A. F. Gladstone and R. O. C. Norman, *J. Chem. Soc.*, (*C*), **1966**, 1536.

benzene afforded white needles, *cis*-1-acetyl-5-phenylpyrazoline compound (VI), mp 168°C.

Found: C, 80.49; H, 4.69; N, 9.00%. Calcd for $C_{21}H_{16}ON_2$: C, 80.75; H, 5.16; N, 8.97%.

The Reaction of Va with Phenyl Isocyanate. To a solution of Va (500 mg) in ether (15 m*l*), a solution of phenyl isocyanate (410 mg) in ether (10 m*l*) was added, drop by drop, at room temperature. The reaction mixture was then stirred at room temperature for 30 min; during this time white crystals appeared. After the crystals had been collected by filtration, recrystallization from a dioxane - benzene mixture to give the 1 : 2 adduct (VII) as white grains, mp 225—226°C. Yield, 870 mg (96%).

Found: C, 74.98; H, 4.67; N, 10.53%. Calcd for $C_{33}H_{26}O_3N_4$: C, 75.20; H, 4.94; N, 10.64%.

The Hydrolysis of VII. After a suspension of VII (200 mg) in 15% hydrochloric acid (10 m*l*) had been heated at 100°C for 3 min, crystals were collected by filtration. These crude crystals were extracted with dioxane, leaving 35 mg (34%) of *N*,*N*′-bis(phenylcarbamoyl)hydrazine as white needles, mp 270°C; this compound was identical with the authentic sample prepared from the reaction of phenyl isocyanate with hydrazine.

The dioxane extract was concentrated *in vacuo* to afford the 1,2-bis(phenylcarbamoyl)-3-phenylpyrazoline compound (VIII) as orange yellow grains, mp 227—229°C. Yield, 85 mg (44%).

Found: C, 77.61; H, 4.63; N, 10.92%. Calcd for $C_{33}H_{24}O_2N_4$: C, 77.93; H, 4.76; N, 11.02%.

General Method for the Preparation of Pyrazoline Compounds (X). A solution of equimolar amounts of I and phenylhydrazines III (each 1.5 mmol) in 20 m*l* of ethanol containing a few drops of concentrated sulfuric acid was heated on a water-bath for 10 min. The crystals were then collected and purified by recrystallization. The yields of X were quantitative in all cases.

The physical properties and results of the elemental analyses of X are summarized in Table 1.

The Oxidation of the Pyrazoline (X) to the Pyrazole (XI). To a suspension of 240 mg of Xg (R=Cl, R′=R″=NO_2) in 6 m*l* of dichloromethane, a solution of 250 mg of lead tetraacetate in 3 m*l* of dichloromethane was added at room temperature. After the mixture had been stirred at room temperature for 24 hr, it was decomposed with acetic acid and hydrazine hydrate to give a tarry material. The benzene solution of the product was chromatographed on alumina, affording yellow crystals. Recrystallization from ethanol gave 140 mg (60%) of pyrazole (XIc), mp 270°C.

Similar oxidations of Xd and Xf gave the corresponding pyrazoles, XIa and XIb. The yields, physical properties, and elemental analyses of XI are listed in Table 2.

The Reaction of Phenacylideneacenaphthenone (IV) with II. A solution of 200 mg of IV and 1.5 equimolar amounts of II in 10 m*l* of ethanol was refluxed for 30 min. After the mixture had been concentrated *in vacuo*, it was allowed to stand overnight, thus giving crystals. Recrystallization from ethanol gave 65 mg (33%) of 3-phenylacenaphtho[1,2-*c*]pyridazine (XII) as yellow needles, mp 147°C.

Found: C, 85.85; H, 3.99; N, 10.03%. Calcd for $C_{20}H_{12}N_2$: C, 85.69; H, 4.32; N, 9.90%.

The Reaction of IV with 2,4-Dinitrophenylhydrazine (IIIc). A solution of 280 mg of IV and 200 mg of IIIc in 10 m*l* of ethanol containing two drops of concentrated sulfuric acid was refluxed for 15 min. After the reaction mixture had then been cooled, crystals were collected by filtration. Recrystallization from dioxane gave 350 mg (75%) of 1-(2,4-dinitrophenyl)-5-benzoylacenaphtho[1,2-*c*]pyrazoline (XIV) as reddish-brown needles, mp 235°C.

Found: C, 67.31; H, 3.52; N, 11.83%. Calcd for $C_{26}H_{16}O_5N_4$: C, 67.23; H, 3.47; N, 12.06%.

BULLETIN OF THE CHEMICAL SOCIETY OF JAPAN VOL. 42 191—193 (1969)

Synthesis of Albonoursin

Chung-gi SHIN, Yasuhiro CHIGIRA, Mitsuo MASAKI and Masaki OHTA

Laboratory of Organic Chemistry, Tokyo Institute of Technology, Ookayama, Meguro-ku, Tokyo

(Received May 11, 1968)

Treatment of the ester of 2-(2-chloroacetamido)-2-alkenoic acid with ammonia led to the formation of 3-alkylidene-2,5-piperazinedione. By using this method, total synthesis of albonoursin was accomplished. 2-(2-Chloroacetamido)-4-methyl-2-pentenoic acid, derived from the condensation of 4-methyl-2-oxopentanoic acid with chloroacetonitrile or the pyrolysis of 2,2-bis(2-chloroacetamido)-4-methylpentanoic acid, was converted to the ethyl ester, which was treated with ammonia to give 3-isobutylidene-2,5-piperazinedione. The piperazinedione was also synthesized by the esterification of 2-(2-aminoacetamido)-4-methylpentenoic acid, followed by a cyclization of the ester. Condensation of the piperazinedione with benzaldehyde yielded 3-benzylidene-6-isobutylidene-2,5-piperazinedione, and its physical constants are virtually identical with those recorded for the natural albonoursin.

In 1963, Khoklov and Lokshin isolated a new product from the culture filtrates of two *Streptomyces* species, *i.e.*, *St. albus var. fungatus* and *St. noursei*, and designated it as albonoursin.[1] Before the year, Brown and Kelley had reported that *St. noursei* produced a substance, "component 2."[2] Also Rao and Cullen isolated a substance "B-73," from the culture filtrate of *St. albus*.[3] These two substances have been revealed to be identical with albonoursin.[1] The structural investigations were made independently by Khoklov and Lokshin,[1] Brown *et al.*,[4] and Vondracek and Vanek,[5] respectively, and all of them have assigned the 3-benzylidene-6-isobutylidene-2,5-piperazinedione structure (I) for albonoursin.

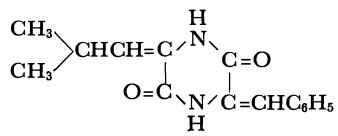

I

Although albonoursin has no special biological activity, it seems of much interest to investigate the synthetic method, since the structure may be regarded as the first cyclic dehydrodipeptide isolated from a natural origin.

In a previous paper,[6] we have described a method for the synthesis of 3-isopropylidene-6-aralkylidene-2,5-piperazinediones. The method consists in the treatment of methyl 2-amino-3-methylcrotonate with phthaloylglycyl chloride, giving methyl 3-methyl-2-phthaloylglycylaminocrotonate, which, after removal of the phthaloyl group, was cyclized to yield 3-isopropylidene-2,5-piperazinedione. The condensation of the piperazinedione with aromatic aldehydes gave 3-isopropylidene-6-aralkylidene-2,5-piperazinediones.

It was also shown, however, that methyl 2-amino-3-methylcrotonate could be obtained by the reduction of the corresponding 2-nitro compound with aluminum amalgam, while analogous reduction of other 2-nitro-2-alkenoic acid esters resulted in the formation of the 2-oximino-alkanoic acid esters as the isolated products.

In the present paper, we wish to report an alternative and more general route for the synthesis of 3-alkylidene-2,5-piperazinediones and the total synthesis of albonoursin.[7]

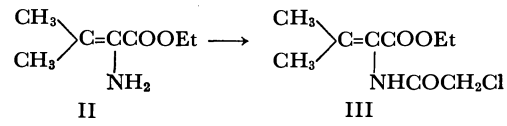

II III

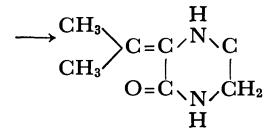

IV

1) A. S. Khoklov and G. B. Lokshin, *Tetrahedron Letters*, **1963**, 1881.

2) R. Brown and C. Kelley, *Annual Report of the New York State Department of Health Albany*, 10 (1957), 47 (1958), 52 (1959), 50 (1960), 40 (1961).

3) K. U. Rao and W. P. Cullen, *J. Am. Chem. Soc.*, **82**, 1127 (1960).

4) R. Brown, C. Kelley and S. E. Wiberley, *J. Org. Chem.*, **30**, 277 (1965).

5) M. Vondracek and Z. Vanek, *Chem. & Ind.*, **1964**, 1686.

6) C. Shin, M. Masaki and M. Ohta, *J. Org. Chem.*, **32**, 1860 (1967).

7) A part of this work was preliminarily communicated: C. Shin, Y. Chigira, M. Masaki and M. Ohta, *Tetrahedron Letters*, **1967**, 4601.

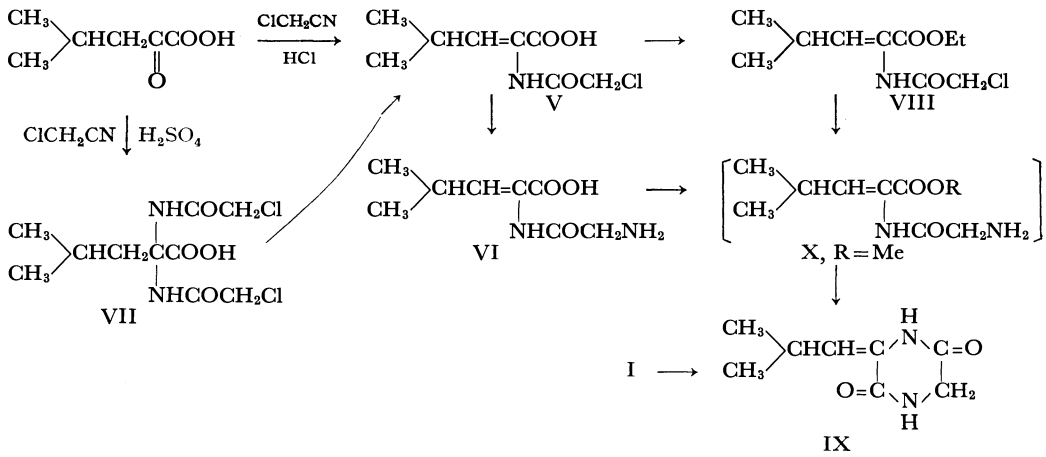

TABLE 1. PHYSICAL CONSTANTS OF 3-BENZYLIDENE-6-ISOBUTYLIDENE-2,5-PIPERAZINEDIONE

Product	Mp, °C	Infrared ν_{max}, cm^{-1}	Ultraviolet λ_{max}, mμ (log ε)
Synthesized	271—271.5	3180, 3080—3030, 1680, 1635, 1420, 1355, 690[a]	320.5 (4.4)[b]
Natural	272[c]	3184, 3080—3030, 1680, 1638, 1424, 1358, 690[c]	234 (3.9), 318 (4.4)[c]
	275—276[d]		
	263—265[e]		201, 236, 316[e]

a) In KBr. b) In dimethylformamide. c) Reference 4. d) Reference 3.
e) Reference 5.

Treatment of ethyl 2-amino-3-methylcrotonate (II) with chloroacetyl chloride in an aqueous solution in the presence of sodium hydrogencarbonate afforded ethyl 2-(2-chloroacetamido)-3-methylcrotonate (III) in 47% yield. When the ester III was treated with ammonia in methanol at room temperature for 2 days, the amination and the subsequent or spontaneous cyclization reactions occurred to yield 3-isopropylidene-2,5-piperazinedione (IV).

In an extension of this method to the synthesis of albonoursin, the ester of 2-(2-chloroacetamido)-4-methyl-2-pentenoic acid is required. Meister and Greenstein have reported that the condensation reaction of α-ketoisocaproic acid with chloroacetonitrile in the presence of hydrogen chloride gave a mixture of 2-(2-chloroacetamido)-4-methyl-2-pentenoic acid (V) and chloroacetamide. The acid V has not been isolated but characterized by its conversion to 2-(2-aminoacetamido)-4-methyl-2-pentenoic acid (VI).[8] However, our modification of the method led to the isolation of V in a pure state (see Experimental). The acid V was also obtained by heating 2,2-bis(2-chloroacetamido)-4-methylpentanoic acid (VII) in acetic acid for 3 hr. The acid V was identified by a comparison with the sample obtained in the preceding paper[9] from 2-chloromethyl-4-isobutylidene-5-oxazolone.

The acid V was transformed into the corresponding ethyl ester (VIII) in 26% yield by heating in ethanol in the presence of sulfuric acid and *p*-toluenesulfonic acid.[10] Treatment of the ester with ammonia in methanol afforded 3-isobutylidene-2,5-piperazinedione (IX).

In an alternative route, 2-(2-aminoacetamido)-4-methyl-2-pentenoic acid (VI) derived from V was refluxed in methanol in the presence of hydrogen chloride to give the corresponding methyl ester (X). By heating in aqueous solution, the ester X gave also the piperazinedione IX in 28% yield.

When the piperazinedione IX was condensed with benzaldehyde in the presence of acetic anhydride and sodium acetate, 3-benzylidene-6-isobutylidene-2,5-piperazinedione (I) was obtained in 56% yield. The identity of the product was confirmed by elemental analysis as well as infrared and ultraviolet spectra. The spectral data and other properties indicate the identity of the natural albonoursin, as shown in Table 1.

Experimental[11]

Ethyl 2-(2-Chloroacetamido)-3-methylcrotonate

8) A. Meister and J.P. Greenstein, *J. Biol. Chem.*, **195**, 849 (1952).

9) H. Kurita, Y. Chigira, M. Masaki and M. Ohta, This Bulletin, **41**, 2758 (1968).

10) In general, the esterification of this type of compounds is difficult. *N*-Acetyl-dehydroalanine has been reported to be esterified by means of the use of diazomethane in 10% yield and of dimethyl sulfate or methyl iodide in 40—50% yield: T. Wieland, G. Ohnacker and W. Ziegler, *Chem. Ber.*, **90**, 194 (1957).

11) All melting points were determined in a liquid bath and are uncorrected.

(III). Chloroacetyl chloride (0.8 g) was added portionwise, with vigorous stirring at room temperature, to ethyl 2-amino-3-methylcrotonate (1 g) suspended in a solution of sodium hydrogencarbonate (0.6 g) in water (15 m*l*). After stirring for 30 min, crystalline precipitates were collected and washed with water. Recrystallization from 50% aqueous ethanol afforded colorless needles (0.7 g, 47%), mp 117—118°C. The product was identical in melting point and infrared spectrum with the sample obtained in the preceding paper.[9]

3-Isopropylidene-2,5-piperazinedione (IV). A solution of III (0.6 g) in methanol (15 m*l*) was saturated with dry gaseous ammonia under cooling. When the solution was allowed to stand at room temperature for 3 days, crystalline substance precipitated. The methanol was evaporated under reduced pressure and the residual crystalline product was washed with cold water. Recrystallization from water afforded colorless prisms (0.26 g, 61%), mp 260°C (decomp.). The infrared spectrum was superimposable on that of the authentic 3-isopropylidene-2,5-piperazinedione.[6]

2,2-Bis (2-chloroacetamido)-4-methylpentanoic Acid (VII). The same directions were followed as that used for 2,2-bis(2-chloroacetamido)propionic acid.[12]

By a reaction of 4-methyl-2-oxopentanoic acid (5 g) and chloroacetonitrile (6 g) in concentrated sulfuric acid (30 m*l*), followed by a recrystallization of the crude product from water, there were obtained colorless prisms (5.6 g, 50%), mp 183—184°C (lit.[13] mp 134°C).

Found: C, 40.41; H, 5.34; N, 9.20%. Calcd for $C_{10}H_{16}N_2O_4Cl_2$: C, 40.13; H, 5.35; N, 9.36%.

2-(2-Chloroacetamido)-4-methyl-2-pentenoic Acid (V). *A) From 4-Methyl-2-oxopentanoic Acid.* The procedure was modified from the method of Meister and Greenstein.[8] A mixture of 4-methyl-2-oxopentanoic acid (4 g) and chloroacetonitrile (2 g) was saturated with dry hydrogen chloride at 0°C, and then allowed to stand in a refrigerator for 3 days. The mixture was treated with dry ether and the crystalline substance, chloroacetamide, was filtered off. The filtrate was concentrated to give a yellow viscous residue (*residue A*), which was dissolved in water (20 m*l*). The pH of the solution was adjusted to 8 with a sodium bicarbonate solution and an insoluble oil formed was removed by extraction with ether. The aqueous layer was acidified to pH 3 with 3 N hydrochloric acid and well extracted four times with ether. The ethereal extract was dried over anhydrous sodium sulfate and then evaporated. Addition of di-*n*-butyl ether to the residual oil gave a crystalline product. Recrystallization from di-*n*-butyl ether afforded colorless needles (0.7 g, 14%), mp 128—129°C. The product was identical with the sample prepared in the preceding paper.[9]

B) From VII. A suspension of VII (3 g) in acetic acid (12 m*l*) was gently refluxed for 3 hr, and the resultant dark brown solution was concentrated under reduced pressure to give a yellow viscous residue, which was treated in the same manner as for the *residue A* in the method A, giving colorless needles (0.7 g, 36.8%), mp 128—129°C. The product was identical, in melting point and infrared spectrum, with the sample obtained by the method A.

Ethyl 2-(2-Chloroacetamido)-4-methyl-2-pentenoate (VIII). A suspension of V (4.8 g) in ethanol (20 m*l*) and benzene (20 m*l*) was refluxed in the presence of concentrated sulfuric acid (0.5 g) and *p*-toluenesulfonic acid (0.5 g) for 5 hr. The resultant solution was concentrated under reduced pressure to give an oily residue. Ether was added to the residue and then the insoluble *p*-toluenesulfonic acid was filtered off. The ethereal solution was washed successively with aqueous sodium bicarbonate and with water, and dried over anhydrous sodium sulfate. After evaporation of the ether, the residue was distilled to give a colorless viscous oil (1.4 g, 25.6%), bp 135—137°C/2 mmHg. Upon addition of petroleum ether, the oil gradually solidified. Recrystallization from petroleum ether afforded colorless prisms, mp 64—67°C.

Found: C, 51.36; H, 6.68; N, 6.10%. Calcd for $C_{10}H_{16}NO_3Cl$: C, 51.39; H, 6.85; N, 6.00%.

2-(2-Aminoacetamido)-4-methyl-2-pentenoic Acid (VI). The procedure was modified from the method of Meister and Greenstein.[8] A solution of V (2.0 g) in methanol (30 m*l*) was saturated with gaseous ammonia under ice cooling and then left to stand at room temperature overnight. The solution was concentrated under reduced pressure: the residual oily product solidified partially upon addition of methanol to give colorless needles (0.5 g), mp 266—267°C (decomp.).[14]

3-Isobutylidene-2,5-piperazinedione (IX). *A) From VIII.* A solution of VIII (0.6 g) in methanol (10 m*l*) was saturated with gaseous ammonia and the resultant mixture was treated in a manner analogous to the case of IV. Recrystallization from water gave colorless needles (0.25 g, 59%), mp 277—278°C (decomp.). ν_{max}^{KBr} 3170, 3050, 1700 and 1640 cm^{-1}. λ_{max}^{KBr} 220 mμ (ε =16600), 240 (14100).

Found: C, 56.81; H, 7.01; N, 16.85%. Calcd for $C_8H_{12}N_2O_2$: C, 57.13; H, 7.19; N, 16.66%.

B) From X. A suspension of VI (0.4 g) in methanol (15 m*l*) was refluxed, while dry hydrogen chloride was passed through the mixture for 2 hr. The solution was concentrated under reduced pressure to dryness giving the methyl ester hydrochloride (X·HCl) as a crystalline residue, which was used without further purification. A solution of the crude X and sodium bicarbonate (0.1 g) in water (10 m*l*) was heated on a steam bath for 3 hr. Crystals gradually precipitated from the solution. The precipitates were collected and recrystallized from 50% aqueous methanol to give colorless needles (0.1 g) mp 277—278°C. The product was identical, in melting point and infrared spectrum, with the sample obtained in method A.

3-Benzylidene-6-isobutylidene-2,5-piperazinedione (I). A mixture of IX (0.05 g) and benzaldehyde (0.2 g) in acetic anhydride (2 m*l*) was heated at 140°C for 5 hr. The mixture was treated with water (4 m*l*) and ether (2 m*l*), giving crystalline precipitates. The precipitates were collected, dissolved in acetic acid and then reprecipitated by addition of water. Recrystallization from acetone afforded colorless needles (0.03 g, 40%).

Found: C, 70.02; H, 6.39; N, 11.00%. Calcd for $C_{15}H_{16}N_2O_2$: C, 70.29; H, 6.29; N, 10.93%.

12) J. P. Greenstein and M. Winitz, "Chemistry of Amino Acids", Vol. 2, John Wiley and Sons, Inc., New York, 1961, p. 849.

13) S.-C. J. Fu, L. Levintow, V. E. Price and J. P. Greenstein, *Arch. Biochem.*, **28**, 440 (1950); *Chem. Abstr.*, **45**, 5625g (1951).

14) Unfortunately the mp was not recorded in literature 13.

BULLETIN OF THE CHEMICAL SOCIETY OF JAPAN VOL. 42 194—199 (1969)

The Synthesis of Cyclic α-Amino Acids. II

Mitsuhiro KINOSHITA, Hiroaki YANAGISAWA, Shuhei Doi, Eisuke KAJI and Sumio UMEZAWA

Department of Applied Chemistry, Faculty of Engineering, Keio University, Koganei-shi, Tokyo

(Received May 23, 1968)

The reaction of substituted derivatives of α-nitrocinnamates bearing a nitro group or a chlorine atom at the *p*- or *m*-position with cyclopentadiene produced corresponding cyclic α-nitro esters (adducts) in a good yields. The reaction of ethyl α-nitrocrotonate with cyclohexadiene gave ethyl 3-methyl-2-nitrobicyclo[2.2.2]-5-octene-2-carboxylate. In the case of an adduct, ethyl 2-nitro-3-(*p*-nitrophenyl)bicyclo[2.2.1]-5-heptene-2-carboxylate, there could be isolated four diastereoisomers as crystalline forms by column chromatography and fractional recrystallization. The stereochemistry of the four isomeric adducts were established by NMR spectroscopy. The readily available three of those isomers were converted to corresponding pure isomers of amino acids by reduction followed by hydrolysis. From the other adducts the major amino acid isomers or the amino acid mixtures were obtained in an analogous route.

A recent publication[1] from this laboratory described the synthesis of cyclic α-amino acids from α,β-unsaturated α-nitro esters, which were used as dienophiles in the Diels-Alder reaction. The present paper is concerned with an extension of this work and presents the syntheses of 2-amino-3-(*p*- or *m*-substituted phenyl)bicyclo[2.2.1]heptane-2-carboxylic acids (IV, XI, XII) and 2-amino-3-methylbicyclo-[2.2.2]octane-2-carboxylic acid (XV) (Fig. 1).

The Diels-Alder reaction of ethyl α,*p*-dinitrocinnamate[2] (I) which was confirmed to be a single isomer by NMR, with excess cyclopentadiene in benzene at 120°C for 1.5 hr gave ethyl 2-nitro-3-(*p*-nitrophenyl) bicyclo[2.2.1]-5-heptene-2-carboxylate (II) in quantitative yield. The semicrystalline adduct II was shown to be a mixture of two fractions, II_1 (R_f, 0.5) and II_2 (R_f, 0.4), by thin layer chromatography. These fractions were effectively separated from each other by silica gel column chromatography. The ratios of II_1 to II_2 observed in several batches of II fell in a range of 1 : 9—1 : 10 by weight. The NMR spectra of II_1 and II_2 showed that both of them were mixtures of diastereoisomers. The fractional recrystallization of II_1 and II_2 resulted in the separation of the diastereoisomers. The components IIA and IID separated from II_1, and the other components IIB and IIC from II_2 were characterized as the pure diastereoisomers of the adduct II (Table 1). The ratios of IIA to IID and of IIB to IIC were estimated to be about 3.5 : 1 and 4 : 1 on the basis of NMR analysis, respectively.

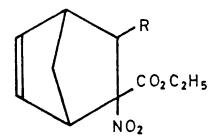

II: R=$C_6H_4NO_2$ (*p*)
VII: R=$C_6H_4NO_2$ (*m*)
VIII: R=C_6H_4Cl (*p*)

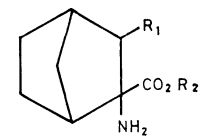

III: R_1=$C_6H_4NH_2$ (*p*), R_2=C_2H_5
IX: R_1=$C_6H_4NH_2$ (*m*), R_2=C_2H_5
X: R_1=C_6H_4Cl (*p*), R_2=C_2H_5
IV: R_1=$C_6H_4NH_2$ (*p*), R_2=H
XI: R_1=$C_6H_4NH_2$ (*m*) R_2=H
XII: R_1=C_6H_4Cl (*p*), R_2=H

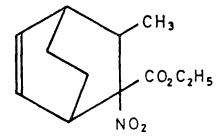

XIII

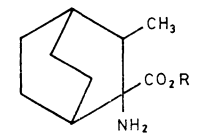

XIV: R=C_2H_5
XV: R=H

Fig. 1.

The stereochemistry of the four diastereoisomers was established by NMR as shown in Fig. 2. Spectral features were assigned on the basis of chemical shifts, integrated area, magnitudess of plittings, and decoupled splitting patterns.[3] The assigned chemical shifts and coupling constants are listed in Tables 2 and 3, respectively.

1) S. Umezawa, M. Kinoshita and H. Yanagisawa, This Bulletin, **40**, 209 (1967).

2) A. Dornow and H. Menzel, *Ann.*, **588**, 40 (1954).

3) J. C. Davis, Jr., and T. V. Van Auken, *J. Am. Chem. Soc.*, **87**, 3900 (1965).

Table 1. Adducts

Compound	Reaction condition °C	Reaction condition hr	Mol ratio*	Mp °C or Bp °C (mmHg)	n_D^{21}	Formula	Calcd, % C	Calcd, % H	Calcd, % N	Found, % C	Found, % H	Found, % N
IIA	120	1.5	8.1	119—120		$C_{16}H_{16}O_6N_2$	57.83	4.82	8.43	57.58	5.09	8.24
IIB				107—108						57.93	5.12	8.34
IIC				79—80						57.87	5.05	8.13
IID				81—81.5						57.81	4.72	8.30
VIIA	120	2.0	8.1	101—102						58.05	4.64	8.26
VIII	110	6.0	8.1	130—140 (0.5)		$C_{16}H_{16}O_4NCl$	59.73	5.01	4.37	59.19	4.64	4.42
XIII	130	12.0	5.9	89—97 (1.0)	1.4830	$C_{12}H_{17}O_4N$	60.24	7.16	5.85	60.47	7.11	5.77

* Diene/dienophile

Table 2. Chemical shift (τ) of adduct II and VII

Compound \ H	5 (q)*	6 (q)	3x (d)*	3n (d)	1 (s)*	4 (s)	7a	7s	CH_2 (q)	CH_3 (t)*
IIA	3.27	3.83	—	5.83	6.20	6.72	7.23(d)	8.00(d)	6.28	9.14
IIB	3.48	3.27	5.27	—	6.28	6.80	8.28(s)		5.66	8.70
IIC	3.29	3.84	—	5.83	6.35	6.77	7.20(d)	7.92(d)	5.69	8.70
IID	3.47	3.27	5.13	—	6.12	6.76	8.27(s)		6.23	9.24
VIIA	3.25	3.83	—	5.84	6.22	6.75	7.15(d)	7.92(d)	6.28	9.17
VIIB	3.45	3.27	5.28	—	6.28	6.78	8.27(s)		5.65	8.70

* s=singlet; d=doublet; t=triplet; q=quartet.

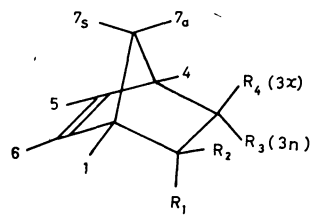

IIA: $R_1=NO_2$, $R_2=CO_2C_2H_5$, $R_3=3n$, $R_4=C_6H_4NO_2(p)$
IIB: $R_1=NO_2$, $R_2=CO_2C_2H_5$, $R_3=C_6H_4NO_2(p)$, $R_4=3x$
IIC: $R_1=CO_2C_2H_5$, $R_2=NO_2$, $R_3=3n$, $R_4=C_6H_4NO_2(p)$
IID: $R_1=CO_2C_2H_5$, $R_2=NO_2$, $R_3=C_6H_4NO_2(p)$, $R_4=3x$
VIIA: $R_1=NO_2$, $R_2=CO_2C_2H_5$, $R_3=3n$, $R_4=C_6H_4NO_2(m)$
VIIB: $R_1=NO_2$, $R_2=CO_2C_2H_5$, $R_3=C_6H_4NO_2(m)$, $R_4=3x$

A letter *n* is added to the number of a hydrogen to denote an *endo* hydrogen and *x* is used to denote an *exo* hydrogen. For the 7-hydrogens the letter *s* specifies the hydrogen *syn* to the double bond and theletter *a* designates the *anti* hydrogen.

Fig. 2.

The bridgehead protons (1,4) are assigned by their broad patterns resulting from several coupling interactions. The bridgehead peak (6.80—6.76τ) at higher field in the isomer IIB and IID can be ascribed to the 4-proton by its coupling constant ($J_{3x,4}=3.3$ cps). It is ascertained that there is no coupling between the bridgehead protons (6.28—6.12τ) in lower field and the 3*x*-protons (doublet centered at 5.27—5.13τ). The olefinic protons (5, 6) in IIB and IID can be assigned by an existence of a remarkable coupling with the bridgehead protons (4, 1). Decoupling shows that the upfield-half of the eight-line pattern of the olefinic protons is coupled ($J_{4,5}=3.0$ cps) with the peak assigned as 4-proton.

In IIA and IIC, both of bridgehead protons show no detectable coupling with 3*n*-proton (doublet centered at 5.83τ). The zero coupling constant ($J_{3n,4}$) can be explained by the deformation of the vicinal dihedral angle[4,5] between 3*n*- and 4-proton. On the other hand, the bridgehead peak at lower field can be assinged to 1-proton as well as in the cases of IIB and IID on the basis of the electronegativity effect[5] of the nearby substituents R_1 and R_2. Decoupling shows that the upfield-half

4) F. A. L. Anet, *Can. J. Chem.*, **39**, 789 (1961).
5) P. Laszlo and P. von R. Schleyer, *J. Am. Chem. Soc.*, **85**, 2709 (1963); W. E. Noland, B. A. Langarger, J. W. Manthey, A. G. Zacchei, D. L. Petrak and K. L. Fian, *Can. J. Chem.*, **45**, 2969 (1967).

TABLE 3. COUPLING CONSTANTS (cps) OF ADDUCT II

Compound	$J_{5,6}$	$J_{4,5}$	$J_{1,6}$	$J_{3n,4}$	$J_{3x,4}$	$J_{7s,3n}$	$J_{7s,7a}$
IIA	5.8	3.0	3.0	0	—	3.0	10.0
IIB	6.0	3.0	3.0	—	3.3	—	?
IIC	5.5	3.1	3.1	0	—	3.0	10.0
IID	6.0	3.0	3.4	—	3.3	—	?

of the eight-line pattern of the olefinic protons in IIA and IIC is coupled ($J_{1,6}=3.0$—3.1 cps) with the peak assigned as 1-proton.

It is interesting that the methylene bridge (7-protons) appear as the characteristic four-line pattern for the spin-spin coupling of two nonequivalent protons in the isomer IIA and IIC, and the geminal coupling constants are equal in both isomers ($J_{7s,7a}=10.0$ cps). However in both IIB and IID, the methylene bridge protons appear as a single peak (8.27—8.28τ) with barely detectable fine structure. In the adduct IIA and IIC, the upfield-doublet (7.92—8.00τ) of this pattern is further split into discernible features, while the downfield-doublet (7.20—7.23τ) is relatively unsplit. Decoupling shows that the upfield-pattern is coupled with the peak assigned as 3*n*-proton, and is attributed to 7*s*-proton. The long-range coupling constant ($J_{7s,3n}=3.0$ cps) falls in the range reported.[3,6,7] The downfield-doublet is then assigned to 7*a*-proton. A downfield shift for hydrogens *syn* to an *exo* substituent has been noted previously by Davis and Van Auken[3] in some *exo*-norbornene derivatives. The downfield shift for 7*a*-proton in IIA and IIC may be attributed to anisotropic effect of the *exo*-substituted *p*-nitrophenyl ring.

The above-mentioned NMR studies for the bridgehead protons, methylene bridge protons and 3-protons of the four isomeric adducts establish the following configurations of 3-*p*-nitrophenyl groups in the addcuts; *exo* in IIA and IIC, while *endo* in IIB and IID. The configurations of 2-carbethoxy groups in the addcuts are deduced on the basis of the chemical shifts of their methyl and methylene protons. Recently, Kleinfelter[8] reported that some phenylnorbornyl *p*-nitrobenzoates in which the *p*-nitrobenzoyl group is in a *cis* relationship with the phenyl group shows a great shielding of one proton pair of *p*-nitrobenzoyl group which is held close to the center of benzene ring. Kleinfelter also reported[9] that a 3-*exo*-phenyl group in 3-phenyl-2-nitrobornanols and their derivatives diamagnetically shields an eclipsed 2-*exo*-proton. A similar effect was observed in *trans*-1,2-diphenylcyclopentane in which the 1- and 2-hydrogens are shielded 0.40 ppm relative to the *cis* isomer.[10] As shown in Table 2, the carbethoxy proton absorptions of the adduct IIA and IID apparently occurred upfield from those of the adduct IIB and IIC. The "*cis*" relationship between the *p*-nitrophenyl and carbethoxy group may exist here in the addcut IIA and IID.

The catalytic hydrogenation of isomers IIA, IIB, IIC and the mixture adduct II with Raney Ni T-4[11] gave three isomers of ethyl 2-amino-3-(*p*-aminophenyl)bicyclo[2.2.1]heptane-2-carboxylate, *i. e.* IIIA, IIIB, IIIC and III, respectively. On hydrolysis with 6 N hydrochloric acid, IIIA, IIIB and IIIC afforded diastereoisomeric 2-amino-3-(*p*-aminophenyl)bicyclo[2.2.1]heptane-2-carboxylic acid, *i. e.* IVA, IVB and IVC, respectively (Table 5). It was interesting that the amino ester IIIA strongly resisted against hydrolysis and, especially, it suffered no hydrolysis in methanolic barium hydroxide solution at 37°C for eighty hours, while the other amino esters IIIB and IIIC were smoothly hydrolyzed. This fact supported the structure of the adduct IIA in which the 2-carbethoxy group undergoes more steric interference owing to the *cis*-3-*p*-nitrophenyl group. The dihydrochloride of major amino acid IVB was sparingly soluble in a cold 6 N hydrochloric acid as compared with its isomeric amino acid dihydrochlorides. On this basis, a convenient preparation of major amino acid IVB was accomplished with 40% overall yield by starting from the mixture adduct II.

In addition, two other amino acids 2-amino-3-(*m*-aminophenyl)bicyclo[2.2.1]heptane-2-carboxylic acid (XIB) and 2-amino-3-(*p*-chlorophenyl)bicyclo-[2.2.1]heptane-2-carboxylic acid (XII) of the above-mentioned type have been synthesized by a similar route. The reaction of cyclopentadiene with ethyl *a*,*m*-dinitrocinnamate (V) and ethyl *a*-nitro-*p*-chlorocinnamate[2] (VI) gave ethyl 2-nitro-3-(*m*-nitrophenyl)bicyclo[2.2.1]-5-heptene-2-carboxylate (VII) and ethyl 2-nitro-3-(*p*-chlorophenyl)bicyclo-[2.2.1]-5-heptene-2-carboxylate (VIII) in a good yield, respectively (Table 1).

6) D. Laszlo and P. von R. Schleyer, *J. Am. Chem. Soc.*, **86**, 1171 (1964).
7) J. Meinwald and Y. Meinwald, *ibid.*, **85**, 2514 (1963).
8) D. C. Kleinfelter, *J. Org. Chem.*, **32**, 3526 (1967).
9) D. C. Kleinfelter, *ibid.*, **32**, 1734 (1967).
10) D. Y. Curtin, H. Gruen and B. A. Shoulders, *Chem. Ind. (London)*, **1958**, 1250; D. Y. Curtin, H. Gruen, Y. G. Hendrickson and H. E. Knipmeyer, *J. Am. Chem. Soc.*, **83**, 4838 (1961).
11) S. Nishimura, This Bulletin, **32**, 61 (1959).

TABLE 4. CYCLIC α-AMINO ESTERS AND THEIR HYDROCHLORIDES

Compound	Mp °C or Bp °C/mmHg	Solvent for Recrystallization (or n_D^{21})	Formula	Calcd, %				Found, %			
				C	H	N	Cl	C	H	N	Cl
IIIA·2HCl	228 (decomp.)	a	$C_{16}H_{24}O_2N_2Cl_2$	55.34	6.97	8.07	20.42	55.51	7.06	7.93	20.25
IIIB·2HCl	250—252 (decomp.)	b						55.66	6.98	8.12	20.20
IXB·2HCl	224—226 (decomp.)	b						54.87	6.90	7.70	20.06
IIIC	94—95.5	c	$C_{16}H_{22}O_2N_2$	70.04	8.08	10.21		70.36	8.32	9.88	
IXB	83—84	c						69.93	8.08	10.37	
X′	95.5—96	d	$C_{16}H_{20}O_2NCl$	65.41	6.86	4.77		65.53	6.75	4.74	
X′·HCl	207—208 (decomp.)	b	$C_{16}H_{21}O_2NCl_2$	58.19	6.41	4.24	21.47	58.44	6.58	4.20	21.41
XIV	74—81/1	(1.4915)	$C_{12}H_{21}O_2N$	68.21	10.02	6.63		68.70	9.72	6.54	
XIV·HCl	177—178	e	$C_{12}H_{22}O_2NCl$	58.17	8.95	5.65		58.05	8.79	5.77	

a=ethanol/diisopropyl ether; b=ethanol/ether; c=petroleum ether (bp 40—60°C); d=*n*-hexane; e=butanone

TABLE 5. HYDROCHLORIDE OF CYCLIC α-AMINO ACIDS

Compound	Mp °C (decomp.)	pK_a	Formula	Calcd, %				Found, %			
				C	H	N	Cl	C	H	N	Cl
IVA·2HCl	275	2.3, 5.0, 9.9	$C_{14}H_{20}O_2N_2Cl_2$	52.67	6.32	8.77	22.21	52.67	6.71	8.39	21.96
IVB·2HCl	270	2.3, 4.4, 9.5						52.51	6.73	8.29	22.44
IVC·2HCl	296	2.4, 4.4, 9.1						52.80	6.59	8.42	22.26
XIB·2HCl	238	2.3, 4.3, 9.5						52.76	6.20	8.55	22.23
XII·HCl	242—245		$C_{14}H_{17}O_2NCl_2$	55.64	5.67	4.63	23.46	55.88	5.72	4.59	23.35
XV·HCl	258—260		$C_{10}H_{18}O_2NCl$	54.67	8.26	6.37	16.14	54.49	8.17	6.67	16.41

The NMR analysis showed that the dienophile V is a single isomer. The NMR spectrum of the adduct VII which was very similar to the pattern of the adduct mixture II, showed the presence of two pairs of isomeric adducts, *i. e.*, VIIB—VIIC (major) and VIIA—VIID (minor) corresponding to the adduct pairs IIB—IIC and IIA—IID, respectively. The presence of about 70% of the main isomer VIIB in VII was also suggested on the basis of the relative intensity of the 3*x*-proton. The separation of the main isomer VIIB by chromatography and recrystallization was unsuccessful, however, sometimes, spontaneous partial separation of VIIA in pure crystalline state was observed. Its NMR spectrum was found to be closely similar to that of the adduct IIA with exception of pattern due to aromatic protons (Tables 1 and 2). The structures of VIIA and VIIB were assigned as shown in Fig. 2.

The hydrogenations of VII and VIII with Raney Ni T-4 gave ethyl 2-amino-3-(*m*-aminophenyl)-bicyclo[2.2.1]heptane-2-carboxylate (IX) and ethyl 2-amino-3-(*p*-chlorophenyl) bicyclo[2.2.1]heptane-2-carboxylate (X), from which crystalline amino esters, IXB and X′ were obtained respectively. The hydrolysis of IXB and X with 6 N hydrochloric acid or barium hydroxide afforded hydrochlorides of corresponding amino acids XIB and XII, respectively (Table 5).

The Diels-Alder reaction of ethyl α-nitrocrotonate[1,12] with 1,3-cyclohexadiene gave an adduct, ethyl 3-methyl-2-nitrobicyclo[2.2.2]-5-octene-2-carboxylate (XIII) in 25% yield. The gas chromatogram of XIII showed three peaks. Hydrogenation of XIII with Raney Ni T-4 gave ethyl 2-amino-3-methylbicyclo[2.2.2]octane-2-carboxylate (XIV), which, on hydrolysis with barium hydroxide, afforded 2-amino-3-methylbicyclo[2.2.2]octane-2-carboxylic acid(XV).

Experimental

Thin layer chromatography (TLC) was conducted by the use of silica gel (Daiichi Pure Chemicals Co., Inc.). The prepared plates were activated at 110°C. The spray reagent used was concentrated sulfuric acid and 0.25% pyridine solution of ninhydrin. Silica

12) S. Umezawa and S. Zen, This Bulletin, **36**, 1143 (1963).

gel column chromatography was carried out by the use of silica gel (Kanto Chemicals Co., Inc.) activated at 110°C before use. The pK_a values were determined by the method of Parks and Davis.[13] Gas-liquid chromatographic analysis was carried out with a Shimadzu-Kotaki Gas Chromatograph, Model GU-21. The NMR spectra were taken with a Japan Electron Optics JNM-H-60 spectrometer at a frequency of 60 Mc by using about 10—20% solution of the sample in deuteriochloroform with tetramethylsilane as an internal standard. Spin decoupling experiments were carried out by using Japan Electron Optics JNM-4H-100 spectrometer and JNM-SD-30 spin decoupler.

Ethyl 2-Nitro-3-(*p*-nitrophenyl)bicyclo[2.2.1]-5-heptene-2-carboxylate (II) (A typical example of the general procedure). A mixture of ethyl α,*p*-dinitrocinnamate (mp 108—109°C from ether) (1.0 g, 3.76 mmol), freshly distilled cyclopentadiene (2.0 g, 30.3 mmol) and dry benzene (2 m*l*) was heated for 1.5 hr at 120°C in a sealed tube. Unchanged cyclopentadiene and benzene were removed in a vacuum. The resulting red-brown oil was placed on a silica gel column (20 g, 2×15 cm) and eluted with 25% petroleum ether in benzene. The first effluent (*ca.* 90 m*l*) containing dicyclopentadiene was discarded. The second effluent (180 m*l*) gave the adduct II (1.26 g, 100%) as a pale-yellow crystalline solid. TLC (6 : 1 *n*-hexane/ethyl acetate) of II showed two spots having R_f-values of 0.5 and 0.4.

The other adducts VII, VIII and XIII were prepared by the general procedure (Table 1). The preparations of VIII and XIII, however, were carried out without solvent and purification was done by distillation. The gas chromatographic analysis of XIII on polyester-succinate column (1-m long) at 180°C with helium (40 m*l*/min) showed three peaks with elution times of 20.0, 22.0 and 26.4 min.

The Separation of Diastereoisomers of the Adduct II and VII. Separation of the Fraction II_1 and II_2. A sample of 1.04 g of II in a small amount of ethyl acetate was placed on a silica gel column (100 g, 3×38 cm) and eluted with 6 : 1 *n*-hexane/ethyl acetate in the flow rate of 12 m*l*/hr. Fractions (*ca.* 4 m*l*) were collected and examined by TLC with the same solvent system as the column chromatography. Fractions 80—118 (150 m*l*) gave II_1 (R_f 0.5; 70 mg, mp 74—114°C). Fractions 124—190 (270 m*l*) gave II_2 (R_f 0.4; 676 mg, mp 71—79°C) and fractions 119—123 (20 m*l*) gave a II_1-II_2 mixture (15 mg). Total yield was 73.2% based on the original adduct II.

Adduct IIA: Recrystallization of the fraction II_1 (230 mg) from methanol gave IIA (115 mg), colorless needles, mp 119—120°C.

Adduct IID: The separation of the adduct IID from its isomer IIA was a laborious work. The mother liquor separated from the first crop of IIA was evaporated to give a yellow crystalline mass melting at 64—70°C. A sample (30 mg) of the material was dissolved in hot methanol (0.6 m*l*). After inoculation of pure IID as a seed, the solution was allowed to stand overnight in a refrigerator to afford colorless large plates of IID (9 mg) which was partly contaminated by the needles of IIA. The plates (4 mg) of IID were picked out with a tweezer from the mixture; mp 79—80°C. The products from similar twelve batches were pooled (50 mg) and recrystallized from methanol to yield 33 mg of an analytical sample, mp 81—81.5°C.

Adduct IIB: A sample (656 mg) of the above-mentioned fraction II_2 was recrystallized from hot methanol (12 m*l*) by inoculation of pure crystals of IIB to give granular crystals (425 mg) of IIB melting at 104.5—106.2°C. Recrystallization afforded an analytical sample, mp 107—108°C. An additional crop (64 mg) of IIB was obtained from the mother liquor; total yield, 489 mg (74.5%).

Adduct IIC: The mother liquor separated from the second crop of IIB was evaporated to give a crystalline mass, which was recrystallized from methanol by inoculation of seed crystals of IIC to afford granular crystals (105 mg) melting at 78.5—80.0°C. An analytical sample of IIC was obtained by one recrystallization from methanol, mp 79—80°C.

Adduct VIIA: (A rare example of the separation of of VIIA). When a mixture adduct VII (1.20 g) prepared by above-mentioned general procedure was triturated with 3 m*l* of ethanol and the triturated mixture was allowed to stand for several hours in a cold place, there separated the crystals of VIIA; yield, 470 mg, mp 82—92°C. Two recrystallizations from ethanol afforded an analytical sample, mp 101—102°C.

Ethyl 2-Amino-3-(*p*-aminophenyl)bicyclo[2.2.1]-heptane-2-carboxylate (IIIB) (A typical example of the general procedure). A solution of ethyl 2-nitro-3-(*p*-nitrophenyl)bicyclo[2.2.1]-5-heptene-2-carboxylate (IIB) (1.5 g) in ether (25 m*l*) was shaken with Raney Ni T-4 (7 m*l*) at 20—25°C and 120 kg/cm² for 5 hr in an autoclave. The contents were then filtered to remove the catalyst and the solution was evaporated in a vacuum. A solution of the resulting oil (1.08 g) in ether (30 m*l*) was extracted with 1 N hydrochloric acid (9 m*l*), and the ethereal solution was washed with water (10 m*l*×4). The aqeuous layer and washings were combined, washed with ether (10 m*l*) and made alkaline by addition of a 50% potassium carbonate solution (2.5 m*l*). The liberated oil was extracted with ether (10 m*l*×4), and the ethereal extract was dried over potassium carbonate. After evaporation of the solvent, the amino ester IIIB was obtained as a pale-yellow viscous oil; yield, 967 mg (77.8%).

The other amino esters, III (isomeric mixture), IIIA, IIIC, IX, X and XIV were prepared by the general procedure. The hydrogenations of X and XIV were carried out in ethanol instead of in ether. The crystalline amino esters IXB and X′ were isolated from the corresponding mixed ester IX and X in a yield of 46.4% and 15%, respectively (Table 4).

The hydrochlorides of IIIA, IIIB, IIIC, IXB, X′, and XIV were obtained from their ethanolic hydrogen chloride solution by dilution with absolute ether (Table 4).

2-Amino-3-(*p*-aminophenyl)bicyclo[2.2.1]heptane-2-carboxylic Acid Dihydrochloride (IVB·2HCl) (A typical example of the general procedure). A solution of IIIB (220 mg) in 6 N hydrochloric acid (5.5 m*l*) was heated in a sealed tube at 110—120°C for 8 hr. After refrigeration of the reaction mixture, the precipitated dihydrochloride of IVB was collected and washed with acetone to afford colorless fine crytals; yield, 218 mg (85.2%). By concentration of the mother

13) T. V. Parke and W. W. Davis, *Anal. Chem.*, **26**, 642 (1954).

liquor the second crop of IVB·2HCl (42 mg) was obtained. Tow recrystallizations from methanol-diisopropyl ether gave an analytical sample, granular crystals; mp 270°C (decomp.).

The dihydrochlorides, IVC·2HCl and XIB·2HCl were prepared by the general procedure, but the isolation of IVC·2HCl was accomplished by evaporation of the reaction mixture, because of its high solubility in cold hydrochloric acid. An analytical sample of IVC·2HCl was obtained by recrystallization from absolute methanolic hydrogen chloride-diisopropyl ether.

2-Amino-3-(*p*-aminophenyl)bicyclo[2.2.1]heptane-2-carboxylic Acid Dihydrochloride (IVA·2HCl). A solution of IIIA (220 mg) in 6 N hydrochloric acid (5.0 ml) was heated in a sealed tube at 110—120°C for 16 hr. The resulting mixture was evaporated in a vacuum to give a solid mass, which was washed with ether and acetone. The yellow powdery product (180 mg) was placed on a silica gel column (1.5×30 cm) and developed with a solvent system of ethyl acetate-pyridine-methanol (3 : 1 : 1) until the yellow band of amino acid was separated completely from the orange band of unchanged amino ester on the column. The silica gel containing amino acid band in a upper portion of the column was scraped out and extracted out with methanol. The methanol extract was evaporated to give an oil which crystallized by trituration with absolute ether; yield, 130 mg (64%). Recrystallization from absolute ethanolic hydrogen chloride-diisopropyl ether afforded an analytical sample of IV·2HCl, mp 232°C(colored)—275°C(decomp.).

2-Amino-3-(*p*-chlorophenyl)bicyclo[2.2.1]heptane-2-carboxylic Acid (XII) and 2-Amino-3-methylbicyclo[2.2.2]octane-2-carboxylic Acid (XV). XII and XV were prepared from X and XIV, respectively by hydrolysis with 0.45 N barium hydroxide in aqueous methanol at 36—37°C for 20 hr, by the similar method as reported previously.[1] The hydrochlorides of XII and XV were obtained from their ethanolic hydrogen chloride solution by dilution with absolute ether.

Ethyl α,*p*-Dinitrocinnamate[2] (I). The NMR signals were observed at $\tau(CDCl_3)$: 2.04 (center of A_2B_2 pattern, aromatic protons); 2.35 (a singlet, β-proton); 5.53 (a quartet, ester methylene protons); and 8.62 (a triplet, ester methyl protons).

Ethyl α,*m*-Dinitrocinnamate (III). Prepared from *m*-nitrobenzylidene-*n*-butylamine[14] and ethyl nitroacetate by the same method as reported by Dornow and Menzel[2]; yield, 61%, mp 101—102°C (from ether). The NMR signals were observed at $\tau(CDCl_3)$: 2.28 (a singlet, β-proton); 5.54 (a quartet, ester methylene protons); and 8.59 (a triplet, ester methyl protons).

Found: C, 49.85; H, 3.95; N, 10.43%. Calcd for $C_{11}H_{10}O_6N_2$: C, 49.63; H, 3.79; N, 10.52%.

The authors are indebted to Professor Shoji Hara, Tokyo College of Pharmacy and Dr. Keishi Kotera, Tokyo Tanabe Seiyaku Co. for the measurement of NMR spectra, and Mr. Saburo Nakada for the microanalyses.

14) S. Zen, Ph. D. Thesis, Keio University, 1963.

BULLETIN OF THE CHEMICAL SOCIETY OF JAPAN VOL. 42 199—202 (1969)

A New Synthesis of Tephrosic Acid*1

Kenji FUKUI, Mitsuru NAKAYAMA and Teruo HARANO

Department of Chemistry, Faculty of Science, Hiroshima University, Higashi Sendamachi, Hiroshima

(Received May 27, 1968)

2′-Carboethoxymethoxy-4′,5′-dimethoxy-7-hydroxyisoflavone was prepared from 7-benzyloxy-4′,5′-dimethoxy-2′-hydroxyisoflavone *via* the corresponding 2′-carboethoxymethoxyisoflavone. The hydrolysis of the 7-hydroxyisoflavone with dilute alkali gave tephrosic acid (2,4-dihydroxyphenyl 2-carboxymethoxy-4,5-dimethoxybenzyl ketone) in a good yield.

Tephrosic acid (I) is an important intermediate in synthesizing rotenoids (*e. g.*, elliptone (II) and munduserone (III)). This acid, I, has been prepared from resorcinol and ethyl (2-cyanomethyl-4,5-dimethoxyphenoxy)acetate (IV) by the Hoesch reaction.[1] However, the preparation of the ester IV has been found to be disadvantageous because of either a poor over-all yield or the tediousness of separating an intermediate difficult to crystallize. The present paper will describe a convenient method of synthesizing I from 7-benzyloxy-4′,5′-dimethoxy-2′-hydroxyisoflavone (V)[2] according to a modification of a procedure reported earlier by the present

*1 The results of this investigation were presented at the 20th Annual Meeting of the Chemical Society of Japan, Tokyo, April, 1967.

1) A. Robertson, *J. Chem. Soc.*, **1932**, 1163.

2) K. Fukui, M. Nakayama, T. Harano and H. Tsuge, 10th Symposium on the Chemistry of Natural Products, Symposium Papers, Tokyo (Oct., 1966), p. 145; K. Fukui, M. Nakayama and T. Harano, This Bulletin, **42**, 233 (1969).

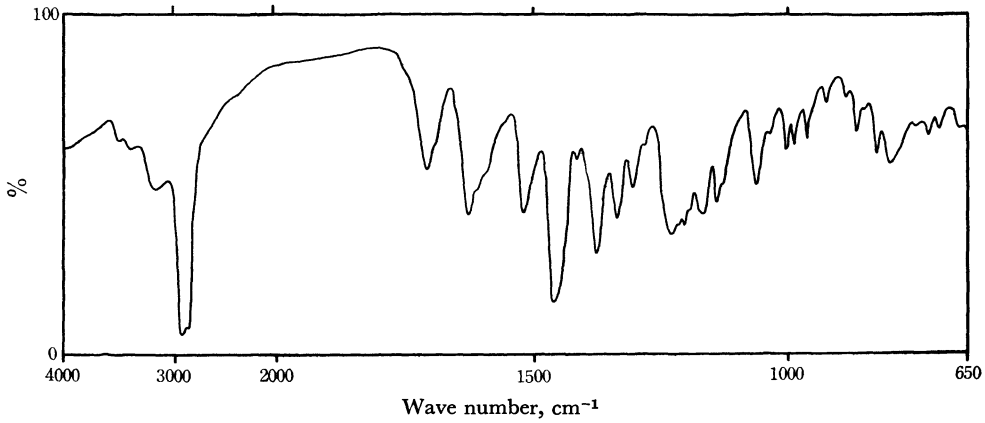

Fig. 1. IR spectrum of I (Nujol).

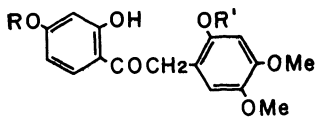

I R = H R' = CH_2CO_2H

VIII R = R' = Me

IX R = Me R' = CH_2CO_2Me

X R = Me R' = CH_2CO_2H

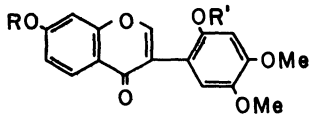

V R = $C_6H_5CH_2$ R' = H

VI R = $C_6H_5CH_2$ R' = CH_2CO_2Et

VII R = H R' = CH_2CO_2Et

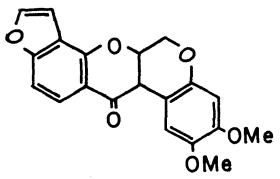

II

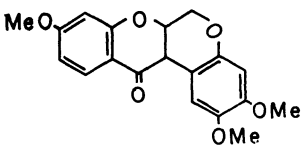

III

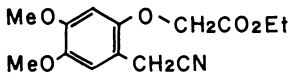

IV

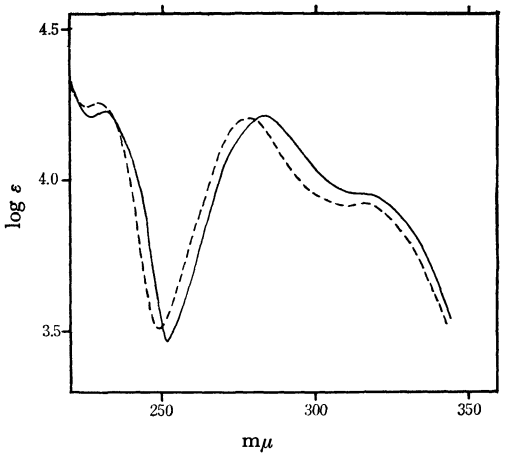

Fig. 2. UV spectra of I (——) and IX (------) in ethanol.

authors[3] and also be Chandrashekar *et al.*[4]

The reaction of the 2'-hydroxyisoflavone V with ethyl bromoacetate in the presence of anhydrous potassium carbonate afforded 7-benzyloxy-2'-carboethoxymethoxy-4',5'-dimethoxyisoflavone (VI) in a good yield. By catalytic hydrogenolysis over palladium-charcoal, the 7-benzyloxyisoflavone VI gave 2'-carboethoxymethoxy-4',5'-dimethoxy-7-hydroxyisoflavone (VII), which was then easily converted into its monoacetate by conventional methods. The treatment of VII with alcoholic potassium hydroxide gave the desired acid, I, in a good yield. This was identified with an authentic

3) K. Fukui, M. Nakayama and T. Harano, *Experientia*, **23**, 613 (1967).

4) V. Chandrashekar, M. Krishnamurti and T. R. Seshadri, *Tetrahedron*, **23**, 2505 (1967).

specimen[5] by a mixed-melting-point determination and by infrared and ultraviolet spectral comparisons (Figs. 1 and 2).

The partial methylation of the acid I with diazomethane gave a methyl ester. A comparison of the NMR spectrum of the ester with that of the 2-hydroxy-4-methoxyphenyl 2,4,5-trimethoxybenzyl ketone (VIII)[6] (Table 1) indicated that the methylated specimen should be represented as 2-hydroxy-4-methoxyphenyl 2-carbomethoxymethoxy-4,5-dimethoxybenzyl ketone (IX). Finally, the hydrolysis of IX with dilute alkali gave tephrosic acid monomethyl ether (X), which had previously been obtained by an alternative route.[3]

Since the synthesis of (±)-II from I has already been carried out,[5] this paper completes the presentation of a new synthesis of (±)-II.

Table 1. The NMR spectra of 2-hydroxyphenyl benzyl ketones VIII and IX*

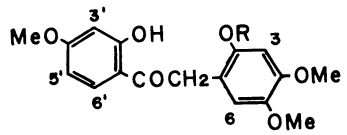

Compound	VIII R=Me	IX R=CH_2CO_2Me
Arom. C_3-H	6.55 s	6.49 s
C_6-H	6.75 s	6.75 s
$C_{3'}$-H	6.40 d	3.68 d
$C_{5'}$-H	6.40 q	6.47 q
$C_{6'}$-H	7.84 d′	7.94 d′
Ar.-CH_2-CO-Ar.	4.17 s	4.29 s
Ar.-O-CH_2-CO_2Me		4.62 s
Ar. -OMe and -CO_2Me	3.82 (3H)	3.75 (3H)
	3.85 (6H)	3.85 (9H)
	3.90 (3H)	
OH	12.68	12.67

* The NMR spectra were measured with a Hitachi Model R-20 NMR spectrometer (60 MHz), using tetramethylsilane as an internal standard (δ-values in $CDCl_3$; s, singlet; d, doublet (J_{meta} 2 Hz); d′, doublet (J_{ortho} 9 Hz); q, quartet (J_{meta} 2 Hz; J_{ortho} 9 Hz).

Experimental*2

7-Benzyloxy-2′-carboethoxymethoxy-4′,5′-dimethoxyisoflavone (VI). To a solution of isoflavone (V: mp 172—173°C)[2] (400 mg) and ethyl bromoacetate (200 mg) in anhydrous acetone (50 m*l*), anhydrous potassium carbonate (1.5 g) was added; the mixture was then refluxed for 24 hr. After the inorganic salts had been filtered off, the solution was concentrated to 5 m*l* and then diluted with water. The separated solid was collected and recrystallized from ethanol to give VI as colorless needles, mp 112—113°C; yield, 370 mg (77%). IR: 1736, 1640, 1620 cm^{-1} (C=O). UV: λ_{max} mμ (log ε); 248 (4.39), 296 (4.29).

Found: C, 68.38; H, 5.27%. Calcd for $C_{28}H_{26}O_8$: C, 68.57; H, 5.30%.

2′-Carboethoxymethoxy-4′,5′-dimethoxy-7-hydroxyisoflavone (VII). A solution of VI (320 mg) in ethyl acetate (100 m*l*) was submitted to catalytic hydrogenolysis at room temperature in the presence of Pd-C (10%: 90 mg). After the catalyst had been filtered off, the filtrate was evaporated under a vacuum; the residue was then recrystallized from ethanol to give VII as colorless microneedles, mp 217.5—218.5°C (lit.[7] mp 217—218°C); yield, 240 mg (92%). IR: 3250 (OH), 1735, 1633 cm^{-1} (C=O). UV: λ_{max} mμ (log ε); 255 (4.53), 296.5 (4.28), 336 (4.01).

Found: C, 63.08; H, 5.13%. Calcd for $C_{21}H_{20}O_8$: C, 62.99; H, 5.04%.

The acetate: acetic anhydride-anhydrous sodium acetate method; mp 137—138°C (colorless microneedles from ethanol). IR: 1768, 1733, 1655, 1625 cm^{-1} (C=O). UV: λ_{max} mμ (log ε); 294 (4.12).

Found: C, 62.19; H, 4.93%. Calcd for $C_{23}H_{22}O_9$: C, 62.44; H, 5.01%.

Tephrosic Acid (2,4-Dihydroxyphenyl 2-Carboxymethoxy-4,5-dimethoxybenzyl Ketone) (I). To a solution of VII (200 mg) in ethanol (50 m*l*), a 10% aqueous potassium hydroxide solution (20 m*l*) was added; the mixture was then refluxed for 2 hr. After the solvent had been removed as much as possible, the residue was acidified with 10% hydrochloric acid. The separated solid was collected and recrystallized from aqueous ethanol to give I as colorless microcrystals, mp 193—195°C (lit., mp 197°C,[1] mp 192.5—194°C,[5] mp 196°C[8]); yield, 100 mg (56%). It gave a reddish-brown color with an alcoholic ferric chloride solution. IR: 3530, 3430, 3230 (OH), 1715, 1638 cm^{-1} (C=O). UV: λ_{max} mμ (log ε); 231 (4.22), 282 (4.21), 314$_i$ (3.96).*3

Found: C, 58.07; H, 5.37%. Calcd for $C_{18}H_{18}O_8 \cdot \frac{1}{2}H_2O$: C, 58.22; H, 5.15%.

2-Hydroxy-4-methoxyphenyl 2-Carbomethoxymethoxy 4,5-dimethoxybenzyl Ketone (IX). I (25 mg) in ether (30 m*l*) was treated with an excess of diazomethane in ether. After standing at room temperature for 24 hr, the mixture was evaporated under a vacuum to dryness. The residue was recrystallized from ethanol to give IX as colorless needles, mp 125—126°C; yield, 25 mg (94%). It gave a reddish-brown color with an alcoholic ferric chloride solution. IR: 1740, 1635 cm^{-1} (C=O). UV: λ_{max} mμ (log ε): 229 (4.25), 278 (4.20), 316 (3.92).

Found: C, 61.62; H, 5.57%. Calcd for $C_{20}H_{22}O_8$: C, 61.53; H, 5.68%.

Tephrosic Acid Monomethyl Ether (2-Hydroxy-4-methoxyphenyl 2-Carboxymethoxy-4,5-dimeth-

5) H. Fukami, G. Sakata and M. Nakajima, *Agr. Biol. Chem.*, **29**, 82 (1965); the authentic sample of I was kindly supplied by Professor Hiroshi Fukami, Kyoto University.

6) K. Fukui, M. Nakayama, M. Hatanaka, T. Okamoto and Y. Kawase, This Bulletin, **36**, 397 (1960).

*2 All melting points are uncorrected; the infrared spectra were measured in Nujol, while the ultraviolet spectra were measured in ethanol.

7) H. Fukami, private communication.

8) E. P. Clark, *J. Am. Chem. Soc.*, **54**, 3000 (1932).

*3 i=inflection point.

oxybenzyl Ketone) (X). A mixtur of IX (10 mg), ethanol (10 m*l*), and a 10% aqueous potassium hydroxide solution (3 m*l*) was treated by a method similar to that used for I; mp 205—206°C (colorless microcrystals from ethanol) (lit. mp 206—207°C,[3] mp 205—206°C,[4] mp 204—205°C[9]). It gave a reddish-brown color with an alcoholic ferric chloride solution. IR: 3250 (broad) (OH), 1735, 1635 cm^{-1} (C=O). UV: λ_{max} mμ (log ε); 229.5 (4.27), 277 (4.24), 316 (3.97).

Found: C, 60.64; H, 5.28%. Calcd for $C_{19}H_{20}O_6$: C, 60.63; H, 5.36%.

9) N. Finch and W. D. Ollis, *Proc. Chem. Soc.*, **1960**, 176.

The authors are grateful to Professor Hiroshi Fukami, Kyoto University, for his gift of tephrosic acid. This work was supported in part by a grant-in-aid from the Ministry of Education.

BULLETIN OF THE CHEMICAL SOCIETY OF JAPAN VOL. 42 202—205 (1969)

Studies of the Organic Reactions of Metal Carbonyls. XV.*1 The Reaction of Potassium Iron Carbonylates with Various Kinds of Olefin Oxides

Yoshinobu TAKEGAMI, Yoshihisa WATANABE, Takeaki MITSUDO and Hiromitsu MASADA

Department of Hydrocarbon Chemistry, Faculty of Engineering, Kyoto University, Sakyo-ku, Kyoto

(Received May 27, 1968)

The reaction between potassium iron carbonylates ($KHFe(CO)_4$, $K_2Fe(CO)_4$ and $K_2Fe_2(CO)_8$) and different olefin oxides has been studied. 1,2-Olefin oxides generally react with these carbonylates and carbon monoxide under an atmospheric pressure and at 30°C. This reduction gives the corresponding terminal olefins and the internal olefins which are formed from the 1-olefins by isomerization. Internal olefin oxides do not react with the carbonylates under the reaction conditions employed. The reduction reaction seems to compete with the carbonylation reaction. A mechanism for the reduction reaction is suggested.

Ethylene oxide and propylene oxide react with potassium iron carbonylates ($KHFe(CO)_4$, $K_2Fe(CO)_4$ and $K_2Fe_2(CO)_8$) and carbon monoxide;[1] carbon monoxide is readily absorbed, and carbonylated products, β-hydroxy esters, are obtained by the treatment of the reaction mixture with an alcoholic solution of iodine. The yield of the esters, however, is very low. Previously it has been shown that styrene oxide also reacts with these iron carbonylates and carbon monoxide to give styrene, α- and β-phenylethyl alcohol, and carbon dioxide, but no carbonylated compound.[2] These facts show that the structure of olefin oxides has a relatively large effect on this reaction. The present work will describe and interpret the reaction, mainly the reduction, o various olefin oxides with the iron carbonylates.

Experimental

The Preparation of Potassium Iron Carbonylates, $KHFe(CO)_4$, $K_2Fe(CO)_4$, and $K_2Fe_2(CO)_8$. The alcoholic solutions of these salts were prepared under a carbon monoxide atmosphere according to the method described in a previous paper:[1] a 50-m*l* portion of a 0.22 M $KHFe(CO)_4$, $K_2Fe(CO)_4$, or 0.11 M $K_2Fe_2(CO)_8$ solution was used in each run.

When $K_2Fe(CO)_4$ is prepared, two equivalent moles of water are formed:[3]

$$Fe(CO)_5 + 4KOH \xrightarrow{\text{in alcohol}} K_2Fe(CO)_4 + K_2CO_3 + 2H_2O \quad (a)$$

Therefore, when a dry solution of $K_2Fe(CO)_4$ was required, the solvent of the $K_2Fe(CO)_4$ solution was distilled off once under a vacuum and then 50 m*l* of a new dry solvent was added.

Materials. The ethylene oxide was obtained from ethylene chlorohydrin and alkali. The propylene oxide,

*1 Presented at the 21st Annual Meeting of the Chemical Society, Osaka, April, 1968. Part XIV: Y. Takegami, Y. Watanabe, I. Kanaya, T. Mitsudo, T. Okajima, N. Morishita and H. Masada, This Bulletin, **41**, 2990 (1968).

1) Y. Takegami, Y. Watanabe, H. Masada and I. Kanaya, This Bulletin, **40**, 1456 (1967).

2) Y. Takegami, Y. Watanabe, T. Mitsudo, I. Kanaya and H. Masada, *ibid.*, **41**, 158 (1968).

3) P. Krumholz and H. M. A. Stettiner, *J. Am. Chem. Soc.*, **71**, 3035 (1949).

the butylene oxides, the iron pentacarbonyl, and the other compounds employed in this study were commercial products.

Reaction Procedures. To the solution of potassium iron carbonylate described above, 2.6 g of propylene oxide was added; the mixture was then agitated vigorously at 30°C under an atmospheric pressure of carbon monoxide or nitrogen. The amount of carbon monoxide absorbed was determined volumetrically. After a certain reaction time, the reaction flask was connected to a cold trap immersed in liquid nitrogen, which was joined with a vaccum pump. The gases were collected in the trap at 30 mmHg for five minutes. The trap was allowed to warm to room temperature and then heated to 80°C, and the gas evolved was analyzed. The reaction mixture was analyzed at the same time. The reactions of other olefin oxides with $K_2Fe(CO)_4$ were carried out similarly.

Analytical Procedure. The reaction products were analyzed by gas chromatography and by means of their infrared spectra, which had been taken on a Shimadzu model IR-27 infrared spectrometer.

Results

The Reaction of $K_2Fe(CO)_4$ and $KHFe(CO)_4$ with Ethylene Oxide. The results of the reaction are summarized in Table 1. The reactions were carried out at 5°C for 5 hr. Ethylene oxide readily reacts with $K_2Fe(CO)_4$ and carbon monoxide, while the reaction solution turns from light yellow to dark red brown. Ethylene is obtained as the reaction product in the amount of 0.5 mol*2 (Exp. 1). As a previous paper has shown,[1] 0.2 mol of a carbonylated product, β-hydroxypropionate, is obtained when the reaction mixture is treated with iodine and alcohol. The reaction also proceeds under nitrogen, but the yield of ethylene is low, 0.2 mol (Exp. 2). $KHFe(CO)_4$ is less reactive than $K_2Fe(CO)_4$ (Exp. 3).

Table 1. The reaction of ethylene oxide with potassium iron carbonylates*1

Exp. No.	Iron carbonylate	Atmosphere	CO absorbed	Yield of ethylene
			mol/mol-$Fe(CO)_4^{2-}$	
1	$K_2Fe(CO)_4$	CO	1.2	0.50*2
2	$K_2Fe(CO)_4$	N_2	—	0.20
3	$KHFe(CO)_4$	CO	1.1	0.33

*1 At 5°C under atmospheric pressure. Reaction time: 5 hr. Solvent: EtOH. Ethylene Oxide/$Fe(CO)_4^{2-}$=5.5.
*2 β-Hydroxypropionate (0.2 mol/mol-$Fe(CO)_4^{2-}$) is obtained simultaneously.

Table 2. The reaction of propylene oxide with potassium iron carbonylates*1

Exp. No.	Iron carbonylate	Atmosphere	CO absorbed	Yield of propylene
			mol/mol-$Fe(CO)_4^{2-}$	
4	$K_2Fe(CO)_4$	CO	2.2	0.65*2
5	$K_2Fe(CO)_4$	N_2	—	0.32
6	$KHFe(CO)_4$	CO	1.8	0.47

*1 At 30°C under atmospheric pressure. Reaction time: 4 hr. Solvent: EtOH. Propylene Oxide/$Fe(CO)_4^{2-}$=4.0.
*2 β-Hydroxybutyrate (0.4 mol/mol-Fe $(CO)_4^{2-}$) is obtained simultaneously.

The Reaction of $K_2Fe(CO)_4$ and $KHFe(CO)_4$ with Propylene Oxide. The results of these reactions are summarized in Table 2. The reactions were carried out at 30°C for 4 hr. As Table 2 shows, propylene (0.65 mol) is obtained from the reaction of propylene oxide with $K_2Fe(CO)_4$ and

Table 3. The reaction of 1,2-butylene oxide with potassium iron carbonylates*1

Exp. No.	Iron carbonylate	Reaction conditions: Solvent	Atmosphere	hr	CO absorbed	Yield: 1-Butene	*trans*-2-Butene	*cis*-2-Butene	Total
						mol/mol-$Fe(CO)_4^{2-}$			
7	$K_2Fe(CO)_4$	EtOH	CO	0.5	0.7	0.08	0.24	0.09	0.41
8	$K_2Fe(CO)_4$	EtOH	CO	1	1.1	0.12	0.28	0.10	0.50
9*2	$K_2Fe(CO)_4$	EtOH	CO	4	2.0	0.04	0.30	0.10	0.44
10	$K_2Fe(CO)_4$	EtOH	N_2	0.5	—	0.01	0.21	0.09	0.31
11	$KHFe(CO)_4$	EtOH	CO	2	1.2	0.05	0.07	0.02	0.14
12	$K_2Fe_2(CO)_8$	EtOH	CO	4	1.4		trace		
13	$K_2Fe(CO)_4$	dry EtOH	CO	2	1.2	0.31	0.18	0.05	0.54
14	$K_2Fe(CO)_4$	dry EtOH	CO	4	1.8	0.25	0.26	0.08	0.59
15	$K_2Fe(CO)_4$	Acetone	CO	2	0	0	0	0	0

*1 1,2-Butylene Oxide/$Fe(CO)_4^{2-}$=3.2
*2 Carbonylated product (0.1 mol/mol-$Fe(CO)_4^{2-}$) and 0.13 mol/mol-Fe $(CO)_4^{2-}$ of *s*-butyl alcohol are obtained simultaneously.

*3 "Mol" means mole per gatom of Fe, which is present as iron carbonylate.

carbon monoxide. The carbon monoxide absorbed amounts to more than 2 mol, and 0.4 mol of a carbonylated product, β-hydroxybutyrate, is formed simultaneously. The reactions with $K_2Fe(CO)_4$ under nitrogen (Exp. 5) and with $KHFe(CO)_4$, (Exp. 6) have a tendency similar to those of the reactions of ethylene oxide (Exps. 2, 3).

The Reaction of $K_2Fe(CO)_4$, $KHFe(CO)_4$, and $K_2Fe_2(CO)_8$ with 1,2-Butylene Oxide. *In an Ethanol Solvent (Including 2 mol of H_2O).*[*3] The results are summarized in Table 3. 1,2-Butylene oxide is also reduced with $K_2Fe(CO)_4$ and carbon monoxide to give butenes. More than 2 mol of carbon monoxide is absorbed in several hours, but the formation of butenes ceases after 1 hr and its yield is 0.5 mol at the maximum. The major product is not 1-butene, the corresponding olefin, but 2-butenes, which may be derived from 1-butene by isomerization. In Exp. 9, a carbonylated product (0.10 mol) and *s*-butyl alcohol (0.13 mol) were also detected, and 2.0 mol of carbon dioxide was evolved when the reaction mixture was acidified with concentrated hydrochloric acid.

The reduction reaction also proceeds under nitrogen, but the yields of butenes are low (Exp. 10), and $KHFe(CO)_4$ is less reactive than $K_2Fe(CO)_4$ (Exp. 11). $K_2Fe_2(CO)_8$ also reacts with 1,2-butylene oxide, absorbing carbon monoxide rapidly, but hardly any butenes are detected (Exp. 12).

In a Dry Ethanol Solvent. When a dry ethanol solvent is used, the total yield of the olefins increases and the major product is 1-butene, showing that the isomerization to 2-butenes is fairly well retarded (*cf.* Exp. 9 and Exp. 13).

In an aprotic solvent such as acetone, 1,2-butylene oxide does not react with the iron carbonylates (Exp. 15).

TABLE 4. THE REACTION OF OTHER EPOXIDE COMPOUNDS WITH $K_2Fe(CO)_4$

Exp. No.	Epoxide	Reaction conditions: Atmosphere	Reaction conditions: hr	CO absorbed mol/mol-$Fe(CO)_4^{2-}$	Yield of propylene mol/mol-$Fe(CO)_4^{2-}$
16	Epichlorohydrin	CO	2	1.5	0.53
17	Epichlorohydrin	N_2	2	—	0.41
18	Allyl glycidyl ether	CO	3	2.4	0.54
19	Glycidol	CO	3	1.5	0.06

Solvent, EtOH at 30°C
Epichlorohydrin/$Fe(CO)_4^{2-}$=5.8
Allyl glycidyl ether/$Fe(CO)_4^{2-}$=3.2
Glycidol/$Fe(CO)_4^{2-}$=4.5

The Reaction of $K_2Fe(CO)_4$ with Epichlorohydrin, Allyl Glycidyl Ether, and Glycidol. The results are summarized in Table 4. These epoxide compounds also react with $K_2Fe(CO)_4$, absorbing a significant amount of carbon monoxide rapidly. Propylene, as the reaction product, is produced in any case, but allyl chloride, diallyl ether, and allyl alcohol, the corresponding reduction products, are not detected in the reaction mixture.

The Reaction of $K_2Fe(CO)_4$ with Internal Olefin Oxides. Internal olefin oxides, such as 2,3-butylene oxide and cyclohexene oxide, do not react with $K_2Fe(CO)_4$ under the conditions employed.

Discussion

The results obtained here show that 1,2-olefin oxides generally react with $K_2Fe(CO)_4$ and carbon monoxide to give not only the carbonylated products, but also the corresponding olefins. Further, the large amount of carbon monoxide absorbed suggests that some other reaction occurs. This complexity of the reaction was not observed in the reaction of $KCo(CO)_4$ with olefin oxides, which gives the carbonylated products selectively.[1]

The mechanism of the formation of olefin is not yet clear. One probable scheme is suggested below. The facts that $K_2Fe(CO)_4$ is the most active in the formation of olefins and that only the 1,2-olefin oxides react under the reaction conditions employed seem to support the following reaction scheme: in the first step, $Fe(CO)_4^{2-}$ makes a nucleophilic attack on the terminal carbon atom of 1,2-olefin oxide to give complex (I). In the reaction of internal olefin oxides, the nucleophilic attack of $Fe(CO)_4^{2-}$ may be retarded, mainly by a steric hindrance.

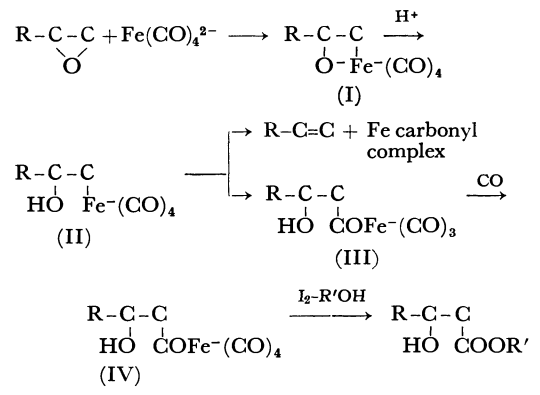

The complex (I) abstracts a proton from water or a solvent to give the complex (II). Olefin seems to be derived by the decomposition of the complex (II). This interpretation is supported by the fact that even under nitrogen the olefin is formed. Some iron carbonyl complex produced by the decomposition seems to regenerate iron carbonylate (Fe-

*3 *Cf.* Eq. (a).

$(CO)_4^{2-}$), with the absorption of CO, which then further reacts with olefin oxide. This scheme is supported by the fact that the yield of olefin under carbon monoxide is larger than that under nitrogen. From the complex (II), β-hydroxyacyliron carbonylate (III and IV) may also be derived to give a β-hydroxy ester when treated with an alcoholic solution of iodine.

In the reaction of 1,2-butylene oxide with $K_2Fe(CO)_4$, a dry ethanol solvent is favorable to the formation of butenes. This effect can also be observed in the reaction of styrene oxide with $K_2Fe(CO)_4$.[2] In a dry and moist ethanol solvents, the major products are 1-butene and 2-butene respectively. This fact can be explained by assuming that an equilibrium between $K_2Fe(CO)_4$ and $KHFe(CO)_4$ exists in the reaction solution; the reaction of $K_2Fe(CO)_4$ gives the corresponding olefin, and the reaction of $KHFe(CO)_4$ gives the isomerized olefin. Cramer and Lindsey showed that $KHFe(CO)_4$ is active in the isomerization of 1-butene to 2-butene.[4]

$$K_2Fe(CO)_4 + H_2O \rightleftarrows KHFe(CO)_4 + KOH$$

From allyl glycidyl ether, glycidol, and epichlorohydrin, the corresponding olefins, allyl ether, allyl alcohol, and allyl chloride, are not detected. However, propylene is formed in a relatively good yield. The fact that allyl ether and ally alcohol react with $K_2Fe(CO)_4$ with much difficulty indicates that these compounds are not the intermediates of the formation of propylene from allyl glycidyl ether and glycidol.

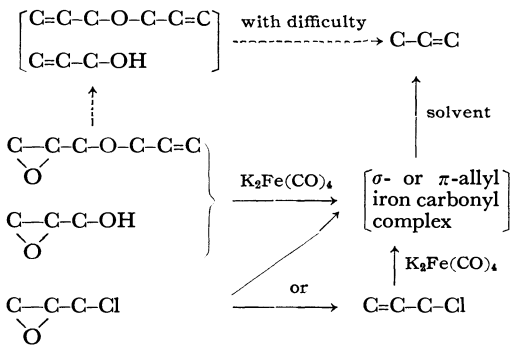

On the other hand, allyl chloride and its derivatives react with $K_2Fe(CO)_4$ very readily to give olefins such as propylene.[2,5] These reactions may be considered to proceed *via* σ- and π-allyl iron carbonylate. In the light of this fact, the reaction of allyl glycidyl ether and glycidol with $K_2Fe(CO)_4$ seems to proceed *via* a kind of allyl iron carbonyl complex. The reaction of epichlorohydrin involves two possible routes; one is *via* allyl chloride, while the other involves some other step to the formation of a π- or σ-allyl iron carbonyl complex, as in the reaction of allyl glycidyl ether and glycidol.

This work was supported in part by The Kawakami Foundation, to which our thanks are due.

4) R. Cramer and R. V. Lindsey, Jr., *J. Am. Chem. Soc.*, **88**, 3534 (1966).

5) Y. Takegami, Y. Watanabe, I. Kanaya, T. Mitsudo, T. Okajima, N. Morishita and H. Masada, This Bulletin, in press.

BULLETIN OF THE CHEMICAL SOCIETY OF JAPAN VOL. 42 206—210 (1969)

Studies of the Organic Reactions of Metal Carbonyls. XVI.*1 Solvent Effects on the Hydroformylation of Propylene and on the Reaction of Cobalt Hydrocarbonyl with 1-Pentene

Yoshinobu TAKEGAMI, Yoshihisa WATANABE, Hiromitsu MASADA and Takeaki MITSUDO

Department of Hydrocarbon Chemistry, Faculty of Engineering, Kyoto University, Sakyo-ku, Kyoto

(Received July 7, 1968)

In the reaction of cobalt hydrocarbonyl with 1-pentene at 10°C, solvents have a great effect on the distribution of the products, caproylcobalt carbonyl (I) and α-methylvalerylcobalt carbonyl (II). The I-to-II ratio is 72 : 28 in toluene, in toluene-dioxane (1 : 1 in volume), and in toluene-ethyl acetate. The percentage of II increases to 40—66% in toluene-diethyl ether, -tetrahydrofuran, -acetone, -ethyl alcohol, and -acetonitrile. In the hydroformylation of propylene, the distribution of the products, *n*- and isobutyraldehyde, is also affected by the solvents. In toluene, the *n*-to-iso ratio is about 75 : 25, while in dioxane and in butyl acetate the percentage of the *n*-aldehyde increases to 79—83%. In methyl alcohol, dimethyl acetals of the aldehydes and *n*- and isobutyrate are formed. The *n*-to-iso ratio is the highest in the esters (3.2—8.5), followed by the acetals (0.7—1.6) and the aldehydes (0.4).

Several workers have reported on the influence of the reaction variables on the hydroformylation reaction of olefins, mainly on the composition of the products.[1] In the course of hydroformylation, a cobalt catalyst is considered to react with olefins as cobalt hydrocarbonyl to give alkyl- and acylcobalt carbonyls as the reaction intermediates.[2]

Previous studies of the hydroformylation of ethyl acrylate in this laboratory have shown that the isomerization of alkyl- and acylcobalt carbonyls has a remarkable effect on the isomeric distribution of the products.[3] Some of the present authors have also shown that the isomerization of *n*- and isobutyrylcobalt carbonyl is highly affected by the solvents; in dioxane only the iso isomer is isomerized; in ethyl acetate both isomer are isomerized, in a 7 : 3 *n*-to-iso ratio, and in toluene the isomerization is very slow.[4] On the basis of these results, the solvents can reasonably be considered to have a marked effect on the hydroformylation of olefins, particularly on the isomeric distribution of the products.

In the present study, the effects of different solvents on the hydroformylation of propylene and on the reaction of 1-pentene with cobalt hydrocarbonyl have been examined in detail.

Experimental

Reaction Procedures. Hydroformylation. An autoclave of a 300 m*l* capacity, made of 18-8 nickel-chrome steel and equipped with a magnetic stirrer, was used. Eighty milliliters of the solvent and 8 m*l* of a dicobalt octacarbonyl solution (containing 1.9 mmol of $Co_2(CO)_8$) were put into the autoclave. After the air in the autoclave had been replaced with hydrogen, 20 m*l* of liquid propylene was put into it, and then hydrogen and carbon monoxide were introduced at certain pressures using a compressor. The autoclave was kept at a certain temperature by electrical heating, but the heating was turned off when the gauge pressure ceased to decline.

Reaction with $HCo(CO)_4$. The reaction of 1-pentene with cobalt hydrocarbonyl was carried out

*1 Presented in part at the 19th Annual Meeting of the Chemical Society of Japan, Yokohama, April, 1966. Part XV: This Bulletin, Y. Takegami, Y. Watanabe, T. Mitsudo and H. Masada, **42**, 202 (1969).

1) a) V. L. Hughes and I. Kirshenbaum, *Ind. Eng. Chem.*, **49**, 1999 (1957). b) S. Brewis, *J. Chem. Soc.*, **1964**, 5014. c) P. Pino, F. Piacenti and P. P. Neggiam, *Chem. & Ind.*, **1961**, 1400. d) P. Pino, S. Pucci and F. Piacenti, *ibid.*, **1963**, 294. e) M. Johnson, *ibid.*, **1963**, 684; *J. Chem. Soc.*, **1963**, 4859. f) F. Piacenti, P. Pino, R. Lazzaroni and M. Bianchi, *J. Chem. Soc., (C)*, **1966**, 488.

2) R. F. Heck and D. S. Breslow, *J. Am. Chem. Soc.*, **83**, 4023 (1961).

3) a) Y. Takegami, C. Yokokawa, Y. Watanabe, H. Masada and Y. Okuda, This Bulletin, **37**, 1190 (1964). b) Y. Takegami, C. Yokokawa and Y. Watanabe, *ibid.*, **39**, 2430 (1966).

4) a) Y. Takegami, C. Yokokawa, Y. Watanabe, H. Masada and Y. Okuda, *ibid.*, **38**, 787 (1965). b) Y. Takegami, Y. Watanabe, H. Masada, Y. Okuda, K. Kubo and C. Yokokawa, *ibid.*, **39**, 1495 (1966).

in the way described in a previous paper.[3a)]

Analysis of the Products. The products were identified by a mixed gas chromatography with authentic samples. A column three meters long and 3 mm in diameter, and filled with dilauryl phthalate on cerite, was used. The column temperature was 70 to 80°C, and the flow rate of the carrier gas (hydrogen) was 60 ml/min. The infrared absorption spectrum was taken on a Shimadzu Model IR-27 spectrophotometer.

Materials. The propylene, toluene, dioxane, butyl acetate, and other organic compounds were commercial products which had been proved to be sufficiently pure by gas chromatography. As authentic samples, the following commercial compounds were used: *n*- and isobutyraldehyde, *n*- and isobutyl alcohol, methyl caproate, and methyl α-methylvalerate. The dicobalt octacarbonyl solution was prepared according to the method given in a previous paper.[5)]

Results and Discussion

The Reaction of 1-Pentene with Cobalt Hydrocarbonyl. The results are summarized in Table 1. The reaction was carried out at 10°C for 4 hr in a mixed solvent (toluene: other solvent = 1 : 1 in volume). The 1-pentene reacts with cobalt hydrocarbonyl to give caproyl- and α-methylvalerylcobalt carbonyl, which then give the corresponding esters upon treatment with an iodine and alcohol.[2)]

Table 1. The reaction of 1-pentene with cobalt hydrocarbonyl*

Exp. No.	Mixed solvent toluene-other solvent (1:1 in volume)	CO absorbed (mol/mol-$HCo(CO)_4$)	Product** Yield (mol/mol-$HCo(CO)_4$)	Product** α-Methyl valerate %
1	Toluene	0.53	0.5	28
2	Ethyl acetate	0.53	0.5	28
3	Dioxane	0.55	0.4	28
4	Tetrahydrofuran	0.51	0.5	39
5	Diethyl ether	0.53	0.5	50
6	Acetone	0.50	0.4	50
7	Ethyl alcohol	−0.1***	0.2	45
8	Acetonitrile	−1.2	0.2	66

* Under carbon monoxide at 10°C for 4 hr. 1-Pentene used: 10 mol/mol-$HCo(CO)_4$.

** Ethyl caproate and ethyl α-methylvalerate.

*** Gas was evolved.

As Table 1 shows, the solvents have a great effect on the distribution of the two isomers. In toluene the isomer with a straight chain structure predominates (72%); this percentage is almost independent of the solvents in such mixtures as toluene-ethyl acetate and toluene-dioxane (Exps. 1—3). However, in toluene-acetonitrile, α-methylvalerate with a branched chain structure is

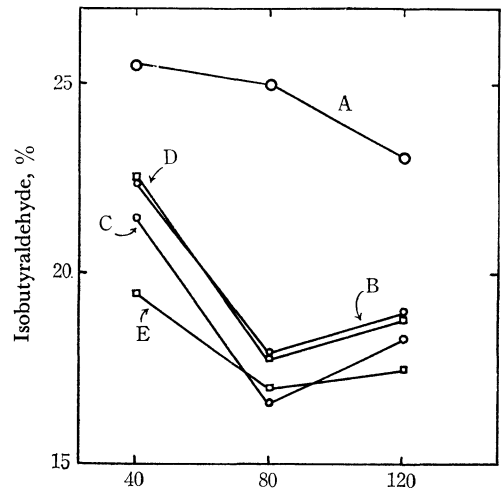

Partial pressure of carbon moroxide, atm

Fig. 1. The percentage of isobutyraldehyde *vs.* the initial partial pressure of carbon monoxide plots for the hydroformylation of propylene (P_{H_2}=80 atm).
A: in toluene at 100°C
B: in dioxane at 100°C
C: in dioxane at 90°C
D: in butyl acetate at 100°C
E: in butyl acetate at 90°C

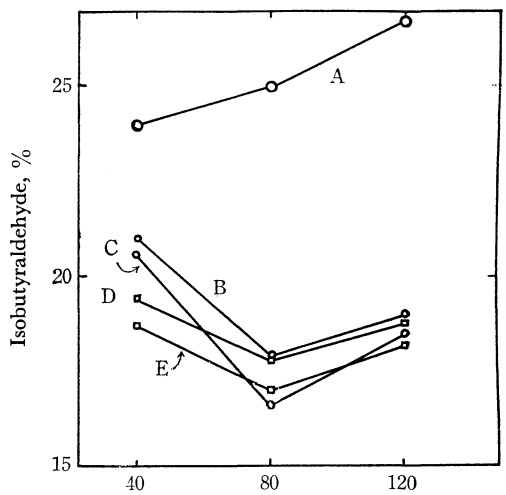

Partial pressure of hydrogen, atm

Fig. 2. The percentage of isobutyraldehyde *vs.* the initial partial pressure of hydrogen plots for the hydroformylation of propylene (P_{CO}=80 atm).
A: in toluene at 100°C
B: in dioxane at 100°C
C: in dioxane at 90°C
D: in butyl acetate at 100°C
E: in butyl acetate at 90°C

5) Y. Takegami, C. Yokokawa and Y. Watanabe, *ibid.*, **37**, 677 (1964).

dominant. Tetrahydrofuran, acetone, diethyl ether, and ethyl alcohol are also a little more favorable to the formation of α-methylvalerate. In this reaction, the factors determining the distribution of the two isomers are the direction of the addition of cobalt hydrocarbonyl to the double bond of 1-pentene and the isomerization between the C_6-acylcobalt carbonyls. However, this iso-

TABLE 2. THE HYDROFORMYLATION OF PROPYLENE IN DIFFERENT SOLVENTS

2a. IN TOIUENE

Exp. No.	Reaction conditions				Gas absorption rate**	Distribution of products	
	Temp. (°C)	Partial pressure* H_2 (atm)	Partial pressure* CO (atm)	Time (min)		Isobutyr-aldehyde (%)	*n*-Butyr-aldehyde (%)
9	100	80	80	30	2.0	25.0	75.0
10	100	80	120	120	0.37	23.1	76.9
11	100	80	40	30	2.3	25.5	74.5
12	100	120	80	30	2.1	26.8	73.2
13	100	40	80	130	0.35	24.0	76.0
14	90	80	80	160	0.25	22.8	77.2
15	110	80	80	20	2.6	26.5	73.5
2b. IN DIOXANE							
16	110	80	80	60	0.75	19.6	80.4
17	100	80	80	100	0.52	17.9	82.1
18	100	40	80	160	0.23	21.0	79.0
19	100	120	80	50	0.87	19.0	81.0
20	100	80	120	180	0.33	19.0	81.0
21	100	80	40	30	0.87	22.4	77.6
22	90	80	80	180	0.22	16.6	83.4
23	90	80	120	250	0.15	18.3	81.7
24	90	40	80	220	0.11	20.6	79.4
25	90	120	80	160	0.27	18.5	81.5
26	90	80	40	140	0.34	21.5	78.5

* Initial pressure.

** Calculated from pressure drops (atm/min).

2c. IN BUTYL ACETATE

Exp. No.	Reaction conditions				Gas absorption rate	Distribution of products	
	Temp. (C°)	Partial pressure H_2 (atm)	Partial pressure CO (atm)	Time (min)		Isobutyr-aldehyde (%)	*n*-Butyr-aldehyde (%)
27	100	80	80	90	0.66	18.7	82.2
28	100	80	40	30	1.5	22.5	77.5
29	100	80	120	160	0.37	18.8	81.2
30	100	120	80	50	0.86	18.8	81.2
31	100	40	80	170	0.34	19.4	80.6
32	90	80	80	180	0.31	17.0	83.0
33	90	80	40	90	0.66	19.5	80.5
34	90	80	120	250	0.16	17.5	82.5
35	90	120	80	140	0.39	18.3	81.7
36	90	40	80	250	0.16	18.7	81.3
2d. IN ACETONE AND DIETHYL ETHER							
37*	100	80	80	30	2.0	34.3	65.7
38*	110	80	80	20	2.5	35.4	64.6
39**	100	80	80	15	5.0	40.0	60.0

* In acetone.

** In diethyl ether.

TABLE 3. THE HYDROFORMYLATION OF PROPYLENE IN METHYL ALCOHOL

Exp. No.	Reaction conditions: Temp. (C°)	Partial pressure* H_2 (atm)	Partial pressure* CO (atm)	Time (min)	Distribution of products**: Aldehydes %	Aldehydes n/iso	Acetals %	Acetals n/iso	Esters %	Esters n/iso	Percentage*** of iso-isomers
40	100	80	80	220	5.3	0.36	80.4	1.6	13.3	7.5	36.2
41	110	80	40	150	7.7	0.40	73.5	1.2	18.8	6.6	41.4
42	110	80	80	130	8.0	0.36	79.3	1.2	12.7	6.5	42.8
43	120	80	20	100	3.3	0.44	67.9	1.0	28.8	5.9	40.5
44	120	80	10	110	0	—	43.8	0.72	56.2	5.0	34.9
45	130	80	10	50	0	—	42.7	0.94	57.3	5.2	31.3
46	130	40	10	40	0	—	66.2	0.86	33.8	3.2	43.5
47	130	120	10	45	0	—	43.4	0.94	56.6	5.4	31.0
48	130	80	5	90	0	—	30.0	1.0	70.0	5.6	26.5
49	150	80	10	30	0	—	46.6	0.94	53.4	5.1	32.5

* Initial pressure.

** *n*- and isobutyraldehyde, *n*- and isobutyraldehyde - dimethyl acetal, and methyl *n*- and isobutyrate.

*** (iso-isomers/products) × 100.

merization occurs with much difficulty under the conditions employed.[4] Thus, the results obtained here show that the direction of the addition of cobalt hydrocarbonyl to the olefin is highly affected by the solvents.

Hydroformylation of Propylene. The effects of variables, especially solvents, on the distribution of the products were also examined. The results are summarized in Tables 2 and 3 and in Figs. 1 and 2. Under the conditions employed, butyraldehydes were obtained in 93—97% yields, while butyl alcohols were also produced as minor products in 3—7% yields. The reaction is considered to proceed as follows:

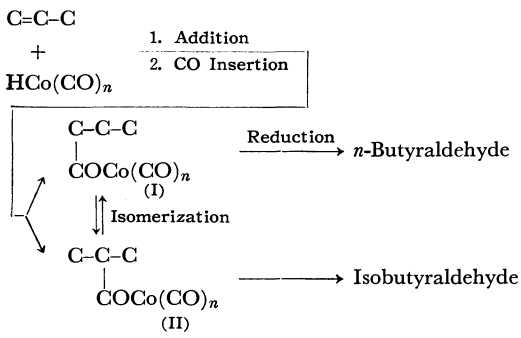

In Toluene. The percentage of *n*-butyraldehyde changes over the 73—77% range at 100°C. In the light of the fact that *n*- and isobutyrylcobalt carbonyl isomerize with much difficulty in toluene,[4a] the distribution of the two aldehydes may be determined mainly by the direction of the addition of cobalt hydrocarbonyl.

In Dioxane. Under any conditions, the percentage of *n*-butyraldehyde grows larger in dioxane (79—82% at 100°C) than in toluene (73—77% at 100°C). Dioxane has a great promoting effect on the isomerization of isobutyrylcobalt carbonyl to the *n*-isomer at room temperature.[4a] Under hydroformylation conditions in dioxane, such an isomerization can reasonably be considered to occur, thus affecting the distribution of the products. This consideration seems to be supported by the fact that dioxane has no effect on the addition of cobalt hydrocarbonyl to 1-pentene, as has been described above.

In Butyl Acetate. As Table 2b shows, butyl acetate is also a more favorable solvent for the formation of *n*-butyraldehyde than toluene. Acetate also promotes the isomerization of the isobutyrylcobalt carbonyl[4a] and has no effect on the addition of cobalt hydrocarbonyl to 1-pentene. Thus, it is possible to interpret the effect of butyl acetate by employing arguments similar to those presented for dioxane.

In Acetone and Diethyl Ether. The percentage of isobutyraldehyde increases to 35 and 40% in acetone and in diethyl ether respectively. This tendency is consistent with the fact that these are taken to be more favorable solvents for the formation of a compound with a branched chain structure in the reaction of cobalt hydrocarbonyl with 1-pentene. Under hydroformylation conditions in these solvents, isobutyrylcobalt carbonyl may be formed more readily by the addition of cobalt hydrocarbonyl to propylene.

Effects of Partial Pressures of Carbon Monoxide and Hydrogen. As Figs. 1 and 2 show, at 100°C in toluene the percentage of isobutyraldehyde decreases with an increase in the partial pressures of carbon monoxide, but increases with an increase in the partial pressures of hydrogen. In dioxane or butyl acetate, however, the percentage of the iso-aldehyde has a minimum at 80 atm of the initial partial pressures of both carbon monoxide and hydrogen. This phenomenon seems to be partly due to the tendency of butyrylcobalt carbonyls

to isomerize in these polar solvents. The distribution of the products is considered to depend in part on two competitive reactions, the reduction and the isomerization of butyrylcobalt carbonyls. Larger partial pressures of carbon monoxide have an inhibitory effect on these reactions,[2,4] but larger partial pressures of hydrogen seem to promote the reduction. The reason why the minimum is observed is, however, not completely clear.

In Methyl Alcohol. As Table 3 shows, in methyl alcohol *n*- and isobutyraldehyde (0—8%), *n*- and isobutyraldehyde-dimethyl acetal (30—80%), and methyl *n*- and isobutyrate (13—70%) are obtained. Under any conditions employed, the aldehydes are readily converted to the corresponding acetals. At low pressures of hydrogen the esters predominate, but at high pressures of hydrogen the acetals predominate. These compounds may be formed according to the following reaction scheme:

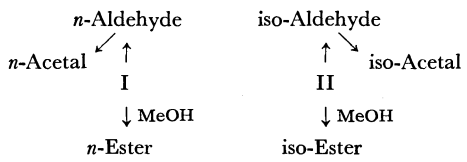

The *n*-to-iso ratio is the highest in the esters (3.3—8.5), followed by the acetals (0.7—1.6) and the aldehyde (0.4). In the light of this fact, the esterification of *n*-butyrylcobalt carbonyl (I) to *n*-butyrate may be said to occur more readily than that of the iso-isomer (II), but the reduction rate of the *n*-isomer is alsmost comparable with that of the iso-isomer. In the stage of the addition of cobalt hydrocarbonyl, equimolar amounts of the *n*- and iso-isomer seem to be formed in methyl alcohol.*2 Thus, under the conditions favorable for the formation of the esters, the fast esterification of I seems to promote the isomerization of II to I, and then the *n*-to-iso ratio of the products increases greatly (Exp. 48).

This work was supported in part by The Kawakami Foundation, to which our thanks are due. We are also grateful to Professor Y. Takezaki and Dr. N. Sugita for their permission to use the compressors.

*2 1-Pentene gives *n*- and iso-C_6-acylcobalt carbonyls in a 1-to-1 ratio in ethyl alcohol.

BULLETIN OF THE CHEMICAL SOCIETY OF JAPAN VOL. 42 210—214 (1969)

Photolysis of Nitrosobenzene

Rikuhei TANIKAGA

Department of Chemistry, Faculty of Science, Kyoto University, Sakyo-ku, Kyoto

(Received May 27, 1968)

The mechanism of the photochemical reaction of nitrosobenzene (I) has been investigated. The irradiation of I leads to the formation of a phenyl radical and nitric oxide. The reaction of the phenyl radical with I yields diphenylnitroxide, which is then easily reduced to diphenylamine. The reaction of diphenylamine with the nitric oxide gives *C*-nitrosodiphenylamines, which are then photochemically oxidized to *C*-nitrodiphenylamines. On the other hand, I is oxidized to nitrobenzene and is, at the same time, reduced to azoxybenzene and azobenzene. Azoxybenzene is photochemically rearranged to 2-hydroxyazobenzene.

Nitrosobenzene (I) is known to be photochemically unstable.

Bamberger reported that azoxybenzene (II), 2-hydroxyazobenzene (III), 4-hydroxyazobenzene, 2-hydroxyazoxybenzene, nitrobenzene, aniline, and other minor products were obtained by the photolysis of I in benzene with sunlight,[1] but it is not clear whether or not his products other than II and III were really formed by the photolysis, because his assignment was doubtful and his analytical methods involved such improper procedures as treatment with heat, an acid and a base.

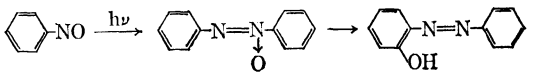

I II III

We found, by means of the ESR technique that the irradiation of I in tetrahydrofuran with a high-pressure mercury lamp led to the fission of the phenyl-nitroso bond and yielded diphenylnitroxide (IV).[2]

1) E. Bamberger, *Ber.*, **35**, 1606 (1902).

2) K. Maruyama, R. Tanikaga and R. Goto, This Bulletin, **37**, 1893 (1964).

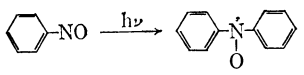

I IV

Recently Shamma *et al.* irradiated I in ethanol at 253.7 mμ and obtained diphenylamine and *C*-nitrodiphenylamines by means of column chromatography; they then, without proof, assumed that the formation of diphenylamines could be followed by that of *N*-nitrosodiphenylamine.[3]

A principal objective of this work is to clarify the mechanism of the photochemical reaction of I by assigning the products.

Results and Discussion

An ethanolic solution of nitrosobenzene (I) (10^{-1} M) in a Pyrex tube was irradiated with a high-pressure mercury lamp. The results are given in Table 1.

Table 1. Irradiation of nitrosobenzene (10^{-1}M) at 25.0±0.1°C

Irradn. time (hr)	Yields of products (%) 2	10
Nitrosobenzene (I)	85.4	63.9
Diphenylnitroxide (IV)	2.0	1.2
Diphenylamine (V)	2.9	6.4
4-Nitrosodiphenylamine (VI)	0.1	0.2
4-Nitrodiphenylamine (VII)	0.4	1.0
2-Nitrodiphenylamine (VIII)	0.6	1.5
Azoxybenzene (II)	3.9	5.4
2-Hydroxyazobenzene (III)	1.8	5.0
Azobenzene (IX)	0.9	3.1
Nitrobenzene (X)	—	*ca.* 1.0
Aniline (XI)	—	<0.5

No remarkable differences from the above results were found upon the irradiation of I in benzene under a nitrogen atmosphere. VI and IX had not previously been obtained.

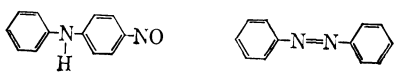

VI IX

Thin layer chromatography (TLC) of the irradiated solution showed that the expected β-phenylhydroxylamine, *N*-nitrosodiphenylamine, and 3-nitrodiphenylamine were not formed; on the other hand, tarry materials and smaller amounts of by-products were present, especially after a long irradiation. Hence, irradiation for many hours is not desirable in the investigation of the photolysis of I.

Although the photolysis involves very complex reactions, it seems to be possible to divide these reactions into the following three classes:

i) Reaction Process A: The bimolecular reaction of nitrosobenzene (I), followed by a phenyl-nitroso bond-rupture, affords diphenylnitroxide (IV), diphenylamine (V), 4-nitrosodiphenylamine (VI), 4-nitrodiphenylamine (VII), and 2-nitrodiphenylamine (VIII).

ii) Reaction Process B: The bimolecular reaction of I, followed by a N–O bond-rupture, affords azoxybenzene (II), 2-hydroxyazobenzene (III), and azobenzene (IX).

iii) Reaction Process C: The oxidation or the reduction of monomeric I affords nitrobenzene (X) or aniline (XI).

The mechanisms of these processes will be described below.

Reaction Process A:

Scheme A:

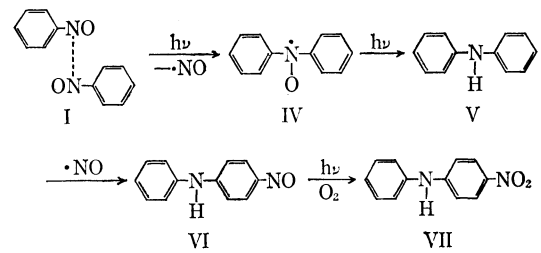

The photochemical reaction of I to IV was described in a previous paper.[2] Later, a similar reaction of nitrosoalkane was reported.[4,5] The finding that no benzene was obtained suggests that the dimeric or a similar form gave rise to the formation of IV.[6] This result is also consistent with the fact that no IV is formed from the photolysis of I with red light,[5] with which only the monomeric form could be excited.

IV is known to be unstable and has been supposed to give V in connection with aryl-*t*-butylnitroxides.[7] Indeed, the irradiation of IV in ethanol produces V easily.

In order to discuss the V-to-VI process, *N*-nitrosodiphenylamine (XII), which had been

3) M. Shamma, J. K. Whitesell and P. L. Warner, Jr., *Tetrahedron Letters*, **1965**, 3869.

4) E. T. Strom and A. L. Bluhm, *Chem. Commun.*, **1966**, 115.

5) A. Mackor, T. A. J. W. Wajer, T. J. de Boer and J. D. W. van Voorst, *Tetrahedron Letters*, **1966**, 2115; T. A. J. W. Wajer, A. Mackor, T. J. de Boer and J. D. W. van Voorst, *Tetrahedron*, **23**, 4021 (1967).

6) It has been discussed which form, monomeric[5] or dimeric[4] form, of nitrosoalkane gives rise to the formation of nitroxide upon the irradiation.

7) A. R. Forrester and R. H. Thomson, *Nature*, **203**, 74 (1964); A. Calder and A. R. Forrester, *Chem. Commun.*, **1967**, 682.

assumed to be an intermediate by Shamma *et al.*,[3] was chosen as a model compound for two reasons. One reason was that XII was expected to give both V and nitric oxide, as in the photolysis of *N*-nitrosamides.[8] The other was that no XII was obtained from the photolysis of I; therefore, it had to be decided whether XII was not an intermediate, or whether the photochemical reaction of XII was so fast that no XII could be detected.

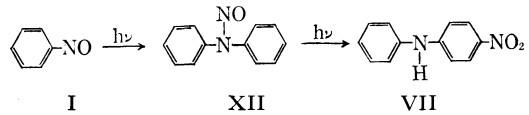

I XII VII

An ethanolic solution of XII (10^{-2} M) was irradiated with a Pyrex filter. The results are given in Table 2.

TABLE 2. IRRADIATION OF *N*-NITROSODIPHENYLAMINE (XII) (10^{-2}M) AT 25.0±0.1°C FOR 3 hr

Compd.	Yields of products (%)		
	Air	N_2	Degassed
XII	33.4	60.0	60.5
V	25.7	9.8	12.5
VI	0.5	1.7	0.0
VII	3.6	0.3	0.0
VIII	4.5	0.1	0.0
Carbazole	2.3	1.0	0.1

Table 2 shows that the N–N bond of XII was broken, and that then the nitric oxide intermolecularly attacked V to give VI. The homolytic fission of the N–N bond was also confirmed by the formation of tetraphenylhydrazine by the photolysis of a saturated ethanolic solution of XII.

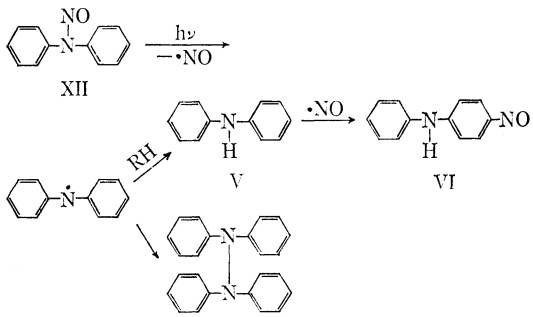

XII V VI

Neither nitroso- nor nitro-diphenylamines were obtained in a degassed state. This finding can be explained by the removal of nitric oxide from the solution.

The well-known photochemical cyclization of V to carbazole[9] will not be discussed.

Under a nitrogen atmosphere, no nitro-compounds were obtained. This suggests that the nitrosodiphenylamine was photochemically oxidized to nitrodiphenylamine. In order to discuss this novel photochemical oxidation of a nitroso-compound to a nitro-compound, an ethanolic solution of VI (10^{-3} M) was irradiated with a Pyrex filter. The results are given in Table 3.

TABLE 3. IRRADIATION OF 4-NITROSODIPHENYLAMINE (10^{-3}M) AT 25.0±0.1°C

	Yields of products (%)		
Irradn. time	3 hr	3 hr	5 min
Sensitizer	—	V (10^{-2}M)	Ph_2CO (10^{-2}M)
VI	46.0	20.3	23.1
VII	13.8	17.3	24.4

Table 3 shows that VI underwent a photosensitized oxidation to VII, and that V could be a sensitizer, though not as efficient a one.

The results described above support Scheme A. XII cannot be an intermediate of I to nitrodiphenylamines, because the irradiation of I never afforded XII, whereas the photochemical reaction of XII was not fast enough.

Reaction Process B:

Scheme B:

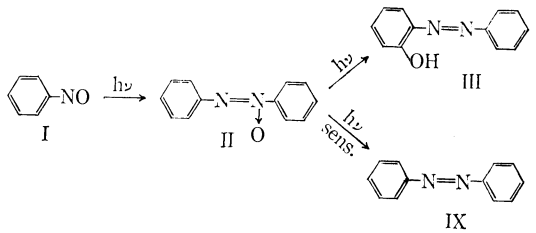

I II III IX

III is formed from the excited singlet state of II,[10] and IX is formed from the excited triplet state of II,[11] as has been reported in previous papers. Although IX was never obtained upon the direct irradiation of II without a sensitizer, IX was obtained upon the irradiation of I. This finding can probably be explained in terms of sensitization of I through its excited triplet state.

Mauser *et al.*[12] postulated, without proof, the following mechanism for the photochemical reduction of I:

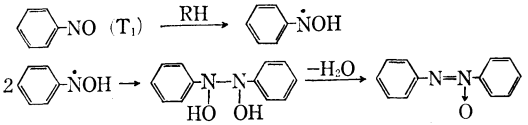

8) L. P. Kuhn, G. G. Kleinspehn and A. C. Duckworth, *J. Am. Chem. Soc.*, **89**, 3858 (1967).

9) D. C. Neckers, "Mechanistic Organic Photochemistry," Reinhold Publishing Corp., New York, N. Y. (1967), p. 239.

10) R. Tanikaga, This Bulletin, **41**, 2151 (1968).

11) R. Tanikaga, K. Maruyama, R. Goto and A. Kaji, *Tetrahedron Letters*, **1966**, 5925; R. Tanikaga, This Bulletin, **41**, 1664 (1968).

12) H. Mauser and H. Heitzer, *Z. Naturforsch.*, **20b**, 200 (1965).

This mechanism may be probable in view of the mechanisms for the photochemical reduction of nitrobenzene[13,14] and the base-catalyzed reduction of I.[15,16]

Since nitrosobenzene in a solution exists in an equilibrium of a monomeric form (I) and a dimeric form (XIII),[17] the other possible mechanism is that II is formed from the excited triplet state of dimeric nitrosobenzene.

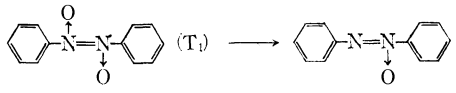

XIII II

This mechanism, similar to that for the photochemical reduction of II to IX *via* the excited triplet state,[11] may be supported by the findings that the irradiation of solid nitrosobenzene with a XIII structure also yielded II, and that an ethanolic solution of benzo[*c*]cinnoline 5,6-dioxide (XIV) with a structure similar to XIII underwent photochemical reduction of benzo[*c*]cinnoline 5-oxide (XV) in the presence of benzophenone.

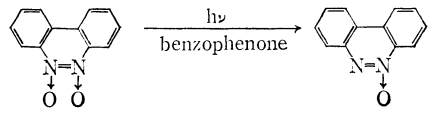

XIV XV

However, it is impossible to decide which mechanism is more reasonable, because the reaction is very complex.

Reaction Process C:

Scheme C:

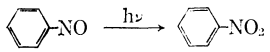

I X

I as well as VI was slightly oxidized, but the unimolecular reaction of I rarely occurred. This result is in contrast with that of the photolysis of I with hydrochloric acid, in which primary amines were obtained as the major products.[18]

At any rate, the dimeric or a similar form may be assumed to be important in the photolysis of nitrosobenzene.

13) R. L. Ward, *J. Chem. Phys.*, **38**, 2588 (1963).
14) R. Hurley and A. C. Testa, *J. Am. Chem. Soc.*, **88**, 4330 (1966).
15) C. J. W. Gutch and W. A. Waters, *Proc. Chem. Soc.*, **1964**, 230.
16) G. A. Russell and E. J. Geels, *J. Am. Chem. Soc.*, **87**, 122 (1965).
17) W. Lüttke, *Z. Elektrochem.*, **61**, 976 (1957) and other references cited therein.
18) S. Hashimoto, J. Sunamoto and K. Kano, Preprints for the 20th Annual Meeting of the Chemical Society of Japan (Tokyo, 1967), Vol. III, p. 179.

Conclusion

The mechanism of the photolysis of nitrosobenzene (I) is as follows:

i) I undergoes the homolytic fission of a nitrosophenyl bond. The phenyl radical formed reacts with I to yield diphenylnitroxide, which is then reduced to diphenylamine. The nitric oxide reacts with diphenylamine to afford *C*-nitrosodiphenylamines, which are photochemically oxidized to *C*-nitrodiphenylamines.

ii) I is reduced to azoxybenzene, which is rearranged to 2-hydroxyazobenzene. Azoxybenzene undergoes a photosensitized reduction to azobenzene.

iii) I is slightly oxidized to nitrobenzene.

Experimental

Materials. Nitrosobenzene (I) was prepared by the reduction of nitrobenzene and was then recrystallized from ethanol (mp 68.0°C).[19] The authentic materials shown in Table 4 were also synthesized in order to determine the products.

Table 4. Melting points and absorption spectra of authentic materials

Compd.	Mp (°C)	$\lambda_{max}^{CHCl_3}$ (mμ)	$\varepsilon_{max}^{CHCl_3}$	Ref.
II	35.5	326	14800	20
III	84.0	325	18000	21
IV	61.5	314	17500	22
V	54.0	290	17000	—
VI	145.0	414	26000	23
VII	134.5	380	19000	24
VIII	75.5	263	14500	—
IX	68.0	319	18500	—
XII	66.5	292	7650	25
Carbazole	245.5	292	17100	—

Photolysis of Nitrosobenzene (I). The irradiation source was a 100-W high-pressure mercury arc lamp fitted with a water-cooled immersion well (Eikosha Halos PIH-100). An ethanolic solution (2 m*l*) of I (10^{-1} M) was irradiated in a Pyrex tube (inner diameter; 13 mm) attached directly to the lamp, and was then thermostated at 25.0±0.1°C. The R_f values and the

19) G. H. Coleman, C. M. McCloskey and F. A. Stuart, "Organic Syntheses," Coll. Vol. III, p. 668 (1955).
20) A. Lachman, *J. Am. Chem. Soc.*, **24**, 1180 (1902).
21) W. M. Cumming and G. S. Ferrier, *J. Chem. Soc.*, **127**, 2375 (1925).
22) H. Wieland and M. Offenbächer, *Ber.*, **47**, 2114 (1914).
23) O. Fischer and E. Hepp, *ibid.*, **19**, 2994 (1886).
24) I. Goldberg, *Chem. Zentr.*, **1907-II**, 957.
25) L. Vanino, "Handbuch der Präparativen Chemie," Vol. II, Verlag von Ferdinand Enke, Stuttgart (1937), p. 672.

color reactions with concentrated sulfuric acid upon the TLC (silica gel) of the solution showed the compounds, II—IX, in Table 1, but no β-phenylhydroxylamine, *m*-nitrodiphenylamine, *N*-nitrosodiphenylamine, and carbazole. The minor products other than II—IX could not be assigned. A small amount of nitrobenzene was detected by gas chromatography (Yanagimoto GCG-5DH, polyethylene glycol, He), but no aniline was. On the other hand, when the solution was diazotized and treated with 2-naphthol or NW-acid (1-naphthol-4-sulfonic acid), no coupling compound with aniline was detected on TLC. Since it was difficult to detect benzene in ethanol, I in cumene was irradiated in the same manner as has been described above for the detection of benzene, but the gas chromatography of the solution showed the absence of any benzene, while its TLC showed the presence of II—IX.

The yield of the product was determined as follows. After the irradiation, 2-hydroxy-4,4′-dichloroazobenzene ($\lambda_{max}^{CHCl_3}=339$ mμ, $\varepsilon_{max}^{CHCl_3}=19500$) was added to the solution as an internal standard. Each component was separated by TLC (Merck silica gel G, *n*-hexane - chloroform (3 : 1)) and then extracted with chloroform. The yield was determined from the intensity of the maximum absorption of the extract in an electronic spectrum, whose extinction coefficient had previously been determined by means of an authentic sample, as is shown in Table 4.

The amount of I unreacted was determined as follows. After the irradiation, ethanol (*ca.* 50 m*l*) was added to the solution; both ethanol and I were then distilled *in vacuo* at the room temperature and trapped in a receiver cooled by dry ice-acetone. The same procedure was repeated until no further I was distilled. The amount of I was determined from the intensity of the maximum absorption of the distillate (*ca.* 250 m*l*).

Photolysis of N-Nitrosodiphenylamine (XII). An ethanolic solution (2 m*l*) of XII (10^{-2} M) was irradiated in a Pyrex tube at 25.0±0.1°C for 3 hr. TLC (silica gel G, *n*-hexane - benzene (2 : 1)) showed the presence of V—VIII, carbazole, and some minor products not identified. Their yields were determined by the method described above. III was used as the internal standard.

When benzene was used as a solvent, the amounts of nitroso- and nitro-derivatives were larger.

Photolysis of 4-Nitrosodiphenylamine (VI). An ethanolic solution (2 m*l*) of VI (10^{-3} M) was irradiated in a Pyrex tube at 25.0±0.1°C. III or 1-benzeneazo-2-naphthol ($\lambda_{max}^{CHCl_3}=317$ mμ, $\varepsilon_{max}^{CHCl_3}=7470$) was added as an internal standard, and then VI and VII were separated by TLC (silica gel G, benzene - *n*-hexane (4 : 1)). Their yields were determined as above. The assignment of the other products was not attempted.

The author wishes to express his thanks to Professor Ryozo Goto for his helpful discussions and encouragement throughout the course of this work, and to Professor Aritsune Kaji for his valuable discussions. He is also indebted to Mr. Kiyomi Sakurai for assistance with part of the experimental work.

BULLETIN OF THE CHEMICAL SOCIETY OF JAPAN VOL. 42 215—220 (1969)

Some Observations on Photolysis of Fused Cyclopentyl Nitrites[1)]

Hiroshi SUGINOME, Norio SATO and Tadashi MASAMUNE

Department of Chemistry, Faculty of Science, Hokkaido University, Sapporo

(Received May 31, 1968)

The results of photolysis of three fused cyclopentyl nitrites, Ib, VIIIb, XIV, all of which have 22,27-imino-17,23-oxidojervane framework, are described. In all three cases, competition among the reactions of 11-alkoxyl radical, which led to a variety of products, has been observed. However, the cleavage of α,β carbon-carbon bond to the nitrosoxyl group in these compounds is not the major course of the reaction. It has been found that whenever sterically possible (*e. g.*, Ib), 11-alkoxyl radical in these nitrites is capable of achieving the Barton reaction and the reaction leads to relatively few products. In two cases of these photolyses, the reaction is accompanied by epimerization of the relevant alkoxyl radicals. Some aspects of these transformations are considered in the light of other available data.

In connection with other investigations we were interested in the photolysis of 11-ol nitrites in C-nor-D-homosteroid framework which can be derived from readily-available veratrum alkaloid jervine.

In this paper, we shall describe the results of photolysis of three nitrites, all of which have 22,27-imino-17,23-oxidojervane framework, and will discuss some aspects of the observed transformations which are summarized in annexed charts.

We first examined photolysis of 3-*O*,*N*-diacetyl-22,27-imino-17,23-oxidojerv-5-ene-3β,11β-diol 11-nitrite (Ib). The reaction of 11β-ol (Ia)[2)] with nitrosyl chloride in pyridine[3)] readily afforded the corresponding stable nitrite (Ib), mp 208—210°C. This was photolyzed in toluene by a 150 W high pressure mercury arc lamp for 3 hr. The three major compounds produced (see Experimental) were isolated by preparative thin layer chromatography*[1] to afford a new compound (III), mp 234.5—235°C, (5%), 3-*O*,*N*-diacetyl-22,27-imino-17,23-oxidojerv-5-ene-3β,11α-diol (VI)[2)] (27%), and 3-*O*,*N*-diacetyl-22,27-imino-17,23-oxidojerv-5-en-3β-ol-11-one (VII)[4)] (24%). The new compound had a molecular formula $C_{31}H_{46}O_6N_2$ and could immediately be formulated as a 19-oximino derivative (III) of 3-*O*,*N*-diacetyl-22,27-imino-17,23-oxidojerv-5-ene-3β,11β-diol by the NMR spectrum which retained all signals between τ 9.13 and τ 7.5 except that of C-19 methyl protons in the 11β-ol (Ia) and showed a singlet absorption at τ 2.3 due to a methine proton at C-19.[5)]

The second nitrite photolyzed was *N*-acetyl-22,27-imino-17,23-oxidojerv-4-en-11β-ol-3-one 11-nitrite (VIIIb), in which A and B rings of Ib were modified. This nitrite was easily obtainable by partial acetylation of the 11β-alcohol (VIIIa)[2)] followed by nitrosation in usual way. Photolysis was carried out under comparable conditions with the photolysis of Ib. Contrary to the photolysis of Ib, the composition of the reaction product was complex (at least 8 spots on thin layer) and three major products, 11-ketone (IX), 11β-ol (X) and 11α-ol (XI) were isolated after extensive preparative thin layer chromatography in the yield of 3%, 23% and 2%,

1) a) Photoinduced Transformations. V. Part of this work has been reported. H. Suginome, N. Sato and T. Masamune, *Tetrahedron Letters*, **1967**, 1557. Part IV. H. Suginome, M. Murakami and T. Masamune, This Bulletin, **41**, 468 (1968). b) Regarding stereochemistry of jervine, see. J. W. Scott, L. J. Durham, H. A. P. deJongh, U. Burckhardt and W. S. Johnson, *Tetrahedron Letters*, **1967**, 2381. G. N. Reeke, Jr., R. L. Vincent and W. N. Lipscomb, *J. Am. Chem. Soc.*, **90**, 1663 (1968). S. M. Kupchan and M. I. Suffness, *ibid.*, **90**, 2730 (1968). c) The configurations at C-12 and C-13 of dihydrojervine (12αH, 13αH) and hence those of 11β-ol (Ia)were proposed by Wintersteiner and Moore (*Tetrahedron*, **20**, 1947 (1964)). However, our recent work shows that C-12 hydrogen of dihydrojervine is preferably β-configuration (T. Masamune, A. Murai, H. Ono, K. Orito and H. Suginome, *Tetrahedron Letters*, in press). Therefore, in this paper, a series of compounds derived from dihydrojervine will be formulated on the basis of this new evidence.

2) T. Masamune, N. Sato, K. Kobayashi, Y. Yamazaki and Y. Mori, *Tetrahedron*, **23**, 1591 (1967).

*1 Yields of the pure compounds from this photolysis are not the same as those described in the preliminary communication.[1)]

3) R. H. Pickard and H. Hunter, *J. Chem. Soc.*, **1923**, 434.

4) W. A. Jacobs and C. F. Heubner, *J. Biol. Chem.*, **170**, 635 (1947).

5) W. D. Phillips, *Ann. N. Y. Acad. Sci.*, **70**, 817 (1958).

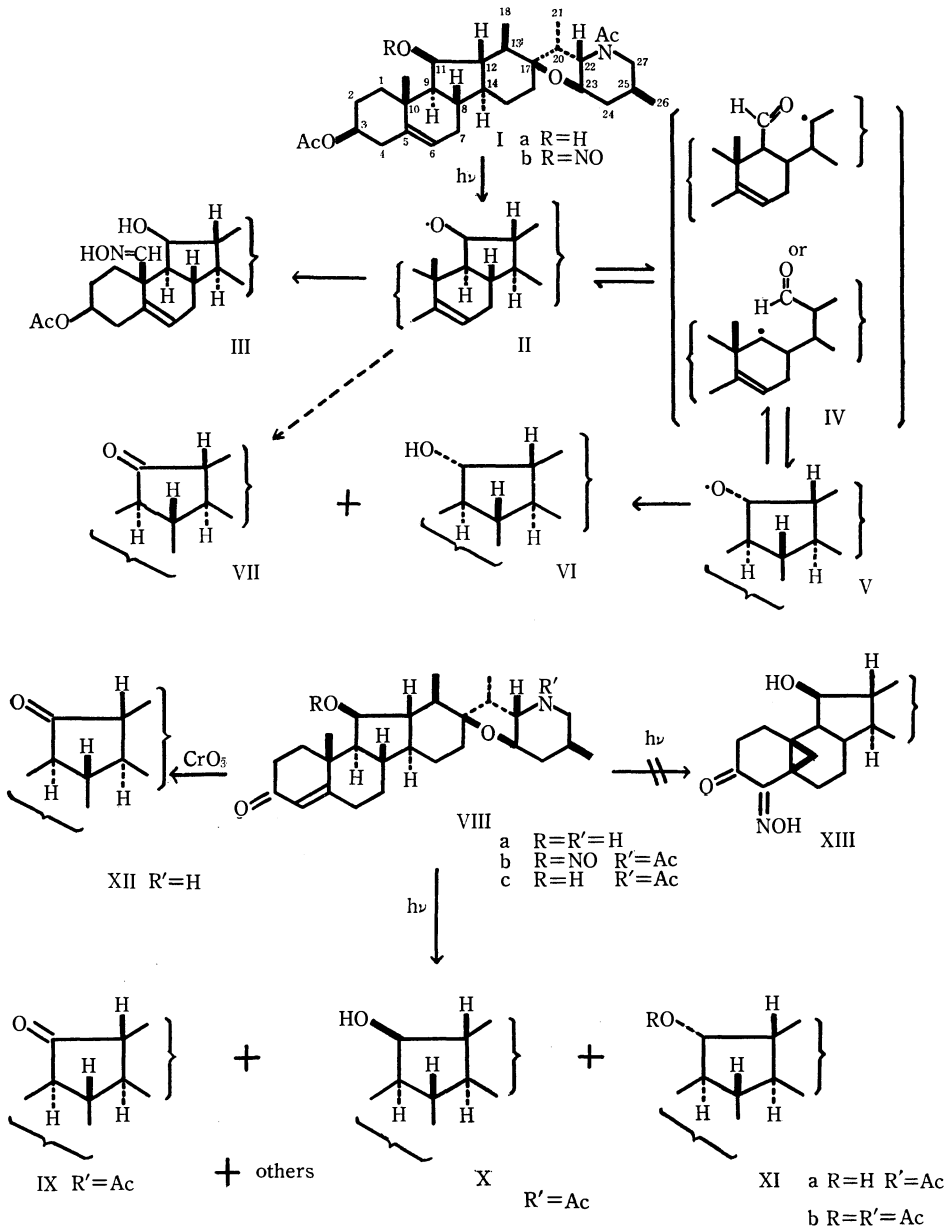

respectively.[6] The compounds IX and XI were new compounds and after the spectroscopic identification these were identified by direct comparison with those newly prepared. Thus, VIIIa[2] was oxidized with chromic anhydride-sulfuric acid in DMF to yield the corresponding 11-ketone (XII). The ketone was then acetylated to yield the corresponding *N*-acetyl derivative (IX) which was identical with the ketone obtained from photolysis.

The 11α-ol (XIa), on the other hand, was prepared by brief hydrolysis of the corresponding diacetyl derivative (XIb).[2]

Various pathways[7-11] have been found in

6) All other products were minor and ill-defined, but the absence of 19-oximino compound or substances having cyclopropane ring, was proved by the NMR spectra of the crude product.

7) For reviews, see a) A. L. Nussbaum and C. H. Robinson, *Tetrahedron*, **17**, 35 (1962). b) M. Akhtar in "Advances in Photochemistry," Vol. II, ed. by W. A. Noyes, G. S. Hammond and J. N. Pitts, Jr., Interscience Publishers, New York, N. Y. (1964), p. 263.

8) C. H. Robinson, O. Gnoj, A. Mitchell, R. Wayne, E. Townley, P. Kabasakalian, E. P. Oliveto and D. H. R. Barton, *J. Am. Chem. Soc.*, **83**, 1771 (1961).

photolysis of nitrites of cyclopentanol derivatives, and the competitive nature of β-scission and inter- or intramolecular hydrogen abstraction in simple alkoxyl radical reactions has been extensively investigated.[12]

It is interesting to note that in the two experiments above mentioned and the photolysis of the 11α-ol nitrite XIV (*vide infra*) none of the products which arise from the scission of α,β-carbon-carbon bond of alkoxyl radicals on five-membered ring[8,11] were found in noticeable amounts, and instead, products of the competition among epimerization, hydrogen abstraction and presumed scission of α,β-carbon-hydrogen bond of alkoxyl radicals were observed.

The formation of 11α-ols, VI, XIa, in these reactions would seem to necessitate inquiry into the possible mode of the transformation.

The most likely mechanism for this epimerization would be one involving reversible aldehyde formation such as IV and this pathway has recently been suggested by Wettstein and co-workers[13] and by Akhtar[7b] to interpret an epimerization[9] from α-caryophyllene alcohol nitrite to epi-α-alcohol, which is the only precedent for this type of transformation.[14]

On the other hand, if we assume that reacting cyclopentyl radicals are planer[15] or that they rapidly invert, other pathways such as *via* a rearrangement of the secondary alkoxyl radical, $RR'CH\text{-}O\cdot \rightarrow RR'\dot{C}\text{-}OH \rightarrow RR'CHOH$, or regeneration of the secondary alcohol followed by the loss of α-hydrogen,[16] $RR'CH'\text{-}O\cdot \rightarrow RR'CHOH \rightarrow RR'\dot{C}\text{-}OH \rightarrow RR'CHOH$, should also be considered, since these pathways can lead to the formation of both 11α and 11β-ols. In fact, two examples[9] of epimerization, including one of the present experiments, resulted in the isolation of both epimers although the ratio of isolated α- and β-epimers was quite different in each case.[17]

However, in regard to these alternatives, we may point out that if the latter mechanisms operate, alkoxyl radicals in six-membered rings must likewise suffer epimerization. Although a considerable number of results have been accumulated on the photolysis of nitrite esters in the field of normal steroids, epimerization of alkoxyl radical in six-membered ring has never been observed[7] and the epimerizations so far found have all been concerned with nitrite on five-membered rings in which a number of scission reactions has been observed.[8,9,11]

This seems to be in favor of the epimerization *via* reversible process as shown in the chart.

It has been found that no 18-oximino derivatives of 22,27-imino-17,23-oxidojervanes were formed in these photolyses. Exclusive attack by the O-radical on the C-19 methyl suggests that the C-18 methyl is not located in the range of attack of the 11-alkoxyl radical. Inspection of the Dreiding model of the 11β-ol (Ia)[1c] indicates that a plausible conformation of the D ring of this molecule, would be a chair form in which the C-18 methyl would occupy an equatorial position. This conformation leads the C-19 methyl to a nearer position than the C-18 methyl with respect to the 11β-alkoxyl radical,

In the NMR spectra of steroid, additivity of group effects for C-18 and C-19 proton signals was well established[18] and this principle has recently been shown to hold for those protons in jervine derivative.[2] It was expected that the present exclusive attack of the 11β-alkoxyl radical on the C-19 methyl might be correlated to these group effects. In 22,27-imino-17,23-oxidojervane derivatives, the deshielding effect of the 11β-hydroxyl for the C-18 proton signals is only 0.11 ppm and has virtually the same value as that of the 11α-hydroxyl group. However, the deshielding effect of the 11β-hydroxyl group for the C-19 methyl has been found to be 0.295 ppm which is close to the corresponding effects of the 11β-

9) A. Nickon, J. R. Mahajan and F. J. McGuire, *J. Org. Chem.*, **26**, 3617 (1961).

10) P. Kabasakalian and E. R. Townley, *ibid.*, **27**, 2918 (1962).

11) P. Kabasakalian and E. R. Townley, *ibid.*, **27**, 3562 (1962); M. Nakazaki and K. Naemura, This Bulletin, **37**, 532 (1964).

12) P. Gray and A. Williams, *Chem. Revs.*, **59**, 239 (1959); J. K. Kochi, *J. Am. Chem. Soc.*, **84**, 1193 (1962); C. Walling and A. Padwa, *ibid.*, **85**, 1593 (1963).

13) C. Meystre, K. Heusler, J. Kalvoda, P. Wieland, G. Anner and A. Wettstein, *Helv. Chim. Acta*, **45**, 1317 (1962), footnote 38.

14) Similar epimerization of 11β-hydroxyl group of normal steroid by oxidation with lead tetraacetate has been reported. K. Heusler, J. Kalvoda, G. Anner and A. Wettstein, *Helv. Chim. Acta*, **46**, 352 (1963); G. B. Spero, J. L. Thompson, W. P. Schneider and F. Kagan, *J. Org. Chem.*, **28**, 2225 (1963).

15) W. A. Pryor, "Free Radicals," McGraw-Hill, New York, N. Y. (1966), p. 30.

16) M. S. Kharasch, J. L. Rowe and W. H. Urry, *J. Org. Chem.*, **16**, 905 (1951).

17) If these mechanisms operate, open-chain optically active secondary nitrites will produce racemic secondary alcohol on photolysis. The result of thermal decomposition of optically active 2-octyl nitrites in liquid phase (N. Kornblum and E. P. Oliveto, *J. Am. Chem. Soc.*, **71**, 266 (1949)) might be relevant at this point and we cited this in the preliminary communication.[1] However, since a recent investigation by Barton and co-workers demonstrated that the pyrolysis of nitrites in the molten state or solution may proceed *via* an ionic mechanism, this fact would not be relevant to the present argument. D. H. R. Barton, G. C. Ramsay and D. Wege, *J. Chem. Soc.*, (*C*), **1967**, 1915.

18) R. F. Zürcher, *Helv. Chim. Acta*, **46**, 2054 (1963). N. S. Bhacca and D. H. Williams, "Application of NMR Spectroscopy in Organic Chemistry," Holden-Day, San Francisco (1964), p. 13.

hydroxyl group in normal steroids. The difference in deshielding effects for the C-19 and C-18 methyls by the 11β-hydroxyl group is consistent with the results of the photolysis. The corresponding reaction in normal steroids, in which the 11β-hydroxyl group has almost the same deshielding effects (0.258 and 0.242 ppm) for the 19 and 18-methyl groups, leads to the formation of the oximino derivatives in both C-19 and C-18 methyls.[19] The correlation between the substituent effects and nitrite photolysis has recently been found in 3α,5α-cyclocholestan-6-ol nitrites.[20] It should be noted that in photolysis of VIIIb, the reaction which led to α-oximino-ketone (XIII) or 19-oximino derivative of 11β-ol (VIIIc) was not, at least, major. In the corresponding 11β-ol nitrite of the normal steroid having Δ^4-3-one, photolysis resulted in the formation of cyclopropane rings.[21]

In photolysis of 3-*O*,*N*-diacetyl-22,27-imino-17,23-oxidojerv-5-en-3β,11β-diol 11-nitrite (Ib) the formation of large amounts of 11-ketone (VII) together with 11α-ol (VI) would be rather distinctive. These can be produced before and (or) after epimerization *via* either disproportionation or α-hydrogen fission. Since a hydrogen on 11-carbon of this molecule is sterically very hindered, 11-ketone (VII) probably arises largely from α-hydrogen fission.[22]

Finally, photolysis of 3-*O*,*N*-diacetyl-22,27-imino-17,23-oxidojerv-5-ene-3β,11α-diol 11-nitrite (XIV), mp 146°C, which can be prepared quantitatively by nitrosation of the corresponding 11α-ol, is described. The irradiation of this compound in toluene for 3 hr led to a complex product mixture consisting of as many as 8 component as revealed by thin layer chromatography. 3-*O*,*N*-Diacetyl-22,27-imino-17,23-oxidojerv-5-en-3β-ol-11-one (VII) (7%), *N*-acetyl-22,27-imino-17,23-oxidojerv-5-en-3β-ol-11-one (XV) (8%), and a new compound melting at 279—281°C, (14%) could be separated by preparative thin layer chromatography. This compound was identified as *N*-acetyl-22,27-imino-17,23-oxidojerv-5-ene-3β,11α-diol (XVI) by direct comparison of its acetyl derivative with the corresponding 3-*O*,11-*O*,*N*-triacetyl derivative. Although it would appear that species generated from NO radical are playing a role in this facile deacetylation at 3 position, additional experimental work would be required before we could make any comments on this.

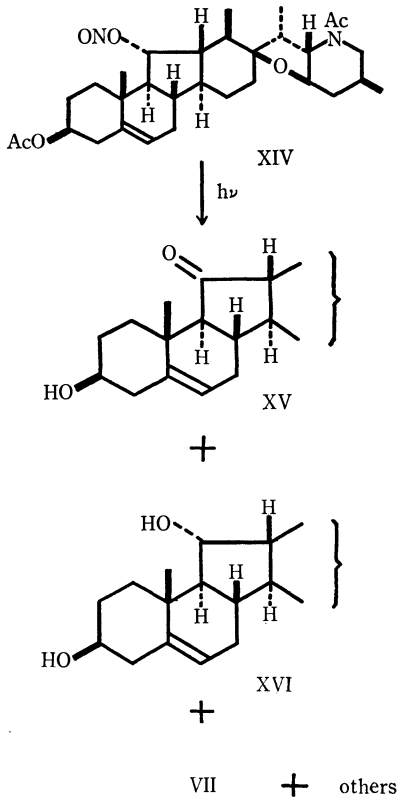

Experimental

Unless otherwise stated, infrared spectra were determined in Nujol using a Nihonbunko DS-402G type spectrophotometer or Jasco Model IR-E spectrophotometer. NMR spectra were determined on a Japan Electron Optics 3H-60 high resolution NMR spectrometer in deuteriochloroform solution using tetramethylsilane as an internal reference. The courses of reactions were followed by thin layer chromatography by using Wakogel B-5, unless stated otherwise.

3-*O*,*N*-Diacetyl-22,27-imino-17,23-oxidojerv-5-en-3β,11β-diol 11-Nitrite (Ib). This nitrite was prepared by nitrosation of 3-*O*,*N*-diacetyl-22,27-imino-17,23-oxidojerv-5-ene-3β,11β-diol in the usual way. The nitrite was recrystallized from chloroform-acetone mixture. Mp 209—210°C $[\alpha]_D$+33.7° *2 (*c* 1.9, chloroform). IR: ν_{max} 1734 (OAc), 1643 (N-Ac), 1725, 1621 (N-O), and 785 cm^{-1} (O-N). NMR: τ 8.95 C-19 methyl).

Found: C, 68.60; H, 8.50; N, 5.33%. Calcd for $C_{31}H_{46}O_6N_2$: C, 68.60; H, 8.54; N, 5.16%.

Photolysis of the Nitrite Ester Ib. The nitrite ester Ib (450 mg) in dry toluene (15 m*l*) under an atmosphere of dry nitrogen was irradiated with a 150-W high pressure mercury arc lamp for 3.5 hr. After evaporation of solvent, the residue was extracted with chloroform and the chloroform solution was washed with water. The residue (538 mg) gave 6 spots on thin

19) D. H. R. Barton and J. M. Beaton, *J. Am. Chem. Soc.*, **84**, 199 (1962).

20) H. Suginome. T. Tsuneno and T. Masamune, *Tetrahedron Letters*, **1967**, 4605.

21) D. H. R. Barton and J. M. Beaton, *J. Am. Chem. Soc.*, **83**, 4083 (1961).

22) Although, in the preliminary communication,[1] we took the view that the formation of the 11-ketone (VII) might be attributed largely to disproportionation, this speculation might prove to be wrong on the basis of further experimental work.

*2 In the preliminary communication, this was reported as $[\alpha]_D$−30°.

layer chromatogram. Among these spots, second, third and sixth spots from the highest one were very minor (Merck aluminum oxide G, type E was used after adding a further 5% of gypsum. A mixture of methanol and ether (1 : 50 vol%) was used as solvent). Preparative thin layer chromatography afforded the following amounts of residues corresponding to each band. The highest band, 103 mg (A), second band, 17 mg (B), third band, 26 mg (C), fourth band, 117 mg (D), fifth band, 61 mg (E). The residue (A) showed mp 210—212°C and was identical with authentic 11-ketone, (VII).[8] R_f value of the residue (B) corresponded to that of Ia. However, this did not afford crystalline material and it has not yet been possible to identify it. The residue (C) was also minor and could not be identified. The residue (D) showed mp 236—238°C and was identical with authentic 11α-ol (VI). The residue (E) (61 mg) was separated into two substances by preparative thin layer chromatography. One (22 mg) melted at 234.5—235°C and was 19-oximino derivative III. IR: ν_{max} 1735 (OAc), 1668 (N-Ac), 3406, and 3205 cm^{-1} (OH). NMR: τ 2.35 (methine at C-19).

Found: C, 68.48; H, 8.47; N, 5.18%. Calcd for $C_{31}H_{46}O_6N_2$: C, 68.60; H, 8.54; N, 5.16%.

The other (5 mg) melted at 197—200°C and has not been identified.

N-Acetyl-22,27-imino-17,23-oxidojerv-4-en-11β-ol-3-one (VIIIC). 22,27-Imino-17,23-oxidojervan-4-en-11β-ol-3-one (500 mg) was dissolved in 22 m*l* of pyridine and 17 m*l* of acetic anhydride and set aside for 1.5 hr at room temperature. After work-up as usual chloroform-acetone solution of the residue yielded crystals of the *N*-acetyl derivative. 450 mg mp 240—242°C. IR: ν_{max} 1625 (N-Ac), 1652 (α,β-unsaturated ketone), and 3458 cm^{-1} (OH). NMR: τ 8.59 (C-19 methyl), τ 7.90 (*N*-acetyl) and τ 4.31 (C-4H).

Found: C, 73.86; H, 9.28; N, 2.84%. Calcd for $C_{29}H_{43}O_4N$: C, 74.16; H, 9.23; N, 2.98%.

N-Acetyl-22,27-imino-17,23-oxidojerv-4-en-11β-ol-3-one 11-Nitrite (VIIIb). *N*-Acetyl-22,27-imino-17,23-oxidojerv-3-en-11β-ol-3-one (300 mg) in pyridine (5m*l*) was cooled to −20——30°C. To this solution there was added dropwise nitrosyl chloride-pyridine mixture while stirring until the solution turned brown. The solution was further stirred for 20 min and was poured into water. Resultant precipitates were collected, dried and recrystallized from acetone-ether. Mp 175—180°C $[\alpha]_D$+186.2° (*c* 0.73, chloroform). IR: ν_{max} 1696 (α,β-unsaturated ketone), and 1662 cm^{-1} (N-Ac). NMR: τ 8.82 (C-19 methyl) and τ 7.95 (*N*-acetyl).

Found: C, 69.70; H, 8.68; N, 5.28%. Calcd for $C_{29}H_{42}O_5N_2$: C, 69.85; H, 8.49; N, 5.62%.

Photolysis of the Nitrite Ester VIIIb. The nitrite ester (828 mg) in dry toluene (13 m*l*) at room temperature and under an atmosphere of dry nitrogen was irradiated with 150-W high pressure mercury arc lamp for 2 hr. After removal of the solvent, the residue was extracted with chloroform. The chloroform solution was washed with water and dried over anhydrous sodium sulfate. The residue was a complex mixture and revealed at least 8 spots on thin layer chromatogram. The preparative thin layer chromatography (Wakogel B5) was carried out as follows: the reaction product was twice developed with a mixture of methanol and ether (1 : 15 vol%). The highest band (least polar compound) afforded the residue (82 mg). This was again purified by thin layer chromatography (solvent: ether), yielding crystals of IX, (16 mg), mp 223—225°C (acetone-ether). $[\alpha]_D$+94° (*c*, 1.5, chloroform). IR: ν_{max} 1652 (α,β-unsaturated ketone), 1729 (5-membered ketone), and 1642 cm^{-1} (N-Ac). NMR: τ 8.81 (C-19 methyl) and τ 7.88 (*N*-acetyl).

Found: C, 74.06; H, 9.00; N, 2.89%. Calcd for $C_{29}H_{41}O_4N$: C, 74.48; H, 8.84; N, 3.00%.

The second band which was major one was eluted to afford oil (120 mg) from which crystals (106 mg) were obtained. This was identical with 11β-ol (VIIIc). All but the above two bands were eluted and combined. The residue was developed twice with methanol and ether (1 : 10 vol%). The least polar compound (11 mg) melted at 249—252°C (acetone-ether). This was identified as 11α-ol (XIa) by comparison with the substance synthesized as below. $[\alpha]_D$ +93° (*c* 2.0, chloroform). IR: ν_{max} 1653 (α,β-unsaturated ketone), 3432 (OH), and 1642 cm^{-1} (N-Ac). NMR: τ 8.86 (C-19 methyl) and τ 7.89 (*N*-acetyl).

Found: C, 74.01; H, 9.20; N, 3.18%. $C_{29}H_{43}O_4N$: C, 74.16; H, 9.23; N, 2.98%.

The NMR spectrum of the crude substance obtained from the rest of the bands above revealed an absence of signals due to a methine proton on carbon bearing an oximino function.

N-Acetyl-22,27-imino-17,23-oxidojerv-4-en-11α-ol-3-one (XI). 11-*O*,*N*-Diacetyl-22,27-imino-17,23-oxidojerv-4-en-11α-ol-3-one (20 mg) in 5% aqueous ethanolic potassium hydroxide (10 m*l*) was refluxed for 40 min. After removal of the solvent, the residue was extracted with chloroforom and water. From the chloroform layer, 11α-ol (8 mg) was obtained. Mp 249—252°C (acetone-ether). This was identical with the product obtained from the photolysis above.

N-Acetyl-22,27-imino-17,23-oxidojerv-4-en-3,11-dione (IX). a) To 22,27-imino-17,23-oxidojerv-4-en-11β-ol-3-one (100 mg) and chromic anhydride (150 mg) in dimethylformamide (11 m*l*), there was added 3 drops of concentrated sulfuric acid and the mixture was stirred for 44 hr at room temperature. After decomposition of the excess chromic anhydride with aqueous saturated sodium bisulfite, tetrahydrofuran was added to the solution and the solution was filtered. Acetone was added to the residue obtained and the solution was again filtered. Removal of the solvent and the extraction of the residue with chloroform yielded crude diketone which was purified by preparative thin layer chromatography to yield amorphous 22,27-imino-17,23-oxidojerv-4-ene-3,11-dione (70mg). IR: ν_{max} 1730 (5-membered ketone), 1667 (α,β-unsaturated ketone), and 3441 cm^{-1} (NH). NMR: τ 8.80 (C-19 methyl).

Found: C, 73.83; H, 9.21; N, 3.04%. Calcd for $C_{29}H_{41}O_4N$: C, 74.48; H, 8.84; N, 3.00%.

This (30 mg) was acetylated in the usual way to yield *N*-acetyl-22, 27-imino-17, 23-oxidojerv-4-ene-3, 11-dione (18 mg), Mp 223—225°C. This was identical with the product obtained from the photolysis above. b) *N*-Acetyl-22,27-imino-17,23-oxidojerv-4-en-11α-ol-3-one (50 mg), chromic anhydride (50m g) and two drops of concentrated sulfuric acid in dimethylformamide (7 m*l*) were stirred for 44 hr at room temperature. After work-up as in the case of the procedure a) above, the residue was purified by preparative thin layer chromato-

graphy to yield diketone IX (20 mg). Mp 223—225°C. This was identical with the specimen obtained by a) above.

3-*O*, *N*-Diacetyl-22, 27-imino-17, 23-oxidojerv-5-en-3β,11α-diol 11-Nitrite (XIV). VI in pyridine was nitrosated at −30°C in usual way. The product was recrystallized from acetone-ether. Mp 146°C.

Found: C, 69.17; H, 8.86; N, 5.00%. Calcd for $C_{31}H_{46}O_6N_2$: C, 68.60; H, 8.54; N, 5.16%.

IR: ν_{max} 1731 (OAc), 1633 (N-Ac), 1644 (N-O), 764, and 777 cm^{-1} (O-N); NMR: τ 8.82 (C-19 methyl).

Photolysis of the Nitrite XIV. The nitrite above (450 mg) in dry toluene (15 m*l*) was irradiated under dry nitrogen at room temperature for 3 hr. After removal of the solvent under reduced pressure, the residue was extracted with chloroform. After usual work-up, the residue (556 mg) obtained was a complex mixture and at least 8 spots were observed on thin layer chromatogram. The three major compounds were isolated by preparative thin layer chromatography (Merck, aluminum oxide G, gypsum content 15%) as follows:

The reaction product was developed with ether. The highest band (least polar compound) afforded the residue (48 mg) from which pure 11-ketone, (VII), mp 210—212°C (from acetone), 30 mg, was obtained. Products from the second and third bands were minor and could not be identified. The residues from the fourth and fifth bands (172 mg) were combined and developed again. The fourth band afforded 42 mg of oily residue. Recrystallization from ether afforded 30 mg of crystals (mp 188°C) which was identified as *N*-acetyl-22,27-imino-17,23-oxidojerv-5-en-3β-ol-11-one, (XV). The residue (65 mg) from the fifth band afforded crystals of 54 mg, mp 279—281°C (from acetone), which was shown to be *N*-acetyl-22,27-imino-17,23-oxidojerv-5-ene-3β,11α-diol (XVI) by converting it into the diacetyl derivative. IR: ν_{max} 1647 (N-Ac) and 1677 cm^{-1} (trisubstituted double bond). NMR: τ 7.89 (N-Ac) and τ 8.98 (C-19 methyl).

Found: C, 73.43; H, 9.41; N, 2.77%. Calcd for $C_{29}H_{45}O_4N$: C, 73.84; H, 9.62; N, 2.97%.

Acetylation of *N*-Acetyl-22,27-imino-17,23-oxidojerv-5-en-3β,11α-diol. Photoproduct XVI was acetylated in usual way. The acetylated product was identical with 3-*O*,11-*O*,*N*-triacetyl-22,27-imino-17,23-oxidojerv-5-ene-3β,11α-diol in every respect.

The authors are indebted to Mr. S. Shimokawa for the measurements of NMR spectra and to the staff of the Laboratory for microanalyses, the Faculty of Pharmaceutical Science of Hokkaido University, for the elemental analyses.

BULLETIN OF THE CHEMICAL SOCIETY OF JAPAN VOL. 42 220—223 (1969)

The Cyclization of Benzoylacetonitrile and Ketones by Ammonium Acetate

Akio SAKURAI and Hiroshi MIDORIKAWA

The Institute of Physical and Chemical Research, Komagome, Bunkyo-ku, Tokyo

(Received June 6, 1968)

Several heterocyclic compounds, such as dihydropyridine, pyridine, tetrahydroquinoline and hexahydroquinoline derivatives, were prepared by the reaction of benzoylacetonitrile with such ketones as acetone, cyclopentanone, cyclohexanone, alkylcyclohexanone, alkylidenecyclohexanone, and aromatic α,β-unsaturated ketone in the presence of ammonium acetate.

In previous paper,[1-3] the syntheses of various nitrogen heterocyclic compounds by means of cyclization between active methylene compounds (ethyl cyanoacetate, ethyl acetoacetate, and malononitrile) and ketones in the presence of ammonium acetate have been reported.

The present paper will deal with the syntheses of similar heterocyclic compounds containing nitrogen by means of the reaction of benzoylacetonitrile with ketones in the presence of ammonium acetate.

Benzoylacetonitrile and acetone in the presence of ammonium acetate reacted in a 2 : 1 molar ratio to give 3,5-dicyano-2,2-dimethyl-4,6-diphenyl-1,2-dihydropyridine (I), with the elimination of three moles of water, as is indicated in the following scheme:

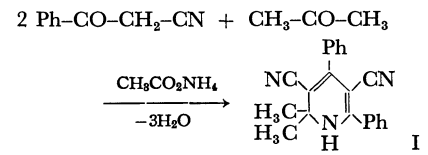

I

1) A. Sakurai and H. Midorikawa, This Bulletin, **40**, 1680 (1967).
2) A. Sakurai and H. Midorikawa, *ibid.*, **41**, 165 (1968).
3) A. Sakurai and H. Midorikawa, *ibid.*, **41**, 430 (1968)

The condensations of benzoylacetonitrile with cyclic ketones are considered to proceed similarly to that of acetone. In these reactions, spiro compounds of such pyridine derivatives as 3,5-dicyano-4,6-diphenyl-1,2-dihydropyridine-2-spiro-1′-cyclopentane (II) and 3,5-dicyano-4,6-diphenyl-1,2-dihydropyridine-2-spiro-1′-cyclohexane (III) were prepared from cyclopentanone and cyclohexanone respectively. On the other hand, the reaction with such an alkylcyclohexanone as 4-methylcyclohexanone was abnormal, and afforded a spiro compound of hexahydroquinoline such as 3-cyano-6,4′-dimethyl-2-phenyl-1,4,5,6,7,8-hexahydroquinoline-4-spiro-1′-cyclohexane (IV), with the elimination of three moles of water from two moles of ketone, one mole each of benzoylacetonitrile and ammonia, as is illustrated below. In this

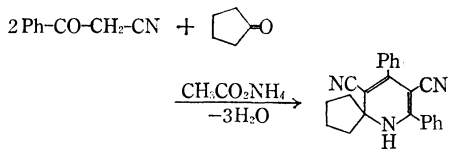

II

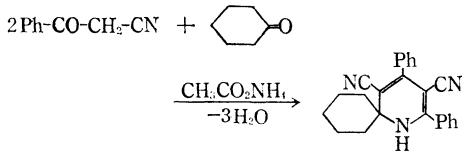

III

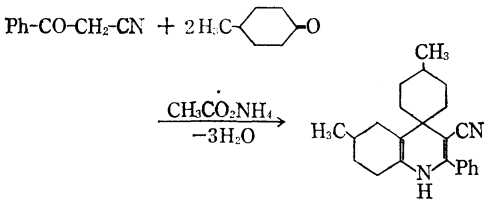

IV

reaction, it was considered that two moles of 4-methylcyclohexanone first condensed, and then cyclized through a Michael reaction such as those of such alkylidenecyclohexanones as 2-benzylidenecyclohexanone and 5-methyl-2-isopropylidenecyclohexanone described below, while the reaction with 2-methylcyclohexanone did not give the dihydropyridine or hexahydroquinoline derivative under similar conditions.

Infrared spectra of compounds I, II and III revealed the absorption bands of imino groups (*ca.* 3200—3290 cm^{-1}) and conjugated cyano groups (*ca.* 2180—2200 cm^{-1}).

The structure of IV was supported by the IR and NMR spectra. Furthermore, the hydrolysis of the cyano group of IV by heating with 60% sulfuric acid gave 6,4′-dimethyl-2-phenyl-1,4,5,6,7,8-hexahydroquinoline-4-spiro-1′-cyclohexane sulfate, melting at 213—215°C with decomposition.

Attempts to prepare the corresponding dihydropyridine derivatives by condensations with such aliphatic higher ketones as methyl ethyl ketone, methyl *n*-propyl ketone, and diethyl ketone or such aromatic ketones as acetophenone and *o*-hydroxyacetophenone were unsuccessful under similar conditions. In these cases, the same compound as that prepared by the self-condensation of benzoylacetonitrile was obtained.

The reaction of benzoylacetonitrile with an α,β-unsaturated ketone such as benzalacetone in the presence of ammonium acetate in a 1 : 1 molar ratio took place, and the pyridine derivative was obtained through a Michael addition, with the elimination of two moles of water and one mole of hydrogen, as is illustrated below:

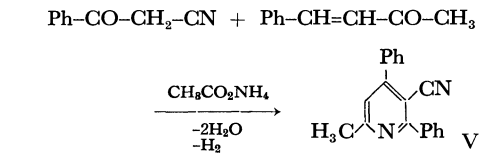

V

The condensations of benzoylacetonitrile with alkylidenecyclohexanones were considered to proceed similarly to that of the α,β-unsaturated ketone (molar ratio 1 : 1). From the reaction with 2-ethylidenecyclohexanone, 3-cyano-4-methyl-2-phenyl-5,6,7,8-tetrahydroquinoline (VI) was prepared through a Michael addition, with the elimination of two moles of water and one mole of hydrogen. On the other hand, the reactions with 2-benzylidenecyclohexanone or 5-methyl-2-isopropylidenecyclohexanone afforded hexahydroquinoline derivatives, such as 3-cyano-2,4-diphenyl-1,4,5,6,7,8-hexahydroquinoline (VIIa) and 3-cyano-4,4,7-trimethyl-2-phenyl-1,4,5,6,7,8-hexahydroquinoline (VIIb). The scheme of these reactions is indicated as follows:

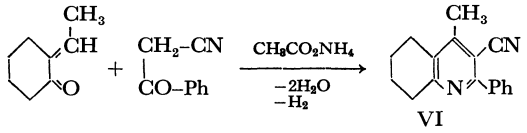

VI

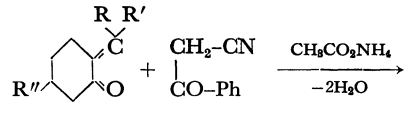

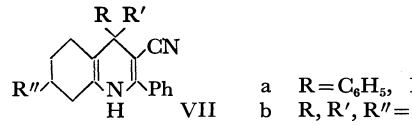

VII a $R=C_6H_5$, $R', R''=H$
b $R, R', R''=CH_3$

The infrared spectra of VIIa and VIIb exhibited the absorption bands of an imino group (3380—3260 cm^{-1}), but the compound VI gave no absorption band in this region. Also, the compounds VI, VIIa, and VIIb revealed the absorptions at 2200—2180 cm^{-1} due to the presence of a conjugated

cyano group. The NMR spectra supported these structures.

The hydrolysis of the cyano group of VI by heating with 60% sulfuric acid gave the corresponding amide melting at 217—219°C.

Benzoylacetonitrile afforded a pyridine derivative by self-condensation in the presence of ammonium acetate. When benzoylacetonitrile was heated with ammonium acetate in glacial acetic acid or alcohol, 6-amino-3-cyano-2,4-diphenylpyridine (VIII) was formed, with the elimination of two moles of water from two moles of benzoylacetonitrile and one mole of ammonia, as is indicated below:

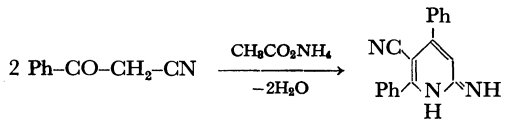

VIII

This compound was also obtained when the reaction was carried out in another solvent, such as benzene or toluene, or without any solvent. The NMR spectrum of the compound VIII showed signals at 7.22 ppm (1H) and 7.85 ppm (1H) due to the presence of imino groups. This fact seems to indicate that the imino form is predominant over the amino form.

The reaction of mesityl oxide with benzoylacetonitrile did not give the expected pyridine derivative, but the same compound as that obtained by the reaction with acetone.

Experimental

All the melting points are uncorrected.

The infrared spectra were determined by means of pressed potassium bromide disks.

The NMR spectra were determined in trifluoroacetic acid or deuteriodimethylsulfoxide at a frequency of 60 Mc, using tetramethylsilane as an internal standard. The chemical shifts are given as ppm downfield from tetramethylsilane.

The Reaction of Benzoylacetonitrile with Ammonium Acetate. A mixture of benzoylacetonitrile (3 g, 0.02 mol) and ammonium acetate (1.6 g, 0.02 mol) was heated in 7 m*l* of alcohol for 4 hr. After it had then been cooled, a crystalline precipitate was obtained; the precipitate was collected and washed with water, dried, and treated with hot alcohol. It was divided into two parts: a hot alcohol-soluble part (A) and a hot alcohol-insoluble part (B). A small amount of water was added to the hot alcohol solution A. After standing overnight at room temperature, pale yellow crystals precipitated out. Recrystallization from dilute alcohol gave 6-amino-2,4-diphenylnicotinonitrile (VIII) melting at 217—218°C[4]; yield, 2 g (35%).

Found: C, 79.91; H, 4.82; N, 15.36%. Calcd for $C_{18}H_{13}N_3$: C, 79.68; H, 4.83; N, 15.49%.

IR: 3460, 3330 (ν NH), 2210 (ν C≡N), 1620, 1590, 1575, 1535, and 1500 cm^{-1} (hetero ring and C_6H_5).

NMR [$(CD_3)_2SO$]: 6.55 (–CH=, singlet, 1H), 7.22 (NH, singelt, 1H), 7.85 (NH, singelt, 1H), and 7.57 ppm (C_6H_5, singlet, 10H).

The hot alcohol-insoluble precipitate, B, was recrystallized from pyridine and a small amount of dilute methanol to give 0.7 g of yellow crystals, melting at 313—315°C. Its structure could not be confirmed.

3,5-Dicyano-2,2-dimethyl-4,6-diphenyl-1,2-dihydropyridine (I). To a mixture of benzoylacetonitrile (2.5 g, 0.017 mol) and acetone (1 g, 0.017 mol), ammonium acetate (1.2 g, 0.016 mol) was added. When the reaction mixture was then heated for 4 hr, a yellow crystalline matter precipitated. After it had been cooled at room temperature, the crystals were collected and washed with an ether-methanol solution and then with water. Recrystallization from glacial acetic acid afforded pale yellow needles, mp 282—284°C; yield, 1.5 g (56%).

Found: C, 81.17; H, 5.18; N, 13.46%. Calcd for $C_{21}H_{17}N_3$: C, 81.00; H, 5.50; N, 13.50%.

IR: 3250, 3200 (ν NH), 2195, 2205 (ν C≡N), 1640, 1580, and 1500 cm^{-1} (hetero ring and C_6H_5).

NMR (CF_3CO_2H): 1.7 (CH_3, singlet, 6H), 7.24 (NH, broad, 1H), and 7.6 ppm (C_6H_5, singlet, 10H).

3,5-Dicyano-4,6-diphenyl-1,2-dihydropyridine-2-spiro-1′-cyclopentane (II). To a mixture of benzoylacetonitrile (2.5 g, 0.017 mol) and cyclopentanone (1.5 g, 0.017 mol), ammonium acetate (1.2 g, 0.016 mol) was added, and the solution was refluxed for 3 hr. After the reaction mixture had been cooled, a crystalline precipitate was formed. It was collected and washed with acetone and then with water. Recrystallization from glacial acetic acid afforded 1 g (34%) of pale yellow needles, mp 281—283°C.

Found: C, 81.39; H, 5.23; N, 12.58%. Calcd for $C_{23}H_{19}N_3$: C, 81.87; H, 5.68; N, 12.45%.

IR: 3250, 3210 (ν NH), 2200 (ν C≡N), 1640, 1580, 1500, and 1480 cm^{-1} (hetero ring and C_6H_5).

NMR (CF_3CO_2H): 1.7—2.6 (ring CH_2, complex multiplet, 8H), 7.25 (NH, singlet, 1H), and 7.52 ppm (C_6H_5, singlet, 10H).

3,5-Dicyano-4,6-diphenyl-1,2-dihydropyridine-2-spiro-1′-cyclohexane (III). A mixture of benzoylacetonitrile (1.5 g, 0.01 mol), cyclohexanone (1 g, 0.01 mol), and ammonium acetate (0.6 g, 0.008 mol) was heated for 3 hr. The reaction mixture was then left to stand in a refrigerator overnight. The crystalline matter thus formed was separated on a filter, washed with an ether-methanol solution, and dried. It was recrystallized from alcohol-glacial acetic acid to give 1.5 g (27%) of pale yellow crystals metling at 224—227°C.

Found: C, 81.99; H, 5.96; N, 11.85%. Calcd for $C_{24}H_{21}N_3$: C, 82.02; H, 6.02; N, 11.96%.

IR: 3290, 3240 (ν NH), 2195, 2180 (ν C≡N), 1630, 1605, 1575, and 1490 cm^{-1} (hetero ring and C_6H_5).

3-Cyano-6,4′-dimethyl-2-phenyl-1,4,5,6,7,8-hexahydroquinoline-4-spiro-1′-cyclohexane (IV). A mixture of benzoylacetonitrile (2.9 g, 0.02 mol), 4-methylcyclohexanone (2.24 g, 0.02 mol), and ammonium acetate (2.3 g, 0.03 mol) was heated for 3 hr. After being left standing for several hours, a pale yellow precipitate began to separate from the solution. The precipitated crystals were collected and washed with ether-methanol and then with water. Recrystallization from alcohol gave 1.5 g (22.5%) of white needles, mp

4) S. Checchi and P. Papini, *Gazz. Chim. Ital.*, **90**, 46 (1960).

196—199°C.

Found: C, 82.76; H, 8.20; N, 8.15%. Calcd for $C_{23}H_{28}N_2$: C, 83.08; H, 8.49; N, 8.43%.

IR: 3280 (νNH), 2180 (ν C≡N), 1670, 1590, 1570, and 1500 cm^{-1} (hetero ring and C_6H_5).

NMR [$(CD_3)_2SO$]: 1.00 (CH_3, doublet, 6H), 1.3—2.4 (ring CH_2 and –CH–, complex multiplet, 16H), 7.55 (C_6H_5, singlet, 5H), and 8.95 ppm (NH, broad, 1H).

Hydrolysis of 3-Cyano-6,4′-dimethyl-2-phenyl-1,4,5,6,7,8-hexahydroquinoline-4-spiro-1′-cyclohexane (IV). To a solution of 95% sulfuric acid (19.2 g) and water (10.8 g), IV (1.5 g) was added, and the mixture was heated for 1 hr. After it had then cooled, a pale yellow crystalline matter separated. It was collected and recrystallized from dilute alcohol to give 0.8 g of 6,4′-dimethyl-2-phenyl-1,4,5,6,7,8-hexahydroquinoline-4-spiro-1′-cyclohexane sulfate melting at 213—215°C with decomposition.

Found: C, 64.87; H, 7.61; N, 3.49; S, 7.71%. Calcd for $C_{22}H_{31}O_4NS$: C, 65.16; H, 7.71; N, 3.45; S, 7.89%.

6-Methyl-2,4-diphenylnicotinonitrile (V). A mixture of benzoylacetonitrile (2 g, 0.014 mol), benzalacetone (2 g, 0.014 mol), and ammonium acetate (1 g, 0.013 mol) was refluxed in 5 m*l* of glacial acetic acid for 5 hr. After cooling, a small amount of water was added to the reaction mixture and it was allowed to stand in a refrigerator overnight. The crystalline matter which was precipitated was collected on a filter and recrystallized from alcohol to afford 1.2 g (32%) of pale yellow needles, mp 150—151°C.

Found: C, 84.40; H, 5.17; N, 10.61%. Calcd for $C_{19}H_{14}N_2$: C, 84.42; H, 5.22; N, 10.36%.

IR: 2220 (ν C≡N), 1590, 1575, 1535, and 1500 cm^{-1} (hetero ring and C_6H_5).

NMR (CF_3CO_2H): 3.07 (CH_3, singlet, 3H), 8.05 (–CH=, singlet, 1H), and 7.8 ppm (C_6H_5, singlet, 10H).

3-Cyano-4-methyl-2-phenyl-5,6,7,8-tetrahydroquinoline (VI). A mixture of benzoylacetonitrile (2 g, 0.014 mol), ethylidenecyclohexanone (1.73 g, 0.014 mol), and ammonium acetate (1 g, 0.013 mol) was refluxed in 5 m*l* of glacial acetic acid for 6 hr. After cooling, the reaction mixture was neutralized with sodium carbonate and allowed to stand overnight at room temperature. A crystalline matter separated from the solution. It was collected and washed with water and then with dilute methanol. Recrystallization from alcohol gave 1.7 g (50%) of colorless needles, mp 127—129°C.

Found: C, 82.53; H, 6.50; N, 11.24%. Calcd for $C_{17}H_{16}N_2$: C, 82.22; H, 6.50; N, 11.28%.

IR: 2220 (ν C≡N), 1585, 1550, and 1500 cm^{-1} (hetero ring and C_6H_5).

NMR (CF_3CO_2H): 2.05 (ring CH_2, broad, 4H), 2.85 (CH_3, singlet, 3H), 2.97, 3.28 (ring CH_2, broad, 4H), and 7.75 ppm (C_6H_5, singlet, 5H).

Hydrolysis of 3-Cyano-4-methyl-2-phenyl-5,6,7,8-tetrahydroquinoline (VI). To a solution of 95% sulfuric acid (9.6 g) and water (5.4 g), VI (0.5 g) was added, and then the mixture was heated for 1 hr.

After being cooled, the solution was poured into ice water. The white precipitate which deposited was collected and dissolved in water, and a few drops of a 10% sodium hydroxide solution were added to it. The precipitated product was washed with water and recrystallized from dilute alcohol to give 0.2 g of 3-carbamoyl-4-methyl-2-phenyl-5,6,7,8-tetrahydroquinoline melting at 217—219°C.

Found: C, 76.48; H, 6.53; N, 10.41%. Calcd for $C_{17}H_{18}ON_2$: C, 76.66; H, 6.81; N, 10.52%.

3-Cyano-2,4-diphenyl-1,4,5,6,7,8-hexahydroquinoline (VIIa). A mixture of benzoylacetonitrile (2 g, 0.014 mol), 2-benzylidenecyclohexanone (2.6 g, 0.014 mol), and ammonium acetate (1.23 g, 0.016 mol) was heated for 5 hr. After the mixture had been left standing for several days, a crystalline mass separated. It was washed with ether, a small amount of a methanol mixture, and then with water. Recrystallization from dilute alcohol afforded 1.5 g (34%) of colorless crystals, mp 132—134°C.

Found: C, 84.42; H, 6.37; N, 8.98%. Calcd for $C_{22}H_{20}N_2$: C, 84.58; H, 6.45; N, 8.97%.

IR: 3380 (ν NH), 2180 (ν C≡N), 1695, 1610, 1600, 1575, 1550, 1505, and 1495 cm^{-1} (hetero ring and C_6H_5).

3-Cyano-4,4,7-trimethyl-2-phenyl-1,4,5,6,7,8-hexahydroquinoline (VIIb). A mixture of benzoylacetonitrile (2 g, 0.014 mol), 2-isopropylidene-5-methylcyclohexanone (2.1 g, 0.014 mol), and ammonium acetate (1.5 g, 0.02 mol) was refluxed in 5 m*l* of glacial acetic acid for 6 hr. After it had stood overnight, a crystalline matter separated; it was collected on a filter, washed with water, and recrystallized from glacial acetic acid to afford 0.9 g (24%) of colorless needles melting at 195—198°C.

Found: C, 81.81; H, 7.84; N, 10.04%. Calcd for $C_{19}H_{22}N_2$: C, 81.97; H, 7.97; N, 10.06%.

IR: 3260 (ν NH), 2180 (νC≡N), 1685, 1615, 1600, 1575, 1515, and 1495 cm^{-1} (hetero ring and C_6H_5).

NMR (CF_3CO_2H): 1.2 (7-CH_3, doublet, 3H), 1.45 (4-CH_3, doublet, 6H), 1.8—3.5 (ring CH_2 and –CH–, complex multiplet), and 7.55 ppm (C_6H_5, singlet, 5H).

The Reaction of Benzoylacetonitrile with Mesityl Oxide. To a mixture of benzoylacetonitrile (1.45 g, 0.01 mol) and mesityl oxide (0.98 g, 0.01 mol), ammonium acetate (0.77 g, 0.01 mol) was added, and the mixture was heated for 5 hr. After the reaction mixture had been left to stand at room temperature, a crystalline matter precipitated. It was collected on a filter, washed with water, and recrystallized from glacial acetic acid and water to afford 0.8 g (26%) of 3,5-dicyano-2, 2-dimethyl-4, 6-diphenyl-1, 2-dihydropyridine (I) as yellow needles, mp 278—281°C.

Found: C, 80.62; H, 4.98; N, 13.68%. Calcd for $C_{21}H_{17}N_3$: C, 81.00; H, 5.50; N, 13.50%.

This substance was identified with the compound obtained by the reaction between acetone and benzoylacetonitrile by a comparison of their infrared spectra.

The authors wish to express their thanks to Dr. Taro Hayashi and Dr. Tatsuo Takeshima for their kind advice. Thanks are also due to Dr. Haruo Homma and his staff for their microanalyses, to Mr. Jun Uzawa for his measurements of the NMR spectra, and to Mr. Hironori Ogawa for his measurements of the IR spectra.

BULLETIN OF THE CHEMICAL SOCIETY OF JAPAN VOL. 42 224—228 (1969)

Syntheses and Reactions of *N*-(Phenylpyruvoyl) Amino Acids

Yasuhiro CHIGIRA, Mitsuo MASAKI and Masaki OHTA

Laboratory of Organic Chemistry, Tokyo Institute of Technology, Ookayama, Meguro-ku, Tokyo

(Received September 11, 1968)

α-Ethoxy- and α-acetoxycinnamoyl chlorides were synthesized by treatments of α-ethoxy- and α-acetoxycinnamic acid with thionyl chloride and oxalyl chloride, respectively, and reactions of amino acid esters with the cinnamoyl chlorides were investigated in order to seek for a synthetic method of *N*-(phenylpyruvoyl) amino acids. *N*-Hydroxy- or *N*-benzyloxy-DL-alanine esters prepared from 2-bromopropionic esters and hydroxylamine or benzyloxyamine were treated with α-ethoxycinnamoyl chloride to give the corresponding *N*-(α-ethoxycinnamoyl) derivatives. Treatment of L-leucine ethyl ester with α-acetoxycinnamoyl chloride afforded *N*-(α-acetoxycinnamoyl)-L-leucine ethyl ester, the removal of the acetyl group from which was readily accomplished under mild, basic conditions, and *N*-(phenylpyruvoyl)-L-leucine ester was obtained. Treatment of the ester with ammonia yielded 3-benzylidene-6-isobutyl-2,5-piperazinedione.

There have been known several synthetic routes to *N*-pyruvoyl amino acids. Bergmann and his coworkers reported the formation of *N*-pyruvoylglycine or *N*-pyruvoylalanine on the acid hydrolysis of 3-methylene-2,5-piperazinediones prepared from *N*-glycyl- or *N*-alanylserine.[1] They have also described that some *N*-pyruvoyl or *N*-(phenylpyruvoyl) amino acids were prepared by the reaction of 4-acetamido-2,4-dimethyl- or 4-benzylidene-2-methyl-5-oxazolone with amino acids followed by acid hydrolysis of the resultant 2,2-diacetamidopropionyl[2] or α-acetamidocinnamoyl amino acids.[3] Direct condensations of pyruvic acid with amino acid esters by means of dicyclohexylcarbodiimide or phosphorus oxychloride have been reported by Stoll *et al.*[4] and Wieland *et al.*[5]

In our approach to the synthesis of *N*-(phenylpyruvoyl) α-hydroxyamino acids, the coupling methods of phenylpyruvic acid and α-hydroxyamino acids were studied. This paper deals with the preparation of α-ethoxy- and α-acetoxycinnamoyl chlorides and those reactions with α-amino and α-hydroxyamino acids.

α-Hydroxyamino acids have been reported to be prepared by the reaction of α-halo acids with hydroxylamine,[6] the hydrolysis of α-hydroxyamino nitriles,[7] or the hydrolysis of nitrones.[8] *N*-Hydroxy-DL-alanine *t*-butyl ester (Ia) was prepared in 98% yield by heating *t*-butyl 2-bromopropionate with hydroxylamine in methanol in the presence of triethylamine for 20 hr. Analogously, *N*-benzyloxy-DL-alanine *t*-butyl ester (Ib) and *N*-benzyloxy-DL-alanine ethyl ester (Ic) were readily prepared by condensations of the esters of 2-bromopropionic acid with benzyloxyamine in acetonitrile in 42% and 59% yield, respectively.

Some attempted reactions of 4-benzylidene-2-methyl-5-oxazolone with *N*-benzyloxy-DL-alanine ethyl ester (Ic) failed to give the *N*-(α-acetoamidocinnamoyl) derivative of the latter, but led only to recovery of the starting materials, possibly owing to the weakness of the nucleophilicity of the amine (Ic). The acid chloride method was then adopted for the coupling reaction. In order to protect the ketonic group of phenylpyruvic acid for such a reaction, the enol ether and the enol ester were employed.

α-Ethoxycinnamic acid was treated with thionyl chloride to give α-ethoxycinnamoyl chloride (II) in 92% yield, which was characterized by conversion to the corresponding anilide. Treatment of L-leucine ethyl ester (III) with the chloride (II) gave *N*-(α-ethoxycinnamoyl)-L-leucine ethyl ester (V), which was characterized by its conversion to the corresponding acid or amide. The hydrolysis of the enol ester moiety was attempted by treating with glacial acetic acid-hydrochloric acid, but the

1) a) M. Bergmann, A. Miekeley, F. Weinmann and E. Kann, *Heppe-Seyler's Z. physiol. Chem.*, **143**, 108 (1925); b) M. Bergmann, A. Miekeley and E. Kann, *ibid.*, **146**, 247 (1925).

2) M. Bergmann and K. Grafe, *ibid.*, **189**, 196 (1930).

3) J. S. Fruton and M. Bergmann, *J. Biol. Chem.*, **166**, 449 (1946).

4) A. Stoll, A. Hofmann, H. G. Leemann, H. Ott and H. R. Schenk, *Helv. Chim. Acta*, **39**, 1165 (1956).

5) T. Wieland, B. Heinke and K. H. Shin, *Chem. Ber.*, **91**, 483 (1958).

6) A. H. Cook and C. A. Slater, *J. Chem. Soc.*, **1956**, 4130.

7) a) W. Traube, *Ber.*, **27**, 1507 (1894); b) L. Neelakantan and W. H. Hartung, *J. Org. Chem.*, **23**, 964 (1958).

8) E. Buehler and G. B. Brown, *ibid.*, **32**, 265 (1967).

starting material was recovered.

Acylation of *N*-hydroxy-DL-alanine *t*-butyl ester (Ia) with the chloride (II) yielded *N*-(*α*-ethoxycinnamoyl)-*N*-hydroxy-DL-alanine *t*-butyl ester (IVa) which gives a positive ferric chloride reaction characteristic of hydroxamic acid. The product IVa was confirmed by elemental analysis and the infrared spectrum. Analogously, treatment of *N*-benzyloxy-DL-alanine *t*-butyl ester (Ib) with the chloride (II) afforded *N*-benzyloxy-*N*-(*α*-ethoxycinnamoyl)-DL-alanine *t*-butyl ester (IVb) as an oily product in 69% yield, which was characterized by the infrared spectrum. When the ester IVb was treated with trifluoroacetic acid at room temperature for a day, both *t*-butyl and ethyl groups were removed and *N*-benzyloxy-*N*-(phenylpyruvoyl)-DL-alanine (VI) was obtained in 25% yield. Treatment of *N*-benzyloxy-DL-alanine ethyl ester (Ic) with the chloride (II) afforded *N*-benzyloxy-*N*-(*α*-ethoxycinnamoyl)-DL-alanine ethyl ester (IVc) as an oily product. Hydrolysis of the ester (IVc) with 20% aqueous sodium hydroxide failed to give the corresponding acid but furnished *α*-ethoxycinnamic amide (VII).[9] The catalytic hydrogenation of IVc gave *N*-(2-ethoxy-3-phenylpropionyl)-*N*-hydroxy-DL-alanine ethyl ester (VIII).

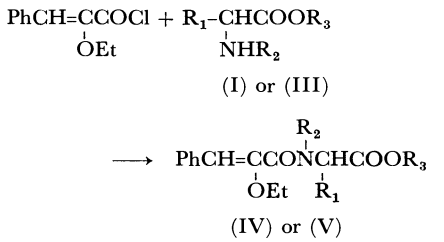

I and IV
a $R_1=CH_3$, $R_2=OH$, $R_3=t$-Bu
b $R_1=CH_3$, $R_2=OC_7H_7$, $R_3=t$-Bu
c $R_1=CH_3$, $R_2=OC_7H_7$, $R_3=Et$
III and V
$R_1=i$-Bu, $R_2=H$, $R_3=Et$

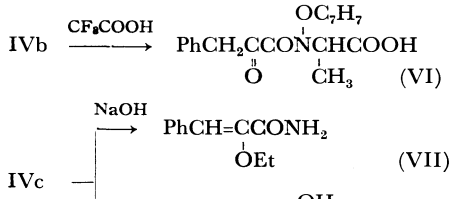

α-Acetoxycinnamoyl chloride (IX) was synthesized in 79% yield by treating *α*-acetoxycinnamic acid with oxalyl chloride. The chloride was characterized by conversion into the corresponding anilide. Acylation of L-leucine ethyl ester (III) with the chloride (IX) afforded *N*-(*α*-acetoxycinnamoyl)-L-leucine ethyl ester (X) in 82% yield. The acetyl group was readily removed by treatment with aqueous sodium bicarbonate or with one equivalent of piperidine, and *N*-(phenylpyruvoyl)-L-leucine ethyl ester (XIa) was obtained in a good yield. The ester (XIa) was characterized by conversion to the 2,4-dinitrophenylhydrazone.

When the ester (XIa) was treated with ammonia in methanol, 3-benzylidene-6-isobutyl-2,5-piperazinedione (XII) was formed in 24% yield. The piperazinedione (XII) was directly obtained by treatment of X with ammonia in methanol. *N*-(Phenylpyruvoyl)-L-leucine prepared by the method of Bergmann *et al.*[3] was heated in methanol in the presence of hydrogen chloride to give the methyl ester (XIb), which, upon treatment with ammonia, also afforded the piperazinedione (XII).

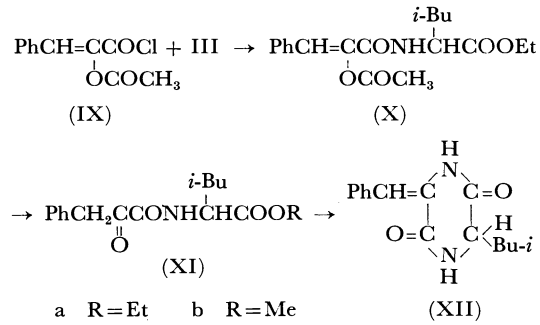

a R=Et b R=Me

α-Acetoxycinnamoyl chloride appears to be the most convenient reagent for the synthesis of *N*-(phenylpyruvoyl) amino acids since the coupling reaction with amines and the removal of the protecting group are accomplished under milder conditions than those used in the aforementioned conventional method.

Experimental[10]

***N*-Hydroxy-DL-alanine *t*-Butyl Ester (Ia).** A solution of hydroxylamine prepared from the hydrochloride (7 g) and sodium (2.3 g) in methanol (90 m*l*) was added to a solution of *t*-butyl 2-bromopropionate (21.0 g) and triethylamine (10.1 g) in methanol (30 m*l*). The resultant solution was refluxed for 20 hr and then concentrated. Ether was added to the residue, and the insoluble substance, triethylamine hydrobromide (18 g), was filtered off. Evaporation of the ether afforded a crystalline residue which was treated with petroleum ether (bp 30—60°C) and collected. Yield was 16.0 g (98%). The product was recrystallized

9) The probable mechanisms for the reaction will be discussed in a subsequent paper.

10) All melting points were determined in a liquid bath and those and all boiling points are uncorrected. All concentrations and evaporations were carried out under reduced pressure. Infrared spectra were determined on a Hitachi EPI-S2 spectrophotometer as thin films of liquids, unless otherwise indicated. NMR spectra were recorded on JUM4H-100 spectrometer (Japan Electron Optics Laboratory Co.).

from petroleum ether (bp 50—90°C) to give colorless needles, mp 72.5—73.5°C.

Found: C, 52.05; H, 9.23; N, 8.34%. Calcd for $C_7H_{15}NO_3$: C, 52.15; H, 9.38; N, 8.69%.

IR (KBr): 3350 (OH), 3200 (NH), 1750 (COOBu-*t*) and 1170 cm^{-1}.

NMR ($CDCl_3$): τ 8.8 (d, 3H), 8.5 (s, 9H), 6.4 (q, 1H) and 3.5 (s, 2H).

***N*-Benzyloxy-DL-alanine *t*-Butyl Ester (Ib).** To a solution of *t*-butyl 2-bromopropionate[11] (10.0 g) in acetonitrile (100 m*l*) were added triethylamine (5.0 g) and benzyloxyamine[12] (6.0 g), and the solution was refluxed for 20 hr. After cooling, the resultant colorless needles (6.0 g) were filtered off. The filtrate was concentrated and the residue was dissolved in a mixture of ether and water. The ethereal layer was washed twice with water and dried over anhydrous sodium sulfate. After removal of the ether, the colorless oily residue was distilled to give a colorless oil (5.0 g, 42%), bp 126—127°C/2 mmHg.

Found: C, 67.15; H, 8.41; N, 5.53%. Calcd for $C_{14}H_{21}NO_3$: C, 66.90; H, 8.42; N, 5.57%.

IR: 3240 (NH), 1730 (COOBu-*t*), 1370, 1225, 1160 and 700 cm^{-1}.

***N*-Benzyloxy-DL-alanine Ethyl Ester (Ic).** The procedure is essentially the same as for Ib. The product was obtained in 59% yield, bp 123—125°C/3.5 mmHg.

Found: C, 64.84; H, 7.52; N, 6.42%. Calcd for $C_{12}H_{17}NO_3$: C, 64.55; H, 7.68; N, 6.27%.

IR: 3250 (NH), 1730 (COOEt), 1320, 1180, 1020 and 700 cm^{-1}.

NMR (CCl_4): τ 8.9 (d, 3H), 8.8 (t, 3H), 6.45 (q, 1H), 5.85 (q, 2H), 5.4 (s, 2H) and 2.7 (s, 5H).

α-Ethoxycinnamoyl Chloride (II). A mixture of α-ethoxycinnamic acid[13] (8.5 g) and thionyl chloride (18 m*l*) was refluxed for 30 min to afford a yellow clear solution. The excess thionyl chloride was evaporated and the residual oil was distilled to give a dark orange oil (8.6 g, 92%), bp 109°C/4 mmHg.

α-Ethoxycinnamic Anilide. A solution of II (1 g) in ether (10 m*l*) was added to a solution of aniline (0.4 g) and pyridine (0.35 g) in ether (10 m*l*). The mixture was treated with water and the insoluble crystalline product was collected. Recrystallization of the product from carbon tetrachloride gave colorless needles (1.1 g, 85%), mp 125°C.

Found: C, 76.03; H, 6.56; N, 5.24%. Calcd for $C_{17}H_{17}NO_2$: C, 76.38; H, 6.41; N, 5.24%.

α-Ethoxycinnamic Amide (VII). A solution of II (0.5 g) in ether was saturated with gaseous ammonia under ice cooling and allowed to stand for 2 hr at room temperature. The mixture was treated with water and the crystalline precipitates were collected and recrystallized from benzene to give colorless needles (0.3 g, 66%), mp 144°C.

Found: C, 69.30; H, 6.97; N, 7.62%. Calcd for $C_{11}H_{13}NO_2$: C, 69.09; H, 6.85; N, 7.33%.

IR (KBr): 3300, 3150 (NH_2), 1670 (C=C), 1620 (CONH), 1410, 1100, 1025 and 690 cm^{-1}.

N-(α-Ethoxycinnamoyl)-L-leucine Ethyl Ester (V). A solution of II (1.5 g) in absolute ether (10 m*l*) was added portionwise, with stirring at 0°C, to a solution of L-leucine ethyl ester (1 g) and pyridine (0.6 g) in absolute ether (10 m*l*). After stirred at room temperature for additional 2 hr, the mixture was treated with water. The ethereal layer was washed successively twice with water, aqueous sodium bicarbonate, water, 1 N hydrochloric acid and finally twice with water, and dried over anhydrous sodium carbonate. Evaporation of the ether afforded a pale yellow oil (1.5 g, 63%), which was used without further purification.

IR: 3300 (NH), 1735 (COOEt), 1670 (C=C), 1635 (CONH) and 1515 (CONH) cm^{-1}.

N-(α-Ethoxycinnamoyl)-L-leucine. A mixture of V (1 g) and 20% aqueous sodium hydroxide (10 m*l*) was stirred for 2 hr and water was added to the mixture until it became to a solution. Next day the aqueous solution was acidified with 3 N hydrochloric acid to afford a viscous oil. The oil was allowed to stand for 3 days in a refrigerator, when it had crystallized. Recrystallization from ligroin gave colorless needles (0.3 g, 33%), mp 101—102°C.

Found: C, 66.97; H, 7.51; N, 4.81%. Calcd for $C_{17}H_{23}NO_4$: C, 66.86; H, 7.59; N, 4.59%.

N-(α-Ethoxycinnamoyl)-L-leucine Amide. A solution of V (1 g) in methanol (40 m*l*) was saturated with gaseous ammonia. The solution was heated at 70°C in the presence of ammonium chloride (0.3 g) in a sealed tube for 2 days and concentrated to dryness. The residue was dissolved in a mixture of ether and water, and the ethereal layer was washed twice with water and dried over anhydrous sodium sulfate. Removal of the ether gave a yellow oil which gradually crystallized. Recrystallization from carbon tetrachloride afforded colorless needles (0.3 g, 32%), mp 114.5—115.5°C.

Found: N, 9.47%. Calcd for $C_{17}H_{24}N_2O_3$: N, 9.20%.

N-Benzyloxy-N-(α-ethoxycinnamoyl)-DL-alanine *t*-Butyl Ester (IVb). The procedure is essentially the same as for V. The product was obtained as a yellow oil in 69% yield, which was used without further purification.

IR: 2950, 1740 (COOBu-t), 1670 (C=C), 1660 (CON<), 1160 and 700 cm^{-1}.

N-Benzyloxy-N-(α-ethoxycinnamoyl)-DL-alanine Ethyl Ester (IVc). The procedure is essentially the same as for V. The product was obtained as a yellow oil in 63% yield, which was used without further purification.

IR: 2950, 1740 (COOEt), 1660 (broad, C=C and CON<), 1210 and 700 cm^{-1}.

NMR (CCl_4): τ 8.8 (t, 3H), 8.7 (d, 3H), 8.5 (t, 3H), 6.0 (q, 2H), 5.9 (q, 2H), 5.15 (m, 1H), 5.05 (s, 2H), 3.9 (S, 1H), 2.8 (s, 5H) and 2.6 (m, 5H).

N-(α-Ethoxycinnamoyl)-N-hydroxy-DL-alanine *t*-Butyl Ester (IVa). A solution of II (4.2 g) in absolute ether (30 m*l*) was added portionwise, with stirring, to a solution of Ia (3.2 g) and pyridine (1.6 g) in absolute ether (20 m*l*). After a day, the precipitated pyridine hydrochloride (1.9 g) was filtered off and the ethereal filtrate was washed twice with water and dried over anhydrous sodium sulfate. Evaporation of the ether afforded a pale yellow oil, which crystallized upon being allowed to stand in a refrigerator. Recrystallization from *n*-hexane gave pale yellow needles (3.4 g, 51%), mp 107—108°C. The product gave a wine red color with a methanolic ferric chloride solution.

11) A. Vollmar and M. S. Dunn, *J. Org. Chem.*, **25**, 387 (1960).

12) M. Masaki and M. Ohta, *ibid.*, **29**, 3165 (1964).

13) T. Gröger and E. Waldmann, *Monatsh. Chem.*, **89**, 370 (1958).

Found: C, 64.54; H, 7.62; N, 4.18%. Calcd for $C_{18}H_{25}NO_5$: C, 64.46; H, 7.51; N, 4.18%.

IR (KBr): 3300 (OH), 1740 (COOBu-*t*), 1660 (C=C), 1620 (CON<), 1450, 1160 and 690 cm^{-1}.

N-Benzyloxy-N-(phenylpyruvoyl)-DL-alanine (VI). The crude IVb (1.0 g) was dissolved in trifluoroacetic acid (3 m*l*) and allowed to stand at room temperature for a day. Removal of the trifluoroacetic acid gave a pale black oil. The oil was dissolved in 1 N aqueous sodium hydroxide, and the solution was washed with ether, treated with activated charcoal and then acidified with 3 N hydrochloric acid. The precipitated oil was extracted with ether and the ethereal extract was dried over anhydrous sodium sulfate. Evaporation of the ether afforded the product as a yellow oil which was treated with petroleum ether (bp 30—60°C), thereby it crystallized gradually. The crystalline product (0.2 g, 25%) was collected and recrystallized from carbon tetrachloride into colorless powder, mp 107—108°C.

Found: C, 66.71; H, 5.54; N, 4.02%. Calcd for $C_{19}H_{19}NO_5$: C, 66.85; H, 5.61; N, 4.10%.

IR (KBr): 1750 (C=O), 1720 (COOH), 1630 (CON<), 1200 and 700 cm^{-1}.

NMR ($CDCl_3$): τ 8.5 (d, 3H), 6.0 (s, 2H), 5.15 (s, 2H) and 2.8 (s, 10H).

Reaction of IVc with Sodium Hydroxide. A mixture of IVc (1.0 g) and 20% aqueous sodium hydroxide (10 m*l*) was stirred at room temperature for 2 hr, and water was added to the mixture until it became to a solution. After a day, the aqueous solution was poured on water to afford α-ethoxycinnamic amide (VII) as crystalline precipitates (0.3 g, 62%). Recrystallization from carbon tetrachloride gave colorless needles which was identical, in melting point and infrared spectrum, with the sample obtained from the reaction of II with ammonia, mp 144°C.

N-(2-Ethoxy-3-phenylpropionyl)-N-hydroxy-DL-alanine Ethyl Ester (VIII). The crude IVc (1 g) was reduced with hydrogen-5% palladium on charcoal (0.5 g) at 50 kg/cm^2 initial pressure in methanol (50 m*l*). After hydrogen absorption had ceased, the catalyst was removed and the solution was concentrated. A solution of the residue in ethyl acetate was treated with activated charcoal and reprecipitated by the addition of petroleum ether (bp 30—60°C). The product (0.2 g, 26%) was recrystallized from carbon tetrachloride to give colorless needles, mp 121.5—122.0°C.

Found: C, 62.30; H, 7.69; N, 4.62%. Calcd for $C_{16}H_{23}NO_5$: C, 62.12; H, 7.49; N, 4.53%.

IR (KBr): 3400 (OH), 1740 (COOEt), 1630 (CON<), 1220, 1190 and 705 cm^{-1}.

α-Acetoxycinnamic Acid. The procedure was modified from the method of Hemmerlé.[14] A suspension of phenylpyruvic acid (2 g) in acetic anhydride (5 m*l*) was refluxed for 2 hr in the presence of *p*-toluenesulfonic acid (0.1 g). On cooling, the resultant clear solution afforded colorless needles (2.0 g, 79%) which was collected and recrystallized from ethyl acetate to give colorless needles, mp 170.5—171.5°C (lit. 168°C,[14] 171—173°C[15]).

α-Acetoxycinnamoyl Chloride (IX). A suspension of the acid (2.0 g) in oxalyl chloride (5 m*l*) was refluxed for 2 hr. The resultant clear solution was concentrated and distilled to give a yellow oil (2.0 g, 92%), bp 105°C/0.07 mmHg.

Found: C, 59.05; H, 4.27%. Calcd for $C_{11}H_9O_3Cl$: C, 58.81; H, 4.04%.

α-Acetoxycinnamic Anilide. The procedure was essentially the same as for α-ethoxycinnamic anilide. Colorless needles from ethyl acetate, mp 171—172°C.

Found: C, 72.35; H, 5.38; N, 5.09%. Calcd for $C_{17}H_{15}NO_3$: C, 72.58; H, 5.37; N, 4.98%.

N-(α-Acetoxycinnamoyl)-L-leucine Ethyl Ester (X). A solution of IX (3.7 g) in absolute ether (20 m*l*) was added portionwise with stirring to a solution of L-leucine ethyl ester (III) (2.6 g) and pyridine (1.14 g) in absolute ether (20 m*l*), and the mixture was stirred for 4 hr. The precipitated pyridine hydrochloride was filtered off and the ethereal filtrate was washed successively with water, aqueous sodium bicarbonate, water, 1 N hydrochloric acid and finally twice with water, and dried over anhydrous sodium sulfate. Evaporation of the ether afforded a crystalline residue which was recrystallized from *n*-hexane to give the product (4.7 g, 82%) as colorless scales, mp 94—96°C.

Found: C, 65.43; H, 7.21; N, 4.27%. Calcd for $C_{19}H_{25}NO_5$: C, 65.69; H, 7.25; N, 4.03%.

IR (KBr): 3320 (NH), 1755 (CH_3COO), 1730 (shoulder, COOEt), 1670 (C=C), 1640 (CONH), 1515, 1185, 1150 and 690 cm^{-1}.

N-(Phenylpyruvoyl)-L-leucine Ethyl Ester (XIa). To a solution of X (1 g) in tetrahydrofuran (10 m*l*) was added a solution of sodium bicarbonate (0.24 g) in water (10 m*l*) and methanol (2 m*l*). The resultant clear solution was stirred for 2 hr and concentrated. The residue was dissolved in ether and treated with 1 N hydrochloric acid. The ethereal layer was washed twice with water and dried over anhydrous sodium sulfate. Removal of the ether gave the product (0.8 g, 91%) as a pale yellow oil, which was used without further purification.

IR: 3300 (NH), 1740 (COOEt), 1700 (COCO), 1530, 1200 and 700 cm^{-1}.

2,4-Dinitrophenylhdrazone of XIa. Orange prisms from ethanol, mp 156—157°C.

Found: C, 56.73; H, 5.35; N, 14.53%. Calcd for $C_{23}H_{27}N_5O_7$: C, 56.90; H, 5.61; N, 14.43%.

N-(Phenylpyruvoyl)-L-leucine Methyl Ester (XIb). A solution of *N*-phenylpyruvoyl-L-leucine[1] (3.0 g) in methanol (30 m*l*) was refluxed in the presence of *p*-toluenesulfonic acid (0.5 g) for 4 hr and concentrated. Ether was added to the residue and then insoluble crystalline precipitates were filtered off. The ethereal filtrate was washed twice with water and dried over anhydrous sodium sulfate. Evaporation of the ether gave a pale yellow oily product (2.3 g, 73%), a portion of which was converted into the 2,4-dinitrophenylhydrazone.

IR: 3300 (NH), 1740 (COOMe), 1685 (COCO), 1530 (CONH), 1200, 1150 and 700 cm^{-1}.

2,4-Dinitrophenylhydrazone of XIb. Yellow prisms from methanol, mp 161°C.

3-Benzylidene-6-isobutyl-2,5-piperazinedione (XII). *From XIa.* A solution of the crude XIa (1 g) in methanol (20 m*l*) was saturated with gaseous ammonia under cooling and allowed to stand at room temperature for 24 hr. The crystalline precipitates were collected

14) R. Hemmerlé, *Ann. chim.* (*Paris*), **7**, 226 (1917).
15) Z. Jerzmanowska and L. Pijewska, *Roczniki Chem.*, **36**, 653 (1962); *Chem. Abstr.*, **59**, 523 (1963).

and sublimed at 230°C under reduced pressure (2 mmHg). Recrystallization of the product from ethanol gave colorless needles (0.2 g, 24%), mp 237—238°C.

Found: C, 69.73; H, 6.70; N, 11.25%. Calcd for $C_{15}H_{18}N_2O_2$: C, 69.74; H, 7.02; N, 10.85%.

IR (KBr): 3200, 3050 (2NH), 1680 (C=C), 1630 (CONH), 1440, 1390 and 700 cm^{-1}.

From XIb. The crude XIb (1.5 g) in methanol (20 m*l*) was treated with gaseous ammonia in a manner analogous to the case of XIa to yield 0.4 g (30%) of the product. The product was identical, in melting point and infrared spectrum with the sample obtained from XIa.

From X. The piperazinedione (XII) was obtained in 15% yield from X by treating with ammonia in a manner analogous to the case of XIa.

BULLETIN OF THE CHEMICAL SOCIETY OF JAPAN VOL. 42 228—232 (1969)

Reaction of *N*-(α-Acetoxycinnamoyl)-*N*-hydroxy Derivatives of DL-Alanine Esters. Formation of Imidazolidinone and Its Transformations into Pyrrolidinedione and Oxazolidinone

Yasuhiro CHIGIRA, Mitsuo MASAKI and Masaki OHTA

Laboratory of Organic Chemistry, Tokyo Institute of Technology, Ookayama, Meguro-ku, Tokyo

(Received June 11, 1968)

Treatment of *N*-benzyloxy-DL-alanine ethyl ester (I) with α-acetoxycinnamoyl chloride (II) gave *N*-(α-acetoxycinnamoyl)-*N*-benzyloxy-DL-alanine ethyl ester (III), which was treated with aqueous sodium bicarbonate, piperidine or hydroxylamine to afford *N*-benzyloxy-*N*-(phenylpyruvoyl)-DL-alanine ethyl ester (IV). Reaction of III or IV with ammonia afforded 5-benzylidene-2-methyl-4-oxo-2-imidazolidinecarboxylic acid (V), which was transformed into 5-methyl-4-phenyl-2,3-pyrrolidinedione (VI) by treatment with aqueous sodium hydroxide and into methyl 5-benzylidene-2-methyl-4-oxo-2-oxazolidinecarboxylate (VII) by treatment with methanolic hydrogen chloride. VI was also derived from III or IV by treatment with sodium hydroxide. *N*-(α-Acetoxycinnamoyl)-*N*-hydroxy-DL-alanine *t*-butyl ester prepared from *N*-hydroxy-DL-alanine *t*-butyl ester and II, was treated with aqueous sodium hydroxide to give *t*-butyl 5-benzylidene-2-methyl-4-oxo-2-oxazolidinecarboxylate.

In the preceding paper we described the preparation of 3-benzylidene-6-isobutyl-2,5-piperazinedione by the reaction of esters of *N*-(α-acetoxycinnamoyl)-L-leucine with ammonia.[1] In an extention of the reaction to *N*-(α-acetoxycinnamoyl)-*N*-benzyloxy-DL-alanine ethyl ester, it might be expected that 1-benzyloxy-3-benzylidene-6-methyl-2,5-piperazinedione would be formed. This paper deals with an unexpected formation of imidazolidinone in such a reaction and its transformations into pyrrolidinedione and oxazolidinone.

Reaction of *N*-benzyloxy-DL-alanine ethyl ester (I) with α-acetoxycinnamoyl chloride (II) gave *N*-(α-acetoxycinnamoyl)-*N*-benzyloxy-DL-alanine ethyl ester (III), which was confirmed by infrared and NMR spectrum. The acetyl group of III could be easily removed by treatment with aqueous sodium bicarbonate, piperidine or hydroxylamine, and *N*-benzyloxy-*N*-(phenylpyruvoyl)-DL-alanine ethyl ester (IV) was obtained. The product was characterized by its conversion to the 2,4-dinitrophenylhydrazone.

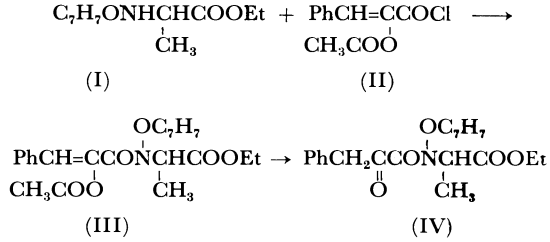

(I) (II)

(III) (IV)

Treatment of IV with ammonia failed to give the expected 2,5-piperazinedione but instead furnished a crystalline product with mp 228—229°C in 60% yield. This compound was also obtained directly from III by treatment with ammonia. Elemental analysis and determination of molecular weight indicated a molecular formula, $C_{12}H_{12}N_2O_3$ for the product, which gives a negative ferric chloride reaction and is insoluble in 1 N hydrochloric acid and in aqueous sodium bicarbonate. These properties as well as the infrared and NMR spectrum revealed the product to be 5-benzylidene-2-methyl-4-oxo-2-imidazolidinecarboxylic acid (V). The

1) Y. Chigira, M. Masaki and M. Ohta, This Bulletin, **42**, 224 (1969).

infrared spectrum showed absorption bands at 3440, 3250 (NH), 3170 (NH), 1710 (COOH), 1690 (CONH), 1680 (C=C) and 1360 cm^{-1}, and the NMR spectrum exhibited signals at τ 8.3 (s, 3H), 7.95 (s, 1NH), 3.85 (s, 1H), 2.6, 2.25 (m, 5H), 2.3 (s, 1NH) and −0.1 (s, 1COOH).[2] 4-Imidazolidinones have been reported to show the infrared absorptions at 1690—1710 (C=O) and 1400—1420 cm^{-1}.[2d]

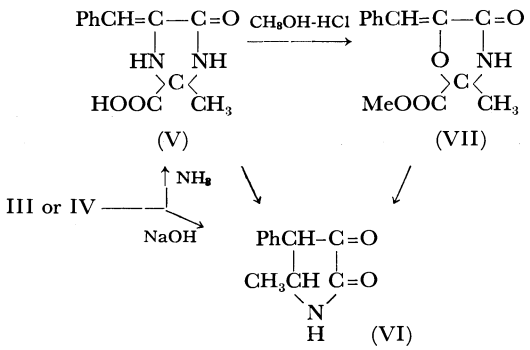

A probable pathway for this reaction would involve an initial elimination of benzyl alcohol from IV, followed or accompanied by the reaction of the ketonic group with ammonia to give ethyl 2 - (2 - imino - 3 - phenylpropionylimino)propionate (VIII) which then cyclized to the ethyl ester of V, and hydrolysis of the ester would yield V. The elimination of benzyl alcohol from IV appeared to be an unexpected reaction, since hydroxamic acids or *N*-acyl-*N*-(benzyloxy)amines are generally stable under the conditions used in the above reaction. However the ease with which benzylalcohol was eliminated from *N*-acyl-*N*-benzyloxy amino acid esters was supported by our previous observation: the alkaline treatment of ethyl *N*-(α-ethoxycinnamoyl)-*N*-benzyloxy-DL-alanine ethyl ester (IX) gave α-ethoxycinnamic amide (X).[1] This reaction was also explained by initial elimination of benzyl alcohol from IX followed by hydrolysis of the resultant ethyl 2-(α-ethoxycinnamoylimino)-propionate (XI) to give the amide (X).

When V was dissolved in aqueous sodium hydroxide and then neutralized with hydrochloric acid, the imidazolidinone (V) could not be recovered but instead pyrrolidinedione (VI) was obtained in 80% yield. The structure of VI was derived from elemental analysis, a positive ferric chloride reaction and spectral studies. The ultraviolet spectrum

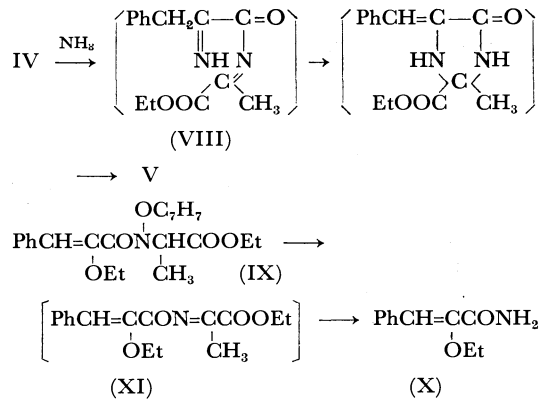

showed absorption maxima at 221, 227 and 287 mμ and the infrared spectrum showed absorption bands at 3200 (NH), 1710 (C=O) and 1670 (CONH) cm^{-1}. This infrared absorption pattern is virtually identical with that described for pyrrolidinediones, *i. e.*, 1700—1730 (C=O) and 1670 (CONH) cm^{-1}.[3] The NMR spectrum exhibited a three-proton doublet at τ 8.8, a one-proton multiplet at 5.45 and a six-proton multiplet at 2.5. The transformation of V into VI would be reasonably explained by an initial hydrolytic fission of carbon-nitrogen bond of the enamine moiety in V accompanied by loss of ammonia to give 2-(phenylpyruvoylimino)-propionic acid (XII), a cyclization of which followed by the decarboxylation yielded VI. The involvement of the intermediate XII in this reaction was supported by the direct formation of VI from III or

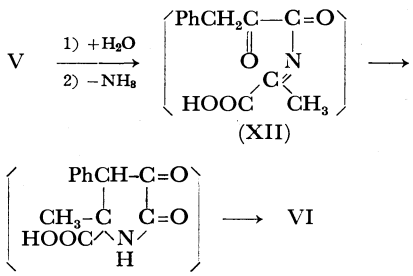

IV. When III or IV was dissolved in 20% aqueous sodium hydroxide and then acidified with hydrochloric acid, pyrrolidinedione (VI) was obtained in 44% and 49% yield respectively.[4] In these reactions, the initial elimination of benzyl alcohol with base would give the ester of XII as intermediate.

A pyrrolidinedione would be obtained if a α-

2) 4-Imidazolidinones have been prepared by desulfurization of thiohydantoins or by the condensations of α-amino nitriles or α-amino acid amides with carbonyl compounds: a) J. T. Eduards and E. F. Matlem, *Chem. Ind.*, **1954**, 193; b) K. Freter, J. Rabinowitz and B. Witkop, *Ann.*, **607**, 174 (1957); c) A. C. Davis and A. L. Levy, *J. Chem. Soc.*, **1951**, 3479; d) U. Zehavi and D. Ben-Ishai, *J. Org. Chem.*, **26**, 1097 (1961).

3) a) P. L. Southwick and E. F. Barnas, *ibid.*, **27**, 98 (1962); b) P. L. Southwick and J. A. Vida, *ibid.*, **27**, 3075 (1962).

4) 2,3-Pyrrolidinediones have been known to be synthesized by the condensations of α-keto acids or its esters with aldehydes and aromatic amines: a) H. Keskin, *Rev. faculté sci. univ. Istanbul*, **11A**, 1 (1946); *Chem. Abstr.*, **40**, 5427 (1946); b) J. R. Merchant, R. J. Shah and R. M. Bhandarkar, *Rec. Trav. Chim.*, **81**, 131 (1962).

ketoacylimine was formed by an alternative route. Treatment of 1,1-diphenylmethylenimine with α-acetoxycinnamoyl chloride (II) afforded *N*-(α-acetoxycinnamoyl)-1,1-diphenylmethylenimine (XIII) which was unstable and decomposed gradually with atomospheric moisture at room temperature to yield α-acetoxycinnamic amide and benzophenone. When XIII was treated with sodium ethoxide, deacetylation followed by cyclization occurred and 4,5,5-triphenyl-2,3-pyrrolidinedione (XIV) was obtained as expected.

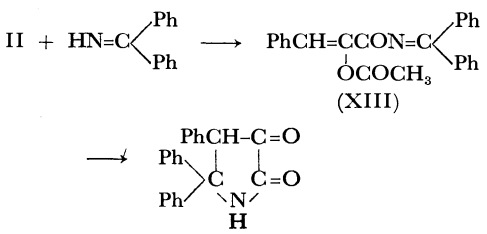

(XIII)

(XIV)

When V was treated with hydrogen chloride in methanol, methyl 5-benzylidene-2-methyl-4-oxo-2-oxazolidinecarboxylate (VII) was obtained in 38% yield. The structure was derived from elemental analysis and spectral studies. The infrared spectrum showed absorption bands at 3070 (NH), 1730 (COOMe), 1710 (CONH) and 1670 (C=C) cm^{-1}. The NMR spectrum exhibited signals at τ 8.15 (s, 3H), 6.2 (s, 3H), 3.65 (s, 1H), 2.6, 2.25 (m, 5H) and 1.05 (s, 1NH).[5] The transformation of V into VII would be rationalized as follows: an initial esterification of V would give the methyl ester (XV) and water, which reacted in the presence of proton to afford methyl 2-phenylpyruvoyliminopropionate (XVI). In contrast to the cyclization of XII into VI under a basic condition, XVI was cyclized to VII in the presence of acid. Treatment of VII with 1 N aqueous sodium hydroxide resulted in the transformation into the pyrrolidinedione (VI) quantitatively. The transformation of

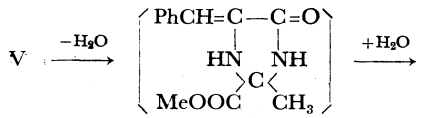

(XV)

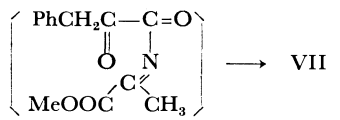

(XVI)

VII into VI would involve again the intermediate XII.

In an analogous fashion, *N*-(α-acetoxycinnamoyl)-*N*-hydroxy-DL-alanine *t*-butyl ester (XVII) was prepared by treatment of *N*-hydroxy-DL-alanine *t*-butyl ester with α-acetoxycinnamoyl chloride (II) in the presence of pyridine. Reaction of XVII with 1 N aqueous sodium hydroxide afforded *t*-butyl 5-benzylidene-2-methyl-4-oxo-2-oxazolidinecarboxylate (XVIII). The structure of XVIII was confirmed by elemental analysis and spectral studies. The infrared spectrum showed absorption bands at 3250 (NH), 1735 (COOBu-*t*), 1710 (CONH) and 1680 (C=C) cm^{-1}. The NMR spectrum exhibited a nine-proton singlet at τ 8.5, a three-proton singelt at 8.2, a one-proton singlet at 3.7 and five-proton multiplets centered at 2.3 and 2.7. These absorption patterns were virtually identical with those of VII.

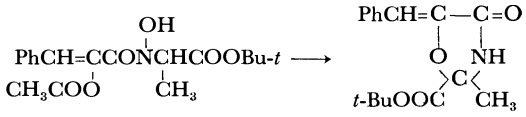

(XVII) (XVIII)

The formation of XVIII from XVII would be also rationalized by dehydration from the hydroxamic moiety of XVII and hydrolysis of the acetoxy moiety followed by a cyclization of the resultant *t*-butyl ester of XII. It is of contrast that the oxazolidinone (XVIII) was formed from *t*-butyl ester of XII under alkaline conditions, while XII was cyclized into the pyrrolidinedione (VI) under similar conditions. The difference should be attributed to the bulkiness of the *t*-butyl group: the formation of pyrrolidinedione from XVII would be impossible since the steric hindrance between phenyl and *t*-butyl groups is so strong that the imino carbon of *t*-butyl ester of XII can not be attacked by the methylene group flanked by phenyl and carbonyl groups, while the steric hindrance would not be so effective in the case of the formation of XVIII.

It is of interest that α-(*N*-acylimino) acid esters (VIII, XI and the esters of XII) were readily formed, but as intermediates, from *N*-acyl derivatives of *N*-benzyloxy- or *N*-hydroxy-DL-alanine esters (IV, IX and XVII) by elimination of benzyl alcohol or water under basic conditions.

Experimental[6]

N-(α-Acetoxycinnamoyl)-N-benzyloxy-DL-alanine Ethyl Ester (III). A solution of α-acetoxycinnamoyl

5) 4-Oxazolidinones have been prepared by the condensations of carbonyl compounds with α-hydroxy nitriles or α-hydroxy acid amides: a) K. Eichenberger, E. Ganz and J. Druey, *Helv. Chim. Acta*, **38**, 284 (1955); b) J. B. Bicking, S. F. Kwong, M. H. Fisher and W. H. Nicholson, *J. Med. Chem.*, **8**, 95 (1965); *Chem. Abstr.*, **62**, 5262 (1965).

6) All melting points were determined in a liquid bath. These and all boiling points are uncorrected. All concentrations and evaporations were carried out under reduced pressure. Infrared spectra were determined on a Hitachi EPI-S2 spectrophotometer as

chloride[1] (II) (3.5 g) in absolute ether (40 ml) was added in portions, with stirring under ice cooling, to a solution of *N*-benzyloxy-DL-alanine ethyl ester[1] (I) (3.5 g) and pyridine (1.2 g) in absolute ether (40 ml). After stirring for 1 hr, the precipitated pyridine hydrochloride (2.1 g) was filtered off. The filtrate was washed successively with water, aqueous sodium bicarbonate, twice with water, 1 N hydrochloric acid, and finally twice with water, and dried over anhydrous sodium sulfate. Evaporation of the ether yielded the product (5.2 g, 81%) as a sirup, which was homogeneous in thin-layer chromatography on silica gel [developed with benzene-alcohol (4:1) or ethyl acetate].

IR (liquid film): 2950, 1765 (CH_3COO), 1740 (COOEt), 1665 (C=C), 1645 (CON<), 1210 and 700 cm^{-1}.

NMR (CCl_4): τ 8.8 (t, 3H), 8.5 (d, 3H), 7.85 (s, 3H), 5.85 (q, 2H), 5.0 (s, 2H), 4.95 (q, 1H), 3.1 (s, 1H), 2.7 (s, 5H) and 2.6 (m, 5H).

***N*-Benzyloxy-*N*-(phenylpyruvoyl)-DL-alanine Ethyl Ester (IV).** *A)* To 1 N methanolic hydroxylamine solution (10 ml) was added III (2.0 g) and the resultant solution was allowed to stand at room temperature for 3 days and then heated at 50—60°C on a water bath for 2 hr. After removal of the methanol, the oily residue was dissolved in ether (20 ml). The ethereal solution was washed successively with water, aqueous sodium bicarbonate, water, 1 N hydrochloric acid and finally with water, and dried over sodium sulfate. The ether was evaporated to afford the product (1.35 g, 75%) as a sirup.

IR (liquid film): 2950, 1740 (COOEt), 1720 (C=O), 1675 (C=C), 1620 (CON<) and 700 cm^{-1}.

2,4-Dinitrophenylhydrazone of IV. To a solution of the product (0.3 g) in methanol (5 ml) was added a methanolic solution of 2,4-dinitrophenylhydrazine sulfate. After a day, the precipitated oily product was separated by decantation and washed twice with methanol. The oily product was dissolved in boiling methanol and the solution was allowed to stand for a week to afford crystalline precipitates. Recrystallization from ethanol afforded yellow needles (0.5 g), mp 135—136°C.

Found: C, 58.97; H, 5.25; N, 12.88%. Calcd for $C_{27}H_{27}N_5O_8$: C, 59.01; H, 4.95; N, 12.75%.

B) A solution of III (1.0 g) and piperidine (0.21 g) in tetrahydrofuran (25 ml) was allowed to stand at room temperature for a day. After removal of the tetrahydrofuran, the oily residue was treated in a manner analogous to the method A to give IV in 70% yield.

C) A solution of III (1.0 g) in tetrahydrofuran was added to a solution of sodium bicarbonate (0.2 g) in water (25 ml) and methanol (2 ml). After a day, the tetrahydrofuran was removed and the aqueous solution was extracted with ether and the ethereal extract was treated in a manner analogous to the method A to give IV in 68% yield.

5-Benzylidene-2-methyl-4-oxo-2-imidazolidinecarboxylic Acid (V). *A) From IV.* A solution of IV (0.8 g) in methanol (20 ml) was saturated with gaseous ammonia under cooling and allowed to stand at room temperature for a day. After removal of the methanol, the crystalline residue was treated with ether. Recrystallization from acetonitrile yielded colorless needles (0.3 g, 60%). A portion of the product was recrystallized from isopropyl alcohol into colorless needles and then from 80% aqueous methanol into colorless prisms, mp 228—229°C.

Found: C, 61.59; H, 5.05; N, 12.07%; mol wt 220. Calcd for $C_{12}H_{12}N_2O_3$: C, 62.06; H, 5.21; N, 12.06%; mol wt 232.

B) From III. A solution of III (0.6 g) in methanol (30 ml) was saturated with gaseous ammonia under cooling and allowed to stand for 2 days. After removal of the methanol, ethyl acetate was added to the residual mixture of an oil and crystals. The insoluble crystals were collected (0.15 g, 44%) and recrystallized from acetonitrile, mp 227—228°C. The product was identical, in melting point and infrared spectrum, with the sample obtained in method A.

5-Methyl-4-phenyl-2,3-pyrrolidinedione (VI). *A)* The imidazolidinone V (0.4 g) was dissolved in 1 N sodium hydroxide (10 ml) and allowed to stand at room temperature overnight. The solution was acidified with 1 N hydrochloric acid to afford gradually crystalline precipitates. The solid was collected and recrystallized from benzene into colorless needles (0.26 g, 80%), mp 228—229°C (with sublimation).

Found: C, 69.45; H, 5.82; N, 7.43%. Calcd for $C_{11}H_{11}NO_2$: C, 69.82; H, 5.86; N, 7.40%.

B) From III. A suspension of III (1.0 g) in 20% aqueous sodium hydroxide was stirred for 6 hr. The resultant clear solution was washed with ether, treated with activated charcoal and acidified with 3 N hydrochloric acid. The precipitated oily product was extracted twice with ether. The ethereal extract was dried over anhydrous sodium sulfate and then evaporated. Addition of carbon tetrachloride to the residual oil gave gradually crystalline product (0.2 g, 44%). Recrystallization from benzene afforded colorless needles, mp 228—229°C. The product was identical, in melting point and infrared spectrum, with the sample obtained by method A.

C) From IV. A suspention of IV (0.6 g) in 20% aqueous sodium hydroxide was treated in a manner analogous to method B to afford the product (0.15 g, 49%).

***N*-(α-Acetoxycinnamoyl)-1,1-diphenylmethylenimine (XIII).** A solution of α-acetoxycinnamoyl chloride (II) (1.5 g) in absolute ether (40 ml) was added in portions, with stirring under ice cooling, to a solution of 1,1-diphenylmethylenimine[7] (2.44 g) in absolute ether (20 ml). After stirring for 2 hr, the precipitated 1,1-diphenylmethylenimine hydrochloride (1.7 g) was filtered off, and the ethereal filtrate was concentrated to dryness. The crystalline residue was treated with dry petroleum ether (bp 30—60°C) to give colorless crystalline product (2.1 g, 84%). A portion of the product was recrystallized from di-*n*-butyl ether to give colorless prisms, mp 98.0—98.5°C.

Found: C, 77.23; H, 5.20; N, 4.35%. Calcd for $C_{24}H_{19}NO_3$: C, 78.03; H, 5.18; N, 3.79%.

KBr disks, unless otherwise indicated. NMR spectra were recorded on JUM4H-100 spectrometer (Japan Electron Optics Laboratory Co.) with tetramethylsilane as internal standard. Molecular weight was measured with a Hitachi-Perkin-Elmer 115 apparatus in dimethylformamide.

7) A. Lachman, "Organic Syntheses," Coll. Vol. II, p. 234 (1943).

IR: 1765 (CH_3COO), 1675 (C=C), 1635 (CON=), 1600, 1210 and 700 cm^{-1}.

This compound is very unstable and decomposed on recrystallization into benzophenone and α-acetoxycinnamic amide. The latter compound was recrystallized from benzene to give colorless needles, mp 143°C.

Found: C, 64.64; H, 5.38; N, 7.01%. Calcd for $C_{11}H_{11}NO_3$: C, 64.38; H, 5.40; N, 6.83%.

4,5,5-Triphenyl-2,3-pyrrolidinedione (XIV). A solution of XIII (0.7 g) in methanol (20 m*l*) was added to sodium methoxide solution [from sodium (0.05 g) and methanol (10 m*l*)] with stirring at room temperature. After a day, the crystalline solid was collected, washed with ether, and then suspended in 1 N hydrochloric acid (10 m*l*). The suspension was extracted with ether and the ethereal extract was dried over anhydrous sodium sulfate. Evaporation of the ether afforded the crystalline product, which was recrystallized from benzene to give colorless needles (0.45 g, 73%), mp 257—258°C.

Found: C, 80.01; H, 5.23; N, 4.55%. Calcd for $C_{22}H_{17}NO_2$: C, 80.71; H, 5.23; N, 4.28%.

IR: 3250 (NH), 1690 (C=O), 1430, 1300, 890, 760 and 700 cm^{-1}.

NMR ($CDCl_3$-DMSO-d_6): τ 6.6 (s, 1H), 2.7 (15H) and 1.65 (s, 1H).

Methyl 5-Benzylidene-2-methyl-4-oxo-2-oxazolidinecarboxylate (VII). A solution of V (0.1 g) in absolute methanol (10 m*l*) was refluxed for 1 hr, while dry hydrogen chloride was passed through the solution, and allowed to stand at room temperature overnight. After removal of the methanol, ether was added to the crystalline residue and the insoluble ammonium chloride (0.035 g) was filtered off. The ethereal filtrate was evaporated to give the crystalline product (0.04 g, 38%). Recrystallization from di-*n*-butyl ether afforded colorless needles, mp 124.5—125.0°C.

Found: C, 62.88; H, 5.36; N, 5.88%. Calcd for $C_{13}H_{13}NO_4$: C, 63.15; H, 5.30; N, 5.69%.

Reaction of VII with Sodium Hydroxide. A solution of VII (0.13 g) in 1 N aqueous sodium hydroxide (5 m*l*) was allowed to stand at room temperature overnight. Neutralization of the solution with 3 N hydrochloric acid afforded crystalline precipitates (0.1 g, 100%) which were collected and recrystallized from benzene, mp 228—229°C. The product was identical, in melting point and infrared spectrum, with the pyrrolidinedione (VI) obtained from V.

***N*-(α-Acetoxycinnamoyl)-*N*-hydroxy-DL-alanine *t*-Butyl Ester (XVII).** A solution of II (1.3 g) in absolute ether (20 m*l*) was added portionwise, with stirring, to a solution of *N*-hydroxy-DL-alanine *t*-butyl ester (0.93 g) and pyridine (0.4 g) in absolute ether (20 m*l*). After 1 hr, water was added to the mixture and the ethereal layer was washed successively with water, aqueous sodium bicarbonate, water, 1 N hydrochloric acid, and finally twice with water, and dried over anhydrous sodium sulfate. The ether was evaporated to afford the product as a pale yellow sirup (1.5 g, 74%), which gives a deep red color with a methanolic ferric chloride solution. The product was used in a succeeding reaction without further purification.

IR (liquid film): 1780 (CH_3COO), 1730 (COOBu-*t*), 1675, 1370, 1160 and 700 cm^{-1}.

***t*-Butyl 5-Benzylidene-2-methyl-4-oxo-2-oxazolidinecarboxylate (XVIII).** A solution of XVII (1 g) in 1 N aqueous sodium hydroxide was allowed to stand at room temperature overnight. The solution was washed twice with ether, treated with activated charcoal and then saturated with carbon dioxide to separate a mixture of crystals and a yellow oil, which was extracted four times with ether. The combined ethereal extracts were dried over anhydrous sodium sulfate and concentrated to give a crystalline residue (0.3 g, 36%). Rapid recrystallization from di-*n*-butyl ether (lower than 90°C) yielded colorless needles, mp 154.5—155.5°C.

Found: C, 66.20; H, 6.24; N, 4.87%. Calcd for $C_{16}H_{19}NO_4$: C, 66.42; H, 6.62; N, 4.84%.

BULLETIN OF THE CHEMICAL SOCIETY OF JAPAN VOL. 42 233—236 (1969)

The Synthesis of 3-Hydroxy-8,9-dimethoxypterocarpan*1

Kenji FUKUI, Mitsuru NAKAYAMA and Teruo HARANO

Department of Chemistry, Faculty of Science, Hiroshima University, Higashi Sendamachi, Hiroshima

(Received June 12, 1968)

7,2′-Dihydroxy-4′,5′-dimethoxyisoflavone was obtained from 7-hydroxy-2′,4′,5′-trimethoxyisoflavone by selective demethylation with aluminum chloride in acetonitrile. By partial benzylation, the dihydroxyisoflavone then gave 7-benzyloxy-4′,5′-dimethoxy-2′-hydroxyisoflavone. The subsequent treatment of the latter with sodium borohydride afforded 3-hydroxy-8,9-dimethoxypterocarpan *via* its 3-benzyloxy-compound.

In connection with the investigation of the syntheses of natural pterocarpans (*e.g.*, (±)-maackiain (I)[1] and (±)-pterocarpin (II)[2]), the syntheses of the same oxygenated analogues and the spectral comparisons of these compounds were attempted. This paper will describe the syntheses of 3-hydroxy-8,9-dimethoxypterocarpan (III)*2 and related compounds from 7-hydroxy-2′,4′,5′-trimethoxyisoflavone (IV).[3]

The selective demethylation at the 2′-position[4] of the 7-hydroxyisoflavone (IV) or of its 7-benzyl derivative (V) in acetonitrile with aluminum chloride afforded 7,2′-dihydroxy-4′,5′-dimethoxyisoflavone (VI) in a good yield; the product then gave a diacetate with acetic anhydride. The partial benzylation of VI at room temperature yielded 7-benzyloxy-4′,5′-dimethoxy-2′-hydroxyisoflavone (VII), which was then easily converted to a monoacetate by a usual method. The treatment of VII with sodium borohydride in absolute alcohol-tetrahydrofuran furnished a product (VIII), $C_{24}H_{22}O_5$, mp 142—143°C, in a good yield. This product (VIII) shows no infrared absorption due to hydroxyl or carbonyl groups (Fig. 1). A comparison of the NMR spectrum (Fig. 2, Table 1)*3 of the product (VIII) with those of pterocarpan derivatives reported in the literature[5] indicates

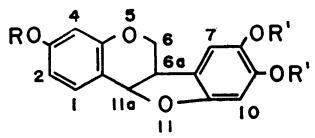

I R = H R′-R′ = CH2
II R = Me R′-R′ = CH2
III R = H R′ = Me
VIII R = C6H5CH2 R′ = Me
X R = CH3CO R′ = Me
XI R = R′ = Me

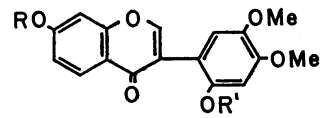

IV R = H R′ = Me
V R = C6H5CH2 R′ = Me
VI R = R′ = H
VII R = C6H5CH2 R′ = H

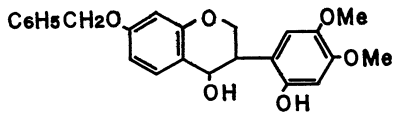

IX

*1 Presented at the 10th Symposium on the Chemistry of Natural Products, Tokyo, Oct., 1966. Symposium papers, p. 145.

1) K. Fukui, M. Nakayama, H. Tsuge and K. Tsuzuki, *Experientia*, **24**, 536 (1968).

2) K. Fukui and M. Nakayama, *Tetrahedron Letters*, **1966**, 1805.

*2 The numbering of pterocarpan is according to S. H. Harper *et al.* (*Chem. Commun.*, **14**, 309 (1965).)

3) K. Fukui, M. Nakayama, M. Hatanaka, T. Okamoto and Y. Kawase, This Bulletin, **36**, 397 (1963).

4) a) K. Aghoiamurthy, A. S. Kukla and T. R. Seshadri, *J. Indian Chem. Soc.*, **38**, 914 (1961); b) V. K. Kalra, A. S. Kukla and T. R. Seshadri, *Indian J. Chem.*, **5**, 287 (1967); c) V. Chandrasheker, M. Krishnamurti and T. R. Seshadri, *Tetrahedron*, **23**, 2505 (1967); d) K. Fukui, M. Nakayama and T. Harano, *Experientia*, **23**, 613 (1967).

*3 The NMR spectra were measured with a Varian A-60 and a Hitachi R-20 spectrometer, using tetramethylsilane as the internal standard (δ-value in $CDCl_3$).

5) a) J. B-son Bredenberg and J. N. Shooley, *Tetrahedron Letters*, **1961**, 285; b) H. Suginome, This Bulletin, **39**, 1529 (1966); c) K. Fukui, M. Nakayama

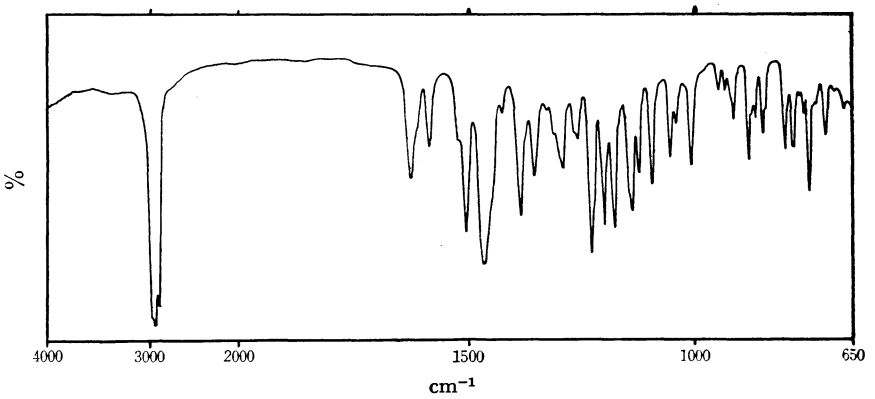

Fig. 1. IR spectrum of VIII (Nujol).

that the broad band at 5.35—5.55 (1H) is due to the C-11a proton, while the complex multiplet at from 3.5–4.5 (3H) surrounding the methoxy resonance is to be assigned to the C-6 protons and the C-6a proton. Accordingly, the structure of VIII is formulated as 3-benzyloxy-8,9-dimethoxypterocarpan. The reaction of the 2′-hydroxyisoflavone (VII) with sodium borohydride to the pterocarpan (VIII) can be postulated as proceeding through an intermediary, a 2′-hydroxyisoflavan-4-ol derivative, 7-benzyloxy-4′,5′-dimethoxy-2′-hydroxyisoflavan-4-ol (IX), followed by dehydration. Attempts to isolate the intermediate (IX) were, however, unsuccessful. The debenzylation of VIII with hydrogen afforded the desired pterocarpan, III, which was also obtained from the 7,2′-dihydroxyisoflavone (VI) by a similar method.

The structure of III is confirmed by the NMR spectra of III, its acetate (X), and methyl ether (XI), which were easily obtained by usual methods. These data are collected in Table 1. The representative NMR spectrum of the acetate (X) is shown in Fig. 3. The aromatic protons are assigned by comparing the data on them with the previously reported data on related compounds, the known values of substituent effects on chemical shifts in aromatic molecules,[6] and the characteristic magnitudes of the aromatic proton-proton splittings.[7]

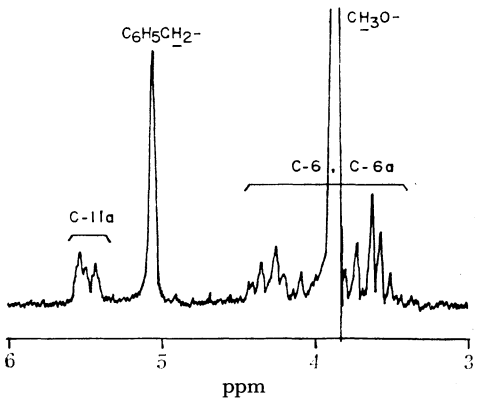

Fig. 2. NMR spectrum of VIII ($CDCl_3$).

TABLE 1. THE NMR SPECTRAL DATA OF PTEROCARPANS*3,4

Proton	Compound VIII	III	X	XI
Arom. C-1	7.45 d	7.33 d	7.51 d	7.40 d
C-2	6.68 q	6.45m	6.78 q	6.62 q
C-4	6.53 d′		6.71	6.48 d′
C-7	6.82 s	7.08	6.83 s	6.82 s
C-10	6.50 s	6.80	6.50 s	6.50 s
C-11a	5.48m	5.55	5.48m	5.48m
C-6—C-6a	3.5—4.4m	3.5—4.4m	3.5—4.4m	3.5—4.4m
CH_3O	3.84 s	3.92 s	3.81 s	3.77 s
	3.87 s		3.82 s	3.81 s
				3.83 s
$C_6H_5CH_2$	7.39 s			
$C_6H_5CH_2$	5.05 s			
CH_3CO			2.26 s	

*4 s, singlet; d, doulet (J_{ortho}=8.5 Hz); d′, doublet (J_{meta}=2.5 Hz); q, quartet (J_{ortho}=8.5 Hz; J_{meta}=2.5 Hz); m, multiplet.

T. Harano and H. Tsuge, 10th Symposium on the Chemistry of Natural Products, Oct., 1966. Symposium papers, p. 145; d) K. G. R. Pachler and W. G. E. Underwood, *Tetrahedron*, **23**, 1817 (1967).

6) J. A. Pople, W. G. Schneider and H. J. Bernstein, "High-resolution Nuclear Magnetic Resonance," McGraw-Hill Book, Co., New York (1959), p. 259.

7) H. S. Gutowsky, C. H. Holm, A. Saika and G. A. Williams, *J. Am. Chem. Soc.*, **79**, 4596 (1957); G. A. Williams and H. S. Gutowsky, *J. Chem. Phys.*, **25**, 1288 (1956).

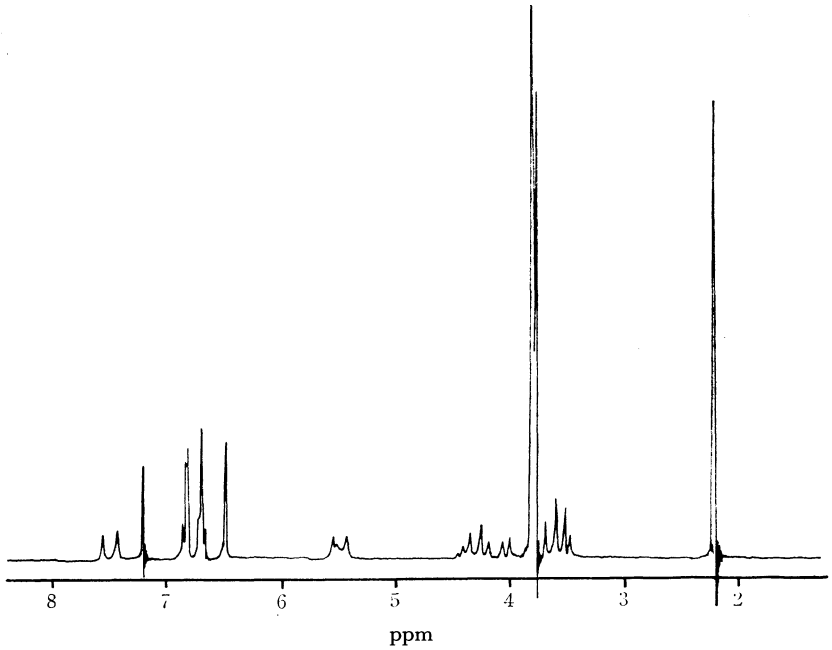

Fig. 3. NMR spectrum of X ($CDCl_3$).

Experimental*5

7-Benzyloxy-2′,4′,5′-trimethoxyisoflavone (V). A mixture of the isoflavone IV[3] (1.5 g), anhydrous potassium carbonate (5.0 g), and benzyl chloride (1.0 g) in anhydrous acetone (80 m*l*) was refluxed for 6 hr. The reaction mixture was then treated in a usual manner. The resulting solid was collected and recrystallized from ethanol to give colorless plates of V, mp 143—144°C (lit.[8] mp 144—145°C); yield, 1.5 g. IR: 1641 cm^{-1} (C=O). UV: λ_{max} mμ (log ε); 247.5 (4.40), 296.5 (4.32).

Found: C, 71.81; H, 5.43%. Calcd for $C_{25}H_{22}O_6$: C, 71.76; H, 5.30%.

7,2′-Dihydroxy-4′,5′-dimethoxyisoflavone (VI). *a) From IV.* A mixture of IV (1.2 g) and anhydrous aluminum chloride (4.0 g) in anhydrous acetonitrile (30 m*l*) was refluxed for 12 hr. After the solvent had been removed, the residue was treated with 10% hydrochloric acid. The resulting solid was collected, washed with water, and recrystallized from ethanol to give light yellow needles of VI, mp 236—237°C; yield, 1.0 g. IR: 3460 (OH), 1619 cm^{-1} (C=O). UV: λ_{max} mμ (log ε); 249_i (4.30),*6 265_i (4.22), 301 (4.28).

Found: C, 64.74; H, 4.58%. Calcd for $C_{17}H_{14}O_6$: C, 64.96; H, 4.49%.

The diacetate: hot acetic anhydride-anhydrous sodium acetate method; mp 152—153°C (colorless needles from ethanol). IR: 1755, 1640 cm^{-1} (C=O). UV: λ_{max} mμ (log ε): 245.5_i (4.38), 290 (4.06).

Found: C, 63.26; H, 4.60%. Calcd for $C_{21}H_{18}O_8$: C, 63.31; H, 4.55%.

b) From V. By a reaction similar to that described above, V (1.2 g), anhydrous aluminum chloride (4.0 g), and anhydrous acetonitrile (30 m*l*) gave VI, mp 236—237°C, which was identical with the sample derived by the above-described method a); yield, 0.85 g.

7-Benzyloxy-2′-hydroxy-4′,5′-dimethoxyisoflavone (VII). Dihydroxyisoflavone VI (0.4 g), benzyl chloride (0.15 g), and anhydrous acetone (100 m*l*) were kept at room temperature for 32 hr while being stirred. After the potassium salts and acetone had then been removed, the water was added to the residue. The resulting solid was collected and recrystallized from ethanol to give yellow needles of VII, mp 172—173°C; yield, 0.3 g. IR: 1622 cm^{-1} (C=O). UV: λ_{max} mμ (log ε); 245_i (4.35), 267 (4.27), 299 (4.32).

Found: C, 70.97; H, 4.98%. Calcd for $C_{24}H_{20}O_6$: C, 71.28; H, 4.99%.

The acetate: hot acetic anhydride-anhydrous sodium acetate method; mp 154—155°C (colorless needles from ethanol). IR: 1750, 1640, 1630 cm^{-1} (C=O). UV: λ_{max} mμ (log ε); 248 (4.40), 293.5 (4.19), 304_i (4.12).

Found: C, 70.13; H, 5.03%. Calcd for $C_{26}H_{22}O_7$: C, 69.94; H, 4.97%.

3-Benzyloxy-8,9-dimethoxypterocarpan (VIII). A solution of sodium borohydride (0.4 g) in absolute ethanol (10 m*l*) was added, drop by drop to a solution of the isoflavone VII (0.3 g) in anhydrous tetrahydrofuran (50 m*l*). The reaction mixture was then kept for 50 hr at room temperature while being stirred. After acetone (20 m*l*) had been added to decompose the excess reducing agent, the solvent was removed under reduced presusre, and 10% hydrochloric acid was added. The separated solid was collected, washed with water, and recrystallized from ethanol to give colorless plates of VIII, mp 142—143°C; yield, 0.22 g. IR: 1627, 1583, 1505 cm^{-1}

*5 All the melting points are uncorrected; the infrared spectra were measured in Nujol, while the ultraviolet spectra were measured in an ethanol solution.

8) K. Fukui and M. Nakayama, This Bulletin, **38**, 1803 (1965).

*6 i=inflection point.

(phenyl). UV: λ_{max} mμ (log ε); 287 (3.88), 298 (3.85).

Found: C, 73.99; H, 5.63%. Calcd for $C_{24}H_{22}O_5$: C, 73.83; H, 5.68%.

3-Hydroxy-8,9-dimethoxypterocarpan (III). *a) From VIII.* A solution of VIII (0.1 g) in acetic acid (40 ml) was submitted to catalytic hydrogenolysis at room temperature in the presence of Pd-C (10%: 0.04 g). After the catalyst had been filtered out, the filtrate was evaporated under reduced pressure; the residue was then recrystallized from dilute ethanol to give colorless crystals of III, mp 209—211°C; yield, 0.06 g. IR: 3460 (OH), 1625, 1595, 1515, 1495 cm^{-1} (phenyl). UV: λ_{max} mμ (log ε); 288 (3.85), 298 (3.85).

Found: C, 65.91; H, 5.68%. Calcd for $C_{17}H_{16}O_5 \cdot \frac{1}{2}H_2O$: C, 66.01; H, 5.54%.

b) From VI. By a reaction similar to that described above, VI (0.6 g) and sodium borohydride (0.7 g) were treated in ethanol - tetrahydrofuran for 60 hr, giving III, mp 209—211°C, which was identical with a sample derived by the above-described method a); yield, 0.5 g.

The acetate (X): hot acetic anhydride - anhydrous sodium acetate method; mp 146—147°C (colorless crystals from ethanol). IR: 1757 (C=O), 1620, 1592, 1501 cm^{-1} (phenyl). UV: λ_{max} mμ (log ε); 288_i (3.76), 300 (3.83).

Found: C, 66.63; H, 5.33%. Calcd for $C_{19}H_{18}O_6$: C, 66.66; H, 5.30%.

The methyl ether (XI): methyl iodide - anhydrous potassium carbonate-acetone method; mp 136—137°C (colorless needles from ethanol). IR: 1616, 1570, 1505, 1492 cm^{-1} (phenyl). UV: λ_{max} mμ (log ε); 288 (3.83), 300 (3.83).

Found: C, 68.49; H, 5.82%. Calcd for $C_{18}H_{18}O_5$: C, 68.78; H, 5.77%.

The authors wish to express their thanks to Professor Shô Itô, Tohoku University, for his NMR spectra measurements. This work was supported in part by a grant-in-aid from the Ministry of Education.

NOTES

BULLETIN OF THE CHEMICAL SOCIETY OF JAPAN VOL. 42 237—240 (1969)

Spectrophotometric Determination of Iron(III) with Rhodamine B and Confirmation of the Composition of Its Complex*1

Hiromu IMAI and Tadahiko YAMADA

Faculty of Engineering, Kansai University, Senriyama, Suita-shi

(Received September 21, 1967)

Rhodamine B (RHCl) has been used in the spectrophotometric determination of gallium(III), gold(III), thallium(III), and antimony(V), forming a complex which can be extracted with organic solvents. Iron(III) also forms a complex with rhodamine B. Consequently, iron(III) in a sample solution interferes with the determination of the above metals.[1-3] It is reported that the iron complex could not be extracted from a 1 N hydrochloric acid solution with benzene by Snell and Snell,[4] or from a 6 N hydrochloric acid solution with isopropyl ether by Onishi and Sandell.[5] However, when a certain organic solvent was used, this complex could be extracted under satisfactory conditions. For these reasons, the spectrophotometric determination of iron(III) based on this color reaction was attempted in a previous work by extraction from a 6 N hydrochloric acid solution with benzene,[6] but this method was not satisfactory because of the lower sensitivity.

The purpose of the present work is to study the determination of a trace of iron(III) with high sensitivity by improving the procedure reported in the previous paper,[6] and to confirm the composition of this complex by employing the method of continuous variation, and that of Molland.

Experimental

Reagents. *Standard Iron(III) Solution.* The stock solution of iron(III) was prepared by dissolving about 3 g of a reagent-grade iron(III) chloride in 250 m*l* of 1 N hydrochloric acid. The concentration of iron in this solution was determined by the oxine method.[7]

Rhodamine B Solution. The solution was prepared by dissolving 0.3 g of RHCl (JIS special grade) dried at 110°C for about 3 hr in 100 m*l* of distilled water.

Extracting Agents. The organic solvents were used after they had been purified by the usual method.[8]

Butyl Cellosolve (BC) Solution. This solution was prepared by dissolving 100 m*l* of ethylene glycol monobutyl ether (butyl cellosolve of Wako Pure Chemicals) in 200 m*l* of distilled water.

Apparatus. A Hitachi photometric photometer, model FPW-4, and an Ito spectrophotometer, model QU-3, were empolyed for all the absorbance measurements, using a 1 cm glass cell.

Standard Procedure for the Determination. A given amount of RHCl, a small amount of BC, and a desired amount of hydrochloric acid were added to a 50 m*l* volumetric flask containing an iron(III) solution, and then mixture was diluted to the mark with water. A 25 m*l* portion of this solution pipetted in a 250 m*l* separating funnel was shaken vigorously with 10 m*l* of an adequate organic solvent for 2 min. The organic layer containing this complex was then completely separated from the aqueous layer by centrifugation. The absorbance of the colored organic layer was measured at 550 mμ or 562 mμ (absorption maximum) against a reference organic solvent treated by the same procedure.

Results and Discussion

The Effects of Extracting Agents. The rhodamine B-iron(III) complex can be extracted from a 6 N hydrochloric acid solution with benzene. The absorption maximum of the colored complex has been known to appear at 558 mμ.[6] If this

*1 This work was presented at the 20th Annual Meeting of the Chemical Society of Japan, Tokyo, April, 1967.

1) E. B. Sandell, "Colorimetric Determination of Traces of Metals," Interscience Publishers, New York, N. Y. (1959), p. 276.

2) L. Luck, *Anal. Chem.*, **31**, 1680 (1959).

3) F. Feigl, "Spot Test in Inorganic Analysis," Elsevier Publishing Company, Amsterdam, London, New York, Princeton (1958), p. 106.

4) F. D. Snell and C. T. Snell, "Colorimetric Method of Analysis," Vol. IIA, D. van Nostrand Co., Toront, New York, London (1959), p. 125.

5) H. Onishi and E. B. Sandell, *Anal. Chim. Acta*, **13**, 159 (1955).

6) H. Imai, *Tech. Reps. of Kansai Univ.*, **4**, 59 (1962).

7) R. Berg, *Z. Anal. Chem.*, **76**, 197 (1929).

8) K. Hata, N. Sugiyama, S. Kobayashi, M. Ota and M. Ōki, "Kagaku Jikken Ho," Kagaku Zokan 6, Kagaku Dojin, Tokyo (1961), pp. 16, 31, 39, 41, 43, 50.

9) H. Imai and K. Nakayama, *Nippon Kagaku Zasshi* (*J. Chem. Soc. Japan, Pure Chem. Sect.*), **87**, 1187 (1966).

Table 1. Effect of extracting agent

Fe(III): 41.63 μg/50 ml, HCl: 6 N, BC: 2 ml/50 ml. Extracting solvent: 10 ml/Sample soln. 25 ml. Wavelength: 550 mμ

0.3% RHCl (ml/50 ml)	Solvent (ml)	Absorbance	0.3% RHCl (ml/50 ml)	Solvent (ml)	Absorbance
15	Bn:MIBK=9.5:0.5	0.442	2	Bn:DON=9.5:0.5	0.038
15	Bn:MIBK=9.0:1.0	0.866	2	Bn:DON=9.0:1.0	0.041
15	Bn:MIBK=8.5:1.5	1.31	2	Bn:EA=9.5:0.5	0.043
5	Bn:MIBK=9.5:0.5	0.208	2	Bn:EA=9.0:1.0	0.078
5	Bn:MIBK=9.0:1.0	0.502	2	Bn:IAA=9.5:0.5	0.037
5	Bn:MIBK=8.5:1.5	0.814	2	Bn:IAA=9.0:1.0	0.064
2	Bn:MIBK=9.5:0.5	0.091	2	Bn:Ac=9.5:0.5	0.033
2	Bn:MIBK=9.0:1.0	0.230	2	Bn:Ac=9.0:1.0	0.086

Bn: Benzene, MIBK: Methyl isobutyl ketone, DON: Dioxane, EA: Ethyl acetate, IAA: Isoamyl acetate, Ac: Acetone

complex was extracted with benzene only, the sensitivity of determination was relatively low compared the case with other methods. Then, the investigation of adding several mixed solvents to benzene was attempted, while varying the absorbance. The results are shown in Table 1.

The maximum degree of extraction of the complex formed in the aqueous solution was obtained by using the mixed solvent of benzene-MIBK. The reference solvent, when treated with the same procedure, gradually colored, while the MIBK concentration increased. As it is best for the color of the reference solvent to be colorless for the spectrophotometric determination, this complex was extracted with benzene containing 10 per cent MIBK by volume.

Effect of Hydrochloric Acid Concentration on the Extraction. The effect of acid concentration on the extraction was examined by using the above solvent.

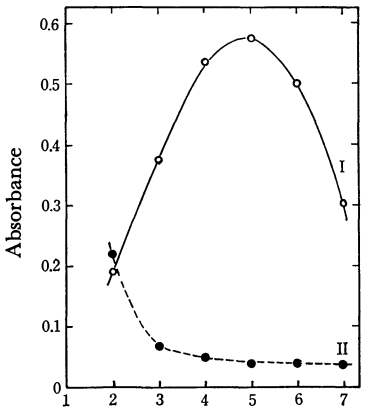

Fig. 1. Effect of acid concentration on absorbance.
Fe(III): 41.63 μg/50 ml, BC: 2 ml/50 ml, 0.3% RHCl: 5 ml/50 ml. Extracting solvent: Bn 9 ml+MIBK 1 ml/Sample soln. 25 ml. Wavelength: 550 mμ
I: Absorbance of this complex in the solvent
II: Absorbance of the reference solvent

From the curves shown in Fig. 1, it can be seen that the maximum absorbance is obtained when this complex was extracted from 5 N hydrochloric acid solution.

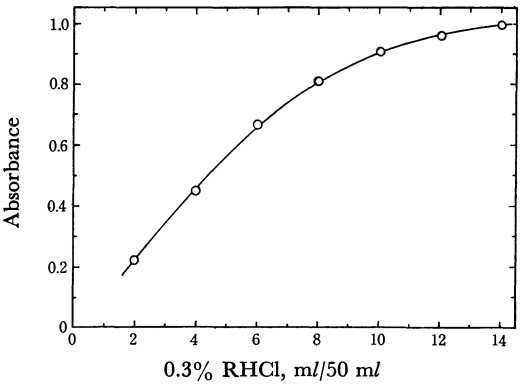

Fig. 2. Effect of RHCl concentration.
Fe(III): 41.63 μg/50 ml, HCl: 5 N, BC: 2 ml/50 ml. Extracting solvent: Bn 9 ml+MIBK 1 ml/Sample soln. 25 ml. Wavelength: 550 mμ

Effects of the Amounts of RHCl and BC. The effect of adding the RHCl concentration to the aqueous layer on the absorbance was also investigated.

As is shown in Fig. 2, the absorbance depends on the concentration of RHCl. The reference solvent was observed to color gradually with an increase in the RHCl concentration. In view of the color of the reference solvent, we used 10 ml of 0.3% RHCl in one further experiments.

The effect of the amount of BC on the absorbance was studied. The results are shown in Fig. 3.

The absorbance increased with an increase in the amount of BC. When more than 2.5 ml of BC was added, the reference solvent colored considerably, this color intensity was observed to change gradually, when the solvent was permitted to stand.

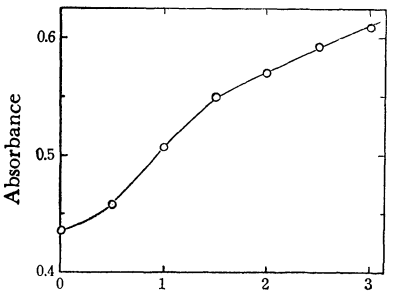

Amount of BC, m*l*/50 m*l*

Fig. 3. Effect of the amount of BC on absorbance. Fe(III): 23.75 μg/50 m*l*, HCl: 5 N, 0.3% RHCl: 10 m*l*/50 m*l*. Extracting solvent: Bn 9 m*l*+MIBK 1 m*l*/Sample soln. 25 m*l*. Wavelength: 550 mμ

Therefore, in further experiments, 2 m*l* of BC were used.

Effect of Time of Standing. The stability of the color intensity of the complex present in the mixed solvent was determined by measuring the absorbance of the organic layer after known periods of time. In such measurements, the absorbance remained almost constant for about 1.5 hr after extraction.

Absorption Spectra and Calibration Curve for Iron(III). Figure 4 shows the absorption spectra of the complex which was extracted from the solution prepared by the addition of varying amounts of 0.3% RHCl to a given amount of iron(III).

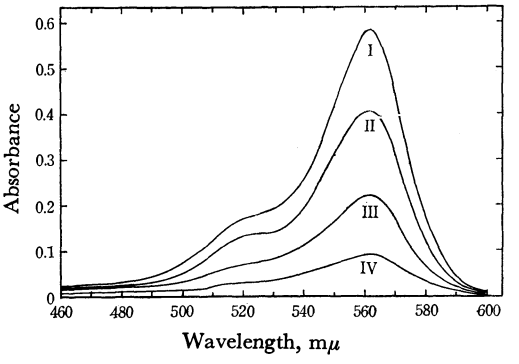

Wavelength, mμ

Fig. 4. Absorption spectra of complex. Fe(III): 23.75 μg/50 m*l*, HCl: 5 N, BC: 2 m*l*/50 m*l*. Extracting solvent: Bn 9 ml+MIBK 1 m*l*/Sample soln. 25 m*l*, 0.3% RHCl (m*l*/50 m*l*): I, 6.0; II, 4.0; III, 2.0; IV, 0.8

The maximum absorption wavelength in the range of RHCl concentration investigated was found at 562 mμ, this result indicated the presence of only one form of the complex.

The calibration curve for the iron(III) determination was prepared at the wavelengths of 550 mμ and 562 mμ in the manner described above.

In all the curves shown in Fig. 5, linear relationships between the absorbance and the concentration are found to be held up to 14 μg of iron(III) in 25 m*l* of the sample solution. The sensitivities of the determination at 562 mμ and 550 mμ were 0.0016 μg and 0.0021 μg iron(III) respectively per cm^2 for $\log(I_0/I)=0.001$. The determination at 562 mμ gives an approximately five-fold increase in the sensitivity compared with the previous investigation.[6]

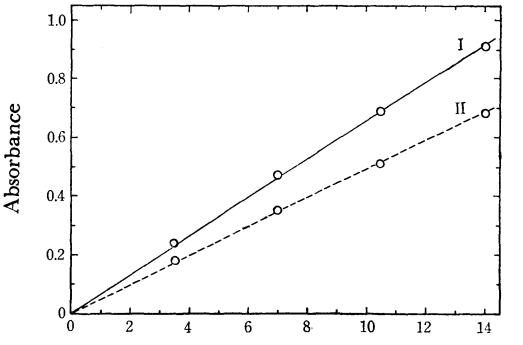

Fe(III), μg/Sample soln. 25 m*l*

Fig. 5. Calibration curves. HCl: 5 N, BC: 2 m*l*/50 m*l*, 0.3% RHCl: 10 m*l*/50 m*l*. Extracting solvent: Bn 9 m*l*+MIBK 1 m*l*/Sample soln. 25 m*l*. Wavelength: I, 562 mμ; II, 550 mμ

The Effect of Diverse Ions. The interference of diverse metallic ions reacting with RHCl in the determination of iron(III) was studied under the conditions used in the proposed procedure. The results are summarized in Table 2.

It was found that gallium(III), gold(III), and thallium(III) interfered even in the smallest concentrations examined, while antimony(V) (in concentrations of more than about 7 μg/25 m*l*). Mercury(II), bismuth(III), and tin(IV) did not do so markedly.

The Composition of the Complex. The composition of the rhodamine B-iron(III) complex was determined by the two methods used in the determination of the compositions of rhodamine B-gold(III)[9] and -gallium(III) complex.[10]

The Method of Continuous Variation. The absorbance of the complex extracted from the aqueous layer, in which the total concentration of iron (III) and RHCl was 79.89×10^{-5} mol/*l* or 39.91×10^{-5} mol/*l* throughout, was plotted against [Fe]/([Fe]+[RHCl]).

Only one complex, 1 to 1, was recognized as being formed, because the average value of the intersecting points obtained from the curves shown in Fig. 6 was 0.51.

10) H. Imai, *Nippon Kagaku Zasshi* (*J. Chem. Soc. Japan, Pure Chem. Sect.*) **87**, 123 (1966).

Table 2. Effect of diverse ions

Fe(III) taken: 6.94 μg/25 m*l*. Condition: measured at same condition as in Fig. 5. Wavelength: 562 mμ

Diverse ions		Fe found	Deviation	Diverse ions		Fe found	Deviation
Kind	μg/25 m*l*	μg/25 m*l*	μg/25 m*l*	Kinds	μg/25 m*l*	μg/25 m*l*	μg/25 m*l*
Hg(II)	3694	6.85	+0.09	Tl(III)	5.38	12.76	+5.86
Ga(III)	1.08	7.82	+0.88	Bi(III)	1270	6.96	+0.02
Ga(III)	4.30	10.50	+3.56	Bi(III)	12700	7.88	+0.94
Au(III)	1.83	7.78	+0.84	Sn(IV)	1710	6.83	+0.11
Au(III)	3.65	10.14	+3.02	Sb(V)	7.33	6.80	−0.14
Tl(III)	2.69	8.76	+1.82	Sb(V)	14.66	8.02	+1.08

Deviation = Fe found − Fe taken

Table 3. Molland method

Condition: measured at same condition as in Fig. 5. Wavelength: 550 mμ

1			2			As_1/As_2
Fe(III) mol/*l*	RHCl mol/*l*	As_1	Fe(III) mol/*l*	RHCl mol/*l*	As_2	
9.94×10^{-5}	6.27×10^{-4}	0.380	6.27×10^{-4}	9.94×10^{-5}	0.436	1.15
9.94×10^{-5}	7.52×10^{-4}	0.415	7.52×10^{-4}	9.94×10^{-5}	0.508	1.22
9.94×10^{-5}	8.77×10^{-4}	0.485	8.77×10^{-4}	9.94×10^{-5}	0.588	1.21
9.94×10^{-5}	10.0×10^{-4}	0.550	10.0×10^{-4}	9.94×10^{-5}	0.650	1.18
9.94×10^{-5}	11.3×10^{-4}	0.610	11.3×10^{-4}	9.94×10^{-5}	0.711	1.17
9.94×10^{-5}	12.5×10^{-4}	0.660	12.5×10^{-4}	9.94×10^{-5}	0.792	1.20
					Average value	1.19

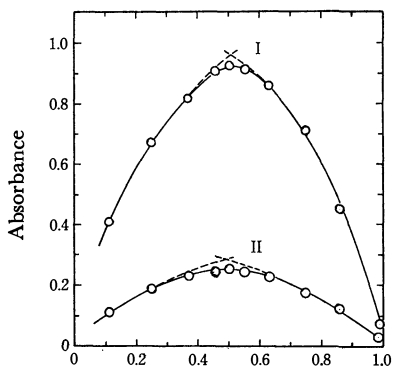

Fig. 6. Method of continuous variation.
Condition: measured at same condition as in Fig. 5. Wavelength: 550 mμ, [Fe]+[RHCl]: I, 79.89×10^{-5} mol/*l*, II, 39.91×10^{-5} mol/*l*

The Molland Method.[11] The formation of the rhodamine B-iron(III) complex can be represented by the following equation[12]:

$$n\mathrm{RH}^+ + m\mathrm{FeCl_4}^- \rightleftarrows (\mathrm{RH})_n\text{-}(\mathrm{FeCl_4})_m \quad (1)$$

Therefore, the absorbance (As_1) of the complex extracted from the solution prepared by the addition of an RHCl solution (b mol/*l*) to a solution containing iron(III) (a mol/*l*) can be written:

$$As_1 = \varepsilon l x_1 \simeq \varepsilon l a/m \quad (2)$$

where ε is the molar extinction coefficient of the complex, l, the thickness of the cell in cm, and x, the concentration of the complex formed.

On the contrary, the absorbance (As_2) obtained from the solution containing iron(III) (b mol/*l*) and RHCl (a mol/*l*) in the same manner as above can be given by:

$$As_2 = \varepsilon l x_2 \simeq \varepsilon l a/n \quad (3)$$

The ratio of n to m may be determined by taking the ratio of the absorbance obtained from both solution:

$$As_1/As_2 = n/m \quad (4)$$

The results obtained from this method are shown in Table 3.

Since the average value of the ratio of As_2 to As_1 obtained from Table 3 was 1.19, this complex was recognized as being 1 to 1.

11) J. Molland, *J. Am. Chem. Soc.*, **62**, 541 (1940).
12) H. Imai, *Nippon Kagaku Zasshi* (*J. Chem. Soc. Japan, Pure Chem. Sect.*), **88**, 227 (1967).

BULLETIN OF THE CHEMICAL SOCIETY OF JAPAN VOL. 42 241—243 (1969)

Asymmetric Hydrogenation of C=O Double Bond with Modified Raney Nickel.*1 XI

Yoshiharu IZUMI, Masami IMAIDA, Tadao HARADA, Tadashi TANABE, Shinichi YAJIMA and Toshio NINOMIYA

Division of Organic Chemistry, Institute for Protein Research, Osaka University, Kita-ku, Osaka

(Received March 1, 1968)

A series of studies of the asymmetric hydrogenation of methyl acetoacetate with the catalysts prepared from Raney nickel catalyst by modifications with aqueous solutions of various optically-active compounds has already been reported by the present authors.[1-11] The effect of the structure of the modifying reagent on the asymmetric activity of the catalyst has been extensively discussed. However, the relationship between the structure of the substrate and the asymmetric yield in the hydrogenation has not yet been reported. In order to clarify the mechanism of asymmetric hydrogenation with a modified Raney nickel catalyst, various substrates were examined with catalysts modified with D-tartaric acid, L-glutamic acid, and some other amino acids. In the present paper, a part of the accumulated results of this study will be given as a basis for future discussion.

TABLE 1.

No.	Substrate	Amount of R-Ni (as alloy) g	Modification: Modifying reagent	Modification: Temp. °C	Modification: pH	Modification: Time hr	Optical rotation of product $[\alpha]_D^{20}$	Absolute config.	Asymmetric yield %
1	Methyl ethyl ketone 0.2 mol	1.5	1%-D-Tartaric acid	100	5.10	1.5	+1.0	-S[a)]	7.7
2	Methyl ethyl ketone 0.15 mol	1.5	2%-L-Glutamic acid	0	4.62	1.5	−0.05	-R	0.4
3	Methyl ethyl ketone 0.15 mol	1.5	2%-L-Glutamic acid	0	4.89	1.5	−0.09	-R	0.7
4	Methyl ethyl ketone 0.15 mol	1.5	2%-L-Glutamic acid	0	5.05	1.5	−0.11	-R	0.8
5	Methyl ethyl ketone 0.15 mol	1.5	2%-L-Glutamic acid	0	5.20	1.5	−0.06	-R	0.5
6	Methyl ethyl ketone 0.15 mol	1.5	2%-L-Glutamic acid	0	7.85	1.5	−0.10	-R	0.8
7	Methyl ethyl ketone 0.15 mol	1.5	2%-L-Glutamic acid	100	4.79	1.5	−0.09	-R	0.7
8	Methyl ethyl ketone 0.15 mol	1.5	2%-L-Glutamic acid	0	5.00	1.5	−0.29	-R	2.2
9	Methyl ethyl ketone 0.15 mol	1.5	2%-L-Glutamic acid	0	8.80	1.5	−0.21	-R	1.6
10	Methyl ethyl ketone 0.15 mol	1.5	2%-L-Alanine	0	6.2	1.5	+0.15	-S	1.1
11	Methyl ethyl ketone 0.15 mol	1.5	2%-L-Alanine	100	—	1.5	+0.27	-S	2.1

*1 Papers I–X were entitled "Asymmetric Hydrogenation with Modified Raney Nickel."

1) H. Fukawa, Y. Izumi, S. Komatsu and S. Akabori, This Bulletin, **35**, 1703 (1962).

2) Y. Izumi, M. Imaida, H. Fukawa and S. Akabori, *ibid.*, **36**, 21 (1963).

3) Y. Izumi, M. Imaida, H. Fukawa and S. Akabori, *ibid.*, **36**, 155 (1963).

4) S. Tatsumi, M. Imaida, Y. Fukuda, Y. Izumi and S. Akabori, *ibid.*, **37**, 846 (1964).

5) Y. Izumi, S. Akabori, H. Fukawa, S. Tatsumi, M. Imaida, Y. Fukuda and S. Komatsu, Proc. of the 3rd Int. Cong. on Catalysis, Vol. 2, 1364 (1964).

6) Y. Izumi, S. Tatsumi, M. Imaida, Y. Fukuda and S. Akabori, This Bulletin, **38**, 1206 (1965).

7) Y. Izumi, S. Tatsumi, M. Imaida, Y. Fukuda and S. Akabori, *ibid.*, **39**, 361 (1966).

8) Y. Izumi, S. Tatsumi and M. Imaida, *ibid.*, **39**, 2223 (1966).

9) S. Tatsumi, *ibid.*, **41**, 409 (1968).

10) Y. Izumi, T. Tanabe and S. Yajima, *ibid.*, **41**, 941 (1968).

11) Y. Izumi, K. Matsunaga, S. Tatsumi and M. Imaida, *ibid.*, to be published.

12	Methyl ethyl ketone 0.4 mol	1.5	2%-L-Phenylalanine	—	—	1.5	0.22	—	1.7
13	Acetophenone 0.15 mol	1.5	2%-L-Glutamic acid	0	5.16	1.5	+0.93	R[b]	2.1
14	Diacetyl 0.18 mol	1.5	2%-D-Tartaric acid	0	5.0	1.5	−0.06	R[c]	0.5
15	Ethyl pyruvate 5 g	0.5	D-Tartaric acid	0	5.0	1.5	+0.26	L–S[d]	2.5
16	α-Ketoglutaric acid 0.5 mol	1.5	2%-L-Glutamic acid	0	5.1	1.5	0	—	—
17	Diethyl α-ketoglutarate 10 g	1.5	2%-L-Glutamic acid	100	5.2	1.5	0	—	—
18	Diethyl α-ketoglutarate 10 g	1.5	2%-D-Tartaric acid	100	5.0	1.5	0	—	—
19	Ethyl acetoacetate 0.15 mol	1.5	2%-D-Tartaric acid	0	5.1	1.5	−2.97	D–R[e]	18
20	Ethyl acetoacetate 0.15 mol	1.5	2%-D-Tartaric acid	100	5.1	1.5	−4.30	D–R	27
21	*n*-Propyl acetoacetate 0.15 mol	1.5	2%-D-Tartaric acid	0	5.1	1.5	−2.28	D–R	16
22	Isopropyl acetoacetate 14 g	1.5	2%-D-Tartaric acid	0	4.0	2.0	−0.58	D–R	4
23	Isopropyl acetoacetate 14 g	1.0	2%-D-Tartaric acid	0	5.0	2.0	−0.76	D–R	5
24	Isopropyl acetoacetate 14 g	1.0	2%-D-Tartaric acid	100	5.1	2.0	−1.58	D–R	11
25	Ethyl benzoylacetate 0.065 mol	1.0	L-Glutamic acid	0	5.12	0.4	+1.90	D–R	8.3[f]
26	Acetylacetone 0.2 mol	1.5	D-Tartaric acid	0	5.0	1.5	−14.83	—	—[g]
27	DL-2-Pentanol-4-on 5 g	1.5	2%-D-Tartaric acid	0	5.0	1.5	−1.15	—	—[g]
28	Diacetonealcohol 13 g	1.5	2%-L-Glutamic acid	0	5.0	1.5	0	—	—
29	Levulinic acid 3 g	1.5	D-Tartaric acid	0	3.5	1.5	0	—	—
30	Methyl levulinate 10 g	1.0	D-Tartaric acid	0	5.2	1.5	−0.40	D–R	3.1[h]
31	Methyl levulinate 10 g	1.0	D-Tartaric acid	100	6.5	1.5	−0.44	D–R	3.4
32	Methyl levulinate 10 g	1.0	L-Glutamic acid	0	5.1	1.5	0	—	0
33	Methyl levulinate 10 g	1.0	L-Glutamic acid	100	5.4	1.5	+0.12	L–S	0.9
34	Methyl 3-acetoxy-crotonate 14 g	1.5	D-Tartaric acid	0	5.2	1.5	Decomposed	—	—
35	Ethyl 3-ethoxycrotonate 15 g	1.5	D-Tartaric acid	0	5.0	1.5	$NO-H_2$-uptake at 60°C	—	—

a) J. Kenyon, H. Phillips and V. P. Pittman, *J. Chem. Soc.*, **1935**, 1077.
b) J. A. Mills, W. Hyne, "Progress in Stereochemistry," Vol. 1, Butterworth, London (1954), p. 187.
c) K. Freudenberg, *Ber.*, **47**, 2027 (1914).
d) A. F. McKay, R. H. Meen and G. F. Wright, *J. Am. Chem. Soc.*, **70**, 430 (1948).
e) The asymmetric yield was calculated from the conversion of methyl 3-hydroxybutyrate to the corresponding ester.
f) G. Senter, A. M. Ward, *J. Chem. Soc.*, **125**, 2142 (1924). The product was hydrolyzed and the asymmetric yield was measured in alcohol.
g) The product is 2,4-pentanediol and the optical resolution of it is in progress.
h) Pure methyl levulinate could not be obtained and the asymmetric yield was calculated by induction of the product to γ-valerolactone.

Experimental

The procedures for the preparation of modified Raney nickel catalyst and for the hydrogenation of the substrate were the same as have been reported in previous papers. The hydrogenation products were purified by distillation, and the optical rotations of the products were measured without dilution in a 1-dm tube. Esters of acetoacetic acid were prepared from diketene and the corresponding alcohols.[12]

12) A. Treibs and K. Hintermeier, *Chem. Ber.*, **87**, 1163 (1954).

Results and Discussion

The modifying conditions and the results are shown in Table 1. In general, it will be seen that better results are obtained in the asymmetric hydrogenation of β-ketoesters or β-diketone, such as esters of acetoacetic acid, ethyl benzoylacetate, and acetylacetone, the enol isomers of which are fairly stable. On the other hand, the asymmetric yields are very low in the hydrogenation of ketones without a β-carbonyl group and, hence, without the stable enol isomer, ketones such as mono-

ketone, ethyl pyruvate, diethyl α-ketoglutarate, methyl levulinate and diacetyl.

In the asymmetric hydrogenation of monoketone, the effect of the modifying pH on the asymmetric activity of the catalyst shows a tendency similar to that observed in the asymmetric hydrogenation of methyl acetoacetate. In the hydrogenation of the esters of acetoacetic acid, those esters with a bulkier alkoxyl moiety gave lower asymmetric yields of the products, the esters of 3-hydroxybutyric acid.

Recently, Petrov *et al.*[13] have reported the asymmetric hydrogenation of ethyl acetoacetate, following the methods of our studies with methyl acetoacetate and using a catalyst prepared by our method. Some of their results agree with those included in the present table, confirming that our results are reproducible.

More detailed results and a discussion of the mechanism of the asymmetric hydrogenation of the carbonyl group will be presented in this Bulletin in the near future.

This research was supported by the Kawaken Fine Chemicals Co., Ltd., Tokyo.

13) Yu. I. Petrov, E. I. Klabnovskii and A. A. Balandin, *Kinetika i Kataliz*, **8**, 814 (1967).

BULLETIN OF THE CHEMICAL SOCIETY OF JAPAN VOL. 42 243—244 (1969)

Contact Potential in Vacuum for Titanium Dioxide Powder

Takeaki IIDA and Hiroshi NOZAKI

The Institute of Industrial Science, The University of Tokyo, 7-2-1, Roppongi, Tokyo

(Received March 15, 1968)

Titanium dioxide is well-known as a pigment. It is considered that the chalking phenomena of titanium dioxide paint have something to do with the behavior of adsorbates on the pigment surface. In the case of zinc oxide, both the photoelectric and the thermoelectric work function have already been determined by measurements of the external photoelectric effect[1] and contact potential[2] respectively, while the behavior of adsorbates has been considerably clarified by many experimental results.[3] However, in the case of titanium dioxide, the surface potential and the surface photovoltage have not been studied, and the behavior of adsorbates has not been clarified as yet. Hence we measured changes in the contact potential and the surface photovoltage of titanium dioxide powder by changing the atmosphere around the layer. These phenomena have significance especially in discussing the surface behavior of titanium dioxide powder.

Experimental

Titanium dioxide powder, which is of a special grade (the impurities are given as follows: Fe$<$0.001%, Pb$<$0.002%, As$<$0.0005%) and the crystal size of which is about 0.1—0.5μ, was dispersed in alcohol and spread uniformly on a 7×7 cm^2 aluminum plate. These specimens were dried at 100°C for 2 hr, and then left in a dark chamber for 48 hr or more. These layers were between 15 and 25 μ thick. The contact potential was measured by the Kelvin method using a nesa glass electrode. The sample was placed in a vacuum vessel, in which there was silicone grease and where a diffusion pump was used. The nesa glass electrode was vibrated by an oscillator at 1 kc/sec. The specimen was exposed to a tungsten lamp without any filters. All the measurements were made at room temperature by the following procedures. After the air in the vessel had been slightly evacuated, the pressure was kept at a given pressure for 2 hr. When the surface potential reached a stable value, we measured the surface potential. The pressure range studied was from normal air pressure to 10^{-5} mmHg. After evacuation to 10^{-5} mmHg, foreign gas was introduced into the system, and the photovoltage of the layer was measured by illuminating the sample surface with a white light of 480 lux.

Results

Figure 1 shows the curves of the surface potentials of rutile and anatase in the dark against the air pressure. The dotted line represents the potential of gold, which corresponds to the work function of 4.8 eV. It may be seen that the surface potential of rutile has a minimum at a pressure around 40 mmHg, and that the surface potential increases with the decrease in air pressure between 10 and

1) F. I. Vilesov, *Soviet Phys. Doklady*, **6**, 1078 (1962); F. I. Vilesov, *Naturwiss.*, **46**, 167 (1959).

2) A. Terenin and J. Akimov, *Z. Phys. Chem. (Leipzig)*, **217**, 307 (1961).

3) W. Doerffler and K. Hauffe, *J. Catalysis*, **3**, 156 (1963).

10^{-4} mmHg, gradually reaching 50—100 mV above the Au-potential at a pressure of 10^{-5} mmHg. The surface potential of anatase was about 400 mV higher than that of the rutile layer in atmospheric air, and monotonously increased with the decrease in air pressure.

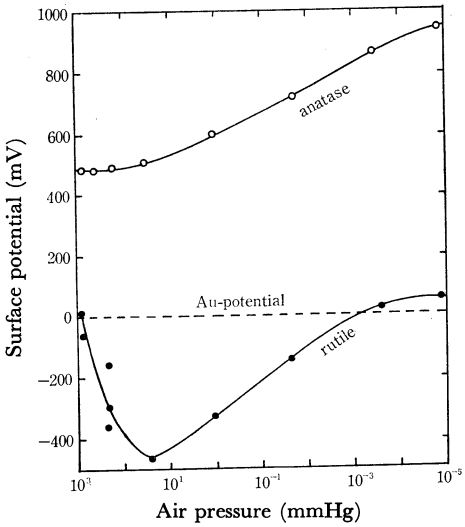

Fig. 1. Surface potential of the rutile and anatase layers in the dark against the air pressure.

In Fig. 2, the surface photovoltages of the rutile layer in various ambients are shown. On irradiation, a large photovoltage, 500 mV, was observed with a quick response in the vacuum of 3×10^{-4} mmHg. However, in dry air at normal pressure, the photovoltage amounted to 240 mV. Moreover, in wet air (relative humidity of 75%), the photovoltage has a very small value, 30 mV.

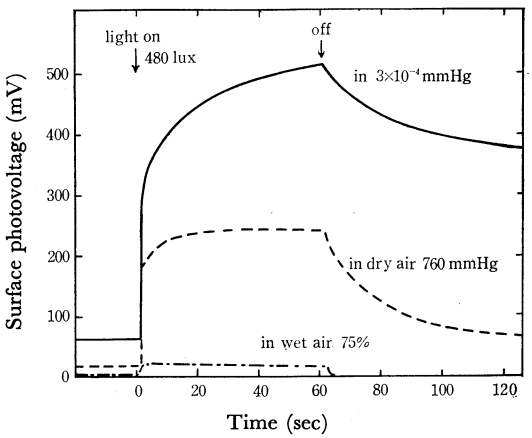

Fig. 2. Surface photovoltage of the rutile layer in various ambients.

Discussion

The adsorbates on the titanium dioxide surface at normal air pressure are considered to be oxygen and water. It has been recognized by ESR that oxygen chemisorbs on the titanium dioxide surface as a negative ion, O_2^-.[4] Therefore, if the air pressure around the layer is decreased, the adsorption equilibrium of oxygen slightly deviates from that at the normal air pressure. Then the surface potential increases with a decrease in air pressure. On the other hand, the behavior of water on the titanium dioxide surface has not yet been clarified. However, in the case of zinc oxide, the behavior of water on the surface has been studied to some extent, and it has been recognized that water chemisorbs on the zinc oxide surface donatively.[5] We assume that the same is the case with titanium dioxide. Therefore, the surface potential decreases if water desorbs from the surface. Figure 1 shows that the change in the surface potential of rutile resembles that of zinc oxide.[6] Therefore, the change in the surface potential of rutile in Fig. 1 means that the water on the surface desorbs first; after that, a part of the oxygen gradually desorbs from the surface. On the basis of these results only, we can not determine the absolute work function of titanium dioxide, because some other adsorbates remain on the suface even at the pressure of 10^{-5} mmHg. In the case of anatase, the minimum peak is not observed. This fact can not be explained easily on the basis of these results only.

The photovoltages observed under the illumination of a white light may be attributed to the desorption of oxygen. Therefore, these phenomena greatly depend on the ambient atmosphere around the layer. In the case of a vacuum of 3×10^{-4} mmHg, the photovoltage reaches a value as high as 500 mV. In wet air, however, the photovoltage greatly decreases. These phenomena indicate that the surface of titanium dioxide is greatly affected by the adsorption of water. Moreover, the rate of the dark decay of the surface photovoltage is slow in a vacuum, but quick, at normal air pressure. It may be said that the rate of the readsorption of oxygen, which is desorbed by light, is low in a vacuum and high at normal air pressure.

The authors wish to thank Mr. Isao Tashiro of the Rikoh Co., Ltd., for giving many useful suggestions about the measurement of the contact potential.

4) R. D. Iyengar, M. Codell, J. S. Karra and J. Turkevich, *J. Am. Chem. Soc.*, **88**, 5055 (1966).

5) H. Hasebe and E. Inoue, *Nippon Kagaku Zasshi (J. Chem. Soc. Japan, Pure Chem. Sect.)*, **87**, 332 (1966).

6) I. Tashiro, T. Kimura, M. Kuwahara and G. Ohno, *Electrophotography*, **8**, 2 (1967); Y. Takahashi and S. Miyaki, *ibid.*, **6**, 16 (1965).

BULLETIN OF THE CHEMICAL SOCIETY OF JAPAN VOL. 42 245—247 (1969)

A Systematic Cation Exchange Separation with Oxalate

Toru NOZAKI, Osamu HIRAIWA, Chujiro HENMI and Kunji KOSHIBA

Department of Industrial Chemistry, Faculty of Engineering, Ehime University, Matsuyama-shi

(Received April 1, 1968)

A few years ago, one of the authors had an interest in oxalatocomplexes and reported spectrophotometric[1-3] and polarographic[4] investigations of several oxalato complexes. Recently, knowledge on stability constants of oxalato metal complexes has accumulated,[5] while only relatively few cation exchange separations with oxalate as an eluting agent have been reported.[6] The present paper contains a systematic, preliminary study of cation exchange separations of nineteen metallic elements with oxalate as an eluting agent. This investigation covered the range of pH 2 to 5 and concentration 0.01 to 0.5 M for the eluant.

It was found that these elements can be roughly classified into three groups according to their ion-exchange behavior. As examples, mutual separations of several metals were carried out.

Experimental

Standard Solutions of Metals. Perchlorates of Be, Al, Ga(III), In(III), Zr, Hf, Th, Fe(III), Co(II), U(VI), Cu(II), Zn, Cd, Mn(II) and Ni, chlorides of Sn(IV), Ti(IV) and Cr(III) and the nitrate of Pb(II) were dissolved in water containing minimum amounts of perchloric, hydrochloric and nitric acid, respectively, sufficient to suppress their hydrolysis and diluted to the concentration of 1×10^{-2} M with distilled water.

Eluting Agents. Oxalate solutions of 0.01, 0.02, 0.05, 0.1, 0.2, 0.4 and 0.5 M adjusted to pH 2.0, 3.0, 4.0 and 5.0, respectively, using a pH meter, were used. All reagents used were of guaranteed grade.

Resin and Column. The resin used was 60—100 mesh "Amberlite IR-120" in ammonium form. The resin bed of the column was 10 cm in height and 0.9 cm in diameter. Each column was preconditioned with 2 N hydrochloric acid, and 0.2 M ammonium chloride solution was passed through the resin bed for conversion to the ammonium form.

Decomposition of Oxalic Acid. For the chelatometric or colorimetric determination of the metals, except for Zn, Mn(II) and Cd, interfering oxalate in solution was eliminated. Various investigations indicated that the method of decomposition of oxalic acid by oxidation with ammonium peroxodisulfate was most suitable. Into a 100-ml flask, 10 ml of 0.1 M oxalate solution and 2.5 ml of 10% ammonium peroxodisulfate was taken, and about 40 ml of distilled water added. Being boiled for 5 to 10 min, the oxalate decomposed. Further, heating was continued for about an hour to decompose excess ammonium peroxodisulfate.

Methods for the Determination of the Metals. The concentrations of Be, Ti(IV) and Cr(III) were determined colorimetrically by the quinalizarine, hydrogen peroxide and chromate methods, respectively. For the other elements, chelatometric titration was used.

Distribution Coefficients. In order to find favorable conditions and a criterion for the separation of the metals adsorbed in the resin bed by elution with oxalate solution, the magnitude of the distribution coefficients

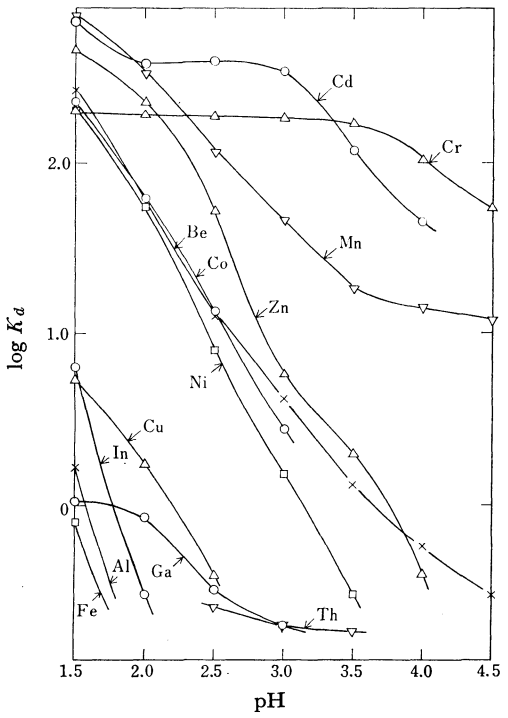

Fig. 1. Distribution coefficients in 0.1 M oxalate.

1) T. Nozaki and H. Kurihara, *Nippon Kagaku Zasshi (J. Chem. Soc. Japan, Pure Chem. Sect.)*, **82**, 707 (1961).

2) H. Kurihara and T. Nozaki, *ibid.*, **83**, 708 (1962).

3) H. Kurihara and T. Nozaki, *ibid.*, **83**, 1246 (1962).

4) T. Nozaki, T. Mise, T. Akiyama and K. Yamamoto, *ibid.*, **86**, 925 (1965).

5) K. V. Krishnamurty and G. M. Harris, *Chem. Revs.*, **61**, 213 (1961).

6) H. Kakihana and K. Narita, "Saishin Ion Kokan (The Newest Ion Exchange)," Hirokawa Shoten, Tokyo (1961).

7) J. I. Watters and R. de Witt, *J. Am. Chem. Soc.*, **82**, 1333 (1960).

Table 1. Classification of metallic elements

	pH of eluant	Elution range (m*l*)	log K_d	Elements
Group I	2.0	0—120	<1	Cu(II), Al, Ga, In, Fe(III), Sn(IV) Ti(IV), Zr, Hf, U(VI), (Th)
Group II	3.0	10—180	<1	Be, Zn, Ni, Co(II)
Group III	3.0	220—	>1	Cd, Mn(II), Pb(II)

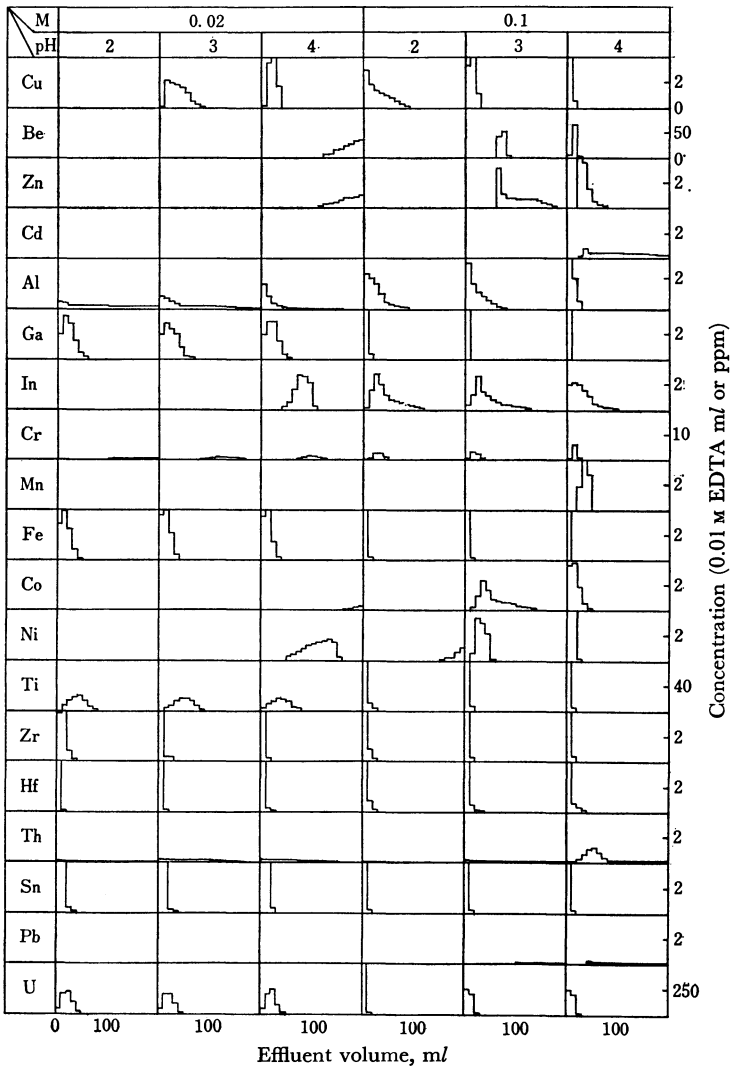

Fig. 2. Elution curves.

was measured by a batch method at varying concentrations and values of pH of oxalate solution. Into a 50-m*l* volumetric flask, 30 m*l* of the oxalate solution of varying concentration from 0.01 to 0.4 M and 10 m*l* of standard metal solution were taken, followed by adjustment of pH to a value between 2.0 and 4.0 with ammonia-water or perchloric acid, and 500 mg of air-dried resin was added and the solution diluted to the mark with distilled water. After standing for 24 hr at 25°C, the concentration of the metal in the aqueous phase was determined.

Elution Curves. Each solution containing about 10^{-4} mol of a metallic element was added to the top of the column. After washing the column with 2 m*l* of water twice, the eluant was passed through the column at a flow rate of 0.5 m*l*/min, and 10 m*l* of the effluent collected with a fraction collector. Each fraction being transferred to a 100-m*l* flask, the concentration of the metal in the fraction was determined after decomposition of the oxalato complex and excess oxalate with ammonium peroxodisulfate.

Results and Discussion

Some of the results on the distribution coefficients and elution curves are shown in Figs. 1 and 2, respectively. The elements investigated can be roughly classified into three groups in Table 1 according to their ion-exchange behavior which is reflected in the pH-distribution coefficient curves.

As shown in Fig. 2, there are many cases where mutual separation seems possible. As examples, the results of mutual separations of several metals are shown in Fig. 3.

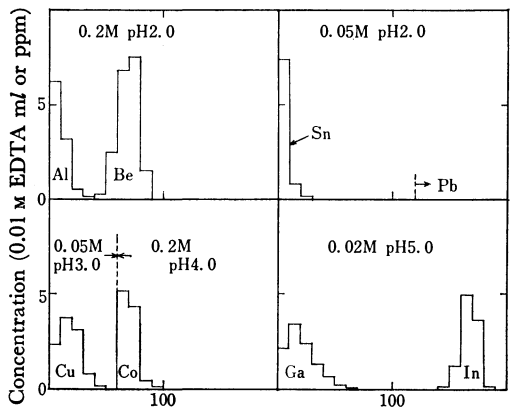

Fig. 3. Mutual separations.

Effect of pH. With 0.1 M eluant at pH 2.0, Be, Zn, Co(II), Mn(II) and Cd were not eluted until 200 m*l*, and Ni was not removed until 150 m*l* of effluent was reached. The rise in pH from 2.0 to 3.0 caused the beginning of elution of Be and Zn from 60 m*l*, and the elution of Ni and Co(II) from 20 m*l*, but Mn(II) and Cd did not elute until 200 m*l*.

Increasing the pH value to 4.0, Mn(II) and Cd began to elute from 30 m*l*.

Thus, the elutions of Be, Zn, Ni, Co(II) and Mn(II) were most sensitive to the pH value of the eluant, and next, those of Cu(II), Cd and Al were most sensitive. In addition, a shortening of the elution range with increase in pH of eluant to 3.0 or 4.0 was found especially with Cu, Zn, Al and Co(II).

Effect of Concentration. As shown in Fig. 2, the effect of concentration of eluant was not found to be great over the concentration range 0.2 to 0.05 M, but considerable delay in elution with 0.02 M eluant was found for In, Be, Zn, Co and Ni. In the case of Al, tailing was small with 0.2 M eluant at pH 2.0, whereas a decrease in concentration at the same pH caused greater tailing.

Table 2. Stability constants of metal-oxalato complexes

Metal	log K_1	log K_2	log K_3	Literature
Cd	2.78	1.60	0.98	4
Zn	5.15	2.21	1.15	5
Co(II)	4.7	2.0	3.0	5
Mn(II)	2.60	2.04	—	4
Ni	4.1	3.1	1.3	7
Al	7.25	5.75	3.3	5
Fe(III)	10.2	7.2	3.6	1
U(VI)	7.3	6.0	5.1	3

The elements in group 1, which are sharply eluted in 0—30 m*l* with 0.1 M eluant at pH 2.0, have large successive stability constants, whereas some elements in group 3 which show large tailing have smaller stability constants, as given in Table 2. Because of this for the latter elements, precipitates seem to form in the column and take much time to dissolve in the eluant at pH 3.0. Detailed mutual separations of the elements will be reported later.

The authors wish to thank Mr. M. Matsunaga and Mr. T. Kuribayashi for their assistance in the experimental work.

BULLETIN OF THE CHEMICAL SOCIETY OF JAPAN VOL. 42 248—250 (1969)

Interaction between Aldehyde and Tris(trimethylsiloxy)aluminum

Takeo SAEGUSA, Takashi UESHIMA and Sadao KITAGAWA

Department of Synthetic Chemistry, Kyoto University, Sakyo-ku, Kyoto

(Received April 10, 1968)

The syntheses and properties of aluminum silanolates and organoaluminum silanolates have been reported by several workers.[1-3] We have now compared their catalytic properties with those of metal alkyls and metal alcoholates in the polymerizations of aldehydes and cyclic ethers.[4,5] Tris(trimethylsiloxy)aluminum (I), $Al(OSiMe_3)_3$, was compared with aluminum *t*-butoxide (II) as a catalyst for the Tishchenko reaction,[6] which is closely related to the aldehyde polymerization.[7-9]

The Tishchenko reaction proceeds through a cycle of four steps:[7-9]

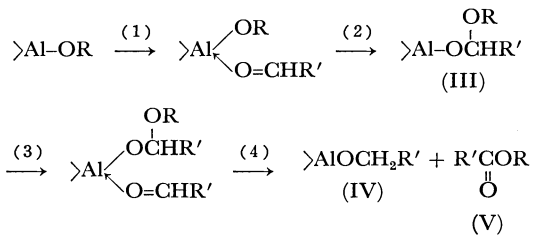

(1) The coordination of aldehyde with an aluminum alcoholate. (2) The transfer of the alkoxyl group to the carbonyl of aldehyde to form an aluminum alcoholate of hemiacetal (III). (3) The coordination of the second aldehyde molecule to the hemiacetal alcoholate. (4) Hydride transfer from the hemiacetal alcoholate onto the second aldehyde to produce an aluminum alcoholate (IV) and ester (V). After the first cycle, the so-called Tishchenko ester, $R'CO_2CH_2R'$ (VI), is continuously produced. We[5] disclosed previously that the reaction on *n*-butyraldehyde with I did not produce the silyl ester of *n*-butyric acid, which was expected from the above scheme, but did give the *n*-butyrate of the aldol of *n*-butyraldehyde as a by-product.[6] In this reaction aldol was first formed; it was then reacted with I to give its aluminum alcoholate, which in turn acted as an initiator of the Tishchenko reaction of *n*-butyraldehyde, producing *n*-butyl *n*-butyrate.

The present study was designed to examine the interaction of I with aldehyde along the lines of the above scheme of the Tishchenko reaction.

The coordination of *n*-butyraldehyde with I was demonstrated by the shift of the IR carbonyl band of aldehyde, $\Delta\nu_{C=O}$, caused by I (145 cm^{-1}); this shift was even greater than that caused by II (140 cm^{-1}). The corresponding values of $\Delta\nu_{C=O}$ for CCl_3CHO were 125 cm^{-1} and 114 cm^{-1} respectively. The coordination was also indicated by NMR; *i. e.*, the chemical shift of aldehyde hydrogen in the NMR of a mixture of benzaldehyde and I was found to depend upon their ratio. This observation corresponds to that in the NMR spectrum of the acetone-aluminum isopropoxide system.[10]

The siloxyl transfer from I to aldehyde was examined by means of study by the NMR spectrum. We have demonstrated previously that the hydrogen of the aluminum alcoholate of hemiacetal III shows a chemical shift different from that of the formyl hydrogen of the starting aldehyde.[11] In the NMR spectrum of a mixture of I and benzaldehyde in *n*-heptane at 20°C, no new signal was detected after 3 days. This observation may be taken as obviating the transfer of the siloxyl group to benzaldehyde. In chloral, however, the transfer of the siloxyl group to chloral does take place, as is indicated by the formation of $CCl_3CO_2SiMe_3$. The difference in reactivity between benzaldehyde and chloral toward the siloxyl transfer may be explained by the electron-withdrawing effect of the trichloromethyl group; *i. e.*, chloral is more electrophillic, and hence it is more reactive.

1) T. Saegusa, T. Ueshima, T. Nakajima and J. Furukawa, *Kogyo Kagaku Zasshi* (*J. Chem. Soc. Japan, Ind. Chem. Sect.*), **68**, 2514 (1965).

2) T. Saegusa, T. Ueshima and K. Kato. This Bulletin, to be published.

3) T. Saegusa, S. Kitagawa and T. Ueshima, *ibid.*, **40**, 1960 (1967).

4) J. Furukawa and T. Saegusa, "Polymerization of Aldehydes and Oxides," John Wiley & Sons, New York (1963).

5) J. Furukawa, T. Saegusa and H. Fujii, *Makromol. Chem.*, **44/46**, 398 (1961).

6) T. Saegusa, K. Hirota, E. Hirasawa and H. Fujii, This Bulletin, **40**, 967 (1967).

7) V. J. Shiner and D. Whittaker, *J. Am. Chem. Soc.*, **85**, 2337 (1963).

8) T. Saegusa, T. Ueshima, K. Kauchi and S. Kitagawa, *J. Org. Chem.*, in press.

9) T. Saegusa, K. Hirota, E. Hirasawa and H. Fujii, This Bulletin, **40**, 967 (1967).

10) V. J. Shiner and D. Whittaker, *J. Am. Chem. Soc.*, **85**, 2337 (1963).

11) T. Saegusa, T. Ueshima, K. Kauchi and S. Kitagawa, *J. Org. Chem.*, **33**, 3657 (1968).

Table 1. Reaction between aldehydes and aluminum compounds

Aldehyde	Reaction condition	Products (%) I		Products (%) II	
C_6H_5CHO	a	No reaction		$C_6H_5COOCH_2C_6H_5$	98
		No reaction		$C_6H_5COOC(CH_3)_3$	1.2[d]
CCl_3CHO	b	$CCl_3COOCH_2CCl_3$ (VII)	70.6	(VII)	0
		$CCl_3COOSi(CH_3)_3$ (VIII)	0.2[d]	$CCl_3COOC(CH_3)_3$ (IX)	0
				$>AlOCH(CCl_3)OC(CH_3)_3$[e]	41[d]
CCl_3CHO	c	VII	29.4		0.3
		VIII	0.2[d]		0.1[d]

a) Aldehyde 0.1 mol, aluminum compound 0.01 mol, *n*-heptane 10 m*l*, 20°C 3 days.
b) Aldehyde, aluminum compound, each 0.1 mol, *n*-heptane 40 m*l*, 30°C 13 days.
c) Aldehyde 0.1 mol, aluminum compound, 0.01 mol, benzene 50 m*l*, 80°C 10 hr.
d) Yield (%) based upon the initial aluminum.
e) The quantity was determined by the method described in the experimental section.

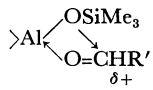

The hydride transfer from the alcoholate of silyl-hemiacetal to the coordinating aldehyde seems to occur quite easily. The formation of trimethylsilyl trichloroacetate from chloral and I implies the transfer of the hydrogen of the alcoholate of silyl-hemiacetal, $>AlOCHOSiMe_3$, to chloral in spite of the electron-withdrawing trichloromethyl group in the alcoholate. Therefore, the absence of the formation of n-$C_3H_7COOSiMe_3$ in the reaction of I with n-C_3H_7CHO may be ascribed to the lack of siloxyl transfer, but not to the lack of a hydride transfer reaction.

In the scheme from (1) to (4), the ester (V) consisting of the alkoxyl (or siloxyl) group which is originally attached to the catalyst was the key compound. The possibility of an ester exchange reaction between the catalyst alkoxyl group and the ester (VI) producing V has been eliminated by reference experiments; *i. e.*, a mixture of I or II and the VI ester under the same conditions did not give V. Furthermore, trimethylsilyl *n*-butyrate was found to be fairly stable; it does not decompose during the reaction.

In conclusion, the difference in catalyst behavior between I and II is due to the difference in transfer reactivity between siloxyl and alkoxyl groups. The lower reactivity of siloxyl transfer may be ascribed to a decreased nucleophilicity of the siloxyl group because of the electron-withdrawing effect of silicon through the $d\pi$-$p\pi$ bond. This assumption is supported by the lower basicity of trimethylsilanol compared with trimethylcarbinol.[12]

12) R. West and R. H. Baney, *J. Am. Chem. Soc.*, **81**, 6145 (1959).

Experimental

Materials. I and II were prepared and purified by procedures described before.[6] The benzaldehyde and chloral were commerical reagents which had been purified by repeated fractional distillations. Trimethylsilyl trichloroacetate, $CCl_3CO_2SiMe_3$, was prepared from sodium trichloroacetate and chlorotrimethylsilane by a procedure described before.[6]

$CCl_3CO_2SiMe_3$ is quite vulnerable to moisture and is readily hydrolyzed. The product was identified as follows. The NMR spectrum of $CCl_3CO_2SiMe_3$ shows a sharp singlet at 0.40 ppm (δ) assignable to protons of Si–CH_3. The product, 0.5375 g, was decomposed with water, and hexamethyldisiloxane was extracted with ethyl ether and analyzed by vpc. The CCl_3CO_2H in the water layer was titrated with 1/10 N NaOH. $Me_3SiOSiMe_3$.

Found: 0.1834 g. Calcd: 0.1852 g. Acidity, Found: 2.298×10^{-3} mol. Calcd: 2.282×10^{-3} mol.

The 2,2,2-trichloroethyl trichloroacetate was prepared by the method described in the literature.[13]

Products Analyses. The products were identified by vpc using two columns (PEG 20000 and Silicone DC 550). Silicone DC 550 and dioctyl phthalate were used for the identification of $CCl_3CO_2SiMe_3$.

Reactions of Chloral. A representative procedure was as follows. A mixture of 0.01 mol of chloral, 0.01 mol of I, and 40 m*l* of *n*-heptane was kept in a sealed tube at 30°C for 13 days. In order to avoid the hygroscopic decompsotion of the products, the reaction mixture was directly analyzed by vpc. The products were $CCl_3CO_2CH_2CCl_3$ (70.6%) and $CCl_3COOSiMe_3$ (0.21%). In the case of the reaction with aluminum *t*-butoxide, no reaction product was detected by vpc analysis. When the reaction system was treated with excess acetic anhydride and was subjected to vacuum distillation, 41% of $AcOCH(CCl_3)OCMe_3$ was obtained.

Found: C, 36.71; H, 5.18; Cl, 40.46%. Calcd for $C_8H_{13}O_3Cl_3$: C, 36.46; H, 4.97; Cl, 40.36%.

The NMR and IR spectra were compatible with this structure. The formation of this compound clearly

13) R. Dworzak, *Monatsh*, **47**, 11 (1927).

indicates the presence of $>Al-O-\underset{\underset{CCl_3}{|}}{\overset{\overset{H}{|}}{C}}-OCMe_3$.

Reaction of Benzaldehyde. A procedure similar to the above was adopted. After the reaction, the products were identified and determined quantitatively by vpc analysis without any after-treatment. In the case of I, no reaction product was found. In the NMR spectrum of the I-benzaldehyde system after the reaction, no signal except for those assignable to the starting reagents was recognized.

BULLETIN OF THE CHEMICAL SOCIETY OF JAPAN VOL. 42 250—252 (1969)

Reaction of Tetraethyl α-Phosphonodicarboxylates with Carbonyl Compounds

Kikumasa SATO, Masao HIRAYAMA and Takashi INOUE

Department of Applied Chemistry, Faculty of Engineering, Yokohama National University, Minami-ku, Yokohama

and Shoji KIKUCHI

Konishiroku Photo Industry Co., Ltd., Hino, Hino-shi, Tokyo

(Received April 20, 1968)

While the reaction of triethyl phosphonoacetate with carbonyl compounds has been well investigated,[1a-c] little attention has been paid to the reaction of tetraethyl α-phosphonodicarboxylates (I) with carbonyl compounds. Wadsworth[2] has reported the reaction of tetraethyl α-phosphonosuccinate with benzaldehyde to give diethyl α-benzylidenesuccinate. On the other hand, a survey of the literature has indicated that a general procedure for preparing diethyl α-alkylidenedicarboxylates (IV) has not yet been reported. Although α-alkylidenesuccinates[3] and glutarates[4] have been prepared by the Stobbe condensation reaction in a single-stage, the preparations of higher α-alkylidenedicarboxylates have dealt almost exclusively with the Reformatskii[5a,b] and Grignard[6] reactions. However, these methods have the disadvantage of low yields.

In connection with the total synthesis of phytol,[7] we have demonstrated that the triethyl phosphonocrotonate anion reacts with carbonyl compounds to give the corresponding α,β-,γ,δ-unsaturated esters. These studies suggest that tetraethyl α-phosphonodicarboxylate anions (II) may also condense with carbonyl compounds to give IV in a single-stage; if so, this reaction would be a more useful method for preparing IV. In the present paper, we have studied the reaction of I with carbonyl compounds in order to develop a new method of preparing IV.

The Michaelis-Arbuzov reactions of diethyl α-bromodicarboxylates with triethyl phosphite were all carried out at 155—160°C; they gave I (n=2, 3,7) in 59—75% yields. These compounds were identified by their elemental analyses and by a study of their infrared spectra. The results are summarized in Table 1.

Table 1. Reaction of diethyl α-bromodicarboxylates with triethyl phosphite

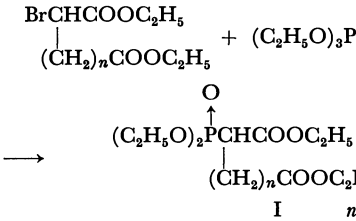

I n=2, 3, 7

I n	Bp °C/mmHg	Yield %	n_D^{20}	Analysis, % Found C	Found H	Calcd C	Calcd H
2	124/0.2	59	1.4445	47.87	8.15	48.15	7.77
3	150/0.5	75	1.4403	49.33	8.73	49.70	8.04
7	106/0.1	59	1.4479	54.98	8.95	54.81	8.94

1) a) H. Takahashi, K. Fujiwara and M. Ohta, This Bulletin, **35**, 1498 (1962). b) B. G. Kovalov, L. A. Yanovskaya and V. F. Kucherov, *Izv. Akad. Nauk SSSR, Otd. Khim. Nauk*, **1962**, 1876. c) L. A. Yanovskaya and V. F. Kucherov, *Izv. Akad. Nauk SSSR, Ser. Khim.*, **1964**, (7) 1341.

2) W. S. Wadsworth and W. D. Emmons, *J. Am. Chem. Soc.*, **83**, 1733 (1961).

3) B. Wojcik and H. Adkins, *ibid.*, **56**, 2424 (1934).

4) W. H. Puterbaugh, *J. Org. Chem.*, **27**, 4010 (1962).

5) a) W. Treibs and G. Leichssenring, *Chem. Ber.*, **84**, 52 (1951). b) R. Gelin and S. Gelin, *Compt. Rend.*, **255**, 1400 (1962).

6) R. Mayer and W. Treivs, *Chem. Ber.*, **87**, 349 (1954).

7) K. Sato, S. Mizuno and M. Hirayama, *J. Org. Chem.*, **32**, 177 (1967).

When phosphonate anions II (n=2,3,7), prepared by adding I to a slurry of sodium hydride in dry tetrahydrofuran (THF), were treated with carbonyl compounds, the corresponding α-alkylidenedicarboxylates, IV (n=2,3,7), were obtained in 10—86% yields. Phosphonate anions, II, reacted exothermically with benzaldehyde even at low temperatures to give the corresponding α-benzylidenedicarboxylates (IVa) (n=2,3,7) in good yields. Similarly, the reactions of II with aldehydes, such as propionaldehyde and p-toluoxyacetaldehyde, were carried out smoothly to give the corresponding α-propylidene- (IVb) and α-(p-toluoxyethylidene)-dicarboxylates (IVc) (n=2,3,7) in good yields. In contrast, the reaction with acetone resulted in a low yield of diethyl α-isopropylidenedicarboxylates (IVd) (n=2,3,7), and acetophenone failed to react with II at all. The results are summarized in Table 2.

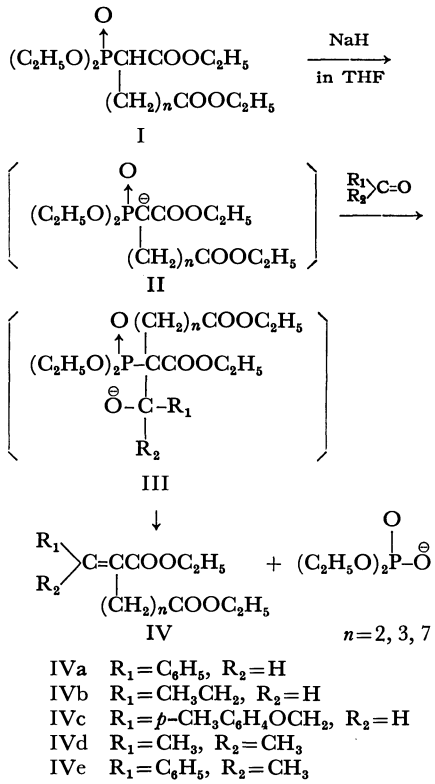

IVa $R_1=C_6H_5$, $R_2=H$
IVb $R_1=CH_3CH_2$, $R_2=H$
IVc $R_1=p\text{-}CH_3C_6H_4OCH_2$, $R_2=H$
IVd $R_1=CH_3$, $R_2=CH_3$
IVe $R_1=C_6H_5$, $R_2=CH_3$

Recently Yanovskaya and her co-workers[1c] reported that triethyl phosphonoacetate did not react with diisopropyl ketone or di-t-butyl ketone, and that the reaction of triethyl phosphonoacetate with methyl t-butyl ketone gave ethyl 3,4,4-trimethyl-2-pentenoate in a poor yield. In explaining their data and also the results summarized in Table 2, the mechanism suggested by Wadsworth[2] can be applied to the behavior of carbonyl compounds toward II; such an application indicates that II is less reactive to ketones, which can find it difficult to take the intermediate III because of the steric hindrance, than to aldehydes, which can readily take III. The products IV (n=2,3,7) were confirmed by their elemental analyses and by a study of their infrared spectra, which showed two ester carbonyl absorptions of the α,β-unsaturated ester carbonyl group and the normal ester carbonyl group, in addition to the double-bond absorption.

In comparison with the Reformatskii reaction, the reaction using phosphonate anions, II, proceeds smoothly under mild conditions and, especially in the case of the reactions with aldehydes, gives the products in good yields. Therefore, the reaction is a useful method of preparing IV.

Table 2. Reaction of tetraethyl α-phosphonodicarboxylates (I) with carbonyl compounds

I, n	Aldehydes or ketones		Reaction condition		Product	Yield, %
	R_1	R_2	Temp., °C	Time, hr		
2	C_6H_5	H	0—5	3	IVa	84
	CH_3CH_2	H	0—5	2	IVb	53
	$p\text{-}CH_3C_6H_4OCH_2$	H	−25——20	1	IVc	70
	CH_3	CH_3	−10—5	15	IVd	21
	C_6H_5	CH_3	−10—room temp.	15	IVe	0
3	C_6H_5	H	0—5	3	IVa	86
	CH_3CH_2	H	0—5	3	IVb	54
	$p\text{-}CH_3C_6H_4OCH_2$	H	−20——15	2	IVc	77
	CH_3	CH_3	−10—5	15	IVd	10
	C_6H_5	CH_3	−10—room temp.	15	IVe	0
7	C_6H_5	H	0—5	3	IVa	79
	CH_3CH_2	H	0—5	3	IVb	56
	$p\text{-}CH_3C_6H_4OCH_2$	H	−20——15	2	IVc	61
	CH_3	CH_3	−10—5	15	IVd	35
	C_6H_5	CH_3	−10—room temp.	15	IVe	0

Experimental[8]

Materials. The triethyl phosphite was prepared by the procedure described by Ford-Moor and Perry.[9] The diethyl α-bromodicarboxylates were obtained by the method of Teichmann[10] in 30—40% yields.

Tetraethyl α-Phosphonoadipate (I, $n=3$). Typical Procedure for a Tetraethyl α-Phosphonodicarboxylates (I). A mixture of diethyl α-bromoadipate (26.4 g, 0.094 mol) and triethyl phosphite (20 g, 0.12 mol) was heated with stirring for 5 hr at 150—160°C. The distillation gave a 74.8% yield of (I, $n=3$), bp 150°C/0.5 mmHg, n_D^{20} 1.4403.

Found: C, 49.33; H, 8.73%. Calcd for $C_{14}H_{27}O_7P$: C, 49.70; H, 8.04%.

The Reaction of Tetraethyl α-Phosphonoadipate with Benzaldehyde. Typical Procedure for the Reaction of Tetraethyl α-Phosphonodicarboxylates with Carbonyl Compounds. Tetraethyl α-phosphonoadipate (15 g, 0.044 mol) was added, drop by drop at 0—5°C, to a slurry of 50% sodium hydride (2.4 g, 0.05 mol) in 100 m*l* of dry THF. After the addition, the mixture was stirred for 2 hr until the evolution of hydrogen gas had ceased. Benzaldehyde (4.7 g, 0.044 mol) was then added to the mixture at the same temperature, and the mixture was stirred for 3 more hr. The excess THF having been evaporated, the mixture was taken up in an excess of water, neutralized, and extracted with ether. The ether layer, after being dried over calcium chloride and evaporated, gave a liquid residue. The residue was then distilled, giving 11.1 g of a clear liquid, bp 150°C/0.22 mmHg (lit.[5a] 169°C/1.5 mmHg), 86% yield n_D^{20} 1.5170. The infrared spectrum of the product contained bands at 1620 cm^{-1} (C=C), 1730, and 1705 cm^{-1} (C=O).

Found: C, 70.39; H, 7.98%. Calcd for $C_{17}H_{22}O_4$: C, 70.32; H, 7.64%.

Table 3. Physical constants and analytical characteristics of products

Compound		Bp °C/mmHg	n_D^{20}	IR cm^{-1}			Analyses, %			
				C=O	C=O (conju.)	C=C	Found		Calcd	
							C	H	C	H
$n=2$	IIIa	126/0.2	1.5231	1735	1710	1630	69.40	7.63	69.55	7.30
	IIIb	80/0.2	1.4510	1740	1710	1650	62.98	8.85	63.14	8.83
	IIIc	155/0.2	1.5072	1735	1710	1650	67.25	7.84	67.38	7.55
	IIId	81/0.4	1.4496	1740	1715	1630	63.34	9.04	63.14	8.83
$n=3$	IIIa	150/0.2	1.5170	1730	1705	1630	70.39	7.98	70.32	7.64
	IIIb	95/0.4	1.4493	1730	1705	1635	64.33	9.45	64.44	9.15
	IIIc	156/0.2	1.4950	1730	1710	1645	68.08	8.14	68.24	7.84
	IIId	94—94.5/0.3	1.4486	1735	1710	1635	64.17	9.26	64.44	9.15
$n=7$	IIIa	161/0.15	1.5029	1740	1715	1635	72.80	8.73	73.30	8.94
	IIIb	125/0.3	1.4564	1740	1715	1635	68.32	10.13	68.42	10.13
	IIIc	188/0.2	1.4976	1735	1710	1650	70.09	9.06	69.81	9.05
	IIId	137/0.2	1.4592	1735	1710	1635	68.46	10.39	68.42	10.13

8) All boiling points are uncorrected. Infrared spectra were recorded on a Hitachi Model EPI-S2 spectrophotometer. Gas chromatographic analyses were carried out on a Shimadzu Model GC-1C chromatograph.

9) A. H. Ford-Moor, "Organic Syntheses," Coll. Vol. IV, p. 955 (1963).

10) B. Teichmann, *Z. Chem.*, **5**(1), 18 (1965).

BULLETIN OF THE CHEMICAL SOCIETY OF JAPAN VOL. 42 253—255(1969)

Electrolytic Separation with Glassy-Carbon Electrodes Prior to Emission Spectrography: Determination of Traces of Silver in High-Purity Zinc

Atsushi MIZUIKE, Nobuhiko MITSUYA and Kunio YAMAGAI

Faculty of Engineering, Nagoya University, Chikusa-ku, Nagoya

(Received April 22, 1968)

In ultratrace analysis by emission spectrography, various chemical or physical separation methods are often used to remove matrix elements prior to the excitation step. These preconcentrations[1] are effective in improving sensitivity, precision and accuracy beyond those which direct excitation of the sample would achieve, provided that the separation loss and contamination due to reagents, vessels and the atmosphere are negligible. This paper describes electrolysis with glassy-carbon cathodes for concentrating 0.01 to a few ppm of silver in zinc metal prior to emission spectrography. Glassy-carbon,[2] a new form of carbon, has been employed in the electrodes for electrolytic separation[3,4] and emission spectrography,[5,6] because of its desirable properties compared with other carbonaceous electrode materials. In the proposed technique, traces of silver are electrodeposited on the end of a glassy-carbon rod from 0.5 to 1.5 N nitric acid solutions in greater than 90% yields, leaving about 99.999% of zinc in the electrolyte. The cathode is then used as an electrode for spark emission spectrography. After completion of the work, the authors found a report[7] describing a similar technique using high-purity graphite or pyrolytic graphite by Alvarez (presented at the 1st Materials Research Symposium held at the NBS, Gaithersburg, Md., in October 1966), although detailed information was not available.

Experimental

Apparatus. A Shimadzu quartz Littrow spectrograph QL-170 (Slit width used: 15μ). A Shimadzu universal excitation source SA-1 (The Feussner circuit was used at 10 kV, 0.0066μF, 0.08 mH and 10Ω). A Rigaku Denki microphotometer CM-1A.

Electrodes, Reagents, *etc.* Glassy-carbon electrodes: Tokai Electrode Manufacturing Co. GC-30S; 4 mmϕ × 40 mm cathodes and 5 mmϕ × 50 mm anodes, unless otherwise stated. They were polished with a series of emery papers of increasing fineness, then with a chromium oxide suspension (0.5 μ) on a rotary table polisher, and washed with nitric acid (1 : 1), followed by water. The cathode was inserted in open-ended polyvinyl chloride tubing (30 mm long) to limit the working area of the surface to the end (0.13 cm^2).

Counter electrodes: Hitachi spectroscopic graphite electrodes (regular, 6.15 mmϕ) were machined into a 60° cone.

Photographic plates: Fuji process panchromatic 101 mm × 252 mm plates.

Standard silver solutions: Prepared from silver nitrate. ^{110m}Ag solution: The Radiochemical Centre Amersham. $AgNO_3$ in HNO_3.

Purified zinc nitrate solution: A 25-m*l* solution containing 11.5 g of $Zn(NO_3)_2 \cdot 6H_2O$ was electrolyzed with two glassy-carbon electrodes (5 mmϕ × 100 mm with no plastic sheath; working cathode area ~5 cm^2) at the total applied voltage of 2.0 V for 24 hr to remove traces of silver. This solution was used to prepare synthetic samples. The Ag/Zn ratio in this solution was found to be 6×10^{-9}, or less than was found by a procedure described later.

All reagents used were of reagent grade. Water purified by distillation and ion exchange was used throughout the work.

Procedure. Place 5.0 g of zinc metal in a 100-m*l* beaker, add 44 m*l* of 6.5 N nitric acid and heat to dissolve. Cool the solution and dilute to 50 m*l* with water. Transfer an aliquot (1 to 5 m*l*) of the solution to an electrolysis cell (23 mm in diameter and 55 mm in height), and add water and 6.5 N nitric acid to give 8 m*l* of 1 N nitric acid solution. Insert two glassy-carbon electrodes into the cell, immersing them 5 mm into the solution. Cover the cell with a sheet of filter paper, stir the solution with a magnetic stirrer and apply 2.0 V *d. c.* between the electrodes using crocodile clips for electrical connections. After 20 hr of electrolysis, remove the cathode without breaking the current. Rinse the lower part of the cathode with water, remove

1) A. Mizuike, "Trace Analysis: Physical Methods," ed. by G. H. Morrison, Interscience, New York (1965), p. 103.
2) S. Yamada and H. Sato, *Nature*, **193**, 261 (1962).
3) A. Mizuike and N. Mitsuya, *Bunseki Kagaku* (*Japan Analyst*), **17**, 1259 (1968).
4) A. Mizuike, K. Fukuda and N. Mitsuya, *Radioisotopes* (*Tokyo*), **17**, 199 (1968).
5) G. Dümecke and J. Wiegmann, *Silikattechnik*, **16**, 287 (1965).
6) K. Morita, H. Sunahara, T. Ishizuka, N. Nakayama and S. Yamada, *Bunko Kenkyu*, **16**, 169 (1967).
7) G. H. Morrison, "Trace Characterization: Chemical and Physical," ed. by W. W. Meinke and B. F. Scribner, (Natl. Bur. Std. Monograph 100)(1967), p. 417.

the plastic sheath, rinse with water again and allow to air-dry. Prepare calibration standards by electrolyzing 1 N nitric acid containing known amounts (0.003, 0.01, 0.03, 0.1, 0.3, 1, 3μg) of silver by the same procedure as described above. Spark through a 3-mm gap between the silver-deposited and the counter (upper) electrode for 60 sec, and record the spectrum in the range of 2460 to 3480 Å on a photographic plate. Record the spectra of the calibration standards on the same plate. After photographic processing, measure the relative transmittance of the silver line 3280.683 Å against the background. Determine the amount of silver present by reference to a calibration curve (Seidel function *vs.* logarithm of quantity of silver) prepared from the calibration standards.

Results and Discussion

Electrolytic Separation of Silver. The conditions of electrolysis in the present work were developed from previous experiments.[3] In order to investigate the deposition rate and the recovery of silver, synthetic samples prepared from purified zinc nitrate, ^{110m}Ag and standard silver solutions were electrolyzed under conditions described previously. Aliquots (0.2 or 1 m*l*) were taken from the electrolyte during electrolysis, or from the 10-m*l* solution obtained by treating the cathode with 5 m*l* of hot nitric acid and water after electrolysis, and their gamma activities measured by means of a well-type scintillation counter. The results are shown in Fig. 1 and Table 1. Greater than 90% yields were achieved for 0.01 to a few μg of silver. About 2% of the total silver was adsorbed on the plastic sheath, and less than 1% deposited on the side of the cathode. Zinc accompanying silver was determined by square wave polarography, and found to be 4 μg when 500 mg of zinc was present before electrolysis.

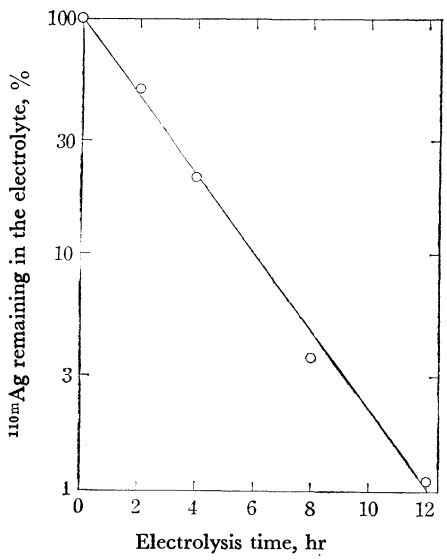

Fig. 1. Electrodeposition of silver on a glassy-carbon cathode from 8 m*l* of 1 N HNO_3 solution containing 0.05 μg of silver and 0.5 g of zinc.

Table 1. Electrodeposition of silver from nitric acid solutions

Free HNO_3 N	Zn present g	Ag present μg	Ag recovery* %
0.5	0	0.01	101
1	0	0.01	91
1.5	0	0.01	91
1	0	2	97
1	0.5	0.01	96
1	0.5	2	93

* By radioactivity measurement. error <3%.

Table 2. Determination of silver in synthetic samples

Zn present: 0.50 g. Analyses made on two separate days.

Ag added μg	Ag found μg
0	<0.003, 0.003
0.010	0.012
0.030	0.026
0.20	0.22
0.30	0.32*

* GC-20 grade glassy-carbon was used.

Table 3. Determination of silver in high-purity zinc metal

Zinc metal	Sample taken, g	Ag found μg	Ag in sample, ppm
99.999% purity*	0.10	0.18	1.8
	0.10**	0.30	2.0
	0.20	0.42	2.1
	0.50	1.00	2.0
			(av. 2.0)***
99.9998% purity	0.10	0.019	0.19
	0.20	0.054	0.27
	0.50	0.12	0.24
			(av. 0.23)

* Analyses made on two separate days.
** 0.10 μg of Ag was added before electrolysis.
*** 2.1 ppm by the photometric *p*-dimethylaminobenzylidenerhodanine method.[3]

Determination of Silver in Zinc. Synthetic samples prepared from purified zinc nitrate and standard silver solutions, and two samples of commercial high-purity zinc metal were analyzed, with the results given in Tables 2 and 3. The blank value through the entire procedure was less than 0.003 μg of silver. The calibration curves were linear over the range 0.003 to 3 μg of silver,

with a deviation of about ±10%. Although autoradiographs indicated that more silver electrodeposited near the circumference of the electrode, almost all the silver was evaporated from the electrode in the first 5-sec period of sparking. The lower limit of determination and the accuracy of the present method are about 0.01 ppm of silver in zinc, and about ±10% at the fractional to a few ppm level, respectively.

The authors are indebted to Dr. Kiyoshi Morita for help in part of the emission spectrography.

BULLETIN OF THE CHEMICAL SOCIETY OF JAPAN VOL. 42 255—257 (1969)

Reactive States of Acridine in Alcohols and the pK Value of T(n–π^*) State as judged from the pH Dependence of the Photoreduction Quantum Yield

Katsumi NAKAMARU, Shigeya NIIZUMA and Masao KOIZUMI

Department of Chemistry, Faculty of Science, Tohoku University, Katahiracho, Sendai

(Received April 23, 1968)

Previous work[1–5] on the photoreduction of acridine (A) in various alcohols has established that the reactive states are in general the singlet excited state S* and the triplet n–π^* state T_2 and that for each reactive state there are molecular (M) and radical (R) mechanisms; therefore generally speaking, four schemes, S*R, S*M, T_2R and T_2M participate in the reaction.

In this paper the similar problem is attacked from a different point of view for methanol, ethanol and isopropanol. As is well-known, pK_A of the ground state, S* and triplet π–π^*, T_1 are respectively 5.45,[6] 10.65[6] and 5.6[7] (for T_2, not known) and the acridinium ion (AH^+) is non-reactive;[8] hence, it is expected that the pH dependence of the photoreduction quantum yield, Φ reflects the pK_A's of the reactive state, provided the equilibrium state were realized in the excited state.

With such a view, the pH depencence of fluorescence and of Φ was investigated at first, using the water-alcohol mixture buffered with (CH_3COONa, HNO_3), (KH_2PO_4, Na_2HPO_4) and (Na_2CO_3, $NaHCO_3$). Taking into account the effect of alcohol on pH-values and Φ in the water-alcohol mixture, the volume ratio of water and alcohol was chosen as 2 : 1. The concentration of acridine was 1×10^{-4} M. Fluorescence was measured by an Aminco Bowman spectrofluorimeter. Since the fluorescence of AH^+ (peak at 470 nm) is very weak at the peak position of A (420 nm), the intensity at 420 nm was taken as the intensity of A. Reaction rate was investigated by illuminating the solution by 365 nm light and by measuring the intensity

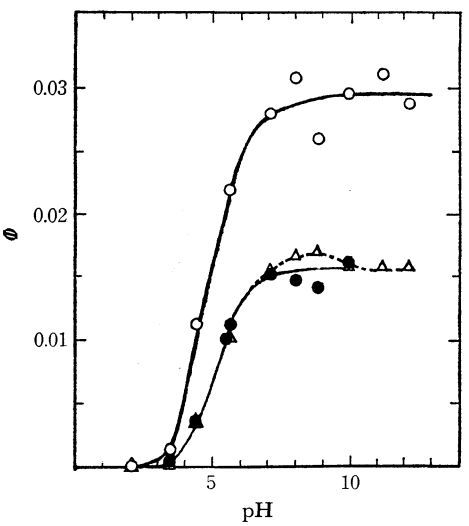

Fig. 1. pH dependence of Φ and I_F in water-ethanol (2:1 in vol).
[A] = 1×10^{-4} M Temperature: 25°C
—○— Φ, deaerated solution
—●— Φ, aerated solution
···△··· I_F, aerated solution

1) A. Kira, S. Kato and M. Koizumi, This Bulletin, **39**, 1221 (1966).
2) A. Kellmann, *J. chim. phys.*, **63**, 936 (1966).
3) A. Kira, Y. Ikeda and M. Koizumi, This Bulletin, **39**, 1673 (1966).
4) M. Koizumi, Y. Ikeda and H. Yamashita, *ibid.*, **41**, 1056 (1968).
5) M. Koizumi, Y. Ikeda and T. Iwaoka, *J. Chem. Phys.* **48**, 1869 (1968).
6) A. Weller, *Z. Elektrochem.*, **61**, 956 (1957).
7) G. Jackson and G. Porter, *Proc. Roy, Soc.*, **A260**, 13 (1961).
8) V. Zanker and H. C. Cnocloch, *Z. Naturforsch.*, **176**, 819 (1962).

of the transmitted 365 nm light.*1 In all cases $\ln(e^D-1)$ - t plot (D, optical density) was satisfactorily linear at least in the initial stage, showing that the reaction is simple with the rate only proportional to the light absorption.

The results, as shown in Fig. 1, clearly show the sharp change around pH ~5 for both the fluorescence intensity (I_F) and Φ. These results indicate that with the usage of the ordinary buffer solutions, the equilibrium in the ground state is still maintained in the excited state. A small change of I_F around pH 9.5 may be due to the quenching action of some inorganic ions. Twice as large Φ in the degassed solution as that in the aerated solution is interpreted to be due to the participation of S*R mechanism and perhaps also of T_2R in the reaction.

Since the acid-base equilibrium specific to the excited state was not realized in the ordinary buffer solution, it has been undertaken next, following Weller,[6] to use NH_4^+ as a proton donor for accelerating the proton transfer and to investigate the effect of $[NH_4^+]$ upon the fluorescence and upon Φ. Fixing $[NH_3]/[NH_4^+]=0.1$ (buffer consisting of NH_3 and NH_4NO_3, pH=8.2, $\log [AH^+]/[A]=-2.75$ in the ground state), the concentration of NH_4^+ was changed from 0.01 M to 2 M.

It was found that with the increase of $[NH_4^+]$, the fluorescence spectrum gradually changes from that of A to AH^+ with a clear isosbestic point, indicating the occurrence of Reaction $A^*+NH_4^+ \rightarrow AH^{+*}+NH_3$. The quenching constants of NH_4^+ for the fluorescence of A, in methanol, ethanol and isopropanol were respectively 2.7, 1.7 and 1.2.*2 Oxygen showed no quenching action. Φ was found also to decrease significantly by the increase of $[NH]_4^+$, as shown in Fig. 2. In this figure, I_F's (I_F at $[NH_4^+]=0.01$ M being normalized to the Φ-value at the same NH_4^+ concentration) are also plotted.

The very good agreement of the I_F- and Φ-plots for the aerated solutions for all alcohols, indicates that the reactive state in the aerated solution, is only S* (see below also). This is in complete agreement with the conclusion given in the previous paper.[4] In the aerated solution, radical mechanisms being eliminated, only S*M and T_2M mechanisms are possible, but the present results rule out the latter.

For the degassed solution, the S*R process contributes to the reaction, but this does not cause

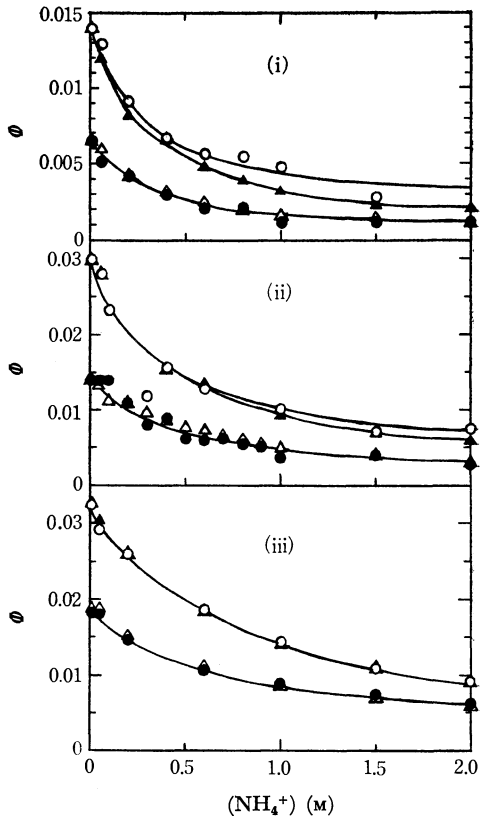

Fig. 2. Dependence of Φ and I_F on the concentration of buffer (NH_4NO_3-NH_3).
[A] = 1×10^{-4} M Temperature: 25°C
(i) water-methanol (2:1 in vol.)
(ii) water-ethanol (2:1 in vol.)
(iii) water-isopropanol (2:1 in vol.)
—○— Φ, deaerated solution
—●— Φ, aerated solution
—▲— I_F, deaerated solution
—△— I_F, aerated solution

any difference between the I_F- and Φ-plots; hence it is only necessary to discuss the participation of T_2. When T_2 participates in the reaction in addition to S*, Φ at $[NH_4^+]=0.01$ M and at an arbitrary value of $[NH_4^+]$ may be put as follows,

$$\Phi_0 = (k_r + k_{ST}f^0)/k_e + k_d + k_r \quad \text{for 0.01 M of } [NH_4^+] \qquad (1)$$

$$\Phi = (k_r + k_{ST}f + k_Q[NH_4^+]\varphi'_{ST}f')/ k_e + k_d + k_r + k_Q[NH_4^+] \qquad (2)$$

where k_e, k_d, k_r and k_{ST} are respectively the rate constant for emission, deactivation (including intersystem crossing), photoreaction and for intersystem crossing and where k_Q is the rate constant for Process $A^*+NH_4^+ \rightarrow AH^{+*}+NH_3$*3 and φ'_{ST} is

*1 The reaction product was judged from UV spectra to be acridan or the like in the aerated solution while in the degassed solution, diacridan was also produced, as judged from the appearance of white precipitate.

*2 These values may be correlated with the viscosity of the solvents (Viscosities of the three alcohols at 30°C are 0.51, 1.00 and 1.76 in the above sequence).

*3 The contribution of the backward reaction, $AH^+ + NH_3 \rightarrow A + NH_4^+$ may be neglected, since the I_{F_0}/I_F-$[NH_4^+]$ plot does not deviate much from the Stern-Volmer plot even at high NH_4^+ concentrations.

the intersystem crossing probability for AH^+. f_0 is a probability (an eventual fraction) for one A_{T_2} molecule produced from S*, to undergo reaction at $[NH_4^+]=0.01$ M. $f(f')$ is the similar probability for A_{T_2} ($AH^+{}_T$) (as to the assignment of $AH^+{}_T$, see below) at $[NH_4^+]>0.01$ M and $f=f_0$ ($f'=0$) or $f<f_0$ ($f'>0$), depending upon whether A_{T_2} ($AH^+{}_T$) produced from S* has no probability or some probability of going to $AH^+{}_T$ (A_{T_2}). The situations can be described quantitatively as follows. The ratio of the quantities of A_{T_2} and $AH^+{}_T$ produced from S* (per unit time), may be approximated as $k_{ST}/k_Q[NH_4^+]\varphi'_{ST}$ and according to the relation,

$$k_{ST}/k_Q[NH_4^+]\varphi'_{ST} \lessgtr ([A_{T_2}]/[AH_T^+])_{eq} = K_{T_2}/[H^+] \quad (3)$$

the values of f and f' will be specified as follows,

$$\begin{cases} f=f_0 \\ f'>0 \end{cases} (\text{for} <) \quad \begin{cases} f=f_0 \\ f'=0 \end{cases} (\text{for} =) \quad \begin{cases} f<f_0 \\ f'=0 \end{cases} (\text{for} >) \quad (4)$$

From (1) and (2) the following relation can be derived straightforwardly.

$$(\Phi/\Phi)/(I_F/I_{F_0}) = \frac{k_r + k_{ST}f + k_Q[NH_4^+]\varphi'_{ST}f'}{k_r + k_{ST}f_0} \quad (5)$$

Three cases are discriminated from (5),

case a): $(\Phi/\Phi_0) > (I_F/I_{F_0})$

case b): $(\Phi/\Phi_0) = (I_F/I_{F_0})$

case c): $(\Phi/\Phi_0) < (I_F/I_{F_0})$

depending upon the following criterion,

$$k_{ST}f + k_Q[NH_4^+]\varphi'_{ST}f' \lessgtr k_{ST}f_0 \quad (6)$$

which in turn, depends upon (4) and accordingly upon (3).

The correlation between (3) and (4) is, however, purely mathematical, and from the practical viewpoint, one may safely say as follows from (6) in conjunction with (3) and (4).

i) Case a) occurs when pK_{T_2} is much smaller than ~ 8 and φ'_{TS} is not so small. ii) Case b) occurs when pK_{T_2} is similarly small and $\varphi'_{ST} \approx 0$, or when S* is an only reactive state.*4

Turning back to the experimental results, case a) fits for methanol and ethanol, and case b) for isopropanol. From the above criterion, it is concluded that for isopropanol S* is an only reactive state and for methanol and ethanol, T_2 also participates in the reaction. The larger difference between (Φ/Φ_0) and (I_F/I_{F_0}) for methanol than for ethanol, as seen in Fig. 2, implies the larger contribution of T_2 in the former case. All these conclusions are in complete agreement with the ones in the previous paper.[4]

Furthermore, the present investigation strongly suggests that pK_{T_2} is much less than ~ 8. This view is further supported from the holding of case a) or case b) throughout the whole range of $[NH_4^+]$, because if pK_{T_2} is near ~ 8, (6) requires the change from case c) to case b) and further to case a) with the increase in $[NH_4^+]$.

The values of $k_Q\varphi'_{ST}f'/(k_r+k_{ST}f_0)$, as estimated from the plot $(\Phi/\Phi_0)/(I_F/I_{F_0})$ *vs.* $[NH_4^+]$ is 0.2—0.3 for methanol. Although these values are not very reliable, yet, there is no doubt that both φ'_{ST} and f' are quite large. This is very important for characterizing $AH_T{}^+$. Firstly, a large value of f' implies the rapid occurrence of Reaction $AH^{+*} \rightarrow A_{T_2} + H^+$, and this is only possible *via* some higher $T(\pi\text{-}\pi^*)$ state or $T(\sigma\text{-}\pi^*)$ state of AH^+. The former, however, is very unlikely, because Process $AH^+{}_T(\pi\text{-}\pi^*) \rightarrow A_T(n\text{-}\pi^*) + H^+$ is the one between different electronic states and may not favorably compete with the transition to the lowest $AH^+{}_T(\pi\text{-}\pi^*)$. Then the quite large value of φ'_{ST} implies that the $T(\sigma\text{-}\pi^*)$ state which in general is highly located, is in the present case, at least lower than AH^{+*}. It is worth while to add that the present technique, at least in principle, enables us to determine the pK value pertaining to $AH^+{}_T(\sigma\text{-}\pi^*) \rightleftarrows A_T(n\text{-}\pi^*) + H^+$.

The authors are gratefull to Professor H. Kokubun for fruitful discussion.

*4 Case c) holds when pK_{T_2} is much larger than 8 and φ'_{ST} is not so large.

BULLETIN OF THE CHEMICAL SOCIETY OF JAPAN VOL. 42 258—260 (1969)

Studies of Heteroaromaticity. XX.[1] Novel Thermal 1,3-Dipolar Cycloaddition of 5-Nitrofuran-2-carbohydroxamoyl Chloride with Diketene and Dicyclohexylcarbodiimide

Tadashi SASAKI and Toshiyuki YOSHIOKA

Institute of Applied Organic Chemistry, Faculty of Engineering, Nagoya University, Chikusa-ku, Nagoya

(Received April 30, 1968)

Ketenes sometimes undergo 1,3-dipolar cycloaddition reactions, but with such typical 1,3-dipoles as nitrones[2] and *N*-oxides,[3] diphenylketene reacts in a different manner, affording an isoxazolone derivative.[4] However, there have been no reports concerning the similar reactions of nitrile oxides with diketene, presumably because of its inertness. Since ketene is generally generated by the pyrolysis of diketene,[5] we attempted the thermal 1,3-dipolar cycloaddition of 5-nitrofuran-2-carbohydroxamoyl chloride (I)[6] to diketene. I was heated in toluene with an equivalent amount of diketene until the evolution of hydrogen chloride gas had ceased; this afforded a crystalline product, II, in a 20% yield, in addition to the recovered I, after purification on a silica-gel (Mallinckrodt, 100 mesh) column. The yield of II was improved to 60% by adding excess amounts of diketene at intervals. The results of elemental analysis and the spectral data support the identification of II as 3-(5-nitro-2-furyl)-5-methylisoxazole, an isomer of 3-(5-nitro-2-furyl)-4-methylisoxazole,[7] mp 146—149°C; it could unambiguously be discriminated from II by an NMR spectral comparison.[8] It is noteworthy that the thermal procedure proceeded, presumably through an expectable intermediate adduct, III, followed by the elimination of carbon dioxide, thus affording an isoxazole derivative, II, instead of isoxazolone. 5-Nitrofuran-2-carbonitrile *N*-oxide did not react at all with diketene under the reaction conditions given by Minami and Matsumoto.[7] Similar treatments of *m*- and *p*-nitrobenzcarbohydroxamoyl chloride with diketene afforded only intractable tars, though the evolution of hydrogen chloride gas was observed in the course of the reactions.

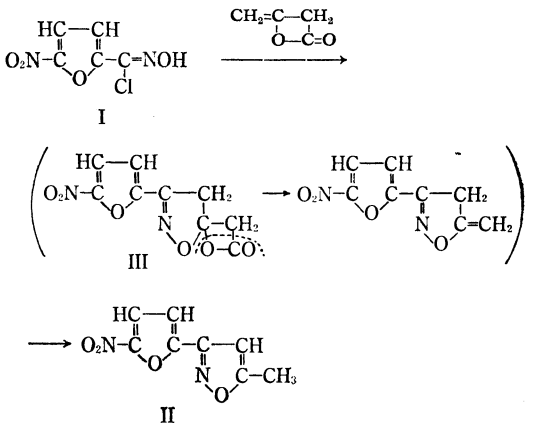

Another interesting example was observed in the 1,3-dipolar cycloaddition reaction of I with carbodiimides. Carbodiimides as dipolarophilic heterocumulenes are known to react with dipolar compounds like hydrazoic acid, diazomethane, and nitrile imines,[9] and quite recently, the addition of aromatic nitrile oxides to diphenylcarbodiimide in the presence of boron trifluoride etherate as a catalyst has been reported to afford a spiro-1,2,4-oxadiazole, IV, *via* a 1 : 1 adduct, V.[10]

I was heated in toluene with an equivalent amount of dicyclohexylcarbodiimide (DCC) until the evolution of hydrogen chloride gas had ceased. The worked-up product (VI) consisted of yellow crystals; the results of the elemental analysis and the spectral data support the idea that VI is 1,4-dicyclohexyl-3-(5-nitro-2-furyl)-4,5-dihydro-5-oxo-1*H*-triazole. This was further confirmed by its chemical conversion to the known *N*,*N*′-dicyclo-

1) Part XIX of this series: T. Sasaki and T. Yoshioka, This Bulletin, **41**, 2212 (1968).

2) C. H. Hassall and A. E. Lippman, *J. Chem. Soc.*, **1953**, 1059; H. Staudinger and K. Miescher, *Helv. Chim. Acta*, **2**, 554 (1919).

3) T. Koenig, *Tetrahedron Letters*, **1965**, 3127.

4) R. Scarpati and P. Sorrentino, *Gazz. Chim. Ital.*, **89**, 1525 (1959).

5) S. Andreades and H. D. Carlson, *Org. Synth.*, **45**, 50 (1965).

6) T. Sasaki and T. Yoshioka, This Bulletin, **40**, 2604 (1967).

7) S. Minami and J. Matusmoto, *Chem. Pharm. Bull. (Tokyo)*, **15**, 366 (1967).

8) NMR ($CDCl_3$) τ: 1.67 (doublet, 5-C–H).

9) H. Ulrich, "Cycloaddition Reactions of Heterocumulenes," Academic Press, New York, N. Y. (1967), p. 260, and the references cited therein.

10) C. Grundman and R. Richter, *Tetrahedron Letters*, **1968**, 963.

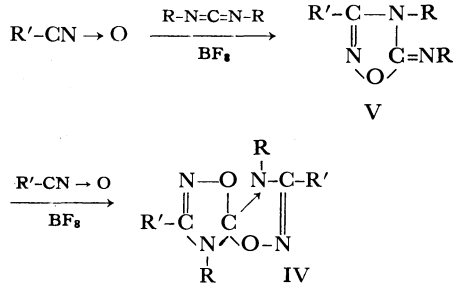

hexylurea[11] when its ethanolic solution was refluxed with sodium ethoxide. The similar thermal treatment of 5-nitrofuran-2-carboxaldehyde oxime (VII) with DCC and the normal treatment of 5-nitrofuran-2-carbonitrile oxide (VIII) with DCC in ether at room temperature both afforded 5-nitrofuran-2-carbonitrile (IX),[12] and no cyclization occurred. Considering the results given by

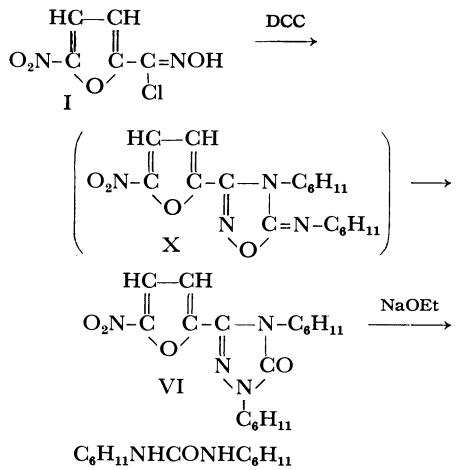

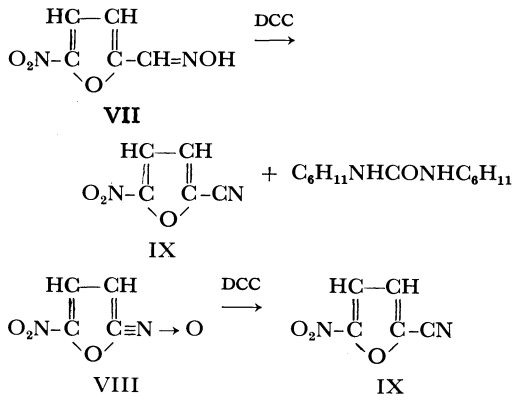

Grundman and Richter,[10] it seems reasonable to assume, in the reaction of I with DCC, that a 1 : 1 adduct like X might be produced as the first step and that this might then be thermally rearranged to VI. However, such a thermal rearrangement of oxadiazole to triazole has never been documented. Therefore, further investigation is necessary before the mechanism can be discussed in detail; this investigation is now being undertaken.

Experimental[13]

3-(5-Nitro-2-furyl)-5-methylisoxazole (II). I (0.88 g; 0.4 mmol) was treated with 1.0 g of diketene and 20 m*l* of toluene at reflux temperature for 18 hr, until the evolution of hydrogen chloride gas had ceased. After the removal of the solvent, the residue was dissolved in chloroform and chromatographed on a silica-gel column. 0.17 g (20%) of yellow crystals, mp 143—144°C, was obtained from the first fraction*1 after recrystallization from ethanol. UV λ_{max}^{EtOH} mμ (ε): 320 (14500). NMR ($CDCl_3$) τ: 2.56 (doublet, J=3.8 cps, 4-C–H of nitrofuran), 2.96 (doublet, J=3.8 cps, 3-C–H of nitrofuran), 3.53 (quartet, J=0.2 cps, 4-C–H), 7.46 (doublet, J=0.2 cps, 5-C–CH_3).

Found: C, 49.38; H, 3.17; N, 14.25%. Calcd for $C_8H_6O_4N_2$: C, 49.47; H, 3.12; N, 14.43%.

1,4-Dicyclohexyl-3-(5-nitro-2-furyl)-4,5-dihydro-5-oxo-1*H*-triazole (VI). I (0.95 g; 0.5 mmol) was refluxed with 1.0 g (0.5 mmol) of DCC in 20 m*l* of toluene for 7 hr, until the evolution of hydrogen chloride gas had ceased. After the removal of the solvent under reduced pressure, the residue was dissolved in chloroform and chromatographed on a silica-gel column. 0.7 g (40%) of VI, mp 146—148°C, was obtained from the first fraction after recrystallization from ethanol. UV λ_{max}^{EtOH} mμ (ε): 350 (3400, shoulder), 295 (9000). IR (KBr) cm^{-1}: 1700 (ν_{CO}). NMR ($CDCl_3$) τ: 2.58 (doublet, J=3.8 cps, 4-C–H of nitrofuran), 2.86 (doublet, J=3.8 cps, 3-C–H of nitrofuran), around 6.2 and 8.5 (multiplet, $-CH_2$).

Found: C, 60.10; H, 6.63; N, 15.71%. Calcd for $C_{18}H_{24}O_4N_4$: C, 59.68; H, 6.71; N, 15.55%.

Conversion of VI to *N,N'*-Dicyclohexylurea. A mixture of 0.23 g of VI, 0.1 g of sodium ethoxide, and 20 m*l* of ethanol was refluxed for 6 hr. After the ethanol had been removed under reduced pressure, the residue was made acidic by adding dilute hydrochloric acid, and then it was extracted with chloroform. After drying a chloroform layer over sodium sulfate, a chloroform solution was chromatographed on a silica

11) Mp 242°C. Found: C, 69.82; H, 11.04; N, 11.92%. Calcd for $C_{13}H_{24}ON_2$: C, 69.60; H, 10.78; N, 12.49%. IR (KBr) cm^{-1}: 3350 (νNH), 1630 (νCO). *Cf.* C. A. Dekker and H. G. Khorana, *J. Org. Chem.*, **76**, 3522 (1954).

12) Mp 62—64°C. T. Sasaki and T. Yoshioka, *Yuki Gosei Kagaku Kyokaishi* (*J. Synth. Org. Chem. Japan*), **25**, 665 (1967).

13) All melting points were determined on a Yanagimoto micromelting-point apparatus and have not been corrected. The ultraviolet spectra were run on a JASCO Model ORD/UV-5 optical rotary dispersion recoder, while the infrared spectra were measured on a JASCO Model IR-S spectrophotometer. The NMR spectra were taken on a Varian A-60 apparatus, with tetramethylsilane as an internal standard, and their chemical shifts are presented in terms of τ values.

*1 From the second fraction, I was recovered in a 56% yield.

column. 0.05 g (50%) of dicyclohexylurea[11] was obtained from the first fraction after recrystallization from benzene - petroleum ether.

N-Nitrofuran-2-carbonitrile (IX). *From 5-Nitrofuran-2-carboxaldehyde Oxime (VII).* A solution of 0.8 g of VII and 1.03 g of DCC in 25 m*l* of toluene was refluxed for 10 hr. After cooling, the resulting precipitates were filtered and washed with hot benzene to afford 1.0 g (87%) of dicyclohexylurea,[11] which was identified by infrared spectral comparison with an authentic specimen. The filtrate was condensed, redissolved in chloroform, and then chromatographed on a silica-gel column. 0.6 g (85%) of VIII[12] was obtained from the first fraction; it was identified by infrared spectral comparison with an authentic specimen.

From 5-Nitrofuran-2-carbonitrile Oxide (VIII). To a stirred solution of 0.8 g of I and 0.91 g of DCC in 30 m*l* of ether, there was added a solution 1 m*l* of triethylamine in 10 m*l* of ether at room temperature. Stirring was continued for 1 hr, after which the resultant triethylamine hydrochloride was filtered and washed with ether. The ether washings were combined with the filtrate and chromatographed on a silica-gel column, using chloroform as an eluent. From the first fraction a very small amount of IX was obtained, while from the third fraction, 0.5 g of dicyclohexylurea[11] was obtained; the other parts were intractable tars hard to characterize.

BULLETIN OF THE CHEMICAL SOCIETY OF JAPAN VOL. 42 260—262 (1969)

Halogenation Reaction of Bis(dithioacetylacetonato) Complexes of Cobalt(II) and Nickel(II)*1

Akiko FURUHASHI, Kunihiko WATANUKI*2 and Akira OUCHI*2

Department of Chemistry, College of Engineering and Science, Aoyama Gakuin University, Megurisawa, Setagaya, Tokyo

(Received May 7, 1968)

Reactions of halogenation reagents with acetylacetonato complexes have already been studied,[1,2] with the successful halogenation of the chelate ring. This reaction is one proof of the aromaticity of the acetylacetonato chelate ring. Thus, the halogenation of dithioacetylacetonato complexes is very interesting, and the chlorination or bromination of $M(L_{SS})_2$ type compounds (where M is Ni(II) or Co(II), HL_{SS} is dithioacetylacetone) prepared by a method given in a previous paper[3] was examined. However, in these cases the products obtained were another type of dithioacetylacetonato complex; *i. e.* $M(L_{SS})_2X_n$.[4,5] The chloro complexes thus obtained were green $M(L_{SS})_2Cl_4$, and the bromo complexes yellow $M(L_{SS})_2Br_6$. All are new compounds. Anlayses and the magnetic moments of these compounds are given in Table 1, IR spectral data between 1800 and 600 cm^{-1} in Table 2 and UV spectra of the methanolic solutions in Table 3. Assignments of the IR spectra are only tentative.[4,8]

The magnetic moments of these chloro compounds are a little higher than those calculated from the formula $\sqrt{n(n+2)}$. In the case of cobalt(II) complexes, these higher values are rather common for octahedral configurations. Although these higher values are not common in the case of nickel(II) octahedral complexes,[6,7] it is not probable that only the nickel complex has a structure different from the other $M(L_{SS})_2Cl_4$ type complexes.[8] As the general properties of complexes having the same general formula, including IR spectral data, are very similar, the structure of the Ni(II) and Co(II) complexes are as follows (shown in a previous paper[8]): four chlorine atoms are directly bonded to the central metal atom, and two dithiolium[9] ions to the metal as a mono-dentate. Their infrared spectra are very similar to those of usual $M(L_{SS})_2X_4$ type complexes. Although methanol decomposes these complexes into the metal, dithiolium and halogen ions, their methanol solution shows two characteristic peaks in the ultraviolet range due to dithiolium ion produced by solvolysis. The wave

*1 Presented at the 21st Annual Meeting of the Chemical Society of Japan, Osaka, March 1968.

*2 College of General Education, University of Tokyo, Komaba, Meguro, Tokyo.

1) R. W. Kluiber, *J. Am. Chem. Soc.*, **82**, 4839 (1960).

2) J. P. Collman, R. A. Moss, H. Maltz and C. C. Heindel, *ibid.*, **83**, 331 (1961).

3) A. Ouchi, M. Hyodo and Y. Takahashi, This Bulletin, **40**, 2819 (1967).

4) A. Furuhashi, K. Watanuki and A. Ouchi, *ibid.*, **41**, 110 (1968).

5) K. Knauer, P. Hemmerich and J. D. W. Van Voorst, *Angew. Chem. Intern. Ed. Engl.*, **6**, 262 (1967).

6) B. N. Figgis, *Nature*, **182**, 1568 (1958).

7) F. A. Cotton and D. M. L. Goodgame, *J. Am. Chem. Soc.*, **82**, 5771 (1960).

8) A. Furuhashi, T. Takeuchi and A. Ouchi, This Bulletin, **41**, 2049 (1968).

9) M. Schmidt, H. Schulz, *Chem. Ber.*, **101**, 277 (1968).

TABLE 1. ANALYSES AND MAGNETIC MOMENTS OF COMPLEXES (HL_{SS} means dithioacetylacetone)

	Magnetic moments (B.M.)		Analyses (%) M	C	H	S	X
$Co(L_{SS})_2Cl_4$	4.51	Calc.	12.73	25.92	3.02	27.07	30.69
		Obs.	12.59	25.36	3.05	26.60	29.93
$Co(L_{SS})_2Br_6$	4.40	Calc.	7.36	15.00	1.75	16.00	59.90
		Obs.	7.85	15.40	2.08	17.04	59.50
$Ni(L_{SS})_2Cl_4$	3.81	Calc.	12.72	25.93	3.03	27.07	30.70
		Obs.	13.09	25.50	3.34	26.68	30.22
$Ni(L_{SS})_2Br_6$	3.16	Calc.	7.35	15.00	1.75	16.00	59.91
		Obs.	7.38	14.77	2.02	15.43	59.50

TABLE 2. INFRARED SPECTRA OF THE COMPLEXES

Figures are given in cm^{-1}, HL_{SS} means dithioacetylacetone.

$Fe(L_{SS})_2Cl_4$[4]	$Co(L_{SS})_2Cl_4$	$Co(L_{SS})_2Br_6$	$Ni(L_{SS})_2Cl_4$	$Ni(L_{SS})_2Br_6$	Tentative Assignments
		1600m		1595 s	
1470 s	1480 s	1480 s 1440w	1480 1470 s	1480 s	ν(C=C) + δ(C–H)
1443 1420 m	1410w	1410w	1410w	1410w	$\delta(CH_3)$
1375 1353 s	1365m	1370m	1368m	1370m	$\delta(CH_3)$
1230m	1230w	1237w	1230w	1226w	δ(C–H), ν(C=S)
1200 s	1206 s	1207 s	1203 s	1203 s	$\nu(C–CH_3)$ or mixture of them
1093w	1095w	1080w	1073w	1075w	$\rho(CH_3)$
	1015w	1015w	1015w		
1007m	1008 s	1008 s	1010m	1016m	
997m	1000w	995w	1000w	990w	$\nu(C–CH_3)$
982w	983w	980w	977w	975w	
	983w	890w	878w	885w	$\nu(C–CH_3)$, ν(C=S) or the
860 s	863 s	860 s	862 s	865 s	mixture of them
710w					ring deformation or others
696 s	703m	702m	705m	710m	

δ: bending ν: stretching ρ: rocking s: strong m: medium w: weak

TABLE 3. ULTRAVIOLET SPECTRA OF THE COMPLEXES DISSOLVED IN METHANOL

(After 30 min at 15°C, 10^{-6}—10^{-5} mol/l)
Figures are given in cm^{-1} for wave numbers and log ε for intensities (in parentheses). HL_{SS} is dithioacetylacetone.

$Fe(L_{SS})_2Cl_4$[4]	$Co(L_{SS})_2Cl_4$	$Co(L_{SS})_2Br_6$	$Ni(L_{SS})_2Cl_4$	$Ni(L_{SS})_2Br_6$	$(L_{SS})ClO_4$[9]
34500	34800	34700	34700	34700	34300
(4.19)	(4.08)	(4.31)	(3.96)	(4.18)	(3.91)
37700	37700	37800	38100	37750	37330
(4.13)	(4.05)	(4.22)	(3.90)	(4.11)	(3.76)

numbers and absorption coefficients of the absorption maxima are very similar to those of dithiolium perchlorate reported in Schmidt's paper.[9] In the visible region only a broad band and a d-d band of the metal ion produced are observed in each case, as is usual for $M(L_{SS})_2X_4$ complexes.[8]

The bromo-complexes thus obtained contain six bromine atoms per metal atom, but from electrovalence consideration,[5] two of them should not be ionic. But it is not a mixture of two compounds,

as $M(L_{SS})_2Br_6$ (where M is Ni(II) or Co(II)) is yellow and the analyses and color do not change even after repeated washing with benzene or carbon tetrachloride; on the other hand, $Co(L_{SS})_2Br_4$ is green. All bromine is titrated by the Volhard method in an aqueous nitric acid solution. These compounds oxidize potassium iodide in aqueous acetic acid solution.

In the case of $Co(L_{SS})_2Br_6$, two atoms of bromine react very soon, but the reaction continues even after that and two more atoms of bromine react very slowly at room temperature. In the case of the nickel compound, the reaction is slow from the beginning but about four atoms of bromine per molecule react in a few hours at 20°C. The role of the dithiolium ion must be considered in the oxidation-reduction reaction too. Although dithiolium perchlorate does not liberate iodine from potassium iodide in aqueous acetic acid solution, the salt changes to orange yellow. Then the oxidation-reduction reaction of the complex is not simple, but at least the existence of labile bromine in it is recognized. $M(L_{SS})_2X_4$ complexes do not react with iodide under the same condition.[5]

These hexabromo complexes decompose rapidly at about 100°C, and slowly even at room temperature. At room temperature, $Co(L_{SS})_2Br_6$ evolves bromine and changes into $Co(L_{SS})_2Br_4$ in several months, but at higher temperatures it loses more, probably due to a second step reaction by evolved bromine. The nickel compound decomposes into bromine and a black product both at room temperature and 100°C. On the other hand, the usual $M(L_{SS})_2X_4$ complexes are far more stable.

The magnetic moments of these hexabromo-complexes are a little lower than those of the corresponding chloro-complexes, as shown in Table 1.

The infrared spectra of these hexabromo-complexes show a sharp peak at about 1600 cm^{-1} but other than that their general features are almost the same as those of usual $M(L_{SS})_2X_4$ type complexes; the ν(C=C) band near 1480 cm^{-1} also appears. (In the case of acetylacetonates, the ν(C=C) band near 1500 cm^{-1} disappears through halogenation though other parts of the spectra do not change seriously.[2]) The electronic spectra of their methanol solutions are almost the same as the usual tetrahalogeno complexes.

From these observations, although the two excess bromine atoms may bond to γ-carbon of the chelate or to β-carbon as proposed by Knauer in the case of $Fe(L_{SS})_2Cl_4$,[5] the bonds are very weak. Then it is reasonable to assume that these compounds are adducts of Br_2 to $M(L_{SS})_2Br_n$.

Milder halogenation reactions using *N*-chlorosuccinimide or *N*-bromosuccinimide were also tried with nickel(II) or cobalt(II) dithioacetylacetonate. Some adducts containing these reagents precipitated immediately, and from the filtrate, tetrachlorobis(dithioacetylacetonato)-cobalt(II) was obtained. But from the cobalt(II) complex and NBS or from the nickel complex and NCS or NBS, the products obtained by the same process were contaminated with the adduct of NXS, and the pure product was hardly obtained.

When solid mixture of sodium borohydride and halogeno complexes were treated with a little water, the starting $M(L_{SS})_2$ type complexes (where M = Co(II) or Ni(II)) were obtained. The yield was about 30%. These products were identified through their analyses, IR spectra and UV spectra of the methanolic solutions. This method is a new convenient synthesis of dithio-β-diketonato complexes.

Experimental

IR spectra were obtained through the nujol and hexachloro-1,3-butadiene mull procedure, using a DS 301 type infrared spectrophotometer of the Japan Spectroscopic Co., Ltd. Ultraviolet spectra were obtained with a Hitachi EPS-2 Spectrophotometer. Magnetic susceptibility measurements were carried out with a Gouy's balance at room temperature (15°C).

Synthesis of Tetrachlorobis (dithioacetylacetonato)nickel(II). Five hundred milligrams (1.56 mmol) of bis(dithioacetylacetonato) nickel(II) was suspended in 20 m*l* of carbon tetrachloride, and chlorine gas was bubbled in while stirring and cooling with ice. A green precipitate was obtained. The product was washed with carbon disulfide, chloroform, carbon tetrachloride and petroleum ether in that order. Recrystallization was not successful. The reaction was almost quantitative and the yield was 700 mg (1.52 mmol).

Other compounds were obtained by almost the same method.

The authors wish to thank the Analytical Division of the Department of Pharmacy for the elemental analyses and the Biochemistry Section of our college for the infrared spectra measurements. The useful discussions of Professor Yukichi Yoshino, Professor Yasumasa Hayakawa and colleagues of our laboratory are also gratefully acknowledged.

BULLETIN OF THE CHEMICAL SOCIETY OF JAPAN VOL. 42 263—265 (1969)

Space Effects of Tetra-*n*-alkyl Ammonium Ions on the Electrical Conduction of Tetracyanoquinodimethane Salts

Hideaki KUSAKAWA and Kazuko AKASHI*1

Mitsubishi Electric Corporation, Central Research Laboratory, Amagasaki, Hyogo

(Received May 24, 1968)

Several papers have been reported on the electrical properties of several kinds of TCNQ complexes,[1,2] but little attention has been paid to the effects of the molecular structure of paired ion on their electrical conduction.[3]

In this work we investigated how the electrical conductivities of TCNQ salts and complexes depend on the size of ammonium ions. Seven sorts of simple salts and six sorts of complex salts of TCNQ were prepared with various tetra-*n*-alkyl ammonium ions as the paired cation, and the space effects of these ammonium ions on the electrical conductivity were investigated. It was found that the electrical conductivities decrease with an increase in the number of carbon atoms in *n*-alkyl groups for the simple salts: on the other hand, for the complex salts the minimum resistivity appears when the tetra-*n*-butyl ammonium ion is used.

Experimental

Formation of Simple Salts. Tetra-*n*-alkyl ammonium halides and equimolar K^+ $TCNQ^-$ were dissolved and mixed in acetonitrile or ethyl acetate. After the potassium halide and solvent had been removed, the crude salt crystals were collected. These crystals were washed with water and dried, and were purified by means of recrystallization from the solvent used in the preparation.

Simple salts of tetra-*n*-amyl and tetra-*n*-hexyl ammonium were pasty and could not be dried completely even under reduced pressure for a long time.

The analytical results and preparation conditions of simple salts are summarized in Table 1.

Preparation of Complex Salts. TCNQ simple salt and equimolar neutral TCNQ were crushed into powder, mixed completely in an agate bowl, and dissolved in dried acetonitrile. After this had been kept at 70°C for one hour, blue-black plate crystals of complex salt were precipitated. Their elementary analytical data are listed in Table 2.

Measuring of Electrical Conductivity. The electrical conductivities of these specimens were measured by a method reported previously.[4]

Results and Discussion

TCNQ Simple Salts. Their electrical resis-

TABLE 1. TCNQ SIMPLE SALTS CONTAINING TETRA-*n*-ALKYL AMMONIUM CATION

Product	Cation source	Solvent used for preparation	Condition of preparation		Elementary analysis			
NH_4·TCNQ	NH_4Cl	*			Calcd Found	64.9 63.9	3.6 3.7	31.5 31.1
$(CH_3)_4N$·TCNQ	$(CH_3)_4N$·Br	CH_3CN	80°C	2 hr	Calcd Found	69.1 68.2	5.8 5.6	25.2 24.5
$(C_2H_5)_4N$·TCNQ	$(C_2H_5)_4N$·Br	CH_3CN	70°C	2 hr	Calcd Found	71.9 71.6	7.2 7.4	21.0 20.7
$(C_3H_7)_4N$·TCNQ	$(C_3H_7)_4N$·I	$CH_3COOC_2H_5$	r.t.	2 hr	Calcd Found	73.8 74.2	8.2 8.3	17.9 16.9
$(C_4H_9)_4N$·TCNQ	$(C_4H_9)_4N$·I	$CH_3COOC_2H_5$	r.t.	2 hr	Calcd Found	75.8 75.3	9.1 8.9	15.7 14.9
$(C_5H_{11})_4N$·TCNQ	$(C_5H_{11})_4N$·Br	CH_3CN	70°C	2 hr	Calcd Found	76.5 77.0	9.6 10.0	13.9 13.7
$(C_6H_{13})_4N$·TCNQ	$(C_6H_{13})_4N$·I	$CH_3COOC_2H_5$	r.t.	4 hr	Calcd Found	77.4 77.4	10.0 10.5	12.5 11.9

* Equimolar NH_4Cl and KTCNQ were ground into powder by an agate bowl and extracted with $CH_3COOC_2H_5$.

*1 Now resigned Mrs. Kazuko Uesaka.

1) W. J. Siemons, P. E. Bierstedt and R. G. Kepler, *J. Chem. Phys.*, **39**, 3523 (1963).

2) H. Scott, P. L. Knonick, R. Chairge and M. M. Labes, *J. Phys. Chem.*, **69**, 1740 (1965).

3) P. Dupuis and J. Neel, *C. A. Acad, Sci. Paris, Ser C.*, **265**, 688 (1967).

4) S. Nishizaki and H. Kusakawa, This Bulletin, **36**, 1681 (1963).

TABLE 2. TCNQ COMPLEX SALTS CONTAINING TETRA-*n*-ALKYL AMMONIUM CATION

Product	Elementary analysis					
	Calcd			Found		
	C	H	N	C	H	N
$(CH_3)_4N\cdot(TCNQ)_2$	69.7	4.1	26.1	70.2	4.3	25.5
$(C_2H_5)_4N\cdot(TCNQ)_2$	71.3	5.2	23.4	71.1	5.3	23.3
$(C_3H_7)_4N\cdot(TCNQ)_2$	72.7	6.1	21.2	72.6	6.1	21.1
$(C_4H_9)_4N\cdot(TCNQ)_2$	73.8	6.8	19.4	74.0	6.6	19.5
$(C_5H_{11})_4N\cdot(TCNQ)_2$	74.8	7.4	17.9	74.9	7.2	17.5
$(C_6H_{13})_4N\cdot(TCNQ)_2$	75.6	7.9	16.5	75.5	8.1	16.2

tivities at room temperature and the temperature dependence (activation energy) of the resistivity are summarized in Table 3. As Table 3 shows, tetra-*n*-alkyl ammonium-TCNQ simple salts can be classified into three groups; ammonium, tetramethyl- and tetraethylammonium salts belong to

TABLE 3. ELECTRICAL RESISTIVITY AND ACTIVATION ENERGY OF TCNQ SIMPLE SALTS

Simple salt	Resistivity at 20°C (Ωcm)	Activation energy E (eV)
$NH_4\cdot TCNQ$	4.3×10^4	0.22
$(CH_3)_4N\cdot TCNQ$	3.4×10^5	0.22
$(C_2H_5)_4N\cdot TCNQ$	$1.0+10^6$	0.28
$(C_3H_7)_4N\cdot TCNQ$	1.6×10^9	0.87
$(C_4H_9)_4N\cdot TCNQ$	4.8×10^{10}	0.88
$(C_5H_{11})_4N\cdot TCNQ$	non reproducible	
$(C_6H_{13})_4N\cdot TCNQ$	non reproducible	

the first, tetra-*n*-propyl- and tetra-*n*-butylammonium salts to the second, and tetra-*n*-amyl- and tetra-*n*-hexylammonium salts to the last group. The activation energies of salts in the first group are approximately 0.22 eV, and their resistivities become higher as the constructing-cation size increases. Of the second group of salts both the resistivity and the activation energy are much larger in magnitude in the first. The resistivities of the third group of salts could not be obtained with a good reproducibility. For tetra-*n*-alkylammonium-TCNQ simple salts a lower resistivity appears on the salt with a smaller ammonium ion size.

TCNQ Complex Salts. The resistivity and activation energies for the complex salts are listed in Table 4. In Fig. 1 the magnitudes of both the resistivity at 20°C and the activation energy of resistivity are plotted *vs.* the number of carbon atoms in the alkyl group.

For complex salts both the resistivity and the activation energy gradually decrease in magnitude with an increase in the ammonium ion size, the minimum values appearing at tetra-*n*-butylammonium complex salt. After this minimum points, each value rapidly increases again.

TABLE 4. ELECTRICAL RESISTIVITY AND ACTIVATION ENERGY OF COMPLEX SALTS

Complex salt	Resistivity at 20°C (Ωcm)	Activation energy E (eV)
$(CH_3)_4N\cdot(TCNQ)_2$	1.1×10^6	0.37
$(C_2H_5)_4N\cdot(TCNQ)_2$	3.3×10^4	0.34
$(C_3H_7)_4N\cdot(TCNQ)_2$	9.9×10^3	0.33
$(C_4H_9)_4N\cdot(TCNQ)_2$	9.7×10^1	0.21
$(C_5H_{11})_4N\cdot(TCNQ)_2$	1.0×10^7	0.75
$(C_6H_{13})_4N\cdot(TCNQ)_2$	4.6×10^8	0.93

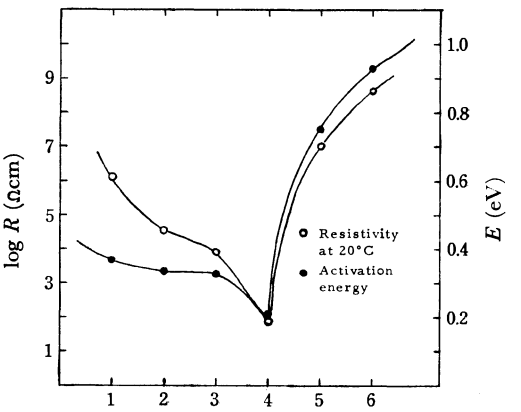

Fig. 1. Relation between resistivity and activation energy and carbon number of *n*-alkyl group in ammoniumion contained in TCNQ complex salts.

The crystal formation and electrical conductivity of complex salts are affected by the size of the paired ammonium ions. The crystal of ammonium complex salt could not be obtained, and the preparation of tetramethyl- and tetra-*n*-hexylammonium complex salts was difficult. It seems that the ammonium ion size influences the arrangement of TCNQ molecules in the complex crystal and that the overlapping of the molecular orbitals on TCNQ is varied. When the paired cation in the complex crystal is the tetra-*n*-butylammonium ion, the arrangemetn of the TCNQ molecule reaches the optimum for electrical conduction. As the

ion size of the paired cation is either smaller or larger than with tetra-*n*-butylammonium, the overlapping of moleculals on TCNQ decreases, thus leading to lower electrical conductivity.

BULLETIN OF THE CHEMICAL SOCIETY OF JAPAN VOL. 42 265—266 (1969)

On the Behavior of the Mixture of Trimethylstibine Sulfide and Tin(IV) Halides in Solution

Mizuo SHINDO, Yoshio MATSUMURA and Rokuro OKAWARA

Department of Applied Chemistry, Osaka University, Yamadakami, Suita, Osaka

(Received May 31, 1968)

In the previous papers[1,2] we have reported that the complexes, $R_2SnX_2 \cdot 2(CH_3)_3SbS$ ($R=CH_3$ or C_2H_5; $X=Cl$ or Br), change completely into three species with the exchange of the anionic ligands in $CHCl_3$ or CH_2Cl_2 as shown in (1).

$$R_2SnX_2 \cdot 2(CH_3)_3SbS \rightarrow (CH_3)_3SbS + (CH_3)_3SbX_2 + \tfrac{1}{3}(R_2SnS)_3 \quad (1)$$

This paper reports additional studies of these particular exchange reactions in $CHCl_3$ or CH_2Cl_2 with the mixtures of $(CH_3)_3SbS$ and R_3SnCl ($R=CH_3$ and C_6H_5) or $(C_6H_5)_2SnCl_2$, although we have not been able to isolate the complexes between the stibine sulfide and the tin chlorides.[2]

Experimental

The materials used in the present experiments and the experimental methods were described in the previous paper.[2]

Results and Discussion

The IR spectra of the mixtures of $(CH_3)_3SbS$ and $(CH_3)_3SnCl$ in various ratios were measured in solution and the relevant IR frequencies of a mixture of $(CH_3)_3SbS$ and $2(CH_3)_3SnCl$ in $CHCl_3$ are given in Table 1.

The spectrum can plausibly be interpreted as a superposition of the four compounds observed independently in $CHCl_3$; $(CH_3)_3SbS$,[2] $(CH_3)_3SnCl$, $(CH_3)_3SbCl_2$[2] and $[(CH_3)_3Sn]_2S$.

The NMR spectrum shown in Fig. 1 also supports this result.

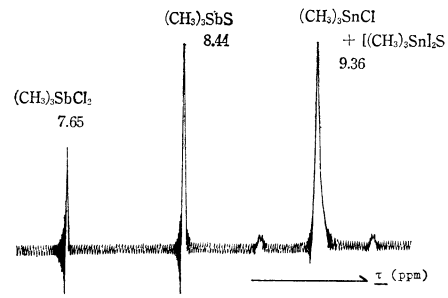

Fig. 1. The NMR spectrum of the mixture of $2(CH_3)_3SnCl$ and $(CH_3)_3SbS$ in $CHCl_3$ at 60 Mc/sec at 20°C.

For the antimony compounds the corresponding

TABLE 1. THE IR FREQUENCIENS OF THE MIXTURE OF $(CH_3)_3SnCl$ AND $(CH_3)_3SbS$ IN $CHCl_3$ (600—400 cm^{-1} region)

$2(CH_3)_3SnCl + (CH_3)_3SbS$	$[(CH_3)_3Sn]_2S$	$(CH_3)_3SnCl$	$(CH_3)_3SbS$[2]	$(CH_3)_3SbCl_2$[2]	Possible assignment
572 vw				572 m	Sb–C deg. str.
—*			551 m		Sb–C deg. str.
545 s		545 s			Sn–C deg. str.
532 m	533 s		531 m		Sb–C sym. str. + Sn–C deg. str.
515 w		514 w			Sn–C sym. str.
509 w(sh).	508 m				Sn–C sym. str.
433 m			433 m		Sb–S str.

* Masked by the strong band at 545 cm^{-1}.

1) M. Shindo and R. Okawara, *Inorg. Nucl. Chem. Letters*, **3**, 75 (1967).

2) M. Shindo, Y. Matsumura and R. Okawara, *J. Organometal Chem.*, **11**, 299 (1968).

two signals were observed. However, the tin compounds showed only one signal at 9.36 ppm. This signal is due to the rapid exchange of chlorine-sulfur atoms or methyl groups between $(CH_3)_3SnCl$ and $[(CH_3)_3Sn]_2S$, for the signal moves to higher field to approach that of $[(CH_3)_3Sn]_2S$ with decreasing ratio of $(CH_3)_3SnCl$ to $[(CH_3)_3Sn]_2S$. The same IR and NMR results were obtained in the case of a mixture of $(CH_3)_3SbCl_2$ and $[(CH_3)_3Sn]_2S$.

From these findings it is clear that the four species exist in equilibrium as shown in (2).

$$2(CH_3)_3SnCl + (CH_3)_3SbS \rightleftarrows (CH_3)_3SbCl_2 + [(CH_3)_3Sn]_2S \quad (2)$$

The molar concentrations of $(CH_3)_3SnCl$ and $[(CH_3)_3Sn]_2S$ can be determined from the intensity ratio of methyl protons of $(CH_3)_3SbS$ to those of $(CH_3)_3SbCl_2$ and Eq. (2). From these results the equilibrium constant, $K=[Me_3SbCl_2]\,[(Me_3Sn)_2S]/[Me_3SnCl]^2[Me_3SbS]$, of Eq. (2) was calculated to be 0.14 (l/mol) at 20°C. Similarly, in cases of $(C_6H_5)_3SnCl$ and $(C_6H_5)_2SnCl_2$, the equilibrium constants are 80(l/mol) and ∞(l/mol)$^{2/3}$, respectively. It can be understood that in the case of $(C_6H_5)_2SnCl_2$ the equilibrium goes, just in the cases of Eq. (1), too much toward the right side. From these it can be concluded that, in general, the equilibrium constant increases as the electron acceptor properties of the tin com- pounds increase.

$$(CH_3)_3SnCl < (C_6H_5)_3SnCl < (CH_3)_2SnCl_2 \sim (C_6H_5)_2SnCl_2$$

BULLETIN OF THE CHEMICAL SOCIETY OF JAPAN VOL. 42 266—268 (1969)

A Comparative Study of Electron Capture by Solutes in γ-Irradiated 2-Methyltetrahydrofuran Glass at 77°K

Terunobu WAKAYAMA, Toyoaki KIMURA, Tetsuo MIYAZAKI, Kenji FUEKI and Zen-ichiro KURI

Department of Synthetic Chemistry, Faculty of Engineering, Nagoya University, Chikusa-ku, Nagoya

(Received June 5, 1968)

It is generally believed that the behavior of electrons produced by the γ-irradiation of molecular compounds depends upon the states of aggregation; the electrons in the liquid phase are solvated and their reactions are mostly diffusion-controlled,[1-3] while they are, of course, free in the gas phase. A study[4] made of the reaction of electrons with a number of organic halides in 2-methyltetrahydrofuran (MTHF) glass at 77°K has led to the conclusion that electrons behave as quasi-free electrons*1 in the solid phase.

These studies of the behavior of electrons were, however, undertaken by different experimental techniques and the interrelation between electrons in the different phases is not clear at present.

It is widely accepted that nitrous oxide reacts with an electrons:

$$e^- + N_2O \longrightarrow N_2 + O^- \qquad (1)$$

Recently it has been shown by kinetic studies involving the analysis of final products that Reaction (1) alone is not sufficient to explain the yield of nitrogen.[5-8]

In the present work, we have studied, by the spectrophotometric method, the reactivities of N_2O, SF_6, and CO_2 with electrons in MTHF glass at 77°K and compared the results with those in the liquid and gas phases.[3,9] We have also studied the reaction of nitrous oxide with electrons by analyzing the final products in connection with the measurements of the reaction intermediates.

When MTHF glasses containing biphenyl are irradiated with γ-rays at 77°K, a fraction of the

1) F. Williams, *J. Am. Chem. Soc.*, **86**, 3954 (1964).
2) G. R. Freeman and J. M. Fayadh, *J. Chem. Phys.*, **43**, 86 (1965).
3) S. Sato, T. Terao, M. Kono and S. Shida, This Bulletin, **40**, 1818 (1967).
4) K. Fueki, N. Kato and Z. Kuri, presented at the 10th Symposium on Radiation Chemistry, Oct., 1967, Hiroshima, Japan.
*1 The term "quasi-free electron" in the solid phase was used for a nearly free electron, one whose interaction with a solvent is minor compared to that of a trapped or solvated electron.
5) G. R. A. Johnson and J. M. Warman, *Nature*, **203**, 73 (1964).
6) W. J. Holtslander and G. R. Freeman, *Can. J. Chem.*, **45**, 1661 (1967).
7) R. A. Holroyd, *J. Phys. Chem.*, **72**, 759 (1968).
8) T. Kimura, T. Miyazaki, K. Fueki and Z. Kuri, This Bulletin, in press (1968).
9) W. J. Holtslander and G. R. Freeman, *J. Phys. Chem.*, **71**, 2562 (1967).

electrons produced are captured by biphenyl to form biphenyl anions. The anion gives a sharp absorption band with $\lambda_{max}=410$ mμ and a broad band with $\lambda_{max}=660$ mμ. The absorption bands attributed to the biphenyl anion decrease in the presence of another electron scavenger (X) in the system. The relative electron attachment cross-section can be obtained from the following relation:[10]

$$\frac{1}{G(C_{12}H_{10}^-)} = \frac{1}{G(C_{12}H_{10}^-)_0} + \frac{\sigma_X[X]}{G(C_{12}H_{10}^-)_0\sigma_{C_{12}H_{10}}[C_{12}H_{10}]}$$

where $G(C_{12}H_{10}^-)_0$ is the yield of the biphenyl anion in the absence of the second solute (X) and where σ is the electron attachment cross-section. When the concentration of biphenyl is taken to be constant, $1/G(C_{12}H_{10}^-)$ is linearly related to the concentration of the second solute (Fig. 1). From the slopes and intercept of straight lines in Fig. 1 the relative electron-attachment cross-sections of SF_6, N_2O and CO_2 in MTHF glass are obtained; they are listed in Table 1. The electron attachment

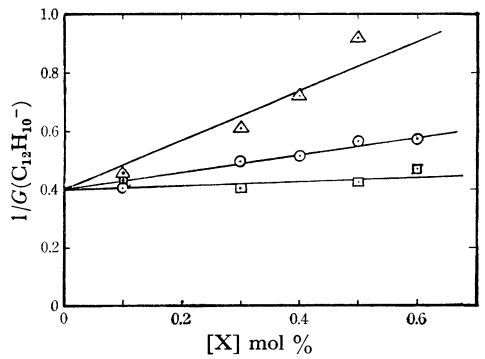

Fig. 1. $1/G(C_{12}H_{10}^-)$ *vs.* M% second solutes (X) in γ-irradiated MTHF solutions containing 0.2 M% biphenyl at 77°K.
△, SF_6; ⊙, N_2O; ⊡, CO_2

Table 1. Relative electron-attachment corss-sections of SF_6, N_2O, and CO_2

	Solid	Gas[9]	Liquid[3]
SF_6	2.3	10	1.0
N_2O	1.0	1.0	1.0
CO_2	0.3	0	1.0

cross-sections of SF_6, N_2O and CO_2 differ in the solid phase, while they are the same in the liquid phase. It has previously been proposed that the electron in the liquid phase is solvated and that its reactions with electron scavengers are diffusion-controlled.[1-3] The electron-attachment cross-sections of SF_6, N_2O and CO_2 in the solid phase are in the same order as those in the gas pahse. This implies that electrons are quasi-free electrons*1 in the solid phase, as has been suggested in previous studies.[4,8]

The reactions of nitrous oxide with biphenyl anions and with electrons in MTHF glass have been investigated by both the spectrophotometric measurement of biphenyl anions and the analysis of nitrogen. The absorption spectra of the biphenyl anion were measured after γ-irradiation to a dose of 8.49×10^3 rad, and nitrogen was measured at room temperature on the samples γ-irradiated at 7°K (dose: 3.91×10^5 rad) by a gas burette connected to a Toepler pump and a cupric oxide furnace kept at 240°C. The yield of biphenyl anions increases linearly with the dose, 8.49×10^3 to 3.91×10^5 rad. The effect of nitrous oxide on the yields of biphenyl anions and nitrogen is shown in Fig. 2. The yield of nitrogen increases rapidly

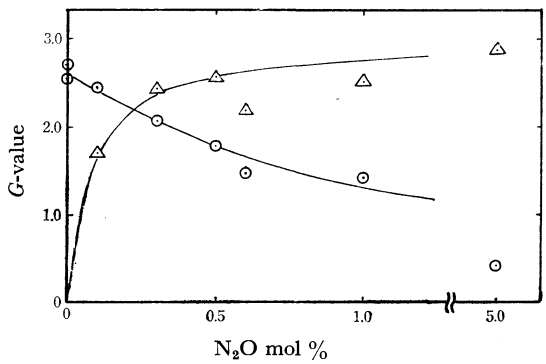

Fig. 2. Effect of nitrous oxide on the yields of biphenyl anion and nitrogen.
Concentration of biphenyl: 0.2 mol%
⊙—⊙, biphenyl anion
△—△, nitrogen

with an increase in the nitrous oxide and becomes constant at concentrations of nitrous oxide higher than 0.5 mol%, while the yield of biphenyl anions gradually decreases with an increase in the nitrous oxide. Though the decrease in biphenyl anions represents the amount of electrons captured by nitrous oxide, it does not correspond to the yield of nitrogen. The yield of nitrogen at high concentrations of nitrous oxide is about 2.6 (G unit), which is approximately equal to the yield of biphenyl anions in the absence of nitrous oxide. These results may be explained by the following scheme:

$$MTHF\text{-}\wedge\!\vee\!\wedge\!\rightarrow MTHF^+ + e^- \quad (2)$$

$$e^- + C_{12}H_{10} \longrightarrow C_{12}H_{10}^- \quad (3)$$

$$e^- + N_2O \longrightarrow N_2 + O^- \quad (1)$$

$$C_{12}H_{10}^- + N_2O \longrightarrow N_2 + O^- + C_{12}H_{10} \quad (4)$$

Reaction (4) probably occurs while the sample is

10) J. P. Guarino, M. R. Ronayne and W. H. Hamill, *Radiation Res.*, **17**, 379 (1962).

being warmed to room temperature. Reaction (4) requires that the electron affinity of nitrous oxide is greater than that of biphenyl, 0.41 eV. It may be concluded that nitrous oxide reacts with an electron to form one nitrogen molecule in MTHF glass

BULLETIN OF THE CHEMICAL SOCIETY OF JAPAN VOL. 42 268—269 (1969)

The Spectrophotometric Determination of Anions by Solvent Extraction with Metal Chelate Cations. V.*1 Thiocyanate with Tris(1,10-phenanthroline)iron(II) Chelate

Yuroku YAMAMOTO, Tsunehiko TARUMOTO and Yasuko HANAMOTO

Department of Chemistry, Faculty of Science, Hiroshima University, Higashisenda, Hiroshima

(Received June 15, 1968)

A number of methods have been reported on the determination of thiocyanate. Aldridge[1] and Baker *et al.*[2] proposed colorimetric methods with a pyridine-benzidine mixture, both of which require quite tedious procedures. Kruse and Mellon[3] used copperpyridine as a color developer, the reaction mechanism of which is still obscure. Winkhaus and Uhrig[4] presented a spectrophotometric method by solvent extraction with di-π-cyclopentadienyltitanium(IV) which, though simple and sensitive, is effective only in a very narrow pH range in the acidic media. Koh and Iwasaki[5] recently reported another spectrophotometric method based on solvent extraction with methylene blue which attained very high sensitivity and was yet influenced to some extent by the reagent concentrations used in the experiment.

Here, we present a new and consistent method for the determination of a small amount of thiocyanate anions, in which thiocyanate as low as 2×10^{-6} in molar concentration was extracted from aqueous solution into nitrobenzene as tris(1,10-phenanthroline)iron(II) thiocyanate and determined spectrophotometrically.

Experimental

All the reagents used in this experiment were of analytical reagent grade and a Hitachi 139 spectrophotometer with 10 mm glass cells was used for measurement.

Recommended Procedure. Take 5 m*l* of thiocyanate solution of concentration ranging from 1×10^{-5} to 2×10^{-4} M in a 50 m*l* beaker. Add 5 m*l* of 0.02 M 1,10-phenanthroline solution, 5 m*l* of 5×10^{-3} M iron(II) solution prepared from Mohr's salt and 5 m*l* of phosphate buffer solution to adjust the pH of this mixture to 5—10. Transfer this into a separatory funnel and dilute to 25 m*l* with distilled water.

Add 10 m*l* of nitrobenzene previously equilibrated with water and shake the funnel for about 5 min. About 30 min after extraction, remove the organic layer and dehydrate with anhydrous sodium sulfate, allowing the mixture to stand another 10 min. Measure the absorbance of the organic phase at 516 mμ with the reagent blank as a reference.

Results and Discussion

The absorption spectrum of the extract is shown in Fig. 1. The absorption maximum was identical with that of tris(1,10-phenanthroline)iron(II) thiocyanate salt dissolved in nitrobenzene. The chemical formula of the extracted species was confirmed to be $[Fe(phen)_3](NCS)_2$ also by continuous variation method, where phen represents 1,10-phenanthroline. This species shows a constant absorbance when extracted from aqueous phase with a wide pH range of 5 to 10, indicating that the degree of extraction was maximum in this pH range. The percentage of the extraction was found to be 52% (*i. e.*, $D=2.7$) by referring the absorbance of the extract to that of a standard solution prepared by dissolving crystalline $[Fe(phen)_3](NCS)_2$ in nitrobenzene. The color was stable for about three hours before slight fading was observed.

Increasing the quantity of tris(1,10-phenanthroline)iron(II) against that of thiocyanate did not affect the degree of extraction, provided the former was 15 times more concentrated than the latter.

*1 Part IV of this series: Y. Yamamoto, K. Kotsuji, S. Kinuwaki and H. Sawamura, *Nippon Kagaku Zasshi* (*J. Chem. Soc. Japan, Pure Chem. Sect.*), **85**, 59 (1964).

1) W. N. Aldridge, *Analyst*, **69**, 262 (1944).

2) M. O. Baker, R. A. Foster, B. G. Post and T. A. Hiett, *Anal. Chem.*, **27**, 448 (1955).

3) J. W. Kruse and M. G. Mellon, *ibid.*, **25**, 446 (1953).

4) G. Winkhaus and H. Uhrig, *Z. Anal. Chem.*, **200**, 14 (1964).

5) T. Koh and I. Iwasaki, This Bulletin, **40**, 569 (1967).

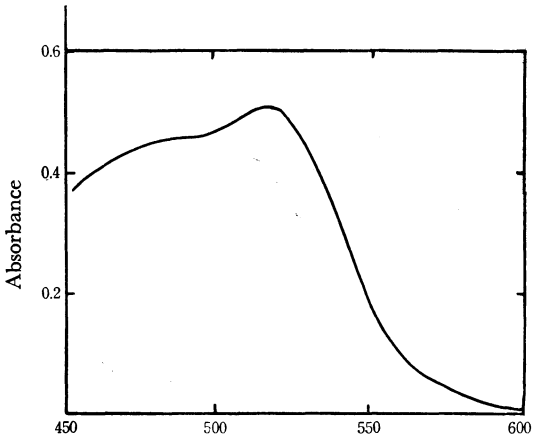

Fig. 1

Fig. 1. Absorption Spectrum of Tris(1,10-phenanthroline)iron(II) thiocyanate in Nitrobenzene Extract.
Tris(1,10-phenanthroline)iron(II) concentration $= 1.0 \times 10^{-3}$M
Thiocyanate concentration $= 4.0 \times 10^{-5}$M
Extraction was done according to the recommended procedure.
Reference : Reagent Blank.

Thus, the tris(1,10-phenanthroline)iron(II) concentration was kept at least 25 times in excess throughout the experiment.

A plot of absorbance in nitrobenzene phase *vs.* thiocyanate concentration in aqueous phase gave a linear relationship over the range of 2×10^{-6} to 4×10^{-5} M thiocyanate. As for the interference of diverse ions, metals highly reactive with thiocyanate, for example, cobalt, nickel, zinc or copper caused comparatively high negative errors when present in amounts equal to the thiocyanate concentration. Sodium, calcium, magnesium and manganese had negligible effects, even when 100 times the amount of thiocyanate was present. Perchlorate, as previously reported,[6] was the most extractable species and therefore its interference was serious. As to other anions, iodide and nitrate form ion pairs with tris(1,10-phenanthroline)iron(II) and therefore produce positive errors, while bromide, chloride, sulfate and phosphate had no appreciable effects even when present in considerable amounts, as may be seen in Table 1.

Table 1. Effect of diverse anions*2

Anion added as sodium salt	Concentration M	Relative error %
F^-	4×10^{-2}	0
Cl^-	2×10^{-3}	0
Br^-	2×10^{-4}	+10.8
I^-	2×10^{-5}	+69.5
NO_3^-	2×10^{-5}	+11.6
SO_4^{-2}	2×10^{-3}	+1.0
$H_2PO_4^-$	2×10^{-3}	0

*2 All the solutions are 2×10^{-5} M in thiocyanate concentration.

The interference of some cations may be easily masked with EDTA, but the interfering anions should be separated prior to the extraction of thiocyanate by proper methods like ion exchange.

6) Y. Yamamoto, K. Kotsuji, S. Kinuwaki and H. Sawamura, *Nippon Kagaku Zasshi* (*J. Chem. Soc. Japan, Pure Chem. Sect.*), **85**, 59 (1964).

BULLETIN OF THE CHEMICAL SOCIETY OF JAPAN VOL. 42 270—272 (1969)

Poisoning Effect of Carbon Disulfide on the Liquid-phase Hydrogenation of Acetone over a Raney-Nickel Catalyst

Sanae KISHIDA and Shiichiro TERANISHI

Department of Chemical Engineering, Faculty of Engineering Science, Osaka University, Machikaneyama-cho, Toyonaka, Osaka

(Received June 17, 1968)

Recently the present authors have reported[1] that the liquid-phase hydrogenation of open-chain ketones over a Raney-nickel catalyst could reasonably be interpreted by the rate equation derived from the Langmuir-Hinshelwood mechanism;

$$v = k \cdot a \cdot C_R/(1 + a \cdot C_R), \quad (1)$$

where k refers to the rate constant; C_R, the concentration of reactant to be hydrogenated, and a, the equilibrium constant concerning the adsorption strength of hydrogen and the reactant.*1

In a previous paper[2] the authors also studied the hydrogenation of mesityl oxide over a Raney-nickel catalyst poisoned by potassium iodide, and found that the equilibrium constant, a, and the rate constant decrease upon the poisoning. The authors, therefore, pointed out that not only the behavior of the rate, but also the change in the kinetics due to the poisoning, has to be taken into account in considering a mechanism of the poisoning in heterogeneous catalysis.

In the present study, the kinetics of acetone hydrogenation over a Raney-nickel catalyst progressively poisoned by carbon disulfide is investigated in detail. A poisoning curve and a mechanism of the poisoning are then discussed accordingly.

Experimental

Catalyst. 1.00 g of Raney-alloy (50.0% Ni) was leached with 50 m*l* of a 20% sodium hydroxide solution at 100°C for 60 min. The sample was then washed 5 times with 100 m*l* of water, 5 times with 25 m*l* of isopropyl alcohol, and 10 times with 25 m*l* of *n*-hexane under hydrogen. The sample was then poisoned by CS_2, and diluted with *n*-hexane. The concentrations were so low that the CS_2 in solution was completely adsorbed by the catalyst. The sample was then washed 5 more times with 25 m*l* of *n*-hexane.

Apparatus and Procedure. For the rate measurements they were as previously reported.[1]

Results

The concentration dependence of the initial rates at 30°C over the catalyst progressively poisoned are shown in Fig. 1. The peak shifts to higher concentrations with the progressive poisoning. The

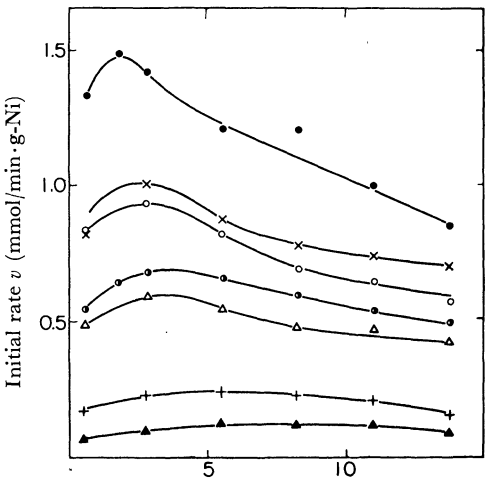

Fig. 1. Acetone hydrogenation over Raney-nickel catalyst progressively poisoned by CS_2.
The amount of CS_2 adsorbed are; ●, 0.0; ×, 0.0167; ○, 0.0474; ◑, 0.0660; △, 0.0835; +, 0.1885; ▲, 0.2505 mmol/g-Ni.

values of k and a for the poisoned catalyst were evaluated from the plots of $\sqrt{C_R/v}$ *vs.* C_R. It was found that k and a decrease in an exponential manner with the amount of carbon disulfide adsorbed, as is shown in Fig. 2; that is, k and a over the poisoned catalyst can be expressed as;

$$k = k_0 \exp(-\beta \cdot x),$$

$$a = a_0 \exp(-\alpha \cdot x),$$

where k_0 and a_0 refer to the rate constant and the equilibrium constant respectively over the un-

1) S. Kishida, S. Kajimoto and S. Teranishi, *Shokubai (Catalyst)*, **9**, 58 (1967); *J. Catalysis*, in printing.

*1 The accurate definition of a is: $a=(1/C_H) \cdot \exp(-\delta\Delta G/RT)$, where C_H refers to the liquid-phase concentration of hydrogen and where $\delta\Delta G$ is the difference in the free energies of the adsorption of hydrogen and a reactant. See Refs. 1 and 2.

2) S. Kishida and S. Teranishi, This Bulletin, **41**, (1968).

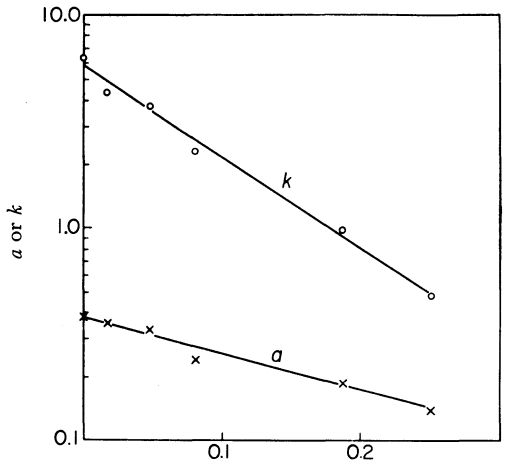

Fig. 2. Plotts of the logarithms of k and a *vs.* x.

poisoned catalyst, and x, the amount of carbon disulfide adsorbed. The β and α can be termed the poisoning coefficients for k and a respectively. From Fig. 2, the values of α and β are found to be 1.04 and 2.47 respectively. By substituting the above relations into Eq. (1), the rate equation available for the unpoisoned and poisoned catalyst can be obtained as:

$$v(x) = \frac{k_0 \cdot \exp(-\beta \cdot x) \cdot a_0 \cdot \exp(-\alpha \cdot x) \cdot C_R}{(1 + a_0 \cdot \exp(-\alpha \cdot x) \cdot C_R)^2}, \qquad (2)$$

where $v(x)$ is the reaction rate over the catalyst poisoned with x mmol of carbon disulfide per gram of Ni.

Discussion

The experimental finding that the peak of the rate *vs.* concentration plot shifts upon the poisoning seems to indicate that the adsorption coefficients of acetone or/and hydrogen are influenced in the presence of carbon disulfide.

Recently, Kishi, Ikeda and Hirota[3] have observed that the ultraviolet and visible absorption bands of acetylacetone adsorbed on evaporated iron shift in the presence of oxygen or water vapor. Eischens and Pliskin[4] reported many observations that the addition of a gas to a chemisorbed CO system shifts the frequency of the CO stretching bands. Blyholder[5] has lately proposed a qualitative interpretation of the phenomenon, applying the molecular orbital theory to a carbon-oxygen-metal system. He has shown that the shift of absorption could be explained as a result of the adsorption of a gas, by which an electron is added to or removed from the metal, with a consequent addition or removal of an electron from the chemisorbed CO. These results indicate an interaction among the adsorbed molecules.

It is necessary to mention that the hydrogenation of benzaldehyde over a Raney-nickel catalyst is markedly promoted in the presence of trimethylamine.[6] This indicates that the reaction rate of heterogeneous catalysis does not always decrease in the presence of a "poison." This so-called promoting effect must also be taken into account in discussing a poisoning mechanism.

As has been previously reported by the present authors[7] in connection with hydrogenation of isobutyl methyl ketone, the fractional surface coverage of adsorbed hydrogen during the reaction is increased by the poisoning. This phenomenon was interpreted as being due to the change in the adsorption strength of the ketone or/and hydrogen, a change caused by the potassium iodide adsorbed.

It seems that these and other phenomena can be reasonably explained and correlated by recognizing that adsorbed molecules interact directly or through the catalyst.[8] The poisoning can then be considered as a phenomenon caused by the interaction of "third material" with reacting molecules,*2 with a consequent change in the adsorption strength and hence, in the reactivity of the latter.

In view of this, a reaction rate over a catalyst progressively poisoned can generally be given by Eq. (2), which also gives a poisoning curve when $v(x)$ is plotted *vs.* x by fixing C_R. If $a_0 \cdot C_R \ll 1$, Eq. (2) becomes; $v(x) = k_0 \cdot a_0 \cdot C_R \cdot \exp(-(\beta+\alpha)x)$, and if $a_0 \cdot C_R \gg 1$, $v(x) = (k_0/a_0 \cdot C_R) \cdot \exp(-(\beta-\alpha)x)$. These are generally written as: $v(x) = (\text{constant}) \times \exp(-\gamma \cdot x)$, which can be expanded as:

$$v(x) = (\text{Constant}) \times (1 - \gamma \cdot x) \qquad (3)$$

in a small range of x, indicating that the rate first falls in a linear manner with poisoning if γ is positive. The poisoning curve of a flexed linear type[9] can now be reasonably interpreted by considering that Eq. (3) does not hold as x increases. Equation

3) K. Kishi, S. Ikeda and K. Hirota, *J. Phys. Chem.*, **71**, 4384 (1967).

4) R. P. Eischens and W. A. Pliskin, *Advan. Catalysis*, **10**, 1 (1958).

5) G. Blyholder, *J. Phys. Chem.*, **68**, 2772 (1964).

6) D. R. Levering, *J. Am. Chem. Soc.*, **71**, 1515 (1949).

7) S. Kishida, Y. Tanaka and S. Teranishi, *Nippon Kagaku Zasshi* (*J. Chem. Soc. Japan, Pure Chem. Sect.*), **89**, 271 (1968).

8) M. Boudart, *J. Am. Chem. Soc.*, **74**, 3556 (1952).

*2 The fact that the kinetics of acetone hydrogenation are explained by the Langmuir-Hinshelwood mechanism can be interpreted as suggesting that the interactions of acetone-acetone, acetone-hydrogen, and hydrogen-hydrogen are not important enough to be taken into account in discussing the kinetics.

9) J. N. Pattison and E. F. Degering, *ibid.*, **73**, 611 (1951); E. F. G. Herington and E. K. Rideal, *Trans. Faraday Soc.*, **40**, 505 (1944).

(3) is substantially the same as that proposed by Maxted.[10]

The values of α and β are naturally different for different reactions, since they depend on the values of an interaction between a poisoning material and a reacting material. A given poison can, therefore, give different poisoning curves, especially in different types of reactions. In Fig. 3, three types of poisoning curves, predictable when α and β are positive, are shown. It can be seen that the reaction rate does not change or even increases, although the rate constant of a given reaction decreases, in the presence of a poison. It has been believed, according to the so-called "active patch" theory, that two different types of active sites can be experimentally distinguished when a given poison inhibits one reaction but does not influence another one.[11] Figure 3, however, suggests another possibility in interpreting the phenomenon. Since there is a possibility that α and β are negative, three more cases have to be taken into account in order to consider all of the poisoning curves predictable from Eq. (2), that is: (1) $\alpha<0$, $\beta<0$, (2) $\alpha<0$, $\beta>0$ and (3) $\alpha>0$, $\beta<0$. Nine other types of poisoning curves can, then, be deduced.

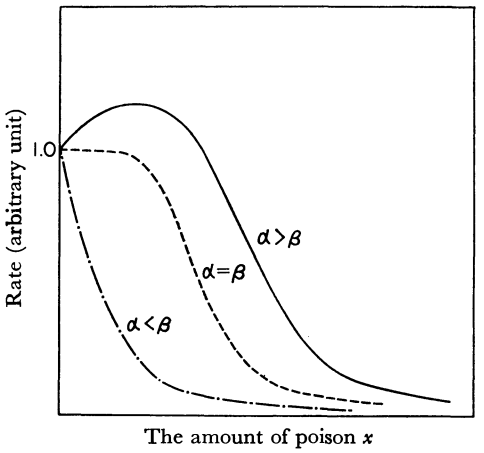

Fig. 3. Poisoning curves predictable from Eq. (2) in the case where α and β are positive

It can now be concluded that various types of observed poisoning curves can be interpreted by considering the poisoning as a phenomenon due to an interaction between a "third material" and the reacting molecules.

10) E. B. Maxted and V. Stone, *J. Chem. Soc.*, **1934**, 672.

11) J. Medema and J. P. W. Houtman, *J. Catalysis*, **6**, 322 (1966); *ibid.*, **8**, 298 (1967).

SHORT COMMUNICATIONS

π Complexes of Vinyl Alcohol and Propenyl Alcohol with Platinum(II)

Yasuo WAKATSUKI, Shun'ichi NOZAKURA and Shunsuke MURAHASHI

Department of Polymer Science, Osaka University, Toyonaka, Osaka

(Received November 4, 1968)

The first description of the vinyl alcohol complex with a transition metal was made by Ariyaratne and Green; it was prepared by the protonation of an oxoalkyl-iron complex.[1]

In the present communication, we wish to report the preparation of vinyl alcohol and propenyl alcohol complexes with Pt(II) in a completely different manner. As is shown below, 1,3-bis-(alkenyl trimethylsilyl ether)-2,4-dichloro-μ-dichlorodiplatinum was synthesized by the replacement of ethylene by alkenyl trimethylsilyl ether, and then the Si–O bond was hydrolyzed to give alkenyl alcohol complexes.

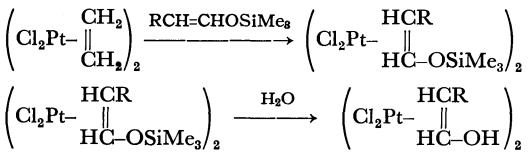

R: H or CH_3

To a suspension of 100 mg of Zeise's dimer, $(Cl_2PtC_2H_4)_2$, in 5 m*l* of toluene, there was added about 0.1 m*l* of vinyl trimethylsilyl ether. The mixture turned orange and became homogeneous shortly after the addition. The toluene and the excess of vinyl trimethylsilyl ether were then evaporated at room temperature to give a yellow powder of $(Cl_2PtCH_2{=}CH{-}OSiMe_3)_2$, which decomposed under nitrogen at 120—122°C. Found: C, 15.77; H, 2.86; Cl, 19.13; Pt, 51.27%. Calcd for $C_5H_{12}Cl_2OSiPt$: C, 15.71; H, 3.16; Cl, 18.55; Pt, 51.04%. This powder was dissolved in 10 m*l* of benzene containing about 200 ppm of water. When the solution was allowed to stand overnight at room temperature, fine yellow crystals of the vinyl alcohol complex precipitated in a 68% yield; these crystals decomposed at 127—131°C. Found: C, 7.91; H, 1.33; Cl, 22.77; Pt, 62.77%. Calcd for $C_2H_4Cl_2OPt$: C, 7.75; H, 1.30; Cl, 22.87; Pt, 62.92%. IR(KBr disk): ν_{O-H} 3200(vs), $\nu_{=C-H}$ 3020(w) and $\nu_{C=C}$ 1548 cm^{-1}(vs).

Since the O–Si bond of the vinyl trimethylsilyl ether complex is extremely sensitive to moisture, the vinyl alcohol complex was also formed when the vinyl trimethylsilyl ether complex was exposed to air (70% humidity) at room temperature for about 10 min.

On the decomposition of the vinyl alcohol complex with pyridine, acetaldehyde was liberated; it was detected by gas chromatography.

A similar reaction of propenyl trimethylsilyl ether gave an orange-yellow powder of $(Cl_2Pt\ CH_3{-}CH{=}CHOSiMe_3)_2$ which decomposed at 118—121°C. Found: C, 18.02; H, 3.42; Cl, 18.68%. Calcd for $C_6H_{14}Cl_2OSiPt$: C, 18.19; H, 3.56; Cl, 17.90%. The hydrolysis was carried out similarly in moist benzene to give brown-yellow crystals of the propenyl alcohol complex after 10 days at room temperature. The yield was 61%. It decomposed at 118—121°C. Found: C, 11.28; H, 1.84; Cl, 22.37; Pt, 60.22%. Calcd for $C_3H_6Cl_2OPt$: C, 11.12; H, 1.87; Cl, 21.88; Pt, 60.20%. IR (Nujol mull): ν_{O-H} 3300(vs), $\nu_{=C-H}$ 3020(w) and $\nu_{C=C}$ 1545 cm^{-1}(s).

These specific absorptions and the absence of carbonyl absorption in the IR spectra are consistent with the proposed structure of the complexes. The NMR spectra were not studied because of the poor solubility of the complexes. The study of the *cis-trans* isomerism of the complexed olefin is now in progress.

1) J. K. P. Ariyaratne and M. L. H. Green, *J. Chem. Soc.*, **1964**, 1.

The Syntheses of Bisdithiobenzoylacetonates and Its Halogeno Derivatives from Dithiolium Salt*1

Yoshiaki TAKAHASHI, Mitsuhisa NAKATANI and Akira OUCHI

Department of Chemistry, College of General Education, The University of Tokyo, Komaba, Meguro-ku, Tokyo

(Received November 6, 1968)

The dithio-derivatives of β-diketonates have very interesting properties and have previously been reported,[1-5] but all of them were then synthesized from metal β-diketonate. As the dithio-β-diketones are so easily dimerized that their monomers have not yet been isolated, these complexes are synthesized by trapping the newly-forming dithio-β-diketone by metal ions before the dimerization occurs.

The present authors previously obtained the dithiolium salts by the method of Schmidt and Schulz from β-diketones,[6] and using the 3-methyl-5-phenyl-1,2-dithiolium perchlorate, the syntheses of some dithio-β-diketonates and halogeno-dithio-β-diketonates have been successful. The bis(dithiobenzoylacetonato)cobalt(II) was synthesized from a mixture of anhydrous cobalt(II) chloride and dithiolium salt by a reduction reaction using sodium borohydride under ice cooling; the product was extracted with chloroform. The nickel(II) complex was obtained by a similar method. The trichlorodithiobenzoylacetonatozinc(II) was synthesized by the reaction of anhydrous zinc(II) chloride and the dithiolium salt in a concentrated hydrochloric acid medium under ice cooling. Other chloro- or bromo-derivatives of the ML_2X_4 and MLX_3 types were obtained by almost the same method. The chemical formulas of the products and their magnetic moments, measured by the Gouy balance method at room temperature, are shown in Table 1. The infrared spectroscopic results of typical compounds are shown in Table 2.

NiL_2 (where HL = dithiobenzoylacetone) obtained by this method was the same as that reported in a previous paper[4] and was isostructural to CoL_2. The CoL_2Cl_4 thus obtained was identical with that reported previously,[4] while the other three ML_2X_4-type complexes seem to be isostructural. The general properties of the MLX_3-type complexes resemble ML_2X_4-type ones.

The further application of this method is now going to be studied in our laboratory; the results will be published elsewhere.

TABLE 1. CHEMICAL FORMULAE OF COMPLEXES CALCULATED FROM THE ANALYSIS AND THE MAGNETIC MOMENTS
(Figures are given in B.M. per 1 mol of metal.)

NiL_2	dia	CoL_2Cl_4	4.63
CoL_2	not measured	CoL_2Br_4	4.64
$MnLCl_3$	6.01	CuL_2Br_4	1.34
$CuLCl_3$	2.09	CdL_2Cl_4	dia
$ZnLCl_3$	dia		

dia = diamagnetic
HL = dithiobenzoylacetone ($C_{10}H_{10}S_2$)

TABLE 2. FREQUENCIES FOUND ABOUT THE COMPLEXES IN INFRARED REGION (Figures are given in cm^{-1}.)

CoL_2	CdL_2Cl_4	$MnLCl_3$
	1590 w	1600 m
1470 s	1493 w	1495 w
1462 sh	1470 s	1478 s
1445 s, sh	1445 sh	1453 w
1360 m	1374 w	1376 w
1344 w	1340 m	1336 m
1293 m	1315 w	1315 w
1270 m	1250 s	1253 s
1220 s	1220 w	1218 w
1210 w		
1180 w		
1157 m	1148 m	1148 m
1108 w	1095 m	1098 m
1075 m	1067 w	1075 w
1025 m	1014 m	1015 m, br
1018 m		
999 m	994 s	995 s
967 w	970 w	973 w
907 w	924 m	928 m
867 w	870 s	870 s
857 m	845 w	840 w
760 s	760 s	767 s
737 s		
693 m	707 w	707 w, sh
	680 s	680 s

*1 This paper was presented at the 18th Symposium on Coordination Chemistry, Kyoto, Oct. 1968.

1) L. Martin and I. M. Stewart, *Nature*, **210**, 522 (1966).
2) K. Knauer, P. Hemmerich and J. D. W. Van Voorst, *Angew. Chem. Intern. Ed. Engl.*, **6**, 262 (1967).
3) A. Furuhashi, K. Watanuki and A. Ouchi, This Bulletin, **41**, 110 (1968).
4) A. Ouchi, M. Nakatani and Y. Takahashi, *ibid.*, **41**, 2044 (1968).
5) A. Furuhashi, T. Takeuchi and A. Ouchi, *ibid.*, **41**, 2049 (1968).
6) M. Schmidt and H. Schulz, *Chem. Ber.*, **101**, 277 (1968).

New Five-coordinate Iridium Complexes

Hiroshi YAMAZAKI, Masahiko TAKESADA and Nobue HAGIHARA

The Institute of Physical and Chemical Research, Yamato-machi, Saitama
The Institute of Scientific and Industrial Research, Osaka University, Yamada-Kami, Suita, Osaka

(Received November 6, 1968)

Recently we have reported the preparation of methyl- and phenyl-(triphenylphosphine)-(1,5-cyclooctadiene)rhodium, and hydrido-tetrakis(triphenylphosphine)rhodium from the reactions of bis(1,5-cyclooctadienerhodium chloride) (I) with methyl, phenyl and isopropyl Grignard reagents in the presence of triphenylphosphine, respectively.[1] In the present communication, we wish to report the preparation of new five-coordinate methyl- and hydrido-iridium complexes resulting from an extended work to the iridium analogue of I.

Bis(1,5-cyclooctadieneiridium chloride) (II) and triphenylphosphine in benzene-ether mixture were treated with methylmagnesium iodide at an ice temperature. After hydrolysis, the organic layer was concentrated and subjected to chromatography on alumina with benzene as eluant. Concentration of the eluate, followed by the addition of hexane to the residue gave pale yellow crystals of methyl-bis(triphenylphosphine)-(1,5-cyclooctadiene)iridium (III) (Yield 17%, mp*1 146—147°C (with decomp). Found: C, 65.12; H, 5.45%. Calcd for $C_{45}H_{45}P_2Ir$: C, 64.34; H, 5.40%. NMR (in C_6D_6): 2.3—3.2τ (C_6H_5), 6.1 and 7.0τ (=CH), 8.1τ (CH_2), 9.44τ (CH_3).). Methyl proton resonance appeared as a singelt and suggested the existence of the phosphine interchange process which could be schematically pictured as:

$$C_8H_{12}Ir(CH_3)P^1 + P^2 \rightleftarrows C_8H_{12}Ir(CH_3)P^1P^2 \rightleftarrows C_8H_{12}Ir(CH_3)P^2 + P^1$$

Phosphine interchange would be rapid enough at room temperature to cause disappearance of P–H coupling. Evidence was obtained by the NMR spectrum at −60°C (in CH_2Cl_2) in which methyl protons showed triplet peaks of 1 : 2 : 1 ratio ($J_{PH}=10$ cps).

Vrieze and Volger[2] pointed out the presence of a five-coordinate short-lived intermediate (diolefin)-$MCl(L)_2$ (M = Rh, Ir and L = Group-V donor lignad) from the NMR studies of ligand exchange reaction of (diolefin)MCl(L), and they isolated $C_8H_{12}IrCl(PPh_3)_2$ when ethanol was used as solvent. It is interesting that the replacement of chlorine by methyl group made the five-coordinate iridium complex easy to isolate.

The reaction of II with isopropylmagnesium bromide in the presence of triphenylphosphine was carried out, in order to compare it with the case of rhodium in which cyclooctadiene was replaced by triphenylphosphine to give hydrido-tetrakis-(triphenylphosphine)rhodium. According to a similar procedure, white needles of hydrido-bis-(triphenylphosphine)-(1,5-cyclooctadiene)iridium (IV) were obtained in almost quantitative yield without loss of a cyclooctadiene ligand (mp*1 162—165°C (with decomp). Found: C, 64.22; H, 5.55; P, 7.33%. Calcd for $C_{44}H_{43}P_2Ir$: C, 63.98; H, 5.25; P, 7.50%). IV was relatively more stable than III. The NMR spectrum (in $CDCl_3$) showed peaks at 2.5—3.0τ (C_6H_5), 6.2 and 6.5τ (=CH, Former peak is broader than the latter), and 8.4τ (CH_2). Additional triplet of 1 : 2 : 1 ratio ($J_{PH}=22$ cps) was found at 23.7τ which was assigned to hydrogen directly bonded to the iridium. It is obvious that the phophine interchange proceed more slowly in this complex than in III.

More detailed studies of this type of complexes are now in progress.

1) M. Takesada, H. Yamazaki and N. Hagihara, *Nippon Kagaku Zasshi* (*J. Chem. Soc. Japan, Pure Chem. Sect.*), **89**, 1121 (1968).

*1 Measured in nitrogen filled capillary tube.

2) K. Vrieze and H. C. Volger, *J. Organometal Chem.*, **11**, 17 (1968).

Radiative and Radiationless Processes in Phthalazine*1

Hiroaki BABA, Iwao YAMAZAKI and Takeshi TAKEMURA

Division of Chemistry, Research Institute of Applied Electricity, Hokkaido University, Sapporo

(Received November 11, 1968)

Although nitrogen heterocyclic compounds generally exhibit strong phosphorescence, *ortho*-diazines such as pyridazine, phthalazine, and 9,10-diazaphenanthrene are known to show either no phosphorescence or very weak phosphorescence. The problem of such puzzling emission properties of the *ortho*-diazines has attracted much attention,[1-4] but remains unsettled. With phthalazine, no emission has been reported, except for a phosphorescence emission in an acidic solution,[5] where the protonation may give rise to an essential change in its emission property. We have recently examined both the radiative and radiationless processes in phthalazine at 77°K. It was found that phthalazine gave no emission in hydrocarbon solvents, but in polar solvents like EPA it did exhibit phosphorescence. In all these cases we were unable to obtain fluorescence from phthalazine.

The phosphorescence spectrum in EPA is shown in Fig. 1, together with the excitation spectrum (corrected). The latter spectrum is seen to be in agreement with the absorption spectrum within experimental errors, indicating that the phosphorescence originates from phthalazine itself. A polarization measurement was made by the photoselection method, with the result that the transition moment of the phosphorescence is parallel to the moment of the 0–0 band of the $^1A \rightarrow {}^1L_b$ absorption; namely, the phosphorescence is polarized along the long axis of the molecule. The lifetime and quantum yield of the phosphorescence were determined to be 0.7 sec and 0.04, respectively.

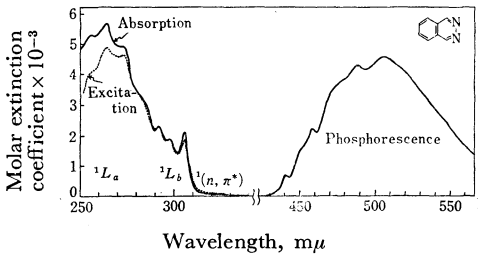

Fig. 1. Phosphorescence, excitation, and absorption spectra of phthalazine in EPA at 77°K.

The radiationless processes in phthalazine were investigated through the phenomenon of the intermolecular T–T energy transfer, with phthalazine as the donor and naphthalene as the acceptor. The solubility of phthalazine in the pure hydrocarbon was so low that a mixture of ether and isopentane (1 : 1) was used as the solvent. In this mixture phthalazine was found to give a phosphorescence emission with a quantum yield of 0.008. The donor(1×10^{-3} M)-acceptor(3.3×10^{-2} M) system was excited at 330 mμ in the region of the $n \rightarrow \pi^*$ absorption of the donor, where the absorption of the acceptor was negligible. An effective energy transfer occurred which led to the sensitized phosphorescence of naphthalene. The overall quantum yield of the acceptor phosphorescence (relative to the donor excitation) amounted to about 0.07. This figure implies that the donor molecule has a considerably high intersystem crossing yield (>0.7), since for naphthalene the ratio of the radiationless triplet-decay rate constant to the radiative constant is known to be large (>10).[1]

These observations lead to the following suggestions. (1) The lack of fluorescence in phthalazine is caused by an efficient intersystem crossing process. (2) The vanishing or low phosphorescence quantum yield of phthalazine results from an anomalously high radiationless rate constant as compared with the radiative rate constant for the $T_1 \rightarrow S_0$ transition. Details of the experiments and further discussions will be presented in a paper to be published later.

*1 Presented in part at the 21st Annual Meeting of the Chemical Society of Japan, Osaka, April, 1968.

1) S. K. Lower and M. A. El-Sayed, *Chem. Revs.*, **66**, 199 (1966).
2) M. A. El-Sayed, *J. Chem. Phys.*, **38**, 2834 (1963); **36**, 573 (1962).
3) B. J. Cohen and L. Goodman, *ibid.*, **46**, 713 (1967).
4) R. M. Hochstrasser and C. Marzzacco, *ibid.*, **45**, 4681 (1966); **46**, 4155 (1967).
5) R. Müller and F. Dörr, *Z. Elektrochem.*, **63**, 1150 (1959).

The Isolation of the Two Isomers of Bis(L-aspartato)cobaltate(III)[1]

Kinya HOSAKA, Hiroaki NISHIKAWA and Muraji SHIBATA

Department of Chemistry, Faculty of Science, Kanazawa University, Kanazawa

(Received November 12, 1968)

There have been only a few investigations of cobalt(III) complexes containing the aspartate anion as a tridentate ligand.[2,3] We have now isolated two isomers of bis(L-aspartato)cobaltate-(III) from a reaction mixture of tricarbonato-cobaltate(III) with L-aspartate.

Monopotassium L-aspartate (31.0 g, 0.2 mol) was added to a solution of tricarbonatocobaltate(III) ($CoCl_2 \cdot 6H_2O$ 23.8 g scale, 0.1 mol), and the mixture was stirred at 60°C for 5 hr.[4] This solution was then acidified with acetic acid and heated on a water bath for 2 hr in order to complete the evolution of carbon dioxide. The resulting solution was treated with methanol to precipitate a red-violet material. This was dissolved in water and used for ion-exchange chromatography. Each portion of the aqueous solution was added to a column (Dowex 1×8, 100—200 mesh, Cl-form, $\phi = 4$ cm, $h = 30$ cm). During elution with a 0.1 M $CaCl_2$ solution, a band at the top of the column separated into two: the first eluted band (red-violet) and the second one (blue-violet). These bands were collected in fractions. Evaporation and the addition of ethanol gave the calcium salts of the desired complex. These were characterized by means of a study of their UV and CD spectra (Fig. 1). The earlier-eluted isomer is designated here as E-1, and the later-eluted one, E-2. The total yields were 5 g (for E-1) and 4 g (for E-2).

Found: C, 23.99; H, 4.76; N, 7.15% for E-1. C, 24.03; H, 4.70; N, 7.17% for E-2. Calcd for $Ca_{0.5}CoC_8H_{17}N_2O_{11.5} = Ca_{1/2}[Co(L\text{-}asp)_2] \cdot 3.5H_2O$: C, 23.77; H, 4.24; N, 6.93%.

The same isomers were also obtained by means of direct synthesis from the components and lead dioxide.

For the bis(L-aspartato)cobaltate(III) ion, three isomers are possible: (a) *trans*(N)·*cis*(O)·*cis*(O_β), (b) *cis*(N)·*trans*(O)·*cis*(O_β), and (c) bis(N)·*cis*(O)·*trans*(O_β), (O_β represents the two β-oxygen atoms). It is considered, from the order of chromatographic elution, that E-2 is either one of the two *cis*(N) isomers, while E-1 is the *trans*(N) isomer or another one of the *cis*(N) isomers. The geometry of our complex ion resembles that of the bis(L-2,3-diamino-propionato)cobalt(III) ion[5] in that they both contain two optically-active tridentate ligands. The CD curve of E-1 is similar, in appearance and magnitude, to that of the L-3*1 isomer of the diaminopropionato complex, and the CD curve of E-2 is similar to that of L-1.*1 The geometry of L-1 has been determined as *trans*(O)·*cis*(N_α)·*cis*(N_β); hence, it seems that E-2 has the corresponding geometry *cis*(N_α)·*trans*(O)·*cis*(O_β). On the other hand, it is impossible to relate the geometry of E-1 to that of L-3, for the latter is not known definitely.

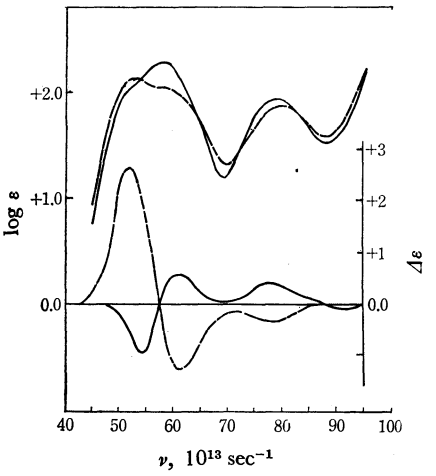

Fig. 1. UV and CD spectra of two isomers of $Ca_{1/2}[Co(L\text{-}asp)_2] \cdot 3.5H_2O$.
—— the ealier-eluted isomer (E-1)
--- the later eluted isomer (E-2)

The E-2 isomer is perhaps the first example of a complex differing in the splitting of the first band from the usual *cis*(N)-$[Co(O)_4(N)_2]$-type complexes.[6] For the *cis*(O)-$[Co(O)_2(N)_4]$-type complexes, such a splitting of the first band appears in the $[Co(L\text{-}asp)(NH_3)_3]^+$ [2] and bis(L-2,3-diamino-propionato)cobalt(III) complexes.[5]

1) Presented in part at the 21st Annual Meeting of the Chemical Society of Japan, Osaka, April, 1968.

2) J. I. Legg and D. W. Cooks, *J. Am. Chem. Soc.*, **89**, 6854 (1967).

3) J. Hidaka, private communication.

4) M. Shibata, H. Nishikawa and K. Hosaka, This Bulletin, **41**, 130 (1968).

5) W. A. Freeman and C. F. Liu, *Inorg. Chem.*, **7**, 764 (1968).

*1 According to the order of chromatographic elution, the isomers are designated as L-1, L-2, and L-3.[5]

6) N. Matsuoka, J. Hidaka and Y. Shimura, This Bulletin, **40**, 1868 (1967).

A Novel Method for the Preparation of *p*-Methoxybenzyloxycarbonyl Amino Acids

Shōsuke Sōfuku, Mitsuo Mizumura and Akira Hagitani

Department of Chemistry, Faculty of Science, Rikkyo (St. Paul's) University Toshima-ku, Tokyo

(Received November 20, 1968)

The *p*-methoxybenzyloxycarbonyl (*p*MZ-) group[1,2] has been widely used as a blocking substituent of the amino moiety of amino acids in peptide synthesis. In the present investigation, it was found that *p*MZ-amino acids were prepared directly from a number of amino acids and *p*-methoxybenzyl chloroformate[3,4] (I) under the conditions of the Schotten-Baumann reaction. The reagent (I) was prepared as follows: a solution of anisyl alcohol (12.4 m*l*, 0.1 mol) in dry ether (100 m*l*) was added to a solution of phosgene (21 m*l*, 0.3 mol) in dry ether (100 m*l*) over a period of 10 min. Then a solution of dimethylaniline (12.7 m*l*, 0.1 mol) in dry ether (100 m*l*) was added dropwise over a period of 1 hr, and the mixture was stirred for 2 hr at −5—−10°C. After filtration of the salt formed in the reaction, the filtrate was evaporated under reduced pressure to an oily residue at below 0°C. Twice more dry ether (100 m*l*) was added and evaporation was repeated to remove excess phosgene. This residue was immediately dissolved in tetrahydrofuran (70 m*l*) and the solution was ready for the next reaction.

The solution of the chloroformate was added little by little over a period of 10 min to a solution of

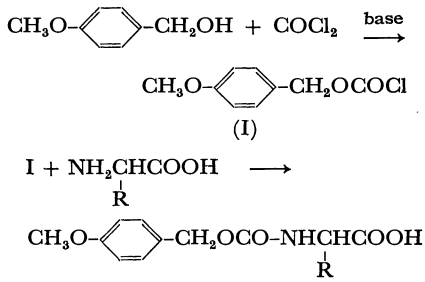

0.05 mol of the amino acid in 200 m*l* of *N* sodium hydroxide (L-glutamic acid: 1.5 N sodium hydroxide) containing tetrahydorfuran (40 m*l*) with vigorous stirring at 0—5°C. This stirring was continued for 2 hr; then the reaction mixture was washed with ether (100 m*l*) and acidified by the addition of solid citric acid. The product was extracted with ethyl acetate (500 m*l*). This layer was washed with water, dried over anhydrous sodium sulfate, and concentrated *in vacuo* to a residue, which was then crystallized from ethyl acetate-petroleum ether. If the product did not crystallize at this stage, the residue was neutralized with a calculated amount of dicyclohexylamine in ether, and the *p*MZ-amino acid was crystallized as the dicyclohexylammonium salt.

By the present method the following compounds were obtained:

*p*MZ-glycine (80.0%), mp 95—98°C*1 (lit.,[3] mp 95—98°C).

*p*MZ-L-alanine (65.4%), mp 78—81°C,*1 $[\alpha]_D^{22}$ −11.5 (*c* 2.0, acetic acid) [lit.,[2] mp 74—75°C, $[\alpha]_D^{22}$ −11.9 (*c* 3.11, acetic acid)]. (Found: C, 56.94; H, 5.83; N, 5.70%. Calcd for $C_{21}H_{15}NO_5$: C, 56.90; H, 5.98; N, 5.54%.)

*p*MZ-L-glutamic acid (46.1%), mp 109—112°C,*1 $[\alpha]_D^{22}$ −5.6 (*c* 2.0, acetic acid) [lit.,[2] mp 109—111°C, $[\alpha]_D^{22}$ −7.44 (*c* 2.02, acetic acid)]. (Found: C, 53.76; H, 5.22; N, 4.58%. Calcd for $C_{14}H_{17}NO_7$: C, 54.00; H, 5.50; N, 4.50%.)

*p*MZ-L-leucine dicyclohexylammonium salt (88.7%), mp 159—162°C,*1 $[\alpha]_D^{21}$ −6.0 (*c* 2.0, methanol) [lit.,[2] mp 162°C, $[\alpha]_D^{24}$ −6.67 (*c* 2.1, methanol)]. (Found: C, 68.04; H, 9.07; N, 6.01%. Calcd for $C_{27}H_{44}N_2O_5$: C, 68.03; H, 9.31; N, 5.88%.)

α-*N*-*p*MZ-δ-*N*-Cbz*2-L-ornithine dicyclohexylammonium salt (33.4%), mp 133—135°C,*1 $[\alpha]_D^{19}$ +6.3 (*c* 2.0, methanol). (Found: C, 66.91; H, 7.91; N, 6.94%. Calcd for $C_{34}H_{49}N_3O_7$: C, 66.75; H, 8.07; N, 6.87%.)

A full report will be presented in a subsequent paper.

1) F. C. McKay and N. F. Albertson, *J. Am. Chem. Soc.*, **79**, 4686 (1957).
2) F. Weygand and K. Hunger, *Chem. Ber.*, **95**, 1 (1962).
3) J. H. Jones and G. T. Young, *Chem. & Ind.*, **1966**, 1722.
4) S. Sōfuku, M. Mizumura and A. Hagitani, *Nippon Kagaku Zasshi* (*J. Chem. Soc. Japan, Pure Chem. Sect.*), **89**, 721 (1968).

*1 All melting points are uncorrected.
*2 Cbz: benzyloxycarbonyl.

BULLETIN OF THE CHEMICAL SOCIETY OF JAPAN VOL. 42 279—284 (1969)

Concentration Polarization Phenomena in Ion-exchange Membrane Electrodialysis. I. Studies of the Diffusion Boundary Layer by Means of Six Different Measurements*1

Toshikatsu SATA, Reiichi YAMANE and Yukio MIZUTANI

Tokuyama Soda Co., Ltd., 1-1 Mikage-cho, Tokuyama, Yamaguchi

(Received December 25, 1967)

The behavior of the diffusion boundary layer in the electrodialysis using ion-exchange membranes, mainly a cation-exchange membrane, was studied by means of six different measurements: 1) the determination of the current-voltage curve or the current-(voltage/current) curve; 2) the relation of the pH change of the solution to the current density; 3) the relation of the charge retention, *i. e.*, the sum of the diffusion potential and the membrane potential generated from the concentration gradient across the membrane immediately after the current is shut off, to the current density; 4) the time required to reach a constant current value, namely, to obtain a stationary diffusion boundary layer, when a constant voltage is supplied to the system, *versus* the current density; 5) the change in the transport number of the counterion in the membrane with the current density, and 6) the relation of the permselectivity between sodium ions and potassium ions to the current density. The interrelation among these results was also examined. The quantity of hydrogen ions or hydroxide ions passing through the membrane increases abruptly at a current density lower than that at which the concentration at the membrane-solution interface in the desalting side attains its minimum. It was newly observed that the results of all the measurements, except for the pH change of the solution, show abnormal phenomena at a current density about twice the limiting current density.

In the electrodialysis using ion-exchange membranes, one of the most important phenomena is the concentration polarization at the membrane-solution interfaces. The concentration gradient is observed on both sides of the membrane-solution interfaces; ions are accumulated or depleted at the interfaces as a result of the difference in the transport numbers in the solution and in the membrane. This phenomenon, called the concentration polarization, is especially important at the membrane-solution interface on the desalting side.

Peers,[1] Rosenberg *et al.*,[2] Frilette,[3] and other investigators studied this phenomenon by observing the current-voltage curve of the membrane-solution system. Uchino *et al.*[4] and Gregor *et al.*[5] observed limiting current density through the relation of the current efficiency to the current density. Cooke[7-9] and Onoue[10] evaluated the interfacial concentration at the membrane-solution interface on the desalting side by determining the charge retention. Though the concentration polarization phenomenon has been studied in the various ways mentioned above, however, there still remain some uncertainties, and the interrelation among the results obtained by means of various measurements is not clear.

In this investigation this phenomenon was observed by means of the following six measurements, with an emphasis on the observation of the current-voltage curve of the membrane-solution system, and the results were compared with each other. The six measurements are: 1) the determina- the pH change of the solution in the electrodialysis system, while Kressman and Tye[6] observed the

*1 Studies on Ion exchange Membranes. XXVII. Presented at the 17th Meeting C.I.T.C.E. (Comite International de Thermodynamique et de Cinetique Electrochimiques) held in Tokyo, Japan, in September 1966.

1) A. M. Peers, *Discussions Faraday Soc.*, **21**, 124 (1956).

2) N. W. Rosenberg, J. A. Kirkham, C. E. Tirrell and N. E. Saliba, *Saline Water Research and Development Progress Report*, No. 1 (U.S. Dept. of Interior), April,

3) V. J. Frilette, *J. Phys. Chem.*, **61**, 168 (1957).

4) T. Uchino, S. Nakaoka, H. Hani and T. Yawataya, *Denki Kagaku* (*J. Electrochem. Soc. Japan*), **26**, 366 (1958).

5) H. P. Gregor and M. A. Peterson, *J. Phys. Chem.*, **63**, 2201 (1964).

6) T. R. E. Kressman and F. L. Tye, *Discussions Faraday Soc.*, **21**, 185 (1956).

7) B. A. Cooke, *Electorchim. Acta*, **3**, 307 (1961).

8) B. A. Cooke, *ibid.*, **4**, 179 (1961).

9) B. A. Cooke, *ibid.*, **5**, 216 (1961).

10) Y. Onoue, *Denki Kagaku* (*J. Electrochem. Soc. Japan*), **30**, 415 (1962).

tion of the current-voltage curve or the current-(voltage/current) curve; 2) the relation of the pH change of the solution to the current density; 3) the relation of the charge retention, *i. e.*, the sum of the diffusion potential and the membrane potential generated from the concentration gradient across the membrane immediately after the current is shut off, to the current density; 4) the time required to reach a constant current value, namely, to obtain a stationary diffusion boundary layer, when a constant voltage is given to the system, *versus* the current density; 5) the change in the transport number of the counterion in the membrane with the current density, and 6) the permselectivity (relative transport number) of potassium ions to sodium ions *versus* the current density.

Experimental

Ion-exchange Membranes. Throughout this investigation, commercial ion-exchange membranes prepared by the "Paste Method," *i. e.*, a cation-exchange membrane, NEOSEPTA CL-2.5T, and an anion-exchange membrane, NEOSEPTA AVS-4T, were used. The characteristics of these membranes are shown in Table 1.

TEBLE 1. CHARACTERISTICS OF ION EXCHANGE MEMBRANES

Name	NEOSEPTA CL-2.5T	NEOSEPTA AVS-4T*1
Type	Strongly acidic cation exchange	Strongly basic anion exchange
Backing	Polyvinyl chloride	Polyvinyl chloride
Thickness (mm)	0.15—0.17	0.15—0.17
Burst strength (kg/cm²)	3—4	4—6
Electric resist.*2 (Ω-cm²)	2.7—3.2	3.7—4.7
Transport number*3	>0.98	>0.98
Water content*4	0.30—0.40	0.25—0.35
Ion exchange cap.*5	1.8—2.0	1.5—2.0

*1 Univalent anion permselective.
*2 Equilibrated with 0.5 N NaCl soln. at 25.0°C.
*3 Measured by electrodialysis with 0.5 N NaCl soln., current density: 10 mA/cm², at 25.0°C.
*4 Equilibrated with 0.5 N NaCl soln., [g H_2O/g Na-form dry memb. (or Cl-form)].
*5 [meq./g Na-form dry memb. (or Cl-form)].

Measurements. 1) *Current-voltage Curve.* The current-voltage curve was observed by using the apparatus shown in Fig. 1, which was also used in the other five measurements. In Fig. 1, 1 and 4 are silver chloride plate electrodes, and 2 and 3 are silver chloride wire probe electrodes which are put close to the membrane (about 2 mm apart). The current was increased automatically by means of a slow moving motor connected with a regulated direct current supply, Metronix Corp. Model 535. As the current-voltage curve varies with an increase in the speed of the current when it is too large, the increase in the speed was adjusted so as not to affect the current-voltage curve. The values

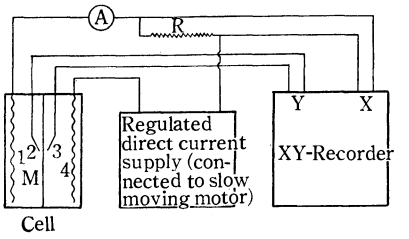

Fig. 1. Equipment used in measurement of current-voltage curve.
R: standard resistance
A: amperemeter
M: membrane
1, 4: silver chloride plate electrodes
2, 3: silver chloride wire probe electrodes

of the current and the voltage were recorded on an X-Y recorder, Watanabe Instruments Corp. Type WX-406.

2) *pH Change in the Solution.* A cell has a cation- or an anion-exchange membrane (4.0 cm² in area) to be examined and shielding cation- and anion-exchange membranes (36 cm² in area). An aqueous 0.500 N sodium chloride solution (3.0*l* in volume) was circulated in the desalting compartment (10 mm thick) at a laminar flow of 4.2 cm sec^{-1}, and an aqueous 2.500 N sodium chloride solution (50 m*l* in volume) was circulated in the concentrating compartment (3 mm thick) at a laminar flow of 1.3 cm sec^{-1}. The pH change in the solution in the concentrating compartment was observed continuously for an hour by using a glass electrode pH-meter, Denki Kagaku Keiki Co. Model MG-1, connected to an X-t recorder, Toa Electronics. EPR-2T, while the current was broken by the dripping of the solution. The difference in the pH of the solution between the starting time and after an hour was evaluated at various current densities at 30.0°C.

3) *Charge Retention.* In preparing Fig. 1 the X-t recorder was used instead of the X-Y recorder, and two turn-over switches were added between the 1 and 4 electrodes and the direct current supply, and between the 2 and 3 electrodes and the X-axis of the X-t recorder. After the membrane-solution system had been electrodialized at a constant current density until a stationary diffusion boundary layer had been obtained, the current was shut off and the charge retention was picked up with the 2 and 3 electrodes. The scanning speed of a pen on the recorder is more than 300 mm/sec, faster than that of turning switches. The decrement curve of the charge retention at various current densities was recorded on the X-t recorder. These measurements were carried out with a natural convection of an aqueous 0.104 N sodium chloride solution by using a membrane 2.0 cm² in area and at 25.0°C.

4) *Transport Number.* The cell was separated into two compartments by a membrane with an area of 2.0 cm². After the electrodialysis had been carried out at a constant current density for an hour using an aqueous 0.104 N sodium chloride solution, the transport number was calculated from the change in the concentration of chloride ions in each compartment and the amount of the electricity was measured with a copper coulometer. These measurements were carried

out with a natural convection and at various current densities at 25.0°C.

5) *Time Required to Obtain a Stationary Diffusion Boundary Layer.* When a constant voltage was supplied to the cell, the current passing through the membrane, as recorded on the X-t recorder, gradually decreased because of the growth of the diffusion boundary layer, the stationary current was then obtained. The time required to reach the constant current value was measured at various constant voltages. The measurements were made with a natural convection of an aqueous 0.104 N sodium chloride solution by using a membrane with an area of 2.0 cm^2 and at 25.0°C.

6) *Permselectivity.* The cell was separated into two compartments by a membrane with an area of 4.0 cm^2. After the system had been electrodialized at a constant current density for an hour using a mixed solution of 0.053 N sodium chloride and 0.053 N potassium chloride, the permselectivity of potassium ions to sodium ions was calculated from the change in the concentration in each compartment. The chloride ions were analysed by the Mohr method, while the potassium ions were analyzed by the gravimetric method using tetraphenylborate. The measurements were made with a natural convection and at various current densities at 25.0°C. The permselectivity is defined as $(t_K^M/t_{Na}^M)/(C_K/C_{Na})$. t_K^M and t_{Na}^M are respectively the transport numbers of the potassium ions and the sodium ions in the membrane, and C_K and C_{Na} are the concentrations of potassium ions and sodium ions respectively in the bulk solution.

Results and Discussion

Typical examples of the current-voltage curve and of the current-(voltage/current) curve obtained with a cation-exchange membrane, NEOSEPTA CL-2.5T, in an aqueous sodium chloride solution are shown in Fig. 2. A similar curve was obtained

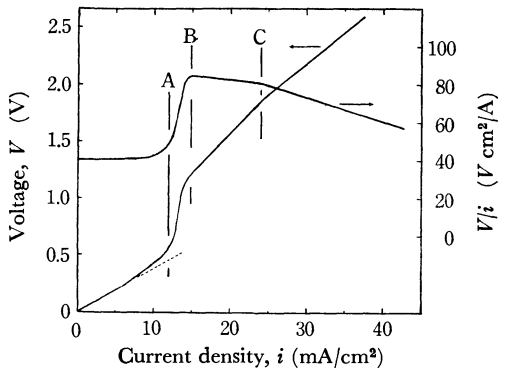

Fig. 2. An example of current-voltage curve and current-V/i curve.
Membrane: CL-2.5T (2.0 cm^2 in area)
Solution: 0.104 N NaCl aqueous solution in natural convection at 25.0°C

with an anion-exchange membrane, NEOSEPTA AVS-4T, in an aqueous sodium chloride solution. In this curve the voltage and the (voltage/current) of the system are anomalous at three different current densities, *i. e.*, A-, B-, and C-points. The current density at the A-point has been defined as the limiting current density.[11] The (voltage/current) ratio shows its maximum value at the B-point, a gradual decrease between the B- and C-points, and an abnormal decrease at the C-point.

The relationship between the pH change of the solution and the current density is shown in Fig. 3, in which the A- and B-points as determined

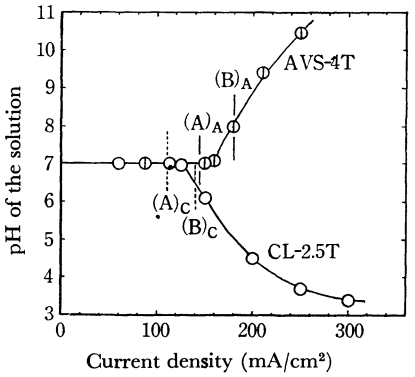

Fi. 3. Relation between pH of the solution in the concentrating side of membrane after current was passed for an hour and current density.
0.500 N NaCl aqueous solution let to flow in the desalting side at 4.2 cm sec^{-1}, and 2.500 N NaCl aqueous solution in the concentrating side at 1.3 cm sec^{-1}.
$(A)_C$, $(B)_C$: A-, B-point in CL-2.5T
$(A)_A$, $(B)_A$: A-, B-point in AVS-4T

from current-voltage curves are added. The pH change in the solution was detected between the A- and the B-points.

The experimental results on the charge retention are shown in Fig. 4. The charge retention is

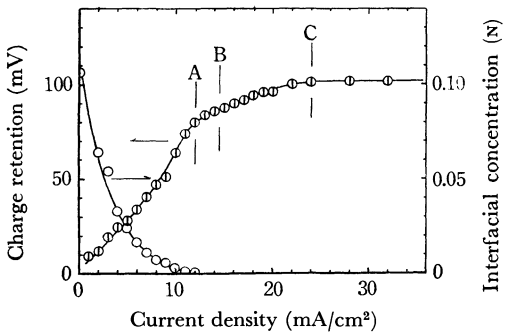

Fig. 4. Relation of charge retention and interfacial concentration in desalting side of membrane evaluated from charge retention to current density.
Membrane: CL-2.5T
Solution: 0.104 N NaCl aqueous solution in natural convection

11) D. A. Cowan and J. H. Brown, *Ind. Eng. Chem.*, **51**, 1445 (1959).

the sum of the diffusion potential and the membrane potential. For example, when the electrodialysis is carried out by using the cation-exchange membrane in an aqueous sodium chloride solution, the charge retention is shown by the following equation[7,10]:

$$E = \frac{RT}{F} 2(\bar{t}_+ - t_+) \ln \frac{(C_0+\Delta C)\gamma_1}{(C_0-\Delta C)\gamma_2} \qquad (1)$$

$\bar{t}_+$ and t_+ are transport numbers of the counterion in the cation-exchange membrane and in the solution, C_0 is the concentration in the bulk solution, ΔC is the difference in the concentration between the membrane-solution interfaces and the bulk solution, and γ_1 and γ_2 are activity coefficients of the counterion at the membrane-solution interfaces on the concentrating side and on the desalting side respectively. The charge retention increases abruptly at current densities lower than the A-point, and increases slowly between the A- and C-points. No change was observed at the B-point, and a constant value was obtained at current densities higher than the C-point. The same results were obtained with the anion-exchange membrane. The concentration at the membrane-solution interface on the desalting side could be calculated from Eq. (1) as long as the quantity of hydrogen ions is negligible in comparison with the quantity of sodium ions in the diffusion boundary layer and in the bulk solution. The calculated values are shown in Fig. 4.

The relation of the transport number to the current density is shown in Fig. 5. The transport

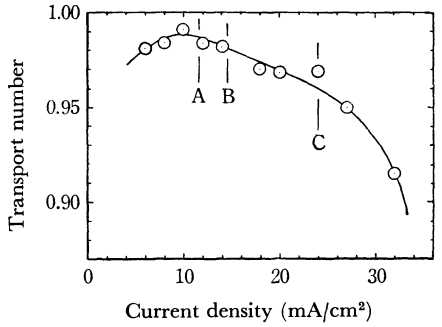

Fig. 5. Relation of transport number to current density.
Membrane: CL-2.5T
Solution: 0.104 N NaCl aqueous solution in natural convection

number shows its maximum value near the A-point; it gradually decreases between the B- and C-points and suddenly above the C-point.

The relation between the time required to obtain a stationary diffusion boundary layer and the current density is shown in Fig. 6. The change in the current with time is shown in Fig. 7 as an

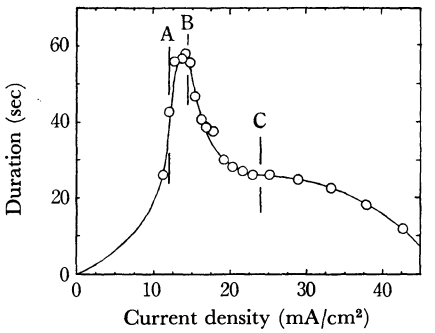

Fig. 6. Relation of duration required to obtain stationary diffusion boundary layer to current density.
Membrane: CL-2.5T
Solution: 0.104N NaCl aqueous solution in natural convection

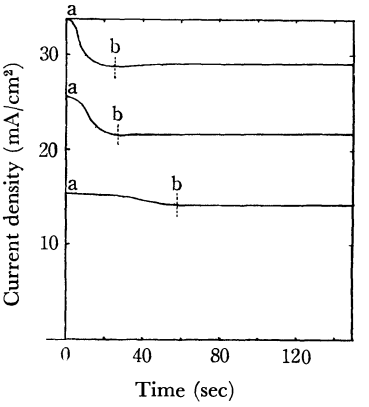

Fig. 7. Decrement curves of current when constant voltage is given to cation exchange membrane-solution system.
Time between a and b is the duration required to obtain the stationary diffusion boundary layer.

example. The time is defined as the time interval between a and b in Fig. 7. No change was observed at the A-point, the maximum was obtained near the B-point, and the duration decreased abruptly at current densities higher than the C-point. The stationary diffusion boundary layer was achieved on balancing the flux of ions passing through the membrane with that of ions transporting to the membrane-solution interface on the desalting side. When the current density increases, the concentration at the membrane-solution interface on the desalting side decreases and the time increases. When the interfacial concentration on the desalting side attained its minimum, the time reached its maximum. Thus, the maximum duration is obtained in the vicinity of the B-point. The duration decreases at current densities higher than the B-point. This behavior is analogous to the relation of the transition time to the current density in the chronopotentiometry. The transition time is

shown as follows:[12]

$$\tau^{1/2} = \frac{nF\pi^{1/2}D^{1/2}C}{2i} \quad (2)$$

C is the concentration of the solution; i is the current density; τ is the transition time; D is the diffusion coefficient, and n and F are the valency and the Faraday constant respectively. The $\tau \propto 1/i^2$ relation is inferred at the current densities between the B- and C-points in Fig. 6. However, the decrease in the duration at current densities higher than the C-point is anomalous.

Figure 8 shows the permselectivity of potassium

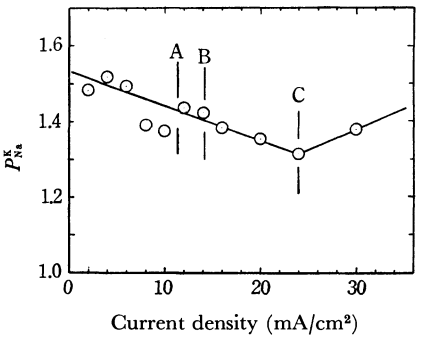

Fig. 8. Reltation of permselectivity between sodium ion and potassium to current density.
Membrane: CL-2.5T
Solution: Mixed solution of 0.053N KCl and 0.053 N NaCl in natural covection
P^{K}_{Na}: Permselectivity between K^+ and Na^+.

ions to sodium ions at several different current densities. As the permselectivity of potassium ions to sodium ions is larger than unity, the concentration of sodium ions becomes larger than that of potassium ions at the membrane-solution interface on the desalting side when the current increases, and so the permselectivity, p^{K}_{Na}, decreases. In Fig. 8 no change is observed at the A- and B-points, but some change is observed at current densities higher than the C-point.

The relation among the six experimental results mentioned above will now be discussed with emphasis on the interpretation of the A-, B-, and C-points. Near the A-point, the voltage of the membrane-solution system suddenly begins to increase, the increase in the charge retention becomes slower, the period required to obtain a stationary diffusion boundary layer increases continuously, and the transport number of the counterion in the membrane attains its maximum. The results on the current-voltage curve, the charge retention, and the duration show a further decrease in the concentration at the membrane-solution interface on the desalting side near the A-point. It was reported in a previous paper[6] that the transport number of sodium ions in the cation-exchange membrane decreases at higher current densities after showing its maximum value as a result of the increase in the transport number of hydrogen ions in the membrane. However, the pH change in the solution was detected between the A- and B-points. The pH change in the solution might arise from the following three causes. First, the pH change in the solution may be on account of the increase in the rate of the dissociation of water under a strong electric field; however, this has scarcely any effect on the pH change in the solution because the electric field of 10^4 V/cm increases the dissociation constant by only 1 percent.[13,14] Secondly, the ion-exchange membranes used in this experiment are reinforced with polyvinyl chloride and so would have conjugated double bonds through the decomposition of polyvinyl chloride during the introduction of sulfonic acid groups and other treatments.[15] If there were an electronic conduction based on conjugated double bonds, the ion-exchange membranes would function as electrodes. Therefore, the electrolysis of water could occur at the membrane-solution interfaces and cause the pH change in the solution. However, as the pH change in the solution was nearly constant in the ion-exchange membranes reinforced with other polymers, this effect would scarcely have any relation with the pH change in the solution. Thirdly, when the current density increases, the concentration of sodium or chloride ions on the desalting membrane-solution interface decreases and becomes nearly equal to the concentration of hydrogen or hydroxide ions (10^{-7} mol/l). Consequently, the quantity of hydrogen or hydroxide ions which pass through the membrane increases in comparison with that of sodium or chloride ions. Hydrogen or hydroxide ions pass through the membrane at current densities lower than the A-point, but the pH change in the solution could not be observed because it is too small to be detected by a usual pH-meter. It may be considered that the pH change in the solution in the electrodialysis is caused by the third reason. We attempted to observe the pH change in the solution visibly by adding a pH-indicator to the solution. However, the current-voltage curve observed in the solution with the pH-indicator differs from those in the solution without the pH-indicator and are not reproducible. The adsorption of the pH-indicator on the membrane would change the characteristics of the membrane.

The concentration of the desalting membrane-solution interface attains its minimum at the B-

12) *Denki Kagaku Binran (Handbook of Electrochemistry)*, 344 (1964).

13) H. P. Gregor and I. P. Miller, *J. Am. Chem. Soc.*, **86**, 5689 (1964).

14) L. Onsager, *J. Chem. Phys.*, **2**, 599 (1934).

15) C. Forgacs and G. Stein, *J. Phys. Chem.*, **69**, 4221 (1965).

point. This is unquestionably established by the observation of the current-(voltage/current) curve and the duration time. The pH change in the solution, the charge retention, and the permselectivity, P_{Na}^{K}, do not show any change at the B-point. Figure 2 shows that the current-(voltage/current) curve decreases at current densities higher than the B-point. In order to make clear the reason for this decrease, the current-voltage curve and the current-(voltage/current) curve were observed using the cation-exchange membrane, NEOSEPTA CL-2.5T, in an aqueous hydrochloric acid solution. The results are shown in Fig. 9.

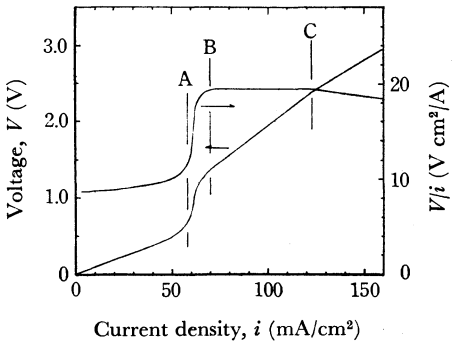

Fig. 9. Current-voltage and current-V/i curve measured in hydrochloric acid solution.
Membrane: CL-2.5T
Solution: 0.100 N HCl aqueous solution in natural convection at 25.0°C

The current-voltage curve does not decrease, but is parallel with the current-axis, between the B- and C-points, while it decreases above the C-point. Accordingly, the decrease in the current-(voltage/current) curve in a sodium chloride solution between the B- and C-points is due to the increase in the transport number of hydrogen ions in the membrane and their high conductivity. At and above the C-point, the current-(voltage/current) curve decreases still more, the duration time decreases abnormally, the decrease in the transport number is great, the permselectivity, P_{Na}^{K}, increases, and the charge retention attains a constant value. This behavior at and above the C-point can not yet be explained.

This paper has mainly described measurements of the cation-exchange membrane. The same results were obtained on the anion-exchange membrane, NEOSEPTA AVS-4T. It was reported in an earlier paper[7] that the extent of the pH change in the solution of the anion-exchange membrane system is larger than that in the cation-exchange membrane system. However, there is no difference between the cation-exchange membrane system and the anion-exchange membrane system in this experiment using NEOSEPTA. Figure 3 shows that the pH of the solution shifts to about 3 in the cation-exchange membrane system and to about 10 in the anion-exchange membrane system at a high current density.

The A-, B-, and C-points measured by means of the six measuring methods are relative values. These points vary with various factors, such as the concentration, the temperature, and the flow velocity of the solution, the structure of the cell, the ionic species, and so on. The effect of these factors on the limiting current density has been studied and will be reported on subsequent papers.

BULLETIN OF THE CHEMICAL SOCIETY OF JAPAN VOL. 42 285—289 (1969)

Shock Induced Reactions of Methane with Nitrous and Nitric Oxides

L. J. DRUMMOND

Australian Defence Scientific Service, Weapons Research Establishment, Salisbury, South Australia

(Received December 5, 1967)

Reflected shock waves, generated in a 5×3 inch shock tube, have been used to ignite mixtures of methane-nitrous oxide and methane-nitric oxide. Monochromators, a pressure transducer and an oscilloscope were used to determine the induction period to ignition (τ) after the reflected wave passed the window. A flash lamp and spectrograph were also used to obtain spectra before and after explosion. For CH_4-N_2O mixtures it was found that the plot of $\log(\tau[N_2O]p_5)$ against inverse temperature was linear and the activation energy was about 60 kcal/mol. This indicates that the rate controlling process was the reaction $N_2O(+M)\rightarrow N_2+O(+M)$. However, the reaction $CH_3+N_2O\rightarrow CH_2+N_2+OH$ may also be important. The results for CH_4-NO mixtures could be expressed by $\log(\tau[NO]p_5)=-10.2+49000/4.58T$ which suggests to the reaction $CH_2+NO\rightarrow CH+HNO$ may be rate controlling. Spectrographic plates showed that CN and OH were present during the induction period but only OH was detected after explosion. This indicates that the reactions $CH+NO\rightarrow CN+OH$ and $CN+NO\rightarrow N_2+CO$ may be a significant mechanism for achieving the reduction of nitric oxide.

The mechanism of methane oxidation with O_2 has been thoroughly examined by Miyama and Takeyama[1] who showed that different reactions governed the induction period to explosion of methane-rich and methane-lean mixtures. For the latter type, OH appeared before the rise in pressure due to exothermic reaction. The temperature dependence of these two induction periods indicated that they were associated with the oxidation of CH_3 and CH_2O respectively.

Our previous work showed that reaction of ammonia[2] and hydrogen[3] with N_2O was rapid and complete. However, with NO, reactions were incomplete even for temperatures of 2000°K and this was believed due to the formation of HNO and subsequent regeneration of NO.

The study is now extended to include methane, the simplest saturated hydrocarbon, as fuel with the hope of identifying the rate-controlling reaction during the induction period and of assessing the influence of the fuel-oxidant ratio on the mechanisms.

Experimental

The shock tube and ancillary equipment have been described.[2] The optical path was 14 mm from the end plate in all experiments. The 1 mm wide beam was split so that the upper half entered a Hilger monochromator set to detect absorption at one wavelength, and the lower half passed to a Bausch and Lomb monochromator set to monitor absorption by OH at 3070 Å. The outputs of the photomultiplier tubes were fed to a Tektronix 555 dual beam oscilloscope. A pressure transducer (Kistler 603 A) was installed in the floor of the shock tube with its centre 2.5 mm from the end plate. Its amplified output was placed on one trace of the oscilloscope set in chopped mode. Alternatively, spectrographic plates were obtained with the use of a Hilger medium quartz spectrograph and a small flash lamp (7.5 μsec duration, 100J). The signal from the detector station due to arrival of the incident shock, instead of triggering the oscilloscope, was fed to a delay unit and then to the flash lamp. With a series of shocks of comparable strength, progressive increase of the delay allowed absorption spectra to be obtained before, at, and after explosion of reactant mixtures which had been processed at comparable temperatures.

The speed of the incident shock (U_s) was measured over 267 mm just before arrival at the end plate. The speed of the reflected shock (U_r) was measured over 135 mm after it had travelled 27 mm from the end plate. An IBM 7090 computer program was used to calculate, for a given value of U_s, the speed of the reflected shock and the pressure (p_5), density and temperature (T_5) of the reactant mixture before reaction occurred. For mixtures containing 80% or more of argon it was possible also to calculate these parameters when reactants had passed instantly to equilibrium products behind this shock.

Helium or hydrogen was used as driver gas, and the initial reactant pressure was 44 Torr in all experiments.

Methane (Phillips, 99.98% pure), nitrous oxide (C.I.G., 99.6% pure) and argon (C.I.G., 99.9% pure) were used directly from cylinders. Nitric oxide, prepared from KNO_2-KI-H_2SO_4, was distilled at low pressure until it was a white solid, melting to a pale

1) H. Miyama and T. Takeyama, This Bulletin, **38** 37 (1965).

2) L. J. Drummond and S. W. Hiscock, *Aust. J. Chem.*, **30**, 815, 825 (1967).

3) L. J. Drummond, *ibid.*, **30**, 2331 (1967).

green liquid.

Mixtures were made up manometrically to 700 Torr pressure and stirred magnetically for two hours before use.

Results

Methane Lean-Nitrous Oxide-Argon Mixtures. Three mixtures (2/8/90, 4/16/80 and 6/24/70) were used. Induction periods (τ_1) were read as the time intervals between the reflected shock passing the window and attainment of maximum [OH] after reaction occurred. Ignition delays, measured to the commencement of N_2O disappearance, were in agreement with τ_1 values. The delay (τ_2) to the pressure rise at the end plate due to the onset of exothermic reaction behind the reflected shock, was somewhat bigger than the corresponding τ_1 value measured 14 mm from the end plate. Results were obtained for $1495 < T_5 < 1935$°K and $2.5 < p_5 < 4.5$ atm. As p_5 was not constant the values of τ_1 and τ_2 were linearly normalised by multiplying by the appropriate p_5 value and Fig. 1 shows logarithmic values of $\tau_1 p_5[N_2O]$ and $\tau_2 p_5[N_2O]$ plotted against $1/T$. Least squares treatment yield the equations

$$\log(\tau_1 p_5[N_2O]) = -(13.82 \pm 0.12) + (60540 \pm 900)/4.58T$$
$$\log(\tau_2 p_5[N_2O]) = -(13.34 \pm 0.25) + (57700 \pm 1900)/4.58T$$

If τ values were not pressure normalised the equations are

$$\log(\tau_1[N_2O]) = -(14.16 \pm 0.16) + (59200 \pm 1200)/4.58T$$
$$\log(\tau_2[N_2O]) = -(13.70 \pm 0.15) + (56500 \pm 1100)/4.58T$$

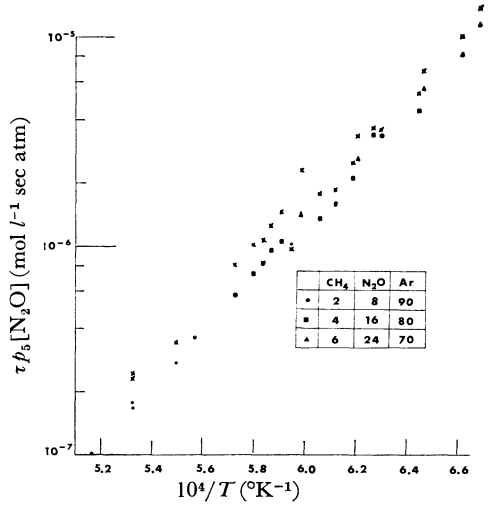

Fig. 1. Plot of $\log(\tau p_5[N_2O])$ against $1/T$ for CH_4 -N_2O-Ar mixtures. Values denoted by X are from pressure records; all others from OH absorption records.

Methane Rich-Nitrous Oxide-Argon Mixtures. Three mixtures (3.3/6.7/90, 6.6/13.4/80 and 10/20/70) were studied for the conditions $1500 < T_5 < 1985$°K and $2.8 < p_5 < 4.6$ atm. Results are summarised as

$$\log(\tau_1 p_5[N_2O]) = -(13.91 \pm 0.21) + (62400 \pm 1600)/4.58T$$
$$\log(\tau_2 p_5[N_2O]) = -(13.53 \pm 0.25) + (60200 \pm 1900)/4.58T$$

If τ values were not pressure normalised the equations are

$$\log(\tau_1[N_2O]) = -(14.22 \pm 0.23) + (60500 \pm 1800)/4.58T$$
$$\log(\tau_2[N_2O]) = -(13.85 \pm 0.18) + (58300 \pm 1400)/4.58T$$

General Obsevations. For each mixture there was a certain driver pressure (and hence T_5 value) below which reaction was not initiated. The pressure records showed that a drop in pressure occurred about the time that reaction should have taken place. The reactant mixture had been chilled by a rarefaction wave reflected back from the zone of collision between reflected shock and contact surface. Thus the shock tube was too short to obtain measurements of long induction periods (about 600 μsec) at temperatures around 1550°K.

The 4/16/80 mixture was studied at a temperature of about 1730°K using the flash lamp and spectrograph. No absorption bands were found during the induction period. At, and after explosion, strong bands due to OH at 2811 and 3064 Å were present.

Measurement of reflected shock speeds were obtained for all mixtures and those for the 3.3/

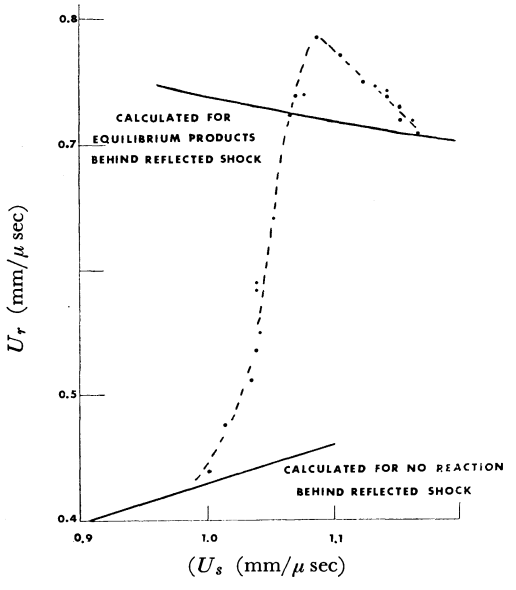

Fig. 2. Shock speed measurements in mixtures of CH_4-N_2O-Ar (3.3/6.7/90).

6.7/90 mixture are shown in Fig. 2.

The phenomenon of "overshoot" (less marked in other mixtures such as 4/16/80) has been seen in other systems,[2,3] and indicates a region in which an overdriven explosion front travels faster than the anticipated combustion-driven wave.

Chemical Reactions. Attempts to identify the rate controlling reaction during the induction period involve choosing a set of reactions such that: the rate determining reaction has an enthalpy change in agreement with the measured activation energy; the number of molecules of fuel (m) and oxidant (n) involved in this reaction agree with the values required for $\log(\tau[\text{fuel}]^m[\text{oxidant}]^n)$ to have a linear relationship with $1/T$; and the remaining reactions in the set should lead to a number of differential equations satisfying the condition that some of the molecules involved in these reactions are in a stationary state condition. A criticism of this method for discerning the rate determining step concerns the assumption that calculations made for non-stationary state conditions are applicable to the steady state. This matter has been discussed recently by Bradley.[4]

However, if we follow the method of Miyama and Takeyama for CH_4-O_2 mixtures, there appear to be two feasible mechanisms for CH_4-N_2O mixtures:

(a) If the reactions

$$N_2O(+M) \longrightarrow N_2 + O(+M) \quad (\Delta H = 40 \text{ kcal}) \qquad (1)$$

$$CH_4 + O \longrightarrow CH_3 + OH \quad (\Delta H = 0 \text{ kcal}) \qquad (2)$$

$$CH_4 + OH \longrightarrow CH_3 + H_2O \quad (\Delta H = -17 \text{ kcal}) \qquad (3)$$

$$CH_3 + N_2O \longrightarrow CH_2 + N_2 + OH \quad (\Delta H = 53 \text{ kcal}) \qquad (4)$$

are of importance during the induction period, then, assuming that O and OH are steady state intermediates and that CH_3 is the principal chain carrier, it is necessary for $k_1[N_2O][M]\tau$ to be constant. Putting $k_1[M] = k'_1 = A\exp(-E/\boldsymbol{R}T)$, the plot of $\log(\tau[N_2O])$ *vs.* $1/T$ should be a straight line, whose slope is the activation energy of reaction (1). We obtained a value of about 60 kcal/mol and previously[2] had measured 57 kcal/mol in a study of the decomposition of nitrous oxide.

(b) If the reactions (3), (4) and

$$CH_4 + N_2O \longrightarrow CH_3 + N_2 + OH \quad (\Delta H = 40 \text{ kcal}) \qquad (5)$$

$$CH_3 + OH \longrightarrow CH_2 + H_2O \quad (\Delta H = -4 \text{ kcal}) \qquad (6)$$

are the important ones, then, assuming that OH is the steady state intermediate and CH_3 is the principal chain carrier, it is necessary for $k_4[N_2O]\tau$ to be constant. Thus $\log(\tau[N_2O])$ *vs.* $1/T$ should be a straight line, whose slope is the activation energy of reaction (4).

Methane - Nitric Oxide - Argon Mixtures. Three mixtures (2/8/90, 4/16/80 and 5/10/85) were used under the conditions $2085 < T_5 < 2810$°K and $3.8 < p_5 < 5.1$ atm. The third mixture (methane-rich) could only be studied over a narrow temperature range due to the low intensity of the OH absorption signal. At these high temperatures there was not a large increase in pressure when reaction occurred and, for this reason, induction periods were only available from OH absorption records. Maximum values of [OH] did not occur rapidly as in a real explosion, but were achieved

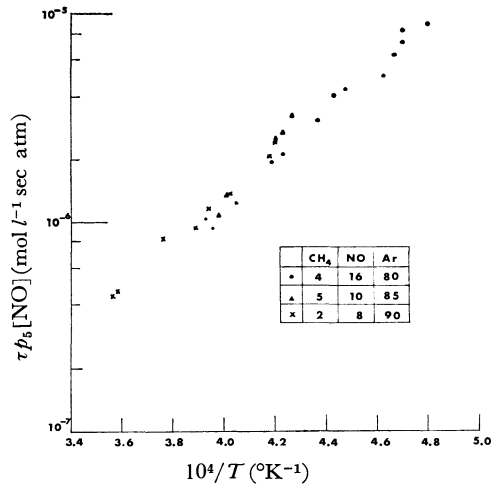

Fig. 3. Plot of $\log(\tau p_5([NO])$ against $1/T$ for CH_4-NO-Ar mixtures.

over tens of micro-seconds after passing through a point of inflexion. A plot of $\log(\tau p_5[NO])$ *vs.* $1/T$ is shown in Fig. 3. Least squares treatment of all data gave the equations

$$\log(\tau\, p_5[NO]) = -(11.20 \pm 0.13) + (49300 \pm 1400)/4.58T$$

$$\log(\tau\, [NO] = -(11.18 \pm 0.16) + (53100 \pm 1800)/4.58T$$

If the methane-rich mixture was ignored

$$\log(\tau\, p_5[NO]) = -(10.17 \pm 0.11) + (49000 \pm 1200)/4.58T$$

$$\log(\tau\, [NO] = -(11.14 \pm 0.17) + (52600 \pm 1800)/4.58T$$

In addition to monitoring OH, monochromator settings of 4320, 3875 and 3360 Å were used. The records indicated that CH and NH were absent but that CN was present during the induction period, disappearing by the time that [OH] had reached about 50% of its maximum value (see Fig. 4). These results were confirmed when the 4/16/80 mixture was studied at a temperature of about 2140°K using the flash lamp and MQ spectrograph. During the induction period the (0,0) and (1,1) bands of the $B^2\Sigma$-$X^2\Sigma$ transition of CN were seen at 3871 and 3883 Å and also,

4) J. N. Bradley, *Trans. Faraday Soc.*, **63**, 2945 (1967).

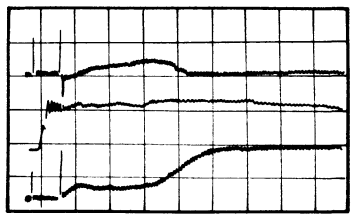

Fig. 4. Oscilloscope record obtained with a mixture of CH_4-NO-Ar (4/16/80). Top trace is absorption at 3875Å, centre trace is pressure, bottom trace is absorption at 3070Å (T_5 is c. 2260°K, 50 μsec/division).

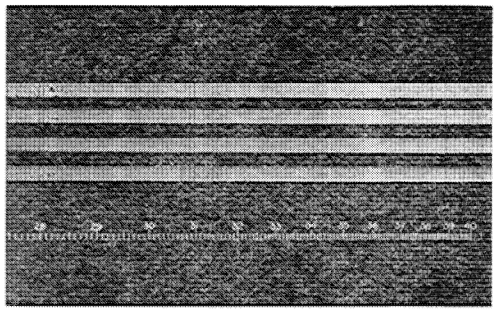

Fig. 5. Spectropgraph obtained with a mixture of CH_4-NO-Ar (4/16/80). First exposure, lamp alone; second, lamp fired 250 μsec after shock passed window; third, delay was 350 μsec; fourth, delay was 450 μsec.

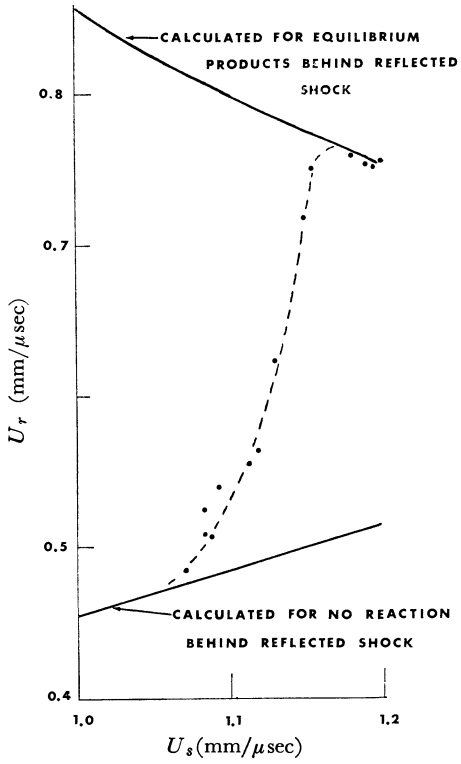

Fig. 6. Shock speed measurements in mixtures of CH_4-NO-Ar (4/16/80).

but faintly, the (0,0) band of OH at 3064 Å. After reaction, only intense bands of OH at 2811 and 3064 Å were seen (Fig. 5).

Figure 6 shows that the measured speed of the fully established combustion-driven shock agrees with that computed for conversion to equilibrium products behind the reaction wave. The initiating reaction for this system could be

$$CH_4 + NO \longrightarrow CH_3 + HNO \quad (\Delta H = 52\,\text{kcal}) \quad (7)$$

At these high temperatures HNO would rapidly decompose and thus further oxidations involving NO and producing HNO could be

$$CH_3 + NO \longrightarrow CH_2 + HNO \quad (\Delta H = 65\,\text{kcal}) \quad (8)$$

$$CH_2 + NO \longrightarrow CH + HNO \quad (\Delta H = 49\,\text{kcal}) \quad (9)$$

The presence of CN and OH during the induction period may be explained by the reaction

$$CH + NO \longrightarrow CN + OH \quad (\Delta H = -45\,\text{kcal}) \quad (10)$$

Assuming that CH_3 is a steady state intermediate and CH_2 is the principal chain carrier it is possible to show that $\log(\tau[NO])$ *vs.* $1/T$ should be a straight line, the slope of which is the activation energy of reaction (9).

Towards the end of the induction period the cyano radical is probably removed by the reaction

$$CN + NO \longrightarrow CO + N_2 \quad (\Delta H = -157\,\text{kcal}) \quad (11)$$

and the heat release of this strongly exothermic reaction causes [OH] to increase, either due to acceleration of reactions (7) through (10) or to reactions such as

$$CH + NO \longrightarrow CO + NH \quad (\Delta H = -101\,\text{kcal}) \quad (12)$$

$$NH + NO \longrightarrow N_2 + OH \quad (\Delta H = -91\,\text{kcal}) \quad (13)$$

Conclusion

Reactions in CH_4 - N_2O mixtures have been initiated by reflected shocks at temperatures above 1500°K. The induction period to explosion, determined from the increase in pressure or achievement of maximum [OH], was inversely proportional to $[N_2O]$. The temperature dependence of the ignition lag indicates that the rate controlling reaction was $N_2O(+M) \rightarrow N_2 + O(+M)$. However the possibility exists that the reaction $CH_3 + N_2O \rightarrow CH_2 + N_2 + OH$ is of importance also. A series of comparable shocks and the use of a spectrograph and flash lamp which was fired at progressively increasing delays after the shock had passed the windows, confirmed that OH was present at, and after, explosion. Measurements of the speed of the combustion-driven shock agreed with those computed for equilibrium conditions behind the shock.

Temperatures above 2080°K were used to induce reactions behind reflected shocks in CH_4 - NO mixtures. Absorption spectroscopy using spectro-

graphic plates showed that CN and OH were present before complete reaction but only OH was detectable afterwards. Absorption records using a monochromator showed that [OH] rose slowly to its maximum value. The induction period tc maximum [OH] was inversely proportional to [NO] and the temperature dependence of the ignition delay indicates that the rate controlling reaction prior to complete combustion is $CH_2+NO\rightarrow CH+HNO$. The detection of CN suggests that the reaction $CN+NO\rightarrow CO+N_2$ may be of importance in accounting for the reduction of nitric oxide.

Dr. I. M. Napier is thanked for assistance in obtaining spectrographic exposures using a lamp of his design. Mr. D. Graham assisted with all shock tube experiments.

BULLETIN OF THE CHEMICAL SOCIETY OF JAPAN VOL. 42 289—291 (1969)

Effect of Ultrasonic Waves on Eriochrome Black T

Sheo PRAKASH and S. K. JAIN

Chemical Laboratories, University of Allahabad, Allahabad, India

(Received March 30, 1968)

Ultrasonic waves of high frequency (1 Mc/sec) have been employed to study the effects on the dilute aqueous solution of Eriochrome Black T. The deaeration of the solution by nitrogen does not greatly affect the rate of decolourization. The process is irreversible and the kinetic study shows it to be unimolecular. Oxidation and subsequent destruction of the dye molecule has been found to be the cause of the fading of the dye solution.

The decolourization of dyes by ultrasonic waves has been reported by Olson and Garden,[1] Azami and Hinohara[2] and Prakash and Prakash.[3-6] The aqueous solutions of various dyes have been found to be decolourized when subjected to the action of light, X-rays and γ-rays. The present paper describes the effect of ultrasonic waves on an aqueous solution of Eriohcrome Black T (abbreviated as EBT).

Experimental

Mullard's high frequency generator type E-7562 having a barium titanate ceramic crystal acting as the transducer was used as the source of ultrasonic power. The work reported here was done at a frequency of 1 Mc/sec. The circuit diagram of generator and ultrasonic bath has been reported earlier.[7]

A stock solution of EBT was prepared by dissolving 0.2306 g of the EBT (BDH) in one litre double distilled water. This was diluted to the desired concentration. The solution was found to be quite stable towards the atmosphere during the period of study.

Twenty-five milliliters of dye solution were irradiated in a round bottom ground stoppered jena bottle which was placed vertically above the transducer so that the sound waves entered the vessel vertically upwards. The solution irradiated for different periods and the change in colorimetric readings noted from Klett Summerson Photoelectric colorimeter, employing the filter No. 55 (transmission 520—600 mμ) which was found to be most suitable for the purpose. The absorption maximum of EBT was 560 mμ and this falls well within the range of this filter. For measuring hydrogen ion concentration a Leeds Northrup A.C. pH meter with glass electrodes was used. In order to see the effect of presence of nitrogen gas on the ultrasonic decolourization of EBT solution nitrogen gas, after passing through suitable traps to remove traces of oxygen, was bubbled for 20 min each time before exposure and then the solutions were irradiated for different intervals of time as usual and change in colour noted.

Results and Dicsussion

Figure 1 is a plot of exposure time *vs.* $-\log(a-x)$ where a is the initial dye concentration and $(a-x)$ its concentration after lapse of exposure time t.

1) A. R. Olson and N. B. Garden, *J. Am. Chem. Soc.*, **54**, 3617 (1932).
2) T. Azami and T. Hinohara, *Nippon Kagaku Zasshi* (*J. Chem. Soc. Japan, Pure Chem. Sect.*), **72**, 453, 515 (1951).
3) S. Prakash and S. Prakash, *J. Acoust. Soc. Amer.*, **32**, 138 (1960).
4) S. Prakash and S. Prakash, *Kolloid. -Z.*, **175**, 50 (1961).
5) S. Prakash and S. Prakash, *Nature*, **191**, 1292 (1961).
6) S. Prakash and S. Prakash, *Z. Phys. Chem.*, (*Leipzig.*) **221**, 145 (1962).
7) S. Prakash, O. Prakash and S. Prakash, This Bulletin, **38**, 1426 (1965).

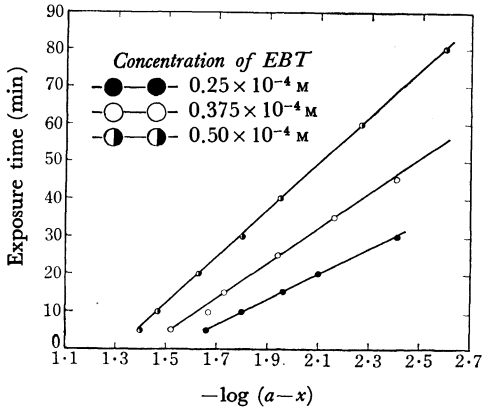

Fig. 1

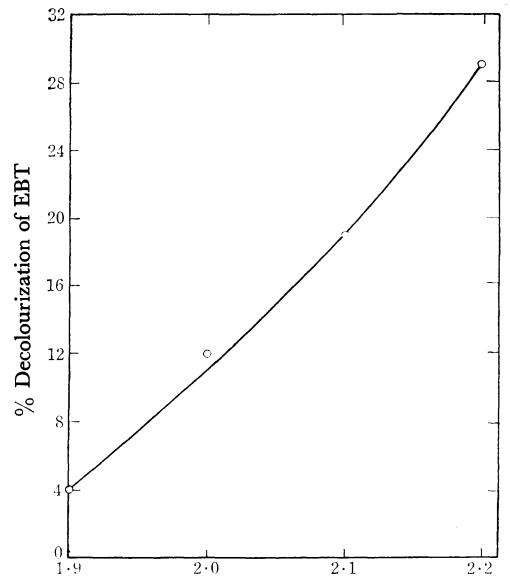

Fig. 2

The decolourisation process has been found to be unimolecular as is evident from the straight line curves obtained. It belongs to the category where the number of molecules of EBT undergoing change per second is proportional to the unreacted molecules present at that instant. This fading varies with change in intensity of the ultrasonic waves (Fig. 2).

The Spectrophotometric studies show that the absorption maximum of the EBT does not change with time of exposure (Fig. 3). Since the molecule breaks up into colourless products which do not exhibit any absorption maximum, the same value is obtained after different intervals of time because of the presence of unbroken EBT molecules.

8) O. Lindstrom and O. Lamm, *J. Phys. Colloid. Chem.*, **55**, 1439 (1951).

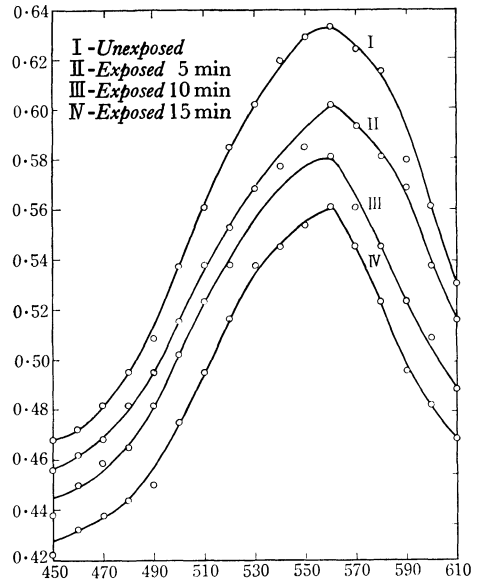

Fig. 3

When an aqueous solution is exposed to ultrasound, hydrogen peroxide is produced along with the formation[8] of H, OH, H_2 and HO_2.

$$H_2O \longrightarrow H, OH, HO_2, H_2O_2$$

A blank experiment was carried out to see whether hydrogen peroxide was responsible for the fading by adding hydrogen peroxide of different concentrations (1.62, 3.25, and 6.5×10^{-2}) to the EBT solution (0.5×10^{-4} M) and keeping it for some time. Even after 24 hr the change was about 6% only. This means that hydrogen peroxide may to some extent be helpful in fading,

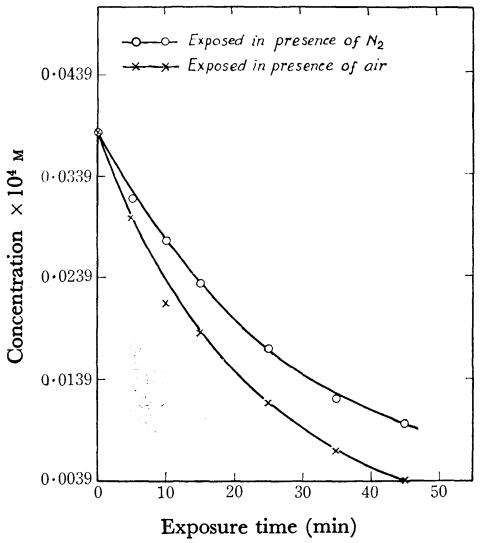

Fig. 4

but is not wholly responsible for it. It is very likely that the fading takes place with a more active reagent prior to the formation of hydrogen peroxide.

When air of the solution was replaced by nitrogen by bubbling the gas before exposure, even then the decolourization occurred, though the rate was reduced considerably (Fig. 4). This is in confirmity with the observations that the ultrasound is able to bring about chemical change even in absence of air or oxygen.

Organic compounds like acetone, dioxane, methyl alcohol, allylthiourea, ether and acrylamide act as inhibitors when they are present in minute quantity (4% by volume). The inhibiting action can be interpreted as due to high vapour pressure, surface tension and internal pressure changes. Most of the sonochemical reactions have been explained on the basis of cavitation, *i. e.*, formation and collapse of the cavity in the solution. The bursting of these cavities generates what is known as cavitational energy and this energy ruptures the bonds of the molecules undergoing change. In presence of substances having high vapour pressure, low surface tension and internal pressure this cavitation is suppressed to a great extent and hence the required energy is not available either to break the molecules of water to produce reactive species H, OH and HO_2 or the reacting molecules themselves.

Unlike photofading of dyes where the primary action is the activation of the molecules, the sonofading is the result of secondary reaction due to the free radicals produced from water by the ultrasonic waves. Also, once the molecule has been decolourized the colour is not restored back, suggesting that the permanent rupture of the molecule takes place. It is oxidation, sometimes reduction or dealkylation which causes the decolourization. However, it is a complex phenomenon and it is difficult to say what is the exact course of the reaction.

BULLETIN OF THE CHEMICAL SOCIETY OF JAPAN VOL. 42 291—298 (1969)

Effect of Cationic Detergents on the Lecithin Stabilized O/W Emulsion

T. G. SASTRY and S. N. SRIVASTAVA

Chemistry Department, Agra College, Agra, India

(Received March 29, 1968)

An oil-in-water system (Nujol being the oil phase) stabilized by the phospholipid, lecithin, has been chosen in this study. The system being negatively charged initially, cationic detergents like lauryl pyridinium chloride (LPC), Cetyl pyridinium bromide (CPB), Phenyl trimethyl ammonium chloride (Ammonyx-200) and Cetyl dimethyl benzyl ammonium chloride (CDBAC) have been employed in order to study their influence on the flocculation and coalescence rates and the degree of aggregation haemocytometrically. Zeta potentials (ξ) have been determined at the corresponding concentrations of the detergents by microcataphoresis and with these values the potential energies and then ultimately the operating van der Waals constant of the system has been determined. From the log C-ξ values it is evident that except Ammonyx-200 which is not an effective cationic detergent, all the others have reversed the charge of the system and their efficiencies are in the order CDBAC>CPB>LPC. The different binding parameters, number of binding sites available for adsorption and free energy of the surface have also been calculated.

The practical utility of detergents in technological field as well as in experimental studies is well known because of their surface activity. Of late much attention is being paid to probe into the more and more complicated structural aspects of these detergents and their molecular orientation on the surfaces and allied aspects. The relative efficiencies of these detergents depend on their carbon chain length and the corresponding adsorbabilities of these complex ions on the surfaces. Cationic surface-active agents are characterised by the fact that the hydrophobic grouping is found in the cation.

In the present studies some of the cationic detergents have been tried in the studies of oil-in-water emulsions stabilised by lecithin, an important phospholipid, which acts as an emulsifying agent in aqueous medium alone and promotes O/W

emulsions in the same way as do proteins. Although many earlier workers[1-7] have tried to use different types of detergents in various O/W-W/O systems, the non-availability of adequate quantitative data with particular reference to the modern theory of colloid stability developed independently by Derjaguin, Verwey and Overbeek (DVO theory),[8-11] prompted us to take up these investigations with the phospholipid as an emulsifying agent in O/W system where Nujol has been chosen as the oil phase. In a previous communication,[12] the effect of inorganic cations has been tried with the same system and this is an extension with complex cationic detergents.

Zeta potentials have been determined at the corresponding concentrations of the detergents where degree of aggregation has been studied haemocytometrically, by microcataphoresis. With these values, the potential energies and then the operating van der Waals constant have been obtained. The binding parameters, number of binding sites available and the free energy of adsorption were also calculated with the electrokinetic data.

Experimental

Materials. The emulsifying agent, lecithin was of BDH quality and the oil phase which consisted of a mixture of Nujol and chlorobenzene were of Ward, Blenkinsop and Co. Ltd., and Polshic Odezymiki Chemiezue, Gliwico (Poland) respectively. Nujol was purified with NaOH.[13]

The detergents lauryl pyridinium chloride (LPC) and cetyl dimethyl benzyl ammonium chloride (CDBAC) were obtained from Industrial Chemical Products, Bombay and further purified with acetone and alcohol respectively. Cetyl pyridinium bromide (CPB) given by I.C.I. (India) was also purified with acetone. Ammonyx-200 (Phenyl trimethyl ammonium chloride) was from Onyx Corporation (U.S.A.) and not further purified. Pyrex galssware and double distilled water were used throughout the studies.

Experimental Methods. The emulsion was prepared by taking 1% of oil (a mixture of 5 parts of Nujol and 6.25 parts of chlorobenzene) containing 1% of emulsifying agent *i.e.*, lecithin with aqueous KCl (0.01 M). The mixture was shaken for a few minutes and homogenised with the hand operated stainless steel homogenizer. (Fisher Scientific Co., U.S.A.). In all the estimations emulsion was prepared under identical conditions.

Flocculation studies were carried out by taking a sample of the emulsion on a double Neubauer model haemocytometer and the counts were taken in 32 squares of the graticule fitted in the eye-picee (each square corresponds to a volume of 7.74×10^{-7} m*l*) with the help of a tally counter under an Olympus microscope (15×62 times magnification). A duplicate counting was always done and the average was taken, the reproducibility being about 5%. The size of the emulsion drops was determined to be 0.70μ dia. from the size frequency analysis of a microphotograph. The electrokinetic potentials were determined by microcataphoresis at a constant temperature of 30°C.

Calculations

The following theoretical aspects were considered before explaining the results of these investigations. In order to apply the D.V.O. theory to the present system, the interaction energy of a colloidal system is given by $V=V_R+V_A$ where V_R is the repulsive energy, V_A is the attraction energy and V is the sum of the two. These two types of energies were calculated with the following Eq.[14]

$$V_R = \frac{\epsilon a \psi_0^2}{2} \ln(1+e^{-\chi H}) \quad (1)$$

$$V_A = \frac{-Aa}{12H} \quad (2)$$

where ψ_0 is the surface potential (assumed equal to the electrokinetic potential for the present system having $\chi a \gg 1$), ϵ the dielectric constant in the double layer (assumed equal to the bulk value 80 of that of water), a the particle radius, H the interparticle distance, χ the Debye-Hückel parameter, and A the van der Waals constant which is taken to be equal to 2.0×10^{-13} erg.

The theoretical degree of aggregation is evaluated as a function of A from the formula.[15]

$$D = 4\pi a^3 n_0 \int S^2 \exp\left(-\frac{V}{kT}\right) ds \quad (3)$$

1) M. Limburg, *Rec. Trav. Chim.*, **45**, 772, 875 (1926).
2) J. Powney and L. J. Wood, *Trans. Faraday Soc.*, (1941).**37**, 152
3) A. E. Alexander, "Colloid Science Course," Cambridge (1945), p. 25.
4) B. D. Powell and A. E. Alexander, *Can. J. Chem.*, **30**, 1044 (1962).
5) Van den Tempel, "Stability of oil-in-water emulsions," Rubber Stichting, Oostingel, 179, Delft (Holland) 1953.
6) R. H. Ottewill, M. C. Rastogi and A. Watanabe, *Trans. Faraday Soc.*, **56**, 854—865 (1960).
7) H. A. Abramson and R. H. Ottewill, R. H. *J. Colloid Sci.*, **17**, 883 (1962).
8) B. V. Derjaguin, *Trans. Faraday Soc.*, **26**, 203, 730 (1940).
9) B. V. Derjaguin, *J. Expt. Theort. Phys. U.S.S.R.*, **11**, 802 (1941).
10) B. V. Derjaguin and L. D. Landau, *Acta Physico. Chim.*, **14**, 633 (1941).
11) E. J. W. Verwey and J. Th. G. Overbeek, "Theory of Stability of Lyophobic Colloids" Elsevier, Amsterdam (1948).
12) T. G. Sastry and S. N. Srivastava, *Ind. J. Chem.* (under publication).
13) D. K. Chattoraj and H. B. Bull, *J. Phys. Chem.*, (1959).
14) B. V. Derjaguin and M. M. Kussakov, *Acta. Phys. Chim., U.R.S.S.*, **10**, 25, 153 (1939).
15) Ref. 11, p. 183.

TABLE 1

Detergent	Formula	Concentration at zero point charge
Ammonyx-200	$C_6H_5N(CH_3)_3Cl$	No reversal of charge even after the addition of 1.0×10^{-1}% (5.83×10^{-3} M)
LPC	$C_{12}H_{25}$–C_6H_5NCl	7.95×10^{-5} M
CPB	$C_{16}H_{33}$–C_6H_5NBr	6.31×10^{-5} M
CDBAC	$C_{16}H_{33}$–$N(CH_3)_2$–CH_2–C_6H_5Cl	1.0×10^{-6} M

where n_0 is the equilibrium number of unassociated particles and $S=2+H/a$. The integration of the above expression is evaluated graphically. The degrees of aggregation thus obtained are plotted against A values and from the graphs correct values of A are determined by interpolation of observed degree of aggregation determined haemocytometrically.

The extent of reversible flocculation can be calculated from the formula.

$$D=\frac{\text{Number of doublets}}{\text{Number of doublets}+\text{Number of singlets}} \quad (4)$$

where D is the number of particles associated with a specific particle *i. e.* the degree of aggregation. Here the singlet means one oil globule which is unassociated and doublet means the combination of two singlets *i. e.*, just flocculated but no coalesced.

From the mobility data, the potentials were calculated by using the Overbeek equation[16] for symmetrical electrolytes, where the relaxation correction has been applied as the particle was small.

$$U=-\frac{\varepsilon\zeta E}{6\pi\eta}\left[f_1(\chi a)-\mathcal{Z}^2\left(\frac{e\zeta}{kT}\right)^2 f_3(\chi a)-\frac{\rho_+-\rho_-}{6\pi\eta e}\left(\frac{e\zeta}{kT}\right)^2 f_4(\chi a)\right] \quad (5)$$

where U, velocity of the particle (average of 10 readings was taken), ρ_+ and ρ_- the friction constants, η the viscosity of the dispersion medium, k the Boltzmann constant, e the electronic charge, $f_1(\chi a)\cdots f_4(\chi a)$ the functions taken from Table 2 (Overbeek *loc. cit.*).

The charge density of an emulsion droplet by adding small quantities of cationic detergents which are likely to adsorb is given by Stern equation.[17]

$$\sigma_s=\frac{\mathcal{N}_1 e z}{1+\frac{55.6}{c}\exp\left(\frac{\Delta G}{kT}\right)} \quad (6)$$

where c is the molar concentration of the added detergent, $\mathcal{N}_1$ the binding sites per cm^2 and ΔG is the free energy of adsorption per molecule. The same equation can be written in the form (*cf.* Wilkins *et al.*[18] and Ottewill *et al.*[6])

$$\sigma_s=\frac{K_1 c}{1+K_2 c} \quad (7)$$

where $K_2=\dfrac{e^{-\Delta G/kT}}{55.6}$ and $K_1=\mathcal{N}_1 K_2 ez$.

K_1 and K_2 are the adsorption constants which have been calculated from the treatment given by Srivastava[19] at zero point of charge which finally yields the following equations.

$$\frac{1}{c}=\frac{4\pi z e\mathcal{N}_1 k_2}{\chi\varepsilon\psi_0\delta}-k_2 \quad (8)$$

$$\left(\frac{d\psi\delta}{d\ln C}\right)_{\psi_0\delta=0}=\left(\frac{\chi\varepsilon\psi\delta}{4\pi ez\mathcal{N}_1}-1\right)_{\psi_0\delta} \quad (9)$$

where z is the valency and $\left(\dfrac{d\psi\delta}{d\ln C}\right)_{\psi_0\delta=0}$ is the slope of the loc C-zeta potential curve (assuming $\psi_0\delta=\zeta$), C the concentration of the detergents at the zero point of charge.

Results and Discussion

(a) Effect of Detergents on Flocculation. The flocculation of the emulsion droplets has been studied by adding different concentrations of the four detergents and counting the number of singlets

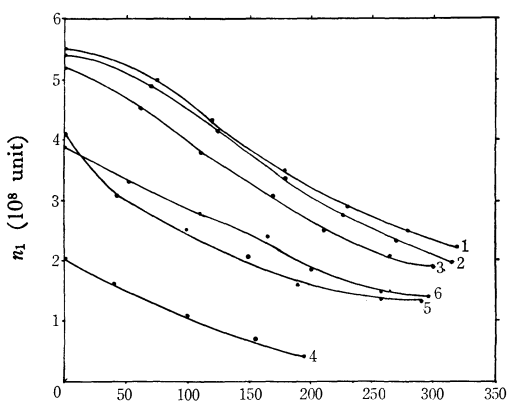

Fig. 1. Plots of time and number of monomers/ml (n: 10^8 unit) (which are not flocculated) at different concentrations of CPB.
(1) 1.0×10^{-6} M (2) 5.0×10^{-6} M (3) 1.0×10^{-5} M (4) 1.0×10^{-4} M (charge reversal range) (5) 5.0×10^{-4} M (6) 1.0×10^{-3} M

16) J. T. G. Overbeek, "Advances in Colloid Science," Vol. III (1950), p. 114.
17) D. J. Z. Stern, *Electro Chem.*, **30**, 568 (1924).
18) Wilkins *et al.*, *J. Theorot. Biol.*, **2**, 173, 186 (1962).
19) S. N. Srivastava, *J. Ind. Chem. Soc.*, **41**, 203 (1964).

and doublets present at various intervals of time. The initial particle concentration of the emulsion was found to be 8.05×10^8 globules/m*l*. Graphs have been plotted between the number of particles (n_1: 10^8 unit) and time. Here only one of the typical graphs (graph 1) obtained from CPB has been given. From the graph it is evident that with increase in concentration of detergent the number of particles decrease gradually and almost attains constancy after some time which shows that reversible flocculation occurs in the system. At comparatively higher concentration the charge reversal takes place and the number of particles suddenly decreases implying thereby that coalescence is appreciable.

(b) Effect on Zeta Potential. Changes in zeta potentials by the addition of these above mentioned cationic detergents have been studied. In our present investigations the pH of the emulsion after the addition of detergents being almost neutral, lecithin is not exhibiting any positive charge as was found by Hanai *et al.*[20] in the acidic range. On the other hand, the slight positive charge of tetramethyl amino group appears to be internally neutralised when it is taken in Nujol and its predominant negative bearing phosphotydal group seems to be contributing to the overall negative charge of the emulsion. So these cationic detergents have been used in flocculation as well as in electrokinetic potential determinations. The corrected zeta values were plotted against the

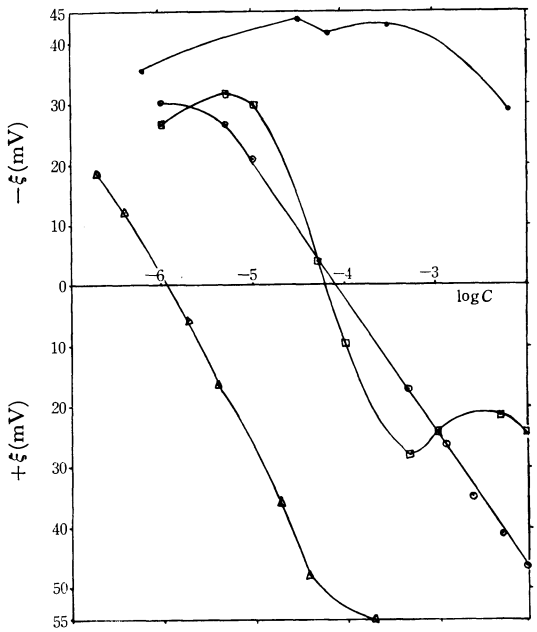

Fig. 2. Plots of log concentration (molar) *vs.* zeta potential (mV) ◎ LPC, ⊡ CPB, ● Ammonyx-200, △ CDBAC.

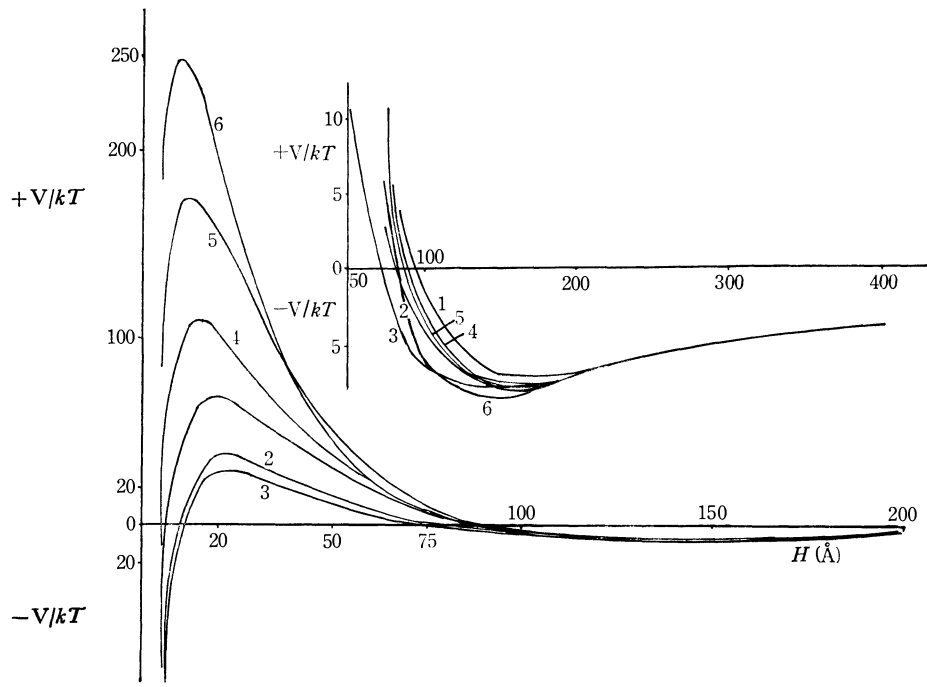

Fig. 3. Plots of distance and potential energy of interaction for LPC at different concentrations showing the heights of maxima and enlarged secondary minima separately. (1) 1.0×10^{-6} M (2) 5.0×10^{-6} M (3) 1.25×10^{-3} M (4) 2.5×10^{-3} M (5) 5.0×10^{-3} M (6) 1.0×10^{-2} M

20) T. Hanai, *et al.*, *J. Theorot. Biol.*, **9**, 378 (1965).

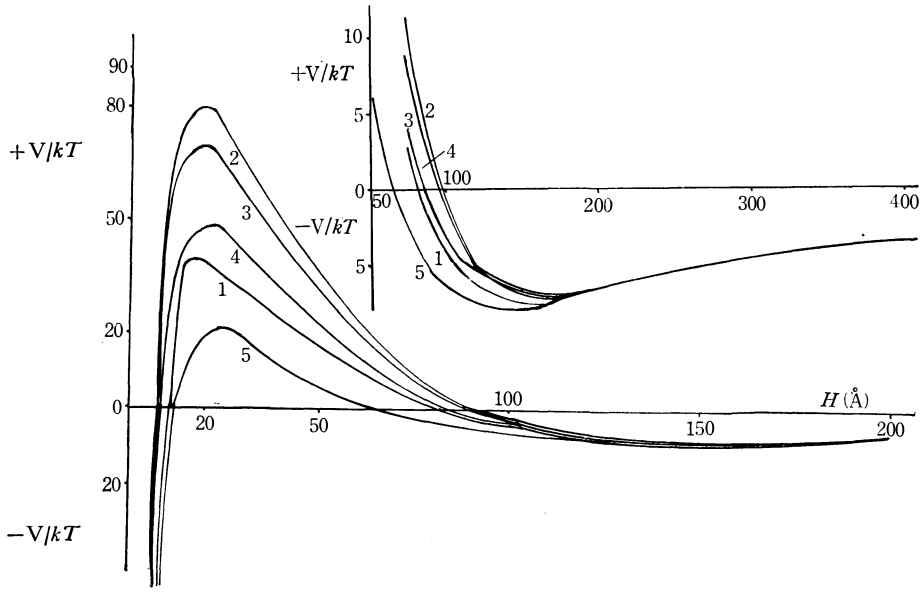

Fig. 4. Plots of distance and potential energy of interaction for CPB at different concentrations showing the heights of maxima and enlarged secondary minima separately. (1) 1.0×10^{-6} M (2) 5.0×10^{-6} M (3) 1.0×10^{-5} M (4) 5.0×10^{-4} M (5) 1.0×10^{-3} M

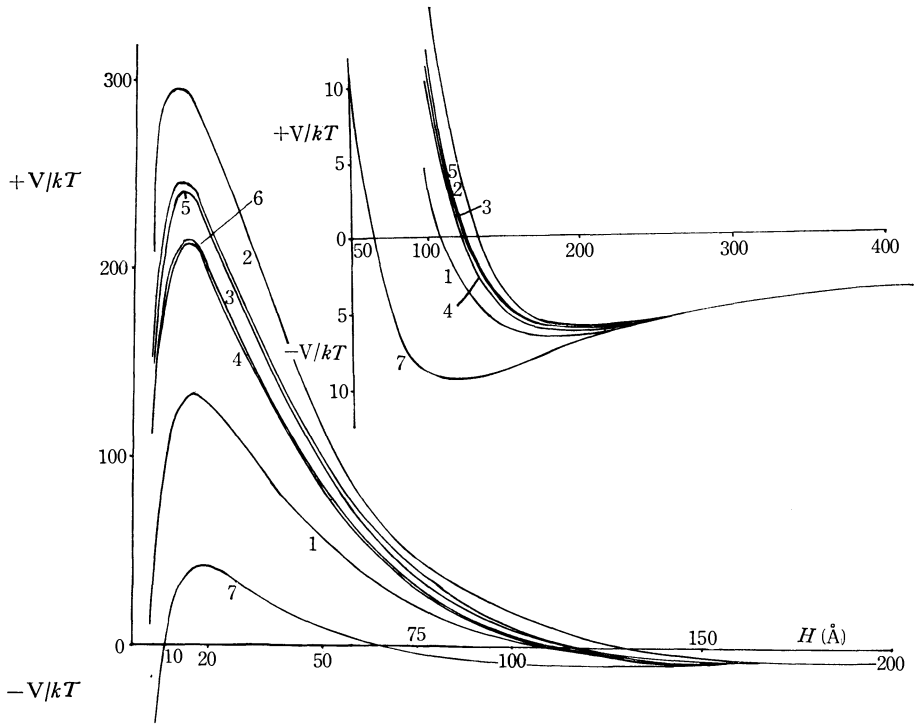

Fig. 5. Plots of distance and potential energy of interaction for Ammonyx-200 at different concentrations showing the heights of maxima and enlarged secondary minima separately. (1) 5.83×10^{-7} M (2) 5.83×10^{-6} M (3) 2.91×10^{-5} M (4) 5.83×10^{-5} M (5) 2.91×10^{-4} M (6) 5.93×10^{-4} M (7) 5.83×10^{-3} M

logarithmic concentrations of the detergents (graph 2). From the graph it is clear that except Ammonyx-200, all the other detergents (LPC, CPB and CDBAC) have reversed the charge of the emulsion globules. The relative efficiencies of these detergents are clearly indicated by the charge reversal concentrations as given in Table 1.

The reversal of charge is due to the adsorption

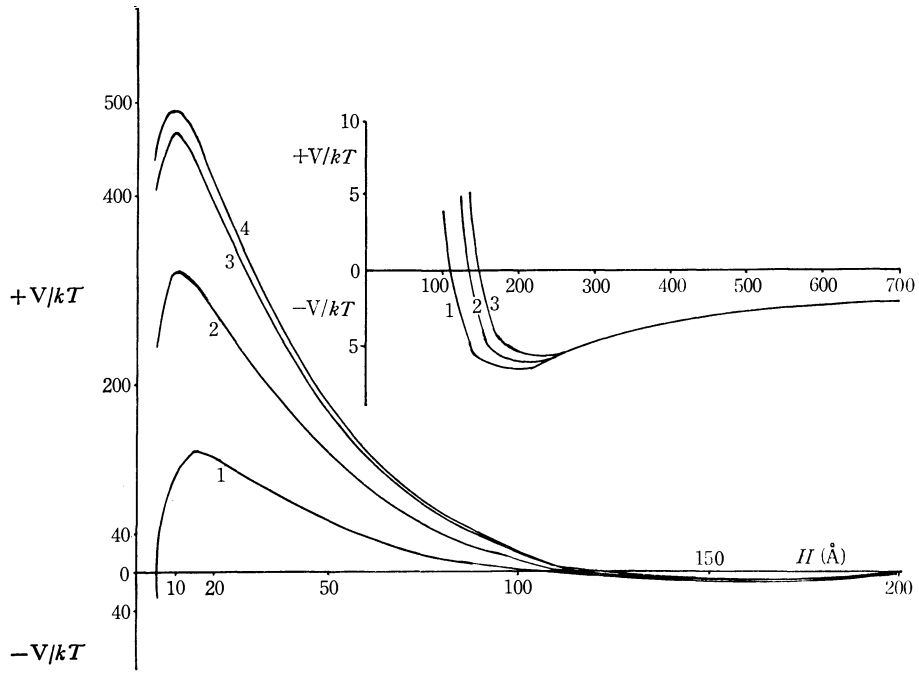

Fig. 6. Plots of distance and potential energy of interaction for CDBAC at different concentrations showing the heights of maxima and enlarged secondary minima separately (1) 1.92×10^{-5} M (2) 2.83×10^{-5} M (3) 1.92×10^{-4} M (4) 3.83×10^{-4} M.

of the cation onto the surface of the lecithin micelles. The flocculation results were also in conformity with the values of zeta potential variations. The efficacy of each detergent could easily be explained by the length of the carbon chain and critical micelle concentration (CMC). The CMC of LPC is determined as 1.66×10^{-2} whereas that of CPB is lower than this. The carbon chain lengths and so flocculating powers are in the increasing order of Ammonyx-200, LPC, CPB and CDBAC.

(c) Interaction Energy Curves and the Stability of Emulsion. In order to test the DVO theory in the present case and also to study the nature of flocculation, the interaction energies V/kT where V comprises of V_R+V_A have been calculated and are plotted as a function of the interparticle distance H (Å) and are presented in graphs 3—6. The high energies exhibited in different systems would naturally indicate the stability of the emulsion and the possibility of only reversible flocculation. When the surface of the emulsion droplet strongly adsorbs the ions of the opposite charge, the coated droplets act as a lyophobic colloid. So the flocculation can be either irreversible in the primary minima or reversible in the secondary minima. In the present investigations under question, the latter aspect seems to be more predominant as evidenced by the high energy above 25 kT and shallow minima of not more than 7 to 8 kT deep at an interparticle distance of 100—150 Å. The enlarged secondary minima portion have also been presented in the same graphs 3—6.

The details of the detergent concentrations and their corresponding zeta potentials, the energy maximum, depth of the secondary minima *etc.* are presented in Table 2.

These results are in conformity with our previous findings with inorganic cations.[12] The only difference which is obvious is that the overall energy barriers have been reduced as compared to the previous ones, presumably, owing to the combined effect of 0.01 KCl+the highly effective cations of the detergents.

By counting the number of singlets and doublets by haemocytometry while doing flocculation studies, the degree of aggregation has been calculated. The theoretical value of the same has also been obtained.[21] These two values did not agree because of the difference in van der Waals constant taken (2.0×10^{-13} erg). So a graph was plotted between different van der Waals constants and the theoretical values of D% (graph 7). From this graph the value of A corresponding to the observed value of D has been noted and found to be 2.6×10^{-13} erg which is almost same as obtained before with electrolytes. This further confirms the range of A obtained by earlier workers.[19-22]

(d) Reversal of Charge and the Binding

21) S. N. Srivastava, *Ind. J. Chem.*, **3**, 376 (1965).
22) J. N. Schunkel and J. A. Kitchener, *Trans. Faraday Soc.*, **56**, 161 (1960).

TABLE 2

Detergent concentration M	Zeta potential in mV	Height of maximum in kT	Interparticle distance at which $V=0$	Depth of secondary minimum
Ammonyx-200				
5.83×10^{-7}	−35.7	134	100—150Å	6.4
5.83×10^{-6}	−47.0	295	100—150Å	6.1
2.91×10^{-5}	−44.1	244	100—150Å	6.2
5.83×10^{-5}	−42.1	213	100—150Å	6.3
2.91×10^{-4}	−44.0	241	100—150Å	6.2
5.83×10^{-4}	−42.4	215	100—150Å	6.2
5.83×10^{-3}	−29.1	41	100—150Å	9.0
LPC				
1.0×10^{-6}	−30.2	69	75—100Å	7.0
5.0×10^{-6}	−26.5	38	75—100Å	7.5
7.95×10^{-5}	Charge reversal			
1.25×10^{-3}	+25.9	29	75—100Å	7.8
2.5×10^{-3}	+34.9	109	75—100Å	7.6
5.0×10^{-3}	+41.1	173	75—100Å	8.0
1.0×10^{-2}	+46.7	248	75—100Å	8.4
CPB				
1.0×10^{-6}	−26.7	38	75—100Å	7.5
5.0×10^{-6}	−31.5	81	75—100Å	6.8
1.0×10^{-5}	−30.5	71	75—100Å	7.0
6.31×10^{-5}	Charge reversal			
5.0×10^{-4}	+28.3	49	75—100Å	6.7
CDBAC				
1.0×10^{-6}	Charge reversal			
1.92×10^{-5}	+35.7	128	100—150Å	6.5
3.83×10^{-5}	+48.3	319	100—150Å	6.0
1.92×10^{-4}	+55.6	467	100—150Å	5.7
3.83×10^{-4}	+56.9	493	100—150Å	5.6

TABLE 3

Detergent	K_1	K_2	N_1 groups/cm²	$-\Delta G$ kcals/mol	Concentration at zero point charge
LPC	1.27×10^{8}	4.50×10^{4}	5.86×10^{12}	6.04	7.95×10^{-5} M
CPB	6.74×10^{7}	3.31×10^{4}	4.24×10^{12}	5.30	6.31×10^{-5} M
CDBAC	4.84×10^{9}	2.24×10^{6}	4.50×10^{12}	5.33	1.0×10^{-6} M

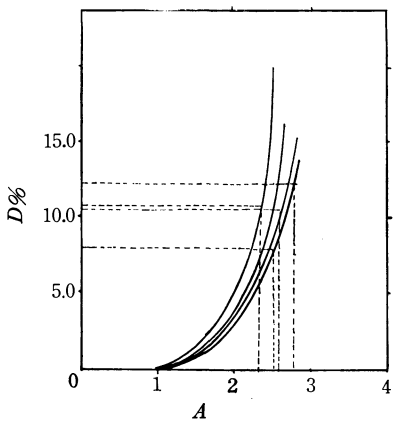

Fig. 7. Plots of Van der Waals constant ($A\times10^{-13}$ erg) and degree of aggregation (D%) at (1) 1.92×10^{-4}M CDBAC, (2) 3.83×10^{-5}M CDBAC (3) 5.0×10^{-6} M CPB (4) 5.83×10^{-6} M Ammonyx-200.

Constants. With the help of the treatment given[17] regarding the calculation of the different binding parameters, number of binding sites available for adsorption and free energy of the surface have been calculated and presented in the Table 3.

From these obtained values it is evident that all these detergents have less number of available sites for adsorption than Ammonyx-200 reported earlier[23] which gives some indication for their capacity to charge reversal. Out of these three presented in the table LPC seems to be weaker than the other as confirmed from the electrokinetic and flocculation measurements. The free energy values are not significantly different from one another.

Finally it may be concluded from the above findings that Ammonyx-200 is not an effective cationic detergent whereas the others are capable of strong adsorption on the lecithin coated oil drops in aqueous KCl so as to cause the charge reversal and their relative efficiencies are in the

23) C. Praksh and S. N. Srivastava, Unpublished data.

order CDBAC>CPB>LPC.

The authors wish to express their thanks to Dr. M. N. Das and Dr. D. K. Chattoraj, Department of Chemistry, Jadavpur University, Calcutta for allowing them to do microelectrophoresis and also to State CSIR, Lucknow for awarding a Fellowship to one of them (T.G.S.).

BULLETIN OF THE CHEMICAL SOCIETY OF JAPAN VOL. 42 298—302 (1969)

Kinetics and Mechanism of the Oxidation of Citric and Glyoxylic Acids by Cerium(IV) Ion

Kalyan K. SENGUPTA

Department of Physical Chemistry, Jadavpur University, Jadavpur, Calcutta-32, India

(Received April 26, 1968)

The mechanism proposed by Waters (*J. Chem. Soc.*, **1955**, 217) for the oxidation of α-hydroxy acids by manganic pyrophosphate accounts for the kinetics of oxidation of citric acid by cerium(IV) ion. The oxidation appears to proceed through the initial formation of complex and subsequently through free radicals.

According to Benrath and Ruland,[1] the reaction between citric acid and cerium(IV) is a complicated one and does not follow the simple kinetic order. Willard and Young[2] oxidized citric acid by ceric sulphate with an idea to find a new method for the quantitative estimation of the hydroxy acid. They oxidized the hydroxy acid up to formic acid. The method described by them was tedious and hence Duke and Smith[3] developed a simpler method using cerium(IV) perchlorate as oxidant. In a more recent communication, Ghosh and Mehrotra[4] showed that the above reaction is a bimolecular one when reactants were of equimolar quantities. According to them both formic acid and formaldehyde are the products of oxidation. It has already been shown that formaldehyde[5] is very sensitive to cerium(IV) ion and two equivalents of cerium(IV) ion were needed per mole of formaldehyde, and so we were suspicious about its existence in the solution specially when it was stored in excess cerium(IV) for several days. Moreover, the stoichiometry of the oxidation reaction reported by different workers was different and the mechanism up to formic acid is not yet known. It was, therefore, intended to reinvestigate the reaction in details. Since glyoxylic acid is one of the possible intermediates of citric acid oxidation, the kinetics of the oxidation of glyoxylic acid has also been studied, the data for which are not available in the literature. A possible mechanism up to formic acid has been suggested.

Experimental

Ceric ammonium sulphate was of E. Merck's (G.R.) grade and the solution of the salt in sulphuric acid was directly made. Ceric ammonium nitrate which was used for the preparation of cerium(IV) perchlorate was of 'AnalaR' grade. Cerium(IV) perchlorate was prepared by the electrolytic oxidation of Ce(III) perchlorate by the method suggested by Smith[3] and finally stored in an ice box until ready for use. Cerium(IV) ion was standardized by the iodometric method.[6] Citric acid was of 'AnalaR' grade whereas glyoxylic acid (Fluka) was purified by recrystallisation. The organic acids were standardized against standard caustic soda. The details of other reagents and experimental set up have been describede lsewhere.[7-9] The reactions have been followed volumetrically and an aliquot part of the reaction mixture was withdrawn at suitable intervals and analysed for residual cerium(IV) by the iodometric method.

1) A. Benrath and K. Ruland, *Z. Anorg. Allgem. Chem.*, **114**, 267 (1920).
2) H. H. Willard and P. Young, *J. Am. Chem. Soc.*, **52**, 130 (1930).
3) F. R. Duke and G. F. Smith, *Ind. Eng. Chem. (Anal. Ed.)*, **15**, 120 (1943).
4) S. Ghosh and R. N. Mehrotra, *Z. Physik. Chem.*, **1/2**, 56 (1963).
5) G. Hargreaves and L. H. Satcliffe, *Trans. Faraday. Soc.*, **51**, 1105 (1955).
6) G. Charlot and D. Bezier, "Quantitative Inorganic Analysis," John Wiley & Sons, New York (1957), p. 60.
7) K. K. Sen Gupta, S. Aditya and B. N. Ghosh, *J. Ind. Chem. Soc.*, **40**, 823 (1963).
8) K. K. Sen Gupta, *Indian J. Chem.*, **2**, 267 (1964).
9) K. K. Sen Gupta and S. Aditya, *J. Electro-Chem. Soc., Japan*, **32**, 200 (1964).

The stoichiometry was determined by allowing reaction mixtures containing a large excess of Ce(IV) ion to stand for several days at 30°C. The excess Ce(IV) ion was then estimated as described previously. It has been found that 14.0 and 2.0 equivalents of cerium(IV) reacted per mole of citric and glyoxylic acids respectively.

The oxidations have been studied mainly in the presence of excess cerium(IV) ions (up to 10 fold excess in the case of citric and 2 fold excess in the case of glyoxylic acids) and the rate was found to be first order in both cases.

Dependence of Rate on Ho in H_2SO_4. The reactions were studied at different sulphuric acid concentrations which retarded the rate of reaction. The plot $\log K$ against $-H_0$ (H_0=Hammett acidity) was linear which was confirmed from two sets of experiments at two different temperatures. (Fig. 1), where the rate constant of first order was denoted by K in sec.$^{-1}$ The values of H_0 at different sulphuric acid concentrations have been taken from the tables of Paul and Long.[10]

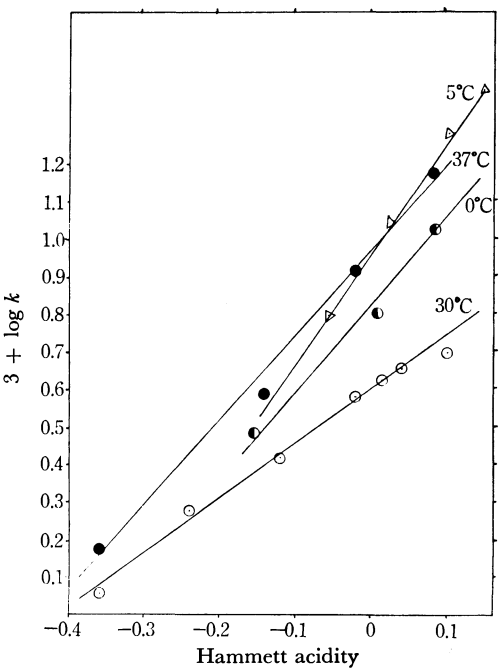

Fig. 1. Variation of $\log k$ against Hammett acidity.
⊙ ● Citric acid
◐ △ Glyoxylic acid

Influence of Salts on the Rate Constants. The reactions have been investigated in the presence of different salts, *e. g.*, potassium chloride, sodium perchlorate, sodium sulphate and magnesium sulphate. Sodium perchlorate had no influence on the rate constant. But there was a slight decrease of rate constant in the case of potassium chloride possibly because of the fact that chloride ion complexes[11] with cerium(IV) thereby decrease the concentration of active species of cerium(IV). Thus no effect of ionic strength has been found on the overall kinetics of the reaction. As usual both sulphate and bisulphate ions retarded the rate of reaction (Tables 1 and 2) and the plots $[SO_4]^{2-}$ against $1/K$ have been shown in Fig. 5. The inhibiting effect of addition of sulphates or sulphuric acid can be explained in the light of the complex nature of ceric sulphate in the solution. This has been discussed in previous communications.[7-9]

Table 1. Oxidation of citric acid by Ce(IV) sulphate
[Ce(IV)]=0.0095 M, [Citric]=0.00376 M, $[H_2SO_4]$=0.251 M, Temp. 30°C

Salt and its concentration	$K \times 10^3$ (sec^{-1})
0	16.32
0.333 M $NaClO_4$	16.32
0.333 M $MgSO_4$	15.35
0.333 M Na_2SO_4	9.212
0.333 M $KHSO_4$	10.45

Table 2. Oxidation of glyoxylic acid by Ce(IV) sulphate
[Ce(IV]=0.01912 M, [Glyoxylic]=0.0144 M, $[H_2SO_4]$=0.7963 M, Temp.=2°C

Salt and its concentration	$K \times 10^2$ (sec^{-1})
0	2.11
8×10^{-2} M $NaClO_4$	2.11
8×10^{-2} M K_2SO_4	1.23

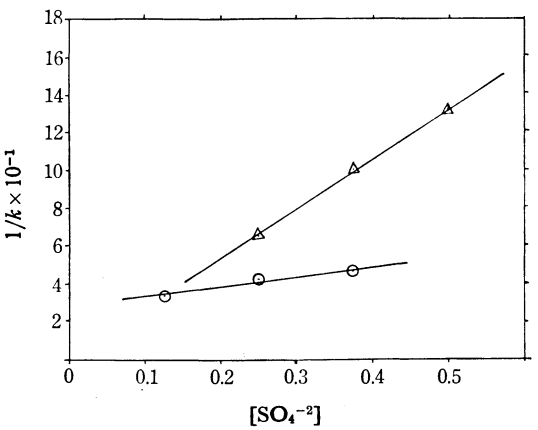

Fig. 5. Oxidation of citric acid by $Ce^{IV}(SO_4)_2$.
$[Ce^{IV}]$=0.0356 M, [Citric]=0.0139 M, $[H_2SO_4]$=0.272 M, Temp=30°C
⊙ $MgSO_4$, △ Na_2SO_4

Influence of Substrate Concentration. The reaction has been studied in various substrate concentrations and the velocity of reaction increased with the increase of substrate concentration. Figure 2 represents the plot of $1/K$ against 1/[Substrate].

Influence of Temperature. The velocity constants have been calculated at different temperatures. Each

10) F. A. Long and M. A. Paul, *Chem. Revs.*, **57**, 1 (1957).

11) K. K. Sen Gupta, S. P. Moulik and P. K. Pal, *J. Ind. Chem. Soc.*, **40**, 217, 429 and 989 (1963).

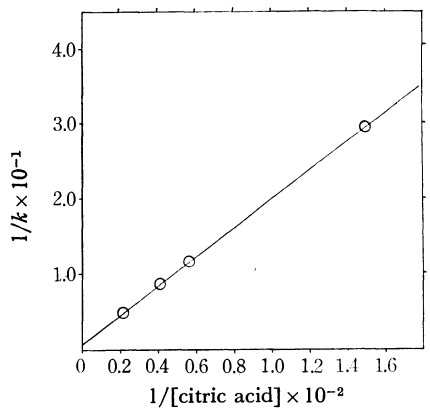

Fig. 2. Variation of substrate on the rate.

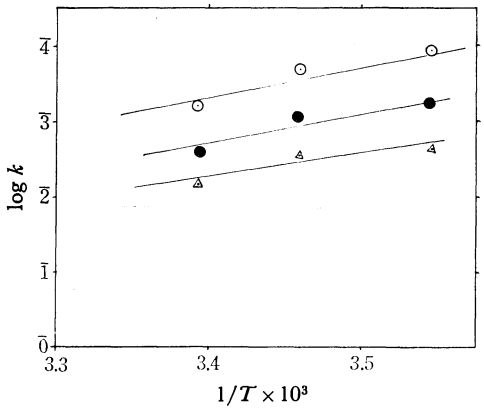

Fig. 3. Oxidation of citric acid by Ce^{IV} perchlorate.

⊙ $[H_2SO_4]=1.920$ M
● $[H_2SO_4]=1.276$ M
△ $[H_2SO_4]=0.869$ M

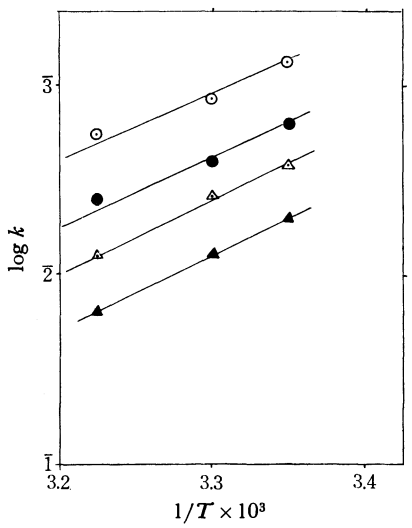

Fig. 4. Oxidation of citric acid by $Ce^{IV}(SO_4)_2$.

⊙ $[H_2SO_4]=1.280$ M △ $[H_2SO_4]=0.587$ M
● $[H_2SO_4]=0.863$ M ▲ $[H_2SO_4]=0.447$ M

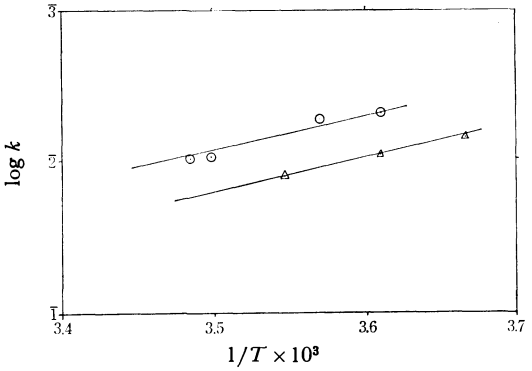

Fig. 6. Oxidation of glyoxylic acid by $Ce^{IV}(SO_4)_2$.

	$[Ce^{IV}(SO_4)_2]$	[glyoxylic]	$[H_2SO_4]$
⊙	0.0196 M	0.0184 M	1.575 M
△	0.0191 M	0.0144 M	1.301 M

TABLE 3. OXIDATION OF THE ACIDS BY Ce(IV) SULPHATE

Acid	E (kcal)	$-\Delta S$ (e. u.)
Citric	18.4	6.1
Malonic	16.1	16.5
Glyoxylic	10.6	29.6

TABLE 4. OXIDATION OF THE ACIDS BY Ce(IV) PERCHLORATE

Acid	E (kcal)	$-\Delta S$ (e. u.)
Citric	16.1	13.3
Malonic	9.2	38.6

experiment was carried out at identical concentrations of sulphuric acid and the reactants. The results have been plotted (Figs. 3, 4 and 6). From the plot of log K *vs.* $1/T$, the activation energy has been calculated. The values of the activation energy and entropy of activation for the different cases of oxidation have been recorded in Tables 3 and 4.

Discussion

On oxidation of citric acid by cerium(IV) ion, CO_2 is evolved and formic acid remains in solution. When large excess of cerium(IV) ion was present (about 20 times excess) a total of about 14 equivalents of cerium(IV) was destroyed per mole of citric acid and this confirms the observation of Smith,[3] and 1.95 mol of formic acid were produced per mole of the citric acid. When Ce(IV) perchlorate was used as oxidant, the reaction was completed within an hour at 30°C up to formic acid which remained unaffected even in excess of cerium(IV) ion. Therefore,

$$C_6H_8O_7 + 14Ce(IV) + 5H_2O \longrightarrow 4CO_2 + 2HCOOH + 14H + 14Ce\ (III)$$

would represent the stoichiometry of the equation. The presence of formic acid was confirmed by

chromotropic acid reaction which was estimated by the usual procedure.[12] Finally, an attempt was made to distinguish between mechanisms (a) and (b).

$$\text{(a)}\quad \mathrm{Ce(IV)} + \mathrm{HCl} \overset{K_1}{\rightleftharpoons} \mathrm{Ce(IV)\cdot HCi}.$$

$$\mathrm{Ce(IV)\cdot HCi} \xrightarrow{K'} \mathrm{Ce\ (III)} + \text{product}$$

(subsequent steps fast)

$$\text{(b)}\quad \mathrm{Ce(IV)} + \mathrm{HCi} \xrightarrow{K_2} \mathrm{Ce\ (III)} + \text{product}$$

(subsequent steps fast)

The immediate change in colour from orange to red (the colour was more prominent when ceric perchlorate was used as oxidant) which again changes to its original colour clearly shows the occurrence of an unstable chelate at the initial stage. A few attempts were made to investigate the complex by Job's method of continuous variation but failed owing to its highly unstable character. The kinetic evidence only indicates that citric acid is oxidized *via* complex formation and the plot $1/K$ against 1/[substrate] labels[13] the corresponding $1/K$ axis indicating information of a complex. This shows that the rate dependence is according to (a)

$$\frac{-\mathrm{d[Ce(IV)]}}{\mathrm{d}t} = \frac{K'K[\mathrm{Ce(IV)}][\mathrm{HCi}]}{1+K[\mathrm{HCi}]}$$

and not the simple dependence (b)

$$-\frac{\mathrm{d[Ce(IV)]}}{\mathrm{d}t} = K[\mathrm{Ce(IV)}][\mathrm{HCi}]$$

The complex finally decomposes to give a free radical[14] the formation of which was tested by induced reduction of mercuric chloride. During the oxidation of citric acid by Ce(IV) ion, mercuric chloride was found to be reduced indicating the formation of a reducing intermediate,[15] *e. g.*, free radical. The reduction was more prominent in concentrated solutions of citric acid and Ce(IV) ion. The free radical further picks up Ce(IV) ion and is oxidised in the following manner.

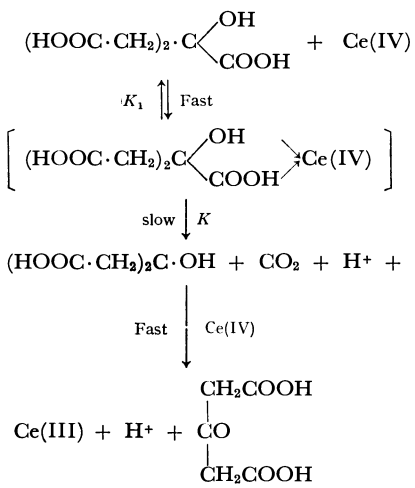

The subsequent steps up to formic acid are also considered to be very fast and an attempt was made to investigate the initial rates of the expected intermediates under comparable conditions. The concentration of the oxidant was three times that of the substrate and the experiments were carried out at 30°C and at sulphuric acid concentration of 0.5 M. The values of K_{Citric} and K_{Malonic} were found to be 4.99×10^{-3} ($\mathrm{sec^{-1}}$) and 10.07×10^{-3} ($\mathrm{sec^{-1}}$) respectively. Again under the same experimental condition glyoxylic acid was instantaneously oxidized and with two fold excess of the oxidant at 5°C, $K_{\mathrm{glyoxylic}}$ was found to be 1.84×10^{-2} ($\mathrm{sec^{-1}}$). The comparison of the values of activation energy of Table 3 also shows the following order:

$$K_{\mathrm{citric}} < K_{\mathrm{malonic}} < K_{\mathrm{glyoxylic}}$$

The oxidation of expected acetone dicarboxylic acid may now take place either through acetone which is formed by the successive decarboxylations of two carboxyl groups as in the case of the oxidation of citric acid[16] by potassium permanganate or by the cleavage of C–C bond of citric acid molecule. It is interesting to examine which of the paths explains the following experimental results. In the oxidation of acetone by Ce(IV) sulphate, Hinshelwood and Shorter[12] found that 8.6 equivalents of Ce(IV) ion are required per mole of acetone even at 70°C. So if acetone dicarboxylic acid is to give acetone and then subsequently oxidized it would need only 8.6 equivalents with the overall consumption of 10.6 equivalents of the oxidant. This rules out the possibility that CH_3-$COCH_3$ is an intermediate. Therefore acetone dicarboxylic acid is oxidized to give one mole of malonic acid and one mole of glyoxylic acid with the overall consumption of four equivalents of Ce(IV) ions in the following way (Scheme 1.)

The formation of glyoxylic acid *via* glycollic acid is not possible as the oxidation of glycollic acid is too slow.[9] The oxidation[17] of malonic acid by cerium(IV) ion may be represented stoichiometrically by the equation:

$$\mathrm{CH_2(COOH)_2} + 6\mathrm{Ce(IV)} + 2\mathrm{H_2O} \longrightarrow 2\mathrm{CO_2} + \mathrm{HCOOH} + 6\mathrm{Ce(III)} + 6\mathrm{H^+}$$

The possible mechanism of the above reaction has already been discussed in the previous communi-

12) C. N. Hinshelwood and J. Shorter, *J. Chem. Soc.*, **1950**, 3276.
13) H. Lineweaver and D. Burke, *J. Am. Chem. Soc.*, **56**, 81 (1934).
14) W. A. Waters and P. Levesley, *J. Chem. Soc.*, **1955**, 217.
15) A. Y. Drummond and W. A. Waters, *ibid.*, **1953**, 2836.
16) G. V. Bakore and R. Shanker, *Indian J. Chem.*, 1963 (1693).

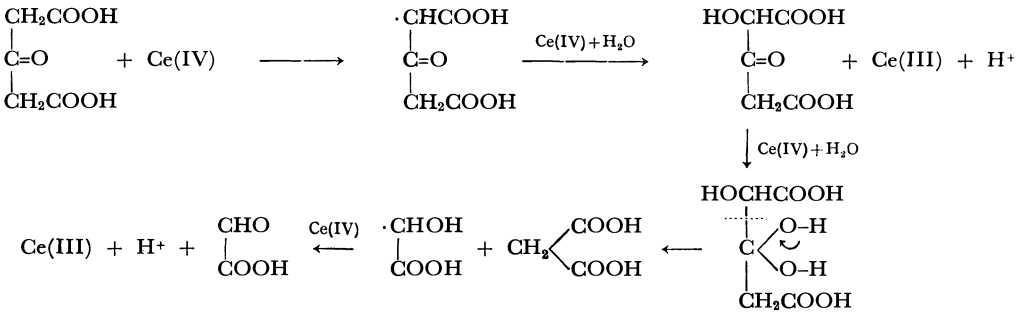

Scheme 1

cation.[17] Malonic acid is oxidized initially to give tartronic acid which by fast steps is further oxidized to produce glyoxylic acid. Glyoxylic acid is then hydrated and oxidized instantaneously at 30°C to give formic acid with the consumption of two equivalents of Ce(IV) ion.

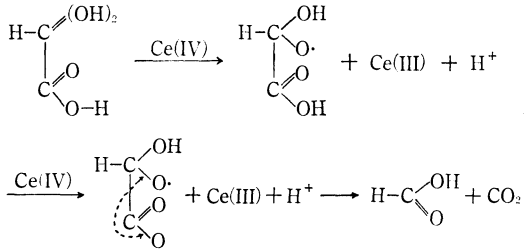

The other mole of glyoxylic acid which has been obtained from acetone dicarboxylic acid has also been oxidized in the above manner to give other mole of formic acid.

While discussing the mechanism through which the reaction proceeds, it has been suggested that the first step is the formation of a complex between ceric ion and the substrate. The question that would occur is why one prefers to assume an initial complex formation and then an electron abstraction by ceric ion to give cerous ion. The possible alternative would be to assume the initiation step as in the case of the oxidation by hydrogen peroxide or a more plausible analogue than by Co^{3+} salt. In cases of both these oxidation processes, formic acid is found to be oxidized, whereas in the oxidation by Ce(IV) salt, formic acid is never oxidized but constitutes one of the products of oxidation reaction. The choice, therefore, falls on the mechanism in which the initiation of the reaction through the formation of a complex and abstraction of electron by ceric ion, is a general first step. The radical would next be involved in reactions be lost, before it can be stabilized. That the reaction is not ionic is supported by the fact that ionic strength had no effect on the rate of oxidation in systems contain- ing perchlorates.

It has been observed that when the oxidant is in excess, the reaction (the consumption of ceric) follows a first order rate. This has been explained on the basis that a steady state concentration[18] of free radical is attained and this finally reacts with ceric ion.

When the organic acid is equivalent or in excess the radical will react with the complex (if it is stable) and then the reaction is apparently a second order one. This is possibly what has been observed by Ghosh and Mehrotra.[4] On the other hand, if the complex is weak the radical will react with ceric ion and the reaction will continue to be the first order. Thus if the organic acid forms a stable complex with the ceric ion, the reaction will pass to one of second order when it goes from excess oxidant to excess of the substrate. Thus stability of the complex plays a role in determining the order of the reaction.

Concerning the thermodynamic constants in the presence of different oxidants, it has been observed that the activation energy in the case of the oxidation by Ce(IV) perchlorate is less than that of the Ce(IV) sulphate. This is possibly due to the fact that sulphate ion forms strong complexes with Ce(IV) ion while perchlorate ion is a weak complex forming anion. Therefore Ce(IV) sulphate will react more slowly with the substrate than Ce(IV) perchlorate. This may also be explained in the light of oxidation potential of Ce(IV)—Ce(III) system which depends on acidity as well as on the kinds of anion present. The oxidation potential of Ce(IV) perchlorate (1 M—2 M acid) is 1.87 V whereas that of Ce(IV) sulphate in sulphuric acid (1M—2 M acid) is 1.44 V which shows that the oxidizing capacity of Ce(IV) sulphate should be less than that of Ce(IV) perchlorate. On the other hand the reaction should be retarded in Ce(IV) sulphate solution requiring a greater energy in the medium.

Thanks are due to Prof. B. N. Ghosh and Dr. M. N. Das for providing laboratory facilities.

17) K. K. Sen Gupta and S. Aditya, *Z. Physik. Chem.*, **38**, **1/2**, 25 (1963).

18) M. Bodenstein, *ibid.*, **85**, 329 (1913).

BULLETIN OF THE CHEMICAL SOCIETY OF JAPAN VOL. 42 303—308 (1969)

The Structure Theory of Water. I. Two State Theory

Kiyoshi ARAKAWA and Katsutaka SASAKI

Research Institute of Applied Electricity, Hokkaido University, Sapporo

(Received March 29, 1968)

A statistical thermodynamic theory was successfully applied to liquid water, based on the two state model which consists of an ice-like structure (class I) and unbonded monomers (class II). The resulting partition function was formulated and calculated using the two quantities, the energy difference between class I and class II, ε, and the free volume per molecule, v_f, as the adjustable parameters which were varied within the physically-reasonable range. The magnitudes of ε and v_f were estimated to be 3 kcal/mol and 4.0×10^{-25} cm^3 respectively to give the best fit of calculated values to the experimental data. From the partition function obtained, the Helmholtz energy, the internal energy, the entropy, and the specific heat were calculated. The agreement between the calculated values and the experimental data was found to be satisfactory. From the obtained result it may be concluded that the simple two state model is adequate to explain the thermodynamical data for liquid water.

A number of studies have been made on the structure of liquid water since Bernal and Fowler[1] proposed a pseude crystal model based on the tetragonal structure in water. However, many problems are left unsolved at present. Morgan and Warren[2] gave the radial distribution curve for water from their X-ray diffraction data, and estimated the average number of first nearest neighbors to be 4.4—4.9 at temperatures from 1.5 to 83°C.

The approach to the structure theory of water based on the ice-like structure, as made by Bernal and Fowler, that is, the approach from the viewpoint that the main structure of liquid water is solid-like, has been taken by many workers. The bent-hydrogen-bonding chain theory given by Pople[3] and the structure theory of Davis and Litovitz[4] are typical of the solid-like theory. However, these theories were found to be able to explain the properties of water only partly. On the other hand, Eucken[5] proposed an association theory, in which water was supposed to be an equilibrium mixture of monomer, dimer, tetramer and octamer.

In 1948, Hall[6] presented a two state theory of water, which was based on the assumption that liquid water was composed of an ice-like structure ("open structure") and unbonded water molecules ("close-packed structure"), in order to explain the ultrasonic absorption data. Hall's theory succeeded in the interpretation of ultrasonic absorption data, but was pointed out by Litovitz and Carnevale[7] to be unsatisfactory for the explanation of the pressure dependence of ultrasonic absorption. Since then, the two state theory of liquid water has been developed in various ways by a number of authors. Some of them, the theories of Samoilov,[8] Frank and Quist,[9] *etc.* were found to emphasize the solid-like structure. On the other hand Frank and Wen[10] proposed a flickering cluster model based on the cooperative nature of hydrogen bonding formation, and pointed out the life time of the cluster to be as short as 10^{-10} or 10^{-11} sec from the relaxation data. According to the suggestion of Frank and Wen, Némethy and Scheraga[11] have presented a refined statistical theory, in which water is assumed to be an equilibrium mixture of flickering clusters and unbonded molecules. The clusters are supposed to be composed of tetra-, tri-, di-, and singly-hydrogen-bonded water molecules, and therefore, Némethy and Scheraga's theory is also regarded as a five state theory.

1) J. D. Bernal and R. H. Fowler, *J. Chem. Phys.*, **1**, 515 (1933).
2) J. Morgan and B. E. Warren, *ibid.*, **6**, 666 (1938).
3) J. A. Pople, *Proc. Roy. Soc.*, **A205**, 163 (1951).
4) C. M. Davis and T. A. Litovitz, *J. Chem. Phys.*, **42**, 2563 (1965).
5) A. Eucken, *Zeit. für Elektrochemie*, **52**, 255 (1948).
6) L. Hall, *Phys. Rev.*, **73**, 775 (1948).
7) T. A. Litovitz and E. H. Carnivale, *J. Appl. Phys.*, **26**, 816 (1955).
8) O. Ya. Samoilov and T. A. Nosova, *Zh. Strukt. Khim.*, **6**, 798 (1965).
9) H. S. Frank and A. S. Quist, *J. Chem. Phys.*, **34**, 604 (1961).
10) H. S. Frank and W-Y. Wen, *Discussions Faraday Soc.*, **24**, 133 (1957); H. S. Frank, *Proc. Roy. Soc.*, **A247**, 481 (1958).
11) G. Némethy and H. A. Scheraga, *J. Chem. Phys.*, **36**, 3382 (1962).

After the proposition of Némethy and Scheraga's theory, several studies have been made along this line. Vand and Senior have recently presented a nine-state theory,[12] and, proposed further an energy band theory. Vand and Senior introduced an additional assumption of the energy band into the structure theory of water without any theoretical explanation. This assumption means a continuous distribution of energy for water molecules and also means the introduction of a very large number of states since the energy changes continuously. It is questionable that, when the life time of the hydrogen-bonded region is known to be as short as 10^{-11}—10^{-10} sec, a number of different states within the hydrogen-bonded region could be distinguished each other, for a "state" has to be regarded as corresponding to a "structure." The assumption of the presence of a number of distinguishable states with as short a life time as 10^{-11}—10^{-10} sec may be doubtful, when the energy difference between the states is as small as the energy of thermal motion. It may be generally said that, on constituting the theory, the number of states assumed is desirable to be as small as possible, so long as the increase in the number of states means the increase in the number of parameters.

Therefore, the authors have made a theoretical investigation on the structure of water based on the two state model, and investigated the effectiveness and the limitation of the two state theory.

Theory

Two State Model. It is assumed that liquid water is an equilibrium mixture of two classes of molecules. Class I is constituted by hydrogen-bonded molecules (open structure or ice-like structure) and class II is constituted by unbonded monomers (close-packed structure). The molecules in each class are assumed to be in a uniform state on the average, and the energy level of the molecules in class II is ε ($\varepsilon>0$), taking the level of those in class I as the ground level. A molecule changes its state fluctuationally with lapse of time, and the life time during which a molecule stays in the state of class I is of the order of 10^{-11}—10^{-10} sec, as pointed out by Frank and Wen[10] based on relaxational data concerning the life time of flickering clusters. It is assumed that a molecule acts as in a solid phase while it stays in the state of class I, and that it acts as in a gaseous phase while in class II.

Statistical Treatment. The formulation of the partition function, $\mathcal{Z}$, for the mixture of Nx molecules in class I and $N(I-x)$ molecules in class II is made as follows,

$$\mathcal{Z}=\frac{N!}{(Nx)!\{N(1-x)\}!}(f_{\mathrm{I}})^{Nx}(f_{\mathrm{II}}\mathrm{e}^{-\varepsilon/RT})^{N(1-x)}, \quad (1)$$

where f_{I} and f_{II} are partition functions for each species. The partition function $\mathcal{Z}$ for the equilibrium mixture is equated to the maximum term as usual regarding x as a parameter. The mole fraction x for class I in the equilibrium mixture is determined by the maximization of $\mathcal{Z}$ concerning x as a variable, using Stirling's approximation,

$$\frac{\partial \ln \mathcal{Z}}{\partial x}=0. \quad (2)$$

Introducing Eq. (1) to Eq. (2), we obtain Eq. (3) for the equilibrium value of x,

$$x=\frac{f_{\mathrm{I}}}{f_{\mathrm{I}}+f_{\mathrm{II}}\mathrm{e}^{-\varepsilon/RT}}, \quad (3)$$

and, introducing Eq. (3) into Eq. (1), the partition function, $\mathcal{Z}$ for the equilibrium mixture, is represented as follows,

$$\mathcal{Z}=(f_{\mathrm{I}}+f_{\mathrm{II}}\mathrm{e}^{-\varepsilon/RT})^{N}. \quad (4)$$

The Helmholtz energy, A is obtained from the following equation (5),

$$A=-kT\ln\mathcal{Z}=-NkT\ln(f_{\mathrm{I}}+f_{\mathrm{II}}\mathrm{e}^{-\varepsilon/RT}) \quad (5)$$

and the energy and entropy can be calculated by Eqs. (6) and (7).

$$E=kT^2\frac{\partial\ln\mathcal{Z}}{\partial T}$$
$$=NkT^2\left(\frac{\partial f_{\mathrm{I}}}{\partial T}+\frac{\partial f_{\mathrm{II}}}{\partial T}\mathrm{e}^{-\varepsilon/RT}+\frac{\varepsilon}{RT^2}\mathrm{e}^{-\varepsilon/RT}f_{\mathrm{II}}\right)\Big/ (f_{\mathrm{I}}+f_{\mathrm{II}}\mathrm{e}^{-\varepsilon/RT}) \quad (6)$$

$$S=(E-A)/T \quad (7)$$

The specific heat, C_V, is derived from the energy, E.

$$C_V=\left(\frac{\partial E}{\partial T}\right)_V \quad (8)$$

The partition functions of each species, f_{I} and f_{II}, are given in the following equations, Eq. (9) and Eq. (10),

$$f_{\mathrm{I}}=\prod_{i=1}^{6}\left(\frac{1}{1-\mathrm{e}^{-h\nu_i/kT}}\right) \quad (9)$$

$$f_{\mathrm{II}}=\left\{\left(\frac{2\pi mkT}{h^2}\right)^{3/2}v_f\right\}\left\{\frac{(8\pi^2kT)^{3/2}(\pi ABC)^{1/2}}{2h^3}\right\}, \quad (10)$$

where ν_i is the frequency of translational vibrations and librations in the state of class I, v_f is the free volume[13] available to a molecule in the state of class II, and A, B and C are the principal moments of inertia of water molecule. The factor in the first bracket of f_{II} corresponds to the translational degrees of freedom and that in the second bracket to the rotational ones. The contribution from intramolecular vibrations into f_{I} and f_{II} is ignored, because it may be safely regarded as 1 at temperatures from 0 to 100°C.

12) V. Vand and W. A. Senior, *J. Chem. Phys.*, **43**, 1869, 1873, 1878 (1965).

13) A. Bondi, *J. Phys. Chem.*, **58**, 929 (1954).

Results

Determination of Parameters. The energy difference between two states, ε, and the free volume, v_f, which is available to a molecule in the state of class II, are two main parameters used in this theory. It is impossible to determine the magnitude of ε and v_f precisely from theory at present, and therefore, they have been treated as the adjustable parameters to give the best fit of calculated values to experimental data. The variation of parameters was, of course, limited within the physically reasonable range. In the earlier treatment based on the two state model the magnitude of ε has been estimated to be within the range of 2.5—3.0 kcal/mol. Smith and Lawson estimated the magnitude of ε to be 2.6 kcal/mol from their sound velocity data,[14] and Lawson *et al.* estimated it to be 3 kcal/mol from their thermal conductivity data.[15] Wada used the value of 2.51 kcal/mol in his treatment.[16]

Taking account of the heat of fusion of ice in addition to the estimation described above, we have taken the range of ε to be 2.75—3.15 kcal/mol.

The magnitude of v_f has been found to be of order of 1% of the volume per molecule (molecular volume) for many liquids.[13,17] Némethy and Scheraga used the value of 4.4×10^{-25} cm^3 which was about 1.5% of the molecular volume of water.[11] The magnitude of v_f calculated from the heat of vaporization of water[13] was 1.1×10^{-25} cm^3 (about 0.35%), and the magnitude of "fluctuation volume" calculated from the distance at the second peak in the Morgan and Warren's radial distribution curve[11,13] was 2.6×10^{-25}—4.6×10^{-25} cm^3, when that distance was taken to be 3.1—3.2 Å. Therefore, calculations have been made within the range of v_f from 1.1 to 4.6×10^{-25} cm^3 as the adjustable parameter. It has been found that the best fit of the calculated to the experimental data has been obtained when the magnitudes of ε and v_f have been taken to be 3 kcal/mol and 4.0×10^{-25} cm^3 (about 1.3% of the molecular volume) respectively.

As for the frequencies which have been attributed to intermolecular vibrations a tentative assignment has been made referring to the data from the infrared and Raman spectroscopy: 210 cm^{-1} for three modes of translational vibrations[11,18,19] and 500 cm^{-1} for three modes of librations on the average.[18,20],*1 The principal moments of inertia have been given to be the same as in the vapor state:[21] $A=1.024\times10^{-40}$, $B=1.921\times10^{-40}$, and $C=2.947\times10^{-40}$.

Calculations of Thermodynamic Variables. Using the values of parameters described above calculations of thermodynamic functions have been made over the temperature range from 0—100°C at 10°C intervals. The calculated values of the Helmholz energy, A, the internal energy, E, the entropy, S, and the specific heat at constant volume, C_V, are given in Table 1, and are plotted against temperature in Fig. (1)—(4). The results calculated are compared with the experimental data for water, which are taken from Dorsey.[11,22] The agreement between the observed and the calculated results is very good for the free energy, and is fairly good for the internal energy and the entropy. The values of E and S calculated are a little larger than the observed. The maximum deviation in the energy is 300 cal/mol, which amounts to 10% of the observed, and that in the entropy is 0.8 e.u., which is 4.7% of the observed. The agreement is found to be better at higher temperatures than at lower temperatures for A, E, and S. The circumstances are a little different for the specific heat, C_V. The curve calculated is found to cross at about 40°C with the experimental curve. The maximum percent deviation in C_V is 17%, which is observed at the boiling point. The agreement between the calculated and the observed specific heat is, however, better than for the curve given by Némethy and Scheraga's theory,[11] as it is seen in Fig. 4.

The magnitude of the mole fraction x has been calculated from Eq. (3), and given in Table 2, together with those given by Némethy and Scheraga,[11] and Buijs and Choppin.[23]

Molar Volume of Water. Concerning the molar volume of water, we assume that it is represented by the linear summation of the volume

14) A. H. Smith and A. W. Lawson, *J. Chem. Phys.*, **22**, 351 (1954).
15) A. W. Lawson, R. Lowell and A. L. Jain, *ibid.*, **30**, 643 (1959).
16) G. Wada, This Bulletin, **34**, 955 (1961).
17) J. H. Hildebrand and R. L. Scott, "The Solubility of Non-electrolyte," ACS Monograph No. 17 (Reinhold, New York (1950), 3rd ed., p. 76).
18) P. A. Giguére and K. B. Harvey, *Can. J. Chem.*, **34**, 798 (1956).
19) P. C. Cross, J. Burnham and P. A. Leighton, *J. Am. Chem. Soc.*, **59**, 1134 (1937).
20) C. H. Cartwright, *Phys. Rev.*, **49**, 470 (1936).
*1 Calculations on the basis of another assignment (lit. (18)—(20), Walrafen, *J. Chem. Phys.*, **47**, 114 (1967)), in which 200 cm^{-1} for translational vibrations and 500, 650, and 750 cm^{-1} for librations, have been made for comparison. Practically the same results have been obtained. The magnitude of x has been found within the deviation of ±0.01 from the results given in Table 2.
21) R. P. Marchi and H. Eyring, *J. Phys. Chem.*, **68**, 221 (1964).
22) N. E. Dorsey, "Properties of Ordinary Water Substances," ACS Monograph No. 81 (Reinhold, New York (1940)).
23) K. Buijs and G. R. Choppin, *J. Chem. Phys.*, **39**, 2035 (1963).

Table 1. Thermodynamic variables

Temp. (°C)	$A_{calc.}$ (kcal/mol)	$A_{obs.}$[11,22] (kcal/mol)	$E_{calc.}$ (kcal/mol)	$E_{obs.}$[11,22] (kcal/mol)	$S_{calc.}$ (cal/deg·mol)	$S_{obs.}$[11,22] (cal/deg·mol)	$(C_V)_{calc.}$ (cal/deg·mol)	$(C_V)_{obs.}$[11,12] (cal/deg·mol)
0	−1.06	−1.20	3.04	2.75	15.0	14.5	19.1	18.1_5
10	−1.28	−1.35	3.14	2.93	15.6	15.1	18.9	18.0_3
20	−1.44	−1.50	3.31	3.11	16.3	15.7	18.9	17.8_8
30	−1.61	−1.66	3.54	3.29	17.0	16.3	18.8	17.7_2
40	−1.78	−1.83	3.70	3.47	17.7	16.9	17.6	17.5_4
50	−1.97	−2.00	3.93	3.65	18.3	17.5	16.9	17.2_9
60	−2.15	−2.17	4.09	3.83	18.7	18.1	16.3	17.1_2
70	−2.35	−2.36	4.26	4.01	19.3	18.6	15.5	16.8_9
80	−2.54	−2.55	4.40	4.20	19.7	19.1	14.7	16.5_9
90	−2.74	−2.74	4.54	4.36	20.1	19.6	13.8	16.3_2
100	−2.94	−2.94	4.64	4.55	20.3	20.0	13.5	16.1_8

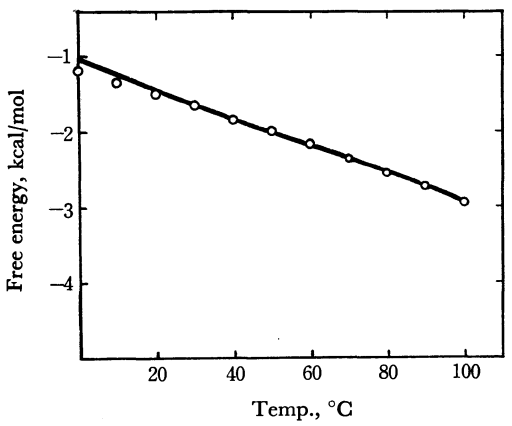

Fig. 1. Free energy, A, for water.
Circle, observed; Solid line, calculated

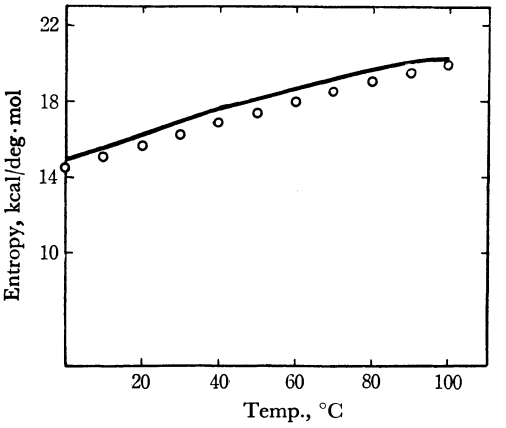

Fig. 3. Entropy, S, for water.
Circle, observed; Solid line, calculated

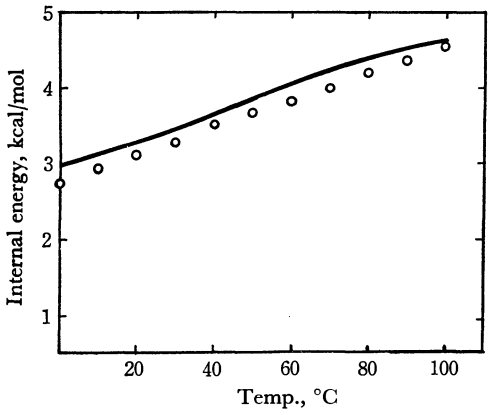

Fig. 2. Internal energy, E, for water.
Circle, observed; Solid line, calculated

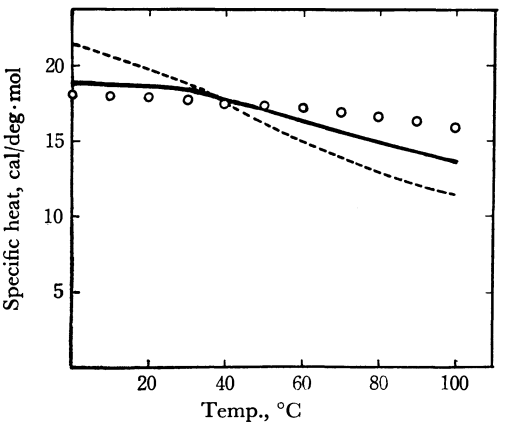

Fig. 4. Specific heat at constant volume, C_V.
Circle, observed; Solid line, calculated by authors;
Dotted line, calculated by Némethy & Scheraga[11]

of two classes of molecules as described below.

$$V = xV_I(1+a_I t) + (1-x)V_{II}(1+a_{II}t) \quad (11)$$

where $V_I \times 19.657$, and $\alpha_I = 1.55 \times 10^{-4}$ which are the values for ice[11,22]; $V_{II} \times 16.252$, $\alpha_{II} = 1.50 \times 10^{-3}$, where V_{II} has been determined by fitting the Eq. (11) to the experimental data at the melting point and α_{II} has been determined in order to obtain the best fit as a parameter. The values of the molar volume calculated are given in Fig. 5

in comparison with the experimental data. The calculated curve is seen to have a minimum at about 4°C. The magnitudes of V_{II} and α_{II} which are for the close-packed structure have been found of reasonable ones,*2 compared with those used by other authors.[11]

Table 2. Fraction of hydrogen-bonded portion, x

Temp. (°C)	Authors	Némethy & Scheraga[11]	Buijs & Choppin[23]
0	0.520	0.528	0.53
10	0.464	0.493	
20	0.415	0.462	
30	0.368	0.434	
40	0.327	0.409	
50	0.293	0.388	0.42
60	0.262	0.370	
70	0.239	0.356	
80	0.215	0.344	
90	0.197	0.334	
100	0.179	0.325	0.35

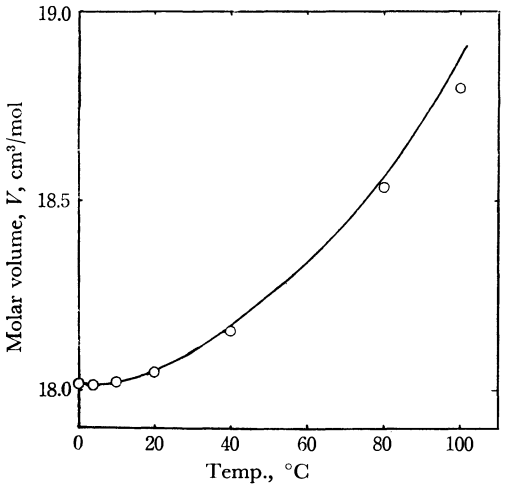

Fig. 5. Molar volume of water.
Solid line, calculated; Circle, observed

Discussions

As seen in Figs. (1)—(5), the results of calculations are found to be satisfactory on the whole, taking into account the simplicity of the model used. This fact supports the idea that the two state model used is an adequate representation of the structure of liquid water in order to describe the thermodynamical behavior. And it is also concluded that thermodynamic data are not sensitive to the detailed structure of each class and are governed by the average character on the whole.

Recently, Eyring and coworkers have proposed the significant structure theory for water.[21,24,26] The earlier theory proposed by Marchi and Eyring[21] used a two state model, but the monomer concentration at the melting point calculated was only 2.5 mol %. This is unreasonably small. The later theory presented by Jhon, Grosh, Ree, and Eyring[24] was a three state theory which assumed that water consists of Ice-I-like structure, Ice-III-like structure, and monomers. The agreement to experimental data was certainly improved in the latter theory,[24] compared with that in the former theory.[21] However, additional assumptions were introduced into the latter theory.

The theory of Némethy and Scheraga may be said to be successful in the approximate description of thermodynamical behaviors of water. However, in the results calculated it is seen that several problems are found left unsolved in addition to the deviation of the magnitude of specific heat from the observed data. The one is the abnormally small magnitude of the mole fraction of di-hydrogen-bonded species, which is unreasonable.[12] Further studies are required.

In the present theory the ice-like structure (class I) is regarded as a uniform state on the average without any further assumption to its structure. Though the present theory has turned out to be successful for the description of thermodynamical behaviors of water, it is, of course, necessary to introduce a further structural assumption concerning the structure of the ice-like region in order to describe the various kinds of relaxational behaviors. From the view-point of relaxational process, it has been proposed, as pointed out by Frank and Wen,[10] that the ice-like structure is composed of flickering clusters.[10,11] It is impossible to determine the size of clusters, exactly speaking, the distribution of the cluster size in the ice-like portion, using the theory based on the two state model which consists of each uniform-structure region, as in the present theory. For the purpose of determining the cluster size the introduction of third state, "the surface state on the cluster" is required, and the investigations by authors along this line are proceeding.

As for the calculation of the partition function concerning f_I (Eq. (9)), the frequency assignment used is, of course, an oversimplification, though the exact assignment has not been determined at

*2 The magnitude of V_{II} corresponds to the molar volume of spherical molecules with the diameter of 3.2 Å, arrayed in b.c.c. lattice, where the void fraction is assumed to be about 10%.

24) M. S. Jhon, J. Grosh, T. Ree and H. Eyring, *J. Chem. Phys.*, **44**, 1465 (1966).
25) H. Eyring and R. P. Marchi, *J. Chem. Educ.*, **40**, 562 (1963).
26) H. Eyring, T. Ree and N. Hirai, *Proc. Natl. Acad. Sci. Am.*, **44**, 683 (1958).

present. This deficiency will be supplemented in the further investigations.

Conclusion

A statistical thermodynamic theory based on the two state model has been successfully applied to liquid water. The two state model firstly proposed by Hall turned out to be an adequate description to the thermodynamical behaviors of water, in spite of its simplicity.

We wish to thank to Miss Yuko Endo for her cooperation in performing this study.

BULLETIN OF THE CHEMICAL SOCIETY OF JAPAN VOL. 42 308—312 (1969)

Anomalous Viscosity of Bitumen Solutions and the Agglomeration of "Molecules"

Katsuya INOUYE,* Junichi TATSUTA*1 and Tsutomu SAKABE**

* *Department of Chemistry, Faculty of Science, Chiba University, Chiba*

** *Resources Research Institute, Kawaguchi*

(Received April 30, 1968)

The flow property of catechol and phenol solutions of 14 bitumen fractions was examined by means of a horizontal viscometer to compare with the molecular weight values of the fractions determined in each solvent. The catechol solutions showed Newtonian flow which corresponds to the homogeneous solutions containing molecules of a limited value of molecular weight. The molecular weight from phenol solutions varies with the fractions, and all fractions showed non-Newtonian (structural) viscosity. The experimental results indicated that bitumens in phenol agglomerate to different extent particular to each fraction. It was presumed that the stress destroys the agglomerated state to a monodisperse state, which is gradually recovered to the original state on standing. It was noted however that the unit particle (or molecule) composing each fraction is not identical in the apparent size in phenol, but varies with fractions.

It has been well recognized that the apparent molecular weight of bitumen fractions extracted from coals or hydrogenated coals showed values within the limited range of 200 to 350, when determined cryoscopically in catechol.[1,2] The fact has consequently led to the concept that the coal or bitumen as coal component is composed of "molecules" of molecular weight of approximately 300. The apparent molecular weight determined by use of other solvents, however, gives different values with fractions. For example, the molecular weight obtained by Weiler *et al.*,[1] determined from the boiling-point elevation of benzene solutions and the freezing-point depression of diphenyl solutions vary considerably with the fractions.

The problem has not been solved if the coal "molecules" of an identical size exist, which may form, in particular situations, their aggregated clusters, or if the varying molecular weights indicate continuously differing dimensions of coal constituting substances.

The present work intends to ascertain the existence of the aggregated state of bitumen "molecules" in the specific solvent by determining the viscosity behavior of the solution. The Newtonian viscosity would be observed, if the "molecules" of the same size or covalently bonded particles of different sizes are dissolved in a solvent, while an anomalous (non-Newtonian) viscosity would appear due to the breaking-down of apparent aggregates with the shear stress in the course of the viscosity measurement.

Experimental

a) Materials. The preparation of fractions has been described in a preceding paper.[3] A Japanese bituminous coal (Yubari) of 83% carbon was ground under 60 Tyler meshes and extracted with benzene

*1 Present address: Nihon Tenkazai Kogyo Co., Ltd., Itabashi, Tokyo.

1) J. F. Weiler, J. J. Ward and H. C. Howard, *J. Am. Chem. Soc.*, **64**, 734 (1942).

2) I. G. C. Dryden, *Fuel*, **31**, 176 (1952).

3) T. Sakabe, K. Inouye, K. Ouchi and H. Honda, *J. Fuel Soc. Japan*, **32**, 610 (1953).

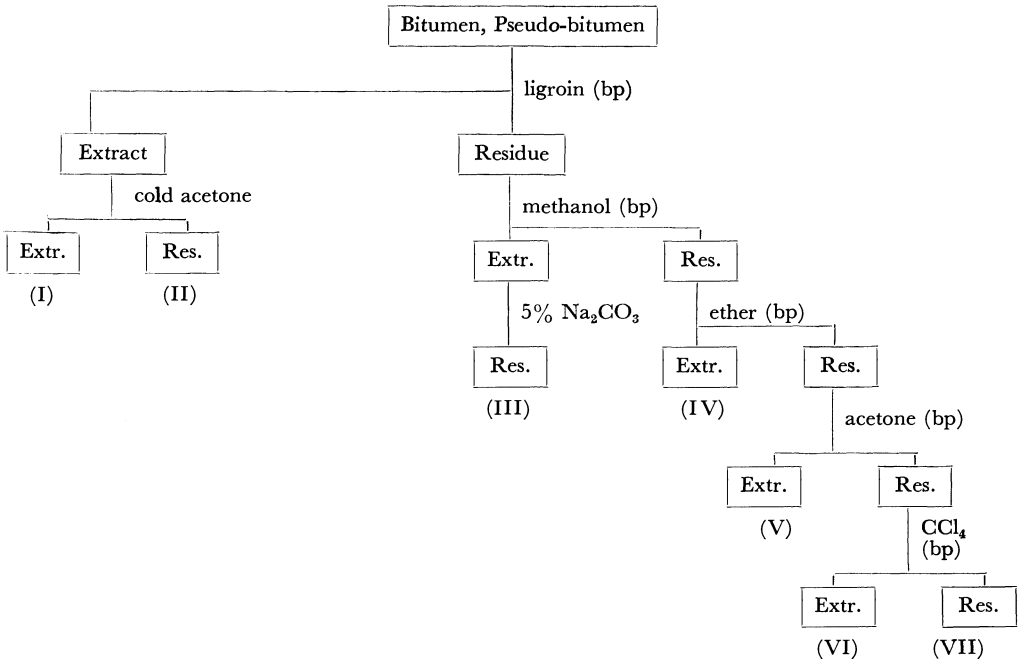

Fig. 1. Fractionation of bitumen and pseudo-bitumen.

at 220—260°C for 15 hr in total in a rotating autoclave. The solid bitumen from the extract, washed repeatedly with petroleum ether, was 7.0% of the original coal (dry-ash-free basis).

The residue of the above extraction was then subjected to catalytic hydrogenation in the autoclave with decalin in the presence of Adkins Ba-Cu-Cr oxide catalyst at 350°C for 6 hr and the initial hydrogen pressure of 100 atm. The product was extracted with benzene at 260°C for 9 hr in total, followed by the separation from the solvent. The pseudo-bitumen obtained was 50.7% of the original coal.

The bitumen and pseudo-bitumen thus obtained were fractionated successively by use of ligroin, methanol, ether, acetone and carbon tetrachloride to give the fractions shown in Fig. 1. Each of the seven fractions from bitumen and pseudo-bitumen is denoted respectively as B-I, -II, -III, -IV, -V, -VI and -VII and PB-I, -II, -III, -IV, -V, -VI and -VII.

Various properties (melting point, ultimate analysis, iodine value, true density, ultraviolet absorption, X-ray diffraction and diamagnetic susceptibility) of the similar fractions have been reported elsewhere.[3]

b) Molecular Weight. The cryoscopic molecular weight in phenol solvent was determined for 4 to 5 solutions of different bitumen concentrations in the range of 0.5 to 2.0%, with much care of avoiding moisture. The melting-point depression value at the zero concentration was obtained by the least-square method. In the case of catechol solvent, the method by Smith and Howard[4] was employed. The molecular depression of 59 was used for the molecular weight calculation.

c) Viscosity Measurement. The viscometer used in this work is a slightly modified Tsuda horizontal viscometer,[5] shown in Fig. 2, with a capillary of 0.5 mm

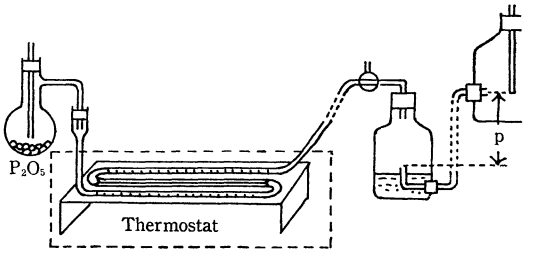

Fig. 2. Horizontal viscosimeter.

inner diameter and 20 cm length. Apart from the original Tsuda viscometer, the moisture absorption into sample solutions was carefully avoided by connecting it with a drying vessel containing P_2O_5.

The absolute viscosity determined by the present viscometer of phenol and catechol was 4.949×10^{-2} poise at 41.0 ± 0.5°C and 3.11×10^{-2} poise at 105 ± 0.5°C, respectively. In case of the determination using catechol solvent, the viscometer was submerged in a liquid-paraffin thermostat.

The time (t) required for 1 cc sample solution to flow through the capillary was measured at various pressure differences (p) supplied from two large water containers, as also schematically illustrated in Fig. 2.

For Newtonian liquids the following relationship is applied:

$$tp = \text{constant.} \quad (1)$$

The product tp is, therefore, independent of p. According

4) R. C. Smith and H. C. Howard, *J. Am. Chem. Soc.*, **57**, 512 (1935).

5) S. Tsuda, *Kolloid-Z.*, **45**, 325 (1928).

to Ostwald,[6] the non-Newtonian "structural" viscosity is well expressed by

$$tp^n = \text{constant } (k), \qquad (2)$$

where the tp value decreases with the increase of p in characteristic manner to the state of secondary "structure" of colloidal particles in the solution. The relationship between log t and log p, which is to be linear, gives the values of n and the constant k in Eq. (2).

Results and Discussion

a) Viscosity of Bitumen Solutions in Catechol. The *pt-p* relationships of catechol solutions in each case gave an identical result that the product *pt* is independent of *p* and consequently that bitumen solutions in catechol show the Newtonian flow.

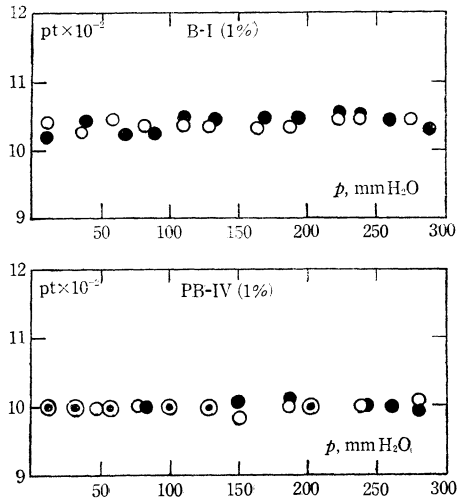

Fig. 3. The *pt-p* relationships of catechol solutions.

Figure 3 shows those of 1.0% solutions of B-I and PB-IV fractions determined at 105±0.5°C. The measurement was performed, at first, in increasing pressure (○), followed then by decreasing pressure (●); no departures were observed between values in the elevating and reversed pressure changes. The results also would indicate the absence of any agglomerates in the solutions.

TABLE 1. ABSOLUTE VISCOSITY AND MOLECULAR WEIGHT OF CATECHOL SOLUTION (1%)

Sample	Absolute viscosity (η), poise	Molecular weight
B-I	3.29×10^{-2}	330
B-VII	3.38×10^{-2}	280
PB-I	3.23×10^{-2}	320
PB-IV	3.23×10^{-2}	360
PB-VII	3.38×10^{-2}	300

6) Wo. Ostwald, *Kolloid-Z.*, **36**, 99 (1925).

Table 1 gives the absolute viscosity calculated from *pt* values at $p=0$ for the solutions of some fractions with respect to the molecular weight determined cryoscopically in catechol solvent. The molecular weight in catechol solvent appears to represent, as discussed by Dryden[2] and Sakabe *et al.*,[3] a more or less degradated state, although the elucidation has not fully been given on the reason why a value of around 300 is usually found.

b) Viscosity of Bitumen Solutions in Phenol. The *pt-p* curves given by the phenol solutions determined at 41±0.5°C, were those of typically non-Newtonian structural viscosity for each solution. There are, however, three types of curves (A, B and C) as illustrated in Fig. 4 as examples. In Type A, the change of *pt* with increasing pressure (○) is almost exactly similar to that with decreasing pressure (●). For the samples of Types B and C, curves of reversed directions do not coincide, but the *pt* values in pressure change of decreasing direction are more or less lower than those in increasing direction. Particularly in Type C, the above mentioned discrepancy is quite apparent so as to indicate that the "structure" in the solution is completely destroyed by the foregoing application of the shearing stress.

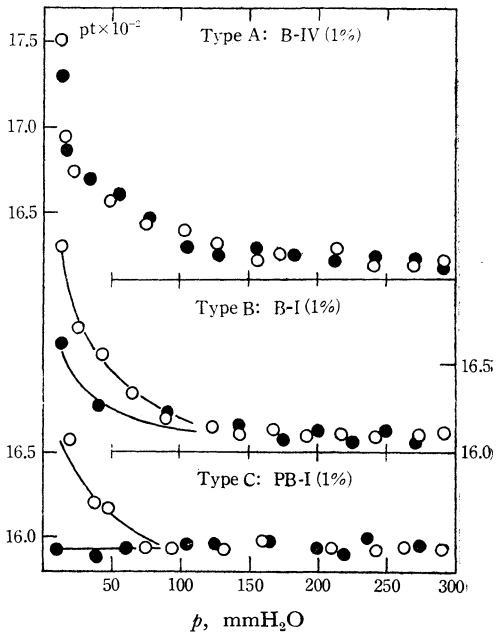

Fig. 4. The *pt-p* relationships of phenol solutions.

If the solutions of Types B and C are subjected to stand at the same temperature after the end of measurement, in other words, after supposed breaking of the secondary structure, the *pt* value increases gradually with the standing time up to the original high value in 24 hr, suggesting that

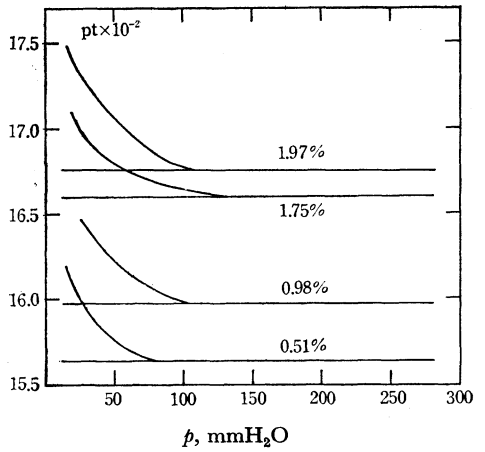

Fig. 5. The variations of *pt-p* relations with concentrations of phenol solutions; sample: PB-I.

Table 2. Absolute viscosity, n, k and molecular weight of phenol solutions (1%)

Sample	Absolute viscosity (η), poise	n	k	Molecular weight
B-I	5.19×10^{-2}	1.01	3.23	347
B-II	5.28×10^{-2}	—	—	350
B-III	5.23×10^{-2}	1.04	3.25	406
B-IV	5.22×10^{-2}	1.05	3.28	522
B-V	5.22×10^{-2}	1.04	3.26	638
B-VI	5.31×10^{-2}	1.08	3.31	1085
B-VII	5.34×10^{-2}	1.08	3.33	1359
PB-I	5.12×10^{-2}	1.03	3.24	396
PB-II	5.21×10^{-2}	1.03	3.25	590
PB-III	5.20×10^{-2}	—	—	392
PB-IV	5.25×10^{-2}	1.04	3.26	539
PB-V	5.34×10^{-2}	1.03	3.26	623
PB-VI	5.32×10^{-2}	1.06	3.30	1085
PB-VII	5.32×10^{-2}	1.09	3.35	1139

the once destroyed structure is ultimately recovered, but in a rather slow process.

Figure 5 gives the influence of concentration on the viscosity behavior (*pt-p* relation) in the case of PB-I fraction. It is suggested that the shape of *pt-p* curve is identical and that the viscosity calculated from *pt* at the non-structural state increases with the concentration.

The values of absolute viscosity (η), n and k in Eq. (2) are tabulated in Table 2 with respect to the molecular weight. Values given were obtained from measurements for the 1% solutions. Values of n are nearly equal to unity, but both the values n and k tend to increase with the molecular weight. It appears that the molecular weight approaches to a value around 300, when n approaches to unity. This result would be plausible, if one assumes that the molecular weight is measured at a state in which agglomerates are incompletely destroyed by the stirring during the course of cryoscopic measurement.

The absolute viscosity, increasing with the molecular weight, is also characterized by the following results. Table 3 gives the η values at different concentrations for some selected fractions as well as the intrinsic viscosity $[\eta]$. Once again, the increase of $[\eta]$ with molecular weight is observed. The linear relationship between $[\eta]$ and the molecular weight, accepted generally for chain polymers, can not however be applied in the present case.

The results shown in Table 3 are also expressed in a different manner. From concentration and pycnometric true density measured at 25.0°C in methanol, the volume fraction (ϕ) occupied by the bitumen was calculated and inserted in the following Einstein equation[7]:

$$\eta = \eta_0(1+\alpha\phi). \quad (3)$$

The value of α obtained from the inclination of linear relationships between η and ϕ, is also

Table 3. Variation of absolute viscosity with concentration of phenol solutions, intrinsic viscosity ($[\eta]$) and Einstein constant (α)

Sample	Molecular weight	Concentration, %	Absolute viscosity (η), poise	Intrinsic viscosity ($[\eta]$), poise	Einstein constant (α)
PB-I	396	0.51	5.02×10^{-2}	3.0×10^{-2}	2.5×10^{-3}
		0.98	5.12×10^{-2}		
		1.75	5.32×10^{-2}		
		1.99	5.37×10^{-2}		
PB-IV	539	0.50	5.07×10^{-2}	5.2×10^{-2}	4.1×10^{-3}
		1.02	5.25×10^{-2}		
		1.52	5.39×10^{-2}		
		2.01	5.54×10^{-2}		
PB-VII	1139	0.50	5.18×10^{-2}	6.8×10^{-2}	5.2×10^{-3}
		1.00	5.32×10^{-2}		
		1.51	5.50×10^{-2}		
		1.99	5.71×10^{-2}		

7) *Cf.* M. Reiner, "Deformation and Flow," H. K. Lewis and Co., London (1949), Chapt. 4.

given in Table 3. The η_0 observed graphically from the similar linear relations at $\phi=0$ was 4.90×10^{-2} poise, which is coincident with the viscosity of pure phenol (4.949×10^{-2} poise).

All these results described above strongly suggest that bitumens in phenol, contrary to the cases of catechol solutions, agglomerate to different extent particular to each fraction. It is generally recognized that the application of shearing stress by the flow dissociates the agglomerated state easily into a monodisperse state, which may be recovered to the original state on standing.

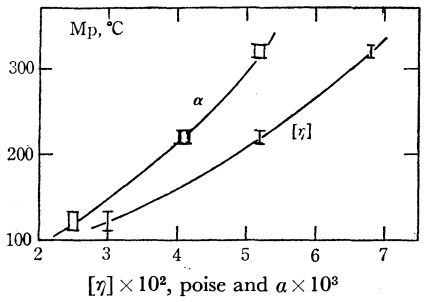

Fig. 6. The increase of melting temperature with intrinsic viscosity and Einstein constant.

However, it is noteworthy that there is no constancy in the values of n and k in Table 2 as well as more apparently of α in Table 3 for different fractions. The fact that these constants show in each case the same tendency to increase with the increase of molecular weight seems to indicate that the unit particle composing each fraction is not identical in the apparent size, but varies from a fraction to another. The increasing tendency described above would mean that the apparent particle size is larger for the fraction which gives larger molecular weight. Also referring to the previously published data,[3] the softening (melting) temperature is almost linearly related with $[\eta]$ and α, as shown in Fig. 6.

It is concluded therefore that the variation of molecular weight obtained by use of phenol solvent is caused partly by the agglomeration of unit particles and partly by the variation of dimension of unit particle. It seems apparent that the dimension of unit particle is larger for the fractions showing larger molecular weights in phenol, and therefore that the molecular weight by phenol is more relevant to the ultimate state of bitumens.

BULLETIN OF THE CHEMICAL SOCIETY OF JAPAN VOL. 42 312—318 (1969)

The Catalytic Activity of Onium Compounds in the Homogeneous Liquid Phase Oxidation of Cumene and α-Pinene

Kenichi FUKUI, Katsutoshi OHKUBO and Tokio YAMABE

Faculty of Engineering, Kyoto University, Sakyo-ku, Kyoto

(Received May 29, 1968)

The catalytic activity of onium compounds was studied in the homogeneous liquid phase oxidation of cumene and α-pinene. The onium salts, particularly sulfonium, phosphonium, selenonium, arsonium and telluronium were found effective. This result is connected to the fact that the central atom in these onium has vacant d orbitals. Among the anions of the onium salts tested, phosphate and sulfate were most effective. The aryl substituents in the central sulfur in sulfonium lessened the activity, while alkyl substituents made it greater. These facts were attributed to charge migration from the substituents and the anionic part to the central atom.

In earlier papers,[1,2] it was reported that phosphonium and sulfonium halides were effective catalysts in the liquid phase oxidation of hydrocarbons such as tetralin, cumene and *p*-xylene, and that the activity of these catalysts was dependent upon the kind of halogen anions involved. Phosphonium and sulfonium tetrafluoroborates were not as effective as halides. Bredereck[3] also reported a similar effect of halogen anions in tetralin oxidation by several alkyl ammonium salts.

It was found later, however, that phosphate and sulfate anions of sulfonium salt were in some cases more active than halogen anions. In addition, the previous papers[1,2] had not discussed the effect of

1) K. Fukui, K. Kanai, T. Takezono and H. Kitano, *Kogyo Kagaku Zasshi* (*J. Chem. Soc. Japan, Ind. Chem. Sect.*), **67**, 1131 (1964).

2) K. Kanai, K. Ohkubo, H. Kitano and K. Fukui, *Bull. Japan Petr. Inst.*, **7**, 52 (1965).

3) H. Bredereck, A. Wagner, R. Blascke, C. Demetriades and K. G. Kottenhahn, *Chem. Ber.*, **92**, 2628 (1959).

the structure of əɥ cation part of onium salts From this point, it was hoped to reinvestigate the catalytic activity of these onium salts in more detail.

It was attempted in the present paper to clarify mainly the role of the cation part of various onium salts in their catalytic action, in connection with the mechanism of interaction of onium catalysts with the oxygen molecule.

In order to investigate the effect of the cation part, the homogeneous liquid phase oxidation of cumene and α-pinene in the presence of tetrafluoroborates of the following oniums was carried out; carbonium, ammonium, oxonium, silyl, phosphonium, sulfonium, arsonium, selenonium and telluronium. The silyl compound was added to the group of onium compounds for comparison's sake. The central atoms of these oniums and their lowest vacant atomic orbitals which might play an important role in interaction with the oxygen molecule (discussed later) are listed in Table 1.

Table 1. The lowest vacant atomic orbitals of central atoms of onium ions

C (2p)	N (3s)	O (3s)
Si (3p)	P (4s, 3d)	S (4s, 3d)
	As (5s, 4d)	Se (5s, 4d)
		Te (6s, 5d, 4f)

It was found that, in these onium salts, phosphonium, sulfonium, selenonium, arsonium, and telluronium were effective; in particular, the first three were outstanding. These compounds are characterized in that the central atoms possess low-lying vacant d orbitals. The order of activity of these onium salts as compared with those with central atoms of elements in the same row of the periodic table was the following:

$$\text{carbonium} < \text{ammonium} < \text{oxonium}$$

$$\text{silyl} < \text{phosphonium} \simeq \text{sulfonium}$$

$$\text{arsonium} (\simeq \text{telluronium}) < \text{selenonium}$$

In order to investigate the effect of the anion part of onium salts, the oxidation of cumene was carried out with various triphenylsulfonium salts as catalysts, such as phosphate, sulfate, nitrate, chromate, perchromate, *etc.* It was found that triphenylsulfonium phosphate and sulfate were more effective than triphenylsulfonium halides in the initial step of oxidation. Furthermore, the effect of substituents of the cation part was investigated using a series of sulfonium tetrafluoroborates. Finally, the mechanism of this homogeneous oxidation with particular reference to the interaction between molecular oxygen nda catalysts was discussed.

Experimental

Material and Method of Oxidation. Cumene was washed with conc. sulfuric acid and dried with anhydrous magnesium sulfate, then distilled to collect the fraction (bp 152.0—152.5°C) which was used for oxidation. α-Pinene was distilled to obtain the 155—156°C fraction. The distillate (10 m*l*) was warmed in the presence of onium salts (0.03 mmol) to 85°C in a nitrogen atmosphere before charging with oxygen. The almost homogeneous solution obtained was subjected to oxidation with the same apparatus and in the same way as reported in a previous paper.[1]

Catalysts. *Triphenylcarbonium Tetrafluoroborate.* Equimolar amounts of triphenylmethyl chloride and silver tetrafluoroborate were mixed in ethyl alcohol and stirred for about 5 hr to form a precipitate of silver chloride. After filtering the precipitate, the filtrate was evacuated to separate reddish yellow crystals of triphenylcarbonium tetrafluoroborate (yield 62%) melting at 207—210°C (dec.).

Found: C, 32.1; H, 6.29%. Calcd for $C_{18}H_{15}CBF_4$: C, 32.4; H, 6.10%.

Tetraethylammonium Tetrafluoroborate. After an equimolar mixture of triethyl amine and ethyl bromide was left standing for about a day in ethyl acetate, a precipitate of tetraethylammonium bromide was obtained, which was filtered and dried *in vacuo*, then, an equimolar mixture of tetraethylammonium bromide and silver tetrafluoroborate was similarly treated to obtain hygroscopic colorless crystals of tetraethylammonium tetrafluoroborate.

Found: C, 44.3; H, 9.22; N, 6.92%. Calcd for $C_8H_{20}NBF_4$: C, 44.2; H, 9.43; N, 6.79%.

Triphenyloxonium Tetrafluoroborate. Phenyldiazonium tetrafluoroborate (10. 5 g) and diphenyl ether (150 g) were refluxed in acetone (300 m*l*) at 80—90°C for half an hour and the solution quenched. The resulting precipitate was dried *in vacuo* to obtain colorless crystals (recrystallized from acetone and ether), melting range between 226 and 227°C (dec.).

Found: C, 28.3; H, 6.17%. Calcd for $C_{18}H_{15}OBF_4$: C, 28.5; H, 6.19%.

Triphenylsilyl Tetrafluoroborate. Tetrachlorosilane (5.7 g) was added to an ether solution of phenylmagnesium bromide (18.1 g) and the mixture refluxed to obtain colorless crystals of triphenylchlorosilane (90% yield), melting at 110—111°C, and equimolar quantities of triphenylchlorosilane and silver tetrafluoroborate were treated in the same way as mentioned above to obtain colorless crystals which were recrystallized from ether and ethyl acetate, mp 314—315°C.

Found: C, 62.4; H, 4.33%. Calcd for $C_{18}H_{15}SiBF_4$: C, 62.1; H, 4.35%.

Triphenylsulfonium-, Tetraphenylphosphonium-, Triphenylselenonium-, and Triphenyltelluronium Tetrafluoroborates. These onium salts were prepared by methods similar to those reported in a previous paper.[4]

4) T. Hashimoto, M. Sugita, H. Kitano and K. Fukui, *Nippon Kagaku Zasshi* (*J. Chem. Soc. Japan, Pure Chem. Sect.*), **88**, 991 (1967).

Compound	Appearance	Mp (°C)	Found		Calcd	
			C (%)	H (%)	C (%)	H (%)
$(C_6H_5)_3S$-$\frac{1}{3}PO_4$	Colorless needles	201—201.5	72.2	5.09	72.0	5.11
$(C_6H_5)_3Se$-$\frac{1}{3}PO_4$	Colorless crystals	178—178.5	63.2	4.39	62.9	4.42
$(C_6H_5)_3Te$-$\frac{1}{3}PO_4$	Colorless crystals	240—240.5	60.5	4.20	60.1	4.41

Triphenylsulfonium-, Triphenylselenonium- and Triphenyltelluronium Phosphate. Twenty milliliters of an aqueous solution of potassium phosphate (0.4 mmol) were added to ethyl alcohol (200 m*l*) solutions of triphenylsulfonium, triphenylselenonium and triphenyltelluronium tetrafluoroborates (1 mmol), and the solutions kept standing for about 24 hr. The precipitates of potassium tetrafluoroborate were filtered off, and the filtrates evacuated in a nitrogen atmosphere. The raw crystals were recrystallized from chloroform and ether. Their appearances and analytical data are listed above.

Tetraphenylphosphonium and Triphenylsulfonium Chlorides. These chlorides were prepared as in previous papers.[1,5] Their appearances and analytical data are listed in the following.

Compound	Appearance	Mp (°C)	Found Cl (%)	Calcd Cl(%)
$(C_6H_5)_4PCl$	Colorless needles	271—272	9.6	9.5
$(C_6H_5)_3SCl$	Colorless needles	297—298	11.6	11.9

Tetraphenylarsonium Tetrafluoroborate. 41.9 g of tetraphenylarsonium chloride (colorless crystals melting at 256—257°C) and 19.47 g of silver tetrafluoroborate were treated similar to the sulfonium fluoroborates. Colorless crystals were obtained, melting at 318—319°C. Found: BF_4, 23.0%. Calcd for $C_{24}H_{20}AsBF_4$: BF_4, 23.4%.

Triphenylsulfonium Nitrate and Tetraphenylphosphonium Nitrate. These salts were prepared by a method similar to that given in a previous paper.[4] The former consisted of colorless needles melting at 225.5—226°C. (Found: C, 66.7; H, 4.71; N, 4.0%. Calcd for $C_{18}H_{15}SNO_3$: C, 66.4; H, 4.65; N, 4.3%), and the latter of colorless crystals melting at 283—284°C. (Found: C, 71.9; H, 5.1; N, 3.7%. Calcd for $C_{24}H_{20}PNO_3$: C, 71.8; H, 5.0; N, 3.5%.)

Triphenylsulfonium Salts. Triphenylsulfonium tetrafluoroborate and potassium salts were treated similar to triphenylsulfonium phosphate. The raw crystals were recrystallized from chloroform and ether. Triphenylsulfonium salts ($(C_6H_5)_3SX$) obtained are described below.

Alkyldiphenylsulfonium Tetrafluoroborate. Equimolar amounts of diphenyl sulfide and silver tetrafluoroborate were kept standing at room temperature to precipitate dark brown crystals which were dried *in vacuo*. Hygroscopic dark brown crystals of diphenyl sulfide-silver fluoroborate complex (90% yield) were obtained which melted at 54—55°C (dec.). (Found: C, 38.5; H, 2.5%. Calcd for $C_{12}H_{10}SBF_4Ag$: C, 37.9; H, 2.6%.) Alkyl iodide (0.08 mol) was added to an ethylene chloride solution of the complex (0.056 mol). The solution was stirred for *ca.* 2 hr at room temperature and left standing overnight to precipitate silver iodide which was removed. After the solvent was removed from the nitrogen atmosphere, crystals were obtained which were recrystallized from chloroform and ether. The products are listed below.

$(C_6H_5)_2RSBF_4$ R	Yield (%)	Mp (°C)	BF_4 Found (%)	BF_4 Calcd (%)
CH_3	44	61—62	30.5	30.9
C_2H_5	40	76—77	28.8	29.4
n-C_3H_7	41	115.5—116.5	27.5	27.7
n-C_4H_9	40	85—86	26.3	27.1

Trialkylsulfonium Tetrafluoroborates. These salts were prepared by the same method as in a previous paper.[5] Analytical data are as follows: $(CH_3)_3SBF_4$ melting at 307—308°C (dec.) (Found: BF_4, 52.3%, Calcd for $C_3H_9SBF_4$: BF_4, 52.9%) and $(C_2H_5)_3SBF_4$ melting at 104—105°C (Found: BF_4, 43.4%, Calcd for $C_6H_{15}SBF_4$: BF_4, 42.1%).

Benzylmethylphenylsulfonium and Dibenzylmethylsulfonium Tetrafluoroborates. Methyl iodide (0.08 mol) was added

$(C_6H_5)_3SX$ X	Appearance	Mp (dec.) (°C)	Found		Calcd	
			C (%)	H (%)	C (%)	H (%)
$\frac{1}{2}SO_4$	Colorless needles	178—179	69.4	4.82	69.7	4.90
$\frac{1}{2}CrO_4$	Colorless needles	181.5—182	67.3	4.67	67.0	4.65
$\frac{1}{2}Cr_2O_7$	Yellow crystals	228.5—239	58.3	4.05	58.7	4.65
$\frac{1}{3}Fe(CN)_6$	Pale green crystals	189—190	71.9	4.49	72.2	4.39
$\frac{1}{2}Ni(CN)_4$	Colorless crystals	164.5—165	68.9	4.31	69.1	4.33
$\frac{1}{2}SeO_4$	Colorless crystals	110—110.5	64.0	4.49	64.4	4.52
$\frac{1}{2}TeO_4$	Colorless needles	191—192	60.0	4.15	60.1	4.21
$\frac{1}{4}P_2O_7$	Colorless needles	190.5—191	70.1	4.81	70.4	4.85
$\frac{1}{2}CO_3$	Colorless needles	189—189.5	75.3	5.52	75.9	5.33

5) K. Fukui, K. Kanai and H. Kitano, *Nippon Kagaku Zasshi* (*J. Chem. Soc. Japan, Pure Chem. Sect.*), **82**, 178 (1961).

to an ethylene chloride solution of equimolar (0.056 mol) amounts of silver tetrafluoroborate and benzylphenylsulfide or dibenzylsulfide. The mixture was treated similar to alkyldiphenylsulfonium tetrafluoroborate, and the following sulfonium tetrafluoroborates obtained: $C_6H_5CH_2(CH_3)(C_6H_5)SBF_4$ melting at 126.5—127.5°C (Found: BF_4, 28.6%. Calcd for $C_{14}H_{15}SBF_4$: BF_4, 29.1%) and $(C_6H_5CH_2)_2CH_3SBF_4$ melting at 214—215°C. Found: BF_4, 29.1%. Calcd for $C_{13}H_{17}SBF_4$: BF_4, 29.7%.

Phenyl-bis-(p-fluorophenyl) sulfonium Tetrafluoroborate. Equimolar quantities of phenylmagnesium bromide and di-*p*-fluorophenylsulfoxide were refluxed in benzene for *ca.* 2 days to precipitate phenyl-bis-(*p*-fluorophenyl) sulfoxymagnesium bromide. The precipitates were triturated with 20% hydrogen tetrafluoroborate and after extraction of the benzene phase by chloroform, followed by the removal of chloroform and recrystallization from chloroform and ether, colorless crystals of phenyl-bis-(*p*-fluorophenyl) sulfonium tetrafluoroborate were ob tained, melting at 185—186°C. Found: BF_4, 22.1%. Calcd for $C_{18}H_{13}SBF_6$: BF_4, 22.5%.

Tribenzylsulfonium Tetrafluoroborate. An equimolar mixture of benzylmagnesium bromide and dibenzylsulfoxide was refluxed in benzene and treated similar to phenyl-bis-(*p*-fluorophenyl)sulfonium tetrafluoroborate. Colorless crystals of tribenzylsulfonium tetrafluoroborate were obtained. Mp 177.5—178.5°C. Found: BF_4, 21.8%. Calcd for $C_{21}H_{21}SBF_4$: BF_4, 22.1%.

Results

The Effect of the Central Atom of the Onium Cation. In order to investigate the effect of a difference in nature of the central atom of the onium cation, the liquid phase oxidation of cumene and α-pinene (10 m*l*) was carried out at 85°C in the presence of 0.03 mmol of triphenyl- or tetraphenyl-onium tetrafluoroborate (except for ammonium, where the tetraethyl derivative was taken), and the amounts of the following main products were determined; cumene hydroperoxide (CHP), dicumyl peroxide (DCP), acetophenone (AP) and α-cumyl alcohol (α-CA) in cumene oxidation products, and hydroperoxides (HPO) containing myrtenyl-, verbenyl- and pinocarveyl hydroperoxides and verbenone (VN) in α-pinene oxidation products. Catalysts used and oxidation products are listed in Tables 2 and 3.

Table 2. The effect of the difference in the onium central atom on cumene oxidation
(Reaction temp.: 85°C, Reaction time: 4.0 hr)

Catalyst	O_2 absorbed (mmol)	$Rate_{max} \times 10^4$ (mol·l^{-1}·sec^{-1})	CHP (%)
$(C_6H_5)_3CBF_4$	2.11	0.26	99.4
$(C_2H_5)_4NBF_4$	4.16	0.34	99.5
$(C_6H_5)_3OBF_4$	5.97	0.67	93.7
$(C_6H_5)_3SBF_4$	10.45	1.12	99.5
$(C_6H_5)_3SeBF_4$	10.35	1.04	99.8
$(C_6H_5)_3TeBF_4$	3.85	0.45	99.7
$(C_6H_5)_4AsBF_4$	2.20	0.22	99.8
none	1.87	0.17	99.5

Table 3. The effect of the difference in the onium central atom on α-pinene oxidation
(Reaction temperature: 85°C)

Catalyst	Reaction time (hr)	O_2 absorbed (mmol)	$Rate_{max} \times 10^4$ (mol·l^{-1}·sec^{-1})	HPO (%)
$(C_6H_5)_3CBF_4$	2.0	3.47	0.52	64.6
$(C_2H_5)_4NBF_4$	2.0	3.86	0.74	61.5
$(C_6H_5)_3OBF_4$	2.0	4.0	0.82	63.4
$(C_6H_5)_3SiBF_4$	2.0	4.24	0.75	99.9
$(C_6H_5)_4PBF_4$	2.0	4.58	0.89	100
$(C_6H_5)_3SBF_4$	2.0	5.82	0.97	99.9
none	3.0	3.21	0.34	31.2

In these and subsequent tables, the percentage of a product (for instance, CHP (%) in Table 2) is defined by

$$\frac{\text{moles of the product cocerned}}{\text{total moles } O_2 \text{ absorbed}} \times 100$$

But in the case of DCP (%), the percentage is defined by

$$\frac{2 \times \text{moles of the product concerned}}{\text{total moles } O_2 \text{ absorbed}} \times 100$$

All products were analyzed according to a procedure similar to that described in the preceding paper. Since all products except DCP mentioned here are formed in the equimolar consumption of oxygen molecules, the total sum of such percentages must be nearly one hundred, as seen in each table.

The approximate order of catalytic activity of these onium tetrafluoroborates was determined as the combined results of cumene and α-pinene oxidations as follows: carbonium<ammonium<oxonium, silyl<phosphonium<sulfonium, arsonium≃telluronium<selenonium. This order was defined by the total sum of oxygen absorbed which almost paralleled the maximum reaction rate at the propagation step, as seen in Tables 2 and 3.

In order to investigate further the effect of the cation central atom, the oxidation of cumene (10 m*l*) was carried out in the presence of tetraphenylphosphonium nitrate and triphenylsulfonium nitrate (0.03 mmol), and α-pinene (10 m*l*) oxidation by triphenylsilyl, tetraphenylphosphonium, triphenylsulfonium and tetraphenylarsonium chlorides (0.03 mmol). The results are listed in Tables 4 and 5.

The oxidation of cumene (10 m*l*) was also carried out with triphenylsulfonium triphenylselenonium and triphenyltelluronium phosphates (0.03 mmol). The results are presented in Table 6.

In these phosphates, the order of activity was found to be the following: sulfonium>selenonium>telluronium. As seen in Table 6, phosphates exhibited remarkable activity in oxygen absorption.

TABLE 4. CUMENE OXIDATION IN THE PRESENCE OF TETRAPHENYLPHOSPHONIUM AND TRIPHENYLSULFONIUM NITRATES
(Reaction temp.: 85°C, Reaction time: 4.0 hr)

Catalyst	O_2 absorbed (mmol)	CHP (%)	AP (%)
$(C_6H_5)_4PNO_3$	7.04	99.6	0.40
$(C_6H_5)_3SNO_3$	7.08	97.3	0.64
none	1.87	99.5	

TABLE 5. α-PINEN OXIDATION IN THE PRESENCE OF ONIUM CHLORIDES AT 85°C

Catalyst	Reaction time (hr)	O_2 absorbed (mmol)	HPO (%)
$(C_6H_5)_3SiCl$	2.3	6.32	57.0
$(C_6H_5)_4PCl$	2.5	9.33	49.8
$(C_6H_5)_3SCl$	2.5	9.75	48.2
$(C_6H_5)_4AsCl$	2.5	4.62	59.8
none	3.0	3.21	31.2

TABLE 6. CUMENE OXIDATION WITH ONIUM PHOSPHATES AT 85°C (Reaction time 4.0 hr)

Catalyst	O_2 absorbed (mmol)	CHP (%)	AP (%)	DCP (%)	α-CA (%)	Total (%)
$(C_6H_5)_3S$-$\frac{1}{3}PO_4$	19.5	64.0	3.92	trace	32.0	99.0
$(C_6H_5)_3Se$-$\frac{1}{3}PO_4$	18.1	79.5	2.38	trace	18.1	99.9
$(C_6H_5)_3Te$-$\frac{1}{3}PO_4$	4.1	100				100
none	1.87	99.1				

Such an effect of the anion part was re-examined in succeeding experiments.

The Effect of Anion Part. A series of triphenylsulfonium (0.03 mmol) with various anion parts was employed for cumene (10 m*l*) oxidation. The results are given in Table 7.

TABLE 7. THE EFFECT OF THE ANION PART UPON CUMENE OXIDATION IN TRIPHENYLSULFONIUM SALT CATALYSTS
(Reaction temp.: 85°C, Reaction time: 4.0 hr)

Catalyst Anion	O_2 absorbed (mmol)	CHP (%)	DCP (%)	AP (%)	α-CA (%)	Total (%)
$\frac{1}{3}PO_4$	19.5	64.0	trace	3.92	32.0	99.9
$\frac{1}{2}SO_4$	6.56	99.1	trace	0.90	trace	100
$\frac{1}{2}CrO_4$	8.10	89.0	8.02	2.84	trace	100
$\frac{1}{2}Cr_2O_7$	6.92	81.0	1.45	3.08	10.5	96.0
$\frac{1}{3}Fe(CN)_6$	3.52	99.9	trace	trace	trace	99.9
$\frac{1}{2}Ni(CN)_4$	8.56	72.4				
$\frac{1}{4}P_2O_7$	14.8	89.6				
$\frac{1}{2}CO_3$	9.65	86.5	11.0	2.32	trace	99.8
NO_3	7.08	99.6				
IO_3	10.15	74.8	22.7	2.16	trace	98.9
ClO_3	0.51	98.0				
Cl	4.88	41.0	1.74	16.7	21.5	96.6
uone	1.87	99.5				

Also, the oxidation of α-pinene (10 m*l*) with triphenylsulfonium sulfate, selenate, and tellurate (0.03 mmol) was carried out. As seen in Table 8, the activity was found to be in the following order: $SO_4^{2-} > SeO_4^{2-} > TeO_4^{2-}$.

TABLE 8. THE OXIDATION OF α-PINENE WITH TRIPHENYLSULFONIUM SULFATE, SELENATE, AND TELLURATE
(Reaction temp.: 85°C, Reaction time: 2.0 hr)

Catalyst	O_2 absorbed (mmol)	HPO (mmol)	HPO (%)	VN (mmol)	VN (%)
$(C_6H_5)_3S$-$\frac{1}{2}SO_4$	22.2	8.0	36.3	5.25	23.6
$(C_6H_5)_3S$-$\frac{1}{2}SeO_4$	13.2	5.30	40.1		
$(C_6H_5)_3S$-$\frac{1}{2}TeO_4$	4.23	3.0	71.0		
none*	3.21	1.00	31.2		

* Reaction time was 3.0 hr.

The Effect of Substituents of the Onium Cation. It is of interest to examine the effect of substituents of the onium cation in connection with knowledge on the nature of the reaction mechanism. The oxidation of α-pinene (10 m*l*) was carried out with sulfonium tetrafluoroborates (0.03 mmol) with

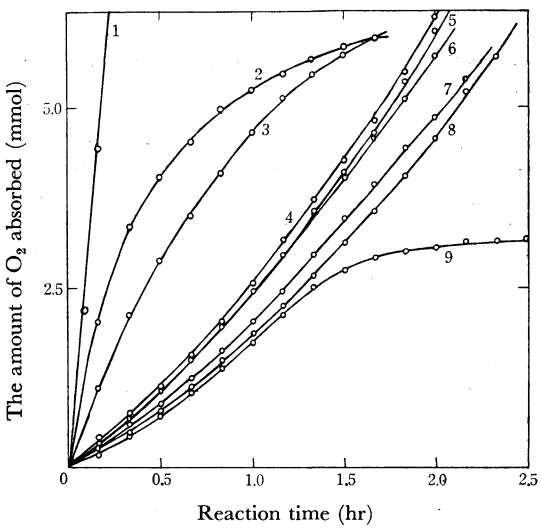

Fig. 1. The oxygen absorption curve of α-pinene the presence of sulfonium tetrafluoroborate $(R_1\text{-}(R_2)(R_3)SBF_4)$.

	1	2	3	4	5
R_1	C_2H_5	$C_6H_5CH_2$	CH_3	$C_6H_5CH_2$	$C_6H_5CH_2$
R_2	C_2H_5	$C_6H_5CH_2$	CH_3	$C_6H_5CH_2$	C_6H_5
R_3	C_2H_5	$C_6H_5CH_2$	CH_3	CH_3	CH_3

	6	7	8	9
R_1	C_6H_5	CH_3	C_6H_5	none
R_2	C_6H_5	C_6H_5	p-F-C_6H_4	
R_3	C_6H_5	C_6H_5	p-F-C_6H_4	

different alkyl or aryl substituents on the sulfur atom. The results are shown in Fig. 1. As shown in Fig. 1, the more aryl substituents attached to the sulfur atom, the lower the activity became.

The oxidation of α-pinene (10 m*l*) was also carried out with alkyldiphenylsulfonium tetrafluoroborates (0.03 mmol) in which the alkyl was methyl, ethyl, *n*-propyl or *n*-butyl at 85°C for 2.5 hr. The results given in Table 9 show that the larger the alkyl group, the higher the catalytic activity became.

The present reaction is a liquid phase (essentially homogeneous) oxidation in which the catalyst structure can be systematically varied, if desired. An investigation of the relation between the structure and the activity of catalysts is expected to supply a clue to the reaction mechanism on a molecular level. It is stressed in this connection that these onium catalysts are, in general, thermally stable and are little oxidized by oxygen molecules, so that we might conclude that they would not act as radical sources in these homogeneous liquid phase oxidations.*1

Discussion

Tables 2 and 3 indicate that the onium salts in which the central atoms are S, Se, Te, P and As are effective catalysts in the liquid phase oxidation of cumene and α-pinene. These atoms are characterized by the fact that they possess vacant d orbitals not far above their valence shells. In view of the widely known participation of d-orbital expansion in the chemistry of sulfur or related atom compounds,[6] it may be worth-while to examine the possibility of relating the outstanding activity of the onium salts to the interaction of their d orbitals.

The electronic state of the onium ion may be thought to be such that the electrons in surrounding alkyl or aryl groups are partially transfered to the spacially far-reaching vacant d orbitals, the energy of which is considerably lowered by the positive charge of the central atom. It is also probable that the anion might take part in this interaction since the "bond" between the anion and the cation part might reasonably be considered to have a more or less covalent nature.

The positive charge on the central atom may thus be partially neutralized by an inflowing electronic charge, and consequently the vacant d orbitals become partially occupied. The resulting electronic state of the onium central atom will, in part, resemble that of the transition metal atoms bearing d electrons properly and exhibiting a variety of catalytic activities in many heterogeneous catalyses.

In this connection, it is of interest to inspect the possibility of interaction between the "partially occupied" d orbital at the onium center considered above and the half-occupied, doubly-degenerate $1\pi_g$ molecular orbitals of the ground-state $^3\sum_g^-$ oxygen molecule. A mode of interaction will become probable when the orbital symmetry relationship becomes favorable.[7]

The circumstances are illustrated in Fig. 2, where the mode of interaction of the oxygen molecule is assumed parallel to the ligand plane. The d orbitals which can be utilized for interaction with O_2 are d_{xy} and d_{xz}. The latter, being of lower energy, would be able to partake in dp–σ type bonding through favorable orbital overlapping. The former d orbital will concern a more labile bond of a dp–π type, also contributing to the bonding interaction between onium and oxygen.

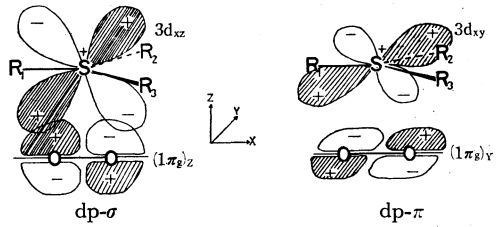

Fig. 2. The interaction between 3d orbital of sulfonium and $1\pi_g$ molecular oxygen.

First comes the depression of catalyst activity by the coexistence of a certain group of compounds which might be thought to possess a stronger affinity to sulfonium salts than molecular oxygen. It is well known[8] that sulfonium halides form stable trihalides in the presence of halogen molecules. Triphenylsulfonium iodide (mp 214—215°C (dec.)) or tetraphenylphosphonium bromide (mp 288—289°C (dec.)) does not initiate cumene oxidation at all at 85°C when used with an equimolar amount of iodine. Also, oxidation proceeding with these sulfonium halides stops completely upon the addition of equimolar iodine. Triphenylsulfonium

*1 In fact, more than 70% of catalysts were recovered from the reaction mixtures, and no appreciable amount of decomposed or oxidized products of catalysts was detected by gas chromatography. Triphenylsulfonium tetrafluoroborate decomposed gradually at 300—350°C to produce fluorobenzene, diphenylsulfide and boron trifluoride. But under the reaction conditions in the present paper, neither sulfide, sulfoxide nor fluorobenzene was detected by gas chromatography. The deactivation of catalysts by the addition of oxidation products was observed, which will be discussed in detail in a subsequent paper.

6) G. Cilento, *Chem. Revs.*, **60**, 147 (1960).

7) K. Fukui, This Bulletin, **39**, 498 (1966) and references cited therein.

8) K. Kanai, T. Hashimoto, H. Kitano and K. Fukui, *Nippon Kagaku Zasshi* (*J. Chem. Soc. Japan, Pure Chem. Sect.*), **86**, 534 (1965).

triiodide (brown crystals, mp 137—138°C) and tetraphenylphosphonium diiodobromide (brown crystals, mp 249—250.5°C) exhibited no activity as catalysts for cumene oxidation.

Such a remarkable deactivation is also seen in the employment of solvents bearing lone-pair electrons. Chloroform, dioxane or acetic acid used as solvent causes the activity of triphenylsulfonium salts to completely disappear. These results might come from the blocking effect of these additives against the interaction of the sulfur d orbital with molecular oxygen.

TABLE 9. α-PINENE OXIDATION BY THE USE OF ALKYL DIPHENYLSULFONIUM TETRAFLUOROBORATE
(Reaction temp.: 85°C, Reaction time: 2.5 hr)

Catalyst	O_2 absorbed (mmol)	HPO (mmol)	HPO (%)	VN (mmol)	VN (%)
$CH_3(C_6H_5)_2SBF_4$	6.37	5.15	80.8	0.56	8.78
$C_2H_5(C_6H_5)_2SBF_4$	6.96	5.05	72.5	0.85	12.2
n-$C_3H_7(C_6H_5)_2SBF_4$	7.04	4.10	58.3	0.92	13.1
n-$C_4H_9(C_6H_5)_2SBF_4$	7.92	4.20	53.0	1.02	13.9
none*	3.12	1.00	31.2	0.69	21.5

* Reaction time was 3.0 hr.

As understood from Fig. 1 and Table 9, the catalytic activity is affected by substituents on the sulfur atom. The mode of partial occupation of d orbital mentioned above may be influenced by substituents. The charge of a d orbital will be increased by electron-donor groups like methyl, ethyl, or larger alkyls attached to the central atom, whereas it will be decreased by such groups as phenyl or *p*-fluorophenyl, so that the interaction of a d orbital with an oxygen molecule may be weakened.

Second, the effect of the anion part should be mentioned. The tetrafluoroborates of such oniums as carbonium, ammonium and oxonium are less active than other onium salts mentioned above. This is probably because their ionic character is too large to transfer electrons from anion to onium, so that interaction between their vacant orbitals and molecular oxygen orbitals is only slight.

In this connection, it is interest to see the relation between the pK_1 value of the acid corresponding to the anion and catalytic activity. An apparent correlation is found in Fig. 3. A suitable range of acidity seems to exist, corresponding to a suitable range of covalent nature of the "bond" between the onium and anion parts.

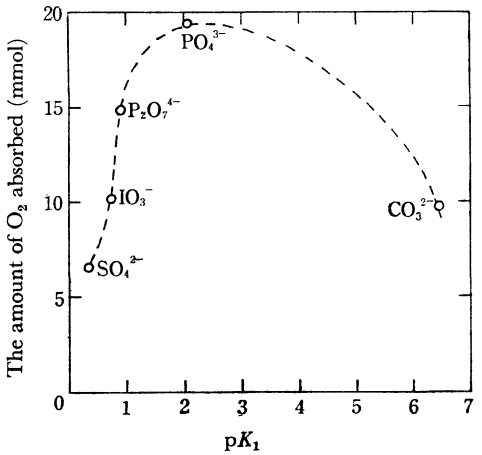

Fig. 3. The effect of pK_1 of the acid corresponding to the anion upon the catalytic activity of triphenylsulfonium salts.

Third, it should be noted that kinetic investigation also seems to favor the molecular oxygen association mechanism, the details of which will be reported in a subsequent paper. The reaction scheme required to satisfy the experimental results involves the interaction of molecular oxygen with the catalyst molecule.

Part of the cost of this investigation was defrayed by a Scientific Research Grant from the Ministry of Education, to which the authors' thanks are due.

BULLETIN OF THE CHEMICAL SOCIETY OF JAPAN VOL. 42 319—322 (1969)

The pNa Study of Sodium Alkyl Sulfates in Aqueous Solutions

Iwao SATAKE, Takashi TAHARA and Ryohei MATUURA

Department of Chemistry, Faculty of Science, Kyushu University, Hakozaki, Fukuoka

(Received May 30, 1968)

The counter-ion activity coefficient of sodium alkyl sulfate with chain length from C_8 to C_{14} was determined in aqueous solutions and in the presence of added magnesium ion. The degree of association of sodium ion to the micelle (β) can be deduced from the concentration dependence of the counter-ion activity. The value of β so determined in the presence of magnesium ion was confirmed to decrease rapidly as the relative concentration of magnesium ion increases. The observed change of counter-ion activity with concentration was found to be interpreted in terms of a lameller micelle model.

The counter-ion activity coefficient in detergent solutions has recently been estimated by applying the membrane electrodes inclusive of the cation sensitive glass electrode. Botré *et al.*[1] used the membrane electrodes of both negative and positive types, and evaluated the degree of dissociation of micelles in aqueous solutions of sodium lauryl sulfate, sodium laurate and laurylamine hydrochloride. Shedlovsky *et al.*[2] used the sodium sensitive glass electrode for estimating the counter-ion activity in mixed solution of sodium alkyl sulfate with chain length from C_{10} to C_{14}. Feinstein and Rosano,[3] using the cationic glass electrode, determined the degree of dissociation of potassium and sodium carboxylate micelles at a constant cation concentration. Further, Stenius and Ekwall[4] obtained the sodium ion activity in a sodium caprylate solution by using the sodium responsive glass electrode.

Although the single-ion activity coefficient is a conventionally defined quantity in nature, the interpretation of which is subject to the same limitations as that of pH, it is of interest to estimate the counter-ion activity coefficient in detergent solutions in order to elucidate the degree of dissociation of the micelle and other related properties.

The present paper is concerned with the determination of counter-ion activities of sodium alkyl sulfates in aqueous solutions with and without added magnesium ion which is almost insensitive to the sodium glass electrode.

1) C. Botré, V. L. Crescenzi and A. Mele, *J. Phys. Chem.*, **63**, 650 (1959).

2) L. Shedlovsky, C. W. Jakob and M. B. Epstein, *ibid.*, **67**, 2075 (1963).

3) M. E. Feinstein and H. L. Rosano, *J. Colloid and Interface Sci.*, **24**, 73 (1967).

4) P. Stenius and P. Ekwall, *Acta Chem. Scand.*, **21**, 1643 (1967).

Experimental

In the present experiment, we used a Horiba pNa meter model N-5 with the following cell:

Na glass electrode | Detergent solution | N NH_4NO_3 | 3.33 N KCl agar bridge | Caromel electrode.

The detergents used were sodium alkyl sulfate with chain length from C_8 to C_{14}, prepared by the esterification of purified long chain alcohols.

It was rather difficult to obtain the reliable e.m.f. when the reference caromel electrode was directly immersed into the detergent solution, on account of the formation of potassium alkyl sulfate which is sparingly soluble in water at the temperature of experiment. The use of N NH_4NO_3 liquid junction, however, permits the precise determination of e.m.f. with an accuracy of ± 0.005 pNa unit. The whole system was maintained at constant temperature of 25°C for C_8 to C_{12} and 35°C for C_{14} and C_{12} with added magnesium ion.

The measurement on the system of sodium dodecyl sulfate (SDS) in salt solutions was performed at a constant mole ratio (R) of $MgSO_4$ to SDS throughout a series of experiment.

The sodium sensitive glass electrode was calibrated with a sodium chloride solution of known activity.[5,6]

Results and Discussion

In Figs. 1—4, the observed values of log a_+ are plotted against the logarithm of total analytical concentration (C) in mol/l of the detergent solutions. In all cases, plots of log a_+ *vs.* log C are nearly linear over the concentration range below the critical micelle concentration (CMC). In this concentration range, the apparent counter-ion activity coefficient (γ_+) defined by a_+/C might be expected to be comparable with that of simple

5) A. S. Brown and D. A. MacInnes, *J. Am. Chem. Soc.*, **57**, 1356 (1935).

6) G. J. Janz and A. R. Gordon, *ibid.*, **65**, 218 (1943).

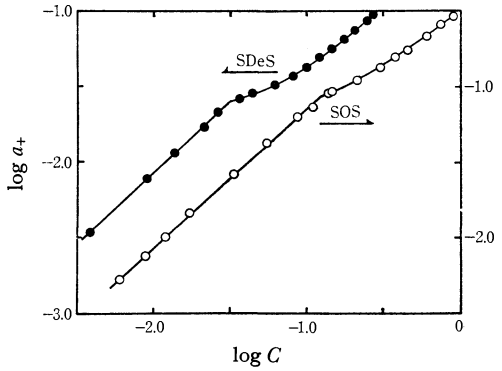

Fig. 1. The plots of log a_+ *vs.* log C for SOS and SDeS at 25°C.

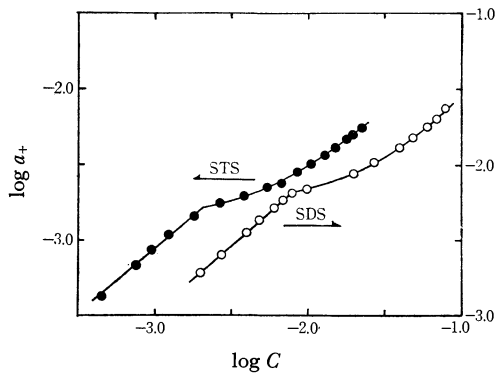

Fig. 2. The plots of log a_+ *vs.* log C for SDS at 25°C and STS at 35°C.

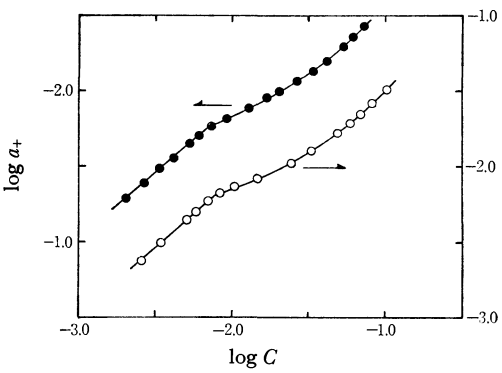

Fig. 3. The plots of log a_+ *vs.* log C for SDS at 35°C.
○: $R = 0$, ●: $R = 0.0467$

electrolyte, *e.g.* NaCl. The experimental fact is, however, not the case. The typical plot of log γ_+ *vs.* $C^{1/2}$ for sodium octyl sulfate (SOS) is given in Fig. 5 together with the value of $\gamma_\pm$ obtained for NaCl by Brown and MacInnes.[5] It will be noted that the value of γ_+ for SOS is considerably small relative to the mean activity coefficient of NaCl in an equivalent solution.

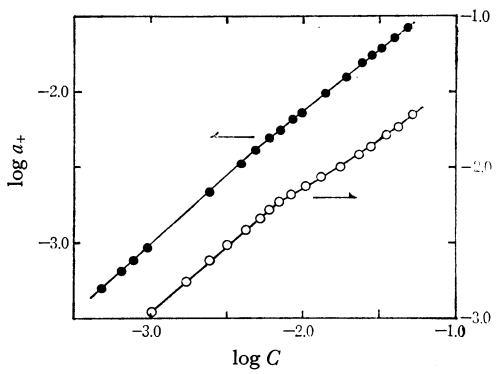

Fig. 4. The plots of log a_+ *vs.* log C for SDS at 35°C.
○: $R = 0.0957$, ●: $R = 0.299$

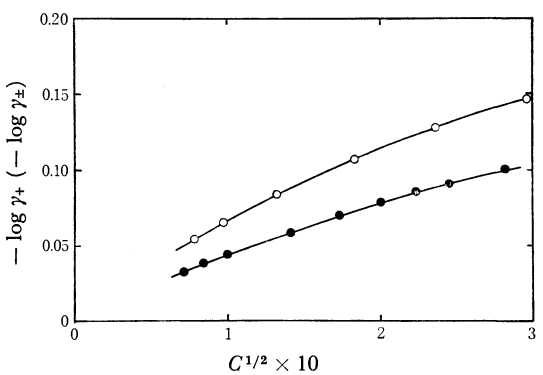

Fig. 5. The plots of $-\log \gamma_+$ *vs.* $C^{1/2}$ for SOS at 25°C.
○: SOS, ●: NaCl ($\gamma_\pm$)[5]

If the Debye-Hückel theory may also be applicable to detergent solutions, the observed deviation must be ascribed either to the increased ional concentration due to the formation of polyvalent aggregates or to the existence of undissociated detergent molecules, *i. e.*, neutral ion pairs. The critical interionic distance for ion pair formation of 1–1 electrolyte is 3.57 Å in water at 25°C. It is, therefore, rather doubtful to assume the formation of neutral ion pairs with such bulky ions as octyl sulfate.

Mukerjee *et al.*[7] suggested the existence of detergent dimer on the basis of conductivity measurement for SDS. In the present case, it is difficult to account for the observed reduction of γ_+ without assuming even higher order association of detergent anions than dimer, *e. g.*, the existence of detergent pentamer. It will be, however, reasonable to assume the existence of small aggregates in the dilute concentration range below CMC, though no conclusive evidence has yet been obtained for such

7) P. Mukerjee, K. J. Mysels and C. I. Dulin, *J. Phys. Chem.*, **62**, 1390 (1958); P. Mukerjee, *ibid.*, **62**, 1397 (1958).

a higher aggregate as pentamer.

The deviation from linearity appearing above the CMC suggests the low degree of dissociation of the micelle. In the presence of the added magnesium ion, a break at the CMC became more obscure as the value of R, the mole ratio of $MgSO_4$ to SDS, increased and no break could be detectable above $R=0.5$. This result indicates that the fraction of sodium ion bound at the micellar surface decreases rapidly as the relative concentration of magnesium ion increases.

In general, the equilibrium distribution of counter-ion is determined by the equality of the electrochemical potential of sodium ion in bulk phase and in the micellar surface region, so that

$$\bar{\mu}_b = \bar{\mu}_s \tag{1}$$

where

$$\bar{\mu}_b = \mu_b^0 + kT \ln a_+ + \varepsilon\psi_b \tag{2}$$

for sodium ion in bulk phase and

$$\bar{\mu}_s = \mu^0{}_s + kT \ln C_s + \mu_s^e \tag{3}$$

for sodium ion bound at the micellar surface. Here, ψ_b is the electrical potential of the bulk phase and ε is the electronic charge. μ_s^e is the electrical part of free energy and C_s is the concentration of bound sodium ion, both at the micellar surface region. We put $\psi_b=0$ according to the common practice. It follows from Eqs. (1), (2) and (3) that

$$\ln a_+ = (\mu_s^0-\mu_b^0)/kT + \ln C_s + \mu_s^e/kT. \tag{4}$$

Suppose that the micelle is lamellar and consists of m alkyl sulfate ions and $m\beta$ sodium ions bound at the micellar surface region V, giving the net charge $-m(1-\beta)\varepsilon$. Then we have

$$C_s = 1000\, m\beta/NV \tag{5}$$

and

$$\psi_s = -(kT/\varepsilon) \ln (2000\pi\sigma^2/DNkTC_b) \tag{6}$$

for the electrical potential at the outer part of Stern layer, where N is the Avogadro number, D the dielectric constant of the medium, σ the surface charge density of the micelle, and C_b the concentration of free sodium ion in the bulk solution, *i. e.*,

$$C_b = C_0 + (1-\beta)(C-C_0). \tag{7}$$

Here, C_0 is the CMC and C is the total analytical concentration of the detergent in mol/l. The expression for the electrical free energy term, μ_s^e, may be obtained by the charging process with respect to the sodium ion charge, q, at the micellar surface.

$$\mu_s^e = \int_0^\varepsilon \psi_s \, dq \tag{8}$$

It follows from Eqs. (6) and (8), with substitution

$$\sigma = -(\varepsilon-\beta q)/A, \tag{9}$$

that

$$\mu^e{}_s = kT[-\ln \{2000\pi\varepsilon^2(1-\beta)^2/DNkTA^2C_b\} + 2\{1+(1/\beta) \ln (1-\beta)\}]. \tag{10}$$

Here, A denotes the area occupied by an alkyl sulfate ion at the micellar surface. Substitution of Eqs. (5) and (10) into Eq. (4) gives

$$\ln a_+ = (\mu_s^0-\mu_b^0)/kT + \ln \{DkTA^2m\beta/2\pi V\varepsilon^2(1-\beta)^2\} + 2\{1+(1/\beta) \ln (1-\beta)\} + \ln\{C_0 + (1-\beta)(C-C_0)\}. \tag{11}$$

If it is assumed that the micellar parameters A, m, V and β are constant throughout the whole concentration range studied, we have

$$a_+ = \text{Const.}\{C_0+(1-\beta)(C-C_0)\}. \tag{12}$$

From the boundary condition that $a_+ \to a_+^0$ $(=\gamma_+C_0)$ when $C\to C_0$, we obtain

$$\gamma_+ = a_+/C = \gamma_+^0\{(1-\beta)+\beta C_0/C\} \tag{13}$$

and

$$\ln \gamma_+^0 = (\mu_s^0-\mu_b^0)/kT + \ln \{DkTA^2m\beta/2\pi V\varepsilon^2(1-\beta)^2\} + 2\{1+(1/\beta) \ln (1-\beta)\}, \tag{14}$$

where, γ_+^0 is the apparent activity coefficient of sodium ion at $C=C_0$. Using Eq. (13), we can estimate the value of β from the slope of γ_+ *vs.* C_0/C plot. It is to be noted that the equation assumed by Botré *et al.*[1] for estimating the degree of dissociation of the micelle can be derived from the lamellar micelle model.

In the presence of added magnesium ion, we assumed that Eq. (13) may also be applicable if the relative concentration of $MgSO_4$ to SDS is small, which is the case for the present experimental condition. Under this condition, the potential determining ion of the diffuse double layer will be assumed to be the sodium ion, since the majority of the added magnesium ion will be bound at the micellar surface on account of the strong coulombic interaction with the micelle. In Fig. 6, the typical plot of γ_+ *vs.* C_0/C is given for sodium tetradecyl sulfate in water at 35°C. The linearity

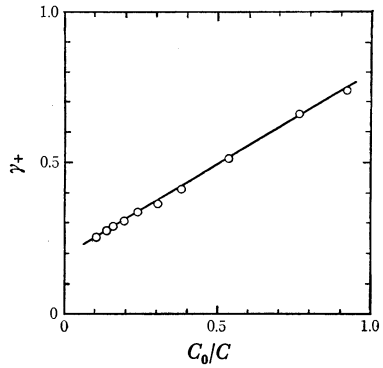

Fig. 6. The polts of γ_+ *vs.* C_0/C for STS at 35°C.

of the line is satisfactory over the whole concentration range studied. In the presence of added magnesium ion, however, the deviation from

linearity is found to appear in higher concentration range above CMC. In these cases, therefore, we used the limiting slope at the CMC in the plot, γ_+ *vs.* C_0/C. The values of β are summarized in Table 1, together with those evaluated by several authors.

TABLE 1. THE VALUES OF β DETERMINED FROM pNa DATA

Detergent*	Temp. (°C)	R	CMC** (mol/l)	β	β(lit.)
SOS	25		1.27×10^{-1}	0.56	
SDeS	25		3.16×10^{-2}	0.62	0.70[2]
SDS	25		7.95×10^{-3}	0.75	0.84,[1] 0.78[2] 0.71,[8] 0.82[9]
STS	35		2.07×10^{-3}	0.76	0.87(25°C)[2]
SDS	35		8.22×10^{-3}	0.72	
SDS+$MgSO_4$	35	0.0467	7.33×10^{-3}	0.52	
SDS+$MgSO_4$	35	0.0957	6.38×10^{-3}	0.42	
SDS+$MgSO_4$	35	0.299	4.83×10^{-3}	0.18	
SDS+$MgSO_4$	35	0.510	3.2×10^{-3}	0.14	

* SOS: Sodium octyl sulfate, SDeS: Sodium decyl sulafte, SDS: Sodium dodecyl sulfate, STS: Sodium tetradecyl sulfate.

** Determined from a break point of log a_+ *vs.* log C plot.

As is clearly shown in Table 1, the value of β increases with increasing chain length and for the same chain length it decreases with increasing temperature. Further, it is confirmed that the addition of magnesium ion to SDS gives rise to the rapid reduction of β.

Once the value of β is determined, we can estimate the specific adsorption energy $\Delta\mu^0$ ($=\mu_s^0-\mu_b^0$) with the additional assumptions for V and A. If it is assumed here that the thickness of the Stern layer is in the order of the diameter (l) of hydrated sodium ion, the available volume for Na^+ ion in the Stern layer may be written as

$$V = mAl. \tag{15}$$

From Eqs. (14) and (15) we have

$$\Delta\mu^0/kT = \ln\{2\pi l\varepsilon^2(1-\beta)^2\gamma_+^{0}/DkTA\beta\} - 2\{1+(1/\beta)\ln(1-\beta)\}. \tag{16}$$

Introducing $A=33$ Å^2 which was determined from the surface adsorption study of tritiated SDS in water,[10] $l=4.6$ Å and $\gamma_+{}^0=0.815$ into Eq. (16), we obtain $\Delta\mu^0=0.85\,kT$ for SDS at 25°C. By using the spherical micelle model, Stigter[11] obtained $\Delta\mu^0=0.5kT$ for the same detergent. The value of $\Delta\mu^0$ estimated above, however, depends on the selected values of A and l, and in fact it tends to zero as the value of A increases. Hence it will be reasonable to assume that the area obtainable by substituting $\Delta\mu^0=0$ into Eq. (16) gives the upper limit of the area per polar head of a detergent anion at the micellar surface. The values of A so determined are 77 Å^2 for SDS, 112 Å^2 for SDeS and 126 Å^2 for SOS at 25°C, respectively. These figures reflect the expanding nature of the micelle with increasing degree of dissociation of the micelle. The true areas will be smaller than these values owing to the definite positive values of $\Delta\mu^0$.

8) D. Stigter and K. J. Mysels, *J. Phys. Chem.*, **59**, 45 (1955).

9) J. N. Philips and K. J. Mysels, *ibid.*, **59**, 325 (1955).

10) G. J. Nilsson, *ibid.*, **61**, 1135 (1957).

11) D. Stigter, *ibid.*, **68**, 3603 (1964).

BULLETIN OF THE CHEMICAL SOCIETY OF JAPAN VOL. 42 323—329 (1969)

Formulas for One- and Two-center Moment Integrals between Slater Type s, p-Orbitals with Integer Effective Principal Quantum Numbers of 1 to 5

Masaru SUZUKI, Yoshimasa NIHEI and Hitoshi KAMADA

Faculty of Engineering, The University of Tokyo, Hongo, Bunkyo-ku, Tokyo

(Received June 6, 1968)

Expansion formulas are presented for one- and two-center moment integrals between Slater type s,p-orbitals with integer effective principal quantum numbers of 1 to 5, together with the procedure. These formulas are useful in the calculation of a dipole moment and a transition moment from a charge distribution calculated by LCAO-MO method. A FORTRAN subprogram containing most of these formulas, which are important in practice, occupies about $7.7K$ of the core memory of a computer, HITAC 5020.

In application of LCAO-MO calculation to the interpretation of the electronic absorption spectra of various molecules, it is useful to compare the calculated values of the intensity as well as the transition energy with the observed values. For this purpose it is necessary to evaluate one-electron moment integrals between all the possible pairs of the atomic orbitals (AO's) taken as bases. Then, these integrals can also be used to calculate the dipole moment of the molecule and to test the accuracy of the calculated charge distribution. Hence it is convenient to write a computer program for the continuous calculation of the dipole moment and the transition moments between any molecular orbitals (MO's) after solving the secular equations for molecules containing any kinds of atoms.

Two-center moment integrals between Slater-type AO's (STO's) with integer effective principal quantum number (n^*) are expressed by formulas similar to those for overlap integrals with auxiliary functions, A_m and B_m with integer m.*1 Some of these formulas for s,p-AO's with small values of n^* (1 and 2) are found,[1,2] but, as far as we know, no adequate table has been published containing STO's with larger values of n^*. This paper will present many of these formulas, together with the procedure.*2

Procedure

MO's, φ's, are taken as linear combination of AO's, χ's, which are centered on the various atoms in the molecule:

$$\varphi_i = \sum_p C_{pi}\chi_p \tag{1}$$

Then the one-electron moment integrals between these MO's are decomposed into integrals with AO's:

$$R_{ij} = \int \varphi_i \, r \, \varphi_j \, d\tau = \sum_{p,q} C_{pi}C_{qj}T_{pq}$$

$$T_{pq} = \int \chi_p \, r \, \chi_q \, d\tau \tag{2}$$

χ_p and χ_q are the AO's centered on atom P and Q respectively, and $\boldsymbol{r}$ is the position vector of an electron relative to an origin fixed in the molecule. When $\boldsymbol{r}_0$ is the position vector of the middle point of P and Q, and $\boldsymbol{r}'$ is of an electron relative to this point, $\boldsymbol{r} = \boldsymbol{r}_0 + \boldsymbol{r}'$, hence:

$$\begin{aligned} T_{pq} &= \int \chi_p \, (\boldsymbol{r}_0 + \boldsymbol{r}') \chi_q \, d\tau \\ &= \int \chi_p \, \boldsymbol{r}_0 \chi_q \, d\tau + \int \chi_p \, \boldsymbol{r}' \chi_q \, d\tau \\ &= \boldsymbol{r}_0 S_{pq} + M_{pq} \end{aligned} \tag{3}$$

where S is an overlap integral, and M is a moment integral relative to the middle point of P and Q. In the following section, three components of $\boldsymbol{r}$, *i. e.*, z, x and y are treated.

Two-center Integrals. Any coordinate systems, (z,x,y), with an origin on PQ, and parallel to the coordinates fixed in the molecule, are transformed by the following transformation matrix to a local coordinate system, (Z,X,Y), with the positive direction of the Z axis from P toward Q as is shown in Fig. 1:

*1 In this paper, a principal quantum number, n, and an effective principal quantum number, n^* $(=n-\delta)$, are distinguished.

1) J. Miller, J. M. Gerhauser, F. A. Matsen, "Quantum Chemistry Integrals and Tables," University of Texas Press, Austin (1959).

2) M. Kotani, A. Amemiya, E. Ishiguro and T. Kimura, "Table of Molecular Integral," II, Maruzen, Tokyo (1963).

*2 For the purpose of convenience some partial overlapping with the books of Miller *et al.*,[1] and Kotani *et al.*,[2] is not avoided.

$$\begin{pmatrix} z \\ x \\ y \end{pmatrix} = \begin{pmatrix} \gamma_z & -\gamma_z\gamma_x/\delta & -\gamma_y/\delta \\ \gamma_x & \delta & 0 \\ \gamma_y & -\gamma_x\gamma_y/\delta & \gamma_z/\delta \end{pmatrix} \begin{pmatrix} \mathcal{Z} \\ X \\ Y \end{pmatrix}$$
$$\delta = (1-\gamma_x^2)^{1/2} \qquad (4)$$

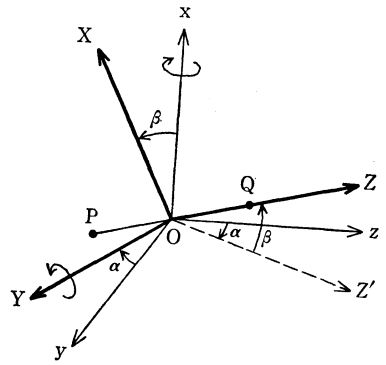

Fig. 1. Transformation to local coordinates.

where γ_z is the direction cosine of $\mathcal{Z}$ axis relative to z axis fixed in a molecule, and so on.

We take STO's as bases, which consist of appropriate combinations of z,x,y and a function of r, where z, x and y are transformed as mentioned above, but r is not. As for the two-center moment integrals relative to the local coordinate system, $(\mathcal{Z},X,Y)$, only those integrals containing none or even numbers of X and/or Y respectively have non-zero values in symmetric property. When only s- and p-AO's are treated, the following nine types are all of the necessary basic two-center integrals:

$(S|\mathcal{Z}|S)$, $(S|\mathcal{Z}|P_Z)$, $(S|X|P_X)$. $(P_Z|\mathcal{Z}|S)$, $(P_X|X|S)$, $(P_Z|\mathcal{Z}|P_Z)$, $(P_Z|X|P_X)$, $(P_X|\mathcal{Z}|P_X)$, $(P_X|X|P_Z)$*3

Any two-center moment integrals between s,p-AO's relative to the original coordinate system are linear combinations of some of the above basic integrals (Table 1).

TABLE 1. DECOMPOSITION OF TWO-CENTER MOMENT INTEGRALS*

$(s\,|\,i\,|\,s) = \gamma_i(S|\mathcal{Z}|S)$
$(s\,|\,i\,|\,p_i) = \gamma_i^2(S|\mathcal{Z}|P_Z) + (1-\gamma_i^2)(S|X|P_X)$
$(p_i\,|\,i\,|\,s) = \gamma_i^2(P_Z|\mathcal{Z}|S) + (1-\gamma_i^2)(P_X|X|S)$
$(s\,|\,i\,|\,p_j) = \gamma_i\gamma_j\{(S|\mathcal{Z}|P_Z) - (S|X|P_X)\}$
$(p_j|\,i\,|\,s) = \gamma_i\gamma_j\{(P_Z|\mathcal{Z}|S) - (P_X|X|S)\}$
$(p_i\,|\,i\,|\,p_i) = \gamma_i[\gamma_i^2(P_Z|\mathcal{Z}|P_Z) + (1-\gamma_i^2)\{(P_Z|X|P_X) + (P_X|\mathcal{Z}|P_X) + (P_X|X|P_Z)\}]$
$(p_i\,|\,j\,|\,p_j) = \gamma_i[(1-\gamma_i^2)(P_Z|X|P_X) + \gamma_i^2\{(P_Z|\mathcal{Z}|P_Z) - (P_X|\mathcal{Z}|P_X) - (P_X|X|P_Z)\}]$
$(p_i\,|\,j\,|\,p_i) = \gamma_j[(1-\gamma_i^2)(P_X|\mathcal{Z}|P_X) + \gamma_i^2\{(P_Z|\mathcal{Z}|P_Z) - (P_Z|X|P_X) - (P_X|X|P_Z)\}]$
$(p_i\,|\,i\,|\,p_j) = \gamma_j[(1-\gamma_i^2)(P_X|X|P_Z) + \gamma_i^2\{(P_Z|\mathcal{Z}|P_Z) - (P_Z|X|P_X) - (P_X|\mathcal{Z}|P_X)\}]$
$(p_i\,|\,j\,|\,p_k) = \gamma_i\gamma_j\gamma_k\{(P_Z|\mathcal{Z}|P_Z) - (P_Z|X|P_X) - (P_X|\mathcal{Z}|P_X) - (P_X|X|P_Z)\}$

* Each of i, j and k denotes either z, x or y.

*3 Integrals with Y are equivalent to those with X.

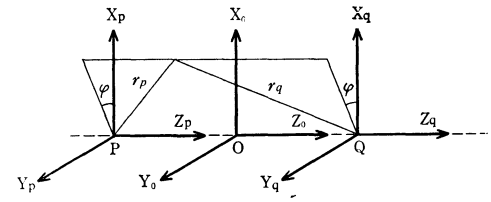

Fig. 2. Local coordinate system.*

* It should be noted that $\mathcal{Z}_p$, $\mathcal{Z}_0$ and $\mathcal{Z}_q$ axes have the same direction.

The actual calculations are performed after the transformation of the local coordinates to the spheroidal coordinate system, (ξ,η,φ). By the use of the latter, each of the basic integrals is expanded into a formula with A_m and B_m as overlap integrals in Ref. 3. Our choice of coordinates (Fig. 2) will result in the folloinwg equations:

$$r_p = R(\xi+\eta)/2, \quad r_q = R(\xi-\eta)/2,$$
$$\mathcal{Z}_p = R(\xi\eta+1)/2, \quad \mathcal{Z}_q = R(\xi\eta-1)/2, \quad \mathcal{Z}_0 = R\xi\eta/2,$$
$$X_p = X_q = X_0 = R\{(\xi^2-1)(1-\eta^2)\}^{1/2}\cos\varphi/2,$$
$$Y_p = Y_q = Y_0 = R\{(\xi^2-1)(1-\eta^2)\}^{1/2}\sin\varphi/2 \qquad (5)$$

where R is the interatomic distance, and:

$$A_m(a) = \int_1^\infty \xi^m e^{-a\xi}\,d\xi$$
$$B_m(b) = \int_{-1}^1 \eta^m e^{-b\eta}\,d\eta$$
$$a = R(\mu_p+\mu_q)/2R_H = (a_p+a_q)/2$$
$$b = R(\mu_p-\mu_q)/2R_H = (a_p-a_q)/2$$
$$a = R\mu/R_H \qquad (6)$$

where R_H is the Bohr radius and μ denotes the exponent of STO. The parameter a and b correspond to p and pt respectively in Ref. 3. When both AO's have integer n^*, m is also an integer, and these expansion formulas are easily obtained with a computer, given the number of each variable as input data. In this work the program was tested by obtaining the corresponding formulas of overlap integrals, in agreement with those in Ref. 3, except the difference in the direction of $\mathcal{Z}_q$ axis.*4

One-center Integrals. One-center moment integrals may be calculated directly in a spherical coordinate system, and only those of the type, $(s|i|p_i)$ or $(p_i|i|s)$ have non-zero values for s,p-AO's, where i denotes either of z,x or y.

Results and Discussion

In Table 2, all expansion formulas of basic two-center moment integrals between s,p-AO's with integer n^*, $1 \leqq n_1^* \leqq n_2^* \leqq 5$, for $b \neq 0$, are presented. Formulas for $b=0$ are derived from the corresponding formulas for $b \neq 0$, by noting that $B_m(0) = 2/(m+1)$ for m even, and $B_m(0)=0$ for m odd. In practice only those for $n_1^* = n_2^*$ are important,

3) R. S. Mulliken, C. A. Rieke, D. Orloff and H. Orloff, *J. Chem. Phys.*, **17**, 1248 (1949).
4) A. Lofthus, *Mol. Phys.*, **5**, 105 (1962).

*4 In Ref. 3, all formulas for $S(n_1p\sigma, n_2p\sigma)$, $n_1=n_2$, should have the opposite sign to those presented there.

TABLE 2. BASIC TWO-CENTER MOMENT INTEGRALS FOR $b \neq 0$

$n_1^* = n_2^* = 1$; $c = (a_1^3 a_2^3)^{1/2} R/8$

$(S\ |\mathcal{Z}|\ S)$: $A_3B_1 - A_1B_3$

$n_1^* = 1, n_2^* = 2$; $c = (a_1^3 a_2^5)^{1/2} R/16$

$(S\ |\mathcal{Z}|\ S)$: $(1/3)^{1/2}(A_4B_1 - A_3B_2 - A_2B_3 + A_1B_4)$

$(S\ |\mathcal{Z}|\ P_Z)$: $A_4B_2 - A_3B_1 - A_2B_4 + A_1B_3$

$(S\ |X|\ P_X)$: $(1/2)\{A_4(B_0 - B_2) + A_2(B_4 - B_0) + A_0(B_2 - B_4)\}$

$n_1^* = 1, n_2^* = 3$; $c = (a_1^3 a_2^7/30)^{1/2} R/16$

$(S\ |\mathcal{Z}|\ S)$: $(1/3)^{1/2}(A_5B_1 - 2A_4B_2 + 2A_2B_4 - A_1B_5)$

$(S\ |\mathcal{Z}|\ P_Z)$: $A_5B_2 - A_4(B_3 + B_1) + A_3(B_2 - B_4) + A_2(B_5 + B_3) - A_1B_4$

$(S\ |X|\ P_X)$: $(1/2)\{A_5(B_0 - B_2) + A_4(B_3 - B_1) + A_3(B_4 - B_0) + A_2(B_1 - B_5) + A_1(B_2 - B_4) + A_0(B_5 - B_3)\}$

$n_1^* = 1, n_2^* = 4$; $c = (a_1^3 a_2^9/105)^{1/2} R/64$

$(S\ |\mathcal{Z}|\ S)$: $(1/3)^{1/2}(A_6B_1 - 3A_5B_2 + 2A_4B_3 + 2A_3B_4 - 3A_2B_5 + A_1B_6)$

$(S\ |\mathcal{Z}|\ P_Z)$: $A_6B_2 - A_5(2B_3 + B_1) + 2A_4B_2 + 2A_3B_5 - A_2(B_6 + 2B_4) + A_1B_5$

$(S\ |X|\ P_X)$: $(1/2)\{A_6(B_0 - B_2) + 2A_5(B_3 - B_1) + A_4(B_2 - B_0) + 2A_3(B_1 - B_5) + A_2(B_6 - B_4) + 2A_1(B_5 - B_3) + A_0(B_4 - B_6)\}$

$n_1^* = 1, n_2^* = 5$; $c = (a_1^3 a_2^{11}/42)^{1/2} R/960$

$(S\ |\mathcal{Z}|\ S)$: $(1/3)^{1/2}(A_7B_1 - 4A_6B_2 + 5A_5B_3 - 5A_3B_5 + 4A_2B_6 - A_1B_7)$

$(S\ |\mathcal{Z}|\ P_Z)$: $A_7B_2 - A_6(3B_3 + B_1) + A_5(2B_4 + 3B_2) + 2A_4(B_5 - B_3) - A_3(3B_6 + 2B_4) + A_2(B_7 + 3B_5) - A_1B_6$

$(S\ |X|\ P_X)$: $(1/2)\{A_7(B_0 - B_2) + 3A_6(B_3 - B_1) + A_5(3B_2 - 2B_4 - B_0) + A_4(3B_1 - B_3 - 2B_5) + A_3(3B_6 - B_4 - 2B_2) + A_2(3B_5 - B_7 - 2B_3) + 3A_1(B_4 - B_6) + A_0(B_7 - B_5)\}$

$n_1^* = n_2^* = 2$; $c = (a_1^5 a_2^5)^{1/2} R/32$

$(S\ |\mathcal{Z}|\ S)$: $(1/3)(A_5B_1 - 2A_3B_3 + A_1B_5)$

$(S\ |\mathcal{Z}|\ P_Z)$: $(1/3)^{1/2}\{A_5B_2 + A_4(B_3 - B_1) - A_3(B_2 + B_4) + A_2(B_3 - B_5) + A_1B_4\}$

$(S\ |X|\ P_X)$: $(1/12)^{1/2}\{A_5(B_0 - B_2) + A_4(B_1 - B_3) + A_3(B_4 - B_0) + A_2(B_5 - B_1) + A_1(B_2 - B_4) + A_0(B_3 - B_5)\}$

$(P_Z|\mathcal{Z}|\ S)$: $(1/3)^{1/2}\{A_5B_2 + A_4(B_1 - B_3) - A_3(B_2 + B_4) + A_2(B_5 - B_3) + A_1B_4\}$

$(P_X|X|\ S)$: $(1/12)^{1/2}\{A_5(B_0 - B_2) + A_4(B_3 - B_1) + A_3(B_4 - B_0) + A_2(B_1 - B_5) + A_1(B_2 - B_4) + A_0(B_5 - B_3)\}$

$(P_Z|\mathcal{Z}|P_Z)$: $A_5B_3 - A_3(B_1 + B_5) + A_1B_3$

$(P_Z|X|P_X)$: $(1/2)\{A_5(B_1 - B_3) + A_4(B_0 - B_2) + A_3(B_5 - B_1) + A_2(B_4 - B_0) + A_1(B_3 - B_5) + A_0(B_2 - B_4)\}$

$(P_X|\mathcal{Z}|P_X)$: $(1/2)\{A_5(B_1 - B_3) + A_3(B_5 - B_1) + A_1(B_3 - B_5)\}$

$(P_X|X|P_Z)$: $(1/2)\{A_5(B_1 - B_3) + A_4(B_2 - B_0) + A_3(B_5 - B_1) + A_2(B_0 - B_4) + A_1(B_3 - B_5) + A_0(B_4 - B_2)\}$

$n_1^* = 2, n_2^* = 3$; $c = (a_1^5 a_2^7/30)^{1/2} R/32$

$(S\ |\mathcal{Z}|\ S)$: $(1/3)(A_6B_1 - A_5B_2 - 2A_4B_3 + 2A_3B_4 + A_2B_5 - A_1B_6)$

$(S\ |\mathcal{Z}|\ P_Z)$: $(1/3)^{1/2}(A_6B_2 - A_5B_1 - 2A_4B_4 + 2A_3B_3 + A_2B_6 - A_1B_5)$

$(S\ |X|\ P_X)$: $(1/12)^{1/2}\{A_6(B_0 - B_2) + A_4(2B_4 - B_2 - B_0) + A_2(2B_2 - B_4 - B_6) + A_0(B_6 - B_4)\}$

$(P_Z|\mathcal{Z}|\ S)$: $(1/3)^{1/2}\{A_6B_2 + A_5(B_1 - 2B_3) - 2A_4B_2 + 2A_3B_5 + A_2(2B_4 - B_6) - A_1B_5\}$

$(P_X|X|\ S)$: $(1/12)^{1/2}\{A_6(B_0 - B_2) + 2A_5(B_3 - B_1) + A_4(B_2 - B_0) + 2A_3(B_1 - B_5) + A_2(B_6 - B_4) + 2A_1(B_5 - B_3) + A_0(B_4 - B_6)\}$

$(P_Z|\mathcal{Z}|P_Z)$: $A_6B_3 - A_5B_4 - A_4(B_1 + B_5) + A_3(B_2 + B_6) + A_2B_3 - A_1B_4$

$(P_Z|X|P_X)$: $(1/2)\{A_6(B_1 - B_3) + A_5(B_4 - 2B_2 + B_0) + A_4(B_5 + B_3 - 2B_1) + A_3(B_2 - B_0 - B_6 + B_4) + A_2(B_1 + B_3 - 2B_5) + A_1(B_6 - 2B_4 + B_2) + A_0(B_5 - B_3)\}$

$(P_X|\mathcal{Z}|P_X)$: $(1/2)\{A_6(B_1 - B_3) + A_5(B_4 - B_2) + A_4(B_5 - B_1) + A_3(B_2 - B_6) + A_2(B_3 - B_5) + A_1(B_6 - B_4)\}$

$(P_X|X|P_Z)$: $(1/2)\{A_6(B_1 - B_3) + A_5(B_4 - B_0) + A_4(B_5 - B_3) + A_3(B_0 + B_2 - B_4 - B_6) + A_2(B_3 - B_1) + A_1(B_6 - B_2) + A_0(B_3 - B_5)\}$

$n_1^* = 2, n_2^* = 4$; $c = (a_1^5 a_2^9/105)^{1/2} R/128$

$(S\ |\mathcal{Z}|\ S)$: $(1/3)(A_7B_1 - 2A_6B_2 - A_5B_3 + 4A_4B_4 - A_3B_5 - 2A_2B_6 + A_1B_7)$

$(S\ |\mathcal{Z}|\ P_Z)$: $(1/3)^{1/2}\{A_7B_2 - A_6(B_3 + B_1) + A_5(B_2 - 2B_4) + 2A_4(B_5 + B_3) + A_3(B_6 - 2B_4) - A_2(B_7 + B_5) + A_1B_6\}$

$(S\ |X|\ P_X)$: $(1/12)^{1/2}\{A_7(B_0 - B_2) + A_6(B_3 - B_1) + A_5(2B_4 - B_2 - B_0) + A_4(B_1 + B_3 - 2B_5) + A_3(2B_2 - B_4 - B_6) + A_2(B_7 + B_5 - 2B_3) + A_1(B_6 - B_4) + A_0(B_5 - B_7)\}$

$(P_Z|\mathcal{Z}|\ S)$: $(1/3)^{1/2}\{A_7B_2 + A_6(B_1 - 3B_3) + A_5(2B_4 - 3B_2) + 2A_4(B_3 + B_5) + A_3(2B_4 - 3B_6) + A_2(B_7 - 3B_5) + A_1B_6\}$

$(P_X|X|\ S)$: $(1/12)^{1/2}\{A_7(B_0 - B_2) + 3A_6(B_3 - B_1) + A_5(3B_2 - 2B_4 - B_0) + A_4(3B_1 - B_3 - 2B_5) + A_3(3B_6 - B_4 - 2B_2) + A_2(3B_5 - B_7 - 2B_3) + 3A_1(B_4 - B_6) + A_0(B_7 - B_5)\}$

$(P_Z|\mathcal{Z}|P_Z)$: $A_7B_3 - 2A_6B_4 - A_5B_1 + 2A_4(B_2+B_6) - A_3B_7 - 2A_2B_4 + A_1B_5$

$(P_Z|X|P_X)$: $(1/2)\{A_7(B_1-B_3) + A_6(2B_4-3B_2+B_0) + 3A_5(B_3-B_1) + A_4(3B_2-B_0-2B_6) + A_3(2B_1-3B_5+B_7) + 3A_2(B_6-B_4) + A_1(3B_5-2B_3-B_7) + A_0(B_4-B_6)\}$

$(P_X|\mathcal{Z}|P_X)$: $(1/2)\{A_7(B_1-B_3) + 2A_6(B_4-B_2) + A_5(B_3-B_1) + 2A_4(B_2-B_6) + A_3(B_7-B_5) + 2A_2(B_6-B_4) + A_1(B_5-B_7)\}$

$(P_X|X|P_Z)$: $(1/2)\{A_7(B_1-B_3) + A_6(2B_4-B_2-B_0) + A_5(B_1-B_3) + A_4(B_0+B_2-2B_6) + A_3(B_7+B_5-2B_1) + A_2(B_6-B_4) + A_1(2B_3-B_5-B_7) + A_0(B_6-B_4)\}$

$n_1^*=2, n_2^*=5$; $c = (a_1^5a_2^{11}/42)^{1/2}R/1920$

$(S|\mathcal{Z}|S)$: $(1/3)(A_8B_1 - 3A_7B_2 + A_6B_3 + 5A_5B_4 - 5A_4B_5 - A_3B_6 + 3A_2B_7 - A_1B_8)$

$(S|\mathcal{Z}|P_Z)$: $(1/3)^{1/2}\{A_8B_2 - A_7(2B_3+B_1) + A_6(2B_2-B_4) + A_5(B_3+4B_5) - A_4(B_6+4B_4) + A_3(B_5-2B_7) + A_2(B_8+2B_6) - A_1B_7\}$

$(S|X|P_X)$: $(1/12)^{1/2}\{A_8(B_0-B_2) + 2A_7(B_3-B_1) + A_6(B_4-B_0) + A_5(2B_1+2B_3-4B_5) + A_4(B_6-2B_4+B_2) + A_3(2B_7+2B_5-4B_3) + A_2(B_4-B_8) + 2A_1(B_5-B_7) + A_0(B_8-B_6)\}$

$(P_Z|\mathcal{Z}|S)$: $(1/3)^{1/2}\{A_8B_2 + A_7(B_1-4B_3) + A_6(5B_4-4B_2) + 5A_5B_3 - 5A_4B_6 + A_3(4B_7-5B_5) + A_2(4B_6-B_8) - A_1B_7\}$

$(P_X|X|S)$: $(1/12)^{1/2}\{A_8(B_0-B_2) + 4A_7(B_3-B_1) + A_6(6B_2-5B_4-B_0) + 4A_5(B_1-B_3) + 5A_4(B_6-B_2) + 4A_3(B_5-B_7) + A_2(B_8-6B_6+5B_4) + 4A_1(B_7-B_5) + A_0(B_6-B_8)\}$

$(P_Z|\mathcal{Z}|P_Z)$: $A_8B_3 - 3A_7B_4 + A_6(2B_5-B_1) + A_5(3B_2+2B_6) - A_4(2B_3+3B_7) + A_3(B_8-2B_4) + 3A_2B_5 - A_1B_6$

$(P_Z|X|P_X)$: $(1/2)\{A_8(B_1-B_3) + A_7(B_0-4B_2+3B_4) + A_6(6B_3-4B_1-2B_5) + A_5(6B_2-B_0-3B_4-2B_6) + 3A_4(B_1-B_3-B_5+B_7) + A_3(6B_6-2B_2-3B_4-B_8) + A_2(6B_5-4B_7-2B_3) + A_1(B_8-4B_6+3B_4) + A_0(B_7-B_5)\}$

$(P_X|\mathcal{Z}|P_X)$: $(1/2)\{A_8(B_1-B_3) + 3A_7(B_4-B_2) + A_6(3B_3-2B_5-B_1) + A_5(3B_2-B_4-2B_6) + A_4(3B_7-B_5-2B_3) + A_3(3B_6-B_8-2B_4) + 3A_2(B_5-B_7) + A_1(B_8-B_6)\}$

$(P_X|X|P_Z)$: $(1/2)\{A_8(B_1-B_3) + A_7(3B_4-2B_2-B_0) + 2A_6(B_1-B_5) + A_5(B_0+B_4-2B_6) + A_4(3B_7+B_5-B_3-3B_1) + A_3(2B_2-B_4-B_8) + 2A_2(B_3-B_7) + A_1(B_8+2B_6-3B_4) + A_0(B_5-B_7)\}$

$n_1^*=n_2^*=3$; $c = (a_1^7a_2^7)^{1/2}R/960$

$(S|\mathcal{Z}|S)$: $(1/3)(A_7B_1 - 3A_5B_3 + 3A_3B_5 - A_1B_7)$

$(S|\mathcal{Z}|P_Z)$: $(1/3)^{1/2}\{A_7B_2 + A_6(B_3-B_1) - A_5(B_2+2B_4) + 2A_4(B_3-B_5) + A_3(B_6+2B_4) + A_2(B_7-B_5) - A_1B_6\}$

$(S|X|P_X)$: $(1/12)^{1/2}\{A_7(B_0-B_2) + A_6(B_1-B_3) + A_5(2B_4-B_2-B_0) + A_4(2B_5-B_3-B_1) + A_3(2B_2-B_4-B_6) + A_2(2B_3-B_5-B_7) + A_1(B_6-B_4) + A_0(B_7-B_5)\}$

$(P_Z|\mathcal{Z}|S)$: $(1/3)^{1/2}\{A_7B_2 + A_6(B_1-B_3) - A_5(2B_4+B_2) + 2A_4(B_5-B_3) + A_3(2B_4+B_6) + A_2(B_5-B_7) - A_1B_6\}$

$(P_X|X|S)$: $(1/12)^{1/2}\{A_7(B_0-B_2) + A_6(B_3-B_1) + A_5(2B_4-B_2-B_0) + A_4(B_1+B_3-2B_5) + A_3(2B_2-B_4-B_6) + A_2(B_7+B_5-2B_3) + A_1(B_6-B_4) + A_0(B_5-B_7)\}$

$(P_Z|\mathcal{Z}|P_Z)$: $A_7B_3 - A_5(2B_5+B_1) + A_3(2B_3+B_7) - A_1B_5$

$(P_Z|X|P_X)$: $(1/2)\{A_7(B_1-B_3) + A_6(B_0-B_2) + A_5(2B_5-B_3-B_1) + A_4(2B_4-B_2-B_0) + A_3(2B_3-B_5-B_7) + A_2(2B_2-B_4-B_6) + A_1(B_7-B_5) + A_0(B_6-B_4)\}$

$(P_X|\mathcal{Z}|P_X)$: $(1/2)\{A_7(B_1-B_3) + A_5(2B_5-B_3-B_1) + A_3(2B_3-B_5-B_7) + A_1(B_7-B_5)\}$

$(P_X|X|P_Z)$: $(1/2)\{A_7(B_1-B_3) + A_6(B_2-B_0) + A_5(2B_5-B_3-B_1) + A_4(B_0+B_2-2B_4) + A_3(2B_3-B_5-B_7) + A_2(B_6+B_4-2B_2) + A_1(B_7-B_5) + A_0(B_4-B_6)\}$

$n_1^*=3, n_2^*=4$; $c = (a_1^7a_2^9/14)^{1/2}R/1920$

$(S|\mathcal{Z}|S)$: $(1/3)(A_8B_1 - A_7B_2 - 3A_6B_3 + 3A_5B_4 + 3A_4B_5 - 3A_3B_6 - A_2B_7 + A_1B_8)$

$(S|\mathcal{Z}|P_Z)$: $(1/3)^{1/2}(A_8B_2 - A_7B_1 - 3A_6B_4 + 3A_5B_3 + 3A_4B_6 - 3A_3B_5 - A_2B_8 + A_1B_7)$

$(S|X|P_X)$: $(1/12)^{1/2}\{A_8(B_0-B_2) + A_6(3B_4-2B_2-B_0) + 3A_4(B_2-B_6) + A_2(B_8+2B_6-3B_4) + A_0(B_6-B_8)\}$

$(P_Z|\mathcal{Z}|S)$: $(1/3)^{1/2}\{A_8B_2 + A_7(B_1-2B_3) - A_6(B_4+2B_2) + A_5(4B_5-B_3) + A_4(4B_4-B_6) - A_3(B_5+2B_7) + A_2(B_8-2B_6) + A_1B_7\}$

$(P_X|X|S)$: $(1/12)^{1/2}\{A_8(B_0-B_2) + 2A_7(B_3-B_1) + A_6(B_4-B_0) + A_5(2B_1+2B_3-4B_5) + A_4(B_6-2B_4+B_2) + A_3(2B_7+2B_5-4B_3) + A_2(B_4-B_8) + 2A_1(B_5-B_7) + A_0(B_8-B_6)\}$

$(P_Z|\mathcal{Z}|P_Z)$: $A_8B_3 - A_7B_4 - A_6(2B_5+B_1) + A_5(2B_6+B_2) + A_4(2B_3+B_7) - A_3(2B_4+B_8) - A_2B_5 + A_1B_6$

$(P_Z|X|P_X)$: $(1/2)\{A_8(B_1-B_3) + A_7(B_0-2B_2+B_4) + 2A_6(B_5-B_1) + A_5(3B_4-2B_6-B_0) + A_4(B_1+3B_3-3B_5-B_7) + A_3(2B_2-3B_4+B_8) + 2A_2(B_7-B_3) + A_1(2B_6-B_8-B_4) + A_0(B_5-B_7)\}$

$(P_X|\mathcal{Z}|P_X)$: $(1/2)\{A_8(B_1-B_3) + A_7(B_4-B_2) + A_6(2B_5-B_3-B_1) + A_5(B_2+B_4-2B_6) + A_4(2B_3-B_5-B_7) + A_3(B_8+B_6-2B_4) + A_2(B_7-B_5) + A_1(B_6-B_8)\}$

$(P_X|X|P_Z)$: $(1/2)\{A_8(B_1-B_3) + A_7(B_4-B_0) + 2A_6(B_5-B_3) + A_5(B_0+2B_2-B_4-2B_6) + A_4(B_3+B_5-B_1-B_7) + A_3(B_8+2B_6-B_4-2B_2) + 2A_2(B_3-B_5) + A_1(B_4-B_8) + A_0(B_7-B_5)\}$

$n_1^*=3, n_2^*=5$; $c = (a_1^7a_2^{11}/35)^{1/2}R/11520$

$(S|\mathcal{Z}|S)$: $(1/3)(A_9B_1 - 2A_8B_2 - 2A_7B_3 + 6A_6B_4 - 6A_4B_6 + 2A_3B_7 + 2A_2B_8 - A_1B_9)$

$(S\ |\mathcal{Z}|P_Z)$: $(1/3)^{1/2}\{A_9B_2 - A_8(B_3+B_1) + A_7(B_2-3B_4) + 3A_6(B_5+B_3) + 3A_5(B_6-B_4) - 3A_4(B_7+B_5) + A_3(3B_6-B_8) + A_2(B_9+B_7) - A_1B_8\}$

$(S\ |X|P_X)$: $(1/12)^{1/2}\{A_9(B_0-B_2) + A_8(B_3-B_1) + A_7(3B_4-2B_2-B_0) + A_6(B_1+2B_3-3B_5) + 3A_5(B_2-B_6) + 3A_4(B_7-B_3) + A_3(B_8+2B_6-3B_4) + A_2(3B_5-2B_7-B_9) + A_1(B_6-B_8) + A_0(B_9-B_7)\}$

$(P_Z|\mathcal{Z}|\ S\ )$: $(1/3)^{1/2}\{A_9B_2 + A_8(B_1-3B_3) + A_7(B_4-3B_2) + A_6(5B_5+B_3) + 5A_5(B_4-B_6) - A_4(B_7+5B_5) + A_3(3B_8-B_6) + A_2(3B_7-B_9) - A_1B_8\}$

$(P_X|X|\ S\ )$: $(1/12)^{1/2}\{A_9(B_0-B_2) + 3A_8(B_3-B_1) + A_7(2B_2-B_4-B_0) + A_6(3B_1+2B_3-5B_5) + A_5(5B_6-4B_4-B_2) + A_4(B_7+4B_5-5B_3) + A_3(5B_4-2B_6-3B_8) + A_2(B_5-2B_7+B_9) + 3A_1(B_8-B_6) + A_0(B_7-B_9)\}$

$(P_Z|\mathcal{Z}|P_Z)$: $A_9B_3 - 2A_8B_4 - A_7(B_5+B_1) + A_6(4B_6+2B_2) + A_5(B_3-B_7) - A_4(4B_4+2B_8) + A_3(B_5+B_9) + 2A_2B_6 - A_1B_7$

$(P_Z|X|P_X)$: $(1/2)\{A_9(B_1-B_3) + A_8(B_0-3B_2+2B_4) + A_7(B_5+2B_3-3B_1) + A_6(2B_2-4B_6+3B_4-B_0) + A_5(B_7-6B_5+3B_3+2B_1) + A_4(B_2-6B_4+3B_6+2B_8) + A_3(3B_5-4B_3-B_9+2B_7) + A_2(B_4+2B_6-3B_8) + A_1(B_9-3B_7+2B_5) + A_0(B_8-B_6)\}$

$(P_X|\mathcal{Z}|P_X)$: $(1/2)\{A_9(B_1-B_3) + 2A_8(B_4-B_2) + A_7(B_5-B_1) + A_6(2B_2+2B_4-4B_6) + A_5(B_7-2B_5+B_3) + A_4(2B_8+2B_6-4B_4) + A_3(B_5-B_9) + 2A_2(B_6-B_8) + A_1(B_9-B_7)\}$

$(P_X|X|P_Z)$: $(1/2)\{A_9(B_1-B_3) + A_8(2B_4-B_2-B_0) + A_7(B_1-2B_3+B_5) + A_6(B_0+2B_2+B_4-4B_6) + A_5(B_7+2B_5-B_3-2B_1) + A_4(2B_8+B_6-2B_4-B_2) + A_3(4B_3-B_5-2B_7-B_9) + A_2(2B_6-B_4-B_8) + A_1(B_9+B_7-2B_5) + A_0(B_6-B_8)\}$

$n_1^*=n_2^*=4$; $c = (a_1^9a_2^9)^{1/2}\,R/53760$

$(S\ |\mathcal{Z}|\ S\ )$: $(1/3)(A_9B_1 - 4A_7B_3 + 6A_5B_5 - 4A_3B_7 + A_1B_9)$

$(S\ |\mathcal{Z}|P_Z)$: $(1/3)^{1/2}\{A_9B_2 + A_8(B_3-B_1) - A_7(3B_4+B_2) + 3A_6(B_3-B_5) + 3A_5(B_4+B_6) + 3A_4(B_7-B_5) - A_3(3B_6+B_8) + A_2(B_7-B_9) + A_1B_8\}$

$(S\ |X|P_X)$: $(1/12)^{1/2}\{A_9(B_0-B_2) + A_8(B_1-B_3) + A_7(3B_4-2B_2-B_0) + A_6(3B_5-2B_3-B_1) + 3A_5(B_2-B_6) + 3A_4(B_3-B_7) + A_3(B_8+2B_6-3B_4) + A_2(B_9+2B_7-3B_5) + A_1(B_6-B_8) + A_0(B_7-B_9)\}$

$(P_Z|\mathcal{Z}|\ S\ )$: $(1/3)^{1/2}\{A_9B_2 + A_8(B_1-B_3) - A_7(3B_4+B_2) + 3A_6(B_5-B_3) + 3A_5(B_4+B_6) + 3A_4(B_5-B_7) - A_3(B_8+3B_6) + A_2(B_9-B_7) + A_1B_8\}$

$(P_X|X|\ S\ )$: $(1/12)^{1/2}\{A_9(B_0-B_2) + A_8(B_3-B_1) + A_7(3B_4-2B_2-B_0) + A_6(B_1+2B_3-3B_5) + 3A_5(B_2-B_6) + 3A_4(B_7-B_3) + A_3(B_8+2B_6-3B_4) + A_2(3B_5-2B_7-B_9) + A_1(B_6-B_8) + A_0(B_9-B_7)\}$

$(P_Z|\mathcal{Z}|P_Z)$: $A_9B_3 - A_7(3B_5+B_1) + 3A_5(B_3+B_7) - A_3(B_9+3B_5) + A_1B_7$

$(P_Z|X|P_X)$: $(1/2)\{A_9(B_1-B_3) + A_8(B_0-B_2) + A_7(3B_5-2B_3-B_1) + A_6(3B_4-2B_2-B_0) + 3A_5(B_3-B_7) + 3A_4(B_2-B_6) + A_3(B_9+2B_7-3B_5) + A_2(B_8+2B_6-3B_4) + A_1(B_7-B_9) + A_0(B_6-B_8)\}$

$(P_X|\mathcal{Z}|P_X)$: $(1/2)\{A_9(B_1-B_3) + A_7(3B_5-2B_3-B_1) + 3A_5(B_3-B_7) + A_3(B_9+2B_7-3B_5) + A_1(B_7-B_9)\}$

$(P_X|X|P_Z)$: $(1/2)\{A_9(B_1-B_3) + A_8(B_2-B_0) + A_7(3B_5-2B_3-B_1) + A_6(B_0+2B_2-3B_4) + 3A_5(B_3-B_7) + 3A_4(B_6-B_2) + A_3(B_9+2B_7-3B_5) + A_2(3B_4-2B_6-B_8) + A_1(B_7-B_9) + A_0(B_8-B_6)$

$n_1^*=4, n_2^*=5$; $c = (a_1^9a_2^{11}/10)^{1/2}\,R/161280$

$(S\ |\mathcal{Z}|\ S\ )$: $(1/3)(A_{10}B_1 - A_9B_2 - 4A_8B_3 + 4A_7B_4 + 6A_6B_5 - 6A_5B_6 - 4A_4B_7 + 4A_3B_8 + A_2B_9 - A_1B_{10})\}$

$(S\ |\mathcal{Z}|P_Z)$: $(1/3)^{1/2}(A_{10}B_2 - A_9B_1 - 4A_8B_4 + 4A_7B_3 + 6A_6B_6 - 6A_5B_5 - 4A_4B_8 + 4A_3B_7 + A_2B_{10} - A_1B_9)$

$(S\ |X|P_X)$: $(1/12)^{1/2}\{A_{10}(B_0-B_2) + A_8(4B_4-3B_2-B_0) + A_6(4B_2+2B_4-6B_6) + A_4(4B_8+2B_6-6B_4) + A_2(4B_6-3B_8-B_{10}) + A_0(B_{10}-B_8)\}$

$(P_Z|\mathcal{Z}|\ S\ )$: $(1/3)\{^{1/2}\,A_{10}B_2 + A_9(B_1-2B_3) - 2A_8(B_4+B_2) + A_7(6B_5-2B_3) + 6A_6B_4 - 6A_5B_7 + A_4(2B_8-6B_6) + 2A_3(B_9+B_7) + A_2(2B_8-B_{10}) - A_1B_9\}$

$(P_X|X|\ S\ )$: $(1/12)^{1/2}\{A_{10}(B_0-B_2) + 2A_9(B_3-B_1) + A_8(2B_4-B_2-B_0) + A_7(2B_1+4B_3-6B_5) + 2A_6(B_2-B_4) + 6A_5(B_7-B_3) + 2A_4(B_6-B_8) + A_3(6B_5-4B_7-2B_9) + A_2(B_{10}+B_8-2B_6) + 2A_1(B_9-B_7) + A_0(B_8-B_{10})\}$

$(P_Z|\mathcal{Z}|P_Z)$: $A_{10}B_3 - A_9B_4 - A_8(3B_5+B_1) + A_7(3B_6+B_2) + 3A_6(B_3+B_7) - 3A_5(B_4+B_8) - A_4(B_9+3B_5) + A_3(B_{10}+3B_6) + A_2B_7 - A_1B_8$

$(P_Z|X|P_X)$: $(1/2)\{A_{10}(B_1-B_3) + A_9(B_0-2B_2+B_4) + A_8(3B_5-B_3-2B_1) + A_7(5B_4-B_2-3B_6-B_0) + A_6(B_1+5B_3-3B_5-3B_7) + 3A_5(B_2-B_4-B_6+B_8) + A_4(B_9+5B_7-3B_5-3B_3) + A_3(5B_6-3B_4-B_8-B_{10}) + A_2(3B_5-B_7-2B_9) + A_1(B_{10}-2B_8+B_6) + A_0(B_9-B_7)\}$

$(P_X|\mathcal{Z}|P_X)$: $(1/2)\{A_{10}(B_1-B_3) + A_9(B_4-B_2) + A_8(3B_5-2B_3-B_1) + A_7(B_2+2B_4-3B_6) + 3A_6(B_3-B_7) + 3A_5(B_8-B_4) + A_4(B_9+2B_7-3B_5) + A_3(3B_6-2B_8-B_{10}) + A_2(B_7-B_9) + A_1(B_{10}-B_8)\}$

$(P_X|X|P_Z)$: $(1/2)\{A_{10}(B_1-B_3) + A_9(B_4-B_0) + 3A_8(B_5-B_3) + A_7(B_0+3B_2-B_4-3B_6) + A_6(B_3+3B_5-3B_7-B_1) + 3A_5(B_8+B_6-B_4-B_2) + A_4(B_9-B_7-3B_5+3B_3) + A_3(3B_4+B_6-3B_8-B_{10}) + 3A_2(B_7-B_5) + A_1(B_{10}-B_6) + A_0(B_7-B_9)\}$

$n_1^*=n_2^*=5$; $c = (a_1^{11}a_2^{11})^{1/2}\,R/4838400$

$$(S\,|\mathcal{Z}|\,S): (1/3)(A_{11}B_1 - 5A_9B_3 + 10A_7B_5 - 10A_5B_7 + 5A_3B_9 - A_1B_{11})$$

$$(S\,|\mathcal{Z}|\,P_Z): (1/3)^{1/2}\{A_{11}B_2 + A_{10}(B_3-B_1) - A_9(4B_4+B_2) + 4A_8(B_3-B_5) + A_7(4B_4+6B_6) + 6A_6(B_7-B_5) - A_5(4B_8+6B_6) + 4A_4(B_7-B_9) + A_3(4B_8+B_{10}) + A_2(B_{11}-B_9) - A_1B_{10}\}$$

$$(S\,|X|\,P_X): (1/12)^{1/2}\{A_{11}(B_0-B_2) + A_{10}(B_1-B_3) + A_9(4B_4-3B_2-B_0) + A_8(4B_5-3B_3-B_1) + A_7(4B_2+2B_4-6B_6) + A_6(4B_3+2B_5-6B_7) + A_5(4B_8+2B_6-6B_4) + A_4(4B_9+2B_7-6B_5) + A_3(4B_6-3B_8-B_{10}) + A_2(4B_7-3B_9-B_{11}) + A_1(B_{10}-B_8) + A_0(B_{11}-B_9)\}$$

$$(P_Z|\mathcal{Z}|\,S): (1/3)^{1/2}\{A_{11}B_2+A_{10}(B_1-B_3) - A_9(4B_4+B_2) + 4A_8(B_5-B_3) + A_7(6B_6+4B_4) + 6A_6(B_5-B_7) - A_5(6B_6+4B_8) + 4A_4(B_9-B_7) + A_3(B_{10}+4B_8) + A_2(B_9-B_{11}) - A_1B_{10}\}$$

$$(P_X|X|\,S): (1/12)^{1/2}\{A_{11}(B_0-B_2) + A_{10}(B_3-B_1) + A_9(4B_4-3B_2-B_0) + A_8(B_1+3B_3-4B_5) + A_7(4B_2+2B_4-6B_6) + A_6(6B_7-2B_5-4B_3) + A_5(4B_8+2B_6-6B_4) + A_4(6B_5-2B_7-4B_9) + A_3(4B_6-3B_8-B_{10}) + A_2(B_{11}+3B_9-4B_7) + A_1(B_{10}-B_8) + A_0(B_9-B_{11})\}$$

$$(P_Z|\mathcal{Z}|P_Z): A_{11}B_3 - A_9(4B_5+B_1) + A_7(6B_7+4B_3) - A_5(6B_5+4B_9) + A_3(B_{11}+4B_7) - A_1B_9$$

$$(P_Z|X|P_X): (1/2)\{A_{11}(B_1-B_3) + A_{10}(B_0-B_2) + A_9(4B_5-3B_3-B_1) + A_8(4B_4-3B_2-B_0) + A_7(4B_3+2B_5-6B_7) + A_6(4B_2+2B_4-6B_6) + A_5(4B_9+2B_7-6B_5) + A_4(4B_8+2B_6-6B_4) + A_3(4B_7-3B_9-B_{11}) + A_2(4B_6-3B_8-B_{10}) + A_1(B_{11}-B_9) + A_0(B_{10}-B_8)\}$$

$$(P_X|\mathcal{Z}|P_X): (1/2)\{A_{11}(B_1-B_3) + A_9(4B_5-3B_3-B_1) + A_7(4B_3+2B_5-6B_7) + A_5(4B_9+2B_7-6B_5) + A_3(4B_7-3B_9-B_{11}) + A_1(B_{11}-B_9)\}$$

$$(P_X|X|P_Z): (1/2)\{A_{11}(B_1-B_3) + A_{10}(B_2-B_0) + A_9(4B_5-3B_3-B_1) + A_8(B_0+3B_2-4B_4) + A_7(4B_3+2B_5-6B_7) + A_6(6B_6-2B_4-4B_2) + A_5(4B_9+2B_7-6B_5) + A_4(6B_4-2B_6-4B_8) + A_3(4B_7-3B_9-B_{11}) + A_2(B_{10}+3B_8-4B_6) + A_1(B_{11}-B_9)+A_0(B_8-B_{10})\}$$

Table 3. Basic two-center moment integrals for $b=0$, and $n_1^*=n_2^*$

$n_1^*=n_2^*=2$; $c=a^5R/240$

$(S\,|\mathcal{Z}|\,P_Z): (1/3)^{1/2}(5A_5-8A_3+3A_1)$

$(S\,|X|\,P_X): (1/3)^{1/2}(5A_5-6A_3+A_1)$

$(P_Z|X|\,P_X): 5A_4-6A_2+A_0$

$n_1^*=n_2^*=3$; $c=a^7R/50400$

$(S\,|\mathcal{Z}|\,P_Z): (1/3)^{1/2}(35A_7-77A_5+57A_3-15A_1)$

$(S\,|X|\,P_X): (1/3)^{1/2}(35A_7-49A_5+17A_3-3A_1)$

$(P_Z|X|\,P_X): 35A_6-49A_4+17A_2-3A_0$

$n_1^*=n_2^*=4$; $c=a^9R/8467200$

$(S\,|\mathcal{Z}|\,P_Z): (1/3)^{1/2}(105A_9-294A_7+324A_5-170A_3+35A_1)$

$(S\,|X|\,P_X): (1/3)^{1/2}(105A_9-168A_7+90A_5-32A_3+5A_1)$

$(P_Z|X|\,P_X): 105A_8-168A_6+90A_4-32A_2+5A_0$

$n_1^*=n_2^*=5$; $c=a^{11}R/8382528000$

$(S\,|\mathcal{Z}|\,P_Z): (1/3)^{1/2}(1155A_{11}-3927A_9+5742A_7-4510A_5+1855A_3-315A_1)$

$(S\,|X|\,P_X): (1/3)^{1/2}(1155A_{11}-2079A_9+1518A_7-814A_5+255A_3-35A_1)$

$(P_Z|X|\,P_X): 1155A_{10}-2079A_8+1518A_6-814A_4+255A_2-35A_0$

Table 4. One-center moment integrals

n_1^*	n_2^*	$M(s\,\|\,i\,\|\,p_t) = M(p_t\,\|\,i\,\|\,s)$
1	2	$32(h_1^3\,h_2^5)^{1/2}/(h_1+h_2)^5$
1	3	$320(h_1^3\,h_2^7/30)^{1/2}/(h_1+h_2)^6$
1	4	$960(h_1^3\,h_2^9/105)^{1/2}/(h_1+h_2)^7$
1	5	$896(h_1^3\,h_2^{11}/42)^{1/2}/(h_1+h_2)^8$
2	2	$160(h_1^5\,h_2^5/3)^{1/2}/(h_1+h_2)^6$
2	3	$640(h_1^5\,h_2^7/10)^{1/2}/(h_1+h_2)^7$
2	4	$2240(h_1^5\,h_2^9/35)^{1/2}/(h_1+h_2)^8$
2	5	$7168(h_1^5\,h_2^{11}/126)^{1/2}/(h_1+h_2)^9$
3	3	$896(h_1^7\,h_2^7/3)^{1/2}/(h_1+h_2)^8$
3	4	$7168(h_1^7h_2^9/42)^{1/2}/(h_1+h_2)^9$
3	5	$21504(h_1^7\,h_2^{11}/105)^{1/2}/(h_1+h_2)^{10}$
4	4	$4608(h_1^9\,h_2^9/3)^{1/2}/(h_1+h_2)^{10}$
4	5	$30720(h_1^9\,h_2^{11}/30)^{1/2}/(h_1+h_2)^{11}$
5	5	$22528(h_1^{11}\,h_2^{11}/3)^{1/2}/(h_1+h_2)^{12}$

which are presented in Table 3. In Tables 2 and 3, each formula is to be multiplied by a parameter c which is common to formulas for a same pair of n_1^* and n_2^*. In Table 4, one-center moment integrals are also collected, where $h=\mu/R_H$.

For $n_1^*>n_2^*$. According to our choice of coordinates (Fig. 2), the following two rules are derived as for basic two-center integrals.

i) Those which contain none or even number of $\mathcal{Z}$ (type 1) do not change the sign through the exchange of two AO's with each other, and the other (type 2) change the sign.

ii) $B_m(b)=B_m(-b)$ for m even, and $=-B_m(-b)$ for m odd.

From the above two rules, the formulas for $n_1^*>n_2^*$ are derived in the following way. When $b\neq 0$, the sign of a term with B_m is changed if m is odd for type 1, and even for type 2, in the formula with two exchanged AO's. When $b=0$, signs of all terms are changed for type 2, and none for type 1. For example:

$$\text{type 2: } (2S|\mathcal{Z}|1S) = (a_1^5\,a_2^3/3)^{1/2}(R/16)(A_4B_1+A_3B_2-A_2B_3-A_1B_4)$$

$$\text{type 1: } (2P_z|\mathcal{Z}|1S) = (a_1^5\,a_2^3)^{1/2}(R/16)(A_4B_2+A_3B_1-A_2B_4-A_1B_3)$$

Other Values of n^*. Basic two-center integrals

for larger values of n^* are derived from formulas of the same type for n^*-1 with the rule presented by Lofthus for overlap integrals.[4] Integrals for non-integer n^* may be evaluated by interpolation from the values for appropriate integer n^*'s, when not so high accuracy is needed.

Programming. Basic moment integrals may be calculated together with corresponding overlap integrals, since values of all parameters are common in both cases. A FORTRAN subprogram including all formulas of one- and two-center moment integrals for s,p-AO's with n^* of 1 to 4 (for $b=0$, only those for $n_1^*=n_2^*$ are included), and an interpolation technique with a parabola, written for a HITAC 5020 computer at the computation center of the University of Tokyo, occupies about $7.7K$ of the core memory, $65K$, while a subprogram for overlap integrals in the same region of n^* occupies about $5K$.

BULLETIN OF THE CHEMICAL SOCIETY OF JAPAN VOL. 42 329—333 (1969)

The Efficiencies of Hydrocarbons and Hydrogen in Quenching Triplet Cadmium Atoms

Shigeru TSUNASHIMA, Shin SATOH and Shin SATO

Department of Applied Physics, Tokyo Institute of Technology, Ookayama, Meguro-ku, Tokyo

(Received June 11, 1968)

The relative efficiencies of sixteen hydrocarbons and of hydrogen in quenching triplet cadmium atoms have been measured at 270±1°C by the competitive quenching method, using the cadmium-photosensitized *cis-trans* isomerization of *cis*-2-butene as a detector reaction. The quenching efficiencies of all the olefins studied and of acetylene were almost the same. The efficiencies of saturated hydrocarbons were, however, very low compared with those of unsaturated ones. Hydrogen was as efficient as unsaturated hydrocarbons.

Electronic energy-transfer reactions in the gas phase are of fundamental interest in chemical kinetics. In spite of many investigations, however, little is understood about the mechanism and the rate-controlling parameters.

Recently, Rebbert and Ausloos measured the efficiencies of various unsaturated hydrocarbons in quenching triplet acetone, and found that the efficiency of olefin depends strongly on its structure.[1] For quenching triplet benzene, Hanninger and Lee found that the efficiencies of ethylene derivatives depend greatly on the number of substitution; *i. e.*, the efficiency of tetramethylethylene is more than ten times as great as that of ethylene.[2] Similar results have been obtained by Morikawa and Cvetanović.[3] In the mercury-photosensitization, however, no such strong dependence has been observed.[4]

In this respect, the measurement of the efficiencies for quenching triplet cadmium atoms should be of interest because a triplet cadmium atom (Cd $5(^3P_1)$; 87.7 kcal) is similar to a triplet mercury atom (Hg $6(^3P_1)$; 112.7 kcal) in its electronic property and is close to triplet benzene (C_6H_6 $(^3B_{1u})$; 84.4 kcal[5]) in its excitation energy.

In cadmium-photosensitization, as was shown in a previous short communication,[6] the quenching efficiencies of ethylene derivatives are almost all the same and the trend of the efficiencies is similar to that obtained by quenching triplet mercury, but is different from those obtained by quenching triplet benzene and acetone. In the present paper, we will present the details of the measurement and of the date obtained after the previous communication was reported.

Experimental

Research-grade acetylene, ethylene, propylene, isobutene, 1-butene, *trans*- and *cis*-2-butenes, trimethylethylene, tetramethylethylene, cyclohexene, methyl-

1) R. E. Rebbert and P. Ausloos, *J. Am. Chem. Soc.*, **87**, 5569 (1965).

2) G. A. Hanninger, Jr., and E. K. C. Lee, *J. Phys. Chem.*, **71**, 3104 (1967).

3) A. Morikawa and R. J. Cvetanović, *Can. J. Chem.*, **46**, 1813 (1968).

4) R. J. Cvetanović, "Progress in Reaction Kinetics," Vol. 2, ed. by G. Porter, Pergamon Press, Oxford (1964), p. 67.

5) D. F. Evans, *J. Chem. Soc.*, **1959**, 2753.

6) S. Tsunashima and S. Sato, This Bulletin, **40**, 2987 (1967).

acetylene, vinylacetylene, 1,3-butadiene, propane, and cyclopropane supplied by the Takachiho Shoji Co. were used after bulb-to-bulb distillations. The gas-chromatographic analyses showed that the impurities were less than 0.5%. *Trans*- and *cis*-2-pentenes supplied by the Takachiho Shoji Co. were used after separating them from each other by gas chromatography. Hydrogen supplied by the Suzuki Shokan Co. was used after passing it through a trap at the temperature of liquid nitrogen. The mass-spectrometric analyses of acetylene-d_2 synthesized from calcium carbide and deuterium oxide, and ethylene-d_4 synthesized from deuterium and acetylene-d_2[7] showed that the isotopical impurities were less than 2%.

The light source and the apparatus were similar to those reported on in a previous paper.[8]

For each experiment, the pressure of *cis*-2-butene was kept almost constant (22—32 mmHg), while the pressure of the quencher was varied. After irradiation with a cadmium lamp at 270±1°C, the products were analyzed by gas chromatography using a column packed with dimethylsulforane on celite (30 m long) supplied by Shimadzu Co. Immediately after each run, the light intensity of the 3261 Å resonance line was measured using the cadmium-photosensitized *cis-trans* isomerization of *cis*-2-butene on the assumption of the quantum yield being 0.5.[8]

Treatment of the Data

The competitive quenching method used is based on the following reactions[8]:

$$\mathrm{Cd} + h\nu \longrightarrow \mathrm{Cd}^* \qquad (1)$$
$$\mathrm{Cd}^* + \mathrm{C} \longrightarrow \mathrm{Cd} + \mathrm{B}^* \qquad k_b \qquad (2)$$
$$\mathrm{Cd}^* + \mathrm{T} \longrightarrow \mathrm{Cd} + \mathrm{B}^* \qquad k_b \qquad (3)$$
$$\mathrm{Cd}^* + \mathrm{X} \longrightarrow \mathrm{Cd} + \mathrm{X}' \qquad k_x \qquad (4)$$
$$\mathrm{B}^* + \mathrm{M} \longrightarrow \tfrac{1}{2}\mathrm{C} + \tfrac{1}{2}\mathrm{T} + \mathrm{M} \qquad (5)$$

where Cd* and B* represent, respectively, a triplet cadmium atom and an excited 2-butene molecule which isomerizes to *cis*- or *trans*-2-butene after collisional deactivation. T and C are *trans*- and *cis*-2-butenes respectively. X is a quencher molecule. As has been suggested in a previous paper,[8] the spontaneous emission process of a triplet cadmium is negligible compared with the process of the isomerization at the higher-than-1 mmHg 2-butene.

The steady-state treatment of the above mechanism gives the following relation;

$$R_0/R = 1 + (k_x/k_b)([\mathrm{X}]/[\mathrm{B}]) \qquad (\mathrm{I})$$

where R_0 and R represent the rates of the isomerization of 2-butene in the absence and in the presence of quencher molecules respectively. k_x and k_b are the efficiencies of a quencher and 2-butene for quenching triplet cadmium atoms respectively.

Equation (I) suggests that the plots of R_0/R as a function of the concentration ratio, [X]/[B], should give a straight line and that the slope of the straight line is relative quenching efficiency of the quencher competitive with 2-butene, k_b/k_x. In the present study, *cis*-2-butene is used as the detector compound.

In order to achieve good analytical accuracy as regards the values of initial rate of the isomerization, it was necessary to make higher conversions. The initial rate of the isomerization was estimated from the raw data using Eq. (II). Equation (II) was derived under the assumptions that the quantum yield of the isomerization of 2-butene is 0.5 and that the efficiency of *trans*-2-butene in quenching triplet cadmium is equal to that of *cis*-2-butene.[8]

$$R = (([\mathrm{C}] + [\mathrm{T}])/2t) \ln (([\mathrm{C}] + [\mathrm{T}])/([\mathrm{C}] - [\mathrm{T}])) \qquad (\mathrm{II})$$

Here, t represents the reaction time. [C] and [T] are the amounts of *cis*- and *trans*-2-butenes respectively obtained after the irradiation.

Results and Discussion

Quenching Data. The presence of quencher molecules retarded the isomerization of 2-butene. The R_0/R ratio was plotted against the concentration ratio, [X]/[B]. Figure 1 shows typical

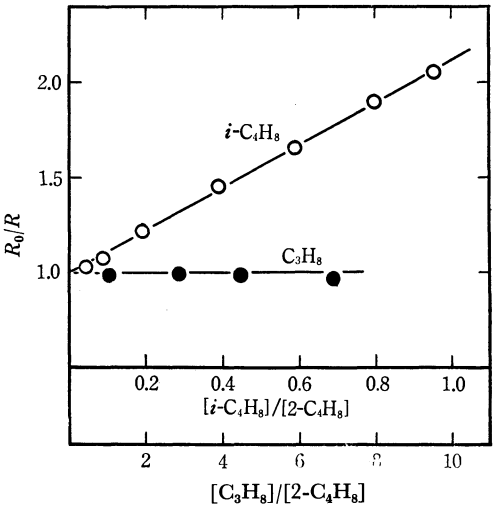

Fig. 1. The ratio of R_0/R as a function of the ratio of the pressure of competing quencher to that of *cis*-2-butene.

results obtained for propane and isobutene as competitive quenchers. Similar plots were obtained with all quenchers examined except for hydrogen. The case of hydrogen will be discussed later. The relative quenching efficiencies calculated from the slopes of the straight lines by the method of least squares are listed in Table 1. Table 1 also shows the relative quenching efficiencies for triplet cadmium,[9] mercury,[4] and

7) Y. Hatano, S. Shida and S. Sato, This Bulletin, **41**, 1120 (1968).

8) S. Tsunashima and S. Sato, *ibid.*, **41**, 284 (1968).

9) E. W. R. Steacie and D. J. LeRoy, *J. Chem. Phys.*, **11**, 164 (1943).

TABLE 1. RELATIVE QUENCHING EFFICIENCIES

Quencher	$Cd(^3P_1)$		$Hg(^3P_1)$	Benzene		Acetone
	This work	a′	b′	c	d	e′
Ethylene	1.03 ± 0.09	1.05	0.90	0.16 ± 0.02	0.25	0.16
Propylene	1.18 ± 0.04	1.06	0.93	0.51 ± 0.04	0.47	0.33
1-Butene	1.08 ± 0.09	1.16		0.50 ± 0.04	0.51	0.33
Isobutene	1.11 ± 0.03		0.95		1.27	0.66
cis-2-Butene	(1.00)	(1.00)	(1.00)	(1.00)	(1.00)	(1.00)
cis-2-Pentene	1.03 ± 0.07					1.4
Trimethylethylene	1.02 ± 0.10			1.7 ± 0.2	1.61	1.4
Tetramethylethylene	0.99 ± 0.11		0.95	3.0 ± 0.3	2.63	8.7
Butadiene	1.13 ± 0.04		0.93		15.	870.
Acetylene	1.03 ± 0.03	0.96	0.83			0.015
Methylacetylene	1.24 ± 0.09					
Vinylacetylene	1.25 ± 0.02					
Cyclohexene	1.02 ± 0.07					0.90
Ethylene-d_4	0.96 ± 0.01					
Acetylene-d_2	0.94 ± 0.10					
Propane	0 ± 0.01	10^{-4}	0.045	~0		
Cyclopropane	0 ± 0.02	0.026	0.033			

a′ Ref. 9, b′ Ref. 4, c Ref. 2, d Ref. 3, e′ Ref. 1

acetone,[1] efficiencies which were determined by the physical method, and also for triplet benzene,[2,3] which were determined by the competitive quenching method. The relative efficiencies for quenching triplet cadmium measured by the present method agree with those obtained by the physical method within the range of experimental error.

Unsaturated Hydrocarbons. In the case of unsaturated hydrocarbons, the experimental accuracy can be expected to be very high, because unsaturated hydrocarbons strongly quench triplet cadmium and small amounts of impurities and/or small amounts of side-reaction products do not affect the main reactions. No measurable amounts of side-reaction products were observed in any case examined except in the cases of methylacetylene and *cis*-2-pentene. In the case of methylacetylene, allene was obtained even in a dark reaction at 270±1°C. In the case of *cis*-2-pentene, *trans*-2-pentene was formed with a high quantum efficiency. The quantum yield of *trans*-2-pentene increased with an increase in the concentration of *cis*-2-pentene (Fig. 2).

More serious systematic errors may arise from the neglect of the following reaction, if they occur:

$$X' + C(\text{or } T) \longrightarrow X + B^* \quad (6)$$
$$X' + M \longrightarrow X + M \quad (7)$$

where X′ represents an energized quencher molecule which is formed by the reaction (4). If the reaction (6) is involved in the mechanism, *i. e.*, if X′ can transfer its energy to 2-butene and cause the *cis-trans* isomerization, the slope of the straight line of the plots of R_0/R *vs.* [X]/[B] does not show the relative quenching efficiency. However, the reaction (6) may be neglected in the case of the quencher examined here, because: (a) the plots of R_0/R as a function of the concentration ratio showed a straight line in every case; (b) in the case of 2-pentene, the total quantum yield of the isomer formations of 2-butene and 2-pentene was 0.5 at various concentration ratios of 2-pentene to 2-butene (Fig. 2); (c) the value of the relative quenching efficiency of 2-pentene as estimated

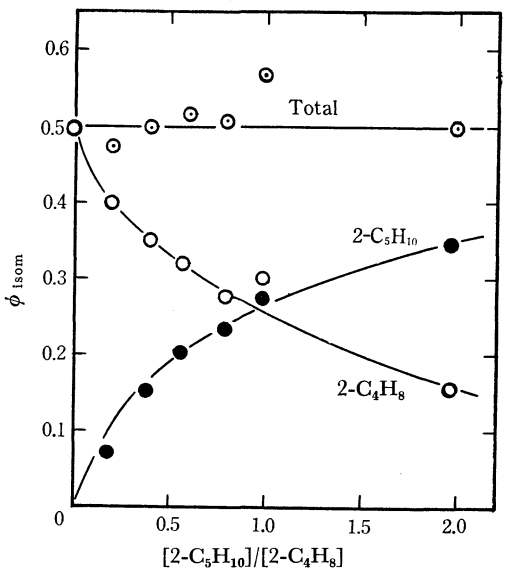

Fig. 2. Quantum yields of isomers formed in the reaction of the mixture of *cis*-2-butene and *cis*-2-pentene photosensitized by triplet cadmium at 270 ±1°C.

from the decrease in the rate of the isomerization of 2-butene is equal to that estimated from the increase in the rate of the isomerization of 2-pentene (Fig. 2); and (d) the quenching efficiencies determined by the present method agree well with those determined by the physical method* (Table 1).

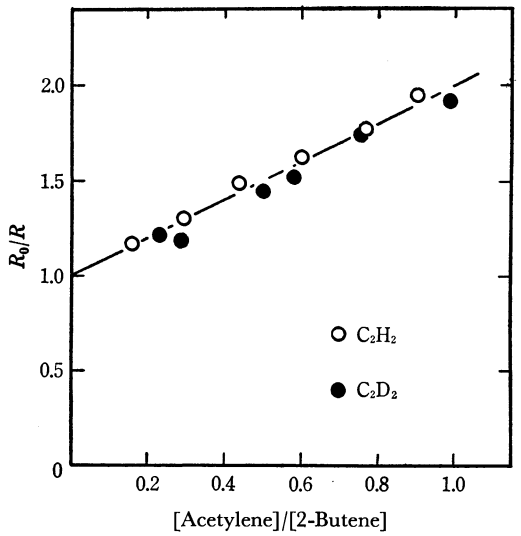

Fig. 3. Isotope effect in the quenching efficiency of acetylene for triplet cadmium atoms at 270±1°C.

Isotope Effects. As is shown in Fig. 3 and in Table 1 the isotope effect in quenching triplet cadmium atoms by acetylene or ethylene is negligibly small.

Comparison with Other Sensitizers. As is also shown in Table 1, the trend of quenching efficiencies obtained in the cadmium-photosensitization is similar to that obtained in the mercury-photosensitization and is different from those obtained in the benzene- and acetone-photosensitizations, in spite of the fact that the energy transferred in the cadmium-photosensitization is close to that transferred in the benzene-photosensitization.

The trend obtained in the acetone-photosensitization was explained by Rebbert and Ausloos as follows[1]: when the energy-transfer process is endothermic,*2 the quenching efficiency increases with a diminishment in the enthalpy change of the reaction. A similar consideration can explain the trend observed in the benzene-photosensitization, but not the trend in the cadmium-photosensitization, even though the quenching measurement of the cadmium-photosensitization were carried out at high temperatures (270±1°C). Morikawa and Cvetanović[3] found that the relative rates of the energy-transfer from the benzene triplet are affected by the temperature and that the apparent activation energy of the quenching efficiency of butadiene is about one kcal smaller than that of *cis*-2-butene. When the relative quenching efficiency of butadiene against *cis*-2-butene is extrapolated to 270°C using their data, it reduces to about 5. However, the relative quenching efficiency of butadiene in comparison with *cis*-2-butene in the cadmium-photosensitization is about unity. Although further experiments are needed, the difference in trend between benzene- and cadmium-photosensitizations is probably not due to the temperature.

Another possible explanation for the difference in the trend is the difference in the electronic property of the photosensitizer, as has been mentioned in a previous short communication.[6]

Saturated Hydrocarbons. The rate of the isomerization of *cis*-2-butene in the cadmium-photosensitization was scarcely affected at all by the addition of propane or cyclopropane. Non-condensible gases at the temperature of liquid nitrogen were not detected in the competitive quenching study. In the cadmium-photosensitized decomposition of pure propane, however, the formation of hydrogen was observed.[10] These results suggest that the quenching efficiency of saturated hydrocarbons is very low compared with that of olefins (Table 1). Therefore, in the reactions of pure saturated hydrocarbons, negligibly small amounts of impurities and side-reaction products may bring about a larger experimental error.

Table 2. Products from the reaction of the mixture of hydrogen and *cis*-2-butene photosensitized by triplet cadmium at 270±1°C[a]

Pressure of hydrogen mmHg	Products μmol				
	C_3H_6	C_4H_{10}	1-C_4H_8	*t*-C_4H_8[b]	*c*-C_4H_8[c]
0	0	0	0	4.70	30.4
8.92	0.60	0.50		4.41	28.5
11.9	0.74	0.57	0.11	4.16	27.6
16.6	0.90	0.77	0.22	4.20	27.9
21.2	1.10	0.82	0.19	3.95	26.7
26.8	1.21	0.97	0.22	3.91	27.6
31.7	1.32	1.13	0.26	3.95	25.5

a) Pressure of *cis*-2-butene: 25.1 mmHg
light intensity: 0.364 μE/min
irradiation time: 30 min
b) *trans*-2-butene
c) *cis*-2-butene

*1 The physical method is based on the measurement of the intensity of phosphorescence.[4]

*2 They compared the vertical triplet energies of olefins with the triplet energy of acetone. In the present authors' opinion, however, the lowest triplet energies of the olefins (which are twisted) should be used for the comparison. In this treatment, therefore, the energy transfer process will always be exothermic. However, their discussion of the trend is still relevant.

10) P. Agius and B. DeB Darwent, *J. Chem. Phys.*, **20**, 1679 (1952).

Hydrogen. As is shown in Table 2, propylene, *n*-butane, and 1-butene were formed together with *trans*-2-butene when a mixture of hydrogen and *cis*-2-butene was photosensitized by triplet cadmium. The quantum yields of the product formations increased with an increase in the pressure of hydrogen. The relative quenching efficiency of hydrogen could not be determined from Eq. (I) because of the large amounts of side-reaction products.

A possible reaction mechanism to account for the formations of propylene and *n*-butane is as follows:

$$Cd^* + C(\text{or } T) \longrightarrow Cd + B^* \qquad k_b \quad (2,3)$$
$$Cd^* + H_2 \rightarrow CdH + H \rightarrow Cd + 2H \qquad k_h \quad (8)$$
$$H + C_4H_8 \longrightarrow CH_3 + C_3H_6 \quad (9)$$
$$\longrightarrow C_4H_9 \quad (10)$$
$$2C_4H_9 \longrightarrow C_4H_8 + C_4H_{10} \quad (11)$$
$$\longrightarrow C_8H_{18} \quad (12)$$

where CdH formation is assumed following Bender and Olsen.[11] This compound, however, may decompose to cadmium and hydrogen atoms through collisions with other molecules, because the heat of the formation of CdH is estimated to be only 15.5 kcal.[10] Usually, the reaction (10) requires a collisional deactivation. Rabinovitch *et al.* found that the efficiency of 2-butene in deactivating the chemically-activated *s*-butyl radicals was much higher than that of hydrogen.[12] Therefore, the reaction (10) may be treated as pressure-independent under the present experimental conditions, *i. e.*, when the pressure of 2-butene is kept constant (25 mmHg) and when the pressure of hydrogen is varied (9—32 mmHg). The C_4H_8 formed by the reaction (11) involves 1-butene, *cis*-, and *trans*-2-butenes. This is the reason that the quenching efficiency of hydrogen can not be calculated with Eq. (I). In this experiment, the amounts of C_8-products formed by the reaction (12) have not been measured. This probably explains the material balance in Table 2.

The steady-state treatment of the above mechanism gives the following equations;

$$1/\phi(C_3H_6) = \tfrac{1}{2}(1+k_{10}/k_9)(1+(k_b/k_h)([B]/[H_2])) \quad (III)$$
$$1/\phi(C_4H_{10}) = (1+k_{12}/k_{11})(1+k_9/k_{10})(1+(k_b/k_h)([B]/[H_2])) \quad (IV)$$

where $\phi(C_3H_6)$ and $\phi(C_4H_{10})$ are the quantum yields of the propylene and *n*-butane formations respectively. k_h is the quenching efficiency of hydrogen, *i. e.*, the rate constant of the reaction (8). The relations of Eqs. (III) and (IV) are plotted in Fig. 4. The intercepts and the slopes of the straight lines in Fig. 4, as calculated by the method of least squares, are listed in Table 3. The

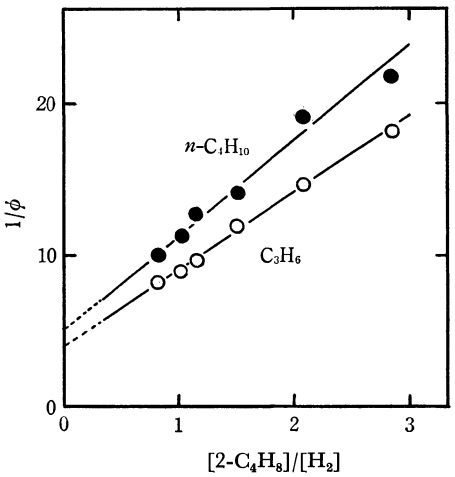

Fig. 4. Plots of the reciprocal of the quantum yields of propylene and *n*-butane formed in the reaction of hydrogen and *cis*-2-butene photosensitized by cadmium as a function of the concentration ratio of *cis*-2-butene to hydrogen.

TABLE 3. THE VALUES OF THE SLOPES AND THE INTERCEPTS OF THE STRAIGHT LINES IN Fig. 5

	Slope	Intercept	Slope/Intercept
$\phi(C_3H_6)$	5.1±0.2	4.0±0.3	1.3±0.1
$\phi(C_4H_{10})$	6.2±0.4	5.2±0.8	1.2±0.3

k_{12}/k_{11} value (the ratio of the disproportionation/recombination of *s*-butyl radicals) is estimated to be ~0.3. This value is appreciably lower than the value estimated by Kraus and Calvert (2.3),[13] but is close to that obtained by Rabinovitch *et al.* (~0.6).[12] The difference may be due to the difference in the source of the radical and/or to the neglect of other possible reactions of *s*-butyl radicals.

From the values of the intercepts and the slopes in Table 3, the relative quenching efficiency of hydrogen against *cis*-2-butene was calculated to be 0.83±0.18 (by using Eq. (IV)) and 0.79±0.08 (by using Eq. (III)). The agreement of these two values is satisfactory. Therefore, it can be said that the quenching efficiency of hydrogen is comparable to those of olefins.

11) P. Bender, *Phys. Rev.*, **36**, 1535 (1930), L. O. Olsen, *J. Chem. Phys.*, **6**, 307 (1938).

12) R. F. Kubin, B. S. Rabinovitch and R. E. Harrington, *J. Chem. Phys.*, **37**, 937 (1962), J. H. Current and B. S. Rabinovitch, *ibid.*, **41**, 2743 (1964).

13) J. W. Kraus and J. G. Calvert, *J. Am. Chem. Soc.*, **79**, 5921 (1957).

BULLETIN OF THE CHEMICAL SOCIETY OF JAPAN VOL. 42 334—343 (1969)

An X-Ray Determination of the Structure of Chamaecynenol

Hirotaka SHIMANOUCHI and Yoshio SASADA

Laboratory of Chemistry for Natural Products, Tokyo Institute of Technology, Ookayama, Meguro-ku, Tokyo

(Received June 12, 1968)

Crystals of chamaecynenol 4-bromo-3-nitrobenzoate, $C_{21}H_{22}O_4NBr$, are monoclinic, with two molecules in a unit cell of the dimensions, $a=10.47$, $b=14.08$, $c=6.75$ Å, and $\beta=101.8°$, and with the space group of $P2_1$. The intensities were recorded on multiple-film equi-inclination Weissenberg photographs and measured visually with a standard scale. The structure was determined by the heavy atom method. The positional and thermal parameters were refined by the least-squares method. The final R factor for the observed reflections is 0.090. The absolute configuration was also determined using anomalous dispersion effect of the bromine atom. It was thus established that chamaecynenol is 7β-ethynyl-4β-hydroxymethyl-10β-methyl-Δ^1-*cis*-octaline in the steroid conformation.

Recently, chamaecynenol $C_{14}H_{20}O$, a novel norsesquiterpenoid, was isolated from the Benihi tree (*Chamaecyparis formosensis* Matsum., Cupressaceae) as a minor constituent.[1] This is an interesting substance as an example of a natural acetylenic compound of terpenoid origin. From chemical and spectroscopic properties, the structure was suspected to be I of the non-steroid *cis*-decalin conformation. However, further chemical investigation was impossible due to too small a quantity of the sample. An X-ray analysis was undertaken in order to reveal such stereochemical details. A heavy atom derivative, chamaecynenol 4-bromo-3-nitrobenzoate, was prepared and supplied by Professor Takase and Dr. Asao.

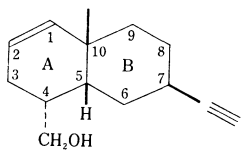

(I)

Experimental

The compound crystallizes from a benzene solution in the form of colorless plates elongated along the c axis. The unit cell dimensions were determined from zero-layer Weissenberg photographs about the b and the c axes, calibrated with superimposed Al powder photographs.

Equi-inclination Weissenberg photographs were taken at room temperature for the layer lines from 0 to 10 about the b axis and from 0 to 4 about c, using Cu$K\alpha$ radiation. The crystals used had the following maximum and minimum dimensions at right angles to the axis of rotation:

0.01 × 0.02 cm for the b axis rotation,
0.01 × 0.03 cm for the c axis rotation.

Intensities were estimated by visual comparison with a standard scale prepared with the same crystals. The multiple-film technique was used to correlate strong and weak reflections, ranging in relative intensities from 8000 to 1. Out of 1982 reflections recorded, about 190 were too weak to be measured. The corrections for the Lorentz and polarization factors were made as usual and those for variation in spot-size in higher layer photographs by the Phillips method.[2] The correction for absorption was neglected.

Crystal Data

The crystallographic and physical data obtained are: Chamaecynenol 4-bromo-3-nitrobenzoate $C_{21}H_{22}O_4NBr$, mp 179—180°C. Monoclinic, $a=10.47$Å, $b=14.08$ Å $c=6.75$ Å, $\beta=101.8°$. Absent spectra, ($0k0$) when k is odd. Space group, $P2_1$. Two molecules per unit cell. Volume of the unit cell, 974.0 Å^3. Density (by flotation), 1.49_4 g·cm^{-3}. Density (calculated), 1.47_4 g·cm^{-3}. Linear absorption coefficient for Cu$K\alpha$ radiation, $\mu=34.5$ cm^{-1}. Total number of electrons per unit cell, $F(000)=444$.

Structure Determination

The x and z coordinates of the bromine atom were obtained from the Harker section and the y coordinate was set arbitrarily as zero. The four images of the benzene ring were easily picked up by inspecting the sharpened Patterson function around the origin, but it was impossible to select the correct one from the two possible positions of the benzene ring which were related to each other by non-crystallographic two-fold axis in the crystal

1) K. Takase, S. Ibe, T. Asao and T. Nozoe, Private Communication.

2) D. C. Phillips, *ActaC ryst.*, **7**, 746 (1954).

through the bromine atom. The minimum function was formed based on Br–Br vector and it gave the peaks for seven carbon atoms (six ring carbons and a carbonyl carbon) and a nitrogen atom. A three-dimensional Fourier synthesis was made with the phases derived from these nine atoms. An approximate mirror plane was found at $y=0$, due to the predominant contribution from the bromine atom to the phases, and each correct light atom peak in the map was accompanied by a peak of considerable height at the position of mirror image. However, it was possible to assemble a plausible molecular model by selecting them. In order to examine more quantitatively the validity of the model, all possible intra- and intermolecular distances less than 4.0 Å were evaluated. Since no unusual surrounding was found for any of the atoms, the second electron-density distribution was evaluated by taking into account the contribution from all atoms. The resulting map clearly showed the peaks of reasonable height for these atoms, very few background noise peaks being observed.

The positional parameters thus obtained, together with isotropic temperature factors, initially set to 4 Å^2, were refined by block-diagonal matrix least-squares method. After three cycles of refinements,

Table 1. Final atomic coordinates and temperature factors

The anisotropic temperature factors are expressed in the form of $\exp\{-(B_{11}h^2+B_{22}k^2+B_{33}l^2+B_{12}hk+B_{13}hl+B_{23}kl)\}$.

Atom	x/a	y/b	z/c	B_{11}	B_{22}	B_{33}	B_{12}	B_{13}	B_{23}
Br	0.1158	0.0000	0.1399	0.01546	0.00456	0.02402	0.00263	−0.00365	0.00423

Atom	x/a	y/b	z/c	B (Å^2)	Atom	x/a	y/b	z/c	B (Å^2)
N	0.1197	0.2255	0.1075	4.26	C(9)	−0.4071	0.0139	−1.3202	3.39
O(1)	−0.1960	0.2078	−0.7406	3.26	C(10)	−0.5027	0.0927	−1.2739	3.01
O(2)	−0.1492	0.3406	−0.5494	3.79	C(11)	−0.2823	0.2685	−0.8920	3.73
O(3)	0.0662	0.2967	0.1661	5.86	C(12)	−0.2752	−0.0784	−0.7848	3.60
O(4)	0.2360	0.2007	0.1772	8.03	C(13)	−0.2461	−0.1349	−0.6531	4.55
C(1)	−0.5175	0.1630	−1.4436	3.83	C(14)	−0.6397	0.0454	−1.2659	5.10
C(2)	−0.4712	0.2503	−1.4307	4.16	C(15)	−0.1412	0.2542	−0.5703	2.94
C(3)	−0.3888	0.2918	−1.2385	4.15	C(16)	−0.0679	0.1908	−0.4100	2.79
C(4)	−0.3364	0.2130	−1.0839	2.81	C(17)	−0.0047	0.2336	−0.2360	2.74
C(5)	−0.4500	0.1386	−1.0672	2.81	C(18)	0.0556	0.1763	−0.0747	2.95
C(6)	−0.4092	0.0672	−0.8981	3.04	C(19)	0.0513	0.0774	−0.0846	3.07
C(7)	−0.3076	−0.0077	−0.9500	3.35	C(20)	−0.0082	0.0350	−0.2665	3.21
C(8)	−0.3675	−0.0604	−1.1503	4.41	C(21)	−0.0662	0.0917	−0.4307	3.31

Table 2. Estimated standard deviations

($\sigma(x)$, $\sigma(y)$ and $\sigma(z)$ in Å, $\sigma(B)$ in Å^2)

Atom	$\sigma(x)$	$\sigma(y)$	$\sigma(z)$	$\sigma(B_{11})$	$\sigma(B_{22})$	$\sigma(B_{33})$	$\sigma(B_{12})$	$\sigma(B_{13})$	$\sigma(B_{23})$
Br	0.0017	0.0032	0.0014	0.00017	0.00006	0.00029	0.00027	0.00035	0.00037

Atom	$\sigma(x)$	$\sigma(y)$	$\sigma(z)$	$\sigma(B)$	Atom	$\sigma(x)$	$\sigma(y)$	$\sigma(z)$	$\sigma(B)$
N	0.0125	0.0128	0.0121	0.24	C(9)	0.0118	0.0147	0.0114	0.24
O(1)	0.0087	0.0092	0.0086	0.16	C(10)	0.0123	0.0125	0.0121	0.22
O(2)	0.0095	0.0096	0.0094	0.18	C(11)	0.0139	0.0142	0.0138	0.25
O(3)	0.0121	0.0130	0.0119	0.26	C(12)	0.0137	0.0143	0.0135	0.24
O(4)	0.0152	0.0162	0.0152	0.36	C(13)	0.0161	0.0167	0.0159	0.30
C(1)	0.0144	0.0146	0.0137	0.26	C(14)	0.0169	0.0168	0.0168	0.34
C(2)	0.0151	0.0159	0.0140	0.28	C(15)	0.0126	0.0126	0.0123	0.21
C(3)	0.0150	0.0158	0.0148	0.27	C(16)	0.0121	0.0119	0.0118	0.20
C(4)	0.0120	0.0125	0.0117	0.20	C(17)	0.0119	0.0119	0.0117	0.20
C(5)	0.0119	0.0122	0.0117	0.21	C(18)	0.0125	0.0122	0.0122	0.21
C(6)	0.0127	0.0127	0.0123	0.22	C(19)	0.0126	0.0127	0.0124	0.22
C(7)	0.0113	0.0177	0.0109	0.21	C(20)	0.0129	0.0127	0.0126	0.22
C(8)	0.0159	0.0160	0.0156	0.29	C(21)	0.0130	0.0132	0.0128	0.23

TABLE 3. OBSERVED AND CALCULATED STRUCTURE FACTORS

H	FO	FC	H	FO	FC	H	FO	FC	H	FO	FC	H	FO	FC	H	FO	FC	H	FO	FC	H	FO	FC
K,L= 0	0		-10	0	4	3	40	37	3	14	9	0	17	15	-10	6	5	-9	12	13	0	3	4	-8	7	8
1	46	61	-9	0	3	4	41	43	4	50	47	1	13	11	-9	3	4	-8	7	6	1	11	11	-7	10	10
2	39	39	-8	0	1	5	22	22	5	21	20	2	10	6	-8	5	4	-7	17	15	2	14	15	-6	7	6
3	18	18	-7	3	2	6	5	3	6	12	12	3	21	20	-7	12	12	-6	17	17	3	7	7	-5	10	11
4	35	35	-6	8	7	7	14	15	7	16	17	4	11	12	-6	12	12	-5	33	32	4	6	6	-4	11	9
5	36	34	-5	13	15	8	19	19	8	14	15	5	10	7	-5	15	15	-4	16	16	5	9	9	-3	9	9
6	10	10	-4	4	5	9	9	11	9	7	8	6	8	9	-4	3	4	-3	35	31	6	15	13	-2	27	30
7	0	3	-3	15	15	10	8	8	10	7	8	7	8	10	-3	23	26	-2	35	33	K,L=	4	7	-1	19	18
8	16	16	-2	30	31	11	6	6	11	0	3	8	7	6	-2	37	38	-1	70	74	-7	2	2	0	4	7
9	3	1	-1	28	25	K,L=	1	3	12	0	1	K,L=	2	6	-1	36	37	0	49	53	-6	0	3	1	25	24
10	3	3	0	19	16	-11	0	2	K,L=	2	1	-9	0	2	0	65	63	1	5	0	-5	0	2	2	25	25
11	0	3	1	28	26	-10	15	18	-12	2	0	-8	0	1	1	24	21	2	51	51	-4	8	10	3	13	13
12	0	1	2	28	24	-9	5	10	-11	5	6	-7	7	8	2	22	22	3	40	43	-3	8	11	4	12	12
K,L= 0		1	3	17	17	-8	18	18	-10	8	8	-6	7	8	3	37	38	4	30	32	-2	0	0	5	7	7
-12	0	4	4	12	11	-7	21	23	-9	0	6	-5	3	4	4	26	28	5	21	22	-1	8	8	6	18	19
-11	0	3	5	9	10	-6	17	18	-8	6	7	-4	14	14	5	6	7	6	12	14	0	11	12	7	7	8
-10	9	11	6	10	9	-5	16	15	-7	6	6	-3	14	13	6	15	15	7	20	22	1	5	7	8	0	1
-9	12	14	7	10	9	-4	19	19	-6	23	20	-2	16	16	7	12	13	8	13	13	2	0	2	9	6	4
-8	8	9	8	2	2	-3	21	20	-5	41	42	-1	12	9	8	3	3	9	0	0	3	6	5	K,L=	5	5
-7	11	14	K,L=	0	6	-2	38	38	-4	37	37	0	24	22	9	4	4	10	3	5	4	5	5	-9	7	8
-6	32	27	-9	0	3	-1	34	31	-3	42	36	1	19	19	10	5	5	11	3	6	K,L=	4	8	-8	10	13
-5	25	25	-8	6	7	0	12	13	-2	65	61	2	12	12	K,L=	3	4	K,L=	4	2	-3	3	2	-7	8	9
-4	12	12	-7	7	8	1	28	27	-1	35	35	3	3	2	-11	4	4	-10	4	6	-2	5	6	-6	7	7
-3	103	104	-6	3	1	2	38	34	0	46	50	4	7	5	-10	0	2	-9	0	0	-1	5	5	-5	10	10
-2	26	25	-5	3	3	3	26	25	1	4	6	5	7	8	-9	0	5	-8	8	8	0	5	6	-4	14	15
-1	41	45	-4	16	17	4	20	19	2	43	42	6	6	7	-8	10	10	-7	20	21	1	4	6	-3	15	15
0	62	62	-3	9	12	5	0	2	3	50	51	7	5	4	-7	9	11	-6	10	9	K,L=	5	0	-2	8	8
1	3	2	-2	20	19	6	22	21	4	16	18	K,L=	2	7	-6	12	14	-5	39	39	1	39	41	-1	16	17
2	48	47	-1	5	6	7	27	25	5	0	2	-9	3	5	-5	0	0	-4	31	28	2	40	42	0	16	16
3	39	43	0	16	13	8	24	21	6	22	22	-8	7	7	-4	20	21	-3	39	41	3	30	28	1	16	18
4	35	41	1	12	10	9	5	6	7	20	22	-7	4	3	-3	34	36	-2	42	45	4	5	3	2	14	12
5	13	11	2	4	4	10	0	4	8	9	10	-6	3	1	-2	20	21	-1	7	7	5	19	18	3	7	6
6	0	1	3	6	2	11	5	5	9	5	3	-5	3	4	-1	2	0	0	26	26	6	28	30	4	11	12
7	25	25	4	3	0	K,L=	1	4	10	7	7	-4	9	8	0	18	18	1	54	52	7	28	29	5	13	11
8	12	10	5	6	6	-11	4	7	11	7	7	-3	6	7	1	37	34	2	82	85	8	0	2	6	7	6
9	7	7	6	13	11	-10	7	10	12	3	5	-2	0	1	2	34	32	3	38	39	9	8	10	7	4	4
10	4	3	7	4	4	-9	0	2	K,L=	2	2	-1	8	7	3	10	11	4	10	10	10	0	3	8	10	7
11	0	3	K,L=	0	7	-8	5	5	-11	5	8	0	8	9	4	7	8	5	11	9	11	4	5	K,L=	5	6
12	5	5	-9	2	3	-7	8	8	-10	3	3	1	7	8	5	11	10	6	16	15	12	0	2	-6	3	3
K,L=	0	2	-8	6	7	-6	14	14	-9	3	3	2	6	6	6	14	16	7	15	15	K,L=	5	1	-5	10	12
-12	3	2	-7	0	2	-5	3	4	-8	22	22	3	7	5	7	7	8	8	7	7	-12	4	7	-4	0	4
-11	3	2	-6	0	6	-4	12	11	-7	18	17	4	9	8	8	3	3	9	6	5	-11	7	7	-3	10	9
-10	4	2	-5	0	2	-3	16	14	-6	41	40	K,L=	2	8	K,L=	3	5	10	7	8	-10	3	3	-2	10	11
-9	12	12	-4	11	12	-2	33	35	-5	19	17	-5	6	8	-10	0	3	11	6	6	-9	8	9	-1	17	18
-8	34	32	-3	11	13	-1	12	11	-4	25	27	-4	2	4	-9	0	2	K,L=	4	3	-8	9	11	0	13	12
-7	21	17	-2	0	0	0	19	16	-3	31	31	-3	0	2	-8	10	10	-10	0	1	-7	15	15	1	8	7
-6	33	26	-1	7	8	1	27	24	-2	21	19	-2	5	6	-7	5	7	-9	4	6	-6	13	13	2	6	6
-5	61	64	0	12	12	2	43	40	-1	24	20	-1	6	7	-6	3	2	-8	20	20	-5	21	17	3	7	8
-4	21	21	1	7	8	3	11	10	0	21	20	0	4	5	-5	0	2	-7	7	6	-4	17	18	4	9	9
-3	4	10	2	8	7	4	14	11	1	8	7	1	2	7	-4	16	15	-6	4	4	-3	68	67	5	4	4
-2	76	73	3	10	9	5	8	9	2	58	54	K,L=	3	0	-3	6	4	-5	11	11	-2	35	36	K,L=	5	7
-1	49	51	4	6	7	6	20	20	3	38	34	1	42	43	-2	0	0	-4	18	18	-1	11	9	-6	4	5
0	28	25	5	12	10	7	5	5	4	14	13	2	66	68	-1	16	15	-3	30	33	0	36	38	-5	3	5
1	56	56	K,L=	0	8	8	0	1	5	25	24	3	37	39	0	11	11	-2	22	23	1	33	35	-4	0	1
2	48	50	-5	4	6	9	4	4	6	16	17	4	19	16	1	24	23	-1	40	39	2	21	25	-3	3	3
3	42	38	-4	0	1	10	5	6	7	9	11	5	13	11	2	3	4	0	36	36	3	20	18	-2	9	9
4	0	1	-3	3	4	K,L=	1	5	8	0	1	6	15	15	3	10	11	1	38	40	4	30	33	-1	4	6
5	10	13	-2	0	4	-8	9	9	9	5	5	7	17	14	4	18	18	2	29	26	5	18	20	0	0	2
6	27	28	-1	9	8	-7	0	5	10	7	6	8	16	18	5	10	12	3	10	9	6	20	19	1	6	6
7	24	21	0	0	1	-6	0	3	11	5	5	9	7	7	6	9	10	4	19	18	7	18	20	2	6	7
8	0	2	1	0	0	-5	15	14	K,L=	2	3	10	5	6	7	2	2	5	27	28	8	10	10	3	12	11
9	15	15	2	6	7	-4	20	21	-11	3	1	11	0	2	8	3	4	6	12	12	9	9	8	4	7	5
10	18	19	K,L=	1	0	-3	19	18	-10	3	2	12	5	6	K,L=	3	6	7	3	4	10	7	8	K,L=	5	8
11	10	9	1	27	22	-2	8	7	-9	3	4	K,L=	3	1	-8	6	8	8	9	8	11	0	2	-3	3	5
K,L=	0	3	2	89	91	-1	17	15	-8	8	6	-12	4	3	-7	3	4	9	10	10	K,L=	5	2	-2	0	2
-12	8	9	3	44	39	0	33	32	-7	14	16	-11	3	4	-6	7	8	10	3	3	-11	0	2	-1	4	4
-11	4	1	4	26	25	1	31	27	-6	0	5	-10	5	6	-5	8	9	K,L=	4	4	-10	3	5	0	5	6
-10	0	2	5	38	34	2	37	32	-5	11	12	-9	6	6	-4	5	4	-10	0	1	-9	10	12	K,L=	6	0
-9	4	5	6	25	26	3	22	18	-4	34	35	-8	7	6	-3	6	6	-9	4	3	-8	11	14	0	43	44
-8	32	34	7	18	19	4	8	7	-3	29	25	-7	11	11	-2	12	11	-8	4	8	-7	0	3	1	37	39
-7	9	7	8	9	11	5	14	13	-2	21	20	-6	19	19	-1	15	15	-7	4	8	-6	15	16	2	16	14
-6	0	1	9	11	11	6	5	5	-1	16	17	-5	34	31	0	13	12	-6	17	19	-5	26	23	3	29	26
-5	21	18	10	5	5	7	0	2	0	15	13	-4	42	41	1	3	4	-5	24	27	-4	19	18	4	34	34
-4	35	32	11	5	5	8	7	6	1	36	34	-3	63	62	2	10	10	-4	25	28	-3	35	33	5	23	24
-3	35	33	12	0	1	K,L=	1	6	2	20	17	-2	33	29	3	15	16	-3	17	17	-2	11	11	6	10	10
-2	11	15	K,L=	1	1	-6	10	12	3	8	6	-1	33	32	4	11	13	-2	11	12	-1	33	37	7	4	5
-1	26	26	-11	0	1	-5	4	5	4	22	20	0	44	54	5	6	6	-1	21	23	0	51	51	8	4	5
0	61	58	-10	4	2	-4	12	12	5	25	25	1	58	62	6	3	3	0	26	25	1	23	24	9	11	12
1	50	52	-9	9	8	-3	4	5	6	14	16	2	49	57	K,L=	3	7	1	7	6	2	18	17	10	0	2
2	20	20	-8	14	14	-2	13	12	7	9	10	3	15	13	-6	6	7	2	5	4	3	24	23	11	0	2
3	7	7	-7	29	28	-1	24	22	8	10	10	4	36	40	-5	0	1	3	24	24	4	37	42	12	0	3
4	26	27	-6	18	16	0	11	9	9	11	13	5	58	60	-4	8	8	4	21	22	5	14	15	K,L=	6	1
5	28	29	-5	31	30	1	9	8	10	2	1	6	28	29	-3	11	10	5	24	22	6	0	2	-12	0	1
6	18	15	-4	58	49	2	8	7	11	3	3	7	9	7	-2	11	11	6	6	4	7	15	15	-11	2	4
7	4	0	-3	100	88	3	13	13	K,L=	2	4	8	0	4	-1	4	6	7	5	5	8	14	14	-10	5	6
8	0	4	-2	157	151	4	13	13	-10	9	11	9	10	11	0	3	1	8	12	11	9	8	8	-9	7	8
9	4	4	-1	26	20	5	3	4	-9	8	9	10	4	4	1	7	6	9	3	3	10	0	3	-8	6	6
10	2	0	0	9	14	6	0	1	-8	3	4	11	0	1	2	11	10	K,L=	4	5	11	0	1	-7	14	14
11	2	0	1	67	66	7	9	5	-7	0	4	K,L=	3	2	3	5	7	-10	6	7	K,L=	5	3	-6	21	20
K,L=	0	4	2	31	27	K,L=	1	7	-6	14	16	-12	6	7	4	6	6	-9	4	2	-11	4	7	-5	24	22
-12	5	5	3	8	6	-6	11	13	-5	17	18	-11	0	1	K,L=	3	8	-8	0	3	-10	0	5	-4	12	9
-11	4	4	4	9	8	-5	0	3	-4	20	19	-10	0	4	-6	2	5	-7	6	7	-9	5	8	-3	17	14
-10	7	9	5	21	22	-4	5	6	-3	12	10	-9	10	10	-5	3	4	-6	13	13	-8	8	10	-2	30	30
-9	3	1	6	21	20	-3	0	4	-2	22	21	-8	7	6	-4	4	3	-5	7	8	-7	0	3	-1	48	50
-8	0	2	7	3	2	-2	13	12	-1	28	28	-7	13	14	-3	4	4	-4	7	9	-6	21	21	0	19	20
-7	0	0	8	3	3	-1	7	8	0	25	23	-6	23	23	-2	4	5	-3	13	15	-5	22	22	1	11	12
-6	10	9	9	11	11	0	3	2	1	7	9	-5	30	33	-1	0	1	-2	14	13	-4	8	10	2	17	19
-5	12	10	10	7	7	1	10	10	2	14	13	-4	31	32	0	3	3	-1	23	25	-3	21	21	3	29	33
-4	11	8	11	4	3	2	6	7	3	25	26	-3	5	7	1	6	8	0	10	8	-2	26	30	4	19	20
-3	0	1	12	6	7	3	8	8	4	28	28	-2	29	34	K,L=	4	0	1	14	13	-1	51	55	5	12	14
-2	16	15	K,L=	1	2	4	3	4	5	14	10	-1	41	46	0	75	96	2	24	23	0	24	22	6	18	19
-1	36	38	-11	3	6	5	6	5	6	12	9	0	61	60	1	47	49	3	12	13	1	18	14	7	14	16
0	34	31	-10	11	12	K,L=	1	8	7	6	6	1	29	28	2	26	27	4	11	11	2	14	16	8	0	1
1	12	11	-9	4	5	-6	5	5	8	9	12	2	19	19	3	8	7	5	4	5	3	16	20	9	7	8
2	13	11	-8	5	5	-5	4	4	9	2	3	3	9	9	4	49	49	6	7	8	4	12	12	10	3	4
3	23	22	-7	13	14	-4	4	5	K,L=	2	5	4	28	31	5	20	20	7	12	10	5	5	7	11	3	4
4	46	45	-6	34	33	-3	7	6	-9	0	1	5	18	19	6	0	1	8	5	4	6	8	11	K,L=	6	2
5	38	33	-5	39	34	-2	0	2	-8	0	1	6	6	6	7	14	17	K,L=	4	6	7	23	23	-12	3	3
6	24	22	-4	40	38	-1	2	0	-7	8	8	7	7	6	8	16	16	-7	0	4	8	8	7	-11	4	5
7	8	6	-3	23	21	0	0	3	-6	13	14	8	8	8	9	14	16	-6	0	2	9	4	6	-10	0	2
8	9	7	-2	9	6	1	8	8	-5	5	5	9	9	10	10	10	11	-5	3	6	10	3	3	-9	3	2
9	9	8	-1	36	36	K,L=	2	0	-4	0	4	10	4	4	11	4	4	-4	6	6	K,L=	5	4	-8	4	3
K,L=	0	5	0	76	73	0	43	54	-3	13	13	11	3	4	K,L=	4	1	-3	15	18	-11	5	7	-7	14	11
-12	0	1	1	32	31	1	7	6	-2	16	13	K,L=	3	3	-11	2	3	-2	3	5	-10	0	5	-6	17	15
-11	0	0	2	17	11	2	59	57	-1	22	19	-11	0	3	-10	10	11	-1	11	10	-9	3	3	-5	20	18

TABLE 3. (Continued)

H	FO	FC	H	FO	FC	H	FO	FC	H	FO	FC	H	FO	FC	H	FO	FC	H	FO	FC	H	FO	FC	H	FO	FC
-4	20	19	7	11	10	0	8	8	8	10	10	2	4	5	7	8	10	1	19	19	-8	4	3	6	7	5	2	7	5
-3	31	32	8	7	7	1	0	4	K,L=	8	5	3	20	23	8	3	3	2	10	8	-7	5	3	7	9	7	3	8	7
-2	33	34	9	4	5	2	4	5	-10	3	5	4	9	9	9	0	1	3	10	9	-6	4	3	K,L=	14	2	4	6	5
-1	18	19	10	2	2	3	11	10	-9	2	1	5	9	8	K,L=	10	3	4	14	15	-5	5	3	-8	0	6	K,L=	16	2
0	15	14	K,L=	7	1	4	9	8	-8	2	3	6	8	10	-9	4	5	5	12	12	-4	6	6	-7	0	4	-5	0	2
1	38	39	-10	4	6	5	5	5	-7	4	6	7	13	13	-8	5	3	6	0	3	-3	6	5	-6	3	4	-4	3	4
2	31	33	-9	6	5	K,L=	7	7	-6	12	13	8	7	7	-7	0	2	7	3	4	-2	3	3	-5	3	1	-3	5	5
3	30	30	-8	12	12	-3	7	8	-5	14	16	9	0	1	-6	0	5	8	6	5	-1	11	11	-4	5	6	-2	11	10
4	12	12	-7	12	12	-2	9	11	-4	7	9	K,L=	9	4	-5	6	7	9	7	5	0	12	13	-3	15	15	-1	3	3
5	2	1	-6	7	4	-1	7	8	-3	8	9	-9	0	1	-4	12	12	K,L=	11	3	1	9	8	-2	15	15	0	3	2
6	25	28	-5	15	14	0	2	3	-2	11	10	-8	6	6	-3	13	13	-10	4	4	2	5	5	-1	8	7	1	5	6
7	10	11	-4	18	18	1	9	7	-1	9	10	-7	8	11	-2	17	19	-9	4	3	3	10	10	0	7	6	2	8	7
8	4	4	-3	15	13	2	6	7	0	9	6	-6	8	10	-1	8	8	-8	2	3	4	15	15	1	12	12	3	8	6
9	10	10	-2	11	7	3	5	8	1	3	4	-5	7	5	0	16	15	-7	3	3	5	4	4	2	9	10	4	0	3
10	3	4	-1	24	23	K,L=	8	0	2	14	15	-4	11	10	1	32	31	-6	0	3	6	4	2	3	5	6	K,L=	16	3
11	3	4	0	24	26	0	23	25	3	12	13	-3	18	19	2	21	23	-5	14	14	K,L=	13	0	4	3	1	-4	5	4
K,L=	6	3	1	34	41	1	21	22	4	5	6	-2	17	16	3	0	1	-4	5	5	1	15	12	5	4	3	-3	5	5
-11	0	2	2	22	23	2	10	7	5	5	4	-1	22	21	4	7	8	-3	7	5	2	27	27	6	12	9	-2	0	1
-10	2	4	3	21	20	3	28	28	6	6	6	0	9	11	5	11	14	-2	15	15	-2	16	15	7	1	5	-1	2	3
-9	7	8	4	19	18	4	23	20	7	8	8	1	14	13	6	9	10	-1	4	2	4	4	5	K,L=	14	3	0	6	6
-8	6	7	5	37	37	5	26	25	K,L=	8	6	2	16	17	7	2	3	0	11	9	5	7	5	-7	0	0	1	5	4
-7	10	9	6	7	8	6	7	4	-8	3	4	3	7	7	8	7	5	1	20	17	6	10	9	-6	5	5	2	7	6
-6	4	3	7	14	15	7	21	20	-7	0	3	4	7	8	K,L=	10	4	2	20	17	7	7	6	-5	2	2	K,L=	17	0
-5	15	15	8	7	7	8	12	13	-6	0	1	5	9	10	-9	3	6	3	22	22	8	0	2	-4	7	8	1	10	8
-4	20	17	9	7	7	9	14	14	-5	3	2	6	10	10	-8	2	4	4	12	12	K,L=	13	1	-3	5	6	2	12	11
-3	34	34	10	2	4	10	6	4	-4	4	5	7	8	7	-7	5	5	5	0	1	-8	4	4	-2	6	6	3	9	8
-2	9	7	K,L=	7	2	11	2	2	-3	6	7	K,L=	9	5	-6	6	6	6	8	7	-7	9	7	-1	2	3	K,L=	17	1
-1	21	23	-10	2	3	K,L=	8	1	-2	4	6	-9	6	6	-5	11	12	7	11	9	-6	3	2	0	10	10	-3	7	7
0	19	19	-9	3	2	-11	7	7	-1	5	5	-8	6	5	-4	13	13	8	6	4	-5	6	7	1	14	14	-2	3	2
1	27	28	-8	4	4	-10	8	8	0	8	10	-7	6	6	-3	10	9	K,L=	11	4	-4	15	15	2	10	9	-1	2	1
2	19	18	-7	7	6	-9	9	9	1	11	13	-6	7	7	-2	19	19	-9	1	3	-3	10	10	3	2	2	0	7	5
3	16	15	-6	4	2	-8	0	1	2	8	9	-5	9	9	-1	26	28	-8	9	7	-2	10	10	4	9	8	1	8	7
4	17	18	-5	17	16	-7	4	4	3	7	7	-4	10	10	0	13	15	-7	7	6	-1	10	9	5	9	9	2	9	8
5	20	23	-4	24	23	-6	14	14	4	7	6	-3	9	8	1	9	9	-6	2	3	0	15	14	K,L=	14	4	K,L=	17	2
6	7	8	-3	11	8	-5	24	24	5	6	5	-2	6	5	2	8	9	-5	6	4	1	14	16	-6	8	1	-3	6	6
7	8	8	-2	18	16	-4	20	18	K,L=	8	7	-1	7	8	3	10	11	-4	10	10	2	14	13	-5	5	6	-2	0	2
8	9	9	-1	30	32	-3	14	12	-6	0	1	0	9	8	4	11	14	-3	12	13	3	5	5	-4	5	6	-1	3	5
9	5	6	0	35	36	-2	19	20	-5	3	4	1	12	12	5	9	9	-2	7	8	4	8	8	-3	0	1	0	7	7
10	5	6	1	19	19	-1	31	31	-4	5	6	2	6	7	6	4	4	-1	10	9	5	13	11	-2	9	7	1	2	3
K,L=	6	4	2	7	7	0	12	12	-3	5	6	3	7	7	7	3	3	0	8	6	6	9	8	-1	10	8	1	2	3.
-11	4	5	3	3	4	1	6	6	-2	0	1	4	8	9	K,L=	10	5	1	13	15	7	9	7	0	10	10			
-10	6	6	4	27	30	2	23	22	-1	4	5	5	10	9	-7	6	5	2	8	9	8	3	3	1	4	4			
-9	4	3	5	23	25	3	14	14	0	6	7	6	9	7	-6	2	3	3	4	4	K,L=	13	2	2	8	7			
-8	6	6	6	7	7	4	16	16	1	7	8	K,L=	9	6	-5	0	1	4	2	3	-9	0	1	3	4	4			
-7	4	4	7	3	4	5	12	11	2	2	2	-7	3	4	-4	6	6	5	7	6	-8	0	3	4	6	7			
-6	11	10	8	5	8	6	13	13	K,L=	9	0	-6	0	3	-3	0	2	6	7	7	-7	3	4	K,L=	15	0			
-5	18	18	9	8	7	7	12	12	1	14	14	-5	5	5	-2	9	10	7	0	4	-6	3	3	1	0	1			
-4	10	10	10	2	2	8	6	7	2	21	24	-4	3	3	-1	9	8	K,L=	12	0	-5	9	9	2	13	13			
-3	14	15	K,L=	7	3	9	6	7	3	19	20	-3	5	4	0	4	4	0	24	25	-4	12	14	3	8	7			
-2	18	18	-9	3	3	10	2	4	4	3	2	-2	7	7	1	7	9	1	15	15	-3	10	10	4	2	3			
-1	23	24	-8	4	5	K,L=	8	2	5	14	13	-1	13	13	2	8	10	2	11	10	-2	9	9	5	4	4			
0	20	20	-7	14	14	-11	0	1	6	19	20	0	8	9	3	9	10	3	16	15	-1	10	9	6	6	5			
1	13	13	-6	15	17	-10	2	4	7	22	22	1	3	3	4	4	4	4	13	12	0	17	17	K,L=	15	1			
2	8	8	-5	15	18	-9	3	1	8	4	3	2	3	5	5	5	5	5	21	20	1	14	13	-7	6	6			
3	4	4	-4	7	4	-8	4	2	9	5	5	3	8	9	6	9	8	6	0	2	2	4	4	-6	3	4			
4	19	19	-3	30	30	-7	11	11	10	4	3	4	11	10	K,L=	10	6	7	8	6	3	13	12	-5	2	2			
5	11	11	-2	6	4	-6	10	11	11	4	5	K,L=	9	7	-7	6	7	8	6	5	4	17	15	-4	3	1			
6	3	3	-1	37	40	-5	8	6	K,L=	9	1	-3	2	4	-6	5	6	9	9	6	5	8	9	-3	8	7			
7	6	6	0	25	24	-4	18	17	-11	5	6	-2	5	6	-5	0	2	K,L=	12	1	6	0	4	-2	12	9			
8	8	8	1	13	14	-3	28	27	-10	7	6	-1	7	7	-4	5	5	-9	0	2	7	0	4	-1	7	6			
9	6	6	2	28	30	-2	28	28	-9	8	9	0	1	0	-3	9	9	-8	3	5	K,L=	13	3	0	17	16			
K,L=	6	5	3	20	19	-1	20	19	-8	7	7	1	0	4	-2	5	6	-7	3	4	-8	0	2	1	13	11			
-9	0	1	4	13	15	0	8	8	-7	11	11	2	2	5	-1	5	4	-6	14	13	-7	4	3	2	11	11			
-8	0	0	5	3	6	1	29	31	-6	11	12	K,L=	10	0	0	6	6	-5	10	11	-6	10	11	3	4	4			
-7	0	1	6	8	7	2	44	47	-5	4	4	0	32	30	1	10	10	-4	9	8	-5	6	6	4	8	2			
-6	9	9	7	4	7	3	30	32	-4	16	16	1	23	25	2	10	9	-3	10	10	-4	3	4	5	7	6			
-5	7	4	8	2	0	4	13	13	-3	32	31	2	8	6	3	0	3	-2	17	15	-3	8	8	6	3	3			
-4	12	12	9	3	1	5	7	6	-2	25	23	3	10	8	K,L=	10	7	-1	18	20	-2	14	14	K,L=	15	2			
-3	12	13	K,L=	7	4	6	15	17	-1	4	1	4	18	19	-3	2	4	0	14	12	-1	14	14	-5	7	7			
-2	18	17	-9	0	3	7	13	14	0	27	30	5	20	19	-2	4	4	1	8	6	0	6	5	-5	3	5			
-1	20	19	-8	4	4	8	0	0	1	36	37	6	13	15	-1	4	5	2	15	15	1	6	4	-4	3	7			
0	10	6	-7	9	9	9	3	2	2	17	18	7	11	11	K,L=	11	0	3	5	6	2	9	10	-3	3	3			
1	10	9	-6	4	2	10	7	6	3	6	6	8	5	5	1	12	11	4	9	7	3	11	13	-2	3	2			
2	16	16	-5	12	11	K,L=	8	3	4	29	31	9	7	8	2	22	22	5	0	3	4	10	9	-1	9	9			
3	15	17	-4	17	18	-11	0	2	5	32	31	10	6	5	3	16	15	6	0	0	5	3	3	0	9	8			
4	8	8	-3	29	30	-10	0	0	6	15	16	K,L=	10	1	4	8	5	7	8	7	6	9	7	1	0	5			
5	4	5	-2	4	2	-9	4	6	7	13	12	-10	2	3	5	6	5	8	6	6	K,L=	13	4	2	3	2			
6	8	9	-1	0	4	-8	7	8	8	6	6	-9	9	9	6	10	12	K,L=	12	2	-7	2	3	3	8	6			
7	7	7	0	12	12	-7	6	7	9	7	8	-8	8	8	7	4	4	-9	0	1	-6	0	1	4	8	8			
K,L=	6	6	1	19	19	-6	8	7	10	3	2	-7	8	7	8	8	6	-8	4	3	-5	0	2	5	8	5			
-9	3	3	2	20	21	-5	17	18	K,L=	9	2	-6	4	3	9	6	5	7	8	10	-4	7	8	K,L=	15	3			
-8	3	3	3	15	16	-4	13	14	-10	0	1	-5	19	19	10	7	7	-6	5	9	-3	7	7	-6	6	7			
-7	6	8	4	4	6	-3	32	32	-9	5	7	-4	6	4	K,L=	11	1	-5	4	7	-2	10	9	-5	6	6			
-6	0	2	5	9	9	-2	4	4	-8	7	7	-3	7	7	-10	0	1	-4	4	5	-1	11	9	-4	4	4			
-5	3	4	6	11	14	-1	21	20	-7	3	4	-2	16	15	-9	8	8	-3	10	9	0	2	3	-3	0	0			
-4	9	7	7	7	8	0	11	12	-6	11	12	-1	31	32	-8	11	10	-2	19	20	1	11	11	-2	2	4			
-3	11	11	8	4	3	1	23	24	-5	18	16	0	23	24	-7	10	11	-1	10	9	2	12	11	-1	5	7			
-2	5	4	K,L=	7	5	2	16	16	-4	18	18	1	9	10	-6	5	3	0	12	9	3	7	7	0	0	3			
-1	5	4	-9	2	2	3	6	6	-3	10	9	2	21	21	-5	8	9	1	10	8	4	5	5	1	6	4			
0	13	13	-8	5	7	4	20	19	-2	8	9	3	29	34	-4	18	18	2	22	20	5	5	5	2	11	9			
1	12	13	-7	4	4	5	13	13	-1	27	29	4	18	20	-3	21	20	3	14	12	K,L=	14	0	3	9	8			
2	10	10	-6	5	5	6	4	6	0	25	26	5	8	8	-2	15	16	4	5	6	0	22	21	4	8	8			
3	6	6	-5	4	2	7	0	0	1	19	20	6	13	13	-1	10	9	5	18	16	1	4	5	K,L=	15	4			
4	0	2	-4	9	10	8	3	5	2	9	9	7	16	17	0	18	18	6	16	13	2	11	9	-4	3	2			
5	8	7	-3	14	16	9	7	7	3	17	17	8	8	8	1	22	22	7	7	6	3	7	5	-3	6	6			
6	8	7	-2	0	2	K,L=	8	4	4	27	31	9	0	3	2	17	16	8	0	3	4	13	13	-2	7	6			
K,L=	6	7	-1	9	9	-11	5	4	5	14	15	10	4	5	3	23	21	K,L=	12	3	5	6	6	-1	0	2			
-5	3	2	0	22	20	-10	4	4	6	4	4	K,L=	10	2	4	12	9	-9	0	3	6	6	5	0	5	5			
-4	7	7	1	12	11	-9	4	5	7	3	2	-10	3	3	5	8	7	-8	6	5	7	6	3	1	5	5			
-3	2	2	2	0	4	-8	4	4	8	8	8	-9	0	2	6	0	2	-7	9	10	8	0	4	2	8	9			
-2	0	1	3	11	12	-7	0	3	9	4	4	-8	6	7	7	6	6	-6	0	3	K,L=	14	1	K,L=	16	0			
-1	5	4	4	14	15	-6	11	12	10	0	2	-7	9	9	8	3	3	-5	8	9	-8	3	4	0	10	9			
0	5	6	5	11	13	-5	17	18	K,L=	9	3	-6	10	9	9	9	9	-4	9	9	-7	2	2	1	7	7			
1	11	11	6	5	6	-4	10	13	-10	0	3	-5	6	4	K,L=	11	2	-3	12	10	-6	7	6	2	3	1			
2	0	1	7	0	1	-3	23	22	-9	2	2	-4	8	6	-10	4	4	-2	0	3	-5	14	14	3	6	6			
3	3	3	K,L=	7	6	-2	4	4	-8	3	4	-3	26	30	-9	4	3	-1	12	13	-4	8	7	4	10	9			
K,L=	6	8	-9	5	4	-1	13	12	-7	7	9	-2	19	18	-8	5	5	0	15	15	-3	8	7	5	7	5			
-2	4	6	-8	3	4	0	19	19	-6	8	8	-1	15	15	-7	4	3	1	10	9	-2	11	11	K,L=	16	1			
K,L=	7	0	-7	3	4	1	9	10	-5	18	19	0	17	18	-6	6	7	2	10	8	-1	14	15	-5	6	4			
1	27	28	-6	5	8	2	11	9	-4	7	6	1	19	18	-5	13	15	3	4	5	0	17	18	-4	7	4			
2	46	48	-5	8	8	3	13	11	-3	12	13	2	18	20	-4	11	10	4	8	7	1	0	2	-3	0	2			
3	33	32	-4	0	1	4	14	15	-2	18	20	3	15	13	-3	6	7	5	6	7	2	5	5	-2	11	9			
4	10	9	-3	3	4	5	11	11	-1	36	36	4	9	7	-2	9	8	6	9	8	3	16	16	-1	10	9			
5	19	17	-2	7	7	6	8	7	0	18	15	5	7	8	-1	13	12	7	5	3	4	10	11	0	8	7			
6	12	11	-1	6	7	7	6	6	1	24	25	6	10	11	0	28	29	K,L=	12	4	5	6	5	1	6	4			

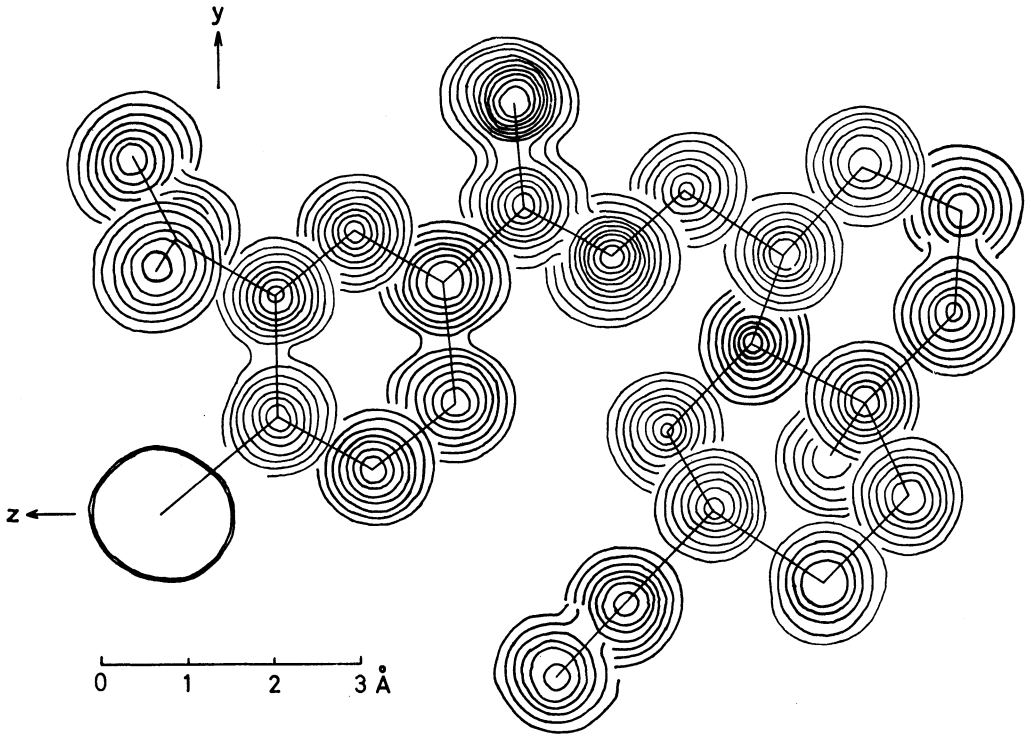

Fig. 1. Composite electron density diagram of sections parallel to (100). The contours are at intervals of 1.0 e. Å^{-3} starting with 1.0 e. Å^{-3}. The contours of the bromine atom are omitted.

the discrepancy factor, $R=\sum \| F_o| - |F_c| / \sum |F_o|$ was about 0.16. At this stage anisotropic temperature factors of the form, $\exp\{-(B_{11}h^2+B_{22}k^2+B_{33}l^2+B_{12}hk+B_{13}hl+B_{23}kl)\}$, were applied for the bromine atom. Four cycles of refinement reduced the R factor to 0.090 for the observed reflections. The atomic scattering factors used in the calculations were taken from the International Tables for X-ray Crystallography (1962).[3] The final atomic coordinates and the temperature factors are given in Table 1, and their standard deviations in Table 2. The observed and calculated structure factors are listed in Table 3. The final three-dimensional electron-density distribution calculated with phases based on these parameters is shown in Fig. 1.

The computations were done on a HITAC 5020 computer in the University of Tokyo with programs written by Dr. T. Ashida.

Determination of Absolute Configuration

After errors caused by neglect of the absorption correction were taken into account, seven sets of Bijvoet pairs were observed to have significantly different intensities in the upper layer photographs around the c axis. For the Bijvoet pairs, $|F(hkl)|$ and $|F(h\bar{k}\bar{l})|$ were calculated using $\Delta f'$ and $\Delta f''$

3) "International Tables for X-ray Crystallography," Vol. 3, Kynoch Press, Birmingham, England (1962), p. 202.

TABLE 4. THE DETERMINATION OF THE ABSOLUTE CONFIGURATION

$h\ k\ l$	Calculated			Observed	
	$\|F(hkl)\|$		$\|F(\bar{h}\bar{k}\bar{l})\|$	$I(hkl)$	$I(\bar{h}\bar{k}\bar{l})$
4 1 0	26.2	>	25.2		<
1 2 0	4.4	<	7.0		>
4 1 1	8.3	>	6.8		<
0 1 2	72.8	>	70.7		<
0 2 2	20.2	<	20.7		>
1 2 2	5.1	<	9.0		>
0 2 3	11.3	<	13.8		>

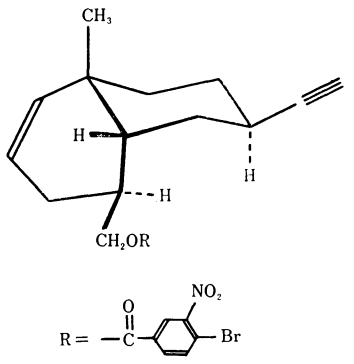

Fig. 2. Absolute configuration and conformation.

for the bromine atom on the basis of the model in a right-handed coordinate system. As shown in Table 4, inequality relations in each pair are the reverse of observed and calculated values, so that model used in the calculations is the mirror image of the actual molecule. Therefore, chamaecynenol has the absolute configuration indicated in Fig. 2. The hydroxymethyl group on C(4) and the ethynyl group on C(7) are in the β orientation.

Results and Discussion

Molecular Structure. From the X-ray analysis described in the preceding paragraphs, the steric structure of the molecule has been determined without any ambiguity. The intramolecular bond lengths and angles are shown in Figs. 3 and 4, respectively. The mean estimated standard deviation in a bond length is about 0.020 Å and in a

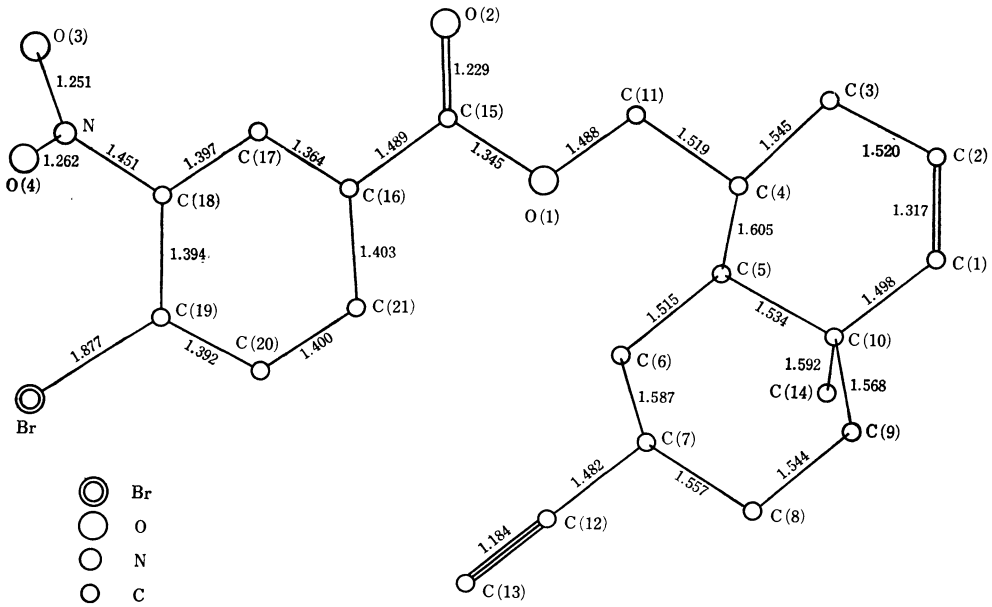

Fig. 3. Bond lengths (Å).

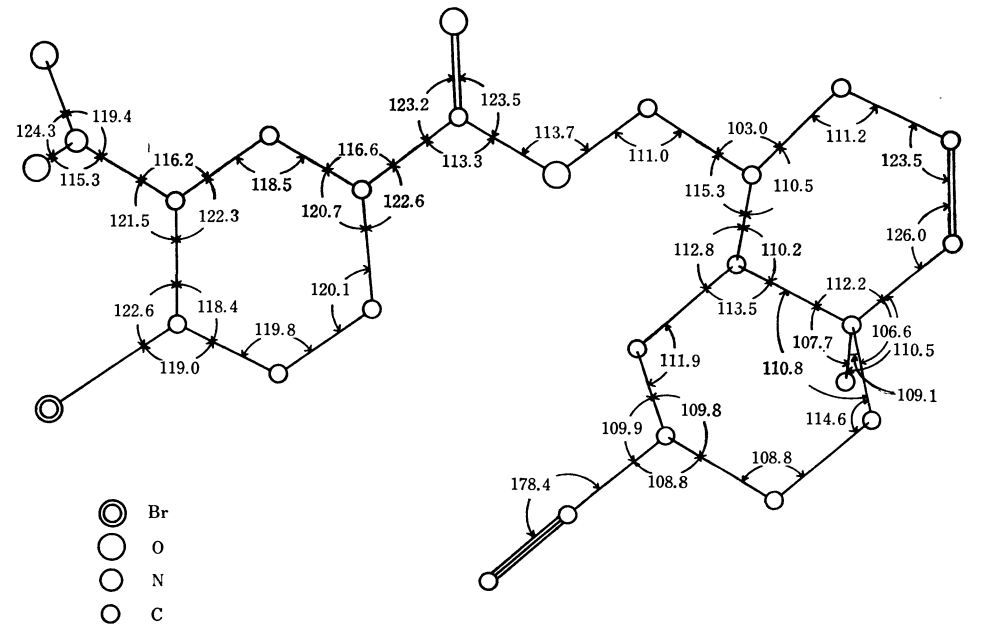

Fig. 4. Bond angles (degrees).

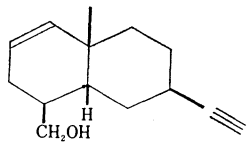

(II)

bond angle about 1.1°. All bond lengths and angles are reasonable within the errors. The locations of the double and the triple bonds are assigned unambiguously, and are the same as those in chamaecynone and isochamaecynone.[4] Thus the chemical structural formula of chamaecynenol has been established as II.

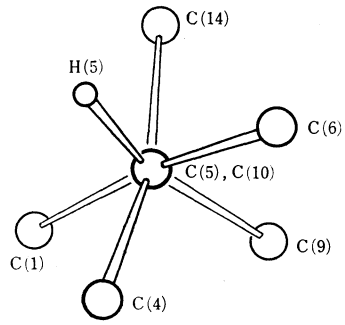

Fig. 5. Conformations about the bond C(5)–C(10).

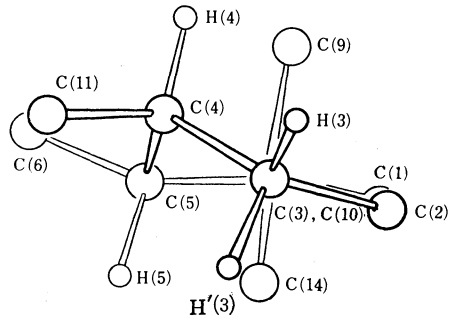

Fig. 6. Ring A, viewed along the line C(3)···C(10).

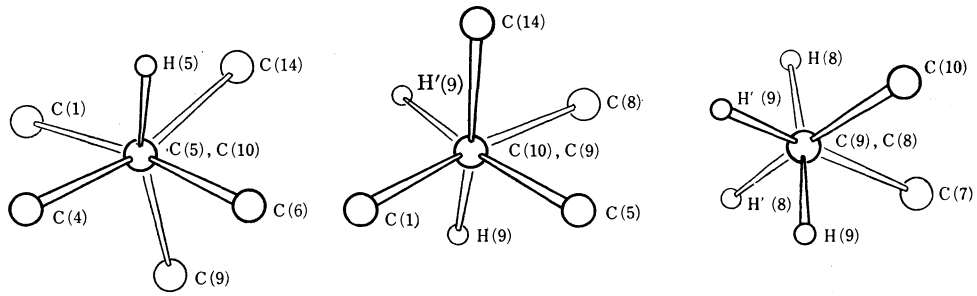

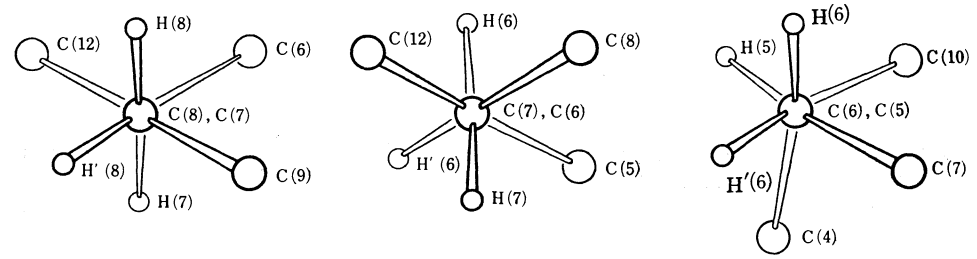

Fig. 7. Conformations about the six single bonds of ring B.

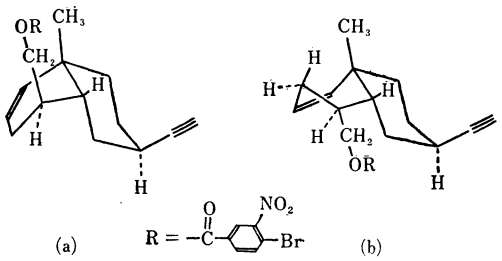

(a) (b)

Fig. 8.

Conformation. A view along C(5)–C(10) in Fig. 5[5] shows that the ring system is cis fused and in the steroid conformation. The ring A is half-chair as shown in Fig. 6. The conformations about the six single bonds in the ring B are shown in Fig. 7; all are seen to be staggered, and the

4) T. Nozoe, Y. S. Cheng and T. Toda, *Tetrahedron Letters*, **1966**, 3663.

5) In the preparation of this and other figures, the positions of the hydrogen atoms were assumed.

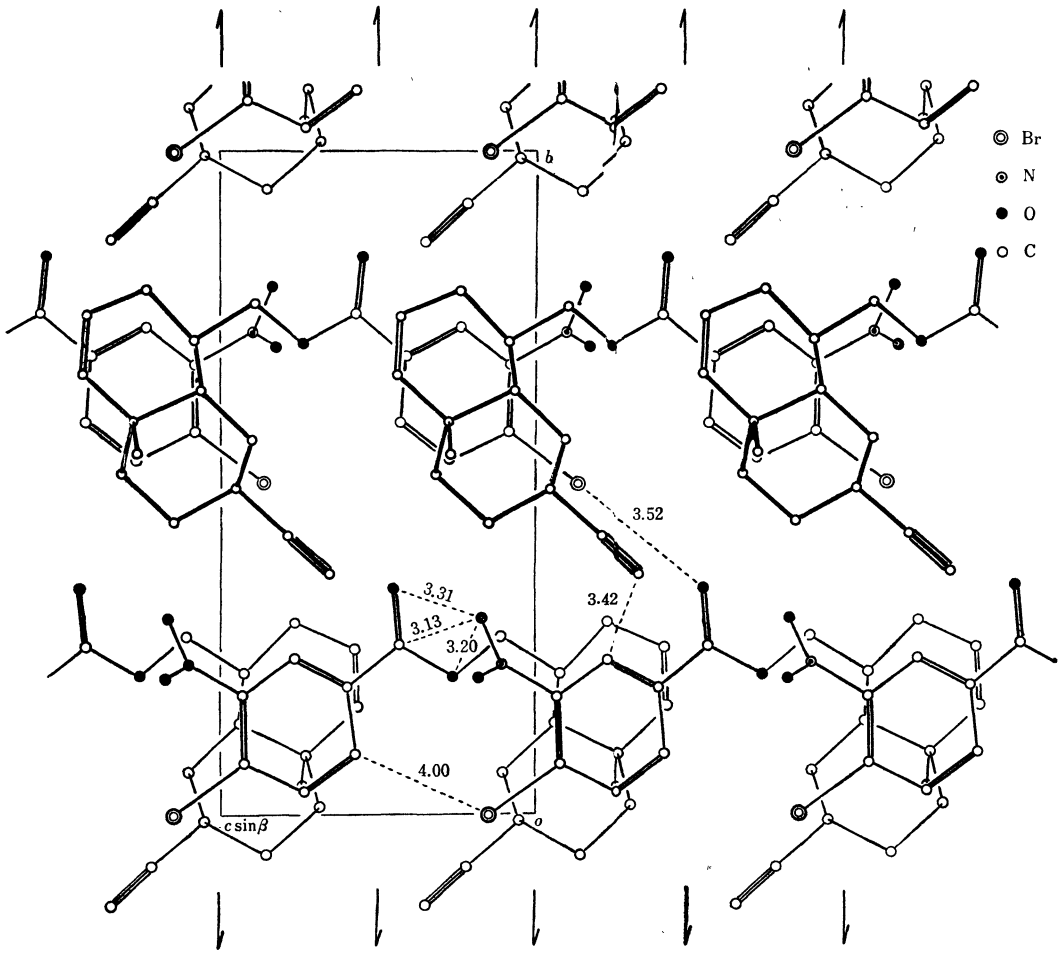

Fig. 9. The crystal structure projected along the a axis and the short intermolecular distances (Å).

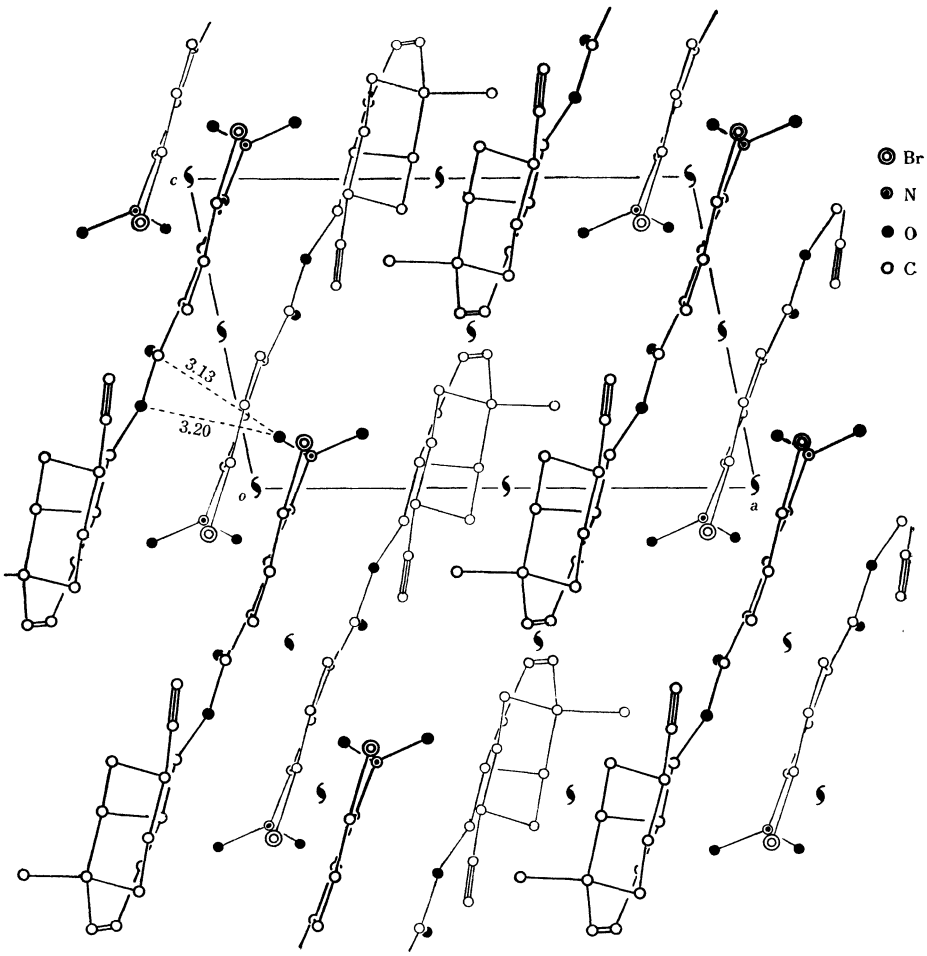

Fig. 10. The crystal structure projected along the b axis and the short intermolecular distances (Å).

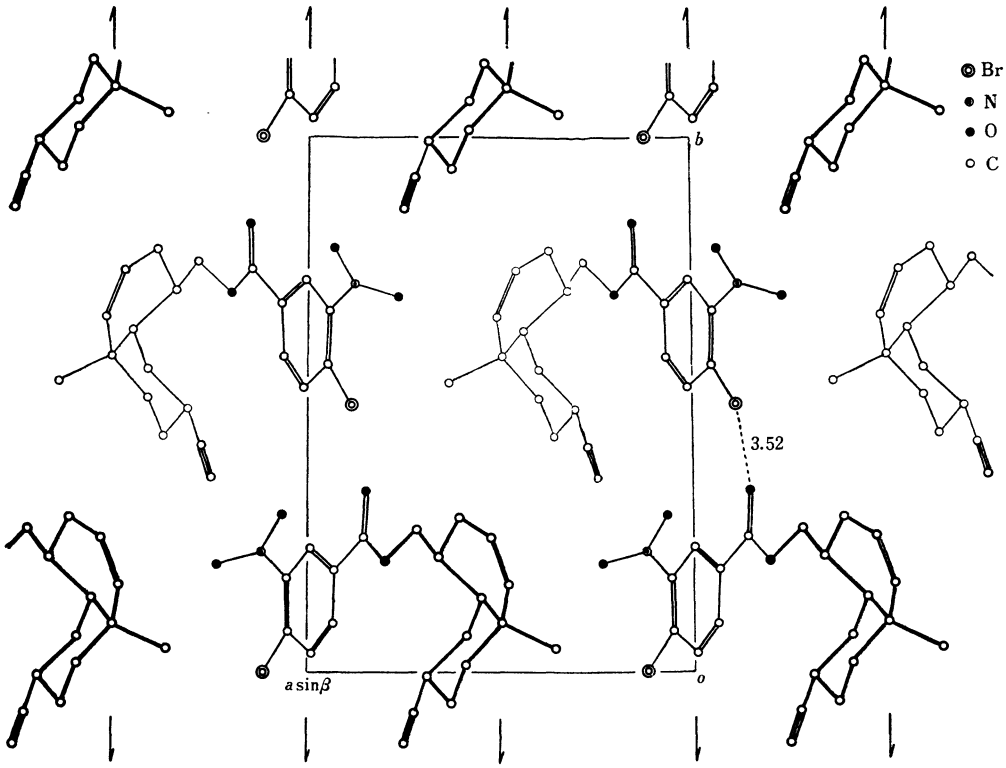

Fig. 11. The crystal structure projected along the c axis and the short intermolecular distances (Å).

ring assumes the chair form. It is indicated that no strain occurs in the ring system.

That the steroid conformation of the present compound is more favorable can be reasonably explained from the stereochemical point of view. If the molecule were forced to take the non-steroid form keeping the chair and the half-chair conformation of the two rings, strong 1,3-diaxial interaction between 4β-hydroxymethyl group and 10β-methyl group would occur as shown in Fig. 8(a). Alternatively, if 4β-hydroxymethyl group were in the equatorial position in order to avoid such 1,3-diaxial interaction, the ring A should be in the less stable half-boat conformation as shown in Fig. 8(b). Consequently, the steroid conformation of this compound is more stable than the non-steroid one. If 4-hydroxymethyl group is in the α orientation, the non-steroid conformation can occur favorably.

Crystal Structure. The packing diagrams of the crystal viewed along the a, b and c axes are shown in Figs. 9, 10 and 11, respectively, together with the short intermolecular distances. The strong dipolar nature of the C=O group may fix the orientation of the nitro group to give the shortest intermolecular carbon-oxygen distance (3.13 Å). The shortest carbon-carbon, oxygen-oxygen, bromine-carbon and bromine-oxygen distances are 3.42 Å, 3.20 Å, 4.00 Å and 3.52 Å, respectively. No unusual short approaches are observed.

The authors are indebted to Professor Kahei Takase and Dr. Toyonobu Asao of Tohoku University for kindly giving us the sample.

BULLETIN OF THE CHEMICAL SOCIETY OF JAPAN VOL. 42 344—348 (1969)

Decomposition of Ammonia and Reactivity of Nitrogen Absorbed on Molybdenum

Susumu TSUCHIYA and Atsumu OZAKI

Research Laboratory of Resources Utilization, Tokyo Institute of Technology, Ookayama, Meguro-ku, Tokyo

(Received June 16, 1968)

Adsorption measurements during the course of ammonia decomposition over molybdenum catalyst have been carried out in a closed circulating system. It was found that most of the nitrogen produced was taken up by molybdenum, and the initial rate of the reaction was independent of the ammonia pressure in a certain region. During the decomposition the nitrogen uptake was several times as much as the amount required to saturate the catalyst surface, which indicates the formation of nitride layers. The catalytic activity of molybdenum trioxide for ammonia decomposition was also observed, and the formation of nitride layers was again suggested. The nitrogen sorbed on molybdenum was removed as ammonia by admitting hydrogen and was displaced by oxygen added afterwards.

Extensive studies[1-4] have been carried out on the ammonia synthesis or decomposition reaction over molybdenum, and the decomposition was found to be zero-order. It is generally admitted that the reaction follows zero-order kinetics when the catalyst surface is fully covered by the reactant or the reaction inermediate. In the case of ammonia decomposition over molybdenum, the zeroth order kinetics might be due to the saturated adsorption of nitrogen on the catalyst surface. The formation of nitride layers was suggested during the decomposition reaction of ammonia on tungsten, which is of zero-order kinetics.[5] Further information on the surface species would be obtained by measuring the adsorption during the ammonia decomposition reaction over molybdenum.

Nitrogen is an inactive element as is well known, and the formation of reactive nitrogen is a subject of interest. The reactant adsorbed must be more reactive than it is in the gas phase, and thus the nitrogen adsorbed on the molybdenum would be reactive.

In this study, the authors also investigated the reactivity of nitrogen sorbed on molybdenum with hydrogen and oxygen, and obtained some information on this system.

Experimental

The apparatus employed is a closed circulating system and the experimental procedures are similar to those described in a previous paper.[6] The amounts of gases sorbed on the catalyst surface were estimated from the amounts of reactants introduced, and the pressure and composition of the circulating gas. The composition of the circulating gas mixture comprised of ammonia, nitrogen and hydrogen was determined by gas chromatography after removing ammonia by means of a trap. The amount of ammonia in the gas phase was estimated from a knowledge of the volume of the system and the decrease in the total pressure by trapping.

Before hydrogen was introduced, the gases were removed by a few minutes' evacuation of the system, assuming that the nitrogen uptake on the surface can hardly be lost by pumping.

The reaction between hydrogen and sorbed nitrogen was carried out in the circulating system with trap cooled in liquid nitrogen. The amount of ammonia thus formed and collected in the trap was estimated from the increase in the total pressure on removal of the liquid nitrogen and a knowledge of the volume of the system.

The ammonia was obtained by distillation from ammonium hydroxide at room temperature and was purified by repeated fractional distillation from dry-ice to liquid nitrogen traps.

The molybdenum-A catalyst was prepared by treating and stabilizing reagent grade commercial molybdenum, with ammonia several times, the decomposition of ammonia taking place. The commercial molybdenum was reduced at 600°C with hydrogen for 50 hr to prepare the molybdenum-B catalyst. No water formed when

1) C. H. Kunsman, *J. Am. Chem. Soc.*, **50**, 2100 (1928).

2) S. Kiperman and M. I. Temkin, *Acta Physicohim. U. S. S. R.*, **21**, 267 (1946).

3) M. R. Hillis, C. Kemball and M. W. Roberts, *Trans. Faraday Soc.*, **62**, 3570 (1966).

4) W. G. Frankenburg, "Catalysis III," ed. by Emmett, Reinhold, New York (1955), p. 185.

5) K. Tamaru, *Trans. Faraday Soc.*, **57**, 1410 (1961).

6) S. Tsuchiya and T. Shiba, *J. Catalysis*, **4**, 116 (1965).

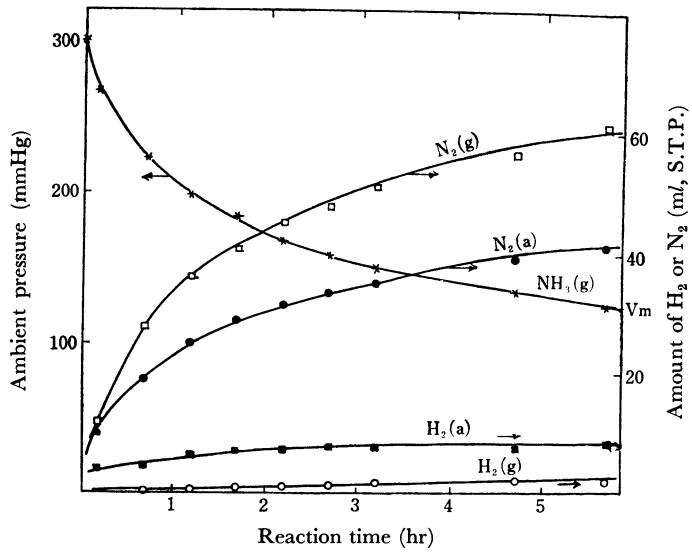

Fig. 1. Decomposition of ammonia over moylbdenum-A at 390°C. *: NH_3 in the gas phase, ○: N_2 in the gas phase, ●: N_2 uptake by the catalyst, □: H_2 in the gas phase, ■: H_2 uptake by the catalyst.

both molybdenum-A and -B were reduced at 500°C with hydrogen. The molybdenum trioxide catalyst was prepared by decomposing ammonium molybdate at 400°C. Before each run, the catalysts were evacuated to 10^{-4} mmHg for four hours at 580°C, and the molybdenum-B catalyst was beforehand treated with hydrogen at 580°C to remove the sorbed nitrogen, the amount of ammonia formed by the treatment being checked. In this way the experimental results were satisfactorily reproducible.

Results

Typical results of ammonia decomposition reaction over molybdenum are shown in Figs. 1 and 2, where the catalysts used were different. (Fig. 1: cat. A 160 g, Fig. 2: cat. B 39.6 g) As the decomposition proceeded, the partial pressure of ammonia decreased with time, and the pressure of hydrogen and nitrogen increased, while the uptake of nitrogen increased, and the amount of hydrogen taken up was very small as shown in Fig. 1. In the case shown in Fig. 2, no uptake of hydrogen was observed. At higher temperatures above 500°C, no uptake of hydrogen took place, even when molybdenum-A was used as the catalyst, and at 560°C the atomic ratio of molybdenum to sorbed nitrogen increased to approximately 0.5. The sample was identified as Mo_2N by X-ray diffraction.

The results for decomposition of various amounts of ammonia are shown in Fig. 3, where the initial rate of increase of the hydrogen pressure due to

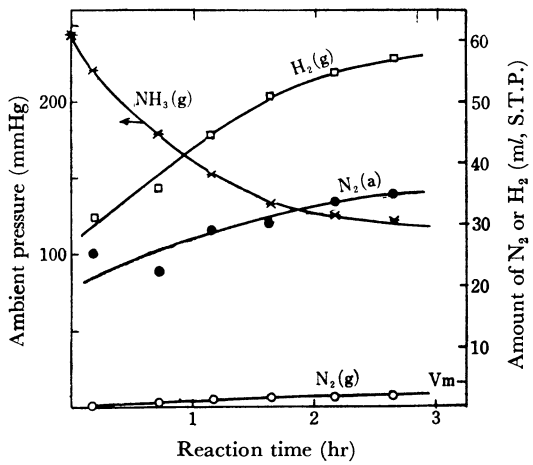

Fig. 2. Decomposition of ammonia over molybdenum-B at 404°C. The symbols used are the same as Fig. 1.

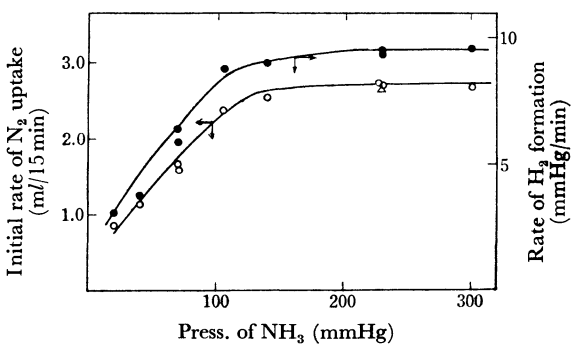

Fig. 3. The plots of the rate of ammonia decomposition (○) and the amounts of nitrogen uptake (●) against the initial partial pressure of ammonia at 454°C (Mo-A).

the ammonia decomposition and the amounts of nitrogen uptake over first fifteen minutes are plotted against the ambient pressure of ammonia. Both the initial rate of the formation of hydrogen and the rate of nitrogen uptake at the initial stage of the reaction were almost independent of the pressure of ammonia above 140 mmHg; rate dependence upon the pressure of ammonia, however, occurs below 140 mmHg.

The apparent activation energies of the ammonia decomposition over the different catalysts, together with those of other workers relevant to the discussion, are given in Table 1, being estimated from the Arrhenius plots (shown in Fig. 4) of the amounts of gas initially evolved. These values are in good agreement with one another.

Table 1. Activation energies for the decomposition of ammonia over molybdenum catalyst

Catalyst	Temperature (°C) range	Activation energy (kcal/mol)
Mo-A	390 — 610	42.6
Mo-B	400 — 440	40.0
MoO_3	400 — 460	43.4
Mo powder[2]	447 — 550	42.5
Mo wire[1]	725 — 850	42.7

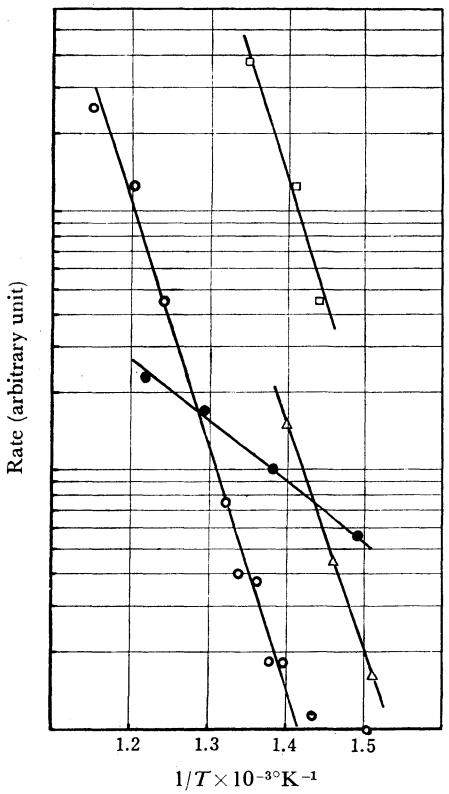

Fig. 4. Arrhenius plots for the ammonia decomposition over different catalyst (○ Mo-A, △ Mo-B, □ Mo oxide) and the reaction between nitrogen sorbed and hydrogen (●).

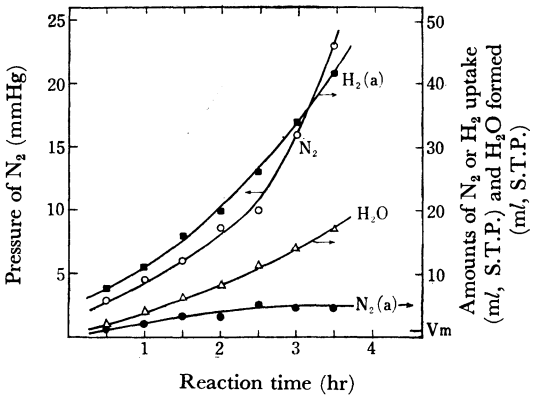

Fig. 5. Decomposition of ammonia over molybdenum trioxide (3.45 g) at 420°C.
△: water vapor formed, the other symbols used are the same as Fig. 1.

When molybdenum trioxide was used as the catalyst, the ammonia was also decomposed, considerable amount of hydrogen and nitrogen was taken up and the formation of water vapor and nitrogen gas was observed, while no hydrogen was detected in the gas phase, as shown in Fig. 5. The hydrogen taken up may exist in the form of H_2O.

The reaction between the hydrogen and nitrogen held on molybdenum was also carried out with the nitrogen-sorbed surface being prepared by decomposition of ammonia and the product observed was identified as only ammonia from its vapor pressure measurement.

The hydrogen pressure dependence of the rate of the hydrogenation of sorbed nitrogen, represented by the cumulative amount of ammonia formed over the first one-hour period, was proportional to $P_{H_2}^{1.5}$ as shown in Fig. 6, where P_{H_2} is the pressure of hydrogen, ammonia being formed linearly with time. The ambient pressure of the hydrogen was represented by the average value over the one-hour period.

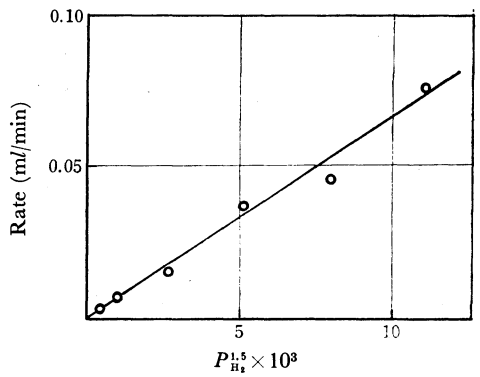

Fig. 6. Dependence of the reaction rate on hydrogen pressure (510°C), the amount of nitrogen uptake being 40 ml (Mo-B).

The rate of the reaction depends on the amount of the nitrogen presorbed on molybdenum as shown in Fig. 7. The rate is proportional to the amount of nitrogen presorbed until the amount reaches eleven times the monolayer value of 4.5 m*l* for the surface.

The apparent activation energy for the hydrogenation was estimated from the Arrhenius plot of the amounts of ammonia formed at fixed conditions of hydrogen pressure (400 mmHg) and nitrogen sorbed (40 m*l*), to be 12 kcal/mol as shown in Fig. 4.

The influence of the oxygen addition to the nitrogen uptake is shown in Fig. 8, and the nitrogen taken up was displaced by successive additions of oxygen where the time intervals between each run were about one-hour. In this case the total displacing ratio of nitrogen to oxygen was approximately ten.

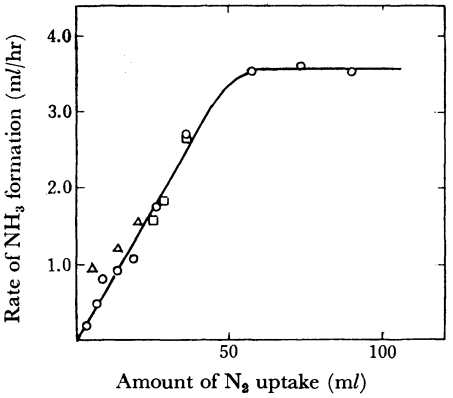

Fig. 7. The dependence of the rate of the reaction upon the amounts of nitrogen uptake at 510°C, the ambient pressure of hydrogen being 400 mmHg (Mo-B).

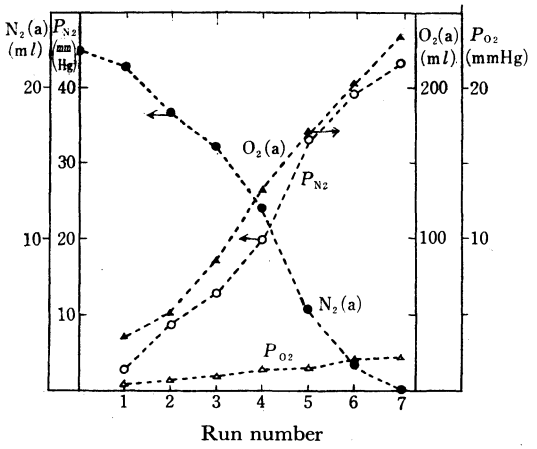

Fig. 8. The effect of oxygen addition to the nitrogen uptake on molybdenum at 400°C. ○: ambient pressure of nitrogen, ●: amounts of nitrogen uptake N_2(a), △: ambient pressure of oxygen, and ▲: amounts of oxygen uptake O_2(a) (Mo-B).

The BET method with nitrogen adsorption revealed the surface area of molybdenum-A to be 0.8 m^2/g, that of molybdenum-B 0.5 m^2/g, and that of molybdenum trioxide, 1.2 m^2/g.

Discussion

1. Decomposition

As shown in Figs. 1 and 2, during the reaction the amounts of nitrogen uptake are greater than V_m in the BET equation, 31.4 m*l*/160 g and 4.56 m*l*/39.6 g, respectively. The results suggest that "surface nitride layers" ate formed of several layers thickness during the ammonia decomposition reaction; the ratio of molybdenum to nitrogen uptake and the result of X-ray diffraction of the sample over which the ammonia was decomposed at higher temperature also support this suggestion.

The decomposition of ammonia over molybdenum may accordingly be shown as

$$NH_3 + 2Mo \rightarrow Mo_2N + 3/2H_2$$

As shown in Fig. 3, the rate of reaction of ammonia with molybdenum is almost independent of the ambient pressure of ammonia above 140 mmHg and seems to be controlled by the rate of diffusion of adsorbed nitrogen into the bulk molybdenum.

The reaction of ammonia with molybdenum trioxide resulted in the decomposition of ammonia to form nitrogen and water vapour, considerable amount of nitrogen being taken up, and the rate of evolution of nitrogen increased with time as shown in Fig. 5. The results may be explained in the following way: molybdenum trioxide is first reduced by ammonia being accompanied by the formation of the nitride; the nitride surface thus formed is active for the decomposition of ammonia and the number of active sites increases with time, while the hydrogen formed may be oxidized immediately to water by molybdenum trioxide.

The agreement in the value of activation energies of the decomposition carried out on the different kinds of catalyst suggests that the active sites on the surfaces are of the same kind and that they exist on a molybdenum nitride surface.

2. The Hydrogenation

The rate of hydrogenation of sorbed nitrogen can be expressed by Eq. (1), as evidenced by the results shown in Figs. 6 and 7.

$$r = k P_{H_2}^{1.5} X_{N_2}$$

where X_{N_2} is the amount of nitrogen taken up, provided that the volume of X_{N_2} is less than 50 m*l*/39.6 g. This dependence of the rate on the amount of nitrogen sorbed is to be noted. Since the monolayer of nitrogen on the surface of the catalyst is 4.6 m*l*, the amount of nitrogen up to 50 m*l* substantially exceeds the V_m value. The fact means that the nitrogen sorbed into the bulk does promote

the rate of hydrogenation of surface nitrogen.

The heat of adsorption of nitrogen on a metal would reasonably be expected to be higher than on a metal nitride, and the stability of the adsorbed nitrogen would be decreased due to the nitride layers. The saturation of the promotion shown in Fig. 7 suggests that the bulk nitride phase is established by sorbed nitrogen.

The interpretation of the reaction order in hydrogen must await further investigation.

The high displacing ratio (such as ten) of nitrogen desorbed to oxygen sorbed must be due to oxygen having a higher affinity than nitrogen for molybdenum, and the formation of bulk oxide is suggested.

The interconversions between metal, nitride and oxide are schematically expressed as follows:

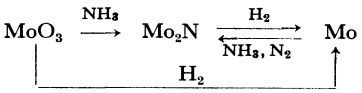

The authors are grateful to Professor M. Taniguchi for his X-ray analysis.

BULLETIN OF THE CHEMICAL SOCIETY OF JAPAN VOL. 42 348—355 (1969)

An MO-Theoretical Study of Several Bimolecular Reactions of Nucleophilic Reagents

Kenichi FUKUI,* Hideyuki HAO** and Hiroshi FUJIMOTO*

* *Department of Hydrocarbon Chemistry, Kyoto University, Kyoto*
** *Ōe Works, Sumitomo Chemical Co., Ltd., Niihama, Ehime*

(Received June 14, 1968)

The relative ease of the occurrence of S_N2 and E2 reactions and the mechanism of related bimolecular processes, such as the base-catalyzed hydrolysis of carboxylic esters and the acid-catalyzed halogenation of aliphatic ketones, are discussed in connection with the MO-theoretical reactivity indices. The results indicate that the valence-inactive populations in the lowest unoccupied (LU) MO are useful reactivity indices for these nucleophilic reactions.

The molecular orbital (MO) theory has been applied by the present authors to the discussion of the mechanism of S_N2 and E2 reactions.[1,2] These two processes are known to take place more or less concurrently, in the reaction of molecules bearing a nucleophilic group with a nucleophilic reagent. In the present paper the relative ease of the occurrence of these two processes is discussed in connection with the MO-theoretical reactivity indices, while a simultaneous discussion of related bimolecular processes, such as the base-catalyzed hydrolysis of carboxylic esters[3a] and the acid-catalyzed halogenation of aliphatic ketones,[3b] is given.

The method of calculation is based on the extended Hückel approach,[4] which has already proved to be useful in the elucidation of the mechanism of many other kinds of reactions.[5–10] As MO-theoretical reactivity indices, the populations of the frontier orbitals[11] are employed, which have been defined in the frame of the extended Hückel approach. For the nucleophilic reactions as treated in the present paper, the valence-inactive population[12] of each position (atom or atomic orbital (AO)) in the lowest unoccupied (LU) MO serves as the frontier electron density. It has been ascertained that this quantity becomes a useful

1) H. Kato, K. Morokuma, T. Yonezawa and K. Fukui, This Bulletin, **38**, 1749 (1965).
2) K. Fukui and H. Fujimoto, *Tetrahedron Letters*, **1965**, 4303.
3) *E. g.*, see E. S. Gould, "Mechanism and Structure in Organic Chemistry," Holt, Rinehart and Winston, New York, a) p. 314; b) 365; c) 374; d) 472 (1959).
4) R. Hoffmann, *J. Chem. Phys.*, **39**, 1397 (1963); **40**, 2474, 2480, 2745 (1964).
5) H. Kato, T. Yonezawa, K. Morokuma and K. Fukui, This Bulletin, **37**, 1710 (1964).
6) H. Kato, K. Yamaguchi, T. Yonezawa and K. Fukui, *ibid.*, **38**, 2144 (1965).
7) T. Yonezawa, O. Yamamoto, H. Kato and K. Fukui, *Nippon Kagaku Zasshi* (*J. Chem. Soc. Japan, Pure Chem. Sect.*), **87**, 26 (1966).
8) H. Fujimoto and K. Fukui, *Tetrahedron Letters*, **1966**, 5551.
9) T. Yonezawa, H. Konishi, H. Kato, K. Morokuma and K. Fukui, *Kogyo Kagaku Zasshi* (*J. Chem. Soc. Japan, Ind. Chem. Sect.*), **69**, 869 (1966).
10) T. Yonezawa, K. Shimizu and H. Kato, This Bulletin, **40**, 456, 1302 (1967).
11) K. Fukui and H. Fujimoto, *ibid.*, **40**, 2787 (1967).
12) K. Ruedenberg, *Rev. Mod. Phys.*, **34**, 326 (1962).

reactivity index in various types of reactions.[13]

Calculations

For the sake of simplicity, chlorine is adopted as a representative of the nucleophilic group throughout the calculations.

The numerical values used in the extended Hückel calculation are given in Table 1. The overlap integrals are evaluated by the use of Mulliken's formula[14] with Slater-type AO's.

Table 1. The effective nuclear charge ($\mathcal{Z}$) of the Slater-type orbitals and the Coulomb integrals (h_{rr})

	H	C	O	Cl	Ref.
$\mathcal{Z}$	1.0	3.25	4.55	6.10	
$h_{rr}(ns)$, eV	−13.60	−21.43	−35.30	−25.23	15
$h_{rr}(np)$, eV	——	−11.42	−13.61	−13.34	15

In order to interpret the experimental data, the following MO-theoretical quantities[16] are calculated and employed:

The partial valence-inactive[12] AO population of AO r in the jth MO:

$$p_r^j = 2(C_r^j)^2$$

The partial valence-inactive atom population of the atom A in the jth MO:

$$p_A^j = \sum_r^A p_r^j$$

The partial atom bond population between the atoms A and B in the jth MO:

$$M_{AB}^j = 2\sum_r^A \sum_s^B C_r^j C_s^j S_{rs}$$

where C_r^j stands for the coefficient of AO r in the jth MO and where $\sum^A$ signifies the summation over all the AO's belonging to the atom A.

The geometry of molecules is determined by the following interatomic distances:

C—H 1.09 Å C—Cl 1.76 Å ^{acyl}C—O 1.36 Å
C—C 1.54 Å C=O 1.22 Å ^{alkyl}C—O 1.46 Å

with the valence angles of carbon and oxygen atoms given by Wheland's monograph,[17] except in chlorine-containing molecules, for which a uniform value, 109°28′, is adopted for carbon for the sake of simplicity.

Results and Discussion

As has been mentioned earlier, it should be noted that the comparison is made between the experimental results, in which the nucleophilic group X is not always a chlorine atom, and the theoretical values calculated with respect to the case where X is equal to chlorine.

1. S_N2 and E2 Reactions. A molecule bearing a nucleophilic group X:

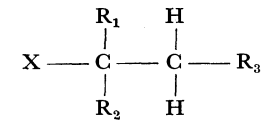

is considered, in which R_1 and R_2 represent a hydrocarbon rest or a hydrogen atom, and in which R_3 is an arbitrary group. The reaction designated as E2[3d] is a double-linkage-forming process by way of the elimination of XH, in which the abstraction takes place dominantly at that hydrogen atom *trans* coplanar with respect to X. This process, which is known as the "*trans*" elimination, has already been treated by the present authors in the frame of the frontier electron method.[2] The experimental results have been interpreted satisfactorily by means of the population of LU MO at each hydrogen atom, p_H^{LU}; the population has completely paralleled the reactivity of many halogenated hydrocarbons, being largest at the β-hydrogen *trans* with respect to the halogen atom.

On the other hand, the S_N2 process is considered to occur by way of the attack of a nucleophile from the backside of the carbon to which the nucleophilic group is attached, leading in general to Walden's inversion. The present authors have already treated[1] this problem MO-theoretically with regard to methyl chloride. The LU MO has been found to localize strongly at the carbon 2p AO lying on the C–Cl axis, extending from the carbon mostly in the direction reverse to the C–Cl bond. This finding reflects the experimental result mentioned above.

It is well known that these two bimolecular processes can frequently take place in a competitive fashion in the same reactant molecule by way of the attack of the same nucleophilic reagent. In order to elucidate the factor determining the readiness of the two processes, the following reactivity indices are employed in interpreting the experimental results.

First, the partial valence-inactive population of the β-hydrogen 1s AO in LU MO, $p_{\beta\text{-}H}^{LU}$, is used for the reactivity index of the β-hydrogen atom in the E2 reaction. As has been mentioned before, this value is expected to parallel the reactivity.

13) For instance, see K. Fukui, "Molecular Orbitals in Chemistry, Physics, and Biology," ed. by P.-O. Löwdin and B. Pullman, Academic Press, New York, N. Y. (1964), and K. Fukui, *Nippon Kagaku Sen-i Kenkyusho Koenshu*, **23**, 75 (1966), and the references cited therein.

14) R. S. Mulliken, C. A. Rieke, D. Orloff and H. Orloff, *J. Chem. Phys.*, **17**, 1248 (1949).

15) H. O. Pritchard and H. A. Skinner, *Chem. Revs.*, **55**, 745 (1955).

16) R. S. Mulliken, *J. Chem. Phys.*, **23**, 1833, 1841, 2338, 2343 (1955).

17) G. W. Wheland, "Resonance in Organic Chemistry," John Wiley & Sons, New York (1955), p. 695.

TABLE 2. THE COMPARISON OF $p^{LU}_{x(C-Cl)}$ AND $p^{LU}_{\beta-H}$ WITH S_N2 AND E2 REACTIVITY

Reactions:

(1) $RBr + C_2H_5O^- \xrightarrow{k_1} ROC_2H_5 + Br^-$ (S_N2)[18b]

(2) $RBr + Cl^- \xrightarrow{k_2} RCl + Br^-$ (S_N2)[18a]

(3) $RCH_2CR'R''Br + C_2H_5O^- \xrightarrow{k_3} RCH{=}CR'R'' + C_2H_5OH + Br^-$ (E2)[18b]

RCl	ε^{LU} (eV)	$\frac{1}{2}p^{LU}_{x(C-Cl)}$	S_N2 reactivity $k_1\times10^5$ at 55°C ($l\,mol^{-1}\,sec^{-1}$)	S_N2 reactivity k_2 relative value	$\frac{1}{2}p^{LU}_{\beta-H}$	E2 reactivity $k_3\times10^5$ at 55°C ($l\,mol^{-1}\,sec^{-1}$)	M^{LU}_{CCl}
CH_3Cl	1.8702	1.0914	——	100	——	——	−1.1392
C_2H_5Cl	1.6242	0.9289	118.2	1.97	0.0793	1.2	−0.9321
$(CH_3)_2CHCl$	1.4873	0.9137	2.1	0.040	0.0862	7.6	−0.9028
$(CH_3)_3CCl$	1.2370	0.8466	small	0.009	0.0911	50	−0.8359

Secondly, the S_N2 process is treated in the following way. The four hybrids belonging to the tetravalent carbon atom attached to the chlorine atom are designated as x_1, x_2, x_3, and x_4; of those, x_1 is taken to be associated with the C–Cl bond. The LU MO obtained by the extended Hückel calculation is transformed into the linear combination of x_1, x_2, x_3, and x_4. The partial valence-inactive AO population of $x_1(=x(C-Cl))$ in LU MO, $p^{LU}_{x(C-Cl)}$, is calculated as responsible for the data being comparable with those of the experimental data. This theoretical index corresponds to the frontier electron density for S_N2 reactivity in the frame of the extended Hückel scheme.

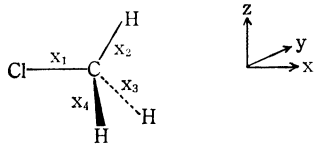

An illustration of the calculations is the case of methyl chloride. The coordinates are taken as indicated. The hybrids are represented by:

$$x_1 = 0.5(2s) - 0.866025(2px)$$
$$x_2 = 0.5(2s) + 0.288675(2px) + 0.816497(2pz)$$
$$x_3 = 0.5(2s) + 0.288675(2px) + 0.707107(2py) - 0.408249(2pz)$$
$$x_4 = 0.5(2s) + 0.288675(2px) - 0.707107(2py) - 0.408249(2pz)$$

The extended Hückel MO of LU level is given by:

$$\psi^{LU} = -0.193928x_{2s} + 1.094344x_{2px} + \cdots$$

which can easily be transformed into:

$$\psi'^{LU} = -1.044694x_1 + 0.218946(x_2+x_3+x_4) + \cdots$$

Hence, the index $\frac{1}{2}p^{LU}_{x(C-Cl)}$ is calculated to be 1.091386.

Such a computation was made with various alkyl chlorides; the results are indicated in Table 2, together with the experimental data. The partial atom bond population between α-carbon and chlorine in LU MO, M^{LU}_{CCl}, is also given in Table 2 in order to explain the reaction mechanism.

The experimental results are taken from the case of alkyl bromides, which can provide abundant data for a comparison with the theory. This substitution is possible as long as one is concerned only with the change in the relative rate resulting from the structural difference of alkyl groups.

From Table 2 it can be seen that, as the alkyl group varies from CH_3 to C_2H_5, i-C_3H_9, and t-C_4H_9, the index $p^{LU}_{x(C-Cl)}$ clearly decreases, while $p^{LU}_{\beta-H}$ increases. This implies that the nucleophilic reactivity of α-carbon diminishes in this order and that the β-proton becomes more and more reactive toward abstraction by nucleophiles; this agrees with our experience that the S_N2 reactivity is $CH_3 > C_2H_5 > i\text{-}C_3H_7 > t\text{-}C_4H_9$, while the E2 reactivity is $C_2H_5 < i\text{-}C_3H_7 < t\text{-}C_4H_9$.

The value of M^{LU}_{CCl} is calculated to be always negative. This means that the C–Cl bond is weakened by the approach of an electron-donor reagent. In addition, the absolute value of M^{LU}_{CCl} decreases in the order of alkyl groups mentioned above; this is consistent with, or, more strictly, not contradictory to, the experimental results in which the S_N2 reactivity decreases in this order.

Table 2 also indicates the energy of LU MO, ε^{LU}. This energy decreases in the order of alkyls stated above. It appears that this implies that the nucleophilic reactivity increases in this order. However, if one assumes the ionization potential of an

18) C. K. Ingold, "Structure and Mechanism in Organic Chemistry," Cornell University Press, Ithaca, New York (1953), a) p. 306; b) p. 419; c) M. L. Dhar, E. D. Hughes, C. K. Ingold and S. Masterman, *J. Chem. Soc.*, **1948**, 2055.

alkoxyl anion to be *ca.* 6—8 eV,[19] the ratio of $\Delta\varepsilon^{LU}$ to $(\varepsilon^{LU}-\varepsilon'^{HO})$, where ε'^{HO} is the energy of the highest occupied (HO) MO of the reagent, is small compared to $\Delta p_r^{LU}/p_r^{LU}$. According to the perturbation theory[20] for the interaction between reactant and reagent, the stabilization energy in an nucleophilic attack is approximately proportional to:

$$\frac{p_r^{LU}}{\varepsilon^{LU}-\varepsilon'^{HO}} \quad (r\text{: } x\text{(C-Cl) or } \beta\text{-H})$$

Therefore, the result reported above implies that in the present case the reactivity can be discussed most conveniently in terms of p_r^{LU}.

The reason for the positive ε^{LU} value should be mentioned here. The basis functions usually adopted in extended Hückel MO's, and in the present case as well, are those AO's in the occupied valence shell only, so the unoccupied MO's are generally calculated to possess an unreasonably high energy. This point is improved by a suitable basis-set extension.[21]

Furthermore, $p_{\beta\text{-H}}^{LU}$ is calculated with respect to various alkyl chlorides and compared with their E2 reactivities in Table 3. Moreover, in this case, the E2 reactivity data are taken from the corresponding bromide reactions. The calculation is carried out with regard to the all-staggered conformation for each compound which is considered to possess the largest existence probability.

The parallel between the calculated results and the experimental results is satisfactory. However, primary alkyl halides like *n*-propyl chloride have no *trans*-hydrogen in the staggered conformation and its β-hydrogen has only a very small $p_{\beta\text{-H}}^{LU}$ value, as may be seen in Fig. 1. On the other hand, the *trans* β-hydrogen appearing in the gauche conformation has a very large $p_{\beta\text{-H}}^{LU}$ value. Although the staggered form is 2.0 kcal more stable than the gauche one, as is indicated in Fig. 1, it is of interest that the gauche form is *ca.* 2.4 kcal more stable than the staggered in the species in which CH_3O^- is placed near the β-hydrogen. This leads one to presume that, in the transition state, the gauche form is more stable instead. For primary alkyl halides, consequently, the values p_r^{LU} of the *trans* β-hydrogen in the gauche conformation have been calculated; they are listed in Table 3.

The Saytzeff rule has already been given a theoretical foundation by the aid of the index $p_{\beta\text{-H}}^{LU}$ with regard to only one case 2-chlorobutane.[2] Here the rule is similarly explained also in the

TABLE 3. PARALLEL OF $p_{\beta\text{-H}}^{LU}$ WITH E2 REACTIVITY[18b]

(1) $R_1R_2CHCH_2Br + C_2H_5O^- \xrightarrow{k} R_1R_2C{=}CH_2 + C_2H_5OH + Br^-$

Compound	R_1	R_2	$\frac{1}{2}p_{\beta\text{-H}}^{LU}$	$k\times10^5$ at 55°C ($l\,mol^{-1}\,sec^{-1}$)
i-BuCl	CH_3	CH_3	0.1289	8.6
n-PrCl	H	CH_3	0.1020	5.3
n-BuCl	H	C_2H_5	0.0663	4.3
n-AmCl	H	*n*-C_3H_7	0.0551	3.5

(2) $RCH_2CH(CH_3)Br + C_2H_5O^- \xrightarrow{k} RCH{=}CHCH_3 + C_2H_5OH + Br^-$

Compound	R	$\frac{1}{2}p_{\beta\text{-H}}^{LU}$	$k\times10^5$ at 25°C ($l\,mol^{-1}\,sec^{-1}$)
2-BuCl	CH_3	0.0909	0.282
i-PrCl	H	0.0862	0.118

(3) $RCH_2C(CH_3)_2Br + C_2H_5O^- \xrightarrow{k} RCH{=}C(CH_3)_2 + C_2H_5OH + Br^-$

Compound	R	$\frac{1}{2}p_{\beta\text{-H}}^{LU}$	$k\times10^5$ at 25°C ($l\,mol^{-1}\,sec^{-1}$)
t-AmCl	CH_3	0.0928	4.20
t-BuCl	H	0.0911	1.00

(4) $CH_3CR_1R_2Br + C_2H_5O^- \xrightarrow{k} CH_2{=}CR_1R_2 + C_2H_5OH + Br^-$

Compound	R_1	R_2	$\frac{1}{2}p_{\beta\text{-H}}^{LU}$	$k\times10^5$ at 25°C ($l\,mol^{-1}\,sec^{-1}$)
t-BuCl	CH_3	CH_3	0.0911	1.00
t-AmCl	CH_3	C_2H_5	0.0909	0.85
i-PrCl	H	CH_3	0.0862	0.118
2-BuCl	H	C_2H_5	0.0842	0.065
EtCl	H	H	0.0793	0.025

(5) $CH_3CH_2CR_1R_2Br + C_2H_5O^- \xrightarrow{k} CH_3CH{=}CR_1R_2 + C_2H_5OH + Br^-$

Compound	R_1	R_2	$\frac{1}{2}p_{\beta\text{-H}}^{LU}$	$k\times10^5$ at 25°C ($l\,mol^{-1}\,sec^{-1}$)
t-AmCl	CH_3	CH_3	0.0928	4.20
2-BuCl	H	CH_3	0.0909	0.282

19) The energy of the HO MO of OH^- is −1.26eV, and that of CH_3O^- is −2.28 eV, according to one calculation (T. Yonezawa, H. Kato and H. Konishi, This Bulletin, **40**, 1071 (1967)). The electron affinity of the OH radical has been reported to be 2.2 eV (H. O. Pritchard, *Chem. Revs.*, **52**, 529 (1953)) or 2.8 eV (F. M. Page, *Discussions Faraday Soc.*, **19**, 87 (1955). Consequently, the ionization potential of the free alkoxyl anion is assumed to be 2—3 eV. The value in the solvated state can be presumed to be 4—5 eV larger.

20) For instance, see K. Fukui, "Ryoshi-Kagaku (Quantum Chemistry)," Asakura-Shoten (1968), p. 407; K. Fukui and H. Fujimoto, This Bulletin, **41**, 1989 (1968).

21) K. Fukui and H. Fujimoto, unpublished paper; K. Fukui and T. Yamabe, unpublished paper.

1. Staggered Form

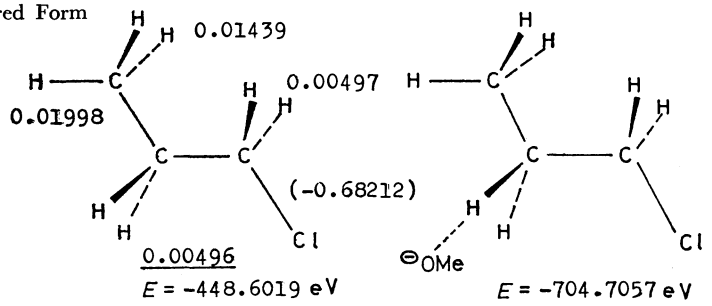

2. Gauche Form

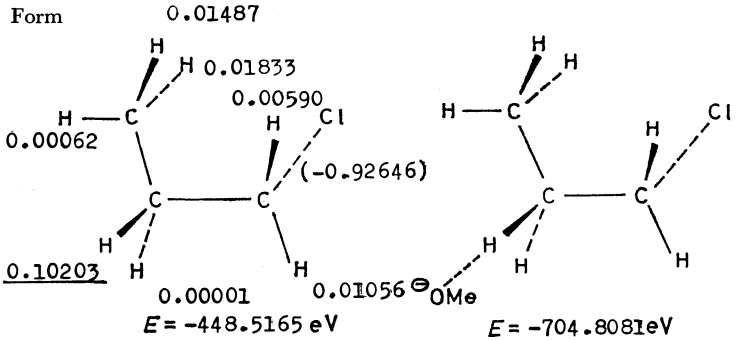

Fig. 1. The transition state E2 reactivity in *n*-PrCl. (The figures without parentheses indicate $\frac{1}{2}p_H^{LU}$; the figures with parentheses stand for M_{CCl}^{LU}; E is the total energy.)

1. 2-Amyl Chloride

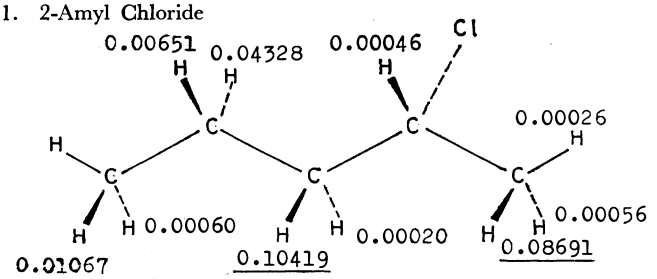

2. *t*-Amyl Chloride

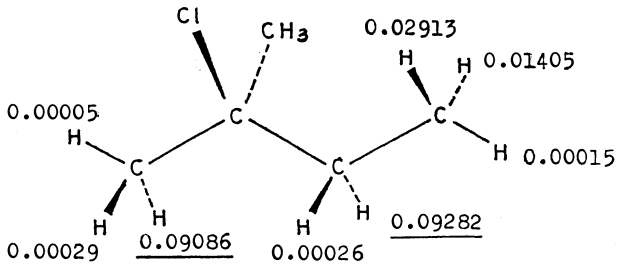

Fig. 2. The $\frac{1}{2}p_H^{LU}$ values of secondary and tertiary alkyl chlorides.

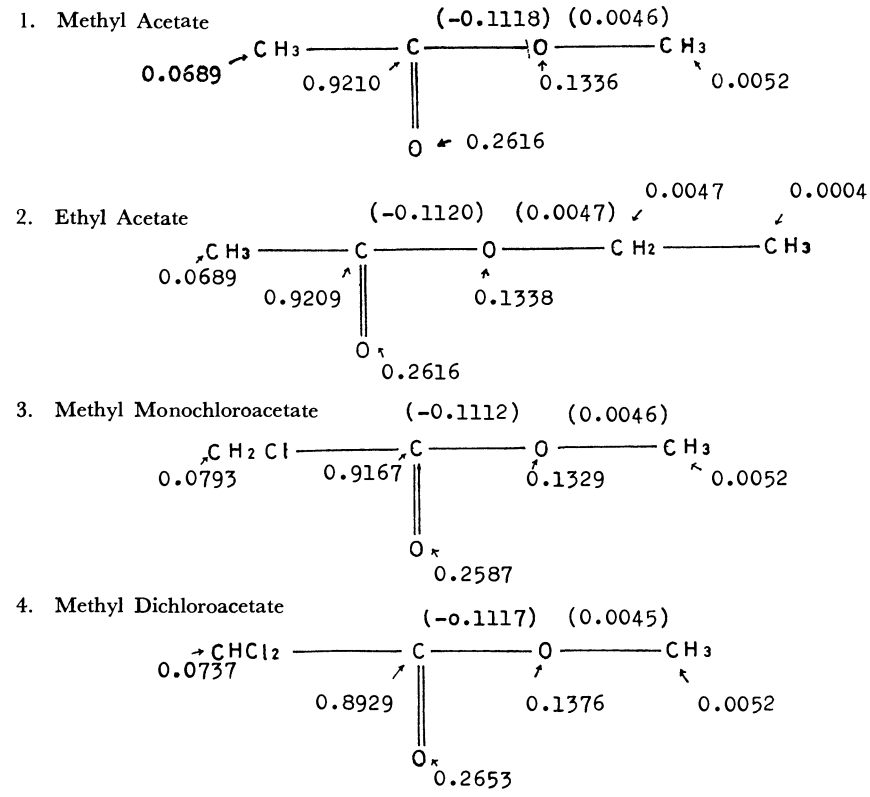

Fig. 3. The values of $\frac{1}{2}p_A^{LU}$ and M_{AB}^{LU} of carboxylic esters. (M_{AB}^{LU} values are in parentheses; $\frac{1}{2}p_A^{LU}$ for CH_2, CH_3, CH_2Cl and $CHCl_2$ are the total sum of the group.)

Table 4. Relation between M_{CCl}^{LU} and total rate of bimolecular nucleophilic reactions[18c]

Reaction: $RBr + C_2H_5O^- \xrightarrow{k}$ Olefin and ROC_2H_5

RCl	M_{CCl}^{LU}	$k \times 10^5$ at 55°C ($l\,mol^{-1}\,sec^{-1}$)
C_2H_5Cl	−0.9321	174
$CH_3CH_2CH_2Cl$	−0.9149	60.0
$CH_3CH_2CH_2CH_2Cl$	−0.6028	43.9
$CH_3CH_2CH_2CH_2CH_2Cl$	−0.3164	39.2

cases of 2-amyl chloride and *t*-amyl chloride, so as to demonstrate a more general applicability of the theory. The results are indicated in Fig. 2, exhibiting the predominance of secondary β-hydrogens over primary ones.

The partial atom bond population of α-carbon and the chlorine atom in LU MO, M_{CCl}^{LU}, is compared to the total rate of S_N2 and E2 reactions in Table 4. As has been pointed out earlier, the LU MO localizes in the C–Cl bond and is antibonding with respect to C–Cl, contributing to the weakening of the bond in the interaction with an electron donor. It should be noted that a parallel can be seen in the table between the absolute value of M_{CCl}^{LU} and the total rate.

2. Base-catalyzed Hydrolysis of Carboxylic Esters. The base-catalyzed bimolecular hydrolysis of carboxylic esters with acyl-oxygen fission ($B_{AC}2$), the mechanism of which was established by the early experiment of Polanyi and Szabo[22] using $H_2{}^{18}O$, is considered to take place through the attack of a nucleophile on the acyl carbon.

The partial valence-inactive atom populations in LU MO, p_A^{LU}, calculated for methyl acetate, ethyl acetate, methyl monochloroacetate, and methyl dichloroacetate are indicated in Fig. 3. The results indicate a distinct population localization at the acyl carbon; this is in accordance with our expectation of the selective attack of a nucleophile at that position.

The values of the partial atom bond population in LU MO, M_{AB}^{LU}, are also shown in the same figure; they indicate the strong antibonding character of this MO at the bond between acyl carbon

22) M. Polanyi and A. L. Szabo, *Trans. Faraday Soc.*, **30**, 508 (1934).

and ester oxygen, whereas this MO is bonding at the alkyl-oxygen bond, in agreement with the experimental results.

3. Acid-catalyzed Halogenation of Ketones. The accelerating effect of acids in the halogenation (and also in the deuteration and racemization) of enolizable ketones is thought to take place by way of an enol intermediate.[3c] Cardwell and Kilner[23] have reported that the Saytzeff rule applies in this process. Recently, Rappe[24] attributed the predominance of the position 3 over the position 1 in the acid-catalyzed halogenation or deuteration of 2-butanone to the difference in stability between the corresponding enol intermediates.

1. Methyl Ethyl Ketone

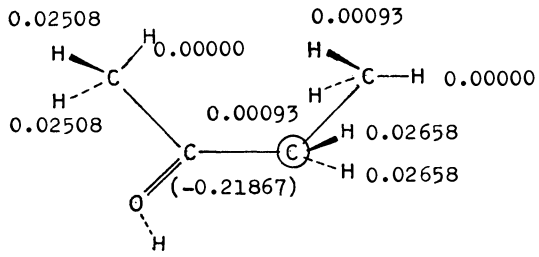

2. Methyl *n*-Propyl Ketone

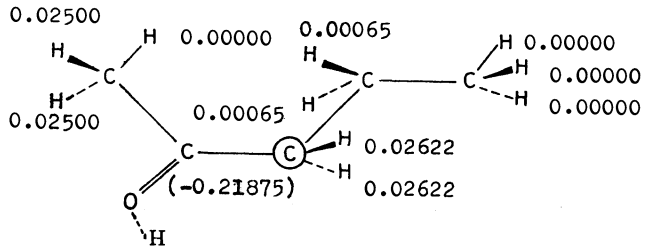

3. 2-Methylcyclohexanone

(a) Equatorial-methyl

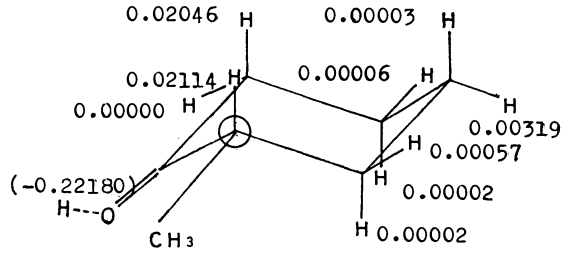

(b) Axial-methyl

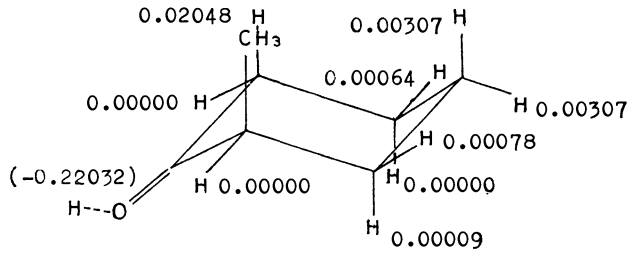

23) H. M. E. Cardwell and A. E. H. Kilner, *J. Chem. Soc.*, **1951**, 2430.

24) C. Rappe, *Arkiv Kemi*, **24**, 321 (1965); *Acta Chem. Scand.*, **20**, 2236 (1966); C. Rappe and W. Sachs, *J. Org. Chem.*, **32**, 3700 (1967); see also A. A. Bothner-By and C. Sun, *ibid.*, **32**, 492 (1967).

4. 3-Methyl Cyclohexanone

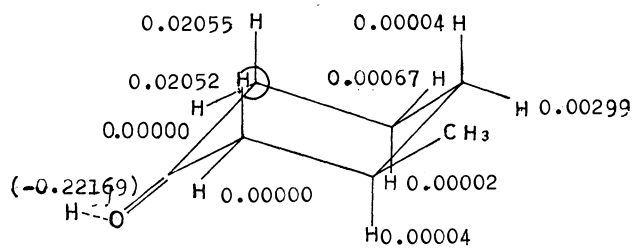

5. Methyl Cyclohexylketone

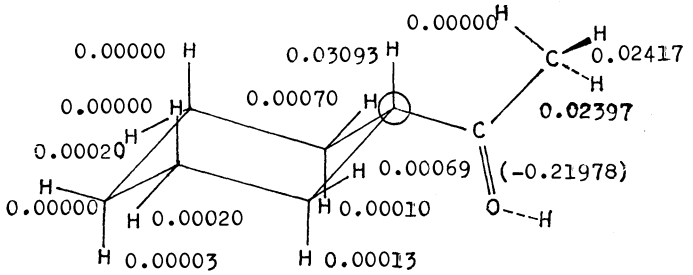

6. 2,5-Dimethyl Clohexanone

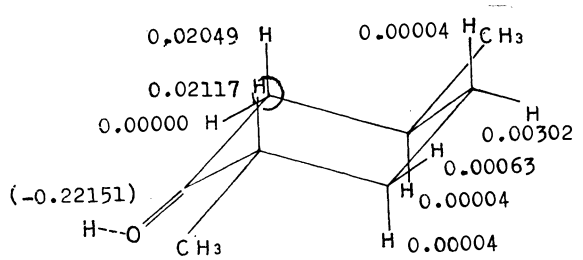

Fig. 4. The $\frac{1}{2}p_H^{LU}$ values of protonated ketones. (The position of proton is 1.1 Å from oxygen in the carbonyl plane, the angle H–O–C being 105°. The figurues in parentheses are M_{AB}^{LU}.)

In connection with this information, the p_H^{LU} values are calculated with respect to the various aliphatic or alicyclic ketones in which a proton is attached to their carbonyl oxygen. Since the location of the proton does not seriously affect the result, it is tentatively taken to be as is indicated in Fig. 4. The methylene hydrogen has a larger p_H^{LU} than the methyl hydrogen in aliphatic ketones, while in alicyclic ketones the p_H^{LU} of the methyne hydrogen is larger than that of the methylene hydrogen.

The site of attack known from experimentation is shown by a circle;[23] this site is easily verified to be consistent with the theoretical result, except in the case of 2,5-dimethylcyclohexanone. As the reagent nucleophile (the acid anion or the base part of a solvent molecule) approaches a hydrogen atom, the carbonyl C–O double bond is weakened and shifts toward a single bond, since LU MO is strongly antibonding in this region. (The M_{AB}^{LU} values are indicated in parentheses in Fig. 4). These circumstances display the orienting effect of the carbonyl group, resembling that of the nucleophilic group in E2 reactions.

It is also of interest to note the reactivity of α-hydrogens in cyclohexanones. As the diagrams for 2-methylcyclohexanone and 3-methylcyclohexanone indicate, axial hydrogens are expected to be more reactive than equatorial ones; this is in accord with Corey's observation of the enolization of 3-β-acetoxycholestan-7-one in hydrobromic acid.[25]

The calculations were carried out on the HITAC 5020 computer at the computation center of the University of Tokyo.

25) E. J. Corey and R. A. Sneen, *J. Am. Chem. Soc.*, **78**, 6269 (1959). The present authors are grateful to Professor Katsuhiko Ichikawa for pointing out this article.

BULLETIN OF THE CHEMICAL SOCIETY OF JAPAN VOL. 42 356—362 (1969)

Mechanism of Intramolecular Energy Transfer in Rare Earth Chelates as Revealed by Infrared Absorption Measurements

Yoshihisa MATSUDA,*1 Shoji MAKISHIMA and Shigeo SHIONOYA

The Institute for Solid State Physics, The University of Tokyo, Roppongi, Minato-ku, Tokyo

(Received June 24, 1968)

The purpose of this paper is to clarify the mechanism of intramolecular energy transfer from the triplet state of the ligand to the excited levels of the central ion in rare earth chelates. As to seven kinds of samarium β-diketonates, the frequency of infrared absorption due to the stretching vibration of the chelate bond, $\tilde{\nu}_{MO}$, and the manner of energy transfer are investigated. The probability of energy transfer is estimated from the ratio of the intensity of the samarium emission to that of the ligand phosphorescence, I_{Sm}/I_{ph}. The overlap integral, S, between the ligand phosphorescence spectrum and the samarium absorption spectrum is obtained. It was found that a linear relation roughly holds between $\log\{(I_{Sm}/I_{ph})/S\}$ and $\tilde{\nu}_{MO}$. On the basis of this fact, one is led, by making some arguments, to the conclusion that intramolecular energy transfer is dominated by the resonance mechanism due to the exchange interaction of the π electron system of the ligand triplet state with the f electron system of the central rare earth ion.

In chelates of rare earths such as europium, intramolecular energy transfer takes place from the ligand to the central rare earth ion, and consequently luminescence of line spectrum due to the f–f transition of the rare earth ion is emitted. The manner and mechanism of this intramolecular energy transfer process has been recently studied by a number of investigators. This has attracted interest also from the viewpoint that these chelates are important as laser materials.

In our previous paper,[1] we have elucidated that after absorption from the ground state to the excited singlet state of the ligand relaxation takes place to the triplet state of the ligand, and then energy is transferred to the central rare earth ion. The purpose of this paper is to clarify the mechanism of this energy transfer process. It is considered that the nature of the chelate bond is closely connected with the efficiency of the energy transfer process. The strength and electron density of the chelate bond will be widely changed with the change of the ligand. This would be strongly reflected to the manner of infrared absorption due to the vibration of the chelate bond. Therefore, it would be useful, for clarifying the mechanism of energy transfer, to investigate the correlation of the efficiency of intramolecular energy transfer with the frequency of the infrared absorption of the chelate bond.

The infrared absorption of metal chelates has been studied by several investigators. Nakamoto and Martell[2] calculated the frequency of the stretching vibration of chelate bond for transition metal acetylacetonates by the normal-coordinate analysis, and made the assignment of observed infrared absorption bands. Misumi and Iwasaki[3] also carried out the normal-coordinate analysis for acetylacetonates of various rare earths, and stated that the force constants for the stretching of rare earth-oxygen (M–O) bond are nearly proportional to the reciprocal values of M–O bond length.

Previously, we have investigated[4] the correlation between the manner of the temperature quenching of the emission of chelated europium ion and the frequency of the M–O bond stretching vibration for seven kinds of europium β-diketonates. It was found in general that the higher the frequency of the M–O bond vibration is, the less quenched the europium emission is with increasing temperature. It was reported by Bhaumik[5] that both the intensity and the lifetime of the emission of chelated europium ion decrease with increasing temperature from 77°K, but that the intensity starts to decrease at lower temperatures than the lifetime does. For instance, in the case of europium

*1 Presently at Department of Organic Synthesis, Faculty of Engineering, Kyushu University, Fukuoka.

1) Y. Matsuda, S. Makishima and S. Shionoya, This Bulletin, **41**, 1513 (1968).

2) K. Nakamoto and A. E. Martell, *J. Chem. Phys.*, **32**, 588 (1960).

3) S. Misumi and N. Iawsaki, This Bulletin, **40**, 550 (1967).

4) S. Shionoya, Y. Matsuda, M. Morita and S. Makishima, a contributed paper at Internatl. Conf. Luminescence, Budapest, 1966, p. 9–84; in press in Proc.

5) M. L. Bhaumik, *J. Chem. Phys.*, **40**, 3711 (1964).

dibenzoylmethide, the intensity starts to decrease at 120°K while the lifetime at 220°K. Similar tendencies were observed for the other europium chelates. From these facts it is suggested that the manner of the temperature quenching is mainly dominated by the temperature dependence of the non-radiative process taking place in the ligand part before intramolecular energy transfer occurs. Then, our results as mentioned above are regarded as indicating that for those europium chelates in which the temperature quenching hardly occurs, the efficiency of intramolecular energy transfer is high and also the frequency of absorption bands due to the M–O bond stretching vibration is high. This was thought to imply that the shorter the M–O bond length is, the higher the efficiency of energy transfer becomes. It was, however, difficult for europium chelates to estimate quantitatively the efficiency of intramolecular energy transfer. If it could be done, it would present more useful information for clarifing the mechanism of intramolecular energy transfer.

It is known that samarium β-diketonates show both the samarium emission and ligand emission, although europium β-diketonates show only the europium emission. Therefore, in case of samarium chelates, it would be possible to estimate the efficiency of energy transfer from the relation between the intensity of the ligand emission and that of the samarium emission. In this paper, as to seven kinds of samarium β-diketonates, infrared absorption due to the vibration of the chelate bond and the manner of intramolecular energy transfer are investigated.

In rare earth chelates, the absorption spectra of the ligand parts show no significant difference in comparison with those of the free ligand molecules,[1] and also the emission spectra of the chelated rare earth ions are very similar to those of the free ions in solutions. Furthermore, energy transfer from the ligand to the rare earth ion is suggested to occur only in a short range, on the basis of the fact, reported by us,[1] that energy transfer does not take place if β-diketone is not coordinated to the rare earth ion in solution. From these facts, the ligand π electron system, *i. e.* energy donor, is considered to interact very weakly with the f electron system of the rare earth ion, *i. e.* energy acceptor. Therefore, it would be inferred that the theory of intermolecular energy transfer due to the resonance mechanism in condensed systems, as developed by Förster[6] and further by Dexter,[7] is also applicable to the intramolecular energy transfer in the present case. It is, therefore, necessary, for discussing the problem along this inference, to take the energy overlap of the ligand triplet level with the excited levels of the chelated rare earth ion into consideration. This energy overlap is estimated from spectral measurements. As will be described below, it has been revealed that the intramolecular energy transfer is governed by the resonance mechanism due to the exchange interaction between the ligand and the central rare earth ion.

Experimental

1) Samples. Hexa-coordinated β-diketonates of samarium were used in this investigation, although octa-coordinated ones were used by many other investigators. The reason is that octa-coordinated chelates are dissociated in solutions so that errors might be caused. The chelates used are listed with their abbreviations in Table 1. These samples were prepared by the following methods.

Table 1. List of samarium β-diketonates, $R_1 \cdot CO \cdot CH_2 \cdot CO \cdot R_2$, used in this investigation

Chelates	Abbreviation	R_1	R_2
Samarium acetylacetonate	SmAA	CH_3	CH_3
Samarium trifluoroacetylacetonate	SmTAA	CF_3	CH_3
Samarium benzoylacetonate	SmB	CH_3	C_6H_5
Samarium trifluorobenzoylacetonate	SmBFA	CF_3	C_6H_5
Samarium dibenzoylmethide	SmD	C_6H_5	C_6H_5
Samarium thenoyltrifluoroacetonate	SmTTA	CF_3	C_4H_3S
Samarium furoyltrifluoroacetonate	SmFTA	CF_3	C_4H_3O

a) SmAA, SmTAA, SmB, SmBFA: About 100 m*l* of xylene solution containing 5 g of β-diketone was refluxed with the stoichiometric quantity of metallic sodium untill all the quantity of sodium had reacted. The precipitate was filtered and was washed with *p*-xylene, benzene and ether in this order. The product, *i. e.* sodium β-diketonate, was dried by air. Aqueous solution of samarium chloride was mixed with aqueous solution of sodium β-diketonate. The precipitate, *i. e.* octa-coordinated chelate, was filtered and washed several times with water. The product was recrystallized in acetone-water, and then was dried under vacuum for 20 hr at 80—100°C in order that it is converted to hexa-coordinated chelate.

b) SmD: The octa-coordinated chelate was prepared by the ordinary piperidine method at first. This was kept under vacuum for 24—30hr at 150°C to obtain hexa-coordinated chelate.[8]

c) SmTTA, SmFTA: Aqueous solution of samarium nitrate was added to toluene solution containing about 30% excess ligand in a separatory funnel. About 50% excess piperidine was added to the solution. This was then shaken and was separated into aqueous and toluene solutions. Normal pentane was added to the toluene solution. The precipitate was collected, and

6) Th. Förster, *Ann. Phys.*, **2**, 55 (1948).
7) D. L. Dexter, *J. Chem. Phys.*, **21**, 836 (1953).
8) R. E. Whan and G. A. Crosby, *J. Mol. Spectry.*, **8**, 315 (1962).

recrystallized in toluene-pentane. The product, *i. e.* octa-coordinated chelate, was kept under vacuum at 120—150°C for 20 hr to obtain hexa-coordinated one.

2) Optical Measurements. *a) Infrared Absorption Spectra.* The measurement was made with a Hitachi EPI-2 infrared spectrophotometer with an NaCl or KBr prism for NaCl or KBr region, respectively, by means of the KBr disk method.

b) Emission Spectra. The measurement was made at liquid nitrogen temperature for methanol-ethanol (1 : 3) solutions of the chelates with the concentration of 5×10^{-3} M. A Kipp & Zonen prism double monochromator and an EMI 9558QB photomultiplier were used. As the exciting light, the 365 mμ line obtained from a 1 kW high pressure mercury lamp combined with a Bausch & Lomb grating monochromator was used.

c) Emission Lifetime. An Edgerton FX-3 type xenon flash lamp (energy: 1 joule/pulse, duration: 2μsec) with an ultraviolet-pass filter was used as the exciting light source. The response of an RCA 931A photomultiplier was fed to an oscilloscope, and decay curve was photographed. All the measuremens were made for methanol-ethanol (1 : 3) solutions of the concentration of 1×10^{-3} M at liquid nitrogen temperature.

Results and Discussions

Infrared absorption spectra were measured for seven kinds of samarium β-diketonates listed in Table 1. As examples, the spectra of SmAA and SmD are shown in Fig. 1.

The assignment of infrared absorption bands for metal acetylacetonate was made, as mentioned already, by several investigators. The theoretical assignment was given first by Nakamoto and Martell[2] for transition metal acetylacetonates. Misumi and Iwasaki[3] carried out a similar calculation for rare earth acetylacetonates. Liang *et al.*[9] also carried out a similar analysis for EuAA. It was pointed out by both of these authors that in rare earth chelates an absorption band in a region of 400 to 450 cm^{-1} is mainly due to the M–O bond stretching, and that another absorption band located at the second place counted from the short wavelength side in a region of 1500 to 1700 cm^{-1} is mainly due to the C–O bond stretching. The assignment for other rare earth β-diketonates was made empirically on the basis of the calculation for acetylacetonate.

Misumi and Iwasaki[3] showed for acetylacetonates of various rare earth ions that the larger the atomic number of the central ion is, the higher the frequency of the absorption band due to the M–O bond stretching is. We measured the frequency of this band in six kinds of β-diketonates, other than acetylacetonates, of lanthanum, samarium, europium and gadolinium, and found that this kind of tendency also holds.

The observed frequency of the absorption bands due to the M–O and C–O bond stretching, $\tilde{\nu}_{MO}$

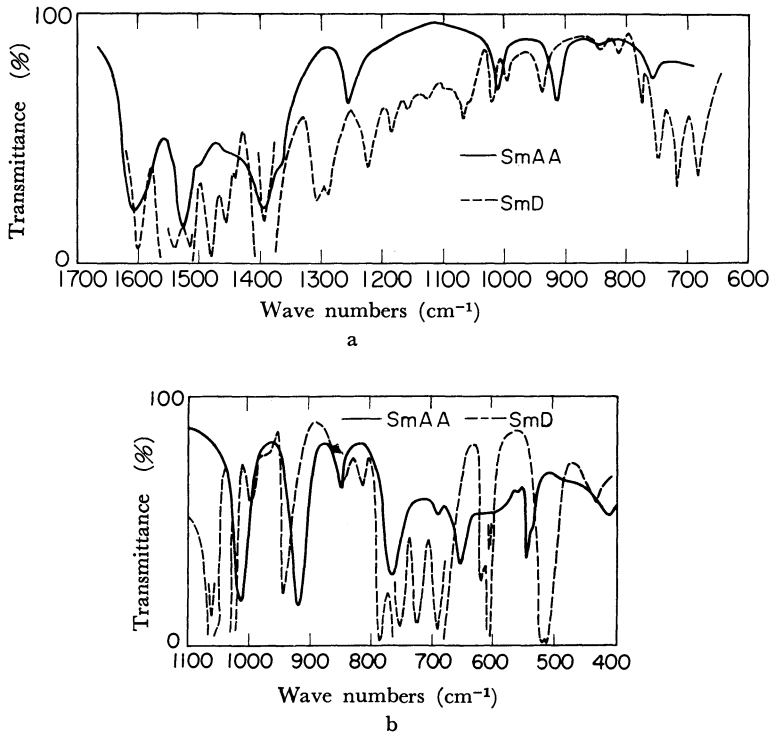

Fig. 1. Infrared absorption spectra of SmAA and SmD, a) obtained by NaCl prims, and b) by KBr prism.

9) C. Y. Liang, E. J. Schimitschek, D. H. Stephens and J. A. Trias, *J. Chem. Phys.*, **46**, 1588 (1967).

and $\tilde{\nu}_{CO}$, for seven kinds of samarium β-diketonates are given in Table 2. The frequency for the M–O bond stretching changes with the change of R_1 and R_2 in β-diketonates. Namely, the value of $\tilde{\nu}_{MO}$ becomes smaller in the order of $C_6H_6 \rightarrow CF_3 \rightarrow CH_3$. On the other hand, the value of ν_{CO} does not show such a systematic change.

TABLE 2. INFRARED ABSORPTION FREQUENCY DUE TO M–O AND C–O BOND STRETCHING, $\tilde{\nu}_{MO}$ AND $\tilde{\nu}_{CO}$, RATIO OF THE INTENSITY OF SAMARIUM EMISSION TO THAT OF LIGAND PHOSPHORESCENCE, I_{Sm}/I_{ph}, OVERLAP INTEGRAL BETWEEN LIGAND PHOSPHORESCENCE SPECTRUM AND SAMARIUM ABSORPTION SPECTRUM, S, AND $(I_{Sm}/I_{ph})/S$, FOR SEVEN KINDS OF SAMARIUM β-DIKETONATES

	$\tilde{\nu}_{MO}(cm^{-1})$	$\tilde{\nu}_{CO}(cm^{-1})$	I_{Sm}/I_{ph}	S	$(I_{Sm}/I_{ph})/S$
SmBFA	438	1530	1.00	0.630	0.444
SmD	430	1538	0.819	0.229	1.00
SmB	433	1523	0.573	1.00	0.160
SmFTA	432	1522	0.242	0.477	0.142
SmTTA	417	1538	0.0296	0.486	0.0170
SmTAA	420	1534	0.0105	0.191	0.0154
SmAA	409	1520	0.00617	0.296	0.00581

Samarium β-diketonates show, under the excitation by ultraviolet light, the emission due to the f–f transitions in the chelated samarium ion, the fluorescence from the excited singlet state of the ligand and the phosphorescence from the triplet state of the ligand. As an example, the emission spectrum of SmAA at liquid nitrogen temperature is given in Fig. 2.

We observed[1] that there is no significant difference between the phosphorescence spectra of lanthanum and gadolinium chelates which do not show the emission of the central ions. This fact indicates that the ligand triplet state is hardly affected by changing the central ion. In Fig. 2, the spectrum of the total ligand emission is separated into the phosphorescence and the fluorescence by referring to their spectra in lanthanum and gadolinium chelates.

The decay times for the samarium emission in seven kinds of samarium β-diketonates were measured by picking a part arround 600 mμ in the spectra up with color filters. It was found that the decay times are in a range of 25 to 35 μsec. The decay times for the phosphorescence were measured for a part arround 490 mμ in the spectra. Those of SmB, SmD and SmBFA were 5, 5 and 7μsec, respectively. For other samarium chelates the measurement could not be made because of low intensities of their phosphorescence.

We reported, as mentioned above, that in rare earth chelates the transfer of excitation energy takes place from the triplet state of the ligand to the excited levels of the chelated rare earth ion. For the samarium chelates studied the probabilities of non-radiative transition within the samarium excited levels would be nearly equal among each other at liquid nitorgen temperature, since there is no significant difference among the lifetimes of the samarium emission. If the transition probability from the triplet state to the ground state of the ligand does not change among these chelates, the probability of intramolecular energy transfer should be proportional to the intensity ratio of the samarium emission to the ligand phosphorescence, I_{Sm}/I_{ph}. However, the transition probability from the triplet to ground state of the ligand cannot be measured for samarium chelates, because of the reason that the lifetime of the triplet state of

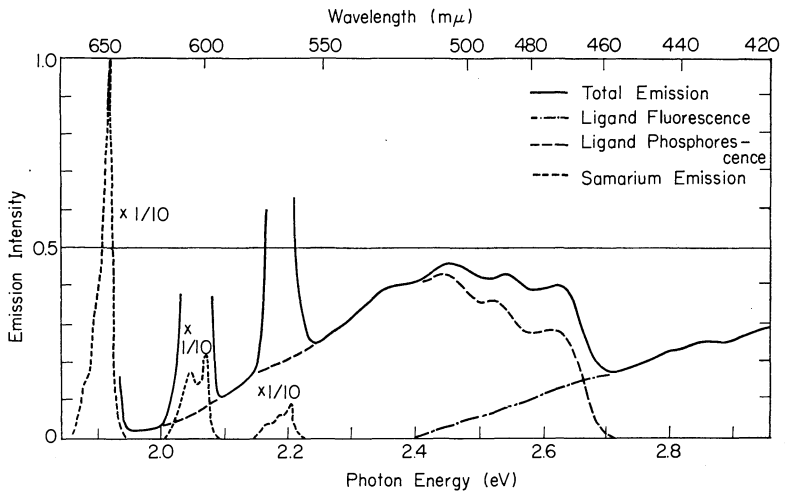

Fig. 2. Emission spectrum of SmAA at liquid nitrogen temperature. The total emission is separated into ligand fluorescence, ligand phosphorescence and samarium emission. "$\times 1/10$" indicates that emission intensity is reduced to one tenth.

samarium chelate is made shorter by the occurrence of intramolecular energy transfer, so that one can not estimate the transition probability from the observed lifetime of the phosphorescence. In the gadolinium β-diketonates, however, intramolecular energy transfer does not occur. Therefore, for seven kinds of gadolinium chelates, the ligands of which are the same as those of samarium chelates under study, the lifetime of the phosphorescence was observed, and was found to be in a range of 35 to 45μsec.

From this it may be considered that these samarium β-diketonates have nearly equal transition probabilities from the triplet to ground state of the ligand. Therefore, the probability of intramolecular energy transfer is regarded to be proportional to I_{Sm}/I_{ph}. The observed values are given in Table 2. Here, I_{Sm} and I_{ph} were obtained, respectively, from the areas of the spectra for the samarium emission and the ligand phosphorescence.

It is clearly observed from the table that the transfer efficiency is enhanced by the fluorination of the ligand or by the enlargement of the conjugate system. Further from the observation of the table, it is very roughly said that in these seven kinds of samarium chelates the larger the value of I_{Sm}/I_{ph} is the higher the frequency of $\tilde{\nu}_{MO}$ is, although there are some exceptions. As for the frequency of $\tilde{\nu}_{CO}$ such a tendency is more obscure.

Since it is inferred, as mentioned already, that the resonance between the π electron system in the ligand and the f electron system in the rare earth ion might be responsible for energy transfer, one has to take the overlap between the spectrum of the phosphorescence from the triplet state of the ligand and that of the absorption of the rare earth ion into consideration for discussing the mechanism of the intramolecular energy transfer. Therefore, the overlap integral, S, as expressed by the following equation was estimated,

$$S = \int I_{ph}(E)\, a(E)\, dE, \qquad (1)$$

where $I_{ph}(E)$ is the phosphorescence spectrum and $a(E)$ is the absorption spectrum of the chelated samarium ion, both being normalized as

$$\int I_{ph}(E)dE = 1 \text{ and } \int a(E)\,dE = 1.$$

Since the absorption spectra of the chelated samarium ions in the chelates used could not be measured because of their very small absorption coefficient, the absorption spectrum of $SmCl_3$ solution was used as a substitute. The absorption and emission spectra of $SmCl_3$ in ethanol solution with the concentration of 1 M are shown in Fig. 3. The absorption measurement was made with a Cary model 14 spectrophotometer at room temperature. This shows an emission spectrum similar to that of the chelated samarium ion; that is, the positions of the emission peaks differ only by 0.006—0.009 eV from those of the chelated samarium ion. The band-width of the phosphorescence spectrum of samarium β-diketonates is about 0.4 eV as seen from Fig. 2. The peak position of the phosphorescence spectrum depends markedly on the kind of the ligand in samarium β-diketonates. It differs at least by 0.25 eV among the seven chelates studied. Therefore, the slight difference of the samarium emission spectra between the chelates and chloride is negligible in comparison with the difference of the phosphorescence spectra. From these facts, it is reasonable to use the absorption spectrum of samarium chloride as a substitute for that of the chelates. The results for S thus estimated are given in Table 2. The values are expressed by normalizing the largest value to be unity.

As is well known Förster[6] investigated the theory of intermolecular energy transfer by resonance mechanism. Dexter[7] developed the theory further to the case where the resonance due to various types of interactions take place. In the case of energy transfer due to exchange interaction, which occurs when energy donor and acceptor are located in close ranges, the probability of transfer, P_t, is approximately given by[7]

$$P_t = \text{const. } S\exp(-2R/L), \qquad (2)$$

where R is the donor-acceptor distance, L is the

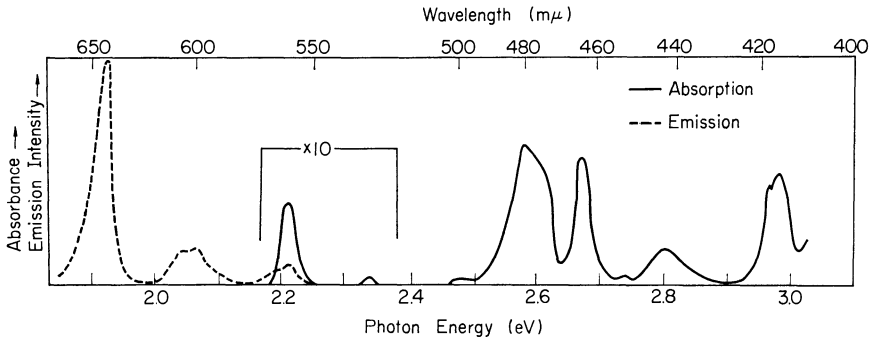

Fig. 3. Absorption spectrum at room temperature and emission spectrum at liquid nitrogen temperature of $SmCl_3$ in ethanol solution. "$\times 10$" indicates that absorbance is ten times magnified.

effective average Bohr radius for the excited and unexcited states of donor and acceptor and S is the overlap integral as defined by Eq. (1). The exponential term of this equation represents the magnitude of the spacial overlap of the wave functions of donor and acceptor.

I_{Sm}/I_{ph} is, as described above, proportional to the probability of intramolecular energy transfer. It was found, after some graphical trial, that a linear relation roughly holds between the values of log $\{(I_{Sm}/I_{ph})/S\}$ and $\tilde{\nu}_{MO}$ as shown in Fig. 4. Namely,

$$I_{Sm}/I_{ph} \propto P_t = a\,S\exp(b\,\tilde{\nu}_{MO}), \tag{3}$$

where a and b are constants.

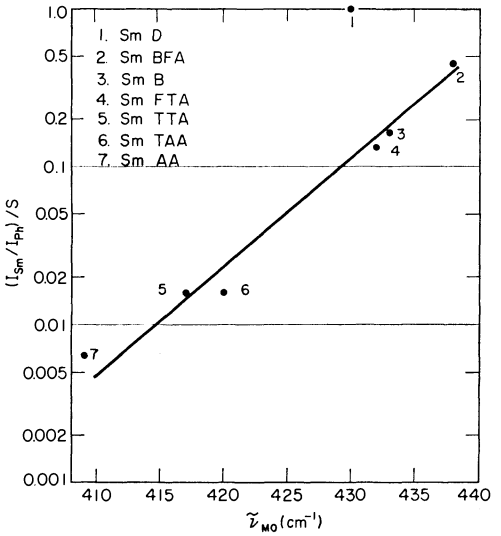

Fig. 4. Plotting of $\tilde{\nu}_{MO}$ *vs.* $(I_{Sm}/I_{ph})/S$ (in logarithmic scale) for seven kinds of samarium β-diketonates.

Let us examine how this experimentally obtained equation is correlated with Eq. (2), the theoretical one for the case of energy transfer due to the exchange interaction. The reduced mass relating with $\tilde{\nu}_{MO}$ in Eq. (3) has the same value for all chelates studied, since M is always samarium. Therefore, $\tilde{\nu}_{MO}$ is proportional to the square root of the force constant of the M–O bond stretching, $\sqrt{k_{MO}}$. Since all the observed values of $\tilde{\nu}_{MO}$ are located in a small range of frequency, *i. e.* in 409 to 438 cm^{-1}, $\tilde{\nu}_{MO}$ can be approximately replaced by k_{MO}. Then, Eq. (3) can be rewritten as,

$$P_t = a'S\exp(b'\,k_{MO}), \tag{4}$$

where a' and b' are constants. It was confirmed that if the plot of $\tilde{\nu}_{MO}{}^2$*vs.* log $\{(I_{Sm}/I_{ph})/S\}$ is made, a rough straight line as in Fig. 4 is obtained.

Several authors studied the correlation of the force constant of chelating bond with the bond length and also with the electron density at the bond. Misumi and Iwasaki[3] reported, as mentioned already, that k_{MO} is nearly proportional to the reciprocal value of the M–O bond length for various rare earth acetylacetonates, if the sum of the ionic radii of oxygen and rare earth ion is taken as the bond length. For the acetylacetonates they studied, the bond length is in the range of 1.43 to 1.56 Å, and $\tilde{\nu}_{MO}$ in the range of 420 to 432 cm^{-1}. The observed values of $\tilde{\nu}_{MO}$ shown in Table 2 change from 409 to 438 cm^{-1}. The M–O bond length in this case, therefore, would be regarded to change a little more widely than the case reported by Misumi and Iwasaki. It would be likely that in various samarium chelates the real length of the M–O bond changes by the change of ligand. Since k_{MO} would be affected by the M–O bond length, r_{MO}, one may assume that the correlation between k_{MO} and r_{MO}, as reported by Misumi and Iwasaki, also holds in this case in which the ligand, but not the central ion, is changed. Since the change of r_{MO} in various samarium chelates is limited only in a narrow range, the inverse proportion of k_{MO} to r_{MO} can be replaced by a simpler dependence, in other words, k_{MO} may be regarded to decrease linearly with the increase of r_{MO}.

Nakamoto *et al.*[10] showed that k_{MO} of transition metal β-diketonates is increased, if the electron density at oxygen in chelate bond is increased by the substitution of R_1 and R_2. Taking it into consideration that k_{MO} is increased with the increase of the electron density at oxygen and also with the increase of electronegativity of the central ion, one can assume that k_{MO} is increased with the increase of electron donation from oxygen to the central ion in chelate bond. The increase of the electron donation would cause the reduction of the bond length.

From the above-mentioned discussion, one may say that k_{MO} is decreased approximately in proportion to the increase of r_{MO}. Therefore Eq. (4) can be rewritten as,

$$P_t = a''S\exp(-b''\,r_{MO}), \tag{5}$$

where a'' and b'' are constants. This equation is equivalent to Eq. (2).

This indicates that the theory of intermolecular energy transfer due to the exchange interaction can be applied also to intramolecular energy transfer in the chelate system. In other words, this indicates that the intramolecular energy transfer under discussion is dominated by the resonance mechanism due to the exchange interaction of the π electron system of the ligand triplet state with the f electron system of the central rare earth ion.

10) K. Nakamoto, Y. Morimoto and A. E. Martell, *J. Am. Chem. Soc.*, **66**, 346 (1962).

Summary and Conclusion

In order to clarify the mechanism of intramolecular energy transfer in rare earth chelates, the correlation of the efficiency of energy transfer with the frequency of the infrared absorption of the chelate bond was investigated. It is known that this energy transfer takes place *via* the triplet state of the ligand. Seven kinds of samarium β-diketonates as shown in Table 1 were used, since samarium chelates show both the samarium emission and ligand emission so that they are more suitable for the present investigation than the chelates of other rare earths. The probability of intramolecular energy transfer was estimated from the ratio of the intensity of the samarium emission to that of the ligand phosphorescence. It is inferred that the theory of intermolecular energy transfer due to the resonance mechanism would be also applicable to the intramolecular energy transfer in the present case. To make discussion along this inference, the overlap integral between the ligand phosphorescence spectrum and the samarium absorption spectrum was estimated.

It was found that an experimental relation as expressed by Eq. (3) roughly holds among the probability of intramolecular energy transfer, the frequency of infrared absorption due to the stretching vibartion of the chelate bond and the overlap integral. By some arguments it was shown that this equation is equivalent to the theoretical equation, Eq. (2), expressing the probability of energy transfer by the resonance mechanism due to the exchange interaction. In conclusion, one can say that intramolecular energy transfer in rare earth chelates is dominated by the resonance mechanism due to the exchange interaction of the π electron system of the ligand triplet state with the f electron system of the central rare earth ion.

The authors wish to thank Mr. M. Morita in this laboratory for his discussion.

BULLETIN OF THE CHEMICAL SOCIETY OF JAPAN VOL. 42 362—365 (1969)

Some Remarks on the Fragmentation of Excited Ions in the Radiolysis of Hydrocarbons

Tetsuo MIYAZAKI

Department of Synthetic Chemistry, Faculty of Engineering, Nagoya University, Chikusa-ku, Nagoya

and Kuniyasu TANNO and Shoji SHIDA

Laboratory of Physical Chemistry, Tokyo Institute of Technology, Meguro-ku, Tokyo

(Received June 26, 1968)

The fragmentation of excited ions in the liquid-phase radiolysis of hydrocarbons is explained by a new mechanism, which involves the fragmentation of a highly excited ion (M^{+**}). The M^{+**} ion is considered here to be the electronic excited states and to decompose by the following mechanism. The electronic excitation energy can spread over all C–C bonds in a molecule before its fragmentation and, when the mean excitation energy per C–C bond exceeds its bond energy, the excited ion decomposes instantaneously in one vibration. Further, the mass spectra of isobutane and isooctane are calculated by a simplified quasi-equilibrium theory by introducing the highly excited ion and are compared with experimental mass spectra and with the calculated values without introducing the highly excited ion.

The mechanism of fragmentation of excited ions in gases at low pressure has usually been studied by an analysis of mass spectra. Quasi-equilibrium theory originally proposed by Rosenstock *et al.*[1] has been developed by several investigators[2] and successfully applied to an interpretation of mass spectra of polyatomic molecules. The theory is based on the fundamental assumption that the

1) H. M. Rosenstock, M. B. Wallenstein, A. L. Wahrhaftig and H. Eyring, *Proc. Natl. Acad. Sci. U. S.*, **38**, 667 (1952).

2) The development of this theory is reviewed by H. M. Rosenstock and M. Krauss in "Mass Spectrometry of Organic Ions," Academic Press, New York, (1963).

Table 1. Fragmentation of excited saturated hydrocarbon ions in the liquid phase

	C CC–C$^+$	C CC–C$^+$ C	C CC–CC$^+$	C C CC–CC$^+$	C C CC–CCC$^+$ C
Bond energy of ion (eV)[a]	0.61	0.35	0.82	0.74	0.56
$G(M^{+*}) + G(M^{+**})$	2.3[c]	1.76[c]	0.83—1.6[d]	1.2—1.8[d]	1.6—1.7[d]
$G(M^{+**})$	1.15	1.0	0.23	0.50	0.36
f[b]	0.50	0.57	0.28—0.14	0.42—0.28	0.22—0.21

a) J. L. Franklin and F. W. Lampe, *Trans. Faraday Soc.*, **57**, 1449 (1961).
b) $f = G(M^{+**})/\{G(M^{+**}) + G(M^{+**})\}$
c) $G(M^{+*}) + G(M^{+**})$ was obtained in the radiolysis of isobutane[6] and neopentane[7] in the gas phase at low pressure.
d) $G(M^{+*}) + G(M^{+**})$ was calculated from the mass spectrum by assuming $W = 25$ eV. The uncertainty in the values is due to the secondary decomposition of fragment ions in the mass spectrometer.

randomization of excitation energy among oscillators occurs before dissociation of the excited ion.

Molecular orbital theory developed by Hirota *et al.*[3] has been successfully applied to the mass spectra of organic compounds.

Recently, the present authors studied the radiolysis of hydrocarbons such as neopentane,[4] isooctane,[4] isobutane,[5] isopentane[5] and 2,3-dimethylbutane[5] in the liquid phase, and found that the fragmentation of excited ions is important. Since collisions between neighboring molecules in a liquid take place roughly in 10^{-13} sec, some of the excited ions must decompose in the period of one vibration ($\lesssim 10^{-13}$ sec) before collisional deactivation. Therefore, the mechanism of such a fast decomposition should be explained by some new theory other than the quasi-equilibrium theory which assumes the randomization of vibrational excitation energy among oscillators.

In the present work, we attempt to explain the fragmentation of excited ions in the liquid phase by a new simple mechanism.

Mechanism of Fragmentation of Excited Ions

It was found by a previous study[6] on the effect of density in the radiolysis of butanes that excited ions are divided into two types. Thus, the ionic fragmentation of a hydrocarbon molecule can be depicted as

$$M \longrightarrow M^{+*} + e \quad (1)$$
$$\longrightarrow M^{+**} + e \quad (2)$$
$$M^{+*} \longrightarrow F^+ + R \quad (3)$$
$$M^{+*} + M \longrightarrow M^+ + M \quad (4)$$
$$M^{+**} \longrightarrow F^+ + R \quad (5)$$

where M is the hydrocarbon molecule, for example, C_4H_{10}, M^{+*} is the excited ion which decomposes slowly and consequently is more efficiently deactivated with increasing density. M^{+**} is another type of ion which is highly excited and decomposes in the period of one vibration, not being susceptible to collisional deactivation even at high densities above 0.1 g cc^{-1}. F^+ is a fragment ion, for example $C_3H_7^+$, and R is a fragment radical, for example CH_3. In order to obtain further information on the fragmentation of highly excited ions, the ionic fragmentation of several hydrocarbons in the liquid phase was studied using ion scavengers. Results reported previously[4,5] are summarized in Table 1. $G(M^{+**})$ represents the yields of ionic fragmentation in the liquid phase, obtained from the yields of carbonium ion (F^+). $G(M^{+*}) + G(M^{+**})$ represents the yields of ionic C–C bond rupture from the total excited ions and can be obtained from radiolysis in the gas phase or from the mass spectrum assuming $W = 25$ eV. The yields of ionic C–C bond rupture from the M^{+**} ion relative to those from total excited ions are represented by $f = G(^{+**})/\{(G(M^{+*}) + G(M^{+**})\}$. Though the bond energy of isobutane is approximately the same as that of isooctane, the f-value of isobutane is much greater than that of isooctane. This indicates that the fragmentation of M^{+**} ion depends upon the number of carbon atoms in the ion. On the other hand, though the number of carbon atoms in neopentane is the same as that of isopentane, the f-value of neopentane is much greater than that of isopentane. This shows that the fragmentation of M^{+**} ion also depends upon the bond energy of ions. The selective C–C bond rupture of M^{+**} ion suggests intramolecular energy transfer within the period of one vibration. It is difficult to attribute the energy transfer in a short time ($\lesssim 10^{-13}$ sec) to the transfer of vibrational energy. Therefore, it is attributed to the transfer of electronic excitation energy. The rate of intramolecular

3) K. Hirota and Y. Niwa, *J. Phys. Chem.*, **72**, 5 (1968). The related papers are cited therein.
4) K. Tanno, T. Miyazaki, K. Shinsaka and S. Shida, *J. Phys. Chem.*, **71**, 4290 (1967).
5) K. Tanno, S. Shida and T. Miyazaki, *ibid.*, **72**, 3496 (1968).
6) T. Miyazaki, *ibid.*, **71**, 4282 (1967).
7) T. Miyazaki and S. Shida, This Bulletin, **39**, 2344 (1966).

transfer of electronic excitation energy is given by the following equation,[8]

$$\Delta n = 2.22 \times 10^{15} |\beta| t \qquad (I)$$

where β is the resonance integral between neighboring carbon atoms in a molecule and Δn the numbers of carbon atoms over which the excitation energy can migrate in t sec. Since β of saturated hydrocarbons amounts to 1—2 eV, we get $\Delta n = 100-200$ at 5×10^{-14} sec. That is, the excitation energy can spread in a time of 5×10^{-14} sec over a large number of atoms, C_{100}–C_{200}. If the highly excited ion (M^{+**}) decomposes from the electronically excited states, it may be reasonable to assume the following mechanism: First, the electronic excitation energy can spread over all C–C bonds in a molecule prior to its fragmentation, even in a highly exicted ion. Second, the excited ion decomposes instantaneously in one vibration, when the mean excitation energy per C–C bond exceeds its bond energy. If the potential energy surfaces for the excited states are repulsive, the second assumption may be valid. In the present study, the distribution function of excitation energy for saturated hydrocarbons is taken from that for *n*-butane, which was obtained experimentally by Chupka and Kaminsky.[9] Since the number of C–C bonds in the isobutane ion is three and the bond energies are 0.61 eV, ions with an excitation energy exceeding 1.83 eV behave as a $C_4H_{10}^{+**}$ ion and ions with an exictation energy of 0.61 eV to 1.83 eV behave as an $C_4H_{10}^{+*}$ ion. The amounts of $C_4H_{10}^{+**}$ and $C_4H_{10}^{+*}$ ions present are obtained from the distribution function of excitation energy. The calculated f is compared with the observed one in Fig. 1. Allowing for

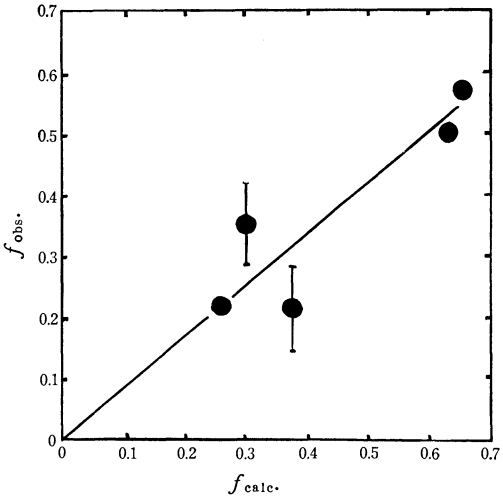

Fig. 1. Comparison of calculated f-values with obseved f-values.

the simplicity of the present treatment and some errors in the experimental values, we may say that the fragmentation of excited ions in the liquid phase is explained by this mechanism. The calculated values of f are slightly higher than the experimental ones. This result suggests that part of excitation energy spreads over C–H bonds, and that about 15% of the total excitation energy may spread over C–H bonds in the short time of rapid decomposition. The distribution of excitation energy in an ion may be related to the initial energy absorption of atoms in the ion. If the initial energy absorption is assumed proportional to the electron density of atoms in the ion, about 70% of the total energy will be absorbed in the carbon atoms in a saturated hydrocarbon ion. It is nescessary in the future to investigate the competing fragmentation reaction with the intramolecular energy transfer from a theoretical as well as an experimental aspect.

Interpretation of Mass Spectra by the Introduction of a Highly Excited Ion (M^{+**})

The mass spectra of saturated hydrocarbons have hitherto been explained by quasi-equilibrium theory.[1] According to a simplified treatment[10] of this theory, the rate constant for dissociation

8) J. L. Magee, "Comparative Effects of Radiation," John Wiley and Sons, Inc., New York (1960), p. 130. The system consists of a chain of N molecules. When the system suffers particle impact, at the initial instant of time $t=0$, the excitation is located on a particular member of the chain, say the p_{th}. The excitation will migrate after a lapse of time. The probability that the excitation will be located on the q_{th} member of the chain at time t is expressed as

$$P(p, q, t) = \left[J_{p-q}\left(\frac{4\pi|\beta|t}{h}\right)\right]^2$$

where $J_{p-q}(4\pi|\beta|t/h)$ is the Bessel function of integral order $p-q$ of the argument $4\pi|\beta|t/h$. β is the resonance integral between neighboring molecules of the chain. If the excitation spreads over Δn units of the chain at time t,

$$(\Delta n)^2 = \overline{(q-p)^2} = \sum_{c=1}^{N}(q-p)^2 P(p, q, t)$$

If we limit our consideration to long chains, it follows that

$$(\Delta n)^2 = \overline{(q-p)^2} = 2\sum_{n=0}^{\infty} n^2 J_n{}^2\left(\frac{4\pi|\beta|t}{h}\right)$$

and it has been found by the use of tabulated Bessel functions that

$$\Delta n = 0.707 \times \frac{4\pi|\beta|t}{h} = 2.22\times10^{15}|\beta|t$$

It is necessary to refer to the original paper by J. L. Magee for more detailed arguments.

9) W. A. Chupka and M. Kaminsky, *J. Chem. Phys.*, **35**, 1991 (1961).

10) D. P. Stevenson, *Radiation Res.*, **10**, 610 (1959).

of a molecule ion with an excitation energy of ε is given by $k(\varepsilon)$:

$$k(\varepsilon) = A\left(1-\frac{\varepsilon_0}{\varepsilon}\right)^{S-1} \qquad \text{(II)}$$

where S is the number of degrees of vibrational freedom of the ion and ε_0 the bond dissociation energy. A is the frequency factor and is taken as 10^{14} sec^{-1} for a simple bond dissociation process. It has been reported that if k is calculated from Eq. (II) using the experimental values of ε_0 and ε and the full number of degrees of vibrational freedom (S), the mass spectrum can not be understood. Several modifications[2] have been undertaken in order to improve the rate constant for fragmentation. For example, it was assumed that the higher transition probability of the excited ion compared with the experimental value was taken in the region of high excitation energy and that the effective number of internal degrees of freedom was considerably less than the full number expected from the molecular structure of the ions.

As proposed in the previous section, the excited ions are divided into two species, M^{+*} and M^{+**}. Since the existence of M^{+**} ion has been hitherto ignored in the calculation of mass spectra by quasi-equilibrium theory, we therefore attempt here to calculate mass spectra introducing the highly excited ion (M^{+**}) in addition to the M^{+*} ion which decomposes according to quasi-equilibrium theory (Calculation A). We also calculate mass spectra by the quasi-equilibrium theory without introducing the M^{+**} ion (Calculation B). Calculations are carried out under the following assumptions.

Calculation A: The excited ion consists of two species M^{+*} and M^{+**}, and the formation of either M^{+*} or M^{+**} is determined by the following two conditions. First, when the mean excitation energy per C–C bond exceeds the bond energy, the excited ion belongs to the M^{+**} ion and decomposes in the period of one vibration.

$$k(\varepsilon) \geqq 10^{13}\,\text{sec}^{-1}, \quad \varepsilon_{max} \geqq \varepsilon > n\varepsilon_0$$

where n is the number of C–C bonds in an ion. Second, when the mean excitation energy per C–C bond does not exceed the bond energy, the excited ion belongs to the M^{+*} ion and decomposes after the accumulation of excitation energy in a particular bond.

$$k(\varepsilon) = \text{Eq. (II)}, \quad n\varepsilon_0 \geqq \varepsilon > \varepsilon_0$$

Calculation B: Only the fragmentation of M^{+*} ion is considered and quasi-equilibrium theory is applied over the whole range of excitation energy.

$$k(\varepsilon) = \text{Eq. (II)}, \quad \varepsilon_{max} \geqq \varepsilon > \varepsilon_0$$

The distribution function of excitation energy for isobutane and isooctane was taken as that of n-butane.[9] For analytical convenience, $k(\varepsilon)$ was calculated from Eq. (II) summing over integrals for all internal energies of 0.5 eV. ε_0 used is given in Tables 2 and 3. The effective number of internal degrees of freedom (S) was determined using the condition $k(\varepsilon_{max}) \leqq 5\times10^{12}$ sec^{-1}. Under this condition, the quasi-equilibrium of vibrational excitation energy among the oscillators may be satisfied. In the present calculation, only the primary decomposition was considered. Actually, the secondary decomposition of fragment ions (reaction (7) and (8)) follows after the primary decomposition (reaction (6)) in a msas spectrometer.

$$i\text{-}C_4H_{10}^+ \longrightarrow C_3H_7^+ + CH_3 \qquad (6)$$
$$C_3H_7^+ \longrightarrow C_3H_5^+ + H_2 \qquad (7)$$
$$C_3H_5^+ \longrightarrow C_3H_3^+ + H_2 \qquad (8)$$

The amount of $C_3H_7^+$ produced in the primary decomposition of isobutane ion can be considered as the sum of $C_3H_7^+$, $C_3H_5^+$ and $C_3H_3^+$. In Tables 2 and 3, the calculated yields of major fragment ions from isobutane ion and isooctane ion are compared with experimental mass spectra. The mass spectra of isobutane are correctly interpreted qualitatively by assuming both M^{+*} and M^{+**} (Calculation A), while the treatment assuming only M^{+*} (Calculation B) fails in a proper interpretation. The mass spectra of isooctane can be understood through both methods of calculation. This is because the ratio of M^{+**} to the total excited ions of isooctane is at best about 25% and the introduction of M^{+**} does not appreciably affect the results, while the corresponding ratio of isobutane amounts to 60%.

Table 2. Fragmentation of i-$C_4H_{10}^+$

	ε_0	Mass spectra	Calculation A[a]	Calculation B[b]
$C_3H_7^+$	0.61 eV	1	1	1
$C_3H_6^+$	0.25 eV	0.23	0.50	1.49

a) Calculated by assuming M^{+**} and M^{+*}
b) Calculated by assuming only M^{+*}

Table 3. Fragmentation of i-$C_8H_{18}^+$

	ε_0	Mass spectra	Calculation A[a]	Calculation B[b]
$C_4H_9^+$	0.56 eV	1	1	1
$C_4H_8^+$	0.40 eV	0.31	0.22	0.25

a) Calculated by assuming M^{+**} and M^{+*}
b) Calculated by assuming only M^{+*}

It has been shown above that the highly excited ion (M^{+**}) is probably important in the radiolysis of hydrocarbons. However, the mechanism of its fragmentation proposed here is too simple and requires revision in the future from a theoretical as well as experimental aspect.

The authors wish to express their appreciation to Professor Zen-ichiro Kuri and Dr. Kenji Fueki for many helpful discussions.

BULLETIN OF THE CHEMICAL SOCIETY OF JAPAN VOL. 42 366—369 (1969)

Electrical Conduction of TCNQ Ion Radical Salts under High Pressure

Ichimin SHIROTANI, Takashi KAJIWARA, Hiroo INOKUCHI and Syun-iti AKIMOTO

The Institute for Solid State Physics, The University of Tokyo, Roppongi, Tokyo

(Received June 28, 1968)

With an increase in the pressure, the electrical resistance of several TCNQ anion radical salts dropped rapidly in the low-pressure region and levelled off at high pressures. The temperature dependence of the resistance of compressed salt was studied over the region from 77°K to 200°K. The values of the activation energy decreased with an increase in the pressure. However, the metallic behaviour was not observed under very high pressures. The conduction mechanism of TCNQ salts was discussed from the point of view of a band scheme.

During the past decade, there has been a great expansion in the amount of high-pressure work, even in the field of molecular crystals.[1,2] Generally speaking, the electrical conductivity of aromatic crystals, typical organic semiconductors, increases with an increase in the pressure. Since the mobility of the charge carriers in the crystal is not very sensitive to applied pressure,[3] the large increase in the conductivity under high pressure is mostly due to the great increment in the concentration of the charge carrier.[4,5] Similar phenomena have also been observed with charge-transfer complexes;[6] the resistance of the less conductive compound has dropped sharply with an increase in the pressure, although that of the high conductive complex had not shown any pronounced effect of the pressure.[7]

Several TCNQ ion radical salts with aromatic cations have a very high conductivity, in one case the highest yet reported for organic semiconductors, and a very small activation energy.[8] The conductivity of these solids arises from the motion of the odd π-electron among the TCNQ sites and they show semiconductive behaviour.[9] As the pressure increases, the resistance of some TCNQ salts falls rapidly in the low-pressure region until it levels off under high pressure.[10] However, the pressure effects on their thermal activation energy are still not known.

In this paper we will report our results on the temperature-dependence measurements of the resistance of several TCNQ salts at high pressure and will discuss their conduction mechanism.

Experimental

The samples used in the experiment were quinolinium-$(TCNQ)_2$ ($Q(TCNQ)_2$), bipyridinium$(TCNQ)_2$ ($BiP(TCNQ)_2$), 4-amino-2, 3, 5, 6-tetramethylanilnium-$(TCNQ)_2$ ($DAD(TCNQ)_2$), cobaltinium$(TCNQ)_2$ ($CoC(TCNQ)_2$), and lithium(TCNQ) (Li(TCNQ)). These compounds were provided by Kondow, who has reported their preparations in detail previously.[9] The samples were studied in the form of powder pressure-fused into flat platelets. The high-pressure cell for resistance measurements was similar as those used previously.[5]

The temperature dependences of the electrical resistance were measured under a constant pressure in the temperature range of 77°K—200°K. The calibration of the pressure with the cell was made using bismuth and lead phase changes at known pressures.

Results

Figures 1 and 2 show the effect of the pressure on the resistance of three TCNQ salts at room temperature. As has been observed in the case of other organic semiconductors, TCNQ complexes showed a decrease in resistance with an increase in the pressure. The decrement was much slower in the high-pressure region. The resistance of less conductive salts such as Li(TCNQ) showed a marked pressure dependence. However, those of

1) H. Inokuchi, This Bulletin, **28**, 570 (1955).
2) H. G. Drickamer, *Solid State Physics*, **17**, 1 (1965).
3) R. G. Kepler, *Phys. Rev.*, **119**, 1226 (1960); T. Kajiwara, H. Inokuchi and S. Minomura, This Bulletin, **40**, 1055 (1967).
4) Y. Harada, Y. Maruyama, I. Shirotani and H. Inokuchi, *ibid.*, **37**, 1378 (1964).
5) I. Shirotani, H. Inokuchi and S. Minomura, *ibid.*, **39**, 386 (1966).
6) Y. Okamoto, S. Snah and Y. Matsunaga, *J. Chem. Phys.*, **43**, 1904 (1965).
7) M. Schwarz, H. W. Davies and B. T. Dobriansky, *ibid.*, **40**, 3257 (1964).
8) W. J. Simons, P. E. Bierstedt and R. G. Kepler, *ibid.*, **39**, 3523 (1963); R. G. Kepler, **39**, 3528 (1963).
9) T. Kondow, K. Siratori and H. Inokuchi, *J. Phys. Soc. Japan*, **21**, 824 (1966); **23**, 98 (1967).
10) R. B. Aust, G. A. Samara and H. G. Drickamer, *J. Chem. Phys.*, **41**, 2003 (1964).

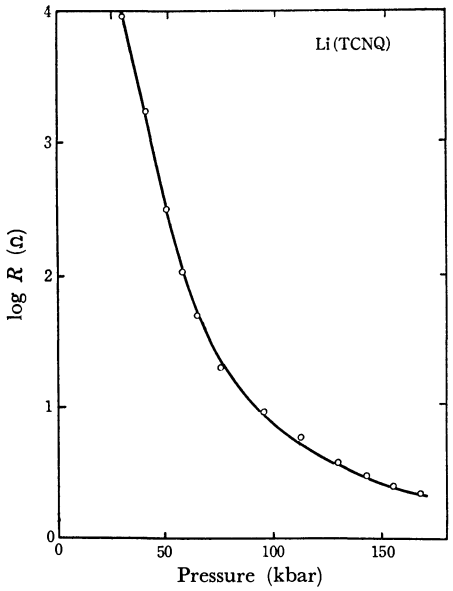

Fig. 1. The pressure dependence of the electrical resistance of Li(TCNQ) salt at room temperature.

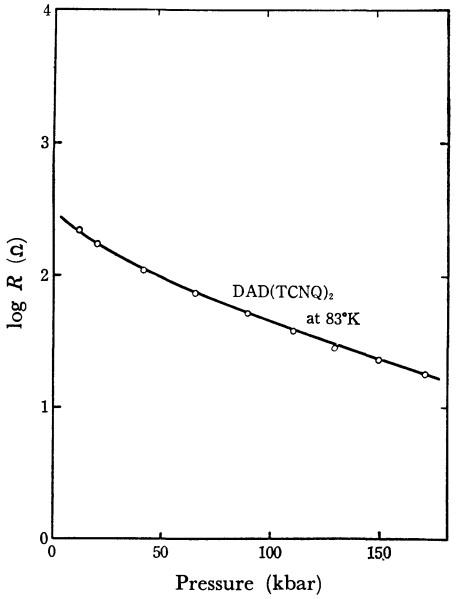

Fig. 3. The pressure dependence of the electrical resistance of $DAD(TCNQ)_2$ salt at 83°K.

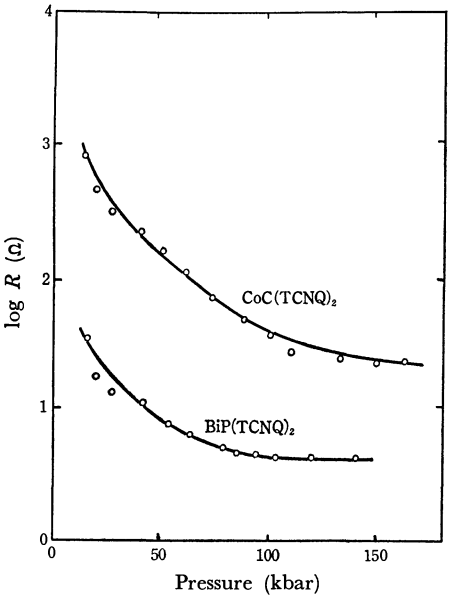

Fig. 2. The pressure resistance curve of TCNQ salts, $CoC(TCNQ)_2$ and $BiP(TCNQ)_2$, at room temperature.

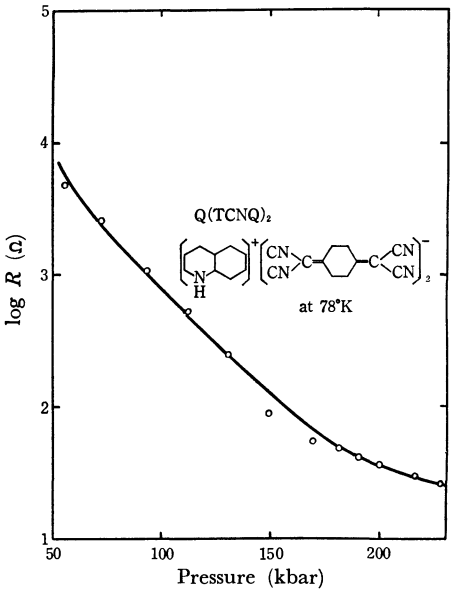

Fig. 4. The pressure resistance curve of $Q(TCNQ)_2$ at 78°K.

TABLE 1. THE ACTIVATION ENERGY OF TCNQ SALTS AT HIGH PRESSURE

Compound	ρ(Ωcm)	Activation energy (eV) at 1 bar	Activation energy (eV) at high pressure
Li(TCNQ)	5×10^5	0.32[a]	0.07 (169 kbar)
$CoC(TCNQ)_2$	6.5	0.034[b]	0.05 (150 kbar)
$DAD(TCNQ)_2$	2	0.08[a]	0.012 (228 kbar)
$BiP(TCNQ)_2$	0.5	——[b]	0.038 (46 kbar) 0.017 (130 kbar)
$Q(TCNQ)_2$	0.25	0.03[a]	0.035 (30 kbar) 0 025 (208 kbar)

a) Ref. 8 (W. J. Simons *et al.*).
b) L. R. Melby *et al.*, *J. Am. Chem. Soc.*, **84**, 3374 (1962).

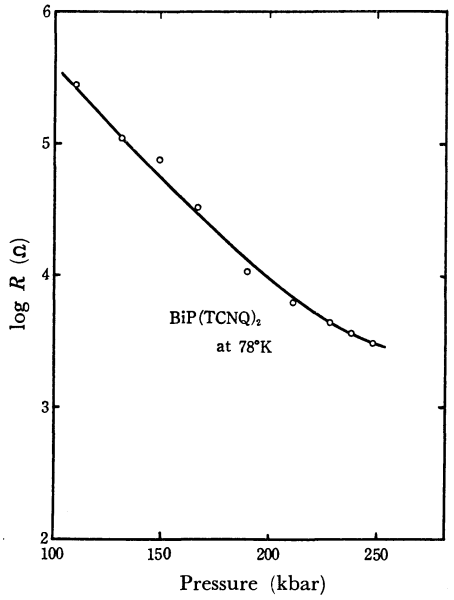

Fig. 5. The relation between pressure and electrical resistance for $BiP(TCNQ)_2$ at 78K°.

the high-conductive salts, such as $Q(TCNQ)_2$ and $DAD(TCNQ)_2$, were insensitive to pressure at room temperature.

Figures 3,4 and 5 show the pressure-resistance curve in the low-temperature region for $DAD(TCNQ)_2$, $Q(TCNQ)_2$ and $BiP(TCNQ)_2$ respectively. Above 100 kbar, the resistance of $Q(TCNQ)_2$ at room temperature rose with an increase in the pressure and drifted upward with time.[10] In the low-temperature region, at 78°K, these phenomena were not found; this means that no chemical reaction occurred.

The activation energies decreased with an increase in the pressure, but did not converge to zero up to 200 kbar. Table 1 shows the values of the activation energies under high pressures.

Discussion

A pressure-induced phase transition to the conducting state has been found for inorganic semiconductors, such as silicon and germanium;[11] their crystal structures change from the diamond type to the white-tin type.[12] However, molecular crystals have not become metallic except for I_2, Se, SnI_4 and pentacene*1 under high pressures. Though the behaviour of the pressure-resistance relation of these exceptional crystals is similar to that of organic semiconductors, the energy gaps become zero without crystal transformation at high pressures.[2]

Kepler *et al.* proposed that $Q(TCNQ)_2$ shows a metallic behaviour at atmospheric pressure: temperature-independent conductivity as high as 10^2 $ohm^{-1}\,cm^{-1}$ and temperature-independent paramagnetic susceptibility.[8] Recently, on the other hand, we have found that $Q(TCNQ)_2$ behaves as a typical semiconductor:[9] it shows a temperature-dependent conductivity of the single crystal, a slightly - temperature - dependent magnetic susceptibility, and also an absorption edge in the far infrared-wavelength region (about 40 cm^{-1}).

In accordance with Mott's criterion for the metal-semiconductor transition,[13] LeBlanc proposed that:

$$2E = C - \Delta \qquad (1)$$

where E is the activation energy, C is the electrostatic energy, and Δ is the band width.[14] When the $C > \Delta$ relation is satisfied, the system is semiconductor, and when $C < \Delta$, the system is metal. The same author estimated the values for TCNQ salts as:

$$\Delta \simeq 0.1\,eV \quad \text{and} \quad C < 0.5\,eV \qquad (2)$$

Since Δ seems to be more sensitive to the pressure than C does in the first approximation, these compounds may be expected to become metals under high pressure. On the contrary, as Table 1 shows, their energy gaps did not reach zero, at least not up to 200 kbar.

Generally, an increase in the pressure results in an increase in the band width. An energy band of a molecular crystal such as anthracene widened 5—6 times at 161 kbar as compared with the value at atmospheric pressure.[4] However, the band width of high-conductive TCNQ salts seems to be less affected by the pressure.*2

In several TCNQ salts with aromatic cations, the line shape of the absorption curve at the edges can be expressed by Eq. (3) at room temperature;[9]

$$k \propto (\nu - \nu_G)^n$$
$$(\nu_G = 36.5\,cm^{-1};\ n = 0.46 \pm 0.05 \text{ for } Q(TCNQ)_2) \qquad (3)$$

where k is the absorption coefficient; ν, the wave number of the incident light, and ν_G and n, the constants. The shape of this absorption edge is due to the direct allowed transition from the valence band to the conduction band. Further, the slightly-tempeature-dependent paramagnetic susceptibility of $Q(TCNQ)_2$ can be explained tentatively in terms of the band theory.[9]

On the other hand, the mobility of the carrier is less than 0.1 $cm^2/V{\cdot}sec$,[8] though the energy gap

11) S. Minomura and H. G. Drickamer, *J. Apply. Phys.*, **34**, 3043 (1963).

12) J. C. Jammison, *Science*, **139**, 762 (1963).

*1 The confirmation of the transition from semiconductor to metal is very difficult, because the chemical change is superposed on the transition.

13) N. F. Mott, *Phil. Mag.*, **6**, 287 (1961).

14) O. H. LeBlanc, *J. Chem. Phys.*, **42**, 4307 (1965).

*2 Their compressibility has not been measured. Probably, they are less compressible than ordinary hydrocarbon solids.

of high conductive TCNQ salts is very small; moreover they have partly-filled bands when considered simply, but they do not show a metallic behaviour even at high pressures. Considering these points, the conduction mechanism can not be explained by the usual band theory. Therefore, on the basis of the experimental results we suggest that even if a conduction band exists, the band width is probably very narrow.

Generally, a presssure coefficient for the optical energy gap of inorganic semiconductors agrees with the value determined by measuring the intrinsic resistivity as a function of the pressure. A similar behaviour has been observed in such molecular crystals as quaterrylene ($C_{40}H_{20}$).[15] If the pressure effect of the far-infrared absorption spectra of TCNQ salts could be studied, these electronic states could be discussed in detail.

The authors wish to thank Dr. T. Kondow for his helpful discussion.

15) I. Shirotani, H. Inokuchi and S. Akimoto, This Bulletin, **40**, 2277 (1967).

BULLETIN OF THE CHEMICAL SOCIETY OF JAPAN VOL. 42 369—372 (1969)

The Formation of Transient Aromatic Ions in Solutions by the Flash Illumination

Kiyoshi KAWAI, Naoto YAMAMOTO and Hiroshi TSUBOMURA

Department of Chemistry, Faculty of Engineering Science, Osaka University, Toyonaka, Osaka

(Received July 1, 1968)

Flash illumination of an oxygen-free acetonitrile solution containing *p*-dimethoxybenzene (DMB) and *s*-trinitrobenzene or chloranil gave a transient absorption spectrum of DMB cation. The decay of the transient absorption spectra follows the second-order reaction kinetics proving that the decay is brought about by the recombination of the anion and the cation after the flash illumination. The formation of the ion-pair may be explained as follows:

$$A + h\nu \longrightarrow A^*$$
$$A^* + D \longrightarrow A^- - D^+$$
$$\downarrow$$
$$A^-_{solv.} + D^+_{solv.} \longrightarrow A + D$$

It was found by Leonhardt and Weller that the fluorescence of perylene in non-polar solvents was quenched by addition of anilines or amines and new fluorescence bands appeared, which were ascribed to the charge transfer fluorescence (CT-fluorescence) emitted from the excited CT-complex formed by an excited perylene and an amine in the ground state.[1,2]

In polar solvents, such CT-fluorescence was not observed and by the flash illumination a transient absorption spectrum attributed to perylene anion was observed. This anion was assumed to be formed *via* the CT-complex of the excited perylene with the ground state amine or *via* a solvent-shared ion pair ($A^-_{solv.}\cdots D^+_{solv.}$).[3]

Though this is a very interesting result, there had been a few reports[1-4] concerning this problem. It is our opinion that further work is needed in order to prove the formation of an ion pair, $A^-_{solv.}$ and $D^+_{solv.}$, by the mechanism proposed by Weller.

Recently, we have found that *N*,*N*,*N'N'*-tetramethyl-*p*-phenylenediamine (TMPD) and α-methylnaphthalene, or other naphthalene derivatives, show similar fluorescence spectrum attributable to the CT-fluorescence in non-polar solvents.[5] In polar

1) H. Leonhardt and A. Weller, *Ber. Bunsenges. Physik. Chem.*, **67**, 791 (1963).

2) H. Leonhardt and A. Weller, *Z. Physik. Chem. N. F.*, **29**, 277 (1961).

3) H. Knibbe, K. Röllig, F. P. Schäfer and A. Weller, *J. Chem. Phys.*, **47**, 1184 (1967); H. Knibbe, D. Rehm and A. Weller, *Ber. Bunsenges. Physik. Chem.*, **72**, 257 (1968).

4) M. Koizumi and H. Yamashita, *Z. Physik. Chem. N. F.*, **57**, 103 (1968).

5) N. Yamamoto, Y. Nakato and H. Tsubomura, This Bulletin, **40**, 451 (1967).

solvents, the same system showed transient absorption spectra assigned to the TMPD cation and naphthalene in the triplet state.[6] This result indicates that excited TMPD and ground state naphthalene derivatives partly form TMPD cation (and probably α-methylnaphthalene anion, though its spectrum was not observed), and partly form the triplet state of α-methylnaphthalene by energy transfer. We have confirmed that the yield of the cation in solution is independent of the light intensity but dependent on the total light input. This finding provides evidence for the generation of the cation by a single-photon process and therefore supports Weller's mechanism.

It was thought to be interesting to find more examples of the ion-pair formation from the donor-acceptor pairs by the flash technique. In the present paper some of the results are reported.

Experimental

The instrument used for the flash illumination has been described elsewhere.[7] The electric energy of a flash was about 250 J and the flash light had the duration time of about 3μsec. A cylindrical quartz sample cell 20 cm long and 1.5cm in diameter was used. Two photolysis flash lamps were made of quartz tube, 20 cm long and 1.0 cm in diameter, with tungsten-electrodes at both ends. These tubes were filled with argon to a pressure of about 100 mmHg. Oxygen in the sample solution was removed by bubbling highly purified nitrogen gas. *p*-Dimethoxybenzene (DMB) used was recrystallized from ethanol and was sublimed. Chloranil was sublimed in vacuum. Acetonitrile was refluxed with phosphorus pentoxide and distilled. Ethanol was dried with calcium oxide and barium oxide and then distilled.

The spectra shown in Fig. 4 were recorded with Cary Spectrophotometer Model 15. All other spectra were obtained by the photographic method followed by recording with a Nalumi microphotometer NLM V11.

Results

***p*-Dimethoxybenzene-*s*-Trinitrobenzene System.** Flash illumination of *s*-trinitrobenzene (2×10^{-3} M) in an oxygen-free acetonitrile solution containing 10^{-3} M *p*-dimethoxybenzene (DMB) gave a transient absorption spectrum showing maxima at 456 mμ and 431 mμ and a shoulder at 414 mμ (Fig. 1a). The transient absorption spectrum was detectable by the photographic measurement until about 50 μsec after the flash illumination. The flash light was filtered by a highly concentrated DMB solution so that only the acceptor molecule, trinitrobenzene, was excited. The sample solution showed no absorption band ascribable to the CT-complex between DMB and trinitrobenzene. In the absence of DMB, no transient absorption spectrum was observed by the flash irradiation of trinitrobenzene in acetonitrile. No transient absorption spectrum attributable to DMB cation was observed by the flash illumination of DMB and trinitrobenzene in non-polar solvents such as benzene or methylcyclohexane.

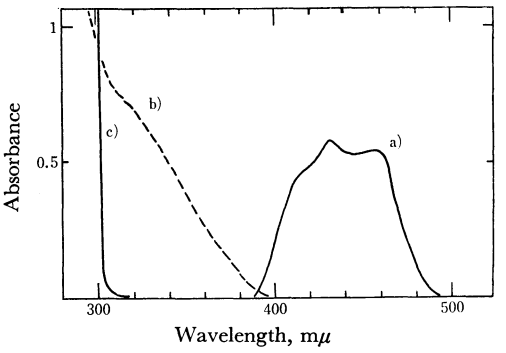

Fig. 1.
(a) Transient absorption spectrum caused by the flash illumination of *s*-trinitrobenzene (2×10^{-3} M) and *p*-dimethoxybenzene (10^{-3}M) in an acetonitrile solution at room temperature. A concentrated *p*-dimethoxybenzene solution was used as a filter.
(b) Absorption spectrum of *s*-trinitrobenze in acetonitrile solution.
(c) Absorption spectrum of *p*-dimethoxybenzene in acetonitrile solution.

***p*-Dimethoxybenzene - Chloranil System.** In the case of the flash illumination of an oxygen-

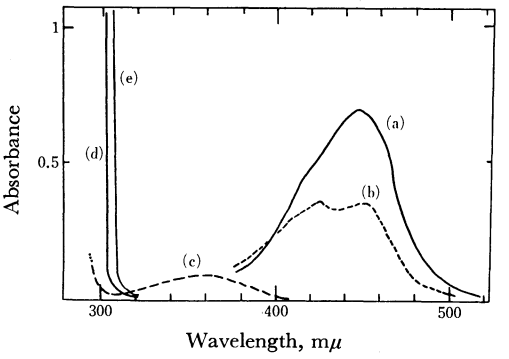

Fig. 2.
(a) Transient absorption spectrum caused by the flash illumination of chloranil (10^{-4}M) and *p*-dimethoxybenzene (10^{-3}M) in an acetonitrile solution.
(b) The same spectrum as above in an ethanol solution.
(c) Absorption spectrum of chloranil in an ethanol solution.
(d) Absorption spectrum of *p*-dimethoxybenzene in acetonitrile solution.
(e) Absorption spectrum of glass filter.

6) Y. Nakato, N. Yamamoto and H. Tsubomura, This Bulletin, **40**, 2480 (1967).
7) N. Yamamoto, Y. Nakato and H. Tsubomura, *ibid.*, **39**, 2603 (1966).

free acetonitrile solution containing about 10^{-3} M DMB and 10^{-4} M chloranil, a transient absorption spectrum was observed with maxima at 446 mμ and a shoulder near 420 mμ as shown in Fig. 2a. A glass filter was used so that only chloranil was excited. The sample solution showed no characteristic band of the CT-complex of DMB and chloranil. The flash illumination of a solution containing only chloranil gave a transient absorption spectrum different from that shown in Fig. 2(a), which may probably be attributable to the semiquinone radical 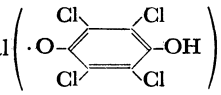 formed by the hydrogen abstraction from solvent on account of the resemblance of the spectrum with that of *p*-benzosemiquinone.

The change of the absorbance of the transient spectrum of Fig. 2(a) was followed by the photographic method until about 300 μsec after the flash illumination. If the transient species formed by the flash illumination is assumed to decay by the second-order reaction kinetics, the absorbance (a) may be represented as follows:

$$\frac{1}{a} = kt + c \quad (k, c\text{: constant}, t\text{: time})$$

Figure 3 shows that the above relation holds well for the absorbance at 446 mμ.

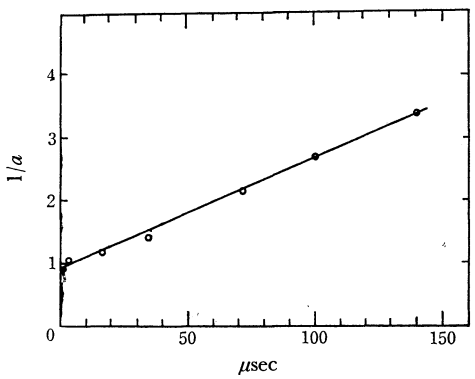

Fig. 3. Relation between the reciprocal of the absorbance (a) of the transient absorption spectrum shown in Fig. 2(a) and the time after the flash. The absorption was measured at 446 mμ.

In the case of an ethanol solution of chloranil and DMB, a flash illumination gave an absorption spectrum with maxima at 428 mμ and 452 mμ and a shoulder at 408 mμ (Fig. 2b).

Spectra of DMB$^+$ and Chloranil$^-$. In order to obtain the spectrum of DMB cation (DMB$^+$), DMB was added to an acetonitrile solution containing a small amount of antimony pentachloride at room temperature. The yellow solution thus obtainde showed a spectrum with maxima at 433 mμ and 458 mμ and a shoulder near 410 mμ as shown in Fig. 4a. The ESR spectrum obtained coincides

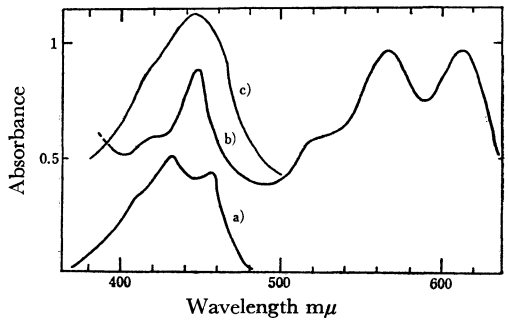

Fig. 4.
(a) Absorption spectrum of *p*-dimethoxybenzene cation formed in the acetonitrile solution containing a small amount of antimony pentachloride.
(b) Absorption spectrum of an acetonitrile solution of *N*,*N*,*N*′,*N*′-tetramethyl-*p*-phenylenediamine and chloranil.
(c) Reproduction of curve (a) of Fig. 2.

well with that of DMB$^+$ measured by Sullivan and Forbes in a sulfuric acid solution of DMB.[8] The visible absorption spectrum (Fig. 4a) also agrees with that of DMB$^+$ formed by the photolysis of DMB in the 1 : 1 mixture of concentrated sulfuric and acetic acid at 77°K.[9]

Figure 4 (b), in the 400—500 mμ region shows the spectrum of chloranil anion prepared by the chemical reduction of chloranil with tetramethyl-*p*-phenylenediamine (TMPD) in the acetonitrile solution at room temperature. The two maxima at 448 mμ and 422 mμ agree with the absorption spectrum of chloranil anion obtained by reducing chloranil with sodium in tetrahydrofuran solution.[10] The spectrum beyond 500 mμ is obviously that for the cation of TMPD.[7]

Discussion

The spectra shown in Fig. 1(a) and Fig. 4(a) agree well in the positions of their maxima and shoulders. If we take into acount of the fact that Fig. 1(a) was obtained by the photographic method followed by recording with a microphotometer and Fig. 4(a) was obtained by the Cary spectrophotometer, we may conclude that the identity of the spectra shown in Fig. 1(a) and Fig. 4(a) are fairly good. These results indicate that DMB

8) W. H. Forbes and P. D. Sullivan, *Canad. J. Chem.*, **44**, 1501 (1966).
9) H. Tsubomura, K. Kimura, H. Yamada and M. Kato, *Tetrahedron Letters*, **47**, 4217 (1965).
10) H. Kainer and A. Ůberle, *Chem. Ber.*, **88**, 1147 (1955).

cation was formed by the flash illumination of *s*-trinitrobenzene in the acetonitrile solution containing DMB and *s*-trinitrobenzene. The formation of DMB cation radical (DMB^+) may be explained by the same mechanism as that proposed by Weller *et al.*[2]:

$$A + DMB \xrightarrow{h\nu} A^* + DMB \longrightarrow (A^* \cdots DMB) \text{ or } (A^{\delta-} \cdots DMB^{\delta+}) \longrightarrow A^-_{solv.} + DMB^+_{solv.}$$

A: *s*-trinitrobenzene (or chloranil)

No spectrum attributable to trinitrobenzene anion was observed. This result shows that trinitrobenzene anion is either very unstable at room temperature or has no absorption band in the visible region.

In the case of DMB-chloranil system, the absorption spectrum obtained (Fig. 2a) is considerably different from that of DMB^+. It seems obvious that this spectrum represent the sum of the absorption spectra of DMB^+ and chloranil anion from the comparison of curves (a), (b) and (c) of Fig. 4.

As stated before, the decay of the transient absorption spectra follows the second order reaction kinetics (Fig. 3). The fact proves that the decay is brought about by the recombination of the anion and the cation after the flash illumination.

In the case of the flash illumination of chloranil in the ethanol solution containing DMB and chloranil, only the transient DMB^+ spectrum appeared, indicating that the chloranil anion is very short-lived in the ethanol solution. To confirm it, the acetonitrile solution containing 10^{-4} M chloranil, 5×10^{-1} M ethanol, and 10^{-3} M DMB was flash illuminated. After the flash illumination the transient spectrum was identical with that shown in Fig. 2 (a) for a time shorter than about 20μsec, then the shape of the transient spectrum gradually changed until about 50μsec after the flash, and finally became identical with that shown in Fig. 2 (b). This experiment shows that chloranil anion formed by the flash illumination reacts very quickly with ethanol.

From the experimental results stated above, it has been unambiguously settled that the cation of *p*-dimethoxybenzene is formed by the flash illumination of it with some acceptors (*s*-trinitrobenzene or chloranil), in polar solvents such as acetonitrile or ethanol. It is well known that these molecules form the charge transfer complexes. But in our experiment the concentrations are so low that essentially all molecules are free from complex formation. In non-polar solvents, no transient ions were observed by similar flash experiments. Leonhardt and Weller showed that the excitation of a donor resulted in the formation of a transient ion of the donor. Our results have shown that the excitation of acceptors also leads to the formation of the transient donor cation.

BULLETIN OF THE CHEMICAL SOCIETY OF JAPAN VOL. 42 372—378 (1969)

Optical and Acoustic Branches and Frequency Distribution of Polyethylene Glycol Chain

Hiroatsu MATSUURA and Tatsuo MIYAZAWA

Institute for Protein Research, Osaka University, Kita-ku, Osaka

(Received July 15, 1968)

Optical and acoustic branches of chain vibrations of polyethylene glycol were treated. The nature of these branches was elucidated on the basis of potential-energy distributions and phase relations. From dispersion curves (frequency *versus* phase difference), the frequency distribution of chain vibrations was calculated, in order to analyze thermal-neutron scattering spectra. Vibrational assignments of scattering peaks in the region 600—200 cm^{-1} were made with reference to the frequency distribution peaks and potential-energy distributions calculated for the single chain.

Infrared absorption, Raman scattering, and neutron inelastic scattering measurements are three important methods for studying chain vibrations of helical polymer molecules. The selection rules for infrared absorption and Raman effect are related with the angle (θ) of rotation, per unit, about the helix axis. Infrared absorption bands arise from vibrations with the phase difference of

$\delta=0$ or θ, while Raman lines arise from vibrations with $\delta=0$, θ, or 2θ.[1,2] For neutron scattering, however, there is no selection rule and chain vibrations for any phase difference contribute to inelastic scattering. Accordingly, frequency distribution peaks give rise to inelastic scattering peaks. For polyethylene glycol, neutron inelastic scattering was observed by Trevino and Boutin[3] and observed scattering peaks were analyzed with reference to the frequency distribution peaks calculated for an isolated chain of polyethylene glycol.[4]

In our previous study,[5] the force field of polyethylene-glycol chain was refined and the nature of observed infrared bands and Raman lines was discussed on the basis of potential-energy distributions. With the refined force field, in the present study, optical and acoustic branches of polyethylene-glycol chain were treated and the nature of these branches was elucidated. Dispersion curves (frequency *versus* phase difference) are useful for analyses of vibrational spectra of model oligomers in the crystalline state.[6] Also, the frequency distribution of chain vibrations was calculated and the nature of neutron scattering peaks was elucidated.

Normal Coordinate Treatment

Polyethylene-glycol chain is in the 7_2 helical conformation (seven units of CH_2CH_2O and two helical turns per fiber period),[7,8] having two twofold axes per unit. One axis bisects the C–O–C bond angle while the other axis intersects the C–C bond at right angle. Accordingly, this polymer chain belongs to dihedral group. A general method for treating helical chain vibrations was described previously.[2,9,10]

Normal vibrations of polyethylene-glycol chain were treated previously for the phase differences of $\delta=0$ (A_1 and A_2) and for $\delta=\theta$ (E_1).[5] In the present study, normal vibrations were treated for the phase differences of $\delta=0°$, 15°,···, 165° and 180°, with the interval of 15°.*1 Bond-stretching, angle-bending, and internal-rotation coordinates were transformed into local-symmetry coordinates; namely σ_{ss} (CH_2 symmetric stretching), σ_{as} (CH_2

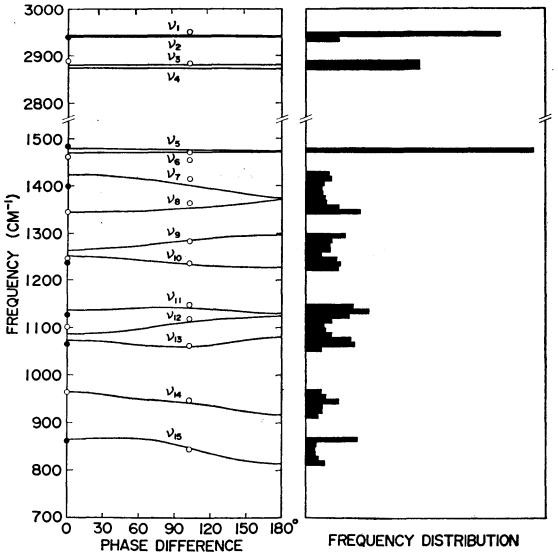

Fig. 1. Dispersion curves for the ν_1—ν_{15} branches and frequency distribution of polyethylene-glycol chain.
○: infrared absorption frequency
●: Raman frequency

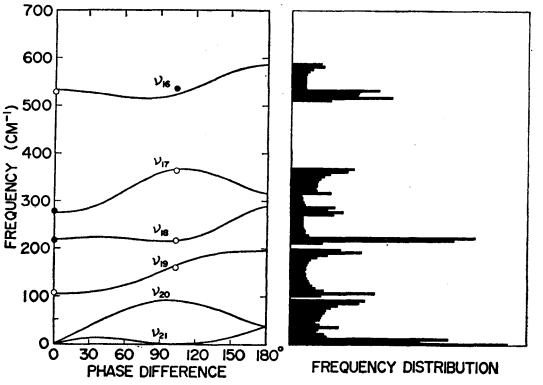

Fig. 2. Dispersion curves for the ν_{16}—ν_{21} branches and frequency distribution of polyethylene-glycol chain.
○: infrared absorption frequency
●: Raman frequency

*1 Only the phase-difference region of $0\leq\delta\leq\pi$ need be treated, since frequenices for $\delta=2\pi+\alpha$ are the same as for $\delta=\alpha$, and frequencies for $\delta=\pi+\beta$ are the same as for $\delta=\pi-\beta$.

1) P. Higgs, *Proc. Roy. Soc.* (*London*), **A220**, 472 (1953).
2) T. Miyazawa, *J. Chem. Phys.*, **35**, 693 (1961).
3) S. Trevino and H. Boutin, *J. Macromol. Sci.*, **A1**, 723 (1967).
4) H. Matsuura and T. Miyazawa, *Rept. Progr. Polymer Phys. Japan*, **9**, 179 (1966).
5) H. Matsuura and T. Miyazawa, This Bulletin, **41**, 1798 (1968).
6) H. Matsuura and T. Miyazawa, Symposium on Molecular Structure, Toyonaka, 1966; *Rept. Progr. Polymer Phys. Japan*, **10**, 187 (1967).
7) T. Miyazawa, *J. Polymer Sci.*, **55**, 215 (1961), addendum; T. Miyazawa, K. Fukushima and Y. Ideguchi, *J. Chem. Phys.*, **37**, 2764 (1962).
8) H. Tadokoro, Y. Chatani, T. Yoshihara, S. Tahara and S. Murahashi, *Makromol. Chem.*, **73**, 109 (1964); T. Yoshihara, H. Tadokoro and S. Murahashi, *J. Chem. Phys.*, **41**, 2902 (1964).
9) T. Miyazawa, *Nippon Kagaku Zasshi* (*J. Chem. Soc. Japan, Pure Chem. Sect.*), **88**, 111 (1967).
10) H. Sugeta and T. Miyazawa, *J. Chem. Phys.*, **47**, 2034 (1967).

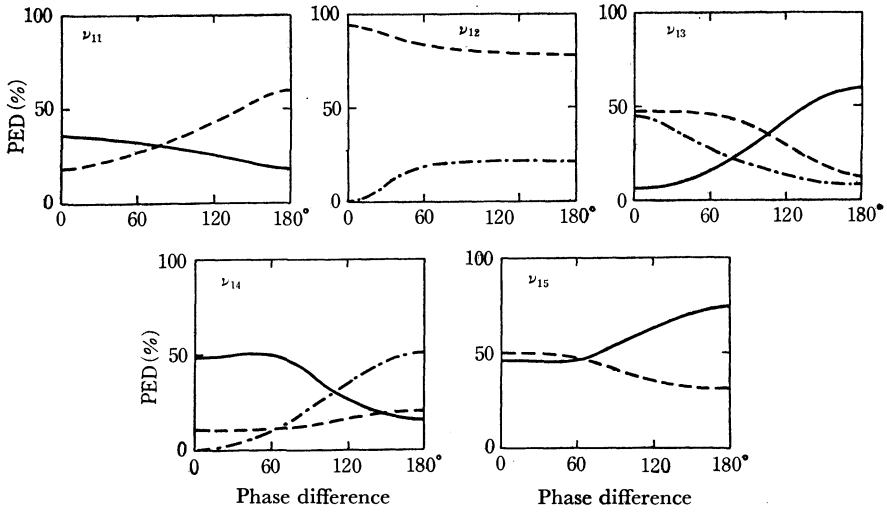

Fig. 3. Dependence of potential-energy distributions (PED) upon phase difference.
—— : σ_{ro}, ------ : $\sigma_{CO\ st}$, —·—·— : $\sigma_{CC\ st}$

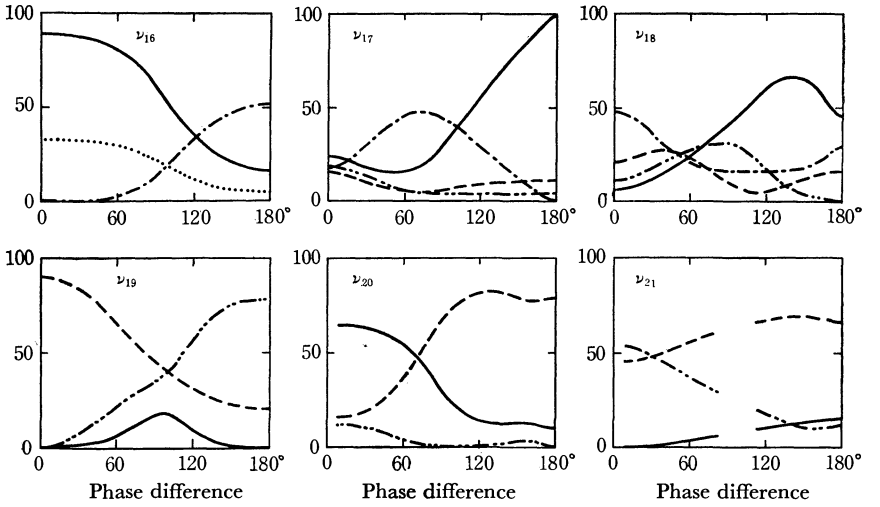

Fig. 4. Dependence of potential-energy distributions (PED) upon phase difference.
····· : σ_{ro}, —— : σ_{CCO}, —·—·— : σ_{COC}, —··—··— : $\sigma_{CC\ to}$, —— : $\sigma_{CO\ to}$

antisymmetric stretching), σ_{sc} (CH_2 scissoring), σ_{wa} (CH_2 wagging), σ_{tw} (CH_2 twisting), σ_{ro} (CH_2 rocking), $\sigma_{CC\ st}$ (C–C stretching), $\sigma_{CO\ st}$ (C–O stretching), σ_{CCO} (C–C–O bending), σ_{COC} (C–O–C bending), $\sigma_{CC\ to}$ (C–C internal-rotation), and $\sigma_{CO\ to}$ (C–O internal-rotation).[5] Inverse-kinetic energy matrices $\boldsymbol{G}(\delta)$ were constructed with the molecular parameters listed previously.[5]

Local-symmetry force constants[11] of polyethylene-glycol chain were refined previously[5] so that frequencies calculated for A_1, A_2 and E_1 vibrations reproduce observed infrared and Raman frequencies with a root-mean-squared deviation as small as 0.9%. The same set of force constants was used in the present study for constructing potential-energy matrices $\boldsymbol{F}(\delta)$.

Vibrational frequencies calculated for $\delta=0°$, 60°, 120°, and 180° are listed*2 in Tables 1 and 2, together with potential-energy distributions (PED) and phase-angle differences[5,9] (phase relations in normal modes of degenerate vibrations). Vibrational modes with $\Delta\varepsilon(OCH_2\text{–}CH_2O) \sim 0°$ and $\sim \pm 180°$ are quasi-symmetric and quasi-antisymmetric, respectively, with respect to the twofold axis that intersects the CH_2–CH_2 bond. Similarly, vibrational modes with $\Delta\varepsilon$(C–O–C) $\sim 0°$ and $\sim \pm 180°$

11) T. Shimanouchi, *Nippon Kagaku Zasshi* (*J. Chem. Soc. Japan, Pure Chem. Sect.*), **86**, 261, 768 (1965); Symposium on Molecular Structure, Tokyo, 1964; Toyonaka, 1966.

*2 A more detailed list is given in Ref. 13, p. 69, including $\delta=30°$, 90° and 150°.

are quasi-symmetric and quasi-antisymmetric, respectively, with respect to the twofold axis that intersects the C–O–C angle. For the phase difference of $\delta=0°$, chain vibrations are classified into A_1 vibrations [$\Delta\varepsilon=0°$] and A_2 vibrations [$\Delta\varepsilon=180°$] while for the phase difference of $\delta=180°$, chain vibrations are classified into B_1 vibrations [$\Delta\varepsilon(OCH_2\text{–}CH_2O)=0°$ and $\Delta\varepsilon(C\text{–}O\text{–}C)=180°$] and B_2 vibrations [$\Delta\varepsilon(OCH_2\text{–}CH_2O)=180°$ and $\Delta\varepsilon(C\text{–}O\text{–}C)=0°$].

Dispersion curves (frequency *versus* phase difference) of twenty-one vibrational branches of polyethylene-glycol chain are shown in Figs. 1 and 2, together with observed infrared and Raman frequencies (excepting ν_{16}, only the infrared frequencies are shown for $\delta=\theta$). Main terms of potential-energy distributions for the branches ν_{11}—ν_{21} are shown in Figs. 3 and 4.

High Frequency Branches

For a helical polymer chain, two branches in the lowest-frequency region are acoustic branches, and other higher-frequency branches are optical branches. For polyethylene glycol, there are seven atoms per repeat unit of CH_2CH_2O, and accordingly chain vibrations consist of twenty-one branches, namely nineteen optical and two acoustic branches (Figs. 1 and 2).

In the highest-frequency region of 3000—2800 cm^{-1}, there are four branches, ν_1—ν_4. The ν_1 and ν_2 branches are associated with CH_2 antisymmetric stretching modes, while ν_3 and ν_4 branches are associated with CH_2 symmetric stretching modes (Table 1). With respect to the local twofold symmetry axis, the ν_1 and ν_3 branches are quasi-antisymmetric ($160°<\Delta\varepsilon\leq180°$) whereas the ν_2 and ν_4 branches are quasi-symmetric ($0°\leq\Delta\varepsilon<20°$). Atomic displacements of these vibrations are highly localized in the CH_2–CH_2 groups so that frequencies of these four branches do not vary with phase difference.

In the polarized infrared spectra of polyethylene glycol, the parallel band at 2890 cm^{-1} is assigned to the $\nu_3(0)$ vibration (A_2), the perpendicular band at 2950 cm^{-1} to the $\nu_1(\theta)$ and $\nu_2(\theta)$ vibrations (E_1), and the perpendicular band at 2885 cm^{-1} to the $\nu_3(\theta)$ vibration (E_1). The medium-intensity Raman line at 2939 cm^{-1} is assigned to the $\nu_2(0)$ vibration while the strong line at 2890 cm^{-1} is assigned to the CH_2 symmetric stretching modes (ν_3 and ν_4).

The ν_5 and ν_6 branches are associated with quasi-symmetric and quasi-antisymmetric scissoring modes, respectively, of CH_2–CH_2 groups (Table 1). Frequencies of these two branches vary little with phase difference. The doublet parallel bands at 1463 and 1457 cm^{-1} are assigned to $\nu_6(0)$ (A_2) and the perpendicular bands at 1470 and 1453 cm^{-1} are assigned to $\nu_5(\theta)$ and $\nu_6(\theta)$ (E_1), respectively. The strong Raman line at 1484 cm^{-1} is assigned to $\nu_5(0)$ (A_1) and weak line at 1449 cm^{-1} to $\nu_6(\theta)$.

Table 1. Calculated frequencies (ν, cm^{-1}), potential energy distributions (PED, %) and phase-angle differences [$\Delta\varepsilon$ (OCH_2-CH_2O)]

δ	ν	PED ($\Delta\varepsilon$)	δ	ν	PED ($\Delta\varepsilon$)
	ν_1 (CH_2 as)			ν_2 (CH_2 as)	
0°	2943 A_2	101(180°)	0°	2940 A_1	101(0°)
60°	2943	101(167°)	60°	2940	101(13°)
120°	2943	101(162°)	120°	2940	101(18°)
180°	2942 B_2	101(180°)	180°	2941 B_1	101(0°)
	ν_3 (CH_2 ss)			ν_4 (CH_2 ss)	
0°	2883 A_2	100(180°)	0°	2874 A_1	101(0°)
60°	2883	100(176°)	60°	2874	100(4°)
120°	2883	100(176°)	120°	2873	100(4°)
180°	2883 B_2	100(180°)	180°	2873 B_1	100(0°)
	ν_5 (CH_2 sc)			ν_6 (CH_2 sc)	
0°	1479 A_1	98(0°)	0°	1470 A_2	100(180°)
60°	1478	99(28°)	60°	1470	100(152°)
120°	1475	100(55°)	120°	1471	100(125°)
180°	1473 B_1	100(0°)	180°	1473 B_2	100(180°)
	ν_7 (CH_2 wa)			ν_8 (CH_2 wa)	
0°	1423 A_1	88(0°)	0°	1344 A_2	107(180°)
60°	1415	90(31°)	60°	1347	107(151°)
120°	1395	97(62°)	120°	1356	106(120°)
180°	1373 B_2	106(180°)	180°	1372 B_1	100(0°)
	ν_9 (CH_2 tw)			ν_{10} (CH_2 tw)	
0°	1264 A_2	81(180°)	0°	1252 A_1	81(0°)
60°	1275	76(73°)	60°	1243	85(112°)
120°	1290	73(30°)	120°	1231	89(156°)
180°	1297 B_1	72(0°)	180°	1226 B_2	92(180°)

The ν_7 and ν_8 branches are due to quasi-symmetric ($0°\leq\Delta\varepsilon<80°$) and quasi-antisymmetric ($100°<\Delta\varepsilon\leq180°$) CH_2 wagging modes, respectively, for $\delta=0$—120°. For the ν_7 branch, the C–C stretching mode contributes to PED by 15—20%. The $\nu_7(0)$ vibration was observed as the Raman line at 1398 cm^{-1} while the $\nu_7(\theta)$ vibration was observed as the perpendicular infrared band at 1415 cm^{-1}. Infrared bands due to $\nu_8(0)$ and $\nu_8(\theta)$ were observed at 1345 cm^{-1} (parallel) and 1364 cm^{-1} (perpendicular), respectively.

The ν_9 and ν_{10} branches are due to CH_2 twisting modes. For $\delta=0°$, the $\nu_9(0)$ and $\nu_{10}(0)$ vibrations are antisymmetric and symmetric, respectively, with respect to the local twofold axis. The parallel infrared band at 1244 cm^{-1} is assigned to $\nu_9(0)$. As δ is increased from 0°, however, phase relations of these vibrations are gradually changed and finally are interchanged for $\delta>45°$. Thus the perpendicular bands at 1283 and 1236 cm^{-1} are assigned to $\nu_9(\theta)$ and $\nu_{10}(\theta)$ which are quasi-symmetric and quasi-antisymmetric, respectively.

The ν_{11}—ν_{15} branches in the region 1200—

TABLE 2. CALCULATED FREQUENCIES (ν, cm^{-1}), POTENTIAL ENERGY DISTRIBUTIONS (PED, %) AND PHASE-ANGLE DIFFERENCES[a] ($\Delta\varepsilon$)

	δ	ν	PED ($\Delta\varepsilon$)		
			CH_2 ro	CO st	CCO
ν_{11}	0°	1137 A_1	36(0°)	18(0°)	11(0°)
	60°	1141	32(41°)	28(42°)	13(− 64°)
	120°	1140	26(79°)	42(20°)	19(−118°)
	180°	1130 B_2	18(180°)	60(0°)	26(−180°)
			CO st	CC st	
ν_{12}	0°	1087 A_2	94(180°)	0	
	60°	1098	83(125°)	18	
	120°	1117	81(143°)	21	
	180°	1124 B_1	78(180°)	21	
			CO st	CC st	CH_2 ro
ν_{13}	0°	1073 A_1	47(0°)	46	7(0°)
	60°	1065	46(104°)	26	16(−128°)
	120°	1063	30(100°)	13	43(− 54°)
	180°	1080 B_1	12(180°)	8	60(0°)
			CO st	CC st	CH_2 ro
ν_{14}	0°	964 A_2	10(180°)	0	49(180°)
	60°	949	10(181°)	10	60(96°)
	120°	936	16(172°)	35	26(26°)
	180°	917 B_1	20(180°)	51	16(0°)
			CO st	CH_2 ro	
ν_{15}	0°	866 A_1	50(0°)	46(0°)	
	60°	868	47(5°)	46(92°)	
	120°	836	36(8°)	63(161°)	
	180°	814 B_2	32(0°)	74(180°)	
			CCO	COC	CH_2 ro
ν_{16}	0°	533 A_2	89(180°)	0	33(−180°)
	60°	518	80(150°)	2	30(−155°)
	120°	540	35(146°)	33	11(−154°)
	180°	587 B_2	16(180°)	52	4(−180°)
			CCO	COC	CO to CC to
ν_{17}	0°	274 A_1	24(0°)	17	16(0°) 19
	60°	322	16(32°)	46	6(44°) 6
	120°	365	57(74°)	29	9(− 23°) 4
	180°	316 B_1	100(0°)	0	10(−180°) 4
			CCO	COC	CO to CC to
ν_{18}	0°	218 A_1	6(0°)	48	22(0°) 11
	60°	221	25(55°)	21	23(34°) 27
	120°	224	60(63°)	16	5(−174°) 17
	180°	289 B_2	44(180°)	30	16(0°) 0
			CO to	CC to	
ν_{19}	0°	105 A_2	90(180°)	0	
	60°	123	65(161°)	22	
	120°	179	31(−150°)	58	
	180°	196 B_1	20(−180°)	78	
			CCO	CO to	
ν_{20}	0°	0 A_1	—	—	
	60°	72	54(11°)	38(45°)	
	120°	86	14(− 35°)	82(69°)	
	180°	38 B_2	10(−180°)	80(0°)	
			CO to	CC to	
ν_{21}	0°	0 A_1	—	—	
	60°	9	56(73°)	36	
	120°	2	67(94°)	19	
	180°	37 B_1	64(180°)	13	

a) Phase-angle differences $\Delta\varepsilon(OCH_2\text{–}CH_2O)$ are shown for CH_2 ro and CCO, while $\Delta\varepsilon$(C–O–C) are shown for CO st and CO to.

800 cm^{-1} are associated with C–O and C–C stretching modes and CH_2 rocking modes (Table 2, Fig. 1). Vibrational coupling among these modes is also shown in Fig. 3.

The ν_{11} and ν_{15} branches arise from vibrational coupling of CH_2 rocking modes and quasi-symmetric C–O stretching modes, although relative contributions of these modes vary with phase difference (Fig. 3). Also phase relations ($\Delta\varepsilon$) of rocking modes of CH_2–CH_2 groups vary with phase difference (δ), from $\Delta\varepsilon=0°$ for $\delta=0°$ to $\Delta\varepsilon=180°$ for $\delta=180°$. The Raman lines at 1126 and 861 cm^{-1} are assigned to $\nu_{11}(0)$ and $\nu_{15}(0)$ and the perpendicular infrared bands at 1149 and 844 cm^{-1} are assigned to $\nu_{11}(\theta)$ and $\nu_{15}(\theta)$, respectively.

The ν_{12} branch around 1100 cm^{-1} is primarily associated with the C–O–C antisymmetric stretching mode ($125°\leq\Delta\varepsilon\leq180°$), in accord with empirical assignments of strong bands around 1100 cm^{-1}. The very strong parallel band at 1102 cm^{-1} and strong perpendicular band at 1119 cm^{-1} are assigned to $\nu_{12}(0)$ and $\nu_{12}(\theta)$, respectively. C–C stretching modes contribute about 20% of PED for $\delta>60°$ (Fig. 3).

The ν_{13} and ν_{14} branches are associated with C–O and C–C stretching modes and CH_2 rocking modes. Frequencies of the ν_{13} branch do not vary much with phase difference (δ), but the nature of ν_{13} vibrations changes markedly with δ. For $\delta=0°$, the $\nu_{13}(0)$ vibration is due to the C–O–C symmetric stretching mode ($\Delta\varepsilon=0°$) and C–C stretching mode. As δ is increased, however, PED contributions of these modes decrease and instead PED of CH_2 rocking modes increases up to 60% for $\delta=180°$ (Fig. 3). The perpendicular infrared band at 1062 cm^{-1} is assigned to $\nu_{13}(\theta)$.

The $\nu_{14}(0)$ vibration is primarily associated with the CH_2 rocking mode ($\Delta\varepsilon=180°$), giving rise to the parallel infrared band at 963 cm^{-1}. As phase difference is increased, PED contribution of C–C stretching modes increases, and for $\delta=\theta$ the $\nu_{14}(\theta)$ vibration is due to the coupling of the quasi-symmetric CH_2 rocking mode and C–C stretching mode, giving rise to the perpendicular band at 947 cm^{-1}.

Low Frequency Branches

In the region below 600 cm^{-1}, there are six vibrational branches, ν_{16}—ν_{21}, as shown in Fig. 2. These branches are associated with C–C–O and C–O–C bending modes and C–O and C–C internal-rotation modes (Table 2 and Fig. 4).

The $\nu_{16}(0)$ vibration is primarily associated with the antisymmetric C–C–O bending mode, giving rise to the parallel band at 529 cm^{-1} with a weak component at 508 cm^{-1}. The doublet splitting is due to Fermi resonance.[5] Because of appreciable contribution of the CH_2 rocking mode (33% of PED), this infrared band is shifted to 444 cm^{-1} (doublet) for perdeuterated species $(-CD_2CD_2O-)_p$. As phase difference is increased, PED contributions of quasi-antisymmetric C–C–O bending mode and quasi-antisymmetric CH_2 rocking mode are gradually replaced with PED of the C–O–C bending mode (Fig. 4). For $\delta=\theta$, the $\nu_{16}(\theta)$ vibration gives rise to the Raman line at 537 cm^{-1}.

The Raman line at 279 cm^{-1} is due to the $\nu_{17}(0)$ vibration of the A_1 species, a coupled vibration of the C–C–O and C–O–C bending modes and C–O and C–C internal-rotation modes (Fig. 4). As δ is increased, PED changes remarkably until finally, for $\delta=180°$, PED is essentially associated with the symmetric C–C–O bending mode. For $\delta=\theta$, $\nu_{17}(\theta)$ is a coupled vibration of the quasi-symmetric C–C–O bending mode and C–O–C bending mode, giving rise to the infrared band and Raman line at 363 cm^{-1}.

The Raman line at 216 cm^{-1} is due to the $\nu_{18}(0)$ vibration, a heavily coupled vibration of bending and internal-rotation modes (Fig. 4). Again PED contributions of the four modes vary markedly with phase difference. The $\nu_{18}(\theta)$ vibration gives rise to the perpendicular infrared band at 216 cm^{-1}.

The parallel far-infrared band at 107 cm^{-1} is due to the $\nu_{19}(0)$ vibration, associated with the antisymmetric internal-rotation mode of C–O bonds. However, as δ is increased, PED contribution of the C–O internal-rotation mode is gradually replaced with PED of the C–C internal-rotation mode (Fig. 4). The $\nu_{19}(\theta)$ vibration gives rise to the perpendicular infrared band at 165 cm^{-1}.

Acoustic Branches

The lowest-frequency branches, ν_{20} and ν_{21}, are the acoustic branches of polyethylene-glycol chain. The non-genuine vibrations $\nu_{20}(0)$ and $\nu_{21}(0)$ correspond to the translation (along the axis) and rotation (about the axis). For $\delta\sim0°$, the longitudinal stretching mode and twisting mode of the chain are coupled to yield the ν_{20} (coupling ratio of 3 : −2) and ν_{21} (ratio of 2 : 3) vibrations.*3 Potential energies of these vibrations are associated largely with quasi-symmetric C–C–O bending mode and with internal-rotation modes of C–C and C–O bonds (quasi-symmetric), respectively.

For $\delta=\theta$, the ν_{21} vibration is reduced to a non-genuine vibration corresponding to the translational mode perpendicular to the chain axis. For $\delta\sim\theta$, the ν_{21} vibration is the bending vibration of the molecular chain. The potential energy of this bending vibration is largely associated with internal-rotation modes of C–O bonds.

Frequency Distribution

For analyses of neutron-scattering peaks, in the present study, the frequency distribution of chain vibrations was calculated from dispersion curves of the twenty-one branches of polyethylene glycol (Figs. 1 and 2). The phase-difference region of $0°\leq\delta\leq180°$ was equally divided into 1800 subsections, and representative phase differences were taken as 0.05°, 0.15°,⋯, 179.85° and 179.95°, for which vibrational frequencies of each branch were calculated.

For the phase-difference region of $0°\leq\delta\leq15°$, vibrational frequencies of the optical branches (ν_1—ν_{19}) were calculated with even functions,

$$\nu(\delta)=\nu(0°)+a_2\delta^2+a_4\delta^4 \quad (1)$$

which satisfy frequencies previously calculated for $\delta=0°$, 15° and 30°, whereas frequencies of the acoustic branches (ν_{20} and ν_{21}) were calculated with odd functions,

$$\nu(\delta)=a_1\delta+a_3\delta^3 \quad (2)$$

which satisfy frequencies for $\delta=0°$, 15° and 30°.

An intermediate phase-difference region was divided into sub-regions of 15—30°, 30—45°,⋯, 135—150°, and 150—165°. For each sub-region of $\delta_0\leq\delta\leq\delta_0+15°$, vibrational frequencies were calculated with the following equation,

$$\nu(\delta)=\nu(\delta_0)+b_1(\delta-\delta_0)+b_2(\delta-\delta_0)^2+b_3(\delta-\delta_0)^3 \quad (3)$$

which satisfies frequencies for $\delta=\delta_0-15°$, δ_0, $\delta_0+15°$ and $\delta_0+30°$.

Finally, for the phase-difference region of $165°\leq\delta\leq180°$, vibrational frequencies were calculated with even functions,

$$\nu(\delta)=\nu(180°)+c_2(180°-\delta)^2+c_4(180°-\delta)^4 \quad (4)$$

which satisfy frequencies for $\delta=150°$, 165° and 180°.

*3 For the polyethylene-glycol chain in the right-handed 7_2 helix, the stretching mode of the chain is accompanied with rotation of the twisting mode in the left-handed and right-handed sense, respectively, for the ν_{20} and ν_{21} vibrations for $\delta\sim0°$.

After vibrational frequencies were calculated for all the branches, the number of vibrations was counted in the frequency sections of 10 cm^{-1} for high-frequency branches ($>700\ cm^{-1}$) and of 5 cm^{-1} for low-frequency branches ($<700\ cm^{-1}$). The frequency-distribution histograms thus obtained are shown in Figs. 1 and 2, together with dispersion curves.

Neutron Scattering Peaks

Thermal-neutron scattering of polyethylene glycol was measured by Trevino and Boutin[3] and inelastic-scattering peaks were observed at 535, 380—310 and 228 cm^{-1} in the frequency region of 600—200 cm^{-1}.*4 Vibrational assignments of these peaks will be made with reference to frequency distribution peaks (and PED) calculated in the present study.

The observed scattering peak at 535 cm^{-1} corresponds to the distribution peaks at 530 and 515 cm^{-1}. These distribution peaks arise from the ν_{16} vibrations for $0° \lesssim \delta \lesssim 110°$ and are largely associated with quasi-antisymmetric C–C–O bending mode. Another distribution peak at 585 cm^{-1} (C–O–C bending) was not resolved in the neutron-scattering measurement.

The broad scattering peak around 380—280 cm^{-1} corresponds to the distribution peaks at 370, 315 and 280 cm^{-1}. The peak at 370 cm^{-1} arises from the maximum portion of the ν_{17} branch for $\delta = 90$—$120°$. As shown in Fig. 4, these ν_{17} vibrations are associated with C–O–C bending and quasi-symmetric C–C–O bending modes. On the other hand, the peak at 315 cm^{-1} arises from the ν_{17} vibrations for $\delta \sim 180°$, and accordingly is due to quasi-symmetric C–C–O bending mode. The distribution peak at 280 cm^{-1} arises from ν_{17} vibrations for $\delta \sim 0°$ and ν_{18} vibrations for $\delta \sim 180°$.

The high distribution peak at 220 cm^{-1} arises from the flat portion of the ν_{18} branch, where vibrational frequencies hardly vary for phase differences of $0° \lesssim \delta \lesssim 120°$ (Fig. 2). In fact, a strong scattering peak was observed at 228 cm^{-1}. These ν_{18} vibrations are coupled vibrations of C–O–C and C–C–O bending modes and C–C and C–O internal-rotation modes.

Thus, neutron-inelastic scattering peaks in the region 600—200 cm^{-1} were assigned, with reference to the frequency distribution calculated for an isolated single chain of polyethylene glycol. However, in the region below 200 cm^{-1}, interchain interactions become significant, so that observed scattering peaks may not be compared with the distribution peaks of an isolated chain. For more realistic analyses of neutron scattering in the low-frequency region, treatments of crystal vibrations are required. Nevertheless, inelastic scattering peaks were observed at 120 and 80 cm^{-1}, apparently corresponding to the Raman lines at 126 and 75 cm^{-1}.[12]

Conclusion

The infrared absorption, Raman scattering, and neutron inelastic scattering spectra of polyethylene glycol were analyzed, on the basis of dispersion curves, frequency distribution and potential-energy distributions calculated for an isolated chain. The dispersion curves are also useful for vibrational analyses of infrared and Raman spectra of model oligomers and for treating heat capacities due to optical branches. The present study was reported, in more detail, in a thesis by Matsuura.[13]

Numerical calculations of the present study were carried out with a HITAC 5020E computer at the University of Tokyo and a NEAC 2200-500 computer at Osaka University.

*4 In the region above 600 cm^{-1}, a scattering peak was observed at 868 cm^{-1}.[3] This scattering peak corresponds to the distribution peak at 870 cm^{-1} (Fig. 1), which is associated with C–O stretching and CH_2 rocking modes.

12) R. F. Schaufele, *Trans. New York Acad. Sci.*, to be published.

13) H. Matsuura, "Vibrational Spectra of Polyethylene Glycol and Related Molecules," Thesis, Chapter II, Osaka University, 1968.

BULLETIN OF THE CHEMICAL SOCIETY OF JAPAN VOL. 42 379—382 (1969)

Structure of Vinylacetylene Determined by Electron Diffraction and Spectroscopy

Tsutomu FUKUYAMA, Kozo KUCHITSU and Yonezo MORINO

Department of Chemistry, Faculty of Science, The University of Tokyo, Hongo, Bunkyo-ku, Tokyo

(Received July 30, 1968)

The average structure of vinylacetylene has been determined by making combined use of the electron-diffraction intensities obtained in the present study and the rotational constants supplied by microwave spectroscopy. The two sorts of data have been found consistent to the uncertainties given below. With the molecular symmetry assumed to be C_s, the following parameters have been obtained in regard to the zero-point average structure: $r(\text{C–C}) = 1.431_0 \pm 0.003_4$, $r(\text{C=C}) = 1.341_6 \pm 0.004_2$, $r(\text{C}\equiv\text{C}) = 1.208_6 \pm 0.002_8$, $r(\text{C–H})_{\text{vinyl}} = 1.087 \pm 0.010$, $r(\text{C–H})_{\text{ethynyl}} = 1.062 \pm 0.018$ Å, $\angle(\text{C=C–C}) = 123.1 \pm 0.5°$, $\angle(\text{C–C}\equiv\text{C}) = 177.9 \pm 1.2°$, $\angle(\text{H–C=C}) = 120.6 \pm 1.5°$, $\angle(\text{C}\equiv\text{C–H}) = 182.3 \pm 3.8°$. There seems to be a significant difference between the C–C length of vinylacetylene and that of propynal. The result has been discussed in terms of the bond-order bond-length correlation.

How does the length of a carbon-carbon bond vary with its environment? This is one of the problems which attract the interest of physical and organic chemists. On the basis of the extensive research by means of rotational spectroscopy, Stoicheff and Costain[1,2] deduced a comprehensive rule, which states that the length of a CC bond is primarily determined by a linear relation depending on the number of atoms adjacent to the carbon atoms at both ends. This rule was shown to hold for a wide range of molecules. For a critical examination of the validity and the limit of applicability of the rule, it is necessary to obtain precise structural parameters of molecules for which neither spectroscopy nor electron diffraction alone can give unique geometry. This requirement was shown to be met in our studies[3-5] by a complementary combination of the two sorts of data. The results of those studies have shown significant deviations from the Stoicheff rule when heteroatoms are present in the system, whereas the rule is valid for pure hydrocarbons.

For butadiene, acrolein, and glyoxal, the central C–C bond increases its length according as it is adjacent to the C=O bond.[3] A similar systematic lengthening has been observed for cyanogen[4] as compared with diacetylene.[6] The first three are conventionally classified as molecules with an sp^2-sp^2 C–C bond, while the latter two are those with an sp-sp C–C bond. It is natural, then, to expect an analogous heteroatom effect in a system containing an sp^2-sp C–C bond. In fact, a deviation from the Stoicheff rule was first observed for an sp^2-sp C–C system by Costain, Stoicheff, and Morton.[1,7] They pointed out that the r_s(C–C) distance of propynal was longer by 0.0025 Å than the value predicted by the linear rule, to which the r_s(C–C) distance of vinylcyanide fitted nicely.

There remains, however, another simple molecule which has a C–C bond of this type: vinylacetylene. No precise structure has been reported for this molecule, although an unpublished work of Bastiansen[8] was cited by Serre,[9] and an r_0 structure was calculated by Whiffen[10] from the rotational constants reported by Morgan and Goldstein.[11] A favorable situation for filling this gap has been brought about by a recent investigation of the microwave spectrum of this molecule by Hirose[12] and by the study of its intramolecular force field by Abe.[13] Taking advantage of these circum-

1) C. C. Costain and B. P. Stoicheff, *J. Chem. Phys.*, **30**, 777 (1959).
2) B. P. Stoicheff, *Tetrahedron*, **17**, 135 (1962).
3) K. Kuchitsu, T. Fukuyama and Y. Morino, *J. Mol. Structure*, **1**, 463 (1968).
4) Y. Morino, K. Kuchitsu, Y. Hori and M. Tanimoto, This Bulletin, **41**, 2349 (1968).
5) K. Kuchitsu, *J. Chem. Phys.*, **49**, 4456 (1968).
6) M. Tanimoto, K. Kuchitsu and Y. Morino, to be published.
7) C. C. Costain and J. R. Morton, *J. Chem. Phys.*, **31**, 389 (1959).
8) O. Bastiansen, unpublished work.
9) J. Serre, *J. chim. phys.*, **53**, 284 (1956).
10) D. H. Whiffen, "Tables of Interatomic Distances and Configuration in Molecules and Ions," ed. by L. E. Sutton, the Chemical Society, London (1958), p. M161.
11) H. W. Morgan and J. H. Goldstein, *J. Chem. Phys.*, **20**, 1981 (1952).
12) C. Hirose, private communication.
13) K. Abe, private communication.

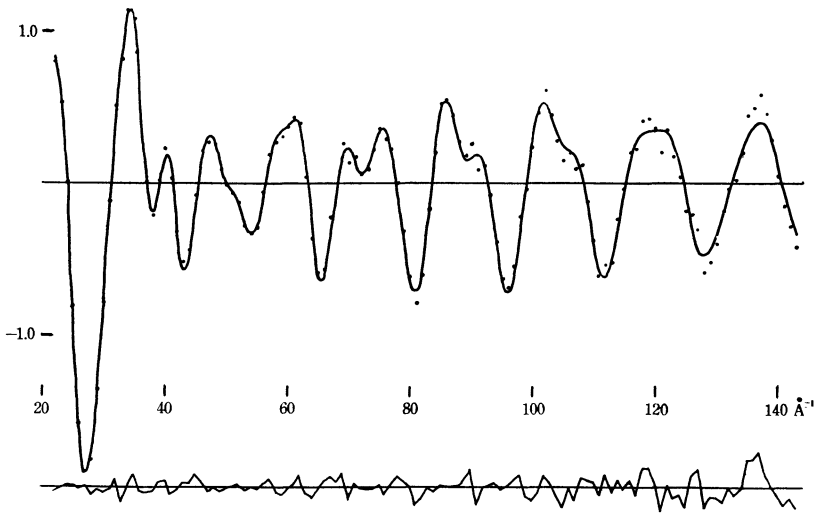

Fig. 1. Molecular scattering intensity. Observed values are shown in dots, and the solid curve represents the best-fit theoretical intensity. The residuals are shown below.

stances, an electron diffraction measurement has been carried out, and the average structure of vinylacetylene has been determined following the procedure applied to butadiene, acrolein, and glyoxal.

Experimental

The vinylacetylene sample supplied by the Tokyo Kagaku Seiki Co., Ltd. as a standard substance for gas chromatography was used without further purification. No impurity line was observed in the infrared spectrum of a freshly supplied sample.[13] Experimental conditions were similar to those described elsewhere.[3] The observed molecular intensity is shown in Fig. 1. Figure 2 illustrates the radial distribution curve.

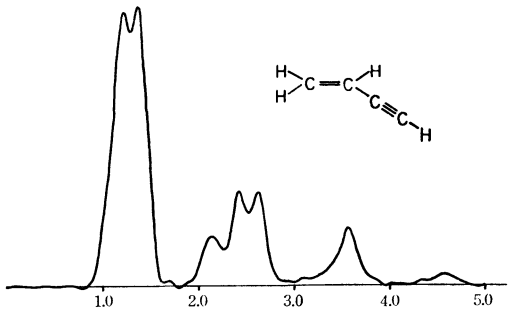

Fig. 2. Radial distribution curve for vinylacetylene.

Analysis

Since the details of the analytical procedure are the same as those described in Ref. 3, only an outline is given here. The calculations have been carried out by a HITAC 5020E Computer at the Computer Center, the University of Tokyo.

It was assumed that the molecule has C_S symmetry, namely that it is planar. With this assumption the number of independent parameters is thirteen for defining the molecular geometry, but in the analysis of the molecular scattering intensity the number of parameters was reduced by the following additional assumptions: Three C–H bond lengths and C=C–H angles in the vinyl group were assumed to be equal. The difference between the C–H bond length in the ethynyl group and those in the vinyl group was fixed at 0.027 Å according to the difference between the r_z(C–H) of acetylene[14] and that of ethylene.[15] Furthermore, the C≡C–H angle was assumed to be 180°. All the above assumptions were applied to the r_α^0 structure, from which the effect of thermal vibrations was removed.

The correction terms for the conversion of r_α into r_α^0 distances were calculated by the procedure given in Refs. 16 and 3. The force constants necessary for the calculation were offered for our use by Abe.

The most probable values of the parameters, r_α^0, obtained by the least-squares analysis are shown in Table 1 with their uncertainties. Table 2 lists the most probable values and the uncertainties of the mean square amplitudes in comparison with the values calculated with the force constants determined by Abe. The agreement is satisfactory. The mean amplitudes for the other atom pairs were fixed at the calculated values throughout the analysis. The parameters of asymmetry κ were estimated as described in Ref. 3, and were fixed at 1.89×10^{-5} and 1.59×10^{-5} Å^{-3} for C–H_{vinyl} and C–$H_{ethynyl}$, respectively.

14) V. W. Laurie and D. R. Herschbach, *J. Chem. Phys.*, **37**, 1687 (1962).
15) K. Kuchitsu, *ibid.*, **44**, 906 (1966).
16) K. Kuchitsu and S. Konaka, *ibid.*, **45**, 4342 (1966).

TABLE 1. STRUCTURE OF VINYLACETYLENE (in Å and degrees)

	r_α^0	σ[d]	r_{av}	σ[d]	Bastiansen[e]
r(C-C)	1.4314	0.0036	1.4310	0.0034	1.430
r(C=C)	1.3414	0.0042	1.3416	0.0042	1.335
r(C≡C)	1.2090	0.0030	1.2086	0.0028	1.206
r(C-H)$_v$[a]	1.087	0.007	1.087	0.010	
r(C-H)$_e$[a]	(1.060)	—	1.062	0.018	
∠(C=C-C)	123.0	0.5	123.1	0.5	123.4
∠(C-C≡C)[b]	177.0	1.7	177.9	1.2	
∠(H_1-C=C)[c]	120.8	1.5	118.7	4.2	
∠(H_2-C=C)			121.6	3.8	
∠(H_3-C=C)			121.7	4.0	
∠(C≡C-H)[b]	(180)	—	182.3	3.8	
k[f]	1.016	0.022	1.012	0.020	

a) Suffices v and e denote vinyl and ethynyl, respectively.

b) The angles are taken as 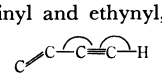

c) Numbering of the hydrogen atoms: 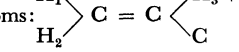

d) 2.5 times the random errors plus the estimates of systematic errors.

e) Ref. 8.

f) Index of resolution.

TABLE 2. MEAN SQUARE AMPLITUDES OF VINYLACETYLENE (in Å)

	$l_{obs.}$		$l_{calc.}$
C-C	0.048	±0.006	0.0473
C=C	0.043_9	±0.004	0.0439
C≡C	0.038	±0.005	0.0367
C-H_v[a]	0.074	±0.006	0.0775
$C_1\cdots C_3$[b]	0.059_4	±0.002	0.0635
$C_2\cdots C_4$	0.053_9	±0.003	0.0520
$C_1\cdots C_4$	0.084	±0.005	0.0867

a) All the vinyl C-H amplitudes were assumed to be equal. Mean amplitudes for C-H_e were varied with fixed difference from those for C-H_v (l(C-H)$_v$ − l(C-H)$_e$=0.0033 Å).

b) Numbering of carbon atoms: C_1=C_2-C_3≡C_4.

The rotational constants B_0 and C_0 for the normal and the deuterated species (deuterated on the ethynyl hydrogen) determined by microwave spectroscopy were communicated by Hirose. After being converted into B_z and C_z, namely into the rotational constants corresponding to the average structure r_z, they were used in the least-squares calculations, in which the rotational constants were combined with the molecular scattering intensity as joint observables. The method is based on the assumption that the r_α^0 structure obtained from electron diffraction and the r_z structure from spectroscopy have essentially the same physical significance so that it is possible to use the two sorts of data to complement one another upon the conversion into those structures. The result is shown in Table 1 as r_{av}. Most of the assumptions with regard to the structure of the vinyl and the ethynyl groups were removed by this procedure. Namely, it became possible to treat the three C=C-H angles, r(C-H)$_{ethynyl}$ and the angle C≡C-H as independent parameters. Although it was not possible to set the C-H distances of the vinyl group free from the restraint that they were equal, this assumption turned out to have no significant effect upon the values of the other parameters: even if any two of the three C-H lengths were assumed to be different by ±0.005 Å, the rest of the parameters changed by not more than 0.001 Å. The isotopic difference r_{av}(C-H) − r_{av}(C-D) was assumed to be 0.0012±0.0020 Å, the value calculated by Eq. (5) of Ref. 5. The observed rotational constants B_0 and C_0, B_z and C_z derived from B_0 and C_0, and the best-fit B_z and C_z are shown in Table 3. The consistency

TABLE 3. OBSERVED AND CALCULATED ROTATIONAL CONSTANTS (in MHz)

	CH_2=CHC≡CH		CH_2=CHC≡CD	
	B	C	B	C
B_0, C_0, obs	4744.95	4329.81	4403.97	4037.86
B_z, C_z, obs	4740.74	4329.93	4400.44	4038.15
B_z, C_z, calc	4740.65	4330.20	4400.50	4037.94

of the electron-diffraction and spectroscopic data is seen by the comparison of the r_α^0 structure with the r_{av} structure in Table 1. The uncertainties in the parameters were estimated in a way similar to that described in Ref. 3. They consist of 2.5 times the random errors plus the estimates of systematic errors.

The r_g structure of vinylacetylene was derived from the r_{av} structure of Table 1 by using the

TABLE 4. COMPARISON OF STRUCTURES (in Å and degrees)

		r(C–C)	r(C=C)	r(C≡C)	r(C–H)$_{vinyl}$	r(C–H)$_{ethynyl}$
Vinylacetylene	(r_g)	1.434 ± 0.003	1.344 ± 0.004	1.215 ± 0.003	1.106 ± 0.010	1.090 ± 0.018
Vinylcyanide	(r_s)	1.426 ± 0.001	1.339 ± 0.001	——	1.086 ± 0.001	——
Propynal	(r_s)	1.445 ± 0.001	——	1.209 ± 0.001	——	1.055 ± 0.001
Ethylene	(r_g)	——	1.337 ± 0.002	——	1.103 ± 0.002	——
Acetylene	(r_g)	——	——	1.209 ± 0.001	——	1.077 ± 0.002
		∠(C=C–C)	∠(C–C≡C)	∠(C=C–H)		
Vinylacetylene	(r_{av})	123.1 ± 0.5	177.9 ± 1.2	120.6 ± 1.5[a]		
Vinylcyanide	(r_s)	122.6	——	121.7		
Propynal	(r_s)	——	178.4 ± 0.2	——		
Ethylene	(r_a^0)	——	——	121.4 ± 0.6		

a) Average value of the three angles.

calculated difference $r_g - r_a^0$. It is shown in Table 4. This structure is considered to be appropriate for comparison of the bond lengths for different molecules.[5] On the other hand, the angles are given in the r_{av} structure, which is suitable for the description of the shape of a molecule.[5]

Discussion

The structure of vinylacetylene shown in Table 1 is close to that given by Bastiansen, although it is not clear whether they are of comparable physical significance.

Table 4 lists the structures of vinylacetylene, vinylcyanide, and propynal. It must be emphasized that the latter molecules are described in the r_s structure whereas the parameters for vinylacetylene are given in the r_g or r_{av} structure. Although no quantitative relation connecting the r_g with the r_s distances has been set forth, there is little doubt in that the former is longer than the latter. The difference is expected to be in the range of several thousandths of an angstrom. In this consideration, it is probable that the r_g(C–C) of propynal is longer than that of vinylacetylene by more than 0.01 Å. Thus the present system provides another example of the lengthening of a C–C bond adjacent to a heteroatom. On the other hand, it is premature to draw any conclusion about whether or not a similar heteroatom effect also exists between vinylacetylene and vinylcyanide, since the r_g(C–C) of vinylcyanide may be close to 1.430 Å. In order to elucidate this point, and to grasp the heteroatom effect more quantitatively, an electron-diffraction investigation of vinylcyanide and propynal is now under way in our laboratory.

It is interesting in this connection to note that molecular-orbital calculations of bond orders have been reported by Moffat,[17] who has shown that the bond order for the C–C bond in vinylacetylene is smaller than that for the corresponding bond in vinylcyanide. According to his calculations, the C–C bond of vinylacetylene should be longer than that of vinylcyanide. He has asserted the agreement of his prediction with the experimental results by comparing directly the electron-diffraction structure of vinylacetylene with the r_s structure of vinylcyanide. This comparison may not be justified in view of the difference between r_g and r_s stated above. Our preliminary calculation by the Pariser-Parr-Pople method shows that the relative magnitude of the C–C bond orders for these molecules depends on the integral parameters, and especially, on the core resonance integral β used in the calculation. It is likely, however, that for any choice of parameters the difference in the observed sp^2-sp C–C bond lengths is larger than that predicted by the bond order-bond length correlation curve proposed by Julg and Pellégatti.[18] The same tendency has been pointed out for butadiene, acrolein, and glyoxal.[3]

The lengths of C=C and C≡C are slightly larger than those of ethylene and acetylene, respectively. A similar lengthening of the C=C double bond has been observed for butadiene (r_g(C=C) = 1.345± 0.002 Å[3]), and that of the triple bond for diacetylene (r_g(C≡C) = 1.218±0.001 Å[6]). These results are suspected as indications of the conjugation effect. On the other hand, the C–H lengths and C=C–H angles are close to those in ethylene or acetylene. The angles C=C–C in butadiene and acrolein are different beyond the limit of uncertainty, as pointed out in Ref. 3. (123.3° and 121.0°, respectively). The corresponding angle in vinylacetylene is found to be close to the former. A slight bend is observed in the C–C≡C chain of vinylacetylene, while C≡C–H is linear within the limit of error. The ethynyl group of propynal has been shown to have a similar r_s structure.[7]

The authors are indebted to Dr. Chiaki Hirose for providing them with the rotational constants for vinylacetylene before publication. Their thanks are also due to Mr. Koichi Abe who offered the vinylacetylene sample and who supplied the force constants for the molecule before publication.

17) J. B. Moffat, *Can. J. Chem.*, **42**, 1323 (1964).

18) A. Julg and A. Pellégatti, *Theoret. chim. Acta*, **2**, 396 (1964).

BULLETIN OF THE CHEMICAL SOCIETY OF JAPAN VOL. 42 383—386 (1969)

Gravimetric Determination of Palladium, Silver, Mercury and Copper with 2-Mercaptomethylbenzimidazole

Bimal C. BERA*1 and M. M. CHAKRABARTTY

Research and Control Laboratory, Durgapur Steel Plant, Durgapur-3, West Bengal, India

(Received May 17, 1968)

New selective methods are described for the gravimetric determination of palladium, silver, copper and mercury with 2-mercaptomethylbenzimidazole. In the presence of EDTA or tartrate, palladium, silver and mercruy are determined at pH of 4—5. Copper is determined as the copper-(I) complex in the same pH range using cyanide as a reducing and complexing agent. Thermogravimetric studies reveal adequate thermal stability of the complexes. X-Ray studies confirm the identity of the end products in the thermolysis of the copper(I) and copper(II) complexes.

2-Mercaptobenzimidazole (A) is a widely used organic precipitant for cations,[1] and has been employed in the gravimetric,[2] spectrophotometirc,[3,4] amperometric[5] determination of palladium and spectrophotometric determination of osmium.[6] Though extensively used as an analytical reagent it is highly non-specific.[7] As part of an investigation on the analytical applications of some analogous heterocyclic thiols, 2-mercaptomethylbenzimidazole (B) was selected. As in this compound the thiol group is linked to the ring system through an additional carbon atom, it may form five-membered chelates with metal ions and may exhibit a greater degree of selectivity compared to (A). The compound forms chelates[8] with nickel and copper and has been used in the spectrophotometric determination[9] of palladium and in the amperometric titration[10] of palladium, silver and copper.

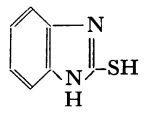

(A)

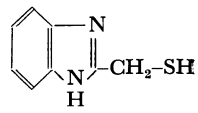

(B)

The present study shows that the reagent can be successfully utilised for the gravimetric determination of palladium, silver and mercury in the pH range of 4—5 by weighing their 1:2, 1:1 and 1:2 complexes respectively. Copper can be determined in the same pH range as the copper(I) complex, because the precipitate of the copper(II) complex is finely divided and is difficult to work with.

In the presence of tartrate or EDTA most of the common ions do not interfere in the determination of palladium, silver and mercury. Interferences of Pt^{4+}, Cu^{2+}, Ag^{+} or Hg^{2+} in the determiantion of palladium are obviated by masking palladium with cyanide. Copper, silver and mercury interfere mutually. The selectivity for copper is achieved by using cyanide as a masking and reducing agent.

Thermogravimetric studies indicate that the complexes have adequate thermal stabilities. The complexes of palladium and silver are decomposed into metals. The mercury complex is converted into metallic mercury which finally escapes. The complexes of copper leave a residue which is a mixture of Cu(I) and Cu(II) oxides as confirmed by X-ray analysis.

Experimental

Apparatus. Measurements of pH were made with a Beckman model G pH meter. A Chevenard thermobalance of type 3 of ADAMEL[11] (Paris) was used for thermal analysis. X-Ray studies were performed in

*1 Present address: Chemistry Department, Asutosh College, Calcutta-26, India.

1) F. J. Welcher, "Organic Analytical Reagents," Vol. IV, Van Nostrand, New York (1948), p. 127.

2) A. K. Majumdar and M. M. Chakrabartty, *Z. anal. Chem.*, **162**, 101 (1958).

3) J. Xavier, *ibid.*, **164**, 250 (1958).

4) A. K. Majumdar and M. M. Chakrabartty, *Anal. Chim. Acta*, **20**, 379 (1959).

5) A. K. Majumdar and M. M. Chakrabartty, *ibid.*, **20**, 386 (1959).

6) B. C. Bera and M. M. Chakrabartty, *Anal. Chem.*, **38**, 1419 (1966).

7) B. C. Bera and M. M. Chakrabartty, *Z. anal. Chem.*, **223**, 169 (1966).

8) G. K. Hughes and F. Lions, *J. Proc. Roy. Soc., (New South Wales)*, **71**, 209 (1937—1938).

9) B. C. Bera and M. M. Chakrabartty, *Mikrochim. Acta*, **1966**, 1094.

10) B. C. Bera and M. M. Chakrabartty, *Talanta*, **13**, 1186 (1966).

11) C. Duval, "Inorganic Thermogravimetric Analysis," 2nd Ed., Elsevier Publishing Co., Amsterdam (1963).

Siemens Krystalloflex-4 using copper target at 35 kV and 16 mA. The exposure time was 3 hr with a 114.6 mm dia. camera.

Reagent Solution. 2-Mercaptomethylbenzimidazole was prepared as described[8] and a 0.5% (W/V) solution in 50% (V/V) aqueous ethanol was employed.

Standard Solutions. Stock solutions of palladium, silver and mercury were prepared and standardised as described earlier.[12] For the standard solution of copper an accurately weighed amount of electrolytic copper (99.99% pure) was dissolved in nitric acid and the excess acid was expelled from the solution.

Preparation of the Complexes. Moderate excess of the reagent was added to the solution of metal ions, buffered with sodium acetate and acetic acid in the pH range of 4—5. The precipitates were allowed to settle, filtered, washed with water and dried in air. The palladium complex was yellow and the copper(II) complex was blue in colour. The other complexes were light yellow.

For preparation of the copper(I) complex, sufficient quantity of saturated sodium sulphite solution or 5% solution of an alkali cyanide was added to copper(II) solution and the pH of the solution was adjusted to 4—5. The solution was heated on the water bath and copper was precipitated as the yellow copper(I) complex. The precipitate was filtered, washed with hot water and dried in air.

Composition of the Complexes. The air dried complexes were dried at 110°C for at least 1 hr and were preserved in a desiccator. The sulphur contents of all the complexes and the metal contents of the palladium, silver and mercury complexes were determined in the same way as reported earlier.[12]

The copper(I and II) complexes were decomposed with concentrated nitric acid. Excess nitric acid and the oxides of nitrogen were expelled by carefully evaporating the solutions with concentrated sulphuric acid and copper was determined iodometrically.

The compositions were as follows:

Found: Pd, 24.56; S, 14.66%. Calcd for $Pd(C_8H_7N_2S)_2$:Pd, 24.58; S, 14.85%. Found: Ag, 39.72; S, 11.70%. Calcd for $Ag(C_8H_7N_2S)$: Ag, 39.80; S, 11.82%. Found: Hg, 37.80; S, 11.93%. Calcd for $Hg(C_8H_7N_2S)_2$: Hg, 38.06; S, 12.17%. Found: Cu, 16.18; S, 16.26%. Calcd for $Cu(C_8H_7N_2S)_2$: Cu, 16.30; S, 16.44%. Found; Cu, 28.10; S, 14.10%. Calcd for $Cu(C_8H_7N_2S)$: Cu, 28.02; S, 14.14%.

Thermal Studies of the Reagent and the Complexes. Aliquots (50—100 mg) of the reagent and the complexes were separately taken in a micro crucible and heated in the thermobalance at the rate of 5°C per minute. The thermogravimetric analysis cruves are shown in Fig. 1.

The reagent started decomposing around 170°C and the destruction of the organic matter continued till 620°C, when the crucible was empty.

The palladium complex remained stable up to 200°C, thereafter underwent slow decomposition till 410°C. Above this point the decomposition was rapid and the level of metallic palladium appeared near 500°C.

The silver complex was stable up to 165°C, then

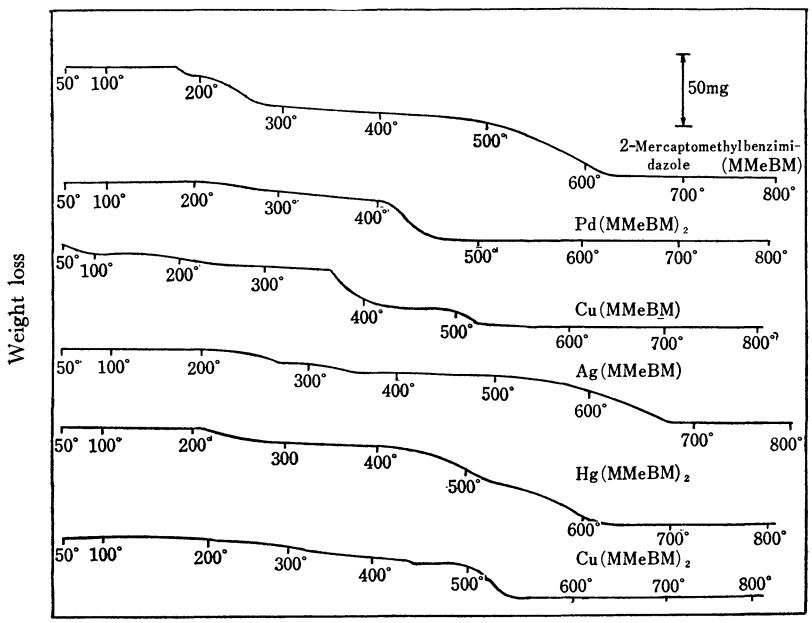

Fig. 1. Thermogravimetric analysis curves.

12) B. C. Bera and M. M. Chakrabartty, *Indian J. Appl. Chem.*, **29**, 75 (1966).

TABLE 1. EFFECT OF pH ON THE DETERMINATION OF PALLADIUM, SILVER, MERCURY AND COPPER

Pd taken = 12.70 mg, Ag taken = 31.40 mg, Hg taken = 38.14 mg, Cu taken = 20.54 mg

Wt. of Pd ppt. (mg)	Pd found (mg)	Wt. of Ag ppt. (mg)	Ag found (mg)	Wt. of Hg ppt. (mg)	Hg found (mg)	Wt. of Cu(I) ppt.(mg)	Cu found (mg)	pH
48.6	11.95	73.2	29.14	90.0	34.26	66.5	18.63	2.0
50.0	12.29	74.6	29.69	95.0	36.31	68.7	19.25	3.0
50.2	12.33	76.6	30.48	89.0	37.25	70.8	19.84	3.5
50.8	12.48	77.4	30.80	98.8	37.61	71.8	20.12	3.7
51.4	12.64	78.6	31.28	99.7	37.95	73.0	20.46	4.0
51.8	12.74	78.7	31.32	100.2	38.15	73.0	20.46	4.3
52.0	12.78	79.0	31.45	100.2	38.15	73.3	20.54	4.5
52.0	12.78	79.2	31.52	100.5	38.23	73.3	20.54	4.8
52.1	12.80	79.2	31.52	100.7	38.31	73.6	20.63	5.0
52.4	12.88	80.0	31.83	101.4	38.60	74.3	20.81	5.2
53.2	13.10	82.4	32.79	102.4	38.97	75.8	21.24	5.5
53.8	13.26	84.6	33.65	104.0	39.60	77.0	21.58	6.0
55.0	13.52	86.2	34.30	106.5	40.53	79.5	22.28	8.0
57.0	14.01	88.5	35.22	109.0	41.48	82.7	23.17	10.0

decomposed slowly till 500°C and rapidly thereafter till 658°C where the horizontal due to metallic silver appeared.

The mercury complex began to lose weight slowly above 180°C till about 400°C when the rate became rapid and the crucible was empty at 640°C. Probably around 400°C mercury was set free from the complex and the rapid loss in weight was due to the escape of mercury and destruction of organic matter.

The initial slope in the T.G.A. profile of the copper-(II) complex was due to the loss of adsorbed moisture. The short horizontal of 105—130°C was due to the diligand complex. The decomposition over the range fo 130—577°C appeared stepwise but there was no strict horizontal. The residue was a mixture of copper(I and II) oxides as confirmed by X-ray studies.

The copper(I) complex was stable up to 170°C, then slowly decomposed till 500°C. Above this point, the rate of decomposition was rapid and a horizontal appeared at 560°C. The residue was again a mixture of the two oxides of copper.

The limiting temperatures of the initial horizontals in the respective thermograms exhibit a decreasing order, such as, Pd(200°C)>Hg(180°C)>Cu^{I}(170°C)>Ag(165°C). This may be taken to be a rough order of the relative thermal stabilities of the complexes. Properties, such as, ionic radii[13] or atomic weights of the metals do not conform to such an order. However, the "ionic potentials" (the ratio of charge to ionic radius) decrease in the order $Pd^{2+}>Hg^{2+}>Cu^{+}>Ag^{+}$ which is in agreement with the above sequence of thermal stability. But the exclusion of the copper(II) complex is not clear. Though the "ionic potential" of Cu^{2+} is higher than that of Hg^{2+}, the complex exhibits the least thermal stability.

Procedure for Palladium, Silver and Mercury. Sufficient amount of 10% (W/V) EDTA. (disodium salt) or tartaric acid solution was added to the solution of a metal ion. The solution was made just alkaline, diluted to about 150 m*l* and the pH was adjusted to 4—5 by adding dilute sodium hydroxide or acetic acid. Moderate excess of the reagent was added with stirring. The precipitates was allowed to settle, filtered through a weighed gooch crucible (G_3 or G_4), washed with hot water (the mercury precipitate was washed with cold water), dried at 110°C and weighed. The results are recorded in Table 1.

Procedure for Copper. To an aliquot of the copper (II) solution 5 m*l* of 5% sodium or potassium cyanide solution was added and the pH was adjusted as usual. The solution was heated to around 70°C on a water bath, copper was precipitated and the mixture was left on the water bath for 10—15 min. The precipitate was filtered, washed with hot water, dried at 110°C and weighed. The results are shown in Table 1.

The metal ions were quantitatively precipitated in the pH range of 4—10, but the precipitates conformed to the above formulas at a pH 4—5. The high results beyond this range were due to the insolubility of the reagent while the values at lower pH were due to the solubility of the complexes.

The reagent not being very soluble a large excess of it was avoided. Generally, 10 m*l* of the reagent solution was sufficient for complete precipitation of 10 mg of palladium or copper and 20 mg of silver or mercury.

Effect of Diverse Ions. Excess EDTA or tartrate solution was added to the palladium, silver or mercury solution containing the diverse ions. The volume of the solution was made to 150 m*l* and the pH was adjusted to 4—5. The metal ions were precipitated with the requisite amount of the reagent. The precipitates were filtered, dried and weighed as usual. Interferences of Pt^{4+}, Cu^{2+} Ag^{+} and Hg^{2+} in the determination of palladium were obviated by complexing palladium with cyanide and precipitating the above ions with the reagent. The filtrate was then evaporated carefully to decompose the cyanide. After complete removal of the cyanide as detected by the copper acetate-benzidine

13) L. E. Sutton, Ed., "Tables of Interionic Distances and Configuration of Molecules and Ions," Chemical Society, London (1958).

acetate reagent,[14] palladium was determined in the solution as usual. Copper, silver and mercury interfered mutually. Effects of diverse ions are presented in Tables 2—5.

Table 2. Effect of diverse ions on the determination of palladium

Pd taken (mg)	Ions added	Amount added (mg)	Wt. of Pd ppt. (mg)	Pd found (mg)
12.70	Pt^{4+}	41.5	52.3	12.86
12.70	Ag^{+}	31.4	52.1	12.80
12.70	Hg^{2+}	38.1	52.2	12.83
12.70	Cu^{2+}	41.0	52.2	12.83
12.70	Pb^{2+}, Cd^{2+}	40 each	51.8	12.74
12.70	Pb^{2+}, Cd^{2+}	60 each	52.2	12.83
15.24	Mn^{2+}, Zn^{2+}, Mg^{2+}	40 each	62.1	15.26
15.24	Mn^{2+}, Zn^{2+}, Mg^{2+}	80 each	62.7	15.41
15.24	Co^{2+}, Ni^{2+}	50 each	61.8	15.19
15.24	Co^{2+}, Ni^{2+}	100 each	62.6	15.39
19.05	Ca^{2+}, Sr^{2+}, Ba^{2}_{+}	50 each	77.3	19.00
19.05	Ca^{2+}, Sr^{2+}, Ba^{2}_{+}	100 each	78.1	19.20
12.70	Fe^{3+}, Cr^{3+}	50 each	52.2	12.83
19.05	Al^{3+}, Be^{2+}, Ti^{4+}	40 each	77.5	19.07
19.05	Al^{3+}, Be^{2+}, Ti^{4+}	80 each	78.4	19.27
15.24	Th^{4+}, Zr^{4}, UO^{2+}	40 each	62.6	15.39
12.70	As^{3+}, Sb^{3+}, Bi^{3+}	50 each	52.1	12.80
12.70	Mo^{6+}, V^{5+}	40 each	51.4	12.64

Table 3. Effect of diverse ions on the determination of silver

Ag taken (mg)	Ions added	Amount added (mg)	Wt. of Ag ppt. (mg)	Ag found
31.40	Pd^{2+}	30.48	78.6	31.28
31.40	Pb^{2+}, Cd^{2+}	60 each	79.1	31.48
31.40	Pb^{2+}, Cd^{2+}	120 each	79.7	31.73
31.40	Mn^{2+}, Zn^{2+}, Mg^{2+}	60 each	78.9	31.41
31.40	Mn^{2+}, Zn^{2+} Mg^{2+}	120 each	79.3	31.56
47.25	Co^{2+}, Ni^{2+}	80 each	118.9	47.33
47.25	Co^{2+}, Ni^{2+}	120 each	119.5	47.55
31.40	Ca^{2+}, Sr^{2+}, Ba^{2+}	60 each	79.1	31.48
31.40	Ca^{2+}, Sr^{2+}, Ba^{2+}	120 each	79.5	31.64
47.25	Fe^{3+}, Cr^{3+}	80 each	119.7	47.61
31.40	Al^{3+} Be^{2+}, Ti^{4+}	80 each	79.6	31.66
31.40	Th^{4+}, Zr^{4+}, UO_2^{2+}	50 each	79.3	31.56
31.40	As^{3+}, Sb^{3+}, Bi^{3+}	06 each	79.6	31.66
47.25	Mo^{6+}, V^{5+}	80 each	119.5	47.55

14) F. Feigl, "Qualitative Analysis by Spot Tests," 5th Ed., Elsevier Publishing Co., New York (1958), p. 276.

Table 4. Effect of diverse ions on the determination of mercury

Hg taken (mg)	Ions added	Amount added (mg)	Wt. of Hg ppt. (mg)	Hg found (mg)
19.07	Pb^{2+}, Cd^{2+}	60 each	50.4	19.18
19.07	Pb^{2+}, Cd^{2+}	90 each	50.5	19.23
19.07	Mn^{2+}, Zn^{2+}, Mg^{2+}	50 each	50.2	19.11
19.07	Mn^{2+}, Zn^{2+}, Mg^{2+}	100 each	50.5	19.23
38.14	Co^{2+}, Ni^{2+}	80 each	100.4	38.21
38.14	Co^{2+}, Ni^{2+}	120 each	100.7	38.32
38.14	Ca^{2+}, Ba^{2+}, Sr^{2+}	60 each	100.4	38.31
38.14	Ca^{2+}, Ba^{2+}, Sr^{2+}	120 each	100.7	38.32
19.07	Fe^{3+}, Cr^{3+}	80 each	50.6	19.26
45.77	Al^{3+}, Be^{2+}, Ti^{4+}	80 each	120.6	45.88
19.07	Th^{4+}, Zr^{4+}, UO_2^{2+}	50 each	50.4	19.18
38.14	As^{3+}, Sb^{3+}, Bi^{3+}	60 each	100.7	38.32
19.07	Mo^{6+}, V^{5+}	60 each	50.5	19.23

Table 5. Effect of diverse ions on the determination of copper

Cu taken (mg)	Ions added	Amount added (mg)	Wt. of Cu ppt. (mg)	Cu found (mg)
20.54	Pb^{2+}, Cd^{2+}	80 each	73.6	20.60
20.54	Pb^{2+}, Cd^{2+}	160 each	74.0	20.73
30.81	Mn^{2+}, Zn^{2+}, Mg^{2+}	100 each	110.0	30.82
30.81	Mn^{2+}, Zn^{2+}, Mg^{2+}	150 each	110.5	30.96
30.81	Co^{2+}, Ni^{2+}	100 each	110.0	30.82
30.81	Co^{2+}, Ni^{2+}	150 each	110.6	30.96
30.81	Ca^{2+}, Sr^{2+}, Ba^{2+}	150 each	110.6	30.95
20.54	Fe^{3+}, Cr^{3+}	80 each	73.7	20.65
41.08	Al^{3+}, Be^{2+}, Ti^{4+}	150 each	147.0	41.19
20.54	Th^{4+}, Zr^{4+}, UO_2^{2+}	50 each	73.5	20.60
20.54	As^{3+}, Sb^{3+}, Bi^{3+}	80 each	73.8	20.68
20.54	Mo^{6+}, V^{5+}	60 each	73.6	20.63

The authors are indebted to the Council of Scientific and Industrial Research (India) for awarding a Fellowship to B.C.B. They are also grateful to the authorities of Durgapur Steel Plant and Jadavpur University, Calcutta-32, for providing all facilities.

BULLETIN OF THE CHEMICAL SOCIETY OF JAPAN VOL. 42 387—393 (1969)

The Yields of Photonuclear Reactions in Titanium and Vanadium with Bremsstrahlung up to 60 MeV

Yoshinaga OKA, Toyoaki KATO and Nobuyoshi SATO

Department of Chemistry, Faculty of Science, Tohoku University, Katahira-cho, Sendai

(Received June 6, 1968)

The yields of a number of radioactive nuclei produced by (γ,xnyp) reactions on titanium and vanadium targets have been determined at four different bremsstrahlung maximum energies, 30, 45, 55 and 60 MeV, with the aid of radiochemical methods and gamma-ray spectrometric measurements. The linear electron accelerator of Tohoku University was the bremsstrahlung source. Yields have been expressed as production rates of given radioactive end-products relative to that of the $^{12}C(\gamma,n)^{11}C$ process. Over the range of energies investigated, the yield of each nuclide increases with increasing maximum energy. The yield of a reaction with the emission of more than one nucleon appeared to be strongly energy dependent. Reaction paths leading to the formation of each nuclide were investigated. The photoproduction of ^{47}Ca from titanium has been observed.

In previous work,[1-6] a number of problems involving reaction yields and applicabilities of induced activities to the activation analysis of many elements have been investigated in the energy region of 20 MeV bremsstrahlung. This energy corresponds to giant resonance for photon absorption and, in this energy region, the main nuclear events are the emission of one neutron, one proton, or occasionally one alpha-particle. The excitation of a nucleus by gamma-rays with higher energies gives rise to more complex events. Apart from reactions with the emission of a single particle, those involving the emission of just two or more nucleons become important. Studies of production rates or yields of such photonuclear reactions are helpful in understanding the processes by which particle emissions take place, as well as in considering the applicability of the resultant activities to activation analysis.

Titanium and vanadium, on the other hand, when irradiated with high-energy photons, undergo photodisintegrations leading to the production of ^{45}Ti, ^{48}V, $^{46-48}Sc$ and other nuclides, which are convenient for the gamma-ray spectrometric determinations of these elements. Abe[7] reported methods for the determination of titanium in iron and vanadium, utilizing the 20 MeV linear electron accelerator. Since yield is a strong function of photon energy, it should be noted that higher sensitivities are expected with an accelerator capable of producing bremsstrahlung radiation of higher energies.

Although a number of studies have been performed on photonuclear reactions in the region of medium weight nuclei,[8-12] relatively little has been determined with regard to photonuclear properties of titanium and vanadium at energies beyond giant resonance.

Sherwood *et al.*[13] determined the cross-sections, integrated to 31 MeV, of photonuclear reactions involving titanium nuclides, and Pai *et al.*[14] measured the yields of protons ejected from titanium nuclides irradiated by 22 and 30 MeV bremsstrahlung.

The present report describes some experimental details on the relative yields of various nuclides

1) Y. Oka, T. Kato, K. Nomura and T. Saito, This Bulletin, **40**, 575 (1967).
2) Y. Oka, T. Kato, K. Nomura, T. Saito and H-T. Tsai, *ibid.*, **41**, 380 (1968).
3) Y. Oka, T. Kato, K. Nomura, T. Saito and H-T. Tsai, *ibid.*, **41**, 2660 (1968).
4) Y. Oka, T. Kato and A. Yamadera, *ibid.*, **41**, 1606 (1968).
5) Y. Oak, T. Kato, K. Nomura and T. Saito, *J. Nucl. Sci. Technol.*, **4**, 346 (1967).
6) Y. Oka, T. Kato and I. Nagai, *ibid.*, **4**, 300 (1967).
7) S. Abe, *Nippon Kagaku Zasshi* (*J. Chem. Soc. Japan, Pure Chem. Sect.*), **87**, 710 (1966); **87**, 714 (1966).
8) R. J. Debs, J. T. Eisinger, A. W. Fairhall, I. Halpern and H. G. Richter, *Phys. Rev.*, **97**, 1325 (1955).
9) I. Halpern, R. J. Debs, J. T. Eisinger, A. W. Fairhall and H. G. Richter, *ibid.*, **97**, 1327 (1955).
10) T. T. Sugihara and I. Halpern, *ibid.*, **101**, 1768 (1956).
11) J. M. Wyckoff, B. Ziegler, H. W. Koch and R. Uhlig, *ibid.*, **137**, 576 (1965).
12) C. B. Fulmer, I. R. Williams and T. H. Handley, *Phys. Rev. Letters*, **19**, 522 (1967).
13) T. R. Sherwood and W. E. Turchinetz, *Nucl. Phys.*, **29**, 292 (1962).
14) H. L. Pai and K. G. McNeill, *Can. J. Phys.*, **45**, 3235 (1967).

resulting from the irradiation of titanium and vanadium targets by bremsstrahlung with energies up to 60 MeV. The linear electron accelerator of Tohoku University was used as the bremsstrahlung source, and yields were measured for each nuclide at just four different maximum energies, 30, 45, 55 and 60 MeV, with the aid of radiochemical methods.

Experimental

Target Materials. The target materials used were titanium of 99.9% purity, in the form of the elemental powder, and "specpure" grade vanadium pentoxide. A definite amount of each sample (approximately 100 mg) was wrapped in thin aluminum foil and made into a small disk with a diameter of 7 mm and a thickness of 3 mm.

Linac and Irradiation. The 300 MeV linear electron accelerator of Tohoku University was the bremsstrahlung source. The machine was operated with the "High Current" accelerating section which provided a high intensity electron current, the peak current being at least 100 mA with energies up to 100 MeV.[15] The beam was deflected 90° from the original beam path of the accelerating section, and again deflected 45° onto the beam exit window. The spread of electron energies in this operating condition is 3% from the selected value. The electron beam produced bremsstrahlung in a platinum converter with a thickness of 3 mm located 3 cm from the beam exit window. In the energy range from 30 to 60 MeV, used in these experiments, the average beam current was at least 30μA, measured at the position of the converter using a current monitor. Targets were set in a water-cooled target holder on the bremsstrahlung beam axis immediately behind the converter. A typical irradiation was terminated in 1 to 2 hr. The bremsstrahlung flux was monitored using a thin sheet of gold (10μ thick, 7 mmφ) adjacent to the samples.

Radiochemical Separations. After irradiation, the target materials were dissolved along with the addition of scandium and calcium carriers, and subjected to separation procedures diagrammed in Tables 1 and 2. The final precipitates were packed in a small glass tube having an internal diameter of 4 mm for the determination of chemical yield and for gmama-ray counting.

Radioactivity Measurement. For measurements of gamma-ray spectra, a 3″ dia. × 3″ NaI(Tl) detector coupled to a 800-channel pulse-height analyzer made

TABLE 1. SEPARATION SCHEME FOR TITANIUM, SCANDIUM AND CALCIUM ACTIVITIES FROM IRRADIATED TITANIUM TARGET

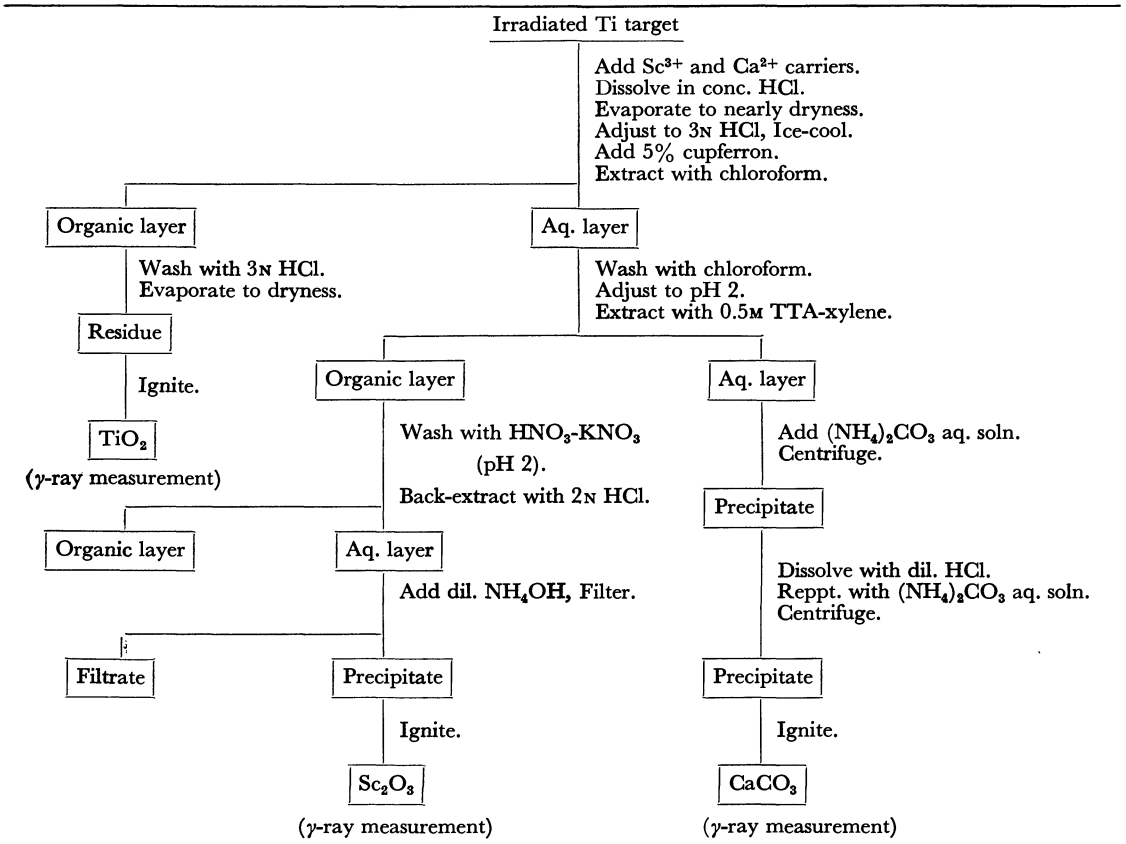

15) In many cases, the pulse repetition rate was 200 pps with a pulse width of 3μ sec.

TABLE 2. SEPARATION SCHEME FOR VANADIUM, SCANDIUM AND CALCIUM ACTIVITIES FROM IRRADIATED VANADIUM TARGET

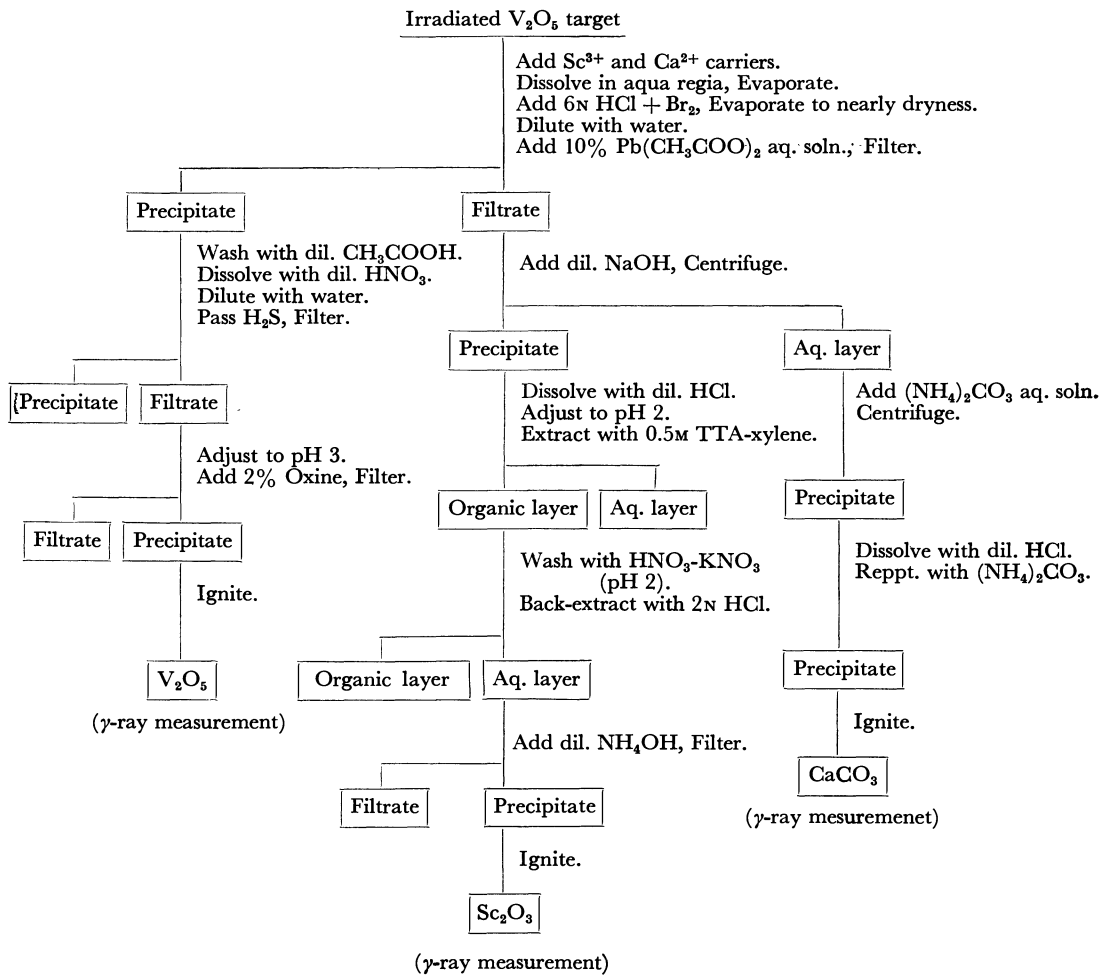

by Tokyo Shibaura Electric Co. Ltd., was employed. Counting efficiencies had been previously determined as a function of source distance and gamma-ray energy. The sample to be measured was centered in a Lucite cylinder with walls thick enough to absorb positions from the decay of any positron emitters. Decay curve analyses were performed to distinguish and to separate the undesired activities. The gamma-ray energies used in the yield determination are given in Table 3.

Yield Determination. Yield is defined as the production rate of a given radioactive end-product per atomic weight of the target element when a standard amount of bremsstrahlung radiation with a given maximum energy is passed through the target during the irradiation period. The initial rates of the various activities present were determined from a decay curve analysis of the counting rate of the relevant photopeak area. Corresponding saturation rates were computed and normalized for bremsstrahlung intensity, which was measured by the amount of ^{196}Au activity in a gold foil irradiated together with the target. After correcting for chemical yields, counting efficiencies, branching

TABLE 3. SOME NUCLEAR DATA FOR NUCLIDES USED FOR YIELD DETERMINATION

Nuclide	Half-life	Gamma-ray used	
		Energy (MeV)	Branching ratio (%)
^{45}Ti	3.09 hr	0.511[a)]	168
^{44}Sc	3.92 hr	0.511[a)]	188
^{46}Sc	83.9 d	1.12	100
^{47}Sc	3.43 d	0.160	73
^{48}Sc	1.83 d	1.31	100
^{47}Ca	4.53 d	1.30	76.3
^{48}V	16.0 d	1.31	97

a) Annihilation radiation.

ratio[16] and the internal conversion electrons,[17] data were expressed as yields.

These yields were expressed relative to that of the $^{12}C(\gamma,n)^{11}C$ process, which was measured by the amount of 0.511 MeV gamma-rays arising from the annihilation of positrons in a standard carbon disk[18] irradiated together with the target.

Results and Discussion

Gamma-Ray Spectra. Figures 1—3 show gamma-ray spectra obtained for separated activities obtained from a titanium target irradiated with 60 MeV bremsstrahlung. A typical gamma-ray spectrum of a titanium fraction is shown in Fig. 1. The decay curve of the area under the 0.511 MeV photopeak showed a half-life of 3.09 hr, which agrees with the literature value of ^{45}Ti. The gamma-ray spectra of the scandium fraction separated from an irradiated titanium target show ones composed of ^{44}Sc, ^{46}Sc, ^{47}Sc and ^{48}Sc. The production of ^{47}Ca from a titanium target is revealed by the characteristic gamma-ray photopeaks at 0.49, 0.81 and 1.30 MeV, as shown for a typical gamma-ray spectrum in Fig. 3.[19]

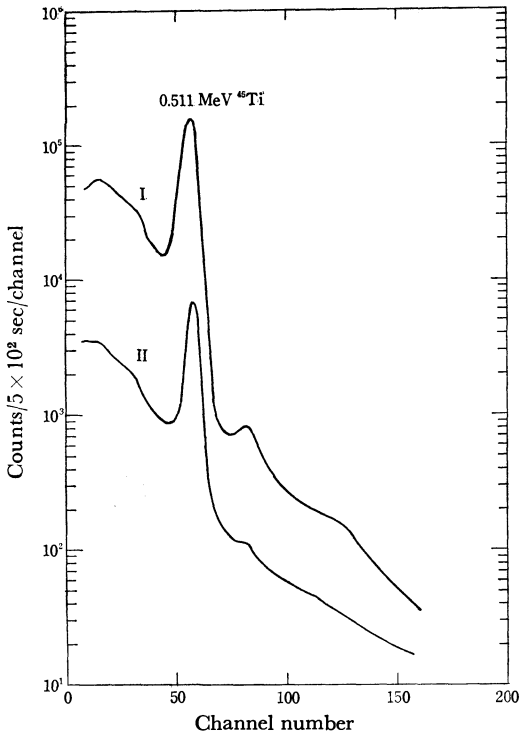

Fig. 1. Gamma-ray spectra of titanium activities.
Irradiation: 60 MeV (45 μA); 1 hr
Source distance:
8 cm from 3″ dia. ×3″ NaI(Tl) crystal
I : 8.8 hr after irradiation
II: 24 hr after irradiation

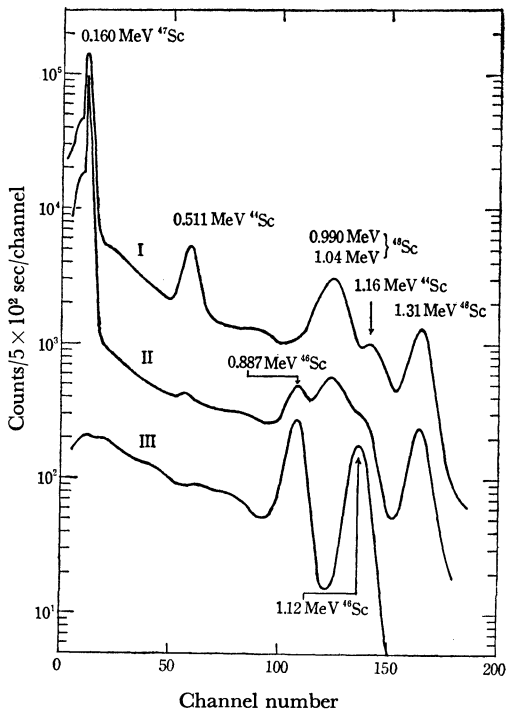

Fig. 2. Gamma-ray spectra of scandium activities separated from titanium target.
Irraidation: 60 MeV (45 μA); 1 hr
Source distance:
8 cm from 3″ dia. ×3″ NaI(Tl) crystal
I : 17.1 hr after irradiation
II : 5.2 d after irradiation
III: 38 d after irradiation

The gamma-ray spectra of the vanadium and scandium fractions from a vanadium target irradiated with 60 MeV bremsstrahlung are shown in Figs. 4 and 5. Photoproductions of vanadium activities other than 16.0-day ^{48}V could not be observed, and no ^{44}Sc activities occurred to any appreciable amount in an irradiated vanadium target under the present experimental conditions. In addition, no gamma-activity could be detected in the calcium fraction.

Reaction Path. The most abundant naturally

16) The decay schemes used were those listed in C. M. Lederer, J. M. Hollander and I. Perlman, "Table of Isotopes," sixth Ed., John Wiley & Sons, Inc., New York (1967).

17) The tables in M. E. Rose, "Internal Conversion Coefficients," North-Holland Publ. Co., Amsterdam (1958), were used.

18) From the carbon rod used as an electrode in emission spectroscopy, small pieces 7 mm ϕ × 3 mm were cut out and used.

19) The gamma-ray at 0.160 MeV is due to the growth decay of ^{47}Sc, the daughter nuclide of ^{47}Ca.

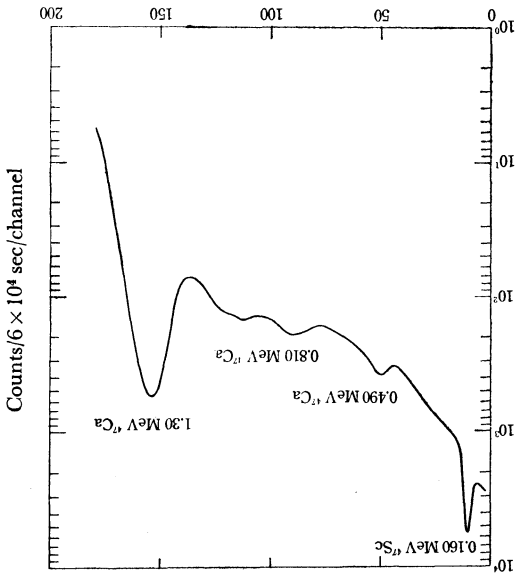

Fig. 3. Gamma-ray spectrum of calcium activities.
Irradiation: 60 MeV (45 μA); 1 hr
Source distance:
5 cm from 3″ dia × 3″ NaI(Tl) crystal
3.0 d after irraditation

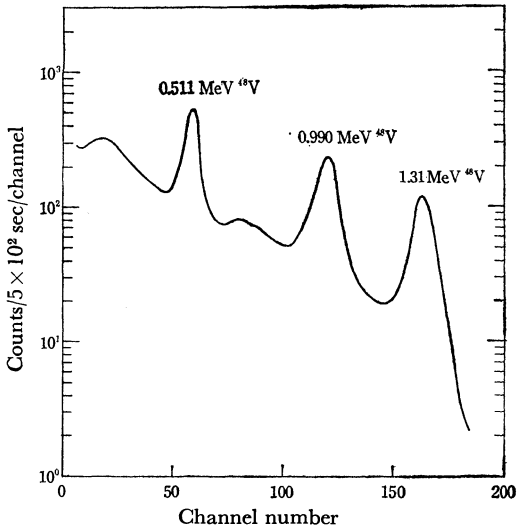

Fig. 4. Gamma-ray spectrum of vanadium activities.
Irradiation: 60 MeV (45 μA); 1 hr
Source distance:
8 cm from 3″ dia × 3″ NaI(Tl) crystal
5.2 d after irradiation.

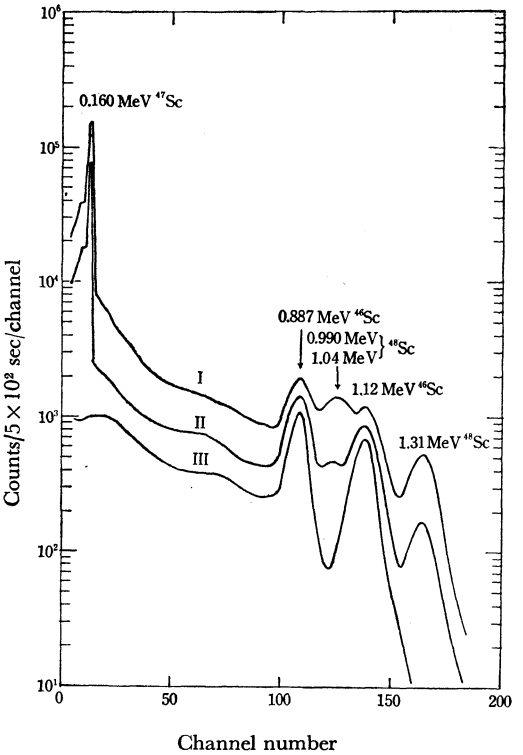

Fig. 5. Gamma-ray spectra of scandium activities separated from vanadium target.
Irradiation: 60 MeV (45 μA); 1 hr
Source distance:
8 cm from 3″ dia. × 3″ NaI(Tl) crystal
I : 2.5 d after irradiation
II : 5.2 d after irradiation
III: 33 d after irradiation

occurring isotope of vanadium is ^{51}V (99.76%). This fact makes the assignments of parent isotopes for observed radionuclides convenient. Titanium, on the other hand, has five naturally occurring isotopes: ^{46}Ti (7.93%), ^{47}Ti (7.28%), ^{48}Ti (73.94%), ^{49}Ti (5.51%) and ^{50}Ti (5.34%). Competitive nuclear reactions should occur in the energy region covered in this experiment. In Tables 4 and 5 are listed the possible nuclear reactions together with their calculated mass thresholds[20] for the production of each radioactive end-product from both elements with natural compositions. In many cases, radionuclides can be formed through several different reaction paths. Photoproduction of ^{45}Ti from vanadium was excluded by considering the natural abundances and threshold energies. Almost all reactions leading to the photoproduction of ^{44}Sc from the parent ^{51}V have threshold energies greater than 50 MeV. This fact makes unlikely a detectable contribution from photonuclear reactions in vanadium to scandium gamma-ray spectra. Finally, the production of ^{47}Ca from vanadium is also unlikely. The reactions producing ^{47}Ca are: ^{50}V $(\gamma,3p)^{47}$Ca, $-Q=28.71$ MeV; ^{51}V$(\gamma,3pn)^{47}$Ca, $-Q=39.75$ MeV; ^{51}V$(\gamma,2pd)^{47}$Ca, $-Q=37.52$ MeV; and ^{51}V$(\gamma,^3Hep)^{47}$Ca, $-Q=32.03$ MeV. Restric-

20) Nuclidic mass values used were those listed in G. Friedlander, J. W. Kennedy and J. M. Miller, "Nuclear and Radiochemistry," 2nd Ed., John Wiley & Sons Inc., New York (1964), p. 533.

TABLE 4. CALCULATED MASS THRESHOLDS FOR PHOTONUCLEAR REACTIONS ON TITANIUM NUCLEI

Reaction	$E_{th}(-Q)$ (MeV)	Reaction	$E_{th}(-Q)$ (MeV)
^{46}Ti(γ, n)^{45}Ti	13.19	^{47}Ti(γ, p)^{46}Sc	10.45
^{47}Ti(γ, 2n)^{45}Ti	22.07	^{48}Ti(γ, pn)^{46}Sc	22.07
^{48}Ti(γ, 3n)^{45}Ti	33.70	^{48}Ti(γ, d)^{46}Sc	19.86
^{49}Ti(γ, 4n)^{45}Ti	42.77	^{49}Ti(γ, p2n)^{46}Sc	30.23
^{50}Ti(γ, 5n)^{45}Ti	52.78	^{49}Ti(γ, dn)^{46}Sc	28.08
		^{49}Ti(γ, t)^{46}Sc	21.75
^{46}Ti(γ, pn)^{44}Sc	21.67	^{50}Ti(γ, p3n)^{46}Sc	41.31
^{46}Ti(γ, d)^{44}Sc	19.44	^{50}Ti(γ, d2n)^{46}Sc	38.95
^{47}Ti(γ, p2n)^{44}Sc	30.56	^{50}Ti(γ, tn)^{46}Sc	32.70
^{47}Ti(γ, dn)^{44}Sc	28.33		
^{47}Ti(γ, t)^{44}Sc	22.07	^{48}Ti(γ, p)^{47}Sc	11.44
^{48}Ti(γ, p3n)^{44}Sc	42.18	^{49}Ti(γ, pn)^{47}Sc	20.36
^{48}Ti(γ, d2n)^{44}Sc	39.95	^{49}Ti(γ, d)^{47}Sc	17.35
^{48}Ti(γ, tn)^{44}Sc	33.69	^{50}Ti(γ, p2n)^{47}Sc	30.52
^{49}Ti(γ, p4n)^{44}Sc	50.32	^{50}Ti(γ, dn)^{47}Sc	28.30
^{49}Ti(γ, d3n)^{44}Sc	48.09	^{50}Ti(γ, t)^{47}Sc	22.04
^{49}Ti(γ, t2n)^{44}Sc	41.84		
^{50}Ti(γ, p5n)^{44}Sc	61.27	^{49}Ti(γ, p)^{48}Sc	11.35
^{50}Ti(γ, d4n)^{44}Sc	59.04	^{50}Ti(γ, pn)^{48}Sc	22.29
^{50}Ti(γ, t3n)^{44}Sc	52.79	^{50}Ti(γ, d)^{48}Sc	20.07
		^{49}Ti(γ, 2p)^{47}Ca	20.77
		^{50}Ti(γ, 2pn)^{47}Ca	31.70
		^{50}Ti(γ, pd)^{47}Ca	29.48
		^{50}Ti(γ, ^{3}He)^{47}Ca	23.99

TABLE 5. CALCULATED MASS THRESHOLDS FOR PHOTONUCLEAR REACTIONS ON VANADIUM NUCLEI

Reaction	$E_{th}(-Q)$ (MeV)	Reaction	$E_{th}(-Q)$ (MeV)
^{50}V(γ, 2n)^{48}V	20.88	^{50}V(γ, 2pn)^{47}Sc	27.52
^{51}V(γ, 3n)^{48}V	31.93	^{50}V(γ, pd)^{47}Sc	25.31
		^{50}V(γ, ^{3}He)^{47}Sc	19.81
^{50}V(γ, 2p2n)^{46}Sc	38.17	^{51}V(γ, 2p2n)^{47}Sc	38.56
^{50}V(γ, pdn)^{46}Sc	35.95	^{51}V(γ, pdn)^{47}Sc	36.34
^{50}V(γ, 2d)^{46}Sc	33.72	^{51}V(γ, 2d)^{47}Sc	34.11
^{50}V(γ, ^{3}Hen)^{46}Sc	30.46	^{51}V(γ, ^{3}Hen)^{47}Sc	30.84
^{50}V(γ, pt)^{46}Sc	29.69	^{51}V(γ, pt)^{47}Sc	30.08
^{50}V(γ, α)^{46}Sc	9.88	^{51}V(γ, α)^{47}Sc	10.26
^{51}V(γ, 2p3n)^{46}Sc	49.21		
^{51}V(γ, pd2n)^{46}Sc	46.99	^{50}V(γ,2p)^{48}Sc	19.29
^{51}V(γ, 2dn)^{46}Sc	44.76	^{51}V(γ, 2pn)^{48}Sc	30.33
^{51}V(γ, ^{3}He2n)^{46}Sc	41.50	^{51}V(γ,pd)^{48}Sc	28.10
^{51}V(γ, ptn)^{46}Sc	40.73	^{51}V(γ,^{3}He)^{48}Sc	22.62
^{51}V(γ, dt)^{46}Sc	38.51		
^{51}V(γ, d, n)^{46}Sc	20.92		

tions posed by the high potential barriers are inherent in these reactions.

Reaction Yield. The yields relative to ^{12}C (γ,n)^{11}C obtained in this experiment are given as a function of the bremsstrahlung maximum energy in Fig. 6. The cross-sectional curve for the reaction ^{12}C(γ,n)^{11}C, reported by Cook *et al.*,[21] has a sharply-peaked resonance centered at 23 MeV, and shows a high energy tail extending at least to 60 MeV. The energy range used herein is well beyond the giant resonance of the ^{12}C(γ,n)^{11}C reaction, and the yield curve for this reaction exhibits a slight increase with increasing energy. Over the range of energies investigated, the relative yield of reactions involving the emission of a single particle do not vary significantly. The yield of a reaction with the emission of more than one nucleon seems likely to be strongly energy dependent.

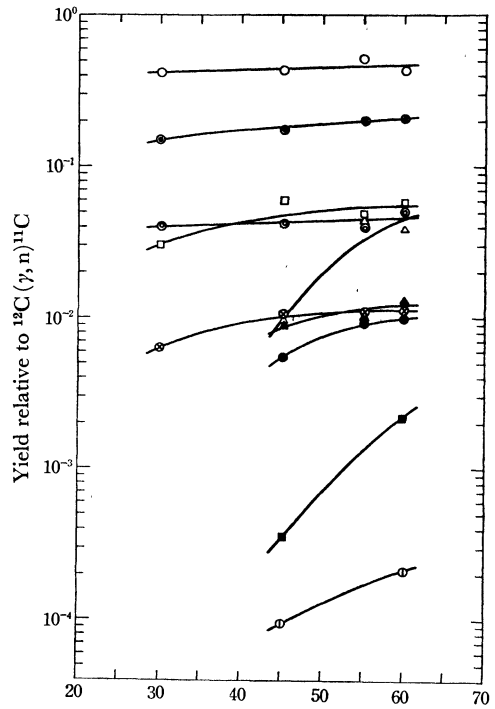

Fig. 6. The yield relative to ^{12}C(γ,n)^{11}C as a function of bremsstrahlung maximum energy.

○ : ^{45}Ti from titanium
● : ^{44}Sc from titanium
◎ : ^{46}Sc from titanium
⊙ : ^{47}Sc from titanium
⊗ : ^{48}Sc from titanium
△ : ^{48}V from vanadium
▲ : ^{46}Sc from vanadium
□ : ^{47}Sc from vanadium
■ : ^{48}Sc from vanadium
◫ : ^{47}Ca from titanium

^{45}Ti from Titanium. The main reaction which can be attributed to the production of ^{45}Ti is the (γ,n) reaction on ^{46}Ti. With high energies, however, contributions from both the ^{47}Ti(γ,2n)^{45}Ti and ^{48}Ti(γ,3n) ^{46}Ti reactions to the total production rate should be taken into account.

$^{44,46-48}$Sc from Titanium. Since ^{44}Sc activity could

21) B. C. Cook, J. E. E. Baglin, J. N. Bradford and J. E. Griffin, *Phys. Rev.*, **143**, 724 (1966).

Table 6. The relative yields for (γ, p) reactions on titanium nuclei expressed as those per mole

Reaction	Yield per mole relative to $^{12}C(\gamma, n)^{11}C$			
	30 MeV	45 MeV	55 MeV	60 MeV
$^{47}Ti(\gamma, p)^{46}Sc$	5.4×10^{-1}	5.8×10^{-1}	5.4×10^{-1}	6.3×10^{-1}
$^{48}Ti(\gamma, p)^{47}Sc$	2.0×10^{-1}	2.4×10^{-1}	2.8×10^{-1}	2.8×10^{-1}
$^{49}Ti(\gamma, p)^{48}Sc$	1.2×10^{-1}	2.1×10^{-1}	2.2×10^{-1}	2.1×10^{-1}

not be detected from irradiated titanium in the energy region of 30 MeV bremsstrahlung, its production rate due to the reactions $^{46}Ti(\gamma,d)^{44}Sc$, $^{46}Ti(\gamma,pn)$ ^{44}Sc and $^{47}Ti(\gamma,t)$ ^{44}Sc would be very small. The upward trend of the yield curve for ^{44}Sc with increasing energy is likely attributable to the reactions (γ,tn), (γ,d2n) and (γ,p3n) in ^{48}Ti.

In this experiment, the gamma-activity attributed to ^{44m}Sc is too weak to be clearly distinguished from those due to the decay of ^{44}Sc and other products. The reason responsible for this behavior is the spin difference between the two isomeric states. In many cases in which an excited state of the residual nucleus can decay to either isomer through intermediate states in gamma-cascades, gamma-transitions of low multipolarity are accorded preference over those of high multipolarity.[4] The spins and parities in ^{44}Sc and ^{44m}Sc are 2^+ and 6^+, respectively, and those of the target nuclides are $0^+(^{46}Ti)$, $5/2^-(^{47}Ti)$ and $0^+(^{48}Ti)$. Since the spin in ^{44}Sc is closer to that of the target nuclides than in ^{44m}Sc, the relative probability of forming these two states is expected to be favorable of ^{44}Sc. The main reaction producing ^{46}Sc from titanium may by the (γ,p) reaction on ^{47}Ti. The $^{48}Ti(\gamma,pn)^{46}Sc$ and $^{48}Ti(\gamma,d)^{46}Sc$ reactions would occur by a considerable amount at higher energies. By taking the abundance of ^{48}Ti into account, almost all ^{47}Sc comes from the parent ^{48}Ti through the (γ,p) process, though a considerable amount may be due to the $^{50}Ti(\gamma,pn)^{48}Sc$ reaction.[22]

Assuming that all of the observed ^{46}Sc, ^{47}Sc and ^{48}Sc indeed arise from the parent nuclides through (γ,p) processes it is possible to convert each yield to that per mole of target nuclide, instead of the yield per atomic weight of target element. In Table 6 are given the results thus obtained. The yield values for the production rates of ^{46}Sc, ^{47}Sc and ^{48}Sc decrease in that order.[23] These results are consistent with the fact that the cross-section for photoproton emission from a neutron excess nuclide is expected to be small.

^{47}Ca from Titanium. The formation of ^{47}Ca could not be attributed to a unique reaction, but to the competitive reactions listed in Table 4. The yields amount to about 1—2 per cent of those for the reaction producing ^{48}Sc, which can be taken as equivalent to the emission of one excess proton from a parent nuclide.

^{48}V from Vanadium. An irradiated vanadium target did not show any ^{48}V activity at 30 MeV, but its production rate increases markedly with increasing maximum energy. It seems likely that almost all of the ^{48}V comes from ^{51}V through the (γ,3n) process.

$^{46-48}Sc$ from Vanadium. For the production of ^{47}Sc and ^{46}Sc from ^{51}V, the only paths which have mass thresholds below 30 MeV are the (γ,α) and (γ,αn) reactions. Of the reaction pathways leading to the production of both nuclides, these two seem to be most important in the energy range investigated. The yield ratios for the production of ^{46}Sc and ^{47}Sc from vanadium have been found to be about 0.2. The reaction which gives rise to ^{48}Sc is about 3—17 per cent as possible as that yielding ^{46}Sc, and is about 0.6—4 per cent as possible as that yielding ^{47}Sc in the energy region from 45 to 60 MeV. The reaction leading to the production of ^{48}Sc from vanadium corresponds to that of ^{47}Ca from titanium. The yields of these reactions can be considered to be low. It appeared unlikely, just as in the case of the titanium target, that any ^{44m}Sc was produced in the irradiation of vanadium.

For analytical purposes, the lower limits of detection under the present experimental conditions were estimated. One mg of titanium gives an activity under the 0.511 MeV photopeak of 4.4×10^4 cpm,[24] so the lower limit of the titanium determination can be set at 1 μg. For vanadium, the limits of detection of 2 mg from the 1.31 MeV peak of ^{48}V and 60μg from the 0.160 MeV peak of ^{47}Sc are obtained.

22) The relative yields reported by Pai *et al.*[14] for the $^{49}Ti(\gamma,p)$ ^{48}Sc, $^{50}Ti(\nu,pn)^{48}Sc$ and $^{50}Ti(\gamma,pn)^{48}Sc$ reactions are 1.5, 0.17 and 0.37, respectively, at 30 MeV.

23) The same order in yield values was obtained in the irradiation of titanium with 20 MeV bremsstrahlung.[2]

24) The corrected value at the end of one-hour irradiation with 60 MeV bremsstrahlung (average beam current, 45μA): The geometry is 10% with a 3″ dia. × 3″ NaI(Tl) crystal.

BULLETIN OF THE CHEMICAL SOCIETY OF JAPAN VOL. 42 394—399 (1969)

Polarographic Study of Copper(II)-*N*-(2-Hydroxyethyl)ethylenediamine-*N*,*N*′,*N*′-triacetate and -2,2′-Ethylenedioxybis-[ethyliminodi(acetate)] Chelates

Mutsuo KODAMA and Yayoe TOMINAGA

Department of Chemistry, Ibaraki University, Mito, Ibaraki

(Received June 8, 1968)

D.c. polarographic behavior of copper(II) ion in *N*-(2-hydroxyethyl)ethylenediamine-*N*,*N*′,*N*′-triacetate (EDTA-OH) and 2,2′-ehtylenedioxybis[ethyliminodi(acetate)] (GEDTA) solutions was studied systematically. In an EDTA-OH solution, copper(II) ion gave invariably a single well-defined wave corresponding to the following two-electron reduction.

$$CuX^- + nH^+ + Hg + 2e^- \rightleftarrows Cu(Hg) + H_nX^{n-3}$$

On the other hand, in a GEDTA solution, two waves were obtained. The height of the first wave, which is reversible in nature, increases with increasing pH of the solution at the expense of the height of the irreversible second wave. From the relation between the half-wave potential and the concentrations of hydrogen ion, GEDTA and acetate ion, determined experimentally, the compositions and the stability constants of copper(II)-GEDTA chelates in solution were determined and the electrode reaction mechanism established:

$$\begin{array}{c} CuZ(Ac)^{3-} \\ \uparrow\downarrow \\ CuZ_2^{6-} \rightleftarrows CuZ^{2-} + nH^+ + Hg + 2e^- \rightleftarrows Cu(Hg) + Ac^- + H_nZ^{n-4} \\ \uparrow\downarrow \\ CuHZ^- \end{array}$$

Copper(II) ion has been reported to form stable chelates with several polyaminocarboxylic acids.[1] Generally, copper(II) ion and its chelates behave reversibly in polarographic electrolysis. Therefore, the polarographic method is well suited to the study of copper(II) chelates.

In this paper, results of a polarographic study of copper(II) chelates of *N*-(2-hydroxyethyl)ethylenediamine-*N*,*N*′,*N*′-triacetic acid (EDTA-OH) and 2,2′-ethylenedioxybis [ethyliminodi (acetic acid)] (GEDTA) are presented.

Experimental

Reagents. Purification of EDTA-OH and GEDTA and the preparation of their solutions were as described previously.[2] Preparation and standardization of copper(II) perchlorate solution are also given is a previous paper.[3] All other chemicals were analytical reagent grade, and were used without further purification. The ionic strength of the sample solutions was adjusted to 0.30 by adding $NaClO_4$ solution.

Apparatus and Experimental Procedure. All apparatus (manual and pen-recording polarographs, and the dropping mercury electrode (DME)) and experimental procedures were as employed previously.[4]

Results and Discussion

D. C. Polarographic Behavior of Copper(II)-*N*-(2-Hydroxyethyl) ethylenediamine-*N*, *N*′, *N*′-triacetate Chelate. The d. c. polarographic behavior of copper(II) ion in an EDTA-OH solution was studied systematically in the pH range 3.80 to 5.90. To maintain the pH of the solution constant, acetate buffer (total concentration of acetate = 0.10 M) was used. As illustrated by the curve in Fig. 1, copper(II) ion in an EDTA-OH solution gave invariably a single well-defined wave over the entire pH range studied. The plot of $\log(i/(i_d-i))$ *versus* potential E gave a straight line with a slope of -32 mV (Fig. 2). Here, i_d and i denote the limiting current and current at potential E, respectively.

The limiting current i_d was exactly proportional to the bulk concentration of copper(II) ion and to the square-root of the effective pressure on the dropping mercury electrode (Tables 1 and 2). These facts clearly imply that the electrode reaction of copper(II) ion in an EDTA-OH solution proceeds reversibly in the usual polarographic sense, corre-

1) L. G. Sillen and A. E. Martell, "Stability Constants of Metal-Ion Complexes," The Chemical Society, London (1964).

2) M. Kodama, C. Sasaki, and T. Noda, This Bulletin, **41**, 2033 (1968).

3) M. Kodama and H. Ebine, *ibid.*, **40**, 1857 (1967).

4) M. Kodama and A. Kimura, *ibid.*, **40**, 1637 (1967).

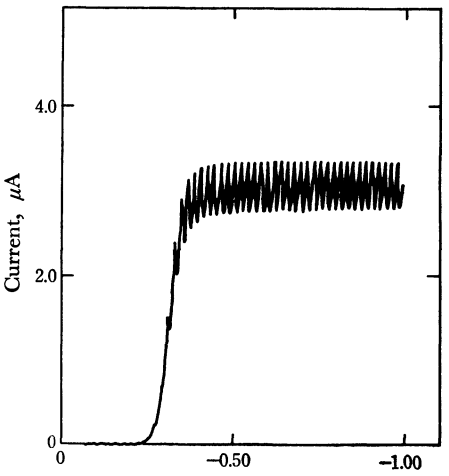

Fig. 1. D.c. polarogram of copper(II)-EDTA-OH chelate.
pH=5.62 (acetate buffer, 0.10M), μ=0.30
Concentration of EDTA-OH=20.0 mM
Concentration of copper(II)=0.682 mM

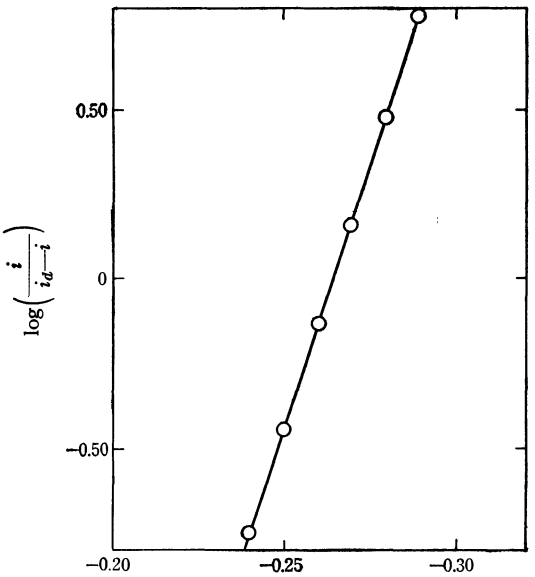

Fig. 2. The d. c. log-plot analysis.
pH=5.62 (acetate buffer, 0.10M), μ=0.30
Concentration of EDTA-OH=20.0 mM
Concentration of copper(II)=0.682 mM

sponding to a two-electron reduction.

When the bulk concentration of uncomplexed EDTA-OH is constant, the half-wave potential $(E_{1/2})_{CuX}$ shifts linearly to negative potentials with decreasing $\log(a_H)_x$ value of EDTA-OH, obeying the following relation (Fig. 3).

$$\frac{\Delta(E_{1/2})_{CuX}}{\Delta \log (a_H)_x} = 31 \text{ mV} \quad (1)$$

Here, $(a_H)_x$ is given by

$$(a_H)_x = 1 + \frac{[H^+]}{k_3} + \frac{[H^+]^2}{k_3 \cdot k_2} + \frac{[H^+]^3}{k_3 \cdot k_2 \cdot k_1} \quad (2)$$

where k's are dissociation constants of EDTA-OH.

When the hydrogen ion concentration of solution was kept constant, $(E_{1/2})_{CuX}$ also shifted to negative potentials with increasing concentration of uncomplexed EDTA-OH, obeying the following relation (Table 3),

$$\frac{\Delta(E)_{1/2})_{CuX}}{\Delta \log [X]_f} = -31 \text{ mV}, \quad (3)$$

but was independent of acetate ion concentration (Table 4).

Table 1. Dependence of the wave-height on the concentration of copper (II)
pH = 5.86, μ = 0.30
Concentration of EDTA-OH = 20.0 mM
Height of mercury column = 60.0 cm

Concentration of Cu(II), C^0_{Cu}, mM	Limiting current i_d, μA	i_d/C^0_{Cu} μA/mM
0.682	2.94_5	4.32
1.36_4	5.88_0	4.31
2.72_8	11.78_0	4.33

Table 2. Dependence of the wave-height on the effective height of mercury column
pH = 5.86, μ = 0.30
Concentration of EDTA-OH = 20.0 mM
Concentration of copper(II) = 1.36_4 mM

Effective height of mercury column h_c, cm	Limiting current id, μA	$i_d/h_c^{1/2}$
49.2	5.33_8	0.761
59.2	5.88_0	0.765
79.2	6.84_1	0.768

Table 3. Dependence of the half-wave poteetial on the ccncentration of EDTA-OH
pH = 5.62, μ = 0.30
Concentration of copper(II) = 0.682 mM
Concentration of acetate ion = 0.10 M

Concentration of EDTA-OH mM	Half-wave potential V vs. SCE	$\Delta E_{1/2}$, mV Calcd	Obsd
10.0	−0.290	0	0
20.0	−0.300	9.0	10
40.0	−0.310	18.0	20

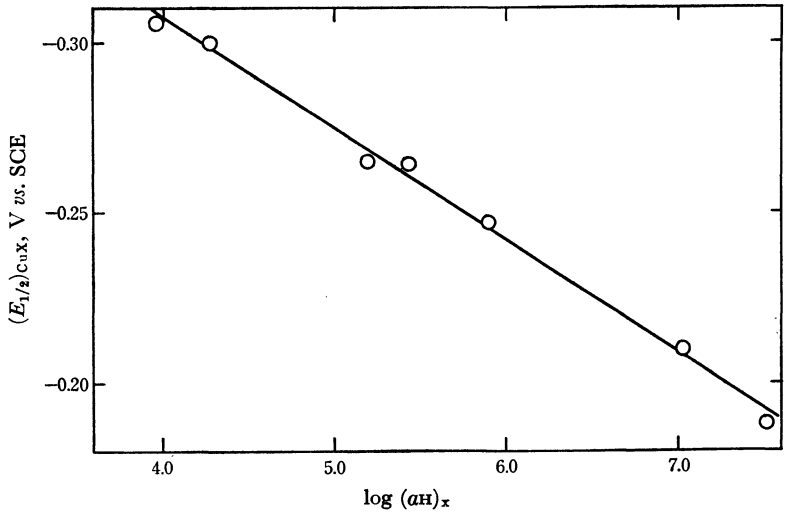

Fig. 3. The relation between the half-wave potential and the pH. μ=0.30
Concentration of EDTA-OH=20.0 mM
Concentration of copper(II)=0.682 mM

TABLE 4. DEPENDENCE OF THE HALF-WAVE POTENTIAL ON THE CONCENTRATIONS OF ACETATE ION OR COPPER(II) ION

pH = 4.85, μ = 0.30
Concentration of EDTA-OH = 20.0 mM

Concentration of acetation M	Concentration of copper(II) mM	Half-wave potential V *vs.* SCE
0.05	0.682	−0.265
0.10	0.682	−0.263
0.10	1.36$_4$	−0.264
0.20	0.682	−0.264

From the above facts, it can be safely concluded that copper(II) ion forms only a normal chelate of 1 to 1 composition with EDTA-OH under the present experimental conditions, and not a protonated chelate or mixed ligand chelate involving acetate ion. The above conclusion was also confirmed by the fact that $(E_{1/2})_{CuX}$ was independent of the concentration of copper(II) ion, provided that the concentration of EDTA-OH and the pH of the solution were kept constant (Table 4).

From the above experimental results and discussion, it is evident that the electrode reaction of copper(II) ion in EDTA-OH solution can be expressed as

$$CuX^- + nH^+ + Hg + 2e \rightleftarrows Cu(Hg) + H_nX^{n-3}, \quad (4)$$

with the half-wave potential $(E_{1/2})_{CuX}$, corresponding to:

$$(E_{1/2})_{CuX} = E^0_{Cu} + 0.0296[\log f_{Cu^{2+}} + \log \frac{k_{Cu(Hg)}}{k_{CuX}} + \log(a_H)_x - \log K_{CuX} - \log[X]_f], \quad (5)$$

where E^0_{Cu} denotes the standard potential, K_{CuX} the stability constant of copper(II)-EDTA-OH chelate, k's the diffusion current constants, $f_{Cu^{2+}}$ the activity coefficient of copper(II) ion at μ=0.30 and $[X]_f$ the bulk concentration of uncomplexed EDTA-OH.

As stated already, the relations between the half-wave potential and the concentrations of acetate ion, EDTA-OH and hydrogen ion, predicted from Eq. (5), were verified satisfactorily by the experimental results.

For the reversible two-electron reduction of copper(II) ion at the mercury electrode, the half-wave potential can be derived as

$$(E_{1/2})_{Cu^{2+}} = E^0_{Cu} + 0.0296\left[\log \frac{k_{Cu(Hg)}}{k_{Cu^{2+}}} + \log f_{Cu^{2+}}\right] \quad (6)$$

Therefore, the shift of the half-wave potential of copper(II) due to the chelate formation with EDTA-OH becomes

$$\Delta(E_{1/2}) = (E_{1/2})_{Cu^{2+}} - (E_{1/2})_{CuX} = 0.0296\left[\log K_{CuX} + \log \frac{k_{CuX}}{k_{Cu^{2+}}} + \log[X]_f - \log(a_H)_x\right] \quad (7)$$

Using the $\Delta(E_{1/2})$ value at $(a_H)x=1$, log K_{CuX} was calculated to be 16.96*1 with the aid of Eq. (7). This agrees well with the value reported by Moeller and Ferrus,[5] and confirms the above explanation.

D. C. Polarographic Behavior of Copper(II)-

*1 This value corresponds to 17.41 at ionic strength 0.10.

5) T. Moeller and R. Ferrus, *J. Inorg. Nuclear Chem.*, **11**, 261 (1961).

2,2'-Ethylenedioxybis[ethyliminodi(acetate)] Chelate. The polarographic behavior of copper(II) ions in a GEDTA solution was studied under experimental conditions similar to those employed in the EDTA-OH system. Copper(II) ion in EDTA-OH solutions gave invariably a well-defined single wave over the entire pH range studied. However, copper(II) ion in a GEDTA solution gave two waves, the heights of which were exactly proportional to the bulk concentration of copper(II) ion and to the square-root of the effective mercury pressure on DME at a given pH (Fig. 4).

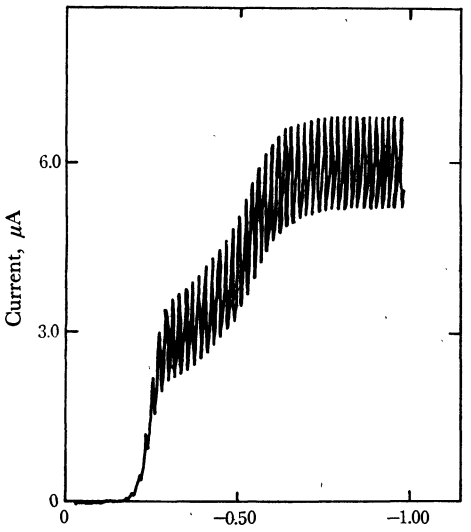

Fig. 4. D. c. polarogram of copper(II)-GEDTA chelate.
pH=5.54 (acetate bufier, 0.10M), μ=0.30
Concentration of GEDTA=18.6 mM
Concentration of copper(II)=1.36$_4$ mM

The height of the first wave, which is reversible in nature, increases with increasing concentration of hydrogen ion at the expense of the height of the irreversible second wave. The sum of two wave heights is almost constant under the experimental conditions employed (3.30<pH<6.00, acetate buffer). When the pH value of the solution is kept constant, with increasing concentration of acetate ion or of GEDTA, the first wave height also increases and the half-wave potential shifts to more negative potentials.

As shown in Fig. 5, a plot of $\log[i/(i_l-i)]$ *vs.* E for the first wave gave a straight line with a slope of −31 mV, corresponding to the two-electron reversible reduction. Here i_l means the limiting current.

These facts may suggest that the first wave corresponds to a two-electron reduction involving copper(II)-GEDTA chelates and the electrode reaction can be expressed as

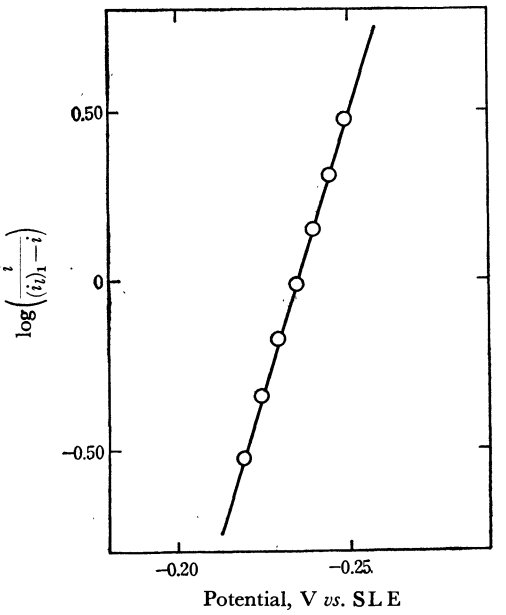

Fig. 5. The d. c. log-plot analysis of the first wave.
pH=5.54 (acetate buffer, 0.10M), μ=0.30
Concentration of GEDTA =18.6 mM
Concentration of copper(II)=1.36$_4$ mM

$$\begin{array}{c} \mathrm{CuZ(Ac)^{3-}} \\ \uparrow\downarrow \\ \mathrm{CuZ_2^{6-}} \rightleftarrows \mathrm{CuZ^{2-}} + n\mathrm{H^+} + \mathrm{Hg} + 2\mathrm{e^-} \rightleftarrows \\ \downarrow\uparrow \\ \mathrm{CuHZ^-} \end{array}$$

$$\mathrm{Cu(Hg)} + \mathrm{Ac^-} + \mathrm{H}_n\mathrm{Z}^{n-4} \qquad (8)$$

where $CuHZ^-$ denotes the protonated chelate, $CuZ(Ac)^{3-}$ the mixed chelate involving acetate ion, CuZ^{2-} and CuZ_2^{6-}, normal chelates of 1 to 1 and 1 to 2 compositions and Z^{4-} completely de-protonated GEDTA anion.

For the above electrode reaction, one can derive the following relation thermodynamically by assuming that all diffusion current constants of copper(II) GEDTA chelates are the same.

$$(E_{1/2})_{CuZ} = E^0_{Cu} - 0.0296\Big[\log K_{CuZ}\Big(1 + K^{H}_{CuZ}[H^+] + K^{Ac}_{CuZ}[Ac^-] + K^{Z}_{CuZ}\frac{[Z]_f}{(\alpha_H)_z}\Big) - \log(\alpha_H)_z + \log[Z]_f + \log\frac{k_{CuZ}}{k_{Cu(Hg)}} + \log f_{Cu^{2+}}\Big], \qquad (9)$$

where $(\alpha_H)_z$ is the (α_H) value of GEDTA and other notations used are defined as follows.

$$K^{AC}_{CuZ} = \frac{[CuZ(Ac)^{3-}]}{[CuZ^{2-}]\cdot[Ac^-]}, \quad K^{H}_{CuZ} = \frac{[CuHZ^-]}{[CuZ^{2-}]\cdot[H^+]}$$

$$K^{Z}_{CuZ} = \frac{[CuZ_2^{6-}]}{[CuZ^{2-}]\cdot[Z^{4-}]}$$

Equation (9) indicates that if the above electrode reaction mechanism proposed is correct, it would be possible to calculate K^{H}_{CuZ}, K^{Ac}_{CuZ} and K^{Z}_{CuZ} values, at least from six $(E_{1/2})_{CuZ}$ values observed at various

concentrations of three species, namely, hydrogen ion, acetate ion and GEDTA. The three K values thus estimated should explain satisfactorily the change in height of the first wave with change in concentrations of the above three species.

K^{H}_{CuZ}, K^{Ac}_{CuZ} and K^{Z}_{CuZ} values were calculated using the half-wave potentials given in Tables 5, 6 and 7, and are listed in Table 8.

Table 5. Dependence of the half-wave potential and the wave-height on pH

μ = 030, Concentration of GEDTA = 18.6 mM
Totoal concentration of acetate = 0.10 M
Concentration of copper(II) = 1.36_4 mM

pH	$E_{1/2}$ of the first wave, V *vs.* SCE	Wave-height, μA		$(i_l)_1/(i_l)_2$ ratio	
		$(i_l)_1$	$(i_l)_2$	Calcd	Obsd
3.80	-0.160_5	5.67_5	0.54_0	13.0	12.1
4.80	-0.200	3.66_0	2.54_0	1.61	1.64
5.54	-0.235	2.75_2	3.17_1	1.00	1.00

Table 6. Dependence of the half-wave potential and the wave-height on the concentration of acetate ion

pH = 5.54, μ = 0.30
Concentration of GEDTA = 18.6 mM
Concentration of copper(II) = 1.36_4 mM

Total concn. of acetate, M	$E_{1/2}$ of the first wave V *vs.* SCE	Wave-height μA		$(i_l)_1/(i_l)_2$ ratio	
		$(i_l)_1$	$(i_l)_2$	Calcd	Obsd
0.10	-0.235	2.75_2	3.17_1	1.00	1.00
0.30	-0.245	3.24_5	2.64_7	1.40	1.40

Table 7. Dependence of the half-wave potential and the wave-height on the concentration of GEDTA

pH = 5.54, μ = 0.30
Total concentration of acetate = 0.10 M
Concentration of copper(II) = 1.36_4 mM

Concn. of GEDTA mM	$E_{1/2}$ of the first wave V *vs.* SCE	Wave-height, μA		$(i_l)_1/(i_l)_2$ ratio	
		$(i_l)_1$	$(i_l)_2$	Calcd	Obsd
13.6	-0.228	2.41_1	3.41_0	1.00	1.00
18.6	-0.235	2.75_2	3.17_1	1.12	1.22
38.6	-0.249	3.11_5	2.85_7	1.53	1.54

Since the half-wave potential of the second wave also shifts to more negative potentials with increasing concentration of GEDTA and pH, this step also corresponds to the reduction of copper(II)-GEDTA chelate. If two species of copper(II)-GEDTA chelates, which show different polarographic behavior, co-exist in equilibrium in solution, the following relation would be expected on the assumption of equal diffusion current constants.

$$\frac{(i_l)_1}{(i_l)_2} = \frac{[CuZ^{2-}]+[CuHZ^{-}]+[CuZ(Ac)^{3-}]+[CuZ_2^{6-}]}{[Cu(II)\text{-}GEDTA^*]} = \frac{1+K^{H}_{CuZ}[H^+]+K^{Ac}_{CuZ}[Ac^-]+K^{Z}_{CuZ}[Z]_f/(a_H)_z}{K}, \quad (10)$$

where $(i_l)_1$ and $(i_l)_2$ denotes the limiting currents of the first and second steps, respectively, and K the equilibrium constant defined as $K=[Cu(II)\text{-}GEDTA^*]/[CuZ^{2-}]$. Here, Cu(II)-GEDTA* means the species which corresponds to the second step.

The ratios $(i_l)_1/(i_l)_2$'s, calculated using K^{H}_{CuZ}, K^{Ac}_{CuZ} and K^{Z}_{CuZ} are listed in Tables 5, 6 and 7 together with observed values. The calculated values agree well with those observed. Although there may be some small doubt about the presence of normal copper(II)-GEDTA chelate of a 1 to 2 composition, this agreement supports the above explanation.

With the aid of Eqs. (6) and (9), log K_{CuZ} was also calculated to be 17.44 (μ=0.10) using the K^{H}_{CuZ}, K^{Ac}_{CuZ} and K^{Z}_{CuZ} values. This also agrees well with the reported value,[6] giving further confirmation to the above explanation.

Table 8. Numerical values

A) Dissociation constants (μ=0.30, mixed constants)
 i) EDTA-OH*
 $pK_1 = 2.35$, $pK_2 = 5.26$, $pK_3 = 9.74$
 ii) GEDTA*
 $pK_1 = 1.96$, $pK_2 = 2.57$, $pK_3 = 8.66$, $pK_4 = 9.19$
 iii) Acetic acid
 $pK_a = 4.75$

B) Stability constants (μ=0.30)
 i) Copper(II)-EDTA-OH chelate
 log K_{CuX} = 16.96**, 16.95[5],*
 ii) Copper(II)-GEDTA chelate
 log K_{CuZ} = 16.77**, 16.73[6],*

C) Equilibrium constants (μ=0.30)**

$$K^{H}_{CuZ} = \frac{[CuHZ^-]}{[CuZ^{2-}]\cdot[H^+]} = 3.87 \times 10^5$$

$$K^{Ac}_{CuZ} = \frac{[CuZ(Ac)^{3-}]}{CuZ^{2-}]\cdot[Ac^-]} = 11.5$$

$$K^{Z}_{CuZ} = \frac{[CuZ_2^{6-}]}{[CuZ^{6-}]\cdot[Z^{4-}]} = 4.34 \times 10^8$$

* Those values were calculated from the related constants in solutions of ionic strength 0.10 and the activity constants of the ions calculated by means of Davies equation.[7]

** These values were obtained by the present authors.

6) J. H. Holloway and C. N. Reilley, *Anal. Chem.*, **32**, 249 (1960).

7) J. N. Butler, "Ionic Equilibrium," Addison-Wesley Publishing Co., Inc., Reading, Massachusetts (1964), p. 437.

Since there is little reason to believe that the two ether oxygens in GEDTA can not partake in the chelate formation of GEDTA, it can not rule out the possibility that there exist two species of copper(II)-GEDTA chelates. Because of its irreversibility, further systematic studies on the nature of the second step were not conducted in this investigation, but to get an insight into the precise nature of the chelate corresponding to the second wave, further systematic investigations by the methods other than polarography should be carried out.

BULLETIN OF THE CHEMICAL SOCIETY OF JAPAN VOL. 42 399—404 (1969)

The 1:1 Complexes of Pyridine-2-carboxamide with Bivalent Metals

Masao SEKIZAKI, Masakazu TANASE and Kazuo YAMASAKI

Inorganic Chemistry Laboratory, Faculty of Science, Nagoya University, Nagoya

(Received June 7, 1968)

The 1 : 1 complexes of pyridine-2-carboxamide (piaH) with the bivalent metals, nickel, copper, cobalt, zinc and cadmium, were prepared and their structures determined through measurements of diffuse reflectance spectra, magnetic moments and infrared spectra. In these complexes, MX_2-(piaH) (X=halogen), pyridine-2-carboxamide is likely to be coordinated to the metal through N(pyridine) and O(amide) atoms with two halogen atoms in the cis-position.

In preceding reports,[1-5] the 1 : 2 complexes of pyridine-2-carboxamide (picolinic acid amide, piaH) with nickel, copper, cobalt, iron and palladium having the general formulae, $[M(pia)_2]$ and $[M(H_2O)_2(piaH)_2]Cl_2$ were studied by various methods. The former complex had N(pyridine) and N(amide) coordination, while the latter N(pyridine) and O(amide) coordination. The 1 : 1 complexes, however, have scarcely been studied except for a copper complex.[6] In the present paper, the syntheses, properties and structures of the 1 : 1 complexes of nickel, copper, cobalt, cadmium and zinc with pyridine-2-carboxamide will be reported.

Experimental

Materials. Pyridine-2-carboxamide is the product of Tokyo Kasei Co. and was used without further purification.

Preparation of Complexes. 1) $CuCl_2(piaH)$*1: This complex was prepared by mixing together an ethanolic solution of 2.4 g (0.02 M) of the ligand and that of 3.4 g (0.02 M) of copper(II) chloride dihydrate.[6] A blue-green powder precipitated. Yield 4 g.

Found: Cu, 24.87; N, 11.35%. Calcd for $C_6H_6N_2OCuCl_2$: Cu, 24.76; N, 10.92%.

2) $CuBr_2(piaH)$: To an ethanolic solution of 2.2 g (0.01 M) of copper(II) bromide, 1.2 g (0.01 M) of the ligand dissolved in ethanol was added. The reddish-brown powder which precipitated was washed with ethanol. Yield 3 g.

Found: Cu, 18.45; N, 8.04%. Calcd for $C_6H_6N_2OCuBr_2$: Cu, 18.39; N, 8.11%.

3) $NiCl_2(piaH)\cdot 2.5H_2O$: Four grams (0.017 M) of nickel chloride hexahydrate, which had been partially dehydrated at 40°C for an hour, was dissolved in ethanol and an ethanolic solution of the ligand (1.2 g, 0.01 M) was added. The mixed solution was concentrated on a water bath until yellowish-green crystals precipitated. Yield 1.4 g.

Found: Ni, 19.88; N, 9.38; Weight loss *in vacuo* at 150°C: 15.33%. Calcd for $C_6H_6N_2ONiCl_2 2.5H_2O$: Ni, 19.78; N, 9.43; H_2O, 15.18%.

4) $CoCl_2(piaH)\cdot 2H_2O$: To an ethanolic solution of 10 g (0.04 M) of cobalt chloride hexahydrate, 1.2 g (0.01 M) of the ligand dissolved in ethanol was added. The purple powder which precipitated on concentrating the solution on a water bath was washed with ethanol. Yield 2 g.

Found: Co, 20.40; N, 9.44; Weight loss *in vacuo* at 150°C: 12.94%. Calcd for $C_6H_6N_2OCoCl_2 2H_2O$: Co,

*1 Dichloro(pyridine-2-carboxamide) copper(II). Other complexes are named in a similar way.

1) K. Yamasaki and M. Sekizaki, This Bulletin, **38**, 2206 (1965).

2) M. Sekizaki and K. Yamasaki, *Nippon Kagaku Zasshi* (*J .Chem. Soc. Japan, Pure Chem. Sect.*), **87**, 1053 (1966).

3) M. Sekizaki and K. Yamasaki, *Spectrochim. Acta*, in press.

4) A. Masuko, T. Nomura and Y. Saito, This Bulletin, **40**, 511 (1967).

5) Y. Nawata, H. Iwasaki and Y. Saito, *ibid* **40**, 515 (1967).

6) K. Nagano, H. Kinoshita and A. Hirakawa, *Chem. Pharm. Bull.*, **12**, 1198 (1964).

20.46; N, 9.73; H_2O, 12.51%.

5) $ZnCl_2$(piaH): Ethanolic solutions of 3 g (0.02 M) of zinc chloride and of 1.2 g (0.01 M) of the ligand were mixed together. The white powder which precipitated after one day was washed with ethanol. Yield 0.9 g.

Found: Zn, 25.03; N, 10.57%. Calcd for $C_6H_6N_2OZnCl_2$: Zn, 25.30; N, 10.84%.

6) $CdCl_2$(piaH): To an aqueous solution of 1.2 g (0.01 M) of the ligand, an aqueous solution of 2.5 g (0.01 M) of cadmium chloride was added. White crystals which precipitated were recrystallized from water. Yield 2.3 g.

Found: Cd, 36.58; N, 9.11%. Calcd for $C_6H_6N_2OCdCl_2$: Cd, 36.80; N, 8.77%.

The deuterated complex, $CdCl_2$(piaD) was prepared by recrystallizing $CdCl_2$(piaH) from 99.75% D_2O.

7) $CdBr_2$(piaH): This complex was prepared in a similar way to the corresponding chloro complex.

Found: Cd, 28.48; N, 7.16%. Calcd for $C_6H_6N_2OCdBr_2$: Cd, 28.50; N, 7.10%.

8) CdI_2(piaH): This complex was prepared in a similar way to the corresponding chloro complex.

Found: Cd, 22.85; N, 5.87%. Calcd for $C_6H_6N_2OCdI_2$: Cd, 23.02; N, 5.74%.

9) $Cd(NCS)_2$(piaH): To a mixture of 2.6 g (0.01 M) of cadmium sulfate 8/3 hydrate and 1.2 g (0.01 M) of the ligand dissolved in warm water, a warm aqueous solution of 2 g (0.02 M) of potassium thiocyanate was added. White crystals which precipitated were recrystallized from water. Yield 1.9 g.

Found: Cd, 32.26; N, 15.90%. Calcd for $C_6H_6N_2OCd(NCS)_2$: Cd, 32.05; N, 15.98%.

Magnetic and Spectroscopic Measurements. Magnetic moments were determined by the Gouy method at room temperature (17.5—20°C). Diffuse reflectance spectra were obtained using a Hitachi EPU-2A spectrophotometer equipped with attachments. Infrared spectra were measured with a JASCO DS-402G spectrophotometer (4000—700 cm^{-1}) and a Hitachi EPI-L spectrophotometer (700—200 cm^{-1}) using Nujol or hexachlorobutadiene mulls.

Results and Discussions

1. General Properties of the Complexes. Among the 1 : 1 complexes studied, only the cadmium complexes (Nos. 6—9) are soluble in water, while the others (Nos. 1—5) are all insoluble and readily decompose in water. All complexes are difficult to dissolve in ethanol and stable in air up to 150°C.

2. Magnetic Moments. The magnetic moments measured are listed in Table 1. The values for nickel and cobalt complexes correspond to two and three unpaired electrons, respectively, and suggest octahedral structures.[7] The values for the copper complexes are normal, indicating square planar or distorted octahedral structures without interaction between copper atoms. Zinc and cadmium complexes are all diamagnetic.

Table 1. Magnetic moments of the 1 : 1 complexes (17.5—20°C)

	Complex	Moment observed	Moment calcd. by the spin-only formula
1	$CuCl_2$(piaH)	1.88 B.M.	1.73 B.M.
2	$CuBr_2$(piaH)	1.82	1.73
3	$NiCl_2$(piaH)·$2.5H_2O$	3.21	2.82
4	$CoCl_2$(piaH)·$2H_2O$	4.97	3.88
5	$ZnCl_2$(piaH)	diamagnetic	
6	$CdCl_2$(piaH)	diamagnetic	
7	$CdBr_2$(piaH)	diamagnetic	
8	CdI_2(piaH)	diamagnetic	
9	$Cd(NCS)_2$(piaH)	diamagnetic	

3. Diffuse Reflectance Spectra. The diffuse reflectance spectra of the nickel complexes are shown in Fig. 1. The bands at 1300, 700 and 415 mμ for the 1 : 1 complex are assigned to the transitions $^3A_{2g} \rightarrow {}^3T_{2g}$ $^3A_{2g} \rightarrow {}^3T_{1g}(F)$ and $^3A_{2g} \rightarrow {}^3T_{1g}(P)$, respectively.[8] The corresponding bands for the 1 : 2 complex, $[Ni(H_2O)_2(piaH)_2]Cl_2$ appear at 875, 625 and 350 mμ.

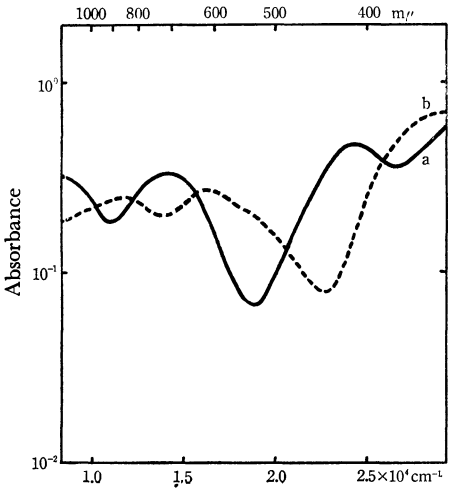

Fig. 1. Diffuse reflectance spectra of the nickel complexes.
a: $NiCl_2$(piaH)·$2.5H_2O$
b: $[Ni(H_2O)_2(piaH)_2]Cl_2$

The diffuse reflectance spectra of the cobalt complexes are shown in Fig. 2. Spectroscopic and magnetic data for the 1 : 1 complexes strongly suggest the octahedral coordination of cobalt compared with the 1 : 2 complex, $[Co(H_2O)_2(piaH)_2]Cl_2$. Absorption bands beyond 1100 mμ and at 550 mμ are assigned to the transitions

7) N. S. Gill and R. S. Nyholm, *J. Inorg. Nucl. Chem.*, **18**, 88 (1961).

8) J. R. Miller, "Advances in Inorganic Chemistry and Radiochemistry," Vol. 4, ed. by Emeleus and Sharpe, 133 (1962).

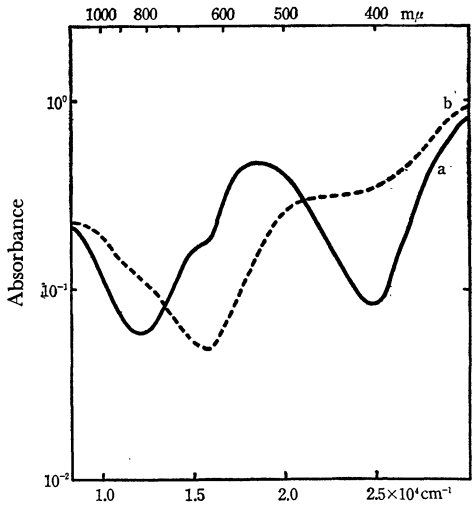

Fig. 2. Diffuse reflectance spectra of the cobalt complexes.
a: $CoCl_2(piaH)\cdot 2H_2O$
b: $[Co(H_2O)_2(piaH)_2]Cl_2$

$^4T_{1g}\rightarrow{}^4T_{2g}$ and $^4T_{1g}\rightarrow{}^4T_{1g}(P)$, respectively, and the shoulder at 650 mμ to the transition $^4T_{1g}\rightarrow{}^4A_{2g}$, which is weak because of the two-electron jump.[9]

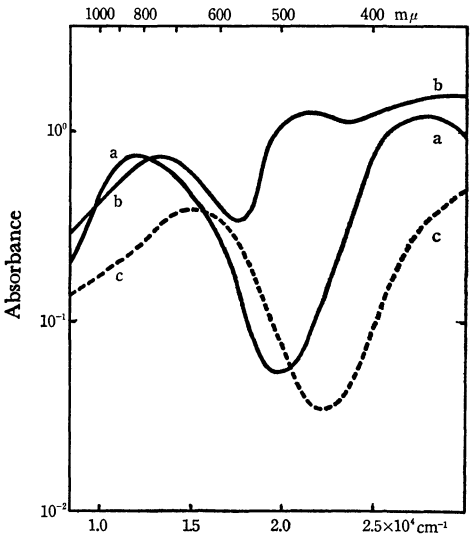

Fig. 3. Diffuse reflectance spectra of the copper complexes.
a: $CuCl_2(piaH)$, b: $CuBr_2(piaH)$,
c: $[Cu(H_2O)_2(piaH)_2]Cl_2$

All the 1 : 1 complexes of nickel and copper show d–d transition bands at longer wavelengths than the corresponding 1 : 2 complexes. This may be due to the coordination of two halogen atoms in the 1 : 1 complexes instead of a pyridine-2-carboxamide molecule.

As shown in Fig. 3, the 1 : 1 complexes of copper, $CuX_2(piaH)$, give two bands in the visible region. The band at 370 mμ for the chloro complex shifts to 470 mμ for the bromo complex and this band is not found for the 1 : 2 complex, $[Cu(H_2O)_2(piaH)_2]Cl_2$. Therefore this band may be assigned to a charge transfer band related to the coordination of halogen atoms. The band due to the d–d transition is observed at 830 mμ for the chloro complex, at 750 mμ for the bromo complex and at 660 mμ for the 1 : 2 complex. These 1 : 1 copper complexes are all thought to be of distorted octahedral or square planar structures, but it is difficult to decide from spectroscopic and magnetic data alone.

Zinc and cadmium complexes show no absorption bands in the visible region.

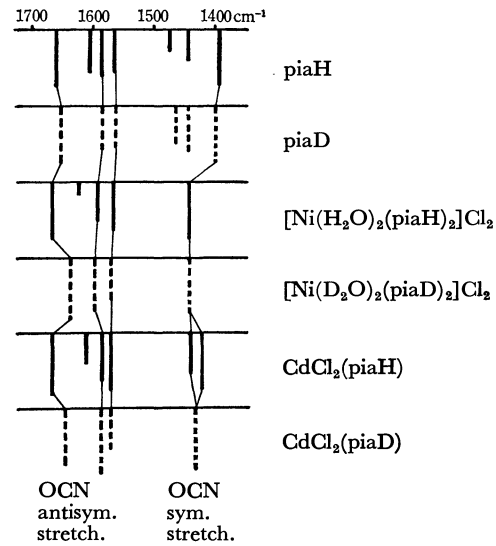

Fig. 4. Infrared spectra of ligands, nickel (1 : 2) and cadmium (1 : 1) complexes.

4. Infrared Spectra. Infrared spectra of the 1 : 1 complexes shown in Figs. 4, 5 and 6 are similar to each other, indicating similar structures; namely octahedral structures for nickel, cobalt, zinc and cadmium complexes, and probably for copper complexes as well.

In the region 4000—700 cm^{-1} some characteristic bands due to the amide group of the ligand are observed. The spectra of the free ligand, the 1 : 1 complexes $MX_2(piaH)$ and 1 : 2 complexes $[M(H_2O)_2(piaH)_2]X_2$,[3] and their deuterated compounds are shown in Fig. 4 and Table 2. In comparing the amide bands of the 1 : 1 complexes with those of the 1 : 2 complexes which had been found to be N and O coordination, a close similarity is observed in the following points: (1) Upon

9) S. Koide, *Phil. Mag.*, [8], **4**, 243 (1959).

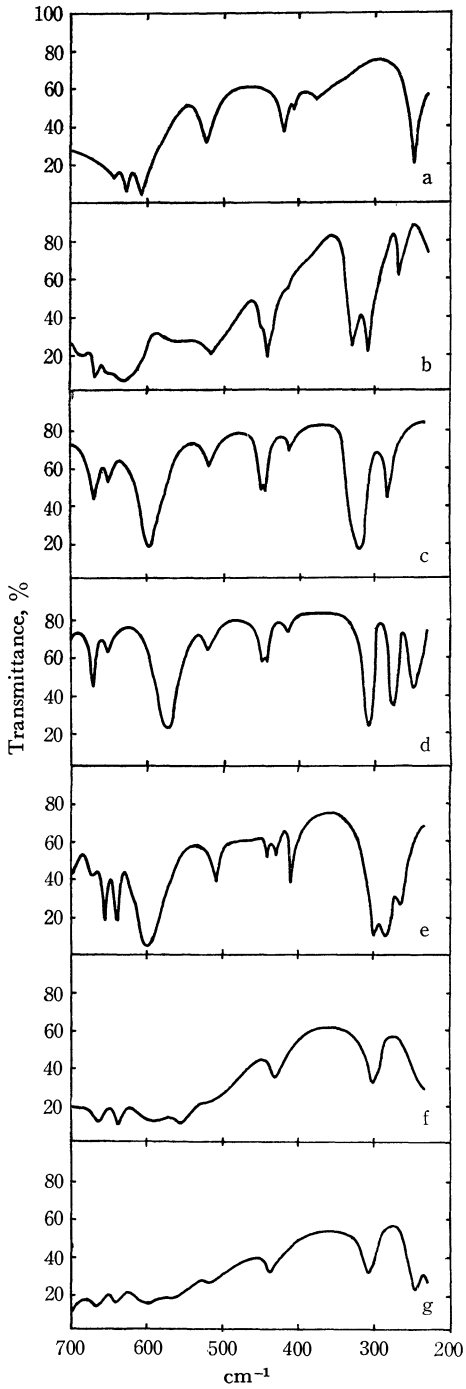

Fig. 5. Far infrared spectra.
a: piaH, b: $[Ni(H_2O)_2(piaH)_2]Cl_2$, c: $CuCl_2$-(piaH), d: $CuBr_2(piaH)$, e: $ZnCl_2(piaH)$, f: $CoCl_2(piaH)\cdot 2H_2O$, g: $NiCl_2(piaH)\cdot 2.5H_2O$

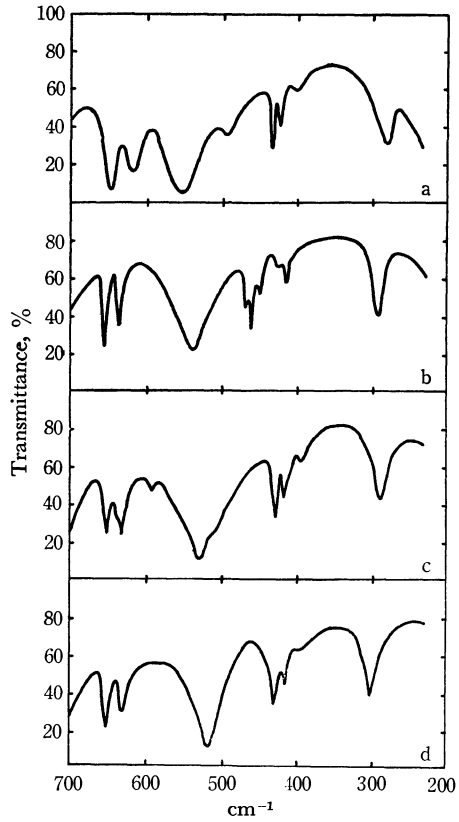

Fig. 6. Far infrared spectra.
a: $CdCl_2(piaH)$, b: $Cd(NCS)_2(piaH)$, c: $CdBr_2(piaH)$, d: $CdI_2(piaH)$

deuteration, the band of OCN antisymmetric stretching vibration mode of both the 1 : 1 and 1 : 2 complexes at 1670—1640 cm^{-1} shifts to lower frequency by 20—30 cm^{-1}, while the shift for the free ligand is small; (2) The band of OCN symmetric stretching vibration mode at 1440-1410 cm^{-1} is observed in a region higher than that of the free ligand by about 40 cm^{-1}, and the shift upon deuteration is small; (3) The band at about 1600 cm^{-1}, which is due to NH_2 scissoring is observed almost at the same position for various complexes. The close similarity of spectra between the 1 : 1 and 1 : 2 complexes suggests similar structures, *i. e.* N(pyridine) and O(amide) coordination for the 1 : 1 complexes, $MX_2(piaH)$, as well as for the 1 : 2 cationic complexes, $[M(H_2O)_2$-$(piaH)_2]X_2$. Entirely different spectra for the 1 : 2 non-ionic complexes, $M(pia)_2$, reported earlier,[3] rule out the possibility of N(pyridine) and N(amide) coordination for the 1 : 1 complexes.

Far infrared spectra (700—200 cm^{-1}) are shown in Figs. 5 and 6 and Table 3, with tentative assignments. The spectra of the 1 : 2 complexes of nickel and the free ligand[3] are also shown for comparison. In this region two characteristic bands due to the amide group are found at about 600 and 500 cm^{-1}. The former band is assigned to the CO in-plane bending mode and the latter to the CO out-of-plane bending mode. The frequency of

TABLE 2. INFRARED SPECTRA OF AMIDE GROUPS IN THE REGION 4000—700 cm^{-1}

1	piaH	3420 s	3155 s	1659 s	1602 m	1391 s	1164 w	1097 s
2	piaD	2550 s	2360 s	1650 s	1204 m	1400 s	920 s	
3	$[Ni(H_2O)_2(piaH)_2]Cl_2$	3300 s	3120 s	1664 s	1616 w	1434 s	1132 w	1109 w
4	$[Ni(D_2O)_2(piaD)_2]Cl_2$	2490 s	2300 s	1636 s	1221 m	1438 s	935 s	
5	$NiCl_2(piaH)\cdot 2.5H_2O$	3320 br	3200 br	1670 s	1610 w	1431 s	1183 w	1110 m
6	$CuCl_2(piaH)$	3395 s	3275 s	1643 s	1608 m	1432 s	1182 w	1123 m
7	$CoCl_2(piaH)\cdot 2H_2O$	3325 br	3195 br	1666 s	1625 m	1430 s	1181 w	1112 m
8	$ZnCl_2(piaH)$	3390 s	3290 s	1660 s	1612 m	1427 s	1177 w	1113 m
9	$CdCl_2(piaH)$	3460 s	3370 s	1666 s	1612 m	1438 m 1414 s	1176 w	1116 w
10	$CdCl_2(piaD)$	2580 s	2430 s	1644 s	1219 w	1427 s	926 w	914 w
	Assignment	NH_2 anti sym. stretch.	NH_2 sym. str.	OCN anti sym. str.	NH_2 sciss.	OCN sym. str.	NH_2 in-plane bend.	

Data for 1—4 were taken from Ref. 3.

TABLE 3. FAR INFRARED SPECTRA OF THE COMPLEXES IN THE REGION 700—200 cm^{-1}

1	piaH	627 s	645 m	607 s	520 m		420 m	411 w		252 s	
2	$[Ni(H_2O)_2](piaH)_2]Cl_2$	667 s	652 sh	632 s	515 m	440 s			328 s 311 s	269 m	230 s
3	$NiCl_2(piaH)\cdot 2.5H_2O$	664 br	641 br	600 br	560 br	436 m			307 m	245 s	
4	$CuCl_2(piaH)$	667 m	650 w	597 s	517 w	445 m 448 m		411 w	321 s	282 m	
5	$CuBr_2(piaH)$	670 m	650 w	576 s	518 w	443 m 447 m		410 w	307 s	275 s	251 m
6	$CoCl_2(piaH)\cdot 2H_2O$	662 br	637 br	595 br	555 br	431 m			302 m	235 s	
7	$ZnCl_2(piaH)$	653 m	639 m	600 s	509 m	439 w	428 w	410 m	300 s	286 s	270 m
8	$CdCl_2(piaH)$	646 s	617 m	552 s	495 w	434 m	422 w	400 w		282 m	
9	$CdBr_2(piaH)$	653 s	634 s	527 s	510 sh	430 s	418 m	396 w		290 m	
10	$CdI_2(piaH)$	655 s	633 m	519 s		430 m	417 w	397 sh		303 m	
11	$Cd(NCS)_2(piaH)$*4	656 s	635 m	538 s	467 w	452 w	415 w			294 m	
	Assignment	NH_2 twist.		CO in-plane bend.	CO out- of-plane bend.	py. ring out- of-plane bend.			*1	*2	*3

*1 chelate ring vibration.
*2 pyridine-amide torsion
*3 chelate ring vibration + M–X stretching (X = halogen)
*4 $Cd(NCS)_2(piaH)$ shows a band at 461 cm^{-1} due to the NCS bending

the CO in-plane bending mode for the 1 : 1 chloro complexes decreases in the following order: Ni~Zn>Co≥Cu>Cd. If the corresponding band is compared for different halogen-substituted complexes of the same metal, the frequency decreases in the following order for copper and cadmium: Cl>NCS>Br>I. On the other hand, frequencies of the CO out-of-plane bending mode show only small differences from each other, and there is no regularity in the shift. Therefore, some correlation between the coordination of halogen atoms and the CO in-plane bending mode seems to exist. Based on the above results, the structure shown in Fig. 7 is proposed for the 1 : 1 complexes, in which the metal, halogen atoms and the am ide group of the ligand are all situated in the same plane.

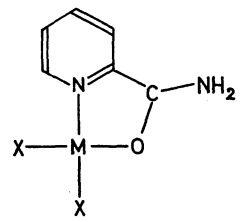

Fig. 7. The proposed structure for the 1 : 1 complex.

Several strong bands observed in the region 320—200 cm^{-1} are assigned to the skeletal vibration correlated with the chelate ring vibration. Of these bands, the one observed for the free ligand at 252 cm^{-1} and the band observed for 1 : 1 complexes at 235—303 cm^{-1} are assigned to the pyridine-amide torsional mode. Several bands are observed at 300 and 250—200 cm^{-1} for the 1 : 1 complexes, but not for the free ligand. These bands are mainly due to the metal - N (pyridine) or metal - O(amide) stretching vibration modes coupled with metal - halogen stretching. For the nickel and cobalt complexes, strong and broad absorptions due to the libration of lattice waters are present in the region 800—200 cm^{-1}.

Far infrared spectra were measured in the laboratory of Professor Shimanouchi, the University of Tokyo, and in the Naka Works, the Hitachi Ltd. The present authors wish to thank for their kindness shown during the measurements, and the Ministry of Education for a research grant.

BULLETIN OF THE CHEMICAL SOCIETY OF JAPAN VOL. 42 404—406 (1969)

The Effect of Acetate Ion on the Rate of the Reaction between Cobalt(II) and Manganese(II)-Ethylenediaminetetraacetate Complexes

Masaru KIMURA

Department of Applied Chemistry, Yamagata University, Yonezawa, Yamagata

(Received June 14, 1968)

The kinetics of the substitution reactions of cobalt(II) ions and manganese(II)-ethylenediaminetetraacetate complexes have been studied in acetate buffer solutions at 25°C and at ionic strength of 0.2. The reaction was treated as to proceed through both hydrated metal ions and monoacetato complexes. The rate constants for six elementary reaction paths, three of which involve hydrated cobalt(II) ions and the others, monoacetatocobalt(II) complexes, were determined. The values obtained indicate that all the reactions proceeding through monoacetatocobalt(II) complexes are about three times faster than the corresponding reactions proceeding through hydrated cobalt(II) ions.

In the previous papers on substitution reactions involving copper(II)-nitrilotriacetate (NTA) complexes[1] and lead(II)-ethylenediaminetetraacetate (EDTA) complexes,[2] it has been shown that monoacetatocopper(II) ions and monoacetatolead(II) ions react more slowly with NTA anions and EDTA anions respectively, than the corresponding hydrated metal ions do. However, recently, Tanaka and Kimura[3] have shown that monoacetatonickel(II) ions react with NTA anions faster than hydrated nickel(II) ions do. Tanaka and Sakuma,[4] and Bydalek,[5] who studied the effect of acetate ions on reactions involving nickel(II) ion, obtained results similar to those reported by Tanaka and Kimura.[3] It seemed to be important and interesting that the effect of acetate ions on the reactions involving nickel(II) ions is the reverse of that on the reactions involving copper(II) and lead(II) ions. This fact was considered to be due to the characteristics of acetatometal complexes, but not of NTA or EDTA; confirmation was sought in the present study. The behavior of the acetatocobalt(II) ions used in the present study was considered to be similar to that of acetatonickel(II) ions.

The substitution reactions between cobalt(II) ions and manganese(II)-ethylenediaminetetraacetate complexes have been investigated in acetate buffer solutions at an ionic strength of 0.2 at 25°C, and the rate constants of the paths by which the reactions proceed through hydrated cobalt(II) ions and monoacetatocobalt(II) complexes have been determined and compared with those of the corresponding reactions of other metal ions.

Experimental

The solution of disodiumethylenediaminetetraacetate

1) N. Tanaka and M. Kimura, This Bulletin, **41**, 2375 (1968).
2) N. Tanaka and H. Ogino, *ibid.*, **36**, 175 (1963).
3) N. Tanaka and M. Kimura, *ibid.*, **40**, 2100 (1967).
4) N. Tanaka and Y. Sakuma, *ibid.*, **32**, 578 (1959).
5) T. J. Bydalek, *Inorg. Chem.*, **4**, 232 (1965).

was standardized by using a standard copper(II) solution by amperometric titration using a dropping-mercury electrode as the indicator electrode. A standard solution of manganese(II) nitrate was prepared from the guaranteed reagents and was standardized amperometrically by the standard solution of EDTA. The preparation and standardization of all the other chemicals and solutions used were the same as have been described in a previous paper.[3]

The rate of the reaction between cobalt(II) ions and manganese(II)-EDTA complexes was determined by measuring the polarographic limiting-diffusion current of cobalt(II) ions in acetate buffer solutions at 25°C and at an ionic strength of 0.2. The ionic strength was adjusted with potassium nitrate. Polyoxyethylene lauryl ether (LEO) (2×10^{-6} M) was added as a maximum suppressor. The pH of the solution was measured after polarographic measurements with a Hitachi-Horiba Model F-5 pH meter.

Results and Discussion

In a solution containing acetate ions up to a concentration of 0.2 M, the overall substitution reaction of cobalt(II) ions and manganese(II)-EDTA complexes can be expressed as follows:

$$\left\{\begin{array}{c}Co^{2+}\\ \downarrow\uparrow\\ CoOAc^{+}\end{array}\right\} + MnY^{2-} \overset{V^{+}_{0,app}}{\rightleftharpoons} CoY^{2-} + \left\{\begin{array}{c}Mn^{2+}\\ \downarrow\uparrow\\ MnOAc^{+}\end{array}\right\} \quad (1)$$

where Y^{4-} denotes a tetravalent EDTA anion.

The apparent concentrations of cobalt(II) ions that can be determined polarographically, $[Co^{2+}]_{app}$ are give by

$$[Co^{2+}]_{app} = [Co^{2+}] + [CoOAc^{+}] \quad (2)$$

Under the present experimental conditions, the rate of the substitution reaction between Co(II) and Mn(II)-EDTA complexes was so slow that the apparent initial rates of the reactions, $-\Delta[Co^{2+}]_{0,app}/\Delta t$, could be measured accurately; the subscript 0 indicates the initial state.

The apparent initial rates of the forward reaction (1), $V^{+}_{0,app}$ were obtained at various pH's with two different concentrations of Mn(II) and acetate ions. The plots of $V^{+}_{0,app}/([Co^{2+}]_{0,app}[MnY^{2-}]_0)$ *versus* $[H^+]$ gave straight lines as is shown in Fig. 1.

On the basis of these facts, the following mechanisms can be suggested for reaction (1).

(i) $$Co^{2+} + MnY^{2-} \overset{k^{+}_{1h}}{\rightleftharpoons} CoY^{2-} + Mn^{2+} \quad (3)$$

$$CoOAc^{+} + MnY^{2-} \overset{k^{+}_{1s}}{\rightleftharpoons} CoY^{2-} + MnOAc^{+} \quad (3')$$

(ii) $$MnY^{2-} + H^{+} \rightleftharpoons MnHY^{-} \quad (4)$$

$$Co^{2+} + MnHY^{-} \overset{k^{+}_{11h}}{\rightleftharpoons} CoHY^{-} + Mn^{2+} \quad (5)$$

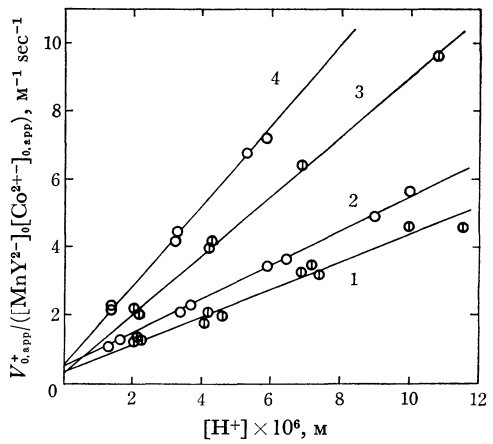

Fig. 1. $V^{+}_{0,app}/([MnY^{2-}]_0[Co^{2+}]_{0,app})$ as a function of hydrogen ion concentration in acetate buffer-potassium nitrate solutions of ionic strength 0.2 at 25°C.
Initial concentrations are $[MnY^{2-}]_0 = 0.378$ mM; $[Co^{2+}]_{0,app} = 0.193$ mM; $[Mn^{2+}]_{0,app} = 4.875$ mM (cruves 3 and 4) and 12.04 mM (curves 1 and 2). Concentrations of acetate ions are 0.039 M for ①, and 0.168 M for ○.

$$CoOAc^{+} + MnHY^{-} \overset{k^{+}_{11s}}{\rightleftharpoons} CoHY^{-} + MnAOc^{+} \quad (5')$$

$$CoHY^{-} \rightleftharpoons CoY^{2-} + H^{+} \quad (6)$$

(iii) $$MnY^{2-} + H^{+} \rightleftharpoons HY^{3-} + \{Mn^{2+} \rightleftharpoons MnOAc^{+}\} \quad (7)$$

$$Co^{2+} + HY^{3-} \overset{k^{+}_{111h}}{\rightleftharpoons} CoY^{2-} + H^{+} \quad (8)$$

$$CoOAc^{+} + HY^{3-} \overset{k^{+}_{111s}}{\rightleftharpoons} CoY^{2-} + H^{+} + OAc^{-} \quad (8')$$

In the experimental treatment, it was assumed that the equilibria between hydrated ions and acetato complexes were maintained while the substitution reactions took place. From the same treatment in principle as in the previous papers,[1-3] Eq. (9) was obtained as the rate equation of reaction (1).

$$V^{+}_{0,app} = \frac{[Co^{2+}]_{0,app}[MnY^{2-}]_0}{1+\beta_{CoOAc}[OAc^-]}\left\{k^{+}_{1h} + k^{+}_{1s}[OAc^-] + (k^{+}_{2h} + k^{+}_{2s}[OAc^-])[H^+] + (k^{+}_{3h} + k^{+}_{3s}[OAc^-])\frac{1+\beta_{MnOAc}[OAc^-]}{[Mn^{2+}]_{0,app}}[H^+]\right\} \quad (9)$$

where: $k^{+}_{1s} = k^{+}_{1s}\beta_{CoOAc}$, $k^{+}_{2h} = k^{+}_{11h}K^{H}_{MnHY}$,
$k^{+}_{2s} = k^{+}_{11s}\beta_{CoOAc}K^{H}_{MnHY}$, $k^{+}_{3h} = k^{+}_{111h}/(K_{MnY}K_{HY})$,
$k^{+}_{3s} = k^{+}_{111s}\beta_{CoOAc}/(K_{MnY}K_{HY})$ (9')

β_{CoOAc} and β_{MnOAc} represent the overall formation constants of the acetatocobalt(II) and acetatomanganese(II) complexes respectively. K^{H}_{MnHY} represents the equiliblium constant of reaction (4), K_{MnY} the formation constant of MnY^{2-}, and K_{HY} the fourth dissociation constant of EDTA. In these equations, the changes in the initial concentrations during the measurements of the initial reaction rates were considered to be negligibly small under these experimental conditions.

The rate constants in Eq. (9) were obtained from an analysis of the plots in Fig. 1; they are given in Table 1.

TABLE 1. RATE CONSTANTS IN EQ. (9) OBTAINED AT IONIC STRENGTH 0.2 AT 25°C

	Rate constant	
k^{+}_{1A}	0.3	$l\,mol^{-1}sec^{-1}$
k^{+}_{1a}	1.3	$l^{2}\,mol^{-2}sec^{-1}$
k^{+}_{2A}	$\sim 6\times10^{4}$	$l^{2}\,mol^{-2}sec^{-1}$
k^{+}_{2a}	$\sim 7\times10^{4}$	$l^{3}\,mol^{-3}sec^{-1}$
k^{+}_{3A}	3.3×10^{3}	$l\,mol^{-1}sec^{-1}$
k^{+}_{3a}	1.1×10^{4}	$l^{2}\,mol^{-2}sec^{-1}$

The rate constants for reactions (3), (3′), (5), (5′), (8), and (8′) were calculated from the relations given in Eqs. (9′) and are given in Table 2. The values of β_{CoOAc},[6] β_{MnOAc},[6] K_{MnY},[7] K_{HY}[7] and K^{H}_{MnHY}[7] which have been used in the calculation

TABLE 2. RATE CONSTANTS FOR REACTIONS, (3), (3′), (5), (5′), (8) AND (8′) AT IONIC STRENGTH 0.2 AT 25°C

Rate constant, $l\,mol^{-1}sec^{-1}$

k^{+}_{IA}	k^{+}_{Ia}	k^{+}_{IIA}	k^{+}_{IIa}	k^{+}_{IIIA}	k^{+}_{IIIa}
0.3	1.1	—6—0	~60	1×10^{7}	3×10^{7}

are 1.2, 1.6, $10^{13.79}$, $10^{-10.22}$, and $10^{3.1}$ respectively.

The rate constants in Table 2 indicate that all the reactions proceeding through Co^{2+} (hydrated ions) are slower than the corresponding reactions proceeding through $CoOAc^{+}$ ions. Similar phenomena have been found in the complex-forming reactions of Ni(II)-NTA complexes[3] and Ni(II)-EDTA complexes,[4] and in substitution reactions between nickel(II) and copper(II)-EDTA complexes.[5] It is noteworthy that these phenomena are unlike those obtained in reactions involving copper(II) ions[1] and lead(II) ions.[2]

The author wishes to thank the Ministry of Education for the financial support granted for this research.

6) H. Ogino, Ph. D. thesis, Tohoku University, (1965).

7) G. Schwarzenbach, R. Gut and G. Andereg, *Helv. Chim. Acta*, **37**, 937 (1954).

BULLETIN OF THE CHEMICAL SOCIETY OF JAPAN VOL. 42 407—411 (1969)

The Effect of Phthalate Ion and Acetate Ion on the Rate of the Reaction between Nickel(II) and Cobalt(II)-Nitrilotriacetate Complexes

Masaru KIMURA

Department of Applied Chemistry, Yamagata University, Yonezawa, Yamagata

(Received June 14, 1968)

A kinetic study of the substitution reactions of nickel(II) ions and cobalt(II)-nitrilotriacetate complexes in phthalate and in acetate buffer has been carried out using a procedure previously reported. The reaction was made to proceed through both hydrated nickel(II) ions and monophthalatonickel(II) complexes or monoacetatonickel(II) complexes. The rate constants for eight elementary reaction paths, four of which involve the hydrated nickel(II) ions, while the others involve the monophthalatonickel(II) complexes (the monoacetatonickel(II) complexes in the case of the measurements in acetate media), were determined at an ionic strength of 0.2 at 25°C. The values obtained indicate that all the reactions proceeding through the monophthalatonickel(II) complexes are slower than the corresponding reactions proceeding through hydrated nickel(II) ions; however, all the reactions proceeding through monoacetatonickel(II) complexes are faster than the corresponding reactions proceeding through hydrated nickel(II) ions. Thus, the kinetic reactivity is in the order of: $NiOAc^+ > Ni^{2+} > NiPh$, where Ph^{2-} indicates a bivalent phthalate anion.

A previous study[1] showed that monoacetatocobalt(II) ions react with ethylenediaminetetraacetate (EDTA) anions and Mn(II)-EDTA complexes faster than with hydrated cobalt(II) ion. This trend has been considered to be due to the characteristics of $CoOAc^+$, the value of the stability constant of which is rather small, and not to those of EDTA and cobalt(II); confirmation was sought in the present study. Since it seems to be important and necessary to extend the study to the investigation of the effect of various anions on the rates of the reactions, and to compare the corresponding reactions, the effect of the phthalate ion and of the acetate ion on the rate of the reaction between nickel(II) and cobalt(II)-nitrilotriacetate (NTA) complexes was examined in the present study.

Experimental

For potassium biphthalate, guaranteed reagents were used without further purification. All the other chemicals and solutions were prepared and standardized in ways described in a previous paper.[2] The method and the procedure employed in the present study were, in principle, the same as those described in previous papers.[1,2]

Results

Under the conditions of the present experiments, the formation of complexes with a metal-to-ligand ratio of 1 : 2 was considered to be negligible. Therefore, the overall substitution reactions between nickel(II) and cobalt(II)-NTA complexes are expressed by:

$$\left\{\begin{matrix} Ni^{2+} \\ \uparrow\downarrow \\ NiZ^{(2-z)+} \end{matrix}\right\} + CoX^- \overset{V^+_{0,app}}{\rightleftharpoons} NiX^- + \left\{\begin{matrix} Co^{2+} \\ \uparrow\downarrow \\ CoZ^{(2-z)+} \end{matrix}\right\} \quad (1)$$

where Z^{z-} indicates a bivalent phthalate anion (Ph^{2-}) or an acetate ion (OAc^-) and X^{3-}, a tervalent NTA anion.

The apparent concentrations of nickel(II) ions, $[Ni^{2+}]_{app}$ that can be determined polarographically are given by:

$$[Ni^{2+}]_{app} = [Ni^{2+}] + [NiZ^{(2-z)+}] \quad (2)$$

In a previous paper,[2] kinetic studies of the reactions between nickel(II) ions and Co(II)-, and Cu(II)-NTA complexes in acetate media were reported. On the basis of the same treatment as in previous studies,[1,2] the reactions of Eq. (1) may be considered to proceed through the following reaction paths:

$$\text{(i)} \quad Ni^{2+} + CoX^- \overset{k^+_{1h}}{\rightleftharpoons} NiX^- + Co^{2+} \quad (3)$$

$$NiZ^{(2-z)+} + CoX^- \overset{k^+_{1s}}{\rightleftharpoons} NiX^- + CoZ^{(2-z)+} \quad (3')$$

$$\text{(ii)} \quad CoX^- + H^+ \rightleftharpoons CoHX \quad (4)$$

1) M. Kimura, This Bulletin, **42**, 404 (1969).
2) N. Tanaka and M. Kimura, *ibid.*, **40**, 2100 (1967).

$$Ni^{2+} + CoHX \overset{k^{+}_{IIh}}{\rightleftharpoons} NiHX + Co^{2+} \quad (5)$$

$$NiZ^{(2-z)+} + CoHX \overset{k^{+}_{IIz}}{\rightleftharpoons} NiHX + CoZ^{(2-z)+} \quad (5')$$

$$NiHX \rightleftharpoons NiX^{-} + H^{+} \quad (6)$$

(iii) $$CoX^{-} \rightleftharpoons X^{3-} + \left\{ \begin{matrix} Co^{2+} \\ \uparrow\downarrow \\ CoZ^{(2-z)+} \end{matrix} \right\} \quad (7)$$

$$Ni^{2+} + X^{3-} \overset{k^{+}_{IIIh}}{\rightleftharpoons} NiX^{-} \quad (8)$$

$$NiZ^{(2-z)+} + X^{3-} \overset{k^{+}_{IIIz}}{\rightleftharpoons} NiX^{-} + Z^{z-} \quad (8')$$

(iv) $$CoX^{-} + H^{+} \rightleftharpoons HX^{2-} + \left\{ \begin{matrix} Co^{2+} \\ \uparrow\downarrow \\ CoZ^{(2-z)+} \end{matrix} \right\} \quad (9)$$

$$Ni^{2+} + HX^{2-} \overset{k^{+}_{IVh}}{\rightleftharpoons} NiHX \quad (10)$$

$$NiZ^{(2-z)+} + HX^{2-} \overset{k^{+}_{IVz}}{\rightleftharpoons} NiHX + Z^{z-} \quad (10')$$

On the basis of this reaction mechanisms, Eq. (11) is obtained from reaction (1):

$$V^{+}_{0,app} = \frac{[CoX^{-}]_0 [Ni^{2+}]_{0,app}}{1+\beta_{NiZ}[Z^{-z}]} \Big\{ k^{+}_{1h} + k^{+}_{1z}[Z^{z-}] + k^{+}_{2h}[H^{+}] + k^{+}_{2z}[Z^{z-}][H^{+}] + (k^{+}_{3h} + k^{+}_{3z}[Z^{z-}] + k^{+}_{4h}[H^{+}] + k^{+}_{4z}[Z^{z-}][H^{+}]) \frac{1+\beta_{CoZ}[Z^{z-}]}{[Co^{2+}]_{0,app}} \Big\} \quad (11)$$

where: $k^{+}_{1z} = k^{+}_{1z}\beta_{NiZ}$, $k^{+}_{2h} = k^{+}_{IIh}K^{H}_{CoHZ}$, $k^{+}_{2z} = k^{+}_{IIz}\beta_{NiZ}K^{H}_{CoHZ}$
$k^{+}_{3h} = k^{+}_{IIIh}/K_{CoX}$, $k^{+}_{3z} = k^{+}_{IIIz}\beta_{NiZ}/K_{CoX}$,
$k^{+}_{4h} = k^{+}_{IVh}/(K_{CoX}K_{HX})$, $k^{+}_{4z} = k^{+}_{IVz}\beta_{NiZ}/(K_{CoX}K_{HX})$ (11')

TABLE 1. $V^{+}_{0,app}$ FOR THE SUBSTITUTION REACTIONS BETWEEN Ni(II) AND Co(II)-NTA COMPLEXES IN PHTHALATE BUFFER-POTASSIUM NITRATE SOLUTION AT IONIC STRENGTH 0.2 AT 25°C
$[Ni^{2+}]_{0,app}$ = 0.202 mM and 0.404 mM for *

$[Ph^{2-}]$ M	pH	$[CoX^{-}]_0$ mM	$[Co^{2+}]_{0,app}$ mM	$V^{+}_{0,app} \times 10^{7}$ M sec^{-1}
0.02	4.98	1.17	0.41	2.87
0.02	4.98	1.17	0.79	1.78
0.02	4.98	1.17	1.18	1.24
0.02	4.98	1.17	1.56	1.00
0.02	5.06	1.17	0.41	2.57
0.02	5.06	1.17	0.79	1.47
0.02	5.06	1.17	1.18	1.15
0.02	5.06	1.17	1.56	0.84
0.02	5.25	1.36	0.57	3.35*
0.02	5.25	1.36	0.95	2.24*
0.02	5.25	1.36	1.34	1.68*
0.02	5.25	1.36	1.72	1.28*
0.02	5.50	1.36	0.57	3.23*
0.02	5.50	1.36	0.95	2.02*
0.02	5.50	1.36	1.34	1.70*
0.02	5.50	1.36	1.72	1.30*
0.02	5.90	1.36	0.57	2.37*
0.02	5.90	1.36	0.95	1.52*
0.02	5.90	1.36	1.34	1.08*
0.02	5.90	1.36	1.72	0.94*
0.04	5.06	1.17	0.41	3.60
0.04	5.06	1.17	0.79	2.00
0.04	5.06	1.17	1.18	1.87
0.04	5.06	1.17	1.56	1.38
0.04	5.17	1.17	0.41	3.43
0.04	5.17	1.17	0.79	1.97
0.04	5.17	1.17	1.18	1.36
0.04	5.17	1.17	1.56	1.38
0.04	5.40	1.36	0.57	4.00*
0.04	5.40	1.36	0.95	2.70*
0.04	5.40	1.36	1.34	2.20*
0.04	5.40	1.36	1.72	1.59*
0.04	5.56	1.36	0.57	3.79*
0.04	5.56	1.36	0.95	2.63*
0.04	5.56	1.36	1.34	1.85*
0.04	5.56	1.36	1.72	1.48*
0.04	5.98	1.36	0.57	2.74*
0.04	5.98	1.36	0.95	1.82*
0.04	5.98	1.36	1.34	1.42*
0.04	5.98	1.36	1.72	1.08*
0.06	5.17	0.68	0.49	2.55
0.06	5.17	0.68	0.86	1.58
0.06	5.17	0.68	1.25	1.25
0.06	5.17	0.68	1.63	0.97
0.06	5.18	0.68	0.49	2.21
0.06	5.18	0.68	0.86	1.33
0.06	5.18	0.68	1.25	1.11
0.06	5.18	0.68	1.63	0.67
0.06	5.18	0.68	0.49	2.39
0.06	5.18	0.68	0.86	1.51
0.06	5.18	0.68	1.25	1.29
0.06	5.18	0.68	1.63	0.90
0.06	5.35	1.17	0.41	3.29
0.06	5.35	1.17	0.79	2.14
0.06	5.35	1.17	1.18	1.71
0.06	5.35	1.17	1.56	1.24
0.06	5.36	0.68	0.49	1.91
0.06	5.36	0.68	0.86	1.27
0.06	5.36	0.68	1.25	0.97
0.06	5.36	0.68	1.63	0.67
0.06	5.46	1.36	0.57	5.17
0.06	5.46	1.36	0.95	3.21
0.06	5.46	1.36	1.34	2.61
0.06	5.46	1.36	1.72	2.00
0.06	5.65	1.36	0.57	4.80
0.06	5.65	1.36	0.95	2.92
0.06	5.65	1.36	1.34	2.37
0.66	5.65	1.36	1.72	1.66
0.06	6.05	1.36	0.57	3.10
0.06	6.05	1.36	0.95	1.84
0.06	6.05	1.36	1.34	1.60
0.06	6.05	1.36	1.72	1.20

TABLE 2. $V^{+}_{0,app}$ FOR THE SUBSTITUTION REACTIONS BETWEEN Ni(II) AND Co(II)-NTA COMPLEXES IN ACETATE BUFFER-POTASSIUM NITRATE SOLUTIONS AT IONIC STRENGTH 0.2 AT 25°C
$[Ni^{2+}]_{0,app} = 0.202$ mM, $[CoX^{-}]_0 = 0.68$ mM and 1.36 mM for *

[OAc⁻] M	pH	$[Co^{2+}]_{0,app}$ mM	$V^{+}_{0,app} \times 10^7$ msec^{-1}	[OAc⁻] M	pH	$[Co^{2+}]_{0,app}$ mM	$V^{+}_{0,app} \times 10^7$ msec^{-1}
0.02	4.94	0.49	1.78	0.10	4.99	0.86	2.43
0.02	5.10	0.49	1.50	0.10	4.99	1.25	2.17
0.02	5.27	0.49	1.18	0.10	4.99	1.63	1.56
0.02	5.74	0.57	1.35*	0.10	5.14	0.49	3.14
0.02	5.74	0.72	0.84*	0.10	5.14	0.86	2.03
0.02	5.74	1.34	0.79*	0.10	5.14	1.25	1.70
0.02	5.74	1.72	0.63*	0.10	5.14	1.63	1.25
0.02	4.94	0.86	1.09	0.10	5.30	0.49	2.62
0.02	4.94	1.25	0.84	0.10	5.30	0.86	1.57
0.02	4.94	1.63	0.76	0.10	5.30	1.25	1.18
0.02	5.10	0.86	1.00	0.10	5.30	1.63	1.02
0.02	5.10	1.25	0.88	0.10	5.56	0.57	3.04*
0.02	5.10	1.63	0.72	0.10	5.56	0.73	1.77*
0.02	5.27	0.86	0.79	0.10	5.56	1.34	1.65*
0.02	5.27	1.25	0.62	0.10	5.56	1.73	1.15*
0.02	5.27	1.63	0.50	0.10	5.91	0.57	2.01*
0.04	4.97	0.49	2.35	0.10	5.91	0.73	1.45*
0.04	4.97	0.86	1.60	0.10	5.91	1.34	1.08*
0.04	4.97	1.25	1.31	0.10	5.91	1.73	1.00*
0.04	4.97	1.63	1.03	0.20	5.17	0.86	2.92
0.04	5.12	0.49	1.94	0.20	5.17	1.25	2.11
0.04	5.12	0.86	1.22	0.20	5.17	1.63	1.68
0.04	5.12	1.25	1.03	0.20	5.36	0.49	3.66
0.04	5.12	1.63	0.81	0.20	5.36	0.86	2.31
0.04	5.29	0.49	1.62	0.20	5.36	1.25	1.70
0.04	5.29	0.86	1.05	0.20	5.36	1.63	1.42
0.04	5.29	1.25	0.97	0.20	5.58	0.49	2.83
0.04	5.29	1.63	0.70	0.20	5.58	0.86	1.63
0.04	5.50	0.57	1.93*	0.20	5.58	1.25	1.17
0.04	5.50	0.73	1.29*	0.20	5.58	1.63	0.91
0.04	5.50	1.34	0.99*	0.20	5.95	0.57	2.80*
0.04	5.50	1.73	0.70*	0.20	5.95	0.73	1.86*
0.04	5.83	0.57	1.44*	0.20	5.95	1.34	1.33*
0.04	5.83	0.73	1.01*	0.20	5.95	1.72	1.12*
0.04	5.83	1.34	0.77*				
0.04	5.83	1.73	0.77*				

The apparent initial rates were measured under varied conditions. The results are given in Tables 1 and 2.

Equation (11) indicates that, if the values of $V^{+}_{0,app}/([CoX^{-}]_0[Ni^{2+}]_{0,app})$ are plotted against $1/[Co^{2+}]_{0,app}$ under conditions at which all quantities but $[Co^{2+}]_{0,app}$ are kept constant, a straight line should be obtained with a slope given by:

$$\frac{1+\beta_{CoZ}[Z^{z-}]}{1+\beta_{NiZ}[Z^{z-}]}\left\{k^{+}_{3h}+k^{+}_{3z}[Z^{z-}]+(k^{+}_{4h}+k^{+}_{4z}[Z^{z-}])[H^{+}]\right\} \quad (12)$$

The slopes obtained from the plots of $V^{+}_{0,app}/([CoX^{-}]_0[Ni_0{}^{2+}]_{0,app})$ *versus* $1/[Co^{2+}]_{0,app}$ were plotted against the hydrated ion concentration according to Eq. (12). These plots gave straight lines, as is shown in Fig. 1.

The rate constants in Eq. (11) were obtained by analyzing the plots of Fig. 1 and the data given in Table 1 and Table 2; they are given in Table 3.

The rate constants for reactions (3), (3′), (8), (8′), (10), and (10′) calculated from the relations given in Eq. (11′), are given in Table 4. The formation constants, K_{CoX}, β_{CoOAc}, β_{NiOAc}, β_{CoPh}, and β_{NiPh}, and the dissociation constant, K_{HX}, which were used in these calculations are given in Table 5.

The values of β_{NiOAc}[3] and β_{CoOAc}[4] were

3) Y. Saito, Ph. D. thesis, Tohoku University (1967).
4) H. Ogino, *ibid.*, (1965).

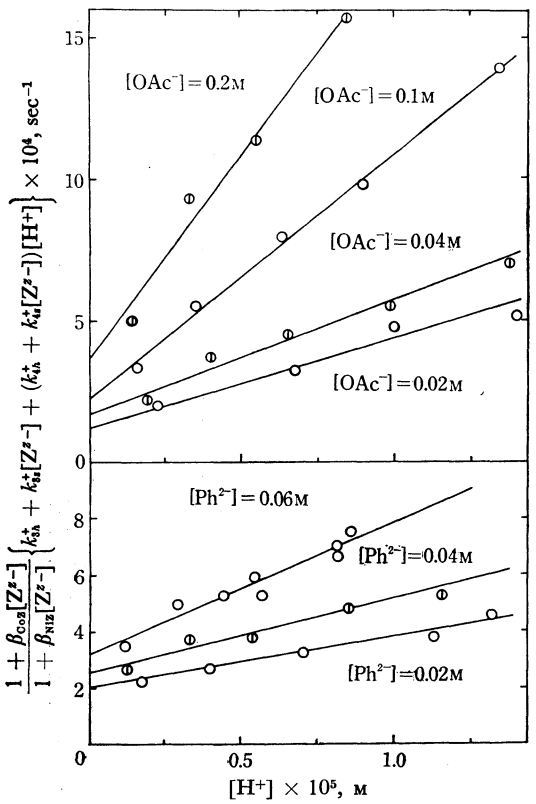

Fig. 1. Eq. (12) as a function of the hydrogen ion concentration.
The conditions are the same as in Tables 1 and 2.

determined by the polarographic method at an ionic strength of 0.2 at 25°C. The value of β_{NiPh} determined at an ionic strength of 0.1 at 25°C by Yasuda *et al.*[5] was used after correction for the ionic strength. The value of β_{CoPh} determined at an ionic strength of 0.4 at 18—25°C by Bobtelsky and Bar-Godda[6] was used without any correction. The thermodynamic constant of K_{HX} determined by Hughes and Martell[7] at 0, 10, 20, and 30°C was used after correction for the temperature and the ionic strength. The value of K_{CoX} determined at an ionic strength of 0.1 at 20°C by Schwarzenbach and Gut[8] was used after correction for the ionic strength.

Discussion

The values in Table 4 indicate that the kinetic reactivity of nickel is in the order of: $NiOAc^+ > Ni^{2+} > NiPh$. This may be compared with the results obtained in the case of the substitution reactions involving cobalt(II) ions,[1] copper(II) ions,[9] and lead (II) ions.[10] The ratios of the rate constant for the two reactions:

$$M^{2+} + L^{3-} \xrightarrow{k^L_M} ML^-$$

$$MZ^{(2-z)+} + L^{3-} \xrightarrow{k^L_{MZ}} ML^- + Z^{z-}$$

can now be discussed. Previous studies dy the present author showed that the comparison of

Table 3. Rate constats in Eq. (11) obtained for the substitution reactions at ionic strength 0.2 at 25°C

Reaction system	Rate constant*							
	k^+_{1h}	k^+_{1z}	k^+_{2h}	k^+_{2z}	k^+_{3h}	k^+_{3z}	k^+_{4h}	k^+_{4z}
NiPh-CoX⁻	$\sim 3\times10^{-2}$	~ 3	$\sim 2\times10^{4}$	$\sim 2\times10^{6}$	1.5×10^{-4}	3.3×10^{-3}	~ 7	$\sim 7\times10^{2}$
$NiOAc^+$-CoX⁻	$\sim 6\times10^{-2}$	$\sim 2\times10^{-1}$	$\sim 3\times10^{4}$	$\sim 1\times10^{5}$	1.1×10^{-4}	2.3×10^{-3}	2×10	9×10^{2}

* Units of rate constants: sec^{-1} for k^+_{3h}; $l\ mol^{-1}sec^{-1}$ for k^+_{1h}, k^+_{3z} and k^+_{4h}; $l^2mol^{-2}sec^{-1}$ for k^+_{1z}, k^+_{2h} and k^+_{4h}; $l^3mol^{-3}sec^{-1}$ for k^+_{2z}.

Table 4. Rate constants for forward reactions of reactions (3), (3′), (8), (8′), (10) and (10′) obtained at ionic strength 0.2 at 25°C

Reaction system	Rate constant, $l\ mol^{-1}sec^{-1}$					
	k^+_{Ih}	k^+_{Iz}	k^+_{IIIh}	k^+_{IIIz}	k^+_{IVh}	k^+_{IVz}
NiPh-CoX⁻	$\sim 3\times10^{-2}$	$\sim 3\times10^{-2}$	$3._2\times10^{6}$	$1._0\times10^{6}$	~ 40	~ 40
$NiOAc^+$-CoX⁻	$\sim 6\times10^{-2}$	$\sim 6\times10^{-2}$	$2._4\times10^{6}$	$1._3\times10^{7}$	80	1×10^{2}

5) M. Yasuda, K. Suzuki and K. Yamasaki, *J. Phys. Chem.*, **60**, 1649 (1956).
6) M. Bobtelsky and I. Bar-Godda, *Bull. Soc. Chim. France*, **1953**, 276.
7) V. L. Hughes and A. E. Martell, *J. Am. Chem. Soc.*, **78**, 1319 (1956).
8) G. Schwarzenbach and R. Gut, *Helv. Chim. Acta*, **34**, 1589 (1956).
9) N. Tanaka and M. Kimura, This Bulletin, **41**, 2375 (1968).
10) N. Tanaka and H. Ogino, *ibid.*, **36**, 175 (1963).

TABLE 5. FORMATION CONSTANTS AT IONIC STRENGTH 0.2 AT 25°C

$\log K_{CoX}$[8]	10.34	β_{NiOAc}[3]	3.7
pK_{HX}[7]	9.62	β_{CoOAc}[4]	1.2
		β_{NiPh}[5]	91
		β_{CoPh}[6]	65

the rate constant is $k^{HY}_{Co} < k^{HY}_{CoOAc}$,[1] but that, on the contrary, $k^{X}_{Cu} > k^{X}_{CuOAc}$.[9] Recently, however, Tanaka and Ogino[10] reported on the kinetics of the substitution reaction between lead(II) and zinc(II)-EDTA complexes. Their results showed that the comparison of the rate constant is $k^{HY}_{Pb} > k^{HY}_{PbOAc}$.

Since it seems important and interesting to investigate the relations between the stability constant of $MZ^{(2-z)+}$ and the ratios of the rate constants, k^{L}_{M}/k^{L}_{MZ}, the plots of k^{L}_{M}/k^{L}_{MZ} against β_{MZ} are given in Fig. 2 together with the results obtained by other researchers.

Figure 2 indicates that the kinetic reactivity of the weak complexe, *i. e.*, $MZ^{(2-z)+}$, may be mainly due to the stability of the weak complex. Inner-sphere complexes, such as $MZ(H_2O)_{n-z}$, which may correspond with $CuOAc^+$, NiPh, and $PbOAc^+$ in Fig 2, seem to have less kinetic reactivity than the corresponding hydrated metal ions. However, outer-spher complexes, that is outer-spher ion-association complexes, such as $M(H_2O)_n^{2+}$–Z^{z-}, or outer-sphere hydrogen-bonding complexes, such as $M(H_2O)^{z+}_n O\langle^{H}_{H}\rangle Z^{z-}$, seem to have larger kinetic reactivities than the corresponding hydrated metal ions. Monoacetatonickel(II) and monoacetatocobalt(II) complexes may be considered to be outer-sphere complexes on the basis of their stability constants.

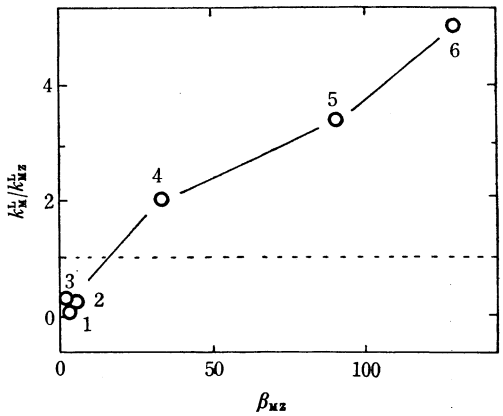

Fig. 2. The relation between k^{L}_{M}/k^{L}_{MZ} and β_{MZ}.
1: Ref. (2) 4: Ref. (9)
2: The present study 5: The present study
3: Ref. (1) 6: Ref. (10)

The author wishes to thank the Ministry of Education for the financial support granted for this research.

BULLETIN OF THE CHEMICAL SOCIETY OF JAPAN VOL. 42 411—416 (1969)

Stability Constants of Some Uranyl Complexes. II

S. RAMAMOORTHY and M. SANTAPPA

Department of Physical Chemistry, University of Madras, Madras-25, India

(Received April 10, 1968)

Stability constants of complexes of uranyl ion with various carboxylic acids were determined by the pH titration method at 31°C and $\mu=0.1$ ($NaClO_4$) in the pH range 2.5—3.5. The 1 : 1 and 1 : 2 complexes were formed with crotonic, pyruvic, malonic, and diglycolic acids and only the 1 : 1 complex with formic, propionic, succinic, adipic, maleic, fumaric acids. The effect of ring size and presence of oxygen atom as keto or ether oxygen or that of double bonds in the ligand acids on the stabilities of the corresponding complexes are discussed.

Recently Rajan and Martell[1] in a potentiometric study of chelates of uranyl perchlorate with carboxylic acids reported the stability constants of uranyl ion-maleate complexes (1 : 1 and 1 : 2), uranyl ion-succinate complex (1 : 1) and uranyl ion-maleate complex (1 : 1) in the pH range 2—4 at 25°C and $\mu=1$ M(KNO_3). As a part of our studies on the complexes of uranyl ion with various organic acids, systems of uranyl ion with formic, propionic, crotonic, pyruvic, malonic, succinic, adipic, maleic, fumaric and diglycolic acids were studied by the pH titration method at 31°C ±0.1°C and $\mu=0.1$ ($NaClO_4$) with a view to determine the

1) K. S. Rajan and A. E. Martell, *J. Inorg. Nucl. Chem.*, **29**, 523 (1967).

TABLE 1. VALUES OF v', v'' AND v''' FROM THE pH TITRATION DATA AND EVALUATION OF $\bar{n}_H$, $\bar{n}$ AND pL FOR THE URANYL ION-FORMIC ACID SYSTEM

v', v'' and v''' are volumes of sodium hydroxide (0.9416 M) added for the titration of (i) 0.022 M $HClO_4$ (100 ml), (ii) 0.022 M $HClO_4$ + 0.025 M formic acid (100 ml), and (iii) 0.022 M $HClO_4$ + 0.025 M formic acid + 0.00497 M uranyl ion (100 ml) respectively for the same pH values, as obtained from an enlarged graph.

μ=0.1 ($NaClO_4$)
T=31 ± 0.1°C

pH	v'	v''	v'''	$\bar{n}_H$	$\bar{n}$	pL
2.4	2.063	2.213	2.413	0.944	0.411	2.860
2.5	2.200	2.365	2.563	0.939	0.414	2.792
2.6	2.300	2.500	2.700	0.925	0.424	2.701
2.8	2.425	2.725	2.963	0.887	0.522	2.532
2.9	2.475	2.838	3.100	0.864	0.594	2.453
3.1	2.525	3.100	3.375	0.783	0.687	2.310
3.2	2.550	3.225	3.500	0.746	0.723	2.230
3.4	2.575	3.550	3.800	0.633	0.777	2.100
3.6	2.600	3.900	4.125	0.510	0.869	1.996
3.7	2.600	4.075	4.333	0.444	1.056	2.274

pK of formic acid from the plot of $\bar{n}_H$ *versus*-log[H^+]=3.539
log K_{ML_1} from the plot of $\bar{n}$ *versus* pL (Fig. 1)=2.61

compositions and stability constants of the complexes in the pH range 1.5—3.5 in which hydrolysis of uranyl ion may completely be neglected[2] and the effect of ring size on stabilities of the complexes and coordinating tendencies of ligands containing oxygen atoms as keto or ether oxygen. The effects of various oxygen donor compounds on the stabilities of the metal chelates are compared with the chelating behaviour of compounds containing no additional coordinating group other than carboxylate group.

Experimental

Materials. Preparation of uranyl perchlorate as well as other reagents and their estimations have been given earlier.[3] Formic (M and B; AnalaR), propionic (B.D.H.; AnalaR), crotonic (Chem. pure; AnalaR), pyruvic (Ingelheim, Germany; pure), malonic (Fluka; purum), succinic (Riedel; pure), adipic (Fluka; purum), maleic (Riedel; pure), fumaric (Fluka; purum) and diglycolic (Fluka; purum) acids were used as such for ligands. These acids were standardized with sodium hydroxide solution (0.1 M).

Procedure. The details of apparatus and of experimental technique used to obtain the Bjerrum-Calvin titration curves and methods of calculation of dissociation constants of ligand acids, and stability constants of complexes by Irving and Rossotti's difference method[4] were outlined in our earlier paper.[3] Acid dissociation constants, pK, of monobasic acids were evaluated from the value of $-\log[H^+]$ at $\bar{n}_H=0.5$, utilising a value of 0.83 for the activity coefficient[5] of 0.1 N [H^+] (Table 1 and Fig. 1A) and K_1 and K_2 of dibasic acids were determined more conveniently by the method of slope and intercept due to Irving and Rossotti[6] (Table 2 and Fig. 2). Stability constants of the complexes, log K_{ML_1} and log K_{ML_2} evaluated from the values of pL ($-\log$ [Ligand]) at $\bar{n}$ (formation function)=0.5 and 1.5 respectively from the formation curves of the systems (Table 1 and Fig. 1B) were only approximate when they did not differ greatly in magnitude (<2.5 log units)[6]; exact values were determined by Eq. (1) according to Irving and Rossotti[6] (Table 3).

where K_{ML_1}, K_{ML_2},..., K_{ML_n} are successive stability constants, [L]=free ligand anion concentration, $\bar{n}=$

$$\frac{\bar{n}}{(\bar{n}-1)[L]} = K_{ML_1} + K_{ML_1}\cdot K_{ML_2}\cdot\frac{(2-\bar{n})[L]}{(1-\bar{n})} + \sum_{n=3}^{N} K_{ML_1}, K_{ML_2}\ldots\ldots K_{ML_n}\cdot\frac{(n-\bar{n})[L]^{n-1}}{(1-\bar{n})} \quad (1)$$

formation function of the system. The formation of only 1 : 1 complex was obvious from the plots of $\bar{n}/(1-\bar{n})[L]$) *versus* $((2-\bar{n}))[L]/(1-\bar{n})$ which was parallel to abscissa (Fig. 2) and in the plots of pL *versus* $\bar{n}$ (Fig. 1B) magnitude of the latter was less than unity, even when $[T_L]/[T_M]$ was 1 to 10, T_L and T_M being total

2) J. Sutton, *J. Chem. Soc.*, (Suppl) 2, S-275 (1949); St. Ahrland, S. Hietanen and L. G. Sillen, *Acta Chem. Scand.*, **8**, 1907 (1954); S. Hietanen and L. G. Sillen, *Acta Chem. Scand.*, **13**, 1828 (1959); M. Bartusek and L. Sommer, *Z. Phys. Chem.*, **226**, 309 (1964).

3) S. Ramamoorthy and M. Santappa, This Bulletin, **41**, 1330 (1968).

4) H. M. Irving and H. S. Rossotti, *J. Chem. Soc.*, **1954**, 2904.

5) J. Kielland, *J. Am. Chem. Soc.*, **59**, 1675 (1937).

6) H. Irving and H. S. Rossotti, *J. Chem. Soc.*, **1953**, 3397; F. J. C. Rossotti and H. S. Rossotti, *Acta Chem. Scand.*, **9**, 1166 (1955).

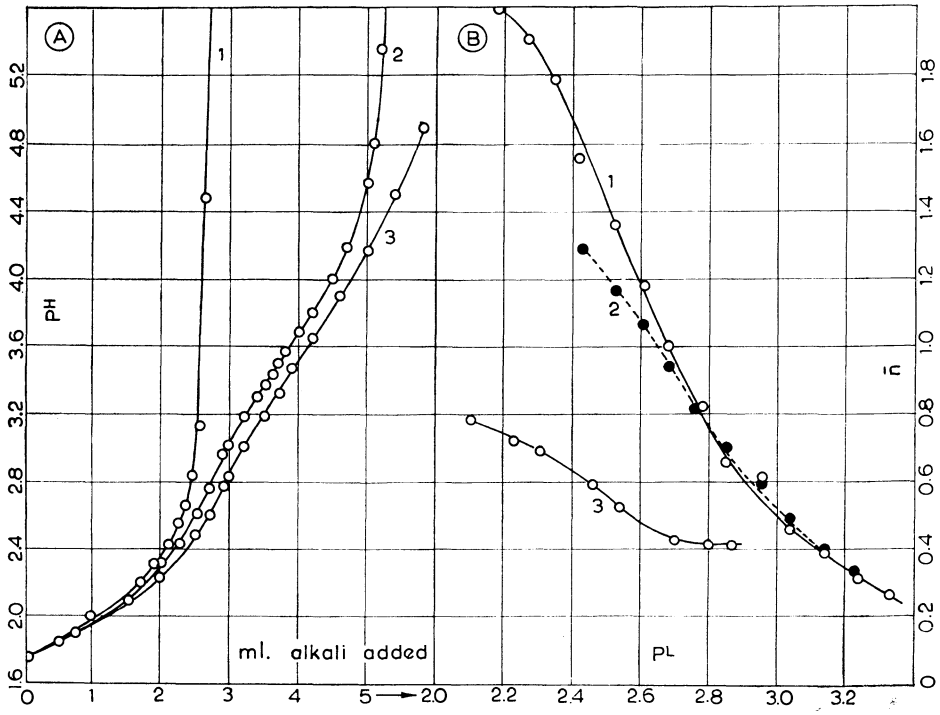

Fig. 1.

(A) uranyl ion-formic acid system.
Plot of pH *versus* ml of alkali added.
(i) $HClO_4$ (0.022 M) + $NaClO_4$ (0.1 M)
(ii) $HClO_4$ (0.022 M) + $NaClO_4$ (0.1 M) + formic acid (0.025 M)
(iii) $HClO_4$ (0.022 M) + $NaClO_4$ (0.1 M) + formic acid (0.025 M) + uranyl ion (0.005 M)

(B) (1) Plot of $\bar{n}_{exp.}$ *versus* pL for the uranyl ion-crotonic acid system.
(2) Plot of $\bar{n}_{calcd.}$ *versus* pL for the uranyl ion-crotonic acid system.
(3) Plot of $\bar{n}$ *versus* pL for theuranyl ion-formic acid system.

TABLE 2. ACID DISSOCIATION CONSTANTS OF THE LIGANDS AND THE STABILITY CONSTANTS OF URANYL COMPLEXES

$\mu=0.1(NaClO_4)$
$T=31\pm0.1°C$

	Ligand	Authors' value				Literature	
		pK_1	pK_2	log K_{ML_1}	log K_{ML_2}	log K_{ML_1}	log K_{ML_2}
1	Formic acid	3.54		2.61			
2	Benzoic acid	4.01		2.57			
3	Phenylacetic acid	4.12		3.21			
4	Propionic acid	4.62		3.03			
5	Phenoxyacetic acid	2.96		2.59			
6	Pyruvic acid	2.39		2.15	0.59		
7	Malonic acid	2.81	5.14	5.28	4.01	5.66	4.00[1]
8	Succinic acid	3.87	5.12	4.48		3.68[1]	
9	Adipic acid	4.12	5.04	4.08			
10	Itacoic acid	3.61	4.98	4.86			
11	Thiomalic acid	2.95	4.45	3.71			
12	Maleic acid	1.95	6.16	5.15		4.46[1]	
13	Fumaric acid	2.89	4.11	3.05			
14	Diglycolic acid	2.77	3.88	4.90	2.84		
15	Crotonic acid	4.53		2.74	2.53		

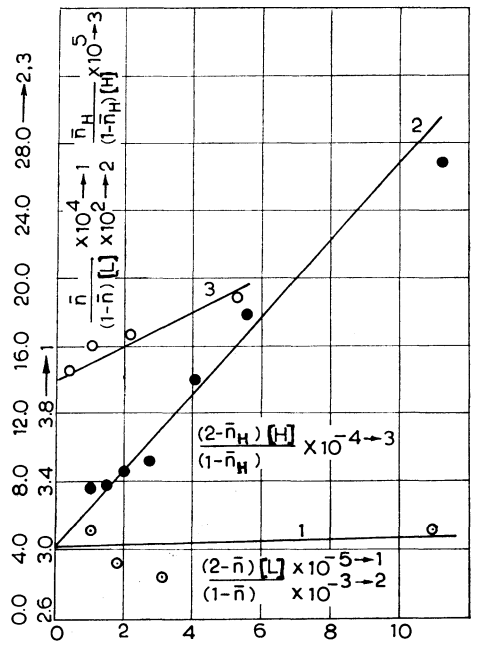

Fig. 2.

(1) Plot of $\frac{\bar{n}}{(1-\bar{n})[L]}$ *versus* $\frac{(2-\bar{n})[L]}{(1-\bar{n})}$
for the uranyl ion-succinic acid systems.

(2) Plot of $\frac{\bar{n}}{(1-\bar{n})[L]}$ *versus* $\frac{(2-\bar{n})[L]}{(1-\bar{n})}$
for the uranyl ion-crotonic acid system.

(3) Plot of $\frac{\bar{n}_H}{(1-\bar{n}_H)[H]}$ *versus* $\frac{(2-\bar{n}_H)[H]}{(1-\bar{n}_H)}$
for the uranylion-malonic acid system.

TABLE 3. EVALUATION OF STABILITY CONSTANTS (K_{ML_1}, K_{ML_2}) FOR THE URANYL ION-CROTONIC ACID SYSTEM

μ=0.1 ($NaClO_4$) $T=31\pm0.1$°C

$\frac{\bar{n}}{(1-\bar{n})[L]}$ ×10⁻²	$\frac{(2-\bar{n})[L]}{(1-\bar{n})}$ ×10³	$\frac{\bar{n}}{(1-\bar{n})[L]}$ ×10⁻²	$\frac{(2-\bar{n})[L]}{(1-\bar{n})}$ ×10³
7.603	1.111	−25.880	−11.890
7.447	1.434	−12.350	− 5.352
8.407	1.914	− 7.372	−22.914
9.105	2.597	− 5.037	− 1.225
14.090	4.027	− 3.866	− 0.563
17.840	5.489	− 3.059	− 0.250
26.350	11.230	− 2.517	− 0.109

Intercept = 5.5×10^2; $\log K_{ML_1}$ = 2.74
Slope = 1.9×10^5; $\log K_{ML_2}$ = 2.53

concentrations of the ligand and the uranyl ion respectively. In such cases, the log K_{ML_1}, calculated graphically from the $\bar{n}$ *versus* pL curves agreed very well with those calculated from Eq. (1). The formation of higher complexes was indicated by the value of $\bar{n}$ going beyond unity in some of the systems studied

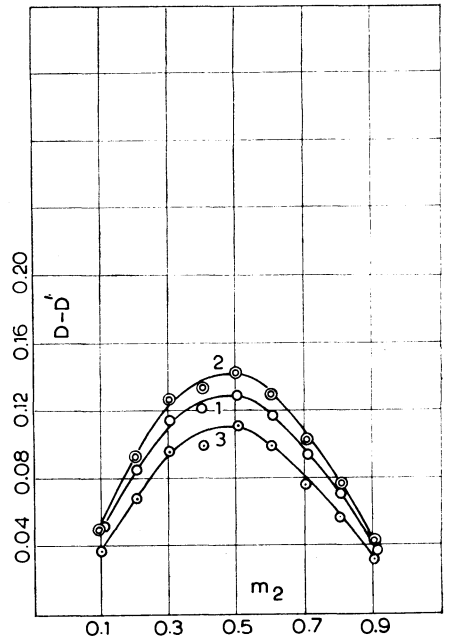

Fig. 3.

Plot of $D-D'$ (observed optical density-optical density calculated for no complexation) *versus* m_2, mole fraction of the uranyl ion.
Total Concentration = [uranyl ion + diglycolic acid] = 0.04 M.
μ=0.1 $T=31\pm0.1$°C
λ=430 mμ (curve 1),
440 mμ (curve 2), and 460 mμ (curve 3).

(uranyl ion-malonic, uranyl ion-pyruvic, uranyl ion-crotonic and uranyl ion-diglycolic acids) (Fig. 1B). In such cases, K_{ML_1} and K_{ML_2} were evaluated from Eq. (1) by the least squares treatment (Table 3). It may be mentioned that since the pH measurements and consequently log K_{ML} values are accurate to ±0.02 units, the log K_{ML_1} and log K_{ML_2} values from half integral values of pL will also be accurate[7] to −log 0.02 units even if log (K_1/K_2) is <2.5. The K_{ML} values reported (Table 2) are concentration (stoichiometric) stability constants as concentrations were used in place of activities. The data at values of pH> 3.5 were not used in the calculation of stability constants. Formation curves which were constructed from the values of pL and $\bar{n}_{calculated}$ using values of log K_{ML_1} and log K_{ML_2} obtained from Irving and Rossotti's equation (1) showed very slight deviations from the formation curves of pL *versus* $\bar{n}_{exp.}$ within the limits of experimental errors. For values of pH>3.5, $\bar{n}_{exp.}$ deviated greatly from $\bar{n}_{calc.}$ probably due to considerable hydrolysis of uranyl ion (Fig. 1B).

Results

The titration curves for (i) perchloric acid-

7) K. E. Jabalpurwala, K. A. Venkatachalam and M. B. Kabadi, *J. Inorg. Nucl. Chem.*, **26**, 1011, 1027 (1964).

sodium perchlorate, (ii) perchloric acid-ligand acid-sodium perchlorate and (iii) uranyl perchlorate - ligand acid - perchloric acid - sodium perchlorate systems against sodium hydroxide are presented for the uranyl ion - formic acid system in Fig. 1A. The $\bar{n}_H$, $\bar{n}$ and pL values are given in Table 1.

Discussion

Most of the data reported in the present paper were obtained for the first time, though reported data on the stability constants in the case of malonic, succinic and maleic acids were obtained under somewhat different experimental conditions of ionic strength (1 M KNO_3) and temperature (25°C). Results for systems of uranyl ion with itaconic, thiomalic, benzoic, phenylacetic and phenoxyacetic acids are taken from the previous paper[3] for comparison and discussion.

(a) Uranyl Ion-Simple Monocarboxylic Acids (Formic, Propionic, Benzoic and Phenylacetic Acids). Dissociation constants of ligand acids are listed in Table 2. The pK of the ligand acid increases in the order formic<benzoic< phenylacetic<propionic acids and K_{ML_1} increases in the order, formic=benzoic<phenylacetic>propionic acids (Table 2). It may be mentioned that $\bar{n}$ did not exceed unity even when $[T_L]/[T_M]$ was 1 to 10 in all the four systems. The formation of only 1 : 1 complex was also obvious from the plots of $\bar{n}/((1-\bar{n})\ [L])$ *versus* $((2-\bar{n})([L])/(1-\bar{n})$ which was parallel to the abscissae (Fig. 2). The stability constants calculated from $\bar{n}$ *versus* pL curve agreed very well with those calculated from Eq.(1). The substitution of H atom in formic acid by a phenyl group caused no change in the stability of the corresponding uranyl complex, while substitution by a benzyl group as well as an ethyl group increases the stability of the respective complexes. This kind of increase was not observed in the case of copper(II) complexes (formic, acetic and propionic acids)[8] and there the alkyl substitution caused no detectable effect on the values of stability constants of the complexes.

b) Uranyl Ion-Monocarboxylic Acid Containing -O- and -CO- linkages (Phenoxyacetic and Pyruvic Acids). From acid dissociation constants (Table 2), it is obvious that pK's of phenoxyacetic and pyruvic acids are very much lower than the corresponding acids, phenylacetic acid and acetic acid[9] (pK=4.64 at μ=0.2 (KCl) and T=20°C) (without -O- and -CO- groups). The stability constants were obtained from the plots of $\bar{n}$ *versus* pL as well as from $\bar{n}/(1=\bar{n})\ [L])$ versus $((2-\bar{n})\ [L])/(1-\bar{n})$ since the difference between log K_{ML_1} and log K_{ML_2} determined from half integral values was less than 2.5 log units. However the half integral values would be in error by -0.02 log units, when the difference in $\log(K_1/K_2)$ is 1.78. The system of uranyl ion-phenoxyacetic acid differed very much from the uranyl ion-pyruvic acid system in number of complexes formed as well as the stability range of the latter; for the former, the value of $\bar{n}$ did not exceed unity even with excess of ligand, [ligand]/[uranyl ion]=1 to 10, indicating the absence of formation of higher complexes, while for the latter, the value of $\bar{n}$ was as high as 0.7 at pH 1.80 and reached 2.0 at pH 3.00. The log K_{ML_1} value of the uranyl ion pyruvic acid system in consistent with the fact that pK of pyruvic acid is lower than that of phenoxyacetic acid. From the orders of stability constants (log K_{ML_1}) of the systems uranyl ion-pyruvic acid, uranyl ion-phenoxyacetic acid, uranyl ion-benzoic, uranyl ion-formic acid complexes etc., it is obvious that neither the phenoxy oxygen in phenoxy-acetic acid nor keto oxygen in pyruvic acid was involved in complexation. However, from the observation that precipitation in the system uranyl ion-pyruvic acid did not occur till pH 10.5, coupled with the fact that complexation was considerable even at low pH, it might be inferred that the keto oxygen stabilized the complex probably through coordination to the uranyl ion. The ether oxygen atom of phenoxyacetic acid has very little tendency for coordination with uranyl ion compared with carbonyl oxygen atom of keto group of pyruvic acid.

c) Uranyl Ion-Simple Dicarboxylic Acids (Malonic, Succinic and Adipic Acids). It may be seen that the difference between pK_1 and pK_2 of the ligand acids (Table 2) decreases as the number of carbon atoms separating the two COOH groups increases *i. e.* malonic→succinic→adipic acids. In other words, the basicity of the first COOH group increases in the same order. It is evident from the log K_{ML_1} values (Table 2) that, of the three ligands malonic acid forms the most stable chelate with uranyl ion with a six membered ring and the stability of the chelate ring decreases with the increase in ring size *i. e.*, from six→seven→ nine memered ring, from malonic→succinic→adipic acids. Though the basicity of the first carboxyl group increases from malonic acid to adipic acid as evident from the pK_1 values, the increasing ring size from malonic acid to adipic acid decreases the stabilities of the chelates in the same order (*i. e.* malonic acid→adipic acid). The formation of the 1 : 2 complex was favoured only in the uranyl ion-malonic acid system (six membered rings), but not in the uranyl ion-succinic acid or uranyl ion-adipic acid system. The difference between the authors' values and those of Rajan

8) S. Ramamoorthy and M. Santappa, *J. Inorg. Nucl. Chem.*, **30**, 2393 (1968).

9) R. K. Cannan and A. Kibrick, *J. Am. Chem. Soc.*, **60**, 2314 (1938).

and Martell (Table 2) may be due to the somewhat different experimental conditions; the latter were measured in 1 M KNO_3 and at 25°C, while authors' values were at 0.1 M $NaClO_4$ and at 31°C. The stability decrease in the series, uranyl ion-malonic acid→uranyl ion-succinic acid→uranyl ion-adipic acid, is consistent with the earlier observations with other metal ions.[10]

d) Uranyl Ion-Substituted Dicarboxylic Acids (Thiomalic and Itaconic Acids). From the results with succinic acid, it was obvious that the formation of the 1 : 2 complex was not indicated with thiomalic (mercapto succinic) and itaconic (methylene succinic) acids. Moreover, from comparison of stability order of thiomalic acid and malic acid complexes, and then itaconic acid and succinic acid complexes, it is believed that the chelate ring is stabilized by the presence of a double bond or by an SH group, and more so by the former.

e) Uranyl Ion-*cis* and *trans* Dicarboxylic Acids (Maleic and Fumaric Acids). The pK_1 and pK_2 values for maleic and fumaric acids (Table 2) calculated by the least squares treatment of Irving and Rossotti's equation indicate the obvious fact that the two COOH groups are well separated in maleic acid, while they are overlapping in fumaric acid. Both the ligands form only 1 : 1 complexes with uranyl ion. From the results (Table 2) of stability of the uranyl ion-maleic acid and uranyl ion-fumaric acid complexes, it was evident that maleic acid formed a seven membered chelate ring with uranyl ion through the two carboxyl groups, while fumaric acid being a trans isomer of maleic acid with two COOH groups separated farther away, formed only a complex (not a chelate) with uranyl ion through one COOH group only. The stability range of the uranyl ion-fumaric acid complex (log K_{ML_1}= 3.05) (*cf.* log K_{ML_1} of the uranyl ion-formic acid complex, 2.61) also supported this argument. If there were no chelate ring in the uranyl ion-maleic acid complex, the stability of the uranyl ion-maleate complex would have been lower than the uranyl ion-fumarate complex from considerations of different pK_1 values of these two ligand acids. On the other hand, the stability of the uranyl ion-maleate system is comparable to any seven-membered chelate ring structure such as the uranyl ion-succinic acid system.

f) Uranyl Ion-Diglycolic Acid System (Dicarboxylic Acid Containing–O–Linkage). The pK_1 and pK_2 values obtained from the slope and intercept method are given in Table 2. Successive formation of the 1 : 1 and 1 : 2 complexes of the uranyl ion-diglycolic acid system was evident from the fact that $\bar{n}$ value reached 1.5 at pH 3.50. It is very interesting that log K_{ML_1} (4.90) is very high for the chelate structure with the eight-membered ring involving two COO^- groups for coordination to metal (*cf.* log K_{ML_1} of the uranyl ion-adipic acid system=4.08 or the uranyl ion-glutaric acid system) and it is comparable to the stabilities of the chelates with five or six-membered rings (*cf.* log K_{ML_1} of the uranyl ion-malonic acid system=5.28). The most probable structure for the uranyl ion-diglycolic acid chelate, therefore, might involve two COO^- groups with additional stabilisation through the –O– group. In fact, Suzuki and Yamasaki[11] showed that diglycolic acid chelates were much more stable than the glutaric acid chelates (absence of –O– groups). The Job's method of continuous variations (Fig. 3) for the uranyl ion-diglycolic acid system gave a peak at m_2 (mole fraction of uranyl ion)=0.5, indicating the 1 : 1 complex. The formation of a higher complex (1 : 2) was shown by a slight shoulder at m_2=0.33. This observation indicated the absence of free carboxylate ion in the uranyl ion-diglycolic acid chelate. It is to be noted that in the copper(II)-malic acid system a 2 : 1 complex was formed as the second carboxylate group was free.[12] **g) Uranyl Ion-Unsaturated Carboxylic Acids; Crotonic Acid.** The values of pK and log K_{ML_1} and K_{ML_2} are listed in Tables 2 and 3. The higher stability of the uranyl ion-crotonic acid complex is due to the hig her basicity of the ligand (*cf.* log K_{ML_1}=2.61 for the uranyl ion-formic acid complex) due to the inductive effect of the methyl group as well as the presence of the double bond in the structure.

From the results, it may be concluded that basicities of the monodentate ligands have very little influence on the stabilities of the corresponding uranyl ion complexes. Steric factors and ring size presumably determine the metal chelate stabilities with bidentate ligands. In general, the uranyl-carboxylate chelates are more stable than the corresponding copper chelates conforming to the extended Irving-Williams order in which uranyl ion occupies a higher place over copper(II).[13]

10) H. Irving, R. J. P. Williams, D. J. Ferret and A. E. Williams, *J. Chem. Soc.*, **1954**, 3494.

11) K. Suzuki and K. Yamasaki, *J. Inorg. Nucl. Chem.*, **28**, 473 (1966); K. Yasuda, K. Yamasaki and H. Ohcaki, This Bulletin, **33**, 1077 (1970).

12) S. Ramamoorthy and M. Santappa, *J. Inorg. Nucl. Chem.*, **30**, 1855 (1968).

13) F. Basolo and R. G. Pearson, "Mechanism of Inorganic Reactions," John Willey & Sons, Inc., New York (1958), p. 16.

BULLETIN OF THE CHEMICAL SOCIETY OF JAPAN VOL. 42 417—431 (1969)

Magnetic Moments and d–d Bands of Copper(II) Halide Complexes with Substituted Pyridine *N*-Oxides and Some Related Ligands*1

Yoneichiro MUTO,* Michinobu KATO,** Hans B. JONASSEN*** and Louis Chopin CUSACHS***

* *Department of Chemistry, Saga University, Saga*
** *Aichi Prefectural University, Mizuho-ku, Nagoya*
*** *Department of Chemistry, Tulane University, New Orleans, La., U.S.A.*

(Received June 17, 1968)

In order to test the substituent effect or the effect of variations in chemical structures on the demagnetization and d–d band shift in dimeric copper(II) halide complexes with pyridine *N*-oxides and some related ligands, a variety of electron-donating or electron-withdrawing substituents attached in 2-, 3- and 4-positions in the pyridine ring of the ligand were extensively studied. In these dimeric complexes, no correlation was observed between the Hammett's σ constants and the observed d–d band positions or magnetic moments. However, irrespective of the nature of the substituents, a linear relation was observed to exist between the d–d band positions and the magnetic moments, indicative of a magnetochemical support for the interpretation of the spectrochemical series through the idea of symmetry-restricted covalency. For the monomeric complexes with the same ligands, a linear relation exists between Hammett's constants and the d–d band positions for each series of the electron-donating and electron-withdrawing substituents. Experimental results indicate that the most important factor determining the non-applicability of Hammett's Rule in these dimeric complexes is the steric condition of the metal ions which shields them from the influence of other molecules or ions. The larger demagnetization effect of the bromide ion compared to the chloride ion has been interpreted as due to its larger nephelauxetic effect. On the basis of the established structure of the parent compound, two pathways for superexchange interaction have been proposed. The importance of a σ type orbital overlap compared to the π type is discussed.

Recently a large number of copper(II) complexes have been reported which have subnormal magnetic moments at room temperature. Quagliano and his coworkers[1] noticed a low magnetic moment, 0.85 B.M., for the 1 : 1 complex of copper(II) chloride with pyridine *N*-oxide. Many studies have been undertaken on this compound and its homologues in order to elucidate the relations between the chemical structures or substituent effects on the demagnetization mechanism. The structure of the parent compound which has recently been determined by X-ray analysis,[2-5] is an excellent model to examine these correlations for the following reasons:

1) Since pyridine *N*-oxide is a monodentate ligand, its coordinate bond to the metal ion is not involved in any other metal ligand bond. This

*1 A part of this study was presented a) by Y. Muto, M. Kato, H. N. Ramaswamy and H. B. Jonassen at the 19th Annual Meeting of the Chemical Society of Japan, Tokyo, April, 1966, Proceedings Vol. II, p. 134; b) by Y. Muto, M. Kato and H. B. Jonassen at the 16th Conference on Coordination Chemistry of the Chemical Society of Japan, Tokyo, December, 1966, Proceedings, p. 66; c) by Y. Muto, M. Kato, H. B. Jonassen and F. Itabe at the 20th Annual Meeting of the Chemical Society of Japan, Tokyo, April, 1967, Proceedings Vol. II, p. 76; d) by Y. Muto, M. Kato, H. B. Jonassen, H. N. Ramaswamy and K. Imai at the 10th International Conference on Coordination Chemistry, Nikko, September, 1967, Proceedings, p. 337; e) by Y. Muto, M. Kato, H. B. Jonassen and H. N. Ramaswamy, This Bulletin, **40**, 1535 (1967); f) by M. Kato, Y. Muto and H. B. Jonassen, *ibid.*, **40**, 1738 (1967), and g) by Y. Muto, M. Kato, H. B. Jonassen and K. Kakiuchi at the 21th Annual Meeting of the Chemical Society of Japan, Osaka, April, 1968, Proceedings Vol. II, p. 1119.

1) J. V. Quagliano, J. Fujita, G. Franz, D. J. Phillips, J. A. Walmsley and S. Y. Tyree, *J. Am. Chem. Soc.*, **83**, 3770 (1961).
2) C. M. Harris, E. Kokot, S. L. Lenzer and T. N. Lockyer, *Chem. Ind. (London)*, **1962**, 651.
3) M. Kubo, Y. Kuroda, M. Kishita and Y. Muto, *Australian J. Chem.*, **16**, 7 (1963).
4) H. L. Schäfer, J. C. Morrow and H. M. Smith, *J. Chem. Phys.*, **42**, 504 (1965).
5) R. S. Sager, R. J. Williams and W. H. Watson, *Inorg. Chem.*, **6**, 951 (1967).

TABLE 1. ANALYTICAL DATA

Ligand (L)	Complex	C%		H%		N%		Cu%	
		Found	Calcd	Found	Calcd	Found	Calcd	Found	Calcd
Pyridine *N*-oxide	$CuL_4(ClO_4)_2$	37.44	37.37	3.18	3.14	8.67	8.72	9.62	9.88
4-Methylpyridine *N*-oxide	$CuL_4(ClO_4)_2$	41.15	41.24	4.02	4.04	8.09	8.02	8.86	9.09
3-Chloropyridine *N*-oxide	$CuLCl_2$	22.81	22.75	1.70	1.53	5.36	5.31	24.12	24.07
	$CuLBr_2$	17.08	17.02	1.25	1.14	4.06	3.97	17.94	18.00
	$CuL_4(ClO_4)_2$	30.69	30.77	2.04	2.07	7.26	7.18	8.13	8.14
3-Bromopyridine *N*-oxide	$CuLBr_2$	15.30	15.11	1.21	1.02	3.56	3.53	15.72	15.99
Nicotinic acid *N*-oxide	$CuLCl_2$	26.63	26.34	1.91	1.84	5.17	5.12	23.18	23.23
Ethylnicotinate *N*-oxide	$CuLCl_2$	31.86	31.86	3.01	3.01	4.62	4.64	21.24	21.07
	$CuLBr_2$	24.71	24.60	2.44	2.32	3.70	3.59	16.21	16.27
	$CuL_4(ClO_4)_2$	41.32	41.28	4.02	3.90	5.97	6.02	6.75	6.82
Ethylisonicotinate *N*-oxide	$CuLCl_2$	31.59	31.86	3.08	3.01	4.65	4.64	21.14	21.07
	$CuLBr_2$	24.68	24.60	2.47	2.32	3.41	3.59	16.30	16.27
	$CuL_4(ClO_4)_2$	41.25	41.28	3.94	3.90	6.08	6.02	6.76	6.82
3-Acetylpyridine *N*-oxide	$CuLCl_2 \cdot \frac{1}{2}C_2H_5OH$	32.44	32.61	3.41	3.42	4.77	4.75	21.34	21.57
	$CuLBr_2 \cdot \frac{1}{2}C_2H_5OH$	25.17	25.05	2.39	2.63	3.77	3.65	16.79	16.57
	$CuL_4(ClO_4)_2$	41.52	41.47	3.43	3.48	7.02	6.91	7.79	7.83
4-Acetylpyridine *N*-oxide	$CuL_4(ClO_4)_2$	41.48	41.47	3.51	3.48	6.94	6.91	7.81	7.83
4-Nitropyridine *N*-oxide	$CuLCl_2$	21.45	21.87	1.60	1.47	10.07	10.20	23.32	23.14
	$CuLBr_2$	16.22	16.52	1.04	1.11	7.63	7.71	17.46	17.48
	$CuL_4(ClO_4)_2$	29.38	29.19	2.08	1.96	13.59	13.62	7.69	7.72
3-Cyanopyridine *N*-oxide	$CuL_4(ClO_4)_2$	38.82	38.80	2.21	2.17	15.05	15.08	8.40	8.55
4-Cyanopyridine *N*-oxide	$CuLCl_2$	28.21	28.31	1.79	1.58	11.01	11.00	24.58	24.96
	$CuLBr_2$	20.83	20.98	1.17	1.17	8.37	8.16	18.44	18.50
	$CuL_4(ClO_4)_2$	38.96	38.80	2.23	2.17	15.21	15.08	8.23	8.55
3-Hydroxypyridine *N*-oxide	$CuLCl_2$	24.52	24.46	2.12	2.05	5.72	5.70	25.73	25.88
	$CuLBr_2$	18.22	17.96	1.54	1.51	4.24	4.19	18.73	19.00
4-Hydroxypyridine *N*-oxide	$CuLCl_2 \cdot H_2O$	23.07	22.79	2.58	2.68	5.56	5.31	24.17	24.11
	$CuLBr_2 \cdot \frac{1}{2}C_2H_5OH$	20.11	20.14	2.57	2.24	3.86	3.92	17.57	17.78
2-Ethylpyridine *N*-oxide	$CuLCl_2$	32.70	32.64	3.63	3.52	5.51	5.44	24.68	24.67
	$CuLBr_2$	24.83	24.26	2.61	2.62	4.06	4.04	18.32	18.34
3-Ethylpyridine *N*-oxide	$CuLCl_2$	32.40	32.64	3.46	3.52	5.48	5.44	24.70	24.67
	$CuLBr_2$	24.13	24.26	2.53	2.62	4.02	4.04	18.47	18.34
4-Ethylpyridine *N*-oxide	$CuLCl_2$	32.61	32.64	3.50	3.52	5.49	5.44	24.72	24.67
	$CuLBr_2$	24.16	24.26	2.54	2.62	3.85	4.04	18.44	18.34
2,4-Lutidine *N*-oxide	$CuLCl_2$	32.47	32.64	3.56	3.52	5.57	5.54	24.67	24.67
	$CuLBr_2$	24.44	24.26	2.64	2.62	4.11	4.04	18.50	18.34
2-Hydroxymethylpyridine *N*-oxide	$CuLCl_2$	27.66	27.76	2.72	2.72	5.30	5.40	24.48	24.48
	$CuLBr_2$	20.15	20.68	2.20	2.02	3.90	4.02	18.02	18.23
3-Hydroxymethylpyridine *N*-oxide	$CuLCl_2$	27.76	27.76	2.57	2.72	5.31	5.40	24.36	24.48
	$CuLBr_2$	20.46	20.68	2.07	2.02	4.05	4.02	18.22	18.23
4-Hydroxymethylpyridine *N*-oxide	$CuLCl_2$	28.01	27.76	2.73	2.72	5.44	5.40	24.42	24.48
	$CuLBr_2$	20.98	20.68	2.01	2.02	4.07	4.02	18.26	18.23
Quinoline *N*-oxide	$CuLCl_2$	38.73	38.66	2.46	2.52	5.15	5.01	22.74	22.72
	$CuLBr_2$	29.41	29.33	1.89	1.91	3.78	3.80	17.27	17.24
4-Methylquinoline *N*-oxide	$CuLCl_2$	41.12	40.90	2.90	3.09	4.59	4.77	21.40	21.64
	$CuLBr_2$	31.77	31.40	2.21	2.37	3.56	3.66	16.33	16.61
Isoquinoline *N*-oxide	$CuLCl_2$	38.57	38.66	2.53	2.52	5.02	5.01	22.52	22.72
	$CuLBr_2$	29.41	29.33	2.02	1.91	3.63	3.80	17.15	17.24

eliminates the possible complexity in the demagnetization mechanism which may occur if a similar coordinate bond were part of a chelate ring.

2) The electronic effect of the substituents on the pyridine ring should transmit directly to the N-oxide oxygen atom which is an atom in the superexchange pathway, Cu–O–Cu.

3) Pyridine N-oxide is presently the only ligand which is monodentate and gives dimeric copper(II) complexes with a variety of substituents on the pyridine ring. As the experimental data for these pyridine N-oxide complexes have accumulated, it has become obvious that the relation between the magnetic properties of the complexes and the electronic nature of the substituents is much more complex than was anticipated earlier.

In order to clarify some of the causes which bring about a lack of correlation between the demagnetization or the d–d band positions and the electronic effects of the substituents, we have extended our previous studies.*[1,6] We have recently prepared a number of copper(II) halide complexes of pyridine N-oxides with a variety of electron-donating and electron-withdrawing substituents attached in 2-, 3- and 4-positions of pyridine ring. For purposes of comparison, some monomeric complexes of the type, $[Cu(X\text{-}PyO)_4](ClO_4)_2$, were also prepared and their spectral properties were characterized in connection with the Hammett's constants.

Experimental

Materials. Pyridine N-oxide, and 2-hydroxymethyl-, 3-hydroxymethyl-, 4-hydroxymethyl-, 4-methyl- and 4-nitro-pyridine N-oxides were obtained commercially. 3-Chloro-, 3-bromo-, 3-acetyl-, 4-acetyl-, 3-cyano-, 4-cyano-, 3-hydroxy-, 2-ethyl-, 3-ethyl- and 4-ethylpyridine N-oxides, and nicotinic acid-, ethylnicotinate-, ethylisonicotinate-, 2,4-lutidine-, quinoline-, 4-methylquinoline- and isoquinoline-N-oxides were prepared by oxidation of the corresponding pyridines by the method of Ochiai.[7] 4-Hydroxypyridine N-oxide was prepared by reaction of 4-nitropyridine N-oxide with dimethylaniline according to Ochiai's direction.[7] All these ligand materials were recrystallized from chloroform or benzene for use of the preparation of the copper(II) complexes.

The Preparation of the Copper(II) Complexes. *1 : 1 Complexes.* These complexes were prepared by heating the mixture of anhydrous copper(II) halide and the stoichiometric amount of ligand in ethanol on a hot plate for a short time. Purification was obtained by recrystallizing them from ethanol or N,N-dimethylformamide. Copper(II) chloride complexes with 2-hydroxymethylpyridine N-oxide, which crystallized as a yellowish green material from ethanol, exhibited a

Table 2. Magnetic data of 1 : 1 complexes

Ligand	$CuCl_2$ complex				$CuBr_2$ complex			
	$10^6 \cdot \chi_g$[a] (c.g.s., e.m.u.)	Temp. (°K)	μ_{eff} (B.M.)	$\mu_{eff}^{25°C}$ (B.M.)	$10^6 \cdot \chi_g$[a] (c.g.s., e.m.u.)	Temp. (°K)	μ_{eff} (B.M.)	$\mu_{eff}^{25°C}$ (B.M.)
3-Cl·PyO[b]	−0.12	297	0.46	0.46	−0.31	291	0.25	0.27
3-Br·PyO					−0.19	287	0.42	0.45
3-COOH·PyO	0.00	294	0.53	0.54				
$3\text{-}COOC_2H_5\cdot PyO$	−0.14	297	0.48	0.48	−0.24	297	0.39	0.39
$4\text{-}COOC_2H_5\cdot PyO$	−0.12	297	0.50	0.50	−0.32	296	0.28	0.29
$3\text{-}CH_3CO\cdot PyO$	0.02	303	0.58	0.57	−0.11	304	0.52	0.50
$4\text{-}NO_2\cdot PyO$	1.72	303	1.21	1.20	−0.12	298	0.45	0.45
4-CN·PyO	1.05	296	0.95	0.96	0.38	297	0.79	0.79
3-OH·PyO	−0.24	286	0.33	0.37	−0.22	287	0.34	0.37
4-OH·PyO	−0.29	291	0.31	0.33	−0.34	294	0.22	0.23
$2\text{-}C_2H_5\cdot PyO$	−0.35	286	0.29	0.32	−0.32	286	0.28	0.31
$3\text{-}C_2H_5\cdot PyO$	−0.19	286	0.42	0.46	−0.27	288	0.34	0.37
$4\text{-}C_2H_5\cdot PyO$	0.03	285	0.55	0.59	−0.24	286	0.38	0.41
$2,4\text{-}(CH_3)_2\cdot PyO$	−0.29	289	0.34	0.37	−0.29	289	0.32	0.35
$2\text{-}CH_2OH\cdot PyO$	−0.24	292	0.37	0.39	−0.24	286	0.36	0.40
$3\text{-}CH_2OH\cdot PyO$	−0.08	292	0.48	0.50	−0.22	283	0.38	0.42
$4\text{-}CH_2OH\cdot PyO$	−0.09	281	0.47	0.53	−0.20	285	0.40	0.44
QNO[c]	−0.35	286	0.30	0.33	−0.33	284	0.29	0.33
$4\text{-}CH_3\cdot QNO$	−0.32	283	0.36	0.40	−0.34	285	0.30	0.33
iso-QNO	−0.18	280	0.45	0.51	−0.25	284	0.39	0.43

a) magnetic susceptibility per gram b) PyO: pyridine N-oxide c) QNO: quinoline N-oxide

6) Y. Muto and H. B. Jonassen, This Bulletin, **39**, 58 (1966).

7) E. Ochiai, *J. Org. Chem.*, **18**, 548 (1953).

normal magnetic moment, 1.88 B.M. at 11°C. The color of this compound gradually changed to yellow on standing in air for a week. The yellow compound was then transferred to a desiccator over silica gel for one month. After this period a very low magnetic moment, 0.37 B.M. at 19°C, was observed.*2

1 : 4 Complexes. These complexes were precipitated immediately from the ethanol solution of stoichiometric mixtures of copper(II) perchlorate hexahydrate and the ligands. They were purified by repeated washing with ethanol.

The preparation was repeated at least twice for each of the 1 : 1 and 1 : 4 complexes. The results of elementary analysis of the complexes are listed in Table 1.

Magnetic Susceptibility Determinations. These data were obtained by the Gouy method at room temperature. The effective magnetic moment, μ_{eff}, per copper atom was calculated from the expression $\mu_{eff} = 2.83\sqrt{\chi_M \cdot T}$ B.M. where χ_M is the molar susceptibility corrected using Pascal's constants[8] for the diamagnetism of the other atoms in the compounds. The magnetic moments observed at room temperature were corrected for minor room temperature variations to those at 25°C, $\mu_{eff}^{25°C}$, by using Bleaney and Bowers' equation[9] assuming $g=2.2$.[10] These results are presented in detail in Table 2.

TABLE 3. d–d BAND MAXIMA OF 1 : 1 COMPLEXES

Ligand	$CuCl_2$ complex λ_{max} (mμ)	$CuBr_2$ complex λ_{max} (mμ)
3-Cl·PyO	820	775
3-Br·PyO		825
3-COOH·PyO	885	
3-$COOC_2H_5$·PyO	825	820*
4-$COOC_2H_5$·PyO	830*	790*
3-CH_3CO·PyO	900*	840
4-NO_2·PyO	1100*	830
4-CN·PyO	805	800
3-OH·PyO	795	780
2-C_2H_5·PyO	763	765*
3-C_2H_5·PyO	810*	812
4-C_2H_5·PyO	820*	820
2,4-$(CH_3)_2$·PyO	765	760
2-CH_2OH·PyO	800*	812
3-CH_2OH·PyO	813	817
4-CH_2OH·PyO	818*	823
QNO	733	735
4-CH_3·QNO	750	745
iso-QNO	810	807

* broad

TABLE 4. d–d BAND MAXIMA OF 1 : 4 COMPLEXES

Complex	λ_{max} (mμ)
$(PyO)_4Cu(ClO_4)_2$	675
$(4\text{-}CH_3\cdot PyO)_4Cu(ClO_4)_2$	670
$(3\text{-}Cl\cdot PyO)_4Cu(ClO_4)_2$	695
$(3\text{-}COOC_2H_5\cdot PyO)_4Cu(ClO_4)_2$	685
$(4\text{-}COOC_2H_5\cdot PyO)_4Cu(ClO_4)_2$	770
$(3\text{-}CH_3CO\cdot PyO)_4Cu(ClO_4)_2$	685
$(4\text{-}CH_3CO\cdot PyO)_4Cu(ClO_4)_2$	760
$(4\text{-}NO_2\cdot PyO)_4Cu(ClO_4)_2$	710
$(3\text{-}CN\cdot PyO)_4Cu(ClO_4)_2$	700
$(4\text{-}CN\cdot PyO)_4Cu(ClO_4)_2$	735

Diffuse Reflectance Spectra. The diffuse reflectance spectra of some compounds were measured in 400—1200 mμ region on a Hitachi spectrophotometer of Model EPU-2A. Magnesium oxide was used as the standard of light reflectance and as the base material to dilute the compounds to obtain appropriate intensities in the reflected light. The spectra of other compounds were recorded in 340—1000 mμ region on a Hitachi spectrophotometer of Model EPS-3T without diluting the compounds with the base. The band maxima are recorded in Tables 3 and 4.

Results and Discussion

I. Nonapplicability of Hammett's Rule to Dimeric Complexes. The early studies of the effect of the ring substituent on the spin-spin coupling mechanism in the dimeric copper(II) halide complexes with pyridine *N*-oxides, the electronic natures of the substituents seemed to correlate well with the demagnetization.[6,11,12] However, the magnetic data of recently prepared complexes with a variety of substituents on the 3- and 4-positions in the pyridine ring revealed that no definite correlation exists between the electronic nature of the substituents in terms of Hammett's σ constants and the extent of the demagnetization or the d–d band positions.

Although some doubt had been thrown on the validity of the commonly used Hammett substituent constant,[13,14] Jaffé and coworkers[15] reported a linear relationship between the basicity

*2 The details of the two modifications with normal and subnormal magnetic moments will be reported shortly.

8) G. Foëx, C. J. Gorter and L. J. Smits, "Constantes Sélectionnées, Diamagnétisme et Paramagnétisme, Relaxation Paramagnétique," Masson & Cie, Paris (1957), p. 222.

9) B. Bleaney and K. D. Bowers, *Proc. Roy. Soc. (London)*, **A214**, 451 (1952).

10) M. Kato, Y. Muto, H. B. Jonassen, K. Imai and A. Harano, This Bulletin, **41**, 1864 (1968).

11) W. E. Hatfield and J. S. Paschal, *J. Am. Chem. Soc.*, **86**, 3888 (1964).

12) W. E. Hatfield and J. C. Morrison, *Inorg. Chem.*, **5**, 1390 (1966).

13) Y. Yukawa and Y. Tsuno, *Nippon Kagaku Zasshi (J. Chem. Soc. Japan, Pure Chem. Sect.)*, **86**, 873 (1965).

14) Y. Yukawa, *Kagaku to Kogyo (Chem. & Chem. Ind., Tokyo)*, **18**, 1298 (1965).

15) H. H. Jaffé and G. O. Doak, *J. Am. Chem. Soc.*, **77**, 4441 (1955).

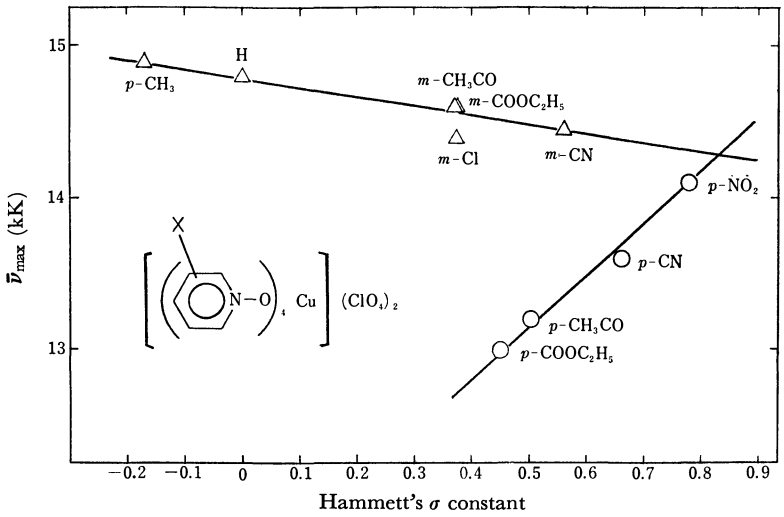

Fig. 1. The plot of the wave numbers ($\bar{\nu}_{max}$ in kK) of d–d band positions of copper(II) perchlorates with substituted pyridine *N*-oxides against Hammett's σ constant.

of a series of substituted pyridine *N*-oxides and the σ values.

Among the infrared active modes of substituted pyridine *N*-oxides,[16-18] Shindo[18] found that the N–O stretching frequencies of a variety of pyridine *N*-oxides derivatives correlate well with the Hammett's constant. Recently Kubota and Miyazaki[19] reported that a plot of the half-wave reduction potentials of substituted pyridine *N*-oxides against Hammett's σ constant gave a good linear relation.

II. Validity of Hammett's Rule in Monomeric Complexes. Recently, metal complexes with pyridine *N*-oxides were reported to confirm the correlation of physicochemical properties of the complexes with the electronic nature of the substituents.[6,11-12,20-27] The correlations were studied for complexes with substituents at the 4-position of the *N*-oxide molecules, where the electronic effect is transmitted to the *N*-oxide oxygen atom by a mesomeric mechanism. However, no test of correlations has been made for the copper(II) complexes with substituents attached in 3-position of the pyridine ring. In these studies furthermore the substituent constants used were σ in some cases and σ^+ or σ^- in others.[28] Hatfield and his coworkers[27] prepared the complexes of the type, $[Cu(X\text{-}PyO)_4](ClO_4)_2$, with X at 4-position in pyridine ring. They found that the d–d bands correlated with the σ^+ value of X.

We prepared the same type of complexes with X of electron-donating and electron-withdrawing nature at the 4- and 3-positions in pyridine ring. For these complexes, two linear relations between the d–d band positions, $\bar{\nu}_{max}$(kK), and Hammett's σ constant, were observed. One has a negative and the other a positive slope (*cf.* Fig. 1).[29] The line with the negative slope is for the compounds with substituents in the 3-position. This line further includes two more compounds, one with *p*-CH_3 and the other with H (standard). This linear relation in this case can be explained if it is assumed that the ligand field band positions are determined mainly by the electron density of the coordinating

16) A. R. Katritzky and J. N. Gardner, *J. Chem. Soc.*, **1958**, 2192.
17) A. R. Katritzky, A. M. Monro, J. A. T. Beard, D. P. Dearnaley and N. J. Earl, *ibid.*, **1958**, 2182.
18) H. Shindo, *Chem. & Pharm. Bull.*, **6**, 117 (1958).
19) T. Kubota and H. Miyazaki, This Bulletin, **39**, 2057 (1966).
20) S. I. Shupack and M. Orchin, *J. Am. Chem. Soc.*, **85**, 902 (1963).
21) W. E. Hatfield, Y. Muto, H. B. Jonassen and J. S. Paschal, *Inorg. Chem.*, **4**, 97 (1965).
22) P. D. Kaplan and M. Orchin, *ibid.*, **4**, 1393 (1965).
23) D. W. Herlocker, R. S. Drago and V. I. Meek, *ibid.*, **5**, 2009 (1966).
24) D. S. Dyer and R. O. Ragsdale, *ibid.*, **6**, 8 (1967).
25) F. E. Dickson, E. W. Gowling and F. F. Bentley, *ibid.*, **6**, 1099 (1967).
26) P. Schmidt and M. Orchin, *ibid.*, **6**, 1260 (1967).
27) R. Whyman, W. E. Hatfield and J. S. Paschal, *Inorg. Chim. Acta*, **1**, 113 (1967).
28) J. Hine, "Physical Organic Chemistry," 2nd ed., McGraw-Hill Book Co., INC., New York, N. Y. (1962), p. 81.
29) J. R. Joy and M. Orchin, *J. Am. Chem. Soc.*, **81**, 305 (1959).

oxygen atoms. Therefore as Hammett's σ constant decreases, these substituents produce larger electron densities on the oxygen atoms. This in turn leads to stronger ligand fields accompanied by higher wave numbers for the ligand field bands.

The line with the positive slope is for the compounds with 4-substituents of great electron-withdrawing power. This linear relation can be explained if it is assumed that back-bonding from the metal to the π-electron systems of ligand molecules[23,30-33] determines the band positions. The back-bonding is considered to take place through resonance structure B,[6] the weight of which should increase with the increase in the electron-withdrawing nature of the substituents.

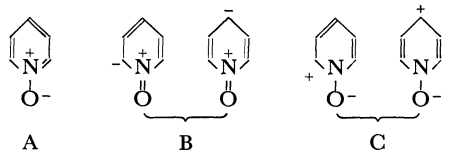

A B C

III. Linear Relation between d–d Band Positions and Corrected Magnetic Moments.

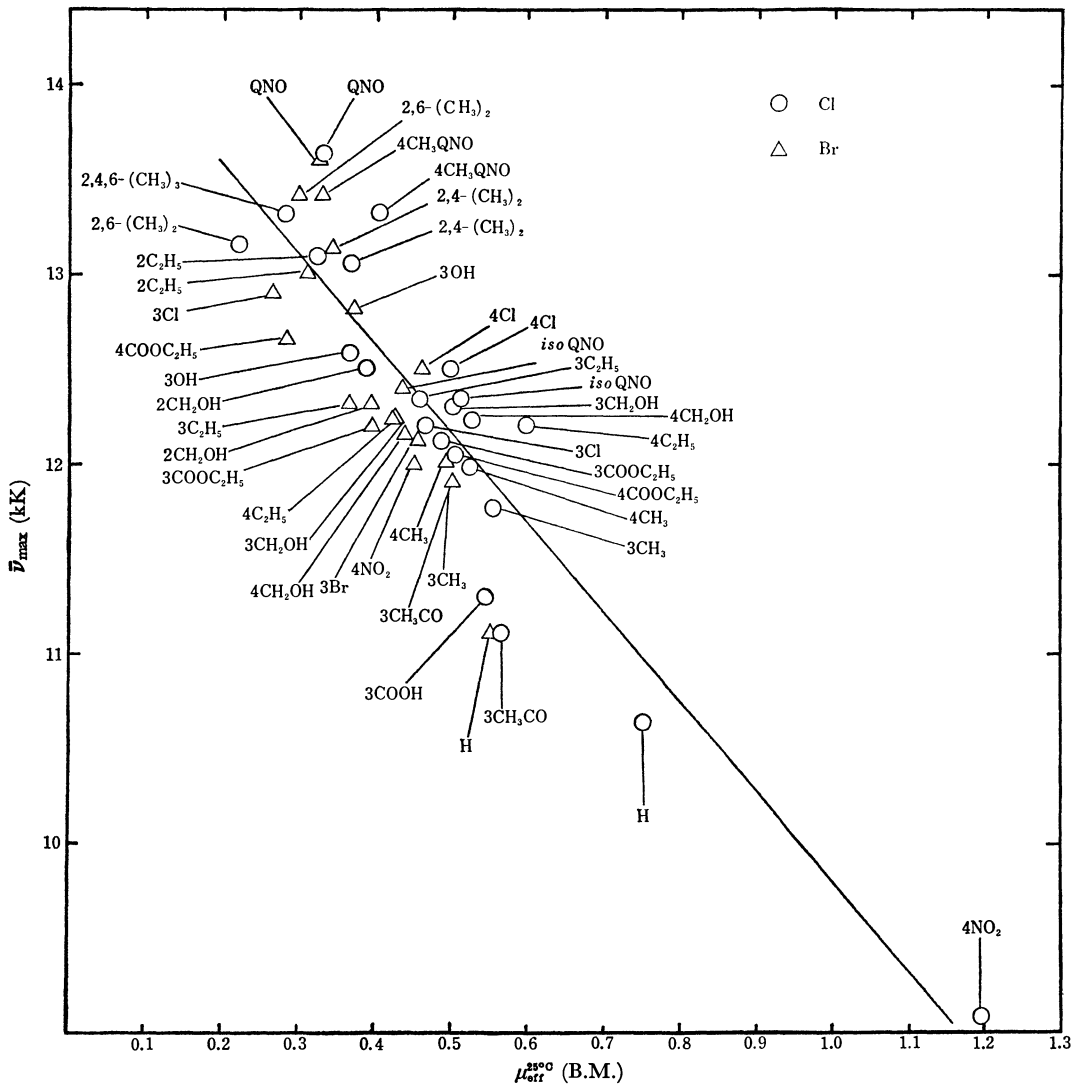

Fig. 2. The plot of the wave numbers ($\bar{\nu}_{max}$ in kK) of d–d bands of copper(II) halide complexes with substituted pyridine *N*-oxides against the corrected magnetic moments ($\mu_{eff}^{25°C}$ in B.M.).
○ and △ indicate the chloro and bromo complexes respectively.

30) N. S. Gill, R. H. Nuttall, D. E. Scaife and D. W. A. Sharp, *J. Inorg. Nucl. Chem.*, **18**, 79 (1961).
31) W. R. May and M. M. Jones, *ibid.*, **24**, 511 (1962).
32) M. Goldstein, E. F. Mooney, A. Anderson and H. A. Gebbie, *Spectrochim. Acta*, **21**, 105 (1965).
33) L. Morpurgo and R. J. P. Williams, *J. Chem. Soc.*, (*A*), **1966**, 73.

The nonapplicability of Hammett's rule in the dimeric copper(II) halide complexes with pyridine *N*-oxides, could possibly indicate that no correlation between any physicochemical quantities exist. However, it was found that both for bromo and chloro complexes, a linear relation exists between the d–d band positions, $\tilde{\nu}_{max}$(kK), and the corrected magnetic moments, $\mu_{eff}^{25°C}$ (*cf.* Fig. 2). It would be more favorable to use J values, the separation energy between singlet and triplet state than $\mu_{eff}^{25°C}$. J values calculated from the observed magnetic moments assuming $g=2.2$, fitted a good linear relation with the d–d band positions ($\tilde{\nu}_{max}$ in kK). However, J values were not used in this paper because the J values calculated as above may be somewhat different from those determined from χ *versus* T curves. On the other hand, the values of $\mu_{eff}^{25°C}$ which were calculated from the χ values observed for the same compound at different temperatures, coincided well with each other within experimental errors.

This relation shows that greater demagnetization is accompanied with greater shift of d–d bands toward shorter wavelengths. This linear relationship between the ligand field bands and the magnetic moments can be cited as a magnetochemical support for the recent correlation of the spectrochemical series to the idea of symmetry-restricted covalency.[34-37] The spin-spin coupling mechanism should occur through the overlap of metal and ligand orbitals, giving a very symmetrically restricted covalency.

IV. Reasons for the Nonapplicability of Hammett's Rule in Dimeric Complexes. (*A*) *Steric Effects Previously Observed.* It was observed that, in many cases, irrespective of the polar effect of the substituents, the magnetic moments of complexes with 3-substituted ligands are smaller than those of the corresponding compounds with 4-substituted ligands. This observation seems to suggest a mechanism by which a greater magnetic interaction is produced between the copper(II) ions in a pair when a substituent is attached at a position closer to the central metal ion.

A similar trend was obtained in the study of the dimeric copper(II) complexes of the formula, $[Cu(\overset{2}{O}\cdot C_6H_4\cdot\overset{1}{C}H{=}N{-}R)Cl]_2$, where R is a mono- or di-substituted aryl group (*cf.* Fig. 3).[38,39]

Chatt and Shaw[40,41] described the metal complexes of the types, $[(PR'_3)_2NiRX]$ and $[(PR'_3)_2MR_2]$, where M=Ni, Co, Fe, and R=substituted aryl or

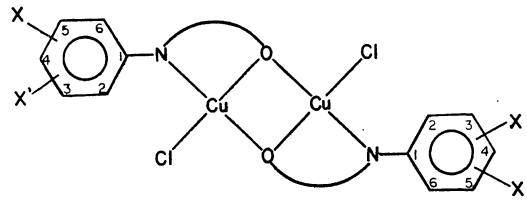

Fig. 3. X=H, Cl, CH_3 and NO_2

some other aromatic groups. They observed that the stability of these complexes has much increased when substituents were attached in the *ortho*-position of R. One of the causes for such additional stabilization of the *ortho*-substituted aryl complexes compared to the meta- or para-substituted aryl compounds, was attributed to the shielding effect of the metal atoms by the *ortho*-substituents.

Such shielding becomes most effective when the aryl group is rotated about the M–C bond such that its plane is perpendicular to that of the complex. Such perpendicular orientations of the aromatic ring with respect to the plane of the complex were observed in molecular models constructed for Chatt's complexes and those reported in this study. Such a stereochemical arrangement is postulated to play an important part in the stabilization of these complexes.

A stabilization of metal complexes by *ortho*-substituents was also observed by Yamada and Miki[42] in their mixed complexes of copper(II) with succinimide and picolines or lutidines.

(*B*) *Recent Results Indicative of Steric Effects.* In order to examine the contribution of the steric effect of substituents on the demagnetization or the d–d band shifts the effect of substituting methyl and ethyl groups in the 2-, 3- and 4-positions was first compared. The methyl group has a greater electron donating power than ethyl group at the 4-position. The Hammett's σ constants of these groups at this position are -0.170 and -0.151 respectively. In the 3-position, two σ values are proposed for ethyl group, -0.043 and -0.07.[43,44] The smaller value, -0.07, is nearly the same as that for the 3-methyl group, -0.069. The methyl group should therefore have almost the same or

34) C. K. Jørgensen, "Absorption Spectra and Chemical Bonding in Complexes," Pergamon Press, New York, N. Y. (1962).

35) C. K. Jørgensen, "Progress in Inorganic Chemistry," Vol. IV, ed. by F. A. Cotton, Interscience Publishers, New York, N. Y. (1962), p. 73.

36) S. Kida, *Kagaku*, **20**, 510 (1965).

37) S. Yamada and S. Komorita, *Kagaku no Ryoiki*, **20**, 645 (1966).

38) M. Kato, Y. Muto, H. N. Ramaswamy, H. B. Jonassen and K. Imai, paper presented at the 16th Conference on Coordination Chemistry of the Chemical Society of Japan, Tokyo, December, 1966, Proceedings, p. 68.

39) Y. Muto, M. Kato, H. B. Jonassen and K. Imai, unpublished data.

40) J. Chatt and B. L. Shaw, *J. Chem. Soc.*, **1960**, 1718.

41) J. Chatt and B. L. Shaw, *ibid.*, **1961**, 285.

42) S. Miki and S. Yamada, This Bulletin, **37**, 1044 (1964).

43) H. H. Jaffé, *Chem. Revs.*, **53**, 191 (1953).

44) D. H. McDaniel and H. C. Brown, *J. Org. Chem.*, **23**, 420 (1958).

a greater electron-donating power than ethyl group in the 3-position. Shindo and Kubota successfully correlated the Hammett's σ values with the N–O stretching frequencies[18] and the half-wave reduction potentials[19] of substituted pyridine *N*-oxides. They used the larger σ value, -0.043, for the 3-substituted ethyl group. The ethyl group which has less electron-donating power but a bulkier size produces a larger effect on the demagnetization or d–d band blue shift than the methyl group which has greater electron-donating power but smaller size. This indicates that the substituent effect in the dimeric copper(II) complexes is at least partly due to a steric factor. Furthermore, since the nature of the polar effect of alkyl groups is mainly inductive, the interpretation of the experimental results observed for the compounds with these substituents is less ambiguous than for those compounds where the substituents have both inductive and mesomeric properties.

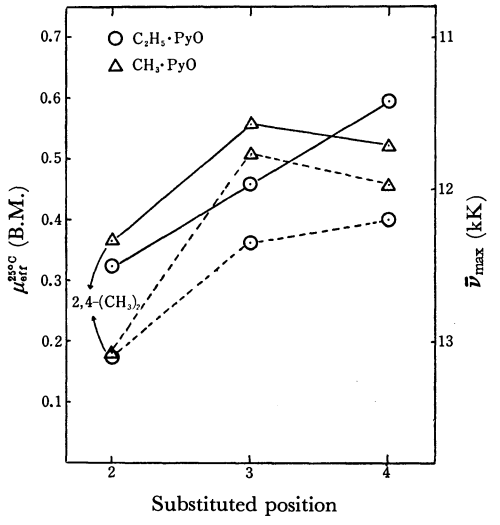

Fig. 4. Variations of magnetic moments ($\mu_{eff}^{25°C}$ in B.M.) and d–d band positions ($\bar{\nu}_{max}$ in kK) of copper(II) chloride complexes with methyl- and ethyl-pyridine *N*-oxides with substituted positions. Solid line is for magnetic moments and dashed line for d–d band positions. △ and ○ indicate complexes with methyl- and ethyl-pyridine *N*-oxides respectively.

The experimental results for chloro complexes are graphically given in Fig. 4. In the 4-position, the methyl group has a greater effect on the demagnetization and the d–d band blue shift than the ethyl group. This is as expected on the basis of the polar effect of substituents in terms of Hammett's constant. The steric effect of the ethyl group which should be larger because of its larger size still however seems not to be operative.

At the 3-position, the magnetic moment of the methyl compound increases to 0.55 B.M. from 0.52 B.M. of the 4-methyl compound as expected from the Hammett's σ values of this substituent. This indicates that, at this position, the steric effect of methyl group can not be observed.

However, at the same position, the magnetic moment value of the 3-ethyl compound decreases from that of the 4-ethyl compound, indicating a larger demagnetization in the 3-substituted compound. The demagnetization of 3-ethyl compound is larger compared to those of 4-methyl and 3-methyl compounds. These observations definitely indicate that the ethyl group in these complexes exerts a steric effect at 3-position. It is remarkable that of substituents with large size, they produce a larger demagnetization, even in the 4-position, than in the parent complex with pyridine *N*-oxide even when their electronic nature is electron-withdrawing in both inductive and mesomeric effects as is the case for $COOC_2H_5$, CH_3CO, *etc.* This seems to indicate stronger metal-ligand bonds in these complexes. Such strengthening of the metal-ligand bonds may occur through back-bonding, metal to ligand, which was observed in the monomeric compounds with pyridine *N*-oxides having the same electron-withdrawing substituents (*cf.* sect. II). However, the established structure of the parent complex is hardly suitable for such back-bonding mechanism (*cf.* sect. VII).

For substitution at 2-position, 2,4-dimethyl compounds were studied instead of the 2-methyl compounds because of the synthetic difficulty of preparing the pure 2-methyl compounds.[45-47]

The magnetic moment of this compound is much smaller than that of the 3-compound as well as that of the 4-compound. It is obvious that the methyl group in the 2-position has a large steric effect on the demagnetization phenomenon.

The magnetic moment of the 2-ethyl compound, 0.32 B.M., is even smaller than that of 2,4-dimethyl-compound, 0.37 B.M. The demagnetization effect of the 4-methyl group in the chloride complexes is estimated to be about 0.2 B.M. in a range from 0.5 to 0.7 B.M., the difference between the values of the 4-methyl and that of the parent complexes. These data indicate that in these dimeric complexes the 2-ethyl group because of its greater steric effect exerts a much greater demagnetization effect than the 2-methyl group.

Molecular framework models were built according to the established structures of the parent complex.[4,5] They indicate that when ethyl groups are attached in the 2-position of the pyridine rings which are almost perpendicular to the copper oxygen plane

45) M. R. Kidd, R. S. Sager and W. H. Watson, *Inorg. Chem.*, **6**, 946 (1967).
46) R. Whyman and W. E. Hatfield, *ibid.*, **6**, 1859 (1967).
47) Y. Muto, unpublished data.

they are located above or below the plane shielding the fifth and the sixth coordination site (*cf.* Fig. 9).

In accordance with the linear relation between the d–d bands and the magnetic moments, the d–d band positions of the methyl and ethyl compounds vary in the same way as the magnetic moments, as the substitution positions are changed. In contrast to the smooth variation in magnetic moments with substituted positions, the blue shift of d–d bands is much greater between 2- and 3-positions than between 3- and 4-positions, indicating that the ligand fields of 2-alkyl compounds are much greater than those of 3- and 4-alkyl compounds. This becomes apparent in the reflectance spectra of copper(II) chlorides with ethylpyridine *N*-oxides (*cf.* Fig. 5). Such discrepancy between the extents of the variations in magnetic moments and d–d band positions should be improved if the energy differences between singlet and triplet states were used instead of the magnetic moments.

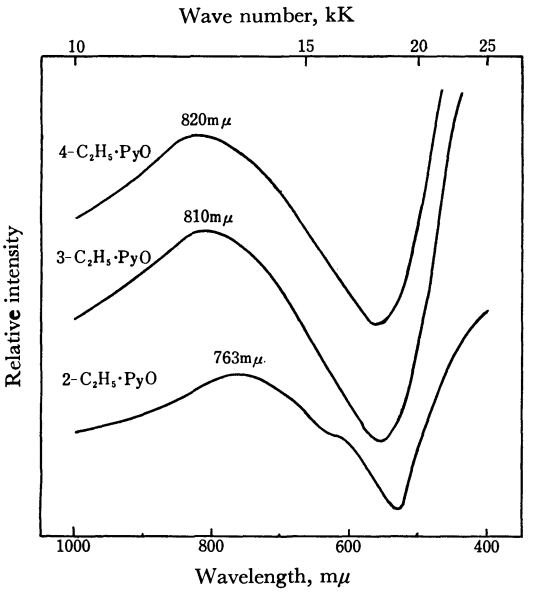

Fig. 5. Reflectance spectra of (ethylpyridine *N*-oxide)-copper(II) chloride.

The variations in spectral and magnetic properties of bromo complexes with changes in substitution positions are essentially the same as those observed for the chloro complexes. However, some interesting differences exist between bromo and chloro complexes in the relative magnitudes of the magnetic moments and the d–d band positions: 1. The magnetic moments of the 4-ethyl bromo complex is smaller than that of the 4-methyl bromo complex. 2. The slope of the line for the variations of magnetic moments with substitution positions is smaller for bromo complexes than for chloro complexes.

(*C*) *Interpretation of Steric Effect.* Yamada and Miki[48] reported that the d–d band of bis(*N*,*N*-diethylethylenediamine)copper(II) perchlorate appears at a much shorter wavelength than expected from its position in the spectrochemical series. They attributed this to the special steric condition of the ligand, which will make it more difficult for other ligands or molecules to approach the fifth and sixth coordination sites of copper(II) ion. It is well known that the quadri-coordinate, planar type of copper(II) complexes display the ligand field bands at much shorter wavelengths than those of sexa-coordinate or pseudo-sexa-coordinate copper(II) complexes. The very large value of the tetragonality ratio $R(\gamma_{Cu}/\gamma_{N_i})$ for this compound was pointed out by Jørgensen.[49,50] It is very probable that on the basis of Pauling's electroneutrality principle[51] the increase in the tetragonality of the complex with *N*-alkylethylenediamine compared to that of the parent ethylenediamine complex produces an increase in the strength of the coordinate bonds in the CuN_4 plane. If bonds to the fifth and sixth coordination position perpendicular to the CuN_4 plane which are present to some extent in the parent ethylenediamine complex, are broken or much weakened, extra electron migration from the ligands to the metal should occur through the bonds in the CuN_4 plane. According to the electroneutrality principle, any rearrangement of electron migration must keep the total electron flow-in as constant as possible.

This can also be described in terms of electron affinity. When the longer bonds perpendicular to the CuN_4 plane present in the parent compound are broken or weakened for some reason, the electron affinity of the metal should be increased. Such an increase in electron affinity of the metal, in turn, increases the strength of the four bonds in the plane.

In dimeric copper(II) halide complexes with pyridine *N*-oxides, the increased tetragonality of the complex due to the steric effect of the substituent, will produce stronger metal-ligand bonds, through which the super-exchange mechanism operates. This steric effect may provide a direct way for the determination of the variation of coordinate bond strength caused by changes in the stereochemistry of complexes. This steric factor which weakens the influence of other ions or mole-

48) S. Yamada and S. Miki, This Bulletin, **36**, 680 (1963).
49) W. E. Hatfield, T. S. Piper and U. Klabunde, *Inorg. Chem.*, **2**, 629 (1963).
50) C. K. Jørgensen, "Biochemistry of Copper," ed. by J. Peisach, P. Aisen and W. E. Blumberg, Academic Press Inc., New York, N. Y. (1966), p. 1.
51) L. Pauling, "The Nature of the Chemical Bond," 3rd ed., Cornell Univ. Press, Ithaca, New York (1960), p. 172.

cules on the fifth or sixth coordination position does not seem to be the only cause bringing about an increase in metal-ligand bond strength or the d–d band blue shift in copper(II) halide pyridine *N*-oxide complexes. The other factor seems to be due to the partial tetrahedral stereochemistry of these complexes which may call for less orbital overlap between metal and ligand. However, as the tetragonality increases with various substitutions on the pyridine ring, the tetrahedral nature decreases.

The combination of these two effects – the steric effect and the electronic effects of the substituents on the pyridine ring – are the prime factor which determines the nonapplicability of Hammett's rule to the magnetic and spectral properties of these dimeric copper(II) halide pyridine *N*-oxide complexes. The enhancement of stability of planar nickel(II) complexes by steric conditions compared to the octahedral ones have also been discussed recently.[52]

V. Further Experiments Indicative of the Steric Effect. (*A*) *Complexes with Quinoline N-Oxide.* In order to examine the steric effect in complexes with ligands other than pyridine *N*-oxides, copper(II) halide complexes with quinoline *N*-oxide, 4-methylquinoline *N*-oxide and isoquinoline *N*-oxide were prepared. The magnetic moments of the complexes with quinoline *N*-oxide, a ligand corresponding 2,3-disubstituted pyridine *N*-oxide, are smaller than those of the complexes with isoquinoline *N*-oxide, a ligand corresponding 3,4-disubstituted pyridine *N*-oxide. The behavior of the d–d band shift of these complexes followed the changes in the magnetic moments, as is demonstrated for bromo complexes in Fig. 6. On the other hand, however, the magnetic and spectral properties of 4-methylquinoline *N*-oxide complexes are not those expected from both steric and electronic considerations. Even though 4-methylquinoline *N*-oxide has a greater steric factor and greater electron-donating power than quinoline *N*-oxide, its complexes show smaller demagnetization and d–d band positions at larger wavelengths than those of quinoline *N*-oxide. Hatfield and coworkers[53,54] encountered the same situation in their study of methyl quinoline complexes.

One possible explanation for this may be that steric factors other than those mentioned above are encountered. A methyl group attached to a ligand of large size probably interferes with the smooth packing in the crystal compared to that of the complex of the parent ligand molecule. Such strains would also produce strains in the chemical bonding of the complex.

(*B*) *Complexes with Hydroxymethylpyridine N-Oxides.* If the group substituted on the pyridine ring also has some coordinating ability, the substituent effect might be opposed by the coordination effect. Under such conditions very little change in physical properties might be observed as the substitution positions on the ring are changed.

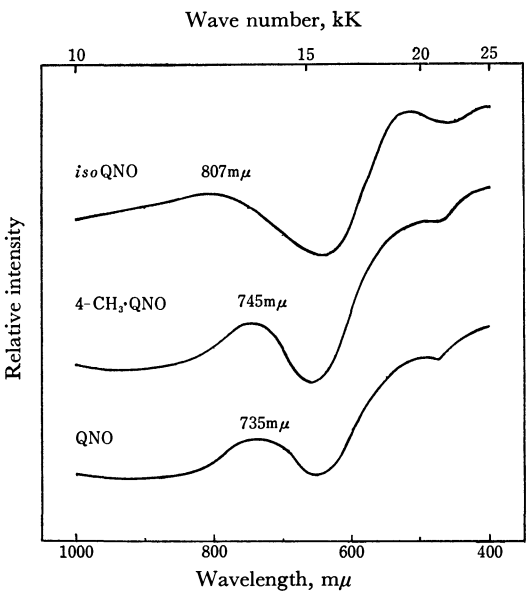

Fig. 6. Reflectance spectra of (quinoline *N*-oxide)-copper(II) bromides.

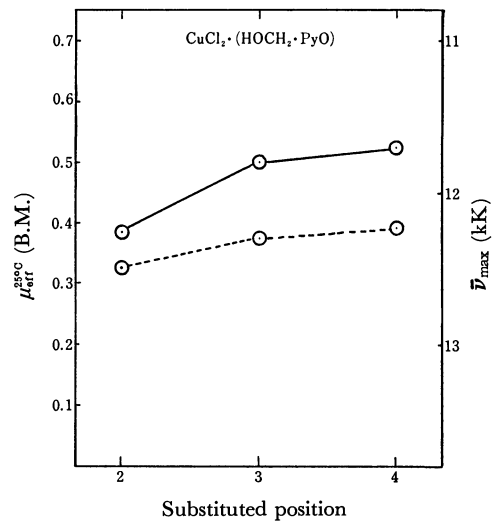

Fig. 7. Variations of magnetic moments ($\mu_{eff}^{25°C}$ in B.M.) and d–d band positions ($\bar{\nu}_{max}$ in kK) of (hydroxymethylpyridine *N*-oxide)-copper(II) chlorides with substituted positions. Solid line is for magnetic moments and dashed line for d–d band positions.

52) C. K. Jørgensen, "Inorganic Complexes," Academic Press Inc., New York, N. Y. (1963), p. 69.

53) W. E. Hatfield, D. B. Copley and R. Whyman, *Inorg. Nucl. Chem. Letters*, **2**, 373 (1966).

54) R. Whyman, D. B. Copley and W. E. Hatfield, *J. Am. Chem. Soc.*, **89**, 3135 (1967).

This was indeed observed for the complexes with hydroxymethylpyridine N-oxide. Figure 7 shows a plot of the data for the chloro complexes. The slopes of the two lines are not as steep as those for the corresponding methyl and ethyl compounds in Fig. 4 indicating that the two effects have at least partially cancelled each other. In Fig. 8 the spectral curves for these complexes are given.

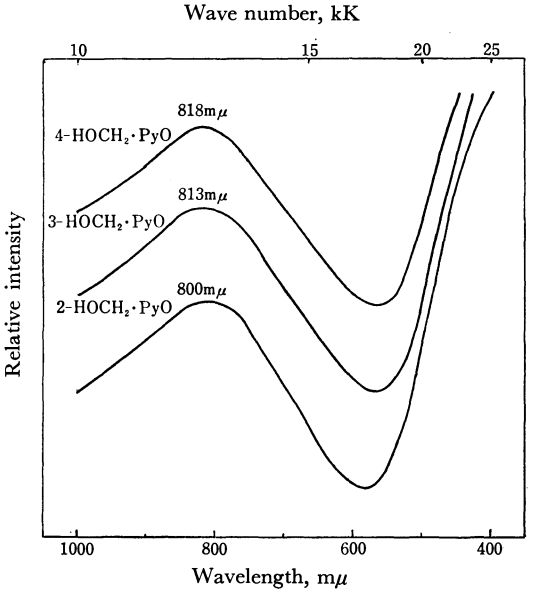

Fig. 8. Reflectance spectra of (hydroxymethylpyridine N-oxide)-copper(II) chlorides.

VI. Influence of Halogen Ions on d-d Band and Magnetic Moment. The influence of halide ions on the d–d band positions and the demagnetization in the chloro and bromo complexes is not what would be expected from the positions of these ions in spectrochemical series.

In almost all cases, the magnetic moments of bromo complexes are smaller than those of the corresponding chloro complexes.*[1f,12] Hatfield and coworkers[12] suggested that this phenomenon may be due to the difference in spin-orbit coupling and temperature independent paramagnetism between the chloro and bromo complexes. In a previous paper,*[1f] we suggested that the difference in nephelauxetic effects[34-37] of the chloride and bromide ions produces such differences in magnetic moments. The greater cloud expanding effect of the bromide ions will produce a greater overlapping of the relevant orbitals of the metal ions and the ligand molecules. This would give a greater covalency in their bonds and should give smaller magnetic moments for the bromo complexes.

Recently, Figgis and Nyholm summarized the contributions of the temperature independent paramagnetism and the spin-orbit coupling in metal complexes.[55,56] With a few exceptions, the d–d bands of bromo complexes with pyridine N-oxides appear at shorter wavelengths than those of the corresponding chloro complexes. The ligand fields of these bromo complexes are larger than those of the corresponding chloro complexes, suggesting smaller contribution, to spin-orbit coupling. The X-ray determinations of crystal structures of Cs_2CuCl_4 and Cs_2CuBr_4[57,58] revealed that these complexes contain flattened tetrahedral configurations with greater flattening for the bromocuprate ion in spite of its larger ionic size and its earlier position in the spectrochemical series.

Recent studies of copper(II) chloride and bromide complexes with aromatic amines revealed that, in some cases, their d–d bands appear where expected from the positions of these ions in the spectrochemical series whereas in others, the band positions appear in the reverse order.[59-63] Uhlig and Staiger[64] reported copper(II) chloride and bromide complexes of aminoalcohols with dimeric structures whose d–d band positions appear from compound to compound in the two different orders in the spectrochemical series as above. An explanation for such anomalous behavior of bromide and chloride ions in the order of spectrochemical series may be found in the recent concept of softness and hardness of metal ions and ligands.[65,66] However, at present, the physical basis of this concept is still somewhat ambiguous which makes a thorough discussion of this phenomenon difficult.[67,68]

55) B. N. Figgis, "Introduction to Ligand Fields," Interscience Publishers, New York, N. Y. (1966), p. 253.
56) R. S. Nyholm, "The Plenary Lecture at Xth International Conference on Coordination Chemistry," Tokyo, September 12, 1967; The Japanese Translation by Y. Saito, *Kagaku to Kogyo (Chem. & Chem. Ind., Tokyo)*, **21**, 338 (1968).
57) L. Helmholz and R. F. Kruh, *J. Am. Chem. Soc.*, **74**, 1176 (1952).
58) B. Morosin and E. C. Lingafelter, *Acta Cryst.*, **13**, 807 (1960).
59) I. S. Ahuja, D. H. Brown, R. H. Nuttall and D. W. A. Sharp, *J. Inorg. Nucl. Chem.*, **27**, 1105 (1965).
60) I. S. Ahuja, D. H. Brown, R. H. Nuttall and D. W. A. Sharp, *ibid.*, **27**, 1625 (1965).
61) W. R. McWhinnie, *ibid.*, **27**. 2573 (1965).
62) A. E. Underhill, *J. Chem. Soc.*, **1965**, 4336.
63) D. E. Billing, A. E. Underhill, D. M. Adams and D. M. Morris, *J. Chem. Soc.*, (*A*), **1966**, 902.
64) E. Uhlig and K. Staiger, *Z. Anorg. Allgem. Chem.*, **346**, 21 (1966).
65) St. Ahrland, "Structure and Bonding," Vol. I, ed. by C. K. Jørgensen, J. B. Neilands, R. S. Nyholm, D. Reinen and R. J. P. Williams, Springer-Verlag, Berlin (1966), p. 207.
66) C. K. Jørgensen, *ibid.*, p. 234.
67) C.K. Jørgensen, The Symposium on Soft and Hard Acids and Bases organized by Professor M. J. Frazer, Northern Polytechnic, Holloway, London N7, March 29—31, 1967; Reports of Cyanamid European Research Institute, Cologny, Switzerland, CERI-TIC-P 130.
68) G. Klopman, the same symposium and the same reports as in Ref. 67; CERI-TIC-P 141.

Ito[69] investigated the anomalous phenomenon that ligands in copper(II) complexes are often out of order in the spectrochemical series. He[70] successfully classified, in conformity with the sense of the series, these ligands into three groups according to the stereochemistry of the complexes; planar-, octahedral- and the intermediate-type. Unfortunately, halide ions were not included in his classification. His classification also does not include the steric shielding effect discussed in this paper.

Since the copper(II) ion has one unpaired electron in any of these stereochemistries, a continuous variation from one stereochemistry to another seems to be possible.[71] Under such conditions, the large size of the bromide ion could display a steric shielding effect different from that of the smaller chloride ion. The cooperation of both factors, large size and cloud expanding, could produce the observed large effect of the bromide ion on the demagnetization and the d–d band blue shift.

It is interesting to note that a plot of the differences of the d–d band positions of the bromide and the chloride complexes with the same ligands, $\bar{\nu}_{max}$ (bromide) $-\bar{\nu}_{max}$ (chloride), against $\bar{\nu}_{max}$ (chloride) decreases from a large value for the 4-nitro compounds to a small value(approximately zero) for the complexes with the largest $\bar{\nu}_{max}$ values. The same type of convergency was observed for the differences in the magnetic moments of chloride and bromide complexes.

VII. Superexchange Pathways. The extent of the spin-spin coupling in dimeric copper(II) complexes varies significantly with the type of structure. Complexes of one structural type may reveal a considerable amount of demagnetization while others of a different structural type display little demagnetization. A part of this demagnetization is attributed to direct metal-metal exchange interaction. The magnetic moments of cupric acetate monohydrate, acetylacetone-mono-(*o*-hydroxyanil)copper(II), and (pyridine *N*-oxide)copper(II) chloride are 1.43 B.M., 1.37 B.M. and 0.77 B.M. at room temperature respectively[72] whereas the metal-metal distances in the established structures are 2.64 Å, 2.99 Å and 3.25 Å respectively. This fact seems to indicate that the observed demagnetization for copper(II) halide complexes with pyridine *N*-oxides is mainly produced by a superexchange mechanism involving bridging oxygen atoms. It is rather surprising that these pyridine *N*-oxide complexes reveal very low magnetic moments despite the fact that they contain rather weak metal-ligand bondings through which a superexchange mechansim must operate. One of the factors which enhances the electron exchange must be the magnitude of orbital-overlap between the related atoms or ions existing in the superexchange pathway.

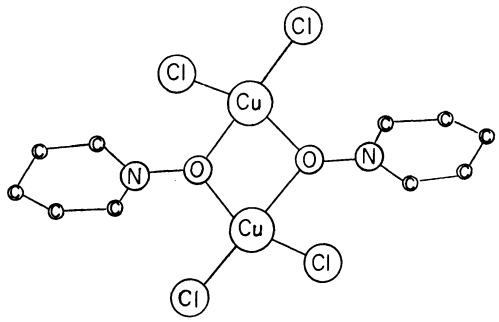

Fig. 9. Structure of (pyridine *N*-oxide)-copper(II) chloride.

On the basis of the known structure of the parent compound (*cf.* Fig. 9),[4,5] we suggest the following two pathways as the most likely ones in dimeric copper(II) halide complexes with pyridine *N*-oxides; one is a σ type- and the other a π type pathway (*cf.* Figs. 10a, 10b and 10c). Figure 10a

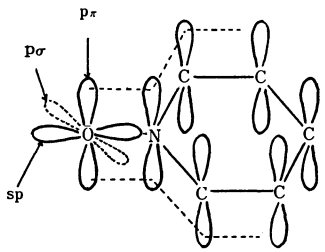

Fig. 10a. Ligand orbital representation in complex.

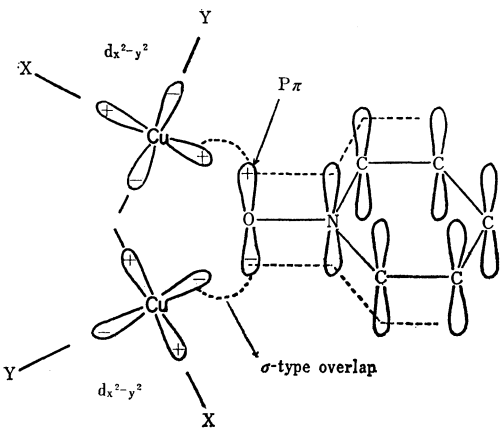

Fig. 10b. Electron exchange pathway of σ-type.

69) H. Ito, *Nippon Kagaku Zasshi* (*J. Chem. Soc. Japan, Pure Chem. Sect.*), **77**, 1395 (1956).
70) H. Ito, "Jikken Kagaku Koza (Zoku)," Vol. VI, ed. by M. Kotake *et al.*, Maruzen, Tokyo (1965), p. 384.
71) M. Kato, *Bull. Aichi Gakugei Univ.*, **9**, 95 (1960).
72) M. Kato, H. B. Jonassen and J. C. Fanning, *Chem. Revs.*, **64**, 99 (1964).

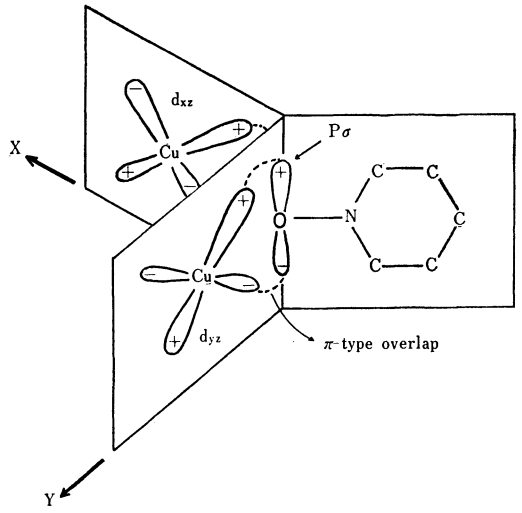

Fig. 10c. Electron exchange pathway of π-type.

provides a representation of the ligand orbitals necessary for describing electron exchange. Orbital-overlap schemes for electron exchange pathways of a σ-type and a π-type are given in Fig. 10b and 10c, respectively. For simplicity, the orbital-overlap schemes in these figures are drawn in idealized form. The actual mode of the orbital-overlapping may differ, in details, from this. The bond angles and other structural parameters should vary somewhat with the nature of the attached substituents or with the packing conditions of the individual molecules. In the structure of the parent complex,[4,5] determined by X-ray analysis, the plane of pyridine ring becomes nearly perpendicular to the Cu$\langle^{O}_{O}\rangle$Cu plane by rotation about the N–O bond, giving an angle of 70 degrees between these two planes. However, the figures were drawn for the two planes falling at essentially 90 degrees. This angle should vary somewhat from complex to complex.

Another orbital overlap of the σ type should also be examined for electron migration (second type). This is set up with the $3d_{x^2-y^2}$ or $3d_{z^2}$ orbitals of copper and an s orbital of oxygen. This orbital overlap has the characteristic of being rather insensitive to the bond angles.[73-75]

The sigma framework of complex molecules is often discussed in terms of localized bonds among hybrid atomic orbitals. This basis is intentionally avoided in Fig. 10 because it obscures the overlap patterns determining the geometric criteria for superexchange.

Of these two pathways the σ type is considered more effective for electron migration for the following reasons: 1. The orbital overlap in a σ type pathway is expected to be greater than those of a π type pathway. 2. Dubicki and Martin[76] suggested that, in copper(II) acetate or in the related compounds, the exchange between metal atoms in a molecule becomes operative *via* the bridging π system by mixing of metal d_{xy} and $d_{x^2-y^2}$ orbitals through spin-orbit coupling.[77] This can be applied to the electronic system of the complexes discussed here. Spin-orbit coupling may be decreased with an increase of the ligand field strength. However, the experimental evidence shows that greater ligand fields produce greater demagnetizations, suggesting that in these complexes the π pathway is less important. 3. The linear relation between the magnetic moments and d–d band positions is taken as evidence of greater importance of a σ pathway compared to a π pathway. Since in these complexes the strength of a σ type bond is believed to be the main factor determining the d–d band positions, it is very probable that the apparent parallelism between magnetic moments and d–d band positions, indicates that spin-spin coupling takes place primarily through the σ bonds. 4. The comparison of (pyridine *N*-oxide)-copper(II) chloride and acetylacetone-mono-(*o*-hydroxyanil)copper(II) whose structures have been determined by X-ray analysis is very useful in the examination of the relative importance of the factors controlling the exchange phenomenon for the following reasons: On the basis of its pK values, a phenolic oxygen produces a much stronger σ type bond than pyridine *N*-oxide's oxygen atom.[6,78] Nevertheless, the *N*-oxide complex and its related compounds display much larger demagnetization than the anil copper(II) complex and its related compounds.[72] This indicates that the most important factor in determining the electron exchange is the bond angles rather than the bond strengths in a pathway, though the latter should be the main factor when complexes with the same bond angles are compared. The importance of bond angles implies that the exchange mechanism operates *via* a σ type of orbital overlap rather than a π type. If electron migration takes place through a π type of orbital overlap, the demagnetization should not be sensitive to variations in bond angles. For a σ type of orbital overlap to be most effective, the bond angles, C–O–Cu_1 and C–O–Cu_2 in Fig. 11a or N–O–Cu_1 and N–O–Cu_2 in Fig. 11b, should be the same. The observed bond

73) L. C. Cusachs, M. Kato and H. B. Jonassen, *Chem. Revs.*, **64**, 122 (1964).
74) J. Kanamori, *J. Phys. Chem. Solids*, **10**, 87 (1959).
75) J. B. Goodenough, "Magnetism and the Chemical Bond," Interscience Publishers, New York, N. Y. (1963), p. 165.
76) L. Dubicki and R. L. Martin, *Inorg. Chem.*, **5**, 2203 (1966).
77) C. J. Ballhausen, "Introduction to Ligand Field Theory," McGraw-Hill Book Co., Inc., New York, N. Y. (1962), p. 113.
78) Ref. 52, p. 108.

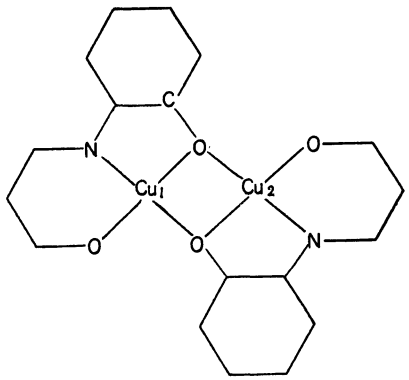

Fig. 11a. Schematic representation of bond angles of acetylacetone-mono-(*o*-hydroxyanil)copper(II).

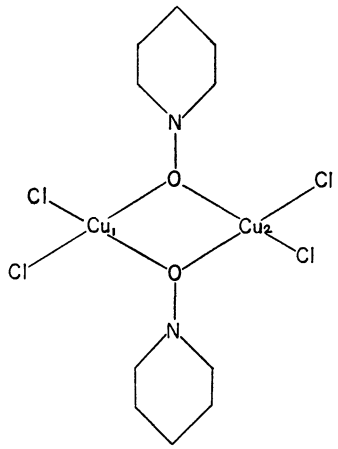

Fig. 11b. Schematic representation of bond angles of (pyridine *N*-oxide)-copper(II) chloride.

angles of the *N*-oxide complex, 127° and 123°,[4,5] are nearly equal. On the other hand, the bond angles of the anil copper(II) differ quite a bit (130° and 111°).[79,80] However, the difference in bond angles in the latter is still not great enough to prevent completely the utilization of a σ type of orbital overlap for electron migration.

The effectiveness of a π pathway and the aforementioned second type of σ pathway for electron migration may be approximately equal in both complexes. It is of interest that among the anil copper(II) and its related complexes, salicylal-*o*-hydroxybenzylamine copper(II) has an extraordinary small magnetic moment, 0.87 B.M.[3,79,81-85] Nearly all tri-coordinated units of these complexes are composed of one *five* and one *six* membered rings. Only the hydroxybenzylamine copper(II) contains two six membered rings in the unit. Molecular framework models indicate that the condition of the equality of the C–O–Cu_1 and C–O–Cu_2 bond angles necessary for an effective σ pathway is best satisfied in this complex (*cf.* Fig. 12). Recent studies of *N*-*n*-propanolsalicylaldiminato-copper(II) and its related complexes[10,86,87] have shown that these complexes all have very low magnetic moments, *ca.* 0.5 B.M. They have tricoordinate units of six-membered rings. Molecular models again indicate only that the condition of similar size bond angle in these complexes is satisfied.

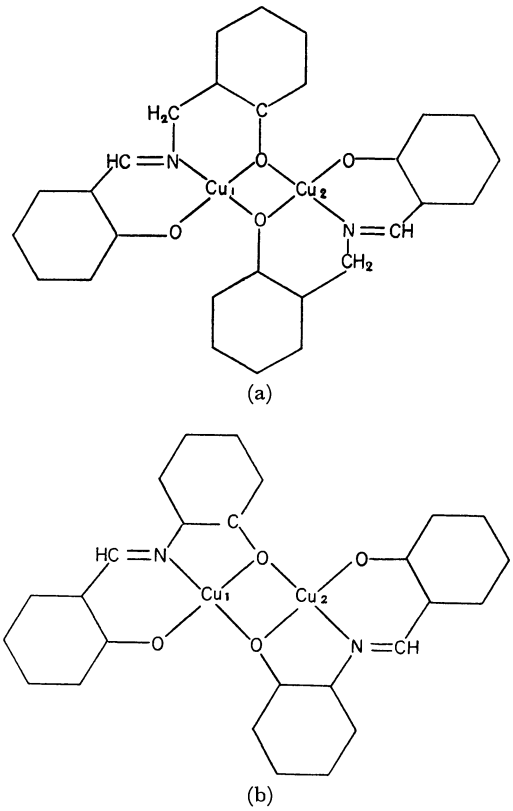

Fig. 12. Schematic representations of the structures fitted (a) and unfitted (b) for the equality condition of bond angles, C–O–Cu_1 and C–O–Cu_2.

79) G. A. Barclay, C. M. Harris, B. F. Hoskins and E. Kokot, *Proc. Chem. Soc.*, **1961**, 264.

80) G. A. Barclay and B. F. Hoskins, *J. Chem. Soc.*, **1965**, 1979.

81) M. Kishita, Y. Muto and M. Kubo, *Australian J. Chem.*, **10**, 386 (1957).

82) M. Kishita, Y. Muto and M. Kubo, *Naturwissenschaften*, **44**, 372 (1957).

83) M. Kishita, Y. Muto and M. Kubo, *ibid.*, **44**, 612 (1957).

84) M. Kishita, Y. Muto and M. Kubo, *Australian J. Chem.*, **11**, 309 (1958).

85) W. E. Hatfield and F. L. Bunger, *Inorg. Chem.*, **5**, 1161 (1966).

86) S. Yamada, Y. Kuge and K. Yamanouchi, *Inorg. Chim. Acta*, **1**, 139 (1967).

87) A. Nakahara and his coworkers, paper presented at the 17th Conference on Coordination Chemistry of the Chemical Society of Japan, Hiroshima, December, 1967, Proceedings, p. 29.

From this, it may be concluded that the large demagnetization observed in copper(II) halide complexes with pyridine *N*-oxides is caused by the availability of the σ type of pathway for electron migration, and the comparatively small amount of demagnetization in acetylacetone-mono-(*o*-hydroxyanil)copper(II) and its related compounds is attributable to the decreased efficiency for utilization of the σ pathway.

Two interesting features can be deduced from the orbital overlap schemes in Fig. 10: 1. The mesomeric effect of substituents attached to pyridine ring is transmitted to a p_π orbital through the π electron system of ligand molecule. In this way, the mesomeric effect of substituents becomes associated with the demagnetization mechanism. The inductive effect of substituents will be transmitted to s or p orbitals of oxygen atom by field effect, π inductive effect, or other effects.[88] 2. In this idealized picture, back-bonding through d_{xz} or d_{yz} orbitals of metal atom is not necessary since the p_σ orbital on the oxygen atom which overlaps these d orbitals is not in conjugation with the π electron system of the pyridine ring. This may be different from the situation to be found in the monomeric copper(II) perchlorate complexes with pyridine *N*-oxides in section II.

The relative effectiveness of direct metal-metal interaction and superexchange interaction in demagnetization should vary with the type of compounds.[2,5,6,12,54,72,79,80,85,89,90] For the latter interaction, the relative importance of the σ and π pathways is a problem for research and, it is expected to vary depending upon the structure of the compounds. It is a surprising fact that the magnetic moments of a great number of copper(II) alkanoates and benzoate fall at about 1.4 B.M.[72,76,91,92]

Molecular orbital calculations suggested by Cusachs, Kato and Jonassen[73] have been carried out for a model complex:[93] Copper(II) formate in the copper acetate cage structure. Although the direct Cu–Cu orbital overlap integrals are entirely insignificant, the two highest, singly occupied, molecular orbitals are of the sigma type with respect to the planes containing the copper and neighboring oxygen atoms, and dominate the computed orbital-orbital coupling terms. The orbital energies of these two molecular orbitals differ by only about 0.3 eV, so it is to be expected that there would be extensive configuration interaction, much as in the case of the ground state of H_2 at large internuclear distances. Coupling was calculated for the asymptotic limit of complete configuration interaction, or localization of a single electron in each half of the molecule, and found to vanish. It may be argued that these one-electron model calculations oversimplify the electron interaction terms quite severely, but no other method is currently available for such large molecules that does not do violence to some of the more important one- and two-electron contributions. These calculations do clearly support the present interpretation of the demagnetization mechanism as proceeding by coupling through the extended *sigma* framework of the molecule.

Progress in the study of spin-spin coupling mechanism in dimeric copper(II) complexes will require more examples of X-ray structural determination along with ESR and NMR experiments.[76]

88) M. J. S. Dewar and P. J. Grisdale, *J. Am. Chem. Soc.*, **84**, 3539 (1962).

89) R. L. Martin and H. Waterman, *J. Chem. Soc.*, **1959**, 1359.

90) T. Watanabe, *J. Phys. Soc. Japan*, **16**, 1677 (1961).

91) J. Lewis, Y. C. Lin, L. K. Royston and R. C. Thompson, *J. Chem. Soc.*, **1965**, 6464.

92) W. E. Hatfield, C. S. Fountain and R. Whyman, *Inorg. Chem.*, **5**, 1855 (1966).

93) L. C. Cusachs, B. L. Trus and J. R. Linn, Jr., unpublished calculations of the type described by L. C. Cusachs and B. B. Cusachs, *J. Phys. Chem.*, **71**, 1060 (1967).

BULLETIN OF THE CHEMICAL SOCIETY OF JAPAN VOL. 42 432—436 (1969)

Studies of Actinium(III) in Various Solutions. II. Distribution Behavior of Lanthanum(III) and Actinium(III) in Some Chelate Extraction Systems

Tatsuya SEKINE, Yasuaki KOIKE and Yuko HASEGAWA

Department of Chemistry, Science University of Tokyo, Kagurazaka, Shinjuku-ku, Tokyo

(Received June 20, 1968)

Distribution behavior of lanthanum(III) and actinium(III) at tracer concentrations was studied in metal chelate extraction systems where the organic phase was chloroform containing dibutylphosphate, thenoyltrifluoroacetone (TTA), β-isopropyltropolone or 5,7-dichloroxine. The separation factors for this pair of ions by extraction with these four chelating ligands were determined. The distribution behavior was also studied in the adduct chelate extraction systems where the organic phase was carbon tetrachloride containing mixed ligands, TTA-tributylphosphate (TBP) or TTA-methyl isobutyl ketone (MIBK). The adduct formation constants for actinium(III)-tris-TTA chelate with these neutral ligands were determined. Results were compared with previous results on the distribution behavior of other trivalent actinide and lanthanide ions in these systems. It was concluded that the separation of lanthanum-actinium was somewhat different from the separation of europium-americium in the same chelate extraction systems. The stabilities of the first adducts with TBP or MIBK of actinium TTA chelate were smaller than those of americium TTA chelate, but the stabilities of the second adducts showed just the reverse order. This tendency in adduct formation is the same as that observed among the lanthanum and europium adduct TTA chelates in previous work. Finally, the use of TTA-TBP mixture was recommended for the extraction of lanthanum(III) or actinium(III) at tracer concentrations based on the fact that the use of these mixed ligands resulted in much better recovery of material and better reproducibility of results than a single chelating ligand.

Little is known about the solvent extraction behavior of actinium except for the early studies of Hagemann,[1] who prepared actinium-227 using a TTA (thenoyltrifluoroacetone) extraction method, and of Peppard, Mason, Gray and Mech,[2] who studied the extraction of this element with TBP (tributylphosphate).

In the present paper, the authors measured the liquid-liquid distribution behavior of actinium(III) and lanthanum(III) in some metal chelate extraction systems in which Sekine and Dyrssen[3,4] previously studied the solvent extraction of europium(III) and americium(III). It was further intended to compare the liquid-liquid distribution behavior of the trivalent lanthanides and actinides.

Experimental

Tracer. Actinium-228 tracer was prepared by the method described in Part I of this series[5] just before use. Lanthanum-140 tracer was prepared from barium-140 by a method similar to actinium-228 as follows: A carrier-free barium-140 solution was stored a few days and adjusted to pH 5—6 using acetate buffer. The lanthanum-140 produced in the solution was extracted with 0.1 M TTA in chloroform. The organic layer was once washed with a fresh buffer solution at pH 5—6 and then the lanthanum-140 was back-extracted by shaking the organic layer with 0.1 M perchloric acid. The aqueous layer thus obtained was then washed with chloroform and used as a stock solution of this isotope.

Reagents. A mixture of DBP (dibutylphosphate) and monobutylphosphate was obtained from Tokyo Kasei Co. DBP was separated and purified by a solvent extraction method.[6] TTA was obtained from Dojindo & Co., IPT (β-isopropyltropolone) from Takasago Perfumery Co. and 5,7-dichloroxine from Tokyo Kasei Co. These chelating reagents were used without further purification. TBP and MIBK (methyl isobutyl ketone) were obtained from Tokyo Kasei Co. They were washed with 0.1 M perchloric acid, water and 0.1 M sodium hydroxide, in that order, and then

1) F. T. Hagemann, *J. Am. Chem. Soc.*, **72**, 768 (1950).

2) D. E. Peppard, G. W. Mason, P. R. Gray and J. F. Mech, *ibid.*, **74**, 6081 (1952).

3) T. Sekine and D. Dyrssen, *Talanta*, **11**, 867 (1964).

4) T. Sekine and D. Dyrssen, *J. Inorg. Nucl. Chem.*, **29**, 1481 (1967).

5) T. Sekine, Y. Koike and M. Sakairi, *J. Nucl. Sci. and Tec.*, **4**, 308 (1967).

6) D. Dyrssen and L. D. Hay, *Acta Chem. Scand.*, **14**, 1100 (1960).

several times with water. Chloroform was washed three times with water. Other reagents were of an analytical grade.

Procedures. All procedures were carried out in a thermostatted room at 25±0.5°C. Lanthanum(III) carrier (initial concentration in the aqueous phase, 5×10^{-5} M) was added to the aqueous phase except for the TBP adduct experiments when the TBP concentration was low. A small amount of sulfanilate, acetate or carbonate (initial concentration in the aqueous phase, 0.01 M) was added to the aqueous phase when a buffer was necessary. It was confirmed that no change in extraction was caused by these buffers at this concentration. A 5 m*l* portion of the aqueous phase and a 5 m*l* portion of the organic phase were placed in tubes with glass stoppers (volume 20 m*l*) and agitated mechanically for 30 min and centrifuged. A 2 m*l* portion was pipetted from each phase and transferred to small glass test tubes and the γ-radioactivity measured with a well-type (NaI) scintillation counter. A small portion was also taken from the aqueous phase and the hydrogen ion concentration measured potentiometrically using a standard solution containing 0.0100 M perchloric acid and 0.09 M or 0.99 M sodium perchlorate as the standard of $-\log[H^+]$ 2.00 in 0.1 M or 1 M perchlorate media. When the hydrogen ion concentration exceeded 0.01 M, it was determined by a titration method.

The net distribution ratio of the trivalent metal ions M^{3+} was defined and determined as follows;

$$D = [M(III)]_{org,\ total}/[M(III)]_{total} = \frac{\gamma\text{-count-rate per ml org. phase}}{\gamma\text{-count-rate per ml aq. phase}}$$

Results

A) Extraction of Metal Chelates. In the extraction of metal chelates, the aqueous phase was kept at 0.1 M perchlorate. The organic phase was chloroform containing 0.1 M DBP, TTA or IPT, or chloroform containing 0.05 M 5,7-dichloroxine.

Assuming that extraction takes place by the following reaction (HA denotes the chelating acid),

$$M^{3+} + (3+n)HA(org) \rightleftarrows MA_3(HA)_n(org) + 3H^+ \quad (1)$$

$$D = \sum[MA_3(HA)_n]_{org}/[M^{3+}] \quad (2)$$

an equilibrium constant for the extraction may be defined if the chelate concentration is kept constant as

$$K = D[H^+]^3 \quad (3)$$

However, when the chelate concentration is not constant, a more involved equation[7] should be used.*1 In the present study, the chelate concentration was kept constant in each series of experiments, and thus Eq. (3) could be used.

Table 1 summarizes the separation of lanthanum(III) and actinium(III) by chelate extraction into chloroform. This table also summarizes previously reported data on the separation of europium(III) and americium(III).[3] The constants $D[H^+]^3$ were calculated from data obtained from the range of the distribution ratio $10>D>0.1$, because the values $D[H^+]^3$ for all the chelate extraction systems were approximately constant only in this range.

In the hydrogen ion concentration region where the distribution ratio is greater than 10, some decrease in the slope of the extraction curve from +3 was observed in the IPT system. This discrepancy was assumed due to aqueous chelate formation.[9] When the distribution ratio is less than 0.1, some decrease in the slope from +3 was also observed in actinium(III) chelate extraction systems, but no explanation can be given for this deviation.

The slope log$D$ *vs.* $-\log[H^+]$ plot for the 5,7-dichloroxine system was found to be +3 at least when $-\log[H^+]$ was below 7. This indicates that the hydrolysis of these ions is not very important

Table 1. Separation of La^{3+} and Ac^{3+} in 0.1M (Na, H)ClO_4 at 25°C by solvent extraction with some chelating acids in chloroform together with previous data on that of Eu^{3+} and Am^{3+} under the similar conditions[3]

Reagent (HA)	$[HA]_{org}$	log $SF_{La^{3+}-Ac^{3+}}$	log $SF_{Eu^{3+}-Am^{3+}}$	log $D_{La^{3+}}[H^+]^3$	log $D_{Ac^{3+}}[H^+]^3$	log $SF_{Eu^{3+}-La^{3+}}$	log $SF_{Am^{3+}-Ac^{3+}}$
Dibutylhydrogen-phosphate (DBP)	0.1M	+0.64	+1.36	−4.92	−5.56	+2.01	+1.29
2-Thenoyltrifluoro-acetone (TTA)	0.1M	+1.84	+0.48	−14.06	−15.90	+2.38	+3.70
β-Isopropyltropolone (IPT)	0.1M	+1.82	−0.01	−13.60	−15.42	+3.70	+5.53
5,7-Dichloroxine (DCOX)	0.05M	+1.71	−0.99	−17.81	−19.52	+4.08	+6.78

7) T. Sekine and D. Dyrssen, *J. Inorg. Nucl. Chem.*, **26**, 1727 (1964).

*1 Actually the chelate complex of europium(III) with IPT in chloroform was found to be of the form EuA_3HA,[8] and it is most probable that the actinium IPT complex also exists in the form AcA_3HA.

8) T. Sekine and D. Dyrssen, *ibid.*, **29**, 1457 (1967).

9) T. Sekine, A. Koizumi and M. Sakairi, This Bulletin, **39**, 2681 (1966).

10) F. J. C. Rossotti and H. Rossotti, "The Determination of Stability Constants," McGraw-Hill Co., Inc., New York (1961), p. 233.

11) G. Biedermann and L. Ciavatta, *Acta Chem. Scand.*, **15**, 1347 (1961).

if the hydrogen ion concentration is kept above 10^{-7} M.[10,11]

B) Extraction of Adduct Metal Chelates. The adduct formation of actinium(III)-tris-TTA chelate with TBP or MIBK was studied in carbon tetrachloride. In these experiments, the aqueous phase was adjusted to 1 M (H, Na)ClO_4 in order to compare results with the previous data.[4]

As a statistical treatment of adduct chelate formation in a solvent extraction system has been already given in a previous paper,[12] only a brief description will be given here. When metal tris-TTA chelate MA_3 forms adduct chelate complexes with an organophilic neutral ligand L, the reaction and formation constants may be described by

$$MA_3(org) + nL(org) \rightleftarrows MA_3L_n(org) \quad (4)$$

$$\beta_n = [MA_3L_n]_{org}/[MA_3]_{org}[L]^n_{org} \quad (5)$$

When these adduct chelates are formed in the organic phase and M^{3+} is the only metal species in the aqueous phase, the net distribution ratio may be generally written.

$$D = \frac{[MA_3]_{org} + [MA_3L]_{org} + [MA_3L_2]_{org} + \cdots}{[M^{3+}]} \quad (6)$$

When the net distribution ratio of the metal chelate extraction in the absence of the adduct forming ligand can be described as $D_0 = [MA_3]_{org}/[M^{3+}]$, the following equation is obtained from Eqs. (5) and (6) if the chelating ligand and hydrogen ion concentrations are kept constant;

$$D/D_0 = 1 + \beta_1[L]_{org} + \beta_2[L]^2_{org} + \cdots \quad (7)$$

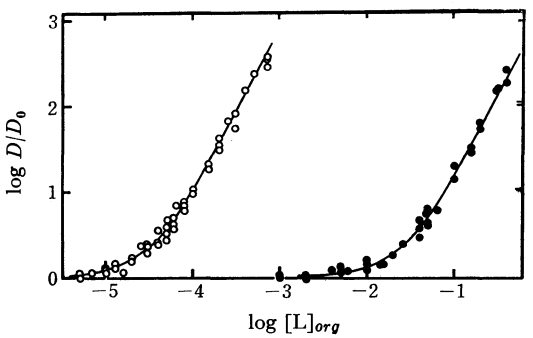

Fig. 1. The increase in the TTA extraction of actinium(III) by the adduct fromation shown as a function of the concentration of the adduct forming ligand.
Organic phase: Carbon tetrachloride containing 0.1 M TTA and TBP (open circles) or MIBK (closed circles).
Aqueous phase: 1M $NaClO_4$.
The solid curves were drawn as follows.
TBP: $Y = \log(1 + 10^{4.2}[L]_{org} + 10^{8.9}[L]^2_{org})$
MIBK: $Y = \log(1 + 10^{1.3}[L]_{org} + 10^{3.1}[L]^2_{org})$

Figure 1 shows the $\log D/D_0$ *vs.* $\log[L]_{org}$ plot of actinium(III)-tris-TTA chelate in carbon tetrachloride when the neutral ligand was TBP or MIBK.

The formation constants were determined in the same manner as described in Ref. 12 and are given in Table 2 together with the formation constants of lanthanum(III), europium(III), lutetium(III) and americium(III) tris-TTA chelates under the same experimental conditions as in Ref. 7. The solid curves in Fig. 1 are calculated from the formation constants given in Table 2.

TABLE 2. ADDUCT FORMATION OF TRIS-TTA CHELATES IN CARBON TETRACHLORIDE AT 25°C (AQUEOUS PHASE, 1M $NaClO_4$)

(a) Extraction constants with pure TTA in carbon tetrachloride
$K_{ex_0} = [MA_3]_{org}[H^+]^3/[M^{3+}][HA]^3_{org}$

Metal ion	log K_{ex_0}	Ionic radius Å**
Ac^{3+}	−12.90	1.11
La^{3+}*	−10.95	1.04
Am^{3+}*	−8.88	0.99
Eu^{3+}*	−8.57	0.96

(b) Adduct formation constants of tris-TTA chelate in carbon tetrahcloride at 25°C
$\beta_1 = [MA_3L]_{org}/[MA_3]_{org}[L]_{org}$
$\beta_2 = [MA_3L_2]_{org}/[MA_3]_{org}[L]^2_{org}$
$K_2 = \beta_2/\beta_1 = [MA_3L_2]_{org}/[MA_3L]_{org}[L]_{org}$

Metal chelate	MIBK			TBP		
	logβ_1	logβ_2	logK_2	logβ_1	logβ_2	logK_2
AcA_3	1.3	3.1	1.8	4.2	8.9	4.7
LaA_3*	2.0	2.9	0.9	4.8	9.3	4.5
AmA_3*	1.8	2.5	0.7	5.1	8.9	3.8
EuA_3*	1.8	2.4	0.6	5.2	8.9	3.7

* taken from Ref. 4.
** taken from W. H. Zachariesen, "The Actinide Elements," NNES-14A McGraw-Hill, New York (1954).

It was found that the results on the extraction of carrier-free lanthanum(III) and actinium(III) were not very reproducible. The addition of non-radioactive lanthanum(III) (initial concentration in the aqueous phase, 5×10^{-5} M) improved the reproducibility very much, especially that of actinium extraction. The extraction of carrier-free actinium(III), however, was very reproducible when a mixture of TTA and TBP in carbon tetrachloride was employed as extractants instead of a single chelating agent.

12) T. Sekine and M. Ono, This Bulletin, **38**, 2087 (1965).

Discussion

The results are summarized as follows;

A) The extraction of actinium(III) with the four chelating reagents was always inferior to that of lanthanum(III). The separation of lanthanum(III) from actinium(III) using TTA, IPT or 5,7-dichloroxine was better than that of europium(III) from americium(III) with the same reagent, but the difference in extraction of lanthanum(III) and actinium(III) using DBP was inferior to that of europium(III) and americium(III). In a previous study,[3] americium(III) was extracted with 5,7-dichloroxine ten times better than europium(III), but the separation of actinium(III) from lanthanum(III) with this reagent, on the other hand, showed just the reverse tendency; lanthanum(III) extracted fifty times better than actinium(III).

B) In a previous work,[4] it was pointed out that the stability of the first adducts MA_3L was greater in the increasing order of extractability of the tris-TTA metal complexes $LaA_3L < EuA_3L < LuA_3L$, but the stability of the second complexes MA_3L_2 was greater in the reverse order $LaA_3L_2 > EuA_3L_2 > LuA_3L_2$. A similar tendency of stability was also observed in TBP adducts of actinide TTA chelates; the formation constants of the first adducts of actinium TTA chelate were smaller than those of americium TTA chelate. On the other hand, the stepwise formation constants K_2 of actinium adducts were larger than those of americium adducts.

The similarity in chemical properties of lanthanides and actinides has been explained in terms of their electronic configurations; the 4f orbitals (lanthanides) or 5f orbitals (actinides) are filled successively by electrons with increase in atomic number. In the case of lanthanum and actinium, however, a contribution from the 4f and 5f electrons to their chemical properties is not expected, and thus the chemical properties of these pairs of elements could be different to some extent.

Separation of two metal ions by a metal chelate extraction method is influenced by many factors. The separation factor (*SF* in Table 1) is defined,

$$SF = \frac{D_{La^{3+}}[H^+]^3}{D_{Ac^{3+}}[H^+]^3} \quad \text{(when } [HA]_{org} \text{ is the same)}$$

this equation can be altered as follows (*cf.* also Ref. 13).

The distribution ratio in a metal chelate extraction system can generally be written,

$$D = \frac{[MA_3]_{org} + [MA_3(HA)]_{org} + \cdots + [MA_3(HA)_n]_{org}}{[M^{3+}] + [MA^{2+}] + [MA_2^+] + [MA_3] + \cdots + [MA_n^{3-n}]} \quad (8)$$

13) T. Wakahayashi *et al.*, *J. Inorg. Nucl. Chem.*, **26**, 2255, 2265 (1964); **27**, 1141 (1965).

Let us discuss the case where only the MA_3 species is extracted into the organic phase for simplicity (a general discussion will also be possible). When we define the stability constants of metal chelates produced in the aqueous phase and the distribution constant of the non-charged metal chelate as follows,

$$\beta_n = \frac{[MA_n^{3-n}]}{[M^{3+}][A^-]^n} \quad (9)$$

$$K_{DM} = \frac{[MA_3]_{org}}{[MA_3]} \quad (10)$$

the distribution ratio can be described as

$$D = \frac{K_{DM}\beta_3[A^-]^3}{1 + \beta_1[A^-] + \beta_2[A^-]^2 + \beta_3[A^-]^3 + \cdots + \beta_n[A^-]^n} \quad (11)$$

The separation factor of two metal ions (denoted M_a and M_b) can be written from Eq. (11) as (the subscripts "*a*" and "*b*" denote the constants for M_a and M_b);

$$\frac{Da}{Db} = \frac{K_{DMa}\beta_{3a}}{K_{DMb}\beta_{3b}} \times \frac{1 + \beta_{1b}[A^-] + \beta_{2b}[A^-]^2 + \beta_{3b}[A^-]^3 + \cdots}{1 + \beta_{1a}[A^-] + \beta_{2a}[A^-]^2 + \beta_{3a}[A^-]^3 + \cdots} \quad (12)$$

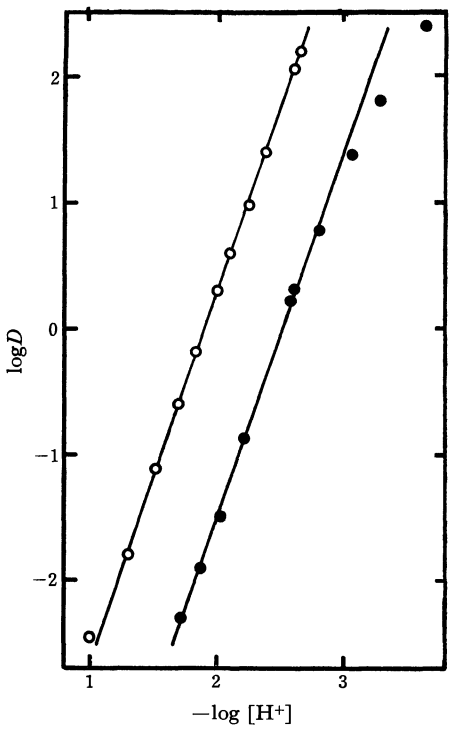

Fig. 2. Extraction of lanthanum(III) (open circles) and actinium(III) (closed circles) with mixed solvents as a function of the hydrogen ion concentration.
Organic phase: carbon tetrachloride containing 0.2 M TTA and 0.2 M TBP.
Aqueous phase: 1 M aqueous sodium perchlorate.

We see from Eq. (12) that the separation factor will not be constant over all hydrogen ion concentrations, but in the region where no aqueous chelate complexes are formed (where the slope of the plot log$D$ *vs.* $-\log[H^+]$ is $+3$), the separation factor can be written

$$SF = \frac{Da}{Db} = \frac{K_{DMa}\beta_{3a}}{K_{DMb}\beta_{3b}} \qquad (13)$$

Equation (13) shows that the separation of these two metal ions is concerned only with the stability and the extractability of the third chelate complexes.

No previous information on these factors for lanthanide and actinide chelate seems to have been reported. Further discussion on the separation of lanthanides and actinides by metal chelate extraction would be possible if we could obtain the K_{DM} and β_3 values of the chelates.

In Ref. 4, the general tendency of the stability of the adduct metal chelates was explained in terms of the residual coordination power of metal ions which is decreased if they form more stable complexes with the chelating ligands. This tendency is again found in the present results. The extractability of actinium(III) with TTA is smaller than that of lanthanum(III) or americium(III). This fact indicates a smaller β_3 value for actinium(III) than for the others.*2 Thus we may expect a larger residual coordination power in actinium tris-TTA chelate than in the other which causes the actinium tris-TTA chelates to form less stable first adducts and more stable second adducts.

As described, the extraction of carrier-free lanthanum or actinium in liquid-liquid systems containing only a chelating acid is not reproducible. When it is necessary to treat these ions at tracer concentrations, we recommend the use of mixed extractant systems. The extraction of carrie-free actinium was conveniently carried out with the use of TTA-TBP mixtures. Figure 2 shows the log$D$ *vs.* $-\log[H^+]$ plot of these ions when the organic phase was carbon tetrachloride containing 0.2 M TTA and 0.2 M TBP. In this system, the separation factor is 1.80 and the recovery of the materials almost quantitative. The reproducibility of the experimental results was excellent.

*2 As no information on the magnitude of K_{DM} values is available, we can not discuss the stabilities of these tris-TTA chelate, β_3, except from the extraction constants as seen from Eq. (13). However, it would not be unreasonable to assume that the separation factor is concerned more with β_3 than with K_{DM}, or the organophilic tendencies of the metal chelates would resemble each other because the metal ions in the chelate complex molecules are surrounded by three common organophilic molecules.

BULLETIN OF THE CHEMICAL SOCIETY OF JAPAN VOL. 42 436—439 (1969)

Chemical Effects Associated with β-Decay Process. III. The Chemical Behavior of ^{144}Pr Decayed from ^{144}Ce(III)-EDTA Complexes in the Solid Phase

Takanobu SHIOKAWA, Hiroshi KUDO*1 and Takashi OMORI

Department of Chemistry, Faculty of Science, Tohoku University, Katahira-cho, Sendai

(Received June 22, 1968)

The chemical behavior of ^{144}Pr formed by the β^--decay of ^{144}Ce in crystals of ^{144}Ce(III)-EDTA complexes has been investigated by means of ion-exchange techniques. The initial yield of $^{144}Pr^{3+}$ ion, which reflects the distribution of the ^{144}Pr atoms in the crystal, is independent of the dissolving condition, but is affected by the amount of hydration in the crystal. Abnormal behavior of ^{144}Pr atom has not been found in the ammonium salt. These results suggest that in the solid phase $^{144}Pr^{3+}$ or its precursor may be produced as a result of multiple charging of the daughter following electron shake-off and internal conversion of γ-rays.

A number of studies have been carried out on the chemical consequences of molecules resulting from the β^--decay of a constituent atom. The chemical behavior of the radioactive daughter atom depends on its recoil energy, charge and and electronic excitation resulting from the change in nuclear charge. Therefore, a change in oxidation

*1 Present address: Japan Atomic Energy Research Institute, Tokai, Ibaraki.

state of the radioactive daughter atom has become of interest. Cerium-praseodymium-144 possesses several advantages in its nuclear and chemical properties for a study of the chemical behavior of the radioactive daughter atoms formed by β^--decay. Several authors[1-4] reported the chemical behavior of ^{144}Pr in this system previously.

In an earlier paper,[2] the present authors investigated the chemical behavior of ^{144}Pr formed by β^--decay of the ^{144}Ce labeled cerium(III)-ethylenediaminetetraacetate (^{144}Ce(III)-EDTA) complex in the liquid phase. The results suggested that an increase in the nuclear charge of ^{144}Pr plays the most important role in the process of β^--decay of ^{144}Ce(III)-EDTA complex, and leads to the disruption of the complex molecule *via* intramolecular electron-transfer. The kinetic study[3] indicated the existence of an intermediate, produced as a result of β^--decay.

The present investigation was undertaken in the solid phase to obtain further information on the chemical behavior of ^{144}Pr formed by β^--decay of ^{144}Ce(III)-EDTA complex.

Experimental

Chemicals. Reagents used are as reported previously.[2]

The sodium salt of ^{144}Ce(III)-EDTA complex (Na-$^{144}CeY \cdot mH_2O$) was synthesized by the reaction of cerium(III) nitrate and the disodium salt of EDTA (Na_2H_2Y) in aqueous solution at pH 6.5. The solution was concentrated by evaporation and placed in an ice bath. The resulting crystalline product was recrystallized from a 90 per cent ethanol solution. In the process of recrystallization, the carrier-free ^{144}Ce was added. The ammonium salt of ^{144}Ce(III)-EDTA complex (NH_4-$^{144}CeY \cdot 5H_2O$) was prepared in a similar way, except that the ammonium salt of EDTA was used instead of the sodium salt.

The solid chelates were analyzed for Ce^{3+} and Y^{4-}, and then the hydration number of the crystal calculated by difference.[5]

Apparatus and Procedures. The solid complex, allowed to stand for more than three hours at 0°C, was dissolved in a 0.4 M sodium acetate buffer solution. The ionic strength was adjusted to 0.5 with sodium chloride. The final concentration of the complex ion was 1×10^{-3} M. The solution was placed in a bath at the desired temperature. To separate the free-ion, an aliquot of the solution was withdrawn through a Dowex 50W-X8 column (8 mm$\phi \times$10 mm, 50—100 mesh). The resin used had been treated with a proper buffer solution before use. All procedures were performed at 0 ± 0.5°C.

The yield of the free-ion fraction was obtained by counting the γ-activities of both the resin phase and the combined effluents, as described previously.[2] The pH of the solutioh was measured with a glass-electrode pH meter to an accuracy of ± 0.01.

Results

It was found that the yields of $^{144}Pr^{3+}$ ion, which represent the extent of molecular disruption due to β^--decay of ^{144}Ce(III)-EDTA complex increase or decrease with time after dissolution. As an example, Fig. 1 shows an increase in the apparent yield of $^{144}Pr^{3+}$ ion up to the plateau value in a neutral solution. It should be noticed that the cerium is also adsorbed to some extent on the resin under this condition. Since the adsorbability of the cerium(III) ion is independent of the lapse of time after dissolution, it is ascribed to the transfer of the EDTA complex to the cationic fraction on separation. Thus, the net yield of $^{144}Pr^{3+}$ ion formed by β^--decay of ^{144}Ce(III)-EDTA complex could be obtained by subtraction of the normal distribution from the apparent yield. Figure 2 shows the net yield curves for $^{144}Pr^{3+}$ ion at various pH values.

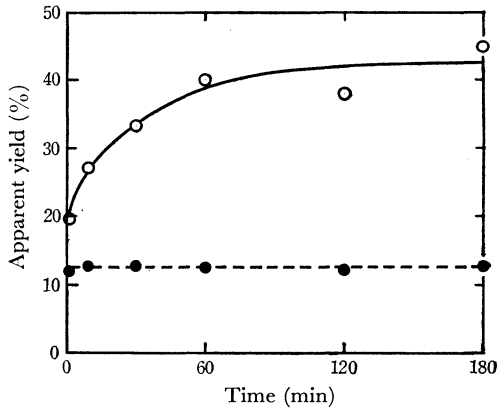

Fig. 1. Apparent yield of $^{144}Pr^{3+}$ and $^{144}Ce^{3+}$ in Na-$^{144}CeY \cdot 7H_2O$ dissolving at pH 7.08.
○: $^{144}Pr^{3+}$; ●: $^{144}Ce^{3+}$

The plateau yield of $^{144}Pr^{3+}$ ion increases in the neutral regions, pH 6.5, whereas it decreases in low pH regions. The distribution of the plateau yields of $^{144}Pr^{3+}$ ion as a function of pH is shown in Fig. 3.

The initial yield of $^{144}Pr^{3+}$ ion, which is defined as the yield just after dissolution of the crystal, could be obtained by extrapolation of the yield of $^{144}Pr^{3+}$ ion to zero time. The initial yield of $^{144}Pr^{3+}$ ion for a given crystal is quite independent

1) R. R. Edwards and C. D. Coryell, TID-13363 (1961).
2) T. Shiokawa, H. Kudo and T. Omori, This Bulletin, **38**, 1340 (1965).
3) T. Shiokawa and T. Omori, *ibid.*, **38**, 1892 (1965).
4) P. Glentworth and B. Wiseall, "Chemical Effects of Nuclear Transformations (Proc. Symp. Vienna)," Vol. II. IAEA, Vienna (1965), p. 483.
5) N. P. Kusakina and E. M. Yakinets, *Russ. J. Inorg. Chem.*, **10**, 457, 459 (1965).

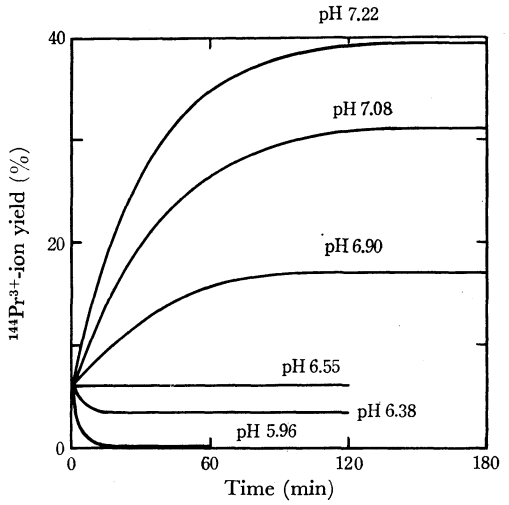

Fig. 2. Yield of $^{144}Pr^{3+}$ ion in $Na^{144}CeY \cdot 7H_2O$ dissolving at various pH.

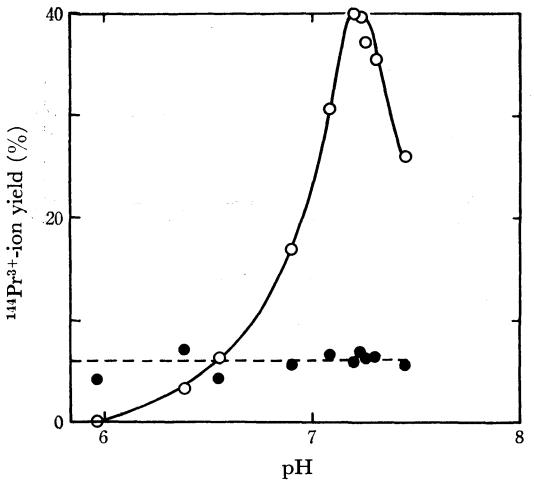

Fig. 3. Yield of $^{144}Pr^{3+}$ ion in $Na^{144}CeY \cdot 7H_2O$ as a function of pH of the aqueous solution.
○: plateau yield; ●: initial yield

of the dissolving condition of the aqueous solution, while it is significantly affected by the hydration number of the crystal. The results are summarized in Table 1.

TABLE 1. INITIAL YIELD OF $^{144}Pr^{3+}$ ION RESULTING FROM β^--DECAY OF ^{144}Ce IN THE CRYSTAL OF EDTA COMPLEXES

Crystal	Initial yield (%)
$Na^{144}CeY \cdot 4H_2O$	3.9±0.4
$NH_4{}^{144}CeY \cdot 5H_2O$	4.7±0.4
$Na^{144}CeY \cdot 6H_2O$	5.4±0.4
$Na^{144}CeY \cdot 7H_2O$	6.0±0.4
$Na^{144}CeY \cdot 12H_2O$	9.1±0.3

Discussion

The general aspect of the distribution curve of the plateau yields of $^{144}Pr^{3+}$ ion as seen in Fig. 3 is similar to that observed in the liquid system.[3] Thus, the plateau yield of $^{144}Pr^{3+}$ ion could be explained by application of the mechanism proposed previously[2,3]; that is, tetrapositive ^{144}Pr produced as a result of simple β^--decay of ^{144}Ce(III)-EDTA complex would be reduced to a tripositive state by intramolecular electron-transfer. The tripositive praseodymium still forms an intermediate complex with an oxidation product of EDTA, but is liberated by proton attack as the free-ion form.

In a given crystal, however, the initial yields obtained under different dissolving conditions are essentially constant, as shown in Fig. 2. From Table 1, one can also see that the initial yield of $^{144}Pr^{3+}$ ion increases with hydration number of the crystal. These results strongly suggest the existence of a chemical species other than the intermediate in the solid state; *viz.*, $^{144}Pr^{3+}$ ion or a precursor, which transforms to $^{144}Pr^{3+}$ ion just after dissolution. In the solid phase, the intermediate is thought to be rather stable, and its contribution to the initial yield of $^{144}Pr^{3+}$ ion would be of minor importance. A possible alternative explanation could be that the initial molecular ion, ^{144}Pr(IV)-EDTA, can exist in the crystal, or that it can be stabilized to ^{144}Pr(III)-EDTA complex by intermolecular electron-transfer.

As pointed out above, the daughter atom formed by β^--decay will have a positive charge of one unit higher than the parent atom, and tetravalent ^{144}Pr may cause the disruption of EDTA complex *via* an intermediate. On the other hand, further ionization resulting from electron shake-off will take place, so that the daughter atom will have a positive charge greater than +5. In addition, multiple charging of ^{144}Pr will take place in consequence of the internal conversion of γ-rays. The yield is estimated to be 13% from the internal conversion coefficient.[6]

In comparison with theoretical estimates, relatively small values for the initial yields predict that all multiply charged species do not transform to the free praseodymium ion or its precursor. However, it should be noticed that in the solid phase the chemical effect associated with the β^--decay of ^{144}Ce is mainly attributed to the multiple

6) I. Pullman and P. Axel, *Phys. Rev.*, **102**, 1366 (1956).

7) J. L. Hoard, E. Willstandter and J. V. Silverton, *J. Am. Chem. Soc.*, **87**, 1611 (1965).

8) For example, R. E. Cleary, W. H. Hamill and R. R. Williams, *J. Am. Chem. Soc.*, **74**, 4675 (1952); K. J. McCallum and A. G. Maddock, *Trans. Faraday Soc.*, **49**, 1150 (1953); G. Harbottle, *J. Chem. Phys.*, **22**, 1083 (1954).

charging of the daughter atoms following electron shake-off and Auger processes, so long as it is discussed in terms of the initial yield of $^{144}Pr^{3+}$ ion.

In order to understand the fate of the ^{144}Pr atom in the solid phase, it is very important to investigate the effect of the hydration number of the solid complex on initial yield. On the basis of a structural investigation of rare earth-EDTA complexes,[7] it seems reasonable to estimate that the structural formula of the sodium salt of ^{144}Ce-(III)-EDTA complex is $NaCeY(O_2H)_4 \cdot mH_2O$. Since the hydration numbers of the solid complexes used in this experiment varied from four to twelve, the complexes have fundamentally identical structures, being different in outer-sphere hydration. Accordingly, a linear increase in initial yields with hydration numbers of the EDTA complexes would suggest that water molecules in the outer-sphere affect either the decomposition of the EDTA complex resulting from the highly charged ^{144}Pr ion or the stabilization reaction of liberated ^{144}Pr ion in the solid phase.

It appeared of interest to study the initial yield of $^{144}Pr^{3+}$ ion in the ammonium salt of ^{144}Ce(III)-EDTA complex. In the (n,γ) reaction, retentions of the ammonium salts are always abnormally low.[8] No discrepancy, however, has been found in this system, as seen in Table 1. This fact suggests that because of the low recoil energy of the β^--decay of ^{144}Ce, ^{144}Pr could not interact with ammonium ion.

The chemical consequences of the β^--decay of the ^{144}Ce(III)-EDTA complex has been discussed hitherto mainly from the point of veiw of thermodynamical instability of the daughter molecular ion.[2,3] However, the present investigation in the solid phase reveals that the multiple charge of the daughter plays an important role in determining the chemical behavior of the ^{144}Pr atom.

BULLETIN OF THE CHEMICAL SOCIETY OF JAPAN VOL. 42 439—442 (1969)

Long-term Integration of Polarographic Currents and Its Analytical Application

Kiyoshi MATSUDA and Reita TAMAMUSHI

The Institute of Physical and Chemical Research, Yamato-machi, Saitama

(Received June 26, 1968)

The integral readout technique was applied to the accurate determination of average polarographic currents. The long-term integration of polarographic currents provides a useful method of compensating residual currents and thus of increasing the sensitivity and accuracy of the d. c. polarographic analysis. The analytical utility of the proposed method was tested with cadmium, lead, and zinc ions in chloride solutions; these ions were found to be determined with reasonable accuracy even at concentrations as low as 10^{-6} M. Depolarizers at concentrations of the order of 10^{-4} M can be determined accurately in air-saturated solutions. The present method has the considerable merit that its sensitivity is not affected by the degree of reversibility of the electrode reaction. The integral technique was also applied successfully to the compensation of residual currents by the twin-cell system, in which a pair of dropping mercury electrodes is not necessarily synchronized.

Increase in sensitivity and accuracy is an urgent requirement to the instrumental methods of analysis. The recent development in the modified alternating current (a.c.) polarography, the radio-frequency polarography, and the anodic stripping voltammetry has made it possible to determine the depolarizers at concentrations as low as 10^{-8} M. Their absolute accuracy, however, is not very high, and the sensitivity is low when the electrode reaction is slow.

The diffusion current in the direct current (d.c.) polarography has the advantage of good reproducibility and high accuracy, when applied to the determination of depolarizers. In the conventional d.c. polarographic method, however, the measurement of diffusion currents at lower concentrations becomes increasingly difficult because of the large contribution of residual currents. Many attempts have been made to eliminate the residual current and to increase the signal-to-noise

ratio; typical examples are the differential polarography, the derivative polarography,[1] and the tast polarography.[2] These methods generally require careful synchronization of a pair of dropping mercury electrodes (DME) or elaborate electronic instruments, and their practical usefulness is very much limited.

The application of integral readout methods is expected to be effective to overcome some of the above-mentioned difficulties and to increase the sensitivity and accuracy of the d.c. polarographic measurement. Booman *et al.* measured the charge transferred during a short period of electrolysis at solid electrodes by using a precision current integrator; they stated that a linear relation between the concentration and the charge transferred was obeyed to within 1%.[3] The integration of single sweep oscillopolarograms was proposed by Christie, Lauer, and Osteryoung.[4] Lauer and Osteryoung[5] reported that the integration of polargoraphic currents during a life of a single mercury drop is a suitable method for separation of capacitive and faradaic currents and for trace analysis.

The present paper deals with a new technique in which the polarographic current is integrated electronically over a long period of time (about 10 min) at a given electrode potential. The experimental results demonstrated the usefulness of the proposed technique for the elimination of residual currents and accurate measurement of average polarographic currents.

Experimental

Apparatus. The basic circuits of the apparatus used are shown in Fig. 1; both circuits (a) and (b) gave essentially the same results.

The principle of circuit (a) is similar to that of a linear bridge. The polarographic current, i_p, at a given electrode potential is integrated by the integrator, I_1, for a certain period of time (*e. g.*, about 10 min), while a constant current, i_c, is integrated by the other integrator, I_2; the sign and the magnitude of i_c are adjusted so that the output voltage of the inverter, INV, is opposite in its sign and exactly equal in its magnitude to the integrated value of the residual current at the given potential. The addition of both the signals from

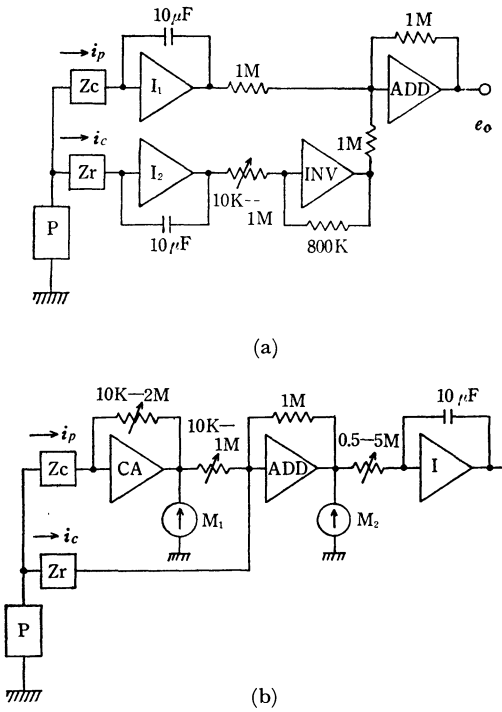

Fig. 1. Basic circuits of the plarographic current integrator with the residual current compensation: P, applying d. c. potentiometer; Z_c, polarographic cell; Z_r, variable resistance or a polarographic cell with supporting electrolyte solutions; I, integrator; ADD, adder; CA, current-to-voltage converter; INV, inverter; M, voltmeter. Chopper-stabilized operational amplifiers (Asia Seisakusho) were used in circuit (a), and solid-state differential operational amplifiers (Model 9814, Aiko Denki, Co., Ltd.) were used in circuit (b).

I_1 and INV by the adder, ADD, then eliminates the contribution of the residual current.

In circuit (b), the sign and the magnitude of the polarographic current, i_p, are changed by the current-to-voltage converter, CA; the residual current component is eliminated from the polarographic current by introducing a properly adjusted, constant current, i_c, to the summing point of the adder, ADD. The output signal of ADD is then integrated by the integrator, I, for a given period of time. In this circuit the adder, ADD, may be omitted by applying i_c directly to the summing point of the integrator, I.

The output voltage, e_o, of the apparatus was found to be strictly proportional to the input current over the wide range of current from a few nanoamperes to about 0.2 μA, the standard deviation of the slope being about 0.5%.

Cell and Reagents. The polarographic cell used was a glass beaker of a 100 cc capacity with a rubber stopper. The conventional DMEs of usual drop time and flow rate of mercury served as working electrodes. Either an internal mercury pool or an external saturated calomel electrode (SCE) was used as the counter electrode; the electric contact between the cell solution and the SCE was made by means of an agar bridge with a sintered glass tip.

1) For example, D. J. Fisher, W. L. Belew and M. T. Kelley, "Polarography 1964," Vol. 1, ed. by Graham J. Hills, MacMillan, London (1966), p. 89.

2) K. Kronenberger, H. Strehlow and A. W. Elbel, *Leybold polarograph. Ber.*, **5**, 62 (1957) through L. Šerák, "Progress in Polarography," Vol. 2, ed. by P. Zuman and I. M. Kolthoff, Interscience Publishers, New York (1962), p. 546.

3) G. L. Booman, E. Morgan and A. L. Crittenden, *J. Am. Chem. Soc.*, **78**, 5533 (1956).

4) J. H. Christie, G. Lauer and R. A. Osteryoung, *J. Electrochem. Soc.*, **111**, 1420 (1964).

5) G. Lauer and R. A. Osteryoung, *Anal. Chem.*, **39**, 1866 (1967).

The solutions were prepared from redistilled water and analytical reagent grade chemicals. When the measurement was carried out with a deaerated solution, purified nitrogen gas was passed over the solution.

All measurements were made in a water thermostat of 25.0 ±0.1°C.

Results and Discussion

Theory. At a given constant potential in the diffusion current plateau the instantaneous polarographic current, $i_p(t)$, at time t during the growth of a spherical mercury drop is given by

$$i_p(t) = k_1 nCD^{1/2}m^{2/3}t^{1/6} + k_2\sigma m^{2/3}t^{-1/3} \quad (1)$$

where k_1 and k_2 are constants, σ is the surface charge density at the given potential, and the other symbols have their usual meaning. Integration of Eq. (1) then gives the charge, $Q(t_d)$, transferred during the growth of a single mercury drop with a drop time of t_d,[5]

$$Q(t_d) = \frac{6}{7}k_1 nCD^{1/2}m^{2/3}t_d^{7/6} + \frac{3}{2}k_2\sigma m^{2/3}t_d^{2/3} \quad (2)$$

Multiplying Eq. (2) by θ/t_d we obtain the following equation representing the charge, $Q(\theta)$, transferred during the period of time of θ ($\theta \gg t_d$),

$$Q(\theta) = (\bar{i}_d + \bar{i}_r)\theta \quad (3)$$

$$\bar{i}_d = \frac{6}{7}k_1 nCD^{1/2}m^{2/3}t_d^{1/6}$$

$$\bar{i}_r = \frac{3}{2}k_2\sigma m^{2/3}t_d^{-1/3}$$

where $\bar{i}_d$ and $\bar{i}_r$ are the average diffusion current and the average charging current, respectively, over the drop life.

The output voltage, e_o, of the present apparatus, being proportional to $Q(\theta)$, is expected to give the average diffusion current when the contribution of the charging current is properly eliminated.

Compensation of Residual Currents. The long-term integration of polarographic currents almost completely eliminates the oscillation due to the periodical renewal of the mercury drop; this makes it possible to compensate the residual current by applying a constant current, i_c, in the way as described before.

The most important factor which determines the accuracy of the present method, when the method is applied to trace analysis, is the constancy of residual currents. Let us consider for example the determination of 1×10^{-6} M of cadmium in a 1 M potassium chloride solution. At the DME used, the residual current at −0.85 V *vs.* SCE in the deaerated supporting electrolyte solution was about 6×10^{-8} A when a SCE was used as an external counter electorde, and it was about ten times larger than the diffusion current of cadmium. Therefore, only 1% fluctuation in the residual current will result in an error of about 10% in the determination of cadmium.

The magnitude and constancy of residual currents in a deaerated potassium chloride solution were very much affected by the nature of the counter electrode and also by the purity of mercury of the DME. The residual current with an internal mercury pool was several times greater than that with the external SCE, and it increased gradually during the measurement, probably because of the dissolution of mercury. The increase in the residual current with an internal mercury pool was more remarkable in solutions saturated with air. When the external SCE was used, the residual current fluctuated slightly for a short period of time, but it reached a reasonably constant value after 1/2 to 1 hr. Therefore, the use of an external counter electrode such as a SCE is strongly recommended for trace analysis. The mercury of high purity should be used for the DME, because a slight contamination of mercury seems to increase the magnitude and instability of residual currents.

The complete compensation of residual currents, as shown in Fig. 2 (curve 1), was achieved by the careful adjustment of the magnitude of applying constant current, i_c. The differential polarography technique with a twin-cell system was also successful for compensating residual currents. The long-term integration method, when applied to the twin-cell system, has the advantage that it obviates the complication of synchronizing the two DME's. By using the twin-cell system, the residual current of an air-saturated potassium chloride solution with an external SCE was perfectly eliminated over the wide potential range from zero to −1.4 V, when the adjustment had been made at the potential of −0.85 V. The twin-cell technique seems to have another possibility of determining accurately the concentration of major component if a solution of a known concentration is used as the reference.

Relationship between the Output Voltage and the Concentration. The output voltage *vs.* concentration relationship was examined with cadmium, lead, and zinc ions in 1 M chloride solutions over the concentration range of 10^{-6}—10^{-3} M according to the following procedure. The constant current, i_c, necessary to compensate the residual current was determined first with the supporting electrolyte solution of a given volume. A known amount of the concentrated solution of the depolarizer was then added successively to the supporting electrolyte solution from a precision micro-syringe; the total volume of the added solution was always less than 1% of the initial volume of supporting electrolyte solution. When deaerated solutions were subjected to analysis, the purified nitrogen gas was bubbled through the solution for about 10 min after each addition of the depolarizer solution.

In each case, the output voltage of the apparatus increased linearly with the time of integration as

shown in Fig. 2, and the output voltage, $e_o(\theta)$, at a given time of integration (*e. g.* $\theta=640$ sec) was found to be perfectly proportional to the concentration of the depolarizer except for the deviation at the lowest concentrations. Figure 3 shows a typical example of the $e_o(\theta)$ *vs.* C (concentration) relationship. The significant deviation from the linearity at very low concentrations ($C<3\times10^{-6}$ M) is thought to be due to the adsorption of depolarizer on glass surfaces of the cell.

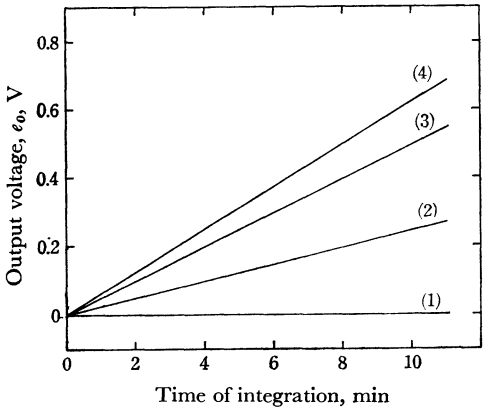

Fig. 2. Relation between the output voltage, e_o, and the time of intergration in deaerated 1 M KCl solutions with an external SCE: (1) 1 M KCl, (2) 4×10^{-5} M Cd(II) +1 M KCl, (3) 8×10^{-5} M Cd(II)+1 M KCl, (4) 1×10^{-4} M Cd(II)+1 M KCl. The residual current was compensated by applying constant current, i_c.

The accuracy of the present method, when the method was applied to the determination of cadmium, lead, and zinc ions in chloride solutions, is demonstrated in Table 1 in terms of the quantity, $(s_b/b)\times100$, where b is the slope of the $e_o(\theta)$ *vs.* C relationship and s_b the standard deviation of the slope.

Conclusion. The present study shows that the long-term integration of polarographic currents provides a very useful method of determining depolarizers in solutions with a relatively large but constant background. With this technique the diffusion current as small as one tenth of the residual current can be measured with reasonably high accuracy. The application of the twin-cell system to the present method seems to be very promising for compensating the residual current and for determining the major component. The present method, when compared with the conventional a.c. polarography, has similar sensitivity but higher accuracy; the method also has the advantage

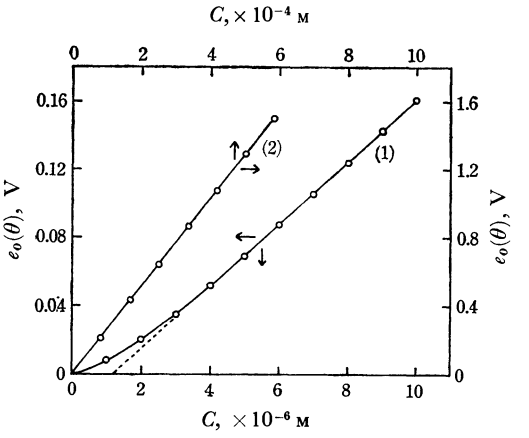

Fig. 3. Relationship between the output voltage, $e_o(\theta)$, at $\theta=640$ sec and the concentration, C, of cadmium ions in deaerated 1 M KCl solutions with an external SCE: (1) concentration range of 1×10^{-6} —1×10^{-5} M, (2) concentration range of 1×10^{-4}—6×10^{-4} M. The residual current was compensated by applying constant current, i_c. The $e_o(\theta)$ values for (1) and (2) are not calibrated for the sensitivity of the apparatus.

TABLE 1. STANDARD DEVIATION, s_b, FOR THE SLOPE, b, OF THE $e_o(\theta)$ *vs.* C RELATIONSHIP

System	Concn. range	$(s_b/b)\times100$
Cd(II) in deaerated 1M KCl at −0.85 V *vs.* SCE	$(1-10)\times10^{-6}$M	1.83
	$(2-10)\times10^{-5}$M	0.544
	$(1-6\ )\times10^{-4}$M	0.484
Cd(II) in air-saturated 1M KCl at −0.85 V *vs.* SCE	$(1-7\ )\times10^{-4}$M	0.458
Pb(II) in deaerated 1M KCl contg. 0.01N HCl and 5×10^{-6}M LEO at −0.65 V *vs.* SCE	$(1-14)\times10^{-6}$M	0.219
	$(2-14)\times10^{-5}$M	0.578
Zn(II) in deaerated 1M KCl contg. 2×10^{-6}M LEO at −1.20 V *vs.* SCE	$(2-14)\times10^{-6}$M	0.560

LEO: polyoxyethylene lauryl ether.

that its sensitivity is not affected by the degree of reversibility of the electrode reaction. From the standpoint of theoretical application, the long-term integration technique will provide a useful method of measuring the true average current at the DME. The accuracy of measurements may be increased by the use of a digital readout equipment.

The authors wish to thank Dr. Gen P. Satô of Sophia University for the valuable discussions and suggestions.

BULLETIN OF THE CHEMICAL SOCIETY OF JAPAN VOL. 42 443—446 (1969)

π-Allylic Coordination of Ethyl Acetoacetate to Palladium(II)*1

Yoshisato TEZUKA,*2 Tetsuya OGURA and Shinichi KAWAGUCHI*3

Department of Chemistry, Faculty of Science, Osaka City University, Sumiyoshi-ku, Osaka

(Received June 28, 1968)

The ethanolysis of diketene is accelerated by the addition of sodium tetrachloropalladate(II). Yellow crystals separated in the end of this reaction were identified as di-μ-chlorobis(π-1-ethoxycarbonyl-2-hydroxyallyl)dipalladium(II) on the ground of analytical data, molecular weight and infrared spectrum. The same complex was also prepared directly by the reaction of palladium(II) chloride with ethyl acetoacetate in water.

A number of π-allylic complexes have been synthesized from palladium(II) chloride and various mono-olefins or conjugated diolefins,[1] but those of unsaturated ketones and esters have been rather few. Tsuji and Imamura[2] prepared π-allylic palladium(II) complexes from α,β- and β,γ-unsaturated esters, Parshall and Wilkinson[3] from α,β-unsaturated ketones such as mesityl oxide, and Kasahara *et al.*[4] from α,β-unsaturated cyclic ketones. This paper reports a novel type of π-allylpalladium(II) complex containing ethoxycarbonyl and hydroxy groups as substituents at 1 and 2 positions, respectively.

In a previous paper[5] we reported copper(I) chloride complex of acrolein, the structure of which has been studied by X-ray and found to contain each acrolein molecule serving as a bridging group between two copper atoms *via* the double bond and the carbonyl oxygen atom.[6] As an extention of this series an unsaturated lactone, diketene was employed as a ligand, and its reactions with several metal compounds have been studied. In the course of these studies sodium tetrachloropalladate(II) was found to catalyze the alcoholysis of diketene and deposit the plladium(II) complex of the reaction product, ethyl acetoacetate.

Experimental

Materials. Diketene supplied by Daicel, Ltd. was used immediately after distillation under reduced pressure. Commercial palladium(II) chloride was evacuated at 300°C. A mixture of palladium(II) chloride and sodium chloride in the mole ratio of 1 : 2 was dissolved in ethanol. The solvent was then evaporated up to dryness and sodium tetrachloropalladate(II) thus prepared was further dried at 100°C *in vacuo*. Dichlorobis(benzonitrile)palladium(II) was prepared by the direct reaction between palladium(II) chloride and benzonitrile according to the Kharasch's method.[7] Dichloromethane, benzene and alcohols were purified by standard methods.[8]

Measurements. Palladium was determined gravimetrically as the dimethylglyoximato complex and chlorine as the silver salt.[9] The molecular weight was determined by the method of boiling point elevation of benzene. The ultraviolet absorption spectra were measured with a Hitachi EPS-2 recording spectrophotometer, and the infrared absorption spectra by means of a Hitachi infrared spectrophotometer EPI-2 or a Shimadzu infrared spectrophotometer IR-27. The proton magnetic resonance spectra were measured with a 60 Mc spectrometer, model JNM 3H 60 of Japan Electron Optics Laboratory, Ltd.

Reaction of Sodium Tetrachloropalladate(II) with Diketene in Ethanol. To a solution of sodium tetrachloropalladate(II) (5.6×10^{-3} mol) in ethanol (70 ml) was added gradually an ethanol solution of diketene

*1 Presented at the 20th Annual Meeting of the Chemical Society of Japan, Tokyo, March, 1967.

*2 On leave from Toyama University, Faculty of Literature and Science.

*3 To whom communications should be addressed.

1) For example, M. L. H. Green and P. L. I. Nagy, "Advances in Organometallic Chemistry," Vol. 2, ed. by F. G. A. Stone and R. West, Academic Press, New York (1964), p. 325; R. Hüttel, *et al.*, *Chem. Ber.*, **98**, 1753 (1965); M. S. Lupin, J. Powell and B. L. Shaw, *J. Chem. Soc.*, (*A*), **1966**, 1687.

2) J. Tsuji and S. Imamura, This Bulletin, **40**, 197 (1967).

3) G. W. Parshall and G. Wilkinson, *Inorg. Chem.*, **1**, 896 (1962).

4) A. Kasahara, K. Tanaka and K. Asamiya, This Bulletin, **40**, 351 (1967).

5) S. Kawaguchi and T. Ogura, *Inorg. Chem.*, **5**, 844 (1966).

6) Y. Kushi, T. Ogura, S. Kawaguchi and H. Kuroya, Presented at the 20th Annual Meeting of the Chemical Society of Japan, Tokyo, April, 1967.

7) M. S. Kharasch, *J. Am. Chem. Soc.*, **60**, 882 (1938).

8) J. A. Riddick and E. E. Toops, Jr., "Organic Solvents," 2nd ed., Interscience, New York, (1955).

9) F. P. Treadwell and W. T. Hall, "Analytical Chemistry," Vol. 2, 9th ed., Wiley, New York (1942), pp. 140, 291.

(1.18×10^{-2} mol) under stirring at room temperature. Together with white sodium chloride yellow palladium complex precipitated, which was recrystallized from benzene. The yield of light yellow needles was about 20% on the base of palladium employed.

Found: C, 26.79; H, 3.29; Cl, 12.8; Pd, 39.33%. Calcd for $C_6H_9O_3ClPd$: C, 26.56; H, 3.32; Cl, 13.1; Pd, 39.27%.

If a more dilute solution of sodium tetrachloropalladate(II) is employed, the ethanolysis of diketene is catalyzed by palladium(II), resulting in ethyl acetoacetate, but the ester complex is not separated due to its solubility. In one experiment a solution of 2.5 mg (8.5×10^{-6} mol) of sodium tetrachloropalladate(II) and 0.25 m*l* (3×10^{-3} mol) of diketene in 2 m*l* (40×10^{-3} mol) of ethanol was kept for 5 hr at 15°C. The gas chromatogram of this solution showed three peaks ascribable to diketene, ethanol and ethyl acetoacetate, and the conversion of diketene was estimated to be 90%. When a diketene solution in ethanol without the palladium(II) catalyst was kept standing overnight at room temperature, no trace of ethyl acetoacetate was found in the solution. The ethanolysis of diketene can thus be concluded not to proceed without a catalyst under these conditions.

Reaction of Palladium(II) Chloride with Ethyl Acetoacetate in Water. Palladium chloride (5.6×10^{-3} mol) was dissolved in 100 m*l* of water, to which ethyl acetoacetate (4.6×10^{-2} mol) was added. The mixture was kept at 40—60°C under stirring for about 40 hr. Brown precipitate formed was filtered off and the filtrate was kept standing for about 70 hr at room temperature. Yellow precipitate appeared, which was recrystallized from benzene, and the yield was about 20% on the base of palladium. The analytical data agree with values calculated for $PdCl(C_6H_9O_3)$ just as did the complex obtained in the reaction between sodium tetrachloropalladate(II) and diketene in ethanol.

Found: C, 26.88; H, 3.56; Cl, 13.2; Pd, 38.60%.

In a similar way the palladium(II) complex of methyl acetoacetate was prepared in the yield of about 10%. The solubilities of this complex in various solvents are even poorer than those of the complex of ethyl acetoacetate.

Found: C, 23.51; H, 3.02; Cl, 13.9; Pd, 41.00%. Calcd for $(C_5H_7O_3)PdCl$: C, 23.26; H, 3.10; Cl, 13.76; Pd, 41.25%.

Reaction of Dichlorobis(benzonitrile)palladium(II) with Diketene in Benzene. In the nitrogen atmosphere a benzene solution (500 m*l*) of dichlorobis(benzonitrile)palladium(II) (2.6×10^{-3} mol) was kept at around 60°C under stirring, to which 3.6×10^{-2} mol of diketene in 50 m*l* of benzene was added gradually. The solution turned from brown to yellow and yellow precipitate resulted. Yield of the crude product was about 80% on the base of palladium. After reprecipitation from ethanol by addition of petroleum ether the palladium complex gave the following analytical results.

Found: C, 20.71; H, 2.37; Cl, 16.02; Pd, 46.08%. Calcd for $C_4H_5O_2ClPd$: C, 21.15; H, 2.20; Cl, 15.63; Pd, 46.89%.

Reaction of Dichlorodi-μ-chlorobis(ethylene)dipalladium(II) with Diketene in Benzene. The reactant complex was prepared by the reaction between dichlorobis(benzonitrile)palladium(II) and ethylene in benzene according to the Kharasch's method.[7] A suspension of $PdCl_2(C_2H_4)$ (2×10^{-3} mol) in 250 m*l* of benzene was kept in the nitrogen atmosphere at room temperature under stirring, to which 3×10^{-2} mol of diketene in benzene was added gradually. The reaction mixture which was orange yellow at first turned to blue yellow and separated some solid. The precipitate was washed with benzene and dried at 80°C *in vacuo*. Results of the elemental analysis agreed again with values calculated for $PdCl(C_4H_5O_2)$.

Found: C, 20.43; H, 2.47; Pd, 46.07%.

Syntheses of Reference Complexes. Bis(acetylacetonato)palladium(II) was prepared by the reaction between palladium(II) chloride and excess amount of acetylacetone in water at around 60°C. Yellow complex obtained was recrystallized from benzene and dried at 100°C *in vacuo*.

Found: C, 39.57; H, 4.87%. Calcd for $(C_5H_7O_2)_2Pd$: C, 39.42; H, 4.60%.

Nickel(II) complex of ethyl acetoacetate was synthesized by the reaction between the nickel ammine complex and the ester in water. The product was recrystallized from dichloromethane and dried at 100°C *in vacuo*.

Found: C, 40.82; H, 6.27%. Calcd for $Ni(C_6H_9O_3)_2\cdot 2H_2O$: C, 40.24; H, 6.43%.

Results and Discussion

Di-μ-chlorobis(π-1-ethoxycarbonyl-2-hydroxyallyl)dipalladium(II). Light yellow crystals which were produced in the reaction of sodium tetrachloropalladate(II) with diketene in ethanol have the empirical formula $PdCl(C_6H_9O_3)$. When this compound was heated at around 180°C *in vacuo*, partial carbonization occurred and volatile substance was evolved, which was identified as ethyl acetoacetate by means of the gas chromatography and infrared spectra. It was also decomposed by dilute hydrochloric acid to set free ethyl acetoacetate. These results indicate that this is a palladium(II) complex of ethyl acetoacetate.

This complex is slightly soluble in benzene, dichloromethane, methyl and ethyl alcohols (10^{-2}—10^{-3} mol/*l* at room temperature). It is more soluble in dimethyl sulfoxide, but reddish yellow precipitate is separated therefrom on standing, which shows an identical infrared spectrum with what is obtained in the reaction between palladium(II) chloride and dimethyl sulfoxide. Tetrahydrofuran and pyridine also show high solubilities, but decomposition of the complex resulted on standing in either case. The molecular weight of this palladium(II) complex was determined to be 502 by measuring the boiling point elevation of benzene. This value nearly coincides with 541 calculated for the dimer, certifying the molecular formula $[PdCl(C_6H_9O_3)]_2$ and satisfying the usual coordination number four of palladium(II).

The infrared spectra were measured in the region of 400 through 5000 cm^{-1} by the potassium bromide disk method. Characteristic absorption bands are listed in Table 1 together with those for the corresponding complex of methyl acetoacetate. Infrared

Table 1. Characteristic infrared absorption bands of di-μ-chlorobis(π-1-ethoxycarbonyl-2-hydroxyallyl)dipalladium(II) (A) and di-μ-chlorobis(π-1-methoxycarbonyl-2-hydroxyallyl)dipalladium (II) (B) determined in the potassium bromide disk

Compex A, cm^{-1}	Complex B, cm^{-1}	Assignment
3200 m	3160 m	O–H str.
3080 w	3080 w	end methylene str.
1675 vs	1670 vs	C=O str.
1445 s	1435 s	delocalized C–C str.
1205 vs	1220 vs	COC asym. str.
1170 s	1170 s	COC sym. str.
1040 m	1035 m	delocalized C–C str. + C–OH str.
545 m	545 m	skeletal deform.

spectra of ethyl acetoacetate[10] and di-μ-chlorobis-(π-allyl)dipalladium(II)[11] were referred to in assigning absorption bands of the present complex. Although bis(acetylacetonato)palladium(II) is well known to be a usual enolate chelate,[12] corresponding palladium(II) complex of ethyl acetoacetate has not yet been reported. As shown in Table 1, the present complex does not show C=O and C=C stretching bands characteristic for the enolate chelate,[13] but has very strong peaks at 1675 and 1205 cm^{-1} indicating the presence of uncoordinated ethoxycarbonyl group. The peak at 3200 cm^{-1} must be attributed to an OH group. It is a quite novel and rather curious feature that the OH group of an enol form is preserved intact in this β-dicarbonyl complex. On the other hand peaks at 3080 and 1445 cm^{-1} may be ascribed to the stretching vibrations of end methylene and π-allylic C–C bonds, respectively.[11] Furthermore the absorption band at 546 cm^{-1} might be attributable to the skeletal deformation which was assigned by Fritz[11] as characteristic for the π-allyl group. These infrared informations strongly suggest the formula I for the palladium(II) complex of ethyl acetoacetate.

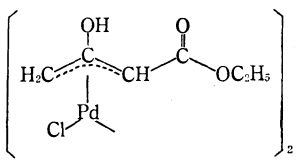

I

The stretching band of OH usually appears[14] at around 3600 cm^{-1}, and that of C=O at 1740 and 1715 cm^{-1} in the case of free ethyl acetoacetate. These bands are observed at 3200 and 1675 cm^{-1}, respectively in case of the present complex. These shifts to the lower frequency side suggest the presence of inter- or intramolecular hydrogen bonding between the two functional groups.

Proton magnetic resonance spectra are frequently utilized as one of the most powerful tools in the structural study of π-allylic metal complexes.[15] Unfortunately, however, suitable inert solvents are not available for the present complex. It is not enough soluble in alcohols or haloalkanes, and reacts with dimethyl sulfoxide and other better solvents. Thus useful informations can not be obtained from these studies. The X-ray analysis of this complex is now in progress and preliminary results[16] clearly support the structure I, and certify the presence of intermolecular hydrogen linkage which constitutes a one-dimensional polymeric structure. The palladium(II) complex of ethyl acetoacetate can now be named as di-μ-chloro-bis-(π-1-ethoxycarbonyl-2-hydroxyallyl)dipalladium(II).

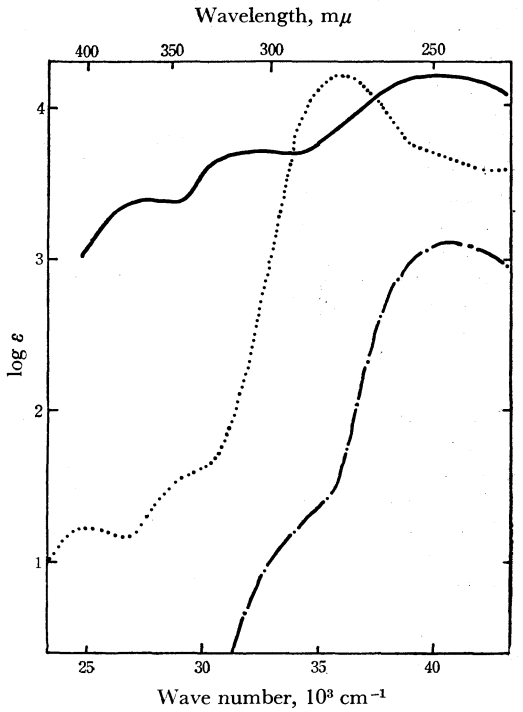

Fig. 1. Ultraviolet absorption spectra of ethyl acetoacetate ($C_6H_{10}O_3$) (-•-•-), $Ni(C_6H_9O_3)_2$ (·····) and $[PdCl(C_6H_9O_3)]_2$ (———).

10) L. J. Bellamy, "The Infra-red Spectra of Complex Molecules," Wiley, New York (1957), pp. 178.
11) H. P. Fritz, *Chem. Ber.*, **94**, 1217 (1961).
12) K. Nakamoto, P. J. McCarthy and A. E. Martell, *J. Am. Chem. Soc.*, **83**, 1272 (1961).
13) G. T. Behnke and K. Nakamoto, *ibid.*, **6**, 433 (1967).
14) p. 95 of Ref. 10.
15) See, for instance, J. K. Becconsall, B. E. Job and S. O'Brien, *J. Chem. Soc.*, (*A*), **1967**, 423; W. B. Wise, D. C. Lini and K. C. Ramey, *Chem. Commun.*, **1967**, 463.
16) K. Oda, N. Yasuoka, N. Kasai, M. Kakudo, Y. Tezuka, T. Ogura and S. Kawaguchi, *Chem. Commun.*, **1968**, 989.

The ultraviolet spectrum of this complex in ethanol is shown in Fig. 1 together with those of ethyl acetoacetate and its nickel(II) complex. A very broad band at around 250 mμ seems to be characteristic of the ligand. The nickel(II) complex of ethyl acetoacetate shows absorption maxima at 690 and 403 mμ, of which the extinction coefficients are both small and attributable to the d–d transition. The present π-allylic complex has very strong bands at 358 (log ε=3.38) and around 310 mμ (log ε=3.69). These absorptions may be related to the π-allylic structure of the complex. The absorption data of a related compound di-μ-chlorobis(π-1-methoxymethylallyl)dipalladium(II) in methanol were reported by Robinson and Shaw,[17] which show maxima at 330 (log ε=2.98), 229 sh (log ε=3.86) and 208 mμ (log ε=4.19). Some correspondence seems to exist between absorption data of these π-allylic palladium complexes, but their exact assignments are not possible.

Uncharacterized Complex $PdCl(C_4H_5O_2)$. The analytical data of the complex obtained in the reaction between dichlorobis(benzonitrile)palladium(II) and diketene nearly coincide with those calculated for $PdCl(C_4H_5O_2)$. It is hardly soluble in benzene or haloalkanes,but dissolves pretty well in methyl and ethyl alcohols. The same compound was also obtained in the reaction between di-chloro-di-μ-chlorobis(ethylene)dipalladium(II) with diketene in benzene. The analytical and infrared data suggest that this is not a complex of diketene itself. The nature of this complex is now under investigation.

The Mechanism of Alcoholysis of Diketene in the Presence of Pd(II). When excess amount of diketene is added to an ethanol solution of sodium tetrachloropalladate(II), color of the solution turns from red to yellow in a few minutes and sodium chloride precipitates at the same time. Then irritative ordor of diketene changes gradually to agreeable one of the ester. Ethyl acetoacetate produced was identified by means of the gas chromatography.

The palladium(II) complex of the ester was deposited in the end of reaction when the tetrachloropalladate(II) was used in a higher concentration. This is a complex of the reaction product, and during the steady course of the catalytic alcoholysis of diketene, the ligand ester must be easily displaced by the substrate, diketene.

Diketene is known to be an acid of medium strength (pK_a=7.1),[18] and will liberate a proton to coordinate to palladium.

$$Na_2PdCl_4 + C_4H_4O_2 \rightleftarrows \underset{\text{II}}{PdCl(C_4H_3O_2)} + HCl + 2NaCl \qquad (1)$$

The intermediate II has not yet been identified but is just presumed here. The strong acidity of the reaction mixture and precipitation of sodium chloride support Eq. (1). The nucleophilic attack of an alcohol molecule on the carbonyl carbon may result in the rupture of the lactone ring.

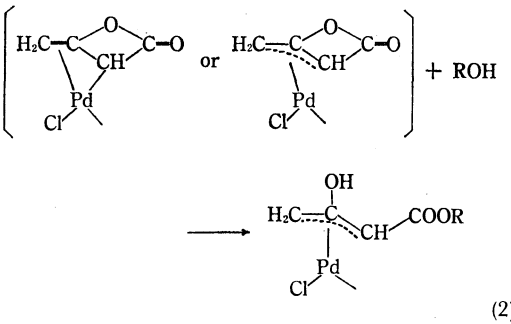

(2)

The relative rate of the Pd(II) catalyzed alcoholysis in various aliphatic alcohols are in the decreasing order of MeOH>EtOH> *n*-PrOH~*i*-PrOH. This is the same tendency as that observed for the acid catalyzed esterification. Detailed informations concerning the mechanism of Pd(II) catalyzed alcoholysis of diketene must await further investigations.

The authors are grateful to Daicel, Ltd. for the generous gift of diketene. Thanks are also due to Mr. Kenichiro Noda for his help in the NMR measurements.

17) S. D. Robinson and B. L. Shaw, *J. Chem. Soc.*, **1963**, 4806.

18) A. Wassermann, *ibid.*, **1948**, 1323.

BULLETIN OF THE CHEMICAL SOCIETY OF JAPAN VOL. 42 447—452 (1969)

Association Involving Optically Active Ions. II. Association Constants of Tris(ethylenediamine)cobalt(III) and Tris(propylenediamine)-cobalt(III) Ions with Some Anions

Kazuko OGINO

Department of Chemistry, Faculty of Science, Tohoku University, Katahira-cho, Sendai

(Received June 30, 1968)

Association constants of [Co en$_3$]$^{3+}$ (en=ethylenediamine) and *d*- and *l*-[Co *d*-pn$_3$]$^{3+}$ (pn=propylenediamine; *d*- and *l*- refer to the sign of optical rotation at sodium D-line) with some anions have been determined spectrophotometrically. Values are as follows: [Co en$_3$]$^{3+}$·SO$_4^{2-}$ 49, [Co-en$_3$]$^{3+}$·glycollate$^-$ ~5, *d*-[Co *d*-pn$_3$]$^{3+}$·SO$_4^{2-}$ 70, *d*-[Co *d*-pn$_3$]$^{3+}$·*d*-tart^{2-} (tart^{2-}=bivalent tartrate anion) 30, *d*-[Co *d*-pn$_3$]$^{3+}$·*l*-tart^{2-} 28, *l*-[Co *d*-pn$_3$]$^{3+}$·SO$_4^{2-}$ 43, *l*-[Co *d*-pn$_3$]$^{3+}$·*d*-tart^{2-} ~7, *l*-[Co-*d*-pn$_3$]$^{3+}$·*l*-tart^{2-} ~16. These association constants are discussed in terms of the microscopic interaction between the ions. The effect of outer-sphere association on the circular dichroism and optical rotatory dispersion is also discussed.

In the outer-sphere association, ionic charges and radii are considered to be of primary importance. It is also known that other effects such as dipole moment and polarizability exert influence. However, few investigations have been made on the effect of microscopic construction of individual ions on the outer-sphere association. In a previous paper,[1] it was shown that stereospecificity exists in the association between tris(ethylenediamine)-cobalt(III), [Co en$_3$]$^{3+}$, and tartrate ions. It can be interpreted only on the basis of microscopic interaction between ions. In order to obtain more distinct information on such an interaction, association involving diastereoisomers of tris(propylenediamine)cobalt(III) ions, *d*- and *l*-[Co *d*-pn$_3$]$^{3+}$ (*d*- and *l*- refer to the sign of the optical rotation at sodium D-line), is investigated in this paper. These systems are considered to be appropriate for the present purpose because the two isomers are different from each other only in the mutual orientation of bonds. Association constants of these complex ions with tartrate and with sulfate are determined spectrophotometrically and effects of association on the circular dichroism (CD) and optical rotatory dispersion (ORD) are investigated.

Experimental

The complexes *d*-[Co *d*-pn$_3$]I$_3$·H$_2$O and *l*-[Co *d*-pn$_3$]Cl·*d*-tart·3H$_2$O (tart^{2-} denotes bivalent tartrate anion) were prepared according to the method reported in the literature.[2] The complex *d*-[Co *d*-pn$_3$]I$_3$·H$_2$O was treated with Na$_3$[Co(CN)$_6$]. The precipitate was washed to be free from iodide and then converted into perchlorate by passing through a column of Dowex 1, X-8 in the perchlorate form. Found: C, 18.10; H, 5.29; N, 14.16%. Calcd for [CoC$_9$H$_{30}$N$_6$](ClO$_4$)$_3$·H$_2$O: C, 18.12; H, 5.40; N, 14.09%. Molecular rotations at sodium D-line, and at peaks of ORD are as follows: $[M]_D$=150°, $[M]_{525}$=2250° and $[M]_{468}$=8000°. The complex *l*-[Co *d*-pn$_3$](ClO$_4$)$_3$ was obtained by the addition of perchloric acid into the solution of *l*-[Co *d*-pn$_3$]Cl·*d*-tart·3H$_3$O. Found: C, 18.92; H, 5.08; N, 14.45%. Calcd for [CoC$_9$H$_{30}$N$_6$](ClO$_4$)$_3$: C, 18.67; H, 5.22; N, 14.50%. $[M]_D$=1500°, $[M]_{515}$=4500° and $[M]_{431}$=5100°. The preparation of *d*-[Co en$_3$]-(ClO$_4$)$_3$ was described in the previous paper.[1]

The electronic absorption spectra were measured with a Shimadzu QV-50 Spectrophotometer, and the ORD and CD spectra were obtained with a JASCO ORD/UV-5 Optical Rotatory Dispersion Recorder. All measurements were carried out at 25°C and μ=0.1 (NaClO$_4$). The pH of the solution was adjusted so that tartrate ions are present as a bivalent anion in the solution. The concentration of the complexes was varied from 0.03 to 1.25 mM.

Results and Discussion

The absorbancy, CD and ORD of many complex ions are affected by the outer-sphere association, which is expressed by

$$M^{m+} + jX^{x-} \rightleftarrows MX_j^{(m-jx)+} \quad (j=1, 2, \cdots, n) \quad (1)$$

where M^{m+} and X^{x-} correspond to the complex ion and the counter ion, respectively. Association constants are defined by

$$K = [MX^{(m-x)+}]/([M^{m+}][X^{x-}]) \quad (2)$$

$$\beta_j = [MX_j^{(m-jx)+}]/([M^{m+}][X^{x-}]^j) \quad (3)$$

1) K. Ogino and U. Saito, This Bulletin, **40**, 826 (1967).

2) F. P. Dwyer, F. L. Garvan and A. Shulman, *J. Am. Chem. Soc.*, **81**, 290 (1959).

In the previous paper,[1] the relation between the association constants and the change of a partial molar quantity on association, Δ, was given in a generalized form (Eq. (12) in Ref. 1):

$$\Delta = \sum_{j=1}^{n} \Delta_{MX_j}\beta_j[X^{x-}]^j/(1 + \sum_{j=1}^{n} \beta_j[X^{x-}]^j) \quad (4)$$

which is valid for any property that is additive for $MX_j^{(m-jx)+}$, *e. g.*, absorbancy, electrical conductivity, *etc.* In the case of absorbancy, Δ and Δ_{MX_j} are defined by

$$\Delta = \varepsilon_{app} - \varepsilon_0 \quad (5)$$

and

$$\Delta_{MX_j} = \varepsilon_{MX_j} - \varepsilon_0 \quad (6)$$

respectively, where ε_0 and ε_{MX_j} are molar extinction coefficients of M^{m+} and $MX^{(m-jx)+}$, and ε_{app} is the apparent extinction coefficient of the solution:

$$\varepsilon_{app} = (\text{absorbancy})/([M^{m+}] + \sum_{j=1}^{n}[MX_j^{(m-jx)+}]) \quad (7)$$

In the case of CD and ORD, Δ and Δ_{MX_j} are defined similarly as in Eqs. (5) and (6):

$$\Delta = (\varepsilon_l - \varepsilon_r)_{app} - (\varepsilon_l - \varepsilon_0)_0 \quad (8)$$

$$\Delta_{MX_j} = (\varepsilon_l - \varepsilon_r)_{MX_j} - (\varepsilon_l - \varepsilon_r)_0 \quad (9)$$

for CD and

$$\Delta = [M]_{app} - [M]_0 \quad (10)$$

$$\Delta_{MX_j} = [M]_{MX_j} - [M]_0 \quad (11)$$

for ORD, where the subscripts *app*, 0 and MX_j have the same meanings as in Eqs. (5) and (6).

Assuming that only the species $MX^{(m-x)+}$ is formed and higher association is absent, Eq. (12) is obtained instead of Eq. (4).

$$\Delta = \Delta_{MX}K[X^{x-}]/(1 + K[X^{x-}]) \quad (12)$$

$$\Delta_{MX} = \varepsilon_{MX} - \varepsilon_0 \quad (13)$$

As has been explained in the previous paper,[1] the association constant K can be determined by use of Eq. (14).

$$[X^{x-}]/\Delta = [X^{x-}]/\Delta_{MX} + 1/(K\Delta_{MX}) \quad (14)$$

By plotting $[X^{x-}]/\Delta$ against $[X^{x-}]$, K is obtained as the ratio of slope to intercept of the resulting straight line. If other species, $MX_2^{(m-2x)+}, \cdots, MX_n^{(m-nx)+}$ were also formed, the plot of $[X^{x-}]/\Delta$ *vs.* $[X^{x-}]$ would not give a straight line, but give a curve dependent on the relative magnitude of Δ_{MX_j} and β_j. Whenever the curvature of the plot is small and can be approximated to be a straight line, an apparent 1 : 1 association constant can be obtained by use of Eq. (14). However, such an apparent constant should be a function of the ratio $\Delta_{MX_j}/\Delta_{MX}$, and since the ratio is expected to depend on the wavelength at which the absorbancy is measured, the apparent constant obtained at different wavelengths will not give a constant value.

Equation (14) was applied to the change of absorbancy of $[Co\,en_3]^{3+}$ on addition of sulfate, and the association constants were obtained to be 49, 47 and 50 from absorbancies at 260, 262 and 265 mμ, respectively. The small deviation of these values suggests that 1 : 1 association occurs predominantly.

The absence of higher association was also examined by the following procedure. When the change of absorbancy, CD or ODR at two concentrations $[X^{x-}]_1$ and $[X^{x-}]_2$ are measured to be Δ_1 and Δ_2 respectively, the ratio Δ_1/Δ_2 is given by

$$\frac{\Delta_1}{\Delta_2} = \frac{(\sum_{j=1}^{n} \Delta_{MX_j}[X^{x-}]_1^j)(1 + \sum_{j=1}^{n} \beta_j[X^{x-}]_2^j)}{(\sum_{j=1}^{n} \Delta_{MX_j}[X^{x-}]_2^j)(1 + \sum_{j=1}^{n} \beta_j[X^{x-}]_1^j)} \quad (15)$$

It is a function of the ratio $\Delta_{MX_j}/\Delta_{MX}$. When only 1 : 1 association takes place, Eq. (15) is simplified as

$$\frac{\Delta_1}{\Delta_2} = \frac{[X^{x-}]_1(1 + K[X^{x-}]_2)}{[X^{x-}]_2(1 + K[X^{x-}]_1)} \quad (16)$$

which does not contain Δ_{MX}, hence Δ_1/Δ_2 should be constant for any properties that are affected by association. This equation was applied to the changes of the absorbancy, ORD and CD of the system *d*-$[Co\,en_3]^{3+}$ and sulfate in the wavelengths where the changes caused by the addition of sulfate could be measured most accurately (*cf.* Figs. 4 and 5). The result for the absorbancy is shown in Table 1. At $[X^{x-}]_1 = 0.025$ M and $[X^{x-}]_2 = 0.01$ M, the value of Δ_1/Δ_2 is calculated to be 1.68 by use of Eq. (16) and $K = 49$. The values in Table 1 agree with it. The ratio for the change

Table 1. The ratio Δ_1/Δ_2 at $[X^{x-}]_1 = 0.025$ M and $[X^{x-}]_2 = 0.010$ M for absorbancy of the system, $[Co\,en_3]^{3+}$ and sulfate

mμ	Δ_1/Δ_2	mμ	Δ_1/Δ_2	mμ	Δ_1/Δ_2
267.5	1.7_0	257.5	1.6_4	216	1.7
265	1.6_4	255	1.6_8	210	1.7
262.5	1.6_7	225	1.6	206	1.6
260	1.6_8	220	1.7		

of ORD at 360—410 mμ and that for CD at 435—470 mμ were also found to agree with the calculated value within the experimental error.

From above observations it may be concluded that only the species $[Co\,en_3]^{3+}\cdot SO_4^{2-}$ are formed predominantly by the association under the experimental condition. Larsson[3] reported the evidence of higher association between $[Co\,en_3]^{3+}$ and sulfate ions. This difference may be due to the differences in sulfate concentrations and ionic strength: In the study by Larsson, sulfate concentration was varied from 0.015 to 1 M and other electrolytes were not added in solution, while in this study the

3) R. Larsson, *Acta Chem. Scand.*, **16**, 2267 (1962).

maximum sulfate concentration was 0.025 M and ionic strength was kept to be 0.1 with sodium perchlorate.

The absorbancy, CD and ORD of [Co *d*-pn_3]$^{3+}$ also changed on the addition of sulfate and tartrate. In Figs. 1 and 2 are shown the changes in the

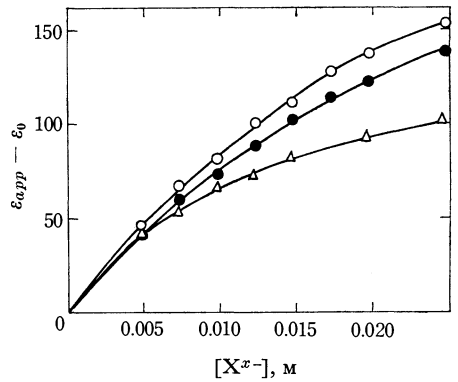

Fig. 1. Variation of the apparent extinction coefficient of *d*-[Co *d*-pn_3]$^{3+}$ at 265 mμ as a function of anion concentration, [X^{x-}], μ=0.1, 25°C.
—○—: X^{x-}=*d*-tart^{2-}, —●—: X^{x-}=*l*-tart^{2-}, —△—: X^{x-}=SO_4^{2-}

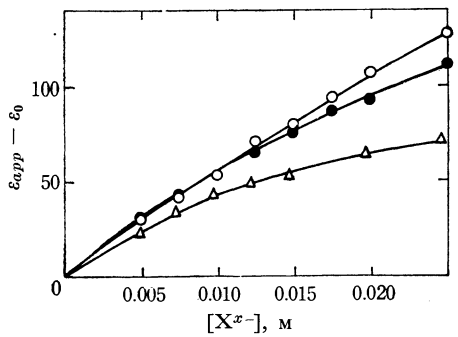

Fig. 2. Variation of the apparent extinction coefficient of *l*-[Co *d*-pn_3]$^{3+}$ at 265 mμ as a function of anion concentration, [X^{x-}], μ=0.1, 25°C.
—○—: X^{x-}=*d*-tart^{2-}, —●—: X^{x-}=*l*-tart^{2-}, —△—: X^{x-}=SO_4^{2-}

apparent extinction coefficient (*cf.* Eq. (5)) at 265 mμ. The changes are neither the same for *d*- and *l*-tartrate, nor for *d*- and *l*-[Co *d*-pn_3]$^{3+}$. From these plots association constants were determined by use of Eq. (14). In Table 2 the constants obtained are given. Using these association constants, the changes of CD and ORD spectra of *d*- and *l*-[Co *d*-pn_3]$^{3+}$ on the addition of sulfate could be explained by Eq. (16). This equation was also applied to the system *d*-[Co *d*-pn_3]$^{3+}$ and tartrate, but was not applied to the system *l*-[Co *d*-pn_3]$^{3+}$ and tartrate because of the limited accuracy of association constants and the small change of CD caused by the addition of tartrate (*cf.* Fig. 9).

It was shown by the X-ray analyses that the absolute configurations of *d*- and *l*-[Co *d*-pn_3]$^{3+}$

Table 2. Association constants at μ=0.1 and 25°C

	Absolute configuration	*d*-tart^{2-}	*l*-tart^{2-}	SO_4^{2-}	glycolate$^-$
d-[Co en_3]$^{3+}$	$\Delta(C_2)$[4]	26±2[1]		49±2	5±2
l-[Co en_3]$^{3+}$	$\Lambda(C_2)$	21±2[1]			
d-[Co *d*-pn_3]$^{3+}$	$\Delta(C_2)$[5]	30±2	28±2	70±2	
l-[Co *d*-pn_3]$^{3+}$	$\Lambda(C_2)$[6]	7±2	16±2	43±3	

are $\Delta(C_2)$[5] and $\Delta(C_2)$[6],*1 respectively, and *d*- and *l*-[Co *d*-pn_3]$^{3+}$ correspond to the "*lel*" type and the "*ob*" type according to Corey and Bailar's notation.[7] In the *lel* conformation, two sets of three N–H bonds are nearly parallel to the C_3 axis of the complex ion,[8] and the anion in the ion pair can be located along the direction of the C_3 axis so as to form hydrogen bonding with N–H hydrogen. On the other hand, in the *ob* conformation orientations of the N–H bonds are not the same to one another. As is seen in Table 2, the association constants for *lel*-$\Delta(C_2)$-[Co *d*-pn_3]$^{3+}$ are substantially larger than those for the *ob*-$\Lambda(C_2)$-isomer. Such a difference will be attributable to the difference in the orientation of N–H bonds in *lel* and *ob* isomer.

The conformations of [Co en_3]$^{3+}$ in the solution are predominantly *lel*. Association constants in Table 2 show that those for [Co en_3]$^{3+}$ are a little smaller than those for *lel*-Δ-[Co *d*-pn_3]$^{3+}$,*2 contrary

4) Y. Saito, K. Nakatsu, M. Shiro and H. Kuroya, This Bulletin, **30**, 795 (1957); *Acta Cryst.*, **8**, 729 (1955).

5) H. Iwasaki and Y. Saito, This Bulletin, **39**, 92 (1966).

6) Y. Saito, Structures and Absolute Configurations of Cobalt(III) Complexes, Plenary Lecture, Xth I.C.C.C., *Pure Appl. Chem.*, IUPAC, to be published.

*1 The complex *l*-[Co *d*-pn_3]$^{3+}$ used in this study is the same sample that was used in the X-ray analysis by Y. Saito *et al.*

7) E. J. Corey and J. C. Bailar, *J. Am. Chem. Soc.*, **81**, 2620 (1959).

8) S. F. Mason and B. J. Norman, *J. Chem. Soc., A*, **1966**, 307.

*2 According to the potential energy difference calculated by Corey and Bailar,[7] *ca.* 64% of the total complex in the solution of tris(diamine)cobalt(III), is in the *lel* conformation, *ca.* 3% in the *ob* conformation, and the rest of the complex is in the intermediate conformations between *lel* and *ob*. The result of the calculation was supported by the experiments by Dwyer *et al.*[9] When it is assumed that the association constant between sulfate and [Co en_3]$^{3+}$ in conformations other than *lel* is about 43/70 (ratio of association constants of *ob*-Λ-[Co *d*-pn_3]$^{3+}$·SO_4^{2-} and *lel*-Δ-[Co *d*-pn_3]$^{3+}$·SO_4^{2-}) of that of [Co en_3]$^{3+}$ in the *lel* conformation, the hypothetical association constant of *lel*-[Co en_3]$^{3+}$·SO_4^{2-} is calculated to be 58, which is still smaller than the association constant of *lel*-Δ-[Co *d*-pn_3]$^{3+}$·SO_4^{2-}.

9) F. P. Dwyer, T. E. MacDermott and A. M. Sargeson, *J. Am. Chem. Soc.*, **85**, 2913 (1963); F. P. Dwyer, A. M. Sargeson and L. B. James, *ibid.*, **86**, 590 (1964).

to the expectation from the electrostatic theory that the larger ions should have smaller association constants. This indicates that the steric hindrance of the methyl group of propylenediamine is not significant in the association with sulfate and with tartrate. It may be because the methyl groups have trigonal orientation nearly perpendicular to the C_3 axis and do not interfere with the approach of anions along the direction of the C_3 axis.

Association constants of $[Co\ en_3]^{3+}$ with tartrate ions were discussed briefly in the previous paper.[1] They are about one half of that with sulfate but much larger than that with univalent glycollate. It suggests that the two carboxylate groups in a tartrate ion take part simultaneously in association. Therefore the two carboxylates in a tartrate ion should not be oriented trans to each other. Between the two gauche conformations of a *d*-tartrate ion in Fig. 3, I is considered to be more stable because

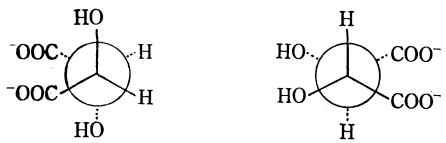

Fig. 3. Conformations of a *d*-tartrate ion viewed along the direction of the bond between two asymmetric carbon atoms.

two hydroxyl groups are trans to each other and hydrogen bonding is possible between $-COO^-$ and $-OH$. Thus, the bond $^-OOC-C-C-COO^-$ in a *d*-tartrate ion is arranged as a right handed screw in an ion-pair, while in an *l*-tartrate ion it is arranged as a left handed screw. The difference in the association constants of *lel*-Δ- and *ob*-Λ-$[Co\ d\text{-}pn_3]^{3+}$ with *d*- and *l*-tartrate ions is supposed to be related to the relative configuration of the

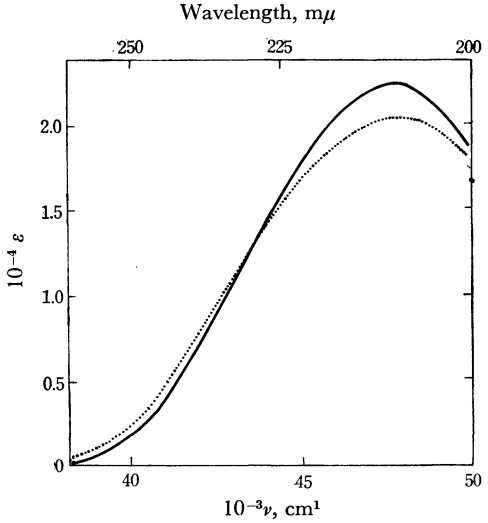

Fig. 4. Electronic absorption spectra in the charge transfer region.
——: $[Co\ en_3]^{3+}$, ·····: $[Co\ en_3]^{3+}\cdot SO_4^{2-}$

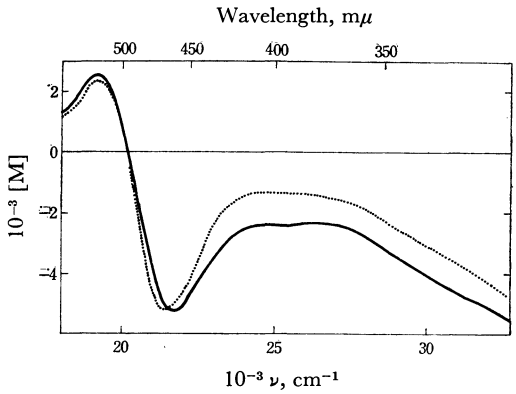

Fig. 5. Optical rotatory dispersion curves.
——: $[Co\ en_3]^{3+}$, ·····: $[Co\ en_3]^{3+}\cdot SO_4^{2-}$

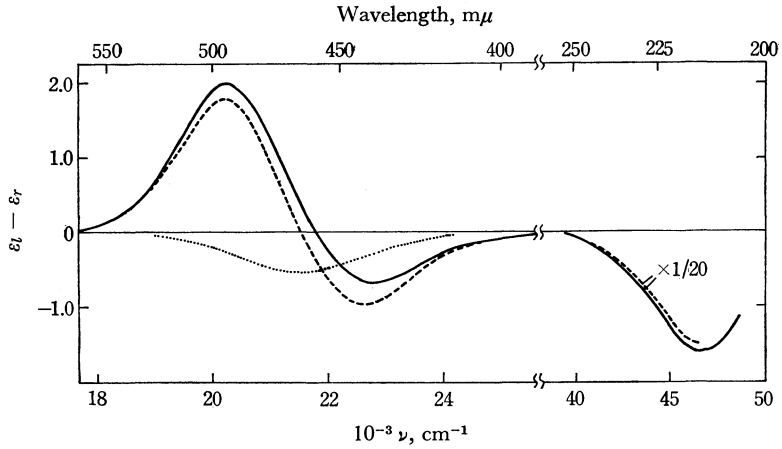

Fig. 6. Effect of sulfate on the circular dichroism curve of Δ-$[Co\ d\text{-}pn_3](ClO_4)_3\cdot H_2O$, $\mu=0.1(NaClO_4)$, 25°C.
——: CD in solution without sulfate, ------: CD in 0.025 M Na_2SO_4 solution,
·····: Difference between CD curves of Δ-$[Co\ d\text{-}pn_3]^{3+}\cdot SO_4^{2-}$ and Δ-$[Co\ d\text{-}pn_3]^{3+}$ (*cf.* Eq. (17)).

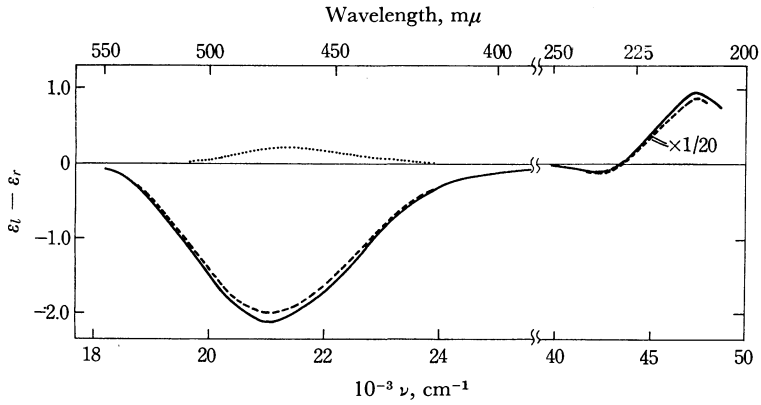

Fig. 7. Effect of sulfate on the circular dichroism curve of Λ-$[Co\ d\text{-}pn_3](ClO_4)_3$, μ=0.1($NaClO_4$), 25°C.
——: CD in solution without sulfate, ------: CD in 0.025 M Na_2SO_4 solution,
……: Difference between CD curves of Λ-$[Co\ d\text{-}pn_3]^{3+}\cdot SO_4^{2-}$ and Λ-$[Co\ d\text{-}pn_3]^{3+}$ (*cf.* Eq. (17)).

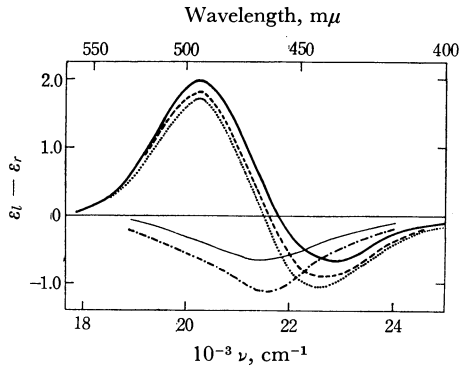

Fig. 8. Effect of tartrate on the circular dichroism spectrum of Δ-$[Co\ d\text{-}pn_3](ClO_4)_3\cdot H_2O$, μ=0.1 ($NaClO_4$), 25°C.
——: CD in solution without tartrate
……: CD in 0.025 M Na_2*d*-tart solution
------: CD in 0.025 M Na_2 *l*-tart solution
-·-·-: Difference between CD curves of Δ-$[Co\ d\text{-}pn_3]^{3+}\cdot d\text{-}tart^{2-}$ and Δ-$[Co\ d\text{-}pn_3]^{3+}$
——: Difference between CD curves of Δ-$[Co\ d\text{-}pn_3]^{3+}\cdot l\text{-}tart^{2-}$ and Δ-$[Co\ d\text{-}pn_3]^{3+}$

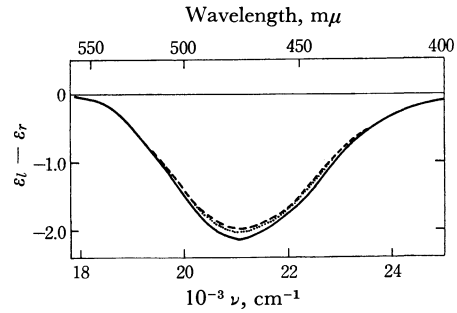

Fig. 9. Effect of tartrate on the circular dichroism spectrum of Λ-$[Co\ d\text{-}pn_3](ClO_4)_3$, μ=0.1($NaClO_4$), 25°C.
——: CD in solution without tartrate
……: CD in 0.025 M Na_2 *d*-tart solution
------: CD in 0.025 M Na_2 *l*-tart solution

complex ion and the ^-OOC–C–C–COO^- screw in the tartrate ion. A consideration with the aid of molecular models reveals that association of *d*-tartrate ion with complex ions of $\Delta(C_2)$ configuration is more preferable to that with complex ions of $\Lambda(C_2)$ configuration. This assumption is in accord with the results in Table 2. The difference in the association constants of tartrate ions with *lel*-Δ- and *ob*-Λ-$[Co\ d\text{-}pn_3]^{3+}$, which have the same charge and nearly the same size, shows the importance of the microscopic construction of ions in the outer-sphere association.

Using the association constant in Table 2, absorption and CD spectra of $[Co\ en_3]^{3+}$ and $[Co\ d\text{-}pn_3]^{3+}$ were analyzed in terms of 1 : 1 association by use of Eq. (12). In Figs. 4 and 5 are shown the absorption spectrum and the ORD curve of the ion-pair $[Co\ en_3]^{3+}\cdot SO_4^{2-}$. The absorbancy increases by association at wavelengths 270—230 mμ, but it decreases at shorter wavelengths. The absorbancy of *lel*-Δ- and *ob*-Λ-$[Co\ d\text{-}pn_3]^{3+}$ change similarly by the association with sulfate as that of $[Co\ en_3]^{3+}$.

Figures 6 and 7 show CD spectra of *lel*-Δ- and *ob*-Λ-$[Co\ d\text{-}pn_3]^{3+}$ in the absence and in the presence of 0.025 M sodium sulfate. The CD bands of these complexes in the absence of sulfate were discussed in a seperate paper.[10] As can be seen in

10) K. Ogino, K. Murano and J. Fujita, *Inorg. Nucl. Chem. Letters*, **4**, 351 (1968).

Figs. 6 and 7 the sign of the change on addition of sulfate (*cf.* Eq. (8)) is negative in the *d–d* abosprtion region and positive in the charge transfer region for *lel*-Δ-[Co *d*-pn_3]$^{3+}$, while the sign of the change is reversed for *ob*-Λ-[Co *d*-pn_3]$^{3+}$. Figures 8 and 9 are CD spectra of *lel*-Δ- and *ob*-Λ-[Co *d*-pn_3]$^{3+}$ in 0.025 M *d*- and *l*-tartrate solutions. The changes in CD produced by the addition of sulfate and tartrate are larger for *lel*-Δ-[Co *d*-pn_3]$^{3+}$ than for *ob*-Λ-[Co *d*-pn_3]$^{3+}$. As can be seen from Eq. (12) such a difference is attributable to differences of both K and Δ_{MX} which is defined by

$$\Delta_{MX} = (\varepsilon_l - \varepsilon_r)_{MX} - (\varepsilon_l - \varepsilon_r)_0 \qquad (17)$$

$(\varepsilon_l - \varepsilon_r)_{MX}$ being the circular dichroism of the ion-pair. Vales of Δ_{MX} were obtained at each wavelength and are also given in Figs. 6 and 7. It is seen that the larger change of CD of *lel*-Δ-[Co *d*-pn_3]$^{3+}$ than that of *ob*-Λ-[Co *d*-pn_3]$^{3+}$ caused by the addition of the same amount of sulfate is due to larger values of both K and Δ_{MX} of the *lel*-$\Delta(C_2)$-isomer. Values of Δ_{MX} were obtained also for the association of *lel*-Δ-[Co *d*-pn_3]$^{3+}$ with tartrate (Fig. 8). The difference of Δ_{MX} values for *lel*-$\Delta(C_2)$- and *ob*-$\Lambda(C_2)$-isomer and for *d*- and *l*-tartrate may be related to the different structure in the outer-sphere association due to different conformations.

The author wishes to thank Professor Kazuo Saito and Dr. Junnosuke Fujita for their helpful advice and encouragement, and Mr. Hide Saito from whom the complex *l*-[Co *d*-pn_3]Cl·*d*-tart·$3H_2O$ was obtained.

BULLETIN OF THE CHEMICAL SOCIETY OF JAPAN VOL. 42 452—456 (1969)

The Stability of Fused Rings in Metal Chelates. IV. Preparation and Relative Stability of Copper(II) Complexes with Tetradentate Schiff Base Ligands

Yasuo NAKAO, Naoki NONAGASE and Akitsugu NAKAHARA

Institute of Chemistry, College of General Education, Osaka University, Toyonaka, Osaka

(Received July 1, 1968)

Relative stability of sixteen aldehyde- and the corresponding ketone-Schiff base chelates has been investigated in terms of their decomposing temperature and half-wave potential against the reduction of copper(II) at the dropping mercury electrode. The previous conclusion, established for copper(II) tridentate Schiff base complexes, that Schiff base chelates of aldehydes are generally less stable than those of corresponding ketones has been proved to be valid also for copper(II) tetradentate Schiff base complexes if there is no serious steric hindrance in the Schiff base ligand. As a result of this investigation, six new copper(II) chelates were synthesized and characterized.

In a previous paper[1] we have pointed out that copper(II) chelates of aldehyde-Schiff bases are generally less stable than those of the corresponding ketone-Schiff bases. This conclusion was, however, drawn only from the comparison of relative stability of some copper(II) chelates with tridentate Schiff bases derived from glyoxylate or pyruvate and various amino acid residues. The investigation has recently been extended to copper(II) chelates with tetradentate Schiff bases derived from some other aldehydes or ketones and various diamines or glycylglycine. Thus the validity of the former conclusion has been reinvestigated on the basis of experimental data on the relative stability of sixteen copper(II) tetradentate chelates.

The carbonyl compounds employed in this work were not only glyoxylate and pyruvate but also salicylaldehyde, benzoylacetone, benzoylacetaldehyde and 2-hydroxyacetophenone. On the other hand, ethylene-, trimethylene- and tetramethylenediamine, and glycylglycine were employed as amino compounds to form Schiff bases with the above described carbonyl compounds. Structural formulae of the sixteen copper(II) - Schiff base chelates derived from those carbonyl and amino compounds are illustrated in Fig. 1, I—XVI. Among those complexes, I, III, IV, V, VII and XVI are new compounds; the complexes shown by the odd numbers are chelates of aldehyde-Schiff bases,

1) Y. Nakao, K. Sakurai and A. Nakahara, This Bulletin, **39**, 1471 (1966).

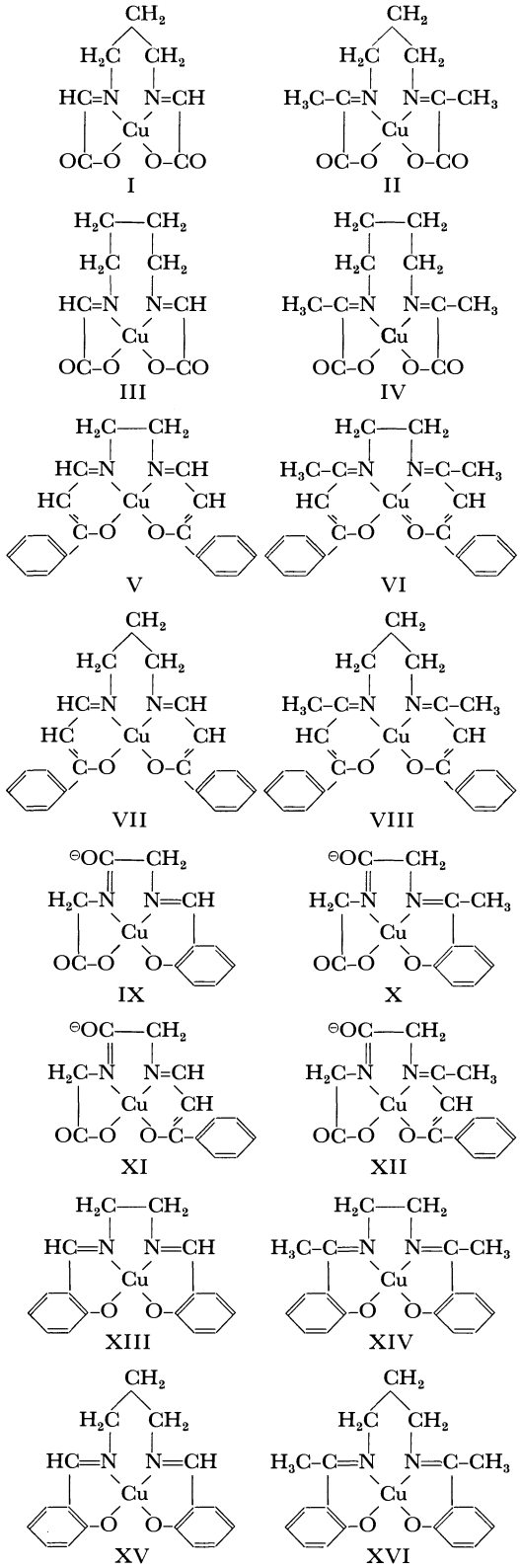

Fig. 1. Structural formulae of copper (II) chelates of aldehyde- and ketone-Schiff bases.

while those shown by the even numbers are of ketone-Schiff bases.

The relative stability of copper(II)-aldehyde- and -ketone-Schiff base complexes has been determined in terms of their decomposing temperature and half-wave potential of the reduction of copper(II) at the dropping mercury electrode.[2] The numerical data are tabulated in Table 1.

Copper(II) Complexes of Schiff Bases derived from Glyoxylate or Pyruvate and Various Diamines (I—IV). The copper(II) complex of Schiff base derived from pyruvate and trimethylenediamine, II, has been reported in a former paper.[2] The corresponding complex of aldehyde-Schiff base derived from glyoxylate and trimethylenediamine, I, has newly been prepared and compared with II. Both of them consist of the same skeletal structure (5-6-5 fused-chelate-ring*[1]) and are blue crystals, but they distinctly differ from each other in decomposing temperature and half-wave potential of the reduction of copper(II). The numerical data tabulated in Table 1 apparently support the previous conclusion that aldehyde-Schiff base complex is less stable than the corresponding ketone-Schiff base complex. The same trend is also observed in the comparison of bis-(glyoxylate)- and bis(pyruvate)-tetramethylenediamine complex, III and IV, in which the fused-chelate-ring is 5-7-5.

Further it may be concluded from the comparison of I and III, or II and IV, that if the carbonyl moiety in Schiff base ligand is same, 5-6-5 fused ring system is more stable than 5-7-5 system. (I<II; III<IV; I>III*[2]; II>IV).

Copper(II) Complexes of Schiff Bases derived from Benzoylacetaldehyde or -acetone and Ethylene- or Trimethylene-diamine (V—VIII). The copper(II) chelates of Schiff base derived from benzoylacetone and ethylenediamine, VI, and that from benzoylacetone and trimethylenediamine, VIII, were reported by Martell *et al.*[3] In the present investigation we have newly prepared the corresponding chelates of aldehyde-Schiff bases, V and VII. As is clear from Table 1, the Schiff base complexes of ethylenediamine, V and VI, are reddish brown, whereas those of trimethylenediamine, VII and VIII, are greenish brown. The

*[1] The abbreviation 5-6-5 indicates the fused-chelate-ring structure containing five-, six- and five-membered ring in clockwise direction.

2) A. Nakahara, H. Yamamoto and H. Matsumoto, This Bulletin, **37**, 1137 (1964).

*[2] Though this particular relation, I>III, does not seem to be decisive because of the fact that the decomposing temperature of the complex I is rather lower than that of the complex III, the conclusion might be supported from the comparison of strain in the fused ring system of the respective chelates.

3) P. J. McCarthy, R. J. Hovey, K. Ueno and A. E. Martell, *J. Am. Chem. Soc.*, **77**, 5820 (1955).

Table 1. Some properties of copper(II) chelates of aldehyde- and ketone-Schiff bases

Chelate	Ligand (Schiff base)	Color of crystals	Melting (or decomposing) temp. °C	Half-wave potential, $E_{1/2}$ *vs.* SCE at 25°C
I	2 : 1 glyoxylate : trimethylenediamine	blue	190—200 (decomp.)	−0.25 V (irrev.)
II	2 : 1 pyruvate : trimethylenediamine	blue	209—219 (decomp.)	−0.49 V (irrev.)
III	2 : 1 glyoxylate : tetramethylenediamine	pale-blue	200—206 (decomp.)	−0.11 V (irrev.)
IV	2 : 1 pyruvate : tetramethylenediamine	pale-blue	207—215 (decomp.)	−0.34 V (irrev.)
V	2 : 1 benzoylacetaldehyde : ethylenediamine	red-brown	227—229 (decomp.)	−0.87 V (irrev.) (50% H_2O-pyridine)
VI	2 : 1 benzoylacetone : ethylenediamine	red-brown	277—281	−0.90 V (irrev.) (50% H_2O-pyridine)
VII	2 : 1 benzoylacetaldehyde : trimethylenediamine	green-brown	153—154 (decomp.)	−0.70 V (irrev.) (50% H_2O-pyridine)
VIII	2 : 1 benzoylacetone : trimethylenediamine	green	194—196 (decomp.)	$E^{(1)}_{1/2}$, −0.52 V (irrev.) $E^{(2)}_{1/2}$, −0.70 V (irrev.) (50% H_2O-pyridine)
IX	1 : 1 salicylaldehyde : glycylglycine	violet	289 (decomp.)	−0.58 V (irrev.)
X	1 : 1 2-hydroxyacetophenone : glycylglycine	violet	326—330 (decomp.)	−0.67 V (irrev.)
XI	1 : 1 benzoylacetaldehyde : glycylglycine	violet	222—225 (decomp.)	−0.60 V (irrev.)
XII	1 : 1 benzoylacetone : glycylglycine	violet	244—246 (decomp.)	−0.68 V (irrev.)
XIII	2 : 1 salicylaldehyde : ethylenediamine	green	276—285 (decomp.)	−0.75 V (irrev.) (50% H_2O-pyridine)
XIV	2 : 1 2-hydroxyacetophenone : ethylenediamine	red-brown	235—242 (decomp.)	−0.63 V (irrev.) (50% H_2O-pyridine)
XV	2 : 1 salicylaldehyde : trimethylenediamine	green-brown	276—280 (decomp.)	−0.53 V (irrev.) (50% H_2O-pyridine)
XVI	2 : 1 2-hydroxyacetophenone : trimethylenediamine	green	242—247 (decomp.)	−0.49 V (irrev.) (50% H_2O-pyridine)

extraordinary difference is also found in their decomposing temperature and half-wave potential. It is noteworthy that even this kind of distinct difference is accompanied by the slight change of fused ring from the 6-5-6 to 6-6-6 system.

The aldehyde-Schiff base complexes are proved, also here, to be less stable than the corresponding ketone-Schiff base complexes; in the comparison of the same two aldehyde-Schiff base chelates, or ketone-Schiff base chelates, the stability of the 6-5-6 fused ring structure is higher than that of the 6-6-6 structure. (V<VI; VII<VIII; V>VII; VI>VIII).

Copper(II) Complexes of Schiff Bases with Glycylglycine (IX—XII). As already reported,[4] copper(II) chelates of Schiff bases derived from salicylaldehyde, 2-hydroxyacetophenone, benzoylacetaldehyde or benzoylacetone and glycylglycine have the structure of 5-5-6 fused ring and appear reddish purple. Thier decomposing temperature and half-wave potential in polarographic measurement are indicated in Table 1, from which the following relation in their relative stability is easily concluded: IX<X; XI<XII. The validity of the previous conclusion that Schiff base chelates of aldehydes are less stable than those of ketones is thus well supported.

Copper(II) Complexes of Schiff Bases derived from Salicylaldehyde or 2-Hydroxyacetophenone and Ethylene- or Trimethylenediamine (XIII—XVI). Bis(salicylaldehyde)-ethylenediimine chelate, XIII, -trimethylenediimine chelate, XV, and bis(2-hydroxyacetophenone)ethylenediimine chelate, XIV, have long been known since the work of Tsumaki *et al.*[5] In addition to those, we have newly prepared bis(2-hydroxyacetophenone)trimethylenediimine chelate, XVI.

Inspection of the numerical data for these chelates in Table 1 reveals that the situation on relative stability of aldehyde- and ketone-Schiff base chelates is the reverse of the cases described above. In other words, the Schiff base complexes of aldehydes are more stable than those of ketone, so far as these particular chelates are concerned. However, the reversal of this kind may be attributed to a steric hindrance resulting from the bulky methyl group of the 2-hydroxyacetophenone moiety. The steric effect of the methyl group can easily be duplicated by using a Stuart Model. Although this effect of methyl group does not seem to be so serious, but still it may be great enough to weaken the coordination of the tetradentate ligand to some extent. For this reason, it may be understood that the ketone Schiff base chelates, XIV and XVI,

4) A. Nakahara, K. Hamada, I. Miyachi and K. Sakurai, This Bulletin, **40**, 2826 (1967).

5) P. Pfeiffer, E. Breith, E. Lübbe and T. Tsumaki, *Ann.*, **503**, 84 (1933).

become less stable than the aldehyde-Schiff base chelates, XIII and XV. In the case of complex X, in which the Schiff base ligand consists of glycylglycine and 2-hydroxyacetophenone, the steric hindrance of the same methyl group has not been necessary to be taken into account. This is because of the reason that the complex X contains only one 2-hydroxyacetophenone moiety in the molecule, and hence the steric effect of methyl group is considered to be not so serious as that in complexes, XIV or XVI.

Thus the previous conclusion that Schiff base chelates of aldehydes are generally less stable than those of corresponding ketones is proved to be valid also for tetradentate chelates, whenever there is no serious steric hindrance in the ligand.

Experimental

Syntheses of Ligands. *Sodium Glyoxylate* was prepared from tartaric acid according to the direction of Metzler *et al.*[6]

Benzoylacetaldehyde was prepared from acetophenone according to the direction in the literature.[7]

Bis(benzoylacetaldehyde)ethylendiimine. To a mixture of 5.2 g of benzoylacetaldehyde and 0.8 g of sodium hydroxide in 80 m*l* of ethanol was added 2.4 g of ethylenediamine dihydrochloride. The mixture was stirred and heated at about 55°C for several hours, and was then filtered. The filtrate was concentrated to some extent and allowed to stand for a few hours in a refrigerator; thereupon yellow crystals were deposited. The product was filtered and recrystallized from ethanol. Mp 143—144°C. Found: C, 74.99; H, 6.17; N, 8.64%. Calcd for $C_{20}H_{20}O_2N_2$: C, 75.00; H, 6.26; N, 8.75%.

Bis(2-hydroxyacetophenone)trimethylenediimine. A mixture of 5.9 g of 2-hydroxyacetophenone and 1.6 g of trimethylenediamine was dissolved in 10 m*l* of ethanol. The mixture was stirred and heated at about 70°C for half an hour. Upon cooling the solution yellow crystals were deposited. This was filtered and recrystallized from ethanol. Mp 127°C. Found: C, 73.17; H, 7.01; N, 8.81%. Calcd for $C_{19}H_{22}O_2N_2$: C, 73.55; H, 7.10; N, 9.03%.

Preparation of Metal Chelates. *Copper(II) Complex of Bis(glyoxylate)trimethylenediimine(I).* To a mixture of 1.8 g of trimethylenediamine and 5.7 g of sodium glyoxylate in 10 m*l* of water was added a freshly precipitated cupric oxide (*ca.* 2 g). The mixture was vigorously stirred at 10°C for about four hours; hereupon a bluish crystalline powder was gradually deposited. This was recrystallized from water. Found: C, 30.25; H, 4.19; N, 10.32%. Calcd for $Cu(C_7H_8O_4N_2)\cdot 1.5H_2O$: C, 30.60; H, 4.01; N, 10.20%.

Copper(II) Complex of Bis(pyruvate)trimethylenediimine(II). Although the method of preparation of this compound had already been reported in the previous paper,[2] the procedure was a little simplified by the use of copper(II) acetate in place of freshly precipitated copper(II) oxide.

Copper(II) Complex of Bis(glyoxylate)tetramethylenediimine (III). To a mixture of 2.2 g of tetramethylenediamine and 5.7 g of sodium glyoxylate monohydrate in 50 m*l* of water was added 5.0 g of copper(II) acetate monohydrate. The mixture was stirred at 20°C for one hour to give a pale blue crystalline powder. This was filtered and washed several times by water. Found: C, 29.79; H, 5.12; N, 8.30%. Calcd for $Cu(C_8H_{10}O_4N_2)\cdot 3.5H_2O$: C, 29.58; H, 5.24; N, 8.62 %.

Copper(II) Complex of Bis(pyruvate)tetramethylenediimine (IV). To a freshly precipitated cupric oxide, obtained from 10 g of copper(II) sulfate pentahydrate in 50 m*l* of water was added 4.4 g of pyruvic acid and 2.2 g of tetramethylenediamine. The mixture was stirred and heated at 40°C for about two hours. After it had been filtered, the solution was, to some extent, evaporated *in vacuo*, and then allowed to stand for a few hours in a refrigerator; hereupon a blue powder was deposited. This was filtered and recrystallized from water. Found: C, 34.93; H, 6.07; N, 8.05%. Calcd for $Cu(C_{10}H_{14}O_4N_2)\cdot 3H_2O$: C, 34.93; H, 5.82; N, 8.17%.

Bisbenzoylacetaldehyde-ethylenediiminocopper(II) (V). To a mixture of 2.2 g of bis(benzoylacetaldehyde)ethylenediimine and 35 m*l* of acetone was added a freshly precipitated copper(II) oxide obtained from 4.0 g of copper(II) sulfate pentahydrate. The mixture was stirred and heated at 60°C for about three hours. After it had been filtered, the solution was cooled to give reddish brown crystals. This was recrystallized from acetone. Found: C, 62.76; H, 4.58; N, 7.31%. Calcd for $Cu(C_{20}H_{18}O_2N_2)$: C, 62.91; H, 4.72; N, 7.34%.

Bisbenzoylacetone-ethylenediiminocopper(II) (VI) and Bisbenzoylacetone-trimethylenediiminocopper(II) (VIII), were prepared according to the method of Martell *et al.*[3]

Bisbenzoylacetaldehyde-trimethylenediiminocopper(II) (VII). Seven grams of benzoylacetaldehyde, 1 g of sodium hydroxide and 3.4 g of trimethylenediamine dihydrochloride were mixed together in 80 m*l* of ethanol. The mixture was stirred and heated at 60°C for three hours. After it had been filtered, the solution was concentrated under vacuum until the volume became to about 20 m*l*. To this solution of bisbenzoylacetaldehyde-trimethylenediimine was added copper(II) oxide, which had been obtained from 10 g of copper(II) sulfate pentahydrate, and 50 m*l* of acetone. The copper(II) chelate, VII, was thus obtained and purified according to the same procedure as described for the preparation of the chelate V. Found: C, 64.19; H, 5.06; N, 6.95%. Calcd for $Cu(C_{21}H_{20}O_2N_2)$: C, 63.72; H, 5.06; N, 7.08%.

Copper(II) Chelates of Glycylglycine-Schiff Bases (IX–XII). The preparation of these chelates were already reported.[4]

Bissalicylaldehyde-ethylenediiminocopper(II) (XIII), Bis-2-hydroxyacetophenone-ethylenediiminocopper(II) (XIV), and Bissalicylaldehyde-trimethylenediiminocopper(II) (XV), were prepared according to the method of Tsumaki *et al.*[5]

Bis-2-hydroxyacetophenone-trimethylenediiminocopper (II) (XVI). Two grams of bis-2-hydroxyacetophenone-trimethylenediimine was dissolved in 40 m*l* of acetone, and was mixed together with freshly precipitated copper(II) oxide, which had been obtained from 4.0 g of copper(II) sulfate pentahydrate. The mixture was stirred and heated at 60°C for four hours. After it had been filtered, the solution was cooled to give green crystals. This was recrystallized from acetone. Found: C, 61.61; H, 5.48; N, 7.56%. Calcd for $Cu(C_{19}H_{20}O_2N_2)$: C, 61.37; H, 5.38; N, 7.54%.

6) D. E. Metzler, J. Olivard and E. E. Snell, *J. Am. Chem. Soc.*, **76**, 647 (1954).

7) Org. Reaction, Vol VIII, p. 126.

Polarographic Measurements. The measurements were carried out by the same method as already described.[1] The solvent used was water for the compounds I—IV and IX—XII, and 50% (by volume) pyridine-water for V—VIII and XIII—XVI.

The authors thank the Ministry of Education for the financial support granted for this research.

BULLETIN OF THE CHEMICAL SOCIETY OF JAPAN VOL. 42 456—459 (1969)

The Spectrophotometric Determination of Thorium(IV) with Bromopyrogallol Red*1,*2

Kôichi Tonosaki* and Takayoshi Sakai**,*3

*Chemical Department, Faculty of Science, Hirosaki University, Bunkyō-chō, Hirosaki

**Hirosaki High School, Shintera-machi, Hirosaki

(Received July 3, 1968)

Bromopyrogallol red reacts with thorium(IV) to form a stable complex with an absorption maximum at 645 mμ against a reagent blank. The maximum absorbance is obtained in the pH range of 5.6 to 5.9 when the solution is heated in a boiling water bath for 20 min. The color system obeys Beer's law in the range 6 to 106 μg of thorium in 25 ml. The molar absorptivity of the complex is calculated to be 5.0×10^4 at 645 mμ. The sensitivity of the reaction is 0.004 μg thorium per cm^2. The complex has the composition 1 to 2 in metal to ligand. The effect of diverse ions on the determination is also examined.

Bromopyrogallol red (5,5′-dibromopyrogallol sulfophthalein), which was first prepared by Vodak *et al.*[1] as a chromogenic dye-stuff, reacts with many metal cations to form colored complexes and has widely been used as a metallochromic indicator in complexometric titrations. The present paper describes a new spectrophotometric method for the determination of thorium(IV), using bromopyrogallol red as a color reagent.

Various dye-stuffs, including thorin,[2] neo-thorin,[2] quinalizarin,[3] naphthazarin,[4] quercetin,[5] eriochrome black T,[6] solochromate fast red,[7] arsenazo III,[8] xylenol orange[9] and methylthymol blue,[9] have been used as color reagents in the spectrophotometric determination of thorium. No work has been reported, however, on the reaction between thorium(IV) and bromopyrogallol red.

It was found that in the presence of excess reagent, thorium(IV) reacts sensitively with bromopyrogallol red under heating to form a stable complex with a metal to ligand ratio of 1 to 2. This work was done to determine optimum conditions for the spectrophotometric determination of thorium(IV).

Experimental

Reagents. *Standard Thorium(IV) Solution.* About 1×10^{-2} M thorium(IV) solution was prepared by dissolving guaranteed reagent thorium(IV) nitrate tetrahydrate in about 0.1 N nitric acid. The solution was

*1 This work was presented at the Tohoku Branch Meeting of the Chemical Society of Japan, Hirosaki, October, 1967.

*2 After this manuscript had been completed, the authors received a report by Vasilenko *et al.*[12] The report was on the spectrophotometric study of the interaction of thorium(IV) with BPR. They applied a sodium acetate-hydrochloric acid medium as the buffer solution. The range of mesurement for thorium was 2 to 60 μg per 25 ml with a 1 to 2 complex at pH 5.0 and 630 mμ. The sensitivity of the reaction and the effect of diverse ions was not given.

*3 Present address: Hachinohe Technical College, Tamonoki, Hachinohe.

1) Z. Vodak and O. Leminger, *Collection Czech. Chem. Commun.*, **21**, 1522 (1956).

2) Nippon Kagakukai "Kagaku Binran (Chemical Handbook)" (in Japanese), Maruzen, Tokyo (1958), p. 1090.

3) P. Purushottam, *Z. Anal. Chem.*, **145**, 245 (1955).

4) T. Moellar and M. Tecotzky, *Anal. Chem.*, **27**, 1056 (1955).

5) O. Menis, D. L. Manning and G. Goldstein, *ibid.*, **29**, 1426 (1957).

6) P. E. Lott, K. L. Cheng and B. C. H. Kwan, *ibid.*, **32**, 1702 (1960).

7) J. Korkisch and G. E. Janauer, *ibid.*, **33**, 1930 (1961).

8) H. Onishi, *Japan Analyst*, **12**, 1153 (1963).

9) M. Otomo, *ibid.*, **14**, 229 (1965).

standardized by EDTA titration using xylenol orange[10] as an indicator. It was diluted with water to desired concentrations.

Bromopyrogallol Red (abbreviated BPR; MW, 558.16 as free acid) *Solution.* A 1×10^{-3} M BPR solution was prepared by dissolving the right amount of Dotite BPR reagent, which has been preserved in a desiccator overnight, in 50%v/v ethanol.

Stock solutions of diverse ions were prepared from their reagent grade chemicals in appropriate concentrations. A 0.25 M acetate buffer solution was also used for pH adjustment.

Apparatus. A Hitachi-Perkin Elmer spectrophotometer, model 139, was used with 1 cm glass cells. A Hitachi-Horiba glass-electrode pH meter, Model M-4, was used for pH measurement.

All measurements were carried out at 25±0.5°C.

Standard Procedure. To a sample solution containing up to 100 μg of thorium in a 50 m*l* Erlemeyer flask, 1.0 m*l* of a 1×10^{-3}M BPR solution and 10 m*l* of 0.25 M acetate buffer solution with a pH of 5.7 were added, and the solution diluted with water to about 20 m*l*. It was heated in a boiling water bath for 20 min. The solution was cooled with running water to room temperature, transferred to a 25 m*l* volumetric flask, and diluted to the mark with water. After the solution had been kept for 20 min at 25°C, the absorbance of the solution was measured at 645 mμ using the reagent blank as a reference.

Results and Discussion

Absorption Curves. The absorption curves of the solutions containing thorium(IV) and BPR at various pH values are shown in Fig. 1. These curves were obtained by measuring the absorbance of the colored solutions against the reagent blank which contained the same amount of BPR.

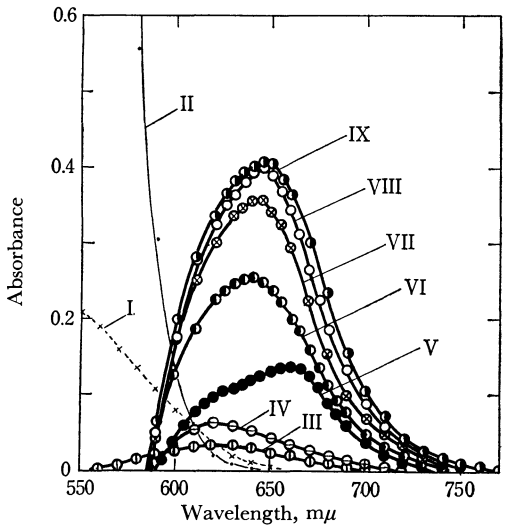

Fig. 1. Absorption cruves of BPR and its thorium complex in the presence of excessive reagent
BPR: 4.01×10^{-5} M, Th(IV): 47.1 μg in 25 m*l* (8.11×10^{-6} M), μ: 0.1. BPR *vs.* water — pH: I, 14.0; II, 6.22. Thorium-BPR complex *vs.* BPR — pH: III, 2.30, 4.10, IV, 4.60; V, 4.78; VI, 5.05; VII, 5.53; VIII, 5.60—5.95; IX, 6.05—6.30.

Below pH 4.6, the solution had an absorption maximum at about 620 mμ. The curves obtained at pH 4.8 (Curve V) had shoulders at about 630 mμ. Between pH 5.5 and 6.3, however, the solutions gave absorption curves with an absorption maximum at about 645 mμ. Therefore, it may be said that in the presence of excess BPR, two complexes are formed between thorium(IV) and the reagent; the complex with an absorption maximum at about 645 mμ was used for the determination of thorium.

The Effect of pH. The absorbance of the solution as a function of pH was measured at 645 mμ. From the curve shown in Fig. 2 (Curve I), it is found that the maximum absorbance is obtained in the pH range 5.6 to 6.2. Between pH 5.6 and 5.9, the absorbance of the solution remained almost unchanged for several hours, while above pH 6.0, the complex showed a tendency to precipitate when the solution was allowed to stand for more than about 2 hr. The color development was, therefore, made at pH 5.7.

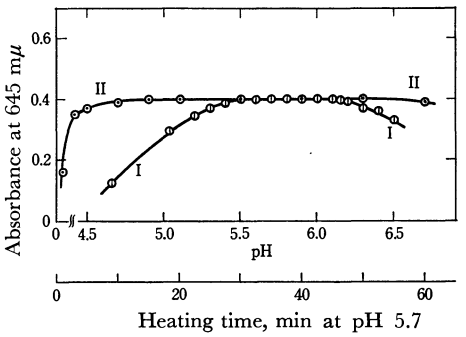

Fig. 2. Effects of pH and heating time.
I: pH, II: Heating time, Th(IV): 47.1 μg. BPR: 4.01×10^{-5} M, μ: 0.1, Reference: Reagent blank

The Effect of Heating Time. The color reaction of BPR with thorium(IV) is very slow at room temperature; several hours were required for complete color development. The effect of heating time on color formation was examined in a boiling water bath at a constant pH of 5.7. As shown in Fig. 2 (Curve II), maximum color development was obtained when the solution was heated for 15 to 40 min.

The Effect of the Amount of Reagent. The effect of the reagent concentration on color development was examined. It is seen in Fig. 3 that constant absorbance is obtained with 0.6 to 1.6 m*l* of a 1×10^{-3} M BPR solution. Therefore, 1.0 m*l* was chosen as the working volume of the reagent.

Color Stability. The absorbance of the solution prepared at pH 5.7 was measured as a function of time following the preparation of the solution.

10) K. Ueno, "Kireto Tekitei (Chelatometric Titration)" (in Japanese), Nankodo, Tokyo (1960), p. 313.

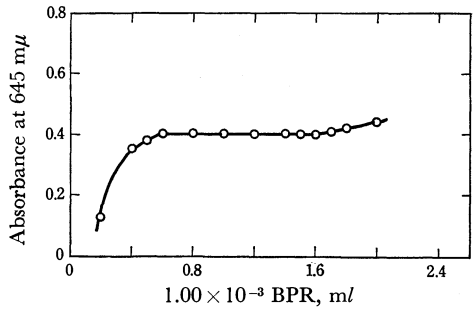

Fig. 3. Effect of addition of BPR.
Th(IV): 47.1 μg, pH: 5.70, μ: 0.1, Reference: Reagent blank

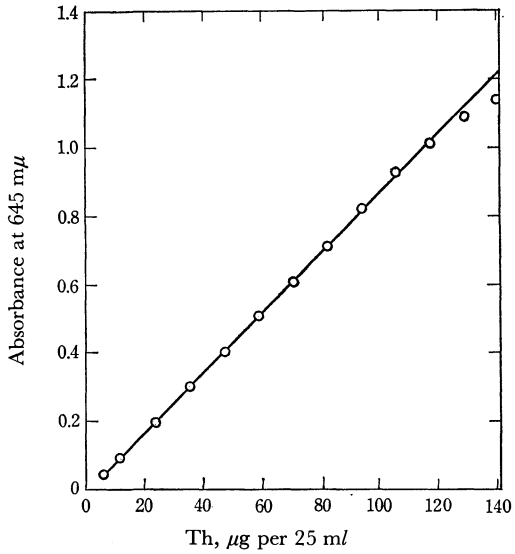

Fig. 4. Calibration curve.
BPR: 4.10×10^{-5} M, pH: 5.70, μ: 0.1, Reference: Reagent blank

Table 1. Comparison with other reagents

Reagent	Molar absorptivity $\times10^4$	Sensitivity μg/cm²
Bromopyrogallol Red	5.08(645 mμ)	0.004
Thorin[2]		0.03(545 mμ)
Neo-thorin[2]		0.02(600 mμ)
Quinalizarin[3]		0.02(590 mμ)
Naphthazarin[4]	2.24(620 mμ)	0.01
Quercetin[5]	3.30(422 mμ)	0.007
Eriochrome Black T[6]	3.50(700 mμ)	0.004
Solochromate Fast Red[7]	1.39(490 mμ)	0.017
Arsenazo III[8]	13.00(665 mμ)	
Xylenol Orange[9]	7.70(568 mμ)	0.003
Methylthymol Blue[9]	3.94(568 mμ)	0.006

There was no change in absorbance over a period of 24 hr.

Calibration Curve. From the foregoing results, a calibration curve for the determination of thorium was prepared in the manner described above. Figure 4 shows that Beer's law is obeyed over the range 6 to 106 μg (0.2 to 4.2 ppm) of thorium at 645 mμ and pH 5.7. According to Sandell's notation,[11] the sensitivity of the reaction is 0.004μg of thorium per cm². The molar absorptivity is calculated to be 5.08×10^4. The latter two values were compared with those of other methods as listed in Table 1. This indicates that the proposed method is less sensitive than the arsenazo III method.[8] However, it compares with the xylenol orange method[9] in sensitivity. The reproducibility of the method was examined using a solution containing 47.6 μg of thorium. From data obtained from twelve determinations, the standard deviation was calculated to be 0.0036 (0.88%) in absorbance.

The Effect of Diverse Ions. The effect of diverse ions on the determination of thorium was examined. The results are summarized in Tables 2 and 3, from which it is seen that cobalt(II), nickel(II), zinc(II), strontium(II), sulfate and chloride ions do not interfere, but many other ions, especially aluminum(III), lanthanum(III), zirconium(IV), yttrium(III), cadmium(II), fluoride,

Table 2. Effect of cations on determination at pH 5.7

Thorium taken: 46.0 μg (0.20 μmol)
Cations added: each 0.20 μmol

Cation	μg Th found	Relative error (%)
Ag(I)	49.2	+ 6.9
Al(III)	0.0	−100.0
Be(II)	42.9	− 6.8
Bi(III)	62.8	+ 36.6
Cd(II)	21.3	− 53.7
Ce(III)	31.9	− 30.7
Co(II)	45.6	− 0.9
Cr(III)	41.6	− 9.6
Cu(II)	60.1	+ 30.7
Fe(III)	36.4	− 20.9
Ga(III)	32.5	− 29.4
Hg(II)	44.1	− 4.1
In(III)	24.5	− 46.8
La(III)	98.6	+114.4
Nd(III)	61.0	+ 32.6
Ni(II)	46.0	± 0.0
Pb(II)	43.6	− 5.2
Sr(II)	44.6	− 3.0
Ti(IV)	24.2	− 47.4
U(VI)	47.8	+ 3.9
V(IV)	41.6	− 9.6
Y(III)	74.1	+ 60.9
Yb(III)	43.7	− 5.0
Zn(II)	45.5	− 1.1
Zr(IV)	91.6	+ 99.1

11) E. B. Sandell, "Colorimetric Determination of Traces of Metals," Interscience Publishers, New York (1950), p. 49.

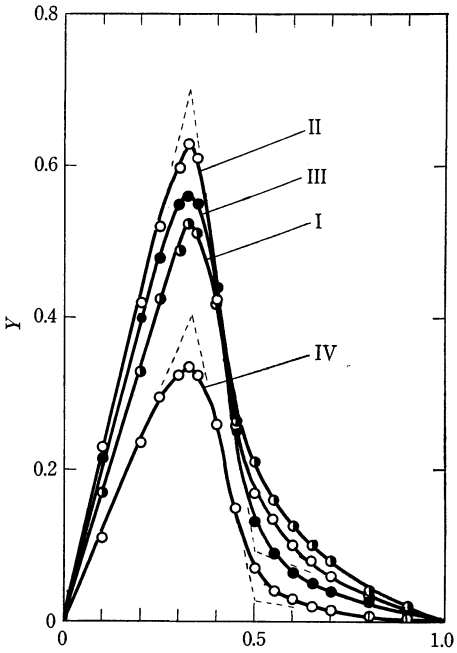

Fig. 5. Continuous variation method.
$[Th]+[BPR]=4.0\times10^{-5}$ M, pH: 5.7, μ: 0.1, I: 620 mμ, II: 640 mμ, III: 660 mμ, IV: 680 mμ, Reference: Water

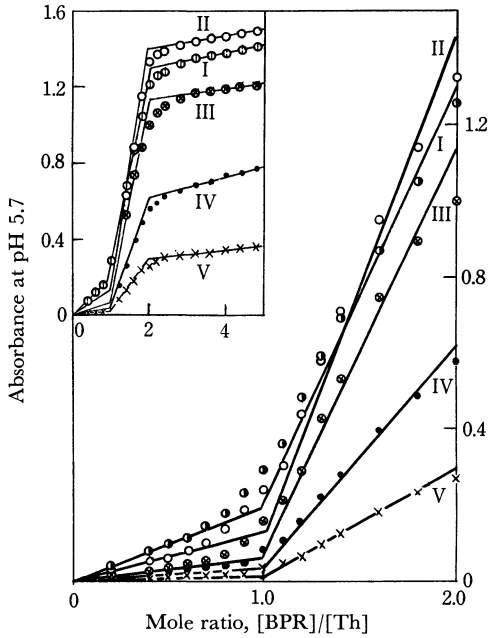

Fig. 6. Mole ratio method.
Th(IV): 2.0×10^{-5} M, μ: 0.1, I: 620 mμ, II: 640 mμ, III: 660 mμ, IV: 680 mμ, V: 700 mμ

oxalate, tartrate, citrate, phosphate, NTA and EDTA do interfere with the determination of thorium.

Table 3. Effect of anions and complexing agents on determination of thorium at pH 5.7
Thorium taken: 46.0 μg (0.20 μmol)

Anion or complexing agent added	Molar excess over thorium	Th found μg	Relative error %
F^-	1	40.5	−12.0
	2	25.5	−46.8
	10	4.4	−90.5
Cl^-	250	46.4	+ 0.9
	500	47.7	+ 3.4
	1000	47.8	+ 3.9
$H_2PO_4^-$	0.1	45.7	− 0.7
	0.5	35.0	−23.9
	1	10.4	−77.5
SO_4^{2-}	500	46.0	± 0.0
	1000	45.0	− 1.1
$C_2O_4^{2-}$	1	40.5	−12.0
	2	34.6	−30.0
	10	31.9	−33.1
Tartrate $C_4H_4O_6^{2-}$	0.5	50.8	+10.4
	1	49.6	+ 7.8
	10	47.4	+ 3.0
	20	42.2	− 8.3
Citrate $C_6H_5O_7^{3-}$	0.1	46.8	+ 1.7
	0.5	37.5	−18.5
	1	20.5	−55.5
NTA	0.1	40.5	−12.0
	0.5	47.3	+ 2.8
EDTA	0.01	44.8	− 2.6
	0.1	43.1	− 6.3

Composition of the Complex. Attempts were made to characterize the thorium(IV)-BPR complex by two usual methods, the continuous variation method and the mole ratio method. These experiments were performed at a constant pH value of 5.7. Absorbance measurements were made at four wavelengths between 620 and 680 mμ. As shown in Fig. 5, the results obtained with the method of continuous variations indicate that thorium(IV) forms chiefly a 1 to 2 complex with BPR at pH 5.7. The results obtained with the mole ratio method (Fig. 6) show that a 1 to 1 complex is also formed under the same conditions. It may be concluded, therefore, that depending on the amount of reagent, two complexes of different compositions, 1 to 1 and 1 to 2, are formed between thorium(IV) and BPR. It was found, moreover, that another 1 to 1 complex with an absorption maximum at 550 mμ was formed in the pH range 1.3 to 4.2.

The authors wish to thank Dr. Makoto Otomo for his discussion and Mr. Kôichi Tanaka and Takaaki Ôsaga for their assistance. This investigation was partly supported by a grant from the Ministry of Education.

12) V. D. Vasilenko, M. V. Shanya and V. I. Bolbas, *Zh. Analit. Khim.*, **22**, 1818 (1967).

BULLETIN OF THE CHEMICAL SOCIETY OF JAPAN VOL. 42 460—464 (1969)

Two-dimensional Dual-band Thin-layer Chromatographic Separation of Polynuclear Hydrocarbons

Hidetsuru MATSUSHITA and Yasutomo SUZUKI

National Institute of Industrial Health, Kizuki-Sumiyoshi, Kawasaki

(Received July 13, 1968)

A two-dimensional dual-band thin-layer chromatographic procedure for the separation of a mixture containing many polynuclear hydrocarbons is described. A chromatoplate composed of two adsorbent layers, aluminum oxide G and acetylated cellulose, is used in this chromatography. A sample containing various polynuclear hydrocarbons is first developed on an aluminum oxide G layer with *n*-hexane - ether (19 : 1, v/v) and then on an acetylated cellulose layer with methanol-ether-water (4 : 4 : 1, v/v). A mixture of 15 polynuclear hydrocarbons was completely separated into its components by this treatment. This method was then applied to the separation of a vacuum-sublimation extract of particulates obtained from Tokyo air. The extract was separated into 69 spots, and it was proved that several hydrocarbons, including benzo(*a*)pyrene, has been isolated in a pure state.

The separation and determination of polynuclear hydrocarbons including benzo(*a*)pyrene, a potent carcinogen, in urban air pollutants is of importance in relation to the rapid increase in lung-cancer mortality in many countries in the world within the last 30 years. Thin-layer chromatography has recently attracted much attention in connection with the separation of the hydrocarbons, and several methods have been reported.[1-12] However, these methods do not seem to give a satisfactory separation for a sample containing many polynuclear hydrocarbons, such as an extract from air pollutants. For example, thin-layer chromatography using aluminum oxide G as the adsorbent and *n*-hexane-ether (19 : 1,v/v) as the developing solvent gives a good separation of a mixture of phenanthrene, pyrene, perylene, and dibenzo(*a*,*h*)anthracene, but it gives only a poor separation for a mixture of benzo(*a*)pyrene, benzo(*b*)fluoranthene, perylene, and benzo(*e*)pyrene. On the other hand, chromatography using a partially-acetylated cellulose as the adsorbent and methanol-ether-water (4 : 4 : 1,v/v) as the developing solvent gives a good separation for the latter mixture, but a poor separation for the former.

This paper is concerned with a new method for the two-dimensional thin-layer chromatographic separation of a complex mixture of polynuclear hydrocarbons. The thin-layer chromatoplate in the present method is composed of two adsorbent layers, aluminum oxide G and acetylated cellulose. The former layer is used in the first development, and the latter, in the second development.

Experimental

Hydrocarbons. The polynuclear hydrocarbons tested were anthracene, phenanthrene, pyrene, benzo(*a*)anthracene, chrysene, benzo(*e*)pyrene, benzo(*b*)fluoranthene, benzo(*a*)pyrene, perylene, anthanthrene, benzo(*ghi*)perylene, dibenzo(*a*,*h*)anthracene, coronene, dibenzo(*a*,*i*)pyrene, and benzo(*k*)fluoranthene. The benzo(*b*)fluoranthene was a kind gift to us from Dr. B. T. Commins (MRC Air Pollution Research Unit, St. Bartholomew's Hospital Medical College, London). The benzo(*e*)pyrene and benzo(*k*)fluoranthene were kindly presented by Professor M. Kuratsune(Kyushu University, Japan). The other hydrocarbons were obtained from the Koch-Light Co., Ltd., London.

Adsorbents. Aluminium oxide G acc. to Stahl (E. Merck) and 26% acetylated cellulose were used

1) E. Sawicki, T. W. Stanley, W. C. Elbert and J. D. Pfaff, *Anal. Chem.*, **36**, 497 (1964).
2) G. M. Badger, J. K. Donnelly and T. M. Spotswood, *J. Chromatog.*, **10**, 397 (1963).
3) Th. Wieland, G. Lüben and H. Determann, *Experientia*, **18**, 432 (1962).
4) N. Kucharczk, J. Fohl and J. Vymetal, *J. Chromatog.*, **11**, 55 (1963).
5) K. Wettig, *Z. Ges. Hyg. Grenzg.*, **10**, 15 (1964).
6) H. Matsushita, Y. Suzuki and H. Sakabe, This Bulletin, **36**, 1371 (1963).
7) H. Kessler and E. Müller, *J. Chromatog.*, **24**, 469 (1966).
8) R. G. Harvey and M. Halonen, *ibid.*, **25**, 294 (1966).
9) R. H. White and J. W. Howard, *ibid.*, **29**, 108 (1967).
10) M. Frank-Neumann and P. Jössang, *ibid.*, **14**, 280 (1964).
11) E. Sawicki, T. W. Stanley, W. C. Elbert, J. Meeker and S. McPherson, *Atomospheric Environ.*, **1**, 131 (1967).
12) J. Janák and V. Kubecová, J. *Chromatog.*, **33**, 132 (1968).

as the adsorbents. The latter adsorbent was prepared by the acetylation of cellulose powder by the method of Wieland, Lüben, and Determann.[3] Camag's cellulose powder D for thin-layer chromatography was dried at 110°C for 30 min and then cooled in a desiccator containing concentrated sulfuric acid. The dried cellulose powder (30 g) was then acetylated in a mixed solution of benzene (675 m*l*), acetic anhydride (225 m*l*), and concentrated sulfuric acid (0.9 m*l*). Twenty-six percent acetylated cellulose was obtained by the reaction at 70°C for 9 hr. The cellulose was washed by methanol and ether and dried completely in an electric furnace at about 80°C.

Applicator and Coating. A chromatoplate with two adsorbent layers of aluminium oxide G and acetylated cellulose was prepared by the use of the applicator shown in Fig. 1. This is analogous to the applicator devised by Gilmore and Cortes.[13] The trough of the applicator (20 cm × 3.6 cm) was divided into two parts by a strip of stainless steel inserted into the grooves of the front and rear gates of the applicator. One part of the divided trough had the dimensions of 16 cm × 3.6 cm, and the other part, 4 cm × 3.6 cm. The strip-end in contact with the glass plate was shaped like a knife edge.

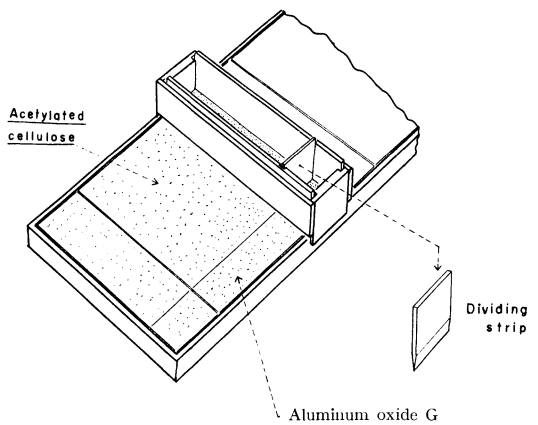

Fig. 1. Applicator for preparing dual band thin layer chromatoplate.

Slurries of the adsorbents were prepared by mixing them with a 10% methanol aqueous solution. The mixing ratio of the adsorbent to the methanol solution was 7 : 11 (g/m*l*) for aluminum oxide G and 10 : 45 (g/m*l*) for acetylated cellulose.

A slurry of aluminum oxide G was poured into the smaller part of the trough, and a slurry of acetylated cellulose, into the larger part of the trough. Then, they were immediately spread over glass plates (20 cm × 20 cm) in a thickness of 300μ. This gave a chromatoplate consisting of an aluminum oxide G layer (4 cm × 20 cm) and an acetylated cellulose layer (16 cm × 20 cm). The boundary line between the two adsorbent layers was very sharp. After having been left for about 3 hr for superficial drying at room temperature, the chromatoplate was activated by heating it at 110°C for 1 hr. The activated plate was then stored in a chamber kept at a relative humidity of about 20%. The humidity was easily controlled by putting a petri-dish containing a saturated potassium acetate aqueous solution on the bottom of the chamber.

Sample Application. A mixture of polynuclear hydrocarbons was applied to the lower left corner of the aluminium oxide G layer at a point 15 mm from the bottom of the layer and 10 mm from the layer boundary. The relative humidity of the atmosphere in the spotting box was kept at about 20% by putting a petri-dish containing a saturated potassium acetate aqueous solution into the box. The amounts applied to the layer were in the range of 0.03—0.4μg for each polynuclear hydrocarbon.

Development and Detection. The first development was carried out on the aluminum oxide G layer in a paper-lined chamber equilibrated with freshly-prepared *n*-hexane - ether (19 : 1, v/v) and also with a saturated potassium acetate aqueous solution. The development was continued until the front of *n*-hexane - ether (19 : 1, v/v) reached 150 mm. The developing time was about 35 min. The plate was then removed from the chamber, air-dried for about 5 min, rotated 90°, and inserted into the second chamber which had been equilibrated with freshly-prepared methanol-ether-water (4 : 4 : 1,v/v). The second development was continued until the solvent front reached 100 mm from the layer boundary. The developing time here was about 55 min.

The spots separated on the chromatoplate were detected by means of their fluorescence under ultraviolet light. All the polynuclear hydrocarbons except chrysene and phenanthrene were detected under long-wave ultraviolet light (365 mμ). Chrysene and phenanthrene were detected under short-wave ultraviolet light (253 mμ). The irradiation time of the short-wave ultraviolet light should be made as short as possible in order to prevent the photochemical decomposition of polynuclear hydrocarbons.

Results

Separation of Polynuclear Hydrocarbons. The R_f values of the 15 hydrocarbons are listed in Table 1. The hydrocarbons which had overlapped each other on the aluminum oxide G layer upon the first development were adequately separated by the second development on the acetylated cellulose layer. This is clearly demonstrated in Fig. 2.

It must be noted that the first development on the aluminium oxide layer should be carried out in a chamber kept at a constant relative humidity of about 20%, because the R_f values of the hydrocarbons are highly affected by the humidity of the atmosphere in a developing chamber.[14,15] Development at a higher or at a lower humidity gave an unsatisfactory separation of the polynuclear hydrocarbons, as is shown in Table 1.

13) D. R. Gilmore and A. Cortes, *J. Chromatog.*, **21**, 148 (1966).

14) H. Matsushita and Y. Suzuki, *Ind. Health*, **4**, 59 (1966).

15) Y. Suzuki and H. Matsushita, *ibid.*, **5**, 65 (1967).

TABLE 1. R_f VALUES OF POLYNUCLEAR HYDROCARBONS ON TWO-DIMENSIONAL DUAL BAND THIN LAYER CHROMATOGRAM*

No.	Substance	Aluminum oxide G			Acetylated cellulose		
		Relative humidity			No. of repeated development**		
		20%	7%	49%	1	2	3
1	Anthracene	0.55	0.31	0.64	0.54	0.61	0.66
2	Phenanthrene	0.54			0.48	0.56	0.60
3	Pyrene	0.49	0.21	0.61	0.43	0.51	0.54
4	Benzo(*a*)anthracene	0.37	0.08	0.56	0.35	0.43	0.46
5	Chrysene	0.35			0.20	0.26	0.29
6	Benzo(*e*)pyrene	0.27			0.47	0.55	0.58
7	Benzo(*a*)pyrene	0.27	0.04	0.51	0.13	0.18	0.20
8	Perylene	0.26			0.39	0.47	0.50
9	Benzo(*k*)fluoranthene	0.25			0.28	0.34	0.37
10	Benzo(*b*)fluoranthene	0.25			0.19	0.25	0.28
11	Anthanthrene	0.18			0.19	0.24	0.27
12	Benzo(*ghi*)perylene	0.17	0.02	0.46	0.52	0.59	0.64
13	Dibenzo(*a,h*)anthracene	0.14			0.42	0.50	0.53
14	Coronene	0.10			0.58	0.66	0.71
15	Dibenzo(*a,i*)pyrene	0.07	0.01	0.36	0.28	0.35	0.38

* R_f values were mean of 3 determinations. Deviation of each R_f value from the mean value was within 0.03. Developing temperature was 18 ± 2°C.

** Repeated development was carried out on acetylated cellulose layer with intermittent drying of 10 min in a room.

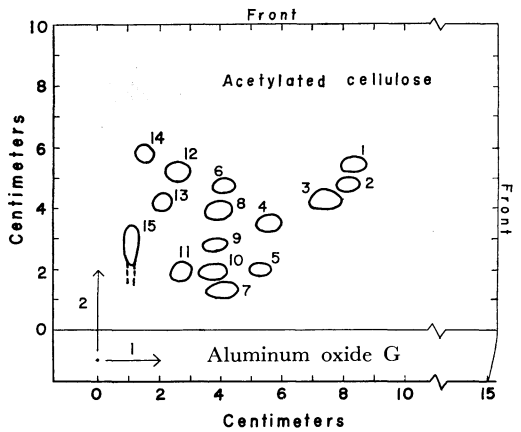

Fig. 2. Two-dimensional dual band thin layer chromatogram of polynuclear hydrocarbons.
The number of each spot corresponds to that of polynuclear hydrocarbon cited in Table 1.

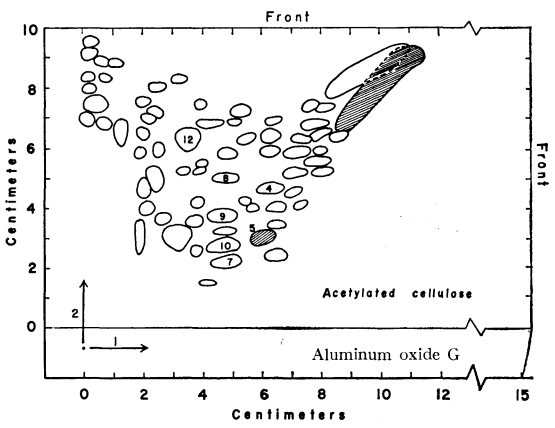

Fig. 3. Two-dimensional dual band thin layer chromatogram of vacuum sublimation extract from suspended particulates in Tokyo air.
Separation on acetylated cellulose layer was carried out by developing the plate three times to the 10 cm mark in methanol-ether-water with intermittent drying of 10 min in a room. The number indicated for several sports corresponds to that of polynuclear hydrocarbons cited in Table 1. The spot with oblique lines is that detected by short-wave ultraviolet light irradiation.

In the second development, spots of polynuclear hydrocarbons on the aluminum oxide G layer migrated rapidly with a rise in the solvent front, were deformed to a very small shape like a hairline on the layer boundary, and then were further separated into several spots on the acetylated cellulose layer. Since the spots separated on the acetylated cellulose layer took small, oval shapes, a high separability and detectability were obtained.

Separation of an Extract from Air Pollutants. The present method was used in the separation of an extract from air pollutants in Tokyo. Suspended particulates in Tokyo air were collected on a glass fibre filter (Gelman A, Gelman Instrument Co.) using a high-volume air sampler (Staplex Co.). The polynuclear hydrocarbons in

the particulates were extracted by vacuum sublimation, which had been proved to be more advantageous than solvent extraction for the extraction of polynuclear hydrocarbons.[16-18] The vacuum sublimation was carried out for about 30 min under conditions of 300°C and 0.007 mmHg for the particulates (185.5 mg) collected on a glass fibre filter. The sublimate which deposited on the narrow range of the inner surface of the sublimation tube (2 mm in inner diameter)was easily dissolved by 180 μl of benzene inserted into the tube by a microsyringe. Two microliters of the solution were used for the separation by the present thin-layer chromatography. Figure 3 shows the chromatogram for the sublimation extract of particulates in Tokyo air. Sixty-nine spots were detected on the chromatogram by means of their fluorescence under long- or short-wave ultraviolet light. A spot containing benzo(*a*)pyrene which had been obtained by the first development was further separated into 9 spots by the second development. The fluorescence and excitation spectra of the benzene extract of the spot corresponding to benzo(*a*)pyrene were entirely coincident with the spectra of the pure benzo(*a*)pyrene solution, as is shown in Fig. 4. Other polynuclear hydrocarbons, such as benzo(*b*)-fluoranthene, benzo(*k*)fluoranthene, perylene, benzo(*ghi*)perylene, chrysene, and benzo(*a*)anthracene, were also proved to be isolated in a pure state from the sublimation extract by spectrofluorometry.

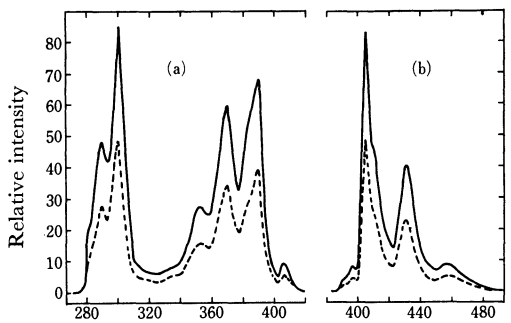

Fig. 4. Excitation and fluorescence spectra of spot 7 and benzo(*a*)pyrene solutions.
(a) Excitation spectra; (b) Fluorescence spectra.
—— Benzene extract of spot 7.
------ Benzo(a)pyrene benzene solution.

Discussion

The present chromatography has some advantages for the separation of polynuclear hydrocarbons over the hitherto-reported thin-layer chromatographies which use a single adsorbent layer.[1-12] The separation efficiency is high, since spots of the hydrocarbons are scattered all over the acetylated cellulose layer in the present method. The high separation efficiency comes from the combined use of the two adsorbent layers which are different in separation characteristics. Another advantage of the present method is the high sensitivity. For example, the minimum detectable value of benzo-(*a*)pyrene is 0.001 μg or less in the present method, while the value is 0.007 μg in the one-dimensional chromatography using silica gel as the adsorbent layer and *n*-hexane - *o*-dichlorobenzene - pyridine (10 : 1 : 0.5,v/v) as the developing solvent.[6] This high sensitivity comes from the combined use of two different chromatographies; adsorption chromatography in the first and partition chromatography in the second development. The adsorption force of aluminium oxide G for the hydrocarbons is very much weakened by the second developing solvent, which contains water as one component, as may easily be understood from the facts that the R_f values of the hydrocarbons on the aluminum oxide layer are highly affected even by the moisture content in a developing chamber and increase remarkably with an increase in the moisture content.[14,15] For these reasons, the spots on the aluminum oxide G layer are rapidly transferred to the boundary between the two adsorbent layers as very small, hairline-like spots and then separated into components on the acetylated cellulose layer with the rise of the second developing solvent. The hairline-like spots cause very small oval spots on acetylated cellulose after the second development, resulting in the enhancement of the sensitivity in the detection of polynuclear hydrocarbons.

Furthermore, the fluorescence intensities of the hydrocarbons on the acetylated cellulose layer are not much reduced even after having been left for a prolonged period in a dark room, although the fluorescences on the aluminum oxide layer change in color and are reduced remarkably in intensity by the same treatment.

In the present method, the two adsorbents should be so selected as to equalize approximately the moving speeds of the first developing solvent on the two layers. If the moving speeds differ markedly, the spots of hydrocarbons on the aluminum oxide layer will be found on a heavily-curved line after the first development, as is illustrated schematically in Fig. 5. This often has an adverse effect on the separation. For this reason, we selected acetylated cellulose prepared from cellulose D (Camag) as the adsorbent in the second development. Acetylated cellulose prepared from cellulose D-O (Camag) and MN 300 acetylated cellulose (M. Nagel) were not suitable for the adsorbent in this method, because the moving speeds of the first developing solvent on these cellulose layers

16) W. L. Ball, G. E. Moore, J. L. Monkmann and M. Katz, *Amer. Ind. Hyg. Assoc. J.*, **23**, 222 (1962).
17) H. Sakabe, *Proc. Roy. Soc. Med.*, **57**, 1005 (1964).
18) H. Arito, R. Soda and H. Matsushita, *Ind. Health*, **5**, 243 (1967).

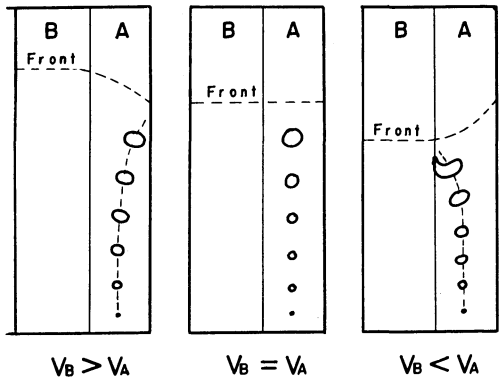

Fig. 5. Schematic representation of the 1st dimensional chromatograms.
A and B indicate aluminum oxide G and acetylated cellulose, respectively. V_A and V_B indicate the moving speed of developing solvent on A and B layers.

were considerably higher than that on the aluminum oxide G layer.

In an accurate determination of the benzo(*a*)pyrene in air pollutants, it should first be isolated completely from the other hydrocarbons. However, the benzo(*a*)pyrene fraction obtained by the column, paper or thin-layer chromatography, which is ordinarily used, is frequently contaminated by other hydrocarbons, some of which interfere with an accurate determination of the benzo(*a*)pyrene. The benzo(*a*)pyrene fraction obtained by the present chromatography was completely isolated from such hydrocarbons as benzo(*k*)fluoranthene, benzo(*e*)pyrene, benzo(*b*)fluoranthene, and perylene, and proved to be spectrofluorometrically pure. Thus, the present method may also make possible an accurate determination of the benzo(*a*)pyrene in air pollutants.

BULLETIN OF THE CHEMICAL SOCIETY OF JAPAN VOL. 42 464—469 (1969)

Effects of the Addition of Chlorohydrocarbons on the Oxidation of Propylene*1; A Consideration of the Negative Temperature Coefficient

Mitsuo MASAI, Etsuro ECHIGOYA*2 and Kiyoshi MORIKAWA*3

Research Laboratory of Resources Utilization, Tokyo Institute of Technology, Ookayama, Meguro-ku, Tokyo

(Received June 15, 1967)

A small amount of allyl chloride, 1,1-dichloroethane, or chloroform was added to the reactant in the oxidation of propylene in an inert fluidized-bed reactor. A negative temperature coefficient is observed in the conversion of propylene and in the formation of various products, but not propylene oxide, in the experiments with allyl chloride or 1,1-dichloroethane added. The results of the chloroform-adding experiments show a positive temperature coefficient in the conversion of propylene and in the formation of gaseous products. The results of the work described here are discussed on the basis of the probable reaction scheme. The results of the chloroform-adding experiments support the proposed catalytic effect of the chlorocarbene on the decomposition of acetaldehyde. It is concluded that the negative temperature coefficient is attributable to the apparent inactivity of acetaldehyde (the branching agent) in the high-temperature region in this reaction atmosphere.

Previous works[1,2] using an inert fluidized-bed reactor have shown that a very pronounced negative temperature coefficient is observed in the conversion of propylene and in the formation of acetaldehyde, propylene oxide, acrolein, propionaldehyde, carbon monoxide, methane, and ethylene in an excess-propylene atmosphere. The purpose of the present paper is to describe the results of oxidation experi-

*1 Part of a discussion presented at the 18th Annual Meeting of the Chemical Society of Japan, Osaka, April, 1965.

*2 Present address: Department of Chemical Engineering, Faculty of Engineering, Tokyo Institute of Technology.

*3 Present address: Japan Gasoline Co., Ltd., New Otemachi Bldg., Otemachi, Chiyoda-ku, Tokyo.

1) E. Echigoya, M. Masai and K. Morikawa, This Bulletin, **41**, 904 (1968).

2) M. Masai, E. Echigoya and K. Morikawa, *ibid.*, **41**, 910 (1968).

ments featuring the addition of allyl chloride, 1,1-dichloroethane, or chloroform to the reactant (propylene and oxygen) using an inert fluidized-bed reactor, and also to discuss the cause of the negative temperature coefficient on the basis of the reaction scheme reported previously.[2,3]

In the same reaction system, Kamiya studied the effects of the addition of chloroform or other halogenated hydrocarbons to the reactant;[4] his results showed the acceleration of the reaction by the addition of these substances. Hurst, Skirrow, and Tipper accounted for the low overall activation energy in terms of the enhanced decomposition of hydroperoxide by the hydrogen bromide added in the oxidation of butene.[5] Seakins demonstrated the strong accelerating effect of chloroform on the chain propagation in the oxidation of propane.[6]

There have been many discussions of the negative temperature coefficient.[7] Among these, Yenikolopyan discussed it in terms of the decrease in branching resulting from the decomposition of the hydroperoxy, the acetyl, and the acetyl peroxy radicals in the oxidation of propylene.[7] Shtern demonstrated that, in the oxidation of propane, the induction period was shortened by the addition of acetaldehyde to the reaction system in the low-temperature region, but no effect was observed in the high-temperature region.[8] McMillane and Calvert showed that the estimated rate constants of the oxidation of the acetyl radical were 0.7×10^{8} $l\cdot mol^{-1}\cdot sec^{-1}$ at 290°C and 3.8×10^{8} at 36°C;[9] these values were obtained on the postulation that the rate constant of the decomposition reaction of the acetyl radical increases normally with an increase in the temperature. Seakins and Hinshelwood discussed the observed maximum of the rate against the temperature on the basis of a kinetic study.[10]

In the present work, experiments featuring the addition of allyl chloride or 1,1-dichloroethane showed a temperature dependence of the reaction results, except in the formation of propylene oxide, similar to that observed in the previous works.[1,2] A different temperature dependence was, however, observed in the chloroform adding experiments. The results obtained will be discussed on the basis of a reaction scheme reported before.[2,3] It will be concluded that the negative temperature coefficient is attributable to the apparent inactivity of acetaldehyde (the branching agent) at a high temperature in this reaction atmosphere.

Experimental

Materials. The allyl chloride and the 1,1-dichloroethane, both of G. R. quality, were obtained from the Tokyo Kasei Kogyo Co., Ltd. (Tokyo). The chloroform, containing 1% of ethanol as a stabilizer, was obtained from the Wako Junyaku Kogyo Co., Ltd. (Osaka). The propylene gas, the oxygen, and the silicon carbide have been described before.[1]

Apparatus. This was as has been described for Exp. A in a previous paper.[2]

Procedures. These were as have been described for Exp. A in a previous paper.[2] The concentrations of the additives were 0.50—0.58 vol% for the allyl chloride, 0.48—0.55 vol% for the 1,1-dichloroethane, and 0.50—0.55 vol% for the chloroform, according to the reaction temperature.

Analysis. This was done as has been described for Exp. A in a previous paper.[2]

Results

The results of the oxidation experiments are shown in Figs. 1—9. In these figures, the full lines with black points are for the oxidation experiments with the additives, while the dotted lines with open points are for the oxidation experiments without the additives (standard experiment).

The additions of allyl chloride and 1,1-dichloroethane gave similar results, as is shown in Figs. 1 and 4, 2 and 5, and 3 and 6. The remarkable difference due to the additives is the increase in the yield of propylene oxide with the rise in the temperature (Figs. 1 and 4). Methane and ethylene are increased by these additives (Figs. 2 and 5). The amount of carbon monoxide and the conversion of propylene are increased by these additives (Figs. 3 and 6). Negative temperature coefficients are observed in these experiments except in the case of propylene oxide (Figs. 1—6).

Considerable differences are observed between the chloroform-adding experiments and the standard experiment as is shown in Figs. 7—9. Acetaldehyde (AA) and propylene oxide (PO) are considerably decreased at a high temperature. While acrolein (Acr) and propionaldehyde (PA) are increased slightly at a higher temperature (Fig. 7), the results for Acr and PA are nearly the same as the results shown in Figs. 1 and 4. The temperature co-

3) M. Masai, E. Echigoya and K. Morikawa, *ibid.*, **41**, 920 (1968).

4) Y. Kamiya, *Sekiyu Gakkai Shi* (*J. Japan Petrol. Inst.*), **5**, 573 (1962).

5) P. Hurst, G. Skirrow and C. F. H. Tipper, *Proc. Roy. Soc.*, **A268**, 405 (1962).

6) M. Seakins, *ibid.*, **A274**, 413 (1963).

7) V. Ya. Shtern, "The Gas-phase Oxidation of Hydrocarbons," English translation by M. F. Mullins, Pergamon Press, Oxford (1964), pp. 105—110, 480—492.

8) N. N. Semenov, "Some Problems in Chemical Kinetics and Reactivity," Japanese translation by T. Kwan and A. Matsuda, Vol. 2, Iwanami Shoten Co., Tokyo (1963), Chap. 12 § 1.

9) G. R. McMillane and J. G. Calvert, "Oxidation and Combustion Reviews," ed. by C. F. R. Tipper, Vol. 1, Elsevier Pub. Co., Amsterdam (1965), pp. 110—111.

10) M. Seakins and C. Hinshelwood, *Proc. Roy. Soc.*, **A276**, 324 (1963).

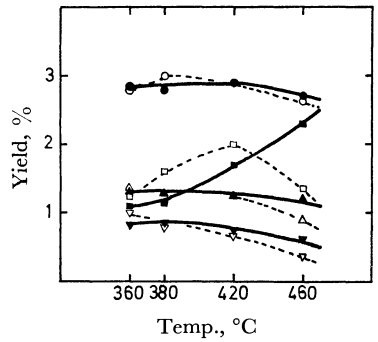

Fig. 1. Yield *vs.* temp. curves with the addition of allyl chloride; under 3.5 atm with mole fraction of O_2, 0.2.
-●-, AA; --○--, AA in standard exp.
-■-, PO; --□--, PO in standard exp.
-▲-, Acr; --△--, Acr in standard exp.
-▼-, PA; --▽--, PA in standard exp.

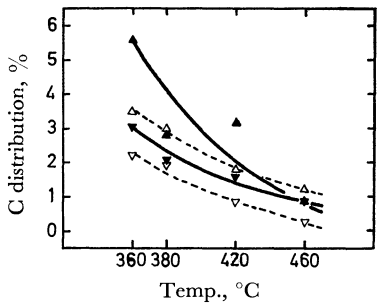

Fig. 2. Carbon distribution *vs.* temp. curves with the addition of allyl chloride; under 3.5 atm with mole fraction of O_2, 0.2.
-▲-, C_2H_4; --△--, C_2H_4 in standard exp.
-▼-, CH_4; --▽--, CH_4 in standard exp.

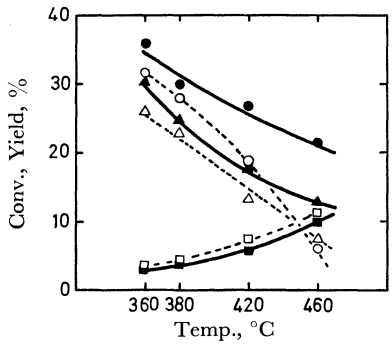

Fig. 3. Conversion and yield *vs.* temp. curves with the addition of allyl chloride; under 3.5 atm with mole fraction of O_2, 0.2.
-●-, conv. of C_3H_6
--○--, conv. of C_3H_6 in standard exp.
-▲-, yield of CO
--△--, yield of CO in standard exp.
-■-, yield of CO_2
--□--, yield of CO_2 in standard exp.

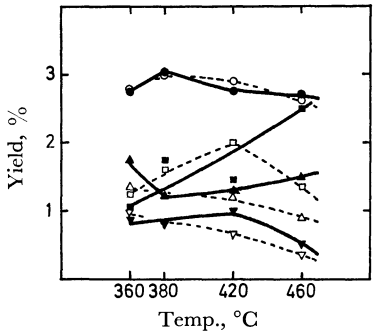

Fig. 4. Yield *vs.* temp. curves with the addition of 1,1-dichloroethane; under 3.5 atm with mole fraction of O_2, 0.2.
-●-, AA --○--, AA in standard exp.
-■-, PO --□--, PO in standard exp.
-▲-, Acr --△--, Acr in standard exp.
-▼-, PA --▽--, PA in standard exp.

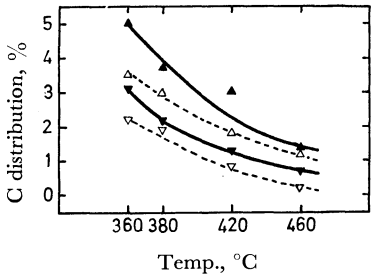

Fig. 5. Carbon distribution *vs.* temp. curves with the addition of 1,1-dichloroethane; under 3.5 atm with mole fraction of O_2, 0.2.
-▲-, C_2H_4; --△--, C_2H_4 in standard exp.
-▼-, CH_4; --▽--, CH_4 in standard exp.

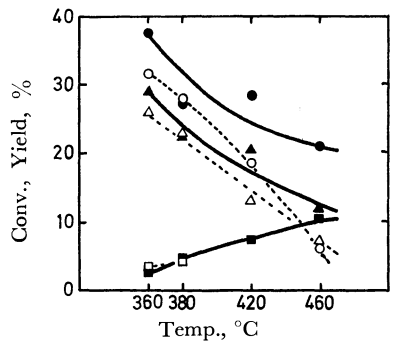

Fig. 6. Conversion and yield *vs.* temp. curves with the addition of 1,1-dichloroethane; under 3.5 atm with mole fraction of O_2, 0.2.
-●-, conv. of C_3H_6
--○--, conv. of C_3H_6 in standard exp.
-▲-, yield of CO
--△--, yield of CO in standard exp.
-■-, yield of CO_2
-□-, yield of CO_2 in standard exp.

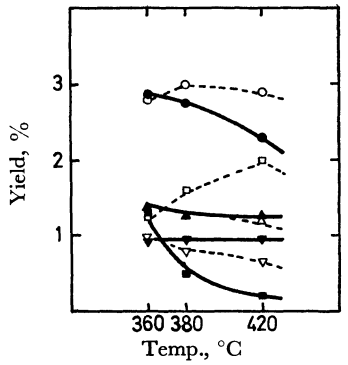

Fig. 7. Yield *vs.* temp. curves with the addition of chloroform; under 3.5 atm with mole fraction of O_2, 0.2.
-●-, AA; --○--, AA in standard exp.
-■-, PO; --□--, PO in standard exp.
-▲-, Acr; --△--, Acr in standard exp.
-▼-, PA; --▽--, PA in standard exp.

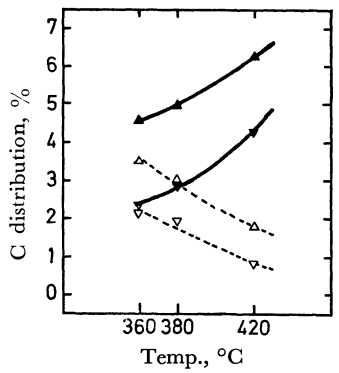

Fig. 8. Carbon distribution *vs.* temp. curves with the addition of chloroform; under 3.5 atm with mole fraction of O_2, 0.2.
-▲-, C_2H_4; --△--, C_2H_4 in standard exp.
-▼-, CH_4 ; --▼--, CH_4 in standard exp.

efficients for the formations of methane, ethylene (Fig. 8), carbon monoxide, and carbon dioxide, and for the conversion of propylene (Fig. 9) are reversed by the addition of chloroform. Ethylene is increased in all the experiments with additives (Figs. 2, 5, and 8).

Discussion

As has been described above, the lowest temperature at which the reaction occurs is not affected by the addition of allyl chloride, 1,1-dichloroethane, or chloroform. These facts indicate that these additives do not affect the initiation step. The considerable differences observed between the results of the adding experiments and the standard experiment show that these additives remarkably affect the reaction in the early steps of the chain.

The results described above will be discussed

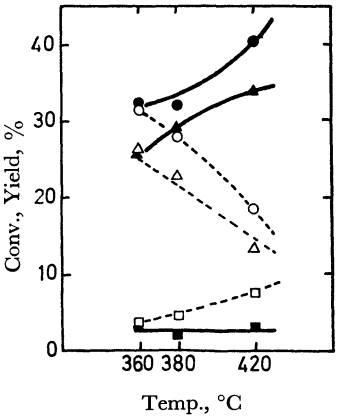

Fig. 9. Conversion and yield *vs.* temp. curves with the addition of chloroform; under 3.5 atm with mole fraction of O_2, 0.2.
-●-, conv. of C_3H_6
--○--, conv. of C_3H_6 in standard exp.
-▲-, yield of CO
--△--, yield of CO in standard exp.
-■-, yield of CO_2
--□--, yield of CO_2 in standard exp.

below on the basis of a reaction scheme reported before.[2,3] The main part of the scheme is shown in Table 1. In this scheme, PO is mainly formed *via* AA in an excess-propylene atmosphere as has been discussed before.[2],*4

Effects of the Addition of Allyl Chloride and 1,1-Dichloroethane. While nearly the same results are obtained by the addition of these two additives, the forms of their decompositions are different; *i. e.*, one is radical, and the other is monomolecular:[11]

$$CH_2{=}CHCH_2Cl \rightarrow CH_2{=}C\dot{H}CH_2 + \dot{C}l$$
$$CH_3CHCl_2 \rightarrow CH_2{=}CHCl + HCl$$

The chlorine atom most likely reacts with propylene to form hydrogen chloride and the allyl radical, and also probably recombines into chlorine. Hydrogen chloride is produced by both these additives.

*4 There may be some objection to this previously obtained conclusion.[2] The objection will be that, under the conditions of Exp. B_1 of the previous paper,[2] bromine or bromine compounds may interfere with the formation of PO. This objection cannot be sustained, however, because the interaction between bromine or bromine compounds and PO can be neglected, as has been discussed in "*4" in a previous paper,[2] and also because the addition reaction of the bromine atom to the double bond of propylene does not interfere with the same addition reaction of the allyl peroxy radical, for an excess of propylene is present in the reaction atmosphere.[2]

11) N. N. Semenov, "Some Problems in Chemical Kinetics and Reactivity," Japanese translation by T. Kwan and A. Matsuda, Vol. 1, Iwanami Shoten Co., Tokyo (1963), Chap. 7 § 4, § 7.

Table 1. The main part of the scheme[2)]

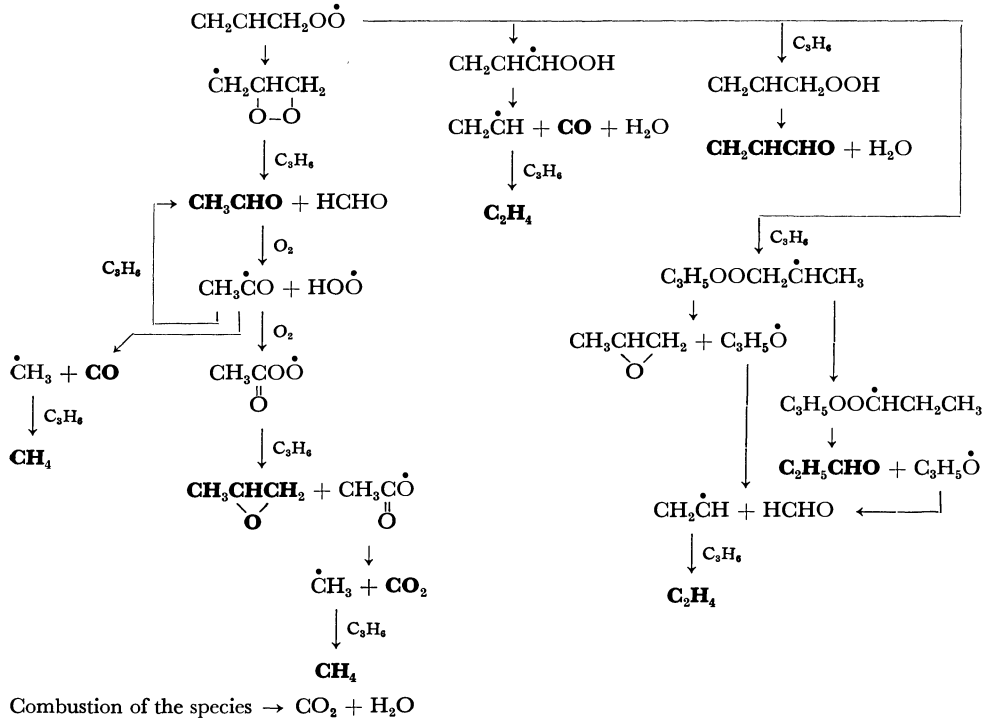

Quite similar results are obtained in these two adding experiments; this suggests that the hydrogen chloride is a predominantly effective species in both these experiments.*5 The increase in the formation of methane and carbon monoxide may be attributed to the enhanced decomposition of AA, as hydrogen chloride is known to accelerate the decomposition of AA slightly.[13)] The yield of AA is little affected by the presence of these two additives or, therefore, by the presence of hydrogen chloride (Figs. 1 and 4). This suggests that the true amount of AA formed should be increased, if we consider the increased consumption of AA resulting from the enhanced decomposition. The amount of ethylene, which is mainly formed from the allyl peroxy radical (Table 1), is also increased (Figs. 2 and 5). These increase in the formation of AA and ethylene may indicate an increased formation of the allyl peroxy radical. If so, the increased conversion of propylene can be explained in terms of the increased formation of the allyl peroxy radical. The degree of the increase in the formation of ethylene is less than those of methane and carbon monoxide at 460°C in the two adding experiments. This indicates that the reaction of the allyl peroxy radical to AA becomes predominant in comparison with the reaction to ethylene at 460°C.

The most notable feature in these two adding experiments is the positive temperature coefficient observed in the formation of PO (Figs. 1 and 4). The positive temperature coefficient observed in the PO formation is mainly due to the increased formation of PO at 460°C in the two adding experiments. This increase can be ascribed to the increased formation of AA, as has been discussed above, because it has been suggested that PO is formed mainly through the addition of the acetyl peroxy radical to the double bond of propylene.[2)] The low yield of PO in the 360—420°C region in the two adding experiments (Figs. 1 and 4) indicates that the increase in the formation of the allyl peroxy radical, discussed above, contributes only a little to the formation of PO. The route to PO *via* the addition of the allyl peroxy radical to the double bond of propylene has already been established to be minor.[2)] The true amount of AA formed is certainly smaller at 360—420°C, as has been discussed above; This is the reason for the low yield of PO in this temperature region.

The Effects of Chloroform. Contrary to the case with the standard experiment, and also to the former two adding experiments, the positive temperature coefficients of the conversion of propyl-

*5 In the case of 1,1-dichloroethane, the presence of vinyl chloride should be considered. The accelerating effect of vinyl chloride on propane oxidation has been reported.[12)] The resemblance of the results of the two adding experiments are so remarkable that it may be reasonable to consider the hydrogen chloride formed as the predominantly effective species.

12) M. Seakins, *Proc. Roy. Soc.*, **A277**, 279 (1964).
13) H. Fromherz, *Z. physik. Chem.*, **B25**, 301 (1934).

ene and of the formation of methane, ethylene, and carbon monoxide are observed in the chloroform-adding experiments. Decrease in the formation of AA and PO are noticed in the higher-temperature region.

For the decomposition of chloroform, two kinds of reactions have been reported.*6 Reaction (1) has been proposed in the presence of peroxide:[14a]

$$CHCl_3 \rightarrow \dot{C}Cl_3 + \dot{H} \qquad (1)$$

Reaction (2) has been reported to have an activation energy of 47 kcal/mol:[12]

$$CHCl_3 \rightarrow :CCl_2 + HCl \qquad (2)$$

The bond-dissociation energy of CCl_3–H is 95.7 kcal/mol.[15] Therefore, reaction (2) is more probably predominant.*7 The chlorocarbene $:CCl_2$ is an electrophilic and relatively stable radical.[14b] The chlorocarbene has been shown to add to double bonds such as C=C and C=N.[14b]

Therefore, it is reasonable to suggest the addition of the chlorocarbene to the carbonyl group of AA. The scheme of this suggested reaction is as follows;

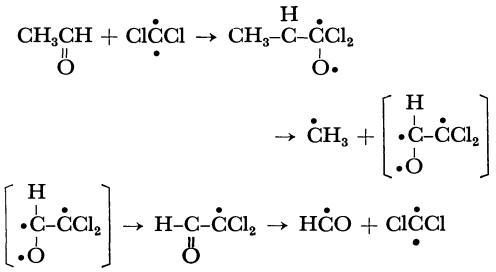

Thus, the chlorocarbene is regenerated. This hypothetical catalytic action of the chlorocarbene on the decomposition of AA is supported by the results of the chloroform-adding experiments and also by a reaction scheme reported earlier[2] (Table 1). Here, the effect of hydrogen chloride is considered to be small in view of the results of the allyl chloride and 1,1-dichloroethane-adding experiments.

Table 2 shows that the addition of chloroform increased the formation of methane considerably in comparison with ethylene and carbon monoxide. In the case of the addition of allyl chloride or 1,1-dichloroethane, the increase in methane is not very obvious in comparison with ethylene and carbon monoxide. As a result of the reaction of the chlorocarbene and AA, only the formation of methane is increased. The decreases in AA and PO also support the catalytic effect of the chlorocarbene.

Table 2. Comparison of the effects of the additives on the formation of methane, ethylene and carbon monoxide at 420°C (the values for the standard experiments are taken as unity)

Product	Additive		
	$CHCl_3$	C_3H_5Cl	CH_3CHCl_2
CH_4	5.8	1.7	2.0
C_2H_4	3.3	1.6	1.7
CO	2.5	1.3	1.5

As has been discussed in the case of the former two additives, hydrogen chloride accelerates the oxidation reaction considerably at 360°C. In the chloroform-adding experiments at 360°C, only the value of ethylene varies from those of the standard experiment. Therefore, the decomposition of chloroform into the chlorocarbene and hydrogen chloride is not as sufficient at 360°C as at 420°C.

As has been shown in the discussions of the former two additives, the negative temperature coefficient of the oxidation reaction is observed in spite of the acceleration by hydrogen chloride. Because of the catalytic effect of the chlorocarbene on AA, which is the degenerate branching agent,[2,3] the main path of the oxidation reaction changed from I to II as below:

$$\text{I} \quad C_3H_5O\dot{O} \rightarrow AA \rightarrow PO$$

$$\text{II} \quad C_3H_5O\dot{O} \rightarrow AA \xrightarrow{:CCl_2} CH_4$$

Therefore, the change in the temperature coefficient from negative to positive is quite reasonable because of the increase in the concentration of the chlorocarbene with the rise in the reaction temperature.

Thus, the catalytic action of the chlorocarbene—though hypothetical—on the decomposition of AA changes these temperature correlations. The hypothetical reaction is the branching reaction, for number of radicals increases in the course of the reaction of AA with the chlorocarbene. This probably shows that the negative temperature coefficient is caused by the retarded reactivity of AA in the high-temperature region in this reaction atmosphere. This accords with Shtern's conclusion[8] described above, that AA does not behave as a branching agent in the temperature region where the negative temperature coefficient is observed. The cause of this inactivity of AA has not yet been elucidated.[8]

The authors wish to thank the Nippon Petrochemicals Co., Ltd., for supplying the propylene gas and also the Mitsui Mining and Smelting Co., Ltd., for supplying the silicon carbide.

*6 The route to $\dot{C}HCl_2$ is not considered here, because $\dot{C}HCl_2$ is not as stable as $\dot{C}HBr_2$[14a] and also because no precise and accurate value of D($CHCl_2$–Cl) can be found.

14) J. I. G. Cadogon and M. J. Perkins "The Chemistry of Alkene," ed. by S. Patai, Interscience Pub., London (1964), a) p. 589; b) pp. 640—642.

15) J. A. Kerr, *Chem. Rev.*, **66**, 465 (1966).

*7 The reverse reaction of reaction (1) is a radical recombination reaction: The activation energy for this reverse reaction is negligible. Therefore, the activation energy of reaction (1) is 95.7 kcal/mol.

BULLETIN OF THE CHEMICAL SOCIETY OF JAPAN VOL. 42 470—474 (1969)

The Reaction of Alcohols and Hydrocarbons in a Silent Electric Discharge. I. The Decomposition of 2-Propanol by the Discharge*1

Teruo HIRAKI

Institute of Commodities, Faculty of Economics, Kagawa University, Takamatsu

(Received April 2, 1968)

The reaction of 2-propanol under a silent electric discharge was studied using two kinds of discharge tubes. One was Siemen's tube, which was used for investigating a silent discharge decomposition of 2-propanol. The other was a special tube that had one side of the walls made of copper or its salts; it was used for studying the effects of the wall on the decomposition. The main liquid products were acetaldehyde, acetone, *dl*-2-butanol, 2-methyl-2-propanol, 2-methyl-2-butanol, and hydrocarbons. The gaseous products were methane, C_2—C_4-hydrocarbons, carbon monoxide, carbon dioxide, and hydrogen. These components were obtained in every run, regardless of the type of tube used. However, the distribution of the products varied with the sort of tube. The formation of 2-methyl-2-butanol can be explained by the addition of a 1-hydroxyisopropyl radical with the ethylene produced; the only product formed by adding this radical to ethylene was the one-to-one adduct. By replacing one side of the glassy walls with a wall of a glass-filter-packed copper or its salts, the yield of 2-methyl-2-propanol was increased relatively, and those of 2-methyl-2-butanol and *dl*-2-pentanol were decreased.

Kawamoto *et al.*[1] found that acrylonitrile and higher cyanides were produced by the reaction of prussic acid with ethylene in a silent electric discharge. The higher cyanides seem to be formed by a chain telomerization.

A similar telomerization may also occur in the discharge reaction of 2-propanol and ethylene, considering Urry's[2] research on the peroxide- and light-induced additions of several alcohols to olefins, and the fact[3,4] that the *α*-C-alkylations of primary and secondary alcohols result not only from peroxide- or light-induced reaction, but also from gamma-ray irradiation.

It would be interesting to ascertain if a silent electric discharge initiates the telomerization. In the present paper, preliminarily, the author wishes to report some observations on the chemical behavior of 2-propanol submitted to silent discharge, including a study of the effects on the reaction of a wall made of copper or its salts.

Experimental

Material. 2-Propanol was purified by column distillation after it had been refluxed over potassium carbonate. No impurity was found by gas chromatographical analysis using a 3-m column of PEG-6000.

Packing. The packing material shown in Table 1 was prepared by the method described in Kawamoto's[5] paper.

Discharge Tubes. The discharge tubes used are shown in Fig. 1-a. Two kinds of tubes, here simply noted as tube 1 and tube 2, were used.

Tube 1 was a Pyrex tube of the Siemen type[6] with a gap length of 2.5 mm and an effective length of 45 cm. The outside (B) of the discharge tube was filled with water, while the inner tube (A) was filled with a 3% $CuSO_4$ solution. Electrodes (C) were inserted into both (A) and (B).

Tube 2 was a Pyrex tube with a glass filter which had an effective length of 30 cm, an outside diameter of 2 cm, and a space gap 2.5 mm long. The outside (B) of the discharge tube and a glass filter (D) were filled with water and 5 g of the packing material respectively. Electrodes (C) were inserted into both (B) and (D).

Apparatus and Procedure. The experiment was performed by using the flow system and the reflux system. The apparatus for the flow system and the reflux system are shown in Figs. 2 and 3. The reduced copper for packing was prepared by passing purified

*1 The major part of this research was presented at the 19th Annual Meeting of the Chemical Society of Japan, Yokohama, April, 1966.

1) K. Kawamoto and S. Tsutsumi, Preprints for the 18th Annual Meeting of the Chemical Society of Japan (1965), p. 173.

2) W. H. Urry, F. W. Stacey, E. S. Huser and O. O. Juveland, *J. Am. Chem. Soc.*, **76**, 450 (1954).

3) T. Kurihara and H. Hotta, This Bulletin, **37**, 1448 (1964).

4) K. Hirota and M. Hatada, *ibid.*, **34**, 1644 (1961).

5) K. Kawamoto, *ibid.*, **34**, 161 (1961).

6) T. Matsuda, K. Oto and K. Sugino, *Nippon Kagaku Zasshi* (*J. Chem. Soc. Japan, Pure Chem. Sect.*), **79**, 324 (1958).

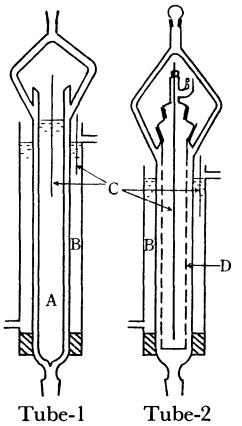

Fig. 1-a. The used discharge tubes.

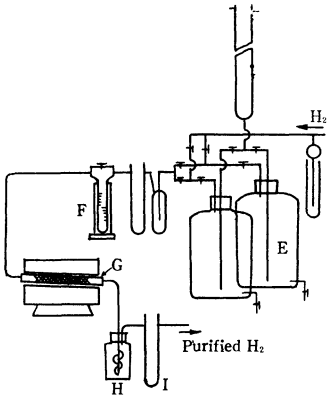

Fig. 1-b. Apparatus for purifying hydrogen.

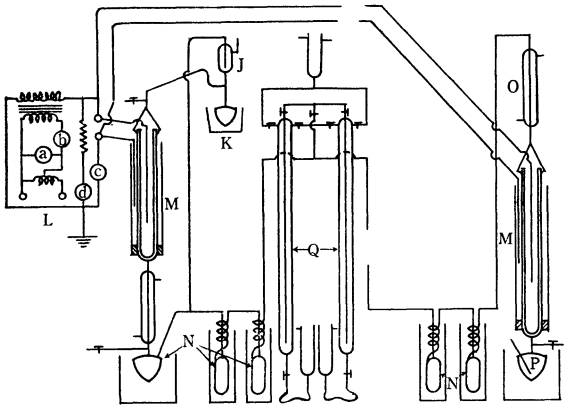

Fig. 2. The apparatus for a flow system.
a) Voltmeter, V
b) Ammeter, A
c) Ammeter, mA
d) Ammeter, μA

Fig. 3. The apparatus for a reflux system.

hydrogen on copper salt for 3—5 hr and at a velocity of 1.0—1.4 *l*/hr through the filter heated to 180°C. The apparatus for purifying hydrogen is illustrated in Fig. 1-b. Hydrogen coming from the reservoir (E) was passed through a tube (G) containing heated copper gauze in order to remove the oxygen in the hydrogen, and then through a bottle (H) containing a 30% sodium hydroxide solution and a solid sodium hydroxide tube (I). The hydrogen flow rate was measured by passing it through a calibrated flowmeter (F).

In the case of the flow system, as soon as the 2-propanol had fallen at a regular velocity from a dropping funnel (J) into a pot, a heater (K) turned it into vapor, which was then introduced into a discharge tube (M). The reaction products that passed through the tube were separated into a condensable part and non-condensable gases by three traps (N) cooled to 0°C.

In the case of the reflux system, 2-propanol in a still pot (P) was vaporized by heating it to 110°C; the vapor was then passed through the discharge tube (M). The reaction products passed through the discharge field were preliminarily separated into a condensable part and non-condensable gases by a condenser (O) kept at 55°C. The condensable products came back to the still pot again. The non-condensable part was further separated from the condensable products by two traps (N) cooled at 0°C. The volume of non-condensable gas was measured by a calibrated gas holder (Q).

The high tension was applied to the discharge tube from a transformer (L; capacity, 15 kV) which used a 60-cycle alternating current.

Analyses. The reaction products were identified by comparing their retention times on gas chromatography with those of authentic samples. The non-condensable products were analyzed by gas chromatography (column, 3 m activated charcoal at 100°C; carrier gas, hydrogen). For the analyses of C_3 and C_4-hydrocarbons and of hydrogen, a 3-m column of HMPA (Hexamethylphosphoric triamide) and a 3-m column of molecular sieve-13X were used at 35°C (carrier gas, helium).

The condensable products were identified not only by gas chromatography (column, tricresyl phosphate, PEG-6000 and silicon DC-550 at 100°C; carrier gas, helium), but also by derivatization. Thus, 2-methyl-2-propanol, obtained as a fraction boiling at 81—82°C, and *dl*-2-butanol (bp 99—100°C) were converted into their 3,5-dinitrobenzoates,*2 the melting points of the derivatives being 140—141°C and 75—76°C respectively. They showed no depression of the melting points when mixed with authentic specimens. The quantitative analysis of the liquid products was performed by gas chromatography (column, 3 m, PEG-6000 at 100°C; carrier gas, He).

Results and Discussion

The decomposition of 2-propanol was performed under the experimental conditions shown in Table 1; the reaction products which have been identified are listed in Table 2. The subscripts A and B in these tables indicate a flow system and a reflux

*2 The 3,5-dinitrobenzoates of 2-methyl-2-propanol and *dl*-2-butanol were prepared according to the procedure of Shriner *et al.*: R. L. Shriner, R. C. Fuson and D. Y. Curtin, "The Systematic Identification of Organic Compounds," 4th ed., John Wiley & Sons, New York (1956), p. 212.

TABLE 1. EXPERIMENTAL CONDITIONS

Exp. No.	1		2		3		4		5		6	7
System of process	A	B	A	B	A	B	A	B	A	B	B	A
Packings*	$Cu(OH)_2$		Reduced Cu-1		$CuCO_3 \cdot Cu(OH)_2$		Reduced Cu-2		Cu		None	None
Second. voltage, kV	15	15	15	15	15	15	15	15	15	15	13.5	15
current, mA	0.9	0.7	0.5	0.8	0.5	0.4	0.5	0.4	0.9	0.4	4.7	2.8
Temp. of discharge tube, °C	85	85	85	85	85	85	85	85	85	85	15 in, 32	85 85
Discharge time, hr	4	4	4	4	4.5	4	4	4	4.5	4	9	4.5
Material:												
2-Propanol												
Amount, g	38.56	38.88	38.85	38.98	38.68	38.92	38.94	38.97	38.60	38.97	38.78	36.99
Velocity, g/hr	9.65	—	9.71	—	8.60	—	9.72	—	8.58	—	—	8.22

* Symbol of reduced Cu-1 or -2 means the reduced copper that prepared by treating copper (II) hydroxide or hydroxide carbonate with hydrogen, respectively (see experimental).

TABLE 2. THE RESULTS

Exp. No.	1_A	1_B	2_A	2_B	3_A	3_B	4_A	4_B	5_A	5_B	6_B	7_A
Amount of liquid products, g	1.68	1.07	1.36	0.90	0.68	0.17	0.58	0.14	0.85	0.08	0.20	2.10
Conversion, %*	4.36	2.75	3.50	2.31	1.76	0.44	1.49	0.36	2.20	0.21	0.52	5.68
Composition of liquid products, %**												
Acetone	29.9	11.0	60.0	11.0	41.0	37.9	62.2	26.0	50.8	45.7	24.3	50.6
Acetaldehyde	5.9	2.6	12.3	3.1	21.0	5.9	10.0	6.9	21.7	1.3	0.3	16.7
dl-2-Butanol	3.0	2.8	3.2	4.0	6.6	8.5	6.7	5.0	6.7	11.3	3.7	6.9
2-Methyl-2-propanol	4.5	4.2	2.7	8.4	8.1	15.6	4.8	8.2	6.4	13.9	9.3	2.0
2-Methyl-2-butanol	0.3	0	0.2	0	0.6	0	0.5	0	0.7	0	2.2	0.6
Isobutyl methyl ketone	0.3	0.7	0.2	0.2	1.6	1.9	1.8	0.9	1.9	4.6	0.6	0
Methyl vinyl ketone	9.6	1.0	0.6	0.8	8.9	8.2	1.2	0	2.2	2.6	1.2	2.8
Hydrocarbons***	43.9	77.7	17.0	72.5	1.4	21.6	8.0	53.0	1.7	17.9	53.0	13.9
dl-2-Pentanol	0.4	0	0.5	0	0.9	0	0.8	0	1.2	0	0	1.2
The others	2.2	0	3.3	0	9.9	0.4	4.0	0	6.7	2.7	5.4	5.3
Gaseous products collected:												
Volume, *l*	2.2	0.5	2.5	1.1	2.5	0.8	1.6	0.5	2.4	0.5	—	—

Components; Methane, Ethylene, Ethane, Acetylene, Propane, Propylene, C_4-Hydrocarbons, Carbon monoxide, Carbon dioxide and Hydrogen.

* The conversion efficiency was given by (grams of reaction product per grams of 2-propanol used) × 100.

** The yields of each compound produced were given by (grams of each compound per grams of total reaction product) × 100.

*** Hydrocarbons contain 2-methylbutane, 2,3-dimethylbutane, *n*-hexane, 1-hexene, *etc.*

system respectively.

In general, the reaction rate was too low under a reflux system to discuss chemismus.

When Siemen's Tube Was Used (Exp. Nos. 6_B and 7_A). The main liquid products formed in the decomposition of 2-propanol at 85°C were acetone, acetaldehyde, *dl*-2-butanol, 2-methyl-2-propanol, and 2,3-dimethylbutane. A small amount of 2-methyl-2-butanol was also formed.

The percentage compositions of compounds shown in Table 2 are the average of three experiments; the fluctuations in the yields of these compounds were less than 1%.

The main gaseous products which were formed in this reaction were methane, ethane, ethylene, acetylene, C_3 and C_4-hydrocarbons, carbon monoxide, carbon dioxide, and hydrogen.

The characteristic of the action of silent discharge on a compound seems to be the electronic excitation of the molecule. Some of the molecules may be transformed by inelastic collisions into vibrationally-excited molecules. The activated molecules thus formed are considered to change into radicals or atoms, and into a very small amount of ionized

TABLE 3. THE ASSUMED RADICALS AND REACTION SCHEME

$CH_3CH(OH)CH_3 + e^*$ (accelerated electron) $\rightarrow$
$CH_3CH(OH)CH_3^*$ (excited 2-propanol) + e (electron decelerated by collision)

$CH_3CH(OH)CH_3^* \rightarrow$

(I) $\rightarrow CH_3\dot{C}(OH)CH_3 + \dot{H}$

$CH_3\dot{C}(OH)CH_3 \xrightarrow{\dot{C}H_3} (CH_3)_3COH$ (1)

$CH_3\dot{C}(OH)CH_3 \xrightarrow{C_2H_4} (CH_3)_2C(OH)\dot{C}_2H_4 \xrightarrow{i\text{-PrOH}} (CH_3)_2C(OH)C_2H_5$ (2)

(II) $\rightarrow CH_3CH(OH)\dot{C}H_2 + \dot{H}$

$CH_3CH(OH)\dot{C}H_2 \xrightarrow{\dot{C}H_3} CH_3CH(OH)CH_2CH_3$ (3)

$CH_3CH(OH)\dot{C}H_2 \xrightarrow{C_2H_4} CH_3CH(OH)CH_2\dot{C}_2H_4 \xrightarrow{i\text{-PrOH}} CH_3CH(OH)CH_2C_2H_5$ (4)

(III) $\rightarrow CH_3\dot{C}HOH + \dot{C}H_3$

$CH_3\dot{C}HOH \xrightarrow{C_2H_4} CH_3CH(OH)\dot{C}_2H_4 \xrightarrow{i\text{-PrOH}} CH_3CH(OH)C_2H_5$ (5)

(IV) $\rightarrow CH_3\dot{C}HCH_3 + \dot{O}H$

$CH_3\dot{C}HCH_3 \xrightarrow{C_2H_4} CH_3CH(\dot{C}_2H_4)CH_3 \xrightarrow{i\text{-PrOH}} CH_3CH(C_2H_5)CH_3$ (6)

$CH_3\dot{C}HCH_3 \xrightarrow{\text{coupling}} (CH_3)_2CHCH(CH_3)_2$ (7)

molecules,*3 as has been reported by many workers.[7] The radicals assumed to be formed from 2-propanol under the silent discharge, and a part of the postulated reaction scheme, are shown in Table 3. The methyl radical can be thought to be formed not only in the formation process of the Radical III in Table 3, but also in the secondary reaction, since more methane*4 than acetaldehyde was produced in every run.

It can be thought that *dl*-2-butanol is formed by two processes: the combination of a methyl radical with a 2-hydroxypropyl radical (Reaction 3), and the addition of a 1-hydroxyethyl radical to the ethylene formed during the reaction (Reaction 5). Although the process of reaction (5) has been proposed in radiolysis,[3] reaction (3) is thought to be the main process for formation of *dl*-2-butanol in the present study, since the yields of C_2-hydrocarbons, including ethylene, are very low.

It has been reported by Bach[8] that the processes induced by the discharge reaction are similar to those induced by radiolysis. However, when present study (Exp. No. 6_B; at 15—32°C) is compared with the study of the radiolysis of liquid 2-propanol,*5 it is found that the glycols which were produced in the radiolysis were not formed by the discharge.

Much acetone and acetaldehyde were obtained in this reaction. This is similar to the case in the radiolysis of 2-propanol.[3] The dehydrogenation of 2-propanol to give acetone in radiolysis or photolysis has been postulated to occur through the 1-hydroxyisopropyl radical by Atkinson and Di,[9] or through the transfer of a pair of hydrogen atoms from 2-propanol by Raphael *et al.*[10] or McDonell.*5 In our reaction, the latter seems to be the main process (but not necessarily the only one) for forming acetone, because, were acetone formed by a process such as has been proposed by Atkinson and Di, some pinacols would be produced at the same time by the great quantity of the 1-hydroxyisopropyl radical formed.

Finally, the liquid hydrocarbons seem to be formed

*3 Devins and Burton found, in the decomposition of ammonia under a silent discharge, that the contribution of ionized molecules was very low; J. C. Devins and M. Burton, *J. Am. Chem. Soc.*, **76**, 2618 (1954).

7) E. G. Linder and A. P. Davis, *J. Phys. Chem.*, **35**, 3649 (1931); S. C. Lind and G. R. Schultze, *ibid.*, **42**, 547 (1938); H. Fujimoto, This Bulletin, **13**, 281 (1938); H. Wiener and M. Burton, *J. Am. Chem. Soc.*, **75**, 5815 (1953); E. Inoue, *J. Electrochem. Soc. Japan (Denki Kagaku)*, **23**, 574 (1955); S. Takahashi, *Nippon Kagaku Zasshi (J. Chem. Soc. Japan, Pure Chem. Sect.)*, **79**, 132 (1958).

*4 The data on the yield of methane is not presented because of the inaccurate data on hydrogen.

8) N. Bach, *Chem. Eng. Progress*, **51**, 478 (1955).

*5 McDonell and Newton have been reported that the *G*-values of the products formed in the radiolysis of liquid 2-propanol were as follows: H_2 (2.71), C_1—C_4-hydrocarbons (1.76), total carbonyl (2.96), *vic*-glycols (0.39); W. R. McDonell and A. S. Newton, *J. Am. Chem. Soc.*, **76**, 4651 (1954). Spinks and Woods have discussed how the products of the radiolysis of liquid methanol are very similar to those of the radiolysis of methanol vapor, and so are those of the radiolysis of ethanol. Therefore, the products of the radiolysis of 2-propanol vapor are thought to be similar to those of the radiolysis of the liquid 2-propanol; J. W. T. Spinks and R. J. Woods, "An Introduction to Radiation Chemistry," John Wiley & Sons, New York (1964).

9) B. Atkinson and M. Di, *Trans. Faraday Soc.*, **54**, 1331 (1958).

10) R. A. Raphael, E. C. Taylor and H. Wynberg, "Advances in Organic Chemistry," Vol. II, Interscience Publishers, New York (1960), p. 355.

through the isopropyl radical, which may be derived from the excited 2-propanol.

Whan a Special Tube Filled with Copper or Its Salts Was Used. It has been discussed in detail by Semenov[11] how, in photolysis, the reaction products are greatly affected by the nature of the substances forming the wall, as well as by the size of the vessel. However, Inoue[12] found, in a discharge reaction, that the size of the vessel had no influence on the reaction rate. In order to check the wall effects on the decomposition of 2-propanol, the reaction was carried out in a tube packed with copper or its salts (all runs except Nos. 6_B and 7_A in Tables 1 and 2).

Comparing the Glassy Wall with a Wall of Copper or Its Salts. The product pattern was somewhat simplified by changing the glassy wall to a copper(II) hydroxide wall. For example, the gas chromatogram showed seventeen peaks for the products from the 7_A run, but only ten peaks for the 1_A run (PEG-6000, 100°C, He). Thus, the former contains more kinds of hydrocarbons and unidentified, high-boiling products than 1_A.

A similar product pattern was obtained in the presence of the other packing materials, too, except in the case of metallic copper. When the reaction was carried out in a tube with a metallic copper wall (Exp. No. 5_A), the percentages of all the liquid products except hydrocarbons and acetaldehyde were almost the same as with 7_A (using glass walls).

The reaction rate and the amounts of 2-methyl-2-butanol, *dl*-2-pentanol, and all the carbonyl compounds except methyl vinyl ketone were greatest when the glassy-wall tube was used.

Effects of Packing Substances. When the two reduced coppers, 1 and 2 (Exp. Nos. 2_A and 4_A respectively), were used as packing, as compared with the original copper salts (Exp. Nos. 1_A and 3_A), the following differences were noticed in the liquid products: (1) the acetone yield increased remarkably; (2) the yields of 2-methyl-2-propanol and methyl vinyl ketone decreased; and (3) the relative yields of *dl*-2-butanol, 2-methyl-2-butanol, and *dl*-2-pentanol were almost the same, regardless of the reduction treatment.

The reason why the 2-propanol excited by the discharge changes almost entirely into acetone in the presence of the reduced coppers is considered to be as follows: Metallic copper and reduced copper are effective catalysts for the dehydrogenation of alcohols.[13] Although these coppers behave excellently as catalysts, usually at a high temperature, Taylor[14] showed that the irradiation of radioactive rays makes a solid catalyst active, even at a low temperature, by destroying the catalyst poison, forming a positive hole on the surface, trapping electrons, *etc.* Similar effects might be brought about by the silent discharge.

2-Methyl-2-propanol, hydrocarbons, and methyl vinyl ketone were obtained in the highest yields when copper(II) hydroxide was used as packing (Exp. No. 1_A). This packing material aids in forming hydrocarbons especially. This fact implies that the C–O-bond breaking in 2-propanol occurs rather preferably in the presence of this material.

On the other hand, relatively much methyl vinyl ketone was produced in the presence of copper salts. This product may be formed by the combination of a vinyl radical with an acetyl radical. The acetyl radical can be thought to be formed by a secondary reaction of the acetone or acetaldehyde produced, since the photolysis[15] and the radiolysis[16] of acetone and acetaldehyde have been known to produce the acetyl radicals. The vinyl radical can be formed by the elimination of a hydrogen atom from the ethylene produced under a silent discharge, as has been suggested by Tsutsumi[17] and by Thomas *et al.*[18] The yields of ethylene, acetylene, 1-butene, and 1,3-butadiene in gaseous products were highest in the presence of copper salts. Therefore, the vinyl radical seems to be increased in those cases. For this reason, the methyl vinyl ketone may be obtained in the highest yield in the presence of copper salts.

The main conclusions to be drawn from these results are as follows: (1) Despite the different kinds of discharge tubes, the liquid products consisted of similar components, but the compositions of the products depend on the kind of tube. (2) The 2-hydroxypropyl radical was regarded as an important intermediate in the reaction. (3) The only radical addition product was the one-to-one adduct. (4) On the wall of copper(II) hydroxide, C–O-bond breaking in the 2-propanol occurred rather preferably upon the discharge. (5) Copper(II) hydroxide and hydroxide carbonate might give more of the vinyl radical than other materials. (6) Generally speaking, the selectivity was a little higher in the presence of packing than in its absence.

11) N. N. Semenov, "On Some Problems of Chemical Kinetics and Reactivity," USSR Academy of Sciences Printing House, Moscow (1958).

12) E. Inoue, *J. Electrochem. Soc. Japan (Denki Kagaku)*, **23**, 76 (1955).

13) P. Sabatier and J. B. Senderens, *Compt. Rend.*, **136**, 738, 921, 983 (1903).

14) E. H. Taylor, *Nucleonics*, **20**, (Jan.), 53 (1962).

15) W. A. Noyes, Jr. and L. M. Dorfman, *J. Chem. Phys.*, **16**, 788 (1948).

16) P. Ausloos and J. F. Paulson, *J. Am. Chem. Soc.*, **80**, 5117 (1958).

17) S. Tsutsumi, *Chem. Ind.*, **16**, 623 (1965).

18) C. L. Thomas, G. Egloff and J. C. Morrell, *Chem. Revs.*, **28**, 1 (1941).

BULLETIN OF THE CHEMICAL SOCIETY OF JAPAN VOL. 42 475—478 (1969)

The Configuration of 6,8(9)-*p*-Menthadien-2,4-diols and *p*-Menthane-2,4-diols

Yoshitsugu SAKUDA

Chemistry Laboratory, Kochi Women's University, Kochi

(Received May 6, 1968)

The 6,8(9)-*p*-menthadien-*trans*-2,4-diol (I) and 6,8(9)-*p*-menthadien-*cis*-2,4-diol (II) were obtained by the oxidation of *l-cis*-carvyl acetate with selenium dioxide. The hydrogenation of each 6,8(9)-*p*-menthadien-2,4-diol gave a different pair of *p*-menthane-2,4-diols, one pair being *p*-menthane-2,4-diols (III and IV) from *trans*-2,4-diol (I) and the other pair being *p*-menthane-2,4-diols (V and VI) from *cis*-2,4-diol (II). The absolute configurations of the *p*-menthane-2,4-diols (III, IV, V and VI) were assigned as follows on the basis of the chemical evidence, the IR and NMR data, and the Cotton-effect sign of the oxidation products of these isomers: III, (1S : 2R : 4S); IV, (1R : 2R : 4S); V, (1R : 2R : 4R) and VI, (1S : 2R : 4R)-*p*-menthane-2,4-diol. The identification of these diastereoisomeric diols III–VI made possible the assignment of a configuration to diols I and II.

In previous papers[1,2] some 8(9)-*p*-menthendiols and 8(9)-*p*-menthen-aldols were prepared by the oxidation of 8(9)-*p*-menthen-ols and those acetates with selenium dioxide. The configuration of the reaction product was assigned on the basis of the chemical evidence and the IR spectra. Now new diols, 6,8(9)-*p*-menthadien-*trans*-2,4-diol (I) and 6,8(9)-*p*-menthadien-*cis*-2,4-diol (II), have been obtained from *l-cis*-carvyl acetate by selenium dioxide oxidation, followed by the saponification of the reaction product.

In a study of the mechanism by which olefins are oxidized with selenium dioxide, Schaefer and Horvath[3] and Olson[4] have shown that selenium dioxide or its conjugate acid acts as an electrophile and attacks a double bond, thus forming a carbonium ion. When Schaefer's mechanism is applied in the case of carvyl acetate the reaction process is as is shown in Fig. 1. This view of the mechanism of the oxidation appears to accord well with that by which the two diols, I and II, are produced.

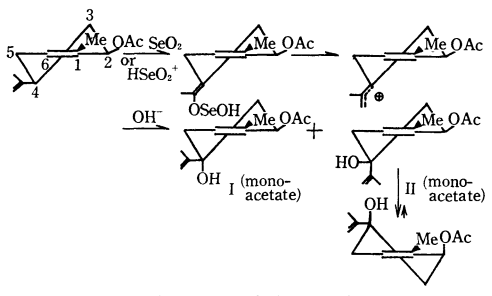

Fig. 1. Oxidation of *l-cis*-carvyl acetate.

The hydrogenation of the unsaturated diols, I and II, yielded four diastereoisomeric *p*-menthane-2,4-diols, III, IV, V, and VI. *p*-Menthane-2,4-diol, mp 93—94°C, was prepared by Wallach[5] by the catalytic hydrogenation of the 6-*p*-menthen-2,4-diol obtained by the hydration of sabinol. However, there has been no experimental evidence with respect to a spatial arrangement of the hydroxyl and methyl groups. This paper will report on the preparation and the configuration of these diols, I—VI.

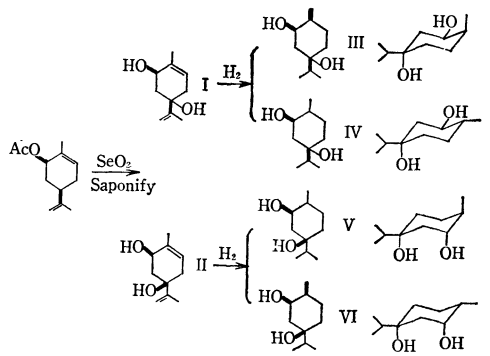

Fig. 2. The configurational assignment of 6,8(9)-*p*-menthadien-2,4-diols (I, II) and *p*-menthane-2,4-diols (III—VI).

1) Y. Sakuda, This Bulletin, **34**, 514 (1961).

2) Y. Sakuda, *J. Sci. Hiroshima Univ.*, **A-II**, **25**, 207 (1961).

3) J. P. Schaefer and B. Horvath, *Tetrahedron Letters*, No. 30, 2023 (1964).

4) D. H. Olson, *ibid.*, No. 19, 2053 (1966).

5) O. Wallach, *Ann.*, **414**, 203 (1917).

6,8(9)-*p*-Menthadien-*trans*-2,4-diol (I) and -*cis*-2,4-diol (II). *l-cis*-Carvyl acetate was oxidized with a solution of selenium dioxide dissolved in *t*-butyl alcohol at room temperature. The diols, I and II, were separated by column chromatography from the saponified product of the less volatile part of the reaction mixture.

6,8(9)-p-Menthadien-trans-3,4-diol (I). The IR spectrum of I showed the bands at 898, 1650, and 3100 cm^{-1} due to the isopropenyl group and that at 3400 cm^{-1} due to the hydroxyl group. The NMR spectrum of I in chloroform-*d*, shown in Fig. 3a, exhibited well-separated signals; this is consistent with that spectrum expected for 6,8(9)-*p*-menthadien-ol.

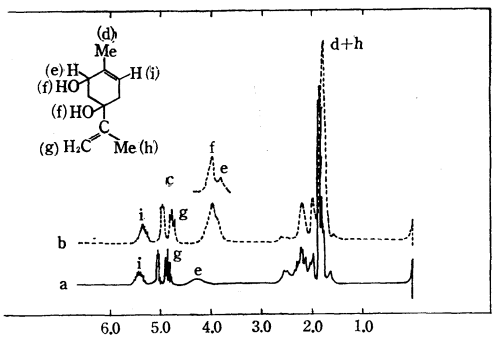

Fig. 3. NMR spectra of (a) I in $CDCl_3$ (——), (b) II in CCl_4 (-----) and (c) fragment of II in CCl_4 + C_6H_6 (-----).

6,8(9)-p-Menthadien-cis-2,4-diol (II). The IR spectrum of II showed the bands at 900, 1647, and 3100 cm^{-1} due to the isopropenyl group and that at 3360 cm^{-1} due to the hydroxyl group. The NMR spectrum of II in carbon tetrachloride shown in Fig. 3b was analogous with that of I except for the signal at δ 3.7—4.1 ppm. The NMR spectrum of II, measured in a mixed solvent of carbon tetrachloride and benzene, showed that the absorption at δ 3.7—4.1 ppm appears as two clear splitting signals, at δ 3.60 ppm due to the carbinol proton at the C-2 position and at δ 3.86 ppm due to two hydroxyl protons (Fig. 3c). It was assumed that a strong intramolecular hydrogen bond exists in II from the fact that the OH proton signal of II appeared at a lower field than that of I. The presence of the intramolecular hydrogen bond in II was further evidenced by the measurement of the IR spectra of I and II.[6] The IR spectrum of I in a dilute solution of carbon tetrachloride showed two bands, at 3635 (ε 49) and 3606 (ε 88) cm^{-1}; the lower-frequency band has a weak shoulder at 3590 cm^{-1}. The band at 3635 cm^{-1} is attributed to the free secondary hydroxyl group, and the band at 3606 cm^{-1}, to the hydroxyl group which interacts with the π-electron of the isopropenyl group.[7,8] The IR spectrum of II showed two bands, at 3612(ε 66) and 3550(ε 69) cm^{-1}; the higher-frequency band has a shoulder at 3595 cm^{-1}. The band at 3612 cm^{-1} is attributed to the free tertiary hydroxyl group, and the band at 3550 cm^{-1}, to the OH–O intramolecularly-hydrogen-bonded hydroxyl group. Considering the value of the difference between free and bonded OH bands, it was assumed that II is a *cis*-cyclohexene-1,3(2,4)-diol.[7a] Thus the NMR and IR data provided adequate evidence for determining the configuration of II to be 6,8(9)-*p*-menthadien-*cis*-2,4-diol. Furthermore, the fact that the configuration of each of the diols, I and II, is 6,8(9)-*p*-menthadien-2,4-diol was confirmed by the hydrogenation of I and II.

***p*-Menthane-2,4-diols III, IV, V and VI.** Upon the hydrogenation of the double bond, each of

TABLE 1. IR AND NMR DATA FOR *p*-MENTHANE-2,4-DIOLS

Diol	Neat	Concn. (mol/*l*)	IR OH, cm^{-1}		NMR, δ ppm		
			CCl_4 soln.		9H	1H	2H
			free(ε)	bonded(ε)	$C\underline{H}_3\times3$	$\underline{H}C$–OH	$O\underline{H}\times2$
III	3280	0.0032	3620(99)		0.88 0.97	4.06[a]	
IV	3280	0.0036	3635(69) 3625(69)		0.88 0.93	3.3[b]	
V	3260	0.0029	3620(69)	3535(90)	0.88 0.97	3.67[a]	3.0[b]
VI	3300	0.0030	3635(48) 3618(48)	3535(100)	0.88 0.97	3.87[a]	3.3[b]

a) Multiplet b) Broad singlet

6) M. Tichy, "Advances in Organic Chemistry," Vol. 5, Interscience Publishers, New York, N. Y. (1965), p. 115.

7) a) L. P. Kuhn, *J. Am. Chem. Soc.*, **74**, 2492 (1952). b) A. R. H. Cole, G. T. A. Müller, D. W. Thornton and R. L. S. Willix, *J. Chem. Soc.*, **1959**, 1218. c) A. R. H. Cole, P. R. Jefferies and G. T. A. Müller, *ibid.*, **1959**, 1222.

8) a) M. Ôki, H. Iwamura, J. Aihara and H. Iida, This Bulletin, **41**, 176 (1968). b) T. Shishibori, *ibid.*, **41**, 1170 (1968).

the diols, I and II, would be expected to give two *p*-menthane-2,4-diols, a pair of diastereoisomers epimeric at the C-1 position. Indeed, the I diol gave two products, III and IV, and the II diol gave V and VI. The IR and NMR data for these four diastereoisomeric *p*-menthane-2,4-diols are shown in Table 1. The IR spectra of V and VI in a dilute solution of carbon tetrachloride showed the band at 3535 cm^{-1} due to the intramolecularly-hydrogen-bonded hydroxyl group. Considering the value of the difference between free and bonded OH bands, it was assumed that V and VI are *cis*-cyclohexane-1,3(2,4)-idol.[7a] The NMR spectra of V and VI, measured after adding one drop of concentrated hydrochloric acid to a chloroform-d solution, showed no broad absorption at δ 3.0 or 3.3 ppm. From this fact, the absorption at δ 3.0 or 3.3 ppm was assigned to the OH proton signal. The fact that the OH proton signals of both the V and VI diols appear at a lower field than those of III and IV can account for the presence of strong intramolecular hydrogen bonds in V and VI.

Then it was confirmed that each of four diols, III, IV, V, and VI was diastereoisomeric *p*-menthane-2,4-diol. The IR spectrum of each of the four compounds obtained by the oxidation of III, IV, V, and VI with Jones' reagent[9] showed the band at 1700 cm^{-1} due to the carbonyl group and that at *ca.* 3400 cm^{-1} due to the hydroxyl group. The IR spectrum of the oxidation product of III coincided with that of the oxidation product of V. Each of the four oxidation products of III, IV, V, and VI gave the same 2,4-dinitrophenylhydrazone (2,4-DNP), which was identified as carvenone 2,4-DNP by a direct comparison with an authentic sample. When a mixture of the oxidation product of IV, ethyl alcohol, and sulfuric acid was left to stand overnight under the same conditions as those under which 2,4-DNP was prepared, dehydration occurred and carvenone produced. This fact confirmed that when a 2,4-DNP was derived from each oxidation product of III, IV, V, and VI, dehydration occurred and that, consequently, only carvenone 2,4-DNP was produced from the four oxidation products. From these facts it was concluded that each original diol, III, IV, V, and VI, is diastereoisomeric *p*-menthane-2,4-diol.

Absolute Configuration of *p*-Menthane-2,4-diols III, IV, V and VI. The optical rotatory dispersion spectra of the three oxidation products of III, V, and VI with Jones' reagent are shown in Fig. 4.

The oxidation product of III exhibits a strong positive Cotton effect, the oxidation product of V exhibits a strong negative Cotton effect, and the oxidation product of VI exhibits a weak negative Cotton effect. Considering the Cotton-effect signs of these oxidation products, it was concluded that the oxidation products of III and V are enantiomer, and that the oxidation product of V possesses an axial methyl group at the C-1 position and that the oxidation product of VI possesses an equatorial methyl group at the C-1 position. Assuming that the conformations of these original diols are maintained throughout the oxidation procedure with Jones' reagent, the absolute configuration of each diol, III, IV, V, and VI, was assigned as is shown in Fig. 1; that is to say, III, IV, V and VI are (1S : 2R : 4S), (1R : 2R : 4S), (1R : 2R : 4R), and (1S : 2R : 4R)-*p*-menthane-2,4-diol respectively.

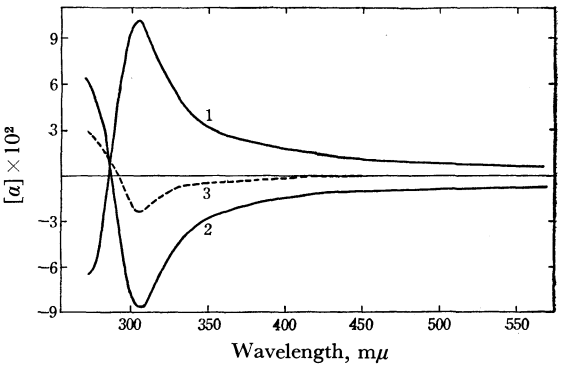

Fig. 4. Cotton effect of the oxidation products of III (curve 1), V (curve 2) and VI (curve 3).

Experimental

The NMR spectra were recorded with a Varian A-60 NMR spectrometer using TMS as the internal standard. The IR spectra in the 2500—4000 cm^{-1} region were determined with a Perkin-Elmer Model 621 grating spectrophotometer using a stoppered sodium chloride cell with a path length of 2.00 cm. The ORD spectra were determined in methanol with a Nippon Bunko ORD/UV-5 spectropolarimeter. The reaction products were analyzed by gas chromatography using a diethylene glycol succinate column at 150 and 190°C.

Samples. *l-cis-Carvyl Acetate.* *l-cis*-Carveol was prepared from *l*-carvone by reduction with lithium aluminium hydride[10] and was purified *via* its 3,5-dinitrobenzoate. Physical constants:[11] mp 23—24°C, bp 81—82°C/2 mmHg, n_D^{25} 1.4955, d_4^{25} 0.9524, $[\alpha]_D$ −24.4. *l-cis*-Carvyl acetate was prepared by refluxing the pure *l-cis*-carveol thus obtained with acetic anhydride and with anhydrous sodium acetate. Bp 90—92°C/2 mmHg, n_D^{25} 1.4731, d_4^{25} 0.9689, $[\alpha]_D$ −42.9.

6,8(9)-*p*-Menthadien-*trans*-2,4-diol(I) and -*cis*-2,4-diol (II). These two diols were prepared from *l-cis*-carvyl acetate by selenium dioxide oxidation as follows.

9) K. Bowden, I. M. Hellbron, E. H. H. Jones and B. C. L. Weedon, *J. Chem. Soc.*, **1946**, 39.

10) R. H. Reitsema, *J. Am. Chem. Soc.*, **75**, 1996 (1953).

11) R. G. Johnston and J. Read, *J. Chem. Soc.*, **1934**, 233.

A solution of *l-cis*-carvyl acetate (97 g, 1/2 mol) in benzene (97 g) was stirred, drop by drop, into a solution of selenium dioxide (28 g, 1/4 mol) dissolved in *t*-butyl alcohol (225 g, 3 mol). The temperature of the reaction mixture rose to 45°C. The mixture was then left to stand at room temperature overnight. After the solvent had been removed, the remaining product was distilled under reduced pressure, giving two fractions: 1 (bp 65—90°C/2 mmHg (28 g)) and 2 (bp 91—110°C/2 mmHg (19.2 g)). Fraction 1 consisted mainly of unchanged carvyl acetate. Fraction 2 was saponified and was then chromatographed on a silica-gel column, giving I and II. The yield of I plus II was 10% based on the sample used. I, mp 107—108°C, $[\alpha]_D$ +20.0 (*c* 3.7, ethanol). Found: C, 71.62; H, 9.87%. Calcd for $C_{10}H_{16}O_2$: C, 71.39; H, 9.58%. II, bp 110—111°C/2 mmHg, n_D^{25} 1.5045, d_4^{25} 1.0508, $[\alpha]_D$ +14.0 (*c* 11.8, ethanol).

(1R : 2R : 4R)-*p*-Menthane-2,4-diol (V) and (1S : 2R : 4R)-*p*-Menthane-2,4-diol (VI). A solution of II (1.6 g) in ethanol (50 cc) containing Raney Ni (*ca.* 2 g) was shaken for 8 hr at 40—60°C under a 100—110 atm. H_2 pressure. The total semisolid hydrogenation product (1.6 g) gave two peaks corresponding in those retention times to V and VI on the gas chromatogram. The area ratio of the peaks of V and VI was 7 : 2. After the filtration of the liquid compound, the remaining crystals were recrystallized from hexane. Three recrystallizations gave needles of V, mp 76.5°C. Found: C, 69.22; H, 11.48%. Calcd for $C_{10}H_{20}O_2$: C, 69.76; H, 11.62%. The liquid filtrate was chromatographed on an alumina column. Elution with a methanol-ether mixture (1 : 30) gave 35 fractions, which were then analyzed by gas chromatography. Fractions 1—16 consisted of the solvent alone. Fractions 17—20 gave the liquid diol, VI. Found: C, 70.30; H, 11.62%. Calcd for $C_{10}H_{20}O_2$: C, 69.76; H, 11.62%. Fractions 21—35 gave mixtures of V and VI.

(1S : 2R : 4S)-*p*-Menthane-2,4-diol (III) and (1R : 2R : 4S)-*p*-Menthane-2,4-diol (IV). *trans*-Diol (I) was hydrogenated in the same way as was *cis*-diol (II) described above. The total crystalline hydrogenation product gave two peaks, corresponding in retention time to the two *p*-menthane-2,4-diols, III and IV, on the gas chromatogram. The area ratio of the peaks of III and IV was 1 : 4. The product was recrystallized from hexane, hexane - ethyl acetate (4 : 1), ether, benzene, and hexane - ethyl acetate (9 : 1) successively. Twenty-three recrystallizations gave white flakes of III, mp 153°C. Found: C, 70.00; H, 11.72%. Calcd for $C_{10}H_{20}O_2$: C, 69.76; H, 11.62%. After the solvent had been removed from the combined mother liquors, the remaining product was chromatographed on an alumina column. Elution with a methanol-ether mixture (1 : 30) gave 55 fractions, which then were analysed by gas chromatography. Fractions 1—16 consisted of the solvent alone. Fractions 17—26 gave white needles of IV, mp 115—116°C. Found: C, 69.84; H, 11.72%. Calcd for $C_{10}H_{20}O_2$: C, 69.76; H, 11.62%. Fractions 27—55 gave mixtures of III and IV.

Oxidation of Four *p*-Menthane-2,4-diols, III, IV, V, and VI, with Chromic Acid. A solution of chromic trioxide (46 mg, 0.46 mmol), concentrated sulfuric acid (0.1 cc), and water (0.5 cc) was added, over a ten minutes period, to a solution of V (38 mg, 0.22 mmol) dissolved in acetone (1 cc), and then cooled to 0°C, while the mixture, cooled in an ice-water bath, was being stirred vigorously. The mixture was then poured into ice water and extracted with ether. The evaporation of the ether gave a viscous oil (35 mg) which showed characteristic absorptions at 1700 cm^{-1} due to the carbonyl group and at 3400 cm^{-1} due to the hydroxyl group. The 2,4-DNP of this carbonyl compound was prepared in the usual way; mp 165—166°C, UV λ_{max}^{alc} 387 mμ. Found: N, 16.69%. Calcd for $C_{16}H_{23}O_5N_4$: N, 16.80%. This 2,4-DNP was identified as carvenone 2,4-DNP by a mixed-melting-point determination and by a direct comparison of the IR spectra. The III, IV, and VI diols were oxidized in the same way as in the case of V. The 2,4-DNP of each of these three oxidation products was prepared and melted at the same mp, 165—166°C; all were identified as carvenone 2,4-DNP.

Dehydration of Oxidation Product of the IV Diol. From the fact that each of the four oxidation products of III, IV, V, and VI gave the same 2,4-DNP, it was assumed that dehydration occurred when the 2,4-DNP was derived. To confirm this, the following experiment was carried out. A solution of the oxidation product (50 mg) of IV with chromic trioxide, ethanol (3 cc), concentrated sulfuric acid (0.2 cc), and water (0.3 cc) was left to stand at room temperature overnight. This conditions were the same as in the case of the derived 2,4-DNP. After water had been added, the reaction mixture was extracted with ether. The extract was chromatographed on a silica-gel column. Elution with petroleum ether - ethyl acetate (9 : 1) gave carvenone as an initial elute; it was identified by its UV spectrum, λ_{max}^{alc} 234 mμ, and 2,4-DNP; mp 165—166°C.

The author wishes to express his deep thanks to Professor Robert D. Stolow of Tufts University for his kind advice and to Professor Shô Ito of Tohoku University and Mr. Tsuyoshi Shishibori of Hiroshima University for their measurement of the NMR, IR, and ORD spectra.

BULLETIN OF THE CHEMICAL SOCIETY OF JAPAN VOL. 42 479—482 (1969)

The Synthesis of Poly-L-arginine Hydrobromide and Copolymers of L-Arginine and Other Amino Acids*1

Tadao HAYAKAWA, Yoshiyuki KONDO, Hiroyuki YAMAMOTO and Yukiko MURAKAMI

Institute of High Polymer Research, Faculty of Textile Science and Technology, Shinshu University, Ueda

(Received May 13, 1968)

Pure crystalline $N^{\omega,\omega'}$-dicarbobenzyloxy-L-arginine N-carboxyanhydride hydrochloride was obtained from $N^{\alpha,\omega,\omega'}$-tricarbobenzyloxy-L-arginine and thionyl chloride. It was polymerized to poly-$N^{\omega,\omega'}$-dicarbobenzyloxy-L-arginine. This polymer was converted to poly-N^{ω}-carbobenzyloxy-L-arginine by treating it with alcoholic potassium hydroxide; also, both carbobenzyloxy groups of the protected polymer were completely removed into poly-L-arginine by treating them with hydrogen bromide in glacial acetic acid. Several copolymers containing L-arginine residue were also prepared by the copolymerization of the above NCA and the NCAs of other amino acids, such as γ-benzyl-L-glutamate, L-alanine, and N^{ε}-carbobenzyloxy-L-lysine.

The natural α-amino acids found in protein give polyamino acids upon the polymerization of all the corresponding α-amino acid N-carboxyanhydride (α-amino acid.NCA) except arginine. Because of the high basicity of the guanido group, the preparation of the pure NCA of L-arginine derivative is difficult and has not been reported in detail.[1,2]

These synthetic methods of producing poly-L-arginine have been reported: (a) poly-L-ornithine prepared by the NCA method was guanidized into poly-L-arginine with 1-guanyl-3,5-dimethylpyrazole or isomethylthiourea,[3,4] and (b) poly-L-nitroarginine prepared by the N-carbothiophenyl method was reduced to poly-L-arginine hydrochloride with stannous chloride in formic acid.[5] In the former case, however, it is very difficult to guanidize quantitatively the ornithyl residues of poly-L-ornithine into poly-L-arginine, and in the latter case, no polymer with a high molecular weight has been prepared. In addition, it is difficult to synthesize copolymers with other amino acids by the use of the above methods.

In this report, the synthesis of poly-L-arginine hydrobromide and copolymers of L-arginine and other amino acids, such as L-glutamic acid, L-alanine, and L-lysine, will be described. The synthetic route of poly-L-arginine (V) is summarized in Eq. (1).

Dicarbobenzyloxy-L-arginine NCA hydrochloride (II) was obtained from tricarbobenzyloxy-L-arginine (I)[6] by the use of thionyl chloride in dioxane. The infrared absorption spectrum of Compound II showed absorptions at 1850 cm^{-1} and 1785 cm^{-1}. These might correspond to the C=O groups in the five-membered ring of NCA. Poly-$N^{\omega,\omega'}$-dicarbobenzyloxy-L-arginine was prepared as follows: NCA hydrochloride (II) was treated with silver oxide in dry acetone to remove any hydrogen chloride and was then polymerized in dioxane by adding triethylamine as an initiator. Polymerization was allowed to proceed at room temperature, the solution became a clear gel after several days. The molecular weight was found to be about 30000 by titration with N/50 CH_3ONa in methanol. Poly-$N^{\omega,\omega'}$-dicarbobenzyloxy-L-arginine (III) was treated with alcoholic potassium hydroxide to convert it into poly-N^{ω}-carbobenzyloxy-L-arginine (IV) by the elimination of one carbobenzyloxy group of the protected guanido group of III. Poly-L-arginine hydrobromide was obtained by treating III or IV with HBr in glacial acetic acid at 50°C. The acid hydrolyzate of poly-L-arginine hydrobromide gave only one spot of arginine upon paper chromatography and showed no racemization of arginine. The copolymerization of $N^{\omega,\omega'}$-dicarbobenzyloxy-L-arginine NCA and other amino acid NCAs (γ-benzyl-L-glutamate, L-alanine and N^{ε}-carbobenzyloxy-L-lysine) was performed. The yield, molecular weight, and amino acid composition of each copolymer were determined. The molar ratio was determined quantitatively by paper chromatography

*1 Presented at the 21th Annual Meeting of the Chemical Society of Japan, Osaka, April, 1968.

1) L. Zervas, M. Winitz and J. Greenstein, *J. Org. Chem.*, **22**, 1515 (1957).

2) T. Hayakawa, C. R. Windsor and S. W. Fox, *Arch. Biochem. Biophys.*, **118**, 265 (1967).

3) S. Ariely, M. Wilchek and A. Patchornik, *Biopolymers*, **4**, 91 (1966).

4) E. Katchalski and P. Spitnik, *J. Am. Chem. Soc.*, **73**, 3992 (1951).

5) T. Hayakawa, Y. Fujiwara and J. Noguchi, This Bulletin, **40**, 1205 (1967).

6) L. Zervas, T. Otani, M. Winitz and J. Greenstein, *J. Am. Chem. Soc.*, **81**, 2878 (1959).

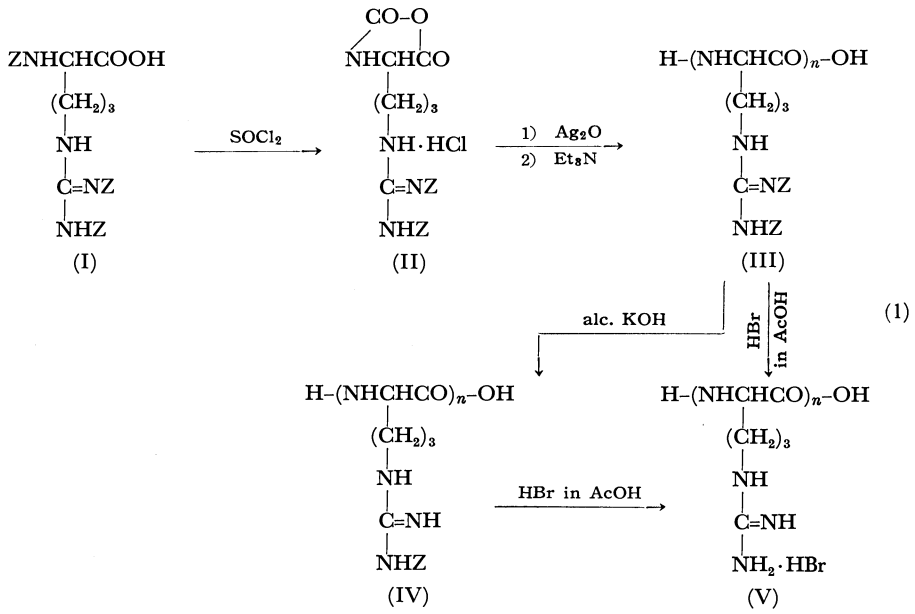

Z: $C_6H_5CH_2OCO-$

after acid hydrolysis. The results of the elemental analyses of these copolymers are shown in Table 1. In a way similar to that of poly-L-arginine synthesis, one carbobenzyloxy group of the arginine residue and the benzyl group of glutamate in these copolymers were removed (see Table 2) by treating them with alcoholic potassium hydroxide. Also, all the protecting groups of the copolymers were removed by treating them with hydrogen bromide in glacial acetic acid. The liberated homopolymer and copolymers were soluble in water and showed positive Biuret and Sakaguchi reactions.

Poly-L-arginine and the copolymers containing a L-arginyl residue provide a valuable model of natural basic proteins, such as salmine and clupeine, which have a high arginine content. The physicochemical properties of these polymers, such as the infrared spectra, X-ray analyses, and optical rotatory dispersion, will be reported in the near future.

Experimental

$N^{\alpha,\omega,\omega'}$-Tricarbobenzyloxy-L-arginine(I). $N^{\alpha,\omega,\omega'}$-Tricarbobenzyloxy-L-arginine (I) was prepared from L-arginine hydrochloride and carbobenzyloxy chloride as has been described by Zervas *et al.*[6]

$N^{\omega,\omega'}$-Dicarbobenzyloxy-L-arginine NCA Hydrochloride (II). To a solution of tricarbobenzyloxy-L-arginine (I) (2.0 g) in 5 m*l* of dioxane, thionyl chloride (1.0 m*l*) was added; the mixture was then allowed to stand for 5 hr at room temperature. When to this mixture dry ether was added, a white precipitate was obtained. This precipitate was filtered, washed with dry ether, and recrystallized from dry acetone and ether. Yield, 1.45 g (83.1%); mp 62°C (decomp.).

Found: C, 54.71; H, 5.37; N, 11.04; Cl, 6.94%. Calcd for $C_{23}H_{25}O_7N_4Cl$: C, 54.71; H, 4.99; N, 11.10; Cl, 7.02%.

$N^{\omega,\omega'}$-Dicarbobenzyloxy-L-arginine NCA. To a solution of $N^{\omega,\omega'}$-dicarbobenzyloxy-L-arginine NCA hydrochloride (II) (1.45 g) in 20 m*l* of dry acetone, dry silver oxide (1.5 g) was added. The mixture was stirred until it showed negative in a chloride test and was then passed through a dry charcoal column to purify it.[7] The acetone in the clear filtrate was removed to dryness *in vacuo*; an oily residue was thus obtained. Yield 1.0 g (83.3 %). The residue was used for immediate polymerization.

Poly-$N^{\omega,\omega'}$-dicarbobenzyloxy-L-arginine (III). To a solution of $N^{\omega,\omega'}$-dicarbobenzyloxy-L-arginine NCA (1.0 g) in 5 m*l* of dioxane, 0.0028 m*l* of triethylamine was added as an initiator; the mixture was polymerized in a sealed tube at room temperature. The polymerization proceeded until a clear gel was obtained. After one week, the reaction mixture was heated in a boiling water bath for 5 hr. After it had been cooled, the mixture was stirred into 100 m*l* of water. The polymer was collected by centrifugation, washed with water, and dried. Yield, 0.8 g (88.0%); $[\alpha]_D^{20}$ +13.1° (*c* 0.6, dioxane) and $[\alpha]_D^{20}$ −20.3° (*c* 0.5, trifluoroacetic acid). Equiv. mol wt≒30000 (by titration of the carboxyl end group with N/50 CH_3ONa in methanol).

Found: C, 62.25; H, 5.79; N, 13.11%. Calcd for $(C_{22}H_{24}O_5N_4)_n$: C, 62.25; H, 5.70; N, 13.20%.

Poly-$N^{\omega,\omega'}$-carbobenzyloxy-L-arginine (IV). To a solution of poly-$N^{\omega,\omega'}$-dicarbobenzyloxy-L-arginine (III) (200 mg) in 1.2 m*l* of dioxane, 1.2 m*l* of 0.6 N potassium hydroxide in 95% ethanol was added and shaken for 2 hr at room temperature. The solution was acidified with acetic acid. After the removal of the organic solvent, the polymer was precipitated by the addition of water. The polymer was collected by centrifugation

7) J. Noguchi, N. Nishi, M. Itaya and S. Tokura, *Kogyo Kagaku Zasshi* (*J. Chem. Soc. Japan, Ind. Chem. Sect.*), **69**, 745 (1966).

and dried. Yield, 102 mg (74.4%); $[\alpha]_D^{20}$ +20.4° (*c* 0.2, 2-chloroethanol) and $[\alpha]_D^{20}$ −28.6° (*c* 0.3. trifluoroacetic acid).

Found: C, 57.89; H, 6.16; N, 19.02%. Calcd for $(C_{14}H_{18}O_3N_4)_n$: C, 57.92; H, 6.25; N, 19.30%.

Poly-L-arginine Hydrobromide (V). (a) Poly-$N^{\omega,\omega'}$-dicarbobenzyloxy-L-arginine (100 mg) was dissolved in 10 m*l* of 6 N hydrogen bromide in glacial acetic acid and stirred for 90 min at 50°C. The reaction mixture was then evaporated to dryness *in vacuo*, and the residue was treated with dry ether. The polymer was collected by centrifugation and washed with ether. This polymer was dissolved in a minimum amount of water and reprecipitated with ethanol. It was then collected by centrifugation, washed with ether, and dried. Yield, 32 mg (57.1%) (b) Poly-N^{ω}-carbobenzyloxy-L-arginine (115 mg) was treated in the way described above. Yield, 57.5 mg (61.2%); $[\alpha]_D^{20}$ −49.2° (*c* 1.0, water).

Found: C, 28.64; H, 5.60; N, 21.56%. Calcd for $(C_6H_{13}ON_4Br\cdot H_2O)_n$: C, 28.25; H, 5.93; N, 21.96%.

Hydrolysis of Poly-L-arginine Hydrobromide. A solution of poly-L-arginine hydrobromide (62.5 mg) in 10 m*l* of 6 N hydrochloric acid was hydrolyzed at 105°C for 24 hr. The hydrolyzate gave only arginine upon paper chromatography. The hydrolyzate was $[\alpha]_D^{20}$ +26.3°, which agrees with the value of authentic L-arginine.

Copoly(γ-benzyl-L-glutamate, $N^{\omega,\omega'}$-dicarbobenzyloxy-L-arginine)(2 : 1). To a solution of γ-benzyl-L-glutamate NCA (0.7 g) and $N^{\omega,\omega'}$-dicarbobenzyloxy-L-arginine NCA (0.62 g) in 13 m*l* of dioxane, 0.0055 m*l* of triethylamine was added as an initiator, and the mixture was polymerized in a sealed tube at room temperature for 5 days. The reaction mixture was heated for 2 hr in a boiling water bath, and then poured into water. The polymer precipitated was collected by centrifugation and dried. Yield, 1.0 g (87.2%). The analytical data and the molecular weight are shown in Table 1.

Other Copolymers. Copoly(γ-methyl-L-glutamate, $N^{\omega,\omega'}$-dicarbobenzyloxy-L-arginine) (2 : 1); copoly(L-alanine, $N^{\omega,\omega'}$-dicarbobenzyloxy-L-arginine) (1 : 1) and (2 : 1); copoly(N^{ε}-carbobenzyloxy-L-lysine, $N^{\omega,\omega'}$-dicarbobenzyloxy-L-arginine) (3 : 2) and (2 : 1) were prepared by the copolymerization of $N^{\omega,\omega'}$-dicarbobenzyloxy-L-arginine NCA and the corresponding amino acid NCAs in the molar ratios presented above. The yields, the molecular weights, and the analytical data are shown in Table 1.

Hydrolysis of Copolymers. A portion of these polymers were hydrolyzed with 6 N hydrochloric acid

Table 1. Copolymers of $N^{\omega,\omega'}$-dicarbobenzyloxy-L-arginine and other amino acids

Copolymer	Amino acid Mole ratio	Yield %	Amino acid composition Mole ratio	Molecular weight	Molecular formula	Found % C	Found % H	Found % N	Calcd % C	Calcd % H	Calcd % N
$N^{\omega,\omega'}$-Di-Z-L-Arg / N^{ε}-Z-L-Lys	2 / 3	84.4	2 / 3.2 [a]	12000	$(2C_{22}H_{24}O_5N_4\cdot 3C_{14}H_{18}O_3N_2)_n$	62.85	6.24	11.92	63.14	6.29	11.99
$N^{\omega,\omega'}$-Di-Z-L-Arg / N^{ε}-Z-L-Lys	1 / 2	96.8	1 / 2.1 [a]	12000	$(C_{22}H_{24}O_5N_4\cdot 2C_{14}H_{18}O_3N_2)_n$	63.18	6.40	11.63	63.28	6.37	11.81
$N^{\omega,\omega'}$-Di-Z-L-Arg / L-Ala	1 / 1	69.7	1 / 1.2	6100	$(C_{22}H_{24}O_5N_4\cdot C_3H_5ON)_n$	60.21	6.03	14.27	60.60	5.90	14.13
$N^{\omega,\omega'}$-Di-Z-L-Arg / L-Ala	2 / 1	70.5	1.8 / 1	17000	$(2C_{22}H_{24}O_5N_4\cdot C_3H_5ON)_n$	61.40	5.89	13.92	61.36	5.81	13.70
$N^{\omega,\omega'}$-Di-Z-L-Arg / γ-Benzyl-L-Glu	1 / 2	68.2	1 / 1.9	6400	$(C_{22}H_{24}O_5N_4\cdot 2C_{14}H_{13}O_3N)_n$	64.69	6.07	9.64	64.02	5.84	9.74
$N^{\omega,\omega'}$-Di-Z-L-Arg / γ-Methyl-L-Glu	1 / 2	75.3	1 / 2.0	5000	$(C_{22}H_{24}O_5N_4\cdot 2C_6H_9O_3N)_n$	57.82	6.05	11.58	57.46	5.96	11.83

a) Determined after dinitrophenylation.

Table 2. Copolymers of N^{ω}-carbobenzyloxy-L-arginine and other amino acids

Copolymer	Amino acid Mole ratio	Yield %	Molecular formula	Found % C	Found % H	Found % N	Calcd % C	Calcd % H	Calcd % N
N^{ω}-Z-L-Arg / N^{ε}-Z-L-Lys	2 / 3	86.4	$(2C_{14}H_{18}O_3N_4\cdot 3C_{14}H_{13}O_3N_2)_n$	61.90	6.84	14.24	61.48	6.63	14.34
N^{ω}-Z-L-Arg / L-Ala	1 / 1	77.2	$(C_{14}H_{18}O_3N_4\cdot C_3H_5ON)_n$	54.07	6.70	18.67	53.82	6.64	18.46
N^{ω}-Z-L-Arg / L-Glu	1 / 2	73.8	$(C_{14}H_{18}O_3N_4\cdot 2C_5H_7O_2N\ H_2O)_n$	53.29	6.28	15.83	53.92	6.41	15.72

Table 3. Copolymers of L-arginine hydrobromide and other amino acids

Copolymer	Amino acid Mole ratio	Yield %	Molecular formula	Found % C	Found % H	Found % N	Calcd % C	Calcd % H	Calcd % N
L-Arg·HBr / L-Lys·HBr	2 / 3	73.0	$(2C_6H_{12}ON_4 \cdot 3C_6H_{12}ON_2 \cdot 5HBr \cdot 2H_2O)_n$	32.24	6.14	16.35	32.07	6.19	16.21
L-Arg·HBr / L-Ala	1 / 1	78.6	$(C_6H_{12}ON_4 \cdot C_3H_5ON \cdot HBr \cdot H_2O)_n$	33.52	5.87	21.63	33.32	6.16	21.41
L-Arg·HBr / L-Glu	1 / 2	83.3	$(C_6H_{12}ON_4 \cdot 2C_5H_7O_2N \cdot HBr \cdot 2H_2O)_n$	38.66	6.04	16.65	38.48	6.26	16.83

at 105°C for 24 hr. The amino acid compositions were determined quantitatively by paper chromatography. The data are shown in Table 1.

Copoly(L-alanine, N^{ω}-carbobenzyloxy-L-arginine) (1 : 1). To a solution of copoly(L-alanine, $N^{\omega,\omega'}$-dicarbobenzyloxy-L-arginine) (1 : 1) (200 mg) in 0.9 m*l* of dioxane, 0.9 m*l* of 0.6 N potassium hydroxide in 95% ethanol was added. The mixture was shaken at room temperature for 2 hr. The mixture was then acidified with acetic acid, and the polymer precipitated by the addition of water. The polymer was collected by centrifugation, washed with water, ethanol, and ether, and dried. The yield and the analytical data are shown in Table 2. Copoly(L-glutamic acid, N^{ω}-carbobenzyloxy-L-arginine) (2 : 1) and copoly(N^{ε}-carbobenzyloxy-L-lysine N^{ω}-carbobenzyloxy-L-arginine) (3 : 2) were prepared in a similar way by treatment with alcoholic potassium hydroxide. The yield and the analytical data are shown in Table 2.

Copoly(L-lysine hydrobromide, L-arginine hydrobromide) (3 : 2). Copoly(N^{ε}-carbobenzyloxy-L-lysine, $N^{\omega,\omega'}$-dicarbobenzyloxy-L-arginine) (3 : 2) (200 mg) was dissolved in 10 m*l* of 6 N hydrogen bromide in glacial acetic acid, stirred for 90 min at 50°C, and evaporated to dryness *in vacuo*. The residue was treated with dry ether. The polymer was collected by centrifugation, washed with ether, and dried. This polymer was redissolved in a minimum amount of water and reprecipitated with ethanol and ether. The yield and the analytical data are shown in Table 3. From the corresponding protected copolymers, copoly(L-glutamic acid, L-arginine hydrobromide) (2 : 1) and copoly(L-alanine, L-arginine hydrobromide) (1 : 1) were prepared in the same way. The yield and the analytical data are shown in Table 3.

The authors wish to express their thanks to Professor Junzo Noguchi of Hokkaido University for his encouragement and valuable disccusions, and are also indebted to the Kaishin Kisei Domei of this Faculty for its financial support.

BULLETIN OF THE CHEMICAL SOCIETY OF JAPAN VOL. 42 482—487 (1969)

Intramolecular Hydrogen Bonds. XIII.[1] The Preferable Conformation of α-Hydroxy-carboxylic and *o*-Hydroxybenzoic Acids

Nobuo Mori, Yuzuru Asano, Toshiko Irie and Yojiro Tsuzuki

Science University of Tokyo, Kagurazaka, Shinjuku-ku, Tokyo

(Received May 21, 1968)

The infrared hydroxyl and carbonyl stretching absorption spectra of salicylic, mandelic, and α-hydroxyisobutyric acids have been measured in dilute carbon tetrachloride solutions. The spectral data indicate that the first two acids exist exclusively in an internally-bonded conformation, one where the phenolic and the alcoholic hydroxyl groups form a hydrogen bond with the carbonyl oxygen atom of the *cis*-carboxyl structure, while the last acid takes, apart from such a conformation, another internally-bonded conformation, one where the hydroxyl group of the *trans*-carboxyl structure interacts with the alcoholic oxygen atom.

It is well known that the carboxyl group in a carboxylic acid takes the *cis*-structure exclusively, a structure in which the carbonyl and the hydroxyl group are *cis* in respect of the C–O bond, but not the *trans*-structure where both groups are *trans*.

1) Part XII: N. Mori, Y. Asano and Y. Tsuzuki, This Bulletin, **41**, 1871 (1968).

An indirect estimation of the stabilization energy indicates the former to be more stable by *ca.* 3 kcal/mol than the latter.[2] When a strong proton-acceptor atom, such as an oxygen or a nitrogen atom, is present close to the carboxyl group, the *trans*-structure can exist to a considerable extent as a result of the hydrogen bond formation between that atom and the carboxyl-OH group; the enthalpy of this hydrogen bond formation is, in general, at most 1.5 kcal/mol with *α*-alkoxyalkanoic acids[3] and at most 3.3 kcal/mol with *o*-alkoxybenzoic acids.[4] These values are comparable to those of ordinary intramolecular OH-to-O hydrogen bonds forming similar 5- or 6-membered rings (*e. g.*, 2.2 and 2.1 kcal/mol with *β*-methoxyethanol and *γ*-methoxypropanol respectively[5]). A simple comparison of these energies seems to suggest that, in *α*-hydroxy-carboxylic and *o*-hydroxybenzoic acids, the carboxyl group may take the *trans*-structure to a significant extent, working through hydrogen bonding with the *α*- or *o*-hydroxyl-oxygen atom. In order to verify this suggestion,we have attempted the infrared investigation of the intramolecular hydrogen bonding in salicylic, mandelic, and *α*-hydroxyisobutyric acids in dilute carbon tetrachloride solutions. The last two acids examined as *α*-hydroxy acids are not indispensable, but they are accessible in the pure, crystalline form.

Experimental

Samples. All the acids were known crystalline compounds; they were prepared and purified by the methods described in the literature, and some known derivatives of them were prepared. Their melting and boiling points were equal to, or very close to, the reported values. The carbon tetrachloride was fractionated over phosphorus pentoxide.

Infrared Measurements. The hydroxyl- and the carbonyl-stretching region were measured at 25°C using a grating, double-beam spectrophotometer, Model DS-403G, of the Japan Spectroscopic Co., Ltd. Since the solubility of each acid in the solvent is very low, in most cases saturated solutions were employed. The concentrations of the derivatived used were 0.002 and 0.001 mol/*l* for the OH and the CO measurements respectively. The cells used were 5.0 and 1.0 cm in optical path length for the OH and the CO measurements respectively. The observed frequencies were calibrated against those of a standard polystyrene film.

Results and Discussion

The OH and the CO spectra of representative acids are shown in Figs. 1—3, while the spectral data of all the compounds are summarized in Tables 1 and 2.

Salicylic Acids (1—6).*1 In the monomeric OH region, each of the acids shows only two bonded OH bands, with maxima around 3530 and 3200 cm^{-1}; the higher frequency band is sharp and almost symmetric, while the lower frequency band is broad and is obscured by the C–H and the dimeric carboxyl-OH bands.

These acids can take the three internally-bonded forms, I, II, and III, shown in Fig. 4. In this figure, the numerical values added to Form I are the observed frequencies of the respective groups, while those in parentheses added to the other

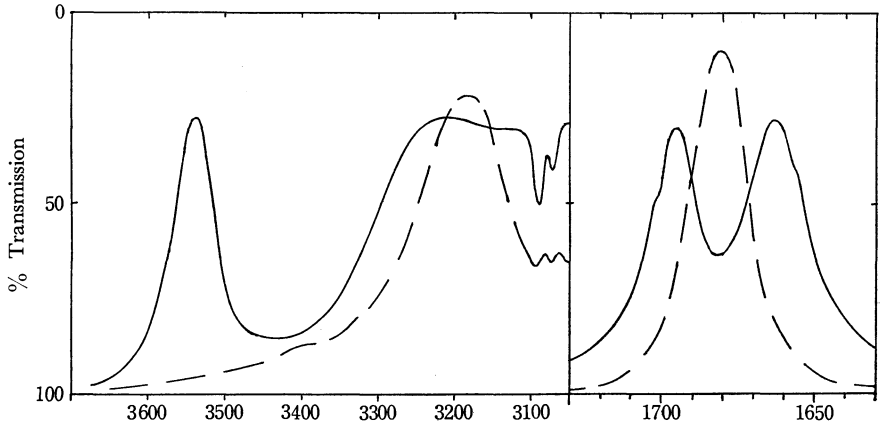

Fig. 1. The IR OH and C=O spectra: salicylic acid (1) ——, methyl salicylate (9) — —.

2) M. Ōki and M. Hirota, *Nippon Kagaku Zasshi* (*J. Chem. Soc. Japan, Pure Chem. Sect.*), **86**, 115 (1965).

3) M. Ōki and M. Hirota, This Bulletin, **36**, 290 (1963).

4) M. Davies, "Hydrogen Bonding," ed. by D. Hadzi, Pergamon Press, London (1959), p. 393; M. Ōki and M. Hirota, This Bulletin, **37**, 209 (1964); M. Ōki, M. Hirota and S. Hirofuji, *Spectrochim. Acta*, **22**, 1537 (1966).

5) L. P. Kuhn and R. A. Wires, *J. Am. Chem. Soc.*, **86**, 2161 (1964).

*1 Brooks and his co-workers[6] have previously reported and discussed the spectral data of some salicylic acids in dilute carbon tetrachloride solutions. However, there have been no discussions of the possibility of the presence of the *trans*-carboxyl structure.

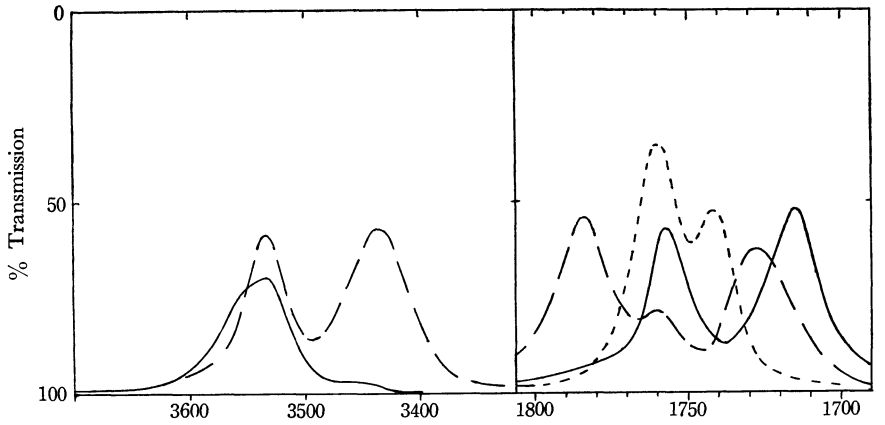

Fig. 2. The IR OH and C=O spectra: mandelic acid (13) ——, α-methoxyphenyl acetic acid (20) — —, methyl α-methoxyphenylacetate (22) – – – – –.

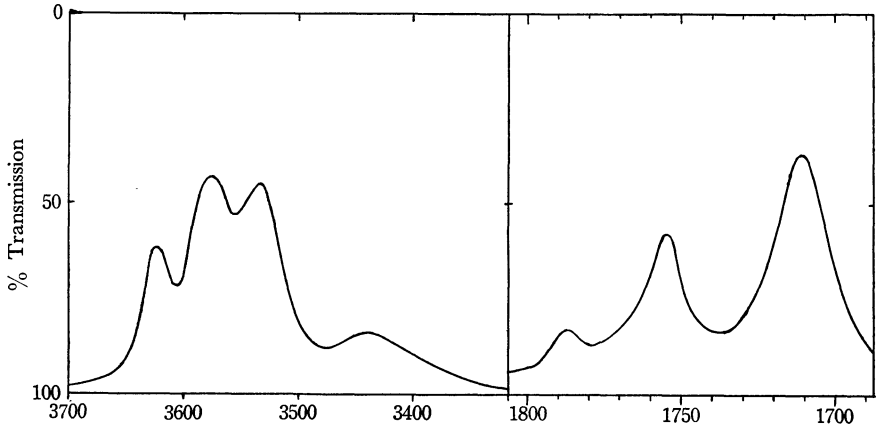

Fig. 3. The IR OH and C=O spectra of α-hydroxyisobutyric acid (23).

Table 1. Spectral data of salicylic acids and some derivatives thereof

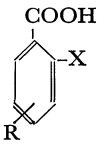

No.	X	R	Monomeric ν_{OH}			Monomeric $\nu_{C=O}$		Dimeric $\nu_{C=O}$
			Free *cis*-COOH	Bonded *trans*-COOH	Bonded phenolic OH*1	Bonded *cis*-COOH	*trans*-COOH	
1	OH	H	3538	—	3205	1695	—	1662
2	OH	4-Me	3540	—	3205	1695	—	1660
3	OH	4-Cl	3531	—	3175	1698	—	1664
4	OH	4-Br	3532	—	3170	1698	—	1665
5	OH	5-Me	3538	—	3215	1696	—	1662
6	OH	5-MeO	3536	—	3227	1698	—	1667
7[7]	H	H	3540	—		1744*2	—	1697
8[7]	MeO	H	3530	3365		1751*2	1760	1702

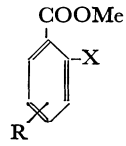

No.	X	R	Bonded phenolic OH	Bonded *cis*-COOMe
9	OH	H	3185	1680
10	OH	4-Cl	3160	1681
11	OH	5-MeO	3222	1684
12[6]	OH	6-OH	3205 3470	1686

*1 Inexact because of overlapping with the C—H and the dimeric COOH absorption band.
*2 Free carbonyl.

TABLE 2. SPECTRAL DATA OF MANDELIC AND α-HYDROXYISOBUTYRIC ACIDS AND OF SOME DERIVATIVES THEREOF

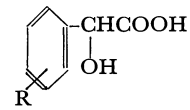

No.	R	Monomeric ν_{OH}					Monomeric $\nu_{C=O}$		Dimeric $\nu_{C=O}$
		Free alcoholic OH	Bonded alcoholic OH	Bonded *cis*-COOH	*trans*-COOH	C=O overtone*1	Bonded *cis*-COOH	*trans*-COOH	
13	H	—	3564*2	3534	—	3445	1756	—	1714
14*4	*p*-NO_2	—		3534					
15	*p*-Br	—	3565*2	3532	—	3445	1758	—	1713
16	*p*-Cl	—	3570*2	3536	—	3445	1759	—	1714
17	*p*-CH_3	—	3566*2	3536	—	3440	1755	—	1709
18	*p*-CH_3O	—	3566*2	3536	—	3445	1756	—	1710
19	*m*-Cl	—	3566*2	3533	—	3445	1759	—	1715
20	$C_6H_5CHCOOH$ OCH_3			3533	3435*5		1760	1784	1728
21	$C_6H_5CHCOOCH_3$ OH	—	3613, 3610[9] 3551, 3536[9]			3455	1737		
22	$C_6H_5CHCOOCH_3$ OCH_3					3500	1759*3 1741		
23	$(CH_3)_2CCOOH$ OH	3623	3575	3537	3436*5		1755	1788	1712
24[3]	$(CH_3)_2CCOOH$ OCH_3			3528.1	3408.8		1762.2	1789.0	
25	$(CH_3)_2CCOOC_2H_5$ OH	—	3606[10] 3544			3460	1732		

*1 The relative intensity to the OH band is about 0.015.
*2 The approximate frequency of the center of the broadened part on the higher frequency side of the monomeric *cis*-COOH band.
*3 These two bands are associated with two rotational isomers (*cis* and gauche form) around the C_1–O bond of the COOMe group.[1]
*4 Very slightly soluble.
*5 This band probably contains the C=O overtone band.

forms are the frequencies which would be expected on the basis of the reported spectral data of the reference compounds, including *o*-methoxybenzoic acid (8), methyl salicylates (9—11), and methyl *o,o'*-dihydroxybenzoate (12).

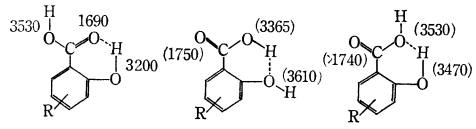

Fig. 4. Internally-bonded forms of salicylic acids.

The appearance of the two OH bands gives evidence of the preferential existence of Form I, since there are no other detectable absorptions corresponding to any of the interacted phenolic and carboxyl OH groups in the other forms. These findings agree completely with those based on the carbonyl data; in the monomeric C=O region these acids show a single absorption due to the internally bonded, *cis*-carboxyl C=O group, but there are no absorptions which correspond to the free carbonyl groups in Forms II and III. The very weak shoulder appearing at 1702 cm^{-1}, which is observed in all the salicylic acids, can not definitely be assigned at the present time.

Mandelic Acids (13—19). In the monomeric OH region, these acids show an intense band at 3535 cm^{-1} and a broadened part centered at *ca.* 3565 cm^{-1}. Apart from these, a very weak absorption band appears near 3445 cm^{-1} with a relative intensity of *ca.* 0.015.

These acids can take the three internally-bonded forms, IV, V, and VI, shown in Fig. 5, where the values in parentheses are the frequencies of the

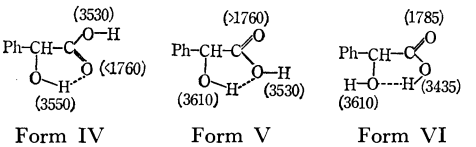

Fig. 5. Internally-bonded forms of mandelic acids.

corresponding groups which would be expected on the basis of the spectral data of the reference compounds, including *α*-methoxyphenylacetic acid (20), methyl mandelate (21), and methyl *α*-methoxyphenylacetate (22). According to these comparisons, only Form IV can reasonably explain the appearance of the two overlapped, strong bands. The very weak band of the lowest frequency can be due either to the carbonyl overtone or to a minor amount of the *trans*-carboxyl group, judging from both the relative intensity and the position at which it appears. However, the carbonyl overtone seems responsible for it, since the observation of carbonyl spectra shows the presence of no *trans*-carboxyl group. The carbonyl spectra each contain only two bands, which correspond to the *cis*-carboxyl and the dimeric carboxyl group; there is no absorption of the *trans*-carboxyl group, which could be expected to appear near 1790 cm^{-1}.

α-Hydroxyisobutyric Acid (23). In the monomeric OH region, this acid shows four bands, at 3623 (weak), 3575 (strong), 3534 (strong), and 3436 cm^{-1} (weak). On the basis of a comparison of these data with those of *α*-methoxyisobutyric acid (24) and ethyl *α*-hydroxyisobutyrate (25), the two strong bands can be assigned to the bonded alcoholic and the *cis*-carboxyl OH group in Form VII (see Fig. 6, in which the frequencies in parentheses are those expected).

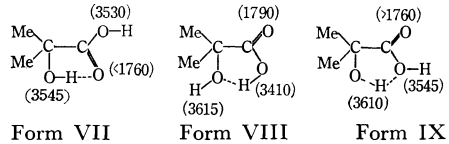

Fig. 6. Internally-bonded form of *α*-hydroxyisobutyric acid.

As for the last band, its intensity is too high for it to be that of a carbonyl overtone; therefore, it may be predominantly due to a *trans*-carboxyl absorption overlapped with the carbonyl overtone. The first weak band may be assigned to either or to both of the two, free and bonded, alcoholic OH species in Forms VIII and IX. In view of the appearance of the weak, *trans*-carboxyl OH and CO band, however, the assignment to the free OH species in Form VIII is rather more reasonable.

In the monomeric C=O region, the acid shows a weak and a strong band at 1788 and 1755 cm^{-1}; these bands can be assigned to the *trans*-carboxyl group in Form VIII and to the *cis*-carboxyl group in Form VII respectively. The precise proportion of the *trans*-carboxyl group to the whole can not be calculated because the respective molecular absorption coefficients are unknown. From the intensity ratio of the apparent bonded OH bands, however, it can be calculated to be approximately 0.16.

It is interesting that the acid takes the *trans*-

6) C. J. W. Brooks, G. Eglinton and J. F. Morman, *J. Chem. Soc.*, **1961**, 661.

7) C. J. W. Brooks, G. Eglinton and J. F. Morman, *ibid.*, **1961**, 106.

8) M. Ōki, and M. Hirota, This Bulletin, **37**, 213 (1964).

9) N. Mori, Y. Tanaka and Y. Tsuzuki, *ibid.*, **39**, 1490 (1966).

10) N. Mori, S. Ōmura, N. Kobayashi and Y. Tsuzuki, *ibid.*, **38**, 2149 (1965).

carboxyl structure VIII to a significant extent, while mandelic and salicylic acids take no such structures. The difference can not decisively be explained at the present time, but it seems attributable to some unknown factors other than steric effects, because the latter two acids, rather than the former, would be expected to meet the steric requirements for taking the *trans*-structures for the following reasons: (1) *α*-hydroxyisobutyric acid may involve the steric repulsion between the two *α*-methyl groups and the free alcoholic OH group in the *trans*-structure (such a repulsion has already been proposed in the cases of *α,α*-dialkylethyleneglycols[11]) and, therefore, it may prefer the *cis*-Structure VII, which involves no such repulsion, while (2) mandelic and salicylic acids may not involve steric effects strong enough to make the presence of *trans*-structures II and VI completely impossible, since even *α*-methoxyphenylacetic and *o*-methoxybenzoic acids prefer the *trans*-structures to an appreciable extent.

Substituent Effects on the OH Frequencies. The alcoholic and carboxyl OH frequencies of mandelic acids are almost constant irrespective of the substituent, while those of salicylic acids change depending on the substituent. The correlation with the ordinary Hammett *σ*-constant[12] is shown in Fig. 7, where the ordinate is the difference in frequency between unsubstituted (γ^{H}_{OH}) and substituted acid (γ^{R}_{OH}), and the abscissa, the Hammett *σ*-constant. In the case of salicylic acids, the relatively large deviation of some phenolic OH plots from the straight line would not be due to the inexactness

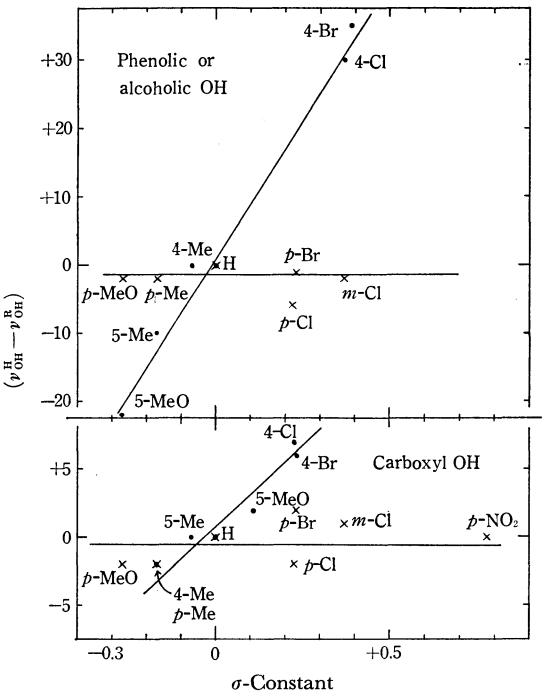

Fig. 7. Correlation of ν_{OH} with Hammett *σ*-constant in salicylic (—•—) and mandelic acids (—×—).

of the frequencies, but, rather, due mainly to the electronic effects of the substituent, influencing the hydrogen bonding through the carbonyl-oxygen atom. A detailed study of this problem is in progress and will be reported in the next part of this series of studies.

11) L. P. Kuhn, *J. Am. Chem. Soc.*, **80**, 5950 (1958).
12) H. H. Jaffé, *Chem. Revs.*, **53**, 191 (1953).

BULLETIN OF THE CHEMICAL SOCIETY OF JAPAN VOL. 42 488—491 (1969)

Intramolecular Hydrogen Bonds. XIV.[1] Correlation of the Hydroxyl and the Carbonyl Frequencies of Methyl Salicylates with Hammett's Substituent Constants

Nobuo Mori, Yuzuru Asano and Yojiro Tsuzuki

Department of Chemistry, Science University of Tokyo, Kagurazaka, Shinjuku-ku, Tokyo

(Received June 5, 1968)

The infrared OH and C=O stretching spectra of methyl 4- or 5-substituted salicylates have been measured in dilute carbon tetrachloride solutions, and the respective peak-frequencies have been correlated with ordinary Hammett's σ-constants. The best linear relationship has been established between the γ_{OH} and the $(\sigma_{OH}-0.38\sigma_{COOMe})$ values and between the $\gamma_{C=O}$ and the $(\sigma_{COOMe}-0.49\sigma_{OH})$ values, where σ_{OH} and σ_{COOMe} are the σ-constants of a substituent with respect to the OH and the COOMe group respectively. Besides, in other internally-bonded phenol systems, including *o*-bromophenols, *o*,*o*'-dihalophenols, and salicylic acids, the plotting of the OH frequencies against the $(\sigma_{OH}-A\sigma_X)$ values gave the best linear relationship, where A is a constant depending on the kind of proton acceptor, X. The value of A can be a measure of the electronic effects of the substituent, influencing the bonded OH frequency through X.

In general, the spectroscopic properties of ring-substituted aromatic compounds can be correlated with the electronic nature of the substituents. In unassociated phenols,[2] benzoates,[3] and benzoic acids,[4] for example, the respective infrared OH and C=O stretching frequencies have been correlated with Hammett's σ-constants.

In internally-associated phenol systems, such as *o*-hydroxybenzaldehyde-anils (mono-substituted in the anil moiety)[5] and *p*-substituted phenylglyoxylic acids,[6] the hydrogen-bonded OH and C=O frequencies change linearly with the σ-constants.

On the other hand, the additivity of electronic effects of substituents has been pointed out,[7] and these effects have been reported with the carbonyl stretching modes of substituted benzoic acids.[8] Accordingly, very interesting is a system of benzene compounds, each of which contains a substituent with electronic effects which contribute to the interaction between two other substituents, both attached to the same benzene ring. An infrared investigation has previously been reported on the substituent effect on the interaction between the OH and the C=O group in 2-hydroxy-5-substituted-acetophenones;[9] in this case, the observed spectral shift, $\Delta\gamma_{OH}$, was correlated with the term of $(\sigma_p+\sigma_m)/2$, suggesting that equal proportions of the two tautomeric structures contribute to the interaction. However, their bonded OH bands appeared in the complex C–H stretching absorption region, thus reducing the accuracy of the reported band frequencies.

The present investigation has been performed on the electronic effects of a substituent exerted on the hydrogen bonding in methyl 4- and 5-monosubstituted salicylates, the bonded OH bands of which can easily and reliably be assigned.[10]

A major work on the chelation in substituted salicylates has been performed by Brooks and his co-workers,[10] but their interest was primarily in the problem of the so-called *o*-effects of adjacent substituents on the chelation.

Another subject of this investigation is the correlation of the OH frequencies with Hammett's σ-constants in the systems of internally-bonded phenolic compounds, such as substituted *o*-halophenols and salicylic acids, which may be expected to have essentially the same mechanism of hydrogen-bond formation.

1) Part XIII: N. Mori, Y. Asano, T. Irie and Y. Tsuzuki, This Bulletin, **42**, 482 (1969).

2) P. J. Stone and H. W. Thompson, *Spectrochim. Acta*, **10**, 17 (1957).

3) J. L. Mateos, R. Cetina, E. Olivera and S. Meza, *J. Org. Chem.*, **26**, 2494 (1961).

4) M. St. C. Flett, *Trans. Faraday Soc.*, **44**, 767 (1948).

5) A. T. Shulgin and A. W. Baker, *Nature*, **182**, 1299 (1958); A. W. Baker and A. T. Shulgin, *J. Am. Chem. Soc.*, **81**, 1523 (1959).

6) A. Schellenberger and G. Oehme, *Tetrahedron Letters*, **1966**, 767.

7) H. H. Jaffé, *Science*, **118**, 242 (1953).

8) N. Fuson, M. L. Josien and E. M. Shelton, *J. Am. Chem. Soc.*, **76**, 2526 (1954).

9) Z. Yoshida and M. Haruta, *Tetrahedron Letters*, **1964**, 2631.

10) C. J. W. Brooks, G. Eglinton and J. F. Morman, *J. Chem. Soc.*, **1961**, 661.

Experimental

Samples. All the esters, except for the 4-bromo-homologue, were known substances and were prepared by the methods described in the literature. The purified esters had almost, or completely, the same melting or boiling points as the reported values. The methyl 4-bromosalicylate was prepared by essentially the same method as the known 4-chloro-compound.

Infrared Measurement. This was carried out in almost the same manner as has been described in the preceding paper,[1] at an operating temperature of *ca.* 25°C, using a grating, double-beam spectrophotometer, Model DS-403G, of the Japan Spectroscopic Co., Ltd. The OH-stretching region was measured in a concentration of 0.002 mol/*l* or less in carbon tetrachloride, while the C=O stretching region was measured in a concentration of 0.001 mol/*l* or less. The cells used were 5.0 and 1.0 cm in optical path-length for the OH and the C=O measurements respectively. At those concentrations, no intermolecular hydrogen bonding was present, as has been described in the literature.[10]

Results and Discussion

The infrared OH and C=O spectra of three representative esters are shown in Fig. 1, while the spectral data of all the esters are summarized in Table 1. In the OH region, each of the esters shows only a very broad, intense, bonded OH band, with a distinct maximum in a frequency range from 3140 to 3222 cm^{-1}; the OH absorption begins near 3500 cm^{-1}, and the lower frequency side merges into the C–H absorption region. The carbonyl bands, which are sharp and, in most cases, almost symmetrical, appear near 1700 cm^{-1}; this frequency is lower than the 1730 cm^{-1} of methyl benzoate but much higher than the 1650 cm^{-1} of tautomeric *o*-hydroxyacetophenones.[9] The relatively small lowering of the carbonyl frequency from 1730 cm^{-1} suggests that the intramolecular hydrogen bonding in these esters can be explained by structure I, but not by a mixture of the two tautomeric structures I and II or by the meso-ionic structure III. In fact, the observation of the infrared spectra has shown none of the absorption bands to be expected for the quinoid-carbonyl (near 1650 cm^{-1}) and the C⋯O half double bond (near 1400 cm^{-1}).

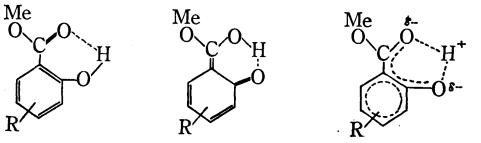

I II III

In these esters, therefore, the conformation of the carbonyl group*1 can be fixed by chelation with the phenolic OH group.[10] In this case, however, the coplanarity of the two substituents and

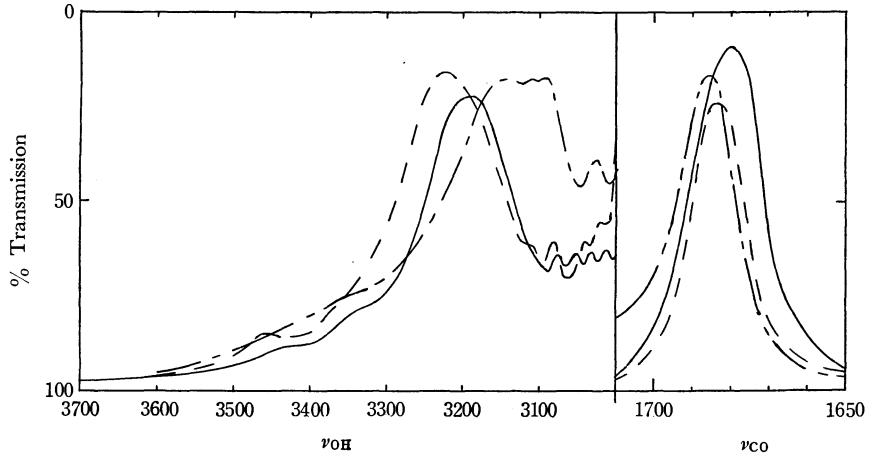

Fig. 1. Infrared OH (left) and C=O spectra (right) of methyl salicylate (——), methyl 5-methoxysalicylate (— — —) and methyl 5-nitrosalicylate (— - —).

*1 In general, a carboxylate ester function itself, while strongly preferring a roughly planar conformation resulting from the resonance interaction between the alkoxy-oxygen and the carbonyl group,[11] may be exclusively in a *cis*-arrangement,[12] where both groups are *cis* in respect of the C–O bond, but not trans, because of the electrostatic repulsion of filled orbitals.[13] Accordingly, the *cis*-arrangement is the normally preferred one.[14]

11) G. W. Wheland, "Resonance in Organic Chemistry," John Wiley and Sons, New York, N. Y. (1955), p. 99.

12) R. J. B. Marsden and L. E. Sutton, *J. Chem. Soc.*, **1936**, 1383; R. Huisgen and H. Ott, *Tetrahedron*, **6**, 253 (1959).

13) D. Cooke, *J. Am. Chem. Soc.*, **80**, 49 (1958).

14) S. Mizushima, "Structure of Molecules and Internal Rotation," Academic Press, New York (1954), p. 88.

Table 1. The physical constants and the infrared data of methyl salicylates

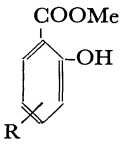

R	Mp,°C (Bp, °C/mmHg)	ν_{OH}	$\nu_{C=O}$	σ_{OH}	σ_{COOMe}
H	(77/5)	3185	1680	0	0
4-CH_3	27.5—28 (88/3)	3188	1678	−0.069	−0.170
4-CH_3O	48—49	3163	1673	+0.115	−0.268
4-Cl	27 (91/3)	3160	1681	+0.373	+0.227
4-Br*	41—42 (97/2)	3155	1682	+0.391	+0.232
5-CH_3	(97—99/5)	3209	1680	−0.170	−0.069
5-CH_3O	(85/1.5)	3222	1684	−0.268	+0.115
5-NO_2	116	3140	1687	+0.778	+0.710

* Anal., Found: C, 3.18; H, 41.84%. Calcd: C, 3.03; H, 41.59%.

the benzene ring is not implied.

In substituted phenols[2] and benzoates,[3] the respective OH and C=O stretching frequencies become lower and higher respectively as the electron-withdrawing by the substituents increases. The substituent effects on both frequencies are interpreted in terms of the changes in the electronegativities of, respectively, the hydroxyl-oxygen and the carbonyl-carbon atom corresponding to the changes in the substituents. That is, as the electron-withdrawal by the substituents increases, the O–H bond of substituted phenols is weakened, resulting in a decreased OH stretching frequency, while the carbonyl double-bond character of substituted benzoates is increased (the contribution of the polar structure, $\overset{+}{C}-\overset{-}{O}$, to the resonance is decreased), resulting in an increased C=O stretching frequency.

In the case of the present salicylates, a substituent is expected to have electronic effects on the characteristics of the O–H and the C=O bond, both being involved in the hydrogen-bonding interaction, and thus to have an effect on the interaction itself. For example, the interaction will be strengthened by the increase in the polarity of the O–H bond and will simultaneously be weakened by the decrease in the polarity of the C=O bond, as the electron-withdrawal by the substituent increases. The sum of the two effects, reversely influencing the interaction in this way, is reflected by the observed bonded OH and C=O frequencies. In the above case, for example, the frequency of the OH group involved in the interaction will be decreased with an increase in the O–H polarity and will be simultaneously increased as a result of the interaction being weakened by the decrease in the C=O polarity.

On the basis of the above considerations, the observed OH and C=O frequencies were plotted against the respective ordinary Hammett's σ-

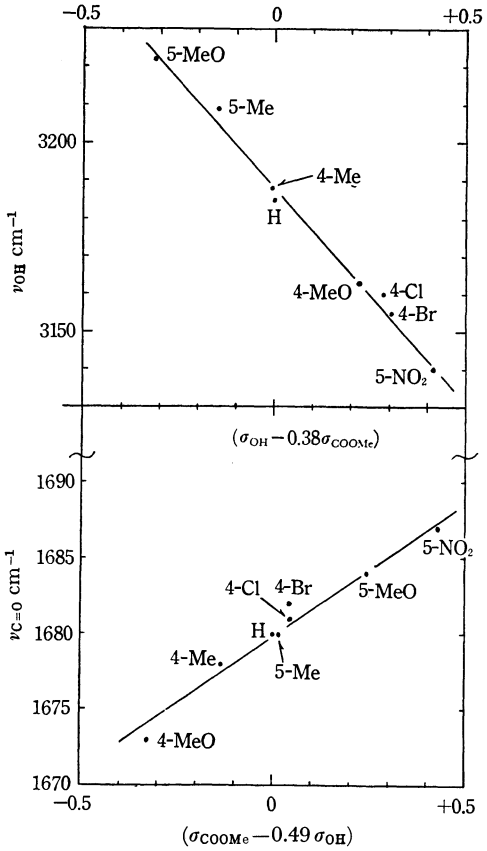

Fig. 2. Correlation of ν_{OH} and $\sigma_{C=O}$ with σ-constant in methyl salicylates.

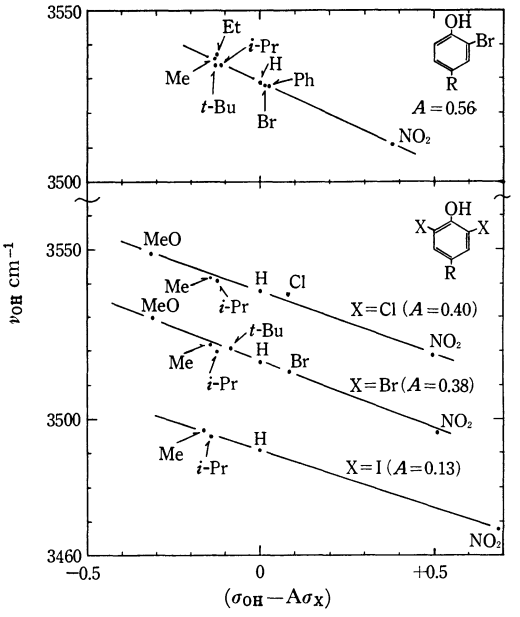

Fig. 3. Correlation of ν_{OH} with σ-constant in o-bromophenols and in o,o'-dihalophenols.

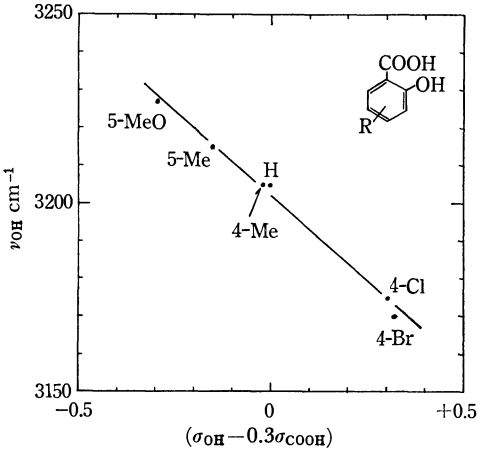

Fig. 4. Correlation of ν_{OH} (phenolic) with σ-constant in salicylic acids.

constants.[15] The best linear relationship has been established between the values of γ_{OH} and $(\sigma_{OH}-0.38\sigma_{COOMe})$ and between those of $\gamma_{C=O}$ and $(\sigma_{COOMe}-0.49\sigma_{OH})$, as is shown in Fig. 2, where σ_{OH} and σ_{COOMe} are the Hammett σ-constants of a substituent with respect to the OH and COOMe groups respectively. In the former relationship, the factor of 0.38 seems to be a measure of the electronic effect of the substituent on the bonded OH frequency, operating through the proton-accepting carbonyl group, while the factor of 0.49 in the latter is a similar measure of the substituent effect influencing the bonded C=O frequency through the proton-donating hydroxyl group.

In some systems of phenolic compounds, including substituted o-bromophenols,[16] o,o'-dihalophenols,[17] and salicylic acids,[1] a linear relationship has been further obtained between the values of γ_{OH} and $(\sigma_{OH}-A\sigma_X)$,*2 as is shown in Figs. 3 and 4, where the OH frequencies used in the plotting are those reported in the literature. However, the reported OH frequencies of o-hydroxyacetophenones[9] have not provided a linear relationship. Accordingly, the intramolecular hydrogen bonding in the former three systems of compounds can probably be explained in terms of essentially the same structure as that of the methyl salicylates.

In the cases of the p-substituted o,o'-dihalophenols, each forming a similar 5-membered ring through the hydrogen bonding, the OH frequency can be determined by the constant of A, which increases with the halogens in the order: I (0.13)<Br(0.38)<Cl(0.40), which is equivalent to the order of their electronegativities. It is well known[18] that, in o-halophenols, the spectral shifts, $\Delta\gamma_{OH}$, increase with the halogens in the order: F<Cl<Br<I, which is the reverse of the order of the electronegativities and is different from that of the hydrogen bond enthalpies. However, the disagreement in the orders has not yet been elucidated. Though the present investigation does not deal with this problem, the value of A seems to imply the operation of another significant factor in the hydrogen-bond formation.

15) H. H. Jaffé, *Chem. Revs.*, **53**, 191 (1953).

*2 The value of A is a constant depending on the kind of proton-acceptor, X, and the terms of σ_{OH} and σ_X are ordinary Hammett σ-constants of a substituent with respect to the OH and X group respectively.

16) I. Brown, G. Eglinton and M. Martin-Smith, *Spectrochim. Acta*, **18**, 1593 (1962).

17) A. W. Baker, H. O. Kerlinger and A. T. Shulgin, *ibid.*, **20**, 1477 (1964).

18) For example, A. W. Baker and A. T. Shulgin, *Can. J. Chem.*, **43**, 650 (1965); D. A. K. Jones and J. G. Watkinson, *J. Chem. Soc.*, **1964**, 2366, and the references cited therein.

BULLETIN OF THE CHEMICAL SOCIETY OF JAPAN VOL. 42 492—498 (1969)

Ethylidenation of L-Sorbose[1-3]

Takashi MAEDA, Masumi KIYOKAWA and Kanji TOKUYAMA

Shionogi Research Laboratory, Shionogi & Co., Ltd., Fukushima-ku, Osaka

(Received June 8, 1968)

The ethylidenation of L-sorbose (I) with acetaldehyde dimethylacetal in the presence of an acid was studied. When the reaction was interrupted at the initial stage, an equilibrium mixture of the two possible cyclic acetals, 1,2-*O*-(III) and 1,3-*O*-ethylidene-*α*-L-sorbopyranose (V), was obtained. When the reaction was allowed to proceed for longer periods of time, 1,3:4,6-di-*O*-ethylidene-*β*-L-sorbofuranose (IX) was mainly isolated; the transformation of this to two diastereoisomeric 2,3:4,6-di-*O*-ethylidene-*α*-L-sorbofuranoses (XV and XVIII) required the use of highly acidic conditions. A pathway of I→(III⇄V)→IX→(XV+XVIII) was tentatively proposed for the ethylidenation of I.

The acetonation of L-sorbose (I) yields 1,2-*O*-isopropylidene-*α*-L-sorbopyranose (II) as the initial product;[4,5] this is then converted into 2,3:4,6-di-*O*-isopropylidene-*α*-L-sorbofuranose (VII) exclusively.[6] Although the presence of an equilibrium between II and 1,3-*O*-isopropylidene-*α*-L-sorbopyranose (IV) at the initial stage of the reaction has reasonably been anticipated from the acetalation of glycerol,[7] IV could not be isolated. This discrepancy must be considered on stereochemical grounds. As has been pointed out by Brown, Brewster, and Schechter,[8] the formation of a six-membered *O*-isopropylidene ketal is inhibited because one of the two methyl groups is necessarily axial in the chair conformation for the six-membered ring. On the other hand, there is no axial methyl group in a six-membered ethylidene acetal, so that 1,3-*O*-ethylidene-*α*-L-sorbopyranose (V) can be expected to be isolated from the ethylidenation of I. The isolation of V may give important information regarding the complicated reaction mechanisms of the acetalation of I.[4,9,10] This paper will report on the ethylidenation of I with acetaldehyde dimethylacetal[11] in the presence of an acid. The products from this reaction were isolated by preparative thin-layer chromatography and were identified on the basis of chemical and proton magnetic resonance (PMR) spectroscopic evidence. The assignment of the PMR spectra shown in Tables 1 and 2 is based on the chemical shifts with reference to the corresponding acetonated compounds.[2,10,12]

The treatment of I with acetaldehyde dimethylacetal in the presence of *p*-toluenesulfonic acid at 40°C for 2.7 hr or under weaker conditions afforded one diethylidene compound (IX) and four monoethylidene compounds, the latter of which were purified as the acetates, IIIa, Va, VIa, and XIIIa. The Va acetate showed bands due to a hydroxyl group in its infrared spectrum. This hydroxyl group was considered to be a tertiary one, because no acetylation occurred with acetic anhydride in pyridine at ordinary temperatures, whereas reduction was observed with a Fehling solution. The methylation of Va with methyl iodide in the presence of silver oxide yielded VIa. This product, VIa, was also obtained by the ethylidenation of methyl *α*-L-sorbopyranoside (XXI),[13] followed by acetylation. Thus, the structures of Va and VIa were determined to be the 4,5-di-*O*-acetates of V and methyl 1,3-*O*-ethylidene-*α*-L-sorbopyranoside (VI). The PMR spectra of Va and VIa in chloroform-d

1) Sorboses. XIII. For Part XII, see Ref. 2.

2) T. Maeda, K. Tori, S. Satoh and K. Tokuyama, This Bulletin, **41**, 2495 (1968).

3) Some of results of this paper have appeared in a preliminary form. T. Maeda and K. Tokuyama, *Tetrahedron Letters*, **1968**, 3079.

4) K. Tokuyama, E. Honda and N. Hōki, *J. Org. Chem.*, **29**, 133 (1964).

5) J. R. Patil and J. L. Bose, *J. Indian Chem. Soc.*, **43**, 161 (1961).

6) T. Reichstein and A. Grüssner, *Helv. Chim. Acta*, **17**, 377 (1934).

7) a) R. V. Lemieux, "Molecular Rearrangements," Part 2, ed. by P. de Mayo, Interscience, New York (1964), p. 214. b) H. Hibbert and J. G. Morazain, *Can. J. Research*, **2**, 214 (1930). c) N. Baggett, J. M. Duxbury, A. B. Foster and J. M. Wegber, *Carbohyd. Res.*, **2**, 216 (1966). d) G. Stefanovic and D. Petrovic, *Tetrahedron Letters*, **1967**, 3153.

8) H. C. Brown, J. H. Brewster and H. Schechter, *J. Am. Chem. Soc.*, **76**, 467 (1954).

9) K. Tokuyama and E. Honda, This Bulletin, **37**, 591 (1964).

10) T. Maeda, *ibid.*, **40**, 2122 (1967).

11) The use of acetaldehyde was not feasible because of the formation of oxidoethylene derivatives.

12) L. D. Hall, *Adv. Carbohyd. Chem.*, **19**, 51 (1964).

13) H. H. Schlubach and G. Graef, *Ann.*, **532**, 211 (1937).

Table 1. Chemical shifts (τ) in chloroform-d[a)]

Compound	H_1 and $H_{1'}$	H_3	H_4	H_5	H_6 and $H_{6'}$	CH_3—CH(O,O)	CH$_3$—CH(O,O)	Other signal
IIIa	6.00, 6.33 (6.03, 6.37)	4.95 (4.78)	4.52 (4.18)	~5.0 (~4.8)	~6.2 (~6.2)	8.55 (8.68)	4.70 (4.77)	OCOCH_3: 7.93, 7.98, 8.00 (8.23, 8.30, 8.35)
Va	6.23, 6.42 (6.45,6.70)	6.52 (6.80)	4.58 (4.18)	5.02 (4.85)	5.97, 6.23 (6.00, 6.23)	8.62 (8.81)	5.25 (5.73)	OCOCH_3: 7.95, 7.98 (8.25, 8.38)
VIa	5.83, 6.67	6.52	4.47 ~ 5.03		6.17, 6.45	8.63	5.27	OCOCH_3: 7.95, OCH_3: 6.67
VIII	5.93, 6.27	5.88	5.6 ~ 5.8		6.08	8.65, 8.67	5.28, 5.35	
XIa	5.73, 6.33 (5.50, 6.65)	5.97 (5.93)	4.73 (4.63)	~5.2 (5.18)	~5.8 (5.7~5.8)	8.67 (8.75)	5.37 (5.73)	OCOCH_3: 7.93(6H), OCH_3: 6.73 (8.30, 8.35) (6.98)
XIIIa	~5.59	4.76	5.6 ~ 6.2			8.68	5.37	OCOCH_3: 7.89, 7.91
XV	~6.4 (~6.1)	5.53 (5.42)	5.70 (5.95)	6.00 (6.53)	5.75, 6.16 (6.00, 6.78)	8.63, 8.70 (8.78, 8.82)	4.57, 5.35 (4.77, 5.84)	OH: 7.77 (7.78)
XVa	5.54, 5.75 (5.20, 5.51)	5.62 (5.46)	5.73 (6.08)	6.00 (6.49)	5.80, 6.16 (6.00, 6.73)	8.65, 8.70 (8.75, 8.80)	4.58, 5.37 (4.75, 5.82)	OCOCH_3: 7.90 (8.31)
XVI	~5.7 (5.48, 5.56)	5.63 (5.52)	b) (~6.2)	6.03 (6.58)	b), 6.25 (~6.1, 6.85)	8.72, 8.80 (8.80, 8.88)	4.62, 5.42 (4.81, 5.90)	ArCH_3: 7.57 (8.15)
XVII	6.38, 6.70 (6.15, 6.35)	5.40 (5.22)	5.57 (6.12)	6.05 (6.53)	5.85, 6.25 (6.02, 6.80)	8.65, 8.90 (8.55, 8.88)	4.52, 5.45 (4.67, 5.87)	
XVIII	~6.15 (~6.08)	5.56 (5.47)	b) b)	b) (6.06)	b), 6.12 (5.97, 6.72)	8.58, 8.70 (8.71, 8.79)	4.82, 5.35 (5.00, 5.83)	OH: 7.72 (7.62)
XVIIIa	b) (5.32, 5.52)	5.67 (5.57)	5.5 ~ 6.0 (6.12)	(6.25)	6.13 (5.97, 6.73)	8.57, 8.70 (8.72, 8.80)	4.83, 5.37 (4.95, 5.83)	OCOCH_3: 7.90 (8.33)
XIX	5.67, 5.80 (5.52, 5.60)	5.65 (5.55)	b) (~6.2)	5.82 (6.72)	b), 6.20 (~6.1, 6.80)	8.68, 8.78 (8.82, 8.87)	4.90, 5.42 (4.92, 5.90)	ArCH_3: 7.57 (8.13)
XX	6.37, 6.67 (6.23, 6.30)	5.48 (5.28)	5.85 (6.10)	5.95 (~6.2)	5.85, 6.72 (5.98, 6.72)	8.58, 8.85 (8.70, 8.85)	4.60, 5.44 (4.70, 5.87)	

a) The values in parentheses were observed in benzene-d_6. b) Obscured.

TABLE 2. COUPLING CONSTANTS (Hz)

Compound	$J_{1,1'}$	$J_{3,4}$	$J_{4,5}$	$J_{5,6}$	$J_{5,6'}$	$J_{6,6'}$	J_{CH_3CH}
IIIa	9.0	9.7	9	a)	a)	a)	5.0
Va	10.5	9.8	9.3	6.2	10.2	11.0	5.0
VIa	12.0	9.8	9	6.2	10.2	11.0	5.0
VIII	12.0	0.5	a)	a)	~2	13	5.0
XIa[b]	12.0	0.6	5.3	a)	a)	a)	5.0
XIIIa	a)	0.6	a)	a)	a)	a)	5.0
XV	a)	0.5	~2	~2	~2	12.8	5.0
XVa	11.8	0.5	~2	~2	~2	12.8	5.0
XVI	10.5	0.5	~2	~2	~2	12.8	5.0
XVII	9.6	0.5	2.5	~2	~2	12.8	5.0
XVIII	a)	0.5	a)	a)	~2	12.8	5.0
XVIIIa	11.8	0.5	~2	~2	~2	12.8	5.0
XIX	10.5	0.5	~2	~2	~2	12.8	5.0
XX	9.6	0.5	~2	~2	~2	12.8	5.0

a) not determinable. b) $J_{1,4}=0.8$

show a doublet due to H_3 at a higher filed (τ 6.52), a doublet-doublet due to H_4 (τ 4.47—4.58) and a multiplet due to H_4 (τ 5.02—5.03) at a lower field; the large coupling constants of $J_{3,4}$, $J_{4,5}$, and $J_{5,6}$, (9.3—10.2 Hz) are consistent with the proposed pyranose structures.[12,14,15]

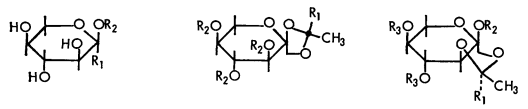

I $R_1 = CH_2OH$, $R_2 = H$
XXI $R_1 = CH_2OH$, $R_2 = CH_3$
XXII $R_1 = CH_2OTs$, $R_2 = H$
XXIII $R_1 = COOCH_3$, $R_2 = H$

II $R_1 = CH_3$, $R_2 = H$
III $R_1 = R_2 = H$
IIIa $R_1 = H$, $R_2 = Ac$

IV $R_1 = CH_3$, $R_2 = R_3 = H$
V $R_1 = R_2 = R_3 = H$
Va $R_1 = R_2 = H$, $R_3 = Ac$
VI $R_1 = R_3 = H$, $R_2 = CH_3$
VIa $R_1 = H$, $R_2 = CH_3$, $R_3 = Ac$

Chart 1

The combined data of elemental analysis, optical rotation, and the infrared spectrum established that IIIa was the tri-*O*-acetate of monoethylidene-*α*-L-sorbose. The PMR spectrum in chloroform-d showed three three-proton singlets due to acetoxyls and signals due to H_3 (doublet), H_4 (doublet-doublet), and H_5 (multiplet) in the H–C–OAc region (τ 4.5—5.0). The large coupling constants of $J_{3,4}$ and $J_{4,5}$ (9—9.7 Hz) indicated its pyranose structure in the 1C conformation. Therefore, the structure of IIIa was determined to be the 3,4,5-tri-*O*-acetate of 1,2-*O*-ethylidene-*α*-L-sorbopyranose (III).

When the ethylidenation was allowed to continue for longer periods of time, the amount of diethylidene derivative (IX) increased at the expense of the monoethylidene compounds. The compound IX was considered to have a tertiary hydroxyl group for the same reasons as was Va. The methylation of IX with methyl iodide in the presence of silver oxide gave a glycoside (X), which was also isolated from the reaction mixture to a limited extent. The PMR spectrum of X in chloroform-d shows two one-proton quartets due to the methine protons of ethylidene groups at τ 5.27 and 5.28. Since the signal due to the methine proton of an ethylylidene ring in chloroform-d appeared at τ 4.70 for five-membered ring of IIIa and at τ 5.25—5.27 for the six-membered rings of Va and VIa, the ethylidene groups of X were assigned to those of six-membered rings. These data and their positive optical rotations apparently established that the structures of IX and X were 1,3:4,6-di-*O*-ethylidene-*β*-L-sorbofuranose, the ethylidene analog of 1,3:4,6-di-*O*-isopropylidene-*β*-L-sorbofuranose (VIII),[10] and methyl 1,3:4,6-di-*O*-ethylidene-*β*-L-sorbo-furanoside, respectively. The partial deacetalation of X with 60% acetic acid gave a monoethylidene sorboside (XI), which was then purified as a diacetate (XIa). The PMR spectrum of XIa in chloroform-d (see Fig. 1) shows singlets at τ 7.93 due to two acetyl methyls and at τ 6.73 due to one methoxy methyl, a doublet at τ 8.67 ($J=5.0$ Hz) due to one ethylidene methyl, and a quartet at τ 5.37 due to one methine proton of a six-membered ethylidene group. The patterns of the remaining protons are quite similar to those of methyl 1,3-

14) a) F. W. Lichtenthaler and H. K. Yahya, *Tetrahedron Letters*, **1965**, 1805. b) F. W. Lichtenthaler and H. K. Yahya, *Chem. Ber.*, **100**, 2389 (1967). c) H. Paulsen, H. Köster and K. Heynes, *ibid.*, **100**, 2669 (1967).

15) The evidence of PMR indicates that the favored conformations of Va and VIa are the 1C chair from.

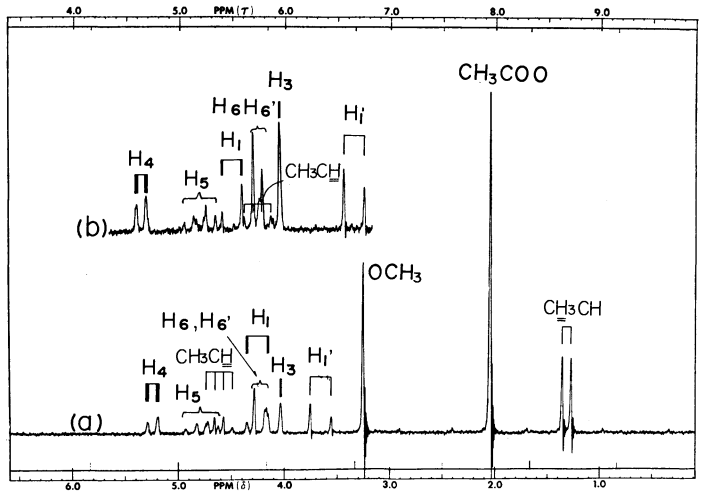

Fig. 1. PMR spectra of XIa in chloroform-d (a) and benzene-d_6 (b) at 60 MHz.

O-isopropylidene-4,6-di-*O*-acetyl-*β*-L-sorbofuranoside (XII), showing a remarkable low-field shift of H_4.[2] Therefore, XI was identified as methyl 1,3-*O*-ethylidene-*β*-L-sorbofuranoside; the formation of XI supports the structure of IX.

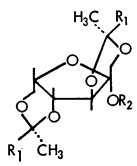

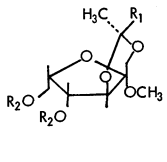

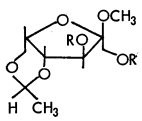

VIII $R_1 = CH_3$, $R_2 = H$

IX $R_1 = R_2 = H$

X $R_1 = H$, $R_2 = CH_3$

XI $R_1 = R_2 = H$

XIa $R_1 = H$, $R_2 = Ac$

XII $R_1 = CH_3$, $R_2 = Ac$

XIII R = H

XIIIa R = Ac

Chart 2

The exclusive formation of IX as compared to the predominant formation of VII from the acetonation of I under similar conditions is noteworthy. This fact suggests that IX is more stable than VIII in an acidic medium. This stability of IX can be attributed to the absence of an axial methyl group in the chair conformations of the *O*-ethylidene group.[8]

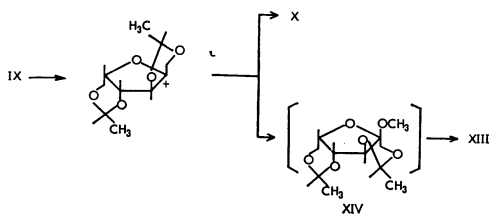

Chart 3

The negative value of optical rotation shows the anomeric configuration of XIIIa to be an *α*-anomer. The PMR spectrum of XIIIa in chloroform-d shows the presence of a six-membered ethylidene ring $\left(CH_3C\underline{H}<^{O}_{O}\ \tau\ 5.37\right)$; the signal due to H_3 is shifted downfield remarkably, while the signal due to H_4 is shifted upfield, in comparison with those observed in the spectrum of XIa. Therefore, the structure of XIII was determined to be methyl 4,6-*O*-ethylidene-*α*-L-sorbofuranoside.[2] The small coupling of $J_{3,4}$ (=0.6 Hz) also supports this furanose structure. The formation of X and XIII was proposed to be as follows: no isolation of 1,3:4,6-di-*O*-ethylidene-*α*-L-sorbofuranose results from its stereochemical instability.

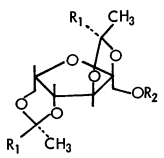

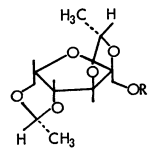

VII $R_1 = CH_3$, $R_2 = H$

XV $R_1 = R_2 = H$

XVa $R_1 = H$, $R_2 = Ac$

XVI $R_1 = H$, $R_2 = Ts$

XVII $R_1 = H$, $R_2 = trityl$

XVIII R = H

XVIIIa R = Ac

XIX R = Ts

XX R = trityl

Chart 4

Drastic conditions were required for the formation of 2,3:4,6-di-*O*-ethylidene-*α*-L-sorbofuranose. When

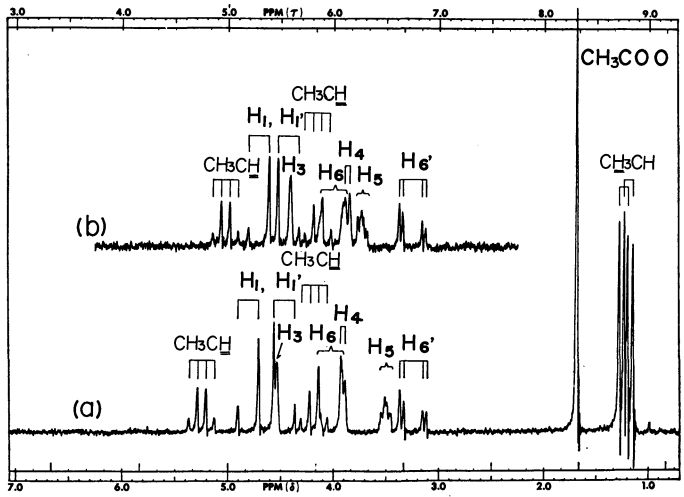

Fig. 2. PMR spectra of XV (a) and XVIII (b) in chloroform-d at 60 MHz.

I was treated with acetaldehyde dimethylacetal using a high concentration of sulfuric acid, a syrup was obtained which contained two isomers (XV and XVIII) with two ethylidene groups and negative optical rotations. Both derivatives, XV and XVIII, easily afforded acetates (XVa and XVIIIa), tosylates (XVI and XIX), and tritylates (XVII and XX respectively), and were both converted into methyl 2-keto-L-gulonate (XXIII) by Reichstein's procedure.[6] Further, XVI (or XIX) was identical with one of the two tosylates derived from the ethylidenation of 1-*O*-tosyl-L-sorbose (XXII).[16] These facts suggested the presence of a C_1-hydroxyl group in both isomers. The PMR spectra of the XVa and XVIIIa acetates (see Fig. 2) included the characteristic signals for a furanose structure, a somewhat broad singlet due to H_3 ($J_{3,4}$=0.5 Hz) and a doublet due to H_4 ($J_{4,5}$=5.8 Hz). Therefore, the structures of XV and XVIII were determined to be the diastereoisomers of 2,3:4,6-di-*O*-ethylidene-*α*-L-sorbofuranose, which differ only at the acetal center of the 2,3-*O*-ring since those methyl groups on the 1,3-dioxanes fused at the 4,6-position of furanose rings have been found to be equatorial in both isomers on the basis of non-bonded interactions[7a] and also on the basis of extensive studies of acetals.[17]

Ethylidene methine protons in chloroform-d appeared as quartets at τ 4.58 and 5.37 for XVa and at τ 4.83 and 5.37 for XVIIIa. Signals at a lower field were assignable to the protons on the dioxolane rings, as has been described above. Since the ethylidene methine proton on the dioxolane ring fused directly to the five-membered cyclic system is deshielded when *endo*,[17-19] XV (τ 4.58) and XVIII (τ 4.83) are assigned the H-*endo* and H-*exo* configurations[20,21] respectively.

As has been mentioned above, the expected 1,3-*O*-ethylidene pyranose V was successfully isolated; this suggested the presence of an equilibrium between 1,2-*O*-acetal (III) and 1,3-*O*-acetal (V) in the initial stage of the acetalation, much as in the acetalation of glycerol.[7] Further, the pathway of IX→(XV+XVIII) was also confirmed. Thus, the reaction pathway of I→(III⇄V)→IX→(XV+XVIII) for the ethylidenation of L-sorbose (I) was established; a detailed discussion of this will be presented elsewhere.

Experimental

Thin-layer chromatography was performed on silica gel using ether - *n*-hexane (2 : 1 v/v) as a solvent. The separated materials were developed with iodine. In the cases of preparative thin-layer chromatography (PTC), the developed zones were extracted with acetone. The evaporation of the acetone under reduced pressure gave the materials.

The PMR spectra were measured on a Varian A-60 spectrometer at 60 MHz in chloroform-d and/or benzene-d_6, using tetramethylsilane as the internal reference at

16) T. S. Gardner and J. Lee, *J. Org. Chem.*, **12**, 733 (1947).

17) N. A. Baggett, K. W. Buck, A. B. Foster and J. M. Webber, *J. Chem. Soc.*, **1965**, 3401, and earlier papers in this series.

18) F. Kametani and Y. Minoura, paper presented at the Annual Meeting of the Pharmaceutical Society of Japan, Tokyo, April, 1968.

19) R. J. Ferrier and L. R. Hatton, *Carbohyd. Res.*, **5**, 132 (1967).

20) The "H-*endo*" and "H-*exo*" diastereoisomers correspond to the R and S configurations respectively. See Ref. 21.

21) R. S. Cahn, C. K. Ingold and V. Prelog, *Angew. Chem. Internat. Edit.*, **5**, 385 (1966); *Experimentia*, **12**, 81 (1956); *J. Chem. Soc.*, **1951**, 612.

the ordinary probe temperature. All the melting points were measured on a Kofler block and were corrected. The optical rotations were determined in a 10 cm microtube in chloroform containing 1% ethanol, and the concentrations were recorded in percentages.

The solvents used were removed under reduced pressure below 40°C.

Ethylidenation of L-Sorbose (I). a) To a mixture of dry, finely-powdered L-sorbose (I) (15 g) and acetaldehyde dimethylacetal (50 ml), dioxane (50 ml) containing *p*-toluenesulfonic acid (TsOH) (1 g) was added. The suspended solution was vigorously stirred for 2.7 hr at 40°C, and then neutralized with potassium carbonate. After the removal of the unreacted L-sorbose (I) (7 g) and the excess potassium carbonate by filtration, the filtrate was concentrated to a yellow syrup (10.5 g). The chloroform solution (100 ml) of the syrup was washed with water (3×15 ml). From the chloroform layer, a di-*O*-ethylidene compound (IX) was isolated by a procedure (c) described below. The combined water was evaporated to a thick syrup (4.14 g). Without purification, the syrup was treated with acetic anhydride (20 ml) in pyridine (25 ml) at 0—5°C. After 3 hr, the solution was evaporated to give a syrup (4.7 g), from which IIIa (R_f 0.5—0.6, 0.27 g), VIa (R_f 0.44—0.51, 0.42 g), and XIIIa (R_f 0.39—0.49, 0.38 g) were then isolated by PTC. IIIa: syrup, $[\alpha]_D^{22}$ −45.7 (*c* 0.341). Found: C, 50.95; H, 6.02%. Calcd for $C_{14}H_{20}O_9$: C, 50.60; H, 6.07%. VIa: needles (recryst. from *n*-hexane), mp 93—94°C, $[\alpha]_D^{24}$ −58.4 (*c* 0.527). Found: C, 51.23; H, 6.59%. Calcd for $C_{13}H_{20}O_8$: C, 51.31; H, 6.63%. XIIIa: syrup, $[\alpha]_D^{23}$ −31.2 (*c* 1.020). Found: C, 51.30; H, 6.60%. Calcd for $C_{13}H_{20}O_8$: C, 51.31; H, 6.63%.

b) A solution of I (3.0 g) and acetaldehyde dimethylacetal (15 ml) in dimethylsulfoxide (15 ml) containing TsOH (0.3 g) was stirred at room temperature. After 3.3 hr, the solution was neutralized with ammonia water and then concentrated to a syrup (4.9 g). Without purification, the syrup was treated with acetic anhydride (20 ml) in pyridine (25 ml) at 0—5°C. After 3 hr, the solution was evaporated to give a syrup (3.9 g), from which IIIa (0.18 g), and Va (R_f 0.16—0.28, 0.16 g) were then isolated by PTC. Va: needles (recryst. from *n*-hexane, mp 140—142°C, $[\alpha]_D^{24}$ −24.7 (*c* 0.458). Found: C, 49.66; H, 6.19%. Calcd for $C_{12}H_{18}O_8$: C, 49.65; H, 6.25%.

c) A suspended solution of I (15 g) and acetaldehyde dimethylacetal (35 ml) in dioxane (50 ml) containing TsOH (1.0 g) was vigorously stirred at 40°C for 4.5 hr. The solution was made alkaline with potassium carbonate and then concentrated to a syrup (16.2 g), whose thin-layer chromatogram showed the presence of IX as the major product and X as the minor one. Several purifications of the syrup by PTC afforded IX (R_f 0.39—0.49, 2.5 g) and X (R_f 0.52—0.61, 0.52 g). IX: syrup, $[\alpha]_D^{24}$ +66.0 (*c* 1.006). Found: C, 51.48; H, 7.02%. Calcd for $C_{10}H_{16}O_6$: C, 51.72; H, 6.94%. X: syrup, $[\alpha]_D^{28}$ +68.1 (*c* 1.036). Found: C, 53.77; H, 7.35%. Calcd for $C_{11}H_{18}O_6$: C, 53.65; H, 7.37%.

d) A mixture of I (4.2 g), acetaldehyde dimethylacetal (30 ml), and sulfuric acid (6 g) was stirred at 30°C for 3 hr. The solution was neutralized with a a sodium carbonate solution and then concentrated to a syrup. The syrup was extracted with acetone, and the acetone removed. The chloroform solution of the residue was washed with water and dried, and the solvent removed. The purification of the residue (6.3 g) by PTC (R_f 0.14—0.27) gave crude crystals (3.9 g). The crystals were then treated with acetic anhydride (25 ml) in pyridine (25 ml) at 5°C. After standing overnight, the reaction mixture was poured over ice water and extracted with chloroform. The chloroform was washed with a sodium carbonate solution and then with water, and dried, after which the solvent was removed. From the residue, XVa (R_f 0.46—0.60, 1.28 g) and XVIIIa (R_f 0.38—0.49, 2.0 g) were isolated by PTC. XVa: plates (recryst. from *n*-hexane), mp 71—72°C, $[\alpha]_D^{20}$ −21.5 (*c* 0.783). Found: C, 52.33; H, 6.54%. Calcd for $C_{12}H_{18}O_7$: C, 52.55; H, 6.62%. XVIIIa; columns (recryst. from *n*-hexane), mp 53—54°C, $[\alpha]_D^{20}$ −24.0 (*c* 0.504). Found: C, 52.59; H, 6.46%. Calcd for $C_{12}H_{18}O_7$: C, 52.55; H, 6.62%.

Methyl 1,3-*O*-Ethylidene-4,6-di-*O*-acetyl-β-L-sorbofuranoside (XIa). A solution of X (1.19 g) in 60% acetic acid (50 ml) was heated at 95°C for 45 min. The solvent was removed twice by the addition of an excess of ethanol and by subsequent concentration. Without further purification, the residual syrup (1.04 g) was acetylated with acetic anhydride (20 ml) and pyridine (30 ml) in a refrigerator for 4 hr. The evaporation of the solvent gave a syrup (1.3 g), which was purified by PTC and then by recrystallization from *n*-hexane. XIa (197 mg) was obtained, mp 61—62°C, $[\alpha]_D^{24}$ +53.7 (*c* 0.536). Found: C, 51.50; H, 6.62%. Calcd for $C_{13}H_{20}O_8$: C, 51.31; H, 6.63%.

(R)-2,3:(R)-4,6-Di-*O*-ethylidene-α-L-sorbofuranose (XV). To a solution of XVa (0.7 g) in methanol (5 ml), 0.1 N methanolic sodium methoxide (150 ml) was added. After the mixture had stood at room temperature for 10 min, the solvent was removed, and then the mixture was extracted with chloroform. The chloroform was washed with water and dried, and the solvent was removed. The recrystallization of the residue from *n*-hexane gave needles (0.43 g), mp 58—59°C, $[\alpha]_D^{20}$ −8.5 (*c* 0.562). Found: C, 51.86; H, 6.96%. Calcd for $C_{10}H_{16}O_6$: C, 51.72; H, 6.94%.

(S)-2,3: (R)-4,6-Di-*O*-ethylidene-α-L-sorbofuranose (XVIII). A mixture of XVIIIa (1.55 g) in methanol (100 ml) and 0.1 N methanolic sodium methoxide (100 ml) was stirred at room temperature for 10 min. XVIII was then obtained in the above-described manner. XVIII: needles (recryst. from ethyl acetate and *n*-hexane), mp 82—83°C, $[\alpha]_D^{20}$ −9.5 (*c* 0.927). Found: C, 51.80; H, 6.85%. Calcd for $C_{10}H_{16}O_6$: C, 51.72; H, 6.94%.

Methyl 1,3-*O*-Ethylidene-4,5-di-*O*-acetyl-α-L-sorbopyranoside (VIa). a) A mixture of Va (0.15 g), methyl iodide (10.5 g), and silver oxide (1 g) was refluxed for 9 hr. The precipitates were removed by filtration, and the filtrate was concentrated to give a syrup. The syrup was purified by PTC (R_f 0.44—0.51), followed by recrystallization from *n*-hexane. VIa (0.1 g) was obtained.

b) A solution of methyl α-L-sorbopyranoside (XXI) (1.4 g), acetaldehyde dimethylacetal (28 ml), and TsOH (0.14 g) was stirred at room temperature. After 2 hr, the solution was neutralized with methanolic sodium methoxide. After the removal of the solvent, the residue was extracted with chloroform and the solvent removed. The residue was treated with acetic anhydride (20 ml) in pyridine (20 ml) at 5°C for 4 hr and then worked up by a procedure similar to that used in the ethylidena-

tion of I (a). VIa (0.1 g) was thus obtained.

Methyl 1,3:4,6-Di-*O*-ethylidene-β-L-sorbofuranoside (X). A mixture of IX (0.14 g), methyl iodide (14 g), and silver oxide (0.5 g) was refluxed for 4.7 hr. The precipitates were removed by filtration, and the filtrate was concentrated to give a syrup. The purification of the syrup by PTC (R_f 0.52—0.61) gave X (0.1 g).

1-*O*-Tosyl-(R)-2,3:(R)-4,6-di-*O*-ethylidene-α-L-sorbofuranose (XVI). A solution of XV (0.2 g) and tosyl chloride (0.5 g) in pyridine (3 ml) was kept overnight at room temperature. The solution was then poured over ice, extracted with chloroform which had been washed with a sodium bicarbonate solution and then with water, dried, and evaporated to dryness. The recrystallization of the residual syrup from methanol and water gave needles (0.26 g), mp 70—72°C (dec.), $[\alpha]_D^{24}$ −8.2 (*c* 0.970). Found: C, 52.84; H, 5.76; S, 8.26%. Calcd for $C_{17}H_{22}O_8S$: C, 52.85; H, 5.70; S, 8.29%.

1-*O*-Tosyl-(S)-2,3:(R)-4,6-di-*O*-ethylidene-α-L-sorbofuranose (XIX). A solution of XVIII (0.3 g) and tosyl chloride (0.5 g) in pyridine (3 ml) was worked up in a procedure similar to the above. XIX (0.35 g) was thus obtained as needles (recryst. from methanol and and water), mp 72.5—73°C, $[\alpha]_D^{24}$ −7.0 (*c* 0.814). Found: C, 53.15; H, 5.61; S, 8.49%. Calcd for $C_{17}H_{22}O_8S$: C, 52.85; H, 5.70; S, 8.29%.

Ethylidenation of 1-*O*-Tosyl-L-sorbose (XXII). A mixture of XXII (1.5 g) and acetaldehyde dimethylacetal (30 ml) was stirred at room temperature in the presence of sulfuric acid (2.2 g) for 3.7 hr and then neutralized with a sodium bicarbonate solution. The solvent was removed to give a syrup, which was then dissolved in chloroform, washed with water, and dried. The evaporation of the chloroform gave a syrup, from which XV (R_f 0.26—0.32, 0.56 g) and XVIII (R_f 0.39—0.45, 0.65 g) were isolated by PTC.

1-*O*-Trityl-(R)-2,3:(R)-4,6-di-*O*-ethylidene-α-L-sorbofuranose (XVII). To a solution of XV (0.3 g) in pyridine (6 ml), trityl chloride (1 g) was added. After standing at room temperature for 8 days, the solution was poured over ice and then extracted with chloroform. The chloroform was washed with a sodium carbonate solution, with hydrochloric acid, and then with water, and the solvent was removed. Crude crystals (1.25 g) were purified by PTC (R_f 0.41—0.49), followed by recrystallization from *n*-hexane. XVII was thus obtained as plates (0.09 g), mp 130—133°C, $[\alpha]_D^{24}$ −32.8 (*c* 2.903). Found: C, 73.69; H, 6.47%. Calcd for $C_{29}H_{30}O_6$: C, 73.40; H, 6.37%.

1-*O*-Trityl-(S)-2,3:(R)-4,6-di-*O*-ethylidene-α-L-sorbofuranose (XX) was obtained from XVIII (0.5 g), by a procedure similar to the above (PTC: R_f 0.54—0.59, 0.42 g). XX: columns (recryst. from *n*-hexane), mp 162—163°C, $[\alpha]_D^{23}$ −35.5 (*c* 0.738). Found: C, 73.43; H, 6.32%. Calcd for $C_{29}H_{30}O_6$: C, 73.40; H, 6.37%.

Oxidation of 2,3:4,6-di-*O*-ethylidene-α-L-sorbofuranoses (XV and XVIII). To a solution of a crude mixture of XV and XVIII (1.95 g) in water (24 ml) containing potassium hydroxide (1.11 g), a potassium permanganate (2.8 g) solution (31 ml) was added, batch by batch, over a 2.5-hr period. After the mixture had then been stirred at 25—26°C for 1.2 hr, the precipitates were removed by filtration, the filtrate was saturated with carbon dioxide, and then the water was removed. The residue was extracted with hot ethanol and the ethanol was concentrated to a powder, which was then dissolved in water (2 ml). The pH of the water was adjusted to 1.0 with hydrochloric acid under cooling. The acidic solution was extracted with ethyl acetate. The removal of the ethyl acetate gave a syrup; this solution in methanol (6 ml) containing one drop of hydrochloric acid was refluxed for 6 hr, and then the solvent was removed without heating to give methyl L-gulonate (XXIII) (0.04 g), mp 151—153°C. This was identical with an authentic sample.[6]

The authors wish to express their gratitude to Professor Toshihiko Okamoto, University of Tokyo, and Dr. Ken'ichi Takeda, Director of this Laboratory, for their encouragement.

BULLETIN OF THE CHEMICAL SOCIETY OF JAPAN VOL. 42 499—501 (1969)

Hydrogenation and Hydrogenolysis. XI.[1] The Hydrogenation of Methoxy- and Ethoxyanilines with a Ruthenium Catalyst*1

Shigeo NISHIMURA and Hisashi YOSHINO

Department of Industrial Chemistry, Tokyo University of Agriculture and Technology, Koganei, Tokyo

(Received June 10, 1968)

Hydrogenation of methoxy- and ethoxyanilines with a ruthenium catalyst was investigated at 80°C under the hydrogen pressure of 80—100 kg/cm^2. The amount of hydrogenolysis which occurred during hydrogenation varied with solvent from 35.1% in methanol to 8.5% in *t*-butyl alcohol in the hydrogenation of *p*-methoxyaniline. With use of *t*-butyl alcohol as solvent, good yields of methoxy- and ethoxycyclohexylamines were obtained from corresponding alkoxyanilines. It was shown that the rate of formation of cyclohexylamine increases with increasing polarity of solvent. *m*-Alkoxyanilines were found to hydrogenolyze more readily than the corresponding ortho or para isomers. For the greater tendency of meta isomers toward hydrogenolysis, an explanation based on the ionic cleavage of the carbon-oxygen bond was suggested.

In the preceding paper,[1] we have reported an effective method of the hydrogenation of methoxy- and ethoxyanilines, the alkoxyl group of which is rather labile to hydrogenolysis, with the rhodium oxide catalyst prepared by the lithium nitrate fusion of rhodium chloride. Over this catalyst, hydrogenolysis occurred only to slight extent and methoxy- and ethoxycyclohexylamines were obtained in excellent yields.

The hydrogenation of alkoxyanilines with ruthenium catalysts is usually accompanied by more extensive hydrogenolysis than with rhodium, although ruthenium has proved to be a useful metal in the catalytic hydrogenation of aromatic amines.[2] Freifelder and Stone[3] hydrogenated various alkoxyanilines with a ruthenium dioxide as catalyst in methyl or ethyl alcohol at elevated temperature and pressure. However, hydrogenation of methoxy- and ethoxyanilines gave only rather low yields of the corresponding alkoxycyclohexylamines under these conditions, except in the case of *o*-ethoxyaniline where 2-ethoxycyclohexylamine was obtained in 78.7% yield.

In this paper, we have investigated the ruthenium-catalyzed hydrogenation of methoxy- and ethoxyanilines, especially with reference to the effect of solvents on accompanying hydrogenolysis. It has been shown that the nature of the solvent used has a profound effect on the extent of hydrogenolysis and that the rate of formation of cyclohexylamine increases with increasing polarity of the solvent.

Experimental

Catalyst. The ruthenium hydroxide, prepared from aqueous solutions of ruthenium chloride and lithium hydroxide according to the procedure described previously,[4] was used as the catalyst throughout the experiments.

Hydrogenation and Analysis of Products. These were carried out in the same way as described in the preceding paper.[1] On direct gas chromatography of the reaction mixture, *n*-butyl alcohol could not be separated from cyclohexylamine and the analysis in this case was done after separation of produced amines from the solvent through their hydrochlorides. Alkoxycyclohexylamines gave two peaks on gas chromatogram, except in the case of 2-methoxy isomer where only one peak was obtained probably because of insufficient separation. The areas of the larger peaks, which probably corresponded to the cis isomers, were 84.3, 67.6, 93.1, 82.3 and 66.7% for 3-methoxy-, 4-methoxy-, 2-ethoxy-, 3-ethoxy- and 4-ethoxycyclohexylamines, respectively.

Solvents. All solvents used in hydrogenations were carefully dehydrated according to the methods recommended in the literature,[5] otherwise small amounts of hydrolysis products, alkoxycyclohexanols, were often formed during hydrogenation.

1) Part X: S. Nishimura, H. Uchino and H. Yoshino, This Bulletin, **41**, 2194 (1968).

*1 Presented at the 21st Annual Meeting of the Chemical Society of Japan, Osaka, April, 1968.

2) P. N. Rylander, "Catalytic Hydrogenation over Platinum Metals," Academic Press, New York (1967), p. 352.

3) M. Freifelder and G. R. Stone, *J. Org. Chem.*, **27**, 3568 (1962).

4) Y. Takagi, T. Naito and S. Nishimura, This Bulletin, **38**, 2119 (1965).

5) "Organic Solvents," 2nd Ed. ("Technique of Organic Chemistry," Vol. VII ed. by A. Weissberger), Interscience Publishers, New York (1955).

TABLE 1. THE EFFECT OF SOLVENTS ON THE RUTHENIUM-CATALYZED HYDROGENATION AND HYDROGENOLYSIS OF *p*-METHOXYANILINE[a]

Solvent	ε[b] at 80°C	Reac. time (hr)	Hydrogenolysis (mol %)	Half-hydrogenation time (min)	Rate of formation of cyclohexylamine ($mol \cdot min^{-1} \cdot g \cdot cat^{-1} \times 10^3$)
MeOH	23.9	5.8	35.1	40	4.4
EtOH	16.8	2.5	30.1	50	3.0
PrOH	13.1	2.0	26.2	50	2.6
i-PrOH	12.2	2.3	16.5	50	1.65
BuOH	11.3	2.5	21.7	60	1.8
s-BuOH	9.4	3.0	13.1	60	1.1
t-BuOH	6.1	2.5	8.5	50	0.85
THF	6.7	5.0	11.3	90	0.63
i-Pr_2O	3.3[c]	6.5	15.6	170	0.46
MCH[d]	1.9	5.5	13.1	110	0.60

a) *p*-Methoxyaniline (0.1 mol) was hydrogenated in 30 m*l* of solvent at 80°C under 80—100 kg/cm² in the presence of 0.1 g of ruthenium hydroxide and 0.01 g of $LiOH \cdot H_2O$.
b) Dielectric constants were obtained by extrapolating the values taken from "Landolt-Börnstein Tabellen," 6 Aufl. II Band, 6 Teil, Springer-Verlag (1959), p. 613.
c) The temperature dependence was approximated by that of ethyl isoamyl ether.
d) Methylcyclohexane.

Results and Discussion

The effect of various solvents was investigated in the hydrogenation of *p*-methoxyaniline at 80°C under the hydrogen pressure of 80—100 kg/cm² in the presence of ruthenium hydroxide and a small amount of lithium hydroxide, which has been shown to be an effective catalyst system for hydrogenation of aniline.[6] The results are summarized in Table 1. It is seen that hydrogenolysis occurred most extensively in methanol and ethanol, and varied considerably with the kind of solvent from 35.1% in methanol to 8.5% in *t*-butyl alcohol. It is noteworthy that hydrogenolysis took place to greater extent in less polar non-alcoholic solvents (isopropyl ether and methylcyclohexane) than in *t*-butyl alcohol. The amount of hydrogenolysis was thus found to be the smallest in *t*-butyl alcohol of the solvents investigated.[7] In Fig. 1 the rate of formation of cyclohexylamine, obtained on the basis of the amount of cyclohexylamine formed during half-hydrogenation time, is plotted *versus* the reciprocal of the dielectric constant of the solvent in which hydrogenation was carried out. It will be seen that the rate of formation of cyclohexylamine is a function of polarity of solvent: the greater the dielectric constant of a solvent is, the larger is the rate of formation of cyclohexylamine in the solvent. As noted above, the extent of hydrogenolysis is not always in the order of polarity of solvent. Generally, hydrogenation proceeded more slowly in non-alcoholic solvents than in alcoholic solvents (see Table 1) and probably this is the reason of rather large amounts of hydrogenolysis obtained in the former solvents notwithstanding their small dielectric constants. If we assume that the effect of solvent on the rate of hydrogenation is similar for alkoxyaniline and for the intermediate allyl-type ethers which probably undergo hydrogenolysis when further hydrogenated,[8] it may be considered that the change in the rate of formation of cyclohexylamine in various solvents represents the effect of solvents on the rate of hydrogenolysis of the alkoxyl group. Thus, the effect of solvents indicated in Fig. 1 can be interpreted as showing the effect of polarity of solvent on the rate of hydrogenolysis of the carbon-oxygen linkage. The observed effect thus suggests that more polarized transition states are involved in hydrogenolysis of the intermediates leading to the formation of cyclohexylamine. This is also in line with the currently accepted mechanism of catalytic hydrogenolysis in which an ionic cleavage of the carbon-oxygen bond is involved.[9]

Since it has been found that hydrogenolysis occurs only to a small extent in *t*-butyl alcohol, isomeric methoxy- and ethoxyanilines have been hydrogenated in this solvent, the results being summarized in Table 2. It is seen that hydrogenolysis is generally at low level and methoxy- and

6) S. Nishimura, T. Shu, T. Hara and Y. Takagi, This Bulletin, **39**, 329 (1966).

7) A similar effect of solvents was reported in hydrogenation of some benzyl alcohols with platinum oxide catalyst, where the amount of hydrogenolysis decreased with solvent in the order : primary>secondary>tertiary alcohol [Y. Ichinohe and H. Ito, This Bulletin, **37**, 887 (1964)].

8) This may be presumed by considering that the hydrogenolysis probably occurs by the S_N type mechanism (see Ref. 9) and such reaction will occur more easily in the allyl-type ether than in the corresponding aryl ether, because the formation of the transition state of carbonium ion character will be much favored in the allyl-type ether.

9) a) W. A. Bonner and J. A. Zderic, *J. Am. Chem. Soc.*, **78**, 3218 (1956). b) S. Mitsui and Y. Nagahisa, *Chem. Ind. (London)*, **1965**, 1975 and references cited therein.

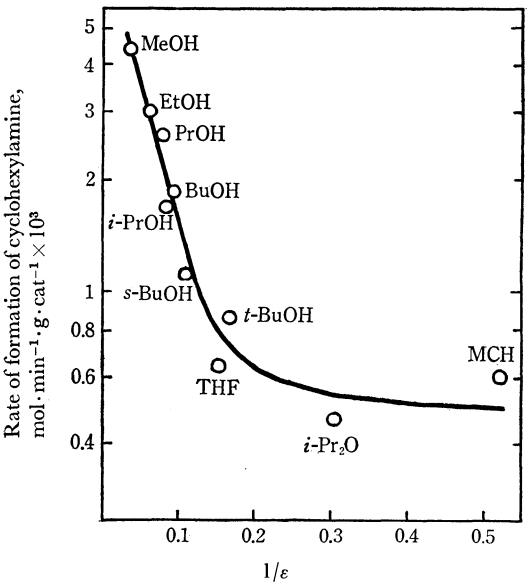

Fig. 1. Effect of solvents on the rate of formation of cyclohexylamine as a function of the reciprocal of dielectric constant in hydrogenation of *p*-methoxyaniline with Ru catalyst.

ethoxycyclohexylamines were obtained in more than 80% yields by distillation of products. Thus, the hydrogenation of alkoxyanilines with ruthenium hydroxide catalyst in *t*-butyl alcohol affords an excellent alternative method for the synthesis of alkoxycyclohexylamines.[10] The relative rates of formation of cyclohexylamine are also listed in the last column of Table 2, taking the rate for *o*-ethoxyaniline as unity. A noteworthy feature of the results is the fact that the meta isomers hydrogenolyze more easily than the corresponding ortho and para isomers. These results are in contrast with those obtained previously with rhodium catalyst in which the rate of formation of cyclohexylamine increased in the order: ortho<meta<para isomer, although differences between meta and para isomers were rather small.[1] The greater tendency of the meta isomer toward hydrogenolysis has been observed also in other hydrogenations.[11] It appears difficult to explain this phenomenon only either by the steric factor or by the probability of the formation of allyl-type ethers.[12] On the basis of an ionic cleavage of the carbon-oxygen bond, it may be suggested that the electron-releasing ability of the amino group at the meta position will stabilize the transition states of carbonium ion character when the allyl-type ethers undergo hydrogenolysis, as shown below in one example of dihydro intermediates. Such an effect will not be expected in the allyl-type intermediates resulting from the hydrogenation of *o*- or *p*-alkoxyaniline.[13]

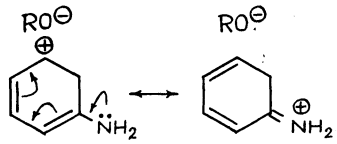

This work was supported by the Mitsubishi Chemical Industries Co., Ltd., to which our thanks are due.

TABLE 2. HYDROGENATION OF METHOXY- AND ETHOXYANILINE WITH RUTHENIUM CATALYST[a]

RO in RO-$C_6H_4NH_2$	Reac. temp. (°C)	Reac. time (hr)	Mol% composition of products[b]				Alkoxycyclohexylamine			Relative rate of formation of cyclohexylamine
			I	II	III	IV	Yield by dist. (%)	Bp (°C/mmHg)	n_D^{25}	
o-CH_3O	80	6.3	83.3	12.7	1.3	2.7				0.739
o-CH_3O	90	2.5	89.2	10.6	0.2	0.0	81.1	67.5—68.5/18	1.4599	
m-CH_3O	80	2.3	86.4	13.6	0.0	0.0	80.9	81—82.5/21	1.4620	1.58
p-CH_3O	80	1.5	93.9	6.1	0.0	0.0	84.8	75—76.2/18.5	1.4630	0.724
o-C_2H_5O	80	1.5	93.1	6.9	0.0	0.0	82.3	78.5—79.5/23	1.4531	1.00
m-C_2H_5O	80	1.3	90.4	8.9	0.7	0.0	81.2	87.5—89.4/24	1.4585	1.13
p-C_2H_5O	80	1.4	95.6	4.4	0.0	0.0	84.7	83—86.5/20	1.4597	0.616

a) Methoxy- or ethoxyaniline (0.1 mol) was hydrogenated in 30 ml of anhydrous *t*-butyl alcohol under 80—100 kg/cm² in the presence of 0.2 g of ruthenium hydroxide and 0.02 g of $LiOH \cdot H_2O$.

b) I: Alkoxycyclohexylamine. II: Cyclohexylamine. III: Secondary products. IV: Alkoxyaniline

10) Although hydrogenolysis occurred more extensively with the ruthenium catalyst than with rhodium oxide catalyst (see Ref. 1), use of the ruthenium catalyst will be advantageous in hydrogenations at a larger ratio of substrate to catalyst because of lesser decrease in the rate during hydrogenation.

11) More extensive hydrogenolysis in meta isomer than in ortho or para isomer has been observed, *e. g.*, in hydrogenation of isomeric dimethoxybenzenes with platinum metal catalysts (Y. Takagi and S. Nishimura, unpublished results). *Cf.* also H. A. Smith and R. G. Thompson, "Advances in Catalysis," Vol. 9, p. 727 (1957).

12) M. Freifelder, Y. H. Ng and P. F. Helgren, *J. Org. Chem.*, **30**, 2485 (1965).

13) *p*-Methoxyaniline was reported to hydrogenolyze to a much greater extent than the meta isomer in hydrogenation with rhodium-on-alumina in the presence of one equivalent of acetic acid.[12] This fact may support the explanation suggested above, but similar results were also obtained in ethanol with ethoxy- and propoxyanilines. For further discussion, a detailed study will be necessary.

BULLETIN OF THE CHEMICAL SOCIETY OF JAPAN VOL. 42 502—505 (1969)

Synthesis of 1- and 2-Piperidinophenazine Derivatives

Hideo ENDO and Masao TADA

The Research Institute for Tuberculosis, Leprosy and Cancer, Tohoku University, Kitayoban-cho, Sendai

and Ken KATAGIRI

Shionogi Research Laboratory, Shionogi & Co., Ltd., Fukushima-ku, Osaka

(Received June 19, 1968)

A number of new piperidinophenazines have been prepared by the reactions of various halogenophenazines and their oxides, including several new compounds, with piperidine. The halogen-activating effect of the oxide groups in 1- or 2-halogenophenazine oxides, which had previously been known, was also observed in the present piperidination. It has been found that 1-chlorophenazine was considerably less reactive than 2-chlorophenazine in the piperidination, that but the 5-oxide group in 1-chlorophenazine-5-oxide enhanced the reactivity of chlorine.

As a part of our general scheme for the synthetic study of phenazine derivatives and the investigation of their biological activities,[1,2] we have carried out the synthesis of 1- and 2-piperidinophenazine derivatives from halogenophenazines. In the present paper, we shall describe our results in full detail.

Landquist reported that the reaction of 2-chlorophenazine-5,10-dioxide (I) with boiling piperidine gave 2-piperidinophenazine-5,10-dioxide (II) and 2-piperidinophenazine-mono-*N*-oxide as dark red crystals (mp 159°C).[3] Investigating this reaction further, we found that the reaction of I with piperidine under the same conditions yielded II and two piperidinophenazine-mono-*N*-oxides: reddish violet crystals (III) (mp 128°C) and reddish orange crystals (IV) (mp 167°C). In an attempt to decide the position of the *N*-oxide group in III and IV, 2-chlorophenazine-5-oxide (V)[4] and 3-chlorophenazine-5-oxide (VI)[4] were treated with boiling piperidine for 8 hr to give III in a 31% yield and IV in a 43% yield respectively. IV was also obtained in a 41% yield from 3-bromophenazine-5-oxide (VII)[5] under the same conditions. II, III, and IV were heated with zinc powder in acetic acid to yield piperidinophenazine (VIII), which was also derived in a 29% yield from 2-chlorophenazine (IX)[4] by treatment with boiling piperidine for 50 hr. VIII was also obtained in a 31% yield from 2-bromophenazine (X).[5] VIII was heated with diluted sulfuric acid at 200°C for 8 hr in a sealed tube to form 2-hydroxyphenazine (XI), which has already been described by Vivian.[6] From these experiments, it is clear that the structures of III and IV are 2-piperidinophenazine-5-oxide and 3-piperidinophenazine-5-oxide respectively.

The treatment of 2-chloro-9-methylphenazine (XII)[7] with piperidine in the presence of cuprous chloride for 50 hr gave 9-methyl-2-piperidinophenazine (XIII). 2-Chloro-9-methylphenazine-5-oxide (XIV) was prepared by the Wohl-Aue reaction of *p*-chloronitrobenzene with *o*-toluidine or by the oxidation of XII with hydrogen peroxide in acetic acid, and was then submitted to piperidination, thus forming 9-methyl-2-piperidinophenazine-5-oxide (XV). XV was reduced with zinc powder in acetic acid to afford XIII. The same treatment of 2-chloro-7-methoxyphenazine (XVI)[8] and 2-chloro-9-methoxyphenazine (XVII)[9] with piperidine for 50 hr in the presence of cuprous chloride afforded 7-methoxy-2-piperidinophenazine (XVIII) and 9-methoxy-2-piperidinophenazine (XIX) respectively. 2-Chloro-7-methoxyphenazine-5-oxide (XX)[4] was treated with piperidine for 25 hr to give a mixture of XVIII and 7-methoxy-

1) H. Endo, M. Tada and K. Katagiri, *Sci. Rep. Res. Inst. Tohoku Univ. Ser. C*, **12**, 53 (1965); *ibid.*, **13**, 12 (1966); *ibid.*, **13**, 197 (1966).

2) K. Katagiri *et al.*, *Ann. Rept. Shionogi Res. Lab.*, **15**, 84 (1965); *ibid.*, **16**, 52 (1966); *ibid.*, **16**, 58 (1966); *ibid.*, **17**, 127 (1967); *ibid.*, **17**, 133 (1967); *ibid.*, **17**, 137 (1967).

3) J. K. Landquist, *J. Chem. Soc.*, **1956**, 2550.

4) I. J. Pachter and M. C. Kloetzel, *J. Am. Chem. Soc.*, **74**, 971 (1952).

5) V. P. Chernetskii and A. I. Kiprianov, *Zh. Obshch. Khim.*, **26**, 3032 (1956); through *Chem. Abstr.*, **51**, 8762 (1957).

6) D. L. Vivian, *J. Am. Chem. Soc.*, **73**, 457 (1951).

7) S. Maffei, S. Pietra and A. M. Rivolta, *Ann. chim. (Rome)*, **43**, 611 (1953).

8) D. L. Vivian, G. Y. Greenberg and J. L. Hartwell, *J. Org. Chem.*, **16**, 1 (1951).

9) I. Yoshioka and R. Ashikawa, *Yakugaku Zasshi*, **79**, 896 (1959).

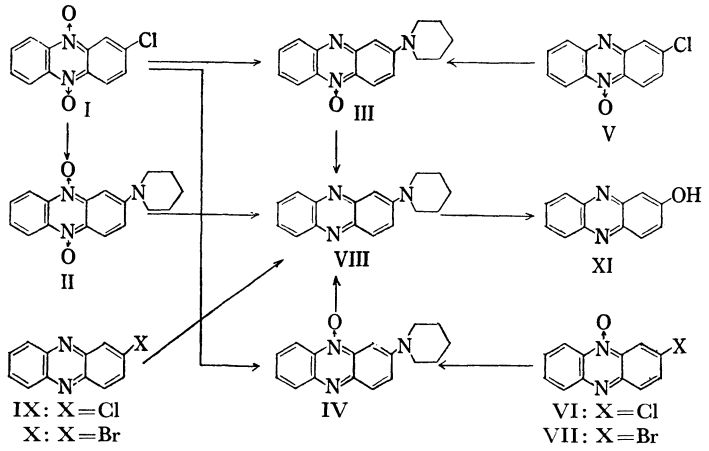

2-piperidinophenazine-5-oxide (XXI). By reduction, XXI was converted into XVIII. The piperidination of 2-chloro-9-methoxyphenazine-5-oxide (XXII), which had been derived from XVII by the oxidation, afforded a mixture of XIX and its *N*-oxide derivative (XXIII). XIX was also obtained from XXIII by reduction.

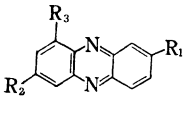

XII: R_1=Cl; R_2=H; R_3=CH_3

XIII: R_1=N⟨⟩; R_2=H; R_3=CH_3

XVI: R_1=Cl; R_2=OCH_3; R_3=H

XVII: R_1=Cl; R_2=H; R_3=OCH_3

XVIII: R_1=N⟨⟩; R_2=OCH_3; R_3=H

XIX: R_1=N⟨⟩; R_2=H; R_3=OCH_3

XXIV: R_1=R_2=H; R_3=Cl

XXV: R_1=R_2=H; R_3=N⟨⟩

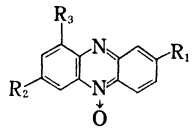

XIV: R_1=Cl; R_2=H; R_3=CH_3

XV: R_1=N⟨⟩; R_2=H; R_3=CH_3

XX: R_1=Cl; R_2=OCH_3; R_3=H

XXI: R_1=N⟨⟩; R_2=OCH_3; R_3=H

XXII: R_1=Cl; R_2=H; R_3=OCH_3

XXIII: R_1=N⟨⟩; R_2=H; R_3=OCH_3

XXVI: R_1=R_2=H; R_3=Cl

XXVII: R_1=R_2=H; R_3=N⟨⟩

The treatment of 1-chlorophenazine (XXIV)[4] with piperidine in the presence of cuprous chloride or cupric chloride for 70 hr gave 1-piperidinophenazine (XXV) in an 8% yield. Thus, although the 1-chloro compound (XXIV) is considerably less reactive to nucleophilic attack than the 2-chloro isomer (IX), it has been found that, in the corresponding 5-oxide (XXVI),[4] the reaction proceeded much more easily. Namely, XXVI was treated with piperidine for 25 hr to give both a 3% yield of XXV and a 28% yield of 1-piperidinophenazine-5-oxide (XXVII), which was then reduced with zinc powder in acetic acid to form XXV.

The halogen-activating effect of the oxide groups in halogenophenazine oxides has already been reported by Pachter and Kloetzel[4] and by Vivian[6] in the case of alcoholysis and hydrolysis. The present experiments reveal that halogens in halogenophenazine oxides, I, V, VI, VII, XIV, XX, XXII, and XXVI, are replaced with piperidine more readily than those of the corresponding phenazines.

We shall report elsewhere on the growth-inhibitory activity of the compounds described above against Crocker Sarcoma 180.[10]

Experimental[11]

The Reaction of 2-Chlorophenazine-5,10-dioxide (I) and Piperidine. A mixture of I (3.0 g) and piperidine (30 m*l*) was submitted to the reaction conditions employed by Landquist[3]: when the mixture was refluxed for 1.5 hr, 2-piperidinophenazine-5,10-dioxide (II) (mp 173—174°C; 1.25 g) was obtained as violet-black needles (from a mixture of benzene and petroleum ether). From the benzene-petroleum ether mother liquor, red crystals (1.0 g) were obtained after the evaporation of the solvent. The crystals were dissolved in benzene, and the solution was then passed through a column of alumina and eluted with benzene. From the first effluent, a mixture of 2- (V) and 3-chlorophenazine-5-oxide (VI) (0.2 g) was obtained. The column was then further eluted with chloroform, yielding crude crystals. Recrystallization from a mixture of benzene and ligroin gave 3-piperidinophenazine-5-oxide (IV) (mp 166—167°C; 210 mg) as reddish-orange needles.

Found: C, 73.37; H, 6.04; N, 14.91%. Calcd for

10) H. Endo, M. Tada and K. Katagiri, *Sci. Rep. Res. Inst. Tohoku Univ. Ser. C*, to be published.

11) All melting points are uncorrected.

$C_{17}H_{17}N_3O$: C, 73.09; H, 6.13; N, 15.04%.

The mother liquor was evaporated to dryness, and the residue was recrystallized from diluted methanol to yield 2-piperidinophenazine-5-oxide (III) (mp 127—128°C; 200 mg) as reddish-violet needles.

Found: C, 73.29; H, 6.05; N, 14.90%. Calcd for $C_{17}H_{17}N_3O$: C, 73.09; H, 6.13; N, 15.04%.

2-Piperidinophenazine-5-oxide (III). A mixture of V (1.5 g) and piperidine (15 ml) was refluxed for 8 hr. After the addition of water (0.5 l) and acetic acid (8 ml), the resulting precipitate was filtered, washed with water, dried, and dissolved in chloroform. The chloroform solution was then passed through a column of alumina and eluted with chloroform. From the first effluent, V (0.4 g) was recovered, while from the second effluent III (560 mg) was obtained.

3-Piperidinophenazine-5-oxide (IV). *a) From VI.* A mixture of VI (1.5 g) and piperidine (15 ml) was refluxed for 8 hr; the reaction mixture was then treated as in the case of III to give IV (780 mg).

b) From VII. A mixture of VII (500 mg) and piperidine (5 ml) was refluxed for 8 hr; then the reaction mixture was treated as in the case of III to yield IV (210 mg).

2-Piperidinophenazine (VIII). *a) From IX.* A solution of IX (1.5 g) in piperidine (15 ml) was refluxed for 50 hr and then poured into water (0.5 l). The crystals thereby separated were dissolved in chloroform. The solution was passed through a column of alumina and eluted with chloroform. From the effluent, orange crystals were obtained; they were recrystallized from methanol to yield VIII (mp 129—130°C; 540 mg) as orange needles.

Found: C, 77.38; H, 6.59; N, 15.98%. Calcd for $C_{17}H_{17}N_3$: C, 77.53; H, 6.51; N, 15.96%.

b) From X. A solution of X (0.5 g) in piperidine (5 ml) was treated as in the case of a) above to afford VIII (160 mg).

c) From II. To a solution of II (200 mg) in acetic acid (10 ml), zinc powder (0.4 g) was added in small portions. The reaction mixture was then warmed on a water bath for 30 min and filtered. The filtrate was diluted with water and made slightly alkaline with diluted ammonium hydroxide. The crystals precipitated were collected, washed with water, dried, and dissolved in chloroform. The solution was passed through a column of alumina and eluted with chloroform. From the effluent, VIII (90 mg) was obtained.

d) From III or IV. To a solution of III or IV (200 mg) in acetic acid (10 ml), zinc powder (0.5 g) was added. The mixture was treated as in the case of the reduction mentioned above to give VIII (100 mg).

2-Hydroxyphenazine (XI). A solution of VIII (200 mg) in 20% sulfuric acid (3 ml) was heated at 200°C for 8 hr in a sealed tube. After cooling, the reaction mixture was diluted with water, made slightly alkaline with diluted sodium hydroxide, and filtered by suction. The filtrate was acidified weakly with diluted acetic acid. The crystals thereby yielded were recrystallized from diluted ethanol to yield red needles (mp 248—250°C (decomp.); 70 mg), which were identified as XI[6] by a comparison of their infrared spectra.

9-Methyl-2-piperidinophenazine (XIII). *a) From XII. i)* A mixture of XII (1.4 g), piperidine (15 ml), and cuprous chloride (0.1 g) was refluxed for 50 hr and then poured into water (1 l). The crystals thereby formed were collected by filtration, washed with water, dried, and dissolved in benzene. The benzene solution was passed through a column of alumina and eluted with benzene. From the effluent, XII (0.5 g) was recovered. When the column was further eluted with chloroform, dark red crystals were obtained. Recrystallization from a mixture of cyclohexane and petroleum ether afforded XIII (mp 76—77°C; 190 mg) as fine, reddish-orange crystals.

Found: C, 77.95; H, 6.95; N, 15.32%. Calcd for $C_{18}H_{19}N_3$: C, 77.94; H, 6.91; N, 15.15%.

ii) A mixture of XII (1.4 g) and piperidine (15 ml) was treated as in the case of i) to give XIII (140 mg). XII (0.8 g) was also recovered.

b) From XV. To a solution of XV (200 mg) in acetic acid (6 ml), zinc powder (0.5 g) was added in small portions. The resulting mixture was treated as in the procedure c) used in the preparation of VIII to afford XIII (50 mg).

2-Chloro-9-methylphenazine-5-oxide (XIV). *a) By the Wohl-Aue Reaction.* To a solution of *p*-nitrochlorobenzene (45 g) and *o*-toluidine (25 g) in toluene (300 ml), powdered potassium hydroxide (60 g) was added, and the resulting mixture was refluxed gently for 5 hr. The toluene solution was filtered while hot and then steam-distilled. The crude product deposited in the remaining aqueous solution was collected, washed with water, dried, and dissolved in chloroform. The solution was then passed through a column of alumina and eluted with chloroform. From the effluent, crystals were obtained. These were recrystallized from benzene to afford XIV (mp 173—174°C; 5 g) as bright yellow needles.

Found: C, 63.59; H, 3.70; N, 11.40%. Calcd for $C_{13}H_9ClN_2O$: C, 63.81; H, 3.71; N, 11.45%.

A mixture of XIV (1 g) and zinc powder (1 g) in acetic acid (20 ml) was treated as in the case of the procedure c) used in the preparation of VIII to give crude crystals. Recrystallization from a mixture of benzene and ethanol afforded yellow needles (mp 152—153°C; 750 mg), which showed no depression of melting point upon admixture with XII.[7] The infrared spectrum was identical with that of XII.

b) By Oxidation. To a solution of XII (1 g) in acetic acid (50 ml), 30% hydrogen peroxide (5 ml) was added. The reaction mixture was warmed at 55°C for 3 hr and then poured into water (1 l). The crystals thus formed were collected by filtration and recrystallized from benzene to give XIV (850 mg).

9-Methyl-2-piperidinophenazine-5-oxide (XV). A mixture of XIV (2 g) and piperidine (10 ml) was refluxed for 16 hr and then poured into water (300 ml) and acetic acid (5 ml). The crystals thereby separated were collected, washed with water, and dried. The product was dissolved in benzene, and the solution was passed through a column of alumina and eluted with benzene. From the first effluent, XII (320 mg) was obtained, while XIV (620 mg) was recovered from the second effluent. When the column was then further eluted with chloroform, dark violet crystals were obtained from the effluent. The recrystallization of these from a mixture of benzene and methanol gave XV (mp 165—166°C; 750 mg) as reddish-violet needles.

Found: C, 73.54; H, 6.63; N, 14.03%. Calcd for $C_{18}H_{19}N_3O$: C, 73.69; H, 6.53; N, 14.33%.

7-Methoxy-2-piperidinophenazine (XVIII). *a)* A

mixture of XVI (1.5 g), piperidine (15 m*l*), and cuprous chloride (0.1 g) was refluxed for 50 hr and then treated as in the case of XV to give XVIII (mp 146—147°C; 160 mg) as bright reddish-orange needles (from a mixture of cyclohexane and benzene); XVI (0.9 g) was also recovered.

Found: C, 73.78; H, 6.45; N, 14.31%. Calcd for $C_{18}H_{19}N_3O$: C, 73.69; H, 6.53; N, 14.33%.

b) A mixture of XVI (1.5 g) and piperidine (15 m*l*) was refluxed for 100 hr; the resulting mixture gave XVIII (200 mg). XVI (1.1 g) was also recovered.

9-Methoxy-2-piperidinophenazine (XIX). A mixture of XVII (1.5 g), piperidine (15 m*l*), and cuprous chloride (0.2 g) was refluxed for 50 hr and then treated as in the case of XV to give dark orange crystals. Recrystallization from diluted methanol yielded XIX (mp 124—125°C; 310 mg) as deep reddish-orange needles. XVII (120 mg) was also recovered.

Found: C, 73.55; H, 6.38; N, 14.06%. Calcd for $C_{18}H_{19}N_3O$: C, 73.69; H, 6.53; N, 14.33%.

7-Methoxy-2-piperidinophenazine-5-oxide (XXI). *a*) A mixture of XX (1.5 g) and piperidine (15 m*l*) was refluxed for 25 hr and then poured into water (1 *l*). After the usual work-up, the crystals obtained were dissolved in benzene. The solution was passed through a column of alumina and eluted with benzene. From the first effluent, XVI (0.7 g) was obtained. XX (200 mg) was recovered from the second effluent. When the column was further eluted with chloroform, XVIII (55 mg) and dark red crystals were obtained. The recrystallization of the crystals from diluted methanol afforded XXI (mp 171—172°C; 150 mg) as fine, red crystals.

Found: C, 69.59; H, 6.14; N, 13.87%. Calcd for $C_{18}H_{19}N_3O_2$: C, 69.88; H, 6.19; N, 13.58%.

b) A mixture of XX (1.5 g) and piperidine (15 m*l*) was refluxed for 16 hr and then treated as in the case of a) above to give XVI (400 mg), XX (350 mg), and XXI (100 mg).

To a solution of XXI (200 mg) in acetic acid (10 m*l*), zinc powder (0.5 g) was added; the mixture was then treated as in the case of the procedure c) used in the preparation of VIII to afford XVIII (110 mg).

2-Chloro-9-methoxyphenazine-5-oxide (XXII). To a solution of XVII (1.4 g) in acetic acid (50 m*l*), 30% hydrogen peroxide (10 m*l*) was added. The resulting solution was warmed at 55°C for 3 hr and then poured into water (2 *l*). The deep yellow crystals which separated were collected and washed with water. The recrystallization of the crystals from a mixture of benzene and ligroin gave XXII (mp 217—218°C (decomp.); 1.2 g) as orange-yellow needles.

Found: C, 60.02; H, 3.49; N, 10.49%. Calcd for $C_{13}H_9ClN_2O_2$: C, 59.90; H, 3.48; N, 10.75%.

XXII was treated with zinc powder in acetic acid to give XVII.

9-Methoxy-2-piperidinophenazine-5-oxide (XXIII). A mixture of XXII (1.5 g) and piperidine (15 m*l*) was refluxed for 24 hr and then treated as in the case of the procedure a) used in the preparation of XXI to give XVII (450 mg), XIX (500 mg), and dark violet crystals. The crystals were recrystallized from diluted methanol to yield XXIII (mp 153—154°C; 250 mg) as deep reddish-violet micro-prisms.

Found: C, 69.73; H, 6.24; N, 13.26%. Calcd for $C_{18}H_{19}N_3O_2$: C, 69.88; H, 6.19; N, 13.58%.

To a solution of XXIII (100 mg) in acetic acid (5 m*l*), zinc powder (0.3 g) was added; the mixture was then treated as in the case of the procedure c) used in the preparation of VIII to afford XIX (50 mg).

1-Piperidinophenazine (XXV). *a*) To a solution of XXIV (1.5 g) in piperidine (15 m*l*), cuprous chloride or cupric chloride (0.2 g) was added. The mixture was refluxed for 70 hr and then poured into water (1 *l*). The resulting precipitate was washed with water, dried, and dissolved in benzene. The benzene solution was passed through a column of alumina and eluted with benzene. From the first effluent, XXIV (500 mg) was recovered, while crude crystals were obtained from the second effluent. Recrystallization from a mixture of cyclohexane and petroleum ether gave XXV (mp 130—131°C; 150 mg) as orange-red needles.

Found: C, 77.25; H, 6.60; N, 15.70%. Calcd for $C_{17}H_{17}N_3$: C, 77.53; H, 6.51; N, 15.96%.

b) A solution of XXIV (1.5 g) in piperidine (15 m*l*) was refluxed for 60 hr and then treated as in a) above to give XXV (50 mg). XXIV (0.9 g) was also recovered.

1-Piperidinophenazine-5-oxide (XXVII). *a*) A mixture of XXVI (1.5 g) and piperidine (15 m*l*) was refluxed for 25 hr and then treated as in the case of XXV to give XXIV (60 mg), XXV (50 mg), XXVI (50 mg), and dark red crystals (500 mg). The crystals were recrystallized from cyclohexane to afford XXVII (mp 161—162°C) as fine, reddish-violet needles.

Found: C, 72.98; H, 6.18; N, 14.90%. Calcd for $C_{17}H_{17}N_3O$: C, 73.09; H, 6.13; N, 15.04%.

b) A mixture of XXVI (1.0 g) and piperidine (10 m*l*) was refluxed for 10 hr and then treated as in the case of a) above to afford XXIV (50 mg), XXVI (650 mg), and XXVII (120 mg).

To a solution of XXVII (100 mg) in acetic acid (5 m*l*), zinc powder (0.3 g) was added; the mixture was then treated as in the case of the procedure c) used in the preparation of VIII to give XXV (25 mg).

BULLETIN OF THE CHEMICAL SOCIETY OF JAPAN VOL. 42 506—507 (1969)

Synthesis of 1- and 2-Morpholinophenazine Derivatives

Hideo Endo and Masao Tada

The Research Institute for Tuberculosis, Leprosy and Cancer, Tohoku University, Kitayoban-cho, Sendai

and Ken Katagiri

Shionogi Research Laboratory, Shionogi & Co., Ltd., Fukushima-ku, Osaka

(Received June 19, 1968)

A number of new morpholinophenazines have been prepared by the reactions of various halogenophenazine derivatives with morpholine. It has been found that the replacement of the halogen atom of halogenophenazine-*N*-oxides with morpholine is accompanied by the removal of the oxide group and that no morpholinophenazine-*N*-oxides are formed in these reactions.

In a previous paper,[1] the reactions of halogenophenazine derivatives with piperidine were reported. The present paper will describe the synthesis of morpholinophenazines.

The reaction of morpholine with 1-chlorophenazine (I) in the presence of cuprous chloride or cupric chloride gave a 17% yield of 1-morpholinophenazine (II), which was also obtained from 1-chlorophenazine-5-oxide (III). The treatment of 2-chlorophenazine (IV) with morpholine gave a 59% yield of 2-morpholinophenazine (V), which was also derived from 2-bromophenazine (VI). Either 2-chlorophenazine-5-oxide (VII) or 3-chlorophenazine-5-oxide (VIII) was treated with morpholine to give V, which was also obtained from 3-bromophenazine-5-oxide (IX) or 2-chlorophenazine-5,10-dioxide (X). V was refluxed with diluted sulfuric acid or heated with diluted sulfuric acid at 200°C in a sealed tube to yield 2-hydroxyphenazine (XI), which had been reported by Vivian.[2]

The above series of reactions reveals that the replacement of the halogen atom with morpholine in halogenophenazine-*N*-oxides is accompanied by

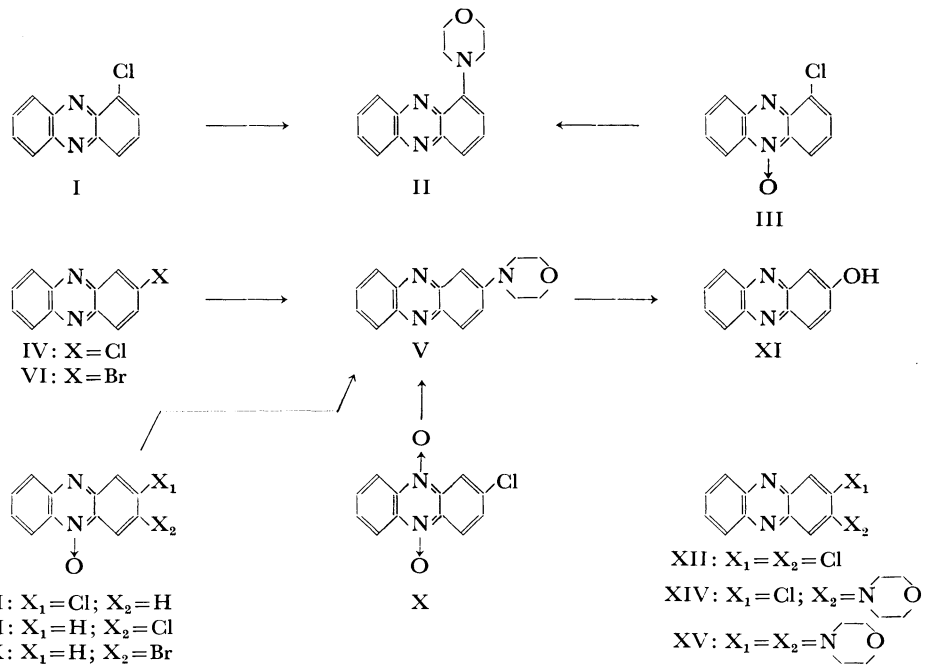

1) H. Endo, M. Tada and K. Katagiri. This Bulletin, **42**, 502 (1969).

2) D. L. Vivian, *J. Am. Chem. Soc.*, **73**, 457 (1951).

the removal of the oxide group in these phenazine-*N*-oxides, as was found during substitution with piperidine by Landquist[3] and by us.[1] However, the present finding, that no *N*-oxides are produced, is in contrast with the corresponding reaction with piperidine.[1]

The reaction of 2,3-dichlorophenazine (XII)[4] or 2,3-dichlorophenazine-5-oxide (XIII)[4] with morpholine afforded both 2-chloro-3-morpholinophenazine (XIV) in a 44% yield and 2,3-dimorpholinophenazine (XV) in a 3% yield. XV was also obtained from XIV. Brackman *et al.* have reported that the reaction of 4,5-dimorpholino-*o*-benzoquinone with *o*-phenylenediamine gave XV.[5] The treatment of 2-chloro-9-methylphenazine (XVI) or 2-chloro-9-methylphenazine-5-oxide (XVII) with morpholine gave 9-methyl-2-morpholinophenazine (XVIII).

The growth-inhibitory activity of these reaction products against Crocker Sarcoma 180 will be reported on elsewhere.[6]

Experimental[7]

1-Morpholinophenazine (II). *a) From 1-Chlorophenazine (I).* A mixture of I (1.5 g) and cuprous chloride or cupric chloride (0.1 g) in morpholine (15 m*l*) was refluxed for 50 hr and then poured into water (300 m*l*). After the addition of acetic acid (8 m*l*), the resulting precipitate was collected, washed with water, sucked dry, and dissolved in benzene. The benzene solution was then passed through a column of alumina and eluted with benzene. From the effluent, I (0.95 g) was recovered. When the column was then further eluted with chloroform, dark orange crystals were obtained. Recrystallization from cyclohexane gave II (mp 165—166°C; 320 mg) as reddish-orange needles.

Found: C, 72.11; H, 5.74; N, 15.73%. Calcd for $C_{16}H_{15}N_3O$: C, 72.43; H, 5.70; N, 15.84%.

b) From 1-Chlorophenazine-5-oxide (III). A solution of III (1.5 g) in morpholine (15 m*l*) was refluxed for 24 hr and then treated as in the case of a) to give both I (1.1 g) and II (100 mg).

2-Morpholinophenazine (V) *a) From 2-Chlorophenazine (IV).* A solution of IV (1.5 g) in morpholine (15 m*l*) was refluxed for 70 hr and then treated as in the case of the procedure a) used in the preparation of II to give dark orange crystals (1.1 g). Recrystallization from benzene afforded V (mp 172—173°C) as yellowish orange needles. IV (0.1 g) was also recovered.

Found: C, 72.22; H, 5.68; N, 16.04%. Calcd for $C_{16}H_{15}N_3O$: C, 72.43; H, 5.70; N, 15.84%.

b) From 2-Bromophenazine (VI). A solution of VI (150 mg) in morpholine (5 m*l*) was refluxed for 50 hr and then treated as in the case of the a) used in the preparation of II to give V (80 mg). VI (20 mg) was also recovered.

c) From 2-Chlorophenazine-5-oxide (VII). A mixture of VII (1.5 g) and morpholine (15 m*l*) was refluxed for 12 hr and then treated as in the case of the a) used in the preparation of II to give both IV (600 mg) and V (450 mg).

d) From 5-Chlorophenazine-5-oxide (VIII). A mixture of VIII (1.5 g) and morpholine (15 m*l*) was refluxed for 12 hr and then treated as in the case of the a) used in the preparation of II to give both IV (150 mg) and V (500 mg).

e) From 3-Bromophenazine-5-oxide (IX). A mixture of IX (150 mg) and morpholine (5 m*l*) was refluxed for 12 hr and then treated as in the case of the a) used in the preparation of II to give V (40 mg).

f) From 2-Chlorophenazine-5,10-dioxide (X). *i)* A mixture of X (1.5 g) and morpholine (15 m*l*) was refluxed for 3 hr and then treated as in the case of the a) used in the preparation of II to give crude crystals (1.1 g), which contained IV (850 mg), V(20 mg), and a mixture (15 mg) of VII and VIII.

ii) A mixture of X (1.5 g) and morpholine (15 m*l*) was refluxed for 12 hr and then treated as in the case of the a) used in the preparation of II to give IV (530 mg) and V (580 mg).

The Reaction of 2,3-Dichlorophenazine (XII) or 2,3-Dichlorophenazine-5-oxide (XIII) with Morpholine. A mixture of XII or XIII (1.5 g), morpholine (15 m*l*), and cupric chloride (0.2 g) was refluxed for 70 hr and then poured into water (1.5 *l*). The crystals thereby separated were collected, washed with water, sucked dry, and dissolved in benzene. The solution was passed through a column of alumina and eluted with benzene. From the first effluent, yellow crystals were obtained. Recrystallization from ethanol gave 2-chloro-3-morpholinophenazine (XIV) (mp 131—132°C; 800 mg) as bright yellow needles.

Found: C, 64.08; H, 4.69; N, 13.87%. Calcd for $C_{16}H_{14}ClN_3O$: C, 64.11; H, 4.71; N, 14.02%.

From the second effluent, dark orange crystals (60mg) were obtained; they were recrystallized from ethanol to form yellow needles (mp 218—219°C; 35 mg), which showed no depression of melting point on admixture with 2,3-dimorpholinophenazine (XV).[5] The infrared spectrum was identical with that of XV. By refluxing XIV (100 mg) in morpholine (5 m*l*) for 70 hr, XV (10 mg) was also obtained.

9-Methyl-2-morpholinophenazine (XVIII). *a) From XVI.* A mixture of XVI (1.5 g), morpholine (15 m*l*), and cupric chloride (0.2 g) was refluxed for 70 hr and then treated as in the case of the a) used in the preparation of II to give orange crystals. Recrystallization from a mixture of benzene and cyclohexane afforded XVIII (mp 185—186°C; 650 mg) as brilliant yellowish-orange needles. XVI (250 mg) was also recovered.

Found: C, 73.00; H, 6.05; N, 15.01%. Calcd for $C_{17}H_{17}N_3O$: C, 73.09; H, 6.13; N, 15.04%.

b) From XVII. A mixture of XVII (1.5 g), morpholine (15 m*l*), and cupric chloride (0.2 g) was refluxed for 70 hr and then treated as in the case of the a) used in the preparation of II to give both XVI (110 mg) and XVIII (850 mg).

3) J. K. Landquist, *J. Chem. Soc.*, **1956**, 2550.

4) V. P. Chernetskii and A. I. Kiprianov, *Zh. Obshch. Khim.*, **23**, 1743 (1953); through *Chem. Abstr.* **48**, 13695 (1954).

5) W. Brackman and E. Havinga, *Rec. Trav. Chim.*, **74**, 937 (1955).

6) H. Endo, M. Tada and K. Katagiri, *Sci. Rep. Res. Inst. Tohoku Univ. Ser. C,* to be published.

7) All melting points are uncorrected.

BULLETIN OF THE CHEMICAL SOCIETY OF JAPAN VOL. 42 508—512 (1969)

Syntheses and Reactions of Functional Polymers. XL. Enhanced Reactivity of Poly(vinyl chloride) by Neighboring-Group Participation of the *N*,*N*-Disubstituted Dithiocarbamate Function*1

Takeshi NAKAI, Hideo KAWAOKA*2 and Makoto OKAWARA

Research Laboratory of Resources Utilization, Tokyo Institute of Technology, Ookayama, Meguro-ku, Tokyo

(Received June 27, 1968)

In order to demonstrate that neighboring-group participation of the *N*,*N*-disubstituted dithiocarbamate function is involved in the substitution reaction of poly (vinyl chloride) (PVC) with the dithiocarbamate anion, the rates of reactions of PVC and the copolymer (vinyl chloride-*S*-vinyl *N*,*N*-diethyldithiocarbamate) with $^{-}$SCS-NEt$_2$ were compared under the same conditions. These polymer reactions were undertaken in dimethylformamide or tetrahydrofuran at 45°C. The rate enhancements with the copolymer were observed in both solvents. From these observations, it was concluded that the chloromethylene groups in PVC neighboring the dithiocarbamate function were activated toward the nucleophile *via* neighboring-group participation. This is the first time that neighboring-group participation involving the polymer main chain might be observed in the polymer reaction. The difference in reaction mechanism between the polymer reaction and the model reaction was discussed.

It is well-known that poly(vinyl chloride) (PVC) is more unsusceptible to nucleophilic substitution (S_N) reactions and more readily eliminates hydrogen chloride, as compared with alkyl chlorides. For that reason, chemical modifications of PVC have been subjected to restriction.

During the course of our studies on preparations of photosensitive polymers containing the dithiocarbamate function by polymer reactions, it was found that PVC reacted readily with dithiocarbamate anions in dimethylformamide (DMF) at 40—50°C without elimination of hydrogen chloride.[1] The remarkable reactivity of PVC under mild conditions might be due to three factors: (i) the enhanced electrophilicity of PVC by the solvation with DMF,[2] (ii) the large nucleophilicity of the dithiocarbamate anion[3] and (iii) enhancement of the nucleophilicity by DMF.[4]

On the other hand, we have reported that neighboring-group participation of the *N*,*N*-disubstituted dithiocarbamate function is involved through the intermediacy of the isolatable anchimeric cation*3 in the reactions of 1,2-dichloroethane[5] and 1,3-dichloropropane (a model compound for PVC)[6] with the dithiocarmate anion, *e. g.*, as shown in Scheme 1.

The present work was undertaken in order to prove that neighboring-group participation of the

*1 Presented at the 17th Annual Meeting of the Society of Polymer Science of Japan, Tokyo, May, 1968.

*2 Present address: Sanshin Chem. Ind. Co., Yanaishi, Yamaguchi-ken.

1) a) M. Okawara, K. Morishita and E. Imoto, *Kogyo Kagaku Zasshi* (*J. Chem. Soc. Japan, Ind. Chem. Sect.*), **69**, 761 (1966); b) T. Nakagawa, Y. Taniguchi and M. Okawara, *ibid.*, **70**, 2382 (1967). For other types of photosensitive polymers containing the dithiocarbamate function, also see M. Okawara and co-workers, *ibid.*, **66**, 1383 (1963); **69**, 766 (1966).

2) S. Yoneda and co-workers [*ibid.*, **68**, 1074, 1077 (1965)] have reported that the electrophilicities of alkyl halides are enhanced by the complex formation with DMF.

3) Dithiocarbamate anions are ranked with the strongest nucleophiles in aqueous solutions: R. E. Davis, "Survey of Progress in Chemistry," Vol. 2, ed. by A. Scott, Academic Press Inc., New York, N. Y. (1964), p. 189; R. E. Davis, H. Nakshbendi and A. Ohno, *J. Org. Chem.*, **31**, 2702 (1966).

4) Rate enhancements of the S_N reactions in dipolar aprotic solvents such as DMF have been reported in many literatures. For reviews on this subject, see A. J. Parker, *Quart. Revs.*, **16**, 163 (1962); "Advances in Physical Organic Chemistry," Vol. 5, ed. by V. Gold, Academic Press Inc., New York, N. Y. (1967), p. 173.

*3 The word "anchimeric cation" stands for the cyclic carbonium ion formed *via* the intramolecular S_N reaction involving the neighboring group, such as 2-dimethylamino-1,3-dithian-2-ylium ion in Scheme 1.

5) T. Nakai, Y. Ueno and M. Okawara, *Tetrahedron Letters*, **1967**, 3831.

6) T. Nakai, Y. Ueno and M. Okawara, Abstracts of papers presented at the 18th Symposium on Organic Reaction Mechanisms, Kyoto, October, 1967, p. 77.

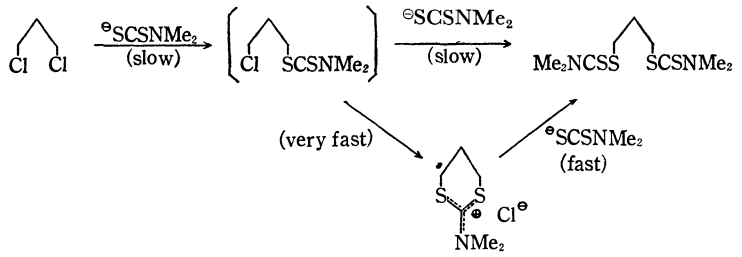

Scheme 1

dithiocarbamate function is certainly involved in the reaction of PVC with *N*,*N*-diethyldithiocarbamate anion ($^{-}$SN). Assuming that the concept of neighboring-group participation might be applied into the polymer reaction of PVC with $^{-}$SN, the reaction should proceed as shown in Scheme 2 to result in the formation of the polymer containing the block-type structure (I).

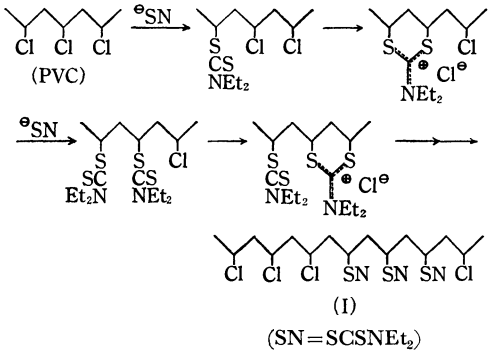

Scheme 2

On the other hand, the copolymer from vinyl chloride (VCl) and *S*-vinyl *N*,*N*-diethyldithiocarbamate (VSN) should be of the random structure as given by the formula (II).

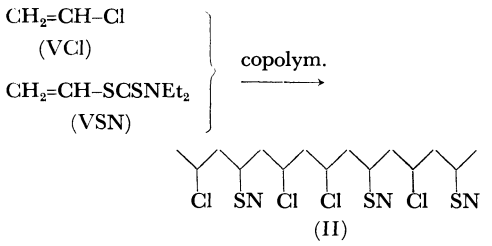

Consequently, it can be said that the polymer (II) apparently contains more chloromethylene (-CHCl-) groups neighboring the dithiocarbamate function than the polymer (I) does. Thus, in order to demonstrate that the neighboring group participates in the polymer reaction, we attempted to compare the rate of reaction of the polymer (I) and $^{-}$SN with that of the polymer (II) under the same reaction conditions.

Results

Reactions of PVC with Sodium *N*,*N*-Diethyldithiocarbamate (NaSN). Reactions of PVC with NaSN (initial molar ratio 2 : 1) were carried out in DMF or tetrahydrofuran (THF) at 45°C. The reaction was followed by the sulfur analysis of the resulting polymer precipitated after a given interval. The results obtained are shown in Table 1. As shown in Fig. 1, the reaction fitted in a

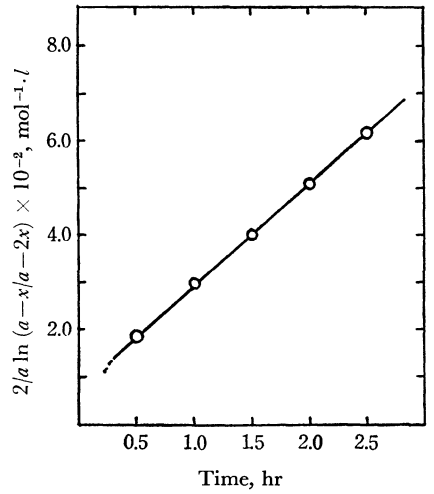

Fig. 1. Second-order rate plot for the reaction of PVC with NaSN in DMF at 45°C.

second-order rate equation (the rate constant= 2.78×10^{-6} mol$^{-1}\cdot l\cdot$sec^{-1}). It may be noted that the rate of reaction in DMF is much larger than that in THF. The fact indicates that the three factors described above have a serious influence on the rate of reaction.

Reactions of the Copolymer (VCl-VSN) with NaSN. *S*-Vinyl *N*,*N*-diethyldithiocarbamate (VSN) was prepared by the vacuum pyrolysis of ethylene bis(*N*,*N*-diethyldithiocarbamate).[7] The copolymerization of VCl with VSN was undertaken in bulk at 45°C using *a*,*a*'-azobisisobutyronitrile

7) T. Nakai, K. Shioya and M. Okawara, *Makromol. Chem.*, **108**, 95 (1967).

TABLE 1. REACTIONS OF PVC WITH NaSN

PVC ($\bar{P}$=400) 7.5 g (0.12 mol); NaSN 10.3 g (0.06 mol)
Solvent 170 ml; Reaction temp. 45±0.5°C

Solvent	Time hr	Resulting polymers	
		Sulfur content %*	Concn. of VSN, mol%
DMF	0.5	5.75	6.23
	1.0	8.23±0.02	9.37
	1.5	9.81±0.01	11.5
	2.0	11.21±0.02	13.6
	2.5	12.25±0.03	15.2
THF	1.5	0.73±0.04	0.721
	2.0	0.84±0.03	0.830
	2.5	1.02±0.04	1.01

* An average and a variation of values obtained by two analyses.

(AIBN) as an initiator. The reactivity ratio of these monomers, r_{VCl} and r_{VSN}, were tentatively calculated using the Q,e values obtained from the respective copolymerization with styrene (VCl

TABLE 2. COPOLYMERIZATION OF VCl WITH VSN

Polym. temp. 45±0.5°C; AIBN 0.130 g

VCl g	VSN g	Time hr	Conv. %	Copolymers	
				Sulfur content* %	Concn. of VSN mol%
11.50	0.54	50	32.3	2.28±0.01	2.25
11.70	0.86	33	22.3	4.44±0.03	4.70
12.69	1.15	48	21.1	5.79±0.00	6.40
12.64	1.58	72	28.1	6.06±0.03	6.65
11.96	1.61	72	30.7	6.46±0.01	7.10
11.31	1.74	33	19.8	9.40±0.02	10.3

* An average and a variation of values obtained by two analyses.

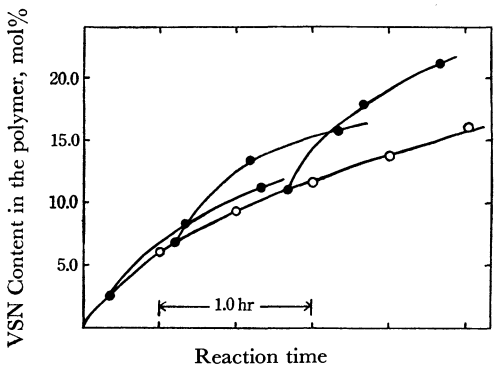

Fig. 2. Reactions of PVC and copolymers with NaSN in DMF.
○: PVC ●: Copolymer

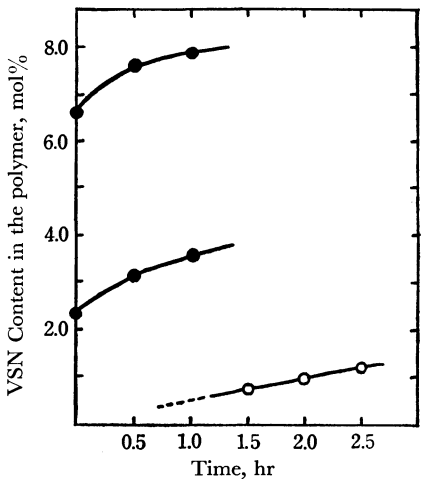

Fig. 3. Reactions of PVC and copolymers with NaSN in THF.
○; PVC ●; Copolymer

TABLE 3. REACTIONS OF COPOLYMERS WITH NaSN

Reaction temp. 45±0.5°C
Initial molar ratio; (VCl in the copolymer+added NaCl): (VSN in the copolymer+added NaSN) =2 : 1

Solvent	Reactant copolymer[a] Concn. of VSN mol%	Time hr	Resulting copolymer	
			Sulfur content %[b]	Concn. of VSN mol%
DMF	2.32	0.5	7.28±0.01	8.16
		1.0	9.34±0.03	10.9
	4.70	1.0	10.43±0.05	13.3
	6.65	0.5	10.42±0.01	13.3
		1.0	12.24±0.02	15.3
	11.0	0.5	13.95±0.03	17.4
		1.0	15.64±0.04	21.1
THF	2.32	0.5	3.05±0.01	3.15
		1.0	3.24±0.00	3.36
	6.65	0.5	6.99±0.02	7.79
		1.0	7.05±0.02	7.87

a) See Table 2
b) An average and a variation of values obtained by two analyses.

Q=0.044, e=+0.20[8]; VSN Q=0.45, e=−1.54[7]). The ratio r_{VCl} and r_{VSN} obtained were 0.069 and 1.426, respectively, indicating that VCl is less reactive than VSN. Thus, in order to prepare the random copolymer such as the formula (II), VSN was copolymerized with VCl from a low range of feed compositions. All copolymers were obtained in the form of solid. The experimental data are shown in Table 2. Concentrations of VSN

8) L. J. Young, *J. Polymer Sci.*, **54**, 411 (1961).

in the copolymers were evaluated by sulfur analyses.

Next, reactions of these copolymers with NaSN were undertaken in DMF or THF under the same conditions as the reaction of PVC described above. Then, in order to compare exactly reactivities of the copolymer and PVC containing the same amount of VSN as the copolymer, the same molar amount of sodium chloride as that of VSN in the copolymer was added to the reactant mixture and the initial molar ratio (VCl in the copolymer+added NaCl)/(VSN in the copolymer+added NaSN) was adjusted to two in all cases. The VSN content of the resulting copolymer precipitated after a given interval was evaluated by the sulfur determination. The results obtained are given in Table 3. The plots of the VSN content in the resulting copolymers against the time are shown in Figs. 2 and 3, together with data for the reaction of PVC as references.

Discussion

Figure 2 shows important facts: (i) the rate enhancement*4 with the copolymer was clearly observed as compared with PVC containing the same concentration of VSN as the copolymer and (ii) the rate enhancement with the copolymer increased with the concentration of VSN in the copolymer. These facts lead substantially to the reasonable conclusion that participation of the neighboring dithiocarbamate function is no doubt involved in these polymer reactions, that is, the chloromethylene groups neighboring the dithiocarbamate function are activated toward the dithiocarbamate anion, as described in Scheme 2. These facts also indicate that the polymer from PVC and $^{-}$SN contains considerably the block-type structure such as the formula (I). This is the first time that neighboring-group participation involving the polymer main chain might be observed in the polymer reaction. The neighboring-group effects in polymer reactions reported so far all involve the polymer side chains. This method for activating PVC may further provide a possibility of a variety of chemical modifications of PVC *via* the S_N reaction with other nucleophiles which resist reaction with PVC itself. We are studying the reaction of the copolymer(VCl-VSN) with other nucleophiles.

Contrany to expectation the solvent effect on the rate enhancement with the copolymer was not particularly predominant (compare Figs. 2 and 3). This finding is in direct contrast to the observation that in the reaction of 1,2-dichloroethane with *N*,*N*-dimethyldithiocarbamate anion, neighboring-group participation of the dithiocarbamate function in THF is about two hundred times as large as that in DMF.[5] Taking it into consideration that the large solvent effect was observed on the rate of reaction of PVC with $^{-}$SN, this fact indicates that the normal S_N2 reaction involving no neighboring-group participation simultaneously occurs in the polymer reactions and that, in contrast to reactions of 1,2-dichloroethane and 1,3-dichloropropane described above, the intramolecular cyclization involving the neighboring dithiocarbamate function is slow for the polymer reaction.

In short, these polymer reactions consist of both the normal S_N2 reaction (pathway a) and the intramolecular cyclization followed by the S_N reaction (pathway b) giving a random polymer and block-type polymer respectively, as shown below.

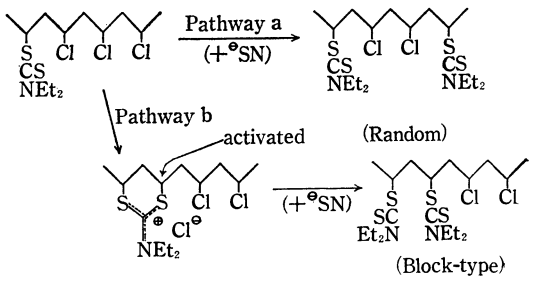

Scheme 3. Copolymer or PVC containig the SN function.

In all cases kinetical observation leads to the conclusion that the S_N reaction involving neighboring-group participation (pathway b) certainly occurs in the polymer reaction.

Experimental

Materials. Commercial NaSN was washed several times with chloroform and then dried *in vacuo*. This salt contains two molecules of coordinated water.[9] Commercial PVC (P=400) was purified by reprecipitating twice (DMF-MeOH). *S*-Vinyl *N*,*N*-diethyldithiocarbamate (VSN) was prepared by the vacuum pyrolysis of ethylene bis(*N*,*N*-diethyldithiocarbamate)[7] and then twice distilled at a reduced pressure (yield 95%); bp 93—94°C/1 mmHg, n_D 1.588 (27°C).

The solvents employed were purified by the usual methods.

Copolymerization Procedure. Commercial VCl was purified as follows: VCl was transferred into a flask cooled in a Dry Ice mixture from a cylinder through

*4 The rate enhancement with the copolymer is related to the ratio $\tan\theta_c/\tan\theta_h$ which was more than one, as illastrated below.

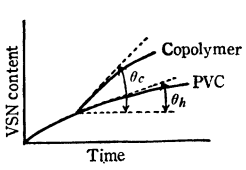

9) T. Nakai and M. Okawara, This Bulletin, **41**, 707 (1968).

a 10% aqueous solution of sodium hydroxide and a soda lime column. Using the usual vacuum system, VCl was further distilled through a soda lime column and then a given amount of purified VCl was condensed into a hard-glass tube of approximately 150 m*l* capacity containing given amounts of VSN and AIBN. The tube was carefully sealed and then immersed into a thermostat maintained at 45±0.5°C. After a given interval, the tube was removed from the thermostat and opened at −78°C. The reaction mixture was poured into a large amount of methanol giving a slightly yellowish precipitate. The copolymer was filtered and dried *in vacuo*. The copolymer was purified by reprecipitation (DMF-MeOH) and then completely dried *in vacuo*. The concentration of VSN in the copolymer was evaluated by sulfur determinations. The experimental results obtained are summarized in Table 2.

Polymer Reaction Procedure. The reaction of PVC with NaSN was undertaken as follows: a solution of 6.30 g (0.10 mol) of PVC and 8.60 g (0.05 mol) of NaSN in 100 m*l* of DMF was stirred in the thermostat maintained at 45±0.5°C. After a given interval, 25 m*l* of the reaction mixture was pippetted out and then poured into approximately 100 m*l* of methanol giving a white precipitate. The resulting polymer was purified by reprecipitation (DMF-MeOH) and dried *in vacuo*. The degree of substitution, that is, the concentration of VSN in the resulting polymer, was evaluated by two sulfur determinations. The experimental results obtained are summarized in Table 1. Infrared spectra of the resulting polymers exhibited no absorption bands due to the carbon-carbon double bond, indicating that no elimination of hydrogen chloride occurred during the reaction.

The reaction of the copolymer prepared above with NaSN was carried out under the same conditions as those of PVC. For example, a solution of 1.00 g of the copolymer (sulfur content 6.06%), 0.055 g of NaCl and 1.10 g of NaSN in 14.3 m*l* of DMF was stirred at 45°C. After a given interval, 7 m*l* of the reaction mixture was poured into methanol to give a slightly yellowish precipitate. The content of VSN in the resulting copolymer was evaluated by sulfur determinations. The results obtained are given in Table 3.

The authors are grateful to Mr. Yoshio Jo, the Nihon Zeon Co., for sulfur determinations.

BULLETIN OF THE CHEMICAL SOCIETY OF JAPAN VOL. 42 512—520 (1969)

The Cooxidation of Hydrocarbons in the Liquid Phase. V. Determination of the Reactivity Ratios

Etsuo NIKI, Yoshio KAMIYA and Nobuto OHTA

Department of Fuel Engineering, The University of Tokyo, Hongo, Tokyo

(Received June 28, 1968)

The cooxidations of cumene (C) and tetralin (T) and of styrene (S) and tetralin were studied in the presence of azobisisobutyronitrile; the reactivity ratios, r, were obtained as $r_C=0.21$ and $r_T=5.0$ for the cumene-tetralin system at 80°C and as $r_S=2.7$ and $r_T=0.49$ for the styrene-tetralin system at 70°C. A new method for the determination of r values from the rates of cooxidation has been developed. The merits and demerits of several methods for the determination of r values are discussed. In cases where a large curvature, preferably a rate minimum, is obtained by plotting the rates against the reactant compositions, the determination from the rates of cooxidation may be most suitable. In other cases, the use of the copolymerization equation may be preferable by product analyses. The hydroperoxide method may be valid for some systems.

In the liquid-phase autoxidation of hydrocarbons, the peroxy radicals play an important role as chain carriers, and the bimolecular reaction of the peroxy radical and the hydrocarbon is the rate-determining step. The reactivities of the hydrocarbons toward the peroxy radicals, however, are hard to ascertain, although much data have been presented on the reactivities of the hydrocarbons toward other free radicals and atoms.[1] The difficulty in obtaining the reactivities toward the peroxy radicals comes mostly from the fact that there are no appropriate sources for the peroxy radicals. The other oxy radical, alkoxy radicals, can be produced by the thermal or photochemical decomposition of dialkyl peroxides,[2] alkyl hypohalites,[3] peroxy oxalates,[4]

1) W. A. Pryor, "Free Radicals," McGraw-Hill Book Co., New York (1966), Chap. 12; K. U. Ingold, International Symposium on Free Radicals in Solution, Ann Arbor, Mich,. Aug., 1966.

or hyponitrites.[5]

The absolute rate constants for the propagation step in the autoxidation of hydrocarbons, k_p, can be determined by either the rotating sector method[6] or the thermocouple method.[7] However, the reactivities of the hydrocarbons toward the peroxy radicals obtained from the absolute rate constants ate those toward the peroxy radicals derived from the hydrocarbons themselves, and the reactivities of the various hydrocarbons toward a specific peroxy radical can not be obtained.

Recently, the cooxidation method has been used in order to get information on this subject. By performing the cooxidations of binary mixtures of standard hydrocarbon and various hydrocarbons, relative reactivities can be obtained from the values of the reactivity ratios. Furthermore, the reactivities and selectivities of the various peroxy radicals may also be obtained from the reactivity ratios together with the knowledge of the absolute k_p values.

Thus, the reactivity ratios are understood to be very important, and several workers have tried to determine them. However, the precise determination of the reactivity ratios is very hard, and some of the values thus far reported are suspect. This paper will present an improved method for the determination of the reactivity ratios from the rates of cooxidation and will discuss the several methods thus far reported.

Results

Cooxidation of Cumene and Tetralin. When this work was started, the reactivity ratios, r, in the cooxidation of cumene (C) and tetralin (T) had been reported to be $r_c=0.043$ and $r_T=16$ at 90°C by Russell,[8] $r_T=10$ at 60°C by Alagy *et al.*,[9] and $r_C=0$ and $r_T=2.5$ at 60°C in a benzene solution by Russell and Williamson.[10] These values seemed inconsistent, and so the cooxidation of this binary system was reinvestigated in order to obtain reliable r values from the rates of cooxidation.[11]

In the oxidation of the binary mixtures of cumene and tetralin, the following six propagation steps and three termination steps are involved:

$$\begin{aligned}
&\text{Propagation:}\quad C\cdot + O_2 \rightarrow CO_2\cdot\\
&\qquad\qquad T\cdot + O_2 \rightarrow TO_2\cdot\\
&\qquad\qquad CO_2\cdot + CH \rightarrow COOH + C\cdot \qquad k_{CC}\\
&\qquad\qquad CO_2\cdot + TH \rightarrow COOH + T\cdot \qquad k_{CT}\\
&\qquad\qquad TO_2\cdot + TH \rightarrow TOOH + T\cdot \qquad k_{TT}\\
&\qquad\qquad TO_2\cdot + CH \rightarrow TOOH + C\cdot \qquad k_{TC}\\
&\text{Termination:}\quad CO_2\cdot + CO_2\cdot \rightarrow \left.\begin{matrix}\\ \\ \end{matrix}\right\} \text{non-radical products} + O_2 \qquad k_{tCC}\\
&\qquad\qquad CO_2\cdot + TO_2\cdot \rightarrow \qquad\qquad\qquad\qquad\qquad\quad 2k_{tCT}\\
&\qquad\qquad TO_2\cdot + TO_2\cdot \rightarrow \qquad\qquad\qquad\qquad\qquad\quad k_{tTT}
\end{aligned}$$

The steady-state treatment gives the following rate equation:[14]

$$-\frac{dO_2}{dt}=\frac{(r_C[C]^2+2[C][T]+r_T[T]^2)R_i^{1/2}}{(r_C^2\delta_C^2[C]^2+2\phi r_C r_T\delta_C\delta_T[C][T]+r_T^2\delta_T^2[T]^2)^{1/2}} \tag{1}$$

where: $r_c = k_{CC}/k_{CT}$, $r_T = k_{TT}/k_{TC}$, $\delta_C = (2k_{tCC})^{1/2}/k_{CC}$, $\delta_T = (2k_{tTT})^{1/2}/k_{TT}$, $\phi = k_{tCT}/(k_{tCC}k_{tTT})^{1/2}$.

It was confirmed that the rates of the cooxidation of cumene and tetralin were independent of the oxygen pressure above 150 mmHg and were proportional to the square root of the initiator concentrations; this demonstrates that only peroxy radicals are involved in the termination reactions and that Eq. (1) is obeyed under the reaction conditions employed.

The reactivity ratios were determined from the rates of cooxidation. Equation (1) has three unknown factors, r_c, r_T and ϕ. The expression:

$$F(r_C, r_T, \phi) = Ar_C^2 + Br_Cr_T\phi + Cr_Cr_T + Dr_T^2 + Er_C + Fr_T + G = 0 \tag{2}$$

where: $A = V\delta_C^2[C]^2-[C]^4$, $B = 2V\delta_C\delta_T[C][T]$, $C = -2[C]^2[T]^2$, $D = V\delta_T^2[T]^2-[T]^4$, $E = -4[C]^3[T]$, $F = -4[C][T]^3$, $G = -4[C]^2[T]^2$, $V = (-dO_2/dt)^2/R_i$,

2) E. G. E. Hawkins, "Organic Peroxides," Spon Ltd., London (1961).

3) C. Walling and B. B. Jacknow, *J. Am. Chem. Soc.*, **82**, 6108 (1960), and the subsequent papers.

4) P. D. Bartlett, E. P. Benzing and R. E. Pincock, *ibid.*, **82**, 1762 (1960).

5) H. Kiefer and T. G. Traylor, *Tetrahedron Letters*, **1966**, 6163; *J. Am. Chem. Soc.*, **89**, 6667 (1967).

6) J. A. Howard and K. U. Ingold, *Can. J. Chem.*, **43**, 2729 (1965).

7) J. A. Howard and J. C. Robb, *Trans. Faraday Soc.*, **59**, 1590 (1963).

8) G. A. Russell, *J. Am. Chem. Soc.*, **77**, 4583 (1955).

9) J. Alagy, G. Clement and J. C. Balaceanu, *Bull. Soc. Chim. France*, 1495 (1960).

10) G. A. Russell and R. C. Williamson, Jr., *J. Am. Chem. Soc.*, **86**, 2364 (1964).

11) Recently, Mayo *et al.*[12] and Howard *et al.*[13] presented reasonable values for this system using different methods from ours: $r_C=0.13$ and $r_T=4.6$ at 60°C; $r_C=0.18$ and $r_T=4.5$ at 56°C, and $r_C=0.11$ and $r_T=8.3$ at 30°C, respectively.

12) F. R. Mayo, M. G. Syz, T. Mill and J. K. Castleman, International Oxidation Symposium, San Francisco, Calif., Aug., 1967.

13) J. A. Howard, W. J. Schwalm and K. U. Ingold, *ibid.*

14) E. Niki, Y. Kamiya and N. Ohta, *Kogyo Kagaku Zasshi* (*J. Chem. Soc. Japan, Ind. Chem. Sect.*), **70**, 42, 1679 (1967). A statistical factor of 2 is included in the cross termination rate constant, k_{tCT}. The definition of $\phi=k_{tCT}/2(k_{tCC}k_{tTT})^{1/2}$ instead based on the treatment of Flory gives the same rate equation.

can be derived from Eq. (1). The runs performed with various initial mixture compositions all give Eq. (2) with various values for each coefficient, A to G. The three unknowns can be calculated from each combination of the three equations, F_1, F_2, and F_3. By eliminating the term $r_c r_T \phi$ and then the term r_T^2, r_T can be expressed with r_C (Eq. (3)):

$$r_T = (u_1 r_T^2 + u_2 r_T + u_3)/(u_4 r_T + u_5) \quad (3)$$

where: $u_1 = a(D_1B_3 - D_3B_1) - d(A_1B_3 - A_3B_1)$,

$u_2 = e(D_1B_3 - D_3B_1) - d(E_1B_3 - E_3B_1)$,

$u_3 = g(D_1B_3 - D_3B_1) - d(E_1B_3 - E_3B_1)$,

$u_4 = -c(D_1B_3 - D_3B_1) + d(C_1B_3 - C_3B_1)$,

$u_5 = -f(D_1B_3 - D_3B_1) + d(F_1B_3 - F_3B_1)$,

$a = A_1B_2 - A_2B_1$, $c = C_1B_2 - C_2B_1$,

$d = D_1B_2 - D_2B_1$, $e = E_1B_2 - E_2B_1$,

$f = F_1B_2 - F_2B_1$, $g = G_1B_2 - G_2B_1$.

The substitution of r_T thus obtained into the equation obtained by eliminating the term $r_C r_T \phi$ yields the fourth-degree equation of r_C (Eq. (4)), which can be solved by substitution or by Newton's method:

$$G(r_C) = v_1 r_C^4 + v_2 r_C^3 + v_3 r_C^2 + v_4 r_C + v_5 \quad (4)$$

where: $v_1 = au_4^2 + cu_1u_4 + du_1^2$,

$v_2 = 2au_4u_5 + cu_2u_4 + cu_1u_5 + 2du_1u_2 + eu_4^2 + fu_1u_4$,

$v_3 = au_5^2 + cu_3u_4 + cu_2u_5 + du_2^2 + 2du_1u_3 + 2eu_4u_5 + fu_2u_4 + fu_1u_5 + gu_4^2$,

$v_4 = cu_3u_5 + 2du_2u_3 + eu_5^2 + fu_3u_4 + fu_2u_5 + 2gu_4u_5$,

$v_5 = du_3^2 + fu_3u_5 + gu_5^2$.

The values of u_i and v_i are functions of [C], [T], δ_C, δ_T, R_i and the rates of oxygen absorption. The substitution of r_C obtained from Eq. (3) gives r_T. Thus, from each of the combination of the three runs performed, r_C and r_T are obtained. The values for r_C and r_T numbering, ${}_nC_3$, can be obtained by performing the cooxidations with n different compositions.[15]

The values of δ were calculated from the rate equation for the oxidation of neat hydrocarbon, RH (Eq. (5)):

$$-dO_2/dt = k_p(2k_t)^{-1/2}[RH]R_i^{1/2} + R_i(1/e - 1)/2 \quad (5)$$

The second term on the right hand of Eq. (5) is the correction for the nitrogen and oxygen evolved and is absorbed in the initiation and termination steps, e being the efficiency of the initiator. The values of 1.52×10^{-4} sec^{-1} and 0.65 were taken for k_t and e respectively at 80°C. The rates of the oxidation of pure cumene and tetralin at 80°C in the presence of 1.00×10^{-2} M of AIBN were 6.00×10^{-5} and 1.09×10^{-4} M/sec respectively, while values of 166 and 94.5 (M sec)$^{-1/2}$ were obtained for δ_C and δ_T respectively. The rates of the cooxidation of cumene and tetralin at 80°C are shown in Table 1.

TABLE 1. RATES OF COOXIDATIONS OF CUMENE AND TETRALIN[a]

Cumene M	Tetralin M	$-dO_2/dt \times 10^5$ M/sec	ϕ[b]
0.00	7.35	10.9	
2.40	4.90	7.72	4.12
3.60	3.68	6.13	4.38
4.80	2.45	4.69	4.39
6.00	1.23	3.49	4.40
6.55	0.668	3.17	4.41
7.20	0.00	6.00	

a) 80°C, [AIBN] = 1.00×10^{-2}M.
b) See text.

Examples of the solution of Eqs. (4) and (3) are shown in Fig. 1. Thus, the reactivity ratios were obtained as 0.21 ± 0.01 and 5.0 ± 0.1 for r_C

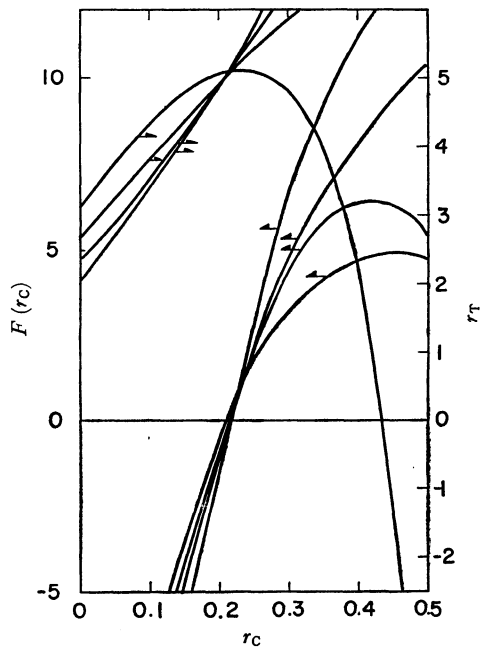

Fig. 1. Determination of r values in the cooxidation of cumene (C) and tetralin (T), 80°C.

15) Alagy *et al.*[9] determined r values from the rates of cooxidation for the first time. They eliminated the term $r_C r_T \phi$ alone to obtain a group of quadratic equations of r_C *vs.* r_T, whose positive intersections being the solution. However, the drawing of the conics is troublesome. On the contrary, in the procedures presented in this paper, the values of two reactivity ratios can be obtained directly from the computer, more easily and more accurately.

and r_T respectively. These values seem reasonable compared with those of Mayo *et al.*[12] and Howard *et al.*[13] reported recently. Equation (1) can be solved for ϕ from a knowledge of the values of r_C and r_T, the two hydrocarbon concentrations, the rate of initiation, and the rate of oxidation. The results are shown in Table 1. A weighed average of 4.3 was taken as the value of ϕ.[16]

Cooxidation of Styrene and Tetralin. The cooxidation of styrene (S) and tetralin (T) was performed at 70°C under an atmospheric pressure of oxygen. This system was employed in order to establish the validity of our rate method for determining the reactivity ratios. Styrene[17] and tetralin are useful hydrocarbons since both of them produce secondary peroxy radicals whose termination reactions are simple compared with those of tertiary peroxy radicals; moreover, as will be discussed below, this system is suitable for the determination of the reactivity ratios by means of product analyses.

Table 2. Rates of cooxidation of styrene and tetralin[a]

Styrene M	Tetralin M	$-dO_2/dt \times 10^5$ M/sec	Kinetic chain length	$(M\,sec)^{-1/2}$	ϕ[b]
8.75	0.00	14.0	272	44.8	
7.30	1.23	10.6	206		3.08
5.83	2.45	8.26	160		2.84
3.50	4.41	4.82	93.5		3.95
2.92	4.90	4.35	84.5		3.95
1.46	6.13	3.54	68.8		3.94
0.795	6.68	3.42	66.5		3.96
0.00	7.35	3.95	76.7	130	

a) 70°C, [AIBN] = 1.00×10^{-2}M.
b) Calculated assuming $r_S = 2.7$ and $r_T = 0.49$.

The rates of the cooxidations of styrene and tetralin are summarized in Table 2. A rate minimum is again observed in this system. The values of 2.7 and 0.49 were obtained for r_S and r_T respectively from the results in Table 2 by a treatment similar to that used for the system of cumene and tetralin. The value of ϕ was obtained as 3.9.

The reactivity ratios in this styrene-tetralin system were also determined by product analyses. In order to avoid high conversions of the oxidants, the oxygen uptake and the hydroperoxide formation were measured by the use of a gas buret and by the iodometric titration of the Wibaut method[18] respectively. The amount of styrene reacted was taken as the difference between the oxygen uptake and the hydroperoxide formed, the latter corre-

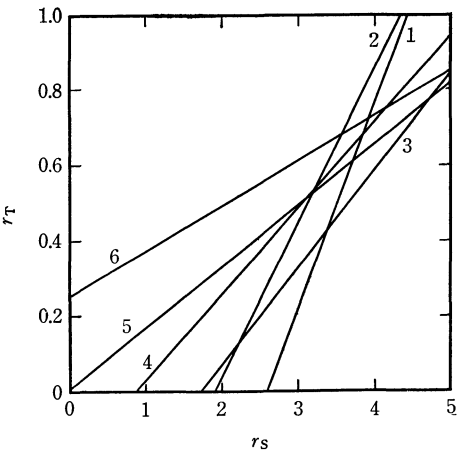

Fig. 2. Determination of r values in the cooxidation of styrene (S) and tetralin (T), 80°C; Mayo-Lewis method.

Table 3. Cooxidations of styrene (S) and tetralin (T)[a]

Run No.	1	2	3	4	5	6	7	8
$[S]_0$	17.50	0.00	10.50	8.76	7.00	5.84	4.36	2.92
$[T]_0$	0.00	15.70	5.88	7.36	8.82	9.80	11.02	12.26
Time, min	44	80	70	95	110	130	140	150
$-O_2$[b]	0.698	0.386	0.606	0.638	0.636	0.606	0.562	0.592
conv., %	3.99	2.62	3.70	3.96	4.01	3.87	3.66	3.90
hpo[c]$=\Delta T$	0.0036	0.370	0.0914	0.144	0.185	0.234	0.276	0.390
ΔS[d]			0.5146	0.494	0.451	0.372	0.286	0.202
$[S]_f$			9.986	8.266	6.549	5.468	4.074	2.718
$[T]_f$			5.788	7.216	8.635	9.566	10.744	12.87

a) 70°C, 760 mmHg of oxygen pressure and 1.00×10^{-2}M of AIBN. Quantities in millimoles. The subscripts o and f represent the initial and final concentrations respectively.
b) After correction.
c) Hydroperoxide determined by the Wibaut method.[18] After correction for hydroperoxide from AIBN.
d) $S = (-O_2) - \Delta T$.

16) Howard *et al.* reported the values of 5.9 and 4.8 for ϕ at 30°C and 56°C respectively.[13]
17) A. A. Miller and F. R. Mayo, *J. Am. Chem. Soc.*, **78**, 1017 (1956); F. R. Mayo, *ibid.*, **80**, 2465 (1958).
18) J. P. Wibaut, H. B. van Leeuwen and B. Van der Wal, *Rec. Trav. Chim.*, **73**, 1033 (1954).

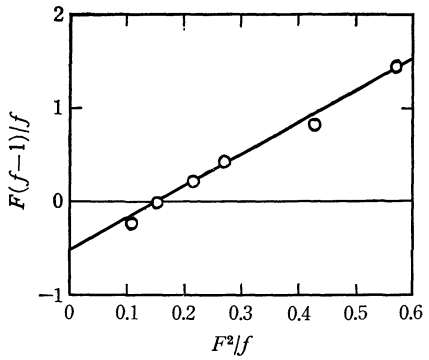

Fig. 3. Determination of r values in the cooxidation of styrene (S) and tetralin (T), 70°C; Fineman-Ross method.
The solid line corresponds to $r_S=3.3$ and $r_T=0.49$.
$F=[S]_0/[T]_0, f=\Delta S/\Delta T$

sponding to the disappearance of tetralin. The oxidation products of styrene are mostly styrene polyperoxide, plus small amounts of benzaldehyde and formaldehyde, under an atmospheric pressure of oxygen and with a long kinetic chain length.[17] The Wibaut method[18] gave little titer for polyperoxide, while the tetralyl hydroperoxide could be determined quantitatively (Table 3). This procedure was first employed by Mayo and his coworkers for the cooxidation of styrene and cumene.[12] The results are summarized in Table 3. The oxidations were performed up to a conversion of approximately 4% based on the oxygen uptake, where 2—7% of the initial hydrocarbons were oxidized. The results in Table 3 were treated by means of the Mayo-Lewis method[19] and the Fineman-Ross method,[20] which are shown in Figs. 2 and 3.

The r values obtained from the Mayo-Lewis method show considerable scatter. This must be mostly because the conversions of both hydrocarbons are very small where, as will be discussed later, a small error in the final concentrations of the hydrocarbons causes a large error in the r values. A Fineman-Ross plot gave the values of 3.3 and 0.49 for r_S and r_T respectively. These values are in reasonably good agreement with those obtained from the rates of cooxidation. Although the conversions were kept low, there still remains some possibility that some loss of precision is involved due to the complicated chain-transfer reaction of tetralyl hydroperoxide with the polystyrylperoxy radical.[21] On the other hand, the reactivity ratios can be determined from the rates of cooxidation at the initial stage of the oxidation.

Discussion

The merits and demerits of several methods for the determination of the reactivity ratios will be discussed in this section.

Determination from the Rates of Cooxidation. The merits of this method are, first, the rates of oxygen absorption can be measured quite easily and accurately, and secondly, they can be obtained at the initial stage of the oxidation. In the present work, the conversions of both hydrocarbons are about only 1% or less. These merits will become more obvious hereafter.

One of the difficulties comes from the complicated termination reactions. The chain termination reactions by secondary and primary peroxy radicals are now fairly well understood to proceed *via* the following cyclic transition state:[22]

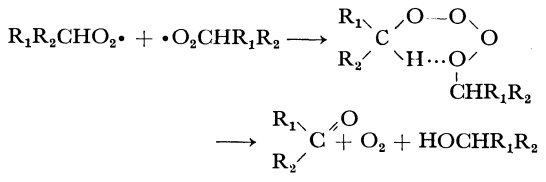

The bimolecular interactions of tertiary peroxy radicals, lacking α-hydrogen, are complicated and have been studied intensively by many investigators recently.[23] As for the interaction between cumylperoxy radicals, it is assumed to produce oxygen and two cumyloxy radicals, a minor portion of which recombines in the cage to form dicumyl peroxide, while the rest undergoes cleavage reaction to give acetophenone and methyl radical. The methylperoxy radical produced from the methyl radical participates in the terminating reaction. This method of determining r values assumes that ϕ is a constant. However, as has been pointed out by Mayo,[12] the ϕ concept is an arbitrary one, and if the methylperoxy radical plays a significant part in the chain termination reaction, the three termination steps listed above may not be enough in themselves and so this method may be unreliable.

The absolute rate constants in the oxidations of cumene[7,13,23-26] and tetralin[27,28] have been de-

19) F. R. Mayo and F. M. Lewis, *J. Am. Chem. Soc.*, **66**, 1594 (1944).
20) M. Fineman and S. D. Ross, *J. Polymer Sci.*, **5**, 259 (1950).
21) R. Hiatt, C. W. Gould and F. R. Mayo, *J. Org. Chem.*, **29**, 3461 (1964). See also discussion in the present text.
22) G. A. Russell, *J. Am. Chem. Soc.*, **79**, 3871 (1957); J. A. Howard and K. U. Ingold, *ibid.*, **90**, 1056 (1968).
23) D. G. Hendry, *ibid.*, **89**, 5433 (1967), and papers cited therein.
24) H. W. Melville and S. Richards, *J. Chem. Soc.*, 944 (1954). The values were corrected by a factor of 1.0/0.65 since Melville and Richards assumed that e was equal to 1.0.
25) J. R. Thomas and C. A. Tolman, *J. Am. Chem. Soc.*, **84**, 2079 (1962).

termined and the extrapolated values of $k_{CC}=1.4$, $k_{tCC}=2.8\times10^4$, $k_{TT}=41$, and $k_{tTT}=9.8\times10^6$ M^{-1} sec^{-1} are obtained at 80°C. The other rate constants in the cooxidation of cumene and tetralin can be calculated by the use of these absolute rate constants, the two reactivity ratios, and the ϕ value. They are $k_{CT}=6.7$, $k_{TC}=8.2$, and $k_{tCT}=2.3\times10^6$ M^{-1} sec^{-1}. From the four propagation rate constants, $k_{TC}/k_{CC}=5.9$ and $k_{TT}/k_{CT}=6.1$; this implies that the tetralylperoxy radical is approximately 6 times as reactive as the cumylperoxy radical toward cumene and tetralin.[29] The steady state concentrations of cumylperoxy and tetralylperoxy radicals can be calculated from Eqs. (6) and (7):

$$[CO_2\cdot] = k_{TC}[C]R_t^{1/2}/(2k_{tCC}k_{TC}^2[C]^2 + 4k_{tCT}k_{CT}k_{TC}[C][T] + 2k_{tTT}k_{CT}^2[T]^2)^{1/2} \quad (6)$$

$$[TO_2\cdot] = k_{CT}[T][CO_2\cdot]/k_{TC}[C] \quad (7)$$

In Fig. 4, the calculated concentrations are plotted against the hydrocarbon compositions, while Fig. 5 shows the rates of each of the four propagation steps. The rates of the individual termination reaction can be computed using the values of the peroxy radical concentrations and the absolute rate constants. The results are shown in Fig. 6. These figures show that the contribution of the bimolecular interaction of cumylperoxy radicals in the chain termination is small even when the concentration of the cumylperoxy radicals is much larger than that of the tetralylperoxy radical; for example, at the 0.90 molar fraction of cumene, the cumylperoxy radical is richer than the tetralylperoxy radical by a factor of 12, but the relative importance of the interaction of cumylperoxy radicals is only 5%, and 80% of the termination is performed by the reaction between cumylperoxy and tetralylperoxy radicals. The crossed interaction

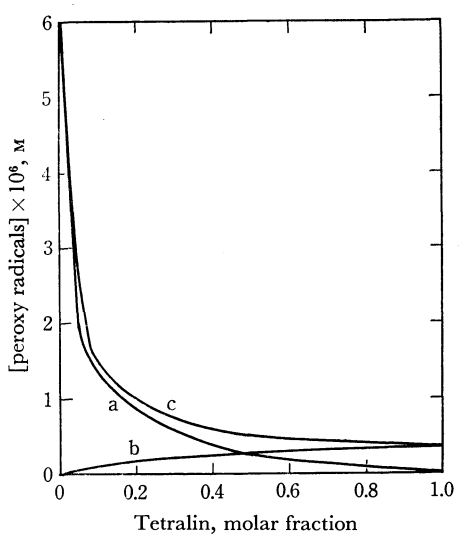

Fig. 4. Concentrations of peroxy radicals in the cooxidation of cumene (C) and tetralin (T), 80°C, [AIBN] = 1.0×10^{-2}.
a: $[CO_2\cdot]$, b: $[TO_2\cdot]$, c: $[CO_2\cdot]+[TO_2\cdot]$

between cumylperoxy and tetralylperoxy radicals is assumed to proceed as follows to really terminate chains without any cleavage reaction to form the methyl radical.[31] Thus, the ϕ value may well be assumed to be constant when the concentration of tetralin is more than 10%.

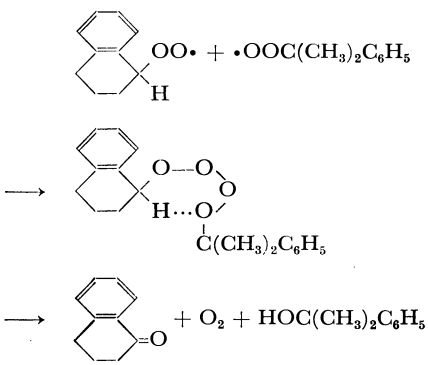

The effects of error in the determination of the reactivity ratios from the rates of cooxidation were examined. Table 4 shows how a 10% error in r values affects the rates of cooxidation. It was confirmed that every group of the calculated rates of cooxidation in Table 4 gave the assumed r values. Since the plots of the oxygen uptake against the time gave an excellent straight line at the initial stage of the oxidation with satisfactory reproducibility, and since it is not difficult to obtain the rates of oxidation within an experimental error of 10%, accurate r values are expected to be obtained from the rates of cooxidation.

26) A. A. Vichutinskii, *Dokl. Akad. Nauk SSSR*, **157**, 150 (1964).
27) J. A. Howard and K. U. Ingold, *Can. J. Chem.*, **44**, 1119 (1966).
28) C. H. Bamford and M. J. S. Dewar, *Proc. Royal Soc.*, **A198**, 252 (1949).
29) If the reactivities of the peroxy radicals, ROO·, are independent of the structure of R, the product of two reactivity ratios is unity. However, it must be noteworthy that the product of two r values being unity does not always imply the identical reactivities of the peroxy radicals independent of their nature. Even if the reactivities are different, the product of two r values can be unity when the *relative* reactivities of the peroxy radicals are same toward the hydrocarbons. Ingold and his collaborators[27,30] suggest that the differences in the reactivities of the peroxy radicals are due to steric factors. But the difference in the electron affinity of the peroxy radicals may be responsible in part.
30) B. S. Middleton and K. U. Ingold, *Can. J. Chem.*, **45**, 191 (1967).
31) A large value of ϕ may also support this concept.

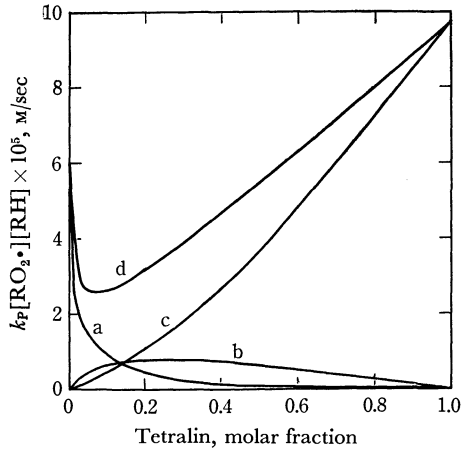

Fig. 5. Rates of propagation steps in the cooxidation of cumene (C) and tetralin (T), 80°C, [AIBN] = 1.0×10^{-2}M.
a: $k_{CC}[CO_2\cdot][CH]$, b: $k_{CT}[CO_2\cdot][TH]=k_{TC}[TO_2\cdot][CH]$, c: $k_{TT}[TO_2\cdot][TH]$, d: a+2b+c

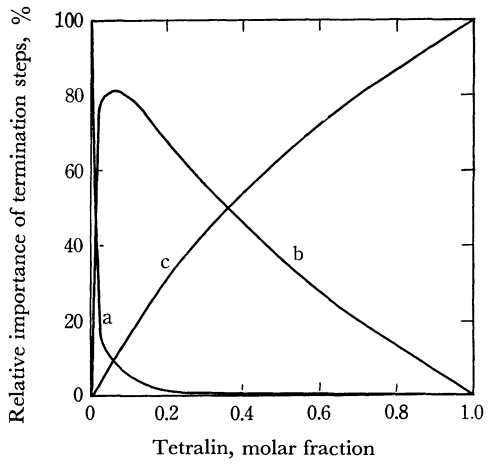

Fig. 6. Relative importance of the termination steps in the cooxidation of cumene (C) and tetralin (T), 80°C, [AIBN] = 1.0×10^{-2}.
a: COO•+COO•
b: COO•+TOO•
c: TOO•+TOO•
} → non-radical products+O_2

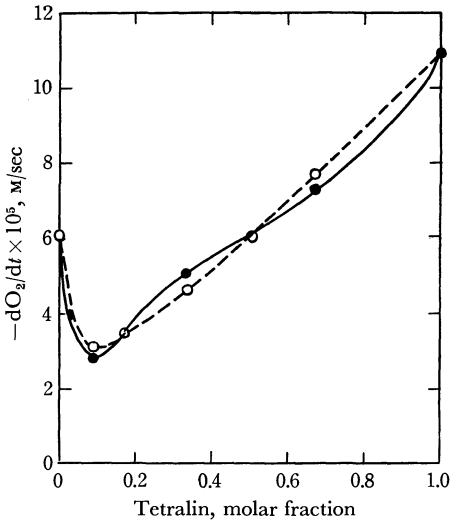

Fig. 7. Rates of cooxidation of cumene and tetralin, 80°C, [AIBN] = 1.0×10^{-2}.
○: observed, ●: assumed (see text)

It was found, however, that when the curve obtained by plotting the rates of oxidation against the hydrocarbon compositions is uneven, a small error in the rate will produce a large error in the reactivity ratios. Figure 7 shows a plot obtained by assuming that Nos. 1,3, and 5 in Table 4 have −10%, +10% and −5% errors respectively in the rates of oxidation. The curve, as may be seen, is uneven. The calculation of the reactivity ratios from Eqs. (4) and (3) using these values gave poor results. For example, Nos. 1, 2 and 4 gave the values of 0.06 and 2.0 for r_C and r_T respectively, while Nos. 1, 3, and 4 gave 0.0 and 0.6. It was also found that the smaller the curvature of the plot, the larger the effects of error in the rate of oxidation on the reactivity ratios (see No. 5 in Table 4).

The above discussion suggests that the determination of the reactivity ratios from the rates of cooxidation is reliable and useful if a smooth plot is obtained between the rates of cooxidation and hydrocarbon compositions and if the curvature is

TABLE 4. EFFECTS OF ERROR IN THF REACTIVITY RATIOS ON THE RATES OF COOXIDATION OF CUMENE AND TETRALIN[a)]

No.	Cumene M	Tetralin M	$(-dO_2/dt)_{obs.}\times10^5$ M/sec	$(-dO_2/dt)\times10^5$ in M/sec calculated by assuming[b)]: r_C=0.21 r_T=5.0	0.21 4.5	0.21 5.5	0.19 5.0	0.19 4.5	0.19 5.5	0.23 5.0	0.23 4.5	0.23 5.5
1	6.55	0.668	3.17	3.20	3.35	3.08	3.21	3.36	3.08	3.20	3.34	3.08
2	6.00	1.23	3.49	3.52	3.65	3.41	3.57	3.71	3.46	3.48	3.61	3.36
3	4.80	2.45	4.69	4.72	4.82	4.63	4.81	4.92	4.72	4.63	4.73	4.55
4	3.60	3.68	6.13	6.15	6.22	6.09	6.25	6.33	6.18	6.06	6.12	6.00
5	2.40	4.90	7.72	7.68	7.72	7.65	7.76	7.82	7.72	7.60	7.64	7.57

a) 80°C, [AIBN] = 1.00×10^{-2}M.
b) $\delta_C = 166$, $\delta_T = 94.5$, $R_i = 1.98\times10^{-6}$ M/sec, and $\phi = 4.3$.

large, preferably when the rate minimum is observed.

Mayo-Lewis Method.[19] This method was derived from the copolymerization equation[32] and was first applied to the cooxidations of benzaldehydes by Walling and McElhill.[33] The initial and final concentrations of both hydrocarbons must be known. The two initial concentrations can be calculated, and the final concentrations are measured experimentally either by analyzing them directly by means, for example, of gas-liquid chromatography or by analyzing the products. Russell and Williamson[10] determined the reactivity ratios for many systems by making use of this method. However, in most cases employed, the reactivity ratios show considerable scatter. The best results were obtained for the system of cumene and *cis*-decalin. Table 5 shows their results and also some values calculated assuming that the errors indicated in the eighth column are involved. The solutions of the results in Table 5 by using the integrated form of the Mayo-Lewis method are shown in Fig. 8, which indicates that a small error

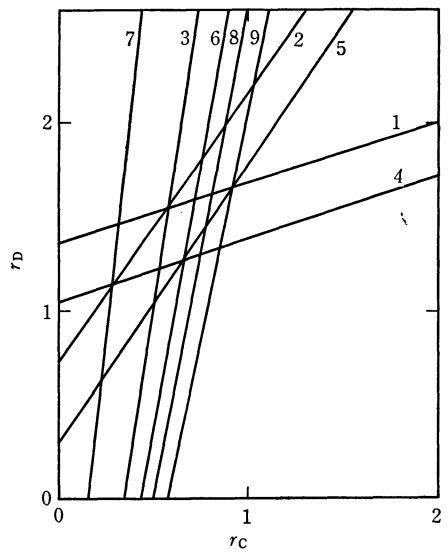

Fig. 8. Cooxidations of cumene (C) and *cis*-decalin (D), 60°C.

will produce a large error in r values. Experimentally, the values of $r_C=0.58$ and $r_D=1.56$ are obtained, but when one of the three concentrations contains an error of 5%, the values of r_C and r_D are 0.70 and 1.7 (Nos. 1, 2, 6); 0.69 and 1.4 (1, 3, 5); 0.48 and 1.3 (2, 3, 4), and 0.39 and 1.4 (1,2,7) respectively. Thus an error of only 5% in one of the three systems will produce a 10—30% error in the reactivity ratios. Furthermore, analyses by gas-liquid chromatography are usually apt to involve a greater error. When the conversions of the hydrocarbons are small, this analytical error may be more critical.

On the other hand, if the oxidation advances and hydroperoxides are built up considerably, the following cross induced decomposition of hydroperoxides by the peroxy radicals complicates the kinetic scheme. The work by Thomas and Tolman[25] and by Howard, Schwalm, and Ingold[13] indicates the possibilities of these reactions:

$$\mathrm{AOOH} + \mathrm{BOO\cdot} \longrightarrow \mathrm{AOO\cdot} + \mathrm{BOOH}$$
$$\mathrm{BOOH} + \mathrm{AOO\cdot} \longrightarrow \mathrm{BOO\cdot} + \mathrm{AOOH}$$

In order to reduce this difficulty, Hendry[34] devised a new technique in which the consumption of the more reactive hydrocarbon and the oxygen uptake are measured. This procedure is especially attractive in cases where reactants have large differences in reactivity. However, even in this procedure, the conversion of the more reactive hydrocarbon is more than 10%, generally between 20—25%.[34]

Table 5. Cooxidations of cumene (C) and *cis*-decalin (D)

No.	$[C]_0$ M	$[D]_0$ M	$[C]_f$ M	$[D]_f$ M	Conv., % C	Conv., % D	Error %[b]
1	0.200	0.800	0.192	0.750	4.0	6.2	
2	0.500	0.500	0.466	0.446	6.8	10.8	
3	0.800	0.200	0.726	0.170	9.2	15.0	
4	0.200	0.800	0.183	0.713			− 5
5	0.500	0.500	0.443	0.424			− 5
6	0.800	0.200	0.690	0.162			− 5
7	0.800	0.200	0.762	0.178			+ 5
8	0.800	0.200	0.654	0.153			−10
9	0.800	0.200	0.581	0.136			−20

a) The values of Nos. 1, 2, and 3 are the results of Russell and Williamson at 60°C in benzene.[10]
b) Assumed.

Fineman-Ross Method.[20] This method was also derived from the copolymerization equation. A limitation of this method is that this can be used only when the conversions of both oxidants are small enough so that the decrease in the concentrations is negligible compared with their initial concentrations. The determination of the variation in the reactants at the very initial stage is very difficult.

Hydroperoxide Method. Recently, Howard, Schwalm, and Ingold[13] proposed a new method for the determination of the reactivity ratios. They

32) F. R. Mayo and C. Walling, *Chem. Revs.*, **46**, 191 (1950).
33) C. Walling and E. A. McElhill, *J. Am. Chem. Soc.*, **73**, 2927 (1951).
34) D. G. Hendry, International Oxidation Symposium, San Francisco, Calif., Aug., 1967.

have oxidized one hydrocarbon in the presence of hydroperoxide derived from another hydrocarbon. In the oxidation of the system of AH plus BOOH, the following elementary steps are involved:[13]

$$\mathrm{AH} \longrightarrow \mathrm{A}\cdot \qquad R_i = \text{Rate of initiation}$$

$$\mathrm{A}\cdot + \mathrm{O_2} \longrightarrow \mathrm{AOO}\cdot$$

$$\mathrm{AOO}\cdot + \mathrm{BOOH} \longrightarrow \mathrm{AOOH} + \mathrm{BOO}\cdot \qquad k_{\mathrm{ABOOH}}$$

$$\mathrm{BOO}\cdot + \mathrm{AH} \longrightarrow \mathrm{BOOH} + \mathrm{A}\cdot \qquad k_{\mathrm{BA}} \ (\ll k_{\mathrm{ABOOH}})$$

$$2\,\mathrm{BOO}\cdot \longrightarrow \text{non-radical products} \qquad k_{t\mathrm{BB}}$$

A steady state treatment gives the following rate equation:

$$-\mathrm{d}O_2/\mathrm{d}t = k_{\mathrm{BA}}[\mathrm{AH}]R_i^{1/2}/(2k_{t\mathrm{BB}})^{1/2} \qquad (8)$$

Since [AH], R_i, and $k_{t\mathrm{BB}}$ are known, k_{BA} can be calculated by measuring the rate of oxidation. If k_{BA} is known, r_{B} can be calculated with the value of k_{BB}, which can be measured separately.

Howard *et al.*[13] assumed that the termination reaction is solely by the interaction of the peroxy radicals which were derived from the hydroperoxide. However, there remains some possibility that a cross termination reaction by AOO· and BOO· radicals as well as the bimolecular interaction of BOO· radicals may also be important, especially when the latter is much slower than the former. Actually, in a mixture of tetralin and cumyl hydroperoxide, the cross termination between cumylperoxy and tetralylperoxy radicals is calculated, from the concentrations of both peroxy radicals and the absolute rate constants, to compose up to 30% of the total. Another limitation is that this method is applicable only for the peroxy radicals whose incipient hydroperoxides can be isolated.

In conclusion, the method for the determination of the reactivity ratios must be carefully chosen depending on the systems. When the rates of cooxidation are plotted against the reactant compositions, three types of lines are obtained: a large curvature, a gently-sloping curve, and a straight line. In cases where a large curvature, preferably a rate minimum, is observed and a smooth line is obtained, the determination from the rates of cooxidation may be most suitable. In other cases, the use of the copolymerization equation may be preferable. A direct determination of the reactants by gas-liquid chromatography is not appropriate, and the measurements of the oxygen uptake and/or hydroperoxide formed, and the analyses of hydroperoxides are more suitable when the copolymerization equation is used. The hydroperoxide method may be valid for some systems.

Experimental

Cumene and tetralin were shaken successively with sulfuric acid, water, alkali, and water, dried with calcium chloride, and then distilled under reduced pressure of nitrogen. Styrene was washed with alkali and then with water, dried, and distilled under reduced pressure of nitrogen. All the hydrocarbons were passed down the activated alumina column immediately before use. Azobisisobutyronitrile was recrystallized from methanol several times. Oxygen was used without further purification.

The rate of oxygen absorption was measured by a manometer in a constant pressure closed system. Stirring was accomplished by means of a magnetic stirrer with a Teflon-coated stirring bar. The volume of oxygen absorbed was read periodically, every one or two minutes, depending on the rate, and was plotted against the time. In every run, more than fifteen points were plotted. No induction period was observed, and a straight line was obtained. The slope was read and was taken as the rate of oxidation. The cell was cleaned by washing successively with a solution of $K_2Cr_2O_7$ plus concentrated sulfuric acid, ammonia, water, acetone, and methanol, and then dried. Hydroperoxide was determined by iodometric titration, the Wibaut method,[18] where hydroperoxide was treated with KI in 80% acetic acid at room temperature.

The calculation was done at the Data Processing Center of the University of Tokyo using a OKITAC 5090 computer.

BULLETIN OF THE CHEMICAL SOCIETY OF JAPAN VOL. 42 521—527 (1969)

The Synthesis of Regular Copolymers of Glycine and Alanine

Sho TAKAHASHI*1

Department of Physics, Faculty of Science, Nagoya University, Chikusa-ku, Nagoya

(Received July 8, 1968)

The synthesis of polypeptides with a repeating sequence of glycines and L-alanines, *i. e.*, poly-(L-Ala-Gly-Gly), poly-(L-Ala-L-Ala-Gly), and poly-(L-Ala-L-Ala-L-Ala-Gly), are reported. Polymerization was achieved by a self-condensation of *p*-nitrophenyl esters of the corresponding tri- or tetrapeptides.

In 1963, Gratzer and Doty[1] reported the remarkable stability of the α-helical conformation of poly-L-alanine. On the other hand, the simplest polyamino acid, poly-glycine, has the so-called β-conformation in the solid state, as is well known.[2] It seemed to us to be very much meaningful to study the conformation of a series of copolymers made from glycine and alanine, since the interactions between their side chains were the simplest to interpret theoretically. To analyze the problem unambiguously, the glycine-alanine copolymers must be sequential. (It has been shown by Nylund and Miller[3] that different monomer reactivity ratios are observed between the beginning and the close of the random copolymerization of glutamic acid- and leucine-*N*-carboxy anhydride). In this paper, we wish to report the synthesis of sequential polypeptides consisting of glycine and L-alanine.

Efforts to obtain sequential copolymers of glycine and alanine have been made by many workers, such as the attempt to get poly-(L-alanyl-glycyl-glycine) from methyl L-alanyl-glycyl-glycinate by Fischer[4] and those to get poly-(D,L-alanyl-glycyl-glycine) from the analogous tripeptide methylester or thiophenylester by Wilson and Pascu[5] and Schramm *et al.*[6] Other references are cited in the review by Katchalsky and Sela.[7] These polymers, however, had rather low molecular weights, and the reproducibility was poor. It was necessary to carry out self-condensation reactions at elevated temperatures because of the relatively low reactivity of peptide alkylesters.

In the past few years, several papers related to the synthesis of sequential polymers of other amino acids have appeared. The methods which have been reported may be classified into two categories: (a) the treatment of a free peptide in solution with a suitable condensing agent (dicyclohexylcarbodiimide,[8a-c] tetraethylpyrophosphite,[8c,9] pyrophosphoric acid,[10] and ethyl metaphosphate[11] have been used as condensing agents.) and (b) the self-condensation of peptide, one of whose terminals has been activated by an adequate substituent towards the attack of the other terminal of another molecule. Noguchi[12] developed the *N*-carbothiophenyl amino acid method and synthesized poly-(L-alanyl-glycine), which has also been synthesized recently by Australian workers.[13a] An active ester method has also been applied; the results are

*1 Present address: Laboratory of Chemistry, National Institute of Health, Bethesda, Md., 20014, U.S.A.

1) W. B. Gratzer and P. Doty, *J. Am. Chem. Soc.*, **85**, 1193 (1963); P. Doty and W. B. Gratzer, in "Polyamino Acids, Polypeptides, and Proteins," ed. by M. A. Stahmann, The University of Wisconsin Press, Madison (1962), p. 111.

2) For instance, A. Elliott, E. M. Bradbury, A. R. Downie and W. E. Hanby, in "Polyamino Acids, Polypeptides, and Proteins," p. 255.

3) R. E. Nylund and W. G. Miller, *J. Am. Chem. Soc.*, **87**, 3537 (1965).

4) E. Fischer, *Ber.*, **39**, 2893 (1906).

5) E. J. Wilson and E. Pascu, *J. Org. Chem.*, **7**, 126 (1942).

6) G. Schramm and G. Thumm, *Z. Naturforsch.*, **3b**, 218 (1948); G. Schramm and H. Restle, *Makromol. Chem.*, **13**, 103 (1954); I. Brunn-Leube and G. Schramm, *Chem. Ber.*, **89**, 2045 (1956).

7) E. Katchalsky and M. Sela, *Adv. Protein Chem.*, **13**, 449 (1958).

8) a) V. Bruckner, M. Szekerke and J. Kovacs, *Naturwissenschaften*, **43**, 107 (1956). b) T. Vajda, *Chem. Ind.*, **1963**, 785. c) H. Kitaoka, S. Sakakibara and H. Tani, This Bulletin, **31**, 802 (1958).

9) S. G. Waley, *J. Chem. Soc.*, **1955**, 517.

10) G. Schramm and H. Wissmann, *Chem. Ber.*, **91**, 1073 (1958).

11) G. Spach, *Angew. Chem.*, **76**, 381 (1964).

12) J. Noguchi and T. Hayakawa, *J. Am. Chem. Soc.*, **76**, 2846 (1954); J. Noguchi *et al.*, *Nippon Kagaku Zasshi* (*J. Chem. Soc. Japan, Pure Chem. Sect.*), **74**, 961 (1953); *ibid.*, **75**, 639 (1954).

13) a) R. D. B. Fraser, T. P. MacRae, F. H. C. Stewart and E. Suzuki, *J. Mol. Biol.*, **11**, 706 (1965). b) F. H. C. Stewart, *Australian J. Chem.*, **18**, 887 (1965).

satisfactory with peptide *p*-nitrophenyl esters[13b,14] or pentachlorophenyl esters.[15]

We selected the *p*-nitrophenyl ester method for the synthesis of sequential polymers of glycine and L-alanine. The principles of the synthesis of such regular polypeptides with high molecular weights are the following: (1) the number of amino acids which build up a polymerization unit must be three or more in order to exclude a primary intramolecular cyclization, since dipeptides may form six-membered ring compounds (diketopiperazine derivatives); (2) in order to avoid an intramolecular cyclization, a satisfactory concentrated solution of reactants must be used.

Results

Synthesis of Polymerizing Units. In order to avoid racemization yielding peptide bonds during the course of the condensation reaction, we always used the so-called azide method if L-alanine was present in a position where the reaction occurred. The azide method is one of the two methods which have been recommended for the coupling of amino acids without racemization[16] (the other one[17] is coupling through 1-hydroxy-piperidine esters). Figure 1 outlines the synthetic steps for the required derivatives of tri- and tetra-peptides.

L-Alanine was ethylated in ethanol saturated with hydrogen chloride, and then converted into the hydrazide of carbobenzoxyalanine according to the method described by Erlanger and Brand.[18] The azide coupling of II with ethyl glycyl-glycinate hydrochloride, which has been derived from the ethanolysis of diketopiperazine (IV) in the presence of hydrogen chloride,[19] gave the ethyl ester of carbobenzoxy-L-alanyl-glycyl-glycine (III). The compound III was also obtained from step-by-step synthesis through the compound VI[18,20] and compound VII. The compound III was hydrolyzed with a slight excess of sodium hydroxide in aqueous methanol; this afforded a free acid (VIII) which was then converted into *p*-nitrophenyl ester (IX) by the use of dicyclohexylcarbodiimide as the condensing agent. Recently, Kovacs[15] recommended the use of a pentachlorophenyl ester instead of a *p*-nitrophenyl ester as the active ester for polymerization, since a pentachlorophenyloxy group is probably a more electron-attracting group than a *p*-nitrophenyloxy group; these catalytic hydrogenation will be used in contrast to the case of a *p*-nitrophenyl ester. We also tried to synthesize a pentachlorophenyl ester of VIII from VIII and pentachlorophenol using dicyclohexylcarbodiimide, but the surprisingly low solubilities of the ester towards general solvents made it very difficult to purify the crude ester. The carbobenzoxy group of the compound IX was smoothly eliminated in the usual manner in acetic acid half-saturated with hydrogen bromide, and the resulting *p*-nitrophenyl-L-alanyl-glycyl-glycinate was recrystallized enough times to obtain a high-molecular-weight polymer.

p-Nitrophenyl L-alanyl-L-alanyl-glycinate hydrobromide and *p*-nitrophenyl (L-alanyl)$_3$-glycinate hydrobromide were synthesized in the same manner. Of the derivatives appearing in Fig. 1, mention should be made of the remarkable crystallizability of the compound XVI. It gave large needles very easily in the presence of a small amount of methanol, even if we started from crude, half-crystalline XV. Elementary analysis confirmed the presence of one mole of methanol as a methanol of crystallization.

Initially we tried to synthesize a *p*-nitrophenyl ester of carbobenzoxy-L-alanyl-(glycyl)$_3$ through a free acid, XXVIII, but the ethyl ester, XXII, showed a striking resistance towards hydrolysis under usual conditions, in great contrast with the other cases.[21] For instance, when treated with 1.3 molar sodium hydroxide in methanol, analogous ethyl esters, III, XIII, and XVIII, were hydrolyzed completely within 20 min. On the contrary, 90% or more of XXII was present even after 48 hr under the same conditions (as confirmed by an infrared spectral analysis). Also, the isobutyl ester, XXVII, was not hydrolyzed. In these cases, the prolonged treatment of the XXII or XXVII esters with alkali or treatment under more drastic conditions resulted in the simultaneous elimination of the carbobenzoxy group. The effort to obtain a *t*-butyl ester of XXVIII from VIII and *t*-butyl glycinate[22] failed; the oily crude material resisted further purification. A *p*-toluenesulfonic acid-catalyzed ester-interchange reaction between XXII or XXVII and a large excess of *p*-nitrophenol in

14) a) D. F. DeTar, W. Honsberg, U. Honsberg, A. Wieland, M. Gouge, H. Bach, A. Tahara, W. S. Brinigar and F. F. Rogers, Jr., *J. Am. Chem. Soc.*, **85**, 2873 (1963). b) S. M. Bloom, S. K. Dasgupta, R. P. Patel and E. R. Blout, *ibid.*, **88**, 2035 (1966). c) R. D. B. Fraser, B. S. Harrap, T. P. MacRae, F. H. C. Stewart and E. Suzuki, *J. Mol. Biol.*, **14**, 423 (1965). d) R. D. B. Fraser, T. P. MacRae and F. H. C. Stewart, *ibid.*, **19**, 580 (1966).

15) J. Kovacs, R. Giannotti and A. Kapoor, *J. Am, Chem. Soc.*, **88**, 2282 (1966).

16) E. Schröder and K. Lübke, "The Peptides," Vol. I, Academic Press, N. Y. (1965), p. 325.

17) S. M. Beaumont, B. D. Handford, J. H. Jones and G. T. Young, *Chem. Commun. (London)*, **1965**, 53.

18) B. F. Erlanger and E. Brand, *J. Am. Chem. Soc.*, **73**, 3508 (1951).

19) E. Fischer and E. Forneau, *Chem. Ber.*, **34**, 2868 (1901) (J. P. Greenstein and M. Winitz, "Chemistry of the Amino Acids," John Wiley, N. Y. (1961), p. 803).

20) M. Bergmann, L. Zervas, J. S. Fruton, F. Schneider and H. Schleich, *J. Biol. Chem.*, **109**, 325(1935).

21) J. P. Greenstein and M. Winitz, "Chemistry of the Amino Acids," John Wiley, N. Y. (1961), p. 1158.

22) E. Taschner, A. Chimiak, B. Bator and T. Sokotowska, *Ann.*, **646**, 134 (1961).

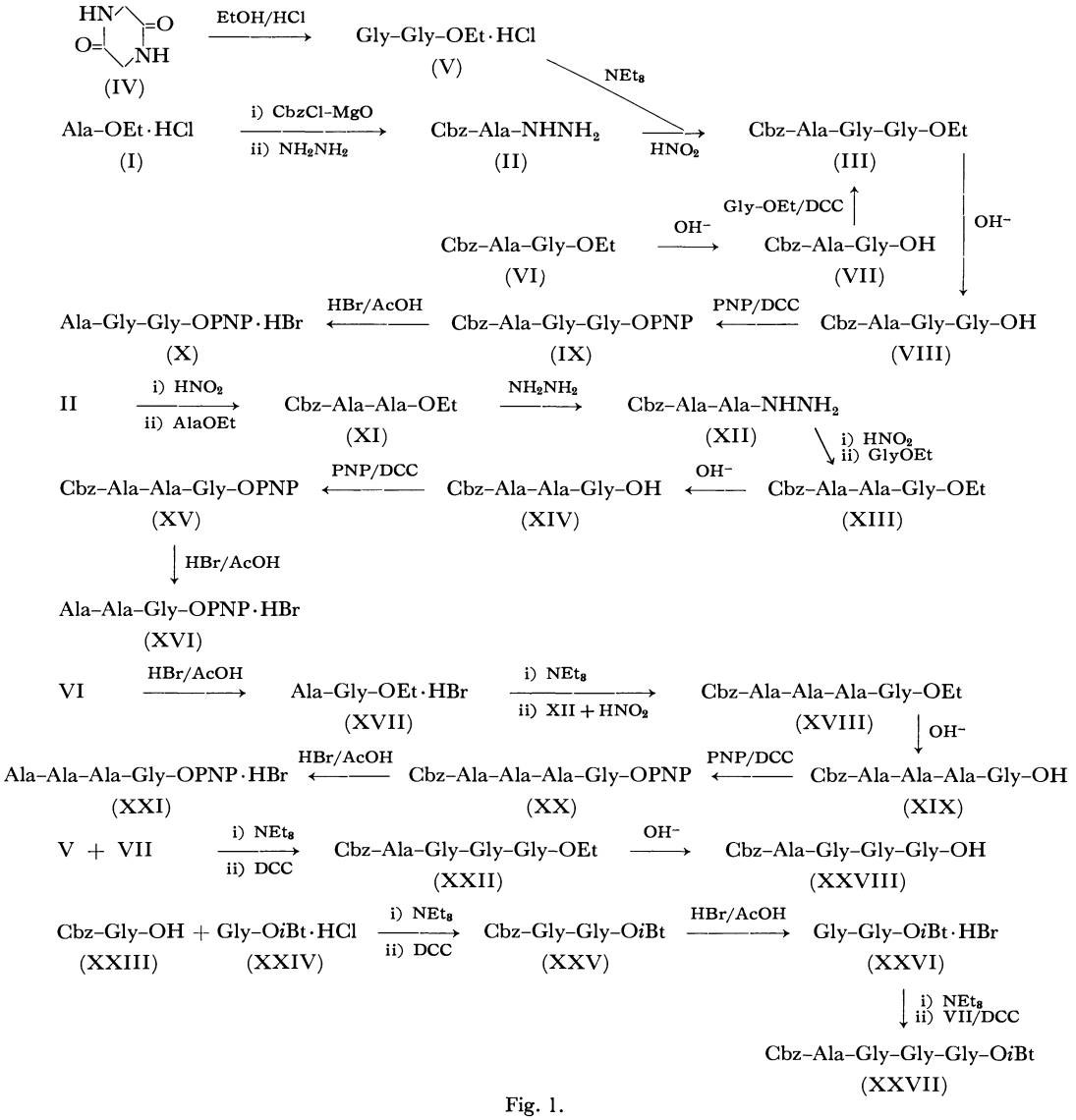

Fig. 1.

tetrahydrofuran also resulted in the accompanying destruction of the carbobenzoxy group.

Polymerization. Polymerization was achieved successfully in dimethyl sulfoxide as the solvent. 30—40% solutions of X, XVI and XXI were reacted with equimolar amounts of triethylamine. The yields of the polymers were in the range of 30—40% of the theory.

Molecular-weight Determinations. Since the polymers dissolved only in dichloroacetic acid or in trifluoroacetic acid, we met very great difficulty in determining the molecular weights of the polymers. Measurements using the ultracentrifuge were impossible because such solvents would corrode the cells.

If we assume the Doty's viscosity-molecular-weight relationships[23] which were obtained in the case of poly-benzyl-L-glutamate in dichloroacetic acid, to be valid in our case also, we can estimate the order of the molecular weights of our polymers by measuring the intrinsic viscosity in dichloroacetic acid. Such measurements give the values of 30000, 35000, and 20000 as the molecular weights for poly-Ala-Gly-Gly, poly-Ala-Ala-Gly, and poly-Ala-Ala-Ala-Gly respectively. There must be, of course, some slight modifications of the coefficient appearing in Doty's viscosity-molecular weights relationship, and the relationship remains to be established for other peptides, but the results obtained above will

23) P. Doty, J. H. Bradbury and A. M. Holtzer, *J. Am. Chem. Soc.*, **78**, 947 (1956).

be not so incredible as a first-order approximation if we remember that most polypeptides exist in the form of a random-coil conformation in dichloroacetic acid (except in the case of poly-L-leucine).[24] For instance, Kovacs calculated the molecular weight of his poly-Glu-Ala-Glu to be 25000 by the sedimentation velocity method using the ultracentrifuge. On the other hand, his sample showed an intrinsic viscosity of 0.3 dl/g in dichloroacetic acid, a value which corresponds to MW 40000 if we apply Doty's relationship. DeTar[14a] also showed that the values obtained by this relationship for the various polymers are at least roughly comparable with those obtained by the Archibald technique or by end-group assays using the DNP method.

Problem of Racemization. It is essential to know whether a racemization reaction has occurred or not. We measured the optical rotatory dispersion curves for the acid hydrolysates of polymers and compared them with that of L-alanine treated under the same hydrolytic conditions. The results showed that the racemization was less than 5%, if it occurred at all.

Experimental

The recorded melting points are determined on a microhotstage and are uncorrected. The infrared spectra were taken with a JASCO DS-402G grating-type spectrometer or with a JASCO IR-S spectrometer with a NaCl prism mounted. The measurements were made with KBr discs. The optical rotatory dispersion measurements were made with a JASCO ORD/UV 5 recording spectropolarimeter. The azide coupling reactions were carried out in a cold room (at 2—3°C). Viscosity measurements were made at 22°C with an Ostwald type viscometer whose flow time for solvent dichloroacetic acid was about 8 min. Elementary micro analysis was carried out at the Faculty of Agriculture in this university, and the mean values of two or three times analysis are reported. The amino acids analysis was carried out with a Beckman-Spinco amino acid autoanalyzer, Model 120, using a 90 cm column. Commercially available dimethyl sulfoxide was distilled under reduced pressure, 90—92°C fraction at 28 mm/Hg was used. L-Alanine was kindly gifted from Ajinomoto Co. Inc., by the courtesy of Professor Y. Hirata.

Ethyl Carbobenzoxy-L-alanyl-glycyl-glycinate (III). *a) Azide Method.* Five grams of carbobenzoxy-L-alanine hydrazide[18] was dissolved in the mixture of 10 m*l* of 5N hydrochloric acid and 100 m*l* of water and cooled to −10°C. A cold solution of sodium nitrite (1.65 g) was added to it, then the oily azide precipitated was extracted with diethyl ether. After washing the extracts with water and 3% sodium bicarbonate and drying over sodium sulfate for a short time, the cold solution of ethyl glycyl-glycinate, which was prepared from 4.2 g of ethyl glycyl-glycinate hydrochloride (V) and 2.75 g of triethylamine in 100 m*l* of diethyl ether and applied filtration of precipitated amine hydrochloride, was added to it. The reaction mixture was stood for overnight at 2—3°C, then washed with 0.5 N hydrochloric acid and 3% sodium bicarbonate solution. The solvent was removed *in vacuo* to leave white crystalline III, which was recrystallized from ethanol. Yield, 4.2 g mp 134—136°C.

Found: C, 56.06; H, 6.11; N, 11.63%. Calcd for $C_{17}H_{23}O_6N_3$: C, 55.88; H, 6.35; N, 11.50%.

IR: 1743 (ester), 1699 (carbobenzoxy) cm^{-1}.

The compound V was prepared by the restricted ethanolysis of diketopiperazine (IV) in the presence of hydrogen chloride.[19]

b) Dicyclohexylcarbodiimide Method. Ethyl carbobenzoxy-L-ananyl-glycinate[18,20] (30 g) was hydrolyzed in 20% aqueous methanol with 130 m*l* (1.2 eq.) of 0.95 N sodium hydroxide. 23 g of the free acid (VII) was obtained as white massive crystals, and recrystallized from methanol-water, mp 129—134°C. 3.8 g of the free acid VII was dissolved in the mixture of 1.9 g of ethyl glycinate hydrochloride and 1.75 g of triethylamine in 40 m*l* of dimethylformamide. 2.8 g of dicyclohexyl-carbodiimide in 5 m*l* of dimethylformamide was then added dropwise under stirring with external cooling. The solution was stirred for 1 day at room temperature. The dicyclohexylurea was filtered off and the solvent was removed at 1 mm/Hg. The resultant solid was washed with water and recrystallized from ethanol to give the tripeptide ester III, mp 133—135°C, which was undepressed on admixture with a sample prepared by method a).

Carbobenzoxy-L-alanyl-glycyl-glycine (VIII). Ethyl carbobenzoxy-L-alanyl-glycly-gylcinate III, 10 g, was hydrolyzed by 37.4 m*l* of 0.95 N sodium hydroxide in 100 m*l* of 90% aqueous methanol. The solution was stood for 20 min and filtered. Acidification of the filtrate with 5 N hydrochloric acid to pH 1 and concentration under reduced pressure gave a solid of free acid (VIII), which was recrystallized from water. An analytical sample showed mp 163°C.

Found: C, 53.43; H, 5.61; N, 12.54%. Calcd for $C_{15}H_{19}O_6N_3$: C, 53.40; H, 5.68; N, 12.46%.

1725 (COOH), 1680 (sh. carbobenzoxy) cm^{-1}.

***p*-Nitrophenyl Carbobenzoxy-L-alanyl-glycyl-glycinate (IX).** To a cooled mixture of carbobenzoxy-L-alanyl-glycyl-glycine (VIII, 5 g), *p*-nitrophenol (2.2 g), and dimethylformamide (90 m*l*), 3.7 g of dicyclohexylcarbodiimide in 10 m*l* of dimethylformamide was added dropwise with magnetically stirring. The stirring was continued at 0°C overnight. The dicyclohexylurea was filtered off and the solvent was removed at 1 mm/Hg. On addition of diethyl ether (50 m*l*) and storage in the refrigerator, *p*-nitrophenyl ester (IX) crystallized, 4 g, mp 147—150°C. The compound was crystallized from ethanol, mp 149—152°C.

Found: C, 55.03; H, 4.81; N, 12.26%. Calcd for $C_{21}H_{22}O_8N_4$: C, 55.02; H, 4.84; N, 12.22%.

1770 (ester), 1700(carbobenzoxy), 1495 and 1355-(NO_2)cm^{-1}.

***p*-Nitrophenyl L-Alanyl-glycyl-glycine Hydrobromide (X).** The compound (IX), 3 g, was dissolved at room temperature in 5 m*l* of acetic acid which was half saturated with hydrogen bromide. After 30 min excess hydrogen bromide was replaced by a nitrogen stream, then the solvent was removed under reduced

24) G. D. Fasman, in "Polyamino Acids, Polypeptides, and Proteins," ed. by M. A. Stahmann, the University of Wisconsin Press, Madison (1962), p. 221.

pressure at 45°C. The resultant oil was washed thoroughly with dry diethyl ether, and dissolved in isopropyl alcohol. On adding dry ether and storage in the refrigerator, the desired ester hydrobromide (X) appeared as fine crystals, 1.5 g, mp 180°C dec., slightly hygroscopic. Further purification of X was carried out with isopropyl alcohol and diethyl ether. The compound X was stored in a dark place, since the compound colored in a brighter place.

Found: C, 38.32; H, 4.40; N, 14.06%. Calcd for $C_{13}H_{16}O_6N_4$: C, 38.53; H, 4.23; N, 13.83%.

1778 (ester), 1361 (NO_2) cm^{-1}.

Ethyl Carbobenzoxy-L-alanyl-L-alanyl-glycinate (XIII). Ethyl carbobenzoxy-L-alanyl-L-alaninate (XI) was derived from carbobenzoxy-L-alanine hydrazide (II) and ethyl L-alaninate hydrochloride (I) by an azide method, and recrystallized from ethyl acetate–*n*-hexane, mp 115—117°C (lit.[18,25] mp 116°C). The compound (XI) was reacted with hydrazine in ethanol to afford carbobenzoxy-L-alanyl-L-alanine hydrazide (XII), which was recrystallized from ethanol, mp 211—213°C (lit.[18] mp 209°C). 10 g of XII was dissolved in the mixture of 5 N hydrochloric acid (15.5 m*l*) and water (300 m*l*), and cooled to −10°C. A solution of 2.7 g of sodium nitrite in 10 m*l* of water was then added to it, and the resultant precipitate was extracted with chloroform (150 m*l* × 2). The combined extracts were washed with water and 3% sodium bicarbonate solution and reacted with ethyl glycinate which was prepared from 7 g of ethyl glycinate hydrochloride and 6.7 g of triethylamine in 100 m*l* of chloroform. After standing overnight at 2—3°C, the reaction mixture was washed thoroughly with 0.5 N hydrochloric acid and 3% sodium bicarbonate solution. The solvent was removed under reduced pressure to give a crystalline tripeptide ethyl ester (XIII), 9.2 g, mp 170°C. Recrystallization twice from ethanol raised the mp to 177—179°C.

Found: C, 57.03; H, 6.41; N, 11.13%. Calcd for $C_{18}H_{25}O_6N_3$: C, 56.98; H, 6.64; N, 11.08%.

IR: 1742 (ester), 1683 (carbobenzoxy) cm^{-1}.

Carbobenzoxy-L-alanyl-L-alanyl-glycine (XIV). Ethyl ester XIII was hydrolyzed in aqueous methanol with 1.3 equivalent of sodium hydroxide as described in the preparation of VIII. It was recrystallized from water or dimethylformamide-chloroform, mp 205—206°C. Yield was about 85%.

Found: C, 54.64; H, 6.05; N, 11.91%. Calcd for $C_{16}H_{21}O_6N_3$: C, 54.69; H, 6.02; N, 11.96%.

IR: 1730 (broad, COOH), 1670 (carbobenzoxy) cm^{-1}.

***p*-Nitrophenyl Carbobenzoxy-L-alanyl-L-alanyl-glycinate (XV).** Five grams of dicyclohexylcarbodiimide in 10 m*l* of chloroform was added dropwise to the mixture of 5 g of the compound XIV, 2.26 g of *p*-nitrophenol, and 90 m*l* of dimethylformamide with magnetically stirring at 0°C. The reaction mixture was stirred overnight at room temperature. A half milliliters of acetic acid was added to it to destroy an excess carbodiimide and stirring was continued for another 2 hr. Dicyclohexylurea was filtered off and the solvent dimethylformamide was removed at 1 mm/Hg until a few milliliters of dimethylformamide remained. On adding 20 m*l* of chloroform and standing for a few hours, the solution separated further amounts of dicyclohexylurea. This step was repeated several times to eliminate cyclohexylurea as possible. The syrup remained was dissolved in a few milliliters of chloroform and kept in the refrigerator to give crystalline XV. Yield, 6.0 g (90% of theory). Crude material was recrystallized from methanol, mp 192—193°C.

Found: C, 55.54; H, 5.15; N, 11.94%. Calcd for $C_{22}H_{24}O_8N_4$: C, 55.93; H, 5.12; N, 11.86%.

IR: 1760 (ester), 1685 (carbobenzoxy), 1345 (NO_2) cm^{-1}.

***p*-Nitrophenyl L-Alanyl-L-alanyl-glycinate Hydrobromide (XVI).** The compound XV was dissolved in 6 m*l* of acetic acid saturated with hydrogen bromide. After the reaction had proceeded for 2 hr, excess hydrogen bromide and acetic acid were removed under reduced pressure at 40°C. The gummy residue was washed thoroughly with dry diethyl ether to be free from the traces of acid. On addition of small amount of methanol, tripeptide ester hydrobromide XVI crystallized out soon, 1.3 g, mp 172—184°C with decomposition. For the polymerization, the material was recrystallized from methanol three times, mp 180—185°C with decomposition.

Found: C, 39.79; H, 4.71; N, 11.91%. Calcd for $C_{14}H_{18}O_6N_4 \cdot HBr \cdot CH_3OH$: C, 39.92; H, 5.14; N, 12.42%.

IR: 1764 (ester), 1492 and 1355 (NO_2) cm^{-1}.

Ethyl Carbobenzoxy-L-alanyl-L-alanyl-L-alanyl-glycinate (XVIII). Ten grams of carbobenzoxy-L-alanyl-L-alanine hydrazide XII was reacted with ethyl L-alanyl-glycinate in the same condition as mentioned in the synthesis of the compound XIII. Ethyl L-alanyl-glycinate was prepared from triethylamine (5.1 g) and XVII (13 g), which in turn was obtained by the deacylation of ethyl carbobenzoxy-L-alanyl-glycinate, VI, in acetic acid saturated with hydrogen bromide. After standing for 24 hr at room temperature, the reaction mixture separated the crystalline XVIII. Filtration and recrystallization from ethanol-water gave a pure product, 9.5 g, mp 235—237°C.

Found: C, 56.03; H, 6.88; N, 12.38%. Calcd for $C_{21}H_{30}O_7N_4$: C, 55.99; H, 6.71; N, 12.44%.

IR: 1748 (ester), 1695 (carbobenzoxy) cm^{-1}.

Carbobenzoxy-L-alanyl-L-alanyl-L-alanyl-glycine (XIX). Tripeptide ethyl ester (XVIII, 7 g) was hydrolyzed with 31 m*l* of 1 N sodium hydroxide in 40% aqueous methanol. On acidification with 7 m*l* of 5 N hydrochloric acid, free acid (XIX) crystallized out as fine needles, 2.6 g, mp 225°C. It was crystallized from ethanol-water, the sample for analysis had mp 232—234°C. The same pure sample was obtained by reprecipitation (after dissolving the material in 1 N sodium hydroxide, the required amount of 5 N hydrochloric acid was added).

Found: C, 54.01; H, 6.31; N, 13.29%. Calcd for $C_{19}H_{26}O_7N_4$: C, 54.02; H, 6.20; N, 13.26%.

IR: 1720 (COOH), 1697 (carbobenzoxy) cm^{-1}.

***p*-Nitrophenyl Carbobenzoxy-L-alanyl-L-alanyl-L-alanyl-glycinate (XX).** 2.1 g of the tetrapeptide free acid XIX was reacted with *p*-nitrophenol (0.85 g) and dicyclohexylcarbodiimide (1.25 g) in 30 m*l* of dimethylformamide. The *p*-nitrophenyl ester XX was crystallized from dioxane-water or ethanol-water. The material from dioxane-water showed slightly higher mp (240°C with decomposition), than that from ethanol-water (mp 236—237°C with decomposition).

25) W. H. Stein, S. Moore and M. Bergmann, *J. Biol. Chem.*, **154**, 191 (1944).

Found: C, 55.46; H, 5.00; N, 12.62%. Calcd for $C_{25}H_{29}O_9N_5$: C, 55.24; H, 5.38; N, 12.89%.

IR: 1672(ester), 1705(sh. carbobenzoxy), 1353(NO_2) cm^{-1}.

p-Nitrophenyl L-Alanyl-L-alanyl-L-alanyl-glycine Hydrobromide (XXI). The compound XX was deacylated in hydrogen bromide-saturated acetic acid as described in the case of XVI. The resulting oily product was crystallized and recrystallized from isopropyl alcohol and ethyl ether in about 70% yield, mp 153°C (decomposition). This material was highly hygroscopic and labile to light.

Found: C, 41.78; H, 5.91; N, 14.16%. Calcd for $C_{17}H_{23}O_7N_5 \cdot HBr$: C, 41.64; H, 4.93; N, 14.28%.

IR: 1680 (ester), 1360 (NO_2) cm^{-1}.

Ethyl Carbobenzoxy-L-alanyl-glycyl-glycyl-glycinate (XXII). Twenty-two grams of carbobenzoxy-L-alanyl-glycine was dissolved in the mixture of ethyl glycyl-glycinate hydrochloride (19 g), triethylamine (9.8 g), and dimethylformamide (200 m*l*). To this turbid solution, 18 g of dicyclohexylcarbodiimide in dimethylformamide (50 m*l*) was added portionwise under cooling. After stirring for 24 hr at room temperature, the product ester was obtained by the usual manner, and crystallized from ethanol, 21.5 g, mp 168—169°C. Analytical sample which was recrystallized twice from ethanol showed mp 173—175°C.

Found: C, 54.21; H, 6.13; N, 13.29%. Calcd for $C_{19}H_{26}O_7N_4$: C, 54.02; H, 6.20; N, 13.26.

IR: 1740 (ester) 1696 (carbobenzoxy) cm^{-1}.

Attempted Hydrolysis of Tetrapeptide Ester XXII. a) The peptide ester XXII was treated with 1.3 equivalent molar of sodium hydroxide in 50% aqueous methanol for 48 hr at room temperature. On acidifying and concentrating the reaction mixture, the resultant products contained 90% or more of the starting ester XXII (from an infrared spectra). Tetrahydrofuran, in place of methanol, was also used as solvent, but showed no significant effects.

b) The peptide ester XXII was boiled for 15 min under the same medium described as above. The infrared spectra of the products thus obtained showed a significant relative decrease of the peak 1695 cm^{-1} (carbonyl group of benzyloxycarbonyl moiety). Furthermore, the products was oily and resisted towards further attempts to purify them. The same destruction of benzyloxycarbonyl group was observed in the trial for ester interchange reaction. In that case, the peptide ester XXII was refluxed with large amount of *p*-nitrophenol in tetrahydrofuran in the presence of *p*-toluenesulfonic acid.

Isobutyl Glycyl-glycinate Hydrobromide (XXVI). Isobutyl glycinate hydrochloride (XXIV) was prepared in the usual manner from isobutyl alcohol, glycine, and hydrogen chloride. XXIV was coupled with carbobenzoxy-glycine using dicyclohexylcarbodiimide to afford isobutyl carbobenzoxy-glycyl-glycinate (XXV) in 91% yield.

Thirty five grams of XXV was dissolved in 50 m*l* of acetic acid saturated with hydrogen bromide. After 30 min, the separated crystalline hydrobromide XXVI was filtered. Filtrate gave further crop of XXVI on concentration under reduced pressure. The combined material was recrystallized from isobutyl alcohol, 24.2 g (83% of theory), mp 184—188°C.

Found: C, 35.67; H, 6.19; N, 9.99%. Calcd for $C_8H_{16}O_3N_2 \cdot HBr$: C, 35.69; H, 6.36; N, 10.41%.

IR: 1743(ester) cm^{-1}.

Isobutyl Carbobenzoxy-L-alanyl-glycyl-glycyl-glycinate (XXVII). To the cold suspension of carbobenzoxy-L-alanyl-glycine (VII, 10 g), isobutyl glycyl-glycinate hydrobromide (XXVI, 11.5 g) and triethylamine (4.33 g) in dimethylformamide (100 m*l*), 8.1 g of dicyclohexylcarbodiimide in 30 m*l* of dimethylformamide was added dropwise at 0°C with magnetically stirring. Stirring was continued for 24 hr at room temperature. Following filtration through Hyflo "Super-Cel", solvent was evaporated under reduced pressure at 45°C. Scratching and trituration with water induced crystallization. The product (XXVII) was filtered off and recrystallized from ethyl acetate or aqueous tetrahydrofuran. There were slight differences in the fingerprint region of infrared spectra between the product crystallized from ethyl acetate and that from tetrahydrofuran and water; the former had higher mp (141—145°C), the latter lower mp (122—128°C). Elementary analysis was taken with the product from ethyl acetate.

Found: N, 12.01%. Calcd for $C_{21}H_{30}O_7N_4$: N, 12.44%.

IR: 1719 (ester), 1699 (carbobenzoxy) cm^{-1}.

The isobutyl ester, XXVII, was not hydrolyzed under the condition shown above.

Polymerization of X, XVI and XXI. Each compound was dissolved in dimethyl sulfoxide to give a 30—40% solution. With vigorous stirring, an equimolar amount of triethylamine was added to it in a portion. Stirring was continued, but after about 30 min, the reaction mixture solidified. After 1 day, the completely solidified mixutre was crushed and washed with dimethyl sulfoxide (5 times, applying a centrifugation) and methanol. The resultant pale yellow powder was dissolved in a few milliliters of dichloroacetic acid, filtered with a glass-filter. Polymer was reprecipitated from this solution with methanol or chloroform. Amino acid analysis: (a) Poly-(L-Ala-Gly_2), Ala : Gly=0.99 : 2; (b) Poly-(L-Ala_2-Gly), Ala : Gly=2.01 : 1; (c) Poly-(L-Ala_3-Gly), Ala : Gly=2.98 : 1.

Elementary analysis: (a) Poly-(L-Ala-Gly_2). Found: C, 45.49; H, 5.79; N, 22.67%. Calcd for $(C_7H_{11}O_3N_3)_n$: C, 45.40; H, 5.99; N, 22.69%. (b) Poly-(L-Ala_2-Gly). Found: C, 47.21; H, 6.27; N, 19.98%. Calcd for $(C_8H_{13}O_3N_3)_n$: C, 48.23; H, 6.58; N, 21.10%. (b) Poly-(L-Ala_3-Gly). Found: C, 47.32; H, 6.80; N, 19.52%. Calcd for $(C_{11}H_{18}O_4N_4)_n$: C, 48.88; H, 6.71; N, 20.73%.

Viscosities in dichloroacetic acid: (a) Poly-(L-Ala-Gly_2); $\eta_{sp}/c=0.235$ ($c=1\%$), $[\eta]=0.22$. (b) Poly-(L-Ala_2-Gly); $\eta_{sp}/c=0.294$ ($c=1\%$), $[\eta]=0.26$. (c) Poly-(L-Ala_3-Gly); $\eta_{sp}/c=0.170$ ($c=1\%$), $[\eta]=0.15$.

Optical Purity. 0.5% solutions of polymers in 6 N hydrochloric acid were heated in refluxing xylene for 24 hr. Hydrolysates were evaporated to dryness in a vacuum desiccator in which potassium hydroxide was placed, and redissolved in 0.1 N hydrochloric acid to make 1% solutions. L-Alanine itself was also treated under the same condition. Optical rotatory dispersion curve was measured on each sample; the value of molecular rotation in the range of 240 mμ to 600 mμ were identical in each case within 5% error. These values are: 518° at 250 mμ, 135° at 300 mμ, 62° at 350 mμ, and 27° at 400 mμ.

The author wishes to express very much thanks to Professor Fumio Oosawa and the members of his laboratory for their encouragements and discussions. Thanks are also due to Professor Yoshimasa Hirata and Ajinomoto Co. Inc., for their interests and supports in this work. Mr. Natsuki Kato arranged the microanalysis, and it is the author's pleasure to acknowledge him.

BULLETIN OF THE CHEMICAL SOCIETY OF JAPAN VOL. 42 527—529 (1969)

Organic Syntheses by Means of Metal Complexes. II.[1] Oxo Reaction Catalyzed by Cyclopentadienyliron Dicarbonyl Dimer

Jiro Tsuji and Yoichi Mori

Basic Research Laboratories, Toyo Rayon Co., Kamakura

(Received July 10, 1968)

It was found that cyclopentadienyliron dicarbonyl dimer is an active catalyst for oxo reaction and the characteristic features of the catalysis have been studied.

Carbonylation reactions of olefins are catalyzed by transition metal carbonyls, and iron, cobalt and nickel carbonyls are commonly used for the reactions. These metal carbonyls catalyze different types of the carbonylation reactions of olefins and acetylenes.[2,3] The relationship between the structure of the metal carbonyls and their catalytic activity seems to be an interesting problem. Metal carbonyls can be classified into mononuclear and polynuclear carbonyls as one way of the classification. Typical mononuclear carbonyls are nickel tetracarbonyl and iron pentacarbonyl. Dicobalt octacarbonyl (I) belongs to the latter and has a cobalt-cobalt bonding. The major difference of the catalytic activity of these two types of metal carbonyls can be explained in the following way from a mechanistic standpoint. It is known that the first step of the carbonylation reactions is the formation of a metal hydride bond in most cases. Dicobalt octacarbonyl forms cobalt tetracarbonyl hydride (II) by splitting the cobalt-cobalt bond by reacting with hydrogen as shown below.

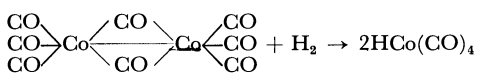

$$+ H_2 \rightarrow 2HCo(CO)_4$$

I II

On the other hand, the carbonylation reaction catalyzed by nickel tetracarbonyl proceeds in the presence of hydrogen halide and the first step of the carbonylation is the oxidative addition of hydrogen halide to nickel tetracarbonyl to form halonickeldicarbonyl hydride (III).[4]

$$Ni(CO)_4 + HX \longrightarrow HNi(CO)_2X + 2CO$$

III

Once these metal hydrides are formed, then follows the insertion of olefin into the metal hydride bond in both cases.

It is possible to convert mononuclear carbonyls into dinuclear carbonyls by the coordination of cyclopentadienyl anion. For example, nickel, iron and molybdenum carbonyls can be converted into the dinuclear ones by reacting with dicyclopentadiene ($C_{10}H_{12}$).

$$2Fe(CO)_5 + C_{10}H_{12} \longrightarrow$$

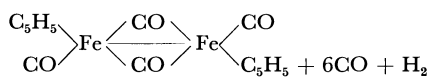

$$+ 6CO + H_2$$

IV

On the other hand, dicobalt octacarbonyl can be converted into the mononuclear cyclopentadienyl cobalt dicarbonyl (V) by the reaction of cyclopentadiene as shown below.

$$Co_2(CO)_8 + 2C_5H_6 \rightarrow 2C_5H_5Co(CO)_2 + 4CO + H_2$$

I V

Thus it seems interesting to investigate the catalytic activity of these mono- and dinuclear carbonyls coordinated with cyclopentadienyl anion. So far no studies have been reported on the catalytic activity of these metal carbonyls coordinated with

1) Part 1. T. Susuki and J. Tsuji, *Tetrahedron Letters*, **1968**, 913.

2) C. E. Bird, *Chem. Revs.*, **62**, 283 (1962).

3) H. Wakamatsu, *Yûki Gôsei Kagaku Kyokaishi* (*J. Soc. Org. Synth. Chem., Japan*), **25**, 999 (1967).

4) R. F. Heck, *J. Am. Chem. Soc.*, **85**, 2013 (1963).

cyclopentadienyl anion. In other words, this study was undertaken to find whether there is any similarity in the catalytic activity between dicobalt octacarbonyl (I) and cyclopentadienyliron dicarbonyl dimer (IV). In this paper the catalytic activity of the complex (IV) in oxo reaction is described.

The oxo reaction, namely the formation of aldehydes from olefins, carbon monoxide and hydrogen, is carried out most satisfactorily by the catalytic action of typical dinuclear carbonyls such as cobalt and rhodium carbonyls. So far, there is no report that any iron carbonyls are active for the oxo reaction. Now it was found that the oxo reaction can be carried out with the complex IV as the catalyst under certain conditions. The reaction of propylene with carbon monoxide and hydrogen to form butyraldehydes was studied under several different conditions.

$$CH_3CH{=}CH_2 + H_2 + CO \xrightarrow{IV} CH_3CH(CHO)CH_3 + CH_3CH_2CH_2CHO$$

Table 1. Effect of pressure[a]

Press. (atm) H_2	Press. (atm) CO	Ratio of iso/*n*-aldehyde	Yield (%)[b]	Higher aldehydes (g)
50	50	2.14	69.5	0.68
100	50	1.45	52.3	0.68
75	75	1.98	45.5	0.79

a) Reactions were carried out with the complex IV (0.7 g), propylene (10 ml), benzene (15 ml), and toluene (2 ml), at 150°C for 40 hr.
b) Total yield of C_4 aldehydes based on the charged propylene.

Table 2. Effect of reaction temperature and time[a]

Reaction Temp. (°C)	Reaction Time (hr)	Ratio of iso/*n*-aldehyde	Yield (%)	Higher aldehydes (g)
175	40	2.52	10.5	0.3
150	40	2.14	69.5	0.68
150	15	2.06	9.1	trace
125	40	—	trace	—

a) Reactions were carried out with the complex IV (0.7 g), propylene (10 ml), benzene (15 ml), hydrogen (50 atm) and carbon monoxide (50 atm).

In Tables 1 and 2, the effects of the reaction temperature, time and pressure on the reaction are shown. From these results, several characteristic features of the catalytic activity of the complex IV are apparent. One of them is that a larger amount of isobutyraldehyde was formed than *n*-butyraldehyde, and higher hydrogen pressure relative to that of carbon monoxide tends to favor the formation of the normal aldehyde. In the usual oxo reaction catalyzed by dicobalt octacarbonyl, several by-products are formed. For example, the hydrogenation of aldehydes to alcohols is observed in a considerable extent by hydrogenating activity of dicobalt octacarbonyl. Also aldol condensation of the aldehydes to form higher unsaturated aldehydes is another side reaction. A strongly acidic cobalt-tetracarbonyl hydride catalyzes the aldol condensation. These side reactions were almost negligible in the oxo reaction catalyzed by the complex IV and the products of the reaction were almost free of the alcohols and aldol condensation products. Therefore, it can be said that the acidic property and hydrogenating activity of the complex IV are weaker than those of dicobalt octacarbonyl.

Table 3. Oxo reaction of butenes[a]

Butene	Ratio of 2-methylbutyraldehyde/*n*-valeraldehyde	Yield (%)[b]	Higher aldehydes (g)
1-Butene	2.03	53.8	0.18
cis-2-Butene	2.59	25.4	0.62
trans-2-Butene	3.02	16.8	0.57

a) Reactions were carried out with the complex IV (0.7 g), butene (10 ml), benzene (15 ml), hydrogen (50 atm), and carbon monoxide (50 atm) at 150°C for 40 hr.
b) Total yield of C_5 aldehydes based on the charged butenes.

Several solvents were tested in the reaction and it was found that ethanol and benzene were most satisfactory. When the reaction was carried out in ethanol, the product was aldehydes and no ester was formed. Then the carbonylation of 1-butene, *cis*- and *trans*-2-butenes was carried out and the results are shown in Table 3. It was observed that 1-olefin is more reactive than 2-olefins, and cis olefin is more reactive than trans olefin as expected. It should be noticed that *n*-valeraldehyde was formed in a considerable amount from 2-butenes and it is apparent that the complex IV catalyzes the isomerization of the inner olefins to the terminal olefins.

It can be said that the catalytic activity of the complex IV is somewhat lower than that of dicobalt octacarbonyl and longer reaction time is necessary. The range of optimum reaction temperature seems to be narrow, and best result was obtained at 150°C. After the reaction, it is possible to recover the catalyst intact by handling the reaction mixture under mild conditions and the recovered catalyst can be used again.

Finally the mechanism of the reaction is proposed in the following way. The first step of the reaction is the splitting of the iron-iron bond with hydrogen to form cyclopentadienylirondicarbonyl hydride (V). The successive insertions of olefin and carbon monoxide are followed to form alkyl (VI) and acyl complex (VII). Finally, the acyl complex (VII) is converted into the aldehyde with the regeneration of the hydride complex (V).

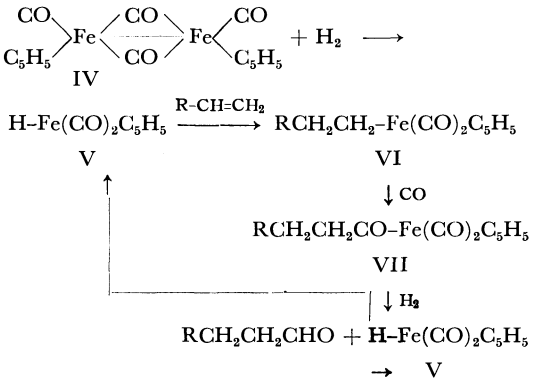

Experimental

Material. Cyclopentadienyliron dicarbonyl dimer was prepared by a known method from iron pentacarbonyl and dicyclopentadiene (red purple crystals, mp 194°C (decomp.).[5]

Oxo Reaction of Propylene. Only typical reaction is described. The complex IV (0.7 g), benzene (15 m*l*) and toluene (2 m*l*) were mixed in a glass vessel equipped with a gas inlet capillary, and the vessel was placed in an autoclave (100 m*l*). Liquid propylene (10 m*l*) was measured in a measuring glass tube and then distilled into the autoclave with cooling in a dry ice bath. Carbon monoxide and hydrogen (50 kg/cm² each) were introduced at room temperature. The reaction was carried out at 150°C for 40 hr with shaking. Pressure drop of 80 kg/cm² was observed during the reaction. The amounts of the aldehydes formed were determined gas chromatographically (squalene at 100°C) and the formation of *n*-butyraldehyde (2.3 g) and isobutyraldehyde (4.93 g) was confirmed. By distillation, 0.68 g of a higher boiling aldehyde was obtained.

5) R. B. King, "Organometallic Syntheses," Vol. 1, Academic Press, New York (1965), p. 114.

BULLETIN OF THE CHEMICAL SOCIETY OF JAPAN VOL. 42 529—533 (1969)

Studies of Aminosugars. XXI. The Total Synthesis of Kanamycin C[1)]

Sumio UMEZAWA, Shinkiti KOTO, Kuniaki TATSUTA and Takayuki TSUMURA

Department of Applied Chemistry, Faculty of Engineering, Keio University, Koganei-shi, Tokyo

(Received July 16, 1968)

4-*O*-(3-*O*-Benzyl-2-carbobenzoxyamino-4,6-*O*-isopropylidene-2-deoxy-*α*-D-glucopyranosyl)-*N*,*N*′-dicarbobenzoxy-2-deoxystreptamine has been prepared from paromamine and condensed with 3-acetamido-2,4,6-tri-*O*-benzyl-3-deoxy-*α*-D-glucopyranosyl chloride by a modified Koenigs-Knorr reaction. The identity of the synthetic *α*,*α*-diglycoside with a substance of the same structure derived from natural kanamycin C was shown. Removal of the masking groups gave the product identical with natural kanamycin C.

In recent years, certain strains of *Streptomyces* have been found to produce aminoglycosidic antibiotics which are entirely carbohydrate in nature, for example, streptomycins, neomycins, kanamycins and paromomycins. Interest in the chemistry of aminoglycosides has recently become widespread and has received added impetus as the recognition of the great importance of the aminoglycosidic antibiotics in medicines and biology has grown. However, none of these carbohydrate-antibiotics has never been synthesized. In this paper we describe the total synthesis of kanamycin C, a member of kanamycin congeners, syntheses of other members, kanamycin A and B, being described in the following papers.

In a previous paper[2)] we prepared the *β*,*β*-

1) Part XXXVI of "Studies on Antibiotics and Related Substances" by Sumio Umezawa. This paper was read before the 21th Annual Meeting of the Chemical Society of Japan, Osaka, April, 1968. (See abstracts of papers of the Meeting, Vol. 3, p. 2212). A part of this work has been briefly communicated: S.Umezawa, S. Koto, K. Tatsuta and T. Tsumura *J. Antibiotics*, **21**, 162 (1968).

2) S. Koto, Y. Ito and S. Umezawa, This Bulletin, **38**, 1447 (1965).

diglycosides, which are kanamycin-analogues, from deoxystreptamine and 3-amino-3-deoxy-D-glucose or 6-amino-6-deoxy-D-glucose by way of the Koenigs-Knorr reaction and found that these compounds showed no antibiotic activity. These results underlined the fact that the approach to the synthesis of aminoglycosidic antibiotics found difficulty in the formation of α-glycosidic linkages. The preparation of α-glycopyranosides in high yields still remains the most important problem of carbohydrate chemistry, and in these circumstances we considered it advisable, as far as possible, to suitably mask 1-halogeno-sugars on one hand, and to partially mask aglycones on the other hand, considering the neighboring groups participation.

Kanamycin C was first discovered by Rothrock *et al.*,[3] and the structure (VIII) was elucidated by Murase.[4] Kanamycin C is composed of 3-amino-3-deoxy-D-glucose and paromamine[5] (I) which is a nonreducing fragment of paromomycin and is an α-glycoside of 2-amino-2-deoxy-D-glucose joined at C-1 to the C-4 of 2-deoxystreptamine. In this paper we described the synthesis of kanamycin C from paromamine. Since we[6] have previously synthesized paromamine, the combined achievements constitute the first synthesis of kanamycin C.

Paromamine was treated with carbobenzoxy chloride in the presence of sodium carbonate in aqueous acetone at about −10°C to give tri-*N*-carbobenzoxy-paromamine (II) in an 88% yield, which was acetonated with 2,2-dimethoxypropane in the presence of *p*-toluenesulfonic acid in *N*,*N*-dimethylformamide (DMF) at 110°C to give the diisopropylidene derivative (III), mp 243—245°C, $[\alpha]_D^{18}$ +71° (*c* 0.59, DMF), in a quantitative yield. According to the finding by Evans *et al.*[7] that the acetal exchange reaction of methyl α-D-glucopyranoside with 2,2-dimethoxypropane mainly gives methyl 4,6-*O*-isopropylidene-α-D-glucoside, the structure of III is considered to include an isopropylidene group attached to C-4 and C-6 in the glucosamine moiety.

Benzylation of III with benzyl bromide in the presence of barium oxide and barium hydroxide in DMF gave IV, mp 160—162°C, $[\alpha]_D^{18}$ +72° (*c* 0.60, DMF), in a 82% yield. Deacetonation of IV by treatment with 80% acetic acid gave quantitatively 4-*O*-(3-*O*-benzyl-2-carbobenzoxyamino-2-deoxy-α-D-glucopyranosyl)-*N*,*N*′-dicarbobenzoxy-2-deoxystreptamine (V), mp 270—271°C (decomp.), $[\alpha]_D^{18}$ +101° (*c* 0.52, DMF).

When V was caused to react with 2,2-dimethoxypropane at room temperature, partial acetonation of V was successful to give monoisopropylidene derivative (VI), mp 239—241°C, $[\alpha]_D^{18}$ +75° (*c* 0.63, DMF), in a 55% yield. It is worth mentioning that the hydroxyl groups of C-4 and C-6 in the glucosamine moiety were acetonated in preference to the hydroxyl groups in deoxystreptamine.

3-Acetamido-2,4,6-tri-*O*-benzyl-3-deoxy-α-D-glucopyranosyl chloride[8] was condensed with VI in the presence of mercuric cyanide and Drierite in benzene-dioxane at 100°C. The product was treated with acetic acid to remove the isopropylidene group, hydrogenated over palladium black in a mixture of dioxane-water-concentrated hydrochloric acid to remove carbobenzoxy and benzyl groups, and de-*N*-acetylated with barium hydroxide to give a ninhydrin-positive product. This was dinitrophenylated with 2,4-dinitrofluorobenzene in the presence of sodium bicarbonate in aqueous ethanol and then *O*-acetylated with acetic anhydride and anhydrous sodium acetate. The product, which showed about four spots with R_f-values of 0.56, 0.45, 0.35 and 0.27 on a thin-layer chromatogram (TLC) with a solvent system: toluene-MEK (2 : 1), was chromatographed on a silica-gel column with the same solvent system. The substance of R_f-value 0.35 was isolated to give synthetic hepta-*O*-acetyl-tetra-*N*-(2,4-dinitrophenyl)-kanamycin C (VII), mp 208—211°C (decomp.), $[\alpha]_D^{18}$ +285° (*c* 0.75, acetone), in a 15% overall yield from VI.

On the other hand, natural kanamycin C was dinitrophenylated and acetylated to give hepta-*O*-acetyl-tetra-*N*-(2,4-dinitrophenyl) derivative of kanamycin C, mp 208—211°C (decomp.), $[\alpha]_D^{18}$ +299° (*c* 0.64, acetone).

The identity of the synthetic VII with the above mentioned derivative of natural kanamycin C was established by elemental analyses, specific rotations, by their failure to depress the mixed melting point and identical mobilities on TLC and infrared spectra.

Hydrolysis of VII with methanolic ammonia followed by treatment with Dowex 1×2 (OH^-) resin gave a crystalline free base of synthetic kanamycin C (VIII), $[\alpha]_D^{18}$ +139° (*c* 0.50, water), which was identical with an authentic sample of the natural kanamycin C. Optical rotations were essentially equal and infrared spectra were superimposable. On descending paper chromatography the R_f-value of the synthetic VIII agreed with

3) J. W. Rothrock, R. T. Goegelman and F. J. Wolf, *Antibiotics Annual*, **1958/59**, 796.

4) M. Murase, *J. Antibiotics*, **A14**, 367 (1961).

5) T. H. Haskell, J. C. French and Q. R. Bartz, *J. Am. Chem. Soc.*, **81**, 3480 (1959).

6) S. Umezawa and S. Koto, This Bulletin, **39**, 2014 (1966).

7) M. E. Evans, F. W. Parrish and L. Long, Jr., *Carbohydrate Research*, **3**, 453 (1967).

8) This compound was reported by S. Umezawa *et al.* at the 20th Annual Meeting of the Chemical Society of Japan, Tokyo, March 31, 1967. (See abstracts of the papers of the Meeting, III, p. 596.) S. Koto, T. Tsumura, Y. Kato and S. Umezawa, This Bulletin, **41**, 2765 (1968).

9) S. Umezawa, S. Koto, K. Tatsuta and T. Tsumura, *J. Antibiotics*, **21**, 163 (1968).

that of natural kanamycin C. The antibiotic spectra[9] and minimal inhibitory concentrations of the synthetic VIII against test organisms were in agreement with those of natural kanamycin C.

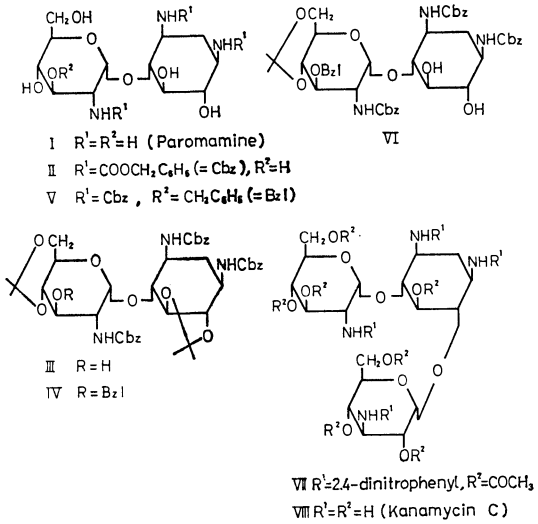

Experimental

General Procedures. Thin layer chromatography (TLC) was performed on "Silica-Rider for TLC" (Daiichi Pure Chemicals Co.) using the following solvent systems: (a) benzene - methyl ethyl ketone (MEK) (4 : 1), (b) benzene - MEK (1 : 1), and (c) toluene - MEK (2 : 1). The 2,4-dinitrophenyl (DNP) derivatives were visualized directly on an air-dried plate as yellow spots, while others were detected by spraying a dried chromatogram with 50% sulfuric acid and heating it at 110°C. Paper chromatography was performed on Toyo filter paper No. 51, using a solvent system: (d) *n*-butanol - pyridine - water - acetic acid (6 : 4 : 3 : 1); ninhydrin in pyridine (0.3%) was sprayed on. Infrared spectra were determined in potassium bromide pellets.

Tri-*N*-carbobenzoxyparomamine (II). To a mixture of paromamine (I) (5 g) and sodium carbonate (15 g) in water (50 m*l*) and acetone (150 m*l*) was added slowly carbobenzoxychloride in toluene (30%, 28 g) under stirring at −10—−5°C. After having been stirred for about 4 hr, the reaction mixture was set aside in a refrigerator overnight. The resulting white solid was shaken with a mixture of water (400 m*l*) and ether (20 m*l*), collected by filtration and pressed between filter papers to remove moisture and oily matters. The waxy product was triturated with 1 N hydrochloric acid (300 m*l*), filtered, washed with water and dried *in vacuo*. Recrystallization from dioxane (400 m*l*) gave a colorless solid, 6.7 g, mp 258°C (decomp.), $[\alpha]_D^{18}$ +64.5° (*c* 0.67, DMF). The mother liquor deposited a further crop, 3.1 g. Total yield 88%. IR spectrum: 3330, 1697 and 1542 cm^{-1} (NHCbz).

Found: C, 59.74; H, 6.28; N, 5.55%. Calcd for $C_{36}H_{43}N_3O_{13}$: C, 59.58; H, 5.97; N, 5.79%.

4-*O*-(2-Carbobenzoxyamino-4,6-*O*-isopropylidene-2-deoxy-*α*-D-glucopyranosyl)-*N*,*N*′-dicarbobenzoxy-5,6-*O*-isopropylidene-2-deoxystreptamine (III). To a solution of II (4.7 g) in anhydrous DMF (30 m*l*) was added *p*-toluenesulfonic acid monohydrate (0.06 g) and 2,2-dimethoxypropane (6.2 m*l*), and the solution was heated at 110°C for 4 hr with occasional stirring. The mixture was neutralized with Amberlite IRA-400 (OH type) washed with methanol before use and filtered. Concentration gave a residue, which solidified when triturated with water. Recrystallization from ethanol; colorless crystals, 5.2 g (98%), mp 243—245°C, $[\alpha]_D^{18}$ +71° (*c* 0.59, DMF), IR spectrum: 3340, 1698 and 1533 (NHCbz), 1167, 1137 and 1047 cm^{-1} (ketal).

Found: C, 62.63; H, 6.50; N, 5.39%. Calcd for $C_{42}H_{51}N_3O_{13}$: C, 62.60; H, 6.38; N, 5.21%.

4-*O*-(3-*O*-Benzyl-2-carbobenzoxyamino-4,6-*O*-isopropylidene-2-deoxy-*α*-D-glucopyranosyl)-*N*,*N*′-dicarbobenzoxy-5,6-*O*-isopropylidene-2-deoxystreptamine (IV). To a solution of III (5.1 g) in anhydrous DMF (80 m*l*) was added pulverized barium oxide (5.2 g) and barium hydroxide octahydrate (6.2 g) with stirring and the mixture was cooled to −10°C. Benzyl bromide (3.7 m*l*) was added drop by drop to the mixture under vigorous agitation. The reaction temperature was allowed to rise gradually to 0°C during 4 hr and then to room temperature during an additional 4 hr. The slightly colored mixture was further stirred continuously for 20 hr at room temperature. Chloroform (150 m*l*) was added and the mixture was filtered through a layer of Celite (thickness 20 mm). The filtrate was evaporated to give a sirup, which was chromatographed on a silica-gel column (400 g, 51 × 510 mm) with a solvent mixture (a). An eluate between 1400—2300 m*l* was evaporated to dryness. The residue was recrystallized from ethanol to give IV; yield 4.7 g (82%), mp 160—162°C, $[\alpha]_D^{18}$ +72.4° (*c* 0.61, DMF), IR spectrum: 3335, 1730—1700 and 1540—1520 cm^{-1} (NHCbz), 1172, 1132 and 1040 cm^{-1} (ketal).

Found: C, 65.47; H, 6.67; N, 4.80%. Calcd for $C_{49}H_{57}N_3O_{13}$: C, 65.68; H, 6.41; N, 4.69%.

4-*O*-(3-*O*-Benzyl-2-carbobenzoxyamino-2-deoxy-*α*-D-glucopyranosyl)-*N*,*N*′-dicarbobenzoxy-2-deoxystreptamine (V). A suspension of IV (3.0 g) in aqueous acetic acid (80%; 100 m*l*) was stirred at 50°C until the solution became clear and then kept at room temperature overnight. The resulting precipitate was collected, washed with water and dried *in vacuo*. Recrystallization from ethanol gave colorless needles of V; yield 2.7 g (98%), mp 270—271°C (decomp.), $[\alpha]_D^{18}$ +101° (*c* 0.52, DMF), IR spectrum: 3340, 1699 and 1538 (NHCbz) 1026 cm^{-1} (*O*-benzyl).

Found: C, 63.08; H, 6.13; N, 5.24%. Calcd for $C_{43}H_{49}N_3O_{13}$: C, 63.30; H, 6.05; N, 5.15%.

4-*O*-(3-*O*-Benzyl-2-carbobenzoxyamino-2-deoxy-4,6-*O*-isopropylidene-*α*-D-glucopyranosyl)-*N*,*N*′-dicarbobenzoxy-2-deoxystreptamine (VI). To a solution of V (2.2 g) in DMF (13 m*l*) was added *p*-toluenesulfonic acid (0.03 g) and 2,2-dimethoxypropane (0.8 m*l*), and the mixture was allowed to stand at room temperature overnight. After neutralization with Amberlite IRA-400 (OH type) washed with methanol before use, the solution was evaporated to give a residue, which showed two spots of R_f values 0.86 and 0.53 on TLC with the solvent system (b). The residue was chromatographed on a silica-gel column (200 g, 50 × 295 mm) with the solvent system (b), the effluent being cut into fractions of 15 m*l* each. The substance of

R_f 0.53 appeared in the fractions of tube Nos. 30—53, which afforded 1.3 g of VI (55%). Recrystallization from ethanol; mp 239—241°C, $[\alpha]_D^{18}$ +75.2° (*c* 0.63, DMF), IR spectrum: 3335, 1697 and 1535 (NHCbz), 1170, 1130 and 1035 (ketal), 1026 cm^{-1} (*O*-benzyl).

Found: C, 64.29; H, 6.11; N, 4.78%. Calcd for $C_{46}H_{53}N_3O_{13}$: C, 64.55; H, 6.24; N, 4.91%.

The diisopropylidene derivative IV (R_f 0.86) was also obtained from the fractions between tube Nos. 31—33 and weighed 0.5 g.

Proof for the Structure of VI. Monoisopropylidene derivative VI (13 mg) in DMF (1 m*l*) was benzylated in the above-mentioned manner with barium oxide (24 mg), barium hydroxide octahydrate (29 mg) and benzyl bromide (18 m*l*). The TLC of the oily product showed that VI completely vanished and a new spot appeared. The oily product was dissolved in hot aqueous acetic acid (80%) and allowed to stand at room temperature for 5 hr. The colorless solid separated was collected, yield 8 mg. The deacetonated product was hydrolyzed in a mixture of glacial acetic acid, methyl cellosolve, water and concentrated hydrochloric acid (10 : 5 : 3 : 2) by heating at 100°C for 10 hr under reflux to remove carbobenzoxy groups and to cleave the glycosidic linkage. On the other hand, a control experiment was carried out with II. The paper chromatogram of the hydrolyzates using the solvent system (d) and ninhydrin-coloration showed that the fully benzylated VI gave neither 2-amino-2-deoxy-D-glucose nor 2-deoxystreptamine, while II gave both of them, indicating that the isopropylidene and benzyl groups are present in the glucosamine moiety of VI.

Synthetic Hepta-*O*-acetyl-tetra-*N*-(2,4-dinitrophenyl)-kanamycin C (VII). A mixture of VI (1.13 g), dried powdery mercuric cyanide (0.46 g) and freshly activated Drierite (3.66 g) in a mixture of dioxane (5.5 m*l*) and benzene (11 m*l*) was heated to reflux for a few minutes under agitation. To the mixture, which was somewhat cooled, was added well dried 3-acetamido-2,4,6-tri-*O*-benzyl-3-deoxy-α-D-glucopyranosyl chloride[8] (1.3 g, 1.7 eq.) and the reaction mixture was stirred vigorously under reflux for 9 hr under anhydrous conditions. During the course of reaction the mixture turned gradually dark and somewhat pasty. The resulting mixture was filtered and thoroughly washed with dioxane and ethyl acetate. The filtrate combined with washings was evaporated to give a sirup, which was extracted with ethyl acetate (150 m*l*). The extract was washed with three 100 m*l* portions of 20% aqueous sodium chloride, dried over anhydrous sodium sulfate and evaporated to give an oily product (1.8 g). Aqueous acetic acid (80%; 20 m*l*) was added and the mixture was warmed to 50°C under stirring until the solution became clear. The solution was allowed to stand for 1 hr and evaporated to give the deacetonated product, which was then hydrogenated over palladium black (0.3 g) in a mixture of dioxane (21 m*l*), water (3.5 m*l*), ethanol (0.5 m*l*) and concentrated hydrochloric acid (2 m*l*), under 3 atm of hydrogen pressure at about 40°C with occasional addition of portions of water whose total volume was 35 m*l*. The hydrogenolysis took 48 hr for completion. After removal of the catalyst, the solution was evaporated at a temperature below 30°C to give a sirup (0.74 g). The ninhydrin-positive sirup was dissolved in 1 N aqueous barium hydroxide (40 m*l*) and heated over a boiling water bath for 2 hr. The mixture was acidified with 3 N sulfuric acid to pH 2 and the mixture was centrifuged to remove barium sulfate. The supernatant was neutralized with Dowex 1×2 (OH type) and evaporated to give a colorless sirup (0.6 g) of free base. Paper chromatography and bioautography of the product showed that the product mainly contained the substance whose R_f-value coincided with that of natural kanamycin C. The product was dinitrophenylated with 2,4-dinitrofluorobenzene (0.84 g) in the presence of sodium bicarbonate (0.4 g) in 50% aqueous ethanol (60 m*l*) at room temperature under stirring overnight. Precipitation of a yellow gummy substance was observed. The resulting mixture was neutralized with 0.1 N hydrochloric acid and followed by evaporation to give a sirup. This was acetylated with acetic anhydride (20 m*l*) and anhydrous sodium acetate (1 g) with stirring at 100°C. After evaporation, the residue was extracted with acetone and the extract was evaporated to give a yellow glass (1.8 g), which showed about four spots with R_f value of 0.56, 0.45, 0.35 and 0.27 on TLC with the solvent system (c). The product was chromatographed on a silica-gel column (150 g, 49×310 mm) with the same solvent system, being cut into fractions of 8 g each. The main product of R_f value 0.35 appeared in fractions of tube Nos. 34—48, which was evaporated and followed by recrystallization from the solvent system (c) to give yellow needles of VII (overall yield from VI, 15%); mp 208—211°C (decomp.), $[\alpha]_D^{18}$ +285° (*c* 0.75, acetone), IR spectrum: 3320, 1620, 1595, 1550, 1525, 1335, 835 and 745 (NHDNP), 1750, 1365 and 1220 cm^{-1} (OAc).

Found: C, 46.68; H, 4.34; N, 11.84%. Calcd for $C_{56}H_{58}N_{12}O_{34}$: C, 46.61; H, 4.05; N, 11.65%.

Synthetic Kanamycin C (VIII). A sample (47 mg) of VII was dissolved in 20 m*l* of methanol saturated with ammonia at 0°C and allowed to stand at room temperature for 4 hr to remove acetyl groups. Evaporation of the reaction mixture *in vacuo* gave a yellow glass (39 mg), which was treated with 0.5 m*l* of Dowex 1×2 (OH type) in moistened acetone (3 m*l*) at room temperature for 4 hr to remove dinitrophenyl groups. The resin was filtered off, and the filtrate was evaporated. The residue was passed through a small column of Dowex 1×2 (OH type) with water to give a colorless solution of pure free base. Evaporation followed by recrystallization from aqueous methanol containing small amount of ethanol gave VIII; $[\alpha]_D^{18}$ +139° (*c* 0.50, water).

Found: C, 44.40; H, 7.28; N, 11.80%. Calcd for $C_{18}H_{36}N_4O_{11}$: C, 44.62; H, 7.49; N, 11.56%.

The natural kanamycin A showed $[\alpha]_D^{18}$ +145° (*c* 0.58, water) [lit.[4] $[\alpha]_D^{18}$ +126° (*c* 1, water)]. On descending paper chromatography by ninhydrin-coloration using the solvent system (d), the R_f-value of the synthetic product (VIII) agreed with that of the natural kanamycin C. Infrared spectra of VIII and the natural specimen were superimposable. The antibiotic spectra[9] and minimal inhibitory concentrations of the synthetic product VIII against test organisms coincided with that of natural kanamycin C.

Natural Hepta-*O*-acetyl-tetra-*N*-(2,4-dinitrophenyl)-kanamycin C. To a solution of natural kanamycin C (50 mg) in water (0.5 m*l*) was added sodium bicarbonate (26 mg) and 2,4-dinitrofluorobenzene (58 mg) in ethanol (0.6 m*l*) and the mixture was vigorously stirred at room temperature for 3 hr. Water (1 m*l*) was

added and agitated overnight to precipitate a yellow solid, which was collected and washed thoroughly with water; yield 95 mg (82%). The *N*-dinitrophenyl derivative (95 mg) was acetylated with acetic anhydride (5 m*l*) and anhydrous sodium acetate (0.5 g) by heating at 110°C under stirring for 2 hr. The resulting mixture was concentrated under reduced pressure and followed by dilution with acetone and filtration. The filtrate was again evaporated and made free from acetic anhydride by co-evaporating with toluene three times to give a yellow glass (140 mg), which was purified by chromatography on a silica-gel column (10 g, 23×100 mm) with the solvent system (c) being cut into 3 m*l* each. The fraction Nos. 8—20 were collected and evaporated to give a yellow solid; 130 mg (89%). Crystallization from the solvent system (c) afforded yellow needles of hepta-*O*-acetyl-tetra-*N*-(2,4-dinitrophenyl)-kanamycin C; mp 208—211°C (decomp.), $[\alpha]_D^{18}$ +299° (*c* 0.64, acetone), IR spectrum: 3320, 1620, 1595, 1550, 1525, 1335, 835 and 745 (NHDNP), 1750, 1365 and 1220 cm^{-1} (OAc).

Found: C, 46.65; H, 4.24; N, 11.78%. Calcd for $C_{56}H_{58}N_{12}O_{34}$: C, 46.61; H, 4.05; N, 11.65%.

The authors are indebted to the Kawasaki-Factory of Meiji-Seika, Ltd., for supplying kanamycin C. Thanks are also due to Mr. Saburo Nakada for microanalyses and to Mr. Yoshio Nishimura and Mr. Hirokuni Hineno for technical assistance.

BULLETIN OF THE CHEMICAL SOCIETY OF JAPAN VOL. 42 533—537 (1969)

Studies of Aminosugars. XXII. The Total Synthesis of Kanamycin A[1]

Sumio UMEZAWA, Kuniaki TATSUTA and Shinkiti KOTO

Department of Applied Chemistry, Faculty of Engineering, Keio University, Koganei-shi, Tokyo

(Received July 16, 1968)

6-*O*-(3-Amino-3-deoxy-*α*-D-glucopyranosyl)-2-deoxystreptamine, which was previously synthesized, was masked with carbobenzoxy, isopropylidene and benzyl groups to give 6-*O*-(2-*O*-benzyl-3-carbobenzoxyamino-3-deoxy-4,6-*O*-isopropylidene-*α*-D-glucopyranosyl)-*N*,*N*′-dicarbobenzoxy-2-deoxystreptamine, with which 2,3,4-tri-*O*-benzyl-6-(*N*-benzylacetamido)-6-deoxy-*α*-D-glucopyranosyl chloride was condensed by a modified Koenigs-Knorr reaction, to give an *α*,*α*-diglycoside compound. The identity of the product with a substance of the same structure derived from natural kanamycin A was shown. Removal of the masking groups gave the synthetic kanamycin A, which was identical to the natural specimen.

Kanamycins[2] belong to a group of water-soluble, basic antibiotics that are entirely carbohydrate in nature and show broad-spectrum antibacterial activity. They were discovered by H. Umezawa *et al.* in cultures of *Streptomyces kanamyceticus* n. sp. Okami *et* Umezawa. Kanamycin A is the major component of kanamycin complex produced by the above-mentioned strain. Cleavage products of kanamycin A are 3-amino-3-deoxy-D-glucose (kanosamine), 6-amino-6-deoxy-D-glucose and 2-deoxystreptamine. The former two kinds of aminosugars had not previously been encountered in natural products. (3-Amino-3-deoxy-*α*-D-glucopyranosyl)-2-deoxy-streptamine[3] and (6-amino-6-deoxy-*α*-D-glucopyranosyl)-2-deoxy-streptamine[4] were also isolated from the partial hydrolysis product. The structure of kanamycin A[5-7] (VIII) was established as *O*-(6-amino-6-deoxy-*α*-D-glucopyranosyl)-(1→4)-*O*-[3-amino-3-deoxy-*α*-D-glucopyranosyl-(1→6)]-1,3-diamino-1,2,3-trideoxy-*myo*-inositol. Absolute configuration of kanamycins

1) Part XXXVII of "Studies on Antibiotics and Related Substances" by Sumio Umezawa. This paper was read before the 160th Research Meeting of Japan Antibiotic Research Association, March 22, 1968. A part of this work has been briefly communicated: S. Umezawa, K. Tatsuta and S. Koto, *J. Antibiotics*, **21**, 367 (1968).

2) H. Umezawa, M. Ueda, K. Maeda, K. Yagishita, S. Kondo, Y. Okami, R. Utahara, Y. Osato, K. Nitta and T. Takeuchi, *J. Antibiotics*, **A10**, 181 (1957).

3) K. Maeda, M. Murase, H. Mawatari and H. Umezawa, *ibid.*, **A11**, 163 (1958).

4) S. Umezawa and T. Tsuchiya, *ibid.*, **A15**, 51 (1962).

5) S. Umezawa, Y. Ito and S. Fukatsu, *ibid.*, **A11**, 120, 162 (1958); This Bulletin, **32**, 81 (1959).

6) M. J. Cron, O. B. Fardig, D. L. Johnson, D. F. Whitehead, I. R. Hooper and R. U. Lemieux, *J. Am. Chem. Soc.*, **80**, 4115 (1958).

7) H. Ogawa, T. Ito, S. Inoue and S. Kondo, *J. Antibiotics*, **A11**, 169 (1958); H. Ogawa, T. Ito, S. Kondo and S. Inoue, *Bull. Agr. Chem. Soc. Japan*, **23**, 289 (1959).

were recently revealed.[8-10]

After having completed structural studies on kanamycin A, we turned to contemplation of its synthesis. There appeared to be two possible routes to kanamycin A, one of which was a route *via* a masked derivative of 6-*O*-(3-amino-3-deoxy-*α*-D-glucopyranosyl)-2-deoxystreptamine (I, 3AD) and the other was a route *via* a masked derivative of 4-*O*-(6-amino-6-deoxy-*α*-D-glucopyranosyl)-2-deoxystreptamine (6AD). We chose the former route, because 3AD is more readily obtainable than 6AD from the partially hydrolyzed product of kanamycin A in order to identify with the synthetic specimen. In the present paper, the total synthesis of kanamycin A and related compounds are described.[11]

The initial phase of the synthesis was thus concerned with the preparation of 3AD, which has very recently been reported.[12] The 3AD now had to be suitably masked. Treatment of 3AD with carbobenzoxychloride in aqueous sodium carbonate gave tri-*N*-carbobenzoxy derivative (II) in a 84% yield. Acetonation of II with 2,2-dimethoxypropane in the presence of *p*-toluenesulfonic acid in dimethylformamide (DMF) at 110°C afforded the diisopropylidene derivative (III), mp 234°C, $[\alpha]_D^{18}$ +53° (*c* 0.67, DMF), in a quantitative yield. Benzylation of III with benzyl bromide in the presence of barium oxide and barium hydroxide in DMF afforded the benzyl derivative (IV), mp 258°C, $[\alpha]_D^{18}$ +43° (*c* 0.67, DMF), which was deacetonated by treatment with 80% acetic acid to give 6-*O*-(2-*O*-benzyl-3-carbobenzoxyamino-3-deoxy-*α*-D-glucopyranosyl)-*N*,*N*′-dicarbobenzoxy-2-deoxystreptamine (V), mp 288°C, (decomp.), $[\alpha]_D^{18}$ +40° (*c* 0.67, DMF), quantitatively. Treatment of V with 2,2-dimethoxypropane at 5°C in the presence of *p*-toluenesulfonic acid in DMF successfully gave monoisopropylidene derivative (VI), mp 240°C, $[\alpha]_D^{18}$ +40° (*c* 0.67, DMF), in a 64% yield. It is worth mentioning that the hydroxyl groups at C-4 and C-6 in the 3-amino-3-deoxy-D-glucose moiety were acetonated in preference to the hydroxyl groups in the deoxystreptamine. This reaction is similar to that carried out in the preparation of the corresponding derivative of paromamine in the case of the total synthesis of kanamycin C in the foregoing report.

We could now proceed along the main synthetic pathway. In analogy to the foregoing studies on kanamycin C, the intermediate VI was condensed with 6-(*N*-benzylacetamido)-2,3,4-tri-*O*-benzyl-6-deoxy-*α*-D-glucopyranosyl chloride[13] in the presence of mercuric cyanide and Drierite in dioxane-benzene. The product was treated with aqueous acetic acid to remove the isopropylidene group, hydrogenated over palladium black to remove carbobenzoxy and *O*-benzyl groups, de-*N*-acetylated with barium hydroxide, and again hydrogenated to remove the *N*-benzyl group. The ninhydrin-positive product was dinitrophenylated with 2,4-dinitrofluorobenzene and then *O*-acetylated with acetic anhydride and anhydrous sodium acetate. The product, which showed about six spots with R_f-values of 0.54, 0.34, 0.30, 0.27 (main), 0.25 and 0.15 on a thin-layer chromatogram (TLC) with a solvent system (e): toluene-MEK (3 : 1), was chromatographed on a silica-gel column with the same solvent. The main product (VII) of the R_f-value 0.27 was isolated as yellow needles in an overall-yield 10.1% from VI.

On the other hand, kanamycin A was dinitrophenylated and acetylated to give hepta-*O*-acetyl-tetra-*N*-(2,4-dinitrophenyl)-kanamycin A.

The synthetic yellow needles (VII), mp 210—213°C (decomp.), $[\alpha]_D^{18}$ +50° (*c* 1.0, acetone), were proved to be identical to the above-mentioned derivative of natural kanamycin A by elemental analyses, specific rotations, by their failure to depress the mixed melting point, identical mobilities on TLC and infrared spectra.

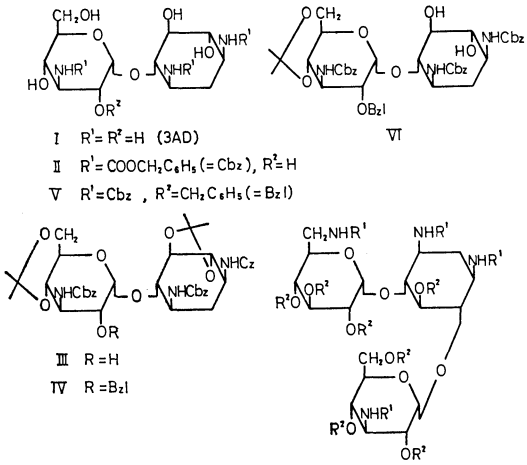

8) M. Hichens and K. L. Rinehart, Jr., *J. Am. Chem. Soc.*, **85**, 1547 (1963).

9) S. Tatsuoka, S. Horii, K. L. Rinehart, Jr., and T. Nakabayashi, *J. Antibiotics*, **A17**, 88 (1964).

10) S. Umezawa, K. Tatsuta and T. Tsuchiya, This Bulletin, **39**, 1244 (1966).

11) For brief report of an alternative, independent synthesis of the kanamycin A, *cf.* M. Nakajima, A. Hasegawa, N. Kurihara, H. Shibata, T. Ueno and D. Nishimura, *Tetrahedron Letters*, **1968**, 623.

12) S. Koto, K. Tatsuta, E. Kitazawa and S. Umezawa, *J. Antibiotics*, **21**, 365 (1968); This Bulletin, **41**, 2769 (1968).

13) This compound was reported by S. Umezawa *et al.* at the 20th Annual Meeting of the Chemical Society of Japan, Tokyo, Mar. 31, 1967. (See abstracts of the papers of the Meeting, Vol. III, p. 596). S. Koto, T. Tsumura, Y. Kato and S. Umezawa, This Bulletin, **41**, 2765 (1968).

Before dinitrophenylation of the ninhydrin-positive product, we made efforts to directly separate the synthetic kanamycin A from the crude product by chromatographic technique, but it was unsuccessful. We found that VII could be separated when the crude product was subjected to dinitrophenylation and acetylation.

Hydrolysis of VII with methanolic ammonia followed by treatment with an excess of Dowex 1×2 (OH^-) resin afforded a free base, which was purified by chromatography on a column of Dowex 1×2 (OH^-) resin and recrystallized from aqueous methanol - ethanol to afford the synthetic kanamycin A of $[\alpha]_D^{18}$ +149° (*c* 0.87, water). The natural kanamycin A showed $[\alpha]_D^{18}$ +151° (*c* 1.0, water). The identity of the synthetic kanamycin A with the natural specimen was further established by elemental analyses, identical mobilities on TLC, superimposable infrared spectra and by their failure to depress the mixed melting point. The antibiotic spectra and minimal inhibitory concentrations[1] of the synthetic kanamycin A against test organisms were in agreement with those of the natural kanamycin A.

Experimental

General Procedures. Thin layer chromatography (TLC) and paper chromatography were carried out similarly as described in the foregoing report, using solvent systems: (a) benzene-ethanol (4 : 1), (b) benzene-methyl ethyl ketone (MEK) (4 : 1), (c) benzene-methanol (4 : 1), (d) benzene-ethyl acetate (1 : 2), (e) toluene-MEK (3: 1), and (f) *n*-butanol - pyridine - water - acetic acid (6 : 4 : 3 : 1).

6-*O*-(3-Carbobenzoxyamino-3-deoxy-α-D-glucopyranosyl)-*N*,*N*′-dicarbobenzoxy-2-deoxystreptamine (II). To a solution of 6-*O*-(3-amino-3-deoxy-α-D-glucopyranosyl)-2-deoxystreptamine (I) (6.0 g) and sodium carbonate (18 g) in a mixture of water (60 m*l*) and acetone (180 m*l*) was added carbobenzoxychloride in toluene (30%, 32 g) under agitation at −10°C during an hour. Having been stirred for about 4 hr, the reaction mixture was set aside in a refrigerator overnight. The resulting solid was shaken with a mixture (600 m*l*) of water and ether (15: 1 v/v), collected and pressed between filter papers. The waxy product was triturated with 1 N hydrochloric acid (300 m*l*), filtered, washed with water and dried. Recrystallization from dioxane (900 m*l*) afforded colorless solid; 9.5 g. The mother liquor gave a second crop; 1.8 g. Total yield 84%; mp 280—282°C (decomp.), $[\alpha]_D^{18}$ +54° (*c* 0.67, DMF), IR spectrum: 3330, 1693 and 1547 cm^{-1} (NHCbz).

Found: C, 59.86; H, 6.25; N, 5.66%. Calcd for $C_{36}H_{43}N_3O_{13}$: C, 59.58; H, 5.97; N, 5.79%.

6-*O*-(3-Carbobenzoxyamino-3-deoxy-4,6-*O*-isopropylidene-α-D-glucopyranosyl)-*N*,*N*′-dicarbobenzoxy-4,5-*O*-isopropylidene-2-deoxystreptamine (III). To a solution of II (4.6 g) in anhydrous DMF (30 m*l*) was added *p*-toluenesulfonic acid monohydrate (0.06 g) and 2,2-dimethoxypropane (7.0 m*l*), and the solution was heated at 110°C for 4 hr with occasional stirring. The mixture was neutralized with Amberlite IRA-400 (OH type; 10 m*l*) washed with methanol before use, filtered and the solution was evaporated *in vacuo* to give a residue, which was solidified by treatment with water; yield 4.9 g (94%). An analytically pure sample was obtained by chromatography on a silica-gel column, using the solvent system (a); mp 233—234°C, $[\alpha]_D^{18}$ +53° (*c* 0.67, DMF), IR spectrum: 3350, 1700 and 1537 (NHCbz), 1175 and 1063 cm^{-1} (ketal).

Found: C, 62.67; H, 6.59; N, 5.35%. Calcd for $C_{42}H_{51}N_3O_{13}$: C, 62.60; H, 6.38; N, 5.21%.

6-*O*-(2-*O*-Benzyl-3-carbobenzoxyamino-3-deoxy-4,6-*O*-isopropylidene-α-D-glucopyranosyl)-*N*,*N*′-dicarbobenzoxy-4,5-*O*-isopropylidene-2-deoxystreptamine (IV). To a solution of III (4.9 g) in anhydrous DMF (80 m*l*) was added pulverized barium oxide (4.9 g) and barium hydroxide octahydrate (5.9 g) with stirring and the mixture was cooled to −15°C. Benzyl bromide (3.5 m*l*) was added dropwise to the mixture under agitation, and the reaction temperature was allowed to raise gradually to 0°C during 4 hr. The mixture was further stirred for 20 hr at room temperature and filtered through a thick layer of Celite. The filtrate and washings were combined and evaporated *in vacuo* to give a sirup, which was taken up into chloroform (200 m*l*) to precipitate a gelatinous mass. This product was transferred to the top of a thick layer of Hyflosupercel (60×60 mm) and washed with chloroform (300 m*l*) and then with hot chloroform (300 m*l*) to afford a fraction containing IV, which was evaporated *in vacuo* to give an analytically pure solid of IV; 4.1 g, mp 258°C; $[\alpha]_D^{18}$ +43° (*c* 0.67, DMF), IR spectrum: 3340, 1700 and 1538 (NHCbz), 1177 and 1066 cm^{-1} (ketal).

Found: C, 65.88; H, 6.66; N, 4.51%. Calcd for $C_{49}H_{57}N_3O_{13}$: C, 65.68; H, 6.41; N, 4.69%.

6-*O*-(2-*O*-Benzyl-3-carbobenzoxyamino-3-deoxy-α-D-glucopyranosyl)-*N*,*N*′-dicarbobenzoxy-2-deoxystreptamine (V). A suspension of IV (4.1 g) in 80% aqueous acetic acid (120 m*l*) was heated at 80°C for a while to give a clear solution, which was kept standing at room temperature overnight to separate a colorless precipitate. This was collected, washed with water and dried to afford a colorless powder of V, mp 286—288°C (decomp.), $[\alpha]_D^{18}$ +40° (*c* 0.67, DMF), IR spectrum: 1695 and 1547 (NHCbz), 1052 cm^{-1} (*O*-benzyl).

Found: C, 63.13; H, 6.32; N, 5.02%. Calcd for $C_{43}H_{49}N_3O_{13}$: C, 63.30; H, 6.05; N, 5.15%.

6-*O*-(2-*O*-Benzyl-3-carbobenzoxyamino-3-deoxy-4,6-*O*-isopropylidene-α-D-glucopyranosyl)-*N*,*N*′-dicarbobenzoxy-2-deoxystreptamine (VI). To a solution of V (2.8 g) in DMF (17 m*l*) was added *p*-toluenesulfonic acid monohydrate (0.03 g) and 2,2-dimethoxypropane (1.2 m*l*), and the mixture was allowed to stand at about 5°C for 16 hr. The mixture was neutralized with Amberlite IRA-400 (OH type; 8 m*l*) washed with methanol before use, and evaporated *in vacuo* to give a sirup, which was solidified by trituration with water. The crude product (2.9 g) was extracted with ethyl acetate (340 m*l*) and the extract was evaporated under reduced pressure. The residue was crystallized from ethanol; yield 1.9 g (64%). Examination of the product by TLC using the solvent system (d) indicated that the product was quite pure, mp 239—240°C, $[\alpha]_D^{18}$ +40° (*c* 0.67, DMF), IR spectrum: 3340, 1698 and 1540 (NHCbz), 1172 and 1063 cm^{-1} (ketal).

Found: C, 64.43; H, 6.09; N, 4.76%. Calcd for

$C_{46}H_{53}N_3O_{13}$: C, 64.55; H, 6.24; N, 4.91%.

Proof for the Structure of VI. The monoisopropylidene derivative VI (26 mg) was benzylated with benzyl bromide (0.036 ml) in the presence of barium oxide (47 mg) and barium hydroxide octahydrate (58 mg), similarly as described for the preparation of IV. TLC using the solvent system (b) showed that VI completely disappeared and a new spot appeared. An oily product (20 mg) was dissolved in a mixture of acetic acid (6.0 ml), methyl cellosolve (3.0 ml), water (1.6 ml) and concentrated hydrochloric acid (1.2 ml) and heated at 100°C for 10 hr. The paper chromatography of the hydrolyzate using the solvent mixture (f) and ninhydrin-coloration showed that hydrolysis of the fully benzylated VI gave neither 3-amino-3-deoxy-D-glucose nor 2-deoxystreptamine, while analogous hydrolysis of II (a control test) gave both of them.

Synthetic Hepta-*O*-acetyl-tetra-*N*-(2,4-dinitrophenyl)-kanamycin A (VII). A mixture of VI (1.65 g), finely pulverized mercuric cyanide (0.7 g) and freshly ignited Drierite (5.4 g) in anhydrous dioxane (10 ml) was heated to reflux for 15 min under stirring and then cooled to room temperature. To the mixture was added well dried 2,3,4-tri-*O*-benzyl-6-(*N*-benzylacetamido)-6-deoxy-α-D-glucopyranosyl chloride (2.2 g; 1.9 eq.) in anhydrous benzene (30 ml) and the mixture was stirred vigorously under reflux for 10 hr to give a brown viscous mixture. The mixture was passed through a bed of Celite and washed with dioxane (100 ml) and ethyl acetate (100 ml). The filtrate and washings were combined and evaporated. The brown residue (6.4 g) was extracted with ethyl acetate (120 ml) and the extract was washed with three 100 ml portions of 20% aqueous potassium bromide and 100 ml of water. After drying over anhydrous sodium sulfate, the solution was evaporated to give an oily product (5.8 g). To the product was added 80% aqueous acetic acid (40 ml) and the mixture was kept standing for 30 min with occasional stirring. Evaporation under reduced pressure afforded a colorless sirup (5.0 g). This deacetonated product was hydrogenated over palladium black (0.5 g) in a solvent mixture of dioxane (30 ml), water (2 ml) and concentrated hydrochloric acid (3 ml) under 3.5 atm of hydrogen pressure at about 40°C with occasional addition of small portions of water whose total volume was 30 ml. After 24 hr, the hydrogenation was completed and the catalyst was filtered off. The solution was evaporated under reduced pressure below 30°C and made free from hydrogen chloride by co-distillation with *n*-butanol to afford a colorless sirup (1.4 g). The product was heated with 1 N barium hydroxide (60 ml) at 100°C for 2.4 hr to remove the *N*-acetyl group. The hydrolyzate was neutralized with 3 N sulfuric acid to pH 2. Inorganic matter was removed by centrifuging and the supernatant was treated with Dowex 1×2 (OH type) to pH about 9.5. After removal of the resin, the solution was evaporated to give a colorless sirup (0.8 g). Finally, the *N*-benzyl blocking was removed by catalytic hydrogenation. The sirup (0.8 g) in water (10 ml) and concentrated hydrochloric acid (0.5 ml) was shaken over palladium black (0.3 g) under 3.5 atm of hydrogen pressure for 48 hr at about 40°C. After removal of the catalyst, the solution was evaporated under reduced pressure at 30°C and followed by co-distillation with *n*-butanol to afford a glassy product (0.9 g). The product was ninhydrin-positive and the major R_f value indicated that the product consisted of the hydrochloride of synthetic kanamycin A. However, attempts to isolate it were unsuccessful. Then the product was dinitrophenylated with 2,4-dinitrofluorobenzene (1.7 g) in 50% aqueous ethanol (60 ml) in the presence of sodium bicarbonate (0.63 g) at room temperature overnight under stirring, whereupon a gummy product separated. Addition of water (80 ml) to the mixture and further agitation made the gummy product powdery. The yellow powder (1.73 g) was acetylated with acetic anhydride (30 ml) in the presence of freshly fused sodium acetate (1.5 g) at 100°C for 10 hr with stirring. The resulting mixture was evaporated *in vacuo* and the residue was extracted with excess acetone. The extract was evaporated and made free from acetic anhydride by co-distillation with toluene to give a yellow glass (2.2 g), which showed a major spot of R_f 0.27 together with several minor spots on TLC using the solvent system (e). The product was chromatographed on a silica-gel column (200 g; 4.7×26 cm) with the same solvent system, the effluent being cut into 10 ml each. The main product having R_f value 0.27 appeared in fractions of Nos. 65—70. Evaporation gave yellow needles, 0.28 g (overall yield from VI 10%), recrystallization from the same solvent system gave VII; mp 210—213°C (decomp.), $[\alpha]_D^{18}$ +50° (*c* 1.0, acetone), IR spectrum: 3340, 1625, 1600, 1550, 1525, 1340, 835 and 745 (NHDNP), 1765, 1370 and 1220 cm^{-1} (OAc).

Found: C, 46.71; H, 4.22; N, 11.58%. Calcd for $C_{56}H_{58}N_{12}O_{34}$: C, 46.61; H, 4.05; N, 11.65%.

The melting point of VII was not depressed by admixture with the hepta-*O*-acetyl-tetra-*N*-(2,4-dinitrophenyl) derivative of natural kanamycin A described below. On TLC with the solvent system (e), the synthetic VII and the above-mentioned derivative of kanamycin A showed identical mobilities and their IR spectra were superimposable.

Synthetic Kanamycin A (VIII). A sample (50 mg) of VII was dissolved in methanol (8 ml) saturated with ammonia at 0°C and the solution was allowed to stand at room temperature for 4 hr. Concentration of the solution *in vacuo* gave a sirup, which was treated with Dowex 1×2 (OH type; *ca.* 2 ml of wet resin) in acetone (9 ml) at room temperature with stirring overnight. After removal of the resin, the solution was evaporated and followed by purification by passing through a small column of Dowex 1×2 (OH type; *ca.* 1 ml) to give a colorless glass, which was treated with aqueous methanol containing ethanol to afford the crystalline free base of synthetic kanamycin A (VIII); yield 47%, $[\alpha]_D^{18}$ +149° (*c* 0.87, water).

Found: C, 44.47; H, 7.69; N, 11.27%. Calcd for $C_{18}H_{36}N_4O_{11}$: C, 44.62; H, 7.49; N, 11.56%.

On descending paper chromatography by ninhydrin-coloration using the solvent system (f), the R_f value of the synthetic product VIII agreed with that of the natural kanamycin A. Infrared spectra of VIII and the natural specimen were superimposable. The antibiotic spectra and minimal inhibitory concentrations[14] of the synthetic product VIII against test organisms coincided with that of natural kanamycin A.

Natural Hepta-*O*-acetyl-tetra-*N*-(2,4-dinitrophenyl)-kanamycin A. To a solution of natural kanamycin

14) S. Umezawa, K. Tatsuta and S. Kto, *J. Antibiotics*, **21**, 367 (1968).

A (0.5 g) in water (5 m*l*) was added sodium bicarbonate (0.2 g) and 2,4-dinitrofluorobenzene (0.45 g) in ethanol (5 m*l*), and the mixture was agitated for 2 hr at room temperature to give a yellow gummy substance, which was rubbed by glass rod with water (15 m*l*) to give a yellow powdery solid; 0.9 g (75%).

The dinitrophenyl derivative was then fully acetylated with acetic anhydride (20 m*l*) in the presence of anhydrous sodium acetate (2 g) by heating at 100°C under stirring for 3 hr. The resulting mixture was evaporated *in vacuo* and followed by dilution with excess acetone. Insoluble matters were filtered off and the solution was evaporated and made free from acetic anhydride by co-evaporation with toluene to give a yellow glass, 1.95 g. The product was purified by silica-gel column chromatography (150 g; 3.5 × 35 cm) with a solvent mixture of benzene-MEK (2 : 1), the effluent being cut into 10 g each. The fraction Nos. 34—37 were combined and evaporated to afford *N*-dinitrophenyl-*O*-acetyl derivative of natural kanamycin A; 0.6 g (41% from the base). Recrystallization from the same solvent system gave yellow needles; mp 210—213°C (decomp.), $[\alpha]_D^{18}$ +52° (*c* 1.0, acetone), IR spectrum: 3340, 1625, 1600, 1550, 1525, 1340, 835 and 745 (NHDNP), 1765, 1370 and 1220 cm^{-1} (OAc).

Found: C, 46.74; H, 4.10; N, 11.69%. Calcd for $C_{56}H_{58}N_{12}O_{34}$: C, 46.61; H, 4.05; N, 11.65%.

We wish to thank Professor H. Umezawa for his helpful advice, Mr. S. Nakada for microanalyses and Mr. T. Tsumura for technical assistance. We also thank the Kawasaki-Factory of Meiji-Seika, Ltd., for supplying kanamycin A.

BULLETIN OF THE CHEMICAL SOCIETY OF JAPAN VOL. 42 537—541 (1969)

Studies of Aminosugars. XXIII. The Total Synthesis of Kanamycin B[1]

Sumio UMEZAWA, Shinkiti KOTO, Kuniaki TATSUTA, Hirokuni HINENO, Yoshio NISHIMURA and Takayuki TSUMURA

Department of Applied Chemistry, Faculty of Engineering, Keio University, Koganei-shi, Tokyo

(Received July 16, 1968)

4-*O*-(3,4-Di-*O*-benzyl-2,6-dicarbobenzoxyamino-2,6-dideoxy-*α*-D-glucopyranosyl)-*N*,*N*′-dicarbobenzoxy-2-deoxystreptamine has been prepared from neamine and condensed with 3-acetamido-2,4,6-tri-*O*-benzyl-3-deoxy-*α*-D-glucopyranosyl chloride by a modified Koenigs-Knorr reaction to give an *α*,*α*-diglycoside. The identity of the product with a substance of the same structure derived from natural kanamycin B was shown. Removal of the masking groups from the product gave the synthetic kanamycin B, which was identical with natural kanamycin B.

Paper chromatography[2] and ion-exchange chromatography[3] of the kanamycin complex revealed the presence of two minor congeners, kanamycin B and C, in addition to kanamycin A. Kanamycin B was isolated by counter-current distribution of the salicylidene derivatives and by chromatography.[4,5] Kanamycin B is composed of 2-deoxystreptamine, 3-amino-3-deoxy-D-glucose and 2,6-diamino-2,6-dideoxy-D-glucose.[4,6] The structure of kanamycin B was established as *O*-(2,6-diamino-2,6-dideoxy-*α*-D-glucopyranosyl)-(1→4)-*O*-[3-amino-3-deoxy-*α*-D-glucopyranosyl-(1→6)]-1,3-diamino-1,2,3-trideoxy-*myo*-inositol.[6,7] In other words, kanamycin B is an *α*-glycoside of neamine[8] (I) and 3-

1) Part XXXVIII of "Studies on Antibiotics and Related Substances" by Sumio Umezawa. A part of this work has been briefly communicated: S. Umezawa, S. Koto, K. Tatsuta, H. Hineno, Y. Nishimura and T. Tsumura, *J. Antibiotics*, **21**, 424 (1968).

2) K. Maeda, M. Ueda, K. Yagishita, S. Kawaji, S. Kondo, M. Murase, T. Takeuchi, Y. Okami and H. Umezawa, *J. Antibiotics*, **A10**, 228 (1957); M. J. Cron, D. L. Johnson, F. M. Palermiti, Y. Perron, H. D. Taylor, D. F. Whitehead and I. R. Hooper, *J. Am. Chem. Soc.*, **80**, 752 (1958).

3) J. W. Rothrock, R. T. Goegelman and F. J. Wolf, *Antibiotics Annual*, **1958/59**, 796.

4) H. Schmitz, O. B. Fardig, F. A. O'Herron, N. A. Rousche and I. R. Hooper, *J. Am. Chem. Soc.*, **80**, 2912 (1958).

5) T. Wakazawa, Y. Sugano, N. Abe, S. Fukatsu and S. Kawaji, *J. Antibiotics*, **A14**, 180 (1961).

6) T. Ito, M. Nishio and H. Ogawa, *ibid.*, **A17**, 189 (1964).

7) M. Hichens and K. L. Rinehart, Jr., *J. Am. Chem. Soc.*, **85**, 1547 (1963).

8) R. L. Peck, C. E. Hoffhine, Jr., P. Gale and K. Folkers, *ibid.*, **71**, 2950 (1949); R. L. Peck, C. E. Hoffhine, Jr., F. H. Gale and K. Folkers, *ibid.*, **75**, 1018 (1953).

amino-3-deoxy-D-glucose. In this paper, we describe the synthesis of kanamycin B from neamine and 3-amino-3-deoxy-D-glucose. Since we[9] have synthesized neamine (I) from paromamine which was synthesized[10] from glucosamine and 2-deoxystreptamine, the combined achievements constitute the total synthesis of kanamycin B.

Neamine was converted into tetra-*N*-carbobenzoxy-neamine (II). Treatment of II with 2,2-dimethoxypropane in the presence of *p*-toluenesulfonic acid in *N*,*N*-dimethylformamide (DMF) at 110°C followed by chromatography on silica gel gave a mixture of monoisopropylidene derivatives (IIIa and IIIb) in a 41% yield. The mixture was benzylated with benzyl bromide in the presence of barium oxide and barium hydroxide in DMF and followed by chromatography on silica gel to afford 4-*O*-(3,4-di-*O*-benzyl-2,6-dicarbobenzoxy-amino-2,6-dideoxy-*α*-D-glucopyranosyl)-*N*,*N*′-dicarbobenzoxy-5,6-*O*-isopropylidene-2-deoxystreptamine (IVa) mp 185°C, $[\alpha]_D^{18}$ +57° (*c* 0.67, DMF) and 4-*O*-(2,6-dicarbobenzoxy-amino-2,6-dideoxy-3,4-*O*-isopropylidene-*α*-D-glucopyranosyl)-5,6-di-*O*-benzyl-*N*,*N*′-dicarbobenzoxy-2-deoxystreptamine (IVb) mp 230—231°C, $[\alpha]_D^{18}$ +33° (*c* 0.67, DMF) in 12% and 37% yield respectively.

Deacetonation of IVa by treatment with aqueous acetic acid gave 4-*O*-(3,4-di-*O*-benzyl-2,6-dicarbobenzoxyamino-2,6-dideoxy-*α*-D-glucopyranosyl)-*N*,*N*′-dicarbobenzoxy-2-deoxystreptamine (V) in an 86% yield, mp 221—222°C, $[\alpha]_D^{18}$ +58° (*c* 0.67, DMF).

The compound V was condensed with 3-acetamido-2,4,6-tri-*O*-benzyl-3-deoxy-*α*-D-glucopyranosyl chloride, which was already utilized for the synthesis of kanamycin C,[11] in the presence of mercuric cyanide and Drierite in benzene-dioxane. The condensation product was hydrogenated in a mixture of dioxane–water–concentrated hydrochloric acid over palladium black to remove the *O*-benzyl and *N*-carbobenzoxy groups, and de-*N*-acetylated with hot aqueous barium hydroxide to give a ninhydrin-positive product. Paper chromatography and bioautography of the product showed that the product mainly contained the substance whose R_f-value coincided with that of natural kanamycin B, however, attempts to isolate it were unsuccessful. Then the product was *N*-dinitrophenylated with 2,4-dinitrofluorobenzene in aqueous ethanol in the presence of sodium bicarbonate and then *O*-acetylated with acetic anhydride and sodium acetate. The product, which showed about four spots of R_f-values 0.40, 0.33, 0.13 and 0.08 on a thin layer chromatogram with a solvent system (c): toluene–methyl ethyl ketone (4 : 1), was chromatographed on a silica gel column with the same solvent system. The substance of R_f-value 0.08 was isolated and proved to be synthetic hexa-*O*-acetyl-penta-*N*-(2,4-dinitrophenyl)-kanamycin B (VI) mp 212—213°C (decomp.), $[\alpha]_D^{18}$ +220° (*c* 0.3, acetone), overall yield from V being 5%.

On the other hand, natural kanamycin B was dinitrophenylated and acetylated by the above-mentioned procedure to afford the hexa-*O*-acetyl-penta-*N*-(2,4-dinitrophenyl) derivative of kanamycin B, mp 217—218°C (decomp.), $[\alpha]_D^{18}$ +240° (*c* 0.4, acetone).

The identity of the synthetic VI to the above-mentioned derivative of natural kanamycin B was established by elemental analyses, specific rotations, by their failure to depress the mixed melting point and identical mobilities on thin layer chromatography and infrared spectra.

We have investigated the above-mentioned removal of *O*-benzyl and *N*-carbobenzoxy groups in some detail and found that treatment of the condensation product with sodium in liquid ammonia instead of catalytic hydrogenation with palladium black gave a better result and the overall yield of VI from V was raised to about 15%.

Finally, ammonolysis of the synthetic VI with methanolic ammonia followed by hydrolysis with excess of Dowex 1×2 (OH^-) resin afforded a free base, which was purified by chromatography on a column of the same resin. The free base melted at 178—182°C (decomp.), $[\alpha]_D^{18}$ +130° (*c* 0.5, water). The identity of the free base to the natural kanamycin B [mp 179—181°C (decomp.), $[\alpha]_D^{18}$ +128° (*c* 0.5, water)] was further established by their failure to depress the mixed melting point,

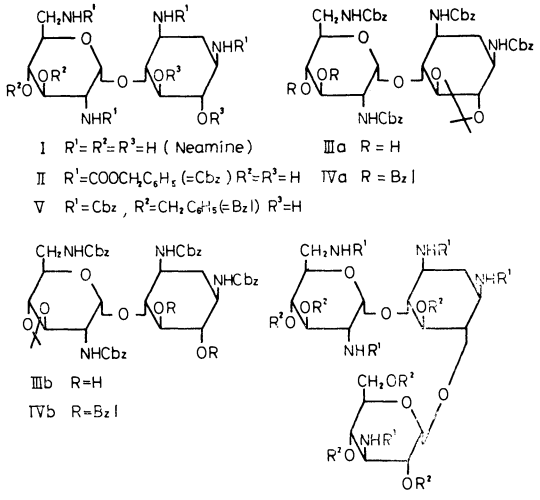

9) K. Tatsuta, E. Kitazawa and S. Umezawa, This Bulletin, **40**, 2371 (1967).

10) S. Umezawa and S. Koto, *ibid.*, **39**, 2014 (1966).

11) S. Umezawa, S. Koto, K. Tatsuta and T. Tsumura, *J. Antibiotics*, **21**, 162 (1968) (brief communication); See the foregoing paper.

identical mobilities on thin layer chromatography and infrared spectra. The antibiotic spectra and minimal inhibitory concentrations[1] of the synthetic kanamycin B against test bacteria were identical with those of the natural kanamycin B.

Experimental

General Procedures. Thin layer chromatography (TLC) was carried out on "Silica-Rider for TLC" (Dai-ichi Pure Chemicals Co.) using three solvent systems: (a) benzene-ethanol (7 : 1), (b) benzene-methyl ethyl ketone (MEK) (4 : 1), and (c) toluene-MEK (4 : 1), as mobile phases. Paper chromatography was performed in the previously described fashion.

Tetra-*N*-carbobenzoxy-neamine (II). To a solution of neamine (I) (15 g) and sodium carbonate decahydrate (39 g) in water (150 m*l*) was added acetone (450 m*l*) under agitation and the mixture was cooled to −5 — −10°C. Carbobenzoxychloride in toluene (30%; 104 g) was added for one hour. After having been vigorously stirred for about 4 hr at −5— −10°C, the reaction mixture was set aside in a refrigerator overnight. The resulting colorless solid was collected by filtration and tightly pressed between filter papers to remove oily matter and moisture. The waxy product was pulverized with 1 N hydrochloric acid (600 m*l*), filtered and dried *in vacuo* to give a colorless powder; yield 43 g. The product was dissolved in a hot mixture of dioxane (850 m*l*) and water (6 m*l*) and insoluble matters were filtered off. When the filtrate was allowed to stand at room temperature overnight, a colorless gelatinous mass precipitated; yield 34 g. The mother liquor deposited a second crop, 1.2 g. Total yield 89%, mp 259°C (decomp.), $[\alpha]_D^{18}$ +44° (*c* 0.67, DMF), IR spectrum (KBr): 1698 and 1538 cm^{-1} (NHCbz).

Found: C, 61.59; H, 5.97; N, 6.64%. Calcd for $C_{44}H_{50}N_4O_{14}$: C, 61.54; H, 5.86; N, 6.52%.

4-*O*-(3,4-Di-*O*-benzyl-2,6-dicarbobenzoxyamino-2,6-dideoxy-α-D-glucopyranosyl)-*N*,*N*′-dicarbobenzoxy-5,6-*O*-isopropylidene-2-deoxystreptamine (IVa) and 4-*O*-(2,6-Dicarbobenzoxyamino-2,6-dideoxy-3,4-*O*-isopropylidene-α-D-glucopyranosyl)-5,6-di-*O*-benzyl-*N*,*N*′-dicarbobenzoxy-2-deoxystreptamine(IVb). A mixture of II (5.2 g), *p*-toluenesulfonic acid monohydrate (0.052 g) and 2,2-dimethoxypropane (1.4 m*l*) in anhydrous DMF (30 m*l*) was heated at 110°C for 4 hr. The resulting reddish-brown solution was cooled and neutralized with about 10 m*l* of Amberlite IRA-400 (OH type) washed with methanol before use. The resin was filtered off and the solution was evaporated. The residue was chromatographed on a silica-gel column (500 g; 47×680 mm) using the solvent system (a) to separate two fractions of R_f-values 0.65 and 0.55 on TLC with the solvent system (a). The fraction of R_f 0.55 appeared between 930 m*l* and 2100 m*l*. The fraction was still a mixture of two kinds of mono-*O*-isopropylidene derivatives (IIIa and IIIb); yield 3.37 g (63%), $[\alpha]_D^{18}$ +42° (*c* 0.67, DMF).

Found: C, 63.03; H, 6.31; N, 6.34. Calcd for $C_{47}H_{54}N_4O_{14}$: C, 62.80; H, 6.05; N, 6.23%.

The mixture (5.28 g) of monoisopropylidene derivatives was dissolved in anhydrous DMF (70 m*l*) and to the solution were added powdery barium oxide (5.04 g) and finely crushed barium hydroxide octahydrate (6.35 g). After being cooled to −10°C, benzyl bromide (5.1 m*l*) was added dropwise into the mixture, and vigorously stirred at 0°C for 4 hr and then at room temperature for an additional 20 hr. The slightly colored mixture was diluted with chloroform (140 m*l*) and the insoluble matters were filtered off. The filtrate was evaporated *in vacuo* and the residue was extracted with chloroform. Concentration of the extract gave an oily substance, which was chromatographed on a column of silica-gel (500 g, 50×695 mm), using the solvent system (b). Each 15 g fraction was examined by TLC. The fractions containing only a substance of an R_f-value 0.50 appeared in tube Nos. 20—29. Evaporation afforded IVa, yield 0.74 g (12%), mp 185°C, $[\alpha]_D^{18}$ +57° (*c* 0.67, DMF), IR spectrum (KBr): 3350, 1700 and 1536 (NHCbz), 1137 and 1060 cm^{-1} (ketal).

Found: C, 68.07; H, 6.32; N, 5.30%. Calcd for $C_{61}H_{66}N_4O_{14}$: C, 67.89; H, 6.16; N, 5.19%.

Fractions (850 m*l*) after tube No. 43 contained the substance of R_f 0.25. Evaporation gave IVb, yield 2.33 g (37%), mp 230—231°C, $[\alpha]_D^{18}$ +33° (*c* 0.67, DMF), IR spectrum (KBr): 3350, 1700 and 1535 (NHCbz), 1157, 1133, 1060 and 1020 cm^{-1} (ketal).

Found: C, 67.43; H, 6.37; N, 5.32%. Calcd for $C_{61}H_{66}N_4O_{14}$: C, 67.89; H, 6.16; N, 5.19%.

4-*O*-(3,4-Di-*O*-benzyl-2,6-dicarbobenzoxyamino-2,6-dideoxy-α-D-glucopyranosyl)-*N*,*N*′-dicarbobenzoxy2-deoxystreptamine (V). A sample (0.74 g) of IVa was dissolved in warm aqueous acetic acid (80%, 25 m*l*), and the solution was kept standing at room temperature overnight. The resulting solid was collected, washed well with water and dried *in vacuo* to give an analytically pure solid of V; yield 0.64 g (90%), mp 221—222°C, $[\alpha]_D^{18}$ +58° (*c* 0.67, DMF), IR spectrum (KBr): 3340, 1699 and 1540 (NHCbz), 1037 cm^{-1} (*O*-benzyl).

Found: C, 66.74; H, 6.41; N, 5.58%. Calcd for $C_{58}H_{62}N_4O_{14}$: C, 67.04; H, 6.01; N, 5.39%.

Proof for the Structure of V. Each sample (10 mg) of V and IVb was dissolved in a mixture of acetic acid (0.6 m*l*) and acetic anhydride (0.1 m*l*) and to the solution was added a mixture of acetic acid and sulfuric acid (5 : 1; 0.07 m*l*) at 0°C. The solutions were stirred at room temperature overnight and then poured onto cracked ices (about 3 g) to separate an oily substance, which was extracted with benzene (6 m*l*). Each extract was washed with aqueous 5% sodium bicarbonate solution and water. After drying over sodium sulfate, each benzene-solution was evaporated and the residue was de-*O*-acetylated by treatment with saturated methanolic ammonia (10 m*l*) in a refrigerator overnight. The mixture was evaporated *in vacuo* and to the residue was added 1 N aqueous barium hydroxide (8 m*l*). After heating at 100°C for 4 hr, each hydrolyzate was neutralized with 3 N sulfuric acid to pH 2 and insoluble matters were removed by centrifuge. Each supernatant was treated with Dowex 1×2 (OH type) to pH 8—9 and the resin was filtered off. Evaporation and drying *in vacuo* afforded a mixture of free bases. Each mixture was examined by paper chromatography with the solvent system of (d) by ninhydrin coloration. 2-Deoxystreptamine was present in the hydrolyzate from V, while IVb did not produce 2-deoxystreptamine.

Synthetic Hexa-*O*-acetyl-penta-*N*(2,4-dinitrophenyl)-kanamycin B (VI). A mixture of V (0.8 g), well pulverized mercuric cyanide (0.31 g) and freshly activated Drierite (3.3 g) in a mixed solvent of benzene (9 m*l*) and dioxane (3 m*l*) was heated to reflux with stirring under anhydrous conditions and then cooled to room temperature. To the mixture was added well dried 3-acetamido-2,4,6-tri-*O*-benzyl-3-deoxy-*α*-D-glucopyranosyl chloride (0.60 g; 1.7 eq.) at once and the mixture was vigorously stirred at reflux temperature for 20 hr. During the course of the reaction the mixture gradually became somewhat thick and brown. After removal of insoluble matters by filtration, the solution was evaporated. The dark brown residue was extracted with ethyl acetate (70 m*l*) and the extract was washed with five 20 m*l* portions of 20% aqueous potassium bromide and then three 20 m*l* portions of water. After being dried over anhydrous sodium sulfate, the ethyl acetate solution was evaporated to give a sirup, 0.75 g. The condensation product was hydrogenated over palladium black (0.3 g) in a mixture (24 m*l*) of dioxane, water, methanol and concentrated hydrochloric acid (20 : 1 : 2 : 1) at about 40°C under 3.5 atm of hydrogen pressure with occasional additions of small portions of water, whose total volume was 5 m*l*. After removal of the catalyst, the hydrogenated solution was evaporated to dryness *in vacuo*. The residue was again hydrogenated over fresh palladium black (0.15 g) in the same manner as mentioned above until the total volume of water reached 10 m*l*. The same hydrogenation procedure was further repeated twice. The total duration of hydrogenation took 150 hr. After removal of the catalyst, the solution was evaporated to give a ninhydrin-positive sirup, 0.55 g, which was hydrolyzed by heating with 1 N barium hydroxide (10 m*l*) on a boiling water water bath for 2.5 hr. After cooling to room temperature, the mixture was neutralized with 3 N sulfuric acid to pH 2 and the insoluble matter was removed by centrifuge. The solution was neutralized with Dowex 1×2 (OH type) to pH 7—8, and the resin was filtered. Evaporation of the filtrate afforded a sirup of a mixture of free bases, 0.51 g. All attempts to obtain kanamycin B from the product in a pure form have so far been unsuccessful.

The mixture (0.5 g) of free bases was dinitrophenylated with 2,4-dinitrofluorobenzene (1.2 g) in the presence of sodium bicarbonate (0.55 g) in a mixture (60 m*l*) of water and ethanol (1 : 1) under stirring at room temperature overnight. The resulting mixture was neutralized with 0.1 N hydrochloric acid and dried up *in vacuo* to give a yellowish-orange residue, from which excess 2,4-dinitrofluorobenzene was removed by co-distillation with *n*-butanol. The residue was fully acetylated by heating with acetic anhydride (20 m*l*) and anhydrous sodium acetate (1.1 g), at 110°C, stirring vigorously for 5 hr. The mixture was dried up *in vacuo* and extracted with acetone. The extract was again evaporated to afford a yellow sirup, 1.5 g, which showed about four spots of R_f-values 0.40, 0.33, 0.13 and 0.08, on TLC, developing with the solvent system (c). The sirup was chromatographed on a column of silica-gel (10 g, 22×55 mm) with the solvent system (c), each fraction of the effluent being 10 g. The substance of R_f-value 0.08 appeared in the fractions of Nos. 12—25, which was evaporated to give yellow needles of VI, 0.06 g (5% overall-yield from V). Recrystallization from the solvent system (c); mp 212—213°C (decomp.), $[\alpha]_D^{18}$ +220° (*c* 0.3, acetone), IR spectrum (KBr): 3350, 3120, 1625, 1600, 1530, 1340, 835 and 745 (NHDNP), 1760 and 1220 cm^{-1} (OAc).

Found: C, 46.16; H, 4.23; N, 12.96%. Calcd for $C_{60}H_{59}N_{15}O_{36}$: C, 46.01; H, 3.80; N, 13.42%.

On TLC the R_f-value of the synthetic VI agreed with that of the hexa-*O*-acetyl-penta-*N*-(2,4-dinitrophenyl) derivative of natural kanamycin B (see below). Infrared spectra of VI and the above derivative were superimposable. The melting point of VI was not depressed by admixture with the above derivative.

We have investigated the above-mentioned removal of *O*-benzyl and *N*-carbobenzoxy groups in some detail. Instead of hydrogenation with palladium black, the condensation product (a sirup 0.7 g) was dissolved in liquid ammonia (60 m*l*) and sodium (0.3 g) was added under cooling in a solid carbon dioxide - methanol bath (−80——85°C). The solution became blue and the reaction was continued for 2 hr with occasional stirring. To the solution was added ammonium chloride until the blue color disappeared. Evaporation of the solution at room temperature left a colorless residue, which was treated with water to precipitate insoluble matters. The mixture was filtered and the solution was evaporated. The resulting colorless, ninhydrin-positive residue was dissolved in 1 N aqueous barium hydroxide solution (50 m*l*) and refluxed at 100°C for 2 hr. After cooling to room temperature, the solution was acidified with 3 N sulfuric acid to pH 2 and the barium salt was removed by centrifuge. The solution was filtered and neutralized with Dowex 1×2 (OH type) to pH about 7. After removal of the resin, the solution was evaporated *in vacuo* to give a colorless sirup. Dinitrophenylation and acetylation followed by chromatography with silica gel were carried out by similar procedure as described above. The yield of VI was 0.18 g (15% overall yield from V).

Synthetic Kanamaycin B (VII). A sample (77 mg) of VI was dissolved in methanol (50 m*l*), saturated with dry ammonia gas at 0°C and the red solution was set aside at room temperature overnight. After evaporation under reduced pressure, the residual yellow sirup was taken up with acetone (5 m*l*) and treated with excess Dowex 1×2 (*ca.* 2 m*l* of wet OH type) at room temperature for 12 hr with stirring. After removal of resin, the solution was evaporated *in vacuo* to give a glassy residue (24 mg) of VII, which was purified by chromatography with a small column of Dowex 1×2 (6× 50 mm). Treatment of the product with ethanol containing a small amount of water gave an analytically pure VII; 17 mg (72%), mp 178—182°C (decomp.), $[\alpha]_D^{18}$ +130° (*c* 0.5, water).

Found: C, 44.90; H, 7.34; N, 14.51. Calcd for $C_{18}H_{37}N_5O_{10}$: C, 44.71; H, 7.71; N, 14.49%.

On a descending paper chromatogram the R_f-value of the synthetic VII was in agreement with that of natural kanamycin B, after developing for 72 hr at room temperature. The antibiotics spectra and minimal inhibitory concentrations[1] of synthetic VII against test organisms coincided with those of natural kanamycin B.

Hexa-*O*-acetyl-penta-*N*-(2,4-dinitrophenyl) Derivative of Natural Kanamycin B. Free base of natural kanamycin B (40 mg) was dinitrophenylated with 2,4-dinitrofluorobenzene (59 mg) in the presence

of sodium bicarbonate (26 mg) in a mixture of water (0.5 m*l*) and ethanol (0.5 m*l*) with vigorous agitation at room temperature overnight. The yellow precipitate was collected and washed thoroughly with water and ethanol; yield 77 mg.

The product (75 mg) was then fully *O*-acetylated by heating with acetic anhydride (7.5 m*l*) in the presence of anhydrous sodium acetate (750 mg) at 110°C for 4 hr under stirring. The mixture was dried up to give a residue, which was extracted with an excess of acetone. The extract was evaporated *in vacuo* to give a yellow product; 99.9 mg. The product was purified on a column of silica-gel (10 g; 22×55 mm) with toluene-MEK (2 : 1), the effluent being cut into 1 m*l* each. After the initial effluent of 24 m*l*, hexa-*O*-acetyl-penta-*N*-(2,4-dinitrophenyl) derivative of natural kanamycin B was eluted in tube Nos. 5—24; 77 mg (49.2%), mp 217—218°C (decomp.), $[\alpha]_D^{18}$ +240° (*c* 0.4, acetone), IR spectrum (KBr): 3350, 3120, 1625, 1600, 1530, 1340, 835 and 745 (NHDNP), 1760 and 1225 cm^{-1} (OAc).

Found: C, 46.31; H, 4.21; N, 13.38%. Calcd for $C_{60}H_{59}N_{51}O_{36}$: C, 46.01; H, 3.80; N, 13.42%.

The authors are indebted to the Kawasaki-Factory of Meiji-Seika Co. Ltd., for supplying kanamycin B. Thanks are also due to Professor Hamao Umezawa of Institute of Microbial Chemistry for helpful advice and to Mr. Saburo Nakada for microanalysis.

NOTES

BULLETIN OF THE CHEMICAL SOCIETY OF JAPAN VOL. 42 542—543 (1969)

Gas Chromatographic Determination of Nitrogen in Metals by Means of Inert Gas Fusion Using Silicon

Jiro KASHIMA and Takuo YAMAZAKI

The Castings Research Laboratory, Waseda University, Totsuka-machi, Shinjuku-ku, Tokyo

(Received March 16, 1968)

Nitrogen in metals has been determined by means of chemical distillation which is a modification of the Kjeldahl method.[1,2] A vacuum fusion method and inert gas fusion method each making use of a platinum bath have also recently come into use. The results obtained by these methods agree with those obtained by the Kjeldahl method.[3,4]

This paper deals with the determination of nitrogen by means of inert gas fusion. We found that when a metal or alloy is melted in a graphite crucible in the presence of silicon, nitrogen and oxygen contained in the metal or alloy are completely set free. The molten product passes into the graphite crucible. Utilizing this fact a new method for the determination of nitrogen was worked out. This method is much simpler than the Kjeldahl method.

A tin capsule containing the sample (10—80 mg) and silicon (100—300 mg) was put in a graphite crucible. The graphite crucible was heated in a stream of argon up to 1900°C by means of a high frequency induction furnace. In less than a minute the molten product passed into the crucible. All of the gases contained in the sample were liberated. The gases were then passed through a column (length=70 cm, inner diameter=0.4 cm), filled with activated charcoal and kept at −20°C, for 3 min. The gases absorbed by activated charcoal were liberated by heating the column up to 140°C, and the amount of liberated gases was determined by means of gas chromatography. The amount of nitrogen was calculated by means of the formula

$$m = A\frac{a-b}{w} \times 100,$$

where m=nitrogen in wt %, A=constant, a=chromatographic area in cm^2, b=chromatographic area in blank test in cm^2, w=weight of sample in gram.

The constant A denotes the weight of nitrogen per square centimeter of chromatographic area. It has the value 1.5 μg per cm^2. The results are shown in Fig. 1. For the construction of the figure, the procedure given in a previous paper was used.[5] Linearity holds up to 5 μg of nitrogen. Deviation from linearity takes place for the values of nitrogen higher than this.

Degassed graphite crucibles were used in the experiment. Degassing was carried out by heating

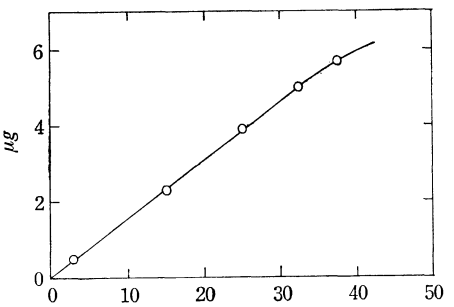

Fig. 1. Relation between the weight of nitrogen and gas chromatographic area.

TABLE 1. BLANK TEST OF GRAPHITE CRUCIBLE

Grade of crucible	Weight in μg	
	Nitrogen	Oxygen
Reactor	0.25	0.14
Spectroscopic	0.80	0.32

1) B. A. Generozov, *Zavodskaya Lab.*, **3**, 314 (1947).
2) National Academy of Sciences, "Report of the Panel on Analytical Problems in Refractory Metals," Rept. MAB-154-M(1), Vol. 11 (1959), p. 17.
3) V. A. Fassel, F. M. Evens and C. C. Hill, *Anal. Chem.*, **36**, 2115 (1964).
4) B. D. Holt and H. T. Goodspeed, *ibid.*, **35**, 1510 (1963).
5) J. Kashima and T. Yamazaki, This Bulletin, **39**, 1448 (1966).

Table 2. Nitrogen content of pure iron prepared by various methods

Preparation of iron	No. of determinations	Nitrogen, wt%		Standard deviations %
		Inert gas fusion	Kjeldahl method	
Iron, melted by arc, melted for the second time in a vacuum furnace	4	0.0008_8	0.0009	0.0001_0
Iron, melted by arc	4	0.0035_5	0.0035	0.00009_6
Iron, open hearth	5	0.0106_0	0.0106	0.0001_3

a crucible containing 100 mg of silicon at 1900°C for 3 min in a stream of argon. Most of the gases were eliminated by this treatment. The treatment was repeated. The amounts of nitrogen and oxygen liberated by the second treatment were determined by means of gas chromatography and were found to be negligibly small. A degassed graphite crucible could be use three times for the determination of nitrogen. The results are given in Table 1.

As an illustration, the results of the determination of nitrogen in pure iron are given in Table 2. The values obtained coincide with those obtained by means of the Kjeldahl method. The results obtained from other metals are summarized in Table 3.

Table 3. Nitrogen content in metals

Metals	No. of determinations	Nitrogen, wt %	Avarage deviation %
Stainless steel (25Cr12Ni)	5	0.0522	±0.003
Nitrogen-doped tungsten (wire)	4	0.0068	0.0008
Nitrogen-doped molybdenum (wire)	3	0.0215	0.002
Pure silicon (on market)	4	0.00043	0.00005
Silicon (on market)	4	0.0010	0.0002

BULLETIN OF THE CHEMICAL SOCIETY OF JAPAN VOL. 42 543—545 (1969)

Preparation of 2-Alkenonitrile by Means of the Pyrolysis of Diethyl 1-Cyanoalkyl Phosphate

Yoshiki OKAMOTO, Tsutomu NITTA and Hiroshi SAKURAI

The Institute of Scientific and Industrial Research, Osaka University, Yamada-kami, Suita-shi, Osaka

(Received April 25, 1968)

In previous papers, it has been reported that the long-chain aliphatic aldehydes and *α*-hydroxycarboxylic acids were prepared from diethyl acylphosphonates by treatment with sodium borohydride or potassium cyanide *via* the following scheme:

$$\mathrm{RCOPO(OC_2H_5)_2} \xrightarrow{\mathrm{NaBH_4}} \mathrm{RCH(OH)PO(OC_2H_5)_2} \xrightarrow{\mathrm{OH^-}} \mathrm{RCHO} + \mathrm{HPO(OC_2H_5)_2} \quad (1)^{1)}$$

$$\mathrm{RCOPO(OC_2H_5)_2} \xrightarrow[2)\ \mathrm{KCN}]{1)\ \mathrm{NaHSO_3}} \mathrm{RCH(OH)PO(OC_2H_5)_2} \xrightarrow{\mathrm{OH^-}} \mathrm{RCH(CN)OPO(OC_2H_5)_2} \xrightarrow[\mathrm{H_2O}]{\mathrm{H^+}} \mathrm{RCH(OH)COOH} \quad (2)^{2)}$$

It has also been reported that 2-butenonitrile was synthesized by the pyrolysis of 1-cyanopropyl acetate, itself prepared by the acetylation of propionaldehyde cyanhydrin.[3] In order to get long-chain 2-alkenonitriles, the corresponding long-chain aliphatic aldehydes were necessary. The preparation of long-chain aldehyde is, however, generally troublesome, and, in addition, the cyanhydrin could not be acetylated in a good yield.

In this note, a convenient method for the preparation of 2-alkenonitrile by means of the pyrolysis of diethyl 1-cyanoalkyl phosphate will be reported.

1) Y. Okamoto and H. Sakurai, *Kogyo Kagaku Zasshi* (*J. Chem. Soc. Japan, Ind. Chem. Sect.*), **70**, 797 (1967).

2) Y. Okamoto, T. Nitta and H. Sakurai, *ibid.*, **71**, 187 (1968).

3) D. L. Macpeek, P. S. Strarcher and B. P. Benjamin, *J. Am. Chem. Soc.*, **81**, 680 (1959).

$$RCH_2\dot{C}H(OPO(OC_2H_5)_2)\dot{C}N \longrightarrow RHC{=}CHCN + HPO(OC_2H_5)_2 \quad (3)$$

Diethyl acylphosphonates were easily prepared in good yields by the reaction of the corresponding acid chloride and triethyl phosphite.[2] The properties and the yields are summarized in Table 1.

Table 1. Preparation of diethyl acylphosphonates ($RCH_2COPO(OC_2H_5)_2$)

R	Yield (%)	Bp (°C/mmHg)	n_D^{25}
CH_3	85	66—67/0.5	1.4245
C_2H_5	90	75—76/1	1.4273
C_4H_9	89	85—86/0.5	1.4326
C_8H_{17}	87	125—126/0.5	1.4392
$C_{10}H_{21}$	88	155—156/1	1.4407

Diethyl 1-cyanoalkyl phosphates could be obtained from the corresponding diethyl acylphosphonate and potassium cyanide in an aqueous solution, but the yields were reduced by the hydrolysis reaction of some of the diethyl acylphosphonates.

$$RCOPO(OC_2H_5)_2 + H_2O \xrightarrow{OH^-} RCOOH + HPO(OC_2H_5)_2 \quad (4)$$

On the other hand, when the sodium bisulfite adduct of diethyl acylphosphonate, which had been prepared by the addition of diethyl acylphosphonate to the saturated aqueous solution of sodium bisulfite, was treated with an aqueous solution of potassium cyanide at pH 8, the corresponding cyanhydrin derivative was obtained as crystals in high yields. The yields and the properties are listed in Table 2. The infrared spectra showed the absortption peak of the hydroxyl group at 3170 cm^{-1}.

Diethyl 1-cyano-1-hydroxyalkylphosphonate isomerized rapidly into diethyl 1-cyanoalkyl phosphate in a large excess of a saturated aqueous solution of potassium cyanide (pH>12). The reaction occurred exothermically, and the diethyl 1-cyanoalkyl phosphate was almost quantitatively separated in an oily layer. After having been washed with water, the phosphate was used for the pyrolysis without further purification. The infrared spectra showed no absorption peak of the hydroxyl group.

Table 2. Preparation of diethyl 1-cyano-1-hydroxyalkylphosphonate ($RCH_2C(OH)(CN)PO(OC_2H_5)_2$)

R	Yield (%)	Mp (°C)		Anal. (%) P	N	C	H
CH_3	85	—	Found	14.01	6.31	43.22	7.11
			Calcd	14.00	6.33	43.88	7.29
C_2H_5	88	68—69	Found	13.00	5.97	46.00	7.79
			Calcd	13.13	5.96	45.89	7.71
C_4H_9	89	25—26	Found	11.52	5.29	50.68	8.59
			Calcd	11.77	5.32	50.19	8.42
C_8H_{17}	87	42—43	Found	10.21	4.41	56.00	9.70
			Calcd	10.01	4.53	55.01	9.76
$C_{10}H_{25}$	90	45—46	Found	8.86	3.93	58.58	10.05
			Calcd	8.92	4.03	58.77	10.03

The pyrolysis was carried out under reduced pressure (2—3 mmHg) in a stainless steel tube (ϕ 3 cm×60 cm) heated at 400—600°C in an electric furnace. The thermal decomposition of diethyl 1-cyanoalkyl phosphate occurred thoroughly above 300°C. The pure 2-alkenonitriles were obtained by the fractional distillation of the pyrolysis products. The yields and the properties of 2-alkenonitriles are listed in Table 3.

Table 3. Preparation of 2-alkenonitrile obtained from 1-cyanoalkyl phosphate (RCH=CHCN)

R	Yield (%)	Bp (°C/mmHg)	n_D^{20}
CH_3	71	103—105	1.4195
C_2H_5	53	44—45/17	1.4301
C_4H_9	52	71—74/22	1.4399
C_8H_{17}	52	86—89/1.5	1.4507
$C_{10}H_{21}$	51	105—109/3.5	1.4549

The purities of the 2-alkenonitriles were checked by gas chromatography (>98%). The infrared spectra indicated that the double bond (C=C) was only in the trans form (965 cm^{-1}).

The yield of 2-butenonitrile from diethyl 1-cyanopropyl phosphate was almost equal to that from 1-cyanopropyl acetate.

Diethyl 1-cyano-2-phenylethyl phosphate gave 3-phenylpropenonitrile in a 76% yield, but diethyl 1-cyanobenzyl phosphate did not give the corresponding 2-alkenonitrile, but rather benzalaldehyde in a 51% yield.

Experimental

Diethyl Acylphosphonate. The diethyl acylphosphonates were prepared by the reaction of the corresponding acyl chlorides with triethyl phosphite according to a procedure described earlier.[2]

Diethyl 1-Cyano-1-hydroxyalkylphosphonate and Diethyl 1-Cyanoalkyl Phosphate. One hundred grams of diethyl acylphosphonate were stirred, drop by drop, into 400 ml of a saturated aqueous solution of sodium bisulfite at 30°C. The reaction mixture came to be viscous; then a saturated aqueous solution of potassium cyanide was stirred in over a period of 1 hr, until the pH of the mixture rose to 8. The oily layer separated was extracted with ether. After the evaporation of the solvent, diethyl 1-cyano-1-hydroxyalkylphosphonate solidified on cooling. It was then recrystallized

from acetone (see Table 2).

Eighty grams of diethyl 1-cyano-1-hydroxyalkylphosphonate were added slowly to 200 m*l* of a saturated aqueous solution of potassium cyanide cooled with ice water. The isomerization reaction occurred exothermically. Then the reaction mixture was stirred for 30 min, and the product was extracted with ether. The ethereal extract was washed with water. After the removal of the solvent under a vacuum, the residue, diethyl 1-cyanoalkyl phosphate, was obtained; it was used for pyrolysis without any further purification.

Pyrolysis of Diethyl 1-Cyanoalkyl Phosphate. Typical Procedure. Thirty grams of diethyl 1-cyanoalkyl phosphate were charged continuously, at the rate of 1 m*l*/min, into the top of a 60 cm stainless steel tube (dia. 3 cm), which was inclined at twenty degrees from the horizontal; the tube was then heated at 600°C under reduced pressure (3—5 mmHg). The products were trapped as solid materials in a tube cooled with liquid nitrogen. Pure 2-alkenonitrile was obtained by fractional distillation in the presence of a catalytic amount of hydroquinone (see Table 3).

BULLETIN OF THE CHEMICAL SOCIETY OF JAPAN VOL. 42 545—547 (1969)

The Crystal Structure of Tetraallyldichromium, $Cr_2(C_3H_5)_4$

Takao Aoki, Akio Furusaki and Yujiro Tomiie†

Faculty of Science, Kwansei Gakuin University, Nishinomiya

and Katsuhiro Ono and Kenjiro Tanaka

Research Institute of Idemitsu Kosan Co., Ltd., Tokuyama

(Received May 6, 1968)

A product of the reaction of anhydrous chromium chloride with allylmagnesium chloride in an ether solution was found to be a potential component of a catalyst for the polymerization of olefins. The product can be recrystallized from hydrocarbon solutions in needle-like crystals, brownish-black in color and with a metallic luster. Though this compound is exceedingly inflamable when exposed to air, we have succeeded in determining its chemical composition by elementary analysis and its molecular weight by the cryoscopic method. From the results of infrared absorption, mass spectroscopic analysis, and nuclear magnetic resonance, it was concluded that the compound is tetraallyldichromium, corresponding to the molecular formula $Cr_2(C_3H_5)_4$, and that the reaction can be written as follows:

$$2CrCl_3+6C_3H_5MgCl \rightarrow Cr_2(C_3H_5)_4+C_6H_{10}+6MgCl_2.$$

The yield of the reaction reaches 90—95% if the temperature is controlled properly.

With a hope to look into the mechanism of the catalytic activity, we have undertaken an X-ray crystal analysis of tetraallyldichromium.

Samples sealed in glass capillary tubes filled with argon gas were used throughout the experiment because of their high sensitivity to air. The single crystals used were prisms elongated along the c-axis, with dimensions of (0.1—0.2)×(0.1—0.2)×(1.5—3.0)mm. The crystal data are as follows: the molecular weight is 268; the unit cell is tetragonal with $a=18.19\pm0.09$, $c=7.50\pm0.05$ Å, and contains eight molecules of $Cr_2(C_3H_5)_4$; the space group is $P\bar{4}2_1c$—D_{2d}^{4}; the density calculated is 1.44 g·cm^{-3}.

X-Ray intensities were visually estimated from multiple-film equi-inclination Weissenberg photographs taken from the zeroth to the fifth layer around the c-axis with Ni-filtered Cu$K\alpha$ radiation. Five oscillation photographs taken using the equi-inclination method were prepared in order to find the scale factors by comparing the structure factors of reflections appearing in each layer with those of the equatorial reflections. The relative intensities of all the six layer reflections put on the same scale were corrected for the Lorentz-polarization factor,

Table 1. The final atomic positions

	X/a	Y/b	Z/c
Cr1	0.2113	0.0524	0.1791
Cr2	0.2819	−0.0290	0.1519
C11	0.3708	0.0294	0.0274
C12	0.3342	0.0923	0.1400
C13	0.2732	0.1377	0.0463
C21	0.2108	0.0955	0.4631
C22	0.1590	0.0452	0.4578
C23	0.1060	0.0351	0.3156
C31	0.1494	0.0267	−0.0600
C32	0.2158	−0.0017	−0.1250
C33	0.2413	−0.0736	−0.0980
C41	0.2616	−0.1439	0.2552
C42	0.2767	−0.0979	0.4104
C43	0.3391	−0.0485	0.4126

† Deceased 31 May, 1967.

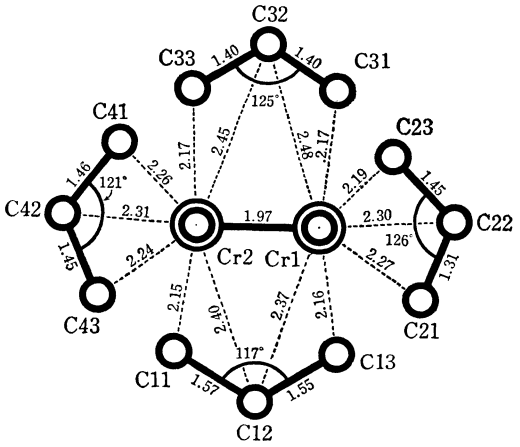

Fig. 1. Interatomic distances (Å) and bond angles (°).

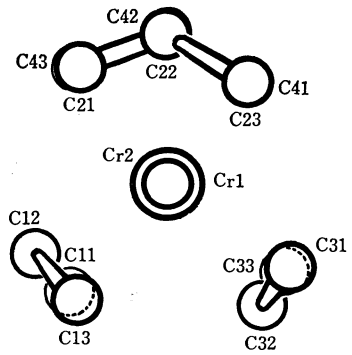

Fig. 2(a). The configuration of the complex, $Cr_2(C_3H_4)$, viewed along the Cr—Cr axis.

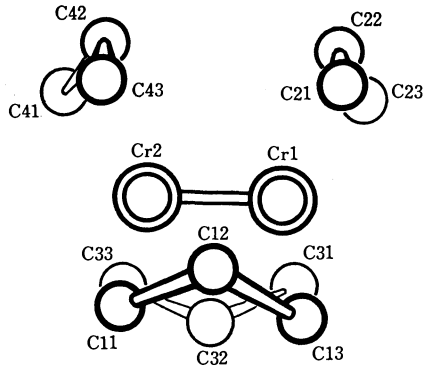

Fig. 2(b). The configuration of the complex, $Cr_2(C_3H_5)_4$, viewed along an axis perpendicular to the Cr–Cr.

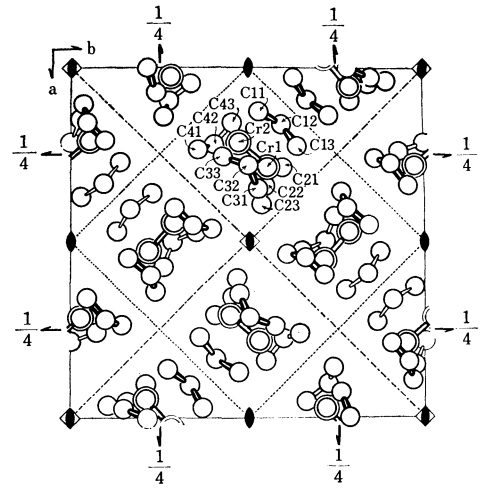

Fig. 3. The packing arrangement of the complex, $Cr_2(C_3H_5)_4$, viewed along the c-axis.

but not for the absorption effect. The relative values of the observed structure factors of 656 independent reflections were converted into an absolute scale by Wilson's method.

The positions of the chromium atoms were determined from a three dimensional Patterson function and refined by the least-squares method. Twelve carbon atoms were found on a Fourier map calculated using the phases of the heavy atoms alone. The fourteen positions thus obtained were refined by the least-squares method, taking into consideration the anisotropic thermal motions of all the atoms and the anomalous dispersion effect of chromium. The final R factor was 11.2%.

The atomic positions thus obtained are given in Table 1; the estimated maximum deviations are 0.06 Å for the carbon and 0.006 Å for the chromium atoms. The interatomic distances and bond angles are shown in Fig. 1. The configuration of the complex, $Cr_2(C_3H_5)_4$, and the packing arrangement in the unit cell are shown in Figs. 2 and 3 respectively. Four allyl ligands make a distorted tetrahedron around the two directly-coupled metal atoms. The Cr–Cr distance, 1.97Å, in the molecule is considerably smaller than that found in metallic chromium, 2.50 Å; it is indeed, the smallest metal-to-metal distance reported so far for organometallic compounds. The four ligands may be divided into two groups on the basis of the mode of coordination. The planes of the C11–C12–C13 and C31–C32–C33 groups are nearly parallel to the Cr–Cr axis and each of these groups is coordinated to both of the chromium atoms. On the other hand, the C21–C22–C23 and C41–C42–C43 groups are approximately perpendicular to the Cr–Cr axis and each is coordinated to one of the chromium atoms. The average bond length of the C–C bond is 1.45 Å, which is comparable with the mean value of the single and double bonds of the carbon atoms. None of the intermolecular interatomic distances are abnormally short, so the molecules are held together by the van der Waals interactions alone.

Because of the unexpected death of one of the present authors (Yujiro Tomiie), this work was completed in the laboratory of Professor Tokunosuké Watanabé, to whom the authors' thanks are also due for his helpful discussions about this manuscript. The authors would like also to thank Mr. K. Echigoya for his assistance in measuring the intensities.

BULLETIN OF THE CHEMICAL SOCIETY OF JAPAN VOL. 42 547—548 (1969)

The Formation of 1,4-Disubstituted Piperazines from 1-Substituted Aziridines

Itaru OKADA, Nobuhiro ITOH and Rokuro SUDO

Laboratory of Organic Chemistry, Tokyo Institute of Technology, Ookayama, Meguro-ku, Tokyo

(Received May 31, 1968)

The dimerization of aziridines to piperazines has received little attention.[1-5] Heine and his coworkers reported that 1-arylsulfonylaziridines and 1-phenylaziridine, on treatment with sodium iodide, were dimerized to the corresponding piperazines.[6] Recently, Dick found the reaction of certain 1-alkylaziridines with alkyl or alkenyl halides gave nearly quantitatively the corresponding 1,1,4-trialkylpiperazinium halides.[7]

In the course of our study we found that the treatment of 1-cyclohexylaziridine with four equivalents of phenylmagnesium bromide gave a 41% yield of 1,4-dicyclohexylpiperazine. The structure of this piperazine was established by a study of the melting point,[8] by its elemental analysis and by a study of its infrared spectrum. Similarly, 1-benzylaziridine was dimerized to the corresponding 1,4-disubstituted piperazine. Control runs in the absence of the Grignard reagent resulted in the recovery of aziridines. Using half an equivalent of magnesium bromide instead of the Grignard reagent, 1-substituted aziridines in refluxing methanol were dimerized to the corresponding 1,4-disubstituted piperazines in 50—70% yields. The dimerization of aziridines also occurred with a catalytic amount of other Lewis acids. These results are summarized in Table 1.

TABLE 1. REACTION OF 1-SUBSTITUTED AZIRIDINES WITH LEWIS ACIDS OR PHEYLMAGNESIUM BROMIDE

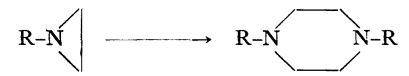

Reaction	Substituent	Catalyst	Yield %	Mp°C or Bp°C/mmHg
1	*i*-C_3H_7	$MgBr_2$	70	97/20
2	*n*-C_4H_9	$MgBr_2$	43	134/27[c]
3	C_6H_{11}	$MgBr_2$	72	117–118[d,e]
4		$SnCl_4$	60	
5		$ZnCl_2$	50	
6		$BF_3O(C_2H_5)_2$	52	
7		$AlCl_3$	66	
8		C_6H_5MgBr	41	
9	$C_6H_5CH_2$	$MgBr_2$[a,b]	66	90–91[f,g]
10		C_5H_6MgBr	15	

	Formula	Elemental analysis Calcd, % C	H	N	Found, % C	H	N
1	$C_{10}H_{22}N_2$	70.53	13.02	16.45	70.20	12.93	16.16
2	$C_{12}H_{26}N_2$	72.66	13.21	14.12	72.78	13.17	13.82
8	$C_{16}H_{30}N_2$	76.74	12.08	11.19	76.66	11.81	10.98
10	$C_{18}H_{22}N_2$	81.16	8.33	10.52	81.01	8.70	10.35

a) THF as solvent. b) See Experimental. c) Lit. bp 114°C/10 mmHg.[7] d) Lit. mp 118°C.[8] e) Recrystallized from acetonitrile. f) Lit. mp 92°C.[9] g) Recrystallized from ethanol.

It is well known that the reaction of ethylene oxide with a Grignard reagent gives a primary alcohol. However, the reaction of aziridines with this reagent did not give secondary amines, but piperazines. The catalytic action of the Grignard

1) W. G. Brab, *J. Chem. Soc.*, **1955**, 2580.
2) L. B. Clapp, *J. Am. Chem. Soc.*, **73**, 2584 (1951).
3) H. Stamm, *Chem. Ber.*, **99**, 2556 (1966).
4) G. K. HelmKamp, R. D. Clark and J. R. Koskinen, *J. Org. Chem.*, **30**, 666 (1965).
5) Y. Iwakura, K. Uno, N. Nakabayashi, T. Tani and W. Chiang, *Kogyo Kagaku Zasshi* (*J. Chem. Soc. Japan, Ind. Chem. Sect.*), **68**, 1222 (1965).
6) H. W. Heine, W. G. Kenyon and E. M. Johnson, *J. Am. Chem. Soc.*, **83**, 2570 (1961).
7) C. R. Dick, *J. Org. Chem.*, **32**, 72 (1967).
8) C. N. Ionescu *et al.*, *Acad. rep. populare Romîne, Studii cercetări chim.*, **5**, No. 1, 7—15 (1957); through *Chem. Abstr.*, **52**, 398i (1968).
9) Heilbron, "Dictionary of Organic Compounds," ed. by A. H. Cook and E. R. H. Jones, Oxford University Press, New York, N. Y. (1953), p. 216.

reagent seems to be the following: Initially, the magnesium of this reagent coordinates to the basic aziridine nitrogen; then the electrophilic ring carbon attacks not the carbon of the Grignard reagent, but another aziridine nitrogen, and a piperazine is formed. The reason for this seems to be that the nucleophilicity of the Grignard reagent is less strong than that of aziridine nitrogen. In view of this, it is obvious that Lewis acids are also more effective catalysts than the Grignard reagent.

Experimental

Reaction of 1-Substituted Aziridines with Phenylmagnesium Bromide. An 80 m*l* portion of a dry ether solution containing 0.16 mol of phenylmagnesium bromide was prepared, and to this solution there was added rapidly 0.04 mol of aziridine dissolved in 50 m*l* of dry ether. The mixture was then refluxed for 7 hr and allowed to stand at room temperature overnight. The solution was decomposed by pouring in 40 g of ammonium chloride and ice. The ether layer was washed with water and dried over anhydrous potassium carbonate. The solvent was evaporated and allowed to stand in a refrigerator overnight. The oily brown residue was treated with 10 m*l* of acetonitrile. A white precipitate was separated by filtration and recrystallized.

Reaction of 1-Substituted Aziridines with Magnesium Bromide. A mixture of 0.02 mol of the aziridine, 1.84 g of magnesium bromide, and 40 m*l* of methanol was refluxed for 7 hr. The solvent was evaporated, and the residue was treated with a slight excess of potassium hydroxide and water. The solution was extracted several times by ether. The ether layer was dried over anhydrous potassium carbonate and evaporated. The crude product was recrystallized or distilled. In the case of 1-benzylaziridine, a white crystal was obtained as a by-product; mp 141—142°C.

BULLETIN OF THE CHEMICAL SOCIETY OF JAPAN VOL. 42 548—550 (1969)

A Correlation between the Magnetic and Optical Properties of Some Cation Radical Salts

Yoichiro SATO, Minoru KINOSHITA, Mizuka SANO*1 and Hideo AKAMATU

Department of Chemistry, Faculty of Science, The University of Tokyo, Hongo, Tokyo

(Received June 5, 1968)

The paramagnetic susceptibilities of the cation radical salts formed by the oxidation of phenothiazine (PT), *N*-methylphenothiazine (MPT), and thianthrene (TA) with antimony pentachloride have been reported in a previous paper.[1] The variation in the susceptibilities for PT·$SbCl_4$ and PT·$SbCl_5$ with temperature has been explained in terms of the linear Ising model; thus, the spin-exchange coupling parameters (J) have been determined to be 0.034 and 0.0042 eV respectively. The susceptibilities for MPT·$SbCl_5$ and TA·$SbCl_5$, on the other hand, obeyed the Curie-Weiss law above 100°K. The Weiss constants (θ) for these salts were found to be -5 ± 10°K and 0 ± 4°K respectively.

In this paper we will report a finding of correlation between the values of the spin-exchange coupling parameter and the intensities of the absorption band in the near-infrared region of the solid cation radical salts. The static susceptibility of phenothiazine bromide (PT·Br), which was prepared by the procedure of Kehrmann and Diserens,[2] was also measured as a function of temperature with a Faraday-type magnetic balance. The absorption spectrum of a solid radical salt was obtained with a powder sample suspended in liquid paraffin.

Results and Discussion

Solid phenothiazine bromide was found to be diamagnetic at room temperature (-14.3×10^{-5} emu/mol). After corrections had been made for the diamagnetism and for a small paramagnetism due to impurities, the intrinsic paramagnetic susceptibility for the bromide was found to be 1.2×10^{-5} emu/mol at 296°K, and to decrease with a decrease in temperature. The change in the paramagnetic susceptibility with temperature was found to fit well the curve calculated from the linear Ising model, for which J was taken to be 0.12 eV.

The values of the spin-exchange coupling parameter for MPT·$SbCl_5$ and TA·$SbCl_5$ were not given explicitly in the previous paper. If we assume that the linear Ising model for which the relation

*1 Present address: Department of Materials Science, The University of Electro-Communications, Chofu, Tokyo.

1) Y. Sato, M. Kinoshita, M. Sano and H. Akamatu, This Bulletin, **40**, 2539 (1967).

2) F. Kehrmann and L. Diserens, *Ber.*, **48**, 318 (1915).

$J=-k\theta$ holds in the temperature region $T \gg J/k$, is applicable to the paramagnetism of the salts, the parameter can be estimated from the observed value of a Weiss constant. The values thus calculated are listed in Table 1.

TABLE 1. EXCHANGE COUPLING PARAMETER FOR THE SALTS STUDIED

Compound	J (eV)
TA·$SbCl_5$*	$\sim$ 0
MPT·$SbCl_5$*	$\sim 4.3 \times 10^{-4}$
PT·$SbCl_5$*	4.2×10^{-3}
PT·$SbCl_4$*	3.4×10^{-2}
PT·Br	$\sim 1.2 \times 10^{-1}$

* The paramagnetism of these salts originates entirely from the respective mono-positive organic molecules and antimony pentachloride is thought to be forming closed shell negative ions.[1]

The absorption spectra for solid TA·$SbCl_5$ and MPT·$SbCl_5$ were found to correspond well to the spectra of the respective solutions in dichloromethane, and no extra band could be observed in the spectra of the solids, as is shown in Fig. 1. This result reveals that the cation radicals in a solid are nearly as free as in a solution. The same conclusion has been derived from the magnetic susceptibility measurements, which have shown negligible values of the spin-exchange coupling parameter for these salts.

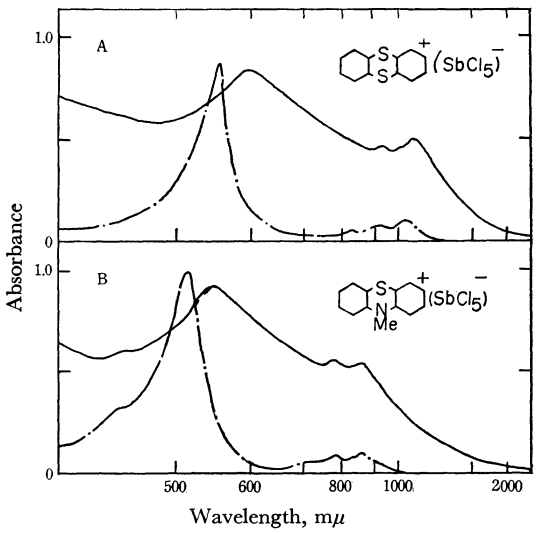

Fig. 1. A, The absorption spectra of thianthrene mono-positive ion. ———— Solid TA·$SbCl_5$, —·—·—·— dichloromethane solution; B, The absorption spectra of *N*-methylphenothiazine mono-positive ion. ———— Solid MPT·$SbCl_5$, ——·——·——·—— dichloromethane solution.

The spin-exchange coupling parameters for the three kinds of radical salts of phenothiazine, PT·Br, PT·$SbCl_4$, and PT·$SbCl_5$, were larger in value than those for MPT·$SbCl_5$ and TA·$SbCl_5$, and their values decreased in this sequence, as Table 1 shows. The solution spectra of all these phenothiazine salts showed the same pattern, a pattern which was also in agreement with that reported for a phenothiazine mono-positive ion by Shine and Mach.[3] When the salts were formed into a solid, they showed extra absorption bands in the near-infrared region, where no absorption was found in the solution spectra. As is shown in Fig. 2, PT·Br, PT·$SbCl_4$, and PT·$SbCl_5$ exhibited new absorption bands at 900, 1070, and 1000 mμ (shoulder) respectively. The band for PT·Br was found to be the strongest in intensity among the salts; this fact is consistent with the fact that the spin exchange coupling parameter for the salt is the largest in value. The absorption bands for the phenothiazine salts decreased in intensity in the same sequence as the spin-exchange coupling parameters, though little difference was found with respect to the position of the absorption band.

The new absorption band is regarded as arising

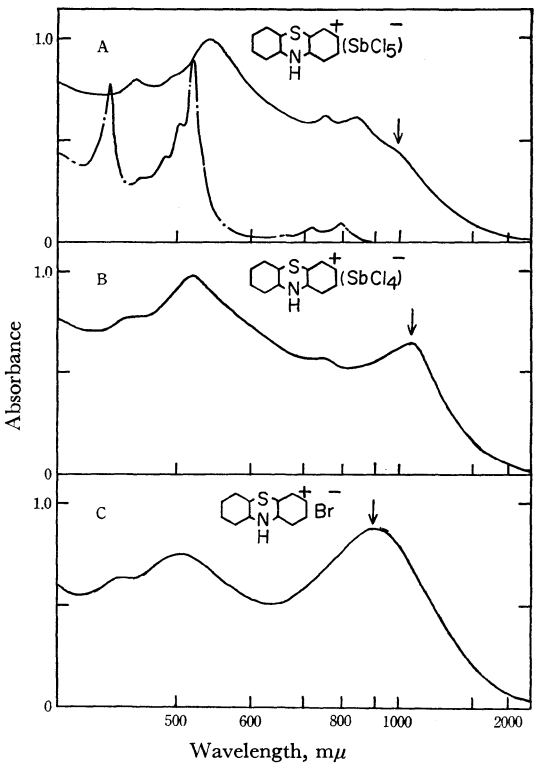

Fig. 2. The absorption spectra of phenothiazine mono-positive ion. A, ———— Solid PT·$SbCl_5$, —·—·—·— dichloromethane solution; B, Solid PT·$SbCl_4$; C, Solid PT·Br. The position of the charge-transfer absorption band for the respective salt is indicated by an arrow.

3) H. J. Shine and E. E. Mach, *J. Org. Chem.*, **30**, 2130 (1965).

from charge-transfer interaction between phenothiazine cation radicals in the solid. When phenothiazine radicals are stacked in a face-to-face manner, forming chain-like arrays of molecules, as is known in the structure of some radical salts,[4] the charge-transfer absorption may be expressed as a transition of the type $\langle\cdots D^+D^+D^+D^+\cdots\rangle \rightarrow \langle\cdots D^+D^{2+}D^0D^+\cdots\rangle$, where D denotes a phenothiazine molecule. The excitation energy of the transition is not greatly influenced by a small change in the intermolecular distance or mutual orientation, for it is essentially determined by the difference between the ionization potential and the electron affinity of the phenothiazine *mono-positive ion* radical (D^+). This is in agreement with the observed insensitivity of the band positions in the three phenothiazine radical salts.

The spin-exchange coupling parameter and the intensity of a charge-transfer band are both thought to be approximately proportional to the square of an overlap integral between neighboring radicals. A relatively small change in the intermolecular distance or mutual orientation may cause a somewhat large change in the overlap integral; this change, in turn, results in the different intensity of the charge-transfer absorption and in the different value of the spin-exchange coupling parameter. This may be what has been observed with the three kinds of phenothiazine radical salts. The same interpretation can be given to the appearance of intense charge-transfer absorption bands with the radical salts, such as *p*-phenylenediamine bromide,[5] Würster's blue perchlorate at 77°K,[5-9] and alkali metal salts of 7,7,8,8-tetracyano-*p*-quinodimethan,[10,11] which exhibit strong antiferromagnetic spin-exchange coupling.

From the observed correlation between the magnetic and optical properties, it may be inferred that the spin-exchange coupling parameter, J, is determined mainly by the charge-transfer interaction in these salts. A qualitative explanation may be made by considering, for the sake of brevity, a particular pair of adjacent radicals in a chain. The pair of identical radicals gives rise to a singlet (non-magnetic) state and a triplet (magnetic) state, for which the relative positions are determined, to a first approximation, by an exchange integral between the paired radicals. The excited charge-transfer configuration specified above, which is usually singlet, will then interact with the ground state and stabilize its energy, while the triplet state remains unaffected, thus leading to a further separation of the singlet-triplet energy gap. This view of the situation, when extended to a linear array of radicals, implies that the charge-transfer configurational interactions also contribute to the determination of the relative energy levels of the magnetic and non-magnetic states. Therefore, it appears that the sign and magnitude of a spin-exchange coupling parameter are sensitively dependent on the relative energies of the exchange interaction and the charge-transfer configurational interaction effects. For the cation radical salts studied here, it is likely that the stabilization energy due to the latter effect is of primary importance rather than that due to the former.

4) a) C. J. Fritchie, Jr., *Acta Cryst.*, **20**, 892 (1966); b) C. J. Fritchie, Jr., and P. Arthur, Jr., *ibid.*, **21**, 139 (1966).

5) K. Uemura, S. Nakayama, Y. Seo, K. Suzuki and Y. Ooshika, This Bulletin, **39**, 1348 (1966).

6) G. R. Anderson, *J. Chem. Phys.*, **47**, 3853 (1967).

7) a) W. Duffy, Jr., *ibid.*, **36**, 490 (1962); b) K. Okumura, *J. Phys. Soc. Japan*, **18**, 69 (1963); c) R. S. Rhodes, *Bull. Am. Phys. Soc.*, **8**, 469 (1963).

8) D. D. Thomas, H. Keller and H. M. McConnell, *J. Chem. Phys.*, **39**, 2321 (1963), and references contained therein.

9) H. Chihara, M. Nakamura and S. Seki, This Bulletin, **38**, 1776 (1965).

10) R. G. Kepler, *J. Chem. Phys.*, **39**, 3528 (1963).

11) Y. Iida and Y. Matsunaga, The work presented at the 20th Annunal Meeting of the Chemical Society of Japan, April, 1967.

BULLETIN OF THE CHEMICAL SOCIETY OF JAPAN VOL. 42 551—553 (1969)

Studies on the Coagulation of Silver Sol: Effect of Dialysis, Non-electrolytes and Ageing on the Constants of Bhattacharya's Equation

Mukhtar SINGH and O. P. BANSAL

Chemical Laboratories, Agra College, Agra, India

(Received April 20, 1968)

Bhattacharya *et al.*[1] established the relation between the electrolyte concentration, C, and the inverse of the corresponding time of coagulation, $1/t$, in the zone of slow coagulation and obtained hyperbolic curves in the majority of cases, although straight lines were obtained in some cases. The relation established by them is,

$$C = a + \frac{m \cdot 1/t}{n + 1/t} \qquad (1)$$

where a, m and n are constants. The equation on simplifying assumes the form:

$$1/(C - a) = (n/m)t + 1/m \qquad (2)$$

Accordingly, a verification of the equation can be made from the coagulation data if the plots between $1/(C-a)$ and t provide a straight line.

In this communication, an attempt has been made to study the variations of the constants, *i. e.*, a, m and n at different periods of dialysis of the sol. The values of the constants have also been evaluated in the presence of different non-electrolytes to throw light on the stabilising or sensitising power of the non-electrolytes used. The effect of ageing on the above constants for the dialysed silver sol using $NaNO_3$, $Ba(NO_3)_2$ and $Al(NO_3)_2$ as coagulating electrolytes, has also been incorporated in this paper.

Experimental

Silver sol was prepared by adding just sufficient ammonia to 20 m*l* of 5% silver nitrate solution to dissolve silver hydroxide formed; the solution was then made upto one litre. 2% solution of tannic acid was then added to the solution, drop by drop with constant stirring, until a dark brown sol was obtained. It was dialysed against running distilled water until free from electrolytes.

Three different samples of the sol were prepapred. One sample was used for the study of the effect of dialysis,the second for the effect of ageing and the third for the study of non-electrolyte effect.

Time of coagulation of the sol, using $NaNO_3$, $Ba(NO_3)_2$ and $Al(NO_3)_3$ as coagulating electrolytes was determined by light extinction method, using a Gallenkamp Photoelectric Colorimeter. For each concentration of the coagulating electrolyte, the extinction was plotted against the time (Fig. 1). Then a straight line parallel to the time axis was drawn so as to cut all the curves at different points, referring to the same state of aggregation in all the different cases.

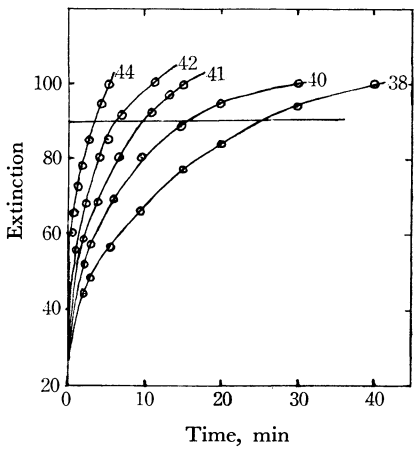

Fig. 1. Coagulation of silver sol- with $NaNO_3$ of various concentrations (mM/*l*)

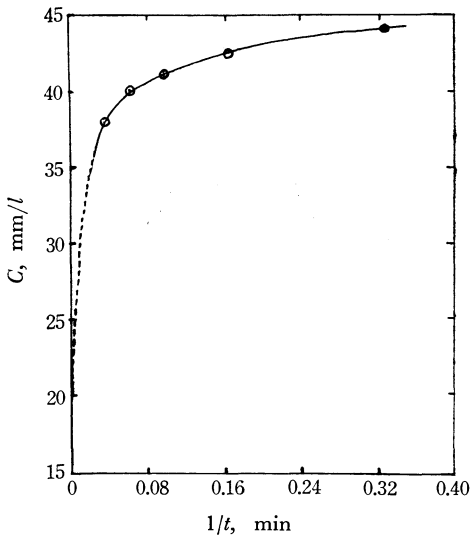

Fig. 2. Relation between the electrolyte concentration and inverse of the coagulation time.

1) A. K. Bhattacharya *et al.*, *J. Ind. Chem. Soc.*, **28**, 179, 638 (1951); **29**, 687, 759 (1952); *J. Colloid Sci.*, **10**, 551 (1955).

TABLE 1. EFFECT OF DIALYSIS

Sol dialysed for(days)	Sp. cond. $\times 10^4$ (mhos) at 30°C	$NaNO_3$			$Ba(NO_3)_2$			$Al(NO_3)_3$		
		a (mM)	*m* (mM)	*n* (min^{-1})	*a* (mM)	*m* (mM)	*n* (min^{-1})	*a* (mM)	*m* (mM)	*n* (min^{-1})
1	3.70	50.0	25.0	0.0312	0.22	0.114	0.0974	0.035	0.023	0.0596
2	2.17	45.0	23.81	0.020	0.71	0.150	0.0638	0.030	0.0212	0.057
3	1.50	40.0	26.31	0.0183	0.16	0.125	0.0642	0.025	0.018	0.0472
5	0.70	30.0	25.0	0.0132	0.14	0.135	0.0554	0.020	0.0169	0.0432
7	0.28	20.0	24.32	0.0123	1.03	0.111	0.0454	0.015	0.020	0.0413
9	0.24	10.0	27.0	0.0110	0.12	0.120	0.0321	0.005	0.0185	0.0355

TABLE 2. EFFECT OF AGEING

Concentration of the sol = 0.203 g silver/*l*

Period of ageing (days)	$NaNO_3$			$Ba(NO_3)_2$			$Al(NO_3)_3$		
	a (mM)	*m* (mM)	*n* (min^{-1})	*a* (mM)	*m* (mM)	*n* (min^{-1})	*a* (mM)	*m* (mM)	*n* (min^{-1})
0	8.0	40.0	0.101	0.08	0.156	0.055	0.019	0.0078	0.0312
10	6.0	25.0	0.0291	0.04	0.180	0.042	0.018	0.0081	0.0300
20	5.0	18.18	0.080	0.03	0.135	0.0325	0.017	0.0085	0.0282
30	2.0	9.09	0.0591	0.010	p.100	0.0261	0.014	0.009	0.0253

TABLE 3. EFFECT OF NON-ELECTROLYTES

Concentration of the sol = 0.3296 g silver/litre

		$NaNO_3$			$Ba(NO_3)_3$			$Al(NO_3)_3$		
		a (mM)	*m* (mM)	*n* (min^{-1})	*a* (mM)	*m* (mM)	*n* (min^{-1})	*a* (mM)	*m* (mM)	*n* (min^{-1})
Ethanol	(0.1 m*l*)	24.5	12.5	0.0270	0.12	0.133	0.053	0.022	0.0071	0.046
Ethanol	(0.2 m*l*)	19.5	10.0	0.0232	0.11	0.080	0.0230	0.021	0.0062	0.036
Ethanol	(0.3 m*l*)	17.0	8.7	0.0217	0.10	0.075	0.0200	0.020	0.0053	0.032
Ethanol	(0.4 m*l*)	14.5	8.0	0.0120	0.09	0.065	0.0182	0.0190	0.0050	0.030
Ethanol	(0.5 m*l*)	13.0	6.0	0.0080	0.08	0.050	0.0140	0.0180	0.0043	0.020
Acetone	(0.1 m*l*)	25.0	10.53	0.0210	0.14	0.120	0.0460	0.021	0.008	0.040
Acetone	(0.2 m*l*)	20.0	11.76	0.0160	0.135	0.100	0.0420	0.020	0.0077	0.038
Acetone	(0.3 m*l*)	18.0	9.00	0.010	0.125	0.100	0.0380	0.0195	0.0077	0.0307
Acetone	(0.4 m*l*)	15.0	7.70	0.0083	0.120	0.092	0.030	0.0190	0.0069	0.0280
Acetone	(0.5 m*l*)	13.0	8.00	0.0062	0.110	0.073	0.0261	0.0180	0.0059	0.0250
Formamide	(0.1 m*l*)	24.0	12.05	0.0120	0.120	0.125	0.048	0.022	0.0075	0.0458
Formamide	(0.2 m*l*)	22.0	13.16	0.0110	0.10	0.110	0.045	0.021	0.0070	0.0420
Formamide	(0.3 m*l*)	22.0	13.16	0.0110	0.095	0.100	0.041	0.020	0.0067	0.0382
Formamide	(0.4 m*l*)	22.0	13.16	0.0110	0.090	0.100	0.0372	0.0195	0.0064	0.0345
Formamide	(0.5 m*l*)	22.0	13.16	0.0110	0.085	0.0909	0.0312	0.0190	0.0062	0.0321
Pure sol	—	26.0	15.87	0.0276	0.150	0.1136	0.0556	0.0260	0.00363	0.052
Urea-5M	(1.0 m*l*)	28.0	18.52	0.0278	—	—	—	—	—	—
Urea-5M	(1.5 m*l*)	30.0	19.23	0.0281	0.155	0.1786	0.091	0.030	0.040	0.056
Urea-5M	(2.0 m*l*)	—	—	—	0.160	0.2272	0.098	0.040	0.05	0.0621

The inverse of the coagulating time thus obtained were plotted against the electrolyte concentration, and the value of a was determined as the concentration extrapolated to $(1/t)\rightarrow 0$, as is shown in Fig. 2. Finally, $1/(C-a)$ was plotted against t; straight lines, as Figs. 3 and 4 show, were obtained, as was to be expected from Eq. (2). The values of m and n can be obtained from these straight lines.[2] The values of the constants obtained for the same stage of coagulation given by the same extinction value for the sol at the different stages of dialysis and ageing, and also in the presence of different amounts of various non-electrolytes have been recorded in Tables 1, 2 and 3.

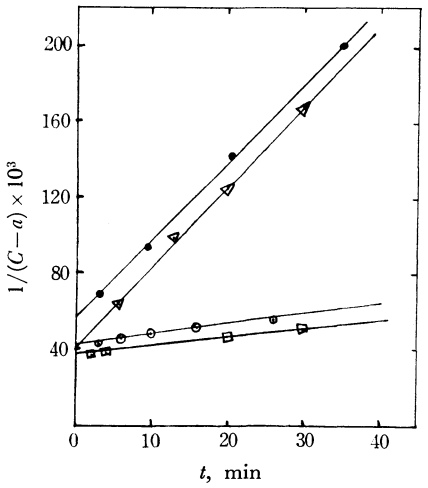

Fig. 3. Coagulation with $NaNO_3$.
⊙ Sol dialysed for 7 days.
⊡ Sol dialysed for 9 days.
△ Sol aged for 10 days.
● Sol aged for 20 days.

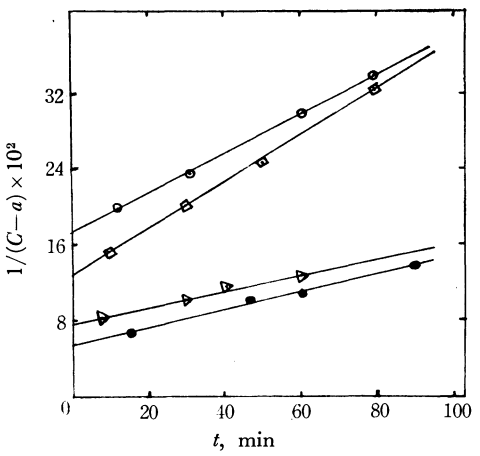

Fig. 4. Coagulation with $NaNO_3$.
⊙ In the presence of ethanol
⊡ In the presence of acetone
△ In the presence of formamide
● In the presence of urea.

2) A. K. Bhattacharya *et al.*, *J. Colloid Sci.*, **11**, 124 (1956); *Agra Univ. J. Res. Sci.*, **12**, 101 (1963).

Discussion

Bhattacharya's equation, in the form of Eq. (2), shows that the plots, $1/(C-a)$ against t should be a straight line and this has actually been observed in all cases of the present studies (Representative Figs. 3 and 4) confirming the applicability of the equation for the coagulation of the sol by electrolytes, in the partially dialysed state and also in the presence of non-electrolytes.

If $1/t$ is made large as compared to n, Eq. (1) takes up the form, $C=a+m$. This means that m is the excess of the electrolyte that should be added above the critical stability concentration, a, in order to cause the immediate coagulation of the sol. It may be said that at $C=a+m$, the region of slow coagulation merges into that of rapid coagulation. From Table 1 it is evident that the value of $(a+m)$ decreases with progressive dialysis of the sol indicating that the region of slow coagulation merges into that of rapid coagulation earlier in the dialysed sol. From this, it is evident that the sol becomes increasingly sensitive with progressive dialysis.

The values of the constants, a, $(a+m)$ and n show a decrease in the presence of ethanol, acetone and formamide but the presence of urea causes an increase. Ethanol, acetone and formamide sensities the sol against mono, di and tri-valent ions, since in the presence of these non-ionic substances the region of slow coagulation merges into that of rapid coagulation earlier as evidenced by the low values of $(a+m)$. Urea stabilises the sol. The extent of stabilisation or sensitisation increases with the increased non-ionic addition.

Ageing results in aggregation of particles which renders the sol unstable and since a, $(a+m)$ and n are connected with the stability, the values of these constants should decrease with the ageing of the sol, and this fact has also been confirmed experimentally.

On examining critically the variations in the values of a, it is found that the variations in the values of a with the valency of the precipitating ion support the law that the coagulating power of the ion increases with the increase in its valency. This law has been stated originally for the lowest electrolyte concentration, $(a+m)$ required for the rapid coagulation, but here the law is applied better to the maximum electrolyte concentration, a, at which even the slow coagulation is expected not to occur.

Thanks are due to Dr. A. K. Bhattacharya, D. Sc., F.R.I.C. (London), Prof. of Chemistry, University of Jammu and Kashmir and Dr. A. Kumar for their valuable suggestions in this work.

BULLETIN OF THE CHEMICAL SOCIETY OF JAPAN VOL. 42 554 (1969)

Zirconium Ethoxide: A New Method of Preparation

S. K. ANAND, J. J. SINGH, R. K. MULTANI and B. D. JAIN

Department of Chemistry, University of Delhi, Delhi-7, India

(Received May 10, 1968)

Meerwein and Bersin[1] could not obtain zirconium tetraethoxide by the interaction between zirconium tetrachloride and sodium ethoxide in anhydrous alcohol due to the formation of $NaH[Zr(OEt)_6]$ which in the presence of dry HCl gas however gave zirconium tetraethoxide. Bradley and Wardlaw,[2,3] prepared $Zr(OEt)_4$ by the action of dry ammonia on solutions of zirconium tetrachloride in appropriate alcohol. The above methods involve the use of anhydrous alcohol, the preparation of which is quite tedious.

It is well known that most of the alkyl esters of fatty acids react with ammonia and form corresponding alcohols and acid amides. This property of the esters has been utilised for the preparation of a number of metal alkoxides. The present communication deals with the preparation of zirconium tetraethoxide by the interaction of anhydrous zirconium tetrachloride in dry benzene with ethyl formate, ethyl acetate or diethyl oxalate in the presence of dry ammonia, whereby the alcohol which is formed in the above reaction is itself used in the formation of metal alkoxide.

Through benzene dried azeotropically, containing anhydrous zirconium chloride and ester-dried over anhydrous magnesium sulphate (quantities given in Table 1) placed in a two necked one litre quickfit flask fitted with a reflux condenser, dry ammonia was passed. As the reaction was exothermic in all cases, ice bath was used to prevent the loss of benzene and the lower esters. On the completion of the reaction and after the removal of dissolved ammonia under reduced pressure, zirconium tetraethoxide was obtained by distillation at 235°C/5.2 mmHg.

Zirconium in the alkoxide was estimated as ZrO_2 and ethoxy group was determined by the chromic acid method.[4,5]

From the analytical data (given in Table 1), the composition of the compound obtained in all the cases studied above corresponds to $Zr(OC_2H_5)_4$.

Although a large number of workers,[6,7] have prepared metal alkoxides by the ammonia method no definite information regarding the role of ammonia in the reaction has been reported and it is generally believed that it acts as a hydrogen chloride acceptor. Fowles and Pollard[8–10] who have studied in detail the behaviour of a number of transition metal halides towards ammonia have reported the formation of various ammoniates and amido chlorides of these metsls. In order to ascertain the role of ammonia in the above reactions the formation of the above intermediates during the preparation of zirconium tetraethoxide by the present method is also under investigation.

TABLE 1

Ester	Ester taken (g)	$ZrCl_4$ taken (g)	Benzene taken (g)	Yield %	Analysis of Zr-ethoxide found	
					%Zr	$\%OC_2H_5$
Ethyl formate	10.5	1.1	550	60—65	33.52	66.25
Ethyl acetate	16.0	1.5	500	54—57	33.65	66.18
Diethyl oxalate	10.0	0.9	400	49—51	33.55	66.25

Calcd for $Zr(OC_2H_5)_4$: Zr, 33.63; OC_2H_5, 66.37%.

1) H. Meerwein and T. Bersin, *Ann.*, **476**, 113 (1929).
2) D. C. Bradley and W. Wardlaw, *Nature*, **75**, 165 (1950).
3) D. C. Bradley and W. Wardlaw, *J. Chem. Soc.*, **1951**, 280.
4) C. A. Adams and J. R. Nicholls, *Analyst*, **54**, 2 (1929).
5) D. C. Bradley, F. M. Abdel Halim and W. Wardlaw, *J. Chem. Soc.*, **1950**, 3450.
6) D. C. Bradley, "Progress in Inorganic Chemistry," Vol. II, ed. by F. A. Cotton, Interscience Publishers, Inc., New York (1960), p. 303.
7) R. C. Mehrotra, Proc. 54th Ind. Sci. Cong. (Hyderabad) Part II, 1967.
8) G. W. A. Fowles and F. H. Pollard, *J. Chem. Soc.*, **1952**, 4938.
9) G. W. A. Fowles and F. H. Pollard, *ibid.*, **1953**, 4128.
10) G. W. A. Fowles and F. H. Pollard, *ibid.*, **1953**, 2588.

BULLETIN OF THE CHEMICAL SOCIETY OF JAPAN VOL. 42 555 (1969)

Spectrophotometric Determination of a Trace Amount of Cobalt(II) in Nickel(II) Solution

Mutsuo KODAMA

Department of Chemistry, Ibaraki University, Mito, Ibaraki

(Received June 8, 1968)

Previously,[1,2] we studied the substitution reactions of Eriochrom Black T (BT) with cobalt(II)- and nickel(II)-EDTA chelates spectrophotometrically, and determined the reaction mechanism and rate constants.

The reaction of BT with cobalt(II)-EDTA chelate was found to proceed much faster than that with nickel(II)-EDTA chelate. In the mixture of nickel(II)- and coblat(II)-EDTA chelates, the reaction of BT may proceed through both nickel(II)- and cobalt(II)-EDTA chelates. Therefore, in nickel(II)-EDTA solution contaminated with a trace amount of cobalt(II)-EDTA chelate, the rate at which the concentration of BT decreases would be much greater than that in the pure nickel(II)-EDTA chelate solution. Hence, even a trace amount of cobalt(II) in the nickel(II)-EDTA solution may be estimated by determining the increase in the apparent rate at which the concentration of BT decreases.

As stated previously,[1,2] both reactions of BT with cobalt(II)- and nickel(II)-EDTA chelate are first-order in BT and first-order in metal(II)-EDTA chelate. Consequently, the initial rate of the substitution reaction, $-(\mathrm{d[BT]}/\mathrm{d}t)_0$, in the mixed solution of nickel(II)- and cobalt(II)-EDTA chelate containing uncomplexed EDTA can be expressed as,

$$-\left(\frac{\mathrm{d[BT]}}{\mathrm{d}t}\right)_0 = (k_{\mathrm{Ni}}\cdot[\mathrm{NiY^{2-}}] + k_{\mathrm{Co}}[\mathrm{CoY^{2-}}])\cdot[\mathrm{BT}]_0 \quad (1)$$

where k_{Ni} and k_{Co} are the conditional second-order rate constants of the reaction of BT with pure nickel(II)-EDTA chelate and that with pure cobalt(II)-EDTA chelate, respectively. Both k_{Ni} and k_{Co} values increase with increasing pH value of the solution.[1,2]

Alternatively, one can define the initial reaction rate as,

$$-\left(\frac{\mathrm{d[BT]}}{\mathrm{d}t}\right)_0 = k\cdot[\mathrm{MY^{2-}}]_t\cdot[\mathrm{BT}]_0 \quad (2)$$

where $[\mathrm{MY^{2-}}]_t = [\mathrm{NiY^{2-}}] + [\mathrm{CoY^{2-}}]$.

Combining the above two equations, one can derive the following relation.

$$[\mathrm{CoY^{2-}}] = \frac{k - k_{\mathrm{Ni}}}{k_{\mathrm{Co}} - k_{\mathrm{Ni}}}[\mathrm{MY^{2-}}]_t \quad (3)$$

This relation clearly shows that when the total concentration of cobalt(II)- and nickel(II)-EDTA chelates is known, the concentration of cobalt(II)-EDTA chelate in the nickel(II)-EDTA chelate solution, $[\mathrm{CoY^{2-}}]$, can be estimated from k, k_{Ni} and k_{Co} values determined experimentally. The concentration of cobalt(II) in the nickel(II)-EDTA solution was estimated with the aid of Eq. (3) using k, k_{Ni} and k_{Co} values determined at pH 9.60. Typical results are given in Table 1, which can be regarded as satisfactory. k_{Ni} and k's used in the calculation of $[\mathrm{CoY^{2-}}]$ were determined from the initial slope of absorbance *vs.* time curves, because the absorbance decreases almost linearly with time in the reaction of BT with pure nickel(II)-EDTA, and with nickel(II)-EDTA contaminated with a small amount of cobalt(II). On the other hand, k_{Co} was estimated from the slope of the linear relation between $\log(A_{\mathrm{D}}/(A-A_{\mathrm{CoD}}))$[1] and time t, because the reaction of BT with cobalt(II)-EDTA chelate proceeds so rapidly that the initial slope cannot be determined accurately.

Table 1. Calculation of $[\mathrm{CoY^{2-}}]$ with the aid of Eq. (3)

$\mu = 0.30$, 15°C
$\lambda = 630\,\mathrm{m}\mu$, pH = 9.60
$k_{\mathrm{Co}} = 1.74\times10^{1}$, $k_{\mathrm{Ni}} = 3.58\times10^{-2}$

k	$[\mathrm{MY^{-2}}]_t$ mM	$[\mathrm{CoY^{2-}}]$ mM	
		added	found
1.98×10^{-1}	5.05	5.0×10^{-2}	4.7×10^{-2}
3.76×10^{-1}	5.10	1.0×10^{-1}	1.0×10^{-1}
7.22×10^{-1}	5.20	2.0×10^{-1}	2.1×10^{-1}
5.28×10^{-2}	10.46	1.0×10^{-2}	1.0×10^{-2}*
7.10×10^{-2}	10.47	2.0×10^{-2}	2.1×10^{-2}
1.24×10^{-1}	10.50	5.0×10^{-2}	5.3×10^{-2}
2.09×10^{-1}	10.55	1.0×10^{-1}	1.1×10^{-1}

* This value is less accurate.

Apparatus, detailed experimental procedures and the preparation of standard solutions used in this study were as described in previous papers.[1,2]

1) M. Kodama, This Bulletin, **40**, 2575 (1967).
2) M. Kodama, C. Sasaki and M. Murata, *ibid.*, **41**, 1333 (1968).

BULLETIN OF THE CHEMICAL SOCIETY OF JAPAN VOL. 42 556—558 (1969)

Studies on Heteroaromaticity. XXIX.[1] Synthesis and Reactions of 1-(5-Nitro-2-furoyl)aziridine Oxime

Tadashi SASAKI and Toshiyuki YOSHIOKA

Institute of Applied Organic Chemistry, Faculty of Engineering, Nagoya University, Chikusa-ku, Nagoya

(Received June 10, 1968)

In the previous papers,[2,3] we have reported the ring-opening reactions of β-(5-nitro-2-furyl)-acryloylaziridine and *N*-[β-(5-nitro-2-furyl)vinyl]-*N'*-ethyleneurea with acid, base or nucleophilic reagents affording oxazoline derivatives similar to general activated aziridine derivatives,[4] but in low yields.

This paper deals with the synthesis and reactions of 1-(5-nitro-2-furoyl)aziridine oxime (I), which was readily prepared from 5-nitro-2-furonitrile oxide[5] and aziridine in ether at 0°C in 80% yield. This structure was confirmed by the elemental analysis and the spectral data; an absorption at 3200 cm^{-1} in the infrared spectrum and a signal at 7.75 τ (singlet, 4H, $-CH_2-CH_2-$) in the NMR spectrum indicate the presence of an OH group and aziridine ring respectively. The aziridine ring in I was comparably stable and it did not react at all with aniline or *p*-toluidine even when it was refluxed in toluene for 8 hr. By addition of a catalytic amount of boron trifluoride etherate to a dry ethereal solution of I and aniline, however, I polymerized even at room temperature. Treatmet of I with acetic anhydride at room temperature, with phenyl isocyanate in refluxing benzene, or with benzoyl chloride in the presence of triethylamine at room temperature, gave the corresponding *O*-substituted oximates, II, III, and IV, in high yields respectively.

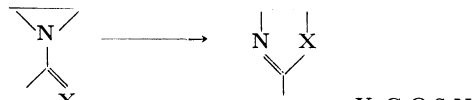

(V) (VI) X: C, O, S, N

Aziridines V possessing unsaturated substituents on the nitrogen are known to undergo ring expansion to yield 1-azacyclopentene derivatives VI.[6] It was of interest to determine whether or not the similar processes would occur in our aziridine oxime.

All attempts for ring-expansion of I by treating it in refluxing ethanol with organic acids like *p*-nitrobenzoic acid or 5-nitro-2-furoic acid were unsuccessful and only resulted in the cleavage of the aziridine ring to form products, VII and VIII, in low yields. The infrared spectra of VII and VIII showed common absorptions at 3500,

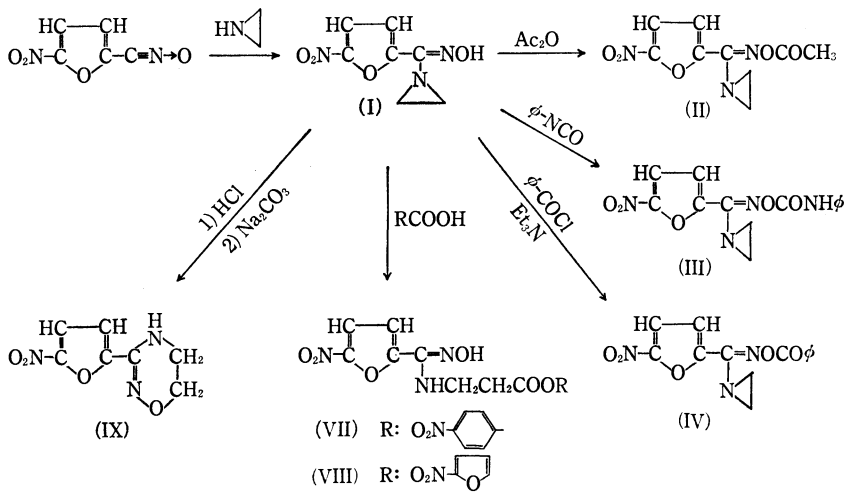

1) Part XXVIII of this series: T. Sasaki and M. Ando, *Yuki Gosei Kagaku Kyokai-shi* (*J. Soc. Org. Synth. Chem., Japan*), **27** 169 (1969).
2) T. Sasaki and T. Yoshioka, *ibid.*, **25**, 658 (1967).
3) T. Sasaki and T. Yoshioka, This Bulletin, **41**, 1258 (1968).
4) G. E. Ham, *J. Org. Chem.*, **29**, 3052 (1964).
5) T. Sasaki and T. Yoshioka, This Bulletin, **40**, 2604 (1967).
6) P. Scheider, *J. Org. Chem.*, **32**, 2628 (1967).

3400 (ν_{NH}), 1720, and 1715 (ν_{CO}) cm^{-1} and their ultraviolet absorption spectra manifested patterns similar to that of *N*-methyl-(5-nitro-2-furan)carbonamidoxime which is known to be a tautomeric mixture between its amino oxime and amino alcohol.[7] However, when I was treated with a mineral acid such as hydrochloric acid in acetone at room temperature for 1 day, an oily product was obtained, which was further treated with an aqueous sodium carbonate solution to afford 3-(5-nitro-2-furyl)-4,5-dihydro-6*H*-1,2,4-oxadiazine (IX), mp 195—197°C, in 51% yield; this structure was confirmed by the elemental analysis and the spectral data. The infrared spectrum showed absorptions at 3200 (sharp, ν_{NH}) and 1620 ($\nu_{C=N}$) cm^{-1} and the NMR signals appeared at around 2.6 τ (broad, 1H, NH), 6.10 (triplet, 2H, $-CH_2O-$) and 6.61 (multiplet, 2H, $-CH_2N-$), all supporting the presence of 4,5-dihydro-6*H*-1,2,4-oxadiazine ring in IX.

About the mechanism of the formation of IX from I, this reaction seems to proceed through two discrete steps; the first step is the cleavage of the ring by acid treatment and the second one is the ring closure by alkaline treatment, as have been reported by Rajagopalan and Talaty.[8]

All the results are summarized in the above scheme.

Experimental[9]

1-(5-Nitro-2-furoyl)aziridine Oxime (I). 5-Nitro-2-furohydroxamoyl chloride[7] (0.95 g) was dissolved in 20 m*l* of dry ether. To this solution was added a solution of 1.0 m*l* of aziridine in 5 m*l* of dry ether with stirring at 0—5°C. After 3 minutes' stirring at the same temperature, aziridine hydrochloride was filtered off and the filtrate was kept standing overnight in an ice box. The precipitates were collected, washed with ethanol and recrystallized from ethanol to afford 0.7 g (80%) of I as light yellow crystals, mp 172°C (decomp). IR (KBr) cm^{-1}: 3200 (broad, ν_{OH}), 1630 ($\nu_{C=N}$). UV λ_{max}^{EtOH} mμ (ε): 348 (11600), 250 (8000). NMR (DMSO-d_6) τ: −1.25 (singlet, 1 H, OH, disappeared on deuteration), 2.28 and 2.92 (each doublet, 1 H, J=3.8 cps, nitrofuran ring protons), 7.65 (singlet, 4 H, $-CH_2-CH_2-$).

Found: C, 42.82; H, 3.73; N, 20.82%. Calcd for $C_7H_7O_4N_3$: C, 42.64; H, 3.58; N, 21.32%.

1-(5-Nitro-2-furoyl)aziridine Oxime *O*-Acetylate (II). A solution of 0.4 g of I in 6 m*l* of acetic anhydride was allowed to stand at room temperature overnight. Removal of the unreacted acetic anhydride *in vacuo* afforded an oil. It was treated with 10 m*l* of water to give yellow precipitates, which were recrystallized from ethanol - petroleum ether to give 0.27 g (55%) of II, mp 129°C. IR (KBr) cm^{-1}: 1760 (ν_{CO}). UV λ_{max}^{EtOH} mμ (ε): 326 (16500), 250 (10200).

Found: C, 44.94; H, 3.69; N, 17.42%. Calcd for $C_9H_9O_5N_3$: C, 45.19; H, 3.79; N, 17.57%.

1-(5-Nitro-2-furoyl)aziridine Oxime *O*-Phenylcarbamate (III). A mixture of 0.23 g of I and 0.3 m*l* of phenyl isocyanate in 20 m*l* of dry benzene was refluxed for 4 hr. After removal of the solvent under reduced pressure, the residue was recrystallized from ethanol to give 0.27 g (71%) of III, mp 145°C. IR (KBr) cm^{-1}: 3360 (ν_{NH}), 1750 (ν_{CO}). UV λ_{max}^{EtOH} mμ (ε): 330 (15500), 237 (22000).

Found: C, 53.00; H, 3.84; N, 18.49%. Calcd for $C_{14}H_{12}O_5N_4$: C, 53.16; H, 3.82; N, 17.72%.

1-(5-Nitro-2-furoyl)aziridine Oxime *O*-Benzoate (IV). A mixture of 0.3 g of I and 4 m*l* of benzoyl chloride was dissolved in a mixture of 10 m*l* of tetrahydrofuran and 10 m*l* of dry ether. To this solution was added 0.4 m*l* of triethylamine in 5 m*l* of dry ether at room temperature with stirring. After stirring was continued for 3 hr, the solids which separated were filtered, washed with water and recrystallized from ethanol to give 0.76 g (80%) of IV as light yellow crystals, mp 166°C. IR (KBr) cm^{-1}: 1735 (ν_{CO}). UV λ_{max}^{EtOH} mμ (ε): 325 (15300), 254 (12100), 232 (14800).

Found: C, 56.05; H, 3.72; N, 13.94%. Calcd for $C_{14}H_{11}O_5N_3$: C, 55.81; H, 3.68; N, 13.95%

Reaction of I with Organic Acids. A solution of 0.4 g of I and 0.35 g of *p*-nitrobenzoic acid in 30 m*l* of ethanol was refluxed for 7 hr. The solvent was removed under reduced pressure and the oily residue was treated with 20 m*l* of ethanol - water (1 : 2). The solids which separated were filtered and recrystallized from ethanol - petroleum ether to give 0.36 g (50%) of VII as yellow crystals, mp 122°C. IR (KBr) cm^{-1}: 3500 (ν_{NH}), 3200 (ν_{OH}), 1720 (ν_{CO}). UV λ_{max}^{EtOH} mμ (ε): 360 (5900), 295 (9600), 254 (19200).

Found: C, 45.88; H, 3.29; N, 15.70%. Calcd for $C_{14}H_{12}O_8N_4$: C, 46.16; H, 3.32; N, 15.38%.

Similarly, 0.25 g (30%) of VIII, mp 134—136°C, was obtained from 0.4 g of I and 0.37 g of 5-nitro-2-furoic acid after 4 hr's refluxing in 15 m*l* of ethanol and worked up as above. IR (KBr) cm^{-1}: 3490 (ν_{NH}), 3400 (ν_{OH}), 1715 (ν_{CO}). UV λ_{max}^{EtOH} mμ (ε): 360 (6200), 294 (16500), 234 (10300).

Found: C, 40.91; H, 2.84; N, 15.92%. Calcd for $C_{12}H_{10}O_9N_4$: C, 40.68; H, 2.85; N, 15.82%.

3-(5-Nitro-2-furyl)-4,5-dihydro-6*H*-1,2,4-oxadiazine (IX). To a solution of 0.4 g of I in 8 m*l* of acetone was added a mixture of 2 m*l* of concentrated hydrochloric acid and 5 m*l* of acetone at 0—5°C for 0.5 hr with stirring. Stirring was continued at room temperature for 1 day. After a distillable fraction was removed under reduced pressure, an oily residue was dissolved in 10 m*l* of water and the solution was made alkaline with an aqueous sodium carbonate solution and then, stored overnight in an ice box. The precipitates were collected, washed with water and recrystallized from

7) T. Sasaki and T. Yoshioka, *Yuki Gosei Kagaku Kyokai-shi* (*J. Soc. Org. Synth. Chem., Japan*), **25**, 665 (1967).

8) P. Rajagopalan and C. N. Talaty, *J. Am. Chem. Soc.*, **88**, 5048 (1966).

9) All melting points were determined on a Yanagimoto electric micromelting point apparatus and uncorrected. All the infrared and ultraviolet spectra were recorded on a JASCO Model IR-S infrared spectrometer and on a Hitachi Model ESP-2 recording spectrometer respectively. The NMR spectra were taken on a Varian A-60 apparatus with tetramethylsilane as an internal standard and the chemical shifts are presented in terms of τ-values.

ethanol to give 0.24 g (51%) of IX as brown crystals, mp 197°C. IR (KBr) cm^{-1}: 3200 (sharp, ν_{NH}), 1620 ($\nu_{C=N}$). UV λ_{max}^{EtOH} $m\mu$ (ε): 348 (7300), 304 (7600), 240 (6800). NMR (DMSO-d_6) τ: 2.88 and 2.90 (each doublet, 1 H, J=3.8 cps, nitrofuran ring protons), 2.6 (broad, 1 H, NH, disappeared on deuteration), 6.10 (triplet, 2 H, J=4.0 cps, CH_2), 6.61 (multiplet, 2 H, CH_2).

Found: C, 42.65; H, 3.50; N, 21.15%. Calcd for $C_7H_7O_4N_3$: C, 42.64; H, 3.58; N, 21.32%.

BULLETIN OF THE CHEMICAL SOCIETY OF JAPAN VOL. 42 558—560 (1969)

Studies on Reactions of Isoprenoids. V.[1] 1,3-Dipolar Cycloaddition Adducts of Myrcene with Benzonitrile Oxide

Tadashi SASAKI, Shoji EGUCHI and Teruhiko ISHII

Institute of Applied Organic Chemistry, Faculty of Engineering, Nagoya University, Furo-cho, Chikusa-ku, Nagoya

(Received June 13, 1968)

In continuing our previous study on the diene reactivity of myrcene,[1] this paper deals with the reactivity of each double bond in myrcene with benzonitrile oxide. Although several 1,3-dipolar cycloaddition reactions with butadiene and its derivatives have been reported,[2,3] there seems no report concerning the 1,3-dipolar cycloaddition reactions with myrcene, 7-methyl-3-methylene-1,6-octadiene.

Results and Discussion

The 1,3-dipolarophilicity of myrcene toward several 1,3-dipoles such as diazomethane, diphenylnitrilimine, phenyl azide, tosyl azide, and benzonitrile oxide was examined, among which, however, only benzonitrile oxide showed enough reactivity to give the corresponding adducts. Myrcene was treated with benzonitrile oxide in refluxing ether and the reaction products were purified on a silica-gel column to give four products, I—IV as shown in Table 1.

As seen from this table, all of these products had the composition corresponding to 1 : 2-adducts. It is interesting that neither 1 : 1-adduct nor 1 : 3-adduct was obtained in the reaction using a 1 : 1-molar ratio[4] of myrcene to benzonitrile oxide, though some of the butadiene derivatives are known to give a 1 : 1-adduct with benzonitrile oxide.[3] This fact might suggest that the reactivity of the three double bonds in myrcene with benzonitrile oxide discriminates an isolated double bond from conjugated ones in the examined conditions as will be supported by the following structural

TABLE 1. 1,3-DIPOLAR CYCLOADDUCTS OF MYRCENE WITH BENZONITRILE OXIDE

Compd.	Mp(°C)	Yield[a] (%)	Formula	Anal. (%) Calcd C	Calcd H	Calcd N	Found C	Found H	Found N
I	113—114	2.0	$C_{24}H_{26}O_2N_2$	76.97	7.00	7.48	77.24	7.05	7.42
II	120—122	0.08	$C_{24}H_{26}O_2N_2$	76.97	7.00	7.48	77.12	7.02	6.79
III	139—141	1.2	$C_{24}H_{26}O_2N_2$	76.97	7.00	7.48	77.24	7.23	7.48
IV	149—151	11.5	$C_{24}H_{26}O_2N_2$	76.97	7.00	7.48	77.36	7.23	7.13

a) The molar ratio of myrcene to benzonitrile oxide was 1 : 1 and the yield was based on benzhydroxamoyl chloride from which benzonitrile oxide was generated.

1) Part IV of this series: T. Sasaki, S. Eguchi and T. Ishii, submitted to *J. Org. Chem.*

2) For a recent review on 1,3-dipolar cycloadditions, see R. Huisgen, R. Grashey and J. Sauer, "Cycloaddition Reactions of Alkenes" in "The Chemistry of Alkenes," ed. by S. Patai, Interscience Publisher, New York, N. Y,. (1964), pp. 806—978.

3) About benzonitrile oxide, see a) A. Quilico, P. Grunanger and R. Mazzini, *Gazz. Chim. Ital.*, **82**, 349 (1952); *Chem. Abstr.*, **48**, 2039d (1954); b) V. N. Chistokletov and A. T. Troshchenko, *Izv. Sib. Otd. Akad. Nauk SSSR, Ser. Khim. Nauk*, **1963**, 147; *Chem. Abstr.*, **59**, 13960h (1963).

4) No 1 : 3-adduct was obtained even in the reaction using a 1 : 2-molar ratio of myrcene to benzonitrile oxide.

elucidation of the four adducts.

The structure of I was assigned as A or B on the basis of its NMR spectrum which had the signals at τ 2.10—2.80 (10 H, m, two phenyl protons), 4.80 (1 H, broad s, C=CH), 5.02 (1 H, unsymmetrical t, J=8.0 Hz, O-C<u>H</u>CH_2- in an isoxazoline ring), 6.54 (2 H, d, J=8.0 Hz, O-$CHC\underline{H}_2$- in an isoxazoline ring), 6.58 (2 H, d, J=3.0 Hz, $-CH_2-$ in an isoxazoline ring),[5] 7.60—8.03 (4 H, complex m, $-CH_2CH_2-$), 8.28 and 8.35 (6 H, s, $C=C(CH_3)_2$).

The structure of II was assumed to be similar to that of I, since its infrared spectrum was superimposable with that of II and the R_f values of I and II on TLC[6] examinations were exactly the same value of 0.43.

The structure of III and IV were also assignable as A or B from their NMR data; III had the signals at τ 2.20—2.78 (10 H, m, two phenyl protons), 4.81 (1 H, broad s, C=CH), 5.04 (1 H, t, J=8.0 Hz, $OC\underline{H}CH_2$- in an isoxazoline ring), 6.56 (2 H, d, J=8.0 Hz, $OCHC\underline{H}_2$- in an isoxazoline ring), 6.64 (2 H, d, J=3.0 Hz, $-CH_2-$ in an isoxazoline ring), 7.65—8.10 (4 H, complex m, $-CH_2CH_2-$), 8.30 and 8.37 (6 H, s, $C=C(CH_3)_2$); IV had the signals at τ 2.10—2.70 (10 H, m, two phenyl protons), 4.85 (1 H, broad s, C=CH), 5.04 (1 H, unsymmetrical t, J=7.5 Hz, $OC\underline{H}CH_2$- in an isoxazoline ring), 6.57 (2 H, unsymmetrical d, J=7.5 Hz, $OCHC\underline{H}_2$- in an isoxazoline ring), 6.60 (2 H, s, $-CH_2-$ in an isoxazoline ring), 7.54—8.10 (4 H, complex m, $-CH_2CH_2-$), 8.27 and 8.35 (6 H, s, $C=C(CH_3)_2$).

The infrared spectra of I—IV were very similar one another, I and II exhibiting absorption bands at 1600, 1570, 1500, 920, 860, 763, and 691 cm^{-1}, and III and IV, at 1600, 1570, 1500, 940, 920, 900, 860, 764, and 693 cm^{-1}. From these data, I and II could be distinguishable from III and IV, since the former group had only one band at 920 cm^{-1} and the latter, three bands at 940, 920, and 900 cm^{-1} in fingerprint regions. On the other hand, the results of TLC[6] examinations of I—IV indicated also the same discrimination[7] in I—IV.

The two possible structure A and B for the isolated four 1 : 2-adducts could now be possibly

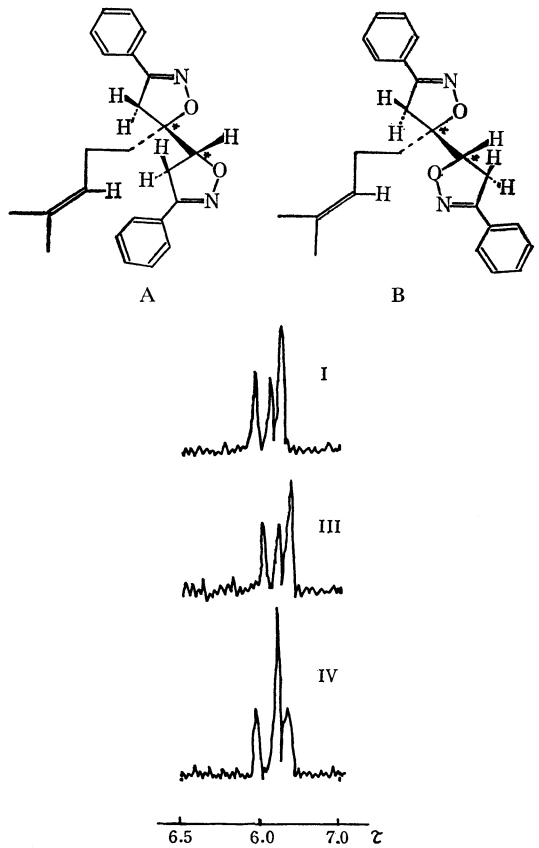

Fig. 1. NMR spectra of I, III, and IV in $CDCl_3$ at 60 Mc. Methylene protons signals of isoxazoline rings.

correlated with the presence of two groups, I and II, and III and IV, in these adducts. However, the observed subtle differences in their infrared and NMR spectra (Fig. 1), and R_f values on TLC were unsatisfactory to distinguish them.[8]

The isolation of the four 1 : 2-adducts could be explained by the presence of the two asymmetric

5) In a strict sense, this signal should be analyzed as an AB q, although both outer signals of an AB q of I at this region were very weak and they were almost hidden in noises as shown in Fig. 1. Only in the spectrum of I, the value of $J_{AB}/_{d\tau}$=0.86 for this q could be obtained.

6) TLC (Thin Layer Chromatography) was carried out by using silica-gel (Wakogel, B-5) plate, benzene as a developing solvent, and iodine as a developing reagent.

7) The R_f values of III and IV on TLC were same each other and 0.32 which was slightly smaller than those (0.43) of I and II.

8) A conjecture that I and II may correspond to an A structure and III and IV, to a B structure, will be favored by the facts that the combined yield of I and II was much lower than that of III and IV, and melting points of I and II were lower than those of III and IV, since A is assumed to be less stable than B because of the electrostatic repulsions of two oxygen atoms.

9) All melting points were determined on a Yanagimoto micro-melting point apparatus and are uncorrected. Microanalyses were carried out on a Yanagimoto C. H. N. Corder Model MT-1. The infrared spectra (KBr) were recorded on a JASCO Model IR-S infrared spectrophotometer and NMR spectra were obtained in $CDCl_3$ with a Hitachi high-resolution NMR spectrometer Model H-6013 at 60 Mc. All NMR data are reported in τ values relative to TMS as an internal standard, and singlet peaks are designated as s, doublet as d, triplet as t, and so on.

carbons in both A and B, which are responsible for diastereoisomers.

Experimental[9]

Reaction of Myrcene with Benzonitrile Oxide. A mixture of 1.50 g (0.011 mol) of myrcene and benzonitrile oxide prepared from 2.0 g (0.013 mol) of benzhydroxamoyl chloride[10] and 1.6 g (0.016 mol) of triethylamine, in 50 m*l* of ether was refluxed for 16 hrs and the crude products were obtained as a sticky residue after removal of the solvent. Purification of the crude products on a silica-gel (Wakogel, C-100-200) column eluted with benzene afforded three main fractions. From the first fraction, crude myrcene was recovered and the second fraction was a mixture of I, II, III, and IV. From the third fraction, a mixture of III and IV was obtained (*ca.* 0.30 g). Further purifications of the second fraction on a silica-gel column afforded *ca.* 0.2 g of a mixture of I and II, and 0.20 g of a mixture of III and IV. Fractional recrystallizations of the mixture of I and II, and the combined mixture of III and IV (0.5 g) from benzene - *n*-hexane afforded finally analytically pure samples of I (0.050 g) as needles, II (0.002 g) as needles, III (0.030 g) as needles, and IV (0.300 g) as needles. Their yields, melting points, and analyses are summarized in Table 1.

10) M. H. Benn, *Can. J. Chem.*, **42**, 2313 (1964) and references cited therein.

BULLETIN OF THE CHEMICAL SOCIETY OF JAPAN VOL. 42 560—561 (1969)

The Photo-Fries Rearrangement of Hydroxyphenyl Cinnamates*1

Heitaro OBARA, Hiroshi TAKAHASHI and Hiromichi HIRANO

Department of Applied Chemistry, Faculty of Engineering, Yamagata University, Yonezawa

(Received June 14, 1968)

Our recent investigation of the photochemical Fries rearrangement of phenyl cinnamate[1] has prompted the present authors to attempt the preparation of the corresponding hydroxychalcones (4, 5, and 6) by the photo-irradiation of *o*-, *m*- and *p*-hydroxyphenyl cinnamates (1, 2, and 3).

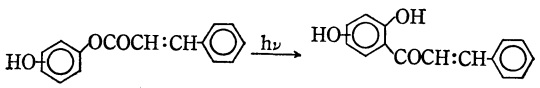

Hydroxyphenyl cinnamates		Dihydroxychalcones	
(1)	*o*-OH	(4)	2′,3′-di-OH
(2)	*m*-OH	(5)	2′,4′-di-OH
(3)	*p*-OH	(6)	2′,5′-di-OH

As we have described in a previous communication,[1] if these photo-Fries rearrangements are successful there may arise the possibility of a light-catalyzed synthesis of the corresponding polyhydroxychalcones from various polyhydroxyphenyl monocinnamates.

o-Hydroxyphenyl cinnamate (1), mp 137—138°C, *m*-hydroxyphenyl cinnamate (2), mp 112—113°C, and *p*-hydroxyphenyl cinnamate (3), mp 166—167°C, were isolated from the reaction mixture obtained by the acylation of catechol, resorcinol, and hydroquinone with cinnamoyl chloride in pyridine. The structures of these compounds were confirmed by the elemental analyses and by a study of their IR spectra.

The yields of these monocinnamates were generally low because there was some difficulty in separating them from the mixture of mono- and di-cinnamates.

The irradiation was carried out in a benzene solution under a nitrogen atmosphere at room temperature using a high-pressure 100 W mercury arc. After irradiation, the benzene was evaporated *in vacuo*, and the residue was chromatographed on a column of silica gel; the resulting chalcones were recrystallized from methanol or benzene.

2′,3′-Dihydroxychalcone (4)[2] was obtained from (1) in a 20% yield; this structure was identified by the elemental analysis, by a study of the IR spectrum, and, furthermore, by its conversion into 8-hydroxyflavanone (7).[2] Similarly, 2′,4′-dihydroxychalcone (5)[3] and 2′,5′-dihydroxychalcone (6)[4] were obtained in 5 and 16% yields respectively; these structures were identified by a comparison of the melting points and UV and IR spectra with those of authentic samples. The formation of 3,′4′-dihydroxychalcone and 2′,6′-dihydroxychalcone from (1) and (2) respectively was expected in these photochemical reactions, but no such chalcones could be isolated from the above irradiation products.

*1 Presented at the Tohoku Local Meeting of the Chemical Society of Japan, Hirosaki, October, 1967.

1) H. Obara and H. Takahashi, This Bulletin, **40**, 1012 (1967).

2) W. I. Awad, M. F. El-Neweihy and S. F. Selim, *J. Org. Chem.*, **25**, 1335 (1960).

3) S. Matsueda, K. Sannohe and Y. Saito, This Bulletin, **36**, 1528 (1963).

4) M. K. Seikel, M. J. Lounsbury and S. Wang, *J. Org. Chem.*, **27**, 2952 (1962).

Experimental

All the melting points are uncorrected.

***o*-Hydroxyphenyl Cinnamate (1).** Into a solution of 8.8 g of catechol in 60 m*l* of pyridine, 13.6 g of cinnamoyl chloride was slowly stirred over a period of about 1 hr at 45°C. The reaction mixture was then poured into cold water and extracted with ether. After the removal of the ether-insoluble crystals, the ether layer was washed with a dilute aqueous sodium hydrogencarbonate solution, dilute hydrochloric acid, and then water. The ether solution was evaporated *in vacuo*, and the residual crystals were dissolved in warm ethanol. After the removal of the ethanol-insoluble crystals by filtration, the filtrate was evaporated *in vacuo*; the resulting white crystals were then recrystallized from benzene. Yield, 4.76 g (24.8%), mp 140—141°C. IR (KBr): 3380 (ν_{OH}) and 1708 cm^{-1} (ν_{CO}). UV: λ_{max}^{EtOH} 283 mμ (log ε=4.49).

Found: C, 75.15; H, 5.32%. Calcd for $C_{15}H_{12}O_3$: C, 74.99; H, 5.03%.

Catechol dicinnamate was obtained from the ether-insoluble part. Yield, 6.3 g (29.6%), mp 126—127°C (from ethanol). IR (KBr): 1730 and 1720 cm^{-1} (ν_{CO}).

Found: C, 77.99; H, 5.03%. Calcd for $C_{24}H_{18}O_4$: C, 77.82; H, 4.92%.

***m*-Hydroxyphenyl Cinnamate (2).** This compound was prepared in a 3.7% yield by the same method as in the case of (1). Mp 112—113°C (from benzene). IR (KBr): 3350 (ν_{OH}) and 1692 cm^{-1} (ν_{CO}). UV: λ_{max}^{EtOH} 284 mμ (log ε=4.42).

Found: C, 75.21; H, 5.21%. Calcd for $C_{15}H_{12}O_3$: C, 74.99; H, 5.03%.

Resorcinol dicinnamate, yield, 22.8%, mp 118—119°C (from ethanol). IR (KBr): 1728 cm^{-1} (ν_{CO}).

Found: C, 77.86; H, 5.11%. Calcd for $C_{24}H_{18}O_4$: C, 77.82; H, 4.92%.

***p*-Hydroxyphenyl Cinnamate (3).** To a stirred solution of 8.8 g of hydroquinone in 60 m*l* of pyridine, there was slowly added 13.6 g of cinnamoyl chloride over a period of about 1 hr at 45°C. The reaction mixture was then poured into cold water and extracted with ether, and the ether layer was washed with a dilute aqueous sodium hydrogencarbonate solution, dilute hydrochloric acid, and then water. The ether solution was evaporated *in vacuo*, and the residual white crystals were dissolved in warm methanol. After the removal of the methanol-insoluble crystals by filtration, the filtrate was evaporated *in vacuo*; the resulting white crystals were recrystallized from ethanol. Yield, 4.0 g (20.8%), mp 167—168°C. IR (KBr): 3389 (ν_{OH}) and 1695 cm^{-1} (ν_{CO}). UV: λ_{max}^{EtOH} 283 mμ (log ε=4.49).

Found: C, 75.04; H, 5.28%. Calcd for $C_{15}H_{12}O_3$: C, 74.99; H, 5.03%.

Hydroquinone dicinnamate was obtained from the above methanol-insoluble part. Yield, 3.3 g (11.0%), mp 186—188°C (from benzene). IR (KBr): 1735 cm^{-1} (ν_{CO}).

Found: C, 78.12; H, 5.19%. Calcd for $C_{24}H_{18}O_4$: C, 77.82; H, 4.92%.

Irradiation of *o*-Hydroxyphenyl Cinnamate (1). A solution of 500 mg of (1) in 300 m*l* of dry benzene was irradiated under a nitrogen atmosphere at room temperature by a high-pressure 100 W mercury arc for 30 hr. After irradiation, benzene was evaporated *in vacuo* and the resulting crude mixture was chromatographed on a 570×30 mm column of silica gel. 2′,3′-Dihydroxychalcone (4) was obtained as orange crystals from the first elution with ligroin-benzene-ethyl acetate (2 : 2 : 1). Yield, 100 mg (20%), mp 149—150°C (from methanol) (lit. mp 151°C[2]). IR (KBr): 3460 (ν_{OH}) and 1632 cm^{-1} (ν_{CO}). UV: λ_{max}^{EtOH} 232 (log ε=4.32), 322 mμ (4.63).

Found: C, 75.22; H, 5.27%. Calcd for $C_{15}H_{12}O_3$: C, 74.99; H, 5.03%.

This chalcone (4) was converted into 8-hydroxyflavanone, mp 191—192°C (lit. mp 192°C[2]), by refluxing it with methanolic hydrochloric acid for 10 hr.

Irradiation of *m*-Hydroxyphenyl Cinnamate (2). A solution of 1.0 g of (2) in 300 m*l* of benzene was irradiated for 30 hr as has been described above. Elution with benzene-ethyl acetate (2 : 1) gave 400 mg of white crystals, which were identified as the unchanged starting materials by a comparison of the IR spectrum with that of (2). The second fraction gave 50 mg of yellow crystals, which were identified as 2′,4′-dihydroxychalcone (5) by a comparison of the IR spectrum with that of an authentic sample. Mp 146—147°C (from benzene) (lit. 150—151°C[3]). The third fraction gave 110 mg of resorcinol, while the fourth fraction, which was eluted with methanol, gave 120 mg of brown, viscous polymeric products.

Irradiation of *p*-Hydroxyphenyl Cinnamate (3). A solution of 1.0 g of (3) in 500 m*l* of benzene was irradiated for 30 hr and then worked up as has been described above. Elution with chloroform-ethyl acetate (10 : 1) gave 160 mg of orange crystals, which were identified as 2′,5′-dihydroxychalcone (6) by a comparison of the IR spectrum with that of an authentic sample. Mp 172—173°C (from methanol) (lit. mp 173—173.5°C[4]). IR (KBr): 3280 (ν_{OH}) and 1637 cm^{-1} (ν_{CO}). UV: λ_{max}^{EtOH} 229 (log ε=4.12), 316 (4.37) and 408 mμ (3.69).

The authors wish to acknowledge the microanalyses of Mr. Jun-ichi Onodera, and the technical assistance of Mr. Norio Moriya.

BULLETIN OF THE CHEMICAL SOCIETY OF JAPAN VOL. 42 562 (1969)

The Preparation of Copper(I) Complex Containing Organic Halide*1

Keisuke WADA and Harukichi HASHIMOTO

Department of Synthetic Chemistry, The University of Tokyo, Hongo, Bunkyo-ku, Tokyo

(Received June 14, 1968)

The copper ion catalysed reactions of organic halides have been extensively studied for their potent utilities in the field of organic synthetic chemistry. One important subject still remaining is the elucidation of the nature of the interaction between organic halide and copper ion. An approach to this problem is the preparation of a relatively stable complex of intermediate character of the reaction between organic halide and copper ion. Organocopper compound that involves copper-carbon bond is a fairly familiar one.[1] Only a little is known, however, about a compound that involves the direct interaction between copper and halogen atom in the organic halide. In 1914, Peters prepared the cuprous cyanide complex coordinated by methyl iodide.[2] Since then no remarkable study has been reported on this type of the compound.

During the course of studies on the redox ligand transfer reaction or organic halide with transition metal complex,[3] we discovered new complexes of general formula CuX (organic halide) $(P\phi_3)_2$. The complexes were obtained by the reaction of cuprous chloride, triphenylphosphine and organic halide in acetonitrile solutions under a nitrogen stream at reflux. The complexes were separated from reaction mixture as precipitates and after repeated washing with ethyl ether, were dried *in vacuo*. Typical of these complexes is that of benzyl iodide.

The same complex was obtained also by the reaction of tris(triphenylphosphine)-copper(I) chloride and benzyl iodide. The yield was nearly stoichiometric in this case.

$$CuCl(P\phi_3)_3 + C_6H_5CH_2I \longrightarrow CuCl(C_6H_5CH_2I)(P\phi_3)_2 + P\phi_3$$

Found: C, 61.98; H, 4.23; Cu, 7.52%. Calcd for $CuCl(C_6H_5CH_2I)(P\phi_3)_2$: C, 61.36; H, 4.43; Cu, 7.55%. The complex is white crystalline and rather sensitive to light but fairly stable against oxygen. The infrared spectrum of the complex gives a sharp strong band at 581 cm^{-1} and several other bands due to triphenylphosphine and benzyl iodide. The 581 cm^{-1} band is assigned to C–I stretching of benzyl iodide coordinated to copper atom, although there remains some uncertainty. The NMR spectrum of methylene proton at elevated temperature gives a signal at 5.08 ppm. The signal of free benzyl iodide at the same condition appears at 5.33 ppm. The ultraviolet spectrum shows a new band at 250 mμ.

The reaction of this complex and ethylenediamine in acetonitrile produces a trace of bibenzyl. The complex of this type may be the precursor of intermediate in the redox ligand transfer reaction of organic halide.[3]

*1 Oxidation-Reduction Reactions by Transition Metal Complexes. IV.

1) H. Hashimoto and T. Nakano, *J. Org. Chem.*, **31**, 891 (1966).

2) W. Peters, *Z. Anorg. Allgem. Chem.*, **89**, 191 (1914).

3) K. Wada and H. Hashimoto, This Bulletin, **41**, 3001 (1968).

BULLETIN OF THE CHEMICAL SOCIETY OF JAPAN VOL. 42 563—564 (1969)

Stochastic Model for Langmuir Isotherm

Kenji ISHIDA

Depatment of Applied Chemistry, Ibaraki University, Hitachi, Ibaraki

(Received June 17, 1968)

A monolayer adsorption isotherm was deduced theoretically by Langmuir on the basis of a kinetic interpretation of the adsorption of gas molecules on a solid surface.[1] On the same assumption as in the classical Langmuir theory, a stochastic model for the adsorption-desorption process in a closed system at constant temperature can be formulated as follows. Let us denote by $p(n)$ the probability of finding n adsorbed molecules in stationary state and by λ and μ the probabilities of adsorption and desorption for one molecule, respectively. The probability $p(n)$ then satisfies the set of difference equations,[2]

$$\lambda\{\gamma-(n-1)\}\{(\sigma-(n-1)\}p(n-1)-\{\lambda(\gamma-n)(\sigma-n)+\mu n\}p(n)+\mu(n+1)p(n+1)=0 \quad (0\leq n\leq\sigma) \tag{1}$$

where γ is the total number of molecules in the system under consideration, σ the number of sites on the surface and $\gamma>\sigma$ and $p(-1)=p(\sigma+1)=0$ have been assumed. The probability $p(n)$ is independent of the initial state of the system and $\sum_{n=0}^{\sigma}p(n)=1$ is satisfied. The set of difference equations, (1), may be solved recurrently. We then have the stationary probability distribution,

$$p(n)=r_n z^n/R_{\sigma,\gamma}(z) \tag{2}$$

where $z=\lambda/\mu$ and $r_n=\binom{\sigma}{n}(\gamma)_n=\binom{\sigma}{n}\gamma!/(\gamma-n)!$ and $R_{\sigma,\gamma}(z)=\sum_{n=0}^{\sigma}r_n z^n$ is called the rook polynomial.[3] The probability distributions for different values of z are illustrated in Fig. 1. It is to be noted, here, that the statistic-mechanical model leads also to the probability distribution,[4]

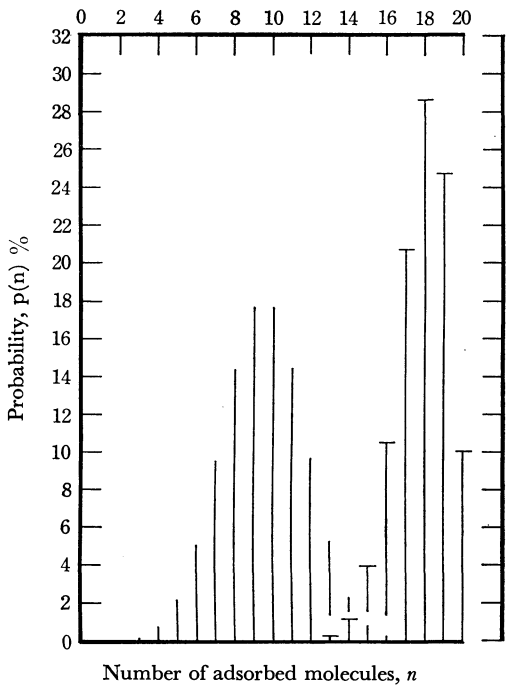

Fig. 1. Probability distribution.
$\gamma=100$, $\sigma=20$; —: $z=10^{-2}$, |—: $z=10^{-1}$

$$p_{\text{S.M.}}(n)=(1/Q)\frac{\sigma!}{n!(\sigma-n)!}q^n\frac{1}{(\gamma-n)!}q_G{}^{\gamma-n}=(q_G{}^{\gamma}/Q\gamma!)\binom{\sigma}{n}(\gamma)_n(q/q_G)^n \tag{3}$$

which is of the same form as (2). In this formula, the quantities q and q_G denote respectively the partition functions of adsorbed and gaseous molecules and the partition function for the whole system,

$$Q=(q_G{}^{\gamma}/\gamma!)\sum_{n=0}^{\sigma}\binom{\sigma}{n}(\gamma)_n(q/q_G)^n$$

1) I. Langmuir, *J. Am. Chem. Soc.*, **38**, 2221 (1916); **40**, 1361 (1918).

2) K. Ishida, *Nippon Kagaku Zasshi* (*J. Chem. Soc. Japan, Pure Chem. Sect.*), **81**, 524 (1960).

3) J. Riordan, "An Introduction to Combinatorial Analysis," John Wiley & Sons, Inc., New York, N. Y. (1958), p. 171.

4) For proof, refer to T. L. Hill, "Introduction to Statistical Thermodynamics," Addison-Wesley Publishing Company, Reading, Massachusetts (1960), Section 10-3.

is regarded as the normalization factor.

It follows from (2) that the mean number of adsorbed molecules, $\langle n\rangle$, is given by

$$\langle n\rangle = z\frac{\mathrm{d}}{\mathrm{d}z}R_{\sigma,\gamma}(z)/R_{\sigma,\gamma}(z) \tag{4}$$

It is convenient to relate $R_{\sigma,\gamma}(z)$ to the confluent hypergeometric function[5] $\Phi(\gamma+1, \gamma-\sigma+1; 1/z)$ by the formula,

$$R_{\sigma,\gamma}(z) = (\gamma)_\sigma z^\sigma \mathrm{e}^{-1/z}\Phi(\gamma+1, \gamma-\sigma+1; 1/z) \tag{5}$$

Substituting (5) into (4) and using the differential relation,

$$z\frac{\mathrm{d}}{\mathrm{d}z}\Phi(\gamma+1, \gamma-\sigma+1; 1/z) = \sigma\Phi(\gamma, \gamma-\sigma+1; 1/z) - (\sigma+1/z)\,\Phi(\gamma+1, \gamma-\sigma+1; 1/z)$$

we obtain

$$\langle n\rangle = \sigma\Phi(\gamma, \gamma-\sigma+1; 1/z)/\Phi(\gamma+1, \gamma-\sigma+1; 1/z) \tag{6}$$

Therefore, the mean number of gas molecules, $\langle n_G\rangle = \gamma - \langle n\rangle$, is given by

$$\langle n_G\rangle = (\gamma-\sigma)\Phi(\gamma, \gamma-\sigma; 1/z)/\Phi(\gamma+1, \gamma-\sigma+1; 1/z) \tag{7}$$

where we have used the recurrence relation,

$$\gamma\Phi(\gamma+1, \gamma-\sigma+1; 1/z) - \sigma\Phi(\gamma, \gamma-\sigma+1; 1/z) = (\gamma-\sigma)\,\Phi(\gamma, \gamma-\sigma; 1/z)$$

It follows from (6) and (7) that the stochastic Langmuir isotherm may be written in the form,

$$\langle n\rangle = \sigma\frac{z\langle n_G\rangle}{1+z\langle n_G\rangle - z(\gamma-\sigma)\Delta} \tag{8}$$

where for brevity we have introduced a quantity Δ defined by

$$\Delta = \Phi(\gamma, \gamma-\sigma; 1/z)/\Phi(\gamma+1, \gamma-\sigma+1; 1/z) - \Phi(\gamma-1, \gamma-\sigma; 1/z)/\Phi(\gamma, \gamma-\sigma+1; 1/z)$$

In deriving (8), we have also used the recurrence relation,

$$(1/z)\,\Phi(\gamma, \gamma-\sigma+1; 1/z) = (\gamma-\sigma)\{\Phi(\gamma,\gamma-\sigma; 1/z) - \Phi(\gamma-1, \gamma-\sigma; 1/z)\}$$

It is possible, however, to connect the quantity Δ with the variance (fluctuation),

$$\langle n^2\rangle - \langle n\rangle^2 = \langle n\rangle + z^2\frac{\mathrm{d}^2}{\mathrm{d}z^2}R_{\sigma,\gamma}(z)/R_{\sigma,\gamma}(z) - \left(z\frac{\mathrm{d}}{\mathrm{d}z}R_{\sigma,\gamma}(z)/R_{\sigma,\gamma}(z)\right)^2$$

Applying (5) to this equation, we obtain, after rather long but straightforward algebra,

$$\langle n^2\rangle - \langle n\rangle^2 = \langle n\rangle(\gamma-\sigma)\Delta \tag{9}$$

where $\Delta > 0$ in the case of $\gamma > \sigma$. By combining (9) with (8), we obtain

$$\langle n\rangle = \sigma\frac{z\langle n_G\rangle}{1+z\langle n_G\rangle}\left\{1+\frac{\langle n^2\rangle - \langle n\rangle^2}{\sigma\langle n_G\rangle}\right\} \tag{10}$$

which can be also deduced directly from (1). Since the inequality $\langle n^2\rangle - \langle n\rangle^2 \ll \sigma\langle n_G\rangle$ holds for ordinary statistical thermodynamic systems, (10) becomes

$$\langle n\rangle \simeq \sigma\frac{z\langle n_G\rangle}{1+z\langle n_G\rangle}$$

which is, in the mean, consistent with the classical Langmuir isotherm. The variance (9), however, may not be negligible in small systems.

5) A. Erdélyi *et al.*, "Higher Transcendental Functions," Vol. I, McGraw-Hill Book Co., Inc., New York, N. Y. (1953), p. 248.

BULLETIN OF THE CHEMICAL SOCIETY OF JAPAN VOL. 42 564—565 (1969)

Stochastic Model for Autocatalytic Reaction

Kenji ISHIDA

Department of Applied Chemistry, Ibaraki University, Hitachi, Ibaraki

(Received June 17, 1968)

In the autocatalytic reaction A→B, the rate of production of B is not only proportional to the concentration of reactant A, but also to the concentration of product B; in other words the reaction catalyzes itself. Hence, this reaction may be regarded as a second-order reaction.

To construct a stochastic model for the autocatalytic reaction, let the random variable $X(t)$ represent the number of molecules of the product B at time t, and let us denote the probability of finding x molecules of B in the reaction system at time t by $P(x\,;t)=\mathrm{Prob}\{X(t)=x\}$, $x=b,\ b+1,\cdots,\ b+a$, where $X(0)=b(\geq 1)$ and $a(\geq b)$ is the total number of molecules of reactant A. If, then, the

transition probability that one B-molecule will be produced in the interval $(t,\ t+\Delta t)$ is given by $k\{a-(x-b)\}x\Delta t+o(\Delta t)$, it follows from the stochastic theory of second-order reaction kinetics[1-3] that the probability $P(x\,;t)$ satisfies the set of differential-difference equations

$$\frac{\mathrm{d}}{\mathrm{d}t}P(x;t) = k\{a-[(x-1)-b]\}(x-1)P(x-1;t) - k\{a-(x-b)\}xP(x;t) \qquad (1)$$
$$(b \leq x \leq b+a)$$

where k is the rate constant and $P(b-1\,;t)=0$ has been assumed for all $t \geq 0$. This is to be solved with the initial conditions

$$P(x;0) = 1 \quad \text{for } x = b$$
$$= 0 \quad \text{otherwise.}$$

We then have the probability distribution, for $b \geq x \geq (a+b)/2$ $(a+b,$ even) or $b \geq x \geq (a+b-1)/2$ $(a+b,$ odd),

$$P(x;t) = \frac{a!(x-1)!}{(a+b-x)!(b-1)!}\sum_{i=b}^{x}(-1)^{i-b}(a+b-2i) \times \frac{(a+b-x-i-1)}{(a-i)!(i-b)!(x-i)!}\exp\{-k(a+b-i)it\}$$
$$= \frac{a!(x-1)!}{(a+b-x)!(b-1)!}\sum_{j=0}^{x-b}(-1)^{j}(a-b-2j) \times \frac{(a-x-j-1)!}{(a-b-j)!j!(x-b-j)!} \times \exp\{-k(a-j)(b+j)t\} \qquad (2)$$

which has been derived by the method of Laplace transform.

The restriction $b \geq x \geq (a+b)/2$ or $b \geq x \geq (a+b-1)/2$ has been assumed for the study of the initial stage of reaction. In this stage, it follows that the approximations

$$\frac{a!}{(a+b-x)!} = a^{x-b}\prod_{i=1}^{x-b-1}\left(1-\frac{i}{a}\right) \simeq a^{x-b}$$

and

$$(a-b-2j)\frac{(a-x-j-1)!}{(a-b-j)!} = a\left(1-\frac{b+2j}{a}\right)\Big/a^{x-b+1}\prod_{i=0}^{x-b}\left(1-\frac{b+j+i}{a}\right) \simeq a^{-(x-b)}$$

hold for sufficiently large $a(\gg b)$. Moreover, we assume that

$$k(a-j)(b+j) = ka\left(1-\frac{j}{a}\right)(b+j) \simeq \lambda(b+j)$$

where ka has been replaced by the new constant λ. By introducing these approximations into (2), we obtain

$$P(x;t) = \frac{(x-1)!}{(x-b)!(b-1)!}\exp(-\lambda bt) \times \sum_{j=0}^{x-b}\frac{(x-b)}{j!(x-b-j)!}\{-\exp(-\lambda t)\}^{j} = \binom{x-1}{x-b}\exp(-\lambda bt)\{1-\exp(-\lambda t)\}^{x-b} \qquad (3)$$

in agreement with Delbrück's treatment.[4] He proposed the differential-difference equation (4) describing the statistical fluctuation of a simple autocatalytic reaction mechanism. We thus see that the probability distribution (3) satisfies the equation,

$$\frac{\mathrm{d}}{\mathrm{d}t}P(x;t) = \lambda(x-1)P(x-1;t) - \lambda xP(x;t) \qquad (4)$$
$$(x=b,\ b+1,\ \cdots)$$

on the assumption that the number of molecules of reactant A is so large that it remains constant through the course of reaction. As long as the initial number of molecules, a, is sufficiently large but finite, (3) is an approximation of (2) and holds only for the initial stage of the autocatalytic reaction. This will become still more clear by comparing the following two rate equations for the means $\langle x \rangle$,

$$\frac{\mathrm{d}}{\mathrm{d}t}\langle x\rangle = k\{a-(\langle x\rangle - b)\}\langle x\rangle - k(\langle x^2\rangle - \langle x^2\rangle)$$

and

$$\frac{\mathrm{d}}{\mathrm{d}t}\langle x\rangle = \lambda\langle x\rangle$$

which can be derived from (1) and (4), respectively.

1) D. A. McQuarrie, C. J. Jachimowski and M. E. Russell, *J. Chem. Phys.*, **40**, 2914 (1964).
2) K. Ishida, *ibid.*, **41**, 2472 (1964).
3) I. G. Darvey, W. Ninham and P. J. Staff, *J. Chem. Phys.*, **45**, 2145 (1966); I. G. Darvey and W. Ninham, *ibid.*, **46**, 1626 (1967).
4) M. Delbrück, *J. Chem. Phys.*, **8**, 120 (1940). See also A. T. Bharucha-Reid, "Elements of the Theory of Markov Processes and their Applications," McGraw-Hill Book Co., Inc., New York, N. Y. (1960), p. 360.

BULLETIN OF THE CHEMICAL SOCIETY OF JAPAN VOL. 42 566 (1969)

Preparation of Carboxymethylthiophenazines

Hideo ENDO and Masao TADA

The Research Institute for Tuberculosis, Leprosy and Cancer, Tohoku University, Kitayoban-cho, Sendai

and Ken KATAGIRI

Shionogi Research Laboratory, Shionogi & Co., Ltd., Fukushima-ku, Osaka

(Received June 19, 1968)

In previous papers,[1,2] the reactions of halogenophenazine derivatives with piperidine and morpholine were reported. In this paper, the reactions of various halogenophenazine derivatives with mercaptoacetic acid will be reported.

Landquist has reported that the reaction of 2-chlorophenazine-5,10-dioxide (I) with sodium mercaptoacetate gave 2-carboxymethylthiophenazine (II).[3] By a modification of this method, we could obtain II from 2-chlorophenazine (III), 2-bromophenazine (IV), 2-chlorophenazine-5-oxide (V), 3-chlorophenazine-5-oxide (VI), and 3-bromophenazine-5-oxide (VII). The reaction of either 1-chlorophenazine (VIII) or 1-chlorophenazine-5-oxide (IX) with sodium mercaptoacetate gave 1-carboxymethylthiophenazine (X). In this case, 1-chlorophenazine was shown to be less reactive toward the reagent than 2-chloro compounds.

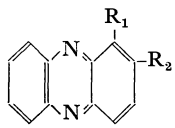

II: R_1=H; R_2=SCH_2CO_2H
X: R_1=SCH_2CO_2H; R_2=H

The enhancement of the reactivity of halogen by the oxide groups in halogenophenazine oxides was also observed in the present experiments.

The growth-inhibitory activity of II and X against Crocker Sarcoma 180 has also been investigated and will be reported on elsewhere.[4]

Experimental[5]

2-Carboxymethyl thiophenazine (II). *a) From III.* To a solution of III (1.7 g) in ethanol (40 m*l*), a sodium mercaptoacetate solution prepared from mercaptoacetic acid (1.5 g) and a 10% sodium hydroxide aqueous solution (14 m*l*) was added. The mixture was refluxed for 17 hr and then poured into water (0.5 *l*). The aqueous solution was filtered, and the filtrate was slightly acidified with diluted hydrochloric acid. The crystals (1.9 g) thereby separated were collected, washed with water, and dried. Recrystallization from ethanol afforded fine, brownish-yellow prisms (mp 255—256°C (decomp.)), which were identified as II[3] by a comparison of their infrared spectra.

b) From IV. To a solution of IV (0.2 g) in ethanol (4 m*l*), a solution of mercaptoacetic acid (150 mg) in 10% sodium hydroxide (1.4 m*l*) was added; the mixture was then treated as in the case of a) to give II (140 mg).

c) From V. To a solution of V (1.9 g) in ethanol (40 m*l*), a solution of mercaptoacetic acid (1.5 g) in 10% sodium hydroxide (14 m*l*) was added; The mixture was then refluxed for 5.5 hr and treated as in the case of a) to give II (1.7 g).

d) From VI. To a solution of VI (1.9 g) in ethanol (40 m*l*), a solution of mercaptoacetic acid (1.5 g) in 10% sodium hydroxide (14 m*l*) was added. The mixture was then refluxed for 5 hr and treated as in the case of a) to afford II (1.8 g).

e) From VII. To a solution of VII (0.2 g) in ethanol (4 m*l*), a solution of mercaptoacetic acid (150 mg) in 10% sodium hydroxide (1.4 m*l*) was added. The mixture was then refluxed for 4.5 hr and treated as in the case of a) to give II (140 mg).

1-Carboxymethylthiophenazine (X). *a) From VIII.* To a solution of VIII (1.7 g) in ethanol (40 m*l*), a solution of mercaptoacetic acid (1.5 g) in 10% sodium hydroxide aqueous solution (14 m*l*) was added. The mixture was refluxed for 20 hr and then poured into water (0.5 *l*). The crystals which separated were filtered and recrystallized from methanol to recover VIII (1.2 g). The filtrate was slightly acidified with diluted hydrochloric acid to give crystals (530 mg). Recrystallization from ethanol afforded X (mp 240—241°C (decomp.)) as fine, brownish-yellow crystals.

Found: C, 62.19; H, 3.96; N, 10.08%. Calcd for $C_{14}H_{10}N_2O_2S$: C, 62.21; H, 3.73; N, 10.36%.

b) From IX. To a solution of IX (1.9 g) in ethanol (40 m*l*), a solution of mercaptoacetic acid (1.5 g) in 10% sodium hydroxide (14 m*l*) was added. The resultant mixture was refluxed for 10 hr and treated as in the case of a) above to yield both X (550 mg) and VIII (1.2 g).

1) H. Endo, M. Tada and K. Katagiri, This Bulletin, **42**, 502 (1969).
2) H. Endo, M. Tada and K. Katagiri, *ibid.*, **42**, 506 (1969).
3) J. K. Landquist, *J. Chem. Soc.*, **1956**, 2550.
4) H. Endo, M. Tada and K. Katagiri, *Sci. Rep. Res. Inst. Tohoku Univ. Ser. C,* to be published.
5) All melting points are uncorrected.

BULLETIN OF THE CHEMICAL SOCIETY OF JAPAN VOL. 42 567—569 (1969)

Protonation of Allene. Evidence for the Formation of 1,1-Diphenyl-3,3-dibromoprop-1-ene

Fumio TODA, Masahiro HIGASHI and Katsuhiko AKAGI

Department of Industrial Chemistry, Faculty of Engineering, Ehime University, Matsuyama

(Received June 21, 1968)

It has been reported[1] that the action of phosphorus tribromide on 1,1-diphenylprop-2-yn-1-ol (I) in acetic acid affords 1,1-diphenyl-3,3-dibromoprop-1-ene (VIII) (mp 82°C) and that the reaction proceeds *via* the bromoallene intermediate II, as is shown in Scheme 1. Recently, Martinet and Doupeux[2] have reported the formation of 1,1-diphenyl-1,3-dibromoprop-2-ene (IX) (mp 81—82°C) by the reaction of hydrogen bromide and 1,1-diphenyl-3-bromopropa-1,2-diene (II), which had been isolated by the action of phosphorus tribromide on I in hexane.

Our treatment of II with hydrogen bromide afforded crystals (mp 82°C) which were identical with those obtained previously.[2] However, some physical data (mp, infrared and NMR spectra) reported[2] for IX were identical with those of VIII. These ambiguous results prompted us to reinvestigate the structure of the dibromide and then the protonation of bromoallene II.

An evidence that the dibromide is allylic *gem*-dibromide (VIII) but not 1,3-dibromide (IX) was obtained by the following cross-addition reactions. 1,1-Diphenyl-3-bromo-3-chloroprop-1-ene (IV) (mp 50—52°C), derived from II and hydrogen chloride, was identical with that obtained from the chloro-analog of II (III) and hydrogen bromide, as is shown in Scheme 1. Since the treatment of II with a large excess of hydrogen bromide or of hydrogen chloride afforded VIII or dichloro-analog V, phosphorus trihalide in acetic acid was used as the source of hydrogen halide in order to avoid the presence of excess hydrogen halide. The bromochloro compound, IV, thus obtained was different from the dichloro-analog, V (mp 23.5—24°C), prepared by the addition of hydrogen chloride to III. The infrared spectra of IV and V were almost identical with that of VIII. The acid- or base-catalysed hydrolysis of IV and V gave 1,1-diphenylprop-1-en-3-al (VI), as in the case of VIII.[1] Finally, the structure of the dibromide reported in two previous articles[1,2] may be identified as allylic *gem*-dibromide VIII.

The above results led us to the following speculation. The cation in which the plus charge is located on C-3, $>C{=}CH{-}\overset{+}{C}HBr$, may be more stable than that in which the charge is on C-1, $>\overset{+}{C}{-}CH{=}CHBr$. The stability of the former may be due to a longer conjugate system for the delocalization of the positive charge.

The ultraviolet spectrum[1] of VIII, 242 (10200), 266 (14700), and 273 mμ (ε, 16500), shows the presence of a conjugate system corresponding to 1,1-diphenylethylene and supports the structure VIII. Martinet and Doupeux have assigned the structure IX to the dibromide on the basis of the infrared and NMR spectra, but not the ultraviolet spectrum. We have tried to identify the infrared and NMR spectral bands of VIII, by which they were misled to determine the structure of the dibromide to be IX.

The infrared spectrum of VIII showed a strong band at 880 cm^{-1}, as is shown in Fig. 1. In order to identify this band, VIII-2-d was prepared by the addition of deuterium bromide to II. In VIII-2-d, the 880 cm^{-1} band shifted to 735 cm^{-1}. Therefore, the band may be assigned to the out-of-plane deformation of $\overset{2}{C}{-}H$. This assignment is reasonable

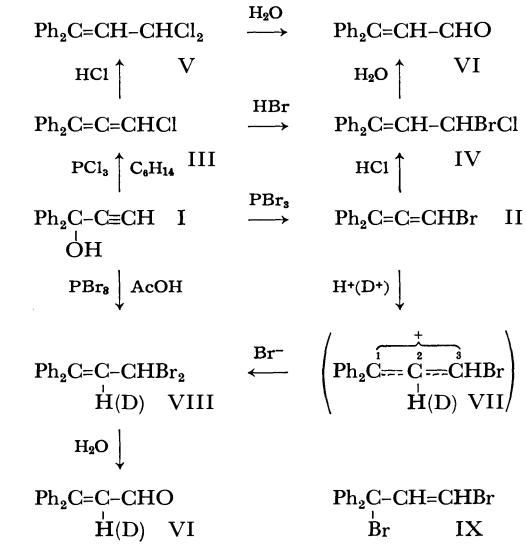

Scheme 1

1) H. Tani and F. Toda, This Bulletin, **37**, 470 (1964).

2) P. Martinet and H. Doupeux, *Compt. rend.*, **261**, 2498 (1965).

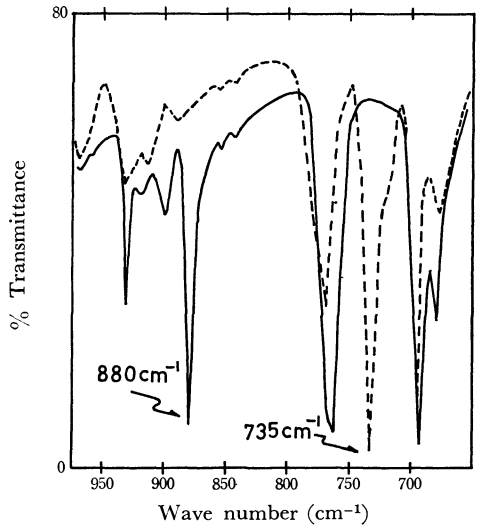

Fig. 1. The infrared spectra of VIII (——) and VIII-2-d (------).

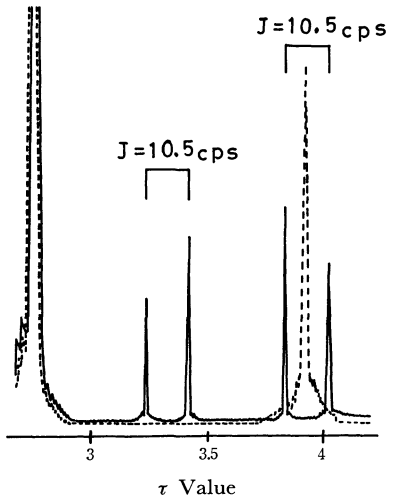

Fig. 2. The NMR spectra of VIII (——) and VIII-2-d (------).

since it is well known[3] that the general frequency for the CH out-of-plane deformation of trisubstituted ethylene, 840—800 cm^{-1}, varies with the change in substituents.

As is shown in Fig. 2, the NMR spectrum of VIII showed a multiplet (centered at 2.70, phenyl) and two doublets (centered at 3.35, $J=10.5$ cps and centered at 3.95τ, $J=10.5$ cps) in the integrated ratio of 10 : 1 : 1. Martient and Doupeux have identified the two doublets as two vinyl hydrogens of IX. However, since the structure VIII instead of IX was confirmed to be correct, the two doublets may be assinged to vinyl and allylic hydrogens. The doublet at the lower field, which disappeared in the spectrum of VIII-2-d (Fig. 2), may be attributed to the vinyl hydrogen. The remaining signal may be due to the allylic hydrogen. The observed value, 3.95τ, of the allylic methine hydrogen agrees fairly well with that calculated, 3.78τ, according to Shoolery's equation[4] using 2.33 and 1.32 ppm as the effective shielding constants of bromine and diphenylethylene respectively.

Experimental[5]

Instrumental Analyses. The infrared spectra were recorded in Nujol mull on a grating spectrophotometer, IR-G, of Japan Spectroscopic Co. The NMR spectra were recorded in carbon tetrachloride on a Japan Electron Optics Laboratory C-60 spectrometer, using TMS as the internal standard.

1,1-Diphenyl-3-bromopropadiene (II) and 1,1-Diphenyl-3-chloropropadiene (III). A solution of I (3.0 g, 15 mmol) in hexane (40 m*l*) was cooled to *ca.* −25°C with a dry ice-methanol bath. Into the solution, phosphorus tribromide (4.0 g, 15 mmol) was stirred over a 20-min period. The stirring was then continued for a further 2 hr at *ca.* −25°C. The crystalline solid recrystallized from hexane afforded II as colorless needles, 3.0 g (74%), mp 74.5—75°C (lit.[2] mp 67—69°C). IR: 1926 cm^{-1} ($\nu_{C=C=C}$).

Found: C, 66.07; H, 3.89%. Calcd for $C_{15}H_{11}Br$: C, 66.38; H, 4.06%.

The treatment of I with phosphorus trichloride in hexane under the conditions employed for the preparation of II afforded III as colorless needles in a 59% yield after recrystallization from hexane, mp 46.5—48.5°C. IR: 1930 cm^{-1} ($\nu_{C=C=C}$).

Found: C, 78.72; H, 4.58%. Calcd for $C_{15}H_{11}Cl$: C, 79.43; H, 4.91%.

1,1-Diphenyl-3,3-dibromoprop-1-ene (VIII) and 1,1-Diphenyl-3,3-dibromoprop-1-ene-2-d (VIII-2-d). The dibromide VIII was prepared by the reaction of I and phosphorus tribromide in acetic acid[1] or by that of II and hydrogen bromide in hexane,[2] mp 82°C (lit.[1] 82°C: lit.[2] 81—82°C). The mixed melting point of the dibromides prepared according to the methods of those two articles showed no depression.

The deuterated dibromide, VIII-2-d, was obtained by the reaction of II and deuterium bromide[6] in hexane; it consisted of colorless prisms, mp 82°C. IR: 2500 ($\nu_{=C-D}$) and 735 cm^{-1} ($\delta_{=C-D}$). NMR: 2.70 (multiplet, phenyl, 10 H) and 3.95τ (singlet, methine, 1H). The acid- or base-catalyzed hydrolysis of VIII-2-d afforded VI-2-d in a quantitative yield. For VI-2-d, the CH out-of-plane deformation of trisubstituted ethylene of VI, 880 cm^{-1}, was shifted to 755 cm^{-1}.

1,1-Diphenyl-3-bromo-3-chloroprop-1-ene (IV). *A*)

3) L. J. Bellamy, "The Infra-red Spectra of Complex Molecules," Methuen, London (1958), p. 31.

4) B. P. Dailey and J. N. Shoolery, *J. Am. Chem. Soc.*, **77**, 3977 (1955).

5) All melting points are corrected.

6) Deuterium bromide was prepared by the reaction of phosphorus tribromide and deuterium oxide, according to the reported procedure: H. Kwart and J. L. Nyce, *J. Am. Chem. Soc.*, **86**, 2601 (1964).

Into an ice-cooled mixture of II (2.58 g, 9 mmol) and acetic acid (5 m*l*), phosphorus trichloride (1.5 g, 10 mmol) was stirred over a 5-min period. The stirring was continued for a further 30 min, and the reaction mixture was decomposed with water and extracted with ether. The ether layer was washed with water and dried over sodium sulfate, and the solvent was evaporated to dryness to leave IV as colorless leaflets, 0.9 g (37%), mp 50—52°C,. IR: 875 cm^{-1} ($\delta_{=C-H}$).

Found:*1 C, 56.96; H, 3.70%. Calcd for $C_{15}H_{12}BrCl$: C, 58.54; H, 3.90%.

B) Into an ice-cooled mixture of III (1.7 g, 7.5 mmol) and acetic acid (5 m*l*), phosphorus tribromide (1.0 g, 3.5 mmol)*2 was stirred over a 5-min period. Crystalline solid 1.3 g (56%), mp 50—52°C. A mixed-melting-point determination with crystals obtained by the procedure A showed no depression. The infrared spectrum was identical with that of crystals obtained by the procedure A. The acid- or base-catalyzed hydrolysis of IV afforded VI in a quantitative yield, mp 44°C. A mixed-melting-point determination with an authentic specimen (lit.[7] mp 44.5—45.5°C) showed no depression.

1,1-Diphenyl-3,3-dichloroprop-1-ene (V). Into an ice-cooled solution of I (3.0 g, 15 mmol) in acetic acid (5 m*l*), phosphorus trichloride (4.0 g, 30 mmol) was stirred over a 5-min period. After 2 days, the reaction mixture was decomposed with water and extracted with ether. The ether layer was washed with water and dried over sodium sulfate. The crude oil remaining after the evaporation of the solvent was distilled to afford V, 2.3 g (65%), bp 134°C/2 mmHg, mp 23.5—24°C. IR: 1617 ($\nu_{C=C}$) and 876 cm^{-1} ($\delta_{=C-H}$). The spectrum was similar to those of VIII and IV.

Found: C, 68.28; H, 4.31%. Calcd for $C_{15}H_{12}Cl_2$: C, 68.44; H, 4.56%.

The acid or base-catalyzed hydrolysis of V afforded VI in a quantitative yield, mp 44°C. A mixed-melting-point determination with an authentic sample (lit.[7] mp 44.5—45.5°C) showed no depression.

The treatment of III with hydrogen chloride in hexane also afforded V in a quantitative yield.

*1 Since the bromochloride IV was converted into dibromide VIII and dichloride V gradually by repeated recrystallizations from hexane, it was difficult to purify it further.

*2 When a large excess of phosphorus tribromide was used, dibromide VIII was isolated as the sole product.

7) H. Lorenz and R. Wizinger, *Helv. Chim. Acta*, **28**, 600 (1945).

BULLETIN OF THE CHEMICAL SOCIETY OF JAPAN VOL. 42 569—570 (1969)

Synthesis of Pipataline

Yoshimori OMOTE, Hinako TAZAWA, Yoshimori FUJINUMA and Noboru SUGIYAMA

Department of Chemistry, Tokyo Kyoiku University, Otsuka, Tokyo

(Received June 27, 1968)

Atal *et al.*[1] have recently reported the isolation of pipataline from *Piper peepuloides* Roxb. and proposed that its structure is 1-(3,4-methylenedioxyphenyl)-1-dodecene (I). In connection with our studies[2-4] of melanin precursors we have synthesized pipataline (I) as a model catechol melanin precursor. The synthesis of pipataline consists of the addition of *n*-undecyl magnesium iodide to piperonal and the removal of the water.

Heating *n*-undecyl magnesiumiodide and piperonal under reflux for one hour gave an alcohol (II) as a colorless liquid, bp 200—220°C/10^{-3}—10^{-4} mmHg, this alcohol was then dehydrated, by aluminum oxide at 200°C for 30 min. The product (I) was extracted with ether and recrystallized from petroleum ether - ethanol to afford colorless crystals, mp 37°C. The spectral data of UV, IR and NMR, are in good agreement with those of natural pipataline.[1]

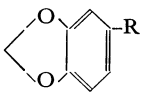

I, R= $CH{=}CH(CH_2)_9CH_3$
II, R= $CH(OH)CH_2(CH_2)_9CH_3$

Experimental

***n*-Undecyl Iodide.** A mixture of *n*-undecyl alcohol (6 g), iodine (5.4 g), and red phosphorus (0.6 g) was heated at 110—120°C for 6 hr and then kept overnight at room temperature. The ethereal extract from the reaction mixture was washed with a 10% aqueous sodium thiosulfate solution and dried over anhydrous sodium sulfate. The removal of the solvent gave *n*-undecyl iodide (6.2 g), which was then distilled at

1) C. K. Atal, K. L. Dhar and A. Pelter, *Chem. & Ind.*, **1967**, 2173.

2) Y. Omote, U. Kurabayashi, A. Momose and N. Sugiyama, *Nippon Kagaku Zasshi* (*J. Chem. Soc. Japan, Pure Chem. Sect.*), **88**, 80 (1967).

3) Y. Omote, H. Yasuda, Y. Fujinuma and N. Sugiyama, *ibid.*, **89**, 594 (1968).

4) Y. Omote, Y. Fujinuma and N. Sugiyama, *Chem. Commun.*, **1968**, 190.

104—110°C/2 mmHg (lit.[5] 125°C/3 mmHg).

1-(3,4-methylenedioxyphenyl)-1-dodecanol (II). Piperonal (2.1 g) dissolved in ether (20 m*l*) was added to *n*-undecyl magnesiumiodide, prepared from magnesium (0.5 g) and *n*-undecyl iodide (3 g) in ether (25 m*l*), under cooling with ice water. The mixture was heated with stirring under reflux for one hour. To the mixture there was then added 3 N hydrochloric acid under cooling. The etheral layer from the acidified mixture was washed with a 40% aqueous sodium bisulfite and then with an aqueous sodium bicarbonate solution. After drying over anhydrous sodium sulfate, the solvent was evaporated, and to the residue there was added ethanol. Then the undissolved precipitates were filtered off and the ethanol solution was evaporated to give the alcohol (II) (0.7 g), which was distilled at 200—220°C/10^{-3}—10^{-4} mmHg in a molecular still. Found: C, 75.54; H, 9.85%. Calcd for $C_{19}H_{30}O_3$: C, 74.47; H, 9.87%. IR ν (liq. film) 3400, 2925, 1610, 1245 and 1043 cm^{-1}. UV λ_{max}^{EtOH} nm 234, 288.

From the insoluble precipitates described above there was obtained a hydrocarbon (0.3 g), mp 43—44°C, mol wt (Rast)=341, IR ν^{KBr} 2900, 2840, 1470 and 718 cm^{-1}. This seems to be docosane (mp 47°C), probably resulting from the reaction of *n*-undecyl magnesiumiodide with *n*-undecyl iodide.

Pipataline (I). The alcohol (II) (0.35 g) was dehydrated by activated aluminum oxide (0.18 g) under a nitrogen atmosphere at 180—200°C for 30 min. The reaction mixture was then extracted with ether. The removal of the solvent and recrystallization from petroleum ether - ethanol gave pipataline as colorless crystals (50 mg), mp 37°C (lit.[1] 38°C). Found: C, 78.62; H, 9.78%. Calcd for $C_{19}H_{28}O_2$: C, 79.12; H, 9.79%. IR ν^{KBr} 2920, 2850, 1605, 1248 and 1040 $cm.^{-1}$ UV λ_{max}^{EtOH} nm (ε) 262 (12700), 269 (12400) and 307 (6100). NMR τ ($CDCl_3$) 3.12(1H), 3.23 (2H, aromatic), 3.40 (1H,d,J=15 cps, olefinic), 3.7—4.1 (complex pattern, olefinic), 4.05 (methylendioxy), 7.6—8.0 (allylic), 8.2—8.9 (methylene), 8.95—9.3 (methyl).

5) "Beilsteins Handbuch der Organischen Chemie," (**1**), 66.

BULLETIN OF THE CHEMICAL SOCIETY OF JAPAN VOL. 42 570—571 (1969)

Infrared Spectra and Molecular Conformations of Poly-γ-methyl-DL-glutamate

Yukio MASUDA

Department of Chemistry, Japan Women's University, Bunkyo-ku, Tokyo

and Tatsuo MIYAZAWA

Institute for Protein Research, Osaka University, Kita-ku, Osaka

(Received June 27, 1968)

Polyamino acids are known to take various conformations, namely the α helix, β-form or disordered form. For conformation diagnoses, the amide I and II bands in the infrared spectra[1] are extensively used. In our previous study, the amide V bands arising from the N–H out-of-plane bending mode were also found useful for conformation studies.[2] With the observed amide bands, the conformations of racemic polyamino acids were analysed in the present study.

Poly-γ-methyl-DL-glutamate (PMDLG) were synthesized by the Leuchs method. Racemic γ-methyl-DL-glutamate (mp 185°C) was converted to *N*-carboxyamino acid anhydride [A] (mp 72°C), which was polymerized in dioxane, with the initiator [I] of sodium methoxide or *n*-hexylamine. The polymer was precipitated by pouring the reaction mixture into diethyl ether, filtered, washed, and dried. The molecular weight of the polymers were estimated by viscosity measurements in dichloroacetic acid.[3] Infrared absorption spectra were observed with solid films cast from chloroform solution or with potassium bromide discs. Hitachi 225 or EPI-L spectrophotometers were used for the infrared measurements.

Fig. 1A shows the infrared spectrum of PMDLG ($A/I=100$). The amide I bands at 1685 and 1625 cm^{-1} indicate the existence of the β-form. However, the strong amide I band at 1655 cm^{-1}, amide II band at 1540 cm^{-1}, and the strong amide V band at 635 cm^{-1} indicate that the predominant conformation of this polymer is the α helix. This observation is similar to the case of copoly-γ-

1) T. Miyazawa and E. R. Blout, *J. Am. Chem. Soc.*, **83**, 712 (1961) and references cited therein.

2) T. Miyazawa, Y. Masuda and K. Fukushima, *J. Polymer Sci.*, **62**, S62 (1962); Y. Masuda and T. Miyazawa, *Makromol. Chem.*, **103**, 261 (1967).

3) P. Doty, J. H. Bradbury and A. M. Holtzer, *J. Am. Chem. Soc.*, **78**, 947 (1956).

methyl-D,L-glutamate (D : L=1 : 1, A/I=200) which exhibits a strong amide V band at 630 cm^{-1}. In the far infrared region, the characteristic band[4] of α-helical polyglutamate esters is also observed at 410 cm^{-1} for PMDLG.

For the low-molecular-weight PMDLG with A/I=20 or 8, the amide I bands were observed at 1690 and 1630 cm^{-1}, amide II bands at 1525 cm^{-1}, and the amide V band at 700 cm^{-1}. Accordingly, these molecules are predominantly in the β-form. On the other hand, Fig. 1B shows the infrared spectrum of PMDLG with A/I=4. The amide I bands at 1695, 1660, and 1633 cm^{-1}, the amide II bands at 1545 and 1530 cm^{-1}, and the amide V bands at about 700 and 670 cm^{-1} indicate that there are some fractions of the disordered form together with the β-form. This conformation of PMDLG (A/I=4) makes contrast with the case of PMLG (A/I=4) which is predominantly in the β-form. Thus infrared observations are useful especially for conformation diagnoses of DL-polypeptides which do not exhibit optical rotatory dispersion.

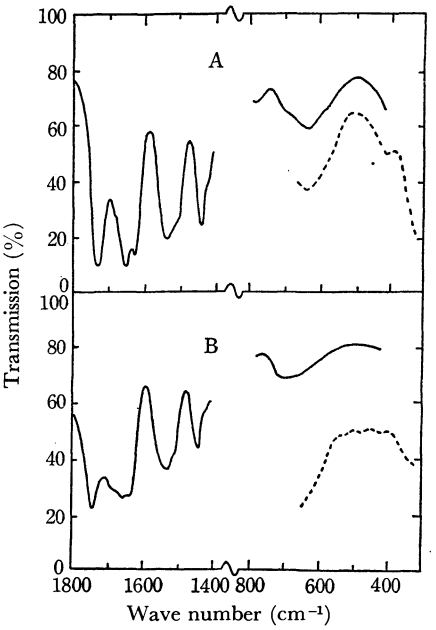

Fig. 1. Infrared Spectra of Poly-γ-methyl-DL-glutamate, A/I=100 (A) and A/I=4 (B); measured with Hitachi 225 (solid line) or EPI-L (broken line).

The authors wish to thank Miss T. Makiguchi for her kind technical assistance and also to Hitachi, Ltd. for the use of infrared spectrophotometers.

4) T. Miyazawa, K. Fukushima, S. Sugano, and Y. Masuda, in "Conformation of Biopolymers," ed. by G. N. Ramachandran, Academic Press, London (1967), p. 557.

BULLETIN OF THE CHEMICAL SOCIETY OF JAPAN VOL. 42 571—572 (1969)

The Cobalt Carbonyl-catalyzed Hydroesterification of Methyl Acrylate with Carbon Monoxide and Methanol

Akio MATSUDA

Government Chemical Industrial Research Institute, Tokyo, Mita, Meguro-ku, Tokyo

(Received July 2, 1968)

In a previous paper it was reported that the cobalt carbonyl-catalyzed hydroesterification of acrylonitrile with carbon monoxide and methanol occurred in the presence of a small amount of hydrogen and a limited amount of pyridine, and that the amount of methyl α-cyanopropionate produced was larger than that of methyl β-cyanopropionate.[1] The present report is concerned with the results obtained when methyl acrylate was used in this reaction instead of acrylonitrile. The reaction procedure and the method of analyses were essentially the same as have been described in the previous report.[1]

Standard samples for the gas chromatographic analyses were obtained as follows. Dimethyl succinate was obtained commercially. Dimethyl methylmalonate was synthesized by the action of methanol and 86% sulfuric acid on methyl α-cyanopropionate, which was the main product of the hydroesterification of acrylonitrile and which had already been identified.[1] Dimethyl γ-ketopimelate was separated by distillation from the reaction product and was purified by recrystallization from cyclohexane.

Identification of Dimethyl γ-Ketopimelate. Mp 53°C. IR spectrum: C=O (ester) 1748 cm^{-1}, C=O (ketone) 1725 cm^{-1}. NMR spectrum at 60 Mc (in carbon tetrachloride, with tetramethyl-

1) A. Matsuda, This Bulletin, **40**, 135 (1967).

silane as the internal standard): α-CH_2 τ 7.42 (triplet), β-CH_2 τ 7.35 (triplet), OCH_3 τ 6.39 (singlet).

Found: C, 53.50; H, 6.96%. Calcd for $C_9H_{14}O_5$: C, 53.46; H, 6.98%.

Results

The hydroesterification of methyl acrylate occurred in the presence of a small amount of hydrogen and pyridine, resulting in a high yield of dimethyl succinate and a very small yield of dimethyl methylmalonate. This exclusive formation of β-methoxycarbonylated product is in contrast to the case of the hydroesterification of acrylonitrile, where α-methoxycarbonylation predominates.[1] Dimethyl γ-ketopimelate was found as a by-product.

The effect of the reaction temperature is shown in Table 1.[2] The reaction rate is almost independent of the temperature in the 120—160°C range. The yield of dimethyl succinate decreases as the temperature increases, whereas the yield of dimethyl γ-ketopimelate increases with the temperature. The α/β ratio, contrary to the case of acrylonitrile,[1] increases along with the temperature.

Table 1. The effect of reaction temperature

1/2 mol methyl acrylate, 2 mol methanol, 4 mmol $Co_2(CO)_8$, 30 mmol pyridine; total pressure 200 kg/cm²; reaction time 1 hr; hydrogen content of the gas used, 5%.

Reaction temp. °C	Rate const. k min^{-1}	Conversion mol %	Products yields (mol %) DM	DS	DK[a]	α/β[b]
120	10×10^{-2}	100	1.9	82	2.3	0.023
140	13×10^{-2}	100	2.0	78	5.5	0.026
160	12×10^{-2}	100	1.9	67	7.8	0.029

a) Abbreviations DM, DS, and DK stand for dimethyl esters of methylmalonic acid, succinic acid, and γ-ketopimelic acid.
b) α/β stands for the mole ratio DM/DS.

The effect of the amount of pyridine is shown in Table 2; the rate constant and the selectivity toward each product are plotted against the amount of pyridine in Fig. 1.[3] The rate constant, k, increases almost in proportion to the amount of pyridine; this indicates that the reaction rate is first order with respect to the pyridine concentration. The selectivity toward dimethyl succinate increases with the amount of pyridine, whereas the selectivity toward dimethyl methylmalonate decreases slightly. The α/β ratio remarkably decreases as the amount of pyridine increases; this trend is again opposite to the case of acrylonitrile, where the methyl α-cyanopropionate/methyl β-cyanopropionate mole ratio increases along with the amount of pyridine.[1] The selectivity toward methyl γ-ketopimelate becomes larger as the amount of pyridine is reduced.

A more detailed study aimed at obtaining enough information to explain the above differences between the results of the hydroesterification of methyl acrylate and that of acrylonitrile will be reported in the future.

Table 2. The effect of the amount pyridine

1/2 mol methyl acrylate, 1/2 mol methanol, 4 mmol $Co_2(CO)_8$; reaction temperature 110°C, total pressure 160 kg/cm²; hydrogen content of the gas used, 7%.

Pyridine mmol	Rate const. k min^{-1}	Reaction time min	Conversion mol %	Products yields (mol %) DM	DS	DK	α/β
1	1.2×10^{-2}	120	60	2.6	29	15	0.090
3	2.3×10^{-2}	120	100	3.2	75	13	0.043
10	8.8×10^{-2}	25	90	2.0	73	7.0	0.027

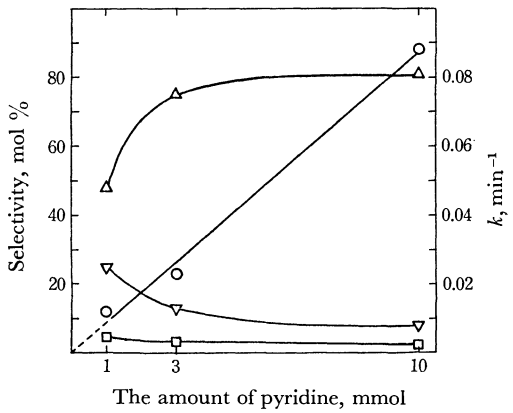

Fig. 1. The plot of k and the selectivity against the amount of pyridine.
-○-: k (min^{-1}).
-△-: Dimethyl succinate (mol %).
-▽-: Dimethyl γ-ketopimelate (mol %).
-□-: Dimethyl methylmalonate (mol %).

2) The overall first-order rate constant, k, was roughly estimated from the amount of gas supplied during the early stages of the reaction. The conversion was also roughly estimated from the total amount of gas supplied during the reaction. Although the product contained small amounts of acetal and methyl propionate resulting from the hydroformylation and hydrogenation of methyl acrylate, their yields are not listed in the table because of the lack of data.

3) The selectivity was calculated from Table 2 by dividing the yield by the conversion.

BULLETIN OF THE CHEMICAL SOCIETY OF JAPAN VOL. 42 573—574 (1969)

The Stability of Fused Rings in Metal Chelates. V. Copper(II) Chelates of the Schiff Base Derived from Pyruvic Acid and *n*-Propanolamine

Akitsugu NAKAHARA, Isao MIYACHI and Toshihiko KOHNO

Institute of Chemistry, College of General Education, Osaka University, Toyonaka, Osaka

(Received July 10, 1968)

Although ethanolamine molecule is provided with two donor groups for chelation, it cannot always be coordinated as a bidentate ligand around a metal ion. The Schiff base derived from salicylaldehyde and ethanolamine is, for instance, coordinated around copper(II) to produce not only the one-to-one type copper(II)-Schiff base complex but also the one-to-two type complex,[1] in which the hydroxyl groups of the ethanolamine moieties are free from coordination. In addition to that, the Schiff base derived from pyruvic acid and ethanolamine reacts with copper(II) to form exclusively the one-to-two type copper(II)-Schiff base complex; consequently the corresponding one-to-one type complex is hardly obtained regardless of the molar ratio of copper(II) to Schiff base employed in the preparation.[2]

These findings are explainable by taking into account the rather weak binding ability of alcohol oxygen in one hand, and the low stability of the 5-5[3] fused-chelate-ring structure on the other hand.[4] If this interpretation is valid, it may well be suggested that the successful preparation of the one-to-one type copper(II)-Schiff base complex of this kind will become easier by adopting *n*-propanolamine instead of ethanolamine moiety, because of its more stable 5-6 fused-chelate-ring structure as indicated in I. On the basis of this consideration, we have recently succeeded in preparing the one-to-one type copper(II) complex of the Schiff base derived from pyruvic acid and *n*-propanolamine, I, as well as the corresponding one-to-two type chelate, II.

The freshly prepared one-to-one type complex is a blue lath-shaped crystal, and is described by the

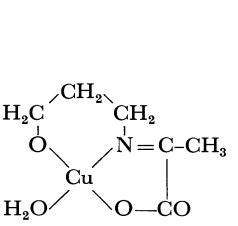

(I)

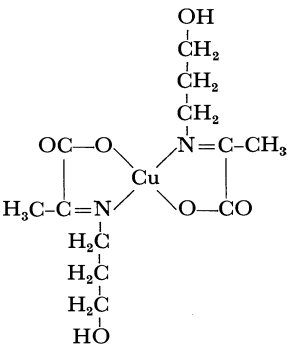

(II)

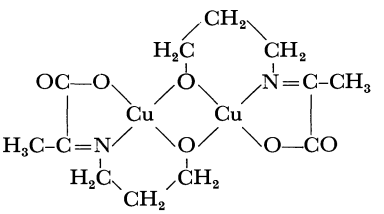

(III)

formula, $[Cu(pyv=propam)(H_2O)]\cdot 4H_2O$, where pyv=propam represents the Schiff base derived from pyruvic acid and propanolamine. However, the complex undergoes a gradual dehydration of itself in atmosphere, resulting a purple crystalline powder, to which a binuclear structure as illustrated in III is easily assigned on the basis of its extremely subnormal magnetic moment (0.7 B. M. for copper atom) and magnitude of molcular weight (428.7) in chloroform. The formation of this binuclear complex is even more accelerated by heating *in vacuo*.

Although we do not have any decisive proof for the particular binuclear structure III, the other possible structure, in which two copper(II) atoms are bridged by carboxylate-oxygen, would be less plausible in some respects. For example, there is a fact that similar type complex of *N*-ethanolsalicylaldimine does not give the corresponding binuclear complex,[1] whereas that of *N*-*n*-propanolsalicylaldimine does to produce a brownish

1) A. Nakahara, H. Yamamoto and H. Matsumoto, *Sci. Rep.* (College of General Education, Osaka Univ.), **12**, 11 (1964).

2) Y. Komiyama and A. Nakahara, to be submitted. The title of paper will be "The Crystal and Molecular Structure of Bis(β-hydroxyethyliminopyruvato)copper-(II) Tetrahydrate."

3) A fused-chelate-ring consisting of two five-membered rings is abbreviated as 5-5 in this paper.

4) A. Nakahara, Y. Yamamoto and Y. Matsumoto, This Bulletin, **37**, 1137 (1964).

Table 1. Magnetic susceptibilities per gram and magnetic moments of copper (II) complexes of γ-hydroxypropyliminopyruvate

Complex	Temp. °C	$10^6\chi_g$	μ(B.M.)
[Cu(pyv=propam$_2$)]·2H$_2$O	16	3.55	1.9
[Cu$_2$(pyv=propam)$_2$]	18	0.45	0.7

purple binuclear complex.[5,6] In other words, the propanol-oxygen seems to take an important role in the formation of binuclear complexes.

The one-to-two type copper(II)-Schiff base complex is a light blue plate, and shows a normal magnetic moment (1.9 B. M. for copper atom). The two alcohol-oxygen atoms must, of course, be free from coordination in the light of the molecular structure of the corresponding chelate with β-hydroxyethyliminopyruvate, determined by X-ray analysis.

Of interest is comparison of the tendency for the formation of binuclear complexes: (1) the one-to-one type complex with salicylideneiminoethanol does not form binuclear complex, (2) the same type complex with salicylideneiminopropanol cannot even be isolated because of high stability of the binuclear complex, (3) similar complex with γ-hydroxypropyliminopyruvate is appropriately stable and, for this reason, complexes of both monomer and dimer structure can be isolated in crystalline state.

Experimental

The Preparation of Copper(II) Complexes of Schiff Base derived from Pyruvic Acid and *n*-Propanolamine. *The One-to-One Type Copper(II)-Schiff Base Complex, I,* [Cu(pyv=propam)(H$_2$O)]·4H$_2$O. A mixture of 1.76 g (0.02 mol) of pyruvic acid and 1.50 g (0.02 mol) of ethanolamine were dissolved in 200 m*l* of aqueous ethanol (50 vol %). To this was added 1.60 g (0.04 mol) of sodium hydroxide and 4 g (0.02 mol) of copper(II) acetate monohydrate. The mixture was stirred and heated at about 70°C for 1.5 hr; hereupon a blue-green solution was obtained. After it had been filtered, the solution was concentrated until the volume of the solution became one third of the initial state. The resulting solution was allowed to stand overnight in a refrigerator. A large amout of blue-green crystals was obtained, which was recrystallized from a small quantity of water. Found: C, 24.06; H, 6.28; N, 4.84. Calcd for [Cu(pyv=propam)(H$_2$O)]·4H$_2$O: C, 24.28; H, 6.45; N, 4.72%. Since the compound readily underwent a dehydration in atmosphere, the elemental analysis had to be performed by uisng freshly deposited crystals.

The One-to-Two Type Copper(II)-Schiff Base Complex, II, [Cu(pyv=propam)$_2$]·2H$_2$O. The almost same procedure as that employed in the above preparation was adopted, but the molar ratio of the reagents was 1 : 2 : 1 copper(II): Schiff base : sodium hydroxide instead of 1 : 1 : 2. mp 188—192°C (decomp). Found: C, 36.51; H, 6.32; N, 7.24%. Calcd for [Cu(pyv=propam)$_2$]·2H$_2$O: C, 37.16; H, 6.24; N, 7.22%.

The Binuclear form of the One-to-One Type Copper(II)-Schiff Base Complex, III. The complex, I, was dehydrated at 80°C *in vacuo* for several hours until the weight became constant. Found: C, 34.69; H, 4.30; N, 6.79%. Calcd for [Cu$_2$(pyv=propam)$_2$]: C, 34.87; H, 4.39; N, 6.78%. Molecular weight in chloroform: 428.9. Calcd for the above formula: 413.4.

Magnetic Measurements. The magnetic susceptibility was determined at room temperature by using a Gouy magnetic apparatus. The results are shown in Table 1. From the observed susceptibilities, the magnetic moments were evaluated per copper atom. The results are shown in Table 1.

The Molecular Weight of the Complex, III, was determined with a Hitachi Model-115 osmometer by using chloroform solution.

The authors thank the Ministry of Education for the financial support granted for this research.

5) S. Yamada, Y. Kuge and K. Yamanouchi, *Inorg. Chim. Acta*, **1**, 139 (1967).

6) M. Kato, Y. Muto, H. B. Jonassen, K. Imai and A. Harano, This Bulletin, **41**, 1864 (1968).

BULLETIN OF THE CHEMICAL SOCIETY OF JAPAN VOL. 42 575—576 (1969)

Gel Filtration of Mixtures of Surfactants on Sephadex. II. Estimation of Micellar Molecular Weights of Mixed Surfactants

Fumikatsu TOKIWA, Kenji OHKI and Isao KOKUBO

Research Laboratories, Kao Soap Company, Minato-Yakushubata, Wakayama-shi

(Received July 10, 1968)

It has been shown in previous works[1,2] that gel filtration is useful as a research tool for studying the micellar properties of surfactants and that it also furnishes a simple means of estimating the micellar molecular weight (MMW) of a single surfactant from the retention volume of the micelle (V_M).

In the present work, the gel filtration of mixtures of two surfactants at different mixing ratios has been studied, together with the determination of the MMW's of the mixtures, in order to establish the relation between V_M and MMW. The surfactants used were sodium dodecyl sulfate (SDS), $C_{12}H_{25}OSO_3Na$, and dodecyl polyoxyethylene ether (DPE), $C_{12}H_{25}O(CH_2CH_2O)_pH$, with a p value of 12.[3]

TABLE 1. MICELLAR PROPERTIES OF THE MIXTURES OF SDS AND DPE

Mixing ratio in mole SDS/DPE	in 0.10 M NaCl				in water	
	V_M/V_0	$D_M \times 10^7$, cm²/sec	ϕ, ml/g	MWM[a] $\times 10^{-4}$	V_M/V_0	MMW[b] $\times 10^{-4}$
100/0	1.90	10.1	1.30	2.65	2.30	1.75
80/20	1.77	9.36	1.44	3.00	2.24	1.90
60/40	1.65	8.02	1.68	4.10	2.29	1.85
40/60	1.53	7.26	1.83	5.08	2.21	1.95
20/80	1.35	6.59	1.94	6.14	1.95	2.70
0/100	1.25	6.42	2.01	6.50	1.30	6.20

a) Calculated from diffusion and viscosity data.
b) Estimated from the log MMW *vs.* V_M/V_0 curve.

Table 1 gives the relative retention volumes of the micelles, V_M/V_0, at different SDS/DPE ratios in the absence and in the presence of 0.10 M NaCl, where V_0 is the void volume of the column used. These values were obtained on Sephadex G-100 by a method previously described.[1] Sephadex G-100 was chosen by taking into account its fractionation range of molecular weight (1×10^3—1×10^5). The V_M/V_0 value in 0.10 M NaCl decreases gradually with a decrease in the amount of SDS, while the value in water is almost constant, independently of the SDS/DPE ratio, in the region from 100/0 to 40/60, and then it decreases steeply with an increase in the amount of DPE. The V_M/V_0 values in the presence of sodium chloride are, in general, smaller than those in water. It has been found in a previous work that there is a linear relation between log MMW and V_M/V_0 for various types of single surfactants, but not for surfactants with a heterocyclic structure.[1] Now, it is of interest and importance to learn whether the linear relation would also be found in the present mixed systems.

The MMW values for the mixed micelles of SDS and DPE at various SDS/DPE ratios are given in Table 1; these values were calculated from the diffusion and viscosity data by the following equation, on the assumption that the micelle is a spherical and rigid particle:[5,6]

$$\mathrm{MMW} = \frac{4\pi r^3}{3} \cdot \frac{N}{\phi}$$

where:

$$r = kT/6\pi\eta D_M$$

Here, r is the radius of the micelle; η, the viscosity of the solvent; D_M, the diffusion coefficient of the micelle, and ϕ, the effective specific volume of the micelle, while N, R, and T have the conventional meanings. The values of ϕ and D_M are given in Table 1. The ϕ was obtained from the relative viscosity of the solution in terms of the Guth-Simha equation[5,7]; in the present case, it was independent of the concentration of the mixture at relatively high concentrations. The MMW value obtained from ϕ and D_M by Eq. (1) for SDS or DPE alone is in agreement with the

1) F. Tokiwa, K. Ohki and I. Kokubo, This Bulletin, **41**, 2285 (1968).
2) F. Tokiwa, K. Ohki and I. Kokubo, *ibid.*, **41**, 2845 (1968).
3) The SDS used was the same sample as that described in Ref. 1; the DPE was prepared from dodecyl alcohol of a high purity by the addition of ethylene oxide.[4]
4) F. Tokiwa and K. Ohki, *J. Phys. Chem.*, **71**, 1343 (1967).
5) T. Nakagawa and H. Inoue, *Nippon Kagaku Zasshi* (*J. Chem. Soc. Japan, Pure Chem. Sect.*), **78**, 636 (1957).
6) T. Nakagawa and K. Shinoda, "Colloidal Surfactants," Academic Press New York (1963), p. 115.
7) E. Guth and R. Simha, *Kolloid-Z.*, **74**, 147 (1936).

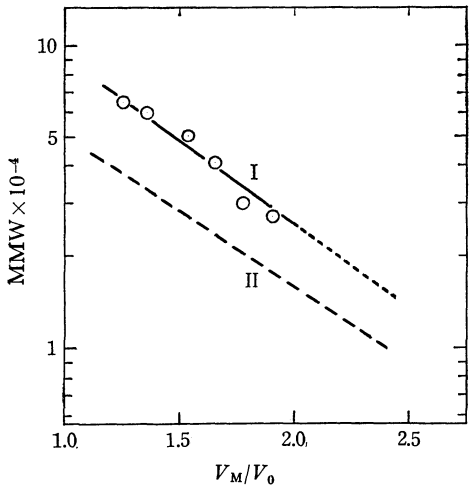

Fig. 1. The relation between log MMW and V_M/V_0 for the mixed micelles of SDS and DPE at various mixing ratios using the Sephadex G-100 column at 25°C (I). For reference, the relation for the various types of single surfactants on Sephadex G-75 is also shown by the broken line II.

published value.[8,9]

The MMW values thus obtained at various SDS/DPE ratios are plotted against V_M/V_0 in Fig. 1. A linear relation is seen between log MMW and V_M/V_0 although the points are somewhat scattered. For reference, the relation for various types of single surfactants obtained in a previous work[1] using Sephadex G-75 is also shown in Fig. 1. From the data presented above, it may be concluded that the gel filtration on Sephadex is a convenient way of roughly estimating the micellar molecular weights of mixed surfactants as well as of single surfactants. The MMW values of the mixed micelles of SDS and DPE in water, estimated from the log MMW *vs.* V_M/V_0 curve (I), are given in Table 1.

Experimental

The gel filtration measurements were performed on Sephadex G-100 by a method previously described, (*cf.* Fig. 1 in Ref. 1). The diffusion coefficients of the micelles were determined by the Schlieren method using a Neurath-type cell with the usual precautions.[4] The calculation of the diffusion coefficients was based on the moment method.[10,11] The viscosities of solutions were measured using a Cannon-Fenske-type viscometer with a flow time of 269 sec for pure water. All the experiments were carried out at 25°C.

The authors wish to express their thanks to Dr. H. Kita, Director of the Research Laboratories, for his encouragement and for the permission to publish this paper.

8) K. J. Mysels and L. H. Princen, *J. Phys. Chem.*, **63**, 1696 (1959).
9) P. Becher, *J. Colloid Sci.*, **16**, 49 (1961).
10) O. Lamm, *Nova Acta Regiae Soc. Sci. Upsal.*, **IV, 10**, No. 6 (1937).
11) K. Tyuzyo, *Kolloid-Z.*, **175**, 40 (1960).

BULLETIN OF THE CHEMICAL SOCIETY OF JAPAN VOL. 42 576—577 (1969)

Magnetic Moments of Copper(II) Diethyldithiocarbamate and Related Compounds

Ken-ichi HARA, Wasuke MORI, Motomichi INOUE, Michihiko KISHITA, and Masaji KUBO

Department of Chemistry, Nagoya University, Chikusa, Nagoya

(Received July 13, 1968)

The X-ray crystal analysis of copper(II) diethyldithiocarbamate[1] and di-*n*-propyldithiocarbamate[2] has shown that the crystals are formed with a binuclear structure having the Cu-Cu distance equal to 3.38—3.59 Å as a unit. Each copper atom has a distorted tetragonal-pyramidal coordination involving four sulfur atoms from two diethyldithiocarbamate groups at the corners of a square and the fifth surfur atom belonging to the other monomeric unit at the apex of the tetragonal pyramid. At room temperature, copper(II) dialkyldithiocarbamates[3] show magnetic moments of 1.75—1.76 B. M., which are smaller than about 1.9 B.M. normally observed for magnetically dilute

1) M. Bonamico, G. Dessy, A. Mugnoli, A. Vaciago and L. Zambonelli, *Acta Cryst.*, **19**, 886 (1965).

2) A. Pignedoli and G. Peyronel, *Gazz. Chim. Ital.*, **92**, 745 (1963).

3) G. Foëx, "Constantes Sélectionnées, Diamagnétisme et Paramagnétisme," Masson, Paris (1957).

TABLE 1. EFFECTIVE MAGNETIC MOMENTS, μ_{eff}, WEISS CONSTANTS, θ, MAGNETIC MOMENTS, μ_C, CALCULATED FROM CURIE CONSTANTS, C, MAGNETIC MOMENTS IN CHLOROFORM, μ_{sol}, AND MAGNETIC MOMENTS, μ_{calc}, CALCULATED FROM SPECTROSCOPIC DATA, Δ_1, OF COPPER (II) DIETHYLDITHIOCARBAMATE AND RELATED COMPOUNDS

Compounds	μ_{eff}, B.M.	θ, °K	C, emu/mol	μ_C, B.M.	μ_{sol}, B.M.	Δ_1, $10^4\,cm^{-1}$	μ_{calc}, B.M.
$Cu[(CH_3)_2NCS_2]_2$	1.75 (23°C)	−4	0.387	1.76	—	2.30	1.79
$Cu[(C_2H_5)_2NCS_2]_2$	1.75 (21°C)	+1	0.380	1.74	1.72	2.28	1.79
$Cu[(n\text{-}C_3H_7)_2NCS_2]_2$	1.76 (21°C)	−1	0.390	1.77	1.74	2.28	1.79

copper(II) compounds. In view of the binuclear structure and the low effective magnetic moments, one would expect the presence of spin coupling within a pair of copper atoms. However, electron spin resonance studies[4,5] yielded $g_\parallel=2.1085$ and $g_\perp=2.0236$, which are smaller than those of a majority of copper(II) complexes. This fact suggests that the low magnetic moments are due to a strong crystal field leading to the quenching of orbital contribution. In order to clarify this point, we have determined the magnetic susceptibilities of copper(II) dimethyldithiocarbamate, diethyldithiocarbamate, and di-*n*-propyldithiocarbamate in the solid state by the Gouy method[6,7] in a temperature range of 80—300°K and also the magnetic moments of these compounds of chloroform solutions.

The materials were prepared from commercial samples of sodium dialkyldithiocarbamates and copper(II) acetate. They were recrystallized from chloroform by adding methanol. The X-ray powder patterns of copper(II) diethyldithiocarbamate and di-*n*-propyldithiocarbamate showed agreement with the data of the complete X-ray crystal analysis.[1,2]

The magnetic susceptibilities of the compounds obey the Curie-Weiss law in the whole range of temperature studied. The Weiss constant and the Curie constant are listed in Table 1. The observed susceptibilities of the solutions of copper(II) diethyldithiocarbamate and di-*n*-propyldithiocarbamate in chloroform at 20°C show a linear relation to the concentration over the range of 0.3—1.2% and 0.4—2.4% by weight, respectively. The magnetic moments of the copper(II) complexes in chloroform were calculated from the slope of the susceptibility *versus* concentration plot and are shown in Table 1. Copper(II) dimethyldithiocarbamate could not be investigated in solutions, because it is sparingly soluble in common solvents.

The very small values for Weiss constants indicate that spin interaction is negligible in spite of the binuclear structure and the low effective magnetic moments. The magnetic moments, $\mu_C=1.74$—1.76 B.M., calculated from the Curie constants are smaller than about 1.9 B.M. for common copper(II) compounds. Since an unpaired electron in the $d_{x^2-y^2}$ orbital gives rise to magnetic polarization, the g-factor is given by

$$g_\parallel = 2\left(1-\frac{4\lambda}{\Delta_1}\right)$$
$$g_\perp = 2\left(1-\frac{\lambda}{\Delta_2}\right) \qquad (1)$$

for a copper(II) ion in a crystal field having D_{4h} symmetry.[8] Here, λ is the spin-orbit coupling constant, and Δ_1 and Δ_2 are energy separations between b_{2g} and b_{1g} states and between e_g and b_{1g} states, respectively. For copper(II) complexes,[9] λ is negative, and its absolute value is 625 cm^{-1}. Since Δ_2 is much greater than Δ_1, the magnetic moments of copper(II) compounds are given by

$$\mu = \left[\frac{1}{3}(g_\parallel{}^2+2g_\perp{}^2)S(S+1)\right]^{1/2}\beta$$
$$= 3^{1/2}\left(1-\frac{4\lambda}{3\Delta_1}\right)\beta \qquad (2)$$

where S is the total spin of a copper(II) ion equal to 1/2 and β denotes the Bohr magneton. Although the crystal field has C_{4v} symmetry in these copper(II) complexes, it can be approximated by D_{4h} symmetry because of a long distance of the apical sulfur atom from the central copper atom. In fact, the magnetic moments of copper(II) diethyldithiocarbamate and di-*n*-propyldithiocarbamate in chloroform agree excellently with those in the solid state as shown in Table 1. We have taken the visible and ultraviolet spectra of the compounds in chloroform and estimated Δ_1 in order to evaluate the magnetic moments by Eq. (2). The good agreement between the observed and calculated magnetic moments indicates that the low magnetic moments are due to the effect of a strong crystal field rather than to spin interaction between copper atoms in the binuclear structure.

4) T. R. Reddy and R. Srinivasan, *J. Chem. Phys.*, **43**, 1404 (1965).

5) H. R. Gersmann and J. D. Swalen, *ibid.*, **36**, 3221 (1962).

6) M. Kondo, M. Kishita, M. Kimura and M. Kubo, This Bulletin, **29**, 305 (1956).

7) M. Inoue, M. Kishita and M. Kubo, *Inorg. Chem.*, **6**, 900 (1967).

8) C. J. Ballhausen, "Introduction to Ligand Field Theory," McGraw-Hill, New York (1962).

9) W. Moffitt and C. J. Ballhausen, *Ann. Rev. Phys. Chem.*, **7**, 107 (1956).

SHORT COMMUNICATIONS

Studies on Photo-polarography. IV. Solvent Effect on Photocurrents

Hideo IMAI and Kazuo YAMASHITA

Department of Chemistry, Faculty of General Education, Hiroshima University, Hiroshima

(Received November 20, 1968)

The photoelectric effect at a metal-electrolyte interface has recently attracted attention in relation to the formation of the solvated electron and its reaction with the scavenger.[1-3] The solvent effect on this process, however, has not yet been reported. The authors have investigated the solvent effect on the photocurrent of nitrate in aqueous-organic solvent solutions containing 0.2 M KCl. The dropping mercury electrode was irradiated by the polychromatic light from a xenon lamp (250—350 mμ with a Toshiba UV-D25 filter), and the photocurrent was produced by the reaction of e_{aq}^- with NO_3^- to form NO_3^{2-} as the intermediate.[4]

The quadratic relationship[2] of the field effect on the photocurrent was proved in the potential region from -1.0 to -1.6 V *vs.* SCE. At a given potential the photocurrent was proportional to the square root of the nitrate concentration (0.1—10 mM) in good accordance with Barker's theory.[1]

According to the Barker model of the process, the photoelectrically emitted electrons are thermalized at around a distance, δ, away from the electrode surface, and are then hydrated (*cf.* Fig. 1). At the distance, δ, the coulombic energy (image force) is in balance with the thermal energy of the electron, *i. e.*,

$$\frac{e^2}{\varepsilon\delta} = kT \qquad (1)$$

where ε is the static dielectric constant of the medium and the other symbols are of their usual significance. It is noteworthy that in Eq. (1) δ is inversely proportional to ε. Our experimental evidence shows that log i_p (i_p, the photocurrent) is proportional to $1/\varepsilon$ as is shown in Fig. 2, *i. e.*,

$$\log i_p = K_1\left(\frac{1}{\varepsilon}\right) + K_2 \qquad (2)$$

where K_1 and K_2 are the constants. Assuming the exponential distribution of emitted electrons along the r axis, equation (3) can be derived as follows;

$$i_p \propto \int_\delta^\infty e^{-r}dr = -e^{-\delta} = -e^{-\frac{e^2}{\varepsilon kT}} \qquad (3)$$

Detailed investigation is now in progress in our laboratory.

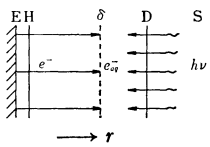

Fig. 1. Schematic representation of irradiated electrode surface.
E: Electrode D: Diffuse double layer
H: Helmholtz plane S: Solution
δ: Deposition plane

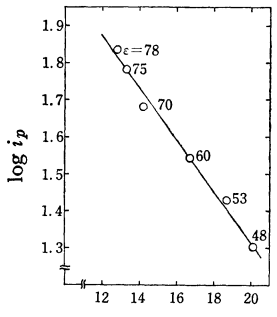

Fig. 2. Variation of log i_p with $1/\varepsilon$.
Solution; ethanol-water mixture containing 0.2 M KCl.
Scavenger of e_{aq}^-; 5 mM NO_3^-.
Applied potential; -1.6 V *vs.* SCE.
The measurements were carried out without altering at all the optical alignment. The values of ε were not corrected for the effect of the electric field and electrolyte.

1) G. C. Barker, A. W. Cardner and D. C. Sammon, *J. Electrochem. Soc.*, **113**, 1182 (1966).
2) P. Delahay and V. S. Srinivasan, *J. Phys. Chem.*, **70**, 420 (1966).
3) V. P. Sharma, P. Delahay, G. G. Susbielles and G. Tessari, *J. Electroanal. Chem.*, **16**, 285 (1968).
4) M. Ottolenghi and J. Rabani, *J. Phys. Chem.*, **72**, 593 (1968).

A Thiocyanato Cobalt(III) Complex: $[Co(SCN)_2dip_2]ClO_4 \cdot 2H_2O$*

Nobufumi MAKI and Shukichi SAKURABA

Department of Chemistry, Faculty of Engineering, Shizuoka University, Johoku, Hamamatsu

(Received November 11, 1968)

As far as the cobalt(III) complexes are concerned, the rhodanato-ligand has been well known to be bound to the central cobalt(III) atom by the nitrogen atom; ideed, the isothiocyanato-cobalt(III) complexes have been more familiar than the thiocyanato-ones, in which the ligand(SCN^-) is bound by the sulfur atom.

Several years ago, the pentacyanocobaltate(III) complex, $K_3[Co(CN)_5SCN]$, was described as belonging to the group of the thiocyanato-complexes.[2] Recently, Stotz *et al.*[2] have reported the synthesis of the isothiocyanato complex, $K_3[Co(CN)_5NCS]$.

In the present communication, the dithiocyanatobis(2,2′-dipyridyl)cobalt(III) complex (a new complex) has been prepared and has been ascertained to be bound by the sulfur atom on the evidence of the absorption spectrum in the visible and infrared regions.

Preparation of $[Co(SCN)_2dip_2]ClO_4 \cdot 2H_2O$. A water solution (100 m*l*) containing 0.46 g of KNCS was stirred, drop by drop, into 300 m*l* of a water solution of *trans*-$[CoCl_2dip_2]Cl$[3] (1.0 g). First, a green precipitate separated from the solution, and then, it turned dark brown. The product was filtered and washed with water several times. The crude complex was twice recrystallized from a hot 60% ethanol-water mixture. Ruby-like red crystals were thus obtained. Found: Co, 9.81; C, 46.90; N, 16.62; H, 3.70%. Calcd for $[Co(SCN)_2dip_2]NCS \cdot 5/2H_2O$: Co, 9.98, C, 46.78; N, 16.60; H, 3.58%.

The perchlorate of the complex was obtained by treating the thiocyanate with 10% $HClO_4$ at 40°C. Found: Co, 9.28; C, 42.30; N, 13.53; H, 3.48%. Calcd for $[Co(SCN)_2dip_2]ClO_4 \cdot 2H_2O$: Co, 9.46; C, 42.42; N, 13.49; H, 3.24%.

The complex is insoluble in water but soluble in ethanol.

Figure 1 shows the absorption spectra of the dithiocyanato-cobalt(III) and its related complexes with 2,2′-dipyridyl. The absorptivity of the first spin-allowed band for the $[Co(SCN)_2dip_2]^+$ ion is seen to be considerably larger than those of the other complexes of the $[CoN_6]$ type. This fact may well be interpreted as being due to the hyperchromic effect of the sulfur-bonded ligand, SCN^-.

The infrared evidence is summarized in Table 1. The values of the C–S stretching-vibration fall within the 690—720 cm^{-1} range characteristic of sulfur-bonded thiocyanato-complexes, while the values for the usual isothiocyanato-ammine and -amine complexes come within the 780—860 cm^{-1} range characteristic of nitrogen-bonded isothiocyanato-complexes.[4]

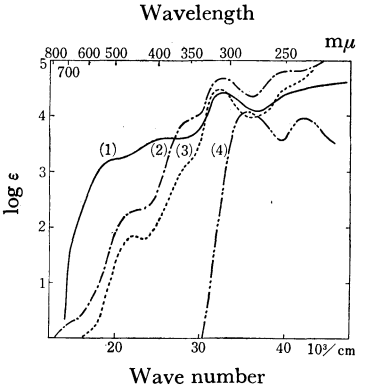

Fig. 1. The absorption spectra of the cobalt(III) complexes with 2,2′-dipyridyl:
(1) —— $[Co(SCN)_2dip_2]ClO_4 \cdot 2H_2O$; (2) –·– $[Co(NO_2)_2dip_2]Cl \cdot 5H_2O$; (3) ------ $[Co\,dip_3](ClO_4)_3 \cdot 3H_2O$; (4) ·–·– 2,2-dipyridyl.

TABLE 1. THE FREQUENCIES OF THE C–N AND C–S STRETCHING VIBRATIONS FOR THE THIOCYANATO- AND ISOTHIOCYANATO-COBALT(III) COMPLEXES IN A SOLID STATE

Compound	C–N	C–S
$[Co(SCN)_2dip_2]ClO_4 \cdot 2H_2O$	2080 s	718 m
$[Co(SCN)_2phen_2]NCS$	2060 s	714 m
cis-$[Co(NCS)_2en_2]Cl \cdot H_2O$	2110 m 2060 s	803 w 788 m
trans-$[Co(NCS)_2en_2]Cl \cdot H_2O$	2120 m 2080 w	788 m

phen=1,10-phenanthroline s=strong; m=medium; w=weak

* dip=2,2′-dipyridyl.

1) N. Maki, J. Fujita and R. Tsuchida, *Nature*, **183**, 458 (1959).

2) I. Stotz, W. K. Wilmarth and A. Haim, *Inorg. Chem.*, **7**, 1250 (1968).

3) F. M. Jaeger and J. A. van Dijk, *Z. Anorg. Allgem. Chem.*, **227**, 273 (1936).

4) A. Turco and C. Pecile, *Nature*, **191**, 66 (1961).

Reversible Oxygenation of Cobalt(II) Complexes on Polyvinylpyridine

Akira MISONO, Seiichiro KODA and Yasuzo UCHIDA

Department of Industrial Chemistry, Faculty of Engineering, The University of Tokyo, Hongo, Tokyo

(Received November 26, 1968)

Several kinds of oxygen complexes have been found recently[1] which are interesting from the point of view of oxidation catalysts and biochemical reactions. Among them, some *bis*- salicylaldehyde-imine-cobalt(II) complexes are well-known oxygen carrier chelates,[2] but the details of the oxygenation and the deoxygenation processes of these complexes and the technological designs of these complexes as solid-state oxidizing catalysts have not yet been fully studied.

The present authors found that an ESR signal appeared when a mixture of *bis*-salicylaldehyde-ethylenediimine cobalt(II) (A: prepared according to Ref. 3, recry. from methanol; the complex thus prepared is, as it stands, stable under air.) and *poly*-4-vinylpyridine (PVP: prepared according to Ref. 4) was exposed to oxygen, while, the signal disappeared when the mixture was placed in a vacuum. Several cycles were tried successfully. The same situation existed with the mixture of *bis*(salicylaldiminato)cobalt(II) (B: prepared according to Ref. 5; stable under air as it stands. The complex thus prepared is, however, suspected

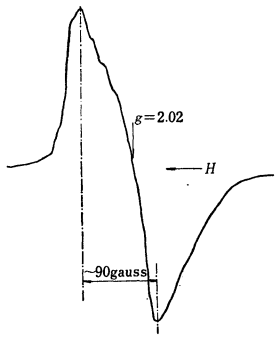

Fig. 1. The ESR signal on the mixture of the complex A and PVP under oxygen (at room temperature).

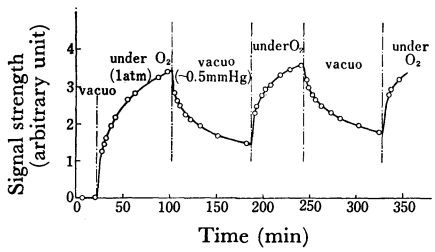

Fig. 2. The reversible cycles of the oxygenation and the deoxygenation of the complex A on PVP (at room temperature).

not to be pure *bis*(salicylaldiminato)cobalt(II) according to Ref. 6; this question remains to be solved in the future). These mixtures were made by mixing one of the complexes with PVP in methanol (for example, at the mole ratio (pyridine ring in the polymer/the complex) of about 50) and by then evaporating the solvent methanol.

Figure 1 shows the ESR signal of a mixture of the A complex and PVP under oxygen (1 atm). The ESR signal of the mixture of the B complex and PVP is almost the same.

The rate of the appearance and the disappearance of the signal may be rather well controlled by the diffusion of oxygen in the polymer film.

The presence of carbon monoxide (examined in the case of the mixture of the A complex and PVP) and that of ethylene (examined in the case of the mixture of the B complex and PVP) had no observable effect on the appearance or disappearance of the signal. When nitric oxide was introduced (examined in the case of the mixture of the B complex and PVP), the signal rapidly disappeared.

The signal cannot be identified exactly, but it may be caused by cobalt(II) coordinated with oxygen (for example, $Co^{II}-O_2 \leftrightarrow Co^{III}-O_2^{\ominus}$).

The oxygen adsorption on these mixtures should be compared with those on metal oxides and haemoglobins.

Some other complexes, such as copper(II) complexes mixed with PVP, are, in parallel, investigated by means of ESR in order to make clear the coordination structure of metal chelates on PVP.

1) Y. Saito, *J. of Synthetic Organic Chem., Japan*, **26**, 943 (1968).
2) L. H. Vogt, Jr., *Chem. Revs.*, **63**, 269 (1963).
3) R. H. Bailes and M. Calvin, *J. Am. Chem. Soc.*, **69**, 1886 (1947).
4) S. Tazuke and S. Okamura, *J. Polymer Sci.*, A**4**, 141 (1966).
5) J. Endo, *Nippon Kwagaku Kwaisi* (*J. Chem. Soc. Japan*), **65**, 424 (1944).
6) H. Nishikawa and S. Yamada, This Bulletin, **37**, 8 (1964).

Photoreaction of 3,4-Diphenyl-1,2,5-oxadiazole[1]

Toshio MUKAI, Toyonari OINE and Akira MATSUBARA

Department of Chemistry, Faculty of Science, Tohoku University, Sendai

(Received December 4, 1968)

Recent progress in the photochemistry of five-membered heterocycles[2] and our studies of the photochemistry of *α*-dioximes[3] have led us to investigate the photoreaction of 3,4-diphenyl-1,2,5-oxadiazole (I). Because very recently Cantrell and Haller reported an extensive study of the photochemistry of I and its related compounds[4], we intend to report our results, although our study has not yet been completed.

The irradiation of I in *benzene* (0.17%) in a Pyrex vessel with a high-pressure mercury lamp afforded benzonitrile (II) (50%), 3,5-diphenyl-1,2,4-oxadiazole (III), mp 106—108°C[5] (10%), and diphenylfuroxan (IV), mp 113—115°C, (14%), in addition to I (25%). Although Cantrell and Haller did not observe the formation of III and IV, the formation of all the photoproducts can be explained by the double-fragmentation process proposed by them.[4] That is, III can be derived by the recombination of II and benzonitrile oxide (V),[6] both of which are fragments from I, while IV is formed by the recombination of two moelcules of V.[7] However, the formation of III can also be explained by the ring contraction-expansion process as was first proposed by Ullman and Singh.[2a]

In order to distinguish between these two pathways, the irradiation of I was carried out in the presence of an excess of benzonitrile (5 equiv. to I). The finding that the formation of III increased very much compared to that of IV (III : IV is *ca.* 3.5 : 1) may suggest that the double fragmentation is the correct path for the formation of III.

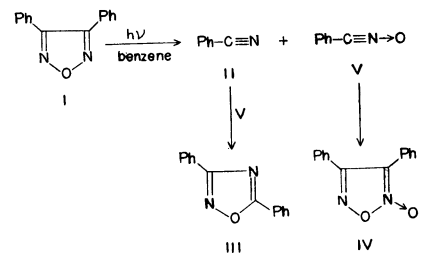

On electron impact, I exhibits the following peaks (m^+/e): 222 (M^+, 95%), 192 ($M-NO^+$, 85%), 151 (17%), 119 ($Ph-C{\equiv}N{\rightarrow}O^+$ and $Ph-N{=}C{=}O^+$, 86%), 103 ($PhCN^+$, 10%), 91 (PhN^+, 34%) and 89 (PhC^+, 100%). Thus, it was made clear that the double fragmentation of I was observed not only in photolysis and thermolysis,[8] but also in electron impact.

On the other hand, the irradiation of I in *methanol* (0.17%) gave methyl benzoate (6%), phenacyl alcohol, mp 84—86°C, (3%), 3,5-diphenyl-1,2,4-oxadiazole (3%), and/or benzamide (2%), in addition to benzonitrile (64%). The formation of these minor products will be discussed elsewhere, because our study is still in progress.

1) Organic Photochemistry. XI. Preceding paper; T. Oine and T. Mukai, *Tetrahedron Letters*, in press.

2) a) E. F. Ullman and B. Singh, *J. Am. Chem. Soc.*, **88**, 1844 (1966); **89**, 6911 (1967). b) H. Wynberg, R. M. Kellog, H. van Driel and G. E. Beekhuis, *ibid.*, **89**, 3501 (1967). c) H. Newman, *Tetrahedron Letters*, **1968**, 2417, 2421.

3) Irradiation of phenanthraquinone-dioxime in methanol afforded phenanthro[9,10-*c*]furazan (30% after 8 hr irr.) or 2,2′-dicyanobiphenyl (8% after 56 hr irr.).

4) T. S. Cantrell and W. S. Haller, *Chem. Commun.*, **1968**, 977.

5) All products are reported in the papers. Their structures have no doubt on the basis of reported mp and observed spectral data.

6) R. Huisgen, W. Mack and E. Anneser, *Tetrahedron Letters*, **1961**, 587.

7) a) A. Werner and H. Buss, *Ber.*, **27**, 2193 (1894). b) H. Wieland, *ibid.*, **40**, 1667 (1907).

8) a) K. V. Auwer and V. Meyer, *Ber.*, **21**, 784 (1888). b) F. D. Dodge, *Ann.*, **264**, 178 (1890).

A New Approach to the Study of the Reactions of Nitrogen Atoms with Hydrocarbons

Takefumi OKA and Shin SATO

Department of Applied Physics, Tokyo Institute of Technology, Ookayama, Meguro-ku, Tokyo

(Received December 10, 1968)

The reactions of nitrogen atoms with various hydrocarbons have been extensively investigated by many investigators using the discharge of nitrogen gas at low pressures.[1-4] The main product observed in their experiments was hydrogen cyanide. Other products, such as ammonia and methyl cyanide, were always found in minor amounts.

Recently, a few groups, including that of our laboratory, used high-energy radiations to produce nitrogen atoms in the gas phase at higher pressures.[5] However, nitrogen-containing product observed was again only hydrogen cyanide, and the reaction mechanism was very much complicated by the participation of nitrogen molecule ions in the reactions.

We have studied the γ-radiolysis of a liquid nitrogen containing small amounts of various hydrocarbons. This short communication will report the preliminary results obtained; these results are quite different from the results obtained in the gas phase.[5]

When a 3-m*l* portion of liquid nitrogen containing 4×10^{-2} mol% of propylene was irradiated at 77°K by γ-rays for three hours at the dose rate of 10^6 R/hr, the products observed were methyl cyanide (0.80 μmol), propane (0.55 μmol), and small amounts of ethane, ethylene, isobutane, 4-methylpentene-1 and ammonia. The absence of hydrogen cyanide was noticeable.

Table 1 summarizes the results for nitrogen-containing products obtained when various hydrocarbons were used. With the hydrocarbons of group 1, various nitrogen-containing products were observed, while with those of group 2 practically no such products were observed. At first sight, this appears to indicate that nitrogen atoms have less reactivity to the hydrocarbons in the group 2.

Table 1. Nitrogen containing products and their approximate *G*-values[a]

Hydrocarbon[b]	Products (*G*-values)	Mp °C
	Group I	
Ethylene	HCN (0.2), CH_3CN (0.1), NH_3 (small)[c]	−169.2
Propane	CH_3CN (0.08)	−189.9
Propylene	CH_3CN (0.13), NH_3 (small)[c]	−185.2
Allene	HCN (small), CH_3CN (0.05), CH_2=CHCN (0.05)	−136.0
Butene-1	HCN (small), CH_3CN (0.05), C_2H_5CN (0.05)	−185.4
	Group II	
Acetylene	no HCN	−81.8
trans-Butene-2	no HCN, no nitril compounds	−105.6
1,3-Butadiene	HCN (small), no nitril compounds	−108.9

a) Estimations are based on the energy absorbed by liquid nitrogen.
b) Mole fraction of each hydrocarbon is in the order of 10^{-4}.
c) After treated with Nessler reagent, analyzed spectrophotometrically at 430 mμ.

However, it may be expected from the melting points listed in the table that the hydrocarbons of the group 1 are more soluble in liquid nitrogen than are those of the group 2. This may be the reason why the hydrocarbons of the group 2 give few nitrogen-containing products.

Experimental. A certain amount of hydrocarbon was frozen in a sample tube at 77°K. When compressed nitrogen gas (1.5 atm) was then introduced into the tube at 77°K, nitrogen was gradually liquefied at the bottom of the tube. This was continued until a required volume of the liquid was obtained. Then the cock of the tube was closed and the tube was removed from the vacuum line. The sample was then vigorously shaken in order to mix its contents. After irradiation, the volatile components were pumped off from the mixture at 77°K and the residue was analyzed by gas chromatography (a 5-m column packed with Carbowax 20 M and a 2-m column of dioctyl phthalate), mass spectrometry, and infrared spectroscopy.

1) H. G. V. Evans, G. R. Freeman and C. A. Winkler, *Can. J. Chem.*, **34**, 1271 (1956).
2) Y. Shinozaki, R. Shaw and N. N. Lichtin, *J. Am. Chem. Soc.*, **86**, 341 (1964).
3) J. T. Herron, *J. Phys. Chem.*, **69**, 2736 (1965).
4) D. R. Safrany and W. Jaster, *ibid.*, **72**, 518 (1968).
5) T. Oka, R. Kato, S. Sato and S. Shida, This Bulletin, **41**, 2192 (1968).

BULLETIN OF THE CHEMICAL SOCIETY OF JAPAN VOL. 42 583—593 (1969)

Study of Wall Effect on the Flow of Polyvinylpyrrolidone Solutions in Capillary*1

Takehiko WATANABE, Takeshi MINESHITA and Sôzaburo ONO

Laboratory of Biophysical Chemistry, College of Agriculture, University of Osaka Prefecture, Sakai, Osaka

(Received June 3, 1968)

Dependence of the viscosity of the polyvinylpyrrolidone ($\bar{M}_v = 4.0 \times 10^4$ and 9.0×10^5) solutions on the bore-size of capillary viscometer has been studied at 35°C, in pure water, in dimethyl sulfoxide (DMSO), in water-DMSO, and in aqueous solution with various cosolutes, at various concentrations (0.5—5.0 g/100 m*l*). Viscosity measurements were carried out with a Maron-Belner type low shear capillary viscometer with various capillary radii (0.0190—0.0761 cm) within the shear stress range of 0.2—20 dyn/cm^2 at the capillary wall. The solutions showed a behavior of non-Newtonian flow and dependence on the size of the capillary. The viscosity of the polymer solutions in DMSO, and in water-DMSO decreased with the decrease in the capillary bore-size within the range of shear stress studied, and that in pure water, although similar phenomena as above were observed in higher shear stress, increased with the decrease in the capillary bore-size at the range of the lower shear stress, and this capillary bore-size dependence could not be observed with the aqueous solutions with cosolutes. The difference in the characteristics of the capillary bore-size dependence of the viscosity may be attributed to the difference in the behavior of the polymer molecules existing near the wall at which the thermal motion of the polymer molecules will be hindered by the existence of the capillary wall. The results were represented by the modified Ree-Eyring generalized flow formula for a flow system containing one Newtonian flow unit and one non-Newtonian one which included the additional terms dependent on the capillary bore-size. The viscosity equation suitable for analysing the dependence of the viscosity on the capillary bore-size at entire ranges of the rate of shear, was derived by assuming the wall layer composed of the double layers (of thickness d_o and $d_i - d_o$) in the flowing liquid in the capillary tube, and by combining this equation with the modified Ree-Eyring equation, the values of d_o and d_i were calculated.

Many papers[1-9] have been published concerning the phenomena that the viscosity of many suspensions, including blood, when measured with the capillary viscometer, decreases with decreasing capillary bore-size. For a similar phenomenon observed with polymer solution, experimental and theoretical treatments[10-11] were made by Oldroyd and Toms. However, as stated in the previous paper,[12] the results obtained with polyvinylpyrrolidone or PVP, solutions, could not be explained satisfactorily with their treatments. The capillary bore-size dependence of the viscosity of PVP in various solvents at the infinite high rate of shear, was treated by assuming the existence of the wall layer (of thickness d_i) in the flowing liquid.

In the present paper, the analysis of the capillary bore-size dependence of the viscosity at entire ranges of rate of shear was attempted.

*1 Partially presented at the 19th Symposium of the Colloid Chemistry, Nagoya, Oct. 1966, and 20th Annual Meeting of the Chemical Society of Japan, Tokyo, April, 1967.

1) R. H. Haynes and A. C. Burton, *Am. J. Physiol.*, **197**, 943 (1959); *ibid.*, **198**, 1193 (1960).
2) R. E. Wells, Jr., *Am. J. Med.*, **31**, 505 (1961).
3) H. W. Thomas, *Biorheology*, **1**, 41 (1962).
4) A. L. Copley and P. H. Staple, *ibid.*, **1**, 3 (1962).
5) E. W. Merril, E. R. Gilliland, G. Cokelet, H. Shin, A. Britten and R. E. Wells, Jr., *Trans. Soc. Rheol.*, **7**, 303 (1963).
6) H. L. Goldsmith and S.G. Mason, *Nature*, **190**, 1095 (1961).
7) R. E. Wells, Jr., and E. W. Merril, *Science*, **133**, 763 (1961).
8) A. L. Copley, "Flow Properties of Blood and Other Biological Systems," (ed. A. L. Copley and G. Stainsby), Pergamon Press (1960), p. 97.
9) T. Watanabe, S. Oka and M. Yamamoto, *Biorheology*, **1**, 193 (1962).
10) J. G. Oldroyd, *J. Colloid Sci.*, **4**, 333 (1949).
11) B. A. Toms, *ibid.*, **4**, 511 (1949).
12) T. Mineshita, T. Watanabe and S. Ono, *J. Polymer Sci.*, Part C, **23(2)** (1969), in press. (Study on Wall Effect for Flow of Polymer Solution in Capillary).

Experimental

PVP used was a commercial product, Luviskol K-90 and K-30 were obtained from Badische Anilin und Soda Fabrik A. G. Other materials were commercial chemicals.

As to the viscosity measurements, a Maron-Belner low shear capillary viscometer with continuous varying pressure head was used.[13-14] The instrumental dimensions of the viscometers are shown in Table 1. Details on viscosity measurements are the same as described in the previous paper.[15]

TABLE 1. THE DIMENSIONS OF THE VISCOMETER

Radius of capillary $R\times10^2$ (cm)	Radius of bulb R_b (cm)	Length of capillary L (cm)	Radius of manometer $R_m\times10$* (cm)
7.61	1.095	27.7	3.99
5.02	1.260	28.7	4.00
3.08	1.245	28.7	1.40
3.02	1.270	28.9	1.44
2.73	1.300	29.4	0.97
2.38	1.250	28.6	1.08
2.28	1.261	28.8	1.44
1.90	1.260	29.0	1.00

* The R_m values of the corresponding viscometer listed in Table 1 of Ref. 15 and in Table 2 of Ref. 12 should read the values listed in this table.

The measurements of extinction angle were carried out by using a Rao Flow Birefringence Viscometer Model No. B-23.

The spectrophotometric measurements were carried out with the use of a Hitachi EPS-3 Recording Spectrophotometer.

Results and Discussion

The plots of viscosity *vs.* rate of shear for K-30 aqueous solution (adjusted to pH=10.4 with KOH) and the aqueous solution with cosolute, *i. e.*, serine, aspartic acid, tryptophan, benzoic acid, and lactic acid, and K-90 aqueous solution with benzoic acid or tryptophan, in various capillaries are shown in Figs. 1(a), 1(b), 1(c), and 1(d). These substances used as cosolutes are known as the agents which induce the change in the dissolved state of the PVP molecules in various ways.[16] The viscosity of the PVP aqueous solution without cosolute shows marked dependence on the capillary bore-sizes, in the same manner as stated in the previous papers.[12,15] However, the viscosity of the aqueous solution with cosolute did not show the observable dependence on the capillary bore-size, in spite of the fact that non-Newtonian nature of the aqueous solution with cosolute, *i. e.*, serine, aspartic acid, and tryptophan, is more enhanced than that in the case without cosolute. The results show that the flow of the non-Newtonian fluids does not always

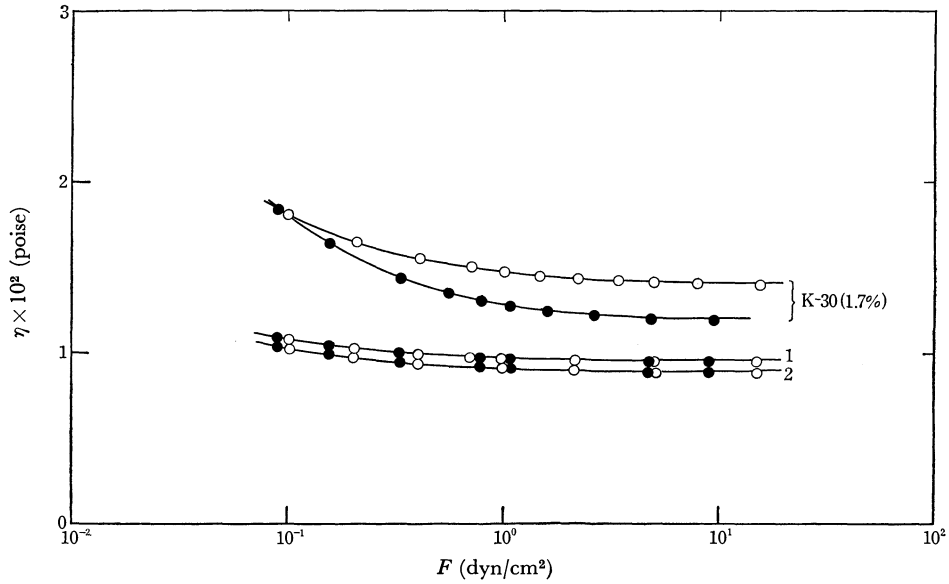

Fig. 1(a). Plots of visocsity *versus* shear stress (log scale) for K-30 (1.7%) aqueous solution with or without cosolute.
○ R=0.0308 cm, ● R=0.0190 cm
(1) cosolute, 0.05 M lactic acid; (2) cosolute, 0.025 M benzoic acid

13) S. H. Maron and R. J. Belner, *J. Appl. Phys.*, **26**, 1457 (1955); *J. Colloid Sci.*, **10**, 523 (1955).
14) I. M. Krieger and S. H. Maron, *J. Appl. Phys.*, **23**, 147 (1952); *ibid.*, **25**, 72 (1954).
15) T. Mineshita, T. Watanabe and S. Ono, This Bulletin, **40**, 2217 (1967).
16) J. Eliassaf, F. Erriksson and F. R. Eirich, *J. Polymer Sci.*, **47**, 193 (1961).

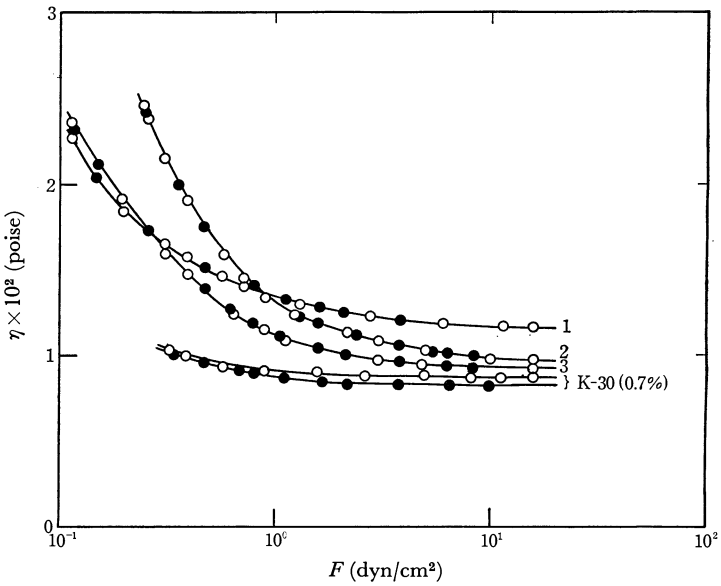

Fig. 1(b). Plots of viscosity *versus* shear stress (log scale) for K-30 (0.7%) aqueous solution with or without cosolute.
○ R=0.0308 cm, ● R=0.0190 cm
(1) cosolute, 0.1 M DL-tryptophan; (2) cosolute, 0.1 M L-aspartic acid; (3) cosolute, 0.1 M DL-serine

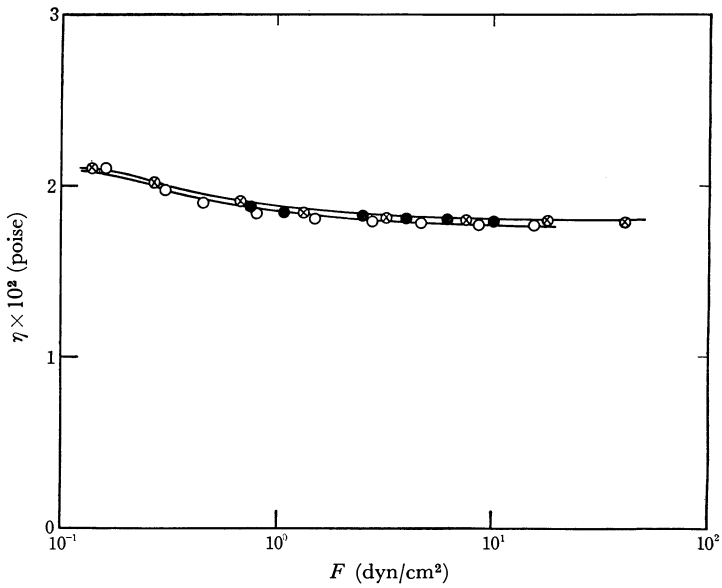

Fig. 1(c). Plots of viscosity *versus* shear stress (log scale) for K-90 (1%) aqueous solution with cosolute.
⊗ R=0.0761 cm, ○ R=0.0308 cm, ● R=0.0190 cm; cosolute, 0.025 M benzoic acid

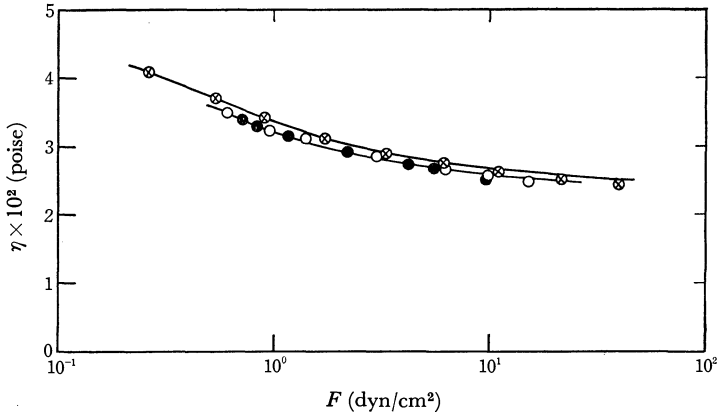

Fig. 1(d). Plots of viscosity *versus* shear stress (log scale) for K-90 (1%) aqueous solution with cosolute.
⊗ R=0.0761 cm; ○ R=0.0308 cm; ● R=0.0190 cm
cosolute, 0.1 M DL-tryptophan.

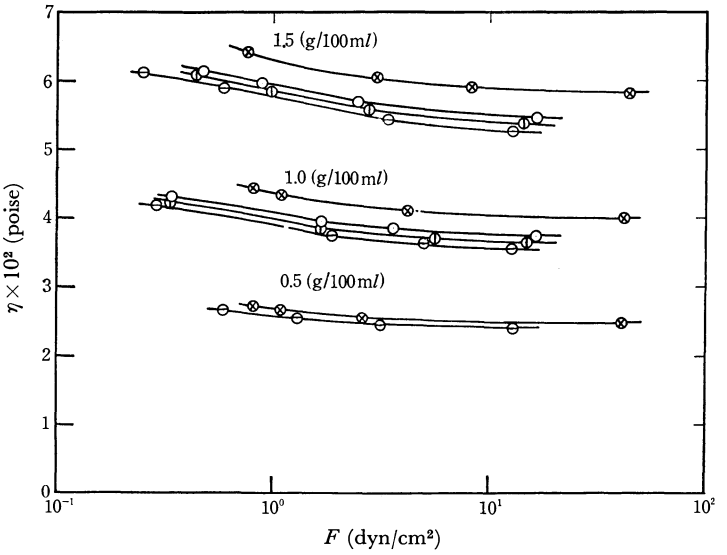

Fig. 2. Plots of viscosity *versus* shear stress (log scale) for K-90 in DMSO.
⊗ R=0.0761 cm, ○ R=0.0308 cm,
⊕ R=0.0273 cm, ⊖ R=0.0238 cm

show the capillary bore-size dependence of the viscosity. The other typical plots of viscosity *vs.* shear stress for K-90 solutions at various concentrations in DMSO in various capillaries are shown in Fig. 2.

Non-Newtonian flow behavior is observed, and the viscosity decreases with the decrease of capillary bore-size in all ranges of shear stress studied. Similar results are obtained with the solutions in water-DMSO mixture and also in *n*-propanol and in water - *n*-propanol mixture as reported in the previous paper.[15]

The experimental results were represented by the modified Ree-Eyring generalized flow formula for a flow system containing one Newtonian flow unit and one non-Newtonian one which includes the additional terms dependent on the capillary bore-size (radius: R) as follows:[15]

$$\eta = \left(\eta_1' - \frac{\sigma_1}{R}\right) + \left(\frac{1}{b_2'} + \frac{\sigma_2}{R}\right)\left(\frac{1}{a_2}\right)\left(\frac{a_2}{G}\right)\sinh^{-1}\left(\frac{G}{a_2}\right) \tag{1}$$

where,

$$\eta_1' - \frac{\sigma_1}{R} = \eta_1, \quad \frac{1}{b_2'} + \frac{\sigma_2}{R} = \frac{1}{b_2},$$

$$\eta_1 = \frac{x_1\beta_1}{\alpha_1}, \quad a_2 = \frac{1}{\beta_2}, \quad b_2 = \frac{a_2}{x_2},$$

TABLE 2(a). PARAMETERS OF EQ. (1) FOR PVP (K-30) AQUEOUS SOLUTIONS (at 35°C)

Solvent	Concentration (g/100 ml)	$R = 0.0308$ (cm)	$R = 0.0302$ (cm)	$R = 0.0238$ (cm)	$R = 0.0228$ (cm)	$R = 0.0190$ (cm)
Pure water without cosolute	0.73	$\eta_1 =$ 8.50	8.49	8.30	8.18	8.09
		$a_2 =$ 2.0	2.0	2.0	2.0	2.0
		$b_2 =$ 93.5	91.7	81.3	80.0	69.0
		$\eta_0 =$ 13.8	13.9	14.5	14.4	15.3
0.1 M DL-Serine	0.73	$\eta_1 =$ 8.92	8.92	8.91	8.91	8.90
		$a_2 =$ 2.0	2.0	2.0	2.0	2.0
		$b_2 =$ 22.7	22.7	22.7	22.7	22.7
		$\eta_0 =$ 31.0	31.0	31.0	31.0	31.0
0.1 M L-Aspartic acid	0.73	$\eta_1 =$ 9.20	9.20	9.20	9.19	9.19
		$a_2 =$ 2.0	2.0	2.0	2.0	2.0
		$b_2 =$ 15.0	15.0	15.0	15.0	15.0
		$\eta_0 =$ 42.5	42.5	42.5	42.5	42.5
0.1 M DL-Tryptophan	0.73	$\eta_1 =$ 11.4	11.4	11.4	11.4	11.4
		$a_2 =$ 2.0	2.0	2.0	2.0	2.0
		$b_2 =$ 29.1	29.1	29.1	29.1	29.1
		$\eta_0 =$ 28.6	28.6	28.6	28.6	28.6
Pure water without cosolute	1.70	$\eta_1 =$ 14.0	13.2	12.8	12.6	11.8
		$a_2 =$ 2.0	2.0	2.0	2.0	2.0
		$b_2 =$ 75.2	75.2	62.5	55.9	50.0
		$\eta_0 =$ 20.7	19.9	20.8	21.6	21.8
0.05 M Lactic acid	1.70	$\eta_1 =$ 9.01	9.01	9.01	9.00	9.00
		$a_2 =$ 2.0	2.0	2.0	2.0	2.0
		$b_2 =$ 200	200	200	200	200
		$\eta_0 =$ 11.5	11.5	11.5	11.5	11.5
0.025 M Benzoic acid	1.70	$\eta_1 =$ 9.50	9.50	9.49	9.48	9.48
		$a_2 =$ 2.0	2.0	2.0	2.0	2.0
		$b_2 =$ 200	200	200	200	200
		$\eta_0 =$ 12.0	12.0	12.0	12.0	12.0

η_1 and η_0: unit in m poise, $\eta_0 = \eta_1 + (1000/a_2 b_2)$.

TABLE 2(b). PARAMETERS OF VISCOSITY EQUATION (at 35°C)

PVP(K-90) 1% aqueous solution with 0.1 M DL-tryptophan, where $a_2 = 5.0$			PVP(K-90) 1% aqueous solution with 0.025 M benzoic acid, where $a_2 = 5.0$		
$R = 0.0761$	$R = 0.0302$	$R = 0.0190$	$R = 0.0761$	$R = 0.0302$	$R = 0.0190$
$\eta_1 = 25.0$	$\eta_1 = 24.2$	$\eta_1 = 24.0$	$\eta_1 = 17.2$	$\eta_1 = 17.2$	$\eta_1 = 17.2$
$b_2 = 10$	$b_2 = 10$	$b_2 = 10$	$b_2 = 50$	$b_2 = 50$	$b_2 = 50$
$\eta_0 = 45.0$	$\eta_0 = 44.2$	$\eta_0 = 44.0$	$\eta_0 = 21.2$	$\eta_0 = 21.2$	$\eta_0 = 21.2$

R: unit in cm; η_1 and η_0: unit in m poise, $\eta_0 = \eta_1 + (1000/a_2 b_2)$.

x=the fractional area on a shear surface occupied by the flow unit, β=the relaxation time of the flow unit, and α=ratio of shear volume to twice the average kinetic energy of the flow unit. Subscripts 1 and 2 of the parameters refer to the Newtonian and non-Newtonian flow units, respectively. $\sigma_1 = -\mathrm{d}(\eta_1)/\mathrm{d}(1/R)$ and $\sigma_2 = \mathrm{d}(1/b_2)/\mathrm{d}(1/R)$ are the slopes of the linear plot of η_1 *vs.* $1/R$ and $1/b_2$ *vs.* $1/R$ respectively, and η'_1 and $1/b'_2$ are the extrapolated values of η_1 and $1/b_2$ at $1/R \to 0$, respectively.

The values of η_1, a_2, b_2, σ_1, σ_2, η_1', and $1/b_2'$ are shown in Tables 2(a), (b), (c) and Tables 3(a), (b).

The flow represented by Eq. (1) becomes Newtonian under the condition of $(G/a_2) \to \infty$, and $(G/a_2) \to 0$, and the values of viscosity, η_∞(at $G/a_2 \to \infty$), and η_0 (at $G/a_2 \to 0$) are respectively reduced to

$$\eta_\infty = \eta_1 = \left(\eta_1' - \frac{\sigma_1}{R}\right) \tag{2}$$

TABLE 2(c). PARAMETERS OF VISCOSITY EQUATION (at 35°C)

	Concentration (g/100 ml)								
	1.5			1.0			0.5		
$R\times10^2$ (cm)	$\eta_1\times10^3$ (poise)	b_2	$(\eta_1+(1/a_2b_2))\times10^3$(poise)	$\eta_1\times10^3$ (poise)	b_2	$(\eta_1+(1/a_2b_2))\times10^3$(poise)	$\eta_1\times10^3$ (poise)	b_2	$(\eta_1+(1/a_2b_2))\times10^3$(poise)
PVP (K-90) in DMSO where $a_2=5.0$									
7.61	57.5	20.8	67.1	40.0	26.7	47.5	25.0	44.4	29.5
3.08	53.4	20.2	63.3	36.6	25.3	44.5	24.5	44.4	29.0
2.73	52.5	19.6	62.7	36.0	24.7	44.1	24.5	44.4	29.0
2.38	51.5	19.4	61.8	35.0	24.4	43.2	24.3	42.6	29.0
PVP (K-90) in 50% DMSO where $a_2=5.0$									
7.61	86.0	14.0	100.3	59.5	20.4	69.3	37.5	40.8	42.4
3.08	82.5	13.3	97.5	57.5	20.0	67.4	35.5	40.0	40.5
2.73	81.5	13.3	96.5	57.4	20.0	67.4	35.0	37.0	40.4
2.38	80.5	13.2	95.7	56.7	19.8	66.8	34.5	36.4	40.0
PVP (K-90) in 20% DMSO where $a_2=5.0$									
7.61	45.8	25.0	53.8	32.7	40.0	37.7	20.0	50.0	24.0
3.08	42.6	21.3	52.0	30.9	35.1	36.6	18.8	42.6	23.5
2.73	42.0	20.8	51.6	30.6	34.5	36.4	18.6	42.6	23.3
2.38	41.0	19.8	51.1	30.0	33.3	36.0	18.2	40.0	23.2

TABLE 3(a). THE VALUES OF η_1', σ_1', $1/b_2'$ AND σ_2 FOR K-30 AND K-90 IN WATER WITH VARIOUS COSOLUTES

$\bar{M}_v\times10^{-4}$	Solvent	Concn. (g/100 ml)	$\eta_1'\times10^3$ (poise)	$1/b_2'\times10^3$ (poise/sec)	$\sigma_1\times10^3$ (poise·cm)	$\sigma_2\times10^3$ (poise·cm/sec)
4	Pure water without cosolute	1.70	16.2	5.0	0.09	0.28
4	0.025 M Benzoic acid	1.70	9.5	5.0	0	0
4	0.05 M Lactic acid	1.70	9.0	5.0	0	0
4	Pure water without cosolute	0.73	8.9	5.0	0.02	0.17
4	0.1 M DL-Serine	0.73	8.9	44.1	0	0
4	0.1 M DL-Aspartic acid	0.73	9.2	66.7	0	0
4	0.1 M DL-Tryptophan	0.73	11.4	34.4	0	0
90	Pure water without cosolute	1.07	36	(−23)	0.4	(1.3)
90	0.1 M DL-Tryptophan	1.0	25.2	100	0.02	0
90	0.025 M Benzoic acid	1.0	17.2	20	0	0

TABLE 3(b). THE VALUES OF η_1', σ_1, $1/b_2'$ AND σ_2 FOR K-90 IN WATER-DMSO MIXTURES AT SEVERAL CONCENTRATIONS

Solvent	Concn. (g/100 ml)	$\eta_1'\times10^3$ (poise)	$\sigma_1\times10^3$ (poise·cm)	$1/b_2'\times10^3$ (dyn/cm²)	$\sigma_2\times10^3$ (dyn/cm)
20% DMSO	1.5	48	0.17	35	0.4
	1.0	34	0.09	23	0.2
	0.5	21	0.06	18	0.2
50% DMSO	1.5	90	0.23	70	0.2
	1.0	61	0.11	49	0.1
	0.5	39	0.10	24	0.1
100% DMSO	1.5	60	0.20	49	0.1
	1.0	42	0.18	37	0.1
	0.5	25	0.03	22	0.1

and

$$\eta_0 = \eta_1 + \frac{1}{a_2 b_2} = \left(\eta_1' - \frac{\sigma_1}{R}\right) + \left(\frac{1}{a_2}\right)\left(\frac{1}{b_2'} + \frac{\sigma_2}{R}\right)$$

$$= \left(\eta_1' + \frac{1}{a_2 b_2'}\right) - \frac{\left(\sigma_1 - \frac{\sigma_2}{a_2}\right)}{R} = \eta_0' - \frac{\left(\sigma_1 - \frac{\sigma_2}{a_2}\right)}{R} \quad (3)$$

In the above equations the values of η_∞, η_0, η_1, η_1', $1/b_2$, and $1/b_2'$ must be positive; however, as stated in the previous paper,[15] the values of $1/b_2'$ obtained with K-90 aqueous solution and those of $MgCl_2$ solution obtained by the extrapolation of the line representing the linear relationship between $1/b_2$ *vs.* $1/R$ at the range of relatively larger values of $1/R$ are negative. Moreover, as shown in Fig. 3 the results obtained with 2.0% K-90 aqueous solution show that the slope of the plots of $1/b_2$ *vs.* $1/R$ changes at a certain radius (R_i). This result shows that Eq. (1) holds strictly in the same manner as in the case of other systems, for the flow of K-90 solutions in water and in $MgCl_2$ solution in the capillary having the radius larger than R_i above which the values of $1/b_2'$ are positive. Therefore, with K-90 solution in water and $MgCl_2$ solution reported in the previous paper[15] the σ_2 values with the slope having a positive $1/b_2'$ will also be expected if the experiment is carried out using the viscometers having much larger capillary radius than those used in the previous study.[15]

As shown in the previous papers,[12,15] the dependence of $\eta_\infty(=\eta_1)$ of the polymer solutions on the value of R will be explained as such a result of the decrease in the relaxation time of the solvent molecules near the wall compared with that of the bulk, because the rotational redistribution of the oriented PVP molecules in the preferred direction under the streamline of the flow may be geometrically hindered by the capillary wall and the resistance of the PVP molecules against the flow of the solvent molecules under the shear stress will become weaker near the wall than that in the bulk. From the above consideration, it may be expected that when the dissolved polymer molecules take a spherical form and have no tendency to orient under the streamline of the flow, the

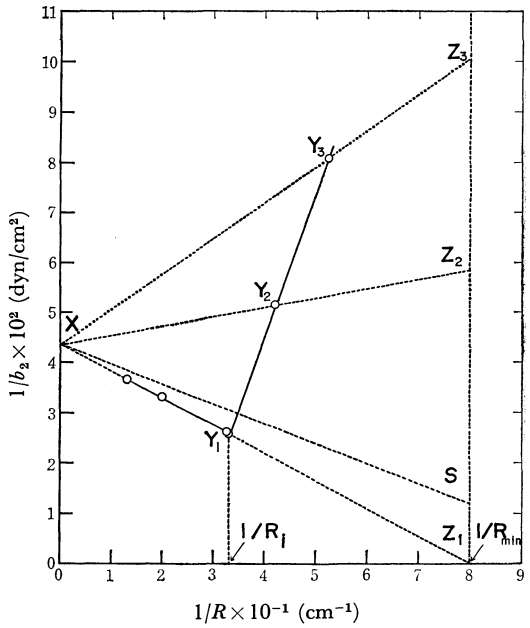

Fig. 3. Plots of $1/b_2$ *versus* $1/R$ for K-90 (2%) in water.

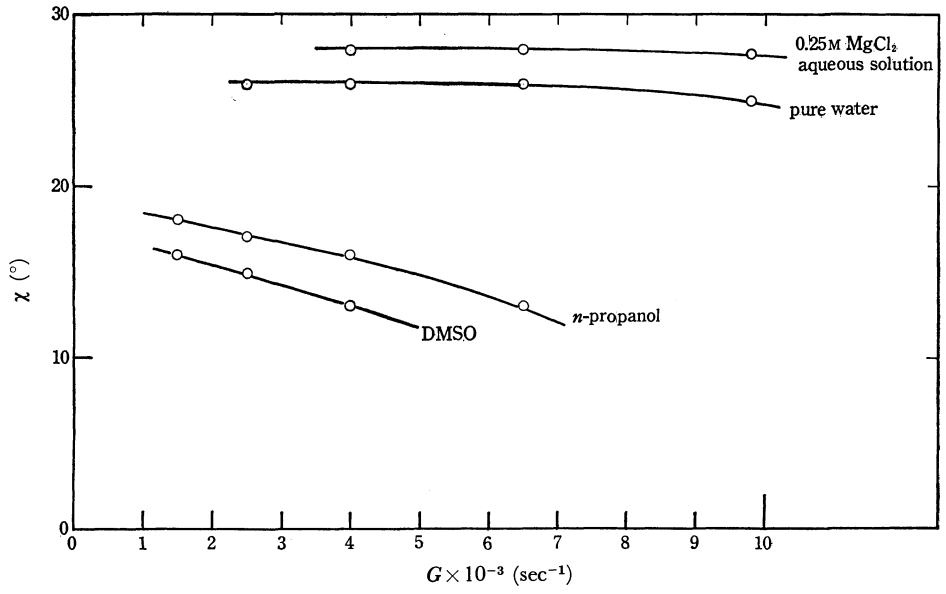

Fig. 4. Plots of extinction angle *versus* rate of shear for K-90 (1%) in various solvents.

observed viscosity would not change with the bore-size of the capillary.

The dependence of the extinction angle on the rate of shear for K-90 (1%) in various solvents is shown in Fig. 4. The PVP molecules in *n*-propanol, and in DMSO, in water and in 0.25M $MgCl_2$ aqueous solution show the tendency to orient under the streamline of flow. On the other hand, in the case of the solutions with the cosolute, the position of the arms of the cross of isocline could not be detected, *i. e.* extinction angle is equal to 45° in all rates of shear, and the orientation under the streamline of flow could not be observed. From these results, the PVP molecules may be expected to interact with the cosolute and to take spherical form in solution, because the degradation of the PVP molecules with the interaction with the cosolute could not be expected. Therefore, it may be concluded that the orientation of the polymer molecules under the streamline of flow is one of the necessary conditions for the appearance of the capillary size dependence of the viscosity.

For the viscosity at a finite rate of shear, the contribution of the non-Newtonian term of Eq. (1) must be considered. The geometric hindrance of the capillary wall to the free rotation of PVP molecules described above, would control the nature of the flow pattern of the polymer solution in the capillary tube independently of the magnitude of the pressure of the streamline. When the contribution of the non-Newtonian term to the solution viscosity depends solely on a compromise between the thermal motion of the PVP molecules and the orienting effect of the streamline, the value of σ_2, will take a value satisfying the following relation

$$-\frac{\sigma_1}{\eta_1'} = \frac{\sigma_2/a_2}{1/a^2b_2'}$$

or

$$\sigma_2 = -\sigma_1(1/b_2')/\eta_1' \qquad (4)$$

When the observed value of σ_2 is more positive than the one expected from Eq. (4), some additional structural formation of the PVP molecules near the wall will be expected to occur and on the contrary when more negative, the slippage of PVP molecules at the wall will occur. The formation of the above structure at the wall will be facilitated by the same geometric hindrance stated above to the thermal motion of the PVP molecules near the wall, because the interaction will be promoted between the wall surface and polymer molecules, *e. g.*, the adsorption of polymers on the wall *etc.*, thus, favoring the subsequent formation of some structure in the neighborhood of the wall.

The adsorption and the subsequent formation of some structure at the wall will be studied by the measurement of the change in concentration of the solution before and after the filtration through the fine sintered glass filter under gravity. The concentration of the PVP was determined by the spectroscopic measurement in the range of the wavelength between 220 and 240 mμ.*2 The first 1 m*l* of the filtrate of the 0.02 g/*l* solutions of PVP in water, in 0.25M $MgCl_2$ aqueous solution and in *n*-propanol showed the decrease in concentration of the magnitude of 5−10% compared with that of the original solution. But in the case of 0.01 g/*l* aqueous solution of PVP with 2.5×10^{-4}M tryptophan or 1.25×10^{-4}M benzoic acid, no appreciable change in the concentration was observed. Therefore, the occurrence of the adsorption of the PVP molecules on the glass wall will be one of the factors which determine the behavior of the flow of the polymer solution in capillary tube.

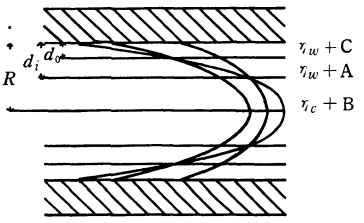

Fig. 5. Schematic model of the flow in the presence of wall layer.

Considering the above stated wall effect of the viscosity of the solutions, the flow model was proposed as shown in Fig. 5. The flowing liquid was assumed to be composed of a liquid layer near the wall (wall layer thickness d_i) and the bulk liquid. The former is divided into two layers at the distance of d_o ($d_o<d_i$) from the wall, one of which is situated on the near side of the wall, having the viscosity of η_w+C, and the other on the far-side, having the viscosity of η_w+A. The latter has the viscosity of η_c+B, to which the influence of the existence of the wall could not reach. The flow of these liquid layers may be represented by Poiseuille's law. Then the flow volume V of the liquid flowing through the tube in the interval of time t (sec) is

$$V=\frac{\pi Pt}{2L}\left[\frac{1}{\eta_w+C}\int_{R-d_o}^{R}(R^2-r^2)r\cdot dr+\frac{1}{\eta_w+A}\int_{R-d_i}^{R-d_o}(R^2-r^2)r\cdot dr+\frac{1}{\eta_c+B}\int_{0}^{R-d_i}(R^2-r^2)r\cdot dr\right.$$

*2 The PVP has the broad absorption peak with high intensity below 210 mμ, however, this range of wavelength could not be used for the concentration determination, because the $MgCl_2$ aqueous solution and *n*-propanol have also the intense absorption peaks in the same range of wavelength.

$$+ (R-d_o)^2\left\{\frac{1}{2(\eta_w+C)}[R^2-(R-d_o)^2] - \frac{1}{2(\eta_w+A)}[R^2-(R-d_o)^2]\right\} + (R-d_i)^2\left\{\frac{1}{2(\eta_w+A)}[R^2-(R-d_i)^2]\right.$$
$$\left. - \frac{1}{2(\eta_c+B)}[R^2-(R-d_i)^2]\right\}\Bigg] \quad (5)$$

where, P: driving pressure and r: distance from the center of tube.
The experimental value of the volume of flow is expressed as follows:

$$V = \pi PtR^4/8L\eta_{exp} \quad (6)$$

where η_{exp} is the viscosity determined experimentally. The values of V of both Eqs. (5) and (6) should be equal. Hence,

$$\eta_{exp} = \frac{(\eta_w+C)(\eta_w+A)(\eta_c+B)}{(\eta_w+C)(\eta_w+A) + (A-C)(\eta_c+B)D_0 + (\eta_c-\eta_w)(\eta_w+C)D_i + (B-A)(\eta_w+C)D_i} \quad (7)$$

where,
$$D_i = 4(d_i/R) - 6(d_i/R)^2 + 4(d_i/R)^3 - (d_i/R)^4$$
$$D_0 = 4(d_o/R) - 6(d_o/R)^2 + 4(d_o/R)^3 - (d_o/R)^4$$

Comparing Eq. (7) with Eq. (3)

$$\frac{\sigma_1 - \frac{\sigma_2}{a_2}}{R} = \frac{(\eta_c+B)\{(A-C)(\eta_c+B)D_0 + (\eta_c-\eta_w)(\eta_w+C)D_i + (B-A)(\eta_w+C)D_i\}}{(\eta_w+C)(\eta_w+A) + (A-C)(\eta_c+B)D_0 + (\eta_c-\eta_w)(\eta_w+C)D_i + (B-A)(\eta_w+C)D_i}$$

when $G \to 0$, $\eta_{exp} = \eta_1 + \frac{1}{a_2 b_2} = \eta_0$, and $\eta_c + B = \eta_1' + \frac{1}{a_2 b_2'} = \eta_0'$ (8)

When $(G/a_2)\to\infty$, the values of A, B, C, in above flow model are zero, *i. e.*, A, B, $C=0$, therefore, the flow model will be reduced to simpler one composed of the wall layer (thickness: d_i) having the viscosity of η_w and the bulk liquid of viscosity η_c as follows.[12]

$$\eta_{exp} = \eta_c[1-\{(\eta_c-\eta_w)D_i\}/\{\eta_w+(\eta_c-\eta_w)D_i\}] \quad (9)$$

where $\eta_c \geq \eta_{exp} \geq \eta_w$, since the values of $\eta_\infty(\eta_1)$ decrease with the decrease of capillary radii. Comparing the Newtonian term of Eq. (1) or Eq. (2) with Eq. (9),

$$\sigma_1 = \eta_c(\eta_c-\eta_w)D_iR/\{\eta_w+(\eta_c-\eta_w)D_i\},$$
$$\eta_{exp} = \eta_\infty = \eta_1 \quad \text{and} \quad \eta_c = \eta_1' \quad (10)$$

Comparing Eq. (10) with Eq. (8)

$$B = 1/a_2 b_2' \quad (11)$$

Under the conditions of $(G/a_2)\to 0$ and $\eta_0 \geq \eta_\infty$, the relations of A, B, $C>0$ and $d_o \leq d_i$ must be satisfied.

For the calculation of the value of d_i and d_o, the value of η_w must be determined. However, there is no satisfactory way, either experimentally or theoretically, of determining the value of η_w. Whenever the polymer molecules near the wall are oriented completely by the geometric hindrance of the capillary wall under the pressure of the streamline at G/a_2 or $G\to\infty$, the expected viscosity value of flowing polymer solution near the wall, could not be lower than that of the solvent or that calculated by the Einstein equation. In the following calculation, the value of the viscosity expected from the Einstein equation was arbitrarily taken as the value of η_w.

Moreover, when the line of the plot of experimental $1/b_2$ *vs.* $1/R$, taking a more negative slope than the one expected from Eq. (4), intersects the $1/R$ axis at a point (where $1/b_2=0$) having a smaller value of $1/R$ than the one corresponding to the η_w value on η_1 *vs.* $1/R$ plots, the value of viscosity corresponding to the $1/R$ where $1/b_2=0$ on the line of η_1 *vs.* $1/R$ plots must be taken as the value of η_w in order to satisfy the condition of $\eta_0 \geq \eta_1\ (\eta_\infty) \geq \eta_w$.

Applying the value of η_w to Eq. (9) with the aid of Eq.(10), values of d_i corresponding to each R will be calculated. The value of $1/R$ corresponding to the η_w above stated, on the line of η_1 *vs.* $1/R$ relation gives the maximum value of $1/R\,(=1/R_{\min})$ where Eq. (1) could hold. Therefore the value of $R_{\min}$ is the minimum radius below which the capillary bore-size dependence of the viscosity could not be observed.

In calculating the value of d_o, the values of A and C must be determined. The value of A is given by the product of $1/a_2$ times the value of $1/b_2$ (*e. g.* point S in Fig. 3) corresponding to the $1/R_{\min}$ on the line drawn from $1/b'_2$ (point X) with a slope of σ_2 satisfied by the Eq. (4). The value of C is obtained from the value of $1/b_2$ corresponding to $1/R_{\min}$ on the slope of experimental $1/b_2$ *vs.* $1/R$ relation. Applying these values of A and C with the value of B obtained with Eq. (11) and the values of η_c, η_w and d_i already obtained, to Eq. (7), the values of d_o corresponding to each R will be calculated.

The relationships between d_o or d_i and R obtained with 2% K-90 in water and 1% K-90 in DMSO are shown in Figs. 6 and 7. In the case of 2% K-90 in water as shown in Fig. 3, where the relation $1/b_2$ *vs.* $1/R$ has been represented by two straight lines crossing at a point of a certain

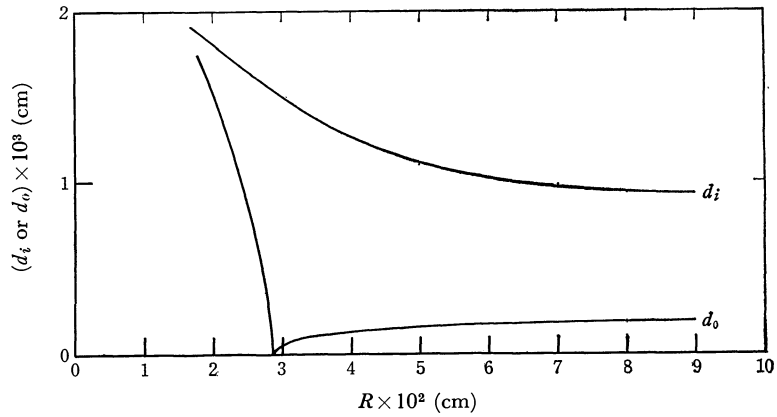

Fig. 6. Relation between d_i or d_o, and R, calculated from Eq. (7) and Eq. (9), with polymer K-90 (2%) in water, where $\eta_w=14.0\times10^{-3}$ (poise), $\eta_c=53.0\times10^{-3}$ (poise), $A=5.8\times10^{-3}$ (poise), $B=22.0\times10^{-3}$ (poise), $C=0$ (where $R > 0.0302$ (cm)) and $C=30\times10^{-3}$ (poise) (at $R=0.0238$ (cm)) and so on.

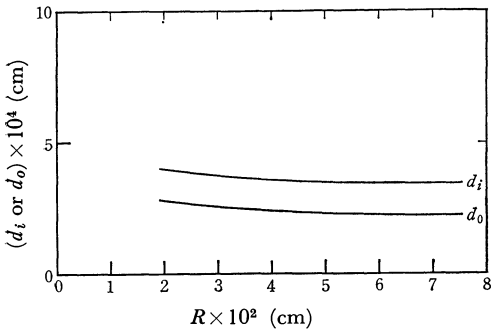

Fig. 7. Relationship between d_i or d_o and R, calculated from Eq.(7) and Eq. (9), with polymer K-90 (1%) in DMSO, where $\eta_w=1.00\times10^{-2}$ (poise), $\eta_c=42.4\times10^{-3}$ (poise), $A=1.63\times10^{-3}$ (poise) $B=6.9\times10^{-3}$ (poise), $C=11.1\times10^{-3}$ (poise).

radius (R_t), the value of C for the range of $1/R$ smaller than the value of $1/R_t$, is given by the product of $1/a_2$ times the value of $1/b_2$ (point Z_1 in Fig. 3) obtained on the extrapolated line from the experimental $1/b_2$ *vs.* $1/R$ relationship (line XY_1) of the corresponding range of $1/R$ as stated above. In the range of $1/R$ above the $1/R_t$, the value of C is obtained from the value of $1/b_2$ (point Z_2 or Z_3) corresponding to $1/R_{min}$ on the straight line drawn from $1/b_2'$ (point X) through the experimental $1/b_2$ (point Y_2 or Y_3); therefore, in this range not only the values of d_o changes with R but also the values of C changes with R. The results obtained with K-90 2.0% aqueous solution show that in a larger capillary bore the nature of capillary dependence of the viscosity of the solution at $G/a_2\rightarrow0$ may be predominantly determined by the slippage of the PVP molecules at the wall, and in a smaller capillary bore it may be determined by the existence of the some structure formed at the wall.

The abnormal phenomenon observed with K-90 in water, may be expected to occur under the conditions as follows. As shown in Figs. 3 and 8, the experimental results that the relation $1/b_2$ *vs.* $1/R$ or η_0 *vs.* $1/R$ must be represented by two straight lines, were obtained with K-90 aqueous solutions in the concentration range of 0.5—2.0%; however, in the case of K-30 aqueous solution, such a result was obtained only with the solution of such a high concentration as 5.6%. On the other hand, the tendency of the increase of η_0 with the decrease of capillary radius is always observed with the aqueous solution of PVP irrespective of molecular weight; therefore, this tendency may be said to be the general character of the flow of the PVP aqueous solution in a capillary and may be brought about

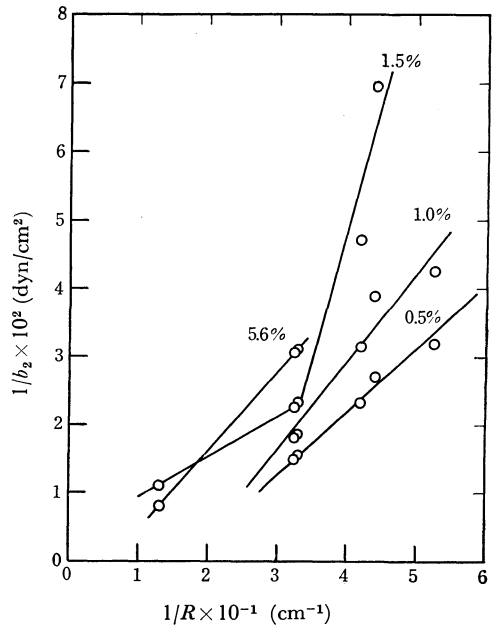

Fig. 8. Plots of $1/b_2$ *versus* $1/R$ for K-90 (1.5%, 1.0%, 0.5%) and K-30 (5.6%) in water.

by the poor nature of water as solvent. In water, compared with the case of good solvent, the adsorption of PVP molecules on the wall surface occurs more easily and subsequent formation of a rather stiff structure is facilitated by the more frequent contacts and the stronger entanglement of PVP molecules under the geometric hindrance of the wall to the thermal motion of the PVP molecules. Such a sturcture at the wall may be formed more easily in a narrower tube than in a wider one, because the geometric hindrance of the wall to the thermal motion of the PVP molecules will be more enhanced in the narrower capillary tube in which the hindrance for the rotational motion of the PVP molecules in the shear surface will occur more frequently than in the case in a wider tube. The flow behavior of the solution in the capillary tube of radius $R_{\min}$ is determined by the structure at the wall as stated above.

On the other hand, when the concentration of PVP in the solution becomes higher or the molecular weight becomes larger, the more frequent contacts and stronger entanglements of PVP molecules in the solution will assist the formation of a certain structure throughout the solution and the PVP molecules near the wall will be forced to move with the adjacent molecules existing at the far-side of the wall, that is, the slippage of the PVP molecules at the wall will occur. Such a slippage will occur in the case of the flow of the solution in the capillary tube of radius larger than R_i.

In the solution flowing through the capillary tube of radius between R_i and $R_{\min}$ the actual behavior of the PVP molecules at the wall will be determined by a compromise between the two effects stated above on the PVP molecules near the wall. A similar situation will also hold with the solution of PVP in $MgCl_2$ aqueous solution.

As shown in Fig. 9, when the value of η_0 is larger than that of η_0', the calculated value of d_o (this distance is designated as d_c) becomes larger than that of d_i and this does not satisfy the prerequisite of $d_o < d_i$. The change of d_i and d_c with R is shown in Fig. 10. This result may be brought about under circumstances where the formation of the structure near the wall extends from the wall to the central bulk liquid beyond the region of the wall layer. The result also shows the development of the very viscous layer (thickness; $d_c - d_i$, viscosity $= (\eta_w + A) + (\eta_w + C) + (\eta_c + B)$) on the far-side of the wall and in contact with the wall layer (thickness; d_i, viscosity $= \eta_w + C$) with the disappearance of the layer of viscosity of $(\eta_w + A)$. Referring to the observation made by Segré and Silberberg[17] with the dilute suspension of macroscopic spherical particles of polymethyl methacrylate in a liquid of high viscosity that the collection of the particles occurs in a thin annular region within the flowing liquid through a tube, such a development of high viscous layer as stated above is not an unrealizable phenomenon. Furthermore by the application of the present treatment to the analysis of the capillary bore-size dependence of the viscosity of blood,[18] which shows a similar characteristics as shown in Fig. 9, a possible mechanism for the above phenomenon will be obtained.

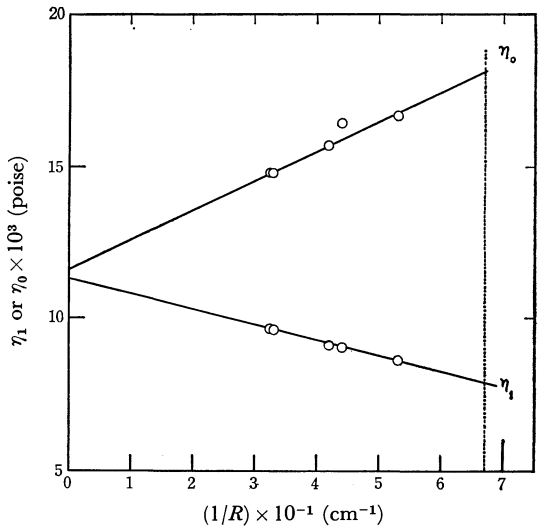

Fig. 9. Plots of η_1 *versus* $1/R$, and η_0 *versus* $1/R$, for K-30 (1%) 0.25 M $MgCl_2$ aqueous solution, where $\eta_w = 7.9 \times 10^{-3}$ (poise), $\eta_c = 11.3 \times 10^{-3}$ (poise), $A = 0.21 \times 10^{-3}$ (poise), $B = 0.3 \times 10^{-3}$ (poise), $C = 10.2 \times 10^{-3}$ (poise).

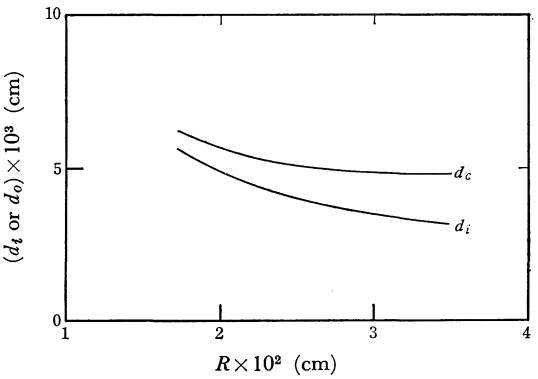

Fig. 10. Plots of d_c or d_i *versus* R for K-30 (1%) 0.25 M $MgCl_2$ aqueous solution.

The authors wish to thank Mr. Seizo Takahashi, Eizaburo Watanabe and Kenji Ueda for their kind assistance in the experiment. The cost of this research has been partly defrayed by a grant of the Ministry of Education.

17) G. Segré and A. Silberberg, *Nature*, **189**, 209 (1961).

18) T. Mineshita, Y. Nakane, T. Watanabe and S. Ono, unpublished work read at the 19th symposium of Colloid Chemistry, Nagoya, Nov. 1, 1966.

BULLETIN OF THE CHEMICAL SOCIETY OF JAPAN VOL. 42 594—599 (1969)

The Flow Properties of γ-Polyglutamic Acid Solutions in Capillary*1

Takeshi MINESHITA, Shigeru MATSUMURA, Hiromi ONO, Takehiko WATANABE and Sôzaburo ONO

Laboratory of Biophysical Chemistry, College of Agriculture, University of Osaka Prefecture, Sakai, Osaka

(Received June 3, 1968)

Dependence of the viscosity of the solution of γ-polyglutamic acid in eater at various pH's on the bore-size of the capillary viscometer has been studied at 25°C at various concentrations (0.01—0.05 g/100 m*l*). Measurements were carried out with a Maron-Belner type low shear capillary viscometer with various capillary radii (1.9×10^{-2}—7.6×10^{-2} cm) within the shear stress range 0.2—20 dyn/cm^2 at the capillary wall. The polymer solutions showed a non-Newtonian flow behavior and a capillary bore-size dependence and both of these properties were diminished with the decreasing of pH. This capillary bore-size dependence may be attributed to the geometric hindrance of the capillary wall to the thermal motion of the polymer molecules near the wall. The dissolved state of the polymer molecules in solutions of various pH's has been studied by means of optical rotatory dispersions, flow birefringence and intrinsic viscosity. The dissolved state of the polymer solution as well as the capillary bore-size dependence were sensitive to pH. The polymer molecule in neutral and alkaline media may be in the form of a highly expanded chain and in acid medium in a contracted form having a some ordered chain conformation.

In the previous papers,[1-3] the dependence of the viscosity of polyvinylpyrrolidone solutions on the bore-size of capillary viscometer was reported and the flow of the polymer solution through the capillary was treated by assuming the existence of the double wall layer which is owing to the geometric hindrance of the capillary wall to the thermal motion of the polymer molecules near the wall in the flowing liquid.

In this paper, the similar treatments as stated above, were attempted to the solution of γ-polyglutamic acid, as an example of polyelectrolytes, and also the study on the dissolved state of γ-polyglutamic acid was made concerning the appearance of the capillary bore-size dependence of the viscosity.

Experimental

Materials. γ-Polyglutamic acid, or γ-PGA is a polymer of glutamic acid linked through the γ-carboxyl and α-amino group and was supplied by Dr. Sawao Murao, Laboratory of Fermentational Chemistry of University of Osaka Prefecture. This polymer is produced by the *Bacillus subtlis uar. polyglutamicum* from glucose and urea and composed of about 60% D-glutamic acid and 40% L-anomer. Molecular weight of the polymer is estimated as more than 1000000. More details for the polymer will be presented by Murao in elsewhere.[4]

Measurements. A Maron-Belner type capillary viscometer[5] suitable for the study of the flow of non-Newtonian fluids at the low shear stress of 0.2 to 20 dyn/cm^2 was used. Details on viscosity measurements was the same as described in the previous paper.[1]

Viscometers used for the determination of intrinsic viscosity were the Ubbelohde dilution type having the efflux time of about 180 sec for water at 25°C at which temperature the measurements were made.

The extinction angle, χ, and the birefringence, Δn, were measured with a Rao Flow Birefringence Viscometer Model No. B-23 over the gradient range from 50 to 5000 sec^{-1} at 25±0.01°C.

Optical rotatory dispersion (ORD) measurements were carried out with a Yanagimoto ORD-185. All measurements were made in quartz cells with an optical path of 0.10, 0.20, or 0.50 cm at 25±0.01°C.

Results and Discussion

The plots of viscosity *vs.* rate of shear of γ-PGA solution (0.05%) at pH 2.2 are shown in Fig. 1(a). Non-Newtonian flow behavior and capillary bore-size dependence were observed in all ranges of

*1 Partially presented at the 20th Symposium of the Colloid Chemistry, Hokkaido, Aug. 31, 1967.

1) T. Mineshita, T. Watanabe and S. Ono, This Bulletin, **40**, 2217 (1967).

2) T. Mineshita, T. Watanabe and S. Ono, *J. Polymer Sci.* Part C, **23(2)** (1969) in press. (Study on Wall Effect for Flow of Polymer Solution in Capillary).

3) T. Watanabe, T. Mineshita and S. Ono, This Bulletin, **42**, 583 (1969).

4) S. Murao, *Kobunshi* (*High Polymers, Japan*), **16**, 1204 (1967); *Nippon Nogeikagaku Kaishi* (*J. Agri. Chem. Soc. Japan*), in press.

5) S. H. Maron and R. J. Belner, *J. Appl. Phys.*, **26**, 1457 (1955).

rate of shear studied for the solution of higher concentration, while in lower concentration, the flow property approaches to one of Newtonian character and the capillary bore-size dependence becomes slight. The other examples of the plots of viscosity *vs.* rate of shear of γ-PGA solution (0.01%) at pH 7.1 in various capillaries are shown in Fig. 1(b). It is obviously shown that both

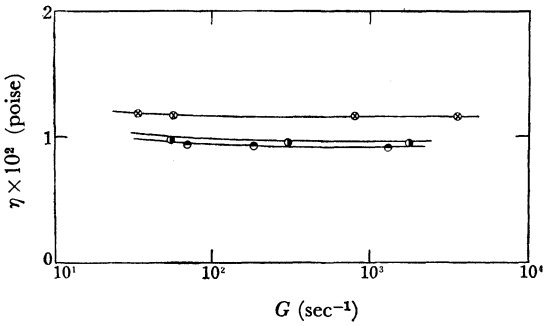

Fig. 1(a). Plots of viscosity *versus* rate of shear for γ-PGA (0.05 g/100 m*l*) aqueous solution (pH= 2.2).
⊗ R=0.0761 cm; ◑ R=0.0302cm;
◓ R=0.0228 cm

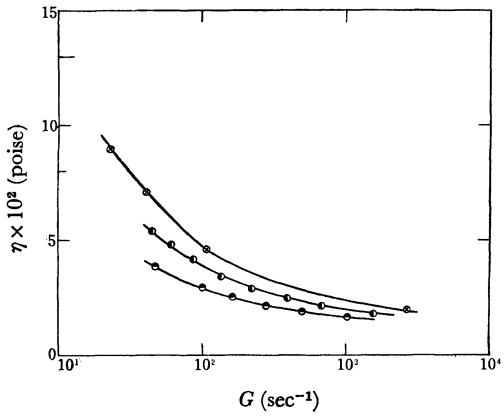

Fig. 1(b). Plots of viscosity *versus* rate of shear for γ-PGA (0.01 g/100 m*l*)aqueous solution (pH=7.1).
⊗ R=0.0761 cm; ◐ R=0.0502 cm;
◓ R=0.0302 cm

the non-Newtonian nature and the capillary bore-size dependence of the viscosity were more enhanced in an neutral solution, especially in lower ranges of shear stress.

The experimental results were expressed by the modified formula of the generalized Ree-Eyring equation[1,6,7] for a flow system containing one Newtonian flow unit and one non-Newtonian unit which includes the additional terms dependent on the capillary bore-size as follows.

$$\eta = \left(\eta_1' - \frac{\sigma_1}{R}\right) + \left(\frac{1}{b_2'} + \frac{\sigma_2}{R}\right)\left(\frac{1}{a_2}\right)\left(\frac{a_2}{G}\right) \sinh^{-1}\left(\frac{G}{a_2}\right) \tag{1}$$

where $\eta_1 = \eta_1' - \frac{\sigma_1}{R}$ and $\frac{1}{b_2} = \frac{1}{b_2'} + \frac{\sigma_2}{R}$,

$\sigma_1 = -\mathrm{d}(\eta_1)/\mathrm{d}\left(\frac{1}{R}\right)$,

$\sigma_2 = \mathrm{d}\left(\frac{1}{b_2}\right)\Big/\mathrm{d}\left(\frac{1}{R}\right)$, $\eta_1 = x_1\beta_1/\alpha_1$,

$a_2 = 1/\beta_2$, and $b_2 = a_2/x_2$,

and x is the fractional area on a shear surface occupied by the flow unit, β is the relaxation time of the flow unit, and α is the ratio of shear volume to twice the average kinetic energy of the flow unit; the subscripts 1 and 2 of the parameters refer to the Newtonian and non-Newtonian flow units, respectively and R is the radius of the capillary tube.

The flow represented by Eq. (1) becomes Newtonian under the condition of $(G/a_2)\to\infty$, and $(G/a_2)\to 0$, and the values of viscosity, η_∞ (at $G/a_2\to\infty$) and η_0 (at $G/a_2\to 0$) are reduced to

$$\eta_\infty = \eta_1 = \eta_1' - \frac{\sigma_1}{R} \tag{2}$$

and

$$\eta_0 = \eta_1 + \frac{1}{a_2 b_2} = \left(\eta_1' - \frac{\sigma_1}{R}\right) + \left(\frac{1}{a_2}\right)\left(\frac{1}{b_2'} + \frac{\sigma_2}{R}\right)$$

$$= \left(\eta_1' + \frac{1}{a_2 b_2'}\right) - \left(\frac{\sigma_1 - \frac{\sigma_2}{a_2}}{R}\right) = \eta_0' - \frac{\left(\sigma_1 - \frac{\sigma_2}{a_2}\right)}{R} \tag{3}$$

The values of η_1, a_2, b_2 and $\eta_0\left(=\eta_1 + \frac{1}{a_2 b_2}\right)$ obtained with Eq. (1) are shown in Table 1.

The relationships between $\eta_1(=\eta_\infty)$ and $1/R$ for γ-PGA solutions at various pHs are shown in Fig. 2. For comparing this relation for γ-PGA with that for PVP solution, one of the typical one obtained with PVP (K-90 0.5%) 0.25M $MgCl_2$ aqueous solution, is also shown in Fig. 2

Plots of η_1 *vs.* $1/R$ show approximately linear relation with negative slope of σ_1 in all examples. Therefore, also in the case of γ-PGA solutions, this dependence of η_1 of the polymer solution on R may be treated as the similar dependence as presented in preceding paper[1] for PVP in various

6) S. Glasstone, K. J. Laidler and H. Eyring, "The Theory of Rate Process," McGraw-Hill, New York (1941), p. 477.

7) T. Ree and H. Eyring, *Rheology* (ed. Eirich), **2**, Chap. 3, p. 83 (1958).

TABLE 1. PARAMETERS OF VISCOSITY EQUATION (at 25°C)

$R\times10^2$ (cm)	$\eta_1\times10^3$ (poise)	b_2	$(\eta_1+(1/a_2b_2))\times10^3$ (poise)
γ-PGA (0.05%) in water (pH=2.2) where a_2=5.0			
7.61	11.6	200	12.6
3.02	9.3	200	10.3
2.28	9.0	200	10.0
γ-PGA (0.01%) in water (pH=7.1) where a_2=5.0			
7.61	16.8	1.3	170.6
5.02	15.7	1.6	140.7
3.02	14.8	2.5	94.8

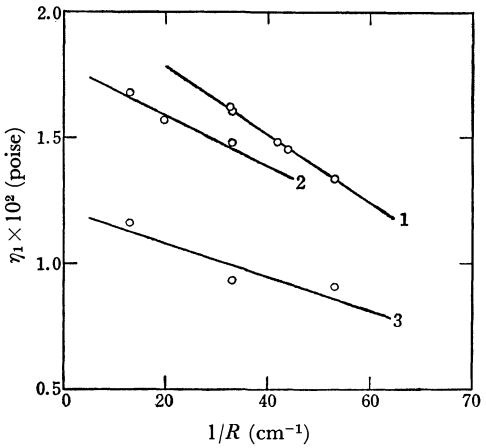

Fig. 2. Plots of η_1 *versus* $1/R$ for γ-PGA and PVP solutions.
(1) K-90 (0.5%) in 0.25 M $MgCl_2$ aqueous solution
(2) γ-PGA (0.01%) aqueous solution (pH=7.1)
(3) γ-PGA (0.05%) aqueous solution (pH=2.2)

solvents. This dependence will be due to the decrease in relaxation time of the solvent molecules near the wall compared with that of the bulk, because of the geometric hindrance of the capillary wall to the thermal motion of the polymer molecules oriented in the preferred direction under the streamline of the flow near the wall. And the resistance of the polymer molecules against the flow of the solvent molecules under the shear stress will become weaker near the wall than that in the bulk; this wall effect on the orientation of the polymer molecules will extend a certain distance from the wall into the central part of the solution in a capillary. Thus, as shown in preceding paper,[1] the viscosity of the solution in the narrower capillary will decrease compared with that in the wider one.

The relationships between $1/b_2$ and $1/R$ for γ-PGA solutions at various pHs are shown in

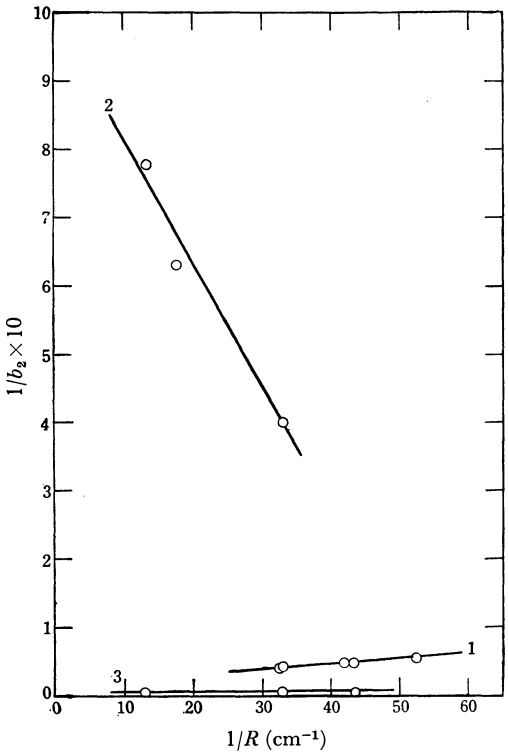

Fig. 3. Plots of $1/b_2$ *versus* $1/R$ for γ-PGA and PVP solutions.
(1) K-90 (1.5%) in *n*-propanol
(2) γ-PGA (0.01%) aqueous solution (pH=7.1)
(3) γ-PGA (0.05%) aqueous solution (pH=2.2)

Fig. 3. A typical plot of PVP obtained with K-90 (1.5%) *n*-propanol solution is compared with that of γ-PGA solution. Plots of $1/b_2$ *vs.* $1/R$ for PVP solution in *n*-propanol show the linear relation, of which slope σ_2 takes a positive value, while the one for γ-PGA solution at pH 7.1 shows a negative one, and $1/b_2$ decreases with the increase of $1/R$.

When no additional effect of the wall on the flow of the polymer solution will occur with the decrease of rate of shear except the one considered in the case of η_∞ (G/a_2 or $G\to\infty$), the following relationship must be held between σ_1 and σ_2.

$$-\frac{\sigma_1}{\eta_1'}=\left(\frac{\sigma_2}{a_2}\right)\Big/\left(\frac{1}{a_2b_2'}\right)$$

or

$$\sigma_2=-\sigma_1\left(\frac{1}{b_2'}\right)\Big/\eta_1' \qquad (4)$$

The experimental value of σ_2 obtained with γ-PGA solutions at pH 7.1 is more negative than the calculated one by Eq.(4). This result suggests the occurence of the slippage of the γ-PGA molecules at the wall because of the existence of the

repulsive force between the negatively charged glass surface and negatively charged γ-PGA molecules owing to the ionization of the carboxyl group of the polymer.

According to the flow equation based on the double wall layer model presented in the previous paper[3] experimental value of viscosity(η_{exp}) is represented as follows;

$$\eta_{exp} = \frac{(\eta_w+C)(\eta_w+A)(\eta_c+B)}{(\eta_w+C)(\eta_w+A) + (A-C)(\eta_c+B)D_o + (\eta_c-\eta_w)(\eta_w+C)D_i + (B-A)(\eta_w+C)D_i} \quad (5)$$

where $D_i=4(d_i/R)-6(d_i/R)^2+4(d_i/R)^3-(d_i/R)^4$ and $D_0=4(d_o/R)-6(d_o/R)^2+4(d_o/R)^3-(d_o/R)^4$

Where $(G/a_2)\to\infty$, the values of A, B, C in above flow equation are zero, *i. e.*, A, B, $C=0$. Therefore, the flow model will reduced to simpler one composing of the wall layer (thickness: d_i) having the viscosity of η_w and the bulk liquid of viscosity η_c, and under the conditions of $(G/a_2)\to 0$, where $\eta_0\geq\eta_\infty$, the relations, A, B, $C\geq 0$ and $d_o\leq d_i$ are held.

Combining Eq. (1) with Eq. (5) as the same manner as stated in the previous paper,[3] the values of d_o and d_i corresponding to each R were calculated as shown in Fig. 4.

With the solution at pH 2.2, the following relationship holds among the viscosity of the each layer $\eta_c+B>\eta_w+C>\eta_w+A$ as in the case of PVP in *n*-propanol and this fact suggests the some structural formation at the wall in the flowing liquid in capillary tube. On the contrary, with the solution at pH 7.1, where $\eta_c+B>\eta_w+A>\eta_w+C$, the slippage of the polymer molecules will occur at the wall surface.

The structural formation at the wall was ascertained by the measurement of the concentration change of the solution between the one before and after the filtration through the glass filter as the same manner as stated in the previous paper.[3]

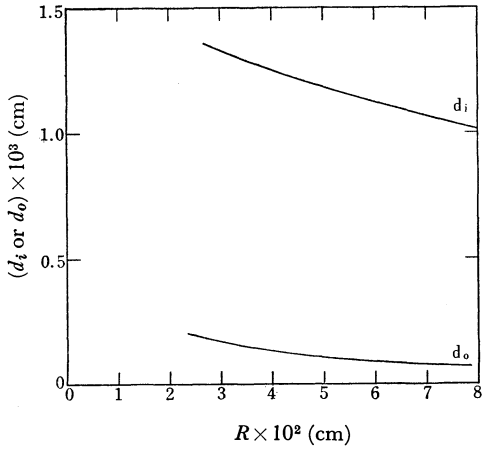

Fig. 4(b). Plots of d_i or d_o *versus* R for γ-PGA (0.01 %) aqueous solution (pH=7.1), where $\eta_w=12.0\times 10^{-3}$ (poise), $\eta_c=18.0\times 10^{-3}$ (poise), $A=125\times 10^{-3}$ (poise), $B=187\times 10^{-3}$ (poise), and $C=0$.

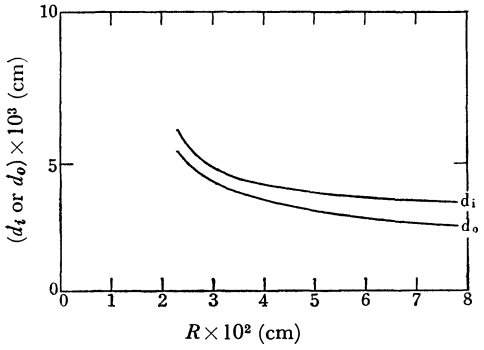

Fig. 4(a). Plots of d_i or d_o *versus* R for γ-PGA (0.05%) aqueous solution (pH=2.2), where $\eta_w=8.0\times 10^{-3}$ (poise), $\eta_c=12.5\times 10^{-3}$ (poise), $A=0.64\times 10^{-3}$ (poise), $B=1.0\times 10^{-3}$ (poise), $C=1.0\times 10^{-3}$ (poise).

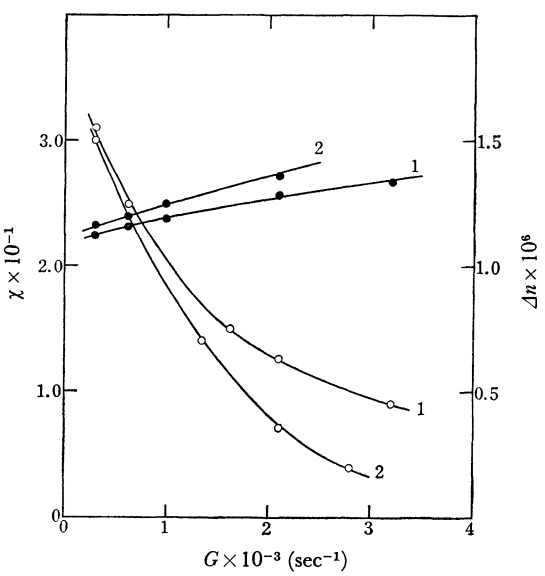

Fig. 5. Relationship between χ and Δn for γ-PGA solutions (○) extinction angle (χ); (●) birefringence (Δn), 1, γ-PGA (0.01%) in water (pH=7.0); 2, γ-PGA (0.01%) in water (pH=11.2).

With neutral solution no appreciable change in concentration was observed in spite of the very high

value of intrinsic viscosity as stated below. Whereas in acid solution the decrease in concentration of γ-PGA by the filtration was observed and this fact will support the above assumption of the some structural formation at the wall in acid medium.

For the interpretation on the cause of the marked difference in flow of the two kinds of solutions (at low pH and neutral or higher pH) the experiments have been made as follows. The plots of extinction angle and the birefringence of the polymer solution against the rate of shear are shown in Fig. 5. The lower extinction angle and higher flow birefringence was observed with the increase of rate of shear for the polymer solution of neutral or higher pH and it obviously shows that the polymer molecules would orient remarkably. However, at lower pH, the position of the arms of the cross of isocline could not be detected in all rates of shear, and the orientation under the streamline of the flow could not be observed. It may be assumed that the γ-PGA molecules in acid medium will actually orient under the streamline of the flow because if the molecules did not show the tendency to orient, the capillary bore-size dependence of the viscosity must disappear as the case of the PVP aqueous solution with cosolute as stated in the previous paper.[3] The change in the degree of the orientation of the polymer molecules at each pH may be due to the change in the dissolved states of the polymer in each solvents.

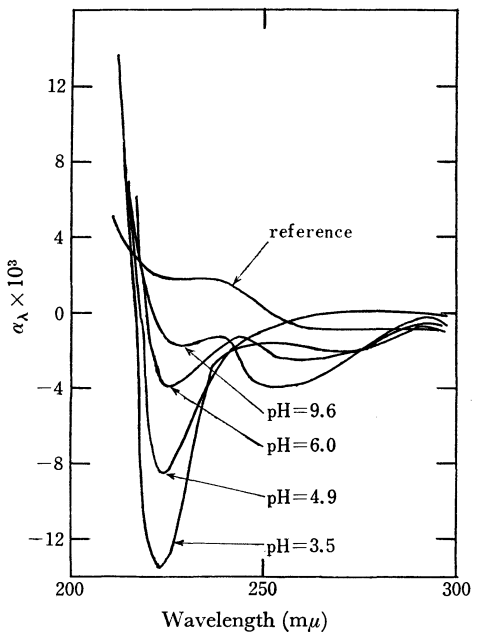

Fig. 6. Optical rotatory dispersion curves for γ-PGA (0.012%) in water.

The change in the conformation of the polymer molecules at various pH's, will be reflected in ORD curves in ultraviolet zone. The curves are shown in Fig. 6. The curves, at the lower pH show a negative Cotton effect with a trough at 225 mμ and the depth of the trough becomes deeper with decreasing in pH. Dependence of the ORD curves on pH values shows obviously the conformation change of the polymer molecules, from the disordered conformation at higher pH to the more ordered one with the decrease of the pH values.

The change in the hydrodynamic volume of the polymer molecules in solution may be estimated by the change in the value of the intrinsic viscosity

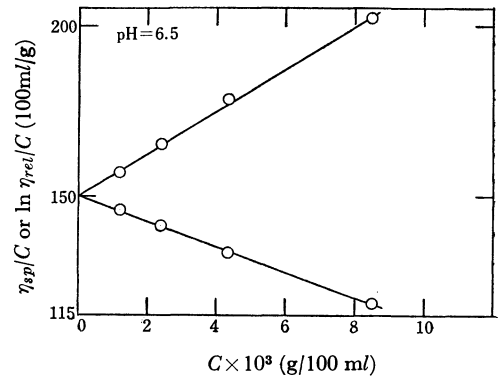

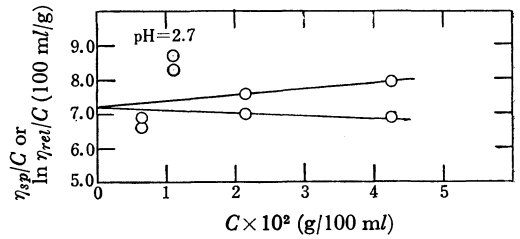

Fig. 7. Plots of η_{sp}/C or ln η_{rel}/C *versus* C for γ-PGA solutions.

between the solutions at pH 2.7 and 6.5. The results are shown in Fig. 7. The intrinsic viscosity at higher pH is very larger compared with that of the lower one: at pH 6.5 about 150 (100 ml/g) and at pH 2.7 about 7.0 (100 ml/g). This fact shows that the polymer molecules in higher pH solution will be dissolved as the more expanded form than that in the lower one.

Thus, from the results of flow birefringence, optical rotatory dispersion, and intrinsic viscosity, the polymer molecule in neutral and alkaline media will be in highly expanded chain conformation while that in the acid medium in contracted form having a some ordered conformation. Therefore, the polymer molecule in neutral and alkaline media will be as the form readily to orient under the

streamline of the flow, while that in the acid medium will be in the contracted form of which the tendency to orient under the streamline of the flow could not be obviously observed by the flow birefringence measurement because the length of the dissolved molecules becomes shorter than the minimum length necessary for the observation with the apparatus. Therefore, it may be said that the measurement of the capillary bore-size dependence of the polymer solution is a sensitive method for the estimation of the anisotropy of the shape of the dissolved polymer molecules.

BULLETIN OF THE CHEMICAL SOCIETY OF JAPAN VOL. 42 599—607 (1969)

Kinetics and Mechanism of Oxidation of D-Glucose and D-Fructose by Potassium Ferricyanide in the Presence of Ammonia

K. C. GUPTA

Chemistry Department, University of Lucknow, India

and M. P. SINGH

Chemistry Department, University of Allahabad, India

(Received January 20, 1968)

The reaction rate is independent of the concentration of ferricyanide ion and directly proportional to both the reducing sugar and ammonia concentration. The reaction is of general basic catalysis in nature. The reaction rate is decreased with the addition of ammonium chloride due to common ion effect. The catalytic constants k_{OH^-} and k_{NH_3} have been calculated graphically. The reaction rate is, also, decreased with the gradual decrease in dielectric constant of the solvent and increased with the gradual increase in ionic strength. The rate expression obtained is as:

$$-\frac{d[Fe\,y^{3-}]}{dt} = k_1[NH_3]\,[\text{Reducing Sugar}]$$

Conant, Aston and Tonberg[1] have studied the oxidation quantitatively of four aldehydes and D-glucose, D-fructose and D-arabinose by alkaline molybdicyanide, tungsticyanide and ferricyanide potentiometrically. They found that more alkaline the solution the more rapid was the reaction. They have also considered that the initial stage of the oxidation of an organic substance by an electron abstracting agent might be fast, reversible and pH dependent. Speakman and Waters,[2] Hinshelwood and Shorter,[3] Drummond and Waters[4] have also reported the enolization to be necessary prior to oxidation of aldehydes and ketones. The most systematic study of the kinetics of oxidation of reducing sugars in alkaline medium by bivalent copper by Singh, Krishna and Ghosh[5] in the presence of complexing agents, Singh and Singh[6] in absence of complexing agents and by alkaline hexacyanoferrate(III) by Nath and Singh[7] has been done. They have reported the reaction rate to be independent of oxidizing agent and directly proportional to reducing sugar and alkali concentration. The similar results have been obtained by Srivastava, Nath and Singh[8a,8b] in the oxidation of aldopentoses and disaccharides.

The present study deals with the kinetics of

1) J. B. Conant, J. G. Aston and C. O. Tonberg, *J. Am. Chem. Soc.*, **52**, 407 (1930).

2) P. T. Speakman, and W. A. Waters, *J. Chem. Soc.*, **1955**, 40.

3) C. Hinshelwood and J. Shorter, *ibid.*, **1950**, 3276.

4) A. Y. Drummond and W. A. Waters, *ibid.*, **1950**, 3425.

5) M. P. Singh, B. Krishna and S. Ghosh, *Z. Physik. Chem.*, **204**, 1 (1955).

6) S. V. Singh and M. P. Singh, *Z. Physik. Chem. (Frankfurt)*, **50**, 1/2 (1966).

7) N. Nath and M. P. Singh, *J. Phys. Chem.*, **69**, 2038 (1965).

8) a) R. K. Srivastava, N. Nath and M. P. Singh, This Bulletin, **39**, 833 (1966). b) R. K. Srivastava, N. Nath and M. P. Singh, *Tetrahedron*, **23**, 1189 (1967).

oxidation of D-glucose and D-fructose by potassium ferricyanide in the presence of weak base ammonia. The effect of solvent (dielectric constant) and ionic strength on the reaction rate has also been studied.

Experimental

The course of the reaction has been followed by estimating unreduced potassium ferricyanide at different intervals of time iodometrically. The reactions were started by mixing the fresh solution of reducing sugar with potassium ferricyanide and ammonia kept in a bottle in an electrically maintained thermostat at constant temperature which has an accuracy of ± 0.1°C.

Potassium ferricyanide, sulphuric acid, sodium thiosulphate, potassium ferrocyanide and D-glucose used were of B.D.H. (Analar) grade. Ammonia, Ammonium chloride B.D.H. (L.R.) and E. Merck sample of potassium iodide and D-fructose were also used. The values for the dielectric constant of alcohol-water mixture were obtained with a cell of 1.68$\mu\mu$f capacity by a dielectrometer (Dielkometer Type TBK No. 53015) working on the principle of heterodyne beat method.

Results and Discussion

The kinetics of oxidation of D-glucose[9] has been done by us. The next series of experiments have been performed by following the kinetics of oxidation of D-fructose by potassium ferricyanide in the presence of ammonia. The results obtained are similar to that of D-glucose except that the D-fructose has a higher rate (4.8 times) of oxidation.

Order of Reaction with Respect to Ferricyanide Ion. The order of the reaction with respect to ferricyanide ion has been determined by keeping the concentration of D-fructose high. The standard zero-order velocity constant (k_s) has been calculated by multiplying k_0 ($\Delta x/\Delta t$) by the strength (s) of sodium thiosulphate used divided by aliquot (v) sucked *i. e.* $k_s = k_0 \times s/v$. The following Tables 1 and 2 and the summarized Table 3 show the same k_s values at increasing concentration of potassium ferricyanide at constant concentration of other reactants. This indicates that the reaction rate is independent of ferricyanide ion. Also, the results of Table 1 have been shown graphically in Fig. A, in which the molar concentration of remaining ferricyanide ion has been plotted against time t. A straight line after slight induction period is obtained. From the slope the k_s value comes out to be 6.66×10^{-5} mol $l^{-1} \cdot min^{-1}$ which is identical to the value of k_s calculated in Table 1. This further confirms that reaction rate is independent of ferricyanide ion.

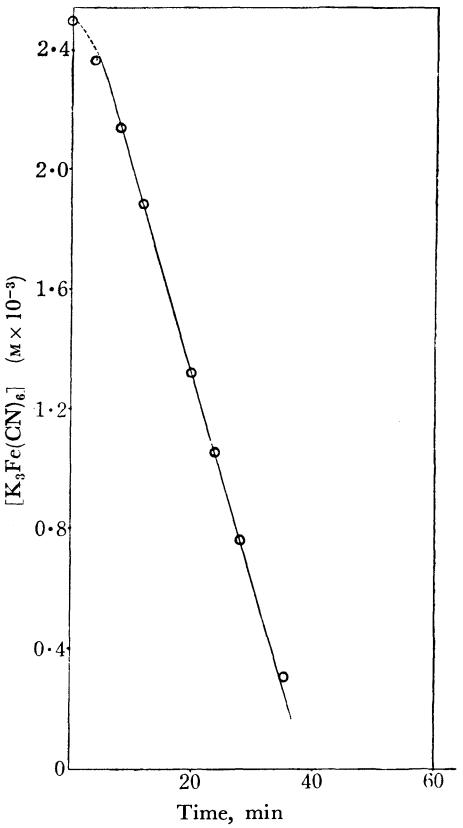

Fig. A

Temperature 40°C
Zero order plot
$[K_3Fe(CN)_6] = 2.50 \times 10^{-3}$M
[D-Fructose] $= 1.00 \times 10^{-2}$M
$[NH_3] = 1.00 \times 10^{-1}$N
Frome slope
$k_s = 6.66 \times 10^{-5}$ mol l^{-1} $^{-1}$mn^{-1}

TABLE 1

Temp.: 40°C
$[K_3Fe(CN)_6] = 2.5 \times 10^{-3}$M, $[NH_3] = 1.00 \times 10^{-1}$N
[D-Fructose] $= 1.00 \times 10^{-2}$M

Time min	N/752 hypo ml	$k_0 = \frac{\Delta x}{\Delta t}$
0	9.40	—
4	8.90	0.125
8	8.06	0.210
12	7.10	0.240
20	5.00	0.262
24	4.00	0.250
28	2.88	0.280
35	1.20	0.240
∞	0.00	

Mean k_0 0.247
(Neg. 1st constant)

$k_s = 6.56 \times 10^{-5}$ moll^{-1}min

9) K. C. Gupta and M. P. Singh, *Z. Physik, Chem.*, **232**, 289 (1966).

TABLE 2

Temp.: 40°C

$[K_3Fe(CN)_6]=3.33\times10^{-3}$M, $[NH_3]=1.00\times10^{-1}$N

[D-Fructose] $=1.00\times10^{-2}$M

Time min	N/752 hypo ml	$k_0=\frac{\Delta x}{\Delta t}$
0	12.46	—
5	11.54	0.184
10	10.60	0.188
15	9.20	0.280
20	8.20	0.200
25	7.20	0.200
30	6.00	0.240
45	3.00	0.200
55	1.50	0.150
∞	0.00	

Mean k_0 0.224

(Neg. 1st two and last constant)

$k_s=5.95\times10^{-5}$ mol l^{-1} min^{-1}

TABLE 3

Temp.: 40°C

$[NH_3]=1.00\times10^{-1}$N, [D-Fructose] $=1.00\times10^{-2}$M

$[K_3Fe(CN_6)]$ M$\times10^3$	μ M	$k_s\times10^5$ mol l^{-1} min^{-1}
2.50	0.015	6.56
3.33	0.020	5.95
4.00	0.024	6.01
5.00	0.030	6.01

TABLE 4

Temp.: 40°C

$[K_3Fe(CN_6)]=2.50\times10^{-3}$M, $[NH_3]=1.00\times10^{-1}$N

[D-Fructos] $=1.00\times10^{-2}$M

$[K_4Fe(CN_6)]$ M$\times10^3$	$k_s\times10^5$ mol l^{-1} min^{-1}
2.50	6.15
3.33	6.78
5.00	6.80
10.00	7.27

Table 4 shows the effect of variation of potassium ferrocyanide on the reaction rate at constant concentration of other reactants. Practically the same k_s values indicate that the reaction rate is not affected by the concentration of the ferrocyanide ion. The slight increase in k_s value at its higher concentration is due to increase in ionic strength.

Order of Reaction with Respect to D-Fructose. In order to determine the order of the reaction with respect to D-fructose, its concentration has been varied keeping the concentration of other reactants constant. The results have been given in summarized form in Table 5. It is observed that zero order velocity constant increases proportionately with the increase in concentration of D-fructose. In the third column, the k_s/[D-fructose] value has been calculated which is fairly uniform. This indicates that the reaction rate is directly proportional to D-fructose concentration.

TABLE 5. EFFECT OF VARIATION OF AMMONIA ON THE REACTION RATE

Temp.: 40°C

$[K_3Fe(CN)_6]=2.50\times10^{-3}$M, $[NH_3]=5.00\times10^{-2}$N

[D-Fructose] M$\times10^2$	$k_s\times10^5$ mol l^{-1} min^{-1}	k/[D-Fructose] $\times10^3$
0.666	2.50	3.75
1.000	3.87	3.87
1.250	4.01	3.20
2.000	6.22	3.11

Table 6 shows the effect of increasing concentrations of ammonia on the reaction rate under identical condition of other reactants at two different temperatures, *i. e.*, 40°C and 35°C. It is observed that k_s value gradually increases with the increasing concentrations of ammonia. Also, the k_s values have been calculated for normal concentration of ammonia. These values gradually decrease with the increase in concentration of ammonia and decrease in hydroxyl ion concentration.

Further, these results have been shown graphically (Fig. 1) by plotting k_s against the concentration of ammonia. It is observed that at lower con-

TABLE 6

$[K_3Fe(CN)_6]=2.50\times10^{-3}$M, [D-Fructose] $=1.00\times10^{-2}$M

Temp. : 40°C			Temp. : 35°C	
$[NH_3]$ N$\times10^2$	$k_s\times10^5$ mol l^{-1} min^{-1}	k_s/$[NH_3]$ $\times10^4$	$k_s\times10^5$ mol l^{-1} min^{-1}	k_s/$[NH_3]$ $\times10^4$
2.00	1.84	9.20	—	—
3.33	2.89	8.67	1.60	4.80
5.00	3.87	7.74	2.10	4.20
10.00	6.56	6.56	3.57	3.57
20.00	9.04	4.52	5.30	2.65

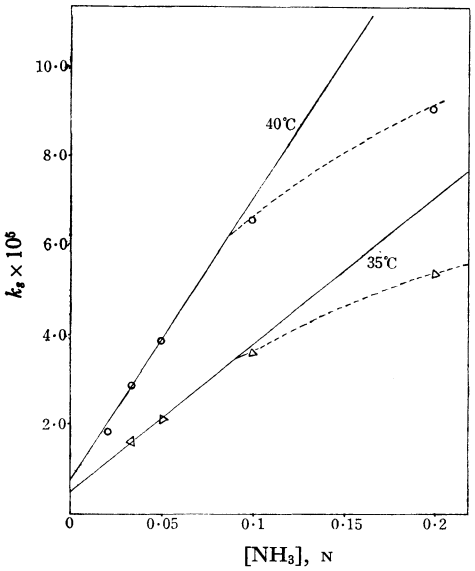

Fig. 1
Variation of NH_3 Conc.
$[K_3Fe(CN)_6] = 2.50 \times 10^{-3}$ M
[D-Fructose] $= 1.00 \times 10^{-2}$ M

centration of ammonia, there is direct proportionality; but at higher concentration there is deviation due to the decrease in dissociation of ammonia.

Common Ion Effect and Catalytic Constants. For reactions involving catalysis by bases there is a secondary salt effect which has to do with the effect of ionic strength on the dissociation of weak bases. Thus the actual degree of dissociation of a weak base such as ammonia can be changed by changing the concentration of salts in solution. Since the rate of reaction depends on the concentration of hydroxyl ions obtained from ammonia, it is clear that the rate of reaction will depend on the salt concentration. Table 7 shows the results at increasing concentrations of ammonium chloride on the reaction rate at constant concentration of other reactants. Due to common ion effect the hydroxyl ion concentration decreases with the increase in ammonium chloride concentration; which

TABLE 7
$[K_3Fe(CN_6)] = 2.50 \times 10^{-3}$M, [D-Fructose] $= 1.00 \times 10^{-2}$M
$[NH_3] = 10.00 \times 10^{-2}$N

	Temp.: 35°C		Temp.: 40°C
$[NH_4Cl]$ M $\times 10^2$	pH	$k_s \times 10^5$ mol l^{-1} min^{-1}	$k_s \times 10^5$ mol l^{-1} min^{-1}
0.00	—	3.57	6.56
0.25	10.4	2.29	4.10
0.50	10.2	1.66	2.63
1.00	10.0	1.20	1.87
2.00	9.7	0.67	1.22

leads to gradual decrease in zero order velocity cononstant.

The reaction between ferricyanide ion and D-glucose (*loc. cit.*) and D-fructose is of general basis catalysis in nature. In order to confirm this the following experiments have been performed at varying concentrations of ammonia and ammonium chloride by keeping their ratio constant. The results have been given in summarized form in Tables 8 and 9.

TABLE 8
$[K_3Fe(CN_6)] = 2.50 \times 10^{-3}$M, [D-Glucose] $= 5.00 \times 10^{-2}$M

$[NH_3]$ N $\times 10^2$	$[NH_4Cl]$ M $\times 10^2$	Temp.: 40°C $k_s \times 10^5$ mol l^{-1} min^{-1}	Temp.: 35°C $k_s \times 10^5$ mol l^{-1} min^{-1}
3.3	0.33	1.01	0.694
	pH 10.0		
5.0	0.50	1.22	0.787
10.0	1.00	1.66	1.07
20.0	2.00	1.99	1.28
3.3	0.166	1.45	0.942
	pH = 10.2		
5.0	0.250	1.70	1.09
10.0	0.500	2.20	1.38
20.0	1.000	3.15	1.90

In Tables 8 and 9 the concentrations of ammonia and ammonium chloride have been gradually increased, keeping their ratios constant (10 : 1 and 20 : 1) in each case at 40°C and 35°C. These

TABLE 9
$[K_3Fe(CN)_6] = 2.50 \times 10^{-3}$M, [D-Fructose] $= 1.00 \times 10^{-2}$M

$[NH_3]$ N $\times 10^2$	$[NH_4Cl]$ M $\times 10^2$		Temp.: 40°C $k_s \times 10^5$ mol l^{-1} min^{-1}	Temp.: 35°C $k_s \times 10^5$ mol l^{-1} min^{-1}
2.00	0.200		1.02	—
3.33	0.333	pH = 10.0	1.17	0.763
5.00	0.500		1.44	0.926
10.00	1.000		1.87	1.200
20.00	2.000		2.34	1.340
3.33	0.166		1.68	1.11
5.00	0.250	pH = 10.2	1.93	1.22
10.00	0.500		2.63	1.66
20.00	1.000		3.85	2.26

results are at constant pOH because pOH of the system is related by the following equation.

$$\text{pOH} = \text{p}K_b + \log \frac{[\text{salt}]}{[\text{base}]} \qquad (1)$$

where $pK_b = \log 1/K_b$, K_b being dissociation constant of the base which is related with the equilibria

$$NH_3 + H_2O \rightleftharpoons NH_4^+ + OH^-$$

From the above equation it is clear that the increase in k_s values is only due to the increase in

TABLE 10.

$[K_3Fe(CN_6)]=2.50\times10^{-3}$M $[K_3Fe(CN)_6]=2.50\times10^{-3}$M
[D-Glucose] $=5.00\times10^{-2}$M [D-Fructose] $=1.00\times10^{-2}$M

	k_{OH^-} mol l^{-1} min^{-1}	k_{NH_3} mol l^{-1} min^{-1}	k_{OH^-} mol l^{-1} min^{-1}	k_{NH_3} mol l^{-1} min^{-1}
40°C	6.77×10^{-2}	1.13×10^{-4}	7.31×10^{-2}	1.47×10^{-4}
35°C	4.50×10^{-2}	0.71×10^{-4}	5.02×10^{-2}	0.87×10^{-4}

undissociated ammonia. This shows that the reaction is of general basic catalysis in nature and in these experiments the total rate (k_s) is governed by the following equation.

$$k_s = kOH^-\cdot[OH^-]+k_{NH_3}\cdot[NH_3] \qquad (2)$$

where k_{OH^-} and k_{NH_3} are the catalytic constants of OH^- and NH_3 respectively. In order to show the validity of Eq. (2) the results of these Tables have been shown graphically in Figs. 2, 3, 4 and 5 by plotting k_s against ammonia concentration and the catalytic constant of OH^- (k_{OH^-}) has been calculated from the value of the intercept of the ordinate and the value of k_{NH_3} has been calculated from the slope of the straight line. The values obtained are given in Table 10.

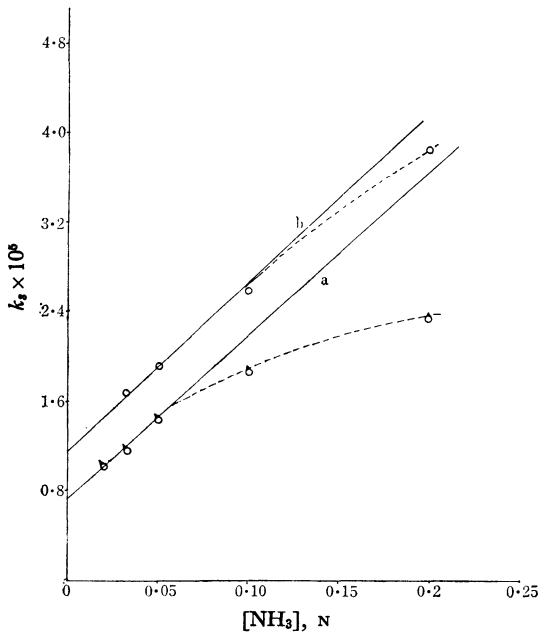

Fig. 2

Tempeature 40°C
Variation of NH_4Cl at fixed ratio
$[K_3Fe(CN)_6]=2.50\times10^{-3}$ M
[D-Fructose] $=1.00\times10^{-2}$ M
a=10 : 1, pH=10.0
$k_{NH_3}=1.45\times10^{-4}$ mol l^{-1} min^{-1}
$k_{OH^-}=7.3\times10^{-2}$ mol l^{-1} min^{-1}
b=20 : 1, pH=10.2
$k_{NH_3}=1.5\times10^{-4}$ mol l^{-1} min^{-1}
$k_{OH^-}=7.32\times10^{-2}$ mol l^{-1} min^{-1}

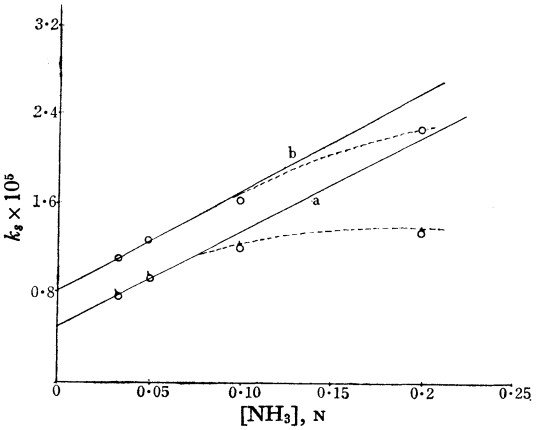

Fig. 3

Temperarure 35°C
Variation of NH_4Cl at fixed ratio
$[K_3Fe(CN)_6]=2.50\times10^{-3}$ M
[D-Fructose] $=1.00\times10^{-2}$ M
a=10 : 1, pH=10.0
$k_{NH_3}=0.86\times10^{-4}$ mol l^{-1}min^{-1}
$k_{OH^-}=5.0\times10^{-2}$ mol l^{-1} min^{-1}
b=20 : 1, pH=10.2
$k_{NH_3}=0.89\times10^{-4}$ mol l^{-1} min^{-1}
$k_{OH^-}=5.10\times10^{-2}$ mol l^{-1} min^{-1}.

From the graph it is clear that linearity is obtained only at lower concentrations of the base and the electrolyte. The deviation at higher concentrations is due to the fact that Eq. (2) is valid only at low ionic strength.

Effect of Dielectric Constant and Ionic Strength. In the reaction between ion-dipolar molecule the logarithm of the velocity constant is a linear function of ionic strength (μ) instead of square root of μ as in the case of reaction between ion-ion. This is only valid when there is a large variation in ionic strength, because under such conditions Debye-Hückel term disappears and only the Hückel term ($b\mu$) becomes prominent. On the other hand, the activity of the hydroxyl ion can be increased by the addition of the neutral salt, and thus the catalytic influence of the hydroxyl ion becomes a function of the concentration of the salt. This is also called a secondary salt effect. In order to show the validity of the above conclusion the effect of varying dielectric constant (by adding ethanol or methanol by volume) and ionic strength on the reaction rate has been studied. The results have been given in the Tables 11, 12

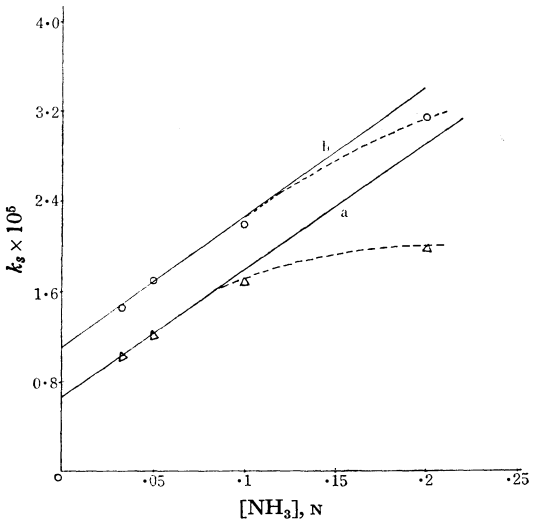

Fig. 4

Temperature 40°C
Varition of NH_4Cl at fixed ratio
$[K_3Fe(CN)_6] = 2.50 \times 10^{-3}$ M
[D-Glucose] $= 5.00 \times 10^{-2}$ M
a = 10 : 1, pH = 10.0 $k_{NH_3} = 1.12 \times 10^{-4}$ mol l^{-1} min^{-1}
$k_{OH^-} = 6.6 \times 10^{-2}$ mol l^{-1} min^{-1}
b = 20 : 1, pH = 10.2 $k_{NH_3} = 1.14 \times 10^{-4}$ mol l^{-1} min^{-1}
$k_{OH^-} = 6.94 \times 10^{-2}$ mol l^{-1} min^{-1}

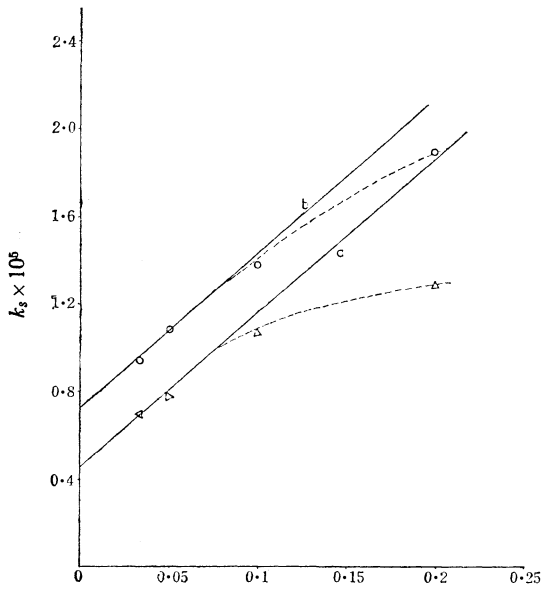

Fig. 5

Temperature 35°C
Variation of NH_4Cl at fixed ratio
$[K_3Fe(CN)_6] = 2.50 \times 10^{-3}$ M
[D-Glucose] $= 5.00 \times 10^{-2}$ M
a = 10 : 1, pH = 10.0 $k_{NH_3} = 0.7 \times 10^{-4}$ mol l^{-1} min^{-1}
$k_{OH^-} = 4.5 \times 10^{-2}$ mol l^{-1} min^{-1}
b = 20 : 1, pH = 10.2 $k_{NH_3} = 0.72 \times 10^{-4}$, mol l^{-1} min^{-1}
$k_{OH^-} = 4.5 \times 10^{-2}$ mol l^{-1} min^{-1}

and 13. In the case of ammonia the reaction rate decreases with the decrease in dielectric constant, but in the case of strong base sodium hydroxide enhanced reaction rates with the decrease in dielectric constant are obtained. On the other hand when neutral salt (KCl) is added at particular dielectric constant the reaction rate increases with the gradual increase in ionic strength.

In the case of ion-ion reactions, the effect of ionic strength and dielectric constant on the reaction rate is expressed by Brönsted-Christiansen-Scatcherd[10] equation. A similar relationship is expressed by Amis and Joffé[11] and Laidler and Eyring[12] in the case of reaction between ion-dipolar molecule. Both the above equations show that logarithm of velocity constant varies as ionic strength instead of square root of ionic strength as in the case of ion-ion reactions. In order to show the validity of the data the log k_s has been plotted against μ (Fig. 6). A straight line with slight deviation at low ionic strength (due to complication of secondary salt effect) is obtained. Further, ln k_0' varies as $1/D$, where k_0' is the velocity constant at zero ionic strength and D is the dielectric constant of the solution. These two equations lead to contradictory results[13] which have been described in the following lines.

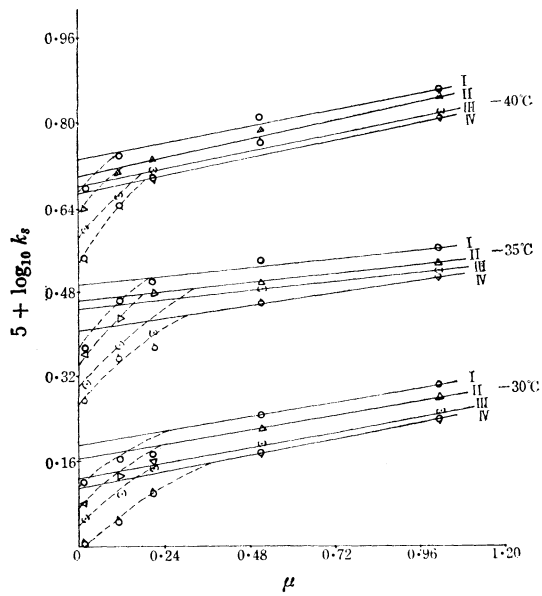

Fig. 6

Variation of ionic strength
$[K_3Fe(CN)_6] = 2.50 \times 10^{-3}$ M
$[NH_3] = 1.00 \times 10^{-1}$ N
[D-Glucose] $= 5.00 \times 10^{-2}$ M

10) Edawrd S. Amis, "Kinetics of Chemical Change in Solution," The Macmillan Company, N. Y. (1949), p. 77.

11) Edward S. Amis and H. H. Jaffé, *J. Chem. Phys.*, **10**, 598 (1942).

12) K. J. Laidler and H. Eyring, *Ann. New York Acad. Sci.*, **39**, 299 (1940).

	For positive ion effect of increasing		For negative ion effectof increasing	
	dielectric constant	ionic strength	dielectric constant	ionic sterngth
Author	decrease	increase	increase	decrease
Amis and Jaffé				
Laidler and Eyring	decrease	increase	decrease	increase

From the above results it is clear that both the equations predict the same results in the case of reaction between positive ion and dipolar molecule, but there is difference in the case of reaction between negative ion and dipolar molecule. Now in the present reaction between negative ion and dipolar molecule (reducing sugar) in presence of ammonia the effect of variation of ionic strength on the reaction rate is in agreement with the result predicted by Laidler and Eyring. Now, when the dielectric constant has been decreased, an increase in the reaction rate is observed in the presence of sodium hydroxide and decrease in the presence of ammonia. Thus the results obtained in the case of sodium hydroxide are again in agreement with Eyring's equation. The contradictory result obtained in the presence of ammonia is due to the fact that the decrease in the dielectric constant of the medium results in the decrease in hydroxyl ion and increase in NH_3 concentration. This has been shown graphically in Fig. 7 by plotting log k_s against $1/D$. A straight line with relative slope

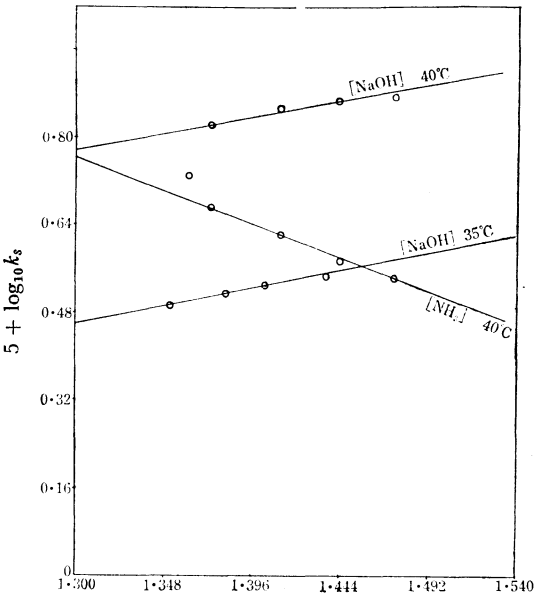

Fig. 7
Variation of dielectric (Methanol) constant
$[K_3Fe(CN)_6]=2.50\times10^{-3}$ M
[D-Glucose] $=5.00\times10^{-2}$ M
$[NH_3]=1.00\times10^{-1}$ N

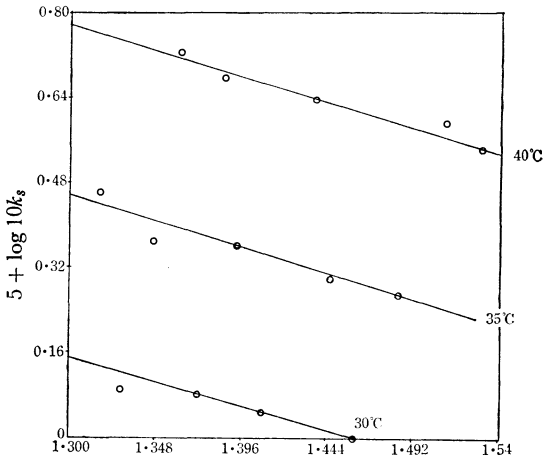

Fig. 8
Variation of dielectric (Ethanol) Constant
$[K_3Fe(CN)_6]=2.50\times10^{-3}$ M
$[NH_3]=1.00\times10^{-1}$ N
[D-Clucose] $=5.00\times10^{-2}$ M
$\mu=0.015$ M

TABLE 11

Temp.: 40°C
$[K_3Fe(CN_6)]=2.5\times10^{-3}$M $[K_3Fe(CN_6)]=2.5\times10^{-3}$M
$[NH_3]=1.00\times10^{-1}$N $[NaOH]=6.66\times10^{-3}$N
[D-Glucose] $=5.00\times10^{-2}$M [D-Glucose] $=1.00\times10^{-2}$M
$\mu=0.015$ M $\mu=1.0216$ M

Percentage of methanol by vol.	D	$k_s\times10^5$ mol l^{-1} min^{-1}	$k_s\times10^5$ mol l^{-1} min^{-1}
5	72.77	4.70	6.62
10	70.83	4.17	7.10
15	69.21	3.72	7.30
20	67.82	3.48	7.51

TABLE 12

Temp. : 35°C
$[K_3Fe(CN)_6]=2.5\times10^{-3}$M, $[NaOH]=6.66\times10^{-3}$N
[D-glucose] $=1.00\times10^{-2}$M
$\mu=0.0616$ M

Percentage of methanol by vol.	D	$k_s\times10^5$ mol l^{-1} min^{-1}
5	73.93	3.13
10	72.33	3.26
15	71.23	3.39
20	69.59	3.51

13) Edward S. Amis, "Kinetics of Chemical Change in Solution," The Macmillan Company, N. Y. (1949), p. 174.

Table 13

$[K_3Fe(CN_6)]=2.50\times10^{-3}$M, $[K_3Fe(CN)_6]=2.5\times10^{-3}$M, $[NH_3]=1.00\times10^{-1}$N, $[NH_3]=1.00\times10^{-1}$N, [D-Glucose]$=5.00\times10^{-2}$M, [D-Fructose]$=1.00\times10^{-2}$M

Percentage of ethanol by vol.	D	μ M	$k_s\times10^5$ mol l^{-1}. min^{-1}	$k_s\times10^5$ mol l^{-1}. min^{-1}	Percentage of ethanol by vol.	D	μ M	$k_s\times10^5$ mol l^{-1}. min^{-1}	$k_s\times10^5$ mol l^{-1}. min^{-1}
	Temp: 40°C						1.015	3.44	4.60
0	73.38	0.015	5.35	6.56	15	69.36	0.015	2.01	2.40
5	72.06	0.015	4.78	5.75	III		0.115	2.36	3.12
I		0.115	5.52	6.61			0.215	2.52	3.26
		0.215	—	7.02			0.515	3.08	3.86
		0.515	6.47	7.52			1.015	3.32	4.21
		1.015	7.27	8.28	20	67.32	0.015	1.87	2.16
10	69.53	0.015	4.36	4.92	IV		0.115	2.26	2.92
II		0.115	5.10	5.86			0.215	2.34	3.15
		0.215	5.42	6.35			0.515	2.87	3.63
		0.515	6.12	7.03			1.019	3.24	3.92
		1.015	7.10	8.20		Temp.: 30°C			
15	66.16	0.015	3.95	4.31	0	77.25	0.015	1.50	2.01
III		0.115	4.64	5.36	5	75.15	0.015	1.32	1.74
		0.212	5.16	5.91	I		0.115	1.47	1.91
		0.515	6.16	6.61			0.215	1.49	2.20
		1.015	6.63	7.50			0.515	1.75	2.40
20	65.32	0.015	3.51	3.83			1.015	2.01	2.57
IV		0.115	4.48	5.01	10	72.83	0.015	1.21	1.68
		0.212	5.03	5.69	II		0.115	1.36	1.74
		0.515	5.84	6.43			0.215	1.44	2.02
		1.015	6.46	7.23			0.515	1.66	2.22
	Temp.: 35°C						1.015	1.91	2.45
0	76.03	0.015	2.90	3.57	15	70.95	0.015	1.12	1.51
5	74.15	0.015	2.35	3.06	III		0.115	1.25	1.68
I		0.115	2.92	3.60			0.215	1.41	1.82
		0.215	3.21	3.84			0.515	1.55	2.03
		0.515	3.47	4.40			1.015	1.80	2.31
		1.015	3.66	4.93	20	68.44	0.015	1.00	1.37
10	71.67	0.015	2.30	2.72	VI		0.115	1.11	1.49
II		0.115	2.69	3.43			0.215	1.25	1.65
		0.215	3.02	3.72			0.515	1.50	1.92
		0.515	3.13	4.32			1.015	1.73	2.17

is obtained. This fact is supported by Harned.[14] He has reported in the case of acetic acid that logarithm of ionization constant varies as $1/D$. Thus in our case there would have been an increase with the decrease in dielectric constant as observed in the case of sodium hydroxide (Fig. 8) and the decrease in the reaction rate observed is only due to decrease in dissociation constant.

Mechanism of the Reaction

A careful study of the oxidation of reducing sugars (D-glucose and D-fructose) indicates that the rate expression is of the form:

$$-\frac{d[Fe\ y^{3-}]}{dt}=k[NH_3][s] \qquad (1)$$

where [s] represents the concentration of reducing sugar and [Fe y^{3-}] the ferricyanide ion. The above equation indicates that the reaction velocity is independent of the concentration of ferricyanide ion and directly proportional to both the ammonia and reducing sugar concentration. For any given concentration of alkali, if the concentration of reducing sugar is comparatively larger than ferricyanide ion, the rate expression takes the form

$$-\frac{d[Fe\ y^{3-}]}{dt}=k_s=\frac{\Delta x}{\Delta t}$$

where

$$k_s=k[NH_3][s] \qquad (2)$$

where k_s is the standard zero velocity constant and k the specific rate constant.

From the results it appears that first step involves the action of alkali on the reducing sugar (*loc. cit.*)

14) H. S. Harned, *J. Phys. Chem.*, **43**, 275 (1939).

forming an intermediate 1,2-enediol, which is subsequently oxidized by the ferricyanide ion. The latter being a comparatively faster process, so that the reaction becomes independent of ferricyanide ion concentration.

Thus

$$[S] + [NH_3] \underset{k_{-1}}{\overset{k_1\,(slow)}{\rightleftharpoons}} \underset{R}{\overset{H}{\overset{|}{C}}}\!\!-\!\!OH \;\; \underset{|}{C}\!\!-\!\!OH \qquad \text{(1st step)}$$

1,2-enediol (en)

$$[en] + [Fe\ y^{3-}] \xrightarrow{k_2\,(fast)} [FeOY^{4-}] + \text{other reaction products} \qquad \text{(2nd step)}$$

considering the stationary state for enediol and $k_2 \gg k_{-1}$ the final rate expression comes out to be

$$-\frac{d[Fe\ y^{3-}]}{dt} = k_1[NH_3][S] \qquad (3)$$

where k_1 is identical with k of Eq. (1). Equation (3) confirms our experimental findings. Further, this leads to the conclusion that the rate of enolization is the rate of oxidation of the reducing sugar.

One of the authors (K. C. Gupta) is thankful to C.S.I.R., Government of India for financial assistance and to the Head of the Chemistry Department, University of Allahabad for providing the necessary facilities to carry out the research work.

BULLETIN OF THE CHEMICAL SOCIETY OF JAPAN VOL. 42 607—614 (1969)

Measurement of Negative Ions Formed by Electron Impact. I. Negative Ion Mass Spectra of Nitroalkanes

Satoru TSUDA, Akira YOKOHATA and Michihiro KAWAI

Department of Chemistry, Faculty of Engineering, Hiroshima University, Senda-machi, Hiroshima

(Received June 17, 1968)

The negative ion mass spectra of nitroalkanes (nitromethane, nitroethane, 1-nitropropane and 2-nitropropane) have been mesaured with a mass spectrometer under electron energies of 80 eV, 40 eV, 9.5 eV and 4.5 eV in the range of pressure used for usual analysis. The spectral intensities of negative ions were compared with those of positive ions. In 80 or 40 eV electron impact experiments, *m/e* 16 (O^-), 46 (NO_2^-), 26 (probably, CN^-) and 42 (probably, CNO^- or $C_2H_4N^-$) ions were commonly found. Their yields showed good linearity against pressure under the present experimental conditions. The peaks of *m/e* 61 (parent ion; $CH_3NO_2^-$) in nitromethane, of *m/e* 25 (C_2H^-) in nitroethane, 1-nitropropane and 2-nitropropane, and a relatively strong peak of *m/e* 60 ($CH_2NO_2^-$) in 1-nitropropane were characteristic. For lower electron energies, the strong dependency of the yield of negative ions on the electron energy was confirmed. The yield of negative ions as compared with positive ions for 80 eV and 40 eV of electron energy was lower by a factor of $\sim 10^4$. On the other hand, the comparison of the yield of positive ions for 15 eV electrons with that of negative ions for 9.5 eV electrons gave the value of ~ 0.2. In addition, of the role these negative ions in radiolysis has been briefly discussed.

In the last few years studies involving positive ion mass spectra have been carried out with a great variety of organic compounds. However, only a few papers have been published with respect to negative ion mass spectrometry. Also, discrepancies are seen between the published experimental results, which demonstrate the need for further work. In general, the mechanisms for formation of negative ions by electron impact can be classified into the following processes:[1] (a) The radiative capture of a free electron by a neutral atom ($e + A \rightarrow A^- + h\nu$). (b) Capture of a free electron by an atom with a third body taking up the excess energy ($e + A + B \rightarrow A^- + B +$ kinetic energy). (c) Capture of a free electron by a molecule, with the vibrational excitation of the molecular ion and its subsequent stabilization by a collision with another molecule ($e + XY \rightarrow (XY)^{-*}$; $(XY)^{-*} + A \rightarrow XY^- + A +$ kinetic energy). (d) Dissociative attachment: capture of a free electron by a mol-

1) E. W. McDaniel, "Collision Phenomena in Ionized Gases," John Wiley & Sons, Inc., New York (1964), p. 368.

ecule, the excess energy going into dissociation of the molecule ($e + XY \rightarrow (XY)^{-*} \rightarrow X + Y^-$). (e) Ion-pair production: noncapture dissociation of a molecule into positive and negative ions ($e + XY \rightarrow e + X^+ + Y^-$). (f) Transfer of one or more electrons to a neutral structure or a positive ion in a collision with another particle ($A + B \rightarrow A^- + B^+$; or $C^+ + D \rightarrow C^- + D^{2+}$).

Under ordinary laboratory conditions, and excluding charge-changing collisions, processes (b), (c) and (d) would be the most probable. For electron with energies in excess of about 7—20 eV, (e) will also become important.

As these processes are pressure dependent in different ways,[2] the relative intensities of negative ion mass spectra can be expected to change with sample pressure. A further complication is the low yield of negative ions as compared with positive ions in the range of 50 eV to 70 eV of electron energy. However, the recent developements of detection method and apparatus have overcome considerably these difficulties.

Moruzzi *et al.*[3] have surveyed the negative-ion species produced in oxygen and some gases containing oxygen for various pressures and E/P conditions*1 using an rf mass spectrometer coupled to an electron drift tube operating at pressures up to 5 mmHg. Compton *et al.*[4] have studied the non-dissociative electron capture in complex molecules and negative-ion lifetimes with a modified Bendix mass spectrometer. Melton *et al.*[5] have published the results of measurement for individual and total cross sections for the production of positive ions, negative ions and free radicals by using the modified dual electron beam method. Also, Christophorou and Compton[6] have reviewed the electron swarm and electron beam techniques under the subject of interaction of low energy electrons with polyatomic molecules.

On the other hand, the role of negative ions has recently drawn increasing attention in the field of radiation chemistry. Cundall *et al.*[7] have pointed out the importance of negative ions in the radiolysis of nitroalkanes. Warman[8] has elucidated the occurrence of the ion-molecule reactions of negative oxygen atom ions with the additives such as carbon dioxide and acetone in the radiolysis of alkane-nitrous oxide systems.

Also, in the silent discharge reactions in the gas phase with which a part of our recent works are concerned, the role of negative ions has been suggested to be important.[9]

At the present stage when the negative ion mass spectra were only measured for limited compounds, further work on negative ions is strongly required. The present work deals with the negative ion mass spectra of nitroalkanes,*2 especially in relation to the electron energy effect.

Experimental

This investigation was carried out using a standard Hitachi RMU-6D mass spectrometer equipped with a T-2M ion source having a straight line rhenium filament. The ion detection circuit consisted of a ten stage electron multiplier having Ag-Mg dynode and a Faraday collector. All the spectra were measured with an ionizing current of 80 μA and a constant accelerating voltage of 1.8 kV, under the ionizing energies of 80 eV, 40 eV, 9.5 eV and 4.5 eV.

The electron energy was calibrated by the vanishing current method as compared to the ionization potential of argon[10] or the appearance potential[11] of m/e 16 (O^-) from carbon monoxide.

The polarity of the collector ion lens was reversed for negative ion measurement. The electron multiplier was always operated at 1.4 kV.

The research grade nitroalkanes (nitromethane, nitroethane, 1-nitropropane and 2-nitropropane) were used without further purification. Data for each of the compounds were taken at a pressure of $\sim 10^{-6}$ mmHg in the source.

Results and Discussion

Nitromethane. In 80 eV electron impact experiments, negative ions of m/e 16 (O^-), 46 (NO_2^-), 26 (CN^-) and 42 (CNO^-) have mainly been observed (Fig. 1a). The result was consistent with that of Aplin *et al.*,[12] except that the relative intensity of m/e 16 (O^-) ion to m/e 26 (CN^-) ion was reversed.

It is probable that differences in the source

2) C. E. Melton in "Mass Spectrometry of Organic Ions," F. W. McLafferty, Ed., Academic Press, Inc., New York, N. Y. (1963), p. 163.

3) J. L. Moruzzi and A. V. Phelps, *J. Chem. Phys.*, **45**, 4617 (1966).

*1 E: electric field strength. P: pressure.

4) R. N. Compton, L. G. Christophorou, G. S. Hurst and P. W. Reinhardt, *J. Chem. Phys.*, **45**, 4634 (1966).

5) C. E. Melton and P. S. Rudolf, *ibid.*, **47**, 1771 (1967).

6) L. G. Christophorou and R. N. Compton, *Health Physics*, **13**, 1277 (1967).

7) R. B. Cundall, A. W. Locke and G. C. Street, *Nature*, **210**, 1354 (1966).

8) J. M. Warman, *ibid.*, **213**, 382 (1967).

9) A. Yokohata and S. Tsuda, Presented at the 10th Conference on Radiation Chemistry, Hiroshima, October, 1967.

*2 Negative ion mass spectra have not yet been measured, except nitromethane which is measured only at an electron energy of 70 eV. (See Ref. 12)

10) K. Watanabe, T. Nakayama and J. Mottl, *J. Quant, Spectrosc. Radiat. Transfer.*, **2**, 369 (1962).

11) M. A. Fineman and W. Petrocelli, *J. Chem. Phys.*, **36**, 25 (1962).

12) R. T. Aplin, H. Budzikiewiez and C. Djerassi, *J. Am. Chem. Soc.*, **87**, 3180 (1965).

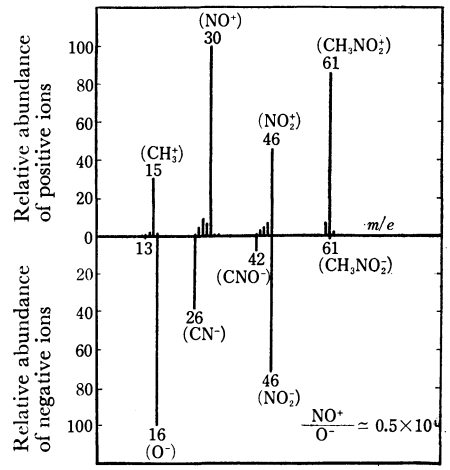

Fig. 1a

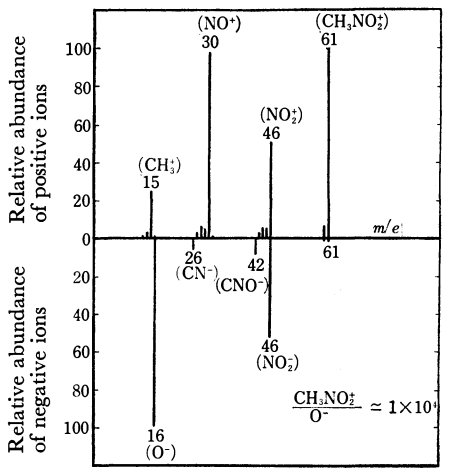

Fig. 1b.

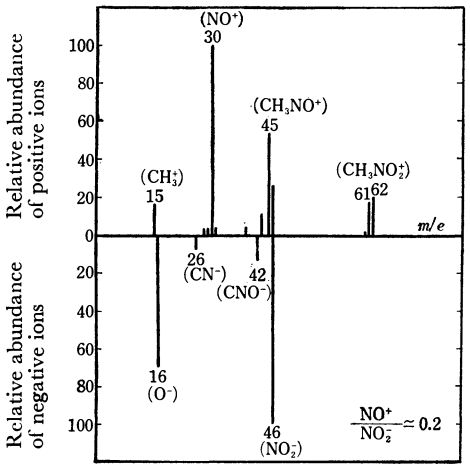

Fig. 1c.

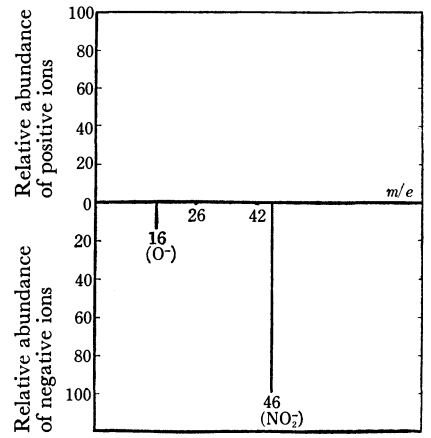

Fig. 1d.

Fig. 1. Positive and negative ion mass spectra of nitromethane (source pressure: $\sim 10^{-6}$ mmHg).
a 80 eV b 40 eV c 15 eV for positive ions, 9.5 eV for negative ions d 4.5 eV

pressure and in the geometry of the ion source are responsible for this discrepancy, which emphasizes the much greater sensibility of negative ion mass spectrometry toward the change in experimental conditions as compared with positive ion mass spectrometry.

As in alcohols[2] the most intense peak was the *m/e* 16 (O^-) ion. Also, it might be mentioned that it is one of the characteristics found frequently in the compounds containing oxygen atoms. When the yield of O^- ion was compared with that of positive ion of *m/e* 30 (NO^+) (the most intense peak among the positive ions), NO^+/O^- was $\sim 0.5 \times 10^4$.

For 40 eV electrons (Fig. 1b), the pattern of the negative ions did not differ so much from that for 80 eV electrons except the decrement in the intensity of *m/e* 26 (CN^-) ion, and the ratio of $CH_3NO_2^+$ to O^- was $\sim 1 \times 10^4$.

The comparison of the yield of *m/e* 46 (NO_2^-) ion obtained with 9.5 eV electrons with that of positive ion of *m/e* 30 (NO^+) obtained with 15 eV electrons*3 (Fig. 1c; C condition) gave a value

Table 1. Minor negative ions from CH_3NO_2

m/e	Relative intensities for electron energies of		
	80 eV*	9.5 eV**	4.5 eV**
12	0.2		
13	1.1	0.2	
26			1.2
42			2.5
60	0.7		
61	1.8		

* Normalized to O^- (yield=100)
** Normalized to NO_2^- (yield=100)

*3 Since the species of positive ions produced by the impact of 9.5 eV electrons are very limited, the data for 15 eV electrons were conveniently used for comparison.

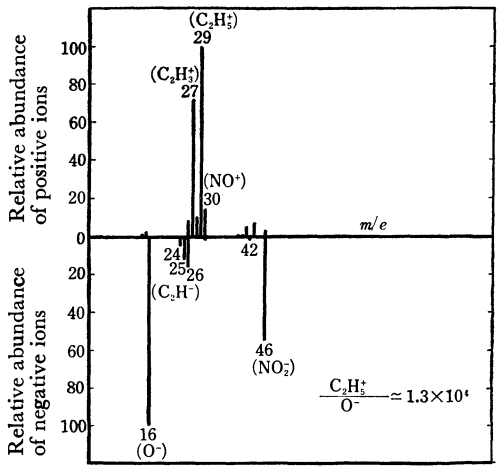

Fig. 2a.

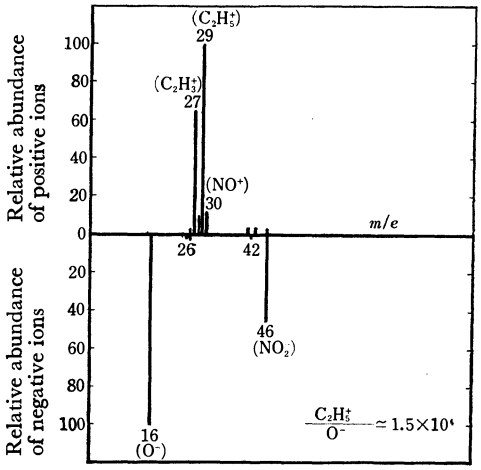

Fig. 2b.

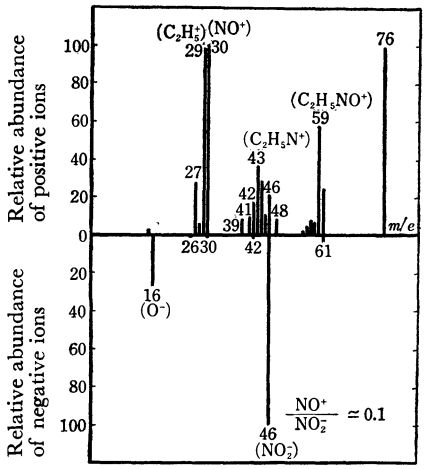

Fig. 2c.

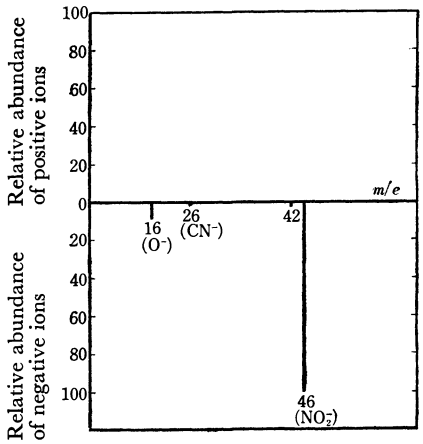

Fig. 2d

Fig. 2. Positive and negative ion mass spectra of nitroethane (source pressure: $\sim 10^{-6}$ mmHg).
a 80 eV b 40 eV c 15 eV for positive ions, 9.5 eV for negative ions d 4.5 eV

of ~0.2 for NO^+/NO_2^-. It should be noted that under this condition the yield of NO_2^- is somewhat higher than NO^+.

For 4.5 eV electrons (Fig. 1d) *m/e* 46 (NO_2^-) ions predominated over other negative ions.

Table 1 shows the yields of the minor negative ions for 80 eV, 9.5 eV and 4.5 eV. For 80 eV, a relatively high yield of *m/e* 13 (CH^-) among the negative ions arising from the methyl group is consistent with that in methyl alcohol.[2] It is also of interest that the *m/e* 61 ($CH_3NO_2^-$) ion has been observed.

Nitroethane. For the impact of 80 eV electrons (Fig. 2a) negative ions of *m/e* 16 (O^-), 46 (NO_2^-), 26 (probably, CN^-), 25 (C_2H^-), 24 (C_2^-) and 42 (probably, CNO^- or $C_2H_4N^-$) have been observed. The peak of parent ion ($C_2H_5NO_2^-$) has not been found. When the yield of O^- ion was compared with that of $C_2H_5^+$ (the most intense peak among the positive ions), $C_2H_5^+/O^-$ was $\sim 1.3 \times 10^4$. A relatively large peak of *m/e* 25 (C_2H^-) among the negative ions arising from the ethyl group is quite similar to the situations in ethane or ethyl alcohol.[2]

TABLE 2. MINOR NEGATIVE IONS FROM $C_2H_5NO_2$

m/e	Relative intensities for electron energies of		
	80 eV*	9.5 eV**	4.5 eV**
25		0.1	
26		1.1	1.0
30	1.2	0.8	0.4
40		0.1	
42	1.6	1.9	0.4
47		0.2	
48		0.2	

* Normalized to O^- (yield=100)
** Normalized to NO_2^- (yield=100)

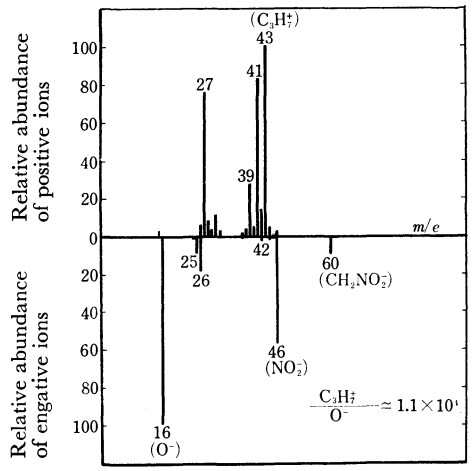

Fig. 3a

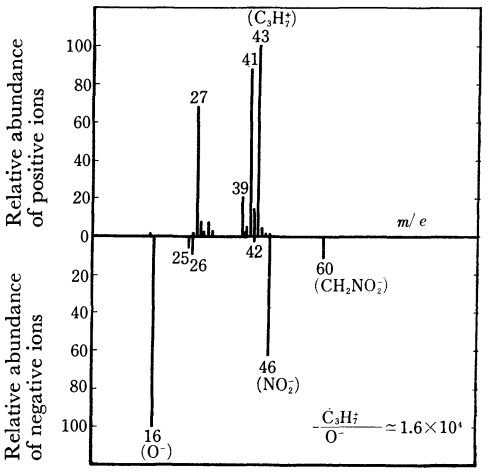

Fig. 3b

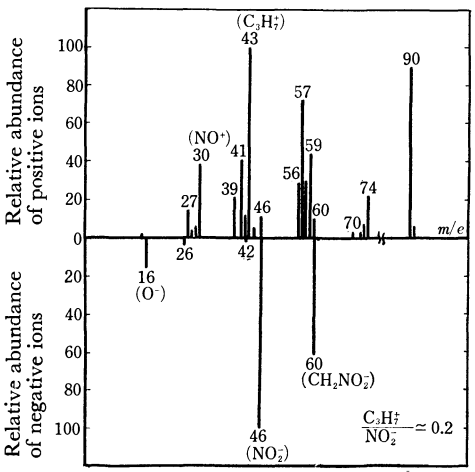

Fig. 3c

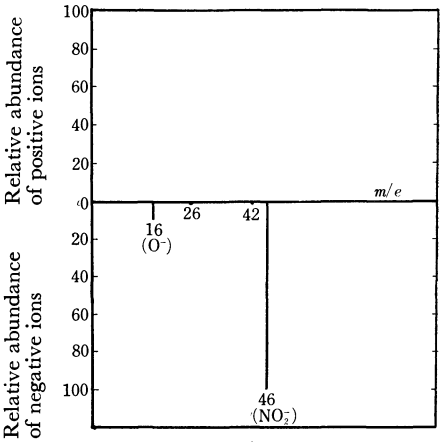

Fig. 3d.

Fig. 3. Positive and negative ion mass spectra of 1-nitropropane (source pressure: $\sim 10^{-6}$ mmHg).
a 80 eV b 40 eV c 15 eV for positive ions, 9.5 eV for negative ions d 4.5 eV

Mass spectra for 40 eV (Fig. 2b) were not so different from those of 80 eV except the decrement of peaks of *m/e* 26 (CN^-), 25 (C_2H^-) and 24 (C_2^-) ions. The ratio $C_2H_5^+/O^-$ was $\sim 1.5\times 10^4$.

For 9.5 eV and 4.5 eV (Figs. 2c and 2d), the *m/e* 46 (NO_2^-) ion predominated over other negative ions. Under C condition NO^+/NO_2^- was $\sim$0.1.

Table 2 shows the yields of the minor negative ions in relation to the electron energy. It can be seen that the ions formed extend over the range of *m/e* 25 to 48 and their variety is relatively small in both cases of 80 eV and 4.5 eV.

1-Nitropropane and 2-Nitropropane. For the impact of 80 eV and 40 eV electrons (Figs. 3a, 4a and 3b, 4b), 1-nitropropane and 2-nitropropane gave almost the same negative ions; *m/e* 16 (O^-), 46 (NO_2^-), 26 (CN^-) and 25 (C_2H^-), except for the appearance of *m/e* 60 ($CH_2NO_2^-$) in 1-nitropropane.

It is of great interest that in 1-nitropropane a relatively strong peak of *m/e* 25 (C_2H^-) ion has been observed as one of negative ions arising from the propyl group. This was consistent with the situation in *n*-propyl alcohol.[2)]

The comparison of the yield of O^- ion with that of $C_3H_7^+$ (the most intense peak among the positive ions) gave the following values for $C_3H_7^+/O^-$; $\sim 1.1\times 10^4$ at 80 eV and 1.6×10^4 at 40 eV for 1-nitropropane, $\sim 1.0\times 10^4$ and $\sim 1.4\times 10^4$ for 2-nitropropane, respectively.

Patterns obtained for 9.5 eV and for 4.5 eV (Figs. 3c, 4c and 3d, 4d) were similar respectively for the two samples, except a large peak of *m/e* 60 ($CH_2NO_2^-$) for electron impact of 9.5 eV on 1-nitropropane.

The ratio of the yield of $C_3H_7^+$ to O^- under the C condition; $C_3H_7^+/O^-$ were $\sim$0.2 for 1-nitropropane and $\sim$0.3 for 2-nitropropane.

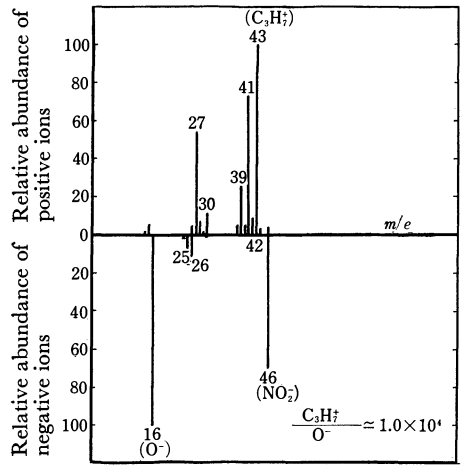

Fig. 4a

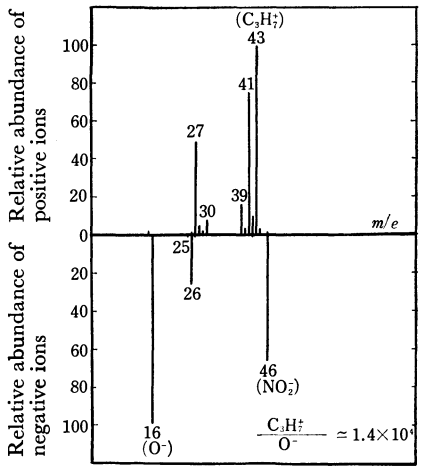

Fig. 4b

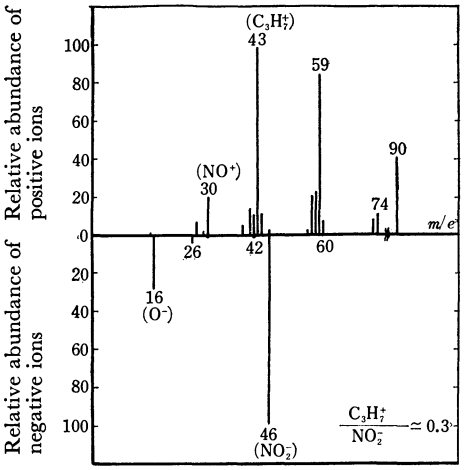

Fig. 4c

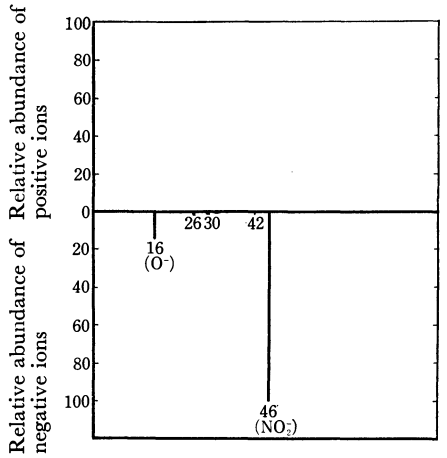

Fig. 4d

Fig. 4. Positive and negative mass spectra of 2-nitropropane (source pressure: $\sim10^{-6}$ mmHg).
a 80 eV b 40 eV c 15 eV for positive ions, 9.5 eV for negative ions d 4.5 eV

TABLE 3. MINOR NEGATIVE IONS FROM 1-$C_3H_7NO_2$

m/e	Relative intensities for electron energies of		
	80 eV*	9.5 eV**	4.5 eV**
12	0.2		
13	0.4		
14	0.2		
24	1.1		
26			0.2
27		0.1	
30	0.7	0.5	
36	0.2		
37	0.2		
42		2.1	0.4
44		0.4	
47		0.4	
48		0.2	
58		0.2	
61		0.8	
62		0.1	

* Normalized to O^- (yield=100)
** Normalized to NO_2^- (yield=100)

Tables 3 and 4 show the yields of minor negative ions for 1-nitropropane and 2-nitropropane respectively in relation to the electron energy.

Effect of Pressure. Figure 5 shows the relation between yields of *m/e* 46 (NO_2^-), 16 (O^-), 26 probably CN^-) and 42 (probably, CNO^- or $C_2H_4N^-$) ions and the pressure for each sample (5a for *m/e* 46 ion, 5b for *m/e* 16 ion, 5c for *m/e* 26 ion and 5d for *m/e* 42 ion) under the electron energy of 80 eV.

All the results showed good linearity against the pressure under a given experimental condition. Also, this linear relationship was independent of the electron energy as shown in Fig. 6 where the yields of *m/e* 46 (NO_2^-) ion from nitromethane are shown as an example. A similar linear relationship had been reported for *m/e* 1 (H^-) ion produced from hydrogen[13] under the electron energies of 6.8 eV, 10.0 eV and 14.2 eV in the range of pressure

13) G. J. Schulz, *Phys. Rev.*, **113**, 816 (1959).

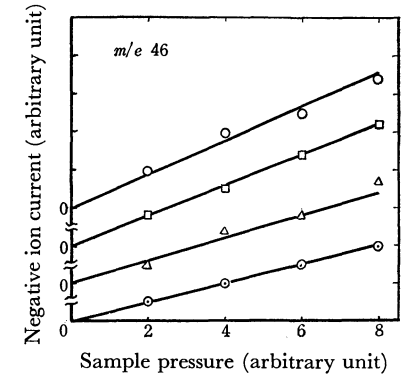

Fig. 5a

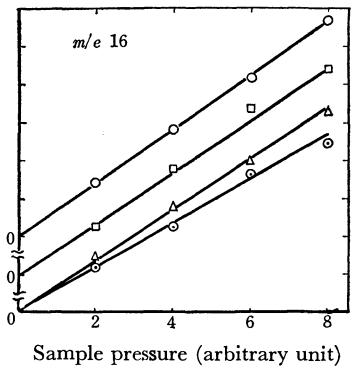

Fig. 5b

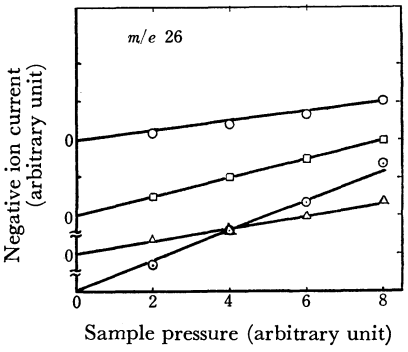

Fig. 5c

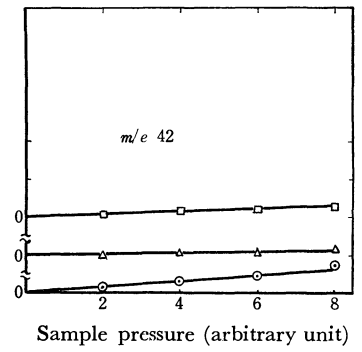

Fig. 5d

Fig. 5. Plot of negative ion current against pressure (Electron energy: 80 eV).
○ 2-$C_3H_7NO_2$ □ 1-$C_3H_7NO_2$ △ $C_2H_5NO_2$ ⊙ CH_3NO_2

Table 4. Minor negative ions from 2-$C_3H_7NO_2$

m/e	Relative intensities for electron energies of		
	80 eV*	9.5 eV**	4.5 eV**
14	0.3		
24	0.9		
26			0.2
30	1.1	1.1	
36	0.4		
37	0.4		
38	0.4		
39	0.4		
40		0.1	0.1
41	0.2		0.4
42		0.4	<0.1
47		0.2	
48		0.3	

* Normalized to O^- (yield=100)
** Normalized to NO_2^- (yield=100)

from 1×10^{-4} mmHg to 4×10^{-4} mmHg and for *m/e* 39 (CH_3CC^-) ion from methylacetylene in the range of pressure[14] up to about 5×10^{-5} mmHg. Of course, the pressure dependency may become complicated at higher pressures because of the occurrence of ion-molecule reactions. In the

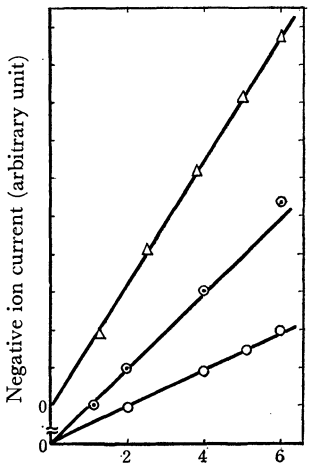

Fig. 6. Plot of negative ion current (NO_2^-) against pressure in CH_3NO_2.
△ 4.5 eV ⊙ 9.5 eV ○ 40 eV

14) T. Sugiura, T. Seguchi and K. Arakawa, This Bulletin, **40**, 2992 (1967).

present work, however, such a study was not made because of instrumental difficulties.

Role of Negative Ions in Radiolysis. The results obtained in this work suggest clearly the importance of the role of negative ions in the radiolysis of these compounds, at least in the primary process.

Indeed, in the radiolysis of nitromethane, the importance of the following reactions has been pointed out.[7]

$$CH_3NO_2 + e \longrightarrow CH_3 + NO_2^- \quad (1)$$
$$\longrightarrow CH_3^- + NO_2 \quad (2)$$
$$\longrightarrow CH_3NO + O^- \quad (3)$$
$$\longrightarrow CH_3NO^- + O \quad (4)$$

The finding that neither CH_3^- nor CH_3NO^- ions can be found, however, shows that the reactions (2) and (4) are to be rejected. Instead, the reaction (5) is to be taken into consideration, as presumed from the measurement of appearance potential of O^- ion from nitromethane.*4

$$CH_3NO_2 + e \longrightarrow CH_3N + O + O^- \quad (5)$$

Besides the above reactions, the reactions (6) and (7) accompanied with the formation of CN^- and CNO^- should be also added.*5

$$CH_3NO_2 + e \longrightarrow H_2O + OH + CN^- \quad (6)$$
$$CH_3NO_2 + e \longrightarrow H_2O + H + CNO^- \quad (7)$$

Furthermore, in 1-nitropropane the reaction (8) accompanied with the formation of $CH_2NO_2^-$ ion appears to be significant.*4

$$C_3H_7NO_2 + e \longrightarrow H + C_2H_4 + CH_2NO_2^- \quad (8)$$

Also, a relatively strong peak of $CH_2NO_2^-$ ion might provide an useful method for the identification of 1-nitropropane.

*4 to be discussed in the 2nd report of this series.
*5 to be published.

BULLETIN OF THE CHEMICAL SOCIETY OF JAPAN VOL. 42 614—618 (1969)

Measurement of Negative Ions Formed by Electron Impact. II. The Ionization Efficiency Curves of Negative Nitro, Oxygen Atom and Nitromethylene Ions from Nitroalkanes

Satoru TSUDA, Akira YOKOHATA and Michihiro KAWAI

Department of Chemistry, Faculty of Engineering, Hiroshima University, Senda-machi, Hiroshima

(Received June 17, 1968)

The ionization efficiency (IE) curves of NO_2^-, O^- and $CH_2NO_2^-$ ions from nitroalkanes (nitromethane, nitroethane, 1-nitropropane and 2-nitropropane) have been measured with a Hitachi RMU-6D mass spectrometer. Based on each authorized value of *IP*(CH_3, C_2H_5, C_3H_7, O and H), *D*(C–NO_2, C–H, C–C, NO–O and N–O), *EA*(NO_2 and O) and the excitation energy of CH_3, the respective onsets observed for the electron energies above ~3 eV on the IE curves were suggested to be interpreted as appearance potentials of the following reactions. For NO_2^- ions, $RNO_2+e\rightarrow R^*+NO_2^-$, $RNO_2+e\rightarrow R^++NO_2^-+e$; for O^- ions, $RNO_2+e\rightarrow RNO+O^-$, $RNO_2+e\rightarrow RN+O+O^-$, $RNO_2+e\rightarrow RN^++O+O^-+e$; for $CH_2NO_2^-$ ions, $CH_3NO_2+e\rightarrow H^+ CH_2NO_2^-+e$, $RNO_2+e\rightarrow H+R_1+CH_2NO_2^-$. On the other hand, the strong peak of NO_2^- ions due to the dissociative electron capture process ($RNO_2+e\rightarrow R+NO_2^-$) was observed at the lower electoron energy. Furthermore, a value of *EA*(CH_2NO_2) was presented to be ~0.5 eV.

Recently, several studies have been reported on the measurement of negative ion mass spectra by the electron impact method.[1-5] However, they have only been made for the limited kinds of compounds. Furthermore, the data of the ionization efficiency (IE) curves of negative ions are very limited. On the other hand, the role of negative ions is attracting increasing attention in the field of radiation chemistry.[6] Especially, the compounds containing nitrogen and oxygen atoms are of

1) C. E. Melton in "Mass Spectrometry of Organic Ions," ed. by F. W. Mclafferty, Academic Press, Inc., New York, N. Y. (1963), p. 163.

2) E. W. McDaniel, "Collision Phenomena in Ionized Gases," John Wiley & Sons, Inc., New York (1964), p. 368.

3) R. T. Aplin, H. Budzikiewez and C. Djerassi, *J. Am. Chem. Soc.*, **87**, 3180 (1965).

4) C. E. Melton and P. S. Rudolf, *J. Chem. Phys.*, **47**, 1771 (1967).

5) T. Sugiura, T. Seguchi and K. Arakawa, This Bulletin, **40**, 2992 (1967).

interest.

The present work provides information on the IE curves of negative nitro, oxygen atom and nitromethylene ions (NO_2^-, O^- and $CH_2NO_2^-$) from nitroalkanes for which, as far as the authors know, few reports have been published.

Experimental

The investigation was carried out using a Hitachi RMU-6D mass spectrometer equipped with a T-2M ion source having a straight line rhenium filament. The ion detection circuit consisted of an electron multiplier and of a Faraday collector.

All experiments were made with an ionizing current of 80 μA down to the electron energy of ~3 eV, though it decreased considerably in intensity at lower energies. The accerelating voltage used was always 1.8 kV and the electron multiplier was operated at 1.4 kV. The energy scale was corrected by using the values (9.4 eV and 20.9 eV) of appearance potential of O^- ions from carbon monoxide[7] and those (4.4 eV and 17.3 eV) of O^- ions from oxygen.[8] The reliability of this work, however, is restricted to electron energies above ~3 eV, because of instrumental difficulties.

The research grade nitroalkanes (nitromethane, nitroethane, 1-nitropropane and 2-nitropropane) were used without further purification. Measurements for each of the compounds were made at a pressure of about 1×10^{-6} mmHg in the source and a pressure of about 2×10^{-7} mmHg in the analyzer tube.

Results and Discussion

Formation of NO_2^- Ion. Figures 1A-a, 1B-a, 1C-a and 1D-a show respectively the IE curves of NO_2^- ions produced from nitromethane, nitroethane, 1-nitropropane and 2-nitropropane. Figures 1A-b, 1B-b, 1C-b and 1D-b show the same curves, respectively, in the range of electron energy from 3 eV to 15 eV on an expanded scale.

Through all the samples, three resonance peaks were commonly found. In addition, for nitromethane a small peak at 12 eV was found. The first resonance peak lies at a considerably lower electron energy, the second at 4.6 eV for nitromethane, 5.4 eV for nitroethane, 5.5 eV for 1-nitropropane and 5.5 eV for 2-nitropropane, and the last at 8.5 eV, 9.7 eV, 9.8 eV and 9.9 eV, respectively.

These facts show clearly that three processes contribute to the formation of NO_2^- ions. The first process can be easily understood as the dissociative electron capture. Because $D<EA$ (D:

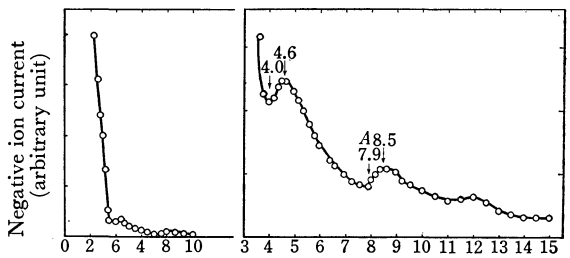

Fig. 1A-a Fig. 1A-b

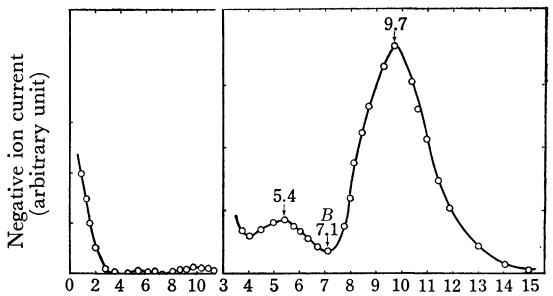

Fig. 1B-a Fig. 1B-b

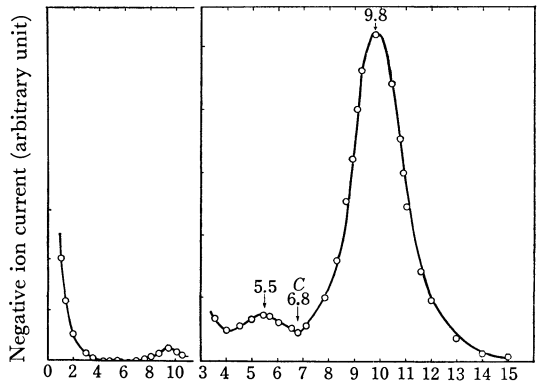

Fig. 1C-a Fig. 1C-b

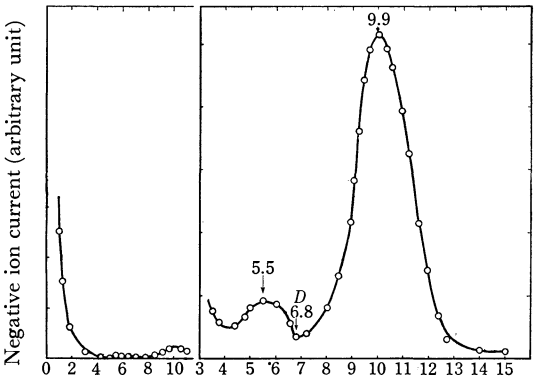

Fig. 1D-a Fig. 1D-b

Fig. 1. Ionization efficiency curves of NO_2^- from nitroalkanes.

A CH_3NO_2 B $C_2H_5NO_2$
C 1-$C_3H_7NO_2$ D 2-$C_3H_7NO_2$

6) R. B. Cundall, A. W. Locke and G. C. Street, *Nature*, **210**, 1354 (1966).

7) M. A. Fineman and A. w. Petrocelli, *J. Chem. Phys.*, **36**, 25 (1962).

8) D. c. Frost and C. A. McDowell, *J. Am. Chem. Soc.*, **80**, 6183 (1958).

dissociation energy of C–N bond, *EA*: electron affinity of NO_2), the dissociative electron capture is energetically possible even with thermal electrons. The appearance potential of NO_2^- ions due to this process can be expected to be below zero, *e. g.*, for nitromethane, -1.4—-1.6 eV.*1

The second process which can be expected to appear at 4.0 eV is not well known. Following Schulz's interpretation made for the formation of H^- ions from hydrogen,[9] however, it seems to correspond to the process of $R^*+NO_2^-$ (R^*: excited state of radical). If a value of 4.0 eV in nitromethane is taken as the value of appearance potential of $CH_3^*+NO_2^-$, the excitation energy of methyl radical can be estimated to be 5.4—5.6 eV. The agreement with the value (5.7 eV) reported by Herzberg *et al.*[10] is relatively good. Of course, this interpretation is a tentative one which demonstrates the need for further work.*2

The third process seems to correspond to that of an ion pair formation $[R^+ + NO_2^-]$. Each value marked by B, C and D in Fig. 1 coincides well with the corresponding value[11] obtained by one of the authors except for nitromethane. Thus, the third process can be concluded as the ion pair formation. For nitromethane an ion pair seems to appear at ~7.9 eV (the value marked by A in Fig. 1) which is not inconsistent with the value (8.2 eV) estimated by taking $D(C\text{–}NO_2)=2.3$ eV, $IP(CH_3)=9.8$ eV and $EA(NO_2)=3.9$ eV. A small change in negative ion current around 8 eV, however, suggests that the cross section for ion pair formation is very small compared with that of other nitroalkanes.

The present work confirms also that the IE curve for 2-nitropropane is the same as that for 1-nitropropane. It is of interest that the peak due to the ion pair formation process has been found in ~8.5 eV for nitromethane and ~9.8 eV for other three compounds irrespective of the change of alkyl group. These results indicate that the cross section for ion pair formation $[R^+ + NO_2^-]$ varies strongly with the electron energy and has a maximum value around 8.5 eV or 9.8 eV.

The relative intensity of NO_2^- ions produced from each compound is shown in Table 1. The peak height of the third process in nitromethane was almost the same as that of negative oxygen atom ions (O^-)*3 produced from carbon monoxide under the same experimental condition. Therefore, the cross section for negative nitro ion formation due to the first process should be very large.

TABLE 1. RELATIVE INTENSITY OF NO_2^- IONS PRODUCED FROM NITROALKANES

Compound \ Process	Relative intensity of peak by each process*		
	1st process	2nd rpocess	3rd process
CH_3NO_2	(> 240)	~ 3	~ 3.5
$C_2H_5NO_2$	(> 130)	1	~ 6
$1\text{-}C_3H_7NO_2$	(> 150)	~ 1	~ 8
$2\text{-}C_3H_7NO_2$	(> 200)	~ 1.5	~ 8.5

* Normalized to the peak of 2 nd process in IE curve of NO_2^- from $C_2H_5NO_2$ (yield=1).

Formation of O^- Ion. Figures 2A, 2B, 2C and 2D show respectively the IE curves of O^- ions from nitromethane, nitroethane, 1-nitropropane and 2-nitropropane. Although the negative ions of *m/e* 16 may be assigned to the species (*e. g.* NH_2^-) other than O^- ion, their possibility might be ruled out in the range of low electron energy because the complicated rearrangement is necessary for its formation.

All of the results show the possibility of three processes. The first process appears at ~3.1 eV and peaks at ~ 6.6 eV irrespective of the compounds. Thus, this process seems to be the dissociative electron capture for which the reaction (1) or (2) can be expected.

$$RNO_2 + e \longrightarrow RNO + O^- \quad (1)$$
$$\longrightarrow RN + O + O^- \quad (2)$$

However, the reaction (2) would require much higher energy than ~3.1 eV, because the values of D(RNO–O) and D(RN–O) are expected to be higher than D(NO–O) and D(N–O)[12] respectively, as pointed out by Kandel.[13] At this stage we would prefer the reaction (1), although this problem is not fully resolved.

The second process seems to appear at ~8.3 eV for nitromethane, at ~8.6 eV for other three compounds and peaks at 9.5 eV and ~10.1 eV respectively. Possibly, this corresponds to the reaction (2). Then, the values of $D(CH_3NO_2 \rightarrow CH_3N+O+O)$ and $D(RNO_2 \rightarrow RN+O+O)$ are estimated to be ~9.8 eV and ~10.1 eV respectively.

*1 $D(CH_3\text{–}NO_2) \simeq 2.5$—2.3 eV (R. I. Reed, "Ion Production by Electron Impact," Academic Press, London (1962), p. 35). $EA(NO_2) \simeq 3.9$ eV (See Ref. 11).

9) G. J. Schulz, *Phys. Rev.*, **113**, 816 (1959).

10) G. Herzberg and J. Shovsmith, *Can. J. Phys.*, **34**, 523 (1956).

*2 Although a series of optical absorption bands for nitrite ions (NO_2^-) from 330 mμ to 390 mμ has been measured by Pringsheim, this does not fit the value of 5.4≃5.6 eV; P. Pringsheim, *J. Chem. Phys.*, **23**, 369 (1955).

11) S. Tsuda and W. H. Hamill, *Advan. Mass. Spectry.*, **3**, 249 (1965).

*3 Cross section: 1.6×10^{-19} cm² (G. J. Schulz, *Phys. Rev.*, **128**, 178 (1962)).

12) V. I. Vedeneyev, L. V. Gurvich, V. N. Kondrat'yev, V. A. Medvedev and Ye. L. Frankevich, "Bond Energies, Ionization Potentials and Electron Affinities," Bulter Tanner Ltd., London (1966), p. 29: D(NO–O)≃3.2 eV, D(N–O)≃6.6 eV.

13) R. J. Kandell, *J. Chem. Phys.*, **23**, 84 (1955).

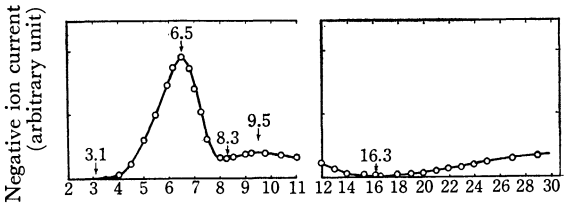

Fig. 2A-a Fig. 2A-b

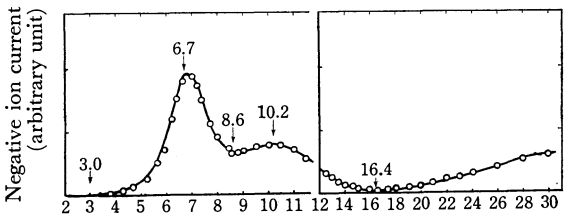

Fig. 2B-a Fig. 2B-b

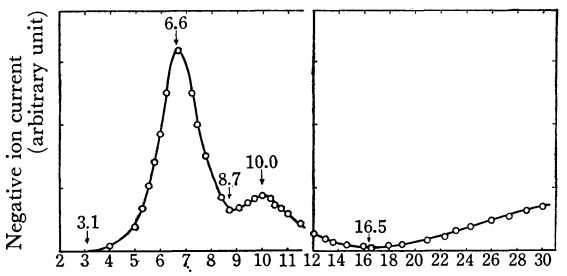

Fig. 2C-a Fig. 2C-b

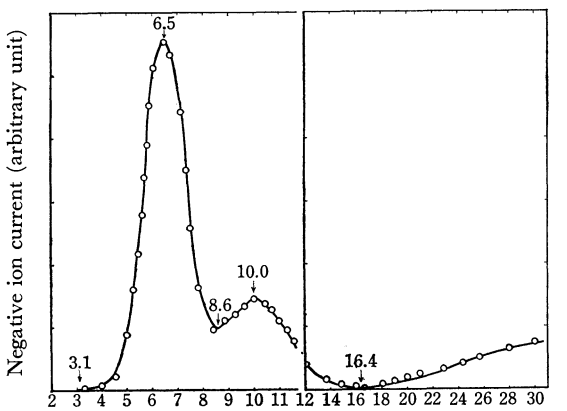

Fig. 2D-a Fig. 2D-b

Fig. 2. Ionization efficiency curves of O^- from nitroalkanes.

A CH_3NO_2 B $C_2H_5NO_2$
C $1\text{-}C_3H_7NO_2$ D $2\text{-}C_3H_7NO_2$

The third process appears to ~16.4 eV irrespective of the compounds. The following ion pair formation might be considered.

$$RNO_2 + e \longrightarrow RN^+ + O + O^- + e \qquad (3)$$

For nitromethane the appearnace potential of the reaction (3) can be etimated to be ~16 eV, taking $\Delta H_f(CH_3N^+) \simeq 11.4$ eV,[14] $\Delta H_f(CH_3NO_2) \simeq -0.8$ eV,[13] $\Delta H_f(O) \simeq 2.6$ eV[15] and $EA(O) = 1.45$ eV.[16] It agrees approximately with 16.3 eV observed for nitromethane.

Table 2. Relative intensity of O^- ions produced from nitroalkanes

Compound \ Process	Relative intensity of peak due to each process*	
	1st process	2nd process
CH_3NO_2	~3.2	~0.8
$C_2H_5NO_2$	~3	~1.3
$1\text{-}C_3H_7NO_2$	~5	~1.5
$2\text{-}C_3H_7NO_2$	~8.5	~2.5

* Normalized to the peak of 2nd process in IE curve of NO_2^- from $C_2H_5NO_2$ (yield=1).

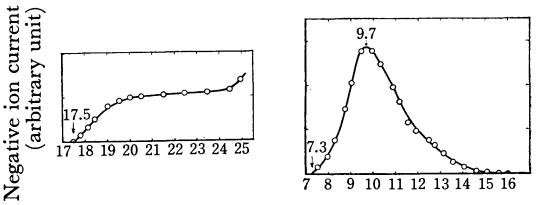

Fig. 3A Fig. 3B

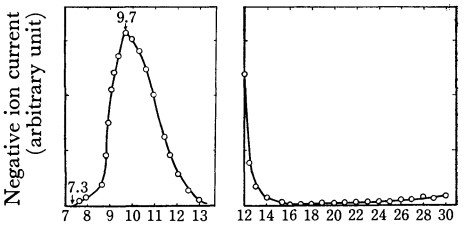

Fig. 3C-a Fig. 3C-b

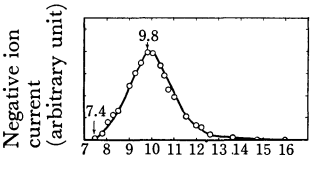

Fig. 3D

Fig. 3. Ionization efficiency curves of $CH_2NO_2^-$.

A CH_3NO_2 B $C_2H_5NO_2$
C $1\text{-}C_3H_7NO_2$ D $2\text{-}C_3H_7NO_2$

14) F. H. Field and J. J. Franklin, "Electron Impact Phenomena," Academic Press Inc., New York (1957), p. 274.

15) R. R. Bernecker and F. A. Long, *J. Phys. Chem.*, **65**, 1565 (1961).

16) D. C. Frost and C. A. McDowell, *J. Am. Chem. Soc.*, **80**, 6183 (1958).

Table 2 shows the relative intensity of the peaks of O^- ions produced from each compound.

Formation of $CH_2NO_2^-$ (m/e 60) Ion. Figures 3(A), 3(B), 3(C) and 3(D) show respectively the IE curves of $CH_2NO_2^-$ ions*4 from nitromethane, nitroethane, 1-nitropropane and 2-nitropropane. All of the results except for nitromethane showed a broad resonance peak in the range of electron energy from 7.3 eV to ~16 eV. The peaks were respectively at 9.7 eV for nitroethane, at 9.7 eV for 1-nitropropane, and at 9.8 eV for 2-nitropropane.

A relatively high value of appearance potential (~7.3 eV) rules out the possibility of the dissociative electron capture process; $R+CH_2NO_2^-$ (R: radical).

In the discussion on IE curves of NO_2^- ions, the authors pointed out the possibility of ion pair formation in the range of electron energy from 6.8 eV to 15 eV. If the process of ion pair formation corresponds also to a value of ~7.3 eV, the electron affinity of CH_2NO_2 radical can be estimated to be 4.5 eV from the reaction (4) by using the values of $D(C_2H_5\text{–}CH_3)=3.5$ eV[12] and $IP(C_2H_5)=8.3$ eV[17]

$$1\text{-}C_3H_7NO_2 + e \longrightarrow C_2H_5^+ + CH_2NO_2^- + e \quad (4)$$

On the other hand, the reaction (5)[17] gives the value of 6.1 eV.

$$C_2H_5NO_2 + e \longrightarrow CH_3^+ + CH_2NO_2^- + e \quad (5)$$

In addition to their high values, their inconsistency rules out the possibility of the ion pair formation. Then, the possibility of reaction (6) or (7) is expected.*5

$$RNO_2 + e \longrightarrow H + R_1 + CH_2NO_2^- \quad (6)$$
$$RNO_2 + e \longrightarrow CH_3 + CH_2 + CH_2NO_2^- \quad (7)$$

However, the same value*6 of onset suggests the possibility of the reaction (6).

For 1-nitropropane in which the formation of $CH_2NO_2^-$ ions was successively observed for the electron energies higher than ~17 eV, the onset of ion pair formation might be expected in this range. Because of a very slow slope of IE curve (Fig. 3 C-b), however, it was very difficult to determine the value of onset.

On the other hand, a high onset value (17.5 eV) in nitromethane suggests strongly the possibility of the following ion pair formation.

$$CH_3NO_2 + e \longrightarrow H^+ + CH_2NO_2^- + e \quad (8)$$

Then, the electron affinity of CH_2NO_2 radical can be estimated to be 0.5 eV, by using $D(C\text{–}H)=4.4$ eV and $IP(H)=13.6$ eV. This value is also consistent with the value (0.6 eV) estimated from reaction (6), by taking $D(C\text{–}H)=4.4$ eV, $D(C\text{–}C)=3.5$ eV. However, because of a very small yield of $CH_2NO_2^-$ ion the reliability of this value is not so high.

TABLE 3. RELATIVE INTENSITY OF THE PEAKS OF $CH_2NO_2^-$ IONS

Compound	Relative intensity*
$C_2H_5NO_2$	~0.05
$1\text{-}C_3H_7NO_2$	~5
$2\text{-}C_3H_7NO_2$	~0.12

* Normalized to the peak of 2nd process in IE curve of NO_2^- from $C_2H_5NO_2$ (yield=1).

Table 3 shows the relative intensity of the peaks of $CH_2NO_2^-$ ion from each compound.*7 It should be emphasized that the intensity of $CH_2NO_2^-$ from 1-nitropropane is much stronger (about 100—40 times) than that from nitroethane and 2-nitropropane. This might be useful for the identification of 1-nitropropane.

The authors are indebted to Professor William H. Hamill, Radiation Laboratory, University of Notre Dame, Indiana, U. S. A. for helpful suggestions and discussions.

*4 The possibility of $C_2H_4O_2$ ion may be ruled out, because (1) in spite of the complicated rearrangement required for the formation of $C_2H_4O_2^-$ from $1\text{-}C_3H_7NO_2$, a relatively large peak of m/e 60 ion was found, and (2) the appearance potential observed cannot be explained with the formation of this ion.

17) C. E. Melton and W. H. Hamill, *J. Chem. Phys.*, **41**, 3464 (1964).

*5 The $CH_2NO_2^-$ ion from 2-nitropropane is considered to be the rearrangement ion.

*6 The appearance potential of the reaction (6) is shown as follows.

$AP=D(C\text{–}H)+D(C\text{–}C)-EA(CH_2NO_2)$

where the excess kinetic energy of fragment ions is ignored.

*7 The relative intensity of $CH_2NO_2^-$ ion from CH_3NO_2 was very samll (~0.02) in the range of electron energy from 20 eV to 23 eV.

BULLETIN OF THE CHEMICAL SOCIETY OF JAPAN VOL. 42 619—624 (1969)

Infrared Spectra of Acylureas and *NN'*-Deuterated Acylureas

Toyozo Uno, Katsunosuke Machida, Kazuhiko Hanai and Yutaka Saito

Faculty of Pharmaceutical Sciences, Kyoto University, Sakyo-ku, Kyoto

(Received July 3, 1968)

The infrared spectra of seven monoacylureas and their *NN'*-deuterated compounds have been measured in the region between 3600 and 450 cm^{-1}. A number of characteristic absorption bands of the $-CONHCONH_2$ and $-CONDCOND_2$ groups have been found and assigned by referring to the infrared spectra of related compounds and the isotopic frequency shifts. Partial deuteration by mixtures of water and heavy water has been made to distinguish the absorptions due to the NH and NH_2 groups from each other. The features of infrared spectra of monoacylureas can be explained by regarding them as composite spectra of aliphatic imides and urea. From the effect of the alkyl frame-work vibrations for the imide III frequency, it is suggested that the RCONH– group of monoacylureas takes the *trans* conformation.

The infrared spectra of monosubstituted amides and related compounds have been the subject of a large number of systematic investigation.[1] The coupling between the CN stretching vibration and the NH in-plane deformation vibration of monosubstituted amides has been proved to be related closely to the conformation of the –CONH– group. The amide II and III bands arising from this coupling are observed only for the *trans* conformation.[2] A similar effect of the structure on the vibrational coupling has been reported for the aliphatic imides in which two C=O bonds are connected to a NH bond.[3] It is desirable to extend the analysis of the amide type vibrational coupling to more complicated combinations of the C=O and NH bonds, since they are involved in many biologically important compounds.

The present paper deals with the infrared spectra of seven monoacylureas, $RCONHCONH_2$ [R = CH_3, C_2H_5, *n*-C_3H_7, *i*-C_3H_7, *n*-C_4H_9, *i*-C_4H_9, $(C_2H_5)_2CH$] and their *NN'*-deuterated derivatives. The assignment of the characteristic frequencies of the $-CONHCONH_2$ and $-CONDCOND_2$ groups was given on the basis of the spectral change on deuteration and comparison with related compounds such as urea,[4] monosubstituted amides[5] and aliphatic imides.[6]

Experimental

Acetylurea[7] and propionylurea[8] were prepared by heating a mixture of corresponding acid, acid anhydride, urea and trace sulfuric acid. The usual method of acylation with acyl chloride in dry benzene was used for preparing *n*-butyryl, *i*-butyryl-, *n*-valeryl, *i*-valeryl and diethylacetyl ureas.[8] These acylureas were recrystallized several times from ethyl alcohol. The *NN'*-deuterated compounds were prepared by recrystallization from a mixture of dioxane and heavy water, and partially deuterated compounds from a mixture of dioxane, water and heavy water.

The infrared spectra were recorded on a Koken DS 301 infrared spectrophotometer equipped with NaCl (4000—700 cm^{-1}) and KBr (700—450 cm^{-1}) prisms. The samples were subjected to the measurement in the form of solid dispersed in Nujol and H. C. B. (hexachlorobutadiene). The absorption frequencies are listed in Tables 1 and 2.

Results and Discussion

The Region above 2000cm^{-1}. Acylureas have both the NH_2 and NH groups, and three absorption bands due to the stretching vibrations of these groups are observed near 3430, 3320 and 3230 cm^{-1}. Watson *et al.* assigned the bands near 3420 and 3320 cm^{-1} to the NH_2 antisymmetric and symmetric stretching vibrations, respectively, and the band near 3230 cm^{-1} to the NH stretching vibration.[9]

1) L. J. Bellamy, "The Infrared Spectra of Complex Molecules," 2nd Ed., Methuen & Co., Ltd. London, John Wiley & Sons, Inc., New York (1958), p. 203.

2) T. Miyazawa, T. Shimanouchi and S. Mizushima, *J. Chem. Phys.*, **29**, 611 (1958).

3) T. Uno and K. Machida, This Bulletin, **36**, 427 (1963)

4) A. Yamaguchi, T. Miyazawa, T. Shimanouchi and S. Mizushima, *Spectrochim. Acta*, **10**, 170 (1957); A. Yamaguchi, *Nippon Kayaku Zasshi* (*J. Chem. Soc. Japan, Pure Chem. Sect.*), **78**, 1319, 1467 (1957).

5) T. Miyazawa, T. Shimanouchi and S. Mizushima, *J. Chem. Phys.*, **24**, 408 (1956).

6) T. Uno and K. Machida, This Bulletin, **34**, 551 (1961).

7) E. A. Werner, *J. Chem. Soc.*, **109**, 1127 (1916).

8) R. W. Stoughton, *J. Org. Chem.*, **2**, 514 (1938).

9) J. R. Watson and M. Pernaroski, *J. Associ. Offici. Agri. Chemists*, **45**, 609 (1962).

We investigated the infrared spectra of partially deuterated samples obtained by exchange reaction with the mixture of water and heavy water in various proportions, and interchanged Watson *et al.*'s assignments of the bands near 3320 and 3230 cm^{-1} on the basis of the intensity change of these bands on the progress of deuteration. One may assume that the isotopic change on the NH_2 and NH groups hardly affects the vibrational frequencies of each other, and that the intensities of the NH_2 and the NH stretching bands are determined by the total concentration of the molecules involving the corresponding group. The concentration of the NH_2 group in the partially deuterated samples decreases more steeply than that of the NH group as the concentration of heavy water in the mixed solvent increases, since the former has two exchangeable protons while the latter has one. Such difference in the rate of concentration changes is expected to give rise to the difference in the rate of intensity changes between the NH_2 and the NH stretching bands, although one must be careful in taking account of the interference of bands due to the NHD group.

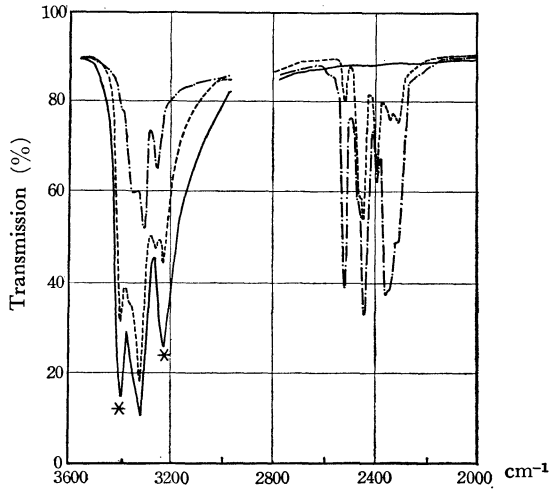

Fig. 1. Infrared spectra of propionylurea (———), partially deuterated propionylurea from 25% D_2O (--------) and partially dueterated propionylurea from 75% D_2O (– – – –).
* the band due to the NH_2 species.

In Fig. 1, the infrared spectra of partially deuterated propionylureas between 3800 and 2200 cm^{-1} are shown. The intensities of the bands at 3424 and 3252 cm^{-1} (labeled*) decrease more rapidly than the intensity of the band at 3342 cm^{-1} on the progress of deuteration. This result suggests that the bands at 3424 and 3252 cm^{-1} are due to the NH_2 antisymmetric and symmetric stretching vibrations, respectively, and that the band at 3342 cm^{-1} is due to the NH stretching vibration. Similarly, for the deuterated compounds the bands at 2550 and 2390 cm^{-1} are assigned to the ND_2 antisymmetric and symmetric stretching vibrations, respectively, and the band at 2466 cm^{-1} to the ND stretching vibration. The intensity changes of these bands on successive deuteration are just what are expected from the concentration changes of the ND_2 and the ND groups. The bands at 3370 and 3278 cm^{-1} are observed only for the partially deuterated samples. They are attributed to the NH stretching vibrations of the NHD group, and their contributions to the peak intensities of the NH_2 and the NH stretching bands are estimated to be small. The presence of two NH stretching bands of the NHD group may be due to the presence of the NH bonds in *trans* and *cis* conformations against the C=O bond. The partially deuterated samples show also the ND stretching bands of the NHD group at 2475 and 2413 cm^{-1}.

The Region between 2000 and 1500 cm^{-1}. Figures 2—8 show the representative infrared spectra of seven monoacylureas and their *NN'*-deuterated compounds in the region between 1900 and 400 cm^{-1}. The infrared spectra between 1800 and 1500 cm^{-1} of the presently investigated acylureas may be classified into two types distinguishable from each other by the feature of the C=O stretching and the NH_2 bending absorptions. The type I spectra are shown by acetyl-, propionyl-, *i*-butyryl- and diethylacetylureas, and the type II spectra by *n*-valeryl-, *n*-butyryl- and *i*-valerylureas.

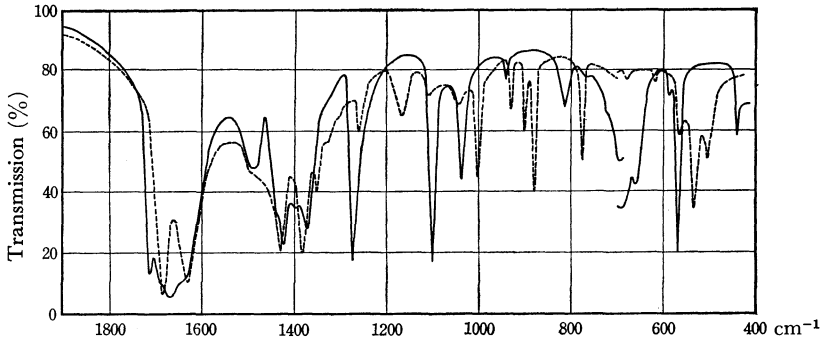

Fig. 2. Infrared spectra of acetylurea (solid line) and acetylurea-d_3 (broken line).

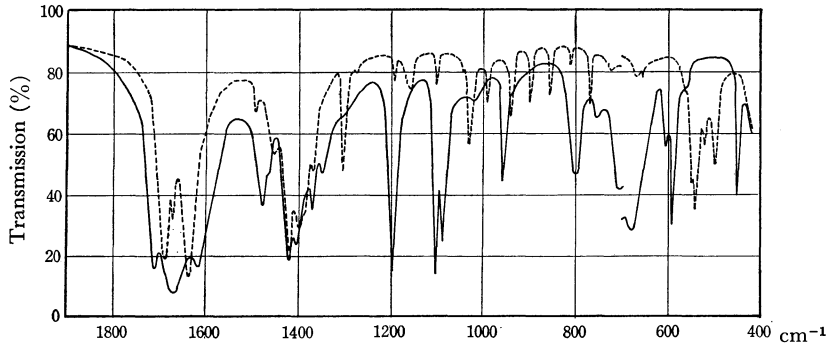

Fig. 3. Infrared spetra of propionylurea (solid line) and propionylurea-d_3 (broken line).

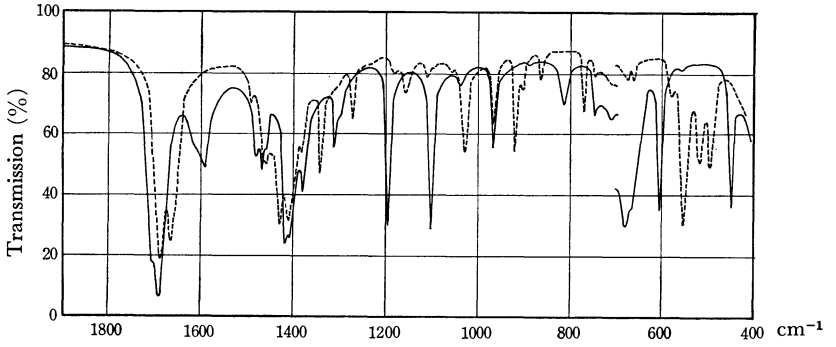

Fig. 4. Infrared spectra of *n*-butyrylurea (solid line) and *n*-butyrylurea-d_3 (broken line).

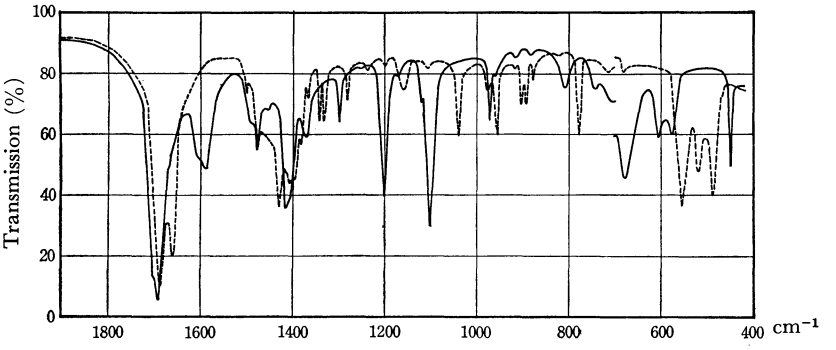

Fig. 5. Infrared spectra of *i*-butyrylurea (solid line) and *i*-butyrylurea-d_3 (broken line).

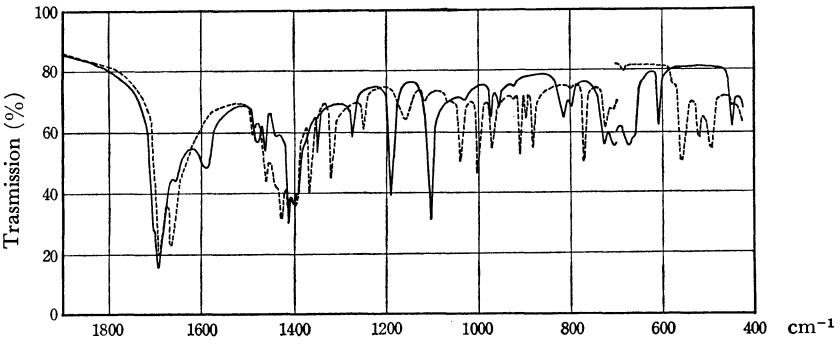

Fig. 6. Infrared spectra of *n*-valerylurea (solid line) and *n*-valerylurea-d_3 (broken line).

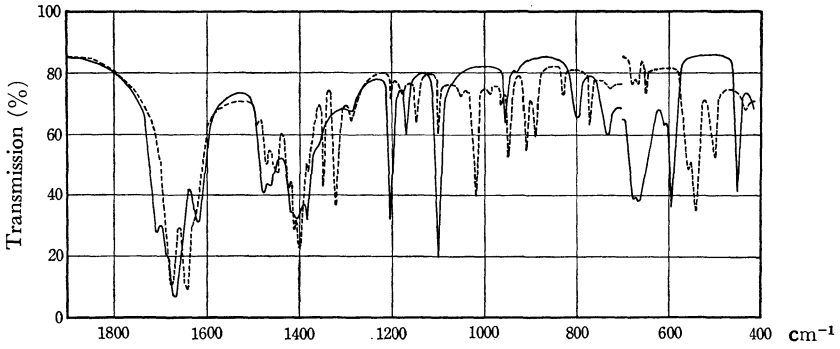

Fig. 7. Infrared spectra of *i*-valerylurea (solid line) and *i*-valerylurea-d_3 (broken line).

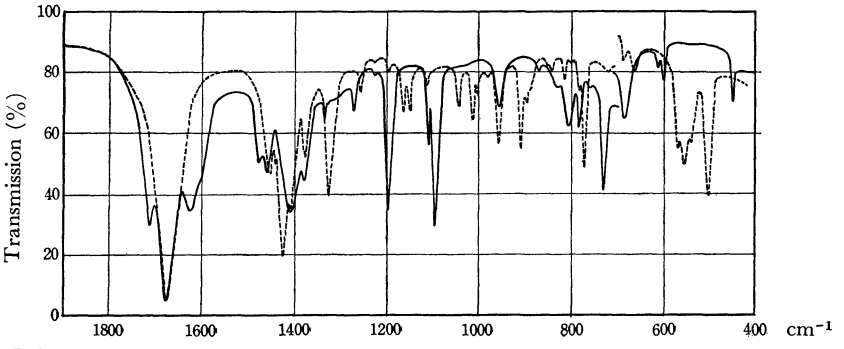

Fig. 8. Infrared spectra of diethylacetylurea (solid line) and diethylacetylurea-d_3 (broken line).

In the type II spectra, the C=O stretching absorptions, observed as a sharp and strong band near 1690 cm^{-1} and its shoulder near 1705 cm^{-1}, are separated clearly from the NH_2 bending absorption near 1590 cm^{-1} which disappears on *NN'*-deuteration. In the type I spectra, on the other hand, the C=O stretching and the NH_2 bending absorptions overlap with each other and give rise to a strong composite band with three peaks near 1710, 1680 and 1620 cm^{-1}. The spectral change on *NN'*-deuteration gives no definite clue to identify the absorption due to the NH_2 bending vibration. We tentatively assigned the 1620 cm^{-1} peak to this vibration from analogy to the type II spectra. The difference between the type I and II spectra may result from the difference in the scheme of hydrogen bonds involving the C=O and the NH_2 groups. Although this spectral difference is rather empirical at the present stage, it should be noted that a preliminary survey of infrared spectra of a number of α-brominated acylureas has also shown the presence of the two types I and II. The C=O stretching absorption of the *NN'*-deuterated acylureas splits mostly into two distinct peaks, around 1680 and 1640 cm^{-1} for the type I and around 1690 and 1665 for the type II. Only diethylacetylurea shows a single peak at 1681 cm^{-1}.

The Region between 1500 and 850 cm^{-1}. The spectral change on *NN'*-deuteration is complicated in this region since many deformation vibrations of the NH_2, NH, ND_2 and ND groups show their frequencies in this region and they couple often with other vibrations. Acetylurea shows a medium band at 1485 cm^{-1} and two sharp and fairly strong bands at 1260 and 1098 cm^{-1}, all of which disappear on *NN'*-deuteration. The 1485 cm^{-1} and the 1098 cm^{-1} bands persist in the spectra of other acylureas, but the 1260 cm^{-1} band is replaced by a similar band near 1200 cm^{-1} on the change of the acyl group from acetyl to the others. In some cases involving large acyl groups, the presence of the 1480 cm^{-1} is obscured by the overlap of the CH_3 and CH_2 deformation absorptions, and is confirmed only by the comparison with the corresponding *NN'*-deuterated compounds. Instead of these bands, the *NN'*-deuterated acylureas show commonly four weak to medium bands around 1330, 1170, 1050 and 900 cm^{-1}. We assigned the 1100 cm^{-1} band of the undeuterated compounds to the NH_2 rocking vibration from analogy to acetamide,[10] urea[4] and biuret,[11] and the 1170 cm^{-1} band and the 900 cm^{-1} band of *NN'*-deuterated compounds to the ND_2 bending and ND_2 rocking vibrations, respectively, from analogy to

10) I. Suzuki, This Bulletin, **35**, 1279 (1962).
11) M. Takimoto, *Nippon Kagaku Zasshi* (*J. Chem. Soc. Japan, Pure Chem. Sect.*), **85**, 168 (1964).

Table 1. The infrared characteristic frequencies of $-CONHCONH_2$ group

CH_3-	CH_3CH_2-	$CH_3CH_2CH_2-$	$(CH_3)_2CH-$	$CH_3(CH_2)_3-$	$(CH_3)_2CH_2CH_2-$	$(C_2H_5)_2CH-$	Assignment
3425 vs*	3424 vs	3419 vs	3414 s	3408 s	3419 s	3394 s	NH_2 asym. stretching
3354 vs	3342 vs	3338 vs	3325 vs	3335 s	3339 s	3321 s	NH stretching
3232 s	3252 s	3238 m	3248 m	3232 m	3238 m	3230 m	NH_2 sym. stretching
1712 s	1712 vs	1707 vs	1705 vs	1704 vs	1705 vs	1714 vs	C=O stretching
1674 vs	1680 vs	1693 vs	1668 vs	1690 vs	1690 vs	1681 s	C=O stretching
1637 s	1620 s	1595 m	1619 s	1593 m	1593 m	1624 m	NH_2 bending
1485 m	1476 m	1479 m	1481 m	1480 w	1483 w	1476 m	Imide II band
1414 vs	1407 vs	1415 s	1410 s	1414 s	1412 m	1412 s	CN stretching (?)
1260 s	1198 vs	1193 s	1203 s	1187 s	1198 vs	1198 s	Imide III band
1098 s	1098 s	1098 s	1100 s	1098 s	1100 s	1096 s	NH_2 rocking
942 vw	956 m	966 m	953 w	971 w	968 w	957 w	CN stretching
815 w	800 m	815 w	802 w	815 w	812 w	808 w	C=O out-of-plane deformation (urea part)
725, 695 mb	700 mb	710 mb	735 mb	732, 704 mb	715 mb	740 mb	NH out-of-plane deformation
660 mb	680 mb	680 mb	675, 665 mb	680 mb	680 mb	685 mb	NH_2 wagging
589 vw, 569 vs	607 vw, 595 s	650 m	609 vw, 593 m	608 m	603 w, 577 w	600 w	CO in-plane or out-of-plane deformation (amide part)

Table 2. The infrared characteristic frequencies of $-CONDCOND_2$ group

CH_3-	CH_3CH_2-	$CH_3CH_2CH_2-$	$(CH_3)_2CH-$	$CH_3(CH_2)_3-$	$(CH_3)_2CH_2CH_2-$	$(C_2H_5)_2CH-$	Assignment
2544 s	2550 s	2545 m	2551 s	2542 m	2542 m	2545 m	ND_2 asym. stretching
2474 m	2466 s	2466 m	2466 s	2468 m	2468 m	2465 m	ND stretching
2393 s	2390 m	2377 m	2396 s	2379 m	2380 m	2386 m	ND_2 sym. stretching
1682 vs	1691 vs	1691 vs	1680 vs	1690 vs	1687 vs	1681 vs	C=O stretching
1637 vs	1640 vs	1666 s	1641 vs	1666 vs	1664 vs		C=O stretching
1425 s	1421 vs	1430 s	1415 s	1430 s	1431 s	1425 s	CN stretching (?)
1348 m	1307 s	1342 m	1319 m	1321 s	1332 m	1328 m	Imide II′ band
1169 vw	1160 vw	1159 vw	1156 w	1158 w	1167 w	1170 w	ND_2 bending
1112 vw	1032 m	1030 w	1021 w	1041 m	1038 m	1047 m	Imide III′ band
933 w	946 w	964 w	950 w	967 m	955 m	957 m	CN stretching
879 m	899 w	904 m	908 w	910 m	906 w	910 m	ND_2 rocking
772 w	770 w	772 w	772 w	771 m	773 m	773 m	C=O out-of-plane deformation (urea paprt)
534 wb	549 sh, 542 s	551 s	563 m, 548 m	559 s	558 m	573 m	C=O in-plane or out-of-plane deformation (amide part)
563 w	518 m	521 w	544 m	517 m	525 w	554 s	ND out-of-plane deformation
505 m	495 m	496 m	501 w	495 s	494 s	501 s	ND_2 wagging

* vs: very strong, s: strong, m: medinm, w: weak, vw: very weak, b: broad

acetamide-d_2[10] and urea-d_4.[4] The remaining deuteration sensitive absorption frequencies are quite analogous to those reported for aliphatic acylic imides, RCONHCOR′ (R, R′=alkyl), and their *N*-deuterated derivatives.[6] The imide II band near 1500 cm^{-1} and the imide III band between 1240 and 1180 cm^{-1} of aliphatic acylic imides are replaced on deuteration by the imide II′ band near 1330 cm^{-1} and the imide III′ band near 1000 cm^{-1}. By the normal coordinate analysis of diacetamide,[3] it has been confirmed that the imide II and III bands arise from the coupling between the NH in-plane deformation vibration and the CN stretching vibrations of the –CONHCO– group, just as in the well known case of the amide II and III bands of monosubstituted amides. The imide II′ band of the deuterated acylic imides is mainly due to the CN stretching vibration and the imide III′ band due to the ND in-plane deformation vibration. From the structural analogy between acylureas and acylic imides, the 1480 cm^{-1} band of the presently investigated acylureas is identified immediately as the imide II band and the 1260 cm^{-1} of acetylurea and the 1200 cm^{-1} band of the other acylureas as the imide III band. The 1330 cm^{-1} and the 1050 cm^{-1} bands of the *NN′*-deuterated acylureas correspond probably to the imide II′ and III′ bands, respectively. These empirical assignmengs of the deuteration sensitive bands of acylureas are given support to by the infrared spectra of the partially deuterated samples. On the increase of the relative amount of heavy water in the solvent for the exchange reaction, the 1100 cm^{-1} band shows faster intensity decrease than the 1480 cm^{-1} band and the 1200 cm^{-1} band (1280 cm^{-1} for acetylurea), whereas the 1170 cm^{-1} and the 900 cm^{-1} bands show slower intensity increase than the 1330 cm^{-1} and the 1050 cm^{-1} bands. The partially deuterated samples show only a few additional absorptions appearing as satellite peaks of the above mentioned bands, although these samples are mixtures of many isotopic molecules with respect to the number and positions of deuterium atoms.

For aliphatic acylic imides it has been reported that the vibrations of alkyl groups contribute to the imide III band through the coupling with the CN stretching vibrations, and this coupling gives rise to the low frequency shift of the imide III frequency of aliphatic acylic imides from 1240 cm^{-1} to 1180 cm^{-1} on the change of alkyl frameworks from methyl to ethyl and larger alkyl groups. Similarly, the effect of the alkyl framework on the imide III frequency of acylureas presently observed indicates that the CN stretching vibration of the RCONH– group of acylureas couples with the NH in-plane deformation vibration as well as with the vibrations of the alkyl framework. It is well known that the coupling between the CN stretching and the NH in-plane deformation vibrations occurs only for the trans –CONH– group.[2] Accordingly, the RCONH– group of acylureas is probably in the trans conformation.

Besides the CN stretching vibration of RCONH– group participating in the imide II and III bands, acylureas have two more degrees of freedom for those arising from the $-NHCONH_2$ group. We assigned the weak or medium band near 950 cm^{-1} observed commonly for the presently investigated acylureas and their *NN′*-deuterated compounds to one of these two CN stertching vibrations. This absorption frequency is comparable with the CN symmetric stretching frequency of urea itself at 1000 cm^{-1}.[4] The remaining CN stretching band is then supposed to appear around 1450 cm^{-1} by analogy with the CN antisymmetric stretching frequency of urea (1660 cm^{-1}).[4] The interference of the CH deformation bands of alkyl groups makes it difficult, however, to identify this band. The strong bands near 1410 cm^{-1} for acylureas and near 1440 cm^{-1} for the *NN′*-deuterated compounds were tentatively assigned to this CN stretching vibration.

The Region between 850 and 450 cm^{-1}. For the undeuterated acylureas, four bands around 810, 700, 680 and 570 cm^{-1} are commonly observed between 850 and 450 cm^{-1}. Referring to the C=O out-of-plane deformation frequency of urea, we assigned the slightly broad band near 810 cm^{-1} of undeuterated acylureas to the corresponding vibration of the $-NHCONH_2$ group. On *NN′*-deuteration, this band is replaced by the sharp band at 770 cm^{-1}, the frequency being almost independent of the alkyl group. The broad bands around 700 and 680 cm^{-1} of acylureas disappear on deuteration and are assigned to the NH_2 wagging and the NH out-of-plane deformation, vibration respectively, from analogy with urea and aliphatic imides. For the *NN′*-deuterated compounds, the corresponding ND_2 wagging and the ND out-of-plane deformation bands are found near 550 and 500 cm^{-1}, respectively. These assignments were given support to again by the change in the relative intensities on partial *NN′*-deuteration.

The group frequencies so far left unassigned in this region are the C=O in-plane and out-of-plane deformation vibrations of the RCONH– group and the C=O in-plane deformation vibration of the $-NHCONH_2$ group. By comparison with the available data for monosubstituted amides,[5] imides[6] and urea,[4] these vibrations are expected to have their frequencies around 600 cm^{-1}. The strong band near 570 cm^{-1} of acylureas may therefore be taken as an overlapped absorption contributed by these vibrations. The corresponding band for *NN′*-deuterated compounds is observed around 530 cm^{-1}.

Thanks are due to the members of the Microanalytical Center of Kyoto University for elemental analysis.

BULLETIN OF THE CHEMICAL SOCIETY OF JAPAN VOL. 42 625—630 (1969)

Photochemistry of Acridine and Acridan. Two Isomeric Forms of Acridine Semiquinone

Akira KIRA

The Institute of Physical and Chemical Research, Yamatomachi, Saitama

and Masao KOIZUMI

Department of Chemistry, Faculty of Science, Tohoku University, Sendai

(Received July 11, 1968)

A transient species characterized by the absorption peaks at 350 mμ and 560 mμ has been found in the flash photolysis of acridan in both benzene and methanol solutions. This species has been proved to be different from the acridine semiquinone reported already, but has been identified as another acridine semiquinone radical on the basis of its direct conversion to acridine and also from its low reactivity to oxygen which denies the possibility of being triplet acridan. Thus it is concluded that two isomeric forms of acridine semiquinone exist. From the result of the flash photolysis of biacridan, the one reported previously has been identified definitely with a radical having a hydrogen atom attached to the nitrogen atom of acridine. Therefore, the newly discovered one is most likely a radical with a hydrogen atom attached on the 9 carbon atom of acridine.

In previous papers,[1,2] acridine semiquinone with the absorption maxima at 278 mμ and ~520 mμ has been found in flash photolysis studies of acridine in alcohols. Judging from the results of steady-illumination studies,[3] the formation of semiquinone was also expected in the photoreduction of acridine by acridan (dihydroacridine) in inert solvents, but the transient species in this case showed some difference against the semiquinone described above both in its spectral and in kinetic features.[4] Under such circumstances, it is most desirable to study further the transient absorption spectra observed in the photoreduction of acridine in various conditions, and in particular, in the photodehydrogenation of acridan.

In the present work, the photoreaction of acridan was studied with the flash method in a non-polar solvent, benzene and also in a polar solvent, methanol, both of which had been used in the previous investigations. In addition, the transient species produced photochemically in benzene solutions of acridine and acridan was investigated in more detail. It has been found that the results are interpreted satisfactorily by regarding a new transient band from acridan as an isomer of the acridine semiquinone. Furthermore, the structure of the semiquinone found in the photoreduction of acridine was determined by comparing its spectrum with the transient spectrum in the photolysis of biacridan.

Experimental

Apparatus. A flash photolysis apparatus used in the present work was constructed recently at the Institute of Physical and Chemical Research.

The excitation source consisting of two U-shaped xenon flash lamps connected in series were fired with the electric charge stored in two or three 1 μF-capacitors at 6 to 10 kV. A half-intensity duration was 15 μs at 9 kV and 3 μF. A quartz cylinder 10 cm in length and with an inner diameter of 8 mm, was used as a sample cell. Liquid or solution filters were set between the lamps and the cell; filter cells were of quartz with a size of $106 \times 52 \times 8$ mm^3. Details of the apparatus are described elsewhere.[5]

Illumination Conditions. Samples were illuminated by the 64 to 94 J flash through filters. Methanol solutions were excited through a plastic filter with a ~250 mμ cut off. For benzene solutions of acridan, a liquid benzene filter was employed to eliminate the photo-excitation of the solvent. In the solutions of acridine and acridan, only the former was excited by using a Toshiba UV-D2 filter. Biacridan dissolved in dimethylsulfoxide (DMSO) was illuminated through the plastic filter described above. Although the solvent, DMSO, absorbs considerably under this condition, the excitation of the solvent did not disturb the observation of the transient spectra.

Samples. Acridan was prepared by reducing acridine with sodium amalgam and recrystallized three times from a methanol-water mixture after removing insoluble

1) A. Kira, S. Kato and M. Koizumi, This Bulletin, **39**, 1221 (1966).
2) A. Kira, *Sci, Rep. Tohoku Univ.*, **49**, 129 (1966).
3) S. Niizuma, Y. Ikeda and M. Koizumi, This Bulletin, **40**, 2249 (1967).
4) A. Kira and M. Koizumi, *ibid.*, **40**, 2486 (1967).
5) A. Kira and K. Nishi, *Rep. IPCR*, **44**, 56 (1968) (in Japanese).

precipitates. Acridine was recrystallized three times from an ethanol-water mixture.

Biacridan was photochemically prepared and recrystallized from dimethylsulfoxide.[6]

Benzene fractionally distilled from a guaranteed reagent of Wako Pure Chemicals Co. was used throughout the present work; it gave slower decays of the transient species in the photolysis of acridan than a Dotite "Primasol" benzene without further purification.

A G. R. methanol submitted to the fractional distillation was used; a "spectral" methanol which we purchased was found to contain some amines as a stabilizing agent.

Dimethylsulfoxide was twice fractionally crystallized from a Wako reagent grade reagent.

Solutions were degassed by the usual freeze-pump-thaw method. The procedure was repeated at least three times. When the distillation of a soluent between two traps was made as the method of degassging, some acridan was converted to acridine in the case of methanol.

Results and Discussion

Comparison of the Transient Spectra in Various Systems.

Transient absorption spectra for acridan are shown in Figs. 1 and 2. The peaks are situated at 352 and 557 mμ in a benzene solution and at 350 and 564 mμ in a methanol solution. Hereafter, we will call them the 350 mμ- and the 560 mμ-band respectively. These two bands decay similarly in the second order, as will be described later, and it appears that they are ascribed mainly to the one same species. They were also observed in the aerated solutions, though the intensities were somewhat reduced. The decay of the transient absorption in aerated solutions had duration times of the order of 10^{-4} sec. This suggests that a species giving rise to these bands has low reactivity to oxygen, because, if it were to react with oxygen with the diffusion-controlled rate constant, 10^{10} M^{-1} sec^{-1}, the duration time in aerated solutions containing $\sim 2\times 10^{-3}$M oxygen (for both solvents) would be of the order of 10^{-7} sec. The predominant final product was identified with acridine from its absorption spectra; an example for benzene solution is shown in Fig. 3. Furthermore, in methanol which is transparent in the near UV region, an intense maximum at 250 mμ characteristic of acridine was also observed. As shown in Fig. 4, the formation of acridine was found to proceed in parallel with the fade-out of the transient absorption at 560 mμ, in both deaerated and aerated methanol solutions.

According to previous papers,[1,2] the spectra of acridine semiquinone obtained in the photoreduction of acridine in deareated alcohol solutions have the maxima at ~480 and ~520 mμ in the visible

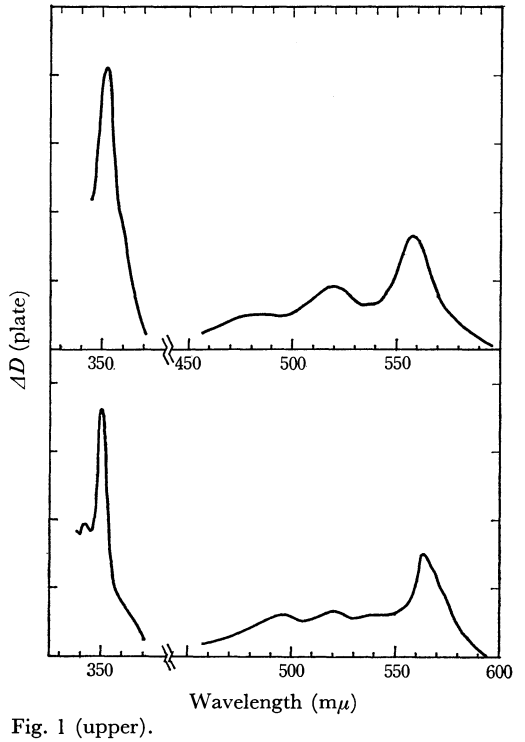

Fig. 1 (upper).
A transient spectrum observed in a deaerated benzene solution of 1×10^{-4} M acridan (t: 50 μsec), and
Fig. 2 (lower).
One observed in a deaerated methanol solution of 5×10^{-5} M acridan (t: 50 μsec). Both spectra were photographed on the same plate. The wavelength response of the plate (Fuji, Neopan.) is not corrected (also for Figs. 5 and 6).

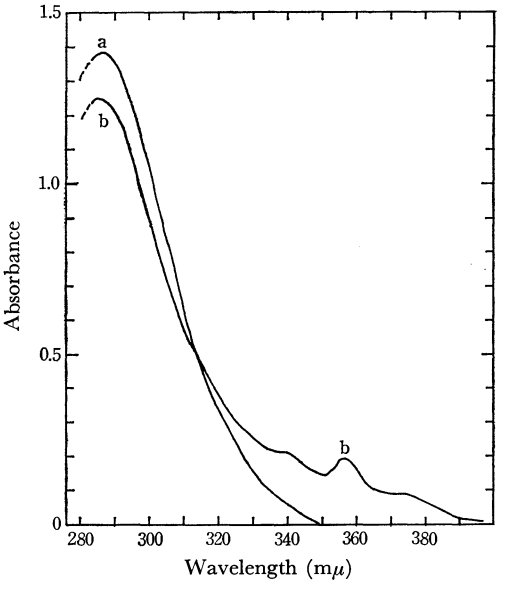

Fig. 3. The original (a) and final (b) spectra in the illumination of 1×10^{-4} M acridan in a deaerated benzene solution. The sample was illuminated 6 times with a 9 kV-3 μF flash.

6) F. Mader and V. Zanker, *Chem. Ber.*, **97**, 2418 (1964).

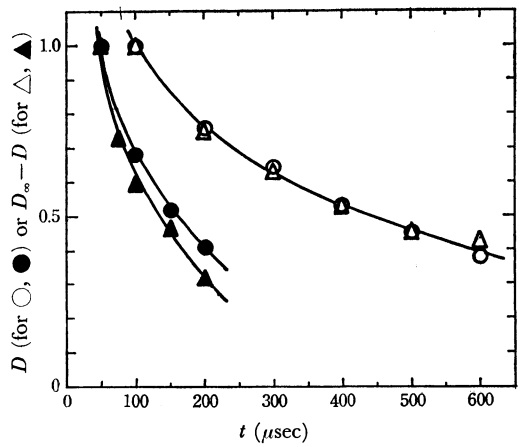

Fig. 4. The decay in the transient absorption (564 mμ) and the increase in the acridine absorption (250 mμ).
●, 564 mμ and ▲, 250 mμ for deaerated solution; ○, 564 mμ and △, 250 mμ for aerated solution. Each pair of curves is normalized at the initial measuring point. (In methanol, the reaction proceeds faster in the deaerated condition than in the aerated one).

region, but no appreciable band near 560 mμ. This semiquinone is so sensitive to oxygen that its spectrum completely vanishes in aerated solutions. Thus, the predominant transient species with 350 and 560 mμ bands found in the present investigation is quite distinguished from the acridine semiquinone previously reported.

As seen in Fig. 1, a weak maximum is perceived at 520 mμ in deaerated benzene solutions. Upon aeration, the intensity at 520 mμ was reduced to one eighth of the deaerated one, while the intensity at 560 mμ to one fourth. This suggests that the 520 mμ band in the present system is partially ascribed to the transient species reported in the previous paper. A maximum at 520 mμ was not observed clearly in a methanol solution.

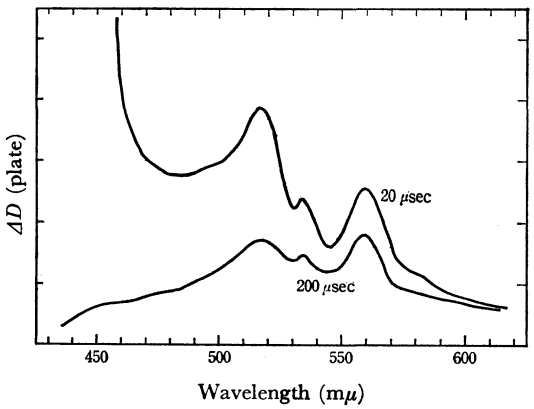

Fig. 5. Transient spectra in the photoreaction of acridine with acridan in deaerated benzene solution.

It was reported, in another previous paper,[4] that when acridine was excited by a flash in the benzene solutions containing acridan, a band with a maximum near 560 mμ as well as the 520 mμ band appeared. In that paper, however, both 520 and 560 mμ bands were attributed, tentatively or rather implicitly, to a single transient species. Hence the transient spectra in this system were examined in more detail under the condition that acridine was selectively excited. The spectra in the deaerated solutions given in Fig. 5 reconfirm the previous result. Thus the short-lived transient absorption is the T-T absorption of acridine with an intense peak at 440 mμ,[4] and the long-lived one consists of the 520 and 560 mμ bands. However, in view of the findings already described, a more reasonable interpretation is that the transient species consist of two components, the oxygen-sensitive and the oxygen-insensitive ones. This has actually been proved in the following way. The intensity ratio of the 520 mμ band to the 560 mμ band was examined in various oxygen concentrations. The results are given in Table 1, which shows definitely that oxygen attacks the 520 mμ band more efficiently.

Biacridan (Compound III in Fig. 7), which is hardly soluble in methanol and benzene, was dissolved in DMSO and its transient spectrum

Table 1. The dependence of the transient absorption intensity on the oxygen concentration

1×10^{-4}M Acridine and 1×10^{-4}M acridan in benzene solutions

$[O_2]$ (M)	D^{520}	D^{560}	D^{520}/D^{560}
0	0.416	0.301	1.38
6.3×10^{-5}	0.254	0.242	1.05
1.3×10^{-4}	0.095	0.100	0.95
2.2×10^{-4}	0.044	0.052	0.85

D is the optical density for 10 cm path and the superscript denotes the wavelength (mμ).

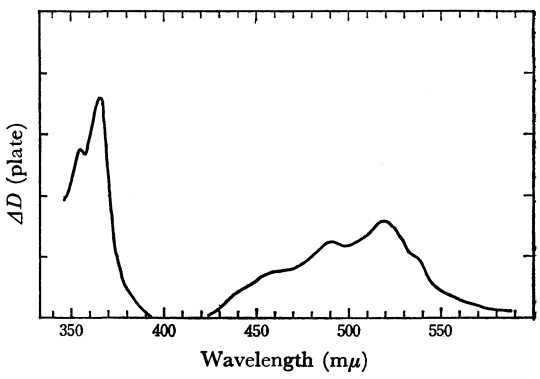

Fg. 6. A transient spectrum from biacridan in a deaerated DMSO solution (t: 200 μsec).

obtained upon flashing was examined. As Fig. 6 shows, the spectrum lacking the 560 mμ band, agrees with that obtained in the photoreduction of acridine in alcohols. The two bands located at ~520 mμ and at 350 mμ decay in a similar way and may be attributed to the same species. The bands in Fig. 6 were not observed in aerated solutions. The main final product was identified with acridine from the absorption spectrum. The yield of acridine was found to increase by a factor of two by the aeration. This is similar to the previous observation made in the photoreduction of acridine in alcohols. These findings substantiate the conclusion that the same transient species are produced in the photolysis of biacridan and in the photoreduction of acridine in alcohols.

Assignment of the Two Species. It is clear from the above experimental facts, that there are two kinds of long-lived species other than T-states, that is, the one without the 560 mμ band and the other with the 560 mμ band. Only the former is produced in the photolysis of biacridan and in the photoreduction of acridine in alcohols, while in benzene solutions both are produced in the reaction of excited acridine and acridan and, in the photolysis of acridan the latter is the main species.

Since there is no other type of dissociation conceivable for biacridan than the following one,

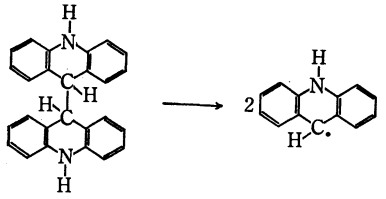

Biacridan (III) C-radical (I)

Fig. 7

the above results unambiguously lead to the assignment that the transient species without 560 mμ band is the radical with an unpaired electron on 9-carbon atom (C-radical).

Hitherto most workers[6-8] have considered, perhaps from chemical intuition, that the acridine semiquinone is the C-radical. In fact, the production of biacridan has been ascertained[6,9-11] in the photoreduction of acridine in hydrogen donating solvents and this may be regarded to support the formation of the C-radical as an intermediate. But the first confirmative evidence that only the C-radical is produced in the photoreduction of acridine in alcohols has been afforded in the present work.

As for the other transient species, it is most reasonable to assign it as an isomeric semiquinone with an unpaired electron on nitrogen atom (N-radical), because it is produced accompanied with the C-radical in the course of the photochemical reaction between acridine and acridan in inert solvents; the C-radical, in analogy with the photoreduction of acridine in alcohols, may be produced from acridine through a hydrogen atom transfer from acridan to acridine. This hydrogen atom is the one located either in 9-carbon or nitrogen atom in acridan and one may say, to be consistent with the experimental result, that the latter is more easily detached than the former. The main reaction may then be written as follows.

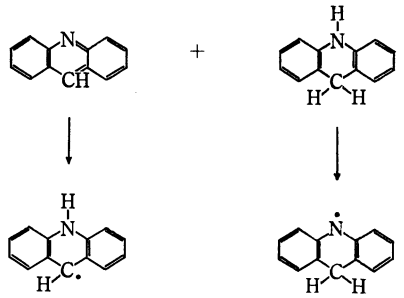

C-radical N-radical (II)

Fig. 8

This interpretation is also supported by the type of hydrogen abstraction in the photolysis of acridan in which the species with 560 mμ band seems to be the principal intermediate. The view that the 560 mμ band is ascribed to an isomeric semiquinone is also supported by the fact that, in the photolysis of acridan, the formation of acridine proceeds in parallel with the fade-out of the 560 mμ band.

More direct proof for the above assignment of the N-radical analogous to the proof for the C-radical was attempted but was unsuccessful, since appropriate compounds which may give rise to the N-radical, for example, *N,N'*-biacridan or *N*-halogenated acridan were not available. Attempts for preparing the N-radical by the radiolysis method are now in progress.

Although there is scarcely any doubt that the 560 mμ band is due to the N-radical, it might be added that all other conceivable assignments can be rejected from the experimental facts. These will be described below briefly.

Firstly, this species can not be assigned as the triplet acridan, because in the photoreaction of acridine with acridan, the triplet energy transfer,[12]

7) R. C. Kaye and H. I. Stonehill, *J. Chem. Soc.*, **1951**, 27.

8) R. A. Jackson and W. A. Waters, *ibid.*, **1958**, 4632.

9) A. Kellmann, *J. Chim. Phys.*, **63**, 936 (1966).

10) M. Giurgea, G. Mihai, V. Topa and M. Musa, *ibid.*, **61**, 619 (1964).

11) H. Göth, P. Cerutti and H. Schmid, *Helv. Chim. Acta*, **48**, 1395 (1965).

12) F. Wilkinson, "Advances in Photochemistry," Vol. III, Interscience Pub., New York (1964), p. 241.

$$A^T + AH_2 \longrightarrow A + AH_2^T$$

where a superscript T represents the triplet state, is, in all probabilities, not possible, since the energy levels of the triplet state are for acridine[13] and acridan[14] respectively 14800 cm^{-1} and 24200 cm^{-1}. In addition, the poor reactivity of this species to oxygen, does not agree with the generally accepted properties of the triplet state of organic molecules.

The second conceivable possibility is the formation of radical cation from acridan; but the absorption spectrum of acridan cation produced by a radiolysis method was found to be quite different.[15]

The final possibility is the formation of a certain molecular complex of the C-radical with acridine or acridan or alternatively dimerization of the C-radical. These possibilities are, however, safely denied from the concentration effect of certain substances on the relative intensity ratio of 560- to 520 mμ-band. For example, values of this ratio were 0.7 in the direct excitation of a benzene solution of 1×10^{-4}M acridan and 1.6 in the acridine excitation of a benzene solution containing 1×10^{-4}M acridine and 1×10^{-4}M acridan. In these experiments, the initial optical densities at 520 mμ were 0.40 and 0.15 respectively. These results preclude the possibility of the 560 mμ species being the radical dimer, because if it were the case, the dimer concentration should be proportional to the square of the monomer concentration in contradiction to the above data.

Some Aspects of the Kinetic Behaviors of the Two Semiquinones. Acridine-Acridan in Benzene. In the previous paper,[4] the second order rate constant for the decay of acridine semiquinone in the deaerated condition was estimated by analyzing the change in the optical density at 520, 560 and 350 mμ. The rate constant was interpreted to be related with Processes

$$2AH \longrightarrow (AH)_2$$
$$2AH \longrightarrow A + AH_2$$

The semiquinone treated in the previous paper, however, was the species produced by the reaction between acridine and acridan in benzene solutions and it has been proved by the present work that the species is not a single species but consists of the C-radical (AH) and N-radical (AH'). Hence the rate constants reported in that paper should be considered to be a kind of averaged one for the following processes,

$$AH + AH \longrightarrow AH_2 + A$$
$$\longrightarrow (AH)_2$$
$$AH + AH' \longrightarrow A + AH_2$$
$$AH' + AH' \longrightarrow A + AH_2$$
$$(\longrightarrow (AH')_2?) \quad etc.$$

Some of the ε-values are also concerned with both AH and AH'. It is impossible to analyze the data according to the above scheme.

As for the aerated solution, an attempt to evaluate the rate constant for $AH+O_2\rightarrow A+HO_2$ was unsuccessful in the previous paper. This was attributed to the complicated nature of the reaction. For instance, Reaction $AH+O_2\rightarrow A+HO_2$ and Reaction $AH_2+O_2^*\rightarrow AH+HO_2$, where O_2^* is the singlet oxygen, occur simultaneously. Besides the real situations are even more complicated because there are two radical species AH and AH'. It will practically be impossible to evaluate the rate constants for $AH+O_2\rightarrow A+HO_2$ and $AH'+O_2\rightarrow A+HO_2$ separately as long as the acridine-acridan system is concerned.

Acridan in Benzene. In Figs. 9 and 10 some of the typical decay curves of the transient absorption in benzene solutions of acridan are shown. The decay curves are drawn in terms of $D-D_{A\infty}$, where D is the observed optical density and $D_{A\infty}$, the one of acridine produced by one flash (at $t=\infty$), since the following relation holds where ε_R and ε_A

$$D - D_{A\infty} = l(\varepsilon_R - \varepsilon_A)[R]$$

are respectively the molar extinction coefficient of a radical and acridine.*1 It is evident that the decay obeys the second order satisfactorily. The rate constants at 560 mμ and at 356 mμ can be compared from the slopes in Fig. 10 and the values of D_i and D_A; it was found that the value at the former wavelength was always larger by about several ten %. This suggests that the C-radical, which also absorbs at 356 mμ, might be somewhat more stable than the N-radical in the deaerated condition. It is interesting that the above result eliminates the quick conversion of the type $AH \rightleftarrows AH'$ in this case. Because, if for instance, AH' converts to AH by the following reaction with a high rate,

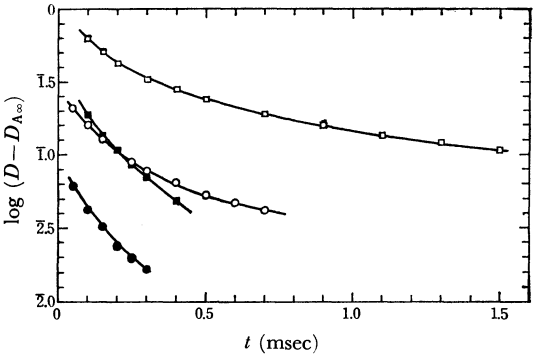

Fig. 9. Decay curves of the transient absorption in a benzene solution of acridan.
□, 356 mμ and ○, 560 mμ in deaerated solution,
■, 356 mμ and ●, 560 mμ in aerated solution.

13) D. F. Evans, *J. Chem. Soc.*, **1957**, 1351.
14) H. Kokubun and K. Kikuchi, private communication.
15) T. Shida and A. Kira, to be published.

*1 At 560 mμ, both $D_{A\infty}$ and ε_A are zero, since acridine does not absorb.

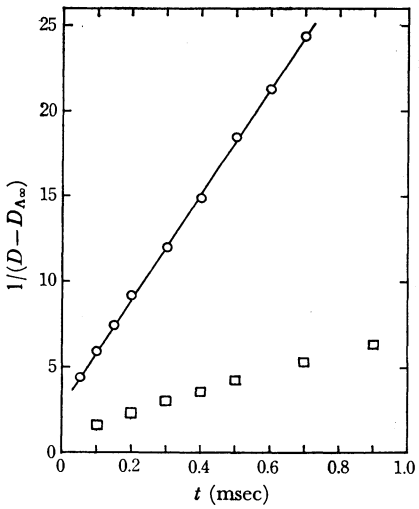

Fig. 10. The second-order plots for the decay curves given in Fig. 9. The symbols are the same as those in Fig. 9.

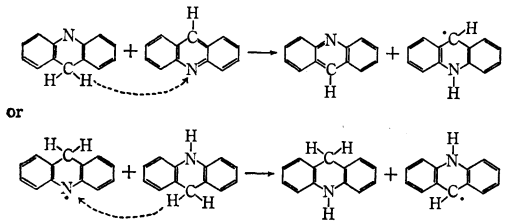

the apparent decay at 560 mμ should not obey a simple second order.

The true second order rate constant can be evaluated if one assumes that AH′ disappears according to the reaction

$$AH' + AH' \longrightarrow A + AH_2 \qquad (1)$$

If this is correct, ε^{560} (AH′) can be estimated from the value of D_∞^{356} (for acridine). The result was $1.3\times10^4 M^{-1}cm^{-1}$ and the rate constant for Reaction (1) was found to be $k_1\sim4\times10^9 M^{-1}sec^{-1}$. However there is no assurance that all AH′ disappears according to Reaction (1); on the contrary, it is more likely that a certain radical species produced by the reaction of hydrogen atoms with the solvent molecules participates in the reaction. In fact the k-value found for the methanol solution was different and appreciably larger than for the benzene solution. Therefore, it is also doubtful whether the above rate constant is concerned with only Reaction (1).

In the aerated solution, such a complication is supposed to be largely eliminated, because oxygen is likely to attack such radical species, and the disappearance of AH′ may perhaps occur mainly through Reaction $AH'+O_2\rightarrow A+HO_2$ (2) and Reaction (1). In fact, the decay curves under the aerated condition was found to be practically the same in benzene and in methanol. From the above reasoning, it may be allowed to put the rate formula as follows,

$$-\frac{dD}{dt}=\frac{2k_1}{\varepsilon_R l}D^2+k_2[O_2]D \qquad (3)$$

where k_1 and k_2 are the rate constants of Reactions (1) and (2) respectively. Dividing Eq. (3) by D, one gets

$$-\frac{d\log D}{dt}=\frac{2k_1}{\varepsilon_R l}D+k_2[O_2] \qquad (4)$$

Hence the plot of the gradient in Fig. 9 against the optical density gives $k_2[O_2]$ as an intercept on the ordinate. The value of k_2 thus obtained is $2\times10^5 M^{-1}sec^{-1}$ for both benzene and methanol solutions. According to the previous paper,[1] the corresponding value for the C-radical in ethanol is $1.2\times10^9 M^{-1}sec^{-1}$. The value of k_2 for the N-radical is not very reliable, and yet it is quite certain that the reactivity of C- and N-radical against oxygen is profoundly different.

The authors are grateful to Dr. Masashi Imamura for generous support and helpful discussions, and to Dr. Tadamasa Shida for useful suggestions.

Note Added after the Preparation of This Paper. We have found in a newly arrived Zeit. für physik. Chem. N. F., a paper of Zanker *et al.*[16] They gave some evidence for the photochemical formation of N-radical of some acridan derivatives in the rigid ethanol at low temperatures. For example, the transient band with the 575 mμ max for 9-C_2H_5 and 9-CH_3 acridan corresponds most likely to the 560 mμ band of our N-radical of acridine and also to the 570 mμ band in alcohols at low temperatures, reported by Niizuma and Koizumi.[17]

16) V. Zanker, E. Erhardt and H. H. Mantsch, *Z. physik. Chem., N. F.*, **58**, 1 (1968).

17) S. Niizuma and M. Koizumi, This Bulletin, **41**, 1090 (1968).

BULLETIN OF THE CHEMICAL SOCIETY OF JAPAN VOL. 42 631—634 (1969)

Polymerization of *N*-Vinylcarbazole in the Presence of β-Cyanoacrolein

Hiroshi SUMITOMO and Ichiro TAKEMURA

Faculty of Agriculture, Nagoya University, Chikusa, Nagoya

(Received July 15, 1968)

It was found that *N*-vinylcarbazole (VCZ) initiated the polymerization in the presence of β-cyanoacrolein (CAL) even in air at room temperature. The polymerization of VCZ induced by CAL was investigated in benzene at 60°C. Polymer formed was found to be VCZ homopolymer. The rate of polymerization attains to a maximum at the mole fraction of CAL of about 0.65 in the monomer mixture. The products obtained from the terpolymerization in the system of CAL-VCZ-Styrene in benzene at 60°C contain no CAL unit and exclusively consist of the VCZ component. The composition curve of the copolymer is contrasted with that of a radical initiated copolymer. In view of these results, as well as the *Q-e* values of both CAL and VCZ, it seems possible that the cationic polymerization of VCZ is induced by some donor-acceptor type interaction between VCZ and CAL.

Since the publication of papers by Scott *et al.* and Ellinger (1963) it has often been shown that the polymerization of *N*-vinylcarbazole (VCZ) is easily induced by electron acceptors, although the mechanism of the initiation is still a matter of controversy.[1)]

We have observed that VCZ starts the polymerization immediately after mixing with β-cyanoacrolein (NC–CH=CH–CHO, CAL) even in air at room temperature. In the present note it is elucidated that the polymerization of VCZ is initiated cationically by some kind of interaction between a donor (VCZ) and an acceptor (CAL).

Experimental

Materials. CAL was prepared by dehydrogenation of β-cyanopropionaldehyde (CPA).[2),3)] VCZ (B.A.S.F. Chemicals Ltd.) was recrystallized from methanol (mp 65.5—66°C) after distillation under a reduced pressure (bp 142—142.5°C/2 mmHg). Styrene (St) was washed with an aqueous solution of sodium thiosulfate, water, 5% aqueous solution of potassium hydroxide and then water, drying on anhydrous sodium sulfate, before distillation at reduced pressure. Bp 46.7—47.0°C/22 mmHg. Azobisisobutyronitrile(AIBN) was recrystallized from ethanol. Benzene was distilled after drying with sodium.

Polymerization. The polymerization at different compositions of VCZ and CAL was investigated in air at 60°C. Terpolymerization of VCZ, CAL and St was also carried out at different molar ratios of VCZ to St, at the constant molar ratio, VCZ : CAL, of unity, and at the total monomer concentration of 4 mol/*l* in benzene, in air and at 60°C. Resulting polymer was precipitated into a larger amount of methanol, purified by the reprecipitation in the system of benzene (solvent) - methanol (precipitant), and then dried at room temperature under vacuum.

Determination of Polymer Composition. Infrared absorption spectra were measured for polymerization products, which were compared with those for parent monomers and their homopolymers. No St homopolymer was extracted with use of carbon tetrachloride from the product of the terpolymerization.

Polymer compositions were determined from nitrogen contents by the Kjeldahl method for the products in VCZ-CAL system and by an elementary analysis using C.H.N. Corder (Yanagimoto Co., Ltd.) for those in VCZ-CAL-St system. There is a good agreement between the results obtained in the nitrogen analysis by these different methods.

Viscometry. Viscosity numbers, η_{sp}/c, of polymers were measured at the concentration of 0.3 g/100 m*l* in benzene at 25±0.05°C with use of an Ostwald viscometer.

Results and Discussion

The results of the preliminary test are shown in Table 1.

VCZ alone gives no polymer in the present conditions, but the addition of CAL results in the formation of the polymer in higher yield even in air at room temperature. There appears no influence of the presence of a radical initiator. The nitrogen contents of the products show the agreement with the value calculated for VCZ homopolymer (PVCZ). An agreement between the infrared spectra (KBr disk), as shown in Fig. 1, of the product and of PVCZ which was obtained by AIBN initiated polymerization, also indicates

1) J. Pac and P. H. Plesch, *Polymer*, **8**, 237 (1967).
2) H. Sumitomo and K. Azuma, *J. Polymer Sci.*, **B4**, 883 (1966).
3) S. Motoki, S. Satsumabayashi and T. Matsuda, This Bulletin, **39**, 1519 (1966).

TABLE 1. POLYMERIZATION OF VCZ IN THE PRESENCE OF CAL[a]
EFFECTS OF SOLVENT AND RADICAL INITIATOR

Expt. No.	Monomer VCZ g	Monomer CAL g	Monomer CPA g	Mole fractn. of CAL (or CPA)	Wt. ratio of benzene : monomer	AIBM mol% to monomer	Temp. °C	Time hr	Convn. %	Nitrogen content[b] %
101	0.48	—	—	—	2	—	24.0—24.5	3	0	—
102	0.48	—	—	—	2	0.5	24.0—24.5	3	0	—
130	0.48	0.21	—	0.5	—	—	27.5—27.9	3	34.6	7.22
131	0.48	0.21	—	0.5	—	0.5	27.5—27.9	3	34.2	7.24
134	1.93	0.81	—	0.5	2	—	27.5—27.9	5	1.5	7.23
135	1.93	0.81	—	0.5	2	0.5	27.5—27.9	5	1.0	7.25
—	1.93	—	0.83	0.5	—	—	21.5	3	0	—

a) In air.
b) Calculated for poly (*N*-vinylcarbazole), 7.25%.

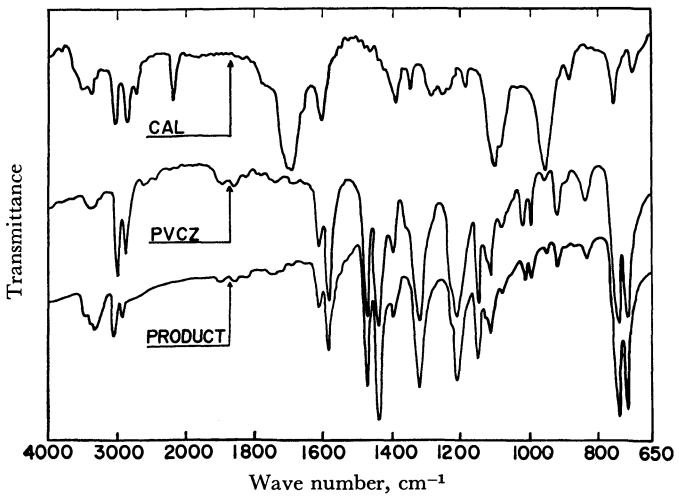

Fig. 1. Infrared absorption spectra of β-cyanoacrolein (CAL), poly(*N*-vinylcarbazole) (PVCZ) and a product obtained in the experiments shown in Table 1.

TABLE 2. POLYMERIZATION OF VCZ IN THE PRESENCE OF CAL[a]
EFFECT OF COMPOSITION OF MONOMER MIXTURE

Expt. No.	Monomer VCZ g	Monomer CAL g	Mol fractn. of CAL	Time hr	Convn. %	Rate %/hr	η_{sp}/c[b]
217	3.47	0.16	0.1	2.8	1.8	0.62	0.14
218	3.09	0.32	0.2	5.2	4.6	0.87	—
219	2.70	0.48	0.3	3.5	4.5	1.29	0.29
220	2.32	0.64	0.4	3.0	5.7	1.88	0.31
221	1.93	0.81	0.5	2.3	9.2	3.95	0.35
222	1.54	0.97	0.6	2.2	10.9	5.00	—
223	1.16	1.13	0.7	3.7	18.5	5.04	0.29
224	0.77	1.30	0.8	3.2	15.7	4.96	0.22
225	0.39	1.46	0.9	4.5	15.6	3.47	0.29

a) In benzene, [CAL]+[VCZ]=2mol/*l*, 60°C, in air.
b) Benzene, c=0.3 g/100 m*l*, 25°C. η_{sp}/c of radical initiated polymer, 1.1.

TABLE 3. CAL-VCZ-St TERPOLYMERIZATION[a]

Expt. No.	Monomer VCZ g	Monomer CAL g	Monomer St g	Mol fractn. of VCZ in VCZ+St	Time hr	Convn. %	Mol fractn. of VCZ in copolymer[b]
513	2.84	0.64	13.60	0.1	16	1.00	0.817
514	2.59	0.54	5.56	0.2	2	0.91	0.876
515	3.58	1.50	4.48	0.3	9	2.63	0.917
519	2.22	0.93	1.78	0.4	6	7.63	0.952
516	2.59	1.09	1.38	0.5	2	5.72	0.934
520	3.34	2.88	0.46	0.8	0.3	3.64	0.923
506	1.84	0.77	0.11	0.9	0.3	2.81	1.000

a) [CAL]+[VCZ]+[St] = 4 mol/*l*, [CAL]/[VCZ] = 1, benzene, in air, 60°C.
b) Determined by elementary analysis.

that no CAL unit was detectably incorporated into the polymer chain.

Figure 2 summarizes the results of the polymerization of VCZ in the presence of different mole fractions of CAL at the constant total monomer concentration of 0.4 mol/*l* in benzene at 60°C.

The polymerization starts without any induction period. The rate of polymerization seems to attain to a maximum at the mole fraction of CAL of about 0.65. Similar behaviors can be seen in Table 2 in which the polymerization is investigated at the total monomer concentration of 2 mol/*l*. All of the solution viscosity numbers, η_{sp}/c, of polymer are much lower than those of a radical polymer.

In Fig. 3 are plotted the rate as well as the viscosity numbers against the mole fraction of CAL in monomers to show the remarkable tendencies in graphical form. It is conceivable from these facts that there may be some donor-acceptor type of interaction between VCZ and CAL.

Table 3 includes the results of terpolymerization in the system of CAL-VCZ-St at the constant mole ratio of CAL to VCZ of unity in the total monomer concentration of 4 mol/*l* in benzene at 60°C.

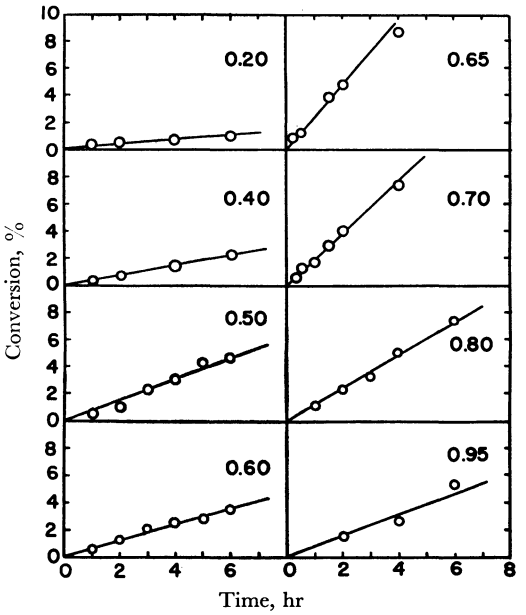

Fig. 2. Polymerization of VCZ in the presence of CAL.
Effect of composition in monomer mixture (numbers in figures show mole fraction of CAL).
[CAL]+[VCZ]=0.4 mol/*l*, benzene, 60°C, in air.

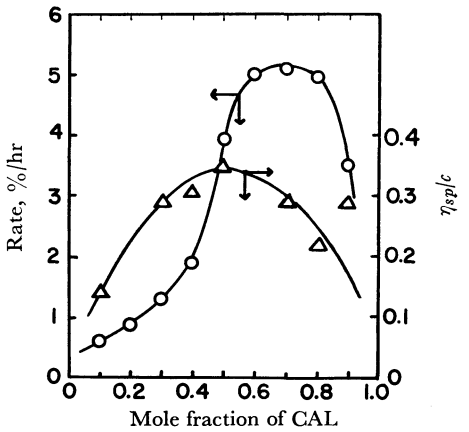

Fig. 3. Polymerization of VCZ in the presence of CAL.
Effect of composition in monomer mixture.
[VCZ]+[CAL]=2 mol/*l*, benzene, 60°C, in air.

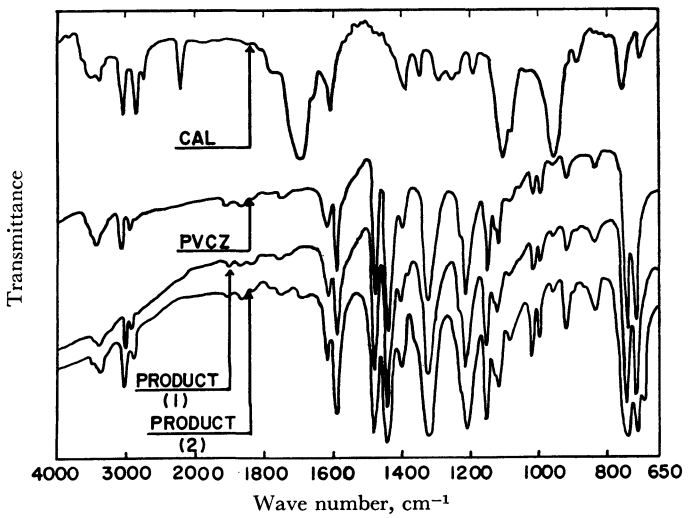

Fig. 4. Infrared absorption spectra of CAL monomer, PVCZ, a product (1) obtained from the experiments other than Expt. No. 513 and the product (2) obtained from Expt. No. 513.

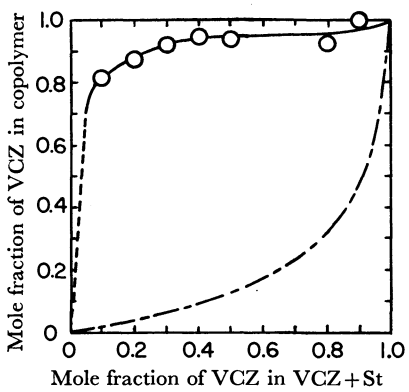

Fig. 5. Composition of copolymer as a function of monomer composition in CAL-VCZ-St system. [CAL]+[VCZ]+[St]=4 mol/*l*, [VCZ]/[CAL]=1, Benzene, 60°C, in air. ——: radical copolymerization of VCZ with St (R. Hart (1961)).

The infrared spectra of the Product 1, starting from the mole fraction of VCZ higher than 0.1 in the total amount of VCZ and St (any product excepting expt. No. 513), and of the Product 2 from that of 0.1, are compared with those of PVCZ and of CAL monomer in Fig. 4.

The spectra of both products are not different from that of PVCZ, excepting that an absorption by styrene appears slightly at 700 cm^{-1} in the spectrum of product 2, and do not represent any absorption peak of CAL.

In Fig. 4 the compositions of the copolymers obtained here are plotted against the monomer compositions. From the fact that the copolymers consist exclusively of the VCZ component and also that the curve is contrasted with that for the radical copolymer given by Hart,[4] it may be suggested that the copolymerization in the present system takes place cationically.

Q-e values of CAL are determined to be $Q=0.53$ and $e=2.07$[5] and those of VCZ are presented to be $Q=0.41$ and $e=-1.40$.[6] It seems possible, therefore, that there may exist some donor-acceptor type interaction between CAL and VCZ inducing the cationic polymerization of VCZ.

4) R. Hart, *Macromol. Chem.*, **47**, 134 (1961).
5) I. Takemura and H. Sumitomo, This Bulletin, **42**, 634 (1969).
6) G. E. Ham, ed., "Copolymerization," Interscience Publishers, New York (1964), p. 862.

BULLETIN OF THE CHEMICAL SOCIETY OF JAPAN VOL. 42 634—636 (1969)

Copolymerization of β-Cyanoacrolein with Acrylonitrile

Ichiro TAKEMURA and Hiroshi SUMITOMO

Faculty of Agriculture, Nagoya University, Chikusa, Nagoya

(Received July 15, 1968)

Radical initiated copolymerization of β-cyanoacrolein (CAL, M_2) with acrylonitrile (M_1) in benzene at 60°C was investigated. The monomer reactivity ratios were determined to be $r_1=3.2$ and $r_2=0$. The copolymerization behavior is discussed in comparison with that in the system of styrene and CAL previously described. The Q and e values of CAL were also estimated to be 0.53 and 2.07, respectively, which were compared with those of other polar monomers.

In preceding papers,[1,2] the radical copolymerization of the new monomer, β-cyanoacrolein (CAL), with styrene (St) was investigated to give monomer reactivity ratios and to demonstrate the existence of a penultimate effect. It was also described that CAL induced the polymerization of *N*-vinylcarbazole even in air at room temperature and that there may be some donor-acceptor type interaction between *N*-vinylcarbazole and CAL in solution leading to initiate the cationic polymerization of *N*-vinylcarbazole.[2] The purpose of the present study is to determine the monomer reactivity ratios and *Q-e* values in the radical copolymerization of CAL with acrylonitrile (AN).

Experimental

Materials. CAL was prepared according to the same method as that previously described.[1] Commercial AN was twice distilled in a stream of nitrogen after drying over potassium carbonate. Bp 77.0—77.3°C.

1) H. Sumitomo and K. Azuma, *J. Polymer Sci.*, **B4**, 883 (1966).

2) H. Sumitomo and I. Takemura, This Bulletin, **42**, 631 (1969).

TABLE 1. AN(M_1)-CAL(M_2) RADICAL COPOLYMERIZATION[a]

Expt. No.	Monomer AN(M_1) g	AN(M_1) mol	CAL(M_2) g	CAL(M_2) mol	Mol fraction of AN	Initiator[b]	Time hr	Yield g	Conversion %	Copolymer composition[c] mol fraction of AN
13	0.59	0.011	8.11	0.100	0.10	AIBN	18	0.12	1.40	0.608
36	1.06	0.020	6.48	0.080	0.20	Bz_2O_2	25	0.16	2.09	0.640
37	1.33	0.025	6.08	0.075	0.25	Bz_2O_2	20.5	0.19	2.55	0.673
38	1.59	0.030	5.67	0.070	0.30	Bz_2O_2	15	0.20	2.78	0.707
39	1.86	0.035	5.27	0.065	0.35	Bz_2O_2	12.5	0.26	3.61	0.757
33	2.12	0.040	4.86	0.060	0.40	Bz_2O_2	4.5	0.09	1.26	0.760
34	3.18	0.060	3.24	0.040	0.60	Bz_2O_2	1.5	0.11	1.70	0.860
35	4.24	0.080	1.62	0.020	0.80	Bz_2O_2	0.5	0.10	1.69	0.930
27	4.78	0.090	0.81	0.010	0.90	AIBN	0.25	0.16	2.93	0.971

a) In benzene at 60°C. The weight ratio of benzene to monomer, 2.
b) 0.5 mol% to monomer.
c) Determined by nitrogen contents by the Kjeldahl method.

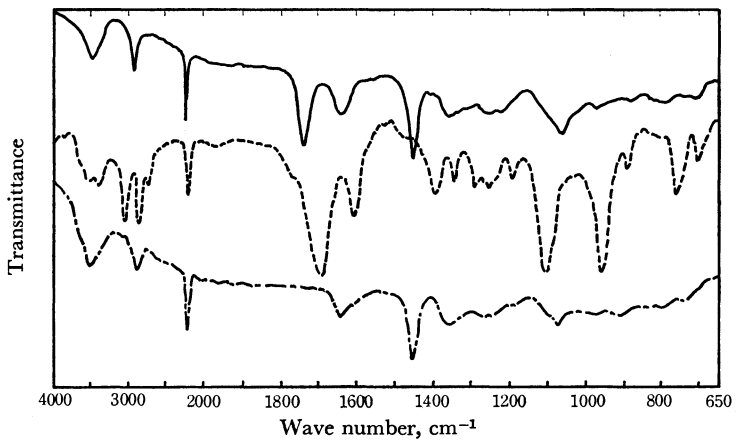

Fig. 1. Infrared absorption spectra of β-cyanoacrolein-acrylonitrile copolymer (solid curve), β-cyanoacrolein monomer (broken curve) and polyacrylonitrile (dot-dash-curve).

Azobisisobutyronitrile (AIBN) was recrystallized from ethanol. Benzoyl peroxide (Bz_2O_2) was purified by the reprecipitation from its chloroform solution into methanol. Benzene and dimethyl formamide (DMF) were purified in the usual way.

Polymerization. In a glass tube were placed initiator, CAL, AN and solvent in this order. The tube was sealed under vacuum after repeating freezing and thawing. Polymerization was conducted at 60± 0.1°C. The resulting copolymer was precipitated in a larger amount of methanol and then purified by the reprecipitation in the system of DMF-methanol.

Copolymer Composition. The compositions of copolymers were determined from nitrogen contents by the Kjeldahl method.

Results and Discussion

The results of the copolymerization of AN (M_1) with CAL (M_2) are summarized in Table 1. Figure 1 shows the infrared absorption spectra of the copolymer, AN homopolymer and the CAL monomer.

In Fig. 2 are plotted the compositions of the initial copolymers against the initial monomer compositions. No homopolymerization of CAL was experimentally found to occur in the present condition. Hence the monomer reactivity ratio r_2 can be estimated at 0. The solid curve shown in Fig. 2 are drawn adopting values of $r_1=3.2$ and $r_2=0$ to the conventional Lewis-Mayo equation and it agrees very closely with the experimental data. Included in Fig. 2 for comparison is the data obtained in the previous St (M_1)-CAL (M_2) system.[1]

There is a remarkable difference between the monomer reactivity ratios obtained in these copolymerization systems. The value of r_1 is larger than

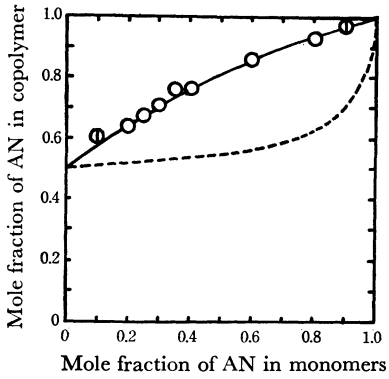

Fig. 2. Composition curve of St(M_1)-CAL(M_2) copolymerization ○, Bz_2O_2; ①, AIBN.
Solid curve, calculated by using $r_1=3.2$, $r_2=0$.
Broken curve shows St(M_1)-CAL(M_2) system ($r_1=0.09$; $r_1'=0.27$; $r_2=r_2'=0$).[1)]

unity in the AN (M_1)-CAL (M_2) system, whereas $r_1<1$ in the system of St (M_1)-CAL (M_2).

It has also been noticed in our experiments that, for example, the mixture of equal moles of St and CAL gives the copolymer at 5.7% conversion in 5.2 hr at 60°C, even in air without any other initiator. It is conceivable that there may be some donor-acceptor type interaction between St and CAL.

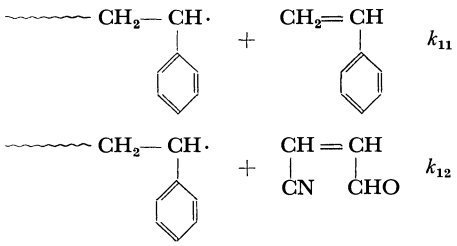

In the present copolymerization system, it may be suggested from the r_1 value that there exists stronger repulsion being attributed to the polar substituted groups between the growing AN radical and the coming CAL monomer rather than the AN monomer.

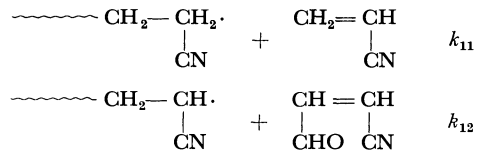

The values of Q and e for CAL calculated from the copolymerization data are shown in Table 2. Table 2 also includes the Q-e values for the related polar monomers.

TABLE 2. THE Q-e VALUES OF POLAR MONOMERS

Monomers		Q	e	Ref.
Maleic anhydride	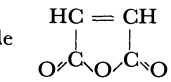	0.23	2.25	3)
CAL	NC–CH=CH–CHO	0.53	2.07	This paper
Fumaronitrile	NC–CH=CH–CN	0.80	1.96	3)
Acrylonitrile	CH_2=CH–CN	0.60	1.20	3)
Acrolein	CH_2=CH–CHO	0.85	0.73	3)

It can be seen from the e values in Table 2 that the polar effect of substituted groups in CAL is comparable with that in fumaronitrile, larger than that in AN and acrolein, and smaller than that in maleic anhydride.

3) G. E. Ham ed., "Copolymerization," Interscience Publishers, New York (1964), p. 845.

BULLETIN OF THE CHEMICAL SOCIETY OF JAPAN VOL. 42 637—643 (1969)

Electronic Spectra of Crystalline TCNQ Anion Radical Salts. II. Complex Salts*1

Yôichi IIDA

Department of Chemistry, Faculty of Science, Hokkaido University, Sapporo

(Received July 17, 1968)

The present paper deals with crystalline TCNQ anion radical "complex" salts of $(M^+)_2(TCNQ)_3^{-\cdot}$ and $M^+(TCNQ)_2^{-\cdot}$ composed of the formally-neutral TCNQ and its anion radical $TCNQ^{-\cdot}$. Their crystalline electronic spectra were measured in the range between 4.0 and 30.8 kK by diffuse reflectance and in the 0.65—4.0 kK range by transmittance. None of their spectra except those of the (2 : 3) compounds were found to bear any resemblance to those in the simple salts. Although the spectra of the (2 : 3) compounds are similar to those of the simple salts with low conductivities, the former exhibit an additional weak absorption in the range lower than 6 kK. The (1 : 2) compounds with intermediate conductivities show a strong band around 3 kK, and those with high conductivities, around 2.0—2.5 kK. Their spectra are discussed on the basis of the interaction among unpaired electrons in connection with their electrical and magnetic properties. The difference in the interaction modes of the ion radicals between "simple" and "complex" salts is also speculated upon.

Our primary interest is in studying the interactions among unpaired electrons in the solid state of ion radical salts. Along this line, we have investigated the crystalline electronic spectra of Würster's cation radical salts[1] and 7,7,8,8-tetracyanoquinodimethane (TCNQ) anion radical simple salts.[2] It has been concluded that their crystalline spectra arise from charge-transfer interaction between ion radicals. Furthermore, the spectra have been proved to have a close correlation with their electrical and magnetic properties. In TCNQ simple salts, the charge-transfer bands have been observed around 9 kK in low-conductivity compounds and at 4.3 kK in high-conductivity compounds. On the other hand, TCNQ forms new classes of complex salts of $(M^+)_2(TCNQ)_3^{-\cdot}$ and $M^+(TCNQ)_2^{-\cdot}$ as well as simple salts of $M^+TCNQ^{-\cdot}$, where M^+ represents a diamagnetic counter cation.[3,4] Thus, the complex salts include the formally-neutral TCNQ besides the anion radical $TCNQ^{-\cdot}$. The complex salts range from semimetal-like substances with a temperature-independent paramagnetism to intermediate-conductivity compounds with triplet-exciton systems.[3-8] The purpose of the present paper is to study the electronic states of the complex salts in the solid state by means of their crystalline electronic spectra. This study also involves the effects of the introduction of neutral TCNQ molecules on the modes of the interaction among unpaired electrons previously investigated in the simple salts.[2]

Experimental

Materials. The TCNQ complex salts under investigation are classified below.

The (2 : 3) Compounds. $(Cs^+)_2(TCNQ)_3^{-\cdot}$ and $(Morpholinium^+)_2(TCNQ)_3^{-\cdot}$.

The (1 : 2) Compounds with Intermediate Conductivity. Methyltriphenylphosphonium$^+$(TCNQ)$_2^{-\cdot}$, Methyltriphenylarsonium$^+$(TCNQ)$_2^{-\cdot}$, Ethyltriphenylphosphonium$^+$(TCNQ)$_2^{-\cdot}$, Ethyltriphenylarsonium$^+$(TCNQ)$_2^{-\cdot}$, Trimethylphenylammonium$^+$(TCNQ)$_2^{-\cdot}$, Triethylammonium$^+$(TCNQ)$_2^{-\cdot}$, Triethylphenylammonium$^+$(TCNQ)$_2^{-\cdot}$, Tetraethylammonium$^+$(TCNQ)$_2^{-\cdot}$, Ethyltri-*n*-propylammonium$^+$(TCNQ)$_2^{-\cdot}$, and Tetra-*n*-propylammonium$^+$(TCNQ)$_2^{-\cdot}$.

The (1 : 2) Compounds with High Conductivity. Quinolinium$^+$(TCNQ)$_2^{-\cdot}$, *N*-Methylquinolinium$^+$(TCNQ)$_2^{-\cdot}$, *N*-Ethylquinolinium$^+$(TCNQ)$_2^{-\cdot}$, *N*-(*n*-Propyl)quinolinium$^+$

*1 Presented in part at the 20th Annual Meeting of the Chemical Society of Japan, Tokyo, April, 1967, and at the Symposium on Molecular Structure, Sapporo, October, 1967.

1) Y. Iida and Y. Matsunaga, This Bulletin, **41**, 2615 (1968).
2) Y. Iida, *ibid.*, **42**, 71 (1969).
3) L. R. Melby, R. J. Harder, W. R. Hertler, W. Mahler, R. E. Benson and W. E. Mochel, *J. Am. Chem. Soc.*, **84**, 3374 (1962).
4) W. J. Siemons, P. E. Bierstedt and R. G. Kepler, *J. Chem. Phys.*, **39**, 3523 (1963).
5) R. G. Kepler, *ibid.*, **39**, 3528 (1963).
6) D. B. Chesnut and W. D. Phillips, *ibid.*, **35**, 1002 (1961).
7) D. B. Chesnut and P. Arthur, Jr., *ibid.*, **36**, 2969 (1962).
8) M. T. Jones and D. B. Chesnut, *ibid.*, **38**, 1311 (1963).

$(TCNQ)_2^-$, *N*-Methylisoquinolinium$^+(TCNQ)_2^-$, *N*-Ethylisoquinolinium$^+(TCNQ)_2^-$, Quinaldinium$^+(TCNQ)_2^-$, *N*-Methylquinaldinium$^+(TCNQ)_2^-$, *N*-Ethylquinaldinium$^+(TCNQ)_2^-$, Lepidinium$^+(TCNQ)_2^-$, *N*-Methyllepidinium$^+(TCNQ)_2^-$, *N*-Ethyl-2,6-dimethylquinolinium$^+(TCNQ)_2^-$, and *N*-Methylacridinium$^+(TCNQ)_2^-$.

These compounds were prepared by a direct reaction between TCNQ and the iodides in acetonitrile.[3] The compositions of the compounds, which have not yet appeared in the literature, were determined on the basis of the intensity-ratios of some absorption bands measured in acetonitrile.[3]

Measurements. The measurements of the absorption spectra in acetonitrile were carried out under the conditions presented in a previous paper.[2] The crystalline electronic spectra were measured in the range between 4.0 and 30.8 kK by means of diffuse reflectance and were plotted using the Kubelka-Munk equation $f(R)=(1-R)^2/2R$, where R is the reflectance. The details were the same as in previous papers.[1,2] The absorption spectra in the solid state were recorded in the range between 0.65 and 4.0 kK as Nujol mulls.

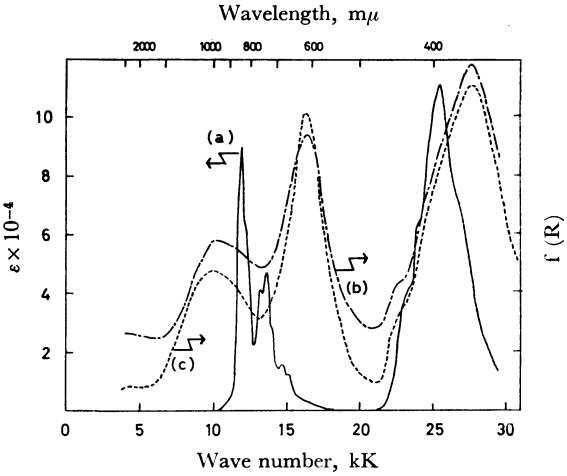

Fig. 1. Electronic spectra of $(Cs^+)_2(TCNQ)_3^{--}$ in acetonitrile solution (a), $(Cs^+)_2(TCNQ)_3^{--}$ in the solid state (b) and (Morpholinium$^+)_2(TCNQ)_3^{--}$ in the solid state (c).

Results and Discussion

The absorption spectra of neutral TCNQ and anion radical $TCNQ^-$ in acetonitrile have been illustrated in a previous paper.[2] As for the complex salts in acetonitrile, the components have been found to be completely dissociated, thus giving a spectra consisting of those of independent TCNQ and $TCNQ^-$ molecules. However, in the solid state, TCNQ molecules form "supermolecules" composed of their unique groups.[4-9]

These complex salts may be divided into (2 : 3) and (1 : 2) salts on the basis of the ratio of cations to TCNQ molecules. It is further possible to divide the (1 : 2) salts into intermediate- and high-conductivity compounds on the basis of their electrical properties.[4] These classifications allow correlation with the optical and magnetic properties in the complex salts to be discussed below.

The (2 : 3) Compounds. They are restricted to $(Cs^+)_2(TCNQ)_3^{--}$ and (Morpholinium$^+)_2$-$(TCNQ)_3^{--}$, which were obtained in the form of large blue-black crystals. They have conductivities of the order of 10^{-3}—$10^{-5}\Omega^{-1}\,cm^{-1}$ or less and activation energies as high as 0.3 eV.[3,4]

$(Cs^+)_2(TCNQ)_3^{--}$. According to Fritchie and Arthur,[9] this salt crystallizes with the symmetry of the space group $P2_1/c(C_{2h}^5)$ and with two formula units per cell. TCNQ molecules pack face-to-face to form somewhat irregular columns parallel to the b-axis, with a unique grouping of charge-transfer-bonded triads. The inter-planar spacing is 3.22 Å within a triad and 3.26 Å between triads.

The absorption spectrum of the salt in acetonitrile is shown in Fig. 1, curve a. The crystalline spectrum illustrated in Fig. 1, curve b, is found to resemble that of the $TCNQ^-$ dimer in an aqueous solution[10] or those of the simple salts with low-conductivities.[2] The crystalline spectrum of the Cs salt comprises peaks at 10.1, 16.2 and 27.5 kK, a weak band in the region less than 6 kK and extending to 4 kK, and a slight shoulder around 23 kK. These three peaks almost correspond to those at 8.5, 16.4, and 27.8 kK respectively in the simple potassium salt.[2] The high-energy peaks at 16.2 and 27.5 kK in the Cs salt may also well be compared with those at 15.6 and 27.0 kK respectively in the dimer.[10] Neutral TCNQ in acetonitrile has a band peak at 25.3 kK with a molar extinction coefficient as high as 65000,[2] therefore, if this band makes some contribution to the band at 27.5 kK in the Cs salt, the appearance of a shoulder or a remarkable increase in the intensity relative to that at 16.2 kK may be expected. However, the spectrum of the Cs salt shows that this appears not to be the case. The shoulder around 23 kK is too slight to be the expected one; it is probably due to a non-interacting TCNQ or $TCNQ^-$ monomer in some kind of defects. Thus, the band due to TCNQ may be regarded as appreciably blue-shifted, thus making only a small contribution to the band at 27.5 kK. Therefore, for the same reason as with the simple salts,[2] the bands at 16.2 and 27.5 kK in the Cs salt should mainly be assigned to the shifted bands of the $TCNQ^-$ monomer, while the band at 10.1 kK must be the charge-transfer band between $TCNQ^-$ molecules (*cf.* Ref. 11). Finally, the weak low-energy band characteristic of the (2 : 3) salts may be regarded as due to charge-transfer interaction between $TCNQ^-$ and

9) C. J. Fritchie, Jr., and P. Arthur, Jr., *Acta Cryst.*, **21**, 139 (1966).

10) R. H. Boyd and W. D. Phillips, *J. Chem. Phys.*, **43**, 2927 (1965).

TCNQ, for it appears only upon the introduction of TCNQ.

The finding that the crystalline spectrum is due almost entirely to the pair-by-pair interaction between unpaired electrons in the Cs salt is probably associated with its magnetic properties. According to Chesnut and Arthur,[7] its paramagnetism is to be attributed to a triplet-exciton state lying 0.16 eV above a singlet state.[8] Understandably, the pair-by-pair interaction leads to the singlet-triplet energy separation. However, the addition of neutral TCNQ to the $TCNQ^-$ dimer may contribute to a reduction of the localized triplet character, producing a triplet exciton in the crystal. The reason for this is as follows. With respect to the unpaired electrons, the dimer in the (2 : 3) salt corresponds to the doubly-charged TCNQ triad. The interacting distance between two unpaired electrons in the triplet state of the triad may be longer than that in the dimer without neutral TCNQ, because the lowest-triplet configuration is not mixed with the charge-transfer configuration and, consequently, the two electrons in the triplet state may be regarded as mutually repulsive.[2,11] Thus, the introduction of neutral TCNQ should decrease the intra-dimer interaction and increase the inter-dimer interaction in the triplet state, at least to some extent, thus resulting in the triplet exciton. On the other hand, the electronic transitions conceived here occur among singlet states, where the mixing of the lowest singlet configuration with the charge-transfer configuration in the triad is quite significant. Therefore, the pair-by-pair interaction may be regarded as strong in the singlet states, giving rise to the spectral resemblance to the dimer without neutral TCNQ. At any rate, the presence of additional TCNQ to this salt seems to perturb weakly the pair-by-pair interaction of ion radicals. This effect may make a small contribution to the increase in electrical conductivity. The conductivity of the complex Cs salt ($1\times10^{-5}\,\Omega^{-1}\,cm^{-1}$ at 23°C, compaction measurement) should be compared with that of the simple salt with the same cation (5×10^{-4}).[4]

(Morpholinium$^+$)$_2$(TCNQ)$_3^{-}$. The crystalline spectrum (Fig. 1, curve c) consists of peaks at 10.0, 16.3, and 27.6 kK, and a weak band in the region from less than 6 kK to 4 kK. These bands agree well with the corresponding bands in the Cs salt. Furthermore, the spectrum of the complex morpholinium salt bears a close resemblance, except the weak low-energy band, to that in the simple salt with the same cation,[2] which has peaks at 9.5, 16.3, and 27.7 kK. The band at 9.5 kK in the simple salt has been ascribed to the inter-radical charge-transfer transition, to which the band at 10.0 kK in the complex salt is also regarded as due. Again, in these morpholinium salts, the weak low-energy band is also characteristic of the complex salt. Although the electrical conductivity of the complex salt ($2\times10^{-4}\,\Omega^{-1}cm^{-1}$, single-crystal measurement)[3] is larger than that of the simple salt (1×10^{-9}),[4] the former is classified as part of the group with intermediate conductivity. Accordingly, the perturbation due to the introduction of TCNQ is certainly weak. There are many reasons to believe that the complex morpholinium salt possesses a crystal structure similar to that of the Cs salt and exhibits magnetic properties based on a triplet exciton.[6]

The (1 : 2) Intermediate-Conductivity Compounds. The counter cations of these compounds, such as methyltriphenylphosphonium (Ph_3PCH_3) or methyltriphenylarsonium (Ph_3AsCH_3), usually have a nearly spherical form and a relatively large size. These salts are obtained in the form of well-developed blue-black crystals. They have conductivities of the order of $10^{-2}\,\Omega^{-1}\,cm^{-1}$ or less, and activation energies as high as 0.3 eV.[3,4] In the following paragraphs, the results of some representative samples will be discussed in detail.

(Ph_3XCH_3)$^+$(TCNQ)$_2^-$ (X=P or As). These salts have almost identical electronic properties except for the occurrence of a phase transition in the phosphonium salt at 40°C.*2 The crystal structures of these salts have not yet been ascertained. The absorption spectrum of the phosphonium salt in acetonitrile and its crystalline spectrum are given

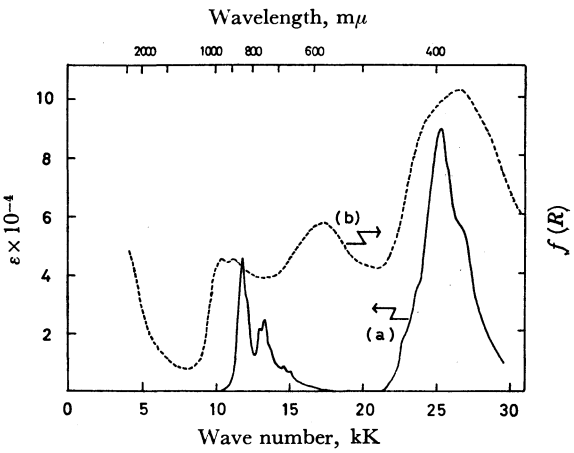

Fig. 2. Electronic spectra of $(Ph_3PCH_3)^+(TCNQ)_2^-$ in acetonitrile solution (a) and in the solid state (b).

11) K. H. Hausser and J. N. Murrell, *ibid.*, **27**, 500 (1957).

*2 In the phosphonium salt, a phase transition occurs at 40°C, where an abrupt and reversible change in ESR intensity and electrical conductivity has been observed. The measurement of the thermal analysis has also been carried out. See Y. Iida, M. Kinoshita, M. Sano and H. Akamatu, This Bulletin, **37**, 428 (1964); Y. Iida, M. Kinoshita, A. Kawamori and K. Suzuki, *ibid.*, **37**, 764 (1964).

in Fig. 2 by curve a and curve b respectively. Quite similar electronic spectra in acetonitrile and in the solid state were obtained in the arsonium salt. The crystalline spectrum of the phosphonium or the arsonium salt, on the other hand, bears no resemblance to the dimer spectrum, consisting of peaks at 10.4, 11.4, 17.2, and 26.3 kK, and an intense band with its peak in the region less than 4 kK. Although the locations of the bands at 17.2 and 26.3 kK nearly correspond to those at 15.6 and 27.0 kK respectively in the dimer,[10] the band at 26.3 kK should comprise not only that due to the dimer but also that due to neutral TCNQ, because the band at 26.3 kK has an appreciably larger intensity than that at 17.2 kK and even has its shoulder around 24 kK. There has been no contribution of the band due to TCNQ in the (2 : 3) salts. The pair-by-pair interaction as to the unpaired electrons in the phosphonium or the arsonium salt is decreased compared to that in the (2 : 3) salts, but it still remains, because the peak at 17.2 kK almost certainly to be ascribed to the dimer spectrum[10] is relatively diffused and continuously overlaps with other bands. The decrease is probably caused by the presence of more TCNQ in the (1 : 2) salt than in the (2 : 3) salt. Whether the doublet bands at 10.4 and 11.4 kK are due to two different electronic transitions or to one with vibrational structures is not clear. Furthermore, it is difficult to decide whether they are shifted bands of the $TCNQ^-$ monomer or charge-transfer bands between $TCNQ^-$ molecules. However, it can be said that, although the charge-transfer band is expected to appear around 10 kK, the band splitting may make the latter possibility improbable. On the other hand, the location of the band peak in the range less than 4 kK was not determined by the diffuse reflectance spectrum. Therefore, we examined the infrared absorption spectrum, which indicates that this intense electronic band partially screens the vibrational spectrum and has its peak around 2.9—3.3 kK. It is not clear whether this band is to be ascribed to the charge-transfer band between $TCNQ^-$ and TCNQ, or to the direct transition from the valence state to the electrical conduction state. Possible support for the former possibility is that similar low-energy bands, although weak in intensity, have been observed in the (2 : 3) salts and that, here, they are remarkably increased in intensity by the further introduction of TCNQ. However, they appear in the compounds with relatively high electrical conductivities. Therefore, we believe that they are closely correlated with their high conductivities.

The paramagnetism of the phosphonium or the arsonium salt is based on a triplet-exciton state lying 0.062 eV above the singlet state.[6] Therefore, the mode of interaction among the ion radicals is certainly by pairs. However, the delocalization of the triplet exciton in these salts is increased (*i. e.*, there is an increase in the triplet-exciton band width) and its singlet-triplet energy separation is decreased, compared with the values in the Cs salt.[12] This change can probably be said to be caused, by an extension of the reason mentioned above for the Cs salt, by the presence of the additional TCNQ. However, in these (1 : 2) salts, the presence of this TCNQ still appreciably modifies the crystalline electronic spectrum with a pair-by-pair character. Such was not the case with the (2 : 3) salts, where the change is relatively slight. Furthermore, the presence of neutral TCNQ in the (1 : 2) salts causes a remarkable increase in the electrical conductivity. For example, the complex phosphonium salt has $2\times10^{-2}\ \Omega^{-1}\,cm^{-1}$ at 23°C (single-crystal measurement), a value which is markedly larger than the 2×10^{-11} of the simple salt with the same cation.[4] The former should also be compared with the 1×10^{-3} value of the complex Cs salt (single-crystal measurement),[4] where, on the contrary, the effect has been regarded as weak.

It may be concluded that, in the phosphonium or the arsonium salt, the perturbation due to the introduction of TCNQ is relatively strong. Nonetheless, one can still picture the TCNQ molecules as existing in unique groups of four (*i. e.*, two $TCNQ^-$ and two TCNQ molecules) along a one-dimensional column in the solid state.

The Other Compounds. All of the other compounds belonging to this group bear, more or less, an optical resemblance to those of the phosphonium or the arsonium salt. The band peaks of their crystalline spectra are designated as shown in Fig. 3, which also gives an example of the spectrum of

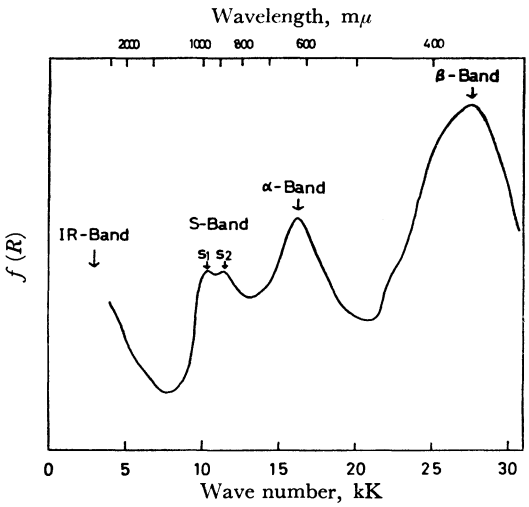

Fig. 3. Electronic spectrum of Triethylammonium$^+$-$(TCNQ)_2^-$ in the solid state, together with the designation of its band peaks.

12) Z. G. Soos and R. C. Hughes, *J. Chem. Phys.*, **46**, 253 (1967).

the triethylammonium salt. The features of the low-energy band (IR-band), the splitting (~1 kK) of the doublet S_1- and S_2-bands, and the rather sharp α-band relative to the (1 : 2) high-conductivity compounds (see below) should be noted. The locations of the IR-bands in these intermediate-conductivity compounds are estimated to be in the same range as in the phosphonium salt (*i. e.*, 2.9—3.3 kK). The other peaks are listed in Table 1. Evidently, the corresponding band peaks are

TABLE 1. THE DATA FOR THE BAND PEAKS EXCEPT THE IR-BAND IN THE CRYSTALLINE ELECTRONIC SPECTRA OF THE (1 : 2) INTERMEDIATE-CONDUCTIVITY TCNQ COMPLEX SALTS

Cation*	S-Band(kK)		α-Band (kK)	β-Band (kK)
	S_1	S_2		
$MePh_3P$	10.4	11.4	17.2	26.3
$MePh_3As$	10.3	11.4	17.2	26.7
$EtPh_3P$	11.3		17.2	27.0
$EtPh_3As$	11.3		16.9	26.7
Me_3PhN	10.2	11.5	16.4	26.3
Et_3HN	10.3	11.4	16.4	27.2
Et_3PhN	10.5	11.4	16.0	27.5
Et_4N	10.0	11.4	17.0	27.2
$Et(n\text{-Pro})_3N$	9.9	11.3	16.3	26.7
$n\text{-Pro}_4N$	9.9	11.3	16.3	27.0

* Substituents of methyl, ethyl, *n*-propyl and phenyl are abbreviated as Me, Et, *n*-Pro and Ph, respectively.

shifted slightly by the change in the cations; on this change, however, depends the sharpness of the α-bands related to the degree of pair-by-pair interaction of ion radicals. The triethylammonium salt is found to have an especially sharp and strong α-band, exhibiting, on the other hand, magnetic properties based on a triplet exciton.*3

In all events, in the (1 : 2) intermediate-conductivity compounds, the pair-by-pair interaction of ion radicals is relatively decreased by the further introduction of TCNQ. However, we believe that that interaction mode will still not be changed.

The (1:2) High-Conductivity Compounds. The counter cations of these compounds are aromatic or heterocyclic cations such as quinolinium. These compounds come out of the solution in the form of small blue-black needles. The quinolinium salt, for example, exhibits an electrical conductivity as high as 100 Ω^{-1} cm^{-1} and an activation energy as low as 0.03 eV (single-crystal measurement).[4] In the following paragraphs, the results of the crystalline spectra in some representative samples will be discussed in detail.

Quinolinium$^+(TCNQ)_2^-$. The crystal structure of this salt has not yet been ascertained. The absorption spectrum in acetonitrile, shown by curve a of Fig. 4, is essentially the same as those of the (1 : 2) intermediate-conductivity compounds. Al-

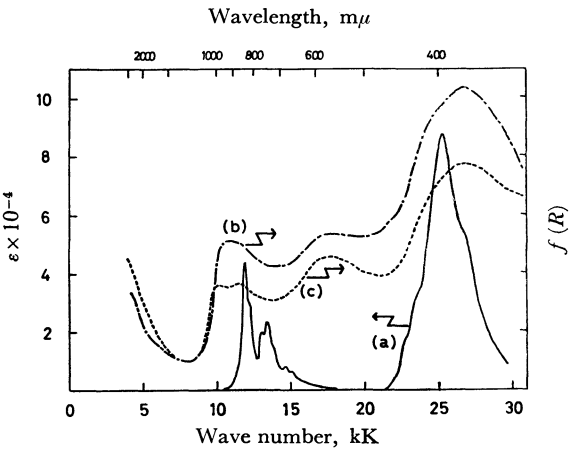

Fig. 4. Electronic spectra of Quinolinium$^+$ $(TCNQ)_2^-$ in acetonitrile solution (a), Quinolinium$^+$ $(TCNQ)_2^-$ in the solid state (b) and *N*-(*n*-Propyl)quinolinium$^+$ $(TCNQ)_2^-$ in the solid state (c).

though the crystalline spectrum illustrated by curve b of Fig. 4 bears a rough resemblance to those of the intermediate-conductivity compounds, some differences may be noted. The crystalline spectrum of the quinolinium salt has peaks at 10.5, 17.4, and 26.7 kK, and an intense band with its peak in the range less than 4 kK. The last band peak was not determined by means of the diffuse reflectance, so we have also examined the absorption spectrum, which shows, in this case, that the vibrational spectrum is completely screened by this intense electronic transition. The location of the peak is thus estimated to be around 2.0—2.5 kK. This band may be connected with that observed in the far infrared region by Kondow *et al.*[13] It should also be mentioned that this band is not exactly the same as the IR-band in the intermediate-conductivity compounds, which is around 2.9—3.3 kK. In connection with the contrast of their conductivities, this difference in their lowest-energy bands implies a difference in the interaction modes of unpaired electrons between high- and intermediate-conductivity compounds (see below). Furthermore, there is reason to believe that these bands in both the groups may arise from a transition from the valence band to the electrical conduction band.[13]

*3 In explaining the temperature dependence of the magnetic susceptibility of the triethylammonium salt, Soos and Hughes' theory (see Ref. 12) has supported the model of a weakly alternating antiferromagnet rather than that of almost isolated triplets. However, in the crystalline spectrum presented here, the especially sharp and strong α-band may imply a strongly pair-by-pair interaction of ion radicals in this salt.

TABLE 2. THE DATA FOR THE BAND PEAKS EXCEPT THE LOWEST-ENERGY BAND IN THE CRYSTALLINE ELECTRONIC SPECTRA OF THE (1 : 2) HIGH-CONDUCTIVITY TCNQ COMPLEX SALTS. THE DESIGNATION OF THE BANDS NEARLY CORRESPONDS TO THAT IN Fig. 3

Cation	S-Band (kK)		α-Band (kK)	β-Band (kK)
	S_1	S_2		
Quinolinium	10.5		17.4	26.7
N-Methylquinolinium	10.2	11.4	16.3	27.4
N-Ethylquinolinium	10.0	11.6	16.9	26.7
N-(*n*-Propyl)quinolinium	10.0	11.6	17.8	26.7
N-Methylisoquinolinium	10.4	11.4	18.2	25.8
N-Ethylisoquinolinium	10.3	11.6	16.3	—
Quinaldinium	10.5		17.7	26.3
N-Methylquinaldinium	10.7		17.8	27.5
N-Ethylquinaldinium	10.2	11.6	16.1	27.0
Lepidinium	12.0		17.5	26.3
N-Methyllepidinium	10.0	11.4	16.4	27.0
N-Ethyl-2,6-dimethylquinolinium	10.4	11.8	18.0	—
N-Methylacridinium	11.2		17.8	27.5

The quinolinium salt has one band, around 10.5 kK, corresponding to the S_1- and S_2-bands in the intermediate-conductivity compounds. Usually, the spectra of the compounds with high conductivities are found to comprise one band with no such splitting, whereas the splitting tends to appear with a decrease in the conductivity. Accordingly, the nature of the band at 10.5 kK depends on its conductivity. However, its origin is not clear. The band at 17.4 kK, probably related to the pair-by-pair interaction of ion radicals, is more diffused than the α-band in the intermediate-conductivity compounds and is remarkably overlapped with other bands. These findings imply that the pair-by-pair interaction would almost vanish in the quinolinium salt. On the other hand, the band around 26.7 kK rather resembles the β-band in the intermediate-conductivity compounds. These observations provide us with some reasons for the more-than-pair-by-pair interaction of ion radicals in this salt. As in the cases with some TCNQ salts,[7,9,14,15] the TCNQ molecules in the quinolinium salt should form a one-dimensional column, so each unpaired electron should interact equally and strongly with two neighbors. In this respect, the (1 : 2) high-conductivity compounds are different from the (1 : 2) intermediate-conductivity compounds. The more-than-pair-by-pair interaction of the ion radicals in the quinolinium salt causes the delocalization of the unpaired electrons, which, in turn, brings about its high electrical conductivity and the low activation energy. Also, in this case, the presence of neutral TCNQ makes some contribution to the delocalization. The mode of the interaction is, except for the exclusion of the neutral molecules, similar to those of some Würster's salts with a more-than-pair-by-pair and strong interaction[1] or that of the high-conductivity TCNQ simple salt of *N*-methylphenazinium.[2] In view of these facts, we believe that the magnetic property of the quinolinium salt with an almost temperature-independent paramagnetism ($\chi = 4.3 \pm 0.2 \times 10^{-7}$ emu/g)[5] may be based on a non-alternating linear chain antiferromagnet. However, we hesitate to accept the idea of a complete Heisenberg antiferromagnet because of the delocalization of the unpaired electrons.

The Other Compounds. All the other compounds belonging to this group show crystalline spectra essentially like that of the quinolinium salt. However, it is noteworthy that a splitting of the doublet bands around 10 kK appears, and that the sharpness of the band around 17 kK is increased, with a decrease in their electrical conductivities. The band peaks of their crystalline spectra, nearly corresponding to S-, α-, and β-bands in the intermediate-conductivity compounds, are listed in Table 2. The spectrum of the *N*-(*n*-propyl)quinolinium salt, as an example, is illustrated by curve c of Fig. 4. The decrease in the conductivities depends largely on the size and the shape of the cations. For example, the introduction of a substituent as bulky as *n*-propyl to the quinolinium cation decreases 100 Ω^{-1} cm^{-1} at 23°C of the quinolinium salt[4] to 2 of the *N*-(*n*-propyl)quinolinium salt.[3] Therefore, the introduction of bulky substituents to the flat cations (*e. g.*, aromatic or heterocyclic) leads to intermediate conductivities,

13) T. Kondow, K. Siratori and H. Inokuchi, *J. Phys. Soc. Japan*, **21**, 824 (1966); **23**, 98 (1967).

14) G. R. Anderson and C. J. Fritchie, Jr., Second National Meeting, Society for Applied Spectroscopy, San Diego, October 14, Paper 111 (1963).

15) C. J. Fritchie, Jr., *Acta Cryst.*, **20**, 892 (1966).

and the doublet bands around 10 kK and a rather sharp and strong α-band come to be clearly observed. Accordingly, it may be concluded that those introductions of substituents contribute, to varying degrees, to the change of the more-than-pair-by-pair interaction of ion radicals into the pair-by-pair interaction. It is expected that this change in the interaction modes will greatly affect their magnetic properties, again producing triplet excitons.

The author wishes to express his thanks to Professor Yoshio Matsunaga for his generous support to this work and to Mr. Nobuhiko Miyajima for his technical assistance.

BULLETIN OF THE CHEMICAL SOCIETY OF JAPAN VOL. 42 643—650 (1969)

The Etherification Reactions of Allyl Alcohol Catalyzed by the Copper(I) Chloride Complex*1

Tetsuya OGURA, Nobuo FURUNO*2 and Shinichi KAWAGUCHI

Department of Chemistry, Faculty of Science, Osaka City University, Sumiyoshi-ku, Osaka

(Received July 17, 1968)

Diallyl ether was produced exclusively when an allyl alcohol solution containing copper(I) chloride and ammonium chloride was heated in the absence of air. A mixture of allyl and ethyl alcohols gave diallyl and ethyl allyl ethers, but no trace of diethyl ether. The tracer experiment employing ^{18}O-enriched allyl alcohol showed that the C–O bond in allyl alcohol was ruptured in the ethyl allyl ether formation. The kinetic study of these etherification reactions showed that the rate determining step would include the nucleophilic attack of an allyl or ethyl alcohol molecule on the catalyst-substrate complex. A novel allyl alcohol complex, $(NH_4)_2Cu_2Cl_4(C_3H_6O)_2$, was isolated and characterized, but the active catalyst species was assumed to be $(NH_4)_2Cu_4Cl_6$. Methyl derivatives of allyl alcohol were also allowed to react in the presence of the same catalyst and the possible mechanism of etherification was discussed.

Copper(I) chloride was found by Berthelot[1] to enhance the solubilities of olefins such as ethylene and propylene in aqueous solutions. This fact suggests the specific interaction between copper(I) and the olefinic double bond. Gilliland *et al.*[2] succeeded later in synthesizing these complexes under pressure of olefins.

In our laboratory syntheses and reactions of metal complexes of substituted olefins have been studied, and crystalline complexes of copper(I) chloride with acrolein,[3] allyl alcohol[4] and allylamine[5] were prepared by direct reactions. This paper reports the catalytic action of copper(I) chloride complex for the etherification reactions of allyl alcohol, and a possible reaction mechanism is presented based on the kinetic and tracer experiments.

Experimental

Materials. Copper(II) chloride dihydrate was mixed with excess copper powder and heated to 110°C under reduced pressure. After the dehydration, the mixture was heated to 500°C resulting in liquid copper(I) chloride, which was cooled to room temperature. The crude product was crushed and purified by distillation at 500°C *in vacuo*. The highly pure specimens of copper(I) chloride for the kinetic experiments were prepared by distilling more than three times. Ammonium chloride of analytical grade was further purified by sublimation. Allyl alcohol was dried with molecular sieves, Type 3A (Linde Co.) and distilled through a 30 cm Widmer column. Commercial methylallyl alcohols were used

*1 Presented at the 17th Symposium on the Chemistry of Metal Coordination Compounds of the Chemical Society of Japan, Hiroshima, December, 1967.

*2 Present address: Research Department, Nippon Paint Co., Ltd., Neyagawa, Osaka.

1) M. P. E. Berthelot, *Ann. chim. phys.*, **23**, 32 (1901).

2) E. R. Gilliland, J. E. Seebold, J. R. Fitz Hugh and P. S. Morgan, *J. Am. Chem. Soc.*, **61**, 1960 (1939); E. R. Gilliland, H. L. Bliss and C. E. Kip, *ibid.*, **63**, 2088 (1941).

3) S. Kawaguchi and T. Ogura, *Inorg. Chem.*, **5**, 844 (1966).

4) T. Ogura, N. Furuno and S. Kawaguchi, This Bulletin, **40**, 1171 (1967).

5) T. Ogura, T. Hamachi and S. Kawaguchi, *ibid.*, **41**, 892 (1968).

without further purification. Ethyl alcohol was dried employing magnesium ribbon.

Stoichiometry Determination of the Etherification Reactions. Into an ampoule containing 0.1—1 g of copper(I) chloride and 0.05—0.5 g of ammonium chloride was distilled 5 g of allyl alcohol or a mixture of allyl and ethyl alcohols *in vacuo*. The ampoule was sealed off, put into an autoclave together with water whose vapor pressure is very similar to that of allyl alcohol, and heated to 160—180°C.

Volatile reaction products were collected in a trap by vacuum distillation and separated by vapor phase chromatography (abbreviated as VPC) using a 1 m column packed with 30% triethanolamine on Chamelite CS of Kishida Chemicals, Ltd. (60°C, H_2 flow of 80 m*l*/min). The water content was determined by the Karl Fischer method.

Preparation and Reaction of Allyl Alcohol Enriched with ^{18}O. Twenty five grams of silver perchlorate was dissolved in 20 m*l* of ^{18}O-enriched (2%) water, to which 8 g of allyl chloride was added gradually under vigorous agitation in an ice bath. An exothermic reaction occurred separating out silver chloride. In order to neutralize perchloric acid produced, sodium hydrogen carbonate was added occasionally until yellow silver carbonate began to appear. The reaction mixture was kept standing for two days at room temperature. Volatile products were collected by distillation under reduced pressure and dried with anhydrous copper(II) sulfate. Allyl alcohol was separated from the by-product, diallyl ether, by means of VPC.

A mixture of labeled allyl alcohol (0.4 g), unlabeled ethyl alcohol (1.6 g), copper(I) chloride (0.05 g) and ammonium chloride (0.02 g) was allowed to react in an ampoule at 160—180°C. Calcium chloride was added to the product mixture to separate the ether layer. Ethyl allyl ether was fractionated through the VPC column and submitted to the mass spectrometric analysis.

Kinetic Studies. Since the reaction system containing copper(I) chloride is very sensitive to air, the whole procedure was performed under rigorous exclusion of air. A desired number of ampoules containing a reaction mixture of the same composition were prepared using the apparatus depicted in Fig. 1. The reaction mixture (30—40 m*l*) was made up by vacuum distillation of allyl alcohol into a large ampoule (A) containing a mixture of copper(I) chloride and ammonium chloride. The ampoule (A) was attached to the vacuum line in an inverse fashion. A small portion (about 2 m*l*) of the solution was transfered to each small ampoule (C) evacuated in advance through the tap (B). The ampoule (C) was then fused off at D. Many ampoules thus prepared were immersed in a liquid paraffin bath and maintained at a constant temperature between 120—180°C. Each ampoule was picked up at appropriate time intervals and quenched. The extent of reaction was determined by measuring the water content by means of the Karl Fischer method.

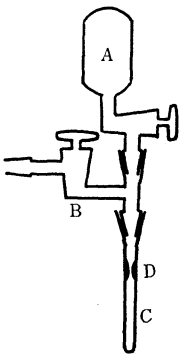

Fig. 1. The apparatus for preparing ampoules containing the reaction mixture of the same composition.

When a mixture of allyl and ethyl alcohols was allowed to react in the presence of copper(I) chloride and ammonium chloride, the produced ethers were separated through the VPC column. Diallyl and ethyl allyl ethers were identified, but no trace of diethyl ether was found. Preliminary calibration experiments revealed that the mole ratios of diallyl ether to allyl alcohol and ethyl allyl ether to ethyl alcohol in their mixture are proportional in the region below 0.05 to the respective peak height ratios on a vapor phase chromatogram (Fig. 2.) Many ampoules containing allyl and ethyl alcohols in various ratios together with copper(I) chloride and ammonium chloride were kept at a constant temperature of 148.1°C. The reaction was quenched at 0.01—2% conversion in either case, and amounts of diallyl and ethyl allyl ethers were determined by means of Fig. 2.

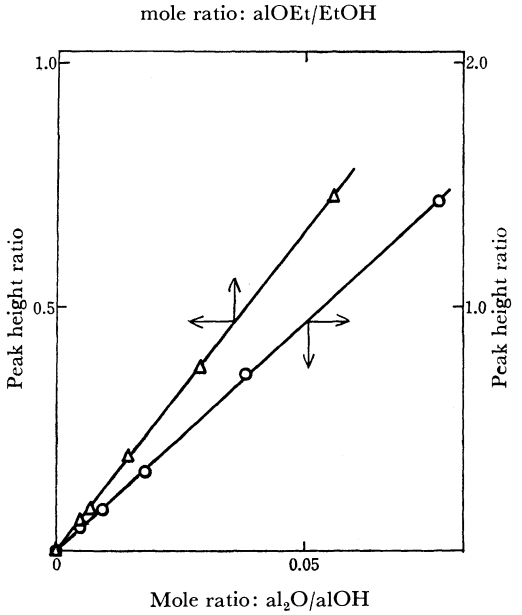

Fig. 2. Calibration lines between the mole ratio and the peak height ratio on a gas chromatogram of diallyl ether to allyl alcohol and ethyl allyl ether to ethyl alcohol.

Etherification of α-, β- and γ-Methylallyl Alcohols. To promote the elucidation of the reaction mechanism, the etherification reaction of substituted allyl alcohols were performed and the products distribution was measured in each case. In 3 m*l* of a methylallyl alcohol, 30 mg of copper(I) chloride and 10 mg of

ammonium chloride were dissolved and allowed to react at 92°C for 2.5—16 hr to attain 1—7% conversion. Reaction products were fractionated through a VPC column containing polyethylene glycol (1 m) and triethanolamine (1 m) at 96°C using hydrogen gas flow of 40 ml/min. The nature of each fraction was identified by means of its infrared and proton magnetic resonance spectra. Table 1 summarizes reaction products from each methylallyl alcohol and their relative rates of formation.

Table 1. Reaction products from methyl-substituted allyl alcohols in the presence of copper(I) chloride catalyst*

Substrate	Products	Relative rates of formation
α OH	γ OH	< 0.1
	α ₂O	1.2
	α O γ	1
β OH	β ₂O	1
γ OH	α OH	1
	α O γ	1
	γ ₂O	~0.03

* α, β and γ denote α-methylallyl (CH_2=CH–CH(CH_3)–), β-methylallyl (CH_2=C(CH_3)–CH_2–) and γ-methylallyl (CH(CH_3)=CH–CH_2–) radicals, raspectively.

Synthesis of the Crystalline Complex $(NH_4)_2Cu_2Cl_4(C_3H_6O)_2$. An allyl alcohol solution (30 ml) containing copper(I) chloride (0.531 g, 5.36 mmol) and ammonium chloride (0.287 g, 5.37 mmol) was heated at 80°C for 3 hr, and most of excess alcohol was distilled off. White crystals resulted were dried completely by distillation of the remaining solvent *in vacuo* at the temperature difference between 5 and 0°C for 3 days.

Found: Cu, 29.9; Cl, 33.4; C_3H_6O, 28.2%; Calcd for $(NH_4)_2Cu_2Cl_4(C_3H_6O)_2$: Cu, 30.1; Cl, 33.6; C_3H_6O, 27.6%.

Measurements. Copper was determined by the electrolysis, chloride gravimetrically as the silver salt, and allyl alcohol by the brominating method.[4] The infrared spectra were measured in Nujol with a Hitachi infrared spectrophotometer EPI-2, and NMR spectra with a 60 MC spectrophotometer, model JNM 3H60 of Japan Electron Optics Laboratory, Ltd. The mass analysis was performed with a Hitachi mass spectrometer RMU-6.

Results

The Stoichiometry of Diallyl Ether Formation. When allyl alcohol containing copper(I) chloride and ammonium chloride was heated for several hours at 160—180°C, the mixture separated into two liquid layers. The upper layer consisted of dially ether containing a small amount of copper(I) chloride, and the lower aqueous layer included copper(I) chloride, ammonium chloride and remaining allyl alcohol. In an experiment at 180°C for 24 hr, 93% of allyl alcohol employed (90.2 mmol) was converted to diallyl ether (42.1 mmol) and water (42.0 mmol), and no side reaction occurred. The mass balance can thus be represented by Eq. (1).

$$2CH_2{=}CH{-}CH_2OH \longrightarrow (CH_2{=}CH{-}CH_2)_2O + H_2O \quad (1)$$

When allyl alcohol containing highly pure copper(I) chloride alone was heated under the same conditions, no allyl ether was produced. Ammonium chloride alone does not work either. The effective catalyst must be composed of copper(I) chloride and a certain amount of chloride ions since calcium chloride works as well as ammonium chloride and lithium chloride is also effective though to a lesser extent. Silver perchlorate and nitrate were examined. Diallyl ether was produced in these cases, too, but some side reactions also proceeded depositing metallic silver.

Kinetics of the Diallyl Ether Formation. With any catalyst composition a first order linear plot was obtained before the extent of reaction attained to 25% (Fig. 3). The reaction rate is

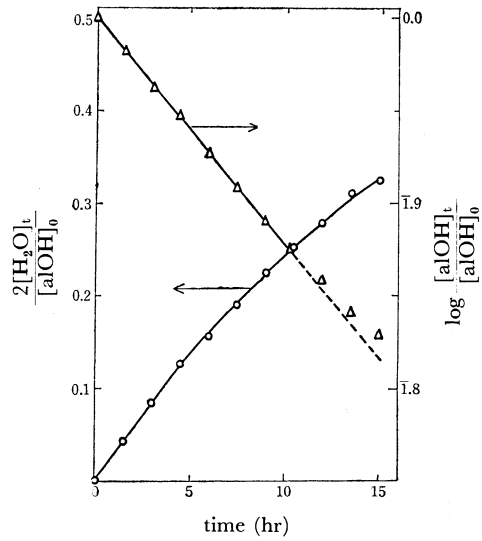

Fig. 3. The pseudo first order plot of the etherification reaction of allyl alcohol at 144.8°C. $[Cu_2Cl_2]_0$=0.0630, $[NH_4Cl]_0$=0.0581 mol/kg solvent

thus represented by Eq. (2). At a higher extent of the reaction the mixture separated into two layers

$$\frac{d[H_2O]}{dt} = -\frac{1}{2}\frac{d[C_3H_5OH]}{dt} = k_1[C_3H_5OH] \quad (2)$$

and the first order rate law did not hold any more.

The pseudo first order rate constant k_1 changed with concentrations of both copper(I) chloride and ammonium chloride. When the concentration of ammonium chloride was kept constant and that

of copper(I) chloride increased, the recation rate increased linearly as shown in Fig. 4. It should be noticed that the straight line intersects the abscissa. On the other hand the dependence of k_1 upon the concentration of ammonium chloride was rather complicated as illustrated in Fig. 5. A maximum appeared at a concentration of ammonium chloride about half that of copper(I) chloride in the monomer unit.

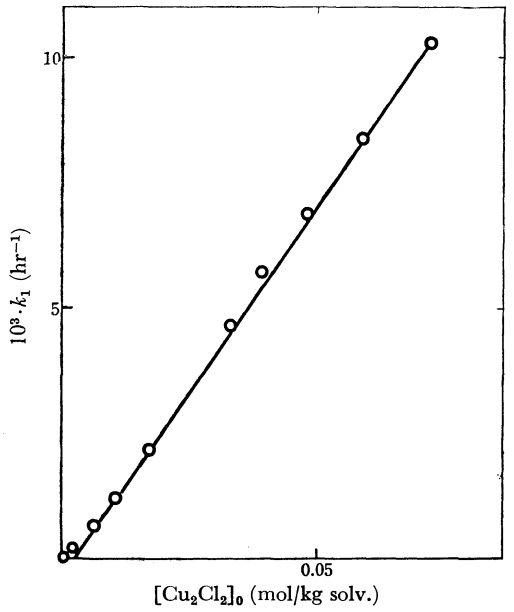

Fig. 4. Dependence of the pseudo first order rate constant (Eq. (1)) upon the concentration of copper(I) chloride at 148.6°C.
$[NH_4Cl]_0$=0.00916 mol/kg solvent

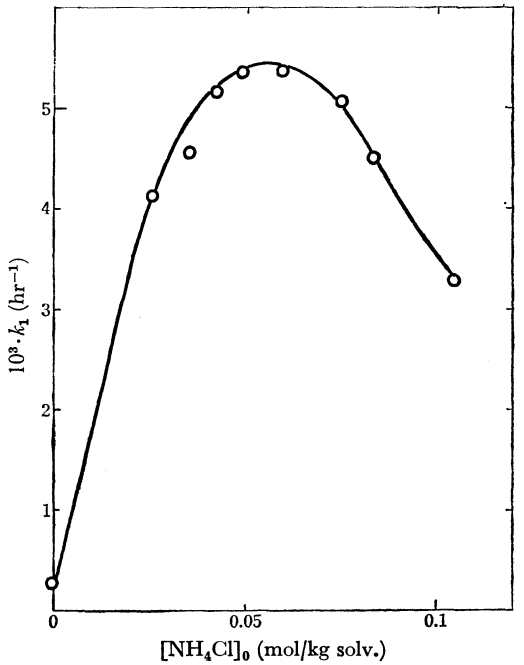

Fig. 5. Dependence of the pseudo first order rate constant (Eq. (1)) upon the concentration of ammonium chloride at 135.0°C.
$[Cu_2Cl_2]_0$=0.0546 mol/kg solvent

Adduct Formation of Copper(I) Chloride with Ammonium Chloride in Allyl Alcohol. The solubility of copper(I) chloride in water is very low, but is much enhanced by the coexistence of ammonium chloride and the formation of adducts, $CuCl \cdot NH_4Cl$ and $2CuCl \cdot NH_4Cl$ was reported.[6] On the other hand the solubility of ammonium chloride in allyl alcohol is very low (0.246 g in 100 g solvent at 20°C), but is enhanced by the presence of copper(I) chloride. For instance 0.685 g of ammonium chloride dissolves in 100 g of allyl alcohol at 10°C containing 1.26 g of copper(I) chloride. The mole ratio of the two solutes is close to unity suggesting the formation of 1 : 1 adduct in allyl alcohol.

The state of aggregation of copper(I) chloride by itself and also in the coexistence of ammonium chloride was investigated by measuring the boiling point elevation of allyl alcohol in nitrogen atmosphere with the modified Cotrell apparatus.[7] The molal elevation constant of boiling point of allyl alcohol was determined to be 1.615°C employing naphthalene as a reference solute. (Value of the constant calculated using 10.1 kcal/mol as the molar heat of vaporization[8] is 1.57°C.) Table 2 summarizes the results obtained. In each case the molality of solution found is nearly half of that employed, revealing that copper(I) chloride exists as a dimer in boiling allyl alcohol.[9] It should be noticed that

TABLE 2. DEGREE OF DIMERIZATION OF COPPER(I) CHLORIDE IN ALLYL ALCOHOL IN THE ABSENCE AND PRESENCE OF AMMONIUM CHLORIDE DETERMINED BY THE BOILING POINT ELEVATION

Molality employed $\times 10^3$		Molality found $\times 10^3$	Degree of dimerization
CuCl	NH_4Cl		
5.48	0	2.71	1.01
3.94	0	2.17	0.90
3.44	0	1.84	0.93
3.19	0	1.66	0.96
5.06	2.67	2.66	0.95
2.71	2.18	1.37	0.99
			Mean 0.96

6) I. S. Morozov and G. V. Ustavschikova, *Bull. acad. sci. USSR, Classe sci. chim.*, **1944**, 451; *Chem. Abst.*, **39**, 3199 (1945).
7) F. G. Cotrell, *J. Am. Chem. Soc.*, **41**, 721 (1919).
8) D. R. Stull, *Ind. Eng. Chem.*, **39**, 517 (1947).
9) The report in a previous paper (Ref. 4) that copper(I) chloride exists as a monomer in boiling allyl alcohol was in error.

the degree of dimerization of copper(I) chloride is not affected by the presence of ammonium chloride up to the equimolar amount. This fact indicates that the equilibrium constant of the adduct formation (Eq. (3)) is very large and also that this adduct is not ionized appreciably in boiling allyl alcohol.

$$Cu_2Cl_2 \cdot xC_3H_6O + 2NH_4Cl \rightleftarrows (NH_4)_2Cu_2Cl_4 \cdot xC_3H_6O \quad (3)$$

The crystalline adduct $(NH_4)_2Cu_2Cl_4 \cdot (C_3H_6O)_2$ was in fact isolated as described in the Experimental Section. The characteristic infrared absorption bands of this complex are listed in Table 3 together

Table 3. Characteristic infrared absorption bands in Nujol (cm^{-1})

$(NH_4)_2Cu_2Cl_4 \cdot (C_3H_6O)_2$	1630	1010	~3400	1700
$Cu_2Cl_2 \cdot (C_3H_6O)_2$	1550	1015	3340	——
C_3H_6O	1645	1030	3340	——
Assignment	ν(C=C)	ν(C–O)	ν(O–H)	$\delta(NH_4)$

with those for dimeric copper(I) chloride complex with allyl alcohol.[4] In the latter complex coordination of the double bond of allyl alcohol is evidenced by the large shift of C=C stretching frequency to the lower frequency side. The coordination of OH group was also concluded by a slight shift of C–O stretching frequency in comparison with the allyl alcohol complex of calcium chloride,[4] and the dimeric structure of I was assigned to this complex. On the other hand the infrared absorption data in Table 3 indicate that in the present complex containing ammonium chloride, allyl alcohol is linked to copper as a unidentate ligand solely *via* the oxygen atom as shown by II.

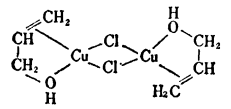

I

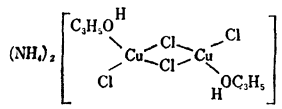

II

In the aqueous solution of copper(I) chloride together with ammonium chloride, the water molecule may take the position of allyl alcohol, and the reported complex[10] $KCuCl_2 \cdot H_2O$ may be considered to have a dimeric structure like II.

Etherification Reactions in the Mixture of Allyl and Ethyl Alcohols. The rates of formation of diallyl and ethyl allyl ethers were calculated assuming the pseudo first order kinetics, and data thus obtained were plotted against each alcohol concentration. Straight lines were obtained as shown in Fig. 6 indicating that these reactions obey the following rate equations:

$$\frac{d[al_2O]}{dt} = k_1[alOH] = (k_a'[Cu_2Cl_2]_0[NH_4Cl]_0)\,[alOH] \quad (4)$$

$$\frac{d[EtOal]}{dt} = k_2[EtOH] = (k_e'[Cu_2Cl_2]_0[NH_4Cl]_0)\,[EtOH] \quad (5)$$

Here alOH denotes allyl alcohol. Figure 6 also indicates that the rate of formation of ethyl allyl ether is somewhat larger than that of diallyl ether: $k'_a = 17.9$, $k'_e = 29.2$ (kg·solvent)^2/mol^2·hr.

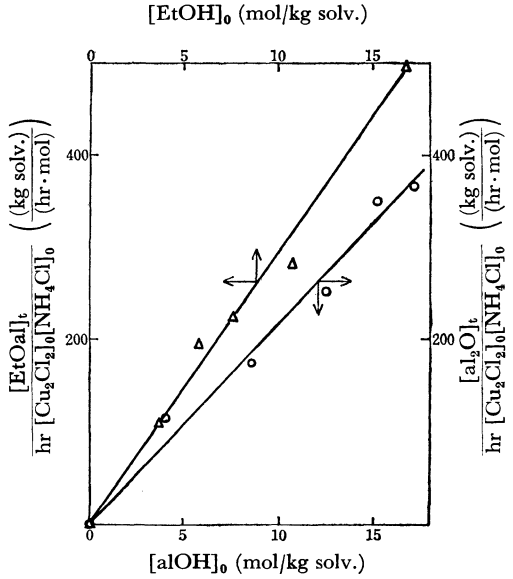

Fig. 6. Dependences of rates of diallyl and ethyl allyl ether formations upon the composition of mixtures of allyl and ethyl alcohols at 148.1°C.

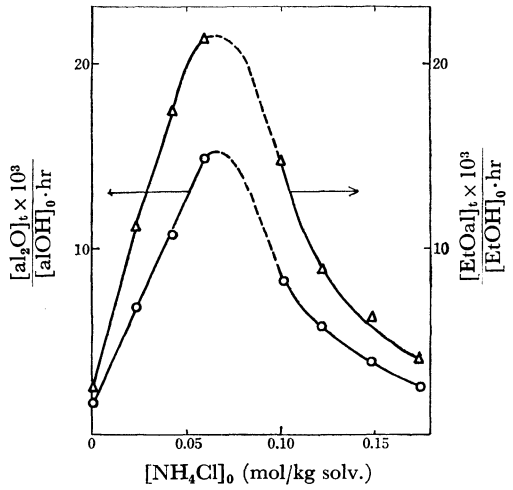

Fig. 7. Dependences of the pseudo first order rate constants of diallyl and ethyl allyl ether formations upon the concentration of ammonium chloride at 148.1°C.
$[Cu_2Cl_2]_0 = 0.0654$ mol/kg solvent

10) J. J. P. Valeton and W. Frömel, *Z. anorg. u. allg. Chem.*, **137**, 91 (1924).

Data plotted in Fig. 6 were obtained in the region of low concentrations of ammonium chloride, and Eqs. (4) and (5) hold only at these conditions. If the concentration of copper(I) chloride is kept constant and that of ammonium chloride is changed, the pseudo first order rate constants k_1 and k_2 change in the fashion shown in Fig. 7. Again, maximum rates are attained when the concentration of ammonium chloride is about half as large as that of copper(I) chloride in the monomer unit. These are the same features as that observed in the case of allyl alcohol alone (Fig. 5).

Tracer Experiments. In the etherification reaction between allyl and ethyl alcohols one molecule of water is eliminated. In order to elucidate the reaction mechanism, it is very important to find out from which alcohol the oxygen atom of water molecule originates. Allyl alcohol containing 1.83 atom % of ^{18}O was allowed to react with natural ethyl alcohol and ethyl allyl ether produced was submitted to the mass analysis. If the ether molecule has oxygen atom from allyl alcohol, the peak height ratio of mass 88 to mass 86 should be 18.8×10^{-3}. On the other hand if the oxygen atom in the ether molecule originated from ethyl alcohol, the ratio is expected to be 4.5×10^{-3}. Natural isotopic abundances of carbon, hydrogen and oxygen were taken into account in these calculations. Ethyl allyl ether produced in the reaction between natural allyl and ethyl alcohols showed the value of 4.4×10^{-3} as this ratio. The reaction product from the ^{18}O-enriched allyl alcohol and natural ethyl alcohol gave the ratio value of 4.6×10^{-3}, clearly indicating the following reaction.

$$C_3H_5{}^{18}OH + C_2H_5OH = C_3H_5OC_2H_5 + H_2{}^{18}O \quad (6)$$

Discussion

Effective Catalyst Species. It should be concluded that the complex I does not catalyze the reaction since highly pure copper(I) chloride alone was found to be ineffective. The points lying on the ordinates in Figs. 5 and 7 were brought about by copper(I) chloride which had been exposed to air for a while. Partial oxidation of copper(I) might have occurred resulting in a a mixture of copper(II) chloride and oxide playing a role of the chloride source. Figures 5 and 7 suggest that the most effective catalyst may have the composition of $Cu_2Cl_2\cdot NH_4Cl$. In Fig. 5 an appreciable activity is observed at the catalyst composition of $Cu_2Cl_2\cdot 2NH_4Cl$. This may be due either to the true activity of the complex II, or to a small amount of the above catalyst $Cu_2Cl_2\cdot NH_4Cl$ existing in equilibrium with the ineffective complex II. The rate profiles of diallyl ether formation in Figs. 5 and 7 were determined at different conditions, but calculations utilizing the dependences of rate upon temperature and the catalyst composition show that the maximum rates are nearly equal in both cases, indicating absence of the appreciable solvent effect upon the rate process. On the other hand, the rate of diallyl ether formation at the catalyst composition of $Cu_2Cl_2\cdot 2NH_4Cl$ in a mixture of allyl and ethyl alcohols (Fig. 7) is much lower than that at the corresponding conditions in allyl alcohol alone (Fig. 5). This fact might suggest that the complex II may not be appreciably effective, but the equilibrium forming the true catalyst $Cu_2Cl_2\cdot NH_4Cl$ may be unfavorable in the mixed solvent.

Now we assume that the following two equilibria are attained in allyl alcohol or in a mixture of allyl and ethyl alcohols.

$$Cu_2Cl_2 + 2NH_4Cl \overset{K_1}{\rightleftarrows} (NH_4)_2Cu_2Cl_4 \quad (7)$$

$$(NH_4)_2Cu_2Cl_4 + Cu_2Cl_2 \overset{K_2}{\rightleftarrows} (NH_4)_2Cu_4Cl_6 \quad (8)$$

Allyl alcohol molecules in the coordination sphere of copper(I) are omitted in these formulas. Equilibrium quotients are represented by

$$K_1 = \frac{y}{(a-2x-y)(b-2x-2y)^2} \quad (9)$$

$$K_2 = \frac{x}{y(a-2x-y)} \quad (10)$$

where $a=[Cu_2Cl_2]_0$, $b=[NH_4Cl]_0$, $x=[(NH_4)_2Cu_4Cl_6]$, and $y=[(NH_4)_2Cu_2Cl_4]$. If the active catalyst species is presumed to be $(NH_4)_2Cu_4Cl_6$, that is

$$k_1 = k_a x \quad (11)$$

the optimum activity should be shown when the maximum value of x is attained at appropriate b. Differentiating Eq. (10) with b,

$$\left(\frac{1}{K_2}+2y\right)\frac{dx}{db} = (a-2x-2y)\frac{dy}{db}$$

Here $dy/db\neq0$ and the maximum of x is realized when

$$a - 2x - 2y = 0 \quad (12)$$

From Eqs. (9) and (12)

$$|a-b| = \frac{1}{\sqrt{K_1}} \quad (13)$$

As is evidenced by the data in Table 2 and the fact that the complex $(NH_4)_2Cu_2Cl_4(C_3H_6O)_2$ was isolated as crystals, K_1 must be very large and hence Eq. (13) indicates that the maximum rate will be observed at $[NH_4Cl]_0$ near $[Cu_2Cl_2]_0$. This feature was in fact observed in Figs. 5 and 7.

From Eqs. (10) and (11)

$$k_1 = k_a K_2 y(a-2x-y)$$

If $K_1 \gg 1$, then $y \fallingdotseq b/2$ and if $K_2 \ll 1$, then $a-y \gg 2x$, and hence

$$k_1 \fallingdotseq k_a K_2 \frac{b}{2}\left(a-\frac{b}{2}\right)$$
$$= k_a K_2([NH_4Cl]_0/2)([Cu_2Cl_2]_0-[NH_4Cl]_0/2) \quad (14)$$

This relation is reconciled with the observed results in Fig. 4. The straight line really intersects the abscissa at $[Cu_2Cl_2]_0 \fallingdotseq [NH_4Cl]_0/2$. When $[Cu_2Cl_2]_0 \gg [NH_4Cl]_0/2$ Eq. (14) may be approximated by Eq. (4). The facts that the formation of ethyl allyl ether shows a similar rate profile with respect to the ammonium chloride concentration (Fig. 7) and obeys a similar rate law (Eq. (5)) suggest that this reaction also is promoted by the same catalyst species and goes through the same pathways as the diallyl ether formation.

The temperature dependence of k_aK_2 was measured and the apparent activation energy of 19.9 kcal/mol was obtained from the Arrhenius plot in Fig. 8. However the activation energy referring

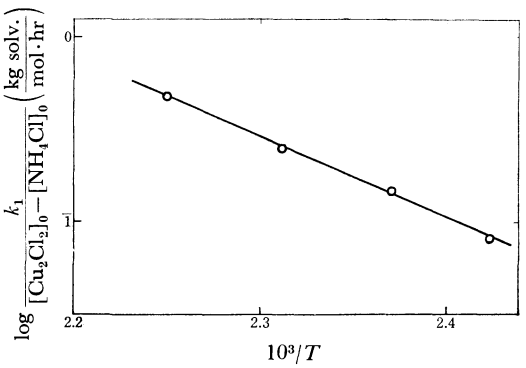

Fig. 8. The Arrhenius plot of the composite rate constant k_aK_2 (Eq. (14)) at a fixed concentration of ammonium chloride, 0.00916 mol/kg solvent.

to k_a can not be determined since the heat of formation of the catalyst-substrate complex is unknown.

The effective substrate-catalyst complex here assumed, $(NH_4)_2Cu_4Cl_6 \cdot x(C_3H_6O)$ looks like a tetrameric species. Unfortunately this complex has not been isolated due to its low stability, or may be due to far larger stability of $(NH_4)_2Cu_2Cl_4(C_3H_6O)_2$. However, several examples of tetrameric copper(I) chloride complexes have been reported so far. Wilkins and Burkin[11] synthesized copper(I) halide complexes with long-chain aliphatic amines such as n-$C_{18}H_{37}NH_2$, n-$C_{12}H_{25}NH_2$ and n-$C_8H_{17}NH_2$. Monoamine complexes $CuX(RNH_2)$, where X=Cl, Br, I, were all tetrameric and substituted by pyridine to form $[CuXpy]_4$. The molecular weight of copper(I) chloride in diethylamine was determined by Clifton and Yoke to be tetrameric.[12] Furthermore the molecular structure of tetrameric copper(I) chloride complex of norbornadiene was determined with X-ray by Baenziger, Haight and Doyle to contain an eight-membered ring composed of copper and chlorine atoms.[13]

The reason is not clear at present why copper(I) chloride alone is not effective, but a little excess amount of chloride (Cu : Cl=2 : 3) is needed to realize the highest activity, and more excess amount of chloride is retarding. Chloride ions coordinated to copper(I) atom might modify the electronic state of the metal very delicately. Further comparative studies using fluoride, bromide or other ligands are needed.

Reaction Pathways. The etherification of alcohols is usually catalyzed by protonic acids and is believed to proceed *via* carbonium ions.[14] This view is supported by the fact that other Lewis acids such as zinc chloride, boron trifluoride and aluminum chloride also convert alcohols to ethers. However it is quite certain that the present copper(I) chloride catalyst is not playing the same role as these simple Lewis acids, but is activating the double bond mainly since diethyl ether was not produced at all. Tracer experiments employing ^{18}O-enriched allyl alcohol clarified that the C–O bond in allyl alcohol was ruptured in the etherification with ethyl alcohol. Furthermore the observed kinetics was interpreted to be first order with respect to the copper(I) complex of allyl alcohol and also first order concerning allyl or ethyl alcohol.

There still remain two possibilities whether the alkoxy group adds to the α-carbon III, or attacks the γ-carbon from the back side IV. In order to obtain a clue to this question allyl alcohol derivatives containing a methyl substituent at each carbon atom were used as substrates.

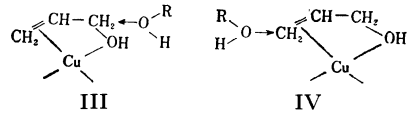

In the etherification of γ-methylallyl alcohol, α-methylallyl γ-methylallyl ether was produced exclusively, bis(γ-methylallyl) ether being a very minor product (Table 1). This result strongly supports the supposition that the nucleophilic attack of the alcohol molecule occurred on the γ-carbon accompanying migration of the double bond (S_N2') and cleavage of the C–O bond. On the contrary α-methylallyl alcohol produced both bis(α-allylmethyl) ether and α-methylallyl γ-methylallyl ether in nearly equal amounts.

The solvolysis reactions of allylic chlorides have

11) R. G. Wilkins and A. R. Burkin, *J. Chem. Soc.*, **1950**, 127, 132.

12) J. R. Clifton and J. T. Yoke III, *Inorg. Chem.*, **5**, 1630 (1966).

13) N. C. Baenziger, H. L. Haight and J. R. Doyle, *ibid.*, **3**, 1535 (1964).

14) E. R. Alexander, "Principles of Ionic Organic Reactions," Wiley, New York, N. Y. (1950), p. 214.

15) R. H. DeWolfe and W. G. Young, "The Chemistry of Alkenes," ed. by S. Patai, Interscience Publishers, New York, N. Y. (1964), p. 681.

been studied very extensively.[15] The data on solvent effects indicate that the solvolysis of allyl chloride is closest to the bimolecular end of the mechanistic range, and that the mechanism shifts toward limiting S_N1 in the sequence $CH_2=CHCH_2Cl$, $CH_2=C(CH_3)CH_2Cl$, $CH_3CH=CHCH_2Cl$, $CH_3CHClCH=CH_2$, ------$(CH_3)_2CClCH=CH_2$. Thus, γ-methylallyl chloride is solvolyzed mainly *via* S_N2 path in ethanol resulting in γ-methylallyl alcohol in 91% yield. The electronic effect of γ-substituent is interpreted to greatly favor the normal S_N2 pathway. It is very interesting that quite the opposite result was obtained in the present etherification reaction. The ligation of the double bond to copper atom might decrease the electron density around γ-carbon so much as to favor the S_N2' pathway. The fact that the etherification of either methylallyl alcohol is about a hundred times faster than that of allyl alcohol suggests the specific character of the copper(I) catalysis.

In the case of allyl alcohol itself almost extreme S_N2' mechanism might be realized. The partial labeling of hydrogen atoms in allyl alcohol and NMR assays of the product ether will answer this question. On the other hand α-methylallyl chloride lies at the righthand side than γ-methylallyl chloride in the above mechanistic sequence from S_N2 to S_N1, and the products composition in Table 1 suggests that α-methylallyl alcohol may follow an intermediate mechanism between S_N2' and S_N1 and the polarized structure V of the copper complex may accept the nucleophilic atttack of the alcohol molecule on both α-and γ-carbon atoms.

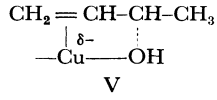

V

The isomerization of methylallyl alcohol proceeds remarkably in the case of γ-methylallyl alcohol. The mechanism is not yet certain at all, but the trend agrees with the previous finding[15] that α-, β- and γ-methyl substituents on the allylic system increase the rate of isomerization of allylic alcohols by factors of 10^2, 10^1 and 10^3, respectively.

The authors are grateful to Professor Nobukazu Okazaki of the Nara Women's University for his kind gift of ^{18}O-enriched water. They also wish to thank Dr. Yoshio Hirose, Director of the Institute of Food Chemistry, for the mass spectrometric measurements.

BULLETIN OF THE CHEMICAL SOCIETY OF JAPAN VOL. 42 650—657 (1969)

Electron Spin Resonance Study of Radicals Formed by Abstracting Hydrogen from Amides*1

Teijiro YONEZAWA, Isao NODA and Takashi KAWAMURA

Department of Hydrocarbon Chemistry, Faculty of Engineering, Kyoto University, Sakyo-ku, Kyoto

(Received July 25, 1968)

Electron spin resonance (ESR) studies were made on various radicals formed from formamide, acetamide, *N*-methylformamide, *N*-methylacetamide, *N*,*N*-dimethylformamide and propionamide by hydrogen abstraction with hydroxyl radicals produced by the reaction of hydrogen peroxide and titanium trichloride in aqueous solution, using a rapid flow technique. In each case, except for formamide, various π-electron radicals were found. For formamide, *N*-methylformamide, and *N*,*N*-dimethylformamide, carbamoyl and its methyl substituted σ electron radicals were detected. The g factor of the σ electron radical is qualitatively discussed.

It is well known that acyl type radicals, thought to be σ electron radicals, are formed as intermediate species in radical reactions of aldehydes or formamides.[1] In the reaction of aldehydes with a hydroxyl radical in aqueous solution, the expected acyl type radicals were not detected with electron

*1 This work was presented at the Sixth Symposium on ESR Spectroscopy, Kyoto, Oct., 1967.

1) C. Walling, "Free Radicals in Solutions," John Wiley & Sons, Inc., N. Y. (1957).

spin resonance (ESR) spectroscopy. Buley and Norman[2] have proposed a reaction mechanism, in which the hydrated aldehyde R–CH$(OH)_2$ behaves as a reactant.[3] It is expected that acyl radicals will be observed when formamides, which barely exist in the form of hydrates NRR′–CH$(OH)_2$ in aqueous solution, react with a hydroxyl radical. An ESR study on intermediate radicals in the oxidation of simple amides with hydroxyl radical at room temperature was carried out using a rapid flow technique with a hydrogen peroxide and titanium trichloride redox system in aqueous solution. In each case, except for formamide, various π electron radicals formed by hydrogen abstraction were found, and for formamide and its *N*-methyl derivatives, ESR spectra attributed to acyl type σ electron radicals (carbamoyl radicals, CONRR′) were observed. It is our purpose here to investigate the properties of intermediate radicals, especially carbamoyl radicals. Recently, Livingston and Zeldes[4] reported an ESR study of free radicals formed from ultraviolet irradiation of a solution of an amide containing either hydrogen peroxide or acetone. A comparative discussion with their results is made in the present paper.

Experimental

The ESR spectrometer employed was a JEOL JES-3BSX instrument operating at a nominal frequency of 9.4 GHz with a 100 kHz field modulation with a TE_{011} cylindrical mode cavity. The static magnetic field was generated by a JES electromagnet with a nominal homogeneity of 1×10^{-6}/sample volume. For measurement of the *g* factor and hyperfine couplings, a glass capillary was attached to the sample tube. The capillary was filled with a reference compound, an aqueous solution of potassium peroxylamine disulfonate. The *g* factor and the hyperfine coupling constant of ^{14}N of the reference compound is 2.00559 ± 0.00001 and 13.07 ± 0.05 gauss, respectively. Estimated error limits are ±0.00002 and ±0.1 gauss for measured *g* factors and hyperfine coupling constants, respectively; otherwise probable errors are cited.

The rapid flow system consists of a JES-SM-1 mixing chamber and a JES-LC-0l capillary sample tube for aqueous solutions. The reagent solutions used were: (A) Acidified (0.1 M H_2SO_4) aqueous titanous chloride solution (0.02M); (B) aqueous hydrogen peroxide (0.2M). The substrate was added to solution (A) and its concentration varied within the range 0.3—3M, so as to obtain a sufficiently intense absorption.

Results and Discussion

The results obtained for each amide are presented separately and discussed. Hyperfine couplings are designated by the letter *a* with a superscript to indicate the magnetic nucleus and a subscript only where ambiguity would otherwise result. In the case of σ electron radicals, *g* factors are useful for the identification of radical structures, and are discussed later.

1. Formamide. The ESR spectrum of the radical formed by the reaction of formamide with hydroxyl radical is shown in Fig. 1. Parameters of this radical are summarized in Table 1. It has

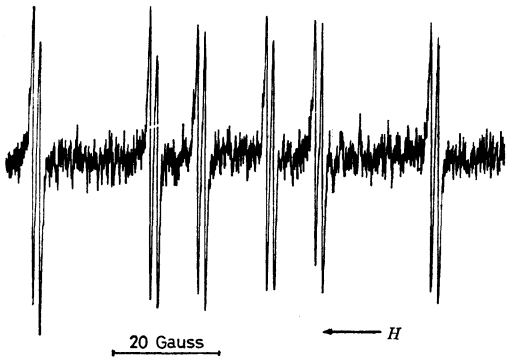

Fig. 1. The ESR spectrum of the radical obtained from formamide.

Table 1. ESR parameters of the radical[a] resulting from hydrogen abstraction from formamide

	This work	Livingston and Zeldes[b]	Smith and Wood[c]
g	2.00167	2.00155	2.0016
a^{N}[d]	21.8	21.69	21.65
$a^{H}_{NH,t}$[d]	30.8	30.41	30.55
$a^{H}_{NH,c}$[d]	1.3	1.27	1.22

a) This radical is assigned to carbamoyl radical (See text). b) Ref. 4. c) Ref. 9. d) In unit of gauss.

a characteristic *g* factor smaller than that of the free spin (2.00232), like vinyl ($g=2.00220$)[5] and formyl ($g=2.0009$)[6] σ electron radicals. In general, *g* factors of π electron radicals are greater than 2.00232.[7]

Therfore the radical obtained from formamide is

2) A. L. Buley and R. O. C. Norman, *Proc. Chem. Soc.*, **1964**, 225.

3) Aldehydes have been found not to give ESR signals due to acyl radicals even in non-aqueous systems (probably because of their high reactivities). H. Zeldes and R. Livingston, *J. Chem. Phys.*, **47**, 1465 (1967).

4) R. Livingston and H. Zeldes, *ibid.*, **47**, 4173 (1967).

5) R. W. Fessenden and R. H. Schuler, *ibid.*, **39**, 2147 (1963).

6) F. J. Adrian, E. L. Cochran and V. A. Bowers, *ibid.*, **36**, 1661 (1962).

7) a) H. M. McConnell and R. E. Robertson, *J. Phys. Chem.*, **61**, 1018 (1957); b) A. J. Stone, *Mol. Phys.*, **7**, 311 (1963).

expected to be a σ electron radical. Possible structures for the σ electron radical with two nonequivalent protons and one nitrogen nucleus formed from formamide is I, II or III.

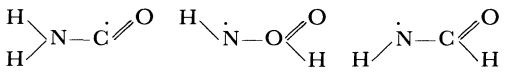

I II III

As shown later, σ electron radicals which have g factors and ^{14}N couplings with values approximately the same as those in Table 1 are formed from *N*-methylformamide and *N,N*-dimethylformamide. From the former, methylcarbamoyl radical (derivative of I) and the radical formed by N–H hydrogen abstraction (derivative of II or III) are possible. The only σ electron radical possible by abstracting hydrogen from *N,N*-dimethylformamide is dimethylcarbamoyl radical (dimethyl derivative of I), which shows that the σ electron radical formed from formamide should be the carbamoyl radical (I). This assignment of the radical formed from formamide is consistent with that of Livingston and Zeldes,[4] who have concluded that a hydroxyl radical formed through UV irradiation abstracts hydrogen bonded to the carbon atom of formamide resulting in a "non $-\pi$" radical. This identification also coincides with the theoretical conclusion of the present authors.[8]

On the other hand, Smith and Wood[9] perfomed an experiment similar to the present one and remarked that the radical of Table 1 is HCONH, formed by abstraction of hydrogen bonded to nitrogen. However, both experimental[4] and theoretical[8] evidence, together with the discussion given above, show that the radical of Table 1 is a carbamoyl σ electron radical. Referring to the calculated results,[8] the proton splitting constants are assigned as

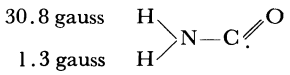

This assignment is reasonable in comparison with those of vinyl[10] and iminoxy[11] radicals.

Fessenden[12] has reported the ^{13}C coupling constant of the β-carbon in a vinyl radical to be ± 8.55 gauss. When the spin density on the 2s atomic orbital is unity, ^{13}C and ^{14}N isotropic splitting constants are calculated to be 1110 gauss and 549 gauss, respectively.[13] The observed ^{14}N isotropic coupling constant of 21.8 gauss in the carbamoyl radical seems somewhat large when compared with the ^{13}C splitting constant of the vinyl radical if both radicals are considered to be planar.[14] The large ^{14}N coupling constant of the carbamoyl may be explained in the following way. When the CNH_2 group in the carbamoyl radical is a shallow pyramid[15] or the amino group is somewhat twisted around the N–C bond from the CNO plane, thus forming a non-planar structure of carbamoyl radical, the odd electron may delocalize into a lone pair orbital on the nitrogen. The odd electron density of the lone pair orbital of the nitrogen will induce a positive spin density at the nitrogen nucleus through spin polarization as well as through the s-nature of the lone pair orbital, resulting in a large isotropic ^{14}N hyperfine coupling constant. From the above, it is thought that the carbamoyl radical does not have a planar structure.

2. *N*-Methylformamide. Radicals formed by the reaction of *N*-methylformamide, $TiCl_3$ and H_2O_2 gave an asymmetric spectrum as shown in Fig. 2a. It is clear that more than one radical

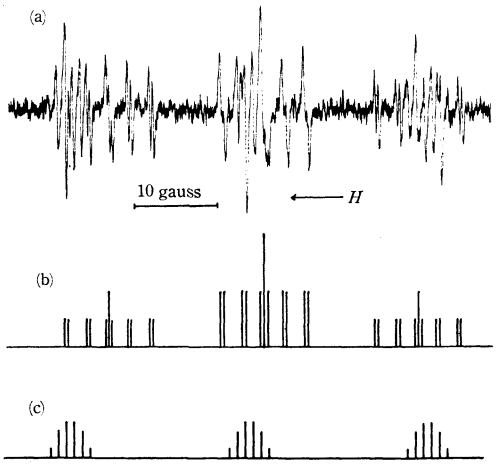

Fig. 2. (a) The ESR spectrum of radicals formed by abstraction of a hydrogen from *N*-methylformamide.
(b) The stick spectrum constructed with parameters of Table 2 for HCONH-($\dot{C}H_2$).
(c) The stick spectrum for the methylcarbamoyl radical constructed with parameters listed in Table 3.

8) T. Yonezawa, I. Noda and T. Kawamura, This Bulletin, **41**, 766 (1968).
9) P. Smith and P. B. Wood, *Can. J. Chem.*, **44**, 3085 (1966).
10) a) E. L. Cochran, F. J. Adrian and V. A. Bowers, *J. Chem. Phys.*, **40**, 213 (1964); b) F. J. Adrian and M. Karplus, *ibid.*, **41**, 56 (1964).
11) M. Kashiwagi and Y. Kurita, *J. Phys., Soc. Japan*, **21**, 558 (1966).
12) R. W. Fessenden, *J. Phys., Chem.*, **71**, 74 (1967).
13) J. R. Morton, *Chem. Revs.*, **64**, 453 (1964).
14) The calculated isotropic hyperfine coupling constant of ^{14}N in carbamoyl radical with an assumed planar structure is 8.0 gauss, which is small when compared with the observed value. See Ref. 8.
15) Costain and Dowling concluded from their microwave spectrum study that the CNH_2 group in formamide has a shallow pyramid structure. C. C. Costain and J. M. Dowling, *J. Chem. Phys.*, **32**, 158 (1960).

Table 2. Measured parameters for $HCONH(\dot{C}H_2)$

	This work	Livingston and Zeldes[a]
g	2.00288	2.00283
$a^{H}_{CH_2}$[b]	19.2[c]	$a^{H}_{CH_{2,1}} = 19.05$, $a^{H}_{CH_{2,2}} = 18.92$
a^{H}_{CH}[b]	5.1	4.83
a^{H}_{NH}[b]	0.4	0.32
a^{N}[b]	2.6	2.50

a) Ref. 4. b) In unit of gauss. c) Coupling constants of two protons in the $-\dot{C}H_2$ group are not strictly the same as is seen from the comparison between line shaps of the low-field side doublet in the high-field cluster and the low-field side doublet in the central cluster of Fig. 2a.

Table 3. Parameters of methylcarbamoyl radical (V)

g	2.00182
a^{H}_{NH}[a]	2.0
$a^{H}_{CH_3}$[a]	1.0
a^{N}[a]	22.2

a) In unit of gauss.

is present. This spectrum can be analyzed as two superimposed spectra shown in Figs. 2b and 2c, constructed with the parameters given in Tables 2 and 3. The radical of Table 2 (*i. e.* Fig. 2b) can be assigned to a π electron radical $HCONH(\dot{C}H_2)$. Livingston and Zeldes[4] have observed essentially the same spectrum as in Fig. 2b during photolysis of a 30% aqueous solution of *N*-methylformamide containing 1% H_2O_2, and identified the radical as $HCONH(\dot{C}H_2)$, with the possible structure

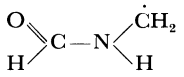

IV

The radical of Table 3 (*i. e.* Fig. 2c), which was not observed in the ESR-photolysis-study of Livingston and Zeldes,[4] is identified as a methyl carbamoyl σ electron radical with the configuration

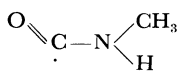

V

This assignment is based on following results: (1) the g factor of this radical (2.00182) is smaller than the spin-only value (2.00232) and resembles that of the carbamoyl radical formed from formamide (Table 1); (2) the ^{14}N coupling constant is nearly equal to that of the carbamoyl radical: (3) this radical should have a configuration with the NH bond *cis* to the odd electron σ orbital, otherwise the value of a^{H}_{NH} should be of the same order as $a^{H}_{NH,t}$= 30.8 gauss of the carbomoyl radical; (4) in the case of σ electron radicals, it is reasonable that the coupling constant of the methyl proton decreases from 30.8 gauss ($a^{H}_{NH,t}$ of the carbamoyl radical, Table 1) to 1.0 gauss ($a^{H}_{CH_3}$ of the methylcarbamoyl radical, Table 3) when the hydrogen in the amino group is substituted by a methyl group.

The NMR and IR studies[16] showed that *N*-methylformamide has its formyl hydrogen *trans* to the NCH_3. It is interesting that the abstraction of formyl hydrogen from *N*-methylformamide by a hydroxyl radical does not change the conformation of the skelton of O=C–N–C.

3. *N,N*-Dimethylformamide. Radicals formed from the reaction between *N,N*-dimethylformamide and hydroxyl radicals prepared by the redox reaction of $TiCl_3$ and H_2O_2 give a very complex ESR spectrum, as shown in Fig. 3a. The spectrum consists of three clusters of lines. All three clusters of lines were measured in considerable detail, and it was clear that three radical species resulting from abstraction of a hydrogen atom from a methyl or formyl groups were present. The spectrum of Fig. 3a consists of three spectra, Figs. 3b, 3c and 3d, constructed with the parameters listed in Tables 4, 5 and 6, respectively. The radicals in Table 4 and 5 (*i. e.* Figs. 3b and 3c) are easily identified as geometrically isomeric π radicals, $HCON(\dot{C}H_3)(\dot{C}H_2)$, formed by the abstraction of methyl hydrogen. A comparison of the parameters of Tables 2, 4 and 5 suggests that the radical of Table 5 has the same coformation as the radical from *N*-methylformamide. Assuming that $HCONH(\dot{C}H_2)$ has the conformation of IV in the preceding section, the radicals of Tables 4 and 5 may have the conformations VI and VII shown below, respectively.

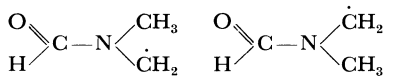

VI VII

The radical of Table 6 with a small g factor is identified as dimethylcarbamoyl σ electron radical VIII.

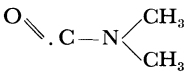

VIII

The proton coupling constant of 0.7 gauss is assigned to the protons of the methyl group *trans* to the odd electron orbital in comparison with *N*-methylcarbamoyl radical formed from *N*-methylformamide. The proton coupling of the methyl group *cis* to the odd electron orbital is small and not resolved.

16) a) V. J. Kowalewski and D. G. de Kowalewski, *J. Chem. Phys.*, **32**, 1272 (1960); b) R. L. Jones, *J. Mol. Spectry.*, **2**, 581 (1958) and references cited therein.

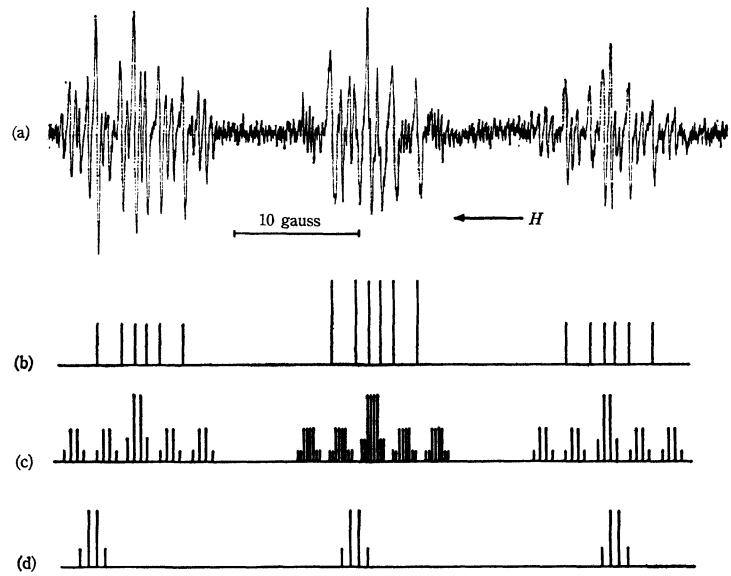

Fig. 3. (a) The ESR spectrum observed during the reaction of *N,N*-dimethylformamide and hydroxyl radical.
(b) The reconstructed spectrum with parameters of Table 4.
(c) The reconstructed spectrum with parameters listed in Table 5.
(d) The stick spectrum constructed with parameters given in Table 6 for dimethylcarbamoyl.

TABLE 4. PARAMETERS FOR THE RADICAL (VI) FORMED BY ABSTRACTING A HYDROGEN FROM METHYL GROUP *cis* TO THE FORMYL HYDROGEN OF *N,N*-DIMETHYLFORMAMIDE

	This work	Livingston and Zeldes[a]
g	2.0030[b]	2.00296
$a^{H}_{CH_3}$[c]	18.7[d]	$a^{H}_{CH_2\cdot 1} = 18.46$, $a^{H}_{CH_2\cdot 2} = 18.33$
a^{H}_{HC}[c]	3.0[d]	2.72
$a^{H}_{CH_3}$[c]	~ 0[d]	0.32
a^{N}[c]	1.9[d]	1.58

a) Parameters for Isomer II of $HCON(CH_3)(\dot{C}H_2)$ of Livingoston and Zeldes. Ref. 4.
b) Probable erorr: ±0.0001. c) In unit of gauss.
d) Probable error: ±0.3 gauss.

TABLE 5. PARAMETERS FOR THE RADICAL (VII) FORMED BY ABSTRACTING A HYDROGEN FROM CH_3 *TRANS* TO THE FORMYL HYDROGEN OF *N,N*-DIMETHYLFORMAMIDE

	This work	Livingston and Zeldes[a]
g	2.0029[b]	2.00284
$a^{H}_{CH_2\cdot 1}$[c]	19.0[d]	18.54
$a^{H}_{CH_2\cdot 2}$[c]	18.5[d]	18.37
a^{H}_{CH}[c]	5.2[d]	4.72
$a^{H}_{CH_3}$[c]	0.5[d]	0.76
a^{N}[c]	2.6[d]	2.25

a) Parameters for isomer I of $HCON(CH_3)(\dot{C}H_2)$ of Livingston and Zeldes. Ref. 4.
b) Probable error: ±0.0001. c) In unit of gauss.
d) Probable error: ±0.3 gauss.

TABLE 6. PARAMETERS MEASURED FOR *N,N*-DIMETHYLCARBAMOYL RADICAL (VIII)

g	2.0020[a]
$a^{H}_{CH_3,t}$[b]	0.7[c]
$a^{H}_{CH_3,c}$[b]	~ 0[c]
a^{N}[b]	20.8[c]

a) Probable error: ±0.0001. b) In unit of gauss.
c) Probable error: ±0.3 gauss.

4. Acetamide. The radical obtained from acetamide gave a well-resolved spectrum, as Fig. 4. The ESR spectrum of this radical formed by abstraction of a hydrogen atom by OH radical has been reported by Livingston and Zeldes (OH radical prepared by photolysis of H_2O_2)[4] and by Smith and Wood (OH radical prepared from the redox reaction between $TiCl_3$ and H_2O_2).[9] This radical is $\dot{C}H_2CONH_2$ π electron radical and its parameters are summarised in Table 7.

Two amino-group protons of this radical are not equivalent, as seen in Table 7. It is interesting that the difference between the coupling constants of these two protons are very large relative to their magnitude (about 16% of their mean value). This difference may be interpreted as follows; (1) polarizabilities of two NH σ bonds are not equal mainly because of the difference in NH bond lengths;[17] thus, the σ-π exchange interaction

17) Two NH bond lengths of formamide are 1.002 Å and 1.014 Å, respectively (Ref. 15).

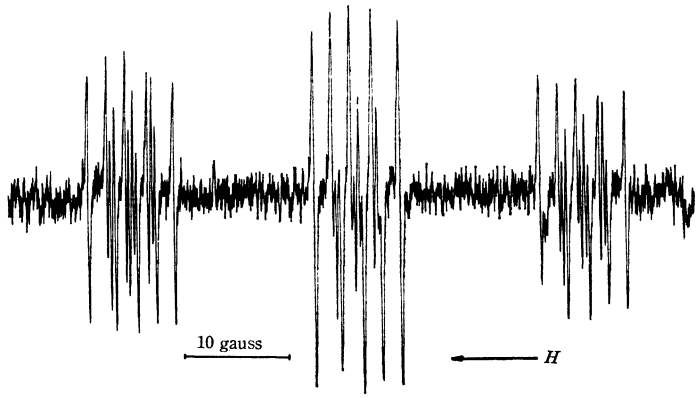

Fig. 4. The ESR spectrum of $\dot{C}H_2CONH_2$ formed by a hydrogen abstruction from acetamide.

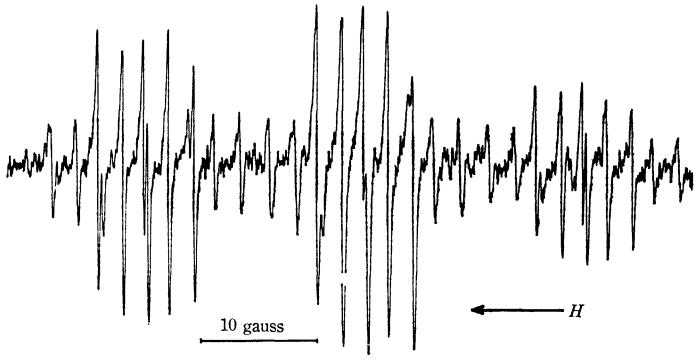

Fig. 5. The ESR spectrum of the radical formed by abstracting hydrogen from *N*-methylacetamide.

induces, at positions of amino-protons, different spin densities and/or (2) amino protons are out of the molecular plane with different angles,[18] then, the odd electron which delocalizes into the two NH σ bonds causes unequal spin densities at the amino-proton positions.

5. *N*-Methylacetamide. Figure 5 shows the spectrum of the radical obtained from *N*-methylacetamide. The ESR parameters are listed in Table 8 along with the parameters reported by Livingston and Zeldes.[4]

The radical was formed by abstraction of a hydrogen atom from a methyl group; there is ambiguity as to which methyl group lost the hydrogen, the choices are $OC(CH_3)NH(\dot{C}H_2)$ and $OC(\dot{C}H_2)NH(CH_3)$. A comparison of parameters of Table 8 with those for π electron radicals from methyl substituted formamides (Tables 2, 4 and 5) and acetamide (Table 7) gives some preference for $OC(CH_3)NH(\dot{C}H_2)$. Friedman and Shechter[19]

18) In the case of formamide, $\angle$(H'NC plane)(NCO plane)$=7\pm5°$ and $\angle$(H''NC plane)(NCO plane)$=12\pm5°$, where H' and H'' designate proton in the NH_2 group. Ref. 15.

19) L. Friedman and H. Shechter, *Tetrahedron Letters*, **1961**, 238.

Table 7. Measured parameters for $\dot{C}H_2CONH_2$

	This work	Livingston and Zeldes[a]	Smith and Wood[b]
g	2.00304	2.00298	2.0034
$a^{H}_{CH_2}$ [c]	21.5	21.34	21.28
$a^{H}_{NH_{s.t}}$ [c]	2.6	2.43	2.53
$a^{H}_{NH_{s.s}}$ [c]	2.2	2.04	1.96
a^{N} [c]	1.8	1.72	1.96

a) Ref. 4. b) Ref. 9. c) In unit of gauss.

Table 8. Parameters measured for the radical formed by abstructing a hydrogen from *N*-methyl group of *N*-methylacetamide

	This work	Livingston and Zeldes[a]
g	2.00282	2.00277
$a^{H}_{CH_2}$ [b]	19.1	18.89 and 18.95
$a^{H}_{CH_3}$ [b]	4.0	3.85
a^{N} [b]	2.2	2.07
a^{H}_{NH} [b]	~ 0	~ 0

a) Ref. 4. b) In unit of gauss.

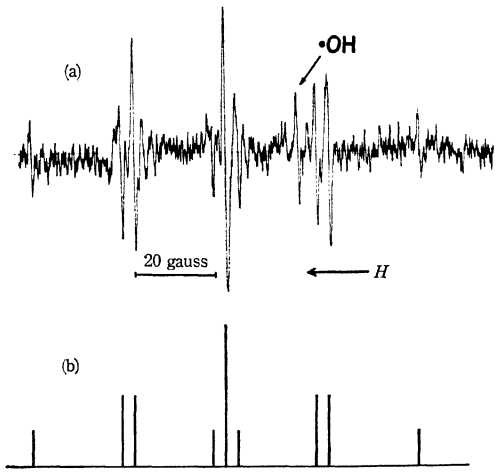

Fig. 6. (a) The ESR spectrum of radicals formed by the reaction of propionamide and hydroxyl radical. The line with an arrow is the signal of remaining hydroxyl radical.
(b) The stick spectrum constructed with parameters of Table 9 for $\dot{C}H_2CH_2$-$CONH_2$.

reported that radical-dimerization of *N*-methylacetamide by *t*-butyl peroxide yields *N*,*N*′-diacetylethylenediamine (71% yield). This implies that the hydrogen atom in the *N*-methyl group is more easily abstracted than the hydrogen in the acetyl group by radical reactions. Therefore, the radical from *N*-methylacetamide is identified as $OC(CH_3)$-$NH(\dot{C}H_2)$, which agrees with the identification proposed by Livingston and Zeldes.[4]

6. Propionamide. Radicals formed by the reaction of propionamide with hydroxyl radicals gave the spectrum in Fig. 6a. The spectrum contains three triplets as in Fig. 6b, constructed from the parameters given in Table 9. The radical of Table 9 can be assigned to the radical $\dot{C}H_2CH_2$-$CONH_2$. The remaining lines can not be analyzed because of their low intensity.

TABLE 9. PARAMETERS MEASURED FOR $\dot{C}H_2CH_2CONH_2$

g	2.00275
$a^{H}_{CH_2\text{-}}$ a)	22.4
$a^{H}_{\text{-}CH_2\text{-}}$ a)	25.6

a) In unit of gauss.

7. *g* Factor of σ Electron Radical. Stone[20] has derived the following expression for one of the diagonal components of the *g* tensor;

$$g^{zz} = g_e + \Delta g^{zz}, \tag{1}$$

where g_e is the free electron *g* factor, 2.00232, and Δg^{zz} is given by

$$\Delta g^{zz} = 2\sum_{n\neq p} \frac{\sum_k \sum_{\mu,\nu} C^{(p)}_{k\mu} C^{(n)}_{k\nu} < \chi_{k\mu}|l^z_k|\chi_{k\nu} > \sum_{k'} \sum_{\mu'\nu'} C^{(n)}_{k'\mu'} C^{(p)}_{k'\nu'} < \chi_{k'\mu'}|l^z_{k'}|\chi_{k'\nu'} > \zeta_{k'}}{\varepsilon_p - \varepsilon_n} \tag{2}$$

Here, l_k is the angular momentum about the *k*-th nucleus, ε_p and ε_n are the energies of molecular orbitals $\varphi^{(p)}$ and $\varphi^{(n)}$ and ζ_k is the spin-orbit coupling constant for the *k*th atom. Molecular orbitals $\varphi^{(p)}$ (half-occupied MO) and $\varphi^{(n)}$ (vacant or doubly occupied MOs) are expessed as linear combinations of the μth atomic orbital of the *k*th atom, $\chi_{k\mu}$, as

$$\varphi^{(p)} = \sum_k \sum_\mu C^{(p)}_{k\mu} \chi_{k\mu} \quad \text{and} \quad \varphi^{(n)} = \sum_k \sum_\mu C^{(n)}_{k\mu} \chi_{k\mu}. \tag{3}$$

Similar expressions give the other diagonal components. The *g* factor of a radical in solution is given as the arithmetic mean of the three diagonal elements of the *g* tensor,

$$g = g_e + \Delta g \tag{4}$$

$$\Delta g = \frac{1}{3}(\Delta g^{xx} + \Delta g^{yy} + \Delta g^{zz}). \tag{5}$$

In the case of σ electron radicals, MO's with π symmetry give large contributions to Δg, since the value of $\varepsilon_p - \varepsilon_n$, which appears in Eq. (2), is small. The odd electron orbital of σ radicals are generally localized on one atom. Therefore, the numerator of Eq. (2) often has a positive value, and the sign of Δg of Eq. (5) is, with some exceptions, determined by the energy differences between the half-occupied and lower vacant orbitals, and between the half-occupied and higher doubly occupied orbitals. When the former is smaller than the latter, Δg becomes negative and *vice versa*. Therefore it is expected that for the σ electron radical, which has an odd electron localized mainly on the less electronegative atom in that radical and has a higher half-occupied orbital energy, the *g* factor is expected to be smaller than the spin-only value (2.00232). Experimental *g* factors of such σ electron radicals as discussed above are summarized in Table 10. On the other hand, iminoxy radicals have been reported[11,21] to have *g* factors ranging from 2.005 to 2.008, which are much larger than the free-spin *g* factor. The odd electron of the iminoxy radical is mainly localized on the electronegative atoms (oxygen and nitrogen)

20) A. J. Stone, *Proc. Roy. Soc.*, **A271**, 424 (1963); *Mol. Phys.*, **7**, 311 (1963).
21) M. C. R. Symons, *J. Chem. Soc.*, **1963**, 1189.

TABLE 10. REPORTED g FACTORS OF σ ELECTRON RADICALS WHICH ARE SMALLER THAN OR NEARLY EQUAL TO 2.00232

Radical	g Value	Reference
Vinyl radical	2.00220	Fessenden and Schuler[a)]
1-Methyl-1-vinyl radical	2.00222	Fessenden and Schuler[a)]
HCN anion radical	2.0022	Root *et al.*[b)]
Formyl radical	2.0009	Adrian *et al.*[c)]
2-Pyridyl radical	2.001	Bower *et al.*[d)]
Carbamoyl radical	2.00167	This work
Methylcarbamoyl radical	2.00182	This work
Dimethylcarbamoyl radical	2.0020	This work

a) R. W. Fessenden and R. H. Schuler, *J. Chem. Phys.*, **39**, 2147 (1963).
b) K. D. J. Root, M. C. R. Symons and B. C. Weatherley, *Mol. Phys.*, **11**, 161 (1966).
c) F. J. Adrian, E. L. Cochran and V. A. Bowers, *J. Chem. Phys.*, **36**, 1661 (1962).
d) H. J. Bower, J. A. McRae and M. C. R. Symons, *Chem. Commun.*, **1967**, 542.

of the radical, and the energy level of the odd electron orbital is expected to be low.

Although the above discussions are highly qualitative, they are sometimes useful for the identification of σ electron radicals. It is noteworthy that the substitution of a methyl group into vinyl and carbamoyl radicals enlarges their g factors, as seen in Table 10. Substitution of a methyl group into these radicals elevates energy levels of π orbitals. On the other hand, the energy level of the odd electron σ orbital might be scarcely affected by a methyl substitution. The energy difference between the vacant π and the half-occupied σ orbitals of methyl substituted carbamoyl (or vinyl) radical is larger than that of the carbamoyl (or vinyl) radical. Differences between orbital energies of the half-occupied σ and doubly occupied π orbitals of methyl substituted carbamoyl (or vinyl) radicals are smaller than those of carbamoyl (or vinyl) radical. Both effects enlarge g factors of methyl substituted carbamoyl and vinyl radicals. These explanations for the g factors of carbamoyl, methylcarbamoyl and dimethlcarbamoyl radicals also confirm the present identification of σ electron radicals formed from formamide and its *N*-methyl and *N*,*N*-dimethyl derivatives.

BULLETIN OF THE CHEMICAL SOCIETY OF JAPAN VOL. 42 658—663 (1969)

Solvated Electron Formed in Water by the Silent Electric Discharge in Argon Atmosphere

Akira YOKOHATA

Department of Chemistry, Faculty of Engineering, Hiroshima University, Senda-machi, Hiroshima

(Received July 25, 1968)

Based on radiation chemistry of water a study on the chemical changes resulting from the silent electric discharge of aqueous solution under argon atmosphere was made for the purpose of elucidating the nature of the reducing species formed. In the neutral aqueous $ClCH_2COOH$ system the effects of such additives as CH_3OH and NO_3^- on the yield of Cl^- and in the system containing NO_3^- the yield of NO_2^- were investigated. Moreover, in the alkaline aqueous $K_3Fe(CN)_6$ system emphasis was placed on the yield of aquocomplex. In view of the non-dependence of the yield of Cl^- on the concentration of additive NO_3^- and of the low yields of NO_2^- and $Fe(CN)_5OH_2^{3-}$ produced, it was concluded that in the silent electric discharge the yield of solvated electrons which react with solutes in the bulk of water is very small ($G \lesssim 0.06$). Reasons for the low yield of solvated electrons are briefly described.

The chemical effects of silent electric discharge and those of high energy radiations have been demonstrated to be identical in many respects.[1-4] Silent electric discharge may be considered to be a peculiar particle-accelerator of low energy having the following characteristics.

(1) The electrons at one atmospheric pressure have an energy distribution from just above zero to a value slightly higher than the ionization potential of the gas in which the discharge occurs.[5,6]

(2) Relatively low voltages (10—15 kV) result in the high currents (~1 mA). From the point of view of total power, the dose rate can be expected to be considerably high.

Consistent with theoretical considerations, our recent studies[4] have proved that most of the reactions of aqueous solutions induced by the silent electric discharge in the inert gas atmospheres can be well interpreted with an indirect effect of the slow electrons to water molecules, the primary one being the radiolysis of water to give the intermediates, reducing radical or hydroxyl radical.

The apparent dose rate under our experimental conditions was 7.2×10^6 R/hr as reported previously[4] and each primary G value of radicals was estimated as follows:

$$^sG(\mathrm{Red}) = 0.6, \quad ^sG(\mathrm{OH}) = 0.7 \qquad (1)^{*1}$$

They were almost independent of pH within the experimental error. The content of $^sG(\mathrm{Red})=0.6$, however, is yet unknown. The present investigation was undertaken to estimate the yield of solvated electrons. Neutral aqueous monochloroacetic acid and alkaline aqueous potassium ferricyanide solutions were both selected as the reaction systems suitable for this purpose.

Experimental

The discharge tube and the electrical circuit used were identical with those previously described.[4] A discharge tube of the ozonizer type (Fig. 1) was composed of two coaxial hard-glass tubes; the tin foil wrapped

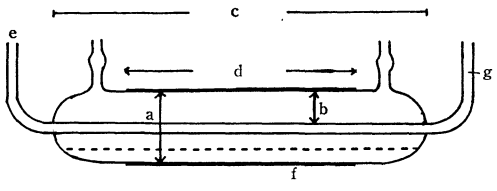

Fig. 1. Schematic diagram of discharge tube.
a, 26 mm b, 8 mm c, 300 mm
d, 230 mm e, 10 mmϕ f, tin foil
---- surface of solution

1) M. Freund and G. Földiak, *Erdöl und Kohle*, **10**, 758 (1957).

2) H. J. Pasman, J. C. Vlugter and C. J. Breukink, *Brenstoff-chemie*, **46**, 271 (1965).

3) Z. Paàl and G. Földiak, "Radiation Chem. Proceedings of the 1962 Tihany Symposium," Akademiai Kiado, Budapest (1964), p. 445.

4) A. Yokohata and S. Tsuda, This Bulletin, **39**, 46, 53, 1636 (1966); **40**, 294, 1339, 2502, 2507 (1967).

5) L. B. Loeb, "Basic Processes of Gaseous Electronics," Univ. of California Press., Berkeley (1955), p. 269.

6) N. R. Dibelius, J. C. Fraser, M. Kawahata and C. D. Doyle, *Chem. Eng. Progress*, **60**, 41 (1964).

*1 The symbol ^sG means the effective G value in the silent electric discharge. $^sG(\mathrm{Red})$means the ^sG value of total reducing species.

around the outer was used as one electrode (f) and dilute sulfuric acid in the inner tube (g) as the other electrode (the high-tension side). After pouring the sample solution into the discharge tube, discharge was made by applying high tension to these two electrodes with argon flowing through the gas space of the discharge tube at a velocity of about 120 ml/min.

All experiments were made at a constant solution volume of 10 ml, at room temperature after removing the dissolved oxygen from the solution by bubbling argon gas into the solution, and at a constant discharge current of I=1 mA.

The discharge tube was washed with a mixture of methylalcohol and a saturated aqueous solution of sodium hydroxide besides the usual cleaning solution, and dried by evacuation.

Gamma-ray irradiations were carried out using a 260 curie ^{60}Co source. The dose rate (1.57×10^5R/hr) was determined by the Fricke dosimeter, taking $G(Fe^{3+})$ =15.5.

Materials. Reagents used were of the reagent grade. Argon gas (pyrity: 99.998%) was used without further procedure. Triply-distilled water was used in all the runs.

Analysis. Microquantities of chloride were determined by the turbidimetric method.[7] The turbidity was measured at 350 mμ with a spectrophotometer. Nitrite ions were determined colorimetrically at 540 mμ.[8]

The aquopentacyanide ion, $Fe(CN)_5OH_2^{3-}$, was determined spectrophotometrically by the method using NaN_3.[9,10] A calibration curve was obtained by the following procedure: $Na_3Fe(CN)_5OH_2$ was prepared according to the method of Hofmann[11] and was purified by passing through an alumina chromatographic column and eluting with water. Its content in the eluted solution was determined by the ceric titration. An aliquot (2 ml) of the solution containing the various amounts of $Na_3Fe(CN)_5OH_2$ was pipetted in a 10 ml-volumetric flask to which 0.3 M CH_3COOH-0.3 M NaN_3 was added, and after 15—20 min the optical density at 560 mμ was measured. The molecular extinction coefficient thus obtained was 1.4×10^3 M^{-1} cm^{-1} at pH 4—6. The presence of $Fe(CN)_6^{4-}$ and $Fe(CN)_6^{3-}$ did not interfere with this measurement.

Results and Discussion

Neutral Monochloroacetic Acid Solution. It is well known[12] that in the field of γ-radiolysis the formation of inorganic chloride on irradiation of deaerated solution of $ClCH_2COOH$ is a result of reaction of the reducing species (mainly e_{aq}^-) with the solute. The reaction of OH radicals has been believed to result in dehydrogenation rather than dechlorination. The H-radicals among the reducing species induce principally the hydrogen abstraction reaction with a small possibility of dechlorination.[13] The reaction mechanism is shown as follows.

$$e_{aq}^- + ClCH_2COO^- \longrightarrow Cl^- + CH_2COO^- \quad (2)$$
$$H + ClCH_2COO^- \longrightarrow H_2 + ClCHCOO^- \quad (3)$$
$$\searrow Cl^- + H^+ + CH_2COO^- \quad (4)$$
$$OH + ClCH_2COO^- \longrightarrow H_2O + ClCHCOO^- \quad (5)$$

The silent electric discharge also leads to the formation of inorganic chloride. Figure 2 shows the relationship between the yield and the duration of discharge, in which a good linear correlation can be seen. The yield of Cl^- was independent of the solute concentration in the range from 1×10^{-3} to 1×10^{-2}M (pH=6.5).

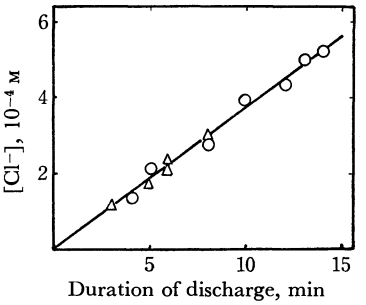

Fig. 2. Silent electric discharge of neutral aqueous solution of $ClCH_2COOH$.
○, 0.01 M $ClCH_2COOH$
△, 0.001 M $ClCH_2COOH$

If the above-mentioned mechanism can be accepted and reaction (4) can be ignored because $k_4=0.09\ k_3$,[13] the yield of e_{aq}^- should equal the yield of Cl^-. Our recent work, however, showed the formation of inorganic chloride in a considerable amount even under the experimental conditions in which reaction (2) could not be expected to

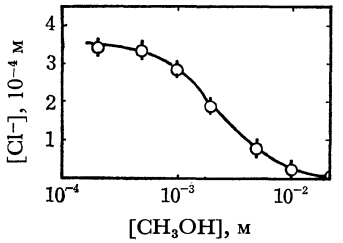

Fig. 3. Effect of CH_3OH on Cl^- yield in the silent electric discharge of neutral aqueous solution of $ClCH_2COOH$ (1×10^{-2} M).

7) E. N. Luce, E. C. Denice and F. E. Akerlund, *Ind. Eng. Chem.*, **15**, 365 (1943).
8) T. Rigg, G. Scholes and J. Weiss, *J. Chem. Soc.*, **1952**, 3034.
9) O. Baudisch, *Ber.*, **62**, 2706 (1929).
10) S. Ohno, This Bulletin, **40**, 1765 (1967).
11) G. Brauer, "Handbuch der Präparativen Anorganischen Chemie" Ferdinand Enke Verlag, Stuttgart (1954), 1363.
12) E. Hayon and A. O. Allen, *J. Phys. Chem.*, **65**, 2181 (1961).
13) J. Jortner and J. Rabani, *J. Am. Chem. Soc.*, **83**, 4868 (1961); *J. Phys. Chem.*, **66**, 2078, 2081 (1962).

occur.*2 This finding is noteworthy in that the possibility of dechlorination reaction due to OH is suggested. Thus, a more detailed experiment was undertaken.

Figure 3 shows the effect of additive CH_3OH on the yield of Cl^- obtained by the silent electric discharge with discharge current at 1 mA and duration at 10 min. It is of great interest that there was a strong suppressive effect of CH_3OH.

When $[CH_3OH]/[ClCH_2COOH]<2$, CH_3OH cannot compete with the $ClCH_2COO^-$ for e_{aq}^-, because the rate constant of reaction of e_{aq}^- with $ClCH_2COO^-$, $k_2=3.8\times10^9 M^{-1}\,sec^{-1}$,[14] is much larger than that with CH_3OH, $k_{e_{aq}^-+CH_3OH}<10^7\ M^{-1}\,sec^{-1}$.[15] These findings lead to the possibility that in the case of silent electric discharge the radicals (*i. e.* OH, H) to be scavenged by CH_3OH play an important role in the formation of Cl^-. Thus, the competition of (6) with (7) and of (4) with (8) should be expected.

$$OH + ClCH_2COO^- \longrightarrow Cl^- + X \quad (6)$$
$$OH + CH_3OH \longrightarrow CH_2OH + H_2O \quad (7)$$
$$H + CH_3OH \longrightarrow CH_2OH + H_2 \quad (8)$$

where X means the reaction product. However, since the yield of Cl^- observed ($^sG(Cl^-)=0.3$) is much larger than the yield expected ($^sG(Cl^-)=0.06$) to be produced *via* reaction (4) on the basis of $^sG(Red)=0.6$ and $k_4=0.09\ k_3$ the contribution of hydrogen atom may not be considered to be significant. Thus, the possibility of (6) is strongly suggested.

If the occurrence of reaction (6) is possible, the considerable yield of Cl^- should be expected even by the addition of electron scavengers such as NO_3^-. Indeed, as shown later, experiments of γ-ray irradiation came up to our expectation. This residual amount is too much to be expected from H atoms and can be suppressed almost completely by the addition of 0.1 M CH_3OH. These findings tend to confirm the possibility of the occurrence of reaction (6).

Our study provides further evidence that Cl^- can be formed by the reaction of the Fenton reagent with $ClCH_2COOH$ but also be suppressed by the addition of CH_3OH.

In the absence of electron scavenger, however, there was hardly any effect of additive CH_3OH on the γ-radiolysis. This suggests that reaction (6) is important only in little or no presence of e_{aq}^-. In the present stage, the reaction scheme must await further study.*3 In any event, the main point here is that most of Cl^- produced by the silent electric discharge is due to the reaction of the active species (mainly OH) other than e_{aq}^- with $ClCH_2COO^-$.

Effect of Nitrate Ions Added in the $ClCH_2COOH$ System. Figure 4 shows the effect of NO_3^- on the yield of Cl^- and NO_2^- in the γ-irradiated solution of 0.01 M $ClCH_2COOH$ (deaerated, pH 6.5). The increment in NO_2^- yield and the decrement in Cl^- yield with an increasing NO_3^- concentration suggest the competition of (2) with (9), followed by (10) and (11).[16]

$$e_{aq}^- + NO_3^- \longrightarrow NO_3^{2-} \quad (9)$$
$$NO_3^{2-} + H^+ \longrightarrow NO_2 + OH^- \quad (10)$$
$$2NO_2 + H_2O \longrightarrow NO_2^- + NO_3^- + 2H^+ \quad (11)$$

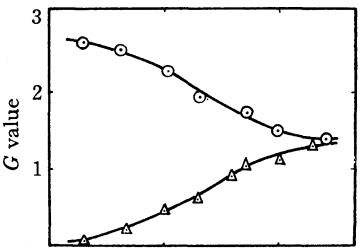

Fig. 4. Effect of KNO_3 on G (Cl^-) and G (NO_2^-) in γ-radiolysis of neutral aqueous solution of $ClCH_2COOH$ (1×10^{-2} M).
⊙, G (Cl^-) △, G (NO_2^-)

If above mechanism is accepted, Eq. (12) can be derived in the presence of sufficient amount of NO_3^- to scavenge all of e_{aq}^-.

$$G(NO_2^-) = 0.5\,G(e_{aq}^-) \quad (12)$$

Reaction (13) might be also expected, since $k_{H+NO_3^-}\approx10^7 M^{-1}\,sec^{-1}$ [17] and $k_{H+ClCH_2COO^-}=1.9\times10^6 M^{-1}sec^{-1}$ [18].

$$H + NO_3^- \longrightarrow HNO_3^- \quad (13)$$

However, as the yield of NO_2^- below pH 3 where a considerable amount of H could be expected by the reaction of e_{aq}^- with H^+ was negligibly small, HNO_3^- disappears probably through the reactions with solute or intermediates to yield products other than NO_2^-.

If, as discussed above, NO_2^- is produced *via* reactions (9)—(11), a simple competition of (2) with (9) leads to Eq. (14).

$$\frac{1}{G(NO_2^-)} = \frac{2}{G(e_{aq}^-)} + \frac{2}{G(e_{aq}^-)}\,\frac{k_2[ClCH_2COO^-]}{k_9[NO_3^-]} \quad (14)$$

*2 Presented at the 21th Annual Meeting of the Chemical Society of Japan, Osaka, March, 1968.

14) D. M. Brown, F. S. Dainton, J. P. Keene and D. C. Walker, *Proc. Chem. Soc.*, **1964**, 266.

15) E. J. Hart, J. K. Thomas and S. Gordon, *Radiation Res. Suppl.*, **4**, 74 (1964).

*3 The rate constant of (6) and additional details will be considered in a publication of the radiolysis of the system containing CH_3OH and N_2O.

16) J. T. Allan, *J. Phys. Chem.*, **68**, 2697 (1964).

17) T. J. Sworski, "Proceedings of the Fifth Informal Conference on the Radiation Chemistry of Water," Univ. of Notre Dame, Indiana (1966), p. 28.

18) M. G. Scholes and M. Simic, *J. Phys. Chem.*, **68**, 1738 (1964).

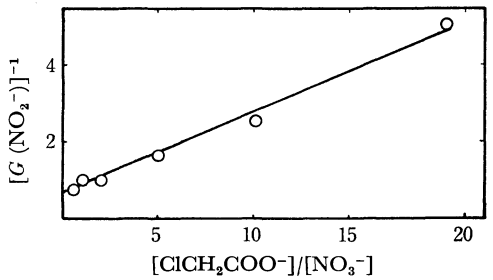

Fig. 5. A plot of $1/G(NO_2^-)$ against $[ClCH_2COO^-]/[NO_3^-]$ (Eq. (14)).

In Fig. 5 $1/G(NO_2^-)$ is plotted against $[ClCH_2COO^-]/[NO_3^-]$. A straight line in Fig. 5 supports the validity of the simple competition mentioned above. Thus, $k_2/k_9=0.15$ can be estimated by using a value of $G(e_{aq}^-)=2.8$. $K_9=1.1\times10^{10}$ M^{-1} sec^{-1} [19] gives $k_2=1.7\times10^9$ M^{-1} sec^{-1}, which is almost consistent with other workers (3.8 or 1.2×10^9 M^{-1} sec^{-1}).[14,20]

On the other hand, nitrite ion was also formed in the silent electric discharge. Figure 6 shows the relationship between the yield of NO_2^- and duration of discharge for aqueous solution of 0.01M $ClCH_2COO^-$+0.1M NO_3^- (pH=6.5). Figure 7 shows the dependence of the yield of Cl^- and NO_2^- on

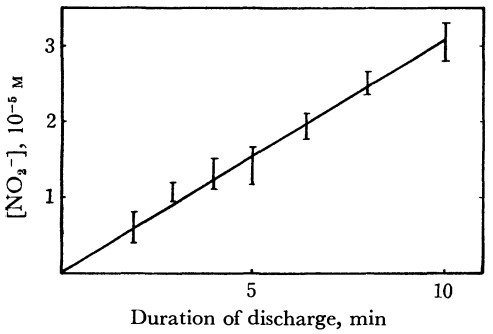

Fig. 6. Silent electric discharge of neutral aqueous solution of 0.01 M $ClCH_2COOH$+0.1 M KNO_3.

the NO_3^- concentration. A linear curve in Fig. 6 gives ${}^sG(NO_2^-)\approx0.03$, which is very small when compared with ${}^sG(\text{Red})=0.6$. Because $k_2/k_9=0.15$, most of the e_{aq}^- should react with NO_3^- to yield NO_2^- in the experimental conditions where $[ClCH_2COO^-]/[NO_3^-]<0.1$. Of course, H atoms may make a small contribution to this yield. Thus ${}^sG(e_{aq}^-)$ estimated by Eq. (12) gives the maximum value.

$$ {}^sG(e_{aq}^-) \lesssim 0.06 \qquad (15) $$

Non-dependence of the yield of Cl^- on the additive NO_3^- known as a strong electron scavenger (Fig. 7) is of interest. It is one of other evidences

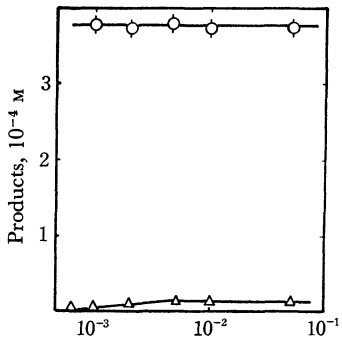

Fig. 7. Dependency of yields of Cl^- and NO_2^- on $[NO_3^-]$ in the silent electric discharge.
Initial concentration of $ClCH_2COOH$, 1×10^{-2} M (pH=6.5)
○, Cl^- △, NO_2^-

that in the silent electric discharge the yield of the solvated electrons can be concluded to be very small.

Alkaline Aqueous Solution of Potassium Ferricyanide. In order to secure a further evidence on the yield of solvated electrons, a study was extended to another system, $K_3Fe(CN)_6^{3-}$-0.1N NaOH solution. In this system the attention was directed toward the reaction of e_{aq}^- to $Fe(CN)_6^{3-}$.

It has been recently reported by Haïssinsky *et al.*[21] that aquopentacyanide is formed *via* following competitive reaction.

$$ e_{aq}^- + Fe(CN)_6^{3-} \longrightarrow Fe(CN)_6^{4-} \qquad (16) $$
$$ \searrow Fe(CN)_5OH_2^{3-} + CN^- \qquad (17) $$
$$ H + Fe(CN)_6^{3-} \longrightarrow Fe(CN)_6^{4-} + H^+ \qquad (18) $$
$$ \searrow Fe(CN)_5OH_2^{3-} + CN^- + H^+ \qquad (19) $$

More recently, Burchill *et al.*[22] reported that the product which gives a colored complex with nitrosobenzene ($Fe(CN)_5PhNO^{3-}$) is diminished by the presence of oxygen or N_2O, and therefore the product may be formed by Eq. (17). On the other hand, the formation of aquopentacyanide was also confirmed[23] by using NaN_3 instead of nitrosobenzene.

In the present work, the NaN_3 method was applied for the determination of the solvated electrons formed by the silent electric discharge.

In the silent electric discharge,*4 the product which gives a colored complex with NaN_3 was also found. Figure 8 shows that the relation of the yield of product to the duration of discharge is linear

19) J. K. Thomas, S. Gordon and E. J. Hart, *ibid.*, **68**, 1524 (1964).
20) M. Anbar and E. J. Hart, *ibid.*, **69**, 271 (1965).
21) M. Haïssinsky, A. M. Koulkès and É. Masri, *J. Chim. Phys.*, **63**, 1129 (1966).
22) C. E. Burchill, F. S. Dainton and D. Smithies, *Trans. Faraday Soc.*, **63**, 932 (1967).
23) S. Ohno and G. Tsuchihashi, *Radioisotopes (Japan)*, **16**, 434 (1967).
*4 The disappearance of ferricyanide ions has been reported[4] to be ${}^sG(-Fe(CN_6^{3-})=2.8$.

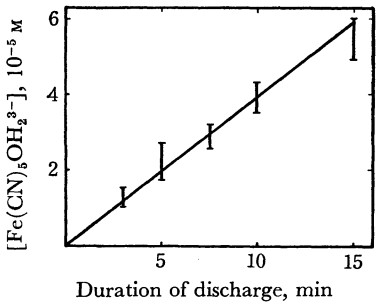

Fig. 8. Silent electric discharge of alkaline aqueous solution of 5×10^{-3} M $Fe(CN)_6^{3-}$ (0.1N NaOH).

and that the yield is independent of the concentration in the range from 5×10^{-3} M to 1×10^{-2} M $Fe(CN)_6^{3-}$ within the experimental error. Then the ${}^sG$ value of the product can be estimated to be about 0.03.

In clarifying the relation between $G(e_{aq}^-)$ and the G value of the product, the γ-ray experiment of the deaerated system was done in the same concentration range. The yield of the product ($G(Fe(CN)_5OH_2^{3-})=1.4$) was almost independent of the concentration in the range from 5×10^{-3} M to 1×10^{-2} M $Fe(CN)_6^{3-}$ and larger than the yield in lower concentration.*5

On the other hand, the strong suppressive effect of N_2O on the yield of the product was also confirmed in this experiment (Fig. 9). Thus, there seems to be no doubt that the product originates mostly from the reaction of e_{aq}^- with $Fe(CN)_6^{3-}$.

Therefore, in the range from 5×10^{-3} M to 1×10^{-2} M $Fe(CN)_6^{3-}$, Eq. (20) can be obtained by using a value of $G(e_{aq}^-)=2.8$.

$$G(e_{aq}^-)\approx 2G(Fe(CN)_5OH_2^{3-}) \qquad (20)$$

By applying the yield of the product obtained in the silent electric discharge (${}^sG(Fe(CN)_5OH_2^{3-})=0.03$) to Eq. (20), ${}^sG(e_{aq}^-)$ can be estimated to be about 0.06. A part of the yield, however, might be due to the H atom. Thus, this gives a maximum value.

$${}^sG(e_{aq}^-)\lesssim 0.06 \qquad (21)$$

General Discussion. In the case of the silent electric discharge clusters of intermediates will be formed densely on the surface of water by the impact of low energy particles (mainly e^-). In the clusters, the primary main product will be an excited water molecule since the energy of the electron is most probably less than the ionization

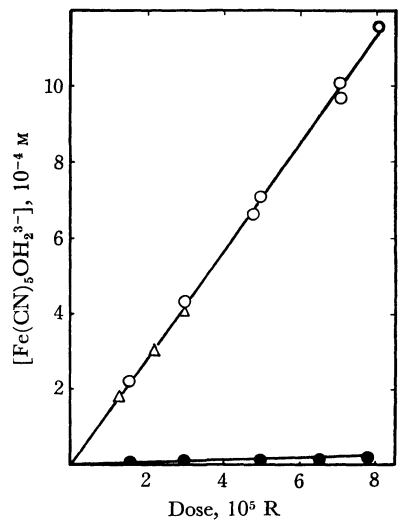

Fig. 9. γ-Ray radiolysis of alkaline aqueous solution of $K_3Fe(CN)_6$ (0.1 N NaOH).
○, 5×10^{-3} M $Fe(CN)_6^{3-}$
△, 1×10^{-2} M $Fe(CN)_6^{3-}$
●, 5×10^{-3} M $Fe(CN)_6^{3-}+2\times10^{-2}$ M N_2O

potential of water molecule. Thus the main reducing species produced from radiolysis by the silent electric discharge can be considered to be hydrogen atom formed mainly through the excitation of water molecule:

$$e_p^- + H_2O \longrightarrow H_2O^* + e_s^- \qquad (22)$$

(e_p^-: primary electron, e_s^-: secondary electron)

$$H_2O^* \longrightarrow H + OH \qquad (23)$$

In addition, the formation of negative ions would be also naturally expected[24] although they (H^- and O^-) would disappear *via* reactions (27) and (28).

$$e^- + H_2O \longrightarrow H + OH^- \qquad (24)$$
$$e^- + H_2O \longrightarrow H^- + OH \qquad (25)$$
$$e^- + H_2O \longrightarrow O^- + 2H \qquad (26)$$
$$H^- + H_2O \longrightarrow H_2 + OH^- \qquad (27)$$
$$O^- + H_2O \longrightarrow OH + OH^- \qquad (28)$$

A part of the primary or secondary electrons might also probably disappear *via* neutralization reaction with the positive ions M^+ (Ar^+, *etc.*) on the surface of water:

$$e_s^-(\text{ or } e_p^-) + M^+ \longrightarrow M \qquad (29)$$

Of course, a part of them might be also solvated to give e_{aq}^-, but most of the solvated electrons produced are expected to combine *via* reaction (30) before they escape from the clusters of intermediates to react with the solute in the bulk.

$$e_{aq}^- + e_{aq}^- \longrightarrow H_2 + 2OH^- \qquad (30)$$

The foregoing, although speculative, may provide an adequate explanation for the small yield of

*5 We confirmed that at a relatively low concentration of $Fe(CN)_6^{3-}$(*e. g.* 5×10^{-4}M), the yield of the product which gives a coloured complex with NaN_3 ($G(Fe(CN)_5OH_2^{3-})=0.5$) is approximately consistent with that[22] of nitrosobenzene method, and that the product has a dependency on the concentration of $Fe(CN)_6^{3-}$ as pointed out by Haïssinsky.

24) M. Burton, "Comparative Effect of Radiation," John Wiley & Sons, New York (1960), p. 152.

the solvated electron in the bulk of water.

In the present stage, however, it is very difficult to discuss quantitatively the fate of slow electrons.

It is our conclusion that in the silent electric discharge the yield of solvated electrons which react with solutes in bulk of water is very small ($^{s}G \lesssim 0.06$).

The author wishes to thank Professor S. Tsuda, Faculty of Engineering of Hiroshima Univ., for many helpful discussions and suggestions during this work. Thanks are also due to Professor M. Miura, Faculty of Science of Hiroshima Univ., for his continuing interest and encouragement.

BULLETIN OF THE CHEMICAL SOCIETY OF JAPAN VOL. 42 663—666 (1969)

The Microwave Spectrum, Structure, and Dipole Moment of Ethylene Episulfoxide

Shuji SAITO

Sagami Chemical Research Center, Sagamihara, Kanagawa

(Received August 1, 1968)

The microwave spectra of the normal species as well as the ^{13}C and ^{34}S isotopic molecules of ethylene episulfoxide have been observed. The rotational constants thus obtained lead to the following structural parameters: S–O=1.483±0.003 Å, C–S=1.822±0.003Å, ∠OSC=111°1′±10′, ∠CSC=48°46′±10′, on the assumption that the C–H distance and the ∠HCH and ∠H_2CC angles are the same as those of ethylene sulfide. From the Stark shifts, the dipole moment has been determined to be μ_a=3.61±0.04 D, μ_c=0.89±0.01 D and μ_{total}=3.72±0.04 D. The bond nature of S–O and C–S has then been discussed on the basis of these data.

Ethylene episulfoxide, a three-membered ring compound, was initially prepared by Hartzell and Paige[1] by the direct oxidation of ethylene sulfide with sodium metaperiodate. They reported that ethylene episulfoxide undergoes dethionylation to yield ethylene and sulfur monoxide at a temperature near 100°C.[1] Dodson and Sauers carried out the thermal decomposition of ethylene episulfoxide in the presence of dienes and obtained cyclic sulfoxides.[2] Among the several sulfoxides reported,[1-5] dimethyl sulfoxide is well-known as a useful reactant for the oxidation of various functional groups to carbonyl compounds,[6] and as an excellent solvent for various organic and inorganic compounds. Compared with dimethyl sulfoxide, ethylene episulfoxide is far too unstable and more reactive even under mild conditions.

As ethylene episulfoxide is one of the simplest alkyl sulfoxides, it would be interesting to determine its molecular structure. The accumulated data on the structures of alkyl sulfoxides give a way of understanding the stability and reactivity of these compounds. Accurate r_e structures of the SO[7] and SO_2[8] molecules were obtained from the microwave spectra in the vibrationally-excited states. Pierce and Hayashi[9a] and Dreizler and Rudolph[9b] determined the r_s structure of dimethyl sulfide by analyzing the rotational spectra of various isotopic species. The r_0 structures of dimethyl sulfoxide[10] and ethylene sulfide[11] were obtained

1) G. E. Hartzell and J. N. Paige, *J. Am. Chem. Soc.*, **88**, 2616 (1966).

2) R. M. Dodson and R. F. Sauers, *Chem. Commun.*, **1967**, 1189.

3) D. C. Dittmer and G. C. Levy, *J. Org. Chem.*, **30**, 636 (1965).

4) G. E. Hartzell and J. N. Paige, *ibid.*, **32**, 459 (1967).

5) R. C. Krug and D. E. Bosewell, *J. Heterocyclic Chem.*, **4**, 309 (1967).

6) a) N. Kornblum, J. W. Powers, G. J. Anderson, W. J. Jones, H. O. Larson, O. Levand and W. M. Weaver, *J. Am. Chem. Soc.*, **79**, 6562 (1957). b) F. W. Sweat and W. W. Epstein, *J. Org. Chem.*, **32**, 835 (1967).

7) a) T. Amano, E. Hirota and Y. Morino, *J. Phys. Soc. Japan*, **22**, 399 (1967). b) F. X. Powell and D. R. Lide, Jr., *J. Chem. Phys.*, **41**, 1413 (1964). c) M. Winnewisser, K. V. L. N. Sastry, R. L. Cook and W. Gordy, *ibid.*, **41**, 1687 (1964).

8) a) S. Saito, *J. Mol. Spectry.*, to be published. b) Y. Morino, Y. Kikuchi, S. Saito and E. Hirota, *J. Mol. Spectry.*, **13**, 95 (1964).

9 a) L. Pierce and M. Hayashi, *J. Chem. Phys.*, **35**, 479 (1961). b) H. Dreizler and H. D. Rudolph, *Z. Naturforsch.*, **17a**, 712 (1962).

10) H. Dreizler and G. Dendl, *Z. Naturforsch.*, **19a**, 512 (1964).

11) G. L. Cunningham, Jr., A. W. Boyd, R. J. Myers and W. D. Gwinn, *J. Chem. Phys.*, **19**, 676 (1951).

by microwave spectroscopy. The purpose of this research is to determine the structure and the dipole moment of ethylene episulfoxide from its microwave spectrum.

Experimental

The sample of ethylene episulfoxide, prepared by the oxidation of ethylene sulfide using perbenzoic acid, was kindly provided by Fukuyama and Sato.[12] The microwave spectrum of ethylene episulfoxide was studied in the region from 8000 MHz to 36000 MHz with a conventional sinusoidal Stark-modulated spectrograph. Most of the measurements were carried out with a 3-m absorption cell at room temperature.

Microwave Spectrum

A tentative molecular model was first drawn by inference from analogous compounds, such as dimethyl sulfoxide[10] and ethylene sulfide.[11] The model was found to be a nearly prolate symmetric top with a dipole moment whose a and c components are about four and one Debyes respectively. Thus, strong a-type R branch transitions would be observed near every 11000 MHz, and weak c-type Q branch transitions would cover the whole region. The Stark effects should be rather large.

Table 1. Observed microwave transition frequencies of ethylene episulfoxide (C_2H_4SO) in the ground state (MHz)

Transition	f_{obs}	Δf[a]
a-type		
$1_{01} \leftarrow 0_{00}$	10519.30[b]	0.00
$2_{11} \leftarrow 1_{10}$	21258.84[b]	0.00
$2_{02} \leftarrow 1_{01}$	21033.96[b]	−0.16
$2_{12} \leftarrow 1_{11}$	20817.60[b]	0.00
$3_{12} \leftarrow 2_{11}$	31885.13[b]	0.36
$3_{21} \leftarrow 2_{20}$	31573.30[b]	0.46
$3_{22} \leftarrow 2_{21}$	31556.76[b]	0.42
$3_{03} \leftarrow 2_{02}$	31540.36[b]	0.38
$3_{13} \leftarrow 2_{12}$	31223.13[b]	0.17
c-type		
$1_{10} \leftarrow 0_{00}$	19477.78[c]	0.00
$2_{11} \leftarrow 1_{01}$	30216.64[c]	−0.68
$2_{02} \leftarrow 1_{10}$	12075.41[b]	−0.23
$3_{03} \leftarrow 2_{11}$	22357.24[c]	0.47
$1_{11} \leftarrow 1_{01}$	8737.19[b]	−0.69
$2_{12} \leftarrow 2_{02}$	8521.67[b]	0.32
$2_{21} \leftarrow 2_{11}$	26212.58[d]	−0.93
$2_{20} \leftarrow 2_{12}$	26879.98[d]	0.48

a) $\Delta f = f_{obs} - f_{calc}$. b) Accuracy ± 0.1 MHz.
c) Accuracy ± 0.2 MHz. d) Accuracy ± 0.4 MHz.

12) A. Negishi, K. Sato, S. Saito and M. Fukuyama, Preprints for the 21st Annual Meeting of the Chemical Society of Japan, Suita (April, 1968).

A search was made, using an oscilloscope, in the 10—12 GHz region, where the $1_{01} \leftarrow 0_{00}$ transitions were expected to occur on the basis of the molecular model described above. A good absorption candidate was located at 10519 MHz; this absorption showed a typical $J=1 \leftarrow 0$ Stark effect. The assignment of this line to the $1_{01} \leftarrow 0_{00}$ transition was confirmed by the observation at about 21 GHz of three $J=2 \leftarrow 1$ transitions which showed Stark patterns characteristic of the $J=2 \leftarrow 1$ transitions. From the a-type transitions thus assigned, the c-type transitions were predicted and searched for by means of a strip-chart recorder. The observed frequencies are given in Table 1. Subsequent measurements were made on the a-type transitions of the S-34 and C-13 species in natural abundance; the results are shown in Table 2.

Table 2. Observed microwave transition frequencies of $C_2H_4{}^{34}SO$ and $^{13}CCH_4SO$ (MHz)

Transition	f_{obs}	Δf[a]
$C_2H_4{}^{34}SO$		
$2_{11} \leftarrow 1_{10}$	21135.38[b]	0.00
$2_{02} \leftarrow 1_{01}$	20936.94[b]	0.00
$2_{12} \leftarrow 1_{11}$	20745.20[b]	0.00
$^{13}CCH_4SO$		
$2_{02} \leftarrow 1_{01}$	20675.92[b]	0.00
$2_{12} \leftarrow 1_{11}$	20440.96[b]	0.00
$1_{01} \leftarrow 0_{00}$	10340.52[b]	0.00

a) $\Delta f = f_{obs} - f_{calc}$. b) Accuracy ± 0.1 MHz.

Table 3. Rotational constants and centrifugal distortion constants of ethylene episulfoxide (MHz)

C_2H_4SO	
A	= 14107.86 ± 0.30
B	= 5369.99 ± 0.10
C	= 5149.37 ± 0.10
D_J	= 0.015 ± 0.010
D_{JK}	= 0.006 ± 0.015
$C_2H_4{}^{34}SO$	
B	= 5332.74 ± 0.10
C	= 5137.66 ± 0.10
$^{13}CCH_4SO$	
B	= 5290.14 ± 0.10
C	= 5050.44 ± 0.10

The rotational constants for the normal species were obtained by using three low-J transitions. In the analysis of the spectra, the centrifugal distortion effect was calculated by the following symmetric-top expression:

$$W(J,K_1,K_1) = E(J,K_{-1},K_1) - D_J J^2(J+1)^2 - D_{JK} J(J+1) K_{-}^2 - D_K K_{-}^4$$

where $W(J,K_{-1},K_1)$ denoted the rotational energy including centrifugal effects; $E(J,K_{-1},K_1)$ the rigid rotor rotational energy, and the other terms the usual centrifugal terms. This treatment is possible because the ethylene episulfoxide molecule is very close to a prolate symmetric top: $b_p=-0.01247$. The rotational spectra for the S-34 and C-13 species were analyzed in a similar way, using the centrifugal distortion corrections determined from the analysis of the normal species. The rotational constants and the centrifugal distortion constants are listed in Table 3.

Dipole Moment

Stark effect coefficients were measured for the $M=0$, $1_{01}\leftarrow 0_{00}$ transition and for the $M=1$ and 0 components of the $2_{02}\leftarrow 1_{01}$ transition. The Stark displacements were compared with those of the OCS molecule, for which the dipole moment was taken to be 0.7124 D.[13] The observed Stark coefficients and the comparison with the calculated values are shown in Table 4. μ_a was determined

Table 4. Stark coefficients and dipole moment of ethylene episulfoxide

Transition		$\Delta\nu/E^2$(MHz)/(V/cm)$^2\times 10^4$ obs	obs-calc
$1_{01}\leftarrow 0_{00}$	$M=0$	1.696	0.000
$2_{02}\leftarrow 1_{01}$	$M=0$	−0.463	0.000
	$M=1$	0.437	0.001
$\mu_a=3.61\pm0.04$ D		$\mu_c=0.89\pm0.01$ D	
$\mu_{total}=3.72\pm0.04$ D			

to be 3.61±0.04 D and μ_c, to be 0.89±0.01 D. They yield a value of 3.72±0.04 D for the total dipole moment, which makes an angle of 13°51′ with *a* principal axis. The orientation of the dipole moment relative to the molecular framework was not uniquely determined. The structural calculation described in the next section indicates that the S–O bond axis makes an angle of 42°2′ with the *a* axis, and the plane containing the C_2S ring, an angle of 24°46′ with the *a* axis, so that there are two possibilities, 28°11′ and 55°53′, for the angle between the S–O bond and the total dipole moment. In view of the fact that the dipole moment of ethylene episulfoxide is composed mainly of one S–O and two C–S bond moments, the former possibility, 28°11′, seems preferable to the latter. Figure 1 thus shows only the former configuration.

Molecular Structure

Seven structural parameters are necessary for specifying the molecular structure of ethylene episulfoxide. Fortunately, seven rotational constants have been obtained: three for the normal, two for the S-34, and two for the C-13 species. It seems inadequate to use the rotational constants, *B* and *C*, of the S-34 species for the determination of the structure, because the sulfur atom is so near the center of gravity that the structure derived from the rotational constants of the S-34 species is apt to be affected by zero-point vibrations.

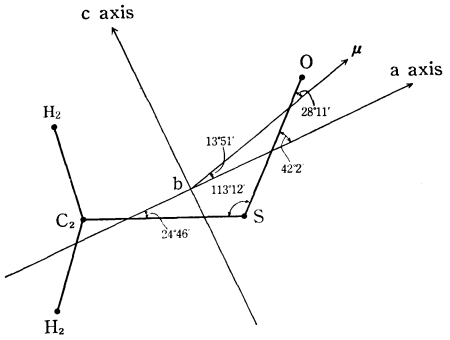

Fig. 1. Structure of ethylene episulfoxide.

Among the seven structural parameters, the most interesting ones are those which describe the episulfoxide part of the molecule. It can be expected that the ethylene part of ethylene episulfoxide is almost the same as that of ethylene sulfide. This prediction is understandable in view of the structures of dimethyl sulfide[9] and dimethyl sulfoxide[10] studied by microwave spectroscopy. Moreover, as a result of the small mass of the hydrogen atom, the moments of inertia depend only slightly on any assumption concerning the configuration of the ethylene part. Hence, we assume that the ethylene part of ethylene episulfoxide is the same as that of ethylene sulfide, that is, that C–H=1.078 Å, ∠HCH=116°0′, and $\angle H_2CC=151°43'$.[11] The four remaining parameters, the S–O and C–S distances, and the ∠OSC and ∠CSC angles are determined to give the five observed rotational constants for the normal

Table 5. r_0 structure of ethylene episulfoxide

r(S–O)	1.483 ± 0.003 Å
r(C–S)	1.822 ± 0.003 Å
∠OSC	110° 1′ ± 10′
∠CSC	48°46′ ± 10′
r(C–C)[a]	1.504 ± 0.003 Å
assumed parameters	
r(C–H)	1.078 Å
∠HCH	116° 0′
$\angle H_2CC$	151°43′

a) r(C–C) distance is not independent of the other parameters listed above.

13) S. A. Marshall and J. Weber, *Phys. Rev.*, **105**, 1502 (1957).

and C-13 species. The structure thus obtained is given in Table 5.

Discussion

The molecular structure of ethylene episulfoxide determined above gives some clue for understanding the properties of alkyl sulfoxides, which have rarely been discussed. The S–O and C–S bond distances of the related compounds previously reported are compared in Table 6 with those of ethylene episulfoxide obtained in this work. The S–O and C–S bond moments of ethylene episulfoxide can be evaluated from the values of the total dipole moment given in Table 4 if the C–H bond moments are disregarded. These results are also listed in Table 6, along with the bond moments

TABLE 6. S–O and C–S BOND DISTANCES AND BOND MOMENTS IN VARIOUS COMPOUNDS

Molecule		r(S–O)	μ(S–O)	r(C–S)	μ(C–S)
$(CH_2)_2SO$[a]	r_0	1.483 Å	2.53 D	1.822 Å	1.06 D
$(CH_3)_2SO$[b]	r_0	1.47_7 Å	2.70 D	1.81_0 Å	1.47 D
$(CH_2)_2S$[c]	r_0	.....	.....	1.819 Å	1.01 D
$(CH_3)_2S$[d]	r_s	.....	.....	1.802 Å	1.15 D
$(CH_3)_2S_2$[e]	r_0	.....	.....	1.81_0 Å	1.38 D
SO[f]	r_e	1.48108 Å	1.55 D	.....	.....
SO_2[g]	r_e	1.4308 Å	1.58 D[i]	.....	.....
S_2O[h]	r_0	1.465 Å	1.58 D	.....	.....

a) This work. b) Ref. 10.
c) Ref. 11. d) Ref. 9.
e) D. Sutter, H. Dreizler and H. D. Rudolph, *Z. Naturforsch.*, **20a**, 1676 (1965).
f) Ref. 7. g) Ref. 8.
h) D. J. Meschi and R. J. Myers, *J. Mol. Spectry.*, **3**, 405 (1959). i) G. F. Grable and W. V. Smith, *J. Chem. Phys.*, **19**, 502 (1951).

of related compounds, which were calculated in a similar way. It may be seen that the S–O bond length of ethylene episulfoxide is longer than those of SO_2 and S_2O, and almost equal to that of SO. As was expected prior to the measurements, ethylene episulfoxide has nearly the same S–O bond distance as dimethyl sulfoxide. The C–S bond length of ethylene episulfoxide is a little longer than those of dimethyl sulfide, dimethyl disulfide, and dimethyl sulfoxide, and is almost equal to that of ethylene sulfide. This comparison indicates that the S–O bond of ethylene episulfoxide is almost a double bond, while the C–S bond is almost a single bond.

On the other hand, the C–S bond moment of ethylene episulfoxide is quite normal and is nearly the same as that of ethylene sulfide within the limits of experimental error, whereas the S–O bond moment is considerably larger than those of SO, SO_2, and S_2O. The unusual polarity of the S–O bond can be understood by means of the molecular orbital calculations made by Moffitt.[14] Using the self-consistent LCAO method, he calculated the bond order and the formal charge distribution in the SO, SO_2, SO_3, R_2SO, and R_2SO_2 molecules. He predicted that the dipole moments for alkyl sulfoxides would be about 3.5 D; according to the difference between the electronegativities of the alkyl groups and the sulfur atom, the positive charge moves considerably farther from the negatively-charged oxygen atom, and the C–S bonds of alkyl sulfoxides are weaker than those in alkyl sulfones and alkyl sulfides because the former has hardly any 3*s* electrons of the sulfur atom.

The weakness of the C–S bond has been demonstrated by the experimental finding that ethylene episulfoxide decomposes near 100°C.[1] This has also been confirmed by microwave spectroscopy detecting the rotational lines of sulfur monoxide in the ground state. The thermal decomposition of ethylene episulfoxide will be reported in a separate paper.

The author would like to express his hearty thanks to Professor Yonezo Morino for his encouragement and for the valuable advice given throughout this work. He also wishes to thank Dr. M. Fukuyama and Mr. K. Sato for providing a sample of ethylene episulfoxide.

14) W. Moffitt, *Proc. Roy. Soc.* (*London*), **A200**, 409 (1950).

BULLETIN OF THE CHEMICAL SOCIETY OF JAPAN VOL. 42 667—670 (1969)

Detection of Sulfur Monoxide in the Pyrolysis of Ethylene Episulfoxide by Microwave Spectroscopy

Shuji SAITO

Sagami Chemical Research Center, Sagamihara, Kanagawa

(Received August 8, 1968)

Microwave spectroscopy has been applied to the study of the pyrolysis of ethylene episulfoxide in the vapor phase. The rotational lines of SO in the electronic ground state, $^3\sum^-$, were observed with a good signal-to-noise ratio. The pyrolyzed sample of ethylene episulfoxide was analyzed semi-quantitatively by the use of the microwave spectra. It turned out that ethylene episulfoxide really decomposed into ethylene and sulfur monoxide. The mechanism of the thermal decomposition is discussed in detail.

Alkyl sulfoxides are interesting and important molecules, but only a few examples have been reported, for they are unstable.[1-7] Hartzell and Paige[3] and Negishi, Sato, Saito, and Fukuyama[7] synthesized ethylene episulfoxide by the direct oxidation of ethylene sulfide. Hartzell and Paige[3] observed, by means of mass spectrometry and differential thermal analysis, that it decomposed into ethylene and sulfur monoxide near 100°C. Dodson and Sauers[4] carried out the controlled thermal decomposition of ethylene episulfoxide in the presence of dienes and thus obtained cyclic sulfoxides. They suggested that the sulfur monoxide generated in the pyrolysis might be in the $^1\sum^+$ state or even in the $^1\Delta$ state. By observing and analyzing the rotational spectra of ethylene episulfoxide, Saito[8] determined the molecular structure and discussed the S–O and C–S bonds.

The microwave spectroscopy of free radicals has made considerable progress in recent years following a long pause after Dousmanis, Sanders, and Townes reported the OH radical.[9] Powell and Lide,[10] and Winnewisser, Sastry, Cook and Gordy[11] observed SO. Amano, Hirota and Morino[12] determined the r_e structure of SO. ClO[13] and SN[14] have also recently been studied by means of microwave spectroscopy.

The present work is concerned with the study of the pyrolysis of ethylene episulfoxide. The main purpose is to confirm the existence of SO in the pyrolyzed sample by means of microwave spectroscopy and, moreover, to ascertain the state in which the sulfur monoxide is generated in order to understand the mechanism of the thermal decomposition.

Experimental

The reaction vessel and the Stark absorption cell used are shown in Fig. 1. The reaction vessel was made of a quarz tube 15 mm in diameter and 300 mm long; the temperature of the vessel was controlled by varying the voltage applied to the heater. The temperature of the vessel was measured at the outer surface of the tube by a chromel-alumel thermometer. The vessel was connected by a Teflon coupler 8 mm in inner diameter with the Stark absorption cell of the microwave spectrograph. The absorption cell was made of an X-band waveguide 800 mm long; this waveguide was split in two in the centers of the narrow sides. The two pieces of the split waveguide were separated and fixed by Teflon spacers of the **H** form so as to serve as Stark electrodes. The inner dimensions of the electrodes were made equal to those of the X-band waveguide.

1) S. B. Soloway, U. S. Pat. 2694073, *Chem. Abstr.*, **49**, 3465 (1955).
2) D. C. Dittmer and G. C. Levy, *J. Org. Chem.*, **30**, 636 (1965).
3) G. E. Hartzell and J. N. Paige, *J. Am. Chem. Soc.*, **88**, 2616 (1966).
4) R. M. Dodson and R. F. Sauers, *Chem. Commun.*, **1967**, 1189.
5) G. E. Hartzell and J. N. Paige, *J. Org. Chem.*, **32**, 459 (1967).
6) R. C. Krug and D. E. Boswell, *J. Heterocyclic Chem.*, **4**, 309 (1967).
7) A. Negishi, K. Sato, S. Saito and M. Fukuyama, Preprints for the 21st Annual Meeting of the Chemical Society of Japan, Suita (April, 1968).
8) S. Saito, to be published.
9) G. C. Dousmanis, T. M. Sanders, Jr., and C. H. Townes, *Phys. Rev.*, **100**, 1735 (1955).
10) F. X. Powell and D. R. Lide, Jr., *J. Chem. Phys.*, **41**, 1413 (1964).
11) M. Winnewisser, K. V. L. N. Sastry, R. L. Cook and W. Gordy, *ibid.*, **41**, 1687 (1964).
12) T. Amano, E. Hirota and Y. Morino, *J. Phys. Soc. Japan*, **22**, 399 (1967).
13) T. Amano, E. Hirota and Y. Morino, *J. Mol. Spectry.*, to be published.
14) T. Amano, private communication.

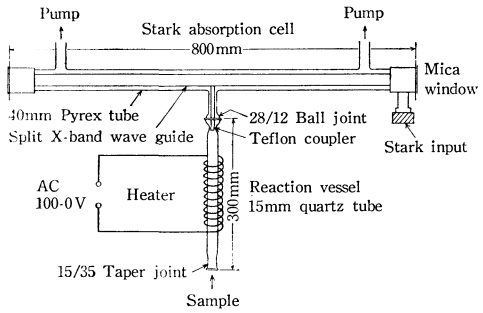

Fig. 1. Schematic diagram of reaction vessel and Stark absorption cell.

To prevent the decomposition and reaction of unstable molecules and radicals on the surface of the electrodes, the inner sides of the electrodes were coated with *"corning K"* coat.[10] The whole electrodes were then fixed in a Pyrex tube 40 mm in diameter by means of Teflon holders. The microweave spectrograph used was a conventional one with 110 kHz sinusoidal Stark modulation.[8] After passing through the absorption cell, the sample gas was led to a trap cooled to the temperature of liquid nitrogen, and then pumped by a rotary pump at the rate of 150 *l*/min.

The sample of ethylene episulfoxide, prepared by the oxidation of ethylene episulfide using perbenzoic acid, was kindly provided by Fukuyama, Sato and Makino.

Pyrolysis

The pyrolysis was done in the range from room temperature to 780°C and at pressures of from 0.01 to 0.1 mmHg. When the temperature of the reaction tube was raised gradually, at about 185°C the rotational line of sulfur monoxide in the electronic ground state, $^3\sum^-$, $J,K=1,0\leftarrow 0,1$ at 30001.58 MHz,[10] was observed by the use of a strip-chart recorder, as is shown in Fig. 2. With a further rise in the temperature, the absorption line of the SO became stronger, until above 250°C it was observable on a CRO. Above 560°C, the intensity of the line remained stationary. The variation in the intensity with the temperature is presented in Fig. 3. Under similar conditions of pyrolysis, the intensity of the transition of ethylene episulfoxide, $3_{03}\leftarrow 2_{02}$, at 31540.36 MHz[8] was followed. The temperature variation in the intensity is also shown in Fig. 3. It is clear that, above 560°C, ethylene episulfoxide decomposed by about 100%. The maximum signal-to-noise ratio of the absorption line of SO was about 5000, at 580°C and at 0.05 mmHg; this value was about twice as large as that of the SO generated in the reaction of atomic oxygen and OCS.[10,11]

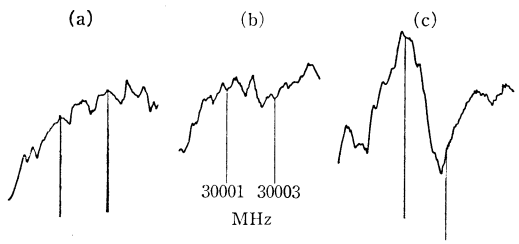

Fig. 2. Recorder tracings of the $J,K = 1,0 \leftarrow 0,1$ transition of the SO molecule in the $^3\sum^-$ state, generated in the pyrolysis of ethylene episulfoxide.
Frequency ≒ 30002 MHz
Stark DC bias = 500 V/cm
Stark mod. = 300 V/cm
Pressure = 0.02 mmHg
(a) At 180°C, the line of SO is not observed.
(b) At 187°C, the line is detected with the S/N of about one to two.
(c) At 200°C, the line has the S/N of about seven.

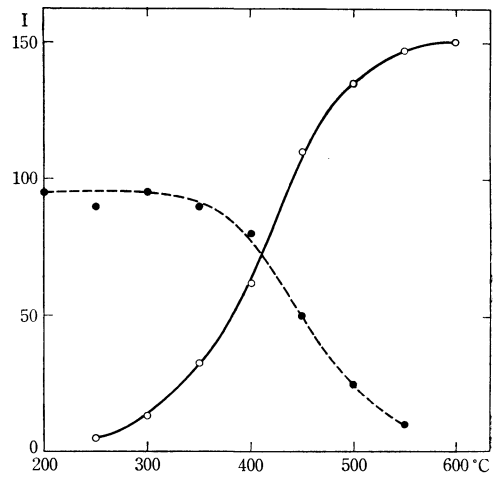

Fig. 3. Temperature variation of the absorption intensities of the lines for SO ($^3\sum^-$) and ethylene episulfoxide.
○ denotes the intensity of the $J,K = 1,0 \leftarrow 0,1$ transition of SO at 30002 MHz.
● denotes the intensity of the $3_{03} \leftarrow 2_{02}$ transition of ethylene episulfoxide at 31540 MHz.

Experimental Results

The sample pyrolyzed at 580°C and 0.02 mmHg was analyzed semi-quantitatively by the use of the microwave spectra. The absorption lines of $(CH_2)_2SO$, SO, SO_2, and H_2CO were measured on a CRO, and those of $(CH_2)_2S$ and $(CH_2)_2O$, on a strip-chart recorder. The concentrations of the stable molecules, such as $(CH_2)_2SO$, SO_2, H_2CO, $(CH_2)_2S$, and $(CH_2)_2O$, were determined by comparison with the corresponding standard samples.[15] The concentrations of the unstable

15) Y. Morino and E. Hirota, *Nippon Kagaku Zasshi* (*J. Chem. Soc. Japan, Pure Chem. Sect.*), **85**, 535 (1964).

Table 1. The composition of the pyrolyzed sample of ethylene episulfoxide

Molecule	Percentage	Method	Ref. to Mw spectra
$(CH_2)_2SO$	2	CRO	a)
SO	~3	CRO	b)
SO_2	20	CRO	c)
S_2O	~24	CRO	d)
H_2CO	0.8	CRO	e)
$(CH_2)_2S$	≤ 0.3	Reorder	f)
$(CH_2)_2O$	≤ 0.04	Reorder	f)

a) Ref. 8. b) Ref. 10.
c) Y. Morino, Y. Kikuchi, S. Saito and E. Hirota, *J. Mol. Spectry.*, **13**, 95 (1964). d) Ref. 16.
e) T. Oka, K. Takagi and Y. Morino, *J. Mol. Spectry.* **14**, 27 (1964).
f) G. L. Cunningham, Jr., A. *W.* Boyd, R. J. Myers and W. D. Gwinn, *J. Chem. Phys.*, **19**, 676 (1951).

molecules, SO[10] and S_2O,[16] were estimated by calculating the absorption intensity using the reported values of the microwave spectra. The results are listed in Table 1.

The final products of the pyrolysis were collected with a trap cooled at the temperature of liquid nitrogen; after vaporization, they were analyzed by the use of their infrared and microwave spectra. The main components of the products were ethylene and SO_2. The mole ratio between ethylene and SO_2 turned out to be about two.

Mechanism of Thermal Decomposition

It is interesting to consider the mechanism of the thermal decomposition of ethylene episulfoxide. The concentrations of ethylene sulfide and ethylene oxide were found to be less than 0.3% and 0.04% respectively, as is shown in Table 1. Thus, the abscission reaction of the S–O bond, which gives theatomicoxygen:

$$(CH_2)_2SO \longrightarrow (CH_2)_2S + O \qquad (1)$$

is probably not the main one in the thermal decomposition.

Prior to discussing the other mechanisms in detail, it is necessary to know the energy levels of ethylene and SO, and the heat of the decomposition. According to Evans,[17] Mulliken,[18] and Kuppermann and Raff,[19] the lowest triplet state of planar ethylene, $^3B_{3u}$, is about 4.6 eV ($\fallingdotseq$37100 cm^{-1}) above the ground state, ^1A_g. Rabinovitch, Douglas, and Looney[20] obtained the energy value of the lowest singlet state of perpendicular ethylene as the activation energy of the *cis-trans* isomerization of 1,2-di-deutero-ethylene. The $^1B_1$ state is located 2.66 eV ($\fallingdotseq$21500 cm^{-1}) above the ground state of the planar ethylene. There has been no observation of the lowest triplet state of the perpendicular ethylene, but the calculations for the electronic states of ethylene by various MO methods[21] suggest that the lowest triplet state, $^3A_2$, is below the singlet state, $^1B_1$, by from 0.1 to 0.3 eV. Hence, it is reasonable to assume that the $^3A_2$ state is located somewhere between 2.36 and 2.56 eV ($\fallingdotseq$19100 and 20700 cm^{-1}) above the ^1A_g state.

Unfortunately, there is no reliable data on the electronic states of SO. On the basis of the discussions made by Carrington *et al.*,[22] and on the basis of the energy levels of the oxygen molecule,[23–25] it is plausible to estimate that the $^1\Delta$ state of SO is located near, or less than 8000 cm^{-1} above, the ground state, $^3\Sigma^-$.

On the other hand, the heat of the decomposition of ethylene episulfoxide to ethylene and SO in the vapor phase can be calculated by the use of the heat of the formation of dimethyl sulfoxide on the assumption that the heat of the formation of ethylene episulfoxide from dimethyl sulfoxide by dehydrogenation is equal to that of ethylene sulfide from dimethyl sulfide.[26] The decomposition, $(CH_2)_2SO \rightarrow CH_2=CH_2+SO$, was found to be an exothermic reaction of about 39 ± 10 kcal/mol. (The uncertainty is mainly due to the assumption made above.)

The relative energies considered are shown schematically in Fig. 4. It is evident that the heat of decomposition is not enough to take the electronically-excited states of ethylene into the reaction path. The two possible reactions which yield both ethylene and sulfur monoxide in the ground states are as follows:

$$(CH_2)_2SO(^1A') + M \longrightarrow CH_2=CH_2(^1A_g) + SO(^3\Sigma^-) + M \qquad (2)$$

$$(CH_2)_2SO(^1A') \longrightarrow CH_2=CH_2(^1A_g) + SO(^1\Delta, {}^1\Sigma^+)$$

$$SO(^1\Delta, {}^1\Sigma^+) + X \longrightarrow SO(^3\Sigma^-) + X \qquad (3)$$

16) D. J. Meschi and R. J. Myers, *J. Mol. Spectry.*, **3**, 405 (1959).
17) D. F. Evans, *J. Chem. Soc.*, **1096**, 1735.
18) R. S. Mulliken, *J. Chem. Phys.*, **33**, 1596 (1960).
19) A. Kuppermann and L. M. Raff, *ibid.*, **37**, 2497 (1962); *Discussions Faraday Soc.*, **35**, 30 (1963); *J. Chem. Phys.*, **39**, 1607 (1963).
20) B. S. Rabinovitch, J. E. Douglas and F. S. Looney, *J. Chem. Phys.*, **20**, 1807 (1952).
21) U. Kaldor and I. Schavitt, *ibid.*, **48**, 191 (1968).
22) A. Carrington, D. H. Levy and T. A. Miller, *Trans. Faraday Soc.*, **62**, 2994 (1966).
23) H. D. Babcock and L. Herzberg, *Astrophys. J.*, **108**, 167 (1948).
24) L. Herzberg and G. Herzberg, *ibid.*, **105**, 353 (1947).
25) R. M. Badger, A. C. Wright and R. F. Whitlock, *J. Chem. Phys.*, **43**, 4345 (1965).
26) "Landolt-Börnstein, Zahlenwerte und Funktionen," Vol. II, Part 4, ed. by K. Schäfer and E. Lax, Springer-Verlag, Berlin (1961).

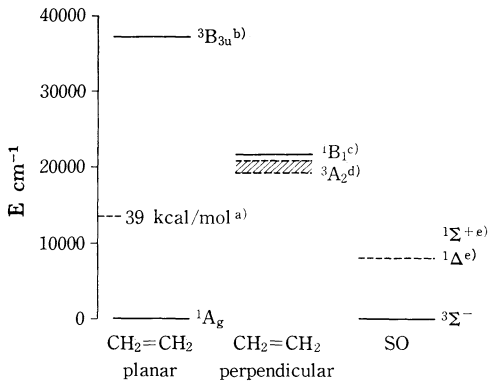

Fig. 4. Energy levels of ethylene and SO.
a) The caluclated values of the heat of decomposition in the vapor phase, $(CH_2)_2SO \rightarrow CH_2{=}CH_2 + SO$
b) Refs. 17—19.
c) Ref. 20.
d) Assumed from the calculated values by the various MO methods.[21]
e) Assumed with inference for the oxygen molecule.[22-24]

The process (2) means the direct decomposition of ethylene episulfoxide into ethylene and sulfur monoxide by a collision with a third body, such as the hot surface of the reaction tube. Spin conservation[27] may be violated by such a collision. The reaction (3), however, is a reaction path which initially sets free the ethylene in the ground state and the sulfur monoxide in the excited singlet states. Then, the SO in the singlet states passes into the ground state under the influence of a third body.

According to Uehara,[28] no electron paramagnetic resonance lines of the SO in the $^1\Delta$ state[29] were detected in the pyrolysis of ethylene episulfoxide under conditions similar to those described above. The sensitivity of the spectrograph he used was about 1×10^{-11} spins/gauss. The lifetime of $^1\Delta$ SO should be rather long because the transition between the $^1\Delta$ and $^3\sum^-$ states is forbidden. Really, in the case of oxygen, the radiative lifetime of the O_2 in the $^1\Delta_g$ state is about 45 min.[25] Hence, the reaction (3) can not be the main process.

As a result, the main reaction of the thermal decomposition of ethylene episulfoxide must be (2): ethylene episulfoxide decomposes on the hot surface of the reaction tube to yield both the ethylene and SO molecules in the ground states.

In the above consideration, many unestablished assumptions have been used, such as those concerning the term energies of ethylene and SO, the heat of the decomposition of $(CH_2)_2SO$, and the sensitivity of the EPR spectrometer. The possibility of the reaction (3) should not, therefore, be excluded completely. To understand the mechanism further, it will be helpful to determine the heat of the decomposition of ethylene episulfoxide and to locate the $^1\Delta$ and $^1\sum^+$ states of SO.

The SO molecule thus generated is unstable. The decomposition of the SO molecule has been studied by many investigators. Schenk and Steudel have reviewed the research into this problem up to 1964.[30] The reaction of SO has not been specifically investigated in this study, but it is meaningful to refer to the decomposition of SO, especially since the present system of reaction is almost free from the oxygen atom and the oxygen molecule. As Table 1 shows, the rotational lines of SO_2 and S_2O were observed immediately after the pyrolysis. It was also noticed that solid sulfur adhered to the inner walls of the reaction tube and the trap. These facts can be explained by the following reactions, which have already been discussed[30,31]:

$$SO + SO \longrightarrow SO_2 + S$$
$$SO + S \longrightarrow S_2O$$

Schenk and Steudel[30] pointed out that the S_2O molecule was stable in the vapor phase, but that it polymerized in the cold trap and the polysulfur oxide decomposed into solid sulfur and SO_2 at room temperature. Thus, all of the oxygen atoms initially contained in the ethylene episulfoxide molecules passed into the SO_2 molecules. This mechanism explains why the ratio between ethylene and SO_2 in the final products of the pyrolysis was about two, by means of the following overall reaction:

$$6(CH_2)_2SO \longrightarrow 6CH_2{=}CH_2 + 3SO_2 + 3S$$

The author would like to thank Professor Yonezo Morino for his encouragement and valuable advice throughout this work. He also wishes to thank Dr. H. Uehara and Mr. Y. Nakano for their helpful discussions, and Dr. M. Fukuyama and Mr. K. Sato, who supplied the sample of ethylene episulfoxide.

27) G. Herzberg, "Electronic Spectra of Polyatomic Molecules," D. Van Nostrand Co., Inc., Princeton, N. J. (1966), p. 276.
28) H. Uehara, private communication.
29) A. Carrington, D. H. Levy and T. A. Miller, *Proc. Roy. Soc.*, **A293**, 108 (1966); *J. Chem. Phys.*, **47**, 3801 (1967).
30) P. W. Schenk and R. Steudel, *Angew. Chem., Intern. E. Engl.*, **4**, 402 (1965).
31) K. Hoyermann, H. Gg. Wagner and J. Wolfrum, *Ber. Bunsenges. Physik. Chem.*, **71**, 603 (1967).

BULLETIN OF THE CHEMICAL SOCIETY OF JAPAN VOL. 42 671—676 (1969)

The Charge-transfer Bands in the Crystal Spectra of Molecular Compounds of Tetramethylbenzidine and Those of Benzidine

Takako AMANO, Haruo KURODA and Hideo AKAMATU

Department of Chemistry, Faculty of Science, The University of Tokyo, Hongo, Tokyo

(Received August 7, 1968)

The polarized absorption spectra in the 280—1100 mμ region have been observed for the single crystals of eight molecular compounds which involve *N,N,N′,N′*-tetramethylbenzidine and benzidine as the electron donor and *p*-chloranil, TCNQ, 1,3,5-trinitrobenzene, and *p*-benzoquinone as the electron acceptor. The donor and acceptor molecules are not in the ionic states in the ground states of these molecular compounds, in spite of the low ionization potentials of tetramethylbenzidine and benzidine. The observed spectra are composed of absorption bands associated with intramolecular transitions in the constituent molecules and those associated with the charge transfer from the donor to the acceptor. It was found that the polarization of the second charge-transfer band is almost perpendicular to that of the first one in the case of chloranil and TCNQ compounds of benzidine and tetramethylbenzidine. In other cases, the first and second charge-transfer bands were confirmed to be polarized nearly parallel to each other as in a usual charge-transfer molecular compound.

Aromatic amines generally behave as a good π-electron donor. They form solid molecular compounds by the interaction with a variety of π-electron acceptors. These molecular compound crystals have been often found to be an organic semiconductor of relatively good electrical conductivity.[1,2] In a previous paper,[3] we have studied the electronic spectra of single crystals of molecular compounds which are formed by aromatic amines with chloranil. We have shown that a strong donor such as *N,N,N′,N′*-tetramethyl-*p*-phenylenediamine (TMPD) gives a salt-like, solid consisting of the positive ions of donor and the negative ions of acceptor, whereas a "charge transfer" molecular compound, where the constituent molecules are essentially in the non-ionic state, is formed by an aromatic amine of not very strong donor property. The molecular compound of *N,N,N′,N′*-tetramethylbenzidine with chloranil is anomalous in this respect. Although tetramethylbenzidine must be a strong donor with an ionization potential comparable to that of TMPD, this molecular compound has been reported to have a non-ionic structure.[1] Interestingly tetramethylbenzidine forms a non-ionic molecular compound even with a very strong π-electron acceptor such as 7,7,8,8-tetracyanoquinodimethane (TCNQ).[4]

In view of this unusual situation found for the molecular compounds of tetramethylbenzidine, we have attempted to obtain informations concerning the charge-transfer interaction in these molecular compounds by observing the electronic spectra of single crystals. In the present paper, we shall report the polarized absorption spectra in the visible and ultraviolet region observed for the molecular compound crystals which involve tetramethylbenzidine or benzidine as the donor and TCNQ, *p*-chloranil, 1,3,5-trinitrobenzene, and *p*-benzoquinone as the acceptor.

Experimental

Molecular compound crystals were obtained from benzene or carbon tetrachloride solutions containing appropriate amounts of donor and acceptor. The composition of each molecular compound was determined by the elementary analysis of the crystalline powder.

The infrared spectrum was examined on each molecular compound by use of the Nujol-mull method for the purpose to know if the component molecules are in the ionic state or not. The observed infrared spectra of molecular compounds were compared with those of the neutral molecules and ions of the components. We examined also the electron spin resonance absorption. All these results led us to conclude that none of the molecular compounds studied here is an ion-radical salt.

The polarized absorption spectra of single crystals, in the 280—1100 mμ region, were measured with a

1) Y. Matsunaga, *Nature*, **205**, 72 (1965).

2) H. Kuroda, K. Yoshihara and H. Akamatu, This Bulletin, **35**, 1604 (1962).

3) T. Amano, H. Kuroda and H. Akamatu, *ibid.*, **41**, 83 (1968).

4) Y. Matsunaga, Preprint of the 20th annual meeting of the Chemical Society of Japan, 1M 011 (1967).

microspectrophotometer, a modification of OLYMPUS MSP-A-IV. The details of the apparatus and experimental procedures have been already described elsewhere.[5] The measurement was carried out at the room temperature on the developed face of a crystal microscopic size, which have been carefully selected out from a freshly prepared crystalline powder. When we noticed the presence of several different crystal habits, the absorption spectra were observed on each type of crystal. The absorption spectra of the Nujol mulls of crystalline powders were also observed to obtain information concerning the low-energy absorption bands.

Results

The experimental results are shown in Figs. 1—9, where the polarized absorption spectra measured on one typical crystal only are shown for each molecular compound.

(a) Tetramethylbenzidine-Chloranil (1 : 1) Compound. The spectra shown in Fig. 1 indicate the presence of a strong band with an absorption maximum at a wave number below 9 kK. By examining the Nujol-mull spectrum of the crystalline powder, it was found that the maximum of this band is located at 8—9 kK and probably is the lowest-energy electronic band of this molecular compound crystal. This band is exclusively polarized in the direction parallel to one of the edges of a parallel piped crystal, which is denoted "X" in Fig. 1. The next band is found at 18.3 kK, which exhibits a polarization quite different from that of the first band, namely the absorption occurs strongly as the incident light is polarized in the Y-direction, *i. e.* a direction perpendicular to X. The polarization ratio, I_Y/I_X, was found to be about 4. These two bands can not be attributed to any intramolecular transition since the lowest transition is at 32.9 kK ($B_{1u}\leftarrow A_g$, π–π^*) in tetramethylbenzidine and at 27 kK (forbidden π–π^* transition) in chloranil. We shall tentatively assign them as the first and second charge-transfer bands. Seemingly the broad band in the 25—30 kK region is a local excitation band associated mainly with the 32.9 kK transition of tetramethylbenzidine.

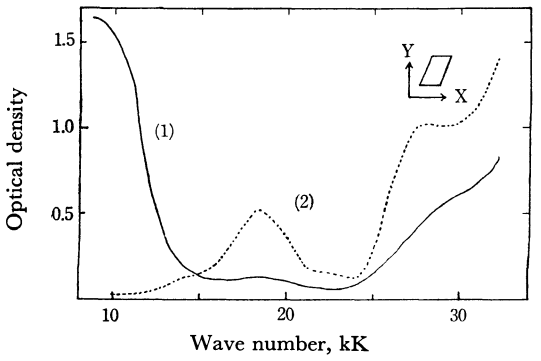

Fig. 1. Absorption spectra of tetramethylbenzidine-chloranil compound.
(1) X-spectrum, (2) Y-spectrum

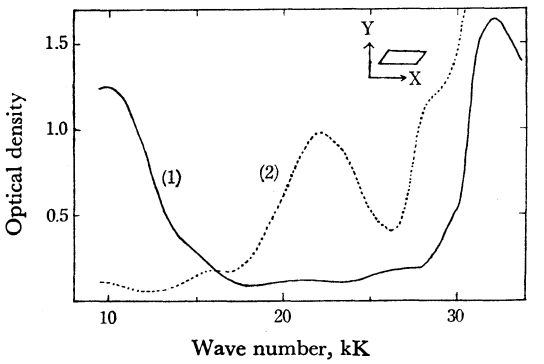

Fig. 2. Absorption spectra of benzidine-chloranil compound.
(1) X-spectrum, (2) Y-spectrum

(b) Benzidine-Chloranil (1 : 1) Compound. The spectra of this molecular compound are similar in many respects to those of the tetramethylbenzidine-chloranil compound. There are two bands in the region where we can expect no band due to intramolecular transition. We assign them as the first and second charge-transfer bands. The maxima of these bands are located respectively at 10 and 22.2 kK. These bands are polarized almost perpendicular to each other as in the tetramethylbenzidine-chloranil compound. A strong peak at 32 kK is probably due to the 35 kK π–π^* transition ($B_{1u}\leftarrow A_g$) of benzidine and/or the 35 kK π–π^* transition ($B_{1u}\leftarrow A_g$) of chloranil. Then we have to consider that these transitions have been shifted to lower energy by about 3 kK in the molecular compound crystal. Presumably a small shoulder at 28 kK is associated with the 27 kK transition (π–π^*, forbidden) of chloranil.

(c) Tetramethylbenzidine-TCNQ (1 : 1) Compound. As is well known, TCNQ is a very

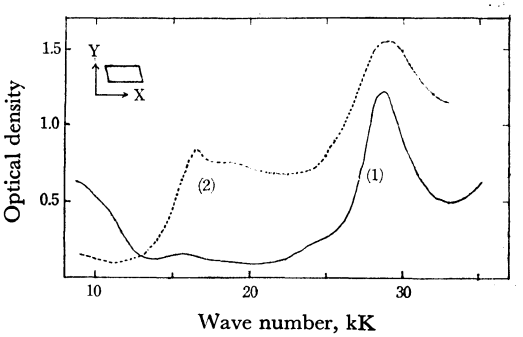

Fig. 3. Absorption spectra of tetramethylbenzidine-TCNQ compound.
(1) X-spectrum, (2) Y-spectrum

5) H. Kuroda, T. Kunii, S. Hiroma and H. Akamatu, *J. Mol. Spectry.*, **22**, 60 (1967).

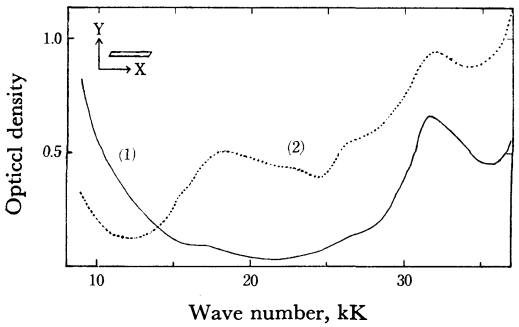

Fig. 4. Absorption spectra of benzidine-TCNQ compound.
(1) X-spectrum, (2) Y-spectrum

strong acceptor, which forms ion-radical salts with a variety of electron donors. In effect, the TMPD-TCNQ compound is composed of $TMPD^+$ ion and $TCNQ^-$ ion, between which there exists a relatively strong charge-transfer interaction.[6] In the case of the tetramethylbenzidine-TCNQ compound, however, all experimental results suggest that the component molecules are essentially in the neutral states. We believe that this molecular compound can be regarded as a non-ionic molecular compound. The high-energy tail of an absorption band can be seen at the low wavenumber limit of the observed spectra shown in Fig. 3. The absorption maximum of this band was found to be located at 7.5 kK in the Nujol-mull spectrum of the powder. The second band is very broad and markedly asymmetric, the maximum of which is located at 16.5 kK. The polarization direction is nearly perpendicular to each other between these two bands. We assign them as the charge-transfer bands. The third band located at about 29 kK is likely to be a local-excitation band associated with the 32.9 kK transition of tetramethylbenzidine. An alternate assignment would be to attribute it to the lowest π–π^* transition of TCNQ (25.3 kK, $B_{1u} \leftarrow A_{1g}$). But the former assignment seems more plausible when we compare the spectrum in this region with that of the benzidine-TCNQ compound.

(d) Benzidine-TCNQ (1 : 1) Compound. Similar to the tetramethylbenzidine-TCNQ compound, we can assign the lowest-energy band at 8 kK and the next band at 18 kK as the first and second charge-transfer bands respectively. In the 25—35 kK region, there is a peak at 32 kK and a shoulder at about 26 kK. It should be noted that the benzidine-chloranil compound also exhibits a strong absorption band at 32 kK while the compound of tetramethylbenzidine with chloranil and that with TCNQ give a band at 29 kK. Therefore the 32 kK band in the benzidine compounds seems to be mainly associated with the intramolecular transition of benzidine, and not due to TCNQ. Presumably the 26 kK shoulder is associated with the 25.3 kK transition of TCNQ.

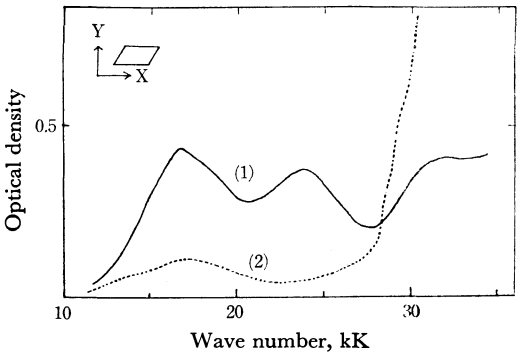

Fig. 5. Absorption spectra of tetramethylbenzidine-trinitrobenzene compound.
(1) X-spectrum, (2) Y-spectrum

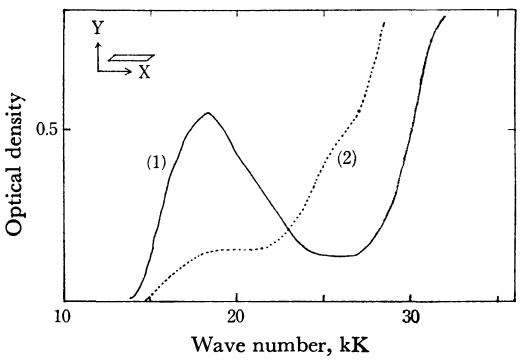

Fig. 6. Absorption spectra of benzidine-trinitrobenzene compound.
(1) X-spectrum, (2) Y-spectrum

(e) Tetramethylbenzidine-Trinitrobenzene (1 : 2) Compound. The two absorption bands, at 16.7 kK and 23.9 kK, can be assigned as the first and second charge-transfer bands. In this case, the polarization is not significantly different between these two charge-transfer bands. In this respect, this molecular compound is markedly different from the chloranil- and TCNQ-compounds mentioned above, but is similar to usual charge-transfer compounds. In order to obtain more precise information concerning the polarization direction, we observed the variation of optical density with the direction of polarization of incident light. The results obtained at the wavenumbers corresponding to the absorption maxima of the two charge-transfer bands are shown in Fig. 7, which indicates that the principal axis of absorption is slightly different between the two bands.

(f) Benzidine-Trinitrobenzene (1 : 1) Compound. The orientation of a trinitrobenzene molecule relative to a benzidine molecule in the

6) H. Kuroda, S. Hiroma and H. Akamatu, This Bulletin, **41**, 2855 (1968).

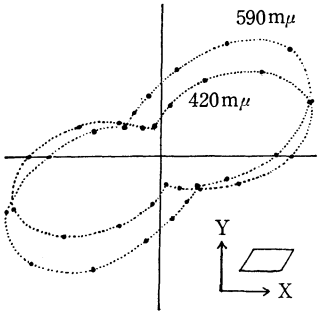

Fig. 7. Variation of optical density with the direction of polarization of incident light, measured for tetramethylbenzidine-trinitrobenzene compound.

crystal of this molecular compound has been reported to be as follows by Wallwork[7]: The benzidine and trinitrobenzene molecules are alternately stacked face-to-face on each other along a crystal axis, but the molecular center of trinitrobenzene is shifted sideway from the position where it would be directly over that of benzidine. In this sence, the arrangement of molecules in this molecular compound is analogous to those in a typical charge-transfer compound. This compound can be obtained in the form of a needle crystal, the elongated axis of which corresponds probably to the direction of the alternate stacking of donor and acceptor molecules. As shown in Fig. 6, we denoted this elongated direction as "X". The absorption band found at 18.3 kK is strongly polarized along the X-direction. This can be assigned as the first charge-transfer band. The second charge-transfer band is not clearly observed. In the Y-polarized spectrum, there is a weak shoulder around 26 kK, which might be due to the second charge-transfer band. If this is the case, we have to consider that there is a significant difference in the polarization direction between the first and second charge-transfer bands. But it is also possible that this 26 kK shoulder is

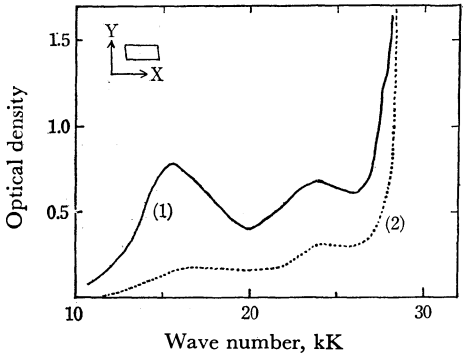

Fig. 8. Absorption spectra of tetramethylbenzidine-*p*-benzoquinone compound.
(1) X-spectrum, (2) Y-spectrum

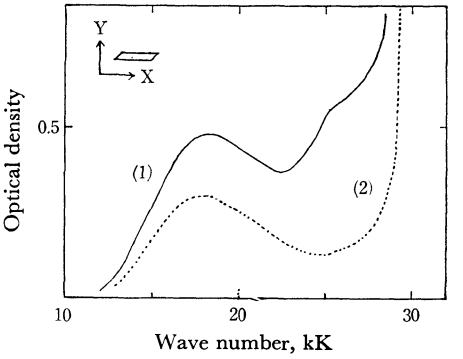

Fig. 9. Absorption spectra of benzidine-*p*-benzoquinone compound.
(1) X-spectrum, (2) Y-spectrum

associated with a local excitation, not with the charge transfer.

(g) Tetramethylbenzidine-*p*-Benzoquinone (1 : 2) Compound. The 15.6 kK and 23.8 kK bands in Fig. 8 can be assigned as the first and second charge-transfer bands respectively. The polarization direction is not appreciably different between these bands. The mole ratio of donor to acceptor is found to be 1 : 2. In these respects, the general situation seems to be similar to the tetramethylbenzidine-trinitrobenzene compound.

(h) Benzidine-*p*-Benzoquinone (2 : 1) Compound. Although the molecular size of benzidine is almost twice that of *p*-benzoquinone, the mole ratio was found to be 1 : 2. This fact seems to suggest that this molecular compound possesses some peculiar crystal structure. The 18kK band in Fig. 9 can be regarded as the first charge-transfer band. The polarization ratio I_X/I_Y is about 1.7 in this band. Presumably a weak shoulder at about 25 kK in the X-polarized spectrum corresponds to the second charge-transfer band.

Discussion

As we have shown above, most of the solid molecular compounds of tetramethylbenzidine and benzidine exhibit two absorption bands in the region where we can expect no local excitation band. We have tentatively assgin them as the first and second charge-transfer bands. The energies of these bands are plotted in Figs. 10 and 11 against the electron affinity of acceptor.*1 These plots clearly demonstrate that the excitation energies are, in fact, almost linearly dependent of the electron affinity of acceptor as expected for a band associated with the charge transfer from a donor molecule to an acceptor molecule.

In solution, tetramethylbenzidine and benzidine

7) S. C. Wallwork, *J. Chem. Soc.*, **1961**, 494.

*1 We have adopted here the values of electron affinity which have been proposed by Briegleb.[8]

8) G. Briegleb, *Angew. Chem.*, **76**, 326 (1964).

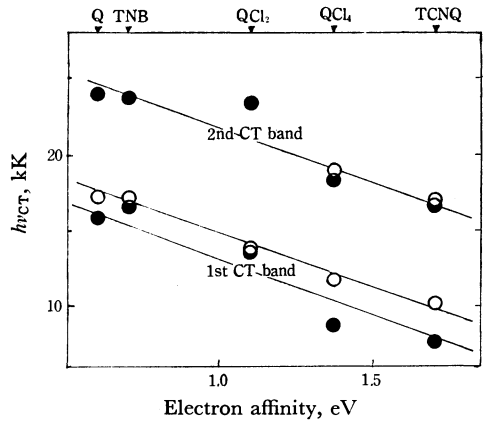

Fig. 10. Energy of charge transfer excitation and electron affinity of acceptor for tetramethylbenzidine compounds.
The acceptor is indicated at the top of the figure.*
○ solution, ● crystal

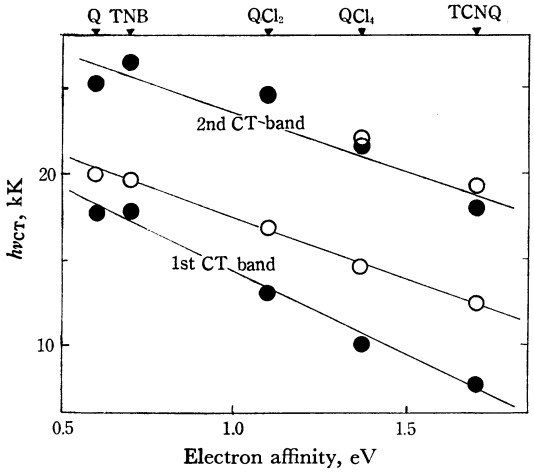

Fig. 11. Energy of charge transfer excitation and electron affinity of acceptor for benzidine compounds.*
○ solution, ● crystal

form molecular complexes with π-electron acceptor, in which the donor and acceptor molecules are in face-to-face contact with each other. The energies of the charge-transfer bands observed for these complexes are also plotted in Figs. 10 and 11. The first charge-transfer band of a molecular compound crystal is a little lower in energy compared with the corresponding band of the molecular complex formed in solution. The energy of the second charge-transfer band of a molecular compound crystal, however, nearly coincides with that of the corresponding band of the complex in solution.

* The following abbreviations are used; Q: *p*-benzoquinone, TNB: 1,3,5-trinitrobenzene, QCl_2: 2,5-dichloro-*p*-benzoquinone and QCl_4: chloranil.

As is well known, there is a simple relation between the ionization potential, I, of the donor and the energy of the charge-transfer band, $h\nu_{CT}$, of the 1 : 1 complex which is formed in solution between a donor molecule and an acceptor molecule. Briegleb and Czekalla have proposed the following empirical equation for a series of chloranil complexes.[9]

$$h\nu_{CT} = I - 5.7 + 0.44/(I-5.7) \quad [\text{eV}] \qquad (1)$$

We have reexamined the relation, and found that the energy of a charge-transfer band of a chloranil complex can be well expressed as follows.

$$h\nu_{CT} = 0.87I - 4.46 \quad [\text{eV}] \qquad (2)$$

We have calculated the self-consistent-field molecular orbitals (SCF-MO's) for the π-conjugated systems in benzidine and tetramethylbenzidine by the variable-β modification of Pariser-Parr-Pople method.*2 The energy and symmetry of the calculated SCF-MO are given in Table 1.

Table 1. Energies of SCF MO's of benzidine and tetramethylbenzidine

Level	Symmetry*	Orbital energy (eV)		
		Benzidine	Tetramethylbenzidine	
1	b_{3u}	−13.56	−13.46	occupied
2	b_{2g}	−13.29	−13.15	
3	b_{3u}	−12.14	−11.95	
4	b_{2g}	−10.97	−10.75	
5	a_u	− 9.90	− 9.85	
6	b_{1g}	− 9.86	− 9.81	
7	b_{3u}	− 9.15	− 8.88	
8	b_{2g}	− 8.05	− 7.84	
9	b_{3u}	− 1.19	− 1.11	unoccupied
10	a_u	− 0.63	− 0.57	
11	b_{1g}	− 0.58	− 0.52	
12	b_{2g}	0.35	0.42	
13	b_{3u}	2.01	2.07	
14	b_{2g}	2.85	2.92	

* The long axis of benzidine molecule is taken as Z axis.

From these calculations, we can predict the ionization potential as 7.0 and 6.8 eV respectively in benzidine and tetramethylbenzidine.[10] Substituting these values in Eq. (1) as well as in Eq. (2), we estimated the energy of the first charge-transfer band for the chloranil complexes of these amines. The energy of the second charge-transfer

9) G. Briegleb and J. Czekalla, *Z. Elektrochem.*, **63**, 6 (1959).

*2 The procedures of SCF-MO calculation are described elsewhere.[10] The calculation was carried out by using HITAC 5020E at the computer center of The University of Tokyo.

10) T. L. Kunii and H. Kuroda, *Theoret. Chim. Acta*, **11**, 97 (1968).

band was estimated by assuming that its energy difference from the first band is equal to the separation between the highest occupied and second highest occupied orbitals of donor. The results are given in Table 2, which are in satisfactory agreement with the observations. Therefore we can conclude that, in the case of these complexes in solution, the first and second charge-transfer bands are associated respectively with the charge transfer from the highest occupied orbital of donor to the lowest vacant orbital of acceptor and that from the second highest occupied orbital of donor.

TABLE 2. CALCULATED AND OBSERVED FREQUENCIES OF THE FIRST AND SECOND CHARGE-TRANSFER BANDS OF BENZIDINE AND TETRAMETHYLBENZIDINE COMPLEXES WITH CHLORANIL IN SOLUTION (kK)

	Calcd		Obsd
	by Eq. (1)	by Eq. (2)	
Benzidine-Chloranil			
First CT band	13.2	13.2	14.2
Second CT band	22.1	22.0	22.0
Tetramethylbenzidine-Chloranil			
First CT band	12.1	11.8	11.7
Second CT band	20.4	20.2	19.7

In the molecular compound crystal, the electronic processes responsible for the charge-transfer bands could be different from those in the 1 : 1 complex in solution since a donor molecule is surrounded by several acceptor molecules in the crystal state. In this case, the charge transfer could take place from a donor molecule not only to the nearest acceptor molecule but also to the second nearest acceptor molecules or others. However, we can safely conclude that the first charge-transfer band of the crystal is associated with the charge transfer from the highest occupied orbital of donor molecule to the lowest vacant orbital of the nearest acceptor molecule since its excitation energy is a little lower than the first charge-transfer band of the corresponding complex formed in solution.

The situation is a little complicated in the second charge-transfer band. In the crystal of a typical charge-transfer compound, the donor and acceptor molecules are alternately stacked along one of the crystal axes. In such a case, an absorption band associated with the charge transfer from a donor molecule to the nearest acceptor molecule should be polarized parallel to this stacking axis unless it is markedly mixed with a local excitation. In effect the observed direction of polarization is in accord with this prediction for the first charge-transfer bands as well as for the second one in a variety of molecular compounds. However, in the molecular compounds of tetramethylbenzidine or benzidine with chloranil and in those with TCNQ, the second charge-transfer band in the crystal spectrum is polarized in the direction almost perpendicular to the polarization direction of the first charge-transfer band. This polarization of the second charge-transfer band could not be explained if we attribute the band to the charge transfer from a donor molecule to the neareast acceptor molecule as in the first charge-transfer band.*3

Presumably the second charge-transfer band is associated with the charge transfer from a donor molecule to the second-nearest acceptor molecule whereas the first one is associated with the charge transfer to the nearest acceptor molecule. If the distance of the second-nearest acceptor molecule from the donor is markedly larger than that of the nearest acceptor molecule, the band due to the charge transfer to the second-nearest acceptor molecule should be of extremely small intensity. This is not the case as can be seen in the spectra shown in Figs. 1—4. We have to consider therefore that the second-nearest acceptor molecule is also in a close contact with the donor molecule.

Then the large energy difference between the first and second charge-transfer bands could not be attributed to the difference in the Coulomb energy term only. A possible explanation would be as follows: the relative orientation of a donor molecule to the nearest acceptor molecule allows the charge transfer from the highest occupied orbital of donor to the lowest vacant orbital of acceptor, but not that from the next occupied orbital of donor, whereas the latter can effectively occur between a donor molecule and the second-nearest acceptor molecule. In other words, the second chrage-transfer band is mainly associated with the charge transfer from the second highest occupied orbital of a donor molecule to the lowest vacant orbital of the second nearest acceptor molecule. Thus the energy difference between the first and second charge-transfer band would be mainly determined by the energy difference between the highest two occupied orbitals of the donor. Anyway, the crystal structure analysis has to be carried out on one of these molecular compounds in order to clarify the validity of the above posturated explanation for the charge-transfer bands. It is now in progress in our laboratory on the tetramethylbenzidine-chloranil (1 : 1) compound.

The polarized crystal spectra of benzidine-TCNQ molecular compound shown in this paper was measured by Mr. S. Hiroma of our laboratory, to whom the authors' thanks are due.

*3 We can exclude the possibility that the first and second bands correspond to the factor group components of a single transition because they are separated from each other as large as 1 eV or more.

BULLETIN OF THE CHEMICAL SOCIETY OF JAPAN VOL. 42 677—681 (1969)

Solubility of Ag_2O in Na_2O-B_2O_3 Melts

Takashi MAEKAWA, Toshio YOKOKAWA and Kichizo NIWA

Department of Chemistry, Faculty of Science, Hokkaido University, Sapporo

(Received August 8, 1968)

The solubility of silver oxide in Na_2O-B_2O_3 melts was determined as a function of the Na_2O contents, the temperature (825°C—935°C), and the oxygen partial pressures. The results show that the silver oxide dissolves in a borate as a network modifier, just like alkali metal oxides, which destroy the B–O–B bonds to produce four coordinated boron as well as three. In the Ag_2O-B_2O_3 binary system, the solubility of silver oxide increases with an increase in the oxygen partial pressures. In the Ag_2O-Na_2O-B_2O_3 ternary system, the solubility of Ag_2O decreases with an increase in the Na_2O contents. This shows that the silver oxide is a weaker base than sodium oxide. The activity of the oxygen ion, $a_{O^=}$, was determined from the iso-activity lines of silver oxide. In a constant basic oxide content, $a_{O^=}$ increases with an increase in the Na_2O content. By extrapolating the Ag_2O contents to zero, the oxygen-ion activity in the Na_2O-B_2O_3 melt was determined.

Molten oxides are quite interesting because of their special structures and have been studied from various aspects. The borates are especially distinguishable from such other mixed oxides as phosphates and silicates because of their structures. The boron atom can coordinate four oxygen atoms as well as three. Therefore, the borate melts show an exceptional behavior known as the boron anomaly.

Various attempts to explain the structure of molten oxides have been made. Lux and Flood[1,2] explained the thermodynamic properties in terms of acidity and basicity. Krogh-Moe[3,4] and Bray *et al.*[5], studied the structure of borate with techniques of X-ray, NMR, and phase diagrams and measured the ratio of four to three-coordinated boron atoms with various contents of alkali metal oxide. Shartsis *et al.*,[6,7] measured the density, viscosity, and electrical resistivity of molten alkali borates.

The present work was performed in order to clarify whether silver oxide dissolves in a boron oxide as a network modifier and in order to examine the behavior of silver oxide in the presence of sodium oxide. The solubility of silver oxide in B_2O_3 has already been measured by Willis and Hennessy.[8]

Another aim of this investigation was related to the basicity of oxide melts. The oxygen-ion activity in an oxide melt is an important factor, since the basicity of the melts, which varies with the melt composition and kind of basic oxide, is supposed to be determined by this quantity. Pearce[9] measured the solubility of carbon dioxide and obtained the oxygen-ion activity in soda-silica melts. In this work the oxygen-ion activity was determined from the solubility measurements of Ag_2O in the Na_2O-B_2O_3 system.

Experimental

(a) Material and Preparation. Samples were prepared from commercial chemicals of a guaranteed reagent grade. Their impurities were as follows; $SO_4<0.003\%$, heavy metals$<0.001\%$, and $Fe<0.002\%$ for B_2O_3; $SO_4<0.002\%$, $Cu<0.0005\%$, and $Fe<0.002\%$ for $AgNO_3$; $Cl<0.001\%$, $SO_4<0.002\%$, and $PO_4<0.002\%$ for borax.

To prepare the Na_2O-B_2O_3 mother melt, a suitable quantity of boric oxide and borax were melted in a platinum crucible.

(b) Chemical Analysis. For the determination of silver, a weighed sample of glass was dissolved in dilute HNO_3 and then the solution was titrated with standardized KSCN. The B_2O_3 was determined in the following way. The sample was dissolved in dilute nitric acid and the pH was adjusted with *p*-nitrophenol. Glycerol was then added, and the B_2O_3 was titrated with an NaOH standard solution.

1) H. Lux, *Z. Elecrochem.*, **45**, 303 (1939).
2) H. Flood and T. Forland, *Acta Chem. Scand.*, **1**, 592 (1947).
3) Krogh Moe, *Acta Cryst.*, **18**, 77 (1965).
4) Krogh Moe, *Phys. Chem. Glasses*, **3**(**1**), 1 (1962).
5) P. Bray and A. Silver, "Modern Aspect of the Vitreous State," Vol. 1, Butterworths, London (1960).
6) L. Shartsis, W. Capps and S. Spinner, *J. Am. Ceram. Soc.*, **36**(**2**), 35 (1953).
7) L. Shartsis, W. Capps and S. Spinner, *ibid.*, **36**(**10**), 319 (1953).
8) G. Willis and F. Hennessy, *Trans. A.I.M.E.*, **197**, 1367 (1953).
9) M. Pearce, *J. Am. Ceram. Soc.*, **47**(**7**), 342 (1964).

(c) **Oxygen Pressure.** A gas mixture of oxygen and nitrogen, the oxygen partial pressure of which has previously been determined by being introducing it into the gas chromatograph at appropriate time intervals, was bubbled through the melt during each run.

(d) **Temperature.** The temperature was controlled with an Okura EC-51-type controller. During every run, the temperature was kept constant within ±1°C.

(e) **Procedure.** The method of Willis and Hennessy was employed. The sample melt was inserted in an Ag crucible and heated in an atmosphere containing oxygen of various partial pressures.

The solution reaction can be expressed by:

$$2Ag + \tfrac{1}{2}O_2 = Ag_2O \text{ (in borate)} \qquad (1)$$

The equilibrium constant, K, is defined by:

$$K = a_{Ag_2O}/\sqrt{P_{O_2}}\, a_{Ag}^2 \qquad (2)$$

at a given temperature.

Since a_{Ag} is set at unity under the present experimental condition, a_{Ag_2O} is directly proportional to the square root of the equilibrium oxygen partial pressure. Further, it is convenient to define the standard state of Ag_2O as the melt which is in equilibrium with 1 atm of oxygen. Therefore, the activity of Ag_2O is given simply by $\sqrt{P_{O_2}}$ when P_{O_2} is expressed in terms of atmosphere. The diameter of the silver crucible is 2 cm, and it is 4 cm deep. The sample in the crucible was maintained at the desired temperature in a tubular resistance furnace. An oxygen-nitrogen gas mixture was bubbled through the silver tube into this sample. The rate of the reaction (1) is very slow to the right direction, since the reaction proceeds one-dimensionally along the circle where the three phases are in contact. On the other hand, the backward reaction proceeds two-dimensionally on the surface of the melt, where the excess silver precipitates from the melt. The preliminary experiments showing this situation are represented in Fig. 1. The backward reaction required only about 20 hr, while it took more than 100 hr for the forward reaction to approach equilibrium. Therefore, the solubility of Ag_2O was measured mostly from the backward reaction.

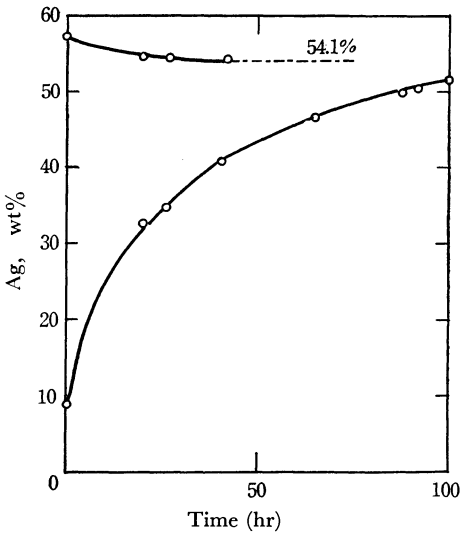

Fig. 1. Preliminary experiment of solution equilibrium of the reaction; $2Ag+\frac{1}{2}O_2=Ag_2O$ (in borate) at 900°C under 1 atm of oxygen. The equilibrium value is 54.1%.

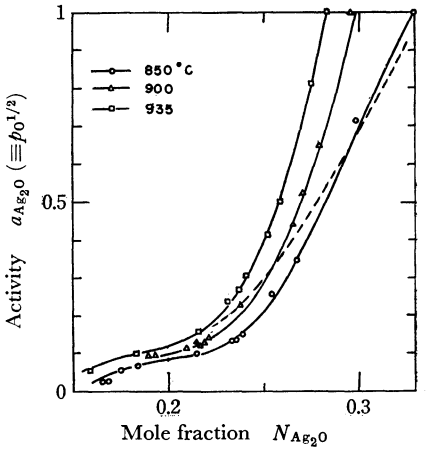

Fig. 2. The activity of Ag_2O, $a_{Ag_2O}(\equiv P_{O_2})$, at 850°C, 900°C, and 935°C. The dotted curve represents the Willis and Hennessy's data at 850°C. The standard state for Ag_2O is the melt in equilibrium with silver and oxygen at 1 atm.

Results and Discussion

(1) Ag_2O-B_2O_3 Binary System. Figure 2 shows the activity of Ag_2O as a function of the composition of Ag_2O at a constant temperature. The dotted curve represents the Willis and Hennessy data at 850°C. It should be noted first that the solubility of silver oxide increases with the oxygen pressure in accordance with Eq. (1). The curve of Willis and Hennessy agrees fairly well with that of the present binary system.

The partial-molar Gibbs free energy of the solution of Ag_2O is obtained from the relation:

$$\bar{G}_{Ag_2O} = RT \ln a_{Ag_2O} \qquad (3)$$

$\bar{G}_{Ag_2O}$ is plotted in Fig. 3 as a function of the Ag_2O concentration. Here one should note that the standard state is the solution in equilibrium with one atmosphere of oxygen.

From the temperature dependence of the partial-molar free energy of a solution, the partial-molar heat of the solution was derived; it is plotted as a function of the composition in Fig. 4. Because of the narrow temperature ranges, the values of the heat of solution are uncertain within the limits of error of ±1 kcal/mol.

The partial molar entropy is obtained from the equation;

$$\bar{S}_{Ag_2O} = (\bar{H}_{Ag_2O} - \bar{G}_{Ag_2O})/T \qquad (4)$$

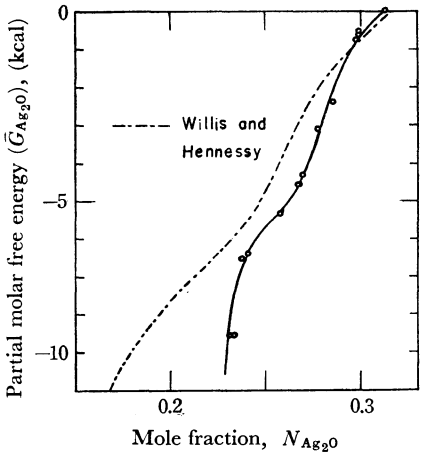

Fig. 3. Partial molar free energies of Ag_2O ($\bar{G}_{Ag_2O}$) in Ag_2O-B_2O_3 melts at 850°C.
The dotted curve represents the Willis and Hennessy's data. The standard state for Ag_2O; Silver and oxygen at 1 atm.

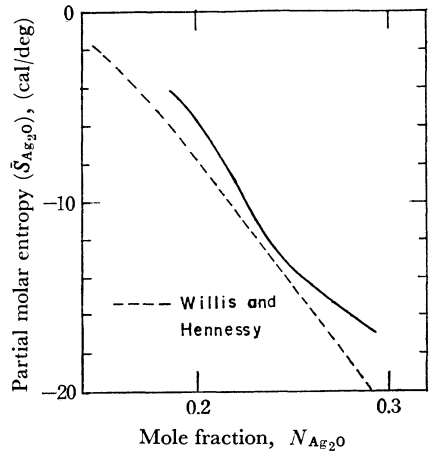

Fig. 5. Partial molar entropies of Ag_2O ($\bar{S}_{Ag_2O}$) in Ag_2O-B_2O_3 melts.
The dotted curve represents Willis and Hennessy's data. Standard state for Ag_2O: Silver and oxygen at 1 atm.

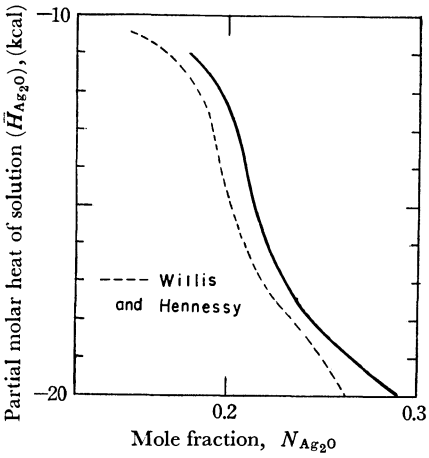

Fig. 4. Partial molar heat of solution of Ag_2O ($\bar{H}_{Ag_2O}$) in Ag_2O-B_2O_3 melts.
The dotted curve represents the Willis and Hennessy's data. Standard state for Ag_2O: silver and oxygen at 1 atm.

it is shown in Fig. 5.

In all cases there is an inflection at $N_{Ag_2O}=0.2$. These phenomena indicate that the structure of Ag-borate changes significantly around this composition. In the alkaline borate melts, the destruction of the network proceeds by means of the following reaction;

$$2\ \begin{matrix}O\\ O\end{matrix}\!\!>\!B\text{–}O\text{–} + O^{=} = 2\ \begin{matrix}O\\ O\end{matrix}\!\!>\!B\!<\!\begin{matrix}O^{-}\\ O\end{matrix} \quad \text{or} \quad 2\ \begin{matrix}O\\ O\end{matrix}\!\!>\!B\text{–}O^{-} \qquad (5)$$

The ratio of four- to three-coordinated boron atoms and the behavior of non-bridging oxygen ions, in the above reaction have been discussed by Beekenkamp[10] in the case of alkali borate glasses. He proposed the equation;

$$N_4 = X_4(X/1-X) \qquad (6)$$

where X_4 is defined by;

$$X_4 = [1+\exp(-\Delta G/KT)]^{-1} \qquad (7)$$

where ΔG is the thermodynamic potential difference between the BO_3-M unit and the BO_4-M unit, and where X is the mole fraction of alkali oxide. The same mechanism seems to be applicable in the present system. Thus, the inflection around $N_{Ag_2O}=0.2$ can be explained in terms of the equilibrium of the BO_3 unit and BO_4. If one follows the above line of approach, these experimental results seem to show that the formation of four-coordinated boron atoms is predominant to $N_{Ag_2O}=0.2$, while after this composition non-bridging oxygen ions gradually begin to be formed.

The infrared absorption spectra[11] and the electric conductivity[12] in the Ag_2O-B_2O_3 system, which have been determined in our laboratory, also support this view.

(2) Ag_2O-Na_2O-B_2O_3 Ternary System. Figure 6 shows the square root of the oxygen partial pressure, *i. e.*, a_{Ag_2O}, as a function of the composition, it also shows the Na_2O content at 850°C. The iso-activity lines in the Ag_2O-Na_2O-B_2O_3 ternary composition diagram are shown in Fig. 7. The solubility of silver oxide decreases with an

10) P. Beekenkamp, *Phys. Chem. Glasses*, **9(1)**, 14 (1968).

11) H. Kodama, Y. Kimura, T. Yokokawa and K. Niwa, This Bulletin, **42**, 681 (1969).

12) M. Honda, *Hokkaido Kyoiku Daigaku Kiyo* (*J. Hokkaido Univ. of Education*), **2A 17(1)**, 33 (1966).

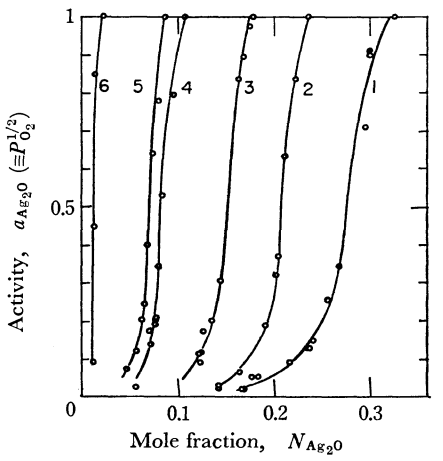

Fig. 6. The activity of Ag_2O, a_{Ag_2O} ($P_{O_2}{}^{1/2}$), at 850°C as a function of Na_2O contents.
Curve 1, 2, 3, 4, 5, and 6 refer respectively to the ratio of $N_{Na_2O}/N_{B_2O_3}$ = 0, 1/18, 1/9.0, 1/5.0, 1/4.8, and 1/2.

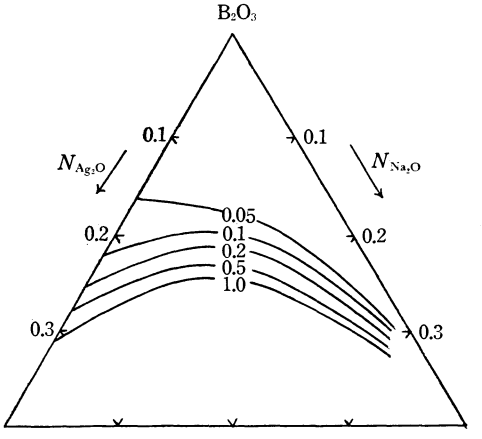

Fig. 7. The iso-activity lines of Ag_2O in Ag_2O-Na_2O-B_2O_3 ternary composition diagram at 850°C.
The standard state for Ag_2O is the melt in equilibrium with silver and oxygen at 1 atm.

increase in the Na_2O contents. This indicates that the silver oxide is a weaker base than sodium oxide. This is due to the fact that, while the silver ion and the sodium ion are both monovalent and are comparable in their ionic radii, the silver ion has a large polarizability and its bond to oxygen shows a somewhat covalent character. From Fig. 7 the following fact is shown: when the Ag_2O contents are small, the a_{Ag_2O} value increases with the increase in the Ag_2O contents at a constant composition of B_2O_3, but on the Ag_2O-rich side the inverse relation occurs. This might be explained by a possible strong negative interaction among silver ions when the Ag_2O contents increase. However, this idea is not acceptable in view of the fact that in the Ag_2O-B_2O_3 binary system Ag_2O behaves much like Na_2O. In molten oxide systems, it has been proposed that the strength of the base can be expressed in terms of the oxygen ion activity. This is an idea similar to that of the hydrogen ion concentration in aqueous solutions. An acid-base equilibrium was porposed by Lux and Flood to result from the following reaction;

$$\text{Base} = \text{Acid} + O^= \tag{8}$$

Therefore, the higher the oxygen ion activity in a melt, the stronger its basicity. The basicity of the melts will change with the relative contents of Ag_2O and Na_2O due to the difference in the oxygen-ion activity of the two components, even in the melts with an equal composition of total basic oxides. Thus Fig. 7 shows that the oxygen-ion activity of Ag-borate is smaller than that of Na-Borate. If Ag_2O and Na_2O dissociate perfectly in the melts, the following relations hold;

$$a_{Ag_2O} = a_{Ag^+}^2 \cdot a_{O^=} = N_{Ag^+}^2 \cdot \gamma_{Ag^+}^2 \cdot a_{O^=} = N_{Ag^+}^2 \cdot A \tag{9}$$

Here the A quantity is defined by;

$$A = a_{Ag_2O}/N_{Ag_2O} = \gamma_{Ag^+}^2 \, a_{O^=} \tag{10}$$

where;

$$N_{Ag^+} = N_{Ag_2O}/(N_{Ag_2O} + N_{Na_2O}) \tag{11}$$

Figure 8 shows the relation between A and N_{Ag} at a constant composition of basic oxides. From Fig. 8 it may be seen that, even at a constant basic oxide composition, A increases with the increase in the proportion of Na_2O to Ag_2O. If

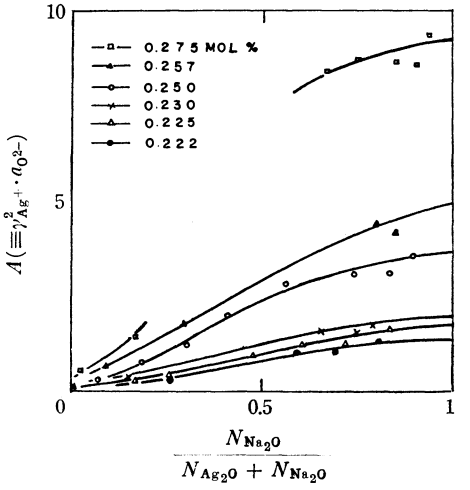

Fig. 8. The quantity $A(=\gamma_{Ag^+}^2 \cdot a_{O^{2-}})$ as a function of $N_{Na}(=N_{Na_2O}/(N_{Ag_2O}+N_{Na_2O})$ at constant basic oxide concentration at 850°C.

it is assumed that γ_{Ag^+} is independent of the composition. A becomes proportional to $a_{O^=}$. γ_{Ag^+} will be assumed to be constant at the lower limits

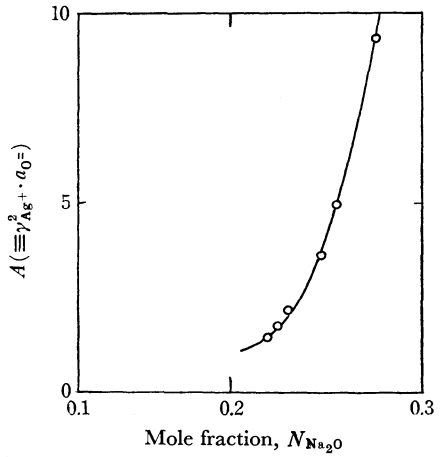

Fig. 9. The oxygen ion activity in arbitrary unit in Na_2O-B_2O_3 binary melt at 850°C.

of the Ag_2O concentration, even though this assumption is not acceptable over the complete range of the compositions. Therefore, the value of A extraporated to $N_{Ag_2O}=0$ indicates a quantity proportional to the activity of oxygen ions in the Na_2O-B_2O_3 binary system. This relation is plotted in Fig. 9. The oxygen-ion activity increases rapidly with an increese in the Na_2O contents.

(3) **Metallic Silver.** It has long been considered that the silver in a glass is in a metallic colloidal state, and that this causes the coloration. However, the fact that the definite solubility exists as a function of the temperature, the oxygen pressure, and the Na_2O content shows that the silver mostly dissolves in a glass as Ag_2O as far as a thermodynamic treatment is concerned. Another piece of evidence to support this view is the electric conductivity of this system, which will be reported on a separate paper. The electrical conductance of Ag-borate is similar to that of Na-borate in its absolute value as well as in its activation energy.

The color of this glass is yellow; it turns red with the increase in the Ag_2O content. This coloration is probably due to the covalent character of the Ag–O bond.

BULLETIN OF THE CHEMICAL SOCIETY OF JAPAN VOL. 42 681—685 (1969)

Electrical Conductance of Molten Salt Systems: Ag_2O-B_2O_3 and Ag_2O-Na_2O-B_2O_3

Hiroshi KODAMA, Yoshihiro KIMURA, Toshio YOKOKAWA and Kichizo NIWA

Department of Chemistry, Faculty of Science, Hokkaido University, Sapporo

(Received August 8, 1968)

The electrical resistance of the Ag_2O-B_2O_3 and Ag_2O-Na_2O-B_2O_3 systems has been measured in the approximate temperature range from 750 to 1000°C. The equivalent conductance at 900°C and the activation energy of the conductance for the Ag_2O-B_2O_3 system were calculated. They were then compared with the corresponding values of alkali borate melts. The results led to the conclusion that the silver ion is not bound to the oxygen ion in the melt, but behaves like Li^+, Na^+, and K^+ which are known to be monovalent network modifiers and to be free to move in the melt.

Various physico-chemical properties of alkali borate melts have been reported by several groups of workers.[1] Electrical conductance, one of them, has been measured by a few investigators.[2,3] Silver oxide, as well as alkali metal oxide, dissolves into molten boron trioxide at high temperatures to form a silver borate melt.[4,5] Therefore, it seemed of interest to study the silver borate melt from the kinetic point of view. Thus, a comparison of the electrical conductance of the melts, of both Ag_2O-B_2O_3 and Ag_2O-Na_2O-B_2O_3, with that of alkali borate melt will provide important knowledge concerning the conduction mechanism in the silver-containing melt. Two possible, contradictory

1) J. D. Mackenzie, "Modern Aspect of the Vitreous State," Vol. 1, 2, 3, Butterworths, London (1964).

2) J. Kinumaki and K. Sasaki, *Repts. Research Insts. Tohoku Univ., Ser. A*, **3**, 285 (1951).

3) L. Shartsis, W. Capps and S. Spinner, *J. Am. Ceram. Soc.*, **36**, 319 (1953).

4) G. M. Willis and F. L. Hennessy, *J. Metal*, 1367 (1953).

5) T. Maekawa, T. Yokokawa and K. Niwa, This Bulletin, **42**, 677 (1969).

results may be anticipated; One might expect to obtain data analogous to that on the conduction of the binary alkali borate melt, because the silver ion, which is considered to be the sole electric carrier, has the same charge as the sodium ion, and, moreover, their ionic radii are nearly the same. On the other hand, the silver ion might display, notwithstanding these similarities, quite a different behavior since the silver ion has a stronger covalency than the alkali metal ion.

This report will present data on the electrical conductance of the binary melt, Ag_2O-B_2O_3 as well as the ternary melt, Ag_2O-Na_2O-B_2O_3, in the approximate temperature range from 750 to 1000°C. Further, the equivalent conductance will be estimated for the binary melt with the aid of the density data.[6]

Experimental

Materials and Reagent. The silver borate melt was prepared in the following way. Anhydrous boron trioxide of a guaranteed reagent grade was put into a platinum crucible (34 mm in diameter and 38 mm high) and heated in an air atmosphere at about 1000°C for long enough for the water to be driven off from the oxide melt. Then, $AgNO_3$ of a guaranteed reagent grade was added in its melt. Silver nitrate decomposed with NO_2 fumes and reacted immediately with the molten boron trioxide to produce the silver borate. The melt of the required Ag_2O content was stirred sufficiently with a silver rod in order to achieve a uniform composition. The ternary melt, Ag_2O-Na_2O-B_2O_3, was made by adding $AgNO_3$ to the Na_2O-B_2O_3 binary melt which had been prepared by melting the required amounts of alkali carbonate and anhydrous boron trioxide in a platinum crucible. The samples were analyzed for B_2O_3 content by titration with a 0.1N NaOH aqueous solution and for Ag_2O content by titration with a KSCN solution.

Apparatus and Procedure. A diagramatic sketch of the apparatus for measuring electrical resistance is given in Fig. 1. A dipping electrode arrangement was used to measure the melt resistance. It consisted of a pair of parallel Pt wires. An alternating current signal was supplied to a Kohlrausch Bridge (Yokogawa Electric Works type K-1) by means of an Audio Frequency Oscillator (Trio Corporation Type AG-10). The output of the resistance bridge was fed into the vertical input of a cathoderay oscillograph (Daimatsu Electric Company Type LBO 3A). 20 mm of the electrodes were dipped into the melt in the cell, the immersion depth being fixed precisely by a device in the electrodes' connection with a cathetometer. Since the resistance was shown to be independent of the frequency between 1 and 10 kc, the measurements were made at 10 kc. The determination of the cell constant was made at 25°C by means of a 0.1N KCl solution.

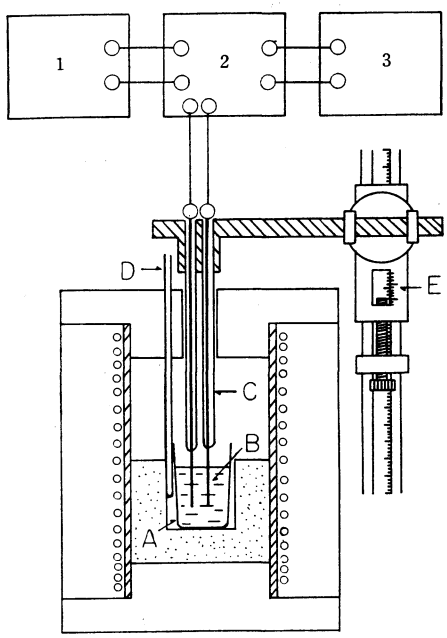

Fig. 1. Apparatus for measurement of electrical resistance.
A: Pt-crucible, B: Pt-electrode, C: electrode-holder (quartz tube), D: thermocouple-sheath, E: cathetometer.
1: Oscillograph, 2: Kohlrausch Bridge, 3: Oscillator

Results and Discussion

Binary Liquid, Ag_2O-B_2O_3. For each melt, the electrical resistance values were obtained at about every 20°C. Figure 2 shows a plot of the logarithmic specific conductance (κ) against the functions of the reciprocal absolute temperature

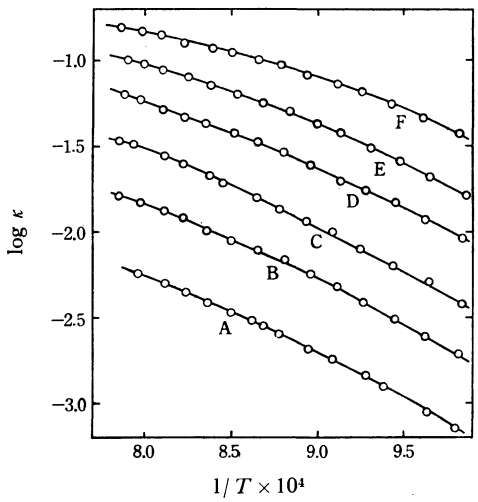

Fig. 2. Relation between specific conductance and temperature for silver borate melts.
A: 3.49 mol% Ag_2O B: 5.32 mol% Ag_2O
C: 8.35 mol% Ag_2O D: 11.74 mol% Ag_2O
E: 15.86 mol% Ag_2O F: 20.44 mol% Ag_2O

6) Y. Ono *et al.*, Unpublished.

$(1/T)$. These conductance-temperature relations are analogous to those of the sodium borate melt in magnitude as well as in the temperature coefficient, which had been measured by Shartsis.[3] Since an alkali borate melt is an ionic conductor, the present results suggest that the silver borate melt is also an ionic conductor.

It is clear in Fig. 2 that the graphs can be represented by curves rather than straight lines. A recent investigation[7] has established that the temperature dependence of the conductance at low temperatures can be described rather accurately by a modified form of the Arrhenius equation;

$$\Lambda = AT^{-1/2} \exp\left(\frac{-k}{T-T_0}\right)$$

where Λ is the equivalent conductance and where A, k, and T_0 are constants. This empirical equation has been supported by the theoretical treatment, too.[8,9] In the present investigation, $\log \Lambda + 1/2 \log T$ was tentatively plotted as a function of $\log (1/T - T_0)$ with various values of T_0. Although this procedure gave a better linear relation than the graphs in Fig. 2, a definite value of T_0 could not be evaluated from the data on the temperature range covered. Thus, the further consideration of T_0 was abandoned in the present study. The activation energy of the conductance was, therefore, estimated with an Arrhenius-type equation for the higher temperature range. The activation energy is shown in Fig. 3 as a function of the silver oxide concentration. In Fig. 3 the decrease in the activation energy with the increase in the amount of silver oxide is interpreted as the effect of the silver oxide's modification of the borate network structure as well as the effect of the change

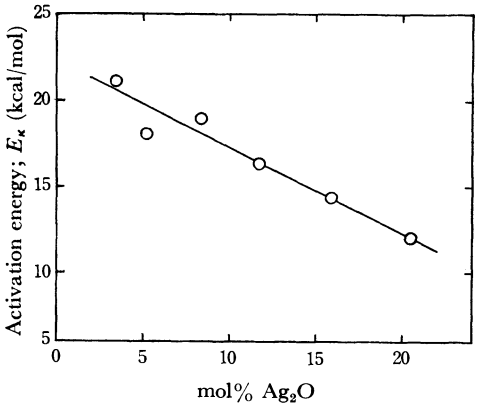

Fig. 3. Relation between activation energy and composition of silver borate melts at 900°C.

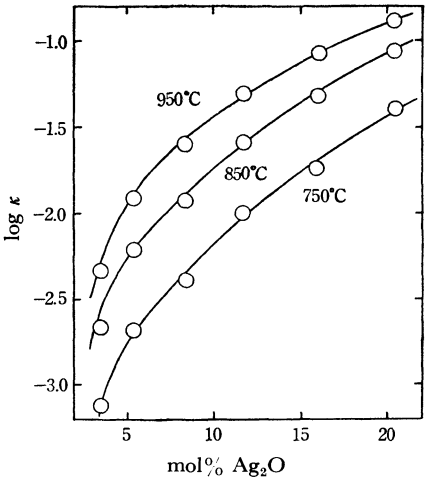

Fig. 4. Relation between specific conductance and composition of silver borate melts.

in thermal expansibility with the change in composition. The value of the activation energy for silver borate and the rate of its decrease are similar to those for alkali metal borates. In Fig. 4 $\log \kappa$ is plotted agnist the silver oxide contents. The conduction-composition isotherms show that the addition of silver oxide increases the conductance of the liquid. An increase similar to this has already been found in the case of alkali metal oxides (see also Fig. 9). For a discussion of the mehcanism of conductance, it is necessary to employ a equivalent conductance which is independent of the ionic concentration per unit of volume. For a system in which the conductance is due to a single ionic species, the equivalent conductance is given by:

$$\Lambda = \frac{100kM}{\rho nzx}$$

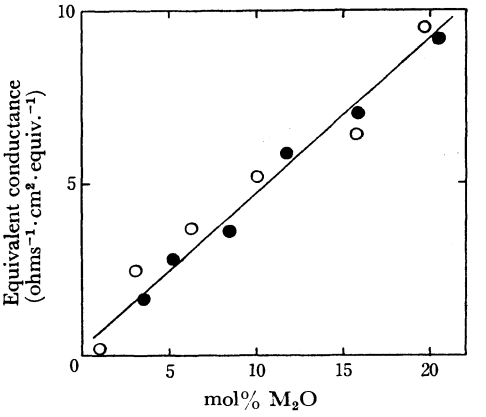

Fig. 5. Equivalent conductance isotherms for silver borate melt and sodium borate melt as functions of composition at 900°C.
● M=Ag ○ M=Na

7) C. A. Angell, *J. Phys. Chem.*, **70**, 2793 (1966).
8) G. Adam and J. Gibbs, *J. Chem. Phys.*, **43**, 139 (1965).
9) P. B. Macedo and T. A. Litovitz, *ibid.*, **42**, 245 (1964).

where ρ is the density of the melt; n, the wt% of the melta oxide; M, the molecular weight of M_xO_y; z, the charge on M, and x, the number of M atoms per molecule of M_xO_y. In the present case, since only the silver ion contributes to the conductance, this equation is valid. Making use of the density data of Ono *et al.*,[6] the equivalent conductance was then calculated from the above equation.

Figure 5 shows the equivalent conductance isotherm for 900°C as a function of the concentration of silver oxide (with the concentrations ranging from zero to 20 mol%), as well as the corresponding value of sodium borate, determined by Shartsis *et al.* From this agreement of the concentration dependence of the two borates, it is evident that the gradual increase in the equivalent conductance with the increase in the silver oxide contents can be interpreted in terms of the "network-destruction effect."

Ternary Melts; Ag_2O-Na_2O-B_2O_3. As has been stated previously, silver oxide was added to

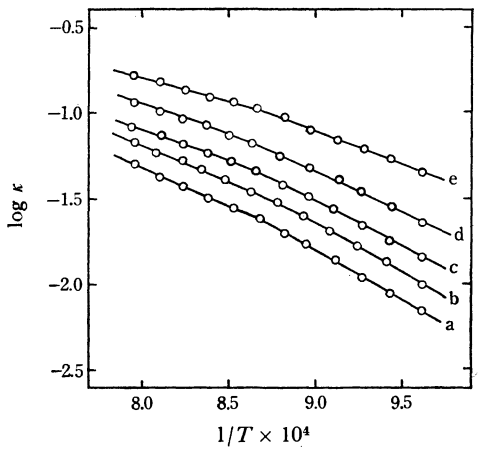

Fig. 6. Relation between specific conductance and temperature for Ag_2O-Na_2O-B_2O_3 system (series A, having a molar ratio $Na_2O/B_2O_3=3.97$).
a : 7.03 mol% Ag_2O b : 9.02 mol% Ag_2O
c : 10.42 mol% Ag_2O d : 13.42 mol% Ag_2O
e : 17.24 mol% Ag_2O

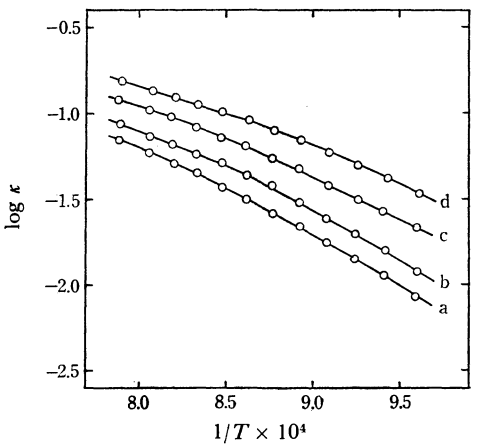

Fig. 7. Relation between specific conductance and temperature for Ag_2O-Na_2O-B_2O_3 system (series B, having molar ratio $Na_2O/B_2O_3=7.91$).
a : 2.63 mol% Ag_2O b : 5.33 mol% Ag_2O
c : 8.90 mol% Ag_2O d : 11.61 mol% Ag_2O

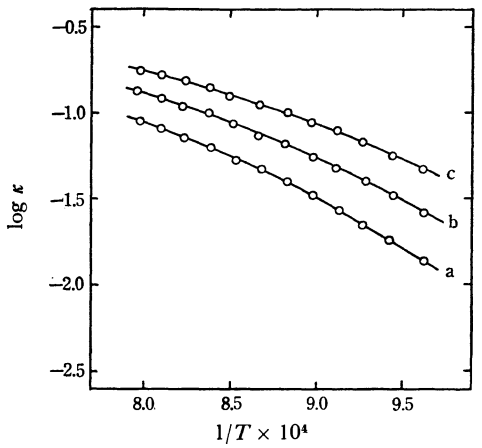

Fig. 8. Relation between specific conductance and temperature for Ag_2O-Na_2O-B_2O_3 system (series C, having a molar ratio $Na_2O/B_2O_3=18.96$).
a : 1.95 mol% Ag_2O b : 6.07 mol% Ag_2O
c : 10.66 mol% Ag_2O

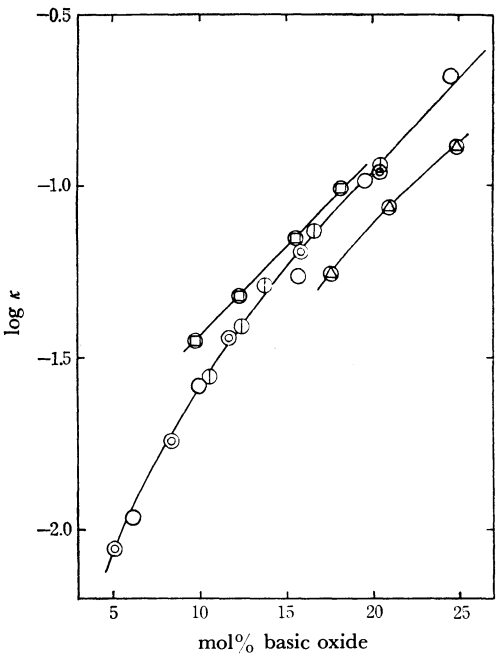

Fig. 9. Relation between specific conductance and basic oxide compositions, which are given by mol% of Ag_2O or Na_2O for the binary borate and by their sum for the ternary systems.
○, Na_2O–B_2O_3; ◎, Ag_2O–B_2O_3; ①, series A; ⊡, series B; ⊿, series C

a Na_2O-B_2O_3 binary system, and the resistance was then measured for the region from 750 to 1000°C. This procedure was repeated several times. The starting compositions for binary systems were 3.97 (Series A), 7.91 (Series B), and 18.96 (Series C) at the molar ratio of Na_2O/B_2O_3. Plots of log κ against the functions of $1/T$ are shown in Figs. 6, 7, and 8. In Fig. 9 the log κ isotherms of both binary and ternary systems at 900°C are plotted as a function of the sum of the mole percents of Na_2O and Ag_2O. This figure shows that the data of Series A coincide with those of Na_2O-B_2O_3 or Ag_2O-B_2O_3, while Series B and C show some deviation. Considering the effect of the molar volume, this shows that the conductance is nearly additive with respect to silver and sodium ions. It may be concluded from the results of this conductance investigation that, when silver oxide dissolves in borate melt, silver oxide dissociated almost perfectly in silver- and oxygen-ions; that is, silver oxide acts as a network modifier of boric oxide and the silver ion shows a conductance behavior very similar to that of potassium, sodium, and lithium ions.

BULLETIN OF THE CHEMICAL SOCIETY OF JAPAN VOL. 42 685—689 (1969)

Zeeman Effect of Phosphorescence. II. Intensity Considerations on Pyrazine Phosphorescence

Tohru AZUMI, Mitsuo ITO and Saburo NAGAKURA

The Institute for Solid State Physics, The University of Tokyo, Roppongi, Minato-ku, Tokyo

(Received August 10, 1968)

The Zeeman splitting of pyrazine phosphorescence is observed. The amount of splitting is 1.4 cm^{-1} under the magnetic field of 15 kilogauss. This magnitude is just what one expects for the free spin, which means that the zero-field splitting parameters are small compared with the observed splitting. On the assumption of random orientations of the pyrazine molecules in the sample, the phosphorescence intensities from the three split subcomponents are expected to be in the ratio of $13g_1 : 16g_0 : 13g_{-1}$ where g's represent populations. This expectation is roughly manifested in the experimental observation. Finally, the theoretical calculation of the zero-field splitting parameters, D and E, is attempted, and the results are interpreted in terms of the experimental data.

Phosphorescence of organic molecules was interpreted by Terenin[1] and by Lewis and Kasha[2] to be the multiplicity forbidden emission; namely, for majority of organic molecules where the ground state is singlet, Jablonski's "phosphorescent state"[3] was identified as the triplet state. Since then, considerable efforts have been devoted to date to substantiate the mechanism suggested by these authors. It is at present the usual notion that the triplet nature of the phosphorescent state is fairly well established. However, it seems not unworthy to recall these efforts and to judge how much the usually accepted notion is founded.

Probably, the most direct works reported so far along this line are the measurements of paramagnetic susceptibility[4] in earlier days and the recent ESR measurements of the excited triplet state.[5] These works have revealed that the triplet state is produced by irradiation of solid solution of organic molecules by ultraviolet light and that it decays in a manner nearly identical to phosphorescence. The triplet state is considered simultaneously the phosphorescent state because of the *approximate* identity of the decay mode. Other evidence which shows the spin forbidden character of the phosphorescence comes from the heavy-atom effect, both intramolecular and intermolecular: McClure[6] found that the

1) A. Terenin, *Acta Physicochem. USSR*, **18**, 210 (1943).

2) G. N. Lewis and M. Kasha, *J. Am. Chem. Soc.*, **66**, 2100 (1944).

3) A. Jablonski, *Z. Physik*, **94**, 38 (1935).

4) G. N. Lewis and M. Calvin, *J. Am. Chem. Soc.*, **67**, 1232 (1945).

5) C. A. Hutchison and B. W. Mangum, *J. Chem. Phys.*, **29**, 952 (1958); J. H. van der Waals and M. S. de Groot, *Mol. Phys.*, **2**, 333 (1959); W. A. Yager, E. Wasserman and K. M. R. Cramer, *J. Chem. Phys.*, **37**, 1148 (1962).

6) D. S. McClure, *J. Chem. Phys.*, **17**, 905 (1949).

introduction of heavy atoms such as halogen and sulfur to hydrocarbon molecules decreases the phosphorescence lifetime considerably, and that this lifetime decrease is quantitatively explained by the increase of spin-orbit coupling in the presence of heavy atom. The decrease of the phosphorescence lifetime in the heavy atom containing solvents is also interpreted by McGlynn[7] in a similar manner.

As is seen in the two examples cited above, the phosphorescence *lifetime* data have frequently been presented as evidence supporting the identity of the phosphorescent state to the triplet state. However, conclusions based on lifetime data are not unique, and can not be served as a conclusive evidence. For, it is not certain whether the phosphorescent state is simultaneously the triplet state itself or is a certain kinetically rate-limiting state or species produced *via* the triplet state. In view of the long lifetime of the triplet state and its potency to photochemical reactions this suspicion does not seem too unrealistic. A pertinent example is delayed thermal fluorescence,[8] or *alpha*-phosphorescence[9] in the widely used, but somewhat misleading, terminology.[10] This emission consists of thermal excitation to the singlet excited state followed by fluorescence emission. Even though its lifetime is identical to that of the phosphorescence, the emission starts out actually from the singlet state and not from the triplet state.

As described above many experiments carried out to date do not necessarily present conclusive evidence of the triplet nature of the phosphorescence. One might suppose that a Zeeman splitting of the phosphorescence would provide the most unambiguous verification of the triplet nature of the phosphorescent state. This experiment was already suggested by Weisman and Lipkin[16] in 1942; however, no attempts have been reported to date. The lack of such attempts is probably due to the difficulty in observing the phosphorescence spectrum sharp enough to resolve the Zeeman slpitting.

As reported in a previous paper[17] we have succeeded to observe the Zeeman splitting of the phosphorescence of pyrazine crystal. The pyrazine crystal was chosen because it emits fairly intense and quite sharp phosphorescence at 4.2°K. Moreover, for n,π^* triplet excited states of aza-aromatics ESR measurements have never been succeeded, and the phosphorescence measurements under magnetic field are likely to be the only means of identifying the three spin subcomponents. The present paper concerns the detailed analyses of this observation.

Experimental

Pyrazine was purified by repeated (seven times) sublimations in vacuum between room temperature and the dry ice temperature. After the final step of sublimation, the sample was transferred to a quartz cell and the cell was sealed off. All procedures were carried out in vacuum and a contact with air was rigorously avoided.

The emission was taken at 4.2°K in a polycrystalline form. A liquid helium cryostat was placed between the poles of a JEOL JM210 magnet. The magnetic field applied was 15400 gauss. Excitation was effected to the region of $^1B_{2u}(\pi,\pi^*)$ excited state with light from a 500 W high pressure mercury lamp passed through a following filter combination: (1) Toshiba's glass filter UV-D2, (2) 1 cm path of 10^{-3}M K_2CrO_4 aqueous solution, and (3) 1 cm path of $NiSO_4$ and $CoSO_4$ mixed aqueous solution (0.55M and 0.15M, respectively). Because of the geometrical limitations a phosphoroscope was not used. The emission spectrum thus obtained was identical to that obtained with a Becquerel type phosphoroscope and without any filters. The emission was photo graphed on a Kodak 103a-F plate in the second order of a 1200 grooves/mmg rating (blaze at 5000 Å) mounted on a Spex Spectrometer Model 1700-II.

Results

The detailed analyses of the phosphorescence spectrum as well as of the singlet to triplet absorption spectrum will be published elsewhere. Our

7) S. P. McGlynn, M. R. Reynolds, G. W. Daigre and N. Christodouleas, *J. Chem. Phys.*, **66**, 2499 (1962); S. P. McGlynn, J. Daigre and F. J. Smith, *ibid.*, **40**, 507 (1964).

8) S. P. McGlynn, T. Azumi and M. Kinoshita, "The Molecular Spectroscopy of the Triplet State," Prentice Hall, New Jersey (1968).

9) G. N. Lewis, D. Lipkin and T. T. Magel, *J. Am. Chem. Soc.*, **63**, 3005 (1941).

10) There have been numerous terminologies for this process and is sometimes confusing. In earlier days Pringsheim[11] merely called this process "phosphorescence," while Förster[12] called it "high temperature phosphorescence." Terminologies used in recent days are: "*alpha*-phosphorescence" by Lewis, Lipkin, and Magel,[9] "E-type delayed fluorescence" by Parker and Hatchard,[13] "slow fluorescence" by Windsor,[14] and "*alpha*-delayed fluorescence" by Lower and El-Sayed.[15] We use the term "delayed themal fluorescence" following the suggestion of Ref. 8.

11) P. Pringsheim, "Fluorescence and Phosphorescence," Interscience Publishers, New York (1949).

12) Th. Förester, "Fluoreszenz Organischer Verbindungen," Vandenhoeck Ruprecht, Göttingen (1951).

13) C. A. Parker and C. G. Hatchard, *Trans. Faraday Soc.*, **57**, 1894 (1961).

14) M. W. Windsor, "Physics and Chemistry of the Organic Solid State," Vol. 1, Interscience Publishers, New York (1964).

15) S. K. Lower and M. A. El-Sayed, *Chem. Revs.*, **66**, 199 (1966).

16) S. I. Weisman and D. Lipkin, *J. Am. Chem. Soc.*, **64**, 1916 (1942).

17) T. Auzmi, Y. Udagawa, M. Ito and S. Nagakura, *J. Chem. Phys.*, **47**, 4850 (1967).

18) M. Ito and T. Shigeoka, *ibid.*, **44**, 1001 (1966).

interest is now focussed on the four emission lines near the onset of the spectrum which are quite sharp and intense, and are consequently suited to Zeeman effect experiments. The group of these four lines are repeatedly found in progressions of 606, 759, 953, and 1254 cm^{-1}. In view of the agreement of these progressions with the Raman frequencies,[18] the above mentioned four lines are interpreted to be due to pyrazine.[19] The effect of magnetic field on these lines is shown in Fig. 1.

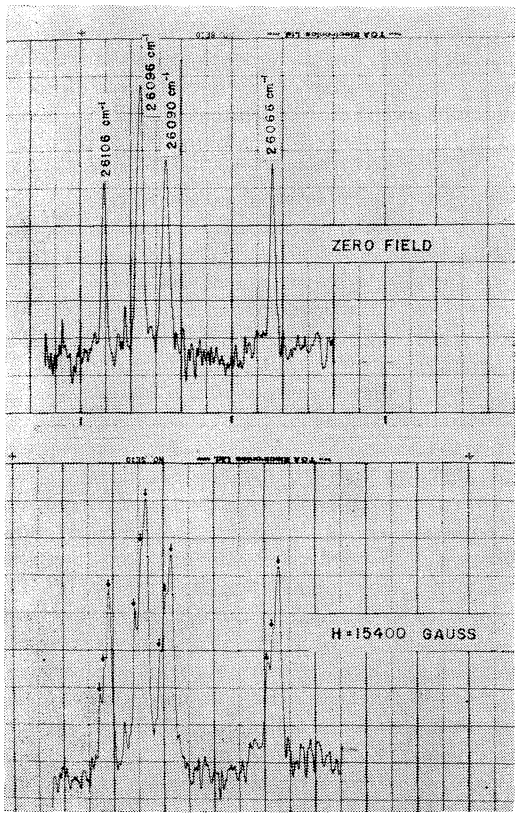

Fig. 1. Zeeman effect of the phosphorescence of pyrazine crystals.

It is immediately clear that magnetic field splitts the emission lines into the three subcomponents, as are indicated by arrows. For all the four lines, separation between two nearest subcomponents is approximately 1.4 cm^{-1}. Also, Fig. 1 clearly indicates that the lower energy subcomponent emitts more intensely than the higher one. This marked difference in intensity might at first seem quite natural in view of the population differences. However, noting that the phosphorescence intensities are determined not only by population but also, more importantly, by the matrix elements connecting the upper and the lower levels, one needs to consider further. The following discussion concerns this point.

Discussion

In analyzing the above results we have, in principle, to consider the effect of magnetic field on the triplet excitons. However, the nature of the triplet excitons is not sufficiently enough understood for pyrazine crystal to warrant detailed analysis. Further, it is believed that the intermolecular interaction is not very significant as compared with the effect of magnetic field. Hence, as a preliminary approach, in the following, we neglect any intermolecular interaction.

Let the lowest triplet state be produced by an excitation of an electron from a molecular orbital ϕ_a to a molecular orbital ϕ_b.[20] We choose the following zeroth order triplet eigenfunctions:

$$\begin{aligned} |T_x\rangle &= 2^{-1/2}(|\bar{\phi}_a\bar{\phi}_b| - |\phi_a\phi_b|) \\ |T_y\rangle &= 2^{-1/2}(|\bar{\phi}_a\bar{\phi}_b| + |\phi_a\phi_b|) \\ |T_z\rangle &= 2^{-1/2}(|\phi_a\bar{\phi}_b| + |\bar{\phi}_a\phi_b|) \end{aligned} \quad (1)$$

The Hamiltonian for Zeeman effect is represented by

$$\mathcal{H} = g\beta\mathrm{H}(lS_x+mS_y+nS_z) + DS_z^2 + E(S_x^2-S_y^2) \quad (2)$$

where l, m, and n are direction cosines of molecular axes, x, y, and z, respectively, with the field direction, and D and E are the zero-field splitting parameters. The displacement of the triplet levels due to (2) should be asymmetric because of the terms involving D and E. However, as pointed out above, within the accuracy of our experiments both the higher and the lower energy subcomponents are displaced from the middle component by 1.4 cm^{-1}. Furthermore, the amount of 1.4 cm^{-1} is just one expects from the term $g\beta$H under the magnetic field of 15400 gauss. It is consequently assumed that the terms involving D and E may be neglected. The eigenvectors $|T_1\rangle$, $|T_0\rangle$, and $|T_{-1}\rangle$ are then easily obtained as

$$\begin{pmatrix} |T_1\rangle \\ |T_0\rangle \\ |T_{-1}\rangle \end{pmatrix} = \begin{pmatrix} \sqrt{\frac{1-l^2}{2}} & \frac{n+ilm}{\sqrt{2(1-l^2)}} & \frac{-(nl+im)}{\sqrt{2(1-l^2)}} \\ l & im & n \\ \sqrt{\frac{1-l^2}{2}} & \frac{n-ilm}{\sqrt{2(1-l^2)}} & \frac{-(nl-im)}{\sqrt{2(1-l^2)}} \end{pmatrix} \begin{pmatrix} |T_x\rangle \\ |T_y\rangle \\ |T_z\rangle \end{pmatrix} \quad (3)$$

For the spin-forbidden phosphorescence to be observed, there must be a singlet state, or states, which may mix with the lowest triplet state by

19) These lines, however, do not coincide with the onset of the singlet to triplet absorption. Detailed examinations have revealed that these are due to the pyrazine molecule at some crystalline defects. T. Auzmi, Y. Nakano and M. Ito, to be published.

20) Here, configuration interactions with other singly excited or with doubly excited configurations are not considered. However, the inclusion or them does not alter the conclusions.

spin-orbit interaction, and further may have a dipole allowed transition to the ground state. Alternatively, one may consider a mechanism in which the singlet ground state mixes with a triplet state by the spin-orbit interaction. However, as far as group theoretical considerations are concerned, these two mechanisms result in identical conclusions; hence, in the following treatment, only the perturbation to the lowest triplet state is considered. Spin-orbit interaction is, in general, expressed as the sum of one-electron and two-electron operators;[21] however, only the former is considered here. Specifically,

$$\mathcal{H}_{so} = \sum_i \xi_i l_i s_i \tag{4}$$

Restricting the spin-orbit interaction to one-electron operator, the singlet state which may mix with the triplet state is only of the type

$$|S\rangle = 2^{-1/2}(|\phi_a\bar{\phi}_c| + |\phi_c\bar{\phi}_a|) \tag{5}$$

here the molecular orbital ϕ_c is chosen so that the transition between $|S\rangle$ and the ground state is dipole-allowed. The matrix elements for the spin-orbit interaction are now readily obtained as follows:

$$\begin{aligned} \langle S|\mathcal{H}_{so}|T_x\rangle &= -(h/4\pi)\xi\langle\phi_c|l_x|\phi_b\rangle \\ \langle S|\mathcal{H}_{so}|T_y\rangle &= i(h/4\pi)\xi\langle\phi_c|l_y|\phi_b\rangle \\ \langle S|\mathcal{H}_{so}|T_z\rangle &= -(h/4\pi)\xi\langle\phi_c|l_z|\phi_b\rangle \end{aligned} \tag{6}$$

In the expansion of the integrals over *molecular orbitals* in (6) in terms of integrals over *atomic orbitals*, we choose to neglect all multi-center integrals other than the one-center terms. With this approximation, and further if the molecular axes are chosen[22] as shown in Fig. 2, it is immediately

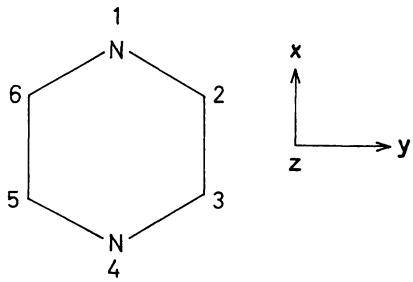

Fig. 2. Molecular axes and the numbering of atoms in pyrazine molecule.

clear that the first and the third integrals in (6) necessarily vanish since the operator l transform like rotation. It is, therefore, concluded that only the $|T_y\rangle$ component is emissive.

Let the phosphorescence intensities from the three subcomponents, $|T_1\rangle$, $|T_0\rangle$, and $|T_{-1}\rangle$ be denoted by I_1, I_0, and I_{-1}. Then from (3)

$$I_1 : I_0 : I_{-1} = [(1-m^2)/2]g_1 : m^2 g_0 : [(1-m^2)/2]g_{-1} \tag{7}$$

where g_1, g_0, and g_{-1} denote the population of the three subcomponents.

The relationship expressed by (7) may be verified using an oriented sample; this is the subject we are presently attempting to work. In the present case, however, the sample is polycrystalline and the above relationship can not be used as it is. In what follows intensity relationship is derived on the assumption that our polycrystalline sample is randomly oriented. The discussion closely follows that of photoselection by Albrecht.[24] Two sets of coordinates are defined, the laboratory-fixed set (a, b, c) and the molecule-fixed set (x, y, z). Assigning these a common origin we then specify the orientation of a molecule in using Eulerian angles θ, ϕ, and ψ. The cosines of the angles between the axes of the two sets of coordinates are denoted by t_{ax}, *etc.*

Let unpolarized exciting light be incident along b axis onto the ac face, and the phosphoresecnce is viewed also along b axis. In our experimental setup the magnetic field is applied along c axis, and therefore $m^2 = t_{cy}^2$. The exciting light is absorbed mainly to $^1B_{2u}(\pi,\pi^*)$ state (y axis). As determined by Krishna and Goodman,[25] phosphorescence is polarized along x axis. In the case of $^1B_{2u}(\pi,\pi^*)$ excitation, the probability that a single molecule at θ, ϕ, and ψ is photoselected is $(t_{ay}^2+t_{cy}^2)/2$, while the probability of viewing the phosphorescence with unpolarized light is $(t_{ax}^2+t_{cx}^2)/2$. Then, the phosphorescence intensities from the three subcomponents are expressed as:

$$\begin{aligned} I_1 : I_0 : I_{-1} = {} & g_1(t_{ay}^2+t_{cy}^2)(t_{ax}^2+t_{cx}^2)(1-\tfrac{1}{2}t_{cy}^2) : \\ & g_0(t_{ay}^2+t_{cy}^2)(t_{ax}^2+t_{cx}^2)t_{cy}^2 : \\ & g_{-1}(t_{ay}^2+t_{cy}^2)(t_{ax}^2+t_{cx}^2)(1-\tfrac{1}{2}t_{cy}^2) \end{aligned} \tag{8}$$

This expression should be integrated over the Eulerian angles

$$\int_0^{\pi}\sin\theta\,d\theta\int_0^{2\pi}d\phi\int_0^{2\pi}d\psi$$

The final results for $^1B_{2u}(\pi,\pi^*)$ excitation is

$$I_1 : I_0 : I_{-1} = 13g_1 : 16g_0 : 13g_{-1} \tag{9}$$

Similarly for $^1B_{1u}(n,\pi^*)$ excitation,

$$I_1 : I_0 : I_{-1} = 8g_1 : 5g_0 : 8g_{-1} \tag{10}$$

If these ratios are calculated with the Boltzmann distribution at 4.2°K for three substates that are 1.4 cm^{-1} apart successively,

21) H. A. Kramers, "Quantum Mechanics," North-Holland Publishing Co., Amsterdam (1957).

22) This choice of axes, which is different from that of Mulliken's recommendation,[23] is convenient since the familiar form of Eq. (2) is consistent with the condition, $D>3E>0$.

23) R. S. Mulliken, *J. Chem. Phys.*, **23**, 1997 (1955).

24) A. C. Albrecht, *J. Mol. Spectry.*, **6**, 84 (1961).

25) V. G. Krishna and L. Goodman, *J. Chem. Phys.*, **36**, 2217 (1961).

$$I_1 : I_0 : I_{-1} = 1.0 : 0.76 : 0.38 \quad \text{for } {}^1B_{2u}(\pi,\pi^*) \text{ excitation} \tag{11}$$

and

$$I_1 : I_0 : I_{-1} = 1.0 : 0.39 : 0.38 \quad \text{for } {}^1B_{1u}(n,\pi^*) \text{ excitation} \tag{12}$$

It is, at this stage, impossible to obtain the accurate intensity ratio from Fig. 1, for there is, to a certain extent, a band overlap, and also the ordinate in the microphotometer tracing is not calibrated to intensity scale. Moreover, our polycrystalline sample can not be expected to be perfectly random. Yet, it is evident from Fig. 1 that the intensity relationship is more in conformity with the ${}^1B_{2u}$-(π,π^*) excitation, which is just we expect from our experimental condition. (*vide supra*).

Conclusions and Remarks

The Zeeman splitting of the phosphorescence was observed for pyrazine and thereby the triplet nature of the phosphorescence is definitely substantiated. The observed intensities of the three phosphorescence subcomponents are roughly in agreement with theoretical predictions. It may also be concluded that the population of the three triplet subcomponents is governed by the Boltzmann distribution at 4.2°K.

In the above discussions we have adopted a number of approximations. In the first place our discussion is confined to the case of the pyrazine solution in which solutes are oriented randomly. Although this treatment is in principle unjustified for polycrystalline sample, it may be justified in rough estimates. More detailed analysis on triplet excitons are the subject of future investigations. We have further neglected the zero-field splitting parameters, D and E. This approximation was based on our experimental data on energy splitting. However, it is not immediately certain if this assumption is also valid when intensities are evaluated in a manner discussed above. Unfortunately, there have not been any ESR observations for pyrazine triplet state, and no data are available, at present, for the zero-field splitting parameters. In view of the lack of data, theoretical evaluations of these values are of interest and are attempted in Appendix.

We wish to express our appreciation to Professor Shigeo Shionoya and his associates for their kindness in letting us use the magnet and the cryostat. We are also grateful to Mr. Yasuo Udagawa for experimental assistance and for stimulating discussions.

Appendix

Calculations of the Zero-Field Splitting Parameters. The purpose of this calculation is to obtain an order of magnitude of D and E values, and hence, semi-empirical approach is adopted.

The molecular orbitals are obtained by the usual Pariser-Parr-Pople method. The coordinates of atoms in pyrazine molecule are taken from the results of an X-ray analysis by Wheatley.[26] Ionization potentials and electron affinities are taken from the table of Pilcher and Skinner.[27] Zero-differential overlap is assumed throughout and penetration integrals are neglected. Two-center repulsion integrals are calculated by uniformly charged sphere model formula given by Pariser and Parr.[28] Core resonance integrals between adjacent atoms are chosen to proportional to overlap integrals, and

$$\beta_{CC} = -2.526\,\text{eV}, \quad \beta_{CN} = -2.162\,\text{eV} \tag{A1}$$

The lowest vacant SCF molecular orbital, π_4^*, thus obtained[29] is

$$\pi_4^* = -0.5349(\chi_1+\chi_4) + 0.3270(\chi_2+\chi_3+\chi_5+\chi_6) \tag{A2}$$

where χ_r is $2p\pi$ atomic orbital on rth atom and where numbering of atoms is shown in Fig. 2.

The lowest triplet state may be successfully expressed by a single configuration of the type (n_-,π_4^*), where n_- represents the minus combination of the two nitrogen nonbonding orbitals. Only configuration which has the same symmetry species with this is of the type (n_+, π_6^*), but because it locates at higher energy, the mixing may well be neglected.

The one-center integrals are computed exactly from the SCF atomic orbitals expanded in Slater orbitals by Clementi and Roothaan[30] by means of analytical formulas given by Higuchi.[31] The final results are[32]

$$D = 0.31\,\text{cm}^{-1} \text{ and } E = 0.01\,\text{cm}^{-1}.$$

The value of D thus obtained is a little larger than the D values for π,π^* triplet states of aromatic hydrocarbons, and is roughly in the same order of magnitude as those of n,π^* ground state obtained experimentally[33,34] and theoretically.[31] It is consequently believed that the calculated values are not much off.[35] If this asertion is correct, the zero-field splitting is not very significantly small compared with the Zeeman splitting, and might be observed in a high resolution work.

---

26) P. J. Wheatley, *Acta Cryst.*, **10**, 182 (1957).

27) G. Pilcher and H. A. Skinner, *J. Inorg. Nucl. Chem.*, **24**, 937 (1962).

28) R. Pariser and R. G. Parr, *J. Chem. Phys.*, **21**, 767 (1953).

29) The computations were carried out with a HITAC 5020 in Computer Center, The University of Tokyo. We are grateful to Mr. Fumihiko Hirota in this laboratory for a computer program for SCF.

30) E. Clementi and C. C. J. Roothaan, *Phys. Rev.*, **127**, 1618 (1962).

31) J. Higuchi, *J. Chem. Phys.*, **38**, 1237 (1963).

32) The use of a single Slater orbital, the exponent being determined by the Slater recipe, in calculating the one-center terms yields: D=0.16 cm^{-1} and E= 0.02 cm^{-1}.

33) A. M. Trozzolo, R. M. Murray and E. Wasserman, *J. Am. Chem. Soc.*, **84**, 4990 (1962).

34) G. Smolinsky, E. Wasserman and W. A. Yager, *J. Am. Chem. Soc.*, **84**, 3220 (1962).

35) Rough estimate given by Sternlicht yields: $D=2E$=0.78. H. Sternlicht, *J. Chem. Phys.*, **38**, 3216 (1963).

BULLETIN OF THE CHEMICAL SOCIETY OF JAPAN VOL. 42 690—693 (1969)

A Spectrophotometric Study of the Uranyl Chelate of 2-(1,8-Dihydroxy-3,6-disulfo-2-naphthylazo)-phenoxyacetic Acid

Yasuaki SHIMOISHI*1

Department of Chemistry, Faculty of Science, Okayama University, Tsushima, Okayama-shi

(Received June 8, 1968)

2-(1,8-Dihydroxy-3,6-disulfo-2-naphthylazo)-phenoxyacetic acid reacts with the uranyl ion in an acidic medium to form a violet chelate. The composition of the chelate is 1:1 in the molar ratio. The apparent stability constants over the pH range from 3.4 to 5.2 and the formation constant of the chelate, are estimated spectrophotometrically at 25°C and an ionic strength of 0.1 by the use of KNO_3. The value of the formation constant was calculated as 1.25×10^{10} from the apparent stability constants.

A new chelating agent, 2-(1,8-dihydroxy-3,6-disulfo-2-naphthylazo)-phenoxyacetic acid [PAC],[1] one that was first introduced by our laboratory, reacts with several metal ions to give its colored chelates. The apparent stability constants of a stable 1 : 1 chelate with the thorium ion, and the use of the chelate in the determination of micro amounts of the fluoride ion, have been reported in previous papers.[2,3]

This paper will describe the properties of the reagent and the reaction between the reagent and the uranyl ion. The acid form of the reagent has three molecules of the water of crystallization; it loses two of them at 135°C, and one at 175°C. Moreover, the anhydride gradually decomposes above 190°C. The reagent forms a 1 : 1 violet chelate with the uranyl ion between the pH values of 3.4 and 5.2; the apparent stability constants, log K', of the chelate over that pH range are measured spectrophotometrically.

In the pH range measured, the reagent exists predominantly as the diprotonated form, considering the value of its acid dissociation constants. From the relation between log K' and pH, however, it was found that the uranyl ion displaces one proton from the reagent in that pH range to form a chelate. This fact shows that the other proton existing between two oxygen atoms of chromotropic acid does not take part in the formation of the chelate.

The formation constant of the chelate is calculated from the values of the apparent stability constants to be 1.25×10^{10} at 25°C and at an ionic strength of 0.1 (KNO_3).

Experimental

Reagent. A pure reagent, 2-(1,8-dihydroxy-3,6-disulfo-2-naphthylazo)-phenoxyacetic acid·$3H_2O$, was obtained in the form of black violet needles after purification from a concentrated hydrochloric acid. The purity was checked by flame analysis and elementary analysis.

Found: C, 39.13; H, 3.65; N, 5.07%. Calcd for $C_{18}H_{20}O_{14}N_2S_2$: C, 39.13; H, 3.73; N, 5.15%.

Uranyl Nitrate Solution. A standard stock solution of uranyl was prepared by dissolving the uranyl nitrate (E. Merck's guaranteed-grade reagent) in deionized distilled water. The standardization of the uranyl solution consisted of the precipitation of the hydrous oxide, followed by ignition to oxide.[4]

Apparatus. *Spectral and pH Measurements.* A Hitachi Model EPS-2 automatic recording spectrophotometer was used for the measurement of the absorption spectra. For quantitative measurements a Hitachi Model 139 spectrophotometer with 1-cm glass cells was used. The pH was measured by using a Towa-Denpa Model HM-8 glass electrode pH meter.

Thermal Analysis. The thermal analysis was carried out using a thermal balance and a differential thermal analyzer, both made by Rigaku Denki.

Procedure. The uranyl chelate solution at various pH values was prepared as follows. Five mililiters of a 2.7×10^{-4}M uranyl nitrate solution and the same volume of a 2.7×10^{-4}M reagent solution were placed in a 50-m*l* volumetric flask; then a 1M potassium nitrate solution was added to maintain the ionic strength at 0.1. The pH of the solution was then adjusted from 3.4 to 5.2 by the addition of nitric acid or of a sodium hydroxide solution. The solution was finally diluted to 50 m*l* with deionized distilled water. After the solutions had been allowed to stand for one hour at

*1 Present address: School for X-ray Technicians, Faculty of Medicine, Okayama University, Oka, Oakayama-shi.

1) K. Tôei, H. Miyata, T. Shibata and S. Miyamura, This Bulletin, **38**, 334 (1965).

2) H. Miyata, *ibid.*, **40**, 1875 (1967).

3) T. Hayami and Y. Shimoishi, *ibid.*, **40**, 1139 (1967).

4) W. W. Scott, "Standard Methods of Chemical Analysis," D. van Nostrand Co., Inc., New York (1939), p. 1022.

25°C, their absorbances for water and the pH of the solutions were measured.

Results and Discussion

The Water of Crystallization of the Reagent. In order to confirm the water of crystallization of the reagent, a thermal analysis was employed. As is shown in Fig. 1, the curve from a thermal

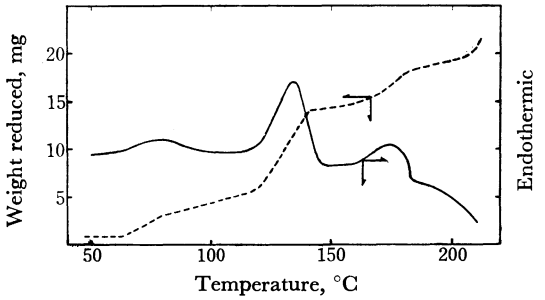

Fig. 1. Thermal analysis of the reagent.
--- Thermal balance curve
—— Differential thermal curve

balance had inflection points in changes in the sample weight over the temperature range between 50 and 210°C. The thermal differential curves showed four changes, at 80, 135, and 175°C corresponding to an endothermic change, and above 190°C, corresponding to a exothermic change. The first endothermic change, at 80°C, corresponds to the elimination of the hydrated water of the reagent, while the second and the third changes denote the elimination of the water of crystallization. However, the reagent after the treatment at 60°C in a vacuum has no inflection points in changes in weight below 180°C. From these results, it was found that the reduced weight of the sample at 135°C and 175°C includes the weight of three moles of water of crystallization. Above 190°C, the reagent gradually decomposes.

The Acid Dissociation Constants. The reagent dissociates in water as follows:

$$H_3R^{2-} \rightleftharpoons H_2R^{3-} + H^+$$
$$H_2R^{3-} \rightleftharpoons HR^{4-} + H^+$$

and

K_{a1} and K_{a2} represent, respectively, the dissociation of the carboxyl group and that of one of the naphtholic hydroxyl groups in the reagent. The values of pK_{a1} and pK_{a2} were found to be 2.99 and 9.76[2] respectively at 25°C and μ= 0.1.

Absorption Spectra. The absorption spectra of the solutions containing uranyl and the reagent in a molar ratio of 1 : 1 are shown in Fig. 2 over the pH range from 3.4 to 5.2. The curves show that the absorbance at 600 mμ becomes higher with an increase in the pH value.

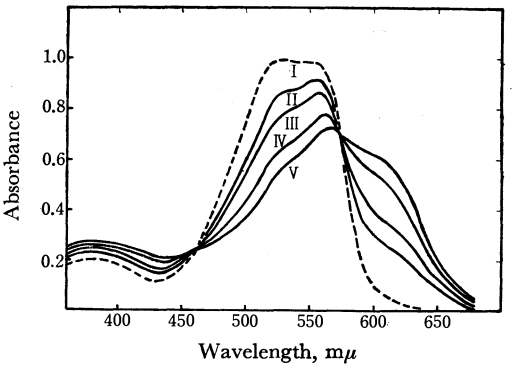

Fig. 2. Absorption spectra of the reagent (broken line) and its uranyl complex (solid line).
I 2.7×10^{-5} reagent solution at pH 5.69
II—V The solution containing uranyl and the reagent (1 : 1) at pH's 3.87, 4.01, 4.52 and 5.02 respectively.

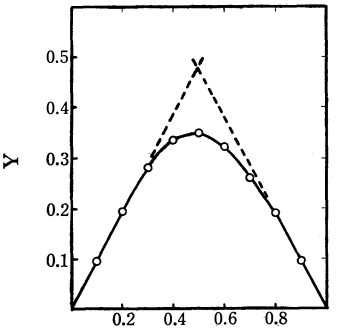

Fig. 3. Continuous variation method.
at 605 mμ, pH 5.2.
Total uranyl and the reagent concn. = 2.7×10^{-5} mol/l

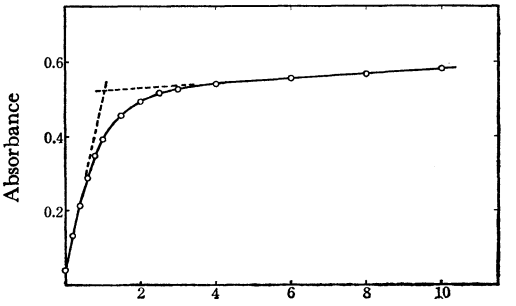

Fig. 4. Mole-ratio method.
at 605 mμ, pH 5.2.
The reagent concn. = 2.7×10^{-5} mol/l
Uranyl concn. varied

The Stability of the Color. The color of the complex reached its maximum within a few minutes after mixing; the absorbance then remained almost constant for at least two hours.

The Composition of the Chelate. Figure 3 shows the results obtained by the continuous variation method, the maximum absorbance of the chelate being obtained at a molar ratio of 1 : 1. The molar-ratio method in Fig. 4 was also employed at pH 5.1 for various uranyl concentrations. The results again clearly indicated the formation of a 1 : 1 chelate.

The Apparent Stability Constants. The apparent stability constant, K', and the acid dissociation constants, K_{a1} and K_{a2}, are expressed as follows:

$$K' = [MHR]/[M][H_3R + H_2R + HR] \quad (1)$$
$$K_{a1} = [H][H_2R]/[H_3R] \quad (2)$$
$$K_{a2} = [H]/[HR]/[H_2R] \quad (3)$$

where the ionic charge was neglected for the sake of convenience. The total concentrations of the reagent and uranyl are given as:

$$C_R = [H_3R] + [H_2R] + [HR] + [MHR] \quad (4)$$
$$C_M = [M] + [MHR] \quad (5)$$

where [M] represents the uranyl ion concentration. Under the experimental conditions studied, at pH values below 6 [HR] can be disregarded, judging from the pK_{a2} value (9.76[1]).

On the other hand, the absorbance of the chelate solution, E, is given by Eq. (6). The uranyl ion gives no absorption at around 605 mμ and $\varepsilon_M[M]$ can be neglected.

$$E = \varepsilon_{H_3R}[H_3R] + \varepsilon_{H_2R}[H_2R] + \varepsilon_{MHR}[MHR] \quad (6)$$

where ε_{H_3R}, ε_{H_2R}, and ε_{MHR} are the molar absorption coefficients of the reagent and the uranyl chelate respectively. The value of ε_{MHR} was calculated from the absorbance of a solution in which an excess amount of uranyl was added to the reagent; the complete formation of the chelate from the reagent could be assumed.

The apparent stability constant was estimated from the following equation by substituting Eqs. (2)—(6) into Eq. (1):

$$K' = [C_R - A]/[C_M - (C_R - A)]A \quad (7)$$

where:

$$A = (1 + K_{a_1}/[H])(E - \varepsilon_{MHR} C_R)/[\varepsilon_{H_3R} + \varepsilon_{H_2R}(K_{a_1}/[H]) - \varepsilon_{MHR}(1 + K_{a_1}/[H])]$$

The constants, log K', estimated from Eq. (7) are listed in Table 1.

The Relation between the Apparent Stability and the Acid Dissociation Constants. Owing to the existence of a strong hydrogen bridge between two oxygen atoms of the chromotropic acid of the reagent, the remaining naphtholic hydroxyl group, corresponding to K_{a3}, does not dissociate under ordinary experimental conditions. Therefore, the reagent may be considered to be a tetrabasic acid; the reaction steps and the probable structure of chelate are:

$$UO_2^{2+} + H_2R^{3-} \rightleftarrows UO_2HR^{2-} + H^+,$$

TABLE 1. APPARENT STABILITY CONSTANT AND STABILITY CONSTANT OF THE URANYL CHELATE (25°C, μ=0.1)

$C_R = C_{UO_2} = 2.70 \times 10^{-5}$ M

Values of constants employed in the calculation.

$K_{a_1} = 1.002 \times 10^{-3}$ $\quad \varepsilon_{H_3R} = 9.778 \times 10^2$

$K_{a_2} = 1.738 \times 10^{-10}$ $\quad \varepsilon_{H_2R} = 1.463 \times 10^3$

$\varepsilon_{MHR} = 2.230 \times 10^4$

pH	E	log K'	log K
3.41	0.090	3.64	10.13
3.48	0.105	3.76	10.16
3.66	0.126	3.94	10.13
3.92	0.175	4.19	10.05
4.11	0.214	4.39	10.07
4.44	0.289	4.73	10.07
4.54	0.310	4.82	10.07
4.85	0.361	5.06	10.09
5.03	0.380	5.16	10.09
5.19	0.394	5.23	10.11

under the present experimental conditions (in the pH range between pK_{a1} and pK_{a2}).

In these experimental conditions (pH values from 3.4 to 5.2), the reagent exists predominantly in the diprotonated form and uranyl ion may displace one proton to form a 1 : 1 chelate.

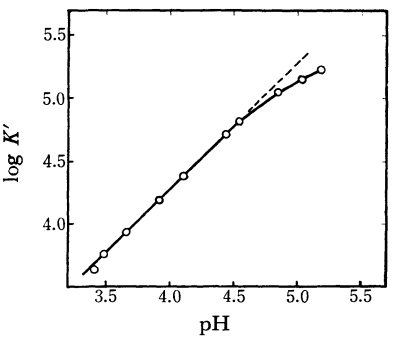

Fig. 5. Relationship between pH and log K. at 25°C, μ = 0.1.

In Fig. 5, the value of log K' is plotted against the pH value. The experimental data obtained are in good agreement with the curve whose slope was 1. This supports the assumption of the above equation, that only a UO_2HR^{2-} chelate is formed. Above pH 4.8, uranyl hydroxide begins to precipitate, so the value of log K' gradually becomes smaller.

The Formation Constant. The formation constant of the uranyl chelate, K, was represented as follows:

$$K = [MHR]/[M][HR] \quad (8)$$
$$K = K'\alpha_M\alpha_H \quad (9)$$

where:

$$\alpha_M = 1 + [OH][M]K^{OH}_{M_2(OH)} + [OH]^2[M]K^{2OH}_{M_2(OH)_2} \quad (10)$$

$$\alpha_H = 1 + K_{a_2}/[H] + K_{a_1}K_{a_2}/[H]^2 \quad (11)$$

As to α_M, the second and third terms of Eq. (10) can be neglected when the pH value is lower than 4.5 ($\alpha_M = 1$), but they cannot be neglected above pH 4.5, as the hydroxo uranyl complexes $M_2(OH)$ and $M_2(OH)_2$ are formed. Therefore, the values of α_M above pH 4.5 were calculated from Eq. (10) using the values of $K^{OH}_{M_2(OH)} = 1.2 \times 10^{10}$ and $K^{2OH}_{M_2(OH)_2} \times 1.0 \times 10^{22}$.[5]

α_H was calculated from Eq. (11), using the values of $K_{a1} = 1.002 \times 10^{-3}$ and $K_{a2} = 1.738 \times 10^{-10}$.[2]

Thus, the values of the formation constant were calculated from Eq. (9). They are also listed in Table 1. The average value of the constant is found to be 1.25×10^{10}.

The author is indebted to Dr. Kyoji Tôei for his guidance, to Dr. Tadashi Hayami for his encouragement, and to Mr. Tatsuo Higashimaya for the measurement of the thermal balance.

5) S. Ahrland, S. Hietanen, L. G. Sillen, *Acta Chem. Scand.*, **9**, 177 (1955).

BULLETIN OF THE CHEMICAL SOCIETY OF JAPAN VOL. 42 693—695 (1969)

Emission Spectrographic Analysis of Metal Solid Samples with Plasma Jet Flame. I. Application of Nitrogen Plasma Flame*1

Kichinosuke HIROKAWA and Hidehiro GOTÔ

The Research Institute for Iron, Steel and Other Metals, Tohoku University, Sendai

(Received June 20, 1968)

A small plasma jet burner for direct excitation of metal solid samples was developed. The optimum operating conditions are as follows; d.c. arc current about 15 A, flow rate of nitrogen tangentially introduced gas about 1.5—2 *l*/min, and that of atomizer gas about 3.5—4 *l*/min. The limit of detection of some elements were determined with solution samples. Satisfactory calibration curves were also obtained for analyses of alloying elements in some solid form alloys.

For the plasma jet flame of emission spectroscopic source,[1] argon or helium gas are used as plasma gas, and a high current of approximately one to a few hundred amperes are employed to excite solution samples. They can be also excited by wall stabilized d. c. arc plasma. Further in usual solution methods, the preparation of standard samples is not necessary. For the solution method, however, the effects of water (solvent), acid, alkali and impurities in the solution on the property of plasma flame must be considered. Therefore, sometimes, the direct excitation of solid sample is desired, and a plasma burner for solid samples was assembled. The small burner developed in our laboratory works with the usual power supply for spectrographic d. c. arc. Nitrogen was employed as tangentially introduced gas and as atomizer gas, so that temperature of plasma flame becomes considerable low, and spectra of low back ground and sharp atom lines are obtained. After the limit of detection for some elements had been studied with solution samples, application of this plasma flame to the analyses of solid metal samples was tried.

Experimental and Results

Instruments. The spectrograph was Shimadzu's Fastie-Ebert type spectrograph GE-340 with a grating of 3000 Å blased. The excitation source was the d. c. arc power supply of Shimadzu High

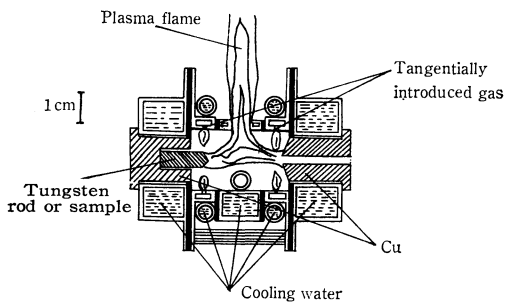

Fig. 1. Cross sectional drawings of plasma burner used.

*1 This paper was read at the 21th Annual Meeting of the Chemical Society of Japan, Osaka, April, 1968.

1) E. Kranz, "XII Colloquium Spectroscopicum Internationale, Exeter," Hilger & Watt, London (1965), p. 574.

Precision Source Unit. The cross sectional drawing of the burner is given in Fig. 1 and photographs of its before and after assembling are shown in Fig. 2.

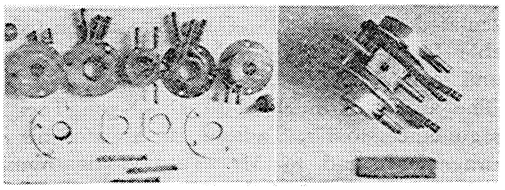

Fig. 2. Plasma burner before and after assembling.

Characteristics of the Plasma Burner and Tests with Solution Sample. The optimum operating conditions of the nitrogen plasma burner must be strictly controlled. An example of good condition is shown in Table 1. With tangentially introduced gas flow rate of about 2 *l*/min, condenser voltage of about 230 V and arc current of 15 A, a stable flame as Fig. 3 was obtained. With a flow rate of below about 1 *l*/min, however, a small flame as Fig. 4 and with a flow rate of over 2.5 *l*/min, a turbulent flame as Fig. 5 was obtained. Then the properties of plasma flame obtained with

TABLE 1. AN EXAMPLE OF OPERATING CONDITION OF PLASMA JET BURNER*

Flow rate of tangentially introduced gas (*l*/min)	Condenser voltage (V)	Arc current (A)	Arc voltage (V)	*Cf.*
1.0	215	16	65	Fig. 4
1.3	215	15	65	
1.5	220	15	74	Fig. 3
1.9	230	15	80	
2.3	228	14	110	Fig. 5

* Primary voltage: 200 V
Flow rate of atomizer gas: 3.5 *l*/min.

Fig. 3. Plasma flame obtained with an optimum condition.

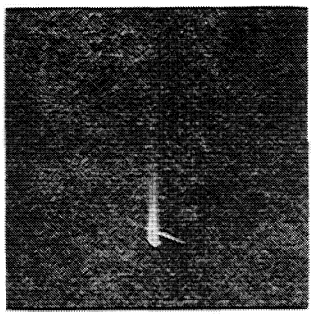

Fig. 4. Short plasma flame obtained with small flow rate of tangentially introduced gas.

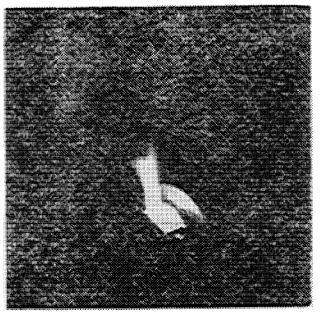

Fig. 5. Turbulent plasma flame obtained with large flow rate of tangentially introduced gas.

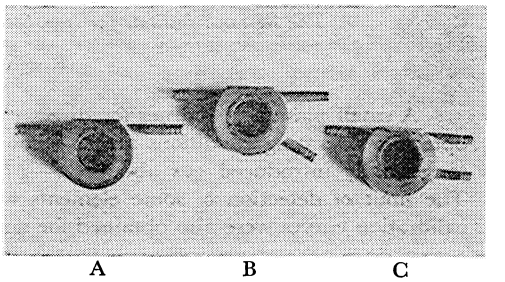

Fig. 6. Three types of center parts of plasma burner examined.

TABLE 2. DETECTION LIMIT OF SOME ELEMENTS IN μg/ml

Center part of burner used	A	B	C
Mode of sample charging	Vertically to the axis of plasma flame	Into center part of plasma core	Into the same direction of tangentially introduced gas
Flow rate of tangentially introduced gas (*l*/min)	1.9	1.5	1.5
Flow rate of atomizer gas (*l*/min)	2.0	4.0	4.0
Al I 3961.5 Å	18	1.4	1.1
Mn I 4031 Å	4.5	1.3	1.2
Fe I 3581 Å	6.7	1.0	1.4
Fe I 3720 Å	2.7	0.95	1.1
Co I 3453.5 Å	4.4	0.92	1.1
Ni I 3414.8 Å	4.5	1.3	1.5
Pb I 4057 Å	11.0	—	1.2

three modes of sample charging (*cf.* Fig. 6 and Table 2) were tested. One tenth normal nitric acid solution of each element in Table 2 was introduced into the plasma flame with an ultrasonic nebulizer, and limits of detection[2] of the elements were studied under optimum conditions as shown in Table 2 in each case. The measurements were carried out by photographic method with slit width of 50 μ and exposure time of 90 sec. Fuji spectrographic photoplates were developed with F.D. 131 at 20°C for 4 min. The discharge conditions were as follows; primary excitation voltage 200 V, condenser voltage 230—240 V, arc current 13—14 A. The coefficient of variation for iron of 0.8 mg/m*l* with Fe I 3720 Å was about 5 per cent. When the solution was introduced into the flame, the flame temperature, measured with the two line method, was around 5500°K.

Application to Metal Solid Samples. In the present experiment, pin-form metal samples were employed as anodes (*cf.* Fig. 1). The operating conditions were the same as the case of c in Table 2, but the flow rate of atomizer gas was 3.5 *l*/min. The time-intensity curve for chromium in chromium steel was obtained as given in Fig. 7-a, and those for chromium, niobium and molybdenum in S-816 alloy (Mn: 1.5, Cr: 20.0, Ni: 20,0, Co: 43.0, Mo: 4.0, W: 4.0, Nb: 4.0, Fe: 3%) were as in Fig. 7-b. After 30 sec pre-discharge,

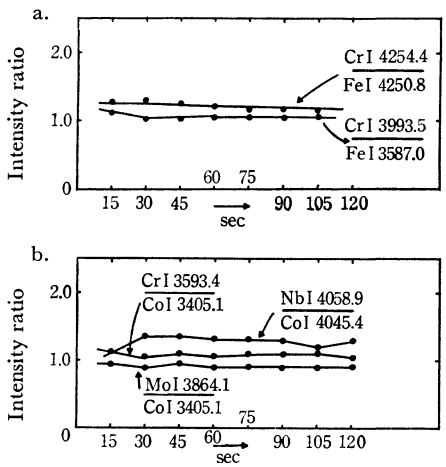

Fig. 7. Time-intensity curve for Cr in Cr-steel (a) and of some elements in S-816 alloy (b).

a nearly constant spectral line intensity ratio was obtained in each case. The calibration curve for chromium in chromium steel was prepared under the following conditions: sample 15 mm in length, 5 mm in diameter, polarity anode, excitation 230 V and 15 A, tangentially introduced gas flow rate 1.5 *l*/min, atomizer gas flow rate 3.5 *l*/min, slit width of the spectrograph 30 μ, pre-discharge time 30 sec and exposure time 10 sec. A calibration curve with good linearity was obtained in a wide concentration range of chromium in steel (Fig. 8).

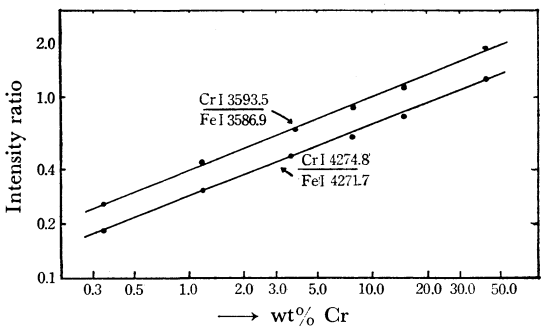

Fig. 8. Calibration curve for Cr in Cr-steel.

In this case the plasma temperature was about 6100°K. For the small amounts of elements in aluminum alloys, time-intensity curves were given as shown in Fig. 9 and the calibration curve for iron in aluminum alloy was given as in Fig. 10.

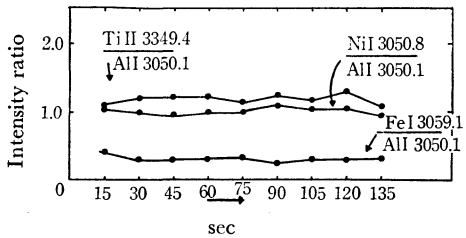

Fig. 9. Time-intensity curve for Ti, Ni and Fe in Al.

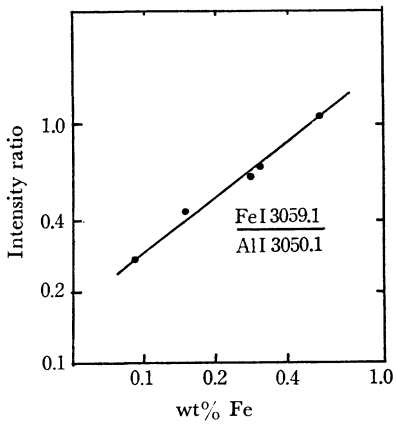

Fig. 10. Calibration curve for Fe in Al.

In this case, however, the operating conditions were the same except the exposure time of 15 sec. In the analyses of aluminum alloys with this nitrogen plasma flame, aluminum reacts with nitrogen and sputters as aluminum nitride, so that the precision for the determination of alloying elements in aluminum alloys is not satisfactory.

2) H. Kaiser, *Spectrochim. Acta*, **3**, 40 (1947).

BULLETIN OF THE CHEMICAL SOCIETY OF JAPAN VOL. 42 696—701 (1969)

Chemical Effects Associated with β-Decay Process. IV. Kinetic Studies of the Chemical Behavior of ^{144}Pr Decayed from the ^{144}Ce(III)-Diethylenetriaminepentaacetate Complex

Takanobu SHIOKAWA and Takashi OMORI

Department of Chemistry, Faculty of Science, Tohoku University, Katahira-cho, Sendai

(Received June 22, 1968)

The chemical behavior of ^{144}Pr as a result of the β^--decay of the ^{144}Ce(III)-diethylenetriaminepentaacetate (^{144}Ce(III)-DTPA) complex was investigated in detail on the basis of the substitution reaction mechanism. The experimental results, represented in terms of the yield of the ^{144}Pr(III)-DTPA complex, were explained quantitatively by the application of Bateman's equation. An increase in the nuclear charge in the β^--decay of the ^{144}Ce(III)-DTPA complex may result in the formation of ^{144}Pr(IV)-DTPA, which would then be reduced to an intermediate complex of ^{144}Pr(III) by an intramolecular electron-transfer. The mechanisms and the rate constants are established for the decomposition of the intermediate leading to the formation of the uncomplexed ion. It was also suggested that the uncomplexed ^{144}Pr(III) ion is produced directly by an exhaustive bond-rupture of the daughter complex ion, without any formation of the intermediate. The ratio of bond-rupture was determined to be 0.25; this value is in accordance with the theoretical value for the formation of the multiply-charged ^{144}Pr ion due to electron shake-off and the internal conversion of γ-rays, followed by the Auger process.

In a previous paper,[1] the chemical behavior of ^{144}Pr produced by the β^--decay of the ^{144}Ce(III)-EDTA complex was investigated on the basis of kinetic considerations. The kinetic treatment indicated that the decomposition rate of an intermediate complex produced as a result of an increase in the nuclear charge in the β^--decay of the ^{144}Ce(III)-EDTA complex, is very important in determining the yield of the ^{144}Pr(III)-EDTA complex.

Recently, Glentworth and Wiseall[2] extensively investigated the chemical behavior of ^{144}Pr in various aminopolycarboxylate complex systems, but the model they proposed does not necessarily account for all of their results.

It appeared necessary to investigate further the stabilization process of ^{144}Pr decayed from the ^{144}Ce(III)-aminopolycarboxylate complexes. As the chelating agent, diethylenetriaminepentaacetic acid (DTPA) was chosen, for with it the lanthanide ions form more stable complexes than with EDTA.[3] In the present paper, the chemical behavior of ^{144}Pr will be discussed in terms of the yield of the ^{144}Pr(III)-DTPA complex, and on the basis of the exchange reaction mechanisms of both $^{144}Ce^{3+}$ and $^{144}Pr^{3+}$ with the cerium(III)-DTPA complex in aqueous solutions.

Experimental

G. R.-grade DTPA was used without further purification. An approximately 10^{-2}M stock solution of Na_3H_2DTPA was prepared by the partial neutralization of the directly-weighed acid with carbonate-free sodium hydroxide. The chelating agent solution was standardized against a standard zinc (II) solution by volumetric titration, using Eriochrome Black T as an indicator.

All the other chemicals and the experimental procedures employed here were substantially the same as those described previously.[1]

Results

Isotopic Exchange Reaction. The exchange rates and mechanisms for the following systems were established:

$$^{144}Ce^{3+} + CeY^{2-} \rightleftharpoons {}^{144}CeY^{2-} + Ce^{3+} \quad (1)$$

$$^{144}Ce^{3+} + PrY^{2-} \rightleftharpoons {}^{144}CeY^{2-} + Pr^{3+} \quad (2)$$

where Y^{5-} indicates the pentavalent DTPA anion. The isotopic exchange rate, R, between the uncomplexed ^{144}Ce(III) ion and the cerium(III)-DTPA complex ion in the pH range of 4.8—5.8 can be expressed as:

$$R = k_{Ce}[H^+]^2[CeY^{2-}] \quad (3)$$

1) T. Shiokawa and T. Omori, This Bulletin, **38**, 1892 (1965).

2) P. Glentworth and B. Wiseall, "Chemical Effects of Nuclear Transformations," Vol. II, IAEA, Vienna (1965), p. 483.

3) L. G. Sillén and A. E. Martell, "Stability Constants of Metal-Ion Complexes," The Chemical Society, London (1964).

Glentworth *et al.*[2] have found that, in the DTPA complex system, the exchange rate is expressed as follows:

$$R = k_{Ce}[H^+]^2[CeY^{2-}] + k'_{Ce}[Ce^{3+}][CeY^{2-}] \quad (3')$$

However, the contribution to the exchange rate of the second term on the right hand of Eq. (3') is fairly small and seems to have little importance in a discussion of the reaction mechanism. Therefore, further study was not made of this effect.

When the equilibrium constant, K, for the reaction expressed by Eq. (2) and k_{Ce} for Eq. (3) are known, the rate constant, k_{Pr}, can be calculated by using the following relation[1]:

$$K = \frac{[Pr^{3+}]_e[^{144}CeY^{2-}]_e}{[PrY^{2-}]_e[^{144}Ce^{3+}]_e} = \frac{k_{Pr}}{k_{Ce}} \quad (4)$$

where the subscript e indicates the chemical equilibrium. The equilibrium constant, K, was determined to be 0.28_7 in the presence of an 0.04M acetate buffer and 0.3M sodium chloride at 25°C. Also, the isotopic exchange rate constants were found to be:

$$k_{Ce} = 7.7_5 \times 10^8\ l^2mol^{-2}min^{-1}$$
$$k_{Pr} = 2.2_3 \times 10^8\ l^2mol^{-2}min^{-1}$$

Substitution Reaction of $^{144}Pr^{3+}$ with the Ce(III)-DTPA Complex Ion. According to the results obtained in the preceding section, the rate of the substitution reaction of $^{144}Pr^{3+}$ and the cerium(III)-DTPA complex may be expressed as:

$$\ln(1-F) = \ln\left\{\frac{[^{144}PrY^{2-}]_e - [^{144}PrY^{2-}]}{[^{144}PrY^{2-}]_e}\right\} = -\left\{k_{Ce}\frac{[CeY^{2-}]}{[Ce^{3+}]} + k_{Pr}\right\}[H^+]^2t \quad (5)$$

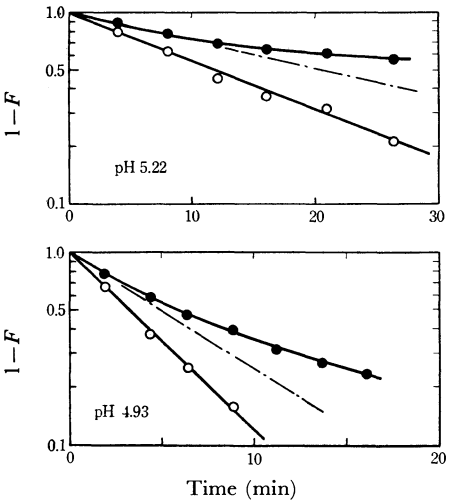

Fig. 1. Relation between $(1-F)$ values and time in the substitution reaction of $^{144}Pr^{3+}$ with cerium-(III)-DTPA complex(I).
25°C; $[Ce^{3+}] = [CeY^{2-}] = 1.00 \times 10^{-4}$ M
●: ^{144}Pr; ○: ^{144}Ce
Dashed lines were calculated by Eq. (5).

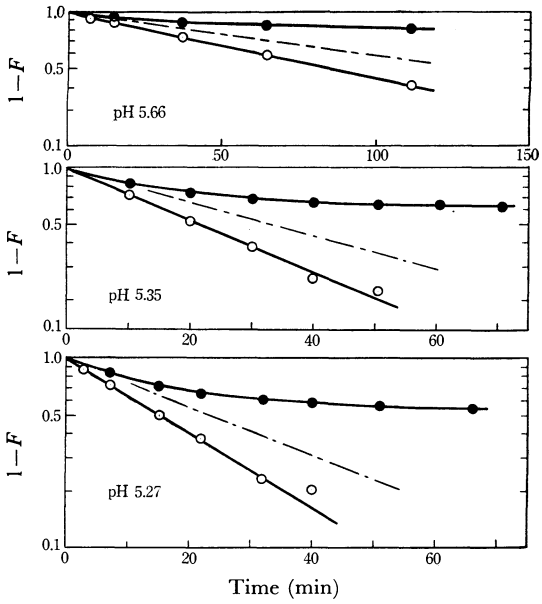

Fig. 2. Relation between $(1-F)$ values and time in the substitution reaction of $^{144}Pr^{3+}$ with cerium-(III)-DTPA complex(II).
25°C; $[Ce^{3+}] = [CeY^{2-}] = 1.00 \times 10^{-4}$ M
●: ^{144}Pr; ○: ^{144}Ce
Dashed lines were calculated by Eq. (5).

where F indicates the fraction of the reaction.

Figures 1 and 2 show plots of the $(1-F)$ values against the reaction time, t. In all cases the discrepancy of $(1-F)$ values from those calculated by Eq. (5) increases with the lapse of time. This is partly to be ascribed to the accumulation of the ^{144}Ce(III)-DTPA complex with the reaction time.

In a previous paper,[1] the chemical behavior of ^{144}Pr was analyzed satisfactorily by using the average life of ^{144}Pr as the reaction time; however, the results obtained at pH 4.8 cannot be rigorously explained by using the average life of ^{144}Pr. It is clearly desirable to introduce a more complete treatment for the stabilization mechanism of ^{144}Pr.

The Chemical Behavior of ^{144}Pr. After a complete equilibration with respect to ^{144}Ce had been attained chemically, the $^{144}PrY^{2-}$-yield, which is defined as the ratio of the γ-activity of the eluate to the total activity, was obtained at 25 and 5°C. As is shown in Figs. 3 and 4, the $^{144}PrY^{2-}$-yield curves have characteristic shapes in comparison with those obtained in the EDTA complex system.[1] The $^{144}PrY^{2-}$-yield at 25°C decreases abruptly up to pH 5.6, while above this point it increases gradually with the pH. At 5°C the minimum point in the $^{144}PrY^{2-}$-yield curve would shift to the lower pH region, and above pH 5.6 the $^{144}PrY^{2-}$-yields are higher than those at 25°C.

It should be noted that, throughout the investigated pH range, the $^{144}PrY^{2-}$-yields obtained

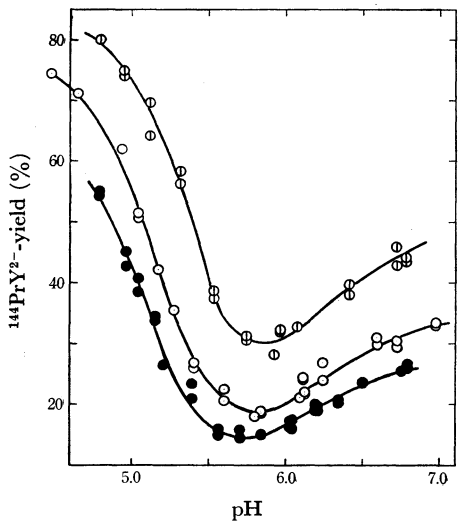

Fig. 3. Dependence of the $^{144}PrY^{2-}$-yield on pH at 25°C.

	$[CeY^{2-}]$	$[Ce^{3+}]$
ⓘ:	2.50×10^{-4} M	1.00×10^{-4} M
○:	1.00×10^{-4} M	1.00×10^{-4} M
●:	1.00×10^{-4} M	1.50×10^{-4} M

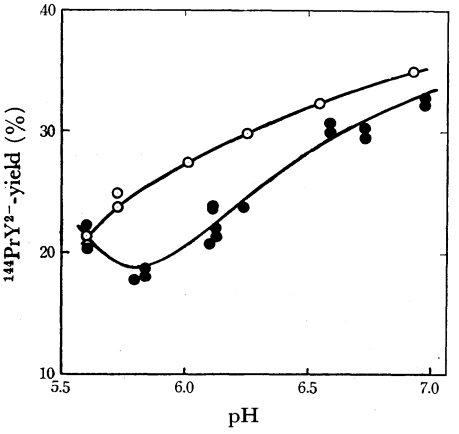

Fig. 4. Dependence of the $^{144}PrY^{2-}$-yield on pH at 5°C.
$[CeY^{2-}] = [Ce^{3+}] = 1.00\times10^{-4}$ M
○: 5°C; ●: 25°C

are less than the equilibrium values to be expected from the relation expressed by Eq. (4).

Chemical Properties of Ce(IV)-DTPA and Its Reduced Complexes. Although a knowledge of the chemical properties of the ^{144}Pr(IV)-DTPA complex is necessary, the higher oxidation potential Pr^{3+} to Pr^{4+}, reported to be −2.86 V,[4] makes this subject difficult to investigate. Thus, some experiments have been carried out on the cerium(IV)-DTPA complex system, on the supposition that the results obtained may be applicable to the ^{144}Pr(IV)-DTPA complex system.

The absorption spectra of the cerium(IV)-DTPA complex and its reduced complex are shown in Fig. 5, together with that of the cerium(III)-DTPA

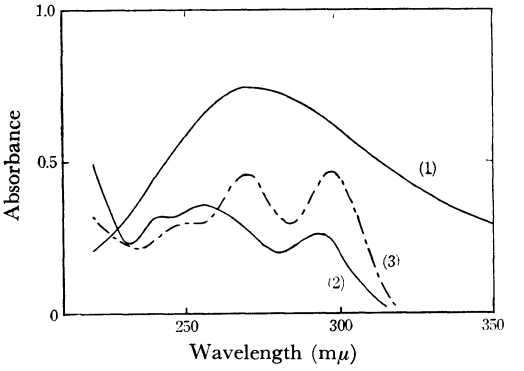

Fig. 5. Absorption spectra of cerium complexes.
(1) Ce(IV)-DTPA (1.00×10^{-4} M)
(2) Ce(III)Z (8.00×10^{-4} M)
(3) Ce(III)-DTPA (8.00×10^{-4} M)

complex. Spectrophotometric investigation showed that the cerium(IV)-DTPA complex is relatively stable in the dark. The decomposition rate is first order with respect to the concentration of the cerium(IV)-DTPA complex. A slight dependence of the rate on the concentration of the hydrogen ion was observed above pH 4.5. The apparent rate constant was obtained as $10^{-2.6}$ min^{-1} at 25°C in the dark.

The cerium(III) complex with an oxidation product of DTPA, Ce(III)Z, is stable in an aqueous solution, but it is converted into the DTPA complex in the presence of excess DTPA. The cerium(III) complex produced by the reduction of the ^{144}Ce-(IV)-DTPA complex is not adsorbed on the cation exchange resin above pH 6, though an abrupt increase in the adsorption coefficient is observed below pH 6, indicating that the formation constant of Ce(III)Z is not very large.

Discussion

Unusual chemical behavior of ^{144}Pr decayed from ^{144}Ce was observed more remarkably in the DTPA complex system than in the EDTA complex system. These results indicate that the chemical behavior of ^{144}Pr in the DTPA complex system cannot be explained sufficiently by the deactivation process proposed in the EDTA complex system.[1]

In order to treat the chemical behavior of ^{144}Pr more strictly, let us re-examine the assumption proposed in the EDTA complex system.

a) Life Time of the ^{144}Pr(IV)-DTPA Complex. The cerium(IV)-DTPA complex is fairly stable compared to the cerium (IV)-EDTA com-

4) L. Eyring, H. Lohr and B. B. Cunningham, *J. Am. Chem. Soc.*, **74**, 1186 (1952).

plex.[5] Although the praseodymium(IV)-DTPA complex must be reduced to a tripositive state because of its thermodynamical instability, it may have a finite life time, with several possibilities.

b) Decomposition Processes of ^{144}Pr(III)Z. Cerium(III)Z is stable in the aqueous solution, but its stability constant may be fairly small compared to the corresponding DTPA complex. The trace amount of ^{144}Pr(III)Z, therefore, apparently decompose when a large excess of the DTPA complex is present.

c) Adsorbability of ^{144}Pr(III)Z on the Cation Exchange Resin. The ^{144}Pr(III)Z which may be produced by an intramolecular electron-transfer of the ^{144}Pr(IV)-DTPA complex still has a negative charge. Consequently, it will not be adsorbed on the resin.

d) Chemical Behavior of ^{144}Pr Decayed from $^{144}Ce^{3+}$. ^{144}Pr will be reduced instantaneously to a tripositive state and exhibits the normal substitution reaction described above.

In view of these considerations, the introduction of Bateman's equation[6] has been undertaken in order to establish rigidly the stabilization process for the ^{144}Pr decayed from ^{144}Ce. The chain mechanism for the stabilization of ^{144}Pr can be expressed as follows:

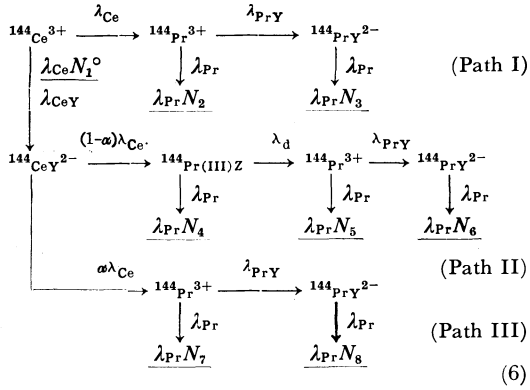

(6)

where λ_{Ce} and λ_{Pr} are the decay constants of ^{144}Ce and ^{144}Pr respectively; λ_{CeY} and λ_{PrY} denote the respective exchange rate constants of $^{144}Ce^{3+}$ and $^{144}Pr^{3+}$ with the cerium(III)-DTPA complex; λ_d, is the decomposition rate constant of an intermediate complex, and α is the ratio of bond-rupture, which is defined as the ratio of the $^{144}Pr^{3+}$ produced directly from the ^{144}Ce(III)-DTPA complex without any formation of the intermediate.

Since the system considered here possesses a radiochemical equilibrium on the whole, the disintegration rate of ^{144}Ce, $\lambda_{Ce}N_-$, is equal to the sum of the disintegration rates of the respective fractions of ^{144}Pr, *i.e.*, to $\sum_{n=2}^{8}\lambda_{Pr}N_n$. For the sake of simplicity, it is assumed that in the introduction of the chain mechanism, the tetrapositive praseodymium produced by the β^--decay is promptly reduced to a tripositive state, and that the intermediate is not transferred to the cationic fraction upon separation. In Eq. (6), therefore, only the $\lambda_{Pr}N_3$, $\lambda_{Pr}N_4$, $\lambda_{Pr}N_6$, and $\lambda_{Pr}N_8$ fractions give any yield of $^{144}PrY^{2-}$. Thus, the solutions of Bateman's equation can be obtained for each fraction as follows:

i) The substitution reaction of the $^{144}Pr^{3+}$ initially present with the cerium(III)-DTPA complex gives the $^{144}PrY^{2-}$. After a lapse of time, t, the fraction of $^{144}PrY^{2-}$ is given by the following equation:

$$(\lambda_{Pr}N_3)_I = \lambda_{Ce}N_1^\circ(e^{-\lambda_{Pr}t} - e^{-(\lambda_{Pr}+\lambda_{PrY})t})\frac{[^{144}PrY^{2-}]_e}{[^{144}Pr^{3+}]_e + [^{144}PrY^{2-}]_e} \tag{7}$$

ii) Fraction of the formation of $^{144}PrY^{2-}$ by path I:

$$(\lambda_{Pr}N_3)_{II} = \lambda_{Ce}N_1^\circ\left(\frac{\lambda_{Pr}}{\lambda_{Pr}+\lambda_{PrY}-\lambda_{CeY}}\right)\left\{e^{-(\lambda_{Pr}+\lambda_{PrY})t} + \frac{\lambda_{PrY}e^{-\lambda_{CeY}t}}{\lambda_{Pr}-\lambda_{CeY}} - \left(\frac{\lambda_{Pr}+\lambda_{PrY}-\lambda_{CeY}}{\lambda_{Pr}-\lambda_{CeY}}\right)e^{-\lambda_{Pr}t}\right\}\frac{[CeY^{2-}]}{[Ce^{3+}]+[CeY^{2-}]}\cdot\frac{[^{144}PrY^{2-}]_e}{[^{144}Pr^{3+}]_e + [^{144}PrY^{2-}]_e} \tag{8}$$

iii) When ^{144}Ce has reached the chemical equilibrium, it exists in the uncomplexed-ion form in the ratio of $[Ce^{3+}]/\{[Ce^{3+}]+[CeY^{2-}]\}$. Consequently, it is necessary to obtain the fraction of the formation of $^{144}PrY^{2-}$ from $^{144}Ce^{3+}$ in path I without regard to the branches to path II and path III.

$$(\lambda_{PI}N_3)_{III} = \lambda_{Ce}N_1^\circ\left(\frac{\lambda_{PrY}}{\lambda_{Pr}+\lambda_{PrY}}\right)\left\{1+\frac{\lambda_{Pr}}{\lambda_{PrY}}e^{-(\lambda_{Pr}+\lambda_{PrY})t} - \left(\frac{\lambda_{Pr}+\lambda_{PrY}}{\lambda_{PrY}}\right)e^{-\lambda_{Pr}t}\right\}\frac{[Ce^{3+}]}{[Ce^{3+}]+[CeY^{2-}]}\cdot\frac{[^{144}PrY^{2-}]_e}{[^{144}Pr^{3+}]_e + [^{144}PrY^{2-}]_e} \tag{9}$$

iv) Contribution of the intermediate complex:

$$\lambda_{Pr}N_4 = (1-\alpha)\lambda_{Ce}N_1^\circ\left\{\frac{\lambda_{Pr}}{\lambda_{Pr}+\lambda_d} - \frac{\lambda_{Pr}e^{-\lambda_{CeY}t}}{\lambda_{Pr}+\lambda_d-\lambda_{CeY}} - \frac{\lambda_{Pr}\lambda_{CeY}e^{-(\lambda_{Pr}+\lambda_d)t}}{(\lambda_{Pr}+\lambda_d)(\lambda_{CeY}-\lambda_{Pr}-\lambda_d)}\right\}\frac{[CeY^{2-}]}{[Ce^{3+}]+[CeY^{2-}]} \tag{10}$$

5) T. R. Bhat and D. Radhamma, *Indian J. Chem.*, **3**, 151 (1965).

6) H. Bateman, *Proc. Cambridge Phil. Soc.*, **15**, 423 (1910).

v) The degree of formation of $^{144}PrY^{2-}$ by path II:

$$\lambda_{Pr}N_6 = (1-a)\lambda_{Ce}N_1^{\circ}\left\{\frac{\lambda_{PrY}\lambda_d}{(\lambda_{Pr}+\lambda_{PrY})(\lambda_{Pr}+\lambda_d)} - \frac{\lambda_{Pr}\lambda_{PrY}\lambda_d e^{-\lambda_{CeY}t}}{(\lambda_{Pr}-\lambda_{CeY})(\lambda_{Pr}+\lambda_d-\lambda_{CeY})(\lambda_{Pr}+\lambda_{PrY}-\lambda_{CeY})}\right.$$
$$+\frac{\lambda_{Pr}\lambda_{PrY}\lambda_{CeY}e^{-(\lambda_{Pr}+\lambda_d)t}}{(\lambda_{Pr}+\lambda_d)(\lambda_{PrY}-\lambda_d)(\lambda_{CeY}-\lambda_{Pr}-\lambda_d)} - \frac{\lambda_{CeY}e^{-\lambda_{Pr}t}}{\lambda_{CeY}-\lambda_{Pr}} + \left.\frac{\lambda_{Pr}\lambda_{CeY}\lambda_d e^{-(\lambda_{Pr}+\lambda_{PrY})t}}{(\lambda_{Pr}+\lambda_{PrY})(\lambda_d-\lambda_{PrY})(\lambda_{CeY}-\lambda_{Pr}-\lambda_{PrY})}\right\}$$
$$\times\frac{[CeY^{2-}]}{[Ce^{3+}]+[CeY^{2-}]}\cdot\frac{[^{144}PrY^{2-}]_e}{[^{144}Pr^{3+}]_e+[^{144}PrY^{2-}]_e} \tag{11}$$

vi) The degree of formation of $^{144}PrY^{2-}$ by path III:

$$\lambda_{Pr}N_8 = a\lambda_{Ce}N_1^{\circ}\left\{\frac{\lambda_{PrY}}{\lambda_{Pr}+\lambda_{PrY}} - \frac{\lambda_{Pr}\lambda_{PrY}e^{-\lambda_{CeY}t}}{(\lambda_{Pr}+\lambda_{PrY}-\lambda_{CeY})(\lambda_{Pr}-\lambda_{CeY})}\right.$$
$$\left.+\frac{\lambda_{Pr}\lambda_{CeY}e^{-(\lambda_{Pr}+\lambda_{PrY})t}}{(\lambda_{CeY}-\lambda_{Pr}-\lambda_{PrY})(\lambda_{Pr}+\lambda_{PrY})} - \frac{\lambda_{CeY}e^{-\lambda_{Pr}t}}{\lambda_{CeY}-\lambda_{Pr}}\right\}\frac{[CeY^{2-}]}{[Ce^{3+}]+[CeY^{2-}]}\cdot\frac{^{144}PrY^{2-}]_e}{[^{144}Pr^{3+}]_e+[^{144}PrY^{2-}]_e} \tag{12}$$

In deriving these equations, λ_{Ce} is very small compared to λ_{Pr}, λ_{CeY}, λ_{PrY}, and λ_d, and could be considered to be effectively zero. After a sufficient lapse of time, when a chemical equlibrium with respect to ^{144}Ce has been attained and when the $^{144}Pr^{3+}$ initially present has decayed out, only the iii, iv, v, and vi fractions contribute to the $^{144}PrY^{2-}$- yield. In addition, the exponential terms in all the equations become, in effective, zero; hence, the $^{144}PrY^{2-}$-yield is given by the following equation:

$$^{144}PrY^{2-}\text{-yield}(\%) = \left\{\frac{\lambda_{PrY}}{\lambda_{Pr}+\lambda_{PrY}}\cdot\frac{[Ce^{3+}]+a[CeY^{2-}]}{[Ce^{3+}]+[CeY^{2-}]}\cdot\frac{[^{144}PrY^{2-}]_e}{[^{144}Pr^{3+}]_e+[^{144}PrY^{2-}]_e}\right.$$
$$+\frac{(1-a)\lambda_{Pr}}{\lambda_{Pr}+\lambda_d}\cdot\frac{[CeY^{2-}]}{[Ce^{3+}]+[CeY^{2-}]}+\frac{(1-a)\lambda_{PrY}\lambda_d}{(\lambda_{Pr}+\lambda_{PrY})(\lambda_{Pr}+\lambda_d)}$$
$$\left.\times\frac{[CeY^{2-}]}{[Ce^{3+}]+[CeY^{2-}]}\cdot\frac{[^{144}PrY^{2-}]_e}{[^{144}Pr^{3+}]_e+[^{144}PrY^{2-}]_e}\right\}\times 100 \tag{13}$$

where the effect of the disintegration of ^{144}Ce can be ignored; by convention, the value for $\lambda_{Ce}N_1^{\circ}$ is taken as unity. Thus, the $^{144}PrY^{2-}$-yield becomes a constant, independent of the reaction time.

In Eq. (13), since the values for λ_{Pr} and λ_{PrY} have already been established, λ_d and α can be obtained by insertion of the experimental values for the $^{144}PrY^{2-}$-yields. It was found that α is a constant independent of the temperature, while λ_d is a function of the concentration of hydrogen ion; that is,

$$\lambda_d = k_d[H^+] \tag{14}$$

The values for the decomposition rate constants of the intermediate, k_d, and for α obtained which best fit the experimental results are given below:

(25°C) $k_d = (5\pm1)\times10^4\ l\,mol^{-1}min^{-1}$
(5°C) $k_d = (2\pm1)\times10^4\ l\,mol^{-1}min^{-1}$
$\alpha = 0.25$

The experimental and calculated values for the $^{144}PrY^{2-}$-yields are compared in Fig. 3, using the following numerical values:

$\lambda_{Pr} = 0.0396$, $\lambda_d = 10^{4.7}[H^+]$, $\alpha = 0.25$ and
$\lambda_{PrY} = \{10^{8.90}[CeY^{2-}]/[Ce^{3+}]+10^{8.36}\}[H^+]^2$

The values for $(1-F)$ in Eq. (5) were also calculated with Eqs. (7)—(12), as shown in Fig. 6. The good agreement between the experimental and calculated values for the $^{144}PrY^{2-}$-yields supports the proposed decomposition process of the intermediate complex, which is substantially analogous to that proposed in the EDTA complex system.[1]

The theoretical considerations of the β^--decay, in addition to the results of the charge spectrometric studies, would predict that a large fraction of the transformation of a β-active atom in a molecule would leave the daughter molecular ion in a little-excited or not in an excited state at all. Furthermore, in the β^--decay of ^{144}Ce, multiple charging resulting from electron shake-off and the internal conversion of γ-rays is of minor importance, and the maximum amount of internal energy

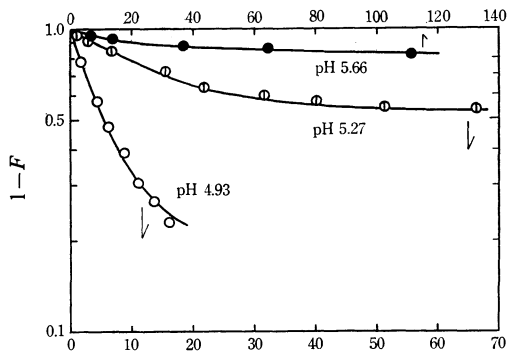

Fig. 6. The $(1-F)$ values calculated by Eqs. (7)—(12).
The circles indicate the experimental values.
The solid curves were calculated by Eqs. (7)—(12).

available from the recoil is less than the bond energies. Thus, the chemical properties of the daughter molecular ion (^{144}Pr(IV)-DTPA complex) play the most important role in determining the fate of the ^{144}Pr decayed from the β^--decay of ^{144}Ce.

Glentworth *et al.*[2] have reported that an attack of the hydrogen ion on the charged excited intermediate molecules ($[^{144}Pr^{IV}Y]^*$) produced by β^--decay results in an enhanced break-up of the daughter complex ion. However, by taking into consideration the facts that the praseodymium(IV) ion is a very powerful oxidizing agent and that inversely, aminopolycarboxylic acids are reducing agents, it is more likely that, before the attack of the hydrogen ion on the ^{144}Pr(IV)-DTPA complex, a unimolecular decomposition resulting from an intramolecular electron-transfer takes place predominantly. Evidence for the reduction by the intramolecular electron-transfer has been found in the cerium(IV)-DTPA complex.

In view of the decomposition mechanism and rate canstants, there is no doubt that the intermediate complex is present. The intramolecular electron-transfer would cause the decarboxylation of a coordinated carboxylate group, and the resultant intermediate complex is possibly less stable than the corresponding parent complex. The value for the rate constant, k_d, is consistent with these considerations.

The multiple charging of the daughter ion resulting from electron shake-off and the internal conversion of γ-rays is of minor importance in the β^--decay of ^{144}Ce, but it cannot be ignored completely.[7] About 18 per cent of ^{144}Pr possesses a charge higher than +5 resulting from the electron shake-off, judging from the results in the β^--decay of ^{133}Xe.[8] Furthermore, the yield of 13 per cent for the multiply-charged species is estimated from the internal conversion coefficient.[9] Consequently, a considerable part of ^{144}Pr might be found in the multiply-charged state, while in about 70 per cent of the events the daughter would be formed in an oxidation state one higher than its parent in the β^--decay of ^{144}Ce. Multiple charging may cause an exhaustive decomposition of the daughter complex, resulting in the liberation of ^{144}Pr in the free-ion form. Indeed, the ratio of the bond rupture of 0.25 corresponds to the extent of the formation of the multiply-charged ^{144}Pr ion.

In addition, in higher pH regions the degree of bond-rupture should give plateau values for the $^{144}PrY^{2-}$-yield curves indepedent of the temperature. As is shown in Fig. 4, both the $^{144}PrY^{2-}$-yields at 25 and 5°C seem to reach the plateau value of 37.5 per cent with an increase in the pH; however, as a result of the hydrolysis of the uncomplexed cerium(III) ion, further investigation could not be carried out.

In conclusion, these considerations lead to a possible stabilization process for the ^{144}Pr decayed from ^{144}Ce, as is illustrated schematically in Fig. 7.

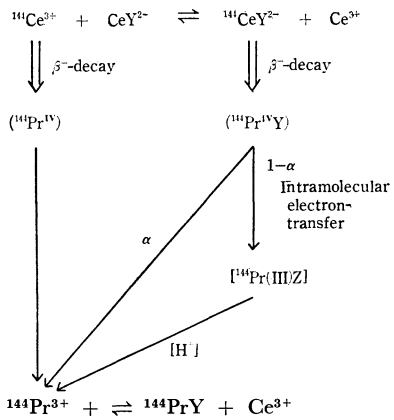

Fig. 7. Stabilization processes of ^{144}Pr produced by β^--decay of ^{144}Ce in the DTPA complex system.

7) T. Shiokawa, H. Kudo and T. Omori, This Bulletin, **42**, 436 (1969).

8) A. H. Snell and F. Pleasonton, *Phys. Rev.*, **111**, 1338 (1958).

9) I. Pullman and P. Axel, *ibid.*, **102**, 1366 (1956).

BULLETIN OF THE CHEMICAL SOCIETY OF JAPAN VOL. 42 702—709 (1969)

Electronic Structure of Tris(1,10-phenanthroline)iron(II) Complex

Tasuku Ito*1 and Nobuyuki Tanaka*2

Department of Chemistry, Faculty of Science, Tohoku University, Katahira-cho, Sendai

and Ichiro Hanazaki and Saburo Nagakura

The Institute of Physical and Chemical Research, Yamato-machi, Saitama
and The Institute forSolid State Physics, The University of Tokyo, Roppongi, Minato-ku, Tokyo

(Received July 13, 1968)

The SCF MO's for the π-electron system of 1,10-phenanthroline have been determined by following the Pariser-Parr-Pople's treatment. For the description of the lower excited states, the configuration interaction among nineteen singly-excited configurations with lower energy has been taken into account. The electronic spectrum of 1,10-phenanthroline has been interpreted on the basis of the results of the theoretical calculation. The SCF MO's for the π-electron system of a coordinated 1,10-phenanthroline in the tris-iron(II) complex have been determined to be self-consistent under the electrostatic potential field of the central metal ion and the other ligand molecules. On the basis of the results for coordinated ligand, the π-electronic structure of tris-(1,10-phenanthroline)iron(II) ion has been investigated from the theoretical point of view. It has been shown that two kinds of the charge-transfer transitions are responsible for an intense absorption band in the visible region, namely electron transfers from the $3d\pi$ orbital of iron to the lowest and the second lowest vacant π MO's of the ligand 1,10-phenanthroline. The discussions have been given on the change of the π–π^* states of 1,10-phenanthroline by the coordination.

The nature of the intensely colored complexes which iron(II) ions form with heterocyclic diamines, such as 2,2′-bipyridine (bipy) and 1,10-phenanthroline (phen), has received much attention and has been extensively studied. The π-bond formation between the central metal atom and the ligand molecules seems to play an important role on the nature of these complexes.[1)]

The π electronic structures of such a type of metal complexes were theoretically treated with success at first on acetylacetonato complexes of metal ions of the first transition series[2)] and then on tris-(2,2′-bipyridine)-[3)] and tris(α-diimine)iron(II)[4)] complexes.

The purpose of the present work is to extend this theoretical treatment to tris(1,10-phenanthroline)-iron(II) ion, $[Fe(phen)_3]^{2+}$. The outline of the calculation will be given, because the method of theoretical treatment was previously described.[2,4)] The integral values characteristic for the present system, however, will be discussed in detail.

Experimental

Materials. Commercial 1,10-phenanthroline monohydrate (Yoneyama Chemical Industries Co., Ltd). was used without further purification. $[Fe(phen)_3]Cl_2 \cdot 7H_2O$[5)] and tris(2,2′-bipyridine)iron(II) perchlorate, $[Fe(bipy)_3](ClO_4)_2$,[6)] were prepared by the standard methods and identified by the chemical analysis.

Measurements. Electronic absorption spectra were measured by a Hitachi recording spectrophotometer Model EPS-3.

SCF MO and Lower Excited States of 1,10-Phenanthroline

The structures of 1,10-phenanthroline and $[Fe(phen)_3]^{2+}$ are shown in Fig. 1 together with the coordinate system used. Also shown are the numbering of the atom and the name of the ligand.

*1 Present address: Department of Chemistry, Faculty of Education, Fukushima University.

*2 Author to whom inquiries should be addressed at the Department of Chemistry, Faculty of Science, Tohoku University, Sendai.

1) D. H. Busch and J. C. Bailar, Jr., *J. Am. Chem. Soc.*, **78**, 1137 (1956).

2) I. Hanazaki, F. Hanazaki and S. Nagakura, *J. Chem. Phys.*, to be published.

3) I. Hanazaki and S. Nagakura, will be reported elsewhere.

4) T. Ito, N. Tanaka, I. Hanazaki and S. Nagakura, This Bulletin, **41**, 365 (1968); *Sci. Repts. Tohoku Univ. Ser. I*, **50**, 168 (1967).

5) K. Madeja and E. König, *J. Inorg. Nucl. Chem.*, **25**, 377 (1963).

6) F. H. Burstall and R. S. Nyholm, *J. Chem. Soc.*, **1952**, 3570.

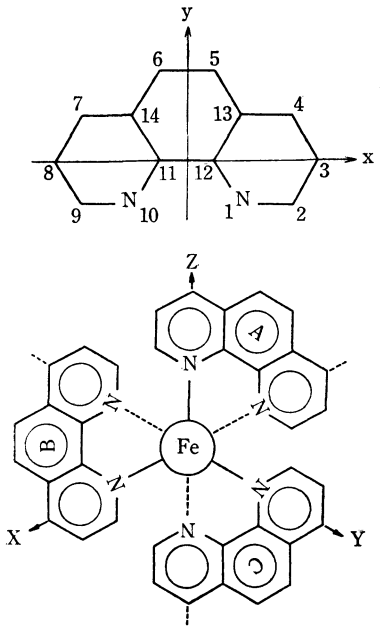

Fig. 1. The geometrical structures of 1,10-phenanthroline and $[Fe(phen)_3]^{2+}$ ion.

Since no experimental work on their geometrical structures has been reported, the bond lengths of all C–C and C–N bonds in the ring were assumed to be 1.39 Å and that of the Fe–N bond was assumed to be 1.97 Å.*3

Free Molecule. The π-electron system of 1,10-phenanthroline, containing 14 π-electrons, was studied by following the Pariser-Parr-Pople's treatment.[8,9]

The valence state ionization potential (I) and the electron affinity (A) were obtained from the table given by Pilcher and Skinner[10] as follows:

$I = 11.22$ eV and $A = 0.62$ eV for carbon
$I = 14.51$ eV and $A = 1.20$ eV for nitrogen

The core resonance integrals between the nearest neighbor AO's (atomic orbitals), β_{ij}, were calculated by the equation,

$$\beta_{ij} = \frac{S_{ij}}{S_0}\beta_0$$

where S_0 (0.248) and β_0 (−2.39 eV) are the overlap integral and the core resonance integral for benzene molecule, respectively. Evaluating the overlap integral, S_{ij}, from the table of Mulliken *et al.*,[11] the core resonance integrals were determined to be

$$\beta_{CN} = -1.879 \text{ eV} \quad \text{and} \quad \beta_{CC} = -2.39 \text{ eV}$$

Table 1 gives the SCF MO's (self-consistent field molecular orbitals) and their orbital energies for 1,10-phenanthroline. The electron densities are given in Table 2. The energies and the wave functions of the lower excited states of 1,10-phenanthroline were obtained by the configuration interaction calculation taking into account nineteen singly-excited configurations with lower energy.

Table 1. SCF MO's and their orbital energies of 1,10-phenanthroline

MO	Symmetry	Orbital energy (eV)	Coefficient*						
			$(\chi_1 \pm \chi_{10})$	$(\chi_2 \pm \chi_9)$	$(\chi_3 \pm \chi_8)$	$(\chi_4 \pm \chi_7)$	$(\chi_5 \pm \chi_6)$	$(\chi_{11} \pm \chi_{12})$	$(\chi_{13} \pm \chi_{14})$
1	b_2	−15.744	0.23463	0.15449	0.17086	0.23452	0.27488	0.35862	0.36431
2	a_2	−14.557	−0.26309	−0.27704	−0.33108	−0.33416	−0.09869	0.17092	−0.30628
3	b_2	−13.305	−0.32703	−0.31232	−0.21055	−0.00639	0.44584	−0.09854	0.20652
4	b_2	−12.452	0.22680	−0.14729	−0.41424	−0.33665	−0.05650	0.37247	0.00336
5	a_2	−12.114	−0.42524	−0.32317	−0.02784	0.27493	0.13640	0.00404	0.34604
6	a_2	−10.890	0.29924	−0.13870	−0.40573	−0.18198	0.14415	−0.29097	0.29672
7	b_2	−10.334	−0.26381	−0.28249	0.00227	0.28025	−0.42221	0.23898	0.19154
8	a_2	− 1.843	−0.24793	0.34863	0.05702	−0.37173	0.36978	0.09243	0.17399
9	b_2	− 1.735	0.38374	−0.11925	−0.30513	0.32295	−0.07944	−0.34154	0.13477
10	b_2	− 0.165	0.19452	−0.42681	0.21735	0.16280	0.16410	0.13016	−0.40297
11	a_2	0.580	0.18580	0.07776	−0.28634	0.27995	0.29351	0.45676	−0.06554
12	a_2	1.102	0.18728	−0.39127	0.34251	−0.12503	0.39047	0.00757	−0.16237
13	b_2	2.047	−0.17852	0.28410	−0.33843	0.34970	0.10474	0.17958	−0.32768
14	a_2	3.817	−0.17129	0.13744	−0.14982	0.21782	0.27483	−0.41094	−0.37078

*) + for b_2, − for a_2

*3 During the development of the present work, the Fe–N bond length was determined to be 1.97 Å by X-ray analysis.[7] Any other detailed description on the bond length and the bond angle was not given.

7) D. H. Templeton, A. Zalkin and T. Ueki, *Acta Cryst.*, **21**, A154 (Supplement) (1966).
8) R. Pariser and R. G. Parr, *J. Chem. Phys.*, **21**, 466, 767 (1953).
9) J. A. Pople, *Proc. Phys. Soc.* (*London*), **A68**, 81 (1955).
10) G. Pilcher and H. A. Skinner, *J. Inorg. Nucl. Chem.*, **24**, 937 (1962).
11) R. S. Mulliken, C. A. Ricke, D. Orloff and H. Orloff, *J. Chem. Phys.*, **17**, 1248 (1949).

Table 2. Electron density of 1,10-phenanthroline

Atom	Electron density
1	1.2453
2	0.8467
3	1.0403
4	0.9346
5	1.0098
12	0.8961
13	1.0273

Table 3. Calculated and observed transition energy (E) and oscillator strength (f) for the absorption spectrum of 1,10-phenanthroline

Calculated			Observed		
Symmetry	E, eV	f	E, eV	ε*1	f*2
A_1	3.83	0.0008	3.85	500	
B_1	4.04	0.10	4.34(sh)*3	~8000	
B_1	4.61	0.73	4.69	27000	0.526
A_1	5.05	0.15			
B_1	5.33	0.30	5.43	40700	0.686
A_1	5.57	0.36			
B_1	5.86	0.90			
A_1	6.19	0.11			

*1 molar extinction coefficient
*2 reported by Favini and Paglia.[12]
*3 shoulder band

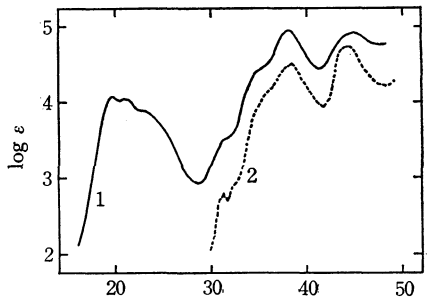

Fig. 2. The absorption spectra of (1) $[Fe(phen)_3]Cl_2 \cdot 7H_2O$ in aqueous solution and (2) 1,10-phenanthroline in ethanol solution.

In Table 3, the predicted π–π^* transition energies and oscillator strengths are presented in comparison with the experimental results. The electronic absorptin spectra of 1,10-phenanthroline and $[Fe(phen)_3]^{2+}$ are shown in Fig. 2. As is seen in Table 3, an agreement between the calculated and the observed results looks satisfactory.

12) G. Favini and E. Paglia, *J. Inorg. Nucl. Chem.*, **8**, 158 (1958).

Badger and Walker[13] found no evidence for n–π^* transition in the absorption spectrum of 1,10-phenanthroline. Their conclusion was based on the absence of solvent effect with variation of solvent polarity. Perkampus and Köhler[14] studied the absorption spectra in methanol and acid methanol solution in detail. They reported that the general structure of the absorption spectrum of phenanthrene was maintained even in 1,10-phenanthroline. Noticeable difference is only the loss of the vibrational structure in the 1,10-phenanthroline spectrum. Consequently, the π–π^* excited states are considered to be similar to these two molecules. Nishimoto and Forster[15] and Skancke[16] gave the assignments for phenanthrene molecule on the basis of the theoretical calculation. Their assignments are similar to the present one for 1,10-phenanthroline. These seem to provide a further support for the present theoretical result.

Coordinated Ligand. The SCF MO's of chelated 1,10-phenanthroline in $[Fe(phen)_3]^{2+}$ were determined, considering not only the field of the 1,10-phenanthroline itself but also the electrostatic potential field due to the central metal atom and the distribution of the π-electrons in the other ligands.*4 Such calculations were carried out for three cases in which the number of the formal charge of iron was assumed to be 0, +1 and +2, since the degree of σ-donation caused by the coordination was not certain. Table 4 shows the result for the case when the formal charge of iron is zero. This was used in the calculation given in this paper. The reason for this is as follows:

Table 4. Calculated transition energy (E) and oscillator strength (f) for coordinated 1,10-phenanthroline in iron complex*

E, eV	Symmetry	f
3.67	A_1	0.009
3.82	B_1	0.004
4.42	B_1	0.853
4.71	A_1	0.327
5.28	B_1	0.109
5.31	A_1	0.109
5.97	B_1	0.153
6.02	A_1	0.186

* Obtained for the case when the formal charge of iron is zero.

13) G. M. Badger and I. S. Walker, *J. Chem. Soc.*, **1956**, 122.
14) H. H. Perkampus and H. Köhler, *Z. Electrochem.*, **64**, 365 (1964).
15) K. Nishimoto and L. S. Forster, *Theoret. Chim. Acta*, **3**, 407 (1965).
16) P. N. Skancke, *Acta Chem. Scand.*, **19**, 401 (1965).
*4 The details of the SCF procedure are referred to Ref. 2.

The energy of an electron transfer from the 3*d* AO of iron to the vacant ligand π-MO depends strongly on the formal charge of iron, in other word, the σ-electron distribution in the metal complex.[17] The parametrization of this energy to the observed value suggested that the formal charge of iron was close to zero.[17] As is seen in Table 4, the spectral feature of a coordinated ligand is not greatly different from that of the free ligand molecule, although the π-electrons of the ligand in the metal complex are conceivably subjected to the strong electrostatic potential field by the central metal atom and the other ligand molecules.

Electronic Structure of Tris(1,10-phenanthroline)iron(II) Complex

The so-called π-electron approximation was adopted in the present study.*5 As component orbitals, π-type 3*d* AO of iron and π-MO's of ligands were taken into account. By placing π-electrons in the appropriate orbitals, the following three types of electronic configurations are obtained: (1) the ground configuration (G), (2) the locally excited configuration (LE) and (3) charge transfer configuration (CT). The π-electronic structure of $[Fe(phen)_3]^{2+}$ was studied by the configuration interaction calculation among these configurations.

Symmetries of Electronic Configurations. The electronic spin of $[Fe(phen)_3]^{2+}$ is singlet in the ground state.[18] Therefore, six *d*-electrons of iron(II) may be in the π-type 3*d* AO, d_{xy}, d_{yz} and d_{zx} with antiparallel spins. The π-electron system of this complex can be divided into four components, namely a π-electron system of iron AO and those of three ligands. The wave function for the ground configuration (G) can be represented as follows:

$$G = |(1\bar{1}2\bar{2}3\bar{3}4\bar{4}5\bar{5}6\bar{6}7\bar{7})^{A}(\ )^{B}(\ )^{C} d_{xy}\bar{d}_{xy}d_{yz}\bar{d}_{yz}d_{zx}\bar{d}_{zx}|$$ *6

where the superscripts A, B and C denote the three coordinated 1,10-phenanthroline molecules shown in Fig. 1. In addition to the ground configuration, thirty six charge transfer (CT) configurations and thirty locally excited (LE) configurations were taken into account, which are given in Table 5. In a way similar to the ground configuration, the wave function for the CT configuration in which an electron is transferred from d_{xy} to φ_8^A is expressed as,

$$CT(d_{xy}\rightarrow\varphi_8^A) = \frac{1}{\sqrt{2}}\left\{\begin{array}{l}|(\ )^{A}(\ )^{B}(\ )^{C}\,8^{A}\bar{d}_{xy}d_{yz}\bar{d}_{yz}d_{zx}\bar{d}_{zx}| \\ +|(\ )^{A}(\ )^{B}(\ )^{C}d_{xy}\bar{8}^{A}d_{yz}\bar{d}_{yz}d_{zx}\bar{d}_{zx}|\end{array}\right\}$$

Table 5. Singly-excited configurations taken into account for the configuration interaction calculation

Configuration	Character	Total number
CT	from $\left\{\begin{array}{l}d_{xy}\\d_{yz}\\d_{zx}\end{array}\right\}$ to $\{\varphi_8, \varphi_9, \varphi_{10}, \varphi_{11}\}$ in each ligand A, B, C	36
LE	lower ten excited states in each ligand A, B, C	30

The wave function for the LE configuration in which only the ligand A is in the μth excited state is expressed as,

$$LE(\Phi_\mu^A) = \sum a_{ij}\frac{1}{\sqrt{2}}\left\{\begin{array}{l}|(\ldots i\bar{j}\ldots)^{A}(\ )^{B}(\ )^{C}d_{xy}\bar{d}_{xy}d_{yz}\bar{d}_{yz}d_{zx}\bar{d}_{zx}| \\ +|(\ldots j\bar{i}\ldots)^{A}(\ )^{B}(\ )^{C}d_{xy}\bar{d}_{xy}d_{yz}\bar{d}_{yz}d_{zx}\bar{d}_{zx})\end{array}\right\}$$

where i and j mean the number of the occupied and the vacant MO of the ground configuration, respectively and a_{ij} means the coefficient of the $(\varphi_i-\varphi_j)$ excited configuration for the μth excited state. The value of a_{ij} was determined in the configuration interaction calculation for coordinated 1,10-phenanthroline. Other CT and LE configurations are expressed in a similar way. The ground, the CT and the LE configurations are classified into the irreducible representations of D_3 symmetry by taking the linear combination, which are given in Table 6.

Configuration Interaction. The matrix elements of the total electronic Hamiltonian between the configurations were calculated in a way similar to the case previously reported.[2,4] The accurate evaluation of the diagonal element of the CT configuration, E_{CT}, is extremely difficult. The difficulty mainly comes from the fact that the value of E_{CT} is very sensitive to the σ-electron distribution, which is uncertain.[2,4] It is also difficult to obtain any reliable value of the π-electron affinity of the coordinated ligand. Therefore, in the present calculation, the diagonal element of the CT configuration with the lowest energy was treated as a parameter. The values of the other CT diagonal elements were determined, considering the difference of the MO's to which an electron is transferred. The diagonal elements of LE configurations are expressed as the sum of the excitation energy in the coordinated 1,10-phenanthroline and the additional term, the latter of which originates from the inter-ligand interaction of the transition dipoles. The interaction energies of the transition dipoles on different ligands, $K'_{\mu\nu}$, were calculated in the same way as previously used.[3] ($K'_{\mu\nu}$ is the interaction energy of the transition dipoles accompanied by the μth transition in ligand A and the νth transition in ligand B). The off-diagonal

17) See Ref. 4.

*5 The applicability of this approximation was already discussed in Ref. 2.

18) F. H. Burstall and R. S. Nyholm, *J. Chem. Soc.*, **1952**, 3570.

*6 The abbreviated notation $(\ )^{\mu}$ means $(1\bar{1}2\bar{2}3\bar{3}4\bar{4}5\bar{5}6\bar{6}7\bar{7})^{\mu}$.

Table 6. Wave functions for G, CT and LE configurations belonging to each irreducible representation of D_3 group*

A_1:

$G=G$

$$CT_1^{A_1}=\frac{1}{\sqrt{6}}\{CT(d_{xy}\to\varphi_8^A)-CT(d_{yz}\to\varphi_8^A)+CT(d_{yz}\to\varphi_8^B)-CT(d_{zx}\to\varphi_8^B)+CT(d_{zx}\to\varphi_8^C)-CT(d_{xy}\to\varphi_8^C)\}$$

$$CT_2^{A_1}=\frac{1}{\sqrt{6}}\{CT(d_{xy}\to\varphi_9^A)+CT(d_{yz}\to\varphi_9^A)+CT(d_{yz}\to\varphi_9^B)+CT(d_{zx}\to\varphi_9^B)+CT(d_{zx}\to\varphi_9^C)+CT(d_{xy}\to\varphi_9^C)\}$$

$$CT_3^{A_1}=\frac{1}{\sqrt{3}}\{CT(d_{zx}\to\varphi_8^A)+CT(d_{yy}\to\varphi_9^B)+CT(d_{yz}\to\varphi_9^C)\}$$

$$CT_4^{A_1}=\frac{1}{\sqrt{6}}\{CT(d_{xy}\to\varphi_{10}^A)-CT(d_{yz}\to\varphi_{10}^A)+CT(d_{yz}\to\varphi_{10}^B)-CT(d_{zx}\to\varphi_{10}^B)+CT(d_{zx}\to\varphi_{10}^C)-CT(d_{xy}\to\varphi_{10}^C)\}$$

$$CT_5^{A_1}=\frac{1}{\sqrt{6}}\{CT(d_{xy}\to\varphi_{11}^A)+CT(d_{yz}\to\varphi_{11}^A)+CT(d_{yz}\to\varphi_{11}^B)+CT(d_{zx}\to\varphi_{11}^B)+CT(d_{zx}\to\varphi_{11}^C)+CT(d_{xy}\to\varphi_{11}^C)\}$$

$$CT_6^{A_1}=\frac{1}{\sqrt{3}}\{CT(d_{zx}\to\varphi_{11}^A)+CT(d_{xy}\to\varphi_{11}^B)+CT(d_{yz}\to\varphi_{11}^C)\}$$

$$LE_1^{A_1}=\frac{1}{\sqrt{3}}\{LE(\Phi_1^A)+LE(\Phi_1^B)+LE(\Phi_1^C)\}$$

$$LE_4^{A_1}=\frac{1}{\sqrt{3}}\{LE(\Phi_4^A)+LE(\Phi_4^B)+LE(\Phi_4^C)\}$$

$$LE_6^{A_1}=\frac{1}{\sqrt{3}}\{LE(\Phi_6^A)+LE(\Phi_6^B)+LE(\Phi_6^C)\}$$

$$LE_8^{A_1}=\frac{1}{\sqrt{3}}\{LE(\Phi_8^A)+LE(\Phi_8^B)+LE(\Phi_8^C)\}$$

$$LE_{10}^{A_1}=\frac{1}{\sqrt{3}}\{LE(\Phi_{10}^A)+LE(\Phi_{10}^B)+LE(\Phi_{10}^C)\}$$

A_2:

$$CT_1^{A_2}=\frac{1}{\sqrt{6}}\{CT(d_{xy}\to\varphi_8^A)+CT(d_{yz}\to\varphi_8^A)+CT(d_{yz}\to\varphi_8^B)+CT(d_{zx}\to\varphi_8^B)+CT(d_{zx}\to\varphi_8^C)+CT(d_{xy}\to\varphi_8^C)\}$$

$$CT_2^{A_2}=\frac{1}{\sqrt{3}}\{CT(d_{zx}\to\varphi_8^A)+CT(d_{xy}\to\varphi_8^B)+CT(d_{yz}\to\varphi_8^C)\}$$

$$CT_3^{A_2}=\frac{1}{\sqrt{6}}\{CT(d_{xy}\to\varphi_9^A)-CT(d_{yz}\to\varphi_9^A)+CT(d_{yz}\to\varphi_9^B)-CT(d_{zx}\to\varphi_9^B)+CT(d_{zx}\to\varphi_9^C)-CT(d_{xy}\to\varphi_9^C)\}$$

$$CT_4^{A_2}=\frac{1}{\sqrt{6}}\{CT(d_{xy}\to\varphi_{10}^A)+CT(d_{yz}\to\varphi_{10}^A)+CT(d_{yz}\to\varphi_{10}^B)+CT(d_{zx}\to\varphi_{10}^B)+CT(d_{zx}\to\varphi_{10}^C)+CT(d_{xy}\to\varphi_{10}^C)\}$$

$$CT_5^{A_2}=\frac{1}{\sqrt{3}}\{CT(d_{zx}\to\varphi_{10}^A)+CT(d_{xy}\to\varphi_{10}^B)+CT(d_{yz}\to\varphi_{10}^C)\}$$

$$CT_6^{A_2}=\frac{1}{\sqrt{6}}\{CT(d_{xy}\to\varphi_{11}^A)-CT(d_{yz}\to\varphi_{11}^A)+CT(d_{yz}\to\varphi_{11}^B)-CT(d_{zx}\to\varphi_{11}^B)+CT(d_{zx}\to\varphi_{11}^C)-CT(d_{xy}\to\varphi_{11}^C)\}$$

$$LE_2^{A_2}=\frac{1}{\sqrt{3}}\{LE(\Phi_2^A)+LE(\Phi_2^B)+LE(\Phi_2^C)\}$$

$$LE_3^{A_2}=\frac{1}{\sqrt{3}}\{LE(\Phi_3^A)+LE(\Phi_3^B)+LE(\Phi_3^C)\}$$

$$LE_5^{A_2}=\frac{1}{\sqrt{3}}\{LE(\Phi_5^A)+LE(\Phi_5^B)+LE(\Phi_5^C)\}$$

$$LE_7^{A_2}=\frac{1}{\sqrt{3}}\{LE(\Phi_7^A)+LE(\Phi_7^B)+LE(\Phi_7^C)\}$$

$$LE_9^{A_2}=\frac{1}{\sqrt{3}}\{LE(\Phi_9^A)+LE(\Phi_9^B)+LE(\Phi_9^C)\}$$

E:

$$CT_1^{E}=\frac{1}{\sqrt{2}}\{CT(d_{xy}\to\varphi_8^B)-CT(d_{yz}\to\varphi_8^C)\}$$

$$CT_2^{E}=\frac{1}{2}\{CT(d_{yz}\to\varphi_8^B)-CT(d_{zx}\to\varphi_8^C)+CT(d_{zx}\to\varphi_8^B)-CT(d_{xy}\to\varphi_8^C)\}$$

$$CT_3^{E}=\frac{1}{\sqrt{12}}\{2CT(d_{xy}\to\varphi_8^A)-CT(d_{yz}\to\varphi_8^B)-CT(d_{zx}\to\varphi_8^C)-2CT(d_{yz}\to\varphi_8^A)+CT(d_{zx}\to\varphi_8^B)+CT(d_{xy}\to\varphi_8^C)\}$$

$$CT_4^{E}=\frac{1}{\sqrt{6}}\{2CT(d_{zx}\to\varphi_9^A)-CT(d_{xy}\to\varphi_9^B)-CT(d_{yz}\to\varphi_9^C)\}$$

$$CT_5^{E}=\frac{1}{\sqrt{12}}\{2CT(d_{xy}\to\varphi_9^A)-CT(d_{yz}\to\varphi_9^B)-CT(d_{zx}\to\varphi_9^C)+2CT(d_{yz}\to\varphi_9^A)-CT(d_{zx}\to\varphi_9^B)-CT(d_{xy}\to\varphi_9^C)\}$$

$$CT_6^{E}=\frac{1}{2}\{CT(d_{yz}\to\varphi_9^B)-CT(d_{zx}\to\varphi_9^C)-CT(d_{zx}\to\varphi_9^B)+CT(d_{xy}\to\varphi_9^C)\}$$

$$CT_7^{E}=\frac{1}{\sqrt{2}}\{CT(d_{xy}\to\varphi_{10}^B)-CT(d_{yz}\to\varphi_{10}^C)\}$$

$$CT_8^{E}=\frac{1}{2}\{CT(d_{yz}\to\varphi_{10}^B)-CT(d_{zx}\to\varphi_{10}^C)+CT(d_{zx}\to\varphi_{10}^B)-CT(d_{xy}\to\varphi_{10}^C)\}$$

$$CT_9^{E}=\frac{1}{\sqrt{12}}\{2CT(d_{xy}\to\varphi_{10}^A)-CT(d_{yz}\to\varphi_{10}^B)-CT(d_{zx}\to\varphi_{10}^C)-2CT(d_{yz}\to\varphi_{10}^A)+CT(d_{zx}\to\varphi_{10}^B)+CT(d_{xy}\to\varphi_{10}^C)\}$$

$$CT_{10}^{E}=\frac{1}{\sqrt{6}}\{2CT(d_{zx}\to\varphi_{11}^A)-CT(d_{xy}\to\varphi_{11}^B)-CT(d_{yz}\to\varphi_{11}^C)\}$$

$$CT_{11}^{E}=\frac{1}{\sqrt{12}}\{2CT(d_{xy}\to\varphi_{11}^A)-CT(d_{yz}\to\varphi_{11}^B)-CT(d_{zx}\to\varphi_{11}^C)+2CT(d_{yz}\to\varphi_{11}^A)-CT(d_{zx}\to\varphi_{11}^B)-CT(d_{xy}\to\varphi_{11}^C)\}$$

$$CT_{12}^{E}=\frac{1}{2}\{CT(d_{yz}\to\varphi_{11}^B)-CT(d_{zx}\to\varphi_{11}^C)-CT(d_{zx}\to\varphi_{11}^B)+CT(d_{xy}\to\varphi_{11}^C)\}$$

$$LE_1^{E}=\frac{1}{\sqrt{6}}\{2LE(\Phi_1^A)-LE(\Phi_1^B)-LE(\Phi_1^C)\}$$

$$LE_2^{E}=\frac{1}{\sqrt{2}}\{LE(\Phi_2^B)-LE(\Phi_2^C)\}$$

$$LE_3^{E}=\frac{1}{\sqrt{2}}\{LE(\Phi_3^B)-LE(\Phi_3^C)\}$$

$$LE_4^{E}=\frac{1}{\sqrt{6}}\{2LE(\Phi_4^A)-LE(\Phi_4^B)-LE(\Phi_4^C)\}$$

$$LE_5^{E}=\frac{1}{\sqrt{2}}\{LE(\Phi_5^B)-LE(\Phi_5^C)\}$$

$$LE_6^{E}=\frac{1}{\sqrt{6}}\{2LE(\Phi_6^A)-LE(\Phi_6^B)-LE(\Phi_6^C)\}$$

$$LE_7^{E}=\frac{1}{\sqrt{2}}\{LE(\Phi_7^B)-LE(\Phi_7^C)\}$$

$$LE_8^{E}=\frac{1}{\sqrt{6}}\{2LE(\Phi_8^A)-LE(\Phi_8^B)-LE(\Phi_8^C)\}$$

$$LE_9^{E}=\frac{1}{\sqrt{2}}\{LE(\Phi_9^B)-LE(\Phi_9^C)\}$$

$$LE_{10}^{E}=\frac{1}{\sqrt{6}}\{2LE(\Phi_{10}^A)-LE(\Phi_{10}^B)-LE(\Phi_{10}^C)\}$$

* The subscript(μ) of LE_μ^s means that LE_μ^s corresponds to the μth excited state of the ligand 1,10-phenanthroline.

matrix elements between G and CT and between CT and LE were accounted for by β, the core resonance integral between the appropriate $3d\pi$ AO of iron and $2p\pi$ AO of nitrogen. It was evaluated with the usual relation,

$$\beta = -S\frac{I_{Fe} + I_N}{2}$$

where S is the overlap integral, and I_{Fe} and I_N are the valence state ionization potentials of iron and nitrogen, respectively. The overlap integral was estimated with the aid of the Slater AO of nitrogen and the double zeta expanded $3d$ AO of iron determined by Richardson *et al.*[19] It was calculated to be 0.090, using the table given by Jaffé.[20] I_{Fe} and I_N are 5.08 eV and 18.68 eV respectively and β amounts to -1.07 eV. In the off-diagonal elements between the CT configurations, only the two-center repulsion integrals of the type $(d_i d_i | \varphi_k^\mu \varphi_l^\mu)$ are taken into account with the point charge approximation. The off-diagonal matrix elements between the LE configurations are expressed in terms of $K'_{\mu\nu}$.

The results obtained by the configuration interaction are shown in Table 7 and the calculated transition energies and the oscillator strengths are given in Table 8 together with the observed ones.

Interpretation of the Electronic Spectrum. From the results given in Tables 7 and 8 it can be concluded that the intense band at the visible region is reasonably assigned to the almost pure CT absorption due to the π-electron migration from the $3d\pi$ AO of iron to the lowest vacant MO, φ_8, of the ligand. The observed absorption bands are too broad and poorly resolved to indicate the components. However, the broad tail appearing

Table 7. Wave functions and energies of the lower electronic states of tris(1,10-phenanthroline)iron(II)ion

	E, eV*1)	Sym.	Wave function*2
W_0	−1.144	A_1	$0.849G-0.449CT_1^{A_1}+0.212CT_2^{A_1}$
W_1	1.429	E	$0.974CT_2^E$
W_2	1.429	A_2	$0.974CT_1^{A_2}$
W_3	1.445	E	$0.974CT_3^E$
W_4	2.564	E	$0.929CT_6^E$
W_5	2.576	A_2	$0.937CT_3^{A_2}$
W_6	2.586	E	$0.941CT_5^E$
W_7	3.696	E	$0.970LE_1^E$
W_8	3.863	E	$0.960LE_2^E$
W_9	3.869	A_2	$0.963LE_2^{A_2}$
W_{10}	4.269	E	$0.695LE_3^E+0.603LE_4^E$
W_{11}	4.458	E	$-0.609LE_3^E+0.529LE_4^E-0.283CT_8^E$ $-0.319CT_9^E$
W_{12}	4.481	A_2	$0.421CT_4^{A_2}-0.611CT_6^{A_2}$ $+0.543LE_3^{A_2}$
W_{13}	4.515	E	$0.834CT_{12}^E+0.223CT_9^E$ $-0.242LE_4^E-0.212LE_5^E$
W_{14}	4.580	A_2	$0.462CT_4^{A_2}+0.703CT_6^{A_2}$ $+0.490LE_3^{A_2}$
W_{15}	4.607	E	$-0.815CT_{11}^E-0.468CT_9^E$
W_{16}	4.648	E	$0.856CT_8^E+0.223CT_{11}^E$ $+0.304CT_{12}^E$
W_{17}	4.733	A_2	$0.726CT_4^{A_2}-0.656LE_3^{A_2}$
W_{18}	4.760	E	$0.204CT_8^E+0.674CT_9^E$ $-0.394CT_{11}^E+0.408LE_4^E$
W_{19}	5.331	E	$0.932LE_6^E-0.212CT_9^E$ $-0.229LE_4^E$
W_{20}	5.429	E	$0.946LE_5^E$
W_{21}	5.438	A_2	$0.952LE_5^{A_2}$
W_{22}	5.948	E	$0.895LE_6^E+0.226LE_7^E$
W_{23}	6.044	E	$0.942LE_7^E-0.246LE_8^E$

*1 The energy of the ground configuration is taken to be zero.
*2 Only main configurations are written.

Table 8. Calculated and observed results on the electronic spectrum of tris (1,10-phenanthroline)iron(II) ion

From W_0 to	Calculated E, eV*2	Calculated f	Observed*1 E, eV*2	Observed*1 log ε
W_1	2.57	0.013		
W_2	2.57	0.030	2.43	4.05
W_3	2.59	0.306		
W_4	3.71	0.231	~2.6*3	~4.0
W_5	3.72	0.321	2.85	3.85
W_6	3.73	0.113		
W_7	4.84	0.064	3.87	3.55
W_8	5.01	0.080		
W_9	5.01	0.059	~4.28*3	~4.4
W_{10}	5.41	1.706		
W_{11}	5.60	0.007		
W_{12}	5.63	0.085		
W_{13}	5.66	0.018	4.66	4.95
W_{14}	5.72	0.129		
W_{15}	5.75	0.005		
W_{16}	5.79	0.265		
W_{17}	5.88	1.074		
W_{18}	5.90	0.378		
W_{19}	6.48	0.162	5.50	4.91
W_{20}	6.57	0.036		
W_{21}	6.58	0.098		
W_{22}	7.09	0.699		
W_{23}	7.19	0.040		

*1 Observed value for tris(1,10-phenanthroline)iron-(II) chloride heptahydrate in aqueous solution.
*3 Transitionn energy.
*3 Shoulder band.

19) J. W. Richardson, W. C. Nieuwport, R. R. Powell and W. F. Edgell, *J. Chem. Phys.*, **36**, 1057 (1962).

20) H. H. Jaffé, *ibid.*, **21**, 258 (1953).

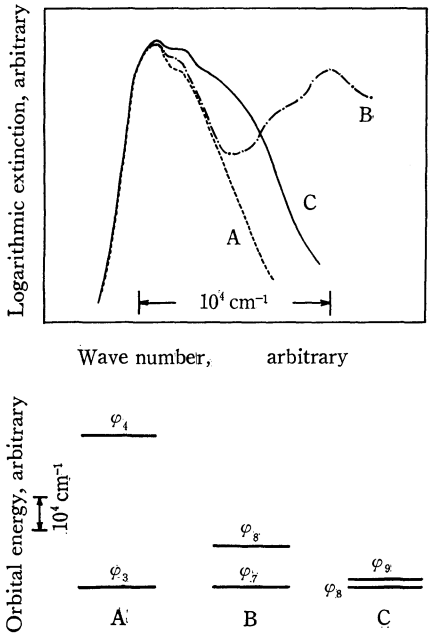

Fig. 3. The CT band shapes and the energies of the two lowest vacant ligand MO's for (A) tris(biacetyl-bis-*N*-methylimine), (B) tris(bipyridine) and (C) tris(phenanthroline) complexes of iron(II).
The spectra are drawn at the appropriate position and on the appropriate intensity scale as the longer wavelength part of the spectrum overlap each other. In the energy level diagram the energy of the lowest vacant orbital is taken equal in order to make easier the comparison of the energy separations between the lowest and the nesxt lowest vacant orbital.

at the shorter wavelength side of this band may be assigned to the overlapping of the second CT band ($3d\pi \rightarrow \varphi_9$). Figure 3 shows the CT band shapes of tris(biacetyl-bis-*N*-methylimine) iron (II), $[Fe(bipy)_3]^{2+}$ and $[Fe(phen)_3]^{2+}$ ions. Also shown are the lowest two vacant MO's for these ligand molecules, to which an electron is transferred. These complexes are considered to have similar electronic structures. As is shown in the previous paper,[4] the CT band of tris(biacetyl-bis-*N*-methylimine)-iron(II) is composed of one kind of CT, namely $3d\pi \rightarrow \varphi_3$. The orbital energy level of the next lowest vacant MO, φ_4, is far from that of φ_3. On the other hand, the lowest two levels are very close to each other for 1,10-phenanthroline and moderately separated for 2,2′-bipyridine. It can be seen in Fig. 3 that the CT band in the visible region is composed of one kind of CT transition for the biacetyl-bis-*N*-methylimine complex, whereas it is composed of two kinds of very closely located CT transitions for the 1,10-phenanthroline complex. It is also clear that such CT bands for the 2,2′-bipyridine complex are resolved into two components.

From great similarities between the absorption curve of 1,10-phenanthroline and $[Fe(phen)_3]^{2+}$, the bands of the complex above 30000 cm^{-1} have been ascribed to the ligand transition beyond reasonable doubt. (See Fig. 2). This was confirmed by the present study. However, it was also shown that the π–π^* transition in the ligand becomes complicated when the ligand is coordinated to form the tris-complex.

One reason for the complication of the absorption bands is that the higher CT bands ($3d\pi \rightarrow \varphi_{10}$ and φ_{11}) appear in the ultraviolet region. They appear in overlap with the LE bands. This situation may be seen clearly in the circular dichroism (CD) spectrum.*7

Since 1,10-phenanthroline has C_{2v} symmetry, the π–π^* transitions should be either y-polarized along the two-fold axis, or x-polarized along the long axis of the ligand molecule (Fig. 1). As has been discussed,[4,21] the x-polarized transition of three ligands in metal complex with D_3 symmetry gives rise to the $A_1 \rightarrow A_2$ and the $A_1 \rightarrow E$ transition while the y-polarized transition gives rise to the $A_1 \rightarrow A_1$ and the $A_1 \rightarrow E$ one, the $A_1 \rightarrow A_1$ transition being symmetrically forbidden. Consequently, if the transition is y-polarized, the resultant electronic absorption spectrum of metal complex consists of single band, which is three times as intense as that of a free 1,10-phenanthroline. On the other hand, if the μth transition is x-polarized, the intensity ratio of the $A_1 \rightarrow E$ to the $A_1 \rightarrow A_2$ transition must be 1 : 2. The transition energy for the $A_1 \rightarrow E$ is smaller by $3K'_{\mu\mu}$ than that for the $A_1 \rightarrow A_2$.*8 Such changes by the coordination take place on each π–π^* level of 1,10-phenanthroline, although the situation becomes more complicated because of the mixing of several LE configurations through the configuration interaction.

The correspondence of the third LE transition theoretically predicted to the observed peak at 37600 cm^{-1} is obvious. The theoretical result shows that this band is intense and x-polarized, which splits into two components in the tris-complex. This splitting is undoubtedly responsible for the observation that an optically active $[Fe(phen)_3]^{2+}$ shows two intense CD peaks with the opposed sign in regard to this absorption band.[22–24]

*7 Two of the present authors (I. H. and S. N.) studied theoretically the CD spectrum of $[Fe(phen)_3]^{2+}$, on the basis of the present results. The details will be reported elsewhere.

21) E. Larsen, S. F. Mason and G. H. Searle, *Acta Chem. Scand.*, **20**, 191 (1966).

*8 $K'_{\mu\mu}$ is the interaction energy of the transition dipoles accompanying the μth transition in ligand A and the same kind of transition in ligand B.

22) A. J. McCaffery and S. F. Mason, *Proc. Chem. Soc.*, **1963**, 211.

23) A. J. McCaffery, S. F. Mason and B. J. Norman, *Proc. Chem. Soc.*, **1964**, 259.

24) J. Hidaka and B. E. Douglas, *Inorg. Chem.*, **3**, 1180 (1964).

The overall agreement of the theoretical transition energy with the observed one is rather poor compared with the case studied previously.[2-4] The calculated transition energies are somewhat high. This discrepancy may probably be attributed to the neglect of the doubly excited LE configurations. In fact, some doubly excited configurations usually appear in a considerably lower energy region, which will possibly bring about a strong effect on the lower singly-excited LE transitions.

The energies of some of the LE transitions are very close to each other in molecules which have the extensive π-electron system such as 1,10-phenanthroline. The transition dipole interaction between the different excited configurations in such a case has an important influence on the electronic states of metal complex through the configuration interaction. The calculated third π-π^* level is close to the fourth one. In metal complex, therefore, the E component of the third level mixes strongly with the fourth one to acquire a larger intensity than what is expected when the configuration interaction is neglected. This fact may partly account for the observation that the lower energy component of the corresponding CD peaks is usually more intense than the higher energy one.*9

Stabilization by the Charge-Delocalization. According to the present theoretical study, $[Fe(phen)_3]^{2+}$ is stabilized by 1.14 eV (26.3 kcal/mol). This stabilization is caused by the mixing of CT configurations into the ground state. In other words, the π-bonding is formed between the iron atom and the ligand molecules. This large stabilization is undoubtedly responsible for the high stability of this complex.

The authors wish to express their thanks to Drs. A. Ishitani and S. Iwata for their kind help in the use of the computer. They also thank the Ministry of Education for the financial support granted for this research.

The numerical calculation was carried out by means of an OKITAC 5090H electronic computer at the Institute of Physical and Chemical Research, a NEAC 2230 at Tohoku University and a HITAC 5020 at the University of Tokyo.

*9 The zero-order rotational strength (R) of these two states is related by the equation, $R(A_2) = -R(E)$.

BULLETIN OF THE CHEMICAL SOCIETY OF JAPAN VOL. 42 709—715 (1969)

Spectroscopy and Magnetic Properties of Nitrosylpentaamminechromium Salts

Hanako KOBAYASHI and Ikuji TSUJIKAWA

Department of Chemistry, Faculty of Science, Kyoto University, Kyoto

and Masayasu MORI and Yoshihisa YAMAMOTO

Faculty of Science, Osaka City University, Osaka

(Received July 23, 1968)

Nitrosylpentaamminechromium chloride (brown), perchlorate (green) and other salts of different colors were studied by visible, IR and ESR spectroscopy and by magnetic susceptibility measurements. The easy shift of visible absorption bands caused by the replacement of outer anions which are responsible for the color difference, ripples observed in one of the absorption bands, *g*-values from ESR and a spin state 1/2 suggested by the susceptibility measurements are interpreted on the basis of a qualitative MO theory for metal nitrosyl complexes.

A series of transition metal nitrosyl compounds $[MNOL_5]X_n$[1] are known, where M is Fe, Mn, Co, Cr or Pt, L is CN, NH_3 or H_2O and X is Cl, Br, NO_3 or ClO_4, *etc.* These compounds are known to be quite peculiar, both from phenomenological and theoretical view points. Most of these compounds have very short M–N distances, for example, 1.63 Å in $[Fe(CN)_5NO]^{2-}$,[2] which

1) W. P. Griffith, J. Lewis and G. Wilkinson, *J. Chem. Soc.*, **1959**, 872; W. P. Griffith, J. Lewis and G. Wilkinson, *ibid.*, **1961**, 775; M. Ardon and J. I. Herman, *ibid.*, **1962**, 507; W. P. Griffith, *ibid.*, **1963**, 3286.

2) P. T. Manoharan and W. C. Hamilton, *Inorg. Chem.*, **2**, 1043 (1963).

shows the existence of π-bonding between M and NO resulting in a strong ligand field around the metal ion. This is confirmed by magnetic measurements, which indicate low spin.

Gray and Ballhausen[3] considered that such a short distance should result in a strong axial destabilization of d orbitals, and gave an orbital energy level scheme for $M(CN)_5NO$ ion based on crystalline field theory. Gray and Bernal[4] treated the same problem by molecular orbital theory, where they considered the formation of strong π-bonds involving the metal nd_{xz} and nd_{yz} orbitals and the nitrosyl $\pi^*(2p_x, 2p_y)$ antibonding orbitals. Recently, a more detailed molecular orbital calculation has been made by Gray, Manoharan, Pearlman and Riley[5] and Manoharan and Gray.[6] Their results suggest that the energy level derived mainly from the nitrosyl antibonding orbital π^* NO (which corresponds to the 4e level of Fig. 4), lies much lower than previously suspected.

Extensive optical spectroscopy[3,6,7] and ESR experiments[8] were carried out on transition metal nitrosyl complexes, especially on $[Fe(CN)_5NO]^{3-}$, $[Cr(CN)_5NO]^{3-}$, $[CrNO(NH_3)_5]^{2+}$ and $[CrNO(H_2O)_5]^{2+}$ ions. Infrared absorptions[9,10] of nitrosyl ligands in these compounds were also well investigated.

It is known that $[CoNO(NH_3)_5]^{2+}$ salts have two isomeric forms, one being the red series and the other the black series. From the rocking frequencies[11] of ammonia ligands in these compounds, it was inferred that the oxidation state of Co ion is three in both the red and black series. The electric conductivity[12] of solutions of these complexes showed that the red series of $CoNO(NH_3)_5$ salts are dimers and the black ones monomers, the latter result being consistent with X-ray data.[13]

Nitrosylpentaamminechromium salts,[14] which are subjects of the present study, also have several characteristic properties. Their color is a function of the outer anions present in the solid state. This suggests considerable effects of outer anions on the ligand field at the metal ion (*cf.* Fig. 1). Thus, solid nitrosylpentaamminechromium chloride, bromide and nitrate are brown, while perchlorate,

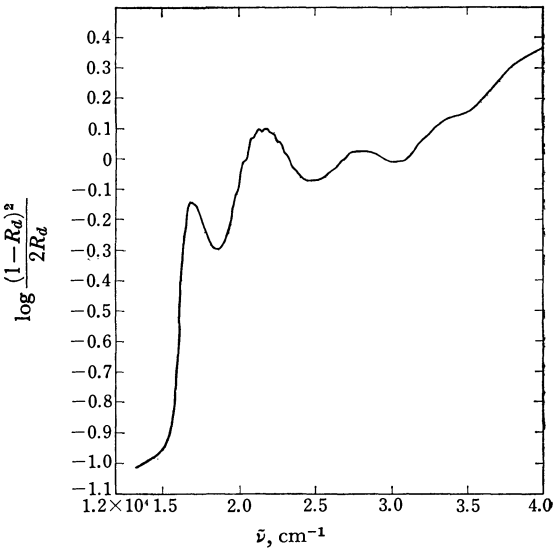

Fig. 1. (a)

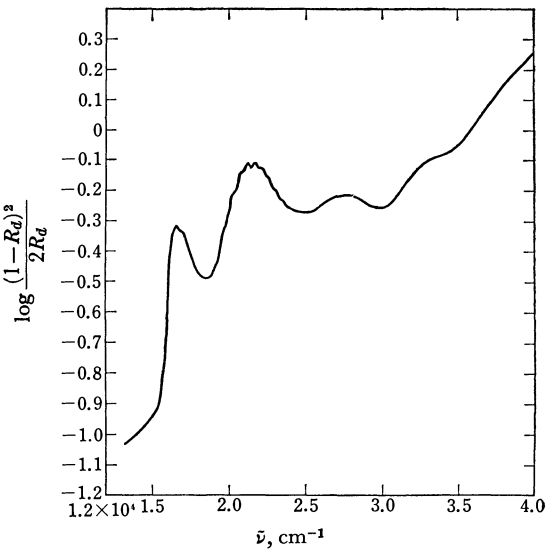

Fig. 1. (b)

3) H. B. Gray and C. J. Ballhausen, *J. Chem. Phys.*, **36**, 1151 (1962).

4) H. B. Gray, I. Bernal and E. Billig, *J. Am. Chem. Soc.*, **84**, 3404 (1962).

5) H. B. Gray, P. T. Manoharan, J. Pearlman and R. F. Riley, *Chem. Commun.*, **1965**, 62.

6) P. T. Manoharan and H. B. Gray, *J. Am. Chem. Soc.*, **87**, 3340 (1965).

7) B. A. Goodman, J. B. Raynor and M. C. R. Symons, *J. Chem. Soc.*, (*A*), **1966**, 994.

8) F. A. Cotton, R. R. Monchamp, R. J. M. Henry and R. C. Young, *J. Inorg. Nucl. Chem.*, **10**, 28 (1959); I. Bernal and S. E. Harrison, *J. Chem. Phys.*, **34**, 102 (1961); J. J. Fortman and R. G. Hayes, *ibid.*, **43**, 15 (1965); I. Bernal, S. D. Robinson, L. S. Meriwether and G. Wilkinson, *Chem. Commun.*, **1965**, 571; J. Danon, H. Panepucci and A. A. Misetich, *J. Chem. Phys.*, **44**, 4154 (1966); J. Danon, R. P. A. Muniz and A. O. Cariae, *ibid.*, **46**, 1210 (1967).

9) J. Lewis, R. J. Irving and G. Wilkinson, *J. Inorg. Nucl. Chem.*, **7**, 32 (1958).

10) W. P. Griffith, J. Lewis and G. Wilkinson, *ibid.*, **7**, 38 (1958).

11) E. P. Bertin, S. Mizushima, T. J. Lane and J. V. Quagliano, *J. Am. Chem. Soc.*, **81**, 3821 (1959).

12) R. D. Feltham, *Inorg. Chem.*, **3**, 1038 (1964).

13) D. Hall and A. A. Taggart, *J. Chem. Soc.*, **1965**, 1359; D. Dale and D. C. Hodgkin, *ibid.*, **1965**, 1364.

14) M. Mori, S. Ueshiba and S. Kawaguchi, This Bulletin, **36**, 796 (1963); W. P. Griffith, *J. Chem. Soc.*, **1963**, 3286.

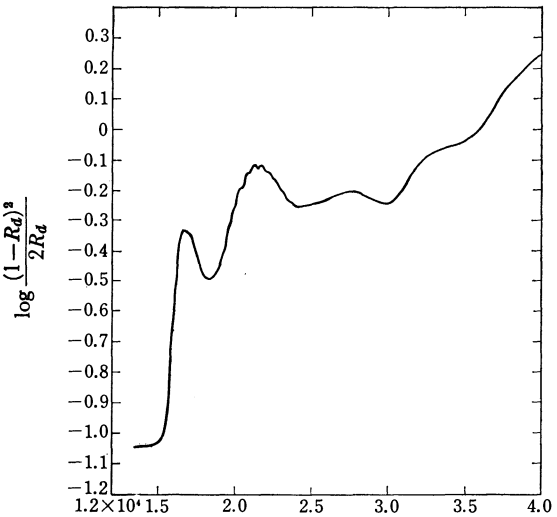

Fig. 1. (c)

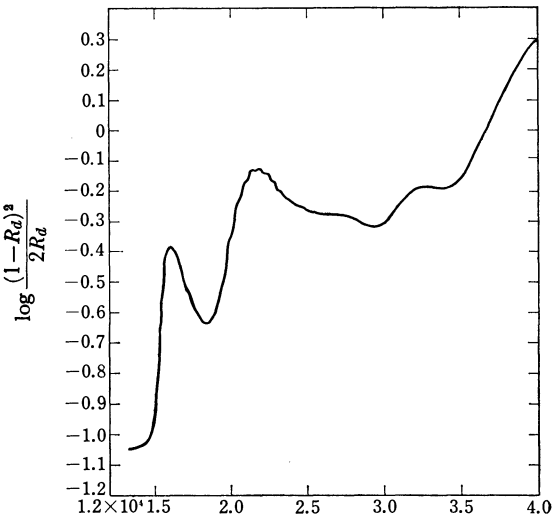

Fig. 1. (d)

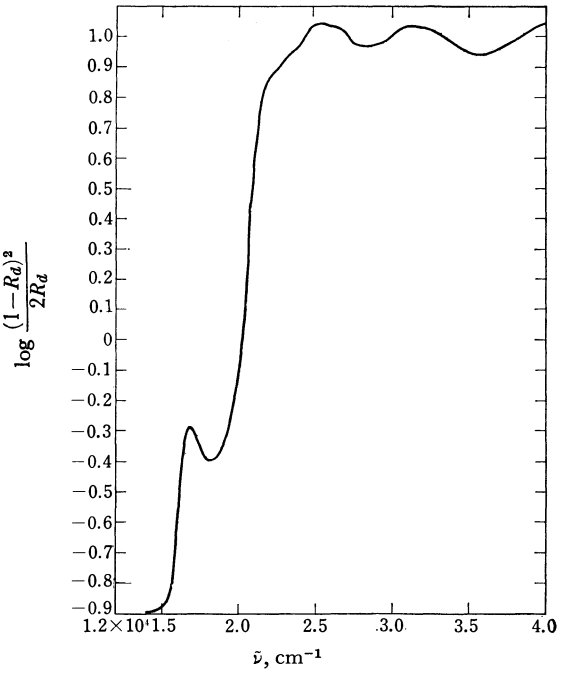

Fig. 1. (e)

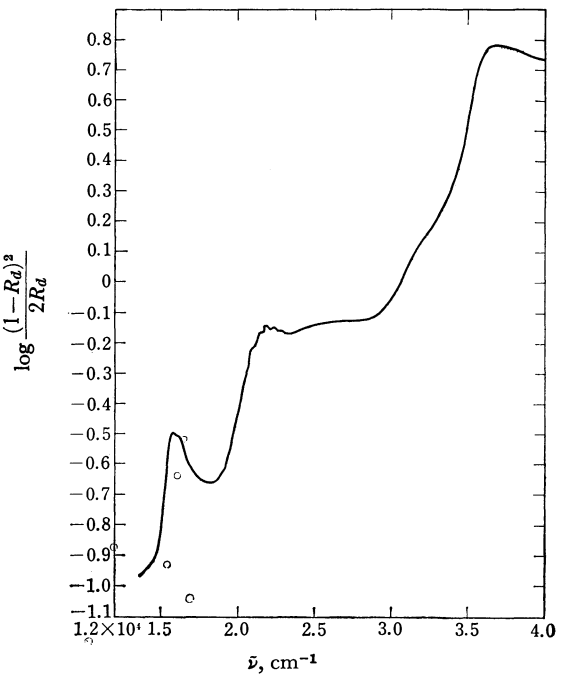

Fig. 1. (f)

Fig. 1. Absorptions found in reflection spectra.

(a): $[CrNO(NH_3)_5]Cl_2$
(b): $[CrNO(NH_3)_5]Br_2$
(c): $[CrNO(NH_3)_5](NO_3)_2$
(d): $[CrNO(NH_3)_5](ClO_4)_2$
(e): $[CrNO(NH_3)_5][B(C_6H_5)_4]_2$
(f): $[CrNO(NH_3)_5][OC_6H_2(NO_2)_3]_2$

tetraphenylborate and picrate are green. The absorption bands of nitrosylpentaamminechromium salts in the visible region have ripples which occur at equal intervals.[15] The salts also are in low spin states even though they are one type of penta-amminechromium salt. The present paper deals

15) M. Mori, Preprints for the 16th Annual Meeting of the Chemical Society of Japan (1963, Tokyo); I. Bernal, S. D. Robinson, L. S. Meriwether and G. Wilkinson, *Chem. Commun.*, **1965**, 571.

with studies of visible reflection, visible absorption, infrared and ESR spectra and of the magnetic susceptibilities of nitrosylpentaamminechromium salts.

Experimental

The nitrosylpentaamminechromium salts were prepared by the method reported by Mori, Ueshiba and Kawaguchi.[14] In this paper, previously unreported tetraphenylborate and the picrate of this complex were prepared by adding the corresponding sodium salt or free acid to aqueous solutions of the chloride.

Found in nitrosylpentaamminechromium picrate: Cr, 8.16; NH_3, 12.80%. Calcd for $[CrNO(NH_3)_5](C_6H_2N_3O_7)_2$: Cr, 8.32; NH_3, 13.58%. Found in nitrosylpentaamminechromium tetraphenylborate: C, 71.69; H, 6.76; N, 9.58%. Calcd for $[CrNO(NH_3)_5][B(C_6H_5)_4]_2$: C, 71.7; H, 6.88; N, 10.44%.

Hexaamminechromium(II) perchlorate was prepared by mixing chromium(II) acetate (prepared from 5 g of potassium dichromate[16]) with 15 g of ammonium perchlorate and 75 m*l*, of 15 M aqueous ammonia in the absence of atmospheric oxygen. The blue precipitate formed was centrifuged or filtered and washed, first with an ammonical aqueous solution of ammonium perchlorate, then with ethanol and finally with petroleum ether. The compound readily oxidizes in air, so that weighing the sample is difficult. However, the atomic ratio was determined to be Cr : NH_3 : ClO_4=1 : 6.10 : 1.97 in a mixed solution prepared by adding the sample wet with petroleum ether to dilute hydrochloric acid. At the same time, the precipitate was shown to be isomorphous with $[M(NH_3)_6](ClO_4)_2$ (M=Mn, Fe, Co, Ni) by an X-ray powder technique. It is thus clear that the blue compound was $[Cr(NH_3)_6](ClO_4)_2$. For the IR study, the mother liquor was further replaced with liquid paraffine. In this liquid, the compound was comparatively stable even between the two plates of sodium chloride used for IR spectroscopy.

The reflection spectra of these complex compounds in powder were obtained using a Hitachi Perkin-Elmer 139 UV-VIS Spectrophotometer. In Fig. 1, such spectra are expressed in terms of $\log[(1-R_d)^2/2R_d]$, where R_d is the diffuse reflectance. This type of curve more clearly shows the relation to absorption spectra. The positions of main maxima in such curves for various

Table 1. Absorption maxima found in reflection spectra of $[CrNO(NH_3)_5]X_2$

X	Absorption maxima (cm^{-1})
Cl	16850, 17200(sh), 21700, 27800, 33300
Br	16600, 17000(sh), 21700, 27700, 33300, 39500
NO_3	16600, 17000(sh), 21700, 27500, 33000
ClO_4	15900, 16300(sh), 21800, 26700, 32500, 40000
$B(C_6H_5)_4$	15700, 16300(sh), 21900, 27000, 32300(sh), 37000 ($B(C_6H_5)_4$)
$OC_6H_2(NO_2)_2$	16800, 17300(sh), ?

Table 2. Infrared absorption maxima of $[CrNO(NH_3)_5]X_2$

Mode of Vibration	$[CrNO(NH_3)_5]X_2$, X= Cl	Br	NO_3	ClO_4	$B(C_6H_5)_4$	$OC_6H_2(NO_2)_3$	
Cr↔NH_3 stretch.	440 m				420 m		
Cr–NO bend.	534 vw*				531 w*		
Cr↔NO stretch.	572 w*				575 vw*		
N–O stretch.	1680 vs	1690 vs	1670 vs	1730 vs	1730	1715	
ClO_4				463 vw, 457 vw			
NH_3 rock.	770 s(B), 730 sh	760 s, 730 sh	770 s, 730 sh	730 s, 760 sh	?	?	
NH_3 sym. deform.	1275 vs(S)	1280 vs	1286 vs	1300 vs(S)	1300 vs	?	
NH_3 stretch.	3300 vs(B)			3410 vs(S), 3340 vs(S)			
NH_3 stretch.	2960 vs(S), 2900 vs(S)			2960 vs(S), 2900 vs(S)			
NH_3 deg. deform.	1610 s			1625 s			

* Assignment by Miki, Ishimori, Yamatera and Okuno.[18]
s: strong, m: medium, w: weak, vw: very weak, sh: shoulder, S: sharp, B: broad, ?: values could not be determined.

Table 3. *g*-Values obtained by ESR for $[CrNO(NH_3)_5]X_2$ in powder and in aqueous solution

X	*g*-Values: Powder r. t.	Solution r. t.	Solution liq. N_2 temperature
Cl	1.989	1.979	
Br	1.985	——	
NO_3	1.986	1.979	
ClO_4	1.982	1.980	
$B(C_6H_5)_4$	1.945($g_{//}$), 2.006($g_\perp$)	1.975×	1.943($g_{//}$)×, 2.004($g_\perp$)×
$OC_6H_2(NO_2)_3$	1.968	1.976×	1.946($g_{//}$)×, 2.005($g_\perp$)×

r. t.: at room temperature,
×: solution in acetone, others are in aqueous, solutions.

16) S. M. Jörgensen, *J. prakt. Chem.*, **30**, 6(1884); "Inorganic Syntheses," Vol. 1, p. 122 (1939); Vol. 3, p. 148 (1950); Vol. 6, p. 145 (1960) and Vol. 8, p. 125 (1966), McGraw-Hill Book Company, Inc., New York and London.

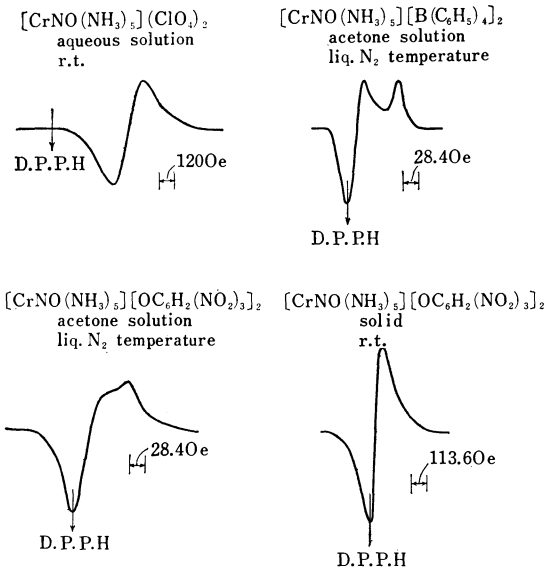

Fig. 2. ESR spectra.

compounds are given in Table 1. The absorption spectra in the visible region of these complex compounds in aqueous solutions were obtained using a Hitachi EPS-2 Recording Spectrometer. In aqueous solutions all compounds showed spectra indistinguishable from each other, irrespective of outer anions.

Infrared absorptions of nitrosylpentaamminechromium salts were observed using a Hitachi EPI infrared Spectrometer. The numerical results are listed in Table 2.

Electron spin resonance spectra were obtained on a Tokyo Denki Seiki T-1000 AX ESR Spectrometer. The results are given in Table 3 and shown in Fig. 2.

The magnetic susceptibilities in the temperature region 1.2°K to 20°K were observed by an alternating current method using a Hartshorn Bridge. The accuracy was ±0.1%. The susceptibilities obeyed the Curie-Weiss law (Fig. 3) and the effective magnetic moments and Curie-Weiss constants were obtained as given in Table 4.

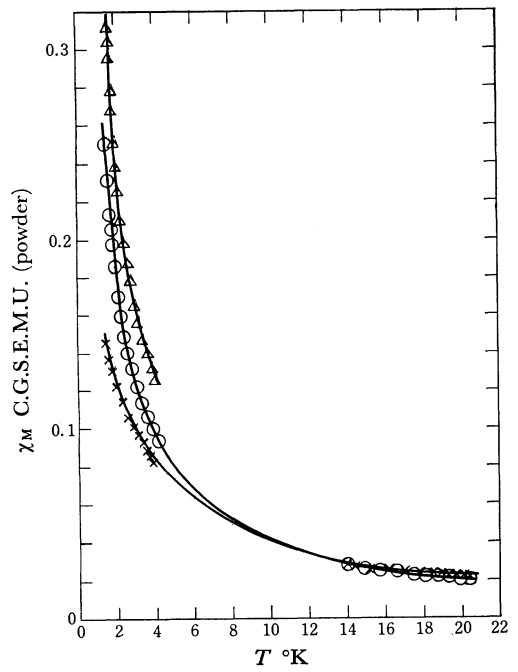

Fig. 3. The molar magnetic susceptibilities (C.G.S. E.M.U.) in powder.

×: $[CrNO(NH_3)_5]Cl_2$, △: $[CrNO(NH_3)_5](NO_3)_2$, ○: $[CrNO(NH_3)_5](ClO_4)_2$

Table 4. The results of the measurements between 1.2°K and 20°K of the magnetic susceptibilities of $[CrNO(NH_3)_5]X_2$ salts

X	Effective Bohr magneton no.	Curie-Weiss const.
Cl	1.9	−1.5°K
Br	2.0	−1.2°K
NO_3	2.0	−0.19°K
ClO_4	1.8	−0.10°K
$B(C_6H_5)_4$	1.6	−0.080°K

Discussion

The magnetic moments obtained at low temperatures (Table 4) indicate that both brown and green salts are in the same spin state of 1/2, and are in agreement with the room temperature data (2.3 Bohr magnetons) reported for the chloride by Griffith.[1] The fact that the susceptibilities obey the Curie-Weiss law down to 1.2°K proves that no dimerization occurs, and in this sense both brown and green salts correspond to the black series of nitrosylpentaamminecobalt salts. However, the Curie-Weiss constants of the brown halides are greater than those of the green salts, suggesting a greater interaction of spins in the former, presumably through anions. As seen from numerical data in Tables 1—4, the various properties, as well as the colors of these chromium complexes, change continuously rather than abruptly from complex to complex. Consequently, such differences in properties, although considerable in some cases, are thought to be due only to a change in the degree of an interaction between the complex cation and the outer anion.

The rocking frequency of ligand ammonia is known to be sensitive to the oxidation state of the central metal ion. The rocking frequency of ammonia ligands in hexaamminechromium(III) perchlorate is 718 cm^{-1}, and that in hexaamminechromium(II) perchlorate, which we newly prepared, was found at 660 cm^{-1}. The rocking frequencies in the nitrosylpentaamminechromium salts (730—770 cm^{-1}, Table 2) fall within the range for Cr(III) complexes, and are considerably higher than that of the Cr(II) complex. Further-

more, the stability in water of our nitrosylpentaamminechromium complexes is comparable to that of Cr(III) ammine complexes. These results may appear to contradict the magnetic data, because the spin state of 1/2 suggests monovalent Cr. However, we note that the same spin state of 1/2 is reached either when we start with monovalent $Cr(3d^5)$ and a NO^+ ligand by considering extensive back donation, or when we start with trivalent $Cr(3d^3)$ and NO^- ligand and consider electron pairing. In any interpretation, the result is the formation of a strong π-bond between Cr and NO as proposed by many investigators, and the concept of oxidation state seems to lose its strict meaning in harmony with Orgel's view.[17] The anomalous bond strength between chromium and nitrosyl is also supported by the fact that the nitrosylpentaamminechromium salts are changed into pentacyanonitrosylchromium salts in KCN solutions without inducing cleavage of the chromium-nitrosyl bond. In this respect, molecular orbital treatment seems to be suitable for a theoretical consideration of the orbital energy levels of these complexes. Manoharan and Gray[6] made a molecular orbital calculation using $[Fe(CN)_5NO]^{2-}$ as the model ion, and the essential features should remain unchanged for $[CrNO(NH_3)_5]^{2+}$ ion. Thus, the general idea of the energy level scheme of the latter ion could be illustrated as in Fig. 4. Here we assume linearity and the arrangement order Cr–N–O, which seem probable from the recent IR study by Miki *et al.*[18]

Clear-cut assignments of the observed absorption spectra seem difficult, but some characteristics of the absorption bands can be treated as follows:

Reflection spectra in powders indicate that the color changes of the above solid complexes are due to a shift of the visible absorption band in the range 16000—17000 cm^{-1} ($\varepsilon=18.2$ in aqueous spectrum). The easy shift of this band can be interpreted by assigning it to a one-electron transition $1b_2(3d_{xy})\rightarrow 4e(\pi^*NO,3d_{xz},3d_{yz})$ (*i. e.*, $B\rightarrow {}^2E$). The excited orbital 4e is a π-type antibonding molecular orbital located mainly on the nitrosyl, and should be easily influenced by an anion. The direction of shift of the absorption band agrees with this assumption, because the chloride ion which is thought to behave as an electron donor and thus raises the π^*NO level by interaction, actually causes the band to shift toward shorter wavelengths.

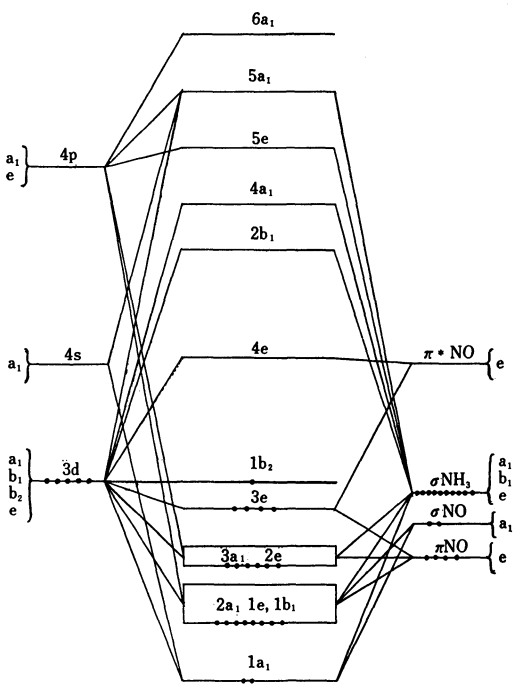

Fig. 4. Molecular orbital energy level for $[CrNO(NH_3)_5]^{2+}$.

The powder spectra also show that the above band is composed of two closely spaced peaks, one of which appears as a shoulder (Fig. 1 and Table 1). This may either be due to a splitting of the 4e level by crystal anisotropy or to the superposition of another band, $3e(3d_{xz},3d_{yz})\rightarrow 4e(\pi^*NO, 3d_{xz},3d_{yz})$ (*i. e.*, $B_2\rightarrow B_2+B_1+A_2+A_1$).

The absorption band near 22000 cm^{-1} ($\varepsilon=101$ in aqueous spectra) is accompanied by ripples spaced at about 480—490 cm^{-1} intervals in aqueous as well as in powder reflection spectra, as shown in Fig. 1, a—f. The wave numbers of small peaks or shoulders in such ripple structures and their spacings are given in Table 5. It seems most probable that the ripple is caused by the coupling of vibrations with the electric dipole transition. We note that vibrational structures on absorption bands have never been reported in other ammine complexes, even when such bands are thought to be allowed only through coupling with vibrational modes. We are thus inclined to think that in this nitrosyl ammine complex there is a special situation in addition to such coupling which made the vibrational structure perceptible in actual spectra. We attribute this to the vibrational stability in the excited state brought about by metal-nitrosyl double bonding, in the sense that there is a well-defined potential minimum even in the excited electronic state. We shall now give some interpretation of a more detailed nature on the problem on these lines.

17) L. E. Orgel, "An Introduction to Transition-Metal Chemistry, Ligand-Field Theory," Methuen and Co. Ltd., London, John Wiley and Sons Inc., New York (1960), pp. 37, 145.

18) E. Miki, T. Ishimori, H. Yamatera and H. Okuno, Proceedings of the Tenth International Conference on Coordination Chemistry, 141 (1967) Tokyo and Nikko, Japan; E. Miki, This Bulletin, **41**, 1835 (1968).

TABLE 5. WAVE NUMBERS AT SMALL PEAKS OR SHOULDERS IN THE RIPPLE STRUCTURE OF 22000 cm^{-1} BAND

$[CrNO(NH_3)_5]X_2$											
X=Cl		Br		NO_3		ClO_4		$B(C_6H_5)_4$		aq. soln.	
cm^{-1}	Δ	cm^{-1}	Δ	cm^{-1}	Δ	cm^{-1}	Δ	cm^{-1}	Δ	cm^{-1}	Δ
23630		23520		23540		23760		23800		23400	
	470		420		420		540		510		480
23160		23100		23120		23220		23290		22920	
	460		480		450		430		410		490
22700		22620		22670		22790		22880		22430	
	460		440		490		470		530		550
22240		22180		22180		22320		22350		21880	
	540		510		470		490		470		470
21700		21670		21710		21830		21880		21410	
	470		470		500		470		480		430
21230		21200		21210		21360		21400		20980	
	480		500		510		460		440		500
20750		20700		20700		20900		20960		20480	
	430		480		490		530		440		510
20320		20220		20210		20370		20420		19970	
	590		520		510		480		510		
19730		19700		19700		19890		19910			
	510						560				
19220						19330					
mean	490		478		480		492		486		490

The band with ripples under discussion (22000 cm^{-1}) is one which undergoes the least change in wave numbers with the substitution of outer anions. This fact, as well as the energy value, suggests the assignment $1b_2(3d_{xy}) \rightarrow 2b_1(3d_{x^2-y^2})$, $(B_2 \rightarrow B_1)$ for this band. This transition must couple with a vibration of E symmetry in order to be allowed. Vibrations of E symmetry observed in IR spectra in the neighborhood of 500 cm^{-1} are a bending vibration of the CrNO skeleton as observed by Miki *et al.*[18] at 531—535 cm^{-1}, and a Cr–NH_3 stretching vibration as observed at 420—440 cm^{-1} by the present authors (Table 2). Although Bernal cited the possibility that the ripple structure on the 22000 cm^{-1} absorption band is due to coupling of the latter vibration, it is felt even more probable to the present authors that it should be due to coupling with the Cr–N–O bending vibration, since the vibrational frequencies are expected to decrease in the excited level. Furthermore, if it were attributable to the Cr–NH_3 E stretching mode as in Bernal's assumption, the ripple structure should appear in other ammine complexes as well, which is not the case. Furthermore, our assumption does not contradict the fact that the excitation $B_2 \rightarrow B_1$ does not break the Cr–N–O linkage.

Other absorption bands, *i. e.*, at 28000 cm^{-1} and 33000 cm^{-1} observed for the perchlorate, also shift toward the violet region by about 1000 cm^{-1} upon substituting the outer anions with halide ions. They probably include transitions $3e(3d_{xz},3d_{zy}) \rightarrow 4a_1(3d_{z^2})(B_2 \rightarrow E)$, $1b_2(3d_{xy}) \rightarrow 4a_1(3d_{z^2})(B_2 \rightarrow A_1)$, *etc.*

The ESR results on nitrosylpentaamminechromium complexes in solution agrees with the results of Bernal and Harrison[8] and Danon, Panepucci and Misetich.[8] Though the nitrosylpentaamminechromium salts could not be obtained as single crystals, powder spectra of tetraphenylborate and of picrate at liquid N_2 temperature gave structures typical of an anisotropic *g*-tensor, and $g_\perp$ and $g_{//}$ were estimated using Kneubühl's method.[19] The situation seems analogous to the case of dimelammonium hexachlorocuprate,[20] which also has a large organic ion exhibiting a dilution effect, enabling one to observe an anisotropic fine structure. The spin-orbit interaction constant calculated from the $g_{//}$ obtained using the energy gap $E(B_{1g} - B_{2g}) = 22000$ cm^{-1} is $\zeta = 158$ cm^{-1}.

Conclusion

Nitrosylpentaamminechromium salts, both the brown and green series, are in low spin states (1/2) and are thus thought to be monomers. The easy shift of the absorption band in the range 16000—17000 cm^{-1}, observed as color differences in powders, is attributable to a rise in energy of the excited level π^*NO cused by a donor-acceptor interaction with anion acting as a donor. Ripples having intervals of about 500 cm^{-1}, observed on the absorption bands near 22000 cm^{-1}, are presumably the result of coupling of vibrational frequencies of the Cr–N–O bending mode (E) with the electric dipole transition $B_1 \rightarrow B_2$.

The authors express their sincere thanks to Professor Ichiro Nakagawa of the University of Tokyo and Professor Hiroshi Tsubomura of Osaka University for their valuable discussions.

19) F. K. Kneubühl, *J. Chem. Phys.*, **33**, 1074 (1960).
20) M. Mori and S. Fujiwara, This Bulletin, **36**, 1636 (1963).

BULLETIN OF THE CHEMICAL SOCIETY OF JAPAN VOL. 42 716—720 (1969)

Geochemical Fractionation of Induced Radionuclides in Fresh Nuclear Debris through the Atmosphere—Np-239 and Co-60

Takeshi SOTOBAYASHI, Toshio SUZUKI and Seitaro KOYAMA

Department of Chemistry, Faculty of Science, University of Niigata, Niigata

(Received July 23, 1968)

The atmospheric fractionation of induced radionuclides is discussed in some detail on the basis of results obtained by making a radiochemical analysis of fresh nuclear debris originating from recent Chinese nuclear test explosions. Among fresh nuclear debris particles collected at Niigata about 4000 km downwind from the Chinese test site, the trend for the enrichment of ^{239}Np was somewhat modified as compared with that derived from an averaged sample collected by a large-scale and high-altitude sampling procedure; more ^{239}Np was present in smaller-size fallout particles. Furthermore, it was found, in rain-water samples collected after the third Chinese nuclear explosion, that the atomic ratio at time-zero of ^{60}Co/^{95}Zr increased with a decrease in the ^{95}Zr-concentration in rain and *vice versa*. This suggests that the atmospheric fractionation of ^{60}Co-rich particles from ^{95}Zr-rich ones takes place during the travel of atomic clouds around the world.

Several papers[1–3] have been published on the atmospheric fractionation of nuclear debris of known origin. We have made a preliminary discussion of the unique fractionation behavior of ^{239}Np in fresh nuclear debris particles of a larger size which originated from the May 9, 1966, Chinese nuclear test explosion.[4] In this paper we will discuss in more detail the geochemical fractionation behavior of ^{239}Np. Furthermore, by comparing the fallout pattern of an induced nuclide ^{60}Co with that of a refractory fission product ^{95}Zr, we have established the geochemical fractionation of another induced nuclide, ^{60}Co; measurements of the variation in the ^{60}Co/^{95}Zr ratio, in fact, yielded experimental evidence for the geochemical fractionation of nuclear debris during the global circulation of the atomic clouds.

Experimental

Particle samples were collected on the roof of the 8-story Niigata City Hall; the roof surface was carefully surveyed by a G-M counter, and radioactive particles were picked off the roof, possibly along with a small amount of inactive dust material, and isolated under a microscope. Rain samples were collected by a stainless-steel funnel (1 m^2 in area) installed on the campus of the Niigata University. The radiochemical separation of each radionuclide was carried out by a combination of conventional precipitation, ion-exchange, and liquid-liquid extraction methods. The measurements of the radioactivity were made using a gas-flow counter or a NaI(Tl) scintillation detector (1¾ in × 1 in or 3 in × 3 in) with a 200-channel pulse-height analyzer.

Results and Discussion

Physical Properties of Hot Particles from the May 9, 1966 Explosion. A large number of highly-radioactive nuclear debris particles were detected within 36 hr of the third Chinese nuclear test on May 9, 1966. The individual particles, collected on May 11, ranged in total β-activity over a factor of 100, while the particles ranged in size from 5 to 24 μ in diameter. Particularly, sixteen single particles were carefully examined under a microscope; they were reddish-brown, and the particle ranged in size from 8 to 24 μ in diameter. The ^{95}Zr-content varied from 10^7 to 10^9 atoms/particle (Fig. 1), and the specific activity, from 2.3 to 7.3×10^{17} ^{95}Zr-equivalent fissions per gram. The average specific activities of surface-burst debris has been reported to be of the order of 10^{14} ^{95}Zr-equivalent fissions per gram, and air-burst debris particles are believed to have specific activities from 10^4 to 10^7 times higher.[5] Thus, the specific activity of the 16 single particles was

1) P. K. Kuroda, K. K. Menon and B. D. Palmer, "La pollution Radioactive Des Milieux Gazeux," Vol. 1, Saclay, France (1965), p. 105.

2) P. K. Kuroda, Y. Miyake and J. Nemoto, *Science*, **150**, 1289 (1965).

3) M. Thein and P. K. Kuroda, *J. Geophys. Res.*, **72**, 1673 (1967).

4) T. Sotobayashi, T. Suzuki and S. Koyama, This Bulletin, **40**, 1555 (1967).

5) E. C. Freiling and M. A. Kay, *Nature*, **209**, 236 (1966).

confined within a narrow range, the highest one among the reported specific activities observed in the case of a land-surface burst.

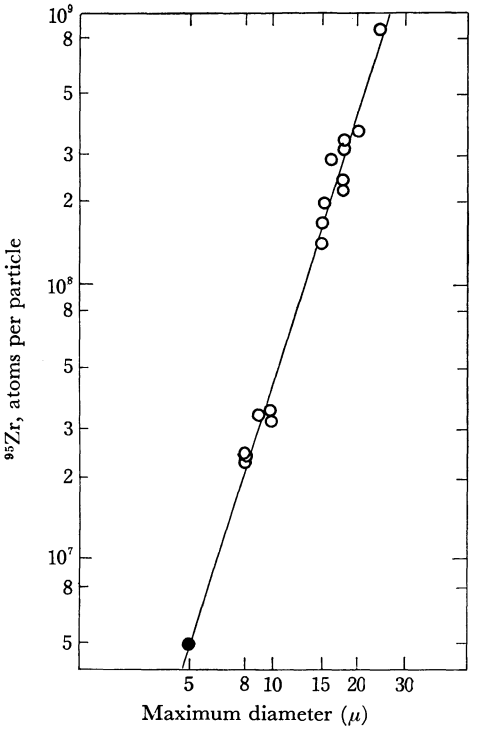

Fig. 1. Correlation between the number of ^{95}Zr atoms and the maximum diameter for 16 single particles collected on May 11, 1966.
●, the average number of atoms/particle for a combined sample of 9 particles.

Figure 1 shows the correlation between the particle size and the number of ^{95}Zr atoms for the 16 single particles. The number of ^{95}Zr atoms is plotted on a logarithmic scale as a function of the logarithm of the maximum diameter of an individual particle. In this graph the data points seem to lie near a solid line with a slope of 3.2. This finding implies that the atoms of ^{95}Zr are incorporated into a single particle with a uniform density. Moreover, the number of ^{95}Zr atoms could, in this case, be used for making a rough estimate of the particle size of nuclear debris.

Unique Fractionation Behavior of ^{239}Np. The debris particles of a larger size were strongly fractionated; concerning short-lived fission products (half-life, 1—3 days), the collected particles, about 250 particles, were all rich in refractory fission products, ^{97}Zr, ^{99}Mo and ^{143}Ce, and poor in ^{132}Te-^{132}I and ^{133}I, as would be expected from their chemical and nuclear properties in such larger particles. Most of the particles were poor in ^{239}Np, but some of them (less than 10 percent) were markedly rich in ^{239}Np, with no detectable amount of the ^{132}Te-^{132}I and ^{133}I in them, while a rain sample collected on May 10—11 was rich in volatile fission products, as is shown in Fig. 4. Figure 2 shows two γ-ray spectra of such two extreme-type particles, A and B; the total β-activity of the A particle was 1.1×10^5 pCi, and that of the B particle, 3.6×10^5 pCi, on May 11. Here the two spectra are normalized to equal the activity level of radiozirconium. The γ-ray spectrum obtained by plotting the difference in counts per channel between the two spectra had a shape similar to the γ-ray spectrum of ^{239}Np, as is shown in the inset. Figure 2 seems to suggest quite similar fractionation behavior in ^{97}Zr, ^{99}Mo, and ^{143}Ce in spite of the difference in ^{239}Np content.

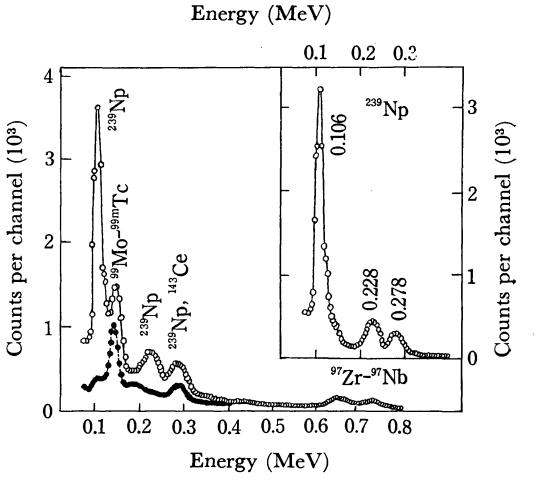

Fig. 2. Gamma-ray spectra of two extremely fractionated hot particles collected on May 11, 1966.
—○—, Particle A; —●—, Particle B

First, this result may be explained by the tentative assumption that the ^{239}Np found in A-type particles is not incorporated into debris particles simultaneously with such refractory fission products as ^{97}Zr at the earlier stages of the debris formation processes, but precipitates a little later on the surface of particles which had condensed at the earlier stages.[6] Further, according to the extensive studies by Freiling[5] and Crocker[7] on the radionuclide fractionation in nuclear debris particles, ^{239}Np originating from a land-surface shot seems to behave like a refractory group. The May 9, 1966, Chinese nuclear explosion was believed to have been blasted near the land surface; this belief is based on the fractionation data for the fallout particles collected in the lower stratosphere.[8] On the other hand, in the present observations, ^{239}Np

6) T. Mamuro, K. Yoshikawa, T. Matsunami and A. Fujita, *Health Physics*, **12**, 757 (1966).
7) G. R. Crocker, *Nature*, **210**, 1028 (1966).
8) H. W. Feely, C. Barrientos and D. Katzman, *ibid.*, **212**, 1303 (1966).

seemed to be present along with refractory fission products in less than 10 percent of the total particles collected. Here it should be mentioned that the particle samples studied in the present work were collected at ground level, at a particular location far away from the place of their formation and shortly after the explosion. Taking these points into consideration, such a unique distribution pattern of ^{239}Np and the observed narrow range of specific activity in the present samples may result mainly from the particular sampling conditions. From an alternative point of view, the present data may suggest the gravitational and meteorological forces and the differences in size and density among the debris particles combine to cause particle separation during the travel of the atomic cloud through the atmosphere. The fractionation behavior of ^{239}Np in this case seemed to be somewhat modified as compared with that seen in an averaged sample collected by a large-scale and high-altitude sampling procedure using air craft.

Variation in the ^{239}Np Content with Particle Size. We have presented the γ-ray spectra of two composite samples in order to examine the change in the enrichment of ^{239}Np with the particle size; the particles were grouped in terms of their total β-activity. A combined sample (I) of 9 particles ranged in total β-activity from 10^3 to 10^4 pCi/particle 2 days after the explosion. Their average size was estimated to be 5μ in diameter by comparing their average atom number of ^{95}Zr per particle with a point on the experimental line (the solid circle in Fig. 1, 4.6×10^6 atoms/particle). The single particles of another composite sample (II) of 8 particles all had more than 10^5 pCi/particle when two days old; their average number of ^{95}Zr-atoms/particle was 2.1×10^8 atoms/particle, and their average diameter was estimated to be 16μ. Figure 3 shows the γ-ray spectra of the two combined samples measured 7 days after the explosion; these spectra are also normalized so as to be equal to the activity level of ^{95}Zr-^{95}Nb. These two composite samples were also poor in volatile fission products. The γ-ray spectrum shown in the inset of Fig. 3 was, as in Fig. 2, plotted by subtracting the γ-ray spectrum of the 9-particle sample from that of the 8-particle one. The spectrum in this inset indicates that the smaller-size particles were, on the average, richer in ^{239}Np than the larger ones. The 9-particle sample (I) belonged to the smallest-size range (5μ) among all the particles collected. Thus, the trend toward the enrichment of ^{239}Np may be believed to depend greatly upon the size of the debris particles.

It should be noted in Fig. 3 that smaller particles were also richer in nuclides with the photopeak at 0.14 MeV, mainly ^{99}Mo-^{99m}Tc, relative to ^{95}Zr-^{95}Nb. This, for reasons to be given below, may present a unique fractionation picture—that one

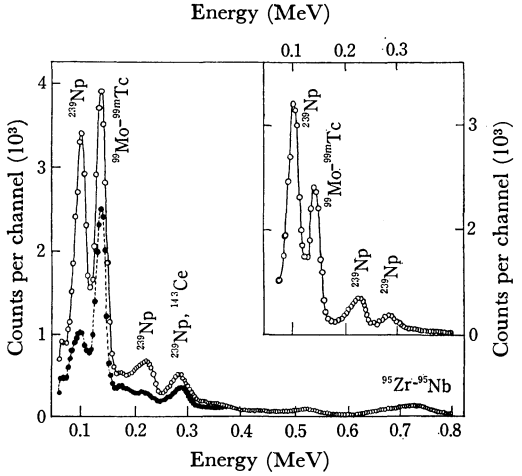

Fig. 3. Gamma-ray spectra of two composite particle samples, I and II.
—○—, Sample (I) of 9 paritcles;
—●—, Sample (II) of 8 particles.

of the most refractory nuclides, ^{99}Mo, shows the same enrichment trend as an induced nuclide, ^{239}Np; (1) the first member of the 99, mass chain, is the completely refractory 35.5-s ^{99}Zr (bp, 4750°C) and an earlier member of mass chain 95, with a significant half-life value, is a less refractory nuclide, 0.7-m ^{95}Sr (bp, 1366°C); (2) the time required for fission products to condense and to form a hot particle at earlier stages of particle formation processes is, on the average, 40 sec or less;[9] (3) larger particles are richer in more refractory fission products.[10] Taking these points into consideration, it may be expected that larger particles will be richer in ^{99}Mo than in ^{95}Zr. The present observations, however, exhibited quite the reverse tendency (Fig. 3).

It is tempting to make a somewhat speculative assumption on the origin of ^{99}Mo in order to explain this finding. Molybdenum metal is present as a minor constituent in the structural material of a nuclear-weapons device, and the isotopic abundance of ^{98}Mo for the element is 23.4%. Some fraction of the total ^{99}Mo observed might be produced by a ^{98}Mo(n,γ)^{99}Mo reaction which takes place during the nuclear fission. The ^{99}Mo fraction may then additionally precipitate on smaller-size particles in a way similar to that in which an induced nuclide, ^{239}Np, is deposited on smaller ones, as has been described above. This assumption is considered to be compatible with the fact that the fractionation correlation parameter of ^{99}Mo is dependent upon the total yield of a nuclear-weapons device.[5]

9) R. S. Clark, K. Yoshikawa, M. N. Rao, B. D. Palmer, M. Thein and P. K. Kuroda, *J. Geophys. Res.*, **72**, 1793 (1967).

10) S. H. Cassidy and R. G. Crocker, USNRDL-TR-67-70 (1967).

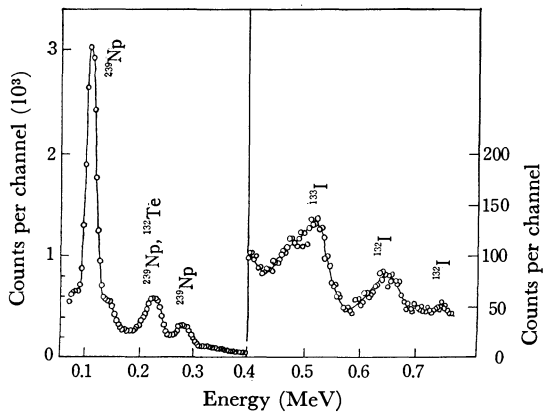

Fig. 4. The γ-ray spectrum of a rain sample (20 l) collected on May 10—11, 1966.

Np-239 in a Rain Sample. It is of interest to note that a rain sample (20 l) collected between 21 : 00 hr on the 10th and 5 : 00 hr on the 11th of May, 1966, before highly-radioactive particles were found in surface air at Niigata, had a unique radiochemical composition, consisting mainly of ^{239}Np, ^{132}Te-^{132}I and ^{133}I, with no detectable amount of refractory fission products, as is shown in Fig. 4. First, it is obvious in this figure that the ^{239}Np in the rain sample behaved nearly volatilely, while in the rain sample of May 15—16 the enrichment behavior of ^{239}Np was similar to that seen in the above-mentioned sample of 9 smaller-size particles. Secondly, this finding suggests that upper-air-borne particles rich in ^{239}Np, perhaps fine in size, first appeared in the atmosphere over Japan and that a part of them fell to the ground by means of wash-out in rain. Therefore, the observation of such rainwater activities also indicates that particle separation may have taken place to a considerable extent in the course of the 1.5-day travel of the atomic cloud from the Chinese test site to Japan.

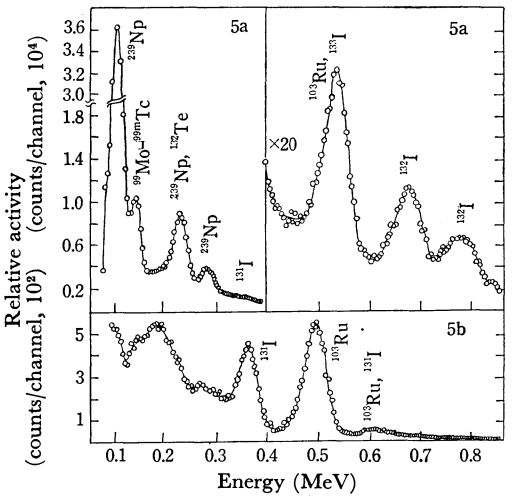

Figs. 5a and 5b. Gamma-ray spectra of a hot particle collected on Dec. 28, 1966.
5a: A γ-ray spectrum measured 2 days after the explosion.
5b: A γ-ray spectrum measured 28 days after the explosion.

Np-239 in Hot Particles from the December 28, 1966, Explosion. More recently we have measured on December 30 the radioactivities of fresh nuclear debris; this debris evidently resulted from the fifth Chinese nuclear test explosion, on December 28, 1966. The highest total β-activity among all the single fallout particles collected was 4.9×10^4 pCi/particle 2 days after the explosion; most of the collected particles had a total β-activity of the order of $\sim 10^3$ pCi/particle an age of 2 days. Figures 5a and 5b show two γ-ray spectra for one such particle, measured 2 and 28 days after the explosion respectively. In Fig. 5a the two photopeaks at 0.67 and 0.78 MeV should be ascribed to ^{132}I, the daughter of ^{132}Te, and the contribution from ^{97}Zr-^{97}Nb radiations to the photopeaks is negligibly small. For this reason, the spectrum in Fig. 5b shows no discernible photopeaks arising from ^{95}Zr-^{95}Nb radiations with a half-life of 65 d in the 0.66—0.80 MeV range and only the well-defined photopeaks resulting from ^{103}Ru are recorded at 0.50 and 0.62 MeV. As a result, the measured particle consisted mainly of ^{239}Np and some volatile fission products, such as ^{131}I, ^{132}Te-^{132}I, ^{133}I, and ^{103}Ru. Thus, in this case, ^{239}Np behaved completely like the volatilely-behaving fission products observed in the rain sample collected on May 11, 1966 (Fig. 4).

Time Variation of the ^{60}Co/^{95}Zr Ratio in Rain Samples. Table 1 shows the experimental

Table 1. Atom numbers at time-zero of ^{95}Zr and ^{60}Co and their ratio in rain samples

Period of collection 1966	Sample volume (l)	^{95}Zr (10^7 atoms)	^{60}Co (10^8 atoms)	^{60}Co/^{95}Zr
10—11 May	20	nd*		
15—16	24	1.9		
22—24	9	0.2		
28—29	32	31.4	15.3	4.9
5—6 June	18	12.5	16.3	13.0
9—11	18	4.8	23.8	49.7
20—22	23	8.7	4.7	5.4
24—27	15	4.7	1.4	3.0
28	48	16.9	0.8	0.5
2—3 July	32	4.8	2.2	4.6
7—9	36	2.5		
13	46	nd*		
15—18	174	6.4		
1—15 Aug.	16	3.6	0.2	0.6

* less than detection limits.

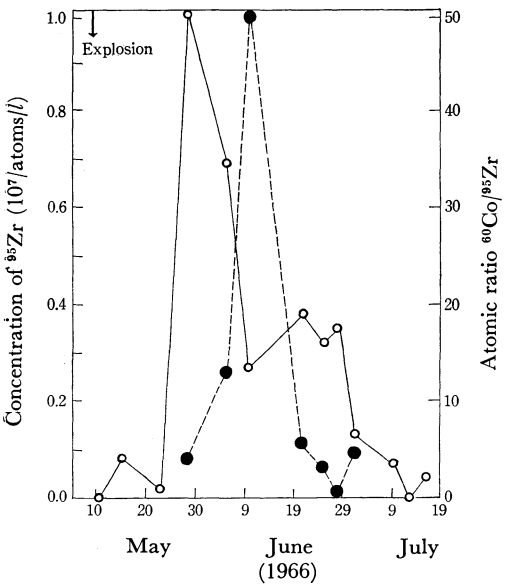

Fig. 6. Time variation of ^{95}Zr concentration and ^{60}Co/^{95}Zr in rainwater between May 11 and July 18, 1966.
—○—, ^{95}Zr concentration; ---●---, ^{60}Co/^{95}Zr

data on ^{60}Co and ^{95}Zr in rain samples collected between May 11 and August 15, 1966. Since no discernible photopeaks for these nuclides were found in the γ-ray spectra of rain samples collected before May 9, it was believed that the two nuclides originated only from the May 9, 1966, Chinese nuclear explosion. Figure 6 shows the ^{60}Co/^{95}Zr ratio at time-zero and the number of ^{95}Zr atoms/liter as a function of the time. First, it should be noted that no measurable amounts of ^{60}Co could be found in any particle or rain sample collected between May 11 and 24, shortly after the explosion. This still remains a puzzling question. It may, however, be seen from Fig. 6. that the ^{60}Co/^{95}Zr atomic ratio in rain increased with a decrease in the ^{95}Zr concentration, and *vice versa*. On the other hand, the first arrival at Niigata of the atomic clouds from the May 9, 1966, event brought about rainfalls with a very low concentration of ^{95}Zr (less than 10^6 atoms/l) on May 10—11, 16, and 24, but the two peak values of the ^{95}Zr concentration in the rain were found 19 and 40 days after the first arrival, as is shown in Fig. 6. The time taken for the atomic cluouds to circulate around the world has been estimated to be 3—4 weeks in spring and summer by measuring the time variation of some fission product ratios.[2] As a result, these two peaks (Fig. 6) can possibly be ascribed to the second and perhaps even the third arrivals of the atomic clouds of the Chinese nuclear explosion, although the second peaks, around June 24, was not well defined. From these findings it is expected that the different distribution patterns between ^{95}Zr-rich and ^{60}Co-rich particles would be established in the rain-producing layers of the atmosphere during their fairly long travel of more than 20 days through the atmosphere. This suggests that the separation of ^{60}Co-rich particles from ^{95}Zr-rich particles would take place during their travel, and that the ^{60}Co-rich particles would remain a longer time than the particles rich in ^{95}Zr. This, therefore, provides evidence that ^{60}Co would be richer in smaller-size particles in the same way that ^{239}Np is.

BULLETIN OF THE CHEMICAL SOCIETY OF JAPAN VOL. 42 721—724 (1969)

Polarographic Study of Thallium(I) Chelates of 2,2′-Ethylenedioxybis[ethyliminodi(acetic acid)] and Cyclohexane-1,2-diamine-*N*,*N*,*N*′,*N*′-tetraacetic Acid

Mutsuo KODAMA and Yayoe TOMINAGA

Department of Chemistry, Ibaraki University, Mito, Ibaraki

(Received July 24, 1968)

D.c. polarographic behavior of thallium(I) ion in 2,2′-ethylenedioxybis[ethyliminodi(acetate)] (GEDTA) and cyclohexane-1,2-diamine-*N*,*N*,*N*′,*N*′-tetraacetate (CyDTA) solutions was studied systematically. Compositions and stability constants of thallium(I)-GEDTA and CyDTA chelates were determined from the shift of the half-wave potential. In both GEDTA and CyDTA systems, thallium(I) ion gave a single well-defined wave corresponding to the following reversible one-electron reduction.

$$\begin{array}{ccc} TlZ^{3-} + Hg + e^- = Tl(Hg) + Z^{4-} \\ \uparrow\downarrow H^+ \qquad\qquad \uparrow\downarrow nH^+ \\ TlHZ^{2-} \qquad\qquad H_nZ^{n-4} \end{array}$$

In contrast to the finding of Anderegg and Bottari, thallium(I) ion was found to form not only a normal chelate but also a protonated chelate with CyDTA.

In a previous paper,[1] both the d.c. and a.c. polarographic behaviors of thallium(I) ion in diethylenetriaminepentaacetate (DTPA) solution were studied systematically, and the electrode reaction mechanism determined. From the shift of the half-wave potential or the a.c. peak potential due to complex formation, the composition and stability constant of thallium(I)-DTPA chelate were also estimated.

In this paper, the d.c. polarographic behavior of thallium(I) chelates of 2,2′-ethylenedioxybis-[ethyliminodi(acetic acid)] (GEDTA) and cyclohexane-1,2-diamine-*N*,*N*,*N*′,*N*′-tetraacetic acid (CyDTA) are dealt with, and their compositions and stability constants determined. Thallium(I) ion was found to form not only a normal chelate but also a protonated chelate with these chelating reagents.

Experimental

Reagents. The preparation and standardization of GEDTA and CyDTA solutions were described previously.[2,3] The preparation of thallium(I) perchlorate solution was also described in a previous paper.[1] All other chemicals were of analytical reagent grade and used without further purification. The ionic strength of the sample solution was adjusted to 0.30 by adding an appropriate amount of $NaClO_4$.

Apparatus and Experimental Procedures. All apparatus and experimental procedures were as employed previously.[1,4]

Results and Discussion

D. c. polarographic behavior of thallium(I)-GEDTA chelate was studied with a solution containing an excess of un-complexed GEDTA in the pH range 8.00 to 10.00. Since, in this pH range, a solution containing an excess of un-complexed GEDTA has enough buffer capacity to keep the pH value of the solution constant, no buffer reagent was used. In the CyDTA system, to avoid equilibrium complexity due to the presence of other complex-forming substances, all experiments were conducted with solutions containing an excess of CyDTA in the pH range 10.0 to 11.70.

As shown in Figs. 1 and 2, both thallium(I)-GEDTA and -CyDTA chelates invariably gave single well-defined waves. In both cases, a log-plot gave a linear relation with a slope of −60 mV corresponding to a one-electron reversible reduction. Furthermore, the wave height was exactly proportional to the square-root of the effective pressure on the dropping mercury electorde (DME) and the bulk concentration of thallium(I) ion in both cases. Results are not shown here.

1) M. Kodama, T. Noda and M. Murata, This Bulletin, **41**, 354 (1968).

2) M. Kodama, C. Sasaki and T. Noda, *ibid.*, **41**, 2033 (1968).

3) M. Kodama and H. Ebine, *ibid.*, **40**, 1857 (1967).

4) M. Kodama and A. Kimura, *ibid.*, **40**, 1639 (1967).

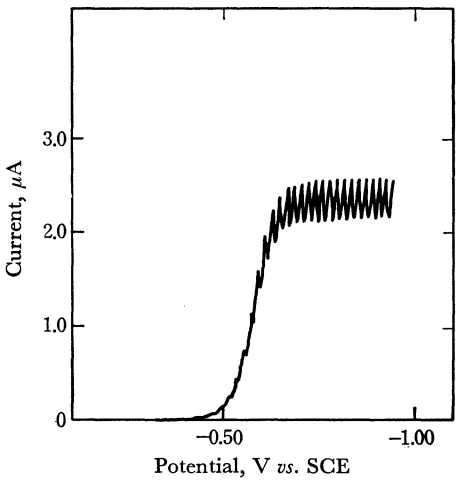

Fig. 1. D. c. polarogram of thallium(I)-GADTA chelate.
pH=8.60, μ=0.30
Concentration of GEDTA=40.0 mM
Concentration of thallium(I)=1.09 mM

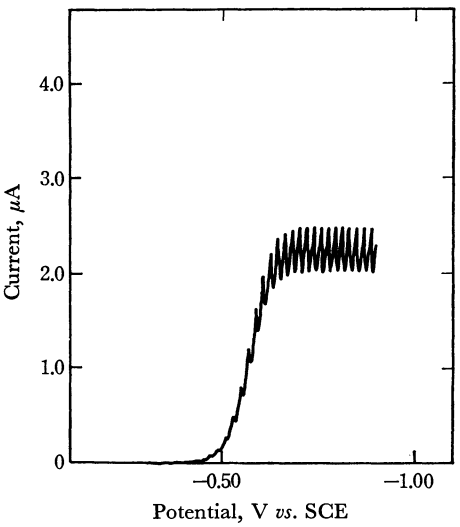

Fig. 2. D. c. polarogram of thallium(I)-CyDTA chelate.
pH=10.68, μ=0.30
Concentration of CyDTA=47.2 mM
Concentration of thallium(I)=1.09 mM

As illustrated by data in Table 1, the half-wave potential, $(E_{1/2})_{TlZ}$, was shifted to more negative potentials with increase in the bulk concentration of un-complexed chelating reagent (GEDTA or CyDTA) according to relation (1), but was independent of thallium(I) concentration.

$$(E_{1/2})_{TlZ} = \text{constant} - 0.0591 \log [Z]_f \qquad (1)$$

where $[Z]_f$ is the concentration of the un-complexed chelating reagent.

In GEDTA solution, $(E_{1/2})_{TlZ}$ was also shifted

Table 1. Dependence of $(E_{1/2})_{TlZ}$ on the concentration of chelating reagent
μ=0.30, Concentration of thallium(I)=1.09 mM

A: GEDTA system pH=8.60

Concentration of GEDTA mM	$(E_{1/2})_{TlZ}$ V *vs.* SCE	$\Delta E_{1/2}$, mV Calcd	Obsd
20.0	−0.553	0	0
40.0	−0.583	−33	−30

B: CyDTA system pH=10.68

Concentration of CyDTA mM	$(E_{1/2})_{TlZ}$ V *vs.* SCE	$\Delta E_{1/2}$, mV Calcd	Obsd
15.0	−0.550	0	0
27.2	−0.567	−16	−17
47.2	−0.581	−29	−31

to more negative potentials with increasing pH of the solution, but no linear relation could be found between $(E_{1/2})_{TlZ}$ and $\log(\alpha_H)_Z$ (Fig. 3). Here, $(\alpha_H)_Z$ is expressed as:

$$(\alpha_H)_Z = 1 + \frac{[H^+]}{k_4} + \frac{[H^+]^2}{k_4 \cdot k_3} + \frac{[H^+]^3}{k_4 \cdot k_3 \cdot k_2} + \frac{[H^+]^4}{k_4 \cdot k_3 \cdot k_2 \cdot k_1} \qquad (2)$$

where k's are the dissociation constants of GEDTA.

The magnitude of deviation from the linear relation of +60 mV slope expected theoretically for the reversible one-electron reduction of a normal chelate increases with decreasing pH (increasing $(\alpha_H)_Z$ value). In the case of the CyDTA system, $(E_{1/2})_{TlZ}$ was almost independent of the pH value under present experimental conditions (10.00 <pH<11.70) (Fig. 3). Since CyDTA has the

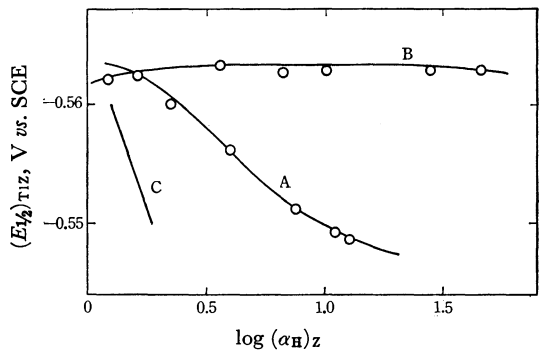

Fig. 3. The relation between $(E_{1/2})_{TlZ}$ and $\log (\alpha_H)_Z$.
μ=0.30
Concentration of thallium(I)=1.09 mM
A: GEDTA system, Concentration of GEDTA=20.0 mM
B: CyDTA system, Concentration of CyDTA=23.6 mM
C: The line theoretically predicted

pK_4 value of 11.43 (μ=0.30), if only a normal chelate is formed between thallium(I) and CyDTA, the half-wave potential should shift simply to more negative potentials with decreasing pH according to the following relation.

$$(E_{1/2})_{TlZ} = \text{constant} + 0.0591 \log (\alpha_H)_Z \quad (3)$$

where $(\alpha_H)_Z$ is the (α_H) value of CyDTA.

Thermodynamically, the formation of a protonated chelate always means an increase in the conditional formation constant, and hence, a negative shift of the half-wave potential. Therefore, the above facts clearly indicate that thallium(I) ion forms not only a normal chelate, TlZ^{3-}, but also a protonated chelate, TlH_nZ^{n-3}, with both GEDTA and CyDTA. Thus, from the above experimental results and discussion, the following electrode reaction can be assumed,

$$\begin{array}{ccc} TlZ^{3-} + Hg + e^- = Tl(Hg) + Z^{4-} & & \\ \updownarrow nH^+ & & \updownarrow nH^+ \\ TlH_nZ^{n-3} & & H_nZ^{n-4} \end{array} \quad (4)$$

with the half-wave potential expressed as:

$$(E_{1/2})_{TlZ} = E^0_{Tl} - 0.0591\left[\log K_{TlZ}(1 + K^H[H^+] + \cdots + K^{nH}[H^+]^n) - \log (\alpha_H)_Z - \log f_{Tl^+} + \log [Z]_f + \log \frac{k_{Tl(Hg)}}{k_{TlZ}}\right] \quad (5)$$

where K_{TlZ} is the formation constant of a normal thallium(I) chelate, $K^{nH}=[TlH_nZ^{n-3}]/[TlZ^{3-}]\cdot[H^+]_n$, n, 1,2,3,$\cdots$, and other symbols have their usual meanings.[1,4]

As discussed previously on the polarography of thallium(I)-DTPA chelate,[1] when normal and protonated chelates are formed and the electrode reaction is reversible, the following relation can be expected.

$$K_{TlZ}(1+K^H[H^+]+\cdots+K^{nH}[H^+]^n) = \text{antilog}\left[\frac{\Delta E_{1/2}}{0.0591} - \log [Z]_f + \log \frac{k_{Tl^+}}{k_{TlZ}} + \log (\alpha_H)_Z\right] \quad (6)$$

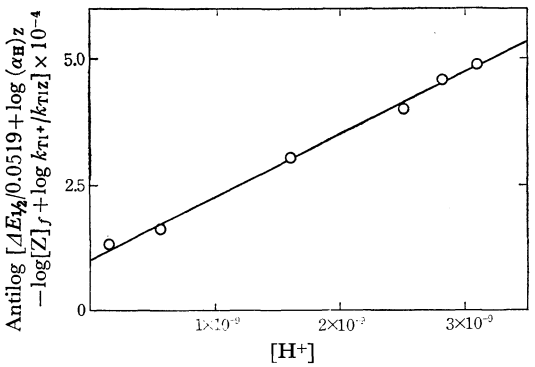

Fig. 4. The relation between antilog [$\Delta E_{1/2}$/0.0591 + log $(\alpha_H)_Z$ − log $[Z]_f$ + log (k_{Tl^+}/k_{TlZ})] and the hydrogen ion concentration.
GEDTA system: μ=0.30,
Concentration of thallium(I) = 1.09 mM

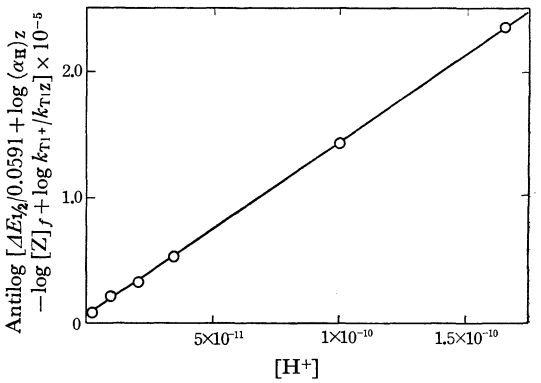

Fig. 5. The relation between antilog [$\Delta E_{1/2}$/0.0591 + log $(\alpha_H)_Z$ − log $[Z]_f$ + log (k_{Tl^+}/k_{TlZ})] and the hydrogen ion concentration.
CyDTA system: μ=0.30,
Concentration of thallium(I) = 1.09 mM

where $\Delta E_{1/2}$ denotes the shift of the half-wave potential due to complex formation.

With the aid of Eq. (6), the composition and stability constants of thallium(I)-GEDTA and -CyDTA chelates were determined using some typical $\Delta E_{1/2}$ values. Results are shown in Figs. 4 and 5. These results clearly show that, in both

Table 2. Equilibrium constants* (μ=0.30)

i) Dissociation constants (mixed constants)*1

	pK_1	pK_2	pK_3	pK_4
GEDTA[6]	1.96	2.57	8.86	9.19
CyDTA[7]	2.39	3.41	5.93	11.43

ii) Stability constants

	log K_{TlZ}	
Tl(I)-GEDTA chelate	4.0	
Tl(I)-CyDTA chelate	3.8_5	6.7^{5} (μ=0.10)

iii) K^H values (mixed constants)

	log K^H
Tl(I)-GEDTA system	9.09
Tl(I)-CyDTA system	11.29

*1 These values were calculated from the related constants in solution of ionic strength 0.10 and the activity coefficients of the ions calculated by means of Davies equation.[8]

5) G. Anderegg and E. Bottari, *Helv. Chim. Acta*, **50**, 2341 (1967).
6) G. Schwarzenbach, H. Senn and G. Anderegg, *ibid.*, **40**, 1866 (1957).
7) G. Schwarzenbach and H. Ackermann, *ibid.*, **32**, 1682 (1949).
8) J. N. Butler, "Ionic Equilibrium," Addison-Wesley Publishing Co., Inc., Reading, Massachusetts (1964), p. 437.

GEDTA and CyDTA systems, thallium(I) ion forms chelates with the compositions TlZ^{3-} and $TlHZ^{2-}$. From the intercepts and slopes of the linear relation between the right hand side of Eq. (6) and the hydrogen ion concentration, K_{TlZ} and K^{H} values were determined and given in Table 2 together with k values used in the calculation of $(\alpha_H)_Z$.

The finding that thallium(I) ion forms normal and protonated chelates with CyDTA is in contrast to the results of Anderegg and Bottari.[5] They have studied the complexation reaction of thallium(I) with CyDTA employing a pH titration method and concluded that thallium(I) ion forms only a normal chelate with a 1-to-1 composition (log $K_{TlZ}=6.7$, $\mu=0.10$); no detailed experimental results were given, and thus, no satisfactory explanation for this discrepancy can be given.

BULLETIN OF THE CHEMICAL SOCIETY OF JAPAN VOL. 42 724—727 (1969)

Polarographic Studies of Copper(II) Chelates of Ethylenediamine-*N*,*N*,*N*′,*N*′-tetrapropionic Acid and Diethylenetriamine-pentaacetic Acid

Mutsuo KODAMA and Yayoe TOMINAGA

Department of Chemistry, Ibaraki University, Mito, Ibaraki

(Received July 24, 1968)

D. c. polarographic behavior of copper(II) in ethylenediamine-*N*,*N*,*N*′,*N*′-tetrapropionate (EDTP) and diethylenetriaminepentaacetate (DTPA) solutions was studied systematically. In EDTP solution, copper(II) ion invariably gave a single well-defined wave corresponding to the following reduction.

$$CuX^{2-} + nH^+ + Hg + 2e^- = Cu(Hg) + H_nX^{n-4}$$

In the DTPA solution, copper(II) ion gave a single wave reversible in nature at pH below 5.0, corresponding to the following electrode reaction.

$$\begin{array}{l} CuZ^{3-} + nH^+ + Hg + 2e^- = Cu(Hg) + H_nZ^{n-5} \\ \quad\quad\quad\quad \uparrow\downarrow H^+ \\ \quad\quad\quad\quad CuHZ^{2-} \end{array}$$

At higher pH, however, two waves could be observed. The second step was irreversible and its wave-height increased with increasing pH at the expense of the height of the first step.

In a previous paper,[1] d.c. polarographic behavior of copper(II)-*N*-(2-hydroxyethyl)-ethylenediamine *N*,*N*′,*N*′-triacetate and -2,2′-ethyldioxybis[ethyliminodi(acetato)] chelates was studied systematically. In *N*-(2-hydroxyethyl)-ethylenediamine *N*,*N*′,*N*′-triacetate (EDTA-OH) solution, copper(II) ion was found to form only a normal chelate with a 1-to-1 composition with EDTA-OH, and to give invariably a single well-defined wave over the entire pH range covered. In 2,2′-ethylenedioxybis[ethyliminodi(acetate)] (GEDTA) solution, however, copper(II) ion gave two waves. The first wave was reversible in nature, but the second irreversible. The precise nature of the first step could be satisfactorily described by assuming that a normal copper(II)-GEDTA chelate of a 1-to-1 composition, which is in equilibrium with a normal chelate of a 1-to-2 composition, a protonated chelate and a mixed ligand chelate involving an acetate ion in solution, undergoes a reversible two-electron reduction at the mercury electrode.

In the present paper, results of a d.c. polarographic study on copper(II) chelates of ethylenediamine-*N*,*N*,*N*′,*N*′-tetrapropionic acid (EDTP) and diethylenetriaminepentaacetic acid (DTPA) are presented.

Experimental

Reagents. The preparation and standardization of copper(II) perchlorate solutions were described previously.[2] The purification of EDTP and DTPA and the preparation of their solutions were also described previously.[3] All other chemicals were of analytical reagent grade and used without further purification. The ionic strength of the sample solution was adjusted to 0.30 by adding an appropriate volume of 1.0 M $NaClO_4$ solution.

Apparatus and Experimental Procedures. All apparatus and experimental procedures were as employed

1) M. Kodama and Y. Tominaga, This Bulletin, **42**, 721 (1969).

2) M. Kodama and H. Ebine, This Bulletin, **40**, 1857 (1967).

previously.[3,4]

Results and Discussion

D.C. Polarographic Behavior of Copper(II) Ion in EDTP Solution. D. c. polarographic behavior of copper(II)-EDTP chelate in solutions containing an excess of un-complexed EDTP was studied systematically in the pH range 3.46 to 7.80. In the pH range from 3.46 to 5.80, an acetate buffer (total concentration of acetate, 0.10 M) was used in order to maintain the pH of the solution at a constant value. At pH above 5.80, no buffer reagent was used because in this pH region, the present system containing un-complexed EDTP is considered to have enough buffer capacity to keep the pH constant.

As in the EDTA-OH system,[1] copper(II) ion in EDTP solution gave a single well-defined wave, the height of which was exactly proportional to the bulk concentration of copper(II) ion and the square-root of the effective pressure on the dropping mercury electrode (DME). The result is not shown here. A typical polarogram and the result of a log-plot are shown in Figs. 1 and 2. These results clearly indicate that the copper(II) ion in the EDTP solution undergoes a reversible, two-electron reduction at the mercury electrode. As shown in Fig. 3, the half-wave potential, $(E_{1/2})_X$, was found to shift to more negative potentials with increasing pH of the solution according to the

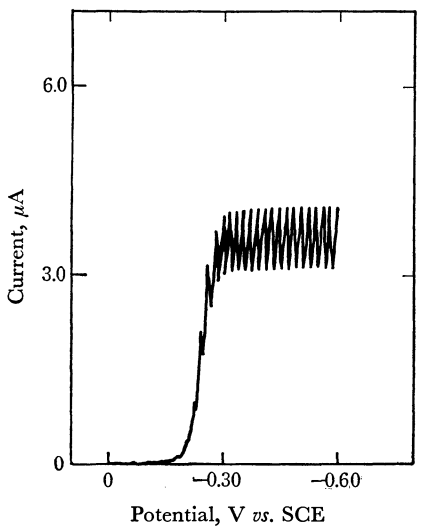

Fig. 1. D.c. polarogram of copper(II)-EDTP chelate.
pH=5.46, μ=0.30
Concentration of EDTP=20.0 mM
Concentration of copper(II)=0.682 mM

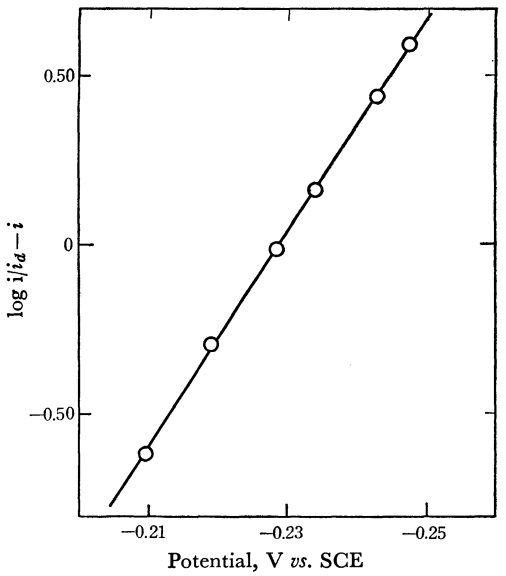

Fig. 2. The d.c. log-plot analysis.
pH=5.46, μ=0.30
Concentration of EDTP=20.0 mM
Concentration of copper(II)=0.682 mM

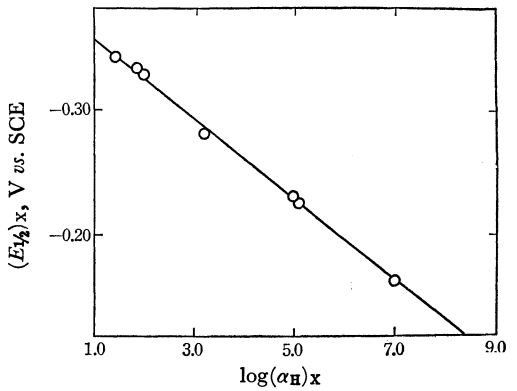

Fig. 3. The relation between the half-wave potential and the pH value.
μ=0.30
Concentration of EDTP=20.0 mM
Concentration of copper(II)=0.682 mM

following relation.

$$(E_{1/2})_X = \text{constant}_1 + 0.0296 \log (\alpha_H)_X \quad (1)$$

where $(\alpha_H)_X = 1+[H^+]/k_4+[H^+]^2/k_4 \cdot k_3+[H^+]^3/k_4 \cdot k_3 \cdot k_2+[H^+]^4/k_4 \cdot k_3 \cdot k_2 \cdot k_1$, and k's are the dissociation constants of EDTP.

The half-wave potential also shifted to more negative potentials with increasing concentration of un-complexed EDTP, $[X]_f$, according to the following relation,

$$(E_{1/2})_X = \text{constant}_2 - 0.0296 \log [X]_f \quad (2)$$

but it is independent of the concentration of acetate and copper(II) ions. Results are given in Table 1.

3) M. Kodama and A. Kimura, *ibid.*, **40**, 1639 (1967).
4) M. Kodama, T. Noda and M. Murata, *ibid.*, **41**, 354 (1968).

TABLE 1. DEPENDENCE OF $(E_{1/2})_X$ ON THE CONCENTRATION OF EDTP OR ACETATE ION
pH=5.33, μ=0.30
Concentration of copper(II)=0.682 mM

A) Dependence of $(E_{1/2})_X$ on the concentration of EDTP.
Total concentration of acetate=0.10 M

Concentration of EDTP mM	$(E_{1/2})_X$ V *vs.* SCE	$\Delta(E_{1/2})_X$, mV Calcd	Obsd
15.0	−0.229	3.6	4.0
20.0	−0.233	0	0
40.0	−0.241	−9.0	−8.0
40.0*1	−0.242	−9.0	−9.0

*1 Concentration of copper(II)=1.364 mM

B) Dependence of $(E_{1/2})_X$ on the concentration of acetate.
Concentration of EDTP=20.0 mM

Concentration of acetate, M	$(E_{1/2})_X$ V *vs.* SCE
0.05	−0.233
0.10	−0.233
0.30	−0.231

From the above experimental results, it can be safely concluded that copper(II) ion forms only a normal 1-to-1 chelate with EDTP under the present experimental conditions and the electrode reaction can be expressed as,

$$CuX^{2-} + nH^+ + Hg + 2e^- = Cu(Hg) + H_nX^{n-4} \quad (3)$$

with the half-wave potential corresponding to:

$$(E_{1/2})_X = E^0_{Cu} + 0.0296[\log f_{Cu^{2+}} + \log\frac{k_{Cu(Hg)}}{k_{CuX}} + \log(\alpha_H)_X - \log K_{CuX} - \log[X]_f] \quad (4)$$

where CuX^{2-} and H_nX^{n-4} refer to copper(II)-EDTP chelate and incompletely dissociated EDTP anion, respectively, and $f_{Cu^{2+}}$, $k_{Cu(Hg)}$, k_{CuX}, K_{CuX} and E^0_{Cu} have their usual meanings. Therefore, as discussed previously,[1] the shift of the half-wave potential of copper(II), $\Delta E_{1/2}$, by complex formation with EDTP, can be given by:

$$\Delta E_{1/2} = 0.0296[\log K_{CuX} + \log\frac{k_{CuX}}{k_{Cu^{2+}}} + \log[X]_f - \log(\alpha_H)_X] \quad (5)$$

where $k_{Cu^{2+}}$ has the same meaning as in a previous paper.[1]

With the aid of Eq. (5), log K_{CuX} value was calculated to be 15.1 from the $\Delta E_{1/2}$ value at $(\alpha_H)_X=1$. In the calculation, $k_{CuX}/k_{Cu^{2+}}$ determined experimentally as 1/1.20 was used. The logK_{CuX} value thus obtained agreed well with the reported one (14.80 at μ=0.30).[5] This agreement lends strong support to the above explanation.

D. C. Polargraphic Behavior of Copper(II) Ion in Diethylenetriaminepentaacetate Solution. Polarographic behavior of copper(II)-DTPA chelates was also studied under experimental conditions similar to those in the EDTP system. At pH below 5.0, copper(II) ion in DTPA solutions invariably gave a single well-defined wave, the height of which was exactly proportional to the concentration of copper(II) ion and the square-root of the effective mercury pressure on the DME. The plot of $\log(i/(i_d-i))$ against applied d. c. potential, E, gave a linear relation with a slope of −31 mV, suggesting a reversible two-electron reduction. The results are not shown here. As shown by the curve in Fig. 4, at pH above 5.0,

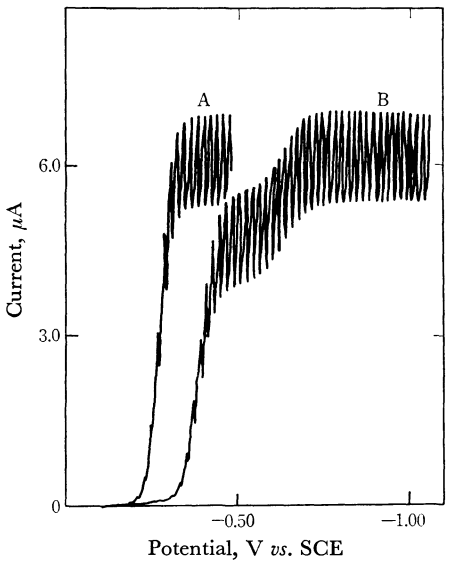

Fig. 4. D.c. polarogram of copper(II)-DTPA chelate.
μ=0.30
Concentration of DTPA=20.0 mM
Concentration of copper(II)=1.364 mM
A: pH=4.15 B: pH=6.01

however, copper(II) ion gave two waves. The first wave is reversible to such an extent that a log-plot gave a linear relation with a slope of −45 mV, and the wave-height increases with increase in hydrogen ion concentration at the expense of the second wave height. The second wave was irreversible in nature. Therefore, in the present study, results obtained mainly at pH below 5.0 will be given. At pH below 3.50, no buffer reagent was used because a system containing a large excess of un-complexed DTPA has enough buffer capacity to maintain the pH value of the solution constant.

As in the EDTP system, at a given pH, the half-wave potential of copper(II)-DTPA chelate, $(E_{1/2})_Z$, shifted to more negative potentials with increase in the bulk concentration of DTPA, $[Z]_f$ according to the following relation:

$$(E_{1/2})_Z = \text{constant}_3 - 0.0296\log[Z]_f \quad (6)$$

but, it is independent of the concentrations of acetate and copper(II) ions. The results are shown in Table 2. These facts clearly indicate that copper(II) ion forms only a normal chelate of a 1-to-1 composition with DTPA under the present experimental conditions. The half-wave potential also shifted to more negative potentials with increasing pH of the solution. But, in contrast with findings in the EDPT system, the plot of $(E_{1/2})_Z$ *vs.* $\log(\alpha_H)_Z$ did not give a linear relation with a slope of +30 mV. Here, $(\alpha_H)_Z$ is the (α_H) value of DTPA.

As discussed previously on the polarography of thallium(I)-DTPA chelate,[4] when copper(II) ion forms both normal and mono-protonated chelates with DTPA, and when the electrode reaction can be expressed as,

$$\begin{array}{l} CuZ^{3-} + nH^+ + Hg + 2e^- = Cu(Hg) + H_nZ^{n-5} \\ \quad\uparrow\downarrow H^+ \\ CuHZ^{2-} \end{array} \qquad (7)$$

the following relation can be expected thermodynamically.

$$K_{CuZ}(1+K^H_{CuZ}\cdot[H^+]) = \text{antilog}\left[\frac{\Delta(E_{1/2})_Z}{0.0296} + \log(\alpha_H)_Z - \log[Z]_f + \log\frac{k_{Cu^{+2}}}{k_{CuZ}}\right] \qquad (8)$$

where $\Delta(E_{1/2})_Z$ is the shift of the half-wave potential due to chelate formation with DTPA, K_{CuZ} the formation constant of copper(II)-DTPA chelate and $K^H_{CuZ}=[CuHZ^{2-}]/[CuZ^{3-}]\cdot[H^+]$. This relation was examined using some experimental data. The result shown in Fig. 5 clearly confirms the above explanation given by the present authors. From

Table 2. Dependence of $(E_{1/2})_Z$ on the concentration of DTPA or acetate ion

pH = 3.80, μ = 0.30

Concentration of copper (II) = 0.682 mM

A) Dependence of $(E_{1/2})_Z$ on the concentration of DTPA.

Total concentration of acetate = 0.10 M

Concentration of DTPA, mM	$(E_{1/2})_Z$ V *vs.* SCE	$\Delta(E_{1/2})_Z$, mV Calcd	Obsd
10.0	− 0.229	5.6	5.0
15.0	− 0.234	0	0
20.0	− 0.239	− 3.9	− 5.0
20.0*1	− 0.239	− 3.9	− 5.0
40.0	− 0.245	− 9.1	− 11.0

*1 Concentration of copper (II) = 1.364 mM

B) Dependence of $(E_{1/2})_Z$ on the concentration of acetate.

Concentration of DTPA = 20.0 mM

Concentration of acetate, M	$(E_{1/2})_Z$, V *vs.* SCE
0.05	− 0.244
0.10	− 0·245
0.30	− 0.243

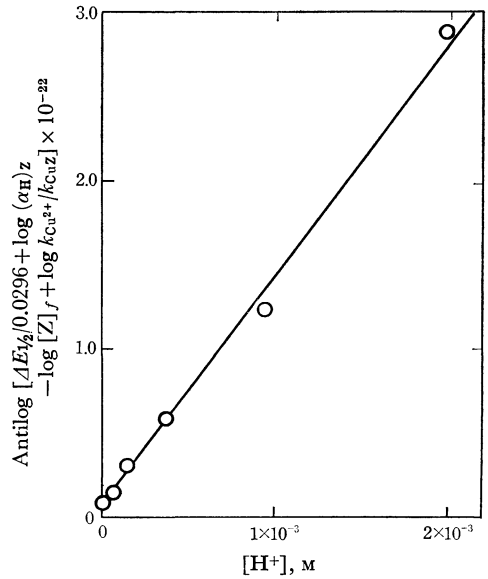

Fig. 5. The relation between antilog $[\Delta(E_{1/2})/0.0296 + \log(\alpha_H)_Z - \log[Z]_f + \log(k_{Cu^{2+}}/k_{CuZ})]$ and the concentration of hydrogen ion.
μ=0.30
Concentration of copper(II) = 0.683 mM

Table 3. Equilibrium constants (μ=0.30)

i) Dissocidation constants (mixed constants)

	pK_1	pK_2	pK_3	pK_4	pK_5
EDTP[5]**	2.96	3.32	6.58	9.33	—
DTPA[6]**	1.82	2.68	4.10	7.74	10.14

ii) Stability constants

	log K_{CuZ}	
Copper(II)-EDTP chelate	15.10*	14.80[5]**
Copper(II)-DTPA chelate	21.00*	20.78[7]**

iii) Equilibrium constant (mixed constant)

Cu(II)-DTPA chelate:	$\log K^H_{CuZ}(=[CuHZ^{2-}]/[CuZ^{3-}]\cdot[H^+])$	
	4.12*	4.45[7]**

* These values were obtained by the present authors.

** Those values were calculated from the related constants in solutions of ionic strength 0.10 and the activity coefficients of the ions calculated by means of Davies equation.[8]

the slope and intercept of the linear relation between the right-hand side of Eq. (8) and $[H^+]$, K_{CuZ} and K^H_{CuZ} were estimated and given in Table 3 along with the reported value and the pK values of DTPA. The agreement between observed and reported values can be regarded as satisfactory.

5) R. C. Curteny, S. Chaberek, Jr. and A. E. Martell, *J. Am. Chem. Soc.*, **75**, 4814 (1953).
6) E. Wanninen, *Suomen Kem.*, **28B**, 146 (1955).
7) G. Anderegg, P. Nageli, F. Muller and G. Schwarzenbach, *Helv. Chim. Acta*, **42**, 827 (1959).
8) J. N. Butler, "Ionic Equilibrium," Addison-Wesley Publishing Co., Inc., Reading, Massachusetts (1964), p. 437.

BULLETIN OF THE CHEMICAL SOCIETY OF JAPAN VOL. 42 728—731 (1969)

Asymmetric Reactions. II. Anomalous Stereoselectivity of the Grignard Reaction with *N*-Benzyl-2,3-*O*-isopropylidene-D-glyceraldimine

Yoshiaki OHGO, Juji YOSHIMURA and Tetsuo SATO

Laboratory of Organic Chemistry, Tokyo Institute of Technology, Ookayama, Meguro-ku, Tokyo

(Received March 23, 1968)

Stereoselectivity of the organomagnesium reaction with *N*-benzyl-2,3-*O*-isopropylidene-D-glyceraldimine was examined under various conditions (change of molarity, solvent, and composition ratio of reagents). The selectivity was not effected by the molarity of the reagents but by the solvent. When the substrate was treated with a mixture of various ratio of magnesium bromide and diphenylmagnesium, a remarkable effect of the ratio on the stereoselectivity was observed. Maximum ratio of *erythro*/*threo* was obtained at the point of equimolar mixture of magnesium bromide and diphenylmagnesium in ether. The structure of the transition intermediate was discussed.

The authors have reported the difference in stereoselectivity between the Grignard and alkyllithium reactions of *N*-phenyl-3,4;5,6-di-*O*-isopropylidene D-glucosaminonitrile,[1] *N*-substituted 3,4-*O*-isopropylidene-D-tetrosaminonitriles, 2,3-*O*-isopropylidene-D-glyceraldimines,[2] and 2,3-*O*-isopropylidene-D-glyceraldehyde,[3] in which the configuration of the major product in the Grignard reactions was inconsistent with that deduced from Cram's rigid model.[4] This stereoselectivity of the Grignard reaction was explained by two possible models A and B.

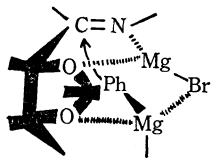

A

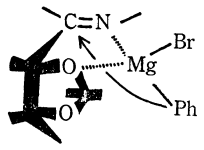

B

A similar steric difference was observed by Stocker *et al.* between phenyllithium and phenylmagnesium halide reactions with α-hydroxyketones or α,β-diketones.[5-7]

The composition of the Grignard reagents under the reaction condition seems to play an important role on such an anomaly. Although the structure of the crystalline Grignard reagent prepared from magnesium and bromobenzene or ethyl bromide in ether was formulated by X-ray diffraction method as $RMgBr \cdot 2Et_2O$ (R=phenyl or ethyl),[8,9] the reagent in the solution exists as an equilibrium mixture of several species as follows. Molecular weight determination by ebullioscopic method showed that the Grignard reagents exist as monomeric species in low molarity in ether solution (10^{-2} M concentration) and are apt to associate in higher molarity,[10,11] while in tetrahydrofuran they exist as monomers even in a higher molarity.[12] IR spectroscopic data suggested that species of the Grignard reagent changes considerably with varying solvent, the nature of the organic part and halogen atom.[13]

The authors examined the effect of the reaction conditions (*i. e.*, change of molarity, solvent and composition ratio of reagents) on the above mentioned stereoselectivity in the reaction of the Grignard reagent with *N*-benzyl-2,3-*O*-isopropylidene-D-glyceraldimine (I), in order to obtain information on the structure of the transition state. Model (A) was found to be more probable.

1) J. Yoshimura, This Bulletin, **35**, 536 (1962).
2) Asymmetric Reactions. I: J. Yoshimura, Y. Ohgo and T. Sato, *J. Am. Chem. Soc.*, **86**, 3858 (1964).
3) This was presented at the 17th Annual Meeting of the Chemical Society of Japan, Tokyo, April, 1964.
4) D. J. Cram and K. R. Kopecky, *J. Am. Chem. Soc.*, **81**, 2737 (1959).
5) J. H. Stocker, P. Sidisunthorn, B. M. Benjamin and C. J. Collins, *ibid.*, **82**, 3913 (1960).
6) J. H. Stocker, *J. Org. Chem.*, **29**, 3593 (1964).
7) J. H. Stocker, *J. Am. Chem. Soc.*, **88**, 2878 (1966).
8) G. Stucky and R. E. Rundle, *J. Am. Chem. Soc.*, **85**, 1002 (1963); *ibid.*, **86**, 4825 (1964).
9) L. J. Guggenberger and R. E. Rundle, *ibid.*, **86**, 5344 (1964).
10) A. D. Vreugdenhil and C. Blomberg, *Rec. trav. Chim.*, **82**, 453 (1963).
11) E. C. Ashby and M. M. Smith, *J. Am. Chem. Soc.*, **86**, 4363 (1964).
12) E. C. Ashby and W. E. Becker, *ibid.*, **85**, 118 (1963).
13) R. M. Salinger and H. S. Mosher, *ibid.*, **86**, 1782 (1964).

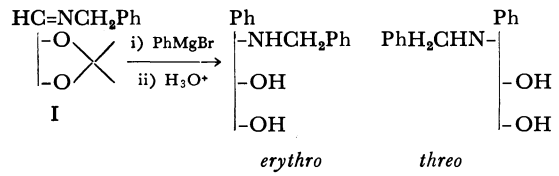

Results

Effects of Concentration and Solvent. I was treated with 3 molar equivalent of organomagnesium compounds under various conditions followed by hydrolysis to give a diastereoisomeric mixture of 1-benzylamino-1-deoxy-1-*C*-phenyl-*threo*- and -*erythro*-D-glyceritols. Diastereoisomeric ratios (*erythro*/*threo*) were calculated from the optical rotations as previously reported.[2)]

The results obtained by changing solvent and molarity are shown in Table 1.

Table 1. Effect of solvent and molarity on the stereoselectivity

Run	Solvent	Molarity	E/T
1	Ether	1.5 M	3.5[2)]
2	Ether	0.081 M	3.4
3	THF	1 M	1.6
4	Benzene	1 M	4.26
5	Ether+TEA[a)]	1.7 M	3.0
6	Ether+TEA[b)]	1.6 M	2.9
7	Ether+TEA[c)]	1.1 M	2.9

a) A mixture of ether (40 m*l*) and triethylamine (3.2 m*l*).
b) A mixture of ether (40 m*l*) and triethylamine (6.4 m*l*).
c) A mixture of ether (40 m*l*) and triethylamine (26 m*l*).

Table 2. Effect of the molar ratio ($MgBr_2/Ph_2Mg$) on the stereoselectivity

Run	Reagent (moles/mole substrate) Ph_2Mg	Reagent (moles/mole substrate) $MgBr_2$	E/T
8	2.15	0	1.56
9	1.29	0.5	3.0
10	1.29	1	4.4
11	1.29	2	5.45
12	1.29	3	4.87
13	1.29	5	3.76
14	1.29	10	2.9

As was shown in runs 1, 2, 5, 6 and 7, the stereoselectivity was not effected by the molarity of the reagents. However, it is worth mentioning that a remarkable difference was found between stereoselectivity in THF solution and in ether solution of lower molarity. No remarkable effect was observed by addition of triethylamine.

Effect of Composition of the Grignard Reagent. I was treated with a mixture of various ratio of magnesium bromide to diphenylmagnesium in ether.

The results are shown in Table 2 and Fig. 1. Figure 1 was obtained by plotting E/T against the molar ratio of magnesium bromide to diphenylmagnesium. It shows that E/T increases steeply with the increase of the ratio of $MgBr_2/Ph_2Mg$ until the ratio reaches about 1, and then begins to decrease gradually with a further increase of the ratio of $MgBr_2/Ph_2Mg$ (>1). Maximum E/T (>5.45) was much greater than that previously obtained by conventional Grignard reagent ($E/T=3.5$).[2)]

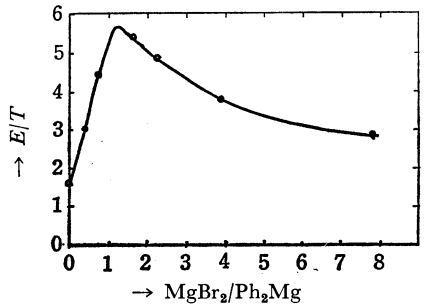

Fig. 1. The effect of the ratio of $MgBr_2/Ph_2Mg$ on the stereoselectivity.

Composition of the Complex formed in the Reaction and the Stereoselectivity by Reverse Addition Mode. In the ordinary Grignard reactions in which the solution of the substrate is added into the Grignard solution, it is observed that a white precipitate appears instantly and then disappears probably on account of being dissolved by excess Grignard solution. If so, a reverse mode of addition in which the reagent is added into the substrate solution should cause precipitation. As expected, the precipitate appeared and increased with the amount of the reagent added till about 1—1.5 equivalent to the substrate, and then began to dissolve with further addition. At the point of the equivalent molar ratio, the precipitate was separated from the solution. The molar ratio of phenylmagnesium bromide to the substrate in precipitate and that in the solution were determined from the content of magnesium and bromide to be 1.5 and 0.16 respectively. This shows that the reagent is considerably concentrated in the precipitate.

Table 3. The stereoselectivities obtained by the reverse addition mode

Run	PhMgBr (moles/mole substrate)	Product E/T
15	1	2.7
16	2	3.16

Two examples of E/T in the reverse addition mode are shown in Table 3. The results show that the stereoselectivity decreased as a whole to some extent, and is apt to increase with an increased amount of the reagent (compare runs 15, 16 and 1).

Discussion

The monomeric Grignard reagent in ether solution [run 2, $E/T=3.4$] gives the same results as the dimeric Grignard ethereal solution [run 1, $E/T=3.5$]. But the result is quite different in THF solution [run 3, $E/T=1.6$] in which the Grignard reagent exists also in monomeric form. This marked difference suggests that species in THF solution differ from those in ether solution, or stronger coordination ability of THF prevents magnesium from bridging between N and C_2-O. The former agrees with the infrared spectroscopic data presented by Salinger and Mosher.[13]

Monomeric species in the Grignard reagent should be diphenylmagnesium, magnesium bromide and phenylmagnesium bromide. In the devised Grignard reaction in which the two monomeric species (magnesium bromide and diphenylmagnesium) are freshly mixed, E/T value increased sharply and linearly with increasing amount of magnesium bromide in the ratio of $MgBr_2/Ph_2Mg<1$ and decreased gradually with increasing amount of magnesium bromide in the region of the ratio >1. The maximum E/T value at $MgBr_2/Ph_2Mg\simeq 1$ was considerably greater than that in the conventional Grignard solution. This result implies that the equimolar mixture of diphenylmagnesium and magnesium bromide is of greater importance than phenylmagnesium bromide to give *erythro* product, and also that alkyl-bromine exchange is not so rapid under the reaction conditions because results with a mixture of magnesium bromide and diphenylmagnesium should be identical with that of conventional Grignard reagent if the exchange is rapid.

From these facts, it may be inferred that the transition state based upon the coordinative interaction (A) plays a greater role for governing the steric direction of the Grignard reaction than that based upon the electrostatic repuslion (B). Here, we must infer a more detailed structure of the possible transition state; which component forms a bridge between C_2-O and nitrogen, and which component coordinates to C_3-O (magnesium bromide or diphenylmagnesium).

Magnesium bromide is more acidic than diphenylmagnesium. Therefore it can be assumed that at first magnesium bromide preferentially makes a bridge between nitrogen and C_2-O by coordination and then diphenylmagnesium coordinates with C_3-O and bromine of the magnesium bromide as shown by C.

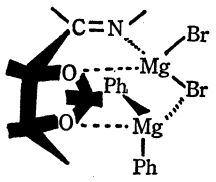

C

Model C explains that an equimolar mixture of magnesium bromide and diphenylmagnesium gives the highest yield of *erythro* derivative, because there is no phenyl group above the five membered ring made by N, C_1, C_2, O and Mg, but under the ring. This model is also in agreement with the results obtained by the reverse addition made. The ratio (reagent/substrate)$=1.5$ in the precipitate implies that half of the substrate is coordinated with dimeric species or two magnesium. It may be considered that the ratio of the substrate coordinated with the dimeric Grignard species increases further on increasing the amount of reagent. Therefore, the stereoselectivity is apt to increase with an increased amount of the reagent (run 15, 16 and 1).

The effect of excess magnesium bromide to lower the E/T can also be explained as follows. When the ratio of magnesium bromide to diphenylmagnesium becomes larger, magnesium bromide will coordinate with C_3-O competitively, and then, Ph-Mg species must approach from above the ring as is shown in diagram D. Consequently, excess magnesium bromide acts to lower the E/T value (run 12, 13, 14 and Fig. 1).

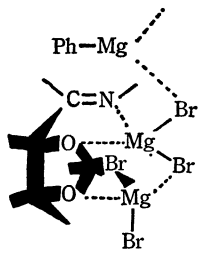

D

Cram *et al.* have explained reversal of the stereoselectivity of phenylmagnesium bromide reaction *vs.* phenyllithium reaction with α,β-diketones or hydroxyketones (Stocker's observation) by dipolar model.[14] However, it cannot be explained by the dipolar model that the reaction with low molar concentration of the Grignard reagent in ether (monomeric reagent) gave almost the same value as that with high molar concentration of the ethereal Grignard reagent (run 1 and 2), and

14) a) D. J. Cram and D. R. Wilson, *J. Am. Chem. Soc.*, **85**, 1245 (1963); b) J. W. Cornforth, R. H. Cornforth and K. K. Maphews, *J. Chem. Soc.*, **1959**, 112.

Table 4. Specific rotations of diastereomeric mixtures

Run	2	3	4	5	6	7	8	9	10	11	12	13	14	15	16
$[\alpha]_D$	+34	+10.5	+39	+31	+30	+30	+9	+31.5	+41	+45	+43	+37	+30	+28	+32

Each specific rotation was measured in ethanol ($c=1.0$, $l=1$).

also that excess of magnesium bromide disturbs formation of *erythro* derivative (Table 2 and Fig. 1).

Experimental

Preparation of the Grignard Reagent in Various Solvent. The Grignard reagent in ether or tetrahydrofuran was prepared as follows.

To a suspension of 1.7 g (0.07 g atom) of magnesium in 100 m*l* of ether or 70 m*l* of tetrahydrofuran was added dropwise a solution of 7.2 m*l* (0.069 mol) of bromobenzene in ether on heating.

The ethereal Grignard solution in low molarity (0.083 M concentration) was prepared by dilution of the above solution with ether (about 700 m*l*; to the final volume of 850 m*l*).

The Grignard benzene solution was prepared by addition of benzene (70 m*l*) to the syrup obtained by removal of ether from ethereal reagent described above.

The Grignard solution with a mixed solvent of ether and triethylamine was prepared by addition of 3.2 m*l*, 6.4 m*l* or 26 m*l* of triethylamine into the ethereal solution described above.

0.25 M Diphenylmagnesium Solution. Diphenylmagnesium was prepared according to the Schlenk method,[15] by shaking 148 g of diphenylmercury and 110 g of magnesium in 1700 m*l* of ether under nitrogen atmosphere for 30 days. Molarity was determined by residual titration with alkali.

2.5 M Magnesium Bromide Solution. An ether solution of magnesium bromide was prepared by the reaction of magnesium with ethylene bromide in ether.[16] The reaction mixture was filtered through glass filter under dried nitrogen atmosphere. The reagent was analyzed by titrating bromine with 0.5 N $AgNO_3$ solution using K_2CrO_3 as an indicator.

A Mixture of Diphenylmagnesium and Magnesium Bromide. In runs 8—14, 120 m*l* of 0.25 M diphenylmagnesium solution was mixed with 4.5 m*l*, 9 m*l*, 18 m*l*, 27 m*l*, 45 m*l* or 90 m*l* of 2.5 M $MgBr_2$ solution respectively, just before the reaction.

General Procedure for the Reaction of *N*-Benzyl-2,3-*O*-isopropylidene-D-glyceraldimine with Various Grignard Reagents. An ether solution of 5 g (0.0228 mol) of *N*-benzyl-2,3-*O*-isopropylidene-D-glyceraldimine was added at 0—5°C under nitrogen atmosphere to the Grignard solution described above. The reaction mixture was stirred at 0—5°C for 1 hr, and then refluxed with stirring for 6—10 hr. It was poured into ice-water containing ammonium chloride covered with 100 m*l* of ether. Ether layer was separated, washed with water, dried, and concentrated *in vacuo* to a syrup. The syrup was treated with 6 N hydrochloric acid (20 m*l*) at 100°C for 3 hr. An insoluble residue was removed by filtration through activated carbon. The filtrate was decolorized with activated carbon, and then extracted four times with 50 m*l* portions of ethyl acetate, after adjustment of the pH to about 10 with sodium hydroxide solution. The combined ethyl acetate solution was washed with water and dried over anhydrous sodium sulfate. The solution was concentrated under reduced pressure to give a diastereoisomeric mixture of the crude 1-benzylamino-1-deoxy-1-*C*-phenyl-D-glyceritol. Thin layer chromatography of each raw product gave a single spot (R_f: 0.63±0.01; solvent=ethanol - benzene mixture (7 : 3)) identical with authentic sample. Analytical values in every case were in agreement with that calculated for $C_{16}H_{19}O_2N$. The specific rotations of the crude products were measured and the results were summarized in Table 4. The mixture was fractionally crystallized from ethanol - acetone to isolate the two pure diastereoisomers. 1-Benzylamino-1-deoxy-1-*C*-phenyl-*threo*-D-glyceritol [mp 101—102°C, $[\alpha]_D$ −81 (*c* 1, ethanol)] and 1-benzylamino-1-deoxy-1-*C*-phenyl-*erythro*-D-glyceritol [mp 89—90°C, $[\alpha]_D$ +68 (*c* 1, ethanol).[2]

Reaction by Reverse Addition Mode. To an ethereal solution of 5 g (0.0228 mol) of I was added an equimolar or two molar equivalent Grignard solution in ether. The reaction mixture was treated by the same procedure as above.

The precipitate appeared on addition of equimolar amount of the reagent (0.00137 mol) into an ethereal solution of I (0.00137 mol) was separated from the solution and washed with ether. The precipitate was dried which weighed 3.15 g. The ether solution was concentrated *in vacuo* to give 1.25 g of a syrup. Combustion of 0.2090 g of the precipitate gave 0.0255 g of magnesium oxide. The ratio of the reagent to the substrate was calculated from this value. The calculated ratio (magnesium/substrate) was 1.5. Similar results were obtained by determination of bromine (using 0.5 N $AgNO_3$ solution). The molar ratio (bromine/substrate) was 1.47.

On the other hand, the ratio (reagent/substrate) in the syrup obtained from the solution was 0.16 by combustion analysis, and 0.35 by bromine determination

15) W. Schlenk, jun., *Ber.*, **64**, 736 (1931).

16) H. O. House, D. D. Traficante and R. A. Evans, *J. Org. Chem.*, **28**, 348 (1963).

BULLETIN OF THE CHEMICAL SOCIETY OF JAPAN VOL. 42 732—737 (1969)

Reaction of Methylsulfinyl Carbanion with Substituted Phthalic Esters

Yoshio Otsuji, Hideo Yabune and Eiji Imoto

Department of Applied Chemistry, Faculty of Engineering, University of Osaka Prefecture, Sakai-shi, Osaka

(Received April 19, 1968)

The treatment of dimethyl 3-nitrophthalate (I) with a mixture of dimethyl sulfoxide and sodium methoxide, followed by the acidification of the resulting mixture with hydrochloric acid, gave azoxybenzene-2,2',3,3'-tetracarboxylic acid (II) and 3-nitrophthalic acid (III). The similar treatment of dimethyl 4-nitrophthalate (IV) afforded 5-methoxy-2-nitroso-1,3-indanedione (V) and 4-methoxyphthalic acid (VI). The similar treatment of dimethyl 4-methoxyphthalate (XV) and dimethyl phthalate gave 2-chloro-2-methylthio-5-methoxy-1,3-indanedione (XVII) and 2-chloro-2-methylthio-1,3-indanedione (XIX) respectively. The general features of these reactions are described.

Becker and Russell[1,2] have recently found that the treatment of diethyl phthalate with methylsulfinyl carbanion and the acidification of the resulting mixture with hydrochloric acid give 2-chloro-2-methylthio-1,3-indanedione, which can then readily be converted to ninhydrin. We have extended this reaction to substituted phthalic esters in the hope of obtaining substituted ninhydrins. During the course of this investigation we have established several new features of this reaction, features which will be reported in this paper.

When dimethyl 3-nitrophthalate (I) was treated in a stream of nitrogen in dimethyl sulfoxide (DMSO) with methylsulfinyl carbanion prepared from DMSO and sodium methoxide, and when the resultant reaction mixture was acidified with hydrochloric acid, azoxybenzene-2,2',3,3'-tetracarboxylic acid (II) and the hydrolysis product, 3-nitrophthalic acid (III), were obtained in 50 and 43% yields respectively.

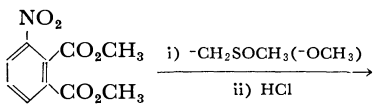

(I)

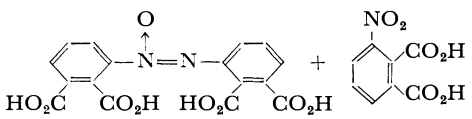

(II) (III)

The similar treatment of dimethyl 4-nitrophthalate (IV) gave 5-methoxy-2-nitroso-1,3-indanedione (V) and 4-methoxyphthalic acid (VI). The yields of V (48—14%) and VI (49—73%) varied to some extent from run to run. In some runs dimethyl 4-methoxyphthalate (VII) was also obtained.

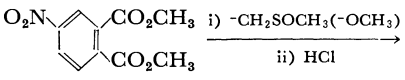

(IV)

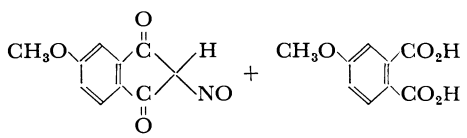

(V) (VI)

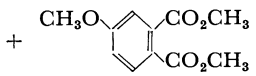

(VII)

The structure of V was established on the basis of its elemental analysis and by a study of its infrared and NMR spectra. The NMR spectrum of V in DMSO-d_6 showed the presence of an acidic proton at $-4.25\ \tau$, suggesting that V exists in the forms of Va, Vb, and Vc in polar solvents.

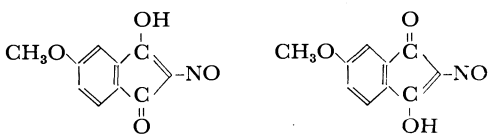

(Va) (Vb)

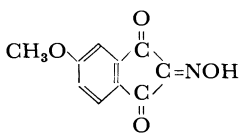

(Vc)

In accordance with this observation, the acetylation of V with acetic anhydride in pyridine gave a mono-acetylated product. The compound V

1) H-D. Becker and G. A. Russell, *J. Org. Chem.*, **28**, 1896 (1963).

2) H-D. Becker, *ibid.*, **29**, 1358 (1964).

also underwent alkaline hydrolysis to give VI. All the properties of the acid VI were identical with those of the acid obtained by the alkaline hydrolysis of the ester VII.

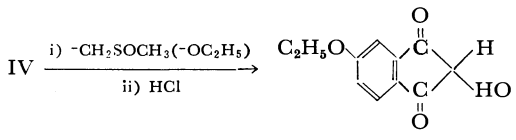

(VIII)

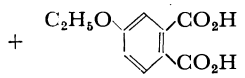

(IX)

The above unexpected behavior of IV was observed even when the anion species was changed from methoxide to ethoxide. Thus, the treatment of IV with methylsulfinyl carbanion prepared from DMSO and sodium ethoxide and a similar work-up of the resultant mixture gave 5-ethoxy-2-nitroso-1,3-indanedione (VIII) and 4-ethoxyphthalic acid (IX) in 51 and 32% yields respectively.

The above reactions of IV have two noticeable features: (1) the replacement of the nitro group by the alkoxyl group, and (2) the formation of nitroso compounds.

The nucleophilic replacement of a nitro group attached to an aromatic ring by an alkoxide ion has been found to occur in the aromatic nitro compounds which are activated by an electron-withdrawing group such as nitro,[3] cyano[4] or carbonyl[5]. In the compound IV two methoxycarbonyl groups act as the activating groups. The failure of the replacement of the nitro group in I may be supposed to be due to a steric hindrance caused by the neighboring methoxycarbonyl group. The following observations are of interest in this connection. When methyl *o*-nitrobenzoate (X) was subjected to the above reaction under similar conditions, azobenzene-2,2'-dicarboxylic acid (XI) and azoxybenzene-2,2'-dicarboxylic acid (XII) were obtained in 44 and 33% yields respectively. On the other hand, methyl *p*-nitrobenzoate (XIII) afforded only the hydrolysis product, *p*-nitrobenzoic acid (XIV).

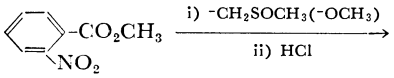

(X)

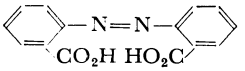

(XII)

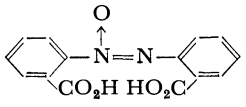

(XII)

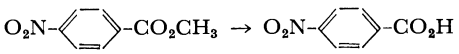

(XIII) (XIV)

These results seem to indicate that at least two methoxycarbonyl groups are needed for the nucleophilic replacement of the nitro group by the alkoxyl group.

The nitroso compounds, V and VIII, were supposed to be formed from dimethyl 4-alkoxyphthalate, which is produced by the replacement of the nitro group in IV by the methoxyl or the ethoxyl group if the nitrite ion is present in the reaction system (the nitrite ion was, in fact, found to be liberated during the course of the reaction leading from IV to V or VIII).

This theory was partly verified by the fact that the treatment of dimethyl 4-methoxyphthalate with methylsulfinyl carbanion prepared from DMSO and potassium *t*-butoxide, the addition of sodium nitrite, and then the acidification of the resultant mixture with hydrochloric acid gave V in a 66% yield. This reaction probably proceeds through an anion of the *β*-keto sulfoxide (XV).

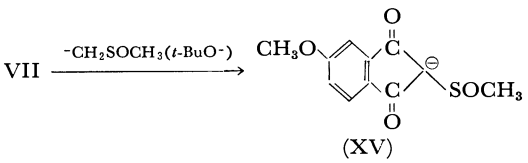

(XV)

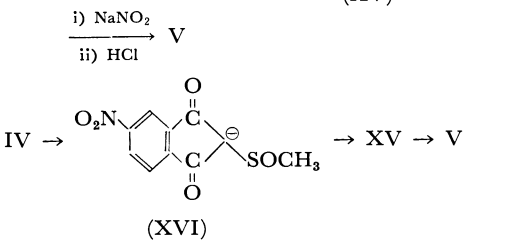

(XVI)

However, another possibility regarding the pathway of the reaction must also be considered. As will be mentioned later, VII did not undergo any condensation reaction leading to XV or its derivatives, but underwent hydrolysis to give the diacid VI when methylsulfinyl carbanion prepared from DMSO and sodium methoxide was used. On the other hand, the nitroso compound was produced from IV even when methylsulfinyl carbanion prepared from DMSO and sodium methoxide was used. Obviously, in the process of the formation of V from IV the condensation of the ester with methylsulfinyl carbanion, which gives an intermediate such as *β*-keto sulfoxide XVI, must be involved. These arguments, therefore, lead to a pathway in which the condensation of IV

3) F. Reverdin, "Organic Syntheses," Coll. Vol. 1, p. 219 (1956).

4) V. V. Richter, *Ber.*, **4**, 21, 459, 553 (1871); **8**, 1418 (1875).

5) J. H. Gorvin, *Chem. and Ind.*, **1967**, 1525.

with methylsulfinyl carbanion may occur prior to the replacement of the nitro group by the alkoxyl group: that is, V, might be formed through 2-methylsulfinyl-5-nitro-1,3-indanedione or its anion (XVI). A detailed examination of the mechanism and a synthetic application of these reactions to afford nitroso compounds are now under way in our laboratory; our results will be published in a separate paper.

The reaction of VII with methylsulfinyl carbanion was then studied in some detail. The treatment of VII with methylsulfinyl carbanion prepared from DMSO and sodium methoxide, and the acidification of the resultant mixture with hydrochloric acid, led to the hydrolysis product, VI. However, when methylsulfinyl carbanion prepared from DMSO and potassium *t*-butoxide was used, 2-chloro-2-methylthio-5-methoxy-1,3-indanedione (XVII) was obtained; upon being refluxed in ethanol, this compound yielded 2-ethoxy-2-methylthio-5-methoxy-1,3-indanedione (XVIII).

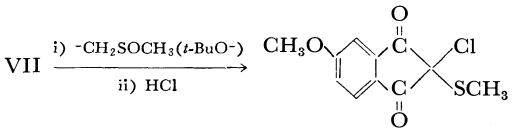

(XVII)

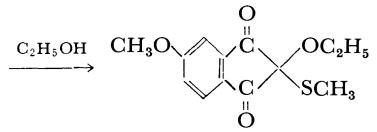

(XVIII)

The structure of XVIII was established on the basis of its elemental analysis, and on a study of its infrared and NMR spectra.

Since, in the above reactions, methylsulfinyl carbanion is formed in the pre-equilibrium stage, the use of a much stronger base would produce a higher concentration of the carbanion. The above results suggest, therefore, that the higher concentration of methylsulfinyl carbanion makes it possible to accomplish the condensation reaction of the carbanion with such compounds as VII, in which the reactivity of the carbonyl group toward nucleophiles is somewhat lowered by the presence of an electron-releasing group.

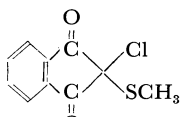

(XIX)

Finally, we repeated the Becker and Russell reaction on dimethyl phthalate using methylsulfinyl carbanions prepared from DMSO and sodium methoxide, and DMSO and potassium *t*-butoxide. In these cases 2-chloro-2-methylthio-1,3-indanedione (XIX) was obtained in yields of 44 and 57% respectively.

Thus, the following conclusions can be drawn from these studies: 1) for the phthalic esters having the nitro group as a substituent, the reaction leads to the reduction of the substituent or the replacement of the substituent by the nucleophiles which are present in the reaction system; 2) for the unsubstituted phthalic esters and phthalic esters with an electron-releasing substituent such as the methoxyl group, a substitution reaction with methylsulfinyl carbanion on the ester carbonyl group takes place.

Experimental

All the melting points are uncorrected. The infrared spectra were obtained with a Hitachi EPI-S_2 infrared spectrophotometer. The NMR spectra were recorded on a Hitachi H-60 high-resolution NMR spectrometer, using tetramethylsilane as the internal standard. Elemental analyses were performed with a Yanagimoto MT-1 CHN Corder.

Reagents. The dimethyl sulfoxide (DMSO) was purified by two distillations over calcium hydride at about 1 mmHg. The sodium methoxide was prepared from sodium and methanol and dried by heating at 100°C under reduced pressure. The sodium ethoxide was prepared from sodium and ethanol and dried similarly. Unless otherwise indicated, the other reagents were of commercial origin or were synthesized by known methods and purified by recrystallization or distillation.

Reaction of Dimethyl 3-Nitrophthalate (I). With DMSO-Sodium Methoxide. A suspension of 5.4 g (0.1 mol) of sodium methoxide in 45 m*l* of DMSO was stirred by introducing a stream of nitrogen into the suspension. A solution of 6.0 g (0.025 mol) of I in 30 m*l* of DMSO was added, drop by drop, to the suspension. The reaction mixture, which soon turned red-brown, was kept under nitrogen at room temperature for 4 hr, and then most of the solvent was evaporated at 1 mmHg. To the residue were added 50 m*l* of ether and 50 m*l* of ice water. The aqueous layer was added, drop by drop, to an ice-cold 100 m*l* of 4 N hydrochloric acid to obtain a precipitate. This precipitate was separated from the aqueous solution (A) by filtration to give 2.4 g (50%) of azoxybenzene-2,2',3,3'-tetracarboxylic acid (II). The analytical sample was obtained by recrystallization from water: mp 236—238°C (decomp); N. E. 93 (calcd 94). The infrared spectrum (in KBr disk) showed hydrogen-bonded multiplet hydroxyl absorptions at 3000—2500 cm^{-1}, and carbonyl absorptions at 1730 and 1680 cm^{-1}.

Found: C, 51.26; H, 2.60; N, 7.32%. Calcd for $C_{16}H_{10}O_9N_2$: C, 51.34; H, 2.69; N, 7.49%.

The acidified aqueous solution, A, was extracted with ether. The ether was evaporated to dryness to give 1.5 g (43%) of 3-nitrophthalic acid (III), which showed a mp of 214—217°C after recrystallization from water. The mixed melting point with an authentic sample prepared by the alkaline hydrolysis of the starting material showed no depression.

Reaction of Dimethyl 4-Nitrophthalate (IV) With DMSO-Sodium Methoxide. An experimental run in which dimethyl 4-methoxyphthalate was obtained will be described as a typical example. A solution of 6.0 g (0.0025 mol) of I in 30 m*l* of DMSO was added to a suspension of 5.4 g (0.1 mol) of sodium methoxide in 45 m*l* of DMSO in a stream of nitrogen. The mixture was kept at room temperature under nitrogen for 4 hr. Most of the solvent was then removed by distillation under reduced pressure. To the residue there were added 50 m*l* of ether and 50 m*l* of water, and the mixture was separated into the aqueous (A) and ether (B) layers. The ether layer, B, was dried over anhydrous sodium sulfate. The ether was removed and the residue was distilled under reduced pressure to give 1.2 g (22%) of dimethyl 4-methoxyphthalate (VII), bp 136—137°C/3 mmHg. The infrared spectrum showed carbonyl absorption at 1725 cm^{-1}. The NMR spectrum (in CCl_4) showed one aromatic proton at 2.28—2.43 τ (1H, broad doublet), two aromatic protons at 3.07—3.20 τ (2H, broad doublet), and two methoxyl singlets at 6.20 and 6.23 τ (the total of the protons due to these two singlets was 9H).

Found: C, 59.04; H, 5.35%. Calcd for $C_{11}H_{12}O_5$: C, 58.92; H, 5.45%.

The aqueous layer A was added to 100 m*l* of cold 4 N hydrochloric acid. The precipitate thus obtained was then separated from the aqueous acid solution (C) by filtration. The precipitate consisted of 0.7 g (13%) of 5-methoxy-2-nitroso-1,3-indanedione (V). The analytical sample of V was obtained by recrystallization from isopropyl alcohol, mp 204—206°C (decomp). The infrared spectrum showed a hydroxyl absorption at 3500 cm^{-1} and carbonyl absorptions at 1730 and 1690 cm^{-1}. The hydroxyl absorption at 3500 cm^{-1} was sometimes missing, and instead a broad absorption appeared at 3150 cm^{-1}. The NMR spectrum (in DMSO-d_6) showed an acidic proton at -4.25 τ (1H, broad singlet), one aromatic proton at 2.02—2.15 τ (1H, broad doublet), two aromatic protons at 2.50—2.65 τ (2H, broad doublet), and a methoxyl singlet at 6.00 τ (3H). The molecular weight, as measured by the Rast method, was 225 (calcd 205).

Found: C, 58.72; H, 3.38; N, 6.65%. Calcd for $C_{10}H_7O_4N$: C, 58.54; H, 3.44; N, 6.83%.

The aqueous acid solution C was extracted with ether. The ether was then evaporated, and the residue was washed with benzene to give 2.8 g (51%) of 4-methoxyphthalic acid (VI). The analytical sample was obtained by recrystallization from water: mp 157—160°C, (lit.[6] mp 168—170°C); N. E. 97 (calcd 98). The acid VI was identical in every respect with the acid obtained by an alkaline hydrolysis of the ester VII.

Found: C, 54.92; H, 4.20%. Calcd for $C_9H_8O_5$: C, 55.10; H, 4.11%.

In a separate experiment, the compounds V and VI were obtained respectively, in 49 and 48% yields while none of the ester VII was isolated.

Acetylation of 5-Methoxy-2-nitroso-1,3-indanedione V. A mixture of 500 mg (0.0024 mol) of V, 5 m*l* of acetic anhydride, and 5 m*l* of pyridine was heated at reflux for 10 min. After cooling, the reaction mixture was subjected to distillation under reduced pressure to remove the unreacted reagents at room temperature. The residue was then washed with cold methanol and recrystallized from benzene to give 280 mg (47%) of a yellow monoacetylated product, mp 185—189°C (decomp). The infrared spectrum showed carbonyl absorptions at 1802, 1747, and 1708 cm^{-1} and absorptions at 1626 (w), 1590 (s), 1492 (s), 1470 (w), and 1436 (w) cm^{-1}. The NMR spectrum showed an aromatic proton at 1.97—2.13τ (1H, broad doublet), two aromatic protons at 2.41—2.57 τ (2H, broad doublet), a signal due to methoxyl at 6.03 τ (3H, singlet), and a signal due to acetyl at 7.72 τ (3H, singlet). The molecular weight, as measured with a Hitachi-Perkin Elmer 115 molecular-weight apparatus, using benzene as the solvent, was 254 (calcd 248).

Found: C, 58.33; H, 3.84; N, 5.68%. Calcd for $C_{12}H_9O_5N$: C, 58.30; H, 3.67; N, 5.67%.

Alkaline Hydrolysis of V. A mixture of 500 mg (2.4 mmol) of V and 4 g of potassium hydroxide in 13 m*l* of methanol and 8 m*l* of water was refluxed for 48 hr, and then most of the solvent was removed by distillation under reduced pressure. The residue was neutralized with hydrochloric acid, extracted with ether, and dried over anhydrous sodium sulfate. The ether was evaporated to give a precipitate. The recrystallization of the precipitate from water gave 400 mg (83%) of 4-methoxyphthalic acid VI, mp 158—160°C, which was identical in every respect with the acid VI obtained above.

Detection of Nitrite Ion Liberated During the Course of the Reaction of IV with DMSO-Sodium Methoxide. The reaction of IV with DMSO-sodium methoxide was carried out in a nitrogen stream as above. The Griess-Romijn reagent[7] was then added to a small portion of the aqueous acid solution C (see above) obtained in this experiment. The ultraviolet spectrum of the resultant solution showed an absorption maximum at 514 mμ, indicating the presence of the nitrite ion.

Reaction of IV with DMSO-Sodium Ethoxide. This experiment was carried out by a method similar to that employed for the reaction of IV with DMSO-sodium methoxide. However, in this case the DMSO-sodium ethoxide system was used for the preparation of methylsulfinyl carbanion. This experiment gave 5-ethoxy-2-nitroso-1,3-indanedione (VIII), mp 174—181°C, and 4-ethoxyphthalic acid (IX), mp 151—154°C, in yields of 51 and 32% respectively. The infrared spectrum of VIII showed a hydroxyl band at 3510 cm^{-1} and carbonyl bands at 1742 and 1694 cm^{-1}. The NMR spectrum (in DMSO) showed an acidic proton at -4.10τ (1H, broad singlet), one aromatic proton at 2.16—2.27 τ (1H, broad doublet), two aromatic protons at 2.59—2.75 τ (2H, broad doublet), two methylene protons in the ethoxyl group at 5.66—6.01 τ (2H, quartet), and three methyl protons in the ethoxyl group at 8.56—8.84 τ (3H, triplet). However, since the analytical data showed that the VIII obtained here was slightly contaminated even after repeated recrystallizations from ethanol - water, the VIII was converted to the *O*-acetyl derivative and the structure was confirmed (see below).

6) S. N. Chakravarti and W. H. Perkin, Jr., *J. Chem. Soc.*, **131**, 196 (1929).

7) F. H. Welcher, "Organic Analytical Reagents," Vol. 11, D. van Nostrand, New York, N. Y. (1948), p. 406.

The structure of IX was established on the basis of the following data. The neutralization equivalent was 101 (calcd 105). The infrared spectrum was consistent with the structure of IX in every respect.

Found: C, 56.92; H, 4.85%. Calcd for $C_{10}H_{10}O_5$: C, 57.14; H, 4.80%.

Acetylation of 5-Ethoxy-2-nitroso-1,3-indanedione (VIII). A mixture of 300 mg of the crude VIII, 3 m*l* of acetic anhydride, and 3 m*l* of dry pyridine was refluxed for 10 min. The unreacted reagents were evaporated at room temperature under reduced pressure. The residue was washed to give 290 mg (96%) of the acetylated product. The analytical sample was obtained by recrystallization from ligroin, mp 137—141°C (decomp). The infrared spectrum showed carbonyl absorptions at 1798, 1748 (w), and 1713 cm^{-1}.

Found: C, 60.00; H, 4.80; N, 5.44%. Calcd for $C_{13}H_{11}O_5N$: C, 59.77; H, 4.24; N, 5.36%.

Reaction of Methyl *o*-Nitrobenzoate (X) with DMSO - Sodium Methoxide. To a suspension of 5.4 g (0.1 mol) of sodium methoxide in 75 m*l* of DMSO, there was added, drop by drop, 4.5 g (0.25 mol) of X in a stream of nitrogen at room temperature. The reaction mixture was kept under the same conditions for 4 hr, and then most of the solvent was evaporated under reduced pressure. The addition of 50 m*l* of ether and 50 m*l* of ice water to the residue, and the subsequent acidification of the aqueous layer with 100 m*l* of 4 N hydrochloric acid, gave a red precipitate. This precipitate was separated from the aqueous acid solution (A) to afford 1.5 g (44%) of azobenzene-2,2'-dicarboxylic acid (XI). The analytical sample of XI was obtained by recrystallization from acetic acid, mp 230—232°C (decomp) (lit.[8] mp 238—239°C (decomp)).

The neutralization equivalent was 135 (calcd 135).

Found: C, 62.60; H, 3.81; N, 10.10%. Calcd for $C_{14}H_{10}O_4N_2$: C, 62.22; H, 3.73; N, 10.37%.

The extraction of the aqueous acid solution A with ether and the evaporation of the ether gave 1.2 g (33%) of azoxybenzene-2,2'-dicarboxylic acid (XII), which, after recrystallization from acetic acid, showed a mp 230°C (decomp) (lit.[9] 253—255°C (decomp)). The neutralization equivalent was 147 (calcd 143).

Found: C, 59.04; H, 3.46; N, 9.32%. Calcd for $C_{14}H_{10}O_5N_2$: C, 58.74; H, 3.52; N, 9.79%.

Reaction of Methyl *p*-Nitrobenzoate (XIII) with DMSO - Sodium Methoxide. The compound XIII was allowed to react with DMSO-sodium methoxide in a manner similar to that described above. By this reaction *p*-nitrobenzoic acid, mp 238—240°C, was obtained in an almost quantitative yield.

Formation of 5-Methoxy-2-nitroso-1,3-indanedione (V) from Dimethyl 4-Methoxyphthalate (VII). Potassium (0.8 g, 0.02 g-atom) was dissolved in 20 m*l* of refluxing *t*-butyl alcohol. After cooling to room temperature, 15 m*l* of DMSO was added and the solution was distilled under a reduced pressure of about 2 mmHg, using a Vigreux column, until the DMSO started to distill out (bp 45°C), and then the solution was cooled. To the partially-solidified residue there was added, drop by drop, 1.0 g (4.5 mmol) of VII in 5 m*l* of DMSO in a stream of nitrogen at room temperature. The reaction mixture was kept for 2.5 hr under nitrogen, and then most of the solvent was evaporated under reduced pressure. Ether (10 m*l*) and ice water (10 m*l*) were added to the residue, and the aqueous layer was separated. To this aqueous solution there was added, drop by drop, a solution of 800 mg of 97% sodium nitrite in 40 m*l* of 4 N-hydrochloric acid under ice-cooling. A yellow precipitate soon appeared; it was separated by filtration to give 630 mg (66%) of V. Recrystallization from isopropyl alcohol showed a mp of 203—206°C (decomp). This material was identical in every respect with that obtained in the reaction of IV with DMSO - sodium methoxide.

Reaction of Dimethyl 4-Methoxyphthalate (VII) with DMSO - Potassium *t*-Butoxide. A mixture of potassium *t*-butoxide in DMSO was prepared from 2.8 g (0.072 g-atom) of potassium, 70 m*l* of *t*-butyl alcohol and 70 m*l* of DMSO as has been described above. To this mixture there was added, drop by drop, 3.5 g (0.016 mol) of VII in 10 m*l* of DMSO in a stream of nitrogen at room temperature. The reaction mixture, which first turned green and then brown, was kept for 3 hr under nitrogen. Most of the solvent was evaporated under reduced pressure, and 36 m*l* of ether and 36 m*l* of ice water were added to the residue. The aqueous layer was separated and acidified with 75 m*l* of 4N-hydrochloric acid. The precipitate thus obtained was separated by filtration to give 3.7 g (92%) of a material which contained sulfur and chlorine atoms. This material, mp 110—115°C, showed absorption bands at 1752, 1713, 1600, 1493 cm^{-1} in its infrared spectrum and the positive Beilstein test. Therefore, the compound was presumed to be 5-methoxy-2-chloro-2-methylthio-1,3-indanedione (XVII). However, no pure sample of this material was obtained because of the difficulty of purification.

Therefore, XVII was converted to 2-ethoxy-5-methoxy-2-methylthio-1,3-indanedione (XVIII). A mixture of 500 mg (2 mmol) of the crude XVII in 5 m*l* of ethanol was refluxed for 3 hr. The solvent was then evaporated under reduced pressure to give an oil which solidified upon standing for 2 days. The recrystallization of the solid from petroleum ether gave 400 mg (80%) of XVIII, mp 73—74.5°C. This compound contained sulfur atoms. The infrared spectrum showed carbonyl absorptions at 1742 and 1707 cm^{-1}. The NMR spectrum (in CCl_4) showed an aromatic proton at 2.10—2.26 τ (1H, broad doublet), two aromatic protons at 2.61—2.76τ (2H, broad doublet), two methylene protons of the ethoxyl group at 5.81—6.16τ (2H, quartet), three methyl protons of the methoxyl group at 6.05τ (3H, singlet), three methyl protons of the methylthio group at 7.84 τ (3H, singlet), and three methyl protons of the ethoxyl group at 8.67—8.91 τ (3H, triplet).

Found: C, 58.90; H, 5.39%. Calcd for $C_{13}H_{14}O_4S$: C, 58.64; H, 5.30%.

Reaction of Dimethyl 4-Methoxyphthalate (VII) with DMSO-Sodium Methoxide. This reaction was carried out in a manner similar to that employed for the reaction of I with DMSO - sodium methoxide, using VII as a substrate. By this reaction 4-methoxyphthalic acid was obtained in an almost quantitative yield.

Reaction of Dimethyl Phthalate with DMSO-Sodium Methoxide and DMSO - Potassium *t*-Butoxide. The reaction of dimethyl phthalate with

8) H. D. K. Drew and J. K. Landquist, *J. Chem. Soc.*, **1938**, 292.

9) J. S. Morley, *ibid.*, **1959**, 2280.

DMSO-sodium methoxide was carried out in a manner similar to that described for the reaction of I with DMSO-sodium methoxide to give 2-chloro-2-methylthio-1,3-indanedione (XIX) in a 44% yield, mp 63—64°C (lit.[1] 63—64°C).

The reaction of dimethyl phthalate with DMSO-potassium *t*-butoxide was carried out in a manner similar to that described for the reaction of VII with DMSO-*t*-butoxide to give XIX in a 62% yield.

BULLETIN OF THE CHEMICAL SOCIETY OF JAPAN VOL. 42 737—740 (1969)

Eine Dienon-Phenol-Umlagerung von 5-Oxo-2-methyl-4,4-dibenzyl-3-äthoxycarbonyl-4,5-dihydro-indol

Tadashi SUEHIRO und Koji EIMURA

Chemisches Institut, Gakushuin Universität, Mejiro, Toshima-ku, Tokio

(Eingegangen am 18. Mai, 1968)

Bei der Einwirkung von Acetanhydrid-Schwefelsäure auf 5-Oxo-2-methyl-4,4-dibenzyl-3-äthoxycarbonyl-4,5-dihydro-indol (I) bei 0°C, findet eine Dienon-Phenol-Umlagerung von I zu 4-Acetoxy-2-methyl-5,6-dibenzyl-3-äthoxycarbonyl-indol (III) statt, dessen Struktur aus der leichten Verseifbarkeit der 3-Äthoxycarbonyl-Gruppe von III und aus den spektroskopischen Befunden der von III abgeleiteten Verbindungen folgte.

5-Oxo-2-methyl-4,4-dibenzyl-3-äthoxycarbonyl-4,5-dihydro-indol (I) lagert sich beim Kochen mit Eisessig-Schwefelsäure unter Abspaltung des Äthoxycarbonyl-Restes zu 5-Hydroxy-2-methyl-4,6-dibenzyl-indol (II) um.[1] In der Kälte findet eine andere Dienon-Phenol-Umlagerung von I statt, und zwar beim Stehen von I in einer Acetanhydrid-Lösung mit etwas Schwefelsäure unter Eis-Kühlung fallen allmählich Kristalle vom Schmp. 224—226°C, zers. (II) in 36% Ausbeute aus. III lässt sich sehr leicht durch 2 stdg. Kochen mit Äthanol-2N Natronlauge in 4-Hydroxy-2-methyl-5,6-dibenzyl-indol-3-carbonsäure vom Schmp. 211—213°C, zers. (IV) verseifen. Die leichte Verseifung des Äthoxycarbonyl-Restes von III weist, wie es nachher erwähnt wird, auf die 4-Acetoxy-Struktur von III hin. IV verliert Carboxyl-Gruppe beim Erhitzen mit Essigsäure und liefert 4-Hydroxy-2-methyl-5,6-dibenzyl-indol vom Schmp. 149—150°C (V). Dieser Schmelzpunkt ist anders als der von II, 111—113°C.[1] Durch Einengen der Mutterlauge von III erhält man in 3% Ausbeute 4-Hydroxy-2-methyl-5,6-dibenzyl-indol-3-carbonsäureäthylester vom Schmp. 232—233°C (VI), dessen Struktur durch Überführung zu IV festgestellt wurde. Aus der Mutterlauge von VI kam bei der Vakuum-Destillation ein dickes Öl vom $Sdp_{0.002}$ 245—260°C (Badtemperature) (VII) über. VII zeigt IR-Bande bei 1755,*1 1735 und 1700/cm im Gegensatz zu III mit 1725 und 1705/cm. VII kann vielleicht ein Zwischenprodukt der Umlagerung sein, dafür konnten wir leider keinen Beweis beibringen und wir haben die Aufarbeitung damit aufgegeben. (Schema 1)

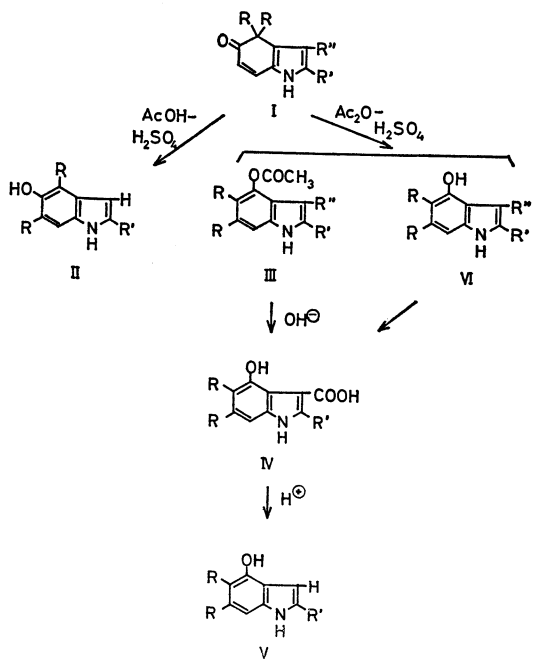

R : $-CH_2C_6H_5$
R′ : $-CH_3$
R″ : $-COOC_2H_5$

Schema 1

*1 *N*-Acetyl-Bande von 5-Methoxy-2-methyl-4-allyl-3-äthoxycarbonyl-1-aceyl-indol liegt bei 1710/cm (Unveröffentlichte Arbeit von Frl. A. Tsubota). 1755-Bande ist wahrscheinlich von *O*-Acethyl-Gruppe.

1) T. Suehiro, *Chem. Ber.*, **100**, 915 (1967).

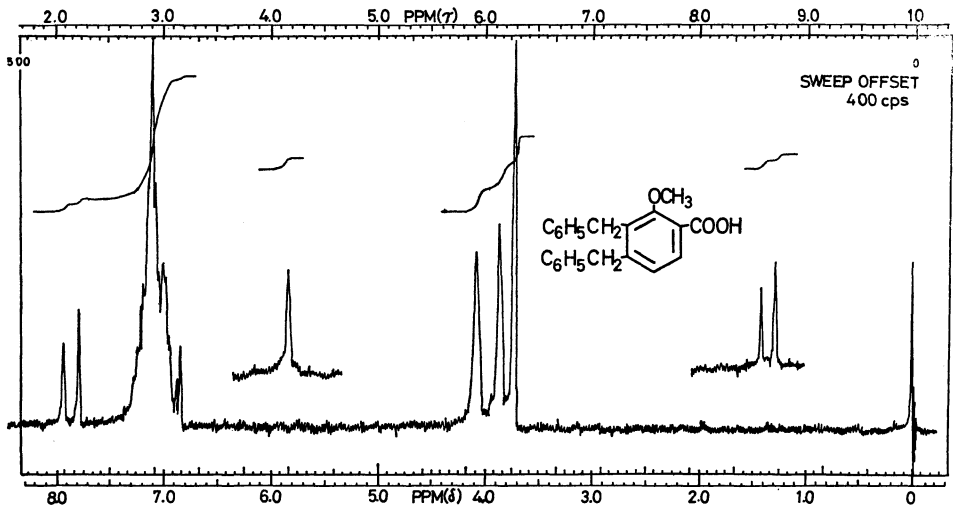

Abbild 1. NMR-Spektrum von XII

Um die Struktur V klar zu machen, haben wir die Abbau-Reaktion von V wie bei dem früheren Fall[1] versucht. V lässt sich zuerst mit Dimethylsulfat und Alkali in den Methyläther vom Schmp. 108—109.5°C (VIII) methylieren. VIII gibt bei der Oxydation mit Acetanhydrid-Wasserstoffsuperoxyd in Gegenwart von Molybdat in 50% Ausbeute 6-Acetamino-2-methoxy-3,4-dibenzyl-benzoesäure vom Schmp. 190—191°C, zers. (IX). IX liefert beim Kochen mit 3 N alkoholischer Salzsäure und anschliessenden Acetylieren 5-Acetamino-2,3-dibenzyl-anisol vom Schmp. 120.5—121.5°C (X). Wenn man IX alkalisch verseift, erhält man 6-Amino-2-methoxy-3,4-dibenzyl-benzoesäure vom Schmp. 124—125°C, zers. (XI), die bei der Deaminierung durch Diazo-Reaktion 2-Methoxy-3,4-dibenzyl-benzoesäure vom Schmp. 119—119.5°C, zers. (XII) gibt. (Schema 2)

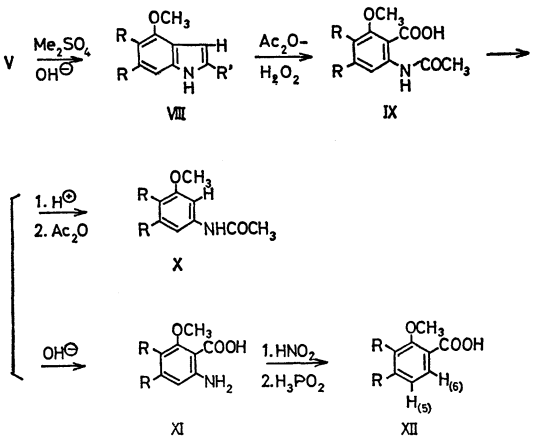

R : $-CH_2C_6H_5$
R' : $-CH_3$

Schema 2

Das UV-Spektrum von X ähnelt denen von 2- und 3-Acetaminoanisole. Man kann daraus aber X nicht eindeutig die Struktur von 2- oder 3-Acetamino-Verbindung zuschreiben. Das NMR-Spektrum von XII (Abbild. 1) zeigt ein Singulett (1H) bei δ 12.5, ein Dublett (1H) bei δ 7.86 (J= 8.4 Hz), ein Multiplett (11H) bei δ 7.10, zwei Singuletts bei δ 4.08 und 3.87 (jede 2H) und ein Singulett (3H) bei δ 3.73. Dem Dublett bei δ 7.86 weisen wir C(6)-H von XII zu, das führt zu dem Schluss, dass XII an C(5) noch ein Wasserstoff-Atom trägt, d. h. V ist an der 7-Stellung frei von dem Substituenten. Zu demselben Schluss kommt man aus den Signalen der aromatischen Protonen von X wieder. Es bleibt noch die Frage, ob die Hydroxyl-Gruppe von V an der 4-oder 6-Stellung steht.

Die 4-Stellung ziehen wir vor für die Hydroxyl-Gruppe nach dem Befunde, dass die 3-Äthoxycarbonyl-Gruppe von III viel leichter als die von 5-Methoxy-2-methyl-4-benzyl-3-äthoxycarbonyl-indol (XIII) verseift wird.[2] Um XIII zu verseifen mussten wir ihn 70 Stdn. bei höheren Temperaturen mit Alkali erhitzen. Unter den Bedingungen, wo III in 63% Ausbeute (Rohprodukt in fast quantitativer Ausbeute) zu IV verseift wird, lässt sich 5-Hydroxy-2-methyl-4-benzyl-3-äthoxycarbonyl-indol (XIV) auch nicht verseifen und in 77% Ausbeute wird die reine Ausgangssubstanz zurückerhalten. Die Schwierigkeit in der Verseifung von XIII und XIV führt zu der Annähme, dass 6-Hydroxy-2-methyl-4,5-dibenzyl-3-äthoxycarbonyl-indol wieder reaktionsträge in der Verseifung ist, weil 5-Hydroxy-indol-3-carbonsäure eine stärkere Carbonsäure als 6-Hydroxy-carbonsäure sein soll,[3] und weil die Estern der stärkeren

2) T. Suehiro, *Chem. Ber.*, **100**, 910 (1967).
3) M. S. Melzer, *J. Org. Chem.*, **27**, 496 (1962).

Carbonsäuren schneller als die der schwächeren Carbonsäuren verseift werden.[4] Auf diesen Betrachtungen soll 6-Hydroxy-2-methyl-4,5-dibenzyl-3-äthoxycarbonyl-indol langsamer als 5-Hydroxyindol - Derivate verseift werden. Die leichte Verseifung von III zu IV ist gut zu verstehen, wenn einmal die Acetoxyl-Gruppe hydrolysiert wird, wie bei den Salicylsäureestern,[5] weil die 4-Hydroxyl- und 3-Äthoxycarbonyl-Gruppen von VI, wie die 1,3-diaxialen Substituenten der Cyclohexan-Reihe, miteinander in Berührung kommen. Für diese sterische Lage sprechen die IR-Banden von VI, ν_{OH} 3160/cm und $\nu_{C=O}$ 1600/cm im Gegensatz zu der monomeren ν_{OH}3630/cm bei V.

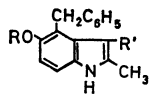

XIII: R=-CH_3, R'=-$COOC_2H_5$
XIV: R=-H, R'=-$COOC_2H_5$

Abbild 2.

Die Bildung von III aus I lässt sich wohl nach dem Schema 3 verstehen, in dessen 3. Stufe die Acetoxyl-Gruppe vorwiegend von der 5- zur 4-Stellung wandert. Die bevorzugte Wandrung vom Acetoxyl Rest findet man in mehreren Beispielen,[6] aber dieses Schema ist nicht ähnlich dem von Marvell und anderen,[6a] nach dem letzternen I 7-Acetoxy-4,5-dibenzyl-indol-Derivat liefern sollte.

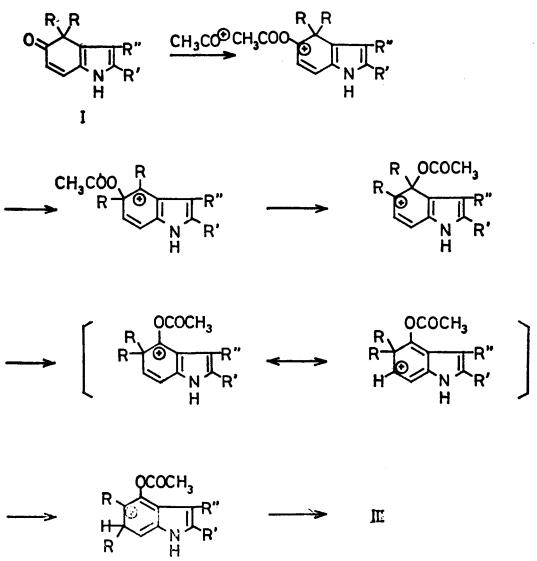

R : -$CH_2C_6H_5$
R' : -CH_3
R'' : -$COOC_2H_5$

Schema 3

Frl. H. Watanabe danken wir für die Mikroanalyse.

Beschreibung der Versuche[*2]

Umsetzung von 5-Oxo-2-methyl-4,4-dibenzyl-3-äthoxycarbonyl-4,5-dihydro-indol (I) mit Acetanhydrid - Schwefelsäure zu 4-Acetoxy-2-methyl-5,6-dibenzyl-3-äthoxycarbonyl-indol (III). Zu einer 2.18 *l* Acetanhydrid Lösung von 106 g (0.27 Mol) I tropft man unter Eis-Kühlung und Umrühren 6.8 ccm konz. Schwefelsäure. Die Farbe der Lösung ändert sich von grün-gelb über orange-rot zu hell braun und in einigen Minuten kommen Kristalle aus. Nach dem Stehenlassen im Kühlschrank über Nächte saugt man die Kristalle ab, wäscht sie mit Wasser und trocknet im Exsiccator. Das Rohprodukt (49.5 g, Schmp. 200—205°C) zeigt nach dem Umkristallisieren aus Essigester den Schmp. 224—226°C. Ausbeute 42.2 g (36%) in farblosen Nadeln. IR-Bande(KBr) bei 3380, 1725, 1705/cm.

Gef.: C, 76.26; H, 6.30; N, 3.17%. Ber. für $C_{28}H_{27}NO_4$: C, 76.17; H, 6.16; N, 3.17%.

4-Hydroxy-2-methyl-5,6-dibenzyl-indol-3-carbonsäure (IV). Man Kocht 8.72 g (0.0198 Mol) III 2 Stdn. unter Rückfluss mit 0.12 *l* 2 N Natronlauge und 0.96 *l* Äthanol. Äthanol destilliert man unter vermindertem Druck ab, verdünnt den Rückstand mit Wasser und säuert mit Essigsäure an, wobei 7.19 g Rohprodukt auskam. Man kristallisiert das Produkt aus Essigester-Äthanol (5 : 1) um und erhält 46 g (63%) farblose Nadeln vom Schmp. 211—213°C, zers. IR-Bande (KBr) bei 3450, 2700—3000, 2630, 2550, 1600/cm.

Gef.: C, 77.65; H, 5.53; N, 3.56%. Ber. für $C_{24}H_{21}NO_3$: C, 77.60; H, 5.70; N, 3.77%.

4-Hydroxy-2-methyl-5,6-dibenzyl-indol (V). Man erhitzt 20 g (53.9 mMol) IV mit 400 ccm Eisessig und 20 ccm Wasser 2 Stdn. auf dem Wasserbad. Die Lösung wird violett. Man engt die Lösung unter vermindertem Druck ein und verdünnt den Rückstand mit Wasser, dabei kamen Kristalle aus. Man reinigt das Rohprodukt durch Florisil-Säule-Benzol und kristallisiert aus Benzol - *n*-Hexan (4 : 1) um. Ausbeute 16.4 g (93%) im farblosen Pulver vom Schmp. 149—151°C. IR-Bande (KBr) bei 3630, 3500/cm.

Gef.: C, 84.45; H, 6.47; N, 4.36%. Ber. für $C_{23}H_{21}NO$: C, 84.37; H, 6.47; N, 4.28%.

4-Hydroxy-2-methyl-5,6-dibenzyl-3-äthoxycarbonyl-indol (VI). Nach dem Entfernen von III aus dem Reaktionsgemisch von 7.5 g I mit Acetanhydrid-Schwefelsäure, zersetzt man die Mutterlauge mit Wasser, engt unter vermindertem Druck ein und verdünnt mit Wasser, wobei ein Öl mit 0.54 g Kristalle

4) C. K. Ingold und W. S. Nathan, *J. Chem. Soc.*, **1936**, 222.

5) M. L. Bender, F. J. Kezdy und B. Zerner, *J. Am. Chem. Soc.*, **85**, 3017 (1963).

6) a) E. N. Marvell und J. L. Stephenson, *ibid.*, **77**, 5177 (1955); b) W. Metlesices, F. Wessely und H. Budzikiewicz, *Tetrahedron*, **6**, 345 (1959); H. Budzikiewicz und W. Metlesices, *J. Org. Chem.*, **24**, 1125 (1959).

*2 Die IR-Spektren wurden mit einem Gerät von Hitachi EPI-S aufgenommen. Die Aufnahme von NMR-Spektrum erfolgte mit dem Gerät A60 der Firma Varian Ass. bei 60 MHz. Die Schemlzpunkte sind nicht korrigiert.

auskam. Umkristallisieren des Produktes aus Essigester gibt 0.21 g farblose Nadeln vom Schmp. 232—233°C. Ausbeute 3%. IR-Bande (Nujol) bei 3400, 3160, 1600/cm, ν_{CH} (3.5×10^{-3} M in CS_2) 3150/cm.

Gef.: C, 77.76; H, 6.74; N, 3.22%. Ber. für $C_{26}H_{25}NO_3$: C, 78.17; H, 6.31; N, 3.51%.

Das Öl, befreit von VI, nimmt man in Benzol auf und wäscht mit Soda-Lösung. Beim Vakuum-Destillation unter 0.002 mmHg kommt bei 245—260°C (Badtemperature) 2.5 g dickes Öl (VII) über. IR-Bande bei 3370, 1750, 1740, 1690/cm. Es wurde weiter nicht erforscht.

Uberführung von VI zu IV. Man kocht 0.11 g VI 4 Stdn. mit 2 ccm Äthanol und 1 ccm 2 N Natronlauge unter Rückfluss. Beim Ansäuern der alkalischen Lösung erhält man 69 mg Kristalle vom Schmp. 212°C, zers., deren IR-Spektrum mit dem von IV übereinstimmt und die Mischprobe zeigte keine Depression.

Versuche der Verseifung von 5-Hydroxy-2-methyl-4-benzyl-3-äthoxycarbonyl-indol[1]. Man kocht 1.0 g (3.24 mMol) von dem Indol (Schmp. 159—160°C) 2 Stdn. unter Rückfluss mit 14.8 ccm 2 N Natronlauge und 110 ccm Äthanol. Nach dem Einengen verdünnt man den Rückstand mit Wasser und säuert mit Essigsäure an, wobei 0.77 g Ausgangssubstanz vom Schmp. 158—160°C auskam.

4-Methoxy-2-methyl-5,6-dibenzyl-indol (VIII). Man methyliert 15 g (46 mMol) V bei Raumtemperatur in einer Mischung von 80 ccm 2 N Natronlauge und 120 ccm Äthanol mit 10 ccm (106 mMol) Dimethylsulfat. Aus dem dunkelvioletten Reaktionsgemisch kommt Rohprodukt (15 g) vom Schmp. 105—108°C aus. Man reinigt es durch eine Kolonne von Florisil-Benzol und kristallisiert aus Benzol - *n*-Hexan (10 : 1) um. Ausbeute 13.5 g in farblosen Blättchen vom Schmp. 108—109.5°C.

Gef.: C, 84.70; H, 6.48; N, 4.15%. Ber. für $C_{24}H_{23}NO_4$: C, 84.42; H, 6.79; N, 4.10%.

6-Acetamino-2-methoxy-3,4-dibenzyl-benzoesäure (IX): Man löst 10 g (29.3 mMol) VIII in 400 ccm Acetanhydrid und tropft dazu unter Eis-Kühlung 1 ccm 1% Molybdat Lösung und dann 90 ccm 30% Wasserstoffsuperoxyd. Man lässt die Mischung 2 Tage im Kühlschrank stehen. Man zersetzt Peroxyd mit wässr. Natriumhydrogensulfid und dampft die Reaktionsmischung ein. Der Rückstand wird beim Stehen fest. Man löst ihn in Sodalösung auf und fällt daraus 6.8 g Rohprodukt vom Schmp. 185—187°C, zers,. durch Ansäuern aus. Umkristallisieren aus 70% Essigsäure gibt 5.6 g (50%) farblose Nadeln vom Schmp. 190—191°C, zers. IR-Bande (KBr) bei 3300, 2700, 1695, 1630, 1600/cm.

Gef.: C, 73.93; H, 5.74; N, 3.49%. Ber. für $C_{24}H_{23}NO_4$: C, 74.02; H, 5.95; N, 3.60%.

5-Acetamino-2,3-dibenzyl-anisol (X). 114 mg (0.293 mMol) IX kocht man mit 5 ccm 6 N Salzsäure und 5 ccm Äthanol 6.5 Stdn. unter Rückfluss. Nach dem Verdünnen mit Wasser und Alkalisch-Machen schüttelt man das Reaktionsgemisch mit Benzol aus. Den Rückstand aus der Benzol-Lösung lässt man über Nacht mit 1 ccm Methanol und 1 ccm Acetanhydrid stehen. Rohprodukt kristallisiert man aus 70% Methanol um und erhält 37 mg (38%) farblose Nadeln vom Schmp. 119.5—120.5°C IR-Bande (KBr) bei 3350, 1655, 1600, 1550, 850/cm. UV-Spektrum (Äthanol) λ_{max} ($\log\varepsilon$): 254 mμ (4.18), 282 (3.66), 286 (3.66), 292 (3.67). NMR-Spektrum(CCl_4 mit TMS Standard) bei δ 7.96s (NH), 7.37d mit J: 2 Hz(arom-H), 6.95m (10H, C_6H_5), 6.38d mit J: 2 Hz(arom-H), 3.78d mit J: 10 Hz (2H, $PhCH_2$), 3.65s (2H, $PhCH_2$), 1.94s (3H, CH_3).

Gef.: C, 79.50; H, 6.63; N, 4.02%. Ber. für $C_{23}H_{23}NO_2$: C, 79.97; H, 6.71; N, 4.06%.

6-Amino-2-methoxy-3,4-dibenzyl-benzoesäure (XI). Man erhitzt 4 g (10.3 mMol) IX in 200 ccm 2 N Natronlauge und 120 ccm Äthanol 5 Stdn. unter Rückfluss. Beim Einengen und Ansäuern mit Salzsäure (Kongo-Rot) fallen 3.4 g Kristalle aus. Umkristallisieren aus 80% Essigsäure gibt 3.1 g farblose Nadeln vom Schmp. 124—125°C, zers. Ausbeute 89%. IR-Bande(KBr) bei 3540, 3450, 2900, 1695, 1650, 1620, 1580, 1535/cm.

Gef.: C, 75.82; H, 6.04; N, 4.20%. Ber. für $C_{22}H_{21}NO_3$: C, 76.06; H, 6.09; N, 4.03%.

2-Methoxy-3,4-dibenzyl-benzoesäure (XII). Man löst 1 g (3 mMol) XI in einer Mischung aus 30 ccm Aceton, 20 ccm Eisessig, 50 ccm hypophosphoriger Säure und 10 ccm 9 N Schwefelsäure auf, und gibt dazu bei 0°C unter Umrühren 2 g festes Natriumnitrit portionsweise und lässt die Lösung 2 Tage im Kühlschrank stehen. Nach dem Entfernen von dem anorganischen Niederschlag engt man die Lösung ein und die ausgeschiedene Kristalle nimmt man in Benzol auf. Man dampft die Benzol-Lösung ab und den Rückstand kristallisiert man aus Petrolbenzin (Sp. 60—80°C) um. Ausbeute 440 mg (47%) in farblosen Nadeln vom Schmp. 119—119.5°, zers. UV-Spektrum(Äthanol): λ_{max} ($\log\varepsilon$) 239 mμ(3.89), 269(3.25), 286(3.11). IR-Bande(KBr) bei 1685, 780/cm. NMR-Spektrum (CCl_4 mit TMS Standard) bei δ 12.5 (1H, COOH), 7.86d mit J: 8.4 Hz(1H, arom-H), 7.10m (11H, $C_6H_5\times2$ und arom-H), 4.08s (2H, $PhCH_2$), 3.87s(2H, $PhCH_2$), 3.73s(3H, OCH_3).

Gef.: C, 79.29; H, 6.04%. Ber. für $C_{22}H_{20}O_3$: C, 79.49; H, 6.06%.

BULLETIN OF THE CHEMICAL SOCIETY OF JAPAN VOL. 42 741—745 (1969)

Reactive Fiber. VII. Preparation and Polymerization of Vinyl Sulfonyl (β-Chloroethyl)amide

Yoshio IWAKURA, Keikichi UNO, Nobuo NAKABAYASHI*1 and Wen-Yen CHIANG

Department of Synthetic Chemistry, Faculty of Engineering, The University of Tokyo, Hongo, Tokyo

(Received June 6, 1968)

Vinyl sulfonyl (β-chloroethyl)amide (III) was prepared from vinyl sulfonyl chloride and aziridine. The monomer reactivity ratios of III (M_2) ($r_1=3.0$, $r_2=0.075$) were determined from the result of copolymerization with styrene (M_1), and Q_2 and e_2 values calculated were 0.13 and 0.42 respectively. Radical polymerization of III gave a polymer with low viscosity and the polymer had good reactivity with nucleophilic reagents. To compare the functional group in polymer chain with that of monomeric compound, methane sulfonyl (β-chloroethyl)amide (IV) was prepared and the reaction between the function and several nucleophiles was studied. Reactive fibers were obtained from copolymers of acrylonitrile and III. Reaction of the fibers with Congo Red was carried out in the presence of pyridine.

The idea of addition reaction was introduced as a reaction species of a reactive polymer which has groups highly reactive to a polymer chain. We reported already several kinds of useful groups to prepare reactive polymers. They are isocyanate,[1] aziridine,[2] epoxide,[3] azlactone,[4] and sulfonyl (β-chloroethyl)amide,[5] *etc.*

In the present paper, the preparation and polymerization of vinyl sulfonyl (β-chloroethyl)amide (III) and the reaction of the resulting reactive polymers are described. Preparation and polymerization of *p*-styrene sulfonyl (β-chloroethyl)-amide have already been published.[6] In order to compare reactive polymer and fiber derived from the styrene derivative with vinyl derivative, we prepared III. The preparation of vinyl sulfonyl aziridine (III') was unsuccessful because of its unstability. Addition of hydrochloric acid to the crude III' gave stable III. The reactivity of sulfonyl (β-chloroethyl)amide with several nucleophilic reagents seemed to be similar to that of sulfonyl aziridine with nucleophiles in the presence of bases.

Experimental

Preparation of Vinyl Sulfonyl (β-Chloroethyl)-amide (III). Into a solution of 44.8 g (0.354 mol) of vinyl sulfonyl chloride in 450 m*l* of methylene chloride was added a mixture of 15.3 g (0.354 mol) of aziridine and 35.8 g (0.354 mol) of triethylamine dropwise with stirring at a temperature of −4°C to 0°C during an hour. The reaction was continued at room temperature for another 30 min. Precipitated triethylammonium chloride was filtrated off and 25 m*l* of concentrated hydrochloric acid was added dropwise into the filtrate with stirring at an ice cooling temperature. Fifteen minutes later the organic layer was taken out and was washed by water several times and dried over calcium chloride. After the evaporation of the solvent *in vacuo* the fraction boiling at 139.5—140.5°C/2 mmHg was obtained. The yield was 20.9 g (34.8%).

Found: C, 28.18; H, 4.50; N, 8.40%. Calcd for $C_4H_8SO_2NCl$: C, 28.32; H, 4.75; N, 8.26%.

Preparation of Methane Sulfonyl (β-Chloroethyl)amide (IV). The compound was prepared by the method of Bestian.[7]

Polymerization of III. III and an initiator, AIBN, were sealed in an ampoule under an atmosphere of nitrogen and the polymerization was carried out at 65—70°C for 20—70 hr. The viscous oily polymer was poured into ether to separate poly-III. The purification of the polymer was performed by reprecipitation technique (THF-ether system). The results are listed in Table 1.

Found: N, 8.16%. Calcd for $(C_4H_8SO_2NCl)_n$: N, 8.26%.

Determination of Monomer Reactivity Ratios. About 2.5—3.5 g of a pair of accurately weighed

*1 Present address: The Institute for Medical and Dental Engineering, Tokyo Medical and Dental University, Surugadai, Tokyo.

1) Y. Iwakura, N. Nakabayashi and H. Suzuki, *Makromol. Chem.*, **78**, 168 (1964).

2) Y. Iwakura, K. Uno, N. Nakabayashi, T. Tani and W. Y. Chiang, *Kogyo Kagaku Zasshi (J. Chem. Soc. Japan, Ind. Chem. Sect.)*, **68**, 1222 (1965).

3) Y. Iwakura, T. Kurosaki and N. Nakabayashi, *Makromol. Chem.*, **44**, 570 (1961).

4) Y. Iwakura, F. Toda and Y. Torii, *J. Polymer Sci.*, **A-1-4**, 2649 (1966).

5) N. Nakabayashi and Y. Iwakura, *Makromol. Chem.*, **81**, 180 (1965).

6) Y. Iwakura, K. Uno, N. Nakabayashi and W. Y. Chiang, *J. Polymer Sci.*, **A-5**, 3193 (1967).

7) H. Bestian, *Ann.*, **566**, 210 (1950).

monomers, styrene (M_1) and III (M_2), were mixed with 5 mg of AIBN in an ampoule cooled with Dry-Ice under an atmosphere of nitrogen and the ampoule was sealed. The copolymerization was carried out at 62°C up to a conversion of 10%. After the copolymerization, the viscous mixture was poured into methanol and white flakes were collected. The reprecipitation was repeated three times. The copolymer was dried *in vacuo*. The composition was determined by elementary analyses.

Styrene - III Copolymer. A mixture of 2.07 g of styrene, 1.37 g of III and 0.01 g of AIBN in an ampoule under an atmosphere of nitrogen was heated at 70°C for 25 hr. The copolymer was dissolved in THF and precipitated in methanol. The purification was repeated three times from THF and methanol system. The yield was 2.1 g (60%). $[\eta]=0.54$ (100 m*l* DMF/g at 30°C).

Acrylonitrile - III Copolymer. *(A) Polymerization in THF.* A solution of 53.0 g (1.00 mol) of acrylonitrile, 2.06 g (0.012 mol) of III and 0.015 g of AIBN in 3.5 m*l* of THF was stirred at 65°C for 90 min under an atmosphere of nitrogen. The reaction mass was put into methanol and the resulting white powder was filtered and washed several times by methanol. The yield was 11.0 g (20.0%). $[\eta]=2.7$ (100 m*l* DMF/g at 30°C). The copolymer contained 0.22% (molar) of III unit based on chlorine analysis, 0.15%.

(B) Slurry Polymerization. A suspension of 53.0 g (1.00 mol) of acrylonitrile and 1.7 g (0.01 mol) of III in 1.0 *l* of distilled water and 7.0 m*l* of 0.1 N of sulfuric acid was stirred at 55°C for 10 min with bubbling nitrogen. A pair of initiators, 1.6 g of ammonium persulfate and 0.80 g of sodium metabisulfite, were separately added into the suspension. The copolymerization was carried out for 2.5 hr at the same temperature. The milky mixture obtained was filtered. The collected white powder was suspended into methanol and separated by filtration and washed with methanol several times. The yield was 51.0 g (92.7%). $[\eta]=1.7$ (100 m*l* DMF/g at 30°C).

Wet Spinning of Acrylonitrile - III Copolymer. Copolymer was dissolved in hot DMF and the solution was allowed to stand overnight at room temperature. The dope was extruded into an ethylene glycol coagulation bath at room temperature by a pressure of 1 atm of nitrogen through a spinneret of six holes (0.12 mm diameter). The extruded fiber was drawn three times in a hot water bath kept at 95—98°C.

Polymer Reaction. *Reaction of Poly-III with Thiophenol.* A solution of 0.08 g of poly-III ,0.15 g of triethylamine and 0.15 g of thiophenol in 1 m*l* of THF was sealed into an ampoule. The reaction was carried out at room temperature for a day and at 100°C for another 4 hr. The polymer solution was concentrated by evaporation of THF *in vacuo* and the residue was poured into distilled water to precipitate the polymer. The obtained polymer was dissolved in THF and the solution was poured into water. The collected one was dried *in vacuo*.

Found: N, 5.72%. Calcd for $(C_{10}H_{13}S_2O_2N)_n$: N, 5.76%.

Reaction of Styrene-III Copolymer with p-Toluidine. A solution of the copolymer, *p*-toluidine and pyridine was refluxed for listed interval in Table 7. Methanol was added into the residue to precipitate the polymer after removal of the solvent from the reaction mixture. The reprecipitation (THF-methanol) was carried out three times. The conversion was calculated from chlorine analyses.

Reaction of Methane Sulfonyl (β-Chloroethyl)-amide with Various Nucleophiles. Typical example: A solution of 1.58 g (0.01 mol) of IV, 1.07 (0.01 mol) of *p*-toluidine, 1.01 g (0.01 mol) of triethylamine in 10 m*l* toluene was refluxed for 10 hr under an atmosphere of nitrogen. After separation of precipitated triethylammonium chloride, oily product was obtained by evaporating the solvent from the filtrate. The etheral solution of the oil gave crystals. The melting point was 68.5—70°C. Analytical data are summarized in Table 4.

Reaction of Fiber (Copolymer of III - AN) and Congo Red. The reaction of fiber and Congo Red are carried out at a ratio of 1 : 125 (0.04 g of fiber in 5 m*l* of dye solution) at a temperature of 95°C for 1 hr. The amount of dye combined chemically with the fiber was determined by measuring the unreacted dye in the solution colorimetrically using a Hitachi Photoelectric Photometer, Type EPO-B.

Results and Discussion

Preparation of Vinyl Sulfonyl (β-Chloroethyl)amide. Vinyl sulfonyl (β-chloroethyl)amide was prepared from ethylene bromide according to the following equations[8-10]:

$$BrCH_2CH_2Br + Na_2SO_3 \rightarrow BrCH_2CH_2SO_3Na$$

$$BrCH_2CH_2SO_3Na + NaOH \rightarrow CH_2{=}CH{-}SO_3Na \quad (I)$$

$$CH_2{=}CH{-}SO_3Na + PCl_5 \rightarrow CH_2{=}CH{-}SO_2Cl + CH_2ClCH_2SO_2Cl \quad (II)$$

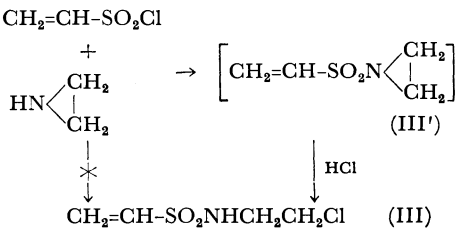

The reaction between sodium vinyl sulfonate and phosphorus pentachloride gave vinyl sulfonyl chloride and 2-chloroethane sulfonyl chloride. Isolation of vinyl sulfonyl aziridine (III'), which is a desirable compound for a reactive monomer, was unsuccessful because of lack of stability. To stabilize the unstable sulfonyl aziridine it was converted to sulfonyl (β-chloroethyl)amide by addition of concentrated hydrochloric acid. The direct preparation of III from II and aziridine was tried, and II was recovered. The infrared absorption spectrum of III showed absorptions of NH at 3280 cm^{-1}, SO_2 at 1333 cm^{-1} and 1150 cm^{-1},

8) W. F. Whitmore and E. D. Landau, *J. Am. Chem. Soc.*, **68**, 1798 (1964).

9) C. S. Marvel, C. F. Bailey and M. S. Sparbey, *ibid.*, **49**, 1833 (1927).

10) E. F. Landau, *ibid.*, **69**, 1219 (1947).

and CH_2=CH at 3080 cm^{-1}, 3050 cm^{-1}, 1610 cm^{-1}, 970 cm^{-1} and 915 cm^{-1}, respectively.

Polymerization and Copolymerization of III. Poly-III was not obtained by UV irradiation. But using a radical initiator gave only low viscosity polymer even after a prolonged polymerization time. The polymer obtained was soluble in tetrahydrofuran (THF), dimethylformamide (DMF), methanol, benzene and acetone but insoluble in ether, water, and chloroform. The polymer of III decomposed at 95—105°C. The infrared absorption spectrum of poly-III showed no absorptions due to C=C double bond bands. The results of the polymerization are shown in Table 1.

Table 1. Polymerization of vinyl sulfonyl (β-chloroethyl)amide (III)

Monomer (g)	Initiator AIBN (g)	Temp. (°C)	Time (hr)	Yield g (%)	η_{inh}[a]
4.59	0.006	65	50	0.2(4.4)	0.29
0.92	0.01	70	20	0.05(5.4)	0.32
0.92	UV	r.t.	18	—	—
1.50	0.01	60	70	0.21(14)	0.39

a) 0.25g/100 m*l* DMF at 30°C.

Table 2. Copolymerization of styrene (M_1) and III (M_2) at 62°C

Expt No.	Mol% in monomer		N% of copolymer	Mol% of copolymer	
	$[M_1]$	$[M_2]$		$[m_1]$	$[m_2]$
1	84.73	15.27	0.86	93.33	6.67
2	80.02	19.98	1.00	92.20	7.80
3	69.97	30.03	1.43	88.61	11.39
4	60.03	39.97	1.90	84.50	15.50
5	50.12	49.88	2.31	80.75	19.25
6	40.11	59.89	3.07	73.35	26.65
7	30.00	70.00	3.79	65.76	34.24
8	20.00	80.00	5.09	50.34	49.66

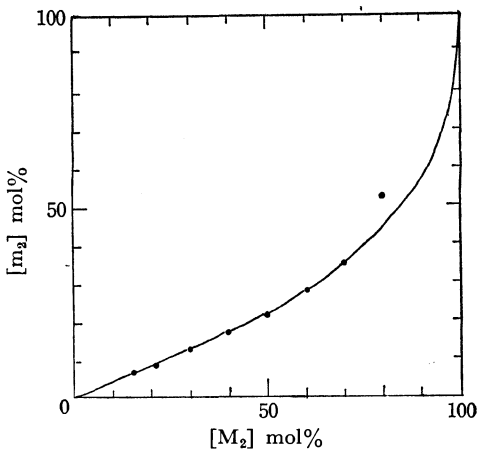

Fig. 1. Copolymerization curve: Styrene (M_1)-III (M_2).
(●) experimental; (—) calculated line based on the r_1, r_2 values

On the copolymerization of III with styrene, monomer feeds and copolymer compositions are shown in Table 2 and Fig. 1. The monomer reactivity ratios of III (M_2) with styrene (M_1) were determined from these data and Q, e values of III were calculated as follows: r_1=3.0, r_2=0.075, Q=0.125, e=0.42.

Reaction of Methane Sulfonyl (β-Chloroethyl)amide with Nucleophiles. As a model of the reaction of poly-III, the reaction of methane sulfonyl (β-chloroethyl)amide (IV) with nucleophiles was carried out. Table 3 shows the results

Table 3. Reaction of methane sulfonyl (β-chloroethyl)amide

Product	IV (mol)	Reagent (mol)	Base (mol)	Toluene (m*l*)	Temp. (°C)	Time (hr)	Yield[a] (%)	Mp (°C)
$CH_3SO_2NH(CH_2)_2S$- (IV-1)	0.01	0.01	0.01	10	reflux	4	13(65)	66.5—67.5
$CH_3SO_2NH(CH_2)_2N$ 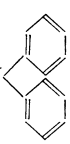 (IV-2)	0.01	0.015	—	—	150	7	7(44)	109—110.0
$CH_3SO_2NH(CH_2)_2NH$- -CH_3 (IV-3)	0.01	0.01	0.01	10	reflux	10	3(53)	68.5—70.0
$CH_3SO_2NH(CH_2)_2NH$- 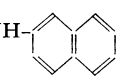 (IV-4)	0.01	0.015	—	—	150	7	17(38)	103—105.0
$CH_3SO_2NH(CH_2)_2NH$- (IV-5)	0.01	0.01	0.01	10	reflux	10	23(78)	48—50.0

a) The yield of purified products is described. Values in parenthesis are the yield of crude products. IR spectra of crude compounds were the same as those of purified samples.

Table 4. Elementary analyses of model compound

Compound	C%		H%		N%	
	Found	Calcd	Found	Calcd	Found	Calcd
IV-1	47.04	46.73	5.83	5.66	6.20	6.06
IV-2	62.30	62.04	6.24	6.25	9.86	9.65
IV-3	52.25	52.61	6.97	7.06	11.99	12.28
IV-4	59.34	59.29	5.92	5.74	10.76	10.64
IV-5	49.60	50.45	6.34	6.54	13.22	13.07

Table 5. The effect of triethylamine on the preparation of $CH_3SO_2NH(CH_2)_2NH$-

IV (mol)	Aniline (mol)	Toluene (ml)	Triethyl amine (mol)	Temp. (°C)	Time (hr)	Yield (%)
0.01	0.01	10	0.01	140	4	78
0.01	0.015	—	—	150	6	37

Table 6. Reaction of poly-III

	Reagent (g)	Poly-III (g)	Solvent THF(ml)	Base[a] (g)	Temp. (°C)	Time (hr)	Yield (%)	Anal. N%	Conversion (%)
Thiophenol	(0.15)	0.08	1	0.15	room 100	24 4	63	5.72	100.7
Aniline	(0.25)	0.07	1	0.20	115	7	70	9.84	32.0
p-Toluidine	(0.05)	0.07	1	0.10	115	6	70	7.97 (Cl)	53.4[b]

a) Triethylamine.
b) Data was calculated from chlorine analysis.

of the reaction. Table 4 shows the elementary analyses of model compounds. From these results, main reaction of IV with nucleophiles may be concluded as a substitution reaction at β-carbon of β-chloroethyl amido group. The reaction is shown as Eq. (1).

$$CH_3SO_2NHCH_2CH_2Cl + RH \rightarrow CH_3SO_2NHCH_2CH_2R + HCl \quad (1)$$

As shown in Table 5, the reaction of IV with aniline proceeded without triethylamine as an acid acceptor and the fact suggests that aniline itself acts as an acid acceptor. When triethylamine was used, the reaction proceeded more smoothly and a high yield of the product was obtained in a short time.

Reaction of Poly-III and Nucleophiles. Poly-III was found to be reactive with nucleophiles such as phenol, aniline and *p*-toluidine like methane sulfonyl (β-chloroethyl)amide. The results are summarized in Table 6.

Table 7. Reaction of copolymer of styrene-III with *p*-toluidine in the presence of pyridine

Exp. No.	Reaction time (min)	Recovered yield (%)	Cl % of reacted polm.	Conversion (%)
1	Original	—	5.42	—
2	5	90	5.28	2.3
3	15	94	5.26	2.7
4	60	75	5.21	3.5
5	120	73	—	6.3[a]
6	240	73	5.08	5.7
7	1800	64	1.05	79.0

a) Conversion was calculated from nitrogen analysis.

Reaction of Copolymer with Nucleophiles. The reaction of styrene-III copolymer with *p*-toluidine was carried out and the results are listed in Table 7. The degree of reaction was calculated by chlorine analysis of the resulting copolymer. The reaction seemed to proceed very slowly. From the values of monomer reactivity ratios of III with styrene, III unit should be placed separately on a copolymer chain. This is very different from homopolymer. The low degree of reaction of the copolymer might reflect the difference of polymer structure.

Polymer of III reacted with thiophenol was soluble in THF, but reaction of polymer III with aniline or *p*-toluidine gave cross-linked polymer. Aniline and *p*-toluidine appeared to act as a bifunctional reagent to make crosslinking as shown in V. The crosslinking presumably disturbs the amine to approach reacting sites and conversion of the reaction becomes low.

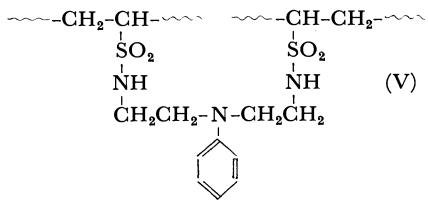

The fiber spun from copolymer of III with acrylonitrile was treated with Congo Red, a kind of amine, in aqueous solution at 95°C for an hour in the presence of pyridine. The amount of dye taken up by the fiber was determined by the colorimetric method. Usual acrylic fibers could not be dyed by Congo Red, a direct dye. The extraction of colored fiber with hot water gave no decoloration. We could conclude that the dye taken up was combined

TABLE 8. REACTION OF POLY-ST-III WITH NUCLEOPHILES

Reagents	Reagent wt. (g)	Poly-St-III[a] (g)	Solvent THF(ml)	Base (ml) Pyridine	Temp. (°C)	Time (hr)	N% (found)	Conversion (%)
Phenol	0.13	0.20	5	1	reflux	2	1.87	18.4
p-Toluidine	0.21	0.20	5	1	reflux	2	2.30	6.3
Congo Red[b]	0.26	0.20	5	1	reflux	2	2.61	4.2

a) Found 2.18 % (N).

b)

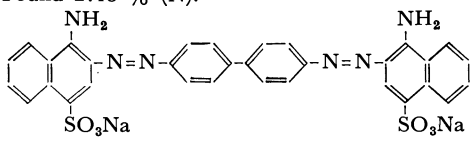

TABLE 9. THE REACTION OF FIBER AND CONGO RED AT VARIOUS CONCENTRATION OF PYRIDINE

Pyridine (%)	Amount of dye (mg/g)	Conversion (%)
2	30	82.3
6	22	60.4
10	25	68.6
14	22	60.4
24	18	49.6
50	14	34.6

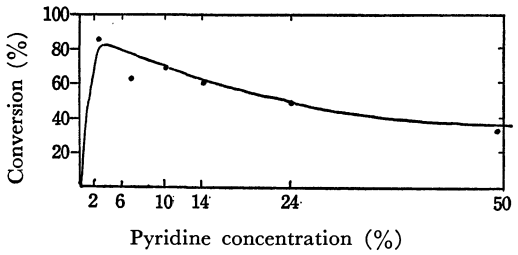

Fig. 2. The effect of pyridine concentration in the dye solution on amount of dye on fiber.

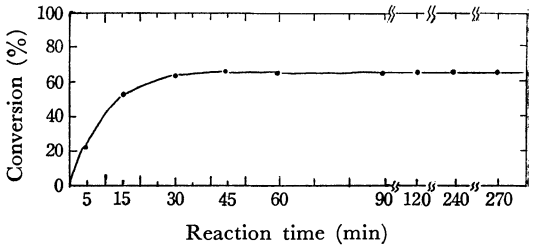

Fig. 3. The relation between the reaction time and the amount of the reaction in the case the dying of the fiber. (Pyridine concn. 10%, at 95°C)

chemically with the fiber. Effect of pyridine concentration in the dye solution on the reaction is shown in Table 9 and Fig. 2. The concentration of pyridine seemed to affect partition coefficient of the dye in the solution and the fiber, which played an important role in the reaction. Finally, we concluded that the reactivity of the sulfonyl (β-chloroethyl)amide groups derivatives of *p*-styrene and vinyl are the same, but the polymerizability and copolymerizability of styrene derivative are better than those of vinyl derivative.

BULLETIN OF THE CHEMICAL SOCIETY OF JAPAN VOL. 42 746—749 (1969)

Deoxygenation of Styrene Oxide by Zinc Metal and Lewis Acid

Sotaro MIYANO, Mitsuhiko HIDA and Harukichi HASHIMOTO

Department of Synthetic Chemistry, The University of Tokyo, Hongo, Tokyo

(Received June 13, 1968)

Styrene oxide was deoxygenated to styrene in 83% yield by zinc metal and zinc chloride in aqueous ether. Under the same reaction conditions phenyl glycidyl ether gave only 2.8% of phenyl allyl ether, and propylene oxide did not give propylene. Effects of the reaction variables on the deoxygenation of styrene oxide were investigated. The yield of styrene was varied with metal halide in anhydrous THF in the following order; $ZnI_2 > ZnCl_2 \sim ZnBr_2 > AlCl_3 > SnCl_4 > FeCl_3 > NaI \gg MgBr_2$. Styrene was formed from styrene oxide by zinc metal and zinc chloride in *ca.* 50% yield in THF, acetone, acetic acid, and aqueous ethanol, but not in anhydrous benzene. The yield of styrene increased almost proportionally with the increase of the molar ratio of zinc chloride to styrene oxide up to 1 : 1. 2-Phenyl-2-chloroethanol gave styrene when treated with zinc metal in the presence or absence of zinc chloride, but 1-phenyl-2-chloroethanol did not. Possible reaction paths of the deoxygenation of styrene oxide by zinc metal and metal halide were discussed.

It is well known that 1,2-epoxides give halohydrins, rearrange to carbonyl compounds, or polymerize to polyethers when treated with Lewis acids.[1] On the other hand, in the course of the investigation of the reaction of zinc-methylene complex with epoxides,[2] we found that styrene oxide is deoxygenated to styrene by zinc metal and Lewis acid. In this paper, we report further investigation of the reaction.

Experimental

Materials. *Epoxides.* Commercial styrene oxide (bp 80°C/16 mmHg). Propylene oxide (Mitsui Chem. Co.) was refluxed and distilled over KOH (bp 34°C). Phenyl glycidyl ether was obtained by conventional method[4] (bp 118—118.3°C/11 mmHg; lit. bp 114—118°C/12 mmHg).

Metal Halides. Anhydrous magnesium bromide was prepared from magnesium turnings and bromine in THF or ether.[5] Anhydrous stannous chloride was prepared by dehydration of $SnCl_2 \cdot 2H_2O$ with acetic anhydride.[6] Zinc halides were either prepared from zinc dust and hydrogen halides, or were of commercial reagent grade.

Styrene Chlorohydrins. 2-Phenyl-2-chloroethanol was obtained by adding HCl gas to styrene oxide in chloroform[7] (bp 97—98.5°C/2.5 mmHg; lit. bp 97—99°C/1.2 mmHg). 1-Phenyl-2-chloroethanol was obtained by the addition of hypochlorite to styrene[8] (bp 106—109°C/7.5 mmHg; lit. bp 110—111°C/6 mmHg).

All solvents were purified as usual before use. Zinc-copper couple was prepared by LeGoff's method[9] and washed several times with the solvent used in the reaction.

Reaction of Styrene Oxide with Zinc Chloride and Zinc-Copper Couple. The reaction was carried out in a 100 m*l*, three necked reaction flask equipped with a dropping funnel, thermometer and reflux condenser topped with calcium chloride drying tube.

Freshly prepared zinc-copper couple obtained from 0.12 g-atom of zinc and 0.5 g of $Cu(OAc)_2 \cdot H_2O$ were mixed with 0.051 mol of zinc chloride and 30 m*l* of THF in a reaction flask. Into the mixture, styrene oxide (0.050 mol) dissolved in 20 m*l* of THF was added for 1 hr at 34—35°C with stirring. After the addition had been completed, reaction was continued for another 5 hr at 35°C with stirring. Then the flask was chilled in ice-water, and the amount of styrene was determined by g.l.c. with *t*-butylbenzene as an internal standard. The reaction mixture was treated as reported previously.[3] Styrene was isolated by distillation and identified by elemental analysis and IR spectrum; bp 58°C/39 mmHg (Found: C, 91.21; H, 7.85%). From the result of g.l.c. analysis the minimum amount of the reacted styrene oxide seemed to be determined, because

1) F. Johnson, "Friedel-Crafts and Related Reactions," Vol. IV, ed. by G. A. Olah, Interscience Publishers, New York-London-Sydney (1965), p. 33.

2) To be published. For the previous work, see Ref. 3.

3) a) S. Miyano, M. Hida and H. Hashimoto, *Kogyo Kagaku Zasshi (J. Chem. Soc. Japan, Ind. Chem. Sect.)*, **69**, 2134 (1966). b) H. Hashimoto, M. Hida and S. Miyano, *J. Organometal. Chem.*, **10**, 518 (1967). c) S. Miyano, M. Hida and H. Hashimoto, *ibid.*, **12**, 263 (1968).

4) K. Furukawa and R. Oda, *Kogyo Kagaku Zasshi (J. Chem. Soc. Japan, Ind. Chem. Sect.)*, **55**, 673 (1952).

5) H. O. House, *J. Am. Chem. Soc.*, **77**, 3070 (1955).

6) J. W. W. Williams, "Organic Syntheses," Coll. Vol. III, p. 627 (1955).

7) G. Berti, F. Bottari, P. L. Ferrarini and B. Macchia, *J. Org. Chem.*, **30**, 4091 (1965).

8) W. S. Emerson, *J. Am. Chem. Soc.*, **67**, 516 (1945).

9) E. LeGoff, *J. Org. Chem.*, **29**, 2048 (1964).

styrene oxide showed all the same retention time on g.l.c. (DOP diasolid column) as phenylacetaldehyde, which may be present in the reaction mixture as the result of rearrangement of styrene oxide.

Reaction of Propylene Oxide with Zinc Metal and Zinc Iodide in Aqueous Ether. Aqueous solution of 57% HI (HI; 0.20 mol, H_2O; 1.09 mol) was added to the zinc dust (0.588 mol) covered with 100 ml of ether with stirring. After the evolution of gas subsided, propylene oxide (0.20 mol) dissolved in 50 ml of ether was dropped to the stirred suspension for 1 hr under gentle reflux (34—35°C). The reaction was continued for another 5 hr at 35°C. Gas evolved during the reaction was introduced with nitrogen into an another flask containing bromine - CCl_4 solution, in which propylene was converted into 1,2-dibromopropane. The dibromide was isolated by distillation, and confirmed by NMR and IR spectra. The yield was determined by g.l.c.

Results and Discussion

Reaction of Epoxides with Zinc Metal and Zinc Halides. Table 1 shows the results of the reaction of styrene oxide, propylene oxide and phenyl glycidyl ether with zinc metal and zinc halide in THF or aqueous ether. Styrene oxide was deoxygenated to styrene in high yields. Propylene oxide gave no propylene, but afforded a 4 : 1 mixture of 1-chloro-2-propanol and 2-chloro-1-propanol (bp 80.5—80.6°C/164 mmHg, 56% based on propylene oxide) (No. 5). When propylene oxide was treated with zinc iodide and zinc, propylene was obtained only in the low yield, but 1-iodo-2-propanol was also isolated in 48% yield based on propylene oxide; bp 76°C/22 mHg (No. 7). On the other hand, propylene was obtained in good yield in the presence of sodium iodide, zinc dust and sodium acetate in aqueous acetic acid, as described by Cornforth *et al.*[10] (No. 9). They reported the deoxygenation of alkylene oxides to alkenes by zinc metal and sodium iodide in acetic acid, and suggested the following reaction mechanism:

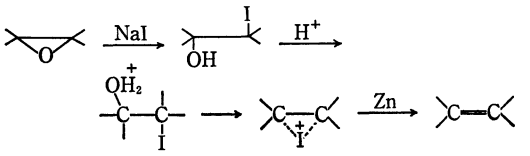

However, in our case, at least in anhydrous THF, the above protonation and dehydration mechanism may not be responsible for the styrene formation from styrene oxide with zinc metal and zinc halides (*vide infra*).

Deoxygenation of Styrene Oxide. *Effect of Metal Halides.* All metal halides except anhydrous magnesium bromide in combination with zinc-copper couple gave fairly good yield of styrene from styrene oxide (Table 2). The inactivity of anhydrous magnesium bromide for styrene formation has not yet been understood clearly. Even sodium iodide gave styrene in a lower yield, but the addition of zinc acetate improved the yield of styrene. In the latter case, it seems that the resultant zinc iodide was an active catalyst. Lower yield of styrene in anhydrous THF compared with that in

Table 1. Reaction of epoxides with zinc metal and zinc halide[a]

No.	Epoxide[b]		Reaction condition		Zn	Olefin (%)[c]	Solvent[d]
1	SO	0.025	$ZnCl_2$ H_2O	0.014 0.107	0.073	83	E 50(ml)
2		0.050	$ZnCl_2$	0.051	0.12[e]	51	T 50
3		0.051	$ZnCl_2$	0.051	—	0	T 50
4		0.050			0.12[e]	1.7	T 50
5	PO	0.020	$ZnCl_2$ H_2O	0.10 0.76	0.49	0	E 150
6		0.10	$ZnCl_2$	0.10	0.51[e]	1.1	T 100
7		0.20	ZnI_2 H_2O	0.10 1.1	0.49	6.5	E 150
8		0.10	ZnI_2	0.10	0.51[e]	6.4	T 100
9		0.20	NaI NaOAc H_2O	0.35 0.21 0.40	0.78	74	A 100
10	PGE	0.10	$ZnCl_2$ H_2O	0.051 0.38	0.26	2.8	E 200

a) 35°C, 6 hr.
b) SO: styrene oxide, PO: propylene oxide, PGE: phenyl glycidyl ether.
c) Based on epoxide used.
d) E; ether, T; THF, A; acetic acid.
e) Zinc-copper couple was used.

10) J. W. Cornforth, R. H. Cornforth and K. K. Mathew, *J. Chem. Soc.*, **1959**, 112.

Table 2. Effect of metal halide on deoxygenation of styrene oxide[a)]

Halide	PhCH=CH$_2$(%)	Minimum conversion of SO (%)
$ZnCl_2$	51	82
$ZnBr_2$	47	82
$ZnBr_2$[b)]	51	
$ZnBr_2$[c)]	49	98
ZnI_2	67	97
$MgBr_2$	0.9	73
$MgBr_2 \cdot 3H_2O$	72	100
$FeCl_3$	17	95
$AlCl_3$	40	100
$SnCl_4$	32	77
NaI	13	73
NaI + $Zn(OAc)_2$[d)]	30	79

a) Styrene oxide: 0.050 mol, solvent: THF 50 *ml*, halide: 0.050 mol, Zn-Cu: 0.12 mol, 35°C, 6 hr.
b) The reaction was carried out in the scale of twice.
c) $ZnBr_2$ was prepared from zinc duct and bromine *in situ*. Reaction was carried out for 3 hr at 60°C.
d) 0.025 mol.

aqueous ether may be due to side reactions such as rearrangement to phenylacetaldehyde.[1)]

Effect of Reagent Molar Ratio. The effect of the amount of zinc chloride on the styrene yield was shown in Fig. 1. No styrene was obtained when styrene oxide was treated only with zinc chloride, or only with zinc metal. The presence of both zinc metal and metal halides is necessary for styrene formation.

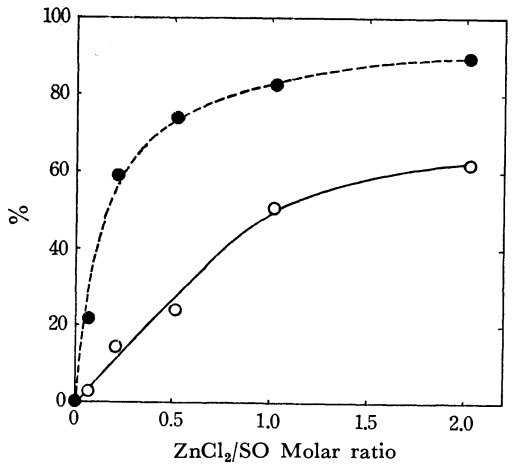

Fig. 1. Effect of the molar ratio of zinc chloride to styrene oxide.
Styrene oxide: 0.050 mol, solvent: THF 50 *ml*, 35°C, 6 hr.
○ Styrene yield.
● Minimum conversion of styrene oxide.

Solvent Effect. Styrene oxide was deoxygenated to styrene by zinc-copper couple and zinc chloride even in protic solvents such as acetic acid and aqueous ethanol, but was not in anhydrous benzene (Table 3). These results may indicate the ionic character of this styrene formation reaction (*vide infra*).

Table 3. Solvent effects for the deoxygenation of styrene oxide[a)]

PhCH=CH$_2$ (%)	Minimum conversion of SO (%)	Solvent
51	82	THF
57	89	acetone
0	42	PhH
55	100	aq. EtOH
43	79	AcOH

a) Styrene oxide: 0.050 mol, Zu-Cu: 0.12 mol, $ZnCl_2$: 0.050 mol, solvent: 50 m*l*, 35°C, 6 hr.

Reducing Reagents Other than Zinc Metal. Zinc metal can be replaced by triphenylphosphine[11)] or magnesium metal, though the yield of styrene was reduced. However, stannous chloride was not effective (Table 4). Magnesium metal was used in the form of turnings, and triphenylphosphine may form acid-base complex with zinc chloride as suggested by Wittig and Haag.[11)] These factors may partly be responsible for the lower yield of styrene.

Table 4. Reducing reagents for the deoxygenation of styrene oxide[a)]

Reducing reagent		PhCH=CH$_2$ (%)	Minimum conversion of SO (%)
Zn-Cu	0.12	51	82
Mg	0.12	16	93
Ph_3P	0.16	38	97
$SnCl_2$	0.060	2.1	47

a) Styrene oxide: 0.050 mol, $ZnCl_2$: 0.050 mol, THF 50 m*l*, 35°C, 6 hr.

Reaction of Styrene Chlorohydrins and Mechanistic Consideration of Deoxygenation of Styrene Oxide. Reactions of 1-phenyl-2-chloroethanol and 2-phenyl-2-chloroethanol with zinc metal in the presence or absence of zinc chloride were compared with those of styrene oxide (Table 5). Though zinc can not eliminate hypochlorite from alkyl chlorohydrins[10,12)] except from those of

11) G. Wittig and H. Haag, *Chem. Ber.*, **88**, 1654 (1955).
12) D. V. Banthorpe, "Elimination Reactions," ed. by E. D. Hughes, Elsevier Pub. Co., Amsterdam-London-New York (1963). p. 136.

special steroidal series,[13] benzylic chloride in 2-phenyl-2-chloroethanol was active enough to give styrene. It may be noticeable that the dechlorohydrination of *erythro*-1,2-diphenyl-2-chloroethanol by zinc dust in acetic acid is well known as the synthetic method of *trans*-stilbene.[14] From these facts the following two reaction paths seem to be probable for the formation of styrene from styrene oxide by zinc metal and metal halides.

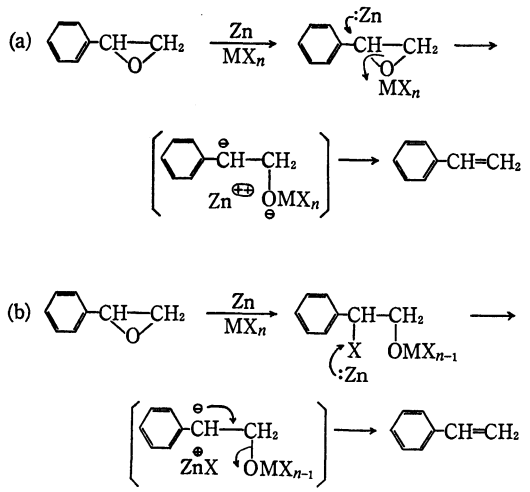

Path (a) shows a concerted electron transfer from zinc to benzylic carbon, followed by an elimination of $OMXn^{-2}$. Path (b) shows the formation of metal salt of 2-phenyl-2-haloethanol as an intermediate. The formation of organozinc intermediate is excluded since no phenethyl alcohol was formed even in acetic acid. Several authors suggested the formation of transient carbanion in the elimination of hypobromite from boromohydrins by zinc metal.[15] Cole and Julian showed that α,β-epoxy ketones and styrene oxide are deoxygenated to olefins by chromous chloride in acetic acid.[16] They suggested the direct attack of chromous ion to α,β-epoxy ketones as follows:

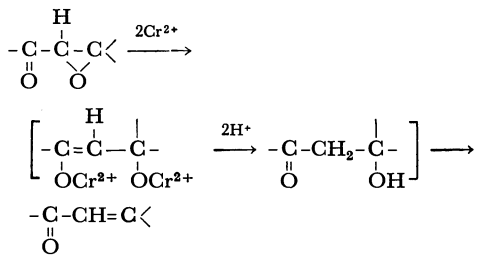

Though they did not mention the mechanism of styrene formation from styrene oxide by chromous chloride, the above two reaction paths (a and b) may be plausible also.[17] Kharasch *et al.* suggested radical chain mechanism for the propylene formation from propylene oxide or two isomers of propylene chlorohydrins by Grignard reagent in the presence of transition metal halide.[18] But styrene was not formed from 2-phenyl-2-chloroethanol by phenylmagnesium bromide in the presence of zinc chloride in THF (Table 5). Further investigation seems to be necessary for the detailed discussion of the reaction of epoxides with zinc metal and metal halide.

Table 5. Comparison of the reaction of styrene oxide and styrene chlorohydrins[a]

Ph-	$\times 10^{-2}$	Reaction condition	$\times 10^{-2}$	Solvent	PhCH=CH_2 (%)
-CH-CH_2 (O)	2.5	Zn / $ZnCl_2$ / H_2O	7.3 / 1.4 / 11	E 50 ml	83
	5.0	Zn-Cu / $ZnCl_2$	12 / 5.1	T 50	51
	5.0	Zn-Cu	12	T 50	1.7
-CH(Cl)-CH_2(OH)	1.6	Zn / $ZnCl_2$ / H_2O	4.6 / 0.75 / 5.6	E 30	58
	1.7	Zn / H_2O	4.6 / 6.2	E 30	3.6
	1.6	PhMgBr / $ZnCl_2$	2.7 / 1.6	T 30	0
-CH(OH)-CH_2(Cl)	1.5	Zn-Cu	6.1	E 30	1.1

a) 35°C, 6 hr.

This work was partly supported by a grant from the Ministry of Education.

13) S. Mori, *Nippon Kagaku Zasshi (J. Chem. Soc. Japan, Pure Chem. Sect.)*, **70**, 257 (1949).

14) L. F. Fieser, "Experiments in Organic Chemistry," D. C. Heath and Co., Boston (1964), p. 219.

15) a) D. R. James, R. W. Rees and C. W. Shoppee, *J. Chem. Soc.*, **1955**, 1370. b) H. O. House and E. S. Ro, *J. Am. Chem. Soc.*, **80**, 182 (1958). c) S. J. Cristol and L. E. Rademacher, *ibid.*, **81**, 1600 (1959).

16) W. Cole and L. Julian, *J. Org. Chem.*, **19**, 131 (1954).

17) Chromous chloride was prepared by the reduction of chromic chloride by zinc metal, and zinc chloride or chromic chloride seems to act as Lewis acid.

18) M. S. Kharasch, L. Biritz, W. Nudenberg, A. Bhattacharya and N. C. Yang, *J. Am. Chem. Soc.*, **83**, 3229 (1961).

BULLETIN OF THE CHEMICAL SOCIETY OF JAPAN VOL. 42 750—755 (1969)

Studies of Purine *N*-Oxides. III. The Synthesis of Purine 3-*N*-Oxides[1]

Hideaki KAWASHIMA and Izumi KUMASHIRO

Central Research Laboratories, Ajinomoto Co., Inc., Suzuki-cho, Kawasaki

(Received June 15, 1968)

6-Methoxy- and 6-ethoxypurine 3-*N*-oxides were obtained by the direct oxidation of the corresponding 6-alkoxypurines with hydrogen peroxide in aqueous acetic acid. 6-Chloropurine was oxidized with monoperphthalic acid in ether to give 6-chloropurine 3-*N*-oxide. These purine 3-*N*-oxides were then converted to hypoxanthine 3-*N*-oxide by hydrolysis with a sodium hydroxide solution. 6-Methoxypurine 3-*N*-oxide and hypoxanthine 3-*N*-oxide were identified with authentic samples unambiguously synthesized from 6-methylsulfonylpurine 3-*N*-oxide, which had itself been obtained by the oxidation of 6-methylthiopurine 3-*N*-oxide. The treatment of hypoxanthine 3-*N*-oxide with hydrochloric acid gave 6,8-dihydroxypurine, 8-chlorohypoxanthine, hypoxanthine, and 2-chloro-4-amino-5-imidazolecarboxamide.

The synthesis of 3-*N*-oxides of purine derivatives by direct oxidation has never been described. Adenine,[2,3] 2,6-diaminopurine,[2] 6-methylpurine,[4] and 6-methyl-8-hydroxypurine[4] are, however, known to be converted to the corresponding 1-*N*-oxides by direct oxidation. Purine[4] and 8-hydroxypurine[4] have been oxidized to mono-*N*-oxides, in which the positions of the *N*-oxide groups are still unknown. Guanine[5,6] was oxidized to guanine 7-*N*-oxide with trifluoroperacetic acid.

Generally, purine 3-*N*-oxides have been synthesized by a cyclization process (*e.g.*, 7-methyladenine 3-*N*-oxide[7] and xanthine 3-*N*-oxide[8]). 6-Mercaptopurine 3-*N*-oxide was obtained from 7-aminothiazolo[5,4-d]pyrimidine 6-*N*-oxide by treating it with a sodium hydroxide solution.[9,10]

In the present paper the synthesis of purine 3-*N*-oxides by direct oxidation will be described. 6-Methoxy purine (Ia) was treated with a mixture of a 30% hydrogen peroxide solution and acetic acid at room temperature. After fifteen days the reaction mixture was evaporated to dryness, and the resulting residue was washed with ethanol and crystallized from water to give fine, colorless crystals. Elementary analysis revealed the composition of the oxidation product (IIa) to be $C_6H_6N_4O_2$, corresponding to that of the expected 6-methoxypurine *N*-oxide. The reduction of this oxidation product (IIa) with hydrogen in the presence of Raney nickel gave 6-methoxypurine (Ia). In addition, IIa possesses a strong absorption maximum in neutral and alkaline solutions near 230 mμ; this is characteristic of purine *N*-oxides in general.[2,11] These properties of this product (IIa) suggest its mono-*N*-oxide structure. 6-Ethoxypurine (Ib) was then similarly oxidized to give a mono-oxidized product (IIb); it had the composition of $C_7H_8N_4O_2$, and showed the properties of purine *N*-oxides.

The direct oxidation of 6-chloropurine has been reported to yield the nonoxidizable hypoxanthine.[9] Since this failure was considered to be due to the presence of water, the oxidation of 6-chloropurine was attempted under an anhydrous condition. 6-Chloropurine (III) partially suspended in an ether solution of monoperphthalic acid was stirred at room temperature for a few days. The resulting precipitation was washed with ether to remove the unchanged 6-chloropurine and the phthalic acid. The ether-insoluble residue showed a new single spot on a paper chromatogram. Since this product was decomposed upon heating in water or some organic solvents, it was reprecipitated from an ammonia-methanol solution by the addition of ether to give pure crystals. The crystals had the

1) Part II of this series: H. Kawashima and I. Kumashiro, This Bulletin, **40**, 639 (1967).
2) M. A. Stevens, D. I. Magrath, H. W. Smith and G. B. Brown, *J. Am. Chem. Soc.*, **80**, 2755 (1958).
3) M. A. Stevens and G. B. Brown, *ibid.*, **80**, 2759 (1958).
4) M. A. Stevens, A. Giner-Sorolla, H. W. Smith and G. B. Brown, *J. Org. Chem.*, **27**, 567 (1962).
5) G. B. Brown, K. Sugiura and R. M. Cresswell, *Cancer Res.*, **25**, 986 (1965).
6) T. J. Delia and G. B. Brown, *J. Org. Chem.*, **38**, 178 (1966).
7) E. C. Taylor and P. K. Loeffler, *ibid.*, **24**, 2035 (1959).
8) R. M. Cresswell, H. K. Maurer, T. Strauss and G. B. Brown, *ibid.*, **30**, 408 (1965).
9) G. Levin and G. B. Brown, *J. Med. Chem.*, **6**, 825 (1963).
10) G. B. Brown, G. Levin, S. Murphy, A. Sele, H. C. Reilly, G. S. Tarnowski, F. A. Schmid, M. N. Teller and C. C. Stock, *ibid.*, **8**, 190 (1965).
11) E. C. Taylor, C. C. Cheng and O. Vogl, *J. Org. Chem.*, **24**, 2019 (1959).

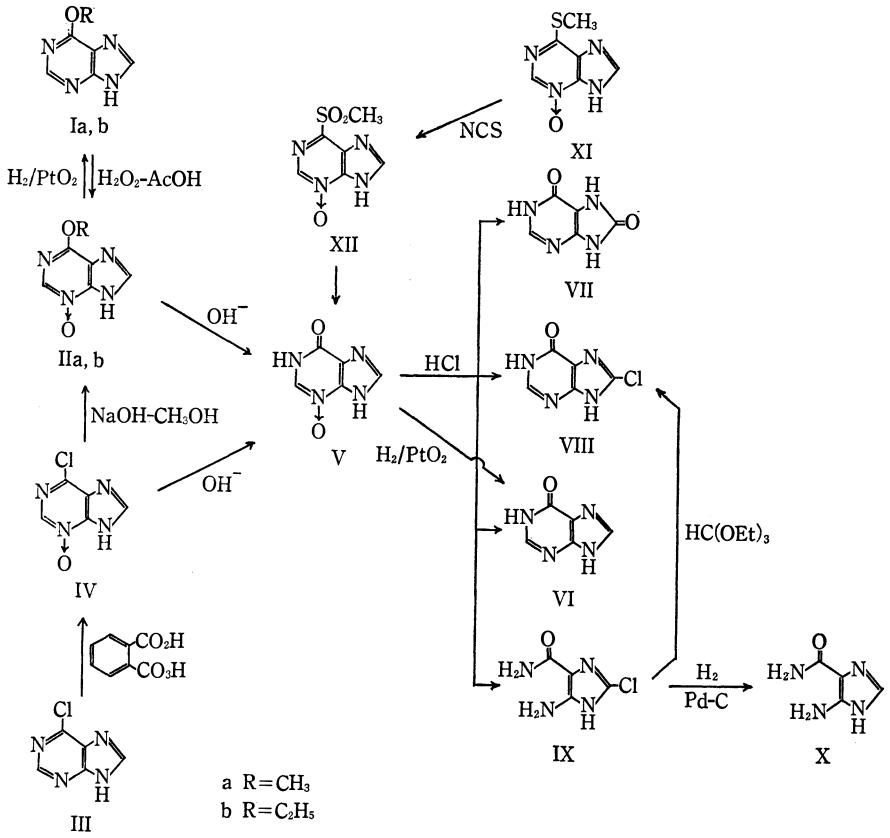

Fig. 1

composition of $C_5H_5N_4OCl \cdot NH_3$ and were convertible to 6-methoxypurine *N*-oxide (IIa) when treated with sodium methoxide. From these properties, the structure of this product was considered to be 6-chloropurine mono-*N*-oxide (IV).

Upon being heated in a 1 N sodium hydroxide solution under refluxing, these 6-alkoxypurine *N*-oxides (IIa, b) and 6-chloropurine *N*-oxide (IV) were both converted to the same new product (V). This new product (V) possessed the composition of $C_5H_4N_4O_2$ and a strong absorption maximum in an alkaline solution at about 230 mμ. Though V was reduced with hydrogen in the presence of Raney nickel to yield hypoxanthine (VI), it was not identified with hypoxanthine 1-*N*-oxide.[11-13] Consequently, V is likely to be hypoxanthine 3-, 7-, or 9-*N*-oxide.

In order to elucidate the structure of V, we attempted the hydrolysis of V with 3 N hydrochloric acid. The hydrolysis products were separated through a Dowex 50 (H^+ type) column to give 6,8-dihydroxypurine (VII), 8-chlorohypoxanthine (VIII), hypoxanthine (VI) and 2-chloro-4-amino-5-imidazolecarboxamide (IX). Compounds VII and VIII were identified with the respective authentic samples.[14]

The structure of IX was determined from the following reactions of IX. The catalytic reduction of IX with hydrogen in the presence of 10% palladium-on-charcoal gave 4-amino-5-imidazolecarboxamide. A cyclization of IX with ethyl orthoformate resulted in the formation of 8-chlorohypoxanthine (VIII).[14]

Purine *N*-oxides have been known, upon hydrolyis in an acid, to give hydroxylaminopyrimidine or -imidazole derivatives by the loss of the carbons adjacent to the *N*-oxide groups. For instance, 2,6-diamino-8-phenylpurine 7-*N*-oxide has been hydrolyzed to give 2,4,6-triamino-5-hydroxylaminopyrimidine,[15] and adenine 1-*N*-oxide has similarly been converted to 4-amino-5-imidazolecarboxamidoxime.[3]

Contrary to expectations, however, the hydrolysis

12) H. Kawashima, T. Meguro and I. Kumashiro, This Bulletin, **39**, 633 (1966).

13) J. C. Parham, J. Fissekis and G. B. Brown, *J. Org. Chem.*, **31**, 966 (1966).

14) R. K. Robins, *J. Am. Chem. Soc.*, **80**, 6671 (1958).

15) G. M. Timmis, I. Cooke and R. G. W. Spickett, "Ciba Foundation Symposium on the Chemistry and Biology of Purines," Little Brown and Co., Boston, Mass. (1957), p. 139.

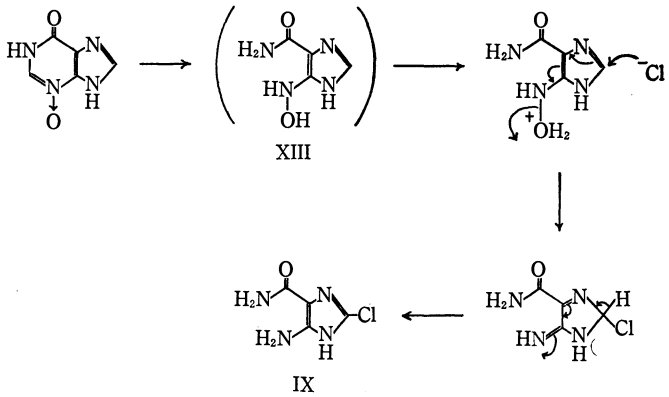

XIII

IX

Fig. 2

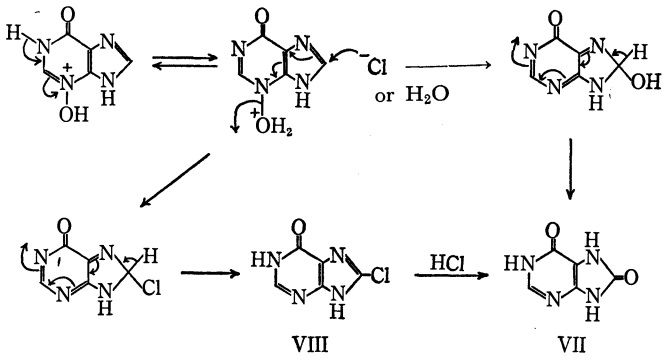

VIII VII

Fig. 3

of hypoxanthine 3-*N*-oxide (V) produced 2-chloro-4-amino-5-imidazolecarboxamide (IX), but not 4-hydroxylamino-5-imidazolecarboxamide (XIII). The opening of the pyrimidine ring of V, with an accompanying loss of 2-carbon, suggests the 3-*N*-oxide structure of V. However, more evidence is desirable.

The identification of V with an authentic hypoxanthine 3-*N*-oxide unambiguously synthesized from 6-mercaptopurine 3-*N*-oxide[9,10] was attempted.

6-Methylthiopurine is known to be oxidized with *N*-chlorosuccinimide to yield 6-methylsulfonylpurine.[16] This method was applied to the synthesis of 6-methylsulfonylpurine 3-*N*-oxide (XII) from 6-methylthiopurine 3-*N*-oxide (XI). XII was treated with a 1 N sodium hydroxide solution to give hypoxanthine 3-*N*-oxide, which was identified with V. Consequently, the 3-*N*-oxide structures of IIa, IIb, IV, and V were confirmed. XII was converted to 6-methoxypurine 3-*N*-oxide (IIa) upon being treated with a solution of sodium hydroxide in methanol.

The route to 2-chloro-4-amino-5-imidazolecarboxamide (IX) from hypoxanthine 3-*N*-oxide (V) upon hydrolysis was estimated to be as follows.

8-Chlorohypoxanthine (VIII), one of the hydrolysis products of hypoxanthine 3-*N*-oxide (V), is not certainly a direct precursor of IX, since VIII is converted to 6,8-dihydroxypurine (VII) upon being refluxed in 3 N hydrochloric acid. At first, prior to the halogenation, V may be hydrolyzed to the presumed ring-opening intermediate (XIII). Then the latter may be attacked by the chloride anion at 2-position to give IX, accompanied by N-O bond breaking (Fig. 2).

Further, the mechanism of the formation of 6,8-dihydroxypurine (VII) and 8-chlorohypoxanthine (VIII) from V upon hydrochloric acid treatment was suggested to be as follows (Fig. 3).

Experimental

6-Methoxypurine 3-*N*-Oxide (IIa). A 30% aqueous hydrogen peroxide solution (150 m*l*) was added to a solution of 6-methoxypurine hemihydrate (15 g) in glacial acetic acid (375 m*l*), and then left to stand at room temperature for 17 days. The volatile materials were removed from the reaction mixture at 40°C under reduced pressure. The yellow residue was washed with ethanol and then twice with hot ethanol to give a white powder of IIa (11.2 g, 72%). The paper chromatogram (solvents A and B) of the

16) M. Ikehara, A. Yamazaki and T. Fujieda, *Chem. Pharm. Bull.*, **10**, 1075 (1962).

TABLE 1. PROPERTIES OF PURINE 3-*N*-OXIDES AND THE RELATED COMPOUNDS

Compound	Mp (°C)	R_f[a]		Spectral deta		
		A	B	pH	λ_{max} mμ	ε
6-Methoxypurine 3-*N*-oxide	215 d[b]	0.63	0.40	1	268	11400
				6	226	24800
					285	10200
				13	228	31600
					282	9300
6-Ethoxypurine 3-*N*-oxide	213 d	0.73	0.59	1	268	12600
				6	226	25000
					285	10800
				13	228	31800
					282	9800
6-Chloropurine 3-*N*-oxide	165 d[c]	0.70	0.45	1	230	20600
					304	7900
				6	231	29000
					308	6700
				13	232	27200
					308	7100
Hypoxanthine 3-*N*-oxide	210—300 d	0.35	0.17	1	261	6500
				6	280	10200
				13	226	25000
					286	10400
6-Methylsulfonylpurine 3-*N*-oxide	197—198 d	0.71	0.36	1	234	10900
					300	3100
					326	4600
				7	234	16100
					305	5100
					330	6500
				13	228	19100
					290	7100
					336	300
2-Chloro-4-aminoimidazole-5-carboxamide	above 150 d[d]	0.57	0.68	1	274	6300
				6	273	9700
				13	284	9700

a) Solvent system, A: *n*-PrOH - aq.NH_4OH - H_2O (20 : 12 : 3 vol/vol); B: *n*-BuOH - AcOH-H_2O (4 : 1 : 1 vol/vol) b) d: decompose c) Ammonium salt d) Hydrochloride

resultant white powder showed a single spot. A portion of this product was crystallized from water to give colorless crystals, mp 215°C (d).

Found: C, 43.30; H, 3.49; N, 33.57%. Calcd for $C_6H_6N_4O_2$: C, 43.37; H, 3.63; N, 33.73%.

Hydrogenation of 6-Methoxypurine 3-*N*-Oxide (IIa). IIa (1 g) was dissolved in a 2 N ammonium hydroxide solution (100 m*l*), and Raney nickel (2 m*l*) was added. The mixture was shaken at room temperature for 35 hr until 145 m*l* of hydrogen had been absorbed. The catalyst was then removed and the filtrate was evaporated to dryness. The residue (600 mg) was crystallized from water; and it was identified with authentic 6-methoxypurine by R_f in solvents A and B, and by a study of the ultraviolet and infrared spectra.

6-Ethoxypurine 3-*N*-Oxide (IIb). A 30% aqueous hydrogen peroxide solution (40 m*l*) was added to a solution of 6-ethoxypurine hemihydrate (4 g) in glacial acetic acid (100 m*l*), and then left to stand at room temperature for 11 days. The reaction mixture was treated in the same manner as the case of 6-methoxypurine 3-*N*-oxide (IIa) to yield IIb (1.5 g, 36%). The resulting powder was crystallized from water to give light-yellow crystals, mp 213°C (d).

Found: C, 46.74; H, 4.80; N, 31.19%. Calcd for $C_7H_8N_4O_2$: C, 46.66; H, 4.48; N, 31.10%.

6-Chloropurine 3-*N*-Oxide (IV). 6-Chloropurine (5 g) was suspended in 1500 m*l* of an ether solution containing 105 g of monoperphthalic acid, and then stirred at room temperature for 12 days. After the reaction, a solid material was collected. From this soild 6-chloropurine and phthalic acid were continuously extracted with ether for 50 hr. The resulting residual light-yellow powder (2.5 g, 45%) showed a single spot on a paper chromatogram (solvents A and B). Methanolic ammonia was then added to the powder, and an insoluble solid was removed by filtration. To the filtrate ether was added to precipitate ammonium salt of 6-chloropurine 3-*N*-oxide (IV). There precipitation

TABLE 2. THE RESULTS OF ION-EXCHANGE COLUMN CHROMATOGRAPHY OF THE HYDROLYSIS PRODUCTS OF HYPOXANTHINE 3-*N*-OXIDE (V) WITH 3 N HCl

Eluting Solvent	Effluent No.	Effluent ml	Compound	Yield g	Yield %	Molecular formura		Anal. % C	Anal. % H	Anal. % N	Anal. % Cl
H_2O	1	1000	none								
	2	1000	6,8-Dihydroxypurine (VII)[a]	1.3	13						
	3	2300	none								
	4	2300	8-Chlorohypoxanthine (VIII)[a]	1.0	8.9	$C_5H_3N_4OCl$	Found	35.01	1.96	32.65	
							Calcd	35.21	1.77	32.85	
	5	1000	none								
1.2 N HCl	6	2450	none								
	7	1850	Hypoxanthine (VI)[a]	0.8	8.9						
	8	500	none								
	9	2400	2-Chloro-4-amino-5-imidazolecarboxamide hydrochloride (IX)[b]	1.0	7.7	$C_4H_5N_4OCl \cdot HCl$	Found	23.81	3.54	28.30	37.0
							Calcd	24.38	3.07	28.44	36.0
	10	1600	none								

a) The effluent was evaporated to dryness. The residue was recrystallized from water, and identified with the authentic sample by R_f (solvents A and B) and ultraviolet and infrared spectra.

b) The effluent was evaporated under reduced pressure at 40°C to dryness. The residue was precipitated from methanol by addition of ether.

was performed once more to yield a colorless powder, mp 165°C (d).

Found: C, 31.87; H, 3.58; N, 36.94; Cl, 18.50%. Calcd for $C_5H_3N_4OCl \cdot NH_3$: C, 32.01; H, 3.22; N, 37.33; Cl, 18.90%.

The Reaction of 6-Chloropurine 3-*N*-Oxide (IV) with Sodium Methoxide. 6-Chloropurine 3-*N*-oxide (1 g) was dissolved in a sodium methoxide solution prepared from 300 mg of sodium and 30 ml of methanol, and then heated to 100°C for 4 hr in a sealed tube. The reaction mixture was evaporated to dryness, and water (20 ml) was added to the residue. The solution was filtered and acidified to pH 4 to precipitate light-yellow crystals. These crystals showed a single spot on a paper chromatogram (solvent A), and the R_f, ultraviolet, and infrared spectra agreed with those of 6-methoxypurine 3-*N*-oxide (IIa).

Hypoxanthine 3-*N*-Oxide (V) from 6-Methoxypurine 3-*N*-Oxide (IIa). 6-Methoxypurine 3-*N*-oxide (8 g) was dissolved in a 1 N sodium hydroxide solution (400 ml), and the mixture was refluxed for 1.5 hr. After the reaction mixture had cooled, concentrated hydrochloric acid was added to adjust the pH to 9, and the mixture was decolorized with charcoal. The solution was acidified to pH 1 to precipitate a light yellow powder of V (6.1 g, 83%). This product was reprecipitated twice with a sodium hydroxide solution-hydrochloric acid, and washed well with water, to yield a fine, colorless powder. The product darkened slowly from 210°C to 300°C.

Found: C, 39.71; H, 2.75; N, 36.68%. Calcd for $C_5H_4N_4O_2$: C, 39.48; H, 2.65; N, 36.84%.

Hypoxanthine 3-*N*-Oxide (V) from 6-Chloropurine 3-*N*-Oxide (IV). 6-Chloropurine 3-*N*-oxide (0.1 g) was dissolved in a 1 N sodium hydroxide solution (5 ml), and the mixture heated under refluxing for 1 hr. The reaction mixture showed a single spot on a paper chromatogram (solvents A and B), and its R_f and ultraviolet spectra agreed with those of hypoxanthine 3-*N*-oxide (V).

Hydrogenation of Hypoxanthine 3-*N*-Oxide (V). Hypoxanthine 3-*N*-oxide (1 g) was dissolved in a 2 N ammonium hydroxide solution (100 ml). Raney nickel (5 ml) was then added, and the mixture was shaken at room temperature with hydrogen at an atmospheric pressure for 22 hr, by which time 160 ml of hydrogen had been absorbed. The catalyst was then removed, and the filtrate was evaporated to dryness. The residue (500 mg) was crystallized from water and identified with hypoxanthine by R_f (solvents A and B), and by a study of the ultraviolet and infrared spectra.

Hydrolysis of Hypoxanthine 3-*N*-Oxide (V) with Hydrochloric Acid. Hypoxanthine 3-*N*-oxide (10 g) was divided into five aliquots. Each of them was dissolved in 3 N hydrochloric acid (100 ml), refluxed for five minutes, and cooled immediately. After being cooled, the five reaction mixtures were combined and passed through a column packed with 1200 ml of Dowex 50WX4 (H^+ type), and then eluted with water and 1.2 N hydrochloric acid. The eluting procedure and the results are presented on Table 2.

Reduction of 2-Chloro-4-amino-5-imidazolecarboxamide (IX). 2-Chloro-4-amino-5-imidazolecarboxamide hydrochloride (50 mg) was dissolved in water (20 ml). To this solution 10% palladium on charcoal (100 mg) was added, and the mixture was shaken for 3 hr at room temperature with hydrogen at atmospheric pressure. The catalyst was then removed by filtration. The filtrate showed a single spot on a paper chromatogram, and its R_f (solvents A and B) and ultraviolet spectrum were identical with those of 4-amino-5-imidazolecarboxamide (X).

Cyclization of 2-Chloro-4-amino-5-imidazolecarboxamide (IX). 2-Chloro-4-amino-5-imidazolecarboxamide hydrochloride (350 mg) was dissolved in a mixture of ethyl orthoformate (10 ml) and acetic anhydride (1 ml), and the resultant mixture was refluxed for 30 min. After being cooled, the reaction mixture

was evaporated to dryness under reduced pressure. The residue was dissolved in water (50 m*l*) passed, through a column packed with 100 m*l* of Dowex 50W X4 (H^+ type), and eluted with water. The first 600-m*l* portion of the effluent was discarded; the next 350-m*l* portion of the effluent was evaporated to dryness under reduced pressure to give 8-chlorohypoxanthine (0.1 g). Its R_f (solvents A and B) and ultraviolet and infrared spectra agreed with those of the authentic sample.

6-Methylsulfonylpurine 3-*N*-Oxide (XII). 6-Methylmercaptopurine 3-*N*-oxide (300 mg) was suspended in 50% methanol (30 m*l*). *N*-Chlorosuccinimide (870 mg) was then added, and the mixture was stirred for 6 hr at room temperature. After the reaction mixture had been left to stand overnight, the precipitated product was filtered and washed with methanol. The crystals obtained (0.2 g, 57%) were recrystallized from water. Mp 197—198°C (d).

Found: C, 33.55; H, 2.76; N, 26.25%. Calcd for $C_6H_6N_4O_3S$: C, 33.64; H, 2.82; N, 26.16%.

Hypoxanthine 3-*N*-Oxide from Methylsulfonylpurine 3-*N*-Oxide (XII). 6-Methylsulfonylpurine 3-*N*-oxide (500 mg) was dissolved in a 1 N sodium hydroxide solution (25 m*l*), and the mixture was refluxed for 2 hr. After being cooled, the reaction mixture was decolorized by adding charcoal and acidified to pH 3 with concentrated hydrochloric acid; this precipitated a light-yellow powder of hypoxanthine 3-*N*-oxide (230 mg, 65%). This product was reprecipitated with a sodium hydroxide solution - hydrochloric acid, and washed well with water, to yield a fine colorless powder. The product darkened slowly above 230°C.

Found: C, 39.62; H, 2.81; N, 36.77%. Calcd for $C_5H_4N_4O_2$: C, 39.48; H, 2.65; N, 36.84%.

6-Methoxypurine 3-*N*-Oxide from 6-Methylsulfonylpurine 3-*N*-Oxide. 6-Methylsulfonylpurine 3-*N*-oxide (0.5 g) was dissolved in a methanol solution (20 m*l*) which contained sodium hydroxide (0.8 g), and the mixture was refluxed for 1 hr. After being cooled, the reaction mixture was neutralized by adding glacial acetic acid and evaporated to dryness. The residue was dissolved in water adsorbed on a column packed with 100 m*l* of Amberlite IR-120 (H^+ type), washed well with water, and eluted with a 1 N ammonium hydroxide solution. The effluent was evaporated to dryness to give 6-methoxypurine 3-*N*-oxide (IIa, 250 mg, 64%), which was then recrystallized from water. This product darkened from 200 to 215°C.

Found: C, 41.93; H, 4.06; N, 33.06%. Calcd for $C_6H_6N_4O_2 \cdot \frac{1}{4}H_2O$: C, 42.23; H, 3.84; N, 32.83%.

The authors wish to thank Mr. Shinichi Motozaki, director of this laboratory for his interest and encouragement. The assistance of Mr. Akio Kakuta throughout this work is also grateful acknowledged.

BULLETIN OF THE CHEMICAL SOCIETY OF JAPAN VOL. 42 755—760 (1969)

Amination of Benzoic Acid in the γ-Radiolysis of Liquid Ammonia

Akihisa SAKUMOTO

Japan Atomic Energy Research Institute, Tokai-mura, Ibaraki

(Received June 25, 1968)

Ammonia and aqueous ammonia solutions of benzoic acid, ^{14}C-carboxyl labeled, were irradiated with ^{60}Co γ-rays at absorbed doses of 1.9×10^{20} and 4.4×10^{20} eV/g respectively. The irradiation temperature was 0°C in both cases. An isotope dilution method was applied to measure the products in irradiated solutions. The *G* values of *o*-, *m*-, and *p*-aminobenzoic acids were 0.016, 0.022, and 0.027 respectively in an ammonia solution. On the other hand, the *G* values of products in an aqueous ammonia solution were 0.011, 0.013, and 0.017 for *o*-, *m*-, and *p*-aminobenzoic acids and 0.029, 0.033, and 0.040 for *o*-, *m*-, and *p*-hydroxybenzoic acids. The disappearance of benzoic acid in an ammonia solution corresponded to a *G* value of about 1.46. From the ratio of the relative partial rate factors, it was deduced that the aminating agent was the amino radical in both cases.

The amination of aromatic compounds has been fairly extensively investigated by using hydroxylammonium chloride in the presence of Friedel-Crafts catalysts,[1] hydroxylamine-*O*-sulfonic acid and some of its derivatives,[2,3] and hydroxylamine-titanous ion in an acid solution.[4] On the other hand, aromatic amination induced by ionizing radiation has received relatively little attention.

The products from radiolysis of liquid ammonia are similar to those from liquid water.[5] The

1) C. Graebe, *Ber.*, **34**, 1773 (1901).

2) R. N. Keller and P. A. S. Smith, *J. Am. Chem. Soc.*, **68**, 899 (1946).

3) P. Kovacic and R. P. Bennett, *ibid.*, **83**, 221 (1961).

4) H. Seaman, P. J. Taylor and W. A. Waters, *J. Chem. Soc.*, **1954**, 4690.

5) D. Cleaver, E. Collinson and F. S. Dainton, *Trans. Faraday Soc.*, **56**, 1640 (1960); F. S. Dainton, T. Skwarski, D. Smithies and E. Wezranowski, *ibid.*, **60**, 1068 (1964); L. Kolditz and U. Prösch, *Z. physik. Chem.*, **218**, 109 (1961).

amination in the nucleus of aromatic compounds, therefore, may be expected to occur during the irradiation of its ammonia solution with ionizing radiation. Puig and Schwarz[6] studied the radiolysis of an ammonia solution of benzene with ^{60}Co γ-rays and found aniline to be formed, corresponding to phenol in an aqueous solution, with a G value of 0.55.

In the mono-substitution of mono-substituted benzene derivatives, the ratio of the products depends upon the degree to which the substituent displays electron-withdrawing or electron-donating properties. The carboxyl group of benzoic acid is particularly interesting as an aromatic substituent because of its *meta*-directional effect on an attacking reagent for the aromatic nucleus. Consequently, some information about an attacking species may be obtained by investigating the ratio of the isomers of substituted benzoic acid.

The aim of this work has been to elucidate the attacking species concerned in the amination reaction in the γ-radiolysis of ammonia solutions. Some results obtained by irradiating ammonia and aqueous ammonia solutions of ^{14}C-carboxyl labeled benzoic acid at a relatively high dose will be described. The reaction products were determined by means of an isotope dilution method. On the basis of the isomeric distribution of the aminobenzoic acids thus obtained, the attacking species participating in the amination reaction in the aromatic nucleus of benzoic acid will be deduced.

Experimental

Materials. The liquid ammonia used was purified in the following manner. An aqueous ammonia solution was placed in a 1 *l* round-bottomed flask fitted with a reflux condenser. The flask was then heated slowly in a water bath. The ammonia gas evolved, after passing through the condenser, was introduced into columns packed with soda-lime and sodium hydroxide; then it was collected into a storage vessel cooled by dry ice-acetone and stored at least for 15 hr as a liquid over metallic sodium. Just before use as a solvent, the ammonia in the storage vessel was distilled under diminished pressure into another vessel immersed in dry ice-acetone in order to eliminate any residual metallic sodium and any other solid impurities; it was then distilled three more times in order to remove any hydrogen formed during purification by metallic sodium.

The water used had been triply distilled, the final distillation being from alkaline potassium permanganate.

The non-radioactive acids used as the carriers of the isotope dilution method were obtained from commercial sources. All of these acids were GR grade and had then been purified further by recrystallization.

Benzoic acid, ^{14}C-carboxyl labeled, was purified by recrystallization from ethyl alcohol - water and then diluted to the specific activities of 1.41×10^{10} dpm/mol and 3.40×10^{10} dpm/mol respectively.

6) J. R. Puig and E. Schwarz, *Industrial Uses of Large Radiation Source*, **1**, 57 (1963).

Preparation of Solutions. In an irradiation vessel there was placed 150 mg of ^{14}C-labeled benzoic acid, with a specific activity of 1.41×10^{10} dpm/mol. Then the vessel was connected to a vacuum line and carefully degassed. After the degasification, 1.52 mol of liquid ammonia, purified by the method described above, was distilled under diminished pressure into a vessel cooled by dry ice-acetone. Then the irradiation vessel with an ammonia solution, cooled by liquid nitrogen, was sealed off.

An aqueous ammonia solution of benzoic acid was prepared by distillating 0.88 mol of liquid ammonia into an irradiation vessel already containing an aqueous benzoic acid solution which had been prepared by adding 150 mg of ^{14}C-labeled benzoic acid (with a specific activity of 3.40×10^{10} dpm/mol) to 0.83 mol of triply-distilled water which has been degassed by repetitions of the freezing-pumping process.

Irradiation. A ^{60}Co γ-rays source of about 16 kCi was used. The ammonia solution was irradiated at the absorbed dose of 1.9×10^{20} eV/g and at the dose rate of 3.5×10^{17} eV/g/min. The total dose given to an aqueous ammonia solution was 4.4×10^{20} eV/g at the dose rate of 6.7×10^{17} eV/g/min. The irradiation temperature of both samples was 0°C, which was controlled with ice-water. The dose rate was measured by Fricke dosimetry, taking $G(Fe^{3+})$ to be 15.5. Appropriate corrections were made for the difference in the electron densities of liquid ammonia and water.

Radioactive Assay. After irradiation, the break-seal of the irradiation vessel was broken. The contents were transferred to a beaker immersed in liquid nitrogen. The irradiation vessel was washed with about 10 cc of demineralized water. After it had stood overnight in order to evaporate any excess ammonia, the combined aqueous solution was diluted to a total volume of 25 cc with demineralized water. An aliquot of the diluted solution was then thoroughly mixed with an accurately-weighed quantity of the carrier acid in ethyl alcohol. The solution was evaporated to dryness, and the precipitate was purified by recrystallization from a suitable solvent until a constant counting rate was obtained. The aminobenzoic acids in products were derived to acetoamidobenzoic acids and purified.

An aliquot of a purified sample was dissolved in the solution of 10 cc of liquid scintillant (4 g of PPO (2,5-diphenyloxazole), 100 mg of POPOP (1,4-bis-2-(5-phenyloxazole)benzene)/*l* of toluene) and 5 cc of methyl alcohol and then counted in a Packard 314 EX-type liquid scintillation spectrometer assembly. A liquid scintillant solution of ^{14}C-labeled benzoic acid (with a specific activity of 3200 dpm/mg) was used as the internal standard for the determination of the counting efficiency.

Results

An ammonia solution of ^{14}C-labeled benzoic acid was irradiated with ^{60}Co γ-rays, and the amount of remaining benzoic acid and the presence of the three mono-aminobenzoic acids and 2,2'-biphenyldicarboxylic acid in the irradiated solution were confirmed by a radioactive-tracer technique. The yield and the G value of each reaction product obtained are summarized in Table 1.

Table 1. Products in γ-radiolysis of ammonia solution of benzoic acid

	Amount mol	Yield %	G
o-Aminobenzoic acid	$(1.31\pm0.06)\times10^{-6}$	0.11	0.016
m-Aminobenzoic acid	$(1.74\pm0.05)\times10^{-6}$	0.14	0.022
p-Aminobenzoic acid	$(2.18\pm0.07)\times10^{-6}$	0.18	0.027
2,2'-Biphenyldicarboxylic acid	$(4.47\pm0.25)\times10^{-7}$	0.07	0.0055
Benzoic acid*1	$(1.110\pm0.003)\times10^{-3}$	90.4	
−Benzoic acid*2	$(1.18\pm0.03)\times10^{-4}$	9.6	1.46

Dose, 1.9×10^{20} eV/g, dose rate, 3.5×10^{17} eV/g/min.
Irradiation temperature, 0°C.
*1 Remaining benzoic acid.
*2 Amounts of the disappearance of benzoic acid.

Table 2. Yields of aminobenzoic and hydroxybenzoic acids in γ-radiolysis of aqueous ammonia solution

	Amount mol	Yield %	G
o-Aminobenzoic acid	$(1.20\pm0.06)\times10^{-6}$	0.10	0.011
m-Aminobenzoic acid	$(1.45\pm0.03)\times10^{-6}$	0.12	0.013
p-Aminobenzoic acid	$(1.84\pm0.04)\times10^{-6}$	0.15	0.017
o-Hydroxybenzoic acid	$(3.22\pm0.08)\times10^{-6}$	0.26	0.029
m-Hydroxybenzoic acid	$(3.67\pm0.03)\times10^{-6}$	0.30	0.033
p-Hydroxybenzoic acid	$(4.42\pm0.14)\times10^{-6}$	0.36	0.040

Dose, 4.4×10^{20} eV/g, dose rate, 6.7×10^{17} eV/g/min.
Irradiation temperature, 0°C.

The remaining benzoic acid in the irradiated solution, 1.11×10^{-3} mol was recovered. This corresponds to 90.4 per cent of the initial amounts of the acid. Consequently, the amount of the total reaction of benzoic acid is 1.18×10^{-4} mol and the G value of the disappearance of the acid, shown as −benzoic acid in Table 1, is calculated to be 1.46. The G value of 1.46 is smaller than that obtained in the case of an aqueous solution of benzoic acid.[7] The G value for mono-aminobenzoic acids were: *ortho*, 0.016; *meta*, 0.022; and *para*, 0.027. The total G value is 0.065, only about a quarter of that of the mono-hydroxybenzoic acids obtained in an aqueous solution.

When the irradiation of an aqueous ammonia solution of benzoic acid was carried out at an absorbed dose of 4.4×10^{20} eV/g, isomers of mono-aminobenzoic acids and of mono-hydroxybenzoic acids were observed as products. The yields are given in Table 2. The total yield of mono-aminobenzoic acids was about 4.5×10^{-6} mol, while that of mono-hydroxybenzoic acids was about 1.1×10^{-5} mol. Therefore, the ratio of mono-aminobenzoic acid to mono-hydroxybenzoic acids is about 1 : 2.4.

From Table 2, the G value of mono-aminobenzoic acids in an aqueous ammonia solution can be seen to be 0.041. In spite of the low G value of mono-aminobenzoic acids in an aqueous ammonia solution, the G value ratio, calculated to be 0.65 : 0.76 : 1 for *o*- : *m*- : *p*-isomers, agrees fairly well with that of 0.59 : 0.81 : 1 in an ammonia solution. The total G value of the mono-hydroxybenzoic acids was 0.10. Although this value is less than a half of that obtained in an aqueous solution, the *o*- : *m*- : *p*-isomer ratio, 0.73 : 0.83 : 1, was similar to that, 0.72 : 0.84 : 1, obtained in an aqueous solution.[7]

Discussion

When an ammonia or aqueous ammonia solution of benzoic acid is subjected to irradiation with ionizing radiation, there is the possibility of some reactions in addition to the amination of the acid. The decarboxylation of ^{14}C-labeled benzoate occurred during the irradiation of a dilute, aerated aqueous solution by ^{60}Co γ-rays.[8,9] Therefore, it may be assumed that a similar decarboxylation occurs in the irradiation of an ammonia solution of benzoic acid. However, no carbon dioxide was measured in this work.

In the γ-radiolysis of an aqueous benzoic acid solution, the ratio of the mono-hydroxybenzoic

7) A. Sakumoto and G. Tsuchihashi, This Bulletin, **34**, 663 (1961).
8) A. M. Downes, *Austr. J. Chem.*, **11**, 154 (1958).
9) R. W. Matthews and D. F. Sangster, *J. Phys. Chem.*, **69**, 1938 (1965).

acids to biphenyldicarboxylic acids produced was about 1 : 3.[7] However, in the γ-radiolysis of an ammonia solution of benzoic acid, the G value of 2,2'-biphenyldicarboxylic acid, the most abundant isomer in an aqueous solution, was smaller than that of any isomer of mono-aminobenzoic acids shown in Table 1. The reason for this is not obvious. When an aqueous solution of *p*-aminobenzoic acid was irradiated with X-rays, 3-hydroxy-4-aminobenzoic acid was observed as the main product, while *p*-hydroxybenzoic acid and aniline were also produced in trace amounts.[10] Therefore, as the production of mono-aminobenzoic acids increases, the similar reaction of the acids will gradually increase in ammonia and aqueous ammonia solutions.

In order to understand the amination reaction of the aromatic nucleus of benzoic acid in the γ-radiolysis of ammonia solutions, consideration must be given to the possibility that the reaction products of the acid with reactive species produced in the γ-radiolysis of ammonia might give aminobenzoic acids. When the pulse radiolysis of an alkaline solution of benzoic acid was carried out using a 15 MeV electron pulse, the acid readily reacted with the hydrated electron produced by the irradiation.[11,12] Nitrobenzene, in which the nitro group has the *meta*-directional effect, also reacted readily with the hydrated electron.[13,14] The hydrated electron scavengers have little or no effect on the yield of *o*-nitrophenol produced in the γ-radiolysis of an aqueous nitrobenzene solution.[15] This means that the product of the electron-nitrobenzene reaction is not a precursor of nitrophenols. Therefore, it may be assumed that there is little possibility of the reaction product of benzoic acid with the solvated electron giving aminobenzoic acids when an ammonia solution is irradiated with ^{60}Co γ-rays.

One of several methods for obtaining information on the attacking reagent involved in a radiation-induced amination reaction is to study the partial rate factors for amination in the nucleus of benzoic acid. It has been evident[16] that, in the further substitution reaction of the mono-substituted benzene derivatives, C_6H_5X, in which the substitutent X is assigned to a $-E$ effect such as that of the carboxyl group, if the entering substituent is an electrophilic heterolytic reagent (*e.g.*, NO_2^+) the partial rate factor at the *meta*-positions with respect to the substituent already present is larger than that at the *ortho*- and *para*-positions. On the other hand, if the mono-substituted benzenes are attacked by a homolytic reagent such as the phenyl radical, a large partial rate factor is obtained at the *ortho*- and *para*-positions rather than at the *meta*-positions. Therefore, a comparison of the partial rate factors will offer information about the attacking reagent participating in the substitution reaction.

When an ammonia solution of benzoic acid was irradiated at the absorbed dose of 1.9×10^{20} eV/g, the amounts of mono-aminobenzoic acids were: *ortho*, 1.31×10^{-6} mol (0.11 per cent of the theoretical amount); *meta*, 1.74×10^{-6} mol (0.14 per cent); *para*, 2.18×10^{-6} mol (0.18 per cent). Unfortunately, the partial rate factor itself for the amination reaction at each nuclear position of benzoic acid can not be obtained from these values. However, in the mono-substituted benzene, C_6H_5X, the partial rate factors at *o*-, *m*-, and *p*-positions with regard to the substituent X are given by the three following expressions respectively:

$$ {}^{X}_{H}k_o = 6\cdot{}^{X}_{H}K\cdot(o)/2 $$
$$ {}^{X}_{H}k_m = 6\cdot{}^{X}_{H}K\cdot(m)/2 $$
$$ {}^{X}_{H}k_p = 6\cdot{}^{X}_{H}K\cdot(p) $$

where (o), (m), and (p) represent the yield of the respective isomers of the reaction products. Therefore, it is possible to use the yield of mono-aminobenzoic acids as a measure of the partial rate factor of the amination reaction at any position in the aromatic nucleus of benzoic acid, if the isomeric distribution accurately reflects the extent of attack by the reagent on the three different positions of benzoic acid. In the case of a radiation-induced reaction, it is preferable to use the G value, used as a measure of the radiation-chemical yields, rather than chemical yields of products. Then, using the G value thus obtained, the relative partial rate factors were calculated to be 0.008, 0.011, and 0.027 for $(o)/2$, $(m)/2$, and (p) in an ammonia solution, as is shown in Table 3. The relative partial rate factor at the *para*-position was larger than that at the *meta*-position. This result demonstrates that the attacking species in amination is uncharged.

Yoshida, Matsumoto, and Oda[17] have reported on the amination of benzoic acid using the hydroxylamine-ferrous ion, which is well known as an aminating reagent with the amino radical. The values they obtained are also presented in Table 3 for the sake of comparison. In this amination, if an aqueous solution of hydroxylamine-ferrous

10) K. F. Nakken, *Radiation Res.*, **21**, 446 (1964).
11) A. Szutka, J. K. Thomas, S. Gordon and E. J. Hart, *J. Phys. Chem.*, **69**, 289 (1965).
12) D. F. Sangster, *ibid.*, **70**, 1712 (1966).
13) E. J. Hart, S. Gordon and J. K. Thomas, *ibid.*, **68**, 1271 (1964).
14) M. Anbar and E. J. Hart, *J. Am. Chem. Soc.*, **86**, 5633 (1964).
15) R. W. Matthews and D. F. Sangster, *J. Phys. Chem.*, **71**, 4056 (1967).
16) D. H. Hey, "Vistas in Free-Radical Chemistry," ed. by W. A. Waters, Pergamon Press, London (1959), p. 209.
17) Z. Yoshida, T. Matsumoto and R. Oda, *Kogyo Kagaku Zasshi (J. Chem. Soc. Japan, Ind. Chem. Sect.)* **65**, 46 (1962).

Table 3. Relative partial rate factors of amination in aromatic nucleus of benzoic acid

	Solvent	(*o*)/2	(*m*)/2	(*p*)
γ-Radiolysis	NH_3	0.008	0.011	0.027
	NH_3-H_2O*1	0.011	0.013	0.033
NH_2OH-Fe(II)*2	H_2O	0.4	0.8	1.2
	96% H_2SO_4	1.45	2.05	3.8

*1 Values from *G* value calculated from the amount of energy absorbed in ammonia in aqueous ammonia solution.
*2 See Ref. 17.

ion was used, 52 per cent of the aminobenzoic acids produced were poly-aminobenzoic acids. On the other hand, if the solvent was 96 per cent sulfuric acid, the poly-aminobenzoic acids composed only 0.9 per cent of the aminobenzoic acids. In spite of this difference in the ratio of poly-aminobenzoic acids to aminobenzoic acids, the large relative partial rate factor was obtained at the *para*-position rather than at the *meta*-position in both cases. It is also clear from Table 3 that the ratio of the relative partial rate factor obtained in the γ-radiolysis of an ammonia solution agrees fairly well with that obtained in amination using the hydroxylamine-ferrous ion.

The reaction rate constants of the hydroxyl radical with the substituted benzenes, C_6H_5Y, are larger than those of the hydroxyl radical with benzene, regardless of Y substituent, if the Y substituent is an electron-donating group.[18] Therefore, it may be assumed that the amination of mono-aminobenzoic acids is easier than that of benzoic acid in the γ-radiolysis of an ammonia solution. When the irradiation of an aqueous benzoic acid solution was carried out, di-hydroxybenzoic acids composed about 15 per cent of the mono-hydroxybenzoic acids, even under conditions favorable for hydroxylation.[7] Accordingly, it is reasonable to presume that there is little formation of poly-aminobenzoic acids in the range of the irradiation. No poly-aminobenzoic acids were measured, so the results obtained cannot be used as an accurate measure of the partial rate factors in the amination reaction. However, it can be deduced from the ratios of the relative partial rate factors summarized in Table 3 that the attacking reagent concerned in the amination reaction during the irradiation of an ammonia solution of benzoic acid is the amino radical.

Returning now to the irradiation of an aqueous ammonia solution of benzoic acid, a lower *G* value of aminobenzoic acids was obtained than that in an ammonia solution. In an aqueous solution of ammonia, the ammonia molecule and the water molecule are attracted to each other by the hydrogen bond, which is roughly 5 per cent of the energy of a covalent bond.[19] Since the energy of activation of such a bond is small, the bond forms and breaks with ease at ordinary temperatures. In a 0.1 molar solution of ammonia, only about a half of the ammonia molecules are hydrated, and although it is possible to isolate two stable crystalline hydrates, $NH_3 \cdot H_2O$ and $(NH_3)_2 \cdot H_2O$, at low temperatures, there is no evidence that undissociated NH_4OH is present.[20] Therefore, it may be assumed that the amount of energy absorbed in each component in an aqueous solution of ammonia is proportional to the total number of electrons in each component when such a solution is irradiated with ^{60}Co γ-rays. Now, by assuming that only ammonia is involved in the formation of aminobenzoic acids in such a solution, the amount of the acids should be related to the amount of energy absorbed in ammonia in the mixture. The determination of the *G* values of hydroxybenzoic acids was also performed in the same manner by assuming that only water is involved in the formation of the acids. The *G* values calculated were 0.021, 0.026, and 0.033 for *o*-, *m*-, and *p*-aminobenzoic acids and 0.060, 0.069, and 0.083 for *o*-, *m*-, and *p*-hydroxybenzoic acids, respectively.

The total *G* value of the aminobenzoic acids was calculated to be 0.080. This value is about 23 per cent larger than that obtained in an ammonia solution. These two *G* values should be in accord with each other provided there is no interaction between the ammonia and water involved in the reaction. The above difference in *G* value, therefore, suggests that there is some interaction between ammonia and water in such a mixture. This suggestion is supported by the enhancement of hydrazine in the γ-radiolysis of an aqueous solution of ammonia.[21] From the proton affinity[22] for ammonia, the proton transfer to ammonia may be expected to occur. If the neutralization of the produced NH_4^+ by solvated electrons were to

18) M. Anbar, D. Meyerstein and P. Neta, *J. Phys. Chem.*, **70**, 2660 (1966).

19) J. B. Davis, *J. Chem. Educ.*, **30**, 511 (1953).
20) F. A. Cotton and G. Willkinson, "Advanced Inorganic Chemistry, A Comprehensive Text, 2nd Ed.," John Wiley and Sons, New York (1966).
21) A. Sakumoto, This Bulletin, **39**, 1349 (1966).
22) J. O'M. Bockris and B. E. Conway, "Modern Aspects of Electrochemistry, No 3," Butterworths, London (1964).

produce amino radicals,[23] some increase in the yields of aminobenzoic acids can be explained. On the other hand, the G value of hydroxybenzoic acids was calculated to be 0.212, slightly less than that obtained in an aqueous solution. Consequently, there might be the possibility of the following interaction:[24]

$$NH_3 + \cdot OH \rightarrow \cdot NH_2 + H_2O$$

If the amino radical is the attacking reagent participating in the amination reaction in an aqueous ammonia solution, the ratio of the relative partial rate factors may be in accord with that obtained in an ammonia solution. On the basis of the assumption that the amount of aminobenzoic acid is proportional to the amount of energy absorbed in ammonia in an aqueous ammonia solution, the relative partial rate factors, $(o)/2$, $(m)/2$ and (p), in such a solution were calculated to be 0.011, 0.013 and 0.033 respectively, as is shown in Table 3. The $(o)/2 : (m)/2 : /(p)$ ratio, 0.32 : 0.38 : 1, is in striking agreement with the ratio, 0.30 : 0.41 : 1, obtained in an ammonia solution. Therefore, it is possible to deduce that the attacking species involved in the amination reaction in an aqueous ammonia solution is also the amino radical.

The ratio of the G value of m-aminobenzoic acid to that of p-aminobenzoic acid was less than 2. This is attributable to some degree of electrophilic character of the amino radical.

The author wishes to thank Dr. G. Tsuchihashi, Sagami Chemical Research Center, for his valuable discussions, and Drs. A. Danno and K. Motojima for their encouragement throughout this work.

23) F. T. Jones and T. J. Sworski, *Trans. Faraday Soc.*, **63**, 2411 (1967).

24) Yu A. Sorokin, V. I. Tsivenko and S. Ya. Pshezhetskii, *Zhur. fiz. Khim.*, **37**, 1871 (1963).

BULLETIN OF THE CHEMICAL SOCIETY OF JAPAN VOL. 42 760—765 (1969)

Reaction of *trans*-Stilbene with *n*-Butyllithium in Tetrahydrofuran

Yoshio OKAMOTO, Masahiko KATO and Heimei YUKI

Department of Chemistry, Faculty of Engineering Science, Osaka University, Toyonaka, Osaka

(Received July 1, 1968)

The reaction of *trans*-stilbene with *n*-butyllithium was investigated in tetrahydrofuran at 0°C. The structures of the products fractionated by column chromatography were determined by elementary analysis, a molecular-weight determination, and a study of the IR, UV, and NMR spectra. The main products were 1,2-diphenylhexane, 1,2-diphenylethane, and 1,2,3-triphenylpropene which was formed by the cleavage of a C-C bond of a product. The reaction mixture showed an ESR signal. The observed results are explained in terms of the anionic copolymerization of *trans*-stilbene and styrene reported previously.

In a previous paper,[1] a study of the anionic copolymerization of styrene and *trans*-stilbene by *n*-butyllithium (*n*-BuLi) has been reported. The results have shown that in tetrahydrofuran (THF) a chain-transfer reaction to the *trans*-stilbene occurs, while in benzene the copolymerization proceeds without any chain-transfer. In the copolymerization, the color of the reaction mixture changes in time; it was followed spectrophotometrically.

The work reported here was carried out in order to clarify two points: the reaction mechanism of the chain-transfer and the change in the color in the copolymerization. Wyman and Altares[2] carried out the same reaction in benzene, but their results differ greatly from ours.

Experimental

Reagent. The preparations and purifications of *trans*-stilbene, *n*-BuLi, and THF were previously described.[1]

Reaction. The reaction was carried out under dry nitrogen in a glass ampoule equipped with a three-way stopcock. To a solution of *trans*-stilbene (10.0 g, 5.56×10^{-2} mol) in THF (250 m*l*), *n*-BuLi (2.83×10^{-2} mol) was added with a syringe over a three-minute period at 0°C. The color of the reaction mixture changed from red to purple in time. After 48 hr, the reaction was terminated by adding methanol (1.1 m*l*, 2.6×10^{-2} mol) until the color of the solution disappeared. The solvent was evaporated *in vacuo*, and then the residue was dissolved in diethyl ether. The ether solution was

1) H. Yuki, M. Kato and Y. Okamoto, This Bulletin, **41**, 1940 (1968).

2) D. P. Wyman and T. Altares, Jr., *Makromol. Chem.*, **72**, 68 (1964).

washed with water and dried over magnesium sulfate; then the ether was removed to give 11.6 g of an oily product.

Fractionation of Product. The fractionation of the above product was carried out by column chromatography with activated alumina, using *n*-hexane, benzene, and methanol as solvents.

Measurements. The measurements of the molecular weight, the elementary analysis, and the IR, UV, and NMR spectra were made according to methods reported previously.[1] The ESR spectrum was measured with a JES-3BX Spectrometer.

Results

Fractionation of Product. Before the fractionation of the reaction product by column chromatography, the product was submitted to sublimation in order to exclude any unchanged *trans*-stilbene. However, no *trans*-stilbene was recovered. The addition of *n*-hexane to the product gave no precipitate of *trans*-stilbene, which is almost insoluble in this solvent at 0°C. The results of the fractionation by column chromatography are shown in Table 1. Fraction 1, which is not shown in the table, was fractionated by subsequent chromatography, using *n*-hexane as a solvent, to give two fractions, 1A and 1B.

Characterization of Each Fraction. The results of the elementary analysis, the molecular weight, and the molecular formula of each fraction are listed in Table 1. The characteristics of the IR and UV spectra, and the ratio of the number of aromatic to that of aliphatic protons (H_{ar}/H_{al}) of the fraction are summarized in Table 2.

Compounds Formed in the Reaction Mixture. Table 3 shows the molecular formulae, the structural formulae, the results of the elementary analyses, the molecular weights, and the ratios of the number of aromatic to that of aliphatic protons (H_{ar}/H_{al}) of the compounds which may be supposed to be the reaction products on the basis of the results.

Structure of Each Fraction. *Fraction 1A.* This fraction was liquid; the results of its elementary analysis and its molecular weight and the molecular formula derived from them were most consistent with those of 1,2-diphenylhexane, Ia, in Table 3. In the NMR spectrum of the fraction 1A (Fig. 1), the chemical shifts of the Ph, $-CH(Ph)-CH_2Ph$, $-CH_2-$, and CH_3-protons, and the relative areas of the peaks, 10.0 : 2.9 : 6.1 : 3.0, also support the above structure. The IR spectrum showed the absence of a C=C double bond, as was also speculated on the basis of the UV spectrum.

Fraction 1B. The melting point of the fraction 1B was 50—52°C. Its molecular formula was similar to that of 1,2-diphenylethane, Ib, in Table 3, the melting point of which is 53°C.[3] The NMR spectrum of this fraction also completely agreed with that of the authentic sample. The NMR spectrum of the fraction 1 indicated that this fraction contained only Ia and Ib in a molar ratio of 3.3.

Table 1. Fractionation of reaction mixture by column chromatography

Fraction	Eluent	Recovery wt%	Elementary analysis C%	Elementary analysis H%	Molecular weight	Molecular formula
1A	*n*-Hexane	38	90.70	9.27	233	$C_{18}H_{21.9}$
1B	*n*-Hexane	9	92.28	7.72	168	$C_{14}H_{13.9}$
2	H/B(95/5)[a]	19	93.37	6.82	264	$C_{21}H_{18.3}$
3	H/B(50/50)[a]	21	92.46	7.64	345	$C_{27}H_{27.0}$
4	Methanol	6	83.27	8.77	291	$C_{22}H_{27.7}$

a) H: *n*-hexane, B: benzene.

Table 2. Characteristics of IR, UV, and NMR spectra

Fraction	IR (cm^{-1})[a] 870	IR (cm^{-1})[a] 1380	IR (cm^{-1})[a] 3300	UV λ_{max} (mμ)	UV ε_{max}	NMR[b] H_{ar}/H_{al}
1A	—	Medium	—	260	411	0.83
1B	—	Weak	—	260	450	2.4
2	Medium	Weak	—	272	14800	5.1
3	Weak	Weak	—	272	5490	2.4
4	Weak	Medium	Strong	—	—	0.68

a) 870: $R_1R_2C=CHR_3$, 1380: CH_3-, 3300: -OH.
b) The ratio of the numbers of aromatic to aliphatic protons.

3) J. S. Buck and S. S. Jenkins, *J. Am. Chem. Soc.*, **51**, 2163 (1929).

Table 3. Compounds supposed to be the products in the reactions

Molecular formula	Structural formula	Composition C%	Composition H%	Molecular weight	H_{ar}/H_{al}[a]	Remarks
$C_{18}H_{22}$	C_4H_9-CH(Ph)-CH_2-Ph	90.76	9.24	238	0.83	Ia
$C_{14}H_{14}$	$PhCH_2CH_2Ph$	92.31	7.69	182	2.5	Ib
$C_{21}H_{18}$	CH_2=C(Ph)-CH(Ph)	93.33	6.67	270	5.0	II
$C_{32}H_{34}$	C_4H_9-(CH(Ph)-CH(Ph))$_2$-H	91.87	8.13	418	1.43	III
$C_{22}H_{30}O$	C_4H_9-CH(Ph)-CH(Ph)-$(CH_2)_4$-OH	85.16	9.68	310	0.5	IV
$C_{28}H_{26}$	CH_2(Ph)-CH(Ph)-CH(Ph)-CH_2(Ph)	92.82	7.18	362	3.3	V

a) The ratio of the numbers of aromatic to aliphatic protons.

Fraction 2. The molecular formula of the fraction 2 was in best accord with 1,2,3-triphenylpropene, II, in Table 3. In the NMR spectra (Fig. 2), the peaks at 3.65 and 6.29 τ were assigned to the methine and methylene protons, respectively, of the *cis*-isomer, judging from the NMR spectra of *cis*- and *trans*-stilbene. The peak at 5.96 τ was assigned to the methylene protons of the *trans*-isomer, while the absorption of its methine proton might overlap with those of aromatic protons near 3 τ. The IR spectrum of the fraction 2 showed an absorption due to a three-substituted olefin at 870 cm^{-1}. A further separation of this fraction by column chromatography gave the *cis*-isomer as the initial fraction; its melting point was 61—62°C (lit.,[4] 62—63°C). The fraction eluted at the later stage of the chromatography was largely composed of the *trans*-isomer, but it always contained a small portion of the *cis*-isomer. In the UV spectra, the absorption maxima of *cis*- and *trans*-1,2,3-triphenylpropene appeared at 260 mμ (ε_{max} 14200) and 273 mμ (ε_{max} 16100) respectively. The molar ratio of the *trans*- to the *cis*-isomer was 1.9; this ratio was calculated from the relative strength of the corresponding absorptions in the NMR spectrum of the fraction 2.

Fraction 3. The molecular weight of the fraction 3 was 345. This rather large value indicates that a compound composed of at least two molecules of *trans*-stilbene must have been a component of this fraction. The sharp peak at 5.96 τ in the NMR spectrum (Fig. 3) suggests that the tailing of *trans*-1,2,3-triphenylpropene, which was present in the fraction 2, is incorporated into this fraction.

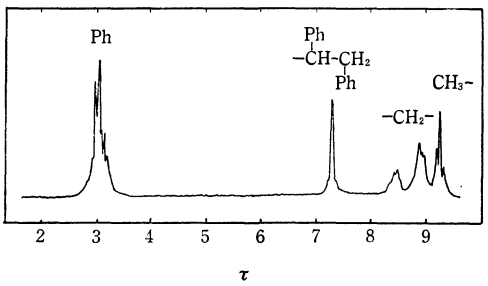

Fig. 1. NMR spectrum of fraction 1A.

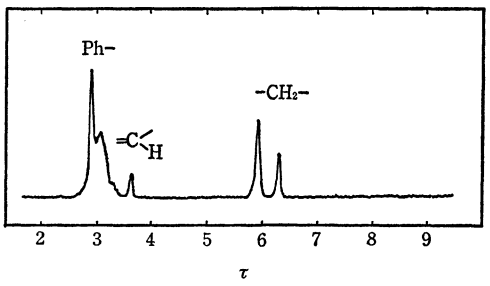

Fig. 2. NMR spectrum of fraction 2.

4) A. Orechoff, *Ber.*, **47**, 89 (1914).

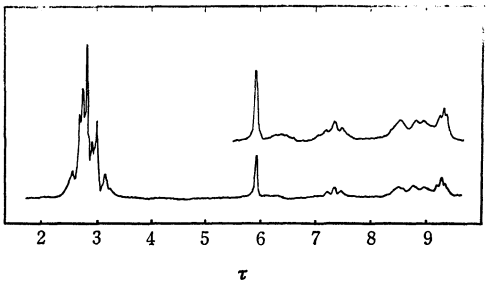

Fig. 3. NMR spectrum of fraction 3.

However, 1,2,3,4-tetraphenyloctane, III in Table 3, must be the main component of this fraction, judging from the absorption at 9.1 τ due to the methyl group and absorptions at 7.5—8.9 τ due to methylene and methine groups in the NMR spectrum, and judging from the molecular weight of this fraction.

This fraction also contained a small amount (about 100 mg) of a compound insoluble in petroleum ether at 0°C; this compound was identified as 1,2,3,4-tetraphenylbutane, V in Table 3. Its melting point was 181—183°C (lit.,[5] 182°C), and the observed H_{ar}/H_{al} ratio in the NMR spectrum was 3.5. Found: C, 92.76; H, 7.24%.

Fraction 4. Judging from the elementary analysis, this fraction consisted of a compound containing oxygen. The IR spectrum suggested the presence of an OH group by means of the strong absorption at 3300 cm^{-1}. Although the NMR spectrum was complicated, the H_{ar}/H_{al} ratio was 0.66. This small value means that there were more aliphatic protons than aromatic ones. The reaction of a carbanion with THF must have formed an alcohol containing the greater portion of the aliphatic protons. A compound such as IV in Table 3 may be proposed as one of the alcohols.

Yields of Product Compounds. The yields of the product compounds identified were calculated from the NMR spectrum of the unfractionated mixture and from the weights of the compounds fractionated by column chromatography. The results are shown in Table 4. The yields of 1,2,3-triphenylpropene (II) and 1,2-diphenylethane (Ib), after reactions of 25 and 180 min carried out under the same conditions as those shown in the Experimental section, were obtained by means of the NMR spectra of the respective reaction mixtures, as are shown in Table 4. The ratios of 1,2,3-triphenylpropene to 1,2-diphenylethane were about 2, regardless of the reaction time.

Table 4. Yields of product compounds[a]
Reaction condition: [Stilbene]/[*n*-BuLi]=2.0, in THF, at 0°C

Reaction time	Ia	Ib	II	III	V
25 min	—	6	16	—	—
180 min	—	16	34	—	—
48 hr	62	18	38	10	2

a) Yield was calculated as per cent of the product (mole) per *n*-BuLi (mole).

5) D. P. Wyman, *J. Org. Chem.*, **27**, 3712 (1962).

Electronic Spectrum of Reaction Mixture. The electronic spectra of the reaction mixtures of *trans*-stilbene and *n*-BuLi in THF at room temperature are shown in Fig. 4. In the reaction of *trans*-stilbene with an excess of *n*-BuLi, the spectrum showed a peak at 332 mμ which was stable for a prolonged time and might be based on a benzyl-type anion, $C_4H_9CH(Ph)-CH(Ph)^-Li^+$. On the other hand, when the molar ratio of *trans*-stilbene to *n*-BuLi was 6.2, new peaks appeared at 555 and 420 mμ in time. When *n*-BuLi was added to the solution of 1,2,3-triphenylpropene in THF, the

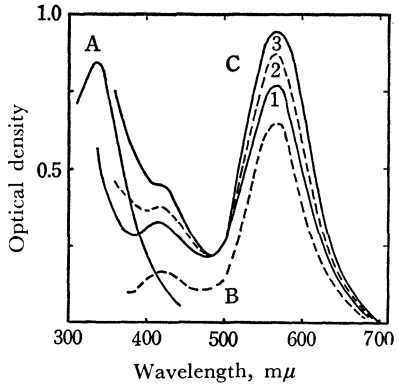

Fig. 4. Electronic spectrum of reaction mixture.
A: [Stilbene]/[*n*-BuLi]=0.25
B: 1,2,3-Triphenylpropene+*n*-BuLi (1 : 1)
C: [Stilbene]/[*n*-BuLi]=6.2
Time: (1) 46 min, (2) 1.4 hr, (3) 2.4 hr

peaks at 555 and 420 mμ appeared instantaneously in the UV spectrum of the solution. Then, 1,2,3-triphenylpropene-3-d_1, was recovered by terminating the reaction with deuterium oxide. This was confirmed by a study of the NMR spectrum.

ESR Spectrum of Reaction Mixture. The ESR spectrum of the reaction mixture in THF was

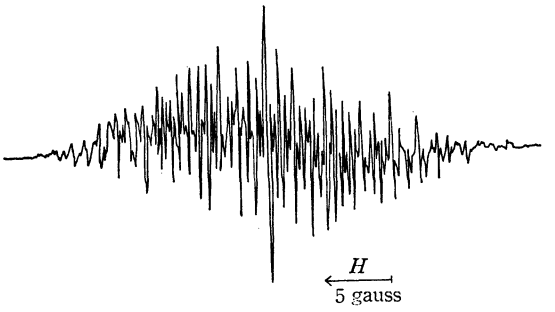

Fig. 5. ESR spectrum of reaction mixture.
[Stilbene]/[*n*-BuLi]=2.0, temp.: room temp.

measured at room temperature, the molar ratio of *trans*-stilbene to *n*-BuLi being 2.0. The spectrum is shown in Fig. 5. In the reaction of 1,2,3-triphenylpropene with *n*-BuLi in THF, however, no ESR signal was observed.

Discussion

The compounds identified as the main products were 1,2-diphenylhexane (Ia), 1,2-diphenylethane (Ib), and 1,2,3-triphenylpropene (II). It is noteworthy that no *trans*-stilbene was recovered and that 1,2-diphenylethane and 1,2,3-triphenylpropene were obtained instead. The mechanisms of the formations of these two compounds cannot be explained by simple addition or abstraction reactions of carbanions. The 1,2,3-triphenylpropene can be produced only by the cleavage of a C–C bond because there is no compound with odd carbons in the starting materials. The molar ratio of the yield of 1,2,3-triphenylpropene to 1,2-diphenylethane was two, regardless of the reaction time; this suggests that the formations of these compounds are interrelated. The following processes (1)—(7) constitute our proposed mechanisms for the production of the above compounds.

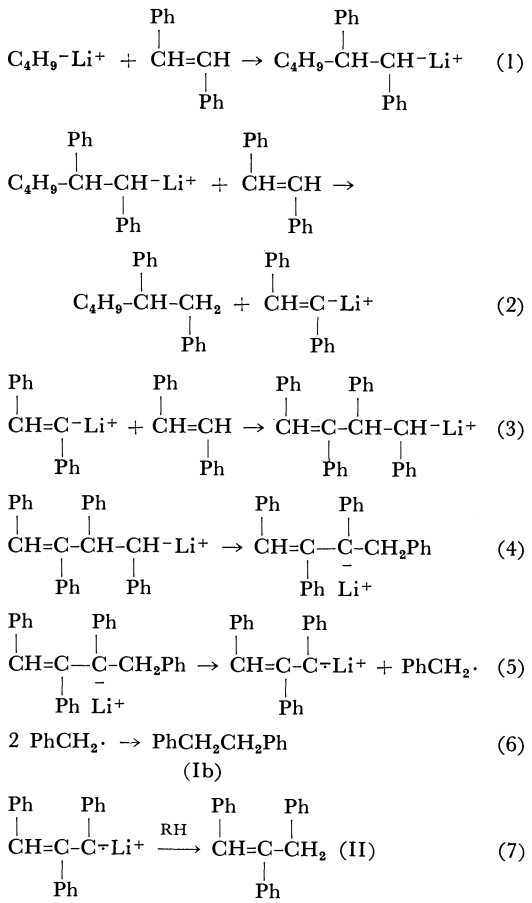

The total product yield indicates that the process (1), which is an addition reaction of *n*-BuLi to *trans*-stilbene, takes place easily. As may be seen from the electronic spectrum of the reaction mixture, the benzyl-type anion formed in the process (1) is stable, if no excess *trans*-stilbene is present. However, the acidity of the methine protons of *trans*-stilbene is rather strong, as is shown by the isomerization of *cis*-stilbene to the *trans*-isomer by a base such as potassium *t*-butoxide.[6] Therefore, if excess *trans*-stilbene is present, the process (2) will occur. This process must be a chain-transfer reaction in the copolymerization of *trans*-stilbene and styrene.[1]

The new anion produced in the process (2) reacts with *trans*-stilbene to give a dimer anion, which may accompany the cleavage of a C–C bond with the production of the benzyl radical and the 1,2,3-triphenylpropenyl radical anion (the process (5)), *via* a proton shift reaction in the process (4). This radical anion may be of new type. The structure of the 1,2,3-triphenylpropenyl radical anion may be represented as shown by RA-II. This radical anion, if present, can be greatly stabilized by the delocalization of an electron on the benzene rings. It has been established that the 1,3-bis(diphenyl)-2-phenylallyl radical, with a similar structure to that of RA-II, is very stable even in air.[7]

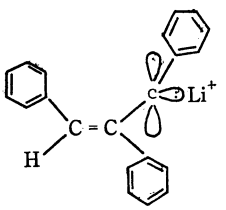

(RA-II)

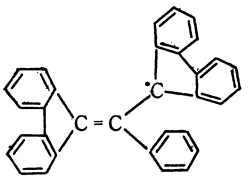

(1,3-Bis(diphenylene)-2-phenylallyl radical)

The reaction mixture of *trans*-stilbene and *n*-BuLi showed an ESR signal (Fig. 5). This might be because of the mono lithium-adduct of *trans*-stilbene. However, no absorption maximum at 480 mμ (ε_{max} 62000)[8] due to the adduct in THF could be observed in the electronic spectrum of the reaction mixture (Fig. 4). The hyperfine structure of the ESR spectrum observed herein suggests the presence of a radical with a rather complicated structure, although it is not certain at present whether or not the ESR signal is due to the radical anion, RA-II. The coupling of benzyl radicals gives 1,2-diphenylethane, as is shown in the process (6).

Although the yield was rather low, 1,2,3,4-tetraphenyloctane was also obtained. This means

6) D. H. Hunter and D. J. Cram, *J. Am. Chem. Soc.*, **88**, 5765 (1966).
7) W. O. Hamilton and G. E. Pake, *J. Chem. Phys.*, **39**, 2694 (1963).
8) E. R. Zabolotny and J. F. Garst, *J. Am. Chem. Soc.*, **86**, 1645 (1964).

that a stilbene anion can add to *trans*-stilbene to give a dimer, even if the reaction is very slow (the process (8)).

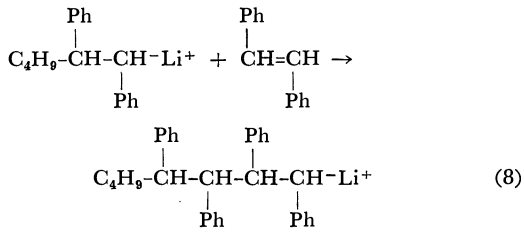

(8)

The formation of a small amount of 1,2,3,4-tetraphenylbutane can be explained by the following process:

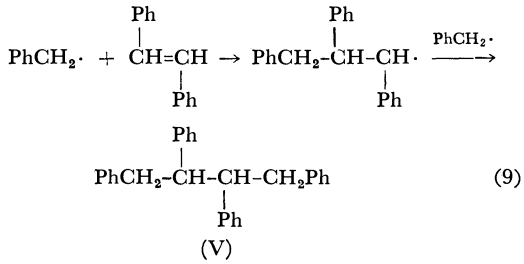

(9)

(V)

The carbinol in the fraction 4 may be produced through the following process:[9,10]

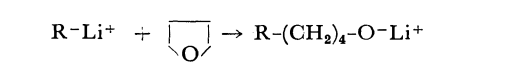

Judging from the yield of each compound obtained in this experiment, *n*-BuLi is considered to be consumed almost quantitatively in the process (1); about 49% of the 1,2-diphenylhexyl anions produced in the process reacted with *trans*-stilbene to give 1,2-diphenylhexane, 1,2,3-triphenylpropene, and 1,2-diphenylethane. About 10% of the 1,2-diphenylhexyl anions were apparently consumed in the formation of 1,2,3,4-tetraphenyloctane, while about 20% of the anions remained free from the subsequent reactions. The residual 1,2-diphenylhexyl anions and also probably a part of the 1,2,3,4-tetraphenyloctyl anions reacted with THF to yield alcohols. The absence of 1,2,3,4-tetraphenylbutene indicates that the anions produced in the processes (3) and (4) are rather unstable.

The reaction mixtures both of *trans*-stilbene with *n*-BuLi and of 1,2,3-triphenylpropene with *n*-BuLi showed the same absorption maxima, at 555 and 420 mμ. It is likely that the A-II anion, which may be produced from RA-II by the abstraction of a hydrogen from any material in the system, will be present in the reaction mixture of *trans*-stilbene and *n*-BuLi. It may be supposed that the radical anion, RA-II, shows the same absorption maxima, at 555 and 420 mμ.

The reaction of 1,2,3-triphenylpropene with *n*-BuLi proceeds as follows:

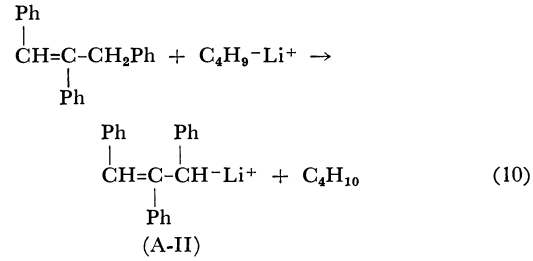

(10)

(A-II)

since the 1,2,3-triphenylpropene with a deuterium at the methylene position is recovered when the reaction is terminated by deuterium oxide.

A distinct solvent effect exists in the reaction of *trans*-stilbene and *n*-BuLi. Wyman and Altares[2] have studied the reaction of *trans*-stilbene and *n*-BuLi in benzene at 60°C. Contrary to the reaction in THF, the main process (11) was found to follow the processes (1) and (8), thus giving the dianions shown below.

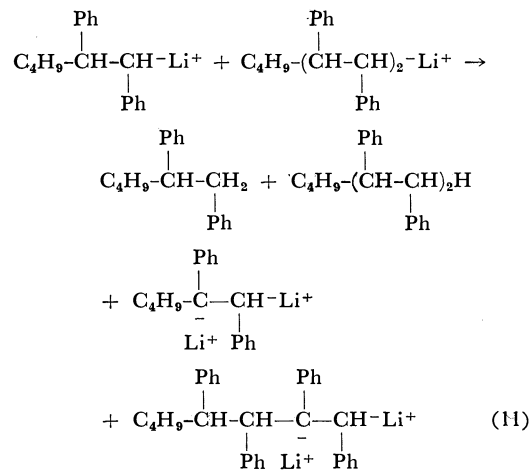

(11)

The results obtained in the present study establish that the chain-transfer in the copolymerization of *trans*-stilbene and styrene occurs by means of the abstraction of a proton from the *trans*-stilbene, as is shown by the process (2), and that the change in the color observed in the copolymerization is associated with the 1,2,3-triphenylpropenyl anion or the radical anion.

9) L. J. Fetters, *J. Polymer Sci.*, **B2**, 425 (1964).
10) Y. Okamoto and H. Yuki, This Bulletin, **41**, 677 (1968).

BULLETIN OF THE CHEMICAL SOCIETY OF JAPAN VOL. 42 766—772 (1969)

Photo-Aryl Coupling and Related Reactions. II. The Formation of Triphenylenes from Halogeno-*o*-terphenyls[1]

Takeo SATO, Shigeru SHIMADA and Kazuo HATA

Department of Chemistry, Faculty of Science, Tokyo Metropolitan University, Setagaya, Tokyo

(Received July 9, 1968)

Electronic effects on the photochemical conversion of *o*-terphenyl to triphenylene were examined by comparing the ultraviolet irraiation reaction, carried out in a benzene solution using iodine as an oxidant, of three classes of *o*-terphenyl derivatives, 4- (**3**) and 4'-substituted (**4**) and 4,4''-disubstituted derivatives (**5**). While a strong electron-withdrawing group such as nitro group, hindered the cyclization reaction to occur, methoxy, fluoro, chloro and bromo compounds afforded the corresponding triphenylene derivatives. With bromo and iodo compounds, however, a complex mixture of the products resulted due to photochemical cleavage of a carbon-halogen bonding, which led to the formation of phenylation products and hence phenyltriphenylenes together with reduction products. Further, with iodo compounds, it was found that no oxidant was necessary to effect the cyclodehydrogenation reaction since iodine was liberated during the photolysis. Possible pathways for the formation of the photolysis products from bromo and iodo compounds were discussed in relation to the relative rates of carbon-halogen cleavage and cyclization reactions. Comparison among three classes of halogeno compounds indicated that, with the exception of iodides, the cyclization reaction occurred more readily with type **4** compound than type **3** compounds, while type **5** compounds reacted only with difficulty.

Recently, we have developed[2] an efficient, quite simple method for the preparation of triphenylene (**2**) employing a photo-aryl coupling reaction of *o*-terphenyl (**1**). By this procedure **2** was obtainable in an optimum yield of 88%. A similar observation has also been announced, in the form of a preliminary account, by Kharasch and co-workers.[3]

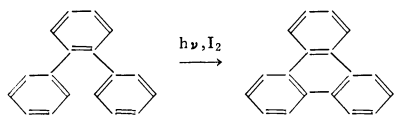

1 **2**

This cyclodehydrogenation reaction, induced by iodine, is regarded as an extention of thoroughly studied *cis*-stilbene - phenanthrene reactions,[4] representing a special case where the central unsaturated linkage of *cis*-stilbene is incorporated into an aromatic system. Mallory and co-workers,[5] during their extensive studies on the photochemistry of stilbenes, have been the first to irradiate **1** but to obtain negative results. Failure could be ascribed, in addition to the problem of a light source, to the choice of cyclohexane as a solvent, since the reaction had been shown to be much slower in this solvent[2] than in benzene in contrast to the *cis*-stilbene case where both solvents are equally suited.

Besides this solvent effect, it has been found[2] that oxygen is ineffective to bring about the cyclization reaction of **1**, thus showing a marked contrast again with the *cis*-stilbene case where iodine, oxygen or preferably a combination of these are employed as the oxidant.

In this paper, electronic effects on the photo-aryl coupling reaction were examined by choosing three representative classes of compounds **3**—**5**. Types **3** and **4** compounds are assumed to give the same product, 2-substituted triphenylene (**6**), whereas

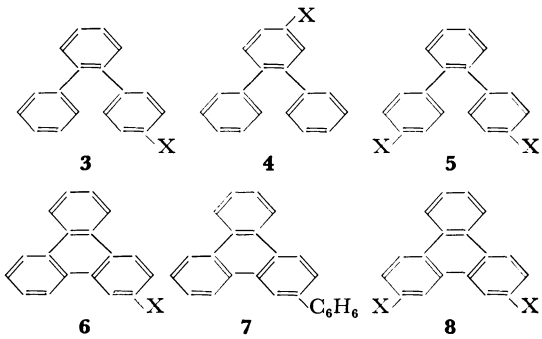

3 **4** **5**

6 **7** **8**

1) For previous paper in this series see, T. Sato, Y. Goto, T. Tohyama, S. Hayashi and K. Hata, This Bulletin, **40**, 2975 (1967).

2) T. Sato, Y. Goto and K. Hata, *ibid.*, **40**, 1994 (1967).

3) N. Kharasch, T. G. Alston, H. B. Lewis and W. Wolf, *Chem. Commun.*, **1965**, 242.

4) F. R. Stermitz in O. L. Chapman ed. "Organic Photochemistry," Vol. 1, Mercel Dekker, Inc., New York (1967), p. 249.

5) F. B. Mallory, C. S. Wood and J. T. Gordon, *J. Am. Chem. Soc.*, **86**, 3094 (1964).

TABLE 1. PHYSICAL PROPERTIES OF SUBSTITUTED *o*-TERPHENYLS

Compound	X	Mp, °C	Formula	Calcd, %			Found, %		
				C	H	Halogen	C	H	Halogen
3	NO_2	112 — 113.5[a]							
3	NHAc	152.5—153[b]							
3	F	77.5 — 79	$C_{18}H_{13}F$	87.07	5.28		87.02	5.51	
3	Cl	82.5 — 83	$C_{18}H_{13}Cl$			13.39			13.78
3	Br	93 — 94[c]	$C_{18}H_{13}Br$	69.92	4.24	25.84	69.60	4.56	25.84
3	I	116 — 116.5	$C_{18}H_{13}I$	60.70	3.68	35.62	61.19	3.50	35.38
3	OCH_3	61.5 — 62.5	$C_{19}H_{16}O$	87.66	6.19		87.73	6.30	
4	NO_2	118.3—118.5[d]	$C_{18}H_{13}NO_2$			(5.09[h])			(5.10[h])
4	Br	103.5—104.5	$C_{18}H_{13}Br$	69.92	4.24	25.84	69.61	4.42	25.68
5	NO_2	213.5—214[e]							
5	Cl	136 — 136.5	$C_{18}H_{12}Cl_2$	72.26	4.04	23.70	72.48	4.25	24.35
5	Br	168 — 170[f]	$C_{18}H_{12}Br_2$	55.65	3.09	41.26	55.34	3.45	41.17
5	I	224 — 226				52.64			52.01
10		151 — 151.5	$C_{24}H_{17}Br$	74.82	4.44		74.18	4.49	
12		144 — 146	$C_{24}H_{17}I$			29.35			28.56
13		181 — 181.5[g]	$C_{30}H_{22}$	94.20	5.80		94.14	5.85	

a) Lit. 105—106°C,[6] 115.5—116.5°C.[7]
b) Lit. (D. H. Hey, M. J. Perkins and G. H. Williams, *J. Chem. Soc.*, **1961**, 749) 159.5—160.5°C.
c) Prepared by the direct bromination of *o*-terphenyl. Formerly, Woods and Scotti[25] prepared the compound from 2-phenyl-2-cyclohexane by the Grignard reaction (reported mp 89—90.5°C).
d) Lit. 118—119°C.[8] Allen and Burness[7] obtained the compound as a by-product on nitration of *o*-terphenyl, but did not determine the position of the nitro group (reported mp 119.5°C).
e) Lit. 218°C.[6]
f) Lit. 170°C.[6] Since 4,4',4''-tribromo derivative[6] also had a similar mp (170°C), the structure was confirmed by elemental analysis.
g) Lit. 182—184°C.[25]
h) Values for nitrogen.

3,6-disubstituted triphenylene (**8**) may be obtained from **5**. In view of difficulties in preparing triphenylene derivatives possessing a definite structure either by ring construction or by substitution method, the present attempt was designed to provide useful synthetic means for them.

o-Terphenyl derivatives used for the photochemical studies are listed in Table 1. Except for bromides (**3**, **5**/Br),*1 which were obtained by the vapor phase bromination[6] of **1**, other types **3** and **5** compounds were prepared by the diazo reaction of amines (**3**,**5**/NH_2).[6,7] 4'-Nitro-[8] and 4'-bromo-*o*-terphenyls (**4**/NO_2, Br) were prepared by the decomposition of 5-substituted 2-(*N*-nitrosoacetamido)biphenyls in benzene solutions.

The ultraviolet irradiation reactions were performed with a 1-kW high-pressure mercury arc lamp housed in a water bucket, into which a sample solution in a quartz tube was immersed. A typical example is illustrated by the case of fluoride (**3**/F): A dilute benzene solution, 1.67×10^{-2} M, containing an equimolar quantity of iodine was irradiated for 96 hr under nitrogen atmosphere. By column chromatography on alumina, there was obtained a 77% yield of 2-fluorotriphenylene (**6**/F).[9] Structural proof was achieved by UV, IR and analytical data. The results of the photochemical reactions are summarized in Table 2. Physical properties and UV data of the triphenylene derivatives are compiled in Table 3.

Whereas chloride (**3**/Cl) reacted similarly to the fluoride to give a 45% yield of 2-chlorotriphenylene (**6**/Cl), bromide (**3**/Br) was found to afford a complex mixture of the products, consisting of starting material (18%), triphenylene (**2**, 6%), 2-bromotriphenylene (**6**/Br, 26%)[10] and 2-phenyltriphenylene (**7**, 28%)[11] listed in the order of elution from alumina column (Exp. 4).

The photolytic cleavage of a carbon-halogen bond is also responsible for the formation of **2** and **7** from iodide (**3**/I). Total triphenylene fraction

*1 The notation means compounds **3** and **5**, where X=Br.

6) C. F. H. Allen and F. P. Pingert, *ibid.*, **64**, 2639 (1942).
7) C. F. H. Allen and D. M. Burness, *J. Org. Chem.*, **14**, 175 (1949).
8) F. H. Case, *ibid.*, **21**, 477 (1956).
9) P. M. G. Bavin and M. J. S. Dewar, *J. Chem. Soc.*, **1956**, 164.
10) C. C. Barker, R. G. Emmerson and J. D. Periam, *ibid.*, **1955**, 4482.
11) D. D. Lawson and C. M. Buess, *J. Org. Chem.*, **25**, 272 (1960).

TABLE 2. ULTRAVIOLET IRRADIATION REACTION OF SUBSTITUTED *o*-TERPHENYLS (**3**—**5**) AND 2-BROMOTRIPHENYLENE (**6**/Br)[a]

Exp.	Compd.	X	mmol	Iodine mmol	Irrad. time, hr	Triphenylenes, %			*o*-Terphenyls, %	
						6	**2**	**7**	**1**	Recovery
1	**3**	NO_2	1.00	1.01	96					94
2	**3**	F	1.01	1.01	96	77				15
3	**3**	Cl	0.51[f]	0.50	96	45				48
4	**3**	Br	1.03	1.02	96	26	6	28		18
5	**3**	Br	1.03		96					67
6	**3**	I	1.00	1.02	48		36	45		10
7	**3**	I[b]	0.52[f]		24		9	17		31
8	**3**	I[c]	0.50[f]		24		9	—	36	45
9	**3**	I[c]	0.50[f]		72		6	—	37	38
10	**3**	I	1.00		48		18	41		
11	**3**	I[d]	0.52[f]		24			—	37	6
12	**3**	OCH_3	1.00	1.02	48	65	1			
13	**4**	NO_2	1.00	1.02	72					88
14	**4**	Br	1.01	0.99	24	66	14	11		
15	**4**	Br	0.50[f]		24					81
16	**4**	Br[c]	1.00	1.00	46	27	27	—	20	11
17	**5**	NO_2	1.01	1.01	96					g)
18	**5**	Cl	0.99	1.01	96					60
19	**5**	Cl	0.52[f]	0.52	120					81
20	**5**	Br	1.01	1.00	20					g)
21	**5**	Br[e]	1.00	1.02	96					35
22	**5**	I[e]	1.01		48					1
23	**6**	Br	0.20[f]	0.25	24	91			—	—
24	**6**	Br	0.50		24	83			—	—

a) Unless otherwise stated, the photochemical reactions in a benzene solution (60 ml) were carried out in a quartz cell using a 1-kW high-pressure mercury lamp under a nitrogen atmosphere.
b) The reaction was carried out under oxygen.
c) Carried out in cyclohexane.
d) Carried out in toluene.
e) Other products are shown in the schemes in the text.
f) Less amount of benzene was used to adjust the concentration to 1.67×10^{-2} M.
g) Infrared spectrum of the product was completely superimposable with that of the starting material.

(**2** plus **7**) amounted to 81% even with shorter irradiation period compared with other halides (Exp. 6). The cleavage of the carbon-iodine bond was so extensive that only isolable iodo compound was a small amount of starting material and no 2-iodotriphenylene (**6**/I) was detected.

The extensive cleavage of the carbon-iodine bond suggested that the liberated iodine might serve as an oxidant to induce the oxidative aryl coupling reaction. That this was indeed the case was confirmed by the experiments carried out in the absence of iodine (Exp. 7—10). The reaction proceeded similarly with irradiation under oxygen (Exp. 7), which itself was ineffective as an oxidant to bring about the cyclization.[2] In contrast, no cyclization occurred when bromides (**3**, **4**/Br) were irradiated in the absence of iodine (Exp. 5, 15).

Although the studies on the photolysis of iodoaromatic compounds date back to 1924 when Job and Emschwiller[12] investigated bond strength of a carbon-iodine bonding, the mechanistic aspects and synthetic applicability have been explored only quite recently.[13] Lately, intermolecular as well as intramolecular aryl coupling reactions induced by the photolysis of iodoaromatics have found wide application not only for the formation of polyphenyls and phenanthrenes but also for the complex natural product[14] and heterocyclic compounds.[15-17]

12) A. Job and G. Emschwiller, *Compt. rend.*, **179**, 52 (1924).
13) W. Wolf and N. Kharasch, *J. Org. Chem.*, **30**, 2493 (1965). Refer to the literatures cited in this paper for earlier studies in this field.
14) S. M. Kupchan and H. C. Wormer, *Tetrahedron Letters*, **1965**, 359; S. M. Kupchan and H. C. Wormer, *J. Org. Chem.*, **30**, 3792 (1965).
15) P. W. Jeffs and J. F. Hansen, *J. Am. Chem. Soc.*, **89**, 2798 (1967).
16) H. S. Thyagarajan, N. Kharasch, H. B. Lewis and W. Wolf, *Chem. Commun.*, **1967**, 614.
17) S. M. Kupchan and R. M. Kanojia, *Tetrahedron Letters*, **1966**, 5353.

Table 3. Physical properties of 2-substituted and 3,6-disubstituted triphenylenes

Compound	X	Mp, °C	Formula	Anal, %	Calcd	Found	λ_{max} (log ε)
6	F	181.5[a]	$C_{18}H_{11}F$	C	87.80	88.05	248(4.85), 257(5.08), 271(4.10),[f] 283(4.08), 303(3.32), 313.5(2.83), 320.5(2.67), 328.5(2.87), 335(2.60), 344(2.84)
				H	4.49	4.49	
6	Cl	143.5—144.5	$C_{18}H_{11}Cl$	C	82.30	82.59	250.5(4.56), 259(4.79), 274.5(3.38), 286(3.83), 305(3.02), 314.5(2.46),[f] 322.5(2.32), 330.5(2.[illegible]0),337.5(2.19), 346.5(1.97)
				H	4.22	4.28	
6	Br	129—131[b]	$C_{18}H_{11}Br$				252(5.18), 260.5(5.41), 275(4.56), 287(4.57), 307.5(3.80), 316(3.10),[f] 323.5(2.96), 331(2.91), 338(2.82), 347(2.48)
6	OCH_3	110—111[c]	$C_{19}H_{14}O$	C	88.34	88.07	254(4.86), 262(5.04), 277(4.20),[f] 287.5(4.16), 320(3.16), 327(2.94), 335(3.26), 343(2.84), 351(3.25)
				H	5.46	5.25	
7		180.5—181[d]	$C_{24}H_{16}$	C	94.70	94.62	260(4.78),[f] 267.5(4.86), 287.5(4.39),[f] 301(4.29)[f]
				H	5.30	5.33	
8	Cl	172—179	$C_{18}H_{10}Cl_2$[e]				
8	Br	232—234	$C_{18}H_{10}Br_2$	C	56.00	56.61	253(3.89), 263(4.12), 277(3.30),[f] 287(3.21),[f] 309.5(2.47),[f] 319(1.94),[f] 326(1.75), 334.5(1.71), 341(1.56), 350(1.43)
				H	2.61	2.79	
11		153—155	$C_{24}H_{15}Br$	C	75.22	75.66	271, 298,[f] 307[f]
				H	3.93	4.01	
14		262—263	$C_{30}H_{20}$	C	94.70	94.52	276, 307[f]
				H	5.30	5.17	

a) Lit. 185—185.5°C.[9]
b) Lit. 131—132°C.[10] No mp depression on admixture with the authentic material obtained by the bromination[10] of **2**.
c) Lit. (W. S. Rapson, *J. Chem. Soc.*, **1941**, 15) 97—98°C.
d) Lit. 183—184°C.[11]
e) Determined by mass spectroscopy, *m/e* 296.
f) Shoulders.

These arylation reactions are assumed[13] to be initiated by the formation of an aryl radical which attacks a benzene nucleus to give an arylcyclohexadienyl radical, dehydrogenation of which with iodine then terminates the reaction. The formation of phenylation products from halogeno-*o*-terphenyls may follow similar steps.

As more closely related studies, Kampmeier and Hoffmeister[18] have shown that the photolysis of 1,2-diiodobenzene in a benzene solution leads to the formation of a small amount of **2** (4% after 175 hr). Similarly irradiation of 2-iodobiphenyl for 60 hr also led to **2** in a small yield.[13,18] The cyclization step leading to **2** and **7** in the present cases would be similar with these.

There are two routes which may account for the formation of **2** and **7**, namely routes a and b:

Route a is initiated by the homolysis of a carbon-halogen bond to give *o*-terphenyl radical, which, *via* *o*-terphenyl (**1**) and 1,1′ : 2′,1″ : 4″,1‴-quaterphenyl (**9**),[3] cyclizes to **2** and **7**. In the alternative route b, cyclization reaction occurs first to afford 2-halogenotriphenylenes (**6**), which then loses a halogen atom by the homolytic cleavage.

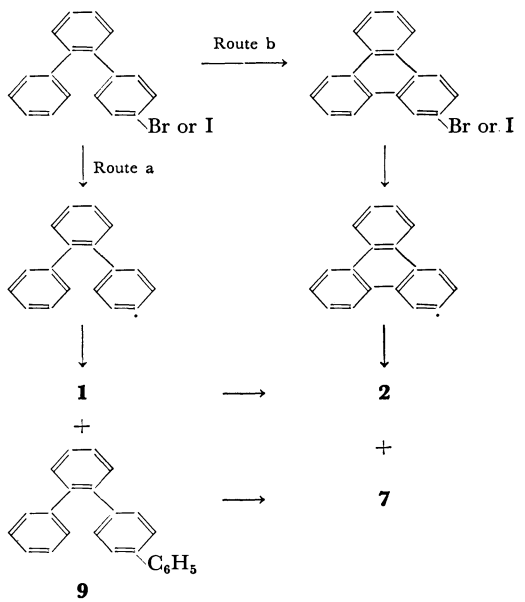

18) J. A. Kampmeier and E. Hoffmeister, *J. Am. Chem. Soc.*, **84**, 3788 (1962).

Hydrogen abstraction and phenylation of triphenylene radical thus formed yield **2** and **7**. Whether a given halogeno-*o*-terphenyl decays after either the two competitive routes a or b is determined by the bond energies of the carbon-halogen linkage and the rate of aryl coupling reaction.

The fact that the ease with which the cyclization occurs is related to the electron density on the terminal benzene rings is illustrated by the extreme cases of three nitro derivatives (**3**—**5**/NO_2), which have been recovered unchanged even after 77—96 hr irradiation (Exp. 1, 13, 17). The results could be compared with a facile reaction of methoxy derivative (**3**/OCH_3), which afforded the expected 2-methoxytriphenylene (**6**/OCH_3) in a 65% yield together with a small amount of triphenylene[19] (Exp. 12). This electronic effect is assumed to be operated among halides **3**, although in a less degree. Another factor, carbon-halogen bond cleavage, however, becomes important only with bromides[23,24] and especially with iodides.[13]

Bond energy considerations favor route a over route b, since a halogen atom is more firmly attached to the resonance-stabilized triphenylene ring than to *o*-terphenyl moiety. Evidence indicated that **2** and **7** arose *via* route a were obtained in the following manner: i) 2-Bromotriphenylene (**6**/Br), the intermediate for route b, was shown to be quite stable (Exp. 23, 24). ii) Obviously, the cyclization of iodide (**3**/I) in the absence of iodine requires the carbon-iodine cleavage as the initial reaction. Further, the fact that the efficiency of the cyclization of the iodide was comparable to **1** itself and was much more rapid than other halides, suggested the loss of iodine in an earlier stage of the reaction.

These results showed that, whereas bromide (**3**/Br) decayed in both ways, the ratio of route a and route b in 3 : 4, iodide (**3**/I) followed most probably after route a and that the cleavage of the carbon-iodine bond ocurred much more rapidly than the cyclization reaction. Comparing between isomeric bromides (**3**, **4**/Br), 4-isomer afforded **6**/Br in a higher yield (66% compared with 26%) even with shorter reaction time (Exp. 4 *vs.* 14).

The reactions in cyclohexane or toluene afforded a reduction product. Thus *o*-terphenyl was isolated in a 36—37% yield by the irradiation of iodide (**3**/I) in a cyclohexane solution (Exp. 8, 9), in which the photo-aryl coupling reaction proceeds more slowly than in benzene (Exp. 10). The photolysis in toluene also afforded a 37% yield of **1** (Exp. 11). Similarly **1** was obtainable in a 20% yield by the irradiation of bromide (**4**/Br) in cyclohexane (Exp. 16).

Ultraviolet irradiation of dihalides (**5**/Cl, Br) revealed that the reactions were even difficult compared with monohalides as evidenced by the higher rates in the starting material recovery (Exp. 18, 19, 20, 21). Dichloride (**5**/Cl) afforded only a trace amount of **8**/Cl, which was characterized by the mass spectrum (parent peak had *m/e* 296).

If the cleavage of a carbon-halogen bond is to occur as above, then, a complex mixture of the products would be expected from the dihalides **5**. The replacement of the halogen atom by a hydrogen or phenyl group would give rise to five *o*-terphenyl structures. They include those *o*-terphenyls **1**, **3**, and **9** of which cyclization and transformation products would be similar to those of the monohalides. New types of *o*-terphenyl derivatives are 4-halogeno-4''-phenyl-*o*-terphenyl (such as **10** and **12**) and 1,1' : 4',1'' : 2'',1''' : 4''',1''''-quinquephenyl (**13**).[25]

Chromatography on alumina of the reaction mixture obtained from dibromide (**5**/Br) afforded four compounds (Exp. 21), among which the starting material was shown to be present in the largest amount (35%). Other compounds, identified by IR, UV and analytical data, were shown in the accompanying scheme (in the order of elution from the column). Diiodide (**5**/I) afforded five compounds which were separated by column chromatography on alumina (Exp. 22). Small amounts of the starting material (1%) and monoiodide (**3**/I, 1%) were eluted first, followed by three compounds as were shown in the scheme. When the reaction was further continued for 7 days, iodo compounds were found to be completely transformed into phenylation and reduction products. Thus only three hydrocarbons were isolated; they were 32% of the quinquephenyl (**13**), 5% of 2-phenyltriphenylene (**7**) and 37% of 3,6-diphenyltriphenylene (**14**). By an independent experiment, the irradiation of **13**, in the presence of iodine, was shown to yield **14** (9% after 92 hr). All the compounds had IR and UV spectra consistent with the assigned structures. Spectral

19) The formation of triphenylene was clearly demonstrated by gas chromatography. It could possibly be formed by carbon-oxygen cleavage of either **3**/OCH_3 or **6**/OCH_3. A small amount of phenolic material was also detected. Photolytic cleavage of ether linkage was noticed by several authors.[20-22] As another model compound having electron-releasing group 4-acetamido-*o*-terphenyl (**3**/$NHCOCH_3$) was irradiated, but soon after the start of the reaction, the compound began to separate out on the wall of the vessel and the reaction had to be discontinued.

20) M. S. Kharasch, G. Stampa and W. Nudenberg, *Science*, **116**, 309 (1952).

21) J. D. Margerum, J. N. Pitts, Jr., J. G. Rutgers and S. Searles, *J. Am. Chem. Soc.*, **81**, 1549 (1959).

22) C. S. Wood and J. B. Mallory, *J. Org. Chem.*, **29**, 3373 (1964).

23) S. M. Kupchan and H. C. Wormer, *Tetrahedron Letters*, **1965**, 359.

24) T. Matsuura and K. Omura, This Bulletin, **39**, 944 (1966).

25) G. F. Woods and F. Scotti, *J. Org. Chem.*, **26**, 312 (1961).

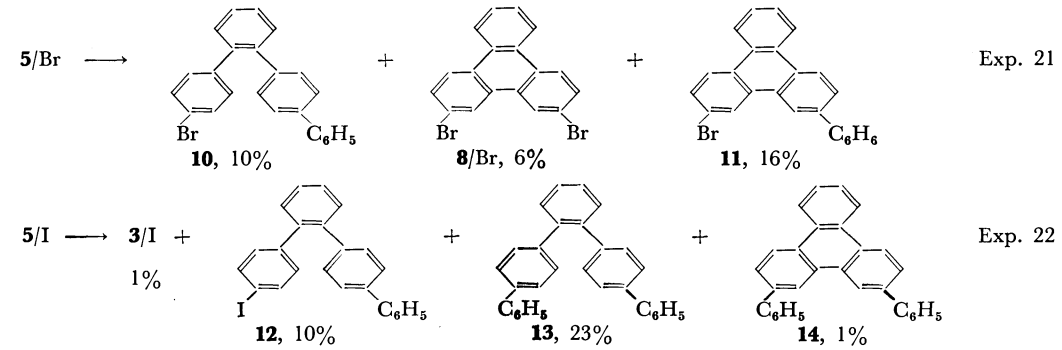

data and analytical figures are compiled in Tables 1 and 3. The formation of **13** and **14** suggested the potential utility of the present method for the synthesis of polyphenyls and their condensation products, such as phenyltriphenylenes.[26]

Of the triphenylene derivatives here obtained, the UV spectra of 2-fluoro- (**6**/F)[8] and 2-phenyltriphenylenes (**7**)[11] were recorded previously. Triphenylene and its derivatives usually display up to ten absorption bands (or shoulders) in the UV region. Slight bathochromic shifts, amounting 2—3 mμ, of each bands occurred with chloride (**6**/Cl) and bromide (**6**/Br) compared with the fluoride. 3,6-Dibromotriphenylene (**8**) showed a quite similar spectrum with the monohalides with slightly more bathochromic shifts (3—6 mμ from **6**/F). Attachment of a phenyl group simplified the spectrum enormously; thus only one peak at 268 mμ, together with three shoulders, were observed for **7**. Similarly, the absorption curves for 3-bromo-6-phenyl- (**11**) and 3,6-diphenyltriphenylenes (**14**) were similar to that of **7**, except that the absorption maximum was shifted to a long wavelength by 3 and 8.5 mμ respectively.

In conclusion, it was found that, with the exception of the iodides, introduction of two halogen substituents at the terminal benzene rings of *o*-terphenyl moiety retards the cyclization reaction significantly, whereas, introduction of one halogen substituent does it only moderately. On the other hand, the presence of a bromine substituent on the central benzene ring does not affect the reaction rate. The fact that benzene is superior over cyclohexane as the solvent for the photo-aryl coupling reaction strongly suggested the importance of the aromatic solvent as a good sensitizer.[13,27,28]

Experimental[29]

Materials. *o*-Terphenyl derivatives subjected to photochemical studies are tabulated in Table 1. Of these, six are known compounds. New syntheses and modifications of known methods will be briefly described.

4-Fluoro-*o*-terphenyl (3/F). To a diazonium chloride solution prepared from 4-amino-*o*-terphenyl (**3**/NH_2),[6] a 42% solution of fluoroboric acid was added. The resulting diazonium fluoroborate was decomposed thermally[30] and the reaction mixture was extracted with benzene. The fluoride (**3**/F) was obtained as colorless prisms, mp 77.5—79°C (recrystallized from *n*-hexane).

4-Chloro- and 4,4''-Dichloro-*o*-terphenyls (3, 5/Cl). They were prepared by the Sandmeyer reaction[31] of amines (**3,5**/NH_2).[6,7] The mono- and dichloride were obtained respectively as colorless plates, mp 82.5—83°C and 136—136.5°C (each recrystallized from *n*-hexane).

4-Bromo- and 4,4''-Dibromo-*o*-terphenyl (3, 5/Br). *o*-Terphenyl was brominated with bromine vapor after the method of Allen and Pingert.[6]

The dibromide was obtained as colorless plates, mp 168—170°C (recrystallized from *n*-hexane). Since 4,4',4''-tribromo-*o*-terphenyl was reported to have a similar mp (170°C), the structure was confirmed by elemental analysis.

The above bromination reaction was stopped when the reaction mixture started to solidify after remaining a viscous liquid. The reaction product in that case was found to be mainly the monobromide, colorless plates, mp 93—94°C (recrystallized from *n*-hexane). The monobromide was formely prepared[25] from 2-phenyl-2-cyclohexanone by the Grignard reaction.

4-Iodo- and 4,4''-Diiodo-*o*-terphenyl (3, 5/I). They were prepared in the usual way by the decomposition of diazonium or bis(diazonium) chloride with potassium iodide.

The monoiodide was obtained as colorless plates, mp 116—116.5°C (recrystallized from *n*-hexane).

The diiodide was obtained as nearly colorless plates, which discolored on standing, mp 224—226°C (recrystallized from benzene).

4-Methoxy-*o*-terphenyl (3/OCH_3). 4-Hydroxy-*o*-terphenyl was prepared by the decomposition of the diazonium sulfate made from **3**/NH_2. Without further

26) The photolytic bisphenylation of diiodopolyphenyls would become a general synthetic method of polyphenyls having two more benzene rings. Studies on this matter will be reported elsewhere.

27) H. Morrison, *J. Am. Chem. Soc.*, **87**, 932 (1965).

28) F. Wilkinson, *J. Phys. Chem.*, **66**, 2569 (1962).

29) All melting points are uncorrected. UV spectra were recorded on a Cary 15 spectrophotometer. The authors are grateful to Mr. H. Kohashi of Osaka University for providing us with the data. Gas chromatography was performed with Hitachi K 53 chromatograph using 5% silicone gum XE-60 on Chromosorb W. column.

30) A. Roe, *Organic Reactions*, **5**, 193 (1957).

purification, it was methylated with dimethyl sulfate, colorless plates, mp 61.5—62.5°C (recrystallized from *n*-hexane).

4'-Bromo-*o*-terphenyl (4/Br). 2-Acetamido-5-bromobiphenyl,[32] mp 130°C, was nitrosated with nitrosyl chloride and was decomposed in a benzene solution in the usual manner.[33] The bromide was purified by passing through alumina column as a benzene solution, and was obtained as colorless plates, mp 103.5—104.5°C (recrystallized from *n*-hexane).

4'-Nitro-*o*-terphenyl (4/NO_2). It was prepared by the decomposition of 5-nitro-2-(*N*-nitrosoacetamido)-biphenyl,[8,34] mp 133°C, in a benzene solution following the method of Case,[8] colorless plates, mp 118.3—118.5°C (recrystallized from *n*-hexane). The compound was reported to be obtainable as a minor product by the direct nitration of *o*-terphenyl and once was referred to as *x*-nitro-*o*-terphenyl, mp 119.5°C.[7]

Photochemical Reactions. *General Procedure.* A sample solution (1.67×10^{-2} M) in a quartz vessel equipped with gas inlet and outlet tubes, was irradiated externally with a 1-kW high-pressure mercury arc lamp (Wako HBC-1000) immersed in a bucket. Cooling was given by running water. During the irradiation a stream of nitrogen (or air) was bubbled through the solution.

The results of photolysis studies are summarized in Table 2. Analysis of the reaction products were performed by column chromatography on alumina, which was eluted with a mixture of *n*-hexane and benzene of varying ratio. A fraction of approximately 100 m*l* was collected. Identification of *o*-terphenyl and triphenylene were also achieved by gas chromatography, though the use of which was limited to a few cases.

The physical properties and UV data of triphenylene derivatives prepared in this study are summarized in Table 3. Since the reaction conditions are given in Table 2, and the work-up procedure of the reaction mixtures from nitro-, fluoro-, chloro-, and methoxy-*o*-terphenyls are straight-forward, only representative experiments on bromides and iodides are briefly mentioned.

4-Bromo-*o*-terphenyl (3/Br). *Exp. 4.* A solution of 319 mg (1.03 mmol) of **3**/Br, 260 mg (1.02 mmol) of iodine in 60 m*l* of benzene was irradiated under nitrogen for 96 hr. After the irradiation reaction was over, the solution was successively washed with sodium thiosulfate solution and water, and was dried over magnesium sulfate. The product was then subjected to column chromatography on alumina using a 10 : 1 mixture of *n*-hexane - benzene as an eluent. By checking the elutes with IR spectra, the products were separated into the following four fractions; 56.5 mg (18%) of **3**/Br, mp 93—94°C (colorless plates from *n*-hexane), 14.2 mg (6%) of **2**, mp 193—194°C (colorless needles from ethanol), 81.3 mg (26%) of **6**/Br,[10] mp 129—131°C (colorless needles from acetone) and 88.2 mg (28%) of **7**,[11] mp 180.5—181°C (colorless needles from ethanol).

Exp. 5. When irradiated in the absence of iodine, the starting material was completely recovered.

4-Iodo-*o*-terphenyl (3/I). *Exp. 10.* A benzene solution of 356 mg (1.00 mmol) of **3**/I was irradiated for 48 hr. By chromatography on alumina, eluted with a 4 : 1 *n*-hexane - benzene mixture, there were obtained 37.1 mg (18%) of **2** (fractions 14—20) and 113 mg (41%) of **7** (fraction 30~).

Exp. 8, 9 and 11. The photolysis in cyclohexane or toluene yielded *o*-terphenyl, which was eluted first from alumina column.

4'-Bromo-*o*-terphenyl (4/Br). *Exp. 14.* A solution of 311 mg (1.01 mmol) of **4**/Br, 250 mg (0.99 mmol) of iodine in 60 m*l* of benzene was irradiated under nitrogen for 24 hr. By chromatography on alumina, eluted with a 9 : 1 *n*-hexane - benzene mixture, there were obtained 31.3 mg (14%) of **2** (fractions 70—76), 204.5 mg (66%) of **6**/Br (fractions 77—120) and 34.2 mg (11%) of **7** (fractions 126—132).

Exp. 16. The irradiation reaction products were first eluted with *n*-hexane, which afforded 44.9 mg (20%) of **1** (fractions 20—30) and 34.9 mg (11%) of **4**/Br (fractions 32—42). The solvent was switched to a 9 : 1 *n*-hexane - benzene mixture to obtain 61.5 mg (27%) of **2** (fractions 61—80) and 83.0 mg (27%) of **6**/Br (fractions 82~).

4,4''-Dibromo-*o*-terphenyl (5/Br). *Exp. 21.* A solution of 388 mg (1.00 mmol) of **5**/Br, 259 mg (1.02 mmol) of iodine in 60 m*l* of benzene was irradiated under nitrogen for 96 hr. The reaction product was analyzed by column chromatography on alumina. After elution with *ca.* 1400 m*l* *n*-hexane, the eluent was changed to a 9 : 1 *n*-hexane - benzene mixture. Starting material (135.2 mg, 35%) came out first (fractions 20—25) which was followed by 39.6 mg (10%) of **10**, mp 151—151.5°C as colorless plates from *n*-hexane (fractions 43—44), 21.8 mg (6%) of **8**/Br, mp 232—234°C as colorless needles from *n*-hexane (fractions 46—48) and 63.0 mg (16%) of **11**, mp 153—155°C, as colorless amorphous material from ethanol (fractions 64—75).

4,4''-Diiodo-*o*-terphenyl (5/I). *Exp. 22.* A solution of 484 mg (1.01 mmol) of **5**/I in 60 m*l* of benzene was irradiated under nitrogen for 48 hr. Since the reaction mixture discolored considerably due to liberated iodine after about 26 hr, it was necessary to remove it by washing the reaction mixture with sodium thiosulfate solution. By column chromatography on alumina, there were obtained five fractions by elution with a 9 : 1 *n*-hexane - benzene mixture; 5.5 mg (2%) of **3**/I (fractions 8—10), 7.2 mg (1%) of **5**/I (fractions 15—19), 42.1 mg (10%) of **12**, mp 144—146°C as colorless plates from *n*-hexane (fractions 39—55), 88.9 mg (23%) of **13**, mp 181—182°C as colorless plates from *n*-hexane (fractions 65—115) and 5.5 mg (1%) of **14** as colorless needles (fractions 116~).

Photochemical conversion of **13** to **14** was confirmed by an independent experiment, in which 50 mg of **13** and 35 mg of iodine in a benzene solution (15 m*l*) was irradiated for 92 hr. By chromatography on alumina, **14**, mp 262—263°C, was isolated in a 9% yield. Quinquephenyl **13** was recovered in 71% yield.

The authors are indebted to the members of the analytical section of the Institute of Physical and Chemical Research for carrying out microanalyses.

31) C. S. Marvel and S. M. McElvain, "Org. Synth.," Coll. Vol. I, p. 170 (1956).

32) H. A. Scarborough and W. A. Waters, *J. Chem. Soc.*, **1927**, 94.

33) W. E. Bachmann and R. A. Hoffman, *Org. Reactions*, **2**, 224 (1957).

34) F. Bell, *J. Chem. Soc.*, **1928**, 2773.

BULLETIN OF THE CHEMICAL SOCIETY OF JAPAN VOL. 42 773—776 (1969)

Photo-Aryl Coupling and Related Reactions. III. The Transannular Dehydrogenation of [2.2]Metacyclophane Induced by Iodine[1]

Takeo SATO,* Meiko WAKABAYASHI,* Shigenari HAYASHI** and Kazuo HATA*

* *Department of Chemistry, Faculty of Science, Tokyo Metropolitan University, Setagaya, Tokyo*
** *Department of Chemistry, Nihon University, Setagaya, Tokyo*

(Received July 9, 1968)

The ultraviolet irradiation of [2.2]metacyclophane (I) with iodine in a cyclohexane solution was shown to afford 4,5,9,10-tetrahydropyrene (II), which, on further dehydrogenation, was led to 4,5-dihydropyrene and pyrene. The transannular reaction leading to II occurred much more rapidly than the subsequent dehydrogenation reactions. Thus II was obtainable in an optimum yield of 62% by the irradiation of I in the presence of an equimolar amount of iodine and an excess of sodium bicarbonate. By ESR and UV spectral studies, 253.7 mμ light was found to be responsible for the transannular reaction.

The origin of pyrene (IV) in coal tar was once questioned and was attributed to *m*-xylene, assuming the intermediacy of either 2,2',6,6'-tetramethylbiphenyl or [2.2]metacyclophane (I).[2] Baker and his co-workers[3] have realized the conversion of I to IV in a 60% yield by the action of palladium charcoal. They also showed hexahydropyrene was obtainable from I by treating it with aluminum chloride. As a related observation, we confirmed smooth conversion of I to 4,5,9,10-tetrahydropyrene (II) by the action of ferric chloride.[4]

Both ionic and homolytic pathways are shown to effect the transannular reaction of I. Thus, electrophilic substitution reactions, such as nitration[5,6] or halogenation reaction[5,7,8] afforded II or its 2-substituted derivatives. Noteworthy is the isolation of II, 4, 5-dihydropyrene (III) and IV from the nitration reaction mixture using benzoyl nitrate.[6] In this case both electrophilic and radical reactions are occurring as competing processes. Photochemical conversion of I to IV was first realized by Lindsay and his co-workers[9] who treated I with bromine under ultraviolet irradiation. We observed that irradiation of I with nitrosyl chloride afforded II in a good yield.[4]

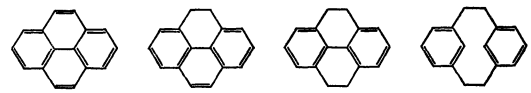

I II III IV

Apart from curiosity in the origin of IV in nature, those reactions involving transannular dehydrogenation or cycloisomerization step are of considerable interest as regards the reaction mechanism and synthetic utility. Whereas some mechanistic studies on the transannular reactions initiated by electrophiles are available,[5,6,8,10,11] only limited studies have been carried out on the photochemical behavior of I.[7,9,12] Our earlier findings that the photo-aryl coupling of I induced by iodine afforded a good yield of II,[7] urged us to study the reaction further in order to find out the optimum reaction conditions and to obtain mechanistic evidence.

The photochemistry of I was examined under selected conditions using a 1-kW high-pressure mercury arc lamp. A cyclohexane solution (0.83×10^{-2} M) contained in a quartz tube was irradiated externally for 20hr under oxygen or nitrogen current. The reaction mixture was analyzed by column chromatography on alumina and the products were characterized by spectroscopic methods or by a direct comparison with the authentic samples. The results are summarized in Table 1.

1) Part II: T. Sato, S. Shimada and K. Hata, This Bulletin, **42**, 766 (1969).
2) W. Baker, J. F. W. McOmie and J. M. Norman, *Chem. & Ind.*, **1950**, 77.
3) W. Baker, J. F. W. McOmie and J. M. Norman, *J. Chem. Soc.*, **1951**, 1114.
4) Unpublished results.
5) N. L. Allinger, M. A. DaRooge and R. B. Hermann, *J. Am. Chem. Soc.*, **83**, 1974 (1961).
6) M. Fujimoto, T. Sato and K. Hata, This Bulletin, **40**, 600 (1967).
7) T. Sato, E. Yamada, Y. Okamura, T. Amada and K. Hata, *ibid.*, **38**, 1049 (1965).
8) T. Sato, M. Wakabayashi, Y. Okamura, T. Amada and K. Hata, *ibid.*, **40**, 2363 (1967).
9) W. S. Lindsay, P. Stokes, L. G. Humber and V. Boekelheide, *J. Am. Chem. Soc.*, **83**, 943 (1961).
10) N. L. Allinger, B. J. Gordon, S.-E. Hu and R. A. Ford, *J. Org. Chem.*, **32**, 2272 (1967).
11) *Cf.* R. W. Griffin, Jr., and R. A. Coburn, *J. Am. Chem. Soc.*, **89**, 4638 (1967).
12) For other attempts of ultraviolet irradiation of I, see R. W. Griffin, Jr., *Chem. Revs.*, **63**, 45 (1963).

TABLE 1. THE PHOTOCHEMICAL REACTIONS OF [2.2]METACYCLOPHANE (I) AND 4,5,9,10-TETRAHYDROPYRENE (II)[a]

No.	Compound, mmol		Iodine mmol	Sodium bicarbonate mmol	Products, %			
					I	II	III	IV
1[b]	I	0.25			100			
2	I	0.25	0.01		17	37	8.2	trace
3	I	0.25	0.25			15	22.4	29.2
4	I	0.25	0.25	0.3		21	28.8	27.4
5	I	0.25	0.125	0.5		38.2	15.0	24.0
6	I	0.25	0.125	0.5[d]		58.4	30.0	10.2
7[b]	I	0.25	0.25	8.3		62.0	26.7	11.3
8[b,c]	I	0.25	0.25	8.3		51.4	48.6	
9	II	0.50	0.25	1.2		54.3	28.2	8.3

a) A cyclohexane solution (30 ml) contained in a quartz tube was irradiated externally with a 1-kW high-pressure mercury are lamp for 20 hr. Except for No. 1, which was carried out under oxygen, all photolysis reactions were performed under a current of nitrogen.
b) Yields are expressed in a product ratio.
c) Ultraviolet irradiation was continued for 40 hr.
d) Instead of sodium bicarbonate, sodium carbonate was used.

First, it was found that oxygen was not effective as the oxidant for the transannular dehydrogenation reaction (No. 1). The rest of the photolyses were thus performed under nitrogen. Addition of a small amount of iodine, however, was shown to lead to the formation of II and III together with a trace amount of IV (No. 2). Higher rate of conversion to pyrene was achieved by the irradiation with an equimolar amount of iodine. In this case the yield of pyrene reached 29.2% (No. 3).

As will be discussed in detail later, the initial product of the reaction is assumed to be II, of which further dehydrogenation may be responsible for the formation of III and IV. This was clearly confirmed by carrying out similar photolysis studies on II itself (No. 9). The compound was found to afford 36.5% of dehydrogenation products. Examination of the effect of base revealed that the presence of an excess of sodium bicarbonate retarded further transformation of II. Thus as high as a 62% yield of II was achieved (No. 7). The fact that only a small amount of iodine is enough to effect the reaction to a significant extent (No. 2) indicates that iodine is regenerated[13] from hydrogen iodide, which is formed in the photolytic dehydrogenation processes. Use of an equimolar amount of iodine and trapping of generated hydrogen iodide thus made this reaction highly specific one.

The photochemical transformation of *cis*-stilbene to phenanthrene[13,14] has been extensively studied and has been extended to the syntheses of phenanthrene derivatives,[15] triphenylenes,[1,16,17] polycondensed ring compounds including phenanthrene system[18-20] and heterocyclic analogs.[21,22] The reaction mechanism has been elucidated beyond doubt by trapping the intermediate compound 4a,4b-dihydrophenanthrene (V), by carrying out ultraviolet irradiation of stilbene solutions in the absence of oxygen.[14,23,24] Oxidation of V with

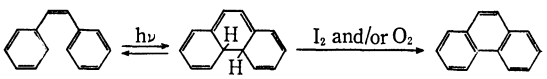

V

oxygen, iodine, or more effectively with the mixture of these two as the dark reaction was assumed to be the final stage of the reaction. Atomic sulfur generated from *cis*-stilbene sulfide was also found to be effective as an oxidant.[25]

It is apparent that no such mechanism formulated above is conceivable for the metacyclophane case,

13) F. B. Mallory, C. S. Wood and J. T. Gordon, *J. Am. Chem. Soc.*, **86**, 3094 (1964).
14) F. R. Stermitz in O. L. Chapman ed. "Organic Photochemistry," Vol. 1, Mercel Dekker, Inc., New York (1967), p. 249.
15) C. S. Wood and F. B. Mallory, *J. Org. Chem.*, **29**, 3373 (1964).
16) N. Kharasch, T. G. Alston, H. B. Lewis and W. Wolf, *Chem. Commun.*, **1965**, 242.
17) T. Sato, Y. Goto and K. Hata, This Bulletin, **40**, 1994 (1967).
18) M. Scholz, M. Mühlstädt and F. Dietz, *Tetrahedron Letters.*, **1967**, 665.
19) W. Carruthers, *J. Chem. Soc.*, (*C*), **1967**, 1525.
20) M. F.-Barbieux, J. Nasielski and K. H. Martin, *Tetrahedron Letters*, **1967**, 743.
21) R. M. Kellogg, M. B. Groen and H. Wynberg, *J. Org. Chem.*, **32**, 3093 (1967).
22) C. E. Loader and C. J. Timmons, *J. Chem. Soc.*, (*C*), **1967**, 1677.
23) W. M. Moore, D. D. Morgan and F. R. Stermitz, *J. Am. Chem. Soc.*, **85**, 829 (1963).
24) K. A. Muskat and E. Fischer, *J. Chem. Soc.*, (*B*), **1967**, 663.
25) T. Sato, Y. Goto, T. Tohyama, S. Hayashi and K. Hata, This Bulletin, **40**, 2975 (1967).

since the two benzene rings in this compound are not in conjugation. Moreover, the fact that oxygen is not effective for cycliaztion suggested that the photo-aryl coupling of I proceeded through an entirely different mechanism from that of *cis*-stilbene-phenanthrene cases.

Recently, Blaschke and Boekelheide[26] prepared [2.2]metacyclophan-1-ene (IV) and observed a photochemical equilibrium (VI⇄VII). They have

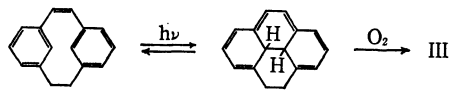

VI VII

noticed that VII is extremely sensitive to oxygen and is easily convertible to III by its presence. The cyclization step in this case is thus similar to the stilbene type and different from ours.

Kinetic studies[27] have revealed that the dehydrogenation reaction of ethylene bridge occurs much more slowly compared with the transannular cyclization step. This permits us to treat the latter process separately from the competing reactions in the initial stage of the reaction. Therefore our effort was concentrated to define the nature of the transannular reaction step.

An ESR signal appeared when a deaerated cyclohexane solution of I containing iodine was irradiated with unfiltered light of a high-pressure mercury lamp at room temperature. The signal was observed as a single line spectrum with a band width of 23 gauss. When, however, I or iodine alone was irradiated under similar conditions no such signal was observable. These facts indicated that a fairly stable radical species was formed by the irradiation of I in the presence of iodine.

It was also found that only 253.7 mμ light was responsible for the formation of the radical intermediate as revealed by the ESR studies using light with various wavelengths. This specificity was further confirmed by the UV spectra measurements under irradiation. The spectral changes under irradiation with 253.7 mμ light are shown in Fig. 1. The appearance of peaks characteristic of II occurring at 260, 268, 280, 292, 320 and 335 mμ after about 3.5hr clearly demonstrated the formation of II. At the same time, if an equimolar or more of iodine was present, the absorbance of the iodine band at 525 mμ showed a marked decrease with the progress of the reaction as shown in Fig. 1. No changes in the spectrum occurred by the irradiation with other lines. From these experiments, it was confirmed that the reaction was initiated by the light of 253.7 mμ and that the excitation of a long wave band of iodine was not effective to bring about the cyclization.

Several mechanisms are conceivable for the facile transannular reaction of I. In view of the appearance of a rather stable radical intermediate, abstraction of 8,16-hydrogen occurred most probably in a stepwise manner. Excited I could react with iodine to give a cation radical or analogous species, of which further dehydrogenation would lead to II.

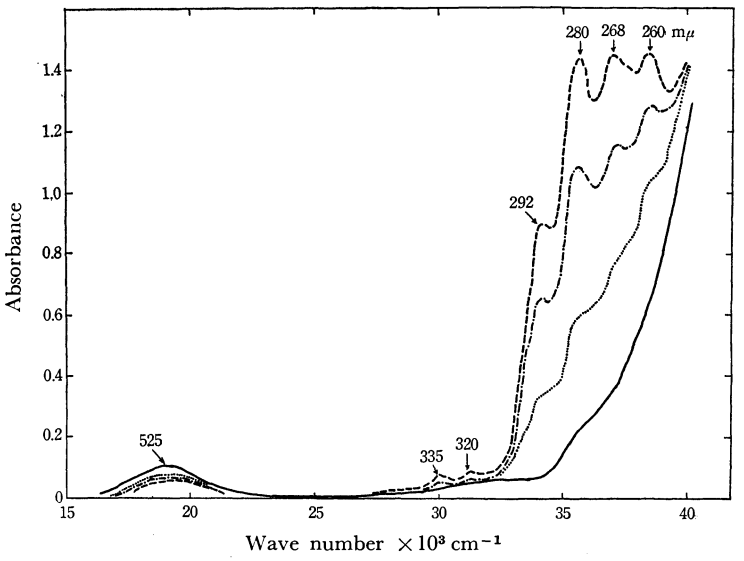

Fig. 1. Change of the absorption spectra of [2.2]metacyclophane (1.3×10^{-4} M) and iodine (0.3×10^{-3} M) in a cyclohexane solution upon irradiation for 69 (·····), 205 (-·-·-) and 330 min (----). The spectrum of the original solution is also shown (——).

26) H. Blaschke and V. Boekelheide, *J. Am. Chem. Soc.*, **89**, 2747 (1967).

27) Details of the kinetic studies will be reported elsewhere by one of the authors (S. H.).

Excitation of iodine at the short wave band might also lead to a similar pathway. Since a mixture of I and iodine in cyclohexane showed a weak charge-transfer band at 280 mμ, excitiation of the complex could also be the initial step of the reaction. On the other hand, the participation of σ-complex would not be likely when one considers the instability of the iodinated aromatic compounds toward irradiation,[1,28] thus our original scheme[7] became unattractive. Although the data at hand strongly suggested the participation of iodine in the initial stage of the reaction, the choice among the absorbing species could not be achieved. The quantum yield of this reaction was found to be 0.016[27] with unfiltered light.

Obviously the cyclization is facilitated by the proximity of two benzene rings which are separated only by 2.689 Å.[29] As expected no reaction occurred when bibenzyl, an open-chain model of I, was irradiated under the conditions described above. The driving force of the reaction might be sought in the highly strained nature of the metacyclophane structure which is relieved by going into bicyclic.

5,13-Dimethyl[2.2]metacyclophane (VIII) has been shown to react similarly to give 2,7-dimethyl-4,5,9,10-tetrahydropyrene (IX).[30] The occurrence of the transannular reaction with the metacyclophane derivative, of which 5- and 13-positions are blocked by methyl groups, also excludes the possibility of the participation of the σ-complex.

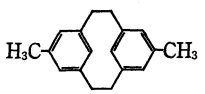

VIII

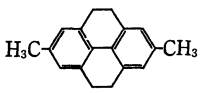

IX

Boekelheide and his co-workers[31] have observed a photochemical equilibrium between *trans*-15,16-dimethyldihydropyrene (X) and 8,16-dimethyl-[2.2]metacyclophane-1,9-diene (XI). It appeared to be of interest to attempt the photocyclization

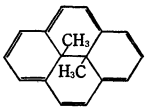

X

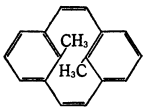

XI

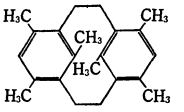

XII

reaction with 8,16-dimethyl derivative such as XII. The hexamethyl[2.2]metacyclophane has, however, been recovered unchanged by the photolysis experiments carried out as above.[30]

Experimental

Light Sources. For preparative experiments, a 1-kW high-pressure mercury arc lamp, Wako HBC-1000, was used. Cyclohexane solutions were irradiated externally in a quartz tube under the selected conditions by being immersed in a water bucket which housed the light source. Cooling was achieved by running water.

For the measurements of the ESR and UV spectra under irradiation a 100-W Toshiba SHL-100 UV lamp was used. The specific lines were selected by using a combination of glass filters (Toshiba and Hoya filters; UV-D25, UV-29, UV-DlC, V-Y48) and nickel sulfate solution (100 g/300 m*l*).

Spectra Measurements. UV spectra were recorded with Shimadzu RS autorecording spectrophotometer or Hitachi EPU-2 spectrophotometer. ESR spectra were recorded with Japan Electron Optics Co., X-band, ESR instrument model JES-3B type. Deaerated cyclohexane solutions were used for the measurements.

The Photolysis of [2.2]Metacyclophane (I). As a typical example, details of experiment No. 7 are given below. A mixture of 50 mg (0.25 mmol) of I, 63 mg (0.25 mmol) of iodine and 70 mg (8.3 mmol) of sodium bicarbonate in 30 m*l* of cyclohexane was irradiated for 20 hr under a nitrogen current. After the reaction was over, the mixture was successively washed with water, sodium thiosulfate solution and water. After drying over magnesium sulfate, the solution was concentrated. By column chromatography on alumina using *n*-hexane as an eluent, there were isolated three fractions, which consisted of 62.0% of II, mp 138°C, 26.7% of III, mp 132°C, and 11.3% of IV, mp 150°C (in the order of elution from the column). They were characterized by NMR and IR spectra and also by a direct comparison with the authentic materials.[6]

The authors are grateful to Professor T. Morita of Gunma University for his continued interest in this work.

28) W. Wolf and N. Kharasch, *J. Org. Chem.*, **30**, 2493 (1965).
29) C. J. Brown, *J. Chem. Soc.*, **1953**, 3278.
30) T. Sato, S. Akabori, N. Muto and K. Hata, *Tetrahedron*, **24**, 5557 (1968).
31) H.-R. Blattmann, D. Menche, E. Heilbronner, R. Molyneux and V. Boekelheide, *J. Am. Chem. Soc.*, **87**, 130 (1965).

BULLETIN OF THE CHEMICAL SOCIETY OF JAPAN VOL. 42 777—779 (1969)

Organic Syntheses by Means of Metal Complexes. III.[1] Cobalt Carbonyl-catalyzed Carbonylation of β-Propiolactone

Yoichi MORI and Jiro TSUJI

Basic Research Laboratories, Toyo Rayon Co., Kamakura

(Received July 10, 1968)

It was found that the carbonylation of β-propiolactone can be carried out in the presence of dicobalt octacarbonyl. Butyrolactone and succinic acid were obtained by the reaction of β-propiolactone with carbon monoxide and hydrogen. Succinic anhydride was obtained by the reaction with carbon monoxide.

β-Propiolactone (abbreviated as PL) is a reactive compound and undergoes many reactions. Its reactions can be classified into two types. One of them proceeds through the *O*-acyl fission (A) which is possible under basic conditions. On the other hand, under acidic conditions, the *O*-alkyl fission (B) occurs.[2]

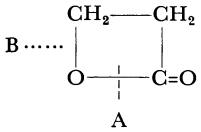

A

It seemed of interest to us to study the reaction of carbon monoxide with highly reactive PL. Carbon monoxide is also reactive and behaves as nucleophile or radical depending on the reaction conditions. It is known that carbon monoxide is activated most effectively by catalytic action of metal carbonyls, among which dicobalt octacarbonyl is well known catalyst of carbonylation of olefins and other unsaturated compounds. In addition, it catalyzes the carbonylation of epoxide which is a highly strained heterocyclic ring.[3] In view of the fact that PL is a highly strained reactive cyclic compound, the carbonylation of PL was attempted by the catalytic action of dicobalt octacarbonyl. It is known that active species in the dicobalt octacarbonyl-catalyzed carbonylation is cobalt tetracarbonyl hydride formed from dicobalt octacarbonyl and hydrogen. The cobalt hydride is strongly acidic. Therefore, it is expected that the carbonylation of PL catalyzed by dicobalt cotacarbonyl

$$Co_2(CO)_8 + H_2 \longrightarrow 2HCo(CO)_4 \qquad (I)$$

via the cobalt hydride in the presence of hydrogen should proceed through the *O*-alkyl fission, and carbon monoxide should be inserted into the *O*-alkyl bond to give a C_4 dicarbonyl compound.

Based on the above assumption, the reaction of PL with carbon monoxide and hydrogen in the presence of dicobalt octacarbonyl in benzene was attempted. In this reaction, hydrogen reacts with dicobalt octacarbonyl to give cobalt tetracarbonyl hydride (I). Once the acidic hydride is formed, then it is reasonable to assume that the *O*-alkyl fission of PL is possible to form a cobalt-alkyl complex, followed by carbon monoxide insertion to give succinic acid aldehyde as final product. However, contrary to the expectation, the product actually obtained by the reaction of PL with carbon monoxide and hydrogen was not the aldehyde. Instead, butyrolactone and succinic acid were isolated from the reaction mixture in a total yield of about 80% based on PL. The ratio of these two products changed depending on the reaction conditions. It is not easy to define which factor favors the formation of either product. The results are shown in Table 1. The result shows that the alcohol and acid were formed instead of the expected aldehyde by the ring opening reaction of PL with carbon monoxide and hydrogen.

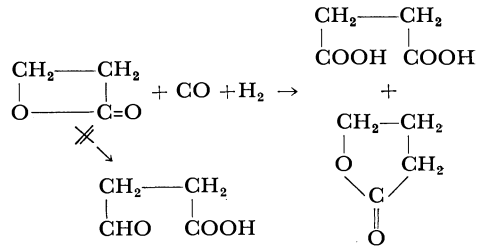

Then the reaction of PL with carbon monoxide in the absence of hydrogen was tried. By the reaction in benzene carried out at 150°C, two products

1) Part II: J. Tsuji and Y. Mori, This, Bulletin, in press.

2) T. L. Gresham, J. E. Jansen, F. W. Shaver and J. T. Gregory, *J. Am. Chem. Soc.*, **70**, 999, 1001, 1003, 1004 (1948).

3) C. Yokokawa, Y. Watanabe and Y. Takegami, This Bulletin, **37**, 667 (1964); J. L. Eisenmann, R. L. Yamartino and J. F. Howard, *J. Org. Chem.*, **26**, 2102 (1961).

Table 1. Reactions of PL with carbon monoxide and hydrogen*

Solvent	Pressure: Carbon monoxide atm	Pressure: Hydrogen atm	Reaction time hr	Products: γ-Butyrolactone g(%)	Products: Succinic acid g(%)
Benzene	50	50	18	2.53(36.9)	2.26(23.9)
Benzene	50	100	18	1.93(28.1)	
Benzene	80	40	18	3.16(45.1)	2.30(24.3)
Benzene	80	40	4	3.12(45.5)	3.63(38.4)
Cyclohexane	80	40	4	0.74(10.8)	5.33(56.5)

* The reactions were carried out with PL (5.75 g), solvent (30 ml) and dicobalt octacarbonyl (0.7 g) at 150°C.

were isolated. One of them was identified as acrylic acid. Apparently acrylic acid was formed by the ring opening of PL without reacting with carbon monoxide. The other product was confirmed to be succinic anhydride. Thus carbon monoxide was inserted into the *O*-alkyl bond.

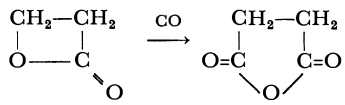

The following mechanisms are proposed for the dicobalt octacarbonyl-catalyzed carbonylation of PL. The reaction of cobalt tetracarbonyl hydride and PL gives the alkyl cobalt complex *via* *O*-alkyl fission. This is reasonable because cobalt hydride is acidic. The alkyl complex is subjected to carbon monoxide insertion to give the acyl complex. The acyl complex is split with either hydrogen or cobalt tetracarbonyl hydride to give aldehyde and dicobalt octacarbonyl. Alcohol is formed by the hydrogenation of the aldehyde or directly from the acyl complex. Then γ-hydroxybutyric acid is converted into the lactone with the liberation of water.

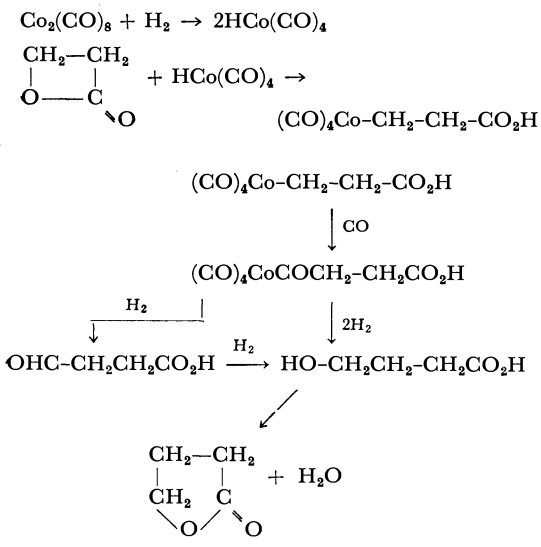

The formation of succinic acid can be explained by the cyclization of the acyl complex as shown below. In the presence of water formed by the lactone formation, succinic anhydride is hydrolyzed to give succinic acid.

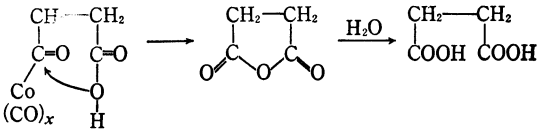

A possible path of the formation of succinic anhydride in the absence of hydrogen is the following. In this reaction cobalt hydride is not formed and the *O*-alkyl fission reaction of PL with dicobalt octacarbonyl gives the following alkyl complex. The carbon monoxide insertion into the alkyl cobalt bond gives acyl complex which cyclizes to give anhydride and dicobalt octacarbonyl.

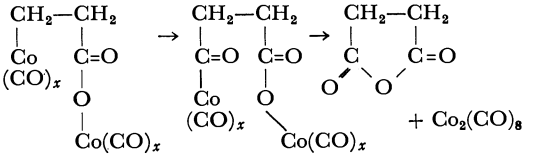

The possibility that the reaction proceeds through the intermediate formation of acrylic acid from PL can be ruled out by the fact that an attempted oxo reaction of acrylic acid under the similar reaction conditions did not proceed and unchanged acrylic acid was recovered almost quantitatively. Therefore the selective introduction of carbon monoxide at β-position of PL should be possible through the intermediate complex formed by the *O*-alkyl fission of PL with cobalt catalyst.

Experimental

Materials. Commercially available PL was used without purification. Dicobalt octacarbonyl was synthesized by the known method.

Reaction of PL with Carbon Monoxide and Hydrogen. Benzene (30 ml), PL (5.75 g) and dicobalt octacarbonyl (0.7 g) were mixed in a glass vessel equipped with a gas inlet capillary and the glass vessel was placed in an autoclave. Carbon monoxide

(80 atm) and hydrogen (40 atm) were charged and the reaction was carried out at 150°C for 4 hr with shaking. A pressure drop of 35 atm was observed. The solvent was removed by distillation from the reaction mixture, and butyrolactone (3.12 g, 45.5%) was isolated by distillation at 91—94°C/20 mmHg. The residue was recrystallized from ether and succinic acid was isolated (3.63 g, 38.4%). Both products were indentified with authentic samples by IR spectra.

Reaction of PL with Carbon Monoxide. Benzene (30 m*l*), PL (5.75 g) and dicobalt octacarbonyl (0.7 g) were mixed in the autoclave as shown above and allowed to react with carbon monoxide (100 atm) at 150°C for 4 hr and pressure drop of 4 atm was observed. Distillation of the reaction mixture gave acrylic acid (1.08 g, 18.8%) and succinic anhydride (2.37 g, 29%, 99°C/2 mmHg). The latter solidified on standing, mp 117—119°C.

BULLETIN OF THE CHEMICAL SOCIETY OF JAPAN VOL. 42 779—781 (1969)

Polymerization of Naphthalene and Reactions of Polynaphthalene

Hiroshi MINATO,[1]* Nobuyuki HIGOSAKI and Chieko ISOBE

Department of Chemistry, International Christian University, Mitaka, Tokyo

(Received July 13, 1968)

Naphthalene was polymerized by use of anhydrous aluminum chloride. The polynaphthalene formed was soluble in various organic solvents. The molecular weight determination suggested that the average degree of polymerization was six. The NMR spectrum indicated the presence of non-aromatic hydrogens, and the elemental analysis roughly corresponded with $(C_{10}H_8)_n$. The reactions of the polymer was examined such as hydrogenation, bromination, thermal dehydrogenation, chloromethylation and epoxidation.

Kovacic and his coworkers reported on the reactions of various aromatic hydrocarbons such as benzene, toluene, xylene and naphthalene with Lewis acids and oxidizing agents.[1)] From benzene, polyphenyls were obtained, which were insoluble and infusible. Naphthalene was let to react in *o*-dichlorobenzene with Lewis acids and oxidizing agents, and 1,1'-, 1,2'- and 2,2'-binaphthayls were obtained.

We have been interested in two-step polymerizations of various compounds, and have examined the possibility of performing the addition and the oxidation separately in order to obtain a soluble and fusible polymer.

It was found that benzene, toluene and xylene yields very little polymer when oxidizing agents were not present. However, it was found that naphthalene was converted into polynaphthalene in quite a good yield when it was let to react with anhydrous aluminum chloride without solvent. The results of this polymerization and the reactions of the polymer obtained will be described in this paper.

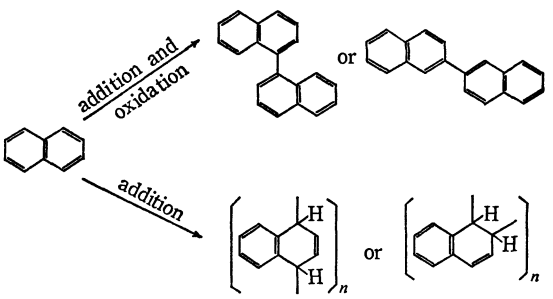

Experimental

Reagents. Naphthalene used was commercially available extra pure grade naphthalene. Anhydrous aluminum chloride used was commercially available extra pure grade.

Polymerization of Naphthalene. *Procedure A.* Naphthalene, 160 g, was ground in a porcelain mortar and placed in a 500 m*l* three-necked round-bottomed flask. Anhydrous aluminum chloride, 11 g, was also finely powdered and added. They were stirred under a nitrogen atmosphere. When the temperature was raised to 70—72°C, the mixture melted and became homogeneous. The reaction was exothermic at the first stage, and no sooner the reaction started than the color of the mixture started to darken. The reaction mixture was kept at 73—72°C for two hours. The

*1 To whom correspondence should be addressed at Department of Chemistry, Tokyo Metropolitan University, Setagaya, Tokyo.

1) P. Kovacic and J. Oziomek, *J. Org. Chem.*, **28**, 968 (1963); P. Kovacic and J. Oziomek, *ibid.*, **29**, 101 (1964); P. Kovacic, F. W. Koch and C. E. Stephan, *J. Polymer Sci.*, **2A**, 1193 (1964); P. Kovacic and M. Kyriakis, *J. Am. Chem. Soc.*, **85**, 456 (1963); P. Kovacic and C. Wu, *J. Org. Chem.*, **26**, 767 (1961); P. Kovacic and F. W. Koch, *ibid.*, **30**, 3176 (1965).

TABLE 1. POLYMERIZATION OF NAPHTHALENE

Procedure	Naphthalene g (mol)	Aluminum chloride, anhydrous g (mol)	Mol% $AlCl_3$	Temp. °C	Time hr	Yield g (%)
A	160 (1.25)	11 (0.0825)	6.2	73—75	2	56.0 (35.0)
B	96 (0.748)	25.5 (0.191)	20.3	80—90	2.5	81.0 (84.4)

black product was a viscous liquid at the reaction temperature and solidified at room temperature. The product was all transferred to a 1-*l* round-bottomed flask to which 500 m*l* of water was added. The naphthalene which remained unreacted was steam-distilled out to a receiver through an air condenser. The steam ditillation was continued for 4 hr. The water was discarded, and another 500 m*l* of fresh water was added to run the second distillation for four hours. The same procedure was carried out for the third distillation. After the third distillation, the black product was added in 200 m*l* of warm benzene, and the product completely dissolved. After cooling anhydrous sodium sulfate was added, and the solution was allowed to stand overnight. After the filtration of the sodium sulfate, benzene was evaporated to yield 56 g of a product. The product was a viscous tar-like substance with cohesive properties. The solubility of the product in petroleum ether was 0.154 g/100 m*l* at 27°C.

Procedure B. The procedure was the same as in Procedure A except the quantities of the reagents and the experimental conditions as Table 1 shows. Analyses of the polymers produced by two procedures indicated that the structure and the properties of these polymers were similar. The polymer produced by Procedure A was subjected to various reactions and analyses.

Purification. Naphthalene polymer, 15 g, was dissolved in 10 m*l* of benzene. The solution was added drop by drop into 200 m*l* of petroleum ether with stirring. The naphthalene polymer was dispersed to yield fine, dark brown precipitates which accumulated at the bottom of the beaker. The precipitates were filtered by use of a glass filter, dried and ground in a mortar. Brown powder, 7.0 g was obtained. The weight percent yield was 47%. Again the brown powder was dissolved in 5 m*l* of benzene, and the benzene solution was added dropwise into a 200 m*l* of stirred petroleum ether. Almost all of the substance was recovered in the second precipitation. For the investigation of the structure, further purification was tried. The polymer, 6.5 g, obtained by the above purification, was shaken three times with 100 m*l* of 5% $NaHCO_3$, three times with 100 m*l* of 5% HCl, and three times with 100 m*l* of distilled water. Anhydrous sodium sulfate was added to the benzene solution, and the solution was allowed to stand overnight. The filtered benzene solution was added dropwise to 400 m*l* of stirred petroleum ether. The benzene solution was dispersed to yield brown precipitates. The precipitates were filtered and dried. The final product obtained was 3.5 g and the percentage yield in this prification was 54%.

Results and Discussion

The Analyses of the Polymer. The NMR spectrum of the naphthalene polymer is shown in Fig. 1. The absorptions at 1.9 ppm and 2.9 ppm are due to aliphatic hydrogens. Since there are two peaks instead of one, the 1,2-dihydro-structure seems to predominate in the polymer. The 1,2-dihydro-structure has two kinds of aliphatic hydrogens and the 1,4-dihydro-structure has one kind of aliphatic hydrogen.

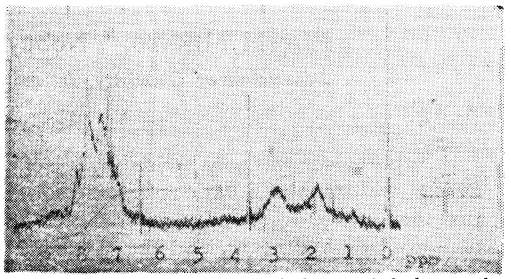

Fig. 1. NMR spectrum of the naphthalene polymer in CCl_4 (reference, tetramethylsilane: 60 Mc).

The results of the elemental analysis of the polymer is summarized in Table 2.

These results indicate the presence of some non-hydrocarbon materials, presumably aluminum chloride. The carbon hydrogen contents correspond with the formula $C_{10}H_{7.37}$. The small difference between this value and theoretical value $C_{10}H_8$ can be ascribed to the dehydrogenation of the polymer, which is likely to take place to some extent even in the absence of any oxidizing agent.

The molecular weight of the polymer was determined by an Osmometer Model 301, Microlab. The determination in chloroform showed that the molecular weight was 761. Since the molecular weight of ($C_{10}H_8$) is 769, the average degree of polymerization of this napthalene polymer is six.

In order to estimate the number of olefinic double bonds, catalytic hydrogenation of the polymer was carried out by use of platinum oxide. The benzene solution of the polymer was treated with hydrogen for three hours at 28°C/1 atm. Two determinations were carried out independently, and it was found that no hydrogen was absorbed in both cases. The failure of the hydrogenation may be ascribed to the bulkiness of the polymer molecule and the steric hindrance as to the olefinic double bonds.

The polymer was brominated with KBr-$KBrO_3$ in acetic acid according to the method of Johnson and Clark.[2] A $C_{10}H_8$ unit absorbed 0.40 bromine

2) H. L. Johnson and R. A. Clark, *Anal. Chem.*, **19**, 869 (1947).

TABLE 2. ELEMENTAL ANALYSIS OF NAPHTHALENE POLYMER

	C%	H%	C%+H%	C%/C%+H%	H%/C%+H%
Found	92.30	5.71	98.01	94.18	5.82
Calcd for $C_{10}H_8$	93.71	6.29	100		
Calcd for $C_{10}H_6$	96.00	4.00	100		

molecule in one hour, but after several hours the absorption only increased to 0.43. Theoretically every $C_{10}H_8$ unit of the polymer should absorb 1.0 molecule of bromine.

When the naphthalene polymer was heated in air, it softened near 60°C, and the color darkened at 160—170°C. While being heated, it apparently was aromatized. At 300°C, it was rather hard solid which could be pressed or moved by a spatula. It was thermally very stable and the weight did not decrease at all when heated for 90 min at 220°C and then for 90 min at 290°C. When it was heated for 6 hr at 320°C, some dehydrogenation took place, and the elemental analysis of the polymer indicated that the structure was $(C_{10}H_{5.82})_n$. The analysis shows that some naphthalene units are bound by more than one linkage.

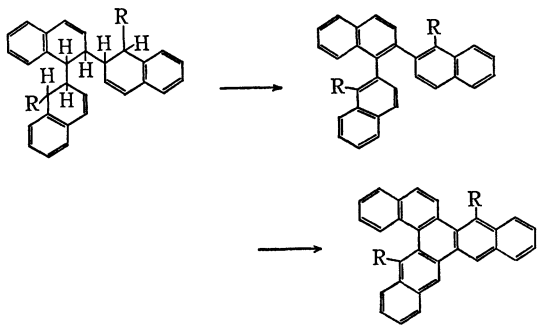

Reactions of the Naphthalene Polymer. *Oxidation with Potassium Permanganate.* The naphthalene polymer was refluxed in an alkaline potassium permanganate solution for 2 hr. The IR spectrum of the product was identical with that of the naphthalene polymer itself. The softening point (about 60°C) of the product was the same as that of the original polymer. It was, therefore, concluded that the naphthalene polymer was not oxidized with the reagent under the conditions mentioned above.

Chloromethylation. The naphthalene polymer was chloromethylated with polyoxymethylene and hydrogen chloride by the usual procedure. The chlorine analysis of the product showed 5.42% chlorine. Since the theoretical value was 20.1%, 27.0% of the initial polymer units was chloromethylated. The IR spectrum showed a new band at 1000 cm^{-1}.

Hydrolysis of the Chloromethylated Polymer. The chloromethylated polymer which was not separated from the unreacted naphthalene polymer was hydrolysed with a potassium carbonate solution. The IR spectrum of the hydrolysis product showed a new band at 1070 cm^{-1} which did not appear in the spectrum of the chloromethylated polymer, while the absorption band at 1000 cm^{-1} in the spectrum of the chloromethylated polymer greatly decreased. The absorption band at 1070 cm^{-1} was assigned to C–O of primary alcohol, and an absorption band due to O–H of primary alcohol appeared at 3400 cm^{-1}.

Epoxidation. The naphthalene polymer was epoxidized according to the method described for the epoxidation of styrene.[3] When the polymer was let to react with perbenzoic acid in benzene at 15°C, the peracid consumed for epoxidation was 71.7% at 113 hr, 78.1% at 165.5 hr and 88.1% at 573.5 hr (after the correction for blanks). In order to remove benzoic acid, the epxoidized polymer solution was treated with 5% sodium bicarbonate solution. Unexpectedly, the epoxidized naphthalene polymer was extracted into the aqueous layer after several extractions. When the alkaline solution was neutralized with hydrochloric acid, brown precipitates were obtained which were benzoic acid and phenolic polymers. Apparently the following reactions took place.

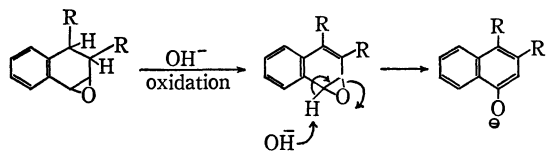

Attempts were made in order to remove benzoic acid without destruction of epoxy group, but in vain. The naphthalene polymer did not form its picrate; the sublimation of benzoic acid resulted in the destruction of the epoxy ring; the column chromatography resulted in the decomposition of the epoxy ring.

In order to have the easier separation of the carboxylic acid after the epoxidation, monoperphthalic acid was used. The rate of epoxidation was a little slower than that with perbenzoic acid, and 39.7% of the peracid was consumed after 44 hr. Phthalic acid precipitated was easily filtered.

The epoxidized naphthalene polymer was mixed with aniline-phenol-formaldehyde resin in the weight ratio of 1 : 0.43, and the mixture was heated at 160°C for 30 min. The mixture solidified completely due to the cross-linking.

3) *Organic Reactions*, **1**, 70 (1954).

BULLETIN OF THE CHEMICAL SOCIETY OF JAPAN VOL. 42 782—789 (1969)

Studies of Peptide Antibiotics. XIV. Analogs of Gramicidin S Containing D-Valine or D-Leucine in Place of D-Phenylalanine

Haruhiko Aoyagi,[1] Tetsuo Kato, Michinori Waki, Okitoshi Abe, Reiko Okawa, Satoru Makisumi and Nobuo Izumiya[2]

Laboratory of Biochemistry, Faculty of Science, Kyushu University, Hakozaki, Fukuoka

(Received July 15, 1968)

Two analogs of gramicidin S, 4,4'-D-valine- and 4,4'-D-leucine-gramicidin S (XVI-A and XVI-B), have been synthesized and tested for the antibacterial properties. The crude product obtained after the cyclization of a linear pentapeptide active ester was composed of the protected monomer and dimer. The pure protected dimer was obtained by a column chromatography of Sephadex LH-20, and the hydrogenolysis of this product in the presence of hydrogen chloride afforded the crystalline hydrochloride of XVI-A or XVI-B. These analogs were as active as natural gramicidin S; the results indicated that the aromatic side chains of the D-phenylalanines in the molecule of gramicidin S can be replaced by the aliphatic side chains without an influence for the activity.

In connection with a series of studies in this laboratory on a significance of the side chains of the amino acid residues of gramicidin S (Fig. 1)

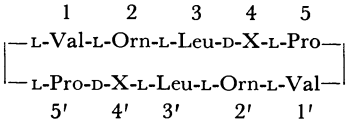

Fig. 1. Structure of gramicidin S (GS) and its analogs. X represents an amino acid residue such as Phe (GS), Val (XVI-A) or Leu (XVI-B).

to its antibacterial activity, it has been reported in the previous paper that an analog of the antibiotics was prepared in which the benzyl groups of D-phenylalanine residues in 4- and 4'-positions of the molecule were replaced by the hydrogens of glycines, and 4,4'-glycine-gramicidin S thus prepared was found to possess almost no activity toward several microorganisms.[3] From this finding, it appeared that the side chains of D-phenylalanines in the sequence of gramicidin S are of considerable importance for an exhibition of the activity. In order to investigate an effect of replacing the benzyl side chains of D-phenylalanines by the aliphatic side chains of D-valines or D-leucines, we attempted to prepare several analogs of gramicidin S. The present paper will describe the syntheses and antibacterial properties of 4,4'-D-valine- and 4,4'-D-leucine-gramicidin S besides the preparations of the cyclic pentapeptides, 4-D-valine- and 4-D-leucine-cyclosemigramicidin S.

It would be noteworthy that D-valine residue is a constituent in several natural antibiotics such as actinomycins and fungisporin, and D-leucine residue in etamycin, esperin and malformin.[4] Some peptide antibiotics such as sporidesmolide I[4] and gramicidin A[5] contain both D-valine and D-leucine as a constiuent. The closely related polymyxin B_1 or E_1 has been shown to be homodetic cyclic decapeptide wherein an amino group of the molecule is acylated with 6-methyl-octanoic acid. Of special interest in connection with the present paper was the fact that polymyxin E_1 differs from polymyxin B_1 in having an D-leucine-residue in place of the D-phenylalanine at 6-position of polymyxin B_1.[6]

Since the cyclization of H-Val-Orn(δ-Z)-Leu-Gly-Pro-ONp[7] afforded exclusively the benzyloxycarbonyl-substituted dimer through the doubling reaction,[3] the syntheses of the protected cyclic decapeptides (XIV-A and -B) were attempted by possible dimerization reaction of the pentapeptide

1) Present address: Department of Chemistry, Case Western Reserve University, Cleveland, Ohio, U. S. A.

2) To Whom the inquiries should be addressed.

3) R. Nagata, M. Waki, M. Kondo, H. Aoyagi, T. Kato, S. Makisumi and N. Izumiya, This Bulletin, **40**, 963 (1967).

4) E. Schröder and K. Lübke. "The Peptides," Vol. 2, Academic Press, New York and London (1966), p. 396.

5) R. Sarges and B. Witkop, *J. Am. Chem. Soc.*, **86**, 1861, 1862 (1964).

6) T. Suzuki, H. Inouye, K. Fujikawa and S. Nagasawa, *J. Biochem.*, **54**, 173 (1963); S. Wilkinson and L. A. Lowe, *Nature*, **204**, 185, 993 (1964).

7) The following abbreviations are from *Biochmistry*, **5**, 2485 (1966); Z-, benzyloxycarbonyl; Z(OMe)-, *p*-methoxybenzyloxycarbonyl; ONp, *p*-nitrophenoxy. Amino acid symbols except D-Phe, D-Val or D-Leu denote the L configuration.

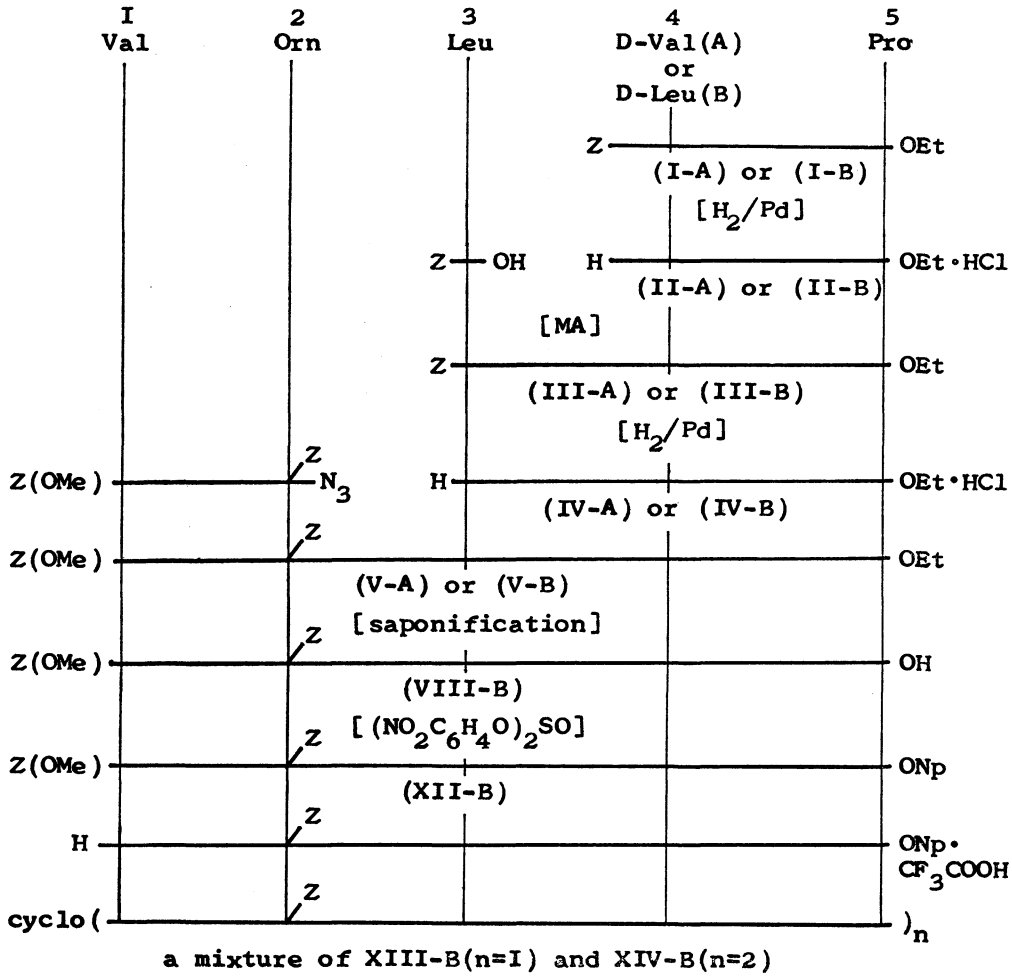

Fig. 2. Cyclization of linear pentapeptide active ester containing D-Leu.

active esters (XII-A and -B) as shown in Figs. 2 and 3. To obtain an acylpentapeptide acid (VIII-A or -B) which is a starting material for the active ester, the corresponding acylpentapeptide ethyl ester was subjected to the saponification; the reaction of the acylpeptide ester (V-B) containing D-leucine proceeded smoothly to afford the acylpeptide acid (VIII-B) in a good yield, whereas the ester (V-A) containing D-valine was found to resist for the saponification reaction. In this connection, it would be noteworthy that several investigators have reported the resistance of a peptide ester containing valine or isoleucine residue for the saponification.[8,9] Therefore, the acylpentapeptide acid (VIII-A) containing D-valine was prepared by the condensation of Z(OMe)-Val-Orn(δ-Z)-N_3 with neutral tripeptide (VII-A). Acyltripeptide acid (VI-A) which is a material for the neutral tripeptide was prepared by the saponification of acylpeptide ester (III-A) without any difficulty though the ester contained a valine residue.

The treatment of an acylpentapeptide acid (VIII-A or -B) with di-p-nitrophenyl sulfite gave an amorphous acylpeptide active ester, and its p-methoxybenzyloxycarbonyl group was removed by the action of trifluoroacetic acid. The pentapeptide active ester trifluoroacetate obtained was treated with a large amount of pyridine (concentration of the ester in pyridine, 3×10^{-3} M). After the evaporation of the reaction mixture, the residue dissolved in aqueous methanol was treated with columns of Dowex 1 and 50 to be free from the undesired products. The subsequent evaporation of the effluent yielded a semi-solid residue which was found to be a mixture of the protected monomer (XIII-A or -B) and dimer (XIV-A or -B). Attempts to separate the components in the residue by the fractional crystallization with methanol-ether failed because of no appreciable difference in solubility between

8) R. Sarges and B. Witkop, *J. Am. Chem. Soc.*, **87**, 2020 (1965).

9) T. Kato and N. Izumiya, This Bulletin, **39**, 2242 (1966).

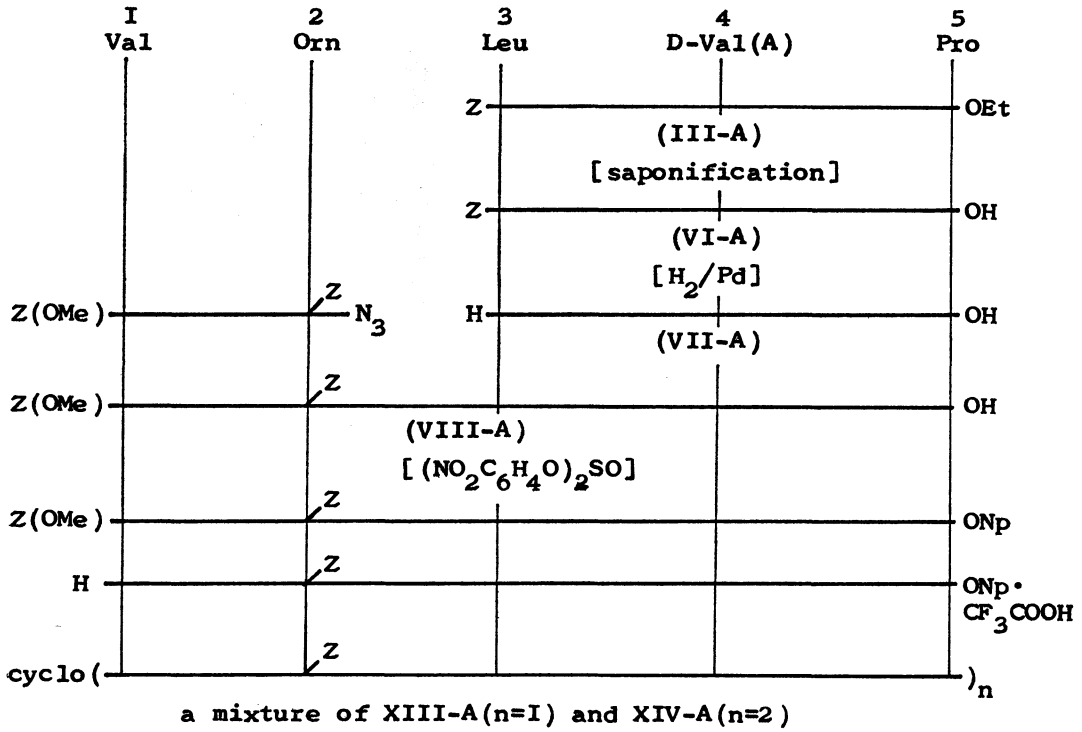

Fig. 3. Cyclization of linear pentapeptide active ester containing D-Val

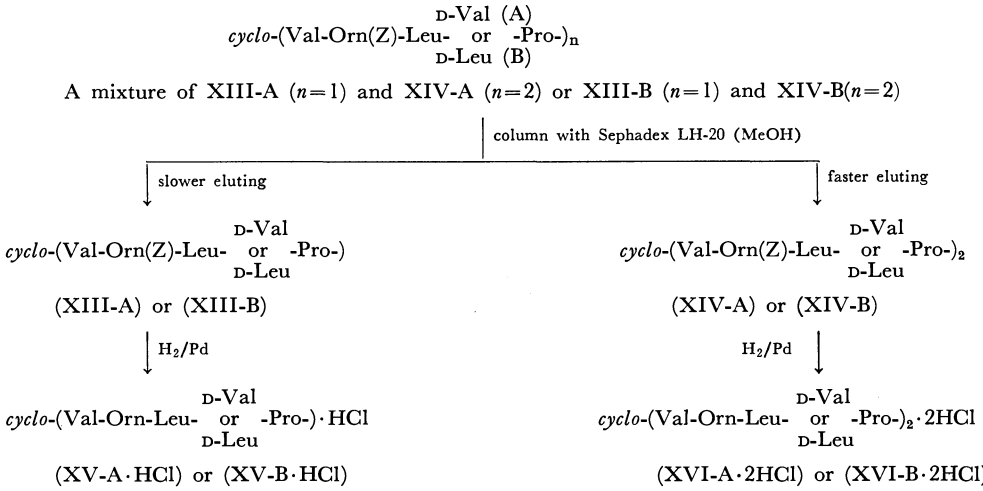

Fig. 4. Separation of the protected monomer and dimer, and preparation of the required GS and cyclosemi GS analogs.

the two components.[10] The separation of the components was achieved by the use of a Sephadex LH-20 column with methanol as an eluting solvent; the protected dimer (XIV-A or -B) was obtained from the faster eluting fraction, and the monomer (XIII-A or -B) from the slower fraction (Fig. 4). The weight ratio of both components calculated

10) In the previous papers, we reported that the pure protected GS,[11] diZ-substituted [Lys$^{2,2'}$]-GS or [Dba$^{2,2'}$]-GS[12] was obtained easily by the fractional crystallization from the mixture of the protected cyclic decapeptide and pentapeptide because of the great difference between their solubilities.

11) M. Waki and N. Izumiya, This Bulletin, **40**, 1687 (1967).

12) M. Waki, O. Abe, R. Okawa, T. Kato, S. Makisumi and N. Izumiya, *ibid.*, **40**, 2904 (1967).

Table 1. Ratio of protected monomer and dimer after cyclization of linear pentapeptide active esters

p-Nitrophenyl ester of[a]	Ratio of compounds in product[b] Z-cyclic monomer	diZ-cyclic dimer
H-Val-Orn(Z)-Leu-D-Phe-Pro-OH[11]	32	68
-Gly-[3]	0	100
-D-Val-	17	83
-D-Leu-	15	85

a) After the first compound listed, only variation of the residue will be shown.
b) The concentrations of linear pentapeptide *p*-nitrophenyl esters in pyridine were $\sim 3 \times 10^{-3}$ M.

are shown in Table 1 with the previous results related to the present paper.

To establish the structure of the protected dimer containing D-leucine derived from the linear pentapeptide active ester, a linear decapeptide active ester was cyclized to yield a benzyloxycarbonyl substituted cyclic decapeptide as shown in Fig. 5. Then the properties of the obtained crystals (XIV-B in Fig. 5) agreed well with that of the protected dimer (XIV-B in Fig. 4).

The hydrogenolysis of each of the protected peptides in the presence of an equivalent hydrogen chloride yielded a crystalline hydrochloride of the required cyclic peptide (XV-A, -B, XVI-A or -B). The antibacterial activities of these peptides toward several microorganisms were further examined (Table 2). It was found that the two cyclosemigramicidin S analogs (XV-A and -B) exhibited no antibacterial activities as same as cyclosemigramicidin S itself[11] and its analogs replaced by glycine[13] or sarcosine[14] at 5-position

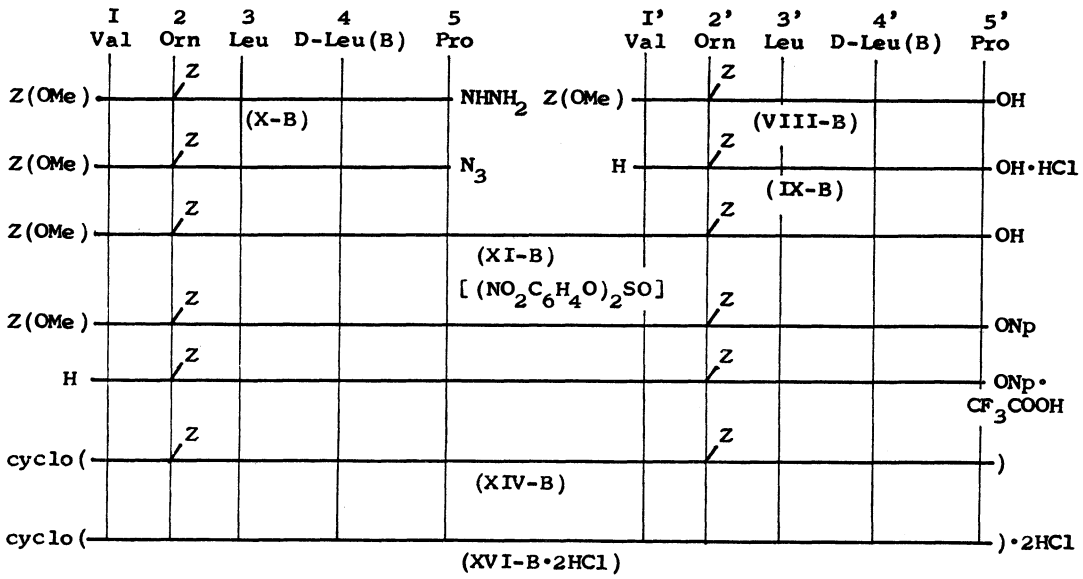

Fig. 5. Cyclization of linear decapeptide active ester.

Table 2. Inhibitory activity of the compounds on microorganisms
Minimum inhibitory concentration, $\mu g/ml$[a]

	Escherichia coli	*Proteus vulgaris*	*Staphylococcus aureus*	*Bacillus subtilis*	*Mycobacterium avium*
GS	>100	>100	5	5	>100
[D-Val[4]]-semiGS (XV-A)	>100	>100	>100	>100	>100
[D-Leu[4]]-semiGS (XV-B)	>100	>100	>100	>100	>100
[D-Val[4,4']]-GS (XVI-A)	>100	>100	10	10	>100
[D-Leu[4,4']]-GS (XVI-B)	>100	>100	10	5	>100

a) The same results were obtained with an usual bouillon agar medium (pH 7.0) and a Stephenson-Whetham's synthetic medium.

13) H. Aoyagi, M. Kondo, T. Kato, S. Makisumi and N. Izumiya, *ibid.*, **40**, 1685 (1967).
14) H. Aoyagi and N. Izumiya, *ibid.*, **39**, 1747 (1966).

of the molecule. On the other hand, 4,4'-D-valine- and D-leucine-gramicidin S were as active as the natural gramicidin S against several microorganisms. The results indicated that the aromatic side chains of D-phenylalanine residues of 4- and 4'-position can be replaced by the bulky aliphatic side chains such as isopropyl and isobutyl groups without any influence in the activity.

Experimental

All melting points are uncorrected.

Z-D-Val-Pro-OEt (I-A). To a solution of benzyloxycarbonyl-D-valine[8] (5.02 g; 20 mmol) and L-proline ethyl ester *p*-toluenesulfonate[15] (6.30 g; 20 mmol) in chloroform (40 ml), there were stirred triethylamine (2.80 ml) and dicyclohexylcarbodiimide[16] (4.12 g) at 0°C. After it had been allowed to stand overnight at 0°C, the mixture was evaporated *in vacuo*, and ethyl acetate was added to the residue. After the dicyclohexylurea was filtered off, the filtrate was washed successively with 4% sodium bicarbonate, 3% hydrochloric acid and water, and dried over sodium sulfate. The filtrate was evaporated *in vacuo*; yield of oil, 3.99 g (58%); R_f, 0.95.[17]

Z-D-Leu-Pro-OEt (I-B). (a) This was obtained from oily benzyloxycarbonyl-D-leucine (6.92 g; 26 mmol) and L-proline ethyl ester *p*-toluenesulfonate (8.20 g; 26 mmol) as described above; yield of oil, 7.48 g (74%); R_f, 0.97.[17] (b) To a solution of benzyloxycarbonyl-D-leucine dicyclohexylammonium salt[18] (4.46 g; 10 mmol) and L-proline ethyl ester *p*-toluenesulfonate (3.15 g; 10 mmol) in chloroform (20 ml), there were stirred dicyclohexylcarbodiimide (2.02 g) at 0°C. After it had been allowed to stand overnight at 0°C, the mixture was treated as described above; yield, 3.06 g (78%); R_f, 0.97.[17]

H-D-Val-Pro-OEt·HCl (II-A). A solution of I-A (3.00 g; 8 mmol) dissolved in 0.48N methanolic hydrogen chloride (17.5ml) was subjected to hydrogenolysis in the presence of palladium black. The filtrate from the catalyst was evaporated to dryness *in vacuo;* yield of oil, 2.20g (99%); R_f, 0.75[17].

H-D-Leu-Pro-OEt·HCl (II-B). This was obtained from I-B (4.70g; 12mmol) as described above; yield of oil, 3.44g (98%); R_f, 0.65.[17]

Z-Leu-D-Val-Pro-OEt (III-A). Benzyloxycarbonyl-L-leucine dicyclohexylammonium salt[19] (3.57g; 8mmol) was coupled with II-A (2.23g; 8mmol) as described for the preparation of I-B (b). Yield of oil, 3.60g (92%); R_f, 0.92.[17]

Z-Leu-D-Leu-Pro-OEt (III-B). This compound was obtained from benzyloxycarbonyl-L-leucine dicyclohexylammonium salt (2.55g; 5.7mmol) and II-B (1.67g; 5.7mmol) as described above. The crude product was recrystallized from ethyl acetate - petroleum ether; yield, 2.02g (71%); mp 135°C; $[\alpha]_D^{22}$ −21.8° (*c* 1, DMF); R_f, 0.97.[17]

Found: C, 64.12; H, 8.30; N, 8.50%. Calcd for $C_{27}H_{41}O_6N_3$: C, 64.39; H, 8.21; N, 8.34%.

H-Leu-D-Val-Pro-OEt·HCl (IV-A). This was obtained from III-A (4.90g; 10mmol) as described for the preparation of II-A; yield of oil, 3.85g (98%); R_f, 0.70.[17]

H-Leu-D-Leu-Pro-OEt·HCl (IV-B). This was obtained from III-B (3.02g; 6 mmol); yield of oil, 2.44 g (100%); R_f, 0.67.[17]

Z(OMe)-Val-Orn(δ-Z)-Leu-D-Val-Pro-OEt (V-A). To a Z(OMe)-Val-Orn(δ-Z)-$NHNH_2$[20] (1.09g; 2mmol) dissolved in a mixture of acetic acid (20ml), dimethylformamide (10 ml) and 1N hydrochloric acid (4.4 ml) was added sodium nitrite (152mg) in water (1ml). After 6 min cold water (100ml) was added to the solution. The azide which precipitated was collected by filtration and washed with 4% sodium bicarbonate and water, and then dried *in vacuo*. The azide was added to a solution of IV-A (0.77 g; 2mmol) and triethylamine (0.28ml) in dimethylformamide (20 ml). The mixture was stirred for 3 days at 0°C and evaporated *in vacuo*. The precipitate which formed upon the addition of water was collected, washed successively with 4% sodium bicarbonate, 10% citric acid and water. It was recrystallized from methanol-dioxane-ether; yield, 1.17 g (69%); mp 180—183°C; $[\alpha]_D^{22}$ −10.8° (*c* 1, DMF); R_f, 0.92.[17]

Found: C, 62.49; H, 7.64; N, 9.92%. Calcd for $C_{45}H_{66}O_{11}N_6$: C, 62.33; H, 7.69; N, 9.69%.

Z(OMe)-Val-Orn(δ-Z)-Leu-D-Leu-Pro-OEt (V-B). The azide derived from Z(OMe)-Val-Orn(δ-Z)-$NHNH_2$ (3.26 g; 6 mmol) was condensed with IV-B (2.44 g; 6 mmol) and triethylamine (0.84 ml) as described above. The crude product was recrystallized from methanol - dioxane - ether - petroleum ether; yield, 4.04 g (77%); mp 142—144°C; $[\alpha]_D^{22}$ −11.0° (*c* 1, DMF); R_f, 0.88.[17]

Found: C, 62.46; H, 7.78; N, 9.76%. Calcd for $C_{46}H_{68}O_{11}N_6$: C, 62.70; H, 7.78; N, 9.53%.

Z-Leu-D-Val-Pro-OH (VI-A). To a solution of III-A (7.20 g; 14.7 mmol) in a mixture of methanol (40 ml) and dioxane (40 ml), 2N sodium hydroxide (11 ml) was added, and the solution was allowed to stand for 5 hr at 30°C. After the addition of 1N hydrochloric acid (23 ml), the solution was evaporated *in vacuo*. The oily product extracted with ethyl acetate (50 ml) and dried over sodium sulfate. The filtrate was evaporated *in vacuo*; yield of oil, 6.5 g (96%); R_f, 0.77.[17]

H-Leu-D-Val-Pro-OH (VII-A). A solution of VI-A (3.35 g; 7.3 mmol) in a mixture of acetic acid (15 ml), methanol (12 ml) and water (3 ml) was subjected to hydrogenolysis in the presence of palladium black. The

15) T. Kato, S. Makisumi, M. Ohno and N. Izumiya, *Nippon Kagaku Zasshi (J. Chem. Soc. Japan, Pure Chem. Sect.)*, **83**, 1151 (1962).

16) J. C. Sheehan and G. P. Hess, *J. Am. Chem. Soc.*, **77**, 1067 (1955).

17) The R_f values refer to the thin-layer chromatography with Merck silica gel G and to the *n*-butanol - acetic acid - pyridine - water (4 : 1 : 1 : 2, v/v) system. Compounds possessing a free amino group were detected by spraying them with ninhydrin, and those with blocked amino groups, by spraying them with 47% hydrobromic acid, and then with ninhydrin.

18) This compound was obtained according to the procedure for the L-isomer; mp 151—152°C, $[\alpha]_D^{22}$ +7.7° (*c* 2, MeOH). Values for the L-isomer;[19] mp 151.5—152°C; $[\alpha]_D^{20}$ −7.86° (MeOH).

19) E. Klieger, E. Schröder and H. Gibian, *Ann.*, **640**, 157 (1966).

20) T. Kato, M. Kondo, M. Ohno and N. Izumiya, This Bulletin, **38**, 1202 (1965).

filtrate was evaporated to dryness *in vacuo*; yield of oil, 2.26 g (95%); R_f, 0.72.[17]

Z(OMe)-Val-Orn(δ-Z)-Leu-D-Val-Pro-OH (VIII-A). The azide derived from Z(OMe)-Val-Orn(δ-Z)-$NHNH_2$ (3.80 g; 7 mmol) was added to a solution of VII-A (2.35 g; 7 mmol) and triethylamine (0.98 m*l*) in dimethylformamide (50 m*l*). The mixture was stirred for 3 days at 0°C and evaporated *in vacuo*. The residue was triturated with 10% citric acid, and the precipitate was collected by filtration and washed with water. It was recrystallized from methanol - ether - petroleum ether; yield, 4.02 g (65%); mp 173—175°C; $[\alpha]_D^{22}$ −12.2° (*c* 1, DMF); R_f, 0.82.[17]

Found: C, 60.41; H, 7.30; N, 10.04%. Calcd for $C_{43}H_{62}O_{11}N_6 \cdot H_2O$: C, 60.18; H, 7.53; N, 9.84%.

Z(OMe)-Val-Orn(δ-Z)-Leu-D-Leu-Pro-OH (VIII-B). To a solution of V-B (4.41 g; 5 mmol) in a mixture of methanol (20 m*l*) and dioxane (20 m*l*), 2 N sodium hydroxide (5 m*l*) was added, and the solution was allowed to stand for 4 hr at 30°C. After the addition of 10% citric acid (75 m*l*) under cooling, the solution was concentrated *in vacuo* at a low temperature, and the precipitate was collected by filtration. This was recrystallized from methanol - ether - petroleum ether; yield, 3.34 g (78%); mp 149—151°C; $[\alpha]_D^{22}$ −20.0° (*c* 1, DMF); R_f, 0.75.[17]

Found: C, 61.53; H, 7.70; N, 9.63%. Calcd for $C_{44}H_{64}O_{11}N_6 \cdot 1/2H_2O$: C, 61.30; H, 7.60; N, 9.75%.

H-Val-Orn(δ-Z)-Leu-D-Leu-Pro-OH·HCl (IX-B). To a solution of VIII-B (3.42 g; 4 mmol) in dioxane (40 m*l*), 4.0 N hydrogen chloride in dioxane (36 m*l*) was added at room temperature. After 2 hr, the solution was evaporated, and the residue was triturated with ether. The crystals were collected with the aid of ether; yield, 2.94 g (98%); mp 163—165°C; $[\alpha]_D^{18}$ −14.0° (*c* 0.5, DMF); R_f, 0.72.[17]

Found: C, 57.63; H, 7.84; N, 11.56%. Calcd for $C_{35}H_{57}O_8N_6Cl$: C, 57.95; H, 7.92; N, 11.59%.

Z(OMe)-Val-Orn(δ-Z)-Leu-D-Leu-Pro-$NHNH_2$ (X-B). To a solution of V-B (3.52 g; 4 mmol) in dimethylformamide (15 m*l*), hydrazine hydrate (4 m*l*) was added and the solution was allowed to stand for 7 days at 30°C. The solution was then concentrated *in vacuo* to a small volume. The hydrazide which precipitated upon the addition of water was collected and recrystallized from dioxane-ether; yield, 3.01 g (87%); mp 147—149°C; $[\alpha]_D^{18}$ −20.4° (*c* 1, DMF); R_f, 0.78.[17]

Found: C, 60.50; H, 7.62; N, 12.50%. Calcd for $C_{44}H_{60}O_{10}N_8 \cdot 1/2H_2O$: C, 60.24; H, 7.71; N, 12.79%.

Z(OMe)-Val-Orn(δ-Z)-Leu-D-Leu-Pro-Val-Orn-(δ-Z)-Leu-D-Leu-Pro-OH (XI-B). The azide derived from X-B (1.04 g; 1.2 mmol) was added to a solution of IX-B (0.87 g; 1.2 mmol) and triethylamine (0.33 m*l*) in dimethylformamide (20 m*l*). The crude product was obtained as described for the preparation of VIII-A and recrystallized from ethyl acetate - petroleum ether; yield, 1.54 g (67%); mp 148—151°C; $[\alpha]_D^{18}$ −34.0° (*c* 0.5, DMF); R_f, 0.80.[17]

Found: C, 61.24; H, 7.89; N, 10.82%. Calcd for $C_{79}H_{118}O_{18}N_{12} \cdot H_2O$: C, 61.54; H, 7.85; N, 10.90%.

Z(OMe)-Val-Orn(δ-Z)-Leu-D-Val-Pro-ONp (XII-A). To a solution of VIII-A (2.04 g; 2.3 mmol) in pyridine (10 m*l*), di-*p*-nitrophenyl sulfite[21] (2.98 g; 9.2 mmol) was added. After the mixture had been allowed to stand overnight at room temperature, it was evaporated *in vacuo*. The residual solid was collected with the aid of a mixture of ether and petroleum ether; yield, 1.73 g. The *p*-nitrophenyl ester content was estimated to be 94% by measuring the optical density at 412 mμ.[22]

Z(OMe)-Val-Orn(δ-Z)-Leu-D-Leu-Pro-ONp (XII-B). The compound VIII-B (0.853 g; 1 mmol) was converted to XII-B (0.890 g) as described above in which *p*-nitrophenyl ester content was estimated to be 111%.

Mixture of *cyclo*-(Val-Orn(δ-Z)-Leu-D-Val-Pro-) (XIII-A) and *cyclo*-(Val-Orn(δ-Z)-Leu-D-Val-Pro-)$_2$ (XIV-A). The compound XII-A (1.73 g) was treated with anisole (2 m*l*) and trifluoroacetic acid (12 m*l*) at 0°C. After 20 min, the solution was evaporated, and the solid was collected with the aid of a mixture of ether and petroleum ether. The pentapeptide *p*-nitrophenyl ester trifluoroacetate thus obtained was dissolved in dimethylformamide (20 m*l*) and acetic acid (1 m*l*). The solution was added dropwise into pyridine (600 m*l*) at 55—60°C during 5 hr and the stirring was continued for additional 2 hr. The solution was evaporated, and the residue was dissolved in a mixture of methanol (25 m*l*), dioxane (25 m*l*) and water (10 m*l*). The solution was treated with columns (1.8×15 cm) of Dowex 1 (OH^- form) and Dowex 50 (H^+ form). The columns were washed with the same solvent (150 m*l*), and the combined effluent was evaporated to dryness. The residual product was collected by filtration with the aid of water and dissolved in 4 m*l* of methanol (solution A). A drop of solution A was subjected to hydrogenolysis, and the electophoresis of the hydrogenated material showed two spots.[23] Half of solution A (2 m*l*) was applied to a column (2.7×52 cm) with Sephadex LH-20, and the development continued with methanol. Elution was carried out at room temperature, at a flow rate of 30 m*l* per hr; a 3 m*l* fraction was collected. The peptide content in the fractions was determined as described previously.[11] The first peak appeared from tube numter 47 to 58, and the second, from 62 to 68. The fractions 59 to 61 contained both components. The other half of solution A was chromatographed; the first peak, 43 to 61 and the second, 64 to 72.

***cyclo*-(Val-Orn(δ-Z)-Leu-D-Val-Pro-) (XIII-A).** The fractions 62—68 and 64—72 were combined and evaporated *in vacuo*, and the product was collected by filtration with the aid of water. The crude product weighed 86 mg. It was recrystallized from methanol - ether - petroleum ether; yield, 68 mg (4.4% from VIII-A); mp 161—163°C; $[\alpha]_D^{22}$ −74.7° (*c* 0.3, DMF); R_f, 0.95.[17]

Found: C, 60.92; H, 7.97; N, 12.43%; mol wt, 704.[24] Calcd for $C_{34}H_{52}O_7N_6 \cdot H_2O$: C, 60.51; H, 8.08; N, 12.46%; mol wt, 675.

***cyclo*-(Val-Orn(δ-Z)-Leu-D-Val-Pro-)$_2$ (XIV-A).** The fractions 47—58 and 43—61 were treated as described above; yield of a crude product, 394 mg. Recrystallization from methanol - ether - petroleum ether gave 346 mg (22% from VIII-A); mp 212—214°C; $[\alpha]_D^{22}$ −137° (*c* 0.3, DMF); R_f, 0.93.[17]

Found: C, 60.38; H, 7.88; N, 12.36%; mol wt,

21) B. Iselin and R. Schwyzer, *Helv. Chim. Acta*, **43**, 1760 (1960).

22) R. Schwyzer and P. Sieber, *ibid.*, **40**, 624 (1957).

23) Each of the hydrogenated materials was designated as XVII-A in this case or XVII-B in the case containing D-leucine, and the results of carboxymethylcellulose column chromatography are shown in Fig. 7.

1372.[24] Calcd for $C_{68}H_{104}O_{14}N_{12}\cdot 2H_2O$: C, 60.51; H, 8.08; N, 12.46%; mol wt. 1350.

Mixture of *cyclo*-(Val-Orn(∂-Z)-Leu-D-Leu-Pro-) (XIII-B) and *cyclo*-(Val-Orn(∂-Z)-Leu-D-Leu-Pro-)$_2$ (XIV-B). Pentapeptide *p*-nitrophenyl ester trifluoroacetate obtained from XII-B (0.887 g) was added to pyridine (200 ml) as described for the preparation of a mixture of XIII-A and XIV-A. A crude product was dissolved in 2 ml of methanol (solution B). A quarter of solution B (0.5 ml) was applied to a column (2.7×52 cm) with Sephadex LH-20 as described. The first peak appeared from tube number 35 to 49, and the second, 53 to 60. The fractions from 50 to 52 contained both components. Other three quarters of solution B were treated similarly.

***cyclo*-(Val-Orn(∂-Z)-Leu-D-Leu-Pro-) (XIII-B).** The four fractions which were eluted slower such as from 53 to 60 were pooled and treated as described for the preparation of XIII-A; yield, 59 mg. It was recrystallized from ethyl acetate - petroleum ether; Yield, 53 mg (7.6% from VIII-B); mp 167—170°C; $[\alpha]_D^{18}$ −30.6° (*c* 0.3, DMF); R_f, 0.96.[17]

Found: C, 60.36; H, 7.97; N, 11.85%; mol wt, 680.[24] Calcd for $C_{35}H_{54}O_7N_6\cdot 3/2H_2O$: C, 60.23; H, 8.23; N, 12.03%; mol wt, 698.

***cyclo*-(Val-Orn(∂-Z)-Leu-D-Leu-Pro)$_2$ (XIV-B).** *(a) From VIII-B.* The four fractions which were eluted faster such as from 35 to 49 were treated as described above; yield, 312 mg. It was recrystallized from ethyl acetate-petroleum ether; yield, 296 mg (43% from VIII-B); mp 205—208°C; $[\alpha]_D^{18}$ −108° (*c* 0.5, DMF); R_f, 0.91.[17]

Found: C, 60.67; H, 8.32; N, 12.34%; mol wt, 1343.[24] Calcd for $C_{70}H_{108}O_{14}N_{12}\cdot 2H_2O$: C, 61.02; H, 8.19; N, 12.20%; mol wt, 1378.

(b) From XI-B. The compound XI-B (0.308 g; 0.2 mmol) was treated with di-*p*-nitrophenyl sulfite (0.65 g) in pyridine (2 ml), and the acyldecapeptide *p*-nitrophenyl ester (0.33 g) was obtained as amorphous powder; its *p*-nitrophenyl ester content, 107%. The product was treated with trifluoroacetic acid (2 ml), and the decapeptide *p*-nitrophenyl ester trifluoroacetate obtained was added to pyridine (100 ml). The effluent from the Dowex 1 and 50 columns was evaporated, and the crystals were collected with the aid of water; yield, 138 mg. This was recrystallized from ethyl acetate-petroleum ether; yield, 123 mg (45% from XI-B); mp 207-210°C; $[\alpha]_D^{18}$ −110° (*c* 0.5, DMF); R_f, 0.91.[17] The mixed mp with XIV-B from VIII-B was not depressed.

***cyclo*-(Val-Orn-Leu-D-Val-Pro-)·HCl (XV-A·HCl).** A solution of XIII-A (20 mg; 0.03 mmol) dissolved in 0.01 N methanolic hydrogen chloride (3.37 ml), was subjected to hydrogenolysis in the presence of palladium black. The solution, after being filtered from the catalyst, was evaporated to dryness *in vacuo*. The crystals were collected with the aid of ether; yield of the air-dried product, 16.2 mg (92%); mp 251—254°C (decomp.); R_f, 0.80[17] and 0.97;[25] amino acid ratios in acid hydrolysate, $Val_{2.1}Orn_{1.0}Leu_{1.0}Pro_{1.1}$.

Found: C, 51.72; H, 8.64; N, 13.47%. Calcd for $C_{26}H_{47}O_5N_6Cl\cdot 2.5H_2O$: C, 52.08; H, 8.49; N, 13.56%.

***cyclo*-(Val-Orn-Leu-D-Leu-Pro-)·HCl (XV-B·HCl).** The compound XIII-B (0.03 mmol) was converted to XV-B as described above; yield of the air-dried product, 90%; mp 240—243°C (decomp.); R_f, 0.75[17] and 0.97;[25] amino acid ratios in acid hydrolysate, $Val_{0.9}Orn_{0.9}Leu_{2.0}Pro_{0.9}$.

Found: C, 51.56; H, 8.93; N, 13.34%. Calcd for $C_{27}H_{49}O_5N_6Cl\cdot 3H_2O$; C, 51.70; H, 8.80; N, 13.40%.

***cyclo*-(Val-Orn-Leu-D-Val-Pro-)$_2$·2HCl (XVI-A·2HCl).** The compound XIV-A (0.05 mmol) was treated

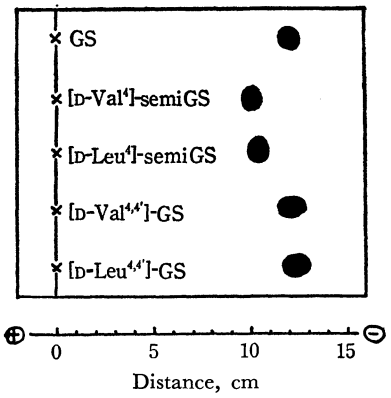

Fig. 6. Paper electrophoresis of the compounds.

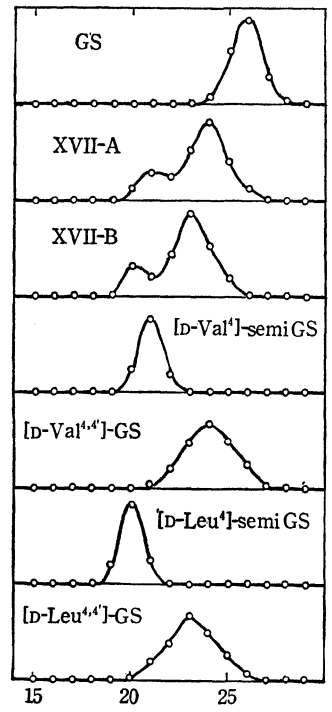

Fig. 7. Carboxymethylcellulose column chromatography of the compounds.
XVII-A or XVII-B, hydrogenated material after cyclization of pentapeptide active ester containing D-Val or D-Leu.

24) The molecular weight was determined on a Hitachi Osmometer, type 115, using methanol as the solvent.

25) The R_f of the paper chromatography with Toyo Roshi No. 52 refers to the *n*-butanol - acetic acid - pyridine - water (4 : 1 : 1 : 2, v/v) system.

as described for the preparation of XV-A; yield of the air-dried product, 96%; mp 275—277°C (decomp.) $[\alpha]_D^{21}$ −133° (*c* 0.3, DMF; R_f, 0.75[17] and 0.97[25]); amino acid ratios in acid hydrolysate, $Val_{1.8}Orn_{0.9}$-$Leu_{1.0}Pro_{0.9}$.

Found: C, 51.78; H, 8.68; N, 13.91%. Calcd for $C_{52}H_{94}O_{10}N_{12}Cl_2 \cdot 5H_2O$: C, 52.08; H, 8.49; N, 13.56%.

The air-dried product lost 8.9% of its weight after drying for 3 hr at 80°C and 2 mmHg. Calcd for $6H_2O$: 8.8%.

***cyclo*-(Val-Orn-Leu-D-Leu-Pro-)$_2$·2HCl (XVI-B·2HCl).** The compound XIV-B (0.04 mmol) was treated as described for the preparation of XV-A; yield of the air-dried product, 86%; mp 256—260°C (decomp.); $[\alpha]_D^{25}$ −100° (*c* 0.3, DMF); R_f, 0.73[17] and 0.95;[25] amino acid ratios in acid hydrolysate, $Val_{0.9}Orn_{1.0}$-$Leu_{2.0}Pro_{0.9}$.

Found: C, 51.72; H, 8.95; N, 13.30%. Calcd for $C_{54}H_{98}O_{10}N_{12}Cl_2 \cdot 6H_2O$: C, 51.70; H, 8.80; N, 13.40%.

The air-dried product lost 6.9% of its weight after dried for 3 hr at 80°C and 2 mmHg. Calcd for $5H_2O$; 7.2%.

Electrophoresis and Carboxymethylcellulose (CMC) Chromatography. Electrophoresis on Toyo Roshi No. 52 paper was carried out with a solvent system, formic acid-acetic acid-methanol-water (1 : 3 : 6 : 10, v/v; pH 1.8) for 2.5 hr at 600 v/30 cm. Figure 6 shows that XVI-A and XVI-B migrate toward the cathode faster than XV-A and XV-B, and that mobilities of XVI-A and XVI-B were comparable with that of gramicidin S. In CMC column chromatography, a sample (0.5-1 mg) was dissolved in 0.2—0.3 m*l* of 0.2 M pyridinium acetate containing 30% methanol (pH 5.1), the solution was applied to a column (0.9×50 cm) with CMC (Eastman No. 7796), and development was continued with the same solvent. Two-m*l* fractions were collected at flow rate of 20 m*l* per hr. The peptide content in the fractions was determined by the ninhydrin method, and the results are shown in Fig. 7.

Microbiological Assays.[26] The minimum amount of the compounds necessary for the complete inhibition of growth was determined by a dilution method using a bouillon agar medium and a synthetic medium. As is shown in Table 1, [D-Val$^{4,4'}$]- and [D-Leu$^{4,4'}$]-gramicidin S were found to be as active as natural gramicidin S against *Staph. aureus* and *B. subtilis*. Whereas cyclo-semigramicidin analogs, XV-A and -B, exhibited no antibacterial activity against the microorganisms tested.

26) We are indebted to Dr. M. Shibata of Takeda Chemical Industries, Ltd. for the assay.

BULLETIN OF THE CHEMICAL SOCIETY OF JAPAN VOL. 42 789—794 (1969)

The Decomposition of Cyclohexyl Hydroperoxide in the Presence of Cyclohexanone and a Novel Rearrangement Product

Sumio CHUBACHI, Hideo MATSUI, Kiyoshi YAMAMOTO and Sachio ISHIMOTO

Product Development Institute of Teijin Limited, Hinode-cho, Iwakuni-shi, Yamaguchi

(Received July 18, 1968)

One of the major reaction products besides cyclohexanol from the reaction of cyclohexyl hydroperoxide with cyclohexanone was isolated and confirmed as ε-cyclohexyloxycaproic acid. The rate of formation of ε-cyclohexyloxycaproic acid was measured in excess cyclohexanone and found to follow a first order law for cyclohexyl hydroperoxide. The activation energy of 10.1 kcal/mol was found for the formation of the acid. The rate of decomposition of cyclohexyl hydroperoxide in cyclohexane was measured in the presence of various concentrations of cyclohexanone and the rates of formation of cyclohexanol and the free carboxylic acids were also measured. An adduct formation between cyclohexyl hydroperoxide and cyclohexanone followed by homolytic decomposition of the adduct was suggested to explain the experimental results.

The reaction of hydrogen peroxide with cyclohexanone has been studied by Criegee *et al.*[1] and they showed the formation of four rather stable peroxides at 40°C.

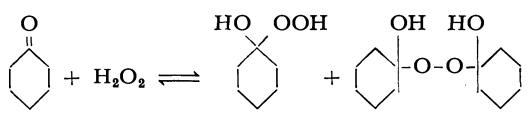

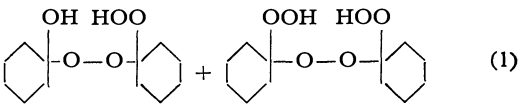

(1)

Denisov *et al.*[2] have studied the free-radical formation in the similar reaction by means of α-naphthylamine technique at 120—140°C. It is also known that alkyl hydroperoxides were strong oxidizing

1) R. Criegee, W. Schnorrenberg and J. Becke, *Ann.*, **565**, 7 (1949).

2) E. T. Denisov, V. V. Kharitonov and E. N Raspopova, *Kinetika i Kataliz*, **5**, 981 (1964).

agents in the presence of alkali hydroxides and cleaved alkyl aryl ketones into corresponding aryl carboxylic acids and alkyl alcohols.[3,4] Cyclohexanone was found to be inert on treatment with *t*-butyl hydroperoxide in the presence of an alkali hydroxide.[3] On the other hand, cyclohexanone reacts readily with peracids to produce ε-caprolactone.[5,6]

This report deals with the decomposition of cyclohexyl hydroperoxide in the presence of cyclohexanone and a novel rearrangement product, namely ε-cyclohexyloxycaproic acid, $C_6H_{11}\cdot O\cdot(CH_2)_5\cdot COOH$ (I). Some kinetic investigations were carried out to estimate the reaction mechanism to this reaction and the characteristic nature of the decomposition of cyclohexyl hydroperoxide in the presence of cyclohexanone was elucidated.

Experimental

Reagents. Commercial cyclohexane and cyclohexanone were fractionated using 2 feet Vigreaux column, bp 80.7°C for cyclohexane and bp 156—156.5°C for cyclohexanone.

Cyclohexyl hydroperoxide was prepared by the following procedure. The air-oxidation of cyclohexane was carried out using an aluminum walled autoclave at 140°C for three hours by passing approximately one *l*/min of air, and the oxidate solution was concentrated by evaporating cyclohexane at a room temperature under a reduced pressure employing a water aspirator until approximately 0.3 mol/*l* of the hydroperoxide concentration was attained. The conecntrated oxidate solution was washed with an equal volume of aqueous 10% Na_2CO_3 solution to remove free acids. The amount of the hydroperoxide in the solution was determined by an iodometric titration of an aliquot of the solution. Two equivalents of NaOH as 40% aqueous solution were added dropwise to the oxidate solution with vigorous stirring at around 5°C. The precipitated salt of hydroperoxide was separated by means of a centrifuge and washed with cyclohexane several times and dried in a desiccator under the reduced pressure of 10mmHg. Dried precipitate was dissolved in the least volume of ice-water and neutralized with 50% acetic acid to pH 6. The solution was extracted with an equal volume of diethyl ether three times. The ether layer was dried and ether was evaporated at a room temperature under the reduced pressure of 3 mmHg.

Isolated cyclohexyl hydroperoxide was 85—90% pure and stored in a refrigerator. The identity of the hydroperoxide was established by an infrared and an NMR spectra. IR spectrum (Hitachi model EPI-S2) (γ_{max}, 1450, 1365, 1160, 1150, 1020, 950 and 840 cm^{-1}). NMR spectrum (Nihon Denshi model JNM 3H-60) measured at 60 Mc (2.16τ(−OOH)(singlet)(1H), 6.08τ (=CH–O–)(multiplet)(1H) and mutiplets centerd around 8.5 τ (–CH_2–)(10H)).

Methyl-ε-cyclohexyloxycaproate. A mixture of cyclohexanone and cyclohexyl hydroperoxide (1:1 molar ratio) was heated at 140°C for 2 hr in a round bottom flask. The reaction mixture was treated with an ethereal solution of diazomethane and the methyl esters of the produced acids were analyzed on the gas liquid partition chromatography, glpc, (Hitachi model KGL-2B), using a 2 m column packed with silanized kieselguhr (30—60 mesh) impregnated with 25% diethyleneglycol succinate operating at 160°C with helium as a carrier gas. A few mg of the comparatively pure unknown compound was obtained by repeated condensation of the eluted vapor corresponding to one of the two major products besides cyclohexanol and identified as methyl-ε-cyclohexyloxycaproate, $C_6H_{11}\cdot O\cdot(CH_2)_5COOCH_3$ (II).

Found: C, 68.2; H, 8.8% (F & M glpc type analyzer). Calcd for $C_{13}H_{24}O_3$; C, 58.4; H, 10.5%.

Infrared spectrum (ν_{max}, 2980, 2920, 1750, 1460, 1440, 1370, 1200, 1180, 1110, 1025 and 955 cm^{-1}). NMR spectrum (6.32τ(−$COOCH_3$)(sing.) (3H), 6.53τ (–CH_2O–)(tripl.)(2H), 7.70τ(–CH_2COO–) (tripl.)(2H), multiplets centerd around 8.5τ(–CH_2–) (16H) and multiplet around 6.35τ(=CHO–)(1H) seemed to be overlapped with the methyl singlet). The structure of the unknown compound was confirmed by the comparison with the spectra of authentic methyl-ε-cyclohexyloxycaproate. The other major product was identified as dimethyl adipate. The total carboxylate content was determined by the use of potentiometric automatic titrater (Hiranuma Sangyo model RA-1) after saponification of the reaction mixture.

Synthesis of Methyl-ε-cyclohexyloxycaproate. In a 500 m*l* round bottom flask 200 g of cyclohexanol was heated with 5.8 g (0.25 mol) of metallic sodium for several hours until homogeneous solution was obtained. ε-Chlorocaproic acid, 15.1 g (0.1 mol), was then added dropwise with vigorous stirring to the solution and heating was continued further for one hour after the addition. The excess cyclohexanol was removed under a reduced pressure and the residue was digested with 150 g of water. Unreacted alkoxide was neutralized by bubbling sufficient volume of carbon dioxide gas through the solution, which was then evaporated to dryness. The solid residue was dissolved in 100 m*l* of water, washed with ether and then acidified. The aqueous solution was extracted with ether. The ether layer was dried and treated with the ethereal diazomethane, and ether was removed to give crude methyl ester of ε-cyclohexyloxycaproic acid, which was then fractionated, bp 115°C at 2 mmHg. Yield 16.4 g (72% of the theoretical yield).

Found: C, 68.4; H, 10.5%. Calcd for $C_{13}H_{24}O_3$: C, 68.4; H, 10.5%.

The IR and NMR spectra of this compound agreed with those of the unknown compound.

Decomposition of Cyclohexyl Hydroperoxide. Thermal decomposition of cyclohexyl hydroperoxide in cyclohexane in the presence of cyclohexanone was studied in an aluminum walled autoclave at 130°C under a stream of nitrogen (1.5 *l*/min). Cyclohexane solutions (300 m*l*) containing *ca.* 0.15 mol of cyclohexyl hydroperoxide and three different concentrations of cyclohexanone were placed in the autoclave, heated to 130°C with vigorous stirring (800 rpm) and maintained at that temperature. Aliquots were withdrawn at specified

3) K. Maruyama, R. Goto and H. Suzuki, *Nippon Kagaku Zasshi, (J. Chem. Soc. Japan, Pure Chem. Sect.)*, **80**, 521 (1959).

4) K. Maruyama, This Bulletin, **34**, 102, 105 (1961).

5) S. L. Fries and P. E. Frankenberg, *J. Am. Chem. Soc.*, **74**, 2679 (1952).

6) M. F. Hawthorne and W. D. Emmons, *ibid.*, **80**, 6398 (1959).

intervals through a sample outlet device. The hydroperoxide concentrations in the aliquots were determined by the iodometric titration and the total free carboxylate contents were determined by the use of potentiometric automatic titrater. The total carbonyl contents were estimated by the method described in an earlier publication.[7] Cyclohexanone and cyclohexanol contents in the aliquots were determined by glpc (Hitachi model KGL-2A), using a 3 m column packed with kieselguhr (30—60 mesh) impregnated with 25% of polyethyleneglycol 3000 operating at 140°C with helium as a carrier gas. Chlorobenzene was used as an inner standard. Since the remaining cyclohexyl hydroperoxide in the sample decomposed on glpc and also gave cyclohexanone and cyclohexanol, their amounts should be deduced from the measured values to obtain true concentrations of cyclohexanone and cyclohexanol in the samples. Glpc of 91 mmol/*l* and 183 mmol/*l* of cyclohexyl hydroperoxide solution in cyclohexane gave 52 mmol/*l* and 97 mmol/*l* of cyclohexanone and 42 mmol/*l* and 92 mmol/*l* of cyclohexanol respectively.

Results and Discussion

The decomposition of cyclohexyl hydroperoxide (100 mmol) in 1 mol of cyclohexanone at 140°C for three hours gave 3 mmol of adipic acid and 3.9 mmol of ε-cyclohexyloxycaproic acid. The total carboxylate content after saponification of the reaction mixture was 34.2 meq. There was some indication of the presence of a higher boiling substance which was revealed by glpc using a capillary column, but no dodecanedioic acid was found in the reaction mixture.

The rates of formation of ε-cyclohexyloxycaproic acid were followed at the three different temperatures, (see Table 1) and an over-all activation energy for the first order rate constants was calculated as 10.1 kcal/mol.

Table 1. Rate constants of ε-cycolhexyloxycaproic acid formation*

Temp. (°C)	$k\times10^{-6}$ (sec^{-1})
105	4.60
120	7.80
130	10.44

* Initial cyclohexyl hydroperoxide concentration is 775 mmol/kg in cyclohexanone.

The rates of decomposition of cyclohexyl hydroperoxide in the presence of three different concentrations of cyclohexanone in cyclohexane solution at 130°C were followed by iodometry, and the rates of formation of cyclohexanone, cyclohexanol and the total free acids in the reaction mixture were also measured. (see Tables 2, 3)

The rate of formation of the total free acids (expressed in meq) was found to obey the equation,

$$\frac{d(FA)}{dt} = k_1\cdot(CHPO)\cdot(ANON), \qquad (2)$$

Table 2. Decomposition of cyclohexyl hydroperoxide in cyclohexane in the presence of cyclohexanone at 130°C

Run No.	Time (min)	CHPO (mmol)	ANON* titd. (mmol)	ANON* glpc** (mmol)	ANOL (mmol)	Free Carboxylic Acids (meq)
A-19	0	150.6	207	194.7	42.7	4.4
	40	99.9	210	205.1	88.1	13.6
	80	62.3	220	214.9	122.9	25.5
	120	41.9	229	227.1	147.1	31.5
	160	27.2	226	226.4	161.4	36.6
A-18	0	156.1	381	384.0	50.0	4.5
	40	79.5	383	382.3	108.3	20.2
	84	41.9	380	402.1	147.1	35.2
	120	23.0	385	402.5	164.5	43.1
	160	12.9	382	395.5	174.5	47.6
A-20	0	148.8	677	653.6	45.6	4.6
	40	62.3	670	659.9	112.9	28.5
	80	27.7	662	650.2	144.2	48.4
	120	12.6	662	657.7	160.7	48.4
	160	6.6	672	660.7	166.7	59.3

* Initial cyclohexanone concentrations; 0.22 mol/*l* for A-19; 0.38 mol/*l* for A-18; 0.67 mol/*l* for A-20.
** ANON (glpc) and ANOL (glpc) were corrected by considering the decomposition of CHPO on glpc.

7) S. Siggia, "Quantitative Organic Analysis *via* Functional Groups," (Japanese Edition), Maruzen, Tokyo (1957), p. 26.

Table 3. Formation of cyclohexanol and total free acids in the decomposition of cyclohexyl hydroperoxide in cyclohexane in the presence of cyclohexanone at 130°C

Run No.	Time (min)	CHPO (Decd.) (mmol)	ANON (Formed) titd. (mmol)	ANON (Formed) glpc (mmol)	ANOL (mmol)	Free Carboxylic Acids (meq)
A-10	0	0.0	0	0.0	0.0	0.0
	40	50.7	3	10.4	45.4	9.2
	80	88.3	13	20.2	80.2	21.2
	120	108.7	22	32.4	104.4	27.1
	160	123.4	19	31.7	118.7	32.2
A-18	0	0.0	0	0.0	0.0	0.0
	40	76.6	2	−1.7	58.3	15.7
	84	114.2	−1	18.1	97.1	30.7
	120	133.1	4	10.5	114.5	35.6
	160	143.2	1	11.5	124.5	43.1
A-20	0	0.0	0	0.0	0.0	0.0
	40	86.5	−7	6.3	67.3	23.9
	80	121.1	−15	−3.6	98.6	43.8
	120	136.2	−15	4.6	115.1	53.4
	160	142.2	−5	7.1	121.1	54.7

where, FA, total free acids; CHPO, cyclohexyl hydroperoxide; ANON, cyclohexanone. (see Figs. 1, 2)

It might be expected that cyclohexyl hydroperoxide forms an adduct (III) with cyclohexanone-like hydrogen peroxide.

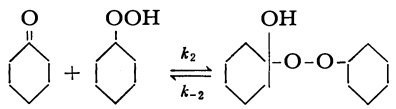

(III) (3)

The formation of ε-cyclohexyloxycaproic acid can be explained by the probable –O–O– bond scission of the adduct followed by β-scission of α-hydroxy-

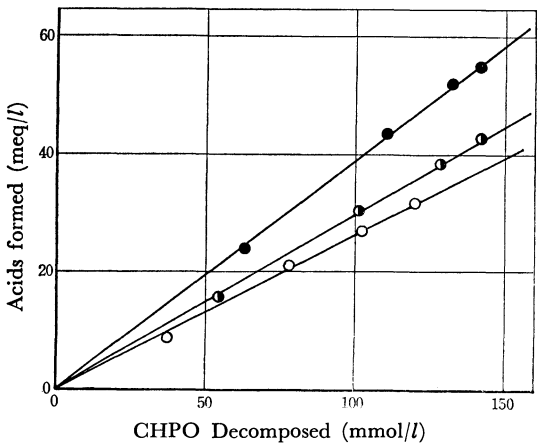

Fig. 1. Relationship between decomposed cyclohexyl hydroperoxide and free acids formed.
●, cyclohexanone 0.67 mol/l; ◑, cyclohexanone 0.38 mol/l; ○, cyclohexanone 0.22 mol/l

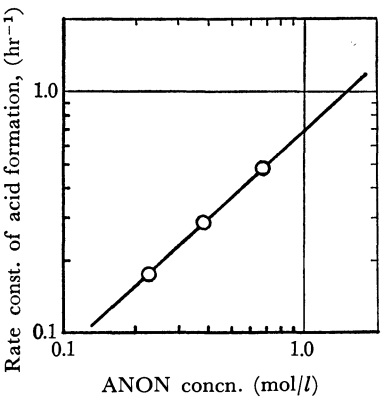

Fig. 2. Relationship between rate constants of acid formation and cyclohexanone concentrations.

alkoxy free radical (IV) to produce a rearranged free radical (VI) and the cage recombination of the radical (VI) with incipient alkoxy radical (V).

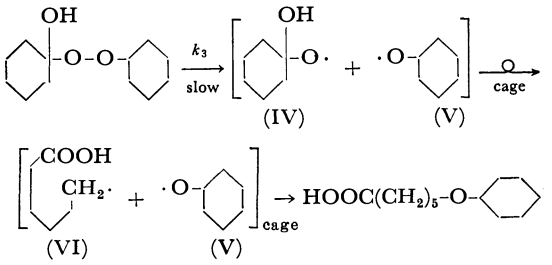

(4)

This process may be either stepwise or a concerted one. If the whole course of the reaction scheme involved the fast pre-equilibrium of the adduct

formation and the slow decomposition of the adduct, the rate of formation of ε-cyclohexyloxycaproic acid would be expressed as follows.

$$\frac{d(CCA)}{dt} = K \cdot k_3 \cdot f \cdot (CHPO) \cdot (ANON), \quad (5)$$

where, CCA, ε-cyclohexyloxycaproic acid; K, equilibrium constant ($K=k_2/k_{-2}$); k_3, decomposition rate constant; f, fraction of radicals to form CCA.

Hence, the over-all activation energy for this reaction will be expressed by,

$$E_a = E_{k2} - E_{k-2} + E_{k3}, \quad (6)$$

where, E_{k2}, activation energy for forward reaction; E_{k-2}, activation energy for backward reaction; E_{k3}, activation energy for decomposition reaction.

Denisov *et al.*[2] reported the value of the heat of formation of the cyclohexanone-H_2O_2 adduct as 6.7 kcal/mol and value of an activation energy for the decomposition rate constant of that adduct as 16.2 kcal/mol. Thus an over-all activation energy of that process would be around 9.5 kcal/mol, which is close to that of ε-cyclohexyloxycaproic acid formation.

The β-scission of the radical (IV) will also be able to give cyclohexanone and hydroxy radical (·OH), but the recombination of hydroxy radical with the alkoxy radical (V) only produces cyclohexyl hydroperoxide and reverses the adduct formation. The main products of the decomposition of cyclohexyl hydroperoxide in the presence of cyclohexanone are clearly cyclohexanol and the carboxylic acids. (see Table 3) This is incompatible with the approximate 1 : 1 formation of cyclohexanone and cyclohexanol in the decomposition of cyclohexyl hydroperoxide on glpc.

The diffusion of the radicals (IV), (V) and hydroxy radical out of the solvent cage may cause the formation of cyclohexanol and the other acidic substances. The initial rate of the formation of cyclohexanol is expressed as

$$\left[\frac{d(ANOL)}{dt}\right]_{initial} = k_4 \cdot (ANON)^{0.51}, \quad (7)$$

where, ANOL, cyclohexanol. (see Fig. 3)

The chain reaction mechanism for the formation of cyclohexanol can be suggested by the approximate one half order dependence of the rate on cyclohexanone concentration and illustrated by the following reaction scheme.

$$\left.\begin{aligned} &\text{Adduct} \rightarrow RO\cdot + R'\cdot, \\ &R'\cdot + ROOH \rightarrow \\ &\quad ROO\cdot + R'H \text{ or } RO\cdot + R'OH, \\ &RO\cdot + ROOH \rightarrow ROO\cdot + ROH, \\ &2ROO\cdot \rightarrow 2RO\cdot + O_2, \\ &2RO\cdot \rightarrow \text{molecular products,} \end{aligned}\right\} \quad (8)$$

where, RO·, $C_6H_{11}O\cdot$; R'·, other radicals; ROOH, $C_6H_{11}OOH$.

The rate of disappearance of cyclohexyl hydroperoxide was observed to be

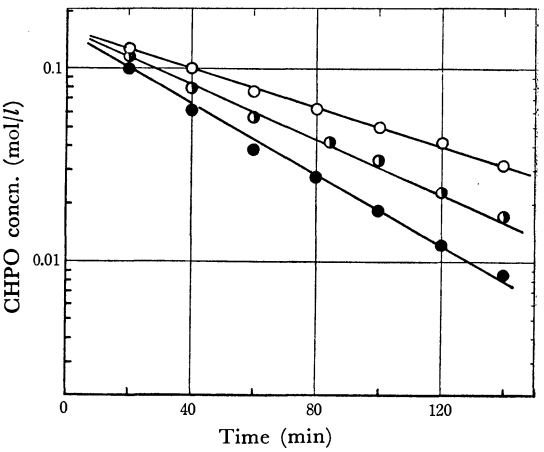

Fig. 4. Disappearance of cyclohexyl hydroperoxide in the presence of cyclohexanone.
●, cyclohexanone 0.67 mol/*l*; ◑, cyclohexanone 0.38 mol/*l*; ○, cyclohexanone 0.22 mol/*l*

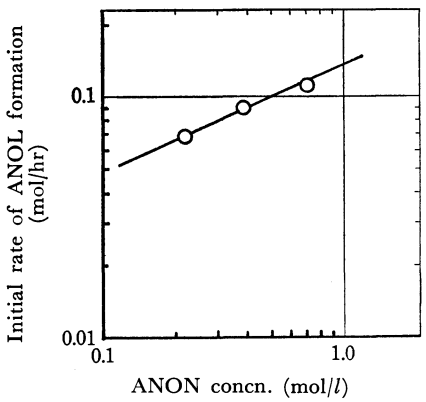

Fig. 3. Relationship between initial rates of cyclohexanol formation and cyclohexanone concentrations.

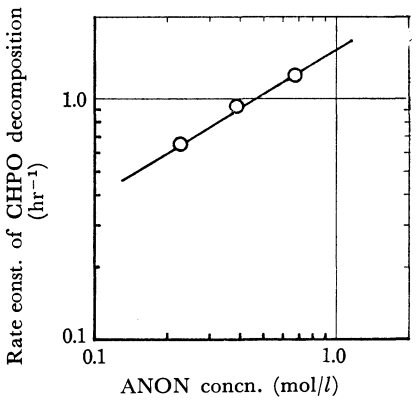

Fig. 5. Relation between decomposition rate constants of cyclohexyl hydroperoxide and cyclohexanone concentrations.

$$-\frac{d(CHPO)}{dt} = k_5 \cdot (CHPO) \cdot (ANON)^{0.67}. \quad (9)$$

(see Figs 4, 5)

The catalytic effect of the produced acids (up to 35 meq) on the rate of disappearance of cyclohexyl hydroperoxide was examined by the addition of a small amount of carboxylic acids (up to 100 mq) to the reaction mixture and found to be not very significant in our experimental condition. (see Table 4)

Table 4. Effects of acid concentration on the rate constants

Run No.	Acid conc. (meq)	k_d* (hr^{-1})	
SA-30	110±13	1.15	Caproic acid was added.
SA-29	38±12	0.93	Adipic acid was added.
SA-31	21±14	0.85	Produced acid only.
SA-21	19±15	0.84	Produced acid only.
SA-34	18±13	0.84	Produced acid only.
---- Extrapolated to zero, 0.78			

Temperature, 130°C; Cyclohexanone concentration, 0.37 mol/l.

* $-\frac{d(CHPO)}{dt} = k_d \cdot (CHPO)$

Consequently, the rate equation of disappearance of cyclohexyl hydroperoxide is considered to involve several independent terms

$$-\frac{d(CHPO)}{dt} = k_6 \cdot (CHPO) + K \cdot k_3 \cdot (CHPO) \cdot (ANON) + k_7 \cdot (CHPO)^m \cdot (ANON)^n, \quad (10)$$

where, k_6, first order rate constant for the decomposition of cyclohexyl hydroperoxide; k_7, rate constant for the induced decomposition of cyclohexyl hydroperoxide.

Farkas *et al.*[8] reported the rate constant of the disappearance of cyclohexyl hydroperoxide in cyclohexane (k_6; 0.000143 min^{-1} at 130°C). The presence of cyclohexanone is found to increase the rate of disappearance of cyclohexyl hydroperoxide (k_{obs}; $0.042+(ANON)^{0.67}$ min^{-1} at 13°C). The observed over-all rate enhancement of disappearance of cyclohexyl hydroperoxide in the presence of cyclohexanone would be the consequence of the combined effect of the terms in the Eq. (10.)

We are indebted to Teijin Limited who granted us permission of publication.

8) A. Farkas and E. Passaglia, *J. Am. Chem. Soc.*, **72**, 3333 (1950).

BULLETIN OF THE CHEMICAL SOCIETY OF JAPAN VOL. 42 794—797 (1969)

Photochemical Ethoxycarbonylmethylation of Benzene with Ethyl Haloacetates[1)]

Yoshiro OGATA, Teruo ITOH and Yasuji IZAWA

Department of Applied Chemistry, Faculty of Engineering, Nagoya University, Chikusa-ku, Nagoya

(Received July 18, 1968)

The ultraviolet light-induced reaction of ethyl haloacetate with an excess benzene gives ethyl phenylacetate (1.7%) and diethyl succinate (1.6%) as main products, while the same reaction of excess chloroacetate with benzene gives ethyl phenylacetate higher yield (optimum 78.4%). Addition of aluminum chloride to the reaction mixture using an excess benzene gives ethyl phenylacetate as a sole product (11.5%). The effect of reaction conditions on the yield is examined.

In the Friedel-Crafts reactions of ordinary carboxylic acids and esters with aromatic compounds, the carbon atom of carbonyl group is the main electrophilic site. In general, the substitution of aromatic rings by $-CH_2COOH$ (carboxymethylation) and by $-CH_2COOR$ (alkoxycarbonylmethylation) are difficult and the papers on these reactions are few.[2)] For example, the condensation of naphthalene with chloroacetic acid affording α-naphthaleneacetic acid in the presence of ferric oxide needs *ca.* 20 hrs' refluxing at 218°C.[2a)] The photo-induced reaction of this type has been

1) Contribution No. 113.

2) a) Y. Ogata and J. Ishiguro, *J. Am. Chem. Soc.*, **72**, 4302 (1950). b) Y. Ogata, J. Ishiguro and Y. Kitamura, *J. Org. Chem.*, **16**, 239 (1951). c) R. L. Lehmann and J. Linter, U. S. Patent 2617822 (1952); *Chem. Abstr.*, **48**, 725 (1954). d) N. K. Bhattacharyya, S. Singh, O. P. Vig and S. M. Mukherji, *Science and Culture (India)*, **18**, 341 (1953); *Chem. Abstr.*, **48**, 2019 (1954).

reported by Kharasch,[3] who succeeded in the carboxymethylation of benzene and cyclohexene with iodoacetic acid, but he provided no detail discussions.

The present paper describes our results on the photochemical ethoxycarbonylmethylation of benzene with ethyl chloroacetate or ethyl bromoacetate in the presence and absence of aluminum chloride.

$$C_6H_6 + ClCH_2COOC_2H_5 \xrightarrow{h\nu} C_6H_5CH_2COOC_2H_5 + HCl$$

Results and Discussion

The ultraviolet irradiation of a solution containing ethyl haloacetate and benzene gave ethyl phenylacetate (I), diethyl succinate (II) and a trace of biphenyl. These products were identified by means of GLC. The results are shown in Table 1 and Fig. 1.

Table 1. The yield of ethyl phenylacetate and diethyl succinate in the photochemical reaction of ethyl haloacetate with benzene in excess at 30°C[a]

$[ClCH_2CO_2Et]$ M	$[C_6H_6]$ M	Yield, %[b] I	Yield, %[b] II	Recovery, %[b] $ClCH_2CO_2Et$
0.1	Solvent	1.7	1.6	—
0.1[c]	Solvent	1.8	0.4	96
0.1[d]	Solvent	2.5	Trace	93
0.1[e]	Solvent	3.0	1.3	69
0.1[f]	0.1	0	0	—
0.1[g]	0.1	0	0	—

a) Irradiation by immersion-type high-pressure Hg lamp for 30 hr.
b) On the basis of added ethyl chloroacetate.
c) Low-pressure Hg lamp was used.
d) Temperature was 65°C.
e) $BrCH_2CO_2Et$ was used.
f) Acetone solution.
g) Methanol solution.

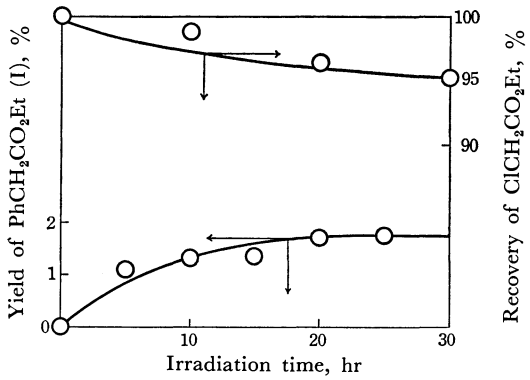

Fig. 1. Typical conversion curves for the reaction of ethyl chloroacetate with benzene.

Irradiation of a benzene solution of 0.1 M ethyl chloroacetate with high-pressure Hg lamp gave I, but in a poor yield (1.7%), while the reaction did not take place in the dark even at refluxing temperature. Almost no further photochemical reactions of I and II occurred.

Since both ethyl chloroacetate and benzene show an absorption band below 2600 Å, a low-pressure Hg lamp which emits almost exclusively 2537 Å light was used under similar conditions, but there was no appreciable effect on the yield of ethyl phenylacetate.

Irradiation at higher temperature (65°C) slightly increased the yield of ethyl phenylacetate. A slight increase in the yield of I was observed, when bromoacetate was used in place of chloroacetate probably because of the lower bond energy of C–Br than that of C–Cl, but the yield was still poor. Generally, the reaction in a solution of an excess benzene gave I in a poor yield, which may be due to the inner filter behavior of solvent benzene.

Further, the irradiation of an acetone or methanol solution of 0.1 M ethyl chloroacetate and 0.1 M benzene gave neither I nor II.

On the other hand, it was of interest to note that the irradiation of 0.1 M benzene in ethyl chloroacetate as solvent gave considerable yields of I and II as main products. In contrast to the reaction in a benzene solution, the yield of I is increased to 78.4%, while that of biphenyl also increases (Table 2). In addition, two other products were detected, neither of which has yet been identified.

Table 2. The yield of ethyl phenylacetate in the photochemical reaction of excess ethyl chloroacetate with benzene at 25°C[a]

$[ClCH_2CO_2Et]$ M	$[C_6H_6]$ M	Yield, %[b] I	Yield, %[b] II[d]
Solvent[c]	0.1	78.4	1.1
Solvent	0.1	39.5[e]	0.9
		48.2[f]	1.6
		45.4	1.1

a) External irradiation by high-pressure Hg lamp for 30 hr.
b) On the basis of added benzene.
c) Immersion-type lamp.
d) Molar ratio of II to I.
e) Oxygen was added.
f) Iodine was added.

A probable primary process of this light-induced reaction may be the bond fission of excited ethyl haloacetate. The following types of bond cleavage have been considered to occur in the photolysis

3) a) N. Kharasch and L. Göthlich, *Angew. Chem.*, **74**, 651 (1962). b) N. Kharasch, P. Lewis and R. K. Sharma, *Chem. Commun.*, 435 (1967).

of alkyl esters[4]; (a) γ-H abstraction by an oxygen atom of carbonyl group and concerted alkyl-oxygen bond fission, (b) acyl-oxygen bond fission and (c) carbonyl-carbon fission. Fission of type (b) occurs mostly at shorter wavelengths (2380 Å and 1870 Å), while fissions of the types (a) and (c) take place at longer wavelength.

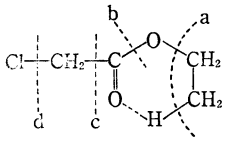

Since a high-pressure Hg lamp was used as the light source in the present reaction, fissions of the types (a) and (c) seem to be more probable. The formation of phenylacetate indicates the occurrence of another type of fission (d) (halogen-carbon bond fission).

The formation of diethyl succinate indicates the formation of ethoxycarbonylmethyl radical (III). In addition, hydrogen chloride was detected in the reaction products by the silver nitrate test. On the basis of these data and available postulates[3,5] of similar radical substitutions on benzene ring, probable reaction pathways to account for the observed products can be presented as follows.

$$ClCH_2CO_2Et \overset{h\nu}{\rightleftharpoons} Cl\cdot + \underset{(III)}{\cdot CH_2CO_2Et} \quad (1)$$

$$\bigcirc + \cdot CH_2CO_2Et \longrightarrow \underset{(IV)}{\bigcirc\!\!\begin{matrix}CH_2CO_2Et\\H\end{matrix}} \quad (2)$$

$$\underset{(IV)}{\bigcirc\!\!\begin{matrix}CH_2CO_2Et\\H\end{matrix}} + Cl\cdot \longrightarrow \underset{(I)}{\bigcirc CH_2CO_2Et} + HCl \quad (3)$$

$$2\cdot CH_2CO_2Et \longrightarrow \underset{(II)}{\begin{matrix}CH_2CO_2Et\\|\\CH_2CO_2Et\end{matrix}} \quad (4)$$

Scheme 1

This scheme involves a σ-complex IV as an unstable intermediate. If the hydrogen atom abstraction from IV (Eq. (3)) would be the rate-determining step, addition of oxygen or iodine as an oxidizing agent to the system should tend to increase the yield of I, but this tendency was virtually not observed; *i. e.*, the addition of oxygen, which may quench the excited chloroacetate, somewhat decreased the yield of **I**, while the addition of iodine slightly increased the yield.

Interestingly, the mixture of 0.1 M aluminum chloride with a benzene solution of 0.1 M ethyl chloroacetate gave on irradiation ethyl phenylacetate as a sole product (Table 3). The yield of I was made better than that without aluminum chloride. These improvements in selectivity and yield of I seem to indicate the participation of an ionic mechanism similar to the ordinary Friedel-Crafts reaction.

TABLE 3. THE YIELDS OF ETHYL PHENYLACETATE IN THE PHOTOCHEMICAL REACTION OF ETHYL CHLOROACETATE WITH EXCESS BENZENE IN THE PRESENCE OF ALUMINUM CHLORIDE AT 25°C[a]

$[ClCH_2CO_2Et]$ M	$[C_6H_6]$	$[AlCl_3]$ M	Yield of $PhCH_2CO_2Et$ %[b]
0.1[c]	Solvent	0.1	11.5
0.2	Solvent	0.1	1.7
0.1	Solvent	0.1	3.2
0.1	Solvent	0.2	3.2

a) Irradiation by high-pressure Hg lamp for 30 hr.
b) On the basis of added ethyl chloroacetate.
c) Deposit on the wall of reaction vessel was cleaned at appropriate interval of time.

The ordinary Friedel-Crafts reaction of benzene with ethyl acetate in the dark gives acetophenone, ethylbenzene and *p*-ethylacetophenone.[6] In the similar dark reaction of benzene with ethyl chloroacetate, the formation of ethylbenzene, diethylbenzene and triethylbenzene has been reported.[7] It has been shown that the activity of halogen atom in ethyl chloroacetate was suppressed by the presence of carbonyl group. The closer the carbonyl group is located to the halogen atom, the more effective is the suppression; *e. g.*, ethyl ω-chloropropionate and ω-chlorobutyrate can react at the halogenated carbon atom in the Friedel-Crafts reaction.[7] However, the halogenated carbon atom is the reaction site in our photo-Friedel-Crafts reaction. This difference may be explained by the photo-excitation of the carbonyl group. If the carbonyl oxygen atom of the ester would gain a positive formal charge through its n–π^* excitation by irradiation, a coordination of aluminum

4) a) P. Ausloos, *Can. J. Chem.*, **36**, 383 (1958). b) P. Ausloos, *J. Am. Chem. Soc.*, **80**, 1310 (1958).

5) a) J. M. Blair, B. Bryce-Smith and B. W. Pengilly, *J. Chem. Soc.*, **1959**, 3174. b) G. E. Corbett and G. H. Williams, *ibid.*, **1964**, 3437.

6) a) L. I. Kashtanov, *Zh. Obsch. Khim.*, **2**, 515 (1932). b) I. G. Farbensindustrie A.-G. Geran Patent 637384 (1936); *Chem. Abstr.*, **31**, 703 (1937). c) J. F. Norris and B. M. Sturgis, *J. Am. Chem. Soc.*, **61**, 1413 (1939). d) J. F. Norris and P. Arthur, Jr., *ibid.* **62**, 874 (1940).

7) I. P. Tsukervanik and I. V. Terenteva, *Dokl. Akad. Nauk SSSR*, **50**, 257 (1945); *Chem. Abstr.*, **43**, 4638 (1949).

chloride to halogen rather than carbonyl should occur, hence the halogenated carbon atom should become the attacking site.

No spectral evidence for a coordination compound between ethyl chloroacetate and aluminum chloride has been reported, while aluminum chloride is shown to coordinate to the carbonyl oxygen atom of ethyl acetate in view of the shift of the carbonyl stretching absorption from 1741 cm^{-1} in ethyl acetate to 1622 cm^{-1} in the complex.[8] Characteristic IR absorption bands of a mixture of aluminum chloride and ethyl chloroacetate are listed in Table 4. Observed shift of ν_{C-Cl} and $\nu_{C=O}$ suggests that aluminum chloride coordinates with both halogen and carbonyl in the ground state, but the halogenated carbon atom can be the more reactive site in the n–π^* excited state of the carbonyl because of its reverse π-electron polarization to that in the ground state.

$$AlCl_3 + ClCH_2CO_2Et \xrightarrow[n-\pi^*]{h\nu} \left[\overset{\delta-}{AlCl_3}\cdots\overset{\delta+}{Cl}CH_2CO_2Et\right]$$

These speculations are rationalized by the photochemical formation of ethyl phenylacetate alone in the presence of aluminum chloride.

Table 4. Infrared spectra (cm^{-1}) of ethyl chloroacetate and its complex with aluminum chloride at 20°C

$ClCH_2CO_2Et$ (liquid)	$ClCH_2CO_2Et \cdot AlCl_3$	Assignment
1770	1740	$\nu_{C=O}$
1195	1215	ν_{CO-O}
1030	1025	ν_{O-Et}
570	490	ν_{C-Cl}

The participation of 1 : 1 complex between ethyl chloroacetate and aluminum chloride in this reaction is suggested by the following experiments. When the molar ratio of chloroacetate to aluminum chloride was varied, the yield of I reached to a maximum value at 1 : 1 of the molar ratio (Table 3).

On mixing ethyl chloroacetate with aluminum chloride, new absorption bands appear at 2750 Å and 3650 Å. These bands may be assigned to the complexes (Va and Vb) of ethyl chloroacetate and aluminum chloride, *i. e.*,

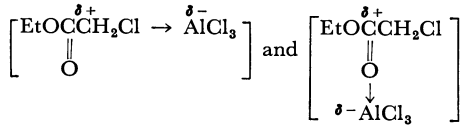

Va

Vb

Therefore, the excitation of these complexes (perhaps C-T complex) also might play an important role as well as the n–π^* excitation of carbonyl in this light-induced primary process, *i. e.*,

$$>C=O \xrightarrow{h\nu} >\overset{\delta-}{C}-\overset{\delta+}{O}\cdot$$

But the excitation of the C-T complexes cannot explain the selective formation of I. Therefore, it is probable that the n–π^* excitation of carbonyl group participates more than that of C-T complexes.

Experimental

Materials. Ethyl bromacetate[9] was prepared by the conventional esterification of bromoacetic acid with ethanol catalyzed by concentrated sulfuric acid, bp 158.5—159°C, ν_{max} 1730, 1185 and 1028 cm^{-1}. Ethyl chloroacetate, bp 52—53°C/21 mmHg, ν_{max} 1770, 1195, 1030 and 570 cm^{-1}, authentic ethyl phenylactate, bp 115—116°C/22 mmHg, ν_{max} 1740, 1605, 1500, 1155 and 1030 cm^{-1}, and authentic diethyl succinate, bp 108—108.5°C/19 mmHg, ν_{max} 1740, 1160 and 1030 cm^{-1}, were also prepared by the similar esterification of the corresponding acids. The IR spectra were measured by a Perkin-Elmer Model 337 spectrophotometer.

General Procedure. A Halos high-pressure 300 W Hg lamp and a low-pressure 30 W Hg lamp with a water-cooling quartz jacket were used as light sources. The reaction mixture was placed in a cylindrical quartz vessel (30×300 mm), N_2 gas being bubbled into the mixture. The vessel together with the lamp was immersed into a water bath at a distance of 5 cm.

For the immersion type irradiation, the light source was immersed in a reaction mixture in a reactor equipped with a N_2 gas inlet, a thermometer and a condenser.

The reaction mixture was irradiated for 30hr. At appropriate intervals of time, aliquots were taken out, each yield being estimated by means of GLC.

Analysis of Products. The identification of products was done by means of GLC employing a Yanagimoto Model GCG-220 operated with a column (1 m× 4 mm) packed with Silicone DC 550 (30 wt %) on Celite 545 of 80—100 mesh using H_2 as a carrier gas (40 ml/min) at 180°C or a Yanagimoto Model GCG-550 F equipped with a hydrogen-flame ionization detector, operated with a column (0.75 m×3 mm) packed with DEGS (13 wt %) on Celite 545 of 80—100 mesh using N_2 as a carrier gas (30 ml/min) at 60—180°C (6°C/min). The yields of products I and II were also estimated by means of GLC under the same conditions using *n*-butyl benzoate as an internal standard. The recovery of the ethyl chloroacetate was estimated by means of GLC operated with a column (2 m×4 mm) packed with Apiezon Grease L (3 wt %) on Celite 545 of 80—100 mesh with H_2 as a carrier gas (40 ml/min) at 80°C using anisole as an internal standard.

8) M. F. Lappert, *J. Chem. Soc.*, **1961**, 817.

9) S. Natelson and S. Gottfried, "Organic Syntheses," Coll. Vol. II, p. 381 (1955).

BULLETIN OF THE CHEMICAL SOCIETY OF JAPAN VOL. 42 798—801 (1969)

Nitroalkenylferrocene. II. The Condensation Reaction of Nitroolefins with Aromatic Carbonyl Compounds

Mikio SHIGA, Hiromichi KONO, Izumi MOTOYAMA and Kazuo HATA

Department of Chemistry, Faculty of Science, Tokyo Metropolitan University, Setagaya, Tokyo

(Received July 30, 1968)

The condensation reactions of β-ferrocenylnitroethylene (**1**), with various aromatic aldehydes in the presence of an excess of sodium methoxide were investigated. The main products of these reactions were ferrocenylnitroalkenols (**2**), which were obtained from precursory sodium salts by the acidification of the reaction mixture. Sodium nitroalkanolate (**4**) was postulated as an intermediate in these reactions. On the other hand, the reaction of **1** with acetophenone resulted in a different condensation, one giving 1-benzoyl-2-ferrocenyl-3-nitropropane (**11**) and 1-benzoyl-2-ferrocenylethylene (**12**).

Various reactions of nitroolefins have been reported by several authors,[1-5] but most of these reports were concerned with the reaction of β-carbon of nitroolefins. With a view of getting some information on the reactivity of the α-carbon of nitroolefins, the condensation of β-ferrocenylnitroethylene (**1**)[6] with aromatic aldehydes was investigated for this paper.

The sodium salt of the nitroethylene (1) reacted with aldehyde in methanol solution at 0°C. The reaction mixture, after it had been kept stirring for 20 hr, was poured into water and the excess of aldehyde was removed with benzene. The acidification of the aqueous solution with dilute hydrochloric acid gave 3-ferrocenyl-2-nitro-1-aryl-2-propen-1-ol (**2**). The product (**2**) is considered to exist in the original reaction mixture as its sodium salt. It was found that some of the nitroalkenols are apt to decompose to give formylferrocene during the extraction of the alkaline solution with benzene. Hence, the preferred procedure for obtaining the nitroalkenols (**2**) is to pour the reaction mixture directly into dilute hydrochloric acid and then to extract it with benzene. The results of the condensation reaction are summarized in Table 1. The NMR and IR spectra of the nitroalkenols (**2**) are shown in Tables 2 and 3. The condensation reactions usually produced a small

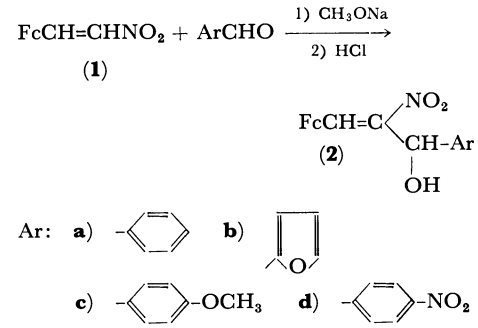

TABLE 1. CONDENSATION REACTION OF β-FERROCENYLNITROETHYLENE WITH AROMATIC ALDEHYDES
(Reaction temp. 0°C. Reaction time 20 hr)

β-Ferrocenylnitroethylene		Aromatic aldehyde			CH_3ONa		Ar in the product (**2**)	Yield	
(g)	(mol)		(g)	(mol)	(g)	(mol)		(g)	(%)
1.28	0.005	Benzaldehyde	2.6	0.025	1.35	0.025	Phenyl (**2a**)	0.93	52
1.28	0.005	Furfural	2.4	0.025	1.35	0.025	2-Furyl (**2b**)	0.62	35
1.28	0.005	*p*-Anisaldehyde	3.4	0.025	1.35	0.025	*p*-Methoxyphenyl (**2c**)	0.83	43
1.28	0.005	*p*-Nitrobenzaldehyde	3.7	0.025	1.35	0.025	*p*-Nitrophenyl (**2d**)	1.17	

1) A. Dornow and F. Boberg, *Ann.*, **578**, 101 (1952).
2) F. Boberg, A. Marei and G. R. Schultze, *ibid.*, **655**, 102 (1962).
3) A. Dornow and F. Borbeg, *Chem. Ber.*, **83**, 261 (1950).
4) D. N. Robertson, *J. Org. Chem.*, **25**, 47 (1960).
5) A. Dornow and A. Frese, *Ann.*, **581**, 211 (1953).
6) M. Shiga, H. Kono, I. Motoyama and K. Hata, This Bulletin, **41**, 1897 (1968).

Table 2. The IR spectra of nitroalkenols (**2**) and its derivatives (**7**), (**8**)

Compound	Frequency (cm^{-1})					
	C=C	NO_2 (asym.)	NO_2 (sym.)	-O-C- ‖ O	C=O	OH
2a	1632	1505	1313			3420
2b	1625	1498	1310			3380
2c	1627	1506	1315			3400
2d	1625	1525	1328			3430
7	1635	1513	1315	1235	1736	
8	1633	1512	1314	1233	1735	

amount of by-products, consisting of formylferrocene and two unidentified ferrocene derivatives, one of which was considered to be a dimer of **1** on the basis of its IR spectrum.

The formation of the nitroalkenol (**2**) from the nitroolefin (**1**) is interpreted as is shown in the scheme. Sodium methoxide reacts with **1** to generate a carbanion (**3**), which then attacks a carbonyl carbon on the aromatic aldehyde to form a sodium nitroalkanolate (**4**). The intermediate (**4**) is converted into the nitroalkenol (**2**), either by the action of sodium methoxide through sodium nitroalkenolate (**5**) (Course A) or by intramolecular hydrogen transfer through the sodium salt of *aci*-nitroalkenol (**6**) (Course B). Course A seems more favorable than Course B when an excess of sodium methoxide is present in the reaction mixture.

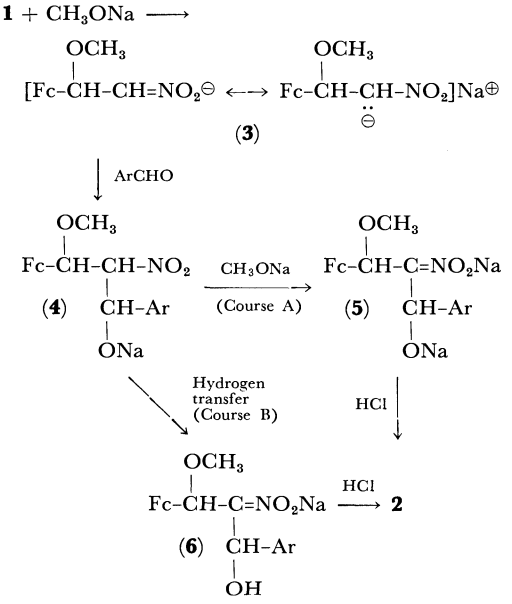

Table 3. The NMR spectra of nitroalkenols (**2**) and its derivatives (**7**) (τ-Value, in $CDCl_3$)

Compound	Cyclopentadienyl ring protons (Subst.)	Cyclopentadienyl ring protons (Unsubst.)	-CH=C(NO2)-	=C(NO2)-CH-	OH	Aromatic ring protons	CH_3
2a	5.38(s)	5.76(s)	1.85(s)	5.96(s)	6.14(s)	2.62(s)	
2b	5.40(s)	5.80(s)	1.91(s)	5.95(s)	6.15(s)	2.61(s)[a] 3.62(s)[b]	
2c	5.40(s)	5.73(s)	2.03(s)	5.93(s)	6.11(s)	2.70(d)[c] 3.11(d)[d]	6.21(s)[e]
7	5.36(s)	5.73(s)	1.82(s)	5.86(s)	—	2.60(s)	7.86(s)[f]

a) and b)

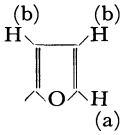

c) and d)

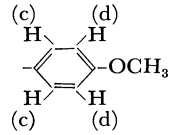

e) Methyl protons of methoxy group.
f) Methyl protons of acetoxy group.

Table 4. Condensation of β-ferrocenylnitroethylene with benzaldehyde

$FcCH=CHNO_2$ (g)	$FcCH=CHNO_2$ (mol)	CH_3ONa (g)	CH_3ONa (mol)	PhCHO (g)	PhCHO (mol)	Solvent	Yield of **2** (%)
1.28	0.005	1.35	0.025	2.6	0.025	Methanol	52
						Pyridine	12
						Tetrahydrofuran	5
						Tetrahydrofuran-Methanol (1:1)	10
1.28	0.005	1.08	0.02	2.0	0.02	Methanol	46
1.28	0.005	0.40	0.0075	0.78	0.0075	Methanol	15

TABLE 5. CONDENSATION OF β-FERROCENYLNITROETHYLENE WITH ACETOPHENONE

Run	$PhCOCH_3$ (g)	$PhCOCH_3$ (mol)	$FcCH{=}CHNO_2$ (g)	$FcCH{=}CHNO_2$ (mol)	CH_3ONa (g)	CH_3ONa (mol)	Product	(g)	(%)
a	3.0	0.025	1.28	0.005	1.35	0.025	**11**	1.57	84
							12	0.07	5
b	9.0	0.075	1.28	0.005	1.35	0.025	**12**	1.35	86
							11	0.05	3

The condensation reactions which were carried out in solvents other than methanol resulted in a low yield of **2** (Table 4). The low yield is probably caused by the insufficient solubilities of the sodium salt (**3**) toward these solvents.

When 3-ferrocenyl-2-nitro-1-phenyl-2-propen-1-ol (**2a**) was treated with acetic anhydride and sodium acetate, two isomeric acetates were obtained. One of them, obtained in a 56% yield, was found by a study of its IR and NMR spectra to be the normal acetylation product (**7**). The other product, obtained in a 6.7% yield, was tentatively identified as the rearrangement product (**8**) from the results of its elemental analysis, but the lack of its NMR data does not permit any conclusive structural assignment.

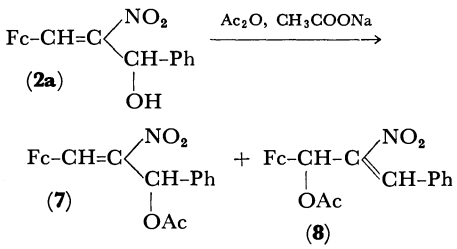

In contrast with the behavior of aldehyde, the similar reaction of the nitroethylene (**1**) with acetophenone gave quite a different result; instead of an analogous nitroalkenol (**9**) or its dehydration product (**10**), 1-benzoyl-2-ferrocenyl-3-nitropropane (**11**) was obtained as the condensation product of a carbanion generated from acetophenone with β-carbon on **1**, together with a small amount of 1-benzoyl-2-ferrocenylethylene (**12**).[7,8]

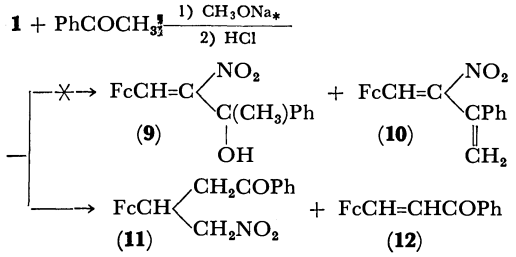

As is shown in Table 5, when a large excess of acetophenone was used (Run b), **12** was obtained in a good yield. It may be assumed that the formation of **12** is to be ascribed to the condensation of the excess acetophenone with formylferrocene, which is itself produced by the following exchange reaction between acetophenone and β-ferrocenylnitroethylene (**1**):

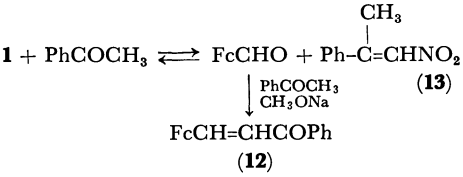

However, this inference is ruled out by the experimental finding that 2-phenyl-1-nitropropene (**13**) could not be detected in the reaction product. A better explanation seemingly lies in the fact that the primary product (**11**) was easily decomposed into 1-benzoyl-2-ferrocenylethylene (**12**) and nitromethane in the presence of sodium methoxide and an excess of acetophenone.

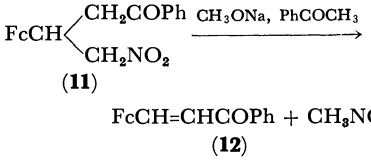

Experimental

General Procedure of Preparing Nitroalkenol (2). The reaction conditions and the products of the condensation reactions of β-ferrocenylnitroethylene with aromatic aldehydes are summarized in Table 1. A typical reaction procedure was as follows: To 1.28 g (0.005 mol) of finely-powdered β-ferrocenylnitroethylene in 7 m*l* of absolute methanol at 0°C, there were added slowly 1.35 g (0.025 mol) of sodium methoxide, which had been freshly-prepared from absolute methanol and sodium metal. Subsequently, 0.025 mol of aromatic aldehyde was added, drop by drop, into the mixture with stirring. After it had been stirred for 20 hr, the reaction mixture was poured into a mixture of 10% hydrochloric acid (100 m*l*) and benzene (30 m*l*), and then stirred for a few more minutes. The benzene layer which separated from the aqueous layer was washed three times with 50 m*l* portions of water and then dried over magnesium sulfate. After the benzene had been removed by distillation under reduced pressure, the residual blue-violet oil was dissolved in 2 m*l* of chloroform and chromatographed on alumina, using chloroform as the solvent, the chromatographic column being covered with aluminum foil in order to prevent the

7) K. Schlögl, *Monatsch. Chem.*, **88**, 601 (1957).
8) J. Boichard, J. P. Monin and J. Tirouflet, *Bull. Soc. Chim. France*, **1963**, 851.

decomposition of unstable nitroalkenol (**2**) by exposure to the light. The first fraction of the chromatography gave the starting material, and the second fraction gave a mixture of **2** and by-products as a blue-violet oil, which was then subjected to further chromatography on Florisil, using benzene as the solvent. Nitroalkenol (**2**) was obtained as a blue-violet oil from the second fraction, whereas the first and the third fraction gave by-products. The nitroalkenol (**2**) thus obtained was purified again by chromatography on Florisil.

3-Ferrocenyl-2-nitro-1-phenyl-2-propen-1-ol (2a). The condensation reaction of β-ferrocenylnitroethylene (**1**) (1.28 g) with benzaldehyde (2.6 g) gave a blue-violet oil of nitroalkenol (**2a**) (0.93 g, 52%).

Found: C, 61.81; H, 4.59; N, 4.11%. Calcd for $C_{19}H_{17}FeNO_3$: C, 62.80; H, 4.68; N, 3.85%.

3-Acetoxy-1-ferrocenyl-2-nitro-3-phenylpropene (7) and 3-Acetoxy-3-ferrocenyl-2-nitro-1-phenylpropene (8). To 400 mg of **2a** in 4 m*l* of acetic anhydride, 0.5 g of anhydrous sodium acetate was added. After it had been heated to 95°C for 3 hr, the reaction mixture was poured into 50 m*l* of water. The blue-brown solid (450 mg) which separated as a precipitate was chromatographed on Florisil, using a mixture of benzene-*n*-hexane (5 : 1) as the solvent. The starting material (**2a**) was recovered as the first fraction. After the starting material had then been completely removed, elution with chloroform gave an acetylated product (**7**), (250 mg, 50% yield as a blue-violet oil.

Found: C, 61.80; H, 4.62; N, 3.02%. Calcd for $C_{21}H_{19}FeNO_4$: C, 62.22; H, 4.62; N, 3. 45%.

A third elution, using a mixture of chloroform and a small amount of methanol as the solvent, afforded the isomeric acetate (**8**), (30 mg, 6.7% yield) as a brown solid (mp 62—64°C).

Found: C, 61.02; H, 4.57; N, 3.40%. Calcd for $C_{21}H_{19}FeNO_4$: C, 62.22; H, 4.62; N, 3.45%.

3-Ferrocenyl-2-nitro-1-(2-furyl)-2-propen-1-ol (2b). The condensation reaction of β-ferrocenylnitroethylene (1.28 g) with furfural (2.4 g) gave 0.61 g (35% yield) of nitroalkenol (**2b**).

Found: C, 58.55; H, 4.02; N, 3.35%. Calcd for $C_{17}H_{15}FeNO_3$: C, 57.79; H, 4. 24; N, 3.96%.

3-Ferrocenyl-2-nitro-1-(*p*-methoxyphenyl)-2-propen-1-ol (2c). *p*-Anisaldehyde condensed with β-ferrocenylnitroethylene to give 0.83 g (43% yield) of nitroalkenol (**2c**).

Found: C, 62.64; H, 4.44%. Calcd for $C_{20}H_{19}FeNO_4$, C: 63.61; H, 4.83%.

3-Ferrocenyl-2-nitro-1-(*p*-nitrophenyl)-2-propen-1-ol (2d). The condensation of β-ferrocenylnitroethylene (1.28 g) with *p*-nitrobenzaldehyde (3.7 g) afforded 1.17 g of crude nitroalkenol (**2d**). A small amount of the by-products could not be removed from the crude **2d** by column chromatography, but the IR spectrum of the crude product clearly showed the existence of **2d**.

1-Benzoyl-2-ferrocenyl-3-nitropropane (11). The condensation reaction of β-ferrocenylnitroethylene (1.28 g, 0.005 mol) with acetophenone (3.0 g, 0.025 mol) was carried out much like that with aldehydes. The first fraction of the chromatographic separation of the crude product on alumina gave a small amount of reddish crystals of 1-benzoyl-2-ferrocenylethylene (**12**) (mp 137—140°C, 0.07 g, 5% yield) upon elution with benzene.

The main product (**11**) was obtained as pale yellow crystals (mp 111—113°C, 1.57 g, 84% yield) by elution with chloroform. The IR spectrum of **11** showed absorption bands at 1670 cm^{-1} (C=O) and at 1549 cm^{-1} (NO_2)

Found: C, 63.80; H, 4.86; N, 3.82%. Calcd for $C_{20}H_{19}FeNO_3$: C, 63.66; H, 5.04; N, 3.71%.

1-Benzoyl-2-ferrocenylethylene (12). a) The condensation reaction described above was carried out in the presence of a large excess (9.0 g, 0.075 mol) of acetophenone. A mixture of **12** and formylferrocene was obtained as the first fraction by the chromatography of the crude product on alumina. After the removal of the formylferrocene by sublimation, **12** was obtained as reddish-orange crystals (1.35 g, 86% yield). The IR spectrum of **12** showed absorption bands at 1655 and 1676 cm^{-1} (C=O).

Found: C, 72.58; H, 5.14%. Calcd for $C_{19}H_{16}FeO$: C, 72.15; H, 5.06%.

b) Acetophenone (6.0 g, 0.05 mol) was added to a solution of **11** (0.74 g, 0.0025 mol) and sodium methoxide (0.54 g, 0.01 mol) in absolute methanol (7 m*l*). After being kept standing overnight, the reaction mixture was poured into 100 m*l* of 10% hydrochloric acid and extracted with benzene. The extract was dried over magnesium sulfate and concentrated. The chromatographic separation of the crude product on alumina gave **12** (0.51 g, 65% yield) from the second fraction.

BULLETIN OF THE CHEMICAL SOCIETY OF JAPAN VOL. 42 802—805 (1969)

The Wolff Rearrangement. V. Kinetic Isotope Effect of α-Diazoacetophenone*1

Yasuhide YUKAWA and Toshikazu IBATA*2

The Institute of Scientific and Industrial Research, Osaka University, Kamiyamada, Suita, Osaka

(Received August 9, 1968)

Kinetic isotope effect of the Wolff rearrangement of carbonyl-^{14}C and phenyl-1-^{14}C labeled α-diazoacetophenone was measured in *t*-butyl alcohol at 30°C, using a solution of silver benzoate in triethylamine as a catalyst. No apparent kinetic isotope effect was observed in both cases within experimental error. These results suggest that the elimination of nitrogen and the migration of phenyl group proceed in two steps in the rate-determining step.

In the previous papers of this series, we have reported the kinetic studies of the Wolff rearrangement of α-diazoacetophenone,[1] and substituent effect of substituted α-diazoacetophenones catalyzed by silver benzoate in alcohols.[2] From these results it was concluded that the rate-determining step of this reaction was that of elimination of nitrogen. In this case following two mechanisms are possible;

a) A concerted one-step mechanism in which elimination of nitrogen and migration of alkyl group proceed synchronously.

b) Two-step mechanism in which the elimination of nitrogen proceeds in the first step, followed by migration of alkyl group.

One-step mechanism

$$[\underset{\text{(I)}}{\overset{\ominus}{\text{RCOC}}=\text{N}_2—\overset{\oplus}{\text{Ag}}\text{N}(\text{C}_2\text{H}_5)_3}] \rightarrow [\underset{\text{(II)}}{\text{R}-\overset{\ominus}{\text{C}}=\text{C}=\text{O}}] + \text{N}_2 + [\text{AgN}(\text{C}_2\text{H}_5)_3]^{\oplus} \quad (1)$$

Two-step mechanism

$$[\underset{\text{(I)}}{\overset{\ominus}{\text{RCOC}}=\text{N}_2—\overset{\oplus}{\text{Ag}}\text{N}(\text{C}_2\text{H}_5)_3}] \rightarrow [\underset{\text{(III)}}{\overset{\ominus}{\text{RCOC}}—\overset{\oplus}{\text{Ag}}\text{N}(\text{C}_2\text{H}_5)_3}] + \text{N}_2 \quad (2)$$

$$[\underset{\text{(III)}}{\overset{\ominus}{\text{RCOC}}—\overset{\oplus}{\text{Ag}}\text{N}(\text{C}_2\text{H}_5)_3}] \rightarrow [\underset{\text{(II)}}{\text{R}-\overset{\ominus}{\text{C}}=\text{C}=\text{O}}] + [\text{AgN}(\text{C}_2\text{H}_5)_3]^{\oplus} \quad (3)$$

The kinetic isotope effect may be useful to distinguish these two mechanisms, in other words, to get the precise information on the transition state of this reaction. In this connection, Fry and his co-workers have studied the kinetic isotope effect of the Curtius rearrangement of phenyl-1-^{14}C, carbonyl-^{14}C and ^{15}N labeled benzazide.[3] We have studied the kinetic isotope effect of the Wolff rearrangement of α-diazoacetophenone-(carbonyl-^{14}C) (IVa) and α-diazoacetophenone-(phenyl-1-^{14}C) (IVb), when triethylamine solution of silver benzoate was used as a catalyst.

Results and Discussion

Kinetic isotope effects of the Wolff rearrangement of (IVa) and (IVb) were determined as follows; Sampling of 10 m*l* of reaction mixture at every ten minutes after the initiation of the reaction, converting the unreacted IV in each sample into a 2,4-dinitrophenylhydrazone of phenacyl chloride by the reaction with 2,4-dinitrophenylhydrazine in the presence of hydrochloric acid, burning the purified hydrazone by modified van Slyke wet-oxidation method,[4] and absorbing the carbon dioxide into an aqueous barium hydroxide solution to give barium carbonate, and counting the radio activity of the barium carbonate by G. M. counter after disk formation. The results obtained were

*1 Presented at the 17th Annual Meeting of the Chemical Society of Japan, Tokyo, April, 1964.

*2 Present address: Department of Chemistry, College of General Education, Osaka University, Toyonaka, Osaka.

1) Y. Yukawa, Y. Tsuno and T. Ibata, This Bulletin, **40**, 2613 (1967).

2) Y. Yukawa, Y. Tsuno and T. Ibata, *ibid.*, **40**, 2618 (1967).

*3 Triethylamine silver ion complex is omitted in V for simplicity, see Refs. 1 and 2.

3) A. Fry, private communication.

4) T. Noguchi, "Experimental Technique on Isotope," Vol. I, Nankodo, Tokyo (1955), p. 95.

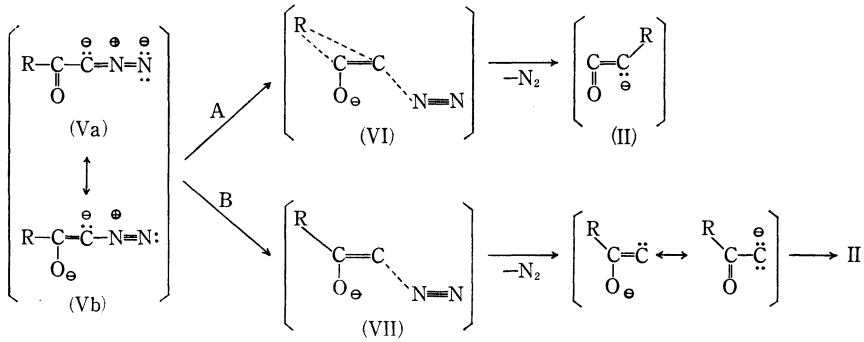

given in Tables 1 and 2. Radio activity of each run was constant within experimental and counting error of ±2%, and no kinetic isotope effect was observed for IVa and IVb.

One of the most important factors of kinetic isotope effect is the variation of the zeropoint energy difference between the transition state and the reaction origin of the rate-determining step by means of heavy and light isotopic compounds. In other words, the partial bond breaking and bond formation with respect to labeled atom in the transition state causes the alternation of the vibrational frequency of that bond and consequently leads to the kinetic isotope effect. Generally, when bond breaking occurs in the transition state the normal kinetic isotope effect is expected, and bond formation causes the reverse one.

It may be considered from our results, in which no kinetic isotope effect was observed in both IVa and IVb, that bond breaking or bond formation with respect to both carbonyl-C-atom and phenyl-1-C-atom of α-diazoacetophenone is not happened in the transition state. Therefore two-step mechanism is preferred. The precise model of the transition state of this reaction may be shown by VII, in which the R-CO bond length is not changed from that of V*[3] (path B). This may suggest that the bond energy effect observed in the substituent effect of para-electron releasing groups, such as *p*-methoxy and *p*-ethoxy, on reaction rate is not attributed to R-CO bond cleavage but to C-N_2 bond cleavage.

Experimental

Materials. *α-Diazoacetophenone-(carbonyl-^{14}C).* A mixture of 1.23 g (0.010 mol) of benzoic-^{14}C acid (sepcific activity 11.8 μc/mmol) and 2.5 g (0.021 mol) of purified thionyl chloride was refluxed for three hours. The excess thionyl chloride was evaporated under reduced pressure, and the last of the reagent was removed by azeotrope with two added 5 m*l* of absolute benzene. Benzoyl chloride obtained was used for diazoacetophenone formation without further purification. To 50 m*l* of etheral solution of diazomethane, prepared by the alkaline decomposition of 7.0 g (0.07 mol) of *N*-nitroso-*N*-methylurea, an etheral solution of previously synthesised benzoyl-^{14}C chloride was added drop by drop under stirring at −5°C. After standing overnight at room temperature, the ether was removed under reduced pressure at room temperature. Yellow crystals of IVa were obtained from the residue on standing in the refrigerator and purified by two recrystallization from petroleum ether. Mp 47.5—48.0°C, yield 0.85 g (58%).

α-Diazoacetophenone(phenyl-1-^{14}C). 1.11 g (0.009 mol) of commercial benzoic acid (phenyl-1-^{14}C labeled) (specific activity 18.7 μc/mmol) was chlorinated by 2.4 g (0.020 mol) of purified thionyl chloride to give phenyl-1-^{14}C labeled benzoyl chloride, according to the same method described in the previous part. IVb was obtained by the reaction of corresponding benzoyl chloride and four equivalents of diazomethane. Mp 47.5—48.0°C, yield 0.83 g (63%). The phenyl-1-labeled α-diazoacetophenone (0.83 g) was diluted isotopically by adding 1.40 g of unlabeled α-diazoacetophenone, and isotopically homogenized by two recrystallization from petroleum ether.

Specific Activity $=18.7\times0.83/(0.83+1.40)=6.96$ μc/mmol

Silver benzoate, t-Butyl Alcohol and Triethylamine. Reagent and solvents used here were prepared and purified by the method previously reported.[1]

Quantitative Determination of α-Diazoacetophenone (IV). When IV was treated with 2,4-dinitrophenylhydrazine (VIII) in alcoholic solution in the presence of hydrochloric acid, 2,4-dinitrophenylhydrazone of phenacyl chloride[5] was precipitated accompanying the evoluation of nitrogen. In order to utilize this reaction for the quantitative determination of unreacted diazoketone in the course of the Wolff rearrangement, it is ascertained that the formation of the hydrazone is almost quantitative under the same condition of the isotope effect determination reaction, as shown in Table 3.

Determination of Rate Constant and Kinetic Isotope Effect of the Wolff Rearrangement of IVa. *Determination of Reaction Rate.* To a solution of 0.813 g (5.5 mmol) of IVa (specific activity, 11.8 μc/mmol) dissolved in 100 m*l* of *t*-butyl alcohol contained in long necked reaction vessel, triethylamine (2.0 m*l*) solution of 0.100 g of silver benzoate was added at a time. After vigorous swirling, reaction vessel was immersed in the thermostated bath at 30.05±0.01°C. A 10 m*l* of alquot of the reaction mixture was pipetted into a 50 m*l* of flask containing 100 mg of VIII and 10 m*l* of concentrated hydrochloric acid and 10 m*l* of ethanol

5) F. Arndt, B. Eistert and W. Partale, *Ber.*, **60**, 1364 (1927).

TABLE 1. REACTION RATE AND KINETIC ISOTOPE EFFECT OF THE WOLFF REARRANGEMENT OF IVa AT 30.05°C

No.	Time (min)	2,4-D weight (mg)	k_1[a] (10^{-4} min^{-1})	G. M. counting[c] (cpm)	counting ratio
1	10[b]	152.8		2636±17	100.0
2	20	136.4	114	2674±10	101.4±1.0
3	30	117.8	130	2636±14	100.0±1.1
4	40	107.0	118	2628±24	99.7±1.5
5	50	97.2	113	2632±26	99.8±1.6
6	60	85.3	117	2664±16	101.1±1.2
7	70	81.7	104	2670±17	101.3±1.2
			$k_1=116\pm6$		

a) Evolution of nitrogen gas accompanied with the reaction causes the error in volume of pipetting and then in rate measurement.
b) Initial sampling was made at ten minutes after the addition of the catalyst, because about ten minutes induction period was observed by the kinetic measurement using azotometer.
c) Counting was made by preset counting method of 10^4 count using Nuclear Chicago G. M. counter attached by Aloka G.M. tube for β-ray (membrane 1.3 mg/cm^2). Each sample was counted six times and average value was listed. These values listed were corrected for natural count (21 cpm).

TABLE 2. REACTION RATE AND KINETIC ISOTOPE EFFECT OF WOLFF REARRANGEMENT OF IVb

No.	Time (min)	2,4-D weight (mg)	k_1[a] (10^{-4} min^{-1})	G. M. counting[c] (cpm)	counting ratio
1	10[b]	150.4	—	1620±10	100.0
2	20	130.6	141	1647± 9	101.7±1.1
3	30	114.9	135	1617±11	99.8±1.3
4	40	102.0	129	1597± 9	98.6±1.1
5	50	90.9	126	1621± 9	100.1±1.1
6	60	81.1	123	—[d]	
7	70	70.8	126	1629± 6	100·6±1.0
			$k_1=130\pm5$		

Following reaction condition was applied:
IVb: 0.910 g, C_6H_5COOAg: 0.100 g, $(C_2H_5)_3N$: 2.00 m*l*, *t*-C_4H_9OH: 100 m*l*, at 30.05±0.02°C
a), b), c) These foot-notes are identical with those in Table 2.
d) Counting of this sample was not measured because of the experimental mistake.

TABLE 3. QUANTITATIVE DETERMINATION OF α-DIAZOACETOPHENONE (IV)

No.	Weight of IV (mg)	Weight of 2,4-D (mg) Calcd	Obs	Obs/Calcd (%)
1	22.8	52.2	52.1	99.8
2	32.5	74.5	75.2	100.9
3	41.8	95.8	95.8	100.0
4	52.0	119.1	119.7	100.6
5	60.6	138.8	139.2	100.3

at the intervals of ten minutes after the addition of the catalyst. The hydrazone solutions were allowed to stand overnight in the bath at 50—60°C, for the purpose of the complete precipitation of the hydrazone and aging of the crystals, then allowed to cool to room temperature, added 10 m*l* of water. Crystals of the hydrazone were collected on the precisely weighed fritted glass funnel, washed with 2 N hydrochloric acid until no yellow color of unreacted VIII-hydrochloride appeared in the filtrate, washed with distilled water and then dried for 12—15 hr at 80—90°C, and weighed.

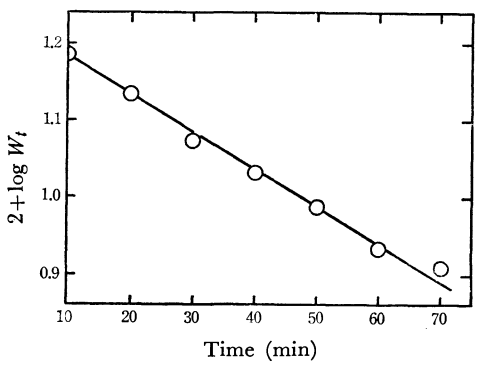

Fig. 1. The linear relationship between log W_t and time in the reaction of IVa.

The linear first-order plot was obtained between log W and time as shown in Fig. 1. The reaction rate k was calculated by the following equation,

$$k_t=2.303\times\log(W_0/W_t)$$

where W_0 and W_t were denoted the weight of the hydrazone at the time of $t=0$ and t respectively, and $t=0$ was

the time of the first pipetting.

Measurement of Kinetic Isotope Effect. The hydrazone obtained from the rate measurement of IVa (shown in Table 1, Nos. 1—7) was recrystallized four times from a mixed solvent of ethyl acetate and ethanol (3 : 1), and solvent was evaporated completely in vacuum desiccator for a few days. About 15—16 mg of purified hydrazone was oxidized by modified van Slyke wet-oxidation method, and carbon dioxide was absorbed by 10 m*l* of saturated barium hydroxide solution to give barium carbonate. Carbon dioxide and barium hydroxide solution was kept separately until oxidation was complete (at 170°C, for 4 hr), in order to homogenize the distribution of carbon fourteen in barium carbonate. Barium carbonate was made as a disk of 1.7 cm in diameter, which had infinite thickness, by filtration (using metallic filter), and radio activity of these barium carbonate samples were counted by G. M. counter after drying.

Determination of Reaction Rate and Kinetic Isotope Effect of the Wolff Rearrangement of IVb. The same procedure described in the case of IVa was used for these measurements. Reaction conditions used and results obtained were given in Table 2 (Fig. 2). It was ascertained that the degree of the contamination of the commercial benzoic acid-(phenyl-1-^{14}C) (IX) used for the synthesis of IVb by the mixing of benzoic acid-(carbonyl-^{14}C) was no more than 0.44%, comparing the radio activity of the barium cabonate obtained by direct oxidation of IX with that obtained by Schmidt rearrangement of IX.

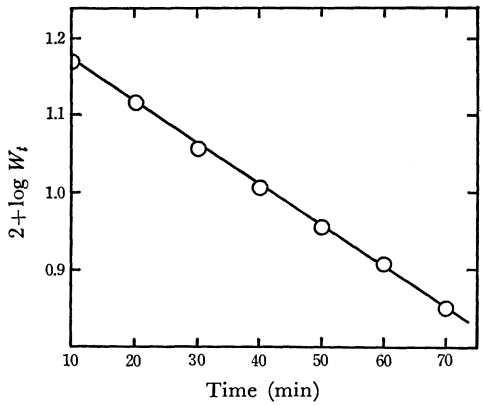

Fig. 2. The linear relationship between log W_t and time in the reaction of IVb.

BULLETIN OF THE CHEMICAL SOCIETY OF JAPAN VOL. 42 805—808 (1969)

Organic Syntheses by Means of Noble Metal Compounds. XXXVIII. Cyclohexanone Oxime Complexes of Palladium[1]

Sinzo IMAMURA, Tsunesuke KAJIMOTO, Yukishige KITANO and Jiro TSUJI

Basic Research Laboratories, Toyo Rayon Co., Kamakura

(Received August 9, 1968)

Ligand exchange reactions of palladium complexes having π-allyl and acetylacetonate as ligands with cyclohexanone oxime were carried out and the formation of several new oxime complexes was reported.

Dioximes as bidentate form stable complexes with various metals, and dimethylglyoxime is a typical example. On the other hand, monoximes do not form a stable complex, and it has been reported that an attempt to prepare a monoxime complex with nickel, iron and cobalt salts gave no stable complex.[2] Formation of stable monoxime complexes with platinum and palladium[2] has been reported briefly. We have found that monoximes form stable complexes with palladium by displacing ligands of various palladium complexes. In this paper the ligand exchange reaction of palladium complexes with cyclohexanone oxime is reported.

Results and Discussion

The formation of a stable complex by the reaction of palladium chloride with two moles of cyclohexanone oxime and its structure have already been reported.[3] The complex can be prepared more easily by treating benzonitrile complex of palladium chloride with the oxime. It was confirmed by X-ray analysis that the complex has a square planar *trans* structure (I). The preparation of the corresponding *cis* complex (II) was attempted

1) Part XXXVII: T. Susuki and J. Tsuji, This Bulletin, **41**, 1954 (1968).

2) A. V. Babaeva and M. A. Mosyagina, *Dokl. Akad. Nauk S. S. S. R.*, **89**, 293 (1953); *Chem. Abstr.*, **47**, 10392 (1953).

3) M. Tanimura, T. Mizushima and Y. Kinoshita, This Bulletin, **40**, 2777 (1967).

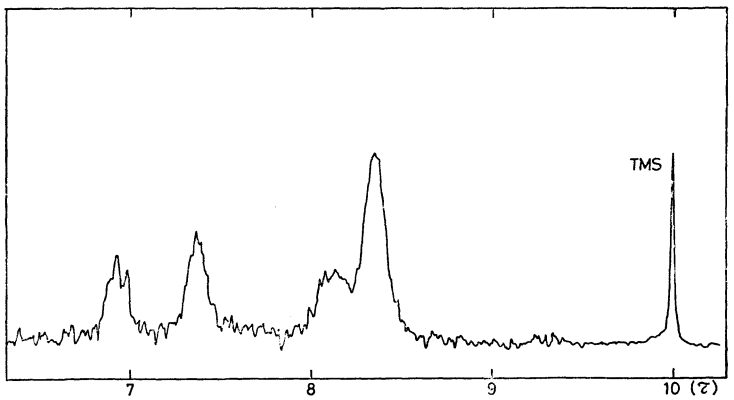

Fig. 1. NMR spectrum of bis(cyclohexanone oxime) palladium chloride (100 Mc/s, in $CDCl_3$).

by the displacement reaction of 1,5-cyclooctadiene-palladium chloride complex with the oxime.

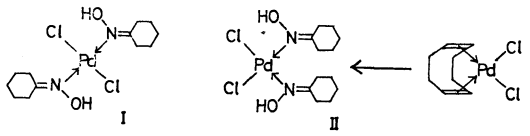

I II

Simple displacement of cyclooctadiene should presumably give the *cis* structure. The complex obtained showed the same IR and NMR spectra as those of the *trans* complex. The only difference was their melting points. The melting point of the *cis* complex, 199°C, was found to be higher than that of the *trans* complex, 184°C. In order to confirm the *cis* structure definitely, the measurement of the dipole moments of both complexes was attempted, but, owing to their low solubilities in benzene, no definite conclusion was obtained. Thus it is not certain whether the complex is really *cis* or not. The NMR spectrum of the *trans* complex is shown in Fig. 1. Two kinds of NMR signals due to the syn and anti α-methylene protons of a cyclohexanone ring are observed at τ 6.91 and τ 7.36. Saito and Nukada[4] reported that, in cyclohexanone oxime hydrochloride, only one kind of α-methylene proton signal is observed, because the paramagnetic anisotropic effect of the hydroxyimino group is eliminated due to the addition of the proton of hydrogen chloride to the lone pair electrons of the nitrogen atom. In the palladium oxime complex, the oxime coordinates to palladium atom with the lone pair electrons of the nitrogen atom, and the separation of the syn and anti proton signals is considered to be attributed to the diamagnetic anisotropic effect of palladium.

From the above mentioned complex formation, it is apparent that cyclohexanone oxime is capable of forming a stable complex with palladium. The oxime complex formation by a ligand exchange reaction of rather stable palladium complexes was attempted. The first example was palladium acetylacetonate, which is a very stable complex. A solution of palladium acetylacetonate in dichloromethane was treated with the oxime at room temperature for 3 min, and a new complex was isolated by the addition of a large amount of ether. The complex showed no IR absorption due to the carbonyl, indicating that the acetylacetone was displaced completely by the oxime. The analysis showed that the complex contained two moles of the oxime anion and two moles of the oxime.

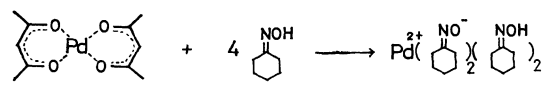

An IR absorption band at 2350 cm^{-1} indicates the presence of hydrogen bonding.[5] The following structure (III) is possible for the complex.

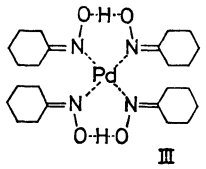

III

π-Allylpalladium chloride was then treated similarly with the oxime in dichloromethane at room temperature. A new complex was isolated by the addition of a large amount of ether. The NMR and IR spectra showed that the complex still retains the π-allyl system and the reaction is not a displacement, but an addition reaction. Analysis showed that one mole of the oxime per two atoms of palladium was incorporated into the complex.

The addition of the oxime molecule by the opening of the bridged structure as shown below (IV) was an expected reaction. The opening of the bridge structure of π-allylpalladium chloride is

4) H. Saito, K. Nukada and M. Ohno, *Tetrahedron Letters*, **1964**, 2164.

5) R. Blinc and D. Hadzi, *J. Chem. Soc.*, **1958**, 4536.

Table 1. Chemical shifts and coupling constants of the π-allyl system of $[Pd(\pi\text{-}C_3H_5)Cl]_2C_6H_{10}NOH$ and $[Pd(\pi\text{-}C_3H_5)Cl]_2$

Complex		τ_1	τ_2	τ_3	J_{12}	J_{13}	Mc/s
$[Pd(\pi\text{-}C_3H_5)Cl]_2C_6H_{10}NOH$	$(CD_3)_2CO$	4.59	5.97	6.96	7.1	11.8	100
	$CDCl_3$	4.56	5.98	6.98	6.8	12.1	60
$[Pd(\pi\text{-}C_3H_5)Cl]_2$[6]	$CHCl_3$	4.55	5.98	7.05	7.1	12.1	40

known with such a ligand as phosphine or amine. Another possibility is the opening of the π-allyl system to form σ-allyl bond (V). If these transformations take place, the complex containing one mole of the oxime per one atom of palladium should be obtained. The analysis clearly indicated that these addition reactions did not take place. Even when an excess of the oxime was allowed to react with π-allylpalladium chloride, only one mole of the oxime per mole of the dimeric π-allyl complex was incorporated.

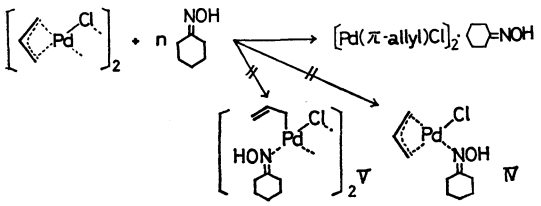

X-Ray crystallographic studies showed that the complex has the structure shown in Fig. 2. Details of the crystallographic studies will be given in a forthcoming paper. In this complex the oxime attaches to one of the palladium atoms by opening the palladium-chlorine bond, forming an unsymmetrical complex. As for the π-allyl system the NMR spectra showed exactly the same pattern as that of the original π-allylpalladium chloride as shown in Table 1. Thus the oxime is quite different from phosphine and other ligands toward π-allyl complex.

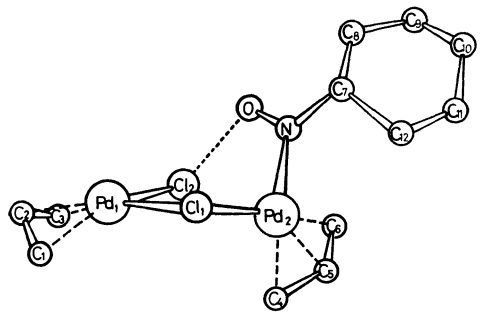

Fig. 2. Schematic drawing of $(Pd(\pi\text{-}C_3H_5)Cl)_2$-$C_6H_{10}NOH$.

From the above experiments, it was found that coordinated acetylacetonate is displaced easily with the oxime, and the π-allyl system remained intact when treated with oxime. The reaction of the oxime with π-allylpalladium acetylacetonate was investigated, with the expectation that the acetylacetonate would be displaced. The preparation of π-allylpalladium acetylacetonate was reported by Shaw[7] by the reaction of π-allylpalladium chloride with thallium acetylacetonate. We have synthesized the same complex by treating the π-allylpalladium chloride with sodium hydroxide solution of acetylacetone.

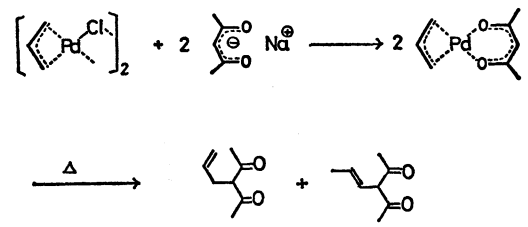

The complex is not stable and decomposes slowly on standing. When heated at 90°C under reduced pressure, the complex decomposed to give 3-allyl-2,4-pentanedione, accompanied by 3-propenyl-2,4-pentanedione. The products were formed by the coupling of the two ligands coordinated to the palladium. A somewhat stable complex was obtained by the reaction of π-(1-ethoxycarbonyl-methyl-3-ethoxycarbonylallyl)palladium chloride with sodium acetylacetonate in benzene.

The reaction of the oxime with π-allylpalladium acetylacetonate in ether proceeded somewhat violently and yellow crystals separated. Infrared spectrum showed the presence of the acetylacetonate system in the new complex. Thus it is apparent that unexpectedly the π-allyl system was displaced with the oxime instead of the acetylacetonate system.

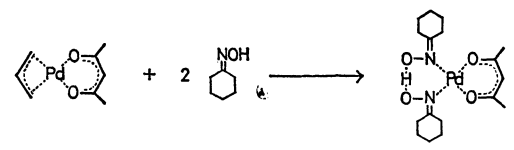

VI

An IR band at 2350 cm^{-1} indicates the presence of hydrogen bonding and the structure (VI) is proposed for the complex.

From the results described in this paper, it is

6) B. L. Shaw and N. Sheppard, *Chem. Ind. (London)*, **1961**, 517.

7) S. D. Robinson and B. L. Shaw, *J. Chem. Soc.*, **1963**, 4806.

apparent that the oxime coordinates to palladium to form stable complexes. Stable ligands such as π-allyl or acetylacetonate can be displaced with the oxime quite easily.

Experimental

Reaction of π-Allylpalladium Chloride with Cyclohexanone Oxime. Bis(π-allyl)palladium chloride (1.83 g) was dissolved in a minimum amount of dichloromethane, and cyclohexanone oxime (0.57 g) was added. The mixture was stirred for 3 min until a complete solution was obtained. Then, a large amount of ether was added to ensure the precipitation to give 2.13 g of a pale yellow complex. The complex was washed well with ether and then recrystallized from a mixture of dichloromethane and ether. On standing in air the complex decomposes slowly. When heated it darkens at 121—131°C and decomposes at 134°C.

Found: C, 30.27; H, 4.56; N, 2.80; Cl, 15.10%. Calcd for $C_{12}H_{21}NOPd_2Cl_2$: C, 30.09; H, 4.42; N, 2.92; Cl, 14.80%.

Reaction of palladium acetylacetonate with cyclohexanone oxime.

Reaction of Palladium Acetylacetonate with Cyclohexanone Oxime. Palladium acetylacetonate (1 g) and cyclohexanone oxime (2 g) were mixed in dichloromethane and the mixture was shaken for 3 min. Pale yellow crystals were obtained by the addition of a large amount of ether. The complex was recrystallized twice from ether-dichloromethane mixture. Mp 167°C. Found: C, 51.65; H, 7.68; N, 9.96%. Calcd for $C_{24}H_{42}N_4O_4Pd$: C, 51.75; H, 7.60; N, 10.05%.

Preparation of π-Allylpalladium Acetylacetonate. Acetylacetone (1 g) and sodium hydroxide (0.4 g) were dissolved in 10 m*l* of water and the solution was poured into a separatory funnel. Then π-allylpalladium chloride (1.83 g) and 30 m*l* of ether were added to the funnel, and the mixture was shaken for 3 min, when the complex dissolved completely. The ethereal layer was separated and the ether was evaporated. From the residue, pale yellow crystals were obtained, which were washed with water. The crystals were purified by subliming twice at 50—60°C/2 mmHg to give colorless crystals; mp 72—73°C. The complex decomposes on standing at room temperature. Found: C, 39.00; H, 4.97%; mol wt, 243. Calcd for $C_8H_{12}O_2Pd$; C, 38.97; H, 4.91%; mol wt, 246.5.

Decomposition of π-Allylpalladium Acetylacetonate. The complex (4.8 g) was heated in an oil bath at 100°C under reduced pressure (30 mmHg), and a liquid (1.2 g) was obtained at 83—90°C/30 mmHg. The liquid was purified by preparative gas chromatography to give 3-allyl-2,4-pentanedione. The structure was determined by NMR and IR spectra. Found; C, 68.71; H, 8.86%; mol wt, 139. Calcd for $C_8H_{12}O_2$: C, 68.54; H, 8.63%; mol wt, 140.18.

Preparation of π-(1-Ethoxycarbonylmethyl-3-ethoxycarbonylallyl)palladium Acetylacetonate. 1-Ethoxycarbonylmethyl-3-ethoxycarbonylallyl palladium chloride (2.55 g) and sodium acetylacetonate (0.92 g) were mixed in 20 m*l* of benzene and the mixture was stirred at room temperature for 30 min. After the reaction, benzene was removed at 2 mmHg and the residue was extracted with ether. By evaporating the ether, pale yellow crystals were obtained, which are more stable than π-allylpalladium acetylacetonate, but decomposes slowly on standing. Found: C, 44.74; H, 5.49%. Calcd for $C_{15}H_{22}O_6Pd$: C, 44.51; H, 5.48%.

Reaction of π-allylpalladium acetylacetonate with cyclohexanone oxime.

Reaction of π-Allylpalladium Acetylacetonate with Cyclohexanone Oxime. π-Allylpalladium acetylacetonate (2.46 g) was dissolved in 25 m*l* of ether, and the oxime (2.16 g) in 15 m*l* of ether was added. The mixture was shaken for 3 min. When it was warmed on a steam bath, a violent reaction was observed and yellow crystals appeared to give 2.9 g of a crude product which was recrystallized from dichloromethane and ether twice to give crystals, mp 149—150°C. Found: C, 47.45; H, 6.57; N, 6.66%. Calcd for $C_{17}H_{18}N_2O_4Pd$; C, 47.40; H, 6.55; N, 6.50%.

The authors would like to thank Mr. H. Saito for helpful discussions on the NMR spectra.

BULLETIN OF THE CHEMICAL SOCIETY OF JAPAN VOL. 42 809—811 (1969)

t-Amyloxycarbonyl as a New Protecting Group in Peptide Synthesis. V. Direct Synthesis of *t*-Amyloxycarbonyl- and *t*-Butyloxycarbonyl-amino Acids Using the Respective *t*-Alkyl Chloroformates

Shumpei SAKAKIBARA, Ichiro HONDA and Katsumi TAKADA

Peptide Center, Institute for Protein Research, Osaka University, Kita-ku, Osaka

Muneji MIYOSHI, Takanobu OHNISHI and Kentaro OKUMURA

Chemical Research Laboratory, Tanabe Seiyaku Co., Ltd., Higashiyodogawa-ku, Osaka

(Received August 12, 1968)

t-Amyloxycarbonylamino acids (Aoc-amino acids) were found to be synthesizable under the conditions of the Schotten-Baumann reaction with *t*-amyl chloroformate in the presence of a water-soluble inert solvent. The procedure was applied to almost all amino acids or their derivatives; the yields of the products and their purities were satisfactory except in the cases of asparagine, glutamine, and nitroarginine. Many *t*-butyloxycarbonylamino acids (Boc-amino acids) were also synthesized successfully using the same procedure. Similarly, *t*-amyl and *t*-butyl carbazates were synthesized in satisfactory yields with these chloroformates and hydrazine hydrate. Thus, the procedure was demonstrated to be the simplest for the preparation of Aoc- or Boc-amino acids and hydrazide.

In this series of studies,[1-4] it has previously been established that *t*-amyl chloroformate (I) is a useful reagent for introducing the Aoc-group into amino acid esters in an organic solvent, and that Aoc-amino acids can be obtained conveniently by the removal of the ester groups. *t*-Amyl carbazate has also been synthesized by the condensation of reagent I with anhydrous hydrazine, and many Aoc-amino acids have been prepared with the carbazate as in the case of the standard method for the synthesis of Boc-amino acids. The Aoc-group thus introduced can be removed during peptide synthesis, as in the case of the Boc-group. The Aoc-method has already been applied to the syntheses of many peptides.[2,5-10]

As was mentioned in the first paper,[1] the introduction of the Aoc-group into free amino acid was unsuccessful with the reagent I when the reaction was carried out under the standard conditions of the Schotten-Baumann reaction. This was attributed to the instability of the reagent I in water. During repeated trials, however, it was found that the addition of an inert water-soluble organic solvent, such as tetrahydrofuran, isopropanol, or methanol, increased the rate of the acylation reaction in comparison with that of the decomposition of I. Finally, new practical conditions were established for the direct preparation of the Aoc-amino acids with the reagent I by the Schotten-Baumann reaction. The reagent I which was synthesized by the ether procedure[1] was preferable for these reactions to that prepared by the toluene method,[4] because the presence of a water-insoluble solvent in the Schotten-Baumann reaction mixture tended to increase the formation of uncertain by-products. Although this procedure was satisfactory for almost all amino acids and their side-chain derivatives, low yields and unsatisfactory purities were observed in the syntheses of Aoc-asparagine, -glutamine, and -nitroarginine, as is shown in Table 1. These phenomena may account for the partial formation of their mixed anhydrides during the reaction, which in these cases may be further transformed to the nitriles or lactams.

The synthesis of *t*-amyl carbazate[4] has been

1) S. Sakakibara, M. Shin, M. Fujino, Y. Shimonishi, S. Inouye and N. Inukai, This Bulletin, **38**, 1522 (1965).
2) S. Sakakibara and M. Fujino, *ibid.*, **39**, 947 (1966).
3) S. Sakakibara and M. Itoh, *ibid.*, **40**, 646 (1967).
4) I. Honda, Y. Shimonishi and S. Sakakibara, *ibid.*, **40**, 2415 (1967).
5) S. Sakakibara and N. Inukai, *ibid.*, **39**, 1567 (1966).
6) S. Sakakibara, Y. Shimonishi, M. Okada and Y. Kishida, "Peptides," Proc. 8th European Peptide Symp. (1966), edited by H. C. Beyermann *et al.*, North-Holland, Amsterdam (1967), p. 44.
7) N. Inukai, K. Nakano and M. Murakami, This Bulletin, **40**, 2913 (1967).
8) N. Inukai, K. Nakano and M. Murakami, *ibid.*, **41**, 182 (1968).
9) S. Sakakibara, Y. Kishida, R. Nishizawa and Y. Shimonishi, *ibid.*, **41**, 438 (1968).
10) S. Sakakibara, Y. Kishida, Y. Kikuchi, R. Sakai and K. Kakiuchi, *ibid.*, **41**, 1273 (1968).

TABLE 1. YIELD AND PHYSICAL CONSTANTS OF AOC-AMINO ACIDS SYNTHESIZED BY THE DIRECT METHOD

Aoc-amino acid	Melting point °C observed	cited[a]	Yield[b] %	$[\alpha]_D$ observed	cited[a]	Temp °C
Gly	84—85.5		74			
		84—85.5				
L-Leu[c]	66—68		75	−17.8° (*c* 2, EtOH)		20
		66—68		−17.3° (*c* 2, EtOH)		20
L-Pro	98—99		88	−47.6° (*c* 1.8, EtOH)		25
		98—99		−47.6° (*c* 2, EtOH)		20
L-Phe[d]	208—210 (decomp.)		77	+38.2° (*c* 0.52, EtOH)		26
		209—211		+40.6° (*c* 0.67, EtOH)		20
L-Asp(NH_2)[e]	151—152 (decomp.)		45	−7.6° (*c* 3.7, DMF)		25
		151.5—152.5		−8.2° (*c* 3.4, DMF)		28
L-Glu(NH_2)[e]	116.5—117.5		36	−17.6° (*c* 3.9, DMF)		25
		115.5—116.5		−19.4° (*c* 4.8, DMF)		20
L-Arg(NO_2)	139 (decomp.)		44	−25.5° (*c* 2.1, pyridine)		25
		139—141 (decomp.)		−28.2° (*c* 2, pyridine)		18
L-Tyr(Bzl)[d]	114—116		85	+42.6° (*c* 4.8, EtOH)		21
		113.5—115.5		+43.1° (*c* 5, EtOH)		21

a) The same lit. as in Ref. 4.
b) Calcd from amino acid after recystallization.
c) Obtained as crystals of mono-hydrate; optical rotation calcd for the hydrate.
d) Obtained as crystals of the dicyclohexylamine salt.
e) Isopropanol (300 m*l*), in stead of methanol, and 3 equivalents of reagent I were used for the reaction.

TABLE 2. YIELD AND PHYSICAL CONSTANTS OF BOC-AMINO ACIDS SYNTHESIZED BY THE DIRECT METHOD

Boc-amino acid	Melting point °C observed	cited	Yield[a] %	$[\alpha]_D$ observed	cited	Temp. °C
Gly	88—89		74			
		88.5—89[b]				
L-Leu[c]	82—83		89	−23.9° (*c* 1.4, AcOH)		25
		67—72[b]		−24.0° (*c* 2, AcOH)[b]		25
L-Phe[d,e]	221—223 (decomp.)		73	−1.7° (*c* 1, AcOH)		25
L-Pro	133—135		90	−60.4° (*c* 2.2, AcOH)		25
		136—137[b]		−60.2° (*c* 2, AcOH)[b]		25
L-Lys(Z)[d]	111—113		66	−7.2° (*c* 1.1, AcOH)		25
		110—111[f]		−9.3° (*c* 1, AcOH)[g,f]		18—25
L-Met[d]	137—139		56	+12.3° (*c* 2.1, MeOH)		25
		138—139[f]		+19.0° (*c* 1, MeOH)[g,f]		18—25

a) Calcd from amino acid after recrystallization.
b) The same lit. as in Ref. 11.
c) Obtained as crystals of mono-hydrate.
d) Obtained as crystals of the dicyclohexylamine salt.
e) Found: C, 69.69; H, 9.85; N, 6.17%. Calcd for $C_{26}H_{42}O_4N_2$: C, 69.92; H, 9.48; N, 6.27%.
f) E. Schnabel, *Ann.*, **702**, 188 (1967).
g) Observed at 578 mμ.

simplified further in the present study; that is, commercially-available hydrazine hydrate (80—90%) was found to be a satisfactory material when the reagent I was slowly added to it for the coupling reaction. The yield of *t*-amyl carbazate was almost the same as that previously reported with anhydrous hydrazine.[4]

The same technique was also applied to the synthesis of Boc-amino acids and of the carbazate. Although Anderson and McGregor[11] abandoned the use of *t*-butyl chloroformate (II)[12] as a reagent for the preparation of Boc-amino acids, these Boc-derivatives were found to be synthesized similarly,

11) G. W. Anderson and A. C. McGregor, *J. Am. Chem. Soc.*, **79**, 6180 (1957).
12) A. R. Choppin and J. W. Rogers, *ibid.*, **70**, 2967 (1948).

and in almost the same yields, as Aoc-derivatives (see Table 2).

One big difference between Aoc- and Boc-derivatives was in their solubilities in water. Although there was no difficulty in extracting Aoc-amino acids or hydrazide from the aqueous reaction media with ether, a strong salting-out was usually necessary to extract the Boc-amino acids or hydrazide from the aqueous reaction mixture. This difference should also be kept in mind when Aoc- or Boc-peptide derivatives are synthesized.

Experimental

All the reactions with the reagent I or the reagent II were monitored by thin-layer chromatography using Silica-gel G; the solvent system was chloroform : methanol : acetic acid (95 : 5 : 3 v/v) or *n*-butanol : acetic acid : water (4 : 1 : 1 v/v). After separation, the spots were located with ninhydrin at 100°C or with iodine vapor at room temperature.

***t*-Amyl Chloroformate (I).** Liquid phosgene was collected and measured (200 m*l*, *ca.* 2.8 mol) in a three-necked flask (capacity 5 *l*), and then a solution of *t*-amyl alcohol (176 g, 2 mol) in dry ether (3 *l*) was added to it. A solution of dry pyridine (150 g, 1.9 mol) in dry ether (1 *l*) was added slowly to the mixture at −20——30°C over a period of 90 min, taking precautions to prevent the introduction of moisture. Efficient stirring was necessary in order to obtain a homogeneous reaction. Stirring was continued for a further 30 min at the same temperature, and then the mixture was kept overnight in a deep freezer at −20°C. The precipitate thus formed was filtered off, again taking care to prevent the introduction of moisture; the filtrate was then concentrated to about 400 m*l* under reduced pressure in an ice-water bath. This solution was used as the stock solution of I without further purification. (It should be kept dry in a deep freezer and use within 10 days.)

***t*-Butyl Chloroformate (II).** Essentially the same procedure was followed with *t*-butyl alcohol (148 g, 2 mol). The final solution was used as the stock solution of II without further purification.

***t*-Amyloxycarbonyl-L-proline** (General Procedure for the Synthesis of Aoc-amino Acids). A stock solution of I (1 mol, calcd from *t*-amyl alcohol) was added slowly to a solution of L-proline (69 g, 0.6 mol) in a mixture of methanol (150 m*l*) and 2 N aqueous sodium hydroxide (600 m*l*) at 0——5°C. The mixture was agitated vigorously with a mechanical stirrer during the addition of I (over about one hour). The stirring was continued for a further 2 hr at 0°C, and then for an additional hour at room temperature. (During the reaction, the solution should be kept above pH 8 by the addition of 4 N aqueous sodium hydroxide. After the addition of I, the extent of the reaction should be checked by thin-layer chromatography; if appreciable proline remains, more reagent should be added.) Then, the reaction mixture was adjusted to pH 2—3 with 1 N hydrochloric acid, and the product was extracted with ethyl acetate (300 m*l*×1, 100 m*l*×3). The combined extract was dried over sodium sulfate. On the concentration of the dried solution, crystals were obtained which were then recrystallized from ethyl acetate and petroleum ether; yield 137 g (88%). The physical constants of the material are shown in Table 1.

***t*-Amyl Carbazate.** Reagent I (1 mol, calcd from *t*-amyl alcohol) was added, over a 3-hr period, to a suspension of 80% hydrazine hydrate (250 g, 4 mol) in ether (1 *l*) at 0——3°C. The slow addition of I and a vigorous stirring of the reaction mixture were essential to obtain a good yield. Stirring was continued at 0°C for an additional 2 hr after the complete addition of I. Then, 4 N sodium hydroxide (250 m*l*) was added to the reaction mixture, the ether layer was separated, and the aqueous layer was extracted with ether (100 m*l*×3). The ether layer and the extracts were combined, washed with a saturated solution of sodium chloride, and dried over sodium sulfate. The removal of ether from the dried solution left an oily material, which was then purified by fractional distillation under reduced pressure; yield, 83 g (57%, calcd from *t*-amyl alcohol), bp 85—86°C/4—5 mmHg. This value was essentially the same as that reported previously.[4]

***t*-Butyloxycarbonylglycine** (General Procedure for the Synthesis of Boc-amino Acids). Glycine (45 g, 0.6 mol) was dissolved in a mixture of methanol (120 m*l*) and 2 N aqueous sodium hydroxide (600 m*l*). The solution was treated with II (1 mol, calcd from *t*-butyl alcohol) following the procedure used for the synthesis of Aoc-L-proline with I. The reaction mixture was acidified to pH 2—3 with 1 N aqueous hydrochloric acid and saturated with sodium chloride; then the product was extracted with ethyl acetate (200 m*l*×2, 100 m*l*×5). The combined extract was washed with a saturated solution of sodium chloride (50 m*l*×2) and dried over sodium sulfate. The concentration of the dried solution left crystals which were then recrystallized from ethyl acetate and petroleum ether; yield, 77 g (74%). The melting point of this compound is shown in Table 2.

***t*-Butyl Carbazate.** The procedure used for the synthesis of *t*-amyl carbazate was followed with the reagent II (1 mol, calcd from *t*-butyl alcohol). The reaction product was extracted with ether (200 m*l*×2, 100 m*l*×5) after the addition of 4 N sodium hydroxide (250 m*l*) and saturation with sodium chloride. The combined ether extract was dried over sodium sulfate, and the dried solution was concentrated to a residue which was purified by fractional distillation; yield, 77 g (58%), bp 92—93°C/10 mmHg, mp 39.5—41.5°C. Reported, bp 120—122°C/15 mmHg, mp 41—42°C.[13]

13) Y. A. Ovchinnikov, A. A. Kiryushkin and A. I. Miroshnikov, *Experientia*, **21**, 418 (1965).

BULLETIN OF THE CHEMICAL SOCIETY OF JAPAN VOL. 42 812—820 (1969)

The Structure and the Stereochemistry of Solidagonic Acid

Shoichi KUSUMOTO, Tomomi OKAZAKI, Akio OHSUKA and Munio KOTAKE

Institute of Organic Chemistry, Faculty of Science, Osaka City University, Kita-ku, Osaka

(Received August 29, 1968)

A new bitter principle, solidagonic acid $C_{22}H_{34}O_4$, was isolated from the root of *Solidago altissima* L. It is a bicyclic diterpene carboxylic acid, having an acetoxyl group and two double bonds, and was formulated as II on the basis of chemical and spectroscopic studies. The other constituents of the root, kolavenic acid (XXIV) and kolavenol (XXVIII) were also isolated, and they were chemically correlated to II. The absolute configurations of II, XXIV and XXVIII were established by application of the octant rule on the ORD curves for some ketonic compounds derived from them.

We have previously reported[1] the isolation and structual elucidation of solidagonic acid, a bitter principle isolated from the root of *Solidago altissima* L. We now present evidences in full detail about its constitution and stereochemistry.

S. altissima L. (Compositae) is a perennial plant native to North America, and now grows all over Japan. Its root has a considerable bitter taste. Several investigations have been reported about the constituents of Solidago species,[2-4] and recently, a diterpene ketone, named solidagenone, was isolated from the root of *S. canadensis* L. and *S. giganitia*. Its structure was deduced as I from spectroscopic and chemical studies.[5] However, nothing has been reported about a bitter principle, and thus our study was undertaken.

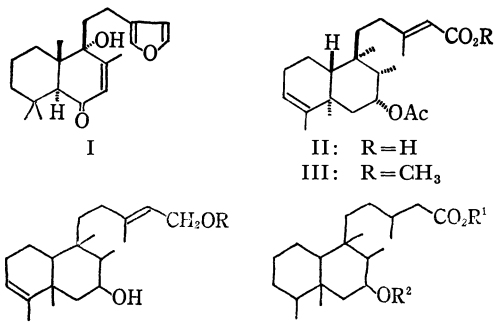

Fig. 1

Results and Discussion

An ethanol extract of the root of *S. altissima* L. was chromatographed repeatedly on silica-gel and silicic acid columns, and a bitter principle was isolated. It was a carboxylic acid and named solidagonic acid (II), $C_{22}H_{34}O_4$, mp 143—144°C, $[\alpha]_D^{12}$ −97.6°. Compound II was treated with diazomethane to give the methyl ester (III) $C_{23}H_{36}O_4$, mp 106.5°C, $[\alpha]_D^{12}$ −98.8°. Later, the method of isolation was improved and III was isolated from the dried root in about a 0.3% yield.

The IR spectrum of II indicated the presence of an ester (ν_{max}^{KBr} 1732, 1237 cm^{-1}) and an α,β-unsaturated acid (3400—2400, 1680, 1637 cm^{-1}). The UV spectra of II and III also suggested the presence of α,β-unsaturated acid (λ_{max}^{EtOH} 217.5 mμ ε 9090) and ester function (217.5 mμ, ε 15400), respectively. The NMR spectrum of II showed the presence of a carboxylic acid (δ 11.75, 1H), an acetyl group (2.00, 3H s), two tertiary methyl groups (0.97 and 1.17, each 3H s), one secondary methyl group (0.92, 3H d J=7 cps) and two olefinic methyl groups (1.59 and 2.18, each 3H slightly splitting singlet). Among them a signal at 2.18 ppm predicted the presence of the $-C(CH_3)=\dot{C}-CO_2H$ group and this was supported by the fact that the signal shifted to 1.65 ppm upon converting III to the diol (IV) by lithium aluminum hydride reduction.

Compound III absorbed 2 mol of hydrogen on catalytic hydrogenation and gave the tetrahydro methyl ester (VI), which proved to be a mixture of stereosiomers (see below). Its NMR spectrum showed the presence of one hydrogen on the carbon atom bearing the acetoxyl group (δ 4.97, 1H broad). Furthermore, calculation of the degree of unsaturation concluded that III has a bicyclic

1) S. Kusumoto, T. Okazaki, A. Ohsuka and M. Kotake, *Tetrahedron Letters*, **1968**, 4325.
2) E. Wada, *Kagaku (Science)*, **22**, 217 (1952).
3) L. Skrzypczakowa, *Acta Polon. Pharm.*, **18**, 39 (1961).
4) K. Stavholt Baalsrud, D. Holme, M. Nestvolt, J. Pliva, J. Stene Sörensen and N. A. Sörensen, *Acta Chem. Scand.*, **6**, 883 (1952).
5) T. Anthonsen, P. H. McCabe, R. McCrindle and R. D. H. Murray, *ibid.*, **21**, 2289 (1967).

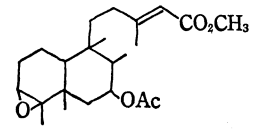

IX

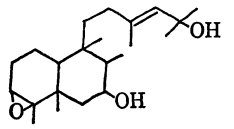

X

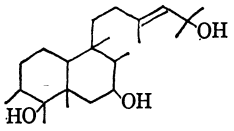

XI

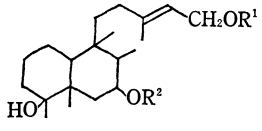

XII: $R^1=R^2=H$
XIII: $R^1=Ac$, $R^2=H$
XIV: $R^1=R^2=Ac$

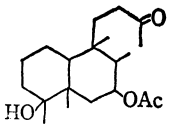

XV

Fig. 2

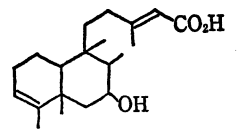

XVI

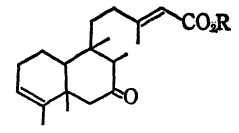

XVII: R=H
XVIII: R=CH_3

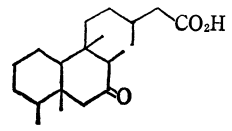

XIX

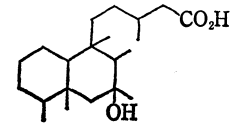

XX

Fig. 3

structure. The carbon skeleton of II is a decaline type since III gave 1,2,5-trimethylnaphthalene when dehydrogenated on selenium or palladium-charcoal.

When III was oxidized with one mole of monoperphthalic acid, a single monoepoxide (IX) $C_{23}H_{36}O_5$, mp 135.5—136.5°C, was obtained. It is clear from the IR and NMR spectra that the terminal α,β-unsaturated ester function remained unchanged (ν_{max}^{KBr} 1715, 1640 cm^{-1}; δ 2.41 3H d $J=1.1$ cps, and 5.53 1H broad singlet), and the other double bond was epoxidized (δ 1.15 3H s, and 2.77 1H triplet like). After introducing a methyl group into the epoxide ring, the product (XI) was dehydrogenated to afford 1,2,5,6-tetramethylnaphthalene, mp 116—117°C. Hence, one of the double bonds in II was fixed at C-3. The monoepoxide (IX) was reduced with lithium aluminum hydride to give the triol (XII) $C_{20}H_{36}O_3$, mp 120—121.5°C. When XII was acetylated with acetic anhydride and pyridine at room temperature, a monoacetate (XIII) $C_{22}H_{38}O_4$, mp 142.5—143.5°C, was obtained. This monoacetate was further acetylated at 100°C to afford an oily diacetate (XIV) (ν_{max}^{Oil} 3500 cm^{-1}; δ 1.97 6H s). Ozonolysis of XIV gave a methyl ketone (XV) $C_{20}H_{34}O_4$, mp 104—105°C, (ν_{max}^{KBr} 1705 cm^{-1}; δ 2.10 3H s). Thus, the structure of another double bond in II was confirmed as $-C(CH_3)=CHCO_2H$

An attempt to establish the position of the acetoxyl group in II was then undertaken. Compound III was hydrolyzed with methanolic potassium hydroxide and the resultant hydroxy acid (XVI), which could not be crystallized, was oxidized with Jones reagent to furnish the keto acid (XVII) which also could not be crystallized. Therefore, XVII was esterified with diazomethane and the product was purified on a silica-gel column to give an oily keto ester (XVIII), which was chracterized as the 2,4-dinitrophenylhydrazone $C_{27}H_{36}O_6N_4$, mp 174°C. When the keto ester (XVIII) was treated with methyl magnesium bromide, an expected product could not be isolated in a satisfactory yield, probably due to further reactions initiated by the ready dehydration of the terminal allylic tertiary alcohol. Thus, this sequence of the reactions was carried out with the tetrahydro series of compounds in the following manner. A crystalline tetrahydro hydroxy acid was obtained by hydrolysis of the tetrahydro derivative (VI) mentioned above, but the yield was poor and a considerable amount of an oil, which could not be crystallized, was obtained from the mother liquor. Therefore, the product of hydrolysis was esterified with diazomethane and two methyl esters were isolated by repeated chromatography on a silica-gel column: VIIa an oil; and VIIb $C_{21}H_{38}O_3$, mp 84—87°C. These esters were hydrolyzed to the corresponding two tetrahydro hydroxy acids: VIIIa $C_{20}H_{36}O_3$, mp 99—100°C; VIIIb $C_{20}H_{36}O_3$, mp 142—144°C. Since the IR spectra of these two acids in chloroform were almost identical, they are considered to be the stereoisomers formed by catalytic hydrogenation. The hydroxy acid (VIIIb) was oxidized with Jones reagent to the keto acid (XIX) $C_{20}H_{34}O_3$, mp 82—83°C. The position of the ketone was marked with methyl Grignard reagent, and the resultant hydroxy acid (XX) was dehydrogenated on selenium to give 1,2,3,5-tetramethylnaphthalene.[6] Thus, the position of acetoxyl group in II was unequivocally defined at C-7.

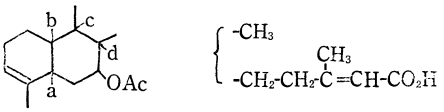

XXI

Fig. 4

6) D. E. A. Rivett, *J. Chem. Soc., (C)*, **1966**, 1892.

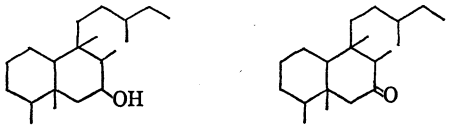

XXII XXIII

Fig. 5

The structure of solidagonic acid (II) proposed on the basis of the foregoing results should have the partial structure represented by XXI, in which the remaining tertiary methyl group and the side chain must be attached to some of the four possible positions *a*—*d*. The positions of the remaining tertiary substituents and the secondary methyl group were determined as follows. The diol (IV) gave the 7-monoalcohol (XXII) on hydrogenation over Adams catalyst in acetic acid - ethanol accompanied with hydrogenolysis of the terminal allylic alcohol. Oxidation of XXII with Jones reagent furnished the 7-ketone (XXIII) $C_{20}H_{36}O$, bp 125—133°C (bath)/1mmHg. The NMR spectrum of XXIII showed the presence of only three hydrogens adjacent to carbonyl group in the region of δ 1.8—2.7 ppm (δ 2.45 1H q J=6.7 cps, δ 1.94 and 2.28 AB type each 1H d J=12 cps). The former was assigned to the hydrogen at C-8 which coupled only with the three hydrogen atoms in the C-8 methyl group. The latter two were assigned to the C-6 methylene protons which coupled only with each other. Consequently the secondary methyl group was fixed at C-8, and it is clear that C-5 and C-9 carry no hydrogen. Although it is not possible to confirm the nature of the remaining two residues attached to C-5 and C-9, the structure represented by II is the most probable one, as judged from the NMR spectra of the two tertiary methyl groups of the various derivatives prepared (see below). Moreover, this structure is the so-called "rearranged labdane skeleton" of the type exhibited by the cascarillins,[7] and it is also reasonably explained on the basis of biogenetic considerations.[8-10] Therefore, the constitution of solidagonic acid is deduced as II.

Kolavenic acid (XXIV) was isolated from a benzene extract of the dried root as its methyl ester (XXV) $C_{21}H_{34}O_2$, bp 151—152°C/1 mmHg, $[\alpha]_D^{26}$ −60.8°. Its IR spectrum suggested the presence of an α,β-unsaturated ester group and its NMR spectrum showed the presence of two tertiary methyl groups (δ 0.76 and 1.02 each 3H s), one

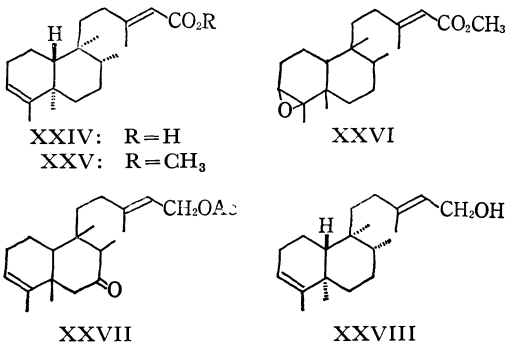

XXIV: R=H
XXV: R=CH_3
XXVI
XXVII XXVIII

Fig. 6

secondary methyl group (0.85 3H d J=6 cps)' two olefinic methyl groups (1.60 and 2.18 each 3H) and two olefinic protons (5.15 1H m, and 5.59 1H broad singlet). The terminal $-C(CH_3)=CH-CO_2H$ group was also expected in XXIV by comparison of these spectra with those of II and III. The compound XXIV was assigned to desacetoxyl solidagonic acid as a result of the following observations: (i) XXV absorbed 2 mol of hydrogen, indicating its bicyclic nature; (ii) dehydrogenation of XXV gave rise to 1,2,5-trimethylnaphthalene; (iii) methylation of the monoepoxide (XXVI) with methyl magnesium bromide followed by dehydrogenation resulted in the formation of 1,2,5,6-tetramethylnaphthalene, indicating that another double bond is at C-3. Compound XXIV was chemically correlated with II as follows. The alcohol formed upon removal of the C-7 oxygen function by Huang-Minlon reduction of the keto acetate (XXVII) was found to be identical with kolavenol (XXVIII), which was prepared by the reduction of XXV with lithium aluminum hydride; the comparison of their IR spectra, $[\alpha]_D$ and the mixed melting point test of their 3,5-dinitrobenzoate. The structure (XXV) thus established is in accordance with the constitution proposed for methyl kolavenate which has been isolated from *Hardwickia pinata* by Dev *et al.*[10] Although direct comparison of both substances has not been possible, it is evident that XXV is identical with methyl kolavenate, since the physical properties of both derivatives are in good agreement. Consequently, XXIV and XXVIII are named kolavenic acid and kolavenol, respectively. Kolavenol itself was also isolated from the dried root as its 3,5-dinitrobenzoate.

The stereochemistry of C-8 was assigned by an examination of solvent effects on the chemical shift of the secondary methyl group in the 7-keto derivatives. Downfield shifts of 0.06 and 0.05 ppm for XXVII and XXIX respectively were observed on changing solvent from carbon tetrachloride to benzene; these values are in reasonable agreement with those for equatorial methyl groups adjacent to a ketone. The equatorial orientation of the

7) T. G. Halsall, A. W. Oxford and W. Rigby, *Chem. Commun.*, **1965**, 218 and references therein.

8) E. J. Corey and J. J. Ursprung, *J. Am. Chem. Soc.*, **78**, 5041 (1956).

9) D. H. R. Barton, H. T. Cheung, A. D. Cross, L. M. Jackmann and M. Martin-Smith, *J. Chem. Soc.*, **1961**, 5061.

10) R. Misra, R. C. Pandey and Sukh Dev, *Tetrahedron Letters*, **1964**, 3751.

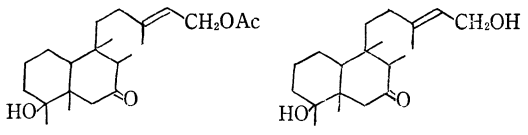

XXIX XXX

Fig. 7

C-8 methyl group was also supported by the fact that the starting ketodiol monoacetate (XXIX) was recovered by the treatment with alkali followed by acetylation.

The C-7 hydrogen appears as broad peaks or broad quartet-like peaks with half height width of 6—8 cps in the NMR spectra for 7-acetoxy or 7-hydroxy derivatives. These values suggest that C-7 hydrogen is in equatorial and thus the acetoxyl group should be axially oriented, since it has been demonstrated that the two adjacent carbon atoms (C-6 and 8) carry axial hydrogens.

The chemical shifts of the two tertiary methyl groups of the various derivatives prepared are summarized in Table 1. Remarkable upfield

Table 1. Chemical shift (δ) of the tertiary methyl groups

Compound	Solv.	C-5 Me	C-9 Me
IV	CCl_4	1.25	0.98
IV	C_6H_5N	1.55	1.21
V	CCl_4	1.25	0.97
XXVII	CCl_4	0.95	0.71
XVI	CCl_4	1.27	1.01
XVIII	CCl_4	0.96	0.72

shifts (about 0.3 ppm) of both of these methyl groups were observed, when the C-7 hydroxyl group was converted to a ketone. Therefore, 1,3-diaxial relations are expected between the methyl groups and the C-7 hydroxyl group.[11] The signals of these methyl groups of the diol (IV) moved downward (0.30 and 0.23 ppm, respectively) when the solvent was changed from carbon tetrachloride to pyridine, in which the downfield shift due to 1,3-diaxial relationship is known to increase.[12] The acetoxyl group in II is in a sterically hindered environment. The evidences for this are based on the following observations; (i) the acetyl group in II and VI resists to alkaline hydrolysis—a period of 10 hr at refluxing temperature was required to complete the reaction in 20% methanolic potassium hydroxide, (ii) the C-7 hydroxyl group could not be acetylated readily and (iii) the triol monoacetate (XIII) was recovered on reduction of the ketodiol monoacetate (XXIX) with sodium borohydride, indicating an attack of the reagent from the opposite side of the original hydroxyl group. These observations lead to the conclusion that the two tertiary methyl groups and the acetoxyl group in II are in a 1,3,5-triaxial relation.

The allylic methyl group in the side chain of III appeared at δ 2.15 ppm in carbon tetrachloride and this signal shifted to 2.20 ppm in benzene. These values are in good agreement with those expected for the allylic methyl group which is *cis* to a carbomethoxyl group.[13]

The ring junction and the absolute configuration were determined by examination of the ORD curves of the 7-ketone (XXIII), the bromoketone (XXXI) and the 2-keto acetate (XXXV). Bromination of XXIII in carbon tetrachloride furnished a monobromoketone (XXXI) $C_{20}H_{35}OBr$,

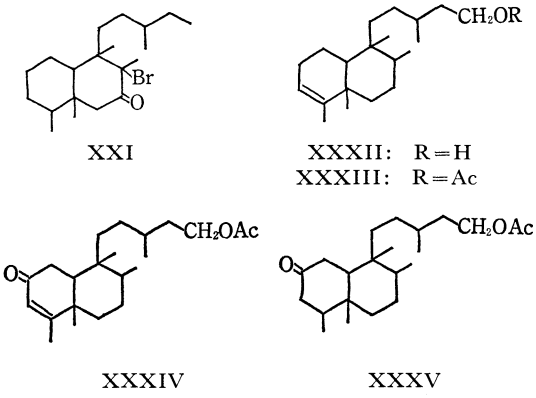

XXI XXXII: R=H
XXXIII: R=Ac

XXXIV XXXV

Fig. 8

which must be the 8-bromide, as the quartet of the C-8 proton disappeared and the singlet of the C-8 methyl group appeared at δ 1.72 ppm in its NMR spectrum. The axial orientation of the bromine was borne out by the facts that only a little shift ($+1\ cm^{-1}$) of the carbonyl band in IR spectrum was observed on bromination,[14] and that the NMR signal of one of the C-6 hydrogens showed a downfield shift which was probably due to the 1,3-diaxial interaction with the bromine atom.[15] This assignment was also confirmed by a bathochromic shift and an increasing amplitude of Cotton effect.[16] The ORD curve of the bromoketone (XXXI) showed a more intense negative Cotton effect ($a=-79.5$) in comparison with the 7-ketone (XXIII) which showed a small negative

11) N. S. Bacca and D. H. Williams, "Application of NMR Spectroscopy in Organic Chemistry," Holden-Day, San Francisco (1964), p. 19.

12) K. Tori and K. Aono, *Ann. Rept. Shionogi Res. Lab.*, **14**, 136 (1964).

13) J. Ronayne and D. H. Williams, *J. Chem. Soc., (C)*, **1967**, 2642.

14) R. N. Jones, D. A. Ramsay, F. Herling and K. Dobriner, *J. Am. Chem. Soc.*, **74**, 2828 (1952).

15) N. S. Bacca and D. H. Williams, "Application of NMR Spectroscopy in Organic Chemistry," Holden-Day, San Francisco (1964), p. 75, 183.

16) C. Djerassi, J. Osiecki, R. Riniker and B. Riniker, *J. Am. Chem. Soc.*, **80**, 1216 (1958).

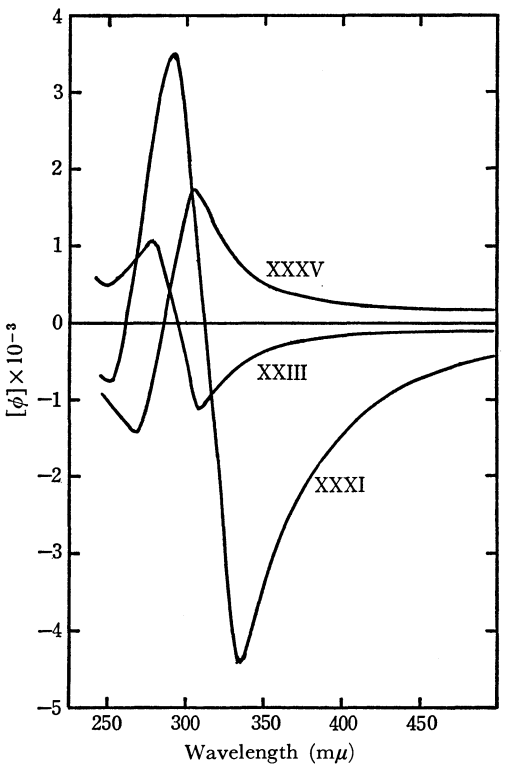

Fig. 9. ORD curves of XXIII, XXXI and XXXV.

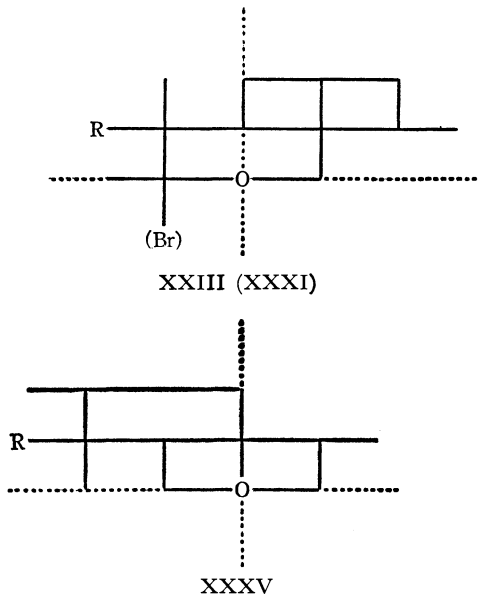

Fig. 10

Cotton effect ($a=-21.5$). Thus the bromine atom is β-oriented according to the axial haloketone rule and the absolute configuration of the B ring, except C-10, should be in the form given by II. The conjugated system in the side chain of methyl kolavenate (XXV) was reduced with metallic sodium in ethanol, and acetylation of the product afforded dihydrokolavenol acetate (XXXIII) $C_{22}H_{38}O_2$, bp 145—150°C (bath)/0.5 mmHg. Compound XXXIII was oxidized with chromium trioxide in acetic acid at 50°C to furnish an α,β-unsaturated cyclohexenone derivative (XXXIV): ν_{max}^{Oil} 1670, 1620 cm^{-1}; λ_{max}^{EtOH} 240 mμ (ε 9800); δ 1.85 3H d $J=1.2$ cps (C-4 methyl) and δ 5.56 1H d $J=1.2$ cps (C-3 proton). The newly introduced carbonyl group must be at C-2 as indicated by these spectral data. The 2-keto acetate (XXXV) $C_{22}H_{38}O_3$ was obtained by hydrogenation of XXXIV and reoxidation of the resultant saturated alcohol. The ORD curve of XXXV showed a positive Cotton effect ($a=+31.5$). Consequently, the *trans* junction of AB ring was established since the absolute configuration of the B ring, except C-10, was determined as mentioned above. Accordingly, the stereochemistry of solidagonic acid was fully established as shown by II.

Experimental

All melting points were measured on a Kofler block and are uncorrected. The NMR spectra were taken on a JEOL C-60 spectrometer in carbon tetrachloride unless otherwise stated; the signals are recorded in ppm from TMS (internal standard) as zero. All rotations were measured in 95% ethanol solution. Petroleum ether had bp 60—70°C. Merck silica-gel (0.05—0.2 mm) was used for chromatography.

Isolation of Solidagonic Acid (II). The sliced fresh root of *S. altissima* L. (11 kg) was extracted with ethanol at room temperature, the ethanol extract concentrated under reduced pressure and the residue extracted with ether. The oily residue (82 g) obtained after removing the solvent was chromatographed on silicagel (400 g) and eluted with benzene - ethyl acetate (95 : 5); 1.4 g of colorless crystals were obtained. The remaining oily portion was rechromatographed on a column of silicic acid (150 g), and eluted with benzene - ethyl acetate (98 : 2); 1.2 g of the crystals. The combined crystalline portion was recrystallized from petroleum ether to give colorless prisms: mp 143—144°C; $[\alpha]_D^{12}$ −97.6° (c 2.07); IR (KBr) 3400—2400, 1732, 1680, 1637, 1237 cm^{-1}; UV λ_{max}^{EtOH} 217.5 mμ (ε 9090); NMR 0.97, 1.17, 2.00 (each 3H s), 0.92 (3H d $J=7$ cps), 1.59, 2.18 (each 3H slightly splitting singlet), near 5.1 (2H broad peak), 5.63 (1H broad singlet), 11.75 (1H s).

Found: C, 72.88; H, 9.51%. Calcd for $C_{22}H_{34}O_4$: C, 72.89; H, 9.45%.

The methyl ester was obtained as granular crystals by esterification with diazomethane in ether and recrystallization from petroleum ether: mp 106.5°C; $[\alpha]_D^{12}$ −98.8° (c 1.80); IR (KBr) 1732, 1720, 1645, 1252, 1145 cm^{-1}; UV λ_{max}^{EtOH} 217.5 mμ (ε 15400); NMR 2.15 (3H d $J=1.2$ cps), 3.63 (3H s); NMR (in benzene) 2.20 (3H d $J=1.2$ cps).

Found: C, 73.22; H, 9.68%. Calcd for $C_{23}H_{36}O_4$: C, 73.36; H, 9.64%.

Isolation of Solidagonic Acid (III) and Kolavenic Acid (XXV) as Their Methyl Esters and of Kolavenol (XXVIII). The dried and crushed root (2.7kg) was

extracted with benzene by allowing to stand at room temperature for 4 weeks. The oily residue (90 g) obtained after removing the solvent under reduced pressure was partitioned between petroleum ether and 80% aqueous methanol.

An oil obtained by the evaporation of the solvent of the methanol-soluble fraction (36 g) was dissolved in ether and treated with an excess of diazomethane. The product was chromatographed on a silica-gel (400 g) column, and eluted with benzene, the eluate concentrated and the residue recrystallized from petroleum ether. Methyl solidagonate (III) was obtained as granular crystals (10 g), mp 106.5°C.

The petroleum ether solution, which had been extracted with 80% methanol, was again extracted with 95% methanol. An oily residue (23 g) left after removal of methanol was treated with an excess of diazomethane in ether. The resultant oil was chromatographed on a silica-gel (280 g) column and eluted with benzene. The first fraction was rechromatographed on a fresh silica-gel (100 g) column with petroleum ether - benzene (1 : 1) as a developing system. Methyl kolavenate (XXV) was obtained as a coloroess oil (8.1 g): bp 151—152°C/1 mmHg; $[\alpha]_D^{26}$ −60.8° (*c* 2.07); IR(oil) 1725, 1645, 1230, 1150 cm^{-1}; NMR 0.76, 1.02, 3.65 (each 3H s), 0.85 (3H d J=6 cps), 1.60 (3H slightly splitting singlet), 2.18 (3H d J=1.2 cps), 5.15 (1H broad), 5.59 (1H broad).

Found: C, 79.05; H, 10.87%. Calcd for $C_{21}H_{34}O_2$: C, 79.19; H, 10.76%.

The second fraction gave a small amount of III.

The third reaction was rechromatographed on a silica-gel column. Its elution with petroleum ether - ethyl acetate (95 : 5) gave an oil (0.5 g), which was treated with 3,5-dinitrobenzoyl chloride in pyridine to furnish kolavenol 3,5-dinitrobenzoate, mp 107°C. It was identified by mixed melting point with an authentic sample (prepared from methyl kolavenate) and by comparison of their IR spectra.

Reduction of III with Lithium Aluminum Hydride. A solution of III (3.5 g) in absolute ether (50 m*l*) was added dropwise to lithium aluminum hydride (1.7 g) in absolute ether (30 m*l*) with stirring, the mixture was stirred for further 4 hr under reflux, and then kept standing overnight. The reaction mixture was treated in the usual manner and the crude product was crystallized from benzene - petroleum ether, the diol (IV) was obtained as needles (2.6 g): mp 93.5—94.5°C; NMR 0.98, 1.25 (each 3H s), near 1.00 (3H d J=*ca.* 7 cps), 1.59 (3H d J=1.5 cps), 1.65 (3H slightly splitting singlet) near 3.94 (1H broad), 4.00 (2H d J=7 cps), 5.06 (1H broad) 5.31 (1H broad triplet J=7 cps); NMR (in pyridine) 1.21, 1.55 (each 3H s), 1.16 (3H d J=7 cps).

Found: C, 78.23; H, 11.16%. Calcd for $C_{20}H_{34}O_2$: C, 78.38; H, 11.18%.

Hydrogenation of III. Compound III (6.4 g) in ethanol (120 m*l*) was hydrogenated over 5% palladium-charcoal (0.6 g) at room temperature and atmospheric pressure; 2 mol of hydrogen was absorbed during 3 hr. The product (VI) (6.4 g) could not be crystallized. NMR 0.92 (6H s), 1.94, 3.60 (each 3H s), 4.97 (1H braod W_h=*ca.* 8 cps).

Dehydrogenation of III. i) A mixture of III (1.0 g) and 10% palladium-charcoal (1.5 g) was heated at 280—300°C under nitrogen for 12 hr, extracted with ether, the solvent evaporated, and a saturated solution of 1,3,5-trinitrobenzene in ethanol added to the residue; the adduct of 1,2,5-trimethylnaphthalene was obtained as orange yellow needles (80 mg), mp 158°C.

Found: C, 59.82; H, 4.68; N, 10.70%. Calcd for $C_{19}H_{17}O_6N_3$: C, 59.53; H, 4.47; N, 10.96%.

ii) Methyl solidagonate (III) (3.0 g) was heated at 270—280°C for 6.5 hr with selenium (3.0 g) under nitrogen, the reaction mixture extracted with ether, the ether extract passed through a column of alumina (20 g) and the solvent of the eluate was evaporated to dryness. A saturated solution of picric acid in ethanol was added to the residue to give 1,2,5-trimethylnaphthalene picrate as reddish orange needles (290 mg), which was recrystallized from ethanol, mp 139—140°C. This picrate was decomposed on a silica-gel column to the corresponding hydrocarbon; NMR 2.40, 2.49, 2.60 (each 3H s).

Styphnate, mp 131°C

Monoepoxide (IX). Monoperphthalic acid (0.485 g, 1.0 equiv.) in ether (22 m*l*) was added to an ether solution of III (1.0 g in 20 m*l*) under stirring in an ice bath and the reaction mixture allowed to stand for 19 hr at room temperature. The reaction mixture was washed successively with a saturated aqueous solution of sodium bicarbonate and water and then dried. The crystalline residue obtained upon evaporation of the solvent was chromatographed on a silica-gel (20 g) column. Elution with benzene - ethyl acetate (95 : 5) gave the monoepoxide (IX) (0.9 g), which was recrystallized from petroleum ether to give colorless prisms: mp 135.5—136.5°C; IR(KBr) 1729, 1715, 1640 cm^{-1}; NMR 0.90 (3H d J=7.1 cps), 0.92, 1.15, 1.19, 1.99, 3.60 (each 3H s), 2.14 (3H d J=1.1 cps), 2.77 (1H triplet like), 5.05 (1H ill resolved quartet, W_h=*ca.* 6 cps), 5.53 (1H broad singlet).

Found: C, 70.40; H, 9.30%. Calcd for $C_{23}H_{36}O_5$: C, 70.37; H, 9.24%.

Grignard Reaction of IX. A solution of IX (3.0 g) in absolute ether (80 m*l*) was added dropwise to a solution of methyl magnesium bromide (which had been prepared from 4.7 g of magnesium in 150 m*l* of absolute ether). The mixture was stirred for 6 hr under reflux, and allowed to stand overnight. The oily product was chromatographed on a silica-gel (90 g) column. Elution with benzene - ethyl acetate (85 : 15) gave the epoxydiol (X) (0.3 g), which was recrystallized from petroleum ether to give colorless prisms: mp 104.5—106°C; NMR 2.80 (1H triplet like).

Found: C, 75.45; H, 11.08%. Calcd for $C_{22}H_{38}O_3$: C, 75.38; H, 10.93%.

Successive elution of the chromatogram with benzene-ethyl acetate (7 : 3) afforded the triol (XI) (0.7 g), which was recrystallized from petroleum ether, mp 85—89°C.

Found: C, 75.69; H, 11.44%. Calcd for $C_{23}H_{42}O_3$: C, 75.36; H, 11.55%.

Dehydrogenation of XI. Compound XI (0.49 g) was heated for 8.5hr at 290—300°C with 10% palladium-charcoal (0.5 g) in a nitrogen atmosphere, the reaction mixture extracted with ether and the solvent removed. The crude oily product upon treatment with picric acid in ethanol gave the picrate (0.08 g), which was decomposed on a silica-gel column to 1,2,5,6-tetramethylnaphthalene; the recrystallized product (from ethanol), mp 116—117°C. NMR 2.41, 2.51 (each 6H s), 7.11, 7.63 (each 2H d J=9 cps).

Found: C, 91.09; H, 8.91%. Calcd for $C_{14}H_{16}$:

C, 91.25; H, 8.75%.

Picrate, mp 155—156°C.

Reduction of IX with Lithium Aluminum Hydride. To lithium aluminum hydride (1.4 g) in absolute ether (20 m*l*) was added a solution of IX (1.0 g) in absolute ether (30 m*l*) during a 30 min period with stirring at room temperature. The mixture was stirred for further 6 hr under reflux and set aside over night at room temperature. The reaction mixture was terated in the usual manner and the crude product was crystallized from benzene, the triol (XII) (0.6 g) was obtained: mp 120—121.5°C; NMR (in $CDCl_3$) 1.70 (3H slightly splitting singlet), 4.14 (2H d J=6 cps), 5.40 (1H broad triplet J=6 cps).

Found: C, 74.12; H, 11.32%. Calcd for $C_{20}H_{36}O_3$: C, 74.02; H, 11.18%.

Triol Monoacetate (XIII). Compound XII (1.0 g) dissolved in pyridine (8 m*l*) was treated with acetic anhydride (4 m*l*), and the reaction mixture set aside 17 hr at room temperature. Recrystallization from benzene gave XIII as prisms (1.0 g): mp 142.5—143.5°C; IR (KBr) 3500, 1712, 1240 cm^{-1}; NMR (in $CDCl_3$) 2.08 (3H s), 4.09 (1H ill resolved quartet), 4.59 (2H d J=7.5 cps), 5.37 (1H broad triplet J=7.5 cps).

Found: C, 72.11; H, 10.52%. Calcd for $C_{23}H_{38}O_4$: C, 72.09; H, 10.45%.

Triol Diacetate (XIV). Compound XIII (1.0 g) in pyridine (10 m*l*) and acetic anhydride (4 m*l*) was heated 100°C for 4hr. The oily product was chromatographed on a silica-gel (30 g) column. Elution with benzene - ethyl acetate (85 : 15) gave the oily diacetate (XIV) (0.85 g): IR(oil) 3500, 1740 (broad), 1230 cm^{-1}; NMR 1.97 (6H s), 5.09 (1H broad.)

Successive elution with the same solvent afforded the starting monoacetate (XIII) (0.2 g).

Ozonolysis of XIV. Ozonized oxygen was passed through a solution of XIV (0.83 g) in chloroform (14 m*l*) under ice-salt cooling for 25 min. The solvent was evaporated *in vacuo* and the oily residue was heated with 20 m*l* of water on a boiling water bath for 30 min. The neutral oil (0.6 g) obtained was chromatographed on a silica-gel (15 g) column with benzene - ethyl acetate (7 : 3) as a developing solvent. The crude methyl ketone (XV) (0.35 g) thus obtained was recrystallized from petroleum ether: mp 104—105°C; IR(KBr) 3540, 1732, 1705, 1232 cm^{-1}; NMR 1.99, 2.10 (each 3H s), 5.05 (1H quartet like W_h=*ca.* 7 cps).

Found: C, 70.75; H, 10.08%. Calcd for $C_{20}H_{34}O_4$: C, 70.97; H, 10.13%.

Keto Ester (XVIII). Compound II (1.0 g) was heated under reflux in 20% methanolic potassium hydroxide (20 m*l*) for 9.5 hr. The hydroxy acid (XVI) obtained as an oil (0.9 g) could not be crystallized after chromatography on a silica-gel column: IR(oil) 3360, 3200—2400, 1685, 1635 cm^{-1}; NMR 1.01, 1.27 (each 3H s), 4.00 (1H broad W_h=7.5 cps).

Jones reagent [a mixture of chromium trioxide (2.7 g) and concentrated sulfuric acid (2.3 m*l*) in water (10 m*l*)] (1.0 m*l*) was added dropwise to a solution of XVI (0.9 g) in acetone (30 m*l*) in an ice bath. The mixture was stirred for 2hr, diluted with water and extracted with ether. The ether solution was concentrated and treated with a solution of diazomethane in ether. Chromatography on a silica-gel (20 g) column with benzene gave the keto ester (XVIII) as an oil (0.65 g): IR(oil) 1710 (broad), 1640, 1225, 1150 cm^{-1}; NMR 0.72, 0.96 (each 3H s).

2, 4-Dinitrophenylhydrazone, mp 174°C.

Found: C, 63.22; H, 7.19; N, 10.86%. Calcd for $C_{27}H_{36}O_6N_4$: C, 63.26; H, 7.08; N, 10.93%.

Tetrahydro-hydroxy Esters (VIIa, b) and hydroxy Acids (VIIIa, b). Compound VI (7.0 g) was heated under reflux in 5% ethanolic potassium hydroxide for 8 hr. The acidic fraction was treated with an excess of diazomethane in ether for 3hr at room temperature. The oily product (6.5 g) obtained by evaporation of the solvent was chromatographed on a silica-gel (150 g) column and eluted with benzene - ethyl acetate (95 : 5). The oily hydroxy ester (VIIa) (3.6 g, a single spot on TLC) was isolated: IR (oil) 3510, 1740, 1200, 1010 cm^{-1}; IR (in CCl_4) 3680, 3500, 1745, 1200, 1010 cm^{-1}.

Successive elution with the same solvent gave a mixture of the two esters (0.8 g) and the crystalline hydroxy ester (VIIb) (1.8 g). The latter was recrystallized from petroleum ether: mp 84—87°C; IR(KBr) 3500, 1720, 1195, 1000 cm^{-1}.

Found: C, 74.69; H, 11.13%. Calcd for $C_{21}H_{38}O_3$: C, 74.51; H, 11.32%.

The IR spectra for VIIa and VIIb in carbon tetrachloride were almost iden tical.

Compound VIIa (2.2 g) was hydrolyzed for 3hr with 8% ethanolic potassium hydroxide under reflux. The hydroxy acid (VIIIa) was isolated in the usual manner and recrystallized from ptroleum ether as colorless plates (2.0 g): mp 99—100°C; IR (in $CHCl_3$) 3600, 3500, 3300—2500, 1710 cm^{-1}.

Found: C, 74.07; H, 11.24%. Calcd for $C_{20}H_{36}O_3$: C, 74.02; 11.18%.

Compound VIIb was hydrolyzed to the hydroxy acid (VIIIb), which was recrystallized from petroleum ether - benzene (8 : 2) as hexagonal plates, mp 142—144°C.

Found: C, 74.28; H, 10.97%.

The IR spectra for VIIIa and VIIIb in chloroform were almost identical.

Oxidation of VIIIb with Jones Reagent. Jones reagent (4.0 m*l*) was added to a solution of VIIIb (3.5 g) in acetone (80 m*l*) during a course of 10 min in an ice bath with stirring and the mixture was stirred for further 30 min at this temperature. The reaction mixture was treated in a usual manner and the crude product was crystallized from petroleum ether. The tetrahydro-keto acid (XIX) was obtained as needles (2.9 g), mp 82—83°C.

Found: C, 74.63; H, 10.71%. Calcd for $C_{20}H_{34}O_3$: C, 74.49; H, 10.63%.

The Reaction of XIX With Methyl Magnesium Bromide. A solution of XIX(3.5 g) in absolute ether was added dropwise to methyl magnesium bromide (which had been prepared from 1.1 g of magnesium) in absolute ether under constant stirring, the mixture heated under reflux for 6 hr, and then the reaction mixture treated as usual. The product was chromatographed on a silica-gel (60 g) column. Its elution with benzene - ethyl acetate (4 : 1) afforded the hydroxy acid (XX) (1.3 g), which was recrystallized from petroleum ether as needles: mp 128.5—130.5°C; IR(KBr) 3460, 3200—2400, 1711 cm^{-1}.

Found: C, 74.45; H, 11.36%. Calcd for $C_{21}H_{38}O_3$: C, 74.51; H, 11.32%.

Dehydrogenation of XX with Selenium. A mixture of XX (1.3 g) and selenium (1.3 g) was heated at 300°C for 10 hr under nitrogen and the reaction mixture

extracted with petroleum ether. The petroleum ether solution was passed through a column of silica-gel (20 g) to give a fraction, which on addition of a saturated solution of picric acid in ethanol, afforded the adduct (192 mg) of 1,2,3,5-tetramethylnaphthalene as orange-red crystals, mp 163—164°C. This adduct was decomposed on a silica-gel column to the corresponding hydrocarbon; NMR 2.32, 2.42, 2.54, 2.62 (each 3H s).

1,3,5-Trinitrobenzene adduct, mp 182—183°C.

Found: C, 60.67; H, 5.12; N, 10.49%. Calcd for $C_{20}H_{19}O_6N_3$: C, 60.45; H, 4.82; N, 10.58%.

7-Ketone (XXIII). Compound IV (2.6 g) in acetic acid (100 m*l*) and ethanol (50 m*l*) was hydrogenated over Adams catalyst (200 mg) at room temperature under atmospheric perssure; about 2.9 mol of hydrogen was absorbed. The oily product (2.6 g) obtained was chromatographed on a silica-gel (20 g) column and eluted with benzene. The 7-monoalcohol (XXII) was obtained as a colorless oil (1.6 g): IR(oil) 3350 cm^{-1}; NMR 3.95 (1H quartet like).

Jones reagent (2.0 m*l*) was added to a solution of XXII (1.6 g) in acetone (30 m*l*) in 3 min in an ice bath, stirred for further 10 min at this temperature, and the reaction mixture worked up in the usual way. Distillation of an oily product under reduced pressure afforded 7-ketone (XXIII) (1.6 g): bp 125—133°C (bath)/1 mmHg; IR(oil) 1708 cm^{-1}; NMR 1.94, 2.28 (each 1H d J=12 cps), 2.45 (1H q J=6.7 cps); ORD $[\phi]_{308}^{\text{trough}}$ −1145°, $[\phi]_{278}^{\text{peak}}$ +1007° (*c* 0.147, in CH_3OH).

Found: C, 82.07; H, 12.35%. Calcd for $C_{20}H_{36}O$: C, 82.12; H, 12.40%.

Dehydrogenation of XXV. Compound XXV (1.6 g) was heated for 10 hr with 10% palladium-charcoal (1.0 g) at 300—320°C under nitrogen and the mixture was extracted with ether. An oil (1.0 g) obtained after removal of the solvent was treated with picric acid in ethanol. Reddish brown crystalls of 1,2,5-trimethylnaphthalene picrate were recrystallized from ethanol; yield 109 mg, mp 136—138°C which was undepressed on admixture with the authentic sample.

Hydrogenation of XXV. Compound XXV (1.6 g) was dissolved in ethanol (50 m*l*) and hydrogenated over Adams catalyst (0.2 g); 2.04 mol of hydrogen was absorbed during a 2.5 hr period. The product was isolated as usual and distilled under reduced pressure: bp 135—140°C (bath)/3 mmHg; IR (oil) 1745, 1160 cm^{-1}.

Methyl Kolavenate Monoepoxide (XXVI). A solution of monoperphthalic acid (3.3 g, 1.1 equiv.) in ether (140 m*l*) was added dropwise to a solution of XXV (5.0 g) in ether (50 m*l*) with stirring in an ice bath. The mixture was set aside for 20 hr at room temperature. Working up in the usual way gave a colorless oil (5.4 g), which was chromatographed on a silica-gel (100 g) column. Elution with benzene - ethyl acetate (95 : 5) afforded the monoepoxide (XXVI) as an oil (4.55 g): IR(oil) 1720, 1645 cm^{-1}; NMR 0.69, 1.06, 1.15, 3.64 (each 3H s), 2.16 (3H d J=1.2 cps), 2.78 (1H triplet like), 5.60 (1H broad singlet).

Grignard Reaction of XXVI Followed by Dehydrogenation. A solution of XXVI (4.3 g) in absolute ether (40 m*l*) was added dropwise to an ice cold solution of methylmagnesium bromide (which had been prepared from 4.7 g of magnesium) in absolute ether (100 m*l*). The mixture was stirred under reflux for 6.5 hr and set aside overnight at room temperature. Working up in the usual way afforded an oily product (4.5 g). A mixture of this oil (2.4 g) and selenium (2.0 g) was heated at 300—320°C for 8 hr under nitrogen and after cooling extracted with ether. The ether solution was passed through a column of alumina and the solvent of the eluate evaporated. The residue was recrystallized from ethanol to give 1,2,5,6-tetramethylnaphthalene; mp 115—116°C, picrate mp 157—157.5°C.

Kolavenol (XXVIII). A solution of XXV (3.2 g) in absolute ether (50 m*l*) was added dropwise to a solution of lithium aluminum hydride (1.0 g) in absolute ether (100 m*l*) in 15 min at room temperature and the mixture refluxed for 3 hr. Working up the reaction mixture in the usual way afforded an oil (3.0 g), which was chromatographed on a silica-gel (60 g) column. Elution with benzene - ethyl acetate (95 : 5) gave kolavenol (XXVIII) as an oil (1.5 g), $[\alpha]_D^{26}$ −57.1° (*c* 2.52).

The 3,5-dinitrobenzoate derivative was prepared by treatment with 3,5-dinitrobenzoyl chloride and pyridine, and recrystallized from ethanol, mp 105.5—106.5°C.

Found: C, 66.90; H, 7.49; N, 5.94%. Calcd for $C_{27}H_{36}O_6N_2$: C, 66.92; H, 7.49; N, 5.78%.

Acetylation of IV Followed by Oxidation. Compound IV (1.0 g) was dissolved in a mixture of pyridine (8 m*l*) and acetic anhydride (4 m*l*) and set aside for 40 hr in a refrigerator. The oily product obtained in the usual way was chromatographed on a silica-gel (19 g) column to remove a small amount of the diacetate. Elution with benzene - ethyl acetate afforded the monoacetate (V) as an oil (1.1 g): IR(oil) 3500, 1740, 1235 cm^{-1}; NMR 0.97, 1.25, 1.97 (each 3H s), 3.96 (1H quartet like), 4.48 (2H d J=7.5 cps).

Compound V (1.1 g) in acetone (25 m*l*) was oxidized with Jones reagent (1.2 m*l*) in an ice bath. Working up the reaction product in the usual way and chromatography on a silica-gel column afforded the keto-acetate (XXVII) as an oil (0.85 g): NMR 0.71, 0.95 (each 3H s), 0.89 (3H d J=*ca.* 7 cps); NMR (in benzene) 0.95 (3H d J=7.2 cps).

Huang-Minlon Reduction of XXVII. A solution of XXVII (0.9 g) in triethyleneglycol (15 m*l*) containing potassium hydroxide (2.5 g) and 80% hydrazine hydrate (5 m*l*) was heated for 1 hr at 130°C, for 2 hr at 150°C and then for 1.5 hr at 210°C. The reaction mixture was extracted with ether and the ether solution was washed thoroughly with water, dried, and evaporated. The residual oil was chromatographed on a silica-gel (16 g) column and eluted with benzene - ethyl acetate (97 : 3); an oily alcohol yield 0.2 g, $[\alpha]_D^{27}$ −55.9°C (*c* 3.04). The IR spectrum of this alcohol was identical with that of kolvavenol (XXVIII) prepared from XXV.

The 3,5-dinitrobenzoate derivative, mp 105—106°C, showed no depression of melting point on admixture with authentic kolavenol 3,5-dinitrobenzoate.

Oxidation of XIII with Jones Reagent. Jones reagent (1.0 m*l*) was added to a solution of XIII (1.0 g) in acetone (20 m*l*) under stirring in an ice bath, and stirred for further 20 min at this temperature. Working up the reaction mixture in the usual way afforded the ketodiol monoacetate (XXIX) as a viscous oil (1.0 g), which could not be crystallized even after

careful chromatography on a silica-gel column. IR (oil) 3500, 1740, 1710, 1240 cm^{-1}; NMR 0.67, 0.91, 1.08, 1.98 (each 3H s), 0.87 (3H d J=6 cps); NMR (in benzene) 0.92 (3H d J=6 cps).

The Alkaline Treatment and Reduction with Sodium Borohydride of XXIX. Compound XXIX (0.7 g) was dissolved in 5% pottasium hydroxide solution in methanol (10 m*l*) and heated under reflux for 2 hr. The solution was concentrated *in vacuo* to half of its volume, diluted with water, and extracted with ether. The ketodiol (XXX) was obtained as a viscous oil (0.5 g), which could not be crystallized.

Compound XXX (0.5 g) was dissolved in pyridine (1 m*l*) and acetic anhydride (2 m*l*) and set aside overnight at room temperature. Working up the reaction mixture in the usual way afforded an oil (0.5 g), and its IR spectrum was identical with that of the starting ketodiol monoacetate (XXIX).

The ketodiol monoacetate (0.5 g) thus obtained was dissolved in methanol (15 m*l*) and sodium borohydride (0.1 g) was added in portions in an ice bath with stirring during 20 min. The mixture was stirred for 2 hr at room temperature, then acidified with acetic acid, and diluted with water to give colorless crystals. Recrystallization from benzene gave the pure crystals (0.4 g), which were found to be identical with authentic triol monoacetate (XIII) as shown by their melting point, mixed melting point and IR spectra.

Bromoketone (XXXI). A solution of bromine (0.10 m*l*) in carbon tetrachloride (4 m*l*) was added dropwise in 20 min to a solution of XXIII (0.5 g) in carbon tetrachloride (20 m*l*) at room temperature under stirring. The solution was stirred for further 30 min, and washed successively with water, aqueous sodium thiosulfate solution and water. Evaporation of the solvent gave a pale yellow oil (0.65 g), which was chromatographed on a silica-gel (14 g) column. Elution with petroleum ether - benzene (1 : 1) afforded the bromoketone (XXXI) as a colorless oil (0.5 g): IR(oil) 1709 cm^{-1}; NMR 1.72 (3H s), 2.21, 3.34 (each 1H d J=12.5 cps); ORD $[\phi]_{335}^{\text{trough}}$ −4450°C, $[\phi]_{292}^{\text{peak}}$ 3500° (*c* 0.119, in CH_3OH).

Found: C, 64.60; H, 9.59%. Calcd for $C_{20}H_{35}OBr$: C, 64.67; H, 9.50%.

Dihydrokolavenol Acetate (XXXIII). Metallic sodium (6 g) was added in portions to a boiling solution of XXV (3.1 g) in absolute ethanol (65 m*l*) during 2 hr. The mixture was kept at 100°C for 1.5 hr (during this period all sodium dissolved), cooled, diluted with water and then extracted with ether. The reddish brown oil (2.1 g) obtained on concentration was acetylated with acetic anhydride and pyridine and the product was chromatographed on a silica-gel (42 g) column with benzene as an eluting solvent. The dihydrokolavenol acetate (XXXIII) was obtained as an oil (1.9 g), which was distilled under reduced pressure: bp 145—150°C (bath)/0.5 mmHg; NMR 1.54 (3H d J=1.6 cps), 1.94 (3H s), 4.01 (2H t J=6.3 cps), 5.08 (1H broad).

Found: C, 79.13; H, 11.26%. Calcd for $C_{22}H_{38}O_2$: C, 78.98; H, 11.45%.

Oxidation of XXXIII with Chromium Trioxide. A solution of XXXIII (1.7 g) and chromium trioxide (1.4 g) in acetic acid (30 m*l*) and water (1.5 m*l*) was heated for 2 hr at 50°C. After an excess reagent was decomposed with ethanol, the solvent was evaporated *in vacuo*. An oily residue was dissolved in ether, the ether solution washed successively with water, a saturated aqueous solution of sodium bicarbonate and water, and dried. The oil obtained on evaporation of the solvent was chromatographed on a silica-gel column and eluted with benzene - ethyl acetate (9 : 1). The 2-keto-3-ene (XXXIV) was obtained as a pale yellow oil (0.5 g): IR(oil) 1738, 1670, 1620, 1235 cm^{-1}; UV $\lambda_{\max}^{\text{EtOH}}$ 240 mμ (ε 9800); NMR 1.85 (3H d J=1.2 cps), 1.96 (3H s), 4.02 (2H t J=6.3 cps) 5.56 (1H d J=1.2 cps).

2-Ketone Acetate (XXXV). Compound XXXIV (0.45 g) in ethanol (20 m*l*) was hydrogenated over Adams catalyst (40 mg) at room temperature and atmospheric pressure; 2.2 mol of hydrogen was absorbed. The product was isolated as a colorless oil (0.4 g), IR(oil) 3400 cm^{-1}.

The hydrogenation product (0.45 g) in acetone (10 m*l*) was oxidized with Jones reagent (0.5 m*l*) in an ice bath. An oily product was chromatographed on a silica-gel (14 g) column and eluted with benzene - ethyl acetate (9 : 1). The 2-ketone acetate (XXXV) was obtained as a colorless oil (0.25 g), which was distilled under reduced pressure: bp 168—173°C (bath)/0.006 mmHg; IR(oil) 1736, 1710, 1235 cm^{-1}; ORD $[\phi]_{305}^{\text{peak}}$ +1740°, $[\phi]_{268}^{\text{trough}}$ −1410° (*c* 0.116, in CH_3OH).

Found: C, 75.18; H, 10.91%. Calcd for $C_{22}H_{38}O_3$: C, 75.38; H, 10.93%.

The authors express their gratitude to Dr. Y. Hirose of the Institute of Food Chemistry for providing facility for the measurement of NMR spectra. They are indebted to Professor K. Naya of Kwansei Gakuin University for the measurement of ORD spectra.

NOTES

BULLETIN OF THE CHEMICAL SOCIETY OF JAPAN VOL. 42 821—823 (1969)

Ultraviolet Spectral Studies in the Esters of Aroylphosphonic Acids

Ken-ichi TERAUCHI and Hiroshi SAKURAI

The Institute of Scientific and Industrial Research, Osaka University, Yamada-Kami, Suita, Osaka

(Received June 22, 1968)

The yellow color and spectral properties of aroylphosphonates are of some interest since the carbon analog benzaldehyde derivatives are colorless and since the phosphorus atom obviously acts as part of the chromophoric system.

The infrared and NMR data[1] provide evidence for a moderately strong conjugation between phosphorus of the phosphoryl group and carbon of the adjacent carbonyl group; more especially, the infrared absorptions of the carbonyl group in Compounds I—VIII (Table 2) show significantly low frequencies (50—65 cm^{-1} less than those[2] of the corresponding aldehydes). Griffin[3] and Berlin[4] have investigated the ultraviolet spectral evidence for d_π–p_π bonding in tri-2-pyrryl-, 2-(1-methylpyrryl),- 2-thienyl-, and 2-furylphosphine oxides, all of which possess a number of *para*-substituents on the aromatic ring, and in some acylphosphonates, respectively. The n–π^* transitions, however, in esters of aroylphosphonic acids have not yet been elucidated. In the present work, the n–π^* bands of Compounds I—VIII have been investigated, and an interesting correlation of the n–π^* band with Hammett substituent constants has been found.

The ultraviolet spectra of benzoylphosphonates were shown in the 320—450 mμ region (Fig. 1). In the ultraviolet and visible regions, the I—VIII benzoylphosphonates have two absorptions (Table 1); that in the 258—295 mμ region is identified as a π–π^* transition (^1A–^1L_a) on the basis of the large extinction coefficients, and the other, occurring in the 373—385 mμ region, identified as an n–π^* transition of the carbonyl group, are involving interaction with the phosphorus d-orbitals. The high intensity π–π^* bands in Compounds I—VIII underwent a bathochromic shift of from 17 to 29 mμ from those of its carbon-analog benzaldehydes.[5] Such a red shift suggests the extended conjugation that electronic excitation would produce an excited electron, one which is probably partially delocalized over the P→O group perhaps through vacant d orbitals on the phosphorus. On the other hand, the n–π^* bands in I—VIII are, of course, at much longer wavelengths. When we compare

TABLE 1. ULTRAVIOLET SPECTRAL DATA FOR AROYLPHOSPHONATES

Compound	R	R′	Transition π–π^* λ_{max}, mμ (log ε_{max})	Transition n–π^* λ_{max}, mμ (log ε_{max})
I	C_6H_5	C_2H_5	258 (4.05)	379 (1.92)
II	C_6H_5	i-C_3H_7	258 (4.11)	379 (1.91)
III	C_6H_5	n-C_4H_9	259 (4.11)	380 (2.01)
IV	C_6H_5	$CH_2CH{=}CH_2$	265 (4.31)	378 (2.18)
V	p-ClC_6H_4	C_2H_5	268 (4.10)	385 (1.97)
VI	p-BrC_6H_4	C_2H_5	271 (4.27)	385 (1.98)
VII	p-$CH_3OC_6H_4$	C_2H_5	294 (4.01)	373 (2.18)
VIII	p-$(CH_3)_3CC_6H_4$	C_2H_5	271 (4.06)	375 (2.16)

the absorption data[6] with those of the benzaldehydes, we find that the n–π^* absorption maxima of benzoylphosphonates show an average bathochromic shift of 50 mμ, suggesting that the orbital on carbon atom overlaps with a vacant d orbital on the phosphorus. Also, the extinction coefficients of benzoylphosphonates are considerably greater than those of the corresponding benzaldehydes. The n–π^* transition of I occurred at a wavelength shorter by 17 mμ in methanol than in cyclohexane (hypsochromic shift). This change follows the pattern

1) K. D. Berlin and H. A. Taylor, *J. Am. Chem. Soc.*, **86**, 3862 (1964).

2) L. J. Bellamy, "The Infrared Spectra of Complex Molecules," John Wiley and Sons, New York, N.Y. (1954).

3) C. E. Griffin, R. P. Peller, K. R. Martin and J. A. Peters, *J. Org. Chem.*, **30**, 97 (1965).

4) K. D. Berlin and D. H. Burpo, *ibid.*, **31**, 1304 (1965).

5) J. C. Dearden and W. F. Forbes, *Can. J. Chem.*, **36**, 1362 (1958).

6) H. E. Ungnade, M. E. Hill and M. J. Kamlet, Ed., "Organic Electronic Spectral Data," Vol. II, Interscience Publishers, Inc., New York (1957), p. 135.

usually observed in carbonyl compounds in changing from non-polar to polar solvents; hence, it substantiate the identification of the spectroscopic transition as n–π^*.

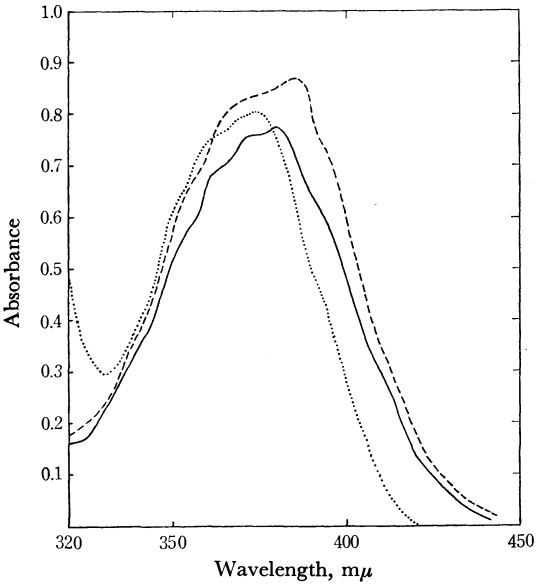

Fig. 1. The electronic spectra of I (——), 928×10^{-5} M; V (– – –), 958×10^{-5} M; and VI (·····), 533×10^{-5} M; all spectra were recorded in cyclohexane.

An interesting correlation between the wavelengths of the most intense n–π^* bands and σ's, the Hammett substituent constants, was also noted (Fig. 2). Although it is recognized that ultraviolet data, which involve both ground and excited states, cannot normally be related to Hammett substituent effects, which involve ground states only, this apparent correlation appears worthy of comment. A linear correlation of wavelengths with σ's was found for benzoylphosphonate and its *p*-*t*-butyl-, *p*-methoxy-, *p*-chloro-, and *p*-bromo derivatives. Unfortunately, no kinetic data involving Hammett correlations in *para*-substituted benzoylphosphonates have yet been reported; however, we believe that this correlation is real and significant.

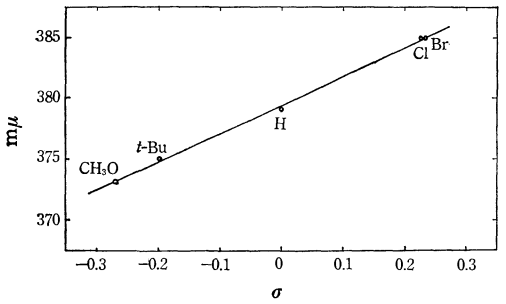

Fig. 2. Carbonyl n–π^* absorption wavelength *vs.* Hammett σ constant for *p*-substituted benzoylphosphonates.

Such a substituent effect prompts the question concerning the preferred conformation in the aroylphosphonates. The NMR data[1] suggest free rotation around the C–P bond. On the other hand, dipole-moment measurements have been reported the values of 2.93 D for I, 3.20 D for VI, and 2.64 D for V.[7]

These values of VI and V, lower and higher, respectively compared to those of the corresponding aldehydes (reported[8] as 3.70 D and 2.03 D respectively) prompt the speculation that the powerful electron inductive abilities of the methoxy and chloro functions cause a change in the electron density on the carbonyl carbon atom. The more the electron density on the carbonyl carbon increases, the more the lifetime of the conformation in which the carbonyl and phosphoryl groups are opposite might increase.

Consequently, it is conceivable that, in Compound V, the interaction of a filled nonbonding orbital on the oxygen of the phosphoryl group with the π-orbital of the carbon atom of the carbonyl group could occur to a greater extent than in Compound VI and could result in the n–π^* band at a longer wavelength. Assuming sp^2-hybridization on the oxygen of the phosphoryl group, the overlap of these orbitals is possible and is probably at a maximum when the P→O bond is perpendicular to the plane composed of the aryl ring, carbon, and phosphorus. It is also known[9] that, when there is a direct (σ-type) interaction of the π-orbital of the carbon atom of the carbonyl group with the lone-pair electron in another group, an intensification of the carbonyl n–π^* band is observed. Therefore, as is shown in Table 1, from the large intensity of the n–π^* band in Compounds I—VIII we will be able to deduce that such a direct

Table 2. Infrared spectra of aroylphosphonates (cm^{-1})

Compd.	C=O	P→O	P–O–C
I	1655	1255	1020
II	1648	1250	998
III	1640	1252	1020
IV	1642	1254	a
V	1645	1251	1015
VI	1640	1250	1014
VII	1630	1245	1021
VIII	1644	1255	1018

a) A broad absorption in the region of 988—1030 cm^{-1}.

7) See Ref. 1. These values are measured in R=CH_3.

8) L. G. Wesson, "Tables of Electric Dipole Moment," The Technology Press, Cambridge, Mass. (1948).

9) J. N. Murrell, "The Theory of the Electronic Spectra of Organic Molecules," John Wiley and Sons, Inc., New York, N.Y. (1963), p. 165.

interaction (overlap effect) exists in benzoylphosphonates. This interactioni is supported by the findings concerning the carbonyl stretching frequency shown in Table 2. However, in view of the ultraviolet data, the p_π–d_π bonding in aroylphosphonates is apparently far less sensitive to rotation around the bond axis than is the p_π–p_π bonding such as that in α-diketones.[10] In arly sulfones, it is known that the formation of p_π–d_π bonds is independent of steric restraints because of the geometry and the large number of 3d orbitals.[11] In compounds of the R_3PO type it has been pointed out that some interaction of 3d orbitals with a π orbital of the chromophoric R group is possible, whatever the orientation of the chromophore plane with respect to the rest of the molecule.[12]

In addition, the β-keto compound diethylphosphonacetophenone has only one high intense band (λ_{max} 245 mμ, log ε 4.32), with no discrenible shoulders in the 220—450 mμ region; this shows the absence of any formation of d_π–p_π bonding.

Experimental

The ultraviolet spectra were determined in spectral-grade cyclohexane on a Hitachi EPU-2 spectrophotometer. The infrared spectra were obtained on a Hitachi EPI-S2 instrument run at a very slow speed in films of the esters of sodium chloride plates. The aroylphosphonates were synthesized by the reaction of trialkyl phosphites with acid chloride.[1] The diethylphosphonacetophenone was prepared by the methods of Borowitz *et al.*[13] Repeated distillation under reduced pressure was used to purify all the compounds needed. Tlc on a 0.25-mm thickness of silica gel, with acetone-chloroform in the volume ratio of 1 : 9, showed only one spot after development for each of the compounds examined.

10) N. J. Leonard and E. R. Blout *J. Am. Chem. Soc.*, **72**, 484 (1950), and references therein.

11) H. H. Jaffe and M. Orchin, "Theory and Applications of Ultraviolet Spectroscopy," John Wiley and Sons, Inc., New York, N.Y. (1962), p. 489.

12) See Ref. 11, p. 474.

13) I. J. Borowitz, M. Anschel and S. Firstenberg, *J. Org. Chem.*, **32**, 1723 (1967).

BULLETIN OF THE CHEMICAL SOCIETY OF JAPAN VOL. 42 823—825 (1969)

Laser-induced Chemical Reaction. I. Reaction of Carbon Vapor Produced by a Pulse Ruby Laser

Ko TAKI, Pil Hyon KIM and Susumu NAMBA

The Institute of Physical and Chemical Research, Yamato-machi, Saitama

(Received July 2, 1968)

An intense laser beam is known to produce a high-temperature region when it hits the surface of a suitable target, resulting in the evaporation of the target material. This note will describe an investigation of the reaction of such a vapor with hydrocarbon.

The target material employed in this work was Shimadzu spectroscopic electrode graphite preheated under a vacuum. The laser used was a pulse ruby laser, the output energy and pulse duration of which were about 3 joules and 0.5 msec respectively.

The laser beam was focused by a lens of 30 mm focal length upon the graphite carbon in a 7-cc Pyrex cell filled with ethylene vapor. After a 10—20 pulse irradiation, the analysis was performed by gas chromatography; the principal products were acetylene, diacetylene, and vinylacetylene. The ratio of C_3 to C_4 products*1 was about 0.03—0.05. The data are listed in Table 1.

TABLE 1. YIELD OF PRODUCTS FROM THE REACTION OF ETHYLENE WITH CARBON VAPOR PRODUCED BY THE LASER BEAM

Product	Yield ($\times 10^{-6}$ mol)
Methane	0.15—0.22
Ethane	0.06—0.08
Ethylene	—
Acetylene	24.0—26.0
Vinylacetylene	0.5
Diacetylene	3.5—4.0
C_3 compounds	0.12—0.15
C_4 compounds	4.0—4.5
C_3/C_4	0.03—0.05

Ethylene: 700 Torr
Carbon consumed: 3.0—4.0 $\times 10^{-5}$ mol
Laser: 10 pulses

*1 All the reaction products were catalytically reduced by PtO_2 and hydrogen, and the propane and butane produced from C_3 and C_4 products were analysed by gas chromatography using a silica gel column; the area ratio was calibrated to the molar ratio.

There have been intensive investigations of the reaction of free carbon atoms produced by nuclear recoil reaction[1,2] and by the photolysis of carbon suboxide[3] and a carbon arc.[4] However, the reaction products and their distributions differ greatly from case to case. In the recoil reaction, it has been shown that the most common primary processes are the additions of the C atom (monoatomic carbon) to C–H and C=C bonds; the resulting adducts then undergo secondary processes. On the other hand, the carbon vapor produced in the carbon arc reacts with butenes to give spiropentane derivatives and bisethanoallene derivatives, which have been suggested to be produced from the reactions of monoatomic carbon (C_1) and triatomic carbon (C_3)[5] respectively, but no formation of acetylene has yet been found. This difference has been considered[6] to be due to the facts that the reaction conditions are not the same, and that, in a recoil reaction, free carbon atoms are apparently reaction species, while in the case of carbon vapor produced in the carbon arc the carbon atoms are complexed on the surface material.

From the fact that the products consist of C_2 and C_4 compounds in the laser-induced reaction, it seems likely that the reaction may involve the interaction of a diatomic carbon intermediate (C_2) with ethylene. There have been a few reports on the reaction of C_2, in which the diatomic carbon intermediate is the precursor of the production of acetylene[7] and other products.[8] It was considered to be highly desirable to confirm the presence of C_2 and, if possible, to observe its chemical properties. Spectroscopically, the presence of C_2 in the carbon vapor produced by laser irradiation was confirmed by the observation of the C_2 Swan bands in the vacuum system, in a hydrogen atmosphere, and in ethylene vapor. The C_2 Swan bands were also observed by Howe[9] and by Mentall and Nicholls[10] in air.

Laser-induced reactions in hydrogen, lower alkanes, butadiene, and butene-1 were also investigated.

In the reaction with hydrogen, the principal product was acetylene (about 80%, based on the carbon consumed), while no ethylene was detected, as is shown in Table 2. On the other hand, a carbon atom was produced by a recoil reaction with hydrogen[11] to produce CH, CH_2, and CH_3 radicals, these radicals undergo further reaction to produce acetylene, ethylene, and other products.

TABLE 2. YIELD OF PRODUCTS FROM THE REACTION OF HYDROGEN WITH CARBON VAPOR PRODUCED BY THE LASER BEAM

Product	Yield ($\times 10^{-6}$ mol)
Methane	0.3—0.4
Acetylene	15.0—20.0
Ethylene	0
C_3 compounds	0.1
C_4 compounds	1.0
C_3/C_4	0.1

Hydrogen: 700 Torr
Carbon consumed: $3.0—4.0 \times 10^{-5}$ mol
Laser: 10 pulses

In the reaction with a hydrogen and ethylene mixture (8 : 1), no pentene-1 was detected. As has been suggested by Wolfgang and his coworkers,[12] the addition of methyne (CH) to an ethylene molecule gives pentene-1. Therefore, the possibility that methyne was a precursor of acetylene may be excluded.

In the reaction with methane, ethane, and cyclopropane, the principal product was acetylene, and only a trace amount of ethylene was formed, as shown in Table 3. A carbon atom has been known to react with methane to produce ethylene and acetylene in an almost equivalent yield by insertion:[13,14]

$$C + CH_4 \rightarrow (CH_3\text{–}\dot{C}\text{–}H) \rightarrow C_2H_4 \text{ and } C_2H_2$$

The reaction of a carbon atom with cyclopropane should give an equivalent amount of acetylene and ethylene[13,15] *via* the carbene formed by the insertion reaction:

In the reaction with 1,3-butadiene and butene-1, neither spiropentane nor bisethanoallene derivatives are detected gas chromatographycally. Thus, monoatomic carbon is not considered to be an

1) M. Marshall, C. MacKay and R. Wolfgang, *J. Am. Chem. Soc.*, **86**, 4741 (1964).
2) H. J. Ache and A. P. Wolf, *ibid.*, **88**, 888 (1966).
3) K. D. Bayes, *ibid.*, **84**, 4077 (1962).
4) P. S. Skell and R. R. Engel, *ibid.*, **88**, 4883 (1966).
5) P. S. Skell, L. D. Wescott, Jr., J. P. Golstein and R. R. Engel, *ibid.*, **85**, 1023 (1963).
6) J. E. Nicholas, C. MacKay and R. Wolfgang, *ibid.*, **87**, 3008 (1965).
7) P. S. Skell and R. F. Harris, *ibid.*, **88**, 5933 (1966).
8) G. J. Pontrelli, *J. Chem. Phys.*, **43**, 2571 (1965).
9) J. A. Howe, *ibid.*, **39**, 1362 (1963).
10) J. E. Mentall and R. W. Nicholls, *ibid.*, **46**, 2881 (1967).
11) C. MacKay, J. Nicholas and R. Wolfgang, *J. Am. Chem. Soc.*, **89**, 5758 (1967).
12) J. Nicholas, C. MacKay and R. Wolfgang, *ibid.*, **88**, 1065 (1966).
13) C. MacKay and R. Wolfgang, *ibid.*, **83**, 2399 (1961).
14) G. Stöcklin and A. P. Wolf, *ibid.*, **85**, 229 (1963).
15) P. B. Shevlin and A. P. Wolf, *ibid.*, **88**, 4735 (1966).

Table 3. Yield of products from the reaction of methane, ethane, and cyclopropane with carbon vapor produced by the laser beam

Substrate	Methane	Ethane	C-Propane
Pressure (Torr)	700	670	680
Product ($\times 10^{-6}$ mol)			
Methane	—	2.9—4.2	2.6—2.8
Ethane	1.1	—	0.1
Ethylene	0	4.2—6.6	2.0—2.3
Acetylene	12.7—17.1	16.1—23.5	22.6—23.2
Propane	—	1.4	—
Propylene	0.31—0.41	—	14.5—16.6
C_3 products	0.5—0.7	1.4—2.7	—
C_4 products	1.8—3.9	3.6—4.0	8.8—10.0
C_3/C_4	0.1—0.4	0.4—0.7	—

Carbon consumed: $3.0—4.0\times10^{-5}$ mol
Laser: 10 pulses

important reactive intermediate in this reaction, since the product patterns are quite different from those in the reaction of the carbon atom.

The yield of C_3 compounds is higher in the reaction with ethane than with ethylene, and the C_3/C_4 ratios in the reaction with ethane and ethylene are 0.7 and 0.04 respectively. If the C_1 atom is the reaction species, C_3 compounds would be formed more easily in ethylene than in ethane.[1,13] In the recoil reaction, the ratio of C_3 compounds to C_4 compounds in ethylene vapor is 2.6.[1,2] These observations suggest that C_2 reacts with ethylene and ethane as follows:

$$C_2H_4 + C_2 \rightarrow (C_2H_4C_2)^* \begin{cases} \nearrow C_3 \text{ compounds} \\ \searrow C_4 \text{ compounds} \end{cases}$$

$$C_2H_6 + C_2 \rightarrow (C_2H_6C_2)^* \begin{cases} \nearrow C_3 \text{ compounds} \\ \searrow C_4 \text{ compounds} \end{cases}$$

In the laser-induced reaction with the mixture of H_2 and D_2 (the D_2/H_2 ratio is 1.1), the isotopic composition*2 of acetylene (C_2H_2 : C_2HD : C_2D_2) was detected to be 1 : 2.1 : 1.3 by mass spectrometrical analysis. From the highest yield of C_2HD, the mechanism of the molecular process, $C_2+H_2\rightarrow C_2H_2$ may be excluded; acetylene may be formed mainly as follows:

$$C_2 + H_2 \rightarrow C_2H + H \qquad \Delta H = -29 \text{ kcal}^{*3}$$

$$C_2H + H_2 \rightarrow C_2H_2 + H \qquad \Delta H = -10 \text{ kcal}$$

Since, in this experiment, the temperature at the surface of graphite carbon irradiated by ruby laser is estimated at 3000—4000°K[18] and since a high concentration of carbon vapor containing C_1, C_2, C_3, *etc.*[10] is produced, reaction product from C_1, C_2, and C_3 should be detected in the reaction. The methane (a small yield) actually formed in the hydrogen atmosphere might be the reaction product of C_1.

In conclusion, diatomic carbon (C_2) is considered to play the dominant role in the laser-induced reaction with olefin (ethylene) and hydrogen to produce acetylene and diacetylene.

The authors wish to acknowledge the valuable assistance of Miss K. Motegi in carrying out this work as well as to express their appreciation to Mr. S. Satooka for his mass spectrometric analysis.

*2 The isotopic composition was determined mass spectrometrically, using the published cracking pattern of C_2HD, C_2D_2, and C_2H_2.[16] The latter two of these compared well with our measured patterns of pure C_2H_2 and C_2D_2.

*3 The C_2H bond energy is from Ref. 17.

16) M. Cowperthwaite and S. H. Bauer, *J. Chem. Phys.*, **36**, 1743 (1962).
17) F. L. Mohler, V. H. Dibeler, L. Williamson and H. Dean, *J. Res. Nat. Beu. Standard*, **48**, 188 (1952).
18) S. Namba, P. H. Kim, S. Nakayama and I. Ida, *Japan. J. Appl. Phys.*, **4**, 153 (1965).

BULLETIN OF THE CHEMICAL SOCIETY OF JAPAN VOL. 42 826—827 (1969)

Studies of Heteroaromaticity. XXIII.[1] 1,3-Dipolar Cycloaddition Reactions of 5-Nitrofuronitrile Oxide and *m*-Nitrobenzonitrile Oxide with Benzyne

Tadashi SASAKI and Toshiyuki YOSHIOKA

Institute of Applied Organic Chemistry, Faculty of Engineering, Nagoya University, Chikusa-ku, Nagoya

(Received July 10, 1968)

Many papers have been published on the electrophilic addition of benzyne to nitrosobenzene,[2] acridine,[3] acetylene derivatives,[4] and on the 1,3-dipolar cycloaddition reactions of benzyne with diazoketones and acyl azides.[5] Also, several kinds of reactive dienes are known as trapping agents of benzyne.[6] However, it seems rather surprising that there has been no report which deals with its 1,3-dipolar cycloaddition reactions with nitrile oxides.

In the course of our studies on the dipolar reactivity of 5-nitro-2-furohydroxamoyl chloride,[7] we have reported that the thermal 1,3-dipolar cycloaddition procedure using hydroxamoyl chlorides has a big advantage over the corresponding nitrile oxide method, especially in the reactions with acetylenic dipolarophiles. Since benzyne is regarded as a cyclic acetylene, we attempted to apply the same procedure to benzyne. The product obtained was yellow crystals and the structure was confirmed to be 3-(5-nitro-2-furyl)benzisoxazole (I) by the elemental analyses and spectral data; the NMR spectrum in $CDCl_3$ showed signals at 1.17τ (multiplet, 1H) and 2.33 (multiplet, 3H), besides those of nitrofuran ring protons at 2.50 (doublet, 1H, J=3.8 cps) and at 2.64 (doublet, 1H, J=3.8 cps).[8] We assigned the signal at 2.33τ to H_B aromatic protons and that at 1.17τ to an H_A proton of the benzene ring. The increased deshielding of H_A compared with that of H_B is explained by the strong paramagnetic anisotropic effect of a neighbouring ether oxygen. The presence of the ultraviolet absorption maximum in ethanol at 327 mμ (ε=10300) indicates that the structure of this product is similar to 3-(5-nitro-2-furyl)-5-substituted isoxazole (II).[7]

Similar treatment of *m*-nitrobenzhydroxamoyl chloride also afforded the corresponding 3-(*m*-nitrophenyl)benzisoxazole (III) in 10% yield. These yields are much lower compared with those in the cases with diazoketones and acyl azides,[5] and these low yields may be explained by the weak electrophilicity of the nitrile oxides formed under the reaction conditions.

Whereas 1,2-dimethoxyethylene is known to be a suitable solvent[9] for the generation of benzyne by the above method, it was used in place of dichloromethane. However, the yields could not be improved so much.

The reaction path may involve the initial coordination of the electronegative oxygen of the nitrile oxide with a triple bond of benzyne to form an oxygen-carbon bonding, followed by cyclization to benzisoxazole as indicated below:

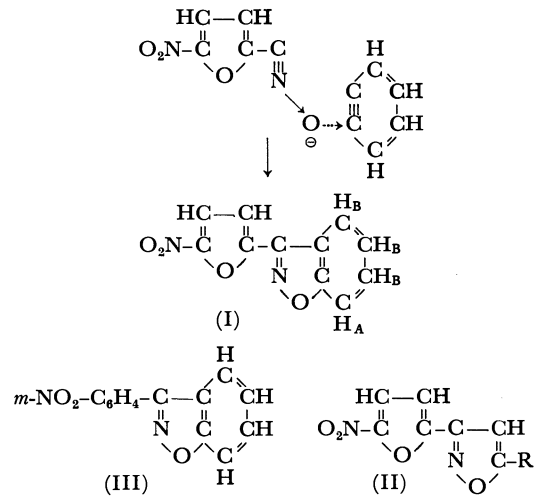

(I) (III) (II)

1) Part XXII of this series: T. Sasaki and M. Ando, This Bulletin, **41**, 2215 (1968).

2) G. N. Steinhoff and M. C. Henry, *J. Org. Chem.*, **29**, 2808 (1964).

3) Private communication from Dr. F. Yoneda (Keio University).

4) M. Stiles and U. Burckhard, *J. Org. Chem.*, **27**, 4715 (1962).

5) W. Ried and M. Schön, *Chem. Ber.*, **98**, 3124 (1965); *Ann.*, **689**, 141 (1965).

6) G. Wittig and A. Krebs, *Chem. Ber.*, **94**, 3260 (1961); G. Wittig and W. R. Hoffmann, *ibid.*, **95**, 2718 (1962); E. Wolthuis, *J. Org. Chem.*, **26**, 2215 (1961); F. M. Beringer and S. J. Huang, *ibid.*, **29**, 445 (1964).

7) T. Sasaki and T. Yoshioka, This Bulletin, **40**, 2604 (1967).

8) T. Sasaki, S. Eguchi and K. Kojima, *J. Heterocyclic Chem.*, **5**, 243 (1968).

9) L. F. Fieser and M. Fieser, "Reagents for Orgranic Synthesis," John Wiley and Sons, Inc., New York, N. Y. (1967), p. 268.

This mechanism is rather interesting when compared with that of benzonitrile oxide with nitrosobenzene[10] and of nitrosobenzene with benzyne,[2] in both of which the reactions are thought to be initiated by a carbon-nitrogen bonding, while the Diels-Alder reaction of benzyne with styrene is recently reported.[11]

Experimental[12]

3-(5-Nitro-2-furyl)benzisoxazole. 5-Nitro-2-furohydroxamoyl chloride,[7] 1.31 g (7 mmol), was dissolved in a mixture of 1 m*l* of isoamyl nitrite and 40 m*l* of dichloromethane. The solution was warmed to 55—60°C and a solution of 1.23 g (9 mmol) of anthranilic acid and 1.2 m*l* of triethylamine in 18 m*l* of acetone was added slowly to this stirred solution at the same temperature in 1 hr. The reaction mixture was refluxed for further 2 hr until the evolution of nitrogen gas had completely ceased. After the solvents were removed under reduced pressure, the residue was dissolved in chloroform and chromatographed on a silica-gel column, using chloroform as the eluent. The first fraction afforded 0.1 g (10%) of yellow crystals, mp 176°C, after recrystallization from ethanol. The main products eluted from other fractions were intractable tars.

Found: C, 57.63; H, 2.62; N, 12.12%. Calcd for $C_{11}H_6O_4N_2$: C 57.40; H, 2.63; N, 12.17%

3-(*m*-Nitrophenyl)benzisoxazole. Similarly, 10% yield of this compound was obtained, mp 176°C. UV λ_{max}^{EtOH} mμ (ε): 285 (6500), 224 (19500).

Found: C, 64.62; H, 3.35; N, 11.45%. Calcd for $C_{13}H_8O_3N_2$: C, 65.00; H, 3.36; N, 11.66%.

10) T. Minisci, R. Galli and A. Quilico, *Tetrahedron Letters*, **1963**, 785.

11) W. L. Dilling, *ibid.*, **1966**, 939.

12) The melting points were determined on a Yanagimoto electric micromelting point apparatus and are uncorrected. All the ultraviolet and infrared spectra were recorded on a JASCO Model ORD/UV-5 optical rotary dispersion recorder and on a JASCO Model IR-S infrared spectrophotometer respectively. The NMR spectra were taken on a Varian A-60 apparatus, with tetramethylsilane as an internal standard, and the chemical shifts are presented in terms of τ values.

BULLETIN OF THE CHEMICAL SOCIETY OF JAPAN VOL. 42 827—828 (1969)

Organic Syntheses by Means of Metal Complexes. IV. Reduction of Nitrobenzene with Carbon Monoxide[1]

Tsunesuke KAJIMOTO and Jiro TSUJI

Basic Research Laboratories, Toyo Rayon Co., Kamakura

(Received July 10, 1968)

Carbon monoxide has been used to reduce many inorganic compounds, but its use in reduction of organic compounds has not been widely explored. This paper reports the reduction of nitrobenzene with carbon monoxide in acetic acid to give acetanilide.

There are several examples of the reduction of nitrobenzene with carbon monoxide. Formation of azobenzene from nitrobenzene and carbon monoxide has been reported.[2] Kmiecik[3] has reported the conversion of 2-nitrobiphenyl to carbazole in the presence of carbon monoxide and iron pentacarbonyl. The synthesis of urethane by the reaction of nitrobenzene and carbon monoxide in alcohols or phenols in the presence of $Rh(CO)_2$-Cl_2 and co-catalyst is known.[4] Hardy and Bennett isolated phenylisocyanate by the reaction of nitrobenzene and carbon monoxide in the presence of Rh/C-$FeCl_3$ catalyst.[5] In these reactions, carbon monoxide behaves as a reducing agent and carbon dioxide is formed. Phenylnitrene may be considered as an intermediate in these reactions.

We attempted nickel carbonyl catalyzed reduction of nitrobenzene with carbon monoxide, and confirmed the formation of acetanilide in high yield. The reaction should be carried out above 300°C, and at 285°C no acetanilide was obtained. When the reaction was done in propionic acid solution, propionanilide was obtained. Somewhat similar catalytic activities were observed with iron pentacarbonyl and dicobalt octacarbonyl. The results are shown in Table 1. Intramolecular condensa-

1) Part III: Y. Mori and J. Tsuji, This Bulletin, **42**, 777 (1969).

2) G. D. Buckley and N. H. Ray, *J. Chem. Soc.*, **1949**, 1154; F. Glaser and R. Van Beneden, *Chem. Ing. Tech.*, **29**, 512 (1957).

3) J. E. Kmiecik, *J. Org. Chem.*, **30**, 2014 (1965).

4) Imperial Chemical Industries, Ltd., Brit. Pat. 993704 and 1080094; *Chem. Abstr.*, **64**, 11126h (1966).

5) W. B. Hardy and R. P. Bennett, *Tetrahedron Letters*, **1967**, 961.

Table 1. Carbonylation of nitrobenzene

Nitrobenzene g	RCOOH R	RCOOH ml	Catalyst		CO* kg/cm²	Reaction Temp, °C	Reaction Time, hr	C_6H_5NHCOR g
7.4	CH_3	30	$Ni(CO)_4$	1.0 ml	100	310	2.0	5.5
9.0	CH_3	25	$Fe(CO)_5$	1.0 ml	100	310	2.0	6.8
9.0	CH_3	25	$Ni(CO)_4$	0.25 ml	100	310	1.5	6.1
3.6	CH_3	10	$Co_2(CO)_8$	0.2 g	50	305	2.0	2.5
4.8	C_2H_5	25	$Ni(CO)_4$	1.0 ml	100	305	2.0	3.1
9.0	CH_3	25	$Ni(CO)_4$	1.0 ml	100	285	2.0	0

* Initial pressure at room temperature.

tion did not occur with *o*-nitrobenzoic acid in toluene solution and nitrobenzene was obtained by decarboxylation.

This reaction may be explained by the following mechanism. At first nitrobenzene is converted into phenylnitrene by giving the oxygen to carbon monoxide. Phenylnitrene is then carbonylated to produce phenyl isocyanate.

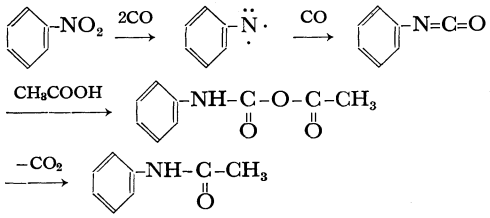

The reaction of isocyanate with acetic acid followed by decarboxylation gives acetanilide. As a related reaction, the formation of acetanilide by the reaction of phenyl thioisocyanate with acetic acid is known.[6]

Experimental

Materials. Commercially available nickel carbonyl and iron carbonyl were used without further purification. Cobalt octacarbonyl was synthesized from cobalt hydroxide by the known method.[7] Nitrobenzene was distilled before use.

Reactions of Nitrobenzene with Carbon Monoxide. Only a typical experiment is described. A stainless steel autoclave (100 ml) was charged with 9 g of nitrobenzene, 25 ml of acetic acid and 0.25 ml of nickel carbonyl. The autoclave was sealed and pressured to 100 kg/cm² with carbon monoxide, and then heated at 310°C for 90 min with stirring. After the reaction, the autoclave was allowed to cool and the reaction product was subjected to distillation. Under reduced pressure, acetanilide (6.1 g, 61%) was collected, which was identified with an authentic sample by mixed melting point determination (112°C) and infrared spectra. At the same time, formation of carbon dioxide was confirmed with a barium hydroxide solution. The other experiments were carried out similarly.

6) B. Pawlewski, *Ber.*, **32**, 1425 (1899).

7) Ajinomoto Co., Inc., Japanese Pat. 265091.

BULLETIN OF THE CHEMICAL SOCIETY OF JAPAN VOL. 42 829—831 (1969)

Metal Acetate- and Alcohol-catalyzed Retropropargyl Rearrangement

Fumio TODA, Masahiro HIGASHI and Katsuhiko AKAGI

Department of Industrial Chemistry, Faculty of Engineering, Ehime University, Matsuyama

(Received July 12, 1968)

A few lithium aluminum hydride-,[1,2] cuprous bromide-,[3] potassium iodide-[3] and silver nitrate-[4] catalyzed retropropargyl rearrangements*1 (Eq. (1)) have been reported. In all these cases, however, the rearrangement was accompanied by isomerization to allene or by reduction to ethylene. It has also been reported that the alkylation of haloallene increases the proportion of the allenic isomer[5] or of the reduction product.[2] We have found that some metal acetates in alcohol and, surprisingly, alcohol itself also act as catalysts for the retropropargyl rearrangement of phenyl-substituted bromoallenes, thus affording alkoxyacetylenes in moderate yields. This is the first finding of the alcohol-catalyzed displacement of a relatively unreactive halogen atom on an unsaturated carbon.

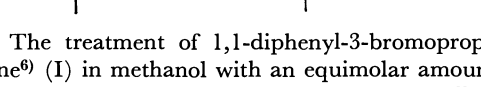

(1)

The treatment of 1,1-diphenyl-3-bromopropadiene[6] (I) in methanol with an equimolar amount of AgOAc at room temperature for 1 hr afforded 1,1-diphenyl-1-methoxyprop-2-yne[7] (IIa) in a 71% yield. By the procedure employed for I, 1,1,6,6-tetraphenyl-3,4-dibromohexa-1,2,4,5-tetraene (IV)[8] was then reacted with methanol in the presence of twice the molar amount of AgOAc; this afforded 1,1,6,6-tetraphenyl-1,6-dimethoxyhexa-2,4-diyne (Va)*2 in a 94% yield. A similar rearrangement was observed with 1,1,4,4-tetraphenyl-3-bromobuta-1,2-diene-4-ol[9] (VI), where the reaction was faster than those of I and IV. The treatment of VI with methanol in the presence of AgOAc for 30 min at room temperature afforded 1,1,4,4-tetraphenyl-1-methoxybut-2-yne-4-ol (VIIa) in a 95% yield. The structure of VIIa was identified by comparing its mp and infrared spectrum with those of an authentic specimen prepared according to the literature.[7]

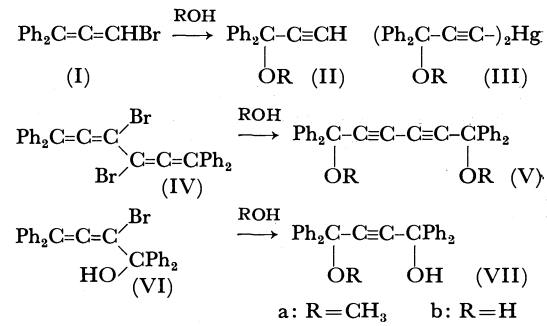

When the AgOAc-catalyzed rearrangements of I, IV, and VI were carried out in aqueous acetone, the corresponding acetylenic alcohols, IIb, Vb, and VIIb, were obtained in quantitative yields.

All of the rearrangements described above were also catalyzed by $Hg(OAc)_2$, whereas the acetates of Cu^{2+}, Zn^{2+}, Cd^{2+}, Pb^{2+}, Cr^{2+}, Co^{2+} and Ni^{2+} were all inert. The treatment of I in methanol with an equimolar amount of $Hg(OAc)_2$ afforded the mercuric acetylide IIIa, whereas the same treatment of IV gave Va. Since IIIa was easily formed by the reaction of IIa and $Hg(OAc)_2$, IIa may be produced initially. The mercuric acetylide IIIa was identical with that prepared according to the usual method.[10] In the case of VI, an unidentified mercuric compound, $C_{30}H_{23}O_3BrHg$, was obtained in a 14% yield in addition to VIIa (54% yield).

The most striking rearrangement was the alcohol-catalyzed one. After standing for a long time at room temperature, a mixture of IV and methanol afforded Va quantitatively. Although the metal acetate-catalyzed rearrangement was done for 1 hr,

1) T. L. Jacobs and W. L. Petty, *J. Org. Chem.*, **28**, 1360 (1963).

2) T. L. Jacobs and R. D. Wilcox, *J. Am. Chem. Soc.*, **86**, 2240 (1964).

3) T. L. Jacobs and W. F. Brill, *ibid.*, **75**, 1314 (1953).

4) Y. R. Bhatia, P. D. Landor and S. R. Landor, *J. Chem. Soc.*, **1959**, 24.

*1 For a recent review, see D. R. Taylor, *Chem. Revs.*, **67**, 317 (1967).

5) T. L. Jacobs, E. G. Teach and D. Weiss, *J. Am. Chem. Soc.*, **77**, 6254 (1955).

6) P. Martinet and H. Doupeux, *Compt. rend.*, **261**, 2498 (1965).

7) J. Godineau, P. Cadiot and A. Willemart, *ibid.*, **246**, 2499 (1958).

8) F. Toda, M. Higashi and K. Akagi, unpublished results.

*2 An authentic sample of Va was prepared by the oxidative coupling of IIa which had been obtained according to the reported method.[7]

9) F. Toda, T. Komoda and K. Akagi, This Bulletin, **41**, 1493 (1968).

10) B. B. Elsner and P. F. M. Paul, *J. Chem. Soc.*, **1951**, 893

a similar reaction without a catalyst afforded unreacted bromoallene. However, the reaction was accelerated by heating; for example, the heating of a mixture of IV and methanol under reflux for 5 hr afforded Va in a 93% yield. The heating under reflux of a solution of I in methanol for 1 hr afforded IIa and 1,1-diphenylprop-1-en-3-al (VIII) in 43 and 46% yields respectively. The latter was identical with that prepared according to the reported method.[11] The same treatment of VI in methanol afforded, quantitatively, 1,1,4,4-tetraphenyl-1,4-dimethoxybut-2-yne (IX), which was identical with that prepared according to a different method.[12] Since the treatment of VIIa in methanol containing a catalytic amount of hydrogen bromide afforded IX quantitatively, it is clear that VIIa was formed initially and that it then reacted further with methanol. The acid-catalyzed replacement of hydroxyl with the alkoxyl group will be reported in a separate paper.

Experimental*3

Silver Acetate-catalyzed Rearrangements in Methanol of Several Bromoallenes. I) A solution of I (2.71 g, 10 mmol) and AgOAc (1.67 g, 10 mmol) in methanol (100 m*l*) was stirred at room temperature for 1 hr. The reaction mixture was then decomposed with water and extracted with ether. The ether layer was washed with water and dried over sodium sulfate. The crude oil remaining after the evaporation of the solvent was distilled to afford IIa, 1.58 g (71%), bp 109°C/3 mmHg. The infrared spectrum was identical with that of an authentic sample prepared according to the literature.[7]

IV) A solution of IV (270 mg, 0.5 mmol) in methanol (10 m*l*) was treated with AgOAc (160 mg, 1 mmol) by the procedure employed for I. The crude crystals obtained by adding water to the reaction mixture were recrystallized from methanol to yield Va as colorless needles, 208 mg (94%), mp 196°C. IR: 2160 ($\nu_{C\equiv C}$) and 1090 cm^{-1} (ν_{C-O}). NMR: a multiplet centered at 2.65 (phenyl, 20H) and a singlet at 6.62τ (methyl, 6H). These spectral data were identical with those of an authentic sample prepared by the oxidative coupling of IIa.

Found: C, 87.15; H, 5.77%. Calcd for $C_{32}H_{26}O_2$: C, 86.88; H, 5.92%.

VI) A solution of VI (453 mg, 1 mmol) in methanol (10 m*l*) was treated with AgOAc (167 mg, 1 mmol) by the procedure employed for I. The curde crystals obtained by adding water to the reaction mixture were recrystallized from petroleum ether (bp 70—80°C) to afford VIIa as colorless needles, 380 mg (95%), mp 112—113°C. IR: 3350 (ν_{OH}) and 1060 cm^{-1} (ν_{C-O}).

Found: C, 85.83; H, 6.12%. Calcd for $C_{29}H_{24}O_2$: C, 86.14; H, 5.94%.

Silver Acetate-catalyzed Rearrangements in Aqueous Acetone of I, IV, and VII. A solution of the bromoallene (I, IV or VII) in 80% aqueous acetone was treated with an equimolar amount of AgOAc by the procedure employed for the rearrangement in methanol. The reaction mixture was decomposed with water and extracted with ether. The ether layer was washed with water, dried over sodium sulfate, and evaporated to dryness to give the corresponding acetylenic alcohol, IIb, VIb, or VIIb, in a quantitative yield in all cases. Each product was recrystallized from acetone to afford the corresponding complex with acetone; each product was identical with the respective authentic sample.[13]

Mercuric Acetate-catalyzed Rearrangements in Methanol of the Following Bromoallenes. I) A mixture of I (271 mg, 1 mmol), $Hg(OAc)_2$ (319 mg, 1 mmol), and methanol (10 m*l*) was stirred at room temperature for 2 hr. Crystals collected by filtration were recrystallized from benzene-petroleum ether (bp 70—80°C) to afford IIIa as colorless needles, 232 mg (72%), mp 211°C. IR: 2160 ($\nu_{C\equiv C}$), and 1185 and 1075 cm^{-1} (ν_{C-O}). NMR: a multiplet centered at 2.63 (phenyl, 20H) and a singlet at 6.64; (methyl, 6H). Those spectral data were identical with those of an authentic sample prepared according to the usual method.[10]

Found: C, 59.72; H, 4.01%. Calcd for $C_{32}H_{26}O_2Hg$: C, 59.76; H, 4.08%.

IV) The same treatment of IV for 5 hr gave Va in a 53% yield.

VI) The treatment of VI (453 mg, 1 mmol) in methanol (10 m*l*) with $Hg(OAc)_2$ (320 mg, 1 mmol) at room temperature for 30 min afforded a crystalline solid. The solid was collected by filtration, washed with methanol, and recyrstallized from acetone to yield an unidentified mercuric compound, 100 mg, (14% as $C_{30}H_{23}O_3BrHg$), mp>270°C.

Found: C, 50.11; H, 3.02%. Calcd for $C_{30}H_{23}O_3$-BrHg: C, 50.63; H, 3.23%.

The combined methanol layer was decomposed with water and extracted with ether. The ether layer was washed with water and dried over sodium sulfate. Crystals obtained by the evaporation of the solvent were recrystallized from petroleum ether (bp 70—80°C) to yield VIIa as colorless needles, 220 mg (54%), mp 112—113°C. A mixed-melting-point determination with an authentic sample prepared by the AgOAc-catalyzed reaction showed no depression.

Alcohol-catalyzed Rearrangements of Several Bromoallenes. I) A solution of I (135 mg, 0.5 mmol) in methanol (10 m*l*) was heated under reflux for 1 hr. After the addition of water, the reaction mixture was extracted with ether. The ether layer was washed with water, dried over sodium sulfate, and

11) H. Lorenz and R. Wizinger, *Helv. Chim. Acta*, **28**, 600 (1945).

12) R. Kuhn and H. Trischmann, *Chem. Ber.*, **94**, 2258 (1961).

*3 All the melting points were uncorrected. The infrared spectra were recorded in Nujol mull on a grating spectrophotometer IR-G of the Japan Spectroscopic Co. The NMR spectra were recorded on a Japan Electron Optics Laboratory C-60 Spectrometer, in $CDCl_3$, using TMS as the internal standard. The vpc analysis was performed on a Hitachi Perkin-Elmer model F6-D instrument at 200°C, using a column containing PEG 6000/Diasolid M.

13) F. Toda and K. Akagi, *Tetrahedron Letters*, **1968**, 3695.

evaporated to dryness to leave an oil, 96 mg. The oil was identified as a mixture of IIa (43% yield) and 1,1-diphenylprop-1-en-3-al[11] (VIII) (46% yield) by vpc analysis using authentic samples.

IV) A solution of IV (135 mg, 0.25 mmol) in methanol (5 m*l*) was heated under reflux for 5 hr to give Va, 103 mg (93%).

VI) The same treatment of VI with methanol for 1 hr afforded IX in a quantitative yield, mp 112—113°C (lit.[12] mp 113—114°C). A mixed-melting-point determination with an authentic sample prepared according to the literature[12] showed no depression. The heating of VIIa with methanol in the presence of a catalytic amount of hydrogen bromide also gave IX in a quantitative yield.

BULLETIN OF THE CHEMICAL SOCIETY OF JAPAN VOL. 42 831—833 (1969)

Reaction of Sulfides with *t*-Butyl Hypochlorite in the Presence of Water, ^{18}O Tracer Study

Kunihiko KIKUKAWA, Waichiro TAGAKI, NORIO KUNIEDA and Shigeru OAE

Department of Applied Chemistry, Faculty of Engineering, Osaka City University, Sugimoto-cho, Sumiyoshi-ku, Osaka

(Received July 20, 1968)

It has been found that *t*-butyl hypochlorite oxidizes organic sulfides to the corresponding sulfoxides or sulfones under suitable reaction conditions, and the synthetic utility of this oxidation to prepare sulfoxide has been examined for series of sulfides.[1-4] However, the mechanistic features have not been fully explored yet. Skell and Epstein obtained sulfoxides by the oxidation of corresponding sulfides at low temperature (−78°C) and suggested the following mechanism (Eq. (1)) which involves an alkoxy sulfonium salt as the intermediate. Walling and Mintz carried out the same reaction in benzene at room temperature, and found that the stoichiometry of the reaction was not 1 : 1 with respect to both the sulfide and the reagent as

$$R_2S + t\text{-}C_4H_9OCl \rightarrow [R_2SOC_4H_9]^+Cl^- \rightarrow R_2SO \quad (1)$$

would be expected from Eq. (1), but the ratio was 1 : 2 and a high yield of sulfoxide and a mixture of products from hypochlorite were obtained. They did not observe any sulfone formation contrary to other reports,[2] and suggested a polar mechanism involving molecular chlorine and diphenyl sulfur dichloride for oxidation of diphenyl sulfide, rejecting free radical mechanisms.

During the courses of our investigation on the oxidation of organic sulfur compounds with halogenating agents, we have been interested in the fate of oxygen atom in the above oxidation. It is obvious that the oxygen atom of the sulfoxide must come from *t*-butyl hypochlorite when the reaction is carried out in non-hydroxylic solvent. Meanwhile, it has been reported that in the presence of water molecular halogen oxidizes sulfides to the corresponding sulfoxides.[5-7] In this oxidation, ^{18}O tracer experiments have demonstrated that the oxygen atom of the sulfoxide comes exclusively from water, and not from any other solvent components such as acetic acid or methanol, *etc.*[7] However, the last possibility of oxygen uptake into sulfoxide from other solvents cannot still be ruled out in some other system.[8]

Therefore, it is interesting to examine the effect of water on the above *t*-butyl hypochlorite oxidation.

Results and Discussion

Oxidation of diphenyl sulfide with an equimolar amount of *t*-butyl hypochlorite in dioxane at room temperature yielded the corresponding sulfoxide. Any intermediate, such as that isolated by Skell and Epstein[2] at low temperature, was not observed.

1) R. J. Gritter and D. J. Carey, *J. Org. Chem.*, **29**, 1160 (1964).

2) P. S. Skell and M. F. Epstein, Abstracts 147th National Meeting of American Chemical Society (Philadelphia, Pa., April 1964,) p. 26N.

3) C. Walling and M. J. Mintz, *J. Org. Chem.*, **32**, 1286 (1967).

4) L. Skattebøl, B. Boulette and S. Solomon, *J. Org. Chem.*, **32**, 3111 (1967).

5) W. Ranky and D. Nelson, "Organic Sulfur Compounds," Vol. I, N. Kharasch, Ed., Pergamon Press, Inc, New York, N. Y. (1961), p. 170.

6) H. Szmant, Ref. 5, p. 154.

7) S. Oae, Y. Ohnishi, S. Kozuka and W. Tagaki, This Bulletin, **39**, 364 (1966) and the related papers.

8) For example, recently Higuchi has shown that in the iodine oxidation of sulfide to give sulfoxide, phosphate and carboxylate anion are effective catalysts, presumably by forming unstable sulfonium intermediate which could decompose to give unlabeled sulfoxide (T. Higuchi and K.-H. Gensch, *J. Am. Chem. Soc.*, **88**, 5486 (1966)).

Table 1. Oxidation of diphenyl sulfide with *t*-butyl hypochlorite

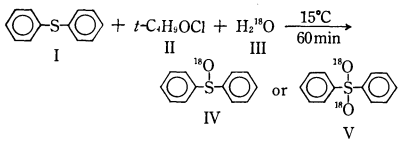

Mole ratio[a]	Yield, %		^{18}O atom %		
I : II : III	IV	V	III	IV	V
1 : 1 : 2	60	—	1.72	1.14	—
1 : 2 : 2	—	80	1.72	—	1.37
1 : 2 : 10	—	90	1.62	—	1.62

a) One gram of I in 30 m*l* of the mixture of II and III.

With twice molar amounts of hypochlorite, diphenyl sulfone was obtained as the main product. The addition of water to the reaction mixture did not change the product composition. The possibility of ^{18}O (of water) incorporation into the products was then examined. The results summarized in Table 1 shows that the ^{18}O incorporation did take place in both sulfoxide and sulfone formation. The amount of incorporation was more than 80% and approached 100% as the amount of water increased. The ^{18}O incorporation has been also examined for the oxidation of sulfoxide to the corresponding sulfone. As shown in Table 2, the oxygen atom of water was again found to be incorporated in the sulfone.

Table 2. Oxidation of diphenyl sulfoxide with *t*-butyl hypochlorite

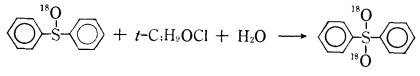

Atom % of ^{18}O in[a]		
Water	Sulfoxide	Sulfone
0.20	1.02	0.62
1.60	1.02	1.25
1.60	0.21	0.78

a) Mole of ratio of sulfoxide : *t*-C_4H_9OCl : H_2O = 1 : 2 : 2

The formation of ^{18}O labeled sulfoxide does not necessarily rule out the possibility that the primary product is the unlabeled sulfoxide which then undergoes an oxygen exchange reaction catalyzed by the hydrogen chloride formed.[9] Therefore, the oxygen exchange reaction of diphenyl sulfoxide was examined by adding hydrogen chloride instead of adding *t*-butyl hypochlorite, although the results in Table 2 indicate that such oxygen exchange reaction must be slow compared to the oxidation reaction. This control experiment also reveals that the oxygen exchange of a sulfoxide is negligible under these conditions (see Experimental).

The above oxidation reaction presumably proceeds through the hydrolysis of either one of the following two different intermediates, VI or VII. For the hydrolysis of VI, there are two possibilities, *i. e.* one is the attack of water on the sulfur atom giving a labeled sulfoxide, the other is the solvolysis of *t*-butyl group giving an unlabeled sulfoxide. The

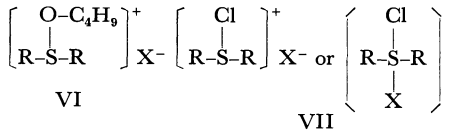

VI VII

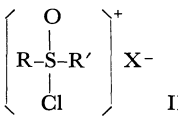

IX

attack of chloride anion on *t*-butyl group would also give an unlabeled sulfoxide. This possibility, however, is not in accord with the above experimental results. Meanwhile it is difficult to consider that the nucleophilic reaction takes place exclusively on the sulfur atom rather than on *t*-butyl group. Therefore, the more likely intermediate is VII which rapidly reacts with water to give a sulfoxide. In the absence of water *t*-butoxy anion would reacts with VII to give VI. The formation of VI and its decomposition to give the sulfoxide would be slower than the formation of VII and its hydrolysis.

The formation of the sulfone and the incorporation of ^{18}O into the sulfone with identical concentration as that of the sulfoxide seem to suggest that the chlorosulfoxonium (IX) is formed as the intermediate which upon quenching with water is converted to the sulfone.

Experimental

Materials. Dioxane was purified by treating with hydrochloric acid and with metallic sodium. Diphenyl sulfide was prepared by Friedel-Crafts reaction of benzene and elemental sulfur according to the method used by Dougherty and Hammond.[10] Diphenyl sulfoxide was prepared by the oxidation of diphenyl sulfide with hydrogen peroxide. *t*-Butyl hypochlorite was prepared by the reaction of *t*-butanol with chlorine in a sodium hydroxide solution according to the method of Leeter and Bell.[11] Diphenyl sulfoxide ^{18}O-labeled was prepared by the oxidation of diphenyl sulfoxide in a mixture of

9) a) K. Mislow, T. Simmons, J. T. Mellilo and A. L. Ternay, *J. Am. Chem. Soc.*, **86**, 1452 (1964). b) K. Kikukawa, W. Tagaki, N. Kunieda and S. Oae, This Bulletin, **39**, 614 (1966).

10) G. Dougherty and P. D. Hammond, *J. Am. Chem. Soc.*, **57**, 117 (1935).

11) H. M. Leeter and E. W. Bell, "Org. Synth.," Coll. Vol. IV, p. 125 (1963).

bromine-$H_2{}^{18}O$-pyridine.[7]

Oxidation of Diphenyl Sulfoxide and Sulfone with *t*-Butyl Hypochlorite in ^{18}O Enriched Water-Dioxane. To a solution of diphenyl sulfoxide in dioxane-water was added *t*-butyl hypochlorite dropwise under stirring at 15°C. After one hour, most of the solvent was removed by concentration under reduced pressure, and water was added to the residue to give crystalline product. The properties and the purity of diphenyl sulfoxide was discussed in the previous papar.[9b] The results are shown in Tables 1 and 2.

Control Experiment. ^{18}O-Labeled diphenyl sulfoxide was treated under the same reaction conditions as in the above oxidation, except that an equimolar amount of hydrogen chloride was added in place of *t*-butyl hypochlorite.

After one hour, diphenyl sulfoxide was recovered and its ^{18}O content was assayed:

Atom % of ^{18}O: Starting sulfoxide, 0.827; recovered sulfoxide, 0.821.

BULLETIN OF THE CHEMICAL SOCIETY OF JAPAN VOL. 42 833—835 (1969)

Kinetics of Multidentate Ligand Substitution Reactions. V. Effects of Ammonia and Thiocyanate Ion on the Substitution Reaction of Eriochrom Black T with Nickel(II)-Ethylenediaminetetraacetate Chelate

Mutsuo KODAMA and Katsumi MIYAMOTO

Department of Chemistry, Ibaraki University, Mito, Ibaraki

(Received July 24, 1968)

In an earlier paper,[1] the substitution reaction of Eriochrom Black T (BT) with nickel(II)-ethylenediaminetetraacetate (Ni(II)-EDTA) chelate was studied spectrophotometrically. The study showed that reaction proceeds through two simultaneous reaction paths involving doubly- and completely-deprotonated BT anions. The present paper deals with the effects of ammonia, thiocyanate and bromide ions on the reaction of BT with Ni(II)-EDTA chelate. Even in the presence of ammonia or thiocyanate, Ni(II)-EDTA chelate showed the same kinetic behavior as in the absence of ammonia or thiocyanate, but the rate of reaction was reduced appreciably. This was ascribed to the fact that the concentration of normal Ni(II)-EDTA chelate, which is reactive in the present situation, is reduced by the formation of a mixed ligand chelate involving ammonia or thiocyanate.

Experimental

Reagents. The preparations of nickel(II) perchlorate and ethylenediaminetetraacetate solutions were described previously.[1] Ammonia and potassium thiocyanate were of analytical reagent grade and used without further purification. A spectrophotometric test showed that the addition of ammonia or thiocyanate did not affect the absorption curve of BT solution (pH=10.0) containing 10.0 mM ethylenediaminetetraacetate. The concentration of ammonia was determined by titrating against standard hydrochloric acid using Methyl Orange as indicator. The concentration of thiocyanate was standardized against a standard silver nitrate solution.[2]

Apparatus and Experimental Procedure. All apparatus and experimental procedures were as described previously.[3] Reactions were followed spectrophotometrically by observing the absorbance at 630 mμ. The ionic strength of sample solutions was adjusted to 0.30 by adding an appropriate amount of sodium perchlorate (ammonia system) or potassium nitrate (thiocyanate or bromide system). A pseudo first-order rate constant, k^+, was obtained from the plot of $\log(A_{HD}/(A-A_{NiD}))$ against time, t, where A_{HD}, A and A_{NiD} have the same meanings as previously.[1]

Results and Discussion

Effects of ammonia and thiocyanate on the substitution reaction of BT with Ni(II)-EDTA chelate were examined at 25°C for solutions containing an excess of ethylenediaminetetraacetate in the pH range 8.50 to 10.50. Therefore, no buffer reagent was used in this study. Even in the presence of ammonia or thiocyanate, nickel(II)-EDTA chelate shows quite the same kinetic behavior as in their absence.[1] However, as illustrated in Fig. 1, ammonia or thiocyanate appreciably reduces the rate of the substitution reaction. The reduction in the pseudo first-order rate constant, k^+,[1] increases

1) M. Kodama, C. Sasaki and M. Murata, This Bulletin, **41**, 1333 (1968).

2) F. P. Treadwell and W. T. Hall, "Analytical Chemistry," Vol. II, John Wiley and Sons, Inc., New York (1951), p. 647.

3) K. Kodama, This Bulletin, **40**, 2575 (1967).

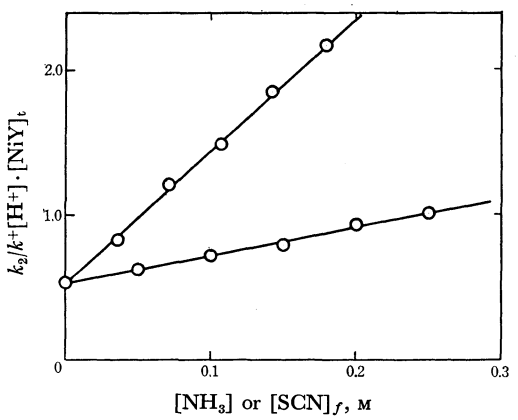

Fig. 1. The relation between $1/k^+$ and the concentration of ammonia or thiocyanate ion.
μ=0.30, 25°C, λ=630 mμ
Concentration of nickel(II)-EDTA=10.45 mM
Concentration of uncomplexed EDTA=10.0 mM

with increasing concentration of ammonia or thiocyanate. All the above facts suggest that the present reaction has the same mechanism as in the absence of ammonia or thiocyanate, but that the concentration of reactive Ni(II)-EDTA chelate in the reaction is reduced by the addition of ammonia or thiocyanate. This can be explained simply by considering the formation of a mixed ligand chelate involving ammonia or thiocyanate which is much less reactive than a normal chelate, NiY^{2-}. If the present reaction proceeded only through NiY^{2-}, the apparent rate constant, k^+, should be given by

$$k^+=\frac{k_2^+\cdot k_2}{[H^+]}\cdot\frac{[NiY]_t}{1+K^{NCS}\cdot[NCS]_f}$$

$$\text{or}\quad \frac{k_2^+\cdot k_2}{[H^+]}\cdot\frac{[NiY]_t}{1+K^{NH_3}\cdot[NH_3]_f} \qquad (1)$$

where k_2^+ and k_2 have the same meanings as in a previous paper,[1] and other notations are defined: $[NiY]_t$, the total concentration of Ni(II)-EDTA chelate; $[NCS]_f$, the concentration of uncomplexed thiocyanate, $[NH_3]_f$,[1]* the concentration of uncomplexed ammonia; $K^{NCS}=[NiY(NCS)^{3-}]/[NiY^{2-}]\cdot[NCS^-]$; $K^{NH_3}=[Ni(NH_3)Y^{2-}]/[NiY^{2-}]\cdot[NH_3]$.

The $k_2[NiY]_t/[H^+]\cdot k^+$ value was plotted against $[NH_3]_f$ or $[NCS]_f$. Results are shown in Fig. 1. The slope *vs.* intercept ratios of the linear relation in Fig. 1 were 17.1 and 3.47 for the ammonia and thiocyanate systems, respectively.

As shown in Fig. 2, the addition of ammonia or thiocyanate results in a change in the absorption curve of Ni(II)-EDTA chelate. This can be ascribed to the formation of a mixed ligand chelate involving ammonia or thiocyanate. From the increase in absorbance, K^{NCS} and K^{NH_3} were determined with

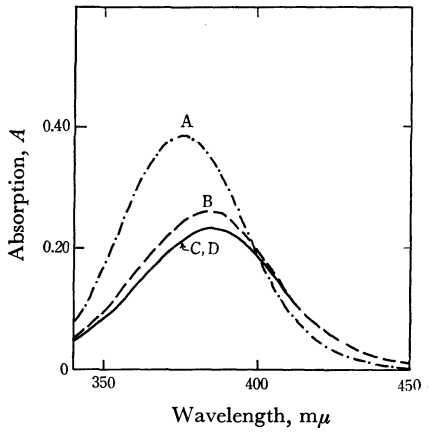

Fig. 2. Absorption curves of nickel(II)-EDTA chelate.
Concentration of nickel(II)-EDTA chelate=10.0 mM
Concentration of uncomplexed EDTA=20.0 mM
μ=0.50, pH=9.70
A: 0.25 M ammonia
B: 0.25 M potassium thiocyanate
C: 0.25 M potassium bromide
D: none

the aid of the following relation derived thermodynamically,

$$\log\frac{A-A_{NiY}}{A_{NiYX}-A}=\log K^X+\log[X]_f \qquad (2)$$

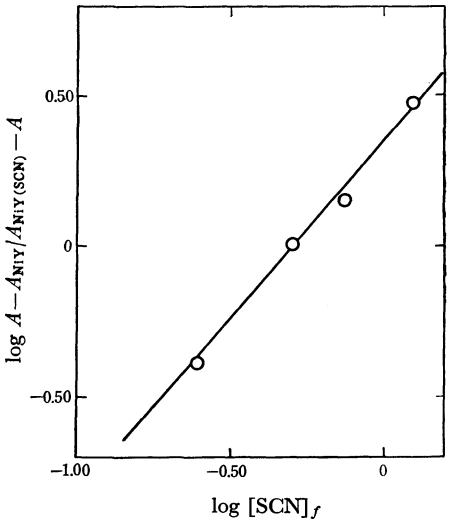

Fig. 3. Determination of K^{SCN}.
μ=2.0, pH=9.70, λ=380 mμ
Concentration of nickel(II)-EDTA=20.0 mM
Concentration of uncomplexed EDTA=20.0 mM
Concentration of thiocyanate ion ranged from 0.25 to 1.25 M

*1 Precisely, $[NH_3]_f$ means the concentration of uncomplexed ammonia.

where K^X denotes K^{NH_3} or K^{NCS} and $[X]_f$, $[NH_3]_f$ or $[NCS]_f$ and where A_{NiY} is the absorbance of a solution containing only NiY^{2-}, A_{NiyX}, the absorbance of a solution in which all Ni(II)-EDTA chelate is present in the form of NiYX, and A the absorbance of a solution containing both Ni(II)-EDTA chelate and ammonia or thiocyanate.

A typical result obtained for the thiocyanate system was given in Fig. 3 (at 380 mμ). The K^{NCS} value was estimated as 3.02 (μ=0.30) from the linear relation. In a similar way, K^{NH_3} was determined as 12.6 (μ=2.0) at 370 mμ, in good agreement with a reported value.[4]

The agreement of the slope *vs.* intercept ratio in the kinetic study with the K^X value determined strongly supports the present authors' explanation that the present reaction proceeds only through NiY^{2-}, and that the mixed ligand chelate involving thiocyanate or ammonia is essentially non-reactive.

In the d^8 octahedral system, any reaction going by the coordination number seven (pentagonal bipyramid) would inevitably lead to a considerable loss in crystal field separation energy, and hence be slow.[5] Therefore, the explanation that ammonia or thiocyanate may form the seventh bond to the nickel(II) ion in the pentagonal bipyramid reaction intermediate, thus making the Ni(II)-EDTA chelate less reactive, is impossible as far as crystal field effects are concerned.

Generally, the rate of dissociation of water from nickel(II) ion is expected to be much faster than that of ammonia. Therefore, if the formation of a Ni(II)-OH_2 bond prior to the formation of the first Ni(II)-BT bond is essentially required in the present reaction, the ammonia coordinated to the nickel(II) ion might considerably reduce the rate of reaction of BT with Ni(II)-EDTA chelate. The same explanation may also be applied to the effect of thiocyanate on the reaction. To understand the precise role of the coordinated ammonia or thiocyanate in the present exchange reaction, further systematic and advanced investigations must be undertaken. The effect of bromide ion which does not form a mixed ligand chelate with NiY^{2-} was also studied, but no practical effect observed.

4) D. W. Margerum and H. M. Rosen, *J. Am. Chem. Soc.*, **89**, 1088 (1967).

5) F. Basolo and R. G. Pearson, "Mechanism of Inorganic Reactions," John Wiley and Sons, Inc., New York (1958), p. 108.

BULLETIN OF THE CHEMICAL SOCIETY OF JAPAN VOL. 42 835—837 (1969)

The Complexation Reaction of 1-(Hydroxy-4-methyl-2-phenylazo)-2-naphthol-4-sulfonic Acid (Calmagite) with Divalent Metal Ions and Use as a Metallochromic Indicator

Mutsuo KODAMA and Katsumi MIYAMOTO

Department of Chemistry, Ibaraki University, Mito, Ibaraki

(Received July 31, 1968)

In previous papers,[1,2] the complexation reaction of 1-(1-hydroxy-2-naphthylazo)-6-nitro-2-naphthol-4-sulfonic acid (Eriochrom Black T, BT) with divalent metal ions in the presence of aminopolycarboxylate was studied spectrophotometrically. In the present paper, solution equilibria between 1-(hydroxy-4-methyl-2-phenylazo)-2-naphthol-4-sulfonic acid (common name, calmagite) and metal(II)-aminopolycarboxylate chelates were dealt with in the same way as in the BT system, and the use of calmagite as a metallochromic indicator in the chelatometric titrations of zinc(II), cadmium(II) and lead(II) was studied.

Apparatus and experimental procedures were those used previously.[1,2] Commercial calmagite was purified by employing the procedure proposed by Lindstrom and Diehl.[3] The C.H.N. analysis and spectrophotometric measurement showed that the purity of calmagite was 93%.

The Complexation Reaction of Calmagite. Typical absorption curves of calmagite and its metal(II) chelates were shown in Fig. 1. In copper(II)-ethylenediaminetetraacetic acid(EDTA), zinc(II)-nitrilotriacetic acid (NTA), lead(II)-NTA and cadmium(II)-*N'*-(hydroxyethyl)-ethylenediamine-*N,N,N'*-triacetic acid (EDTA-OH) systems, the exchange reaction of calmagite with metal(II)-

1) M. Kodama and H. Ebine, This Bulletin, **40**, 1857 (1967).

2) M. Kodama and C. Sasaki, *ibid.*, **41**, 127 (1968).

3) F. Lindstrom and H. Diehl, *Anal. Chem.*, **32**, 1123 (1960).

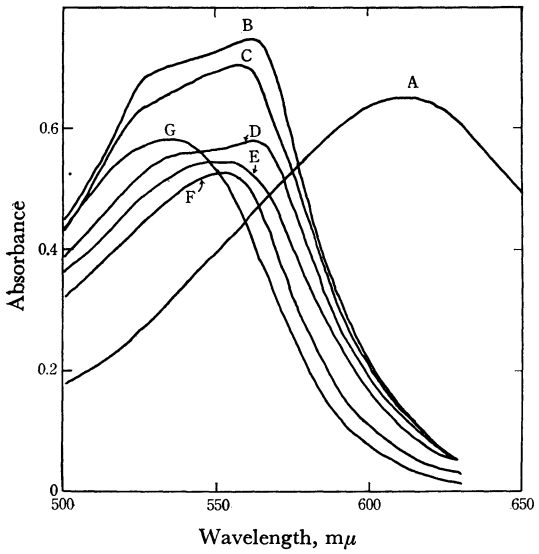

Fig. 1. Absorption curves of calmagite and its metal(II) chelates.
pH=9.79, μ=0.30
Concentration of calmagite=$3.3_0\times10^{-5}$ M
A: no metal(II), 10.0 mM EDTA
B: Ni(II)-NTA chelate 10.0 mM, NTA 10.0 mM
C: Zn(II)-NTA chelate 20.0 mM, NTA 5.0 mM
D: Co(II)-NTA chelate 10.0 mM, NTA 10.0 mM
E: Cd(II) 10.0 mM, ammonia 0.1 M
F: Pb(II)-NTA chelate 30.0 mM, NTA 5.0 mM
G: Cu(II)-NTA chelate 10.0 mM, NTA 10.0 mM

aminopolycarboxylate chelates proceeds very rapidly. Hence, the composition and stability constants of calmagite chelates of these metal(II) ions were determined from $\log(A_{HD}-A)/(A-A_{MD})$ *vs.* $\log[MZ]/([Z]_f\ [1+K_2[Z]_f/(a_H)])$ plots.[1,2] In nickel(II)-EDTA-OH and cobalt(II)-EDTA system, however, the reaction is very slow. Therefore, as in BT system, solution equilibria were determined from a $\log\ [(A_{HD}-A)/(A-A_{MD})[m-(A_{HD}-A)/(A_{HD}-A_{MD})]$ *vs.* $\log\ [Z]_f$ plot.[4,5] The notations here are those used previously.[1,2,4,5] Under the present experimental conditions, calmagite invariably forms chelates of a 1-to-1 composition. Results are given in Table 1. The numerical values used in the calculation of stability constants of calmagite chelates were estimated from the related con-

Table 1. Stability constants, $\log K_{MD}$ (μ=0.30)

	Cu(II)	Ni(II)	Co(II)	Zn(II)	Cd(II)	(Pb(II)
Calmagite	21.70	21.63	21.03	14.73	12.59	12.90
BT[1,2]	21.38	20.8	20.0	12.31	12.74	13.19

Table 2. End point indices (Δ_1 and Δ_2)

System	Metal concentration	Δ_1	Δ_2
Zn(II) ammonia buffer (0.1 M, pH=10.0)	0.1	6.78	3.03
	0.01	5.78	3.03
	0.001	4.78	3.03
Cd(II) ammonia buffer (0.1 M, pH=10.0)	0.1	8.27	4.84
	0.01	7.27	4.84
	0.001	6.27	4.84
Pb(II) 0.1 M tartrate (pH=10.0)	0.1	6.25	6.36
	0.01	5.25	6.36
	0.001	4.25	6.36

Table 3. EDTA Titrations of metal (II) using calmagite as indicator (pH=10.0)

	Concentration of metal(II) M	Volume of metal solution ml	Concentration of EDTA M	Volume of EDTA solution added, ml Calcd	Obsd
Zn(II) ammonia buffer (0.1 M)	1.00×10^{-2}	5.00	$1.38_1\times10^{-2}$	3.62	3.63
		10.00		7.24	7.22
		15.00		10.86	10.83
	1.00×10^{-3}	5.00	$1.38_1\times10^{-3}$	3.62	3.60
		10.00		7.24	7.22
		15.00		10.86	10.85
Cd(II) ammonia buffer (0.1 M)	$0.958_4\times10^{-2}$	5.00	$1.38_1\times10^{-2}$	3.47	3.50
		10.00		6.94	6.90
		15.00		10.41	10.43
	$0.958_4\times10^{-3}$	5.00	$1.38_1\times10^{-3}$	3.47	3.40
		10.00		6.94	6.96
		15.00		10.41	10.43
Pb(II) 0.1 M tartrate	$1.02_4\times10^{-2}$	5.00	$1.38_1\times10^{-2}$	3.71	3.69
		10.00		7.42	7.47
		15.00		11.13	11.17

4) M. Kodama, This Bulletin, **40**, 2575 (1967).

5) M. Kodama, C. Sasaki and M. Murata, *ibid.*, **41**, 2333 (1968).

stants[1-3,6-8] in a solution of ionic strength 0.10 in the same way as previously.[1] On the basis of general relation between stability constant and dissociation constant, the stability constant of metal(II)-calmagite chelate would be larger than that of metal(II)-BT chelate. In contrast to this prediction, log K_{MD} values of cadmium(II) and lead(II) chelates of calmagite were slightly less than those of BT. This abnormal behavior can not be explained in a simple manner, but may partially be attributed to π-back donation, to steric interaction or other effects. It can also be mentioned here that the Irving-Williams series applies to calmagite and BT chelates of copper(II), nickel(II), cobalt(II) and zinc(II).

The Use of Calmagite as an Indicator in Chelatometric Titrations of Zinc(II), Cadmium(II) and Lead(II). Thermodynamically, because of its larger log K_{MD} value, calmagite can not be used as a metallochromic indicator in EDTA titrations of copper(II), nickel(II) and cobalt(II). In the cases of zinc(II), cadmium(II) and lead(II), as shown in Table 2, end point indices, Δ_1 and Δ_2,[9] calculated using stability constants of metal(II)-EDTA,[7] -calmagite, tartrate[10] and ammine[8] complexes, and dissociation constants of EDTA[6] and calmagite,[3] clearly suggest that calmagite can be used successfully as an indicator in EDTA titrations of zinc(II), cadmium(II) and lead(II). This prediction was examined experimentally. At the end point, the color transition from red to bluish-violet occurred sharply. Typical results are given in Table 3. Experimental equivalence points agreed well with stoichiometric ones. Aqueous solutions of calmagite and its metal(II) chelates were much more stable than those of BT, in good agreement with the findings of Lindstrom and Diehl.[3]

6) G. Schwarzenbach and G. Anderegg, *Helv. Chim. Acta*, **40**, 4170 (1957).

7) G. Schwarzenbach, R. Gut, and G. Anderegg, *ibid.*, **37**, 937 (1954).

8) A. Ringbom, "Complexation in Analytical Chemistry," Interscience Publishers, New York (1963), p. 301.

9) C. N. Reilley and R. W. Schmid, *Anal. Chem.*, **31**, 887 (1959).

10) V. E. Panova, *Zhur. neorg. Khim.*, **1**, 422 (1956).

BULLETIN OF THE CHEMICAL SOCIETY OF JAPAN VOL. 42 837—839 (1969)

Radical Copolymerization of Glycidyl Dienecarboxylates with Styrene

Yoshio IWAKURA, Fujio TODA, Reiko IWATA and Yoshinori TORII

Department of Synthetic Chemistry, Faculty of Engineering, The University of Tokyo, Hongo, Tokyo

(Received July 31, 1968)

Extensive studies of the copolymerization of glycidyl acrylate and methacrylate have been undertaken by several investigators in recent years.[1-3] In connection with these works, glycidyl dienecarboxylates such as glycidyl β-vinylacrylate (GV) and glycidyl sorbate (GS) were prepared and copolymerized with styrene in benzene at 60°C, using α,α′-azobisisobutyronitrile as an initiator. The monomer reactivity ratios (r_1, r_2) were determined by the intersection method of Mayo and Lewis[4] and by the method of Fineman and Ross.[5] Then, the Q and e values of both monomers were calculated from these experimental results by means of Alfrey and Price equation.[6] These

TABLE 1. MONOMER REACTIVITY RATIOS AND Q, e VALUES

M_1	M_2	Fineman-Ross Method		Intersection Method		Q	e
		r_1	r_2	r_1	r_2		
Styrene	GV	0.12	4.97	0.13±0.02	4.99±0.14	4.79	−0.05
Styrene	GS	0.81	0.47	0.88±0.07	0.51±0.06	0.56	0.18

1) Y. Iwakura, T. Kurosaki and N. Nakabayashi, *Makromol. Chem.*, **46**, 570 (1961).
2) Y. Iwakura and K. Matsuzaki, *Kobunshi Kagaku* (*J. High Polymers*), **17**, 187 (1960).
3) J. A. Simms, *J. Appl. Polymer Sci.*, **5**, 58 (1961).
4) F. R. Mayo and F. M. Lewis, *J. Am. Chem. Soc.*, **66**, 1594 (1944).
5) M. Fineman and S. D. Ross, *J. Polymer Sci.*, **5**, 259 (1950).
6) T. Alfrey and C. C. Price, *ibid.*, **2**, 101 (1947).

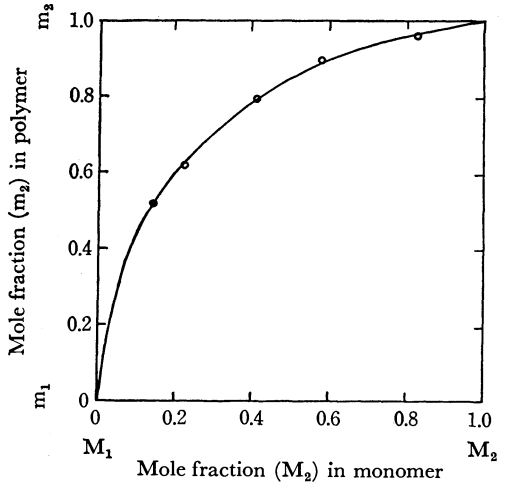

Fig. 1. Styrene - glycidyl β-vinylacrylate.

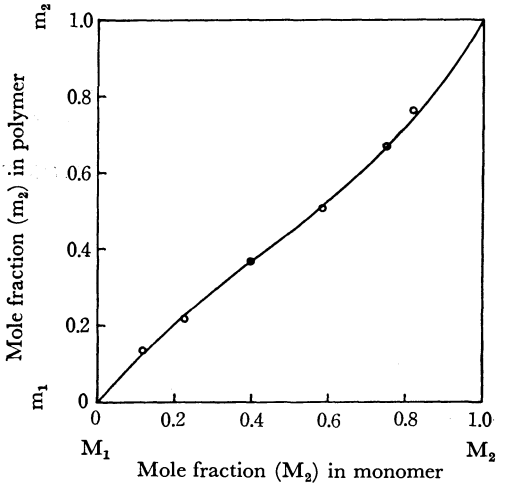

Fig. 2. Styrene - glycidyl sorbate.

values are listed in Table 1. The copolymer composition curves for GV and GS are shown in Figs. 1 and 2. It was found that the apparent rate of copolymerization of GV with styrene was somewhat slow in the region rich in charged styrene components, whereas the situation was reversed in the copolymerization of GS. The copolymer composition curve of GV shows that GV is reactive and is well-incorporated into a copolymer in the monomer mixture richer in styrene components. The copolymer composition curve of GS runs nearly along the 45° line and copolymerization will produce a copolymer possessing almost the same composition as the monomer mixture even at a high conversion.

It has been reported[7] that the replacement of the β-hydrogen of *n*-butyl acrylate by a methyl group brought about a serious decrease in the Q value from 0.50 to 0.007. The difference in Q value between GV and GS is presumably attributable to the same effect in the δ-methyl substitution system. Although the e value was also decreased by β-substitution in the case of butyl acrylate, no influence on the e value by δ-substitution in diene derivatives has been reported in the literature. The small increase in e value by δ-substitution therefore remained unexplained.

Copolymer were found to be soluble in benzene, tetrahydrofuran, dioxane, dimethylformamide, chloroform, and acetone, and insoluble in methanol, *n*-hexane, and water. The copolymers of GV containing a larger amount of GV were gummy materials, however, the other copolymers were white powder.

The infrared absorptions of $\nu_{C=O}$ and δ_{CH} of the *trans*-double bond in the copolymer appeared at 1730 and 970 cm^{-1} and at 1735 and 970 cm^{-1} in the copolymers of GV and GS, respectively. The absorption peaks arising from the phenyl ring of copolymer were exhibited at 1600, 1500, 760, and 700 cm^{-1}. The fact that the absorption maxima of the epoxide group[8] appeared at 900 and 840 cm^{-1} proved that the epoxide ring still remained unattacked in the copolymer. The epoxide contents in copolymers determined by titration corresponded substantially well to those calculated from elemental analyses.

Experimental

Synthesis of β-Vinylacrylic Acid. The procedure of Glushkov[9] was modified for the preparation of β-vinylacrylic acid. Malonic acid (250 g, 2.40 mol) was dissolved in pyridine (350 m*l*). Into the solution, kept at 75—80°C, acrolein (100 m*l*, 1.51 mol) was then added under stirring, drop by drop. The reaction mixture was stirred for 15 min, and then 75 m*l* of acrolein was added, drop by drop. After a few minutes interval, an additional 25 m*l* of acrolein was added to the mixture. After the mixture had been stirred for 30 min, it was poured onto crushed ice and acidified gradually wish 175 m*l* of concentrated sulfuric acid. Yellowish crystals were precipitated in a pulpy state by acidification. The crystals were filtered and washed with cold water. The filtrate was extracted three times with methylene chloride (each 300 m*l*), and the combined extract was dried over sodium sulfate. Yellowish crystals were obtained by the evaporation of the solvent. All the crystals were recrystallized from water, in the presence of hydroquinone as an inhibitor, to yield 66 g (28%) of the product melting at 68.5—70.5°C (lit.,[10] 72°C)

7) L. J. Young and C. C. Kennedy, in "Copolymerization," ed. by G. E. Ham, Interscience Pub., New York (1964), p. 845.

8) L. J. Bellamy, "The Infrared Spectra of Complex Molecules," p. 118, John Wiley & Sons, Inc., New York (1964).

9) R. G. Glushkov and O. Yu. Magidson, *Med. Prom. SSSR*, **16**, No. 3, 27 (1962); *Chem. Abstr.*, **58**, 442c (1963).

10) I. E. Muskat, B. C. Becker, and J. S. Lowenstein, *J. Am. Chem. Soc.*, **52**, 326 (1930).

in the form of needles. Crude crystals seemed to be pure enough for the synthesis of acid chloride. Recrystallization would cause a loss of β-vinylacrylic acid by thermal polymerization.

Synthesis of β-Vinylacryloyl Chloride. β-Vinylacryloyl chloride was synthesized from β-vinylacrylic acid and thionyl chloride in a 68% yield by the method described by Alder.[11] The boiling point was 42—44°C/10 mmHg.

Synthesis of Glycidyl β-Vinylacrylate (GV). In a four-necked flask there was placed glycidol in dry tetrahydrofuran, plus a small amount of an inhibitor. Equimolar amounts of triethylamine and β-vinylacryloyl chloride, each diluted with dry tetrahydrofuran, were added separately through two dropping funnels. Care had to be taken to maintain the reaction mixture in a condition with a slight excess of amine and to keep it below 10°C with an ice bath. After the addition had been completed, the mixture was stirred for 1 hr; the resultant triethylamine hydrochloride was removed by filtration, and the filtrate was dried over sodium sulfate. The product was obtained by distillation under a high vacuum in a 44% yield. The boiling point was 72—73°C/0.4 mmHg. If the bath temperature was raised above 120°C, distillation was impossible because of the thermal polymerization of the liquid phase. IR absorption bands: ν C=O 1715, ν C=C 1640, 1600; *trans*-conjugated diene δ CH 1015; epoxide 905, 840; terminal vinyl δ CH 930 cm^{-1}. λ_{max} 245 mμ in tetrahydrofuran.

Found: C, 62.57; H, 6.61%. Calcd for $C_8H_{10}O_3$: C, 62.32; H, 6.54%.

Synthesis of Sorboyl Chloride. A 500 m*l* flask was charged with 168 g (1.5 mol) of sorbic acid. Phosphorus pentachloride (312 g, 1.5 mol) was then vigorously blended in, portion by portion, using a glass rod. The reaction mixture was liquefied within a short time as the reaction proceeded. After the addition, the hydrogen chloride thus formed was purged from the reaction mixture with an aspirator. The product was separated from phosphorus oxychloride by distillation under reduced pressure with a small amount of a polymerization inhibitor such as *N*-phenyl-β-naphthylamine and purified by redistillation to give a fraction boiling at 70—72.5°C/10 mmHg and weighing 136 g (70% yield[12]). If the bath temperature was raised to over 110°C, the contents of the reaction flask suddenly became a black resinous material.

Synthesis of Glycidyl Sorbate (GS). Glycidyl sorbate was prepared by a method analogous to that used for GV. Toluene was used as the solvent in this case. The precipitated triethylamine hydrochloride was removed by filtration. The crude filtrate showed two carbonyl absorptions at 1720 and 1740 cm^{-1} in the infrared spectrum. The absorption of a higher frequency would indicate the existence of an isomer formed by the migration of the double bond to glycidyl 3,5-hexadienoate in the course of reaction. The crude reaction mixture was then heated together with a small amount of benzylamine at 90°C for 3 hr in order to bring about isomerization to a conjugated structure. The treatment was continued until the absorption at 1740 cm^{-1} disappeared. The solution thus treated was washed successively with dilute sulfuric acid, a sodium bicarbonate solution, and water, and then dried. After the removal of the toluene, vacuum distillation was repeated three times to give GS boiling at 100—102°C/0.3 mmHg[13] in a 42% yield. λ_{max} 259 mμ in tetrahydrofuran.

Found: C, 64.53; H, 7.06%. Calcd for $C_9H_{12}O_3$: C, 64.27; H, 7.19%.

Copolymerization. Polymerization experiments were carried out at 60°C in sealed tubes (10 m*l*) under a nitrogen atmosphere and using α,α′-azobisisobutyronitrile as an initiator. About 2 g of a mixture of precisely weighed styrene and GV was diluted with benzene (5 m*l*; in the case of GS, 2 m*l*) and sealed. The solution was then kept at 60°C for 15—28 hr. The polymer solution was poured into methanol, and the precipitated polymer was collected by filtration and reprecipitated, chloroform being used as the solvent and methanol as the non-solvent. The purified polymers were dried *in vacuo*, and the composition of the copolymer was determined by elemental analyses.

Determination of Epoxide Values. About 300mg of a copolymer sample was precisely weighed and dissolved in 25 m*l* of a HCl-dimethylformamide solution in a glass-stoppered flask.[14] The solution was then kept at 60°C for 64 hr. After the solution had been cooled to room temperature, calcium carbonate (0.5 g), starch solution (1.0 m*l*), and a fluorescein solution (5 drops) were added and the mixture was titrated by a standard silver nitrate solution. The epoxide value was calculated by subtracting the blank titer obtained under the same condition but without a sample.

The epoxy contents of the copolymers are as follows:

Copolymer	From elemental analyses:	From epoxide value:
Styrene-GV	89.1 mol%	84 mol%
Styrene-GS	21.7 mol%	21 mol%

11) K. Alder, M. Schumacher and O. Wolff, *Ann.*, **564**, 79 (1949).

12) T. E. Jones and C. O. Wilson, *J. Am. Pharm. Assoc.*, **42**, 342 (1953).

13) Y. Iwakura, N. Nakabayashi and M. H. Lee, *Makromol. Chem.*, **78**, 157 (1964).

14) L. Shechter, J. Wynstra and R. P. Kurkjy, *Ind. Eng. Chem.*, **48**, 94 (1956).

BULLETIN OF THE CHEMICAL SOCIETY OF JAPAN VOL. 42 840 (1969)

The Near Ultraviolet Absorption Spectrum of Quinoxaline Vapor

Yoshinori HASEGAWA,*1 Yoshito AMAKO and Hiroshi AZUMI

Department of Chemistry, Faculty of Science, Tohoku University, Katahira-cho, Sendai

and Mitsuo ITO and Yoko KAIZU

The Institute for Solid State Physics, The University of Tokyo, Minato-ku, Tokyo

(Received July 31, 1968)

We have measured the n–π^* absorption spectrum of quinoxaline vapor from 20 to 200°C with absorption cells of 40 and 120 cm in length, using a Shimadzu GE-340 grating spectrograph (dispersion in the second order=1.3 Å/mm) and a Jarrell Ash 3.4 m grating spectrograph (dispersion in the second order=2.4 Å/mm).

It has been found in this spectrum,*2 just as had previously been found in the spectrum of pyrazine vapor,[1,2] that the bands consist of two systems, one broad-band system originating at 26016.7 cm^{-1} and with a prominent progression of 525.3 cm^{-1}, and one sharp-band system with a 524.7 cm^{-1} progression with strong false origins at 27496.2 and 27670.1 cm^{-1}. Each band of the sharp system has a clear-cut head on the shorter-wavelength side and degrades toward the longer wavelengths.

Contrary to the case of the pyrazine spectrum, however, we can assign the broad system as an allowed $^1A_1$–$^1B_1$ transition with the 0–0 band at 26016.7 cm^{-1} and the sharp system as a vibronic transition induced by "intensity borrowing" from the $^1A_1$–$^1A_1$ transition, on the basis of the following considerations:

(1) The broad system exhibits a spectral-band feature characteristic of the vibrational structures for an allowed electronic transition, while the sharp system is characteristic of those for a vibronically-induced transition.

(2) In the n–π^* absorption bands of pyrazine,[1,2] the sharp bands have been observed to belong to the parallel bands of a near-oblate symmetric top (the asymmetric parameter, $\kappa \approx +0.7$) and assigned as an allowed electronic transition, while the broad bands, which can be regarded as the perpendicular bands, have been assigned as a vibronic transition. On the other hand, the quinoxaline molecule can be regarded as a near-prolate symmetric top (approximately, $\kappa \approx -0.7$). As is well known,[3] the parallel bands of a prolate symmetric top have nearly the same rotational structures as have of an oblate symmetric top. Therefore, it is natural to suppose that the sharp bands of the quinoxaline spectrum correspond to the parallel bands, (in-plane polarized perpendicular to the N–N axis of the molecule) and the broad bands, to the perpendicular bands, (polarized normal to the molecular plane).

It can not be determined with certainty, however, whether the sharp bands are the "forbidden"[4] bands in the allowed $^1A_1$–$^1B_1$ transition or the electronically-forbidden bands ($^1A_1$–$^1A_2$ transition, a component of the n–π^* splitting), since no hot bands corresponding to the strong false origins at 27496.2 and 27670.1 cm^{-1} appeared at all.*3

If we can regard the two vibrational frequencies, 525.3 and 524.7 cm^{-1}, observed in the broad and sharp system respectively as belonging to one electronic transition, we might assign the sharp bands to the "forbidden" bands in the allowed $^1A_1$–$^1B_1$ transition with the 0–0 band at 26016.7 cm^{-1}. The strong false origins at 27496.2 and 27670.1 cm^{-1} may also be then assigned to 0+1479 and 0+1653 cm^{-1} respectively. It seems, however, that the 1653 cm^{-1} is too high to be a fundamental frequency of the n–π^* state. However, this frequency is unlikely to be a combination.

Although several points remain uncertain, the proposed assignment seems most probable in the light of present knowledge. The vibrational analysis will be reported in detail elsewhere.

---

*1 Present address: College of General Education, Tohoku University, Kawauchi, Sendai.

*2 A part of the photograph of the vapor spectrum has already been presented in Ref. 5.

1) M. Ito, R. Shimada, T. Kuraishi and W. Mizushima, *J. Chem. Phys.*, **26**, 1508 (1957).

2) K. K. Innes, J. D. Simmons and S. G. Tilford, *J. Mol. Spectry.*, **11**, 257 (1963); K. K. Innes and J. E. Parkin, *ibid.*, **21**, 66 (1966).

3) A. C. Allen and P. C. Cross, "Molecular Vibrotor," John Wiley and Sons Inc., New York (1963).

4) A. C. Albrecht, *J. Chem. Phys.*, **33**, 156 (1960); *ibid.*, **33**, 169 (1960).

*3 Previously,[5] three of us (Y.H., Y.A. and H.A.) stated explicitly that the sharp bands of the quinoxaline spectrum are the "forbidden" bands. However, it would be better to state that the assignment is tentative, not conclusive.

5) Y. Hasegawa, Y. Amako and H. Azumi, This Bulletin, **41**, 2608 (1968).

BULLETIN OF THE CHEMICAL SOCIETY OF JAPAN VOL. 42 841—842 (1969)

Formation of 3-Butenoates from Crotonyl Chloride in the Presence of Amines

Yoshio IWAKURA, Fujio TODA, Reiko IWATA*1 and Yoshinori TORII*2

Department of Synthetic Chemistry, Faculty of Engineering, The University of Tokyo, Hongo, Bunkyo-ku, Tokyo

(Received August 5, 1968)

The reaction of acyl halides with alcohols is a conventional method of preparing esters.[1] In the course of applying this method to *trans*-crotonyl chloride in order to obtain unsaturated esters, which are used as monomers in vinyl polymerization, it was found that hydrogen abstraction from the β-methyl group of *trans*-crotonyl chloride occurred and that esters of vinylacetic acid (3-butenoates) were formed, possibly as a result of elimination-addition. In connection with this work, Payne has reported[2] that the dehydrochlorination of 3,3-dimethylacrylyl chloride through the use of tertiary amine occurs by 1,4-elimination to give the intermediate isopropenylketene, which is trapped in a dimeric form. The thermal isomerization of methyl *trans*-crotonate has also been investigated by Butler *et al.*[3]

The dependence of the formation of isomerized esters on various factors, such as the reaction conditions and the kinds of starting materials, was studied by determining by gas chromatography (GC) the ratio of crotonate and 3-butenoate existing in the products. The experimental results are summarized in Table 1. The structural assignment of each ester rests on the infrared and NMR spectra. The experimental results thus far examined show that the product ratio is influenced chiefly by the method of the reaction and by the kinds of reactants, such as alcohols and amines, while it is not so much influenced by the reaction time, the temperature, and the solvents. There was little difference in products ratios between the two methods of addition: 1) the simultaneous addition of acid chloride and amine into alcohol,

TABLE 1. REACTION OF *trans*-CROTONYL CHLORIDE WITH ALCOHOL

Run	Alcohol	Amine	Temp. °C	Solvent	3-Butenoate %	*trans*-Crotonate %	Method of reaction
1	MeOH	TEA	20	THF	76.7	23.3	Amine and acid chloride were added into alcohol.
2	MeOH	TEA	20	THF	74.2	25.8	Amine and acid chloride were added into alcohol, allowed to stand for 18 hr.
3	MeOH	Pyridine	20	THF	8.7	91.3	Amine and acid chloride were added into alcohol.
4	MeOH	DABCO*	20	THF	14.3	85.7	Amine and acid chloride were added into alcohol.
5	MeOH	TEA	20	THF	92.2	7.8	Acid chloride was added into amine and alcohol.
6	MeOH	TEA	−30	THF	92.2	7.8	Acid chloride was added into amine and alcohol.
7	MeOH	TEA	20	Benzene	93.9	6.1	Acid chloride was added into amine and alcohol.
8	MeOH	TEA	20	THF	79.6	20.4	Amine was added into acid chloride and alcohol.
9	*i*-BuOH	TEA	20	THF	98.3	1.7	Acid chloride was added into amine and alcohol.

TEA: Triethylamine THF: Tetrahydrofuran DABCO: Diazabicyclooctane

* On the contrary to our expectation, amount of 3-butenoate in product was small, presumably due to low solubility and basicity of its half-protonated form.

*1 Present address: Government Chemical Industrial Research Institute, Tokyo; Hon-machi, Shibuya-ku, Tokyo.

*2 Present address: Mitsui Toatsu Chemicals Incorporated; Kasumigaseki, Chiyoda-ku, Tokyo.

1) R. B. Wagner and H. D. Zook, "Synthetic Organic Chemistry," John Wiley & Sons, Inc., New York (1961), p. 481.

2) G. B. Payne, *J. Org. Chem.*, **31**, 718 (1966).

3) J. N. Butler and G. J. Small, *Can. J. Chem.*, **41**, 2492 (1963).

and 2) the addition of amine to a mixture of alcohol and acid chloride. However, by the addition of acid chloride to a mixture of amine and alcohol, that is, by a reaction under amine excess conditions, 3-butenoate was predominantly obtained possibly because of elimination-addition. It was noteworthy that a strong base such as triethylamine favored the formation of 3-butenoate, while *trans*-crotonate was mainly given by pyridine under the same reaction conditions. Isobutanol, which is rather bulky, gave a larger amount of isomerized ester than did methanol.

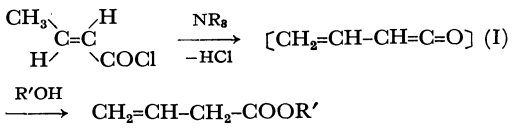

Several mechanisms are possible for the formation of 3-butenoate. The most probable explanation of the reaction scheme is that *trans*-crotonyl chloride is converted to an unstable vinylketene intermediate (I), which then reacts very rapidly with alcohol to give the isomerized ester. This assumption is well in accordance with the description of Payne.[2] The influence of the carbonyl group of α,β-unsaturated acid chlorides on the mobility of β-methyl hydrogen would be extended by conjugation, which has been established in the deuterium exchange reaction of such carboxylic acids as tiglic acid.[4]

Finally, 3-butenoate once formed was stable enough and had little tendency to isomerize to crotonate when the reaction mixture was kept standing at room temperature as long as amine salt did not exist in the system and *vice versa*. However, small amounts of such amines as *n*-butylamine and benzylamine assisted the migration of the double bond of isolated 3-butenoates to the stable conjugated form at elevated temperatures.

4) J. G. Atkinson, J. J. Csakvary, G. T. Herbert, and R. S. Stuart, *J. Am. Chem. Soc.*, **90**, 498 (1968).

Experimental

Synthesis of Standard Materials. The methyl *trans*-crotonate and methyl 3-butenoate (methyl vinylacetate) were synthesized by the esterification of the corresponding acids in excess methanol with a small amount of a *p*-toluenesulfonic acid catalyst: bp; methyl *trans*-crotonate,[5] 120—122°C; methyl 3-butenoate,[6] 111—113°C. The methyl *cis*-crotonate[7] was obtained by courtesy of Professor T. Tsuruta of The University of Tokyo, bp 119°C.

Reaction Conditions. Equimolar amounts (0.1 mol) of alcohol, amine, and *trans*-crotonyl chloride which had been diluted appropriately were allowed to react in a solvent (40 m*l*) for 30 min at a constant temperature. The amine hydrochloride thus precipitated was removed by filtration, and the resultant filtrate was subjected to GC measurement.

Gas chromatography was carried out under the following conditions:

Column PEG 1500, 2 m; He 40 ml/min; Column Temperature 129°C; Sample 1—4 μl.

The retention times of the esters are shown in Table 2. The amounts of the esters were determined from the areas of the peaks in the GC charts. Although they were not measured, the absolute yields were thought to be good enough, since the reactions were carried out under mild conditions.

Table 2. Retention times of each ester in GC

Ester	Retention time	
	min	temp. °C
Methyl *trans*-crotonate	3.08	129
Methyl *cis*-crotonate	2.43	129
Methyl 3-butenoate	2.42	129
Isobutyl 3-butenoate	2.94	155
Isobutyl *trans*-crotonate	3.40	155

5) T. Purdie and W. Marshall, *J. Chem. Soc.*, **59**, 468 (1891).

6) E. J. Corey, *J. Am. Chem. Soc.*, **75**, 2251 (1953).

7) F. Bürki, *Helv. Chim. Acta*, **1**, 231 (1918).

BULLETIN OF THE CHEMICAL SOCIETY OF JAPAN VOL. 42 843—844 (1969)

Isolation of Aplysin, Debromoaplysin, and Aplysinol from *Laurencia Okamurai* Yamada[1]

Toshi IRIE, Minoru SUZUKI and Yoshiki HAYAKAWA

Department of Chemistry, Faculty of Science, Hokkaido University, Sapporo

(Received September 3, 1968)

As part of a continuing search for constituents from *Laurencia* species,[2] we have examined *L. Okamurai* Yamada (Japanese name, Mitsudesozo; Rhodomelaceae). In this paper we will report the isolation of aplysin (I),[3] debromoaplysin (II),[3] aplysinol (III),[3] laurinterol (IV),[2c] and debromolaurinterol (V)[2c] and also a new, unidentified dibromo-compound (VI) from the seaweed.

Methanol extracts of the dried seaweed were evaporated *in vacuo*, and the residue was percolated with ether. The ethereal solution was washed successively with a dilute potassium hydroxide solution, dilute hydrochloric acid, and water, and evaporated. The oily neutral fraction thus obtained was chromatographed on silica gel.

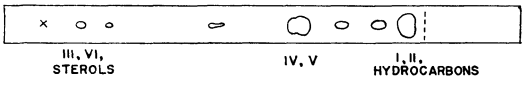

Fig. 1. TLC of the neutral fraction (silica gel, benzene).

From fractions eluted with 9 : 1 *n*-hexane - benzene, there was obtained a crystalline bromo-compound (I), $C_{15}H_{19}OBr$; mp 85—86°C, $[\alpha]_D$ −85°. The UV, IR, and NMR spectra of I were superimposable upon those of aplysin, which was isolated by Yamamura and Hirata[3] from *Aplysia kurodai* (sea rat) and which was also obtained by treatment with *p*-toluenesulfonic acid of laurinterol.[2c] The identity was further confirmed by a comparison of the R_f value on TLC and by a mixed-melting-point determination with an authentic sample.

Fractions eluted with 7 : 3 *n*-hexane - benzene left a colorless oil upon the removal of the solvent; this oil was purified by rechromatography on silica gel to give a pure, oily substance (II), $C_{15}H_{20}O$, $[\alpha]_D$ −63°. The IR and NMR spectra suggest that II is debromoaplysin;[3] this is confirmed by the synthesis from debromolaurinterol (V) shown below.

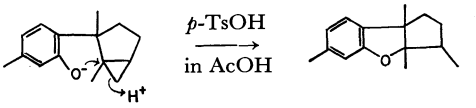

V II

Benzene eluates gave a mixture of alcohols, from which cholesterol, a monobromo-alcohol (III), $C_{15}H_{19}O_2Br$, mp 157—159°C, and a dibromo-compound (VI), $C_{14}H_{20}O_5Br_2$ (M^+ 428), mp 148.5—149°C, were isolated. The compounds III and VI could be purified *via* their acetates, VII, $C_{17}H_{21}O_3Br$, $[\alpha]_D$ −26°, and VIII, $C_{16}H_{22}O_6Br_2$, mp 154—156°C, $[\alpha]_D$ −44°, respectively. Compound III was identified as aplysinol[3] by a comparison of its UV, IR, and NMR spectra with those of an authentic sample. In the IR spectrum, the new dibromo-compound (VI) showed alcoholic group(s) at ν_{max} 3500 cm^{-1}, but no carbonyl function. The IR and NMR spectra of its acetate (VIII) exhibited the presence of an acetoxyl group [ν_{max} 1755 cm^{-1}; τ 7.86 (3H, s)], four tertiary methyl groups (3H, s's at τ 8.82, 8.70, 8.54 and 8.27) (two of which could be assumed to be olefinic and/or attached to epoxide-ring carbon, judging from their chemical shifts), two protons on carbons bearing bromine atoms (τ 5.2—5.8), and a proton on a carbon bearing an acetoxyl group (τ 4.71). The structure elucidation of VI is now in progress.

The principal part of the neutral fraction was eluted with 1 : 1 *n*-hexane - benzene; it was found to consist of laurinterol (IV) and debromolaurinterol (V), which were isolated from *L. intermedia* Yamada.[2c] It is noteworthy that these bromo-compounds have been found in only one seaweed.

Experimental

Isolation. Air-dried seaweed (1.4 kg), collected at Hakata-shima, the Inland Sea of Japan, was extracted with methanol, and then the methanolic solution was concentrated *in vacuo*. The residue was percolated

1) Part XII of "Constituents from Marine Plants." Part XI: T. Irie, T. Suzuki, Y. Yasunari, E. Kurosawa and T. Masamune, *Tetrahedron*, in press.

2) a) T. Irie, M. Suzuki and T. Masamune, *Tetrahedron Letters*, **1965**, 1091; b) T. Irie, Y. Yasunari, T. Suzuki, N. Imai, E. Kurosawa and T. Masamune, *ibid.*, **1965**, 3619; c) T. Irie, M. Suzuki, E. Kurosawa and T. Masamune, *ibid.*, **1966**, 1837; d) T. Irie, M. Izawa and E. Kurosawa, *ibid.*, **1968**, 2901, 2735; e) T. Irie, M. Suzuki and T. Masamune, *Tetrahedron*, **24**, 4193 (1968).

3) S. Yamamura and Y. Hirata, *ibid.*, **19**, 1485 (1963).

with ether, and the ethereal solution was shaken with a 5% potassium hydroxide solution and then with 1N hydrochloric acid to remove the acidic and basic components. After the removal of the solvent, a neutral, brown-colored oil (30 g) was obtained; it was subsequently chromatographed on silica gel.

Aplysin (I). Fractions eluted with 9 : 1 *n*-hexane - benzene left a crystalline substance upon the removal of the solvent. Recrystallization from methanol gave colorless crystals, mp 85—86°C; $[\alpha]_D$ −85° (*c*, 1.25; $CHCl_3$); UV, λ_{max}^{EtOH} 293, 232 mμ (ε 4400, 8100); IR, ν_{max}^{Nujol} 1610, 1580, 1474, 1393, 1380, 1263, 1230, 1100, 1005, 880, 860 cm^{-1}; NMR, τ 8.90 (3H, d, J=6 c/s), 8.75 (3H, s), 8.70 (3H, s), 7.68 (3H, s), 3.48 (1H, s), 2.95 (1H, s). (Found: C, 61.16; H, 6.41%).

The IR and NMR spectra were superimposable upon those of aplysin, and the R_f value on TLC and the mixed-melting-point were the same as those of an authentic sample.

Debromoaplysin (II). Fractions eluted with 7 : 3 *n*-hexane - benzene left an oily substance, which was then purified by rechromatography over silica gel to give a pure, colorless oil, $[\alpha]_D$ −63° (*c*, 1.15; $CHCl_3$); IR, ν_{max}^{film} 1620, 1595, 1500, 1280, 1265, 1120, 1010, 950, 800 cm^{-1}; NMR, τ 8.90 (3H, d, J=6 c/s), 8.75 (3H, s), 8.70 (3H, s), 7.72 (3H, s), 3.60 (1H, broad s), 3.50 (1H, broad d, J=7 c/s), 3.20 (1H, d, J=7 c/s). (Found: C, 82.98; H, 9.20%).

The IR and NMR spectra were superimposable upon those of debromoaplysin, to be described below.

Laurinterol (IV) and Debromolaurinterol (V). From fractions eluted with 1 : 1 *n*-hexane - benzene two compounds, IV, $C_{15}H_{19}OBr$, mp 54—55°C, and V, $C_{15}H_{20}O$ (an oil) were obtained and identified as laurinterol and debromolaurinterol respectively.

Aplysinol (III). Fractions eluted with benzene gave a mixture of alcohols. This mixture was then acetylated with acetic anhydride and pyridine at room temperature. The acetylated product was chromatographed on silica gel to give a pure, colorless oil (VII); $[\alpha]_D$ −26° (*c*, 0.85; $CHCl_3$); UV, λ_{max}^{EtOH} 292, 233 mμ (ε 2600, 5100); IR, ν_{max}^{film} 1750, 1615, 1585, 1490, 1230, 1050 cm^{-1}; NMR, τ 8.93 (3H, d, J=6 c/s), 8.63 (3H, s), 8.07 (3H, s), 7.74 (3H, s), 5.83 (2H, AB-q), 3.44 (1H, s), 2.95 (1H, s).

The acetate VII was saponified with 1.5N methanolic potassium hydroxide under reflux to give the original alcohol (III) in a good yield. Recrystallization from carbon tetrachloride gave colorless crystals, mp 157—159°C; $[\alpha]_D$ −54° (*c*, 0.90; $CHCl_3$); UV, λ_{max}^{EtOH} 292, 233 mμ (ε 5400, 10200); IR, ν_{max}^{Nujol} 3240, 1582, 1490, 1230, 1157, 1102, 1056, 998, 880, 857, 840, 790 cm^{-1}; NMR, τ 8.93 (3H, d, J=6 c/s), 8.54 (3H, s), 7.71 (3H, s), 6.28 (2H, m), 3.47 (1H, s), 2.98 (1H, s).

(Found: C, 57.67; H, 6.17%).

The IR and NMR spectra were superimposable upon those of aplysinol. Aplysinol (III) has also been isolated directly from the original alcoholic mixture by careful rechromatography.

Dibromo-compound (VI). The rechromatography of the afore-mentioned alcoholic mixture led to the isolation of crystals melting at 148.5—149°C (VI); IR, ν_{max}^{Nujol} 3500, 1252, 1080, 1050, 1000, 915, 896, 823, 786 cm^{-1}. Acetate (VIII), colorless crystals, mp 154—156°C (from CCl_4), $[\alpha]_D$ −44° (*c*, 0.75; $CHCl_3$); UV, λ_{max}^{EtOH} 290 mμ (ε 180); IR, ν_{max}^{Nujol} 1755, 1403, 1225, 1082, 1050, 1032, 1012, 942, 878, 828, 790 cm^{-1}; NMR, τ 8.82 (3H, s), 8.70 (3H, s), 8.54 (3H, s), 8.27 (3H, s), 7.86 (3H, s), 7.5—8.2 (2H, m), 7.05 (1H, s), 5.2—5.9 (2H, m), 4.71 (1H, s).

Found: C, 40.65; H, 4.67%. Calcd for $C_{16}H_{22}O_6Br_2$: C, 40.86; H, 4.72%.

The saponification of VIII gave VI in a good yield.

Debromoaplysin (II) from Debromolaurinterol (V). A solution of V (51 mg) and *p*-TsOH (25 mg) in glacial acetic acid (2 ml) was heated at 50°C for 25 hr. After being cooled, the reaction mixture was extracted with ether, and the ethereal solution was washed successively with water, a 5% sodium bicarbonate solution, and a saturated sodium chloride solution, and dried over sodium sulfate. The ether was then removed, and the residual oil was chromatographed over silica gel to give a pure, colorless oil (47 mg),¶ $[\alpha]_D$ −61° (*c*, 0.74, $CHCl_3$); mass spectrum, *m/e* (rel. abund.) 216 (M^+), 202 (15), 201 (100), 187 (11), 173 (18), 160 (31). 159 (50), 145 (14), 119 (9), 91 (9), 77 (6), 55 (4), 43 (5), and 41 (8). The IR and NMR spectra were superimposable upon those of II, and the mass spectral data were identical with those of debromoaplysin reported in the literature.[3]

The authors wish to express their hearty thanks to Professor Yoshimasa Hirata, Nagoya University, for providing them with the IR and NMR spectral charts of aplysinol, and to Professor Toraya Fujiyama, Hiroshima University, for collecting the seaweed. The authors' thanks are also due to Mr. Shigezo Shimokawa and Miss Yoshiko Kishio for their NMR measurements, to Miss Yuko Imai for her measurements of the mass spectra, and to Mrs. Toyoko Toma, Faculty of Pharmaceutical Science, for her microanalyses.

SHORT COMMUNICATIONS

Conformational Dependence of P=O Stretching Vibration Frequency in Six-membered Cyclic Phosphates

Masatsune KAINOSHO, Toshikatsu MOROFUSHI and Asao NAKAMURA

Central Research Laboratories, Ajinomoto Co., Inc., Suzuki-cho, Kawasaki

(Received December 19, 1968)

It has been reported that the P=O stretching frequency ($\nu_{P=O}$) does not show any appreciable dependency on the conformational environments of 1,3,2-dioxaphosphorinane system,[1,2] although the $\nu_{S=O}$ in six-membered cyclic sulfites is quite sensitive to the conformations.[3] NMR and dipole moment studies[4] have shown that the P=O bond is mainly at the equatorial rather than the axial position. The same conformation is also confirmed by the X-ray diffraction method[5] in the crystalline state of several phosphates.

In this communication we wish to present the unequivocal evidence of conformational dependence of $\nu_{P=O}$, which is contrary to previous reports. The infrared spectra of 5,5-dimethyl-2-oxo-2-alkoxy-(or 2-aryloxy)-1,3,2-dioxaphosphorinanes were carefully examined both in solid phase (KBr tablet) and in carbon tetrachloride solution.

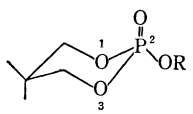

α

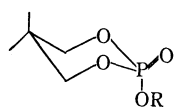

β

In solid phase, all of the compounds examined show a symmetrical single absorption at 1284—1305 cm^{-1} which can be assigned to $\nu_{P=O}$, but in solution an extra band at 1267—1298 cm^{-1} followed by the strong absorption at 1308—1322 cm^{-1} (see Table 1). These bands are assignable to $\nu_{P=O}$ because they were shown to shift by the addtion of phenol possibly due to the formation of hydrogen bonding. The origin of this phenomenon (*i. e.* two $\nu_{P=O}$'s) is attributable to the conformational equilibrium, $\alpha \leftrightarrow \beta$. With I—V, the relative intensity of the higher frequency bands are much stronger than the lower ones, indicating that the former are equatorial and the latter are axial $\nu_{P=O}$. This assignment is compatible with the general trend that the axial stretching frequency is lower than the equatorial one.

TABLE 1.

Compound*	$\nu_{P=O}$ cm^{-1}		
	KBr	CCl_4 sol.	+Phenol
2-Methoxy- (I)	1287	1313	1285
		1272	1234
2-Ethoxy- (II)	—**	1309	1283
		1267	1230
2-Isopropoxy- (III)	1284	1308	1277
		1268	1231
2-*p*-Anisyl- (IV)	1297	1322	1294
		1298	1228
2-(3,5-Dimethyl)phenoxy- (V)	1305	1322	1290
		1294	1228
2-(2,6-Dimethyl)phenoxy- (VI)	1304	1319	1294
		1287	1227
2-(2,6-Di-*t*-butyl-4-methyl)-phenoxy- (VII)	1297	1314	1288
		1286	1230

* Preparation of these compounds will be described elsewhere.

** Liquid at room temperature.

Clearer examples are supplied by VI and VII, in which β-conformation may be expected to have a strong 1,3-diaxial repulsion between the ring hydrogens and the substituents at aryloxy groups. Thus, the intensity ratios of two bands ($\nu_{P=O_{eq}}$: $\nu_{P=O_{ax}}$) are roughly estimated as 4 : 1 and 1 : 1 for VI and VII, respectively. These ratios are in agreement with the NMR results which will be published elsewhere.

1) R. S. Edmundson, *Tetrahedron*, **20**, 2781 (1964).

2) R. A. Y. Jones and A. Y. Katritzky, *J. Chem. Soc.*, **1960**, 4376.

3) H. F. Van Woerden and E. Havinga, *Rec. Trav. Chim. Pays-Bas.*, **86**, 341 (1967).

4) M. Kainosho and T. Shimozawa, *Tetrahedron Letters*, in press.

5) W. Murayama and M. Kainosho, This Bulletin, in press, and references cited therein.

The Electron Spin Resonance of the Trinuclear Vanadyl Pyrophosphate Complex

Akinori HASEGAWA, Yoshio YAMADA and Masaji MIURA

Department of Chemistry, Faculty of Science, Hiroshima University, Higashisenda-machi, Hiroshima

(Received October 30, 1968)

An aqueous solution of the vanadyl pyrophosphate (1 : 1) complex has shown a characteristic ESR spectrum which has never been observed in any other vanadyl complexes. Yakovenko and Mustaev recently proposed $Na_2VOP_2O_7 \cdot 6H_2O$ as the molecular formula for this complex.[1] The observed spectrum (Fig. 1) can not, however, be interpreted in terms of any of the present models of a mononuclear or binuclear complex.

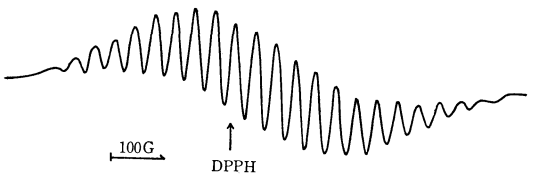

Fig. 1. ESR spectrum of aqueous solution of vanadyl pyrophosphate complex at 25°C

The molecular formula of this system, therefore, has been investigated further by various methods. The amount of water eliminated from the crystal was determined gravimetrically, and that of sodium ions, by atomic absorption spectrophotometry. The molecular weight has been measured by means of a vapor-pressure osmometer with this system. Assuming the complex to be trinuclear, its molecular weight is 1120, a value which is in good agreement with the calculated value, 1077. The results of all these measurements have definitely indicated the trinuclear formula of $[Na_2VOP_2O_7]_3 \cdot 12H_2O$.

Thus, in the trinuclear complex, exchange interaction among three vanadyl ions should be taken into account. The spin Hamiltonian is shown in the form:

$$\mathcal{H} = g\beta H \sum_{i=1}^{3} S^{(i)} + a \sum_{i=1}^{3} S^{(i)} I^{(i)} + \bar{J} \sum_{i>j=1}^{3} S^{(i)} S^{(j)}, \quad (1)$$

where $\bar{J} \gg a$ is assumed. With this assumption and the mixing of the two doublet states with the quartet state, Hudson and Luckhurst showed that the ESR transitions allowed for the quartet state to occur at:[2]

$$h\nu = g\beta H + \frac{a}{3}(m^{(1)} + m^{(2)} + m^{(3)}). \quad (2)$$

The vanadyl pyrophosphate complex may, therefore, be expected to give a spectrum composed of 22 lines and with a splitting of 36.4 gauss. This splitting is one-third of that of 109 gauss observed in vanadyl pyrophosphate (1 : 2), which shows no spin exchange.

Transitions for the two doublet states are also allowed at:

$$h\nu = g\beta H + \frac{a}{3}(m^{(1)} + m^{(2)} + m^{(3)}) \pm \frac{2a}{3}(m^{(1)2} + m^{(2)2} + m^{(3)2} - m^{(1)}m^{(2)} - m^{(2)}m^{(3)} - m^{(3)}m^{(1)})^{1/2}. \quad (3)$$

The spectrum predicted for these transitions is constructed with 144 irregularly spaced lines. As the intensity of these lines is very weak compared with that for the quartet, the quartet state appears predominantly in the spectrum of the trinuclear complex. The spectrum simulated with these assumptions shows a satisfactory agreement with that observed.

Hudson and Luckhurst, using Redfield's theory, explained the distinctive change in the spectrum of the triradical with a rise in the temperature in terms of the spin exchange interaction.[2] In the present case, however, no such change can be observed. This may be attributed to the condition $\bar{J} \gg a$. In order to estimate the value of $\bar{J}$, measurements of the magnetic susceptibility were carried out at various temperatures above 77°K.

According to Kambe's theory,[3] the effective Bohr magneton for this complex obeys the equation:

$$\mu_{eff} = \left[\frac{5\exp(-3\bar{J}/2kT) + 1}{\exp(-3\bar{J}/2kT) + 1}\right]^{1/2}. \quad (4)$$

By comparing this relation with the observed values, $\bar{J} \simeq 30$ cm^{-1} was obtained, where it must be noticed that the sign of $\bar{J}$ is the reverse of the conventional one. This value completely satisfies the condition of $\bar{J} \gg a$, a being 99×10^{-4} cm^{-1}. The large antiferromagnetic exchange interaction may suggest that the spin exchanges through the π bonds of O–P–O in pyrophosphate.

1) R. T. Yakovenko and A. K. Mustaev, *Inst. Neorg. Fiz. Khim.*, **1966**, 30.

2) A. Hudson and G. R. Luckhurst, *Mol. Phys.*, **13**, 409 (1967).

3) K. Kambe, *J. Phys. Soc. Japan*, **5**, 48 (1950).

Mass Spectroscopic Detection of Methyl Radical in the Reaction of Hydrogen Atom with Ethylene

Soji TSUCHIYA, Fukusaburo ISHIHARA, Satsuki TASHIRO and Tsutomu HIKITA

Department of Fuel Technology, Faculty of Engineering, University of Tokyo, Hongo, Tokyo

(Received November 4, 1968)

It is well known[1] that the reaction of hydrogen atom with ethylene produces energy rich ethyl radicals initially, and that those stabilized by collisions with surrounding particles or a wall of a reaction vessel undergo the recombination and the disproportionation reactions. In this communication, we will describe the evidence for the existence of methyl radical, and will suggest the mechanism in a low pressure reaction with a high concentration of hydrogen atom.

Hydrogen atoms, which are produced by a microwave discharge in the mixture of 10% hydrogen in argon, are introduced to the Pyrex reaction tube with a flow velocity of 6 m/sec at 0.45 Torr, and ethylene is added *via* the inner tube that is movable to control the reaction time in the range of 1—15 msec. The reaction products are fed into a TOF mass spectrometer through a pin hole positioned at the end of the reaction tube.

The analysis of the observed mass spectrum shows that ethane and methane are the main reaction products, while butane and propane are minor ones. For example, the reaction at an initial concentrration ratio of $[C_2H_4]_i/[H]_i=5$*1 is expressed by a stoichiometric equation, $C_2H_4+2H=0.77C_2H_6+0.22CH_4+0.07C_3H_8+0.002C_4H_{10}$. In this analysis, the peak intensities of $m/e=15$ and 14 in the spectrum are in excess compared with the ones calculated from the standard mass spectral patterns of the above products. In order to decide what product contributes to the $m/e=15$ peak, the ionization efficiency curve was observed as shown in Fig. 1. The appearance potential is 5.90 eV lower than the ionization potential of argon atom, *i. e.*, 15.76−5.90=9.86 eV. This value is fairly in agreement with that of methyl radical, 9.843 eV.[2] The same experiment to ascertain the existence of ethyl radical was also made. The appearance potential of the $m/e=29$ peak is equal to the ionization potential of ethylene, because the $m/e=29$ peak corresponds to the parent ion of isotopic ethylene $^{13}C^{12}CH_4$. Hence, the concentration of ethyl radical is too small to be detected.

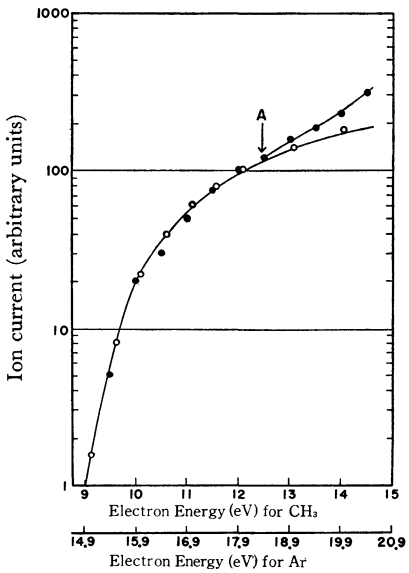

Fig. 1. Ionization efficiency curve of methyl radical in the reaction products.
●: that of CH_3^+ ion from CH_3 radical,
○: for A^+ ion from argon atom; point A shows the beginning of the contribution of CH_3^+ ion from methane in the products.

From the above results, the following reactions are concluded to be dominant in the present condition.

$$C_2H_4 + H \rightleftarrows C_2H_5^* \longrightarrow C_2H_5 \quad (1)$$
$$C_2H_5 + H \longrightarrow C_2H_6 \quad (2)$$
$$\longrightarrow 2CH_3 \quad (3)$$
$$CH_3 + H \longrightarrow CH_4 \quad (4)$$

A very small concentration of ethyl radical is considered due to the fact that the rates of reactions (2) and (3) are much larger than that of (1), and moreover that the collision frequency to stabilize an energy rich ethyl radical is small. The existence of a detectable amount of methyl radical means that reaction (4) is not very fast compared with the reaction (1). The details of the study on the kinetics will be published in the near future.

1) B. A. Thrush, "Progress in Reaction Kinetics," Vol. 3, ed. by G. Porter, Pergamon, New York (1965), p. 65; R. J. Cvetanovic, "Advances in Photochemistry," Vol. 1, ed. by W. A. Noyes, *et al.*, Interscience Publishers, New York (1963), p. 115.

*1 This value is estimated from the relation, $[C_2H_4]_i/([C_2H_4]_i-[C_2H_4]_f)\alpha$, where $[C_2H_4]_f$ is the final concentration of ethylene at the end of the reaction, and α is the stoichiometric ratio of the reaction.

2) G. Herzberg and J. Shoosmith, *Can. J. Phys.*, **34**, 523 (1956).

A Mechanism of the Syndiotactic Polymerization of α-Olefin

Yoshinobu TAKEGAMI and Toshimitsu SUZUKI

Department of Hydrocarbon Chemistry, Faculty of Engineering, Kyoto University, Kyoto

(Received December 5, 1968)

In connection with the initiation step of the polymerization of α-olefin, the insertion reactions of olefins into metal-ethyl bond in Ziegler-type catalysts were studied.[1] An olefin was reacted with a catalyst in a high concentration, and then, after a certain reaction time, the catalyst mixture was decomposed by methanol. The insertion processes of an olefin into a metal-ethyl bond may be formulated as follows:

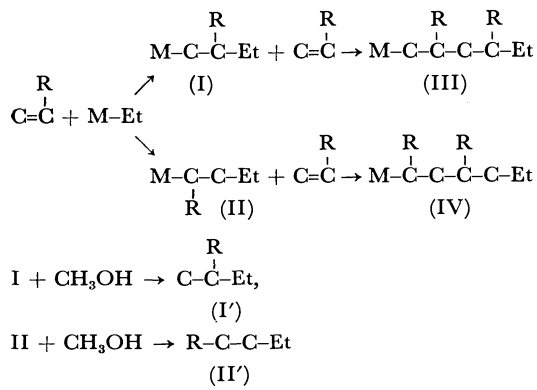

The hydrocarbons thus liberated were identified by gas-liquid chromatography.

The catalyst system containing titanium gave exclusively a metal alkyl (I), which was related to the isotactic polymerization of α-olefins. Unlike as in the titanium system, propylene was polymerized to a syndiotactic polymer with a vanadium catalyst at a low temperature.[2]

The method described in a former paper[1] was used in this vanadium catalyst system. However, in the case of propylene, neither metal alkyl (I) nor (II) were detected at a low temperature. Butene-1 and higher olefins could not be polymerized with this catalyst.[3] Pentene-1 could be reacted with vanadium tetrachloride and diethylaluminum chloride catalysts. After methanolysis, *n*-heptane (from metal alkyl (II)) and a small amount of 3-methylhexane (from metal alkyl (I)) were obtained. The results are summarized in Table 1. At −70°C, where the syndiotactic polymerization of propylene proceeded, almost ten times as much (II) as metal alkyl (I) was obtained. The fact that the yield of the metal alkyls decreased with the reaction time indicates that the second step of the insertion of pentene-1 into metal alkyls (I) and (II) occurred slowly.

Recently Zambelli *et al.*[4] succeeded in copolymerizing ethylene and butene-1 with a syndiospecific catalyst, and they obtained an almost alternating copolymer. This may be explained, in our opinion, by the consideration that the insertion of butene-1 into a sterically-hindered secondary metal alkyl bond is difficult, while ethylene is easily inserted into the secondary metal alkyl bond and forms the primary metal alkyl bond again.

According to this mechanism, almost every experimental result with the syndiospecific catalyst can be clearly explained.

1) A bulky olefin, such as butene-1 or pentene-1, can not be polymerized, for the steric hindrance of the alkyl substituent attached closely to vanadium interrupts the coordination of the approaching monomer.

2) The syndiotacticity in the case of the polymerization of propylene is caused by the monomer attack on the secondary metal alkyl bond from the less hindered site.

3) The addition of anisole to the reaction system increases the tendency of the insertion reaction to the secondary metal alkyl bond, as is shown in Table 1.

TABLE 1. INSERTION REACTION OF PENTENE-1 INTO METAL-ETHYL BOND IN VCl_4-$AlEt_2Cl$ CATALYST

Reaction		Products		
Temp. (°C)	Time (min)	3-Methyhexane(mmol)	*n*-Heptane	Additive (mmol)
−70	5	0.0105	0.0422	
−70	10	0.0126	0.0392	
−70	360	0.0040	0.0141	
−70	10	0.0137	0.135	Anisole 1.0
−70	40	0.0150	0.115	Anisole 1.0
−70	360	0.0022	0.103	Anisole 1.0

VCl_4, 1.00 mmol, $AlEt_2Cl$, 3.00 mmol
pentene-1, 4.5 mmol
Solvent, toluene; Total volume, 10 ml

1) Y. Takegami, T. Suzuki and T. Okazaki, This Bulletin, to be published, No. 4 (1969).

2) A. Zambelli, G. Natta and I. Pasquon, *J. Am. Chem. Soc.*, **84**, 1488 (1962).

3) A. Zambelli, G. Natta and I. Pasquon, *J. Polymer Sci.*, **C4**, 411 (1963).

4) A. Zambelli, A. Lety, C. Tosi and I. Pasquon, *Makromol. Chem.*, **115**, 73 (1968).

Photocycloaddition of Propionaldehyde to Ethyl Vinyl Ether[1]

Kensuke SHIMA and Hiroshi SAKURAI

The Institute of Scientific and Industrial Research, Osaka University, Suita-shi, Osaka

(Received December 6, 1968)

It has been reported that aliphatic aldehyde add to highly-alkylated olefins, such as tri- and tetramethylethylene, to give oxetanes photochemically.[2] However, in the cases of 1-olefins (*e. g.*, 1-hexene or 1-octene) ketones (I) are mainly formed by the radical chain mechanism.[3]

$$R_1CHO + R_2CH{=}CH_2 \xrightarrow{h\nu} R_2CH_2CH_2COR_1 (I)$$

The photoreaction of aliphatic aldehydes with electron-deficient olefins also gives ketones.[4]

In this communication, we wish to report on the photochemical formation of oxetanes from propionaldehyde and ethyl vinyl ether.[5] A solution containing 70 g of ethyl vinyl ether and 32 g of propionaldehyde was irradiated, using a 350-W high-pressure mercury lamp and a Pyrex filter, at 20°C under nitrogen for 20 hr. After the subsequent evaporation of the unreacted materials, a fraction boiling at 60—70°C/27 mmHg was collected; yield, *ca.* 10 g.[6] It contained two main products (more than 85%) and several minor products.[7] A mixture of the two main products (in almost a 1 : 1 ratio) was isolated using a preparative VPC; bp 64°C/27 mmHg, n_D^{28} 1.4133. Found: C, 64.50; H, 11.08%; mol wt,[8] 133. Calcd for $C_7H_{12}O_2$: C, 64.58; H, 10.84%; mol wt, 130.

The structure IIa was assigned on the basis of spectral data. The IR spectrum showed a strong band at 970 cm^{-1} (oxetanes) and neither hydroxyl nor carbonyl absorptions. The NMR spectrum showed resonances at τ 5.3—6.2 (4H, complex multiplet), τ 6.68 (2H, quartet, H^e), τ 8.40 (2H, quintet, H^g), τ 8.88 (3H, triplet, H^f), and τ 9.12 (3H, triplet, H^h).[9] Four hydrogens on the oxetane ring appear at τ 5.3—6.2. If the oxetanes had the structure IIb, $H^{d'}$ would be present in the lower field due to the adjacent two oxygens and would have an appreciably different τ value from those of $H^{b'}$ and $H^{c'}$.[10] On the other hand, if they had the structure IIa, all of the four hydrogens on the ring would be in the α-position relative to the oxygens and would be expected to give complex multiplets because of their similar τ values and because of the complex coupling between them. On the basis of these data, two these oxetanes were confirmed to be *cis*- and *trans*-isomers of IIa.

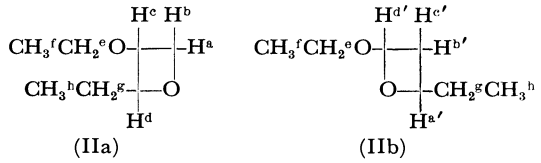

(IIa) (IIb)

Generally, one cannot obtain oxetanes in the photoaddition of aliphatic aldehydes to 1-olefins. This is mainly because of the slow rate of the formation of oxetanes compared with that of the formation of free radicals. It is well established that the formation of oxetanes proceeds *via* the attack by the electrophilic oxygen atoms of the $n\pi^*$ triplet states of carbonyl compounds on olefins with electron-donating groups. Therefore, oxetanes are easily obtained in the photoaddition of propionaldehyde to ethyl vinyl ether. In this case, very few ketones are formed. This may be due to the high probability of polymerization in ethyl vinyl ether. The orientation of the resulting oxetanes is that to be expected from a consideration of the more stable biradical intermediate. It is interesting that 1-olefins, with an electron-donating substituent, give mainly oxetanes upon the photoaddition of aliphatic aldehydes.

1) Organic Photochemical Reactions, Part IX. Part VIII: Y. Nagao, K. Shima and H. Sakurai, *Kogyo Kagaku Zasshi* (*J. Chem. Soc. Japan, Ind. Chem. Sect.*), **72**, 236 (1969).

2) G. Buchi, C. G. Inman and E.S. Lipinsky, *J. Am. Chem. Soc.*, **76**, 4327 (1954); H. Sakurai, K. Shima and S. Toki, *Nippon Kagaku Zasshi* (*J. Chem. Soc. Japan, Pure Chem. Sect.*), **89**, 537 (1968).

3) M. S. Kharasch, W. H. Urry and B. M. Kuderna, *J. Org. Chem.*, **14**, 248 (1949).

4) T. M. Patrick, Jr., *ibid.*, **17**, 1009, 1269 (1952). Recently, it was reported that aliphatic and alicyclic ketones add to electron-deficient olefins to give oxetanes by UV irradiation. The formation of oxetanes probably proceeds *via* $n\pi^*$ singlet ketones. N. J. Turro, P. Wriede, J. C. Dalton, D. Arnold and A. Glick, *J. Am. Chem. Soc.*, **89**, 3950 (1967); J. A. Barltrop and H. A. J. Carless, *Tetrahedron Letters*, **1968**, 3901.

5) We have already reported that the photoaddition of propionaldehyde to styrene gives oxetanes. H. Sakurai, K. Shima and I. Aono, This Bulletin, **38**, 1227 (1965).

6) Residues, 15 g.

7) By VPC, Dinonyl Phthalate, 120°C.

8) VPO method in benzene.

9) Solvent, CCl_4; internal standard, tetramethylsilane.

10) The NMR spectra of oxetanes show the α-hydrogen to oxygen at 5.0—6.0τ; the presence of additional α-oxygen to $H^{d'}$ further lowers its value, while the β-hydrogen to oxygen on the ring occurs at 6.4—7.4τ. D. R. Arnold, R. L. Hinman and A. H. Glick, *Tetrahedron Letters*, **1964**, 1425.

Intrinsic Viscosity of Rigid Complex Molecules*1

Keishiro TSUDA

Textile Research Institute of Japanese Government, Kanagawa-ku, Yokohama

(Received December 16, 1968)

The intrinsic viscosity of a molecule consisting of n elements is expressed in terms of the hydrodynamic force $\boldsymbol{F}_l$ exerted on solvent by an element l as[1)]

$$[\eta] = -\frac{N_0}{M\eta_0\dot{\varepsilon}}\sum_{l=1}^{n}\langle(\boldsymbol{F}_l\cdot\boldsymbol{e}_x)(\boldsymbol{R}_l\cdot\boldsymbol{e}_y)\rangle. \tag{1}$$

Here N_0 is the Avogadro number, M the molecular weight of the solute, η_0 the solvent viscosity, $\dot{\varepsilon}$ the rate of strain, and $\boldsymbol{R}_l$ the position of the indicated element l relative to the molecular center of mass. $\boldsymbol{e}_x$ and $\boldsymbol{e}_y$ are the unit vectors in the x and y directions, respectively. Hence, the unperturbed velocity of the solvent at the point $\boldsymbol{R}_l$ is defined by

$$\boldsymbol{v}_l^0 = \dot{\varepsilon}(\boldsymbol{R}_l\cdot\boldsymbol{e}_y)\boldsymbol{e}_x. \tag{2}$$

The hydrodynamic force $\boldsymbol{F}_l$ is then written as

$$\boldsymbol{F}_l = -\zeta(\boldsymbol{v}_l^0 - \boldsymbol{u}_l) - \zeta\sum_{s=1}^{n}{}'\boldsymbol{T}_{ls}\cdot\boldsymbol{F}_s, \tag{3}$$

where ζ is the friction constant of a single element, $\boldsymbol{u}_l$ the velocity of element l, and the sum extends over 1 to n, but l, with respect to s. $\boldsymbol{T}_{ls}$ represents the Oseen interaction tensor which is defined by

$$\boldsymbol{T}_{ls} = \frac{1}{8\pi\eta_0 R_{ls}}\left(\boldsymbol{I} + \frac{\boldsymbol{R}_{ls}\boldsymbol{R}_{ls}}{R_{ls}^2}\right), \tag{4}$$

where R_{ls} is the distance between elements l and s.

For a solute molecule of rigid structure, we have

$$\boldsymbol{u}_l = (\dot{\varepsilon}/2)[(\boldsymbol{R}_l\cdot\boldsymbol{e}_y)\boldsymbol{e}_x - (\boldsymbol{R}_l\cdot\boldsymbol{e}_x)\boldsymbol{e}_y]. \tag{5}$$

Equation (3) may then be rewritten in the form

$$\boldsymbol{F} = -(\dot{\varepsilon}/2)\zeta\boldsymbol{a}_\beta - \zeta\boldsymbol{T}\cdot\boldsymbol{F}, \tag{6}$$

or in its equivalent form,

$$-(1/\dot{\varepsilon})\boldsymbol{a}_\alpha\cdot\boldsymbol{F} = (\zeta/2)\boldsymbol{g}_{\alpha\beta} + (\zeta/\dot{\varepsilon})\sum_\nu\boldsymbol{a}_\alpha\boldsymbol{a}^\nu\boldsymbol{T}\boldsymbol{a}_\nu\boldsymbol{F}, \tag{7}$$

with the abbreviations,

$$\begin{aligned}\boldsymbol{F} &= \sum_l\boldsymbol{F}_l, \quad \boldsymbol{T} = \sum_l\sum_s\boldsymbol{T}_{ls},\\ \boldsymbol{a}_\beta &= \sum_l[(\boldsymbol{R}_l\cdot\boldsymbol{e}_x)\boldsymbol{e}_y + (\boldsymbol{R}_l\cdot\boldsymbol{e}_y)\boldsymbol{e}_x],\\ \boldsymbol{a}_\alpha &= \sum_l(\boldsymbol{R}_l\cdot\boldsymbol{e}_y)\boldsymbol{e}_x, \quad \boldsymbol{g}_{\alpha\beta} = \boldsymbol{a}_\alpha\cdot\boldsymbol{a}_\beta.\end{aligned} \tag{8}$$

Further, Eq. (7) is transformed to

$$\eta_{\alpha\beta} = (1/2)\zeta\boldsymbol{g}_{\alpha\beta} - \zeta\sum_\nu\boldsymbol{T}_\alpha{}^\nu\eta_{\nu\beta} \tag{9}$$

with

$$\begin{aligned}\eta_{\alpha\alpha} &= -(\zeta\boldsymbol{a}_\alpha/\dot{\varepsilon})[-(\dot{\varepsilon}/2)\boldsymbol{a}_\alpha - \boldsymbol{T}\cdot\boldsymbol{F}],\\ \eta_{\alpha\beta} &= -(\zeta\boldsymbol{a}_\alpha/\dot{\varepsilon})[-(\dot{\varepsilon}/2)\boldsymbol{a}_\beta - \boldsymbol{T}\cdot\boldsymbol{F}],\\ \eta_{\beta\alpha} &= -(\zeta\boldsymbol{a}_\beta/\dot{\varepsilon})[-(\dot{\varepsilon}/2)\boldsymbol{a}_\alpha - \boldsymbol{T}\cdot\boldsymbol{F}],\\ \eta_{\beta\beta} &= -(\zeta\boldsymbol{a}_\beta/\dot{\varepsilon})[-(\dot{\varepsilon}/2)\boldsymbol{a}_\beta - \boldsymbol{T}\cdot\boldsymbol{F}].\end{aligned} \tag{10}$$

Multiplying Eq. (9) by $g^{\gamma\alpha}$, summing the result over α, and using the relation,

$$\sum_\alpha(\eta^{-1})^{\gamma\alpha}\eta_{\alpha\beta} = \delta_\beta^\gamma, \tag{11}$$

we obtain

$$(1/2)(\eta^{-1})^{\alpha\beta} = (g^{\alpha\beta}/\zeta) + T^{\alpha\beta}. \tag{12}$$

Substituting Eq. (12) into Eq. (1), and taking the average over all possible orientations of the solute molecule, we obtain

$$\begin{aligned}[\eta] &= (N_0/M\eta_0)\langle\eta_{\alpha\beta}\rangle\\ &= \frac{N_0}{6M\eta_0}\left(\sum_{l=1}^{n}\zeta R_l^2\right)\left\{1 + \frac{\zeta}{8\pi\eta_0\sum_{l=1}^{n}R_l^2}\sum_{l=1}^{n}\sum_{s=1}^{n}\left\{\frac{R_lR_s\cos\alpha_{ls}}{R_{ls}}\right.\right.\\ &\quad + \frac{1}{10R_{ls}{}^3}[4R_lR_s(R_l^2 + R_s^2)\cos\alpha_{ls}\\ &\quad \left.\left. - R_l^2R_s^2(1 + 7\cos^2\alpha_{ls})]\right\}\right\}\end{aligned} \tag{13}$$*1

with

$$|\boldsymbol{R}_l| = R_l, \quad |\boldsymbol{R}_s| = R_s, \quad (\boldsymbol{R}_l\cdot\boldsymbol{R}_s) = R_lR_s\cos\alpha_{ls}. \tag{14}$$

Let us now show some results obtained by applying the so-called *shell model*[2)] in evaluation of Eq. (13). The first example is a spherical molecule of radius r, whose surface is covered by a number of small spherical elements being in contact with one another. In the limit that the number of small elements approaches infinity while their size tends to zero, the above Eq. (13) yields the Einstein equation,

$$[\eta] = (5N_0/2M)(4\pi r^3/3). \tag{15}$$

The second example is a tetrahedral contact arrangement of four identical spheres which may be regarded as a model of hemoglobin molecule. Thus each sphere may be regarded as a myoglobin molecule. The shell model calculation of Eq. (13) yields

$$[\eta](\text{hemo})/[\eta](\text{myo}) = 1.28. \tag{16}$$

This result is to be compared with the experimental values of $[\eta]$, 4 and 3.6 (cc/g) for hemoglobin,[3,4)] and 3 (cc/g) for myoglobin.[3)] The agreement between theory and experiment seems satisfactory.

More details of the theory will be published later with various applications to other biopolymers and flexible chain polymers.

---

*1 Presented at the 21st Annual Meeting of the Chemical Society of Japan, April 1968, Osaka.

1) J. Riseman and J. G. Kirkwood, "*Rheology*," Vol. 1, ed. by F. R. Eirich, Academic Press, Inc. New York (1956), p. 495.

2) V. Bloomfield, W. O. Dalton and K. E. Van Holde, *Biopolymers*, **5**, 135 (1967).

3) R. F. Steiner, "The Chemical Foundation of Molecular Biology" Van Nostrand, Princeton N. J. (1965), Chap. 6, V. Table 6-2.

4) C. Tanford, "Physical Chemistry of Macromolecules" John Wiley, New York (1961), p. 394.

A Possible Role of Diarylmethanes as the Intermediate for the Disproportionation of Methyl Groups in the Jacobsen Reaction[1]

Hitomi SUZUKI, Yukio TAMURA and Akira SERA

Department of Chemistry, Faculty of Science, Kyoto University, Sakyo-ku, Kyoto

(Received January 9, 1969)

Pentamethylbenzene (I)[2] and chlorotetramethylbenzenes (CTB)[3] are known to undergo disproportionation, in contact with concentrated sulfuric acid, to yield hexamethylbenzene (II) and chloropentamethylbenzene (III), respectively. Under suitable conditions, however, an appreciable amount of diarylmethanes (DAM) has been isolated from these reaction mixtures. Thus, CTB (16.9 g) stirred with sulfuric acid (98 g) for 55 hr at room temperature gave III (5.4—6.3 g) and a higher-melting crystalline product (0.8—1.4 g). The latter was defined as dichloroheptamethyldiphenylmethane (DHD) by analysis ($C_{20}H_{24}Cl_2$), mass spectra (*m/e*: 334(M^+), 319 (M^+–CH_3), 299(M^+–Cl); very strong rearrangement-dissociation peaks characteristic for *o*-methylated DAM at 180 ($C_{11}H_{13}Cl^+$) and 166 ($C_{10}H_{11}Cl^+$)),[4] infrared spectra and PMR spectra (Table 1). Chlorodurene and chloroprehnitene mainly gave a single DAM (IV and VII, respectively), but chloroisodurene yielded an intimate mixture of two isomers (V and VI), where V was the major component. Their structures have been established by the independent syntheses, with the exception of VI, to which the orientation has been allocated on spectral evidences. These DAM were slightly soluble in sulfuric acid, and, when dissolved in methylcyclohexane and stirred with sulfuric acid for a prolonged period, they could slowly be converted into CTB, chlorotrimethylbenzenesulfonic acids and some unidentified, high-melting substances. Besides these products, however, isomeric DHD with substituent groups at 2,2′,6,6′-positions have been found to yield some III under the same conditions, in accord with the findings that DAM are cleft by acid catalyst to give a benzyl cation,[5] which abstracts the hydride ion to be reduced to the corresponding hydrocarbon.[6]

Although an attempt to isolate a definite DAM from the reaction mixture of I has failed due to a complicated character of the by-product, both 2,2′,3,3′,4,4′,5,5′,6- and 2,2′,3,3′,4,4′,5,6,6′-nonamethyldiphenylmethanes have been found to behave similarly toward sulfuric acid, giving I, a little II and tetramethylbenzenesulfonic acids accompanied by amorphous substances. These results may be taken to suggest a possibility of the arylalkyl cation-alkylation mechanism[7] to play some role in the intermolecular migration of methyl groups in the Jacobsen reaction.

TABLE 1. PMR SPECTRA OF DAM FORMED IN THE JACOBSEN REACTION OF MONOCHLOROTETRAMETHYLBENZENES

DAM	Mp (C°)	PMR spectra (in $CDCl_3$, τ)			
		Ar H	CH_2	CH_3	
3′,4-Dichloro-2,2′,3,4′,5,5′,6-heptamethyldiphenylmethane (IV)	213—215	3.77	6.08	7.91 (3)* 7.71 (1)	7.61 (2) 7.52 (1)
2′,5-Dichloro-2,3,4′,4,4′,5′,6-heptamethyldiphenylmethane (V)	219—220	3.76	5.93	7.93 (2) 7.83 (1)	7.76 (2) 7.58 (2)
4′,5-Dichloro-2,2′,3,3′,4,5′,6-heptamethyldiphenylmethane (VI)		3.76	6.08	7.79** 7.67	
2′,6-Dichloro-2,3,3′,4,4′,5,5′-heptamethyldiphenylmethane (VII)	226—227	3.74	5.74	7.92 (2) 7.84 (1) 7.78 (1)	7.72 (1) 7.60 (2)

* Relative intensities in parentheses. ** Others are obscured by strong peaks of V.

1) The Reaction of Polysubstituted Aromatics. Part XII; Part XI: *Nippon Kagaku Zasshi* (*J. Chem. Soc. Japan, Pure Chem. Sect.*), **90**, 105 (1969).

2) O. Jacobsen, *Ber.*, **20**, 896 (1887); L. I. Smith and A. R. Lux, *J. Am. Chem. Soc.*, **51**, 2994 (1929).

3) A. Töhl, *Ber.*, **25**, 1527 (1892); L. I. Smith and C. L. Moyle, *J. Am. Chem. Soc.*, **58**, 1 (1936).

4) S. Meyerson, H. Drews, and E. K. Fields, *ibid.*, **86**, 4964 (1964).

5) C. Serres and E. K. Fields, *ibid.*, **82**, 4685 (1960).

6) H. Suzuki and K. Nakamura, This Bulletin, **41**, 2197 (1968).

7) A. Streitwieser, Jr., and L. Reif, *J. Am. Chem. Soc.*, **86**, 1988 (1964); R. M. Roberts, A. A. Khalaf, and R. N. Green, *ibid.*, **86**, 1609 (1964).

Selective Homogeneous Hydrogenation of 3-Oxo-1,4-diene Steroids with a Ruthenium Complex as Catalyst

Shigeo NISHIMURA and Kiyoshi TSUNEDA

Department of Industrial Chemistry, Tokyo University of Agriculture and Technology, Koganei, Tokyo
Chemical Research Laboratory, Teikoku Hormone Manufacturing Co., Ltd., Shimosakunobe, Kawasaki

(Received January 17, 1969)

Recently, an excellent example of selective homogeneous hydrogenation has been described in the reduction of 3-oxo-1,4-diene steroids to the corresponding 3-oxo-4-enes using chlorotris(triphenylphosphine)rhodium as catalyst.[1,2] Although the hydrogenation with this catalyst seems to proceed quite selectively, it usually does not stop at 3-oxo-4-enes and further hydrogenation to saturated ketones may occur with prolonged reaction period.[1-3]

We have investigated the hydrogenation of 1,4-androstadiene-3,17-dione (I) with a ruthenium complex prepared from hydrated ruthenium chloride and triphenylphosphine,[4] and found that the hydrogenation with this complex is also applicable to the selective reduction of I to 4-androstene-3,17-dione (II). The hydrogenation proceeds rather readily at below 50°C under a high pressure of hydrogen. In contrast to the hydrogenation with the rhodium complex, II was practically not hydrogenated further with this ruthenium complex. A small amount of androstane-3,17-dione (III), the most part of which was the 5α isomer, was produced along with II. The yield of II decreased with elevation of the reaction temperature, although the rate of hydrogenation increased greatly. A noteworthy feature of this hydrogenation is that the selectivity for the formation of II varies considerably with the pressure of hydrogen, as shown in Table 1. Thus, a high yield of II may be obtained by hydrogenating at a relatively low temperature and under a high hydrogen pressure. In a typical run, 750 mg of I was hydrogenated with 150 mg of the catalyst in 15 m*l* of benzene at 40°C under the hydrogen pressure of 125 kg/cm^2 for 10 hr.

Table 1. Effect of hydrogen pressure on the selectivity of hydrogenation of 1,4-androstadiene-3,17-dione (I)[a]

Hydrogen pressure (kg/cm^2)	Reaction time (hr)	% of I converted	Composition of hydrogenated product (%)[b]	
			II	III
10	1.5	12.3	66.4	33.6
30	1.5	19.4	78.9	21.1
50	1.5	26.2	85.8	14.2
100	1.5	45.1	89.5	10.5
162	1.5	64.8	92.5	7.5

a) I (300 mg) was hydrogenated with 300 mg of the ruthenium complex in 60 m*l* of benzene at 50°C.

b) II: 4-androstene-3,17-dione.
III: androstane-3,17-dione, the most part of which was the 5α isomer. The product was analyzed by gas chromatography after evaporation of the solvent followed by extraction with methylcyclohexane.

The product was 94% of II and 6% of III, and contained no starting material, as analyzed by gas chromatography. After the solution was passed through alumina and the solvent removed, recrystallization of the soiid residue from acetone - hexane gave 640 mg of almost pure II, mp 165—169°C, $[\alpha]_D^{22}$ +189 (chloroform). Its infrared spectrum was identical in all respects with that of an authentic sample of II. Under similar conditions, 17β-hydroxy, 17β-acetoxy and 17β-acetyl derivatives of 1,4-androstadien-3-one were also hydrogenated to the corresponding 4-en-3-ones with high selectivity as in the case of I.

Analysis of the product during the course of hydrogenation of I showed that the ratio of the II to III formed was nearly constant throughout the reaction. This indicates that III was produced from I simultaneously with II. A further evidence for this is that a very prolonged hydrogenation of II gave a small amount of III which was a mixture of 5β and 5α isomers. A probable course of the formation of III seems to be the one *via* 5α-androst-1-ene-3,17-dione, which was found to be hydrogenated readily to III under the conditions in which II did not hydrogenate.

Further studies on this hydrogenation are in progress.

1) A. J. Birch and K. A. M. Walker, *J. Chem. Soc.* (*C*), **1966**, 1894.
2) C. Djerassi and J. Gutzwiller, *J. Am. Chem. Soc.*, **88**, 4537 (1966).
3) P. Wieland and G. Anner, *Helv. Chim. Acta*, **51**, 1698 (1968).
4) T. A. Stephenson and G. Wilkinson, *J. Inorg. Nucl. Chem.*, **28**, 945 (1966). The catalyst used in this study was prepared by refluxing hydrated ruthenium chloride (1 g) and triphenylphosphine (6 g) in ethanol (120 m*l*), according to the procedure for the preparation of chlorotris(triphenylphosphine)rhodium [J. A. Osborn, A. H. Jardine, J. F. Young and G. Wilkinson, *J. Chem. Soc.*, (*A*), **1966**, 1711].

Delayed Fluorescence of the DNA-Acridine Dye Complexes in a Frozen Aqueous Solution

Yukio KUBOTA*, Yasuo FUJISAKI* and Masaji MIURA**

*Department of Chemistry, Yamaguchi University, Yamaguchi

**Department of Chemistry, Faculty of Science, Hiroshima University, Hiroshima

(Received December 16, 1968)

In order to obtain further information regarding the energy transfer between the DNA base-dye molecules and between dye-dye molecules in the DNA-acridine dye complexes, the luminescence of the complexes was measured under various conditions by using a Hitachi MPF-2A fluorescence spectrophotometer with an attachment for phosphorescence measurements.[1]

Figures 1 and 2 show typical results obtained for the DNA-proflavine complexes. In the presence of proflavine, the DNA phosphorescence with a peak about 460 mμ diminishes and two new peaks appear; the emissions around 580 mμ and 495 mμ may be ascribed, respectively, to the phosphorescence (P) and delayed fluorescence (DF) of the dye bound to DNA.

The DF observed at a high P/D*1 value seems to be due to the excitation energy transfer from the DNA triplet state to the dye singlet state, as was first suggested by Isenberg *et al.*,[2] in view of the facts that its excitation spectrum is identical with that of the DNA phosphorescence, that the absorption spectra of the complexes overlap to a great extent with the phosphorescence spectrum of DNA, and that the intensity of DF varies proportionally to the intensities of P of DNA and the dye. The intensity of DF decreases with a decrease in the P/D value; this decrease is especially remarkable in the case of denatured DNA.

On the other hand, the DF at a low P/D value appears to be a result of the triplet-triplet annihilation of the dyes, for its excitation spectrum is identical with that of the P of the dye and the intensity of DF is proportinal to the square of the intensity of the P of the dye.[3,4] This type of DF, newly observed in the DNA-dye complexes, becomes remarkable with a decrease in the P/D value. The DF at neither high nor low P/D values decays exponentially. The values of the half-life of DF, an order of 10—60 msec, depend on the P/D value and on the kind of acridine dye. A similar phenomenon of DF was also observed in the cases of acridine orange, acridine yellow, and acriflavine, except that DF due to the photoionization of the dye was additionally observed in the DNA-acriflavine complexes.[5] Further study of the mechanism of DF is in progress.

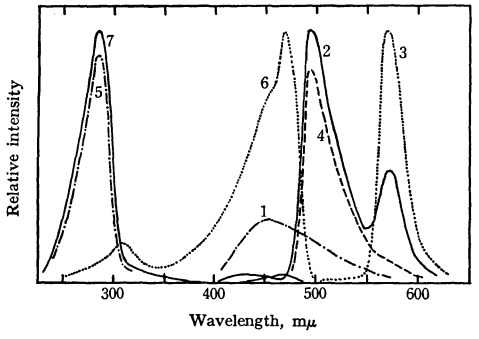

Fig. 1. Excitation (ex.) and emission (em.) spectra of DNA-proflavine complex at 77°K.
Solvent: 0.01 M phosphate buffer + 0.01 M NaCl (pH 7)
DNA: 10^{-2} M in phosphate unit
Proflavine: 10^{-4} M
(1) DNA phosphorescence; long-lived em. spectra of complex excited at (2) 285 mμ and (3) 470 mμ; (4) total em. spectrum of complex; ex. spectra of (5) DNA phosphorescence, (6) phosphorescence of complex, and (7) delayed fluorescence of complx

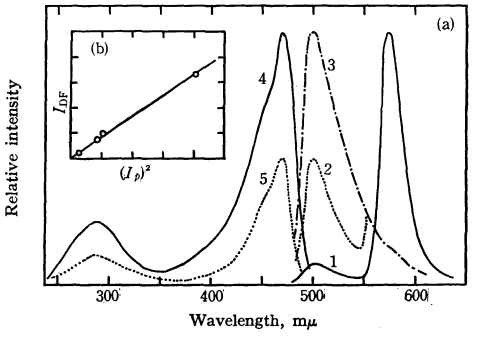

Fig. 2. (a) Excitation and emission spectra of DNA-proflavine complex at 77°K.
DNA: 2.5 × 10^{-4} M in phosphate unit Proflavine: 10^{-4} M
(1) Long-lived em. spectrum of complex excited at 470 mμ; (2) a sextuple sensitivity of (1); (3) total em. spectrum of complex;ex. spectra of (4) phosphorescence and (5) delayed fluorescence of complex
(b) A relationship between I_P and I_{DF}.
I_P : the intensity of phosphorescence at 580 mμ
I_{DF}: the intensity of delayed fluorescence at 500 mμ

1) Y. Kubota and M. Miura, This Bulletin, **40**, 2989 (1967).

*1 The ratio of the number of nucleotides to that of dye molecules.

2) I. Isenberg, R. B. Leslie, S. L. Baird, Jr., R. Rosenbluth and R. Bersohn, *Proc. Natl. Acad. Sci. U.S.*, **52**, 379 (1964).

3) H. Sternlicht, G. C. Nieman and G. W. Bobinson, *J. Chem. Phys.*, **38**, 1326 (1963).

4) T. Azumi and S. P. McGlynn, *ibid.*, **39**, 1186 (1963).

5) Y. Kubota, Y. Fujisaki and M. Miura, *Kogyo Kagaku Zasshi* (*J. Chem. Soc. Japan, Ind. Chem. Sect.*), **72**, 252 (1969).

The Total Synthesis of Dehexyl-deisovaleryloxy-antimycin A_1

Mitsuhiro KINOSHITA and Sumio UMEZAWA

Department of Applied Chemistry, Faculty of Engineeering, Keio University, Koganei-shi, Tokyo

(Received January 23, 1969)

Antimycin A is a complex of at least four closely related antifungal antibiotics (A_1—A_4) produced by *Streptomyces* spp., and the structures of antimycin A_1 (Ib) and A_3 (Ic) were elucidated by van Tamelen *et al.*,[1] Birch *et al.*,[2] Yonehara *et al.*,[3] and Harada *et al.*[4] The most striking characteristic of the structure of antimycin A is its dilactone ring linked *via* an amide bond to 3-formamidosalicylic acid.

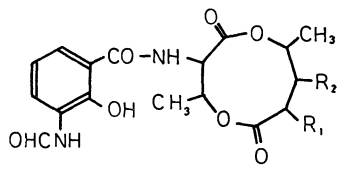

Ia Ib Ic

R_1: H n-C_6H_{13} n-C_4H_9
R_2: H i-C_4H_9COO i-C_4H_9COO

We wish to record the total synthesis of dehexyl-deisovaleryloxy-antimycin A_1 (Ia) which differs from natural antimycin A in that the acyloxy and alkyl substituents of the dilactone ring are replaced by hydrogen atoms.

N-Benzyloxycarbonyl-*O*-*t*-butyl-L-threonine[5] was condensed with *t*-butyl γ-hydroxyvalerate[6] using *N*,*N*′-dicyclohexylcarbodiimide (DCCI) in pyridine to afford *t*-butyl γ-(*N*-benzyloxycarbonyl-*O*-*t*-butyl-L-threonyloxy)valerate (II): $[\alpha]_D^{19}$ −4° (*c* 2, ethanol); yield 42%.

Treatment of II with trifluoroacetic acid gave γ-(*N*-benzyloxycarbonyl-L-threonyloxy)valeric acid

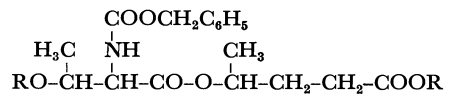

II III

R: t-C_4H_9 H

(III): $[\alpha]_D^{21}$ −16° (*c* 2, ethanol); yield 85.5%. The hydroxycarboxylic acid (III) was cyclized with trifluoroacetic anhydride in benzene (concentration of III in benzene: 4×10^{-2}M) at 75°C for 16 hr to afford colorless crystals of *N*-benzyloxycarbonyl-4-amino-1,5-dimethyl-3,7-dioxo-2,6-dioxacyclononane (IV): mp 105—107°C; $[\alpha]_D^{21}$ +14° (*c* 2, ethanol); MW 335.140 (MS); ν_{max}^{KBr} 3320, 1745, 1693 and 1539 cm^{-1}; yield 32.5%.

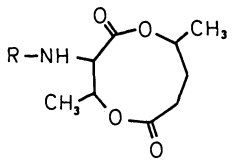

IV V

R_1: $C_6H_5CH_2OCO$ O_2N $OCH_2C_6H_5$

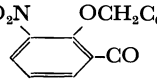

The benzyloxycarbonyl group was removed and the resulting free amino dilactone was *N*-acylated with *O*-benzyl-3-nitrosalicylic acid *N*-hydroxysuccinimide ester to yield *N*-(*O*-benzyl-3′-nitrosalicyloyl)-4-amino-1,5-dimethyl-3,7-dioxo-2,6-dioxacyclononane (V): mp 188—189.5°C; $[\alpha]_D^{28}$ +20° (*c* 2, tetrahydrofuran); ν_{max}^{KBr} 3200, 1743, 1645 and 1532 cm^{-1}; yield 72.4%. Hydrogenation of V over palladium black in methanol, followed by *N*-formylation with 98% formic acid and DCCI afforded dehexyl-deisovaleryloxy-antimycin A_1 (Ia): mp 154—155°C; $[\alpha]_D^{19}$ +70° (*c* 1, chloroform); λ_{max}^{MeOH} 226 (log ε 4.62), 320 mμ (log ε 3.93); $\nu_{max}^{CHCl_3}$ 3435, 1747, 1706, 1647, 1614, and 1531 cm^{-1}; yield 56%. The synthetic product Ia completely inhibited the growth of *Piricularia oryzae* in a concentration of 0.39 mcg/ml by dilution method using bouillon.

1) F. M. Strong, J. P. Dickie, M. F. Loomans, E. E. van Tamelen and R. S. Dewey, *J. Am. Chem. Soc.*, **82**, 1513 (1960); E. E. van Tamelen, J. P. Dickie, M. F. Loomans, R. S. Dewey and F. M. Strong, *ibid.*, **83**, 1639 (1961).

2) A. J. Birch, D. W. Cameron, Y. Harada and R. W. Rickards, *J. Chem. Soc.*, **1961**, 889.

3) H. Yonehara and S. Takeuchi, *J. Antibiotics*, **11A**, 122, 254 (1958).

4) K. Uzu, H. Kato, K. Kumabe and Y. Harada, *ibid.*, **14A**, 209 (1961).

5) E. Schröder, *Ann.*, **670**, 127 (1963).

6) *t*-Butyl γ-hydroxyvalerate was prepared from *t*-butyl levulinate by hydrogenation with Raney Ni.

BULLETIN OF THE CHEMICAL SOCIETY OF JAPAN VOL. 42 855—863 (1969)

Chemiluminescent Reaction between Polyphenols and Ozone in Acetic Acid

Ryôjirô IWAKI

Chemical Laboratories, Hitotsubashi University, Kunitachi-shi, Tokyo

and Isao KAMIYA

Department of General Education, Nagoya University, Chikusa-ku, Nagoya

(Received May 6, 1968)

The chemiluminescence of polyphenols with ozone in acetic acid was investigated in the presence and in the absence of rhodamine B. The emission intensity in the presence of rhodamine B (I_M) was about 100—500 times as large as that in the absence of the dye (I_P). From the measurement of the emission intensity *vs.* the reaction time, it was found that the time required to attain the peak intensity of I_M is almost equal to that required to attain the peak of I_P at equal concentration of polyphenol. A similarity was found in the spectral distributions of I_M and the fluorescence emission of rhodamine B determined under comparable conditions. Rhodamine B was scarcely decomposed for the production of the enhanced emission; this lent support to the conclusion that the enhancement effect of rhodamine B is due to an energy-transfer from an excited species produced by the oxidation of polyphenols to the dye. Determining the changes in the absorption spectra during the luminescent reaction, we also found that the emission results not from the decomposition of polyphenols but from the decomposition of an intermediate compound. On the basis of these results, a reaction scheme was proposed. If the increment of the total light emitted by the enhancement effect, (Δ), is defined as:

Δ=(Total light emitted in the polyphenol+rhodamine B system)−(Total light emitted in polyphenol alone)−(Total light emitted in rhodamine B alone),

the scheme gave the following equation:

$$\Delta = A[\mathrm{R}]_0 \ln(1+[\mathrm{P}]_0/A[\mathrm{R}]_0) \qquad (1)$$

where $[\mathrm{R}]_0$ and $[\mathrm{P}]_0$ are the initial concentrations of rhodamine B and polyphenols respectively. A is the parameter, depending upon the experimental conditions. The values of Δ calculated from Eq. (1) were in fairly good agreement with the measured values.

In connection with the study of the ozonolysis of aromatic compounds, we are interested in the chemiluminescent reaction between ozone and such polyphenols as hydroquinone, resorcinol, catechol, pyrogallol, phloroglucinol, and gallic acid. However, little is yet known as to the mechanism for the chemiluminescent reaction because of the low photon yield.

In 1960, Bersis[1] showed that the emission intensity of the polyphenol chemiluminescence was remarkably enhanced in the presence of rhodamine B. Recently, Kamiya and Iwaki[2] have found that the emission from the reaction of eosin with hydrogen peroxide in an alkaline solution is enhanced by adding uranin. On the basis of kinetic studies, a mechanism involving an energy-transfer from an excited intermediate species*1 produced by the oxidation of eosin to uranin was postulated. Similar effects have been observed by several investigators: Kautsky and Zocher[3] found the effect of rhodamine dyes in the chemiluminescence of siloxen ($Si_6H_3O_6$) with potassium permanganate, and Vasil'ev[4] observed a similar effect of anthracene derivatives in the chemiluminescent autoxidation of hydrocarbon. In all of these reports, an energy-transfer mechanism was postulated to explain the enhanced emission. The present experimental results lend support to the postulation.

The spectral distribution of the enhanced emission agreed with that of the fluorescence emission

1) D. S. Bersis, *Z. Phys. Chem. (Neue Folge)*, **26**, 259 (1960).

2) I. Kamiya and R. Iwaki, This Bulletin, **39**, 269 (1966).

*1 Recently, the present authors have detected the intermediate species by means of a careful measurement of the spectra of the eosin chemiluminescence.

3) H. Zocher and H. Kautsky, *Z. Phys.*, **9**, 267 (1922).

4) R. F. Vasil'ev, *Nature*, **169**, 668 (1962).

of the added fluorescer, which was scarcely decomposed in the production of the enhanced emission.

As has been pointed out by Vasil'ev[5] and by Kasha[6], it is very suggestive that the behavior of excited species in an extremely weak chemiluminescent reaction can be investigated by means of the enhancing technique. In practice, several investigators[7] have carried out studies of weak chemiluminescent reactions by adding suitable fluorescers.

In the present paper, we will describe several experimental results supporting the theory that the enhancement effect of rhodamine B upon the emission of polyphenol chemiluminescence is caused by an energy-transfer excitation. The mechanism for the reaction, based on the kinetic results on the emission intensity, the emission spectra, and the changes in the absorption spectra during the luminescent reactions, will also be discussed.

Experimental

Original concentrated solutions of polyphenols (2.4×10^{-3} mol/l) and rhodamine B (1.6×10^{-3} mol/l) in acetic acid were diluted by adding acetic acid before they were used. Rhodamine B was recrystallized from a 60—70% aqueous ethanol solution. Analytical-grade polyphenols were used without further purification.

Reaction was initiated by introducing ozonized air produced in a Siemens ozonizer. Air was supplied by using a small rotary compressor, to which a manometer and a flowmeter were attached to control the pressure and the flow rate. The air was freed from carbon dioxide by granulated potassium hydroxide and dried by silica gel. Ozonized air was freed from the oxides of nitrogen (if any) by passing it through an aqueous solution of sodium hydroxide. The emitted light was detected with a photomultiplier tube (Toshiba MS9SY) coupled with a linear amplifier, and the output current was lead to a pen-recorder, so that the curves of the emission intensity *vs.* the reaction time could be recorded. Care was taken to keep constant the temperature (30°C) in the ozonizer and in the reaction vessel. The spectra of both the chemiluminescence and fluorescence were measured at 30°C, as has been described in a preceding paper.[8]

The absorption spectra of the reaction systems were measured with a Shimadzu SV-50-type recording spectrophotometer after the dissolved ozone had been removed by passing the systems through nitrogen gas. The concentrations of reactants and products were determined photometrically with a Shimadzu QR-50-type spectrophotometer.

Results

Curves of Emission Instensity *vs.* Reaction Time. The curves of the emission intensity *vs.* the reaction time measured in the rhodamine B system (I_R - t curve), in the gallic acid system (I_P - t

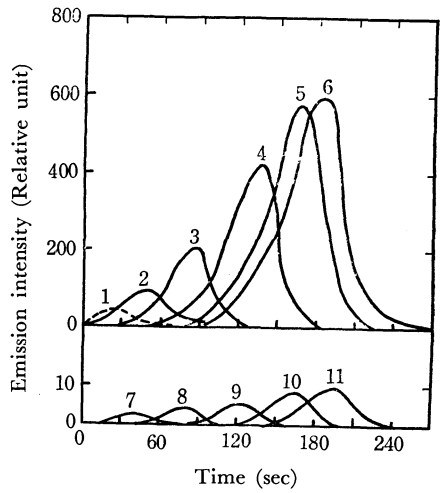

Fig. 1. Curves of emission intensity *vs.* the reaction time in gallic acid systems.
1: I_R (0-1-9), 2: I_M (1-1-8), 3: I_M (3-1-6), 4: I_M (5-1-4), 5: I_M (7-1-2), 6: I_M (9-1-0), 7: I_P (1-0-9), 8: I_P (3-0-7), 9: I_P (5-0-5), 10: I_P (7-0-3), 11: I_P (9-0-1)

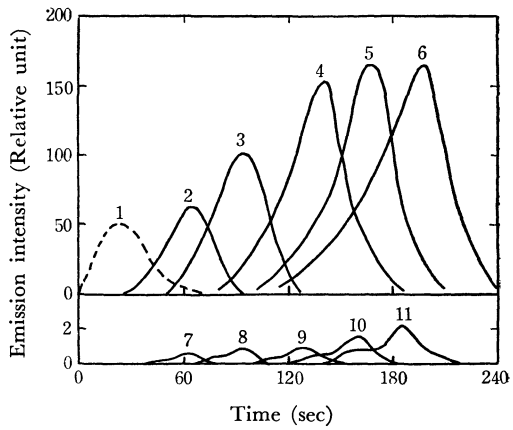

Fig. 2. Curves of emission intensity *vs.* the reaction time in resorcinol systems.
1: I_R (0-1-9), 2: I_M (1-1-8), 3: I_M (3-1-6), 4: I_M (5-1-4), 5: I_M (7-1-2), 6: I_M (9-1-0), 7: I_P (1-0-9), 8: I_P (3-0-7), 9: I_P (5-0-5), 10: I_P (7-0-3), 11: I_P (9-0-1)

5) R. F. Vasil'ev, *Optika i Spectroskopiya (Optics and Spectroscopy)*, **18**, 236, 416 (1965); *Photochem. Photobiol.*, **6**, 35 (1967).

6) A. U. Kahan and M. Kasha, *J. Am. Chem. Soc.*, **88**, 1674 (1966).

7) H. Linschitz, "Light and Life," John Hopkins Press, Baltimore (1961), p. 173; G. Lundeen and R. Livingstone, *Photochem. Photobiol.*, **4**, 1085 (1965); J. Stauff, *ibid.*, **4**, 1199 (1965); L. J. Bollyky, H. H. Whitman, R. A. Clarke and M. M. Rauhut, *J. Org. Chem.*, **32**, 1663 (1967).

8) I. Kamiya and R. Iwaki, This Bulletin, **39**, 264 (1966).

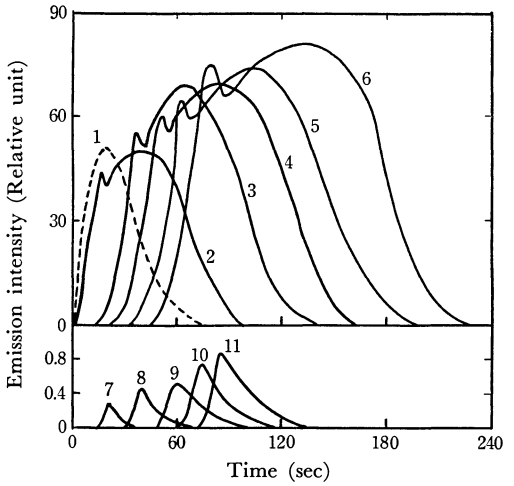

Fig. 3. Curves of emission intensity *vs.* the reaction time in hydroquinone systems.
1: I_R (0-1-9), 2: I_M (1-1-8), 3: I_M (3-1-6), 4: I_M (5-1-4), 5: I_M (7-1-2), 6: I_M (9-1-0), 7: I_P (1-0-9), 8: I_P (3-0-7), 9: I_P (5-0-5), 10: I_P (7-0-3), 11: I_P (9-0-1)

curve), and in the gallic acid system in the presence of rhodamine B (I_M - t curve) are given in Fig. 1, where (x-y-z) refers to the system composed of x m*l* of the polyphenol solution, y m*l* of the rhodamine B solution, and z m*l* of acetic acid. These results indicate that: (1) In both emissions, with and without enhancing, the emission rises to a maximum value (I_{max}) after a period of induction, and then slowly decreases.

(2) In the two systems of equal initial concentrations of polyphenol, the I_{max} of the I_M - t curve is almost 100—500 times as large as that of the I_P-t curve, but the time required to attain the I_{max} (τ) of I_M is nearly equal to that needed to attain that of I_P.

(3) Both values of I_{max} and τ increase with an increase in the concentration of polyphenol.

The curves of the emission intensity measured in resorcinol systems are given in Fig. 2. Similar curves were obtained in catechol systems. Figure 2 shows that the emission characteristics are apparently similar to those in gallic acid, but are not so intense.

Figure 3 shows the emission characteristics measured in hydroquinone systems, demonstrating that I_M - t curves have two emission peaks while I_P- t curves have only one peak. It may be noted that the time required to attain the first peak of the I_P - t curve is almost equal to the time required to attain the I_{max} of I_P - t curve in each pair with equal concentrations of polyphenol.

Similar curves were obtained in the pyrogallol and phloroglucinol systems, but the emission is more intense than that in the hydroquinone system.

The effect of the rhodamine B concentration upon the emission intensity was measured in both the gallic acid system and the hydroquinone system. The results, shown in Figs. 4 and 5 respectively, indicate that the values of I_{max} increase with an increase in the concentration of rhodamine B, but the values of τ hardly vary if the polyphenol concentration is ketp constant.

Figure 6 shows the effect of the rhodamine B concentration upon the I_R - t curve, demonstrating that the induction period is neither so long nor so varied after the change in the initial concentration of rhodamine B as that found in polyphenol chemiluminescence.

Chemiluminescence Spectra. The chemiluminescence spectra were determined in gallic acid and pholoroglucinol system containing rhodamine B, and were compared with the fluorescence spectrum of rhodamine B determined under comparable conditions. As may be seen in Fig. 7 (the gallic acid system) and Fig. 8 (the phloroglucinol

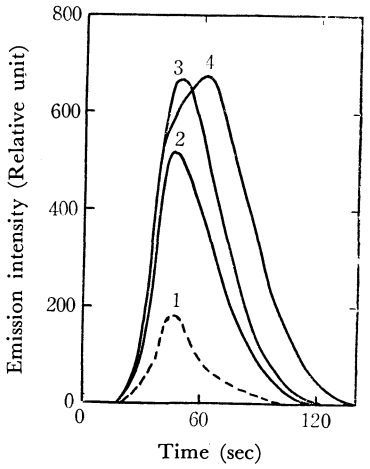

Fig. 4. The effect of rhodamine B concentration upon the I_M - t curves for gallic acid systems.
1: $I_P \times 200$(7-0-3), 2: I_M (7-1-2), 3: I_M (7-2-1), 4: I_M (7-3-0)

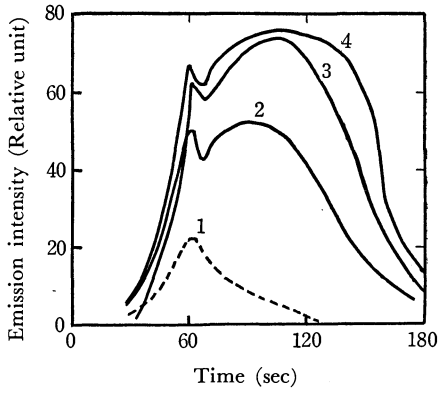

Fig. 5. The effect of rhodamine B upon the I_M - t curves for hydroquinone systems.
1: $I_P \times 200$(7-0-3), 2: I_M (7-1/2-5/2), 3: I_M (7-1-2), 4: I_M (7-2-1)

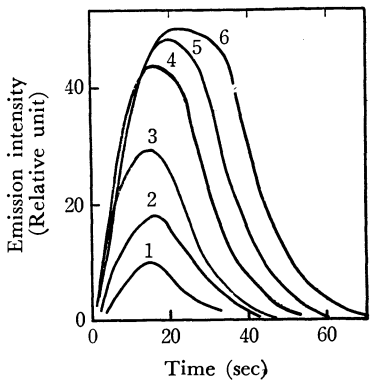

Fig. 6. The effect of rhodamine B concentration upon I_R - t curves.
Curve 1: 8.0×10^{-6} mol/l
Curve 2: 1.6×10^{-5} mol/l
Curve 3: 3.2×10^{-5} mol/l
Curve 4: 6.4×10^{-5} mol/l
Curve 5: 9.6×10^{-5} mol/l
Curve 6: 1.6×10^{-4} mol/l

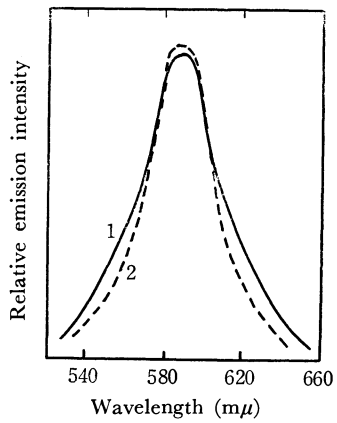

Fig. 7. Chemiluminescence spectrum in gallic acid - rhodamine B system and fluorescence spectrum of rhodamine B.
Curve 1: chemiluminescence
Curve 2: fluorescence

system), similar chemiluminescence and fluorescence spectral distributions were obtained, indicating that the excited singlet of rhodamine B is the emitting species.

Changes in Absorption Spectra of Polyphenol in the Region between 250 mμ and 450 mμ during the Luminescence Reaction. The absorption spectrum of hydroquinone in acetic acid was changed during the oxidation with ozone, as is shown in Fig. 9. The peak at 291 mμ decreased, and simultaneously a new band at about 250 mμ appeared to reach a maximum, which was then decreased by oxidation. The changes can be attributed to both the decomposition of hydroquinone and the formation of an intermediate compound. Figure 10 shows the plots of $\log D_{291}$

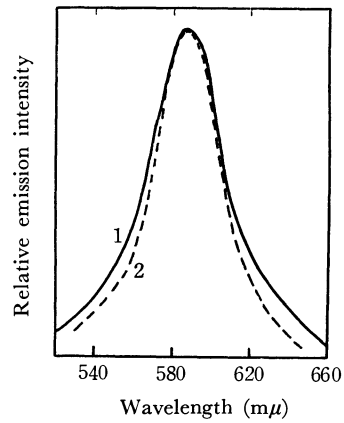

Fig. 8. Chemiluminescence spectrum in phloroglucinol - rhodamine B system and fluorescence spectrum of rhodamine B.
Curve 1: chemiluminescence
Curve 2: fluorescence

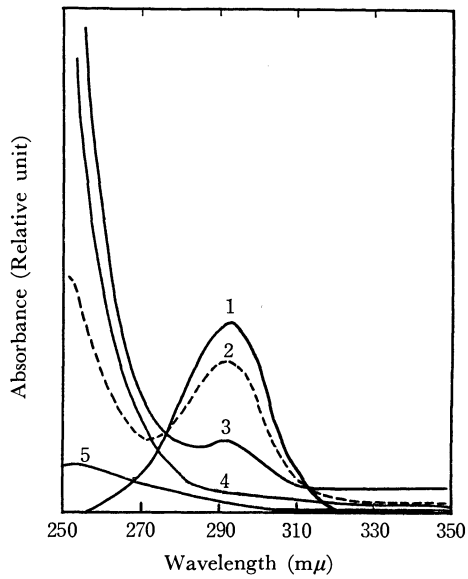

Fig. 9. Change in absorption spectra of hydroquinone system during the luminescent reaction (1→2→3→4→5).

(absorbance at 291 mμ) against the reaction time. The plots on the straight line indicate that the decomposition of hydroquinone from the initial stage of the reaction is first order with respect to the polyphenol concentration. The plots of D_{250} *vs.* reaction time are shown in Fig. 11. It is demonstrated that the decomposition processes are not so simple because the time required to attain the maximum concentration of the intermediate compound increases with an increase in the initial concentration of hydroquinone.

Figure 12 shows the changes in the absorption spectrum of gallic acid during the oxidation with

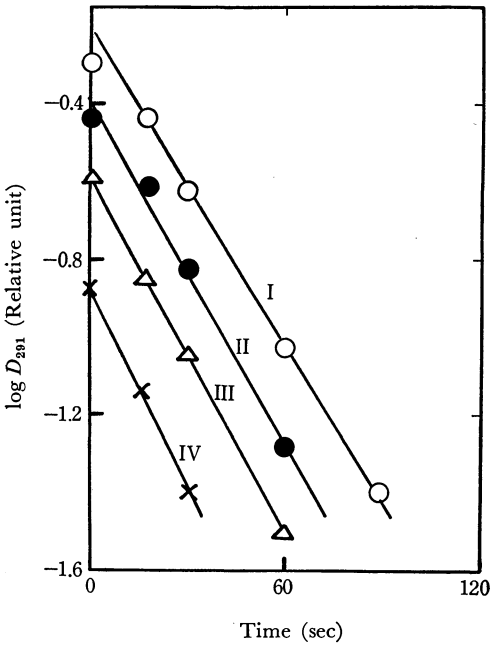

Fig. 10. Plots of log D_{291} against the reaction time in the several systems of various initial concentrations of hydroquinone ($[P]_0$).
Curve I: $[P]_0=2.2\times10^{-3}$ mol/l
Curve II: 1.7×10^{-3} mol/l
Curve III: 1.2×10^{-3} mol/l
Curve IV: 7.2×10^{-4} mol/l

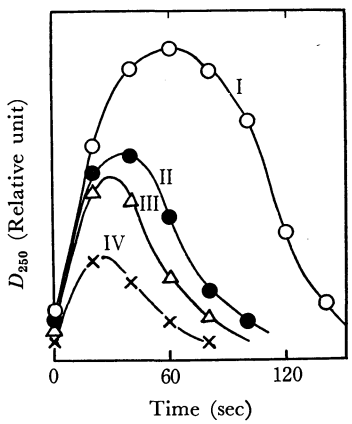

Fig. 11. Plots of D_{250} against the reaction time in the several systems of various initial concentrations of hydroquinone ($[P]_0$).
Curve I: $[P]_0=2.2\times10^{-3}$ mol/l
Curve II: 1.7×10^{-3} mol/l
Curve III: 1.2×10^{-3} mol/l
Curve IV: 7.2×10^{-4} mol/l

ozone. The results show that the peak at 272 mμ decreases without the appearance of a new absorption peak. However, the changes in the absorbance at 340 mμ (D_{340}), shown in Fig. 13, strongly suggest the formation of an intermediate compound. The plots of log D_{272} *vs.* the reaction time, given in Fig. 14, demonstrate that the decomposition of gallic acid at the initial stage is also first order with respect to the polyphenol concentration.

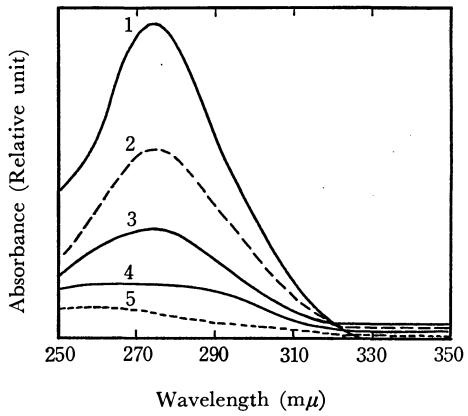

Fig. 12. Changes in absorption spectra of a gallic acid system during the luminescent reaction (1→2→3→4→5).

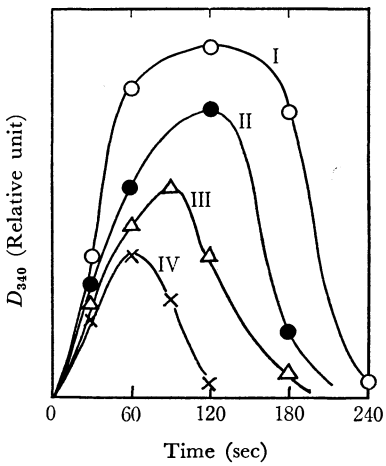

Fig. 13. Plots of D_{340} against the reaction time in the several systems of various initial concentrations of gallic acid ($[P]_0$).
Curve I: $[P]_0=2.2\times10^{-3}$ mol/l
Curve II: 1.7×10^{-3} mol/l
Curve III: 1.2×10^{-3} mol/l
Curve IV: 7.2×10^{-4} mol/l

In resorcinol systems, the changes in the absorption spectrum were not so simple as those in hydroquinone and gallic acid.

Decomposition Rate of Rhodamine B. Figure 15 shows the changes in the concentration of rhodamine B during the luminescent reaction in hydroquinone-rhodamine B systems. It is important and interesting to see that rhodamine B hardly decomposes at all until the hydroquinone decreases upon its oxidation with ozone to a low concentration; this means that the enhanced

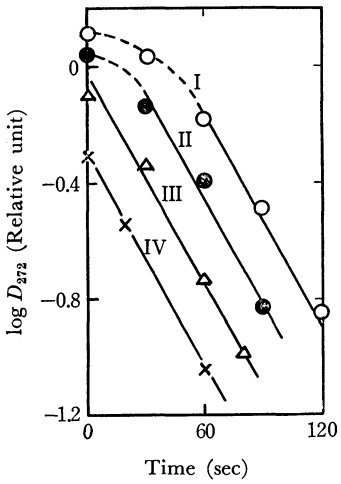

Fig. 14. Plots of $\log D_{272}$ against the reaction time in the several systems of various initial concentrations of gallic acid ($[P]_0$).
Curve I: $[P]_0=2.2\times10^{-3}$ mol/l
Curve II: 1.7×10^{-3} mol/l
Curve III: 1.2×10^{-3} mol/l
Curve IV: 7.2×10^{-4} mol/l

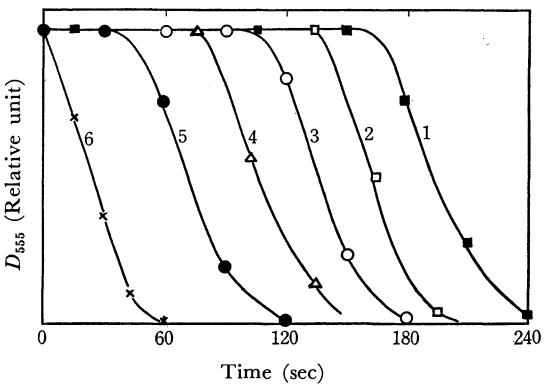

Fig. 15. The concentration of rhodamine B as a function of the reaction time in the several systems of various initial concentrations of hydroquinone.
1: (9-1-0), 2: (7-1-2), 3: (5-1-4),
4: (3-1-6), 5: (1-1-8), 6: (0-1-9)

emission does not result from the decomposition of the dye. The decomposition-curves of rhodamine B measured in other polyphenol-systems are shown in Fig. 16; they demonstrate that all of the polyphenols retard the decomposition of rhodamine B as hydroquinone does.

Discussion

The experimental results apparently indicate that the enhancement effect of rhodamine B upon the chemiluminescence of polyphenols is caused by an energy-transfer from an excited species produced by the reaction of polyphenols to the dye.

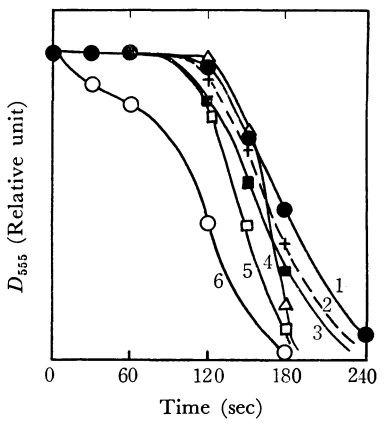

Fig. 16. The concentration of rhodamine B as a function of the reaction time in the several systems of various polyphenols. Initial concentrations of polyphenol and rhodamine B are 2.2×10^{-3} mol/l and 1.6×10^{-4} mol/l, respectively.
1: Catechol, 2: Hydroquinone,
3: Resorcinol, 4: Phloroglucinol,
5: Pyrogallol, 6: Gallic acid

The I_M - t curves with the changes in the concentrations of gallic acid and of the intermediate compound are compared in Fig. 17. It is found that the I_M - t curve does not agree with the decomposition curve of hydroquinone, but does agree with that of the intermediate compound except for the initial stage. This fact indicates that the polyphenol chemiluminescence arises not from the

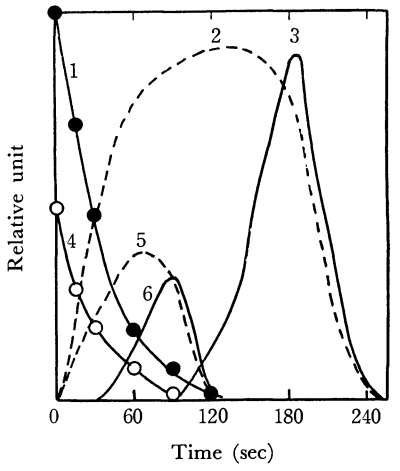

Fig. 17. Comparison between I_M - t curve and concentration curve of gallic acid or intermediate compound in gallic acid systems.
1: $[P]$ - t curve (9-1-0)
2: D_{340} - t curve (9-0-1)
3: I_M - t curve (9-1-0)
4: $[P]$ - t curve (3-1-6)
5: D_{340} - t curve (3-0-7)
6: I_M - t curve (3-1-6)

decomposition of the gallic acid but from the decomposition of the intermediate. The discrepancy for the initial stage in the two curves can be explained by the argument that the decomposition of the intermediate is retarded by polyphenol, as is that of rhodamine B. This argument is supported by the experimental findings to be described below.

A solution of polyphenol was pre-treated for a short duration with ozone in order to lower the concentration of polyphenol; then nitrogen gas was bubbled into it to remove the dissolved ozone. After rhodamine B had been added to the pre-treated solution, ozone was again passed into the solution to initiate the luminescent reaction. The curves of the emission intensity *vs.* the reaction time measured in such pre-treated solutions of gallic acid and hydroquinone are shown in Figs. 18 and 19 respectively. These figures show that the induction periods for the luminescent reactions were shortened by the pre-treatment. Moreover, when small amounts of the polyphenols were added again to the pre-treated solution, the emission was observed after a long induction period, as is shown by dotted curves in Figs. 18 and 19.

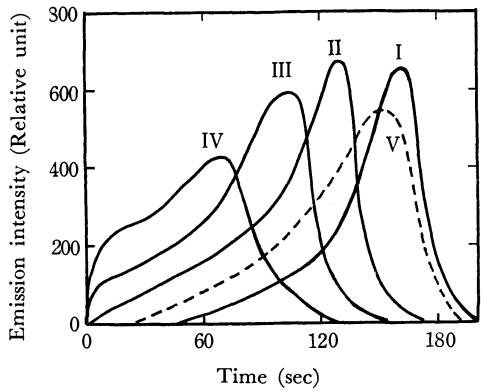

Fig. 18. I_M - t curves measured in gallic acid systems, pre-treated with ozone.
I: non-treated, II: treated for 30 sec, III: 60 sec, IV: 120 sec, V: A small amount of gallic acid was added after pre-treated for 120 sec.

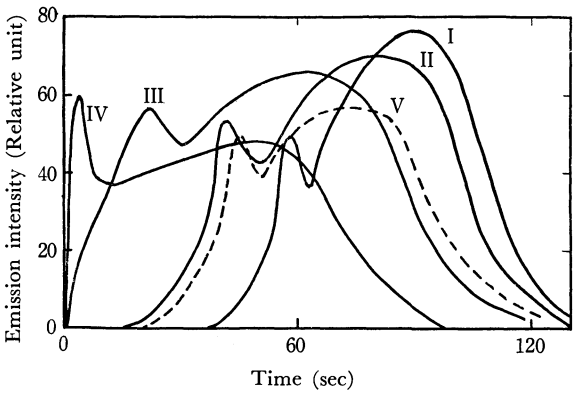

Fig. 19. I_M - t curves measured in hydroquinone systems, pre-treated with ozone.
I: non-treated, II: treated for 30 sec, III: 45 sec, IV: 60 sec, V: A small amount of hydroquinone was added after pre-treated for 60 sec.

As is shown in Fig. 3, the first peak of the I_M - t curves and the peak of the corresponding I_R - t curves are found at the same reaction time. In view of the finding that the polyphenols do retard the decomposition of rhodamine B, it seems liekly that the first peak of the I_M - t curve is to be attributed to the enhanced emission due to an energy-transfer (say, I_{PR}-emission), and the second peak, to the luminescent decomposition of rhodamine B (say, I'_R-emission).

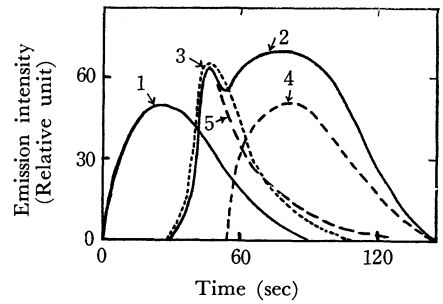

Fig. 20. Curves of I_R, I_M and I_P and shematic curves of I'_R- and I_{PR}-emission in hydroquinone systems.
1: I_R (0-1-9), 2: I_M (5-1-4), 3: I_P (5-0-5)$\times$ 100, 4: I'_R-emission, 5: I_{PR}-emission

If the curve of the I'_R-emission is assumed to be described by the parallel displacement of the I_R - t curve measured for rhodamine B alone, so as to fit the decay part with the I_M - t curve measured in the polyphenol - rhodamine B system, the schematic curve of I_{PR} - emission can be obtained graphically by subtracting the curve of the I'_R-emission from the I_M - t curve. Figure 20 shows the curves of the I'_R-emission and the I_{PR}-emission described in this way, together with the I_P - t curve measured in polyphenol alone. We can see in Fig. 20 that the curve of I_{PR}-emission is very similar to the I_P - t curve.

Two peaks did not appear in the I_M - t curves for gallic acid. This is probably due to the fact that the I'_R-emission falls upon the I_{PR}-emission as a result of the weak retardation for rhodamine B decomposition.

Reaction Scheme

On the basis of the results, the following mechanism seems plausible for the luminescent reaction:

At the initial stage, polyphenol (P) is oxidized with ozone to produce an intermediate compound

(M):

$$P \xrightarrow{O_3} M \qquad [I];\ \text{reaction rate: } k_1.$$

The polyphenol concentration [P] at the reaction time t is given by:

$$[P] = [P]_0 \exp(-k_1 t) \tag{1}$$

where $[P]_0$ is the initial concentration of polyphenol. Taking account of the fact that M does not decompose until [P] becomes small value of $[P]' = [P]_0\exp(-k_1 t')$, we have:

$$[M] = [P]_0\{1-\exp(-k_1 t')\} \tag{2}$$

when $t \leqq t'$. Assuming that t' is nearly equal to τ (the time required to attain I_{max}), the values of [P]' can be calculated from $[P]' = [P]_0\exp(-k_1\tau)$ by using the values of τ measured in hydroquinone systems for various $[P]_0$ and k_1 values; these values are tabluated in Table 1. The values of [P]' are almost constant, which indicates that our presumption is plasusible.

Table 1. The values of [P]' calculated from the equation, $[P]' = [P]_0\exp(-k_1\tau)$ in hydroquinone systems

$[P]_0$ (mol/l)	k_1 (sec^{-1})	τ (sec)	[P]' (mol/l)
2.4×10^{-4}	0.032	17	1.4×10^{-4}
7.2×10^{-4}	0.032	34	2.4×10^{-4}
1.2×10^{-3}	0.032	48	2.6×10^{-4}
1.7×10^{-3}	0.032	60	2.5×10^{-4}
2.2×10^{-3}	0.032	72	2.2×10^{-4}
2.4×10^{-4}	0.045	15	1.2×10^{-4}
7.2×10^{-4}	0.045	27	2.1×10^{-4}
1.2×10^{-3}	0.045	37	2.3×10^{-4}
1.7×10^{-3}	0.045	45	2.2×10^{-4}
2.2×10^{-3}	0.045	52	2.1×10^{-4}

For the sake of simplicity, we may write the production of an excited species (S*) in the following first-order reaction with respect to the concentration of the intermediate compound:

$$M \xrightarrow{O_3} S^* \qquad [II];\ k_2.$$

Thus, when $t>t'$, [M] is given by:

$$[M] = [\{(k_1-k_2)[P]_0 + k_2[P]'\}\exp(-k_2 T) - k_1[P]'\exp(-k_1 T)]/(k_1-k_2) \tag{3}$$

where $T=t-t'$.

S* is deactivated by fluorescence processes or by non-radiative processes:

$$S^* \longrightarrow S + h\nu \qquad [III];\ k_3.$$
$$S^* \longrightarrow S \qquad [IV];\ k_4.$$
$$S^* + M \rightarrow S + M \qquad [V];\ k_5.$$
$$S^* + P \rightarrow S + P \qquad [VI];\ k_6.$$

In the systems involving rhodamine B (R), the processes of energy-transfer from S* to R take place:

$$S^* + R \rightarrow S + R^* \qquad [VII];\ k_7.$$

R* is deactivated by the fluorescence process:

$$R^* \longrightarrow R + h\nu' \qquad [VIII];\ k_8.$$

Although other non-radiative processes of deactivation also take place, our discussion is limited to the process VIII because of the high efficiency of the fluorescence emission of R. The intensity of emission resulting from the energy-transfer (I_{PR}) is given by:

$$I_{PR} = k_8[R^*] = k_7[S^*][R] \tag{4}$$

where [R] is the rhodamine B concentration.

By the steady-state approximation, $d[S^*]/dt=0$, and assuming that $k_5=k_6=k_q$ and $k_3+k_4 \ll k_7[R]+k_q([M]+[P])$, [S*] is given by:

$$[S^*] = k_2[M]/\{k_7[R] + k_q([M] + [P])\} \tag{5}$$

From Eqs. (3), (4), and (5), I_{PR} is given by:

$$I_{PR} = \frac{k_2k_7[R][\{(k_1-k_2)[P]_0+k_2[P]'\}\exp(-k_2T)-k_1[P]'\exp(-k_1T)]}{(k_1-k_2)k_7[R]+k_q[\{(k_1-k_2)[P]_0+k_2[P]'\}\exp(-k_2T)-k_2(P)'\exp(-k_1T)]} \tag{6}$$

The values of Δ (the increment in the total light emitted by the enhancement effect) is defined as:

$$\Delta = \int_0^\infty (I_M - I_P - I_R)dT \tag{7}$$

Using the relations: $I_M = I_{PR} + I'_R$ and $I_M \gg I_P$, and assuming that $\int I_R dT = \int I'_R dT$ and $[R]=[R]_0$ (the initial concentration of rhodamine B), Eq. (7) becomes:

$$\Delta = \int_0^\infty I_{PR}dT = (k_7/k_q)[R]_0\ln\{1+[P]_0/(k_7/k_q)[R]_0\} \tag{8}$$

Equation (8) is reduced to the following convenient form:

$$\Delta = A[R]_0\ln(1+[P]_0/A[R]_0) \tag{9}$$

where $A=k_7/k_q$. Table 2 illustrates the values of Δ measured by using the graphical integration of I_M-t curves and I_R-t curves and the values calculated from Eq. (9) by using a suitable parameter A. The calculated values are in fairly good agreement with the measured values in every polyphenol systems.

A similar chemiluminescence emission and the enhancement effect of rhodamine B were observed

TABLE 2. OBSERVED AND CALCULATED Δ-VALUES IN THE SEVERAL SYSTEMS OF DIFFERENT POLYPHENOLS
$\Delta_{calc.}=A[R]_0\ln(1+[P]_0/A[R]_0)$

Phenol	$[P]_0$ (mol/l)	$[R]_0$ (mol/l)	A	$\Delta_{calc.}\times10^6$	$\Delta_{obs.}\times10^6$
Resorcinol	2.4×10^{-4}	8.0×10^{-6}	5.0	78	81
	2.4×10^{-4}	1.6×10^{-5}	5.0	121	147
	2.4×10^{-4}	3.2×10^{-5}	5.0	147	182
	2.4×10^{-4}	6.4×10^{-5}	5.0	179	166
Catechol	2.4×10^{-4}	8.0×10^{-6}	19	145	145
	2.4×10^{-4}	1.6×10^{-5}	19	175	188
	2.4×10^{-4}	3.2×10^{-5}	19	200	191
	2.4×10^{-4}	6.4×10^{-5}	19	208	225
Hydroquinone	2.4×10^{-4}	8.0×10^{-6}	5.55	83	83
	2.4×10^{-4}	1.6×10^{-5}	5.55	115	117
	2.4×10^{-4}	3.2×10^{-5}	5.55	150	159
	2.4×10^{-4}	6.4×10^{-5}	5.55	189	163
	2.4×10^{-4}	9.6×10^{-5}	5.55	195	179
Phloroglucinol	2.4×10^{-4}	8.0×10^{-6}	40	177	179
	2.4×10^{-4}	1.6×10^{-5}	40	202	207
	2.4×10^{-4}	3.2×10^{-5}	40	207	207
	2.4×10^{-4}	6.4×10^{-5}	40	230	230
	2.4×10^{-4}	1.1×10^{-4}	40	242	251
Gallic acid	1.2×10^{-3}	1.6×10^{-6}	15	69	94
	1.2×10^{-3}	4.0×10^{-6}	15	191	184
	1.2×10^{-3}	8.0×10^{-6}	15	340	288
	1.2×10^{-3}	1.6×10^{-5}	15	432	430
	1.2×10^{-3}	8.0×10^{-5}	15	684	828
	1.2×10^{-3}	1.6×10^{-4}	15	989	971

in the solutions of aminophenols and phenylenediamine in acetic acid, but neither emission nor enhancement effect was observed in the phenol, aniline, nitrophenol, and nitroaniline system. The enhancement effect upon the polyphenol chemiluminescence emission was also observed when anthracene was added in place of rhodamine B, but no enhancement effect was observed in the presence of methylene blue. Further investigation is necessary to elucidate these phenomena.

BULLETIN OF THE CHEMICAL SOCIETY OF JAPAN VOL. 42 864—870 (1969)

A Study on Electron Spin Resonance of the Complex between Metal Ions of Group II and *o*-Quinone Anion*[1]

Keiji KUWATA and Yasuhiro SHIMIZU

Department of Chemistry, Faculty of Science, Osaka University, Toyonaka, Osaka

(Received July 12, 1968)

An electron spin resonance study on the complex formation between *o*-quinone anion and metal ions of group II was undertaken, and the change in *g*-factor and proton hyperfine splittings of *o*-quinone anion by the complex formation were examined in detail. The change in *g*-factor was closely related to both the change in the unpaired electron distribution and the change in energy difference between lone pair orbital of oxygen and unpaired electron orbital. The stabilization of the quinone anion against its coupling reaction was seemed to be related to the shift in *g*-factor by complex formation. The interaction between quinone anion and metal ions was deduced to be partly ionic. An open shell SCF calculation with CI for the free quinone anion was carried out in order to discuss the electronic spectra of the complex.

Besides the electron spin resonance study on the complexes of paramagnetic metal ions, such study on the complex between free radicals or radical ions and diamagnetic metal ions is also efficient in the investigations into the nature of the interaction between ligands and metal ions.

It is well known that the mixture of poly-phenol and alkaline earth metal ion yields green colored complex, and this fact was applied to the qualitative analysis of these ions. During this reaction, a kind of complex between *o*-quinone anion and the metal ions is thought to be produced.

Eaton[1)] studied on the effect of complex formation of *o*-quinone anion with diamagnetic ions of group II and III by the ESR spectra, and found the change in proton hyperfine splitting of the ligand, and the appearance of additional hyperfine splittings due to the nuclear magnetic moment of metal ions in the cases of Y^{3+} and La^{3+} ions.

Since *g*-factor of the ESR spectrum is closely related to the change in the lone pair orbital of oxygen atom in semiquinone anion, it is useful to examine the effects of complex formation of both *g*-factor and proton hyperfine splitting for the investigation into the nature of interaction between ligand and metal ion.

The present work was undertaken in order to examine the change in *g*-factor of *o*-quinone anion and also to reexamine the change in hyperfine splittings in detail, and to make a theoretical discussion on the nature of the interaction between ligand and metal ion.

An attempt to analyze the electronic spectra of *o*-quinone anion was made using an open-shell SCF method of Pople and Nesbet with CI. The effects of complex formation on the reactivity of *o*-quinone anion were also studied.

Experimentals

o-Benzoquinone was prepared by the oxidation of catechol.

The electron spin resonance spectra were measured using a home-made X-band spectrometer of 455-kc/sec field modulation and with a 30 cm electromagnet of

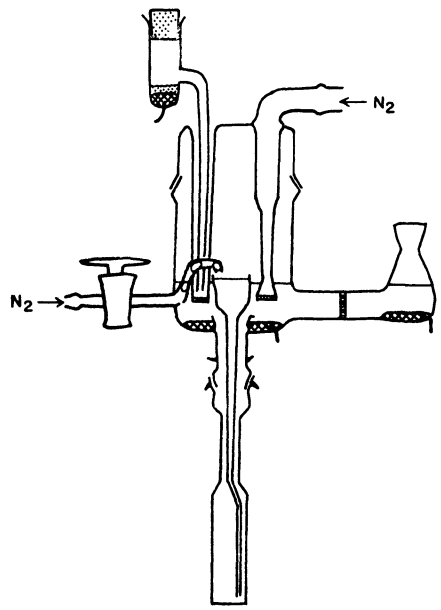

Fig. 1. The electrolytic reduction cell for the measurements of electronic absorption spectra.

*1 This work was presented at the Fourth Symposium on Electron Spin Resonance in 1965, Nagoya.

1) D. R. Eaton, *Inorg. Chem.*, **3**, 1268 (1964).

Japan Electron Optics Laboratory Co. The samples for ESR and UV measurements were prepared as follows. In the case of quinone anions with alkali metal ions, the radicals were prepared using a flow system at a flow rate of about 0.5 ml/sec. In the case of quinone anions with alkaline earth metal ions, three different methods were used: a) the flow method at a flow rate of about 3 ml/min, b) aerial oxidation by shaking the dilute ammonia solution of hydroquinone in contact with air, and deaeration of the solution, c) the electrolytic reduction, the cell for which is shown in Fig. 1.

The electronic absorption spectra were measured using a Hitachi spectrophotometer model EPS-2, under the same condition as that for the measurement of ESR spectra.

For magnetic field calibration, peroxylamine disulfonate was used as a reference with a dual mode (H_{014}) ESR cavity. ^{14}N hyperfine splitting constant and g-factor of peroxylamine disulfonate were taken to be 13.0 G and 2.00550, respectively.[2]

Calculation of Spin Density and g-Factor in Quinone Anion. Hückel MO method and McLachlan's method[3] were used for the calculation of spin density for free and complex quinone anion. In addition, the iterative simple MO method,[4] and the open-shell SCF MO method of Pople and Nesbet[5] with CI were used for free quinone anion.

In the iterative method, the coulomb integrals and the exchange integrals were repeatedly modified according to the values of the total charges and bond orders under the assumption that coulomb and exchange integrals were proportional to the electronegativity of the atom and to the overlap integral between atoms, respectively. The iteration was repeated until the mutual consistency of the assumed set with the calculated set was achieved.

The variation of g-factor in complex quinone anions was analyzed on the basis of theory given by Stone.

Writing the nth molecular orbital ϕ_n as linear combination of atomic orbitals, $\phi_n=\sum_k \chi_k^{(n)}$, where $\chi_k^{(n)}$ is an (un-normalized) atomic orbital on atom k, and using second order perturbation theory with neglecting differential overlap integral, Stone had derived the following expression for g-factor:[6]

$$g_{zz} = 2.00232 + 2\sum_{n\neq p} \frac{\sum_k \langle \chi_k^{(p)}|l_{kz}|\chi_k^{(n)}\rangle \sum_{k'}\zeta_{k'}\langle \chi_{k'}^{(n)}|l_{k'z}|\chi_{k'}^{(p)}\rangle}{E_p - E_n} \quad (1)$$

where l_{kz} is the z-component of angular momentum about the kth atom, ζ_k is the spin orbit coupling constant for the kth atom, E_p is the energy of the odd electron orbital and E_n is the energy of the nth molecular orbital in the molecule.

For the case of quinone anion, Δg can be divided into three parts as follows:

$$\Delta g = g - g_e = \Delta g_{hc} + \Delta g_{co} + \Delta g_n$$

where Δg_{hc}, Δg_{co} and Δg_n are the contributions to Δg from the parts of C-C and C-H σ-orbitals of the skeleton, CO σ-orbitals, and the oxygen lone-pair orbitals, respectively.

In the present study, the iterative simple MO method and the modified extended Hückel MO method were used for π-system and for CO σ-bond, respectively. For simplicity, the bonding between SP^2 hybrid orbital of carbon atom and 2P atomic orbital of oxygen atom was taken as CO σ-bonding. With the above-mentioned orbitals, Δg was calculated using Eq. (1).

Δg_{hc} was estimated from the following equation,[6]

$$\Delta g_{hc} = \sum_i^{\text{carbon}} \rho_i(24.7 - 19.3\Lambda) \times 10^{-5} \quad (2)$$

where Λ is the coefficient of the odd-electron orbital energy, $\alpha+\Lambda\beta$, and ρ_i is the odd-electron density on the ith carbon.

Δg_n could be estimated on the basis of the $n\rightarrow\pi^*$ transition process in quinone anion, so that the contribution from ith lone-pair orbital to Δg_n was given by the following equation, derived from Eq. (1).

$$\Delta g_n{}^i = \frac{2}{3}\frac{\langle \chi_z^{(p)}|l_y|\chi_x^{(n)}\rangle\zeta_O\langle \chi_x^{(n)}|l_y|\chi_z^{(p)}\rangle}{E_p - E_n} = \frac{2}{3}\frac{\zeta_O\rho_O}{E_p - E_n} \quad (3)$$

here, the subscripts x, y and z represent the x, y and z-components of the quantities, respectively, ρ_O is the spin density on oxygen atom and E_p-E_n is the $n\rightarrow\pi^*$ transition energy.

Results

Whereas the hyperfine coupling constants in ESR spectra and the stability of p-benzoquinone anion were not affected by the presence of metal ions, o-benzoquinone anion was fairly affected under the same condition.

The alkali metal ions did not change the hf coupling constants, but slightly increased its signal intensity of the ESR spectrum. Notable effects of the presence of metal ions were seen in the case of alkaline earth metal ions. The coupling constants and g-factor were changed in accordance with the cation species.

Observed hyperfine splittings and g-factors for o-quinone anion are listed in Table 1, together with spin densities derived from experimental proton hyperfine splitting constants using McConnell's relationship: as, $a=Q\cdot\rho$. Here Q was chosen to be 23 gauss.

In addition to the primary o-quinone anion the spectrum which had been attributed to secondary radical was observed in methanol. The latter radical was identified with 4, 5-dimethoxy benzosemiquinone anion radical formed through the substitution of 4 and 5 position of o-quinone anion by methoxy groups.[1]

The observed electronic absorption spectra of

2) J. Q. Adams and J. R. Thomas, *J. Chem. Phys.*, **39**, 1904 (1964).

3) A. D. McLachlan, *Mol. Phys.*, **3**, 233 (1960).

4) Y. Kurita and M. Kubo, This Bulletin, **24**, 13 (1951); S. Nagakura, *ibid.*, **25**, 164 (1952); S. Nagakura and T. Hosoya, *ibid.*, **25**, 179 (1952).

5) J. A. Pople and R. K. Nesbet, *J. Chem. Phys.*, **22**, 571 (1954).

6) A. J. Stone, *Mol. Phys.*, **6**, 509 (1963).

TABLE 1. OBSERVED HYPERFINE SPLITTINGS AND g-FACTORS, TOGETHER WITH SPIN DENSITIES DERIVED FROM EXPERIMENTAL PROTON HF-SPLITTING CONSTANTS BY USING MCCONNELL'S RELATIONSHIP

Counter ion	Solvent	a_3 (gauss)	a_4 (gauss)	ρ_3	ρ_4	g-Factor
NH_4^+	H_2O	0.76	3.77	0.033	0.164	2.00467
Mg^{2+}	H_2O	0.53	4.03	0.023	0.175	2.00423
Ca^{2+}	H_2O	0.66	3.89	0.029	0.169	2.00433
Sr^{2+}	H_2O	0.70	3.82	0.030	0.166	2.00435
Ba^{2+}	H_2O	0.73	3.85	0.032	0.167	2.00400
Zn^{2+}	H_2O	0.49	3.98	0.021	0.173	2.00389
Cd^{2+}	H_2O	0.53	3.93	0.023	0.171	2.00347
Mg^{2+}	DMSO	0.90	3.83	0.039	0.167	2.00442
Ca^{2+}	DMSO	1.03	3.76	0.045	0.163	2.00447
Sr^{2+}	DMSO	1.07	3.67	0.046	0.160	2.00430
Ba^{2+}	DMSO	1.15	3.62	0.050	0.157	2.00386
Zn^{2+}	DMSO	0.77	3.78	0.033	0.164	2.00412

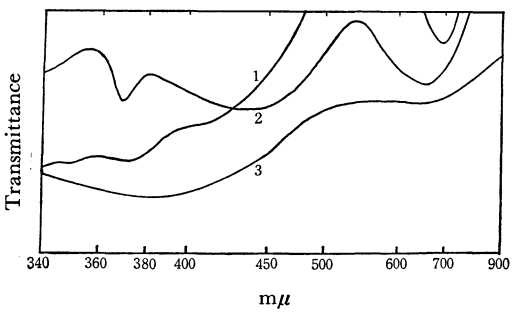

Fig. 2. The electronic absorption spectra of quinone anions.
(1) quinone anion with Mg^{2+} in DMSO
(2) quinone anion with Mg^{2+} in acetonitrile
(3) free quinone anion in acetonitrile

complex radical using an electrolytic reduction are shown in Fig. 2. Three peaks at 370—380 mμ (I), 400—440 mμ (II) and 650—700 mμ (III) were assigned to the complex o-quinone anion radical.

The contour plots of spin densities calculated varying the coulomb integral of oxygen in Hückel MO method and McLachlan's method are shown in Fig. 3.

The spin densities and the odd-electron orbital energy of quinone anion calculated by the iterative simple MO method were as follows.

$$\rho_1 = 0.173,\ \rho_3 = 0.018,\ \rho_4 = 0.104,\ \rho_7 = 0.205,$$

and $E_p = \alpha + 0.574\beta$. $\beta = -2.39$ eV

The unrestricted SCF calculation was carried out until the spin densities became mutually consistent to three decimal places, and the result is shown diagrammatically in Fig. 5, together with the experimental values.

The bonding and antibonding orbitals of a C–O σ-bond were obtained: as,

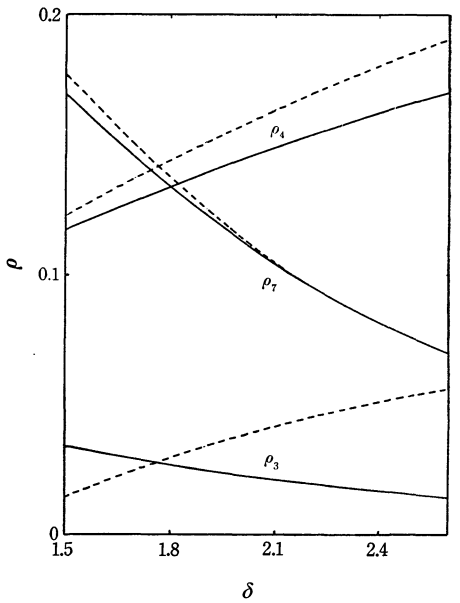

Fig. 3. The contour plots of calculated spin densities.
—— by Hückel MO, ---- by McLachlan's method, in which λ was taken to be 1.2. The axis of abscissa represents δ in coulomb integral $\alpha_O = \alpha + \delta\beta$.

$$\phi^b_{CO} = 0.549\chi_{sp^2} + 0.708\chi_p \quad E^b_{CO} = -22.46\text{ eV}$$

$$\phi^a_{CO} = 0.851\chi_{sp^2} - 0.783\chi_p \quad E^a_{CO} = 2.46\text{ eV}$$

Accordingly, Δg_{hc} and Δg_{co} for the free quinone anion were estimated to be 3.3×10^{-5}, -41.1×10^{-5}, respectively. In aqueous solution, g-factor of the free quinone anion was 2.00467, so that to have such value, the contribution from the lone-pair orbitals, Δg_n should be 273×10^{-5}, and the absorption band for $n\rightarrow\pi^*$ transition was estimated to be at *ca.* 662 mμ using Eq. (3).

Discussion

Hyperfine Coupling Constants of the Complex Radical. As shown in Table 1, hyperfine coupling constants for the ring protons at ortho position decreased as those of meta position increased. The contour plots of calculated spin densities using Hückel MO treatment showed that ρ_4 increased as the δ increased whereas the spin density ρ_3 (at position 3) decreased. Here δ denotes the coefficient of coulomb integral of oxygen atom, $\alpha_O=\alpha+\delta\beta$. This tendency was consistent with that of the change in experimental spin density, accordingly the effect of chelation on the spin density seemed to be equivalent to the value of coulomb integral of oxygen atom where assuming it to be more negative.

Fraenkel *et al.*,[7] showed that McLachlan's method led to an excellent agreement between the observed proton hyperfine splittings and the calculated ones for free *o*-quinone anion, where $\lambda=1.2$, $\alpha_O=\alpha_B+2.1\beta$ and $\beta_{CO}=\beta_{CC}$ were taken as molecular parameters. And in their calculation, while ρ_4 was positive, ρ_3 was negative.

As shown in Fig. 3, McLachlan's method, however, led to such result that not only ρ_4 but also the absolute value of ρ_3 (in this case, ρ_3 was negative) increased as the δ increased. Thus the McLachlan's method was seemingly unsuitable to analyze the experimental result. The present result possibly showed that ρ_3 and ρ_4 were both positive.

In general, spin polarization has a tendency to enhance the spin density at the position where high spin density would be expected by Hückel MO calculation, while it would diminish the spin density at the position where low spin density would be expected by Hückel MO calculation. In fact such tendency was observed so far as ρ_3 and ρ_4 were concerned.

The semiempirical parameter λ in McLachlan's method controls the amount of spin polarization in the radical. If λ is taken to be less than 0.3, the effect of spin polarization still remains small, both ρ_3 and ρ_4 remain positive in the case of δ value less than 2.3 and the tendency of decrease in a_3 and increase in a_4 as δ increases is evident. The turning point of spin density ρ_3 from positive to negative depends on not only λ but δ, *e. g.*, with $\lambda=0.5$, the turning point was at $\delta=1.9$.

On varying the counter ions in the sequence of NH_4^+, Ba^{2+}, Sr^{2+}, Ca^{2+}, Mg^{2+}, ρ_3 decreased, whereas ρ_4 increased. The observed values of ρ_3 and ρ_4 correlated smoothly with electronegativity of the metal atom as shown in Fig. 4, or in other expression the coulomb integral of oxygen in the complex quinone anion seemed to correlate to the electronegativity of metal ion changed. It is noted here that this sequence agreed with the sequence of the stability of the complex quinone anion in solution. This is discussed again in later section.

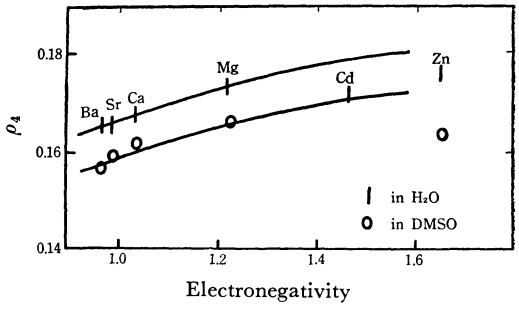

Fig. 4. The relationship between the observed spin density on position 4 and the Pauling's electronegativity of metal atom.

As to the solvent effects, a fact that the complex radical was more stable in DMSO than in water was found. And this was understood by the difference in electrostatic interactions as follows. The dielectric constant of water is larger than that of DMSO, thus in water the radical ion has weaker interaction with metal ion, or the dissociation constant of the complex should be larger than in DMSO. The difference in electrostatic interaction could also relate to the difference in the amount of increase in δ. Figure 4 shows that the oxygen atom had larger value of δ in water than in DMSO, or in other word, in the solvent of larger dielectric constant the value of δ became larger.

***g*-Factor of Complex Radical.** The solvent effect on *g*-factor of diphenyl nitric oxide has been treated as a perturbation of increase in coulomb integral of the oxygen atom through the hydrogen-bonding between solute and solvent.[8] On the other hand, in the present case the addition of metal ion to the oxygen atoms of quinone anion made the coulomb integral of oxygen atom more negative and thus affected on *g*-factor of the anion. Although both the lone pair orbitals of oxygen atom and C-O σ-bond would be likely affected, as the first step of approximation, an assumption that σ-system remains unchanged in the complexes was made. Then the effect of complex formation on *g*-factor could be regarded as a perturbation only on π-electron system. The effect of a change in α_o on the spin density on the rth atom ρ_r, the odd-electron orbital bond order between rth and sth atoms P_{rs} and the odd-electron orbital energy E_p will be expressed using atom-atom polarizability as follows.

7) G. Vincow and G. K. Fraenkel, *J. Chem. Phys.*, **34**, 1333 (1961); G. Vincow, *ibid.*, **38**, 917 (1963).

8) T. Kawamura, S. Matsunami, T. Yonezawa and K. Fukui, This Bulletin, **38**, 1935 (1965).

TABLE 2. *g*-FACTORS FOR COMPLEX QUINONE ANIONS

	Mg^{2+}	Ca^{2+}	Sr^{2+}	Ba^{2+}	Zn^{2+}	Cd^{2+}	NH_4^+
$g_{obs.}$	2.00423	2.00433	2.00435	2.00400	2.00389	2.00347	2.00467
$g_{calc.}$	2.00416	2.00448	2.00454	2.00461	2.00408	2.00420	2.00467
$(g_{obs.}-g_{calc.})\times 10^{+5}$	7	−15	−19	−61	−19	−73	−0

With the molecular orbital calculated by the interative method, these quantities are as follows.

$$\left.\begin{aligned}
\delta E_p &= \rho_7\delta\alpha_7 + \rho_8\delta\alpha_8 = 0.4096\times\delta\alpha_O \\
\delta\rho_1 &= \pi^p{}_{1,7}\delta\alpha_7 + \pi^p{}_{1,8}\delta\alpha_8 = 0.1376\times\delta\alpha_O/\beta \\
\delta\rho_3 &= \pi^p{}_{3,7}\delta\alpha_7 + \pi^p{}_{3,8}\delta\alpha_8 = -0.0184\times\delta\alpha_O/\beta \\
\delta\rho_4 &= \pi^p{}_{4,7}\delta\alpha_7 + \pi^p{}_{4,8}\delta\alpha_8 = 0.0936\times\delta\alpha_O/\beta \\
\delta\rho_7 &= \pi^p{}_{7,7}\delta\alpha_7 + \pi^p{}_{7,8}\delta\alpha_8 = -0.2128\times\delta\alpha_O/\beta \\
\delta P_{17} &= \pi^p{}_{17,7}\delta\alpha_7 + \pi^p{}_{18,8}\delta\alpha_8 = 0.0224\times\delta\alpha_O/\beta
\end{aligned}\right\} \quad (4)$$

Here, the same notation as that in the reference was used.[8]

The effect of complex formation on *g*-factor could be divided into three parts as mentioned in the preceding section, that is to say, $\delta\Delta g_{hc}$, $\delta\Delta g_{co}$ and $\delta\Delta g_n$, which could be expressed by the amount of change in α_o.

$$\left.\begin{aligned}
\delta\Delta g_{hc} &= 1.1\times10^{-5}\times\delta\alpha_O/\beta \\
\delta\Delta g_{co} &= 9.3\times10^{-5}\times\delta\alpha_O/\beta
\end{aligned}\right\} \quad (5)$$

$$\begin{aligned}
\delta\Delta g_n &= \frac{4}{3}\frac{\zeta_O(\rho_O+\delta\rho_O)}{E_p+\delta E_p-E_n} - \frac{4}{3}\frac{\zeta_O\rho_O}{E_p-E_n} \\
&= -140.7\times10^{-5}\times\delta\alpha_O/\beta \\
&\quad -72.9\times10^{-5}\times(\delta\alpha_O/\beta)^2
\end{aligned}$$

Using Eq. (4), the increase in coulomb integral of oxygen atom could be estimated by the deviation of observed hyperfine coupling constants for complex quinone from that for free quinone anion, thus the change in $\delta\Delta g$ was calculated using Eq. (5). Calculated values of *g*-factor are listed in Table 2 together with observed ones.

As seen in Table 2, a trial to explain the variation of *g*-factor of complex quinone anion by considering only about the change in π-system was not necessarily carried out successfully. In the cases of Ba^{2+} and Cd^{2+} there was fairly large disagreement between $g_{cal.}$ and $g_{obs.}$, so that it seemed necessary to consider some additional contributions coming from the change in σ-system.

The contributions from Δg_{hc} and Δg_{co} were estimated to be 3.3×10^{-5} and -41.1×10^{-5}, respectively, and these values are so small that they can be disregarded as compared with Δg_n: the contribution from lone pair orbital.

If the addition of metal ion to oxygen atoms of quinone anion stabilizes lone pair orbital energies of oxygen atoms, the difference between lone pair orbital energy and unpaired electron orbital energy will be enhanced and as a result, the estimated value of *g*-factor will decrease as expected from Eq. (3). Therefore, it may be reasonable to take the difference between the observed value and the calculated one of *g*-factor in Table 2 as the measure of stabilization in lone pair orbital energy of oxygen atom.

The quantity, $g_{obs.}-g_{calc.}$, increased with the stabilization of E_n, so that in this study among the ions of IIa and IIb group elements, the stabilization of lone pair orbital energy was found to increase in the order of $Ba^{2+}>Sr^{2+}>Ca^{2+}>Mg^{2+}$ and $Cd^{2+}>Zn^{2+}$, respectively.

As a conclusion, following mechanisms of the variation of *g*-factor were approved. The change in distribution of unpaired electron in complex quinone anion coming from the increase in coulomb integral of oxygen is partly the origin of the variation of *g*-factor, and the change in energy difference between lone pair orbital of oxygen and unpaired electron orbital is also responsible for the variation of *g*-factor.

Reactivity and Structure of Complex Quinone Anion. Using the alkaline methanol as a solvent for *o*-quinone anion-metal ion system, the spectrum for a secondary radical superimposing on that of primary radical was observed and the secondary radical had been identified as a methoxylated radical (II). This secondary radical was formed by a reaction of primary radical (I) with methanol[1] in the presence of metal ions as catalyst.

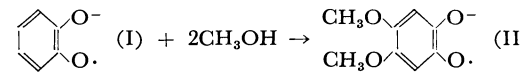

It was shown in Hückel MO treatment that the complex formation brought about the increase in unpaired electron density at position 4 and 5, and also the decrease in total π-electron density at these positions. As a result, the increase in unpaired electron density would make the radical reaction favorable at these positions, and the decrease in total π-electron density would make the negatively charged species more easily to attack at these position too.

The nature of the attacking species was not known at the present stage of experiment, however, it may be suggested that the attacking species is radical or has neagtive charge.

On the other hand, in the absence of metal ions, when the spectrum of *o*-quinone anion in alkaline solution was recorded, the gradual appearance of a triplet spectrum superimposed on the center of original spectrum was observed. This triplet

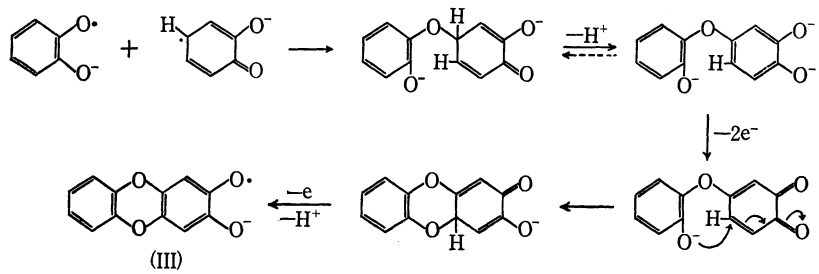

(III)

spectrum was assigned to dibenzo-1,4-dioxin-2,3-quinone anion (III) which was formed through dimerization of *o*-quinone anion.[9]

In this study, however, dimer anion was not observed in the presence of alkaline earth metals. This is probably due to the restriction against dimerization reaction for the complex quinone anion, since oxygen atoms in the complex anion are hindered by a metal ion and are prevented to react with another anion. Upon the addition of various metal ions, the stability of complexed anion against such dimerization reaction increased as the ability of enhancing δ in the coulomb integral of oxygen increased, thus the interaction between oxygen atoms of quinone anion and metal ion played an important role in the selectivity of reaction.

The hyperfine splitting due to the metal nuclei had been observed,[1] and this shows confirmatively that metal ion has an interaction with *o*-quinone anion and the unpaired electron flows into the metal ion, but this amount is estimated to be very small.

For the complex quinone anion, following two structures are possible. a) Metal ion is in the plane of benzene ring and attaches to two oxygen atoms of the quinone anion. b) Metal ion is located above the benzene ring and interacts with whole of the π-electrons of benzene ring.

(a) (b)

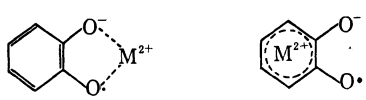

(IV) (V)

In the latter case, the metal ion makes coulomb integrals of all carbon atoms more negative, and this is equivalent to the decrease in δ in coulomb integral of oxygen atoms, and this effect does not agree with experiment, or it will give the wrong tendency in the variation of unpaired electron distribution. Thus, it could be suggested that the *o*-quinone anion-metal complex takes the structure of the former case (a).

Energy Levels of *o*-Quinone Anion. The studies on the electronic spectra of *o*-benzoquinone were reported already,[10] and such an approximate information about the energy levels of the anion tha one or two absorption bands seemingly appear in the wavelength region of 500—800 mμ was derived.

For the detailed discussion on the electronic state of the anion, a calculation based on unrestricted SCF-MO method (UHF) was performed, and three absorption bands in visible region were expected. The energies of the allowed transitions and the oscillator strengths for those transitions are shown in Fig. 5.

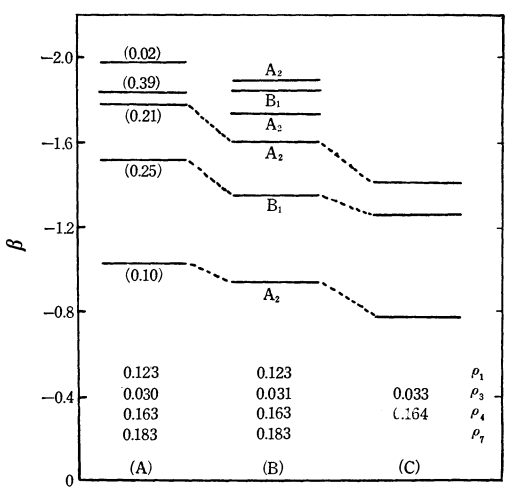

Fig. 5. The spin density and the excitation energy of free quinone anion. (A) by open shell SCFMO (B) by open shell SCFMO-CI. (C) observed values. The numerals in the parentheses indicate the calculated oscillator strengthes.

While the experimental value of oscillator strength could not be determined because of the difficulty in determination of the concentration of the anion, the relative intensities of observed spectra were compared with the calculated oscillator strength, and three observed absorption bands at 370—380 mμ, 400—440 mμ, and 650—760 mμ were assigned to $\pi \rightarrow \pi^*$ transitions.

Figure 5 also shows the result obtained by considering on configuration interaction among twenty

9) F. R. Hewgill, T. J. Stone and W. A. Waters, *J. Chem. Soc.*, **1964**, 408.

10) S. Nagakura and A. Kuboyama, *J. Am. Chem. Soc.*, **76**, 1003 (1954); A. Kuboyama and K. Wada, This Bulletin, **38**, 1709 (1965).

low lying excited doublet states. Since the wave function obtained here was not true eigenfunction of $S=1/2$ state, we should use the annihilation operator and remove the components of higher spin states. The wave function obtained after applying annihilation operator, however, does not satisfy the condition of energy minimum, on the contrary. Even if the higher spin states are excluded, the drastic change of spin density distribution will not be expected because those states are lying in high energy states and the effect from those states will be small. For that reason, only single determinant wave function was used at the starting point. In this CI calculation, we also made an approximation, in which the singly excited states had the same form as those in closed-shell SCF-MO.

In open-shell SCF-MO, electron correlation is already partly included so that the configuration interaction in UHF has different significance from that in restricted HF.

In this study, the result that the configuration interaction scarcely affected on the spin density, whereas it considerably affected on the transition energy was also shown.

The weak absorption band for $n\rightarrow\pi^*$ transition, the energy of which estimated to be approximately 1.8—3.7 eV from the observed values of g-factor using Eq. (3), might be masked by the strong π-π^* transition bands in this region.

The authors wish to express their thanks to Professor Kozo Hirota for his encouragement throughout this work.

Appendix

An Unrestricted SCF MO-CI Calculation of *o*-Quinone Anion. In the closed shell Hartree-Fock wave function, the repulsion between electrons is not accounted for properly because electrons affect each other through their instaneous potentials, not just by their average potentials. The antisymmetry of the wave function itself acts as if there would be a rather strong repulsion between particles with the same spin at small distances, but further correlative effects associated with particles having different spins cannot be treated properly.

On the other hand, in the open shell SCF MO, the orbitals associated with different spins will automatically try to arrange themselves in such a way that particles having antiparallel spins will tend to avoid each other due to their mutual repulsion.

In the present study, the unrestricted Hartree-Fock method (UHF) of Pople and Nesbest was used for free *o*-quinone anion. The ground state wave function was described by:

$$\Psi_g = |\phi_1\bar{\phi}_1\phi_2\bar{\phi}_2\cdots\phi_n\bar{\phi}_n\phi_{n+1}| \tag{6}$$

where $N(=2n+1)$ is the number of π-electrons. The molecular orbitals given by the linear combination of atomic orbitals were chosen to minimize the electronic energy.

$$E=\sum_{i}^{\alpha+\beta}H_i+\frac{1}{2}\sum_{i}^{\alpha+\beta}\sum_{j}^{\alpha+\beta}J_{ij}-\frac{1}{2}\left(\sum_{i}^{\alpha}\sum_{j}^{\alpha}+\sum_{i}^{\beta}\sum_{j}^{\beta}\right)K_{ij}$$

In the calculation of H_i, J_ij and K_ij, the coulomb repulsion integrals, $(\mu\mu|\mu\mu)$ and $(\mu\mu|\nu\nu)$, and the core integrals, α and β were evaluated by the semiempirical procedure analogous to that of Pariser and Parr.[11]

The core integrals were calculated from the next equations:

$$\alpha_\mu=-w_\mu-\sum_{\mu\neq\nu}(\mu\mu|\nu\nu)$$

$$\beta_{CC}=-\frac{17.464}{r^6_{CC}}\text{eV},\quad \beta_{CO}=-\frac{8.8086}{r^6_{CO}}\text{eV}^{12)}$$

where w_μ and $(\mu\mu|\nu\nu)$ were the valence state ionization potential and the coulomb repulsion integral under the neutral electron distribution.

It was assumed that the free *o*-quinone anion was planer and that the ring part and r_{CO} of the radical had the same molecular dimension as that of benzene and 1.23Å, respectively. The one-center coulomb repulsion integral $(\mu\mu|\mu\mu)$ and the two-center coulomb repulsion integral $(\mu\mu|\nu\nu)$ were evaluated from the same procedure as that in Harada's paper.[13]

The best result of calculation, in which core integrals were calculated assuming that each atom of the molecule was neutral but repulsion integral was modified by the result of the iterative simple MO method, is given in Fig. 5.

The configuration interaction between the ground state and the singly excited states in the same spin state as the ground state was considered.

The singly excited states were represented by Slater determinants of the form under our approximation.

$$\left.\begin{aligned}
\psi^{(\mathrm{I})}_{i\rightarrow k}&=|\cdots\phi_i\phi_k\phi_0|(2\alpha\alpha\beta-\alpha\beta\alpha-\beta\alpha\alpha)/\sqrt{6}\\
\psi^{(\mathrm{II})}_{i\rightarrow k}&=|\cdots\phi_i\phi_k\phi_0|(\alpha\beta\alpha-\beta\alpha\alpha)/\sqrt{2}\\
\psi_{i\rightarrow o}&=|\cdots\phi_i\phi_0\bar{\phi}_0|\\
\psi_{o\rightarrow l}&=|\cdots\phi_i\bar{\phi}_i\phi_l|
\end{aligned}\right\} \tag{7}$$

The electronic ground state function was approximated by a linear combination of doublet functions, (6) and (7).

$$\Phi=\sum_i A_i\psi_i$$

11) R. Pariser and R. G. Parr, *J. Chem. Phys.*, **21**, 466, 767 (1953); R. Pariser, *ibid.*, **24**, 250 (1956).
12) H. Kon, This Bulletin, **28**, 275 (1955).
13) Y. Harada, *Mol. Phys.*, **8**, 273 (1964).

BULLETIN OF THE CHEMICAL SOCIETY OF JAPAN VOL. 42 871—874 (1969)

Effect of Potassium Promoter on Iron Oxide Catalysts for Dehydrogenation of Ethylbenzene to Styrene

Katsue SHIBATA and Tadamitsu KIYOURA

Central Research Laboratory, Toyo Koatsu Industries, Inc., Kuden, Totsuka-ku, Yokohama

(Received July 17, 1968)

The catalytic activity and the sintering property of iron oxide catalysts with and without potassium additives have been studied. The potassium oxide acts as a promoter and is effective under given conditions in increasing the activity of the catalyst from four to ten times. The effects of the promoter can be classified thus: (1) Structural promoter: The increase in the apparent bulk density and the shrinkage of the catalyst tablet upon calcination during the preparation of the catalyst are prevented by potassium additives. The differences in the specific surface area and in the pore volume of the catalyst between with and without potassium promoter are slight. These effects on iron oxide appear to be caused largely by the formation of $K_2Fe_{22}O_{34}$. (2) Synergetic promoter: The potassium promoter changes the apparent energy of activation of the dehydrogenation reaction from 28 to 43 kcal/mol. The increase in the catalytic activity is due to the increase in the pre-exponential factor. The increase in the factor can be explained in terms of the higher concentration of the active center produced by the interaction of the potassium promoter with iron oxide. (3) Selectivity promoter: The formation of benzene by a side reaction is retarded by potassium additives.

Alkali metal oxide, especially potassium oxide, is extensively used as a promoter in many catalytic reactions, such as water gas shift, ammonia synthesis, and the dehydrogenation of organic compounds. It is well known that the potassium oxide reduces the amount of carbon deposit on the catalyst surface and causes the deposited carbon to be removed by steaming. In examining an iron oxide catalyst used for the dehydrogenation of butene to butadiene, Kearby[1] has described the characteristics of the potassium promoter. Lee and Holmes[2] studied the relations between the catalytic activity and electronic properties of alkali and alkaline earths promoting iron oxide for the dehydrogenation of ethylbenzene to styrene. However, the effect of alkali on an iron oxide catalyst for the dehydrogenation of organic compounds has not been clarified completely. The present paper describes some results of our study of the promoter action of potassium oxide on the iron oxide catalyst used for the dehydrogenation of ethylbenzene to styrene. The results of our experiments show that potassium acts as both a structural and a synergetic promoter. In addition, the formation of benzene is retarded by potassium oxide additives.

Experimental

Materials. The ethylbenzene was of a reagent grade and was obtained from the Wako Pure Chemicals Company; its purity, tested by gas chromatography, was superior to 99.5%, the remaining part being benzene and toluene. The ferric nitrate and potassium carbonate were reagent-grade chemicals and were used without further purification.

Catalyst Preparation. *Catalyst A*: Ferric hydroxide, prepared by the addition of an aqueous solution of ammonia to a solution of ferric nitrate, was decomposed to ferric oxide at 500°C in air. The ferric oxide powder and a suitable amount of potassium carbonate was mixed by hand grinding in an agate mortar, and then compressed into tablets under a pressure of 100 kg/cm^2. The tablet was calcined at 930°C in an electric furnace for two hours in the presence of air, and then crushed into granules.

Catalyst B: The compressed tablet of the ferric oxide powder without potassium additives was calcined in an electric furnace for two hours at 900°C in air. The calcined tablet was then crushed into granules and impregnated with a suitable amount of an aqueous potassium carbonate solution.

For both Catalyst A and Catalyst B, the fraction passing through a 1.5-mm sieve but not a 1.0-mm sieve was chosen for the activity and apparent-bulk-density mesurements.

Activity Measurements. The catalytic activity was measured with a differential reactor, with the conversion of ethylbenzene being kept below 5%. The distributions of the by-products, benzene and toluene, were measured with an integral reactor.

Preheated ethylbenzene and a 9/1 mol ratio of steam were fed into a stainless-steel reactor (10 mm i.d.) at 1 atm, and the reactor effluent was analyzed by gas chromatography. A thermocouple junction for measuring the reaction temperature was located at a center

1) K. K. Kearby, *Ind. Eng. Chem.*, **42**, 295 (1950).
2) E. H. Lee and L. H. Holmes, Jr., *J. Phys. Chem.*, **67**, 945 (1963).

of the catalyst bed in a stainless steel tube (1.6 mm o.d.) inserted through the bottom of the reactor.

Apparent Bulk Density. A weighed amount of the catalyst granules was placed in an ordinary glass cylinder and then the cylinder was shaken till the granules showed a constant volume.

Shrinkage of the Tablet of the Catalyst. The shrinkage of the tablet (0.5 cm long by 1.00 cm diameter before calcination) by calcination in the process of catalyst preparation was measured by an ordinary micrometer after the tablet had been cooled to room temperature. The maximum variation between samples heated in this way was less than 2%.

X-Ray Diffraction. X-Ray powder diffraction diagrams were recorded by a X-ray diffractometer (Geigerflex). As a X-ray radiation source, vanadium-filtered chrome radiation was used.

Specific Surface Area and Total Pore Volume. The specific surface area was obtained by applying the B. E. T. method to the adsorption isotherm of nitrogen at −196°C. The total pore volume was obtained from the amount of nitrogen adsorbed at the relative pressure of 0.98 in the adsorption of nitrogen at −196°C.

Results and Discussion

Sintering of the Iron Oxide during Catalyst Preparation. The apparent bulk density of the granules of Catalyst A with various concentrations of potassium additives is shown in Fig. 1. The

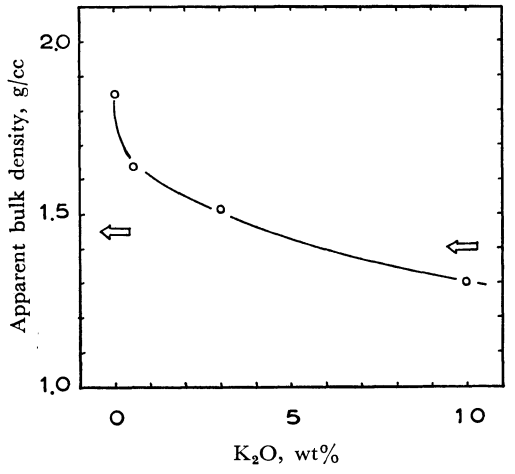

Fig. 1. Apparent bulk density of the iron oxide catalyst with various content of potassium oxide. The arrows indicate the apparent bulk density of catalyst before calcination.

concentration of potassium additives is indicated as a weight percentage of the potassium oxide. The apparent bulk densities of these catalysts before calcination ranged from 1.40 to 1.45 g/cc; after calcination, in the course of preparing a catalyst at 930°C for two hours, the value increased to 1.85 g/cc without potassium additives. The increase in the apparent bulk density upon calcination diminishes progressively with an increase in the concentration of potassium oxide. When the concentration of potassium reaches above about 3%, the apparent bulk density of the catalyst after calcination becomes lower than that of the uncalcined catalyst. Figure 2 shows the effect of the

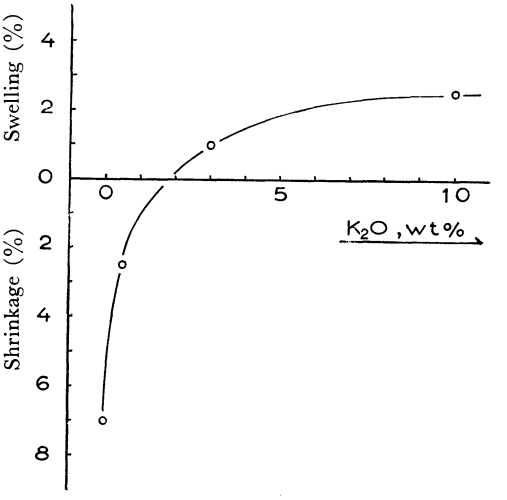

Fig. 2. Shrinkage or swelling of the Catalyst A by calcination in the process of catalyst preparation.

concentration of potassium oxide on the shirnkage or swelling of the Catalyst A tablet in the course of the catalyst preparation. The shrinkage and swelling of the tablet are indicated as changes in the diameter (1.00 cm before calcination). The shrinkage of the tablet without potassium additives is about 7%, whereas a swelling of the tablet is observed when the concentration of potassium oxide reaches above 3%. As is shown in Fig. 3, the

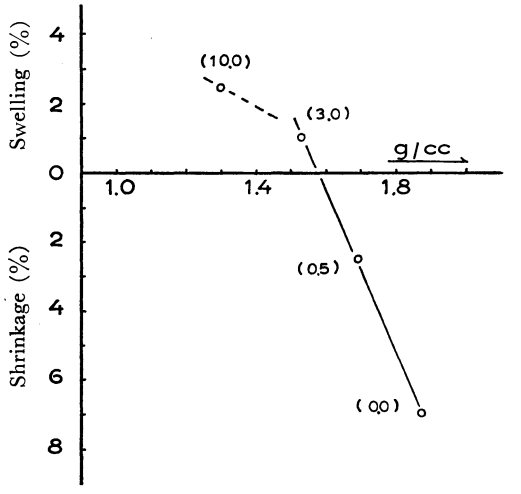

Fig. 3. Relation between apparent bulk density and shrinkage or swelling of the Catalyst A. The numerals in parentheses are the weight percent of potassium oxide.

relation of the shrinkage or swelling to the apparent bulk density is linear except when the concentration of potassium oxide is above 3%. The Table 1 illustrates the specific surface area and the total pore volume of the catalyst with and without a potassium promoter.

Table 1. Surface area and pore volume of the catalyst

	Surface area m^2/g	Pore volume cc/g
Fe_2O_3 uncalcined	28	0.33
Fe_2O_3 calcined	2.5	0.20
Fe_2O_3-K_2O (3 wt%) uncalcined	29	0.33
Fe_2O_3-K_2O (3 wt%) calcined	3.0	0.18

The difference between the specific surface area and the pore volume of the catalyst with and without a potassium promoter is slight. The effect of a potassium promoter in preventing the sintering of the catalyst appears to be caused largely by the formation of $K_2Fe_{22}O_{34}$. The specific gravity of $K_2Fe_{22}O_{34}$ is 4.24,[3,4] whereas that of ferric oxide is 5.13,[5] and it has been reported that $K_2Fe_{22}O_{34}$ is obtained by the calcination of a mixture of ferric oxide and potassium carbonate.[6] X-Ray diffraction diagrams of the iron oxide catalyst with and without potassium additives are shown in Fig. 4. The diagram of iron oxide with potassium additives is essentially the same as that of $K_2Fe_{22}O_{34}$ reported by other workers.[4,7,8] The weight percentage of K_2O in $K_2Fe_{22}O_{34}$ is 5.06; this value is near to the composition where the deviation from the linear relation was observed, as is shown in Fig. 3. The composition of the Catalyst A may be $K_2Fe_{22}O_{34}\cdot nFe_2O_3$ when the content of K_2O is lower than 5.06 wt%; above this concentration the composition may be $K_2Fe_{22}O_{34}\cdot mK_2O$.

Activity Measurements of Catalyst A. To test the stability of the catalyst, the variation of the conversion with the time was tested. After a rapid initial fall of the conversion with the time during the first two hours after ethylbenzene was fed in, the catalyst came to a steady state and the conversion remained constant. The samples used for analyzing the reaction products were withdrawn

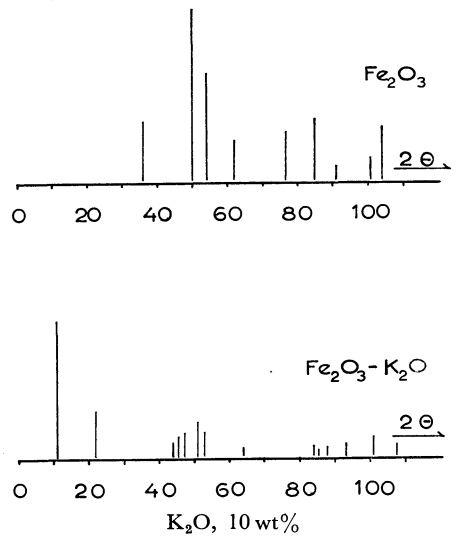

Fig. 4. X-Ray powder diffraction diagrams of iron oxide catalyst with and without potassium promoter. (Radiation: Cr$K\alpha$)

two hours after the start of feeding. Figure 4 shows the temperature dependence of the rate of the dehydrogenation of ethylbenzene using a differential reactor. The reaction rates per unit volume of the catalyst, r, were determined from the $r=(F/V)\cdot X$ relation, where F represents the feed rate of ethylbenzene into the reactor in g-mol per sec, where V represents the volume of the catalyst in ml, and where X represents the fraction of ethylbenzene converted to styrene. The styrene made from the gas-phase reaction in the empty reaction vessel was subtracted from the total conversion. As is shown in Fig. 5, the potassium

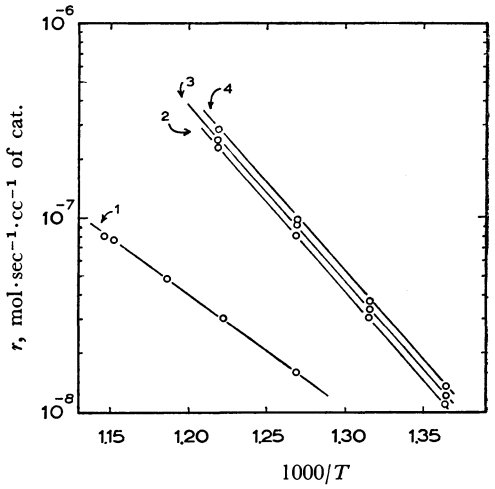

Fig. 5. The effect of temperature on the rate of ethylbenzene dehydrogenation on Catalyst A.
1, Fe_2O_3; 2, Fe_2O_3-K_2O(0.5 wt%);
3, Fe_2O_3-K_2O(3.0 wt%);
4, Fe_2O_3-K_2O(10.0 wt%)

3) V. Cirilli and C. Brisi, *Gazz. Chim. Ital.*, **81**, 50 (1951).
4) Y. Otsubo and K. Yamaguchi, *Nippon Kagaku Zassi (J. Chem. Soc. Japan, Pure Chem. Sect.)*, **82**, 676 (1961).
5) N. A. Lange, "Handbook of Chemistry," Tenth Ed., McGraw-Hill Book Co., New York (1961), p. 251.
6) V. Adelsköld, *Arkiv. Kemi. Min. Geol.*, **12A**, 1 (1938).
7) S. Hilpert and A. Linder, *Z. Phys. Chem.*, **22B**, 395 (1933).
8) E. W. Gorter, *Philips Res. Rep.*, **9**, 259 (1954).

oxide acts as a promoter and is, under given conditions, effective in increasing the activity of the catalyst from four to ten times. The activity of the catalyst is not so sensitive to the potassium oxide concentration in the range from 0.5 to 10.0 wt%, although the rate of dehydrogenation increased slightly with an increase in the concentration of potassium oxide. The apparent energies of activation were obtained from the slopes of the straight lines shown in Fig. 5; they were found to be 28 kcal/mol without potassium additives and 43 kcal/mol with them. Within the limits of experimental error the energy of activation was the same for all the iron oxide catalysts with potassium promoters. The interaction of the potassium promoters with iron oxide is assumed to give an active center which is less reactive than iron oxide without the promoter. The high activity of the potassium-promoted catalyst is caused by a high pre-exponential factor, which compensates for the high activation energy. The increase in the pre-exponential factor can tentatively be explained in terms of the higher concentration of the active center, as the difference between the specific surface area of the catalyst with and without a potassium promoter is slight. It was concluded that the promotion of the iron oxide catalyst by potassium is not only structural but also synergetic in nature. This conclusion was rendered certain by the discovery of the change in the activation energy, since the structural promotion should not alter the temperature coefficient. This conclusion is also supported by the results of the experiments using Catalyst B.

Table 2 shows the distribution of the two by-products, benzene and toluene, together with that of the main product, styrene. These results were measured with an integral reactor.

TABLE 2. DISTRIBUTION OF PRODUCTS
(Reaction temp., 600°C)

Catalyst	Benzene (mol%)	Toluene (mol%)	Styrene (mol%)
Fe_2O_3	2.4	0.55	12.5
Fe_2O_3-K_2O (0.5 wt%)	1.5	2.2	63.9
Fe_2O_3-K_2O (3.0 wt%)	1.1	2.6	65.5
Fe_2O_3-K_2O (10.0 wt%)	1.2	4.3	68.0

As is shown in Table 2, the addition of potassium decreased the catalytic activity of the benzene formation, in spite of the fact that the potassium increased the catalytic activity of the dehydrogenation reaction. Generally, alkylation and dealkylation are catalyzed by an acid. The acidity on iron oxides, if any, must be neutralized by the addition of potassium compounds. Therefore, it is natural to think that the decrease in the activity of benzene formation is mainly due to the neutralization of the acidity of the catalyst by a potassium promoter, rather than to a retardation by the styrene formed.

The formation of toluene increases with an increase in the concentration of potassium oxide. This increase in the activity of toluene formation is partly due to the increased yield of styrene, as the toluene is mainly produced from styrene.

Activity Measurement of Catalyst B. Figure 6 shows the temperature dependence of the rate of the dehydrogenation on Catalyst B. The procedure and the experimental conditions were the same as those of the experiments using Catalyst A. The potassium carbonate-impregnated catalyst showed a drastic change in catalytic performance, displaying sharp increases in the rate of the formation of styrene. The activity of these catalysts was insensitive to the potassium oxide content in the range from 0.5 to 3.0 wt%. The apparent energies of activation were found to be 28 kcal/mol without potassium additives and 46 kcal/mol with them. The high activity of the catalyst with a potassium promoter is caused by a high pre-exponential factor, which compensates for the high activation energy. The increase in the pre-exponential factor is due to the increase in the concentration of the active center which is newly-produced by the interaction of the potassium promoter with iron oxide.

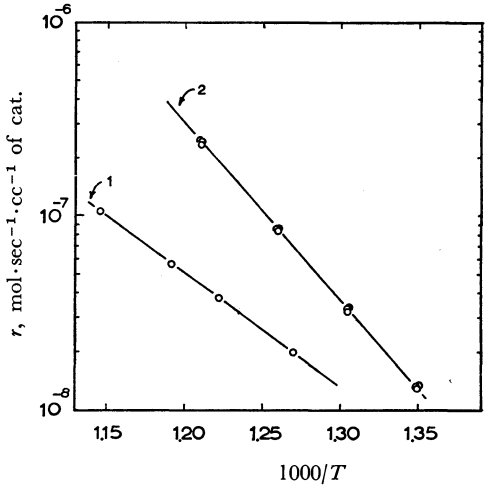

Fig. 6. The effect of temperature on the rate of ethylbenzene dehydrogenation on Catalyst B.
1, Fe_2O_3; 2, Fe_2O_3-K_2O (0.5—3.0 wt%)

As may be seen from the method of preparing Catalyst B, potassium carbonate was impregnated to the calcined iron oxide, and the calcination process was carried out in the absence of potassium carbonate; accordingly, in the case of Catalyst B the effect of the potassium promoter is to enhance the intrinsic activity of the iron oxide catalyst.

BULLETIN OF THE CHEMICAL SOCIETY OF JAPAN VOL. 42 875—880 (1969)

Extraction of Hydrochloric Acid by Tri-*n*-octylamine in Benzene

Takashi KOJIMA, Hiroshi FUKUTOMI and Hidetake KAKIHANA

Research Laboratory of Nuclear Reactor, Tokyo Institute of Technology, Meguro-ku, Tokyo

(Received July 27, 1968)

The equilibria involved in the extraction of HCl by tri-*n*-octylamine (TOA) in benzene have been investigated as a function of the HCl and TOA concentrations. Two distinctly different extractions were observed for two different acidity ranges. From the extraction in the low acidity range (<0.001 M HCl), it has been found that two complexes of TOA·HCl and $(TOA\cdot HCl)_2$ are formed in the organic phase and that the equilibrium constants for the two reactions,

$$TOA(org) + \tfrac{1}{2}H^+(aq) + Cl^-(aq) = TOA\cdot HCl(org)$$

and

$$2TOA(org) + 2H^+(aq) + 2Cl^-(aq) = (TOA\cdot HCl)_2(org),$$

are $K_{11}=(1.51\pm0.02)\times10^4$ and $K_{22}=(2.92\pm0.07)\times10^9$ respectively. For higher concentrations of HCl>3 M, it seems probable that two major complexes of $(TOA\cdot HCl)_2HCl$ and $(TOA\cdot HCl)_3(HCl)_2$ besides the monomer and the dimer, and three minor complexes of $(TOA\cdot HCl)_2(HCl)_2$, $(TOA\cdot HCl)_3HCl$, and $(TOA\cdot HCl)_3(HCl)_3$ are formed in the organic phase.

Since Smith and Page[1] extracted various weak and strong acids with a chloroform solution of methyl-di-octylamine, the extraction of various metal ions from acid solutions by high-molecular-weight amines has been studied and used for various separation processes and analytical techniques. Several reviews[2-4] of this kind of work have been published. On the other hand, although many studies on the extraction mechanism have been reported, in all of these studies except a few,[5-6] the amine salts have been assumed to be monomeric and the possibility of the aggregation of amine salts has been neglected or disregarded.

Since Allen[7] tried to explain the insensitivity of the activity of TOA and di-decylamine sulfates and bisulfates to change in their concentrations by assuming them to form large colloidal aggregates, systematic investigations of the aggregation of several amine salts in the organic phase have been carried out using the methods of light scattering,[8] freezing-point lowering,[9-10] vapor-pressure lowering,[11-12] and two-phase e.m.f. titration.[13] Although it has been found that the amine salts tend to aggregate in an inert solvent with a low dielectric constant, there are still many contradictions in the quantitative treatment of the extraction equilibria.

The main purpose of the work reported here has been to evolve a quantitative description of the extraction equilibria and to find the composition of aggregates of the amine salt in the organic phase. In the present paper, a study of the extraction of HCl from an aqueous solution by TOA in benzene will be reported.

Experimental

Reagents. TOA (supplied by the Kao Saop Co., Tokyo) was purified by vacuum distillation (10 mmHg, and 190—200°C). The other chemicals used were of an analytical grade and were used without further purification. Laboratory-distilled water was used.

Solutions. The TOA solutions were prepared volu-

1) E. L. Smith and J. E. Page, *J. Soc. Chem. Ind. (London)*, **67**, 48 (1948).

2) C. F. Coleman, K. B. Brown, J. G. Moore and K. A. Allen, Paper, No. 510, 2nd United Nations Intern. Conference on the Peaceful Uses of Atomic Energy (1958).

3) F. L. Moore, NAS-NS-3101 (1960).

4) Y. Macus, *Chem. Revs.*, **63**, 139 (1963).

5) P. J. Lloyd and E. A. Mason, *J. Phys. Chem.*, **68**, 3120 (1964).

6) L. Kuca, E. Högfeldt and L. G. Sillen, "Solvent Extraction Chemistry," ed. by D. Dyrseen, J. O. Liljenzin and J. Rydberg, North-Holland Publishing Co., Amsterdam (1967), p. 454; D. Dyrssen and M. De Jesus Tavares, *ibid.*, p. 467.

7) K. A. Allen, *J. Phys. Chem.*, **60**, 239 (1956).

8) K. A. Allen, *ibid.*, **62**, 1119 (1958).

9) V. V. Formin, P. A. Zagorets and A. F. Morgunov, *Zhur. Neorgan Khim.*, **4**, 700 (1959).

10) V. Vdovenko, B. J. Galikin and A. A. Chaikhorskii, *Radiokhmiya*, **3**, 448 (1961).

11) C. D. Strehlow, M. S. Thesis, Dept. of Chem., Massachusetts Institute of Technology (1964).

12) A. S. Kertes, *J. Inorg. Nucl. Chem.*, **27**, 209 (1965).

13) E. Högfeldt, "Ion Exchange," ed. by J. A. Marinsky, Marcel Dekker, New York (1966), p. 153.

metrically from TOA and benzene. Aqueous solutions of hydrochloric acid were prepared by the dilution of 12 M HCl. The ionic strengths of HCl solutions with low concentrations (<TOA concentration) were adjusted with 1 M NaCl in order to keep the mean activity coefficient of HCl in the aqueous phase constant, while no such adjustments were made to solutions with high HCl concentrations (>1 M).

Procedure and Analysis. The TOA solutions were shaken in the extraction tubes with equal volumes of HCl aqueous solutions for 15 min. After centrifuging, suitable aliquots of the aqueous phase and of the organic phase were pipetted out for the determination of HCl concentrations. For the extraction of HCl from a solution of a low acidity, the activities of hydrogen ions in the aqueous phase were measured with a pH meter (Radiometer PHM4c, Copenhagen), the concentrations of HCl extracted into the organic phase were determined from the difference in the HCl concentrations of the aqueous phase before and after the equilibrium. For the extraction of HCl from highly-acidic solutions, the concentrations of HCl in the aqueous phase and in the organic phase were determined titrimetrically by the use of a standard base in an 80% ethanol aqueous solution with a mixed indicator of thymol blue and phenolphthalein. Corrections for the excess HCl extracted by benzene itself were made for the extractions with concentrations higher than 8 M HCl.

The concentrations of TOA solutions were determined titrimetrically by measuring the concentration of HCl which was extracted by shaking with a 1 M HCl aqueous solution. All the experiments were performed in a room with the temperature controlled at 25±1°C.

Results and Discussion

It is convenient to present our results in two parts, since two distinctly different extractions were

TABLE 1. EQUILIBRIUM DATA FOR THE EXTRACTION OF HCl BY TOA IN BENZENE AT 25±1°C AND 1M NaCl (AQ.) IONIC MEDIUM

0.0264 M*		0.0529 M*		0.1064 M*		0.2128 M*	
$-\log(H^+)$	Z	$-\log(H^+)$	Z	$-\log(H^+)$	Z	$-\log(H^+)$	Z
4.936	0.110	4.957	0.110	5.000	0.110	5.063	0.110
4.602	0.221	4.648	0.221	4.688	0.220	4.782	0.220
4.379	0.330	4.425	0.331	4.493	0.330	4.601	0.331
4.197	0.440	4.250	0.441	4.325	0.440	4.440	0.441
4.022	0.549	4.079	0.551	4.158	0.550	4.277	0.551
3.843	0.656	3.900	0.660	3.979	0.660	4.098	0.661
3.633	0.760	3.689	0.768	3.767	0.769	3.885	0.771
3.372	0.859	3.415	0.873	3.480	0.876	3.585	0.880
3.028	0.930	2.942	0.955	2.872	0.967	2.830	0.979
2.717	0.967	2.500	0.989	2.226	0.991	1.948	0.998

* Total concentration of TOA in benzene.

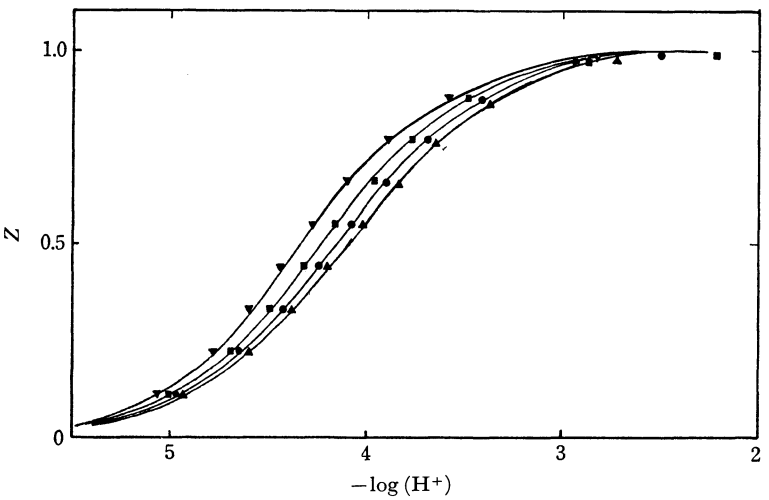

Fig. 1. Z plotted against $-\log(H^+)$ for the extraction of HCl by TOA in benzene from (H, 1 M Na)Cl aqueous solution.
▲ 0.0264 M TOA, ● 0.0529 M TOA, ■ 0.1064 M TOA, ▼ 0.2128 M TOA

observed the two different acidity ranges.

(I) Extraction of HCl the in Low-acidity Range. Since it has been found that the ionic dissociation of amine salts is practically negligible in the low dielectric diluents,[14] a general expression for the extraction of HCl by TOA in benzene can be written by:

$$l\overline{\mathrm{TOA}} + m\mathrm{H}^+ + m\mathrm{Cl}^- = \overline{(\mathrm{TOA})_l(\mathrm{HCl})_m} \quad (1)$$

where the upperlined species are those in the organic phase.

The application of the law of mass action to Eq. (1) gives Eq. (2) on the assumption of ideal behavior in the organic phase:

$$\overline{[(\mathrm{TOA})_l(\mathrm{HCl})_m]} = K_{lm}[\overline{\mathrm{TOA}}]^l(\mathrm{H}^+)^m(\mathrm{Cl}^-)^m \quad (2)$$

where brackets denote the concentration, and parentheses, the activity.

Since the ionic strength in the aqueous phase is adjusted with 1 M NaCl, Eq. (2) is replaced by:

$$\overline{[(\mathrm{TOA})_l(\mathrm{HCl})_m]} = K'_{lm}[\overline{\mathrm{TOA}}]^l(\mathrm{H}^+)^m \quad (3)$$

where:

$$K'_{lm} = K_{lm}(\mathrm{Cl}^-)^m{}_{1\,\mathrm{M\ NaCl}} \quad (4)$$

Using Eq. (3), the following equations can be obtained from the material balance:

$$\overline{[\mathrm{TOA}]}_\mathrm{T} = \overline{[\mathrm{TOA}]} + \sum\sum lK'_{lm}[\overline{\mathrm{TOA}}]^l(\mathrm{H}^+)^m \quad (5)$$

$$\overline{[\mathrm{HCl}]}_\mathrm{T} = \sum\sum mK'_{lm}[\overline{\mathrm{TOA}}]^l(\mathrm{H}^+)^m \quad (6)$$

where $\overline{[\mathrm{TOA}]}_\mathrm{T}$ is the total concentration of TOA and where $\overline{[\mathrm{HCl}]}_\mathrm{T}$ represents that of HCl in the organic phase. Using Eq. (5) and Eq. (6) we can introduce the average number of HCl combined with TOA, Z:

$$Z = \frac{\overline{[\mathrm{HCl}]}_\mathrm{T}}{\overline{[\mathrm{TOA}]}_\mathrm{T}} = \frac{\sum\sum mK'_{lm}[\overline{\mathrm{TOA}}]^{l-1}(\mathrm{H}^+)^m}{1 + \sum\sum lK'_{lm}[\overline{\mathrm{TOA}}]^{l-1}(\mathrm{H}^+)^m} \quad (7)$$

The results of Z and $\log(\mathrm{H}^+)$ for TOA concentrations ranging from 1.25% to 10% by volume are given in Table 1. Plots of Z *vs.* $\log(\mathrm{H}^+)$ are shown in Fig. 1. As may be seen by comparing it with Eq. (7), the disagreement between the plots of Z *vs.* $\log(\mathrm{H}^+)$ for different TOA concentrations indicates that the complexes of $l>1$ are formed.

The concentrations of free amine, $\overline{[\mathrm{TOA}]}$, which can not be determined directly, are obtained as follows. Considering the correlation between Eq. (5) and Eq. (6), the following partial differential equation can be obtained:

$$\left(\frac{\partial \ln b}{\partial \ln a}\right)_B = -\left(\frac{\partial A}{\partial B}\right)_a = -\left\{Z + \left(\frac{\partial Z}{\partial \ln B}\right)_a\right\} \quad (8)$$

where $a=(\mathrm{H}^+)$, $b=\overline{[\mathrm{TOA}]}$, $A=\overline{[\mathrm{HCl}]}_\mathrm{T}$, and $B=\overline{[\mathrm{TOA}]}_\mathrm{T}$.

The integration of Eq. (8) at the B constant gives:

$$\log(b/B) = -\left[\int\left\{Z + \left(\frac{\partial Z}{\partial \ln B}\right)_a\right\}\mathrm{d}\log a\right]_B \quad (9)$$

The values of b determined from graphical integration in Eq. (9), using the values of a, B, and Z in Table 1, were found to be identical with $(B-A)$ regardless of B, as is shown in Fig. 2. This finding leads to the conclusion that the value of $\sum\sum(l-m)K'_{lm}b^la^m$ is equal to zero, *i.e.*, $l=m$.

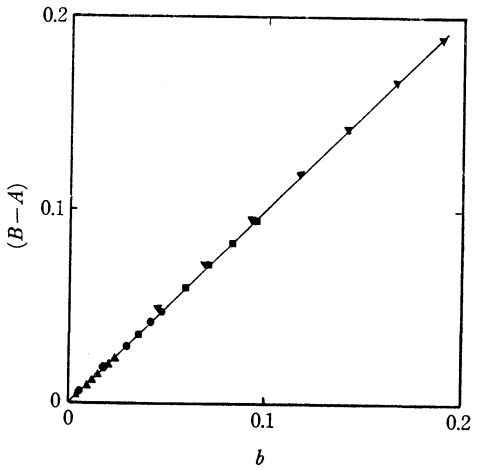

Fig. 2. The comparison between $(B-A)$ and b determined from graphical integration in Eq. (9) using the data in Table 1 where $A=\overline{[\mathrm{HCl}]}_\mathrm{T}$, $B=\overline{[\mathrm{TOA}]}_\mathrm{T}$ and $b=\overline{[\mathrm{TOA}]}$.
▲ 0.0264 M TOA, ● 0.0529 M TOA,
■ 0.1064 M TOA, ▼ 0.2128 M TOA

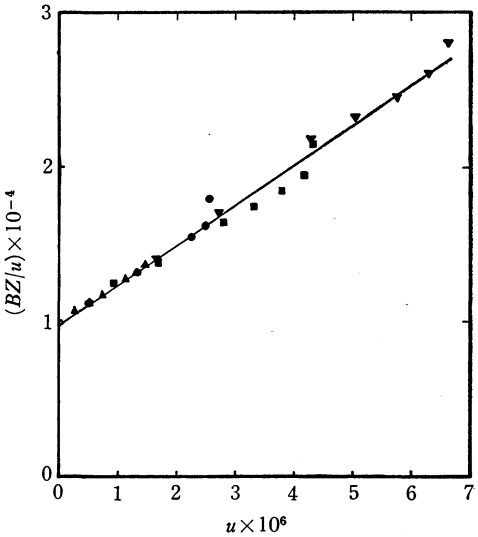

Fig. 3. BZ/u plotted against u for the extraction of HCl by TOA in benzene where $BZ=\overline{[\mathrm{HCl}]}$ and $u=\overline{[\mathrm{TOA}]}(\mathrm{H}^+)$.
▲ 0.0264 M TOA, ● 0.0529 M TOA,
■ 0.1064 M TOA, ▼ 0.2128 M TOA

14) C. Kraus, *J. Phys. Chem.*, **60**, 129 (1956).

Accordingly, Eq. (6) can be rewritten as:

$$A = BZ = \sum lK'_{ll}\, u^l \qquad (10)$$

where $u=ab$ and where $b=(B-A)$. The values of K'_{ll} may be easily determined with the values of BZ and u. The plots of BZ/u *vs.* u give a straight line, as is shown in Fig. 3. This relationship corresponds to the coexistence of two reactions:

$$\overline{\mathrm{TOA}} + \mathrm{H^+} + \mathrm{Cl^-} = \overline{\mathrm{TOA{\cdot}HCl}} \qquad (11)$$

$$2\overline{\mathrm{TOA}} + 2\mathrm{H^+} + 2\mathrm{Cl^-} = (\overline{\mathrm{TOA{\cdot}HCl}})_2 \qquad (12)$$

The values of the equilibrium constants of these reactions have been calculated using the computer program LETAGROP[15] on the data presented in Table 1; the values of $K'_{11}=(9.90\pm0.11)\times10^3$ and $K'_{22}=(1.26\pm0.03)\times10^9$ have also been obtained. By substituting these values into Eq. (4), the values of:

$$K_{11} = (1.51 \pm 0.02) \times 10^4$$

$$K_{22} = (2.92 \pm 0.07) \times 10^9$$

were determined, in which the mean activity coefficient of a 1 M NaCl aqueous solution[16] was used as the activity coefficient of the chloride ion.

The value of $K_{11}=(1.51\pm0.02)\times10^4$ is in good agreement with the corresponding equilibrium constants of $(1.4\pm0.4)\times10^4$ and $(1.3\pm0.3)\times10^4$ when these is no ionic medium and a 2 M LiCl

TABLE 2. EQUILIBRIUM DATA FOR THE EXTRACTION OF HCl BY TOA IN BENZENE AT 25±1°C

0.0527 M*			0.1050 M*			0.2014 M*		
[HCl]	(HCl)	$(Z-1)$	[HCl]	(HCl)	$(Z-1)$	[HCl]	(HCl)	$(Z-1)$
0.97 M	0.64	0.000	1.89 M	3.72	0.000	0.72 M	0.24	0.000
1.98	4.24	0.000	2.82	1.45×10	0.000	1.75	2.97	0.000
2.96	1.79×10	0.002	3.29	2.84	0.005	2.75	1.32×10	0.005
3.89	6.36	0.021	3.79	5.63	0.030	3.78	5.55	0.037
4.87	2.15×10^2	0.070	4.27	1.02×10^2	0.054	4.69	1.72×10^2	0.103
5.90	6.96	0.176	4.75	1.85	0.090	5.49	4.47	0.206
6.82	2.06×10^3	0.336	5.61	5.04	0.186	6.31	1.18×10^3	0.339
7.86	6.81	0.518	6.53	1.46×10^3	0.334	6.67	1.71	0.410
8.72	1.65×10^4	0.650	7.53	4.75	0.492	7.30	3.64	0.495
			7.79	6.31	0.543	7.69	5.68	0.552
			8.60	1.47×10^4	0.655	8.25	1.04×10^4	0.629

* Total concentration of TOA in benzene.

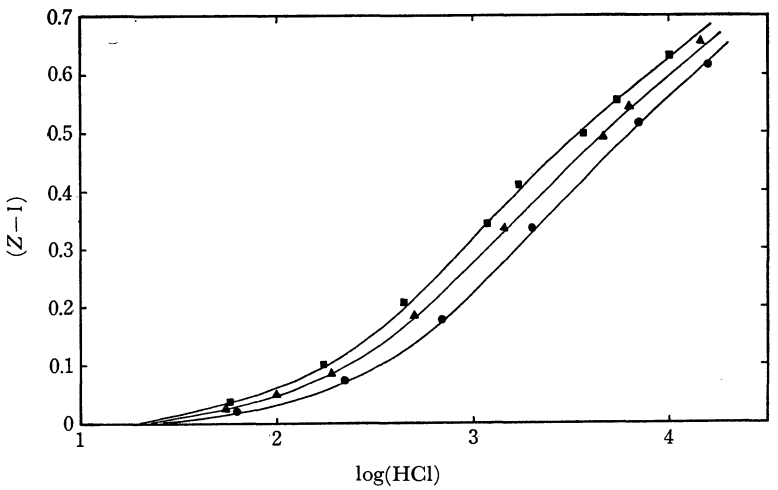

Fig. 4. $(Z-1)$ plotted against log(HCl) for the extraction of HCl by TOA in benzene. ● 0.0527 M TOA, ▲ 0.1050 M TOA, ■ 0.2014 M TOA

15) L. G. Sillén and N. Ingri, *Arkiv Kemi*, **23**, 97 (1964).

16) R. A. Robinson and R. H. Stokes, "Electrolyte Solutions, 2nd ed., Butterworths, London (1959), p. 497.

aqueous solution at 25°C respectively, as reported by Newman and Klotz.[17]

The equilibrium constant, $\bar{\beta}_2$, of the dimer formation expressed by the equation:

$$2\overline{\text{TOA}\cdot\text{HCl}} = \overline{(\text{TOA}\cdot\text{HCl})_2} \qquad (13)$$

was calculated from $\bar{\beta}_2 = K_{22}/K^2_{11}$; the value of $\bar{\beta}_2 = 12.9 \pm 0.5$ was obtained. This value is in close agreement with that of log $\bar{\beta}_2 = 1.1$ (at 25°C) for tri-laurylamine (TLA) chloride in benzene obtained from the measurement of the vapor-pressure lowering by Markovits and Kertes,[18] but it is different from that of $\bar{\beta}_2 = 53$(at 25°C) for TLA chloride in benzene obtained by Scibona *et al.*,[19] using the same method.

(II) Extraction of HCl in the High-acidity Range. As may be seen in the extraction of HCl in the low acidity range, Z values approch unity at $(H^+) \simeq 0.001$ regardless of the TOA concentration, and the relationship of $Z=1$ seems to be satisfied until 3 M HCl. When the concentration of HCl is, however, above 3 M, the Z values increase with the HCl and TOA concentrations; this means that more acid was extracted into amine than corresponds to the 1 : 1 composition. The results are listed in Table 2. The activities of HCl in Table 2 were calculated using the mean activity coefficient.[20] The plots of $(Z-1)$ *vs.* log(HCl) are shown in Fig. 4.

Since the free amine concentrations at high HCl concentrations are supposed to be negligible in view of the values of $K_{11} = (1.51 \pm 0.02) \times 10^4$ and $K_{22} = (2.92 \pm 0.07) \times 10^9$, the expression for the extraction of HCl can be written as:

$$l\overline{\text{TOA}\cdot\text{HCl}} + n\text{HCl} = \overline{(\text{TOA}\cdot\text{HCl})_l(\text{HCl})_n} \qquad (14)$$

Hence, the following equations can be derived from the material balance:

Table 3. The values of [TOA·HCl] determined by graphical integration in Eq. (19) using the data in Table 2

(HCl)	0.0527 M*		0.1050 M*		0.2014 M*	
	$(Z-1)$	$[\overline{\text{TOA}\cdot\text{HCl}}]$	$(Z-1)$	$[\overline{\text{TOA}\cdot\text{HCl}}]$	$(Z-1)$	$[\overline{\text{TOA}\cdot\text{HCl}}]$
1.0×10^2	0.035	0.0289 M	0.052	0.0455 M	0.070	0.0674 M
2.0	0.067	0.0274	0.095	0.0425	0.120	0.0621
3.0	0.095	0.0260	0.130	0.0400	0.160	0.0575
5.0	0.138	0.0238	0.180	0.0358	0.220	0.0510
7.0	0.173	0.0221	0.223	0.0328	0.268	0.0458
1.0×10^3	0.215	0.0201	0.272	0.0291	0.319	0.0404
2.0	0.328	0.0158	0.375	0.0222	0.420	0.0297
3.0	0.390	0.0130	0.435	0.0180	0.475	0.0239
5.0	0.476	0.0101	0.508	0.0137	0.545	0.0179
7.0	0.526	0.0084	0.556	0.0112	0.585	0.0144
1.0×10^4	0.575	0.0067	0.605	0.0089	0.628	0.0114

* Total concentration of TOA in benzene

Table 4. Equilibrium constants for the reaction, $l\overline{\text{TOA}\cdot\text{HCl}} + n\text{HCl} = \overline{(\text{TOA}\cdot\text{HCl})_l(\text{HCl})_n}$ $(t = 25 \pm 1°\text{C})$

Reaction	K_{ln}
$2\overline{\text{TOA}\cdot\text{HCl}} + \text{HCl} = \overline{(\text{TOA}\cdot\text{HCl})_2\text{HCl}}$	$K_{21} = 1.7\times10^{-2}$
$2\overline{\text{TOA}\cdot\text{HCl}} + 2\text{HCl} = \overline{(\text{TOA}\cdot\text{HCl})_2(\text{HCl})_2}$	$K_{22} = 4\times10^{-7}$
$3\overline{\text{TOA}\cdot\text{HCl}} + \text{HCl} = \overline{(\text{TOA}\cdot\text{HCl})_3\text{HCl}}$	$K_{31} = 1.1\times10^{-1}$
$3\overline{\text{TOA}\cdot\text{HCl}} + 2\text{HCl} = \overline{(\text{TOA}\cdot\text{HCl})_3(\text{HCl})_2}$	$K_{32} = 2.2\times10^{-4}$
$3\overline{\text{TOA}\cdot\text{HCl}} + 3\text{HCl} = \overline{(\text{TOA}\cdot\text{HCl})_3(\text{HCl})_3}$	$K_{33} = 5\times10^{-9}$

17) L. Newman and P. Klotz, *J. Phys. Chem.*, **65**, 769 (1961).

18) G. Markovits and A. S. Kertes, "Solvent Extraction Chemistry," ed. by D. Dyrssen, J. O. Liljenzin and J. Rydberg, North-Holland Publishing Co., Amsterdam (1967), p. 390.

19) G. Scibona, S. Basol, P. R. Danesi and F. Orlandini, *J. Inorg. Nucl. Chem.*, **28**, 1441 (1966).

20) R. A. Robinson and R. H. Stokes, "Electrolyte Solutions," 2nd ed., Butterworths, London (1959), p. 504.

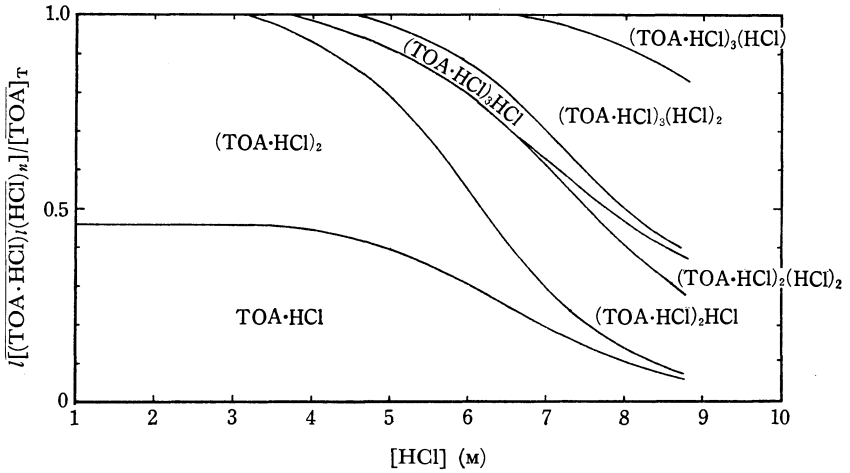

Fig. 5. $l[(\overline{TOA\cdot HCl})_l(\overline{HCl})_n]/[\overline{TOA}]_T$ plotted against [HCl] at $[\overline{TOA}]_T$= 0.1 M. The curves were determined from the material balance using $\bar{\beta}_2$= 12.9 and the values of $\boldsymbol{K}_{ln}$ in Table 4.

$$[\overline{TOA}]_T = [\overline{TOA\cdot HCl}] + 2\bar{\beta}_2[\overline{TOA\cdot HCl}]^2 + \sum\sum l\boldsymbol{K}_{ln}[\overline{TOA\cdot HCl}]^l(HCl)^n \quad (15)$$

$$[\overline{HCl}]_T - [\overline{TOA}]_T = (Z-1)[\overline{TOA}]_T = \sum\sum n\boldsymbol{K}_{ln}[\overline{TOA\cdot HCl}]^l(HCl)^n \quad (16)$$

where $\boldsymbol{K}_{ln}$ is the equilibrium constant of Eq. (14) given by:

$$\boldsymbol{K}_{ln} = \frac{[(\overline{TOA\cdot HCl})_l(\overline{HCl})_n]}{[\overline{TOA\cdot HCl}]^l(HCl)^n} \quad (17)$$

The values of $[\overline{TOA\cdot HCl}]$, which can not be measured directly, are determined as follows. From Eq. (15) and Eq. (16),

$$\left(\frac{\partial \ln b}{\partial \ln a}\right)_B = -\left\{(Z-1) + \left(\frac{\partial(Z-1)}{\partial \ln B}\right)_a\right\} \quad (18)$$

where $a=(HCl)$, $b=[\overline{TOA\cdot HCl}]$, and $B=[\overline{TOA}]_T$.

By integration at the B constant, Eq. (18) becomes:

$$\log(b/b_0) = -\left[\int_{a=a_0}^{a}\left\{(Z-1) + \left(\frac{\partial(Z-1)}{\partial \ln B}\right)_a\right\} d\log a\right]_B \quad (19)$$

where a_0 is the value of a at $Z=1$ and b_0, the value of b at $a=a_0$, which is given by:

$$b_0 = \frac{-1+\sqrt{1+8\bar{\beta}_2 B}}{4\bar{\beta}_2}$$

The values of $b(a,Z-1)_B$ are shown in Table 3; they were determined by graphical integration in Eq. (19) using the data in Table 2. In order to evaluate the values of $\boldsymbol{K}_{ln}$, it is convenient to introduce a new parameter:

$$\boldsymbol{K'}_l = \sum_{n=1}\boldsymbol{K}_{ln}a^n \quad (20)$$

The substitution of Eq. (20) into Eq. (16) yields:

$$A_a = \sum_{l=1} l\boldsymbol{K'}_l b^l \quad (21)$$

where A_a represents the values of $(Z-1)B$ at the a constant.

The method of least squares was used to evaluate the values of $\boldsymbol{K}_{ln}$ fitted to the data in Table 3. Although several combinations of l and n have been tried, the data can be best fitted in with the presence of five species of $(TOA\cdot HCl)_2HCl$, $(TOA\cdot HCl)_2(HCl)_2$, $(TOA\cdot HCl)_3HCl$, $(TOA\cdot HCl)_3(HCl)_2$, and $(TOA\cdot HCl)_3(HCl)_3$. The equilibrium constants for Eq. (14) are given in Table 4. The curves shown in Fig. 3 were determined from the material balance using the values of $\boldsymbol{K}_{ln}$ in Table 4.

As may be seen in Fig. 3, the calculated values of $(Z-1)$ are in good agreement with the experimental values. When the total concentration of TOA and the concentration of HCl in the aqueous phase are given, it should be possible to calculate the concentration of each complex in the organic phase. As an example of the calculation, a graph of $l[(\overline{TOA\cdot HCl})_l(\overline{HCl})_n]/[\overline{TOA}]_T$ against [HCl] at $[\overline{TOA}]_T$=0.1 M is mapped in Fig. 5. From Fig. 5 it may be seen that, besides the monomer and the dimer, the two species of $(TOA\cdot HCl)_2HCl$ and $(TOA\cdot HCl)_3(HCl)_2$ are the major complexes, while the other three species of $(TOA\cdot HCl)_2(HCl)_2$, $(TOA\cdot HCl)_3HCl$ and $(TOA\cdot HCl)_3(HCl)_3$ are the minor complexes.

The authors are deeply grateful to Dr. Erik Högfeldt(Royal Institute of Technology, Stockholm) for performing the LETAGROP calculation and for his stimulating discussions. Thanks are also due to the Kao Soap Co. for its gift of tri-*n*-octylamine.

BULLETIN OF THE CHEMICAL SOCIETY OF JAPAN VOL. 42 881—886 (1969)

The Crystal and Molecular Structure of Bis-(N,N'-π-cyclopentadienyl cobalt)-di-*tert*-butyl Urea, $(\pi\text{-}C_5H_5Co)_2(N\text{-}t\text{-}C_4H_9)_2CO$

Yoshiki MATSUURA,*1 Noritake YASUOKA, Tatzuo UEKI,*2 Nobutami KASAI,*3 and Masao KAKUDO

Department of Applied Chemistry, Faculty of Engineering, Osaka University, Yamada-Kami, Suita, Osaka

(Received July 27, 1968)

The crystals of $(\pi\text{-}C_5H_5Co)_2(N\text{-}t\text{-}C_4H_9)_2CO$ are orthorhombic, and the space group is *Fdd*2, with $a=9.10_1$, $b=17.97_3$, $c=23.61_6$ Å, and $Z=8$. The crystal structure was determined with use of Mo$K\alpha$ counter data, the final R being 0.063 for 578 non-zero reflections. The molecules has a C_2 symmetry, and the carbonyl group lies exactly on the two-fold axis. Unexpectedly, the molecule has the local structure of N,N'-di-*t*-butyl urea, two nitrogen atoms being bridged to two cobalt atoms. The two crystallographically independent Co–N bonds are 1.942 and 1.951 Å, which are equal within the limits cf experimental error. Two cobalt atoms are directly bonded to each other at a distance of 2.371 Å, which is shorter than that of 2.47 Å found in $(CO)_6Co_2(C_2Ph_2)$.

Many polynuclear organometallic compounds which involve metal-metal bonds have been found, and some of them contain nitrogen or sulfur atoms bridging between the metal atoms. The bridge nitrogen or sulfur atoms in these complexes may stabilize the metal-metal bonds.

The $(\pi\text{-}C_5H_5Co)_2(N\text{-}t\text{-}C_4H_9)_2CO$ complex was prepared according to the following reaction[1] (Table 1).

Both complexes, III and IV, are presumed to take trigonal bipyramidal sturctures,[1] having three cobalt atoms in the equatorial plane. Compound II was not identified as N,N'-di-*t*-butyl urea until the structure analysis of the complex I had been completed. According to such recent spectrochemical studies as IR, NMR, and mass spectra, the two structures shown in Fig. 1 have been proposed for the complex I.[1]

To determine the exact structure of this compound involving the feature of coordination around the cobalt atom, the crystal structure analysis of the complex I, $(C_5H_5Co)_2(N\text{-}t\text{-}C_4H_9)_2CO$, was undertaken by means of X-ray diffraction.[2]

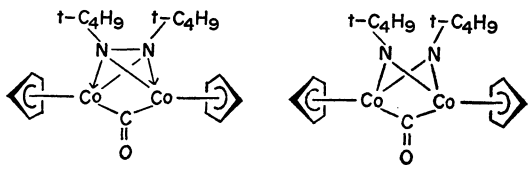

Fig. 1. Two proposed structures for the complex I.

Experimental

The crystal is dark green and has a needle-like shape elongated along the *c* axis. The melting point is 165—168°C, and around this temperature the crystal sublimes appreciably.

The approximate cell dimensions were determined by taking Weissenberg photographs with nickel-filtered Cu$K\alpha$ radiation. The space group was uniquely determined as *Fdd*2 from the following systematic absences

TABLE 1. REACTION BETWEEN $(t\text{-}C_4H_9N)_2S$ AND $\pi\text{-}C_5H_5Co(CO)_2$

				Yield
$(t\text{-}C_4H_9)_2S$		$(\pi\text{-}C_5H_5Co)_2(N\text{-}t\text{-}C_4H_9)_2CO$	(I)	2.1%
+	⟶	+ $(t\text{-}C_4H_9NH)_2CO$	(II)	1.0
		+ $(\pi\text{-}C_5H_5Co)_2S_2$	(III)	22.9
$\pi\text{-}C_5H_5Co(CO)_2$		+ $(\pi\text{-}C_5H_5Co)_3S(CO)$	(IV)	4.7

*1 Present address: Central Research Laboratories, Kurashiki Rayon Co., Ltd., Kurashiki, Okayama.

*2 Present address: Institute for Protein Research, Osaka University, Joancho, Kita-ku, Osaka.

*3 To whom any correspondence should be addressed.

1) S. Otsuka, A. Nakamura and T. Yoshida, *Inorg. Chem.*, **7**, 261 (1968).

2) Y. Matsuura, N. Yasuoka, T. Ueki, N. Kasai, M. Kakudo, S. Otsuka, A. Nakamura and T. Yoshida, *Chem. Commun.*, **1967**, 1122.

of reflections:

hkl; $h + k \neq 2n$, $k + l \neq 2n$;

$0kl$; $k + l \neq 4n$ and

$h0l$; $l + h \neq 4n$

The precise determination of the unit cell dimensions and the collection of the intensity data were carried out by the use of a G. E. XRD-5 diffractometer equipped with a single crystal orienter.*4 Zirconium-filtered Mo$K\alpha$ radiation (λ=0.7107 Å) was used. The crystallographic data of this compound are listed in Table 2.

TABLE 2. CRYSTALLOGRAPHIC DATA OF $(\pi\text{-}C_5H_5Co)_2(N\text{-}t\text{-}C_4H_9)_2CO$

Orthorhombic	$M = 418.1$
$a = 9.10_1$ Å	$Z = 8$
$b = 17.97_3$ Å	$D_m = 1.46$ g·cm^{-3}
$c = 23.61_6$ Å	$D_x = 1.44$ g·cm^{-3}
$V = 3862.9$ Å	Space Group $Fdd2$

Within the limits of $2\theta \leqq 45°$, 641 independent reflections were obtained, but of these 83 were too weak to be measured.

The crystal used had dimensions of 0.10×0.12×0.10 mm. The linear absorption coefficient, μ, was 18.0 cm^{-1}. No correction for absorption was made because of the negligibly small variation in the transmission of X-rays over the observed angular range, while the corrections for Lorentz and polarization factors were made in the usual way.

Structure Determination

As may be seen in Table 2, the unit cell contains eight molecules. Since the general position in the $Fdd2$ space group is sixteen-fold, the whole molecule should possess a C_2 symmetry and the carbonyl group must lie on the two-fold axis.

The position of the cobalt atom was easily found from a three-dimensional Patterson function. A three-dimensional electron density distribution based on the phase of the cobalt atom revealed the positions of all the light atoms other than hydrogen. The positions of these atoms were also confirmed by the minimum function method.

The refinements of the positional and thermal parameters of the 13 non-hydrogen atoms were carried out by means of the least-squares procedure. The first three cycles with isotropic temperature factors for all atoms except hydrogen gave the discrepancy factor of R=0.11 for non-zero reflections. The next three cycles, of a similar refinement, with an anisotropic temperature factor for only the Co atom, gave R=0.083, while five more cycles with anistorpic temperature factors for all the atoms reduced the R to 0.063 (0.093 for all reflections). The quantity minimized was $\sum w(\Delta F)^2$. Throughout the refinement procedure, the following weighting scheme was applied:

$w = 1.0$ for $F_o \geqq 29$, and

$w = 0.2$ for $F_o < 29$ (marked by asterisks in Table 5).

The final atomic coordinates, together with their estimated standard deviations, are listed in Table 3. The thermal parmeters are shown in Table 4,

TABLE 3. ATOMIC COORDINATES AND THEIR STANDARD DEVIATIONS, $\sigma(10^{-3}$ Å)

Atom	x	$\sigma(x)$	y	$\sigma(y)$	z	$\sigma(z)$
Co	0.0852	2	0.0499	2	0.0000	6
N	0.0896	12	−0.0386	11	0.0471	11
C(1)	0.2065	16	−0.0897	16	0.0660	12
C(2)	0.1334	20	−0.1515	17	0.1038	19
C(3)	0.2770	18	−0.1259	18	0.0109	23
C(4)	0.3181	19	−0.0461	21	0.1007	20
C(5)	0.2492	28	0.1301	22	−0.0046	28
C(6)	0.1207	24	0.1581	18	−0.0258	24
C(7)	0.0729	24	0.1140	23	−0.0750	24
C(8)	0.1793	24	0.0580	24	−0.0815	22
C(9)	0.2835	22	0.0720	25	−0.0364	29
C(10)	0.0000	0	0.0000	0	0.0849	24
O	0.0000	0	0.0000	0	0.1348	16

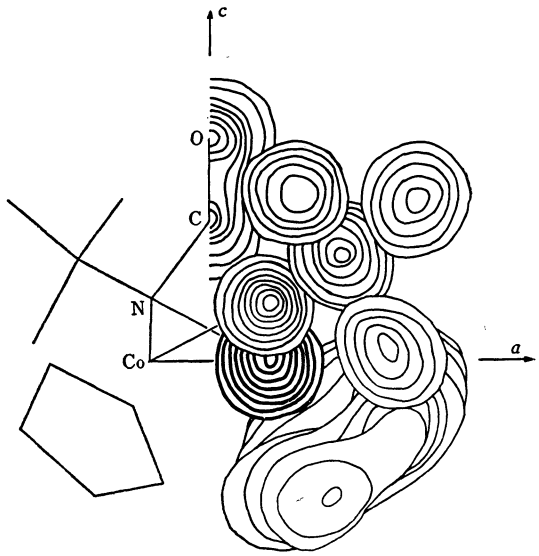

Fig. 2. A composite drawing of the final electron density of a molecule.

while the observed and calculated structure factors are given in Table 5. Figure 2 shows a composite diagram of the three-dimensional electron density distribution viewed along the b axis.

The Patterson function and the minimum function were calculated on a HITAC 5020E computer of the University of Tokyo, with programs written by one of the present authors (N. Y.). The least-squares refinement and other calculations were

*4 The calculations for the goniostat setting were made on a NEAC 2101 computer with a program written by one of the present authors (T. U.).

Table 4. Anisotropic thermal parameters

Parameters are expressed of the form: $\exp\{-(\beta_{11}h^2+\beta_{22}k^2+\beta_{33}l^2+\beta_{12}hk+\beta_{13}hl+\beta_{23}kl)\}$.

Atom	β_{11}	β_{22}	β_{33}	β_{12}	β_{13}	β_{23}	$\bar{B}$*
Co	0.0090	0.0025	0.0020	−0.0003	0.0009	0.0009	3.53
N	0.0092	0.0025	0.0009	0.0020	0.0005	0.0001	2.77
C(1)	0.0116	0.0029	0.0023	0.0045	−0.0016	0.0000	4.27
C(2)	0.0197	0.0030	0.0025	0.0017	0.0023	0.0016	5.36
C(3)	0.0146	0.0042	0.0033	0.0061	0.0036	−0.0007	5.88
C(4)	0.0150	0.0056	0.0028	0.0009	−0.0065	0.0003	6.16
C(5)	0.0376	0.0062	0.0031	−0.0159	0.0069	0.0026	9.13
C(6)	0.0277	0.0028	0.0047	−0.0025	0.0072	0.0051	7.74
C(7)	0.0251	0.0060	0.0034	−0.0060	0.0047	0.0032	7.91
C(8)	0.0250	0.0068	0.0029	−0.0071	0.0072	0.0009	7.82
C(9)	0.0162	0.0078	0.0061	−0.0006	0.0098	0.0053	9.64
C(10)	0.0112	0.0020	0.0021	0.0003	0.0000	0.0000	3.68
O	0.0238	0.0061	0.0012	0.0072	0.0000	0.0000	6.16

* "Equivalent isotropic temperature factor"; obtained by averaging $4\beta_{11}/a^{*2}$, $4\beta_{22}/b^{*2}$, and $4\beta_{33}/c^{*2}$.

carried out on a IBM 7090 computer through the 'UNICON' project and a NEAC 2200 computer of this University with programs written by Dr. Tamaichi Ashida. The atomic scattering factors used in the calculations were taken from those of Hanson and his co-workers.[3]

Results and Discussions

The skeleton of the molecule is shown in Figs. 3 and 4, as viewed along the *b* and *c* axes respectively.

Instead of the previously proposed structure, the complex takes an unexpectedly unique structure. The ligand molecule forms a urea-like structure. The two nitrogen atoms bridge to the two cobalt atoms, and the cobalt atoms are also bonded to each other. These bridge nitrogen atoms are themselves bridged by the carbonyl. Such a urea-like local structure formed in this molecule may be closely related to the formation of *N,N'*-di-*t*-butyl urea during the preparation of this compound; this complex may be regarded as an intermediate in the formation of the above-mentioned urea in the reaction between $(t\text{-}C_4H_9N)_2S$ and $\pi\text{-}C_5H_5Co(CO)_2$ (Table 1). As has been stated before, the whole molecule has a C_2 symmetry, and the carbonyl lies exactly on the two-fold axis. As can be seen in Figs. 3 and 4, there are approximately two verticalmirror planes, perpendicular to each other in the molecule, and the molecule has a quasi-C_{2v} symmetry.

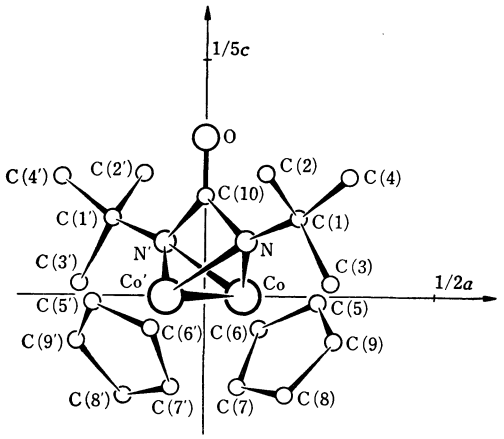

Fig. 3. The molecular structure of $(\pi\text{-}C_5H_5Co)_2\text{-}(N\text{-}t\text{-}C_4H_9)_2CO$.

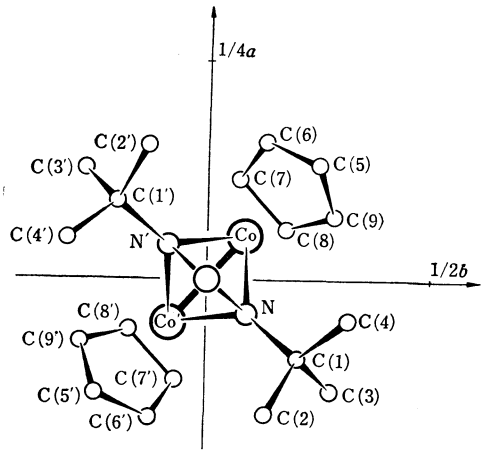

Fig. 4. The skeleton of the molecule; viewed down along the *c* axis.
The molecule has a quasi-C_{2v} symmetry.

The intramolecular bond lengths and angles are summarized in Table 6. In this table, the numbering of atoms is the same as in Figs. 3 and 4.

The Co–Co distance of 2.371 Å is shorter than

3) H. P. Hanson, F. Herman, J. D. Lea and S. Skillman, *Acta Cryst.*, **17**, 1040 (1964).

4) W. G. Sly, *J. Am. Chem. Soc.*, **81**, 18 (1959).

TABLE 5. THE OBSERVED AND CALCULATED STRUCTURE FACTORS ($\times 10$)

L	FO	FC	L	FO	FC	L	FO	FC	L	FO	FC	L	FO	FC	L	FO	FC	L	FO	FC	L	FO	FC
H,K= 0 0			2	515	518	5	63	63	3	192	172	2*	27	20	18	59	64	2*	0	8	4	106	109	14*	28	27
4	402	416	6	131	127	7	116	114	5	86	83	4*	22	28	20*	0	18	4	140	142	6	49	44	H,K=	6	14
8	326	310	10	157	164	9	56	62	7	84	83	6	45	25	H,K=	4	8	6	29	33	8	51	56	8	47	45
12	272	274	14	182	174	11	51	53	9	133	127	8	40	44	0	136	145	8	56	52	10*	28	19	2*	8	13
16	184	178	18	82	91	13	49	59	11	86	93	10*	24	23	2	57	52	10*	0	15	12	57	55	4*	8	28
20	130	127	22	99	99	15	29	31	13	103	97	12*	24	29	4	105	100	12	46	51	14	35	37	6*	8	5
24	90	79	H,K=	2	2	17	54	59	15	56	59	14*	0	20	6	126	130	14*	0	16	16	41	43	8*	8	13
H,K=	2	0	0	127	134	19	65	60	17*	22	32	16*	26	28	8	112	114	16	56	56	18	33	36	H,K=	1	15
2	46	35	2	290	280	21*	27	29	19*	0	21	18*	0	11	10	84	80	18*	0	5	H,K=	4	12	1	56	44
6	94	101	4	132	121	H,K=	7	3	21	40	46	H,K=	8	6	12	86	87	20*	0	36	0	73	71	3	42	44
10	45	48	6	196	183	1	78	81	H,K=	3	5	0	57	57	14	51	56	H,K=	4	10	2	63	60	5	42	35
14	79	80	8	160	153	3	93	76	1	183	175	2	36	39	16	40	44	0	34	30	4	44	44	7*	8	20
18*	23	29	10	157	157	5	70	63	3	73	84	4	73	81	18*	0	32	2	133	132	6	77	78	9*	8	28
22	66	64	12	69	68	7	72	78	5	164	164	6*	0	6	20*	0	32	4	46	46	8*	24	18	11	55	54
H,K=	4	0	14	119	120	9	46	54	7	217	218	8	82	86	H,K=	6	8	6	65	63	10	43	44	13*	8	21
0	129	124	16	55	67	11	47	52	9	200	208	10*	0	22	0	36	37	8*	0	2	12*	25	23	15	55	55
4	124	116	18*	23	30	13	49	51	11	193	189	12	84	71	2	112	113	10	73	71	14*	26	30	H,K=	3	15
8	77	82	20	49	52	15*	0	15	13	129	121	H,K=	1	7	4	33	36	12*	0	17	16*	0	33	1	84	85
12	81	72	22	37	33	17	44	50	15	95	98	1	118	117	6	95	100	14	44	36	H,K=	6	12	3	61	57
16	52	57	24*	27	36	H,K=	9	3	17	93	98	3	177	160	8*	24	18	16*	0	11	0*	0	2	5	80	79
20	35	60	H,K=	4	2	1	32	37	19	75	68	5	134	136	10	63	61	18	47	28	2	124	109	7	85	81
H,K=	6	0	0	155	150	3	66	64	21	37	41	7	158	159	12*	0	5	H,K=	6	10	4*	0	15	9	70	75
2	231	242	2	122	118	5	61	46	H,K=	5	5	9	66	71	14	53	58	0	140	145	6	93	83	11	89	82
6	211	213	4	127	124	7	58	58	1	67	59	11	112	113	16*	0	14	2	30	30	8*	0	7	13	62	53
10	104	99	6	138	137	9	48	44	3	65	56	13	87	89	H,K=	8	8	4	135	137	10	67	58	H,K=	5	15
14	112	106	8	79	80	H,K=	0	4	5	120	112	15	59	72	0	46	55	6*	0	3	12*	0	11	1*	0	27
18	111	104	10	82	82	0	108	93	7	80	73	17	85	85	2	49	50	8	94	97	H,K=	1	13	3	46	38
H,K=	8	0	12	86	89	4	113	104	9	49	37	19*	25	36	4*	26	28	10*	0	5	1	73	82	5	43	33
0	63	57	14	35	48	8	56	64	11	66	68	21*	0	28	6	60	50	12	57	71	3	78	80	7*	8	14
4	49	46	16	78	76	12	39	39	13*	28	27	H,K=	3	7	8	39	37	14*	0	12	5	67	74	9	34	25
8	31	27	18	58	62	16*	0	27	15	58	54	1	82	85	10	52	48	H,K=	8	10	7	54	60	H,K=	8	16
12	38	36	20	32	27	20	55	58	17*	8	10	3	114	123	H,K=	1	9	0*	0	9	9*	0	21	0*	24	19
H,K=	1	1	22	43	35	24*	0	35	19*	0	18	5	152	157	1	153	159	2	33	30	11	42	41	4	35	37
1	337	344	H,K=	6	2	H,K=	2	4	H,K=	7	5	7	225	220	3	165	167	4*	0	10	13	56	60	8	48	52
3	418	416	0	136	140	0	280	267	1	47	41	9	131	125	5	180	181	6*	28	26	15*	26	33	12	47	55
5	120	114	2*	25	19	2	236	226	3	60	62	11	117	121	7	126	135	H,K=	1	11	17	58	62	H,K=	2	16
7	174	173	4	182	189	4	97	120	5	41	45	13	94	93	9	134	132	1	131	136	H,K=	3	13	0	104	99
9	125	121	6*	21	11	6	140	131	7	49	51	15	83	82	11	60	63	3	134	135	1	73	71	2	31	21
11	136	134	8	107	104	8	254	253	9	56	63	17*	0	29	13	88	94	5	139	139	3	75	74	4	79	78
13	135	129	10	49	50	10	44	55	11	48	54	19	48	47	15	72	76	7	111	105	5	72	77	6*	0	7
15	131	129	12	68	69	12	253	244	13	59	54	21	43	34	17	46	54	9	69	69	7	88	85	8	93	91
17	77	73	14*	0	12	14	57	67	15*	0	31	H,K=	5	7	19	63	65	11	62	60	9	58	61	10*	8	11
19	62	68	16	90	87	16	105	98	H,K=	9	5	1	81	75	21	51	52	13	47	53	11	65	57	12	80	78
21	58	58	18*	0	18	18*	0	21	1	64	55	3	84	76	H,K=	3	9	15	61	62	13	52	55	H,K=	4	10
23	67	67	H,K=	8	2	20	73	74	3	67	60	5	68	69	1	68	68	17	44	52	15	47	45	8	32	28
25	44	36	0	63	52	22*	0	28	5	70	63	7	79	77	3	65	54	19	77	66	17*	0	25	2	65	66
H,K=	3	1	2	46	52	24	39	40	7	68	63	9	82	87	5	67	68	H,K=	3	11	H,K=	5	13	4*	8	8
1	146	136	4	50	66	H,K=	4	4	H,K=	0	6	11	55	60	7	61	59	1	42	36	1	83	78	6	88	74
3	61	62	6	31	32	0	39	35	2	148	156	13	30	36	9	75	77	3	55	56	3	54	52	8*	19	18
5	45	40	8	75	77	2	181	198	6	86	82	15	31	45	11*	27	32	5	41	39	5	54	59	H,K=	1	17
7	113	110	10	42	40	4	148	143	10*	25	34	17*	26	33	13*	0	22	7	44	52	7	36	29	1	41	45
9*	28	35	12	57	56	6	208	227	14	70	73	19*	27	30	15	38	32	9*	28	32	9	53	47	3*	0	38
11	40	41	14*	0	18	8	48	54	18	53	50	H,K=	7	7	17*	0	20	11*	0	20	11	33	38	5	45	49
13	68	70	H,K=	1	3	10	143	148	22*	0	14	1	71	79	19*	0	9	13*	0	11	13*	28	35	7	37	42
15*	0	18	1	258	277	12	48	44	H,K=	2	6	3	38	38	21*	0	10	15*	0	16	H,K=	7	13	9	43	47
17	36	45	3	137	119	14	149	139	0	91	91	5	65	69	H,K=	5	9	17*	0	20	1	44	42	11	39	35
19*	24	25	5	337	324	16*	23	38	2	182	186	7	43	48	1	123	130	19*	0	17	3	44	35	H,K=	3	17
21*	0	9	7	106	99	18	81	75	4	71	79	9	70	67	3	92	92	H,K=	5	11	5	49	22	1	46	39
H,K=	5	1	9	145	136	20*	0	31	6	189	188	11	62	58	5	68	68	1	126	125	H,K=	0	14	3	74	68
1	175	180	11	94	101	22	34	37	8	86	80	13	38	37	7	82	88	3	94	91	2	48	51	5	57	54
3	188	189	13	82	90	H,K=	6	4	10	261	262	15	39	40	9	71	78	5	68	68	6	47	54	7	39	45
5	173	176	15	88	90	0	37	26	12	45	57	H,K=	9	7	11	46	50	7	55	62	10*	0	20	9	63	59
7	115	113	17	61	62	2	45	38	14	139	135	1	44	42	13	36	45	9	56	53	14	49	44	H,K=	8	18
9	123	123	19	37	37	4*	21	22	16*	0	21	3	44	38	15*	26	48	11	36	34	H,K=	2	14	2	63	71
11	93	94	21	50	52	6	56	57	18	87	84	H,K=	0	8	17*	0	27	13	65	61	0	32	28	6	61	62
13	45	46	23	46	50	8*	22	10	20*	0	26	0	169	178	H,K=	1	9	15*	27	34	2	110	116	H,K=	2	18
15	41	44	H,K=	3	3	10*	0	19	22	47	46	4	195	195	1	71	65	H,K=	7	11	4	50	44	8	45	51
17	69	73	1	131	130	12*	0	9	H,K=	4	6	8	112	110	3	82	78	1	53	56	6	82	73	2	45	41
19	62	70	3	246	227	14*	0	22	0	101	102	12	121	112	5	54	55	3	49	51	8*	0	12	4	39	31
21	47	57	5	176	168	16*	0	22	2*	23	6	16	89	76	7	74	76	5	57	55	10	109	102	6	59	56
H,K=	7	1	7	38	49	18	38	34	4	212	226	20	86	76	9	42	45	7	33	41	12*	0	10	H,K=	1	19
1	82	81	9	206	199	H,K=	8	4	6	39	39	H,K=	2	8	11	47	47	9	48	43	14	89	75	1	56	49
3	91	92	11	129	135	0*	0	12	8	200	204	0	120	130	13	48	49	H,K=	0	10	16*	0	22	3	52	58
5	90	91	13	132	131	2	71	71	10	54	54	2	116	115	H,K=	0	10	0	153	164	H,K=	4	14			
7	41	41	15	115	105	4	35	23	12	120	118	4	158	166	2	277	289	4	171	177	0	66	58			
9	48	48	17	70	75	6	100	104	14	40	54	6	194	196	6	201	203	8	130	133	2	50	44			
11	47	52	19	30	38	8	37	27	16	95	95	8	133	143	10	187	187	12	108	97	4	102	94			
13	58	54	21	41	43	10	91	94	18*	0	13	10	104	101	14	66	64	16	90	88	6	36	23			
15	63	64	H,K=	5	3	12*	27	6	20	42	43	12	106	112	18	118	115	H,K=	2	12	8	96	85			
17	48	41	1	97	95	H,K=	1	5	H,K=	2	6	14	35	48	H,K=	2	10	0	97	98	10*	0	8			
H,K=	0	2	3	119	116	1*	25	52	0	60	65	16	65	64	0	57	57	2	63	62	12	64	65			

that of 2.47 Å found in $(CO)_6Co_2(C_2Ph_2)$.[4] Such a shortening suggests that the metal-metal bond in this complex may be stabilized by the bridge nitrogens.

All the Co–N bonds, in which two pairs of crystallographically equivalent bonds are included,

(I)

(II)

have the same distances within the limits of experimental error. These four Co–N bonds are in an essentially equal bonding state as a result of the resonance between two canonical structure I and II. The Co–N distances are similar to or somewhat shorter than those found in a number of cobalt-ammine complexes.[5]

The local features of the urea-like part of this compound are listed in Table 7 and compared with those of the urea.

5) Z. Dori, R. Eisenberg and H. B. Gray, *Inorg. Chem.*, **6**, 483 (1967); M. Di Vaira and P. L. Orioli, *ibid.*, **6**, 955 (1967); S. Baggio and L. N. Becka, *Chem. Commun.*, **1967**, 506.

Table 6. Bond distances and angles with their estimated standard deviations, (σ)

Atoms	Distance (Å)	σ (Å)	Atoms	Angle (deg.)	σ (deg.)
Co-Co′	2.371	0.012	N-Co-Co′	52.7	0.4
Co-N	1.942	0.013	N-Co-N′	66.8	0.5
Co-N′	1.951	0.013	N′-Co-Co′	52.3	0.4
N-C(1)	1.474	0.022	Co-N-Co′	75.1	0.5
C(1)-C(2)	1.574	0.027	Co-N-C(1)	134.3	1.0
C(1)-C(3)	1.590	0.029	Co′-N-C(1)	134.2	1.0
C(1)-C(4)	1.521	0.027	Co-N-C(10)	86.9	1.1
N-C(10)	1.394	0.026	Co′-N-C(10)	86.5	1.1
C(10)-O	1.180	0.028	C(1)-N-C(10)	122.5	1.5
Co-C(5)	2.078	0.029	N-C(1)-C(2)	107.8	1.4
Co-C(6)	2.064	0.025	N-C(1)-C(3)	107.3	1.5
Co-C(7)	2.115	0.025	N-C(1)-C(4)	109.0	1.4
Co-C(8)	2.112	0.025	C(2)-C(1)-C(3)	110.2	1.5
Co-C(9)	2.039	0.030	C(3)-C(1)-C(4)	112.5	1.6
C(5)-C(6)	1.369	0.037	C(4)-C(1)-C(2)	109.9	1.5
C(6)-C(7)	1.472	0.034	N-C(10)-N′	100.4	1.6
C(7)-C(8)	1.406	0.034	N-C(10)-O	129.8	2.1
C(8)-C(9)	1.449	0.038	C(5)-C(6)-C(7)	110.0	2.2
C(9)-C(5)	1.323	0.041	C(6)-C(7)-C(8)	105.6	2.1
			C(7)-C(8)-C(9)	104.2	2.2
			C(8)-C(9)-C(5)	113.6	2.6
N···N′	2.142	0.023	C(9)-C(5)-C(6)	106.5	2.5

It seems that the considerably shorter C–O distance, the longer C–N distance, and the smaller NCN angle of this molecule can be interpreted as being mainly due to the strong interaction among the nitrogen and cobalt atoms bound together.

Table 7. The local features of the urea-like part in comparison with urea

	This compound	$(NH_2)_2CO$[6]
C-O	1.18_0	1.26_4 Å
C-N	1.47_4	1.33_6
∠NCN	$100._4$	118.0 deg.

The five carbon atoms of the cyclopentadienyl ring lie almost exactly on a plane; the maximum deviation from the plane being 0.003 Å. The equation of the least-squares plane in terms of rectangular coordinates is:

$$-0.52227X - 0.59808Y + 0.60790Z - 2.64618 = 0,$$

where $X=ax$, $Y=by$, and $Z=cz$.

The carbon atoms in the ring show a marked anisotropy in temperature factors, and these atoms have relatively large "equivalent isotropic temperature factors," as shown in the last column of Table 4. The electron-density distribution of the five carbon atoms of the cyclopentadienyl ring given in Fig. 2 shows a smearing of the electron density along the cyclopentadienyl ring which is similar to that in the ferrocene molecule. From these facts, it may be concluded either that the cyclopentadienyl ring is moving somewhat as a hindered rotator or that there exists an orientational disorder of the rings in the crystal. The

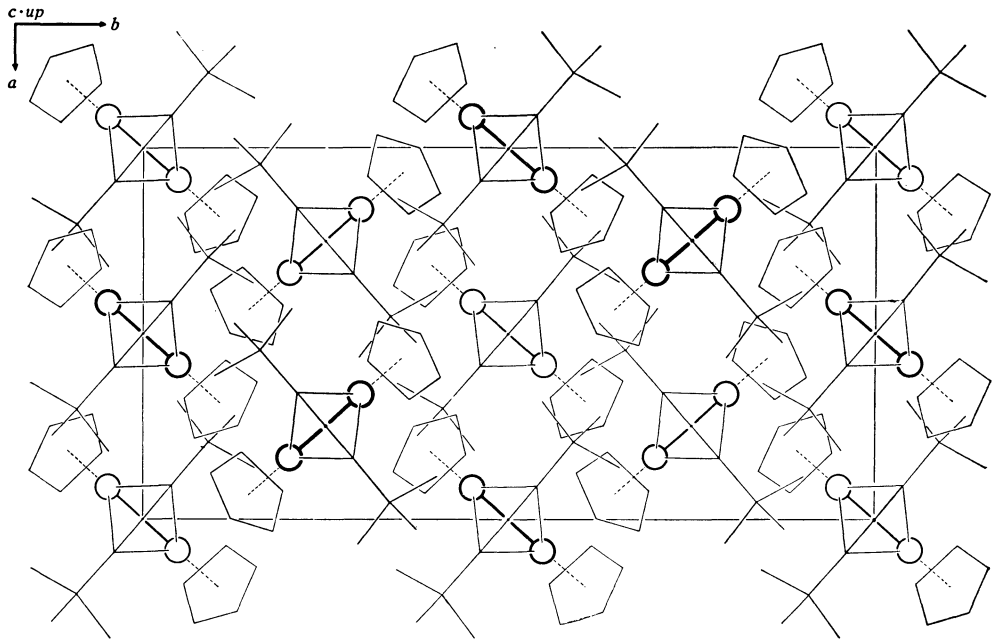

Fig. 5. The crystal structure of $(\pi\text{-}C_5H_5Co)_2(N\text{-}t\text{-}C_4H_9)_2CO$; viewed down along the c axis.

6) N. Sklar, M. E. Senko and B. Post, *Acta Cryst.*, **14**, 716 (1961).

Table 8. Some close intermolecular atomic contacts in the crystal
(those less than 4.0 Å are listed)

	O-C(3^{i})		3.73 Å
	C(4)-C(6^{ii})		3.86 Å
	C(4)-C(7^{ii})		3.72 Å
	O-C(7^{ii})		3.94 Å
	C(2)-C(3^{iii})		3.87 Å
	C(2)-C(8^{iii})		3.70 Å
	O-C(3^{iii})		3.73 Å
Code for superscript:			
i	$0.25-x$,	$0.25+y$,	$0.25+z$;
ii	$0.25+x$,	$0.25-y$,	$0.25+z$;
iii	$-0.25+x$,	$-0.25-y$,	$0.25+z$

plane of each cyclopentadienyl ring is at a distance of 1.704 Å from the cobalt atom.

Figure 5 shows the crystal structure viewed down the c axis. There are seven rather short intermolecular atomic contacts of less than 4.0 Å, the shortest one is 3.70 Å between C(2) and C(8^{iii}) (Table 8). All the other intermolecular distances are far longer than the sum of the van der Waals radii. The sublimation of this crystal around the melting point may be explained by this loose packing of the molecules.

The authors are very grateful to Professor Sei Otsuka and his co-workers of this University who gave them precious specimens.

BULLETIN OF THE CHEMICAL SOCIETY OF JAPAN VOL. 42 886—889 (1969)

K-Band Electron Paramagnetic Resonance of Sulfur Monoxide in the Gaseous Phase

Hiromichi UEHARA

Sagami Chemical Research Center, Sagamihara-shi, Kanagawa

(Received August 2, 1968)

Four K-band electron paramagnetic resonance transitions of $^3\Sigma^-$ $^{32}S^{16}O$ in the gas phase have been observed. One of these occurs between the Zeeman levels of the $K=1$, $J=0\rightarrow K=0$, $J=1$ states and three between the Zeeman levels of the $K=2$, $J=2\rightarrow K=3$, $J=2$ states. The analysis of the spectra has led to the g values of g_s^e, g_l^e, and g_r (in accordance with the notation by Tinkham and Strandberg). Knowledge of the rotational magnetic moment gave the equilibrium internuclear distance of $R_e=1.48101\pm0.00006$ Å.

Two electric dipole EPR transitions of $^3\Sigma^-$ $^{32}S^{16}O$ in the gas phase were first detected by McDonald.[1] Subsequently, another two transitions were observed by Daniels and Dorain[2] and another one by Carrington, Levy and Miller.[3] These five lines occur between levels characterized by $K=1$ and $J=1$ and by $K=2$ and $J=1$, and are observable by using a conventional X-band spectrometer. Several other transitions are expected to be detected at the K-band frequencies. In the present study, four K-band transitions of $^3\Sigma^-$ $^{32}S^{16}O$ were observed among the Zeeman levels of $K=1$, $J=0\rightarrow K=0$, $J=1$ and $K=2$, $J=2\rightarrow K=3$, $J=2$.

Recently, detailed analyses of the X-band spectrum were carried out by Daniels and Dorain[4] and by Carrington, Levy, and Miller[5] using the theory of the oxygen molecule presented by Tinkham and Strandberg.[6,7] Since the sign of the g value of the rotational magnetic moment, g_r, is different between their results, it would be desirable to analyze the K-band spectra independently of the X-band lines, in order thus to determine the sign of g_r. In this study, the g values of the electron spin, the orbital, and the rotational magnetic moments were determined by means of the K-band data. The rotational magnetic moment gave the equilibrium

1) C. C. McDonald, *J. Chem. Phys.*, **39**, 2587 (1963).

2) J. M. Daniels and P. B. Dorain, *ibid.*, **40**, 1160 (1964).

3) A. Carrington, D. H. Levy and T. A. Miller, *Proc. Roy. Soc. (London)*, **A293**, 108 (1966).

4) J. M. Daniels and P. B. Dorain, *J. Chem. Phys.*, **45**, 26 (1966).

5) A. Carrington, D. H. Levy and T. A. Miller, *Proc. Roy. Soc. (London)*, **A298**, 340 (1967).

6) M. Tinkham and M. W. P. Strandberg, *Phys. Rev.*, **97**, 937 (1955). This is referred to as TS I.

7) M. Tinkham and M. W. P. Strandberg, *ibid.*, **97**, 951 (1955). This is referred to as TS II.

internuclear distance, R_e, by the use of the equilibrium *interatomic* distance, r_e, obtained by Amano, Hirota and Morino.[8]

Experimental

A modified Japan Electron Optics Laboratory ESR spectrometer with a 100 kHz field modulation was used in conjunction with a 12-in electromagnet yielding a maximum field of 10000 G. The K-band experiments were performed with a cylindrical TE_{012}-mode detection cavity, the parallel endplates of which were replaced by some with 8 mm-i.d. holes and with collars to prevent any leakage of the cavity radiation. A cavity with a 7.5-mm-o.d. quartz flow tube inserted was adjusted to resonate at 24.9 GHz. The magnetic field was measured with a Hewlett-Packard 5245 L electronic counter by counting the proton magnetic resonance frequency of the water contained in a probe just outside the detection cavity. The field measurements were corrected for the small field differential that existed between the cavity center and the position of the magnetometer probe. The microwave frequencies were determined with reference to the transition frequencies of the atomic hydrogen observed simultaneously with those of SO. The required g factor was taken from the work of Beringer and Heald.[9] A trace amount of hydrogen was added to the oxygen upstream of a microwave discharge cavity in order to generate the atomic hydrogen.

Sulfur monoxide was produced by mixing the product of a microwave discharge in the oxygen gas with carbonyl sulfide at a point just upstream from the detection cavity and was pumped through a quartz flow tube whose inner diameter was 6.5 mm into a K-band spectrometer detection cavity. The gaseous flow through the tube was maintained by means of a Tokuda 500-*l*/min mechanical pump. A waveguide-type discharge cavity was placed 20 cm upstream from the detection cavity and was powered by a Toshiba 2M89 magnetron operated at a frequency of 2450 MHz.

The observation of the SO lines in the K-band region was difficult compared with that in the X-band region. This difficulty was mainly caused by the restriction on the maximum flow rate because of the small size of the flow tube through the K-band cavity. Moreover, the adhesions of sulfur and sulfuric acid inside the flow tube decreased the spectrometer sensitivity and shifted the resonant frequencies, though the sulfur coating was slight at a low partial pressure of carbonyl sulfide. In this study, the partial pressure of carbonyl sulfide was about 3×10^{-2} mmHg, and that of oxygen was about 2×10^{-1} mmHg. Sulfuric acid was formed because of the grease used. By the use of Dow-Corning silicone grease, the sulfuric acid became scarcely discernible. The flow tube was washed with detergent before each measurement. This procedure was indispensable to avoid large noises caused by the free electrons introduced into the spectrometer cavity.

Description and Analysis of the Spectra

Four transitions, $K,J,M=1,0,0\rightarrow0,1,-1$, $2,2,1\rightarrow3,2,2$, $2,2,2\rightarrow3,2,1$, and $2,2,2\rightarrow3,2,2$, were observed in the K-band region. These transitions are shown in Fig. 1. The position of each line was determined as follows: immediately after a transition of SO was measured, a transition of the atomic hydrogen and again the same transition of SO were successively recorded. The frequencies thus determined are listed in Table 1. The experimental uncertainty in the magnetic field is the difference between the two measurements of the field value of a transition of SO plus the error for

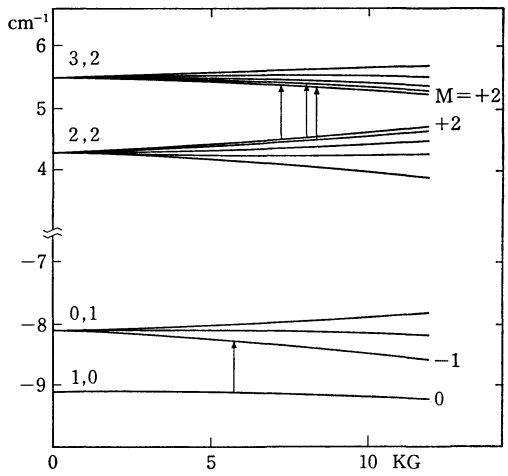

Fig. 1. An energy-level diagram of the magnetic-field splitting of the $K,J=1,0$; $0,1$; $2,2$ and $3,2$ levels of $^{32}S^{16}O$. The observed transitions are indicated.

Table 1. $^3\Sigma^-$ $^{32}S^{16}O$ spectra in the K-band region

K,J,M	H(obs)	ν(obs)	ν(calcd)[a]
$1,0,0\rightarrow0,1,-1$	5743.4±0.4	24932.1±0.3	24931.9
$2,2,2\rightarrow3,2,2$	7240.8±0.2	24906.2±0.3	24906.3
$2,2,2\rightarrow3,2,1$	8026.2±0.2	24901.9±0.3	24901.7
$2,2,1\rightarrow3,2,2$	8333.1±0.2 G	24908.8±0.3 MHz	24908.7 MHz

a) Frequencies were calculated by using $g_s^e=2.00199$, $g_l^e=0.00364$, and $g_r=0.00011$.

8) T. Amano, E. Hirota and Y. Morino, *J. Phys. Soc. Japan*, **22**, 399 (1967).

9) R. Beringer and M. A. Heald, *Phys. Rev.*, **95**, 1474 (1954).

reading the position of a peak. The designated uncertainty in the microwave frequency is based on an estimated error in measuring the position of a peak of atomic hydrogen. Under optimum conditions the strongest band of the 1,0,0→0,1,−1 transition was observed at a 1-sec time constant with a signal-to-noise ratio of 100. The microwave frequency used was 24.9 GHz. The slight difference in microwave frequency for each measurement was due to the slight difference in the position of the quartz-flow tube inserted in the spectrometer cavity. The 2,2,1→3,2,1 and 2,2,1→3,2,0 transitions could not be detected.

The observed spectra were analysed according to the thory of molecular oxygen proposed by Tinkham and Strandberg.[6,7] Recently, Kayama and Baird[10] have shown that several modifications of the theory proposed by Tinkham *et al.* are indispensable. Therefore, we follow the formulation by Tinkham and Strandberg so as not to conflict with the theory of Kayama and Baird. The modifications given by Kayama and Baird will be discussed later. The effective Hamiltonian for $^3\Sigma^-$ molecules were derived[6,7] as:

$$\begin{aligned}\mathscr{H} &= P_R^2/2M + \frac{1}{2}M\omega_e^2R_e^2\xi^2 + b\xi^3 \\ &+ B\mathfrak{R}^2 + \frac{2}{3}\lambda(3S_z^2 - \boldsymbol{S}^2) + \mu\mathfrak{R}\cdot\boldsymbol{S} \\ &+ (g_s^e - g_r)\beta HS_z + g_l^e\beta H\sum_{g=x,y}\phi_{zg}S_g \\ &+ g_r\beta HM, \end{aligned} \tag{1}$$

where:

$$B = B_N - B'',\ \lambda = \lambda' + \lambda''\ \text{and}\ \mu = \mu' + \mu''.$$

Since the Hamiltonian (1) is integrated over the electron coordinates, the ξ dependence of the parameter λ as well as B must be taken into account:

$$B = B_e(1 - 2\xi + 3\xi^2),\quad \lambda = \lambda_e + \lambda_{(1)}\xi + \lambda_{(2)}\xi^2. \tag{2}$$

No similar expansion for the parameter, μ, was found to be necessary for this experiment. The meanings of the various notations used above are the same as those given by Tinkham and Strandberg, except that the gyromagnetic ratios, g_s^e, g_l^e, and g_r, are opposite in sign.

The analysis was carried out by setting up a secular equation of $\mathscr{H}$ with respect to Hund's Case b wavefunctions. The matrix elements off-diagonal in the vibrational quantum number, v, were eliminated by the Van Vleck transformation. This procedure shows that large vibration-dependent terms can be taken out by defining the v-dependent constants, λ_v and B_v, as in the (3) equations:

$$\left.\begin{aligned} B_v &= B_e[1 + (2v+1)(3\varepsilon + 12b\varepsilon^3B^{-1})], \\ \lambda_v &= \lambda_e - 6(2v+1)b\varepsilon^3B^{-1}\lambda_{(1)}, \end{aligned}\right\} \tag{3}$$

although higher-order centrifugal distortion terms cannot be eliminated in this way.

The matrix elements in Hund's Case b representation have been given in Eqs. (52) and (60) of TS I and Eq. (24) in TS II. The elements with $\Delta K = \pm 2$ and $\Delta J = 0, \pm 1$, which are introduced by the term $g_l^e\,\beta H\sum_{g=x,y}\phi_{zg}S_g$ and which are not listed in TS II, are given in the $(K', J', M|\mathscr{H}_{ml}|K, J, M)$ form as:

$$\left.\begin{aligned} &(J-1,J,M|\mathscr{H}_{ml}|J+1,J,M) = \\ &\quad -g_l^e\beta HM/\{(2J+1)[J(J+1)]^{1/2}\} \\ &(J-2,J-1,M|\mathscr{H}_{ml}|J,J,M) = \\ &\quad -g_l^e\beta H[(J^2-1)(J^2-M^2)]^{1/2}/ \\ &\quad \{(2J-1)[J(2J+1)]^{1/2}\}, \\ &(J-1,J-1,M|\mathscr{H}_{ml}|J+1,J,M) = \\ &\quad -g_l^e\beta H[(J^2-1)(J^2-M^2)]^{1/2}/ \\ &\quad \{(2J+1)[J(2J-1)]^{1/2}\} \end{aligned}\right\} \tag{4}$$

where:

$$\mathscr{H}_{ml} = g_l^e\beta H\sum_{g=x,y}\phi_{zg}S_g. \tag{5}$$

The required 19-dimensional matrix for a given value of M was diagonalyzed by using an IBM 7090 computer. The values of field-free parameters used in this study were: $B_{v=0}=21523.6$, $\lambda_{v=0}=158256$, $\mu_{v=0}=-168.5$, and $\lambda_{(1)}=2.1\times10^5$, in units of megahertz. They were obtained by Amano, Hirota, and Morino[8] by analyzing the microwave spectra of $^{32}S^{16}O$.

The computation was made point by point for various values of the field H and of the g values, g_s^e, g_l^e, and g_r. The most probable g values obtained by fitting the K-band $^{32}S^{16}O$ resonances are given in Table 2. The quoted errors reflect the experimental uncertainties both in the magnetic field and in the microwave frequency. The experimental and calculated EPR results are shown in Table 1.

Discussion

It may be seen from Table 1 that the observed EPR transitions in the K-band region can be explained by the theory of Tinkham and Strandberg. Table 2 indicates that the g values, g_s^e, g_l^e, and g_r, obtained in the present study are almost in agreement with those given by Daniels and Dorain. The negative sign of g_r proposed by Carrington, Levy, and Miller[5] does not describe the observed K-band spectra.

All this while the theory of Tinkham and Strandberg was followed. As has been mentioned above, Kayama and Baird pointed out that the contribution of $^1\Sigma_g^+$ to the $^3\Sigma_g^-$ ground state of O_2 cannot be ignored. They re-examined the theory of Tinkham *et al.* by the use of the "true microscopic" spin-orbit interaction Hamiltonian and modified the results given in TS I and II. Their results

10) K. Kayama and J. C. Baird, *J. Chem. Phys.*, **46**, 2604 (1967).

TABLE 2. g VALUES OF SO

g Value	Present study	Daniels and Dorain[4]	Carrington, Levy and Miller[5,a]
g_s^e	2.00199 ± 0.00010	2.00197 ± 0.0001	2.0023
g_l^e	0.00364 ± 0.00020	0.00371 ± 0.0005	0.0040 ± 0.0003
g_r	0.00011 ± 0.00007	0.00019 ± 0.0002	-0.00020 ± 0.00020

a) g Values listed here are all opposite in sign to those of Carrington, Levy and Miller.[5]

revealed that, first, the value of λ'' should be given by the sum of λ''_{Π} and λ''_r, where λ''_{Π} is the contribution to λ'' from the $^3\Pi_g$ symmetry state and λ''_r from the $^{2S+}\Pi^1{}_g$ ($S=0$, 2) and $^{2S+1}\sum_g^+$ ($S=0$, 1, 2) states, and, second, as a result of the mixing of the $^1\sum_g^+$ state with the $^3\sum_g^-$ ground state, the λ_v, μ, and g_l^e parameters in Eqs. (1) and (3) should be interpreted as $\tilde{\lambda}_v$, $\tilde{\mu}$, and $\tilde{g}_l^e$, which depend on the state-mixing as expressed by:

$$\left.\begin{aligned}\tilde{\mu} &= \mu + 2\alpha\left(B_v - \frac{1}{2}\mu\right),\\ \tilde{\lambda}_v &= \lambda_v - \frac{2}{3}\alpha(2\lambda_v + \zeta_v) + \alpha\left(B_v - \frac{3}{2}\mu\right)\\ \tilde{g}_l^e &= g_l^e - \alpha g_s^e,\end{aligned}\right\} \quad (6)$$

where 2α represents the $^1\sum_g^+$ character in the ground state and ζ, the contribution to λ'' from the $^1\sum_g^+$ state.

In the case of sulfur monoxide, there is no g or u symmetry, and the physical interpretation of the parameters introduced by Kayama and Baird must be different from that for the oxygen molecule. Nevertheless, the (6) equations seem valid phenomenologically and we shall not discuss this difference any further. In these circumstances, such physical interpretations of the λ and μ paramters as those given by Daniels and Dorain seem meaningless unless the correct estimates of ζ and μ' or α are made. It is more proper to express the molecular constants, μ' and μ'' in the following form, including α as a parameter:

$$\left.\begin{aligned}\mu' &= -0.0004 + 1.4\alpha \pm 0.0003\\ \mu'' &= -0.0052 - 2.9\alpha \pm 0.0003\ \mathrm{cm^{-1}}.\end{aligned}\right\} \quad (7)$$

Kayama and Baird[10] estimated the 2α value of oxygen to be $(3.0—4.0)\times10^{-4}$. The 2α value for sulfur monoxide should be of the same order of magnitude as that for oxygen. Therefore, the second-order contrubution, $-2Bg_l^e$, constitutes the main part of μ. In fact, the fact that the value, $-2Bg_l^e=-0.0052\pm0.0003\ \mathrm{cm^{-1}}$, determined from the electron resonance is almost equal to the value of $\mu=-0.0056\ \mathrm{cm^{-1}}$ determined through microwave spectroscopy provides a welcome check on the consistency of the electron resonance and the microwave spectra, as was pointed out by Carrington, Levy, and Miller.[5]

The contribution of the electronic mass to the rotational constant is:

$$B'' = B(g_r - g_r^n) = 0.00027 \pm 0.00005\ \mathrm{cm^{-1}}. \quad (8)$$

This leads to the value of $0.721087\pm0.000055\ \mathrm{cm^{-1}}$ of B_{Ne}, the rotational constant of the bare nuclei, when the B_e value of $0.720817\pm0.000005\ \mathrm{cm^{-1}}$ obtained by Amano, Hirota, and Morino is used. The B'' value of $0.00027\ \mathrm{cm^{-1}}$ is a correction of 370 ppm (parts per million). The usual procedure of using atomic rather than nuclear masses reduces this correction 270 ppm, leaving 100 ppm. The equilibrium internuclear distance, R_e, was estimated to be 1.48101 ± 0.00006 Å by using the nuclear masses and the latest values of the universal constants. The difference of 0.00007 Å between r_e and R_e is somewhat larger than the experimental errors. Carrignton, Levy, and Miller[5] concluded that the internuclear distance R_e coincided with the interatomic distance r_e within the limits of experimental error. The contradiction between the two experiments occurs mainly from the different signs of the values obtained for g_r. Most molecules will have $g_r>0$ because the electronic contribution slightly outweighs that of the bare nuclei.[11] A sizable correction of the electronic contribution must be made for the rotational constant, B_e, in order to determine the internuclear distances to the full accuracy of the data. The correction of +370 ppm for B_e in the sulfur monoxide in the present study is of reasonable order of magnitude compared with the correction of +400 ppm in the oxygen molecule.[6]

The author wishes to express his gratitude to Professor Yonezo Morino for his encouragement throughout this work. His thanks are also due to Dr. K. Kayama for helpful suggestions on improving the experimental accuracy.

11) M. Tinkham, "Group Theory and Quantum Mechanics," McGraw-Hill Book Company, Inc., New York (1964), p. 263.

BULLETIN OF THE CHEMICAL SOCIETY OF JAPAN VOL. 42 890—893 (1969)

Basicity of Dimethyl Sulfoxide in an Aqueous Solution as Measured by the Spectrophotometric Indicator Method

Goro WADA

Department of Chemistry, Nara Women's University, Nara

(Received August 10, 1968)

The basic nature of dimethyl sulfoxide (DMSO) has been known in water, and so has its pK_a value, which varies somewhat according to the measuring methods. In the present work, a spectrophotometric method employing thymol blue and *o*-nitroaniline as indicators was applied; the thermodynamical pK_a° value of DMSO was determined to be -1.04 at 25°C. Since there is no dependence of pK_a° upon the temperature, the proton transfer from water to DMSO in water is likely to be athermal.

The nature of dimethyl sulfoxide (DMSO) as a solvent for acid-base equilibria and for other chemical reactions has been well investigated, and the results have been well collected.[1,2] On the other hand, the quantitative basic strength of DMSO as a base itself in an aqueous solution was first found by potentiometric titration by Nylén[3] in 1941, who established that the pK_a° value of DMSO at 20°C was zero, where pK_a° was defined as the thermodynamical dissociation constant of the SH^+ acid, the protonated form of DMSO. Recently, Streuli[4] and Andersen *et al.*[5] determined the pK_a° value to be 1.0 and 0.911 respectively, by similar potentiometric titrations using perchloric acid as the titrant and acetic anhydride as the solvent. More recently, by measuring the chemical shifts of the methyl groups of DMSO as a function of the sulfuric acid concentration, Haake and Cook[6] determined the basicity of DMSO to be -2.7; this value shows a lower basicity than the values previously obtained.

The pK_a° values observed are thus widely scattered between -2.7 and $+1$. The present work was undertaken to estimate it by a method different from those previously adopted. A spectrophotometric method employing two acid-base indicators, thymol blue and *o*-nitroaniline, was applied; it gave -1.04 as pK_a° value, a value which lies nearly at the center between the two extreme values previously determined.

1) I. M. Kolthoff and T. B. Reddy, *Inorg. Chem.*, **1**, 189 (1962).

2) Von D. Martin, A. Weise and H.-J. Nicolas, *Angew. Chem.*, **79**, 340 (1967).

3) P. Nylén, *Z. anorg. u. allgem. Chem.*, **246**, 227 (1941).

4) C. A. Streuli, *Anal. Chem.*, **30**, 997 (1958).

5) K. K. Andersen, W. H. Edmonds, J. B. Biasotti and R. A. Strecker, *J. Org. Chem.*, **31**, 2859 (1966).

6) P. Haake and R. D. Cook, *Tetrahedron Letters*, **1968**, 27.

Experimental

Commercial DMSO was distilled twice under reduced pressure of oxygen-free nitrogen.[7] Anhydrous sodium perchlorate was prepared by recrystalizing a crude wet source from water and drying it to an anhydrous state at a temperature not higher than 300°C. The ionic strength of the solutions presently being investigated, μ, was controlled with this salt. The perchloric acid, thymol blue, and *o*-nitroaniline were used without further purification.

For the measurements of the optical densities of solutions, a Beckman spectrophotometer, Model DU, was used with a thermostated cell compartment and quartz cells with light paths of 1 cm and 10 cm.

Results with Thymol Blue

Ionization Constant and Molar Extinction Coefficients of Thymol Blue. The spectra of thymol blue (thymolsulfonephthalein) at various hydrogen ion concentrations in aqueous solutions are shown in Fig. 1. The figure indicates that the absorption peak at 544 mμ is due to the acid form of the indicator (represented by HIn), while the two absorption peaks at 433 and 335 mμ are due to the base form of the indicator (In^-). Another absorption of the acid form appearing with a peak at 395 mμ (shown by a broken line in Fig. 1) overlaps with the bottom part between the two absorption bands of the base form. Isosbestic points occur at 486 mμ and somewhere between 375 and 390 mμ.

Since the observed absorbance at 540 mμ can be approximately attributed only to the acid form of thymol blue, the molar extinction coefficient of

7) J. Menashi, W. L. Reynolds and G. Van Auken, *Inorg. Chem.*, **4**, 299 (1965).

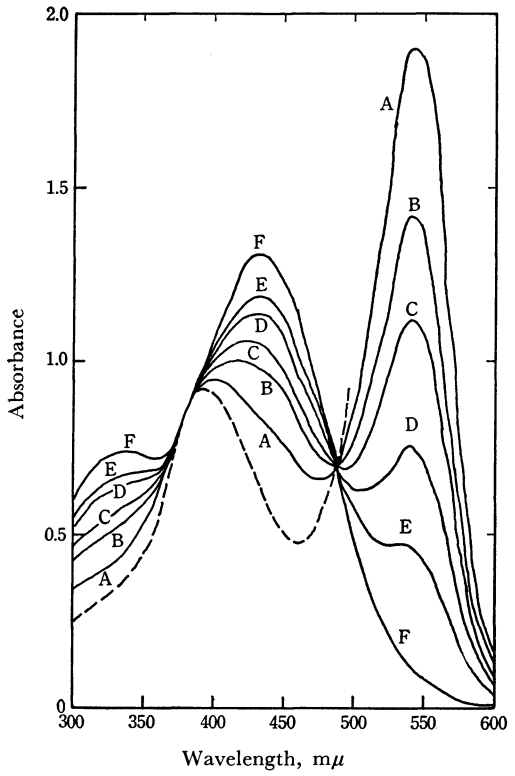

Fig. 1. Absorption spectra of thymol blue at various hydrogen ion concentrations, $[HIn]_0 = 1\times10^{-4}$ M.
A : $[H^+]=0.040$ M, B : 0.020 M, C : 0.013 M
D : 0.0067 M, E : 0.0033 M, F : 10^{-7} M
Broken line : acid from.

the acid form at 540 mμ, ε_A^{540}, can easily be estimated to be 3.13×10^4 $M^{-1}cm^{-1}$, by assuming that of the base form, ε_B^{540}, to be zero.

From the absorbances at 540 mμ at various hydrogen ion concentrations, the respective concentrations of HIn and In^- can be ascertained. Therefore, the ionization constant of the indicator, defined as $K_{HIn}=[H^+][In^-]/[HIn]$, at 25°C is calculated to be $(2.21\pm0.12)\times10^{-2}$ M.

At 540 mμ, ε_A^{540} is so complicatedly affected by the addition of even a small amount of DMSO to the aqueous solution that this wavelength seems less suitable than 433 and 335 mμ for the present purpose of measuring the K_a of the protonated DMSO.

When the solution is neutral, thymol blue may be considered to be completely in the base form.*1 This fact enables us easily to obtain the molar extinction coefficients of the base form, ε_B's. At some acid concentrations, on the other hand, the apparent absorbance of the solution, A, is the sum of those due to the two forms, as is expressed by:

$$A = \varepsilon_A[HIn] + \varepsilon_B[In^-] \quad (1)$$

when either 433 mμ or 335 mμ is employed for the measurement. With the help of the K_{HIn} value, the following data were obtained on the extinction coefficients:

$$\left.\begin{aligned} \varepsilon_A^{433} &= 6.11\times10^3\ M^{-1}\,cm^{-1} \\ \varepsilon_A^{335} &= 2.71\times10^3\ M^{-1}\,cm^{-1} \\ \varepsilon_B^{433} &= 1.31\times10^4\ M^{-1}\,cm^{-1} \\ \varepsilon_B^{335} &= 7.36\times10^3\ M^{-1}\,cm^{-1} \end{aligned}\right\} \quad (2)$$

The ε_A's of thymol blue in an aqueous solution at both 433 and 335 mμ are indifferent to the presence of DMSO at concentrations as high as $[S]_0=0.6$ M within the limits of experimental error, while it was found that the absorption spectrum of the base form of thymol blue has a slight tendency to be lowered in the 350—480 mμ region and raised in that of 300—350 mμ with an increase in the concentration of DMSO at the rates expressed empirically as:

$$\left.\begin{aligned} \varepsilon_B^{433} &= (1.31-0.029[S]_0)\times10^4\ M^{-1}\,cm^{-1} \\ \varepsilon_B^{335} &= (7.36+0.114[S]_0)\times10^3\ M^{-1}\,cm^{-1} \end{aligned}\right\} \quad (3)$$

Calculation of K_a of Protonated DMSO. Since the total concentration of the indicator, $[HIn]_0$, is represented by:

$$[HIn]_0 = [HIn] + [In^-] \quad (4)$$

the following expression can be obtained by combination with Eq. (1):

$$A = \frac{\varepsilon_A[H^+]+\varepsilon_B K_{HIn}}{[H^+]+K_{HIn}}[HIn]_0 \quad (5)$$

When DMSO is added to water to make its total concentration $[S]_0$, with $[HIn]_0$ and $[HClO_4]_0$ kept constant, $[H^+]$ will decrease to $[H^+]'$ due to the protonation of DMSO and, at the same time, ε_B will vary according to Eq. (3). Consequently, A will also alter to A'. By putting the observed A' and calculated ε_B values into Eq. (5), the decrease in the hydrogen ion concentration can be obtained; it is equivalent to the concentration of the protonated DMSO, $[SH^+]$. Since $[S]=[S]_0-[SH^+]$, the value of K_a can easily be calculated. The change in the absorbance caused by the addition of DMSO, $A'-A$, was generally so small compared with A itself that differential spectrophotometry had better be adopted, taking a solution of the indicator in the absence of DMSO as the reference solution.

At comparatively high $[S]_0$ values, the activity of water in the system, a_{H_2O}, is no longer equal to unity but is, rather, reduced to an extent which is assumed to be approximately proportional to its mole fraction in the system. Such a consideration was taken into account in the course of the calculation of K_a.

The values of K_a calculated at various acid and DMSO concentrations at $\mu=0.55$ M and 25°C are listed in Table 1; they give an averaged value

*1 Since thymol blue is dibasic, "the base form" used here must be "the neutral form".

TABLE 1. K_a VALUES AT VARIOUS ACID AND DMSO CONCENTRATIONS AT $\mu=0.55$ M AND 25°C BY USE OF THYMOL BLUE AS AN INDICATOR

$[HClO_4]_0$ M	λ mμ	$[S]_0$ M 0.3	0.4	0.5	0.6	0.7
0.06	433	4.3	4.5	3.7	4.8	4.5
	335	5.0	3.7	4.3	4.2	4.5
0.08	433	4.3	4.2	4.8	4.5	4.5
	335	4.8	4.5	4.8	4.8	4.5
0.10	433	4.8	4.2	5.6	4.2	4.3
	335	5.9	4.3	4.8	5.0	4.8
0.12	433	3.9	4.8	5.6	5.6	5.3
	335	4.3	4.8	4.5	5.0	4.5
0.14	433	3.9	4.8	4.3	3.7	4.8
	335	4.5	4.3	4.8	4.5	5.0
0.16	433	—	5.9	5.6	4.3	5.3
	335	5.9	4.5	4.8	4.5	4.0

Mean 4.7±0.5

TABLE 2. K_a VALUES MEASURED WITH THYMO BLLUE AT VARIOUS TEMPERATURES AT $[S]_0=0.3$—0.7 M, $[HClO_4]_0=0.06$—0.12 M AND $\mu=0.55$ M

T, °C	K_a, M
15	4.5±0.6
25	4.7±0.5
35	4.5±0.6

$K_a=4.7\pm0.5$ M. Table 2 summarizes the averaged K_a values measured in the same way as before at various temperatures; this table indicates that there is almost no variation in K_a with a change in the temperature.

Results with *o*-Nitroaniline

Ionization Constant and Molar Extinction Coefficients of *o*-Nitroaniline. The spectra of *o*-nitroaniline in both the acid and base forms are shown in Fig. 2. Only the base form exhibits a broad absorption band, with a peak at 410 mμ, while the acid form has a maximum absorption at 265 mμ in the ultraviolet region, where the base form has a considerable absorption, too.

Since molecular *o*-nitroaniline is a kind of base, the acid and base forms may be better represented by HIn^+ and In respectively. Then, the ionization constant of the indicator is defined as $K_{In}=[H^+][In]/[HIn^+]$. As to the mass and absorption balances with respect to the indicator, the following two equations are maintained:

$$[In]_0 = [HIn^+] + [In] \quad (6)$$

$$A = \varepsilon[In]_0 = \varepsilon_A [HIn^+] + \varepsilon_B[In] \quad (7)$$

where ε stands for the apparent molar extinction coefficient of the indicator. From these relations, ε is expressed as a function of $[H^+]$:

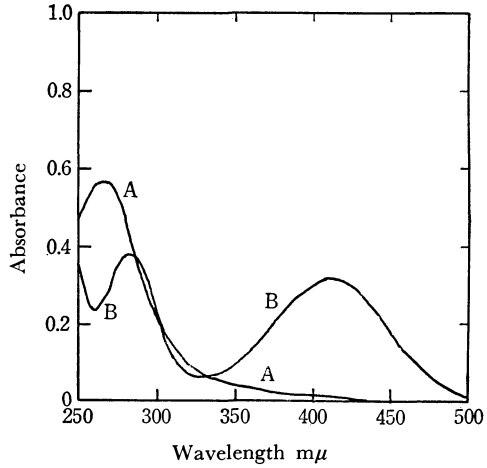

Fig. 2. Absorption spectra of *o*-nitroaniline at $[In]_0=1\times10^{-4}$ M.
A : acid form, B : base form

$$\frac{1}{\varepsilon-\varepsilon_A} = \frac{1}{\varepsilon_B-\varepsilon_A}\left(1+\frac{[H^+]}{K_{In}}\right) \quad (8)$$

If ε_A is negligibly small as compared with ε_B, Eq. (8) is reduced to:

$$\frac{1}{\varepsilon} = \frac{1}{\varepsilon_B} + \frac{[H^+]}{\varepsilon_B K_{In}} \quad (9)$$

This is clearly the case when 380, 410, or 440 mμ is employed for the measurement. The plots of $1/\varepsilon$ *versus* $[H^+]$ at $\mu=0.55$ M and 25°C yield good straight lines at the respective wavelengths, as is shown in Fig. 3, which reveal $\varepsilon_B^{440}=3.48\times10^3$, $\varepsilon_B^{410}=4.47\times10^3$, $\varepsilon_B^{380}=3.16\times10^3$ $M^{-1}cm^{-1}$, and $K_{In}=1.27$ M on the average. The latter value

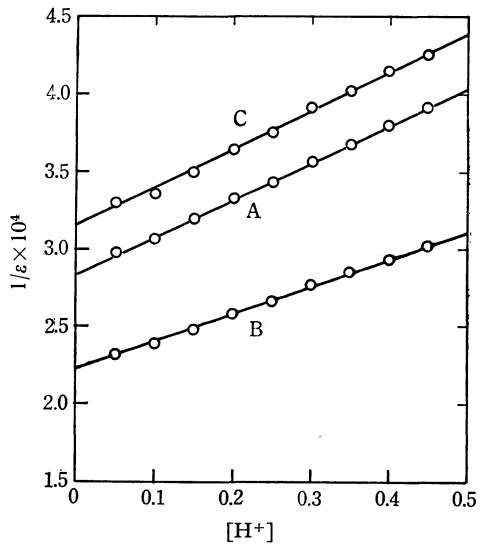

Fig. 3. Linearities of $1/\varepsilon$ of *o*-nitroaniline solution against $[H^+]$ at $\mu=0.55$ M, 25°C.
$[In]_0=1\times10^{-4}$ M, A: 440 mμ, B : 410 mμ, C : 380 mμ

agrees fairly well with the $K_{In}=1.55$ M measured in very concentrated perchloric acid.[8]

In a way quite similar to the case of thymol blue, the ε_B's of *o*-nitroaniline at 440 and 410 mμ were found to be affected by the addition of DMSO, thus:

$$\left.\begin{aligned}\varepsilon_B^{440} &= (3.48+0.138[S]_0)\times 10^3\ M^{-1}\,cm^{-1}\\ \varepsilon_B^{410} &= (4.47+0.113[S]_0)\times 10^3\ M^{-1}\,cm^{-1}\end{aligned}\right\} \quad (10)$$

although ε_B^{380} is almost independent of $[S]_0$.

Calculation of K_a of Protonated DMSO. As in the case of thymol blue, a slight change in A, and, therefore, in ε, upon the addition of DMSO at constant $[HClO_4]_0$ and $[In]_0$ values, observed by means of the differential spectrophotometry, results from the changes in $[H^+]$ and in ε_B (in the case of 440 or 410 mμ) according to Eq. (9). The decrease in $[H^+]$ corresponds to the occurrence of SH^+; this enables us to determine K_a. The calculated results of K_a are summarized in Table 3. The averaged value of K_a at $\mu=0.55$ M and 25°C is found to be 4.6±0.5 M; this value is in good agreement with the results obtained with thymol blue.

Table 3. K_a values at various acid and DMSO concentrations at $\mu=0.55$ M and 25°C by use of *o*-nitroaniline as an indicator

$[HClO_4]_0$ M	λ mμ	$[S]_0$ M 0.2	0.3	0.4	0.5	0.6	0.7
0.3	440	—	4.5	4.8	5.0	5.0	4.8
	410	—	5.3	5.3	5.9	5.6	5.3
	380	—	4.5	4.3	5.3	4.8	4.3
0.4	440	4.8	4.2	4.0	4.5	4.3	4.3
	410	5.0	4.3	4.2	4.8	4.3	4.5
	380	4.8	4.0	3.7	4.0	3.9	3.9

Mean 4.6±0.5

Discussion

The averaged value of K_a as measured by both indicators is 4.7±0.5 M; namely, $pK_a=-0.67$ at $\mu=0.55$ M and 25°C. Through the approximate Debye-Hückel relation:

$$pK_a^\circ = pK_a - 0.5\sqrt{\mu} \quad (11)$$

the thermodynamical basicity strength of DMSO is estimated to be $pK_a^\circ=-1.04$. This pK_a° value is less basic than the values found by the potentiometric titration[4,5] and more basic than that found by the chemical-shifts method.[6] As to the acidic nature, on the other hand, DMSO is an extremely weak acid which yields the CH_3-SO-CH_2^- anion, with a supposed acid dissociation constant of 10^{-31}.[2] In fact, the practical preparation of this anion (methylsulfinyl carbanion) is possible only under very severe conditions.[9]

The fact that the pK_a values of DMSO vary according to the alteration of the measuring methods, namely, about 1 by the potentiometric titration, −1 by the spectrophotometric method and −2.7 by the chemical shifts of the protons, indicates that there may be some variation in the extent of the association between a proton and a DMSO molecule in water. The method of the chemical shifts measures only the closest combination between them, while the electrochemical method finds more associated molecules of DMSO with protons, including those in looser combination. The spectrophotometry discriminates the protonated DMSO from the unprotonated by a way intermediate between the two other methods.

According to the values in Table 2, there is no dependence of K_a upon the temperature; therefore, the enthalpy change associated with the $S+H_3O^+ \rightleftharpoons SH^+ + H_2O$ reaction seems to be zero. This means that the protonation energies of water and DMSO are nearly equal to each other in water.

The experimental part of the work was carried out at the Department of Chemistry, University of Minnesota, U. S. A. The author's sincere thanks are due to Professor Warren L. Reynolds for his helpful discussion.

8) L. P. Hammett and A. J. Deyrup, *J. Am. Chem. Soc.*, **54**, 2721 (1932).

9) E. J. Corey and M. Chaykovsky, *J. Am. Chem. Soc.*, **87**, 1345 (1965).

BULLETIN OF THE CHEMICAL SOCIETY OF JAPAN VOL. 42 894—897 (1969)

Fragmentation of the Excited Isobutane Ion Produced by Charge Transfer from the Nitrogen Molecule Ion

Tetsuo MIYAZAKI, Tadahiko KOHAMA, Kenji FUEKI and Zen-ichiro KURI

Department of Synthetic Chemistry, Faculty of Engineering, Nagoya University, Chikusa-ku, Nagoya

(Received August 12, 1968)

The radiolysis of the N_2-*iso*C_4H_{10} (0.0153 mol/mol of N_2) mixture has been studied by using such ion scavengers as ammonia and sulfur hexafluoride. It was found that the $C_3H_7^+$ ion is formed by the fragmentation of the excited isobutane ion produced by the charge transfer from the nitrogen ion. Although nitrogen is an effective quencher of the excited ion, the yield of the $C_3H_7^+$ ion is constant over the pressure range from 0.66 to 130 atm. It has been concluded that the excited isobutane ion produced by the charge transfer with 5 eV excess energy decomposes very fast and that it can not be deactivated by nitrogen of 130 atm, while it has been reported by other authors that the excited isobutane ion with 1.2 eV excess energy can be deactivated below 1 atm. This difference in the characters of the excited isobutane ions can be explained by the previously-proposed mechanism of the fragmentation.

The fragmentation of the excited ion has been explained by the quasi-equilibrium theory,[1] which is based on the fundamental assumption that the randomization of excitation energy among oscillators occurs before the dissociation of the excited ion.

We concluded in a previous study[2] of the effect of density in the radiolysis of butanes that excited ions can be classified into two types, M^{+*} and M^{+**}. The M^{+*} ion decomposes slowly and can be collisionally deactivated by an increase in the pressure. The M^{+**} ion decomposes in a time of one vibration and can not be deactivated even in the liquid phase. In order to obtain further details on the mechanism, studies[3,4] have been made of the ionic fragmentation in the liquid-phase radiolysis of hydrocarbons, and the following new mechanism of the fragmentation of M^{+**} ion has been proposed[5]: The M^{+**} ion is the electronically-excited ion, and the electronic excitation energy spreads over all the C–C bonds in a molecule prior to its fragmentation. The ion decomposes instantaneously in one vibration at a bond where the mean excitation energy per C–C bond exceeds its bond energy.

The present work studies the effect of pressure on the fragmentation of the excited isobutane ion produced by the charge transfer from the nitrogen ion; the previously-proposed mechanism of the fragmentation is confirmed.

Experimental

The isobutane was supplied by the Takachiho-Shoji Co.; its gas chromatographic analysis showed the presence of 5×10^{-4}% C_2H_6 as an impurity. The ammonia and sulfur hexafluoride were both of high purity and were used without further purification. The nitrogen was 99.99% pure.

The samples were irradiated with γ rays from ^{60}Co at a dose rate of 2.26×10^5 rad/hr and with a total dose of 1.13×10^5 rad at room temperature. The energy absorbed in nitrogen was measured by Fricke dosimetry.

The reaction at a nitrogen pressure of 0.66 atm was carried out in a 350 cc glass cylinder, while those at nitrogen pressures above 1 atm were carried out in a stainless-steel autoclave (45 cc). The products were analyzed by a Hitachi K 53 gas chromatograph equipped with a flame ionization detector (activated alumina column, 2 m, 100°C).

Results and Discussion

Sensitization by Nitrogen. The *G*-value of propane in the radiolysis of N_2(100 atm)-*iso*C_4H_{10} (0.0153 mol/mol of N_2) mixtures amounts to 46 if the value is expressed by the number of product molecules per 100 eV directly absorbed on isobutane. Since the $G(C_3H_8)$ value is 2—3 in the radiolysis of pure isobutane,[2] it may be reasonable to consider that most of the propane in the radiolysis of N_2-*iso*C_4H_{10} mixtures is formed by the sensitization of nitrogen. A similar sensitization was previously

1) H. M. Rosenstock, M. B. Wallenstein, A. L. Wahrhaftig and H. Eyring, *Proc. Natl. Acad. Sci. U. S.*, **38**, 667 (1952).
2) T. Miyazaki, *J. Phys. Chem.*, **71**, 4282 (1967).
3) K. Tanno, T. Miyazaki, K. Shinsaka and S. Shida, *J. Phys. Chem.*, **71**, 4290 (1967).
4) K. Tanno, S. Shida and T. Miyazaki, *ibid.*, **72**, 3496 (1968).
5) T. Miyazaki, K. Tanno and S. Shida, This Bulletin, **42**, 362 (1969).

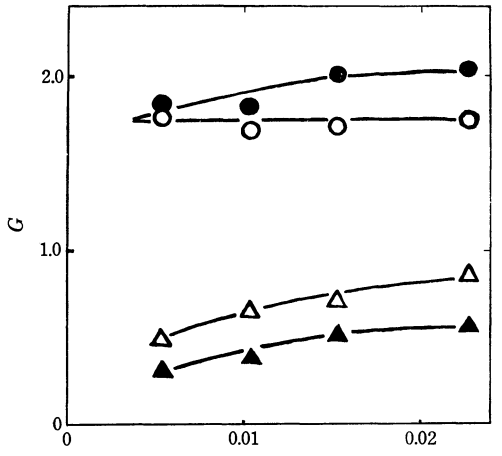

Fig. 1. Effect of increasing concentration of isobutane on the nitrogen sensitization at constant nitrogen pressures of 0.66 and 100 atm.
—●— C_3H_8 at 0.66 atm of N_2
—○— C_3H_8 at 100 atm of N_2
—▲— C_3H_6 at 0.66 atm of N_2
—△— C_3H_6 at 100 atm of N_2

found in the radiolysis of the N_2 - n-C_4H_{10} system.[6] Therefore, the G-values of products are expressed in this paper by the number of product molecules per 100 eV absorbed on nitrogen. The effect of an increase in the concentration of isobutane on the yields of propane above a 0.0153 mol ratio of isobutane suggests that the sensitization by nitrogen may be completed above this concentration (Fig. 1).

Mechanism of Nitrogen Sensitization. The ionic processes of the sensitization were studied by using ammonia as a scavenger of the carbonium ion and sulfur hexafluoride as an electron scavenger. The effect of ammonia on the radiolysis of N_2 (100 atm) - $iso C_4H_{10}$ (0.0153 mol/mol of N_2) - SF_6 (0.003 mol/mol of N_2) mixtures is shown in Fig. 2. Since the neutralization reaction of the stable butane ion ($C_4H_{10}^+$) is suppressed by the presence of sulfur hexafluoride, the reactions of the excited butane ion, such as reactions (3) and (4), can be studied by the addition of ammonia.[3,4] The marked decrease in propane and the increase in propylene upon the addition of ammonia is due to the following reactions of the $C_3H_7^+$ ion with ammonia:

$$N_2 \rightsquigarrow N_2^+ + e \quad (1)$$

$$N_2^+ + i\text{-}C_4H_{10} \rightarrow C_4H_{10}^{+**} + N_2 \quad (2)$$

$$C_4H_{10}^{+**} \rightarrow C_3H_7^+ + CH_3 \quad (3)$$

$$C_3H_7^+ + i\text{-}C_4H_{10} \rightarrow C_3H_8 + C_4H_9^+ \quad (4)$$

6) T. Miyazaki, S. Arai, S. Shida and S. Sunohara, presented at the 16th Annual Meeting of the Chemical Society of Japan, Tokyo, April, 1963.

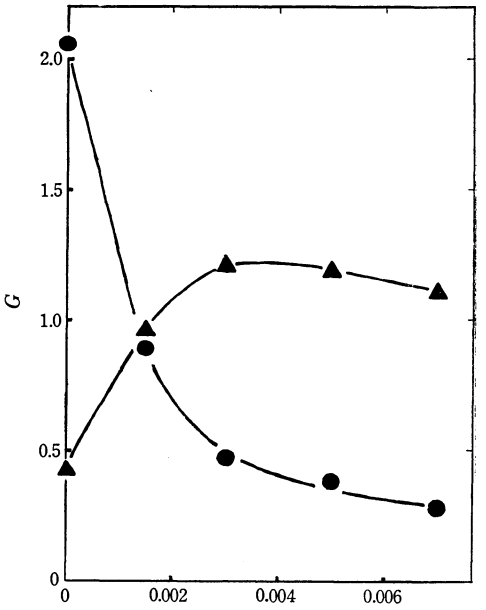

Fig. 2. Effect of ammonia on the radiolysis of N_2(100 atm)-$iso C_4H_{10}$(0.0153 mol/mol of N_2)-SF_6 (0.003 mol/mol of N_2) mixtures.
—●— C_3H_8 —▲— C_3H_6

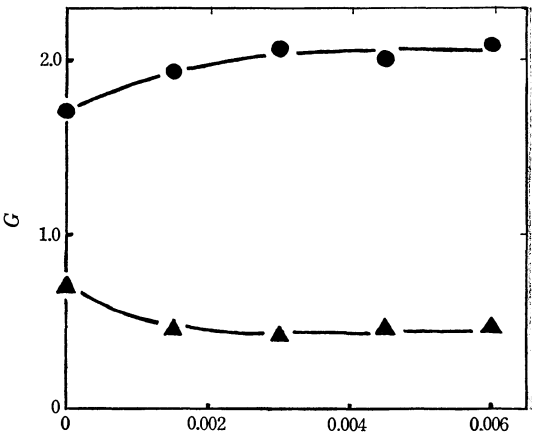

Fig. 3. Effect of sulfur hexafluoride on the radiolysis of N_2(100 atm)-$iso C_4H_{10}$(0.0153 mol/mol of N_2) mixtures.
—●— C_3H_8 —▲— C_3H_6

$$C_3H_7^+ + NH_3 \rightarrow C_3H_6 + NH_4^+ \quad (5)$$
$$\searrow\ C_3H_7NH_3^+ \quad (6)$$

The similar phenomenon was also observed in the gas-phase radiolysis of the n-butane-ammonia system.[7] Since the ionization potential of nitrogen is 15.6 eV, and since that of isobutane is 10.6 eV,

7) T. Miyazaki and S. Shida, This Bulletin, **38**, 2114 (1965).

the $C_4H_{10}^{+**}$ ion formed by the charge transfer from the nitrogen ion has an excitation energy of 5 eV, much higher than the bond energy of the C–C bond (0.61 eV).

The effect of sulfur hexafluoride on the radiolysis of N_2(100 atm) - *iso*C_4H_{10}(0.0153 mol/mol of N_2) mixtures is shown in Fig. 3. Propane increases upon the addition of sulfur hexafluoride, while propylene decreases. The results in Table 1, however, show that propylene does not decrease upon the addition of sulfur hexafluoride in the nitrogen sensitization at 10 and 40 atm, while propane increases. Therefore, the variations in the yields of propane and propylene upon the addition of sulfur hexafluoride may be due to the different mechanisms. One possible mechanism of the slight increase in propane may be as follows:

TABLE 1. EFFECT OF PRESSURE OF NITROGEN ON THE FRAGMENTATION OF ISOBUTANE[a)]

	Pressure of N_2, atm					
	0.66	10	40	70	100	130
	isoC_4H_{10}[b)] system					
C_3H_8	2.01	2.15	2.26	2.22	1.71	1.88
C_3H_6	0.51	0.42	0.55	0.70	0.71	0.89
	isoC_4H_{10}[b)]-SF_6[c)] system					
C_3H_8	2.08	2.36	2.46	2.41	2.06	2.11
C_3H_6	0.60	0.49	0.52	0.45	0.42	0.51
	isoC_4H_{10}[a)]-SF_6[c)]-NH_3[d)] system					
C_3H_8	0.79	0.87	0.89	0.89	0.47	0.52
C_3H_6	0.99	1.19	1.28	1.35	1.21	1.02

a) Yields are expressed as the number of product molecules per 100 eV absorbed in nitrogen.
b) Concentration of *iso*C_4H_{10} is 0.0153 mol/mol of N_2.
c) Concentration of SF_6 is 0.003 mol/mol of N_2.
d) Concentration of NH_3 is 0.003 mol/mol of N_2.

$$N_2 \rightsquigarrow N_2^+ + e \quad (1)$$
$$\rightsquigarrow N_2^* \quad (7)$$
$$N_2^+ + e \rightarrow N_2, 2N \text{ or } N_2^* \quad (8)$$
$$N_2^+ + i\text{-}C_4H_{10} \rightarrow C_4H_{10}^{+**} + N_2 \quad (2)$$
$$e + SF_6 \rightarrow SF_6^- \quad (9)$$

If the recapture of electrons by nitrogen (reaction (8)) is notable even at 10 atm of nitrogen, the reaction (8) is retarded in the presence of sulfur hexafluoride by reaction (9) and reaction (2) is facilitated.

Another possible mechanism of the increase in propane may be as follows: As an excited agron reacts with sulfur hexafluoride,[8)] a highly-excited nitrogen molecule may react with sulfur hexafluoride in a similar fashion to form the nitrogen molecule ion; therefore, the yield of N_2^+, that is, that of $C_4H_{10}^{+**}$, increases upon the addition of sulfur hexafluoride:

$$N_2^* + SF_6 \rightarrow N_2^+ + SF_6^- \quad (10)$$

Effect of Pressure on the Fragmentation of the Excited Butane Ion. The yields of the $C_3H_7^+$ ion are obtained by using the results in Table 1 and the following relationship[4)]:

$$G(C_3H_7^+) = G(C_3H_8) \text{ in the } N_2\text{-}iso C_4H_{10}\text{-}SF_6 \text{ system} - G(C_3H_8) \text{ in the } N_2\text{-}iso C_4H_{10}\text{-}SF_6\text{-}NH_3 \text{ system}$$

$G(C_3H_7^+)$ shows a constant value of 1.55, even if the pressure of nitrogen varies from 0.66 to 130 atm (Fig. 4). In the mass spectrum of isobutane upon the bombardment of electrons with 14—15 eV energy, the fraction of $C_3H_7^+$ amounts to 65% of all the ions.[9)] Taking $W(N_2)$ as 36.3 eV, it may be expected that $G(C_3H_7^+)=1.79$ in the fragmentation of isobutane by nitrogen sensitization. The $G(C_3H_7^+)$ obtained in the sensitization is obviously in agreement with the mass spectrometric value.

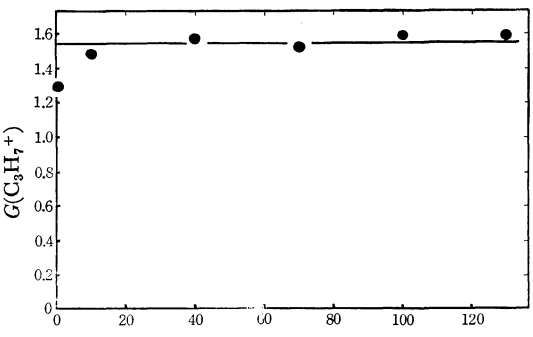

Fig. 4. Effect of pressure of nitrogen on the yields of $C_3H_7^+$ ion formed by the fragmentation of excited isobutane ion.

It has been reported[10)] that nitrogen acts as an efficient quencher of the fragmentation of the excited butane ion which is formed by the photoionization at 1048 A (11.8 eV), and that the quenching cross section of nitrogen is a seventh that of butane. As is shown in Fig. 4, the yield of the $C_3H_7^+$ ion is constant and the following deactivation reaction of the excited isobutane ion does not occur, even at 130 atm of nitrogen:

$$C_4H_{10}^{+**} + N_2 \rightarrow C_4H_{10}^+ + N_2 \quad (11)$$

It may be concluded that the excited isobutane ion with 5 eV excess energy decomposes very fast, probably in the period of one vibration, before the collisons with nitrogen. On the contrary, Ausloos *et al.*[9)] reported that the excited isobutane ion with 1.2 eV excess energy decomposes slowly and is

8) H. Hotop and A. Niehaus, *J. Chem. Phys.*, **47**, 2506 (1967).
9) S. G. Lias and P. Ausloos, *ibid.*, **48**, 392 (1968).
10) P. Ausloos and S. G. Lias, *ibid.*, **45**, 524 (1966).

collisionally deactivated by isobutane of 0.033 atm, which corresponds to a nitrogen pressure of 0.23 atm.

This large difference in the rates of fragmentation of the excited isobutane ions can be explained by the following proposed mechanism[5]: When the ion is highly excited and when the mean excitation energy per C–C bond exceeds its bond energy, the excited ion decomposes in one vibration. When the ion is little excited and when the mean excitation energy per C–C bond does not exceed its bond energy, the excited ion decomposes slowly according to the quasi-equilibrium theory. Since there are three C–C bonds in the isobutane ion, the mean excitation energy per C–C bond of the ion with 5 eV excess energy will be 1.7 eV, higher than the C–C bond energy (0.61 eV), and that of the ion with 1.2 eV excess energy will be 0.4 eV. Consequently, the former excited ion may decompose quickly, in one vibration, while the latter may do so more slowly because of the time lag needed for the accumulation of the excitation energy in a particular bond.

BULLETIN OF THE CHEMICAL SOCIETY OF JAPAN VOL. 42 897—904 (1969)

Infrared Spectra of Partially Deuterated Acetamide

Toyozo UNO, Katsunosuke MACHIDA and Yutaka SAITO

Faculty of Pharmaceutical Sciences, Kyoto University, Sakyo-ku, Kyoto

(Received August 17, 1968)

The infrared spectra of orthorhombic crystals of CH_3CONH_2, CD_3CONH_2, and their *N*-deuterated and partially *N*-deuterated samples have been recorded in the region between 4000 and 400 cm^{-1}. The bands due to the *trans*- and *cis*-NHD species have been assigned by comparing the spectra of various samples containing the NH_2, ND_2 and NHD species in different proportions. In the spectra of the 50% *N*-deuterated samples, the absorption bands near 1530 and 1360 cm^{-1} have been assigned to the amide II and III modes, respectively, of the *trans*-NHD species characteristic of the *trans* conformation of the –CONH– group, and those near 1480 and 1400 cm^{-1} to the NH in-plane deformation and the CN stretching modes, respectively, of the *cis*-NHD species. These assignments were confirmed by the normal coordinates analysis of eight isotopic species of acetamide based on the Urey-Bradley force field.

The hydrogen atoms in the amide group of acetamide are easily substituted by deuterium atoms by the exchange reaction with heavy water. If a mixture of water and heavy water is used in the exchange reaction, the resulting samples should contain the molecular species involving the NH_2, ND_2 and NHD groups. This report presents the assignment of infrared absorption frequencies of the NHD species of acetamide and *C*-deuterated acetamide obtained by this partial *N*-deuteration. As shown in Fig. 1, there are two geometrical isomers of the NHD species arising from the planarity of amide group. Molecular vibrations of these NHD species are of interest because of their structure involving the biochemically important –CONH– group. Our attention was drawn to this point first by observing a strong band near 1520 cm^{-1} in the infrared spectra of incompletely deuterated primary amides and noticing an analogy between this band and the amide II band of *trans*-*N*-monosubstituted amides.

It is well known that the conformation of the C=O and the NH bonds is an important factor determining the vibration modes and frequencies of the –CONH– group. The amide II and III frequencies arising from the coupling between the CN stretching and the NH in-plane deformation vibrations are observed only for the trans conformation.[1] Miyazawa has calculated the normal vibrations of the hypothetical *cis* form of *N*-methylacetamide using the Urey-Bradley force constants which reproduce the observed frequencies of the *trans* form, and has obtained almost pure CN stretching and the NH in-plane deformation vibrations instead of their coupled vibrations.[2] Since the *trans*- and *cis*-isomers of the NHD species in the present study have exactly the same force field with each other, they are expected to afford experimental evidences of the change of vibrational modes given rise to by the purely geometrical effect on the –CONH– group.

1) T. Miyazawa, T. Shimanouchi and S. Mizushima, *J. Chem. Phys.*, **24**, 408 (1956).

2) T. Miyazawa, T. Shimanouchi and S. Mizushima, *ibid.*, **29**, 611 (1958).

Experimental

Commercially available acetamide was purified by the crystallization from ether and ethanol solutions. *C*-Deuterated acetamide was prepared by the reaction between NH_3 gas and CD_3COCl, in ether at −20°C, and was purified by the same way as acetamide. For the preparation of CD_3COCl, commercially available CD_3COOD (Merk AG. Darmstadt) was treated with benzoyl chloride according to Bender's method.[3] These NH_2 compounds were converted into the corresponding ND_2 compounds by the exchange reaction with heavy water. The partially *N*-deuterated samples were prepared by using mixtures of water and heavy water in various proportions.

The infrared spectra were recorded on Koken DS 301 infrared spectrophotometer equipped with sodium chloride (4000—700 cm^{-1}) and potassium bromide (700—400 cm^{-1}) prisms. The measurement was made for the orthorhombic crystal obtained by the crystallization from molten liquid[4] between two potassium bromide plates or between two sodium chloride plates. The crystal form of the partially *N*-deuterated samples prepared in the same way was confirmed to be orthorhombic from the absorptions of the NH_2 species contained in the samples. The absorptions of the ND_2 species in the partially *N*-deuterated samples were then used to identify the crystal form of the almost completely *N*-deuterated samples. It was also found from the comparison of infrared spectra that the orthorhombic crystal was converted into the trigonal crystal on mulling with Nujol or hexachlorobutadiene.

Results and Discussion

A detailed assignment of the infrared absorption bands of acetamide, *C*-deuterated acetamide and their ND_2 species have been given by Suzuki on the basis of the normal coordinates analysis of the a′ vibrations.[5] Although the crystal spectra reported by Suzuki are those of the trigonal form, most of his assignments for the NH_2 and ND_2 species are applicable to the presently investigated orthorhombic form because the infrared absorptions of these two forms are not seriously different from each other.[6] The trigonal form is better than the orthorhombic one to prevent the sample from atmospheric water and to maintain the orginal concentration of the *N*-deuterated species, since the Nujol and hexachlorobutadiene mulls can be prepared more quickly than the crystal film. For investigating the spectral change around 1500 cm^{-1} on successive *N*-deuteration, however, the orthorhombic form was found to be more appropriate since it showed much sharper absorption bands in this region than the corresponding bands of the trigonal form. In Figs. 2—5, the infrared spectra of orthorhombic form of acetamide and *C*-deuterated acetamide obtained from a equimolar mixture of

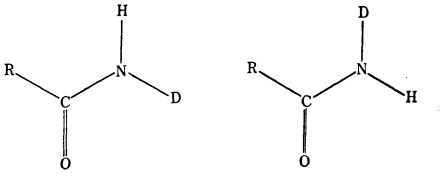

trans-form *cis*-form

Fig. 1. Structurs of the NHD species.

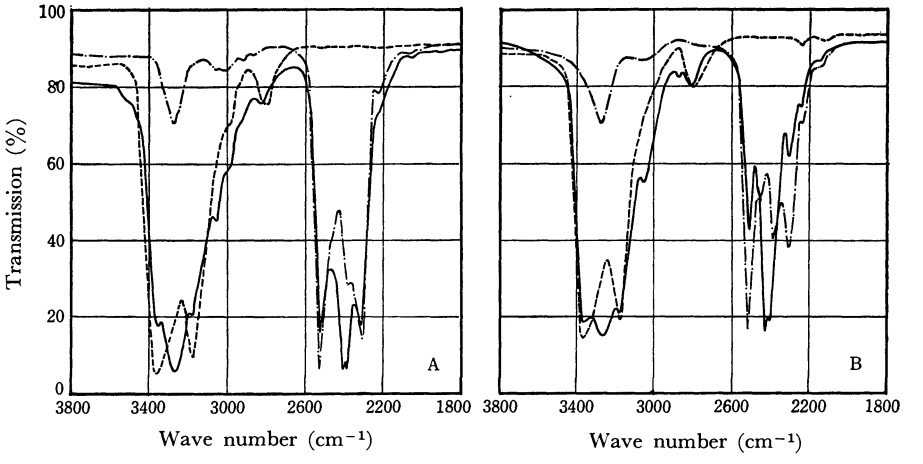

Fig. 2. Infrared spectra of acetamide (A) and *C*-deuterated acetamide (B) in the region between 4000 and 1800 cm^{-1}

--- shows the infrared spectra of the crystal from water,
—— from a equimolar mixture of water and heavy water, —·— from heavy water

3) M. L. Bender and M. S. Feng, *J. Am. Chem. Soc.*, **82**, 6319 (1960).
4) W. C. Hamilton, *Acta Cryst.*, **18**, 866 (1965).
5) I. Suzuki, This Bulletin, **35**, 1279 (1962).
6) W. Kutzelnigg and R. Mecke, *Spectrochim. Acta*, **18**, 549 (1962).

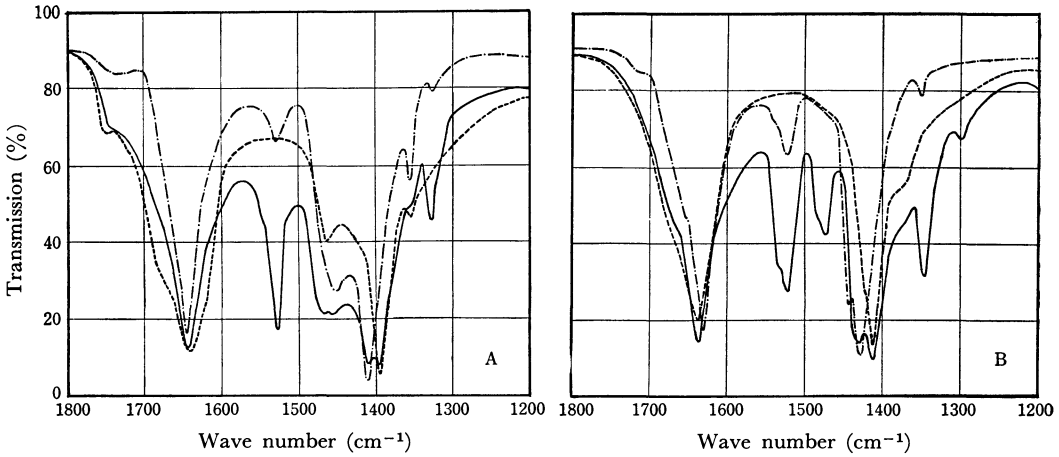

Fig. 3. Infrared spectra of acetamide (A) and *C*-deuterated acetamide (B) in the region between 1800 and 1200 cm^{-1}.
--- shows the infrared spectra of the crystal from water,
—— from a equimolar mixture of water and heavy water, —·— from heavy water

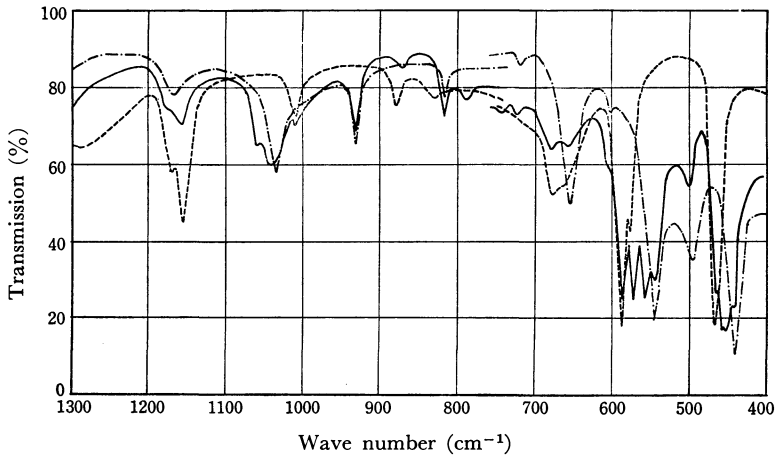

Fig. 4. Infrared spectra of acetamide in the region between 1300 and 400 cm^{-1}.
--- shows the infrared spectra of the crystal from water,
—— from a equimolar mixture of water and heavy water, —·— from heavy water

water and heavy water are shown together with the spectra of the corresponding NH_2 and ND_2 species. We assumed that this mixture gave approximately rise to the deuteration of 50% of amide hydrogen atoms in the whole sample and the resulting crystal included the NHD species in the maximum concentration attainable. The absorption bands due to the NH_2 and ND_2 species appearing in the spectra of this 50% *N*-deuterated samples can be differentiated from those due to the NHD species by referring to the spectra of the NH_2 and ND_2 species. Observed frequencies and assignments are listed in Table 1.

4000—1800 cm^{-1}. The strong bands near 3300 and 2400 cm^{-1} observed for the 50% *N*-deuterated sample of acetamide are assigned to the NH and ND stretching vibrations, respectively, of the NHD compounds. The appearance of these NX (X=H or D) stretching frequencies between the symmetric and antisymmetric NX_2 stretching frequencies is to be expected from the removal of the vibrational coupling between two equivalent NX bonds. The ND stretching band consists of two peaks attributable to the *trans*- and *cis*-NHD species, but the NH stretching band does not show any splitting. A broad band near 2800 cm^{-1} observed for orthorhombic acetamide disappears on *N*-deuteration but does not disappear on *C*-deuteration.

1800—1200 cm^{-1}. In the region between 1700 and 1600 cm^{-1} where the C=O stretching and the NH_2 bending frequencies are expected, the orthorhombic crystal of acetamide shows a strong absorption band consisting of a peak at 1640 cm^{-1} and a

Table 1. Observed frequencies and assignments for *N*-50% deuterated samples

Acetamide		*C*-deuterated acetamide	
3380 m	NH_2 asym. stretching (NH_2)*	3380 m	NH_2 asym. stretching (NH_2)
3270 vs	NH stretching (*trans*- and *cis*-NHD)	3265 vs	NH stretching (*trans*- and *cis*-NHD)
3190 m	NH_2 sym. stretching	3190 m	NH_2 sym. stretching (NH_2)
3055 w	Combination or over-tone (*trans*- and *cis*-NHD)	3050 vw	Combination or over-tone (*trans*- and *cis*-NHD)
3000 vw	CH_3 asym. stretching	2810 w	Combination or over-tone (NH_2)
2930 vw	CH_3 sym. stretching	2527 vs	ND_2 asym. stretching (ND_2)
2815 w	Combination or over-tone (NH_2)	2420 vs	ND stretching (*cis*-NHD)
2530 vs	ND_2 asym. stretching (ND_2)	2400 sh	ND stretching (*trans*-NHD)
2417 vs	ND stretching (*cis*-NHD)	2320 s	ND_2 asym. stretching (ND_2)
2395 vs	ND stretching (*trans*-NHD)	2240 vw	CD_3 asym. stretching
2316 s	ND_2 sym. stretching (ND_2)	2120 vw	CD_3 sym. stretching
1652 vs	C=O stretching NH_2 bending (NH_2)	1634 vs	C=O stretching NH_2 bending (NH_2)
1530 vs	Amide II (*trans*-NHD)	1529 s	Amide II (*trans*-NHD)
1475 sh	NH deformation (*cis*-NHD)	1475 m	NH deformation (*cis*-NHD)
1460 mb	CH_3 deg. deformation	1421 vs	CN stretching (ND_2)
1411 vs	CN stretching (ND_2)	1410 vs	CN stretching (NH_2 and *cis*-NHD)
1398 vs	CN stretching (NH_2 and *cis*-NHD)	1348 s	Amide III (*trans*-NHD)
1358 sh	CH_3 sym. deformation	1187 vw	ND_2 bending (ND_2)
1327 m	Amide III (*trans*-NHD)	1152 w	NH_2 rocking (NH_2)
1175 sh	ND_2 bending (ND_2)	1088 sh	CD_3 sym. deformation (*cis*-NHD)
1154 wb	NH_2 rocking (NH_2)	1084 w	CD_3 sym. deformation (NH_2 and *trans*-NHD)
1060 sh	ND deformation (*trans*-NHD)		
1045 mb	CH_3 rocking (*cis*-NHD)	1070**	CD_3 sym. deformation (ND_2)
1036 sh	CH_3 rocking (ND_2)	1039 m	CD_3 deg. deformation ND deformation (*trans*-NHD)
1010 vw	CH_3 rocking (NH_2)		
933 m	ND deformation (*cis*-NHD) ND_2 rocking (ND_2)	975 wb	ND deformation (*cis*-NHD)
		962 w	ND_2 rocking (ND_2)
871 w	CC′ stretching (*cis*-NHD and NH_2)	831 sh	CC′ stretching (NH_2)
819 w	CC′ stretching (*trans*-NHD and ND_2)	828 vw	CC′ stretching (*cis*-NHD)
680 wb	out-of-plane (NH_2)	812 w	CD_3 rocking
655 wb	out-of-plane (ND_2)	760 vw	CC′ stretching (ND_2 and *trans*-NHD)
586 s	NCO deformation (NH_2)	670 wb	out-of-plane (NH_2)
568 s	NCO deformation (*cis*-NHD)	625 vwb	out-of-plane (ND_2)
556 s	NCO deformation (*trans*-NHD)	566 s	NCO deformation (NH_2)
548 sh	NCO deformation (ND_2)	546 s	NCO deformation (*cis*-NHD)
500 wb	out-of-plane (ND_2)	538 s	NCO deformation (*trans*-NHD)
466 sh	CC′ deformation (NH_2)	526 m	NCO deformation (ND_2)
460 s	CC′ deformation (*trans*-NHD)	490 wb	out-of-plane (ND_2)
455 s	CC′ deformation (*cis*-NHD)		
442 sh	CC′ deformation (ND_2)		

* Parenthesis shows type of amino-group in the molecular species related to the absorption indicated.
** Observed only in the spectra of CD_3COND_2.

shoulder at its high frequency side. Since the assignment of both the peak and the shoulder to fundamentals was found to be necessary from a slight high frequency shift of the apparent absorption maximum on 50% *N*-deuteration, we divided the whole absorption of acetamide into two Lorenz type components, and estimated the position of the unobserved peak of the high frequency component to be 1665 cm^{-1} (Fig. 3-A). Similarly, the high frequency component of the corresponding absorption of *C*-deuterated acetamide was estimated to be 1655 cm^{-1} (Fig. 3-B).

Each of 50% *N*-deuterated samples of acetamide and *C*-deuterated acetamide shows clearly two bands at 1530 and 1328 cm^{-1} attributable to the NHD species. From analogy in the conformation between the *trans*-NHD species and *trans*-*N*-monosubstituted amides, it is conceivable that the CN stretching and the NH in-plane deformation vibrations of the *trans*-NHD species couple appreciably with each other and give rise to the amide II and III bands at 1530 and 1327 cm^{-1},

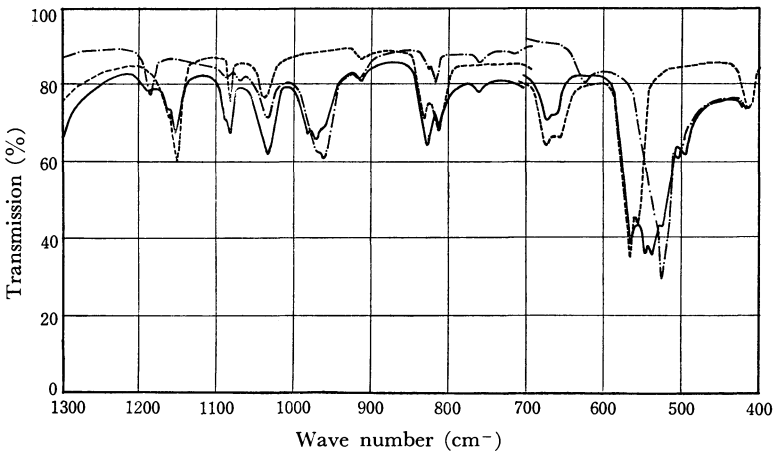

Fig. 5. Infrared spectra of *C*-deuterated acetamide in the region between 1300 and 400 cm^{-1}.
--- shows the infrared spectra of the crystal from water,
—— from a equimolar mixture of water and heavy water, —·— from heavy water

respectively. The frequencies of these bands are comparable with the amide II and the amide III frequencies (1566 and 1301 cm^{-1}, respectively) of *N*-methylacetamide[2] crystal at +15°C. The absorption bands due to the *cis*-NHD species may be found from analogy to *cis*-*N*-monosubstituted amides, for which the coupling between the CN stretching and the NH in-plane deformation vibrations is not appreciable. Supposedly, the NH in-plane deformation frequencies of *cis*-CH_3CONHD and *cis*-CD_3CONHD are not far from the corresponding frequency of diketopiperazine crystal (b_u: 1443 cm^{-1}).[7] For each of 50% *N*-deuterated samples of acetamide and *C*-deuterated acetamide, we observed an absorption band near 1480 cm^{-1} assignable to the NH in-plane deformation vibration of *cis*-NHD species. The intensity change of this absorption on the progress of *N*-deuteration was not obvious for *cis*-CH_3CONHD because of the overlap of the CH_3 degenerate deformation band at 1453 cm^{-1}. It was recognized clearly, however, for *cis*-CD_3CONHD which did not show any interfering fundamental in this region.

1200—400 cm^{-1}. For both acetamide and *C*-deuterated acetamide, most of the bands observed between 1200 and 700 cm^{-1} for the 50% *N*-deuterated samples appear also in the spectra of either the NH_2 or ND_2 species. This result seems to contradict with the fact that the ND in-plane deformation (amide III') mode of both *trans*- and *cis*-NHD species has an intrinsic frequency around 1000 cm^{-1} and is likely to couple with other modes having similar intrinsic frequencies. The normal coordinate analysis discussed in the following section ascertained, however, that the absorptions due to the NHD species overlap considerably with those due to the NH_2 or the ND_2 species.

As seen in Fig. 4, the NCO deformation band of acetamide at 586 cm^{-1} splits into four bands on 50% *N*-deuteration. This fact suggests that the NCO deformation frequencies of the NH_2, ND_2, *trans*-NHD and *cis*-NHD species are different from one another. The middle two bands observed at 568 and 556 cm^{-1} can be assigned to the NHD species. Similar splitting on 50% *N*-deuteration are observed for the NCO deformation band at 566 cm^{-1} of *C*-deuterated acetamide in Fig. 5 and for the CC' deformation band at 466 cm^{-1} of acetamide in Fig. 4.

Normal Coordinate Analysis

On assigning the infrared absorption bands of CH_3CONHD and CD_3CONHD from analogy with *N*-monosubstituted amides, we assumed that the vibrational modes of the –CONH– group were not much affected by the change in the *N*-substituent atom from carbon to deuterium. In order to verify this assumption, we carried out the normal coordinate analysis of the eight isotopic species of acetamide formed by the combination of the CH_3 and CD_3 groups with the NH_2, *trans*-NHD, *cis*-NHD and ND_2 groups. The ***G*** matrices were set up by using the structural parameters based

Table 2. Structural parameter

Bond length, Å		Angle	
R(C=O)	1.260	∠CCN	117.2°
R(C-N)	1.334	∠CCO	119.6°
R(C-C')	1.505	∠NCO	123.2°
R(N-H)	1.02	∠CCH, ∠HCH	109°28'
R(C-H)	1.08	∠CNH, ∠HNH	120.0°

7) K. Fukushima, Y. Ideguchi and T. Miyazawa, This Bulletin, **37**, 349 (1964).

Table 3. Symmetry coordinates for acetamide

Symmetry coordinate	Description of mode	Abbr.
$S_1 = \Delta r_6$	CN stretching	νCN
$S_2 = \Delta r_2$	CC′ stretching	νCC′
$S_3 = \Delta r_1$	C=O stretching	νC=O
$S_4 = \{2\Delta\phi_{78}-(1+\sqrt{3})\Delta\phi_{68}+(\sqrt{3}-1)\Delta\phi_{67}\}/2\sqrt{3}$	*trans*-NH deformation	δ_t-NH
$S_5 = \{2\Delta\phi_{78}-(1+\sqrt{3})\Delta\phi_{67}+(\sqrt{3}-1)\Delta\phi_{68}\}/2\sqrt{3}$	*cis*-NH deformation	δ_c-NH
$S_6 = (2\Delta\phi_{16}-\Delta\phi_{12}-\Delta\phi_{26})/\sqrt{6}$	NCO deformation	δNCO
$S_7 = (\Delta\phi_{26}-\Delta\phi_{12})/\sqrt{2}$	CC′ deformation	δCC′
$S_8 = (2\Delta\phi_{34}-\Delta\phi_{35}-\phi_{45})/\sqrt{6}$	CH_3 degenerate deformation	$\delta_d CH_3$
$S_9 = (\Delta\phi_{23}+\Delta\phi_{24}+\Delta\phi_{25}-\Delta\phi_{34}-\Delta\phi_{35}-\Delta\phi_{45})/\sqrt{6}$	CH_3 symmetric deformation	$\delta_s CH_3$
$S_{10} = (2\Delta\phi_{25}-\Delta\phi_{23}-\Delta\phi_{24})/\sqrt{6}$	CH_3 rocking	ρCH_3
$S_{11} = \Delta r_7$	*trans*-NH stretching	ν_t-NH
$S_{12} = \Delta r_8$	*cis*-NH stretching	ν_c-NH
$S_{13} = (2\Delta r_5-\Delta r_3-\Delta r_4)/\sqrt{6}$	CH_3 antisymmetric stretching	$\nu_a CH_3$
$S_{14} = (\Delta r_3+\Delta r_4+\Delta r_5)/\sqrt{3}$	CH_3 symmetric stretching	$\nu_s CH_3$

Table 4. Product rule and sum rule

Product rule	Obs.	Calcd.	Sum rule	
$\Pi\nu_{i\ NH_2}/\Pi\nu_{i\ ND_2}$*	3.77	3.71	$\sum\nu^2_{i\ NH_2}+\sum\nu'^2_{i\ ND_2}$	8.65×10^7
$\Pi\nu_{i\ cis}/\Pi\nu_{i\ trans}$	1.00	1.00	$\sum\nu^2_{i\ trans}+\sum\nu'^2_{i\ cis}$	8.60×10^7
$\Pi\nu'_{i\ NH_2}/\Pi\nu'_{i\ ND_2}$	3.73	3.73	$\sum\nu^2_{i\ cis}+\sum\nu'^2_{i\ trans}$	8.60×10^7
$\Pi\nu'_{i\ cis}/\Pi\nu'_{i\ trans}$	1.03	1.00	$\sum\nu^2_{i\ ND_2}+\sum\nu'^2_{i\ NH_2}$	8.65×10^7

$\nu_{i\ NH_2}$: infrared absorption frequency of CH_3CONH_2, $\nu_{i\ cis}$: *cis*-CH_3CONHD, $\nu_{i\ trans}$: *trans*-CH_3CONHD, $\nu_{i\ ND_2}$: CH_3COND_2, $\nu'_{i\ NH_2}$: CD_3CONH_2, $\nu'_{i\ cis}$: *cis*-CD_3CONHD, $\nu'_{i\ trans}$: *trans*-CD_3CONHD, $\nu'_{i\ ND_2}$: CD_3COND_2

Table 5. Force constants (md/Å)

Force constant	(md/Å)	Dispersion	Force constant	(md/Å)	Dispersion
K(CN)	5.52_5	0.034	H(HCC)	0.37_9	0.001
K(CO)	7.43_8	0.028	F(HNH)	0.0 (assumed)	—
K(CC)	3.18_7	0.029	F(HNC)	0.37_6	0.003
K(CH)	4.61_7	0.000	F(NCO)	1.22_8	0.021
K(NH)	5.72_8	0.001	F(CCN)	0.13_7	0.016
H(HNH)	0.37_5	0.000	F(CCO)	0.56_3	0.023
H(HNC)	0.40_6	0.000	F(HCH)	0.06_9	0.000
H(NCO)	0.52_1	0.005	F(HCC)	0.36_2	0.001
H(CCN)	0.62_5	0.006	κ	-0.11_8 md Å	0.000
H(CCO)	0.24_7	0.009	P(NH–NH)	-0.14_9	0.000
H(HCH)	0.40_1	0.000			

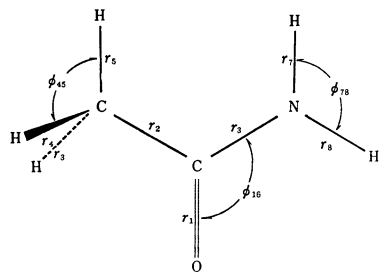

Fig. 6. Molecular structure and internal coordinates of acetamide.

on Hamilton's X ray study[4] as shown in Table 2. The description of the internal coordinates is shown in Fig. 6, and the internal symmetry coordinates are listed in Table 3. A simple Urey-Bradley force field was employed first but an interaction constant between the two NH stretching coordinates in the NH_2 group, P(NH–NH), was introduced after several trial calculations. The stretch-stretch interaction constant of this type was first introduced for methyl group[8] and water[9] as a supplementary

8) I. Nakagawa and T. Shimanouchi, *Spectrochim. Acta*, **18**, 513 (1962).

9) K. Kuchizu and L. S. Bartell, *J. Chem. Phys.*, **36**, 2460 (1962).

Table 6. Fundamental frequencies and main potential energy distributions for CH_3CONH_2 and CD_3CONH_2

	CH_3CONH_2						CD_3CONH_2				
	Obsd	Calcd	Δ(%)	P.E.D. (%)	Abbr.		Obsd	Calcd	Δ(%)	P.E.D. (%)	Abbr.
ν_1	3380	3375	0.2	$S_{11}(49)$, $S_{12}(49)$	ν_aNH_2	ν'_1	3380	3375	0.2	$S_{11}(49)$, $S_{12}(49)$	ν_aNH_2
ν_2	3190	3190	0.0	$S_{11}(51)$, $S_{12}(51)$	ν_sNH_2	ν'_2	3190	3190	0.0	$S_{11}(51)$, $S_{12}(51)$	ν_sNH_2
ν_3	3000	3005	0.2	$S_{13}(100)$	ν_aCH_3	ν'_3	2240	2234	0.3	$S_{13}(100)$	ν_aCD_3
ν_4	2636	2636	0.0	$S_{14}(100)$	ν_sCH_3	ν'_4	2120	2109	0.5	$S_{14}(99)$	ν_sCD_3
ν_5	1665	1670	0.3	$S_3(38)$, $S_4(33)$	νC=O	ν'_5	1655	1660	0.3	$S_3(29)$, $S_4(46)$	νC=O
ν_6	1640	1627	0.8	$S_5(60)$, $S_4(24)$	βNH_2	ν'_6	1639	1620	1.1	$S_5(51)$, $S_3(37)$	βNH_2
ν_7	1470	1471	0.0	$S_8(44)$, $S_{10}(16)$	δ_dCH_3	ν'_7	1413	1414	0.1	$S_1(46)$, $S_2(27)$	νCN
ν_8	1398	1400	0.1	$S_1(32)$, $S_2(22)$	νCN	ν'_8	1152	1151	0.1	$S_5(31)$, $S_4(22)$	ρNH_2
ν_9	1358	1361	0.2	$S_9(83)$	δ_sCH_3	ν'_9	1084	1078	0.7	$S_9(74)$	δ_sCD_3
ν_{10}	1154	1146	0.7	$S_5(32)$, $S_4(21)$	ρNH_2	ν'_{10}	1041	1036	0.5	$S_8(71)$, $S_{10}(17)$	δ_dCD_3
ν_{11}	1010	1018	0.8	$S_{10}(70)$, $S_8(30)$	ρCH_3	ν'_{11}	831	839	1.0	$S_2(20)$, $S_{10}(15)$	νCC′
ν_{12}	878	879	0.1	$S_2(43)$, $S_1(20)$	νCC′	ν'_{12}	813	806	0.8	$S_{10}(53)$, $S_8(20)$	ρCD_3
ν_{13}	586	582	0.7	$S_6(76)$, $S_2(17)$	δNCO	ν'_{13}	566	556	1.8	$S_6(67)$, $S_2(20)$	δNCO
ν_{14}	466	465	0.2	$S_7(87)$	δCC′	ν'_{14}	420	422	0.5	$S_7(80)$	δCC′

$\Delta=(|\nu_{obsd.}-\nu_{calcd.}|/\nu_{obsd.})\times 100$

Table 7. Fundamental frequencies and main potential energy distributions for *trans*-CH_3CONHD and CD_3CONHD

	trans-CH_3CONHD						*trans*-CD_3CONHD				
	Obsd	Calcd	Δ(%)	P.E.D. (%)	Abbr.		Obsd	Calcd	Δ(%)	P.E.D. (%)	Abbr.
ν_1	3270	3293	0.7	$S_{11}(99)$	ν_t-NH	ν'_1	3265	3293	0.9	$S_{11}(99)$	ν_t-NH
ν_2	3000	3005	0.2	$S_{13}(100)$	ν_aCH_3	ν'_2	2424	2397	1.0	$S_{12}(98)$	ν_c-ND
ν_3	2926	2936	0.3	$S_{14}(100)$	ν_sCH_3	ν'_3	2240	2234	0.3	$S_{13}(100)$	ν_aCD_3
ν_4	2395	2397	0.1	$S_{12}(98)$	ν_c-ND	ν'_4	2120	2109	0.5	$S_{14}(100)$	ν_sCD_3
ν_5	1652	1652	0.0	$S_3(59)$, $S_1(17)$	νC=O	ν'_5	1628	1633	0.3	$S_3(67)$, $S_1(17)$	νC=O
ν_6	1530	1534	0.2	$S_5(57)$, $S_1(23)$	Amide II	ν'_6	1529	1531	0.1	$S_5(67)$, $S_1(17)$	Amide II
ν_7	1453	1451	0.1	$S_8(60)$, $S_{10}(14)$	δ_dCH_3	ν'_7	1348	1334	1.0	$S_1(26)$, $S_5(16)$	Amide III
ν_8	1359	1375	1.2	$S_9(88)$	δ_sCH_3						
ν_9	1327	1316	0.8	$S_1(27)$, $S_5(13)$	Amide III	ν'_8	1084	1077	0.6	$S_9(66)$	δ_sCD_3
						ν'_9	1039	1048	0.9	$S_4(30)$, $S_8(18)$	δ_c-ND
ν_{10}	1060	1051	0.8	$S_4(36)$, $S_3(26)$	δ_c-ND	ν'_{10}	1039	1032	0.7	$S_8(53)$, $S_{10}(12)$	δ_dCD_3
ν_{11}	1010	1017	0.7	$S_{10}(70)$, $S_8(30)$	ρCH_3	ν'_{11}	812	819	0.8	$S_{10}(60)$, $S_8(23)$	ρCD_3
ν_{12}	819	818	0.1	$S_2(45)$, $S_4(22)$	νCC′	ν'_{12}	760	767	0.9	$S_2(29)$, $S_4(18)$	νCC′
ν_{13}	556	559	0.5	$S_6(75)$, $S_2(11)$	δNCO	ν'_{13}	538	539	0.2	$S_6(70)$, $S_2(15)$	δNCO
ν_{14}	460	460	0.0	$S_7(85)$	δCC′	ν'_{14}	—	416	—	$S_7(78)$, $S_{10}(11)$	δCC′

$\Delta=(|\nu_{obsd.}-\nu_{calcd.}|/\nu_{obsd.})\times 100$

constant in the Urey-Bradley force field. In the present calculation, this force constant was preferred to the repulsion constant F(HNH) in fitting the NH_2 asym. and sym. stretching frequencies simultaneously. The force constants other than K(NH) and K(CH) were initially taken from Suzuki's work.[5] At the first step of the force constant refinement, only the frequencies of the NH_2 and ND_2 species and the frequencies higher than 1200 cm^{-1} of the NHD species were taken into account, and the values of K(NH), K(CH), K(CO), K(CN) and K(CC) were adjusted by referring to the Jacobian matrix elements. The stretching constants as well as the bending and repulsion constants concerned with hydrogen atoms were refined next by the least squares method for these frequencies. After this refinement, the absorption frequencies below 1200 cm^{-1} attributable to the NHD species were assigned to the vibrational modes of either the *trans* or *cis* species by referring to the calculated frequencies. This assignment was checked by the product rule and independently by the sum rule for isotopic molecules,[10] by as-

10) J. C. Decius and E. B. Wilson, *J. Chem. Phys.*, **19**, 1409 (1951).

Table 8. Fundamental frequencies and main potential energy distributions for *cis*-CH_3CONHD and CD_3CONHD

	cis-CH_3CONHD						*cis*-CD_3CONHD				
	Obsd	Calcd	Δ(%)	P.E.D. (%)	Abbr.		Obsd	Calcd	Δ(%)	P.E.D. (%)	Abbr.
ν_1	3270	3291	0.7	S_{12}(99)	ν_c-NH	ν'_1	3265	3292	0.8	S_{12}(99)	ν_c-NH
ν_2	3000	3005	0.2	S_{13}(100)	$\nu_a CH_3$	ν'_2	2420	2400	0.8	S_{11}(97)	ν_t-ND
ν_3	2926	2935	0.3	S_{14}(100)	$\nu_s CH_3$	ν'_3	2240	2234	0.3	S_{13}(100)	$\nu_a CD_3$
ν_4	2417	2400	0.7	S_{11}(97)	ν_t-ND	ν'_4	2120	2109	0.5	S_{14}(100)	$\nu_s CD_3$
ν_5	1652	1659	0.4	S_3(53), S_1(20)	νC=O	ν'_5	1636	1644	0.5	S_3(57), S_2(20)	νC=O
ν_6	1475	1480	0.4	S_4(51), S_8(25)	δ_c-NH	ν'_6	1475	1469	0.4	S_4(53), S_5(34)	δ_c-NH
ν_7	1453	1460	0.5	S_8(19), S_5(20)	$\delta_d CH_3$	ν'_7	1413	1414	0.1	S_1(45), S_2(27)	νCN
ν_8	1398	1399	0.1	S_1(29), S_8(19)	νCN	ν'_8	1088	1083	0.5	S_9(81)	$\delta_s CD_3$
ν_9	1359	1360	0.1	S_9(84)	$\delta_s CH_3$	ν'_9	1039	1036	0.3	S_8(70)	$\delta_d CD_3$
ν_{10}	1045	1025	1.9	S_{10}(61), S_8(26)	ρCH_3	ν'_{10}	975	966	0.9	S_5(53), S_3(18)	δ_t-ND
ν_{11}	933	952	2.0	S_5(55), S_{10}(10)	δ_t-ND	ν'_{11}	828	828	0.0	S_2(27), S_9(15)	νCC'
ν_{12}	871	875	0.5	S_2(46), S_1(19)	νCC'	ν'_{12}	812	802	1.1	S_{10}(59), S_8(21)	ρCD_3
ν_{13}	568	570	0.4	S_6(75)	δNCO	ν'_{13}	546	545	0.2	S_6(68), S_2(17)	δNCO
ν_{14}	455	449	1.4	S_7(82)	δCC'	ν'_{14}	—	409	—	S_7(77)	δCC'

$\Delta = (|\nu_{obsd.} - \nu_{calcd.}|/\nu_{obsd.}) \times 100$

Table 9. Fundamental frequencies and main potential energy distributions for CH_3COND_2 and CD_3COND_2

	CH_3COND_2						CD_3COND_2				
	Obsd	Calcd	Δ(%)	P.E.D. (%)	Abbr.		Obsd	Calcd	Δ(%)	P.E.D. (%)	Abbr.
ν_1	3000	3005	0.2	S_{13}(100)	$\nu_a CH_3$	ν'_1	2527	2506	0.8	S_{11}(49), S_{12}(48)	$\nu_a ND_2$
ν_2	2926	2936	0.3	S_{14}(100)	$\nu_s CH_3$	ν'_2	2320	2307	0.6	S_{11}(49), S_{12}(51)	$\nu_s ND_2$
ν_3	2530	2506	1.0	S_{11}(49), S_{12}(48)	$\nu_a ND_2$	ν'_3	2240	2234	0.3	S_{13}(100)	$\nu_a CH_3$
ν_4	2316	2307	0.4	S_{11}(49), S_{12}(51)	$\nu_s ND_2$	ν'_4	2120	2109	0.5	S_{14}(99)	$\nu_s CH_3$
ν_5	1644	1645	0.1	S_3(59), S_1(20)	νC=O	ν'_5	1628	1625	0.2	S_3(68), S_1(21)	νC=O
ν_6	1453	1462	0.6	S_8(47), S_{10}(14)	$\delta_d CH_3$	ν'_6	1431	1422	0.6	S_1(50), S_2(30)	νCN
ν_7	1411	1413	0.1	S_1(42), S_2(23)	νCN	ν'_7	1187	1198	0.9	S_4(57), S_5(33)	βND_2
ν_8	1359	1363	0.3	S_9(90)	$\delta_s CH_3$	ν'_8	1070	1068	0.2	S_9(77)	$\delta_s CD_3$
ν_9	1185	1190	1.3	S_4(61), S_5(32)	βND_2	ν'_9	1039	1034	0.5	S_8(69), S_{10}(15)	$\delta_d CD_3$
ν_{10}	1036	1021	1.5	S_{10}(63), S_8(27)	ρCH_3	ν'_{10}	962	954	0.8	S_5(40), S_3(21)	ρND_2
ν_{11}	933	943	1.0	S_5(43), S_1(13)	ρND_2	ν'_{11}	817	808	1.1	S_{10}(62), S_8(23)	ρCD_3
ν_{12}	817	816	0.1	S_2(46), S_3(22)	νCC'	ν'_{12}	760	766	0.8	S_2(31), S_4(18)	νCC'
ν_{13}	548	551	0.5	S_6(73)	δNCO	ν'_{13}	526	531	0.9	S_6(69), S_2(13)	δNCO
ν_{14}	442	444	0.4	S_7(79)	δCC'	ν'_{14}	—	404	—	S_7(75)	δCC'

$\Delta = (|\nu_{obsd.} - \nu_{calcd.}|/\nu_{obsd.}) \times 100$

suming the unobserved CC' deformation frequencies for CD_3COND_2 and *trans*- and *cis*-CD_3CONHD to be the same as the calculated frequencies. The theoretical product rule ratios were obtained from the calculated frequencies. Both the product rule and the sum rule are well satisfied by the assigned frequencies as seen in Table 4. Then at the final step, we added the interaction constant P(NH–NH) with the initial value of zero, fixed the repulsion constant F(HNH) to zero, and refined all other force constants simultaneously to obtain a converged set. The force constants used in the final calculation are shown in Table 5 together with their dispersions. Tables 6—9 show the frequencies calculated from these force constants, the corresponding observed frequencies and the potential energy distributions. The agreement between the calculated and the observed frequencies are quite excellent throughout all isotopic species. It is seen from Table 7 that the coupling between the NH in-plane deformation and the CN stretching vibrations takes place only for the *trans*-NHD species just as shown by the calculation for *N*-methylacetamide.[1)]

Thanks are due to the members of the Computer Center of Kyoto University for the use of a KDC II computer in the normal coordinate analysis.

BULLETIN OF THE CHEMICAL SOCIETY OF JAPAN VOL. 42 905—908 (1969)

Some Experiments on the Triplet State Mechanism of the Spectral Sensitization of Poly(vinyl cinnamate) and Its Application for Searching New Sensitizers*[1]

Minoru TSUDA

Government Chemical Industrial Research Institute, Tokyo, Hiratsuka, Kanagawa

(Received August 17, 1968)

The spectral sensitization of poly(vinyl cinnamate) is considered to occur by the triplet energy transfer from sensitizer to the cinnamoyl group of the polymer. The triplet state mechanism is useful for finding new sensitizers. Some new sensitizer were found on the basis of the theory, and the results may verify the mechanism.

Ultraviolet light irradiation on poly(vinyl cinnamate) reduces the solubility of the polymer according to the dose of light. The main response of cinnamic acid and its esters to photons is believed to be their dimerizations. The dimerization of cinnamoyl groups attached to polymers results in crosslinking of the polymer, which produces the insolubilization of the polymer.

The photosensitivity of poly(vinyl cinnamate) is limited to wavelengths shorter than 340 mμ, but the addition of some organic compounds confers sensitivity on the portion of the spectrum absorbed by those compounds;[1,2] hence, these compounds are spectral sensitizers. The experimental fact that the better sensitizers are aromatic nitro compounds and aromatic cabronyl compounds, suggests that the energy transfer may occur from the triplet state (T-state) of sensitizers to that of the cinnamoyl group (Fig. 1). The proposed mechanism clearly explained the experimental results on the sensitivities of mixed sensitizers which have different lowest triplet levels.[3] In the present paper we will report a search for new sensitizers based on the T-state mechanism; this will be a test for the mechanism.

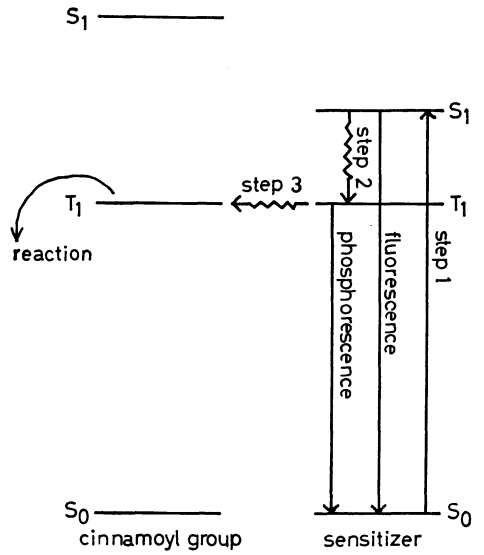

Fig. 1. Energy transfer diagram in spectral sensitization of poly(vinyl cinnamate).

*1 Presented at the International Conference on Photochemistry, Tokyo, August 28, 1965. This paper is a part of the Doctoral Thesis submitted by the author to the University of Tokyo, 1966.

Experimental

Poly(vinyl cinnamate) was prepared by the method reported in previous papers.[4] The polymer was purified by precipitation in methanol.

2,6-Dichloro- and 2,6-Dibromo-*N*,*N*-dimethyl-4-nitroaniline. Br_2(3.7 g) or Cl_2(0.92 g) was added into a methanol (200 ml) solution of *N*,*N*-dimethyl-4-nitroaniline (1.7 g), and the solution was refluxed for 2.5 hr. A large portion of methanol was distilled off, and crystals formed on standing. Recrystallized from ethanol.

Br-Derivative: mp 113.5—114.5°C. Found: C, 29.55; H, 2.40; N, 8.79; Br, 50.88%. Calcd for $C_8H_8N_2O_2Br_2$: C, 29.66; H, 2.49; N, 8.65; Br, 49.33%.

Cl-Derivative: mp 106—107°C. Found: C, 40.72; H, 3.71; N, 11.54; Cl, 29.71%. Calcd for $C_8H_8N_2O_2Cl_2$: C, 40.88; H, 3.43; N, 11.92; Cl, 29.71%.

***N*-Acetyl-4-nitro-1-naphthylamine.** 4-Nitro-1-naphthylamine (2 g) dissolved in acetic anhydride (70 ml) was heated at 100°C for 2 hr. On cooling crystals formed, which were recrystallized from ethanol.

1) Z. Koana, International Congress of Photographic Science, Tokyo (1967).

2) E. M. Robertson, W. P. Van Deusen, L. M. Minsk, *J. Appl. Polymer Sci.*, **2**, 308 (1959).

3) M. Tsuda, *J. Polymer Sci.*, **B2**, 1143 (1964).

4) M. Tsuda, *Makromol. Chem.*, **74**, 174, 183 (1964).

Mp 191.5—192°C. Found: C, 62.75; H, 4.44; N, 11.85%. Calcd for $C_{12}H_{10}N_2O_3$: C, 62.60; H, 4.38; N, 12.16%.

***N*-Benzoyl-4-nitro-1-naphthylamine.** 4-Nitro-1-naphthylamine (1.88 g) dissolved in methyl ethyl ketone (75 m*l*) and benzoyl chloride (1.55 g) were added to 10% aqueous NaOH solution (75 m*l*), and then vigorously agitated for 20 min. After standing, the upper layer was separated and methyl ethyl ketone was distilled off. The residue was recrystallized from ethanol. Mp 238—238.5°C. Found: C, 69.97; H, 4.37; N, 9.55%. Calcd for $C_{17}H_{12}N_2O_3$: C, 69.84; H, 4.14; N, 9.59%.

Other Substances. Guaranteed grade substances from Tokyo Kasei Co., Ltd. were recrystallized. Their melting points agreed with the literature values.

Sensitometry. Gray scale method proposed by Minsk *et al.*[7] was used. The gray scale used was a Kodak Step Tablet No. 2 calibrated by densitometer. The light source was a super high pressure mercury arc lamp (Toshiba SHL-100 UV). Picramide was used as a standard, assuming a relative sensitivity of 400.

Spectroscopy. Emission spectra were measured by a Hitachi EPM-2S type spectrometer, and absorption spectra were measured by Shimadzu IV-50 type spectrometer.

TABLE 1. EMISSION SPECTRA AND SENSITIVITY

Compound	Emission spectra[5,6]	Relative sensitivity
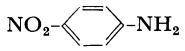	P	410
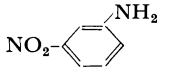	F	0
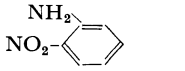	F	0
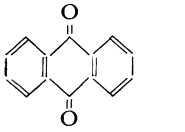	P	130
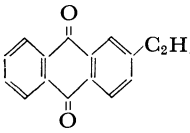	P	360
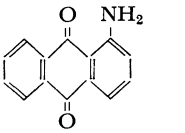	F	0
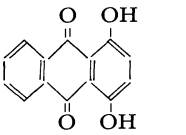	F	0

P: phosphorescence, F: fluorescence

Emission Spectra and Sensitivity

Sensitizers of poly(vinyl cinnamate) may be phosphorescent. It is known that some compounds with similar structures to sensitizers do not sensitize. It was found that they do not phosphoresce but fluoresce as shown in Table 1. The failure to sensitize is easily understood in terms of the T-state mechanism, because, when step 2 in Fig. 1 does not occur, fluorescence only is observed and not phosphorescence.

Heavy Atom Effect

When heavy atoms are introduced into a molecule, step 2 of Fig. 1 is favored by the increase of the spin-orbit interaction. Therefore, we can expect an increase in the sensitizing effect of a sensitizer by the introduction of heavy atoms. At the same time the intensity of phosphorescence of the molecule is expected also to increase.

N,*N*-Dimethyl-4-nitroaniline is a sensitizer having a moderate sensitizing effect. It emits both fluorescence and phosphorescence rather strongly. Therefore, if heavy atoms are introduced into the molecule, we should obtain new sensitizers having

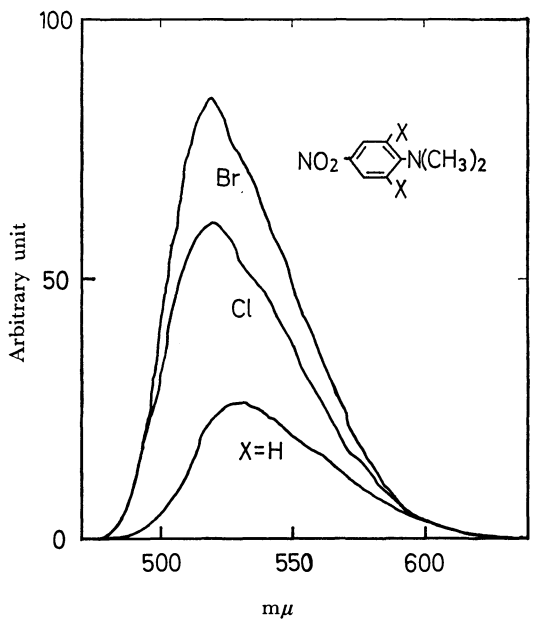

Fig. 2. Phosphorescence spectra of the derivatives of *N*,*N*-dimethyl-4-nitroaniline.
H: *N*,*N*-dimethyl-4-nitroaniline 1.004 mg/cc;
Cl: 2,6-dichloro derivative 1.001 mg/cc;
Br: 2,6-dibromo derivative 1.007 mg/cc;
Solvent: methanol 1 volume, methlcyclohexane 1, ethyl ether 1; Excitation 360 mμ (slit width 40 mμ); Analizer slit width: 2mμ.

5) R. Foster, D. Ll, Hammick, G. M. Hood and A. C. E. Sanders, *J. Chem. Soc.*, **1956**, 4865.
6) H. H. Dearman and A. Chan, *J. Chem. Phys.*, **44**, 416 (1966).
7) L. M. Minck, J. G. Smith, W. P. Van Deusen and J. F. Wright, *J. Appl. Polymer Sci.*, **2**, 302 (1959).

a strong sensitizing effect and showing strong phosphorescence. Phosphorescence spectra of *N,N*-dimethyl-4-nitroaniline (H), and its 2,6-dichloro (Cl), and 2,6-dibromo (Br) derivatives are shown in Fig. 2. The shapes of the spectra are very similar to each other.

It is noticed that the intensity of phosphorescence increases remarkably by replacing H with Cl, or with Br, and the sensitizing effect also increases as expected (Table 2).

Table 2. Heavy atom effect on sensitizers

Sensitizer	Relative sensitivity
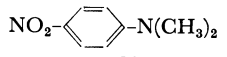	137
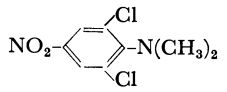	561
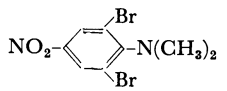	797

As the sensitizing effects are measured by the gray scale method using a super high pressure mercury are lamp as a light source, it may be considered that the exposure is due mainly to 365, 405 and 436 mμ lines considering the absorption spectra of these three sensitizers. The ratio of the intensities of these active lights emitting from the light source is 2.25 : 1 : 2.04, and the transmittances of the gray scale at those wavelengths are 55, 79, and 82%. With those corrections the relative yields of phosphorescence at these three wavelengths are obtained. The sum of the relative yields of phosphorescence at these three wavelengths plotted as the abscissa of Fig. 3 *vs.* the relative sensitivity as the ordinate produced a straight line. The relative sensitivity of the sensitizer is directly proportional to the relative yield of its phosphorescence within the limits of experimental error.

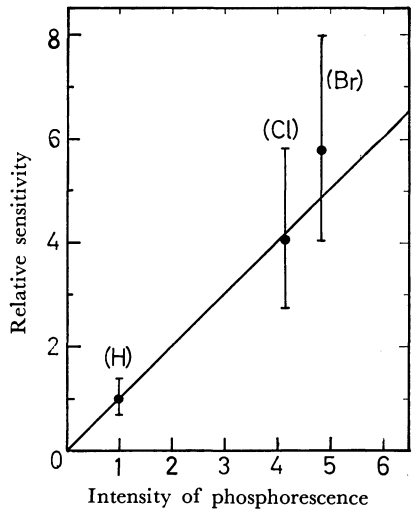

Fig. 3. Relationship between phosphorescence yields and relative sensitivities.

Energy of Triplet State

From the T-state mechanism, the sensitizing effect should be observed only when the energy of T_1 of the sensitizer is equal to or larger than that of the cinnamoyl group (Fig. 1). Therefore, there are some compounds which have not sensitizing effects in spite of their strong phosphorescence. For example, 4-nitro-1-naphthylamine phosphoresces strongly,[5] and its chemical structure is similar to 4-nitroaniline and α-nitronaphthalene (both are strong sensitizers), but it has no sensitizing effect.

Compounds having similar chemical structures may have a constant value of the gap between the peaks of their absorption spectra and the 0–0 bands of their phosphorescence spectra. The values are, for example, about 6000 cm^{-1} for the analogues of 4-nitroaniline and about 10000 cm^{-1} for the analogues of 4-nitrodiphenyl as shown in Table 3. Using this phenomenon, we may expect to change a non-sensitizer, 4-nitro-1-naphthylamine, into a sensitizer.

The peak of the absorption spectrum of 4-nitro-1-naphthylamine shifts toward the shorter wavelength region by *N*-acylation; so, the energy of

Table 3. The gap between the peak of absorption spectrum and the 0–0 band of phosphorescence spectrum

Compound	Gap, cm^{-1}
4-Nitroaniline	7338
N-Methyl-4-nitroaniline	6576
N,N-Dimethyl-4-nitroaniline	6625
4-Nitro-1-naphthylamine	5956
4-Nitrodiphenyl	9262
4,4'-Dinitrodiphenyl	12343
2-Nitrofluorene	9703

Table 4. Sensitizing effect of *N*-acyl-4-nitro-1-naphthylamines

Compound	Relative sensitivity
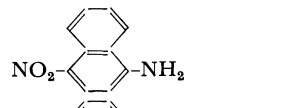	0
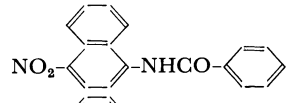	769
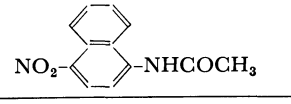	1100

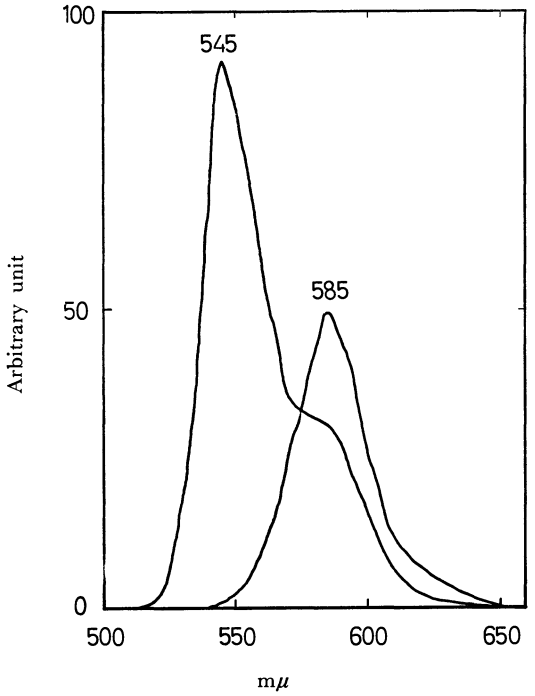

Fig. 4. Phosphorescence spectra of 4-nitro-1-naphthylamine (peak: 585 mμ) and *N*-acetyl-4-nitro-1-naphthylamine (peak: 545 mμ).
Conditions in measurements are different.

T_1 of the *N*-acylated derivative may increase, and get into the sensitizing region. *N*-Acetyl-4-nitro-1-naphthylamine and *N*-benzoyl-4-nitro-1-naphthylamine have really been found to have a strong sensitizing effect (Table 4). The phosphorescence spectra of 4-nitro-1-naphthylamine and its *N*-acetyl derivative are shown in Fig. 4. *N*-Acetyl-4-nitro-1-naphthylamine emits far stronger phosphorescence than 4-nitro-1-naphthylamine though Foster reported[5] that the latter phosphoresces strongly. The excitation spectra of both of them measured under the same conditions are shown in Fig. 5.

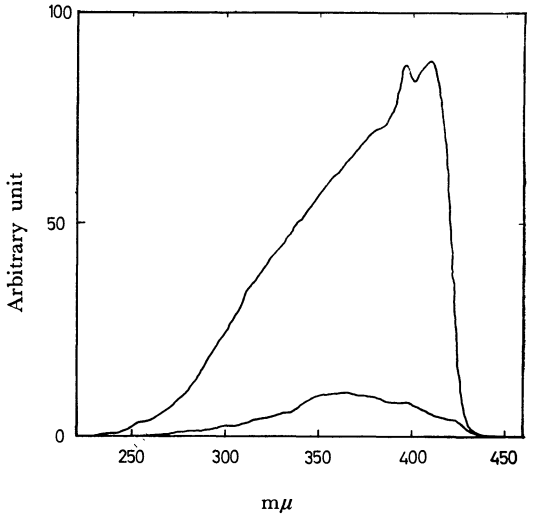

Fig. 5. Excitation spectra of 4-nitro-1-naphthylamine and *N*-acetyl-4-nitro-1-naphthylamine at the same conditions.
Analizer was set at the peak of Fig. 4. Figures of abscissa are the wavelength of excitation light. Conditions: *N*-acetyl-4-nitro-1-naphthylamine 0.944 mg/cc; 4-nitro-1-naphthylamine 0.957 mg/cc; Exciter slit width 3.5 mμ.

Conclusion

It is shown that some deductions from the T-state mechanism agree well with experimental facts. This strongly supports that the spectral sensitization of poly(vinyl cinnamate) occurs by the triplet energy transfer from sensitizers to the cinnamoyl group of the polymer. The theory is also useful for finding new sensitizers.

BULLETIN OF THE CHEMICAL SOCIETY OF JAPAN VOL. 42 909—913 (1969)

Photochemistry of Acetanilide. IV. The Photochemical Reactions in the Vapor Phase and Rigid Matrixes

Haruo SHIZUKA[1] and Ikuzo TANAKA

Laboratory of Physical Chemistry, Tokyo Institute of Technology, Ookayama, Meguro-ku, Tokyo

(Received August 21, 1968)

The photolysis of acetanilide in the vapor phase at 2537 Å and 120°C has been studied by means of mass spectrometry, gas chromatography, and spectrophotometry. In the vapor phase, no such rearrangements of acetanilide as in the liquid phase occurred, only the decomposition of acetanilide. Carbon monoxide and ethane were formed as the main products, and the ratio of carbon monoxide to ethane was about 2. The quantum yield of the predissociation for the N–C bond of acetanilide in the vapor phase was estimated to be 0.28 from the data of the quantum yields for the formations of carbon monoxide and ethane. A small amount of methane and traces of hydrogen and benzene were also detected. The reaction scheme of acetanilide in the vapor phase at 2537 Å and 120°C has been proposed. On the other hand, the photochemical reactions of acetanilide in the rigid matrixes (MP, ME, and EPA) at −196°C and in the PVA sheet at room temperature have also been carried out by the use of a spectrophotometer and an ESR spectrometer. In the rigid matrixes at −196°C, the photochemical rearrangements did not occur, only the back reaction resulting in the distortional structure of acetanilide; this mechanism can be explained by the stiffness of the solvent cage. The cage effect on the photochemical reaction of acetanilide is also discussed.

In previous papers[2-4] on the photochemistry of acetanilide in the liquid phase, it has been shown that the photochemical rearrangement occurs due to the predissociation through the intersystem crossing ${}^3\sigma_0(\text{N–C}) \leftarrow S_1(\pi\pi^*)$, resulting in the fission of the N–C bond and the liberation of anilino and acetyl radicals and, subsequently, the recombination reactions between the pair radicals in a solvent cage.

In the liquid phase, in cyclohexane, for example, the cage effect on the recombination reactions which consist of the back reaction, *o*- and *p*-rearrangements is sufficiently large (the recombination ratio ≈ 0.9).[4] On the other hand, in the vapor phase where the solvent effect may be neglected,[5] it is expected that the recombination reactions do not occur, only the decomposition of acetanilide. However, the vapor pressure of acetanilide at room temperature is very low. In order to obtain a sufficient pressure for the vapor-phase photolysis, acetanilide should be heated at 120°C. Acetanilide does not decompose at 120°C without the radiation of UV light.

On the other hand, it is also interesting to investigate the photochemical reactions of acetanilide in rigid matrixes (MP, ME, and EPA) at −196°C and in a PVA sheet at room temperature, since the solvent cage consisting of these rigid matrixes may be expected to be very stiff.

This paper will report the photolysis of acetanilide in the vapor phase at 2537 Å and 120°C and the photochemical reaction of acetanilide in the rigid matrixes (MP, ME, and EPA) at 2537 Å and −196°C, and in PVA sheet at 2537 Å and room temperature; it will also include a discussion of the reaction schemes in these photochemical reactions.

Experimental

Materials. The acetanilide, ethanol, and ether were the same reagents as have been described in the previous papers.[2-4] The methanol was a Kantokagaku Co. G. R. product. The isopentane was a Tokyo Kasei G. R. product and was purified by passing it through silica gel and by distillation. The polyvinyl alcohol (PVA) was a Koso Chemical Co. G. R. product ($\overline{p} \sim 1500$).

Light Source and Actinometry. A low-pressure mercury lamp with a Vycor glass filter was used as the 2537 Å radiation source. Actinometry was carried out by in the same way as has been described in a previous paper.[2] The light intensity at 2537 Å was 7.85×10^{13} photons sec^{-1} in the vapor-phase photolysis.

1) Present address: Department of Chemistry, Faculty of Engineering, Gunma University, Tenjin-cho Kiryu, Gunma.

2) H. Shizuka and I. Tanaka, This Bulletin, **41**, 2343 (1968).

3) H. Shizuka, *ibid.*, **42**, 52 (1969).

4) H. Shizuka, *ibid.*, **42**, 57 (1969).

5) J. Franck and E. Rabinowitch, *Trans. Faraday Soc.*, **30**, 120 (1934).

Reaction Procedure and Analysis in the Vapor Phase. The cylindrical quartz reaction cell was 10 cm long and 4.3 cm in diameter and had a ground joint and a breakable seal. About 20 mg of acetanilide was put into the reaction cell. After degassing, the reaction cell was sealed off from the vacuum system, which was free from mercury in order to avoid mercury photosensitization. The reaction cell was then heated to 120°C by an electric heater (the vapor pressure of the acetanilide at 120°C was 1.4 Torr), and then the sample was irradiated at 2537 Å.

Acetanilide (mp 115°C, bp 305°C) did not decompose at 120°C without the radiation of UV light. After irradiation, the products were introduced from the reaction cell into the system for analysis. The mixture of noncondensable products at −196°C (carbon monoxide, methane, and hydrogen) was collected into the gas burette of the Toepler gauge and analysed by a mass spectrometer after its quantity had been measured.

The volatile compounds which are condensable in liquid nitrogen (−196°C) were trapped into a LeRoy still. C_2 compounds, such as ethane, ethylene, and acetylene, were then separated from the products with higher boiling points by vacuum distillation, and were collected into the Topeler gauge. After the measurement of their quantities, the mixture was transferred into a small tube with a rubber septum at one end. The C_2 compounds were analyzed by gas chromatography with a silica gel +5% squalane column (2 m long, at 70°C) and with an active-charcoal column (3 m long, at 160°C). The C_n compounds ($n \geq 3$), such as biacetyl and benzene, which had been trapped in the LeRoy still at −150°C, were also transferred into a small tube with a rubber septum at one end. The C_n compounds were analyzed by gas chromatography by means of a dinonyl phthalate column (1 m long, at 70°C) and with a dioctyl phthalate column (1 m long, at 86°C).

The residues of nonvolatile products at room temperature were resolved in ethanol and were measured with a spectrophotometer.

Reaction Procedure and Analysis in Rigid Matrixes. The photochemical reactions of acetanilide were carried out in degassed rigid solvents (MP, EPA, and ME)*1 at 77°K and in polyvinyl alcohol (PVA) sheet*2 at room temperature. The ultraviolet and visible absorption spectra were taken with a Shimadzu SV 50A spectrophotometer. In the photochemical reaction at −196°C, a quartz Dewar flask designed for the spectrophotometry was used as the reaction cell. ESR measurements were also made in degassed rigid solvents (methylcyclohexane and ethanol) at −196°C after irradiation with 2537 Å for 30 min by the use of a JES 3110 X.

In order to disperse acetanilide homogeneously into a PVA sheet (0.17 mm thick), it was immersed in an aqueous solution of acetanilide and then dried at 70°C. The spectral change of the acetanilide in the PVA sheet upon the irradiation at 2537 Å was measured.

*1 MP, methylcyclohexane : isopentane=2 : 1; EPA, ether : isopentane : ethanol=1 : 1 : 1; ME, methanol : ethanol=1 : 1.

*2 PVA sheet was preheated at 80°C. See Y. Tanizaki and S. Kubodera, *J. Mol. Spectry.*, **24**, 1 (1967).

Results and Discussion

Photolysis of Acetanilide in the Vapor Phase. The data on the photolysis of acetanilide in the vapor phase at 2537 Å and 120°C are presented in Table 1 and in Figs. 1 and 2. Table 1 shows the reaction products in the photolysis at a very low conversion (less than 1%).

TABLE 1. REACTION PRODUCTS IN THE PHOTOLYSIS OF ACETANILIDE

Product	Relative yield
CO	100
CH_4	1.4
H_2	Trace
C_2H_6	48
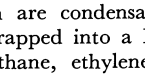	Trace

Carbon monoxide and ethane were obtained as the main products, the ratio of carbon monoxide to ethane was about 2. The amount of methane was about 1.4% that of carbon monoxide. Traces of hydrogen and benzene were also detected, but ethylene, acetylene, biacetyl, and the rearrangement products (*o*- and *p*-amino acetophenones) were not observed.

Figure 1 shows the time dependence of the product formations for carbon monoxide and ethane as a function of the irradiation time. The quantum yields for the formations of carbon monoxide and ethane were 0.28 and 0.14 respectively.

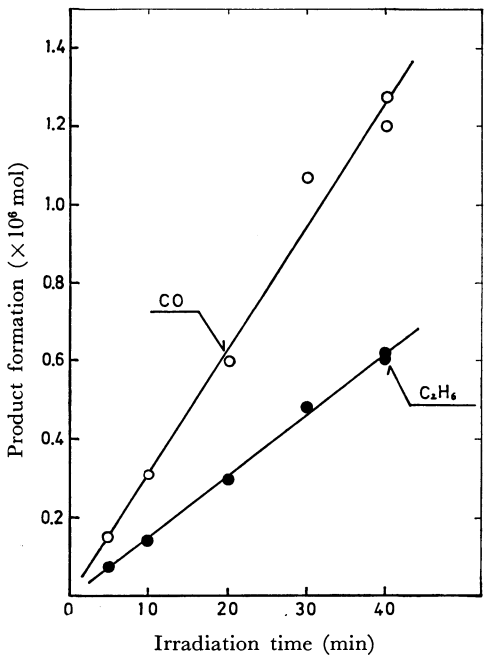

Fig. 1. Time dependence of product formations.

Figure 2 shows the spectral change in acetanilide in this photolysis; no rearrangement of acetanilide occurs in the vapor phase at 2537 Å, judging from the absence of any characteristic absorption bands of *o*- and *p*-amino acetophenones.[2]

Several reactions may be considered as the primary dissociation step in the photolysis of acetanilide:

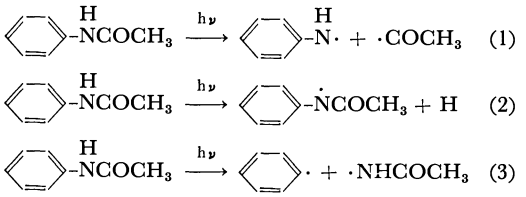

(1)

(2)

(3)

The experimental results on the formations of ethane and carbon monoxide as the main products give very strong evidence for the acetyl radical formation (Eq. (1)). The acetyl radical is known to decompose rapidly and exclusively to the methyl radical and to carbon monoxide above 100°C.[6] All the acetyl radicals formed here by Eq. (1) may, therefore, be assumed to decompose to methyl radicals and carbon monoxide molecules.

The formation of ethane can be explained by the recombination reaction between methyl radicals, and that of a small amount of methane, by the hydrogen-atom abstraction of the methyl radical. When a trace of NO (~0.1 Torr) was added to acetanilide, the formation of ethane was efficiently reduced. This result indicates that the methyl radical is formed in the photolysis of acetanilide and is scavenged by NO.

As has been described above, the rearrangement products of acetanilide were not observed in the vapor-phase photolysis. This means that no recombination reactions between anilino and acetyl radicals, such as the back reaction, *o*- and *p*-rearrangements (Eq. (4)), occurred because of the absence of a solvent cage in the vapor phase.

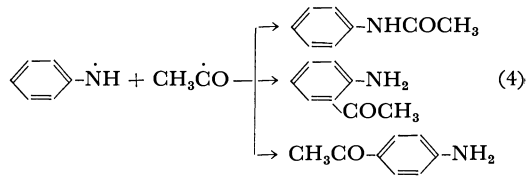

(4)

In view of the quantum yields for the formation of carbon monoxide and ethane, the dissociation quantum yield of acetanilide in the vapor-phase photolysis at 2537 Å and 120°C was estimated to be ~0.28, which is almost the same value as that obtained in the liquid phase (0.25).[4] It may be assumed that the predissociation by the intersystem crossing $^3\sigma_0(\mathrm{N\text{–}C}) \leftarrow S_1(\pi\pi^*)$ occurs in the vapor phase as well as in the liquid phase.

Thus, the reaction scheme of the photolysis of acetanilide in the vapor phase at 2537 Å and 120°C may be represented as follows:

$$S_0 + h\nu \longrightarrow S_2(\pi\pi^*) \quad (5)$$

$$S_2(\pi\pi^*) \xrightarrow{k_{IC}} S_1(\pi\pi^*) \quad (6)$$

$$S_1(\pi\pi^*) \xrightarrow{k_S} S_0 \quad (7)$$

$$S_1(\pi\pi^*) \xrightarrow{k_F} S_0 + h\nu' \quad (8)$$

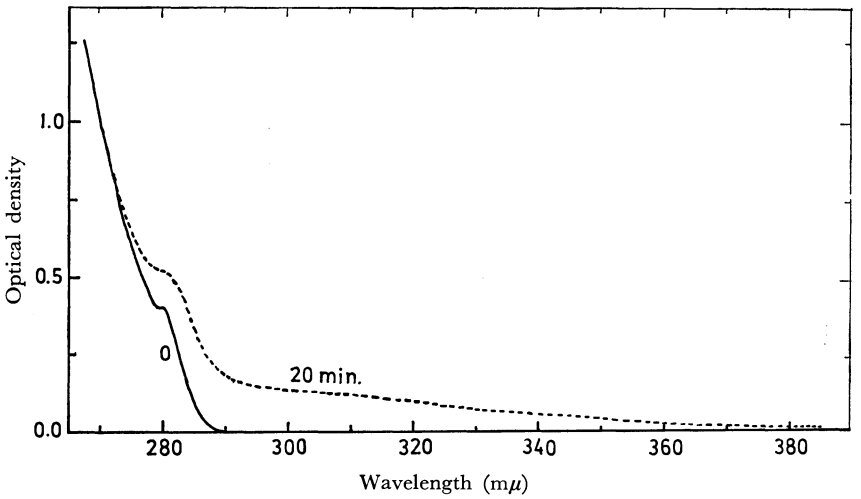

Fig. 2. Spectral change of acetanilide dissolved in ethanol solution after irradiation in the gas phase. —— before, ---- after

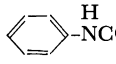 In gas phase (120°C). Irrad. 2537 Å

6) W. A. Noyes, Jr., G. B. Porter and J. E. Jolley, *Chem. Revs.*, **56**, 46 (1956).

$$S_1(\pi\pi^*) \xrightarrow{k_C} T_1(\pi\pi^*) \quad (9)$$

$$S_1(\pi\pi^*) \xrightarrow{k_{dis}} \dot{\phi}\text{-}\dot{N}H + \dot{C}OCH_3 \quad (10)$$

$$\dot{C}OCH_3 \xrightarrow{k_1} \dot{C}O + \dot{C}H_3 \quad (11)$$

$$2\dot{C}H_3 \xrightarrow{k_2} C_2H_6 \quad (12)$$

$$\dot{C}H_3 + RH \xrightarrow{k_3} CH_4 + R\cdot \quad (13)$$

Photochemical Reaction of Acetanilide in the Rigid Matrix. Figures 3(a) and 3(b) show the changes in the UV spectra of acetanilide in MP and ME degassed rigid matrixes at 2537 Å and −196°C respectively. In both cases, absorption band II decreased with the lapse of the irradiation time. The spectral change in acetanilide in the EPA rigid matrix is similar to that in ME. The absorption bands of the anilino radical (3088 Å) and the cation radical (4288 Å) which were observed in the photolysis of aniline[7] did not appear in the case of acetanilide. However, if the reaction cell was warmed up to room temperature after irradiation for 40 min in a MP rigid matrix, the spectral change of acetanilide was scarcely observed in a MP solution. Similar results were also obtained with a ME rigid matrix.

In order to detect the anilino and acetyl radicals, or the cation radical of acetanilide, ESR measurements of acetanilide in the rigid matrixes (degassed methyl cyclohexane and ethanol) at 2537 Å and −196°C were carried out, but no significant ESR signals were observed. The absence of the anilino radical and of the cation radical of acetanilide may be explained as follows:

1) The intersystem crossing $^3\sigma_0(\text{N–C}) \leftarrow S_1(\pi\pi^*)$, which produces anilino and acetyl radicals becomes less feasible at low temperatures due to the temperature dependence of the crossing probability. The acetyl radical can not escape from a solvent cage nor rearrange to the *o*- or *p*-position of the anilino radical. The only possible reaction is the back reaction, because the solvent cage in a glass at a low temperature is quite stiff.

2) The ionization potential of acetanilide (9.07 eV)[3] is larger than that of aniline (7.70 eV).[8]

From these results and considerations, it may be concluded that the spectral change in acetanilide in the rigid matrix at 2537 Å and −196°C was not caused by the *o*- and *p*-rearrangements, but by the back reaction between the pair radicals, resulting in the distorted structure of acetanilide (S_0'), which had only a little π-electron-conjugated system between anilino and acetyl groups. Equations (14) and (15) show the reaction scheme of the photochemical reaction of acetanilide in the rigid matrix at 2537 Å and −196°C.

$$S_1(\pi\pi^*) \xrightarrow{k_{dis}} (\dot{\phi}\text{-}\dot{N}H + \dot{C}OCH_3)\dagger \quad (14)$$

$$(\dot{\phi}\text{-}\dot{N}H + \dot{C}OCH_3)\dagger \longrightarrow S_0' \quad (15)$$

†: a stiff solvent cage.

When the reaction cell was warmed to room temperature, S_0' turned back to the ground state of acetanilide, S_0.

The photochemical reaction of acetanilide in

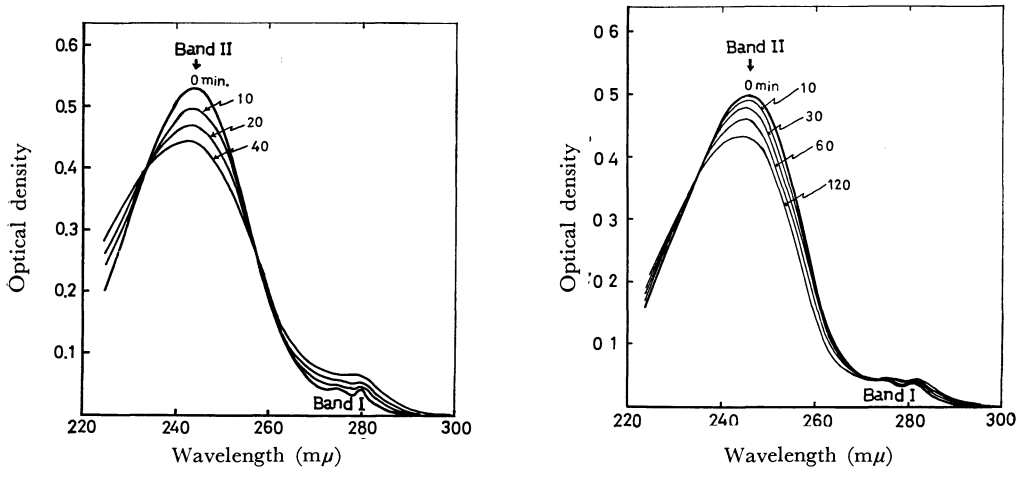

Fig. 3. Spectral change of acetanilide in the rigid matrixes at 2537 Å and −196°C. Numbers refer to time in minutes.
(a) in MP glass (b) in ME glass

7) I. Norman and G. Porter, *Proc. Roy. Soc.* (*London*), **A230**, 399 (1955); E. J. Land and G. Porter, *Trans. Faraday Soc.*, **59**, 2027 (1963).

8) K. Watanabe, *J. Chem. Phys.*, **26**, 542 (1957); R. Bralsfold, P. V. Harris and W. C. Price, *Proc. Roy. Soc.*, **A258**, 459 (1960).

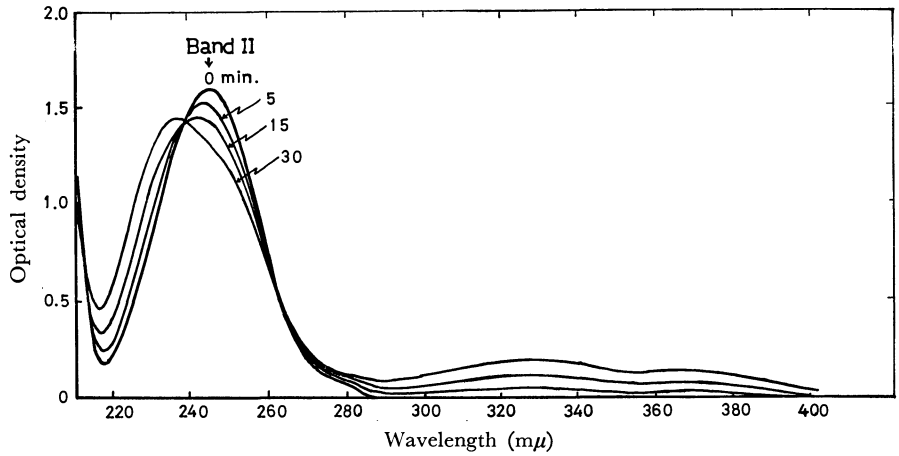

Fig. 4. Spectral change of acetanilide in PVA sheet at 2537 Å and room temperature.

the PVA sheet was observed by spectrophotometry at 2537 Å and at room temperature, as is shown in Fig. 4. Absorption band II decreased and new peaks at 325 and 365 mμ, which correspond to the *o*- and *p*-amino acetophenones respectively, appeared with an increase in the irradiation time. It is assumed that a pair of radicals can rearrange because the PVA matrix at room temperature contains an amorphous structure.

Table 2 shows the quantum yields for the formations of *o*- and *p*-amino acetophenones at 2537 Å in PVA, ethanol, and ME.

Table 2. The quantum yields at 2537 Å in PVA, ethanol, and ME

Solvent	Temp. °C	Quantum yield (Φ)		
		Φ_o	Φ_p	Φ_o/Φ_p
PVA	Room temp.	0.003_8	0.001_6	2.4
Ethanol[a)]	20	0.01_7	0.01_4	1.2
Ethanol	− 70	0.005_1	0.002_1	2.4
ME	−196	0	0	—

a) See Footnote 3.
Φ_o and Φ_p are the quantum yields for the formations of *o*- and *p*-amino acetophenones respectively at 2537 Å.

The quantum yields in the PVA sheet at room temperature decreased considerably in comparison with that in ethanol at 20°C. It seems that the back reaction in the PVA matrix is more predominant than the *o*- and *p*-rearrangements because the solvent cage in the PVA matrix is stiffer than that in ethanol at 20°C. The quantum yields in ethanol at −70°C were smaller than those in ethanol at 20°C. The dependence of the quantum yield in ethanol on the temperature from 20 up to 50°C has previously been described.[3,4)] The viscosity of ethanol in this range of temperature does not change very much, but it increases significantly at lower temperatures (*e.g.*, −70°C).[9)] Therefore, in addition to the effect of the activation energy (E_{dis} ~1.5 kcal/mol in ethanol)[4)] of the photochemical reaction of acetanilide, the cage effect becomes more important at lower temperatures because of the increasing stiffness of the solvent cage.

The ratios of Φ_o/Φ_p in PVA at room temperature and in ethanol at −70°C were about twice that of ethanol at 20°C. This indicates that the dependence of the *p*-rearrangement on the stiffness of the solvent cage is larger than that of the *o*-rearrangement because in a stiff solvent cage the *p*-positions of the anilino radical and the acetyl radical are separated by a longer path.

Conclusion

In the vapor phase at 2537 Å and 120°C, the decomposition of acetanilide took place, forming carbon monoxide and ethane ($CO/C_2H_6 \approx 2$) as the main products, instead of rearrangement. In the rigid matrix at −196°C, the rearrangements do not occur either, only the back reaction. These differences in the photochemical reaction of acetanilide are mainly caused by the cage effect on the recombination reactions between anilino and acetyl radicals formed by the intersystem crossing $^3\sigma_0$ (N–C)←$S_1(\pi\pi^*)$.

The authors are greatly indebted to Associate Professor Yuji Mori of the Tokyo Institute of Technology for his generous and very helpful discussions concerning this paper.

9) See "Kagaku-benran, Kisohen" (Chemical Index of The Chem. Soc. Japan), Maruzen, Tokyo (1966), p. 505. The effect of temperature on the viscosity of ethanol.

Temp., °C	−40	−20	0	10	20	30	40	50
Viscosity, (centi poise)	4.79	2.38	1.78	1.46	1.19	1.00	0.825	0.701

BULLETIN OF THE CHEMICAL SOCIETY OF JAPAN VOL. 42 914—918 (1969)

Solubility of Chlorine in Mixed Solutions of HCl and $CuCl_2$

Fumio HINE and Shusei INUTA

Training Institute for Engineering Teachers, Kyoto University, Uji, Kyoto

(Received August 23, 1968)

The solubility of chlorine in a mixed solution of HCl and $CuCl_2$ under various conditions of concentration, temperature, and partial pressure was determined. The concentration of chlorine in a solution as the sum of Cl_2 and Cl_3^- was found to be proportional to the partial pressure of chlorine in the gas phase; its slope decreased with an increase in the concentration of cupric ions due to the salting-out effect.

The recovery of chlorine from waste HCl is an attractive prospect, but the design engineer in this field requires data on systems consisting of HCl and Cl_2. The present authors have previously reported on the solubility of Cl_2 in concentrated HCl.[1)]

The HCl cell with the oxygen-depolarized cathode developed by Hine *et al.*,[2)] the so-called "Kyoto Process," contains a mixture of HCl and $CuCl_2$ in order to increase the reaction rate at the cathode represented by:

$$4H^+ + O_2 + 4e = 2H_2O \qquad (1)$$

where the cupric ions form a chloride complex such as $CuCl_3^-$ in concentrated HCl.[3)] The solubility of chlorine is, therefore, affected by the concentration of cupric chloride in the solution.

Experimental

The apparatus for vapor-pressure measurements reported by Smith *et al.*[4)] was modified.[5)] The temperature was controlled within a range of ± 0.1 °C; it caused a minor variation in the vapor pressure, but this variation was less than 3 mmHg at 90°C, for example.

The equipment and the flow sheet used for solubility measurements were the same as have previously been described.[1)]

The chlorine gas diluted with nitrogen to be sent to the measurement cell was exactly analyzed, and its moisture and temperature were brought to equilibrium before measurement.

The chlorine dissolved in the solution was titrated by iodometry. Since cupric ions in the solution also reacted on KI, the balance, total amount of KI consumed minus the amount of KI for Cu^{2+}, was taken. The cupric ions were also examined by iodometry. The compositions of the solutions examined are listed in Table 1.

Results and Discussion

Since the pressure of water vapor was not negligible in comparison with the total pressure, it was determined as a function of the temperature and of the composition of the solution. The data obtained are listed in Table 2, while an example of Dühring diagram of a system consisting of HCl and $CuCl_2$ is shown in Fig. 1. The logarithm of the vapor pressure is linear to the reciprocal temperature, $1/T$, as is shown in Fig. 2; therefore, the latent heat seems to be independent of the tempera-

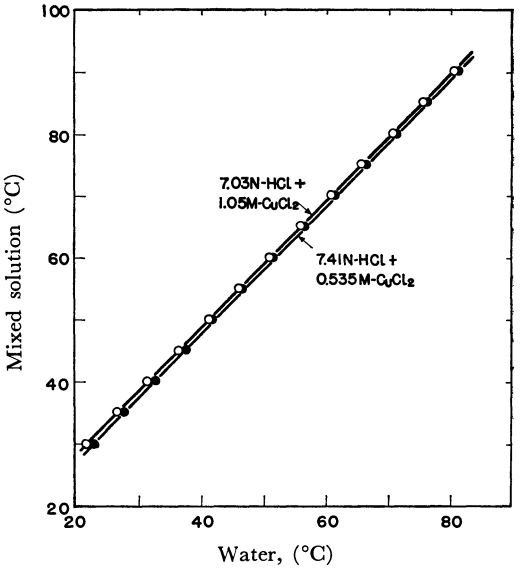

Fig. 1. The Dühring diagram of the mixed solution of HCl and $CuCl_2$ referred to water.

1) F. Hine and S. Inuta, This Bulletin, **41**, 71 (1968).

2) F. Hine, S. Yoshizawa, K. Yamakawa and Y. Nakane, *Electrochem. Techn.*, **4**, 555 (1966).

3) F. Hine and K. Yamakawa, *Electrochim. Acta*, **13**, 2119 (1968).

4) A. Findlay and J. A. Kitchener, "Practical Physical Chemistry," Longmans, Green & Co., London (1955), p. 79.

5) F. Hine and S. Inuta, *Kenkyu Hokoku (Reports of the Training Institute for Engineering Teachers, Kyoto Univ.)*, No. 4, 19 (1968).

Table 1. Analysis of sample solutions

	5 N HCl		6 N HCl		7 N HCl	
Concentration of Cu^{2+}	0.5 M	1.0 M	0.5 M	1.0 M	0.5 M	1.0 M
Concn. of HCl (N)	5.49	5.45	6.25	6.32	7.41	7.03
Concn. of Cu^{2+} (mol/l)	0.516	1.019	0.512	1.038	0.535	1.052

Table 2. Vapor pressure of water over the sample solution

t (°C)	$\frac{1000}{T}$ (1/°K)	5 N HCl				6 N HCl				7 N HCl			
		0.5 M $CuCl_2$		1 M $CuCl_2$		0.5 M $CuCl_2$		1 M $CuCl_2$		0.5 M $CuCl_2$		1 M $CuCl_2$	
		p	t_w	p	t_w	p	t_w	p	t_w	p	t_w	p	t_w
30.0	3.299	20.8	22.8	19.5	21.7	18.2	20.6	17.7	20.2	17.5	20.0	17.5	20.0
35.0	3.245	28.0	27.8	26.3	26.7	24.7	25.7	24.3	25.4	24.0	25.2	24.1	25.2
40.0	3.193	37.0	32.7	34.5	31.4	33.0	30.6	32.5	30.4	32.5	30.4	32.4	30.3
45.0	3.143	48.5	37.6	45.5	36.4	43.0	35.4	42.5	35.1	43.7	35.6	43.0	35.4
50.0	3.095	61.5	42.0	59.0	41.2	56.8	40.5	55.5	40.1	57.8	40.8	55.5	40.1
55.0	3.047	78.5	46.7	76.5	46.2	73.2	45.4	71.3	44.8	74.3	45.6	72.5	45.2
60.0	3.002	100.0	51.6	97.5	51.1	93.7	50.3	91.7	49.8	95.9	50.7	93.6	50.2
65.0	2.957	126.5	56.5	123.7	56.0	119.3	55.2	116.5	54.7	123.4	55.9	119.8	55.3
70.0	2.914	160.0	61.5	155.5	60.9	151.5	60.3	149.0	59.9	159.2	61.4	154.1	60.7
75.0	2.872	199.8	66.4	195.0	65.9	190.8	65.4	188.0	65.1	202.2	66.7	195.0	65.9
80.0	2.832	247.5	71.3	241.5	70.8	238.8	70.5	236.0	70.2	255.0	72.0	247.0	71.3
85.0	2.792	305.7	76.3	298.8	75.8	297.0	75.6	295.3	75.5	320.0	77.5	309.6	76.6
90.0	2.754	376.3	81.4	366.8	80.8	367.2	80.8	365.2	80.7	398.9	82.9	385.4	82.0

p: vapor pressure, in mmHg.
t_w: temperature of water at the vapor pressure p, in °C.

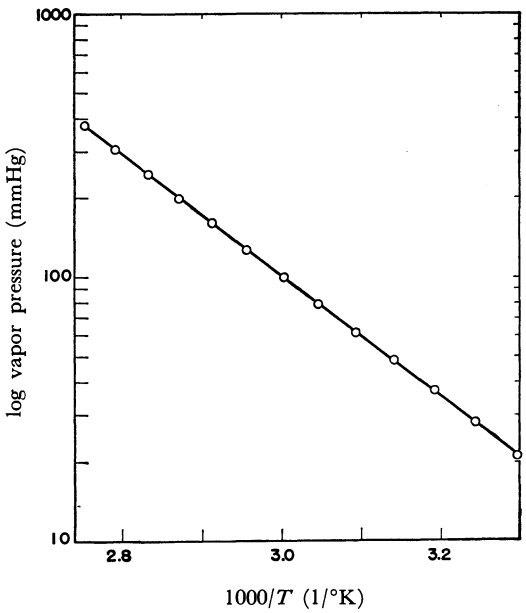

Fig. 2. The vapor pressure of the aqueous solution consisting of 5.49 N HCl and 0.516 M $CuCl_2$ as a function of temperature.

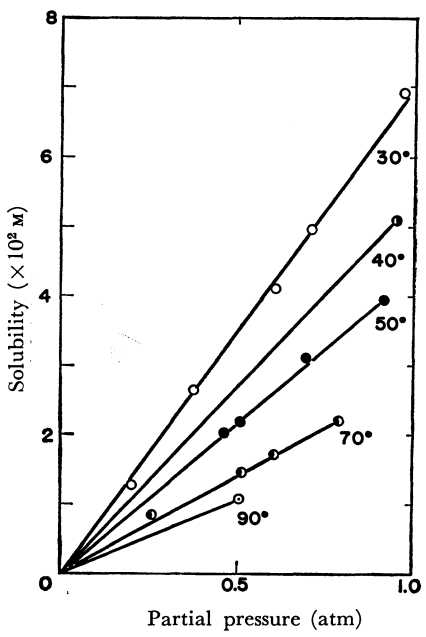

Fig. 3. The solubility of chlorine in 5.49 N HCl +0.516 M $CuCl_2$.

Table 3. Henry's coefficient ($\times 10^2$)

t (°C)	$\frac{1000}{T}$ (1/°K)	5 N HCl		6 N HCl		7 N HCl	
		0.5 M	1.0 M	0.5 M	1.0 M	0.5 M	1.0 M
30	3.2987	6.99	6.57	7.82	6.81	8.07	7.23
40	3.1934	5.37	5.02	5.88	5.31	6.31	5.40
50	3.0945	4.28	3.78	4.60	4.50	4.92	4.12
70	2.9142	2.76	2.36	3.01	2.42	3.04	2.63
90	2.7537	2.15	2.08	2.16	2.40	2.41	2.18

ture between 30 and 90°C.

The solubilities of chlorine at various temperatures and concentrations were plotted against the partial pressure of chlorine. As the example in Fig. 3 shows, it is clear that the following Henry equation can be applied:

$$S_m = H_m \cdot p_{Cl_2} \tag{2}$$

where: S_m: the solubility of chlorine in a mixed solution mol/l
H_m: Henry's coefficient mol/l·atm
p_{Cl_2}: the partial pressure of chlorine atm

The Henry coefficient decreases with an increase in the concentration of cupric ions as is listed in Table 3. However, the slope of the logarithm of the H_m *vs.* $1/T$ curve is independent of the cupric ions, as is shown in Fig. 4. Therefore, the enthalpy change upon the dissolution of chlorine in a mixture of HCl and $CuCl_2$ is equal to that in a solution of HCl.[6]

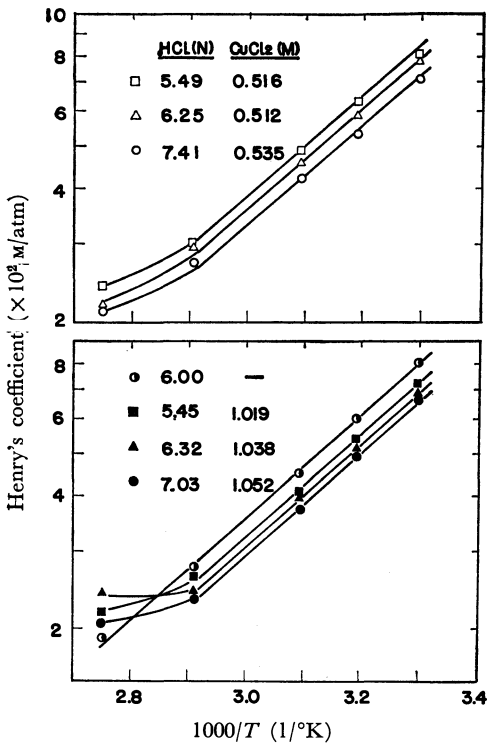

Fig. 4. Henry's coefficient at various conditions of temperature and concentration.

Let us discuss the single solution of HCl first. It is well known that a part of the chlorine forms trichloride complex ions, Cl_3^-, in a chloride solution, and that the other part may dissolve as its molecule, Cl_2.

The total amount of chlorine in HCl, as the sum of Cl_3^- and Cl_2, is a linear function of the HCl concentration and of the partial pressure in the gas phase, as has been described in a previous report,[1] that is,

$$S = H \cdot p_{Cl_2} = (\alpha x + \beta) p_{Cl_2} \tag{3}$$

where: S: the solubility of chlorine mol/l
$H = \alpha x + \beta$: Henry's coefficient mol/l·atm
x: the concentration of Cl^- mol/l
p_{Cl_2}: the partial pressure of Cl_2 atm
α and β: coefficients

Because the system consisting of Cl_2, Cl^-, and Cl_3^- is in a state of equilibrium, the concentration of Cl_3^- is proportional to x as follows:

$$(Cl_3^-) = K \cdot p_{Cl_2} \cdot x \tag{4}$$

where K is the equilibrium constant and where ( ) shows the concentration. Therefore, the concentration of Cl_2 can be represented by the balance of S minus (Cl_3^-); it is also linear to the concentration of Cl^- as follows:

$$(Cl_2) = [(\alpha - K)x + \beta] p_{Cl_2} \tag{5}$$

The effects of the electrolyte on the solubility of gas as its molecule have been studied by many authors[7,8] as the "Salting-Out Effect." They reached the important conclusion that a linear relationship exists between the logarithm of the solubility and the concentration of electrolytes in a solution.

At relatively low concentrations of HCl and in water, the data obtained at 25°C by Sherrill *et al.*[9] agree with Eq. (6), as is shown in Fig. 5.

6) See Eq. (12) in Ref. 1.
7) A. E.. Markham and K. A. Kobe, *Chem. Revs.*, **28**, 519 (1941).
8) H. Hikita, *Kagaku Kogaku (J. Chem. Eng. Japan)*, **23**, 537 (1959).
9) M. S. Sherrill and E. F. Izzard, *J. Am. Chem. Soc.*, **53**, 1667 (1931).

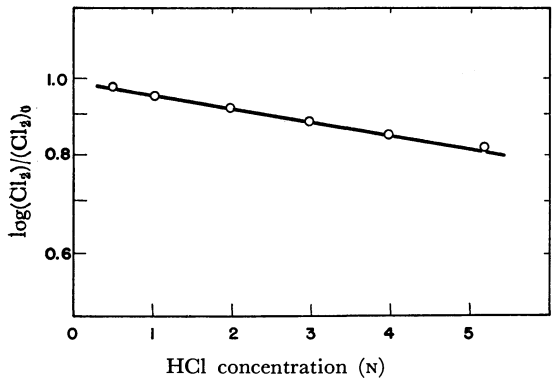

Fig. 5. Concentration of Cl_2 in HCl solution at 1 atm.

That is,

$$\log \frac{(Cl_2)}{(Cl_2)_0} = -kx \qquad (6)$$

where $(Cl_2)_0$ is the solubility of Cl_2 in pure water and where k is a constant and is very small (about 0.0183). Accordingly, the first approximation;

$$(Cl_2) = (Cl_2)_0 \cdot (1 - 2.303kx) \qquad (7)$$

is allowable with a variation of less than 2%. It is essentially the same as Eq. (5).

Zimmerman *et al.*[10] found the equilibrium constant, K, in Eq. (4) or (5) to be 0.01 at 25°C using the spectroscopic method; this value is in good agreement with that of Sherrill.[9] The relationship between K and T has been discussed in the previous report,[1] where the salting-out effect was not considered. Because the slope of the log K *vs.* $1/T$ curve is independent of the concentration of HCl, the value of K and, hence, that of $\alpha - K$ in Eq. (5) at various temperatures between 30 and 90°C can be predicted to be as listed in Table 4.

TABLE 4. K AND $(\alpha - K)$ (in mol/l·atm)

Temperature (°C)	$K \times 10^2$	$-(\alpha - K) \times 10^2$
30	0.845	0.215
40	0.620	0.186
50	0.462	0.158
70	0.273	0.093
90	0.172	0.067

With these values, the concentrations of Cl_2 and Cl_3^- shown in Fig. 6 are obtained. The solid line with open points shows the sum of chlorine dissolved at $p_{Cl_2} = 1$ atm; the data at 25°C, with the closed point, are quoted from the paper by Sherrill *et al.*[9] The thin line represents the concentration of Cl_2 predicted by Eq. (5) at a partial pressure of 1 atm. The closed points with the thin line are also based on Sherrill's data. Accordingly, the concentration of Cl_3^- can be evaluated as the balance of the two lines.

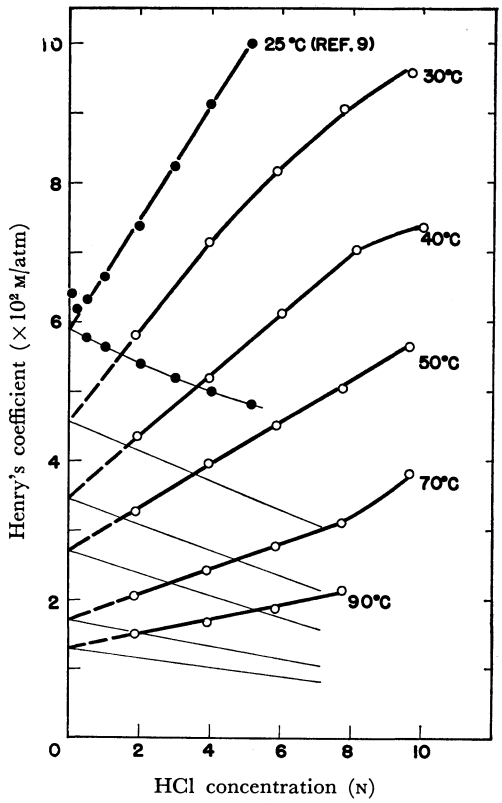

Fig. 6. Henry's coefficient as various conditions of temperature and HCl concentration.

The effect of cupric chloride on the solubility of chlorine in a mixture of HCl and $CuCl_2$ was also examined. The data obtained are shown in Fig. 7, where the ordinate is the Henry coefficient or the solubility at $p_{Cl_2} = 1$ atm and where the abscissa is the concentration of $CuCl_2$ in HCl. The concentrations of Cl_2 and Cl_3^- can be calculated by the procedure described above; the results are listed in Table 5, together with the Henry coefficients.

Now we may consider the mixed solution. It is well known that cupric ions form a chloride complex with HCl as follows:

$$CuCl_2 + Cl^- = CuCl_3^- \qquad (8)$$

This is according to Hine *et al.*,[8] who obtained the coordination number of the complex ion by means of EMF measurements. Therefore, the concentration of Cl^- in the solution decreases with an increase in the cupric ions; that is,

$$(Cl^-) = x - y \qquad (9)$$

where y is the concentration of cupric chloride in mol/l. By substituting this into Eq. (4), the next equation can be obtained:

$$(Cl_3^-) = K \cdot p_{Cl_2}(x - y) \qquad (10)$$

10) G. Zimmerman and F. C. Strong, *ibid.*, **79**, 2063 (1957).

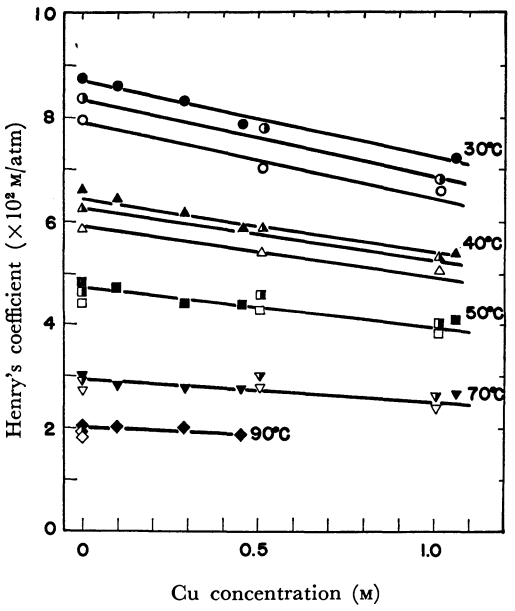

Fig. 7. Henry's coefficient at various conditions of temperature and concentrations of HCl and $CuCl_2$.
Closed point (●): 7.23 N HCl
Semi-closed point (◑): 6.25 N HCl
Open point (○): 5.49 N HCl

Table 5. Solubility of chlorine in 7.23 N HCl at $p_{Cl_2}=1$ atm (mol/l)

Temperture (°C)	$H\times10^2$	$(Cl_2)\times10^2$	$(Cl_3^-)\times10^2$
30	8.80	3.03	5.77
40	6.65	2.13	4.52
50	4.87	1.57	3.30
70	3.02	1.05	1.97
90	2.06	0.81	1.25

We may assume that (Cl_2) decreases with an increase in the concentration of cupric ions due to the salting-out effect, and that it can be represented by the following equation:

$$(Cl_2) = (a - by)p_{Cl_2} \tag{11}$$

where a and b are constants (a should be equal to $(\alpha-K)x+\beta$ because (Cl_2) is represented by Eq. (5) at $y=0$). Accordingly, the solubility of chlorine as the sum of Cl_2 and Cl_3^- can be formulated as follows:

$$S_m = (Cl_3^-)+(Cl_2) = [(\alpha x+\beta)-(K+b)y]p_{Cl_2} \tag{12}$$

From Eqs. (2), (3) and (12), we have:

$$b = \frac{H - H_m}{y} - K \tag{13}$$

Equation (13) represents the salting-out effect due to cupric chloride in the HCl solution on the solubility of chlorine; the data obtained are shown in Fig. 8. The logarithm of b is linear to $1/T$ with the slope of 2.

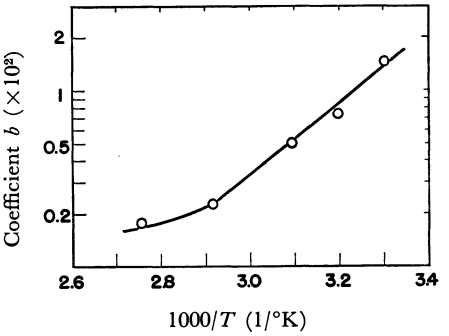

Fig. 8. The coefficient b as a function of temperature.

Equation (11) is an approximation of the next equation:

$$\log\frac{(Cl_2)}{(Cl_2)_0} = -k_m y \tag{14}$$

where k_m is a coefficient. As is shown in Fig. 7, k_m, and, hence, b in Eq. (11) are small and are functions of the temperature.

Summary

The vapor pressure of the aqueous solution consisting of HCl and $CuCl_2$ was measured. The solubility of chlorine in the same solution at a partial pressure of chlorine lower than 1 atm and at 30—90°C was also determined. The enthalpy change upon the dissolution of chlorine in the mixed solution was equal to that in a solution of HCl alone. Henry's Law was found to hold good in this case as well as in pure HCl, while the Henry coefficient decreases with decrease in the HCl concentration and increase in the $CuCl_2$ concentration because of the salting-out effect.

BULLETIN OF THE CHEMICAL SOCIETY OF JAPAN VOL. 42 919—922 (1969)

Fluorescence Lifetime of Acridine in Water-Organic Solvent Mixtures

Hiroshi KOKUBUN*1

Research Institute of Applied Electricity, Hokkaido University, Sapporo

(Received August 23, 1968)

Fluorescence lifetime of acridine has been measured in water-ethanol and water-glycerol mixtures of different composition at 25°C. Remarkable decrease in lifetime value was found as the amount of organic component increases. The lifetime of 10.3 ns was obtained for the aqueous solution. The lifetimes in glycerol and in ethanol were determined as 3.2 and 0.7_2 ns, respectively. The observed ratio of the lifetime in the mixture to the lifetime in water, τ/τ_0, has the same functional dependence on solvent composition as the ratio of fluorescence yield, ϕ/ϕ_0. These quenching phenomena by organic molecules have been interpreted as due to the solvent effects upon the radiationless transition rate. Both static and dynamic mechanisms of quenching are not applicable in the present cases of solvent quenching.

Fluorescence properties of organic compounds in solution are frequently affected by a number of factors depending on the interaction with the solvent molecule. The interaction may be hydrogen-bonding, dipolar forces and so on. Acridine is one of the compounds whose fluorescence quantum yield is strongly dependent on the nature of the solvent. At room temperature acridine emits fluorescence only in the presence of hydroxylic molecule such as water, ethanol or acetic acid.[1] However, when the hydroxylic molecule is such that, like phenol or aniline, the proton donating group X–H is conjugated with an aromatic part, the activation of fluorescence does not occur.[2] The quantum yield of the fluorescence differs considerably from solvent to solvent even when active hydroxylic solvent is employed.

Bowen *et al.*[3,4] found a remarkable reduction of the fluorescence yield of acridine with increasing amount of organic component in water-organic solvent mixtures. For example, in the ethanol solution the quantum yield of the fluorescence is less than 1/10 of that in the aqueous solution. The organic solvent mixed with water shows an effective quenching upon the fluorescence. According to them, the enhanced fluorescence in water-containing solvents is due to the occurrence of the rapid hydrogen-bonding formation between the excited acridine and water, while in the ground state the hydrogen-bonding is negligible. However, this view can be easily ruled out, since the spectroscopic study shows that acridine in the ground state forms the hydrogen-bonded complex with ethanol and other protic molecule substances at rather low concentration of donor molecule.[1,2] In protic solvent acridine may be completely hydrogen-bonded with solvent molecule.

On the other hand, Porter and Vander Donckt[5] explained the low fluorescence yield in ethanol as due to a participation of photoreduction processes in the first singlet excited state. Our recent investigation shows that the contribution of photochemical reaction to the radiationless processes of excited acridine is of minor importance.[6]

For the purpose of establishing the mechanism for this interesting behavior of the fluorescence, measurements have been made of the fluorescence lifetime of acridine dissolved in water-glycerol and water-ethanol mixtures of various compositions. Comparative study of lifetime with spectroscopic and or fluorophotometric study can afford the decisive clue to resolve the mechanisms involved. For example, Schmillen[7] has successfully discriminated the static and dynamic mechanisms of the fluorescence quenching for several dyes.

Experimental

Absorption spectra were measured with a Hitachi EPS-II spectrophotometer. Fluorescence spectra were recorded on a modified Hitachi EPU spectrophotometer. Excitation light source was Ushio USH-100 high pressure mercury lamp combined with Toshiba UV-D1A and UV-35 filters. The spectral calibration factors of this photometer were obtained by the method of

*1 Present address: Department of Chemistry, Faculty of Science, Tohoku University, Sendai.

1) N. Mataga and S. Tsuno, This Bulletin, **30**, 368 (1957).

2) N. Mataga and S. Tsuno, *ibid.*, **30**, 711 (1957).

3) E. J. Bowen and J. Sahu, *J. Chem. Soc.*, **1958**, 3716.

4) E. J. Bowen, N. J. Holder and G. B. Woodger, *J. Phys. Chem.*, **66**, 2491 (1962).

5) E. Vander Donckt and G. Porter, *J. Chem. Phys.*, **46**, 1173 (1967).

6) K. Nakamaru, H. Kokubun and M. Koizumi, to be published.

7) A. Schmillen, *Z. Angew. Phys.*, **6**, 260 (1954).

Lippert *et al.*[8] and were applied to the raw data. Lifetime measurements were made with a phasefluorometer modulated at 10.7 MHz. This device is similar to that reported by Müller *et al.*[9] except for slight simplification and working frequency. The excitation light source was the same as employed in spectral measurements. The delaylines were calibrated with the aid of a standard signal generater and a frequency counter.

Acridine was recrystallized twice from 1 : 1 ethanol-water mixture. G. R. grade glycerol was distilled under reduced pressure prior to use. G. R. grade 99.5% ethanol was used without further purification. In order to avoid the protonation in the excited state,[10] the mixtures were prepared from the aqueous 0.02 N alkaline solution and the organic solution. The concentration of acridine was kept less than 10^{-5} mol/*l* for all solutions prepared, so that the system is free from the undesired concentration quenching. The effect of dissolved oxygen was examined for several solutions, and it was found that the oxygen quenching is negligible. The present results are those for the aerated solutions.

Results and Discussion

Results of lifetime measurements are presented in Fig. 1. As the amount of ethanol or glycerol increases, the lifetime decreases rapidly and then approaches a limiting value for both mixtures. The lifetime in the aqueous solution is 10.3 ns. The limiting values of 3.2 and 0.7_2 ns were obtained respectively for glycerol- and for ethanol-water mixtures. The value for the aqueous solution is close to the value of 13.8 ns obtained by Schmillen,[11] but is not in good agreement. The value of 2.3 ns for 50% ethanol solution is in complete agreement with that obtained by Birks and Dyson.[12] Berlman's value of 0.9 ns[13] for ethanol solution agrees well with the present result. No other literature value which can be compared with the results of the present work is vavailable.

The most striking feature of the present results for ethanol-water mixtures is that the ratio in lifetime, τ/τ_0, as a function of solvent composition is in good agreement with that of quantum yield, ϕ/ϕ_0, obtained by Bowen *et al.*[4] at 18°C except for the small deviation due to the different working temperature and experimental errors. The subscript 0 stands for the values in the aqueous solution. For glycerol-water mixtures the fit of τ/τ_0 curve to that of ϕ/ϕ_0 obtained by Bowen and Sahu[3] is less satisfactory. However, since they did not take into account the effect due to the protonation in the excited state, their results can not be compared strictly with the present results. Hence, it may be considered that the relation, $\tau/\tau_0=\phi/\phi_0$, holds also for glycerol-water mixtures.

In the usual way of interpreting the quenching mechanism, it is a reliable criterion for dynamic quenching that the ratios of quantum yield fit those of lifetime especially for low quecnher concentration. If this is the case, quenching process can be described by the Stern-Volmer equation

$$\phi_0/\phi = \tau_0/\tau = 1 + k\tau_0[Q], \qquad (1)$$

where k and [Q] are the rate constant of quenching process and the quencher concentration, respectively. For both mixtures studied remarkable deviations from the above equation were found as

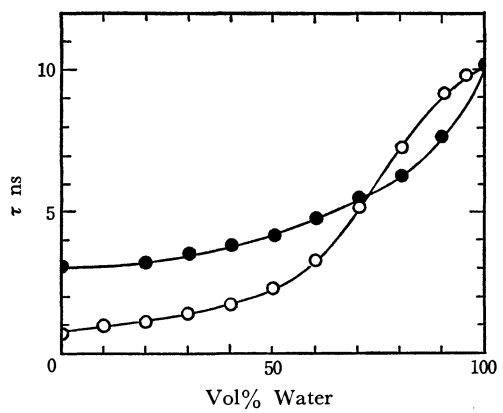

Fig. 1. Fluorescence lifetime of acridine in alcohol-water mixtures at 25°C.
—○—: Ethanol —●—: Glycerol

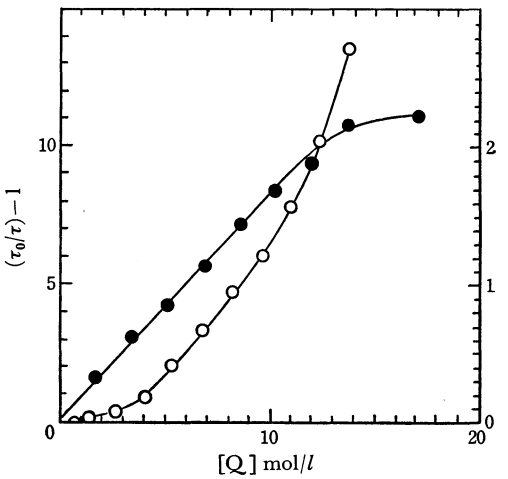

Fig. 2. Stern-Volmer plots.
—○—: Ethanol (left-hand scale)
—●—: Glycerol (right-hand scale)

8) E. Lippert, W. Nägele, I. Seibold-Blankenstein, W. Staiger and W. Voss, *Z. Anal. Chem.*, **170**, 1 (1959).
9) A. Müller, R. Lumry and H. Kokubun, *Rev. Sci. Instr.*, **36**, 1214 (1965).
10) A. Weller, *Z. Elektrochem.*, **61**, 956 (1957).
11) A. Schmillen, in Ref. 10.
12) J. B. Birks and D. J. Dyson, *Proc. Roy. Soc.*, **A275**, 135 (1963).
13) I. B. Berlman, "Handbook of Fluorescence Spectra of Aromatic Molecules," Academic Press, New York (1965).

shown in Fig. 2. In these mixtures, especially for glycerol-water mixtures, strong variation in viscosity might be a cause of the deviations found, since dynamic quenching is a diffusion controlled process. However, no significant relation was found between the apparent quenching constant obtained by the formal application of the Stern-Volmer equation and the viscosity of the corresponding solution. The transient effect is another conceivable factor which causes deviation from the Stern-Volmer equation. Deviation due to this effect is always upward. For glycerol-water mixtures deviation from linearity is contrary to the expected direction. For ethanol-water mixtures it is as expected. However, the value of the slope extrapolated to pure water is almost zero. This means that the dynamic part scarecely contributes to the entire quenching process. Furthermore, the very fact that τ/τ_0 coincides with ϕ/ϕ_0 even for the mixtures rich in organic component (*i. e.*, large quencher concentration), implies a negation of the participation of the dynamic mechanism in quenching process, since the quantum yield measurement detects both dynamic and transient contributions, while the lifetime measurement by phase shift method detects only dynamic contribution. Thus, in every respect it is conclusive that the dynamic collisional mechanism does not participate in the present quenching phenomena.

An alternative is the static quenching, in which the formation of non-fluorescent associate between fluorescer and quencher is an essential origin of quenching. In this case the fluorescence can be emitted only from the free molecule, and the quencher does not affect the decay process of the emitting molecule. No change in lifetime is expected. In the present case, however, we should consider an associate of lower fluorescence yield, *i. e.*, hydrogen bonded acridine with ethanol or glycerol, instead of completely non-fluorescent associate. The number of emitting species is two at least, if the static mechanism is involved in the present system. Although the lifetime to be observed should vary with quencher concentration, τ/τ_0 can in no way be identical with ϕ/ϕ_0. Furthermore, as shown in Fig. 3, the fluorescence spectrum of acridine shifts merely to blue continuously and becomes better structured gradually with the increasing amount of organic component. There is no evidence that the observed fluorescence spectra consist of two components. Hence the static mechanism in a simple form was also excluded.

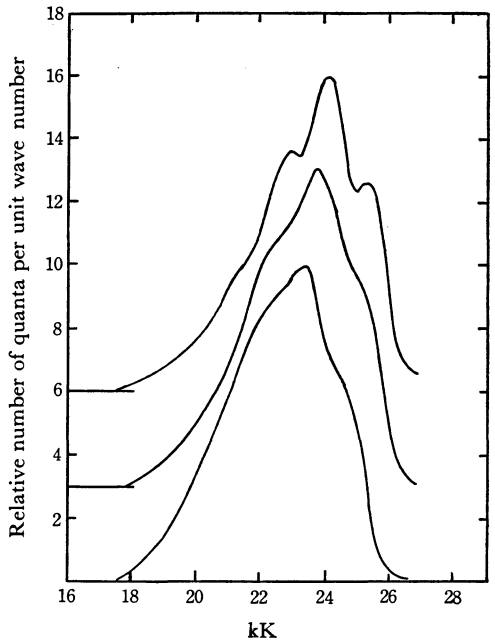

Fig. 3. Fluorescence spectrum of acridine.
Upper: in ethanol
Middle: in 50% ethanol
Lower: in water

Thus it appears that the present result is interpretable only in terms of the solvation in mixed solvents. In the aqueous solution acridine is solvated by water, and all the sites for solvation may be occupied by water molecules. By mixing an organic component into water, the organic molecules replace the water molecules on the solvation sites. This causes the changes in τ and ϕ which are given by

$$\tau = \frac{1}{k_f + k_q} \tag{2}$$

$$\phi = \frac{k_f}{k_f + k_q} \tag{3}$$

respectively. k_f is the rate constant for radiative process, and k_q is that for nonradiative.

Since the absorption intensity of acridine is practically constant in all the solutions studied, k_f can be regarded as constant throughout. Hence, it is clear that the reductions in τ and ϕ are attributed to the increase in k_q. This leads to $\tau/\tau_0 = \phi/\phi_0$ consistent with the experimental finding.

For convenience we write k_8 as a sum of two components,

$$k_q = k_{q0} + k_q(\varphi), \tag{4}$$

where k_{q0} is a radiationless rate constant in the aqueous solution and $k_q(\varphi)$ is the increment of radiationless rate constant upon addition of organic component as a function of volume fraction of organic solvent, φ. Assuming that the $k_q(\varphi)$ is proportional to the concentration, a, of the organic molecules on the acridine surface, we get

$$\frac{k_q(\varphi)}{k_{q\infty}} = \frac{a}{a_\infty} \tag{5}$$

where subscript ∞ describes the quantities for the state completely solvated by the organic molecules. For simplicity, only the first solvation sphere is considered. By means of the similar

procedure as in the treatment of monomolecular-layer adsorption isotherm, we get

$$\frac{a}{a_\infty} = \frac{\phi}{B + \varphi} \tag{6}$$

where B is a constant. Combining Eqs. (2), (4), (5) and (6), we get

$$\frac{\tau}{\tau_0 - \tau} = \frac{B}{k_q \tau_0 \varphi} + \frac{1}{k_{q\infty}\tau_0}. \tag{7}$$

This kind of treatment was first applied by Lippert and Moll[14] to the shift of fluorescence maximum of certain stilbene derivatives in organic mixed solvent.

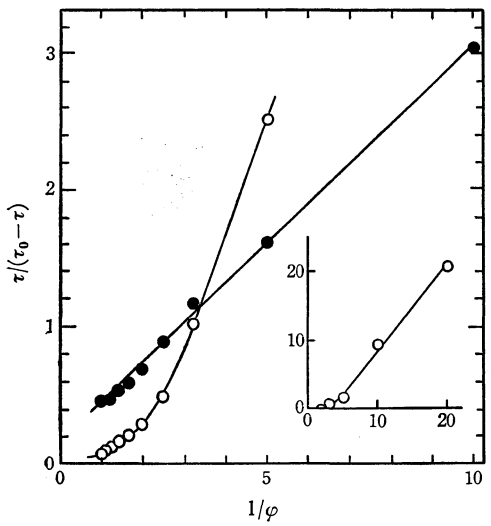

Fig. 4. $\tau/(\tau_0-\tau)$ *vs.* $1/\varphi$ plots.
—○—: Ethanol —●—: Glycerol

Plots of $\tau/(\tau_0-\tau)$ *vs.* $1/\varphi$ are given in Fig. 4. For water-glycerol mixtures the fit to Eq. (7) is quite satisfactory. However, for water-ethanol mixtures the deviation from Eq. (7) is appreciable. What kind of factors are responsible for such a discrepancy between ethanol and glycerol remain inexplicable. Taking the complex nature of these mixtures into account, no further attempt was made to find an equation of better fit.

Thus, the quenching action of organic solvent upon the acridine fluorescence has been interpreted as due to the enhanced radiationless transition produced by solvent effect. The mechanisms based on the simple collision involving two molecules and on the complex formation with definite composition have been completely precluded.

The present experimental data do not discriminate whether intersystem crossing or internal conversion is a dominant cause for the present significant radiationless process. According to Bowen *et al.*[4] the temperature dependence of k_q is well described by an Arrehnius equation for ethanol-water mixtures. The activation energy decreases with increasing ethanol fraction; from 6.59 kcal in 10% ethanol to 4.75 kcal in 50% ethanol solution. That the internal conversion requires activation energy of several kcal is highly improbable, since the density of states is very high. Furthermore, with the above fairly large activation energy the radiationless transition should be inhibited at moderate low temperature. These considerations suggest the minor importance of the internal conversion in the radiationless transitions at the first singlet excited state of acridine.

Although the position of the singlet n–π^* state is not known, it lies above ^1L_a π–π^* state[15] and may be dependent on the solvent composition. It is expected that the organic component lowers the energy of the $(n\text{–}\pi^*)^1$ state. This might be the origin of the solvent dependence of activation energy. The intersystem crossing through the $(n\text{–}\pi^*)^1$ state to the second $(\pi\text{–}\pi^*)^3$ state seems to be most probable.

In connection with present result, the author's attention was called to the work of Medinger and Wilkinson.[16] They found a remarkable deviation from the Stern-Volmer plots in the quenching of 9-phenylanthracene fluorescence in liquid paraffin by bromobenzene. They interpreted this deviation as a result of decreasing activity factor due to very high quencher concentration. However, it seems probable that the quenching by bromobenzene is not a collisional process. High quencher concentration decreases the viscosity of the solution appreciably, nevertheless the deviation from the Stern-Volmer equation is opposite as in the present acridine-glycerol-water system.

Changes in absorption and fluorescence spectra are very small, hence k_f is safely assumed to be practically constant. Equation (7) is easily modified for variables F/F_0 and [B] as follows:

$$\left(\frac{F_0}{F} - 1\right)^{-1} = \frac{C}{k_{q\infty}\tau_0[\mathrm{B}]} + \frac{1}{k_{q\infty}\tau_0} \tag{8}$$

where F/F_0 is the ratio of fluorescence intensity with the presence of bromobenzene to that without quencher, [B] is bromobenzene concentration and C is a constant. The values of F/F_0 found in literature were applied in Eq (8) and a straight line was obtained. Thus, the bromobenzene quenching is explained by the solvent effect upon the radiationless process.

The author wishes to thank Matsunaga Science Foundation for financial support.

14) E. Lippert and F. Moll, *Z. Elektrochem.*, **58**, 718 (1954).

15) G. Coppens, C. Gillet, J. Nasielski and E. Vender Donckt, *Spectrochim. Acta*, **18**, 1441 (1962).

16) T. Medinger and F. Wilkinson, *Trans. Faraday Soc.*, **61**, 620 (1965).

BULLETIN OF THE CHEMICAL SOCIETY OF JAPAN VOL. 42 923—928 (1969)

Semi-Empirical ASMO SCF Method for the Valence Electron System. The Electronic Structures of Protonated Pyridinium and Diazinium Cations

Hiroshi KATO, Hajime KATÔ,*1 Hideyuki KONISHI and Teijiro YONEZAWA

Department of Hydrocarbon Chemistry, Faculty of Engineering, Kyoto University, Sakyo-ku, Kyoto

(Received August 26, 1968)

Using a semi-empirical ASMO SCF method for valence electron systems previously proposed by the present authors, the valence shell electronic structures of various protonated azines are investigated. The compounds treated in the present paper are monoprotonated pyridinium, mono-, and diprotonated diazinium cations. The calculated results show that quite large charge redistributions on both σ and π electron systems in these cations take place in the protonation, while about a 0.7 e charge migrates to the attached protons. As to the transition energies, the lowest π–π^* transitions exhibit slight red shifts, while the n–π^* transitions would be expected to cause large blue shifts by means of protonation. Several models for protonated cations are compared, and the configuration where the proton is situated on the bisector of the CNC(N) angle and in the molecular plane is shown to be the most stable one. The changes in Fock's operators upon protonation are also briefly discussed.

Numerous experimental and theoretical studies of the effect of protonation or hydrogen bonding on the electronic structures of nitrogen heterocycles have been presented in the past decade.[1] Mataga and Mataga treated the protonated pyridinium cation and pyrazinium diion by a semi-empirical SCF method for π electron systems and showed that their calculation were successful in accounting for the electronic spectra of these ions.[2] However, their method is based on the π-approximation and the σ-electronic systems are not taken into account explicitly; that is, the core attraction of the adding proton is considered as a prameter of the perturbation in the π electron systems. Recently, calculations including the π electrons in the compounds containing the nitrogen atoms have been made by several authors, but these treatments have not discussed the electronic spectra and the positions of the added protons.[1g,1,j]

In the present paper, the protonated cations of pyridine and three diazines are calculated by the semi-empirical ASMO SCF method for all valence electron systems previously proposed by the present authors.[3] The changes in the σ and π electronic distributions, the stabilization of the orbitals, and the shift of the electronic transitions caused by the protonation are discussed. Further, the location of the adding proton and the changes in the Fock's operators are investigated. The compounds studied in the present paper are monoprotonated pyridinium and mono- and diprotonated diazinium cations.*2 As to the geometries of these cations, it is assumed that the added proton is situated on the bisector of the CNC angle and in the molecular plane of the compound, which has the same configuration as the free molecule.*2,4,5) The N–H$^+$ bond distance is taken as 1.032 Å, as in the NH_4^- ion, throughout this procedure.[2,5]

Results and Discussion

The Change in the Charge Distribution. The calculated atomic populations of an atom A,

*1 Present address: Department of Chemistry, Faculty of Science, Kobe University.

1) *E. g.*, a) M. Kasha, *Discussions Faraday Soc.*, **9**, 14 (1950); b) J. R. Platt, *J. Chem. Phys.*, **19**, 101 (1951). c) F. Halverson and R. C. Hirt, *ibid.*, **19**, 711 (1951). d) H. McConnell, *ibid.*, **20**, 700 (1952). e) V. G. Krishna and L. Goodman, *ibid.*, **33**, 381 (1961); *J. Am. Chem. Soc.*, **83**, 2042 (1961). f) M. S. Gil and J. N. Murrell, *Trans. Faraday Soc.*, **60**, 248 (1964). g) J. Pugmire and D. M. Grant, *J. Am. Chem. Soc.*, **90**, 679 (1968). h) J. D. Vaughan, D. G. Fullerton and C. Chang, *Int. J. Quantum Chem.*, **2**, 205 (1968). i) J. R. Sabin, *ibid.*, **2**, 23, 31 (1968). j) R. B. Hermann, *ibid.*, **2**, 165 (1968).

2) S. Mataga and N. Mataga, *Naturwissenschaften*, **45**, 333 (1958); *Z. physik. Chem. N. F.*, **19**, 231 (1959); This Bulletin, **32**, 521, (1959).

3) T. Yonezawa, K. Yamaguchi and H. Kato, This Bulletin, **40**, 536 (1967); H. Kato, H. Konishi, H. Yamabe and T. Yonezawa, *ibid.*, **40**, 2761 (1967).

*2 The adopted geometries of free molecules are given in Ref. 4.

4) T. Yonezawa, H. Katô and H. Kato, *Theoret. chim. Acta*, in press.

5) "Tables of Interatomic Distances and Configuration in Molecules and Ions," ed. by L. E. Sutton, The Chem. Soc., London (1956) and (1965).

TABLE 1. THE ATOM POPULATIONS, π AO POPULATIONS AND THEIR DIFFERENCES BETWEEN CATIONS AND FREE COMPOUNDS

Compound*	Position	Q_A**	ΔQ_A	Q_H**	ΔQ_H	$N_{\pi A}$	$\Delta N_{\pi A}$	$\Delta N_{\sigma A}$
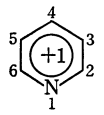	1	5.231	−0.252	0.701	+0.701	1.425	+0.413	−0.665
	2,6	3.784	+0.032	0.896	−0.073	0.879	−0.107	+0.139
	3,5	4.050	−0.068	0.870	−0.043	0.996	−0.021	−0.047
	4	3.966	−0.091	0.881	−0.056	0.824	−0.157	+0.066
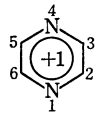	1***	5.148	−0.309	0.709	+0.709	1.381	+0.404	−0.713
	2,6	3.832	+0.010	0.875	−0.075	0.896	−0.115	+0.125
	3,5	3.787	−0.035	0.896	−0.054	0.992	−0.019	−0.016
	4	5.362	−0.095	—	—	0.843	−0.136	+0.041
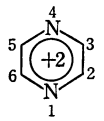	1,4	5.135	−0.322	0.645	+0.645	1.276	+0.298	−0.620
	2,3,5,6	3.780	−0.042	0.829	−0.121	0.862	−0.149	+0.107
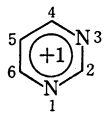	1***	5.316	−0.230	0.680	+0.680	1.455	+0.420	−0.650
	2	3.487	+0.026	0.909	−0.072	0.839	−0.115	+0.141
	3	5.456	−0.090	—	—	1.049	+0.014	−0.076
	4	3.630	−0.103	0.897	−0.060	0.780	−0.183	+0.080
	5	4.119	−0.055	0.863	−0.051	1.032	−0.018	−0.037
	6	3.755	+0.022	0.887	−0.070	0.845	−0.118	+0.140
	1,3	4.267	−0.279	0.635	+0.635	1.446	+0.411	−0.690
	2	3.487	+0.026	0.844	−0.137	0.771	−0.243	+0.269
	4,6	3.665	−0.068	0.832	−0.125	0.694	−0.269	+0.201
	5	4.057	−0.117	0.814	−0.100	1.010	−0.040	−0.077
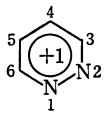	1***	5.002	−0.261	0.693	+0.693	1.401	+0.386	−0.647
	2	5.283	+0.020	—	—	1.056	+0.041	−0.021
	3	3.676	−0.074	0.907	−0.055	0.914	−0.080	+0.006
	4	4.020	−0.084	0.861	−0.060	0.855	−0.137	+0.053
	5	4.040	−0.060	0.873	−0.048	1.013	+0.021	−0.081
	6	3.764	+0.014	0.883	−0.079	0.761	−0.232	+0.246
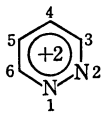	1,2	5.079	−0.184	0.635	+0.635	1.445	+0.430	−0.614
	3,6	3.671	−0.079	0.823	−0.130	0.667	−0.327	+0.248
	4,5	3.965	−0.139	0.816	−0.105	0.889	−0.103	−0.036

* The notation, +1 and +2 indicate to the mono and diprotonated species, respectively. The number for Q_H refers to the position linked with the hydrogen atom.

** The notation, Q_A refers to the atom population of carbon and nitrogen atom, and Q_H to the hydrogen atom. The notation Δ indicates the difference between the values in cation and neutral compound.

*** The protonated nitrogen atom in the monocation.

Q_A and the differences in the charges, ΔQ_A's, in the cation and its neutral molecule are compared in Table 1, where a plus sign indicates an increase in the charge and a minus sign, a decrease in the charge, by protonation. The π atomic orbital (AO) populations and their differences are also listed in the same table, together with σ charge's.

It may be seen from the table that a considerable quantity of the charges migrate to the added proton from the other atoms in the cations, and that the positive charges delocalize in all the positions of the compound. The atomic population of the added proton is equal to the sum of the net charges of the other atoms of its cation. The ratios which

TABLE 2. THE CONTRIBUTION OF VARIOUS TYPE OF ATOMS FOR THE CHARGE OF PROTON (%)

		(%)		
		N	C	H
Monoprotonated	Pyridine	40	25	35
	Pyrazine	58	6	36
	Pyrimidine	47	16	37
	Pyridazine	35	29	35
Diprotonated	Pyrazine	49	13	38
	Pyrimidine	44	18	38
	Pyridazine	29	34	37

are given by the sum of the ΔQ_A's with regard to nitrogen, carbon and hydrogen atoms respectively divided by the atomic population of the proton, are considered to be a measure of the contribution of the transferred charge to the proton from the corresponding atoms. These ratios for the nitrogen, carbon, and hydrogen atoms are listed in Table 2. The results in Table 2 indicate that the charges on the protons in these cations are transferred from all the atoms in the cation; in the monocations, the nitrogen and hydrogen atoms play a important role in the electron transfer, while in the diions, the contribution of the carbon atoms relatively increases. The π electron distributions are also greatly affected by the protonation; for example, the negative charges concentrate on the π AO of the protonated nitrogen atom, and the other carbon atoms almost all bear slightly positive charges. The σ electron redistribution may also be seen in Table 2. Namely, the σ electron populations of the carbon atoms show an alternation of the sign of charge, and at the nearest neighbor carbon its σ electron population increases largely in the cation.

The variations in the AO populations of the nitrogen atoms may be seen in Table 3, where the notation p_n indicates the lone pair 2p AO of the nitrogen atom. The protonation has a remarkable effect on the populations of the p_n and p_π AO's of the nitrogen atom; that is, the p_π AO loses a considerable charge, about 0.7 e, and the p_π AO gains a large negative charge. As a whole, the positive charge on the protonated nitrogen atom is not very large.

Table 3. The AO populations in nitrogen atoms

		s	$p\sigma$	pn	$p\pi$
Pyridine	Neutral	1.85	0.89	1.72	1.01
	Monoion	1.76	1.02	1.00	1.42
Pyrazine	Neutral	1.84	0.89	1.75	0.98
	Monoion N	1.85	0.92	1.75	0.84
	Monoion NH*	1.75	1.00	1.01	1.38
	Diion	1.76	1.02	1.07	1.28

* The protonated nitrogen atom.

Changes in The Total and MO Energies. The proton affinities of these compounds are given as the change in the total energies of the systems, between before and after protonation.[3] The calculated values are collected in Table 4, together with the observed pK_a values and the hydrogen bonding energies.[1e],*3 Unfortunately, there are no observed data on the proton affinities of these compounds; however, the obtained values may be considered slightly large, in view of the observed values for benzene, about 7 eV, and for NH_3, 8 eV.[6] The values given in the table indicate that the order of the proton affinities for the monoprotonation agree with those of the observed pK_a values

Table 4. The proton-affinities, ΔW (eV)

	Calcd ΔW		Obsd[1e]	
	H^{+}*	$2H^{+}$*	pK_a	H.B. energy (kcal/mol)
Pyridine	10.00	—	5.17	—
Pyrazine	9.50	14.07	0.6	4.38
Pyrimidine	9.52	13.96	1.30	4.84
Pyridazine	9.79	13.92	2.33	5.24

* The notations H^+ and $2H^+$ denote to the mono- and diprotonated compounds, respectively.

Pyridine			Pyridinium cation	
No. of MO	ε	No. of MO	ε	$\Delta\varepsilon$
18π b_1	+6.74	18π b_1	+0.93	5.81
17π a_2	+1.22	17π a_2	−4.43	5.65
16π b_1	+0.88	16π b_1	−5.66	6.54
15π b_1	−10.55	15π a_2	−16.27	5.70
14π a_2	−10.57	14π b_1	−16.78	6.32
$13n$ a_1	−10.73	13σ b_2	−17.58	5.62
12σ b_2	−11.96	12σ a_1	−18.41	4.94
11π b_1	−12.69	11σ b_2	−19.52	6.79
10σ b_2	−12.73	10π b_1	−19.53	6.84
9σ a_1	−13.47	9σ a_1	−19.56	5.22
8σ b_2	−14.10	8σ b_2	−19.74	5.64
7σ a_1	−14.34	$7n$ a_1	−20.88	10.15

Fig. 1. The changes of MO energies, (ε) by protonation (eV).

*3 It is noticable that it is necessary to compare the calculated values of proton affinity with those observed in the gas phase, but if the changes in the entropy terms and in the solvent effects by the protonation in these compounds, are constant or are negligibly small, the above comparison is not so unreasonable.

6) F. W. Lampe, J. L. Franklin and F. H. Field, "Progress in Reaction Kinetics," Vol. 1, Pergamon Press, London (1961), p. 67.

TABLE 5. THE SINGLET-SINGLET TRANSITION ENERGIES, ΔE AND OSCILLATOR STRENGTHS, Q

			ΔE_{calcd}			ΔE_{obsd}[2]	Q_{calcd}	
			X*	XH+**	H+XH+**		X*	H+XH+***
Pyridine	π-π*	B_2	5.10	4.99	—	4.83	0.08	0.090
	π-π*	A_1	5.05	5.38	—	5.50****	0.02	0.017
	π-π*	B_2	7.51	7.57	—	—	1.00	0.913
	π-π*	A_1	7.88	7.33	—	—	1.19	0.695
	n-π*	B_1	4.29	8·22	—	—	—	—
	σ-π*	B_1	6.62	6.30	—	—	—	0.008
Pyrazine	π-π*	B_{3u}	5.08	4.86	4.55	4.35	0.02	0.281
	π-π*	B_{1u}	5.22	5.94	5.75	6<	0.02	0.009
	π-π*	B_{3u}	7.42	7.69	8.70	—	0.95	0.935
	π-π*	B_{1u}	8.25	7.51	8.27	—	1.35	1.329
	n-π*	B_{2u}	3.17	3.83	7.34	—	—	—
	n-π*	B_{3g}	4.99	8.22	7.42	—	—	—
	σ-π*	B_{2u}	8.38	—	5.42	—	—	0.003
Pyrimidine	π-π*	B_2	4.80	4.75	4.76	—	0.01	0.138
	π-π*	A_1	5.08	5.11	5.53	—	0.04	0.024
	π-π*	B_2	7.23	6.91	7.48	—	1.16	1.083
	π-π*	A_1	7.20	7.40	7.21	—	0.89	0.710
	n-π*	B_1	3.78	3.73	7.99	—	—	—
	n-π*	A_2	4.80	8.46	8.70	—	—	—
	σ-π*	B_1	6.25	—	5.24	—	—	~0
Pyridazine	π-π*	A_1	5.37	5.43	5.59	—	0.05	0.020
	π-π*	B_2	5.36	5.01	5.04	—	0.01	0.182
	π-π*	B_2	7.13	7.28	7.60	—	0.90	0.652
	π-π*	A_1	7.74	7.41	7.29	—	0.87	0.954
	n-π*	B_1	3.57	3.72	7.98	—	—	—
	n-π*	A_2	3.86	8.12	8.60	—	—	—
	σ-π*	A_2	6.47	—	5.08	—	—	~0

* These calculated values are already given in Ref. 4.
** See note *4.
*** These values are the ones for the monoion (XH^+) in pyridine and for the diion (H^+XH^+) in diazines, respectively.
**** See note *5.

and hydrogen bonding energies, while those for the diprotonation do not. Further, the stabilization energies due to monoprotonation are found to be about twice as large as those of the protonation to a monoprotonated compound. Thus, it may be concluded that the monoprotonations in these diazines occur more easily than do the diprotonations.

The changes in the molecular orbital (MO) energies upon protonation in pyridine are shown in Fig. 1. The pair of MO's in Fig. 1 connected with the arrow line belong to the same irreducible representation and have similar charge distributions. The orbital energy (ε) and the energy difference between these MO's, *i. e.*, the stabilization energy, $\Delta\varepsilon$, are given in Fig. 1. By protonation, all the MO's in a free compound are stabilized about 6 eV; the stabilization of the lone-pair MO (n in Fig. 1) is the largest, 10.12 eV, where the electrons in the MO (n^* in Fig. 1) in cation are mainly localized on the N–H^+ σ bond. That is, this large stabilization is due to the nitrogen lone pair in the n MO participating in the formation of the N–H^+ bond in the n^* MO. Some crossings of energy levels are seen in Fig. 1; particularly a σ MO belonging to the same symmetry as the n MO in free pyridine comes to exist in the higher-energy region in the cation. This result will be discussed in the next section in connection with the transition energy.

Transition Energy. The calculated transition energies obtained by considering the configuration interactions of limited numbers of configurations for various cations are summarized in Table 5, together with those for free molecules which have already been given in Ref. 4. The symmetry shown in this table indicates an irreducible representation of transitions in free and diprotonated compounds; these notations in the case of monoions correspond to the states in which the charge distributions are similar to those of the free and di-

protonated compounds. As may be seen from the table, the lowest π–π^* transitions show a slight red shift, and the n–π^* transitions,*4 a large blue shift, upon protonation. As was pointed out above, the σ–π^* transitions in the dications which belong to the same symmetries as the n–π^* transitions in the parent molecules appear in the lower-energy regions. It is hoped that these σ–π^* transitions in these ions will be identified experimentally. The observed values for lower π–π^* transitions in pyridinium and pyrazinium cations[2] are also listed in the same table. The agreements between the calculated and observed values are fairly satisfactory.*5 The values of the oscillator strength for several π–π^* transitions in several ions were calculated; these values are given in Table 5. The results indicate that the lowest π–π^* transitions in ions are generally intensified by protonation; this finding is in accordance with the experimental results.[2]

The Orientation of Adding Protons. In the present treatment, it is assumed that the proton is situated in the direction of the lone-pair orbital of a nitrogen atom and lies on the molecular plane of a compound. Here, let us investigate the orientation of adding protons. At first, the proton in the pyridinium cation is oriented above the molecular plane, as is shown in Fig. 2. The calculated total energies for various out-of-plane angles, θ, are given in Table 6. The values in this table indicate that the configuration with $\theta=0°$ is the most stable. From the obtained potential curve, the N–H$^+$ bending force constant is calculated to be 0.352 md/Å, compared with the observed value, 0.535 md/Å, in the NH_4^+ ion.[7] Thus, our results seem to be fairly reasonable.

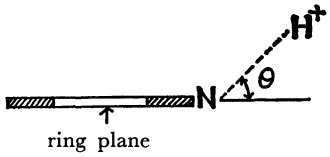

Fig. 2. The orientation of added proton in pyridinium cation.

Table 6. The configuration energies, ΔW for various θ values

θ	0°	30°	55°
ΔW	0	0.32	1.05

The next calculations are made on the monoprotonated pyridazinium cation, in which the proton is located on the vertical bisector of the N–N bond and is on the moleculer plane (B form). The configuration adopted in the previous sections was referred to the A form. These two configurations are shown in Fig. 3. The total energy obtained for the A form is more stable than that for the B form by about 2.8 eV. This destabilization for the B form is mainly due to the lack of any interaction between the proton and the MO which is constituted from the two nitrogen lone pairs and the anti-bonding type between these two lone pairs. This suggestion is supported by the following consideration. In Table 7 are collected the computed atomic dipole and its bond orders of the nitrogen atoms in pyridazine and its various cations.

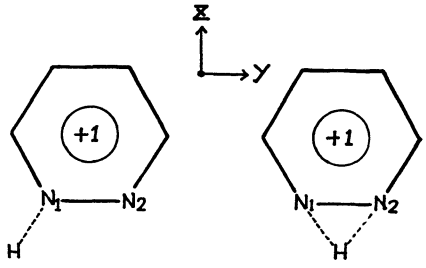

Fig. 3. The two forms in pyridazinium monoion.

Table 7. The atomic dipole values (in unit of debye) and its bond order of nitrogen atom in pyridazine and its ions

		$P_{s_NY_N}$	$P_{s_Nz_N}$	$\mu_A(D)$*
Parent	N_1	−0.137	−0.326	1.33
	N_2	0.137	−0.326	1.33
Monoion B	N_1	−0.151	−0.193	0.92
	N_2	0.151	−0.193	0.92
Monoion A	N_1	0.068	0.011	0.26
	N_2	0.151	−0.342	1.41
Diion	N_1	−0.011	−0.006	0.03
	N_2	0.011	−0.006	0.03

* $\mu_A=[(D_N P_{s_NY_N})^2+(D_N \cdot P_{s_N \cdot z_N})^2]^{1/2}$

$D_N=-e\int \chi_{s_N} r \chi_{p_rN} d\tau \quad (r=x,y,z)$

The listed values show that the large atomic dipoles in the free molecule are diminished by diprotonation. In the monoprotonated ions, the atomic dipole of the protonated nitrogen atom becomes very small and that of the non-protonated nitrogen becomes, inversely, stronger in the A form, whereas in the B form the atomic dipoles of both the nitrogen atoms have considerably large values and are directed toward the outsides of the N–H$^+$ bonds. The magnitudes of the atomic dipoles may be considered to represent the remaining ability of the corresponding lone pair for the bond forma-

*4 The n^*–π^* one in ion in Table 5 refers to the n–π^* transition in a free molecule.

*5 Recently, the second-lowest π–π^* transition energy in the pyridinium cation was estimated to be about 6 eV by Nishimoto (private communication). Our value may be somewhat smaller, as in the case of free molecules (see Ref. 4).

7) I. Nakagawa and S. Mizushima, This Bulletin, **28**, 589 (1955).

tion; so, in the B form, the nitrogen lone pairs still possess considerably strong bonding abilities, in spite of protonation. This is one reason for the lower stabilization of the B form. Accordingly, it may be concluded that, in the most stable configurations of these cations, the proton is situated on the bisector of the C=N–N angle and on the molecular plane, a position compatible with our assumed configurations in previous sections. This fact may be evidence that the nitrogen lone pairs in these compounds can be described approximately as sp^2 hybrids.

The Change in Fock's Operator. Lastly, let us examine the effect of protonation on the Fock's operators. The Fock's operator of the rth diagonal element is represented as follows:

$$F_{rr} = H_{rr} + G_{rr} \tag{1}$$

where H_{rr} is the electron-core interaction terms and G_{rr} is the electron-electron interaction term. With the superscript 0 denoting the free molecule and $+$, the monprotonated species, the differences in the quantities in Eq. (1) between the free and protonated compounds are given by:

$$\left.\begin{aligned} \Delta F_{rr} &= F_{rr}^{+} - F_{rr}^{0} \\ \Delta H_{rr} &= H_{rr}^{+} - H_{rr}^{0} \\ \Delta G_{rr} &= G_{rr}^{+} - G_{rr}^{0} = \Delta G_{rr}^{\sigma} + \Delta G_{rr}^{\pi} \end{aligned}\right\} \tag{2}$$

where ΔG_{rr}^{σ} and ΔG_{rr}^{π} represent the contributions to the electronic interactions between the other σ and π electrons, and the electron in the rth AO, respectively.

For example, the values of Fock's operators for the π AO's and the valence AO's in a nitrogen atom in pyridine and its cation are listed in Table 8. In the table, the ΔH_{rr} values are equal to the core-attraction energies to the rth AO due to the attached proton, and the ΔG_{rr} values are the changes in the electron interaction energies upon the redistribution which is caused by protonation. Here, $\Delta G_{rr}<0$ means the decrease in the electron-repulsion term and $\Delta G_{rr}<0$ is the increase in its term by protonation. From the table, it may be seen that the absolute values of ΔF_{rr} of the π AO's of the C_1 and C_2 positions (the number is the same in Table 1) do not become as much smaller as the values in C_3, contributed by the negative values of ΔG_{rr} terms. Further, it may be noticed that these negative ΔG_{rr} values are mainly contributed from the σ electronic terms. As to the ΔG_{rr} value in the nitrogen π AO, it is found to be nearly equal to zero; this shows that the redistributions in π and σ electrons around this AO result in mutual cancellation, in spite of the large increase in this AO population, as is shown in Table 1. Finally, it may be noticed that the redistributions in σ electron parts cannot be neglected in treating only the π electron systems in this type of cation.

TABLE 8. THE CHANGES OF FOCK'S OPERATOR (eV) BY PROTONATION IN PYRIDINE

AO**	ΔF_{rr}*	ΔH_{rr}	ΔG_{rr}*	$\Delta G^{\pi}{}_{rr}$	$\Delta G^{\sigma}{}_{rr}$
π_1	−4.67	−3.56	−1.11	−0.20	−0.91
π_2	−5.34	−4.03	−1.31	−0.23	−1.08
π_3	−5.66	−5.97	+0.31	+0.96	−0.65
π_4	−9.97	−9.47	−0.50	−0.89	+0.39
n_4	−5.50	−9.47	+4.97	—	—
s_4	−7.72	−9.62	+1.90	—	—

* $\Delta F_{rr}=\Delta H_{rr}+\Delta G_{rr}$, $\Delta G_{rr}=\Delta G^{\sigma}{}_{rr}+\Delta G^{\pi}{}_{rr}$
** The number is the same in Table 1.

The calculations were carried out on the HITAC 5020 E computer at the computer center of the University of Tokyo, whose kindness we hereby acknowledge.

BULLETIN OF THE CHEMICAL SOCIETY OF JAPAN VOL. 42 929—933 (1969)

The Photoconductivity of the Titanium Dioxide Crystal

Takeaki IIDA and Hiroshi NOZAKI

The Institute of Industrial Science, The University of Tokyo, Roppongi, Minato-ku, Tokyo

(Received September 4, 1968)

The photoconductivity of titanium dioxide (rutile type) synthesized by the flame-fusion method was studied. The photoconductivity spectra showed three peaks. The first is the maximum response around the edge of the fundamental absorption of rutile; the second is the peak at 630 mμ (1.98 eV), and the third is the broad-band spectra in the near infrared region of 1.0—1.9 μ. From the facts that Fe is found by chemical analysis to be a major impurity in rutile, that the peak at 630 mμ is enhanced by the increase in Fe concentration from 0.006 mol% to 0.02 mol%, and that the infrared quenching band of photoconductivity is observed at 1.23 μ (1.01 eV) in Fe-doped rutile, it is concluded that this peak at 630 mμ results from the excitation of the electron from the Fe^{3+} level. The broad-band spectra at 1.0—1.9 μ are enhanced by the reduction and are decreased by the oxidation of the crystal, so these excitation spectra are ascribed to lattice defects originating from the non-stoichiometry of TiO_2. These defects have much influence on the photoconductivity of rutile, *i. e.*, on the relation between the photocurrent and the electrical applied field, and on the change the photocurrent *versus* the time.

Titanium dioxide has a conduction band consisting of 2p orbitals of O^{2-}. In the case of rutile, the energy gap of the forbidden band is 3.01 eV—3.05 eV.[1] When titanium dioxide is exposed to the gap light of 420 mμ, it responds quickly to the irradiation with a considerable amount of photocurrent. It is generally considered that a material which has a d-conduction band cannot become a good photoconductor. The reason for this has not yet been clarified and the photoconductivity mechanism of the d-conduction band has not been studied in detail. In view of these points, the photoconductivity of titanium dioxide has many interesting problems. The photoconductivity of the rutile crystal was studied by Cronemeyer.[1] He reported that the photoconductivity spectra of rutile has a maximum response at a wavelength of around 400 mμ. However, he has not mentioned the detailed phenomena of photoconductivity of rutile. Therefore, we have studied the photoconductivity of titanium dioxide in detail, using a single crystal of rutile synthesized by the flame-fusion method. For this report we have studied the photoconductivity spectra for pure rutile, for Fe-doped rutile, and for slightly-reduced rutile, the relation between the photocurrent and the electrical applied field, the change in the photocurrent *versus* the time, and the infrared quenching of photoconductivity for Fe-doped rutile.

Experimental

The single crystal of titanium dioxide was synthesized by the flame-fusion method using highly purified titanium dioxide powder which had been made by firing ammonium-titanil-sulfate at 1000°C. The crystal structure and the direction of the *c*-axis were identified by X-ray deflection. The single crystal was chemically analyzed by spectral analysis. Original crystals grown in an oxyhydrogen flame did not have the stoichiometric composition. Therefore, the crystal was annealed in oxygen gas at 1000°C for 20 hr, and then cooled very slowly to room temperature. The resistivity of this rutile was around 10^{12} Ω cm. After the surface of single crystal plate had been polished with alumina powder to a mirror flatness, the electrodes were attached to this plate by the following procedures. Two parallel zones of silver paste, separated by 5 mm, were painted on one side of the plate, and the sample was heated at 500°C for one hour. Then silver was slightly diffused on the crystal surface, and the electrodes were fixed securely on the surface.

The photoconductivity was measured by the following methods: the sample was mounted on a copper block with silver paste and fixed on the measurement cell. After the air in the cell had been evacuated, the copper block was cooled with liquid nitrogen. The sample was exposed through a quartz window to the monochromic light produced by a monochromator of Carl Zeis, using a 500-W tungsten lamp as the light source. An electric field of 6×10^2 V/cm was applied to the sample, and the photocurrent was measured with an electrometer of the Keithley 610 B type. The infrared quenching spectra of the photoconductivity were measured by the double-beam method; that is, the first excitation light of 400 mμ, which was made by using an interference filter of VV-40 (this filter transmits between 350 mμ and 450 mμ), and the second excitation light of infrared, made by the monochromator, were irradiated on the sample simultaneously, and then the quenching of the photocurrent was measured.

1) D. C. Cronemeyer, *Phys. Rev.*, **87**, 876 (1952).

Results

The general photoconductivity spectra of the rutile crystal are shown in Fig. 1. The maximum of the response is located at the wavelength of 420 mμ at 300°K, but it shifts to 410 mμ at 77°K. The small peak at 630 mμ is observed at any temperature and always has a good reproducibility. The broad response spectrum is observed in the near infrared region of 1.0—1.9 μ at 77°K, but this peak greatly decreases with the increase in the temperature.

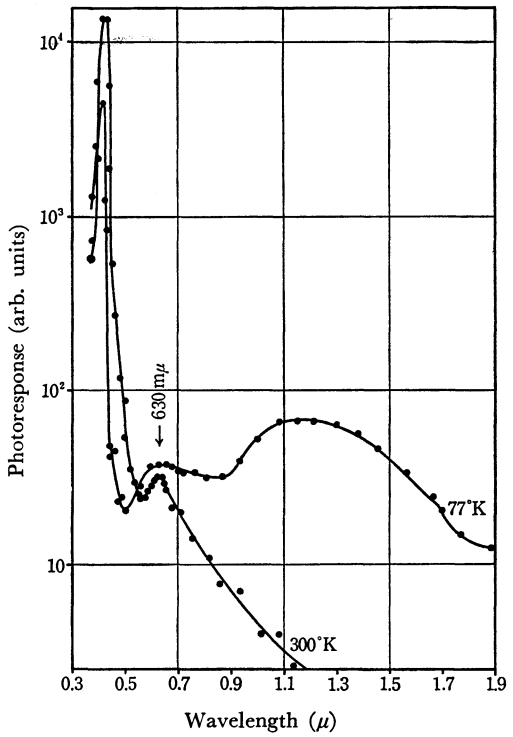

Fig. 1. Photoconductivity spectra for a rutile synthesized by the flame-fusion method.

Chemical analysis of the sample showed that the iron impurity is the major impurity; aluminium, nickel and cobalt are not detected. Therefore, we produced a single crystal doped with 0.02 mol% of iron and measured the photoconductivity spectra. As is shown in Fig. 2, in this sample the peak at 630 mμ is observed clearly, and it is enhanced by the increase in Fe concentration from 0.006 mol% to 0.02 mol%. The broad excitation spectra at 1.0—1.9 μ also appear in the Fe-doped sample, and it can be noticed that the dependence of these broad spectra on the temperature is same as in the case of undoped rutile.

If the rutile crystal is heated at 400°C under the reduced air pressure of 10^{-2} mmHg, the broad response spectra at 1.0—1.9 μ are greatly enhanced. The photoconductivity spectra of slightly-reduced

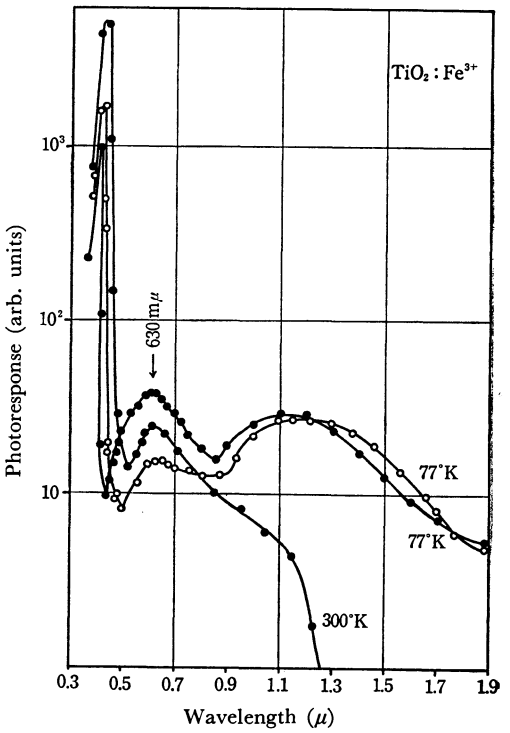

Fig. 2. Photoconductivity spectra for TiO_2 : Fe.
—○—○— TiO_2 : Fe (0.006 mol%)
—●—●— TiO_2 : Fe (0.02 mol%)

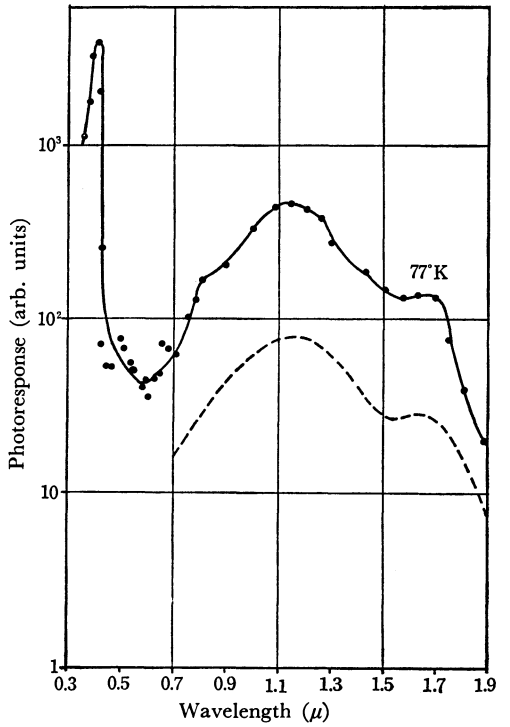

Fig. 3. Photoconductivity spectra for the reduced rutile. The dotted line represents the infrared absorption spectra of the reduced rutile which were reported by Cronemeyer.[2]

rutile, the resistivity of which is around $10^7\ \Omega$ cm, are shown in Fig. 3. It can be noticed that two peaks are found in the broad excitation spectra. One is at 1.2 μ, and the other is at 1.7 μ. The dotted line represents the infrared absorption spectra of reduced rutile measured by Cronemeyer.[2] From these curves it can be recognized that these two peaks, at 1.2 μ and at 1.7 μ, coincide with two peaks of the infrared absorption spectra.

The photocurrent dependencies of rutiles on electrical fields are shown in Fig. 4, using the light of

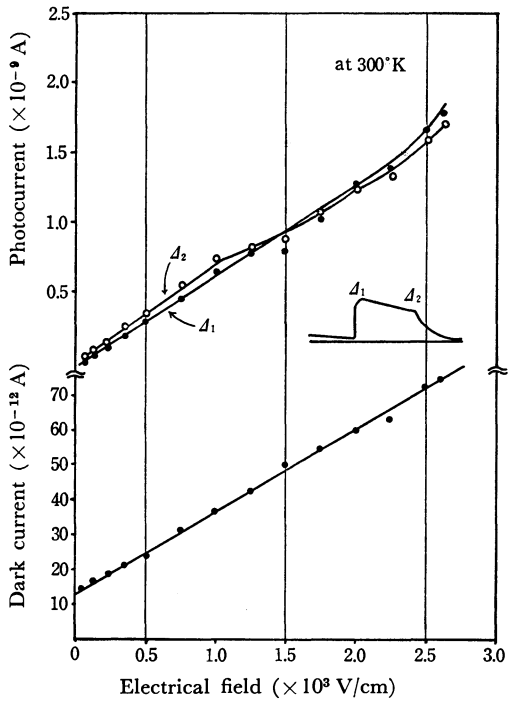

Fig. 4. Photocurrent and dark current dependencies on the electrical field. The notations of Δ_1 and Δ_2 mean the photocurrent measured two seconds and ten seconds respectively after the turn-on of the excitation light.

410 mμ as the excitation beam. The photocurrent increases proportionally to the applied field up to the field strength of 2×10^3 V/cm. The notations Δ_1 and Δ_2 represent the photocurrent measured two seconds and ten seconds respectively after the turn on of the excitation light. The saturation of the photocurrent does not appear even at the field of 2.6×10^3 V/cm. On the contrary, the dark current is exactly proportional to the applied field.

The changes in the photocurrent of a rutile with the time are shown in Fig. 5. As can be seen from the figure, the photocurrent increases rapidly with the time at first, and then it gradually saturates. If these excitations are repeated several times, the

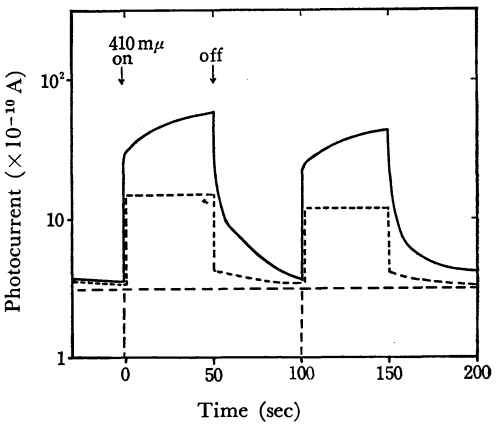

Fig. 5. The change in the photocurrent *versus* the time. The dotted line represents the change in the Fe-doped rutile.

absolute value of the photocurrent decreases gradually. In the case of an Fe-doped rutile, the shape of the photocurrent rather resembles that of the rectangular wave.

In Fig. 6, the infrared quenching spectrum of the photoconductivity of an Fe-doped rutile measured at 77°K by the double-beam method is shown. The infrared quenching band due to the hole trapped at the Fe impurity is observed at 1.23 μ. The dotted line represents the case of pure rutile. This spectrum does not have a quenching band. The degree of infrared quenching is represented by the notation of δ, which is an arbitrary statement of the difference between the full line and the dotted line.

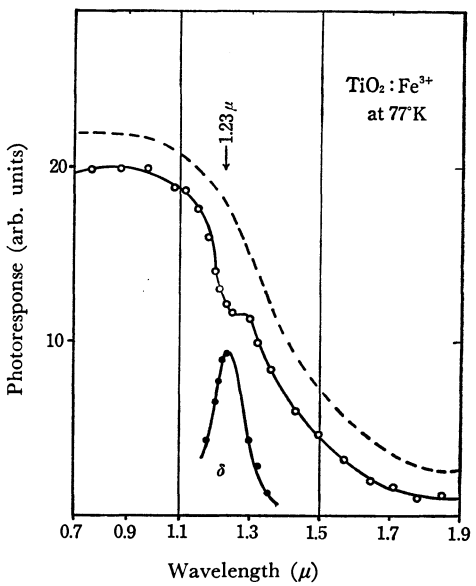

Fig. 6. Infrared quenching spectrum of the photoconductivity for the Fe-doped rutile measured at 77°K.

2) D. C. Cronemeyer, *Phys. Rev.*, **113**, 1222 (1959).

Discussion

The analysis of the conduction mechanism of 3d band is quite complicated because the character of the 3d conduction band has not yet been clarified. Generally speaking, most compounds which are composed of transition elements do not have a photoconductivity. Titanium dioxide has the 3d conduction band of Ti^{3+}, but it has a good response to photoconductivity. This means that the 3d conduction band does not hinder the photoconductivity and that an excited electron can move considerably freely in the 3d conduction band. As a matter of fact, the single crystal produced by the flame-fusion method has many imperfections in its lattice, such as oxygen vacancies[3,4] and interstitial Ti^{3+} ions.[5] These centers become traps or recombination centers, and they have rather more influence on the photoconductivity of titanium dioxide than does the 3d conduction band.

The photoconductivity spectra have three peaks, between 300 mμ and 2.0 μ, as shown in Fig. 1. The first maximum, around 410 mμ, is referred to the edge of the fundamental absorption of rutile, the second small peak, at 630 mμ, has been little influenced by the temperature, while the third peak, at 1.0—1.9 μ, decreases considerably if the temperature increases to 300°K. These latter two maxima may be ascribed to lattice defects in the rutile crystal. Here let us consider what kind of lattice defects exist in the rutile.

It may be said, from Fig. 2, that the peak at 630 mμ results from the excitation of the electron from the Fe impurity to the conduction band of rutile. As a matter of fact, it is very difficult to make a single crystal of rutile containing less than 0.0001 mol% of an iron impurity. Therefore, it can be understood that all the photoconductivity spectra of a single crystal synthesized by the flame-fusion method have a peak of Fe impurity at 630 mμ, and that this impurity acts as a recombination center for the electron and the hole. The ESR measurement for the Fe-doped rutile has been performed by Carter and Okaya.[6] From their ESR results it is clear that Fe occupies the Ti site as a trivalent ion. The ground state of the free Fe^{3+} ion is ^6S. The crystal field of the Ti site is the rhombic field of D_{2h},[7] and the state of ^6S splits into three levels in this crystal field.[8] We can say, from the results of photoconductivity spectra, that the ground state of the Fe impurity lies 1.98 eV (630 mμ) below the conduction band.

From the facts that the broad excitation spectra at 1.0—1.9 μ are enhanced by the reduction and are decreased by the annealment of the crystal in oxygen gas, it may be said that these spectra are due to the lattice defects caused by oxygen deficiency in the rutile crystal. The two peaks, at 1.2 μ and 1.7 μ, ofslightly-reduced rutile coincide with the two peaks of the infrared absorption of reduced rutile as measured by Cronemeyer.[2] He has explained that these two peaks correspond to the ionization energy of two electrons captured by the oxygen vacancy. On the other hand, the measurement of ESR for reduced rutile was performed by Chester,[4] Yamaka[7] and Date,[9] and they concluded that the ESR signal at the g-value of 1.98 is the signal of the interstitial Ti^{3+} ion. Considering these results, we cannot easily deduce defect models with reference to these spectra. The only thing we can say is that the single crystal synthesized by the flame-fusion method has many defects caused by the nonstoichiometry of TiO_2, and that these defects are excited by the light at 1.0—1.9 μ.

Therefore, it is expected that these defects should have much influence on the photoconductivity of rutile. The facts that the photocurrent depends linearly on the electrical field applied up to 1.0×10^3 V/cm, while over that the linear proportionality is not maintained, and the fact that the saturation of the photocurrent at a certain applied field is not observed are general tendencies of a semiconductor which has shallow traps; these facts can be interpreted by saying that the photocurrent observed is due not only to the initial photocurrent but also to the secondary photocurrent caused by the shallow traps.

On the other hand, the linearity of the dark current *versus* the applied field shown in Fig. 4 ensures us a good ohmic contact between the sample and the silver electrodes.

The change of the photocurrent of the rutile *versus* the time, shown in Fig. 5, may be interpreted as follows. The first rise in the photocurrent corresponds to the initial photocurrent, while the next gradual rising process is to be ascribed to the secondary photocurrent resulting from the effect of shallow traps. It the curve of the photocurrent of the Fe-doped rutile *versus* the time (Fig. 5), the effect of the secondary photocurrent does not appear. As we have mentioned above, Fe acts as a recombination center. It might be said that Fe has so large a capture cross-section for the electron and the hole that the effect of shallow traps is very small in the process of the photoconductivity in the Fe-doped rutile.

The impurity center of Fe can also capture a free

3) R. Hashiguti, *J. Phys. Soc. Japan*, **16**, 2223 (1961).
4) H. J. Becker and W. R. Hosler, *ibid.*, **18**, 152 (1963).
5) P. E. Chester, *J. Appl. Phys.*, **32**, 866 (1951).
6) D. L. Carter and A. Okaya, *Phys. Rev.*, **118**, 1458 (1960).
7) E. Yamaka and R. G. Barnes, *ibid.*, **135**, A. 144 (1964).
8) D. L. Carter, *J. Appl. Phys.*, **32**, 2541 (1961).
9) M. Date, *Bussei*, **1**, 22 (1960).

hole from the valence band. If this Fe is excited by the irradiation of the infrared region, the hole captured in Fe is excited to the valence band and it recombines with a free electron in the conduction band, thereby decreasing the photoconductivity. This phenomenon is called the infrared quenching of the photoconductivity. As is shown in Fig. 6, the infrared quenching band appears at 1.23 μ (1.01 eV) in rutile doped with 0.02 mol% of Fe. Therefore, we can find that the energy difference between the impurity level of Fe and the valence band is 1.01 eV. This value agrees with the result obtained from the photoconductivity spectra shown in the second figure.

BULLETIN OF THE CHEMICAL SOCIETY OF JAPAN VOL. 42 933—942 (1969)

The Electronic Structures of Unstable Intermediates. Benzyne and Hetarynes

Teijiro YONEZAWA, Hideyuki KONISHI and Hiroshi KATO

Department of Hydrocarbon Chemistry, Faculty of Engineering, Kyoto University, Sakyo-ku, Kyoto

(Received September 4, 1968)

A semi-empirical SCF MO method for valence electron systems, a modification of our previous method made by introducing the zero-differential overlap approximation except for the one-center exchange integrals, is presented. The results calculated for benzene, pyridine, pyrimidine and thiophene, the parent molecules of benzyne and hetarynes, using this modified method are compared with those obtained by the other calculations and experiments. The unstable intermediates treated in the present paper are benzyne, pyridynes, pyrimidyne and thiophynes. The unknown bond lengths of benzyne and hetarynes are estimated by a semi-empirical relation given in the present treatment. The nature of the carbon-carbon triplet bonds of benzyne and hetarynes is studied on the basis of the bond lengths and the total π bond orders for these bonds. The charge distributions and excitation energies of benzyne and hetarynes, and the chemical reactivity of some hetarynes are also discussed. The lowest triplet states of these intermediates are shown to be close to the singlet ground states.

In our previous series of papers[1-5] a semi-empirical SCF MO treatment for all valence electron systems was presented; this treatment has been shown to be useful in elucidating the electronic structures of various molecules. In the present paper the zero-differential overlap approximation, except for the one-center exchange integrals, is introduced into our previous method[1-5] in order to simplify its procedure and at the same time to make it applicable to large molecular systems.*1 Using this modified method, the electronic structures of benzyne and hetarynes are calculated, and the interatomic distances of these unstable intermediates estimated by a semi-empirical relation. The character of the triple bonds and the ground states of benzyne and hetarynes are discussed.[6]

Theoretical

The molecular orbital (MO) is taken as a linear combination of all the valence atomic orbitals (AO's) centered on the atoms of a molecule. Introducing the zero-differential overlap approximation, except for the one-center exchange integrals, the diagonal elements of the Fock's operator for a closed-shell molecule are given by:

$$F_{rr} = H_{rr} + \frac{1}{2}P_{rr}(rr|rr) + \sum_{r'(\neq r)}^{\text{on A}} P_{r'r'}\left[(rr|r'r') - \frac{1}{2}(rr'|rr')\right] + \sum_{\text{B}(\neq\text{A})} \sum_{s}^{\text{on B}} P_{ss}(rr|ss)$$

(r belonging hereafter to the A atom) (1)

1) T. Yonezawa, K. Yamaguchi and H. Kato, This Bulletin, **40**, 536 (1967).

2) T. Yonezawa, H. Nakatsuji and H. Kato, *ibid.*, **39**, 2788 (1966).

3) T. Yonezawa, H. Konishi and H. Kato, *ibid.*, **40**, 1071 (1967).

4) H. Kato, H. Konishi and T. Yonezawa, *ibid.*, **40**, 1017 (1967).

5) H. Kato, H. Konishi, H. Yamabe and T. Yonezawa, *ibid.*, **40**, 2761 (1967).

*1 The present method differs in the parametrizations of the diagonal and off-diagonal core integrals and one and two-center repulsion integrals from the CNDO method of Pople *et al.* (Ref. 17). Recently, Bene and Jaffé treated benzene, pyridine, and diazines by means of a modified CNDO method (J. D. Bene and H. H. Jaffé, *J. Chem. Phys.*, **48**, 1807 (1968)).

6) Some of these results were reported in a preliminary communication: T. Yonezawa, H. Konishi and H. Kato, This Bulletin, **41**, 1031 (1968).

where $(rr|ss)$ and $(rr'|rr')$ are the two-center Coulomb and one-center exchange repulsion integrals respectively; where $\sum_{r'(\neq r)}^{\text{on A}}$ denotes the summation over all the valence AO's of the A atom except for the rth AO, and where the diagonal core integrals, H_{rr}, are given as follows:[1,5]

$$H_{rr} = U_{rr} + \sum_{B\neq A} (B|rr) \tag{2}$$

$$U_{rr} = -I_r - (N_r - 1)(rr|rr) - \sum_{r'(\neq r)}^{\text{on A}} N_{r'}\left[(rr|r'r') - \frac{1}{2}(rr'|rr')\right] \tag{3}$$

$$(B|rr) = -\sum_{s}^{\text{on B}} N_s(ss|rr) \tag{4}$$

where I_r is the valence state ionization potential of the rth AO and where N_r denotes the number of the valence electrons occupying the rth AO in the valence state. For the valence p AO, U_{rr} is taken as the average value fort he P_x, P_y, and P_z AO's on the same atom.

The off-diagonal elements of the Fock's operator are written in either of two ways, according to whether they are concerned with one-center or two-centers:

$$F_{rr'} = -\frac{1}{2}P_{rr'}\left[(rr|r'r') - 3(rr'|rr')\right]$$

($r \neq r'$, but both on the same atom) (5)

$$F_{rs} = H_{rs} - \frac{1}{2}P_{rs}(rr|ss)$$

($r \neq s$, on different atoms) (6)

where H_{rs} is the core resonance integral, which is given by the following two equations;

$$H_{rs} = -\frac{1}{2}KS_{rs}(I_r + I_s)$$

($r \neq s$, belonging to the adjacent atoms) (7)

$$H_{rs} = 0$$

(otherwise, but $r \neq s$)

where S_{rs} is the overlap integral between the rth and the sth AO's and where K is a constant taken to be 0.8 in the present calculation. This value will be discussed in the later part of this section. The overlap integrals are calculated with the Slater-type AO's, where the exponent values adopted are those obtained by Clementi and Raimondi[7] (shown in Table 1).

Table 1. Slater exponents (ζ_r) and valence state ionization potentials (I_r) of AO's and electron repulsion integrals

		ζ_r[a]	I_r,[b] eV	$(rr\|rr)$,[c] eV	$(rr'\|rr')$,[d] eV
H	1s	1.0000	13.60	12.85	
C	2s	1.6083	21.01	12.10	(2s2p|2s2p)=2.30
	2p	1.5679	11.27	10.93	(2p2p'|2p2p')=0.60
N	2s	1.9237	26.92	12.87	(2s2p|2s2p)=2.99
	2p	1.9170	14.42	11.88	(2p2p'|2p2p')=0.86
S	3s	2.1223	20.08	8.54	(3s3p|3s3p)=1.02
	3p	1.8273	13.32	9.82	(3p3p'|3p3p')=0.60

a) Ref. 7.
b) J. Hinze and H. H. Jaffé *J. Am. Chem. Soc.*, **84**, 540 (1962).
c) Evaluated from the values of I_r and E_r of Ref. b by Eq. (8).
d) Ref. 9.

The one-center Coulomb repulsion integrals are approximated as follows:

$$(rr|rr) = I_r - E_r \tag{8}$$

where E_r is the valence-state electron affinity of the rth AO. The one-center and two-center Coulomb repulsion integrals are calculated by the Ohno approximation:[8],*2

$$(rr|ss) = \frac{1}{2}(1/\sqrt{R_{rs}^2 + 1/(rr|rr)^2} + 1/\sqrt{R_{rs}^2 + 1/(ss|ss)^2}) \tag{9}$$

where R_{rs} is the distance between the atoms to which the two AO's blong.

The one-center exchange integrals are evaluated by the Slater-Condon parameters estimated by Hinze and Jaffé.[9] These values are listed in Table 1, together with the values of I_r and $(rr|rr)$.

For the geomtries of the treated molecules except for benzyne and hetarynes, the data compiled in Ref. 10 are used. An initial set of MO coefficients is obiained by putting F_{rr} as equal to $-I_r$ and by reducing F_{sr} to the H_{rs} term only. The iteration procedure is carried out until the variation in every MO energy remains within 0.001 eV.

Choice of Parameters. The value of K in Eq. (7), which is determined so that the lower calculated

Table 2. Calculated and the experimental π-π^* transition energies of benzene (eV)

State	Calcd	Obsd[a]
$^1B_{2u}$	5.00	4.89
$^1B_{1u}$	5.19	6.14
$^1E_{1u}$	7.36	6.76
$^3B_{2u}$	5.00	5.76
$^3B_{1u}$	4.04	3.66
$^3E_{1u}$	4.52	4.69

a) D. K. Kearns, *J. Chem. Phys.*, **36**, 1608 (1962).

7) E. Clementi and D. L. Raimondi, *J. Chem. Phys.*, **38**, 2686 (1963).
8) K. Ohno, *Theroret. chim. Acta (Berl.)*, **2**, 219 (1964).
*2 When this approximation for the one-center integral (npnp–np'np') is adopted, the rotation invariance to local axes is not exactly preserved. The present results do not differ essentially from the improved results for benzene, pyridine, and benzyne. This improvement will be reported in the near future.
9) J. Hinze and H. H. Jaffé, *J. Chem. Phys.*, **38**, 1834 (1963).
10) "Tables of Interatomic Distances and Configuration in Molecules and Ions," ed. by L. E. Sutton, The Chem. Soc., London (1956 and 1965).

π–π^* transition energies of benzene fit the observed values, is 0.8. The π–π^* transition energies calculated with this value are cited in Table 2, together with the experimental values. This value is adopted throughout these calculations.

Results and Discussion

In this section, some calculated quantities of benzene, pyridine, pyrimidine, and thiophene, the parent molecules of the intermediates treated in this paper, will first be compared with those obtained by other methods of calculation and by other experiments. Second, an empirical relation between the calculated "bond energy" and the bond length will be presented in order to make it possible to estimate the unknown bond lengths of the intermediates. Finally, the electronic structures and configuration of benzyne and hetarynes will be discussed.

Benzene, Pyridine, Pyrimidine, and Thiophene. In Table 3, the occupied MO energies for benzene calculated by the present method are compared with the results of Schulman and Moskowitz[11] and with the experimental ionization potentials assigned by Lindholm and Jonsson.[12] In general, the values of the MO energies of the present calculations are lower than the others. However, the sequence of MO's obtained by our treatments is fairly consistent with the others.

Table 3. Occupied MO energies (eV) for benzene[a]

	Present calcd	Schulman and Moskowitz[b]	Obsd[c]
$e_{1g}(\pi)$	−11.28	−7.83	−9.3
e_{2g}	−13.04	−10.18	−11.4
$a_{2u}(\pi)$	−14.63	−12.30	−12.1
b_{2u}	−14.76	−12.20	−14.7
e_{1u}	−16.00	−12.87	−13.8
b_{1u}	−18.25	−15.31	−15.4
a_{1g}	−20.15	−15.53	−16.9
e_{2g}	−24.59	−19.43	−19.2
e_{1u}	−31.88	−24.42	—
a_{1g}	−36.30	−26.92	—

a) The notation (π) indicates a π molecular orbital.
b) Ref. 11.
c) Ref. 12.

For pyridine, our MO energies are in better agreement with those calculated by Clementi[13] and with the ionization potential measured by the photoionization experiment of Al-Joboury and Turner[14] than is the case with benzene, as is shown in Table 4. The highest occupied (HO) orbital is a nonbonding (n) one in our calculation; this is incompatible with the finding of Clementi[13] and the experimental assignment by Al-Joboury and Turner.[14,15]

Table 4. Occupied MO energies (eV) for pyridine[a]

	Present calcd	Clementi[b]	Obsd[c]
$a_1(n)$	−11.41	−12.66	−10.54
$a_2(\pi)$	−11.55	−12.17	−9.28
$b_1(\pi)$	−11.98	−12.47	−12.22
b_2	−13.49	−15.77	−13.43
$b_1(\pi)$	−15.13	−16.93	−14.44
a_1	−15.18	−17.40	−15.49
b_2	−15.44	−18.23	−16.94
b_2	−16.26	−19.75	−19.39
a_1	−18.09	−19.08	−20.14
a_1	−20.22	−21.20	
b_2	−24.79	−24.61	
a_1	−25.15	−25.08	
b_2	−32.02	−30.21	
a_1	−33.61	−35.50	
a_1	−38.12	−36.13	

a) (n) denotes a non-bonding (lone pair) orbital.
b) Ref. 13.
c) Ref. 14; The assignment of experimental values lower than −10.54 and −9.28 are not definite.

The occupied MO energies for pyridimidine

Table 5. Occupied MO energies (eV) for pyrimidine and thiophene

Pyrimidine		Thiophene	
$b_2(n)$	−11.34	$a_2(\pi)$	−11.00
$a_2(\pi)$	−12.12	$b_1(\pi)$	−11.44
$a_1(n)$	−12.35	$a_1(n)$	−12.78
$b_1(\pi)$	−12.48	a_1	−14.11
a_1	−15.34	b_2	−14.13
b_2	−15.46	$b_1(\pi)$	−14.91
$b_1(\pi)$	−15.58	b_2	−15.43
b_2	−16.18	a_1	−17.47
a_1	−17.66	a_1	−20.75
a_1	−20.43	b_2	−22.34
a_1	−25.14	a_1	−27.37
b_2	−25.56	b_2	−30.37
a_1	−32.94	a_1	−35.35
b_2	−35.22		
a_1	−39.17		

11) J. M. Schulman and J. W. Moskowitz, *J. Chem. Phys.*, **43**, 3287 (1965).
12) E. Lindholm and B.-Ö. Jonsson, *Chem. Phys. Letters*, **1**, 501 (1967).
13) E. Clementi, *J. Chem. Phys.*, **46**, 4731 (1967).
14) M. I. Al-Joboury and D. W. Turner, *J. Chem. Soc.*, **1964**, 4434.
15) By a slight modification of the parametrization, the highest occupied orbital becomes a π MO. This improvement will be described in the near future.

and thiophene, are presented in Table 5. The n orbital of thiophene, localizing mainly on the sulfur atom, is more stable than the higher π orbitals.

The transition energies were calculated for various types of excitations. The calculated values of the π–π^* and n–π^* types for pyridine, pyrimidine, and thiophene are given in Table 6, together with the experimental values. The configuration interactions, including all the π–π^* and n–π^* singly-excited states, are, further, taken into account. When the configuration interactions are considered, a fair agreement between the calculated and observed transition energies and oscillator strengths is observed. The energies of the first π–π^* transitions,

TABLE 6. CALCULATED TRANSITION ENERGIES (eV) OF PYRIDINE, PYRIMIDINE AND THIOPHENE

(a) Pyridine		Calcd		Obsd[a]
Transition	State	(f)	+SECI (f)	(f)
n–π^*	$^1B_1$	4.20(0.0002)	3.97(0.0007)	4.31(0.003)
n–π^*	$^1A_2$	4.74(0)	—	—
π–π^*	$^1B_2$	5.83(0.53)	4.95(0.02)	4.75(0.04)
π–π^*	$^1A_1$	6.30(0.57)	4.99(0.0001)	6.17(0.10)
π–π^*	$^1B_2$	6.45(0.50)	7.32(1.19)	6.82(1.3)
π–π^*	$^1A_1$	6.37(0.58)	7.45(1.35)	
n–π^*	$^3B_1$	3.82(0)	3.50(0)	—
n–π^*	$^3A_2$	4.66(0)	—	—
π–π^*	$^3A_1$	4.28(0)	3.58(0)	3.68
π–π^*	$^3B_2$	4.35(0)	4.29(0)	—

(b) Pyrimidine		Calcd		Obsd[a]
Transition	State	(f)	+SECI (f)	(f)
n–π^*	$^1B_1$	3.66(0.0009)	3.52(0.002)	3.85(0.007)
n–π^*	$^1A_2$	4.15(0)	4.06(0)	—
n–π^*	$^1B_1$	5.16(0.0005)	5.08(0.001)	6.34(0.005)?
π–π^*	$^1B_2$	5.90(0.56)	4.94(0.02)	5.00(0.05)
π–π^*	$^1A_1$	6.20(0.49)	5.04(0.04)	6.49(0.16)?
π–π^*	$^1A_1$	6.31(0.48)	7.23(1.12)	7.25(1.0)
π–π^*	$^1B_2$	6.52(0.52)	7.45(1.24)	
n–π^*	$^3B_1$	3.39(0)	3.15(0)	3.63 —
n–π^*	$^3A_2$	4.00(0)	3.72(0)	—
π–π^*	$^3A_1$	4.25(0)	3.57(0)	—
π–π^*	$^3B_2$	4.30(0)	4.23(0)	—

(c) Thiophene		Calcd		Obsd
Transition	State	(f)	+SECI (f)	(f)
π–π^*	$^1B_2$	5.81(0.41)	5.50(0.23)	5.16—5.90[b] (0.1)[c]
π–π^*	$^1A_1$	6.39(0.62)	6.04(0.16)	6.59—7.25[b] —
π–π^*	$^1A_1$	7.39(0.47)	7.71(1.05)	—
π–π^*	$^1B_2$	7.69(0.17)	7.87(0.41)	—
n–π^*	$^1B_1$	6.37(0.008)	—	—
n–π^*	$^1A_2$	8.58(0)	—	—
π–π^*	$^3B_2$	3.81(0)	3.37(0)	3.89—3.96[d]
π–π^*	$^3A_1$	4.84(0)	4.32(0)	—
n–π^*	$^3B_1$	6.18(0)	—	—
n–π^*	$^3A_2$	8.45(0)	—	—

a) K. K. Innes, J. P. Byrne and I. G. Ross, *J. Mol. Spectroscopy*, **22**, 125 (1967).
b) W. C. Price and A. D. Walsh, *Proc. Roy. Soc.*, **A179**, 201 (1941).
c) J. Sicé *J. Phys. Chem.* **64**, 1572 (1960).
d) M. R. Padbye and S. R. Desai, *Proc. Phys. Soc.*, **A65**, 298 (1952).

$^1A_1 \rightarrow {}^1A_1$, in pyridine and pyrimidine do not agree with the experimental results. These transitions in pyridine and pyrimidine can be correlated with the $^1A_{1g} \rightarrow {}^1B_{1u}$ transition in benzene, the transition energy of which is also in poor agreement with the experimental results, as may be seen in Table 2.

Table 7. AO Charge density for pyridine[a)]

		Present calcd	Clementi[b)]
N	2s	1.561	1.5090
	$2p_x$	0.981	1.0486
	$2p_y$	1.702	1.6608
	$2p_z$	1.183	1.0102
C_2	2s	1.221	1.0472
	$2p_x$	0.793	1.0436
	$2p_y$	0.839	1.0149
	$2p_z$	0.898	1.0048
C_3	2s	1.247	1.0657
	$2p_x$	0.890	1.1138
	$2p_y$	0.911	1.0441
	$2p_z$	1.046	1.0024
C_4	2s	1.245	1.0722
	$2p_x$	0.889	1.0110
	$2p_y$	0.888	1.1444
	$2p_z$	0.931	0.9755
H_2	1s	1.006	0.7783
H_3	1s	0.968	0.7829
H_4	1s	0.986	0.7797

a) y axis is taken as C_2 rotation axis; z axis is taken perpendicular to plane of a molecule.
b) Ref. 13.

Table 8. AO Charge density for pyrimidine and thiophene

Pyrimidine[a)]			Thiophene[a)]		
N	2s	1.578	S	3s	1.702
	$2p_x$	1.489		$3p_x$	1.123
	$2p_y$	1.197		$3p_y$	1.553
	$2p_z$	1.230		$3p_z$	1.755
C_2	2s	1.185	C_2	2s	1.248
	$2p_x$	0.686		$2p_x$	0.835
	$2p_y$	0.823		$2p_y$	0.788
	$2p_z$	0.791		$2p_z$	1.045
C_4	2s	1.225	C_3	2s	1.246
	$2p_x$	0.883		$2p_x$	0.883
	$2p_y$	0.756		$2p_y$	0.876
	$2p_z$	0.828		$2p_z$	1.078
C_5	2s	1.248	H_2	1s	0.974
	$2p_x$	0.923	H_3	1s	0.961
	$2p_y$	0.902			
	$2p_z$	1.093			
H_2	1s	1.021			
H_4	1s	1.002			
H_5	1s	0.950			

a) y is taken as C_2 rotation axis; z is taken perpendicular to plane of a molecule.

These discrepancies may partly be attributed to the evaluation of the two-center Coulomb repulsion by Ohno approximation.[8)] The lowest n–π^* transition energy in thiophene is calculated to be larger than those in pyridine and pyrimidine, and it is also larger than some π–π^* transition energies in thiophene. The fact that the n–π^* transition in thiophene has never been observed may be evidence supporting the present results.

The AO-charge densities for pyridine calculated by the present method are compared with those obtained by Clementi[13)] in Table 7. The formal charge on the nitrogen atom becomes -0.426 in the present calculation, while it was obtained as -0.229 by Clementi.[13)] It may be noted that the large negative charge on the nitrogen atom in the present results is supplies mainly by the σ electrons rather than by the π electrons (the $2p_z$ orbitals in Table 7). The AO-charge densities for pyrimidine and thiophene are also given in Table 8. The $2p_\pi$ AO-charge and atomic charges of the nitrogen atom in pyrimidine are both larger than those in pyridine. This trend for the π charges in two compounds coincides with the finding of McWeeny and Peacock.[16)] The formal charge of the sulfur atom in thiophen, in spite of a considerably large positive value of the $3p_\pi$ net charge, is negative as a result of the back-donation of the σ electrons.

The molecular dipole moments are given approximately by the vector sum of the moment, μ_Q, derived from the net atomic charge and by the atomic dipole moment, μ_{atom}.[17)] The z components in the appropriate Cartesian coordinate are given in Debye units by using Slater-type AO's:

$$\mu_Q(z) = 4.8030 \sum_{A}^{atoms} Q_A z_A$$

$$\mu_{atom(z)} = -\sum_{A}^{atoms} D_n(A) \cdot P_{ns(A)np_z(A)} \times [\zeta_s(A) \cdot \zeta_p(A)]^{n+1/2} \Big/ \left[\frac{\zeta_s(A)+\zeta_p(A)}{2}\right]^{2n+2}$$

where z_A is the z coordinate of the A atom given in units of Å, where $P_{ns(A)np_z(A)}$ is the bond order between the ns and np_z AO's of the A atom, where ζ_s and ζ_p are the orbital exponents for the s and p atomic orbital functions, and where $D_n(A)$ is the constant which is common to the nth row elements, *i. e.*, for $n=2$ and $n=3$, $D_2=7.3370$ Debye and $D_3=10.2718$ Debye. The calculated dipole moments for pyridine and pyridimidine are in fair agreement with the experimental values shown in Table 9. The large calculated dipole moment for thiophene shows that there is still some room for improvement.

16) R. McWeeny and T. E. Peacock, *Proc. Phys. Soc.*, **A70**, 41 (1957).
17) J. A. Pople and G. A. Segal, *J. Chem. Phys.*, **43**, s136 (1965).

TABLE 9. CALCULATED AND OBSERVED DIPOLE MOMENTS (Debye)

	Calcd			Obsd
	μ_Q	μ_{atom}	μ_{total}	μ
Pyridine	1.50	0.78	2.28	2.20[a]
Pyrimidine	1.78	0.91	2.69	2.42[a]
Thiophene	0.49	1.41	1.90	0.55[b]

a) Y. Morino, "Constants of Organic Compounds," Asakura Pub., Tokyo (1963), p. 500.
b) B. Harris, R. J. Le Févre and E. P. A. Sullivan, *J. Chem. Soc.*, **1953**, 1622.

Relation Between Bond Length and E_{AB}. A bond length-bond order relation is usually used to estimate the unknown bond lengths in a π electron approximation.[18] The σ electron contribution is considered to be a constant for every bond in these treatments. In the present paper, a graphical procedure to estimate the bond length of a bond by considering all the valence electrons explicitly is proposed. For this purpose, we utilize the total electronic energy, E_{AB}, of the AB bond as given in Eq. (10) instead of the bond order:

$$E_{AB} = \sum_{r}^{\text{on A}} \sum_{s}^{\text{on B}} P_{rs}(H_{rs}+F_{rs}) \qquad (10)$$

Here $\sum_{r}^{\text{on A}}$ denotes the summation over all the valence AO's belonging to the A atom. We first plot the E_{AB} values *vs.* the observed carbon-carbon bond lengths, R_{AB}, for some typical molecules (for example, C_2H_6, C_2H_4, C_6H_6, and C_2H_2) and also for pyridine, pyrimidine, and thiophene. As may be seen in Fig. 1, a fairly smooth curve can be drawn, and this curve may then be used to predict the lengths of a bond as a semi-empirical relation according to π electron theory. The curves for carbon-nitrogen and carbon-sulfur bonds are obtained similarly (Figs. 2 and 3). These semi-empirical curves will be employed to estimate the bond lengths of benzyne and hetarynes in the next section.

Benzyne and Hetarynes. Benzyne is also called dehydrobenzene and is known to be a typical unstable intermediate on the basis of many experimental results.[19] The electronic structure of benzyne has been discussed from several points of

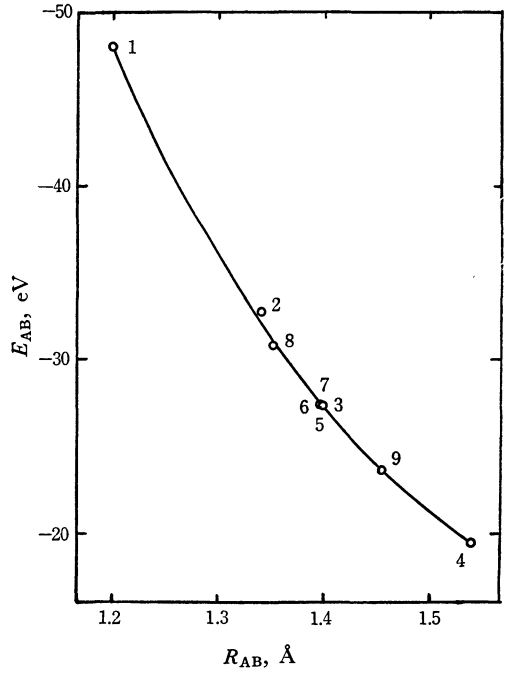

Fig. 1. Values of E_{AB} *vs.* R_{AB} for the carbon-carbon bonds.
1: acetylene 2: ethylene 3: benzene
4: ethane 5: pyridine (2-3)
6: pyridine (3-4) 7: pyrimidine
8: thiophene (2-3) 9: thiophene (3-4)

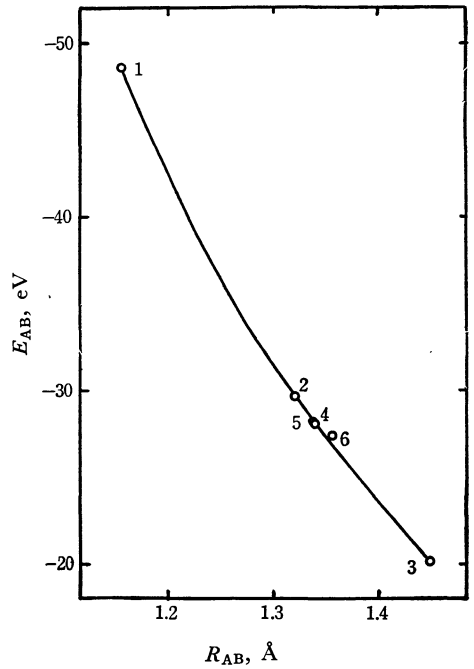

Fig. 2. Values of E_{AB} *vs.* R_{AB} for the carbon-nitrogen bonds.
1: hydrogen cyanide 2: diazomethane
3: methylamine 4: pyridine
5: pyrimidine (1-2) 6: pyrimidine (3-4)

18) C. A. Coulson, *Proc. Roy. Soc.*, **A169**, 413 (1939); for a recent example, *cf.* M. J. S. Dewar and G. J. Gleicher, *J. Chem. Phys.*, **44**, 759 (1966).

19) H. Heaney, *Chem. Revs.*, **62**, 81 (1962).

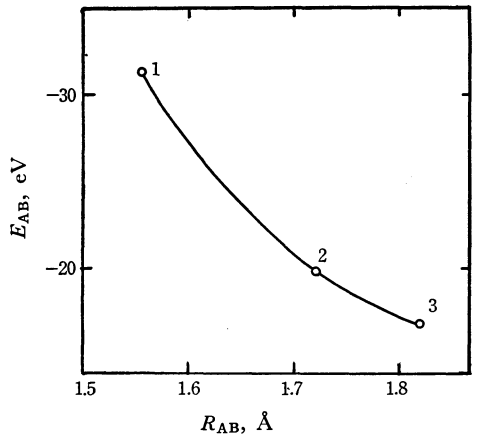

Fig. 3. Values of E_{AB} *vs.* R_{AB} for the carbon-sulfur bonds.
1: carbon disulfide 2: thiophene 3: methyl mercaptan

view by several authors,[20-24] but the electron interation has never explicitly been taken into account in these treatments. Hetarynes and benzyne analogues derives from heteroaromatic compounds, such as 3,4-pyridyne,[25,26] 4,5-pyrimidyne,[25,27] and 2,3-thiophyne,[28] may also be supposed to be unstable intermediates. Calculations on these intermediates and their isomers are performed using the semi-empirical SCF MO method presented in this paper.

Benzyne and hetarynes are so unstable that no information on their geometrical structures has ever been obtained by any experiments. An attempt to estimate the bond lengths of benzyne was made by Coulson by means of a π electron calculation of the Hückel type.[20] He used a semi-empirical bond length-bond order relation. In the present paper, we will use other semiempirical curves relating the bond lengths to the E_{AB}[6]

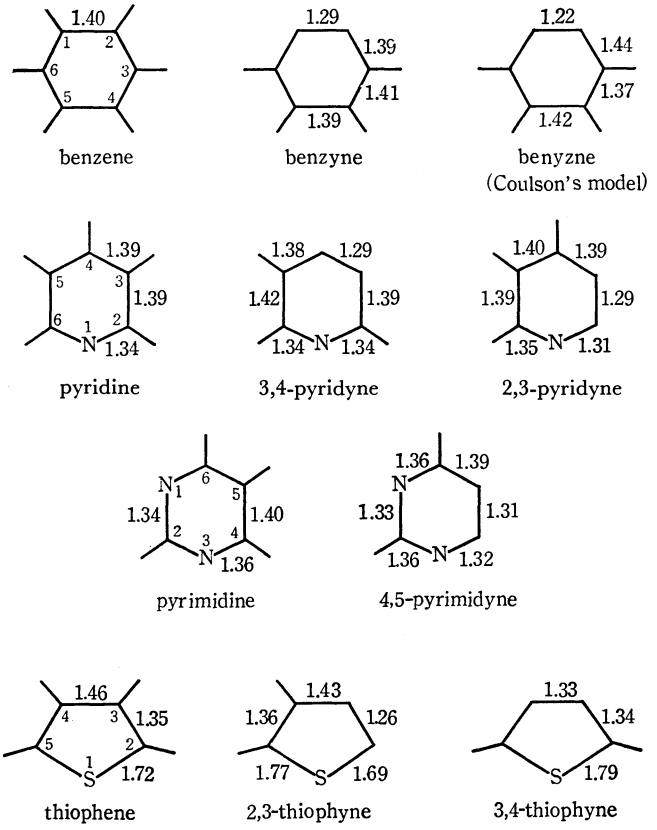

Fig. 4. SCF bond lengths of benzyne and hetarynes.

20) C. A. Coulson, *Chem. Soc. Special Publ. (London)*, **12**, 100 (1958).
21) H. E. Simmons, *J. Am. Chem. Soc.*, **83**, 1657 (1961).
22) R. Huisgen, "Organometallic Chemistry," ed. by H. Zeiss, Reinhold, N. Y. (1960), p. 36.
23) T. Yonezawa, H. Konishi, H. Kato, K. Morokuma and K. Fukui, *Kogyo Kagaku Zasshi (J. Chem. Soc. Japan, Ind. Chem. Sect.)*, **69**, 869 (1966).
24) R. Hoffmann, A. Imamura and W. J. Hehre, *J. Am. Chem. Soc.*, **90**, 1499 (1968).
25) Th. Kauffmann, *Angew. Chem.*, **77**, 557 (1965).
26) Th. Kauffmann and F.-P. Boettcher, *Chem. Ber.*, **95**, 1528 (1962).
27) H. C. van der Plas, *Tetrahedron Letters*, **1965**, 555.
28) G. Wittig, *Angew. Chem.*, **74**, 479 (1962).

(Figs. 1—3).

First, the geometry of the parent molecule with two hydrogen atoms eliminated is adopted for that of an intermediate, and calculation is carried out; secondly, all the bond lengths except for the carbon-hydrogen bonds are estimated at each iteration by using the relation shown in Figs. 1—3. In the course of these iterations, the planarity of a molecule and minimum changes in the bond angles were assumed. The iteration is repeated until a self-consistency within 0.01 Å between the input and the output bond lengths is established.

The SCF bond lengths of the carbon-carbon, the carbon-nitrogen, and the carbon-sulfur bonds in benzyne and hetaynes are shown, together with those of their parent molecules for the sake of comparison, in Fig. 4. The bonds from which the two hydrogen atoms are removed become shorter by about 0.1 Å than parent molecules and take values intermediate between those of the double and triple bonds. For benzyne, the bond lengths estimated by Coulson[20] are also presented in Fig. 4. The present results differ from those of Coulson to some extent. The value of the shortest bond by Coulson is very close to that of the triple bond in acetylene, while our shortest bond is not so short.

The π charge densities for benzyne and hetarynes are presented in Table 10. The variations in the π-charge densities from their parent molecules are not very large except for the C_5 position in 4,5-pyrimidyne.

The values of the π and π' bond orders for benzyne, hetarynes, and their parent molecules in Table 11 show that the shortest bonds of benzyne and hetarnes have quite large $P_{\pi'\pi'}$ values, values which are rather larger than the $P_{\pi\pi}$ values. The total π bond order, the sums of $P_{\pi\pi}$ and $P_{\pi'\pi'}$ for these bonds range from 1.3 to 1.7. From the findings on the bond lengths and the total π bond orders for the shortest carbon-carbon bonds of benzyne and hetarynes, these bonds seem to be normal triple bonds, which may have slightly different bond characters.

It may be noted that all the HO orbitals of

Table 10. π Charge densities for benzyne and hetarynes

a) Benzyne

C_1	C_3	C_4
0.959	1.025	1.016

b) 3,4-Pyridyne

N_1	C_2	C_3	C_4	C_5	C_6
1.217	0.898	0.965	0.913	1.076	0.930

c) 2,3-Pyridyne

N_1	C_2	C_3	C_4	C_5	C_6
1.218	0.931	0.932	0.953	1.038	0.928

d) 4,5-Pyrimidyne

N_1	C_2	N_3	C_4	C_5	C_6
1.191	0.833	1.219	0.760	1.285	0.731

e) 2,3-Thiophyne

S_1	C_2	C_3	C_4	C_5
1.788	0.954	1.104	1.059	1.095

f) 3,4-Thiophyne

S_1	C_2	C_3
1.803	1.089	1.010

Table 11. Values of π and π' bond orders for benzyne, hetarynes and their parent molecules

Bond		$P_{\pi\pi}$	$P_{\pi'\pi'}$*
Benzene	1-2	0.667	—
Benzyne	1-2	0.700	0.819
Pyridine	3-4	0.665	—
Pyridine	2-3	0.667	—
3,4-Pyridyne	3-4	0.700	0.803
2,3-Pyridyne	2-3	0.694	0.770
Pyrimidine	4-5	0.667	—
4,5-Pyrimidyne	4-5	0.690	0.715
Thiophene	2-3	0.853	—
Thiophene	3-4	0.451	—
2,3-Thiophyne	2-3	0.865	0.815
3,4-Thiophyne	3-4	0.483	0.793

* The notation π' represents the component of p orbital which lies in the molecular plane and is perpendicular to the bond axis.

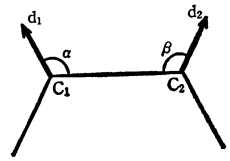

Fig. 5. Directions of the partial atomic dipoles of the carbon atoms in the molecular plane. C_2 is near to a heteroatom in hetaryne.

Table 12. Moments of the partial atomic dipoles of the carbon atoms in the HO and LV orbitals and the angles α and β[a]

		$\lvert d_1\rvert$	$\lvert d_2\rvert$	α(°)	β(°)
Benzyne	HO	0.74	0.74	133	133
	LV	1.31	1.31	123	123
3,4-Pyridyne	HO	0.28	1.38	136	140
	LV	1.34	1.10	122	123
2,3-Pyridyne	HO	1.14	0.01	135	133
	LV	1.19	1.60	121	118
4,5-Pyrimidyne	HO	1.43	0.00	138	141
	LV	0.40	1.90	109	124
2,3-Thiophyne	HO	0.56	0.87	133	134
	LV	1.52	1.73	119	142
3,4-Thiophyne	NHO*	0.76	0.76	128	128
	LV	1.14	1.14	127	127

a) The definition of d_1, d_2, α and β are illustrated in Fig. 5.

* NHO: the next highest orbital.

benzyne and hetarynes except for 3,4-thiophyne and the lowest vacant (LV) orbitals of all the intermediates are highly localized on the carbon atoms from which the two hydrogen atoms are removed. We calculated the partial atomic dipole, d_i, of the ith carbon atom of the triple bond in these MO's. The absolute values of the d_1 and d_2 vectors the α and β angles of the orientation of the partial atomic moment from the C_1–C_2 axis (in Fig. 5) are given in Table 12. The large absolute values of d_1 and d_2 show that the electrons of these MO's are considerably localized at these carbon atoms and that the centers of the negative charge are far from the atom. The values of α and β, which are about 120°, indicate that the HO and LV MO's of benzyne and hetarynes may be described approximately as a linear combination of non-bonding sp^2-type hybrids of the carbon atoms, as has been pointed out by Ingold and King[29] for the excited bent acetylene.

It is well known that benzyne and hetarynes react as intermediates with nucleophilic reagents in the elmination-addition reaction of some substituted benzene and heterocyclic compounds.[19,25] The reactions of hetarynes with nucleophilic reagents generally afford two kinds of isomeric products. The main product of isomers may be predicted from the charge distributions in the LV orbitals of hetarynes. The absolute values of the partial atomic dipole moments in Table 12, which represent the relative strengths of the σ electron-donating power of each carbon atom of the triple bond, can be employed in the present case. From

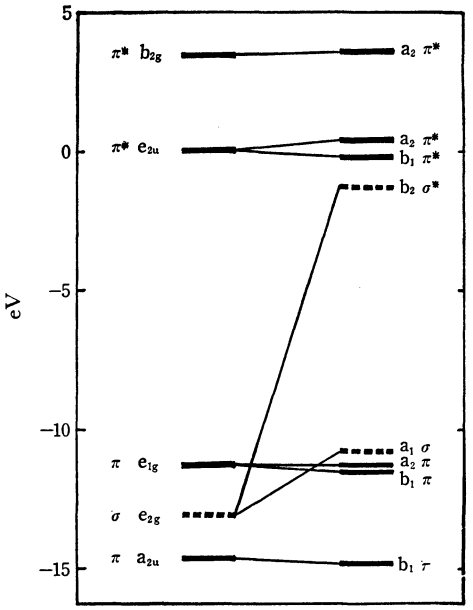

Fig. 6. Relation between the MO levels of benzene and benzynes. The full lines indicate the π MO levels and the dotted line are σ MO levels.

Table 13. Calculated transition energies (eV) of benzyne and hetarynes

Transition	state	(f)	+SECI(f)
Benzyne			
σ-σ*	$^1B_2$	3.73(0.28)	3.01(0.05)
π-σ*	$^1A_2$	3.63(0)	3.33(0)
π-σ*	$^1B_1$	3.57(0.0003)	3.54(0.0003)
π-π*	$^1B_2$	6.13(0.57)	4.87(0.03)
π-π*	$^1A_1$	6.13(0.51)	5.12(0.005)
σ-σ*	$^3B_2$	1.65(0)	1.24(0)
π-π*	$^3B_2$	4.01(0)	3.56(0)
π-π*	$^3A_1$	4.70(0)	4.59(0)
3,4-Pyridyne			
σ-σ*	$^1A'$	3.44(0.20)	2.96(0.05)
n-π*	$^1A''$	5.02(0.0001)	4.66(0.001)
π-π*	$^1A'$	5.91(0.53)	5.04(0.03)
π-π*	$^1A'$	6.17(0.49)	6.06(0.31)
σ-σ*	$^3A'$	1.82(0)	1.67(0)
π-π*	$^3A'$	4.13(0)	3.59(0)
n-π*	$^3A''$	4.68(0)	4.14(0)
2,3-Pyridyne			
σ-σ*	$^1A'$	3.13(0.21)	2.68(0.05)
π-π*	$^1A'$	5.76(0.48)	4.93(0.03)
π-π*	$^1A'$	6.27(0.57)	5.07(0.03)
n-π*	$^1A''$	5.95(10^{-9})	5.57(0.0001)
σ-σ*	$^3A'$	1.60(0)	1.42(0)
π-π*	$^3A'$	4.10(0)	3.57(0)
n-π*	$^3A''$	5.64(0)	5.13(0)
4,5-Pyrimidyne			
σ-σ*	$^1A'$	2.56(0.11)	2.25(0.02)
n-π*	$^1A''$	4.78(10^{-5})	4.61(0.002)
π-π*	$^1A'$	5.72(0.53)	4.99(0.04)
π-π*	$^1A'$	6.21(0.43)	5.34(0.01)
σ-σ*	$^3A'$	1.46(0)	1.33(0)
π-π*	$^3A'$	3.87(0)	3.53(0)
n-π*	$^3A''$	4.54(0)	3.95(0)
2,3-Thiophyne			
σ-σ*	$^1A'$	2.80(0.11)	2.34(0.03)
π-π*	$^1A'$	5.87(0.38)	5.85(0.28)
π-π*	$^1A'$	6.57(0.55)	6.33(0.16)
n-π*	$^1A''$	6.75(0.003)	6.48(0.002)
σ-σ*	$^3A'$	0.85(0)	0.76(0)
π-π*	$^3A'$	3.99(0)	3.49(0)
n-π*	$^3A''$	6.57(0)	6.68(0)
3,4-Thiophyne			
σ-σ*	$^1B_2$	2.91(0.18)	2.65(0.09)
π-π*	$^1B_2$	5.54(0.49)	5.34(0.47)
π-π*	$^1A_1$	6.30(0.51)	6.06(0.21)
n-π*	$^1B_1$	6.19(0.005)	6.20(0.005)
σ-σ*	$^3B_2$	0.86(0)	0.84(0)
π-π*	$^3B_2$	3.28(0)	2.98(0)
n-π*	$^3B_1$	6.01(0)	6.02(0)

29) C. K. Ingold and G. W. King, *J. Chem. Soc.*, **1953**, 2702.

the present calculation, the more reactive sites may be predicted to be as follows: the 4 site for 3,4-pyridyne; the 2 site for 2,3-pyridyne; the 4 site for 4,5-pyrimidyne and the 2 site for 2,3-thiophyne. The only experimental results available for comparison are for 3,4-pyridyne[26] and 4,5pyrimidyne.[25] The reactions of 3-chloro and 3-bromopyridine with lithium piperidide and piperidine give 3- and 4-piperidinopyridine in the 48 : 52 ratio.[25] For the case of 4,5-pyrimidyne, only 4-piperidinopyrimidine was obtained under the same conditions.[25] These experimental results support the predictions based on the present calculations.

Some molecular orbital energy levels of benzyne are illustrated in Fig. 6, combined with those of benzene. The HO and LV orbitals of benzyne are σ-type orbitals (mentioned above), which become unstable because they lack the two hydrogen atoms. The energy changes of the π orbitals are small. The occupied π orbitals of benzene become slightly stable, and also the degeneracy is removed. The other occupied σ-type orbitals of benzyne are more unstable than the corresponding σ orbitals of benzene. Analogous situations also occur in the case of each hetaryne.

The transition energies of benzyne and hetarynes have been calculated, and the configuration interactions further considered among a limited number of singly-excited configurations.[30] The calculated lowest singlet transitions in benzyne and hetarynes, shown in Table 13, are all σ–σ^* type transitions, from the HO to the LV levels. As the experimental value for benzyne, the value of 4.9 eV assigned to the π–π^* transition with the oscillator strength of magnitude of 0.1—0.2[31] has been reported. This energy of the transition is near the value of the lowest singlet π–π^* transition for benzene; this is also shown by the present calculations. The calculated lowest transition energies of the n–π^* type for hetarynes indicate the blue shifts referred to the corresponding ones of their parent molecules (*cf.* Table 6). In addition, the larger shift in 2,3-pyridyne than in 3,4-pyridyne can be recognized. This result may be due to the stronger interaction between the lone pair on the heteroatom and the non-bonding sp^2-type hybrids on the carbon atoms, which are situated nearer each other in the case of 2,3-piridyne than in that of 3,4-pyridyne. A similar tendency is found in the cases of 2,3-thiophyne and 3,4-thiophyne.[32]

A benzyne structure with a triplet state in its ground state was long ago discussed by Müller and Röscheisen,[33] but it was pointed out to be unlikely by Huisgen.[22] In the present calculations, the lowest triplet transitions for benzyne and hetarynes are π–π^*-type transitions. The calculated values for these transitions in Table 13 are extraordinarily small, but they are not negative; therefore, the lowest triplet states of benzyne and hetarynes may lie very close to the ground states, which should be the singlet state.[34]

We are grateful to Professor I. Tabushi for his kind discussion and also to the computation centers of both Tokyo University and Kyoto University, where the present calculations were carried out.

30) The following numbers of configurations, which consist of two groups of AO's (n, π and HO; LV and π^*), are considered: 16 for benzyne; 20 for pyridynes; 24 for pyrimidyne; 15 for thiophynes.

31) R. S. Berry, G. N. Spokes and R. M. Stiles, *J. Chem. Soc.*, **82**, 5240 (1960); **84**, 3570 (1962).

32) In the present calculations, 3,4-pyridyne and 3,4-thiophyne become more stable than 2,3-pyridyne and 2,3-thiophyne respectively, while 2,3-thiophyne has been pointed out by Wittig to be more stable than 3,4-thiophyne (Ref. 28). This disagreement may be attributed to the total energy of the isomers of pyridynes and thiophynes obtained by the point-charge approximation for the core-core repulsion energy.

33) E. Müller and G. Röscheisen, *Chem. Ztg.*, **80**, 101 (1956).

34) Recently, benzyne in the triplet state has been found to make an appreciable contribution in a reaction of benzyne with substituted ethylenes: I. Tabushi, R. Oda and K. Okazaki, *Tetrahedron Letters*, **1968**, 3743.

BULLETIN OF THE CHEMICAL SOCIETY OF JAPAN VOL. 42 943—946 (1969)

Heat of Immersion of Titanium Dioxide in Water. I. The Effect of the Hydration Treatment of Titanium Dioxide

Tetsuo MORIMOTO, Mahiko NAGAO and Teiji OMORI

Department of Chemistry, Faculty of Science, Okayama University, Tsushima, Okayama

(Received September 19, 1968)

On anatase and rutile, three samples which differ in the extent of hydration treatment have been prepared, and the surface area, the water content, and the heat of immersion have been measured. The hydration treatment of the sample increases the water content of the sample and lowers the sintering temperature. These facts suggest that the condensation dehydration of surface hydroxyl groups from the facing surfaces of contacting particles is effective for sintering. The plot of the heat of immersion *vs.* the pretreatment temperature shows a maximum at about 400°C, and the heat of immersion is larger in the sample subjected to heavy hydration treatment. The heat of surface hydration, calculated from the plot of the heat of immersion *vs.* the water content, does not vary with the hydration treatment; it averages 25.2 and 19.0 kcal/mol H_2O for anatase and rutile respectively.

It has been clarified that, on the surfaces of metal oxides, there exist hydroxyl groups which have a great influence on such surface chemical properties as surface electrification, hydrophilicity, adsorbability, and catalytic action. Recently, investigations have been made of the chemical properties of the surface hydroxyl groups themselves from the following two points of view: first, the temperature at which the surface hydroxyl groups start to desorb *in vacuo*,[1,2] and second, the rate at which the surface hydroxyl groups are formed.[3,4] These properties seem to depend on the nature of the substrate oxides. The same situation may also be expected in properties other than those just described.

The value of the heat of immersion of metal oxides is affected by the combination of solid and liquid, and by the origin and the history of the solid. So far it has been discovered that the particle size of the powdered sample and the heat treatment of the sample performed just before the calorimetric measurement greatly influence the heat of immersion, and that these circumstances make it impossible to consider the heat-of-immersion value as inherent in the solid substance.[5,6] Of course, the coatings on the solid surface modify the oxide surface properties.[7] Of these factors, the pretreatment of the sample at elevated temperatures serves to modify the surface properties by removing the surface hydroxyl groups. Most plots of the heat of immersion in water against the pretreatment temperature reveal a maximum.[6,8-11] The appearance of the maximum has been explained in terms of the cooperative effect of the formation of surface hydroxyl groups and the physical adsorption of water on them. By analyzing the heat of immersion, therefore, we can obtain the heat of surface hydration, that is, the heat of the formation of surface hydroxyl groups.

In the present paper the heat of immersion of titanium dioxide in water has been measured in order to investigate the effects of the hydration treatment of the samples on the heat-of-immersion value obtained and on the heat of surface hydration calculated therefrom. As a result, it has been found that the hydration treatment has a great influence on the sintering of particles, and that it causes the heat-of-immersion value to vary considerably, while it scarcely affects the heat of surface hydration.

1) T. Morimoto, M. Nagao and F. Tokuda, This Bulletin, **40**, 2723 (1967).
2) T. Morimoto, M. Nagao and F. Tokuda, *ibid.*, **41**, 1533 (1968).
3) T. Morimoto and M. Nagao, *Kolloid-Z. u. Z. Polymere*, **224**, 62 (1968).
4) to be published.
5) W. H. Wade and N. Hackerman, *J. Phys. Chem.*, **64**, 1196 (1960).
6) W. H. Wade and N. Hackerman, *ibid.*, **65**, 1681 (1961).
7) A. C. Zettlemoyer, R. D. Iyengar and P. Scheidt, *J. Colloid and Interface Sci.*, **22**, 172 (1966).
8) G. J. Young and T. P. Bursh, *J. Colloid Sci.*, **15**, 361 (1960).
9) J. W. Whalen, *Advan. Chem. Ser.*, **33**, 281 (1961).
10) T. Morimoto, K. Shiomi and H. Tanaka, This Bulletin, **37**, 392 (1964).
11) T. Morimoto, M. Nagao and M. Hirata, *Kolloid-Z. u. Z. Polymere*, **225**, 29 (1968).

Experimental

Materials. Both the samples used in the present work, anatase and rutile, presented by the Teikoku Kako Co., had been made from titanium sulfate and were free from coatings. These original samples were treated repeatedly with 0.1 N nitric acid to remove basic impurities, and with 0.1 N ammonia water to remove acidic impurities, and then washed with distilled water; finally, the method of electrodialysis was used to clear them of electrolytes as completely as possible. The resulting samples were dried at 110°C for 10 hr in an oven (AI and RI).

A part of each sample (AI and RI) was treated at 800°C for 4 hr in air, and then exposed to saturated water vapor for 5 days at room temperature (AII and RII).

Another part of each sample (AI and RI) was further immersed in hot water at 80°C for 3 days in order to prepare a highly-hydrated sample (AIII and RIII). The samples AII, AIII, RII, and RIII were finally dried at 110°C for 10 hr as before.

Surface-area Measurement. The specific surface area of the samples was determined by applying the BET theory to the nitrogen adsorption data, assuming the area of a nitrogen molecule to be 16.2 Å^2.

Heat-of-immersion Measurement. The heat of immersion was measured at 25°C by means of a calorimeter equipped with a thermistor as the temperature-sensing element, as has been described previously.[10,11] Prior to the measurement, the glass ampoule containing the sample was treated at a desired temperature in a vacuum of 10^{-5} Torr for 4 hr, sealed off *in vacuo*, and then set in the calorimeter. The technique of the measurement of the heat of immersion was the same as has been described previously.[10,11] It has been pointed out that the heat treatment of titanium dioxide *in vacuo* leads to a partial reduction of the sample, leaving nonstoichiometric and gray-colored surfaces on the sample.[12,13] In the present investigation also, a slight color-change of the sample appeared upon pretreatment at elevated temperatures, but the sample was used for the heat-of-immersion measurement in this state.

Water-content Measurement. In a usual atmosphere water molecules are adsorbed on the surface of titanium dioxide both physically and chemically. The physically-adsorbed water can be removed fairly easily *in vacuo*, even at room temperature, whereas the chemisorbed water can be removed only gradually by heating at higher temperatures. Thus, the water contents at various temperatures were determined by the successive ignition-loss method.[10,11] Since the amount of water expelled above 1000°C was found to be negligible, the water contents at various temperatures were calculated cumulatively by the summation of the amount of water evolved at each temperature, assuming the water content at 1100°C to be zero. In these procedures a small amount of gases other than water vapor was found to be evolved at higher temperatures. This was eliminated from the water-content data in the following way. All the gases evolved at an elevated temperature were trapped in a bulb kept at the temperature of liquid nitrogen, and then measured volumetrically at room temperature after the reevaporation of the trapped gases, using an all-glass apparatus[3] equipped with an oil manometer in order to measure sensitively the minute vapor pressure of water. Next, a part of the gases was retrapped at −72°C. When the gas contained only water vapor, all the gas could be retrapped at −72°C. However, in the gases expelled from the sample at temperatures higher than 300°C, a detectable amount of gases remained uncondensed at −72°C. In such cases, only the condensed gas was again determined in the same way as before, after removing the uncondensed gases by the evacuation of the system. The latter value is illustrated in Fig. 2 as the amount of the water content. The gases other than water which were evolved included, for example, 0.09, 0.18, and 0.29 molecules/100 Å^2 at 300, 400, and 600°C respectively, for the sample RI.

Results and Discussion

In Fig. 1 the specific surface area of titanium dioxide is represented as a function of the temperature of pretreatment. The surface areas of the samples of RI, RII, and AII are almost constant up to 800°C, after that they decrease steeply, indicating the occurrence of sintering. The sintering starts at 700°C with AI, whereas it begins at 600°C with AIII and RIII.

Figure 2 shows the relation between the water content and the temperature of pretreatment, where the former is represented in OH's/100 Å^2. The water content of the rutile obtained is quite small over the whole range examined, as is shown in Fig. 2. This may be explained as follows: the surface hydroxyl groups on rutile can be more easily removed by heating *in vacuo*, and therefore the water content of rutile at 250°C to 400°C is unexpectedly less than those of α-Fe_2O_3 or ZnO.[2]

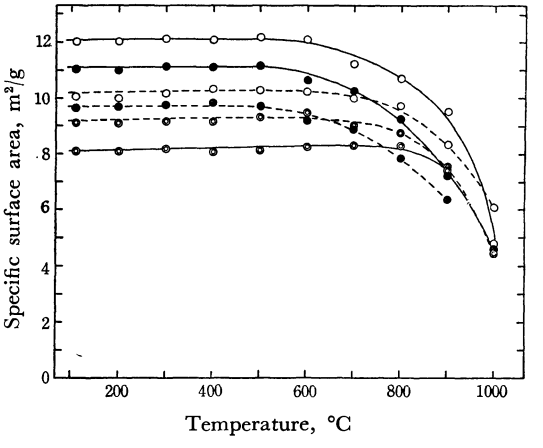

Fig. 1. Dependence of specific surface area of TiO_2 on pretreatment temperature.
—— anatase: ○, AI; ◎, AII; ●, AIII
---- rutile: ○, RI; ◎, RII; ●, RIII

12) J. Gebhardt and K. Herrington, *J. Phys. Chem.*, **62**, 120 (1958).
13) C. M. Hollabaugh and J. J. Chessick, *ibid.*, **65**, 109 (1961).

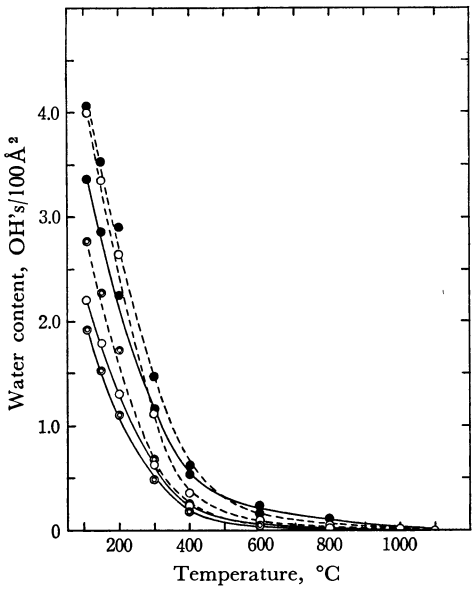

Fig. 2. Water contents of TiO_2 at various temperatures.
—— anatase: ○, AI; ◎, AII; ●, AIII
---- rutile: ○, RI; ◎, RII; ●, RIII

Also, it may be seen from Fig. 2 that the water contents on anatase seems to be slightly less than those on rutile; this may suggest that the surface hydroxyl groups on anatase can be removed as easily as, or more easily than, those on rutile. Furthermore, the water content is the greatest on the samples subjected to heavy hydration treatment in hot water, whereas it is the least on samples exposed to the saturated water vapor after 800°-treatment. In conclusion, the water contents of anatase and rutile decrease in the order: AIII>AI>AII and RIII>RI>RII.

A comparison of Fig. 1 with Fig. 2 leads to an interesting conclusion. On the samples AII and RII, which were once treated at 800°C and then exposed to the saturated water vapor at room temperature, the sintering due to retreatment does not occur below 800°C, but it occurs remarkably over 800°C, as may be expected. On the other hand, the water content of the samples AIII and RIII subjected to heavy hydration procedure in hot water is the largest, and their sintering starts at a lower temperature, 600°C. The temperature at which the sintering of the samples starts rises in the order: AIII<AI<AII and RIII<RI<RII, corresponding to the order of decrease in the water content.

In the present case, the sintering may be initiated by the condensation dehydration of hydroxyl groups from the facing surfaces of contacting particles.[14] The fact that the sintering of the sample with the larger water content starts at a lower temperature seems to support this supposition. When the condensation dehydration occurs from two contacting surfaces facing each other, there is a possibility that a part of the surface hydroxyl groups will be closed into the inner surfaces thus produced. Thus, it is reasonable to consider that it is difficult to remove such surface hydroxyl groups even at elevated temperatures, as is shown in Fig. 2.

The heat of immersion of titanium dioxide is given in Fig. 3 as a function of the temperature of pretreatment. These data show a maximum similar to the results of Wade and Hackerman.[6] The pretreatment temperature at which the maximum appears is about 400°C in the present study, whereas it was between 300°C and 350°C in their experiments. It may be seen from Fig. 3 that the value

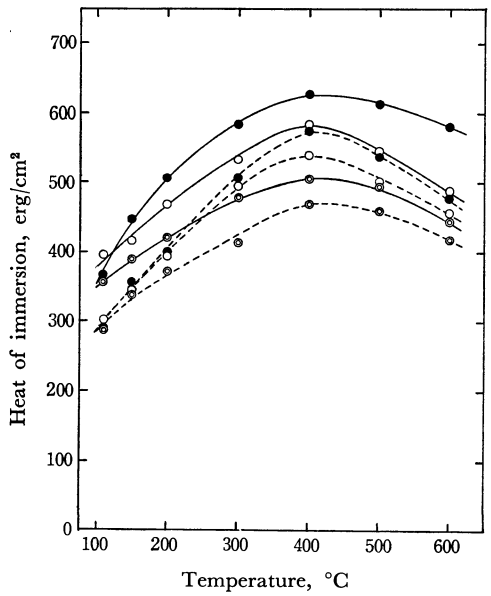

Fig. 3. Dependence of heat of immersion of TiO_2 in water on pretreatment temperature.
—— anatase: ○, AI; ◎, AII; ●, AIII
---- rutile: ○, RI; ◎, RII; ●, RIII

of the heat of immersion varies with the extent of hydration treatment, while in the experiments of Wade and Hackerman it was dependent on the size of the particles used. The heat-of-immersion value decreases in the order: AIII>AI>AII and RIII>RI>RII, parallel with the order of water content.

The heat-of-immersion anomaly, the terms of which imply the appearance of a maximum in the plot of the heat of immersion *vs.* the pretreatment temperature, has been explained as a cooperative effect of the chemisorption and physical adsorption of water: in the range of the steep increase in the heat of immersion, the reversible rehydroxylation (chemisorption of water to form surface

14) P. J. Anderson and P. L. Morgan, *Trans. Faraday Soc.*, **60**, 930 (1964).

hydroxyl groups) occurs on the site dehydrated by the pretreatment at elevated temperatures.[6,8-11] In the range of temperatures higher than the maximum point of the heat of immersion, the reversible rehydroxylation is delayed by the stabilization of the surface oxide structure, so the additional heat evolution by this reaction within the period of the heat-of-immersion measurement (less than 10 min) is decreased.

If we assume that the energy of the physical interaction on the immersion of a powdered sample in water is constant over the whole range of pretreatment temperatures, and that the appearance of the peak of the heat of immersion results from the additional heat evolution by the chemisorption of water, it may be said, as is shown in Fig. 3, that the contribution of the physical interaction varies considerably with the extent of hydration treatment and is larger on a sample which is subjected to a heavy hydration procedure and which is, therefore, rich in water. In general, three kinds of forces may be considered to be concerned with the contribution of the physical interaction on immersing a solid in a liquid: (1) the interaction between the polar surface and the dipole of the liquid molecule, (2) the effect of the induced dipole of the molecule, and (3) the effect of the dispersion force. Since titanium dioxide is known to be one of the most polar substances, it is valid to consider that the first of these three factors is most effective in the present case, being largely influenced by the surface hydroxyl groups.

Figure 4 shows the plots of the heat of immersion against the water content in the range of a steep increase in the heat of immersion in Fig. 3. As has been discussed above, in this range the physical adsorption and the chemisorption of water occur simultaneously, and the slope of this plot implies the energy of formation of a hydroxyl group (heat of surface hydration). The heats of surface hydration obtained are tabulated in Table 1; it is found that the variation in the heat due to the extent of hydration treatment is small, the average value being 25.2 and 19.0 kcal/mol H_2O for anatase and rutile respectively. Thus far the heat of surface hydration has been reported for several metal oxides: 16.1,[8] 3.5—6.5,[9] and 4.66[15] for SiO_2, 15.8 and 9.60 for α- and γ-Al_2O_3,[10] and 23.1 for ZnO.[11] The present data on TiO_2 are found to be comparable with those on ZnO.

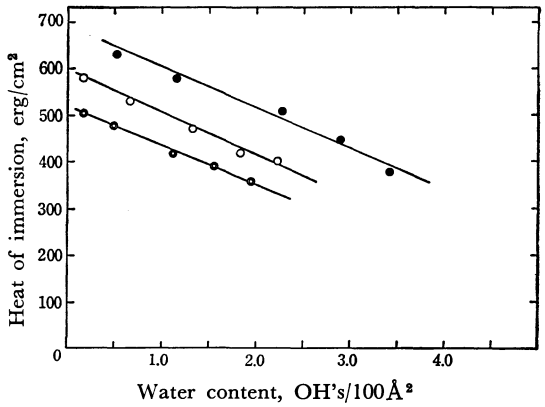

Fig. 4a. Relation between heat of immersion and water content on anatase.
○, AI; ◎, AII; ●, AIII

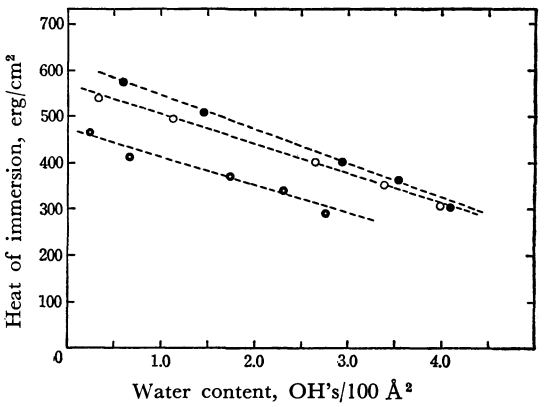

Fig. 4b. Relation heat of immersion and water content on rutile.
○, RI; ◎, RII; ●, RIII

TABLE 1. HEAT OF SURFACE HYDRATION OF TiO_2 (kcal/mol H_2O)

Sample	AI	AII	AIII	RI	RII	RIII
Heat of surface hydration	26.4	24.3	25.0	18.6	18.3	20.1

15) S. Brunauer, D. L. Kantro and C. H. Weise, *Can. J. Chem.*, **34**, 1483 (1956).

BULLETIN OF THE CHEMICAL SOCIETY OF JAPAN VOL. 42 947—951 (1969)

The Chromium(III) Complexes with Anthranilicdiacetic Acid*[1]

Takeshi TOMITA, Eishin KYUNO and Ryokichi TSUCHIYA

Department of Chemistry, Faculty of Science, Kanazawa University, Kanazawa

(Received April 18, 1968)

The following chromium(III) complexes containing the anthranilicdiacetic acid (ATDA) were prepared: $[Cr(atda)^*(H_2O)_2]\cdot 3H_2O$ (reddish-violet) (I), $K[Cr(OH)(atda)(H_2O)]$ (bluish-violet) (II), $[Cr(atda)(phen)^*]\cdot 3H_2O$ (red) (III), $[Cr(atda)(dipy)^*\cdot 2H_2O$ (red) (IV), $[Cr(atda)(en)^*]\cdot 2H_2O$ (red) (V) and $K[Cr(atda)(acac)^*]$ (violet) (VI). From the results of electronic spectra, molar conductivities, chemical and thermal analyses and IR spectra, it was concluded that the Complexes I, II and VI belong to the $[CrO_5N]$, and III, IV and V belong to the $[CrO_3N_3]$ type. ATDA in all these complexes obtained was found to behave only as a quadridentate ligand. The values of the effective magnetic moments were found to be 3.7—3.9 B. M., nearly equal to the spin-only values of the tervalent chromium.
(* atda, phen, dipy, en and, acac are the basic forms of anthranilic acid, *o*-phenanthroline, 2,2'-dipyridyl, ethylenediamine and acetylacetone respectively.)

The syntheses of the chromium(III) complexes with ammoniatriacetic acid (ATA)[1] and with its derivatives, ammoniapropionicdiacetic acid (APDA)[2] and ammoniaisopropionicdiacetic acid (AIPDA)[3] in the solid state have been reported and the coordinating structures of these complexes both in a solid state and in an aqueous solution have been discussed in previous papers. On the other hand, there are few papers on the synthesis of the complexes with the carboxylmethyl derivatives of the anthranilic acid as the aromatic amino acids.

The formation constants in aqueous solution may serve as an important guide for preparing metal coordination compounds. A series of stabilities of the complexes with anthranilic acid and its derivatives have been given by Young *et al.*,[4] who pointed out that the effect of attaching acetic groups to the amino nitrogen upon the stability is seen to grow up in the sequence: anthranilic acid < anthranilicmonoacetic acid < anthranilicdiacetic acid. It may be due to the fact that the number of the chelate rings increases as the carboxylmethyl groups are introduced step by step to anthranilic acid.

In this study, the authors took the anthranilicdiacetic acid (abbreviated as ATDA) as the ligand relating to ATA, but differing from it in that ATDA contains the aromatic ring, and studied the chromium(III) complexes with this ATDA.

The present work was undertaken, i) to prepare the single- and mixed-ligand complexes containing ATDA, ii) to find out how ATDA could behave towards a chromium(III) ion in complex formation, and iii) to discuss their structures based on the comparison with those of the corresponding ATA complexes.

Experimental

Syntheses. *1) Anthranilicdiacetic Acid Hydrochloride* (ATDA·HCl), $C_{11}H_{11}NO_6\cdot HCl$. Anthranilicdiacetic acid hydrochloride was prepared by the reaction of excess monochloroacetic acid with anthranilic acid in the presence of alkali hydroxide solution enough to neutralize the above acids.[4]

2) Anthranilicdiacetatodiaquochromium(III) Trihydrate, $[Cr(atda)(H_2O)_2]\cdot 3H_2O$ (I). To two liters of aqueous solution of 20 g of chromium(III) chloride hexahydrate, 20 g of anthranilicdiacetic acid hydrochloride was added. After the mixture was heated on a boiling water bath for about two hours, the color of the solution gradually turned from green to violet. Evaporating the resulting solution for one hour, the solution was stood at room temperature overnight. Reddish-violet needle crystals precipitated were filtered, and then recrystallization was done in water. Yield, about 12 g. The compound is poorly soluble in both water (M/200) and ethanol.

Found: Cr, 13.08; C, 33.83; H, 4.46; N, 3.46; H_2O, 23.5%. Calcd for $[Cr(C_{11}H_8NO_6)(H_2O)_2]\cdot 3H_2O$: Cr, 13.30; C, 33.68; H, 4.62; N, 3.57; H_2O, 23.0%.

Other complexes newly prepared in the present study were derived from this I as a starting material.

3) Potassium Hydroxoanthranilicdiacetatoaquochromate(III), $K[Cr(OH)(atda)(H_2O)]$ (II). To a solution of 5 g of the Complex I, potassium hydroxide solution was added to adjust the solution to pH 8 and the mixture

*1 Presented at the 17th Symposium on Coordination Compounds, Hiroshima, December, 1967.

1) A. Uehara, E. Kyuno and R. Tsuchiya, This Bulletin, **40**, 2317, 2322 (1967).
2) A. Uehara, E. Kyuno and R. Tsuchiya, *ibid.*, **41**, 2385 (1968).
3) A. Uehara, E. Kyuno and R. Tsuchiya, *ibid.*, **41**, 2393 (1968).
4) A. Young and T. R. Sweet, *J. Am. Chem. Soc.*, **80**, 800 (1958).

was heated on a water bath. After cooling it to room temperature, bluish-violet powder was precipitated and then filtered. The recrystallization was achieved from water. The solubility of this compound in water was about 5 g per liter.

Found: Cr, 13.68; C, 36.66; H, 2.71; N, 3.70%. Calcd for $K[Cr(OH)(C_{11}H_8NO_6)(H_2O)]$: Cr, 13.83; C, 35.11; H, 2.93; N, 3.72%.

4) Anthranilicdiacetato - o - phenanthrolinechromium(III) Trihydrate, $[Cr(atda)(phen)]\cdot 3H_2O$ (III). Five grams of I and 2.5 g of *o*-phenanthroline monohydrate were added to 200 m*l* of water. Heating the mixture on a boiling water bath, pH of the solution was controlled at 8 by dropping the alkali hydroxide solution into it. The color of the solution turned to dark-red from violet in the reaction process. After cooling the solution at 0°C overnight, the red compound was crystallized out. It was filtered and fully washed with water and ethanol. Recrystallization was carried out from the diluted hydrochloric acid solution. Yield, about 1 g. The complex is a little soluble in water.

Found: Cr, 9.74; C, 52.37; H, 4.19; N, 7.97; H_2O, 10.1%. Calcd for $[Cr(C_{11}H_8NO_6)(C_{14}H_{10}N_2)]\cdot 3H_2O$: Cr, 10.03; C, 53.28; H, 4.28; N, 8.14; H_2O, 10.4%.

5) Anthranilicdiacetato-2,2'-dipyridylchromium(III) Dihydrate, $[Cr(atda)(dipy)]\cdot 2H_2O$ (IV). Two grams of 2,2'-dipyridyl were dissolved in 400 m*l* of I solution placed on a boiling water bath. The pH of the mixture was adjusted to about 8 and concentrated for about an hour. After cooling it to 0°C, red crystalline compound was precipitated and was recrystallized from water. Yield, about 1.5 g.

Found: Cr, 10.27; C, 51.07; H, 4.50; N, 8.66; H_2O, 7.8%. Calcd for $[Cr(C_{11}H_8NO_6)(C_{12}H_8N_2)]\cdot 2H_2O$: Cr, 10.52; C, 51.01; H, 4.08; N, 8.50; H_2O, 7.3%.

6) Anthranilicdiacetatoethylenediaminechromium(III) Dihydrate, $[Cr(atda)(en)]\cdot 2H_2O$ (V). Five grams of I were dissolved in 400 m*l* of water and 4 g of ethylenediamine dihydrochloride was added to it. The alkali hydroxide solution was poured drop by drop until a suitable pH was attained and the solution was concentrated to 100 m*l* on a boiling water bath. When the solution was cooled to 0°C, a small amount of red crystals was precipitated. It was filtered and recrystallized from methanol. Yield, about 0.5 g.

Found: Cr, 12.88; C, 39.25; H, 5.32; N, 10.51; H_2O, 9.3%. Calcd for $[Cr(C_{11}H_8NO_6)(C_2H_8N_2)]\cdot 2H_2O$: Cr, 13.05; C, 39.20; H, 5.06; N, 10.60; H_2O, 9.1%.

7) Potassium Anthranilicdiacetatoacetylacetonatochromate(III), $K[Cr(atda)(acac)]$ (VI). Five grams of I were dissolved in 400 m*l* of water, and 4.7 g of potassium acetylacetonate was added. The mixture was warmed on a water bath and then heated in a flask equipped with a reflux condenser for two hours in order to prevent the vaporization of acetylacetone during the reaction. After the solution was concentrated to 200 m*l*, the mixed solution was placed in a desiccator. If the crystal of trisacetylacetonatochromium(III) as the impure substance was deposited, it should be excluded by filtration. When the desired violet powder was precipitated, it was collected on the filter. The recrystallization was carried out from the concentrated aqueous solution. The complex is very soluble in water. Yield, about 0.5 g.

Found: Cr, 11.66; C, 43.71; H, 3.49; N, 2.97%. Calcd for $K[Cr(C_{11}H_8NO_6)(C_5H_7O_2)]$: Cr, 11.50; C, 43.65; H, 3.43; N, 3.18%.

Apparatus. The molar conductivity, the visible, UV and IR spectra, reflectance spectra and the magnetic susceptibility were measured with a Yokogawa Universal Bridge BV-Z-13A, a Hitachi EPS Spectrophotometer, a Jasco DS-301 IR Spectrophotometer, a Hitachi EPU-2A Spectrophotometer equipped with the standard Hitachi Reflectance Attachment and a Gouy Balance, respectively. The quantity of the crystal-water contained in these complexes was estimated from TGA curves measured with a Shimadzu Thermano Balance.

Results and Discussion

Behaviors toward Ion Exchangers and Molar Conductivities. The behaviors of the complexes newly prepared in the present work toward ion exchangers and their molar conductivity data measured in the 1×10^{-3} molar aqueous solution are shown in Table 1. Both the Complexes II and VI were adsorbed by Cl-form exchanger and their molar conductivities were 89.1 and 92.2 mho cm^{-1} respectively. This suggests that both complexes are 1 : 1 valency type and negatively charged electrolytes. All other complexes were adsorbed by neither Na- nor Cl-form exchanger, indicating that all exist as nonelectrolyte state.

Visible and UV Absorption Spectra. The electronic spectra of the Complexes I, II, IV and

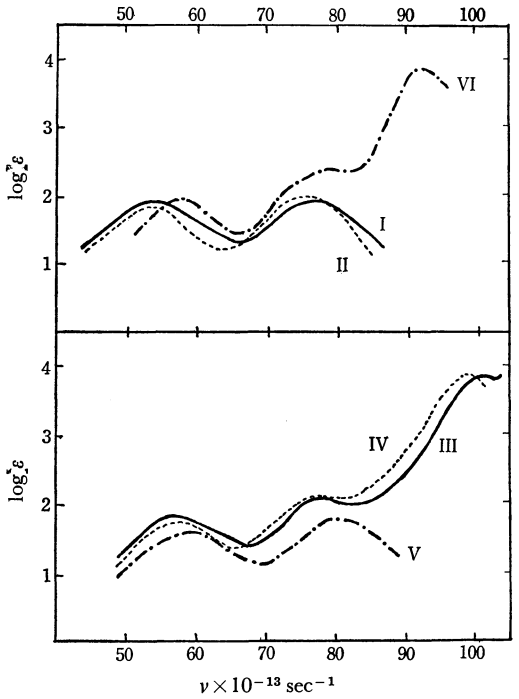

Fig. 1. Electronic absorption spectra.
Measured in aqueous solution for I, II, IV and VI; methanol solution for V; dimethylformamide solution for III.

Table 1. Behavior to the ion exchanger and molar conductivity

	Complex	Color	Adsorption to the ion exchanger		Molar conductivity (mho cm^{-1})
			Na-form	Cl-form	
I	$[Cr(atda)(H_2O)_2]\cdot 3H_2O$	red-violet	−*	−*	
II	$K[Cr(OH)(atda)(H_2O)]$	blue-violet	−	+	89.1
III	$[Cr(atda)(phen)]\cdot 3H_2O$	red	−	−	
IV	$[Cr(atda)(dipy)]\cdot 2H_2O$	red	−	−	
V	$[Cr(atda)(en)]\cdot 2H_2O$	red	−	−	
VI	$K[Cr(atda)(acac)]$	violet	−	+	92.2

* The sign + or − means the possibility or impossibility of the adsorption of the complex species against the exchanger respectively.

Table 2. Absorption maxima

Complex	$\nu_1(10^{13}/sec)$	$(\log \varepsilon_1)$	$\nu_2(10^{13}/sec)$	$(\log \varepsilon_2)$	$\nu_3(10^{13}/sec)$	$(\log \varepsilon_3)$
I	54.9 (56.6)*	(1.93)	75.8 (75.6)	(1.94)		
II	54.1 (56.3)	(1.88)	74.5 (75.2)	(2.03)		
III	57.7 (57.7)	(1.87)	76.9 (76.0)	(2.18)	101.4	(4.02)
IV	57.7 (58.8)	(1.83)	76.7 (76.0)	(2.14)	97.4	(4.02)
V	58.8 (60.9)	(1.83)	79.8 (80.1)	(1.94)		
VI	56.9 (58.7)	(1.96)	78.3 (77.5)	(2.31)	90.9	(3.87)

* The numerals under parentheses indicate the absorption peaks measured by means of the diffuse-reflectance method.

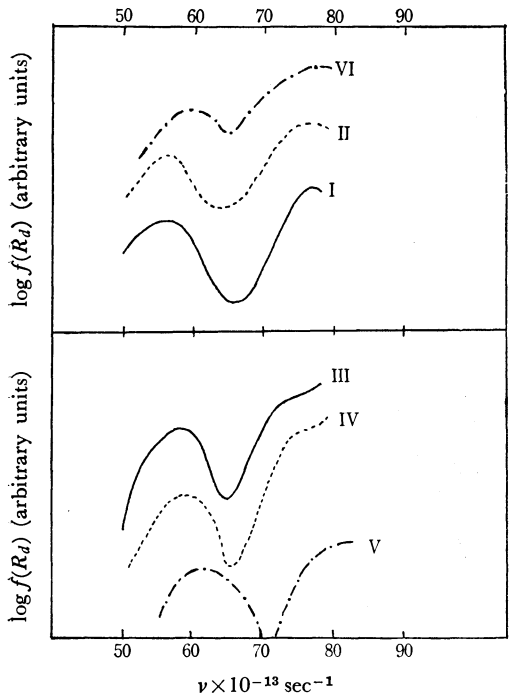

Fig. 2. Absorption spectra measured by the diffuse-reflectance method.
R_d: relative reflectance index

VI measured in aqueous solution and those of the Complexes III and V in DMF and methanol respectively are shown in Fig. 1, and all their absorption spectra obtained by diffuse-reflectance method in the solid state are in Fig. 2. The numerical data of their absorption maxima are summarized in Table 2.

It can be seen from Figs. 1 and 2 that every absorption spectrum in the solution closely coincides with the corresponding one in the solid state. It may indicate that all the complexes concerned exist in analogous form both in solution and in the crystalline state without any decomposition.

It has already been reported that the complexes, $NH_4[Cr(OH)(ata)(H_2O)]\cdot 2H_2O$[1] and $NH_4[Cr(OH)(aipda)(H_2O)]\cdot 4H_2O$,[3] corresponding to the Complex II, easily give rise to conversion to $NH_4[Cr(OH)(ata)(H_2O)_2]$ and $NH_4[Cr(OH)(aipda)(H_2O)_2]$ respectively as soon as dissolved in water and, at the same time, the color changes from purple in the crystal to green in aqueous solution, due to the liberation of nitrogen in ligands from coordination. Taking into account the result that the absorption maxima of II are larger than those of the corresponding ATA and AIPDA complexes cited above, it may be concluded that II is more stable than the ATA and AIPDA complexes.

Complexes III, IV and VI give the characteristic bands probably assigned to 2,2'-dipyridyl, *o*-phenanthroline and acetylacetone coordinated, respectively. When the aqueous solution of V was allowed to stand for several hours, a distinct frequency shift of the absorption peaks to lower wavelength region was observed, probably being attributed to the gradual aquation taking place in the complex.

The conclusion that the nitrogen atom of ATDA always coordinates to chromium(III) ion even in aqueous solution in the complexes concerned in this work, differing from that in the corresponding ATA and AIPDA complexes, may be supported by the information given above.

IR Spectra. The predominant peaks appearing in IR spectra on the complexes obtained are summarized in Table 3. With all complexes, the characteristic bands assigned to the stretching $\nu_{C=C}$ in benzene ring of atda are found near 1600 cm^{-1} and the bands for carboxyl groups of atda coordinated to chromium are shown within the wave number region of 1600—1700 cm^{-1}. By comparing these wave numbers with those observed in ATDA non-coordinated to chromium, 1730 cm^{-1}, it can be deduced that all the carboxyl groups in ATDA in every complex prepared in this work participate in coordination to the metal ion.

TABLE 3. IR DATA (cm^{-1})*

Complex	ν_{O-H}	ν_{N-H}	$\nu_{C=O}$	$\nu_{C=C}$
$atdaH_3$			1680, 1730	1600
I	3320		1620, 1675	1600
II	3240		1660, 1680	1600
III	3380		1675, 1700	1600
IV	3500		1665, 1695	1600
V	3440	3200, 3270	1630, 1680	1600
VI			1665, 1695, 1560	1605, 1530

* Measured in Nujol mull state.

As is indicated in Table 3, Complexes I—V have O–H stretching band and, above all, V shows two band peaks due to N–H stretching vibration rising from ethylenediamine. Complex VI gives two characteristic peaks owing to the acetylacetone coordinated, as is cited in literature.[5]

Magnetic Susceptibility. The effective magnetic moments of the complexes evaluated from the magnetic susceptibility measurement at room temperature are listed in Table 4. All the complexes show the normal magnetic moments, 3.7—3.9 B. M., which are nearly equal to the spin-only values calculated for tervalent chromium.

Thermogravimetric Measurement. The thermogravimetric curves for the complexes are shown in Fig. 3. It can be seen that all the complexes are gradually dehydrated up to about 130°C and then decomposed at about 230—300°C, except for the Complex I which loses stepwise three moles of the crystal-water and then two moles of the coordinated water up to 160°C.

TABLE 4. MAGNETIC MOMENT OF THE COMPLEXES

Complex	Magnetic moment (B. M.)	(Temp. °C)
I	3.76	(18.0)
II	3.80	(19.2)
III	3.80	(29.5)
IV	3.81	(30.0)
V	3.76	(21.3)
VI	3.90	(20.0)

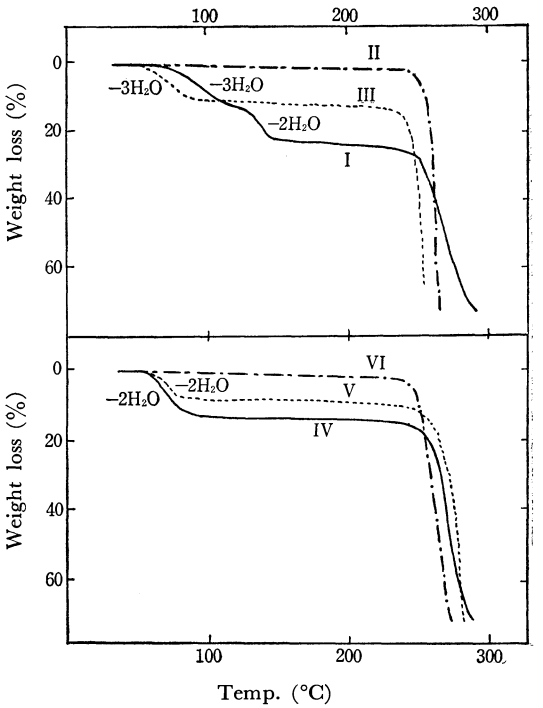

Fig. 3. Thermogravimetric curves.

Discussion on the Structures. The configuration of the ligands, ATA, APDA and ATDA, are sketched in Fig. 4. When ATA behaves toward chromium as a quadridentate ligand, it forms three five-membered chelate rings. However, since there are some steric strains on nitrogen atom, it can be easily left from coordination to chromium, acting as a terdentate one.

In the case of APDA, which is formed by introducing a methylene group into ATA, it can make one six-membered and two five-membered rings. Owing the such configuration, the steric strain focused on the nitrogen atom is, to some extent, reluxed, but one of the carboxyl groups is, in

5) J. P. Collman, R. A. Moss, H. Maltz and C. C. Heindel, *J. Am. Chem. Soc.*, **83**, 531 (1961).

reverse, given the tendency to dislocate from coordination, differing from ATA. In short, both ATA and APDA can behave as terdentate ligands, the former acting without coordination of nitrogen atom and the latter having one of the free carboxyl group.

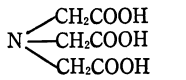

ATA (pK_3, 9.75)

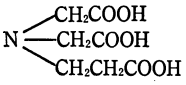

APDA (pK_3, 9.96)

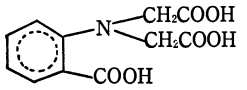

ATDA (pK_3, 7.75)

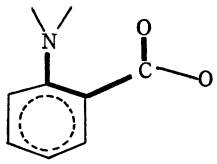

Fig. 4. The configurations of ATDA and related ligands.

On the other hand, ATDA behaves as a quadridentate ligand in all complexes treated in the present study; *i. e.*, it should be emphasized that all the four terminal atoms in the ligand, one nitrogen atom and three oxygen atoms, coordinate to the central metal ion even in an aqueous solution, although APDA sometimes behaves as terdentate ligand despite the fact that it has the analogous skeleton as ATDA. The reason for such difference will be attributed to the presence of the aromatic ring in ATDA. The available resonating interaction among one of the three carboxyls and the tertiary nitrogen group through the benzene ring may result in the shortening of the bond distances (shown by heavy lines in Fig. 4) with some extra stabilization energies and, therefore, the greater chelating power will be generated.[6] Thus, ATDA always behaves as a quadridentate ligand without the easy dissociation of the nitrogen atom from the coordination and without the formation of free carboxyl group even in solution, quite differing from ATA and APDA.

The difference of pK values among these three ligands (shown in Fig. 4) may allow an explanation for such coordinating characteristics in them as mentioned above. For example, the result that even one of the carboxyl groups in ATDA can not be easily released from the central metal in solution may be due to the smaller pK value in it.

In contrast to this stereochemical standpoint, the solubility sequence in water of each starting complex in the syntheses of a series of the mixed complexes, such as $NH_4[Cr(OH)(ata)(H_2O)] > [Cr(OH)(apdaH)(H_2O)] > [Cr(atda)(H_2O)_2]$, may play an important part in their preparation.

6) A. E. Martell and M. Calvin, "Chemistry of the Metal Chelate Compounds," New York Prentice Hall, Inc., New York (1956), p. 156.

BULLETIN OF THE CHEMICAL SOCIETY OF JAPAN VOL. 42 952—955 (1969)

Volumetric Determination of the Iodide Ion with Mercury(II) Ethylenediaminetetraacetate Using Mercury(II)-Methylthymolblue as an Indicator

Toshiaki NOMURA

Department of Chemistry, Faculty of Science, Shinshu University, Asahi, Matsumoto

(Received May 9, 1968)

After 5 m*l* portions of 1×10^{-4} M methylthymolblue (MTB or H_2Me^{4-}) and mercury(II) nitrate solutions had been added to an iodide sample solution adjusted to pH 7.3—8.8, it was diluted to about 50 m*l* with water. This solution was titrated with a 1×10^{-2} M standard mercury(II) ethylenediaminetetraacetate (Hg-EDTA or HgY^{2-}) solution until it turned blue from greenish yellow. The iodide-ion content was calculated by applying the volume of the standard Hg-EDTA solution on the calibration curve determined with solutions of known iodide-ion contents. The iodide ion reacts with HgY^{2-} and with greenish-yellow $HgMe^{4-}$ to form colorless $[HgY(I)]^{3-}$ and blue $[HgMe(I)]^{5-}$ complexes respectively. The $[HgMe(I)]^{5-}$ complex reacts subsequently with the iodide ion to form mercury(II) iodide and greenish-yellow H_2Me^{4-}. It has been found that, except when an excess amount of the iodide ion existed, the $[HgMe(I)]^{5-}$ complex is the most stable among these mixed ligand complexes and mercury(II) iodide. Therefore, the iodide ion can be titrated directly with a Hg-EDTA solution by using $HgMe^{4-}$ as an indicator according to the following equation:

$$HgI_2 + H_2Me^{4-} + HgY^{2-} \rightarrow [HgMe(I)]^{5-} + [HgY(I)]^{3-} + 2H^+$$

Mercury(II) reacts with ethylenediaminetetraacetate (EDTA) to form mercury(II) ethylenediaminetetraacetate (Hg-EDTA or HgY^{2-}), which has no absorption in the visible region. Hg-EDTA reacts further with the iodide ion to form a colorless mixed ligand complex $[HgY(I)]^{3-}$, which does not react with the excess iodide ions any more.[1]

$$HgY^{2-} + I^- \rightarrow [HgY(I)]^{3-} \quad (1)$$

Mercury(II) reacts with colored methylthymolblue (MTB or H_2Me^{4-}) to form mercury(II)-methylthymolblue (Hg-MTB or $HgMe^{4-}$),[2] which has a color similar to that of MTB, and then further reacts with the iodide ion by means of the formation of a blue-colored mixed ligand complex $[HgMe(I)]^{5-}$:[3]

$$HgMe^{4-} + I^- \rightarrow [HgMe(I)]^{5-} \quad (2)$$

The $[HgMe(I)]^{5-}$ complex reacts subsequently with the iodide ion to form mercury(II) iodide and MTB, as the following equation shows:

$$[HgMe(I)]^{5-} + I^- + 2H^+ \rightarrow HgI_2 + H_2Me^{4-} \quad (3)$$

in the way similar to that in which the cyano mixed ligand complex $[HgMe(CN)]^{5-}$ reacts with the cyanide ion to form mercury(II) cyanide and MTB:[4]

$$[HgMe(CN)]^{5-} + CN^- + 2H^+ \rightarrow Hg(CN)_2 + H_2Me^{4-} \quad (4)$$

The order of the stability constants of these iodo mixed ligand complexes and mercury(II) iodide is:

$$[HgMe(I)]^{5-} > [HgY(I)]^{3-} > HgI_2$$

except when excess iodide ions are present in the solution.[5]

When an iodide-ion solution containing a small amount of $HgMe^{4-}$ is titrated with a Hg-EDTA solution, the reaction proceeds as follows.

When a small amount of $HgMe^{4-}$ is added to the iodide-ion solution before the titration, mercury(II) iodide and greenish-yellow H_2Me^{4-} are formed as in Eq. (5), since the excess iodide ions are present:

$$HgMe^{4-} + 2I^- + 2H^+ \rightarrow HgI_2 + H_2Me^{4-} \quad (5)$$

In the begining of the titration of this solution with the Hg-EDTA solution, the free iodide ion reacts with HgY^{2-} to form the $[HgY(I)]^{3-}$ complex as Eq. (1). After the excess iodide ions have been consumed by the Hg-EDTA, the (6) reaction begins and the blue color of $[HgMe(I)]^{5-}$ appears.

$$HgI_2 + HgY^{2-} + H_2Me^{4-} \rightarrow [HgY(I)]^{3-} + [HgMe(I)]^{5-} + 2H^+ \quad (6)$$

1) S. Komatsu and T. Nomura, *Nippon Kagaku Zasshi (J. Chem. Soc. Japan, Pure Chem. Sect.)*, **88**, 63 (1967).

2) N. Iritani and T. Miyahara, *Bunseki Kagaku (Japan Analyst)*, **12**, 1183 (1963).

3) T. Nomura and S. Komatsu, *Nippon Kagaku Zasshi (J. Chem. Soc. Japan, Pure Chem. Sect.)* **90**, 168 (1969).

4) T. Nomura, This Bulletin, **41**, 1619 (1968).

5) T. Nomura and S. Komatsu, unpublished work.

Therefore, the iodide-ion contents in a solution can be titrated with a Hg-EDTA solution, using Hg-MTB as an indicator, if one considers the point at which the color changes from greenish yellow to blue as the end point of the titration.

As a representative method of the volumetric determination of iodide ions, Volhard's method (suitable for a 0.1 M iodide concentration)[6] and iodometry with hypochlorite (suitable for a 0.01 M iodide concentration)[7] have been reported. However, the present, newly-proposed method is especially suitable for the determination of about 0.01 M iodide. It is satisfactorily simple and reproducible.

Experimental

Reagents. All reagents were of an analytical grade and were used without further purification.

Methylthymolblue (MTB) Solution of 1×10^{-4} M. The stock solution of 1×10^{-3} M was prepared by dissolving 390 mg of Dotite MTB in a small amount of water, followed by the addition of 250 m*l* of methanol and by the exact dilution to 500 m*l* with water. This solution was stored in a brown glass bottle.[8] The working solution of 1×10^{-4} M was prepared by dilution with water.

Mercury(II) Nitrate Solution of 1×10^{-4} M. The stock solution of mercury(II) nitrate was prepared by dissolving 3.35 g of mercury(II) nitrate in a small amount of concentrated nitric acid and water, followed by dilution to 1 *l* with water. The precise concentration of this solution was obtained through titration with a 0.01 M standard EDTA solution, using Cu-PAN as an indicator.[9] The working solution of 1×10^{-4} M ($F=1.052$) was prepared by dilution with water.

Standard Iodide Ion Solution of 1×10^{-2} M. The stock solution was prepared by dissolving 16.6 g of potassium iodide and by then diluting to 1 *l* with water. The precise concentration of this solution was determined through titration with Volhard's method.[6] The working solution of 1×10^{-2} M ($F=1.000$) was prepared by dilution with water.

Standard Mercury(II) Ethylenediaminetetraacetate (Hg-EDTA) Solution of 1×10^{-2} M. This solution was prepared by the dissolution of 6.07 g of Dotite Hg-EDTA and by subsequent exact dilution to 1 *l* with water.

Buffer Solutions. Buffer solutions with definite pHs were prepared by properly mixing 0.2 M disodium hydrogenphosphate and 0.2 M potassium dihydrogenphosphate solutions.

Apparatus. The titration of the iodide ion solutions was carried out with a 1/20 graduated microburette. A Hitachi-Horiba M-4-type pH meter was used for the measurement of the pH values.

Procedure. Sample solutions containing up to 30 mg of iodide ions were adjusted to pH 7.3—8.8 with a buffer solution, to which a 5 m*l* portion of both a 1×10^{-4} M MTB and a mercury(II) nitrate solution were added; then they were diluted to about 50 m*l* with water. This solution (greenish yellow) was titrated with a 1×10^{-2} M standard Hg-EDTA solution until the color changed from greenish yellow to blue. The iodide-ion content was calculated by applying the titrated volume of the standard Hg-EDTA solution to the calibration curve obtained from solutions of known iodide-ion contents.

Results and Discussion

$HgMe^{4-}$ Indicator. The molar ratio of mercury(II) to MTB to form $HgMe^{4-}$ is 1 : 1, as has previously been mentioned.[2] Therefore, these reagents should be added to an iodide solution at a 1 : 1 molar ratio. However, because mercury(II) nitrate is insoluble in methanol and MTB is insoluble in water, it is difficult to make a solution which contains the reagents in a 1 : 1 molar ratio in a methanol-water mixture. Although it has been found that these reagents dissolve together in an aqueous buffer solution adjusted at pH 7.0, this solution can not be maintained for a long time because of its unstability. Therefore, each reagent solution should kept separately and added to the sample solution at every titration.

The Amount of Mercury(II) Nitrate Solution. In order to examine the suitable ratio of the mercury-(II) nitrate solution to the MTB solution, various amounts of a mercury(II) nitrate solution and 5 m*l* of a MTB solution were added to an iodide solution which had been adjusted to pH 7.5 and which contained 6.345 mg of iodide ions. The mixture was then diluted to about 50 m*l* with water. This solution was titrated according to the procedure described in the Experimental section. Below 1 m*l* of a mercury(II) nitrate solution, the end point was not clear because the weak blue color of the

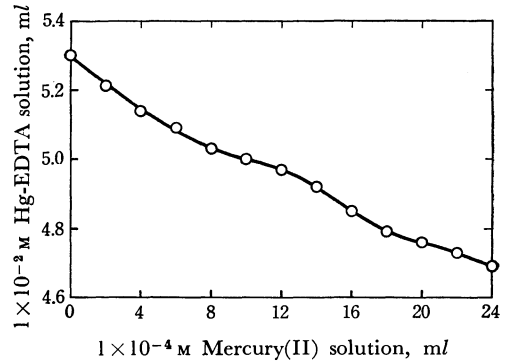

Fig. 1. Amount of mercury(II) solution as an indicator, 6.345 mg of iodide ion, 5 m*l* of 1×10^{-4} M MTB solution, pH 7.5.

6) W. J. Blaedel and V. W. Meloche, "Elementary Quantitative Analysis," Second Edition, John Weatherhill Inc., Tokyo (1966) p. 302.

7) S. Utsumi, T. Okutani, Y. Tamura and I. Iwasaki, *Bunseki Kagaku (Japan Analyst)*, **12**, 951 (1963).

8) T. Nomura, *Nippon Kagaku Zasshi (J. Chem. Soc. Japan, Pure Chem. Sect.)*, **88**, 961 (1967).

9) H. Flaschka and H. Abdine, *Chemist-Analyst*, **45**, 58 (1956).

mixed ligand complex was contradicted by the strong greenish-yellow color of the excess MTB. In the region from 2 m*l* to 5 m*l* of a mercury(II) nitrate solution, the end point was clearly observed despite the excess MTB giving a greenish-yellow color to the solution. From 5 m*l* to 15 m*l* of the mercury(II) nitrate solution, the end point was also clear in spite of the appearance of a yellow-green color just before the end point. However, the amount of the standard Hg-EDTA solution required in the titration was decreased in inverse proportion to the amount of the mercury(II) nitrate solution added. This situation is shown in Fig. 1. Therefore, the amount of the mercury(II) nitrate solution should be kept definite throughout a series of titrations.

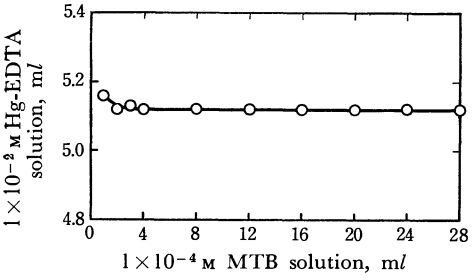

Fig. 2. Amount of MTB solution as an indicator.
6.345 mg of iodide ion, 5 m*l* of 1×10^{-4} M mercury(II) solution, pH 7.5.

The Amount of the MTB Solution. For the same purpose as in the preceding paragraph, various amounts of a MTB solution and 5 m*l* of a mercury(II) nitrate solution were added to the iodide solution under conditions identical to those described above, and this solution was treated similarly. When up to 1 m*l* of the MTB solution was added, the end point could not be determined because scarcely no color change in the solution could be observed. In the range from 6 m*l* to 15 m*l* of the MTB solution added, the greenish-yellow color of the excess MTB remained after the end point had been reached. However, the end point was clearly observed. Over 15 m*l*, however, the end point was not clear because of the strong greenish-yellow color of the excess MTB remaining after the end point. These results are shown in Fig. 2. Therefore, when 5 m*l* of a mercury(II) nitrate solution of 1×10^{-4} M is added, 2 m*l* to 15 m*l* of the MTB solution of 1×10^{-4} M should be added to the iodide sample solution before titration.

As a result of the above examination, the amount of a mercury(II) nitrate solution should be between 2 m*l* and 15 m*l* and the amount of the MTB solution should be from a half to 3 times that of the mercury(II) nitrate solution. In the following experiments, 5 m*l* portions of both mercury(II) nitrate and MTB solutions of 1×10^{-4} M were used.

Effect of pH. After a solution containing 6.345 mg of iodide ions had been adjusted to various pH values with buffer solutions, the solution was treated with the above procedure. The results are shown in Fig. 3. Up to pH 6.7, the end point

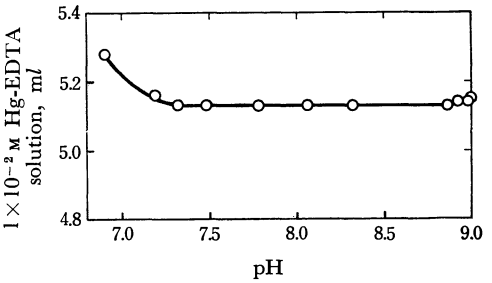

Fig. 3. Effect of pH.
Each 5 m*l* of 1×10^{-4} M MTB and mercury(II) solutions, 6.345 mg of iodide ion.

could not be detected because the yellow of MTB did not change; that is, the mixed ligand complex did not form. Between pH 6.9 and 7.1, the end point could be detected with difficulty. The color change from greenish yellow to blue was very clear between pH 7.3 and 8.8. Furthermore, an identical amount of the standard Hg-EDTA solution was necessary in this pH range. Above pH 8.9, the blue color of MTB in the high-pH region made the end point unobservable. Therefore, the titration should be performed between pH 7.3 and 8.8.

Effect of Standing Time. The interval between the preparation of a sample solution and titration with a standard Hg-EDTA solution was changed in order to study the effect of the standing time. No effect was observed, however, even at titration after 60 min. Therefore, the titration was carried out after a few minutes.

Calibration Curve and Reproducibility of Analytical Results. It is common, in a titration, for the quantity of an ion present in an unknown sample solution to be calculated by multiplicating the Titer by the volume of the standard solution required (titer). In the present method, however, because the standard Hg-EDTA solution contains free mercury(II), the Titer can not be calculated from the volume of the Hg-EDTA solution required to titrate a known amount of iodide ions. If the quantity of iodide ions were calculated with the usual Titer method, any error in the analytical results might be increased in proportion to the difference between a titer and the volume of the standard solution required to determine the Titer. In this experiment, therefore, a calibration curve was made by a procedure which proposed to express the relationship between the iodide-ion content and the volume of the 1×10^{-2} M standard Hg-EDTA solution required (titer). The reap-

Table 1. Reappearance of titer (m*l*) with the proposed procedure

Iodide ions added (mg)	0.317	0.635	1.269	2.538	6.345	12.69	19.04	25.38	31.73
1	0.12	0.41	0.92	1.99	5.13	10.34	15.57	20.83	26.08
2	0.15	0.42	0.94	2.00	5.13	10.33	15.59	20.87	26.12
3	0.15	0.41	0.94	1.99	5.12	10.33	15.61	20.84	26.09
4	0.15	0.41	0.93	1.98	5.12	10.32	15.57	20.83	26.10
5	0.16	0.42	0.93	2.00	5.13	10.33	15.58	20.82	26.10
Standard deviation	0.0063	0.0063	0.0077	0.0077	0.0063	0.0063	0.016	0.017	0.013
Variation coefficient (%)	4.21	1.54	0.83	0.39	0.12	0.06	0.10	0.08	0.05

pearance of titers on the calibration curve was examined; the results are shown in Table 1. The calibration curve is linear from a 0.3 to a 32 mg iodide ion content.

A minor additional comment is necessary regarding this titration. If the sample does not contain any iodide ions at all, the greenish-yellow color of the solution does not change to blue. Therefore, it is recommended that a preliminary test for the presence of iodide ions be made by means of the addition of 5 m*l* of a 1×10^{-4} M iodide solution to the sample. When no iodide is present in the sample, the color of the solution is blue before any of the standard solution is dropped in.

Effect of Diverse Ions. A solution containing 6.345 mg of iodide ions and various foreign ions was titrated by means of the proposed procedure. The results are shown in Table 2. The results that differed more than $\pm2\%$ from the expected volume of the standard Hg-EDTA solution were taken as the criterion for the interference.

The interference of such anions as CN^-, S^{2-}, SCN^-, and Br^- in this titration can be interpreted as originating as follows. The cyanide ion reacts with Hg-EDTA to form mercury(II) cyanide and EDTA, S^{2-} reacts with mercury(II) to form mercury(II) sulfide, and SCN^- and Br^- react with Hg-EDTA or Hg-MTB to form mixed ligand complexes. Cations, such as Co^{2+}, Ni^{2+}, Cu^{2+}, Mn^{2+}, Zn^{2+}, Ca^{2+} and Ag^+, also interfere, since these cations react with MTB to form metal-MTB complexes.

These interfering ions should be separated or masked properly when this procedure is used. A method of separation employing ion-exchange resin has been reported by Takiura *et al.*[10] for anions, and by the author for cations.[8]

Table 2. Effect of diverse ions

Ions	Added as	Tolerance limit	
CN^-	KCN	3 μg	+
S^{2-}	$Na_2S\cdot9H_2O$	7 μg	+
SCN^-	KSCN	150 μg	+
Br^-	KBr	360 μg	+
Cl^-	NaCl	>20 mg	
F^-	KF	>20 mg	
ClO_4^-	$NaClO_4$	>20 mg	
SO_4^{2-}	K_2SO_4	>20 mg	
NO_3^-	$NaNO_3$	>20 mg	
Co^{2+}	$CoSO_4\cdot7H_2O$	20 μg	−
Ni^{2+}	$NiSO_4\cdot7H_2O$	40 μg	−
Cu^{2+}	$CuSO_4\cdot5H_2O$	50 μg	−
Mn^{2+}	$MnSO_4$	80 μg	−
Zn^{2+}	$ZnSO_4\cdot7H_2O$	100 μg	−
Ca^{2+}	$Ca(NO_3)_2$	100 μg	−
Ag^+	$AgNO_3$	200 μg	−
NH_4^+	$(NH_4)_2SO_4$	320 μg	+
Cd^{2+}	$CdSO_4$	350 μg	−
Bi^{3+}	$Bi(NO_3)_3\cdot5H_2O$	600 μg	+
Pb^{2+}	$Pb(NO_3)_2$	1.5 mg	−
Al^{3+}	$Al_2(SO_4)_3$	1.8 mg	+
Fe^{3+}	$Fe(NO_3)_3\cdot9H_2O$	4.3 mg	+
Mg^{2+}	$MgSO_4$	6 mg	+
Ba^{2+}	$Ba(NO_3)_2$	>10 mg	
Sr^{2+}	$Sr(NO_3)_2$	>10 mg	
Th^{4+}	$Th(NO_3)_4\cdot4H_2O$	>10 mg	

(+): positive error, (−): negative error

The author wishes to thank Professor S. Komatsu for his many helpful discussions and suggestions during this work.

10) K. Takiura and Y. Takino, *Bunseki Kagaku (Japan Analyst)*, **10**, 493 (1961).

BULLETIN OF THE CHEMICAL SOCIETY OF JAPAN VOL. 42 956—960 (1969)

Determination of a Small Amount of Iodide by Atomic Absorption Spectrophotometry Using a Cadmium Hollow Cathode Lamp

Takahiro KUMAMARU

Department of Chemistry, Faculty of Science, Hiroshima University, Higashisenda-machi, Hiroshima

(Received June 8, 1968)

A new application of atomic absorption spectrophotometry to the determination of iodide has been proposed. The method is based on solvent extraction into nitrobenzene of the colorless ion-pair formed between tris(1,10-phenanthroline)cadmium(II) and the iodide anion, and the subsequent determination of the cadmium concentration in the extract by atomic absorption in an air-acetylene flame at the 2288 Å cadmium line. The absorbance due to cadmium in the extract shows a linear relationship to the concentration of iodide over the range from 4×10^{-6} to 4×10^{-5} M initially present in the aqueous solution. The optimum conditions for the determination of iodide have been established, and the extraction efficiency and the effect of other anions have also been studied.

Since the resonance lines for most nonmetallic elements occur in the vacuum ultraviolet region, it has been impossible to determine these elements directly by atomic absorption spectrophotometry. Indirect determinations of nonmetals can, however, be readily performed with conventional atomic absorption apparatus. One of these methods is based on the stoichiometric formation of ion-pairs with a cationic metal ion chelate; these ion-pairs can then be isolated and determined by atomic absorption, the results being related quantitatively to the associated nonmetal.

It has been found that iodide anions can be extracted into nitrobenzene if the aqueous solution contains an excess of tris(1,10-phenanthroline)-cadmium(II) cations, and it is possible to determine the iodide by spraying the nitrobenzene solution into the flame of an atomic absorption spectrophotometer, with a cadmium hollow cathode lamp used as the light source. A brief preliminary study of this method has already been reported.[1] The present paper will present a detailed quantitative study undertaken to establish a new application of atomic absorption spectrophotometry. This proposed method for iodide is rapid and accurate, and it is different from the previously known colorimetric methods, which are based on the catalytic action of iodide,[2,3] the starch-iodide reaction,[3] triiodide formation,[3] and red-colored ion-pair formation between the iodide ion and the tris-(1,10-phenanthroline)iron(II) chelate cation.[4]

Indirect methods for the determination of nitrate,[5] pentachlorophenol[6] and phthalic acid,[7,8] based on the same principle, have recently been reported.

Experimental

Apparatus. The atomic absorption was measured with a Hitachi Model EPU-2 spectrophotometer and a Hitachi Model 0420 atomic absorption attachment equipped with a cadmium hollow cathode lamp. An air-acetylene flame was burned with a water-cooled 9-cm slot burner. The pH values were measured with a Hitachi-Horiba Model H-5 pH meter. The shaking for extraction was carried out with an Iwaki Model KM shaker equipped with time control. The gamma ray counting of ^{131}I was performed with an Aloka Model PSM 801 γ-ray spectrometer equipped with a 1 1/2''$\phi\times$1'' NaI(Tl) crystal.

Reagents. All the chemicals used were of an analytical reagent grade.

A phenanthroline-cadmium(II) sulfate solution was prepared by dissolving 1.28 g of cadmium sulfate ($3CdSO_4\cdot8H_2O$) and 3.17 g of 1,10-phenanthroline ($C_{10}H_8N_2\cdot H_2O$) in dilute sulfuric acid and by then diluting the mixture to a volume of 1000 ml with water. The resulting solution (pH 3) is 5.0×10^{-3} M in tris-(1,10-phenanthroline)cadmium(II) sulfate. A cadmium solution for continuous variation plots was prepared by

1) Y. Yamamoto, T. Kumamaru, Y. Hayashi and Y. Otani, *Bunseki Kagaku (Japan Analyst)*, **17**, 92 (1968).

2) I. Iwasaki, S. Utsumi and T. Osawa, This Bulletin, **26**, 108 (1953).

3) B. Zak, "Colorimetric Determination of Nonmetals," ed. by D. F. Boltz, Interscience Publishers, New York (1958), pp. 197—230.

4) Y. Yamamoto and S. Kinuwaki, This Bulletin, **37**, 434 (1964).

5) T. Kumamaru, E. Tao, N. Okamoto and Y. Yamamoto, *ibid.*, **38**, 2204 (1965).

6) Y. Yamamoto, T. Kumamaru and Y. Hayashi, *Talanta*, **14**, 611 (1967).

7) T. Kumamaru, Y. Hayashi, N. Okamoto, E. Tao and Y. Yamamoto, *Anal. Chim. Acta*, **35**, 524 (1966).

8) T. Kumamaru, *ibid.*, **43**, 19 (1968).

the suitable dilution of a cadmium sulfate stock solution (1.0×10^{-2} M) which had been standardized by EDTA titration. A standard stock solution of 1.0×10^{-2} M iodide was prepared from potassium iodide dried at 110°C. The concentration of iodide ions was determined by conventional argentometry. The iodide standard solution for the experiment was prepared by diluting an aliquot of this stock solution with water to give a concentration of 1.0×10^{-4} M. A radioactive iodide solution was also prepared from sodium iodide-^{131}I, which had been obtained from the Japan Radioisotope Association. To make the solution pH 5, a 0.5 M potassium dihydrogenphosphate-disodium hydrogenphosphate solution was employed.

Procedure. Tris(1,10-phenanthroline)cadmium(II) iodide was extracted into nitrobenzene; the organic extract was then aspirated directly into the atomic absorption spectrophotometer.

Five milliliters of the phenanthroline-cadmium(II) sulfate solution (5.0×10^{-3} M), 5 m*l* of a 0.5 M phosphate buffer solution (pH 5), and a measured volume of 15 m*l* or less of the sample solution were placed in a 100-m*l* separatory funnel, and, finally, the aqueous phase volume was adjusted to 25 m*l* with water. After 10 m*l* of nitrobenzene had been poured in, the funnel was shaken for 1 min. The two phases clearly separated within 20 min after the end of the shaking. The organic phase was then dried with 1 g of anhydrous sodium sulfate.

The absorption due to cadmium in the organic phase was then determined with the atomic absorption spectrophotometer against a reagent blank used as a reference, and expressed as the initial concentration of iodide in the aqueous phase, based on stock iodide solution used as standards. The instrument-operating conditions included analysis at the wavelength of 2288 Å, a slit width of 0.4 mm, and a lamp current of 7.5 mA (cadmium lamp). The flow rates of gases for the air-acetylene flame were 8.0 *l*/min of air and 1.6 *l*/min of acetylene. The burner height was adjusted to make the light beam pass 6 mm above the tip of the burner.

Results and Discussion

Atomic Absorption Spectrophotometric Variables. *Lamp Current.* Figure 1 shows the effect of the lamp current in the absorption of cadmium. From five series of results, it can be seen that a low lamp current gives the higher absorbance for the cadmium 2288 Å. However this cadmium hollow cathode lamp could not be used with a current less than 5 mA because of its low light intensity. Therefore, the preferable lamp current was decided to be 7.5 mA.

Air-acetylene Flame. The effects of the variation in the air-acetylene mixture on the absorption were also studied. The results are shown in Fig. 2. For convenience, the gas-flow rates were adjusted so that the burner consumes 8.0 *l*/min of air and 1.6 *l*/min of acetylene in subsequent investigations. Under these flame conditions, it was found that the optimum height for the passage of the light beam from the hollow cathode tube through the reducing flame was 5 to 8 mm above the tip of the burner; higher and lower passage of light gave slightly poorer sensitivities.

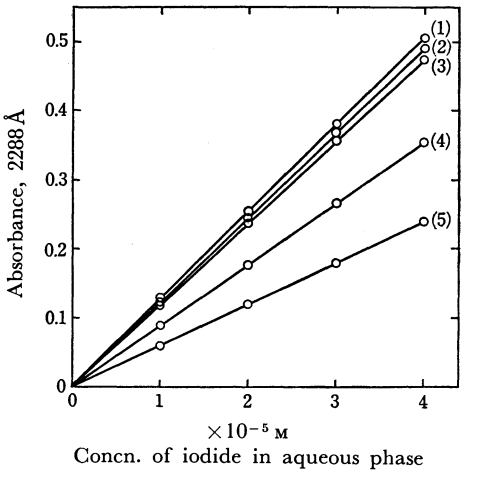

Fig. 1. Calibration curves at various lamp currents.
Lamp current (mA): (1) 5, (2) 7.5, (3) 10, (4) 15, (5) 20
Reference: reagent blank

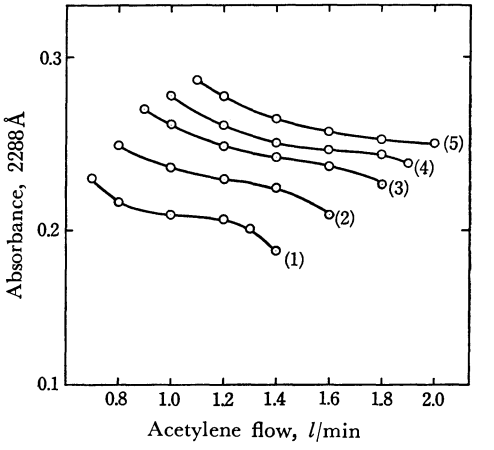

Fig. 2. Effect of variation of air-acetylene mixture on net absorbance for 2.0×10^{-5} M iodide.
Air flow (*l*/min): (1) 6.5, (2) 7.0, (3) 7.5, (4) 8.0, (5) 8.5

Variables of Extraction. *Solvent.* Various kinds of commercially-available organic solvents were tested for the extraction: *n*-butyl alcohol, isoamyl alcohol, isopropyl ether, ethyl acetate, *n*-butyl acetate, methyl isopropyl ketone, methyl isobutyl ketone, chloroform, carbon tetrachloride, 1,2-dichloroethane, cyclohexanone, benzene, chlorobenzene, and nitrobenzene. Only nitrobenzene extracted phenanthroline-cadmium(II) iodide selectively from the aqueous solution. Moreover, nitrobenzene is a suitable solvent for atomic absorption spectrophotometry because it gives a stable flame during the combustion and a higher

sensitivity of measurement.

The extraction percentage of iodide was then determined by the radioactive tracer method using an ^{131}I-labeled iodide solution. One milliliter of each phase was taken after extraction, and the radioactivities of gamma rays were measured with a scintillation counter. The results are shown in Table 1. When the phenanthroline-cadmium(II) chelate cations are absent in the aqueous phase, iodide ions were negligibly extracted into nitrobenzene (~200 cpm).

TABLE 1. EXTRACTION PERCENTAGE

Sample No.	Net cpm (^{131}I)		Extraction percentage, %
	Aqueous phase	Organic phase	
1	7475±89	72760±427	90.7±0.7
2	7513±89	72495±426	90.7±0.7

Organic phase: 10 m*l*, Aqueous phase: 25 m*l*
Initial concentration of iodide: 4.0×10^{-5} M
Initial concentration of tris(phenanthroline)cadmium(II): 1.0×10^{-3} M
pH: 5; buffered with phosphate

pH. The effect of pH on the extraction was studied by extracting the iodide anions from a series of aqueous solutions buffered in the pH range from 2 to 9. In Fig. 3, Curve 2 was obtained by the subtraction of the absorbance in Curve 1 (no iodide) from the total observed absorbance in the sample. The pH variations between 3.5 and 5.5 had practically no effect on the results if the absorbance of the reagent blank was subtracted from the total absorbance at each pH. In the subsequent experiments, the pH of the aqueous phase was adjusted to nearly 5 with a phosphate buffer. The change in the concentration of the phosphate buffer had a negligible effect on the extraction.

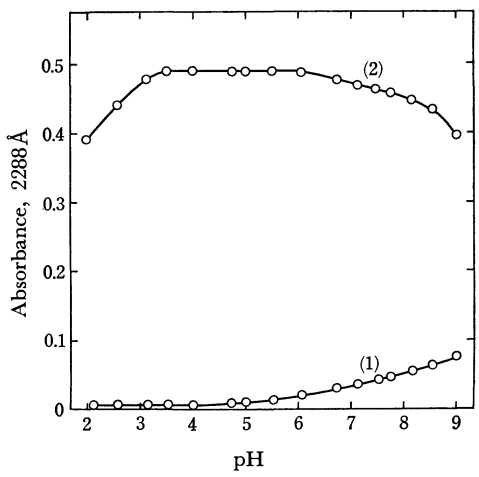

Fig. 3. Effect of pH.
(1) Reagent blank; Absorbance was measured against nitrobenzene.
(2) 4.0×10^{-5} M iodide; Correction in absorbance was made for the reagent blank.

Phenanthroline-Cadmium(II) Sulfate Concentration. As can be seen in Fig. 4, the absorbance of the nitrobenzene phase approached a limit when the chelate concentration was more than 6×10^{-4} M and when the iodide concentration was kept at

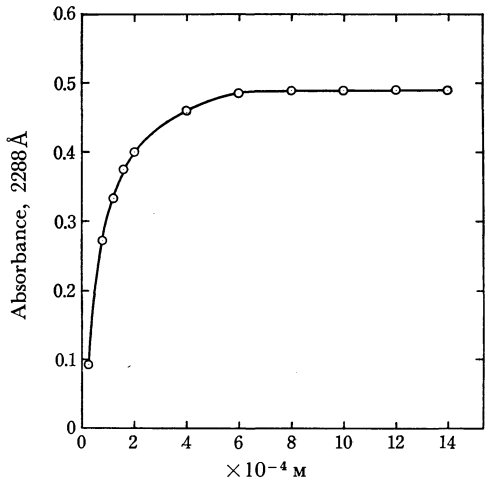

Fig. 4. Effect of chelate concentration on net absorbance for 4.0×10^{-5} M iodide.

4.0×10^{-5} M in the aqueous phase. An excess of at least 15-fold in molar quantity of the phenanthroline chelate to iodide was necessary for quantitative recoveries. Thus the chelate concentration was usually kept at 1.0×10^{-3} M.

Shaking Time. The shaking time for the extraction was varied from 0.5 to 15 min, while the other variables were kept constant. These variations in the shaking time showed that shaking for longer than a 0.5 min did not improve the extraction. Hence, 1 min was employed as the period for the extraction.

Calibration Curve. The standard procedure was decided upon the basis of the above results. The calibration curve was obtained by using varying amounts (1—10 m*l*) of the standard iodide solution (1.0×10^{-4} M). The absorbance due to cadmium in the organic phase showed a linear relationship to the tested concentration range from 4×10^{-6} to 4×10^{-5} M of iodide initially present in the aqueous phase, as is shown in Fig. 1 (Curve 2). This indicates that the high sensitivity of atomic absorption spectrophotometry for cadmium allows the determination of such low concentrations of iodide.

Precision. The reproducibility of the present method was estimated from the results of 10 sample solutions, each 4.0×10^{-5} M in iodide. The average

absorbance was 0.490, and the standard deviation was 0.003 absorbance unit (*i.e.* there was a relative error of 0.6%).

Influence of Diverse Ions. The effect of a series of anions on the extraction of the phenanthroline-cadmium(II) iodide into nitrobenzene was examined. Table 2 shows the degree of interference of diverse ions added to the solution containing iodide in 2.0×10^{-5} M.

Table 2. Effect of diverse anions on the extraction of iodide

Anion	Added as	[Anion]/[Iodide]	Recovery of iodide, %
F^-	NaF	1000	100
		10000	105
Cl^-	NaCl	1	100
		5	104
Br^-	NaBr	0.1	101
		0.5	106
ClO_3^-	$NaClO_3$	0.01	100
		0.1	108
BrO_3^-	$KBrO_3$	1	100
		10	112
IO_3^-	KIO_3	100	100
		1000	104
ClO_4^-	$KClO_4$	0.01	100
		0.1	111
IO_4^-	KIO_4	0.02	99
		0.1	89
		0.5	110
		1	113
CN^-	KCN	10	102
		100	162
NO_2^-	$NaNO_2$	0.1	100
		1	106
NO_3^-	KNO_3	0.1	101
		0.5	110
CO_3^{2-}	Na_2CO_3	1000	100
$B_4O_7^{2-}$	$Na_2B_4O_7$	1000	100

Concentration of iodide: 2.0×10^{-5} M

It is of interest that the halides, when listed in the order of increasing interference with this method, are fluoride, chloride, and bromide, while the oxyacids and the peroxyacids of the halogens are listed, on the contrary, as iodate, bromate and chlorate, and periodate and perchlorate. One rather strange observation was that periodate appeared to interfere in a negative direction when present in a molar quantity lower than 1/10 the level of iodide. A possible reason for this low recovery may be its oxidation effect on iodide ions. Above this amount of periodate, there appeared an increase in the absorbance with an increase in the periodate; this increase might be caused by interference through the extraction of periodate ions with phenanthroline-cadmium(II). Large amounts of phosphate and sulfate, which were present in the reagent solution used, and carbonate, borate, fluoride, and iodate did not interfere with the determination of iodide, while perchlorate and chlorate, even when 1/10 the molar quantity of iodide was present, gave positive errors.

Composition of Extracted Species. In order to examine the composition of the extracted species, continuous variation plots were made in two series of extraction. As for the determination of the chelate formation ratio of phenanthroline to cadmium(II), the concentration of iodide and the total concentration of cadmium(II) and phenanthroline were both kept constant at 2.0×10^{-4} M, and then the extraction was carried out as in the procedure described above with a series of aqueous solutions containing a varying mole ratio of phenanthroline to cadmium(II). The resulting curve [Fig. 5 (Curve 1)], in which the reagent

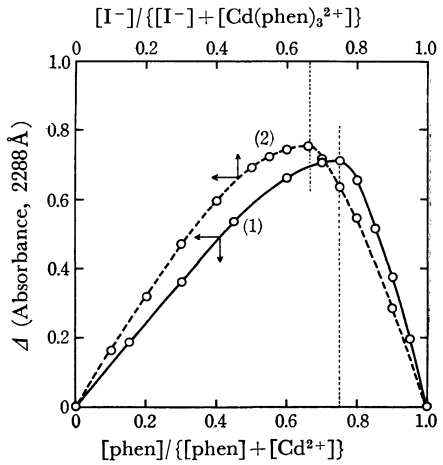

Fig. 5. Continuous variation plots at pH 5.
(1) For phenanthroline-cadmium(II).
Total concentration of phenanthroline and cadmium(II): 2.0×10^{-4} M, concentration of iodide: 2.0×10^{-4} M.
(2) For tris(phenanthroline)cadmium(II) iodide.
Total concentration of tris(phenanthroline)-cadmium(II) and iodide: 1.6×10^{-4} M.
phen=1,10-phenanthroline

blank was subtracted, shows the ratio of phenanthroline to cadmium in the extracted species balances at 3; this indicates that the cationic tris(1,10-phenanthroline)cadmium(II) chelate may take part predominantly in the extraction of the iodide ion as the counter ion. Similar plots to confirm the composition of the tris(1,10-phenanthroline)-cadmium(II) iodide are shown in Fig. 5 (Curve 2). This suggests that a 1 : 2 associated ion-pair is formed in the nitrobenzene phase between the tris(1,10-phenanthroline)cadmium(II) cation and the iodide anion; thus the chemical formula of the extracted species can probably be represented as

[Cd(1,10-phenanthroline)$_3$]·I_2.

The author wishes to express his thanks to Professor Yuroku Yamamoto for his kind guidance and encouragement throughout this work, and also wishes to thank Mr. Yuzuru Otani for his technical assistance in this work.

BULLETIN OF THE CHEMICAL SOCIETY OF JAPAN VOL. 42 960—968 (1969)

Some Thermal Properties of Metal Chelates of *o*-Acylphenols and of Their Ketimine Derivatives*[1]

Seiichiro MATSUMOTO,*[2] Hiroshi KOBAYASHI and Keihei UENO

Department of Organic Synthesis, Faculty of Engineering, Kyushu University, Fukuoka

(Received July 20, 1968)

The beryllium chelates of 2-hydroxy-3-methylacetophenone, 2-hydroxy-3-isopropylisobutyrophenone and 2-hydroxyacetophenone, and the copper- and nickel chelates of the ketimine derivatives of 2-trifluoroacetylphenol and 2-hydroxyisobutyrophenone in addition to the above *o*-acylphenols were synthesized. The thermal stability and relative volatility of these chelate compounds, measured by means of a thermogravimetric method, were found to be strongly increased by introduction of bulky alkyl or trifluoromethyl groups.

In relation to the application of gas-chromatography to the analysis of metal chelates, the great numbers of volatile metal chelates of β-diketones,[1] and of *N*-alkylsalicylaldimines[2] have been synthesized, and especially concerning the homologues of β-diketone, the correlation between the molecular structure of ligands and the volatility of their metal chelates has been intensively investigated.[3] Although no conclusive general rules governing the volatility of metal chelates have been attained yet, an observation has been made that introduction of trifluoromethyl or *t*-butyl group into a β-diketon skeleton strongly increased the volatility of its metal chelates. Except on the β-diketone homologues, however, very few works have been made on volatility of metal chelates and its correlation to the molecular structures of the ligands.

In the hope of obtaining a new type of volatile metal chelates, we synthesized the metal chelate compounds containing aromatic nuclei fused to the chelate rings in a molecule, *e. g.*, metal chelates of salicylaldehyde and of *o*-acylphenols, and investigated their volatilities and thermal stabilities in relation to the effects of aromatic nuclei, and of alkyl groups attached closely to the chelate ring.

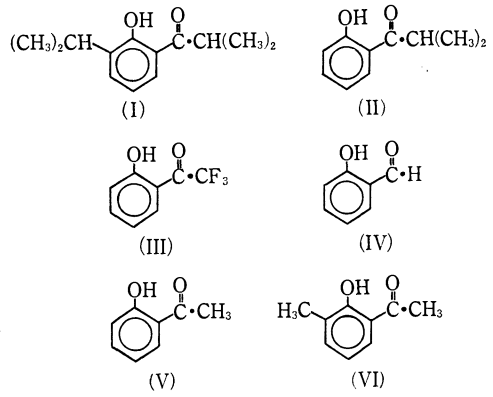

Fig. 1. The structures of the ligands.

*1 Contibution No. 159 from the Department of Organic Synthesis, Kyushu University.

*2 Present address: National Institute for Researches in Inorganic Materials, Fujimicho, Bunkyo-ku, Tokyo.

1) a) R. N. Moshier and R. E. Sievers, "Gas Chromatography of Metal Chelates," Pergamon Press, London (1965). b) M. Arakawa and K. Tanigawa, *Bunseki Kagaku (Japan Analyst)*, **15**, 398 (1966).

2) M. Miyazaki, T. Imanari, T. Kunugi and Z. Tamura, *Chem. Pharm. Bull.*, **14**, 117 (1966).

3) a) E. W. Berg and J. T. Truemper, *J. Phys. Chem.*, **64**, 487 (1960). b) E. W. Berg and H. W. Dowling, *J. Chem. Eng. Data*, **6**, 556 (1961). c) E. W. Berg and J. T. Truemper, *Anal. Chim. Acta*, **32**, 245 (1965). d) K. J. Eisentraut and R. E. Sievers, *J. Inorg. Nucl. Chem.*, **29**, 1931 (1967). e) K. J. Eisentraut and R. E. Sievers, *J. Am. Chem. Soc.*, **87**, 5254 (1965). f) C. S. Springer, Jr., D. W. Meek and R. E. Sievers, *Inorg. Chem.*, **6**, 1105 (1967). g) G. S. Hammond, D. C. Nonhebel and C. S. Wu, *ibid.*, **2**, 73 (1963). h) T. Shigematus, M. Matsui and K. Utsunomiya, This Bulletin, **41**, 763 (1968).

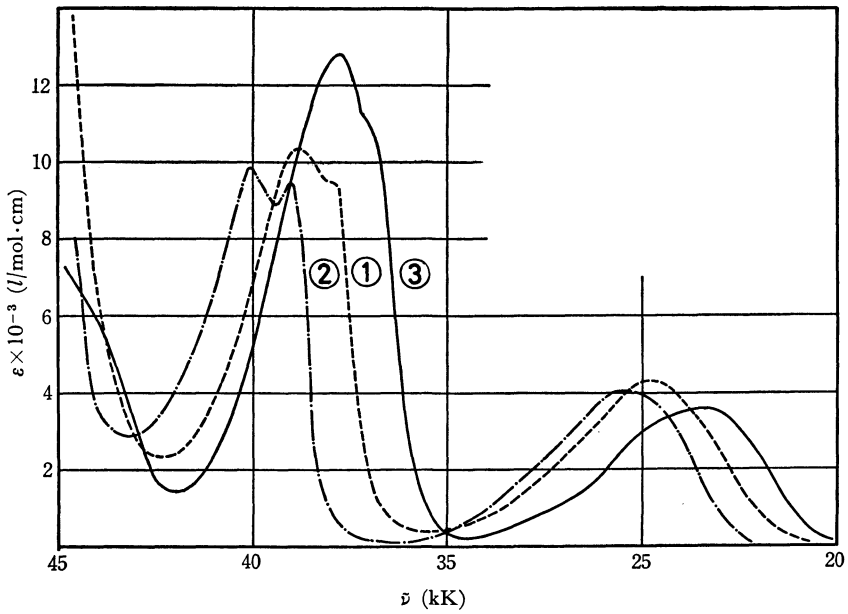

Fig. 2. Ultraviolet spectra of the ligands : Curve 1 for I, 2 for II, and 3 for III, respectively.

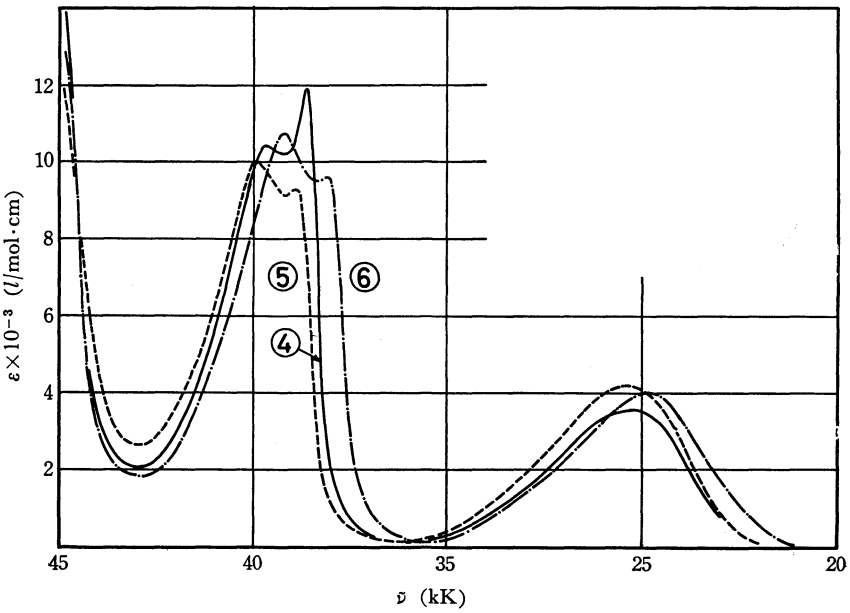

Fig. 3. Ultraviolet spectra of the ligands : Curve 4 for IV, 5 for V, and 6 for VI, respectively.

Results and Discussion

The new ligands synthesized in the present work are 2-hydroxy-3-isopropylisobutyrophenone (I), 2-hydroxyisobutyrophenone (II), and 2-trifluoroacetylphenol (III). In addition to the above, salicylaldehyde (IV), 2-hydroxyacetophenone (V) and 2-hydroxy-3-methylacetophenone (VI) are used as ligands in order to make a comparison with the new ones. The structures of these ligands are shown in Fig. 1.

The new *o*-acylphenols, I, II and III, were synthesized by Fries rearrangement reaction from corresponding phenol acylates, accompanied by formation of isomeric *p*-acylphenols.

Infrared spectrum of I shows a broad diffused band at 3500—2500 cm^{-1} in good contrast with the sharp strong hydroxy band of the isomeric *p*-acylphenol observed at 3310 cm^{-1}. The character and position of this band allow it to be assigned to the stretching vibration of hydroxy group involved

in intramolecular hydrogen bond with carbonyl group sited at *ortho*-position. This is in good agreement with the observation of carbonyl band of I at 1630 cm^{-1} which is at a position of lower wave number as compared with that of the *p*-substituted isomer at 1650 cm^{-1}. 1,2,3-Tri-substituted phenyl moiety in I is ascertained by the nuclear magnetic resonance spectrum, in which three protons on an aromatic nucleus show themselves in a typical ABX pattern ($\delta_A=7.30$ ppm, $\delta_B=7.55$ ppm, $\delta_X=6.70$ ppm, $J_{AX}=J_{BX}=8$ cps, $J_{AB}=2$ cps); a quite similar pattern is observed also concerning three protons in aromatic ring of VI.

Infrared spectra of II and of III also show respectively a broad diffused band assigned to a hydroxy group in an intramolecular hydrogen bond and a band assigned to a lowered carbonyl stretching frequency in comparison with that of each *p*-substituted isomer. The spectra of II and of III reveal respectively a strong band characteristic to *o*-disubstituted benzene ring at about 750 cm^{-1}, and the presence of this band, together with the intramolecular hydrogen bond between the hydroxy and the carbonyl group, indicates *ortho*-acylphenol structures of II and III, which are also ascertained by their abilities of chelate formation with metal ions.

As observed in Figs. 2 and 3, characteristic resemblance to each other in the ultraviolet spectra of all these ligands also indicates that these ligands have the same arrangement of chromophores on a benzene nucleus.

Metal chelates of the *o*-acylphenols were prepared by using beryllium(II), copper(II) and nickel(II) salts. Beryllium ion gave 1 : 2 (metal ion : ligands) chelate compounds (VII) for I, V and VI as shown in Fig. 4, attempts to prepare complexes of III and of IV being unsuccessful. On the other hand, in the cases of copper(II)- and ncikel-(II) ions, usual procedures trying to prepare the complexes of an *o*-acylphenolate afforded, contrary to our intentions, 1 : 2 chelate compounds in which the ligands coordinated in the forms of ketimine derivatives as VIII in Fig. 4. The ketimines

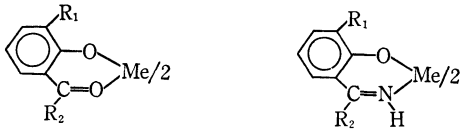

(VII) (VIII)

Fig. 4. The structures of the metal chelates.

seem to arise on the process of chelate formation from the *o*-acylphenols and ammonia added into the reaction media to adjust its pH. Attempts to prepare *o*-acylphenolato-chelate compounds have been unsuccessful.

Thermogravimetric curves of the metal chelates described above are shown in Figs. 5, 6 and 7.

Although a rigorous discussion of volatility of a compound necessitates vapor pressure data at various temperatures and other thermodynamic data, the thermogravimetric method employed in the present work, roughly approximate though it may be, is a convenient procedure for the measurement of thermal stability of a compound and its relative volatility. Results of preliminary experiments on subliming behaviors of the chelates under reduced pressures indicated that the beryllium chelates of I, V and VI were readily sublimed at 150°C/0.5 mmHg, and that the copper- and nickel ketimine chelates of I and III were sublimed at

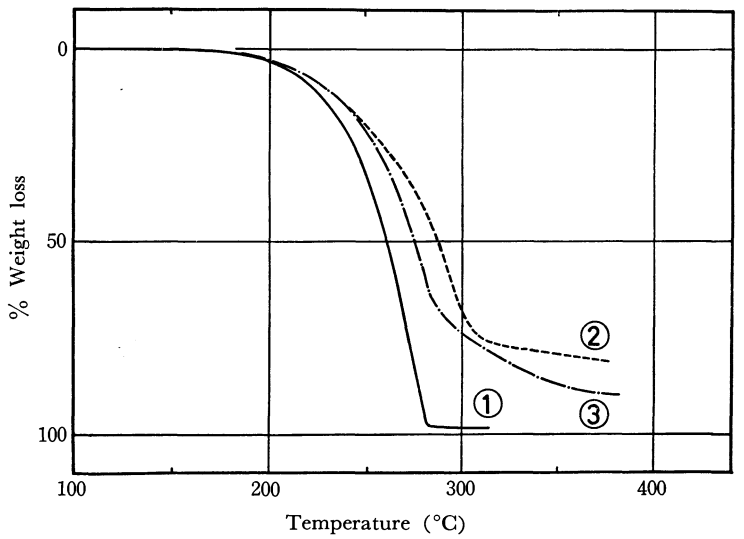

Fig. 5. Thermogravimetric curves of the beryllium chelates: Curve 1 for that of I, 2 for of V, and 3 for of VI, respectively.

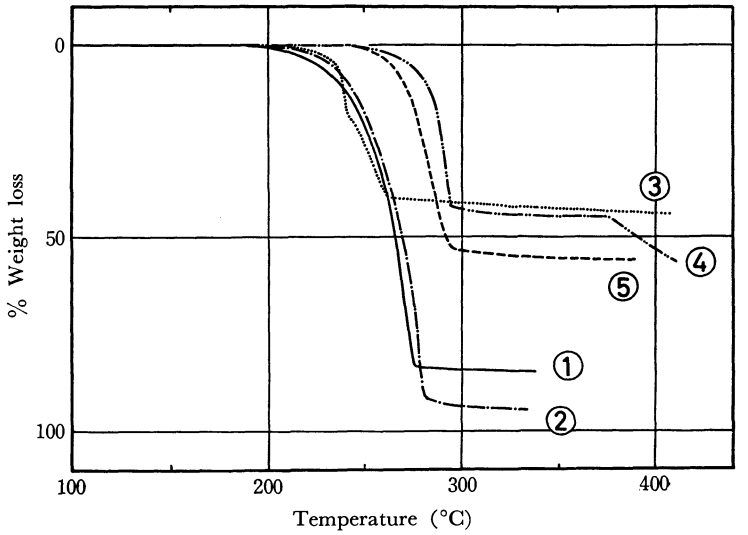

Fig. 6. Thermogravimetric curves of the copper chelates of the ketimine derivatives : Curve 1 for that of I, 2 for of III, 3 for of IV, 4 for of V and 5 for of VI, respectively.

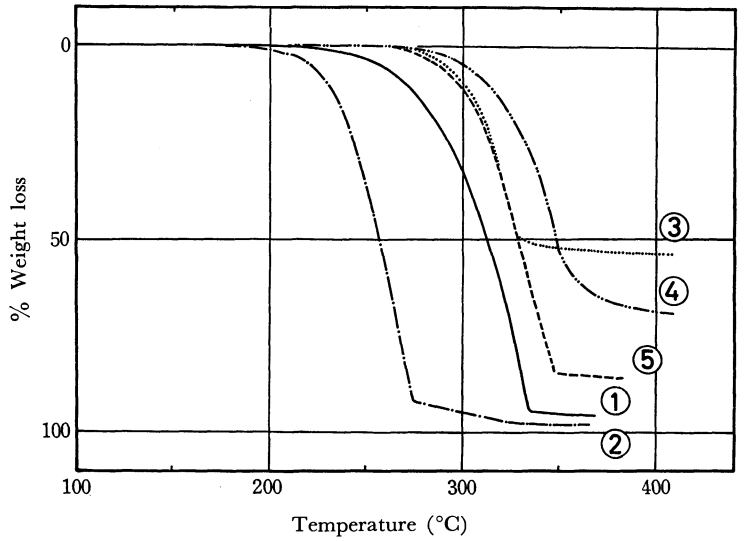

Fig. 7. Thermogravimetric curves of the nickel chelates of the ketimine derivatives : Curve 1 for that of I, 2 for of III, 3 for of IV, 4 for of V, and 5 for of VI, respectively.

about 160°C/0.4 mmHg without any decomposition, while those of IV, V and VI were less sublimable or the sublimation was accompanied with their thermal decomposition.

In the thermogravimetric experiments of these chelate compounds except those of IV, there was observed the deposition of crystalline substances onto the inner wall of the tubular glass part of the apparatus in the initial stage of the weight decrease, and the deposited substance in each experiment was confirmed to be the respective original one intact by infrared spectral comparison. This means that the initial weight decrease is not due to decomposition but to sublimation of the chelate compounds.

Thermogravimetric curves show that the introduction of a methyl group into V to give VI results in slightly easy vaporization of the chelates, and that replacing the methyl groups in VI with isopropyl groups to give I lowers the temperature where vaporization of the chelates begins and subsequently decreases their thermal decomposition as seen in Fig. 5. Thus, among the beryllium chelates only that of I could vaporize completely at a lower temperature without any thermal decomposition. Similar tendencies are observed on the ketimine chelates of copper and of nickel as seen in Figs. 6 and 7; the copper chelate of IV

begins to decompose at about 200°C and no vaporization is observed, the behavior of the nickel chelate also being not far different. Introduction of methyl- or isopropyl groups in the position adjacent to the donor groups in IV to give V, VI or I, makes their chelate compounds increasingly volatile as well as thermally stable, although the vaporization was still accompanied with slight thermal decomposition.

On the other hand, the introduction of trifluoromethyl group lowers the temperature at which vaporization of the complexes begins, as well as suppressing thermal decomposition, as observed in the complexes with the chelating agent III, which shows no thermal decomposition within the temperature range studied here.

Thus, as far as volatility is concerned, the *o*-acylphenols seem to show similar tendencies as those observed in the β-diketones; namely the more crowded groups around the donor atoms in a ligand make its chelate compound more volatile and more stable thermally, and in addition, the introduction of perfluoroalkyl groups into a ligand also makes its metal chelate strongly volatile as well as

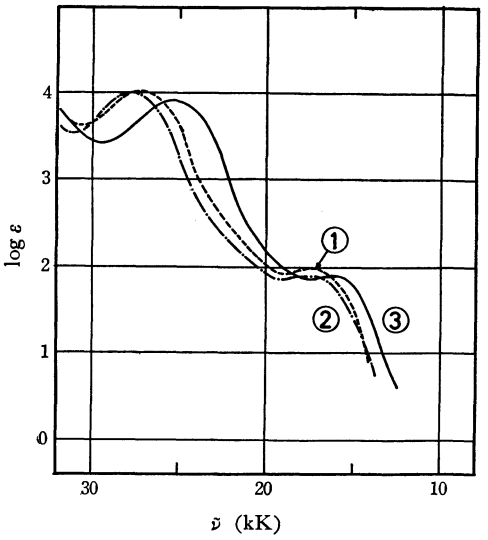

Fig. 8-A

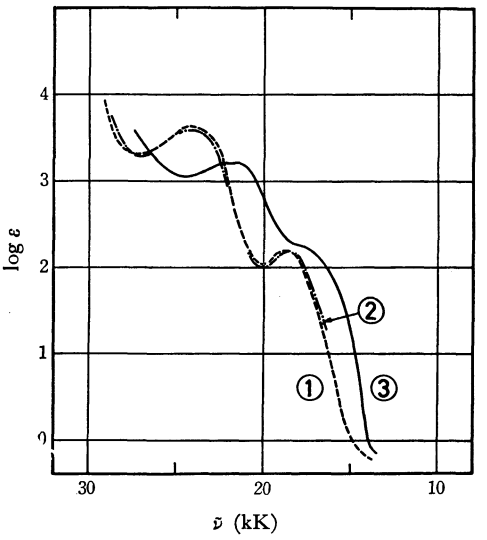

Fig. 9-A

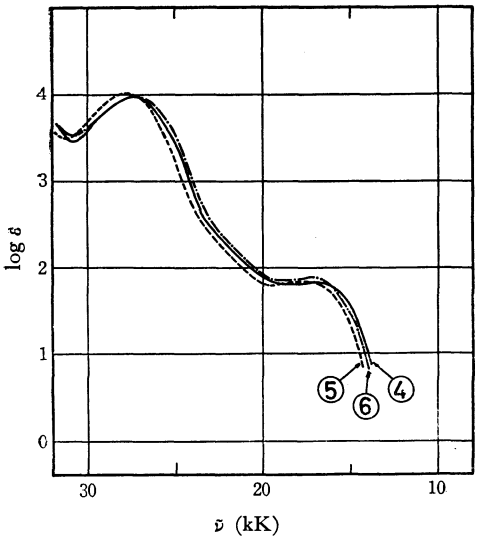

Fig. 8-B

Fig. 8-A, B. Visible spectra of the copper chelates of the ketimine derivatives: Curve 1 for that of I, 2 for of II, 3 for of III, 4 for IV, 5 for of V, and 6 for of VI, respectively.

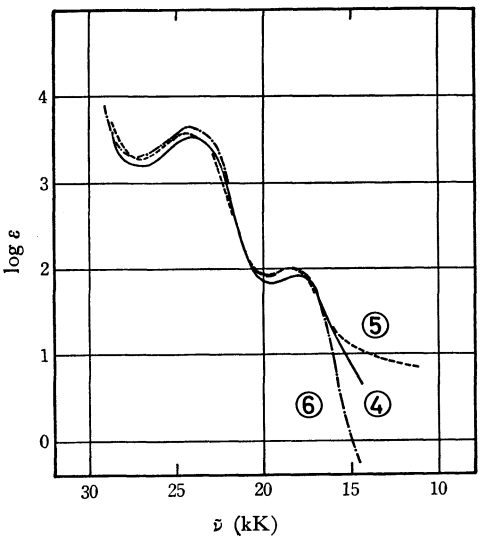

Fig. 9-B

Fig. 9-A, B. Visible spectra of the nickel chelates of the ketimine derivatives: Curve 1 for that of I, 2 for of II, 3 for of III, 4 for IV, 5 for of V, and 6 for of VI, respectively.

thermally stable.

Ultraviolet spectra of the ligands given in Figs. 2 and 3 show that replacing a formyl group with an acyl group (IV→V, *etc.*) causes a characteristic shift on the spectra, although different acyl groups give no significant differences, and the introduction of an alkyl group into the aromatic nucleus (V→VI, or II→I) causes the bathochromic effect, which is still not so intensive as that observed with trifluoromethyl on III. Trifluoromethyl group causes not only strong bathochromic but also hyperchromic effects which are apparent by a comparison of the spectrum of III with that of V.

General features of visible spectra of the copper- and of the nickel ketimine chelates given respectively in Figs. 8 and 9 indicate that they are of a square planar configuration[4] and, although their molecular weights have not been determined, they seem to be all monomeric. Comparisons of their spectra reveal that introduction of alkyl groups into the ligands gives also very little effects on the electronic spectra of their metal complexes, while trifluoromethyl group causes a strong bathochromic shift.

Increased volatility of the chelate compound containing bulky alkyl groups, therefore, seems to be ascribed not to electronic effects by the alkyl groups, but mainly to their steric effects; namely the bulky alkyl groups sterically hinder the polar, or polarizable moieties such as aromatic, and chelate ring from being intermolecularly close to each other, so that consequent intermolecular forces among the chelate molecules seem to decrease to a large extent.

On the other hand, with respect to trifluoromethyl group, the nickel ketimine chelate of III is much more volatile than that of I, and therefore, bulkiness of the ligand or congestion around the central metal ion can not be only a responsible factor for the volatility. In preliminary solubility measurements in chloroform, which is known as one of the nonpolar solvents, the copper ketimine chelate of III has much less solubility than those of I, II, V and VI, though comparable with that of IV. The electronic spectrum of the copper ketimine chelate of III shows the strong red-shift, and the increased volatility of this chelate compound, therefore, must be ascribable not only to steric effects but also particular electronic effects of a trifluoromethyl group.

Whole mechanism of the increased volatility observed here should be very complicated and there remains much to be elucidated.

Experimental

Apparatus and Procedures. All melting points measured are uncorrected. The ultraviolet and visible spectra were measured with a Hitachi EPS-2 recording spectrophotometer, by using *n*-hexane as the solvents for the ligands and chloroform for the metal chelates respectively. The infrared spectra were measured with a JASCO DS-301 recording spectrophotometer. The nuclear magnetic resonance spectra were recorded with a Varian A-60 operating at 60 Mc, by using tetramethylsilane as the internal reference and carbon tetrachloride as the solvent. Thermogravimetric curves were obtained with a Shimadzu automatic recording thermobalance TB-10B under atmospheric pressure. A sample (about 40 mg) was held in a nitrogen stream (flow rate; about 60 ml/min) and heated at a rate of 5°C per minute. Temperatues were measured by alumel chromel thermocouples which were calibrated by the melting points of benzoic acid, succinic acid and anthraquinone.

Synthesis of the Ligands. *2-Hydroxy-3-isopropylisobutyrophenone (I).* 2-Isopropylphenyl isobutyrate[5] (14.7 g) was added dropwise into a suspension of aluminum chloride (10.9 g) in carbon disulfide (20 m*l*) with stirring for 30 min. The mixture was heated with gentle refluxing for an additional hour. After the solvent was distilled, which took about two hours, the temperature of the reaction mixture was gradually raised to 170°C during 30 min, and the mixture was heated keeping this temperature for subsequent 40 min. After cooled to room temperature, the resulting mixture was decomposed with aqueous hydrochloric acid (*ca.* 5 N) and steam-distilled. An organic layer separated from the aqueous distillate was taken into 500 m*l* of ether, and the ethereal solution was washed with 2 N aqueous sodium hydroxide (500 m*l*). The remaining ether layer afforded oily 2-hydroxy-3-isopropylisobutyrophenone (5.3 g) boiling at 109.0—111.0°C/2 mmHg. Found: C, 75.66; H, 8.82%. Calcd for $C_{13}H_{18}O_2$: C, 75.69; H, 8.80%. IR (liquid film): a broad band spreading over during 3500 and 2600 cm^{-1}, a triplet at 2982, 2950, and 2880 cm^{-1}, a sharp carbonyl band having some shoulders at 1632 cm^{-1}, and a sharp singlet at 746 cm^{-1}. NMR (*c* 0.77 M): a doublet at 1.17 and 1.28 ppm (12 protons), a multiplet spreading from 3.0 to 3.8 ppm (2 protons), a triplet centered at 6.70 ppm splitted with 8 cps of *J*-value (1 proton), two quartets (2 protons) centered at 7.30 and 7.55 ppm respectively, each of which is splitted into a quartet with two *J*-values (2 and 8 cps), and a singlet at 12.80 ppm (1 proton). Attempts to prepare a semicarbazone derivative were unsuccessful.

The residue remaining in a still-pot upon the steam-distillation gave the colorless crystals melting at 98.5—99.9°C (from petroleum ether). This crystalline compound was also separated from the alkaline washings after acidified (*ca.* 1 g). Found: C, 75.73; H, 9.01%. Calcd for $C_{13}H_{18}O_2$: C, 75.69; H, 8.80%. IR (potassium bromide disc): a strong band at 3310 cm^{-1}, a doublet at 2974 and 2880 cm^{-1}, a sharp carbonyl band at 1651 cm^{-1}, a prominent doublet at 1608 and 1585 cm^{-1}, and a strong sharp band at 819 cm^{-1}. Semicarbazone is readily formed, mp 199.0—203.0°C. This crystalline compound, though seemed to be 3-isopropyl-4-hydroxyisobutyrophenone, was not confirmed.

2-Hydroxyisobutyrophenone (II). Phenyl isobutyrate[6]

4) C. J. Ballhausen, "Introduction to Ligand Field Theory," McGraw-Hill, New York, N. Y. (1962).

5) A. Spassow, *Ber.*, **75**, 779 (1942).

6) E. H. Man, F. W. Swamer and C. R. Hauser, *J. Am. Chem. Soc.*, **73**, 901 (1951).

(40 g) was added dropwise into a suspension of aluminum chloride (37.3 g) in carbon disulfide (40 ml) with stirring. The mixture was heated in the similar way just as described above. The resulting mixture was decomposed with aqueous hydrochloric acid, and steam-distilled. An organic layer separated from the aqueous distillate was taken into ether, dried and distilled to give a fraction boiling at 79.3—79.5°C/3.5 mmHg (yield: 16.1 g, 40% of the theoretical). IR (liquid film): a broad band spreading over between 3400 and 2600 cm^{-1}, a triplet at 2980, 2940, and 2870 cm^{-1}, a carbonyl band at 1645 cm^{-1}, and two strong bands at 822 and 754 cm^{-1}. Analysis was satisfactory as the metal chelate derivatives, *vide infra*.

2-Trifluoroacetylphenol (III). Phenyl trifluoroacetate[7] (57 g) was added dropwise into a suspension of aluminum chloride (46 g) in carbon disulfide (60 ml) with stirring at room temperature for an hour. The mixture was heated with gentle refluxing for an additional hour. After the solvent was distilled out, which took one and half hour, the temperature of the reaction mixture was gradually rasied to 115°C during 15 min, and the mixture was cooled to 90°C, being kept at this temperature for one and half hour. The resulting mixture, after cooled to room temperature, was decomposed with aqueous hydrochloric acid, and steam-distilled. An organic layer separated from the aqueous distillate was taken into ether, and the ethereal extract was evaporated off. A residual oil was treated with copper acetate and ammonia in aqueous ethanol, giving a copper ketimine chelate (VIII) of the trifluoroacetylphenol (35 g). The ketimine chelate was decomposed with aqueous hydrochloric acid, giving a free ligand, which was extracted with ether, and was rectified to give an oily fraction boiling at 92°C/55 mmHg (yield: 23.8 g, 42% of the theoretical). Found: C, 50.65; H, 2.78%: Calcd for $C_8H_5O_2F_3$: C, 50.54; H, 2.65%. IR (liquid film): a broad band at 3240 cm^{-1}, a carbonyl band at 1684 cm^{-1}, three strong sharp bands at 1155, 950, and 755 cm^{-1}. NMR (*c*, 0.7 M): a triplet at 6.88, 7.03, and 7.17 ppm, a quartet having fine structures at 7.53, 7.67, 7.80, and 7.94 ppm, and a singlet at 11.12 ppm.

Semicarbazone derivative melting at 185.3—188.8°C (from aqueous ethanol). Found: C, 43.60; H, 3.27; N, 16.88%. Calcd for $C_9H_8N_3O_2F_3$: C, 43.73, H, 3.26; N, 17.00%.

From the fraction which did not form a copper ketimine chelate, a small amount of a seemingly *p*-substituted isomeric compound was separated, which was recrystallized from benzene to give colorless needles melting at 105.5—106.0°C. Found: C, 50.48; H, 2.80%. IR (potassium bromide disc): a sharp peak at 3480 cm^{-1} a carbonyl band at 1687 cm^{-1}, and four strong sharp bands at 1160, 951, 855, and 766 cm^{-1}.

2-Hydroxy-3-methylacetophenone (VI).[8,9] It was obtained from *o*-cresyl acetate in a similar manner to that of the ligand II, with accompanied by the *p*-substituted isomer: bp 91.7—91.9°C/5 mmHg. Semicarbazone derivative: mp 240.8—42.6°C.[9] NMR: two singlets at 2.20 and 2.51 ppm (3 protons each), a triplet centered at 6.54 ppm splitted with 7 cps of *J*-value (one proton), two doublets having fine structures, centered at 7.1 and 7.4 ppm respectively, each of which is splitted with 7 cps of *J*-value (one proton each), and a singlet at 12.18 ppm (one proton).

Salicylaldehyde (IV). used here was a commercially available one.

2-Hydroxyactophenone (V) was synthesized from phenyl acetate in a standard procedure, boiling at 113.5—113.8°C/33 mmHg.

Synthesis of the Metal Chelates of Copper and of Nickel. Salicylaldimine chelates of copper and of nickel were synthesized as following. A bis(salicylaldehydato)metal chelate (the copper chelate; 0.50 g, the nickel chelate; 0.50 g), which was prepared according to Tyson and Adams,[10] was added into 10% aqueous ammonia (90 ml for the former chelate and 70 ml for the latter, respectively) and the resulting suspension was stirred at room temperature until the color of the precipitates was changed, which took about an hour. The precipitates, collected by filtration, was washed with methanol, dried and recrystallized from an appropriate solvent. (Yield; 0.50 g for the copper chelate, and 0.41 g for the nickel chelate, respectively). The ketimine chelates of copper and of nickel were synthesized in either of the following procedures.

(A) Into an aqueous alcoholic solution of an ammine metal complex, which was prepared from the aqueous solution of the corresponding metal ion and ammonia in alcohol, was added an alcoholic solution of two moles of an *o*-acylphenol, and the solution was left to stand for a required period of time. Resulting precipitates, collected by filtration, was washed with ammonia and alcohol successively, dried and recrystallized from an appropriate solvent.

(B) Into an aqueous solution of a metal acetate, two moles of an *o*-acylphenol was added, and then alcohol was added so that the mixture made just a homogeneous solution. An appropriate amount of 28% ammonia diluted with alcohol was added into the above solution, and it was left at room temperature until the metal ketimine chelates were precipitated. The resulting precipitates were treated in the similar way just as described above. The details of the amounts of the reagents, the yields and the properties of the chelates are tabulated in Tables 1, 2, 3, and 4.

Synthesis of the Beryllium Chelates. *Bis(2-hydroxy-3-methylacetophenonato)beryllium(II)*. 2-Hydroxy-3-methylacetophenone (1.51 g) dissolved in methanol (5 ml) and 3% methanolic ammonia (8 ml) were added successively into a mixture of a 50% aqueous solution of beryllium nitrate (0.88 g) and methanol (10 ml).

The resulting mixture, after refluxed for several hours, was evaporated to dryness under reduced pressure. The residual solid was dissolved in chloroform, washed with water, and again solidified by evaporation of the solvent. The second solid was recrystallized from petroleum ether to give yellow grains (740 mg) melting at 163.9—65.6°C. Found: C, 70.32; H, 6.04%. Calcd for

7) a) F. Weggand and A. Pöpsch, *Ber.*, **92**, 2095 (1959). b) L. Benoiton, H. N. Rydon and J. E. Willet, *Chem. Ind. (London)*, **1960**, 1060.

8) a) K. von Auwers, M. Lechner and H. Bundesmann, *Ber.*, **58**, 41 (1926). b) K. W. Rosenmund and W. Schnur, *Ann. Chem.*, **460**, 88 (1928).

9) K. von Auwers, H. Bundesmann and F. Wiener, *Ann. Chem.*, **447**, 180 (1926).

10) G. N. Tyson, Jr., and S. C. Adams, *J. Am. Chem. Soc.*, **62**, 1228 (1940).

Table 1. Conditions employed to synthesize the copper ketimine chelates and the results

Ligand	Procedure	Amounts of the reactants and solvents used					Yield (% yield)
		Metal acetate[a]	Ligand	Water	Ethanol	28% Ammonia	
I	B	1.00 g	2.06 g	20 m*l*	80 m*l*	20 m*l*	1.16 g (49%)
II	A	1.00	1.64	25	60	20	1.75 (90)
III	B	0.50	0.96	15	9	1	0.72 (33)
V	B	1.00	1.37	30	—	15	1.38 (83)
VI	A	1.00	1.50	25	70[b]	20	1.70 (94)

a) Copper acetate was in the form of a monohydrate.
b) Methanol was used in the place of ethanol.

Table 2. Conditions employed to synthesize the nickel ketimine chelates and the results

Ligand	Procedure	Amounts of the reactants and solvents used					Yield (% yield)
		Metal acetate[a]	Ligand	Water	Ethanol	28% Ammonia	
I	A	1.25 g	2.06 g	—	35 m*l*	10 m*l*	0.82 g (35%)
II	A	1.24	1.64	20 m*l*	50	10	1.8 (94)
III	B	1.24	1.92	15	18	1.7	1.8 (83)
V	A	1.24	1.37	20	10[b]	10	1.25 (77)
VI	B	2.48	3.00	20	46	4	2.1 (59)

a) Nickel acetate is in the form of a dihydrate.
b) Methanol was used in the place of ethanol.

Table 3. Appearance, melting points and elemental analyses of the copper ketimine chelates

Ligand	Appearance (Solvent used for recryst.)	Mp or (dp) °C	Molecular formula	Elemental analyses					
				Found			Calcd		
				C%	H%	N%	C%	H%	N%
I	G-l(E)[a]	167—170	$C_{26}H_{36}N_2O_2Cu$	66.21	7.79	5.87	66.14	7.69	5.93
II	DG-p(E)[a]	(253—255)	$C_{20}H_{24}N_2O_2Cu$	61.84	6.40	7.13	61.89	6.24	7.23
III	G-n(E)[a]	(260～)	$C_{16}H_{10}N_2O_2F_6Cu$	43.48	2.54	6.28	43.70	2.29	6.37
IV	G-l(E)[a]	(160—170)	$C_{14}H_{12}N_2O_2Cu$	55.74	3.98	9.16	55.35	3.98	9.22
V	G-l(E)[a]	(270—280)	$C_{16}H_{16}N_2O_2Cu$	57.85	4.87	8.46	57.91	4.86	8.44
VI	DG-n(C)[a]	(270—274)	$C_{18}H_{20}N_2O_2Cu$	60.15	5.30	7.73	60.07	5.60	7.78

a) G, green; DG, dark green; l, leaflets; p, fine plates; n, needles; E, ethanol; C, chloroform

Table 4. Appearance, melting points and elemental analyses of the nickel ketimine chelates

Ligand	Appearance (Solvent used for recryst.)	Mp or (dp) °C	Molecular formula	Elemental analyses					
				Found			Calcd		
				C%	H%	N%	C%	H%	N%
I	R-l(E)[a]	163—166	$C_{26}H_{36}N_2O_2Ni$	67.10	7.81	6.04	66.83	7.77	5.99
II	R-g(C)[a]	higher than 300	$C_{20}H_{24}N_2O_2Ni$	61.76	6.09	7.29	62.68	6.32	7.32
III	B-n(C)[a]	(270—280)	$C_{16}H_{10}N_2O_2F_6Ni$	44.12	2.44	6.76	44.18	2.32	6.44
IV	R-l(E)[a]	(280—300)	$C_{14}H_{12}N_2O_2Ni$	55.96	4.00	9.48	56.24	4.05	9.37
V	R-g(C)[a]	higher than 300	$C_{16}H_{16}N_2O_2Ni$	58.30	4.96	8.57	58.77	4.93	8.57
VI	R-g(C)[a]	higher than 300	$C_{18}H_{20}N_2O_2Ni$	61.03	5.42	7.94	60.91	5.64	7.89

a) R, red; B, brown; l, leaflets; g, grains; n, needles; E, ethanol; C, chloroform

$C_{18}H_{18}O_4Be$: C, 70.34; H, 5.90%.

Bis(2-hydroxy-3-isopropylisobutyrophenonato)beryllium(II). 2-Hydroxy-3-isopropylisobutyrophenone (1.05 g) and a 50% aqueous solution of beryllium nitrate (0.45 g) were treated in the same way just as described above to give yellow grains (250 mg) melting at 149.6—52.6°C. Found: C, 74.52; H, 8.24%. Calcd for $C_{26}H_{34}O_4Be$: C, 74.43; H, 8.24%.

Bis(2-hydroxyacetophenonato)beryllium(II). Into a mixture of a 50% aqueous solution of beryllium nitrate (1.3 g), 2-hydroxyacetophenone (2.05 g) and ethanol (5 m*l*) was added a mixture of 28% ammonia (1.2 m*l*) and ethanol (3.8 m*l*). The resulting solution was refluxed for a half an hour, and the solvents were removed as an azeotropic mixture with benzene. The residual solid was recrystallized from benzene, and from a mixture of petroleum ether and benzene successively, to give pale yellow grains (110 mg) melting at 173.1—74.3°C. Found: C, 68.43; H, 5.55%. Calcd for $C_{16}H_{14}O_4Be$: C, 68.81; H, 5.05%.

The authors are grateful to the Ministry of Education for a grant-in-aid for scientific research.

BULLETIN OF THE CHEMICAL SOCIETY OF JAPAN VOL. 42 968—972 (1969)

Spectrophotometric Studies of Ethyl Xanthate Complexes in Aqueous Solutions

Michio NANJO and Taro YAMASAKI

Research Institute of Mineral Dressing and Metallurgy, Tohoku University, Katahira-cho, Sendai

(Received July 22, 1968)

The stability constants of ethyl xanthate complexes of cadmium(II), zinc(II), nickel(II), and cobalt(II) were determined spectrophotometrically in aqueous solutions. Complexes with the 1 : 1 composition, $M(EX)^+$, were found in all cases; the stability constants of these metal complexes were calculated to be 1.2×10^4, 5.2×10, 4.4×10, and 1.1×10 for $Cd(EX)^+$, $Zn(EX)^+$, $Ni(EX)^+$, and $Co(EX)^+$ respectively at an ionic strength of 1.0 and at 25°C. These values were then compared with the stability constants of other metal complexes.

Potassium or sodium ethyl xanthate (KEX or NaEX) has been employed as a flotation agent for sulfide minerals because it gives hardly soluble metal salts in water. Thus, a large number of investigations have been conducted into the behavior of metal xanthates. However, there has been no report on the complex formation reaction between xanthate and metal ions in aqueous solutions. This may be due to the easy formation of insoluble metal xanthates and to the instability of the xanthate ion (EX^-) in an acidic solution. Majima[1] described the formation of soluble complexes, $Pb(EX)_2$, $Ni(EX)_3^-$, and $Co(EX)_3^-$, but his work was limited to studies in acetone-water solutions (1 : 1). In our previous paper[2] we have reported on the formation and properties of a tetracoordinate complex, $Cd(EX)_4^{2-}$, which was formed by the reaction of the cadmium(II) ion with an excess of EX^- in aqueous solutions.

This investigation was undertaken to examine whether other complexes could be formed by varying the concentration ratios of species of metal ions to EX^-.

The 1 : 1 complexes, $M(EX)^+$ (M: Pb, Cd, Zn, Ni, Co), were found to be formed by 3 methods, the spectrophotometric, kinetic, and solubility methods, in aqueous solutions.

This paper will deal with the spectrophotometric studies; the studies by other methods will be discussed in a subsequent paper.[3]

Experimental

Materials. KEX was prepared according to the usual method and was recrystallized three times from ethyl alcohol and ethyl ether. The product was identified by means of its UV and IR spectra. Perchlorates of cobalt, nickel, and lead were prepared by mixing the metal carbonates with perchloric acid and were then recrystallized twice from water. All the other chemicals were of a guaranteed grade and were used without further purification.

Measurements. A Hitachi recording spectrophotometer, Model EPS-3, and a Shimadzu spectrophotometer, Model QR-50, were used for the measurement of the UV absorption spectra. A Toa Model HM-5A pH meter was used for the pH determination. The

1) H. Majima, *Sci. Rep. Res. Inst., Tohoku Univ., Ser. A*, **13**, 433 (1961).

2) T. Yamasaki and M. Nanjo, *Chem. & Ind.*, **1966**, 1530.

3) M. Nanjo and T. Yamasaki, This Bulletin, **42**, 972 (1969).

ionic strength was adjusted to 1.0 by sodium perchlorate, and both the absorbance and the pH were measured at 25°C. This equilibrium measurement was performed at pH 5—7 in order to avoid the decomposition of EX^-.

Results and Discussion

Reaction with the Cadmium(II) Ion. The absorption spectra of a KEX solution recorded in the absence and in the presence of an excess of cadmium(II) ions are presented in Fig. 1. The absorption maxima were found at 226 mμ and 301 mμ. On the addition of cadmium ions a decrease in the absorbance was observed around 301 mμ, but there was no shift in the maximum.

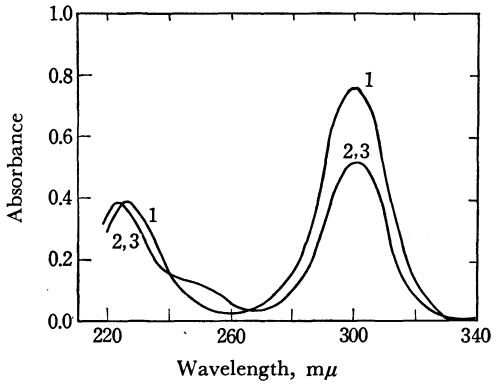

Fig. 1. Absorption spectra of KEX solutions (4.18×10^{-5} M) in the presence of 0.02 M acetate buffer and $CdSO_4$. The contents of $CdSO_4$ are 1) 0, 2) 4.75×10^{-3} and 3) 9.50×10^{-3} M respectively.

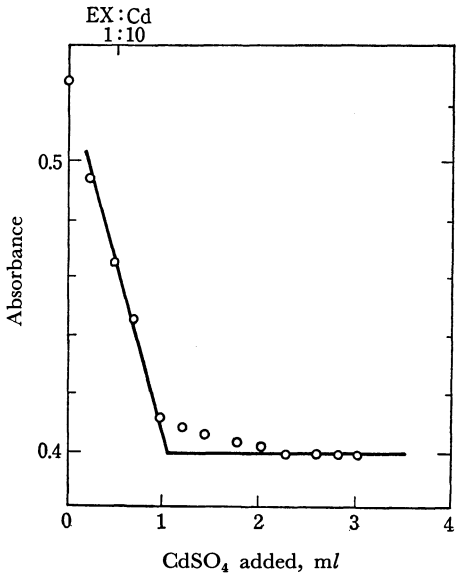

Fig. 2. Photometric titration curve of KEX solution (1.09×10^{-5} M) with $CdSO_4$ (1.02×10^{-2} M) at 301 mμ.

A slight blue shift was observed in the band of 226 mμ, and a new weak absorption band appeared in the region between 240 and 260 mμ; the isosbestic points were also observed at 240 and 265 mμ.

The photometric titration curve of a cadmium sulfate solution with a KEX solution at 301 mμ is given in Fig. 2. In Fig. 2, a plateau of absorbance with an intensity of about 70% of the original absorbance of EX^- was obtained. These changes in the absorption spectrum indicate the formation of a complex before the precipitation of bis-(ethylxanthogenato)cadmium(II), $Cd(EX)_2$, starts (K_{sp}: 2.6×10^{-14} or 5.6×10^{-15}).[4,5]

The composition of the complex was determined by employing the continuous variation method[6] in the presence and in the absence of 0.02 M of an acetate buffer solution. In this system, the mole-ratio method is not applicable because of the instability of the complex ion formed. The differences in absorbance, Δd, between the observed values, d, in a 1 cm cell and the values d_0, calculated by assuming that no complex is formed, were plotted against the mole fractions of EX^-; the results are shown in Fig. 3. The minimum value of Δd lies at a ratio of 0.5; this indicates the formation of a 1 : 1 complex.

The stability constant of the complex was calculated by using the Rose-Drago method.[7] This

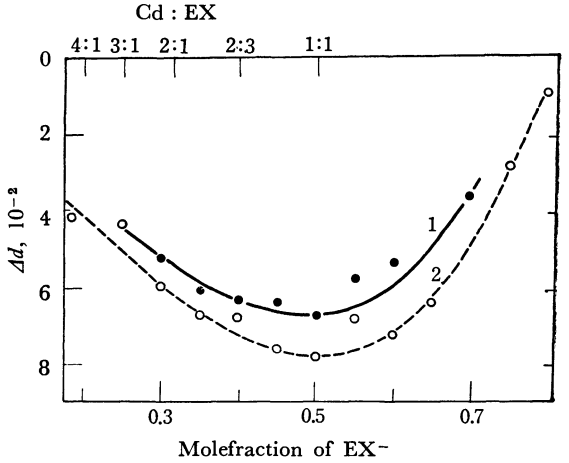

Fig. 3. Continuous variation method. 1) In the absence of acetate buffer, $[EX^-]_t+[Cd^{2+}]_t = 8.0\times10^{-5}$ M. 2) In the presence of 0.02 M acetate buffer, $[EX^-]_t + [Cd^{2+}]_t/1.2 = 8.0\times10^{-5}$ M, on the assumption of $1+K_{CdOAc}[OAc^-] = 1.2$.

4) A. T. Pilipenko, T. P. Varohenko, E. S. Kudelya and A. P. Kostysina, "Soviet Research on Complex and Coordination Compounds," Part II, p. 1325.

5) I. A. Kakovsky, "Second International Congress of Surface Activity," Vol. IV, ed. by J. H. Schulman, Butterworth Scientific Publications, London (1957), p. 225.

6) M. Otomo, This Bulletin, **36**, 137, 889 (1963).

method is applicable when an absorption band of a ligand overlaps with that of a complex, as is shown in Fig. 1. Generally, the equation for the equilibrium is given as follows:

$$M^{2+} + EX^- \overset{K_1}{\rightleftarrows} M(EX)^+. \quad (1)$$

The concentration equilibrium quotient for this reaction can be written as follows:

$$K_1 = [M(EX)^+]/[M^{2+}][EX^-]. \quad (2)$$

The absorption of metal ions at a given wavelength was negligibly small compared with that of the complex and EX^-; therefore, the observed absorbance, d, may be expressed as follows:

$$d = \varepsilon_{EX^-}[EX^-] + \varepsilon_{M(EX)^+}[M(EX)^+], \quad (3)$$

and:

$$d_0 = \varepsilon_{EX^-}[EX^-]_t. \quad (4)$$

The substitution of $[EX^-]$ and $[M(EX)^+]$ from Eq. (3) into Eq. (2) will give the following equation:

$$K_1^{-1} = (d_0-d)/(\varepsilon_{EX^-}-\varepsilon_{M(EX)^+}) - ([EX^-]_t+[M^{2+}]_t) + (\varepsilon_{EX^-}-\varepsilon_{M(EX)^+})([EX^-]_t[M^{2+}]_t)/(d_0-d). \quad (5)$$

In Eq. (3) it is assumed that there are at most two absorbing species which obey Beer's law in the concentration range employed. The isosbestic points observed in Fig. 1 show that two absorbing species are present in the solution and that, as Fig. 2 shows, their absorptions obey Beer's law.

The values of K_1 are plotted against $\varepsilon_{Cd(EX)^+}$ in Fig. 4. This procedure is equivalent to solving a simultaneous equation for all possible pairs (K_1 and $\varepsilon_{M(XE)^+}$) of data. The curves show that they intersect at one point and that there is only one complex ion in the solution. From Fig. 4, K_1 was determined to be 1.2×10^4 in the absence of an acetate buffer, and 1.8×10^4 in the presence of a 0.02 M acetate buffer, the formation of the acetatocadmium(II) complex being taken into consideration.[8,9]

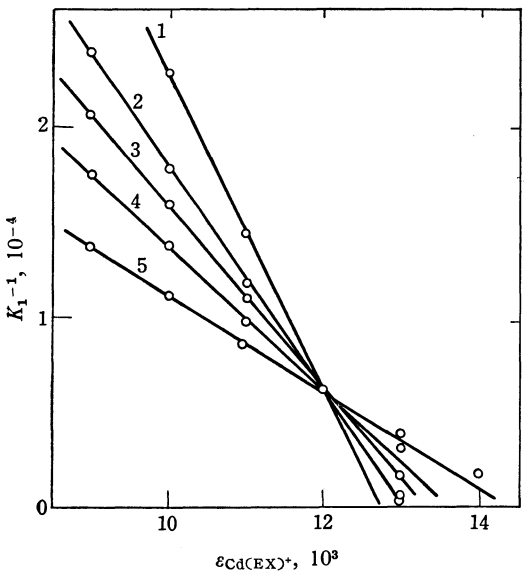

Fig. 4. Rose-Drago's plots at 301 mμ. Each sample solutions contain KEX (3.97×10^{-5} M), 0.02 M acetate buffer and 1) 5.71×10^{-4}, 2) 3.18×10^{-4}, 3) 2.84×10^{-4}, 4) 1.88×10^{-4} and 5) 9.50×10^{-5} M of $CdSO_4$, respectively.

Reaction with Zinc(II) Ions. The experiments were carried out in a 0.2 M acetate buffer solution to prevent the acid decomposition of EX^-. The absorption spectra are shown in Fig. 5. The shapes of the spectra are little different from those of cadmium. The maxima around 301 mμ and 226 mμ show a blue and a red shift respectively, and no new absorption band due to the complex ion could be observed. The isosbestic points were also obtained at 256, 294, and 326 mμ. The absorption of the complex ion obeys Beer's law in an excess of zinc ions. From the Rose-Drago plots, K_1 was determined to be 5.2×10 at 301 mμ, the formation of acetatozinc(II) complex besides the 1 : 1 complex being taken into consideration in a 0.2 M acetate buffer solution.[8] The stability constant employed was 4.6. ($K_{Zn(OAc)^+}$).

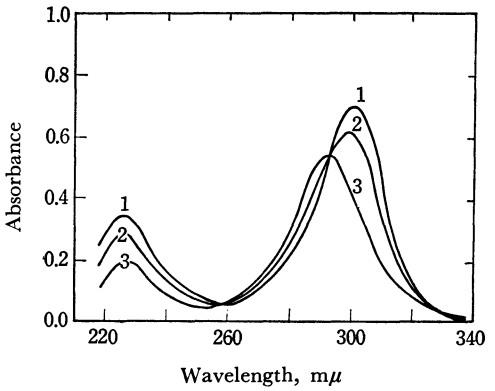

Fig. 5. Absorption spectra of KEX solutions (4.04×10^{-5} M) in the presence of 0.2 M acetate buffer and $Zn(ClO_4)_2$. The contents of $Zn(ClO_4)_2$ in each sample are 1) 0, 2) 4.17×10^{-2} and 3) 1.39×10^{-1} M, respectively.

Reaction with Nickel(II) Ions. The absorption spectra recorded showed a pronounced difference from those of cadmium and zinc, as may be seen in Fig. 6. The isosbestic points were also observed at 285 and 314 mμ, and a new absorption band was obtained around 280 mμ. The absorption band around 301 and 226 mμ showed a red and a blue shift respectively.

7) N. J. Rose and R. S. Drago, *J. Am. Chem. Soc.*, **81**, 6138 (1959).

8) N. Tanaka and K. Kato, This Bulletin, **33**, 417, 1412 (1960).

9) I. Szilard, Dissertation, ETH, Zürich.

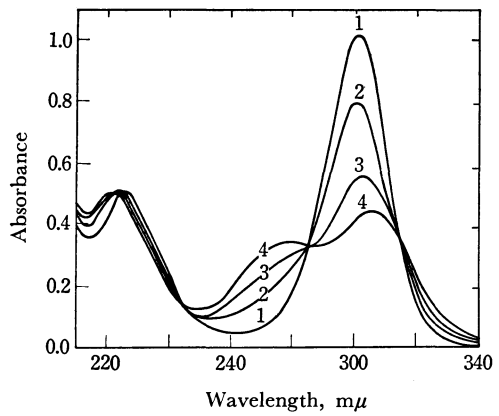

Fig. 6. Absorption spectra of KEX solutions (1.20×10^{-5} M) in the presence of 1) 0, 2) 1.10×10^{-2}, 3) 5.50×10^{-2} and 4) 2.75×10^{-1} M of $Ni(ClO_4)_2$ using 50 mm cells.

Reaction with Cobalt(II) Ions. The sample solution was deairated to protect the cobalt(II) complex from oxidation by air. The absorption spectra are similar in appearance to those of zinc. The band around 301 mμ exhibited a red shift, while the band around 226 mμ showed a blue shift. The isosbestic points were also observed at 240, 288, and 320 mμ, and K_1 was determined to be 1.1×10.

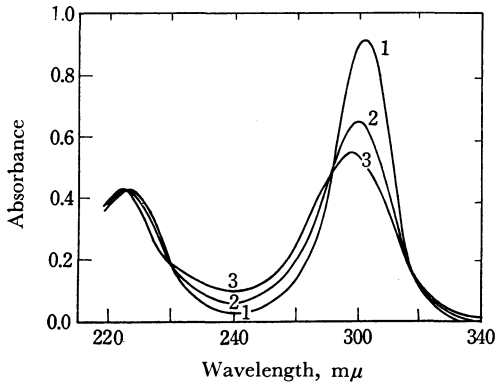

Fig. 7. Absorption spectra of KEX solutions (5.06×10^{-5} M) in the presence of 1) 0, 2) 5.68×10^{-2} and 3) 2.27×10^{-1} M of $Co(ClO_4)_2$ in each sample solutions, respectively.

Reaction with Lead(II), Copper(II), and Magnesium(II) Ions. The dissociation of bis-(ethylxanthogenato)lead(II), $Pb(EX)_2$, was so small that all attempts to obtain K_1 by the Rose-Drago method resulted in failure. The absorption spectra observed in an excess of lead(II) ion are presented in Fig. 8. In the case of copper also, the Rose-Drago method could not be employed because of the formation of dixanthogen, $(C_2H_5O\text{-}CSS)_2$, and ethylxanthogenatocopper(I). However in an large excess of copper(II) ions (10^{-3}—10^{-1} M, $[EX^-]_t=6\times10^{-6}$ M), a well-defined absorption spectra was obtained (Fig. 8). The absorption maxima were observed at 258, 283, 327, and 383 mμ, and the band at 283 mμ obeyed Beer's law ($[EX^-]_t$: 3×10^{-6}—3×10^{-5} M). Those absorption bands may be related to the formation of ethylxanthogenatocopper(II) ($Cu(EX)^+$), because the shape of the spectrum differs markedly from that of dixanthogen and the solubility of ethylxanthogenatocopper(I) has been reported to

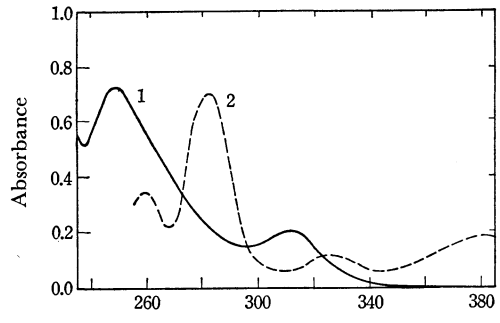

Fig. 8. Absorption spectra of 1) KEX solution (5.0×10^{-5} M) in the presence of 1.34×10^{-3} M of $Pb(ClO_4)_2$ at pH 1.5 and 2) KEX solution (6.55×10^{-6} M) in the presence of 1.24×10^{-1} M of $Cu(ClO_4)_2$ at pH 1.8, using 100 mm cells.

be very low[5] (K_{sp}: 5.2×10^{-23}). A further study by the present authors is in progress; it will be discussed in the near future.

The magnesium(II) ion caused no change in the absorption spectra of EX^-. We failed to prove the formation of any complex by a reaction between magnesium and EX^-.

These results are summarized in Table 1.

Table 1. Stability constants of 1 : 1 complexes 25°C, $\mu=1$ ($NaClO_4$)

Metal ion	K_1
Cd(II)	$(1.2\pm0.1)\times10^4$
	$(1.8\pm0.2)\times10^4$ a)
Zn(II)	$(5.2\pm0.1)\times10$ b)
Ni(II)	$(4.4\pm0.3)\times10$
Co(II)	$(1.1\pm0.1)\times10$
Mg(II)	no complex formed

a) In the presence of 0.02 M acetate buffer.
b) In the presence of 0.2 M acetate buffer.

From the kinetic data,[3] the value of K_1 for $Pb(EX)^+$ was determined to be $(2.5\pm0.4)\times10^4$. The order of K_1 decreases in the series as follows:

$$Pb > Cd \gg Zn > Ni > Co > Mg.$$

10) D. P. Mellor and L. Maley, *Nature*, **159**, 370 (1947).

The Mellow-Maley series,[10] Mg<Mn<Fe<Cd<Zn<Co<Pb<Ni<Cu<Pd, which holds for oxygen and nitrogen ligands, is a direct consequence of their ionization potentials and ionic radii. In the case of Cr(II) and Cu(II), a factor of Jahn-Teller is added to them.

On the other hand, cadmium(II) and lead(II) behave differently toward sulfur of a soft-base compound like EX^-, but they do not belong to the first raw transition series. For these two metal ions the possibility of some degree of L→M π-bonding in the complexes has been pointed out by Irving and Fernelius.[11]

It appears probable that lead(II) and cadmium(II) complexes are stabilized by the π-bonding and do not obey the Mellor-Maley series, because this series was proposed without taking the π-bonding into consideration.

The absorption spectra of EX^- in the presence of an excess of cadmium(II) and lead(II) ions showed a band around 250 mμ which could not be observed in the case of other metals. The absorbance of the ethylxanthogenatolead(II) ion around 250 mμ is stronger than that of cadmium. From these observations and the fact that the stability of the lead complex is highest, the new absorption band around 250 mμ may be explained as a reflection of the L→M π-bonding.

The question whether these absorption bands arose from n–π^* or π–π^* transition in the complexes was not resolved by these studies, but the studies to explain the shift of the absorption bands of EX^- due to the complex formation are in progress by the authors from the view-point of the metal-sulfur bond character, as has been proposed by Pearson.[12]

11) R. J. Irving and W. C. Fernelius, *J. Phys. Chem.*, **60**, 1427 (1956).

12) R. G. Pearson, *J. Am. Chem. Soc.*, **85**, 3533 (1963).

BULLETIN OF THE CHEMICAL SOCIETY OF JAPAN VOL. 42 972—976 (1969)

Acid Decomposition of Metal Xanthate Complexes and Their Stability Constants

Michio NANJO and Taro YAMASAKI

Research Institute of Mineral Dressing and Metallurgy, Tohoku University, Katahiracho, Sendai

(Received July 22, 1968)

The formation of 1 : 1 complexes was confirmed by means of the kinetic method. The acid decomposition of xanthate was delayed by the addition of metal ions because of the decrease in the concentration of ethyl xanthic acid in an equilibrium. By using the rate equation, the stability constants were found to be $(1.0\pm0.2)\times10^4$, $(1.7\pm0.4)\times10$ and $(2.5\pm0.4)\times10^4$ for $Cd(EX)^+$, $Zn(EX)^+$, and $Pb(EX)^+$ respectively.

The behavior of xanthates in solutions has been the subject of numerous investigations because of the complexity of the system.[1-6] Alkali metal xanthates are especially known to be quite unstable in an acidic aqueous solution. This instability of xanthates presents a problem both in research and in the plant operation of mineral flotation with reference to the actual concentration of xanthates remaining in the pulp solution.

The acid decomposition of xanthates has been studied by several investigators. By using a UV spectrophotometer, Iwasaki and Cooke[1] were led to an important implication as to the mechanism of the acid decomposition in the low pH range, where the decomposition is extremely rapid. Majima[2] obtained the same results by using a UV spectrophotometer.

However, there have not yet been any reports that metal ions in the pulps of mineral flotation affect the acid decomposition of xanthate, which is also present in the solution. It should be emphasized that the plant operation of mineral flotation is not conducted in pure water but in

1) I. Iwasaki and S. R. B. Cooke, a) *J. Am. Chem. Soc.*, **80**, 285 (1958); b) *J. Phys. Chem.*, **63**, 1321 (1959); c) *ibid.*, **68**, 2031 (1964).

2) H. Majima, *Sci. Rep. Res. Inst., Tohoku Univ., Ser. A*, **13**, 183 (1961).

3) A. Pomianowski and J. Leja, *Can. J. Chem.*, **46**, 2219 (1963).

4) E. Klein, J. K. Bosarge and I. Norman, *J. Phys. Chem.*, **64**, 1666 (1960).

5) a) C. V. King and E. Dublon, *J. Am. Chem. Soc.*, **54**, 2177 (1932). b) A. Chatenever and C. V. King, *ibid.*, **71**, 3587 (1949). c) M. L. Schochet and C. V. King, *ibid.*, **77**, 4745 (1955).

6) M. A. Cook and J. C. Nixon, *J. Phys. Chem.*, **54**, 445 (1950).

solution, and that the products obtained from xanthate ions with metal ions probably affect the flotation behavior also.

The present paper will show that such metal ions as cadmium, lead, and zinc delay the acid decomposition of potassium ethyl xanthate (KEX) in the low pH range. The reaction can be quantitatively explained by the complex formation between metal ions and the ethyl xanthate ion (EX^-) prior to the rate-determining step.

Experimental

Materials. The KEX and metal perchlorates were prepared and recrystallized by the usual method. All the other chemicals were of a guaranteed grade and were used without further purification. The sodium acetate-acetic acid buffers were prepared by mixing a solution of sodium carbonate and acetic acid.

Procedure. The kinetic measurements were made in 0.2 M buffer solutions or in a concentrated perchloric acid solution. The ionic strength was adjusted to 1.0 with sodium perchlorate through all the measurements. The KEX was dissolved in a dilute sodium hydroxide solution (pH 10—11) to prevent the solution from any acid decomposition before measurements started; then the solution was pipetted into 100 m*l* measuring flasks in which metal ions, sodium perchlorate and sodium acetate - acetic acid buffers or perchloric acid had previously been placed, and the flasks were kept in a thermostat at the temperature of 25°C. The sample solution was then transferred quickly to a quartz absorption cell.

The decomposition of EX^- is easily influenced by the temperature of the solutions,[1-c] so the cell chamber was kept at 25°C by means of a thermostating water jacket.

The decomposition rates were determined by following the absorbance at 301 mμ or 270 mμ employing a Shimadzu Model QR-50 spectrophotometer.

A Toa Model HM-5A pH meter was used for the pH measurements.

Results and Discussion

KEX is readily soluble in water. On dissolving, KEX is dissociated into K^+ and EX^-. Under some conditions, EX^- can be hydrolyzed. Hydrolysis will lead to the formation of xanthic acid:

$$R\text{-}O\text{-}C(S)S^- + H_2O \rightleftarrows R\text{-}O\text{-}C(S)SH + HO^- \quad (R=C_2H_5) \qquad (1)$$

Such a reaction involving ionic combination is known to be extremely rapid.[7] Xanthic acids are very unstable compounds and decompose rapidly into carbon disulfide and alcohols:

$$R\text{-}O\text{-}C(S)SH \rightarrow CS_2 + ROH \qquad (2)$$

The hydrolysis of xanthate anios occurs much faster than does the decomposition of xanthic acid. Consequently, the rate of decomposition depends on the concentration of xanthic acid alone, and anything which affects the hydrolysis of the xanthate anion, such as the concentration of hydrogen ions and metal ions, affects the concentration of xanthic acid in equilibria.

The decomposition rate equation was obtained by Iwasaki and Cooke[1] spectrophotometrically as follows:

$$d[EX^-]_t/dt = -k_3[HEX] = -k_3[EX^-]_t/(1+K_a/[H^+]) \equiv -k_H[EX^-]_t \qquad (3)$$

where $[EX^-]_t$ means the total concentration of the ethyl xanthate species, $[EX^-]_t=[HEX]+[EX^-]$, K_a is a dissociation constant of HEX, and k_3 express a monomolecular decomposition rate constant.

The formation of species other than EX^- and HEX results in a decrease of the concentration of HEX in equilibrium.

By assuming the formation of a stable and water-soluble metal xanthate complex ion, $M(EX)^+$, in place of a insoluble metal xanthate, $M(EX)_2$, in the presence of an excess of metal ions, the decomposition rate equation can be expressed as follows:

$$H^+ + EX^- \overset{\text{fast}}{\rightleftarrows} HEX + M^{2+} \overset{\text{fast}}{\rightleftarrows} M(EX)^+ + H^+$$
$$\downarrow \text{slow}$$
$$EtOH + CS_2 \qquad (4)$$

Since the absorbance at a given wavelength measures the total concentration of EX^-, HEX, and $M(EX)^+$, the decomposition rate may be expressed as follows:

$$d[EX^-]/dt + d[HEX]/dt + d[M(EX)^+]/dt = d([EX^-] + [HEX] + [M(EX)^+])/dt = -k_3[HEX] \qquad (5)$$

By using the dissociation constant of HEX, K_a, and the stability constant of the metal xanthate ion, K_1, Eq. (5) can be rewritten in terms of the total concentration of ethyl xanthate species:

$$d[EX^-]_t/dt = -k_3[HEX] = -k_3[EX^-]_t/(K_a/[H^+]+1 + K_1\cdot K_a\cdot[M^{2+}]/[H^+]) \equiv -k_M[EX^-]_t. \qquad (6)$$

or $$-d\ln[EX^-]_t/dt = k_3/(K_a/[H^+] + 1 + K_1\cdot K_a\cdot[M^{2+}]/[H^+]) \equiv k_M. \qquad (7)$$

were $K_1=[M(EX)^+]/[M^{2+}][EX^-]$

Upon integrating, we have:

$$\log([EX^-]_{t_1}/[EX^-]_{t_2}) = \log(\text{absorbance, } d_1)/(\text{absorbance, } d_2) = k_M(t_2-t_1)/2.303 \qquad (8)$$

Generally, the absorbance for ternary components is represented as follows:

$$d = \varepsilon_{EX^-}[EX^-] + \varepsilon_{HEX}[HEX] + \varepsilon_{M(EX)^+}[M(EX)^+] \qquad (9)$$

where ε_{EX^-}, ε_{HEX}, and $\varepsilon_{M(EX)^+}$ are the molar extinction coefficents of the ethyl xanthate ion, ethyl

7) M. Eigen, *Discussions Faraday Soc.*, **17**, 194 (1954).

xanthic acid, and the complex ion respectively. The absorption of the metal ion is negligibly small at any given wavelength. In the $pH > 1 + pK_a$ range, in which the pK_a is that of HEX ($pK_a = 1.34$),[8] scarcely any undissociated xanthic acid remains in the solution; therefore, the second term in Eq. (9) is negligibly small and the equation may be written as follows:

$$d = \varepsilon_{EX^-}[EX^-] + \varepsilon_{M(EX)^+}[M(EX)^+]. \quad (10)$$

Ethyl xanthic acid is known[3] to have an absorption maximum at 270 mμ ($\varepsilon = 10670$), and the spectrum recorded shows only a weak absorption at 301 mμ ($\varepsilon = 117$). As has been shown in a previous paper,[9] almost all the spectra have an absorption near 300 mμ. Bearing the above facts in mind, the absorbance at 301 mμ may, therefore, be attributed to the total of all the xanthate species except HEX in the high pH range, and the constants for the apparent pseudo first-order rates, k_H and k_M, can easily be obtained from the slope of the logarithm of the absorbance against the time by using Eq. (8). The measurements were made under the conditions of $[EX^-]_t \ll [M^{2+}]_t$ and $[EX^-]_t \ll [H^+]_t$, for which $[H^+]$ and $[M^{2+}]$ were kept constant during the decomposition. When a sodium acetate - acetic acid buffer is used to adjust the pH values, $[M^{2+}]$ is given approximately as follows, taking the formation of acetatometal complexes into consideration:

$$[M^{2+}] = [M^{2+}]_t/(1 + K_{MOAc} \cdot [OAc^-]), \quad (11)$$

in which K_{MOAc} represents the stability constants of acetate complexes.[10,11]

Decomposition in the Presence of an Excess of Cadmium Ions. The absorption spectra of the aqueous solutions of KEX in the presence and in the absence of an excess of cadmium(II) ions were given in a previous paper.[9] The change in the absorption spectra during the acid decomposition in the presence of an excess of cadmium(II) ions is shown in Fig. 1. As can be seen in Fig. 1, an isosbestic point was observed at 216 mμ. There was also a new band at 206 mμ which appeared when recording was done seprately in the higher-frequence region of the spectra. Carbon disulfide is known to absorb at this wavelength. This indicates that

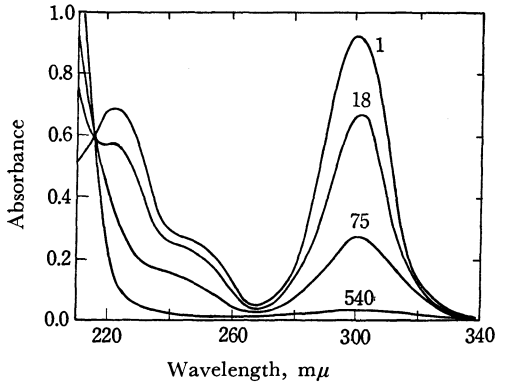

Fig. 1. Absorption spectra of KEX solution (4.32×10^{-5} M), decomposing in the presence of $CdSO_4$ (3.40×10^{-4} M) at pH 0.7. Figures on the curves indicate the standing time of sample solutions in minutes.

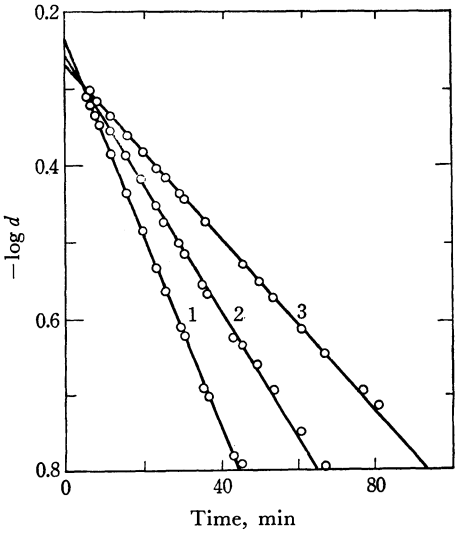

Fig. 2. First order rate plots of an acid decomposition of KEX solution (4.12×10^{-5} M) in the presence of 1) 1.43×10^{-4} M, 2) 2.85×10^{-4} M and 3) 4.75×10^{-4} M of $CdSO_4$ at pH 3.1.

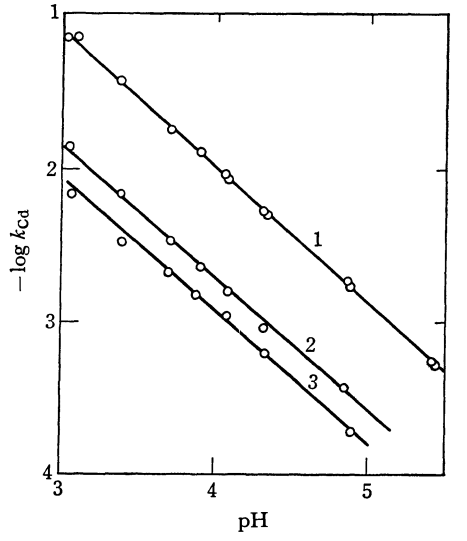

Fig. 3. Relation of pH with $\log k_H$ and $\log k_{Cd}$ in the presence of 0.2 M acetate buffer and 1) 0, 2) 4.8×10^{-4} M, and 3) 9.5×10^{-4} M of Cd(II) ion.*

* Cd(II) ion concentration was kept constant taking the formation of $Cd(OAc)^+$ ion at various pH ranges in consideration.

8) B. Toernell, *Svensk Paperstidn*, **69**, 658 (1966); *Chem. Abstr.*, **66**, 37303 g.

9) M. Nanjo and T. Yamasaki, This Bulletin, **42**, 968 (1969).

the isosbestic point arises from the formation of carbon disulfide and from the decomposition of ethyl xanthate species, and that no other side reactions covered in Eq. (4) occur.

There was no reverse reaction after the decomposition was completed under the conditions employed. Examinations were made at pH 3—5. The first-order plots are given in Fig. 2, the slope may be seen to have been influenced by the pH and by the concentration of cadmium(II) ions. The values of k_H and k_{Cd} were determined from Fig. 2, and the logarithms of k_H and k_{Cd} were plotted against pH (Fig. 3). As can be seen from Fig 3, the slope of the line of k_H was determined to be -0.92, and that of $\log k_3/K_a$, to be 1.69. The slope of k_M was also given as -0.92 at various concentrations of cadmium(II) ions.

These relations demonstrate that our initial assumption of the decomposition mechanism (Eq. (4)) is essentially reasonable; K_1 was also determined to be 1.0×10^4 by using Eq. (12), which was derived from Eqs. (3) and (6) under the condition of $pK_a<pH$:

$$(k_H/k_M) - 1 = [M^{2+}]\cdot K_1, \qquad (12)$$

and $[M^{2+}]$ is calculated by Eq. (11).

In a 0.2M acetate buffer solution, $CdOAc^+$ is the predominant species formed by the reaction of cadmium(II) and acetate ions,[10] ($K_{CdOAc^+}=10$).[11]

Decomposition in the Presence of an Excess of Zinc(II) Ions. The absorption spectra of the zinc(II) complex was given in a previous paper.[9]

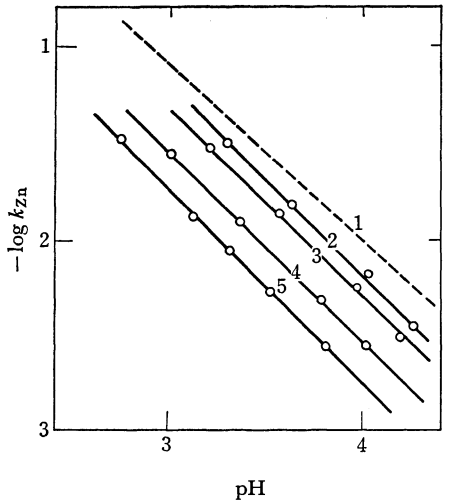

Fig. 4. Relation of pH with $\log k_{Zn}$ in the presence of 0.2 M of acetate buffer and 1) 0, 2) 3.21×10^{-2} M, 3) 6.42×10^{-2} M, 4) 1.61×10^{-1} M and 5) 3.21×10^{-1} M of $Zn(ClO_4)_2$.

10) N. Tanaka and K. Kato, This Bulletin, **33**, 417, 1412 (1960).

11) I. Szilard, Dissertation, ETH, Zürich.

The isosbestic point was found at 216 mμ by the acid decomposition, and nearly the same plots were obtained as those shown in Fig. 3; this indicates a complex formation between zinc(II) and EX^-. The slope of k_{Zn} was determined to be -0.99 (Fig. 4). The zinc(II) ion is less effective in decreasing the decomposition rate than the cadmium(II) ion, which shows that $Zn(EX)^+$ is a less stable ion than that of cadmium.

Decomposition in the Presence of an Excess of Lead(II) ions. The absorption spectra of the lead(II) complex has also been presented in a previous paper[9]; they differed markedly from those of cadmium and zinc. Therefore, kinetic measurements were conducted in highly concentrated solutions of lead(II) ion and perchloric acid in order to avoid the precipitation of $Pb(EX)_2$ and to get the proper conditions for carring out the examinations. In the very low pH range, the formation of HEX should be taken into consideration, so the absorption bands at 270 mμ and 301 mμ were used separately to plot the first-order lines. The resulting values k_{Pb} were the same. This indicates that the absorption spectra are due to the complex ion, which is a very stable ions. The relation between $\log k_{Pb}$ and $\log[Pb^{2+}]_t$ is shown in Fig. 5. The relation between $\log k_{Pb}$ and $\log[H^+]_{add}$ is also represented in Fig. 6, which is derived from Fig. 5. From Figs. 5 and 6, the slopes were determined to be -1.2 and -0.8——-1.0 respectively. These values indicate that, under the present experimental conditions, the

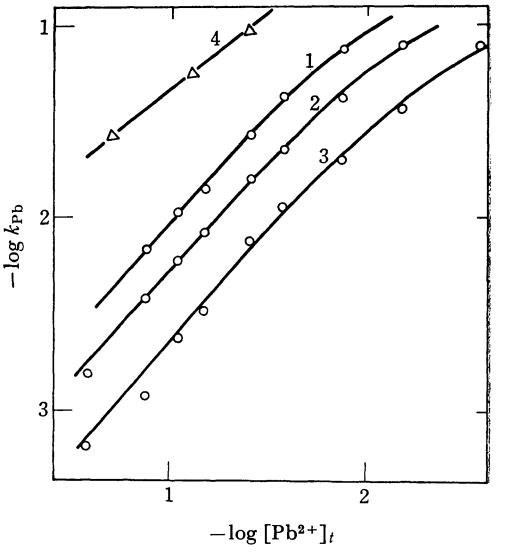

Fig. 5. Relation of $\log[Pb^{2+}]_t$ with $\log k_{Pb}$ in the presence of 1) 5.24×10^{-1} M, 2) 3.00×10^{-1} M and 3) 1.20×10^{-1} M of $HClO_4$.
Curve 4) shows the relation of $\log[Cd^{2+}]_t$ with k_{Cd} in the presence of 3.00×10^{-1} M of $HClO_4$ for the comparison with the curve 2).

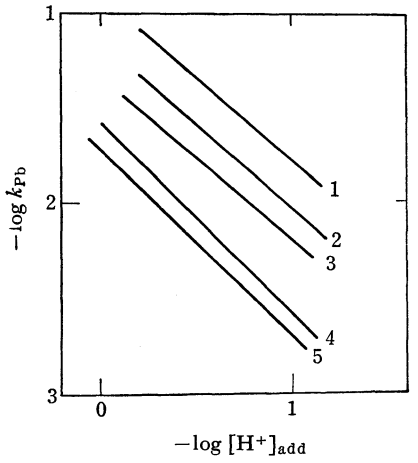

Fig. 6. Relation of $\log [H^+]_{add}$ with $\log k_{Pb}$ in the presence of 1) 1.34×10^{-2} M, 2) 2.68×10^{-2} M, 3) 4.02×10^{-2} M, 4) 6.70×10^{-2} M and 5) 9.38×10^{-2} M of $Pb(ClO_4)_2$.

formation of the complex is the predominant reaction and that the third term of the denominator of Eq. (6), $[M^{2+}]\cdot K_1\cdot K_a/[H^+]$, is larger than the other terms.

In the case of cadmium(II) and zinc(II), the relations between $\log k_M$ and $\log [M^{2+}]$ are not of the first order. They show that the curves are the same as those in Fig. 5 when there is a low concentration of lead(II) ions.

By using Eq. (7), K_1 was calculated from Fig. 5 to be 2.5×10^4; this indicates that the ethylxanthogenatolead(II) complex is more stable than the cadmium(II) complex.

These results are summarized in Table 1. The K_1 values calculated by the kinetic method are in good agreement with those by the spectroscopic method.[9]

Table 1. Stability constants of 1:1 complexes 25°C, $\mu=1(NaClO_4)$

Metal ion	K_1
Pb(II)	$(2.5\pm0.4)\times10^4$
Cd(II)	$(1.0\pm0.2)\times10^4$
Zn(II)	$(1.7\pm0.4)\times10$

The kinetic method is especially useful when the equilibrium method cannot be applied because of the formation of such hydroxides as $Pb(OH)_2$ and $Zn(OH)_2$ in a neutral pH range. Thus, the formation of 1 : 1 complexes is established.

One of the authors (M. N.) wishes especially to thank Professor Nobuyuki Tanaka, Department of Chemistry, Tohoku University, for his many helpful discussions and suggestions during this spectrophotometric and kinetic work.

BULLETIN OF THE CHEMICAL SOCIETY OF JAPAN VOL. 42 976—980 (1969)

The Synergistic Effect in Solvent Extraction. The Effect of Carboxylic Acid on the Solvent Extraction of Europium(III) with Benzoyltrifluoroacetone

Tsunenobu SHIGEMATSU, Masayuki TABUSHI, Masakazu MATSUI and Takaharu HONJYO

Institute for Chemical Research, Kyoto University, Uji, Kyoto

(Received July 25, 1968)

The effects of carboxylic acids, such as formic, chloroacetic, acetic, propionic, butyric and caproic acid, on the extraction of europium with benzoyltrifluoroacetone were studied. The extraction is enhanced by the adduct formation between metal chelates and carboxylic acids in the organic phase, while it is hindered by the formation of metal-complex ions with anions of carboxylic acids in the aqueous phase. Caproic acid acts as an organic Lewis base and shows the synergism, but formic and chloroacetic acids have a masking effect. Acetic acid, propionic acid, and butyric acid behave both as synergists in the organic phase and as masking agents in the aqueous phase. Caproic acid forms more stable adducts than does *n*-hexyl alcohol, and the composition of the chelate adduct is estimated to be $Eu(BFA)_3 \cdot 2CH_3(CH_2)_4COOH$.

As a general procedure for the extraction of metal chelates, a suitable buffer solution is added to the aqueous phase in order to minimize the pH change during the extraction. However, the use of a buffer solution sometimes causes an abnormal distribution of metals as a result of the synergistic effect and the masking effect.

Acetic acid enhances the extraction of thorium

with TTA,[1,2] but inhibits the extraction of lanthanum with TTA[3] or that of uranium[4] and europium[5] with benzoyltrifluoroacetone; it was also observed that the slope of log D *vs.* pH plots decreased upon the addition of acetic acid.[5]

In the present research, the effect of such carboxylic acids as formic, chloroacetic, acetic, propionic, butyric, and caproic acid on the extraction of europium with benzoyltrifluoroacetone in benzene was studied, and the extraction behavior was explained by the adduct formation of the carboxylic acid molecules with europium chelates in the organic phase, and by the complex formation of the acid anions with europium ions in the aqueous phase.

Experimental

Materials. The europium-152, 154 was obtained from the Radiochemical Center, Amersham. The radioisotope was purified by extracting it with 0.05 M benzoyltrifluoroacetone in benzene at pH 5, by back-extracting into 0.1 M perchloric acid, and by evaporating almost to dryness. The residue was dissolved with 0.1 M perchloric acid to make a stock solution. The benzoyltrifluoroacetone was obtained from the Dojindo Co., Ltd. The sodium perchlorate was prepared by adding sodium carbonate to perchloric acid and by subsequent recrystallization from water. All the other reagents were of the G. R. grade and were used without further purification.

Procedure. The experimental procedures were almost the same as have previously been described.[5] Ten milliliters of an aqueous solution containing a few ppm europium ions, 0.1 M sodium perchlorate, and carboxylic acid in a given concentration were shaken with 10 m*l* of 0.05 M benzoyltrifluoroacetone in benzene for one hour at 25±1°C: Each of the carboxylic acids except caproic acid was added in the aqueous phase; caproic acid was added to the organic phase. Aliquots (2 m*l*) of the two phases were pipetted into test tubes, and the distribution ratio of europium was estimated from the gamma counts, as measured with a NaI(Tl) well-type scintillation counter. The pH of the aqueous layer was measured again after the extraction. The partition of the carboxylic acids, such as acetic, propionic, butyric, and caproic acid, between benzene and water was estimated by titrating an aqueous solution containing 0.1 M or 1 M carboxylic acid with a standard sodium hydroxide solution before and after shaking with benzene. The pH of the aqueous layer during the distribution measurement was near 3; therefore, more than 99% of the carboxylic acids may exist in the neutral form. As will be described below, formic acid and chloroacetic acid did not act as synergists, but only as masking agents in the aqueous phase; therefore, the partition was not measured in these cases.

1) R. A. Day, Jr., and R. W. Stoughtom, *J. Am. Chem. Soc.*, **72**, 5662 (1950).
2) G. Goldstein, O. Menis and D. L. Manning, *Anal. Chem.*, **32**, 400 (1960).
3) O. Menis, T. C. Rains and J. A. Dean, *ibid.*, **31**, 187 (1959).
4) T. Shigematsu, M. Tabushi and M. Matsui, This Bulletin, **37**, 1333 (1964).
5) T. Shigematsu, M. Tabushi, M. Matsui and T. Honjyo, *ibid.*, **39**, 165 (1966); *ibid.*, **40**, 2802 (1967).

Theoretical

When the predominant species in the organic phase are MR_3, $MR_3{\cdot}HA$, $MR_3{\cdot}2HA$, $\cdots$, and when those in the aqueous phase are M^{3+}, MA^{2+}, MA_2^{+}, $\cdots$, the distribution ratio of the metal is written as follows:

$$D^* = \frac{\sum_0^m [MR_3 \cdot mHA]_o}{\sum_0^n [MA_n^{(3-n)+}]} \tag{1}$$

where M stands for the metal; MR_3, for the chelate with a chelating agent, HR, and HA, for a carboxylic acid, and where [ ] and [ ]$_o$ indicate the concentration of the relevant chemical species in the aqueous and organic phases respectively.

By introducing the distribution ratio in the absence of the carboxylic acid, D, the equation can be reduced to;

$$\frac{D^*}{D} = \frac{1+\sum_1^m \beta_m [HA]_o{}^m}{1+\sum_1^n k_n [A^-]^n} \tag{2}$$

or;

$$\log D^* - \log D = \log \{1+\sum_1^m \beta_m [HA]_o{}^m\} - \log \{1+\sum_1^n k_n [A^-]^n\} \tag{3}$$

where β_m is the overall stability constant of the adducts formal between the metal chelate and the carboxylic acid, and where k_n is that of the metal complexes with the carboxylic anion; these stability constants are expressed as:

$$\beta_m = \frac{[MR_3 \cdot mHA]_o}{[MR_3]_o [HA]_o{}^m} \tag{4}$$

$$k_n = \frac{[MA_n^{(3-n)+}]}{[M^{3+}][A^-]^n} \tag{5}$$

When the acid dissociation constant of the carboxylic acid, K_A, the partition coefficient of the acid in molecular form, K_d, and the dimerization constant in the organic phase, K_p, are known, the concentration of the monomer species in the organic phase, $[HA]_o$, and of the anionic species in the aqaqueous phase, $[A^-]$, are given from the total concentration of the carboxylic acid, C_{HA}, by the following equations:

$$[HA]_o = \frac{-K_b \sqrt{K_b^2 + 8K_d^2 \cdot K_p C_{HA}}}{4K_d \cdot K_p} \tag{6}$$

$$[A^-] = \frac{K_A(-K_b + \sqrt{K_b^2 + 8K_d^2 \cdot K_p C_{HA}})}{4K_d^2 \cdot K_p \cdot [H^+]} \tag{7}$$

where:

$$K_d = \frac{[HA]_o}{[HA]}, \quad K_p = \frac{[(HA)_2]_o}{[HA]_o^2}$$

and:

$$K_b = 1 + \frac{K_A}{[H^+]} + K_d$$

If the largest portion of the carboxylic acid is distributed into the organic phase, the concentration of the monomer species is obtained by the following equation:

$$[HA]_o = \frac{-1+\sqrt{1+8K_pC_{HA}}}{4K_p} \quad (8)$$

Results and Discussion

The effect of acetic acid on the extraction of europium with benzoyltrifluoroacetone is shown in Fig. 1. With an increase in the concentration of acetic acid, the extraction must be carried out in the higher pH region, and the log D *vs.* pH plot curves concavely. The effect of other carboxylic acids are shown in Fig. 2 (formic and chloroacetic acid), Fig. 3 (propionic acid), Fig. 4 (*n*-butyric acid), and Fig. 5 (caproic acid). Caproic acid enhances, while formic and chloroacetic acid hinder, the extraction. In these cases, the log D *vs.* pH plots are parallel to that obtained in the absence of the carboxylic acids. Propionic acid and *n*-butylic acid increase the extractability in the lower pH region, but decrease the extractability in the higher pH region, indicating convexly-curved log D *vs.* pH plots. Figure 6 presents the change in the distribution ratio of europium as a function of the caproic acid concentration. As is shown in the figure, a straight line with a slope of 1 is obtained when the log D^*/D values are plotted against log C_{HA}, but the slope becomes 2 if they are plotted against log $[HA]_o$. This fact indicates that two moles of caproic acid react with one mole of europium benzoyltrifluoroacetonate to form the $MR_3 \cdot 2HA$-type adduct in benzene, although it is not clear whether caproic acid reacts as the monomer or as the dimer. The overall stability constant of the adduct was esti-

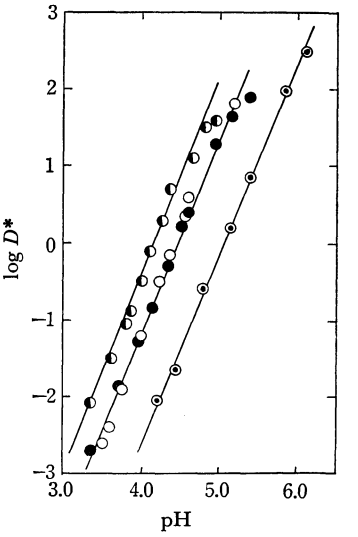

Fig. 2. The distribution ratio of europium(III) as a function of pH in the presence of chloroacetic or formic acid.
Molarity of chloroacetic acid: -◐- none, -○- 0.1 M; formic acid: -◐- none, -●- 0.1 M, -⊙- 1.0 M

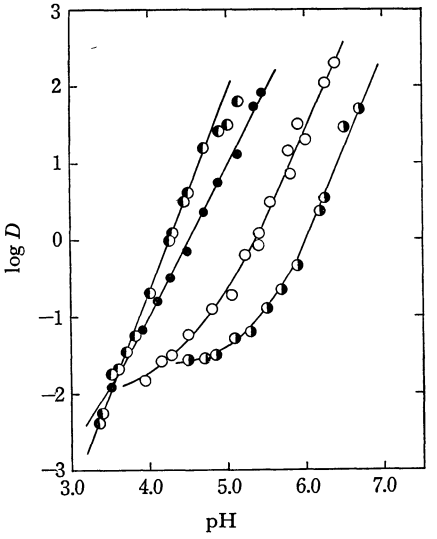

Fig. 1. The distribution ratio of europium(III) as a function of pH in the presence of acetic acid.
Molarity of acetic acid: -◐- none or 0.01 M, -●- 0.1 M, -○- 1.0 M, -◑- 5.0 M

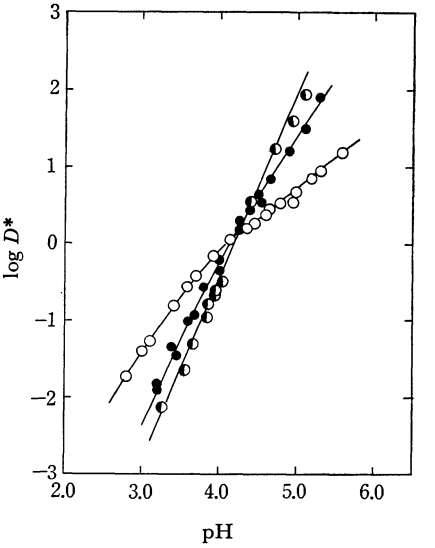

Fig. 3. The distribution ratio of europium(III) as a function of pH in the presence of propionic acid.
Molarity of propionic acid: -◐- none or 0.01 M, -●- 0.1 M, -○- 1.0 M

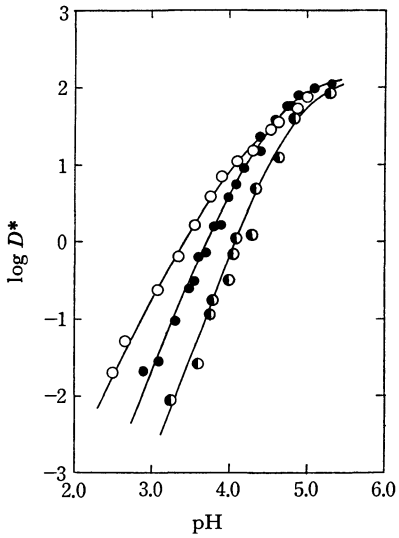

Fig. 4. The distribution ratio of europium(III) as a function of pH in the presence of *n*-butyric acid.
Molarity of *n*-Butyric acid: -◐- none or 0.01 M, -●- 0.1 M, -○- 1.0 M

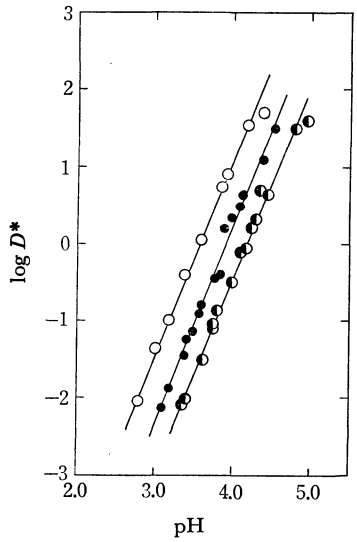

Fig. 5. The distribution ratio of europium(III) as a function of pH in the presence of caproic acid.
Molarity of caproic acid: -◐- none or 0.001 M, -●- 0.01 M, -○- 0.1 M

mated to be $\log \beta_2 = 5.20$. From this value, it may be expected that caproic acid forms more stable adducts with europium benzoyltrifluoroacetonate than does *n*-hexyl alcohol ($\log \beta_2 = 3.10$). In the cases of acetic, propionic, and *n*-butyric acid, some correlation may be observed between the bend point of the $\log D$ *vs.* pH plots and the pK_A value of the carboxylic acid, and between the strength of the synergistic effect and the

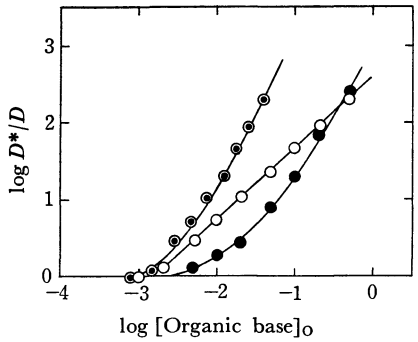

Fig. 6. Variation of the distribution ratio as a function of organic base concentration.
Caproic acid : -○- ($\log D^*/D$ *vs.* $\log C_{HA}$ plot) -⊙- ($\log D^*/D$ *vs.* $\log [HA]_0$ plot)
n-Hexylalcohol: -●- ($\log D^*/D$ *vs.* $\log [n\text{-Hexylalcohol}]_0$ plot)

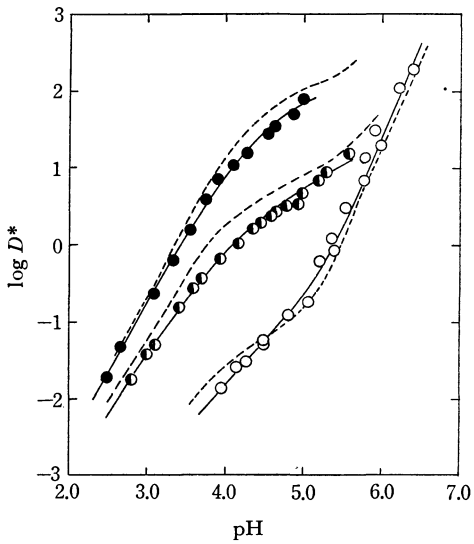

Fig. 7. The extraction curves of europium(III) with benzoyltrifluoroacetone in the presence of 1 M carboxylic acid.
——: experimental, - - -: calculated
Carboxylic acid: -○- Acetic acid, -◐- Propionic acid, -●- *n*-Butyric acid

partition ratio (including K_d and K_p) of the acid. In order to examine why the curious extraction behavior resulted from the distribution equilibrium expressed by Eq. (1), the rough theoretical extraction curves were obtained from the equations described above by introducing various constants of carboxylic acids, which are summarized in Table 1. The K_d and K_p values of *n*-butyric acid were lacking; K_p was assumed to be the same as the values of acetic and propionic acid, and K_d was estimated from the partition of 1M *n*-butyric acid (Ex=72.7%). The extractabilities of acetic and propionic acid obtained experimentally in the present research

TABLE 1. THE CONSTANTS USED FOR THE APPROXIMATE CALCULATION

Carboxylic acid	K_A	K_d	K_p	β_2	k_1	
					0.1 M	1 M
Acetic acid	1.8×10^{-5}	1×10^{-2} a)	1.3×10^{2} a)	1×10^{5} e)	2×10^{2} b)	1×10^{2} f)
Propionic acid	1.3×10^{-5}	5×10^{-2} a)	1.3×10^{2} a)	1×10^{5} e)	1.7×10^{2} b)	8.5×10 f)
n-Butyric acid	1.5×10^{-5}	1.9×10^{-1} d)	1.3×10^{2} c)	1×10^{5} e)	1.4×10^{2} f)	7×10 f)

Carboxylic acid	k_2		% Extrn. of carboxylic acid			
			0.1 M		1 M	
	0.1 M	1 M	Calcd	Exp.	Calcd	Exp.
Acetic acid	8×10^{3} b)	2×10^{3} f)	2	1.7	3	2.5
Propionic acid	6×10^{3} b)	1.5×10^{3} f)	10	9.3	33	30.0
n-Butyric acid	4×10^{3} f)	1×10^{3} f)	42.5	42.5	73	72.7 g)

a) Ref. 6, b) Ref. 7.
c) The value was assumed to be the same with that of acetic and propionic acid.
d) The value was estimated from the K_p value[c] and the extractability[g].
e) The values were assumed from β_2 of caproic acid.
f) The values were assumed from the data presented by Ref. 7.
g) The extractability was used for calculating the K_d value.[d]

were in good agreement with those calculated from the K_d and K_p values previously reported.[6] Also, in the partition of 0.1M *n*-butyric acid, the extractability obtained experimentally agreed well with that derived from the asumed K_d and K_p values. The β_2 values of these acids were uncertain, so $\log \beta_2=5$ was used, the data of caproic acid being referred to. The k_1 and k_2 values used were based on the data in the literature.[7]

Typical calculated extraction curves are indicated in Fig. 7, along with the experimental curves. Since many of the equilibrium constants were roughly estimated, and since the concentration was used instead of the activity in the calculation, the resulting curves were, of course, mere approximations. However, they may not be very wrong, for the vertical scale is logarithmic. Both the extraction curves, those calculated and those experimentally obtained, show a similar shape in each carboxylic acid; this fact indicates that the extraction behavior of europium benzoyltrifluoroacetonate in the presence of carboxylic acid can be explained by Eq. (1). For formic and chloroacetic acid, the first term of Eq. (3) is negligible and only the masking effect appears, while the second term can be neglected and the synergism is observed in the case of cap roic acid.

6) M. Davies, P. Jones, K. Patnaik and E. A. Moywyn-Hughes, *J. Chem. Soc.*, **1951**, 1249.
7) S. P. Sinha; "Complex of the Rare Earths," Pergamon Press, London (1966), pp. 38, 41, 46.

BULLETIN OF THE CHEMICAL SOCIETY OF JAPAN VOL. 42 981—984 (1969)

The Yields of Photonuclear Reactions Leading to the Production of Beryllium-7 with Bremsstrahlung up to 60 MeV

Yoshinaga OKA, Toyoaki KATO and Akira YAMADERA

Department of Chemistry, Faculty of Science, Tohoku University, Katahira-cho, Sendai

(Received July 25, 1968)

Beryllium, boron, carbon, oxygen, and fluorine targets with natural isotopic compositions were irradiated by bremsstrahlung with four maximum energies, 30, 45, 55 and 60 MeV, and the yields of ^{7}Be from each of these targets were determined by means of chemical separation and gamma-ray spectrometric measurements. The yields were obtained relative to the yield of the $^{12}C(\gamma, n)^{11}C$ reaction at each bremsstrahlung energy. The possible reaction pathways leading to the production of ^{7}Be were discussed. The exponential decrease in the yield value against the difference in mass between the target and the product nuclei was observed.

Knowledge of the magnitude and energy dependences of photonuclear reaction yields is basic to an understanding of the interaction of high-energy photons with nuclei. In a previous work,[1] the yields of a number of radioactive nuclei produced by (γ, xnyp) reactions on titanium and vanadium targets have been determined with bremsstrahlung up to 60 MeV. ^{7}Be decays with a half-life of 53 days upon K-capture with a 477 keV gamma-ray, accompanied by a 10.3 per cent in the decay processes.[2] These properties support the idea of obtaining some evidence of the occurrence of high-energy processes in light nuclei through measuring the ^{7}Be activities. ^{7}Be has been observed as a spallation product in a number of high-energy processes with charged particles.[3-7]

Several investigators[8-13] have also shown that ^{7}Be can be produced with high-energy photons from various light elements. However, many of their reports have been only about brief examinations.

In this work, beryllium, boron, carbon, oxygen, and fluorine targets with natural isotopic compositions were irradiated by bremsstrahlung with four different maximum energies, 30, 45, 55 and 60 MeV, and the yields of ^{7}Be from each of these targets were determined by means of gamma-ray spectrometric measurements. The yields were taken relative to the yield of the $^{12}C(\gamma, n)^{11}C$ reaction at each bremsstrahlung energy. The possible reaction pathways leading to the production of ^{7}Be were discussed. The exponential decrease in the yield value against the difference in mass between the target and the product nuclei has also been observed.

Experimental

Target Materials. Target materials of beryllium in the form of metallic flakes, boron in powder form, a carbon spectrograph rod, silica and lithium fluoride were used. All the materials were of a high purity. A definite amount of each sample (100—500 mg) was wrapped in a thin aluminum foil and then made into a small disk 7 mm in diameter and 3 mm thick.

Irradiation. The linear electron accelerator of the Tohoku University was the bremsstrahlung source. The electron beam, accelerated by the "High Current" accelerating section of the machine,[14] produced bremsstrahlung in a platinum converter 3 mm thick located 3 cm from the beam-exit window. Over the energy range investigated, the average beam current was at least 30 μA, measured at the position of the converter by using a current monitor. The targets were set in a water-cooled target holder on the bremsstrahlung beam axis immediately behind the converter. Irradiations were terminated within 1 to 3 hr. The bremsstrahlung

1) Y. Oka, T. Kato and N. Sato, This Bulletin, to be published.

2) C. M. Lederer, J. M. Hollander and I. Perlman, "Table of Isotopes," Sixth Ed., John Wiley & Sons, New York (1967).

3) P. A. Benioff, *Phys. Rev.*, **119**, 316 (1960).

4) I. R. Williams and C. B. Fulmer, *ibid.*, **154**, 1005 (1967).

5) G. Friedlander, J. Hudis and R. L. Wolfgang, *ibid.*, **99**, 263 (1955).

6) M. Honda and D. Lal, *ibid.*, **118**, 1618 (1960).

7) G. V. S. Rayudu, *Canad. J. Chem.*, **42**, 1149 (1964).

8) K. H. Lokan, *Proc. Phys. Soc. (London)*, **A70**, 836 (1957).

9) M. S. Foster and A. F. Voigt, *J. Inorg. Nucl. Chem.*, **24**, 343 (1962).

10) H. Artus, G. Fricke and D. E. von Stein, *Z. Phys.*, **178**, 109 (1964).

11) H. Artus, *Z. Naturf.*, **20a**, 320 (1965).

12) O. L. Garzón and G. G. Rocco, *J. Inorg. Nucl. Chem.*, **29**, 1 (1967).

13) C. B. Fulmer, I. R. Williams, G. F. Dell and L. N. Blumberg, *Bull. Am. Phys. Soc.*, **12**, 499 (1967).

14) The peak current was at least 100 mA with energies up to 100 MeV. In many cases, the pulse repetition was 200 pps, with a pulse width of 3 μsec.

flux was monitored using a thin sheet of gold (10 μ thick, 7 mmϕ) adjacent to the sample.

Radiochemical Separation. To obtain the ^{7}Be spectrum without any contamination by undesirable activities in the irradiated sample, a chemical separation was necessary for all targets except beryllium. After irradiation, each target was dissolved along with 20 mg of a beryllium carrier, and then subjected to separation procedure. Boron powder was dissolved with nitric acid, and silica was dissolved with hydrofluoric acid. Wet oxidation by potassium iodate in a mixture of sulfuric and condensed polyphosphoric acids[15,16] was efficient in decomposing the carbon targets after they had been finely pulverized in a agate mortar. From these solutions, beryllium hydroxide was precipitated by the addition of aqueous ammonia and subsequent centrifuging. The hydroxide was dissolved with a small amount of nitric acid, and beryllium was extracted as its acetylacetonate into chloroform in the presence of EDTA at a pH of 7. The organic layer was back-washed twice, and then evaporated to dryness. The residual organic substances were decomposed by fuming with a sulfuric and perchloric acid mixture. The beryllium hydroxide was again precipitated from this solution by the addition of aqueous ammonia, and then ignited to obtain beryllium oxide.[17] The final oxide was packed in a small glass tube with an internal diameter of 4 mm for the determination of the chemical yield and for the gamma-ray counting.

Radioactivity Measurements. For the measurements of the gamma-ray spectra, a 3'' dia.$\times$3'' NaI(Tl) detector coupled to an 800-channel pulse-height analyzer made by the Tokyo Shibaura Electric Co., Ltd. was employed. Typical gamma-ray spectra are shown in Fig. 1. In each case, the dacay curve followed in the area under the 477 keV photopeak showed a half-life of 53 days, corresponding to the literature value of ^{7}Be.[2] The initial photopeak activity was obtained and used to determine the reaction yield.

Yield Determination. A yield was defined as the production rate of ^{7}Be per atom of a target nucleus when a standard amount of the bremsstrahlung radiation with a given maximum energy was passed through the target during the irradiation period. From the initial activity of the ^{7}Be, the corresponding saturation rate was computed and then normalized for bremsstrahlung intensity, which was measured by the amount of ^{196}Au activity in a gold foil irradiated together with the target. After correcting for chemical yield,[18] counting efficiencies, branching ratio, and internal conversion electrons, the data were expressed in the form of yields. These yields were expressed relative to that of the

TABLE 1. CALCULATED MASS THRESHOLDS FOR THE PHOTOPRODUCTION REACTIONS OF ^{7}Be FROM ^{9}Be, ^{10,11}B, ^{12}C, ^{16}O AND ^{19}F NUCLEI

Reaction	$E_{th}(-Q)$ (MeV)	Reaction	$E_{th}(-Q)$ (MeV)	Reaction	$E_{th}(-Q)$ (MeV)
^{9}Be(γ, 2n)	20.56	^{12}C(γ, αn)	26.27	^{16}O(γ, 2αn)	33.43
		(γ, td)	43.86	((γ, dtα)	51.02
^{10}B(γ, t)	18.67	(γ, ptn)	46.08	(γ, ptαn)	53.24
(γ, p2n)	27.15	(γ, ^{3}He2n)	46.85	(γ, α^{3}He2n)	54.01
(γ, dn)	36.98	(γ, 2dn)	50.11	(γ, 2dαn)	57.28
		(γ, pd2n)	52.34	(γ, pdα2n)	59.50
^{11}B(γ, tn)	30.12	(γ, 2p3n)	54.56	(γ, 2pα3n)	61.73
(γ, p3n)	38.61				
(γ, d2n)	36.38			^{19}F(γ, 2αtn)	45.13
				(γ, d2α2n)	51.39
				(γ, p2α3n)	53.61

TABLE 2. THE REACTION YIELDS LEADING TO ^{7}Be RELATIVE TO ^{12}C(γ, n)^{11}C REACTION

Target nucleus	Relative yield			
	30 MeV	45 MeV	55 MeV	60 MeV
^{9}Be	$(2.9_8\pm0.0_2)\times10^{-2}$(2)	$7.1_1\times10^{-2}$(1)	$8.4_3\times10^{-2}$(1)	$(1.3_9\pm0.1_1)\times10^{-1}$(4)
^{10,11}B	$(6.6_4\pm0.1_0)\times10^{-3}$(2)	$(1.0_3\pm0.0_6)\times10^{-2}$(2)	$1.9_3\times10^{-2}$(1)	$(3.3_9\pm0.2_3)\times10^{-2}$(3)
	$(3.1_2+0.0_5)\times10^{-2}$(2) a)			
^{12}C	$1.3_3\times10^{-3}$(1)	$(2.6_9\pm0.0_9)\times10^{-2}$(2)	$3.2_8\times10^{-2}$(1)	$(3.7_0\pm0.0_7)\times10^{-2}$(2)
^{16}O		$1.0_2\times10^{-3}$(1)		$(3.6_1\pm0.2_4)\times10^{-3}$(2)
^{19}F				$(1.7_6\pm0.0_1)\times10^{-3}$(2)
				$(1.3_4\pm0.0_4)\times10^{-3}$(2) b)

a) Relative yield per mole of ^{10}B. b) The yield relative to ^{19}F(γ, n)^{18}F reaction.

15) T. Kiba, S. Ohashi, T. Takagi and Y. Hirose, *Japan Analyst*, **2**, 446 (1953).
16) M. Ura, *Nippon Kagaku Zasshi* (*J. Chem. Soc. Japan, Pure Chem. Sec.*), **78**, 316 (1957).
17) In the case of ^{7}Be obtained from boron, the present procedure was insufficient for the complete removal of undesired activities; however, these activities could be removed by copper sulfide scavenging before the final hydroxide precipitation.
18) 50—70%.

$^{12}C(\gamma, n)^{11}C$ process, which was measured by the amount of 0.511 MeV gamma-rays arising from the annihilation of the positrons in a standard carbon disk irradiated together with the target.

Results and Discussion

Reaction Path. Beryllium and fluorine are the single-isotopic elements, and the natural isotopic abundances of the most abundant isotopes for carbon and oxygen are 98.893 and 99.759% respectively. Thus, it has been assumed for the sake of simplicity that each of these elements consists entirely of its most abundant isotope. Boron has the natural composition of two isotopes: ^{10}B(19.61%) and ^{11}B(80.39%). The competitive reactions take place on these two isotopes. Table 1 lists the possible nuclear reactions leading to the production of ^{7}Be in the energy region covered in this experiment, together with their calculated mass thresholds.[19] In many cases, ^{7}Be can be formed through several different reaction pathways. At an excitation energy up to 30 MeV, almost all of the ^{7}Be comes from ^{10}B *via* the (γ, t) process, and at this energy, ^{7}Be can be formed from carbon only by the $(\gamma, \alpha n)$ reaction on ^{12}C. For the production of ^{7}Be from ^{16}O, the only pathwhy which has a mass threshold below 45 MeV is the $(\gamma, 2\alpha n)$ reaction, and it may be seen that this reaction is the most probable pathway over the energy range investigated. All of the reactions leading to the photoproduction of ^{7}Be from the parent ^{19}F have threshold energies greater than 45 MeV.

Reaction Yield. The results obtained in this experiment are summarized in Table 2. The numbers in brackets indicate the number of determinations which were made. The errors in these results are less than 5%. For the $^{12}C(\gamma, n)^{11}C$ reaction, the resonance peak lies below 30 MeV, and the yield curve exhibits a slight increases with an increase in the energy.[20,21] The yields of the reactions investigated here appear likely to be strongly energy-dependent. Since ^{7}Be can be formed through competitive reactions on mixed boron targets, except in the irradiation at 30 MeV, the reaction yields were expressed with preference to the per atomic weight of the target element instead of per mole of the target nucleus. The yields are shown in Fig. 2, plotted against the difference in mass between the target and product nuclei at excitation energies of 30, 45 and 60 MeV. For a given energy, the exponential decrease in the reaction yield *versus* the difference in mass is shown. The gradient of the logarithm of the yield against the difference in mass increases as the excitation energy decreases.

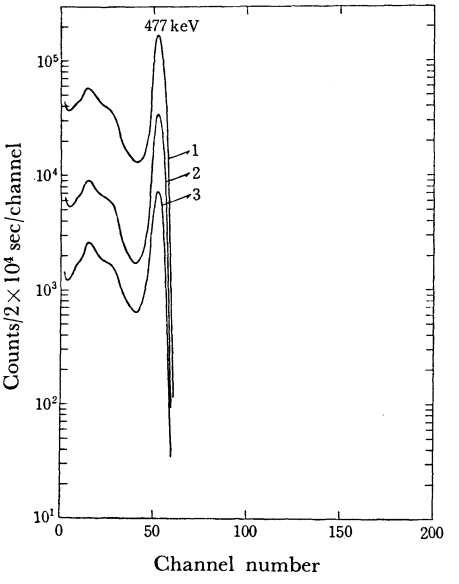

Fig. 1. Gamma-ray spectra of ^{7}Be.
1: Carbon 1.76 g, 32.1 days after irradiation
2: Beryllium 47 mg, 37.5 days after irradiation
3: Boron 77 mg, 49.4 days after irradiation
Irradiation: 60 MeV (45 μA), 3 hr
Measurement: 3″dia.×3″NaI(Tl), source distance=8 cm

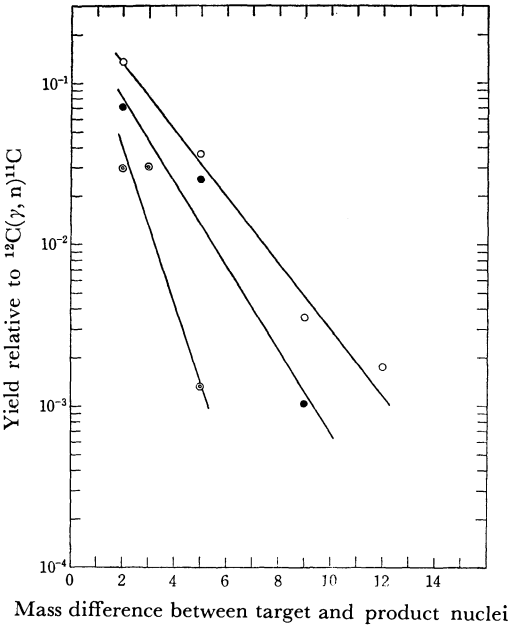

Fig. 2. Relative yield *versus* mass difference between target and product nuclei.
○: 60 MeV ●: 45 MeV ◎: 30 MeV

19) The nuclidic mass values used were those listed by G. Friedlander, J. W. Kennedy and J. M. Miller, "Nuclear and Radiochemistry," 2 nd Ed., John Wiley & Sons, New York (1964), p. 533.

20) W. C. Barber, W. D. George and D. D. Reagan, *Phys. Rev.*, **98**, 73 (1955).

21) B. C. Cook, J. E. E. Baglin, J. N. Bradford and J. E. Griffin, *ibid.*, **143**, 724 (1966).

Walker *et al.*[22] measured the reaction yields for the production of ^{18}F from ^{19}F to ^{32}S targets with 240 MeV bremsstrahlung, and found their exponential decrease when plotted against the number of emitted nucleons.

A similar tendency has been shown in various works of proton-induced spallation reactions,[23-25] and a possible mechanism which would result in this behavior has also been considered. When the total reaction cross-section is distributed among many of the product nuclei, a yield generally favors the product nuclide which is close to the line of the stable nuclei on the isotopic chart. If this is the case, the yield shows the exponential decrease against the difference in mass, as has been determined here. The foregoing presentation may prove useful in a general consideration of photonuclear properties in the energy region up to 60 MeV.

For analytical purposes, the lower limits of detection for beryllium and for boron under the present experimental conditions[26] can be estimated to be 2 and 10 μg respectively. Obviously, these limis of detection will be reduced by a higher bremsstrahlung intensity and by lengthening the time of irradiation.

22) T. G. Walker and W. T. Morton, *Proc. Phys. Soc. (London)*, Vol. LXXV, 4 (1960).

23) S. G. Rudstam, P. C. Stevenson and R. L. Fowler, *Phys. Rev.*, **74**, 442 (1952).

24) S. G. Rudstam, *Phil. Mag.*, **44**, 1131 (1953).

25) R. G. Korteling and A. A. Caretto, Jr., *J. Inorg. Nucl. Chem.*, **29**, 2863 (1967).

26) At the end of a one-hour irradiation with a 60 MeV bremsstrahlung (average beam current: 45 μA), the counting geometry is 10% with a 3'' dia.$\times$ 3'' NaI(Tl) crystal.

BULLETIN OF THE CHEMICAL SOCIETY OF JAPAN VOL. 42 984—988 (1969)

Cobalt(IV) Ammine Complexes with 5-Nitrosalicylato or Similar Ligands. II.*1 Preparation and Properties of Derivatives

Yoshihisa YAMAMOTO and Masayasu MORI

Faculty of Science, Osaka City University, Sumiyoshi-ku, Osaka

and Hayami YONEDA

Chemistry Department, Wakayama University, Masago-cho, Wakayama

and Soichi MISUMI and the Late Kazuo ITO

The Institute of Scientific and Industrial Research, Osaka University, Yamadakami, Suita

(Received July 29, 1968)

Cobalt(IV) compounds of the formulae:

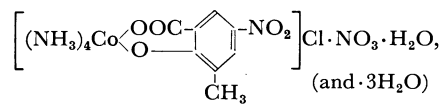

(A)

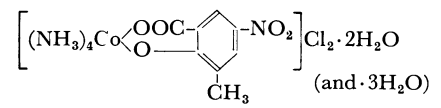

(B)

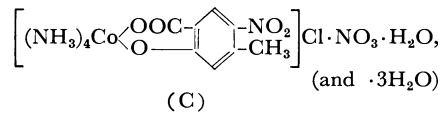

(C)

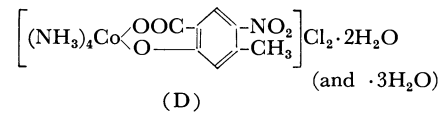

(D)

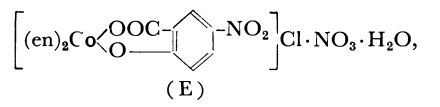

(E)

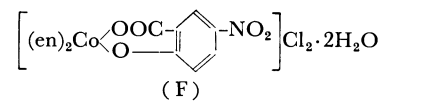

(F)

have been obtained by procedures analogous to that reported for cobalt(IV) ammine complexes with 5-nitrosalicylato ligands.

In the previous work,[1] cobalt(IV) ammine complexes with 5-nitrosalicylato ligands were isolated from the reaction product of salicylatotetraamminecobalt(III) chloride monohydrate and 14 N nitric acid.

In the present report the preparation and some

*1 Presented at the 20th Annual Meeting of the Chemical Society of Japan, Tokyo, 1967.

1) Y. Yamamoto, the Late K. Ito, H. Yoneda and M. Mori, This Bulletin, **40**, 2580 (1967).

fundamental properties of analogous compounds containing ethylenediamine and those containing 3-methyl or 4-methylsalicylato ligands will be described.

Experimental

Preparation. *Salicylatotetraamminecobalt(III) Chloride Monohydrate, Salicylatobis(ethylenediamine)cobalt(III) Chloride Dihydrate, 3-Methylsalicylatotetraaminecobalt(III) Chloride Monohydrate and 4-Methylsalicylatotetraamminecobalt(III) Chloride Monohydrate.* These were prepared by Morgan and Smith's method[2] and recrystallized from water. In the preparation of the latter two compounds, equimolar amounts of the 3-methyl and 4-methylsalicylic acid were used as ligands instead of salicylic acid.

Found in 3-methylsalicylato cobalt(III) ammine complex: C, 29.22; H, 6.23; N, 16.55; Cl, 10.80%. Found in 4-methylsalicylatocobalt(III) ammine complex: C, 28.99; H, 5.81; N, 16.49; Cl, 10.97; NH_3 20.22%. Calcd for $[CoC_8H_{18}N_4O_3]Cl\cdot H_2O$: C, 29.06; H, 6.10; N, 16.94; Cl, 10.72; NH_3, 20.60%.

5-Nitro-3-methylsalicylatotetraamminecobalt(IV) Chloride Nitrate (Abbreviated as A), 5-Nitro-4-methylsalicylatotetraamminecobalt(IV) Chloride Nitrate (Abbreviated as C) and 5-Nitrosalicylatobis(ethylenediamine)cobalt(IV) Chloride Nitrate (Abbreviated as E). The following procedure is an improvement of that reported in paper I for the preparation of 5-nitrosalicylatotetraamminecobalt(IV) salts, and is applicable to the preparation of the original compound as well.

Five milliliters of 14 N nitric acid was added to 5 g of 3-methylsalicylatotetraamminecobalt(III) chloride monohydrate, 4-methylsalicylatotetraamminecobalt(III) chloride monohydrate or salicylatobis(ethylenediamine)cobalt(III) chloride dihydrate. Heat was evolved and the color of the solution changed from russet to green. To the cooled solution was added 10 ml of 14 N nitric acid. The solution was filtered with a glass filter (G4), and the green filtrate was added to acetone. The green substance separated out was filtered with a glass filter (G3), washed with acetone, and dried in a vacuum desiccator. Two grams of this green substance was dissolved in 4 ml of 14 N nitric acid, and the green solution was added into acetone. The precipitated green substance was filtered, washed with acetone and dried. It was reprecipitated twice more by dissolution in 14 N nitric acid and addition of acetone. Yield, 2 g in each case. When dried in a silicagel desiccator, trihydrates were obtained, whereas drying in a desiccator over phosphorus pentoxide yielded monohydrates.

Found in Monohydrate (A): C, 21.99; H, 4.35; N, 19.22; Cl, 7.96; Co, 13.78; NH_3, 15.79%. Found in Monohydrate (C): C, 22.23; H, 4.31; N, 19.10; Cl, 7.98; Co, 13.10; NH_3, 15.60%. Calcd for $[CoC_8H_{17}N_5O_5]\cdot Cl\cdot NO_3\cdot H_2O$: C, 21.955; H, 4.375; N, 19.20; Cl, 8.10; Co, 13.47; NH_3, 15.55%.

Found in Trihydrate (A): C, 20.29; H, 4.41; N, 17.73%. Found in Trihydrate (C): C, 20.10; H, 4.10; N, 17.64%. Calcd for $[CoC_8H_{17}N_5O_5]\cdot Cl\cdot NO_3\cdot 3H_2O$: C, 20.28; H, 4.89; N, 17.74%.

Found in Monohydrate (E): C, 28.17; H, 4.42; N, 18.06; Cl, 7.35%. Calcd for $[CoC_{11}H_{19}N_5O_5]Cl\cdot NO_3\cdot H_2O$: C, 27.77; H, 4.45; N, 17.67; Cl, 7.45%.

5-Nitro-3-methylsalicylatotetraamminecobalt(IV) Dichloride (Abbreviated as B), 5-Nitro-4-methylsalicylatotetraamminecobalt(IV) Dichloride (Abbreviated as D) and 5-Nitrosalicylatobis(ethylenediamine)cobalt(IV) Dichloride (Abbreviated as F). Two grams of substance A, C or E was dissolved in 2 ml of 12 N hydrochloric acid, and the solution was filtered with a glass filter (G4). Acetone was added to the green solution, and the substance separated out was filtered with a glass filter (G3), washed with acetone and dried in a vacuum desiccator. It was reprecipitated from hydrochloric acid solution by addition of acetone. Yield 1.6 g.

When the product was dried in a desiccator over phosphorus pentoxide, dihydrates were formed. In the case of (B) and (D) drying in a silicagel desiccator produced trihydrates.

Found in Dihydrate (B): C, 22.71; H, 4.85; N, 16.37; Cl, 15.58; Co, 14.59%. Found in Dihydrate (D): C, 22.65; H, 4.42; N, 16.21; Cl, 15.67%. Calcd for $[CoC_8H_{17}N_5O_5]Cl_2\cdot 2H_2O$: C, 22.39; H, 4.93; N, 16.32; Cl, 16.52; Co, 13.75%.

Found in Trihydrate (B): C, 21.14; H, 5.06; N, 15.94%. Found in Trihydrate (D): C, 20.66; H, 5.29; N, 15.53%. Calcd for $[CoC_8H_{17}N_5O_5]Cl_2\cdot 3H_2O$: C, 21.49; H, 5.18; N, 15.66%.

Found in Dihydrate (F): C, 28.20; H, 4.97; N, 15.01; Cl, 15.20%. Calcd for $[CoC_{11}H_{19}N_5O_5]Cl_2\cdot 2H_2O$: C, 28.28; H, 4.96; N, 14.99; Cl, 15.18%.

Determination of Organic Ligands. In order to identify the organic ligand, 3 g of A or C was heated in 3 N potassium hydroxide at 60°C for 3 hr. The mixture was filtered and acidified with hydrochloric acid. The ligand acid thus isolated was extracted with ethylether, with subsequent evaporation, to yield the free acid; the acid from A was identified as 3-methyl-5-nitrosalicylic acid and that from C as 4-methyl-5-nitrosalicylic acid by melting point measurements.

Chromatography. In order to examine the purity of the substances, the samples dissolved in mixture solvents of water and acetone (1 : 3 by volume, pH=3 with hydrochloric acid) were chromatographed on acid alumina (Merck, Germany) or silica gel (Wako Pure Chemical Ind., Japan). Each sample was found to contain substantially a single species.

Physicochemical Measurements. The magnetic susceptibilities of the complexes were measured by the Gouy method with a magnetic balance (Shimadzu Seisaku Sho) in the temperature range between 80°K and room temperature.

The visible and ultraviolet absorption spectra were recorded with a recording spectrophotometer, Hitachi EPS-2.

The NMR spectra were recorded at 25+2°C with a Varian A-60-type instrument, and were quoted for a trifluoroacetic acid or deuterium oxide solution using tetramethylsilane as an external standard.

The electric conductivities of the aqueous solutions of the salts were determined by the use of a conductometer, CM-1DB, Toa Denpa Kogyo.

2) G. T. Morgan and J. D. M. Smith, *J. Chem. Soc.*, **1922**, 1956; *ibid.*, **1924**, 1924.

TABLE 1. PROPERTIES OF THE COBALT(IV) AMMINE COMPLEXES

	Magnetic moment μ_{eff}, (B.M.)	Equivalents of iodine liberated per formula weight	Electric conductivity of aqueous solution $\mho$/cm	Absorption bands in slightly acidic (H_2SO_4) solution mμ	ε
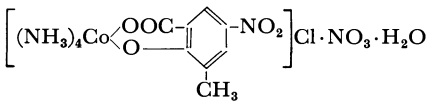 (A)	1.7	1.90	236.2	440 690	2000 6400
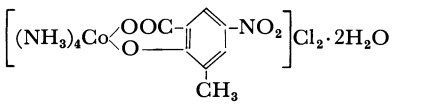 (B)	1.7	1.84		440 690	2100 6800
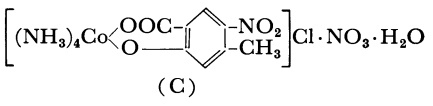 (C)	1.7	1.86	220	440 656	4000 6600
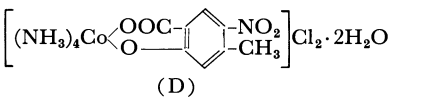 (D)	1.7	1.90		440 656	4300 7000
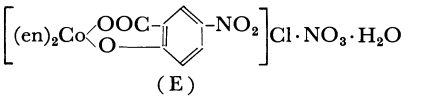 (E)	1.6	1.76		450 682	3200 10000
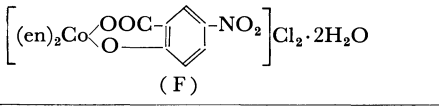 (F)	1.6	1.78		450 682	2800 9800

Result and Discussion

The Constitution of the Compounds. The constitution of each compound was inferred as in the previous study,[1] on the basis of elemental analyses, isolation of the ligand acid (*cf.* Experimental), iodometry, magnetic susceptibility, and the electric conductivity and the absorption spectrum of the aqueous solution. Some of these data are given in Table 1 and Fig. 1.

Recently, Garbett and Gillard[3] studied the reaction of salicylatobis(ethylenediamine)cobalt(III) complex with nitric acid. From the reaction mixture, they obtained a dark green weakly paramagnetic material which, however, they considered impure; they tentatively formulated it as [Co en_2(5-NO-salH)$(NO_3)_2 \cdot 4H_2O$, *i. e.* as a complex containing nitrososalicylate ligand. In its absorption spectrum they found strong absorption maxima at 375 mμ (ε=8700) and 682 mμ (ε=2640). Although the method of preparation of this green material is more or less analogous to the procedure of preparing green complex (E) of the present paper, the spectrum of E (Fig. 1, Table 1) was quite different from their spectra; it showed an absorption peak of much higher intensity (ε=10000) at 682 mμ and also a peak at 450 mμ (ε=3200), but only a very weak peak or a shoulder at 365—375 mμ which was barely perceptible under the strong absorption background (ε=3200) present in this range. It seems possible that the complex of Garbett and Gillard is different from that obtained in the present research. If, instead, their sample were to contain the same green complex as that obtained in the present research, their sample would contain less than 30% of the true green complex as judged from the absorptivity of the peak at 682 mμ. In this latter possibility the very high intensity of the peak at 375 mμ observed by these investigators might be explained as caused by contamination by [Co en_2-(5-NO_2-salH)]$(NO_3)_2 \cdot H_2O$ which ha san absorption peak of very high intensity at this wavelength (374 mμ, ε=21400).

Chromatography of the green complex obtained by the present authors has shown that the material is substantially pure and single. The success in obtaining comparatively pure materials may be due to the fact that all the compounds contained at least one outer chloride ion; complete removal of the chloride ion *e. g.* by use of silver nitrate has been

3) K. Garbett and R. D. Gillard, *Chem. Commun.*, **1967**, 694; *J. Chem. Soc., (A)*, **1968**, 979.

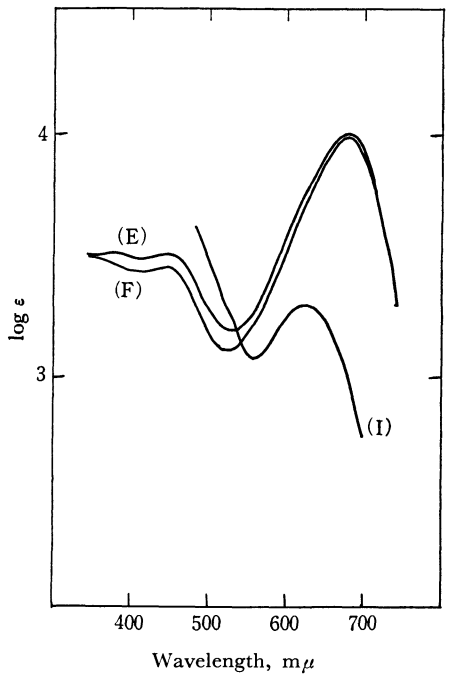

Fig. 1. Absorption spectra of complexes.

(E) $\left[(en)_2Co\langle^{OOC-}_{O}\rangle\!\!\bigcirc\!\!-NO_2\right]ClNO_3\cdot H_2O$

(F) $\left[(en)_2Co\langle^{OOC-}_{O}\rangle\!\!\bigcirc\!\!-NO_2\right]Cl_2\cdot 2H_2O$

(I) $\left[(en)_2Co\langle^{OOC-}_{O}\rangle\!\!\bigcirc\right]Cl\cdot 2H_2O$

found to make the complex very unstable.

In the present paper we shall continue to formulate the compounds as nitro compounds because the only experimental fact so far obtained about this problem was isolation of nitrosalicylic acid or nitrocresotic acid. Of course we can not deny the possibility that the ligand was initially nitroso compound which was oxidized during the treatment with alkalis; the final decision should await further experimental proofs.

There seems to be no ambiguity as to the fact that the formal oxidation state of cobalt is four, this, of course including the possibility that the complex ion as a whole is a free radical carrying one electron vacancy. This can be verified by the effective Bohr magneton number, the charge of +2 and the high oxidizing ability of the complex. Our sample tested neutral in freshly prepared aqueous solution, so that the formulation as the protonated ion is not acceptable.

The magnetic susceptibilities of the compounds obeyed the Curie-Weiss law down to liquid nitrogen temperatures. The effective magnetic moment μ_{eff} in Bohr magnetons (Table 1) was obtained using the formula, $\mu_{eff}=2.84\sqrt{\chi^{cor}_{mol}(T-\theta)}$ where χ^{cor}_{mol} was obtained by correcting the observed molar magnetic susceptibility χ_{mol} for the diamagnetic contribution of the molecule. A more detailed study on the magnetic susceptibilities will be reported elsewhere.

Solubilities. The cobalt(IV) ammine complexes obtained in the present study are soluble in water, dimethylsulfoxide, methanol, nitric acid, hydrochloric acid, trifluoroacetic acid and several acidic solvents, but insoluble in acetone, chloroform, benzene, acetonitrile and other organic solvents of similar nature.

On the other hand, the salts of tetraphenylboric acid, picric acid, 3,5-dinitrosalicylic acid or chloranilic acid are soluble in acetone, chloroform, benzene and similar organic solvents, but are almost insoluble in water.

Stability. The solution of 5-nitrosalicylato-(bisethylenediamine)cobalt(IV) complexes did not undergo any color change after 12 hr, but the solution of 5-nitrosalicylatotetraamminecobalt(IV) complex and its methyl derivatives changed from green to yellowish brown after several hours. The greater stability of the ethylenediamine complexes as compared with the corresponding ammine complexes as shown in this example could be explained in terms of the entropy effect.[4] Another such example is offered by a series of μ-peroxodicobaltammine and μ-peroxodicobalt ethylenediamine complexes, the latter being much more stable toward decomposition.

NMR Spectra. The NMR spectra of 5-nitrosalicylatobis(ethylenediamine)cobalt(IV) chloride

Table 2. The proton magnetic resonance of CH_2 or NH_2 in salicylatoammine cobalt(IV) complex (E)

	Methylene protons		Ammine protons	
	cps		cps	
			*trans**	*cis*
CF_3COOH	106.5	148.0	236.5	284.0
Number of proton	2H	6H	4H	4H
D_2O	121.4	157.4	d. a.	d. a.
Number of proton	2H	6H		

d. a.: Disapppeared signal

*: NMR studies on cobalt(III) ammine complex[5] indicate the proton magnetic resonance for ammonia trans to anion appears on strong field side. We assume that the relation holds in the present case also.

4) A. E. Martell and M. Calvin, "The Chemistry of Metal Chelate Compounds," Prentice-Hall, Inc., Englewood Cliffs, N. J. (1952), p. 149.

5) W. L. Jolly, A. D. Harris and T. S. Briggs, *Inorg. Chem.*, **4**, 1064 (1965).

nitrate were measured in trifluoroacetic acid or deuterium oxide. The spectra had signals at 106.5, 148.0, 236.6 and 284.0 cps for trifluoroacetic acid solution and at 121.4 and 157. 4 cps in the case of deuterium oxide solution (Table 2).

The authors wish to express their gratitude to Mr. Takuzo Fujino, Mr. Junichi Goda and Mr. Tsuneyo Shishido for the elemental analyses, and to Miss Yoshiko Kawashima for the NMR spectra.

BULLETIN OF THE CHEMICAL SOCIETY OF JAPAN VOL. 42 988—994 (1969)

Circular Dichroism of Chromium(III) Complexes. I. L-Tartrato Complexes. Their Stereospecific Formation and Spin-forbidden Absorption Bands

Sumio KAIZAKI, Jinsai HIDAKA and Yoichi SHIMURA

Department of Chemistry, Faculty of Science, Osaka University, Toyonaka, Osaka

(Received August 5, 1968)

Two novel mixed chromium(III) complexes containing L-tartrates and 2,2'-dipyridyl or 1,10-phenanthroline have been prepared, and their electronic absorption and circular dichroism spectra and the rotatory dispersion have been measured in the region of near-infrared to ultraviolet. From the construction of molecular models and from the comparison of the CD bands of the present complexes with those of the resolved oxalato complexes, $(-)_{546}$-$K[Cr(ox)_2(dip)]\cdot 3H_2O$ and $(-)_{546}$-$K[Cr(ox)_2(phen)]\cdot 4H_2O$, it has been concluded that the present complexes have a binuclear structure in which two Cr(III) ions are bridged by two tetradentate L-tartrato ligands and that the absolute configuration of the binuclear complexes is $\Lambda(C_2)$-$\Lambda(C_2)$. Their formation is completely stereospecific and their formulae are represented by $Ba[Cr_2(L\text{-}tart_2H)(dip)_2]_2\cdot 9H_2O$ and $NH_4[Cr_2(L\text{-}tart_2H)(phen)_2]\cdot 6.5H_2O$. The absolute configurations of several complexes which commonly belong to a general type, *cis*-$[Cr(O)_4(N)_2]$ have been determined on the basis of circular dichroism studies of the present binuclear complexes. The circular dichroism in the spin-forbidden absorption band region have also been measured and discussed.

Much evidence has been obtained for the fact that an octahedral metal complex with two or three optically active bidentate ligands has been often stereospecifically formed or isolated; namely, only a limited number of its configurationally optically active isomers has been preferentially formed or isolated.[1] Naturally occuring L-tartrate is one of such bidentate ligands. A definite but not so marked stereospecific formation has been reported in a complex containing one L-tartrate($C_4H_4O_6^{2-}$) and two ethylenediamine ligands.[2] Moreover it is well known that L-tartrate forms various kinds of transition metal complexes which show the so-called anomalous rotatory dispersion in the visible region; most famous and historically important of these is believed to be the tris(L-tartrato)chromium(III) complex,[3] on which the so-called Cotton effect was first observed in 1896 by Cotton.[4] Recently, McCaffery and Mason[5] have shown from their studies using circular dichroism (CD) and rotatory dispersion (RD) techniques that one of the two possible configurationally optically active isomers has been produced in a solution of chromium(III) in 4M potassium L-tartrate at pH 12. That is, the stereospecificity is complete in this tris(L-tartrato) case. In the complexes mentioned above, the L-tartrate ligand is thought to be coordinated as a bidentate ligand, being free from the coordination of two of its four donor groups. Of course, no mononuclear complex which contains a tartrate ion as a tetradentate ligand seems to exist owing to its steric requirement. It has been shown by some X-ray analyses, however, that the tetradentate tartrato ligands exist in some binuclear complexes.[6,7] These binuclear complexes have a

1) F. P. Dwyer, F. L. Garvan and A. Schulman, *J. Am. Chem. Soc.* **81**, 290 (1959); R. G. Denning and T. S. Piper, *Inorg. Chem.*, **5**, 1056 (1966).

2) H. B. Jonassen, J. C. Bailar, Jr., and E. H. Huffman, *J. Am. Chem. Soc.*, **70**, 756 (1948).

3) J.-P. Mathieu, *Ann. Phys.*, [11] **3**, 371 (1935).

4) A. Cotton, *Ann. Chim. Phys.*, [7] **8**, 347 (1896).

5) A. J. McCaffery and S. F. Mason, *Trans. Farad. Soc.*, **59**, 1 (1963).

6) J. G. Forrest and C. K. Prout, *J. Chem. Soc., (A)*, **1967**, 1312; R. E. Tapscott, R. L. Belford and I. C. Paul, *Inorg. Chem.*, **7**, 356 (1968).

7) G. A. Kiosse, N. I. Golovastikov and N. V. Belov, *Soviet Phys. Dokl.*, **9**, 198 (1964); G. A. Kiosse, N. L. Golovastikov, A. V. Ablov and N. V. Belov, *Dokl. Akad. Nauk SSSR*, **177**, 329 (1967); D. H. Templeton, A. Zalkin and T. Ueki, *Acta Cryst.*, **21**, A 154 (1966).

structure in which two five-coordinate metal ions, *i.e.*, antimony(III) or vanadium(IV), are bridged by two tetranegative tartrate anions.

In the persent paper, two new examples of such binuclear complexes will be reported, in which the two central metal ions have octahedral coordination. These are chromium(III) complexes of L-tartrate ($C_4H_2O_6^{4-}$ = tart) and 2,2'-dipyridyl (=dip) or 1,10-phenanthroline (=phen), namely, $Ba[Cr_2(L\text{-}tart_2H)(dip)_2]_2\cdot 9H_2O$ and $NH_4[Cr_2(L\text{-}tart_2H)(phen)_2]\cdot 6.5H_2O$. A preliminary short communication[8] has already been reported for the stereospecific formation of these complexes. The electronic absorption, and CD spectra and RD of these binuclear complexes will be discussed in comparison with those of the corresponding mononuclear complexes, $(-)_{546}$-$K[Cr(ox)_2(dip)]\cdot 3H_2O$ and $(-)_{546}$-$K[Cr(ox)_2(phen)]\cdot 4H_2O$.

Experimental

Preparation. 1) $Ba[Cr_2(L\text{-}tart_2H)(dip)_2]_2\cdot 9H_2O$: To a solution containing 2.3 g of sodium L-tartrate dihydrate ($L\text{-}Na_2H_2tart\cdot 2H_2O$) in 30 m*l* of a boiling dmf water*1 mixture (1 : 1), 3.88 g of $[CrCl_3(dmf)(dip)]$ was added. The reaction mixture was heated at about 120°C for a few minutes in an oil bath. After the color of the solution changed to dark red, the resulting solution was filtered and 1.2 g of $BaCl_2\cdot 2H_2O$ was added to the filtrate. When the solution was cooled in an ice bath, the desired dark crystals began to separate. The crude product was recrystallized from hot water. The pure crystals were filtered off and washed with a little ice water, ethanol and then with ether.

Found: C, 43.51; H, 3.03; N, 7.33; Ba, 9.98%*2. Calcd for $C_{56}H_{42}N_8O_{24}BaCr_4 = Ba[Cr_2(L\text{-}tart_2H)(dip)_2]_2$: C, 43.21; H, 2.73; N, 7.20; Ba, 8.83%. Found: H_2O, 9.24%. Calcd for $Ba[Cr_2(L\text{-}tart_2H)(dip)_2]_2\cdot 9H_2O$: 9.44%.

2) $NH_4[Cr_2(L\text{-}tart_2H)(phen)_2]\cdot 6.5H_2O$: A solution containing 7.7 g of $[CrCl_3(dmf)(phen)]$ and 3.45 g of ammonium L-tartrate ($L\text{-}(NH_4)_2H_2tart$) in 50 m*l* of a dmf-water mixture (1 : 1) was heated at about 120°C in an oil bath for a few minutes, while the color of the solution changed to dark red and the brown complex began to precipitate. It was allowed to stand at room temperature. The product was filtered off, and recrystallized from a hot dmf-water mixture (1 : 1). The pure crystals obtained were washed with a dmf-water mixture, ethanol and then with ether. This complex is sparingly soluble in water, but soluble in a dmf-water mixture (1 : 1).

Found: C, 49.26; H, 3.41; N, 8.46%. Calcd for $C_{32}H_{25}N_5O_{12}Cr_2$: C, 49.55; H, 3.26; N, 9.03%. Found: H_2O, 13.38%. Calcd for the 6.5 hydrate: H_2O, 13.09%.

3) $[CrCl_3(dmf)(dip)]$: This starting complex was prepared by Dwyer's method.[9] The hygroscopic anhydrous chromium(III) chloride, which was used instead of sublimated chromium(III) chloride, was completely dissolved in dry dmf without a trace of zinc dust.[10] To a hot solution of 5 g of chromium(III) chloride in 50 m*l* of dry dmf was added 5 g of 2,2'-dipyridyl. After refluxing the resulting solution for a few minutes, the greenish material began to separate. The reaction mixture was allowed to cool to room temperature. The product was filtered off and washed with cold dmf and then with ether.

4) $[CrCl_3(dmf)(phen)]$: This complex was obtained by the same method as that used for the 2,2'-dipyridyl complex, using 1,10-phenanthroline instead of 2,2'-dipyridyl.

5) $K[Cr(ox)_2(dip)]\cdot 3H_2O$ and $K[Cr(ox)_2(phen)]\cdot 4H_2O$: The preparation and optical resolution of these complexes were carried out by Broomhead's method.[11] The electronic absorption and rotatory dispersion of these complexes obtained coincided with those reported by Bürer.[12]

6) $K[Cr(ox)_2(en)]\cdot 2H_2O$: This was prepared by Werner's method,[13] and resolved by the method of Bushra and Johnson.[14]

Measurements. The electronic absorption spectra Were measured by a Beckman DU spectrophotometer. The CD spectra were recorded with a Roussel-Jouan dichrographe, while the RD curves were obtained with a Yanagimoto Recording spectropolarimeter model-185. The solvent employed for $(-)_{546}$-$K[Cr(ox)_2(dip)]\cdot 3H_2O$, $Ba[Cr_2(L\text{-}tart_2H)(dip)_2]_2\cdot 9H_2O$ and $(+)_{546}$-$K[Cr(ox)_2(en)]\cdot 2H_2O$ was water, and for $(-)_{546}$-$K[Cr(ox)_2(phen)]\cdot 4H_2O$ and $NH_4[Cr_2(L\text{-}tart_2H)(phen)_2]\cdot 6.5H_2O$ a dmf-water mixture (1 : 1). Because the oxalato complexes racemize at moderate rates in aqueous solutions,[11] the measurement for these complexes were made as rapidly as possible using solutions freshly prepared in turn.

Results and Discussion

Spectra of the Visible and Ultraviolet Region. The absorption and CD spectra, and RD of the complexes studied are shown in Figs. 1, 2, 4 and 5, and their characteristics are summarized in Table 1. The data of $(-)_{546}$-$K[Cr(ox)_2(phen)]\cdot 4H_2O$ and of $NH_4[Cr_2(L\text{-}tart_2H)(phen)_2]\cdot 6.5H_2O$ were obtained in a dmf-water mixture (1 : 1), since the L-tartrato complex is sparingly soluble in water. From a comparison of the absorption and CD spectra of $(-)_{546}$-$K[Cr(ox)_2(phen)]\cdot 4H_2O$ in water and in a dmf-water mixture (1 : 1), it was confirmed that the solvent dependence of the spectra of the 1,10-phenanthroline complex is negligibly small.

8) S. Kaizaki, J. Hidaka and Y. Shimura, This Bulletin, **40**, 2207 (1967).

*1 The abbreviation, dmf, represents dimethylformamide.

*2 The content of Ba was determined semi-quantitatively by flame spectrophotometry.

9) F. P. Dwyer and J. A. Broomhead, *Austral. J. Chem.*, **14**, 250 (1961).

10) A. R. Pray, *Inorg. Synth.*, **5**, 153 (1957).

11) J. A. Broomhead, *Austral. J. Chem.*, **15**, 228 (1962).

12) Th. Bürer, *Helv. Chim. Acta*, **46**, 242 (1963).

13) A. Werner, *Ann.*, **406**, 286 (1914).

14) E. Bushra and C. H. Johnson, *J. Chem. Soc.*, **1939**, 1937.

TABLE 1. ABSORPTION (AB) AND CD MAXIMUM DATA OF *cis*-$[Cr(O)_4(N)_2]$ TYPE COMPLEXES
(The wave numbers are given in $10^3\,cm^{-1}$)

K[Cr(ox)$_2$(dip)]		Ba[Cr$_2$(L-tart$_2$H)(dip)$_2$]$_2$*	
AB (log ε_{max})	CD ($\Delta\varepsilon_{ext}$) of $(-)_{546}$-isomer	AB (log ε_{max})	CD ($\Delta\varepsilon_{ext}$)
13.9 ($\bar{1}$.84)	13.8 ($<-0.004_5$)		
ca. 14.4 ($\bar{1}$.80)	14.3 ($>+0.005_4$)		
	14.5 ($>+0.006_6$)		
ca. 14.7 (0.06)	14.8 ($<-0.001_7$)		
	17.0 ($>+0.12$)		15.7 (+0.14)
18.3 (1.87)	19.5 (<-2.22)	18.3 (2.09)	18.3 (−5.10)
ca. 22.5 (1.63)		*ca.* 22.7 (2.10)	
ca. 24.2 (2.10)		*ca.* 24.4 (2.36)	
25.6 (2.21)	25.3 ($>+0.53$)	*ca.* 25.7 (2.50)	25.1 (+0.95)
			28.5 (−0.78)
32.9 (4.01)		33.1 (4.29)	33.6 (+15.0)

K[Cr(ox)$_2$(phen)]		NH_4[Cr$_2$(L-tart$_2$H)(phen)$_2$]	
AB (log ε_{max})	CD ($\Delta\varepsilon_{ext}$) of $(-)_{546}$-isomer	AB (log ε_{max})	CD ($\Delta\varepsilon_{ext}$)
14.1 (0.42)	13.9 ($<-0.03_2$)		
	14.4 ($>+0.003$)		
ca. 14.7 (0.5)	14.7 ($<-0.02_7$)		
	16.4 ($>+0.13$)		15.5 (+0.15)
18.5 (1.89)	19.0 (<-2.46)	18.3 (2.16)	18.3 (−8.11)
24.8 (2.12)	25.6 ($>+0.44$)	24.7 (2.56)	24.5 (+1.21)
28.8 (2.89)		28.0 (3.20)	28.3 (−1.20)
ca. 30.0 (3.10)		*ca.* 30.3 (3.48)	
33.4 (3.90)		33.6 (4.29)	33.6 (+6.00)
36.1 (4.43)		36.0 (4.74)	37.3 (+41.8)

K[Cr(ox)$_2$(en)]	
AB (log ε_{max})	CD ($\Delta\varepsilon_{ext}$) of $(+)_{546}$-isomer
14.5 (0.19)	14.5 ($>+0.007_5$)
ca. 14.9 (0.2)	14.9 ($<-0.010_3$)
	15.3 ($>+0.011_3$)
	16.8 (<-0.05)
18.8 (1.96)	19.4 ($>+2.00$)
25.3 (2.00)	25.3 (<-0.35)

* The intensities are given per one complex ion, *i.e.*, per two chromium(III) ions.

The absorption curves of the L-tartrato and oxalato complexes resemble each other on the whole. It is possible to point out that the new L-tartrato complexes have a geometrical structure similar to that of $[Cr(ox)_2(dip)]^-$ and $[Cr(ox)_2(phen)]^-$. As may be seen in Fig. 1 and Table 1, the 2, 2'-dipyridyl complexes show three narrow inflections in the second spin-allowed absorption band region. In the corresponding region, a few small inversive dispersions are also observed.

The CD spectra and RD of the oxalato and L-tartrato complexes are also similar to each other (Figs. 1 and 2). That is, both the complexes show two CD bands, one positive at about 600 mμ and the other negative at about 520 mμ, in the first spin-allowed d→d absorption band region, and a weak positive CD band (at about 400 mμ) in the second spin-allowed d→d absorption band region. The CD band of the L-tartrato complexes are shifted to longer wavelengths than those of the oxalato complexes in the first spin-allowed absorption band region. Furthermore, the negative CD bands of these complexes are much higher in intensity than the positive one. These facts resemble those of the optically active tris(oxalato) and tris(L-tartrato) chromium(III) complexes in the corresponding region.[5] Assuming that the complexes employed here belong to pseudo D_3 symmetry, the negative CD bands are assigned to the $^4A_2 \rightarrow {}^4E_a$ transition and the positive ones to the $^4A_2 \rightarrow {}^4A_1$ transition as in $(-)_{546}$-[Cr-

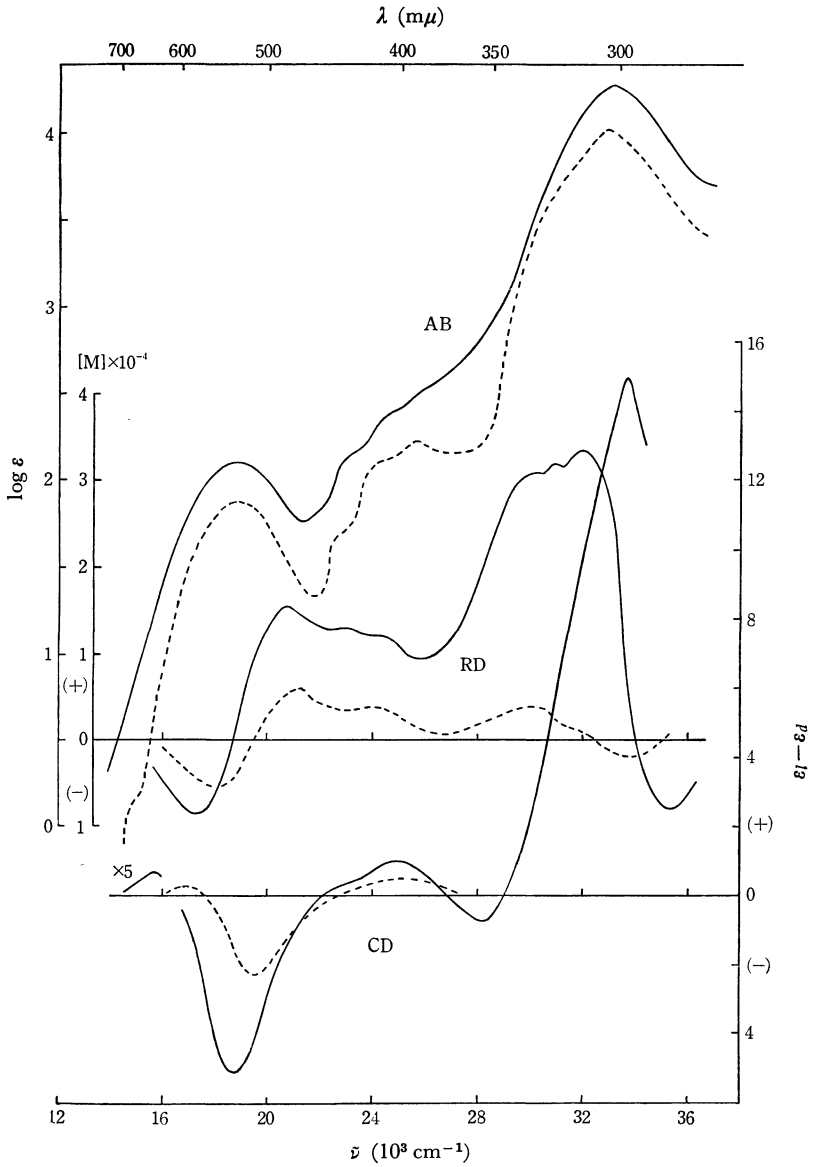

Fig. 1. Absorption (AB), CD and RD curves of, —— $[Cr_2(L\text{-}tart_2H)(dip)_2]^-$ and ---- $(-)_{546}$-$[Cr(ox)_2(dip)]^-$. (AB curves of mononuclear complex was measured for the racemic one.)

$(ox)_3]^{3-}$.[5,15]

From a comparison with the data for the other complexes containing 2,2′-dipyridyl or 1,10-phenanthroline,[16,17] the intense absorption bands at about 300 mμ are assigned to the $\pi \rightarrow \pi^*$ transition originating from the coordinated 2,2′-dipyridyl or 1,10-phenanthroline ligand (Figs. 1 and 2).

Stereospecificity of the L-Tartrato Complexes. The L-tartrato complexes obtained by the reaction of $[CrCl_3(dmf)(dip)]$ or $[CrCl_3(dmf)(phen)]$ with L-tartrate have rather complicated formulae, but the similarity between these complexes and the oxalato complexes are evident. An L-tartrate ion can not span four coordination sites around one metal ion, and the elemental analysis data exclude any possibilities of mononuclear structures for these L-tartrato complexes. It is clear that the optical activity of the L-tartrato complexes is due to a kind of configurational dissymmetry rather

15) A. J. McCaffery, S. F. Mason and R. E. Ballard, *J. Chem. Soc.*, **1965**, 2883.

16) N. Matsuoka, Y. Shimura and R. Tsuchida, *Nippon Kagaku Zasshi (J. Chem. Soc. Japan, Pure Chem. Sect.)*, **82**, 1637 (1961).

17) J. Hidaka and B. E. Douglas, *Inorg. Chem.*, **3**, 1180 (1964).

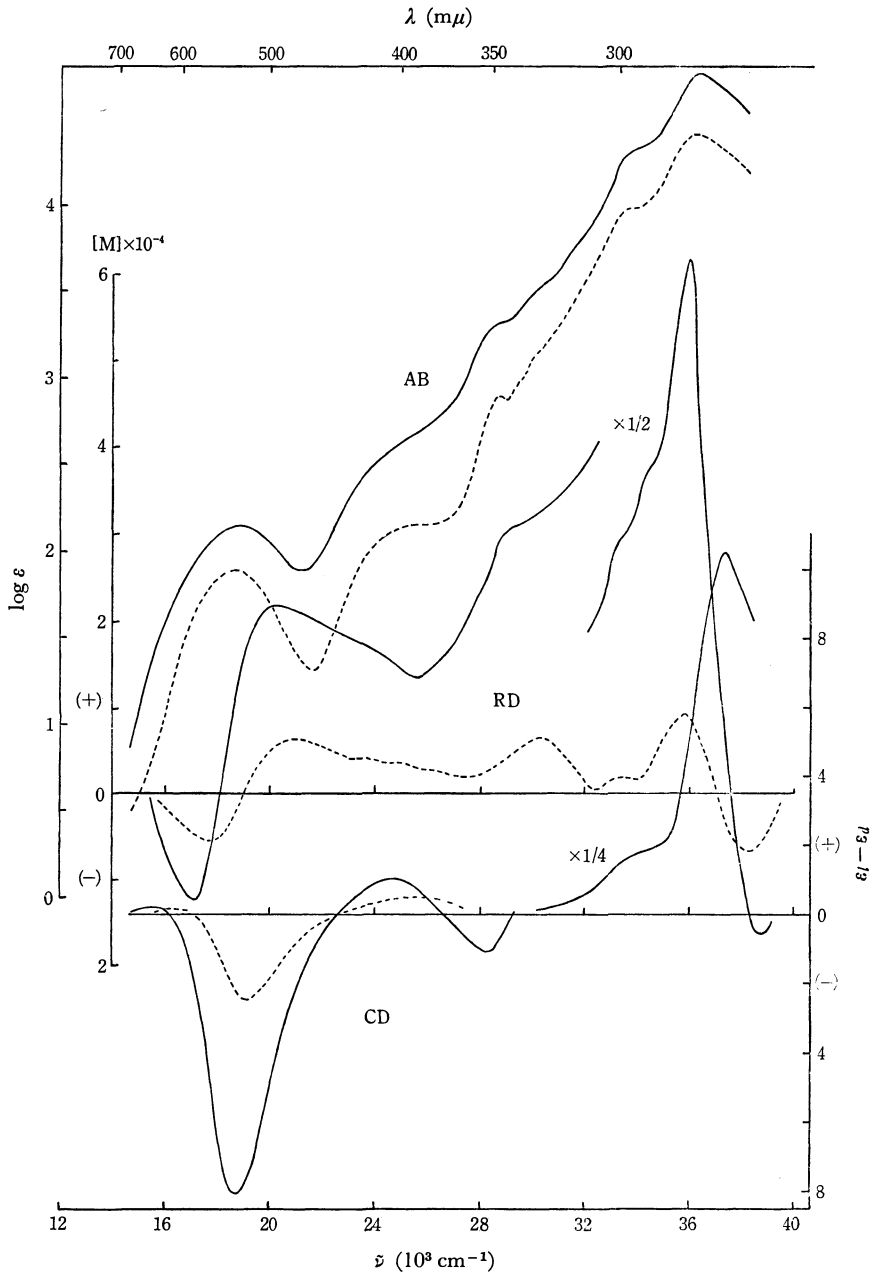

Fig. 2. Absorption (AB), CD and RD curves of, —— $[Cr_2(L\text{-}tart_2H)(phen)_2]^-$, and ---- $(-)_{546}$-$[Cr(ox)_2(phen)]^-$. (AB curve of the mononuclear complex was measured for the racemic one.)

than vicinal contribution of the coordinated L-tartrate ions from following reasons. Firstly, the absorption spectrum, CD and RD of the L-tartrato complexes in the visible region, if calculated per Cr(III) ion, have just the same or stronger intensities than those of the corresponding oxalato complexes. It has been known that the oxalato complexes easily racemize in aqueous solutions with half-lives of about 50 min.[11] On the other hand, the L-tartrato complexes do not racemize at all. Secondly, according to the construction of molecular models, the most probable structure for the experimental formula obtained is a binuclear one in which two chromium (III) ions are bridged by two tetradentate L-tartrate ions, as may be seen in Fig. 3. In this structure, the stereospecificity due to the two dissymmetric ligands is perfect; namely, as far as the L-tartrate is used, the binuclear complex which has an absolute configuration $\Lambda(C_2)$-$\Lambda(C_2)$ about the two tris-chelate type octahedra is the only one possible to be con-

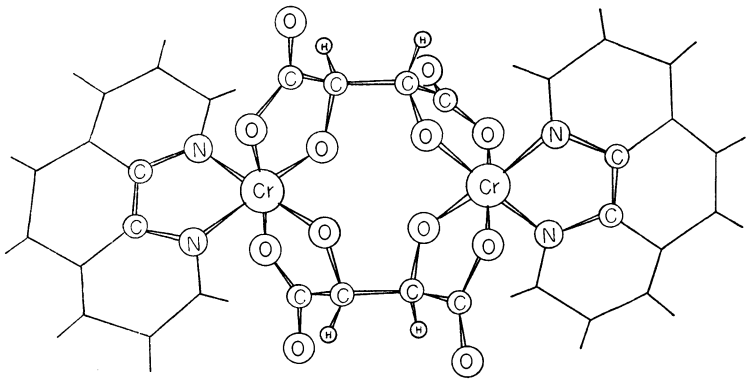

Fig. 3. Proposed structure of the L-tartrato phenanthroline complex (one proton not shown).

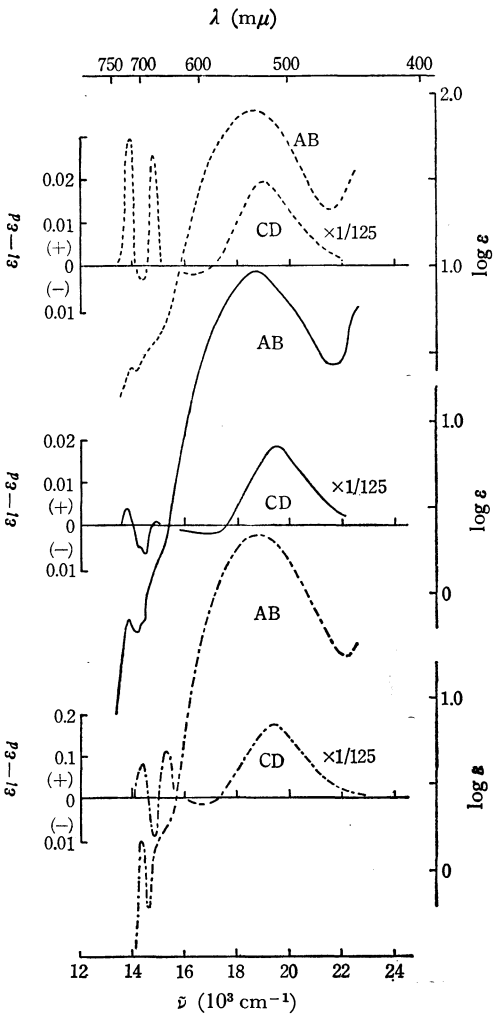

Fig. 4. Absorption (AB) and CD curves of
---- (+)$_{546}$-[Cr(ox)$_2$(phen)]$^-$,
—— (+)$_{546}$-[Cr(ox)$_2$(dip)]$^-$,
·—· (+)$_{546}$-[Cr(ox)$_2$(en)]$^-$.

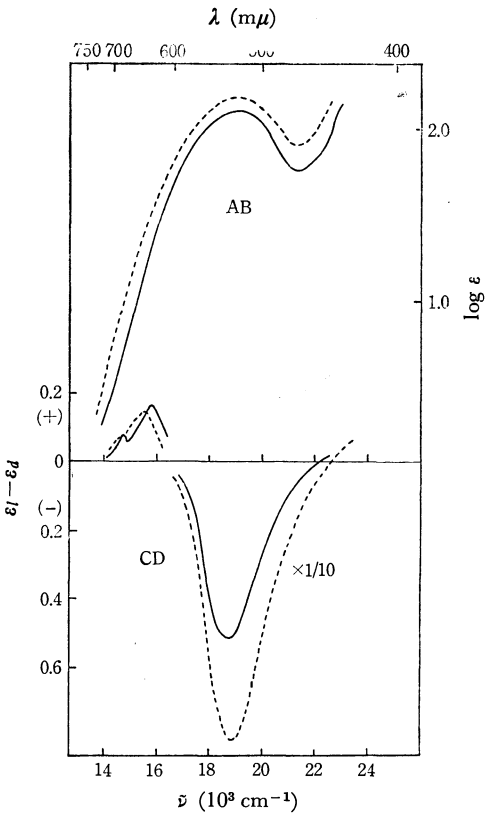

Fig. 5. Absorption (AB) and CD curves of
---- [Cr$_2$(L-tart$_2$H)(phen)$_2$]$^-$,
—— [Cr$_2$(L-tart$_2$H)(dip)$_2$]$^-$.

structed. A similar structure has been revealed for the vanadyl tartrato complexes by the X-ray analyses.[6] In the vanadyl tartrato complexes, the tartrates are tetranegative and tetradentate ligands. On the contrary, it seems likely that in the present chromium(III) complexes, one proton remains undissociated per two tetranegative L-tartrates. Nevertheless, all the L-tartrates seems to be acting as tetradentate ligands. A question remains to be answered about the exact position of this proton or

its role in the binuclear structure.

On the basis that the L-tartrato complexes have the absolute configuration $\Lambda(C_2)$-$\Lambda(C_2)$, it is possible to determine the absolute configurations of the mononuclear complexes which belong to a general type, *cis*-$[Cr(O)_4(N)_2]$, because the similarity of the CD or RD curves between the L-tartrato and the oxalato complexes is quite good. Namely, it can be concluded that $(-)_{546}$-$K[Cr(ox)_2(dip)]\cdot 3H_2O$ and $(+)_{546}$-$K[Cr(ox)_2(phen)]\cdot 4H_2O$, both of which were obtained from the less soluble diastereomers with $(-)_{546}$-$[Co(ox)(en)_2]^+$, have the $\Lambda(C_2)$ and $\Delta(C_2)$ configurations respectively, and that the ethylenediamine complex, $(+)_{546}$-$K[Cr(ox)_2(en)]\cdot 2H_2O$, forming the less soluble diastereomer with brucinium ion, has the $\Delta(C_2)$ configuration.

The $\Lambda(C_2)$ isomers of both the 2,2'-dipyridyl and 1,10-phenanthroline complexes, including the present binuclear complexes show a positive CD band in their ligand $\pi\rightarrow\pi^*$ absorption band region (280—300 mμ). This is also true for another mono-phen-Co(III) complex, $(-)_{546}$-$[Co(en)_2(phen)]I_3$, which shows an intense positive CD band at about 280 mμ and a negative CD band in its first d→d absorption band region.[17]

Spin-forbidden Bands. A few reports have been made on the CD or RD in the region of the spin-forbidden absorption bands of chromium(III) complexes. Kling and Woldbye[18] measured the RD of $(+)_{546}$-$[Cr(en)_3](ClO_4)_3$ and $(+)_{546}$-$[Cr(tn)_3]Cl_3$ in their spin-forbidden bands, and found many sharp inversive dispersions superimposed with each other. McCaffery and Mason[5] measured the CD of tris(L-tartrato)chromium(III) ion in the corresponding region and found a CD band of weak intensity. As may be seen in Figs. 4 and 5, all of the oxalato complexes, $(+)_{546}$-$K[Cr(ox)_2(dip)]\cdot 3H_2O$, $(+)_{546}$-$K[Cr(ox)_2(phen)]\cdot 4H_2O$, and $(+)_{546}$-$K[Cr(ox)_2(en)]\cdot 2H_2O$, show a group of weak CD bands in the spin-forbidden absorption bands. The L-tartrato complexes, $Ba[Cr_2(L\text{-}tart_2H)(dip)_2]_2\cdot 9H_2O$ and $NH_4[Cr_2(L\text{-}tart_2H)(phen)_2]\cdot 6.5H_2O$, also show an apparently positive weak CD band (at about 690 mμ) superposed on the positive CD component (at about 640 mμ) of the first spin-allowed absorption band. Each of the oxalato complexes with the $\Delta(C_2)$ configuration shows three sharp CD peaks, (+), (−), (+) listing from the side of the long wavelengths, though the negative CD peak (at about 690 mμ) of $(+)_{546}$-$K[Cr(ox)_2(dip)]$ splits into two components. The CD intensities of the spin-forbidden bands are one over a few hundred as weak as those of the spin-allowed ones.

The spin-forbidden d→d transition bands which appear in the longer wavelength region than the spin-allowed transition bands should be assigned to the $^4A_{2g}\rightarrow{}^2E_g$ and $^4A_{2g}\rightarrow{}^2T_{1g}$ in a complex of octahedral symmetry. But it seems that the exact assignments of these bands of various chromium(III) complexes are still difficult.[19] The CD band which appears at longest wavelengths for the present complexes may be assigned to the $^4A_{2g}\rightarrow{}^2E_g$ transition under O_h symmetry. In D_3 symmetry, the T_{1g} state breaks down into the E and A_2 states and the E_g state remains as the E state. Since these spin-forbidden transitions acquire their rotational strengths only by borrowing the electric and magnetic moments from the upper quartet state of the same symmetry,[20] the spin-forbidden transitions must have the same sign of the CD bands with that of the spin-allowed transition to the state with the same symmetry. Now, assuming that the present complexes belong to pseudo D_3 symmetry, two positive CD bands of their $(+)_{546}$-isomers may be assigned to the ^2E state and the negative one to the $^2A_2$ state, because the ^4E_a components of the first spin-allowed bands of these complexes have the positive CD sign. However, from the fact that the negative orbitally nondegenerate $^2A_2$ state of $(+)_{546}$-$K[Cr(ox)_2(dip)]$ splits into two CD components, it seems likely that the spin-orbit coupling or vibrational structures must be taken into consideration.

18) O. Kling and F. Woldbye, *Acta Chem. Scand.*, **15**, 704 (1961).

19) H. L. Schläfer, *Z. Phys. Chem. N. F.*, **11**, 65 (1957). C. J. Ballhausen, "Introduction to Ligand Field Theory," McGraw-Hill Book Company, Inc., New York (1962), p. 236.

20) S. F. Mason, *Quart. Rev.*, **27**, 20 (1963).

BULLETIN OF THE CHEMICAL SOCIETY OF JAPAN VOL. 42 995—999 (1969)

The Synergistic Effect in Solvent Extraction. The Effect of the Chelating Ligands on the Stability Constant of Lutetium β-Diketonate Adducts with TOPO

Takaharu HONJYO

Institute for Chemical Research, Kyoto University, Uji, Kyoto

(Received August 7, 1968)

The steric effect and the inductive effect of the functional groups of β-diketones on the adduct formation between lutetium chelates and TOPO in benzene was studied by using various β-diketones with aliphatic groups (acetylacetone, dipropionylmethane, pivaroylacetone, diisobutyrylmethane and dipivaroylmethane), aromatic groups (benzoylacetone, naphthoylacetone and dibenzoylmethane) and fluoromethyl groups (trifluoroacetylacetone, furoyltrifluoroacetone, thenoyltrifluoroacetone, benzoyltrifluoroacetone and hexafluoroacetylacetone). The effect of the temperature on the adduct formation was then estimated. These results may be summarized as follows: (1) The stability of the adduct increases, and the larger synergism appears, as aliphatic groups, aromatic groups, and fluoromethyl groups are successively substituted for the functional groups of β-diketones. This effect may be due to the electron-withdrawing effect of the fluoromethyl group and the conjugation effect (with a metal chelate ring) of the phenyl group. (2) The adducts contain one molecule of TOPO per metal chelate except for the HFA adduct, which contains two molecules of TOPO. The steric hindrance of the terminal groups is hardly recognizable. (3) The extraction constant of the chelates increases, while the stability of the adducts decreases, with a rise in the temperature. The apparent enthalpy change ($-\Delta H$ kcal/mol) upon the adduct formation increases in the order: DPM (5.5)<BzA(5.9)<BFA(8.6) chelates.

During the course of the solvent extraction of metal chelates, an extremely enhanced extraction is often observed in the presence of some neutral Lewis bases. This phenomenon is generally called the synergistic effect and explained by the adduct formation between the metal chelates and the Lewis bases.

The synergism in the extraction of rare earth β-diketonate has been widely investigated;[1-4] solid adducts have been prepared and their properties studied.[5,6] However, the mechanism of the adduct formation and the nature of the metal chelate adducts are not yet completely understood.

Shigematsu and his co-workers have carried out a systematic study of the synergistic extraction of rare earth metals,[7,8] and the following results have been obtained.

(1) In rare earth-benzoyltrifluoroacetone(BFA)-TOPO, TBP and *n*-hexanol systems, the extraction constant of the chelates increases, while the stability of the adducts decreases, with a decrease in the ionic size of the metal. The tendency has also been reported for lanthanum, europium, lutetium-TTA-dimethylsulfoxide, TBP, and hexone systems.[9]

(2) Oxygen-containing Lewis bases, having a stronger donating power of lone-pair electrons, form more stable adducts and therefore show a larger synergism; esters and ketones<alcohols<TBP<TOPO. Organic phosphate and phosphine oxide especially give rise to a large synergism.

(3) Nitrogen-containing Lewis bases, such as amines and heterocyclic compounds, also produce the synergism. The synergistic enhancement of the extraction is of almost the same magnitude as that of oxygen-containing Lewis bases: The effect of the amines is similar to that of alcohols. However, the solid adducts of the former are thermally more stable than the adducts of the latter.

1) H. Irving and D. N. Edgington, *J. Inorg. Nucl. Chem.*, **21**, 169 (1961).
2) T. V. Healy, *ibid.*, **19**, 314 (1961); *ibid.*, **19**, 328 (1961).
3) T. Sekine and M. Ono, This Bulletin, **38**, 2087 (1965).
4) H. Yoshida, *ibid.*, **39**, 1810 (1966).
5) T. V. Healy and J. R. Ferraro, *J. Inorg. Nucl. Chem.*, **24**, 1449 (1962).
6) J. R. Ferraro and T. V. Healy, *ibid.*, **24**, 1463 (1962).
7) T. Shigematsu, M. Tabushi, M. Matsui and T. Honjyo, This Bulletin, **39**, 165 (1966); *ibid.*, **40**, 2807 (1967).
8) T. Shigematsu and T. Honjyo, *Bull. Inst. Chem. Res., Kyoto Univ.*, **25**, 282 (1967).
9) T. Sekine and D. Dyrssen, *J. Inorg. Nucl. Chem.*, **29**, 1481 (1967).

(4) The maximum number of base molecules bound to one molecule of the metal chelate is 2 except in the case of lutetium β-diketonates-TOPO in benzene, where only one molecule of TOPO binds one molecule of the chelates.

In order to obtain more detailed information on this interesting phenomenon, the present research studied the steric effect and the inductive effect of the functional groups of various β-diketones on the adduct formation between lutetium chelates and TOPO.

Experimental

Materials. The radioisotope of lutetium-177 was produced by irradiating pure lutetium oxide in a thermal neutron flux of about 5×10^{12} n/cm²sec in the Research Reactor of Kyoto University. After the irradiated sample had been dissolved in hot hydrochloric acid, the lutetium was extracted at pH 5 with 0.05 M BFA in benzene and stripped into 0.1 M perchloric acid. The resulting solution was evaporated to fumes, and then the residue was dissolved in an appropriate amount of perchloric acid to make a stock solution. The specific activity of the tracer was sufficiently high for this investigation. The sodium perchlorate was prepared from perchloric acid and sodium carbonate and purified by recrystallization from water.

Some substituted β-diketones were synthesized by the acylation of methylketone with aromatic- or aliphatic ethylester in the presence of sodium amide as the base catalyzer.[10] The boiling points and the melting point of these β-diketones were as follows:

Prepared β-diketones

β-Diketones	Bp(°C/mmHg)	Mp(°C)
DPM (dipropionylmethane)	77 — 78/30	—
DIBM (diisobutyrylmethane)	80.5— 81.5/17	—
PvA (pivaroylacetone)	66 — 67/17	—
NtA (naphthoylacetone)	—	79

The other β-diketones, AA (acetylacetone), BzA (benzoylacetone), DBM (dibenzoylmethane), TAA (trifluoroacetylacetone), BFA (benzoyltrifluoroacetone), TTA (thenoyltrifluoroacetone), FTA (furoyltrifluoroacetone), HFA (hexafluoroacetylacetone), DPvM (dipivaroylmethane), and TOPO (tri-*n*-octylphosphine oxide), were obtained from the Dojindo Co. and the Tokyo Kasei Kogyo Co.

Procedure. The experimental procedure was almost the same as has previously been described.[7] To 5 m*l* of an aqueous solution containing lutetium (a few ppm), sodium perchlorate (0.1 M) and acetic acid (0.01 M) and having a desirable pH, 5 m*l* of benzene containing β-diketone (0.05 M or 0.1 M) and various amounts of TOPO were added. Both phases were placed in a 30 m*l* glass-stoppered centrifuge tube and agitated by a mechanical shaker for from one to three hours at a constant temperature in an electric thermostat (−5—30±0.05°C). After centrifugation, 2 m*l* of each phase were pipetted into test tubes (14 mm in diameter), and the γ-radioactivities were measured with a NaI(Tl) well-type scintillation counter. The pH value of the aqueous layers was checked after the extraction.

The extraction constants of the metal chelates, K, and the stability constants of the metal chelate adducts, β_n, can be calculated by the following equations*1:

$$K = [MR_3]_o[H^+]^3/[M^{3+}][HR]_o^3 \quad (1)$$

$$\log K = \log D - 3\log[HR]_o - 3pH \quad (2)$$

$$\beta_n = [MR_3L_n]_o/[MR_3]_o[L]_o^n \quad (3)$$

$$\log D^*/D = \log(1+\sum_{n=1}^{n}\beta_n[L]_o^n) \quad (4)$$

where D and D^* are the distribution ratio in the absence and in the presence of TOPO; M stand for metal, HR for β-diketone, and L for TOPO, and [ ] and [ ]$_o$ designate the concentration of the chemical species in the aqueous and organic phases respectively.

Results and Discussion

Lutetium-β-diketone System. Figure 1 shows the log$D$ *vs.* pH plots in the extraction of lutetium ions with various β-diketones in benzene. With β-diketones with a fluoromethyl group, lutetium can be extracted in the lower pH region. This fact is caused by the inductive effect of the fluoromethyl group, which raises the acidity of the enol form.[11,12] The high extractability can be

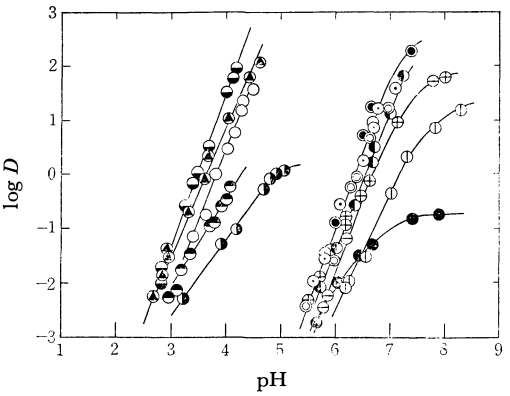

Fig. 1. The distribution ratio of lutetium with various β-diketones as a function of pH.
Organic phase: 0.1 M or 0.05 M β-diketone in benzene
Aqueous phase: 0.1 M $NaClO_4$
0.1 M β-diketone: -●- AA, -⊕- DPM, -◐- DIBM, -⊖- PvA, -⊕- DPvM
0.05 M β-diketone: -◎- BzA, -◉- NtA, -⊙- DBM, -◑- TAA, -○- BFA, -◒- TTA -▲- FTA, -◓- HFA

*1 The treatments of the equations have been interpreted in a previous paper.[7]

10) J. T. Adams and C. R. Hauser, *J. Am. Chem. Soc.*, **66**, 1220 (1944).

11) G. H. Morisson and H. Freiser, "Solvent Extraction in Analytical Chemistry," John Wiley & Sons, New York (1957).

12) J. Stary, "The Solvent Extraction of Metal Chelates," Pergamon Press, Oxford (1964).

attained with β-diketones possessing bulky groups, such as benzoyl-, thenoyl- and pivaroyl groups (*e. g.*, BFA, TTA, and DPvM); this may be due to the hydrophobic structure of the molecule, which prevents the formation of water-soluble complexes[13] and minimizes the solubility of the metal chelates into water. In the extraction with β-diketones which are comparatively soluble in water (*e.g.*, AA, TAA and HFA), the slopes of the log$D$ *vs.* pH plots deviate from 3, the theoretical value, because of the formation of water-soluble complexes.

Figure 1 confirms the general concept that the $pH_{1/2}$ value for the extraction of metal β-diketonates is directly correlative with the pK_D value of the β-diketone.

Lutetium-β-diketone-TOPO System. Figure 2 indicates the log$D$* *vs.* pH plots in the synergistic extraction of lutetium ions with 10^{-3}M TOPO and various β-diketones in benzene. In the presence of TOPO, the extraction of lutetium is very much enhanced by the adduct formation. As may be seen in the figure, the plots of DBM, NtA and BzA curve concavely in the low-distribution region. This curious behavior, however, can not be explained in the present time and was not studied in detail, because it seems not to be very important in this research.

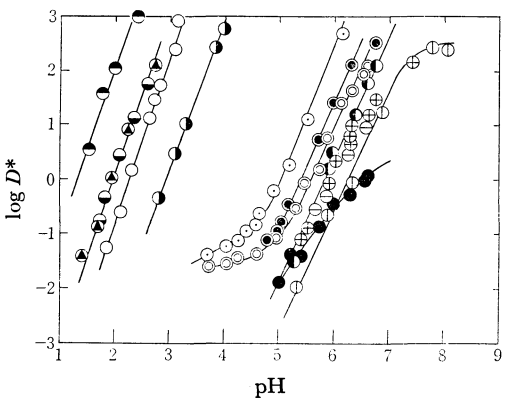

Fig. 2. The distribution ratio of lutetium with various β-diketones in the presence of 0.001 M TOPO as a function of pH. The symbols in the figure are the same as in Fig. 1.

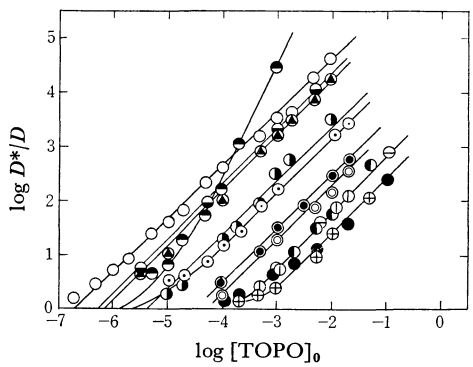

Fig. 3. The distribution ratio of lutetium with β-diketones having various functional groups as a function of TOPO concentration. The symbols in the figure are the same as in Fig. 1.

The effects of the functional groups of various β-diketones on the adduct formation are shown in Fig. 3 as log$D$*/D *vs.* log $[TOPO]_0$ plots. The straight lines with a slope of 1 indicate that one molecule of TOPO binds one molecule of the metal chelate. The HFA chelate adduct contains two molecules of TOPO.

The extraction constants of lutetium β-diketonates, log K, and the stability constants of their TOPO adducts, logβ_n, are summarized in Table 1. The stability of the TOPO adduct with various lutetium β-diketonates increases in the follwing order: aliphatic groups (AA and DPM<PvA, DIBM and DPvM)<aromatic groups (BzA<NtA≪DBM)< fluoromethyl groups (TFA≪FTA<TTA<BFA≪ HFA). In general, the log β_n increases with an increase in the log K value, as is indicated in Fig. 4, and no steric hindrance by terminal aliphatic or aromatic groups upon the adduct formation is observed.

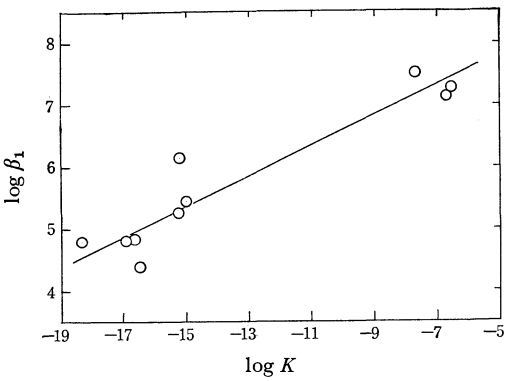

Fig. 4. The stability constant of lutetium β-diketonate TOPO adduct, log β_n as a function of the extraction constant of metal chelate, log K.

As has been described above, the chelates with a fluoromethyl group in the ligand form stable adducts. This may be due to the fact that the electron-withdrawing fluoromethyl group decreases the electron density around the metal ion.[14,15] The fluoromethyl group does not hinder the resonance of the metal chelate ring.[16] The chelates containing the

13) J. F. Suttle and T. K. Keenon, *J. Am. Chem. Soc.*, **76**, 2184 (1954).

14) K. Nakamoto, Y. Morimoto and A. E. Martell, *J. Phys. Chem.*, **66**, 346 (1962).

15) H. F. Holtzclow, Jr., and W. P. Collman, *J. Am. Chem. Soc.*, **79**, 3318 (1957).

16) A. E. Martell and M. Calvin, "Chemistry of the Metal Chelate Compounds," Prentice-Hall, N. Y. (1952).

Table 1. Stability constants of lutetium β-diketonates and their adducts with TOPO

	R	R'	pK_D*	log K	log β_1		R	R'	pK_D*	log K	log β_1
AA	CH_3	CH_3	12.70 (11.27)	—	4.35	DBM			13.75	−15.16	6.15
DPM	CH_2CH_3	CH_2CH_3	—	−16.57	4.35	TAA	CH_3	CF_3	8.70	—	6.25
DIBM	$CH(CH_3)_2$	$CH(CH_3)_2$	(12.48)	−16.57	4.80	BFA		CF_3	9.20	−7.69	7.50
PvA	CH_3	$C(CH_3)_3$	14.20	−16.90	4.80	TTA		CF_3	9.10	−6.56	7.25
DPvM	$C(CH_3)_3$	$C(CH_3)_3$	(14.48)	−18.37	4.80	FTA		CF_3	8.50	−6.78	7.15
BzA	CH_3		12.85	−15.21	5.25	HFA	CF_3	CF_3	6.0	—	6.25
NtA	CH_3		—	−15.06	5.45						(log β_2 =12.50)

* Negative logarithm of the acid dissociation constant of the β-diketone in 75% (V/V) dioxane. L. G. Van Uitert, W. Conard. Fernelius and B. E. Douglas, *J. Am. Chem. Soc.*, **75**, 457 (1953); The values in blacket were obtained by G. S. Hammond, W. G. Borddein and G. A. Guter, *ibid.*, **81**, 4682 (1959).

Table 2. Effect of temperature on stability constant of Lu-β-diketonate-TOPO complexes

	10°C		20°C		30°C		$-\Delta H$ kcal/mol
	log K	log β_1	log K	log β_1	log K	log β_1	
DPM	−16.81	4.75	−16.57	4.35	−15.98	4.25	5.5
BzA	−16.16	5.70	−15.21	5.25	−14.96	5.10	5.9
BFA	− 7.99	8.10	− 7.69	7.50	− 7.37	7.25	8.6

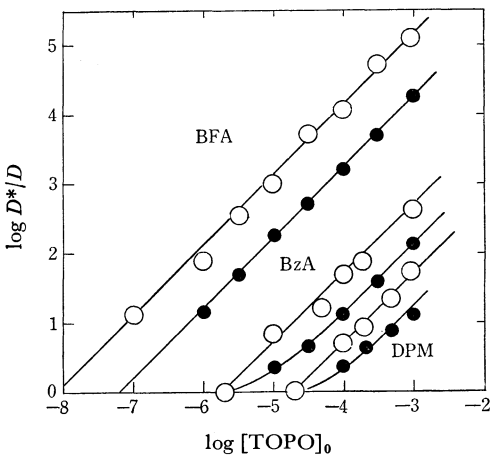

Fig. 5. Variation of the distribution ratio of lutetium as a function of TOPO concentration at 10°C (-○-) and 30°C (-●-).

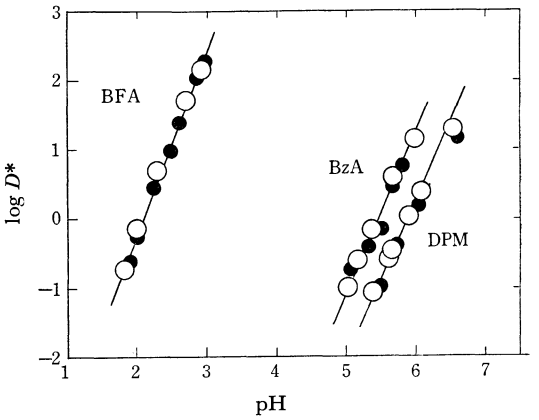

Fig. 6. Logarithm of the distribution ratio of lutetium as a function of pH at 10°C (-●-) and 30°C (-○-).

aromatic group in the ligand also form more stable adducts than those with the aliphatic group do (*e.g.*, TFA<BFA; AA<BvA<DBM). The contribution of the phenyl substitution to the adduct formation may result from the conjugation effect of the groups with the metal chelate rings. Such a conjugation effect may weaken the binding power between the central metals and the coordinated ligand,[17] thereby enhancing the adduct formation. The conjugation effect was also observed in the NMR measurements of metal TTA chelates.[18] As a result of the electron-withdrawing effect of the fluoromethyl group and by the conjugation effect of the phenyl-, thenoyl-, and furoyl-groups, BFA, TTA, and FTA form more stable adducts with TOPO than do other β-diketones. A similar ten-

17) R. L. Belford, A. E. Martell and M. Calvin, *J. Inorg. Nucl. Chem.*, **2**, 11 (1956).
18) J. R. Ferraro, *ibid.*, **26**, 225 (1964).

dency has also been found in the adduct formation between uranyl β-diketonates and TBP.[19]

Figure 5 shows the effect of the temperature on the adduct formation of DPM, BzA, and BFA chelates with TOPO, while Table 2 presents the extraction constants of these chelates and the stability constants of their adducts. The extraction constants of the chelates increase, while the stability of the TOPO adducts decreases, with a rise in the temperature. This phenomenon supports the empirical fact that the more stable a chelate, the less stable the adduct is, because the extraction constant can be taken as a measure of the stability of the metal chelate in the extraction with the same chelating reagent. As may be expected from this fact, the logD^* *vs.* pH plots in the synergistic extraction are little affected by the temperature (in the range from 10°C to 30°C), as is presented in Fig. 6. The apparent enthalpy changes in the adduct formation have been estimated and are presented in Table 2. The value increases in the sequence of DPM, BzA, and BFA.

The author wishes to express his thanks to Professor Tsunenobu Shigematsu (Institute for Chemical Research, Kyoto University) for this guidance throughout this study. Thanks are also due to Drs. Masayuki Tabushi and Masakazu Matsui (Institute for Chemical Research, Kyoto University) for their helpful advice and discussions.

19) K. Batzer, D. E. Goldberg, and L. Newman, *ibid.*, **29**, 1511 (1967).

BULLETIN OF THE CHEMICAL SOCIETY OF JAPAN VOL. 42 999—1006 (1969)

Cobalt(IV) Ammine Complexes with 5-Nitrosalicylato or Similar Ligands. III. Electric Resistivity, Magnetic Susceptibility, and ESR*[1]

Yoshihisa YAMAMOTO

Faculty of Science, Osaka City University, Sumiyoshi-ku, Osaka

(Received August 15, 1968)

The electric and magnetic properties of a series of 5-nitrosalicyclato ammine cobalt(IV) complexes (paramagnetic), the salicylato ammine cobalt(III) complex (diamagnetic), μ-superoxo-dicobalt ammine complexes (paramagnetic), and the μ-peroxodicobalt ammine complex were studied. The resistivity(ρ) at room temperature and the energy gap(ε) for paramagnetic complexes were in the range of, $\rho=7.6\times10^{10}$—1.5×10^{11} Ω cm and $\varepsilon=0.7$—1.1 eV, whereas those for diamagnetic complexes were in the range of $\rho=10^{12}$—10^{14} Ω cm and $\varepsilon=0.75$—1.2 eV. The magnetic susceptibilities of the paramagnetic complexes obeyed the Curie-Weiss law, with comparatively large Curie-Weiss constants (-18—26°K). The g-values and line widths (ΔH_{msl}) in the ESR signals at room temperature were determined for powdered samples of 5-nitrosalicylatotetraamminecobalt(IV) complexes and their derivatives. The ESR parameters obtained were in the range of $g=2.0030$—2.0070 and $\Delta H_{msl}=22.0$—30.6 Oe for powders.

Previous papers have reported on the preparation of cobalt(IV) ammine complexes with 5-nitrosalicylato[1] or similar ligands[2]. Inasmuch as these compounds contain cobalt in the unusual valence state (IV, d^5 in the low spin state), various anomalies are expected in their physical properties. The present paper deals with the results of measurements of the solid electric conductivities, magnetic susceptibilities, and ESR of these compounds.

Experimental

Preparation. *5-Nitrosalicylatotetraamminecobalt(IV) Complexes, 5-Nitrosalicylatobis(ethylenediamine)cobalt(IV) Complexes, 3-Methyl-5-Nitrosalicylatotetraamminecobalt(IV) Complexes, and 4-Methyl-5-Nitrosalicylatotetraamminecobalt-(IV) Complexes.* These complexes were prepared by the methods reported in Papers I[1] and II[2].

The salicylatotetraamminecobalt(III) Complex and its Derivatives and the Salicylatobis(ethylenediamine)-cobalt(III) Complex. These complexes were prepared by Morgan's method.[3]

*1 Presented at the 21st Annual Meeting of the Chemical Society of Japan, Suita, 1968.

1) Y. Yamamoto, the Late K. Ito, H. Yoneda and M. Mori, This Bulletin, **40**, 2580, (1967).

2) Y. Yamamoto, M. Mori, H. Yoneda, S. Misumi and the Late K. Ito, submitted to this Bulletin.

3) G T. Morgan and J. D. Smith, *J. Chem. Soc.*, **1922**, 1956; G. T. Morgan and J. D. Smith, *ibid.*, **1924**, 1924.

The μ-Amido-μ-superoxo-bis(tetraamminecobalt)(4+) Complex. This complex was prepared according to the method of Mori, Weil and Ishiguro.[4]

The μ-Superoxo-bis(pentaamminecobalt)(5+) Complex. This complex was prepared according to the method of Gleu and Rehm.[5]

The μ-Peroxo-bis(pentaamminecobalt)(4+) Complex. This complex was prepared by Werner's method.[6]

Measurements of Electrical Conductivities. The measurements were made with a Toa Denpa Kogyo Microvolt Ammeter, Model PM-18 (for the range 10^{-4}—10^{-12} A), and a Takeda Riken Vibrating Reed Electrometer, Model TR-81 (10^{-7}—10^{-15} A). A fine powder of each complex was compressed into a disk (12 mm in diameter and 1—2 mm thick) under a pressure of about 3×10^2 kg/cm^2. Silver-paste was used as the electrode. The D.C. conductivity was measured in the temperature range from −50 to +120°C. The conductivity vessel, as shown in Fig. 1[7], was evacuated down to 10^{-2} mmHg.

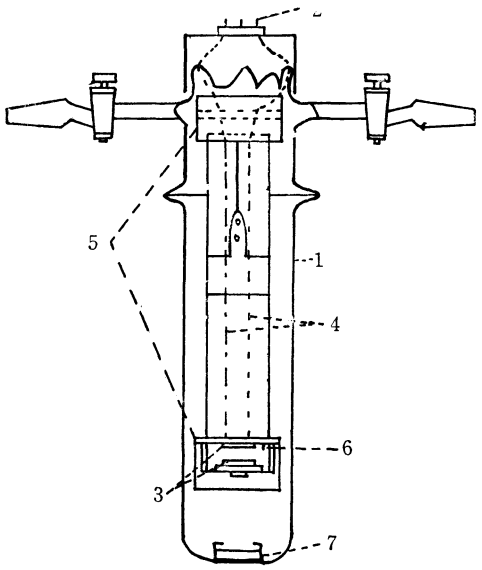

Fig. 1. The apparatus used in measurement of current through powdered sample.

1. Pyrex glass tube
2. Connector of lead line
3. Electrodes
4. Lead line
5. Teflon insulator
6. Thermocouple
7. Dryer

Measurements of Magnetic Susceptibilities. The measurements were made by the Gouy method with a magnetic balance (Shimadzu Seisaku Sho) in the temperature range between 80°K and room temperature. The magnetic susceptibility of 5-nitro-4-methylsalicylatotetraamminecobalt(IV) chloride nitrate was also measured by the AC method, using a Hartshorn bridge in the temperature range between 4.22°K and 1.21°K. The accuracy was ±0.1%.

Electron Spin Resonance. The spectra were recorded at room temperature with a TMF-20305 Tokyo Denki Seiki. Quartz sample tubes 1.5 mm in diameter were used; they were filled with solutions in several kinds of solvent to about 4 cm from the bottom.

Results and Discussion

Electrical Resistivities. An almost linear relationship was observed between the current and the applied voltage up to 15V in the temperature range from −50—+120°C. In most cases the tempera-

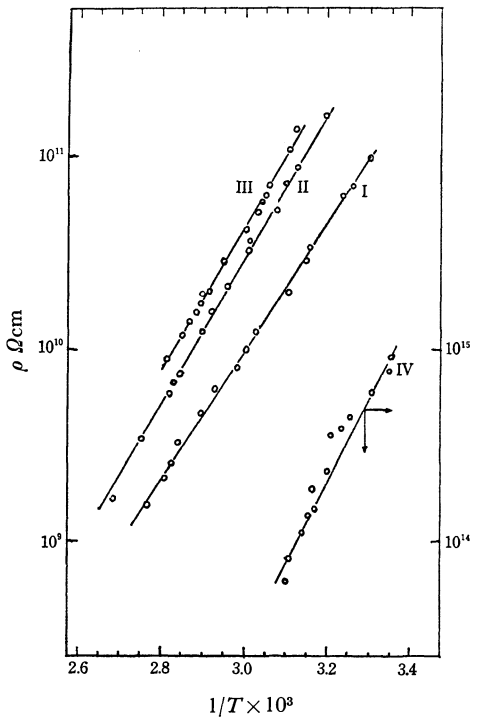

Fig. 2. Resistivity *vs.* $1/T\times10^3$.

(I) $\left[(NH_3)_4Co\langle^{OOC-}_{O-}\!\!\rangle\!-\!NO_2\right]Cl\cdot NO_3\cdot H_2O$ (CH_3)

(II) $\left[(NH_3)_4Co\langle^{OOC-}_{O-}\!\!\rangle\!-\!NO_2\right]Cl_2\cdot 2H_2O$ (CH_3)

(III) $\left[(NH_3)_4Co\langle^{OOC-}_{O-}\!\!\rangle\!-\!NO_2\right]Cl\cdot NO_3\cdot H_2O$ (CH_3)

(IV) $\left[(NH_3)_4Co\langle^{OOC-}_{O-}\!\!\rangle\right]Cl\cdot H_2O$

4) M. Mori, J. A. Weil and M. Ishiguro, *J. Am. Chem. Soc.*, **90**, 615 (1968).

5) K. Gleu and K. Rehm, *Z. Anorg. Allgem. Chem.*, **237**, 79 (1938).

6) A. Werner and A. Mylius, *ibid.*, **16**, 262 (1898).

7) S. Kawai, S. Ito, F. Kanamaru and R. Kiriyama, *Kogyo Kagaku Zasshi (J. Chem. Soc. Japan, Ind. Chem. Sect.)*, **65**, 1757 (1962).

Table 1. Electric properties of cobaltammine complexes

Compound	Specific resistivity at room temperature ρ_{20}, Ωcm	ε, eV (Temp.)
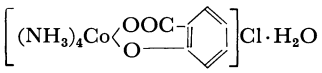	5.7×10^{12}	1.24
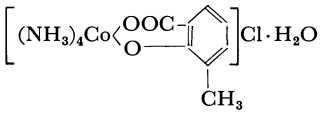	8.7×10^{14}	0.77
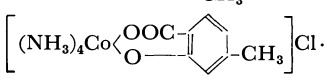	3.5×10^{14}	0.8
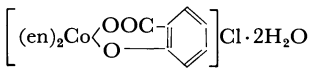	4.1×10^{12}	0.75
$[(NH_3)_5Co\text{-}O_2\text{-}Co(NH_3)_5]\cdot(SO_4)_2\cdot3H_2O$	5.7×10^{11}	1.66
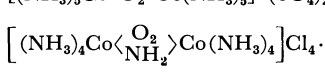	5.2×10^{9}	1.42 (−40—−5°C) 0.34 (−5—+50°C) 0 (+50°C～)
$[(NH_3)_5Co\text{-}O_2\text{-}Co(NH_3)_5]\cdot(SO_4)_2\cdot HSO_4\cdot3H_2O$	1.9×10^{7}	
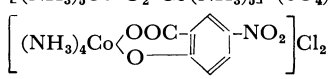	7.55×10^{10}	0.48
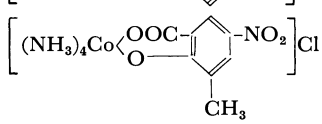	9.8×10^{10}	0.67
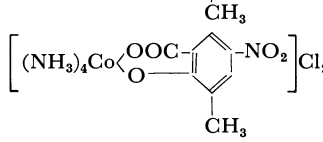	1.5×10^{11}	0.78
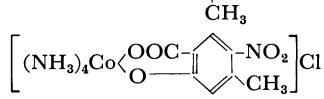	9.6×10^{10}	1.10
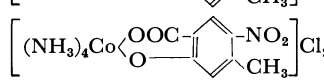	7.5×10^{10}	0.8
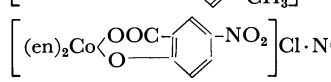	5.2×10^{11}	0.95
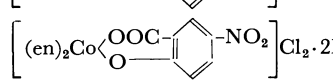	1.5×10^{11}	0.75

ture dependence of the resistivity obeyed the $\rho = \exp(\varepsilon/2\boldsymbol{k}T)$ equation (Fig. 2). The resistivity at 25°C (ρ_{25}) and the apparent energy gap (ε) as calculated from the above equation are tabulated in Table 1.

It should be noted that most of these complexes have the water of crystalliaztion; the influence of this water must be considered in analysing the results of these electric measurements. For the μ-amido-μ-superoxo-bis(tetraamminecobalt) complex, measurement was made in the −40—+80°C range. An almost linear relationship between ρ and $1/T$ was observed between −40 and −10°C, and also between −10°C and +50°C, but the linear relation was not observed above +55°C (Fig. 3). This change in the conductivity behavior is thought to be due to such water molecules. On the other hand, the resistivity of cobalt(IV) complexes showed an almost linear relationship with $1/T$ up to 120°C (*cf.* Fig. 2). This seems to indicate that, in this compound, the water is bound tightly to the carbonyl group of the salicylato ligand. This idea of tightly-bound water was presented by Morgan and Smith[3] for their salicylatotetraamminecobalt(III) salts and was proved by the X-ray analysis of the chloride monohydrate by Hosoo, Kushi, and Kuroya.[8]

Next, let us consider the effect of the number of d-electrons in the cetral metal ion on the electric resistivities of the complexes. Balto and Weiss[9]

8) T. Hosoo, Y. Kushi and H. Kuroya, Presented at the 20th Annual Meeting of the Chemical Society of Japan, Tokyo 1967, *Collection of Résumés*, **2B** 223.

9) B. A. Balto and D. E. Weiss, *Aust. J. Chem.*, **15**, 653 (1962).

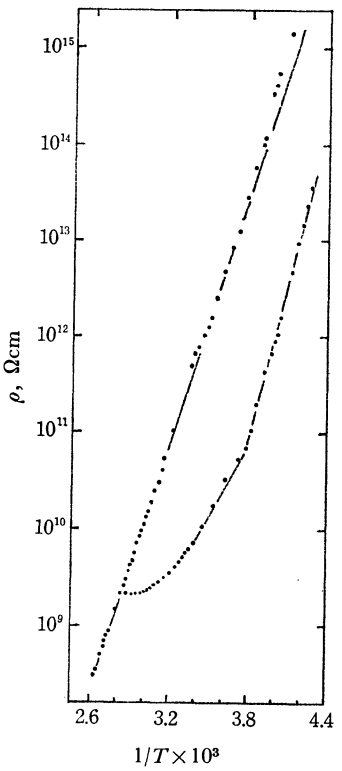

Fig. 3. Resistivity *vs.* $1/T\times10^3$.

(I) $\left[(NH_3)_4Co\langle{}^{OOC-}_{O-}\!\!\rangle\!\!\begin{array}{l}-NO_2\\ CH_3\end{array}\right]Cl_2\cdot2H_2O$

(II) $\left[(NH_3)_4Co\langle{}^{OO}_{NH_2}\rangle Co(NH_3)_4\right]Cl_4\cdot H_2O$

reported the preparation and the resistivity measurements of the iron(III) complex (d^5, 4.7×10^5 Ωcm) and the iron(II) complex (d^6, 3.8×10^4 Ωcm), both with a pentacyclic ligand which had been prepared from chloranil and o-phenylenediamine. Inoue, Hayashi, Takiuchi and Imoto[10] reported on the organic polymer-tin(IV) complex (d^{10}, 3.8×10^{10} Ωcm) and the organic polymer-tin(II) complex ($d^{10}s^2$, 1.76×10^9 Ωcm). Thus, both these groups of investigations found that the number of d or s-electrons in the central metal ion does not have much effect on the electric resistivity, provided that the relevant orbital is sufficiently localized on the central metal ion.

Consequently, if our cobalt compounds contained true tetravalent cobalt atoms, *i.e.*, if the hole produced as the result of oxidation were localized on the cobalt atom, the resistivity should not be much different from that of the normal cobalt(III) ammine complex. Actually, the resistivities of our paramagnetic cobalt(IV) ammine complexes with 5-nitrosalicylato or similar ligands are lower than those of cobalt(III) complexes with similar ligands by factors of 10^2—10^4. Such large differences in the electrical resistivities seem to suggest that the distribution of the electron hole is spread over the entire molecule, or that our green compounds might preferably be regarded as containing free radial complex ions. We might, for comparison, refer to the electrical resistivity of violanthrone-B (a free radical, $\rho_{15}=6.9\times10^6$ Ωcm[11]) and that of violanthrone (with no unpaired spin, $\rho_{15}=1.1\times10^{11}$ Ω·cm[11] or 2.3×10^{10} Ωcm[12]). These results indicate that the radical formation has much effect on the electrical resistivity.

A similar relationship holds between the electrical resistivities of diamagnetic peroxo dicobalt complexes and those of paramagnetic superoxo dicobalt (formerly called peroxo cobalt(III) cobalt(IV)) complexes. The electrical resistivities of paramagnetic μ-superoxo compounds are lower than those of diamagnetic peroxo complexes by factors of 10^2—10^4 (Table 1).

Fielding[13] had reported the resistivity of μ-superoxobis(pentaamminecobalt)(5+) hydrogen trisulfate trihydrate to be $\rho=2\times10^7$ Ωcm at 20°C, which is almost in complete agreement with the measurements made by the present author (Table 1).

Electron Spin Resonance. In the case of superoxo dicobalt complexes, Ebsworth and Weil[14] observed a hyperfine structure with 15 equally-spaced components in the paramagnetic resonance spectra of aqueous solutions: this structure clearly indicated that the unpaired electron spends equal fractions of time on the two cobalt nuclei. Recently, Weil and Kinnaird[15] reported that the ESR spectra of O^{17}-labeled $[(NH_3)_4Co\langle{}^{OO}_{NH_2}\rangle Co(NH_3)_4]^{4+}$ dissolved in very dilute nitric acid showed a hyperfine structure of oxygen-17 in addition to 15 hyperfine lines of cobalt. These ESR spectra show that the unpaired electron is located on the molecular orbital extending over cobalt-oxygen-cobalt.

The present research has revealed that ESR signals are also observable in the green 5-nitrosalicylato cobalt ammine complexes at room temperature. This proves that the complex is actually in a high oxidation state, because coblt(II) compounds known to have too short a relaxation time to allow any ESR signal to appear at room temperature.

10) H. Inoue, S. Hayashi, S. Takiuchi and E. Imoto, *Kogyo Kagaku Zasshi (J. Chem. Soc. Japan, Ind. Chem. Sect.)*, **65**, 1622 (1962).

11) H. Akamatu, T. Maekawa, Y. Iida and M. Kinoshita, This Bulletin **37**, 849 (1964).

12) H. Inokuchi, *ibid.*, **24**, 222 (1951).

13) P. E. Fielding, *J. Chem. Phys.*, **22**, 1153 (1954); P. E. Fielding and D. P. Mellor, *J. Chem. Phys.*, **22**, 1155 (1954).

14) E. V. A. Ebsworth and J. A. Weil, *J. Phys. Chem.*, **63**, 1890 (1959).

15) J. A. Weil and J. K. Kinnaird, *ibid.*, **71**, 3341 (1967).

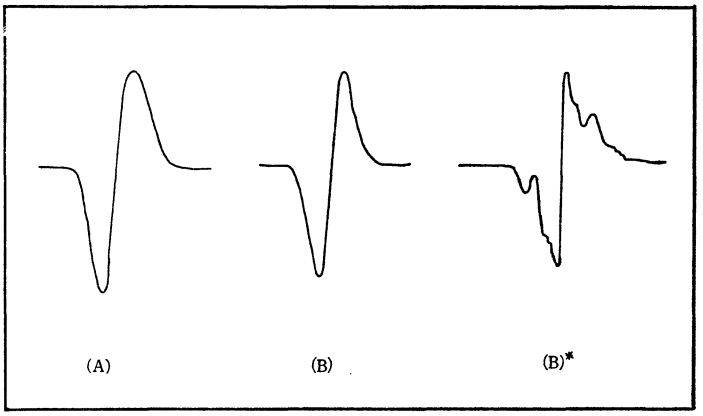

Fig. 4. The ESR spectra of $\left[(NH_3)_4Co\langle^{O}_{OOC}\!\!-\!\!\bigcirc\!\!\bigcirc\!\!-NO_2,\ CH_3\right]X_2$ of powders at 22°C.

(A) : $\left[(NH_3)_4Co\langle^{O}_{OOC}\!\!-\!\!\bigcirc\!\!\bigcirc\!\!-NO_2,\ CH_3\right]Cl_2\cdot 2H_2O$;

(B) and (B*) : $\left[(NH_3)_4Co\langle^{O}_{OOC}\!\!-\!\!\bigcirc\!\!\bigcirc\!\!-NO_2,\ CH_2\right]Cl\cdot NO_3\cdot H_2O$ (B*) : 30 min after preparation.

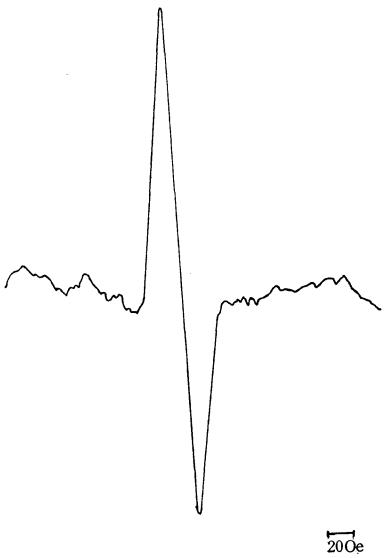

Fig. 5. ESR spectrum of $\left[(en)_2Co\langle^{O}_{OOC}\!\!-\!\!\bigcirc\!\!\bigcirc\!\!-NO_2\right]Cl\cdot NO_3\cdot H_2O$ in aqueous solution at 22°C (about 10^{-1} mol/*l*).

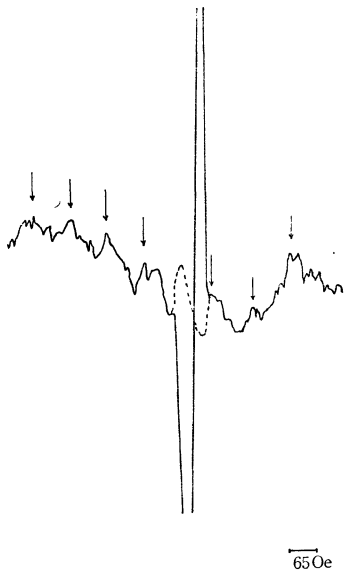

Fig. 6. ESR spectrum of $\left[(en)_2Co\langle^{O}_{OOC}\!\!-\!\!\bigcirc\!\!\bigcirc\!\!-NO_2\right]Cl\cdot NO_3\cdot H_2O$ in aqueous solution at 22°C (about 10^{-2} mol/*l*).

The powder ESR of 5-nitrosalicylatotetraamminecobalt(IV) salts, 3-methyl or 4-methyl-5-nitrosalicylatotetraamminecobalt(IV) salts (Fig. 4), and 5 - nitrosalicylatobis (ethylenediammine) cobalt (IV) salts gave symmetrical spectra; the obtained values of *g*-factor and line width (between points of maximum slope)are given in Table 1.

As has been stated in Paper II,[2] the 5-nitrosalicylatobis(ethylenediamine)cobalt(IV) complex is more stable than the 5-nitrosalicylatotetraamminecobalt-(IV) complex and its methyl derivatives, hence, it is more suitable for the ESR study of solutions.

The solution of 5-nitrosalicylatotetraamminecobalt(IV) salts in water gave spectra without any hyperfine structure and were slightly asymmetric, the high field side being slightly broader. The spectra could be observed for only about an hour

after the dissolution of the samples. Solutions in 35% hydrochloric acid, 20—60% phosphoric acid, and 100% methanol gave no observable spectra.

A solution of 5-nitrosalicylatobis(ethylenediamine)cobalt(IV) complexes in mthanol or 35% hydrochloric acid gave spectra without any hyperfine structure, and the line slope was asymmetric, the high-field side being broader. The aqueous ESR spectra of 5-nitrosalicylatobis(ethylenediamine)-cobalt(IV) salts showed no hyperfine structure, except in a limited range of concentration of about 10^{-1}—10^{-3} mol/l (Fig. 5). At the sample concentration of about 10^{-2}—10^{-3} mol/l, a hyperfine structure of eight lines developed on both field sides of one strong line (Fig. 6). At present, however, it is difficult to assign these hyperfine structures.

One thing that can be said about the obtained spectra described above is that the g-value is always close to the free electron value (Table 2), This seems to be in line with the afore-mentioned assumption of the free-radical nature of the green paramagnetic 5-nitrosalicylatc ammine cobalt complexes.

Magnetic Susceptibilities. The susceptibilities of the compounds were found to be independent of the temperature. χ_{mol}^{cor} was obtained by correcting the observed molar magnetic susceptibility, χ_{mol}, for the diamagnetic contribution of the molecule, which was taken to be 0.000200—0.000220 c.g.s.e. m.u. The effective magnetic moment of the molecule in Bohr magnetons, μ_{eff}, was obtained using the formula:

$$\mu_{eff} = 2.84\sqrt{\chi_{mol}^{cor}(T-\theta)}$$

The Curie-Weiss plots and some related parameters are given in Fig. 7 and Table 2 respectively. The comparatively large Curie-Weiss constants again seem to conform with the free radical nature of the substance as assumed in the foregoing discussion of the electric resistivities. These values might be compared with the Curie-Weiss constants of such free radical as diphenylpicrylhydrazyl (−10°K[16]), diphenylpicrylhydrazyl (in CS_2, −22°K[17]), and violanthron-B (−45°K[11]).

In the case of 5-nitro-4-methylsalicylatotetraamminecobalt(IV) chloride nitrate, the susceptibility measurements were also made at the temperatures of liquid helium; these measurements gave the Curie-Weiss constant of 0°K(Fig. 8) and the

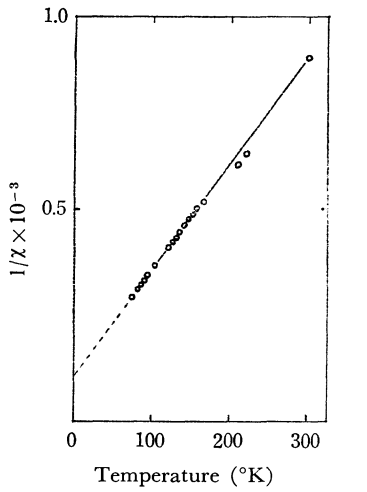

Fig. 7. $1/\chi$ *vs.* temperature diagram.

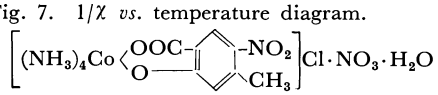

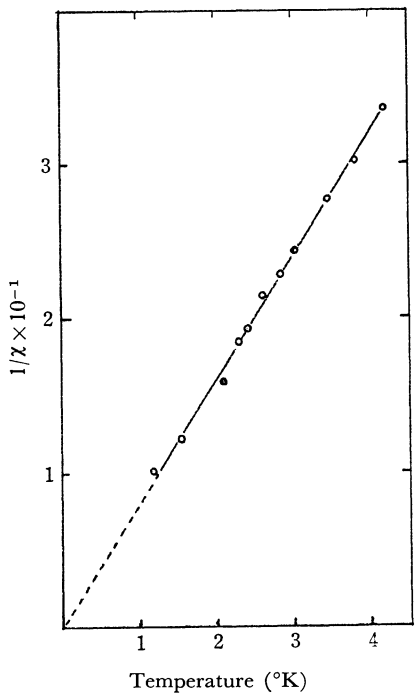

Fig. 8. $1/\chi$ *vs.* Temperature diagram.

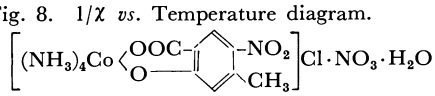

effective Bohr magneton number of 1.05±0.05, in contrast to the values above the temperature of liquid nitrogen, (−18°K, 1.7 B.M., Table 2). This discrepancy between results in different temperature ranges is doubtless due to the bending of the Curie-Weiss plot in the region of very low temperatures.

The author is grateful to Professor Hiroshi Mikawa of Osaka University for his kind offer of conductivity equipment, to Professor Ikuji Tsujikawa and Dr. Hanako Kobayashi of Kyoto University for their kind guidance in the susceptibility measurements, and to Dr. Setsuo Takamuku of Oasaka University for his whole-hearted cooperation in the ESR spectroscopy.

16) J. Turkevich and P. Selwood, *J. Am. Chem. Soc.*, **63**, 1077 (1941).
17) W. Duffy, Jr., *J. Chem. Phys.*, **36**, 490 (1962).

Table 2. The ESR and magnetic properties of cobalt(IV) amminecomplexes with 5-nitrosalicylato or similar ligands

Substance	Form	g-Value	Line-width (Gauss)	Curie-Weiss const. (θ) (°K)	Bohr magneton number (B. M.)
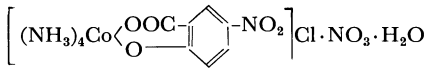	P., sl. sym., r.t.,	2.0046	24.7		1.9
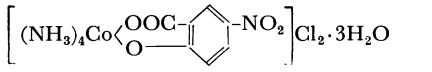	P., asym., r.t.,	2.0046		0	1.7
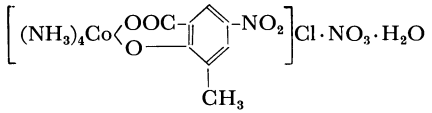	P., asym., r.t.,	2.0036			1.7
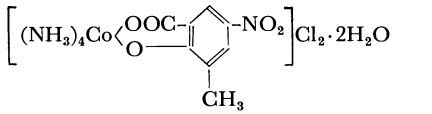	P., asym., r.t.,	2.0036		−20	1.7
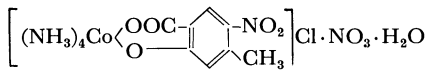	P., sl. sym., r.t.,	2.0070		−18	1.7
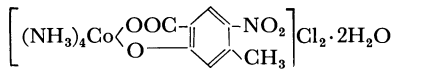	P., asym., r.t.,	2.0070	26.7	−14	1.7
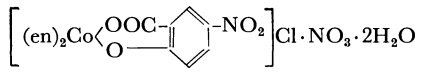	P., sym., r.t., W., sl. sym., r.t., W., sl. sym., liq. N_2	2.0038 2.0030 2.0031	23.6 22.0 25.6	−22	1.6
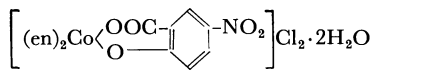	P., sl. sym., r.t., MeOH, asym., r.t., 35% HCl, asym., r.t.,	2.0038 — —	30.6 — —	−26	1.6

sym.: symmetric, sl. sym.: very slightly asymmetric, asym.: asymmetric, P.: powder, W.: in water, r.t.: room temperature

It is also his pleasure to express his indebtedness to Professor Masayasu Mori of Oaska City University for his constant encouragement and for his kindness in looking over the manuscript.

Last but not least, the author should like to emphasize that this series of studies was begun at the suggestion of the late Professor Kazuo Ito of Osaka University and Professor Hayami Yoneda of Wakayama University, to both of whom the author's gratitude is due.

BULLETIN OF THE CHEMICAL SOCIETY OF JAPAN VOL. 42 1006—1010 (1969)

Studies of the Interaction between the Hexyl Anion and Alkali Metal Ions

Shoji Motomizu and Kyoji Tôei

Department of Chemistry, Faculty of Science, Okayama University, Tsushima, Okayama

and Tadashi Iwachido

College of Liberal Arts and Sciences, Okayama University, Tsushima, Okayama

(Received August 17, 1968)

The Hexyl(2,4,6,2′,4′,6′-hexanitrodiphenylamine) anion forms ion-pairs with alkali metal cations to some extent in an aqueous solution. The association constants of these ion-pairs were determined both in nitrobenzene by conductivity measurements and in water by the solvent extraction method. The association constants in nitrobenzene (K_o^{MR}) decrease in the following order: Li>Na>K>Rb>Cs. The plot of log K_o^{MR} against the ionic potential of the alkali metal ions was found to be linear. In nitrobenzene saturated with water, however, the constants vary from 2 to 4. In water the asscoiation constants (K_a^{MR}) vary from about 10 to 400, and the value increases as follows: Li<Na<K<Rb (<Cs). A plot of log K_a^{MR} against the reciprocal of the effective diameter of the hydrated alkali metal ions was found to be linear.

The extraction of alkali metal ions with the Hexyl anion into nitrobenzene has been reported by several authors.[1,2] The mechanism of the extraction is very attractive to us, because many alkali metal salts are well known to be very soluble in water but not in ordinary organic solvents immiscible with water. Generally alkali metal salts, such as chlorides and nitrates, are completely dissociated in an aqueous solution. However, potassium, rubidium, or cesium ions with larger radii than those of other cations, form a precipitate with such a large and symmetric anion as the perchlorate, tetraphenylborate, or Hexyl anion, and this precipitate is occasionally extracted into an organic solvent immiscible with water. This fact implies that the alkali metal ions associate to some extent with a large anion in an aqueous solution to form ion-pairs which can be extracted into nitrobenzene, and that such salts as alkali metal tetraphenylborate or Hexylate would be dissociated in nitrobenzene. In the present paper, the dissociation constants of the Hexyl salts in nitrobenzene were measured by electric conductance measurements. The constants in water were determined by the solvent extraction method.

Experimental

Reagents. Hexyl salt with an alkali metal ion was prepared by dissolving Hexyl into an aqueous solution of an equivalent amount of each alkali metal hydroxide or carbonate. The resulting precipitates were filtered and recrystallized two or three times from ethanol or acetone. The salts were dried at 50°C for 3—5 hr under a pressure of less than 10 mmHg.

The nitrobenzene for the conductivity measurements was prepared by distilling special-grade nitrobenzene which had been dried over anhydrous sodium sulfate. The fraction was collected at 75°C under a pressure of 5 mmHg and was stored in an ampoule to protect it from moisture. The nitrobenzene thus obtained had a specific conductance of $3—5\times10^{-9}$. This value is, however, satisfactory enough for the present purposes.

Potassium chloride for calibrating the conductance cell was purified by recrystallizing it from distilled water and was dried at 45°C in an electric furnace for three hours.

All the other chemicals used were of an analytical reagent grade and were used without further purification.

1) M. Kyrs, *Collection Czechoslov. Chem. Commun.*, **27**, 2380 (1962).

2) T. Iwachido and K. Tôei, This Bulletin, **37**, 1276 (1964).

Electric Conductance Measurements. The electric conductivity of the nitrobenzene solution was determined by the use of a conductometer, CM-1DB, from Toa Electronics Ltd. Measurements were made in a jacketted vessel equipped with platinized platinum electrodes, a thermometer, and a microburet. The jacketted vessel was maintained at 25°C by circulating water from a constant-temperature bath. To a known amount of pure nitrobenzene in the vessel, small quantities of a concentrated nitrobenzene solution of these salts were introduced successively from the microburet.

Extraction Procedure. Twenty milliliters of an aqueous solution of the alkali metal ion (the pH being adjusted to about 11 with each alkali metal hydroxide or carbonate) was shaken moderately with 20 ml of a nitrobenzene solution containing each Hexyl salt for about thirty minutes. After this mixture had been allowed to stand for one or two hours, the organic and the aqueous layers were separated and the Hexyl salt in each phase was determined spectrophotometrically by using a Hitachi-Perkin Elmer Spectrophotometer, Model 139. The final pH of the aqueous phase was 10—11.

All the procedures were made in a constant-temperature room (25±1°C).

Calculations

Association Constants of Hexyl Salt in Nitrobenzene. In non-aqueous systems, where the dielectric constant of the solvent is about 40 or less, to evaluate the limiting conductance, Λ_∞, and the dissociation constant, K_S, from the conductance data, Shedlovsky[3] proposed this equation:

$$\frac{1}{\Lambda S} = \frac{1}{\Lambda_\infty} + \frac{C\Lambda S f^2}{K_S \Lambda_\infty^2} \tag{1}$$

where C is the analytical concentration of 1-1 electrolytes, f is the activity coefficient, $S \equiv \left(\frac{z}{2} + \sqrt{1 + \left(\frac{z}{2}\right)^2}\right)^2$, and z is defined as:

$$z = \alpha\sqrt{C\Lambda}/\Lambda_\infty^{3/2} \tag{2}$$

where α is the Onsager coefficient.

From Eq. (1), $1/\Lambda S$ is found to be linear against $C\Lambda S f^2$ at low concentrations, and Λ_∞ and K_S are obtained from the intercept and the slope.

Hexyl salts are associated in nitrobenzene as follows:

$$M^+ + R^- \overset{K_o^{MR}}{\rightleftharpoons} MR$$

The association constant in nitrobenzene, K_o^{MR}, is written as:

$$K_o^{MR} = \frac{[MR]_o}{[M^+]_o[R^-]_o f_o^2} \left(= \frac{1}{K_S}\right) \tag{3}$$

where the subscript O refers to the organic phase where $[M^+]$, $[R^-]$, and $[MR]$ are the concentrations of the alkali metal ions, the Hexyl anion, and the ion-pairs respectively.

Association Constants of Hexyl Salts in Water. The data of the solvent extraction of Hexyl salts were treated in the following way. Consider the association reaction:

$$M^+ + R^- \overset{K_a^{MR}}{\rightleftharpoons} MR$$

where M^+ represents an alkali metal ion, R^-, a Hexyl anion, and MR, an ion-pair. The association constant of the above equilibrium is:

$$K_a^{MR} = \frac{[MR]_a}{[M^+]_a[R^-]_a f_a^2} \tag{4}$$

Where [ ] indicates the concentration of the substance indicated, where the subscript a refers to the aqueous phase, and where f_a is the activity coefficient.

Besides, at a distribution equilibrium of the two phases, the partition coefficient of the ion-pair MR, D_{MR}, is:

$$D_{MR} = \frac{[MR]_o}{[MR]_a} \tag{5}$$

The distribution ratio of the Hexyl salt, q_R, is written as:

$$q_R \equiv \frac{C_o^R}{C_a^R} = \frac{[MR]_o + [R^-]_o}{[MR]_a + [R^-]_a} \tag{6}$$

where C_o^R and C_a^R represent the total concentrations of the Hexyl salt in the organic and the aqueous phases respectively.

The combination of Eqs. (3), (4), (5) and (6) leads to Eq. (7):

$$\frac{Y}{q_R} = \frac{1}{D_{MR}} + \frac{1}{D_{MR} \cdot K_a^{MR} \cdot f_a^2 [M^+]_a} \tag{7}$$

where:

$$Y \equiv \{0.5 + (0.25 + C_o^R K_o^{MR} f_o^2)^{1/2}\}/C_o^R K_o^{MR} f_o^2 + 1$$

From Eq. (7), a plot of Y/q_R against $(f_a^2[M^+]_a)^{-1}$ should give a straight line and from the intercept and the slope D_{MR} and K_a^{MR} are obtained.

Results and Discussion

Association Constants of Hexyl Salts in Nitrobenzene. The association constants, K_o^{MR}, were calculated from Eq. (1). The starting value of Λ_∞ was determined by the extrapolation of a plot of Λ against $C^{1/2}$. The Λ_∞ was then inserted into Eq. (2), and S and f were calculated. From a plot of $1/\Lambda S$ *vs.* $C\Lambda S f^2$, Λ_∞ and K_S were obtained. The above-mentioned process was repeated (usually three or four times) until a plot of $1/\Lambda S$ against $C\Lambda S f^2$ showed linearity. In Figs. 1 and 2, the equivalent conductances are plotted against the square root of C. In these figures the Λ values at $C^{1/2}=0$ are the calculated Λ_∞ values. From the Λ-$C^{1/2}$ curves, it is obvious that in nitrobenzene, Hexyl salts except Hexyl-Li are very strong electrolytes and that in nitrobenzene almost saturated with water (0.14M) even Hexyl-Li behaves like a very strong electrolyte. Figures 3 and 4 show the

3) T. Shedlovsky, *J. Franklin Inst.*, **225**, 739 (1938).

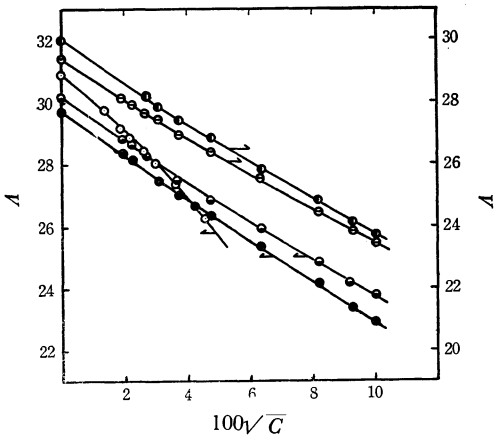

Fig. 1. The Λ-$\sqrt{C}$ curves of Hexyl salts in nitrobenzene.
○ Hexyl-Li, ◐ Hexyl-Rb, ● Hexyl-Na,
⊖ Hexyl-Cs, ◒ Hexyl-K

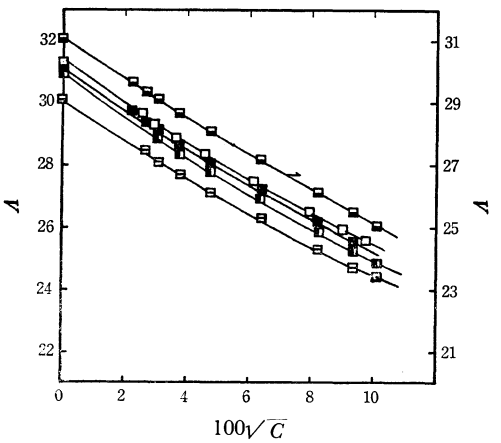

Fig. 2. The Λ-$\sqrt{C}$ curves of Hexyl salts in nitrobenzene saturated with water.
□ Hexyl-Li, ◧ Hexyl-Rb, ■ Hexyl-Na,
⊟ Hexyl-Cs, ◨ Hexyl-K

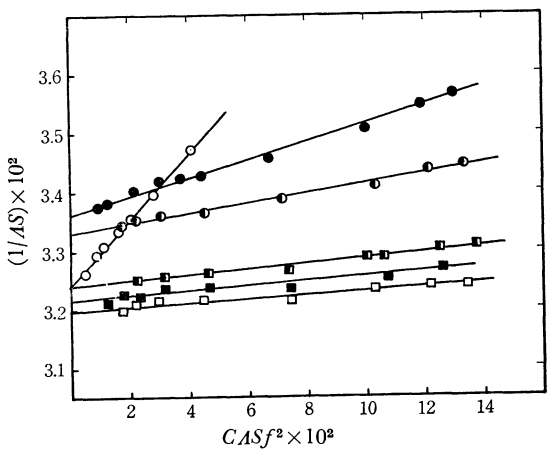

Fig. 3. Shedlovsky plot for Hexyl salts.
The symbols used are the same as those in Figs. 1 and 2.

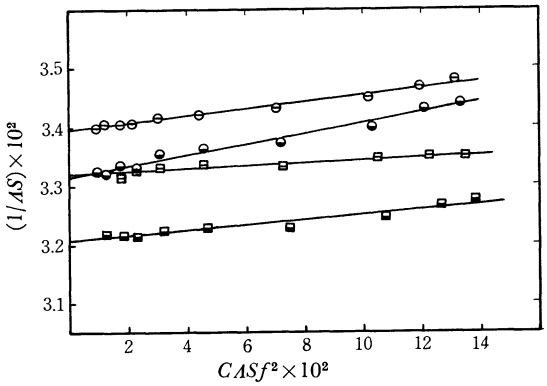

Fig. 4. Shedlovsky plot for Hexyl salts in nitrobenzene saturated with water.
The symbols used are the same as those in Figs. 1 and 2.

plots of $1/\Lambda S$ *vs.* $C\Lambda Sf^2$. The linearity of each plot is very good, and the constants, Λ_∞ and K_0^{MR}, were obtained algebraically by the method of least squares. $\Lambda_{\infty(H_2O)}$ and $K^{MR}_{0(H_2O)}$ refer to Λ_∞ and K_0^{MR} in nitrobenzene almost saturated with water (0.14M) and have been calculated on the assumption that nitrobenzene containing water has the same values of the dielectric constants and viscosity as those of pure nitrobenzene. The constants thus obtained, Λ_∞, $\Lambda_{\infty(H_2O)}$, K_0^{MR} and $K^{MR}_{0(H_2O)}$, are listed in Table 1. In Fig. 5 shows a plot of log K_0^{MR} against the ionic potential of alkali metal (the ratio of the charge to the radius[4] z/r).

In nitrobenzene, the ionic mobilities[5] of hydrogen, sodium, and potassium ions are 23, 17.2, and 19.2 ($cm^2\ sec^{-1}\ V^{-1}$) respectively; that is, the difference between the limiting conductances of Hexyl-Na and Hexyl-K in Table 1 is smaller than expected (~0.5). This result may be ascribed to the residual water in nitrobenzene (~10^{-3}M), because the water saturated in nitrobenzene shows a tendency to increase the limiting conductance and, furthermore, the effect of the water is striking in going from Cs^+ to Na^+, as is shown in Table 1.

It is clear that the larger the radius of the alkali metal ion, the smaller the association constant, K_0^{MR}. However, the association constants, $K^{MR}_{0(H_2O)}$, are

Table 1. The limiting conductance and association constant for hexyl salts in nitrobenzene

MR	Λ_∞	K_0^{MR}	$\Lambda_{\infty(H_2O)}$	$K^{MR}_{0(H_2O)}$	
Hexyl-Li	30.9	52.6	31.3	3.3	
Hexyl-Na	29.7	13.9	31.1	4.0	25[6]
Hexyl-K	30.2	9.5	31.2	4.6	
Hexyl-Rb	30.0	7.7	30.9	4.7	
Hexyl-Cs	29.4	5.2	30.1	2.3	13[6]

4) L. Pauling, "The Nature of the Chemical Bond," 3rd Ed., Cornell Univ. Press, New York (1960).
5) "Kagaku Benran," Maruzen Co., Tokyo (1966).

nearly the same. It seems that these facts are attributable to the solvation of the alkali metal ions with water. In nitrobenzene containing little water, the ion-pairs are formed between non-solvated metal ions and the Hexyl anion. The association constants, K_o^{MR}, have, therefore, a very close relation with the crystal ionic radius of the cation, as is shown in Fig. 5. However, in nitrobenzene containing much water, as the free cation is strongly solvated with water, the ion-pairs will be formed between hydrated metal cations and the Hexyl anion. Therefore, the formation of the ion-pairs will be more difficult than in nitrobenzene containing little water.

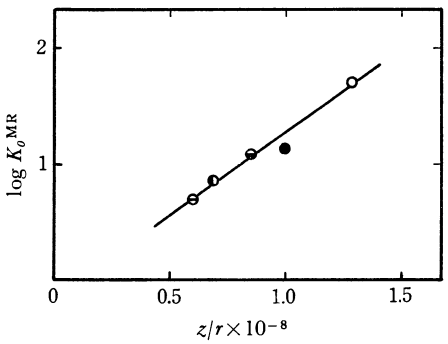

Fig. 5. The plot of $\log K_o^{MR}$ *vs.* z/r.
The symbols used are the same as those in Fig. 1.

These concepts are supported by the following two facts. One is that water is coextracted in nitrobenzene with Hexyl salts, the amount of the coextracted water, as determined by the Karl-Fisher method, decreases in the folowing order: Hexyl-Li (5.5 H_2O mol/Hexyl salts mol)>-Na (3.5)>-K (1.3)>-Rb (0.7), -Cs (0.7), showing that lithium and sodium are solvated very strongly with water. The other fact is that a plot of $\log K_o^{MR}$ *vs.* z/r shows a linearity; that is, the association affinities of Hexyl salts are found to be electrostatic and to be determined chiefly by the ionic radius of the alkali metal.

Kyrš[6] obtained the dissociation constants (K') of Hexyl salts by solvent extraction. His values ($1/K'$) are different from the values ($K^{MR}_{o(H_2O)}$) obtained by the present authors and are closer to the constants, K_o^{MR}, rather than to $K^{MR}_{o(H_2O)}$.

Distribution Ratio of Hexyl Salts. q_R was calculated from C_o^R and C_a^R which had been determined spectrophotometrically. In nitrobenzene, the calibration curves of Hexyl salts follow Beer's law under the conditions of $C_o^R=1—10\times10^{-5}$M at 470 mμ ($\varepsilon=19500$) and $C_o^R=1—10\times10^{-4}$M at 545 mμ ($\varepsilon=885$) and in water follow Beer's law under the conditions of $C_a^R=1—10\times10^{-6}$M at 430 mμ ($\varepsilon=$26200), $C_a^R=1—10\times10^{-5}$M at 505 mμ ($\varepsilon=8920$), and $C_a^R=1—10\times10^{-4}$M at 525 mμ ($\varepsilon=4580$).

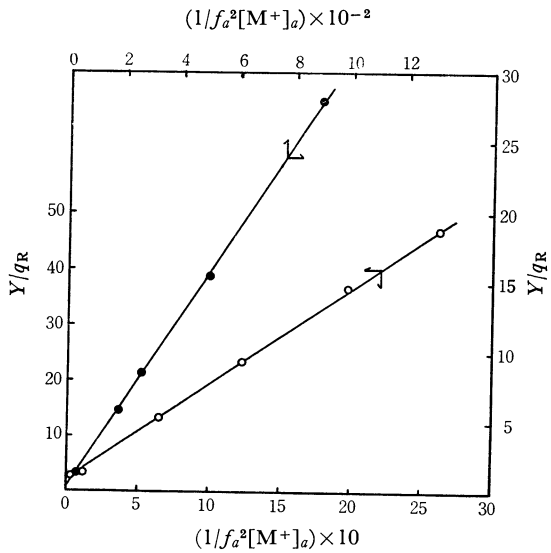

Fig. 6. The plot of Y/q_R *vs.* $1/f_a^2[M^+]_a$.
The symbols used are the same as those in Fig. 1.

In a nitrobenzene solution, the molar extinction coefficients of Hexyl-alkali metal salts are identical; this is also true in water. Besides, no difference between the molar extinction coefficients of the ion-pair and the Hexyl anion was noticed.

Association Constants of Hexyl Salts in an Aqueous Solution. The values of K_a^{MR} can be estimated from Eq. (7). The extractions were carried out by shaking the nitrobenzene solution of Hexyl salts with an aqueous solution containing a known amount of the same kind of alkali metal.

Figures 6 and 7 show the plot of Y/q_R against $1/f_a^2[M^+]_a$. All the straight lines were drawn by means of the method of least squares. In the case of Hexyl-Cs, the association constants could not be obtained, because the distribution ratio is very large, so q_R becomes very uncertain.

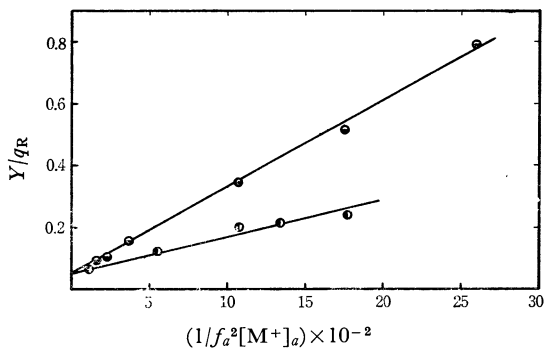

Fig. 7. The plot of Y/q_R *vs.* $1/f_a^2[M^+]_a$.
The symbols used are the same as those in Fig. 1.

6) M. Kyrš and S. Podešva, *Collection Czech. Chem. Commun.*, **27**, 289 (1962).

In Table 2, the constants thus obtained, K_a^{MR} and D_{MR}, are shown; the extraction constants, E_{MR} ($= [MR]_o/[M^+]_a[R^-]_a = D_{MR} \cdot K_a^{MR}$), are also shown in order to compare them with the results obtained by a different method.[6] Though the extraction constant of Hexyl-Cs could not be obtained accurately, $\log E_{CsR}$ was estimated to be more than 5. The values of the extraction constants in the present studies have the same tendency as the results obtained by a different method.

Figure 8 shows a plot of $\log K_a^{MR}$ against z/r_{hyd}, where r_{hyd} is the effective diameter[5] of the hydrated

Table 2. The constants of K_a^{MR}, D_{MR} and $\log E_{MR}$ for hexyl salts

MR	K_a^{MR}	D_{MR}	$\log E_{MR}$	
Hexyl-Li	8.9	0.5	0.76	
Hexyl-Na	9.4	3.4	1.51	2.4[6]
Hexyl-K	174	20.4	3.55	
Hexyl-Rb	365	22.2	3.91	
Hexyl-Cs			(>5)	5.4[6]

alkali metal ions in an aqueous solution. From this plot it is found that, in an aqueous solution, the association affinities depend chiefly upon the hydrated radius of the alkali metal ion, and that ion-pairs will be formed between the Hexyl anion and the hydrated alkali metal cation.

From the association constants of Hexyl alkali metal salts in an aqueous solution, it is found that the larger the constant, K_a^{MR}, the smaller the solubility of the Hexyl salts. When the extraction of the alkali metal is discussed, K_a^{MR}, D_{MR} and K_o^{MR}

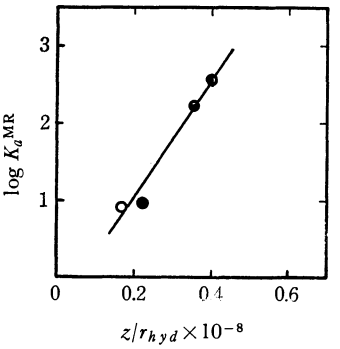

Fig. 8. The plot of $\log K_a^{MR}$ *vs.* z/r_{hyd}.
The symbols used are the same as those in Fig. 1.

are very important. The relation of the distribution ratio, q_M, to these values is shown by Eq. (8):

$$q_M = \frac{C_o^M}{C_a^M} = D_{MR}\left(1 + \frac{1}{K_o^{MR}[R^-]_o f_o^2}\right) \times \left(1 + \frac{1}{K_a^{MR}[R^-]_a f_a^2}\right)^{-1} \quad (8)$$

where C_o^M and C_a^M represent the total concentrations of alkali metal in the organic and aqueous phases respectively. From Eq. (8), it is clear that the extractability of the alkali metal increases with an increase in the values of K_a^{MR} and D_{MR} and with a decrease in the K_o^{MR} value.

The authors are very grateful to Dr. Syozo Sato (Mitsubishi Kasei Co., Ltd.) for his generous gifts of "Hexyl Natrium."

BULLETIN OF THE CHEMICAL SOCIETY OF JAPAN VOL. 42 1011—1016 (1969)

The Spectrophotometric Determination of Palladium with Chromazurol S*[1]

Ryoei ISHIDA

Department of Chemistry, Hakodate Branch, Hokkaido University of Education, Hachiman-cho, Hakodate, Hokkaido

(Received August 21, 1968)

A simple spectrophotometric method for the determination of palladium was studied, using chromazurol S as a reagent. Palladium(II), in a slightly acidic or a nearly neutral solution, reacts with chromazurol S to form blue or red complexes, each consisting of one molecule of the reagent and one atom of palladium. The maximum absorption wavelengths of blue and red complexes are respectively 596 mμ and 500 mμ, against the reagent blanks. The color development of the blue complex formed in a slightly acidic medium is more sensitive, therefore, it was applied to the spectrophotometric determination of palladium. Several conditions for the color development were investigated; a calibration curve was made under the optimum conditions; and the influences of coexisting ions were also investigated. The blue complex gives a maximum absorbance at 596 mμ in the pH range from 4.3 to 5.3. About a 2-fold excess of the reagent over the palladium concentration is necessary in order to obtain the maximum color intensity. The color development is almost instantaneous, and the absorbance remains constant for at least 4 hr. The order of the addition of reagents has no effect upon the absorbance. The color system obeys Beer's law over the concentration range up to 70 μg of palladium per 10 ml. The molar extinction coefficient at 596 mμ is 18600, which corresponds to a sensitivity index of 0.0058 μg/cm^2 for an absorbance of 0.001. Sulfate, chloride, fluoride, phosphate and acetate ions do not interfere with the color reaction. Thiosulfate ion and polycarboxylate ions such as oxalate, citrate and EDTA *etc.* bleach the color of the complex. Cations such as Sc(III), Y(III), Th(IV), U(VI), Be(II), Al(III) and Cu(II) ions cause an over-estimation of palladium; the interference by these cations except copper, however, could be eliminated by the addition of appropriate amounts of either sodium fluoride or sodium phosphate as masking agent.

Chromazurol S reacts with palladous ion in a weakly acidic or a nearly neutral medium to form blue or red complexes according to the pH value of the solution.

In the present paper are described conditions which permit the spectrophotometric determination of palladium at microgram levels.

Dey *et al.*[1,2] and Horiuchi *et al.*[3] have previously proposed methods for determining palladium, using the colored complex with chromazurol S. Their results differ, however, appreciably from the present results and their procedures for the determination are more complicated.

Several conditions for the color development and the composition of the colored complex were investigated. A calibration curve was made under the optimum condition. The influences of coexisting ions were investigated.

Experimental

Apparatus. Spectrophotometric measurements were made with a Shimadzu model QR-50 spectrophotometer, using 1 cm glass transmission cells. All absorbance measurements were carried out at about 20°C. The pH measurements of the solutions were made with a Hitachi-Horiba model M-4 glass electrode pH meter.

Reagents. *Stock Solution of Palladium.* A palladium stock solution was prepared by dissolving palladous chloride powder of analytical reagent grade in a small amount of 1 N perchloric acid, with heating, and then by diluting with distilled water. The resultant solution was standardized by EDTA titration. A standard working solution was prepared by taking an aliquot of the stock solution and diluting it to the desired concentration.

Chromazurol S Solution. About 1.0×10^{-3} M of a chromazurol S solution was prepared by dissolving Dotite Chromazurol S reagent (Dojindo & Co., Kumamoto) in distilled water and then by filtering off the floating residue.

Buffer Solution. Buffer solutions of various pH values were prepared by mixing 1.0 M hexamethylenetetramine and 1.0 N perchloric acid solutions in different ratios.

Other Reagents. All other reagents were of reagent grade.

*1 Presented at the Hokkaido Branch Meeting of the Chemical Society of Japan, Kitami, July, 1967. This paper is a part of the author's doctorate dissertation submitted to Hokkaido University, 1967.

1) S. P. Sangal and A. K. Dey, *Mikrochim. Ichnoanal. Acta*, **1963**, 993.

2) S. P. Sangal and A. K. Dey, *J. Indian Chem. Soc.*, **40**, 464 (1963).

3) Y. Horiuchi and H. Nishida, *Bunseki Kagaku (Japan Analyst)*, **16**, 1018 (1967).

Standard Procedure. Transfer a sample aliquot, containing 10 to 50 μg of palladium, to a 10 m*l* volumetric flask, and then add 0.3 m*l* of a pH 5.0 buffer solution and 1.0 to 1.5 m*l* of a 1.0×10^{-3} M solution of chromazurol S. The solution is diluted to the mark with distilled water, mixed, and allowed to stand for about 1 hr. The absorbance of the solution is measured at 596 mμ by using the reagent blank.

Results and Discussion

Absorption Spectra. The absorption spectrum of the palladium - chromazurol S complex is greatly affected in its shape by pH value of the medium. As described in the following section, however, a spectrum with an absorption maximum at 596 mμ in the pH range between 4.3 and 5.3 was obtained. Figure 1 shows the absorption spectra of chromazurol S and its palladium complex at a pH of 5.0. Chromazurol S is abbreviated as ChS in all figures.

In order to observe the spectral changes cause by varying pH values, a series of solutions containing 32 μg of palladium and 1.0 m*l* of a 1.0×10^{-3} M solution of chromazurol S were prepared at different pH values. The absorption spectrum of each solution was measured against the reagent blank. The results are shown in Fig. 2. In the pH range between 4.3 and 5.3, the maximum absorption wavelength is found at 596 mμ, and the absorption spectra indicate similar shapes. At pH below 4, each peak of the spectrum is shifted toward a longer wavelength; and at pH below 2, a part of the formed complex precipitates. In the pH range between 5.3 and 7.0, the intensity of the absorbance at 596 mμ decreases gradually, in accordance with the increasing pH value of the solution, while an absorption newly appears with a maximum at 500 mμ (curves 7, 6, 5 and 4 in Fig. 2); moreover, these spectra show an isosbestic point at about 545 mμ. It seems that two absorbing species which are in equilibrium with each other have absorption maxima at respectively 596 and 500 mμ. At pH 7.5 or higher, the disappearance of the absorption at 596 mμ is observed, only giving small shoulders. Any absorbance of the complex almost disappears at a pH value of about 8.5.

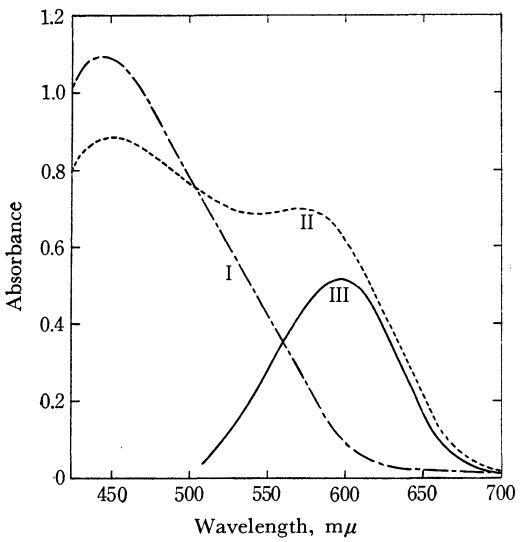

Fig. 1. Absorption spectra of chromazurol S and its palladium complex.
Pd: 3.0×10^{-5} M, ChS: 1.0×10^{-4} M, pH: 5.0
I: ChS *vs.* H_2O, II: Pd-ChS *vs.* H_2O
III: Pd-ChS *vs.* ChS

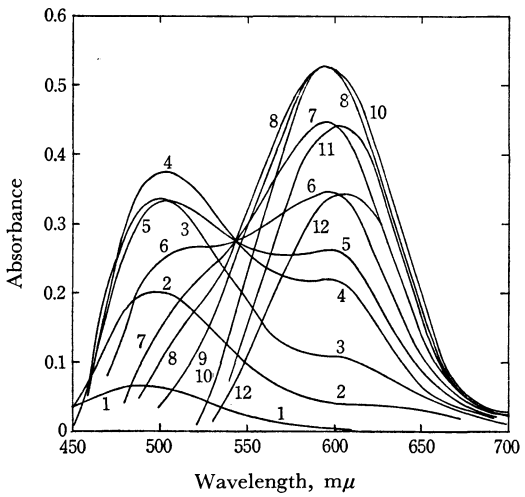

Fig. 2. Absorption spectra of Pd-ChS complex at various pH values.
Pd: 32 μg, ChS: 1.0×10^{-4} M
1: pH 8.2, 2: pH 7.8, 3: pH 7.5, 4: pH 7.1
5: pH 6.9, 6: pH 6.4, 7: pH 5.9, 8: pH 5.3
9: pH 5.0, 10: pH 4.3, 11: pH 3.7, 12: pH 2.7

In the practical spectrophotometric determination of palladium, the complex with absorption maximum at 596 mμ in the pH range between 4.3 and 5.3 was used.

Though the figure is not given, the absorption spectra of solutions containing 0.5 μmol of chromazurol S and palladium added in various amounts up to 5.0×10^{-5} M, show an isosbestic point at about 505 mμ against the water blank at pH 5.0. The occurrence of an isosbestic point indicates that there is only one kind of complex under these conditions.

Effect of pH Value and That of the Amount of the Buffer Solution. The effect of pH on the color development of the palladium complex was studied with solutions varying in pH value from 4 to 8. Figure 3 shows that the maximum and nearly constant absorbance is obtained over the pH range from 4.3 to 5.3.

At a constant pH, the absorbance of the colored solution was measured by varying the amount of the buffer solution. In consequence, the color intensity decreased gradually, by increasing amounts

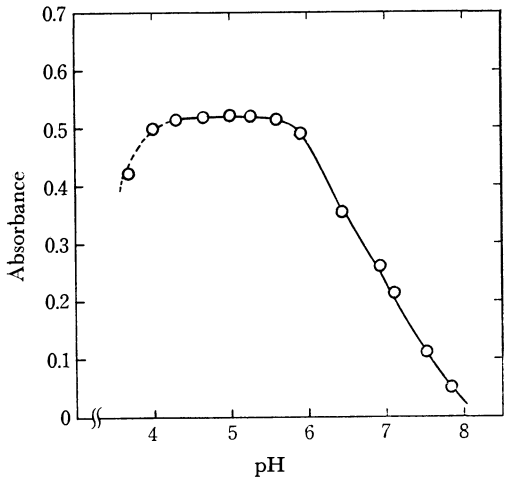

Fig. 3. Effect of pH on color development.
Pd: 3.0×10^{-5} M, ChS: 1.0×10^{-4} M
Wavelength: 596 mμ

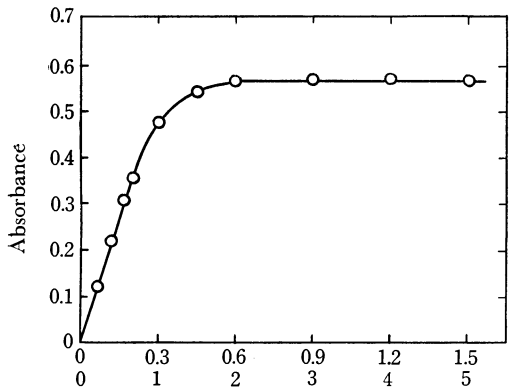

Upper scale: 1.0×10^{-3} M ChS, ml
Lower scale: Mole ratio, [ChS]/[Pd]

Fig. 4. Effect of addition of chromazurol S.
Pd: 0.3 μmol (32 μg), pH: 5.0
Wavelength: 596 mμ

of the buffer solution. In this series of experiments, therefore, 0.3 ml of a 1.0 M buffer solution per 10 ml was always used.

Effect of the Addition of Chromazurol S. In order to study the effect of the concentration of chromazurol S, a series of absorbances was measured under various concentrations of chromazurol S, reagent blanks of same concentration being used as the reference. The results are shown in Fig. 4. The maximum absorbance is obtained by adding more than 0.6 ml of a 1.0×10^{-3} M chromazurol S solution for 0.3 μmol of palladium. Namely, more than a 2-fold excess of the reagent over the palladium concentration is necessary in order to obtain the maximum color intensity.

Effect of Temperature. The absorbance of colored solution was measured at various temperatures. The absorbance gradually decreases with the rise of temperature, and over 30°C the color intensity decreased remarkably. In this series of experiments, therefore, all absorbance measurements were carried out at about 20°C.

Effect of the Order of Adding Reagents. The varying orders in which the reagents were added had no significant effects on the absorbances.

Color Stability. As is shown in Fig. 5, the absorbance of the resultant solution decreased slowly for the first 30 min. After this period, however, it remained practically constant for at least 4 hr.

Calibration Curve. A calibration curve was made under the optimum conditions of those in the sections above-mentioned. The results are

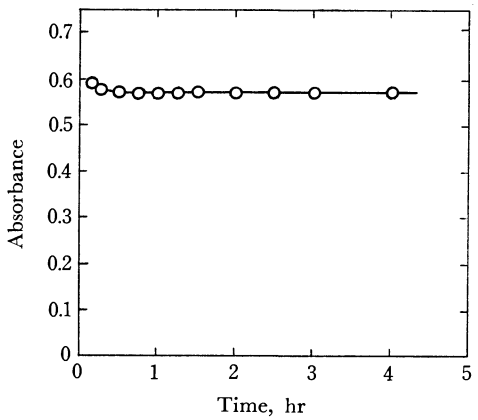

Fig. 5. Color stability.
Pd: 32 μg, ChS: 1.0×10^{-4} M
pH: 5.0, Wavelength: 596 mμ

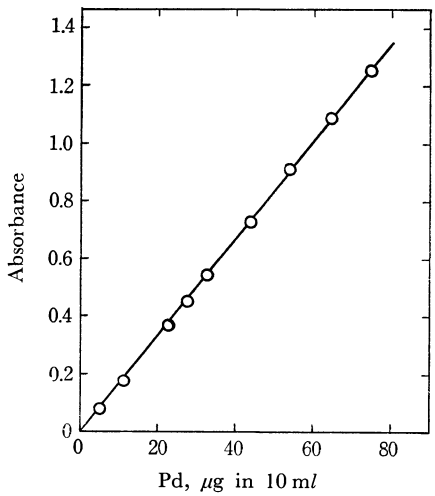

Fig. 6. Calibration curve.
pH: 5.0, Wavelength: 596 mμ

4) A. Ringbom, *Z. Anal. Chem.*, **115**, 332 (1939).
5) E. B. Sandell, "Colorimetric Determination of Traces of Metals," 3rd Ed., Interscience Publishers Inc., New York (1959), p. 80.

shown in Fig. 6. A linear relationship exists between the absorbance and the palladium concentration over the range investigated. The optimum concentration range was then determined by Ringbom's procedure[4] and was found to lie between 10 and 50 μg palladium per 10 ml. Under the conditions of the spectrophotometric determination, the apparent molar extinction coefficient was found to be 18600. The sensitivity of the reaction as expressed by Sandell's notation[5] is 0.0058 μg of palladium per cm^2. This value is about 7-folds more sensitive than that of the data of Dey *et al.*[1]

For the spectrophotometric determination of palladium, several reagents have been used, such as *p*-nitrosodiphenylamine,[6] *p*-nitrosodimethylaniline,[7] mercaptoacetic acid,[8] potassium iodide,[9] ethylenediaminetetraacetic acid,[10] 2-nitroso-1-naphthol,[11] α-furildioxime,[12] xylenol orange,[13] 2-hydroxy-5-methylpropiophenone oxime,[14] and *p*-(mercaptoacetamido)benzenesulfonic acid.[15] The methods using the above reagents, however, in many cases, required the extraction of the complexes into an organic solvent.

The present reagent, chromazurol S, like xylenol orange,[13] has an advantages as a colorimetric reagent for palladium; that is, no extraction of the complex is required, since a palladium-chromazurol S complex is water soluble. This method is comparable in sensitivity with the 2-nitroso-1-naphthol[11] and α-furildioxime[12] methods.

Complex Formation. The combining ratio of palladium and chromazurol S in the complex was studied by the continuous variation method[16] and by the mole ratio method.[17] The results are shown in Figs. 7 and 8. Curves A and B in Figs. 7 and 8 show respectively the plots for the complex having a maximum at 596 mμ, which is formed in a weakly acidic medium, and those for the complex having a maximum at 500 mμ, which is formed in a nearly neutral medium. As is shown in these figures, it may be concluded that palladium forms either of two 1 : 1 complexes, one a red complex with its absorption maximum at 500 mμ and the other a blue complex with its absorption maximum at 596 mμ. From the results of these spectrophotometric studies and the appearance of an isosbestic point, which has already been shown in Fig. 2, it is assumed that the two complex ions are charged differently. It is impossible to obtain definite information on the structures of these palladium-chromazurol S complexes on the basis

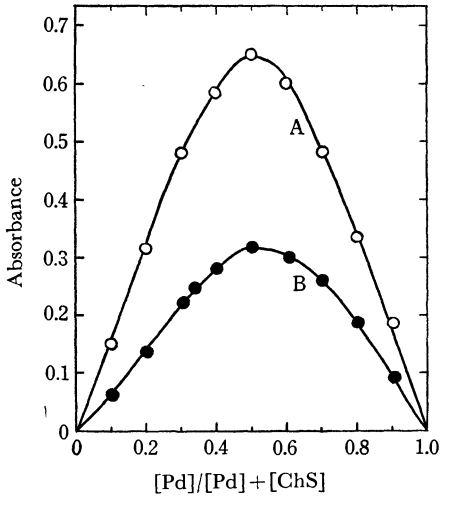

Fig. 7. Continuous variation method.
A: pH, 5.0; Wavelength, 596 mμ;
[Pd]+[ChS]=8.0×10^{-5} M
B: pH, 8.0; Wavelength, 500 mμ;
[Pd]+[ChS]=1.5×10^{-4} M

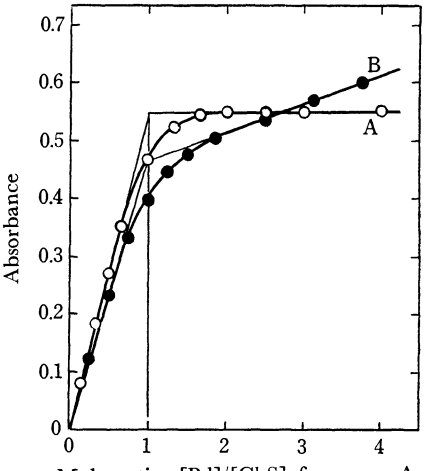

Fig. 8. Mole ratio method.
A: pH, 5.0; Wavelength, 596 mμ;
[ChS]=3.0×10^{-5} M
B: pH, 7.8; Wavelength, 500 mμ;
[Pd]=8.0×10^{-5} M

6) J. H. Yoe and L. G. Overholser, *J. Am. Chem. Soc.*, **61**, 2058 (1939).
7) L. G. Overholser and J. H. Yoe, *ibid.*, **63**, 3224 (1941).
8) O. König and W. R. Crowell, *Mikrochem. ver. Mikrochim. Acta*, **33**, 298 (1948).
9) J. G. Fraser, F. E. Beamish and W. A. E. McBryde, *Anal. Chem.*, **26**, 495 (1954).
10) W. M. MacNevin and O. H. Kriege, *ibid.*, **26**, 1768 (1954).
11) K. L. Cheng, *ibid.*, **26**, 1894 (1954).
12) O. Menis and T. C. Rains, *ibid.*, **27**, 1932 (1955).
13) M. Otomo, This Bulletin, **36**, 889 (1963).
14) S. Prakash, R. P. Singh and K. C. Trikha, *Talanta*, **13**, 1393 (1966).
15) H. K. L. Gupta, M. R. Bhandari and N. C. Sogani, This Bulletin, **40**, 215 (1967).
16) P. Job, *Ann. Chim.*, **9**, 113 (1928).
17) J. H. Yoe and A. L. Jones, *Ind. Eng. Chem. Anal. Ed.*, **16**, 111 (1944).

Table 1. Effect of diverse ions on palladium determination
Palladium taken: 32.0 μg

Ion added, μmol		Palladium found, μg	Ion added, μmol		Palladium found, μg
Sulfate	30	32.3	Ammonium(I)	0.3	31.8
Chloride	3	32.0		3.0	32.2
	15	21.5	Cobalt(II)	0.3	31.7
Fluoride	6	32.1		1.5	31.9
	15	27.1	Molybdenum(VI)	0.3	32.1
Phosphate	1.5	32.2		1.5	32.4
	3	31.8	Calcium(II)	0.3	32.1
	30	30.9		1.5	32.6
Acetate	3	32.2	Iron(II)	0.15	31.9
	15	26.0		0.3	34.8
Carbonate	0.3	31.6	Indium(III)	0.03	34.4
	1.5	24.9		0.3	36.8
Cyanide	0.3	31.9	Yttrium(III)	0.03	32.9
	1.5	21.1		0.3	39.6
Pyroborate	0.3	32.0	Thorium(IV)	0.03	32.0
	1.5	2.5		0.3	47.5
Thiosulfate	0.03	25.7	Copper(II)	0.03	34.5
	0.1	15.8		0.3	47.1
Oxalate	0.03	30.0	Beryllium(II)	0.03	36.0
	0.3	15.0		0.3	59.1
Citrate	0.03	30.1	Scandium(III)	0.03	38.0
	0.3	18.4		0.3	70.2
EDTA	0.03	26.4	Uranium(VI)	0.03	36.9
	0.1	14.2		0.15	57.7
			Aluminium(III)	0.03	41.3
Silver(I)	0.3	32.4		0.15	60.0
	1.0	29.0	Tungsten(VI)	0.3	31.2
Cadmium(II)	0.3	32.0		1.5	21.0
	3.0	31.9	Mercury(II)	0.3	32.2
Lead(II)	0.3	31.9		1.5	28.4
	3.0	31.7	Mercury(I)	0.03	32.3
Manganese(II)	0.3	32.0		0.3	27.6
	3.0	31.8	Tin(II)	0.03	31.7
Nickel(II)	0.3	32.7		0.3	27.0
	3.0	31.7	Neodymium(III)	0.03	31.8
Barium(II)	0.3	32.2		0.15	27.8
	3.0	32.0	Iron(III)	0.03	32.5
Strontium(II)	0.3	31.9		0.15	28.9
	3.0	32.0	Cerium(III)	0.3	32.1
Magnesium(II)	0.3	31.8		0.6	ppt.
	3.0	31.8	Bismuth(III)	0.3	31.3
Zinc(II)	0.3	31.9		0.6	ppt.
	3.0	32.4			

of the experimental results described in the present paper.

Horiuchi *et al.*[3] have indicated that the optimum pH value range for color development is 5.8 to 6.7 and that complexes of 1 to 1 or 1 to 2 are formed, according to the concentration of the reagent used. It seems that the difference between their results and those obtained here may be attributed to the difference between the experimental conditions used.

Effect of Diverse Ions. In order to test the effect of diverse ions upon the palladium determination, absorbance measurements were made for the solutions containing 32.0 μg of palladium and various amounts of particular ion. The results are summarized in Table 1.

Sulfate, chloride, fluoride, phosphate and acetate ions do not interfere, even when present in considerably large amounts. Such anions as carbonate, cyanide and pyroborate ions do not interfere when their amounts are equivalent with palladium; however, these ions give negative errors at higher concentrations. Thiosulfate, oxalate, citrate and EDTA ions inhibit the color formation of the complex, even when added in very small amounts.

Of the 30 cations tested, Fe(II, III), In(III), Y(III), Th(IV), Cu(II), Be(II), Sc(III), U(VI), Al(III), W(VI), Hg(I, II), Sn(II), Nd(III), Ce(III) and Bi(III) interfere with the palladium determination. Among the above cations, Hg(I), Sn(II), Nd(III) and Fe(III) give negative error,

Table 2. Effect of masking agents on palladium determination

Palladium taken: 32.0 μg
Cation added: each 0.3 μmol

Cation	Palladium found, μg Masking agents added:		
	None	Na_3PO_4 3.0 μmol	NaF 6.0 μmol
In(III)	36.8	32.6	33.9
Y(III)	39.6	31.6	32.3
Th(IV)	47.5	31.3	32.3
Sc(III)	70.2	31.1	30.6
Be(II)	59.1	51.0	31.5
Al(III)	73.1	54.0	31.3
U(VI)	75.9	31.9	39.6
Cu(II)	47.1	42.7	45.5

and 0.6 μmol of Ce(III) and Bi(III) precipitate and interfere under these conditions. However, fluoride and phosphate ions, which probably form more stable complexes with many other metal ions to decompose the corresponding chromazurol S complexes, have almost no influence on the complex formation with palladium and chromazurol S unless large amounts are added. Sodium fluoride and sodium phosphate can, therefore, serve as excellent masking agents to prevent the interference of other metals. The results when used fluoride and phosphate ions as masking agent are shown in Table 2.

As is shown in Table 2, among the coexisting ions which introduce positive error with the determination of palladium, metal cations except copper can be effectively masked by either phosphate or fluoride. Accordingly, it is possible to improve selectivity of chromazurol S reagent for palladium.

The author wishes to express his thanks to Miss Kimiko Imai for her assistance in the measurements. Support by the Scientific Research Fund of the Ministry of Education is gratefully acknowledged.

BULLETIN OF THE CHEMICAL SOCIETY OF JAPAN VOL. 42 1016—1020 (1969)

The Crystal Structure of $(-)_D$-Tris(trimethylenediamine)cobalt(III) Bromide Monohydrate*1

Teruo NOMURA,*2 Fumiyuki MARUMO and Yoshihiko SAITO

The Institute for Solid State Physics, The University of Tokyo, Roppongi, Minato-ku, Tokyo

(Received August 22, 1968)

The structure of $(-)_D$-$[Co(tn)_3]Br_3 \cdot H_2O$ (tn: $H_2N-CH_2-CH_2-CH_2-NH_2$) has been solved by the heavy atom method and refined to $R=0.11$ by least-squares analysis based on 1845 three-dimensional data. The substance crystallizes in the monoclinic space group $P2_1$ with unit cell dimensions: $a=16.274$, $b=9.863$, $c=9.489$ Å, $\beta=126.4°$ and $Z=2$. The complex ion in the structure has approximately a three-fold axis of rotation. The three six-membered Co-tn rings are nearly identical and take chair form. The chelate ring is rather flattened out, owing to the strong H-H repulsion. The absolute configuration of $(-)_D$-$[Co(tn)_3]^{3+}$ has been found to be the same as that of $(+)_D$-$[Co(en)_3]^{3+}$.

The absolute configuration of the complex ions, $(+)_D$-$[Co(en)_3]^{3+}$ and $(-)_D$-$[Co(l\text{-}pn)_3]^{3+}$ have been determined by means of X-rays.[1-3] They have five-membered chelate rings. No investigation has, however, been made on the absolute configurations of the complex ions with six-membered chelate rings. One of the simplest of those is tris(trimethylenediamine)cobalt(III) ion, $[Co(tn)_3]^{3+}$. The ORD and CD of $[Co(tn)_3]^{3+}$ have been measured by Woldbye.[4,5] The present investigation of the crystal structure of $(-)_D$-tris(trimethylenediamine)cobalt(III) bromide

*1 Part of this paper is taken from the Doctoral Thesis presented to the University of Tokyo by Teruo Nomura, 1968. Short Communication, This Bulletin, **41**, 530 (1968).

*2 Present address: Department of Chemistry, Rikkyo University, Ikebukuro, Tokyo.

1) Y. Saito, K. Nakatsu, M. Shiro and H. Kuroya, *Acta Cryst.*, **8**, 729 (1955); This Bulletin, **30**, 795 (1957).

2) Y. Saito, H. Iwasaki and H. Ota, This Bulletin, **36**, 1543 (1963).

3) H. Iwasaki and Y. Saito, *ibid.*, **39**, 92 (1966).

4) F. Woldbye, "Optical Rotatory Dispersion of Transition Metal Complexes," European Research Office, U. S. Army, Frankfurt a. M. (1959).

5) F. Woldbye, *Record of Chemical Progress*, **24**, 197 (1963).

monohydrate was undertaken with the purpose of contributing a better knowledge about the relation of the absolute configuration and optical properties of transition metal complexes.

Experimental

$(-)_D$-Tris(trimethylenediamine)cobalt(III) bromide monohydrate was kindly supplied by Professor Woldbye, Technical University of Denmark. Single crystals suitable for X-ray work were grown by slow evaporation of aqueous solution at room temperature. The specimens used for the collection of the intensity data were polished into cylinders of diameter 0.07 cm, the axes being parallel to the *b*- and *c*-axis, respectively. Using Cu$K\alpha$ radiation, equi-inclination Weissenberg photographs were taken of the zero to sixth levels for the crystal rotating about the *b*-axis and the zero to ninth level of the *c*-axis rotation. The intensities were measured visually using standard calibrated scales and were converted to structure amplitude values in the usual way. Correction was also made for absorption by assuming the crystal to be a perfect cylinder. It was soon found that the intensity data obtained with the *c*-axis rotation are not very accurate owing to the ill-formed shape of the specimen, so that they were eliminated from the final set of data used for the refinement. A total of 1845 independent pieces of intensity data were collected.

The crystal data are as follows: $[Co(H_2N\text{-}CH_2\text{-}CH_2\text{-}CH_2\text{-}NH_2)_3]Br_3 \cdot H_2O$, F.W.=538.6, Monoclinic, space group $P2_1$ (No. 4*[3]), a=16.275(10), b=7.863(15), c=9.489(5) Å, β=126.4(1)°, U=970 Å^3, (Cu$K\alpha$ radiation, λ=1.5418 Å), D_m=1.80 g·cm^{-3}, Z=2, D_x=1.79 g·cm^{-3}. Linear absorption coefficient for Cu$K\alpha$ radiation μ=154.0 cm^{-1}.

Determination of the Structure

A three-dimensional Patterson synthesis was calculated, in order to seek the heavy atom-heavy atom vectors. This normal Patterson synthesis was, however, found to be inadequate for this purpose since rather serious overlappings of peaks were observed. To reduce the overlappings a Patterson synthesis was calculated with only the reflections, of which $\sin\theta/\lambda \geq 0.45$. These reflections were supposed to consist mainly of the contributions of the heavy atoms. The peaks were sharpened to a good extent. The interpretation of the Patterson synthesis was not so straightforward because there exist as many as eight heavy atoms in the unit cell (6 Br and 2 Co). After several trials positions of the heavy atoms could be assigned. The coordinates of these atoms were refined by a block-diagonal least-squares method. The discrepancy factor, $R=\sum||F_o|-|F_c||/\sum|F_o|$, decreased to 0.27. A three-dimensional Fourier synthesis with phases determined by the heavy atoms allowed the six nitrogen atoms to be located around the cobalt atom. After further refinements a Fourier synthesis of electron density and a difference synthesis revealed the positions of the rest of all the lighter atoms except those of hydrogen atoms and also indicated that anisotropic temperature factors were required for all the atoms. After several cycles of least-squares refinement with anisotropic thermal parameters, the discrepancy factor was 0.11. The absolute configuration of the complex ion was automatically determined when dispersion corrections were taken into account during the course of the refinement. Part of observed and calculated relations between hkl and $h\bar{k}l$ are compared in Table 1. A final difference Fourier synthesis gave no significant indications of the positions of hydrogen atoms. Atomic scattering factors were taken from International Tables for X-ray Crystallography.[6] Dispersion corrections were also taken from the International Tables. The Fourier synthesis program used is ANSFR-1 written by Dr. H. Iwasaki, in which the anomalous scattering is taken into consideration. The least-squares program is HBLS-III written by Dr. T. Ashida. The weights were assumed as 1 for all

Table 1. Calculated and observed intensity relations between hkl and $h\bar{k}l$

h k l	$Fc^2(hkl)/4$	Obsd	$Fc^2(h\bar{k}l)/4$
1 1 $\bar{2}$	2284	>	2174
3 1 $\bar{2}$	1287	<	1707
3 1 $\bar{4}$	38.1	>	30.9
4 1 $\bar{3}$	330.5	<	533.6
5 1 $\bar{4}$	240.9	>	160.8
5 1 $\bar{9}$	8.4	>	3.4
6 1 $\bar{5}$	170.8	<	199.1
6 1 $\bar{9}$	8.5	<	9.9
7 1 $\bar{6}$	206.8	<	238.1
8 1 $\bar{3}$	634.0	>	448.2
9 1 $\bar{3}$	377.1	<	507.6
10 1 $\bar{3}$	124.3	<	196.0
11 1 $\bar{3}$	173.7	>	110.7
12 1 $\bar{3}$	56.4	<	72.1
2 2 3	98.8	>	92.7
2 2 $\bar{9}$	1.9	<	2.3
3 2 $\bar{4}$	500.0	>	462.3
4 2 $\bar{3}$	390.1	<	411.3
4 2 $\bar{8}$	9.9	>	6.6
4 2 $\bar{9}$	7.8	<	9.5
5 2 $\bar{5}$	576.0	<	653.8
6 2 $\bar{8}$	6.7	<	14.2
7 2 $\bar{7}$	17.4	>	15.0
1 3 3	379.9	>	368.6
2 3 $\bar{3}$	393.6	>	318.6
2 3 3	374.4	>	310.1

*[3] $P2_1/m$ is excluded since the crystal is optically active.

6) International Tables for X-ray Crystallography, Vol. III, Kynoch Press, Birmingham (1962).

reflections in the least-squares refinements. The final three dimensional electron density map is shown in Fig. 1. The final parameters are given in Tables 2 and 3. Agreement between the observed and calculated structure amplitudes is reasonable.*4 The standard deviations of the coordinates, estimated from least-squares results, are 0.005 Å for the bromine and cobalt atoms and 0.03 Å (mean) for others.

TABLE 2. FINAL FRACTIONAL COORDINATES AND THEIR e. s. d.'s

Atom	$x(\sigma(x))\times 10^4$	$y(\sigma(y))\times 10^4$	$z(\sigma(z))\times 10^4$
Co	2373(3)	4587(7)	4293(5)
Br(1)	0683(3)	0000(6)	0958(4)
Br(2)	2704(3)	0730(6)	6770(5)
Br(3)	4111(3)	2083(8)	2622(5)
N(1)	1969(19)	4005(47)	2007(33)
N(2)	2783(16)	5030(36)	6806(28)
N(3)	1305(16)	6401(34)	3412(27)
N(4)	1446(16)	2712(35)	4081(30)
N(5)	3392(15)	2706(35)	5232(29)
N(6)	3386(17)	6386(37)	4913(31)
C(1)	0751(25)	3133(51)	4532(55)
C(2)	0647(22)	6380(52)	3981(43)
C(3)	0060(25)	4692(58)	3524(54)
C(4)	3868(21)	5053(63)	8283(37)
C(5)	4387(20)	3354(46)	8444(36)
C(6)	4415(20)	2978(48)	6882(39)
C(7)	3151(22)	7485(55)	3486(37)
C(8)	1969(21)	5398(46)	0973(34)
C(9)	2972(25)	6419(59)	1964(44)
O	2192(15)	2397(41)	8406(26)

Description of the Structure and Discussion

A projection of the contents of an asymmetric unit onto the plane (010) is presented in Fig. 2. The bond lengths and bond angles with their

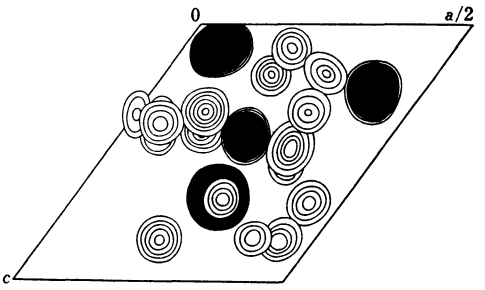

Fig. 1. The final three-dimensional electron density map composed of sections through the atomic centers parallel to (010). The contours are drawn at intervals of 1.0 e.Å^3, starting with 1.0 e.Å^{-3}.

TABLE 3. FINAL THERMAL PARAMETERS AND THEIR e. s. d.*

Temperature factors are of the form: $\exp[-(h^2\beta_{11}+k^2\beta_{22}+l^2\beta_{33}+2hk\beta_{12}+2hl\beta_{13}+2kl\beta_{23})]$.

Atom	$\beta_{11}\times 10^5$	$\beta_{22}\times 10^5$	$\beta_{33}\times 10^5$	$\beta_{12}\times 10^5$	$\beta_{13}\times 10^5$	$\beta_{23}\times 10^5$
Co	00695(0)	02987(2)	02962(1)	00021(0)	00892(0)	−00143(2)
Br(1)	01011(0)	03502(2)	03136(1)	00253(0)	00720(0)	−00089(1)
Br(2)	01293(0)	03155(2)	03779(1)	−00065(0)	01267(0)	−00212(1)
Br(3)	01040(0)	05566(2)	03438(1)	00820(0)	01128(0)	−00032(2)
N(1)	01076(1)	04938(16)	03509(11)	00121(4)	01278(2)	−00120(11)
N(2)	00965(1)	02758(10)	02073(8)	00086(3)	00958(1)	−00152(9)
N(3)	00848(1)	03257(11)	02771(8)	−00277(3)	00975(1)	−00447(8)
N(4)	00924(1)	02729(10)	03554(10)	00035(3)	01263(2)	−00168(8)
N(5)	00726(1)	02986(10)	03197(9)	00098(2)	00906(1)	−00200(8)
N(6)	00897(1)	03835(13)	03401(10)	00167(3)	01165(2)	00612(9)
C(1)	01172(2)	03358(16)	07166(23)	−00042(4)	02239(3)	00726(16)
C(2)	00926(1)	04254(17)	04093(14)	00000(4)	01326(2)	00079(13)
C(3)	01247(2)	03262(17)	07320(23)	00353(5)	02133(3)	00586(18)
C(4)	00958(1)	05319(20)	02964(11)	00497(5)	00797(2)	−00036(15)
C(5)	00828(1)	03242(14)	02801(10)	00157(3)	00651(2)	00384(10)
C(6)	00807(1)	03522(14)	03356(12)	00116(3)	00940(2)	00310(11)
C(7)	01007(1)	04382(17)	03028(11)	00202(4)	01035(2)	−00103(13)
C(8)	01059(1)	03407(14)	02631(10)	−00284(4)	01002(2)	00089(10)
C(9)	01284(2)	05415(22)	03954(14)	−00456(5)	01644(3)	−00189(15)
O	01170(1)	05049(13)	03278(8)	00317(3)	01162(1)	00016(10)

*4 A complete list of the observed and calculated structure factors has been submitted to and is kept as Document No. 6902 at the office of the Bulletin of the Chemical Society of Japan, 1—5 Kanda-Surugadai, Chiyoda-ku, Tokyo. A copy may be secured by citing the Doument number and by remitting, in advance, ¥ 1,600 for photo prints. Pay by check or money order, payable to: Chemical Society of Japan.

e.s.d.'s are listed in Table 4, and pertinent intermolecular contacts (*i. e.*, those less than 4.5 Å) are given in Table 5.

The complex cation, $[Co(tn)_3]^{3+}$, has approximately a three-fold symmetry. A projection of the complex ion along its approximate three-fold axis is shown in Fig. 3. The three chelate rings are nearly but not exactly identical and take chair forms, in contrast to a puckered form of the five-membered chelate rings formed by ethylenediamine. The six-membered ring seems to be more flexible than the five-membered ring. Its conformation may be easily affected by the specific intermolecular forces in the crystal. The chelate ring is rather flattened out due to non-bonded hydrogen interactions. Bond angles Co–N–C are larger than the normal tetrahedral angle, the mean value being 117.4°. This value does not differ significantly from those found in the six-membered ring in *trans*-dichloro(1,4,8,11-tetraazacyclotetradecane)nickel(II).[7] But the mean value of N–C–C and C–C–C angles is 112.8°, which is closer to the normal tetrahedral angle. The N–Co–N angle is larger than 90°, the mean value being 94.5°. The interatomic distances are normal as shown in Table 4. The displacement of the nitrogen atoms from the regular octahedral position is recognized in Fig. 3. The displacements are quite irregular. Distortions of the chelate rings described above and of octahedral coordination appear to make the complex less stable than that with five-membered chelate rings.[8] It is to be noted here that the chair conformation of the metal-trimethylenediamine ring is maintained in various complexes with multidentate chelating agents that contain these amines as their fragments.

A complex cation is surrounded by six bromide anions. Eight closest Br–N approaches occur at distances ranging from 3.24 Å to 3.44 Å. The

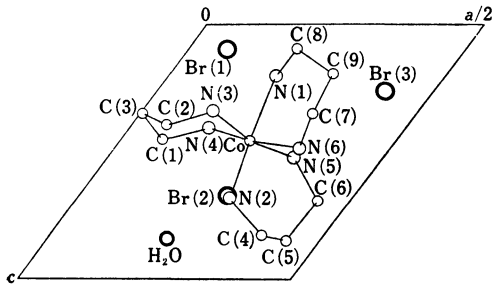

Fig. 2. The structure in an asymmetric unit, viewed along the *b*-axis.

Table 4. The bond lengths and bond angles in the complex ion, $(-)_D$-$[Co(tn)_3]^{3+}$
Their e. s. d.'s are given in parentheses.

Co–N(1)	2.00(3) Å	Co–N(4)	2.00(3) Å
Co–N(2)	2.00(3)	Co–N(5)	2.00(3)
Co–N(3)	2.00(3)	Co–N(6)	2.00(3)
N(1)–C(8)	1.47(5)	N(2)–C(4)	1.47(3)
N(6)–C(7)	1.45(5)	N(4)–C(1)	1.47(7)
N(5)–C(6)	1.48(3)	N(3)–C(2)	1.46(6)
C(8)–C(9)	1.54(5)	C(5)–C(4)	1.54(6)
C(9)–C(7)	1.54(6)	C(1)–C(3)	1.55(5)
C(6)–C(5)	1.54(6)	C(2)–C(3)	1.54(6)
∠N(1)CoN(6)	96(1)°	∠N(1)C(8)C(9)	114(2)°
∠N(2)CoN(5)	92(1)	∠N(6)C(7)C(9)	110(3)
∠N(3)CoN(4)	95(1)	∠N(5)C(6)C(5)	113(3)
		∠N(2)C(4)C(5)	111(3)
∠CoN(1)C(8)	117(2)	∠N(4)C(1)C(3)	114(4)
∠CoN(6)C(7)	118(2)	∠N(3)C(2)C(3)	112(3)
∠CoN(5)C(6)	118(2)		
∠CoN(2)C(4)	119(2)	∠C(7)C(9)C(8)	114(4)
∠CoN(4)C(1)	116(3)	∠C(4)C(5)C(6)	114(3)
∠CoN(3)C(2)	117(2)	∠C(1)C(3)C(2)	114(3)

Table 5. Intermolecular contacts less than 4.5 Å and their e. s. d.'s in parentheses
The following superscripts are used for this table.

'	x,	$y+1/2$,	z
''	$-x$,	$y+1/2$,	$1-z$
'''	$1-x$,	$y+1/2$,	$1-z$

Co–Br(1)	4.533(9) Å	Br(1)–N(1)	3.58(4) Å
Co–Br(2)	4.627(11)	Br(1)–N(4)	3.24(3)
Co–Br(3)	4.510(9)	Br(2)–N(3)	3.44(3)
Co–Br(1'')	4.544(9)	Br(2)–N(5)	3.55(3)
Co–Br(2')	4.183(9)	Br(3)–N(1)	3.52(3)
		Br(3)–N(5)	3.34(3)
O–Co	4.35(3)	Br(1')–N(3)	3.41(3)
O–Br(2)	3.27(3)	Br(2')–N(2)	3.43(3)
O–N(2)	3.04(4)	Br(2')–N(3)	3.44(3)
O–N(4)	3.53(4)	Br(2')–N(6)	3.33(3)
O–N(5)	4.46(5)	Br(3''')–N(6)	3.33(3)

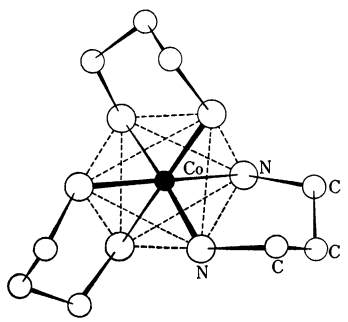

Fig. 3. A drawing of the complex ion, $(-)_D$-$[Co(tn)_3]^{3+}$, viewed along the approximate three-fold axis through the cobalt atom.

7) B. Bosnich, C. K. Poon and M. L. Tobe, *Inorg. Chem.*, **4**, 1102, 1109 (1965).

8) J. C. Bailar, Jr., and J. B. Work, *J. Am. Chem. Soc.*, **68**, 232 (1946).

closest O–N contact occurs at a distance of 3.04 Å between O and N(2), whereas the van der Waals radii are 1.92 Å for Br, 1.50 Å for N and 1.40 Å for O. The molecule of water of crystallization has contact to Br(2) with a distance of 3.27 Å.

The absolute configuration of the complex ion, $(-)_D$-$[Co(tn)_3]^{3+}$, is represented in Fig. 3, which has the same absolute configuration as that of $(+)_D$-$[Co(en)_3]^{3+}$ and may be denoted by Λ.[9] The optical rotatory dispersion and circular dichroism spectra of the complex ion has been measured by Woldbye. Its absolute configuration is enantiomeric to that assigned on the basis of the sign of the prominent Cotton effect.[10,11] Woldbye has assigned correctly its absolute configuration by examining the behavior of CD spectra in the presence of phosphate ions.[12] The complex ions, $(-)_D$-$[Co(tn)_3]^{3+}$ and $(+)_D$-$[Co(en)_3]^{3+}$ have similar circular dichroism spectra and consequently the sign of the Cotton effect of a particular transition does not depend on the N–Co–N ring angle, as some workers suppose.[13]

A simple empirical rule relating the sign of the longer wavelength CD band and the absolute configuration of the chelate ring about the metal atom seems to hold in this case, too.[14]

The rotatory strength of $[Co(tn)_3]^{3+}$ was found to be smaller than that of $[Co(en)_3]^{3+}$ by a factor of ten. This ring size effect seems natural in view of Moffit's model[15] for the tris(bidentate) complexes, in which he ascribed the optical activity to the crowding of the carbon chains of the ligands in space, the crowding becoming greater the shorter the chain. The difference in rotatory strength may also be attributable to the difference in the conformation of the chelate ring. In the cobalt-ethylenediamine ring the two carbon atoms are arranged symmetrically above and below the plane formed by the central metal atom and the two nitrogen atoms, while in the cobalt-trimethylenediamine ring the three methylene groups are located on one side of the plane of the cobalt and the two nitrogen atoms and each chelate ring has approximately a mirror symmetry.

The authors wish to thank Professor Flemming Woldbye for providing the crystals of $(-)_D$-$[Co(tn)_3]Br_3 \cdot H_2O$. This research was partly aided by funds from the Scientific Research Fund of the Ministry of Education to which the authors' thanks are due.

9) IUPAC Information Bulletin, No. 33, p. 68 (1968).

10) R. D. Gillard and G. Wilkinson, *J. Chem. Soc.*, **1964**, 1368.

11) Th. Bürer, *Helv. Chim. Acta*, **46**, 2388 (1963).

12) F. Woldbye, Private Communication, "Studier over optisk Aktivitet," Kap. X Side 11, Thesis, Copenhagen (1968).

13) A. G. Karipides and T. S. Piper, *J. Chem. Phys.*, **40**, 674 (1964); see also T. S. Piper and A. G. Karipides, *Inorg. Chem.*, **4**, 923 (1965).

14) A. G. McCaffery, S. F. Mason and B. J. Norman, *Chem. Commun.*, **1965**, 49.

15) W. Moffitt, *J. Chem. Phys.*, **25**, 1189 (1956).

BULLETIN OF THE CHEMICAL SOCIETY OF JAPAN VOL. 42 1021—1024 (1969)

Polarographic Behavior of Tris(2,2′-bipyridine)chromium(III) and Tris(ethylenediamine)chromium(III) in Acetonitrile Solutions

Yuichi SATO and Nobuyuki TANAKA

Department of Chemistry, Faculty of Science, Tohoku University, Katahira-cho, Sendai

(Received September 10, 1968)

Polarographic behavior of tris(2,2′-bipyridine)chromium(III) perchlorate and tris(ethylenediamine)chromium(III) perchlorate in acetonitrile solutions has been investigated by the measurement of d.c., a.c. and Kalousek polarograms. The bipyridine complex gives a six-step reduction wave when tetraethylammonium perchlorate is used as supporting electrolyte. The limiting currents of the first four steps are all diffusion-controlled, and each of them is of a one-electron reduction process. It has been proposed that at the fourth step univalent tris(2,2′-bipyridine)-chromate anions, $[Cr(bipy)_3]^-$, are formed at the electrode surface in acetonitrile. The limiting current of the one-electron reduction wave of tris(ethylenediamine)chromium(III) is increased upon the addition of 2,2′-bipyridine. It was explained as a reduction of an electroactive species, Cr(II)-bipyridine complex, which was formed by the reaction between Cr(II) produced by the reduction of tris(ethylenediamine)chromium(III) complex and 2,2′-bipyridine at the electrode surface.

As acetonitrile is an aprotic solvent and has less oxidizing power than water, the electrode process in acetonitrile is sometimes quite different in water. Tris(2,2′-bipyridine) complexes of manganese(II),[1] iron(II),[2] cobalt(II)[3] and nickel(II)[4] are reduced to the univalent anions at the dropping mercury electrode(DME). Such a low valent state is expected also in bipyridine complex of chromium.

In the present paper, the electrode processes of tris(2,2′-bipyridine)chromium(III) and tris-(ethylenediamine)chromium(III) are studied and the effect of 2,2′-bipyridine on the reduction wave of the latter complex is discussed. The support on the formation of tris(2,2′-bipyridine)chromate anion, $[Cr(bipy)_3]^-$, at the DME in acetonitrile solutions and an example of electrode process followed by chemical reaction involving electroactive species are presented.

Experimental

Tris(2,2′-bipyridine)chromium(III) perchlorate[5] and tris(ethylenediamine)chromium(III) perchlorate[6] were prepared and identified by elementary analysis. Other reagents were the same as described in a previous paper.[2]

The dropping mercury electrode used had an m value of 0.63_1 mg/sec and a drop time t_d of 4.83 sec when measured in an air-free acetonitrile solutions containing 0.05 M of tetraethylammonium perchlorate, $(C_2H_5)_4NClO_4$ at 25°C and at −0.5 V *vs.* SCE at 50 cm of the height of mercury reservoir. An aqueous saturated calomel electrode(SCE) served as reference electrode. The electrolysis cell and other apparatus are previously reported.[2]

Results

Tris(2,2′-bipyridine)chromium(III) complex gave a six-step reduction wave when tetraethylammonium perchlorate was used as supporting electrolyte. The limiting currents of the first four reduction steps were each found to be proportional to the square root of the mercury pressure between 45 cm and 60 cm on the DME and also to the concentration of the complex. Six reduction steps were also observed at 2.8°C and the ratio of the wave heights was nearly equal to the value at 25°C. The temperature coefficient of the limiting current at 25°C is about 0.8%/deg for each step. No anodic wave was observed at the potentials less positive than about +0.65 V, where the dissolution of mercury started. Upon the addition of free 2,2′-bipyridine to the solution containing 0.5 mM of the complex, the first four steps of the reduction wave were not affected in wave height and reduction potentials, but the wave heights of the fifth and the sixth step were increased. Free 2,2′-bipyridine gave a two-step reduction wave[2] at potentials corresponding nearly to the fifth and the sixth step of the polarogram of the complex. The results of log-plot analysis of the first three

1) Y. Sato and N. Tanaka, This Bulletin, **41**, 2064 (1968).
2) N. Tanaka and Y. Sato, *Inorg. Nucl. Chem. Letters*, **2**, 359 (1966); *Electrochim. Acta*, **13**, 335 (1968).
3) N. Tanaka and Y. Sato, This Bulletin, **41**, 2059 (1968).
4) N. Tanaka and Y. Sato, *Inorg. Nucl. Chem. Letters*, **4**, 487 (1968).
5) B. R. Baker and B. D. Mehta, *Inorg. Chem.*, **6**, 848 (1965).
6) M. Linhard, *Z. Elektrochem.*, **50**, 224 (1944).

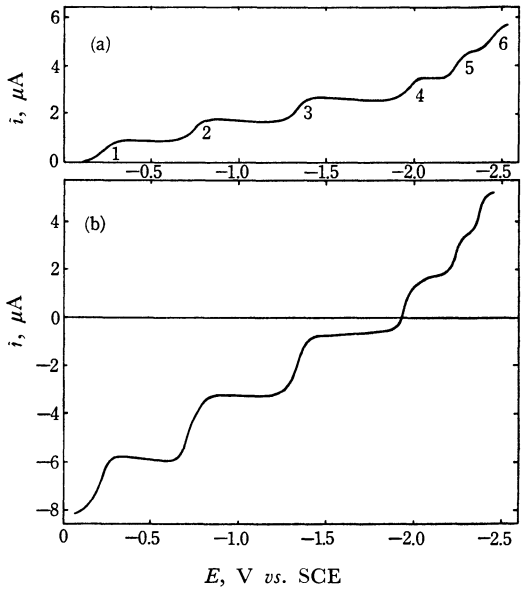

Fig. 1. (a) D.c. and (b) Kalousek polarograms with the solutions containing 0.5 mM $[Cr(bipy)_3](ClO_4)_3$ and 0.05 M $(C_2H_5)_4NClO_4$. E_2 potentials are set up at −2.1 V for curve (b).

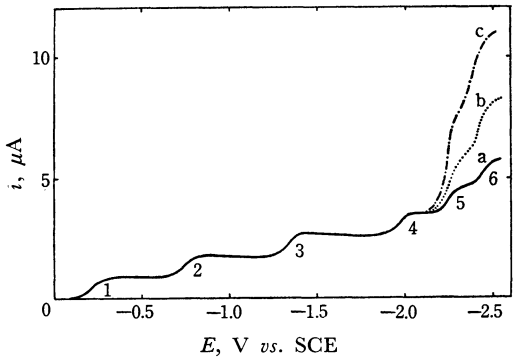

Fig. 2. D.c. polarograms of 0.5 mM $[Cr(bipy)_3](ClO_4)_3$ (a) in the absence and in the presence of (b) 0.028 M, (c) 0.139 M of water. Supporting electrolyte is 0.05 M $(C_2H_5)_4NClO_4$.

steps are given in Table 1. Upon the addition of a small concentration of water, the limiting currents of the fifth and the sixth step were increased, although no influence was found for the first four steps of the polarogram of the complex (see Fig. 2). The reduction wave of free 2,2'-bipyridine is also affected by the addition of a small concentration of water.[2] A. c. polarograms were recorded with solutions containing 0.5 mM of the complex. Six peaks were observed and their peak potentials were found to coincide with the half-wave potentials of the corresponding steps of the d. c. polarogram. The addition of 10 mM of free 2,2'-bipyridine increased the fifth and the sixth peak current, but gave almost no influence on the first four steps.

Table 1. Log-plot analysis for the first three steps of the reduction wave of the chromium(III)-bipyridine complex at 25°C

	$E_{1/2}$, V *vs.* SCE	Slope, mV
1st step	−0.221	61
2nd step	−1.741	58
3rd step	−1.327	51

Electrolytic solutions contain 0.5 mM $[Cr(bipy)_3](ClO_4)_3$, 10.0 mM 2,2'-bipyridine and 0.05 M $(C_2H_5)_4NClO_4$.

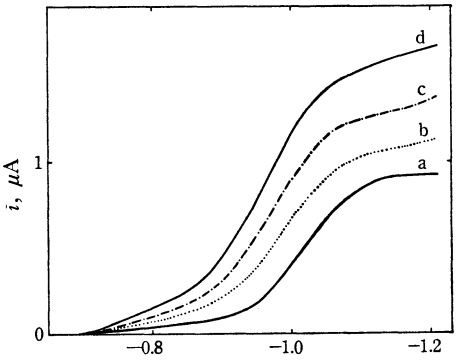

Fig. 3. The effect of 2,2'-bipyridine upon the reduction wave of 0.5 mM $[Cr(en)_3](ClO_4)_3$ containing 0.05 M $(C_2H_5)_4NClO_4$ as supporting electrolyte. 2,2'-bipyridine concentrations are (a) 0, (b) 0.5 mM, (c) 1.0 mM and (d) 3.0 mM.

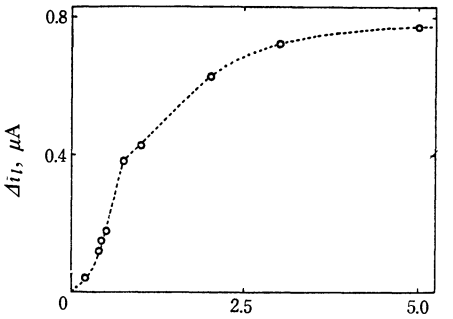

Fig. 4. Relation between the limiting current and the concentration of added 2,2'-bipyridine. Electrolytic solutions contain 0.5 mM $[Cr(en)_3](ClO_4)_3$, 0.05 M $(C_2H_5)_4NClO_4$ and 2,2'-bipyridine. Δi_l is the difference of the limiting current at −1.20 V in the presence and the absence of 2,2'-bipyridine.

The reversibilities of the first four steps were confirmed by the measurement of Kalousek polarograms, when the electrode potentials of the DME were set up at −0.5 V, −1.0 V, −1.6 V and −2.1 V, which are the potentials on the limiting currents of the first, the second, the third and the fourth

Table 2. The relation between the limiting current of the chromium(III)-ethylenediamine complex at −1.20 V and the height of mercury reservoir in the presence of 0.4 mM and 5.0 mM of 2,2'-bipyridine

(A) 0.4 mM 2,2'-bipyridine

h, cm	$\bar{i}_l$, μA	$\bar{i}_l°$, μA	$\Delta\bar{i}_l$, μA
45	1.14	0.91	0.23
50	1.18	0.95	0.23
55	1.21	0.99	0.22
60	1.26	1.03	0.23

(B) 5.0 mM 2,2'-bipyridine

h_{corr}, cm	$\bar{i}_l$, μA	$\bar{i}_l°$, μA	$\Delta\bar{i}_l$, μA	$\sqrt{h_{corr}}$, $cm^{1/2}$	$\Delta\bar{i}_l/\sqrt{h_{corr}}$, $\mu A/cm^{1/2}$
42.86	1.58	0.91	0.67	6.55	0.102
47.86	1.76	0.95	0.81	6.92	0.117
52.86	1.85	0.99	0.86	7.27	0.118
57.86	1.94	1.03	0.91	7.61	0.119

Electrolytic solutions contain 0.5 mM $[Cr(en)_3](ClO_4)_3$, 0.05 M $(C_2H_5)_4NClO_4$ and 2,2'-bipyridine. $\bar{i}_l°$ is the limiting current of the complex in the absence of 2,2'-bipyridine at −1.20 V. $\Delta\bar{i}_l=\bar{i}_l-\bar{i}_l°$

step, respectively. A four-step oxidation wave was obtained, when the electrode potential was set up at −2.1 V (Fig. 1).

Tris(ethylenediamine)chromium(III) perchlorate gave a two-step reduction wave at −1.018 V and −1.650 V when tetraethylammonium perchlorate was used as supporting electrolyte. The ratio in wave height was 1 : 2 and the limiting current of each step was diffusion-controlled. Diffusion current constant, $I_d(=\bar{i}_d/m^{2/3}t_d^{1/6}C)$, for the first step was 1.86, which showed one-electron[1-4] reduction from chromium(III) to chromium(II). Log-plot analysis for the first step was not linear. As 2,2'-bipyridine was added to the solution containing $[Cr(en)_3](ClO_4)_3$ and $(C_2H_5)_4NClO_4$, the limiting current of the first step was increased as shown in Fig. 3. Although the limiting current of the first step was increased with increasing concentration of bipyridine at constant concentration of the complex, $\Delta\bar{i}_l$ (the difference of the limiting current at −1.2 V in the presence and the absence of free bipyridine) was not proportional to the concentration of bipyridine, but approached to the definite value (Fig. 4). The total limiting current of the first step never exceeded twice of the limiting current of the complex. The limiting current ($\Delta\bar{i}_l$) was proportional to the square root of the mercury pressure in the presence of excess bipyridine, whereas it was independent of the mercury pressure when the concentration of bipyridine was smaller than that of the complex (See Table 2). The addition of free anhydrous ethylenediamine to the solution containing the complex and 2,2'-bipyridine depressed the limiting current to the original wave height of the complex only. Kalousek polarograms of 0.5 mM tris(ethylenediamine)chromium(III) which were obtained in the presence and the absence of 2,2'-bipyridine are given in Fig. 5.

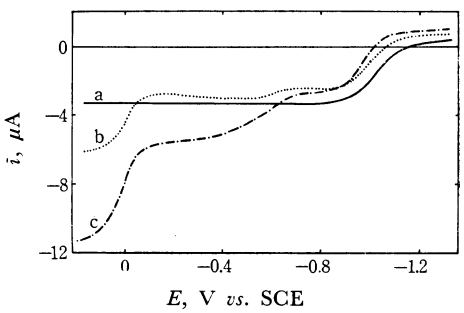

Fig. 5. Kalousek polarograms of 0.5 mM $[Cr(en)_3](ClO_4)_3$ (a) in the absence and in the presence of (b) 0.4 mM, (c) 5.0 mM 2,2'-bipyridine. Supporting electrolyte is 0.05 M $(C_2H_5)_4NClO_4$ and E_2 potentials are set up at −1.20 V.

When the electrode potential was set up at −1.2 V (the potential of the limiting current of the first step of the reduction wave), a one-step oxidation wave was observed in the absence of free bipyridine (curve a in Fig. 5), but two new steps appeared at about 0 V and −0.6 V in the presence of free bipyridine (curves b and c in Fig. 5). The limiting currents of two new oxidation waves were increased with increasing concentrations of bipyridine at the constant concentration of the complex.

Discussion

The limiting current of the first four steps of tris(2,2'-bipyridine)chromium(III) is concluded to be diffusion-controlled from the linear dependence of the wave height on the square root of the mercury pressure and on the complex concentrations and from the temperature coefficient of the limiting currents.[2] The diffusion current constant, $I_d(=\bar{i}_d/m^{2/3}t_d^{1/6}C)$, for the limiting current of the first step is 1.86, which is nearly equal to the value

for the one-electron reduction of various 2,2'-bipyridine complexes in acetonitrile.[1-4] The ratio of the wave heights of the first five steps is $1.00 : 1.1_0 : 1.1_0 : 1.0_7 : 1.8_7$. The fact that the wave heights of the first four steps of the complex are not influenced but those of the last two steps are by the addition of free 2,2'-bipyridine and a small concentration of water shows that the electrode processes of the first four steps and the latter two steps are different in nature. The log-plot analysis and Kalousek polarograms indicate that the electrode processes of the first four steps are reversible. From the same consideration as in the case with the reduction of the iron(II) complex[2] in addition to the fact that the reduction potential of free 2,2'-bipyridine is equal to the potential of the fifth and the sixth step of the reduction wave of the complex, the first four steps are concluded to be each due to the one-electron reduction of the chromium(III) complex itself and the latter two steps, the reduction of free bipyridine liberated from the complex. The first four steps are:

$$[Cr(bipy)_3]^{3+} \underset{-e}{\overset{e}{\rightleftarrows}} [Cr(bipy)_3]^{2+} \underset{-e}{\overset{e}{\rightleftarrows}} [Cr(bipy)_3]^{+} \underset{-e}{\overset{e}{\rightleftarrows}} [Cr(bipy)_3] \underset{-e}{\overset{e}{\rightleftarrows}} [Cr(bipy)_3]^{-} \quad (1)$$

A four-step oxidation wave obtained by Kalousek circuit (Fig. 1) clearly showed the formation of tris(2,2'-bipyridine)chromate anion, $[Cr(bipy)_3]^-$, at the electrode surface in the potential region of the fourth step of the reduction wave. Recently Herzog, Grimm and Waicenbauer[7] prepared $Li[Cr(bipy)_3]\cdot 4THF$ (THF: tetrahydrofuran). The preparations of $Na_2[Cr(bipy)_3]\cdot 7THF$, $Na_3[Cr(bipy)_3]\cdot 7THF$ and $Ca_3[Cr(bipy)_3]\cdot 7NH_3$ were also reported in their paper.[7] In acetonitrile solutions the wave height of the fifth step of the reduction wave is influenced by the addition of water and is larger than that of the first four steps, and the reduction potential of the fifth step coincides nearly to the reduction potential of free bipyridine. Therefore, the formation of stable bivalent or higher valent anions of tris(bipyridine)chromate at the electrode surface seems unlikely. In aqueous solutions some confusing results on the reduction of $[Cr(bipy)_3]^{3+}$ at the DME are obtained.[5,8,9] The result obtained in acetonitrile solution is similar to that obtained by Vlček, but in aqueous solutions only three reduction steps were observed and $[Cr(bipy)_3]$ is the lowest oxidation state.

The increase in wave height of the reduction of tris(ethylenediamine)chromium(III) to chromium(II) by the addition of 2,2'-bipyridine is explained as follows. The limiting current at -1.2 V is considered to be kinetic in nature in the presence of a small concentration of bipyridine from the result that the wave height ($\Delta\bar{i}_l$) is independent of the mercury pressure (Table 2). The fact that the reduction product of $[Cr(en)_3]^{3+}$ is substitution-labile suggests the occurrence of the following substitution reaction at the electrode surface (Eq. (3)).

$$[Cr(en)_3]^{3+} + e \rightarrow [Cr(en)_3]^{2+} \quad (2)$$

$$[Cr(en)_3]^{2+} + p\,bipy \rightleftarrows [Cr(en)_{3-p}(bipy)_p]^{2+} + p\,en \quad (3)$$

$$[Cr(en)_{3-p}(bipy)_p]^{2+} + e \rightarrow [Cr(en)_{3-p}(bipy)_p]^{+} \quad (4)$$

The increase in wave height is owing to the reduction of $[Cr(en)_{3-p}(bipy)_p]^{2+}$ (Eq. (4)), because the half-wave potentials of $[Cr(en)_{3-p}(bipy)_p]^{2+}$ is considered to be nearly equal to that of $[Cr(bipy)_3]^{2+}$ ($E_{1/2}=-0.741$ V as cited in Table 1) and is less negative than that of the first step of $[Cr(en)_3]^{3+}$ ($E_{1/2}=-1.018$ V). The appearance of the new oxidation steps on the Kalousek polarogram (curves b and c in Fig. 5) shows the oxidation of $[Cr(en)_{3-p}(bipy)_p]^{+}$ to higher oxidation states, which is the reduction product of $[Cr(en)_{3-p}(bipy)_p]^{2+}$ formed at -1.20 V. Half-wave potentials of two new steps of the oxidation wave are somewhat less negative than those of the corresponding steps in the case of $[Cr(bipy)_3]^{3+}$ as shown in Fig. 1,

$$[Cr(bipy)_3]^{+} \rightarrow [Cr(bipy)_3]^{2+} + e \quad (5)$$

$$[Cr(bipy)_3]^{2+} \rightarrow [Cr(bipy)_3]^{3+} + e \quad (6)$$

When the concentration of 2,2'-bipyridine added (C_{bipy}) was less than that of the complex, the plot of $\log\Delta\bar{i}_l$ *vs.* $\log C_{bipy}$ was linear and its slope was about 2. This seems to suggest that two bipyridine molecules are coordinated to the electroactive Cr(II) species (namely $p=2$ in Eq. (3)), though electroactive species is not $[Cr(en)(bipy)_2]^{2+}$ but $[Cr(bipy)_2(CH_3CN)_q]^{2+}$. In the case with the reduction of *trans*-$[Cr(NCS)_2(en)_2](SCN)$ in acetonitrile ($E_{1/2}$ is about -1.17 V), a similar phenomenon is also observed in the presence of 2,2'-bipyridine. The depression of wave height ($\Delta\bar{i}_l$) by the addition of free ethylenediamine shows that the rate of the backward reaction of reaction (3) is accelerated. If the above discussion is correct, this is another example of the electrode process followed by chemical reaction involving an electroactive species.[10-12]

The authors wish to thank the Ministry of Education for the financial support granted for this research.

7) S. Herzog, U. Grimm and W. Waicenbauer, *Z. Chem.*, **7**, 355 (1967).

8) A. A. Vlček, *Nature*, **189**, 393 (1961).

9) B. V. Tucker, J. M. Fitzgerald, L. G. Hargis and L. B. Rogers, *J. Electroanal. Chem.*, **13**, 400 (1967).

10) A.A. Vlček, "Progress in Inorganic Chemistry," Vol. 5, ed. by F. A. Cotton, Interscience Publishers, New York (1963), p. 211.

11) N. Tanaka and K. Ebata, *J. Electroanal. Chem.*, **8**, 120 (1964).

12) E. Fischerová, O. Dračka and M. Meloun, *Collection Czechoslov. Chem. Commun.*, **33**, 473 (1968).

BULLETIN OF THE CHEMICAL SOCIETY OF JAPAN VOL. 42 1025—1029 (1969)

On the Viscosity of Liquid Selenium

Shuichi HAMADA, Naosato YOSHIDA and Toshiaki SHIRAI

Department of Chemistry, Faculty of Science, Science University of Tokyo, Kagurazaka, Shinjuku-ku, Tokyo

(Received September, 14, 1968)

The viscosities of liquid selenium and partially-chlorinated liquid selenium were measured in the temperature range from 235°C to 305°C using an Ubbelohde-type tilting viscometer. The "intrinsic" viscosities, η_0, were estimated by extrapolating the values of the viscosities, η_θ, of various rates of shear to a zero rate of shear. The "intrinsic" viscosities of the liquid selenium were estimated to be 20.18, 13.46, 9.11, 6.32, 3.67 and 2.30 poise at 235, 245, 255, 265, 285, and 305°C respectively. The viscosities of the chlorinated liquid selenium decreased with an increase in the chlorine content, but they varied discontinuously at a chlorine content of 0.0125% and then decreased linearly. The apparent activation energy for the viscous flow of the liquid selenium was estimated to be 17.9 kcal/mol. The apparent activation energies for the viscous flow of the chlorinated selenium varied discontinuously at a chlorine content of about 0.0125%, as in the case of the viscosity. The average-chain length of the selenium molecules was considered not to be changed, but the radicals at both ends of the linear chain vanish in forming the bonds with chlorine atoms with an increase in the chlorination below a chlorine content of 0.0125%. Therefore, it is concluded that the presence of radicals at the molecular ends would have an influence upon the viscosity and the apparent activation energy for the viscous flow of selenium. The notable large value of the apparent activation energy of such a non-branched polymer as selenium was attributed to the large amount of energy needed to transport the segments into the holes.

Liquid selenium is considered to be a mixture of Se_8 ring molecules and long chains.[1] The properties of the liquid selenium should be governed by those of the long-chain molecules, since the liquid selenium contains few ring molecules. The number of selenium atoms in a chain of average length was calculated to be 7200 at 230°C by the thermodynamic theory developed by Eisenberg and Tobolsky.[1] The linear chains are considered to be diradical molecules with an unpaired electron at each end of the chain. The presence of radicals in the amorphous selenium was confirmed by Abdullaev *et al.*[2] and Sampath *et al.*[3] on the basis of their ESR studies. Sampath[4] reported that the results obtained by Eisenberg and Tobolsky were supported by the value of the spin concentration in the amorphous selenium. In this study, the effect of radicals on the viscous flow of the liquid selenium was studied.

Experimental

Materials. The selenium and the partially-chlorinated selenium samples were prepared in the manner described in a previous paper.[5]

Procedure. An Ubbelohde-type tilting viscometer[6] was used for the measurements of the viscosities of the liquid samples. The viscosity, η_θ, at the tilting angle, θ, of the viscometer was calculated by the following equation:

$$\eta_\theta = A_\theta \rho t$$

where A_θ, ρ, and t are the parameter of the viscometer, the density of the liquid sample, and the efflux time respectively. The tilting angle, θ, is the angle of the capillary of the viscometer to the vertical line. The parameter, A_θ, of the viscometer was estimated by means of the measurement of the efflux time of glycerol of a known viscosity at 25°C and at various tilting angles, θ. The viscosities, η_θ, of the liquid samples were measured at several tilting angles. The "intrinsic" viscosity, η_0, was estimated graphically by extrapolating the values of the viscosities, η_θ, to a ninety-degree tilting angle, *i.e.*, to a zero rate of shear. The viscosities and the densities of the liquid samples were measured at specified temperatures within an accuracy of ±0.1°C in an electric furnace.

The densimeter is shown in Fig. 1. The volume between the fixed lines, and the diameters of both the capillaries were measured using mercury at 30°C. The height of the liquid selenium column in the capillary was measured with a measuring microscope to an accuracy of 1/100 mm. The linear expansion coefficient of the densimeter is 7.95×10^{-7}°C^{-1} over the temperature

1) A. Eisenberg and A. V. Tobolsky, *J. Polymer Sci.*, **46**, 19 (1960).

2) G. Abdullaev, W. I. Ibragimov, Sh. V. Mamedov, T. Ch. Dzhuvarly and G. H. Aliev, *Dokl. Akad. Nauk Azerb. SSR*, **20**, 13 (1964).

3) P. I. Sampath and R. C. Keezer, *Bull. Am. Phys. Soc.*, **10**, 613 (1965).

4) P. I. Sampath, *J. Chem. Phys.*, **45**, 3519 (1966).

5) S. Hamada, T. Sato and T. Shirai, This Bulletin, **41**, 135 (1968).

6) S. Fujishige, M. Shibayama and J. Kuwana, *J. Polymer Sci.*, **1**, 355 (1963).

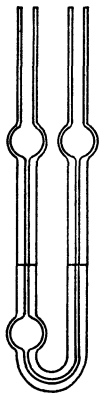

Fig. 1. Densimeter.

range from 20°C to 50°C, and those of the liquid selenium and of the chlorinated liquid selenium are calculated to be from 1.06×10^{-4} to $1.22\times10^{-4}°C^{-1}$ over the temperature range from 230°C to 305°C. Therefore, the expansion of the densimeter is negligible compared with those of the liquid samples.

Results

The Stability of the Chlorinated Liquid Selenium. Figure 2 shows the relationship between the chlorine content of the chlorinated selenium and the heating time at 265°C. The chlorine content decreased linearly with an increase in the heating time until about 3 hr, but the chlorinated selenium was stabilized after 3 hr. Because the escape of chlorine from the chlorinated selenium is considered to be negligible after 3 hrs' heating at 265°C, the viscosities and the densities were measured after 4 hrs' heating at 265°C.

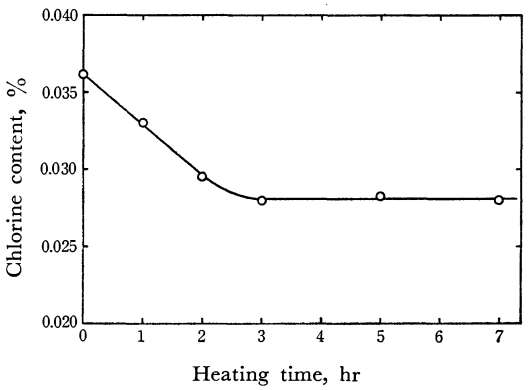

Fig. 2. Variation of chlorine content by heating at 265°C in chlorinated selenium.

The Densities of the Liquid Selenium and of the Chlorinated Liquid Selenium. The density of the liquid selenium was estimated to be 3.9850 g/cm³ at 235°C, and the linear expansion coefficient was calculated to be $1.09\times10^{-4}°C^{-1}$ in the temperature range from 230°C to 305°C, from the temperature dependence of the density. The densities of the chlorinated selenium were estimated to be from 3.9835 to 3.9770 g/cm³ at 235°C in the chlorine-content range from 0.0033 to 0.0257%, and their linear expansion coefficients were calculated to be from 1.08×10^{-4} to $1.19\times10^{-4}°C^{-1}$ in the temperature range from 230°C to 305°C.

The Viscosities of the Liquid Selenium and of the Chlorinated Liquid Selenium. The viscosities, η_θ, of the liquid samples at several tilting angles were measured at temperatures from 230°C to 305°C. Figure 3 shows the dependence of the viscosities, η_θ, of the liquid selenium on the tilting angle, θ, of the viscometer. The viscosity of the liquid selenium decreased with a decrease in the tilting angle of the viscometer, *i. e.*, with an increase in the rate of shear. The viscosities of the chlorinated liquid selenium showed the same appearance as that of the liquid selenium. Both

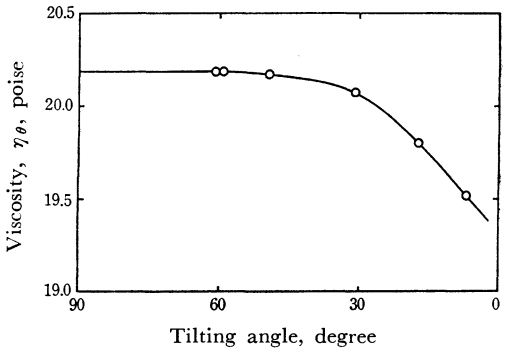

Fig. 3. Dependence of viscosity of liquid selenium on tilting angle.

the liquid selenium and the chlorinated liquid selenium are considered to behave as non-Newtonian liquids. Therefore, the "intrinsic" viscosities, η_0, of the liquid samples were estimated by extrapolating the viscosity values, η_θ, to a zero rate of shear in order to discuss the behavior of their viscous flow.

The "intrinsic" viscosities, η_0, of the liquid samples are given in Table 1.

The dependence of the logarithm of the viscosity, $\log \eta_0$, on the chlorine content at 235°C is shown in Fig. 4. The $\log \eta_0$ values decreased continuously to a chlorine content of 0.0125%, and then more rapidly and linearly with an increase in the chlorine content.

The chlorine content of 0.0125% corresponds to the state when all the radicals at both ends of the linear-chain molecules of selenium vanish in forming bonds with chlorine atoms.[5] The radicals vanish more and more with an increase in the chlorination until 0.0125%, and the average chain length of the chlorinated selenium molecules

Table 1. Viscosities of liquid selenium and of chlorinated liquid selenium

Chlorine Content, %	Viscosities, η_0, poise					
	235°C	245°C	255°C	265°C	285°C	305°C
0	20.18	13.46	9.11	6.32	3.67	2.30
0.0033	17.22	12.40	8.93	6.61	3.76	2.35
0.0053	16.31	11.76	8.48	6.40	3.68	2.20
0.0092	15.95	11.43	8.45	6.25	3.64	2.26
0.0113	15.41	11.11	8.18	6.04	3.54	2.13
0.0126	15.31	10.94	8.06	5.97	3.52	2.10
0.0134	14.83	10.51	7.73	5.82	3.45	2.12
0.0146	14.61	10.19	7.66	5.88	3.39	2.07
0.0197	12.46	8.90	6.73	5.17	3.26	2.06
0.0257	9.84	7.40	5.62	4.28	2.67	1.69

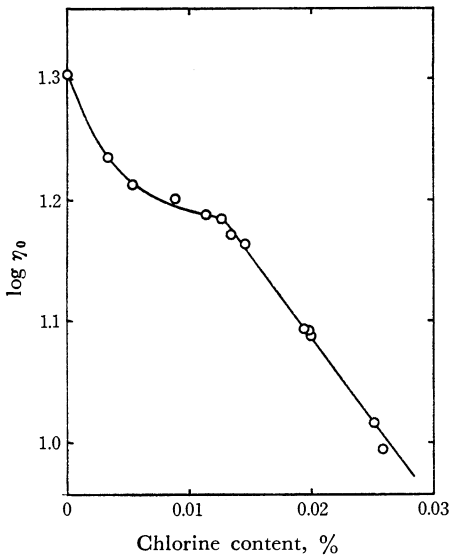

Fig. 4. Plot of log η_0 against chlorine content at 235°C.

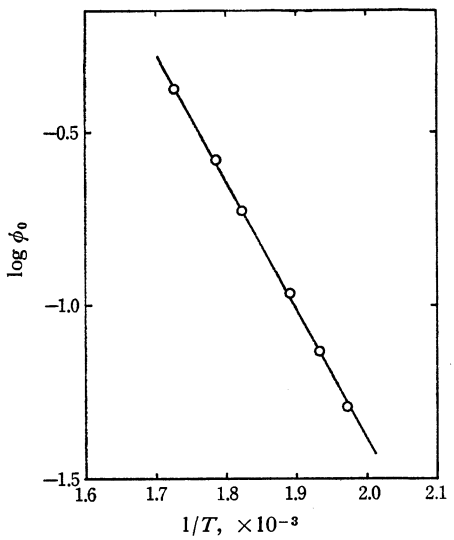

Fig. 5. Temperature dependence of fluidity of liquid selenium.

will not be changed. Therefore, the discontinuous variation in the viscosity at the chlorine content of 0.0125% suggests the influence of the fulfilment of the radicals of the chain ends.

The decreases in the viscosity of the chlorinated selenium above 0.0125% are considered to be due to a cut-off of the chain molecules by chlorine.

The Apparent Activation Energies for the Viscous Flow of the Liquid Selenium and of the Chlorinated Liquid Selenium. Figure 5 shows the relationship between the fluidity, ϕ_0, *i. e.*, $1/\eta_0$, of the liquid selenium and the temperature, T. The log ϕ_0 varied linearly with $1/T$. The temperature dependences of the log ϕ_0 of the chlorinated selenium were similar to that of the liquid selenium. Since the dependences of the log ϕ_0 on the temperature showed an Arrhenius-type variation, the apparent activation energies for the viscous flow, E_{vis}, were estimated from the following equation:

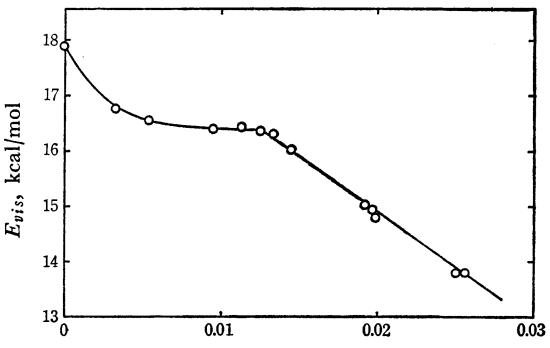

Fig. 6. Dependence of E_{vis} on chlorine content.

$$E_{vis} = -R\mathrm{d}(\ln \phi_0)/\mathrm{d}T$$

The apparent activation energy for the viscous flow of the liquid selenium was estimated to be 17.9 kcal/mol. The dependence of the E_{vis} of

the chlorinated selenium on the chlorine content is shown in Fig. 6. The E_{vis} decreased abruptly with an increase in the chlorine content. The E_{vis} varied discontinuously near the chlorine content of 0.0125%, and then decreased linearly above 0.0125%.

Discussion

The liquid organic-chain polymers, in general, show comparatively small values of E_{vis}, though they increase with an increase in the bulk of the side chains. The E_{vis} values for some organic chain polymers are shown in Table 2.[7] The value of E_{vis} is considerably larger for selenium, though it has no branched chain.

TABLE 2. E_{vis} FOR SOME ORGANIC CHAIN POLYMERS AT A ZERO RATE OF SHEAR

	Ethylene	Propylene	Isobutylene	Styrene
E_{vis} kcal/mol	6.5—7.0	9.0—9.6	12.0—16.2	22.6

The apparent activation energy for the viscous flow consists of two parts. One of them is the energy necessary to produce holes. The other is the energy, ΔE_f which is necessary to drive the segments into the holes. If ϕ_1 and ϕ_2 are the fluidities at a constant volume, that is, the iso-state of a free volume, at temperatures of T_1 and T_2 respectively, ΔE_f can be expressed by the following equation:[8]

$$-\Delta E_f(1/T_1-1/T_2) = \boldsymbol{R}\ln(\phi_1/\phi_2) + \ln(T_1/T_2)/2$$

The relationship between the specific volume of the liquid selenium and the temperature at the specified pressures can be calculated using the values of the thermal expansion coefficient of liquid selenium, $\alpha=3.27\times10^{-4}$, and of the compressibility of liquid selenium,[9] $\beta=1.53\times10^{-5}$ bar^{-1}. From this relationship, certain conditions, *i. e.*, the temperature and the pressure, under which the compressed liquid selenium possesses an iso-volume state can be estimated graphically. Harrison[9] reported the viscosity of liquid selenium over the temperature range from 260°C to 350°C under a compressed system in the range from 1 bar to 1500 bar. The viscosities of the compressed liquid selenium in an iso-volume state at the corresponding temperatures and pressures can be deduced from Harrison's results.

Table 3 shows the viscosities in the case of the iso-volume state of 0.2533 cm^3/g, as an example. The ΔE_f value was calculated to be 11.5 kcal/mol from the data in Table 3. The ΔE_f value for ordinary liquids is, in general, assessed to be within the range from one-tenth to one-fifth of the total apparent activation energy for the viscous flow. A larger amount of energy, however, is necessary to drive the segments into the holes for the viscous flow of the liquid selenium than those of ordinary liquids; this must cause the larger E_{vis} value for the liquid selenium. Moreover, the apparent activation energy for the viscous flow of the liquid selenium shows the character of a "structure activation energy," as in the case of water.

TABLE 3. VISCOSITIES AT ISO-VOLUME STATE $v=0.2533$ cm^3/g

Press., bar	1	500	1000	1500
Temp., °K	533	556	581	605
η, poise	5.69	3.74	2.39	1.61

Bondi[10] expressed the viscosity of the liquid in connection with the v_f and the ΔE_f as follows:

$$\eta = (v_f^{1/3}/v_L)(2\pi m\boldsymbol{k}T)^{1/2}\exp(\Delta E_f/\boldsymbol{R}T)$$

where v_f is the free volume; v_L, the molecular volume in the liquid; m, the mass per molecule, and $\boldsymbol{k}$, the Boltzmann constant. The fraction of v_f at T_g, f_g, defined by Williams, Landel and Ferry,[11] is well known to be 2.5×10^{-2} in usual organic and inorganic polymers. The abnormality of the f_g of the amorphous selenium has been shown by the volume relaxation phenomenon.[5] The f_g value of the amorphous selenium is 6.33×10^{-2}; it is larger than those of the usual polymers, but it decreases with an increase in the chlorination, reaching the normal value, 2.5×10^{-2}, at a chlorine content of more than 0.0125%. Therefore, the free volume of the liquid selenium would be larger than that of the chlorinated liquid selenium. However, the contribution of the free volume term, $(v_f^{1/3}/v_L)$, on the viscosity is not very large. The ΔE_f of the chlorinated selenium could not be established, for the dependence of the viscosity of the chlorinated selenium on the pressure was obscure. However, a decrease in ΔE_f upon the chlorination was suggested by the dependence of the E_{vis}, of the chlorinated selenium on the chlorine content below 0.0125%, as is shown in Fig. 6 (assuming that the chain length of selenium molecules does not change at chlorine contents below 0.0125%). The abrupt decrease in the viscosity of the chlorinated liquid selenium at chlorine contents below 0.0125% is due to the decrease in ΔE_f, in spite of the decrease in the f_g upon chlorination.

7) H. Schott, *J. Appl. Polymer Sci.*, **6**, S29 (1962).
8) S. Glasstone, K. J. Laidler and H. Eyring, "The Theory of Rate Processes," McGraw-Hill, New York (1941), p. 489.
9) D. E. Harrison, *J. Chem. Phys.*, **41**, 844 (1964).
10) A. Bondi, "Rheology: Theory and Applications," F. R. Eirich (ed.), Academic Press, New York (1956), p. 329.
11) M. L. Williams, R. F. Landel and J. D. Ferry, *J. Am. Chem. Soc.*, **77**, 3701 (1955).

The decreases in the viscosity and E_{vis} value of the chlorinated selenium at chlorine contents above 0.0125% are probably due to the shortening of the chain molecules with an increase in the chlorination.

BULLETIN OF THE CHEMICAL SOCIETY OF JAPAN VOL. 42 1029—1036 (1969)

Bipolar Ion-Exchange Membranes Prepared from Blends of Graft Copolymers

Hiroshi KAWABE and Masaya YANAGITA

The Institute of Physical and Chemical Research, Yamato-machi, Saitama

(Received April 12, 1968)

Bipolar ion-exchange membranes were prepared from graft copolymers of polyethylene (PE). Powders of styrene-grafted PE (I) and 4-vinylpyridine-grafted PE (II), or powders of ethyl acrylate-grafted PE (III) and II were blended in various proportions and melt-pressed to films. Ion-exchange groups were then introduced by the sulfonation (100%), alkaline hydrolysis (100%), or *N*-methylation (80—90%) of the blend polymer films. Although, in the titration curves of bipolar membranes, pH regions which apparently resemble the isoelectric point of polyampholytes appeared, no behavior based on the interaction between acidic and basic groups was indicated in the survey of their physico-chemical properties. The dependency of the concentration potential of the membranes (E_m), containing one kind of ionized group, on the mole fraction of the group (F_i) is not remarkable. On the other hand, the E_m of the membranes containing both positively- and negatively-charged groups is strongly dependent on F_i, because of the additive contribution of the oppositely-charged groups to the potential. The bi-ionic potential of the membrane, E_{K-Li}, was found to be a function of $E_m/|E_0|$ ($|E_0|$ is the absolute value of the concentration potential for ideal permselective membranes) in the cases of both I-II and II-III.

The behavior of polyampholites, which characterize many natural substances of biological importance, has long been an object of interest. Recently, some amphoteric ion-exchange membranes have been reported,[1-4] and interaction between acidic and basic groups in the membranes was observed in such phenomena as the membrane potential and the electric conductance.[3]

The gamma-ray-induced vapor-phase grafting of the ionogenic monomer onto polyethylene (PE) affords a convenient way for preparing homogeneous ion-exchange membranes.[4] In the present study, the preparation of bipolar membranes by blending monofunctional graft copolymers, and their physico-chemical properties as a function of the membrane composition, were investigated.

Experimental

Materials. Commercial high-pressure PE powder of 200 mesh (mol wt of 23000) was used. The monomers used were styrene (St), 4-vinylpyridine (VP), and ethyl acrylate (EA), all of commercial grade. Deionized water was used throughout.

TABLE 1. GRAFT COPOLYMERS USED FOR THE PREPARATION OF BLEND FILMS

Code	Monomer	Dose 10^5 R	g %	C_g mmol/g	PMT °C
Ia(A)	ST	1.3	45.6	3.01	195
IIa(G)	VP	14.5	103	4.83	180
IIIa(H)	EA	2.2	58.5	3.69	185
IIb(N)	VP	3.1	43.5	2.89	181
IIIb	EA	2.2	65.0	3.94	185
IIc	VP	2.6	33.6	2.40	181

Preparation of Membranes. The procedures used in the preparation of membranes are shown in Scheme 1. The grafting onto PE powder was carried out by the irradiation of gamma rays in monomer vapor, as has been described in previous papers.[5,6]

1) Y. Onoue, *Denki Kagaku (J. Electrochem. Soc. Japan*, **30**, 225 (1962).
2) P. E. Blatz, *J. Polymer Sci.*, **58**, 755 (1962).
3) H. Jacobson, *J. Phys. Chem.*, **66**, 570 (1962).
4) A. S. Michaels, *Ind. Eng. Chem.*, **57**, 32 (1965).
5) M. Yanagita, H. Kawabe, K. Shinohara and T. Takamatsu, *Sci. Papers I.P.C.R.*, **57**, 10 (1963).
6) M. Yanagita, H. Kawabe, K. Shinohara and T. Takamatsu, *ibid.*, **56**, 218 (1962).

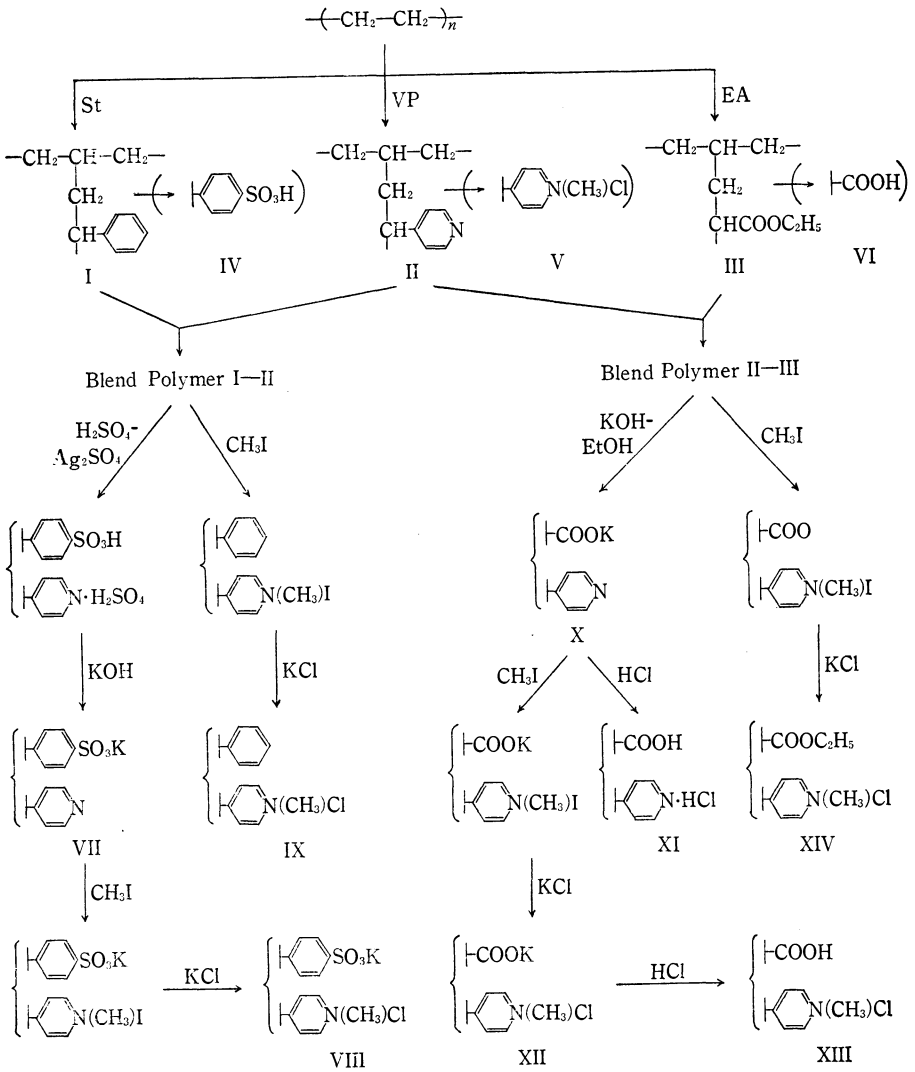

Scheme 1. Preparation of Membranes.

TABLE 2. COMPOSITION OF BLEND POLYMER FILMS[a)]

Code		A	B	C	D	E	F	G
I-II	Ia	3.01	2.54	2.20	1.74	1.22	0.77	0
	IIa	0	0.75	1.29	2.05	2.86	3.59	4.83
Code		H	I	J	K	L	M	N
II-III	IIIa	3.60		2.23	1.61	1.04		0
	IIb	0		1.11	1.61	2.06		2.89
	IIIb		2.79				0.52	
	IIc		0.77				2.08	

a) The composition is expressed in the term of C_g (mmol/g) of both functional groups in the blends.

Three kinds of graft copolymers have been prepared: St-grafted PE (I), VP-grafted PE (II), and EA-grafted PE (III). The degree of grafting (g) (defined by the increase in the weight as $100\times[(W-W_0)/W_0]$), the content of the functional group in the graft copolymer (C_g in mmol/g), and the polymer-melt temperature (PMT) are shown in Table 1. Two kinds of copolymers, I and II or II and III, were well mixed in various ratios, and the blend powders were melt-pressed to film 0.15 mm thick under a pressure of 200 kg/cm^2 at 180°C for ten minutes. The compositions of the copolymers in the blend films are shown in Table 2.

Various kinds of membranes were prepared by the chemical treatments of the blend-polymer films shown in Scheme 1. The sulfonation of the phenyl group, the quaternization of the pyridine group, and the saponification of the ester group in the blend polymers were carried out according to previously-described procedures.[5,6]

Determination of Ion-exchange Capacity. Each group in the bipolar membranes was determined by a combination of the precipitation titration of the halogen ion with acid-base titration, as will be described below.

a) A membrane containing both a carboxylic acid group (a meq) and a pyridine group (b meq) was treated with a potassium hydroxide solution, washed thoroughly with water, and left immersed in 0.1 N HCl (x ml). After the membrane had then been removed, the solution was titrated with 0.1 N NaOH (y ml), and then with 0.1 N $AgNO_3$ (z ml) in the presence of nitric acid. The contents of the groups in membrane are:

$$a = 0.1 \times (z-y);\ b = 0.1 \times (x-y)$$

b) A membrane containing both a sulfonic acid group (a meq) and a pyridine group (b meq) was treated with a hydrochloric acid solution, washed with water, and left immersed in 0.1 N NaOH (x ml). The solution was titrated with 0.1 N HCl (y ml at the equivalent point, and with y' ml added), and then with 0.1 N $AgNO_3$ (z ml).

$$a = 0.1 \times [(x-y) - (z-y')];\ b = 0.1 \times (z-y')$$

c) A membrane containing both a carboxylic or sulfonic acid group (a meq) and a quaternary pyridinium group (b meq) was treated with a hydrochloric acid solution, washed with water, and left immersed in 0.1 N NaOH containing sodium nitrate in a 1 N concentration (x ml). The solution was titrated with 0.1 N HCl (y ml at the equivalent point, and with y' ml added), and then with 0.1 N $AgNO_3$ (z ml).

$$a = 0.1 \times (x-y);\ b = 0.1 \times (z-y')$$

The ion-exchange capacity was calculated for acidic and quaternary pyridinium groups on the basis of the dry weight of the membrane in the salt-form (C_d^K or C_d^{Cl} in meq/g), and also for both the groups on the basis of the wet weight (C_w in meq/g).

Titration Curves of Membranes. The titration curves of monopolar membranes in the presence of sodium chloride were determined in the usual ways reported previously.[7,8] In the case of bipolar membranes, each sample was titrated with a 1 N HCl solution, washed thoroughly, and left immersed in 40 ml of the solution, containing various amounts of sodium hydroxide or hydrogen chloride but no salt, for seven days. The pH of the solution was then measured, and the portions were titrated with 0.1 N HCl or 0.1 N NaOH and with 0.1 N $AgNO_3$. The initial content of chloride ions in the membrane sample was determined separately. The amounts of both sodium and chloride ions in membrane and in solution at each equilibrium were calculated in a way similar to that described in the previous section.

Other Properties of Membranes. The thickness, water content (w in wt%), molality of the ionized group ($\bar{m}$), concentration potential (E_m in mV), and electric conductivity ($\bar{k}$ in $\Omega^{-1}cm^{-1}$) of membranes were measured in the ways described in a previous paper.[6] The bi-ionic potential was measured, in a way similar to the E_m measurement, by using the cell: |0.1 N KCl| membrane|0.1 N LiCl|. The density of the wet membrane (d) was determined by the use of a pycnmeter.

Results and Discussion

Preparation of the Membranes. The blend polymer films, I-II (B–F), containing both phenyl and pyridine groups, were quantitatively sulfonated in a concentrated sulfuric acid containing 1% silver sulfate. The sulfonation of the sample, D, was followed by the capacity measurement and found to be almost completed within an hour at 50°C. The monofunctional film I (A), containing a phenyl group, was sulfonated under the same conditions and found to reach a constant capacity value in five hours. The higher reaction rate of the sulfonation of I-II than of I may be attributed to the swelling effect of ionized pyridine groups in sulfuric acid. The film II (G), containing only pyridine groups, was not sulfonated under the above conditions. The II-III (I-M) films, containing both ester and pyridine groups, were treated with a 1 N KOH - 80% ethanol solution at 75°C for three hours and found to be hydrolysed almost quantitatively. After sulfonation or saponification, the films were treated with methyl iodide - acetone (1 : 1 volume ratio) at 30°C for 5—24 hr; the degree of the quaternization of pyridine groups were found to be 80—90%.

Titration Curves of the Membranes. The titration curves of monopolar membranes were

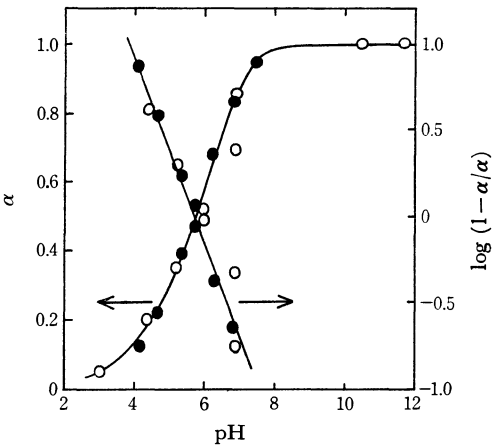

Fig. 1. Titration curves of membrane VI (○) and saponified EA-DVB resin (●) in the presence of 0.1 N NaCl.

7) H. Kawabe, S. Sugimoto and M. Yanagita, *Reports Sci. Res. Inst.* (in Japanese), **30**, 257 (1954).

8) H. Kawabe and M. Yanagita, *J. Sci. Res. Inst.*, **50**, 199 (1959).

first examined. The titration curve of IV (A), containing only sulfonic acid groups, in the presence of 0.1 N NaCl was shown to be typical for strong acid at pH's lower than 7, where the ion-exchange capacity of a dry membrane in the H-form was 2.10 meq/g. The elementary analysis of the membrane showed 7.03% S, which agrees with the value calculated from the capacity at pH 7.

The titration curve of VI (H), containing only carboxylic acid groups, in the presence of 0.1 N NaCl, and that of the saponified EA-divinylbenzene (DVB) copolymer[9,10] containing 5% DVB, are shown in Fig. 1, where α is the degree of ionization. The plots for both the exchangers are, coincidentally, on the same curve. In the figure, the Henderson-Hasselbach-Kathchalsky relation,[11] $pH=pK_a-n'\log[(1-\alpha)/\alpha]$, is also shown, where pK_a and n' are 5.8 and 1.9 respectively. Gregor and Frederic[12] reported that the values of pK_a and n' for the titration of polyacrylic acid with sodium hydroxide were 5.29 and 1.95 in the presence of 0.1 N NaCl, and 6.79 and 2.13 in the absence of any added salt.

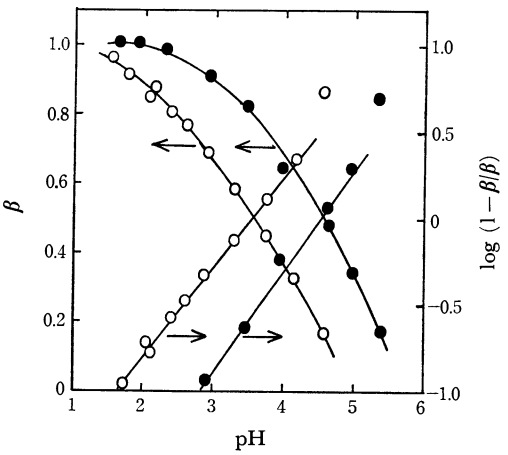

Fig. 2. Titration curves of VP grafted PE film (II) in the presence of 0.1 N NaCl (○) and 1 N NaCl (●).

The titration curves of II, containing only pyridine groups, are shown in Fig. 2, where β is the degree of ionization. From the plots for the $pH=pK_a+n'\log[(1-\beta)/\beta]$ relation, also shown in the figure, the values of pK_a and n' are 3.5 and 1.9 in 0.1 N NaCl, and 4.5 and 1.7 in 1 N NaCl. As may be seen in Fig. 2, the increase in the concentration of added salt (C_s) by $\Delta\log C_s=1$ results in the increase of pK_a by about unity. A similar effect of added salt has been observed in the titration curve of the cross-linked polyacrylic acid resin, though the value of pK_a decreases upon the addition of salt.[10] Since the internal pH of an ion-exchange membrane or resin is different from that of an external solution, it is noticeable that the Henderson-Hasselbach-Katchalsky relation is established for these exchangers. This titration behavior of weak electrolyte-type exchangers may be understood when it is considered that the concentration of salt in the exchangers is quite low as a result of Donnan exclusion and that α or β is directly dependent on the internal pH ($\overline{pH}$), which is a simple function of the external pH, as may be estimated by $(pH+\log a_{Na})$ in the case of cation exchangers and by $(pH-\log a_{Cl})$ in the case of anion exchangers, where a is the activity of the ion in solution.*1

When Figs. 1 and 2 are compared, it may be seen that if both II and VI exist in 0.1 N NaCl, both the groups will ionize at the pH region of 3—5.

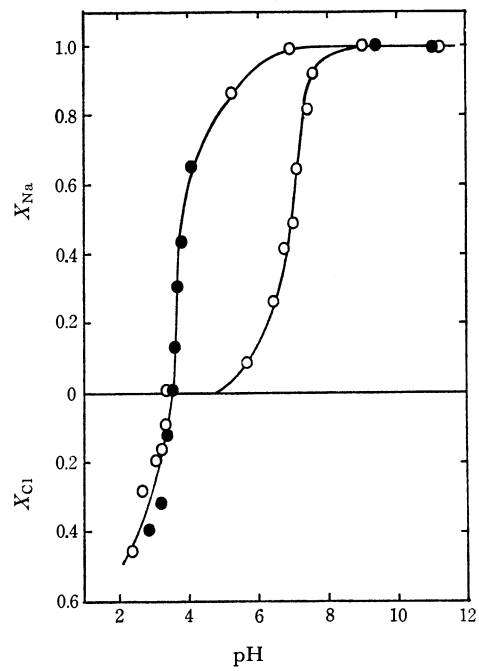

Fig. 3. Titration curves of membranes VII(●) and X (○) in the absence of added salt.

9) H. Kawabe and M. Yanagita, *J. Sci. Res. Inst.*, **53**, 98 (1959).

10) H. Kawabe and M. Yanagita, *ibid.*, **53**, 227 (1959).

11) A. Katchalsky, N. Shavit and H. Eisenberg, *J. Polymer Sci.*, **13**, 69 (1954).

12) H. P. Gregor and M. Frederic, *ibid.*, **23**, 451 (1957).

*1 The relation between the internal pH value and the external pH value of ion-exchange resins has been discussed by Kawabe and Yanagita[8] and by Nagasawa, Ishitani and Kagawa,[13] and quantitatively expressed by Eq. (15) and Eq. (5) of the respective papers.

13) M. Nagasawa, H. Ishitani and I. Kagawa, *Kogyo Kagaku Zassi (J. Chem. Soc. Japan, Ind. Chem. Sect.)*, **61**, 806 (1958).

Such a region will become narrow as the concentration of salt in the solution decreases, because the titration curves of II and VI transfer to lower and higher pH values respectively. It can, then, be predicted that if there is no interaction between acidic and basic groups in the bipolar membrane X (or XI), each group will be separately determined in the titration curve of the membrane at lower salt concentrations, probably lower than 0.01 N. Under such conditions, a pH region which apparently resembles the isoelectric point of polyampholytes may be observed in the titration curve of X, though neither group is ionized in the region in this case. Figure 3 shows the titration curve of X in the absence of any added salt;*2 here the above-mentioned region is observed at pH 3.5—5, where neither group is ionized. The titration curve of the membrane VII, containing both sulfonic acid and pyridine groups, is also shown in Fig. 3. The fact that each titration curve separated by the line, $\overline{X}=0$, is quite similar to that of the corresponding monopolar membrane seems to justify the assumption that there is no interaction between acidic and basic groups in VII and X.

Table 3. General properties of membranes

Code		C_d^K meq/g	C_d^{Cl} meq/g	C_w meq/g	w %	$\overline{m}$	d
VII	A	2.10		1.09	48.2	2.25	1.078
	B	1.94		1.18	39.2	3.01	1.062
	C	1.80		1.08	40.1	2.69	1.074
	D	1.61		0.98	39.0	2.52	1.053
	E	1.16		0.67	42.1	1.60	1.064
	F	0.99		0.63	36.8	1.70	1.066
VIII	B	2.10	0.48	1.55	40.0	3.88	1.081
	C	1.69	0.77	1.21	50.7	2.39	1.050
	D	1.37	1.30	1.44	45.8	3.14	1.089
	E	1.04	1.80	1.30	54.2	2.40	1.028
	F	0.76	1.30	1.60	53.6	2.99	1.039
IX	B		0.54	0.51	4.6	11.0	1.014
	C		0.98	0.87	11.7	7.36	1.046
	D		1.66	1.26	23.8	5.31	1.048
	E		2.20	1.48	32.7	4.54	1.079
	F		2.71	1.65	39.1	4.21	1.046
	G		1.60	1.63	2.99	3.06	
X	H	2.23		1.93	40.0	4.64	
	I	2.47		1.28	48.3	2.64	1.046
	J	2.06		1.11	46.1	2.41	1.040
	K	1.45		0.88	39.6	2.21	1.020
	L	1.02		0.69	32.6	2.12	1.008
	M	0.51		0.43	13.8	3.14	0.986
XII	I	3.35	0.49	1.52	46.8	3.23	1.024
	J	2.00	0.79	1.53	44.9	3.41	1.033
	K	1.37	1.18	1.65	35.2	4.70	1.002
	L	0.91	1.46	1.76	26.0	6.74	0.984
	M	0.48	1.25	1.49	14.7	8.64	0.984
XIII	I		0.43	0.34	21.9	1.53	1.023
	J		0.75	0.53	29.5	1.78	1.021
	K		1.26	0.88	30.4	2.88	1.024
	L		1.57	1.09	30.8	3.54	1.015
	M		1.10	0.92	16.6	5.52	1.009
XIV	I		0.54	0.50	7.3	6.82	1.000
	J		1.13	0.95	16.0	5.91	1.000
	K		1.30	0.96	26.2	3.64	0.986
	L		1.46	1.11	24.5	4.49	0.996
	M		1.58	1.30	17.2	7.61	0.989
	N		2.11	1.43	32.0	4.42	

*2 In Fig. 3, $\overline{X}_{Na}$ and $\overline{X}_{Cl}$ are the mole fractions of exchanged sodium and chloride ions in the bipolar membranes, respectively as defined by $\overline{X}_{Na}=\bar{n}_{RNa}/(\bar{n}_{RH}+\bar{n}_{RNa})$ and $\overline{X}_{Cl}=\bar{n}_{RNHCl}/(\bar{n}_{RN}+\bar{n}_{RNHCl})$, where $\bar{n}_i$ is the number of moles of the species i in the membrane and where RH and RN represent free acidic and basic groups respectively.

General Properties of the Membranes. The properties of the membranes are summarized in Table 3. In the membranes containing oppositely-charged groups (VIII and XII) the properties appear to be attributable to the additive contribution of the two groups and no abnormal behavior based on the interaction between the two groups is indicated.

Electrochemical Properties of the membranes. The relation between the conductivity of a membrane ($\bar{k}$ in $\Omega^{-1}\,cm^{-1}$) in a 1-1-type electrolyte solution and the concentration of the ion ($\overline{C}_i$ in eq/l) in the membrane may be expressed by:

$$\bar{k} = 10^{-3}\sum \bar{\lambda}_i \overline{C}_i \qquad (1)$$

where $\bar{\lambda}_i$ is the equivalent conductivity of the ionic species i. When a membrane is in a dilute solution of electrolytes, since the concentration of sorbed salt in the membrane will be negligible compared with that of exchanged ions, $\bar{\lambda}_i$ may be related to the limiting equivalent conductivity of the species, λ_i^0, by the equation:[14]

$$\bar{\lambda}_i = \lambda_i^0 \phi h A_i F_i' F_i \qquad (2)$$

where ϕ is the pore volume fraction; h, the tortuosity factor, and F_i' and F_i, Ferry and Faxen's drag factors, and where A_i is related to the activation energy for diffusion. Thus, $\bar{k}$ will be strongly dependent on the structural factors of the membrane and on the interactions between the mobile species and its surroundings.

The linear relation between $\bar{k}$ and $\overline{C}$ has been reported for an anion-exchange membrane prepared from ethyleneimine and epichlorohydrin.[15] As is shown in Figs. 4 and 5, in the case of graft copolymer membranes containing one kind of ionized group, the plots of $\bar{k}$ against $\overline{C}$ can be substancially expressed by:

$$\log \bar{k} = a + b\,\overline{C} \qquad (3)$$

where a and b are the experimental constants. This means, in turn, that $\bar{\lambda}_i$ decreases greatly as

14) H. Kawabe, H. Jacobson, I. F. Miller and H. P. Gregor, *J. Colloid Interface Sci.*, **21**, 79 (1966).

15) G. Manecke and K. F. Bohnoeffer, *Z. Electrochem.*, **55**, 475 (1951).

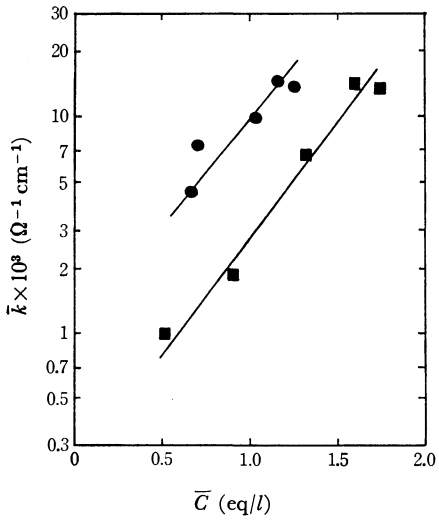

Fig. 4. Dependence of conductivity of membranes VII (●) and IX (■) on concentration of counter ion in membranes.

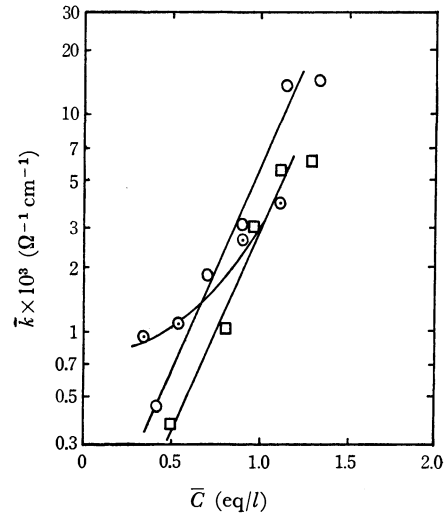

Fig. 5. Dependence of conductivity of membranes X (○), XIII (⊙) and XIV (□) on concentration of counter ion in membranes.

the capacity of the membrane decreases. The exceptionally higher values of $\bar{k}$ of XIII at lower $\bar{C}$ values may be ascribed to the contribution of a carboxylic acid group. In graft copolymer membranes, polar groups are not homogeneously distributed but are concentrated on graft chain; here the exchange-diffusion of ions may take place mainly through the internal polyelectrolyte region, which is composed of ionized groups. Therefore, the lower $\bar{\lambda}$ values at lower $\bar{C}$(or C_w) values, shown in Table 4, are probably attributable mainly to the lower pore-volume fraction and partly to the lower tortuosity factor. In fact, the calculated

Table 4. Equivalent conductance of membranes

Code		$\bar{C}$ eq/l	$\bar{\lambda}$ Ω^{-1}cm^{2}eq^{-1}	$100(\bar{\lambda}/w)$
VII	B	1.25	11	28
	C	1.16	13	31
	D	1.03	9.4	24
	E	0.71	11	26
	F	0.67	6.7	18
IX	B	0.52	1.9	41
	C	0.91	2.0	17
	D	1.32	5.0	21
	E	1.60	8.9	27
	F	1.73	8.0	20
X	I	1.34	26	54
	J	1.15	12	26
	K	0.90	3.4	8
	L	0.70	2.6	8
	M	0.42	1.1	8
XIII	I	0.35	2.7	12
	J	0.54	2.0	7
	K	0.90	2.9	10
	L	1.11	3.5	11
	M	0.93	1.6	10
XIV	I	0.50	0.74	10
	J	0.80	1.3	8
	K	0.95	3.2	12
	L	1.11	5.1	21
	M	1.29	4.7	27

values of $100\times(\bar{\lambda}/w)$ listed in the table seem to be almost independent of $\bar{C}$. In the case of membranes containing oppositely-charged groups (VIII and XII), large values of $\bar{k}$ (around $2\times10^{-2}\Omega^{-1}\cdot$ cm^{-1}) are observed almost independently of the membrane composition.

The concentration potential of a membrane is given by:

$$E_m = -\frac{RT}{F}\left[\bar{t}_K \ln\frac{a_{K''}}{a_{K'}} - \bar{t}_{Cl}\ln\frac{a_{Cl''}}{a_{Cl'}}\right] \qquad (4)$$

where a_i is the activity of the species i in solution ($a'>a''$) and where $\bar{t}_i$ is the transference number of ions in the membrane. The concentration potentials of various membranes placed between 0.1 N KCl and 0.05 N KCl are shown in Fig. 6, in which F_K and F_{Cl} are the mole fractions of ionized acidic and basic groups*3 respectively, and in which $|E_0|$ is the absolute value of the ideal concentration potential as given by the Nernst equation. The absolute values of the concentration potential of VII and XIII increase, and those of IX, X, and XIV, decrease with an in-

*3 The mole fractions F_K and F_{Cl} are defined as follows: $F_K=\bar{n}_{RK}/(\bar{n}_{RK}+\bar{n}_{RN})$ for VII and X; $F_K=\bar{n}_{RK}/(\bar{n}_{RK}+\bar{n}_{RNCl})$ for VIII and XII; $F_{Cl}=\bar{n}_{RNCl}/(\bar{n}_{RK}+\bar{n}_{RNCl})$ for VIII and XII; $F_{Cl}=\bar{n}_{RNCl}/(\bar{n}_{RH}+\bar{n}_{RNCl})$ for IX and XIV, and $F_{Cl}=\bar{n}_{RNCl}/(\bar{n}_{RH}+\bar{n}_{RNCl})$ for XIII, where $\bar{n}_R$ represents the number of moles of an inactive group, such as phenyl and the ester, and where $\bar{n}_{RNCl}$ is that of the quaternary pyridinium group.

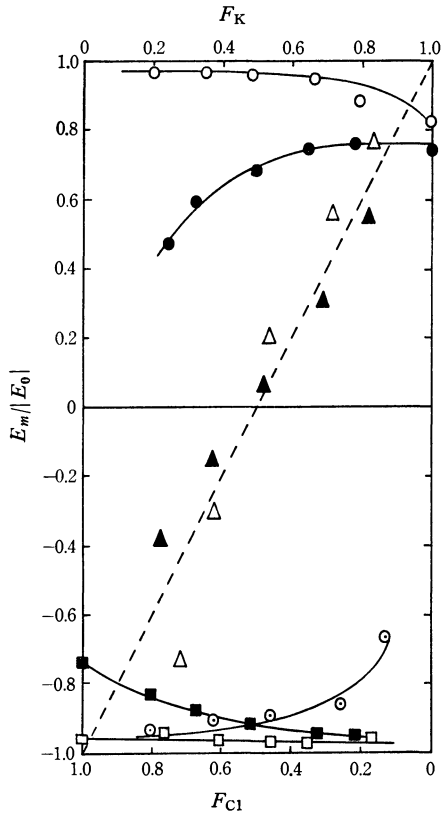

Fig. 6. Dependence of permselectivity of membranes VII (●), VIII (▲), IX (■), X (○), XII (△), XIII (⊙) and XIV (□) on mole fraction of membrane components.

crease in the mole fraction of each ionized group. This is in accordance with the behavior of each membrane except X with respect to the molality of the ionized group described in the previous section. As the Donnan exclusion of salt becomes less effective upon the decrease in $\bar{m}$, the salt content in membrane will increase and the potential will decrease. The sign of the E_m of the membrane XI, containing a carboxylic acid group and a partially-ionized pyridine group, is negative under acidic conditions, but it becomes positive upon repeated washings of the membrane, probably because of the very weak basicity of the pyridine group and the high mobility of the hydrogen ions. Thus, the behavior of X and XI is similar to that of an amphoteric membrane, in which the potential varies from negative to positive depending upon the pH of the solution.[3)]

The plots for VIII and XII, which contain oppositely-charged groups, are on the broken line in Fig. 6. Since E_m is expressed by Eq. (4) and since $\bar{t}_i$ is given by $(\bar{\lambda}_i\bar{C}_i)/(\sum\bar{\lambda}_i\bar{C}_i)$, the potential of VIII and XII will be a linear function of $F_i(=\bar{C}_i/\sum\bar{C}_i)$ provided that there is no interaction between the two groups and provided the mobilities

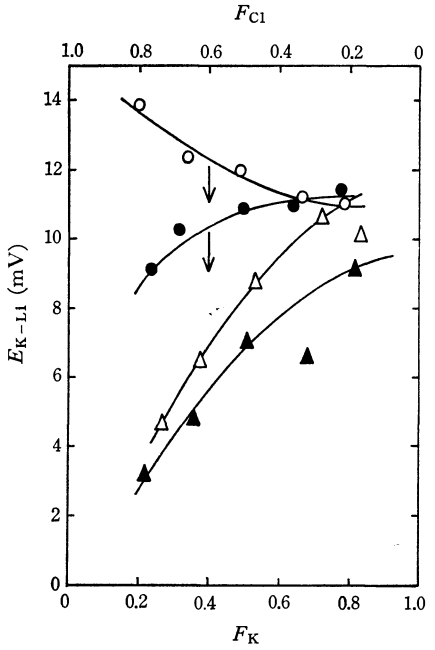

Fig. 7. Dependence of bi-ionic potential of membranes VII (●), VIII (▲), X (○), and XII (△) on mole fraction of membrane components.

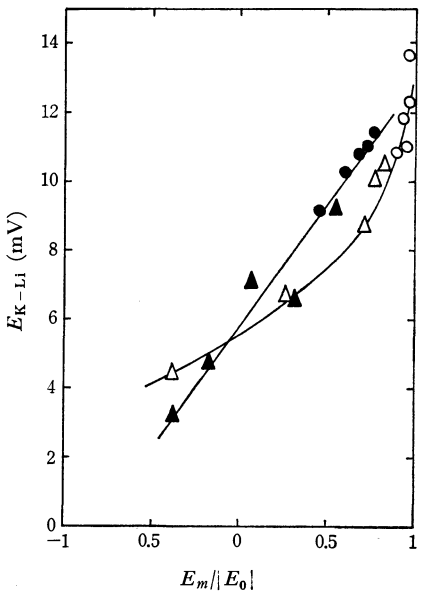

Fig. 8. Dependence of bi-ionic potential of membranes VII (●), VIII (▲), X (○) and XII (△) on permselectivity of the membranes.

of K and Cl ions are equal in a membrane.

The bi-ionic potential of the bipolar membranes for 0.1 N KCl - 0.1 N LiCl, E_{K-Li}, is shown as a function of F_i in Fig. 7. When E_{K-Li} is plotted against $E_m/|E_0|$, a simple relationship is indicated, as is shown in Fig. 8. The fact that E_{K-Li} decreases simply with the decrease in $E_m/|E_0|$

may be understood by considering that chloride ions in a membrane tend to transfer in a direction so as to reduce the bi-ionic potential, which is given for ideal permselective membranes[16] by:

$$E_{K-Li} = \frac{RT}{F} \ln \frac{\bar{D}_K a K' \bar{f}_{Li}}{\bar{D}_{Li} a_{Li}'' \bar{f}_K} \quad (5)$$

where $\bar{D}$ represents the diffusion coefficient of the ions in a membrane; a, the activity of ions in solution, and $\bar{f}$, the activity coefficient of the ions in a membrane. The fact that the E_{K-Li} of the membrane is positive may be qualitatively explained by Eq. (5). Provided that the ion-exchange selectivity coefficient, K_{Li}^K, is expressed by the activity coefficient ratio, $\bar{f}_{Li}/\bar{f}_K$, and that the diffusion coefficient is related to the conductivity through the Nernst-Einstein equation, $D=RT\lambda/F^2$, the following equation is established:

$$E_{K-Li} = \frac{RT}{F} \ln \left[\frac{\bar{k}_K}{\bar{k}_{Li}} K_{Li}^K \right] \quad (6)$$

In the membranes containing a sulfonic acid group (VII and VIII), the selectivity coefficient term seems to be more important, because $\bar{k}_K/\bar{k}_{Li}$ for the membrane VII is less than unity in some regions in Fig. 9. It is known that K_{Li}^K is greater than unity for sulfonic acid-type resins. On the other hand, since the K_{Li}^K of a carboxylic acid-type resin is known to be less than unity, it may be predicted from Eq. (6) that $\bar{k}_K$ will be much higher than $\bar{k}_{Li}$ for the membranes containing a carboxylic-acid group (X and XII). It may be seen in Fig. 9 that $\bar{k}_K/\bar{k}_{Li}$ is greater than 3 for the membrane X.*4

*4 A large difference between sulfonic acid - type membranes and carboxylic acid - type membranes in regard to the conductance of alkali-metal ions was previously observed for monofunctional graft copolymer membranes.[5]

16) F. Helfferich, "Ion Exchange," McGraw-Hill, Inc., New York (1962), p. 380.

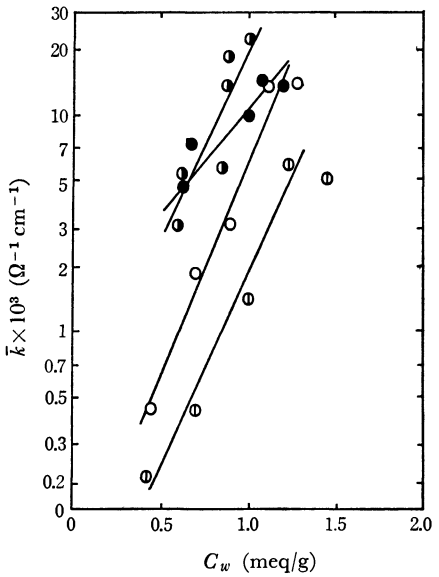

Fig. 9. Conductivities of membrane VII and X.
●: VII in K-form ◑: VII in Li-form
○: X in K-form ⦶: X in Li-form

In reviewing the properties of the membranes prepared from blends of monofunctional graft copolymers, no interaction between acidic and basic groups is indicated, and the concentration potentials of the membranes containing oppositely-charged groups are shown to be additive contributions of the two terms in Eq. (4) in relation to both the groups. This suggests that most of the functional groups of both copolymers in a blend are not brought into contact by the melt-pressed procedure.

The authors wish to express their thanks to Dr. T. Takamatsu for his kind advice in the radiation grafting and to Mr. T. Takeuchi and Mrs. K. Hayashi for their helpful assistance in preparing the samples and carrying out the measurements.

BULLETIN OF THE CHEMICAL SOCIETY OF JAPAN VOL. 42 1037—1047 (1969)

Solvent Effects on ρ Values of the Hammett Equation

Yasuhiko KONDO, Takeki MATSUI and Niichiro TOKURA

Department of Applied Chemistry, Faculty of Engineering, Osaka University, Suita, Osaka

(Received April 15, 1968)

The effects of selvents on ρ values have been systematically treated as a two-variable problem within a linear free-energy relationship framework. It is assumed that the standard activation free energy is a continuous function of σ, a substituent variable, and ξ, a solvent variable. The applicability of the resultant equations is proved by a test of the dissociation constants (obtained from the literature) of benzoic acids in various solvents. As a result, it is proposed that these effects on ρ values can be explained in terms of the interaction or cross-term of σ and ξ. The application to the reaction rates of a typical Menschutkin reaction, obtained by experiments in ten non-aqueous solvents, suggests that the solvent dependence in these reactivities is much more complicated.

Systematic studies of the substituent effects of the dissociation constants of organic acids in solution have been carried out comprehensively by many authors since the proposal of Hammett's equation.[1] The relationships between the ρ values and the environmental changes have also been the subject of some studies.[2,3]

Concerning the effects of solvent on the ρ values, Wynne-Jones[4] discussed the relative acid strengths of some acids in such hydroxylic solvents as water, methanol, and ethanol; he suggested the inverse proportionality of these values to the dielectric constants of the solvents used. Furthermore, Kilpatrick and his co-workers[5] confirmed Wynne-Jones's results on the dissociations of acids in aqueous dioxane; however, they indicated that this relationship was limited to solvents with dielectric constants larger than $\sim$25. In low dielectric solvents (lower than $\sim$25) it did not hold; here the dipole-dipole interaction may dominate. Recently, Grunwald[6] proposed a linearity between the ρ values and his Y_0 values for the dissociation of anilinium ions.

On the other hand, the existence of a linear dependence of ρ values on the reciprocals of the absolute temperatures has also been reported.[2,3] Separating the external contributions to the thermodynamic quantities from the internal ones, Hepler[7] established the dissociation of phenols in an aqueous solution and supported the concept of the existence of a linear relation.

The interest in the effects of solvents on the ρ values, one of the Hammett reaction parameters, has prompted the present authors to initiate this project in the hope of establishing a more systematic treatment of the solvent effects on the Hammett constants. It seems that these problems may be treated as a two-variable problem by considering that both the standard activation free energy for the reaction and the standard free-energy changes in the equilibrium are continuous functions of x and y; x and y standing for the characteristics of the substituent, *i.e.*, σ, and the characteristics of such environmental factors as the solvent properties and the temperatures respectively.

Taylor's expansion theorem is used to treat this problem. Equation (1) represents this theorem for the standard free-energy change, ΔF°, which is a continuous function of foth x and y:[8]

$$\Delta F^\circ(x,y) = \Delta F^\circ(0,0) + \left(\frac{\partial \Delta F^\circ}{\partial x}\right)_{0,0} x + \left(\frac{\partial \Delta F^\circ}{\partial y}\right)_{0,0} y + \left(\frac{\partial^2 \Delta F^\circ}{\partial x \partial y}\right)_{0,0} x \cdot y + \frac{1}{2}\left(\frac{\partial^2 \Delta F^\circ}{\partial x^2}\right)_{0,0} x^2 + \frac{1}{2}\left(\frac{\partial^2 \Delta F^\circ}{\partial y^2}\right)_{0,0} y^2 + 0(x^3, y^3) \quad (1)$$

Here the subscripts indicate the arbitrarily-destinated conditions.

If a linear free-energy relationship is assumed with regard to x and y, the terms of the second and higher powers of x and y, except for the fourth on the right hand side of Eq. (1), can be omitted. Therefore, Eq. (2) can be written as:

1) L. P. Hammett, *J. Am. Chem. Soc.*, **59**, 96 (1937).
2) P. R. Wells, *Chem. Revs.*, **63**, 171 (1963).
3) H. H. Jaffe, *ibid.*, **53**, 191 (1953).
4) W. F. K. Wynne-Jones, *Proc. Roy. Soc. (London)*, **A140**, 440 (1933).
5) J. H. Elliott and M. Kilpatrick, *J. Phys. Chem.*, **45**, 454 (1941).
6) E. Grunwald and B. Gutbezahl, *J. Am. Chem. Soc.*, **75**, 559 (1953).
7) L. G. Hepler, *ibid.*, **85**, 3089 (1963).
8) W. Kaplan, "Advanced Calculus," Addison-Wesley Publishing Co., Massachusetts, U. S. A. (1952), p. 369.

$$\Delta F^\circ(x,y) = \Delta F^\circ(0,0) + \left(\frac{\partial \Delta F^\circ}{\partial x}\right)_{0,0} x + \left(\frac{\partial \Delta F^\circ}{\partial y}\right)_{0,0} y + \left(\frac{\partial^2 \Delta F^\circ}{\partial x \partial y}\right)_{0,0} x \cdot y \quad (2)$$

Then, using Eq. (4), Eq. (2) can be rewritten as follows:

$$\Delta F^\circ(x,y) = \Delta F^\circ(0,0) + A_0 x + B_0 y + \left(\frac{\partial A}{\partial y}\right)_0 x \cdot y \quad (3)$$

$$\left(\frac{\partial A}{\partial y}\right)_0 = \left(\frac{\partial B}{\partial x}\right)_0 \quad (4)$$

Eq. (4) is based on the mathematical theory that the order of differentiation is immaterial because ΔF° is the "property" of the reaction system[9] and because it has been assumed that all the derivatives concerned are continuous in the domain considered.

This equation (3) is essentially the same as that of Miller[10] provided that $\partial A/\partial y$ or $\partial B/\partial x$ is constant. Especially if $\partial A/\partial y$ or $\partial B/\partial x$ is zero, this situation shows that x and y contribute to ΔF° independently; the resultant equation (5) has been useful for the separation of the factors in the substituent effects, *i. e.*, polar, steric, resonance, and so on.[11]

$$\Delta F^\circ(x,y) = \Delta F^\circ(0,0) + A_0 x + B_0 y \quad (5)$$

In order to examine the usefulness of such a treatment of the solvent effects, the dissociation constants of substituted benzoic acids in various aqueous solvents were compared with many literature values, and then the rates of a Menschutkin-type reaction series (I) were followed in various non-aqueous solvents which had not hitherto been studied. This reaction was chosen for the present research because it was expected that the ρ values might be liable to variation in proportion to the solvent changes, since in acetone this value was significantly large.[3,12]

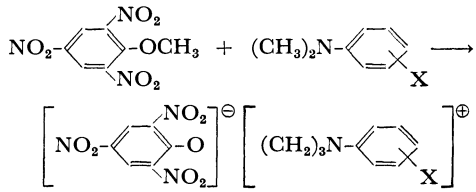

(I)

Results and Discussion

The Application of Eqs. (3) and (4) to the Solvent Effect. Usually, as has been seen in may results, if the Hammett rule holds good in one solvent, it is valid also in other solvents so far as the non-charged substituents are concerned.[3,13] Moreover, if the linear free-energy relationship is assumed also for solvent variation, x and y in Eq. (3) may be replaced by σ and ξ, the characteristic features of a solvent. We can also replace ΔF° with the equilibrium constant, K. Thus Eqs. (3) and (4) yield:

$$\log\left(\frac{K_\sigma^\xi}{K_0^0}\right) = \rho_0 \sigma + \zeta_0 \xi + \left(\frac{\partial \rho}{\partial \xi}\right)_0 \sigma \cdot \xi \quad (6)$$

$$\left(\frac{\partial \rho}{\partial \xi}\right)_0 = \left(\frac{\partial \xi}{\partial \sigma}\right)_0 \quad (7)$$

Now it does not appear that ξ can be uniquely determined by such a special characteristic of a solvent as $1/D$ or $(D-1)/(2D+1)$. Therefore, ξ will be here defined as the logarithmic ratio of the equilibrium constant in a standard solvent to that in others when the unsubstituted reactant is used; that is to say, log $(K_0^{\text{other solv}}/K_0^{\text{reference}})$ (the subscript indicates the substituent and the superscript indicates the solvent). ζ is a measure of the susceptibility of a given reaction series to the ξ defined above.

Equation (6) contains the interaction or the cross term of σ and ξ. This term may be used to explain the solvent effects on ρ and the substituent effects on ζ if these effects are two sides of one thing; that is to say, Eq. (7) is valid. Equations such as Eq. (7) have been frequently used in the form of $pK(H_2O)$ *vs.* pK(other solvent).[14] The arising of this cross-term suggests how the contribution of σ to ΔF° affects the contribution of ξ to ΔF°.

To begin with, the above treatment should be applicable to the thermodynamic equilibrium constants, K_{th}, of benzoic acids in various solvents, for σ may depend on the solvent although it is defined as the logarithmic ratio of the thermodynamic ionization constants of substituted benzoic acid to that of unsubstituted acid in an aqueous solution. Moreover, the thermodynamic values should be used for theoretical treatment.[15] Fortunately, the true acid strengths of benzoic acid and its derivatives have been studied by many workers.

Table 1 shows the ξ values for several solvents, which have been calculated by using the average values of these data taken from the references, together with the dielectric constants (ξ is defined as $\log(K_0^{\text{other solvent}}/K_0^{H_2O})$). Figure 1 represents the plots of $\log(K_\sigma^{\text{other solvent}}/K_\sigma^{H_2O})$ *vs.* ξ. The

9) K. S. Pitzer and L. Brewer, Revised Edition of Lewis and Randall, "Thermodynamics," McGraw-Hill Book Co., New York, N. Y. (1961).
10) S. I. Miller, *J. Am. Chem. Soc.*, **81**, 101 (1959).
11) R. W. Taft, Jr., in "Steric Effects in Organic Chemistry," M. S. Newman, ed., John Wiley and Sons, New York, N. Y. (1956), Chapter 8.
12) E. Hertel and J. Dressel, *Z. Phys. Chem.*, **23**, 281 (1933).
13) C. D. Richie and E. S. Lewis, *J. Am. Chem. Soc.*, **84**, 591 (1962).
14) For example, L. P. Hammett and L. A. Wooten, *ibid.*, **57**, 2289 (1935); B. W. Clare, D. Cook, E. C. F. Ko, Y. C. Mac and A. J. Parker, *ibid.*, **88**, 1911 (1966).
15) J. F. J. Dippy, *Chem. Revs.*, **25**, 151 (1939).

Table 1. ξ Values[a] of solvents for the dissociation of benzoic acid at 25°C

Solvent	H_2O[c,d,g,r]	10 w% MeOH[s]	20 v% MeOH[e,n]	10 w% $(CH_3)_2CO$[h]	20 v% EtOH[e]	20 w% [k,p]	40 v% MeOH[e]	25 w% $(CH_3)_2CO$[h]
ξ	0.00	−0.187	−0.26	−0.25	−0.28	−0.668	−0.744	−0.795
D_{25}[b]	78.6		71.5	73.0	72.7	60.83	63.49	64.0
Solvent	50 v% CH_3OH[e]	40 v% EtOH[e,f]	30 w% [k,p]	50 v% EtOH[e]	60 v% MeOH[n]	40 w% [k,p]	80 v% MeOH[e,n]	70 v% EtOH[e,f]
ξ	−0.95	−1.02	−1.08	−1.34	−1.34	−1.594	−1.093	−1.935
D_{25}[b]	59.03	66.2	51.9	60.8	54.34	43.0	44.43	47.9
Solvent	50 w% [k,p]	80 v% EtOH[e]	90 v% EtOH[e]	95 v% EtOH[e]	61.0 w% [k]	95 v% MeOH[n]	100% MeOH[i,m,g]	100% EtOH[j,l]
ξ	−2.18	−2.25	−2.51	−2.72	−2.80	−3.27	−5.20	−5.94
D_{25}[b]	34.3	43.0	38.75	35.75	25.1	36.04	32.61	24.2
Solvent	*i*-PrOH[u]	*c*-HexOH[u]	50 v% Butyl cellosolve [o]		C_4H_9OH[k]	$(CH_2OH)_2$[k]	$C_6H_5OCH_3$[u]	20% Sucrose[t]
ξ	(−6.72)[v]	(−7.14)[v]	(−1.45)[v]		(−4.41)[v]	(−3.447)[v]	(−1.51)[v]	(+0.02)[v]
D_{25}[b]					17.7	37.7	4.30	

a) ξ is defined as $\log(K_0^{\text{other solvent}}/K_0^{H_2O})$, where $\log K_0^{H_2O}$ has a value of −4.203; average value, Refs. c, d, g, and r.
b) Dielectric constants of aq. EtOH and of aq. dioxane obtained from the interpolation of Timmermans' data; J. Timmermans, "Physico-Chemical Constants of Pure Organic Compounds," Elsevier Publishing Co., Amsterdam, The Netherlands (1950).
c) A. Bieber, *Z. Elektro. Chem.*, **55**, 250 (1951).
d) L. P. Hammett, *J. Am. Chem. Soc.*, **57**, 2289 (1953).
e) W. L. Bright and H. T. Briscoe, *J. Phys. Chem*, **37**, 789 (1933).
f) E. Grunwald and B. J. Berkowitz, *J. Am. Chem. Soc.*, **73**, 4939 (1951).
g) D. H. McDaniel and H. C. Brown, *J. Org. Chem.*, **23**, 420 (1958).
h) J. F. J. Dippy, S. R. C. Hughes and B. C. Kitchiner, *J. Chem. Soc.*, **1964** 1275.
i) H. Goldschmidt, *Z. Physik. Chem.*, **112**, 429 (1924).
j) E. Larsson, "Untersuchungen über die Elektrolytische Dissoziation einiger Elektrolyte in Äthylalkolischer Lösung," Dissertation, Lund (1924).
k) J. H. E. Elliott and M. Kilpatrick, *J. Phys. Chem.*, **45**, 454 (1941).
l) I. D. Tabagua, M. M. Tsurtsumiya and N. A. Izmailov, *Tr. Sukhumsk. Gos. Ped. Inst.*, **15**, 103 (1962); *Chem. Abstr.*, **60**, 14370 (1964).
m) *Ibid.*, **15**, 119 (1962); *Chem. Abstr.*, **60**, 14373 (1964).
n) A. L. Bacarella, E. Grunwald, H. P. Marshall and E. L. Purlee, *J. Org. Chem.*, **20**, 747 (1955).
o) E. Berliner and E. A. Blommers, *J. Am. Chem. Soc.*, **73**, 7479 (1951).
p) H. S. Dunsmore and J. C. Speakman, *Trans. Faraday Soc.*, **50**, 236 (1954).
q) M. Kilpatrick and Arenberg, *J. Am. Chem. Soc.*, **75**, 3812 (1953).
r) R. A. Robinson and A. I. Biggs, *Australian J. Chem.*, **10**, 128 (1957).
s) H. N. Parton and J. Rogers, *Trans. Faraday Soc.*, **38**, 238 (1942).
t) J. F. J. Dippy, *J. Chem. Soc.*, **1944**, 411.
u) (i) V. I. Dulova and D. R. Galieva, *Dolklady Akad. Nauk Uzbek SSR*, **1960**, No. 9, 42-4; *Chem. Abstr.*, **56**, 4140b (1962). (ii) V. I. Dulova and T. A. Maslentsova, *ibid.*, **1960**, No. 2, 27—30; *Chem. Abstr.*, **56**, 8069e (1962).
v) Values in parentheses show the non-thermodynamical ionization constants.

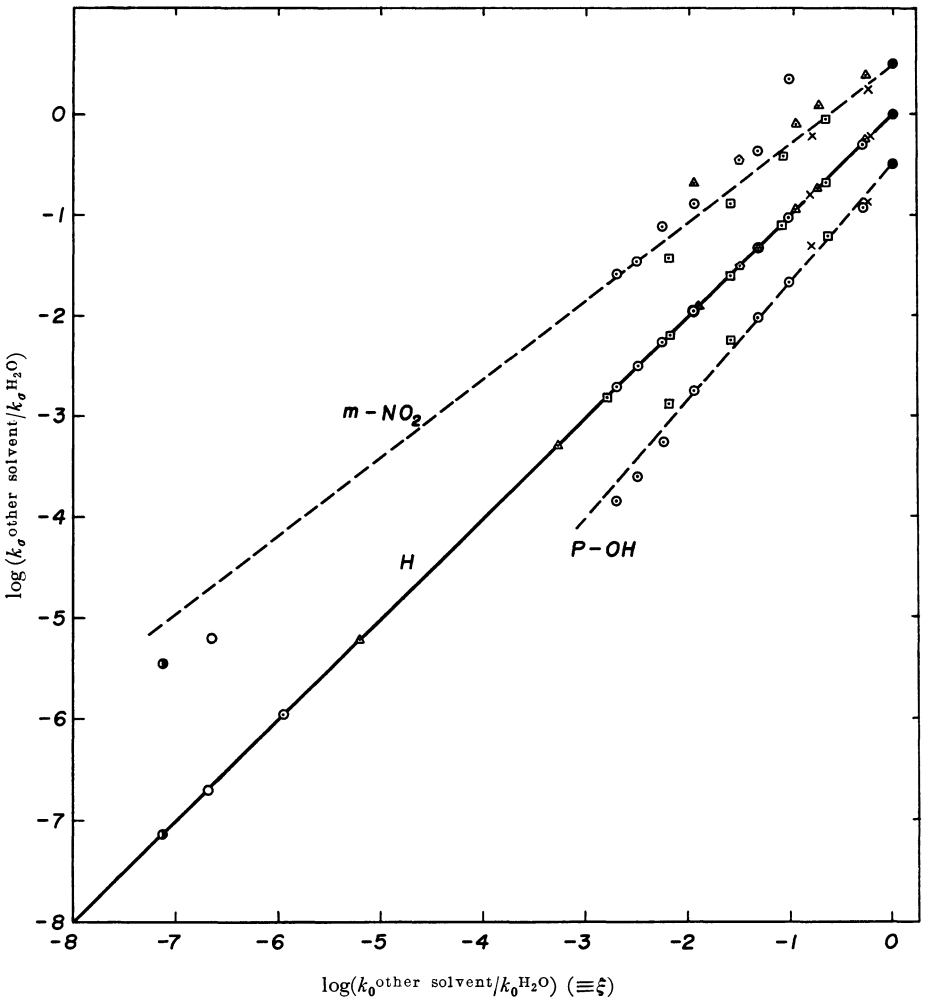

Fig. 1. The representation of linear free energy relationship with regard to solvent variations for the equilibrium constants of benzoic acid and its derivatives at 25°C. The $\log(k_\sigma^{\text{other solvent}}/k_\sigma^{H_2O})$ scale is displaced 0.5 to the upward or downward for m-NO_2 or p-OH derivatives for avoiding confusion. ●, Water; ×, water-acetone mixture; △, water-methanol mixture; ⊙, water-ethanol mixture; ⊡, water-dioxane; ○, isopropanol; ◑, hexanol; ⬠, anisole. See references in Table 1.

slope of this figure results in ζ (ζ_0 is equal to 1.00 according to the definition of ξ). The existence of a relation of the type of Eq. (7) is clearly shown in Figs. 2 and 3; this proves that the variation in the ρ values with the properties of the solvents arises from the cross-interaction of σ and ξ. Figure 2 shows that ρ decreases linearly with an increase in ξ; that is to say, the more polar the solvents are, the smaller this value becomes.

In order to discuss further details of the solvent effect on the ρ value, the relationship between ξ and the dielectric property of the solvent should be examined. As is shown in Fig. 4, an approximately linear relationship exists between ξ and $1/D$, the reciprocal of the dielectric constant, but in aqueous dioxane it is not observed. This is very similar to the situation which Hyne explained as the effect of specific solvation.[16] Judging from this point of view, in this case it may also be considered that dioxane - water mixed solvents have a larger dielectric character than expected and that they affect this equilibrium. The reason why the interaction term has some value is explained if only σ contains some component varying with the solvent.

On the other hand, the effects of the field in which the solute are located are taken as among the most important factors which contribute to the cross - interaction between σ and ξ. Dewar

16) J. B. Hyne, *J. Am. Chem. Soc.*, **85**, 304 (1963).

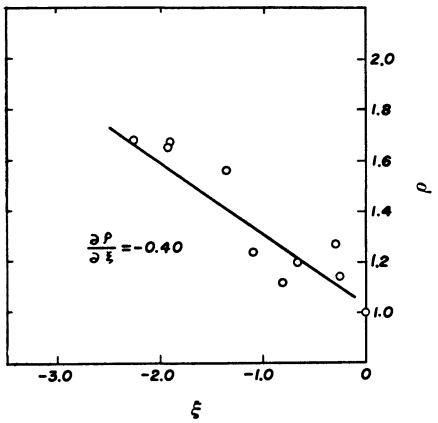

Fig. 2. Plot of ρ *vs.* ξ for the dissociations of benzoic acid and its derivatives.

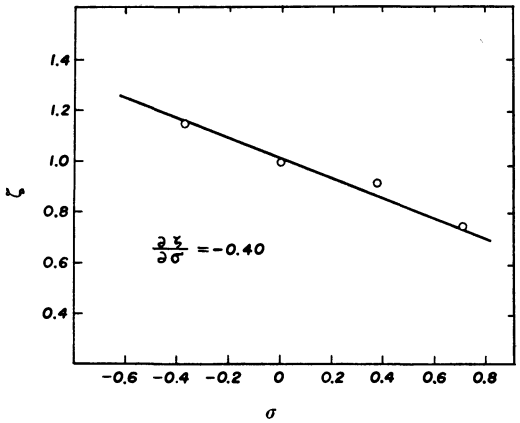

Fig. 3. Plot of ζ *vs.* σ for the dissociations of benzoic acid and its derivatives.

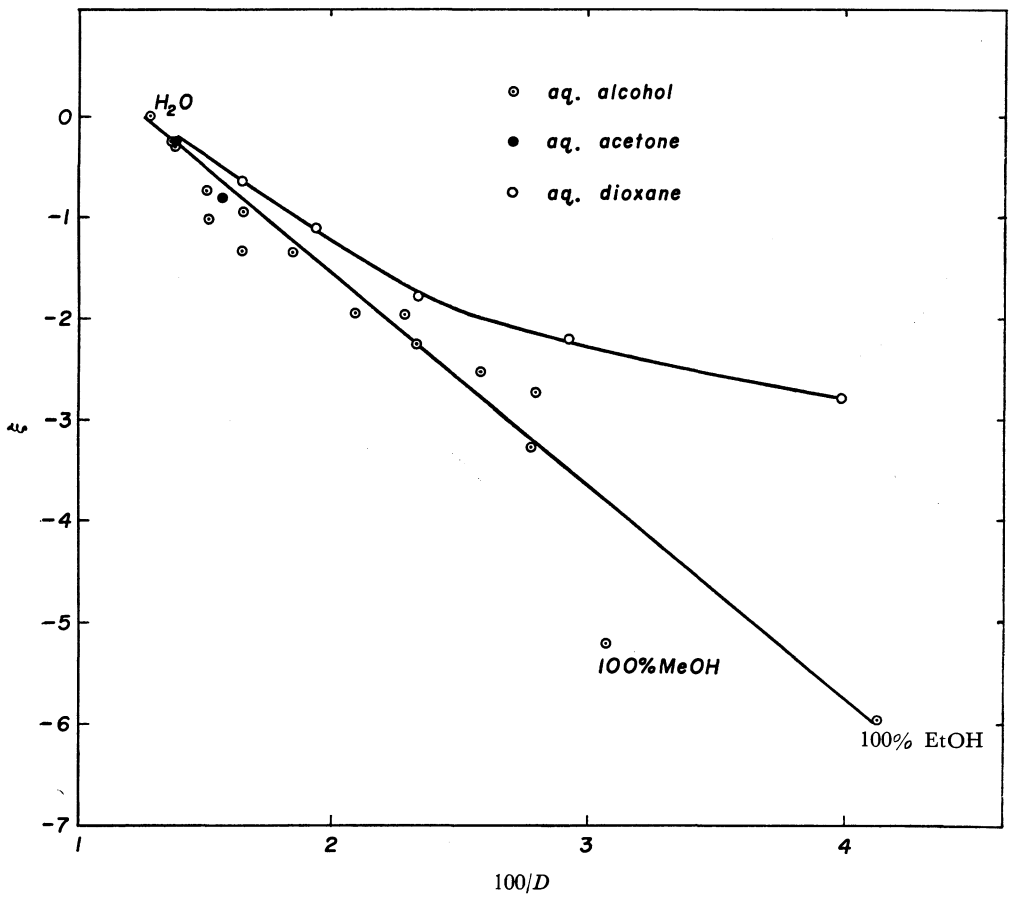

Fig. 4. The relationship between ξ, defined for the dissociation constants of benzoic acid, and $1/D$ for various aqueous solvents.

et al.[17] have emphasized the importance of this factor in a substituent effect. Thus, it seems reasonable that the field effect of each substituent results in the variation in ρ with ξ, as Willi has also suggested.[18]

17) M. J. S. Dewar and P. J. Grisdale, *ibid.*, **84**, 3539 (1962).

18) A. V. Willi, *Helv. Chem. Acta*, **40**, 2032 (1957).

Usually this effect results from both the electrostatic contribution described as $1/D$ and the non-electrostatic (*i. e.*, specific) solvent effect. However, in the equilibrium under consideration, it seems that only the former acts on this effect (Fig. 4). The slope of such a linear plot (Fig. 2) may give a relative measure of the field effect which depends on the type of reaction.

The same treatment is applicable to the other dissociation equilibrium, those of anilinium ions or bicyclo[2.2.2]octane-1-carboxylic acid.[13] Equation (7) holds good for these series. The results of Grunwald showed that the ξ of the former equilibrium is linearly dependent on his Y_0[6] values and then he used the similar equation as Eq. (7) for the prediction of ρ values in several solvents.

On the other hand, the sign of the interaction constant[19] is negative, which seems to be generally true for the equilibrium with a positive ρ value. Over the range of negative ξ values, *i. e.*, in solvents less polar than water, the electron-withdrawing ability of a substituent in this situation increases the force driving for an equilibrium more than that in the additive relation which comes into existence when the interaction term is equal to zero. This can be explained if it is considered that the electron-withdrawing substituent operates to stabilize the carboxylate anion directly through space. The less polar the solvent is, the larger the degree of this effect becomes.

The Non-Aqueous Solvent Effects on ρ Value. It should be noted that the above treatment is also applicable to the variation in the velocity coefficient, k, with both substituents and solvents, using the concept of the theory of the absolute reaction rate;[20] *i. e.*, the standard activation free energy of a reaction is the thermodynamic property. Equation (8) is derived as:

$$\log\left(\frac{k_\sigma{}^\xi}{k_0{}^0}\right) = \rho_0\sigma + \zeta_0\xi + \left(\frac{\partial\rho}{\partial\xi}\right)_0\sigma\cdot\xi \qquad (8)$$

Few systematic studies have been carried out on the non-aqueous solvent effects on the ρ value. Regarding this problem, the present authors have, however, obtained some results of the Menschutkin-type reaction I (Table 2).

Figure 5 shows a Hammett plot based upon some of these data. The correlation coefficient of this plot from Table 2 is good in every solvent except in methanol.[21] This means that the substituent effects on the rates of these reactions can be expressed sufficiently in terms of a simple Hammett substituent constant, and that the reaction mechanisms are not influenced by the change in substituents. Also, it must be emphasized that for even this reaction of the highly hindered system (2,4,6-trinitro substituted reactant), the Hammett relationship holds good. This observation, as has been suggested by Taft,[22] seems to be attributable to the fact that the steric requirement of the reaction is not influenced by the variation in the substituent at the *m*- or *p*-position.

The non-aqueous solvent effects on the ρ value are extremely complex in the reaction under examination, as is shown in Table 2. However, a clear tendency is observed; the ρ values in aromatic solvents are all larger in absolute value than those in other solvents. The above-mentioned treatment has been applied to this reaction. We chose benzene as the standard solvent, and ξ was defined as $\log(k_0{}^{\text{other solvent}}/k_0{}^{C_6H_6})$. The plot of $\log(k_\sigma{}^{\text{other solvent}}/k_\sigma{}^{C_6H_6})$ against ξ (not shown) gives two distinctly different lines, which is equivalent to the fact that the two Hammett plots intersect with each other. The substituents also influence the mode of the variation in the logarithm of the rate constant with the solvent. The solvent constant can not be determined *a priori*. In this respect, the solid and dashed lines in Fig. 6 were drawn in to show that the solvents fall naturally into two groups: group a, along the dashed line in Fig. 6, consists of benzene, *p*-xylene, bromobenzene, and chloroform, while group b, along the solid line in Fig. 6, consists of tetrahydrofuran, methyl ethyl ketone, methanol, and acetonitrile. It goes without saying that Eq. (7) holds for each group. Nitrobenzene shows, however, a deviation from these two lines. The absolute value of ρ decreases with an increase in the solvent polarity in the members of group b, but in the members of group a this tendency is just reversed. In other words, $\partial\rho/\partial\xi$, the measure of the sensitivity to the field effects, is positive in group b and negative in group a since the reaction under consideration has a negative value of ρ.

It is now necessary to review the non-aqueous solvent effects on the kinetics of this type of reaction. A linear dependence of ξ on the $(D-1)/(2D+1)$ function can be expected from the first approximation of Kirkwood's theory[23] for dipole-dipole reactions, but no such simple relationship is observed in group a. Recently Reinheimer *et al.*[24] correlated the abnormally-high reactivity of the

19) The terms $\partial\rho/\partial\xi$ and $\partial\zeta/\partial\sigma$ mean the interaction constants of σ and ξ when it is constant, as is shown in Figs. 2 and 3, judging from the similarity to the estimation of energy levels for polyatomic molecules. See, for example, Ref. 11, p. 503.

20) S. Glasstone, K. J. Laidler and H. Eyring, "Theory of Rate Processes," McGraw-Hill Book Co., New York (1940).

21) As the concurrent methanolysis of the reactant occurs, the pseudo second-order rate constants in methanol must be calculated after a consideration of this solvolysis. For this reason, in methanol the correlation is worse than in other solvents.

22) R. W. Taft, Jr., *J. Am. Chem. Soc.*, **74**, 3120 (1952).

23) J. G. Kirkwood, *J. Chem. Phys.*, **2**, 351 (1934).

24) J. P. Reinheimer, J. D. Harley, and W. W. Meyers, *J. Org. Chem.*, **28**, 1575 (1963).

TABLE 2. RATE CONSTANTS OF THE REACTION BETWEEN *N,N*-DIMETHYLANILINE OR ITS DERIVATIVES AND 2,4,6-TRINITROANISOLE AND ρ VALUES IN VARIOUS SOLVENTS AT 50 ± 0.1°C

Solvent	Substituent — Rate constant,[a] k, $l\cdot mol^{-1}\cdot hr^{-1}$						n[e]	ρ	r[f]
	None	*m*-NO_2	*m*-Cl	*m*-CH_3	*p*-CH_3	*p*-OCH_3			
Benzene	0.112[b]	0.00156[b]	0.0105[b]	0.182[b]	0.375[b,c]	0.701[b]	6	−2.724	−0.999
p-Xylene	0.0821[b]	0.00115[b]	0.00661[b]	0.133[b]			4	−2.669	−0.998
Nitrobenzene	0.7645[c]	0.01095[b]	0.0777[b]	1.15[c]	2.32[c]	4.74[c]	6	−2.67	−0.999
Bromobenzene	0.278[b] (0.317)	0.00267[b]	0.0230[b]	0.521[c]			4	−2.931	−1.000
Acetonitrile	0.579[c]	0.0142[b]	0.0773[b]	0.862[c]	1.59[c]	3.18[c]	6	−2.373	−0.999
Methanol	0.578[c]	0.0169[d]		1.089[c] 1.143[g]		1.726[c] 1.51[g]	4	−2.114	−0.993
Methyl ethyl ketone	0.374[c]	0.00891[b]	0.0461[b]	0.558[c]	0.9865[c]		5	−2.335	−0.999
Tetrahydrofuran	0.2375[b]	0.00551[b]	0.0290[b]	0.393[c]	0.676[c]	1.53[c]	6	−2.463	−0.998
Chloroform	0.419[b]	0.00335[b]	0.0322[b]	0.651[c]			4	−2.947	−1.000
Carbon disulfide		0.0009[b,h]		0.215[b]			2	−3.05	

a) Average value for at least two runs. Deviation of average value not less than 0.5 but not more than 2%.
b) Value by initial rate method.
c) Value by integral rate method.
d) Value obtained without consideration of methanolysis of trinitroanisole.
e) Number of substituents for determination of ρ.
f) Correlation coefficient of Hammett plot.
g) Value obtained by considering methanolysis of trinitroanisole through initial rate method.
h) Less accurate than other.

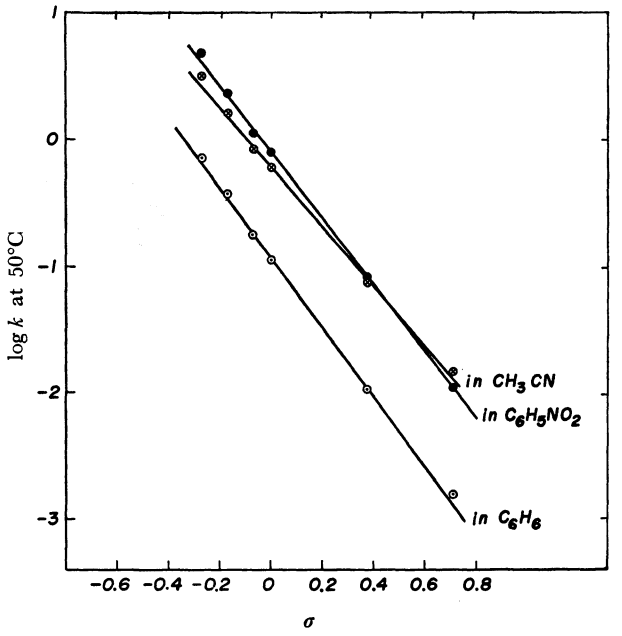

Fig. 5. Hammett plots of the reaction (I), ●, in nitrobenzene; ⊗, in acetonitrile; ⊙, in benzene.

Menschutkin reaction in aromatic solvents with the non-electrostatic properties of these solvents. On examination of the data described in the literature[24] and the data at hand, it can be said that the electron density in the aromatic nucleus seems to play a role in determining the kinetics of this type of reaction in aromatic solvents. There seems to be a specific solvation of a leaving anion in a transition state by aromatic solvents. This effect is clearly in the sequence: nitrobenzene>bromobenzene>benzene>toluene>*p*-xylene. For example, in such aromatic solvents as toluene or *p*-xylene, containing electron-releasing substituents, the rate of this type of reaction is slower than in other solvents.

On the other hand, it has also been noticed that a transition state assumed to be close enough to picrate, the reaction product, may be considerably sensitive to the non-electrostatic or diffusion factor of solvent effects.[25]

These factors may cause a difference in the mode of the variation in ρ with the solvent between the members of group a and those of group b. However, the explanation of this difference must be reserved until it is confirmed that this behavior is not unusual for the Menschutkin type of reaction in non-aqueous solvents; we shall continue our examination on this problem.

Experimental

Kinetic Procedure. It was conductmetrically verified by Hertel and Dressel[12] that the reaction (I) strictly follows the bimolecular rate law and that it is practically completed through the scheme. However, the formation of picrates enabled us to follow the kinetic runs by the convenient spectroscopic technique. The stock solution was introduced into a reaction vessel with a capacity of 50 m*l*, equipped with a slender and long-necked flask, and placed in a thermostat held at 50±0.1°C; then the stock solution of dimethylaniline or its derivatives was added. The sampling solution from this vessel was extracted three times with a constant volume of a water-benzene mixture so that the picrate produced might be obtained as an aqueous solution. This solution was diluted to a concentration favorable for measuring the optical density of the solution. In the experiments using nitrobenzene as the solvent, the water layer was further washed with benzene in order to prevent the contamination by this solvent from markedly affecting the optical densities of the water layer. The optical density of the samples was obtained over the range of 360—400 mμ at intervals of 10 mμ on a Hitachi spectrophotometer EPU-2A, using quartz cells 1.0 cm thick.

These salts appear to be completely dissociated in water. To check this point, the molecular extinction coefficients, ε, of *N,N,N*-trimethylanilinium and *p*-tolyl-*N,N,N*-trimethylanilinium picrate were measured. The calibration curves which were obtained in the range of 360—400 mμ at intervals of 10 mμ obeyed Beer's law excellently in each case. The results are given in Table 3. The table shows that these coefficients are essentially identical with each other, so the data of the *N,N,N*-trimethylanilinium salt were taken for the calculation of the rate constants.

A typical run, the reaction of *m*-methyl-dimethylaniline with 2,4-6-trinitroanisole in tetrahydrofuran at 50°C, is shown in Fig. 7, where D and D_∞ are the

25) E. Grunwald and E. Price, *J. Am. Chem. Soc.*, **86**, 4517 (1964).

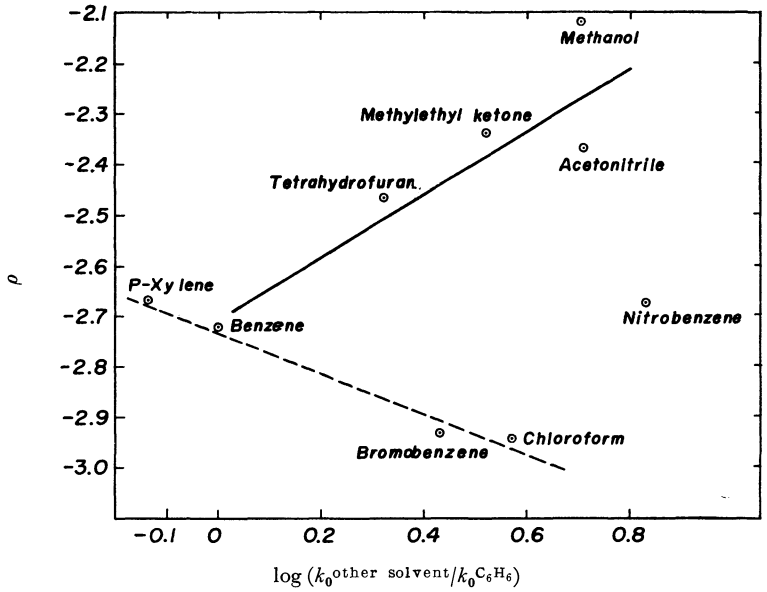

Fig. 6. The relationship between ρ and log ($k_0$other solvent/$k_0C_6H_6$) as the solvent parameter for the reaction (I).

TABLE 3. MOLECULAR EXTINCTION COEFFICIENTS OF SOME PICRATES IN WATER

Picrates, λ, mμ	360	370	380	390	400
Sodium	14080	13090	11730	10780	9870
N,N,N-Trimethylanilinium	13990	12890	12890	11670	9796
p-Methylphenyltrimethyl-ammonium	13960	13050	11850	10860	10010

optical densities of the samples in water at finite and infinite times respectively. Since the optical density is proportional to the concentration of the picrate produced, the second-order rate constant can be obtained by multiplying the slope of such a figure by εl (l indicates the cell length; 10 mm). In the case of slower reactions the method of initial rates was carried out in order to estimate the rate constants by the equation: $dD/dt = (k/\varepsilon l)D^a_\infty \cdot D^b_\infty$. The rate constants obtained by the two procedures agree with each other within 10%, as is shown in the case of bromobenzene in Table 2. The concentrations used in the calculation of the velocity constants were the concentrations at the temperature of the experiment by correcting for solvent expansion. The densities of THF at several temperatures were calculated by the usual manner using one experimental value, d_{20}.[26]

At least one duplicate experiment was always performed with a different initial concentration. As a result, it was observed that the rate coefficient is independent of the concentration. In methanol, however, it was observed that the rate of the methanolysis of trinitroanisole is comparable to the rate of the reaction of *m*-nitro-dimethylaniline with trinitroanisole. The estimation of the rates of the methanolysis of trinitroanisole in methanol was carried out by the initial rate method. The plot of D against t gives a straight line through the zero point. The slope of this plot was $(5.38 \pm 0.21) \times 10^{-3}$ hr^{-1} for the pseudo first-order methanolysis rate (the average value of three independent runs). Using this value, the rate coefficients of the reaction between *m*-methyl- or *p*-methoxy-*N,N*-dimethylaniline and trinitroanisole in methanol were given in the following form:

$$k = \frac{1}{a \cdot b}\left(\frac{dx}{dt}\right)_0 = \frac{k_{\text{methanolysis}}}{b}$$

where $(dx/dt)_0$ was obtained by means of Newton's numerical differential equations.[27]

The rate of the reaction between *m*-nitro-dimethylaniline and trinitroanisole in methanol was obtained by the method of Andrews and Young[28] using the following equation:

$$\frac{(dx/dt)_0}{[\text{TNA}]_0} = k[\text{DMA}]_0 + k_{\text{methanolysis}}$$

A plot of $(dx/dt)_0/[\text{TNA}]_0$ *vs.* $[\text{DMA}]_0$ was a straight line the slope of which gave k.

Table 2 gives the results for the reaction rates in various solvents obtained as has been described above.

26) J. H. Perry, "Chemical Engineer Handbook," 4th ed., McGraw-Hill Book Co., New York (1963).

27) M. Oiwa, "Hanno Sokudo Keisanho, (Measurement of the Reaction Rates)," Asakura Shoten, Tokyo (1962), p. 86.

28) A. A. Frost and R. G. Pearson, "Kinetics and Mechanism," 2nd ed., John Wiley and Sons, New York, N. Y. (1953), p. 369.

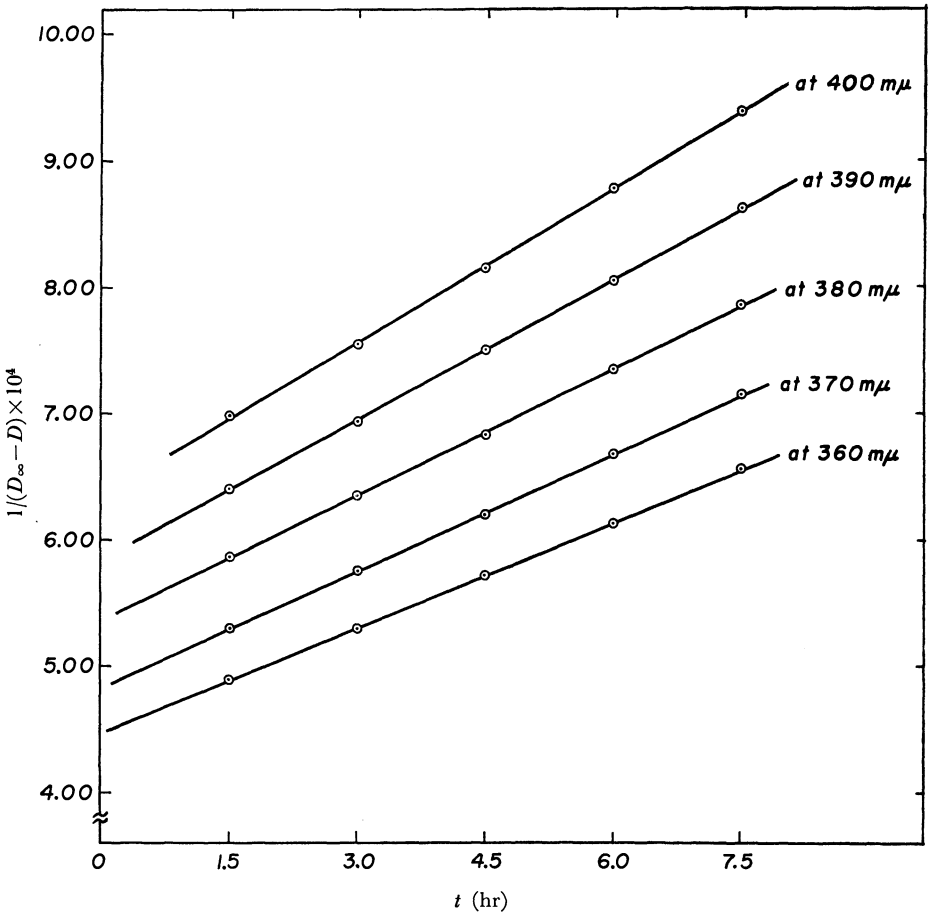

Fig. 7. A typical run for the reaction between *m*-methyl-dimethylaniline and trinitroanisole in tetrahydrofuran at 50°C.

Materials. The *N,N*-dimethylaniline, from Wako Pure Chemicals, was purified according to the procedure described by Fieser[29] and stored in an atmosphere of dry nitrogen until use.

The *p*-methoxy-, *p*-methyl-, *m*-chloro-, and *m*-methyl-*N,N*-dimethylanilines were prepared according to the directions of Fukui *et al.*[30] from commercial *p*-methoxy-, *p*-methyl-, *m*-chloro-, and *m*-methylanilines respectively. The purification of these materials was similar to that of *N,N*-dimethylaniline. The purity of these samples was assured to be sufficient by elemental analysis, infrared spectroscopy, and gas chromatography, in which only a single peak was observed in every case, using two solid supports, P. E. G. 6000 and Silicone D. C. 550.

The *m*-nitro-*N,N*-dimethylaniline was prepared by the usual method of nitration[31] and recrystallized from 95% ethanol at least four times; mp 57—58°C, lit. 57—58°C.[32]

The 2,4,6-trinitroanisole (TNA) was prepared by the reaction[33] of dissolved sodium hydroxide in methanol at 0—5°C with picryl chloride (which was taken from picric acid and phosphorus pentachloride), recrystallized from methanol several times, and dried over silica gel in a desiccator; mp 67—68°C, lit. 67—68°C.[32] Found: C, 34.71; H, 2.35; N, 17.05%. Calcd for $C_7H_5N_3O_7$: C, 34.58; H, 2.0; N, 17.28%.

The *N,N,N*-trimethylanilinium- and *p*-methylphenyltrimethylammonium picrates were prepared from equimolar quantities of amines and anisole at 50°C in THF and were recrystallized from water until a constant melting point was obtained; mp 120—120.5°C and 195—196°C[33] respectively. The sodium salt was prepared from picric acid and sodium hydroxide in boiling water and recrystallized. These salts were dried in an Abderhalden flask for several hours at the boiling point of acetone and then used to obtain the molecular extinction coefficients in water. Benzene, *p*-xylene, and bromobenzene were shaken with concentrated sulfuric

29) L. F. Fieser, "Experiments in Organic Chemistry," Maruzen, Tokyo (1957).

30) K. Fukui, Y. Inamoto, S. Takase and T. Kitano, *Kogyo Kagaku Zasshi (J. Chem. Soc., Japan, Ind. Chem. Sect.)*, **62**, 531 (1959).

31) "Org. Synth.," Coll. Vol. 3, p. 658 (1955).

32) R. C. Farmer, *J. Chem. Soc.*, **1959**, 3425.

33) J. B. Ramsey and E. L. Colichman, *J. Am. Chem. Soc.*, **69**, 3043 (1947).

acid several times until no further discoloration was observed; they were then washed with water, about 10% aqueous potassium hydroxide, and again with water, dried over calcium chloride, and distilled. The center fraction was further distilled twice from phosphorus pentoxide.

The nitrobenzene and methyl ethyl ketone were commercial reagents used without further purification. After drying with calcium chloride and then phosphorus pentoxide, they were distilled three times. The center fraction was collected for use.

The tetrahydrofuran was refluxed with potassium hydroxide and distilled. After drying and refluxing with sodium wire, the center fraction was redistilled. It was stored over sodium wire and then further distilled before use.

The acetonitrile was dired over phosphorus pentoxide, distilled, and treated as before. The center franction was stored over phosphorus pentoxide and distilled before use.

The methanol,[34] chloroform,[35] and carbon disulfide[36] were purified as has been described in the literature.

34) A. A. Maryott, *J. Am. Chem. Soc.*, **63**, 3079 (1941).
35) S. O. Morgan and H. H. Lowry, *J. Phys. Chem.*, **34**, 2385 (1930).
36) E. E. Ogg and J. W. Williams, *J. Am. Chem. Soc.*, **50**, 2894 (1928).

BULLETIN OF THE CHEMICAL SOCIETY OF JAPAN VOL. 42 1047—1051 (1969)

The Anodic Reaction of Acetic Acid in the Presence of Enanthaldehyde, Enanthaldehyde Diethyl Acetal, and 2-Octanone

Akira TAKEDA and Satosi WADA

Department of Synthetics Chemistry

and Sigeru TORII and Yuji MATSUI[1]

Department of Industrial Chemistry, Okayama University, Okayama

(Received June 21, 1968)

The anodic methylation of enanthaldehyde, enanthaldehyde diethyl acetal, and 2-octanone was attempted by electrolyzing a mixture of acetic acid, ethanol (or tetrahydrofuran and/or acetone), water, and potassium hydroxide. The major products from the electrolysis of enanthaldehyde consisted of 2-octanone, 1-heptanol, 3-methyl-2-octanone, and enanthaldehyde diethyl acetal. Similar products were isolated from the reaction mixture of enanthaldehyde diethyl acetal. The anodic methylation of 2-octanone gave 3-methyl-2-octanone as a major product. Possible mechanisms of the formation of these ketones were discussed.

Several workers[2-4] have reported the anodic methylation of aromatic rings, *i. e.*, trinitrotoluene and pyridine, and of double bond of 1,1-diphenylethylene. In the anodic methylation of benzaldehyde in aqueous acetic acid-potassium hydroxide solution,[5] we found the replacement of the hydrogen atom of the formyl group of benzaldehyde by a methyl group to give acetophenone. Such anodic methylation has been found to occur, recently, in the course of the electrolysis of the acetic acid solution containing cinnamic[6] and β-phenylglycidic acids.[7] As an extension of the above

$$\mathrm{Ph{-}\overset{\overset{\mathrm{O}}{\|}}{C}{-}H} \xrightarrow[CH_3COOH]{\text{Anodic Reaction}} \mathrm{Ph{-}\overset{\overset{\mathrm{O}}{\|}}{C}{-}CH_3}$$

method, the anodic methylation of enanthaldehyde and its related compounds were investigated for the preparation of aliphatic methyl ketone.

Results and Discussion

Two platinum foil electrodes were used in the

1) Present address: Department of Applied Chemistry, University of Osaka Prefecture, Sakai, Osaka.

2) F. D. Mango and W. A. Bonner, *J. Org. Chem.*, **29**, 1367 (1964).

3) S. Goldschmidt and M. Minsinger, *Chem. Ber.*, **87**, 956 (1954).

4) L. F. Fieser, R. C. Clapp and W. H. Daudt, *J. Am. Chem. Soc.*, **64**, 2052 (1942).

5) A. Takeda, S. Torii and H. Oka, *Tetrahedron Letters*, **1968**, 1781.

6) A. Takeda, S. Torii and H. Oka, *Memoirs of the School of Engineering, Okayama Univ.*, **3**, 107 (1968).

7) A. Takeda, S. Wada, S. Torii and T. Takaki, unpublished work.

TABLE 1. REACTION PROCEDURES

Substrate (g)	n-$C_6H_{13}CHO$ 22.8	n-$C_6H_{13}CHO$ 25	n-$C_6H_{13}CHO$ 25	n-$C_6H_{13}COCH_3$ 19.2	n-$C_6H_{13}CH(OEt)_2$ 42 (98%)
CH_3COOH* (m*l*)	60+480[a)]	84+600[b)]	84+600[c)]	45+700[d)]	72+600[c)]
Org. Solvent	EtOH	THF	Me_2CO	EtOH	EtOH
(m*l*)	30	100	75	37.5	115
KOH (g)	8.0	8.4	8.4	6.3	8.4
H_2O (m*l*)	40	50	50	37.5	50.0
Reaction time (hr)	210	150	210	210	210
End point (pH)	3.5	3.5	4.0	3.5	4.0
Cell voltage (V)	14—16	16	14—16	14—16	15—16
Electric density (A/cm^2)	0.4—0.6	0.7—0.8	0.33—0.43	0.43—0.80	0.43—0.80
Products					
Neutral (g)	6.5	10.6	12.7	8.6	15.0
Acidic (g)	0.2	0.3	0.7	0.3	0.4

* Additional acetic acid was added as follows: a) 60 m*l* every 26 hr, b) 50 m*l* every 12 hr, c) 50 m*l* every 16 hr, and d) 50 m*l* every 15 hr.

present experiments. Some typical reaction procedures are shown in Table 1. The products of the anodic reaction of enanthaldehyde and its related compounds were separated by chemical procedure into two groups as illustrated in Scheme 1. Both the ketone and aldehyde and the non-ketone and non-aldehyde components were characterized by vapor-phase gas chromatography (vpc). The principal products are summarized in Tables 2 and 3. 2-Octanone and its derivatives, which are expected to be produced from the anodic methylation of enanthaldehyde, were detected. By using the Girard P reagent, the ketone and aldehyde component was separated in about 50% yield. About 64% of the ketone and aldehyde component consisted of 2-octanone. The change of organic solvent had little effect on the constituent of the

TABLE 2. PRODUCTS OF ENANTHALDEHYDE

Constituent[a)]	Neutral portion Peak area (%)	Ketone and aldehyde Peak area (%)
Enanthaldehyde	3.70	6.56
2-Methylenanthaldehyde	0.43	0.78
2-Octanone	36.42	64.51
1-Heptanol	25.81	—
3-Methyl-2-octanone	12.96	22.56
3-Nonanone	1.46	2.59
Enanthaldehyde diethyl acetal	5.65	—
n-Heptyl acetate	4.16	—
Others	9.37 (8 peaks)	4.43 (4 peaks)

a) Separation of the each constituent was carried out by gas chromatography with a 45 m, 10% silicone oil coated Hitachi Golay column Z-45 (SE-30) operating at 75 and 90°C.

TABLE 3. PRODUCTS OF 2-OCTANONE AND ENANTHALDEHYDE DIETHYLACETAL

Constituent[a)]	Substrate (peak area, %) n-$C_6H_{13}CH(OEt)_2$	Substrate (peak area, %) n-$C_6H_{13}COCH_3$
Enanthaldehyde	2.13	—
2-Octanone	28.83	54.60
2-Octanol	—	2.80
3-Methyl-2-octanone	4.65	32.30
3-Nonanone	0.24	2.46
Enanthaldehyde diethyl acetal	14.23	—
2-Octanone diethyl ketal	—	6.45
Others	46.62	1.39

a) Separation was carried out with Hitachi Golay column Z-45 operating at 90°C.

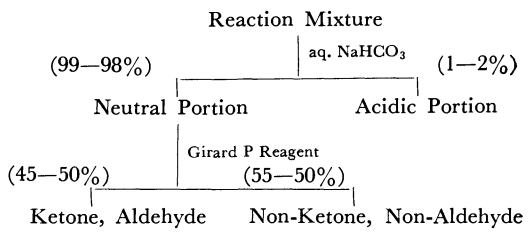

Scheme 1. Separation of the products.

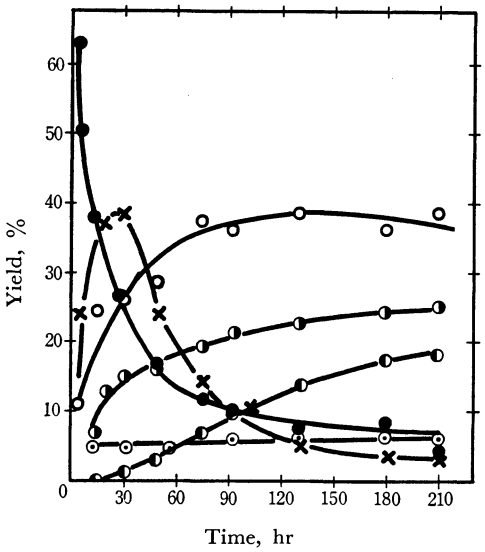

Fig. 1. Relationship between reaction time and yield of constituents in the electrolysis of enanthaldehyde.

● Enanthaldehyde, ○ 2-octanone,
◑ 1-heptanol, ◐ 3-methyl-2-octanone,
⊙ enanthaldehyde diethyl acetal,
× enanthaldehyde ethyl hemiacetal (vpc characterized).

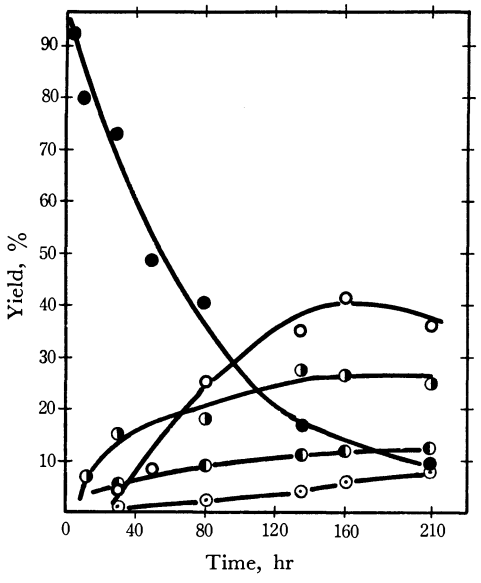

Fig. 2. Relationship between reaction time and yield of constituents in the electrolysis of enanthaldehyde diethyl acetal.

● Enanthaldehyde ethyl hemiacetal,
○ 2-octanone,
◑ enanthaldehyde,
◐ enanthaldehyde diethyl acetal,
⊙ 3-methyl-2-octanone.

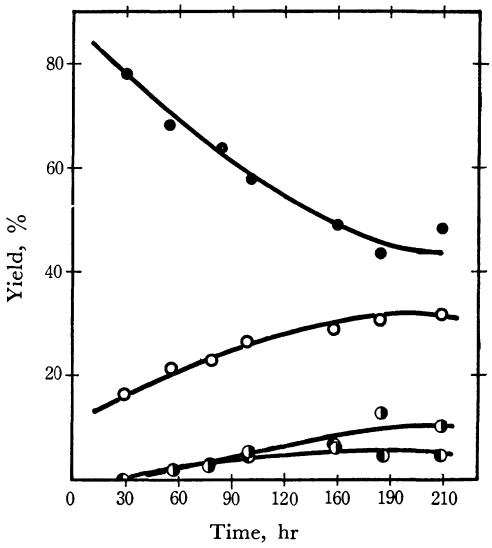

Fig. 3. Relationship between reaction time and yield of constituents in the electrolysis of 2-octanone.

● 2-Octanone,
○ 3-methyl-2-octanone,
◑ 2-octanone diethyl ketal,
◐ 3-nonanone.

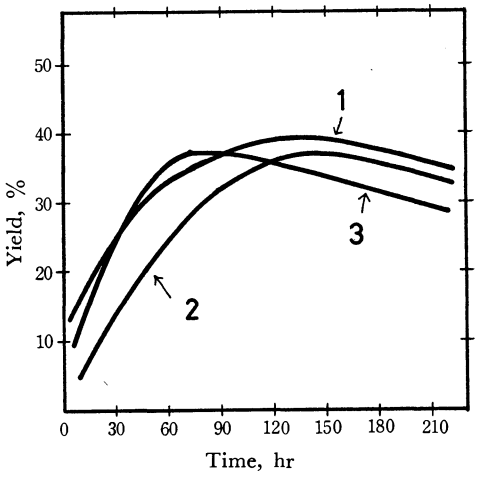

Fig. 4. Relationship between reaction time and yield of 2-octanone, using various solvents.
1 Ethanol, 2 tetrahydrofuran, 3 acetone.

products.

When anodic methylation was carried out in the presence of enanthaldehyde diethyl acetal as a substrate, the constituent of the major products was similar to that described in Table 2. The anodic methylation of 2-octanone afforded 3-methyl-2-octanone as a major product. The results of each reaction which was carried out for 210 hr are illustrated in Figs. 1, 2, and 3. The

results of the formation of 2-octanone in different solvents are shown in Fig. 4.

The results given in Fig. 1 show that the methylation and the reduction of enanthaldehyde proceed principally to afford 2-octanone and 1-heptanol. In the course of this reaction, some enanthaldehyde may be converted into its hemiacetal and diethyl acetal. By electrolyzing 2-octanone in the same media, 3-methyl-2-octanone was produced (Fig. 3). The maximum yield of 2-octanone, in Fig. 1, was estimated when electrolysis was continued for about 140 hr. The line attributed to enanthaldehyde hemiacetal in Fig. 2 shows that the conversion of enanthaldehyde diethyl acetal into the hemiacetal may be performed for a relatively short period. In Fig. 4, it seems that the organic solvent used in the present reaction affected only the rate of the formation of 2-octanone.

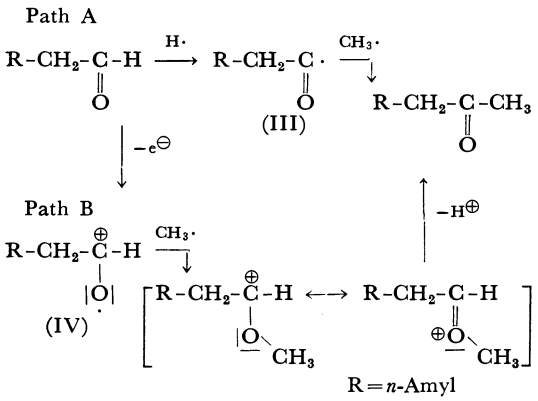

Scheme 2. Formation of 2-octanone.

Path A: The abstraction of a hydrogen atom directly from the formyl group by anodically generated radicals.

Path B: The formation of radical ion (IV) by discharge of the substrate on the anode and the addition of a methyl radical followed by carbonium ion rearrangement.

Recently, Koehl hypothesized[8] that a cation-radical intermediate (I) may be produced, when the triple bond of diphenylacetylene was subjected to discharge at the anode surface. In a previous paper,[5] we also assumed a possibility in which

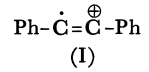

(I)

discharge of the carbonyl group of benzaldehyde at the anode may give cation radical intermediate (IIa and IIb), since no appreciable amount of

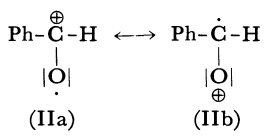

(IIa) (IIb)

8) W. J. Koehl, *J. Org. Chem.*, **32**, 614 (1967).

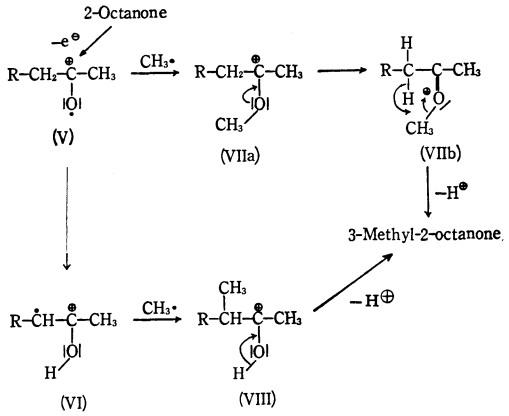

Scheme 3. Formation of 3-methyl-2-octanone.

benzil was detected on the gas chromatogram. Similarly, in the case of enanthaldehyde, absence of dimer of heptanoyl radical (III) was confirmed by vpc. A possible pathway of the formation of 2-octanone may be considered as follows (Scheme 2):

However, considering the mode of attack of a methyl radical to 2-octanone, the assumption of the cation-radical intermediate (IV) seems to be more reasonable. A mechanism of the formation of 3-methyl-2-octanone *via* radical-cation intermediates is outlined in Scheme 3. Considering the facility of the formation of 3-methyl-2-octanone rather than 3-nonanone, it seems that the anodically generated methyl radical[9] may attack radical-cation intermediates (V and VI) to form (VII and VIII), which may further undergo carbonium ion rearrangement giving 3-methyl-2-octanone.

Experimental

All boiling points are uncorrected. The products were analyzed by vapor-phase chromatography (Hitachi F6-D gas chromatograph) using Golay column (Z-45) coated with silicone oil (SE-30).

Apparatus. The electrochemical cell consisted of a cylindrical glass vessel, 7 cm long in diameter and 14 cm high, fitted with a gas lead pipe, a thermometer, and a magnetic stirrer. The vessel was immersed in a water bath, cooled with circulating cold water. The electrodes were two platinum foils (1.5×2.0 cm^2) spaced about 2 mm apart and the current direction was changed every 30 sec by means of a commutator.

Materials. Analytical grade enanthaldehyde, 2-octanone, acetic acid, ethanol, tetrahydrofuran, acetone, and inorganic chemicals were used. The following reference compounds were prepared: enanthaldehyde diethyl acetal,[10] bp 99—102°C/25 mmHg, α-methyl-

9) K. Sugino, T. Sekine and N. Sato, *Electrochem. Technology*, **1**, 112 (1963).

10) E. W. Adams and H. Adkins, *J. Am. Chem. Soc.*, **47**, 1365 (1925).

enanthaldehyde,[11] bp 50—52°C/10 mmHg, 3-methyl-2-octanone,[12] bp 64°C/18 mmHg, 3-nonanone,[13] bp 85—88°C/20 mmHg, 1-heptanol,[14] bp 71—72°C/12 mmHg, 1-heptyl acetate,[15] bp 192°C.

General Procedure. A typical reaction procedure is shown in Table 1. A mixed solution of the substrate, acetic acid, water, the organic solvent, and potassium hydroxide was electrolyzed at Pt electrodes for about 210 hr at 25—35°C, with terminal voltage 14—16 V at a current of 1.2—2.4 A, magnetically stirring, and changing the current direction every 30 sec by means of a commutator. The resulting reaction mixture was diluted with 300 m*l* of water and extracted with ether. The extracts were washed with a saturated aqueous sodium chloride solution and concentrated *in vacuo*. The separation of the products was carried out in the manner shown in Scheme 1. The results of gas chromatography of each experiment are indicated in Tables 2 and 3. The isolation of enanthaldehyde ethyl hemiacetal from the non-ketone and non-aldehyde components through distillation failed. However, we succeeded in detecting the hemiacetal in the high-boiling fraction of the non-ketone and non-aldehyde components both spectroscopically and gas chromatographically: IR (cm^{-1}) 3500—3200 (OH) and 1120—1040 (hemiacetal); vpc with a 1 m, 10% silicone oil (SE-30) coated Chromosorb W (NAW) column operating at 140°C and 0.4 kg/cm^2 (N_2): Retention time 18 min.

11) Brit. Pat. 808880 (1959); *Chem. Abstr.*, **54**, 3319 (1960).

12) S. G. Powell, H. C. Murray and M. M. Baldwin, *J. Am. Chem. Soc.*, **55**, 1153 (1933).

13) P. G. Kletzke, *J. Org. Chem.*, **29**, 1363 (1964).

14) H. T. Clarke and E. E. Dreger, "Organic Syntheses," Coll. Vol. I, p. 304 (1941).

15) U. S. Pat. 2843607 (1958); *Chem. Abstr.*, **52**, 20197c (1958).

BULLETIN OF THE CHEMICAL SOCIETY OF JAPAN VOL. 42 1052—1059 (1969)

The Rotatory Dispersion and Stereochemistry of Organic Compounds. XV.[1] Nitrophenyl Glycosides

Yojiro Tsuzuki, Motoo Koyama, Kazuyuki Aoki, Tatsuo Kato and Koko Tanabe

Department of Chemistry, Science University of Tokyo, Kagurazaka, Shinjuku-ku, Tokyo

(Received September 17, 1968)

It has been reported that some ortho-nitrophenyl glycosides exhibit anomalous optical rotation (Montgomery *et al.*, *J. Am. Chem. Soc.*, **64**, 690 (1942)). To investigate this anomalous effect of the ortho-nitro group the authors have observed the RD spectra on twenty-five derivatives of *o*-nitrophenyl, *p*-nitrophenyl and phenyl glycosides. Every *o*-nitrophenyl derivative (I, IV, VII, XI, XIV, XVII and XX) exhibited a positive Cotton effect near 340 mμ. Furthermore, in order to inquire into this anomaly the authors have observed the CD and UV spectra of these compounds. It follows that the *o*-nitro group is twisted from the benzene ring plane, and that the *o*-nitrophenyl group itself becomes an optical active chromophore, so that the Cotton effects near 340 mμ are caused by the $n\rightarrow\pi^*$ transition of the nitro group. Therefore, the anomaly of *o*-nitrophenyl glycosides in the $[\alpha]_D$ values is concluded to be affected by the strong Cotton effect near 340 mμ.

In the previous paper[1] the rotatory contribution of the nitrophenyl group was reported with diethyl nitrobenzylidene-*d*-tartrates, where the compound with a nitro group in the ortho-position of the phenyl group shows an anomalous rotation in contrast with the corresponding meta and para nitro compounds, whose rotations are normal, and it was really found that the rotatory dispersion (RD) of the *o*-nitro-derivative exhibited such a strong positive Cotton effect near 340 mμ, so that it showed an anomalous rotation affected by the Cotton effect.

The anomaly of the optical rotation due to an *o*-nitro group can be seen in another group of compounds. While the specific rotation $[\alpha]_D$ has been observed with a large number of aryl glycosides,[2-5] only *o*-nitrophenyl glycosides show anomalous rotations, and are exceptions which do not obey the isorotation rule of Hudson.[2,6]

This paper will deal with the studies made with a view of inquiring into the anomalous rotation of *o*-nitrophenyl glycosides by comparing them with those of the tartrates. For that purpose the following twenty-five aryl glycosides have been investigated by means of RD, CD (circular dichroism), as well as UV (ultraviolet absorption) methods and in some cases with the help of NMR method.

Tetraacetyl *o*-nitrophenyl β-D-glucoside (Compound I),
Tetraacetyl *p*-nitrophenyl β-D-glucoside (Compound II),
Tetraacetyl phenyl β-D-glucoside (Compound III),
Tetraacetyl *o*-nitrophenyl β-D-galactoside (Compound IV),
Tetraacetyl *p*-nitrophenyl β-D-galactoside (Compound V),
Tetraacetyl phenyl β-D-galactoside (Compound VI),
Triacetyl *o*-nitrophenyl β-D-xyloside (Compound VII),
Triacetyl *p*-nitrophenyl β-D-xyloside (Compound VIII),
Tetraacetyl *p*-nitrophenyl α-D-glucoside (Compound IX),
Tetraacetyl phenyl α-D-glucoside (Compound X),
Tetraacetyl *o*-nitrophenyl α-D-galactoside (Compound XI),
Tetraacetyl *p*-nitrophenyl α-D-galactoside (Compound XII),
Tetraacetyl phenyl α-D-galactoside (Compound XIII),
o-Nitrophenyl β-D-glucoside (Compound XIV),
p-Nitrophenyl β-D-glucoside (Compound XV),
Phenyl β-D-glucoside (Compound XVI),

1) Y. Tsuzuki, M. Koyama and K. Tanabe, This Bulletin, **41**, 1008 (1968).
2) E. M. Montgomery, M. K. Richtmyer and C. S. Hudson, *J. Am. Chem. Soc.*, **64**, 690 (1942).
3) H. G. Lantham, E. L. May and E. Mosettig, *J. Org. Chem.*, **15**, 884 (1950).
4) B. Capon, W. G. Overend and M. Sobell, *J. Chem. Soc.*, **1961**, 5172.
5) J. A. Snyder and K. P. Link, *J. Am. Chem. Soc.*, **75**, 1758 (1953).
6) W. Pigman, "The Carbohydrates," Academic Press Inc. Publishers, New York (1957), p. 69.

o-Nitrophenyl β-D-galactoside (Compound XVII), *p*-Nitrophenyl β-D-galactoside (Compound XVIII), Phenyl β-D-galactoside (Compound XIX), *o*-Nitrophenyl β-D-xyloside (Compound XX), *p*-Nitrophenyl β-D-xyloside (Compound XXI), *p*-Nitrophenyl α-D-glucoside (Compound XXII), Phenyl α-D-glucoside (Compound XXIII), Phenyl α-D-galactoside (Compound XXIV), and Tetraacetyl 4-nitro-3-methylphenyl β-D-glucoside (Compound XXV).

Results and Discussion

I. Acetylated Glycosides. *Acetylated o-Nitrophenyl β-Glycosides.* In Figs. 1—3 are shown the RD, CD and UV curves of acetyl *o*-nitrophenyl β-D-glucoside (I), -galactoside (IV) and -xyloside (VII). The RD curves of these compounds exhibit complex Cotton effects, the signs of which can be determined by the positive CD_{max} near 325 mμ. The peaks of the positive Cotton effects appear at 370—376 mμ. The two troughs observed at 300—305 mμ and 266—270 mμ can be regarded, in view of the CD curves, to be due to the two negative Cotton effects. As may be seen from Figs. 1 and 2 the UV absorption maxima appear near 255 mμ and 305 mμ.

Acetylated p-Nitrophenyl β-Glycosides. In Figs. 4 and 5 are exhibited the RD, CD and UV curves of tetraacetyl *p*-nitrophenyl derivatives, also showing complex Cotton effects, which are, however, opposite in sign to those of the *o*-nitrophenyl derivatives.

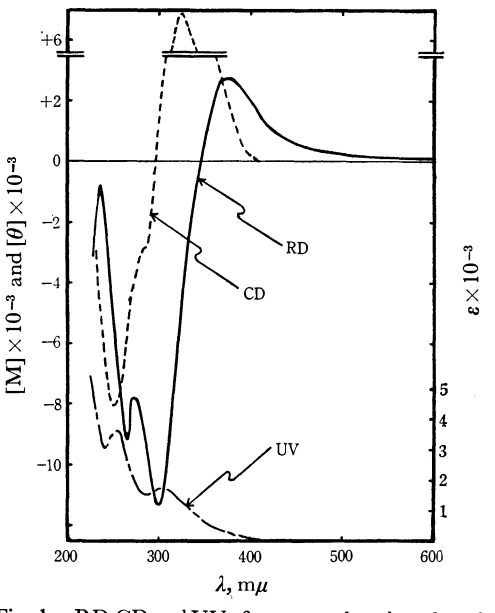

Fig. 1. RD,CD and UV of tetraacetyl *o*-nitrophenyl β-D-glucoside (I).

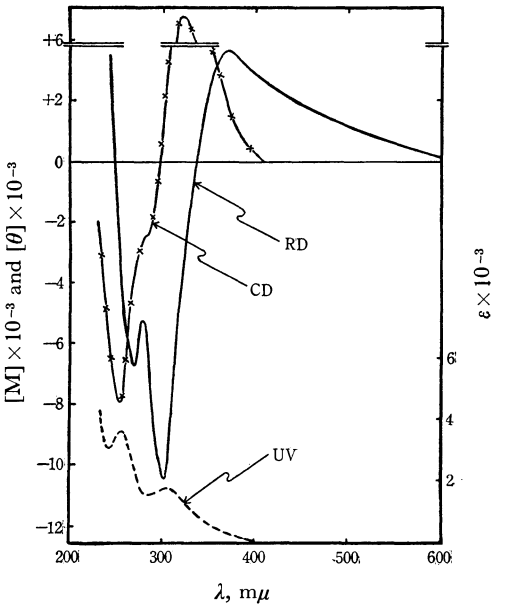

Fig. 2. RD, CD and UV of tetraacetyl *o*-nitrophenyl β-D-galactoside (IV).

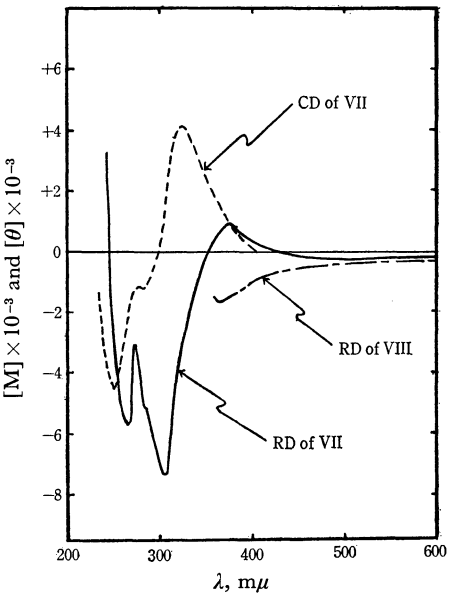

Fig. 3. RD and CD of triacetyl *o*-and *p*-nitrophenyl β-D-xylosides (VII and VIII).

The broad troughs of the RD curves of the compounds II and V may be due to their negative Cotton effects. The same interpretation is also valid for *p*-nitrophenyl xyloside (VIII, Fig. 3). The RD curves of the compounds II and V are, in the longer wavelength region, similar to those of their background compounds with no nitro group III and VI, which, however, exhibit below

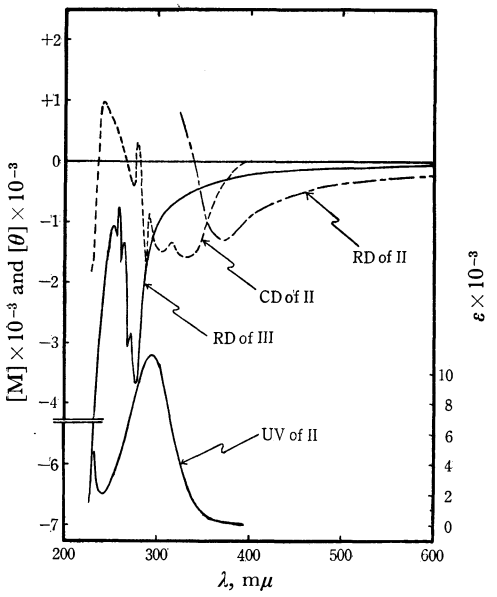

Fig. 4. RD, CD and UV of tetraacetyl aryl β-D-glucosides (II and III).

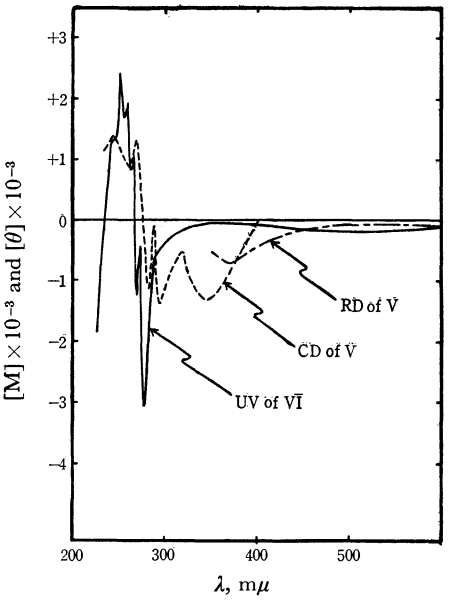

Fig. 5. RD and CD of tetraacetyl aryl β-D-galactoside (V and VI).

270 mμ negative Cotton effects due to the B-band of the phenyl group.

Acetylated o-Nitrophenyl α-Glycoside. Figure 6 represents the RD, CD and UV curves of tetraacetyl o-nitrophenyl α-D-galactoside (XI), where the RD curve shows a positive Cotton effect with a peak around 370 mμ, the shape of which is similar to that of the β-anomer (IV, Fig. 2).

The above stated facts indicate that the RD of

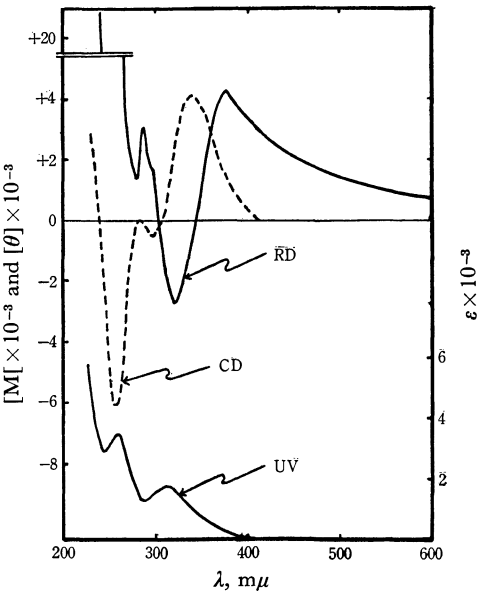

Fig. 6. RD, CD and UV of tetraacetyl o-nitrophenyl α-D-galactoside (XI).

acetylated o-nitrophenyl glycosides are not influenced by the C_1-configuration.

Acetylated p-Nitrophenyl α-Glycosides. The RD curves of tetraacetyl p-nitrophenyl α-D-glucoside (IX) and -galactoside (XII) are given respectively in Figs. 7 and 8. They run in the positive side, quite contrary to those of the β-anomers II and V (Figs. 4 and 5), and rather resemble those of the background RD curves X and XIII (Figs. 7 and 8), but, unlike II and V, show no distinct

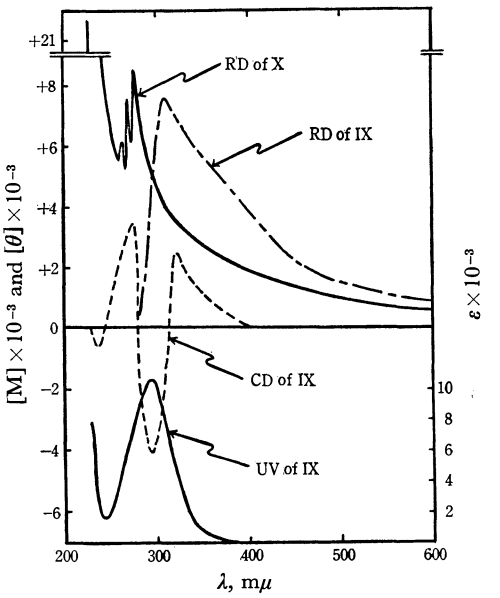

Fig. 7. RD, CD and UV of tetraacetyl aryl α-D-glucosides (IX and X).

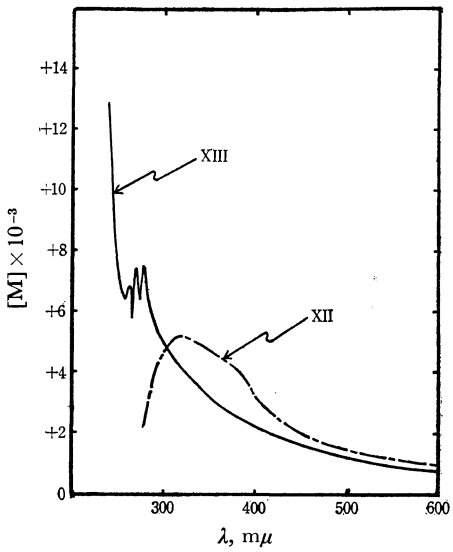

Fig. 8. RD of tetraacetyl aryl α-D-galactosides (XII and XIII).

peaks near 370 mμ, with only a slight shoulder around 370 mμ. This phenomenon can be interpreted as follows, namely, the weak Cotton effect has disappeared under the powerful influence of the strong, positive rotation of the background or of its strong Cotton effect in the shorter wavelength region.

As may be seen from Figs. 7 and 8, the background compounds X and XIII bearing no nitro group really exhibit positive RD curves with positive Cotton effects below 270 mμ attributed to the B-band. The curves contrast finely with the

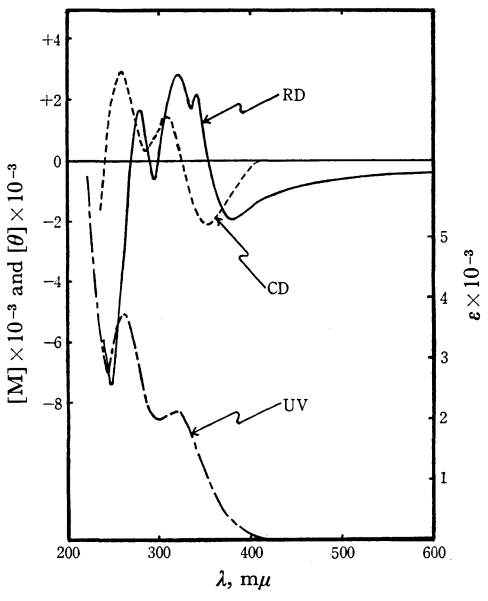

Fig. 9. RD, CD and UV of o-nitrophenyl β-D-glucoside (XIV).

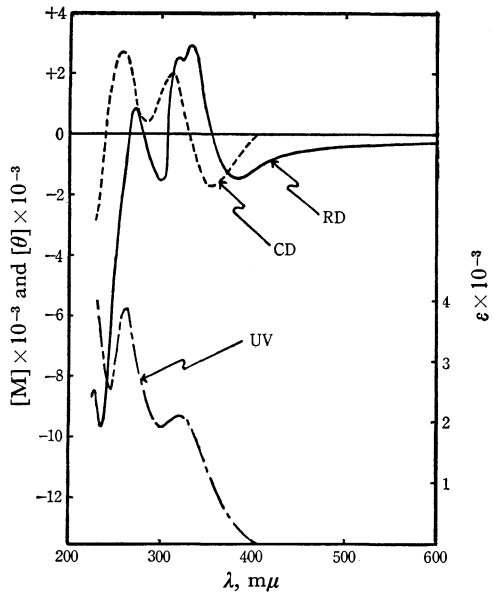

Fig. 10. RD, CD and UV of o-nitrophenyl β-D-galactoside (XVII).

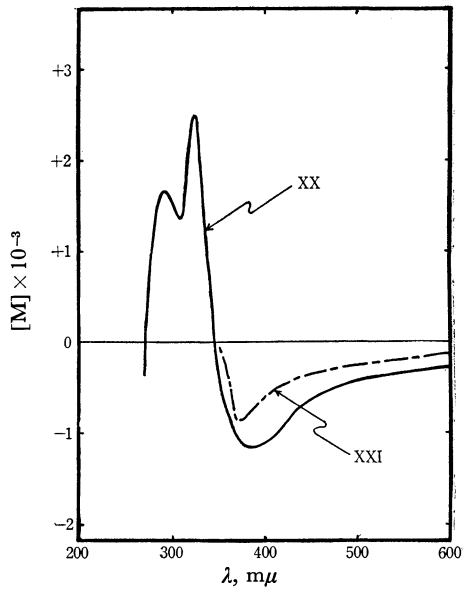

Fig. 11. RD of nitrophenyl β-D-xylosides (XX and XXI).

negative RD curves of the β-anomers III and VI (Figs. 4 and 5). The signs of the Cotton effects agreeing in all cases with the C_1-configurations.

II. Deacetylated Glycosides. *o-Nitrophenyl β-Glycosides.* In Figs. 9—11 are given the RD, CD and UV curves of o-nitrophenyl β-D-glucoside (XIV), -galactoside (XVII) and -xyloside (XX). Each RD curve shows a negative Cotton effect with a trough at 380 mμ. The strengths are estimated from the CD_{max} to be nearly 1/3 of those

of the acetylated derivatives (I and IV), so that these *o*-nitrophenyl β-glycosides show no anomaly in the values $[\alpha]_D$.

And further, these deacetylated *o*-nitrophenyl β-D-glycosides (XIV, XVII and XX) have two positive Cotton effects, as evidenced by the CD_{max} around 310 mμ and 260 mμ, the signs of the Cotton effects are all opposite to those of the corresponding acetylated derivatives (I and IV and VII) and their RD curves are diametrically opposite in each case.

p-Nitrophenyl β-Glycosides. The RD curves of *p*-nitrophenyl β-D-xyloside (XXI), -glucoside (XV) and -galactoside (XVIII) are shown respectively in Figs. 11, 12 and 13, the shapes of which are almost the same with the corresponding acetylated derivatives (VIII in Fig. 3, II in Fig. 4 and V in Fig. 5).

p-Nitrophenyl α-Glycoside. Figure 14 shows the RD, CD and UV curves of *p*-nitrophenyl α-D-glucoside (XXII). While the CD curve (XXII) is similar to that of the acetylated derivative (IX in Fig. 7), the RD curve has a peak around 370 mμ, which corresponds to the slight shoulders observed around 370 mμ in IX as well as in acetylated α-galactoside (XII in Fig. 8). It is to be noted that the RD curve of XII is diametrically symmetrical and opposite to that of the β-anomer (XV). It follows, therefore, that the α-anomer exhibits a positive Cotton effect and the β-anomer a negative one in acetylated as well as in deacetylated derivatives, although the acetyl group enhances the rotation to a certain extent.

Phenyl Glycosides. The CD curves of phenyl β-D-glucoside (XVI), -galactoside (XIX), and of their anomers XXIII znd XXIV are given in Figs. 12, 13 and 14. They all exhibit around 270 mμ Cotton effects due to the B-band, quite likewise the corresponding acetylated derivatives (III, VI, X and XIII), the signs of which are positive in the α-anomers and negative in the β-anomers in accordance with their C_1-configuration.

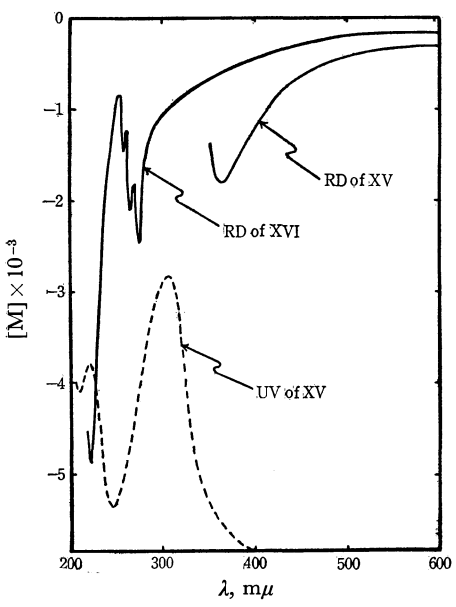

Fig. 12. RD and UV of aryl β-D-glucosides (XV and XVI).

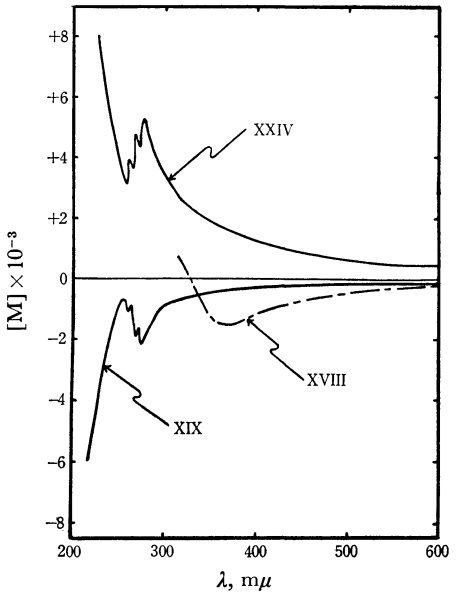

Fig. 13. RD of aryl α- and β-D-galactosides (XVIII, XIX and XXIV).

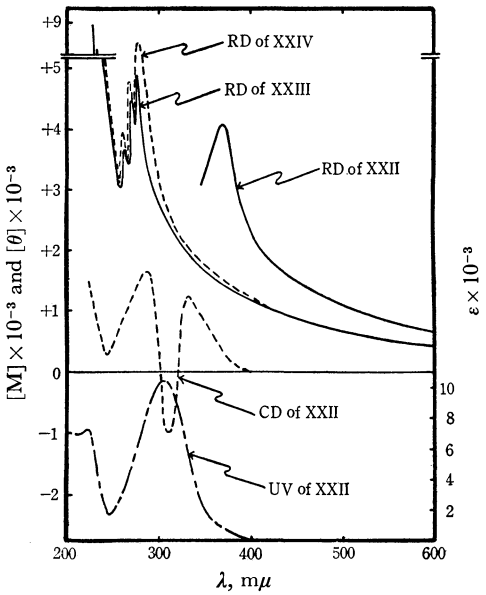

Fig. 14. RD, CD and UV of aryl α-D-glycosides (XXII, XXIII and XXIV).

General Considerations

In the first place the effect of *p*-nitrophenyl

group will be considered. In general the RD curves of *p*-nitrophenyl glycosides exhibit in the region 370—380 mμ more or less distinct Cotton effects or less slight shoulders. A most typical Cotton effect in this region can be seen in a *p*-nitrophenyl β-D-glucoside with an adjacent methyl group (XXV in Fig. 15).

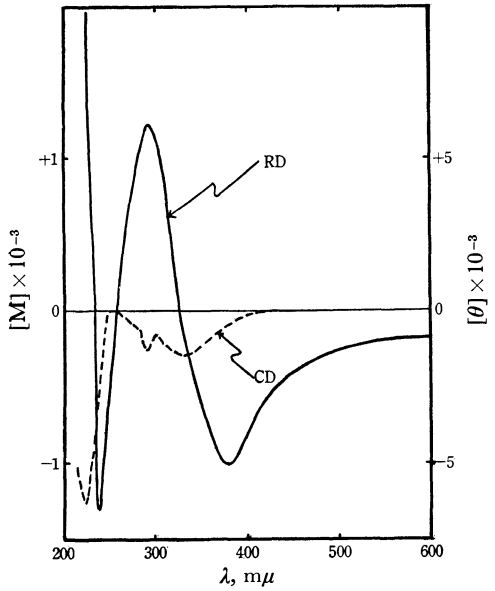

Fig. 15. RD and CD of tetraacetyl 4-nitro-3-methylphenyl glucoside (XXV).

Now, the effect of *o*-nitrophenyl derivatives will be taken into consideration.

The *o*-NO_2 group is regarded to be more twisted from the benzene ring than the *p*-NO_2 group, since the intensity of absorption due to the electronic transition in the molecule is decreased in the former than in the latter. This is evidenced in their UV curves. And since the sugar moiety possesses asymmetry, the nitrophenoxy group is expected to be an asymmetric chromophore in view of the difference in the degrees of twisting toward the right and the left sides.

In the next place, discussions will be made about the following notable facts that acetylated *o*-nitrophenyl glycosides exhibit positive Cotton effects around 340 mμ irrespective of the C_1 configuration, whereas the corresponding deacetylated compounds show negative Cotton effects.

In view of the possibility that the conformation of C_1 may be distorted by the presence of a large group such as *o*-nitrophenoxy group, the conformation of the anomer proton (H_1) has been investigated by means of NMR method.

As the authors' previous reports on the NMR spectra of aryl glycopyranosides,[7] similar results were obtained with tetraacetyl *o*-nitrophenyl galactosides (measured in $CDCl_3$), namely, the H_1 signal of α-galactoside (XI) appears at $\delta=5.89$ ppm, separated from the other signals and the coupling constant is 3.5 Hz, which shows that H_1 is equatorial.

On the other hand, the H_1 signal of β-galactoside (IV) is overlapped with those of H_2, H_3 and H_4, so that the coupling constant can not be obtained. However, since the H_1 signal appears in the magnetic field at least 0.4 ppm higher than in the α-type (XI), the H_1 of the β-glycoside can be concluded to be axial. By these NMR data it has become clear that the C_1-conformation is not distorted and that the anomaly of the *o*-nitro derivatives has another cause.

Hereupon the authors have investigated solvent effects on the optical rotation. In Table 1 are shown the data of studies on tetraacetyl nitrophenyl galactosides.

Table 1. The specific rotation of tetraacetyl nitrophenyl galactosides $\left([\alpha]_{400}^{23}\times\frac{3}{n^2+2}\right)$

Tetraacetyl nitrophenyl galactoside		in CH_3CN (1)	in *s*-$C_2H_4Cl_2$ (2)	(1)−(2)
o-NO_2	α-anomer	664°	544°	120°
	β-anomer	152°	264°	−112°
p-NO_2	α-anomer	507°	504°	3°
	β-anomer	− 83°	− 61°	− 22°

As may be seen in Table 1, the solvent effect is far greater with both the α- and β-anomers in *o*-NO_2 than in *p*-NO_2 derivative. This fact means that a certain interaction between the NO_2 group and the adjacent substituent exerts a significant influence on the optical activity. Furthermore, it is observed that the rotation of the α-anomer is raised with the greater polarity of the solvent, but with the β-anomer the relation is reversed. This indicates that the electrostatic action on the nitro group is in the opposite direction between the α- and β-anomers with respect to the rotation, and that the environment of the nitro group is quite different in the α- and β-anomers. Nevertheless, a series of Cotton effects at 260, 300 and 340 mμ are often nearly equal with the α- and β-anomers (for example, see IV in Fig. 2 and XI in Fig. 6), which suggests, however, that the direct factor making the *o*-nitrophenyl group to be anisotropic really lies in the chromophore. It is then conceivable that the direction of twisting of the nitro group due to a certain stabilized rotamer, one of the possible rotational isomers brought about by the rotation of the *o*-nitrophenoxy group determines the sign of the Cotton effect near 340 mμ, whose high peak affects the value of $[\alpha]_D$.

As to the attribution of the Cotton effects at 260, 300 and 340 mμ the reports of Burawoy *et al.*[8]

7) Y. Tsuzuki and K. Tanaka, This Bulletin, **40**, 1208 (1967).

may be taken into consideration, who observed the UV spectra of nitrophenols. In view of their wavelengths and intensities in absorption, the Cotton effect centered at 260 mμ may be attributed to the K-band of phenyl group, the one at 300—320 mμ to the B-band. And the Cotton effect in the longer wavelength region at 320—355 mμ can be attributed to the $n\rightarrow\pi^*$ transition of the nitro group, as reported in the previous paper.[1]

Finally, mention should be made that each of the derivatives lacking a nitro group (III, VI, X, XIII, XVI, XIX, XXIII and XXIV) exhibits a Cotton effect with a fine structure around 270 mμ irrespective of the presence of acetyl groups. The sign is invariably positive in the α-anomer, and negagive in the β-anomer. The Cotton effect is doubtlessly due to the benzenoid band, as may be evidenced in Fig. 16.

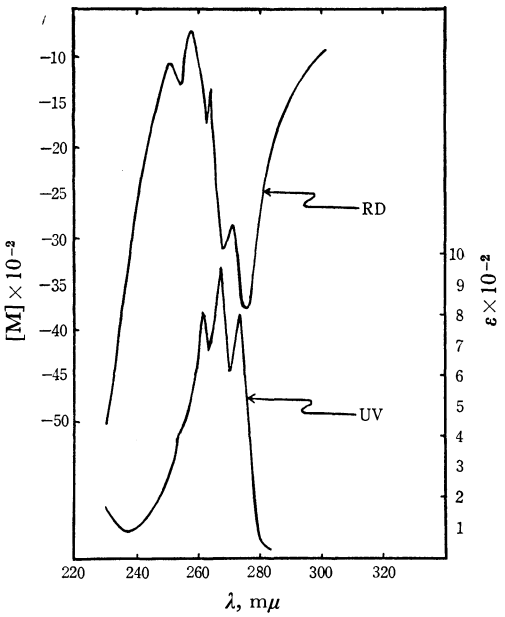

Fig. 16. RD and UV of tetraacetyl phenyl β-D-glucoside (III).

Experimental

The samples were prepared according to the methods described in the literature. The others were also synthesized in a similar way. The rotatory dispersion and the circular dichroism were measured in 1,2-dichloroethane and water at the temperature about 25°C in the wavelength region from 210 to 600 mμ with a JASCO optical rotatory dispersion recorder of the ORD/UV-5 type. The ultraviolet absorption was measured in 1,2-dichloroethane and water with a self-recording spectrophotometer of Hitachi EPU-II type. The NMR spectra were measured with a Varian A-60 spectrometer.

Tetraacetyl *o*-nitrophenyl β-D-glucoside (Compound I).[3] Yellowish needles; mp 159—160°C. The RD was measured at 25°C in 1,2-dichloroethane (*c* 1.152). $[\alpha]_{600}$ +10.0°, $[\alpha]_{589}$ +11.6°, $[\alpha]_{500}$ +44.3°, $[\alpha]_{400}$ +348°, $[\alpha]_{372}$ +591° (peak), $[\alpha]_{300}$ −2420° (trough), $[\alpha]_{274}$ −1660°, $[\alpha]_{266}$ −1950° (trough), $[\alpha]_{236}$ −145°, $[\alpha]_{228}$ −563°. The CD was measured at 25°C in 1,2-dichloroethane (*c* 0.550). $[\theta]_{410}$ +57°, $[\theta]_{324}$ +6920° (peak), $[\theta]_{288}$ −2650°, $[\theta]_{286}$ −2870°, $[\theta]_{284}$ −2870°, $[\theta]_{250}$ −8130° (trough), $[\theta]_{232}$ −2820°. The UV spectrum was measured at 25°C in 1,2-dichloroethane. ε_{max} 1700 at 305 mμ and ε_{max} 3600 at 256 mμ.

Tetraacetyl *p*-nitrophenyl β-D-glucoside (Compound II).[3] Yellowish needles; mp 174°C. The RD was measured at 25°C in 1,2-dichloroethane (*c* 0.906). $[\alpha]_{600}$ −46.3°, $[\alpha]_{589}$ −48.6°, $[\alpha]_{500}$ −75.1°, $[\alpha]_{400}$ −192°, $[\alpha]_{370}$ −285° (trough), $[\alpha]_{320}$ +179°. The CD was measured at 25°C in 1,2-dichloroethane (*c* 0.252). The UV spectrum was measured at 25°C in the same solvent. ε_{max} 11000 at 295 mμ.

Tetraacetyl phenyl β-D-glucoside (Compound III).[3] Colorless needles; mp 122—123°C. The RD was measured at 25°C (*c* 0.509). $[\alpha]_{600}$ −19.1°, $[\alpha]_{589}$ −19.8°, $[\alpha]_{500}$ −34.7°, $[\alpha]_{300}$ −219°, $[\alpha]_{276}$ −873° (trough), $[\alpha]_{271}$ −668°, $[\alpha]_{268}$ −739°, $[\alpha]_{264}$ −311°, $[\alpha]_{263}$ −408°, $[\alpha]_{258}$ −165° (peak), $[\alpha]_{250}$ −266°, $[\alpha]_{226}$ −1590°.

Tetraacetyl *o*-nitrophenyl β-D-galactoside (Compound IV).[9] Yellowish prisms; mp 171—172°C. The RD was measured at 25°C (*c* 1.072). $[\alpha]_{600}$ +37.4°, $[\alpha]_{589}$ +56.7°, $[\alpha]_{500}$ +224°, $[\alpha]_{400}$ +597°, $[\alpha]_{370}$ +785° (peak), $[\alpha]_{350}$ +463°, $[\alpha]_{302}$ −2240° (trough), $[\alpha]_{280}$ −1120°, $[\alpha]_{270}$ −1440° (trough), $[\alpha]_{240}$ +1180°. The CD was measured at 25°C (*c* 0.254). $[\theta]_{400}$ +73.1°, $[\theta]_{322}$ +6760° (peak), $[\theta]_{286}$ −2250°, $[\theta]_{284}$ −2440°, $[\theta]_{282}$ −2500°, $[\theta]_{252}$ −7920° (trough), $[\theta]_{230}$ −1950°. The UV maxima were ε_{max} 1700 at 306 mμ and 3500 at 255 mμ.

Tetraacetyl *p*-nitrophenyl β-D-galctoside (Compound V).[9] Yellowish needles; mp 144°C. The RD was measured at 25°C (*c* 1.024). $[\alpha]_{600}$ −4.89°, $[\alpha]_{589}$ −4.28°, $[\alpha]_{500}$ −9.18°, $[\alpha]_{400}$ −89.9°, $[\alpha]_{370}$ −149° (trough), $[\alpha]_{356}$ −140°. The CD was measured at 25°C (*c* 0.280), $[\theta]_{400}$ −11.1°, $[\theta]_{340}$ −1320° (trough), $[\theta]_{294}$ −1440° (trough), $[\theta]_{288}$ 0°, $[\theta]_{282}$ −1770° (trough), $[\theta]_{268}$ +1330°, $[\theta]_{232}$ +1110°.

Tetraacetyl phenyl β-D-galactoside (Compound VI).[10] Colorless needles; mp 122—123°C. The RD was measured at 25°C (*c* 0.540). $[\alpha]_{600}$ +8.23°, $[\alpha]_{589}$ +7.43°, $[\alpha]_{500}$ +4.53°, $[\alpha]_{400}$ +12.5°, $[\alpha]_{300}$ −43.4°, $[\alpha]_{278}$ −709° (trough), $[\alpha]_{272}$ −60.8°, $[\alpha]_{270}$ −281° (trough), $[\alpha]_{266}$ +315°, $[\alpha]_{263}$ −211° (trough), $[\alpha]_{258}$ +497°, $[\alpha]_{256}$ +432° (trough), $[\alpha]_{252}$ +613°, $[\alpha]_{226}$ −411°.

Triacetyl *o*-nitrophenyl β-D-xyloside (Compound VII).[3] Yellowish prisms; mp 111—112°C. The RD was measured at 25°C (*c* 1.420). $[\alpha]_{600}$ −49.4°, $[\alpha]_{589}$ −50.6°, $[\alpha]_{500}$ −53.5°, $[\alpha]_{400}$ +92.8°, $[\alpha]_{376}$ +228° (peak), $[\alpha]_{306}$ −1850° (trough), $[\alpha]_{274}$ −760° (peak), $[\alpha]_{266}$ −1440° (trough), $[\alpha]_{244}$ +836°. The CD was measured at 25°C (*c* 0.259). $[\theta]_{400}$ +50.6°, $[\theta]_{324}$ +413° (peak), $[\theta]_{300}$ +506°, $[\theta]_{284}$ −1210° (trough),

8) A. Burawoy, M. Cais, J. T. Chamberlain, F. Liversedze and A. R. Thompson, *J. Chem. Soc.*, **1955**, 3721, 3727.

9) M. Seidman and K. P. Link, *J. Am. Chem. Soc.*, **72**, 4324 (1950).

10) B. Helferich and E. Schmits-Hillebrecht, *Ber.*, **66**, 378 (1933).

$[\theta]_{280}$ −1110°, $[\theta]_{254}$ −4500° (trough), $[\theta]_{236}$ −1370°.

Triacetyl *p*-nitrophenyl β-D-xyloside (Compound VIII). Yellowish prisms; 137—138°C. The RD was measured at 25°C (*c* 1.051). $[\alpha]_{600}$ −70.3°, $[\alpha]_{589}$ −71.3°, $[\alpha]_{500}$ −107°, $[\alpha]_{400}$ −249°, $[\alpha]_{366}$ −431°, $[\alpha]_{360}$ −375°.

Tetraacetyl *p*-nitrophenyl α-D-glucoside (Compound IX).[2] Colorless needles; mp 109—110°C. The RD was measured at 25°C (*c* 0.985). $[\alpha]_{600}$ +198°, $[\alpha]_{589}$ +209°, $[\alpha]_{500}$ +329°, $[\alpha]_{400}$ +816°, $[\alpha]_{370}$ +1050°, $[\alpha]_{360}$ +1140°, $[\alpha]_{350}$ +1210°, $[\alpha]_{308}$ +1640° (peak), $[\alpha]_{260}$ −264°, $[\alpha]_{230}$ +1190°. The CD was measured at 25°C (*c* 0.270). $[\theta]_{400}$ +57.3°, $[\theta]_{323}$ +2470°, $[\theta]_{293}$ −4180°, $[\theta]_{276}$ +3140°, $[\theta]_{250}$ +803°, $[\theta]_{230}$ −493°, $[\theta]_{220}$ 0°. The UV maximum ε_{max} was 11000 at 294 mμ.

Tetraacetyl phenyl α-D-glucoside (Compound X).[2] Colorless needles; mp 114°C. The RD was measured at 25°C (*c* 0.517). $[\alpha]_{600}$ +143°, $[\alpha]_{589}$ +151°, $[\alpha]_{500}$ +233°, $[\alpha]_{276}$ +1990° (peak), $[\alpha]_{273}$ +1430°, $[\alpha]_{270}$ +1780°, $[\alpha]_{266}$ +1230° (trough), $[\alpha]_{262}$ +1430°, $[\alpha]_{260}$ +1300°, $[\alpha]_{256}$ +1430°, $[\alpha]_{254}$ +1430°, $[\alpha]_{226}$ +5130°.

Tetraacetyl *o*-nitrophenyl α-D-galactoside (Compound XI). Yellowish prisms; mp 170.5—171°C. The RD was measured at 25°C (*c* 0.985). $[\alpha]_{600}$ +147°, $[\alpha]_{589}$ +157°, $[\alpha]_{500}$ +280°, $[\alpha]_{400}$ +700°, $[\alpha]_{376}$ +910° (peak), $[\alpha]_{320}$ −593° (trough), $[\alpha]_{290}$ +661° (peak), $[\alpha]_{280}$ +284° (trough), $[\alpha]_{240}$ +4420°. The CD was measured at 25°C (*c* 0.247). $[\theta]_{400}$ +313°, $[\theta]_{338}$ +4140° (peak), $[\theta]_{298}$ −576° (trough), $[\theta]_{284}$ 0°, $[\theta]_{282}$ 0°, $[\theta]_{280}$ −75.2°, $[\theta]_{256}$ −6140° (trough), $[\theta]_{230}$ +2760°. The UV maxima ε_{max} were 1800 at 314 mμ and 3500 at 258 mμ.

Tetraacetyl *p*-nitrophenyl α-D-galactoside (Compound XII). Colorless needles; mp 131—132°C. The RD measured at 25°C (*c* 0.955). $[\alpha]_{600}$ +209°, $[\alpha]_{589}$ +218°, $[\alpha]_{500}$ +308°, $[\alpha]_{400}$ +612°, $[\alpha]_{380}$ +815°, $[\alpha]_{350}$ +747°.

Tetraacetyl phenyl α-D-galactoside (Compound XIII). Colorless needles; mp 128—129°C. The RD was measured at 25°C (*c* 0.553). $[\alpha]_{600}$ +170°, $[\alpha]_{589}$ +177°, $[\alpha]_{500}$ +264°, $[\alpha]_{400}$ +496°, $[\alpha]_{300}$ +1160°, $[\alpha]_{278}$ +1770° (peak), $[\alpha]_{274}$ +1570°, $[\alpha]_{238}$ +3020°.

o-Nitrophenyl β-D-glucoside (Compound XIV). Yellowish crystals; mp 198°C. The RD was measured at at 25°C in water (*c* 0.676). $[\alpha]_{600}$ −108°, $[\alpha]_{589}$ −114°, $[\alpha]_{500}$ −179°, $[\alpha]_{400}$ −489°, $[\alpha]_{379}$ −640° (trough), $[\alpha]_{350}$ +228°, $[\alpha]_{320}$ +979° (peak), $[\alpha]_{296}$ −211° (trough), $[\alpha]_{278}$ +560° (peak), $[\alpha]_{248}$ −2460°, $[\alpha]_{240}$ −1830°. The CD was measured at 25°C in water (*c* 0.253). $[\theta]_{400}$ −157°, $[\theta]_{354}$ −2070° (trough), $[\theta]_{350}$ −2040°, $[\theta]_{306}$ +1492° (peak), $[\theta]_{284}$ +314°, $[\theta]_{260}$ +2980° (peak), $[\theta]_{234}$ −1570°. The UV was measured at 22°C in water; ε_{max} was 2100 at 320 mμ and 3800 at 260.4 mμ.

p-Nitrophenyl β-D-glucoside (Compound XV). Colorless needles; mp 163°C. The RD was measured at 25°C in water (*c* 1.150). $[\alpha]_{600}$ −96.3°, $[\alpha]_{589}$ −103°, $[\alpha]_{500}$ −154°, $[\alpha]_{370}$ −609° (trough), $[\alpha]_{314}$ +1140°, $[\alpha]_{300}$ +1060°. The UV spectrum was measured at 22°C in water. The maxima ε_{max} were 8900 at 304 mμ and 6100 at 222 mμ.

Phenyl β-D-glucoside (Compound XVI).[11] White needles; mp 171—172°C. The RD was measured at 25°C in water (*c* 0.600). $[\alpha]_{600}$ −73.4°, $[\alpha]_{589}$ −74.8°, $[\alpha]_{500}$ −110°, $[\alpha]_{300}$ −470°, $[\alpha]_{275}$ −1130° (trough), $[\alpha]_{270}$ −810°, $[\alpha]_{267}$ −930°, $[\alpha]_{263}$ −530°, $[\alpha]_{261}$ −650°, $[\alpha]_{254}$ −370° (peak), $[\alpha]_{222}$ −2170°, $[\alpha]_{220}$ −1990°.

o-Nitrophenyl β-D-galactoside (Compound XVII).[9] Yellowish needles; mp 191—192°C. The RD was measured at 25°C (*c* 0.995). $[\alpha]_{600}$ −65.9°, $[\alpha]_{589}$ −66.7°, $[\alpha]_{500}$ −115°, $[\alpha]_{400}$ −392°, $[\alpha]_{382}$ −499° (trough), $[\alpha]_{334}$ +984° (peak), $[\alpha]_{324}$ +791°, $[\alpha]_{322}$ +841°, $[\alpha]_{300}$ −505° (trough), $[\alpha]_{274}$ +286° (peak), $[\alpha]_{234}$ −3170°, $[\alpha]_{230}$ −2810°, $[\alpha]_{228}$ −2910°. The CD was measured at 25°C (*c* 0.252). $[\theta]_{400}$ −78.8°, $[\theta]_{356}$ −1660° (trough), $[\theta]_{308}$ +1970° (peak), $[\theta]_{280}$ +552°, $[\theta]_{260}$ +2760°, $[\theta]_{240}$ 0°, $[\theta]_{234}$ −2050°, $[\theta]_{228}$ −2520°.

p-Nitrophenyl β-D-galactoside (Compound XVIII). yellowish needles; mp 162—163°C. The RD was measured at 25°C (*c* 0.727). $[\alpha]_{600}$ −77.7°, $[\alpha]_{589}$ −105°, $[\alpha]_{500}$ −164°, $[\alpha]_{400}$ −378°, $[\alpha]_{366}$ −551° (trough), $[\alpha]_{320}$ −105°, $[\alpha]_{270}$ −522°, $[\alpha]_{230}$ −1710°.

Phenyl β-D-galactoside (Compound XIX).[10] Colorless crystals; mp 144°C. The RD was measured at 25°C (*c* 0.484). $[\alpha]_{600}$ −41.1°, $[\alpha]_{589}$ −42.3°, $[\alpha]_{450}$ −82.8°, $[\alpha]_{300}$ −343°, $[\alpha]_{275}$ −965°, $[\alpha]_{274}$ −912°, $[\alpha]_{272}$ −1110° (trough), $[\alpha]_{271}$ −591°, $[\alpha]_{270}$ −815°, $[\alpha]_{266}$ −788°, $[\alpha]_{263}$ −314° (peak), $[\alpha]_{260}$ −443°, $[\alpha]_{256}$ −244°, $[\alpha]_{220}$ −255°.

o-Nitrophenyl β-D-xyloside (Compound XX). Yellowish needles; mp 166—167°C. The RD was measured at 22°C (*c* 0.150). $[\alpha]_{700}$ −66.0°, $[\alpha]_{589}$ −98.7°, $[\alpha]_{500}$ −144°, $[\alpha]_{410}$ −275°, $[\alpha]_{380}$ −418° (trough), $[\alpha]_{325}$ +868° (peak), $[\alpha]_{310}$ +468°, $[\alpha]_{280}$ +1230°, $[\alpha]_{270}$ −92.0°.

p-Nitrophenyl β-D-xyloside (Compound XXI). Yellowish needles; mp 156—157°C. The RD was measured at 22°C (*c* 0.249). $[\alpha]_{600}$ −38.6°, $[\alpha]_{589}$ −55.4°, $[\alpha]_{500}$ −83.5°, $[\alpha]_{380}$ −266°, $[\alpha]_{370}$ −284°.

p-Nitrophenyl α-D-glucoside (Compound XXII). Yellowish needles; mp 216—217°C. The RD was measured at 25°C (*c* 0.249). $[\alpha]_{600}$ +223°, $[\alpha]_{589}$ +232°, $[\alpha]_{500}$ +346°, $[\alpha]_{400}$ +721°, $[\alpha]_{370}$ +1350°, $[\alpha]_{350}$ +1030°, $[\alpha]_{330}$ +2540°, $[\alpha]_{320}$ +1410°. The CD was measured at 25°C (*c* 0.302). $[\theta]_{400}$ +65.8°, $[\theta]_{326}$ +888°, $[\theta]_{310}$ −1010°, $[\theta]_{268}$ +1610°, $[\theta]_{242}$ +296°, $[\theta]_{224}$ +1380°. The UV maxima ε_{max} were 10000 at 306 mμ and 6100 at 222 mμ.

Phenyl α-D-glucoside (Compound XXIII). Colorless needles; mp 153—154°C. The RD was measured at 25°C (*c* 0.522). $[\alpha]_{600}$ +180°, $[\alpha]_{589}$ +190°, $[\alpha]_{500}$ +284°, $[\alpha]_{400}$ +507°, $[\alpha]_{300}$ +1170°, $[\alpha]_{276}$ +2180° (peak), $[\alpha]_{272}$ +1760°, $[\alpha]_{270}$ +1990°, $[\alpha]_{266}$ +1490°, $[\alpha]_{263}$ +1650°, $[\alpha]_{259}$ +1350° (trough), $[\alpha]_{250}$ +1630°, $[\alpha]_{228}$ +3930°.

Phenyl α-D-galactoside (Compound XXIV). Colorless needles; mp 96—97°C. The RD was measured at 25°C in water (*c* 0.543). $[\alpha]_{600}$ +188°, $[\alpha]_{589}$ +195°, $[\alpha]_{500}$ +298°, $[\alpha]_{300}$ +1280°, $[\alpha]_{276}$ +2390° (peak), $[\alpha]_{272}$ +1850°, $[\alpha]_{270}$ +2120°, $[\alpha]_{266}$ +1590°, $[\alpha]_{262}$ +1770°, $[\alpha]_{259}$ +1360° (trough), $[\alpha]_{256}$ +3500°, $[\alpha]_{230}$ +3580°.

Tetraacetyl 4-nitro-3-methylphenyl β-D-glucoside Compound XXV). Colorless needles; mp 138°C. The RD and CD were measured at 25°C in 1,2-dichloroethane (*c* 0.486). $[\alpha]_{600}$ −31°, $[\alpha]_{500}$ −54°, $[\alpha]_{400}$ −168°, $[\alpha]_{380}$ −205° (trough), $[\alpha]_{290}$ +248° (peak), $[\alpha]_{240}$ −269° (trough), $[\alpha]_{220}$ +1490°. $[\theta]_{420}$ 0°, $[\theta]_{330-320}$ −1478°, $[\theta]_{300}$ −800°, $[\theta]_{290}$ −1313°, $[\theta]_{260-250}$ 0°, $[\theta]_{220}$ −5580°.

The authors owe a grant to the Ministry of Education and the measurement of CD to the Japan Spectroscopic Co., Ltd.

BULLETIN OF THE CHEMICAL SOCIETY OF JAPAN VOL. 42 1060—1064 (1969)

The Insertion Reaction of Propylene into Metal-Ethyl Bonds in the Ziegler-Natta Catalyst

Yoshinobu TAKEGAMI, Toshimitsu SUZUKI and Takuya OKAZAKI

Department of Hydrocarbon Chemistry, Faculty of Engineering, Kyoto University, Sakyo-ku, Kyoto

(Received June 30, 1968)

The insertion reaction of propylene into metal-ethyl bonds in $TiCl_4$-$AlEt_3$, $TiCl_3$-$AlEt_3$, $TiCl_3$-$AlEt_2Cl$, and $TiCl_3$-$ZnEt_2$ catalyst systems was studied. The insertion products were converted to the corresponding hydrocarbons by methanolysis, and then analysed by gas-liquid chromatography. From these hydrocarbons, the following three metal alkyls were considered to be formed in the reaction system;

M–C–C–Et (I), M–C–C–Et (II), and M–C–C–C–C–Et (III).
C C C C

These metal alkyls were formed in the solid phase of the catalyst at first and were then transferred to the liquid phase of the catalyst. The amount of the metal alkyls formed in the reaction system was dependent on the catalytic system used. The active polymerization system $TiCl_3$-$AlEt_3$ gave a very small amount of metal alkyls, but the less active $TiCl_3$-$ZnEt_2$ and -$AlEt_2Cl$ systems gave a much greater quantity of the metal alkyls, (I) and (III). In the case of the $TiCl_4$-$AlEt_3$ system, metal alkyl formation was much affected by the Al/Ti molar ratio and the reaction time. Finally, it was concluded that the metal alkyls formed in the system were connected to the polymerization of propylene.

The initiation reaction of the Ziegler-Natta polymerization of α-olefins is considered to be the insertion reaction of the olefin into a metal-alkyl bond in the catalyst.[1] Only a few workers have however, studied the insertion reaction of olefins into metal-alkyl bonds in Ziegler-type catalysts. Vries studied the reaction of isobutene with methyltitanium trichloride. Isobutene was not polymerised by this catalyst, but the formation of neopentane was observed after the hydrolysis of the reaction mixture. In the case of ethylene, no insertion products were obtained and only high-molecular-weight polyethylene was obtained.[2] Azuma and his co-workers found that propylene was formed by the reaction of ethylene with bis(cyclopentadienyl)dimethyltitanium.[3] Shilov studied the reaction of heptene-1 with a soluble Ziegler catalyst ($(C_5H_5)_2TiCl_2$-$AlMe_3$) to give 2-methylheptene-1.[4]

1) Leo Reich and A. Schindler, "Polymerization by Organometallic Compounds," Interscience Publ., New York (1966).

2) H. DE Vries, *Rec. trav. Chim.*, **80**, 866 (1961).

3) K. Shikata, K. Nishino and K. Azuma, *Kogyo Kagaku Zasshi* (*J. Chem. Soc. Japan, Ind. Chem. Sect.*), **68**, 352 (1965).

4) A. E. Shilov, A. K. Shilova and B. N. Bobkov, *Vysokomolekul. Soedin.*, **4**, 1688 (1962).

These results apparently indicate that the insertion reaction of olefins into alkyl-titanium bonds occurs.

The present study deals with the insertion reaction of propylene in the presence of active polymerization catalysts, and discusses the course of metal-alkyl formation.

Experimental

Material. The titanium trichloride (HA grade; hydrogen-reduced $TiCl_4$ and activated by grinding) was obtained from the Stauffer Chemical Co. The titanium tetrachloride was distilled in the presence of a small amount of copper powder under an argon atmosphere.

The alkylaluminum compounds were obtained from the Ethyl Corporation and were used without further purification. The decalin was twice distilled under reduced pressure (bp 70—75°C/25 mmHg).

Reaction Procedure. A three-necked flask was equipped with a magnetic stirrer, a gas inlet, a self-sealing rubber cap, and a gas outlet connected to a mercury manometer and a vacuum system. The gas inlet was connected with a line for propylene, argon, or hydrogen.

To the reaction flask flushed with argon, titanium trichloride, a solvent, and an alkylaluminum compound were added in this order. The catalyst mixture was aged for ten minutes at a certain temperature, the

remaining argon was pumped off, and propylene was introduced to start the reaction. After a certain reaction time, the residual propylene was pumped off and the reaction mixture was cooled to −70°C to prevent any unexpected side reactions (isomerization or a transfer reaction). The reaction mixture was then transferred to the precipitation tube, which had previously been purged by argon, under an argon atmosphere, and separated into solids (titanium trichloride and an insoluble polymer) and liquids (the solvent and alkylaluminum compounds) by means of a centrifuge.

The two phases thus obtained were treated with cold methanolic hydrochloric acid. By this treatment the metal-alkyl bonds formed in the system were converted to the corresponding hydrocarbons. The polymers were filtered off, and the filtrate was subjected to gas-chromatographic analysis.

A Hitachi model F6D gas-liquid chromatograph equipped with a hydrogen flame ionization detector was employed for the quantitative and qualitative analyses of the reaction products. The operating conditions are presented below:

Column	Golay Z45 (SE30)	Golay R45 (PEG)
Size	0.5 mmϕ × 45 m	0.25 mmϕ × 45 m
Temperature	40°C	60°C
N_2 flow rate	1.5 ml/min	0.6 ml/min
Split ratio	1/80	1/150
Sample size	2μl	5μl

Results and Discussion

It is well known that the titanium on the solid surface of the Ziegler-Natta catalyst is ethylated and complexed with alkylaluminum compounds.[5] This metal-ethyl bond is considered to be very reactive, and olefins are easily inserted.

The insertion processes of propylene into metal-ethyl bonds may be formulated as follows:

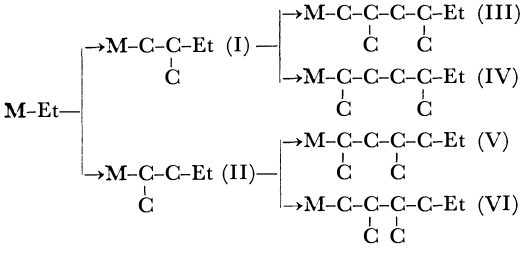

From the end-group analysis of a polymer chain, using ^{14}C-labeled triethylaluminum with titanium trichloride catalyst, it has been said that one end of the polymer chain is an ethyl group,[6] while the other end is a vinylidene double bond as a result of chain transfer to the monomer.[7] These findings lead to the conclusion that the polymerization may proceed *via* primary metal alkyls, (I), (III), and so on.

Identification of the Products. The metal alkyls (I)—(VI) in the catalyst system were converted to the corresponding saturated hydrocarbons by the methanolysis of the reaction mixture. These hydrocarbons were analysed by gas chromatography.

First of all, as a blank test, the catalyst mixture itself ($TiCl_3$-$AlEt_3$ or $TiCl_4$-$AlEt_3$) was decomposed by methanol and then gas-chromatographed. Besides ethane (from ethylaluminum), several small peaks were observed; these were considered to be ethylene oligomers. Three small peaks, which have retention times of 4—5 min were also observed; these have the same retention times as those of isopentane, *n*-pentane, and isopropyl chloride respectively. However, the concentrations of these products were too low for them to be identified more precisely. After the reaction with propylene, three rather remarkable peaks and complex peaks (CP) with retention times of 25—27 min were observed. These peaks were absent in the propylene-free system. Mixing with authentic samples confirmed the formation of isopentane, *n*-pentane, and 2,4-dimethyl-hexane. These hydrocarbons correspond to the methanolysis products of the metal alkyls (I), (II), and (III) respectively. The possibilities of the formation of the metal alkyls (IV), (V), and (VI) were carefully examined in the region of (CP). However, these hydrocarbons were not detected by the gas chromatography.

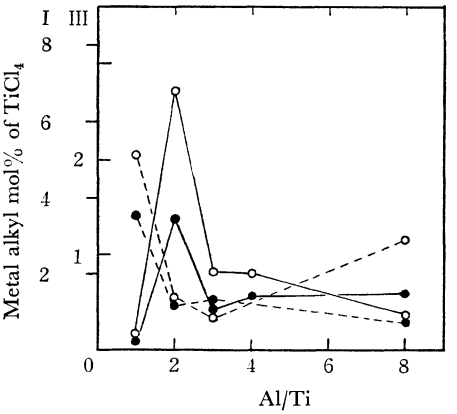

Fig. 1. Effect of Al/Ti molar ratio.
○ metal alkyl (I) ● metal alkyl (III)
bold line at 3 min
dashed line at 15 min
$TiCl_4$ 2.5 mmol, propylene 50 mmol, decalin 50 ml, at 0°C.

5) L. A. M. Rodriguez and H. M. Van Looy, *J. Polymer Sci., Al*, **4**, 1951, 1971 (1966); J. C. W. Chien, *ibid., A*, **1**, 425 (1963).

6) G. Natta, *ibid.*, **34**, 21 (1959).

7) G. Natta and G. Mazzanti, *Advances in Catalysis*, **11**, 1 (1959).

In the presence of aluminum trichloride, propylene gave many C_6-C_8 hydrocarbons, some of which were also observed in the case of titanium-containing catalyst systems. (CP) seemed to be the products from propylene in the presence of a cationic catalyst. This is also supported by the fact that the more acidic $TiCl_4$-containing system gave much (CP).

$TiCl_4$-$AlEt_3$ System. In this catalyst system the polymerization activity of propylene is remarkably affected by the molar ratio of Al/Ti.[8] The amount of the metal alkyls formed in the initial stage (3 or 15 min) is plotted against the molar ratio of Al/Ti in Fig. 1. At 3 min, the quantity of metal alkyls reached a maximum at the Al/Ti molar ratio of 2.0. At 15 min, however, we could not observe the maximum of the metal-alkyl formation at the Al/Ti molar ratio of 2.0. The amounts of the metal alkyls (I) and (III) are almost parallel at any Al/Ti molar ratio at each reaction time.

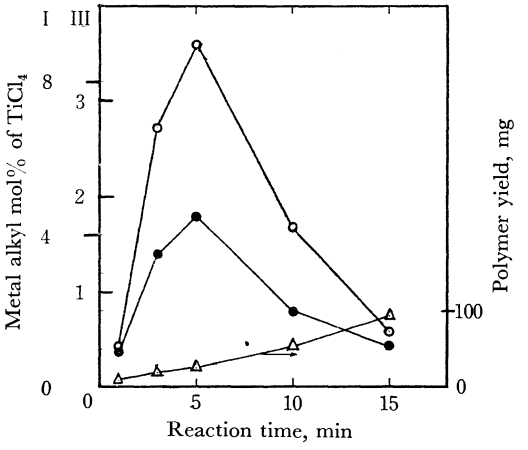

Fig. 2. Metal alkyls *vs.* reaction time.
○ metal alkyl (I) ● metal alkyl (III)
$TiCl_4$ 2.5 mmol, $AlEt_3$ 5.0 mmol,
propylene 50 mmol decalin 50 *ml*, at 0°C

The influence of the reaction time on the course of metal-alkyl formation at the Al/Ti molar ratio of 2.0 is shown in Fig. 2. The amount of the metal alkyls in the solid phase reaches a maximum after about 5 min and then gradually decreases, while the yield of the isotactic polymer increases. In this system transfer reactions of metal alkyls in the solid phase to the liquid phase were also observed (see the next section).

In this catalyst system, the formation of the primary metal alkyls (I) and (III) was observed, while the formation of secondary metal alkyls or cross-inserted metal alkyls was not observed. On the other hand, the insertion reactions of such internal olefins as cyclohexene[9] or pentene-2[10] into metal-ethyl bonds in the Ziegler-Natta catalyst occur under severe conditions. Therefore, we can not rule out the possibility of the formation of secondary metal alkyls in the course of the propylene polymerization; actually, a small amount of the secondary metal alkyl (II) was indeed found in the propylene-polymerization system. Therefore, it becomes an important problem which of these metal alkyls is connected with the isotactic polymerization of propylene.

The behavior of the primary metal alkyls, (I) and (III), in Fig. 2 quite resembles that of the intermediate of a successive reaction. The decrease in metal alkyls with an increase in the reaction time may show that propylene is inserted into these metal alkyls and that the regeneration of these metal alkyl slows or the quantity of metal-ethyl bonds decreases. The same phenomenon was observed in the insertion reaction of isoprene into the metal-ethyl bonds in the $TiCl_4$-$AlEt_3$ catalyst system.[11]

The results obtained from the variation in the Al/Ti molar ratio can be explained by the fact that, at the Al/Ti molar ratio of 1.0, the rate of the insertion reaction of propylene into the metal-ethyl bond and into the metal alkyl (I) is slower than that at the Al/Ti molar ratio of 2.0. The maximum amount of these metal alkyls is about 10 mol% of the titanium used; if all of these metal alkyls are intermediates of the polymerization, this value is too large. As will be discussed below, some of them must be deactivated by being transferred to alkyl-aluminum compounds in the liquid phase and contaminated with an insoluble polymer in the solid phase.

The isotacticity of the polymer obtained in this catalyst system is 50 to 60%. However, no formation of corss-inserted metal alkyls (IV or VI) was detected. This shows the good selectivity of an olefin orientation to a metal-alkyl bond. In the present study we have paid close attention to the structure of the metal alkyls; as Natta has pointed out,[12] the stereospecificity are not a structural problem but a configurational problems in the metal alkyls. Therefore, our findings are not inconsistent with the fact that even in the case of a low-stereospecific catalyst, no cross-inserted metal alkyls were found.

$TiCl_3$-$AlEt_3$ System. In our experiments the

8) G. Natta and P. Pino, *Gazz. Chim. Ital.*, **87**, 549 (1957).

9) Y. Takegami, T. Suzuki and T. Okazaki, *Shokubai (Catalyst)*, **7**, 11 (1965).

10) Y. Takegami, T. Suzuki and T. Okazaki, *Kogyo Kagaku Zasshi (J. Chem. Soc. Japan, Ind. Chem. Sect.)*, **71**, 1719 (1968).

11) Y. Takegami, T. Suzuki and T. Okazaki, *idid.*, **70**, 195 (1967).

12) G. Natta, A. Valvassori, G. Ciampelli and G. Mazzanti, *J. Polymer Sci., A*, **3**, 1 (1965).

rate of the polymerization is almost constant throughout the reaction, and no deactivation of the catalyst is observed.[13] The concentration of the metal alkyls is higher in the solid phase than in the liquid phase. The metal aklyls in the liquid phase are considered to be as a result of the chain-transfer reaction of the metal alkyls formed in the solid phase to alkylaluminum compounds in the liquid phase. This consideration is supported by the fact that after the catalyst mixture had been separated by a centrifuge, and after to the liquid phase thus obtained, propylene had been added and the mixture had then been treated with methanol and submitted to analysis, no metal alkyl formation was observed. The role of metal-ethyl bonds in the solid phase was examined. The solid phase of the catalyst was washed with decalin and centrifuged three times to remove alkylaluminum compounds and then to this solid phase decalin and propylene was added. After the methanolysis small amounts of polypropylene and the metal alkyl (I) were observed in the solid phase of the reaction mixture, but the metal alkyl (III) was not found. These findings indicate that the amount of the metal alkyl (I) in the solid phase is connected with the polymerization.

In Tables 1 and 2 the effect of the Al/Ti molar ratio and the reaction time on the amounts of the metal alkyls is shown. The Al/Ti molar ratio has little effect on the formation of metal alkyls. The metal alkyls do, however, increase slightly with an increase in the reaction time. Usually a few more metal alkyls are found in this system than in the $TiCl_4$-$AlEt_3$ system. This may be attributed to the low concenentration of the metal-ethyl bond and to the higher propagation rate. The $TiCl_3$-$AlEt_3$ system gives a polymer with a molecular weight of 400000 in a 1-min reaction, while the $TiCl_4$-$AlEt_3$ system gives only a 50000-molecular-weight polymer under the same conditions.

$TiCl_3$-$AlEt_3$-H_2 System. The addition of hydrogen to the Natta catalyst caused a remarkable reduction in the molecular weight of the polymer, suggesting that a chain termination by the hydrogenolysis of metal-polymer bonds occurred. The amount of metal alkyls in the solid phase increased slightly upon the addition of hydrogen, as is shown in Table 3. In this case much isopentane and much 2,4-dimethylhexane were observed in the liquid phase, suggesting that the metal alkyls formed are decomposed by hydrogen before methanolysis.

The increase in the amount of the metal alkyls in the solid phase compared to that in the hydrogen-free system may be attributed to the decrease in the propagation rate and to the contamination of the liberated hydrocarbons in the solid phase.

$TiCl_3$-$AlEt_2Cl$ System. In this catalyst system, the so-called settling time[14] was observed. During the settling period the amount of the metal alkyls in the system (in both the liquid and the solid phase) increased with an increase in the polymerization rate (Fig. 3).

The effect of the reaction temperatures on the formation of the metal alkyls is shown in Table 4;

Table 1. The effect of Al/Ti molar ratio on the formation of metal alkyls

Al/Ti	Metal alkyls $\times 10^{-3}$ mmol			Polymer yield
	I	II	III	mg
0.2[a]	0.9	0.1	0.38	190
0.5[a]	0.8	0.1	0.11	205
1.0[a]	1.7	0.2	0.82	205
2.0[a]	6.0	2.1	0.41	175
0.2[b]	1.9	—	0.68	80
0.5[b]	1.2	—	0.24	15
1.0[b]	0.9	—	0.11	40

a) 0°C, 5 min
b) −70°C, 1 min
$TiCl_3$ 13 mmol, $AlEt_3$ variable, decalin 50 ml, $P_{0C_3H_6}$ 710 mmHg (*ca.* 50 mmol)

Table 2. The effect of reaction time on the formation of metal alkyls

Reaction time min	Metal alkyls $\times 10^{-3}$ mmol		Polymer	
	I	III	Yield mg	MW $\times 10^4$
1	0.5	0.31	120	45.2
5	1.0	0.35	380	66.8
15	0.6	0.32	400	58.6
30	2.3	1.09	600	80.4
60	2.6	1.58	960	105

$TiCl_3$ 13 mmol, $AlEt_3$ 6.5 mmol, decalin 50 ml, 0°C, $P_{0C_3H_6}$ 710 mmHg (50 mmol)

Table 3. Effect of hydrogen on the catalytic system $TiCl_3$-$AlEt_3$

P_{0H_2} mmHg	$P_{0C_3H_6}$ mmHg	Reaction time min	Metal alkyls $\times 10^{-3}$ mmol		Polymer	
			I	III	Yield mg	MW $\times 10^4$
0	210	1	0.9	0.41	96	43
500	210	1	4.3	1.40	73	24
0	210	5	1.3	0.39	132	51
500	210	5	4.9	1.92	106	27
640	70	1	3.5	1.51	32	14

$TiCl_3$ 13 mmol, $AlEt_3$ 6.5 mmol, decalin 50 ml, 0°C

13) T. Keii, *Chem. High Polymer* (Tokyo), **22**, 242 (1965).

14) G. Natta and I. Pasquon, *Makromol. Chem.*, **24**, 258 (1957).

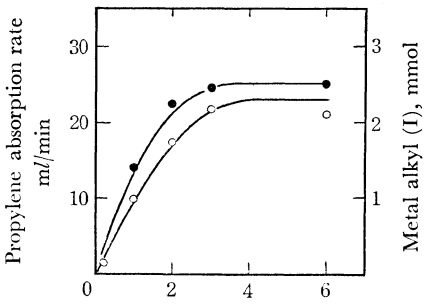

Fig. 3. Metal alkyl and polymerization rate *vs.* reaction time.
○ metal alkyl (I) ● propylene absorption rate
$TiCl_3$ 13 mmol, $AlEt_2Cl$ 6.5 mmol
$P_{C_3H_6}$ 710 mmHg, decalin 50 m*l*, 0°C

TABLE 4. EFFECT OF REACTION TEMPERATURE IN THE CATALYTIC SYSTEM $TiCl_3$-$AlEt_2Cl$

Reaction		Metal alkyls $\times 10^{-3}$ mmol		Polymer yield mg
Temp. °C	Time nim	I	III	
−70	15	0.7	trace	trace
0	15	2.9	0.78	21
30	15[a)]	5.3	1.01	105
30	120[b)]	25.0	12.0	1350
55	15	68.8	5.91	275

$TiCl_3$ 13 mmol, $AlEt_2Cl$ 6.5 mmol, decalin 50 m*l*.
$P_{C_3H_6}$ 710 mmHg const.
a) propylene absorption rate 4.3 m*l*/min
b) propylene absorption rate 13.8 m*l*/min

with a remarkable increase in the polymer yield, the amount of metal alkyls increases.

The electron paramagnetic resonance study of this catalyst[15] has established that the liquid phase of this catalyst contains Ti^{3+} species. The catalyst mixture was separated into liquid and solid phases in the manner described above. To the liquid phase propylene was then added, and after methanolysis, the products were analysed. In this case, contrary to the case of the $TiCl_3$-$AlEt_3$ system,

15) Y. Ono and T. Keii, *J. Polymer Sci., Al*, **4**, 2441 (1966).

TABLE 5. FORMATION OF METAL ALKYLS IN THE CATALYTIC SYSTEM $TiCl_3$-$ZnEt_2$

Reaction		Metal alkyls $\times 10^{-3}$ mmol		Polymer	
Temp. °C	Time min	I	III	Yield mg	MW $\times 10^4$
−70	15	19.2	5.98	—	
0	1	39.2	7.35	—	
0	15	55.2	4.06	trace	
30	15	7.3	4.60	9	2.8
30	240	284	107	786	4.1

$TiCl_3$ 13 mmol, $ZnEt_2$ 6.5 mmol, decalin 50 m*l*, $P_{C_3H_6}$ 710 mmHg const.

the metal alkyls (I) and (III) were found in the reaction mixture.

The titanium contents in the liquid phase were determined by colorimetry. The amount of metal alkyls in the liquid phase corresponds to the amount of titanium in the liquid phase.*1

These findings indicate that, in this catalyst system, the active site for the polymerization is connected with some complex in the liquid phase.

$TiCl_3$-$ZnEt_2$ System. This catalyst system has a very low activity with regard to the polymerization of propylene, while the amount of the metal alkyls formed in the solid phase is rather large. The large amount of the metal alkyls found also in the liquid phase of the reaction mixture indicates that the diethylzinc has a high ability to make chain transfers.[16]

The last two catalytic systems have low activity in the polymerization of propylene at the initial stage of the reaction, but with an increase in the polymerization activity, the metal alkyls increase. The $AlEt_2Cl$ system is usually considered to be a transfer-free polymerization system,[5] however, and it is difficult to confirm our finding. In our opinion this transfer reaction is connected with the activation of the catalyst.

*1 When 13 mmol of $TiCl_3$ and 6.5 mmol of $AlEt_2Cl$ in 20 m*l* of a solvent are used at 30°C, the reaction mixture gives a liquid phase containing 0.06 mmol of titanium. After a 60-min reaction with propylene, this liquid phase gives 0 05 mmol of the metal alkyls (I)+(III).

16) G. Natta, *J. Polymer Sci.*, **34**, 531 (1959).

BULLETIN OF THE CHEMICAL SOCIETY OF JAPAN VOL. 42 1065—1071 (1969)

The Ionic Telomerization of Diene Compounds. IV. The Cationic Telomerization of Butadiene with Its Hydrobromides

Teruzo ASAHARA and Hideo KISE

Institute of Industrial Science, The University of Tokyo, Roppongi, Minato-ku, Tokyo

(Received July 24, 1968)

The cationic telomerization of butadiene with its hydrobromides (1-bromo-2-butene and 3-bromo-1-butene) in the presence of metal halide was investigated. It was found that the molecular weights of the telomers depend on the conversion of the telomerization, initial bromide/butadiene ratio and the solvent used. When halogenated hydrocarbons were used as solvents, telomers with high molecular weights and low unsaturations were obtained. On the other hand, the telomerizations in ether solvents gave telomers with low molecular weights, which contained appreciable amounts of the simple adducts of butadiene and bromobutene. The infrared spectra of the telomers suggested that the addition of butadiene occurred mainly at 1,4-position. On the basis of the analyses of the telomers, the reactivities of the carbonium ion to the basic species which were present in the reaction system were estimated.

The cationic telomerization of butadiene and isoprene with alkyl and alkenyl halides have been investigated by some workers.[1-5] The main subject of the investigations were the development of the method of controlling the molecular weight of the telomers and the clarification of the structures of the telomers.

It was found that the cationic telomerization of butadiene and its hydrochlorides gave their simple adducts and higher telomers (telomers with more than three butadiene units), and the addition occurred both at 1,4 and 1,2 positions of butadiene molecule.[1,2] The structures of higher telomers were very complex because of the multiple reactivities of the carbonium ions. Thus, the telomers had lower degrees of unsaturation and higher chlorine contents as compared with telomers with the ideal formula; $H(C_4H_6)_nCl$.

The amount of the simple adducts of butadiene with chlorobutenes and the average molecular weight of higher telomers depended mainly on the conversion of the reaction and the solvent used.

The present paper refers to the telomerization of butadiene with its hydrobromides in the presence of metal halides. When bromobutene is used as a telogen instead of chlorobutene, there will be some variations in the rate of initiation process; the formation of carbonium ion through the interaction between halogenated butenes and the catalyst. The carbonium ion formed may be surrounded by basic species present in the reaction system, namely, counter-anion, solvent, *etc.*, and the structure of the counter-anion may probably affect the reactivity of the carbonium ion.

Experimental

Materials. Bromobutenes, which were used as telogens, were prepared by the method described in a patent.[6] The reaction of butadiene with hydrobromic acid in the presence of sulfuric acid at 60°C gave two isomeric bromobutenes; 1-bromo-2-butene (crotyl bromide, bp 50—51°C/128 mmHg) and 3-bromo-1-butene (bp 42—43°C/128 mmHg). The total yield of bromobutenes was about 70%, and the content of crotyl bromide in the products was about 80%. As will be described later, the two isomers give telomers with the same structure, though 1-bromo-2-butene enters into the reaction faster than 3-bromo-1-butene. Therefore, the mixture of the isomers was used as telogen except when the difference in the reactivity was estimated. In this paper the mixture of two isomeric bromobutenes is named crotyl bromide (CB).

Butadiene (BD, purity was above 99.3%) was passed before use through columns packed with calcium chloride and sodium hydroxide.

Ethyl bromide was washed several times with a chilled concentrated sulfuric acid and water, dried on

1) A. A. Petrov, Kh. V. Bal'yan, L. I. Bunina-Krivorukova and T. V. Yakovleva, *Zhur. Obshch. Khim.*, **29**, 1576 (1959).

2) T. Asahara and H. Kise, This Bulletin, **39**, 2739 (1966); **40**, 1941 (1967); **40**, 2664 (1967).

3) K. V. Leets, *Zhur. Obshch. Khim.*, **28**, 1823 (1958); **28**, 3090 (1958).

4) A. A. Petrov, Kh. V. Bal'yan, U. I. Kheruze, E. U. Schwarz and L. L. Cherenkova, *ibid.*, **28**, 1435 (1958); **29**, 1876 (1959).

5) L. A. Cherkasova, Kh. V. Bal'yan and L. M. Zubritskii, *ibid.*, **34**, 1917 (1964).

6) A. A. Dolnick, and H. Naidus, U. S. Pat. 2573695 (1951).

calcium chloride, and distilled. Dichloromethane was washed with a dilute aqueous sodium carbonate solution and water, dried on calcium chloride, and distilled. Ethers were dried on sodium and distilled.

Telomerization. Into a 300 ml round-bottomed glass flask, equipped with a sealed stirrer, a thermometer, a condenser and an inlet for gas, definite amounts of the telogen, butadiene and the solvent were placed. Then the catalyst, dissolved in part of the solvent, was slowly added under a stream of nitrogen. The reaction was exothermic, and the rate of the addition of the catalyst solution was adjusted to keep the rise in temperature within 15°C. After the reaction, a small amount of pyridine was added, and the precipitated pyridine/catalyst complex was separated. Then the solution was washed with a 5% sodium carbonate solution, a 5% hydrochloric acid solution, and then water, and dried on anhydrous sodium sulfate. The solvent and the unreacted bromobutene and butadiene were distilled off under a reduced pressure, and the residue was subjected to vacuum distillation to separate the simple adducts of butadiene with bromobutene from the other products.

Analysis. The molecular weights of the telomers were measured with a Mechrolab vapor-pressure osmometer, model 301A, in a benzene solution at 37°C. DDT was used as a standard material.

The infrared spectra of the telomers were taken with a Hitachi-Perkin-Elmer double beam grating spectrophotometer, model 125. The evaluation of the absorption intensity was made by the ordinary base-line method.

The adducts with a 1 : 1 ratio of butadiene with crotyl bromide were analyzed by a gas chromatograph with a flame ionization detector. The separation column was a stainless steel tube packed with Diasolid L; the liquid phase was tricresyl phosphate (10%).

The adducts were isolated by distillation and liquid chromatography through a column packed with activated alumina. The elution was made by carbon tetrachloride or ethyl acetate.

The amounts of unsaturation of the telomers were determined by the Wijs method in the acetic acid solution.

The Alcoholysis of the Telomers. The telomers of butadiene with bromobutene were treated by the 0.5N potassium hydroxide-benzyl alcohol solution at 90°C. Initial ratio of bromine to potassium hydroxide was 0.5. The amounts of the bromine which entered into the reaction were calculated from the titration of the residual alkali with a 0.5N hydrochloric acid solution.

Results and Discussion

1) **Catalyst and Solvent.** The telomerization was carried out in several sorts of solvent in the presence of metal halides (Table 1). The reaction products are yellow or brownish viscous liquid or semisolid. In halogenated hydrocarbons, the reaction is too fast to be controlled. In ethereal solvent, the reaction is mild and reproducible. When ferric chloride is used as a catalyst, the yield of the telomer decreases as follows:

i-Propyl ether>*n*-Butyl ether>Ethyl ether>Dioxane>Ethyl alcohol

A dilute dichloromethane solution of the complex of ferric chloride with ethyl ether had an absorption at 365 mμ. It is known that ethereal compounds form charge transfer complexes with ferric chloride. The result mentioned above may be explained by the differences in the basicity of the solvents. Namely, the catalytic activity of the complexes for the telomerization decreases with the increasing stabilities of the complexes. Elementary analyses and the infrared spectra of the telomers obtained in ethers confirm that any fragment of the solvent molecule is not contained in the reaction products. Accordingly, the dissociation constant, K_2, may be small, and the initiation through the formation

TABLE 1. TELOMERIZATION OF BUTADIENE WITH CROTYL BROMIDE
[CB]/[BD]=1; Reaction temperature, 5—20°C

Catalyst (C)	[C]/[BD] $\times 10^2$	Solvent	Time (min)	Yield[a] (%)	Simple adduct[b] (%)	Av. mol wt[c] (%)	Unsaturation[d] (%)
$FeCl_3$	1.63	$(i\text{-Pr})_2O$	150	49.0	34.8	359	55.5
$FeCl_3$	1.60	$(n\text{-Bu})_2O$	150			319	62.8
$FeCl_3$	3.64	Et_2O	150	42.5	51.4	310	64.7
$FeCl_3$	7.30	Dioxane	150	27.5	45.6	338	62.2
$FeCl_3$	10.3	EtOH	310	0	—	—	—
$AlCl_3$[e]	1.00	EtBr	240	49.1	—	514	39.1
$AlCl_3$[e]	6.21	Et_2O	150	0	—	—	—
$AlCl_3$[e]	10.2	Et_2O	150	0	—	—	—
$AlBr_3$	5.53	Et_2O	240	0	—	—	—
$SnCl_4$	11.6	$(i\text{-Pr})_2O$	150	14.7	36.1	298	66.8
$SnCl_4$	20.5	CH_2Cl_2	310	25.5	11.4	418	50.3

a) The weight percentage of total product based on the initial butadiene and crotyl bromide.
b) The weight percentage of the simple adduct based on the total product.
c) The average molecular weight of higher telomer other than the simple adducts.
d) The percentage of the iodine value of higher telomer to the theoretical iodine value.
e) Reaction temperature, −50—−30°C.

of carbonium ion from the solvent would be neglected.

$$FeCl_3+ROR \underset{K_1}{\rightleftarrows} FeCl_3\cdot OR_2 \underset{K_2}{\rightleftarrows} [FeCl_3\cdot OR]^-+R^+ \quad (1)$$

When aluminum chloride and stannic chloride in halogenated hydrocarbons were used as catalysts, the telomers have high molecular weights and low degrees of unsaturation. As will be discussed later, it is presumed that some side reactions occur concurrently with the main reactions; *e. g.*, the addition of carbonium ion to the double bonds in the telomer or telogen.

The catalytic ability of metal halides in ethers decreases in the order, $FeCl_3>SnCl_4>AlCl_3$. The result is a little different from those of Friedel-Crafts reaction and the telomerizations in halogenated hydrocarbons. The apparent rate of telomerization which is designated by total yield of the telomers would primarily depend on the rate of initiation; the formation of carbonium ion through the interaction of catalyst and crotyl bromide. The strength of the association of metal halide with the solvents may reflect on the catalytic activity of the catalyst solutions.

Table 2. Telomerization of butadiene with two bromobutene isomers

Telogen	Yield (%)	Simple adduct (%)	Av. mol wt of higher telomers
1-Bromo-2-butene	34.8	41.5	285
3-Bromo-1-butene	25.9	51.2	308

Catalyst: $FeCl_3$; Solvent: Et_2O
Reaction time: 150 min
Reaction temperature: 5—15°C

Each of the two isomeric bromobutenes, which were obtained by the hydrobromination of butadiene, was used as telogens (Table 2). It was found that the primary bromide gave a larger amount of telomer than the secondary bromide under the same reaction condition. However, from the infrared spectra of the telomers and the gas chromatogram of the simple adducts, no significant difference in the structures of the telomers from respective bromides was observed. This was also confirmed in the case when chlorobutenes were used as telogens.[2] The fact suggestes that the two isomeric halobutenes form the same carbonium ion with the resonance structures A and B.

$$CH_3\text{-}CH\text{=}CH\text{-}CH_2^+ \text{ (A)} \leftrightarrow CH_3\text{-}\overset{+}{C}H\text{-}CH\text{=}CH_2 \text{ (B)}$$

2) The Effect of Initial CB/BD Ratio. The effects of CB/BD ratio on the yield and the molecular weight of the telomer were investigated. When aluminum chloride in ethyl bromide solution is used, average molecular weight of the telomer mixture decreases monotonously with the increase in the ratio (Fig. 1). However, the yields of the simple adducts of butadiene with crotyl bromide were very low under the conditions. In the region of CB/BD<1, appreciable amounts of insoluble product are obtained, which causes the decrease in the soluble telomers.

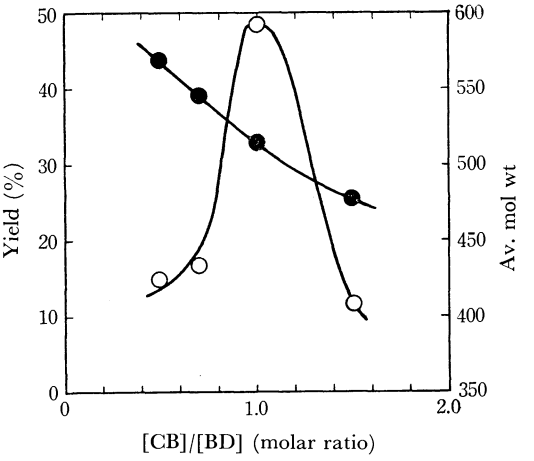

Fig. 1. Effect of the ratio of crotyl bromide to butadiene.
Catalyst, $AlCl_3$; solvent, ethyl bromide.
○, Total yield of telomer; ●, average molecular weight of telomer.
$[AlCl_3]/[BD]=0.01$; reaction temperature, −50°C; reaction time, 4 hr.

On the other hand, when ferric chloride in ether is used, considerable amounts of the simple

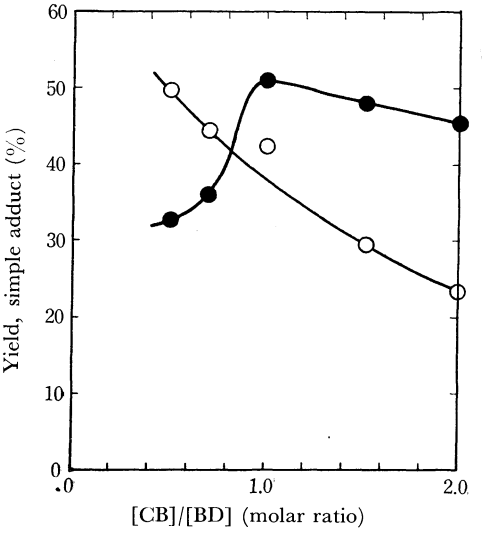

Fig. 2. Effect of the ratio of crotyl bromide to butadiene.
Catalyst, $FeCl_3$; solvent, ethyl ether.
○, Total yield of telomer; ●, simple adduct of butadiene with crotyl bromide.
$[FeCl_3]/[BD]=0.0364$; reaction temperature, 5°C; reaction time, 2.5 hr.

adducts of butadiene with bromobutene are obtained; the maximum yield of the adduct is obtained at CB/BD=1 (Fig. 2). In the region where the ratio is larger than unity, no significant change in the yield ratio of the adduct to the total product is observed. In addition, the average molecular weights of the higher telomers vary little with the variation of the initial CB/BD ratio. It appears that the excess crotyl bromide exists only as a diluent, and does not act as a chain transfer reagent.

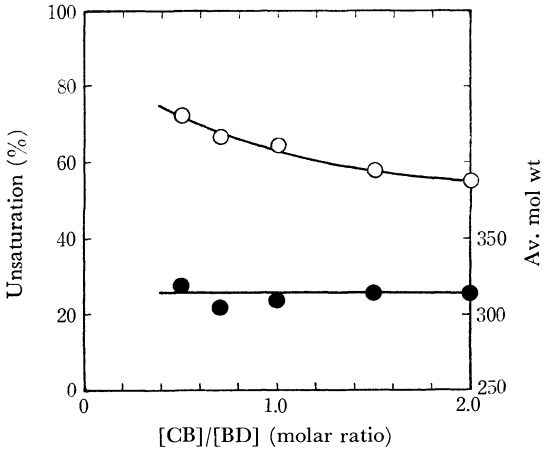

Fig. 3. Effect of the ratio of crotyl bromide to butadiene.
○, Unsaturation of higher telomer; ●, average molecular weight of higher telomer.
Reaction condition is the same as in Fig. 2.

As Fig. 3 shows, however, the increase in the CB/BD ratio causes a decrease in the degree of unsaturation of the higher telomers. It was concluded that the excess crotyl bromide increases the proportion of side reactions (see Section 5). This may be the reason why the simple adduct of butadiene with bromobutene decreases in the region CB/BD>1.

3) The Effect of Catalyst Concentration. As Fig. 5 shows, the average molecular weight of the telomer increases with the increase in the catalyst concentration. This effect may be attributed to the increase in the conversion of the reaction (Fig. 4), because it should be presumed in general that the increase in the catalyst results in the lowering of the molecular weight of the telomer. The relation between the conversion of reaction and the amount of the simple adducts of telogen and taxogen was examined and discussed in the case of telomerizations of butadiene with crotyl chloride[2] and isoprene with prenyl chloride.[3]

4) The Structure of Telomers. The fraction with bp 35—45°C/1 mmHg (I) was separated from the telomer mixture. It was found that the fraction consists of three components from its gas chromatogram. The elementary analysis and the

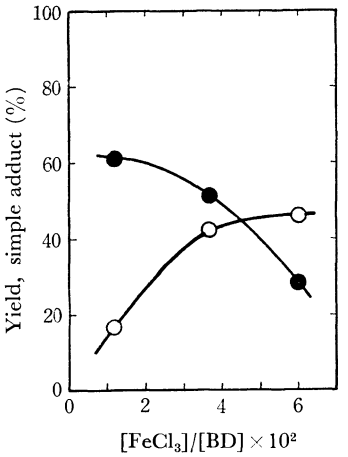

Fig. 4. Effect of the catalyst concentration.
Catalyst, $FeCl_3$; solvent, ethyl ether.
○, Total yield of telomer; ●, simple adduct of butadiene with crotyl bromide.
[CB]/[BD]=1.00; reaction temperature, 5°C; reaction time, 2.5 hr.

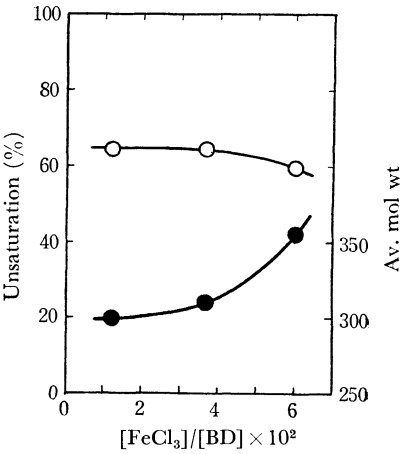

Fig. 5. Effect of the catalyst cocentration.
○, Unsaturation of higher telomer; ●, average molecular weight of higher telomer.
Reaction condition is the same as in Fig. 4.

determination of iodine value indicate that the fraction consists of the simple adducts of butadiene with crotyl bromide.

Found: C, 51.68; H, 7.18; Br, 41.14%. Iodine value, 262.2. Calcd for $H(C_4H_6)_2Br$: C, 50.80; H, 6.94; Br, 42.26%. Iodine value, 268.40.

The fraction I was redistilled into two fractions; bp 35—40°C/1 mmHg (II) and 40—42°C/1 mmHg (III). From the infrared spectra (Figs. 6-2 and 6-3) and NMR spectrum (Fig. 7-2), it was concluded that the fraction II is a mixture of adducts D and E, and the fraction III is adduct C (Fig. 7). The infrared spectrum of II exhibits

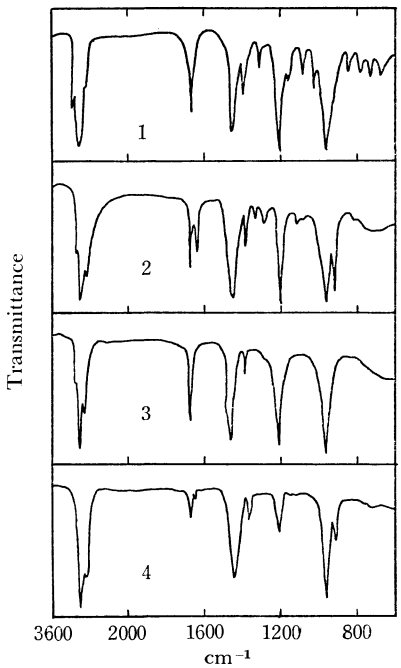

Fig. 6. Infrared spectra of crotyl bromide and telomers.
1, Crotyl bromide; 2, fraction II; 3, fraction III; 4, higher telomer.

the characteristic stretching (1665 cm^{-1}) and deformation (965 cm^{-1}) bands of the internal double bond, as well as the bands of vinyl grouping (1645 and 910 cm^{-1}), while the spectrum of III has only the bands of internal double bond. Adducts D and E, which were contaminated a little by each other, were separated from the fraction II by liquid chromatography. The proportion of C, D and E in the fraction I can be determined from its NMR spectrum (Fig. 7-3) by using the relative intensities of the bands, 8.35/9.00 and 4.55/4.22 (in τ). Thus, the proportions of C, D and E were estimated to be 80%, 10% and 10% respectively. There were found small differences in the value for the adducts obtained under various reaction conditions.

The infrared spectrum of the mixture of telomers other than the simple adducts represents the bands characteristic of internal olefin and vinyl grouping (Fig. 6-4). From the absorption intensities, the ratio of the 1,4 linkage of butadiene unit was calculated to be about 90%.[7]

5) Mechanism of Telomerization. The cationic telomerization of butadiene with crotyl bromide is assumed to proceed as follows:

Initiation:

$$FeCl_3\cdot(Et_2O)_x + CH_3\text{-}CH{=}CH\text{-}CH_2Br \longrightarrow CH_3\text{-}\overset{+}{C}H\text{-}CH{=}CH_2 \leftrightarrow CH_3\text{-}CH{=}CH\text{-}\overset{+}{C}H_2 + [FeCl_3Br]^- + xEt_2O \quad (2)$$

Fig. 7. NMR spectra of crotyl bromide and telomers.
1, Crotyl bromide; 2, fraction III; 3, fraction I.
Assignments:

$$\overset{a}{CH_3}\text{-}\overset{b}{CH}{=}\overset{c}{CH}\text{-}\overset{d}{CH_2}\text{-}\overset{e}{CH_2}\text{-}\overset{f}{CH}{=}\overset{g}{CH}\text{-}\overset{h}{CH_2}Br \quad (C)$$

$$CH_3\text{-}CH{=}CH\text{-}CH_2\text{-}CH_2\text{-}\overset{i}{CH}Br\text{-}\overset{j}{CH}{=}\overset{k}{CH_2} \quad (D)$$

$$CH_2{=}\overset{l}{CH}\text{-}\overset{m}{CH}(CH_3)\text{-}CH_2\text{-}CH{=}CH\text{-}CH_2Br \quad (E)$$

a, 8.35; b and c, 4.55; d and e, 7.87; f and g, 4.22; h, 6.08; i, 5.7; j and k, 4.90; l, 8.15; m, 9.00.

Propagation:

$$CH_3\text{-}CH{=}CH\text{-}CH_2^+ + (n-1)CH_2{=}CH\text{-}CH{=}CH_2 \longrightarrow H(C_4H_6)_{n-1}CH_2\text{-}CH{=}CH\text{-}CH_2^+ \quad (3)$$

Transfer reaction:

$$H(C_4H_6)_{n-1}CH_2\text{-}CH{=}CH\text{-}CH_2^+ + CH_3\text{-}CH{=}CH\text{-}CH_2Br \longrightarrow H(C_4H_6)_nBr + CH_3\text{-}CH{=}CH\text{-}CH_2^+ \quad (4)$$

Termination:

$$H(C_4H_6)_{n-1}CH_2\text{-}CH{=}CH\text{-}CH_2^+ + [FeCl_3Br]^- \longrightarrow H(C_4H_6)_nBr + FeCl_3 \quad (5)$$

It is known that ferric chloride forms a complex with ether in about 1 : 1 ratio.[2] If the solvent used has a smaller basicity than crotyl bromide, ferric chloride may form an adduct with crotyl bromide and subsequently form a carbonium ion, which initiates telomerization. It is deduced that a growing carbonium ion reacts with butadiene or crotyl bromide preferentially in the form with a positive charge on the chain end. Namely, 1,4 addition occurs more predominantly in the present system than the case of butadiene with crotyl chloride.

7) W. S. Richardson, *J. Polymer Sci.*, **13**, 229 (1954).

In the termination reaction (5), the telomer with chlorine atom may be possibly formed. However, analysis by gas chromatograph shows that a very small amount of chlorine cantaining telomer is obtained.

As mentioned above, the increase in the conversion of reaction is followed by the decrease in the proportion of the simple adducts and the increase in the average molecular weight of the higher telomers. The fact may be attributed to the consumption of the simple adducts by retelomerization and/or by side reactions. The τ-values of NMR spectra of 1-position hydrogens in 1-bromo-2-butene and 1-bromoocta-2,6-diene are nearly the same (6.07 and 6.08, Figs. 7-1 and 7-2). This suggests that 1-bromoocta-2,6-diene forms its carbonium ion through the interaction with catalyst as well as crotyl bromide. Thus, the simple adducts and higher telomers once formed may again enter into reactions, which results in the increase in molecular weight of the telomer mixture with the conversion of reaction.

If the telomerization proceeds according to Eqs. (2)—(5), the telomers formed can be represented by $H(C_4H_6)_nBr$. However, it turned out that the telomer mixtures have always higher bromine contents and lower degrees of unsaturation than those expected from the formula shown above. Thus, we represent telomers by $[H(C_4H_6)_\alpha Br]_\beta$; the deviation from $\beta=1$ may be attributed to the side reactions shown below.

Branching:

$$-CH_2-CH=CH-CH_2- + -CH_2^+ \longrightarrow -CH_2-\overset{+}{C}H-\underset{CH_2-}{\overset{|}{C}}H-CH_2- \qquad (6)$$

Cyclization:

$$-CH=CH-\underset{CH_2-CH}{\overset{CH_2-CH_2}{\overset{+}{C}H}} \longrightarrow -\overset{+}{C}H-CH\underset{CH_2-CH}{\overset{CH_2-CH_2}{CH}} \qquad (7)$$

The proton transfer and hydride ion transfer reactions are also plausible,but these reactions have no effect on the average bromine content and the degree of unsaturation. It was found that crotyl bromide itself forms polymers under the action

Table 3. Polymerization of crotyl bromide

Catalyst (C)	[C]/[CB] $\times 10^2$	Solvent	Temp. (°C)	Time (min)	Yield (%)	Av. mol wt
$FeCl_3$	2.43	Et_2O	5—12	150	2.5	327
$AlCl_3$	1.00	EtBr	−49—−41	240	4.6	462

of aluminum chloride or ferric chlorie (Table 3). Therefore, in the telomerization of butadiene and crotyl bromide, a part of crotyl bromide may probably be consumed by the polymerization. The polymerization of crotyl bromide may be included in reaction (6). Reaction (6) increases average bromine content, and reactions (6) and (7) decrease average degree of unsaturation in the telomer mixture. The proportions of the reactions of carbonium ions with basic species were calculated from the analysis of telomers obtained under various reaction conditions[2] (Table 4). It is obvious that the increase in the initial ratio of crotyl bromide to butadiene causes the increase in the probability of branching, while the proportion of cyclization is little affected by the variation of the ratio. In ethereal solvents, the proportion of cyclization varies with the solvent, but the differences are so small that no definite trend can be discerned.

Table 4. Reactivity of carbonium ion

Catalyst	Solvent	[CB]/[BD] (molar ratio)	Yield (%)	Av. mol wt[a]	Proportion of reactions (%)[b]		
					a	*b*	*c*
$FeCl_3$	Et_2O	0.5	49.7	318	76.1	6.2	17.7
$FeCl_3$	Et_2O	2.0	23.5	312	63.6	19.6	16.8
$FeCl_3$	$(i\text{-Pr})_2O$	1.0	49.0	359	65.9	18.0	16.1
$FeCl_3$	$(n\text{-Bu})_2O$	1.0	48.8	319	69.7	11.6	18.7
$AlCl_3$	EtBr	1.0	49.1	514	56.1	20.3	23.6

a) The average molecular weight of higher telomers.
b) *a*, *b* and *c* represent the proportions of reaction (3), (6) and (7) respectively.

When aluminum chloride in ethyl bromide was

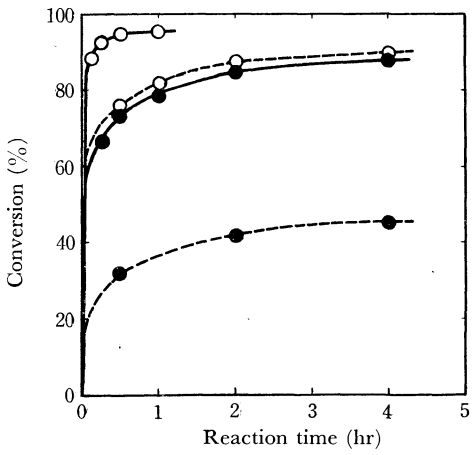

Fig. 8. Time-conversion curves in the reaction of telomers with potassium hydroxide in benzyl alcohol at 90°C.
-○-, Simple adduct of butadiene with crotyl bromide; -●-, higher telomer of butadiene with crotyl bromide; --○--, simple adduct of butadiene with crotyl chloride; --●--, higher telomer of butadiene with crotyl chloride.

used as a catalyst, a marked increase in the proportion of side reactions was found. Namely, the telomers obtained by aluminum chloride in ethyl bromide have structures more branched and cyclized than those obtained by ferric chloride in ethers. The difference may be attributed to the difference in the basicity of the solvent, which interacts with the growing carbonium ions. In other words, reactivities of carbonium ions toward butadiene, crotyl bromide and telomers are influenced by the species of medium in which the carbonium ions exist.

6) Reaction of Telomers with Potassium Hydroxide in Benzyl Alcohol. In order to estimate the reactivities of bromine atoms in the telomers, the telomers were treated with potassium hydroxide in a benzyl alcohol solution. This alcoholysis affords unsaturated ethers with benzene nucleus. As Fig. 8 shows, higher telomers enter into reaction more slowly than 1:1 adducts, which may be ascribed to the steric factor of the telomers. It was also found that the telomers with bromine are more reactive than the telomers with chlorine. That is, the ionic cleavage of carbon–bromine bond is easier than that of carbon–chlorine bond. However, no significant differences were found between the reactivities of crotyl chloride and crotyl bromide in the telomerization. The fact may be explained by the stability of the counter-anions formed through the interaction of crotyl halides and the catalyst. Namely, $[FeCl_3Br]^-$ may be more unstable than $[FeCl_4]^-$, and easily recombines with carbonium ions, which results in the formation of the telomers with lower molecular weights.

BULLETIN OF THE CHEMICAL SOCIETY OF JAPAN VOL. 42 1071—1077 (1969)

Catalysis in Peptide Synthesis with Active Esters. I. Bifunctional Catalysis in the Aminolysis of Benzyloxycarbonyl-L-phenylalanine *p*-Nitrophenyl Ester in Dioxane

Nobuhiro NAKAMIZO*1

Peptide Center, Institute for Protein Research, Osaka University, Kita-ku, Osaka

(Received July 31, 1968)

The aminolysis reaction of benzyloxycarbonyl-L-phenylalanine *p*-nitrophenyl ester (I) with glycine *t*-butyl ester (II) was kinetically investigated in anhydrous dioxane. The spontaneous reaction was confirmed to follow the equation:

$$d[p\text{-nitrophenol}]/dt = k_{obs}[I] = (k_0 + k_{amine}[II])[I][II]$$

The catalytic actions of various additives were studied at a 2×10^{-3}M concentration of I and II, where the amine-catalyzed term could be neglected. Of the many additives, only carboxylic acids and α-pyridone were effective as catalysts. The catalytic effect apparently decreased in the sequence: trimethylacetic acid>acetic acid>α-pyridone>monochloroacetic acid. For these catalyses, a bifunctional, concerted mechanism was proposed which involves an 8-membered transition state.

In recent years, active ester procedures have been widely used in peptide synthesis.[1,2] It is also well-known that some carboxylic acids accelerate the aminolysis reactions of active esters.[3–5] On

*1 Present address: Tokyo Research Laboratory, Kyowa Hakko Kogyo Co., Ltd., Asahi-machi, Machida-shi, Tokyo.

1) E. Schröder and K. Lübke, "The Peptides," Vol. I, Academic Press, New York, N. Y. (1966).

2) M. Bodanszky and M. A. Ondetti, "Peptide Synthesis," Interscience Publishers, New York, N. Y. (1966).

3) R. Schwyzer, M. Feurer and B. Iselin, *Helv. Chim. Acta*, **38**, 83 (1955); B. Iselin, M. Feurer and R. Schwyzer, *ibid.*, **38**, 1508 (1955).

4) a) E. Taschner, G. Błotny, B. Bator and C. Wasielewsky, *Bull. Acad. Polon. Sci., Sér. Sci. Chim.*, **12**, 755 (1964); b) E. Taschner, B. Rzeszotarska and Ł. Lubiewska, *Chem. Ind. (London)*, **1967**, 402.

5) a) S. M. Beumont, B. O. Handford and G. T. Young, *Acta Chim. Acad. Sci. Hung.*, **44**, 37 (1965); b) B. O. Handford, J. H. Jones, G. T. Young and T. F. N. Johnson, *J. Chem. Soc.*, **1965**, 6814.

the other hand, Beyerman *et al.*[6] proposed the use of bifunctional catalysts, such as α-pyridone, 1,2,4-triazole, and succinimide, for the syntheses of peptides *via* some active esters. Little information has, however, been available as to whether carboxylic acids act as simple acid catalysts or as bifunctional catalysts. The present author, therefore, undertook kinetic studies of the catalytic effects of various additives, including some carboxylic acids, on the aminolysis of benzyloxycarbonyl-L-phenylalanine *p*-nitrophenyl ester (I) with glycine *t*-butyl ester (II) in anhydrous dioxane. These studies may also provide an important clue to the general mechanism[7] of the aminolysis of esters.

Experimental

Materials. Dioxane was purified by an ordinary method.[8] Reagent-grade acetic acid was distilled and was fractionally crystallized to a constant mp 16.5°C. Monochloroacetic acid and *p*-nitrophenol were recrystallized from toluene; 1,2,4-triazole, from ether; α-pyridone, from benzene, and tropolone,*2 from cyclohexane. Pentachlorophenol was recrystallized from a mixture of methanol and water after treatment with active carbon; mp 185—188°C. 2,4-Dinitrophenol was recrystallized several times from water, and finally from carbon tetrachloride. Triethylamine was treated with benzyloxycarbonyl-L-phenylalanine *p*-nitrophenyl ester 2 days at room temperature to remove any primary and secondary amines, and then fractionally distilled; bp 89°C. (lit., 89.5°C). Trimethylacetic acid (an extra-pure reagent) and succinimide (a guaranteed reagent) were used without further purification.

Benzyloxycarbonyl-L-phenylalanine *p*-nitrophenyl ester was prepared from benzyloxycarbonyl-L-phenylalanine and *p*-nitrophenol by the dicyclohexylcarbodiimide method; mp 126—127°C (lit. 126—126.5°C)[9]; $[\alpha]_D^{23}$ −24.9 (*c* 2, DMF) (lit., −24.7, *c* 2, DMF).[9] Glycine *t*-butyl ester obtained by the hydrogenolysis of benzyloxycarbonylglycine *t*-butyl ester was fractionally distilled through a 35-cm Vigreaux column under reduced pressure; bp 51—54°C/15 mmHg (lit., 30°C/2 mmHg).[10] The purity of the ester was checked by an amino-group titration with standard hydrochloric acid (100.1% theoretical).

Kinetic Procedure. The reactions were carried out in 50-m*l* graduated flasks immersed in a constant-temperature bath which was controlled to 0.05°C. The reaction mixture was prepared in the following way. Known weights of I and an additive, if any, were placed in the reaction flask, and dioxane was added nearly to the mark. After a thermal equilibrium had been obtained, the mixture was made up with the solvent to exactly 50 m*l*. The reaction was initiated by adding an appropriate volume of a stock solution of II in dioxane. The quantities of both the reactants and the additive were predetermined in order to obtain the desired concentrations when the solution of II was added. Aliquots (0.1 m*l* or 0.2 m*l*) were withdrawn at suitable intervals, diluted to 5 m*l* with dioxane containing an excess anhydrous hydrogen chloride, and analyzed spectrophotometrically. The reactions were followed by the rate of the formation of *p*-nitrophenol. The molar extinction coefficients of I and *p*-nitrophenol were measured at 267 and 304 mμ in anhydrous dioxane; the following data were obtained:

	I	*p*-Nitrophenol
267 mμ	10600 (max)	3430
304 mμ	2250	12150 (max)

The concentrations of *p*-nitrophenol were determined by measuring the absorbance at the two wavelengths and by solving the simultaneous equations. The analysis of the known mixtures of I and *p*-nitrophenol by this method gave an agreement within ±1%. The absorptions of the benzyloxycarbonyl-L-phenylalanylglycine *t*-butyl ester and of the hydrochloride of II can be neglected at these wavelengths. The reference solution was dioxane containing amounts of the additive and hydrogen chloride equal to those in the sample solution. The reaction was generally followed to 60—90% completion with at least 10 readings.

The average deviation from the mean value of the rate constant in duplicate or triplicate experiments was ±3% or less.

Reaction Products and Stoichiometry. The kinetic experiments in dioxane suggested that the reaction of I with II is virtually quantitative. This was checked by the isolation of the benzyloxycarbonyl-L-phenylalanylglycine *t*-butyl ester from a reaction mixture after kinetic measurements. The protected dipeptide ester was recrystallized from ethyl acetate-petroleum ether in a yield of about 90%; mp 88.5—89.5°C. Found: C, 66.99; H, 6.87; N, 6.75%. Calcd for $C_{23}H_{28}O_5N_2$: C, 66.97; H, 6.84: N, 6.79%.

Results

Kinetic studies of the aminolysis reactions of I with II were carried out in anhydrous dioxane in the absence and in the presence of various additives.

6) a) H. C. Beyerman and W. Maassen van den Brink, *Proc. Chem. Soc.*, **1963**, 266; b) H. C. Beyerman and W. Maassen van den Brink, Proc. 6th European Peptide Symposium in Athens, 1963, Pergamon Press, Oxford (1965), p. 85; c) H. C. Beyerman, W. Maassen van den Brink, F. Weygand, A. Prox, W. König, L. Schimdhammer and E. Nintz, *Rec. Trav. Chim.*, **84**, 213 (1965).

7) T. C. Bruice and S. J. Benkovic, "Bioorganic Mechanisms," Vol. I, W. A. Benjamin, New York, N. Y. (1966).

8) L. F. Fieser, "Experiments in Organic Chemistry," 3rd ed., revised, D.C. Heath and Co., Boston (1957), p. 284.

*2 This material was a gift from Professor Takase, Tohoku University, to whom my thanks are due.

9) M. Bodanszky and V. du Vigneaud, *J. Am. Chem. Soc.*, **81**, 6072 (1959).

10) G. W. Anderson and F. M. Callahan, *ibid.*, **82**, 3359 (1960).

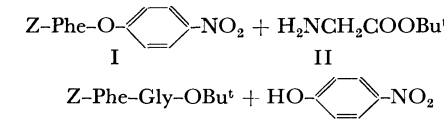

In the presence of a large excess of II, good pseudo-first-order canstants, k^{I}_{obs}, were obtained. In all the kinetic experiments under these conditions the concentration of I was 1.0×10^{-3}M. The second-order rate constants, k^{II}_{obs}, derived from k^{I}_{obs} were variable functions of the concentrations of II, as represented by the following equation:

$$\frac{k^{I}_{obs}}{[II]} = k^{II}_{obs} = k_0 + k_{amine}[II] \qquad (1)$$

where k_0 and k_{amine} are the rate constants for the second- (uncatalyzed) and third-order (amine-catalyzed) processes respectively, and where the superscript I or II denotes the reaction order. This relationship is illustrated in Fig. 1, where

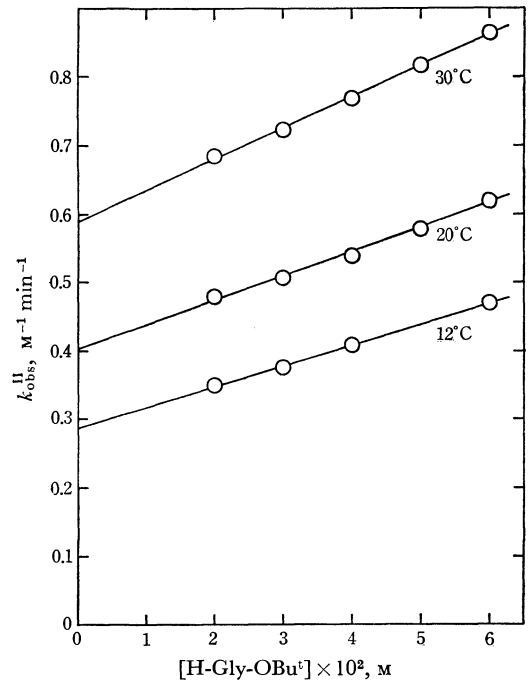

Fig. 1. Effects of the concentration of the amine component on the observed second-order rate constants at different temperatures.

plots of k^{II}_{obs} against the concentration to II give a straight line at each temperature. The values of k_0 and k_{amine} which were calculated from, respectively, the intercepts and slopes of these straight lines by the method of least squares are summarized in Table 1. It follows from these values that the contribution of the amine-catalyzed term to the overall reaction rate is not more than

Table 1. Uncatalyzed and amine-catalyzed rate constants at various temperatures

Temperature, °C	k_0, M^{-1} min^{-1}	k_{amine}, M^{-2} min^{-1}
30	0.59	4.6
20	0.40	3.6
12	0.29	3.1

1% at the concentration of the amine component lower than 10^{-3}M. Thus, in order to simplify the kinetic analysis, all the kinetic runs with additives were carried out at low concentrations where the contribution of the amine-catalyzed term was negligible. Spectrophotometric studies showed that, in anhydrous dioxane, the *p*-nitrophenol formed did not detectably ionize even in the presence of a large excess of II or triethylamine,*3 indicating that the amine component remained in its free form. Accordingly, the formation of *p*-nitrophenol does not disturb the second-order kinetics.

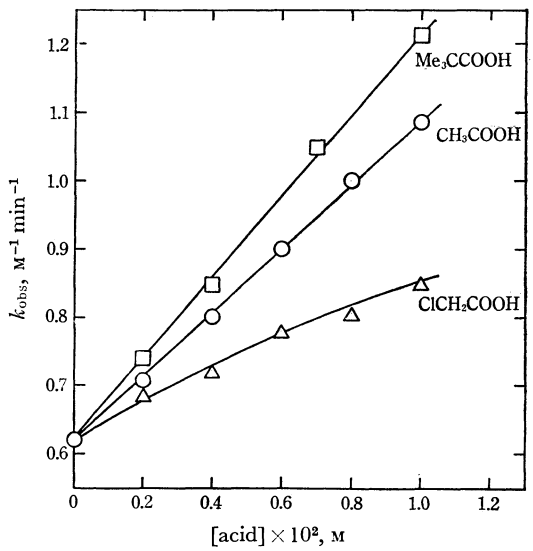

Fig. 2. Effects of the concentration of three carboxylic acids on the observed rate constants at 30°C.

As is shown in Fig. 2, carboxylic acids with a relatively weak acidity, such as trimethylacetic acid and acetic acid, powerfully catalyze the aminolysis of the active ester in dioxane. When

*3 Although it has often been assumed, without any experimental support, that in anhydrous dioxane *p*-nitrophenol ionizes to give the *p*-nitrophenolate anion in the presence of tertiary amine,[11] this is incorrect.

11) a) M. Goodman and L. Levine, *J. Am. Chem. Soc.*, **86**, 2918 (1964); b) M. Goodman and W. J. McGahren, *ibid.*, **87**, 3028 (1965); c) M. Goodman and W. J. McGahren, *Tetrahedron*, **23**, 2031 (1967).

TABLE 2. APPARENT CATALYTIC CONSTANTS OF VARIOUS ADDITIVES AT 30°C

Additive			pka (in aq. soln.)	k_{obs}[a] $M^{-1}\,min^{-1}$	k'_{cat} $M^{-2}\,min^{-1}$
				0.62	
		NEt_3			0
		$MeCONMe_2$			1.8
		H_2O			0
		1,2,4-Triazole	(2.55)	0.63	1.5
		α-Pyridone	11.62 (0.75)	0.71	41
		Succinimide	10.52	0.62	0
	p-$O_2NC_6H_4OH$		7.14	0.61	0
		Tropolone	6.92	0.62	0
		$CCl_3COOH \cdot NEt_3$	5.72	0.50	0
	C_6Cl_5OH		5.3	0.60	0
CMe_3COOH			5.03	0.74	59
CH_3COOH			4.76	0.71	47
	2,4-$(O_2N)_2C_6H_3OH$		4.11	0.57	0
$CH_2ClCOOH$			2.85	0.69	32

[I] = [II] = 2×10^{-3} M

a) The observed rate constants when the concentrations of additives are 2×10^{-3} M.

the acid concentrations were lower than 10^{-2} M, the following relationship was found to hold:

$$k_{obs} = k_0 + k'_{cat}\,[catalyst] \qquad (2)$$

where k'_{cat} was the (apparent)*4 catalyzed constant (Fig. 2). The values of k'_{cat} for each catalyst can be calculated from the slopes of the lines shown in Fig. 2.

Monochloroacetic acid, a slightly stronger acid, also showed a catalytic effect, but a negative deviation*5 from Eq. (2) was observed (Fig. 2).

Such phenols as p-nitro-, pentachloro-, and 2,4-dinitro-phenol did not accelerate, but, rather, came to retard the reaction as their acid strengths increased (*cf.* the 5th column in Table 2).

The trichloroacetate of triethylamine, an acidic salt, also retarded the reaction (Table 2).

α-Pyridone, a classical example of a bifunctional catalyst,[6,12] was almost as effective as acetic acid. Water, triethylamine, succinimide, and tropolone showed little or no catalytic activity. Dimethylacetamide (not as a solvent*6 but as a catalyst) and 1,2,4-triazole showed only a small accelerating effect. Although Bayerman *et al.*[6] found that the catalytic effects of succinimide and 1,2,4-triazole were as large as that of α-pyridone for the syntheses of peptides *via* active esters in acetonitrile or others, the catalytic activities of the former compounds were much smaller than that of the latter under the present conditions. The results mentioned above are summarized in Table 2.

The second-order rate constants observed for the acetic acid-catalyzed reaction at three different temperatures are shown in Table 3.

Table 4 shows the Arrhenius parameters for the uncatalyzed, amine-catalyzed, and acetic acid-catalyzed reactions.

TABLE 3. OBSERVED SECOND-ORDER RATE CONSTANTS FOR THE ACETIC ACID-CATALYZED REACTION AT THE THREE DIFFERENT TEMPERATURES

Acetic acid, M	k_{obs}, $M^{-1}\,min^{-1}$		
	30°C	20°C	12°C
0.000	0.620		
0.002	0.707	0.486	0.360
0.004	0.800	0.565	0.421
0.006	0.900		
0.007		0.685	0.520
0.008	1.000		
0.010	1.085	0.800	0.613

[I] = [II] = 2×10^{-3} M

TABLE 4. ARRHENIUS PARAMETERS FOR THE UNCATALYZED, AMINE-CATALYZED, AND ACETIC ACID-CATALYZED REACTIONS

	Apparent activation energy, kcal/mol	Frequency factor
Uncatalyzed	7.0	6.5×10^4
Amine-catalyzed	3.8	2.8×10^3
Acetic acid-catalyzed	3.4	2.9×10^3

*4 On the meaning of "apparent," see the author's subsequent paper; This Bulletin, **42**, 1078 (1969).

*5 The reason for the negative deviation will be discussed in a subsequent paper (*cf.* *4).

12) C. G. Swain and J. F. Brown, Jr., *J. Am. Chem. Soc.*, **74**, 2538 (1952).

*6 The results of the study on the effect of dimethylacetamide as a solvent will be published in a separate communication.

Discussion

The general acid-base catalysis for the aminolysis of esters is a well-established phenomenon.[7] In the aminolysis (and related reactions) of esters[7] or thiolesters[7] in protic solvents, the kinetic orders of amines in rate expressions are often not unity, because amine components themselves can act as base catalysts. Recently some evidence has been presented for the catalytic actions of the amine components in the acylation of amines with ketenes or esters in aprotic solvents.[13-17] A similar catalysis was found for the present system also.

At a relatively higher concentration of reactants (10^{-2}M), the integrated second-order rate constant decreased with the progress of reaction, indicating the presence of a higher-order process. As has been described in the preceding section, when II was present in at least a twenty-fold excess over I, pseudo-first-order constants, k^{I}_{obs}, were obtained. The second-order rate constants, k^{II}_{obs}, were variable functions of the concentrations of II, as are represented by Eq. (1) and Fig. 1. This finding implies that the reaction consists of two independent processes involving one and two amine molecules. In the latter process the second amine molecule apparently acts as a catalyst.

It is possible to write three transition states, III, IV, and V, for the catalytic process:

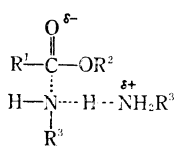

III

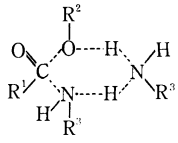

IV

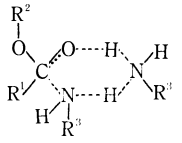

V

In III, the second amine molecule makes the attacking amine more nucleophilic by accepting a proton partly. This process involves a charge creation. The transition state IV, first proposed by Bruice and Mayahi[18] in the ammonolysis of substituted phenyl acetates, is a cyclic, concerted process which involves no charge formation in the transition state. In this cyclic transition state, the catalytic molecule removes a proton from the one undergoing acylation, while there is a simultaneous proton transfer to the leaving group. The transition state V also represents a cyclic mechanism, but it differs from IV in that the carbonyl oxygen atom accepts the proton of the catalyst.

If the first mechanism is correct, a tertiary amine can be expected to exhibit a catalytic effect, because it too can remove a proton from the nucleophile. If a cyclic concerted mechanism, IV or V, is correct, then the tertiary amine should have little effect on the rate, because it cannot participate in the concerted process because of the absence of a labile proton. The author found that triethylamine has little or no catalytic activity in spite of its strong basicity. This fact favors the concerted mechanism. Similar arguments have recently been proposed for the aminolysis of *p*-nitrophenyl acetate in chlorobenzene[15] and for the the acylation of aniline derivatives by ketenes in ether.[13b,c]

It must be remembered, however, that the effectivenesss of a given amine as a general-base catalyst depends not only on its basicity but also on the steric factor. It has been pointed out that the aminolysis by sterically-hindered amines, especially secondary amines, is less susceptible to the general-base catalysis in spite of the availability of a proton.[14,19,20] Therefore, at present, care must be taken in drawing conclusions about the amine-catalyzed mechanism. The cyclic, concerted mechanism is nevertheless very attractive in that, in a nonpolar solvent such as dioxane, the charge creation (ionization) which is required for the mechanism III is not favored.

Even in an aqueous solution much experimental evidence suggestive of cyclic mechanism has been presented in analogous reactions, such as the hydrolysis[7] and ammonolysis[18] of esters.

The validity of this cyclic, concerted mechanism has been more unambiguously demonstrated in the case of carboxylic acid catalysis. As is shown in Table 2, with the single exception of α-pyridone, only carboxylic acids among the many acidic additives examined were more effective as catalysts. Phenols or acidic salts such as triethylammonium trichloroacetate exhibited no effect or a negative effect on the reaction rate, depending on the concentration and strength of the acid. If the reaction proceeds through the simple general-acid catalysis, these acids should possess a catalytic activity similar to that of carboxylic acids. This

13) a) J. M. Briody and D. P. N. Satchell, *Tetrahedron*, **22**, 2649 (1966); b) P. J. Lillford and D. P. N. Satchell, *J. Chem. Soc.*, (*B*), **1967**, 360; c) P. J. Lillford and D. P. N. Satchell, *ibid.*, **1968**, 54.

14) M. G. Dmitrieva and Yu. I. Khurgin, *Izvest. Akad. Nauk SSSR, Ser. Khim.*, **1965**, 1174.

15) F. M. Menger, *J. Am. Chem. Soc.*, **88**, 3081 (1966).

16) A. S. A. S. Shawali and S. S. Biechler, *ibid.*, **89**, 3020 (1967).

17) R. L. Snell, Wo-Kong Kwok and Y. Kim, *ibid.*, **89**, 6728 (1967).

18) T. C. Bruice and M. F. Mayahi, *ibid.*, **82**, 3067 (1960).

19) W. P. Jencks and J. Carriuolo, *ibid.*, **82**, 675 (1960).

20) L. do Amaral, K. Koehler, D. Bartenbach, T. Pletcher and E. H. Cordes, *ibid.*, **89**, 3537 (1967).

is, however, not the case. The possibility that the effect of carboxylic acids may be due to a nonspecific "medium effect" was also eliminated by the finding that water and dimethylacetamide, which have much larger dielectric constants, were far less effective in the acceleration of the reaction.

These facts suggest a specific mechanism, that is, one with a cyclic transition state, as is shown by VI or VII:*7

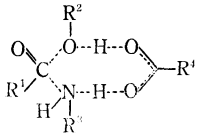

VI

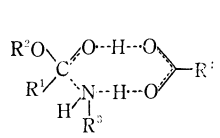

VII

A similar proposal has been made regarding the carboxylic acid-catalysis of the methoxyaminolysis of *p*-nitrophenyl acetate in an aqueous solution on the ground that the catalytic constants for the carboxylic acids are, within the limits of error of the experimental measurements, independent of the acid strength of the catalyst.[20] That Litvinenko and his co-workers established an analogous mechanism of the carboxylic acid catalysis in the acylation of aniline derivatives by carboxylic acid anhydrides or chlorides in a benzene or nitrobenzene solution is particularly noteworthy in this connection.[21-27]

Although the form of this transition state is an eight-membered ring, it should be noted that it perhaps has an atomic configuration analgous to that of the carboxylic acid cyclic dimer. The fact that carboxylic acid and α-pyridone are most effective as catalysts indicates that their atomic configurations are most suitable to the formation of the cyclic transition state. That the geometry of a catalyst (its ability to fit into the eight-membered ring involving two hydrogen atoms) could be an important factor is also supported by the fact that 1,2,4-triazole[6] and tropolone, which would form 7- and 9-membered rings respectively, exhibit little or no catalytic activity (Table 2). Tropolone will prefer forming an intramolecular hydrogen bond of a five-membered ring to acting as a bifunctional catalyst.

Lillford and Satchell,[13b] who recently established the carboxylic acid catalysis for the acylation of aniline derivatives by dimethylketene or isobutyric anhydride in an ether solution, proposed a cyclic transition state such as VIII for the catalysis.

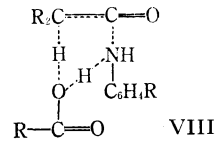

VIII

However, such a formulation cannot explain our finding that phenols do not catalyze the aminolysis of the ester.

Now, there remains a qeutsion which states are correct, IV or V and VI or VIII. In order to answer this question it is necessary to understand the characteristics of the reactions of this type. There is a distinct difference in the characteristics of the reaction between the nucleophilic displacement on the carbonyl carbon and the bimolecular substitution on saturated carbon. In the former the negative charge brought into the reacting site by the attacking nucleophile is once "absorbed" into the carbonyl oxygen, whereas in the latter the charge is directly transmitted to the leaving group. In the former, consequenlty, the factors which assist the "absorption" of the negative charge by the carbonyl oxygen, such as the presence of acid species protonating the oxygen atom (acid catalysis), or the addition of protic solvent which forms a hydrogen bond with the oxygen atom,[28] will promote the formation of an intermediate. The charge "stored" in the carbonyl oxygen atom becomes a driving force to accelerate the decomposition of the intermediate in both forward and backward directions. In this way one cannot speak of the nucleophilic displacement reaction on the carbonyl carbon without considering the role of the carbonyl oxygen. If the formation of the intermediate is the rate-determining step in the presence of the catalyst, as is expected to be indeed

*7 In the aminolysis of the 1-hydroxypiperidine ester and the related compounds, Young *et al.*[5] attributed the accelerating effect of acetic acid to a specific acid catalysis, in which the nitrogen atom of the leaving group is protonated. The acid may, however, act as a bifunctional catalyst, as in the present case.

21) L. M. Litvinenko and D. M. Aleksandrova, *Dokl. Akad. Nauk.*, **118**, 321 (1958).

22) a) L. M. Litvinenko, D. M. Aleksandrova and N. I. Pilyuk, *Ukr. Khim., Zh.*, **25**, 81 (1959); b) L. M. Litvinenko and D. M. Aleksandrova, *ibid.*, **26**, 66 (1960); c) L. M. Litvinenko, and D. M. Aleksandrova and A. A. Zhilinskaya, *ibid.*, **26**, 476 (1960); d) L. M. Litvinenko and D. M. Aleksandrova, *ibid.*, **27**, 212 (1961); e) *ibid.*, **27**, 336 (1961); f) *ibid.*, **27**, 487 (1961); g) L. M. Litvinenko, D. M. Aleksandrova and S. F. Prokopovich, *ibid.*, **27**, 494 (1961); h) L. M. Litvinenko and D. M. Aleksandrova, *ibid.*, **27**, 634 (1961).

23) L. M. Litvinenko and N. M. Oleinik, *Zh. Obshch. Khim.*, **32**, 2290 (1962).

24) L. M. Litvinenko and N. M. Oleinik, *ibid.*, **33**, 2287 (1963).

25) L. M. Litvinenko, *Ukr. Khim. Zh.*, **30**, 317 (1964).

26) L. M. Litvinenko, *Reakt. Sposobnost. Organ. Soedin., Tartsusk. Gos. Univ.*, **2**, 57 (1965); *Chem. Abstr.*, **63**, 17860h (1965).

27) L. M. Litvinenko and N. M. Oleinik, *Ukr. Khim. Zh.*, **32**, 174 (1966).

28) S. L. Jung, J. G. Miller and A. R. Day, *J. Am. Chem. Soc.*, **75**, 4664 (1953), and their preceding papers.

the case,*8 the catalyst must give its proton, not to ether oxygen, but to the carbonyl oxygen atom of the substrate in the transition state. In brief, it follows that the mechanisms which include the transition states V and VII are probably correct. This conclusion is also in accord with the prediction by the "Anthropomorphic rule."[29]

This situation is very similar to that found in the carboxylic acid catalysis for some aromatic nucleophilic substitution reactions; that is, while carboxylic acids catalyzed the aminolysis of cyanuric chloride by aromatic amines,[30] they failed to catalyze the analogous substitution reactions on 2,4,6-trinitrochlorobenzene by amines.[24,30a,31] This fact has been explained as follows. In the former reaction the catalyst accelerates the reaction by protonating the nitrogen atom on the triazine ring, as is shown in IX, but in the latter the catalyst does not accelerate because of the absence of a nitrogen atom.[30a] If the proton of the carboxylic group is directly transferred to the leaving atom (Cl^-), the reaction of 2,4,6-trinitrochlorobenzene will be promoted by carboxylic acids in the same manner as the reaction of cyanuric chloride.

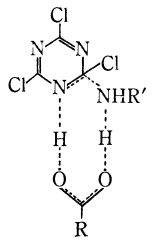

IX

Since the formation of the intermediate is probably a rate-determining step, the collapse rate of the intermediate will be of no importance in the kinetics. However, the carboxylic acid may participate in the collapse process also, as is formulated in X:

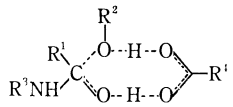

X

The assistance to the nucleophilic attack by catalysts should bring about a lowering of the potential energy barrier. On the other hand, since the catalytic processes represent the higher-order reactions, it may be anticipated that they will have low frequency factors compared with the uncatalyzed process. The Arrhenius parameters for the uncatalyzed, amine-catalyzed, and acetic acid-catalyzed reactions shown in Table 4 reveal that this is indeed the case.

The author would like to express his gratitude to Assistant Professor S. Sakakibara, Osaka University, for his guidance and valuable advice and to Assistant Professor S. Nishida, Osaka University, for his helpful discussions. The author wishes also to thank the Kyowa Hakko Kogyo, Co., Ltd., for the opportunity to conduct this work and publish his resutls.

*8 Since the $-OC_6H_4NO_2$ group is a much better leaving group than the $-NHCH_2COOBu^t$ group, it is probable that the collapse rate of the intermediate to the product is larger than to the starting material, —that, in other words, the second step is of no importance in the kinetics.

29) J. E. Reiman and W. P. Jencks, *ibid.*, **88**, 3973 (1966).

30) a) B. Bitter and H. Zollinger, *Angew. Chem.*, **70**, 246 (1958); b) B. Bitter and H. Zollinger, *Helv. Chim. Acta*, **44**, 812 (1961).

31) L. M. Litvinenko and D. M. Aleksandrova, *Ukr. Khim. Zh.*, **26**, 621 (1960).

BULLETIN OF THE CHEMICAL SOCIETY OF JAPAN VOL. 42 1078—1082 (1969)

Catalysis in Peptide Synthesis with Active Esters. II. Effects of Concentrated Carboxylic Acids on the Aminolysis of Benzyloxycarbonyl-L-phenylalanine *p*-Nitrophenyl Ester in Dioxane

Nobuhiro NAKAMIZO*1

Peptide Center, Institute for Protein Research, Osaka University, Kita-ku, Osaka

(Received July 31, 1968)

The kinetics of the aminolysis reaction of benzyloxycarbonyl-L-phenylalanine *p*-nitrophenyl ester with glycine *t*-butyl ester in dioxane were studied in the presence of high concentrations of several carboxylic acids. Bell-shaped curves were obtained when the rate constants observed for the trimethylacetic acid-, acetic acid-, and monochloroacetic acid-catalyzed reactions were plotted against the logarithms of the reciprocals of the acid concentrations. Cyanoacetic acid and trichloroacetic acid did not accelerate, but, rather, retarded the reaction. In the mathematical derivation the catalyst apparently exhibits no accelerating effect, if $k_0K > k_{cat}$, where k_0 and k_{cat} are the uncatalyzed and the true catalyzed rate constants respectively, and where K is the acid-base equilibrium constant between the nucleophile and the catalyst in a given solvent. The true catalyzed rate constants, k_{cat}, from which the effect of the protonation of the nucleophile had been eliminated were estimated for the trimethylacetic acid- and acetic acid-catalyzed reactions. The fact that the k_{cat} value ($63\text{M}^{-2}\,\text{min}^{-1}$) for trimethylacetic acid, the weaker acid, was greater than that ($53\text{M}^{-2}\,\text{min}^{-1}$) for acetic acid strongly supports the bifunctional, concerted mechanism presented in the preceding paper.

In the preceding paper,[1] evidence was presented that some carboxylic acids act as bifunctional catalysts in the aminolysis of an active ester, benzyloxycarbonyl-L-phenylalanine *p*-nitrophenyl ester (I), in anhydrous dioxane. The catalytic effect apparently decreased in the sequence: trimethylacetic acid>acetic acid>monochloroacetic acid. The apparent effects of these carboxylic acids must, however, be the sum of the accelerating effects due to the catalysis and the retarding effects due to the protonation of the amine component. In order to confirm this supposition, further investigations were undertaken in which the concentrations of the carboxylic acids were varied over wide ranges and the stronger carboxylic acids were used. If the supposition is correct, it is desirable to ascertain the "true" catalytic abilities of these acidic catalysts by substracting the effects due to the protonation of the nucleophile from the apparent effects. The present author has succeeded in estimating the "true" catalyzed constants for some carboxylic acids from the rate data. The present results support strongly the bifunctional, concerted mechanism which was presented in the preceding paper.[1]

Experimental

The cyanoacetic acid and trichloroacetic acid were recrystallized from ether and toluene respectively. The other materials and kinetic procedure were the same as have been described in the preceding paper. All the reactions were conducted at 30°C.

Results

Table 1 summarizes the observed second-order rate canstants in the aminolysis of I with glycine *t*-butyl ester (II) at 30°C in anhydrous dioxane in the presence of trimethylacetic, acetic, monochloroacetic, cyanoacetic, and trichloroacetic acid. The latter two acids did not accelerate, but, rather, retarded the reaction. The constants for trimethylacetic, acetic, and monochloroacetic acid are plotted against the logarithms of the reciprocals of the acid concentrations (p[acid]) in Fig. 1.

The possibilities of the mixed anhydride formation and the acyl exchange reaction between I and carboxylic acid can be ruled out, because benzyloxycarbonyl-L-phenylalanine and acylglycine *t*-butyl esters, which would be formed if these reactions took place, could not be detected by

*1 Present address: Tokyo Research Laboratory, Kyowa Hakko Kogyo Co., Ltd., Asahi-machi, Machida-shi, Tokyo.

1) N. Nakamizo, This Bulletin, **42**, 1071 (1969).

TABLE 1. OBSERVED SECOND-ORDER RATE CONSTANTS FOR THE VARIOUS CARBOXYLIC ACID-CATALYZED REACTIONS AT 30°C

Concentration of acid M	k_{obs}, $M^{-1}\,min^{-1}$				
	CMe_3COOH	CH_3COOH	$CH_2ClCOOH$	$NCCH_2COOH$	CCl_3COOH
0.000	0.62	0.62	0.62	0.62	0.62
0.002	0.74	0.71	0.69	0.61	0.03
0.004	0.85	0.80	0.73	0.58	0.00
0.006		0.90	0.78		
0.007	1.05				
0.008		1.00	0.81	0.57	
0.010	1.21	1.09	0.85		
0.020	1.70	1.51	0.88	0.41	
0.030	2.16	1.88	0.91	0.34	
0.040	2.60	2.23			
0.050	2.98	2.53	0.84	0.26	
0.060	3.34	2.81			
0.080	3.98	3.30			
0.10	4.53	3.73			
0.25		5.09			
0.30	6.45	5.11			
0.50	6.50	4.57			
1.00	4.64	2.48			
pure acid		0.0			

$[I] = [II] = 2 \times 10^{-3}$ M

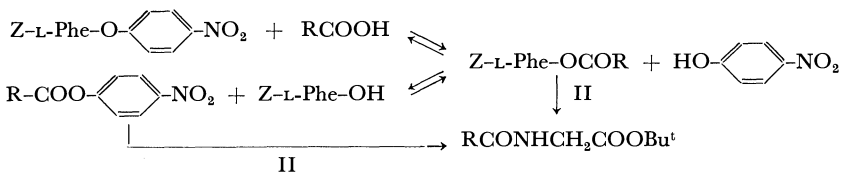

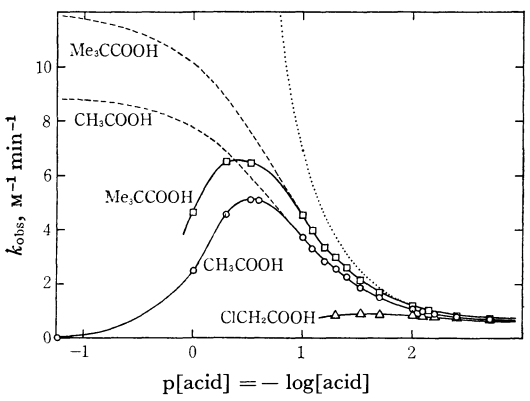

Fig. 1. Dependence of the observed rate constants on the acid concentrations at 30°C.
Solid lines: observed curves; dotted line: theoretical curve for trimethylacetic acid which was calculated from a linear relationship between the k_{obs} and the acid concentration; broken lines: theoretical curves which were derived from the assumption of the acid-base equilibrium.

thin-layer chromatography even at a high concentration of carboxylic acid.

Discussion

As has been shown in the preceding paper,[1] the observed second-order rate constants for the aminolysis reaction of I with II in the presence of trimethylacetic or acetic acid at concentrations lower than 10^{-2}M in dioxane were linearly proportional to the acid concentration. On the other hand, for the monochloroacetic acid - catalyzed reaction, plots of the rate constants against the catalyst concentration showed a negative deviation from the linear relationship. These facts appear to reflect the increase in the protonation of the amine component accompanying the increase in the acid strength and the concentration of the acidic catalyst. If this presumption is correct, similar negative deviations will also appear for the trimethylacetic acid- and acetic acid-catalyzed reactions in higher concentrations of the catalysts. Moreover, for

stronger acids, the apparent catalytic effect may disappear.

The data in Table 1 and Fig. 1 show that this is indeed the case. For example the observed constants for trimethylacetic acid deviated from the calculated curve (dotted line) for which a linear relationship between the rate and the acid concentration was assumed. Furthermore, the values observed at concentrations of more than 0.1M of the acid exhibited a negative deviation even from the calculated curve (broken line) which was based on the assumption that the acidic catalyst partly protonates the amine component to convert it to inactive species, thus resulting in the characteristic bell-shaped curve. For the acetic acid- and monochloroacetic acid-catalyzed reactions also, similar phenomena were observed. The stronger the strength of the acid, the smaller becomes the maximum value of the curve, and the position of the maximum shifts toward a lower acid concentration.*2

In the case of cyanoacetic acid, no maximum was any longer detectable, and the values of k_{obs} for this acid decreased monotonically with an increase in the acid concentration (Table 1). Furthermore, trichloroacetic acid, which is the strongest acid among the catalysts used in the present investigation, inhibited the reaction almost completely when more than one equivalent was added to the amine component (Table 1).

If the apparent effects of the carboxylic acids are the sum of the accelerating effects by the catalysis and the retarding effects by the protonation of the nucleophile, it is necessary to obtain "true" rate constants which do not involve the effects of the protonation.

The acid-base equilibria between carboxylic acids and the amine in a given solvent were assumed to conform to the general equation:

$$RCOOH + H_2N\text{-}R' \overset{K}{\rightleftharpoons} RCOO^- \cdot H_3{}^+N^-R' \quad (1)$$

To simplify, the difference between the free carboxylic acid monomer and the monomer-solvent complex[5] is neglected. With relatively low concentrations (below 0.1M), the presence of the acid dimer in dioxane can be neglected.[6] Then, the ionization constant, K, is written:

$$K = \frac{\alpha}{(c-\alpha b)(1-\alpha)} \quad (2)$$

where b and c are the total concentrations of II and carboxylic acid respectively, and where α is the degree of the ionization of II. When $c \gg \alpha b$, we may write:

$$\alpha = cK/(1+cK) \quad (3)$$

If only free amine is a reactive species, the observed second-order rate constants are represented by:

$$k_{obs} = k_0(1-\alpha) + k_{cat}(1-\alpha)c \quad (4)$$

where k_0 and k_{cat} are the uncatalyzed and the "true" catalyzed rate constant respectively. The substitution of $(1-\alpha)$ from Eq. (3) into Eq. (4) gives:

$$k_{obs} = \frac{k_0 + c \cdot k_{cat}}{1 + cK} \quad (5)$$

Differentiating this with respect to the concentration of the catalyst, we obtain:

$$\frac{dk_{obs}}{dc} = \frac{k_{cat} - k_0K}{(1+cK)^2} \quad (6)$$

Equation (6) reveals that when $k_{cat} > k_0K$, dk_{obs}/dc is positive; that is, the catalyst exhibits a positive effect on the aminolysis reaction in a given solvent. On the other hand, when $k_{cat} < k_0K$, the catalyst apparently shows a negative effect. The right limb of each profile shown in Fig. 1 corresponds to the former case, while the left side of each maximum, and the effects of cyanoacetic and trichloroacetic acid, correspond to the latter.

In order to determine the "true" rate constant, k_{cat}, it is necessary to know the value of K. This information is, however, not available at present. Therefore, the author tried conversely to derive the ionization constants, K, from the rate data obtained here.

Rearranging Eq. (5), we obtain:

$$k_{obs} = \frac{k_{cat}}{K} - \frac{k_{obs} - k_0}{cK} \quad (7)$$

Equation (7) requires that a plot of k_{obs} against $(k_{obs}-k_0)/c$ be a straight line with a slope equal to $-(1/K)$ and an intercept at k_{cat}/K. The resulting plots (Fig. 2) for data below 0.1M of trimethylacetic and acetic acids were satisfactorily linear, with deviations only at the lower catalyst concentrations, where the proximity in the values of k_{obs} and k_0 brings about large uncertainties in the remainder $(k_{obs}-k_0)$. These good linearities may substantiate the validity of the assumptions on which Eq. (7) is based.

*2 Litvinenko *et al.* found that for the acetylation of *p*-nitroaniline with acetic anhydride in mixture of benzene and acetic acid, the maximum of the rate constants appears at about 50%(v/v) of the acid,[2] while for the acylation of *m*-chloroaniline[3,4] or aniline[4] in mixtures of benzene and trichloroacetic acid, the rate constants have maxima at much lower concentrations (~0.01M) of the acid.

2) L. M. Litvinenko and D. M. Aleksandrova, *Ukr. Khim. Zh.*, **27**, 336 (1961).

3) L. M. Litvinenko, D. M. Aleksandrova and S. F. Prokopovich, *ibid.*, **27**, 494 (1961).

4) L. M. Litvinenko and D. M. Aleksandrova, *ibid.*, 634 (1961).

5) N. Muller and P. I. Rose, *J. Phys. Chem.*, **69**, 2564 (1965).

6) J. Lascombe, M. Haurie and M. L. Josien, *J. Chim. Phys.*, **59**, 1433 (1962).

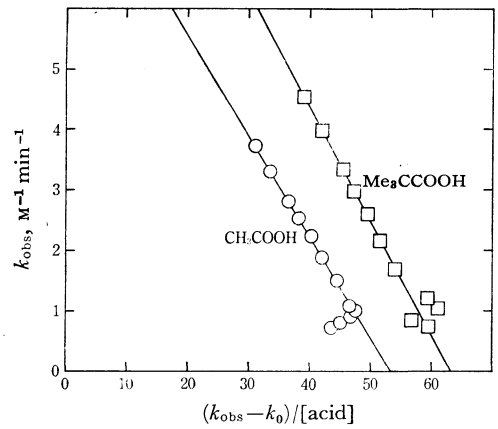

Fig. 2. Plots of Eq. (7), at 30°C.

TABLE 2. THE "TRUE" CATALYZED-RATE CONSTANTS AND THE IONIZATION CONSTANTS FOR TRIMETHYLACETIC ACID AND ACETIC ACID

	k_{cat}, M^{-2} min^{-1}	K, M^{-1}
Trimethylacetic acid	63±2	5.3±0.2
Acetic acid	53±2	6.0±0.2

From the least-squares calculations for the plots, k_{cat} and K values for these two acids were obtained (Table 2).

The theoretical curves calculated from these rate and equilibrium constants are shown as broken lines in Fig. 1.

Similar mathematical treatments were not applicable to other acids because of the larger uncertainties in the values of the remainder $k_{obs}-k_0$.

If the treatments mentioned above are correct, it follows that the weaker trimethylacetic acid (pk_a in H_2O 5.03) has truly, not apparently, a greater catalytic activity than the stronger acetic acid (pk_a 4.76), despite its larger steric requirement. This result, which it is impossible to interpret by a simple general acid catalysis, strongly supports the cyclic, concerted mechanism which was proposed in the preceding paper.[1] When carboxylic acids act bifunctionally, substituents in carboxylic acids will affect the proton-donating powers of the hydroxyl function and the proton-accepting powers of the carbonyl oxygen atom in opposite fashions. As a result, for example, the monomer-dimer equilibrium constants of carboxylic acids in the gas phase are almost independent of their acid strengths.[7]

When they act as bifunctional catalysts, whether the catalytic activities are directly proportional to the acid strengths or whether the reverse is true, will depend on the proportion of the contribution of both the acidic and basic functions to the lowering of the activation free energy. For the mutarotation of tetramethylglucose in a benzene solution, the order of the magnitude of the catalytic ability is as follows: $CCl_3COOH > C_6H_5COOH > \alpha$-pyridone $>$2-aminopyridine.[8] Similarly, for the acylation of aniline derivatives with acetic and benzoic anhydride or benzoyl chloride in benzene, the catalytic effect decreases in the order: $CCl_3COOH > CH_2ClCOOH > C_6H_5COOH > CH_3COOH$.[3,4] In these instances, although carboxylic acids act again as bifunctional catalysts, it seems that their role as acid catalysts rather than as base catalysts is of predominant importance. Bitter and Zollinger[9] found, on the contrary, that for the nucleophilic substitution reaction on cyanuric chloride by aniline in a benzene solution, the catalytic effect increases in the sequence: $CCl_3COOH < CH_2ClCOOH < CH_3COOH < \alpha$-pyridone. On the basis of this finding they considered that the proton-accepting property of a bifunctional catalyst is essential for the catalytic action.

In the present investigation, it may be premature to draw a definitive conclusion, for we still lack the "true" catalytic constants for any catalysts other than trimethylacetic acid and acetic acid. However, the data for the latter two acids seem to show that the proton-accepting ability of the catalyst in the transition complex plays a more important role in the catalysis. It should be noted that, in the transition complex, the proton of the catalyst is transferred to the substrate to a different extent depending on the kind of catalyst; therefore, the basicity of the proton-accepting site on the catalyst is not necessarily parallel to that of the initial catalyst molecule.

As for the bell-shaped, p[acid] - rate profiles illustrated in Fig. 1, a further comment is required. In many organic and enzymatic reactions bell-shaped profiles have been obtained.[10] The reason why such characteristic curves were obtained here, however, appears to be distinct from that for many of the hitherto-known instances in aqueous solutions. No change in the reaction mechanism in both sides of the maximum of the profile, such as those observed in imine formation,[11] nitrone formation,[12]

7) G. C. Pimentel and A. L. McClellan, "The Hydrogen Bonds," W. H. Freeman & Co., San Francisco (1960).

8) C. G. Swain and J. F. Brown, Jr., *J. Am. Chem. Soc.*, **74**, 2538 (1952).

9) a) B. Bitter and H. Zollinger, *Angew. Chem.*, **70**, 246 (1958); b) B. Bitter and H. Zollinger, *Helv. Chim. Acta*, **44**, 812 (1961).

10) T. C. Bruice and S. J. Benkovic, "Bioorganic Mechanisms," Vol. I, W. A. Benjamin, New York, N. Y. (1966).

11) G. E. Lienhard and W. P. Jencks, *J. Am. Chem. Soc.*, **87**, 3855 (1965), and the references cited therein.

12) J. E. Reiman and W. P. Jencks, *ibid.*, **88**, 3973 (1966).

and the aminolysis of imido esters,[13] could be proved in the present case. Of course, the interpretation[10] proposed for the enzymatic reactions with bell-shaped pH-rate profiles are not applicable here either. The author prefers to explain this phenomenon by a change in the nature of the medium. As the concentration of carboxylic acid increases, the ionization "constant" will come not to be constant because of the change from pure dioxane to a mixed solvent of dioxane and carboxylic acid. At such a high acid concentration, the amine component is presumably protonated much more than would be expected from the ionization constant, K, determined above, and consequently the reaction rate decreases. In such a case the extent of the protonation of the amine component will have to be estimated, not by the concentration of the acid, but by the acidity function of the solution.*3 Unfortunately, the acidity function for the dioxane-carboxylic acid system does not seem to have been established. Furthermore, the change in the medium effect on the aminolysis reaction itself, which accompanies the change in the solvent composition, can not be neglected. Therefore, it is difficult to predict theoretically the rate data on the left side of the maximum at the present time.

The author wishes to express his gratitude to Assistant Professor S. Sakakibara of Osaka University for his valuable advice and to Assistant Professor S. Nishida of Osaka University for his helpful discussions.

13) E. S. Hand and W. P. Jencks, *J. Am. Chem. Soc.*, **84**, 3505 (1962).

*3 Such a situation may be analogous to that in hydrolytic reactions at low pH values (below pH 1.0), where maxima in acidity-rate profiles due to a decrease in the activity of water (the nucleophilic species) are sometimes observed.

BULLETIN OF THE CHEMICAL SOCIETY OF JAPAN VOL. 42 1082—1089 (1969)

The Synthesis of Methylacetylene by the Pyrolysis of Propylene. IV. The Pyrolysis of Allyl Chloride

Sango KUNICHIKA,* Yasumasa SAKAKIBARA** and Mamoru TANIUCHI*

* *Institute for Chemical Research, Kyoto University, Gokasho, Uji*

** *Chemical Laboratory of Textile Fibers, Kyoto University of Industrial Arts and Textile Fibers, Kyoto*

(Received August 8, 1968)

Allyl chloride has been pyrolyzed in a flow system over a wide range of conditions (temperature, 800—1200°C; contact time, 0.665×10^{-3}—78.9×10^{-3} sec; concentration, 4.0—13.5 mol%; pressure, atmospheric pressure) to find suitable conditions for producing methylacetylene and allene. In addition, a study on the mechanism of pyrolysis of allyl chloride at high temperatures (800—1200°C) has been made. A total yield of allene and methylacetylene of 14 mol per 100 mol of allyl chloride pyrolyzed was obtained under suitable conditions. By means of the zero conversion method, hydrogen, propylene, allene, diallyl, 1,3-cyclohexadiene, and benzene have been found to be the main reaction products in the early stage of the pyrolysis, while methane, acetylene, ethylene, methylacetylene, butene-1, and butadiene have been found to be the side reaction products. The over-all activation energy of decomposition was 39.4 kcal/mol for an A factor of $10^{8.7}$ sec^{-1}. On the basis of the observed results, a free-radical mechanism has been proposed for the main reactions and the principal side reactions. It was further concluded that the pyrolysis was a radical decomposition initiated by the reaction $C_3H_5Cl\rightarrow C_3H_5\cdot+Cl$ and that the over-all mechanism in the early stage of the pyrolysis was represented essentially by the reaction $2C_3H_5Cl\rightarrow C_3H_5\cdot+\dot{C}_3H_4Cl+HCl$.

In previous papers,[1,2] the authors reported the synthesis of methylacetylene and allene by the pyrolysis of propylene at high temperatures. High temperatures, low conversions, and low pressures

1) a) Y. Sakakibara, This Bulletin, **37**, 1262 (1964); S. Kunichika and Y. Sakakibara, *Bull. Inst. Chem. Res., Kyoto Univ.*, **42**, 270 (1964). b) Y. Sakakibara, This Bulletin, **37**, 1268 (1964).

2) S. Kunichika, Y. Sakakibara and M. Taniuchi, *Bull. Inst. Chem. Res., Kyoto Univ.*, **43**, 469 (1965).

were found to be required for the good production of allene and methylacetylene. Since the C–Cl bond dissociation energy of allyl chloride[3] (58 kcal/mol) is considerably lower than that of α-(C–H) of propylene[4] (85 kcal/mol), the pyrolysis of allyl chloride would be expected to bring about better results under moderate conditions and to give available information about the behavior of allyl radical at high temperatures. In this report, the pyrolysis of allyl chloride under low pressure and high temperature was investigated with the aim of the production of allene and methylacetylene. Although several papers[5–8] have been published on the pyrolysis of allyl chloride, the investigations are mainly carried out below 800°C. Up to the present, it is known that only small amounts of allene and methylacetylene are obtained and that certain products seem to be produced through allene. The reaction products reported by previous investigators are summarized in Table 1.

Table 1. Summary of previous investigations

Reference	Temperature range (°C)	Products
5) Goodall and Howlett	370 to 475	Allene, allene polymers, acetylene, *etc.*
6) Shilov*	594 to 709	Allene, propylene, diallyl, dibenzyl, 4-phenyl-1-butene, *etc.*
7) Porter and Rust	550	Propylene, benzene, C_3H_4, 1,3-cyclohexadiene, hydrogen, methane, ethylene, diallyl, *etc.*
8) Hughes and Yates	540 to 765	Propylene, diallyl, 1,3-cyclohexadiene, benzene, *etc.*

* toluene-carrier technique

Goodall and Howlett first studied the pyrolysis of allyl chloride and concluded that the reaction was a complex homogeneous, heterogeneous process to yield, initially, allene and hydrogen chloride. They found the over-all activation energy of 42.5 kcal/mol for an A factor of $10^{9.10}$ sec^{-1}. They obtained large amounts of allene polymers, but only small amounts of allene were identified, presumably because of the rapid polymerization reaction under the reaction conditions. Shilov, on the other hand, found an activation energy of 59.3 kcal/mol at 623°C for the primary decomposition of allyl chloride in a stream of toluene and proposed that the first step in the pyrolysis was the splitting of the C–Cl bond leading to the formation of Cl atoms and allyl radicals. He obtained allene as the minor reaction product, and the amount of allene was less than 3% of hydrogen chloride.[6b] On the basis of the identification of the products, Porter and Rust, and Hughes and Yates also proposed a mechanism which involved the formation of Cl atoms and allyl radicals in the primary step of the reaction. Both of these authors indicated that allene and methylacetylene were only trace amounts of the pyrolysis products. Moreover, Hughes and Yates obtained 34.7 kcal/mol as the over-all activation energy of the pyrolysis.

The purpose of the present investigation is to determine suitable conditions for the production of methylacetylene and allene by the pyrolysis of allyl chloride and to obtain data on the distribution of the pyrolysis products. Based on the observed experimental results, an effort was made to clarify the reaction mechanism for the pyrolysis at higher temperatures (800—1200°C).

Experimental

Materials. Allyl chloride was prepared from allyl alcohol.[9] Bp 44—45°C; n_D^{22} 1.4135. Cylinder nitrogen of 99.9 mol% purity was used as a diluent.

Apparatus and Procedure. The apparatus is shown in Fig. 1. Dry nitrogen was passed through a rotameter to an allyl chloride mixing bottle which was immersed in a constant temperature oil bath set at about 120°C. Allyl chloride was added to the

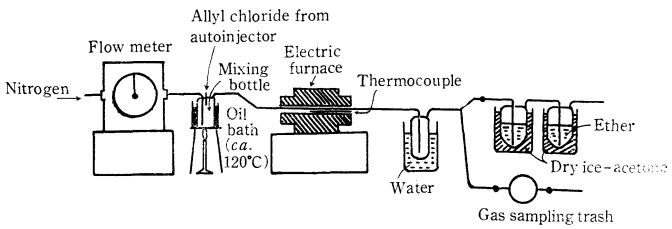

Fig. 1. Apparatus for pyrolysis.

3) M. Szwarc, *Chem. Revs.*, **47**, 75 (1950).
4) J. A. Kerr, *ibid.*, **66**, 465 (1966).
5) A. M. Goodall and K. E. Howlett, *J. Chem. Soc.*, **1954**, 2596.
6) A. E. Shilov, a) *Chem. Abstr.*, **49**, 11605f (1955); b) *J. Phys. Chem.*, **65**, 1088 (1961).
7) L. M. Porter and F. F. Rust, *J. Am. Chem. Soc.*, **78**, 5571 (1956).
8) L. J. Hughes and W. F. Yates, *J. Phys. Chem.*, **64**, 1789 (1960).
9) A. I. Vogel, "A Text-book of Practical Organic Chemistry," 3rd Ed., Longmans, Green and Co., London - New York - Toronto (1956), p. 276.

Columns and conditions	Carrier gas	Products analyzed
Activated charcoal, 2.5 m, 60°C, 25 ml/min	Nitrogen	Hydrogen
Molecular sieve 5-A, 2.5 m, 60°C, 25 ml/min	Hydrogen	Methane, (nitrogen)
30-wt% Dioctyl phthalate, 5.0 m, room temperature, 50 ml/min	Hydrogen	Acetylene, propylene, allene, methylacetylene, butene-1, butadiene
8.0-wt% β,β′-Oxydipropionitrile on silica gel, 2.5 m, 60°C, 25 ml/min	Hydrogen	Ethylene
30-wt% Dioctyl phthalate, 2.5 m, 60°C, 50 ml/min	Hydrogen	(Allyl chloride)
30-wt% Squalane, 2.5 m, 90°C, 50 ml/min	Hydrogen	Diallyl, benzene, 1,3-cyclohexadiene

bottle at a constant rate using an automatic injector. The resulting mixture, containing 4.0—13.5 mol% of allyl chloride, was passed through a short preheater maintained at *ca.* 100°C and then pyrolyzed in a silica reaction tube under the specified conditions at atmospheric pressure. The reactor was heated to the desired temperature while a stream of dry nitrogen was passed through. The electric furnace was made of "Siliconit," and is the same as the one used in a previous investigation.[1a] After the temperature had become stationary the reactant mixture was passed through the reaction tube. The liquid products were collected in a water-trap and then in two dry ice-acetone traps containing 150 ml of ether as an absorbent. After that the gaseous products were collected in a 500 ml sampling flask to which the effluent was bypassed. The water trap was washed twice with 25 ml ether, and then a portion of the ether washed was taken up according to the collection time of the liquid products and was combined with the ether of two dry ice-acetone traps. The pyrolysis was performed under conditions varying over the following wide range; temperature, 800—1200°C; contact time, 0.665×10^{-3}—78.9×10^{-3} sec; concentration of allyl chloride, 4.0—13.5 mol%.

Analysis. Reaction products, consisting of hydrogen and hydrocarbons (mainly from methane up to C_6's), were analyzed by gas chromatography (g.l.c) using six different columns. The columns and their operating conditions are shown in the above table.

Product identification followed careful comparison of the retention behavior of standard hydrocarbons with the unknown products, employing two or more columns with different polarity.

Results

A part of the experimental results is shown in Tables 2 and 3. The yield of each product was given by moles per 100 mol of allyl chloride pyrolyzed. Since methylacetylene and allene are equilibrated rapidly over the isomerization catalysts,[10] their total yield was shown to evaluate conditions for the synthesis of methylacetylene. In order to examine the hydrogen and carbon balance, the percentage of hydrogen and carbon accounted for in the reaction products (H_2 and C_1–C_6 hydrocarbons) was calculated from their yields. Though we tried to identify C_5 components (for example, cyclopentadiene, *etc.*), they were not produced in our experimental conditions.

The Effect of Temperature on Product Yields. For the gaseous products, the results obtained in the conversion range from 18 to 26% are shown in Table 2 and Fig. 2. The yields of

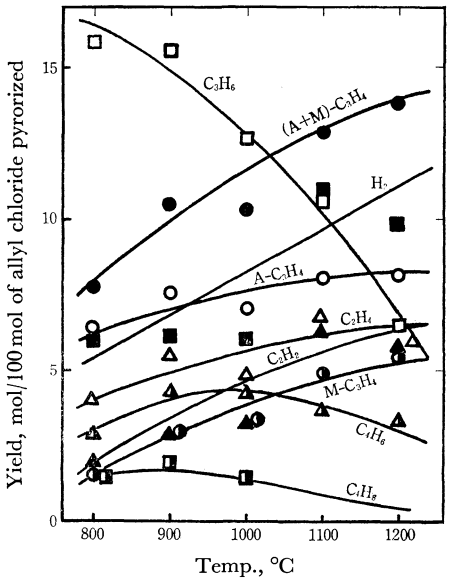

Fig. 2. Effect of temperature on gaseous product yields. Conversion, 18—26%

both methylacetylene and allene increased with the increase of temperature from 800 to 1200°C; the total yield of methylacetylene and allene ranged from 8 mol at 800°C up to 14 mol at 1200°C. Although the total yield increased rapidly at the lower temperatures, the increase was much slower at higher temperatures, ranging from 1100 to 1200°C. Propylene, on the other hand, decreased with an increase in the temperature from 16 mol to 7 mol. At 1000°C, the yield of propylene was much the same as the total yield of allene and methylacetylene. The other main products through C_4 hydrocarbons were hydrogen, methane, acetylene, ethylene, butene-1, and butadiene. The yields of hydrogen, acetylene, and ethylene increased

10) J. F. Cordes and H. Gunzler, *Chem. Ber.*, **92**, 1055 (1959).

Table 2. Pyrolysis of allyl choride at various temperatures

Run No.	1	2	3	4	5	6	7	8	9	10
Temp., °C	800	800	900	900	1000	1000	1100	1100	1200	1200
Contact time, 10^{-3} sec	34.7	42.6	11.3	16.3	2.22	2.58	1.27	1.71	0.665	0.812
Composition of reactant gas, mol %										
Nitrogen	88.7	87.2	92.8	89.8	89.1	87.3	92.9	94.8	96.0	95.2
Allyl chloride	11.3	12.8	7.2	10.2	10.9	12.7	7.9	5.2	4.0	4.8
Rate of expansion	0.962	1.00	0.986	0.974	0.994	0.995	0.985	0.983	0.974	0.975
Conversion, %	25.4	41.2	18.1	34.9	25.7	34.9	25.6	30.6	24.4	36.6
Yield, mol/100 mol of allyl chloride pyrolyzed										
Hydrogen	5.9	4.1	6.1	7.5	6.0	8.2	10.9	10.7	9.8	14.4
Methane	trace	trace	trace	trace	trace	trace	—	trace	—	trace
Acetylene	1.9	1.5	2.8	2.6	3.2	3.6	6.2	5.5	5.8	7.9
Ethylene	3.9	3.8	5.5	5.2	4.7	5.4	6.5	6.2	5.9	3.9
Propylene	15.8	13.8	15.5	13.4	12.6	11.1	10.7	8.5	6.5	5.7
Allene	6.2	4.4	7.5	5.0	7.0	5.5	8.0	8.0	8.1	6.0
Methylacetylene	1.5	1.2	2.9	2.2	3.2	3.2	4.8	5.1	5.7	5.0
1-Butene	1.4	1.0	1.8	1.3	1.4	1.2	trace	trace	trace	trace
Butadiene	2.8	2.2	4.3	3.3	4.2	3.3	3.7	3.4	3.3	2.3
Diallyl	1.3	1.5	2.5	1.7	2.3	1.8	1.1	3.3	1.7	trace
1,3-Cyclohexadiene	6.7	4.3	3.1	3.0	2.4	1.6	1.6	trace	trace	trace
Benzene	19.8	19.1	21.1	20.0	13.2	14.3	12.5	14.8	10.3	9.7
Total yield of methylacetylene and allene	7.7	5.6	10.4	7.2	10.2	8.7	12.8	13.1	13.8	11.0
Total yield of C_6 components	27.8	24.9	26.7	24.7	17.9	17.7	15.2	18.1	12.0	9.7
Percentage of hydrogen and carbon accounted for in products through C_6 components										
Hydrogen	74.0	63.4	77.9	69.4	62.4	59.0	59.2	60.6	49.4	42.0
Carbon	88.5	76.5	92.5	81.7	71.5	67.5	67.2	70.2	56.5	46.9

gradually with an increase in the temperature, reaching 10 mol, 6 mol, and 6 mol, respectively, while the yield of butadiene showed a maximum near 1000°C, and then decreased to 3 mol at 1200°C. The yield of butene-1 decreased gradually from 2 mol at 800°C to the trace amount at 1200°C.

For the liquid products (C_6 components), the results obtained in the conversion range from 18 to 26% are shown in Table 2 and Fig. 3. The yield of benzene decreased with the increase of temperature from 20 mol at 800°C to 10 mol at 1200°C. The yield of 1,3-cyclohexadiene decreased fairly rapidly until 1000°C, and then decreased gradually, ranging from 7 mol at 800°C to 2 mol at 1100°C, while the yield of diallyl was almost constant at about 2 mol all through the temperature examined. Consequently the total yields of C_6 components fell gradually from 28 mol at 800°C to 12 mol at 1200°C.

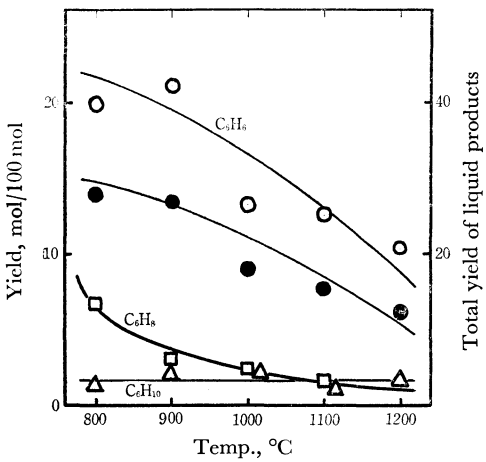

Fig. 3. Effect of temperature on liquid product yields. Conversion, 18—26%
●: total yield of liquid products

On the whole, the polymerization products, C_6 compounds, decreased with the increase in temperature, as is generally known for the decomposition of hydrocarbons (Fig. 3). The carbon and hydrogen balance, however, became remarkably worse at higher temperatures, owing to the increase of tarry and carbonaceous products (Table 2).

The Effect of Conversion on Yields. For the gaseous products, the results of the pyrolysis at 1000°C are shown in Table 3 and Fig. 4. The total yield of methylacetylene and allene decreased with the increasing conversion, ranging from 15 mol at 10% conversion to 4 mol at 90% conversion. In this connection, as the conversion was increased, the yield of allene fell at a considerable rate from 11 mol at 10% conversion to 2 mol at 90% con-

TABLE 3. PYROLYSIS OF ALLYL CHLORIDE AT VARIOUS CONVERSIONS AND CONCENTRATIONS

Run No.	11	12	13	14	15	16	17	18	19	20
Temp., °C	800	1000	1000	1000	1000	1000	1000	1000	1000	1000
Contact time, 10^{-3} sec	21.5	1.36	2.24	9.42	13.7	21.8	23.9	2.44	2.25	2.36
Composition of reactant gas, mol %										
Nitrogen	88.6	93.3	93.3	94.1	91.0	92.1	91.1	95.9	93.3	88.3
Allyl chloride	11.4	6.7	6.8	5.9	9.0	7.9	8.9	4.1	6.7	11.7
Rate of expansion	0.959	0.993	1.00	0.948	1.00	1.00	0.966	1.00	1.00	1.00
Conversion, %	7.1	11.0	21.3	40.1	58.7	86.9	93.5	32.7	29.9	29.1
Yield, mol/100 mol of allyl chloride pyrolyzed										
Hydrogen	—	4.6	6.1	11.8	15.4	21.3	17.9	5.9	4.7	4.6
Methane	—	—	trace	trace	trace	2.0	1.8	—	trace	trace
Acetylene	1.8	3.4	3.3	4.7	4.9	5.3	4.5	3.2	3.3	2.7
Ethylene	2.8	4.4	4.0	4.5	7.3	8.0	7.2	3.7	4.0	4.1
Propylene	17.9	15.5	10.3	9.7	9.4	8.5	7.9	10.9	10.3	10.8
Allene	8.1	10.8	9.6	4.4	3.5	2.3	1.9	7.9	7.2	5.9
Methylacetylene	trace	3.9	3.8	3.5	2.7	2.4	2.0	3.4	3.6	2.6
1-Butene	trace	trace	trace	0.9	0.8	0.7	0.6	—	1.6	1.2
Butadiene	3.4	4.3	4.6	2.8	2.2	1.8	1.5	3.6	4.2	3.4
Diallyl	6.7	6.6	4.2	1.4	trace	trace	trace	2.2	1.9	2.6
1,3-Cyclohexadiene	11.0	6.1	3.0	trace	trace	trace	trace	2.8	2.1	2.3
Benzene	17.9	14.5	15.0	16.6	16.3	20.6	19.2	12.7	15.4	15.7
Total yield of methylacetylene and allene	8.1	14.7	13.4	7.9	6.2	4.7	3.9	11.3	10.8	8.5
Total yield of C_6 components	35.6	27.2	22.2	18.0	16.3	20.6	19.2	17.7	19.4	20.6
Percentage of hydrogen and carbon accounted for in products through C_6 components										
Hydrogen	87.5	86.9	66.6	55.8	54.6	62.6	54.6	57.0	60.6	59.7
Carbon	104.0	95.3	75.5	64.8	59.2	65.7	58.1	67.0	72.5	71.1

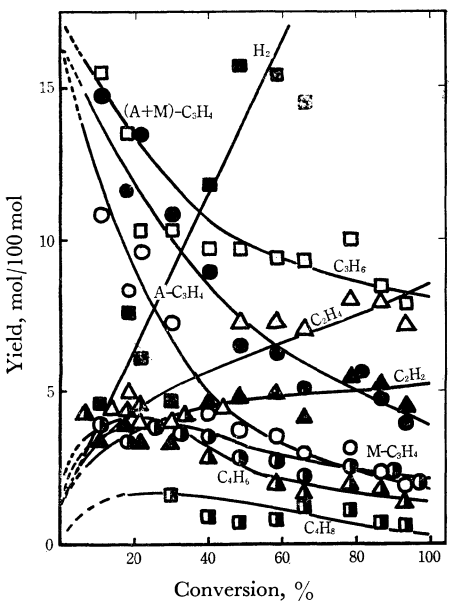

Fig. 4. Effect of conversion on gaseous product yields. Temp., 1000°C

version, while that of methylacetylene was fairly constant at 4 mol in a 10—30% conversion range, and beyond this conversion range, it decreased gradually from 4 mol to 2 mol at 90% conversion. Thus, taking account of an equilibrium relation between methylacetylene and allene, it seems probable that methylacetylene is not a primary product, but a secondary one produced by the isomerization of allene.[1b] The yield of propylene decreased from 15 mol at 10% conversion to 8 mol at 90% conversion. Hydrogen increased from 4 mol at 10% conversion to 20 mol at 90% conversion. The yields of acetylene and ethylene increased gradually from 3 mol and 4 mol at 10% conversion to 5 mol and 8 mol at 90% conversion, respectively. The yield of butadiene decreased gradually from 4 mol at 10% conversion to 2 mol at 90% conversion.

The results for the liquid products at the same temperature are shown in Table 3 and Fig. 5. As the conversion increased, the yield of benzene increased gradually from 14 mol at 10% conversion to 18 mol at 80% conversion, while those of 1,3-cyclohexadiene and diallyl fell rapidly in the lower part of the conversion range from 6 mol at 10% conversion to trace amounts at 60% conversion. As a result, the total yields of C_6 components decreased gradually with the increasing conversion from 26 mol at 10% conversion to 18 mol at 80% conversion.

The amounts of tarry and carbonaceous products

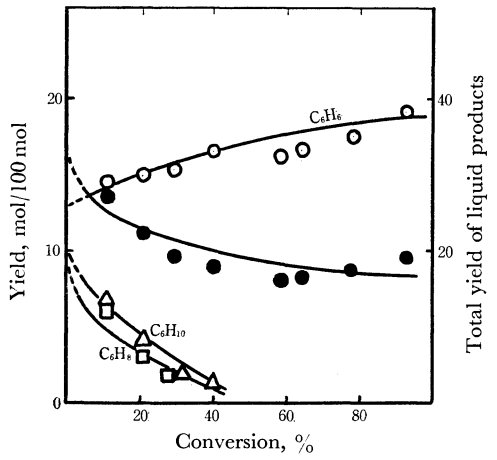

Fig. 5. Effect of conversion on liquid product yields. Temp., 1000°C

●: total yield of liquid products

increased with the increasing conversion to make the material balance remarkably worse, as described in Table 3. Furthermore, it was determined by the zero conversion method that the main products in the early stage of the pyrolysis were propylene, allene, hydrogen, benzene, 1,3-cyclohexadiene, and diallyl, as shown in Figs. 4 and 5.

The Effect of Concentration on Yields. The yields of products obtained in a concentration range of 4 to 12 mol% at 1000°C are shown in Fig. 6 (also in Table 3). When the concentration increased, the yield of propylene was almost constant, being about 11 mol, while the yields of allene and methylacetylene were influenced remarkably and fell from 8 mol to 6 mol and 4 mol to 3 mol, respectively. As a result, the total yield of allene and methylacetylene decreased at a considerable rate with the increasing concentration, ranging from 12 mol at 4 mol% to 9 mol at 12 mol%. The yield of benzene increased from 13 mol to 16 mol with an increase in the concentration. It was further observed that the change of the concentration had no remarkable influence on the yield of any other products, that is, hydrogen, methane, acetylene, ethylene, butene-1, butadiene, diallyl, and 1,3-cyclohexadiene.

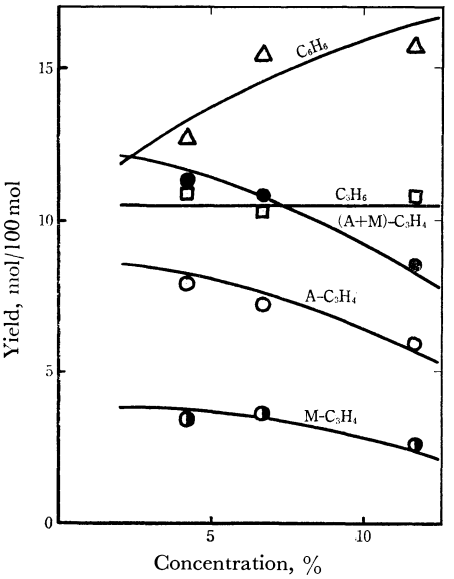

Fig. 6. Effect of concentration on product yields. Temp., 1000°C. Conversion, 29—33%

Kinetics. A rough estimate of the activation energy for the over-all process was made using our data at 800—1200°C. The pyrolysis was found to be first order at a given temperature range. An Arrhenius plot (Fig. 7) of first order

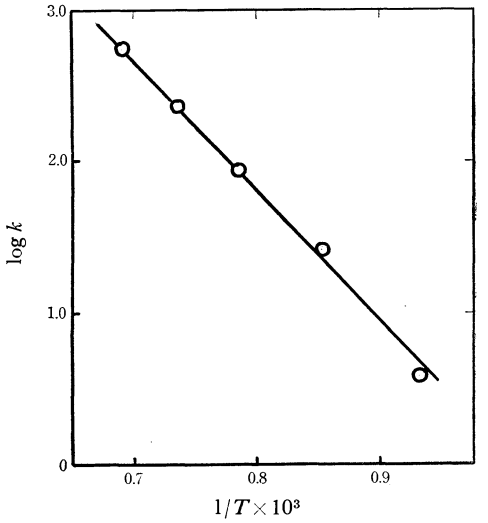

Fig. 7. Plot log k against $1/T$ for allyl chloride.

rate constants based on gas chromatographic analysis for allyl chloride consumed gave a value of 39.4 kcal/mol for the over-all activation energy. This value is much lower than the dissociation energy of allyl chloride, $E_{C_3H_5\text{-}Cl}=58$ kcal/mol.[3] The corresponding A factor was $10^{8.7}$ sec^{-1}. The values of the activation energy and A factor obtained were in good agreement with the values of 42.5 kcal/mol and $10^{9.10}$ sec^{-1} found by Goodall and Howlett. In addition, the activation energy we found was intermediate between those reported by Goodall and Howlett, and Hughes and Yates who reported 34.7 kcal/mol as the over-all activation energy of the pyrolysis.

Discussion

Mechanism. In the present investigation, the reaction products were essentially identical with

those of Porter and Rust, and Hughes and Yates, except that allene and methylacetylene were found as the major products. Thus, the mechanism proposed by both of these authors may be convenient for explaining the experimental results, taking into further consideration the formation steps of allene and methylacetylene. According to the zero conversion method (Figs. 4 and 5), it was concluded that propylene, allene, hydrogen, diallyl, 1,3-cyclohexadiene, and benzene were the main products in the early stage of the pyrolysis. Consequently, a following mechanism may be proposed for the pyrolysis of allyl chloride.

Main Reactions

$$CH_2{=}CH{-}CH_2Cl \rightarrow CH_2{=}CH{-}CH_2\cdot + Cl \quad (1)$$

$$CH_2{=}CH{-}CH_2\cdot + CH_2{=}CH{-}CH_2Cl \rightarrow CH_2{=}CH{-}CH_3 + CH_2{=}CH{-}\dot{C}HCl \quad (2)$$

$$Cl + CH_2{=}CH{-}CH_2Cl \rightarrow HCl + CH_2{=}CH{-}\dot{C}HCl \quad (3)$$

$$CH_2{=}CH{-}CH_2\cdot \rightarrow CH_2{=}C{=}CH_2 + H \quad (4)$$

$$H + CH_2{=}CH{-}CH_2Cl \rightarrow H_2 + CH_2{=}CH{-}\dot{C}HCl \quad (5)$$

$$CH_2{=}CH{-}CH_2\cdot + H \rightarrow CH_2{=}CH{-}CH_3 \quad (6)$$

$$2CH_2{=}CH{-}CH_2\cdot \rightarrow C_6H_{10} \quad (7)$$

$$CH_2{=}CH{-}CH_2\cdot + CH_2{=}CH{-}\dot{C}HCl \rightarrow C_6H_8 + HCl \quad (8)$$

$$2CH_2{=}CH{-}\dot{C}HCl \rightarrow C_6H_6 + 2HCl \quad (9)$$

Side Reactions

Methane

$$CH_3\cdot + RH \rightarrow CH_4 + R\cdot \quad (10)$$

Acetylene

$$CH_3{-}C{\equiv}CH + H \rightarrow HC{\equiv}CH + CH_3\cdot \quad (11)$$

$$\cdot CH{=}CH_2 \rightarrow CH{\equiv}CH + H \quad (12)$$

Ethylene

$$CH_3{-}CH{=}CH_2 + H \rightarrow CH_3\cdot + CH_2{=}CH_2 \quad (13)$$

$$CH_2{=}CH{-}CH_2{-}CH_2{-}CH{=}CH_2 + H \rightarrow CH_2{=}CH_2 + \cdot CH_2{-}CH_2{-}CH{=}CH_2 \quad (14)$$

$$\cdot CH_2{-}CH_2{-}CH{=}CH_2 \rightarrow CH_2{=}CH_2 + \cdot CH{=}CH_2 \quad (15)$$

Propylene

$$CH_2{=}CH{-}CH_2{-}CH_2{-}CH{=}CH_2 + H \rightarrow CH_2{=}CH{-}CH_2\cdot + CH_2{=}CH{-}CH_3 \quad (16)$$

methylacetylene

$$CH_2{=}C{=}CH_2 \rightleftarrows \begin{matrix} CH_2{=}C{=}CH\cdot \\ \uparrow\downarrow \\ \cdot CH_2{-}C{\equiv}CH \end{matrix} + H \rightleftarrows CH_3{-}C{\equiv}CH \quad (17)$$

Butene-1

$$RH + \cdot CH_2{-}CH_2{-}CH{=}CH_2 \rightarrow R\cdot + CH_3{-}CH_2{-}CH{=}CH_2 \quad (18)$$

Butadiene

$$\cdot CH_2{-}CH_2{-}CH{=}CH_2 \rightarrow CH_2{=}CH{-}CH{=}CH_2 + H \quad (19)$$

Hydrogen

$$H + RH \rightarrow H_2 + R\cdot \quad (20)$$

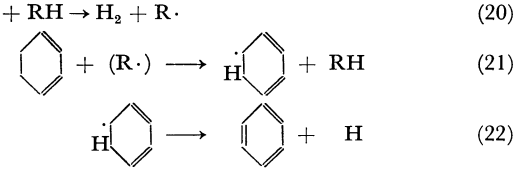

Reactions (1) to (9) are the main reactions in the early stage of the pyrolysis. Reactions (10) to (22) are the principal side reactions, which would be predominant in the higher conversions. The compatibility of the proposed mechanism with the observed experimental data can now be explained.

Main Reactions. Reaction (1) is the initial step which indicates the dissociation of allyl chloride into an allyl radical and a chlorine atom. All the main products, propylene, allene, hydrogen, diallyl, 1,3-cyclohexadiene, and benzene are formed by subsequent Reactions (2) and (6), (4), (5), (7), (8), and (9), respectively. Reaction (4), being the step of the formation of allene from allyl radical,[11,12,1b] appears to be an important course under the conditions studied. Reactions (2), (4), (6), (7), and (8) involving allyl radical proceed competitively with each other. Of these reactions, Reaction (4) appears to become predominant at higher temperature and lower concentration, as supported by the experimental results that allene and methylacetylene increase with an increase in the temperature, and propylene and all C_6 compounds decrease reversely (Figs. 2 and 3). This may be plausible judging from the theoretical foundation that Reaction (4) only is a unimolecular reaction which requires a high activation energy of about 62 kcal/mol.[12a,13] Reactions (8) and (9) are complicated reactions which include combination of allyl and chloroallyl radicals followed by cyclization.[7]

Keeping our mind on Reactions (1) and (3), the over-all reaction in the early stage of the pyrolysis will be represented by the reaction $2C_3H_5Cl \rightarrow C_3H_5 + C_3H_4Cl + HCl$. Consequently, when 100 mol of allyl chloride is decomposed, 50 mol of allyl radical and 50 mol of chloroallyl radical are formed, respectively. Among the reaction products, propylene, allene, methylacetylene, and diallyl are derived certainly from allyl radicals, similarly benzene from chloroallyl radicals, and 1,3-cyclohexadiene from both radicals. As a result, in the early stage of the pyrolysis, the amount of allyl radical should be approximately equal to the sum of the amounts of propylene, allene, methylacetylene, 1,3-cyclohexadiene, and twice of the amounts of diallyl, while the amount of chloroallyl radical should be equal to the sum of the amounts of 1,3-cyclohexadiene and twice of the amounts of benzene. The fact that this relationship is approximately correct can be confirmed from the following results taken from Run 11 at 800°C and Run 12 at 1000°C (Table 3). These observed values 50.4, 46.8, and

11) M. Szwarc, *J. Chem. Phys.*, **17**, 284 (1949).

12) a) A. Amano and M. Uchiyama, *J. Phys. Chem.*, **68**, 1133 (1964); b) K. J. Laidler and B. W. Wojciechowski, *Proc. Roy. Soc.*, **A259**, 257 (1960).

13) K. W. Egger, D. M. Golden and S. W. Benson, *J. Am. Chem. Soc.*, **86**, 5420 (1964); R. J. Ellis and H. M. Frey, *J. Chem. Soc.*, **1964**, 5578; D. M. Golden, A. S. Rodgers and S. W. Benson, *J. Am. Chem. Soc.*, **88**, 3196 (1966).

49.5 are approximate to theoretical value 50.0.

Run 11

$$C_3H_5\cdot \rightarrow C_3H_6 + C_3H_4 + 2C_6H_{10} + C_6H_8$$
$$50.0 \fallingdotseq 17.9 + 8.1 + 2 \times 6.7 + 11.0 = 50.4$$
$$\dot{C}_3H_4Cl \rightarrow C_6H_8 + 2C_6H_6$$
$$50.0 \fallingdotseq 11.0 + 2 \times 17.9 = 46.8$$

Run 12

$$C_3H_5\cdot = 49.5, \quad \dot{C}_3H_4Cl = 35.1$$

The discrepancy between the value of Run 11 and that of Run 12 lies in the difference of temperature. The lower value of chloroallyl radical for Run 12 may be caused by the decomposition of chloroallyl radical to chloroallene and/or $CH_2{=}CH{-}\dot{C}H$ that appears to be probable at higher temperature, though it is not shown in the reaction mechanism. Furthermore, the decrease of carbon and hydrogen balance with the increasing temperature (Table 2) may be discussed in connection with this. Namely, it seems reasonable to presume that the decompositions, followed by association, of allyl and chloroallyl radicals leading to tarry and carbonaceous products may increase remarkably at higher temperature, judging from the fact that benzene is fairly stable under our experimental conditions. From the results mentioned above, it is concluded that the decomposition products in the early stage of the pyrolysis are well accounted for by considering the mechanism comprised mainly reactions of allyl and chloroallyl radicals formed in the pyrolysis.

Side Reactions. Besides the main products, several side reaction products were obtained: methane, acetylene, ethylene, methylacetylene, butene-1, butadiene. The formations of these side reaction products are assumed to proceed largely by Reactions (10)—(15) and (17)—(19). In the experimental results, C_2 compounds, ethylene and acetylene, and C_4 compounds, butene and butadiene, were formed in considerable amounts (Table 2). This fact suggests that diallyl decomposed to give C_2 and C_4 compounds, as shown in Reaction (14). In fact, it was confirmed by our reference experiment that almost the same amounts of C_2 compounds, ethylene and acetylene, and C_4 compounds, butene and butadiene were formed in the pyrolysis of diallyl. Concerning thermal isomerization of allene to methylacetylene, it is reported also by the present authors that allene isomerizes to methylacetylene in fairly good yield at high temperatures.[1] Propylene, hydrogen, and benzene would probably be formed also by Reactions (16), (20), (21), and (22) in addition to the main Reactions (2) and (6), (5), and (9).

As the conversion increases, the pyrolysis reaction would become complex since the participation of hydrogen abstraction by chlorine atom in secondary reactions increases remarkably . Thus, it is difficult to account for the experimental results at high conversions. The rapid decrease in the yields of propylene and allene - methylacetylene with the increasing conversion (Fig. 4) may be responsible for the loss owing to various secondary decomposition and polymerization reactions; the extremely rapid decrease in allene appears to be plausible from the fact that allene is unstable, compared with propylene, and is apt to undergo various secondary reactions including the isomerization Reaction (17). On the other hand, the yield of benzene increases little by little with the increasing conversion (Fig. 5). This may be due mainly to the conversion of 1,3-cyclohexadiene into benzene by Reactions (21) and (22), and to large stability of benzene under our experimental conditions.

As the concentration of allyl chloride increases, bimolecular reactions become more advantageous than unimolecular reactions. The increase in the yield of benzene and the decrease in the yield of allene and methylacetylene with the increasing concentration correspond with this (Fig. 6).

BULLETIN OF THE CHEMICAL SOCIETY OF JAPAN VOL. 42 1090—1094 (1969)

Oxygen Exchange Reaction of Sulfoxides in Dinitrogen Tetroxide[1]

Norio KUNIEDA, Kazuo SAKAI and Shigeru OAE

Department of Applied Chemistry, Faculty of Engineering, Osaka City University, Sumiyoshi-ku, Osaka

(Received August 17, 1968)

Sulfoxides are known to undergo concurrent oxygen exchange and racemization reactions with various reagents (*Bull. Chem. Soc. Japan*, **41**, 1025 (1968)). Especially well studied are the oxygen exchange reactions in acid media. We have found a similar concurrent oxygen exchange and racemization reaction of sulfoxides with liquid dinitrogen tetroxide. The pseudo first order reaction rates of both oxygen exchange and racemization reactions have been determined using both optically active and ^{18}O-labeled sulfoxides. The k_{ex}/k_{rac} value was found to be unity, and the polar effect of substituents on the rates of oxygen exchange of substituted diphenyl sulfoxides was found to be considerably large, and correlated with σ^+ values with $\rho = -1.30$. From these results a plausible mechanism for this reaction has been discussed.

Sulfoxides are of stable pyramidal structure and isoelectronic to carbanions, amines, phosphines, sulfonium ions, *etc.*[2] Therefore, the optical isomerism can exist in sulfoxides, and the stereochemical stability of sulfoxides are known to be far exceeding those of similar sulfonium compounds. Furthermore, unlike those in sulfone group, the S-O linkage of sulfoxides is weak and readily cleaves. These are quite advantageoues for nucleophilic substitutions to occur on the sulfur atom. In fact, there are number of reactions which involve the facile cleavage of the S-O linkage.[3] The concurrent oxygen exchange and racemization reactions of sulfoxides are interesting reactions in these connections, and have attracted considerable attentions in recent years. These oxygen exchange reactions are very convenient for studying the nature of nucleophilic substitution on the trivalent sulfur atom, since one can readily prepare both ^{18}O-labeled and optically active sulfoxides[4] and follow both the loss of ^{18}O-content and the change of optical rotation simultaneously.

There are three types of mechanistic pathways in the nucleophilic substitution on the trivalent sulfur atom. The first type (Type-1) is like an S_N1-type reaction on sp^3 carbon atom, where, the cleavage of the S-O bond takes place in the initial slow step followed by fast recombination with solvent, resulting in the racemization. Among many examples of this type, there are concurrent oxygen exchange and racemization reactions of sulfoxides in concentrated sulfuric acid,[5] in phosphoric acid[6] and in chloroacetic acids.[7] The second type (Type-2) is the mechanism involving an S_N2-like nucleophilic replacement at the sulfur atom forming a new S-O bond while cleaving the old S-O bond at the rate-determining step, resulting in the inversion of configuration of the original sulfoxide. However, unlike the S_N2 reaction on saturated carbon atom there are two possible steric arrangements of both entering and outgoing groups in the nucleophilic substitution involving steric inversion on the sulfur atom, since the intermediate or the incipient complex at the transition state is expected to assume a typical bipyramidal structure. Namely, in addition to the usual S_N2 type arrangement in which both entering and leaving groups assume axial positions, there is another arrangement in which both groups assume radical positions. Both steric arrangements will lead to the net inversion of configuration. Among the former examples are the oxygen exchange reactions of sulfoxides in acetic anhydride[8] and in less concentrated sulfuric acid.[9] The latter example may be found among the reactions of sulfoxides with cyclic oxy-compounds which is now under investigation. There is another type, *i. e.*, (Type-3); when leaving

1) Paper XXVII on Sulfoxides.

2) K. Mislow, "Introduction to Stereochemistry," W. A. Benjamin, Inc., New York, N.Y. (1965), p. 88.

3) For details see; C. C. Price and S. Oae, "Sulfur Bonding," Ronald Press, New York, N. Y. (1962), Chapter 4.

4) a) K. K. Andersen, *Tetrahedron Letters*, **1962**, 93. b) N. Kunieda, K. Sakai and S. Oae, This Bulletin, **41**, 3015 (1968).

5) a) S. Oae, T. Kitao, Y. Kitaoka and S. Kawamura, This Bulletin, **38**, 546 (1965). b) S. Oae and N. Kunieda, *ibid.*, **41**, 696 (1968).

6) N. Kunieda and S. Oae, *ibid.*, **41**, 1025 (1968).

7) S. Oae, M. Yokoyama and M. Kise, *ibid.*, **41**, 1221 (1968).

8) S. Oae and M. Kise, *Tetrahedron Letters*, **1967**, 1409.

9) N. Kunieda and S. Oae, This Bulletin, in press.

Table 1. Oxygen exchange reactions of ^{18}O-labeled sulfoxides in dinitrogen tetroxide at 0°C for 1 hr

Sulfoxide	Atom%-^{18}O of sulfoxide		Ratio of ^{18}O-exchange(%)	Mole ratio of N_2O_4 to sulfoxide	Solvent
	Starting	Recovered			
$C_6H_5SOC_6H_5$	0.98	0.24	97	10	None
	0.66	0.36	79	1.1	CCl_4
$C_6H_5SOCH_2C_6H_5$	1.05	0.40	95	1	$CHCl_3$
$(C_6H_5CH_2)_2SO$	1.68	0.33	91	1	$CHCl_3$
Dibenzothiophene oxide	0.43	0.24	88	10	CCl_4-$CHCl_3$
Phenoxathiin 5-oxide	0.86	0.26	93	10	CCl_4-$CHCl_3$

and entering groups assume axial and radial positions, the oxygen exchange will lead to the retention of configuration. The first example of this type may be the reaction of sulfoxides with DMSO.[10]

Dinitrogen tetroxide is known to be a unique reagent which can oxidize sulfides specifically to the corresponding sulfoxides.[11] Recently we have found that the oxygen exchange reaction of diphenyl sulfoxide readily takes place in liquid dinitrogen tetroxide[12] in similar conditions used for the oxidation of sulfides. Meanwhile Johnson and McCants have also reported that (+)- benzyl *p*-tolyl sulfoxide is rapidly racemized in this reagent.[13] Since dinitrogen tetroxide is a somewhat different oxygen exchange reagent from those used previously, one might expect an entirely different mechanistic route for the oxygen exchange reaction. However, a more careful kinetic study has been desired in order to elucidate a plausible mechanism for this reaction. We now have compiled substantial amounts of kinetic data on this reaction with several sulfoxides in liquid dinitrogen tetroxide and found that this reaction is one of a typical example of Type-1 proceeding through an S_N1-like S–O bond cleavage at the rate-determining step. This paper describes a detailed account of the kinetic study.

Results and Discussion

When a sulfoxide is dissolved in an excess of dinitrogen tetroxide at 0°C, the sulfoxide can be recovered almost quantitatively after an hour without undergoing further oxidation to the sulfone or any other side reaction with dinitrogen tetroxide, and its mp and IR spectrum are completely identical to those of the starting sulfoxide. A few representative results are shown in Table 1. The heteroaromatic sulfoxides, *i. e.*, dibenzothiophene oxide and phenoxathiin 5-oxide, also undergo the oxygen exchange with this reagent.

Earlier Johnson and McCants reported that (+)-benzyl *p*-tolyl sulfoxide is rapidly racemized by liquid dinitrogen tetroxide.[13] We have examined the oxygen exchange reaction of ^{18}O-labeled, optically active ethyl *p*-tolyl sulfoxide in this reagent,[12] and found, as shown in Table 2, that

Table 2. Concurrent oxygen exchange and racemization of (+)- ethyl *p*-tolyl sulfoxide-^{18}O in dinitrogen tetroxide[a]

	^{18}O-concentration (atom%)	Rotation ($[\alpha]_D$ in acetone)
Starting sulfoxide	0.56	+183°
Recovered sulfoxide	0.25[b]	0

a) Mole ratio of sulfoxide to N_2O_4=1 : 10, at 0°C for 1 hr.
b) Ratio of oxygen exhcange=91%.

the racemization is not an independent reaction but accompanies concurrent oxygen exchange reaction in a fashion similar to that in acid media of our previous works.[14]

In the oxidations of sulfides or disulfides with dinitrogen tetroxide, the reaction mixture usually develops a green or blue color, due to the formation of dinitrogen trioxide, and nitric oxide (NO) is evolved.[11]

$$R_2S + N_2O_4 \longrightarrow R_2S{\rightarrow}O + N_2O_3$$
$$N_2O_3 \rightleftarrows NO + NO_2$$

However, when a sulfoxide is dissolved in dinitrogen tetroxide there is no color change or evolution of nitric oxide. Apparently the concurrent oxygen exchange and racemization reactions of sulfoxides proceed without consuming dinitrogen tetroxide. Actually, when 0.997 g of ^{18}O-labeled diphenyl sulfoxide (0.66 atom%-^{18}O) was dissolved in 2.386 g of dinitrogen tetroxide in a vessel connected to

10) S. Oae, M. Yokoyama and S. Oae, *Tetrahedron Letters*, **1968**, 4131.
11) L. Horner and F. Hübenett, *Ann*, **579**, 193 (1953); C. C. Addison and J. C. Sheldon, *J. Chem. Soc.*, **1956**, 2705.
12) S. Oae, N. Kunieda and W. Tagaki, *Chem. & Ind.*, **1965**, 1790.
13) C. R. Johnson and D. McCants, Jr., *J. Am. Chem. Soc.*, **86**, 2935 (1964).
14) Summarized in; N. Kunieda and S. Oae, This Bulletin, **41**, 1025 (1968).

a vacuum line and the solution was kept for 30 min at 0°C, almost quantitative amount of dinitrogen tetroxide (2.379 g) (colorless crystals at the temperature of dry ice-acetone bath) was recovered together with 0.997 g of the oxygen-exchanged sulfoxide (0.25 atom%-^{18}O).

$$\begin{matrix} R \\ R' \end{matrix}\!\!\diagdown\!\!\diagup S^{*}\!\rightarrow {}^{18}O + N_2O_4 \rightleftharpoons O\leftarrow S^{*}\!\!\begin{matrix} \diagup R \\ \diagdown R' \end{matrix} + N_2{}^{18}O_4$$

Since the oxygen exchange reaction accompanies the racemization of sulfoxides, the mechanism of Type-3 is excluded, leaving two other possible mechanistic routes. If the cleavage of S–O bond takes place in the initial slow step followed by fast recombination with solvent according to the Type-1, each oxygen exchange will cause racemization, and then the rate of oxygen exchange becomes identical to that of racemization; $k_{ex}/k_{rac}=1$. The other is the Type-2 mechanism which involves an S_N2-like simultaneous bond forming and cleavage of S–O bond at the rate-determining step, and each oxygen exchange of sulfoxides will result in the inversion of configuration at the central sulfur atom and hence the ratio k_{ex}/k_{rac} becomes 0.5.

The rates of both oxygen exchange and racemization of ^{18}O-labeled and optically active *p*-tolyl phenyl sulfoxide in dinitrogen tetroxide - carbon tetrachloride solution were carefully measured. The results, shown in Table 3, clearly reveal that the rate of the oxygen exchange is identical to that of the racemization, suggesting that the reaction proceeds through the Type-1 mechanism. Furthermore, the rate of this reaction was found to be of first order dependence on the concentration of dinitrogen tetroxide as shown in Fig. 1. The rate constants obtained are of pseudo first order even under the condition when the mole ratio of sulfoxide to dinitrogen tetroxide is atmost 1 : 2—3.

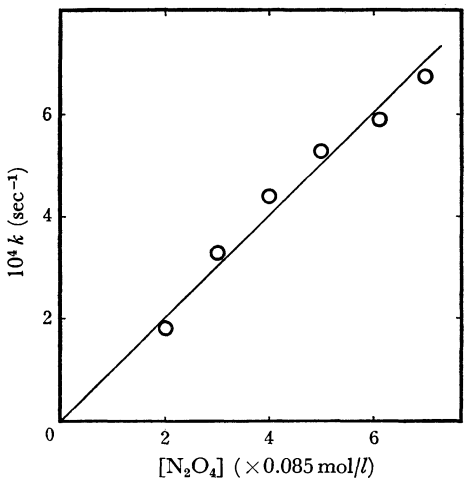

Fig. 1. Rate constants of racemization reaction of (+)- *p*-tolyl phenyl sulfoxide (0.1 mol/l) plotted against mole concentration of dignitrogen tetroxide in carbon tetrachloride at 0°C.
Slope = 1.01 (r=0.993)

It is known that alkyl sulfoxides form molecular addition compounds with dinitrogen tetroxide[15] and the formation of such addition compounds may inhibit further oxidation of sulfoxides to sulfones. The compound formation is considered to be resulted by the interation between electron-rich sulfoxide oxygen and the electron-deficient dinitrogen tetroxide molecule.

TABLE 3. RATE CONSTANTS OF ^{18}O-EXCHANGE AND RACEMIZATION OF *p*-TOLYL PHENYL SULFOXIDE[a] IN DINITROGEN TETROXIDE AT 0°C

Mole concentration of N_2O_4 (mol/l)	10^4k(sec^{-1}) k_{ex}	k_{rac}	k_{ex}/k_{rac}
0.530[b]	6.23±0.12	6.35±0.30	0.983±0.027
0.462[c]	10.4 ±0.1	10.4 ±0.6	1.00 ±0.05
0.281[c]	4.64±0.13	4.80±0.28	0.970±0.030

a) Sulfoxide=0.1 mol/l. b) and c) are media of different batch.

There are two possible structures, *i. e.*, molecular (I) and ionic complex (II), for the addition compounds of sulfoxides.

$$[R_2SO\cdot N_2O_4] \quad [R_2SO\cdots NO]^+ NO_3^-$$
$$\text{(I)} \qquad\qquad \text{(II)}$$

Addison and Sheldon have shown that the molecular complex (I) is favorable in solid state.[15] But in liquid state the ionic structure (II) would be more favorable, since its equilibrium $N_2O_4 \rightleftarrows NO^+NO_3^-$ is also established in the liquid state and the NO^+ ion is also electron deficient, and, morevoer, the sulfoxides are considered to be the donors of medium strength.[16] Therefore, the sulfoxides would form the ionic complex (I) in liquid dinitrogen tetroxide at the initial step of the oxygen exchange and racemization reaction. On the basis of these informations, the following reaction scheme may be constructed, in which the second step of the cleavage of S–O bond is the slow rate-determining step. Path (a) is the heterolysis of the S–O bond to form the doubly positively charged "sulfidonium ion" intermediate. Path (b) is the homolysis to form the cation radical intermediate. If the reaction follows the path (a), the

15) C. C. Addison and J. C. Sheldon, *J. Chem. Soc.*, **1956**, 2705.

16) The classification of structure of dinitrogen tetroxide addition compounds has been offered by Addison and Sheldon [Ref. 15, and H. H. Sisler, *J. Chem. Educ.*, **34**, 555 (1957)], which said a medium strength donors, *e. g.*, carbonyl compounds and sulfoxides, *etc.*, form together ionic and molecular complexes in liquid dinitrogen tetroxide.

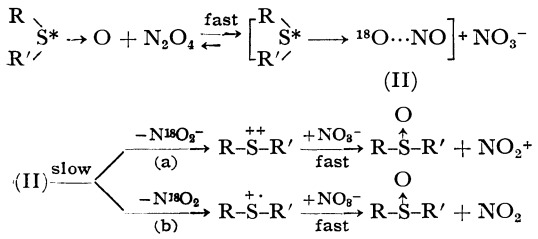

rate would be substantially more effected by polar substituents like in the case of the S_N1-type reaction of carbon compounds than in the case of path (b). Recently, we have found that the most reasonable mechanism for the concurrent oxygen exchange and racemization reactions of diaryl sulfoxides in concentrated sulfuric acid is through the path involving the homolysis of the S–O bond forming the radical cation intermediate. In this case, the polar effects of substituents on the phenyl group are very small and *p*-methyl group accelerates the rate only less than twofold while the electron-withdrawing *p*-chloro group also give a small acceleration.[5b] The rates of the oxygen exchange of several *p*-substituted diphenyl sulfoxides were measured in dinitrogen tetroxide - carbon tetrachloride solution. One finds in Table 4 that the polar effects of *p*-substituents on the rates are considerably large, and the rates are nicely correlated with Brown-Okamoto's σ^+ values and give a considerably large negative ρ value (for σ; $\rho=-1.58$, Correlation coefficient $r=0.948$) (for σ^+; $\rho=-1.30$, $r=0.990$).

Table 4. Kinetics of oxygen exchange of X-C$_6$H$_4$-S^{18}O-C$_6$H$_4$-X[a] with dinitrogen tetroxide[b] in carbon tetrachloride at 0°C

X	$10^4\,k_{ex}$ (sec^{-1})
CH_3O	18.5 ± 0.7
CH_3	4.64 ± 0.13
H	2.50 ± 0.15
Cl	1.04 ± 0.04

a) Sulfoxide=0.1 mol/*l*. b) N_2O_4=0.281 mol/*l*.

Table 5. Oxygen exchange of ^{18}O-labeled diphenyl sulfone[a] in dinitrogen tetroxide at 0°C for 1 hr

	^{18}O-Concentration (atom%)	
	Starting sulfone	Recovered sulfone
Run 1	1.64	1.60
Run 2	1.76	1.71

a) Mole ratio of sulfone to N_2O_4 was 1 : 10.

These rather large polar effect seems to favor the heterolytic cleavage, *i. e.*, path (a) for the reaction.

Diphenyl sulfone was found not to undergo the oxygen exchange in this reagent even without the solvent, as shown in Table 5. This is undoubtedly due to the much strong nature of the S–O bond of sulfones for cleavage in comparison with that of sulfoxides.

Experimental

Materials. *^{18}O-Labeled sulfoxides* were prepared by the oxidation of corresponding sulfides with bromine complex of pyridine and ^{18}O-enriched water in acetic acid by the same procedure as described in our previous paper.[17] Diphenyl sulfoxide; mp 70—71°C (71°C),[18] 0.86_3atom%-^{18}O. Phenyl *p*-tolyl sulfoxide; mp 71—72°C (71—72°C),[18] 1.0_7atom%-^{18}O. Phenyl *p*-chlorophenyl sulfoxide; mp 45—46°C (45—46°C),[18] 1.1_8atom-^{18}O. Phenyl *p*-methoxyphenyl sulfoxide; mp 60°C (55—57°C),[18] 0.57_0atom%-^{18}O. Benzyl phenyl sulfoxide; mp 121—122°C (123°C),[19] 1.0_5atom%-^{18}O. Dibenzyl sulfoxide; mp 136—137°C (133°C),[19] 1.6_8-atom%-^{18}O. Dibenzothiophene oxide; mp 62—67°C, 0.43atom%-^{18}O. Phenoxathiin 5-oxide; mp 151°C (153—154°C),[20] 0.86atom%-^{18}O.

Optically active p-tolyl phenyl sulfoxide was prepared from (−)-menthyl (−)-*p*-toluenesulfinate and phenyl magnesium bromide according to the method developed by Andersen.[4a] Mp 91.5—92°C, $[\alpha]_D=+31.8°$ in CCl_4 ($l=0.5$, $c=1.68$), $[\alpha]_D=+27.8°$ in 96% EtOH ($l=0.5$, $c=1.63$) (lit.[21]); mp 92—93°C, $[\alpha]_D=+27°$ in 95% EtOH).

^{18}O-Labeled optically active ethyl p-tolyl sulfoxide was prepared by Andersen's method[4a] using ^{18}O-labeled (−)-menthyl (−)-*p*-toluenesulfinate which was prepared from ^{18}O-labeled sulfinic acid.[4b] Bp 95—97°C/0.5 mmHg, $[\alpha]_D=+183°$ in acetone ($l=1$, $c=2.1$) (lit[4a]; bp 123—126°C/1.5 mmHg, $[\alpha]_D^{25}=+186°$ in acetone).

^{18}O-Labeled diphenyl sulfone was prepared by the oxidation of diphenyl sulfide with *t*-butyl hypochlorite in the presence of ^{18}O-enriched water by the same procedure as described in our previous paper.[22] Mp 125—126°C (lit.[23]; 124°C), yield 98%.

Dinitrogen tetroxide was prepared by the pyrolysis of dinitrogen pentoxide.[24] The crude oxide was twice distilled over phosphorus pentoxide under faint stream

17) S. Oae, Y. Ohnishi, S. Kozuka and W. Tagaki, This Bulletin, **39**, 364 (1966).
18) C. Modena, *Gazz. Chim. Ital.*, **89**, 834 (1959).
19) R. L. Shriner, H. C. Struck and W. J. Jorison, *J. Am. Chem. Soc.*, **52**, 2060 (1930).
20) H. J. Shine and R. J. Small, *J. Org. Chem.*, **30**, 2140 (1965).
21) K. Mislow, M. M. Green, P. Laur, J. Melillo, T. Simmons and A. L. Ternay, Jr., *J. Am. Chem. Soc.*, **87**, 1958 (1965).
22) K. Kikukawa, W. Tagaki, N. Kunieda and S. Oae, This Bulletin, **42**, 831 (1969).
23) C. A. Buehler and J. E. Masters, *J. Org. Chem.*, **4**, 262 (1939).
24) A. Pedler and F. H. Pollard, "Inorganic Syntheses," Vol. V, ed. by T. Moeller, McGraw-Hill Book Company, Inc., New York, N. Y. (1957), p. 87—90.

of dry oxygen, and then dissolved in pure carbon tetrachloride. The solution was stored in glass vessel with a secured stopper. Concentrations of dinitrogen tetroxide in carbon tetrachloride were determined by titration with a standard alkali solution.

Kinetic Procedure of the Oxygen Exchange and Racemization Reactions of Sulfoxides. An ^{18}O-labeled or an optically active sulfoxide was dissolved in the dinitrogen tetroxide - carbon tetrachloride solution of a predetermined concentration, in such a way as to maintain the concentration of the sulfoxide just about 0.1 mol/*l*, at a preset temperature (0°C). An aliquot portion (7.0 m*l*) of the solution was taken up from time to time for 6—7 times and was quenched witha cold alkaline solution (10% aqueous solution of K_2CO_3). The recovered sulfoxide was extracted with carbon tetrachloride, and the solution was washed with water, and dried over anhydrous sodium sulfate. Finally, carbon tetrachloride was distilled *in vacuo* and then the sulfoxide recovered was subjected to the ^{18}O-analysis or the measurement of optical activity according to the same procedures described in our previous paper[5] using Yanagimoto OR-10 Type polarimater and Hitachi RMU-6E Type mass-spectrometer.

BULLETIN OF THE CHEMICAL SOCIETY OF JAPAN VOL. 42 1094—1098 (1969)

A Study of the Solvent Effect on the Polymerization of *N*-Phenylethyleneimine

Tsutomu KAGIYA, Tomizo KONDO, Kozo NAKAO and Kenichi FUKUI

Faculty of Engineering, Kyoto University, Sakyo-ku, Kyoto

(Received August 21, 1968)

The effect of solvents on the cationic polymerization of *N*-phenylethyleneimine with formic acid catalyst has been studied quantitatively. The polymerization rates in the various solvents used increase in the following order: diethyl ether≃tetrahydrofuran<toluene≃carbon tetrachloride<anisole<methyl acetate<ethylene dichloride<*N*,*N*-dimethylacetamide<dimethyl sulfoxide<epichlorohydrin<acetonitrile. In polar solvents with high dielectric constants, the rates are much larger than those in nonpolar solvents with low dielectric constants. However, in the solvents with similar dielectric constants, such as acetonitrile and *N*,*N*-dimethylacetamide, ethylene dichloride, methyl acetate and tetrahydrofuran, and anisole and diethyl ether, the rates decreased with an increase in the nucleophilicity of the solvents, and the dependence of the polymerization rate on the nucleophilicity of the solvents is much larger in polar solvents than in nonpolar solvents. The propagation rate was markedly influenced by the nature of the solvent, whereas the initiation rate was only a little influenced.

A number of instances have been reported in which the polymerization rate was markedly influenced by the solvents used. No quantitative study of the solvent effect on the polymerization has yet been reported, however. It has been pointed out by many authors that the difference in the rate can not be explained only by the magnitude of the dielectric constant of the solvent, and that the characteristic features of the solvation also affect the reaction rate. As a part of the investigation of the electric nature of the molecule in the liquid phase, we have previously made a quantitative study of the nucleophilic solvation to a deuterium atom of the methanol-d molecule by using the infrared spectroscopic method, and have determined the equilibrium constant, K_D, of various solvents.[1]

1) T. Kagiya, Y. Sumida and T. Inoue, This Bulletin, **41**, 767 (1968).

The purpose of this paper is to investigate quantitatively the effect of the solvent on the polymerization of *N*-phenylethyleneimine by using the equilibrium constants thus obtained.

Experimental

The methods used in the preparation and purification of *N*-phenylethyleneimine have been described in a previous paper.[2] Formic acid and dimethyl sulfoxide of a guaranteed grade were used without further purification. The acetonitrile, epichlorohydrin, anisole, diethyl ether, methyl acetate, *N*,*N*-dimethylacetamide, carbon tetrachloride, toluene and ethylene dichloride were purified by the conventional method.[3] The tetrahydrofuran was distilled in the presence of sodium

2) T. Kagiya, T. Kondo, S. Narisawa and K. Fukui, *ibid.*, **41**, 172 (1968).

3) A. Weissberger *et al.*, "Technique of Organic Chemistry, Vol. VII, Organic Solvents," Interscience Publishers, Inc., New York (1955).

naphthalene after drying over potassium hydroxide and calcium hydride. The methods of the polymerization and molecular-weight determination of the polymer were described in the previous paper. The polymerization was carried out under the following conditions: monomer, 0.005 mol; solvent, 1 ml; catalyst, 2 mol% on monomer; temperature, 0°C.

Results and Discussion

The polymerization of *N*-phenylethyleneimine was carried out in various solvents using formic acid as the catalyst. The plots of the polymer yield against the reaction period are shown in Fig. 1 and Fig. 2. These figures show that the polymerization rate varies markedly with the kind of solvent used. As is shown in Fig. 3 and Fig. 4, the rate of the monomer consumption is expressed by a first-order rate equation with respect to the monomer concentration in the early stages of the polymerization. Considering the fact that the steady-state method is applicable in the polymerization with formic acid in acetonitrile, as has been described in the previous paper, Figs. 3 and 4 may indicate that the concentrations of the propagating species, [P*], are almost constant in the early stages of the polymerization. Moreover, from the fact that the plot of the number-average degree of polymerization is almost proportional to

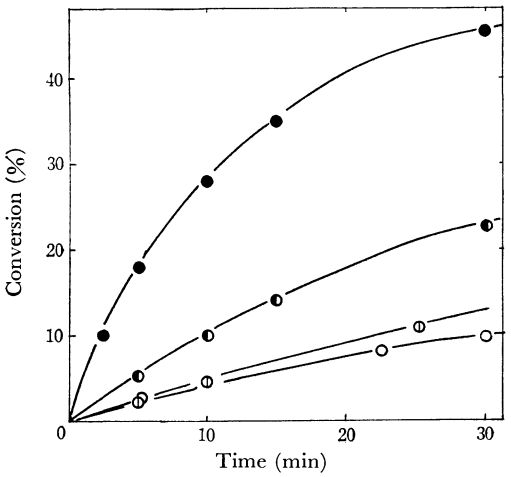

Fig. 1. Polymer yield *vs.* reaction time.
●: Acetonitrile, ◐: Epichlorohydrin
①: Dimethyl sulfoxide
○: *N*,*N*-Dimethylacetamide

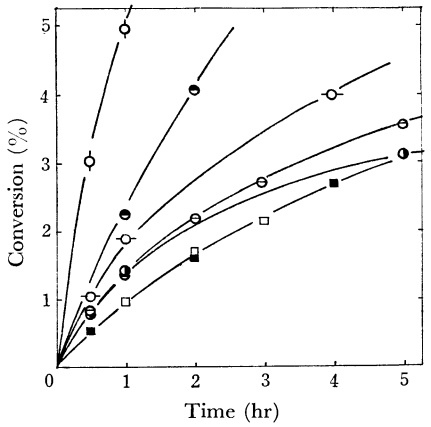

Fig. 2. Polymer yield *vs.* reaction time.
○: Ethylene dichloride, ◓: Methyl acetate
-○-: Anisole, ⊖: Carbon tetrachloride
◑: Toluene, □: Diethyl ether
■: Tetrahydrofuran

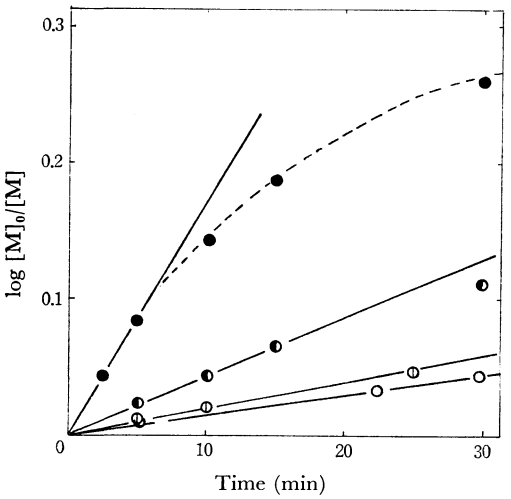

Fig. 3. The plots of log $[M]_0/[M]$ against reaction time.
Notes are the same as in Fig. 1.

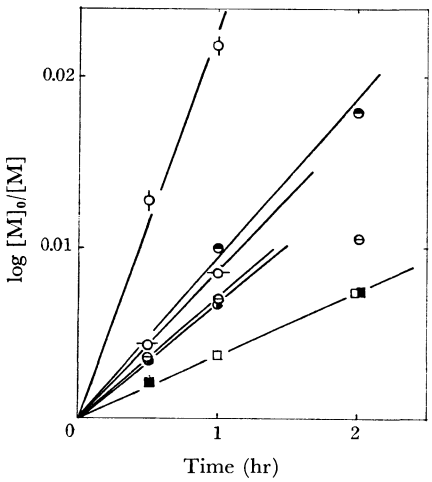

Fig. 4. The plots of log $[M]_0/[M]$ against reaction time.
Notes are the same as in Fig. 2.

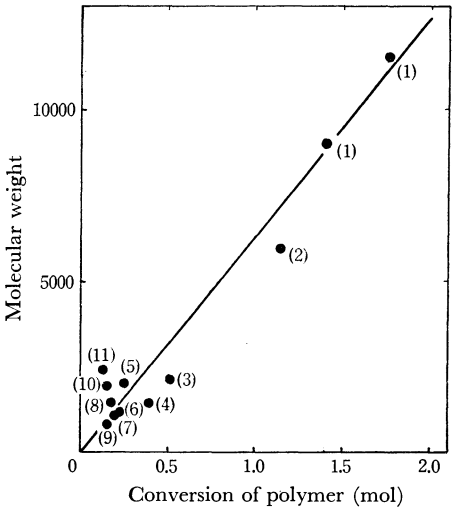

Fig. 5. Plots of molecular weight against conversion of polymer.

Experimental conditions are the same as in Fig. 1 and Fig. 2. (1) Acetonitrile, (2) Epichlorohydrin, (3) Dimethyl sulfoxide, (4) *N,N*-Dimethylacetamide, (5) Ethylene dichloride, (6) Methyl acetate, (7) Anisole, (8) Carbon tetrachloride, (9) Toluene, (10) Tetrahydrofuran, (11) Diethyl ether.

the polymer yield in the solvent used (Fig. 5), the concentration of the propagating species may be constant independently of the kind of solvent. The difference in the slopes of the line in Fig. 3 and Fig. 4 may, then, be due to the differences in the propagation rate between solvents.

From the slopes of the straight line in Fig. 3 and Fig. 4, the products of the rate constant of the propagation reaction, k_p, and the concentrations of the propagating species were obtained. The values of k_p[P*] are summarized in Table 1, along with the physical properties of the solvents. Figure 6 shows the result of plotting the logk_p[P*] value against the dielectric constant of the solvent. Although the polymerization rate tends to increase with an increase in the dielectric constant of the solvent, there was a great difference in the rates, even in solvents with similar dielectric constants, *e. g.*, acetonitrile and *N,N*-dimethylacetamide.

TABLE 1. THE POLYMERIZATION RATES AND THE PHYSICAL PROPERTIES OF THE SOLVENTS

No.	Solvent	k_p[P*] l/min	Dielectric constant ε	K_D
1	Acetonitrile	1720×10^{-5}	37.5	0.352
2	Epichlorohydrin	450	22.6	0.307
3	Dimethyl sulfoxide	210	48.9	2.79
4	*N,N*-Dimethyl acetamide	153	36.7	1.61
5	Ethylene dichloride	43.3	10.4	0.035
6	Methyl acetate	16.7	6.68	0.213
7	Anisole	14.2	4.33	0.136
8	Carbon tetrachloride	11.7	2.24	0.0051
9	Toluene	11.0	2.38	0.0348
10	Tetrahydrofuran	6.25	7.4	1.153
11	Diethyl ether	6.25	4.34	0.854

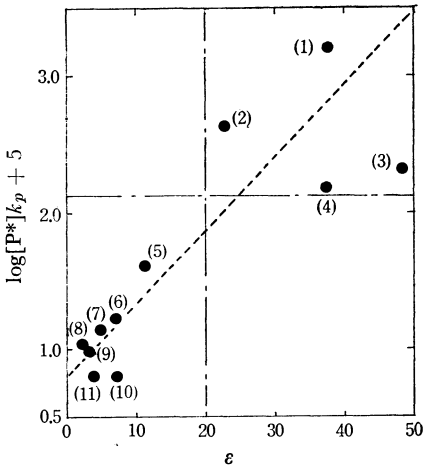

Fig. 6. Relation between log k_p[P*] and dielectric constant of solvents. The numbers of the solvent are the same as in Table 1.

In order to investigate the effect of the electric nature of the solvent on this polymerization, logk_p[P*] was plotted against K_D,[1] where K_D is the nucleophilic equilibrium constant of the solvent in the nucleophilic solvation to a deuterium atom of a methanol-d molecule (Fig. 7). Figure 7 shows

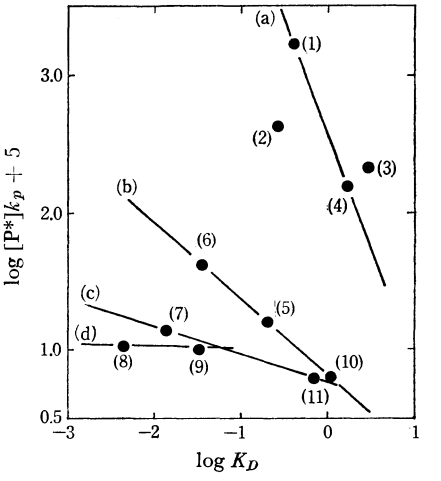

Fig. 7. Relation between log k_p[P*] and logK_D.
Solvents: (a) Acetonitrile and *N,N*-Dimethylacetamide, (ε; 36.6—37.5), (b) Ethylene dichloride, Methyl acetate and Tetrahydrofuran, (ε; 6.68—10.4), (c) Anisole and Diethyl ether, (ε; 4.33—4.34), (d) Carbon tetrachloride and Toluene, (ε; 2.24—2.38). The numbers of the solvent are the same as in Table 1.

that in solvents with similar dielectric constants ((a), (b), (c) and (d)), $k_p[P^*]$ decreased with an increase in the nuculeophilicity of the solvent. This fact indicates that the solvents coordinate competitively to the cationic end group of the polymer and that they depress the propagation rate. Moreover, from the fact that the slope of the straight line increases with an increase in the dielectric constant of the solvent, it is found that the dependency of $k_p[P^*]$ on the nucleophilicity of the solvent is larger in a solvent with high dielectric constant than in one with a low dielectric constant. As has been mentioned in the previous paper, the propagating species are considered to be the dissociated immonium ion and the undissociated immonium ion, which are in equilibrium in a solvent, and the polar solvent is considered to have a larger dissociation constant than the nonpolar solvent. Therefore, the higher dependency of the rate on the electron donability of the polar solvent than on that of the nonpolar solvent may indicate that the solvation of the solvent to the dissociated immonium ion is much larger than that to the undissociated immonium ion.

Mechanism of the Polymerization. From these experimental facts, the mechanism of the polymerization was postulated, with due consideration taken of the solvent effect.

Initiation:

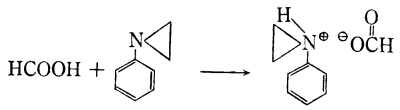

(1)

Propagation:

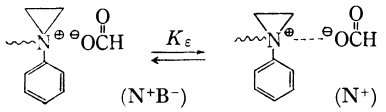

(2)

Propagation by the dissociated immonium ion:

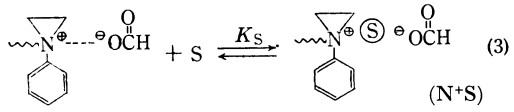

(3)

S: Solvent

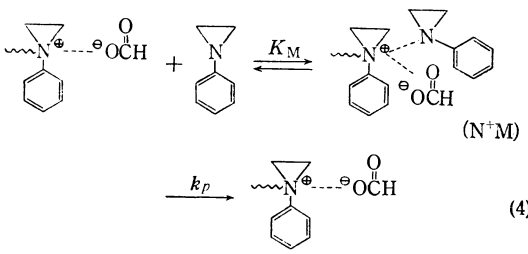

(4)

Propagation by the undissociated immonium ion:

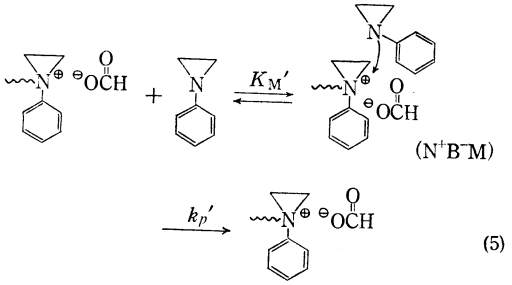

(5)

The initiation reaction is considered to be the reaction of formic acid with *N*-phenylethyleneimine to produce the compound (I). This compound dissociates partially to the immonium ion, and the reaction is in equilibrium. The equilibrium constant is considered to increase with an increase in the dielectric constant of the solvent. Equation (3) shows the solvation of the solvents to the dissociated immonium ion. Since the coordinations of solvents to both propagating species and methanol-d are nucleophilic reactions, the equilibrium constant (K_s) is considered to increase with an increase in K_D. From the facts that, in polar solvents, the propagation rates decrease with an increase in the electron donability of the solvent, propagation is considered to occur by means of a non-solvated immonium ion (Eq. (4)). On the other hand, since in nonpolar solvents, the propagation rate was constant independently of the kind of solvent, it is considered that the coordination of the solvent to the undissociated immonium ion is little, and that propagation occurs as is shown in Eq. (5).

Kinetics. On the basis of the mechanism postulated, the effect of the solvent on the rate of the polymerization (R_p) was quantitatively investigated. When the concentration of compound (I) is expressed by $\alpha[C]_0$, where $[C]_0$ is the initial concentration of the catalyst and whose α is the constant ($0<\alpha<1$), $\alpha[C]_0$ is expressed by Eq. (6):

$$\alpha[C]_0 = [N^+] + [N^+B^-] + [N^+S] + [N^+M] + [N^+B^-M] \quad (6)$$

On the other hand, from Eqs. (2), (3), (4) and (5), Eqs. (7), (8), (9) and (10) were obtained:

$$[N^+]/[N^+B^-] = K_\varepsilon \quad (7)$$

$$[N^+S]/([N^+][S]) = K_S \quad (8)$$

$$[N^+M]/([N^+][M]) = K_M \quad (9)$$

$$[N^+B^-M]/([N^+B^-][M]) = K'_M \quad (10)$$

By combining Eqs. (6), (7), (8), (9) and (10), the concentrations of (N^+B^-M) and (N^+M) are expressed in Eqs. (11) and (12) respectively:

$$[N^+B^-M] = \frac{\alpha[C]_0 K'_M[M]}{1 + K'_M[M] + K_\varepsilon(1+K_M[M] + K_S[S])} \quad (11)$$

$$[N^+M] = \frac{\alpha[C]_0 K_\varepsilon K_M[M]}{1 + K'_M[M] + K_\varepsilon(1+K_M[M] + K_S[S])} \quad (12)$$

The rate of the propagation is expressed in Eq. (13):

$$R_p = -\,\mathrm{d[M]}/\mathrm{d}t = k_p[\mathrm{N^+M}] + k'_p[\mathrm{N^+B^-M}] \quad (13)$$

By substituting Eqs. (11) and (12) into Eq. (13), Eq. (14) is derived:

$$R_p = \frac{(K\varepsilon K_\mathrm{M} k_p + K'_\mathrm{M} k'_p)\alpha[\mathrm{C}]_0}{1 + K'_\mathrm{M}[\mathrm{M}] + K\varepsilon(1+K_\mathrm{M}[\mathrm{M}] + K_\mathrm{S}[\mathrm{S}])}[\mathrm{M}] \quad (14)$$

Considering that K_M and K'_M are much smaller than unity, Eq. (14) may be expressed by Eq. (15):

$$-\mathrm{d[M]}/\mathrm{d}t \fallingdotseq \frac{(K\varepsilon K_\mathrm{M} k_p + K'_\mathrm{M} k'_p)\alpha[\mathrm{C}]_0}{1 + K\varepsilon(1+K_\mathrm{S}[\mathrm{S}])}[\mathrm{M}] \quad (15)$$

Equation (15) shows that the rate of the monomer consumption is expressed by a first-order rate equation with respect to the monomer concentration.

Since, in polar solvents, it is considered that propagation occurs mainly by the dissociated immonium ion, and that k_p is much larger than k_p', Eq. (14) may be expressed approximately by Eq. (16):

$$R_p \fallingdotseq \frac{K\varepsilon K_\mathrm{M} K_p \alpha[\mathrm{C}]_0}{1 + K'_\mathrm{M}[\mathrm{M}] + K\varepsilon(1+K_\mathrm{M}[\mathrm{M}] + K_\mathrm{S}[\mathrm{S}])} \quad (16)$$

By assuming $0 < K\varepsilon < 1$, Equation (16) explains the experimental facts that, in polar solvents, the polymerization rate increases with an increase in the $K\varepsilon$ value (that is, the dielectric constant of the solvent), and that, in a solvent with a similar dielectric constant, the rate decreases with an increase in the K_D (the nucleophilicity of the solvents). Moreover, it can be interpreted by Eq. (16) that the dependency of the rate on the electron donability of the solvent increases as the dielectric constant of the solvent increases. In nonpolar solvents, it is reasonable to consider that the terms of $K\varepsilon K_\mathrm{M} K_p$ and $K\varepsilon(1+K_\mathrm{M}[\mathrm{M}]+K_\mathrm{S}[\mathrm{S}])$ are negligible. Therefore, the rate equation with the use of the nonpolar solvents may be approximately expressed by Eq. (17):

$$R_p \fallingdotseq K'_\mathrm{M}\, k'_p\, \alpha[\mathrm{C}]_0[\mathrm{M}]/(1+K'_\mathrm{M}[\mathrm{M}]) \quad (17)$$

According to Eq. (17), we can explain the experimental finding that, in a nonpolar solvent, the nucleophilicity of the solvent has no effect on the polymerization rate.

BULLETIN OF THE CHEMICAL SOCIETY OF JAPAN VOL. 42 1098—1100 (1969)

Photochemistry of β-Acylacrylic Acids and Their Esters

Noboru SUGIYAMA, Hiroshi KATAOKA, Choji KASHIMA and Kazutoshi YAMADA

Department of Chemistry, Tokyo Kyoiku University, Otsuka, Tokyo

(Received August 23, 1968)

The irradiation of methyl *trans*-β-acetylacrylate (I-A) in methanol or acetone or without any solvent gave the *cis*-isomer (I-B). On the contrary, the irradiation of the free acid of I-A, *trans*-β-acetylacrylic acid (II-A), in methanol or without any solvent gave the angelica lactone, 5-methyl-5-hydroxy-2-oxo-2,5-dihydrofuran (II-C). The irradiation of *trans*-β-pivaloylacrylic acid (III-A) in methanol also afforded the angelica lactone, 5-*t*-butyl-5-hydroxy-2-oxo-2,5-dihydrofuran (III-C). The reaction route from a *cis*-isomer to an angelica lactone was explained in terms of the inductive effect.

In a previous report of this series[1] three isomeric forms of β-acylacrylic acid, the *trans* form, the *cis* form, and the angelica lactone form, were described. We also found that, on irradiation in ether, *trans*-β-benzoylacrylic acid was isomerized to the *cis* form, while in methanol the methanol addition product, β-benzoyl-α-methoxypropionic acid, was obtained.[2-4] Similarly, β-(*p*-toluoyl)-, β-(*p*-anisoyl)- and β-(*p*-bromobenzoyl)-acrylic acids were found to give the methanol adduct.[5] On the other hand, an angelica lactone was obtained as a by-product of the irradiation of β-(*p*-toluoyl)-acrylic acid. Therefore, three reactions are possible in the irradiation of β-aroylacrylic acids: *cis-trans* isomerization, methanol addition, and lactonization.

1) N. Sugiyama, T. Gasha, H. Kataoka and C. Kashima, This Bulletin, **41**, 971 (1968).

2) N. Sugiyama, H. Kataoka, C. Kashima and K. Yamada, *ibid.*, **41**, 2219 (1968).

3) N. Sugiyama, H. Kataoka, C. Kashima and K. Yamada, *ibid.*, submitted for publication.

4) D. V. Rao, V. Lamberti and H. M. Gardner, *Tetrahedron Letters*, **1968**, 1613.

5) Unpublished data.

It seemed of interest to examine the irradiation of methyl *trans*-β-acetylacrylate (I-A), *trans*-β-acetylacrylic acid (II-A), and *trans*-β-pivaloylacrylic acid (III-A).

Methyl *trans*-β-acetylacrylate (I-A) was irradiated in methanol by a high-pressure mercury lamp for 17 hr at room temperature. The structure of the product was determined to be methyl *cis*-β-acetylacrylate (I-B) as follows. New NMR signals observed as an AB quartet at τ 3.84 (J=12.0 c/s) can be assigned to the *cis* olefinic protons, while the two singlet signals at τ 6.27 and 7.72 represent ester methyl and acetyl methyl protons respectively. The yield of the *cis* isomer was 80%. In the reaction mixture, α-methoxylevulinate[6] was not detected.

Methyl *trans*-β-acetylacrylate (I-A) was also irradiated in a solid state and in an acetone solution under the same conditions as have been described above. In a solid state, I-A gradually turned to a liquid. The product in either a solid state or acetone was identified with its *cis*-isomer by means of the NMR spectra as well as by thin-layer chromatography. The yields were 64% in a solid state and 78% in acetone. When the solid state irradiation was continued for a week, no reaction proceeded except the formation of the *cis*-isomer in a yield of 90%.

The methanol solution of *trans*-β-acetylacrylic acid (II-A) was irradiated for 45 hr at room temperature. The photoproduct shows the carbonyl bands at 1760 and 1740 cm^{-1} in the IR spectrum. The NMR spectrum shows the singlet of methyl protons at τ 8.24 and two doublet signals of olefinic protons at τ 2.74 and 3.92 with a coupling constant of 6.0 c/s. These data suggest that the photoproduct is the angelica lactone of II-A, 5-methyl-5-hydroxy-2-oxo-2,5-dihydrofuran (II-C), which is also obtained from II-A by the treatment of thionyl chloride, followed by alkaline hydrolysis.[7]

The most conspicuous feature of NMR data is that the signals of the olefinic protons of methyl *cis*-β-acetylacrylate (I-B) appear in an AB quartet at τ 3.87 with a coupling constant 12.0 c/s, while that of methyl α-methoxylevulinate appears at τ 5.55 with a coupling constant of 6.0 c/s, while no signals of *cis*-isomer or of the methanol adduct are observed in this region. The yield of II-C was calculated for 60% based on the signal intensities of II-A and II-C at τ 3.40 and 3.92 respectively.

When the irradiation of II-A was continued for 115 hr, the yield of II-C reached 85%, while no other products were detected except II-A. This yield is reasonable because II-C is unstable, as has been reported by Scheffold,[7] and so about 15% of II-C might return to II-A.

When II-A was irradiated in a solid state, only II-C was obtained. The yield was 32%.

All the β-acylacrylic acids generally exist in the *trans* form at room temperature except for maleinaldehydic acid, which favors the angelica lactone form.[8] Considering the fact that methyl *trans*-β-acetylacrylate (I-A) is isomerized to the *cis* form I-B by the irradiation, the *trans* form of II-A is expected to isomerized first into *cis*-β-acetylacrylic acid (II-B). The *cis* acid II-B is expected to cyclize easily to the angelica lactone II-C, for the acid carbonyl is close to the acetyl carbonyl and the dissociated proton can attack acetyl carbonyl as is shown in Scheme 1.

If the acetyl group of II-A is replaced by the bulky pivaloyl group, the keto carbonyl group will be inaccessible to the carboxyl group because of the steric hindrance of the pivaloyl group. Thus, the irradiation of *trans*-β-pivaloylacrylic acid (III-A) was examined. A methanol solution of *trans*-β-pivaloylacrylic acid (III-A)[9] was irradiated for

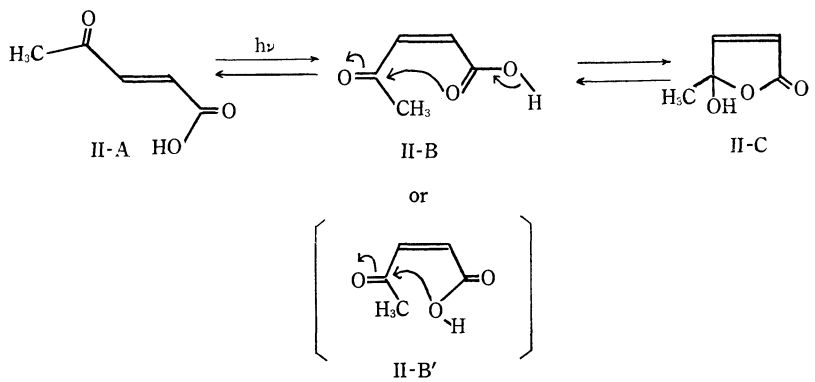

Scheme 1

6) L. Birkofer and R. Dutz, *Ann.*, **608**, 7 (1957).

7) R. Scheffold and P. Dubs, *Helv. chim. Acta*, **50**, 798 (1967).

8) N. Hellström and S. Gronowitz, *Kgl. Lantbruks-Högskol. Ann.*, **25**, 363 (1959). *Cf. Chem. Abstr.*, **54**, 9751f (1960).

9) N. Hellström, *Nature*, **187**, 146 (1960).

55 hr at room temperature. The photoproduct shows the singals characteristic of the angelica lactone, but no signals characteristic of the *cis* form, the methanol adduct, or the starting material, III-A. The angelica lactone III-C was obtained almost quantitatively. The structure of the angelica lactone, 5-*t*-butyl-5-hydroxy-2-oxo-2,5-dihydrofuran (III-C), was confirmed as follows. The IR spectrum shows the lactone carbonyl bands at 1765 and 1740 cm^{-1}, and the olefinic band at 1610 cm^{-1}. The UV spectrum shows the absorption maximum at 204 nm. In the NMR spectrum, the singlet signal of the *t*-butyl group appears at τ 8.96, and the singlet signal of the hydroxyl proton appears at τ 5.15. The two doublet signals at τ 2.62 and 3.84, which were assigned to olefinic protons (J= 6.0 c/s).

These results make it clear that the steric hindrance does not influence the cyclization step, and that the +I effect is more important. This conclusion is also consistent with the fact that β-adamantoylacrylic acid is cyclized to lactone by the irradiation.[10]

Experimental

Instrumentation. The IR and UV spectra were measured on a Hitachi EPI-2-type infrared spectrometer and a Hitachi EPS-3T-type recording spectrometer respectively.

The NMR spectra were recorded in deuterochloroform, with TMS as the internal standard with a Hitachi H-60-type high-resolution nuclear spectrometer.

A Taika 500 W high-pressure mercury lamp was used as the irradiation source, and a Pyrex tube was used as a filter and also as a reaction vessel.

Materials. *trans-β-Acetylacrylic acid* (*II-A*) was prepared by the method previously reported;[11] mp 125—126°C (lit. 126°C).[11]

Methyl trans-β-acetylacrylate (*I-A*) was prepared by the method of Pauly;[12] mp 58.5—60°C (lit. 60°C).[12]

trans-β-Pivaloylacrylic acid (*III-A*) was prepared by the method of Hellström;[9] mp 68—86°C (lit. 70—92°C).[9]

Irradiation of Methyl *trans*-β-Acetylacrylate (I-A). *A) In Methanol.* One hundred milligrams of methyl *trans*-β-acetylacrylate (I-A) were dissolved in 2 m*l* of methanol, after which the mixture was irradiated for 48 hr at room temperature. After the solvent had been removed methyl *cis*-β-acetylacrylate (I-B) was isolated by silica-gel column chromatography and eluted as a yellow oil with benzene. Yield, 80%.

IR (cm^{-1}, liq. film): 1730 (νC=O, ester), 1695 (νC=O, Ac), 1640 (νC=C), 1380, 900, 800 (δCH).

UV (λ_{max}, in EtOH): end absorption.

Found: C, 60.50; H, 7.70%. Calcd for $C_8H_{12}O_3$: C, 61.52; H, 7.75%.

The formation of the methanol adduct, methyl α-methoxylevulinate, was checked by comparing it with an authentic sample which had been synthesized from II-A by treatment with methanol in the presence of sulfuric acid.[6] Neither a study of the NMR spectra nor thin-layer chromatography could detect the adduct.

B) In Acetone. Fifty milligrams of I-A were dissolved in 1 m*l* of acetone, and the mixture was irradiated for 17 hr. Immediately after the solvent had been removed, the NMR spectrum was measured; the yield of I-B was 78%.

C) Without the Solvents. Fifty milligrams of I-A were dissolved in methanol; the solvent was then removed under reduced pressure, and I-A was fixed on the wall of the Pyrex tube. This solid-state I-A was irradiated for 17 hr at room temperature. The reaction mixture was dissolved in deuterochloroform and was measured on a NMR spectrum. I-B was produced in a 64% yield. When the irradiation continued for 1 week, the yield of I-B was raised to 90%.

Irradiation of *trans*-β-Acetylacrylic Acid (II-A). A methanol solution of *trans*-β-acetylacrylic acid (II-A) (500 mg/10 m*l*) was irradiated for 45 hr at room temperature. 5-Methyl-5-hydroxy-2-oxo-2,5-dihydrofuran (II-C) was then obtained as colorless needles from benzene - methanol (10 : 1). Mp 121—124°C (lit. 126°C);[7] yield, 60%. II-C was identified with an authentic sample.[7]

IR (cm^{-1}, KBr): 3500 (νOH), 1770, 1740 (νC=O, angelica lactone), 1650 (νC=C).

UV (λ_{max} nm(ε), in EtOH): 206 (28900).

NMR (τ, in $CDCl_3$): 2.74 (d, J=6.0 c/s, β-olefinic proton), 3.92 (d, J=6.0 c/s, α-olefinic proton), 4.42 (s, hydroxy proton), 8.24 (s, methyl).

When the irradiation was continued for 1 week, the yield of II-C was 85%, while when II-A was irradiated in the solid state for 112 hr, the yield of II-C was only 32%.

Irradiation of *trans*-β-Pivaloylacrylic Acid (III-A). Sixty milligrams of *trans*-β-pivaloylacrylic acid (III-A) were dissolved in 1 m*l* of methanol, after which the mixture was irradiated for 55 hr at room temperature. After removing the solvent, the residue was recrystallized from ether-benzene. 5-*t*-Butyl-5-hydroxy-2-oxo-2,5-dihydrofuran (III-C) was obtained almost quantitatively, as colorless needles; mp 72—74°C.

IR (cm^{-1}, KBr): 3380 (νOH), 1765, 1740 (νC=O, angelica lactone), 1610 (νC=C).

UV (λ_{max} nm(ε), in EtOH): 204 (18600)..

NMR (τ, in $CDCl_3$): 2.62 (d, J=6.0 c/s, β-olefinic proton), 3.84 (d, J=6.0 c/s, α-olefinic proton), 5.15 (broad s, OH), 8.96 (s, *t*-butyl).

Found: C, 60.52; H, 7.70%. Calcd for $C_8H_{12}O_3$: C, 61.52; H, 7.75%.

10) M. Kuchar, *Collection Czech. Chem. Commun.*, **33**, 880 (1968).

11) L. Wolff, *Ann.*, **264**, 246 (1891).

12) H. Pauly, R. Gilmour and G. Will, *ibid.*, **403**, 119 (1914).

BULLETIN OF THE CHEMICAL SOCIETY OF JAPAN VOL. 42 1101—1104 (1969)

Syntheses and Reactions of Functional Polymers. XLV. Synthesis and Properties of Poly(*N*-glycidyl-2-oxazolidone)

Takeshi ENDO, Ryozo NUMAZAWA and Makoto OKAWARA

Research Laboratory of Resources Utilization, Tokyo Institute of Technology, Meguro-ku, Tokyo

(Received August 24, 1968)

N-Glycidyl-2-oxazolidone was synthesized by the reaction of *N*-sodium-2-oxazolidone with epichlorohydrin. *N*-Glycidyl-2-oxazolidone was polymerized with such Lewis acids as boron trifluoride etherate and aluminum chloride to give a white powder. These polymers adsorbed phenol and methyl bromide effectively. In addition, the copolymerization of *N*-glycidyl-2-oxazolidone with styrene was carried out, and the amount of the adsorption of methyl bromide on the copolymers was measured. The amount of the adsorption of methyl bromide increased in the copolymers as the content of 2-oxazolidone moiety increased. A 1 : 1 molar complex of stannic chloride with *N*-glycidyl-2-oxazolidone was isolated; when the complex was heated, poly(*N*-glycidyl-2-oxazolidone) was obtained quantitatively.

It has been previously reported that poly(*N*-vinyl-5-methyl-2-oxazolidone) **I** formed complexes with phenol, halogen alkyls, and halogens.[1]

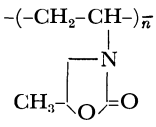

I

Further, we have reported that polyethyleneimine **II**[2] containing 2-oxazolidone moiety in the side chain and poly(*N*-acrylyl-2-oxazolidone)[3] **III** formed complexes with phenols and methyl bromide.

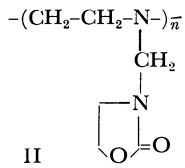

II

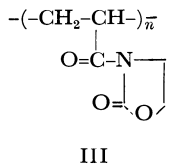

III

In the present investigation, we attempted to prepare a new type of polymer, poly (*N*-glycidyl-2-oxazolidone) **IV**, and to investigate its ability to form complexes with phenol and methyl bromide.

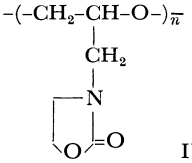

IV

Results and Discussion

Preparation of *N*-Glycidyl-2-oxazolidone (VI). The reactions of active hydrogen compounds with epichlorohydrin using a base[4] or an acid[5] as a catalyst have been reported. Here we tried to synthesize V by the reaction of 2-oxazolidone with epichlorohydrin in the presence of triethylamine, trimethylbenzylammonium chloride, or boron trifluoride etherate, and to prepare VI by treating V with a base. Neither V nor VI could be obtained by these procedures.

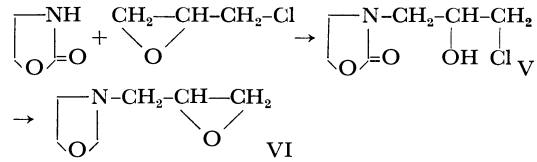

On the other hand, by the reaction of *N*-sodium-2-oxazolidone with epichlorohydrin, VI was obtained in a 41% yield. In this reaction, much residue was obtained, probably due to the polymerization during distillation.

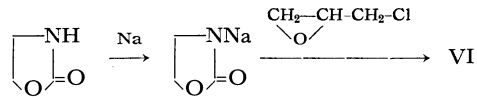

The residue was purified by the reprecipitation (adding benzene to a dimethylformamide (DMF) solution) and identified as poly(*N*-glycidyl-2-oxazolidone) by means of its IR spectrum. The

1) *Ind. & Eng. Chem.*, **52** No. 12 34A (1960); W. E. Walles and W. F. Tousignant, U. S. Pat. 2872321 (1959).

2) T. Endo and M. Okawara, *Makromol. Chem.*, **112**, 49 (1968).

3) T. Endo and M. Okawara Submitted.

4) N. B. Chapman, N. S. Isaacs and R. E. Parker, *J. Chem. Soc.*, **1959**, 1925.

5) L. Shechter, J. Wynstra and R. E. Kurkjy, *Ind. & Eng. Chem.*, **48**, 94 (1956); **49**, 1107 (1957).

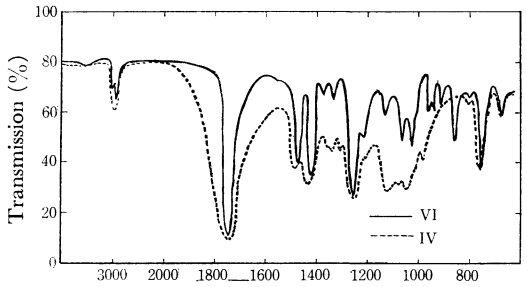

Fig. 1. IR spectra of *N*-glycidyl-2-oxazolidone (VI) and poly (*N*-glycidyl-2-oxazolidone) (IV).

conversion of 2-oxazolidone to VI amounted to 90%, when the polymer produced during distillation was added. VI was identified by an elementary analysis and by means of its IR spectrum. The IR spectrum of VI is shown in Fig. 1. The absorptions of the carbonyl group of cyclic urethane (1745 cm^{-1}) and epoxy ring (910, 850 cm^{-1}) were observed. The results of elementary analysis were in good agreement with the theoretical values.

Polymerization of *N*-Glycidyl-2-oxazolidone (VI). As indicated in Table 1, *N*-glycidyl-2-oxazolidone VI was polymerized at 70°C by such Lewis acids as boron trifluoride etherate and aluminum chloride to give a white powder. At low temperatures, however, VI formed stable complexes with Lewis acids and the polymerization did not proceed appreciably. Anionic catalysts, such as triethylamine and sodium methoxide, were also useless in polymerizing VI. The IR spectrum of IV showed the characteristic C=O absorption band at 1745 cm^{-1} and the absorption attributable to ether linkage (1070 cm^{-1}), as is shown in Fig. 1. On the other hand, the epoxy bands at 910 and 850 cm^{-1} in VI disappeared in the IV polymer. Furthermore, the results of the elementary analysis of IV were in good agreement with the theoretical values. IV was soluble in DMF, dimethyl sulfoxide (DMSO), and formic acid, but it was insoluble in common organic solvents, such as alcohols, ketones, and hydrocarbons. However, the IV polymer of a low molecular weight which was polymerized during distillation was soluble in alcohols and water.

TABLE 1. POLYMERIZATION OF *N*-GLYCIDYL-2-OXAZOLIDONE (VI)
(VI 1.5 g; solvent, dioxane 15 ml; temp., 70°C)

No.	Catalyst[1]	Time (hr)	Yield (%)	$[\eta]$[3]
1	BF_3OEt_2	14	9	0.44
2	BF_3OEt_2	46	33	0.50
3	$AlCl_3$	39	13	0.46
4	Et_3N[2]	46	0	
5	CH_3ONa	46	0	

1) 2 mol% for VI.
2) Triethylamine.
3) Intrinsic viscosity, measured at 30°C in DMF.

Preparation of the Complexes of 2-Oxazolidone-$SnCl_4$ and *N*-Glycidyl-2-oxazolidone (VI)-$SnCl_4$. When stannic chloride was added, drop by drop to a chloroform or methylene chloride solution of 2-oxazolidone at 0°C, a white precipitate was isolated. The structure of the precipitate was determined by means of a study of the IR spectrum and elementary analysis. The carbonyl absorption (1740 cm^{-1}) of 2-oxazolidone shifted to a lower energy region (1710 cm^{-1}). On the contrary, the absorption band due to the N–H linkage (3275 cm^{-1}) of 2-oxazolidone shifted to a high wave number (3420 cm^{-1}). These observations can be interpreted by assuming that the associated 2-oxazolidone changes to the monomeric structure as a result of the formation of a complex with stannic chloride:

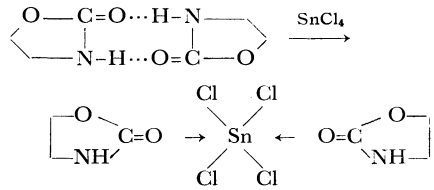

In a similar way, the VI-stannic chloride complex was isolated. The results of the elementary analysis and the IR spectral data of the complex of VI with stannic chloride are summarized in Table 2. The absorption bands due to both C=O and the epoxy ring shifted to lower wave numbers in the complex. From these data, it was concluded that a 1 : 1 molar complex VII of stannic chloride and VI in which two oxygen atoms of VI are coordinated to stannic chloride might be formed as is shown

TABLE 2. THE ELEMENTARY ANALYSES AND IR SPECTRA OF *N*-GLYCIDYL-2-OXAZOLIDONE (VI)-STANNIC CHLORIDE COMPLEX (VII)

	Elementary analyses (%) of VII			
	C	H	N	Cl
Calcd[1]	17.84	2.23	3.47	35.17
Found	17.75	2.30	3.50	35.59

	IR spectral changes (cm^{-1})	
	VI	Complex (XVII)
C=O	1745	1720
epoxy group	850	835

1) Calculated assumig 1 : 1 moar complex of stannic chloride with VI.

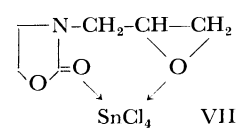

VII

below. When this complex was heated at 60°C for 2 hr, a viscous polymer, IV, was obtained as had been expected.

Copolymerization of *N*-Glycidyl-2-oxazolidone (VI) with Styrene. The copolymerization of *N*-glycidyl-2-oxazolidone with styrene was carried out in dioxane at 70°C using boron trifluoride etherate. The experimental date obtained are summarized in Table 3. The polymers obtained

Table 3. Copolymerization of *N*-glycidyl-2-oxazolidone (M_1) with styrene (M_2) (cat., BF_3OEt_2 2 mol%; temp., 80°C)

No.	$\frac{M_1}{M_1+M_2}\times 100$[1]	Time (hr)	Conversion(%)	N(%) in copolymer	$\frac{m_1}{m_1+m_2}\times 100$[2]
1	17	3.5	3.0	0.41	4.1
2	25	6.0	3.6	1.20	11.7
3	50	8.0	5.6	1.61	16.4
4	75	8.0	6.1	2.85	31.6
5	83	8.0	10.5	6.68	68.1

1) M_1, M_2=initial concentrations of the two monomers (mol).
2) m_1, m_2=concentrations of monomers in the copolymer (mol).

consisted of a white powder. The copolymer composition was determined from the nitrogen content. In the IR spectrum of copolymer, the absorptions of the carbonyl group of the 2-oxazolidone moiety (1745 cm^{-1}), the ether linkage (1070 cm^{-1}) and the phenyl group (1600 and 1490 cm^{-1}) were observed.

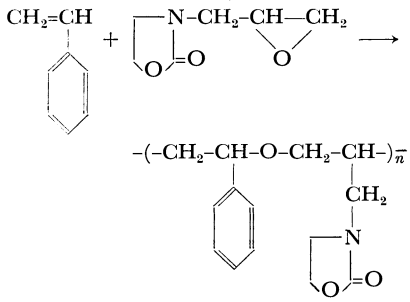

The copolymerization of cyclic ethers with vinyl compounds has been reported.[6]

Complex Formation of Poly(*N*-glydicyl-2-oxazolidone) IV with Phenol and Methyl Bromide. When an aqueous solution of IV with a low viscosity ($[\eta]=0.25$) was added to a phenolic aqueous solution, the complex of IV with phenol was precipitated as a white viscous form; it was then dried under reduced pressure. The amount of phenol in the complex, as determined by the bromide-bromate method, was 19.6 mol%. In the case of IV of a high viscosity ($[\eta]=0.44$,) which was insoluble in water, the polymer was suspended in a phenolic aqueous solution; the solution was then stirred at room temperature for 3 hr. The amount of phenol in the complex, as determined from the amount of decreased phenol in the solution, was 74 mol%. The carbonyl absorption (1745 cm^{-1}) of IV shifted to a lower wave number (1735 cm^{-1}) as a result of the formation of the complex with phenol. Therefore, the bonding force in the IV-phenol complex might be attributable to the hydrogen bonding between the C=O group of the 2-oxazolidone moiety and the hydrogen atom of phenol, as has been discussed before.[3]

In a previous paper,[3] it has been reported that the amount of the adsorption of methyl bromide on the copolymers of *N*-acrylyl-2-oxazolidone and styrene was measured, and that the amount of the adsorption of methyl bromide in the copolymers increased as the content of the 2-oxazolidone group increased. Further, it was suggested the bonding force of the complex formation of the polymers containing a 2-oxazolidone moiety with methyl bromide was the dipole-dipole interaction.

In the present paper, the amount of the adsorption of methyl bromide on the copolymers of *N*-glycidyl-2-oxazolidone VI and styrene was measured at room temperature and 1 atm. The amount of the adsorption of methyl bromide increased as the content of the 2-oxazolidone moiety in the copolymer increased, as is shown in Table 4. Therefore, it was apparent that 2-oxazolidone ring played an important role in the adsorption of methyl bromide on the copolymer.

Table 4. Adsorption of methyl bromide on the copolymer of *N*-glycidyl-2-oxazolidone (M_1) with styrene (M_2) (measured at room temp. and 1 atm)

No.	Copolymer (g)	$\frac{m_1}{m_1+m_2}\times 100$[1]	Values of adsorption Experimental (10^{-5} mol)	Theoretical (10^{-4} mol)
1	0.1	0	0	0
2	0.1	4.1	0.2	0.30
3	0.1	11.7	0.60	0.89
4	0.1	16.7	0.70	1.15
5	0.1	31.7	1.30	1.27
6	0.1	68.1	1.70	4.76
7	0.1	100	2.70	6.45

1) m_1, m_2=concentrations of monomers in the copolymer (mol).
2) Calculated assuming one mole methyl bromide combined with 2-oxazolidone unit mole.

Experimental

Materials. 2-Oxazolidone was prepared by a method reported previously.[3] The sodium dispersion

6) M. Mitoh and Y. Minoura, *Makromol. Chem.*, **110**, 197 (1967).

(content 40%; medium, toluene) was a commercial product (Kawaken Fine Chemicals Co.). The epichlorohydrin was dried on calcium hydride and distilled; bp 116—117°C. BF_3OEt_2, $SnCl_4$ and $AlCl_3$ of a reagent grade were used.

Measurements. The IR spectra and refractive indices were measured on Hitachi infrared EPI-S2 and Erma Abbe-refractometers, respectively.

Synthesis of *N*-Glycidyl-2-oxazolidone (VI). The sodium dispersion (20 g, 0.3 g atom) was stirred drop by drop, into a solution containing 22 g (0.25 mol) of 2-oxazolidone in 50 m*l* of benzene at room temperature. After the stirring had been continued for 5 hr at 40°C, epichlorohydrin (46.3 g 0.5 mol) in 50 m*l* of tetrahydrofuran was stirred drop by drop into this solution at 3—5°C. After the stirring had been continued for 5 hr at 60°C the solvents and the unreacted epichlorohydrin were evaporated and the residue was distilled under reduced pressure to obtain 14.6 g (41%) of VI. The VI was redistilled and analyzed bp 107—108°C/0.1 mmHg n_D^{21} 1.4478. Found: C, 49.82; H, 6.38; N, 9.72%. Calcd. for $C_6H_9O_3N$: C, 50.34; H, 6.34; N, 9.72%. The sizable residue obtained on distillation was dissolved in DMF and poured into benzene. The intrinsic viscosity of the polymer thus obtained was 0.25 in water at 30°C.

Polymerization of *N*-Glycidyl-2-oxazolidone (VI). The polymerization was carried out in sealed tubes at 80°C, using BF_3OEt_2 as the catalyst. After polymerization, the polymer was isolated by pouring the reaction mixture into an agitated acetone-water mixture (20 : 1) and the polymer thus precipitated was dried under reduced pressure.

Found: C, 49.70; H, 6.50; N, 9.70%. Calcd for $C_6H_9O_3N$: C, 50.34; H, 6.34; N, 9.79%. The intrinsic viscosity was measured at 30°C in DMF.

Copolymerization of *N*-Glycidyl-2-oxazolidone (VI) with Styrene. The copolymerization of *N*-glycidyl-2-oxazolidone with styrene was carried out in sealed tubes at 70°C, using BF_3OEt_2 as the catalyst. The copolymer was isolated by pouring the reaction mixture into a methanol-acetone mixture (4 : 1) containing a small amount of water. The white polymer thus precipitated was filtered and dried under reduced pressure. The copolymer compositions were determined by nitrogen analysis.

Preparation of 2-Oxazolidone-Stannic Chloride and *N*-Glycidyl-2-oxazolidone (VI)-Stannic Chloride Complexes. Stannic chloride (13 g, 0.05 mol) in 50 m*l* of chloroform was stirred, drop by drop, into a solution containing 3.5 g (0.04 mol) of 2-oxazolidone in 30 m*l* of chloroform at 0°C. The stirring was then continued for 30 min at 0°C. A white crystalline precipitate was isolated from the solution. After having been washed with chloroform five times, the precipitate was dried under reduced pressure to produce 13 g (93%) of the complex of 2-oxazolidone-stannic chloride, mp 145—146°C.

Found: C, 16.49; H, 2.35; N, 6.42; Cl, 31.53%. Calcd for $C_6H_{10}O_4N_2\ SnCl_4$: C, 16.75; H, 2.30; N, 6.44; Cl, 32.68%.

The VI-stannic chloride complex was prepared in a similar way. Stannic chloride (23.3 g, 0.84 mol) in 50 m*l* of chloroform was stirred drop by drop, into a solution containing 2 g (0.014 mol) of VI in 50 m*l* of chloroform at 0°C. The stirring had been continued for 30 min at 0°C, a white crystalline complex was isolated from the solution. After having been washed with chloroform five times, the complex was dried under reduced pressure to obtaine 5.1 g (90%) of VI-stannic chloride. The complex was heated for 2 hr at 65°C and then extracted with chloroform. After the chloroform had been evaporated, IV was obtained quantitatively. The polymer was dried *in vacuo*. The intrinsic viscosity of the polymer was 0.27 at 30°C in water.

Complex Formation of Poly(*N*-glycidyl-2-oxazolidone) (IV) with Phenol and Methyl Bromide. A solution containing 0.874 g of phenol in 20 m*l* of water was added, drop by drop, to a solution containing 0.05 g of IV ($[\eta]=0.25$) in 10 m*l* of water. A viscous precipitate was then isolated from the solution and dried under reduced pressure. The amount of phenol in the complex was determined by the bromide-bromate method. For a heterogeneous system, 0.1 g of IV ($[\eta]=0.44$) was suspended in a solution containing 0.437 g of phenol in 10 m*l* of water. The solution was then stirred for 3 hr at room temperature.

The amount of phenol in the complex was determined from the decrease in the amount of phenol in the solution.

BULLETIN OF THE CHEMICAL SOCIETY OF JAPAN VOL. 42 1105—1109 (1969)

The Reaction between Hydrocarbon and Hydrogen Cyanide in Silent Electrical Discharge. III.[1] The Reaction of Ethylene or Propylene with Hydrogen Cyanide*1

Kazuaki KAWAMOTO and Yoshiharu NISHIMURA*2

Institute of Commodities, Faculty of Economics, Kagawa University, Takamatsu

(Received August 31, 1968)

The present investigation was undertaken to find out whether or not the relative amounts of acrylonitrile obtained by the reaction between ethylene and hydrogen cyanide in a silent discharge are affected by the substances ($Hg(CN)_2$, Cu, CuCN, Al, Zn and Fe) placed in a glass filter of the special discharge tube, and to examine the possibility of the direct introduction of a cyano radical into propylene by means of the silent discharge. The yield of acrylonitrile depended upon the packing materials in the glass filter. When the discharge wall of the glass filter was filled with $Hg(CN)_2$, the yield of acrylonitrile was at its maximum. When a mixture of propylene and hydrogen cyanide was discharged in an ozonizer in the absence of air, the main liquid products were crotononitrile, methacrylonitrile, and *n*-propyl cyanide. Besides these compounds, the reaction products were confirmed to consist of isopropyl cyanide, acetonitrile, acrylonitrile, 4-methyl-1-pentene, 2,3-dimethylbutane, 1,5-hexadiene, 2-methylpentane, 1-hexene, *n*-hexane, and gaseous products. Judging from the relative concentration of each compound in the reaction products, it may be said that 2-methylvinyl, isopropenyl, propyl, allyl, isopropyl, and cyano radicals are the main intermediates in this reaction system.

In a preceding study,[1] it was found that when a mixture of ethylene and hydrogen cyanide was discharged in an ozonizer, acrylonitrile was obtained in one step. It has been reported by Suzuki[2] and Naito[3] that the formation of ozone is affected by the nature of substances forming the wall of discharge tube; in the case of the commercial processes, one side of the discharge tube is replaced with a wall of stainless steel or aluminum. Further, it has been found by Morinaga and Suzuki[4] that the ozone formation rate is affected by the materials (Soda glass, $2MgO/TiO_2$, TiO_2, $BaTiO_3$ and 95 $BaTiO_3/5SnO_2$) placed in a special-type discharge tube. However, when Sahasrabudhey and Deshpande[5] investigated the influence of wall catalysts on the production of formaldehyde by the interaction of carbon monoxide and hydrogen under the silent discharge, the reaction giving rise to formaldehyde was not affected by the surface catalysts employed.

The reaction of propylene and oxygen under a silent discharge has been investigated by Tsutsumi *et al.*[6] However, no detailed study of the interaction of propylene and hydrogen cyanide in the silent discharge has yet been reported.

The present study has been undertaken to discover how the type of discharge tube influences the reaction between ethylene and hydrogen cyanide; to establish, if possible, the most suitable conditions for the preparation of acrylonitrile, and furthermore, to find out whether or not the direct formation of such cyano-compounds as crotononitrile and methacrylonitrile results from the reaction of propylene and hydrogen cyanide in a silent discharge.

In the case of the reaction between ethylene and hydrogen cyanide, the experiments were carried out in discharge tubes filled with mercuric cyanide, copper, cuprous cyanide, aluminum, zinc, and reduced iron powders using a voltage of 15 kilovolts and a frequency of 60 cycles per second. Propylene and hydrogen cyanide were discharged in a Siemen ozonizer for 9 hr, using a voltage of

1) Part II: K. Kawamoto, This Bulletin, **41**, 2161 (1968).

*1 The major part of these research results were presented at the 19th Annual Meeting of the Chemical Society of Japan, Yokohama, April, 1966.

*2 Present address: Department of Chemistry, Faculty of Education, Kagawa University, Takamatsu.

2) M. Suzuki, *J. Electrochem. Soc. Japan*, **24**, 207 (1956).

3) T. Naito, "Ozonizer Handbook," Korona Co., Tokyo (1960), p. 246.

4) K. Morinaga and M. Suzuki, This Bulletin, **35**, 429 (1962).

5) R. H. Sahasrabudhey and S. M. Deshpande, *J. Indian Chem. Soc.*, **28**, 377 (1951).

6) N. Sonoda, K. Okumura, K. Tauchi and S. Tsutsumi, Preprints for the 19th Annual Meeting of the Chemical Society of Japan (1966), III, 483.

13.5 kilovolts.

Experimental

Materials. The ethylene and propylene used in this experiment showed no impurity in gas-chromatographic analysis. (Columns of activated charcoal, acetonylacetone, and dimethylsulfolane were used.) The hydrogen cyanide was prepared according to the procedure of Brauer.[7]

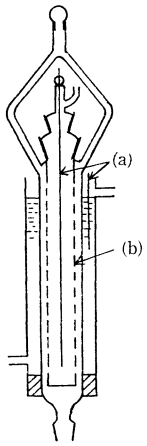

Fig. 1. Discharge tube used in the case of ethylene and hydrogen cyanide.
(a) Electrode (b) Glass filter

Discharge Tube. The discharge tube used for the formation of acrylonitrile is shown in Fig. 1. In this case, two kinds of discharge tubes were used. One was a Pyrex tube (A) with a glass filter (b) 30 cm in length and 2 cm in diameter, and with a space gap of 0.25 cm. The other was a Pyrex tube (B) with a glass filter (b) 10 cm in length and 2 cm in diameter, and with a space gap of 0.25 cm. In the case of propylene and hydrogen cyanide, the discharge tube employed was a Pyrex tube 45 cm in effective length, 4 cm in outside diameter, and with a space gap of 0.25 cm.

Packing. The materials placed in the glass filter in Fig. 1 were mercuric cyanide, copper, cuprous cyanide, aluminum, zinc, and reduced iron; they were used in the powder state.

Apparatus and Procedure. The apparatus employed in the reaction of ethylene and hydrogen cyanide was similar to that used in the passing method in a previous investigation,[8] except that the special tubes described above were used. The glass filter part of the discharge tube was filled with the powder of the packing materials. In the case of propylene, the apparatus was similar to that used in the passing method. These discharge tubes were then maintained at the operating temperature. A mixture of ethylene or propylene and hydrogen cyanide was passed through these discharge tubes at a constant velocity for the period of the reaction. Two moles of hydrogen cyanide were used in each experiment. A current of 60 cycles was sent through a voltage regulator, and the voltage was stepped up by a transformer (Capacity: 15 kV) to give the required value. The reaction products coming out of the discharge tubes were condensed by passing them through A condenser cooled with ice water, and then they were collected by being passed through two ice-cooled traps. The liquid products thus obtained were analyzed by the method described below, while the non-condensable gas was analyzed by gas chromatography at intervals of 30 min.

Identification and Analysis of the Reaction Products. The reaction products obtained by the reaction between ethylene and hydrogen cyanide were identified by the same method as was used in a previous paper.[1] In this case, the gaseous products were found to be hydrogen, ethane, acetylene, *n*-butane, 1-butene, 1,3-butadiene, methane, propane, and propylene.

The liquid products obtained by the reaction between propylene and hydrogen cyanide were identified by comparing their retention times on a gas chromatogram with those of authentic samples.*3 (Tricresyl phosphate, PEG-6000 and silicone DC 550 columns were used for the cyano compounds listed in Table 4, while squalane, β,β'-oxydipropionitrile, tricresyl phosphate and dimethylsulfolane columns were used for the liquid hydrocarbon products.) In addition, the reaction products were fractionally distilled in the presence of a small amount of hydroquinone; the constituents of the fraction were identified by observing the formation of the derivative described below and the infrared absorption.

The fraction boiling at 86—91°C was confirmed to consist mainly of methacrylonitrile by transforming it into the *N-t*-butylmethacrylamide,*4 mp 57—58°C. A mixed-melting-point determination with an authentic sample showed no depression. The infrared spectrum of this fraction agreed with that of the authentic methacrylonitrile.

The crotononitrile and *n*-propyl cyanide were obtained in a fraction boiling at 115—120°C. Upon gas-chromatographic analysis, this fraction showed the same retention time as that of authentic crotononitrile and that of authentic *n*-propyl cyanide.

No allyl cyanide was detected in the reaction products of any experiments. The gas chromatogram (columns: PEG-6000 and tricresyl phosphate) of the liquid products presented three peaks behind the peak of crotononitrile.

7) G. Brauer, "Handbuch der Präparativen Anorganischen Chemie," Ferdinand Enke Verlag, Stuttgart (1954), p. 500.

8) K. Kawamoto, N. Sonoda and S. Tsutsumi, This Bulletin, **41**, 1376 (1968).

*3 The authentic samples were prepared as follows. The crotononitrile (bp 118—119°C, n_D^{20} 1.4221) was prepared by the reaction of crotonamide (mp 158—159°C) and phosphorus pentoxide. The methacrylonitrile (bp 90—91°C, n_D^{25} 1.3979) was prepared from methacrylamide by means of the procedure of Mowry and Morner (D. T. Mowry and R. R. Morner, *J. Am. Chem. Soc.*, **69**, 1831 (1947)). Further, the following commercial chemicals were used for identification; *n*-propyl cyanide, isopropyl cyanide, acetonitrile, acrylonitrile, 4-methyl-1-pentene, 2,3-dimethylbutane, 1,5-hexadiene, 2-methylpentane, 1-hexene, and *n*-hexane.

*4 *N-t*-Butylmethacrylamide was prepared by the method of Plaut and Ritter (H. Plaut and J. J. Ritter, *J. Am. Chem. Soc.*, **73**, 4076 (1951).

From their retention times, hexyl cyanides seem to be present in the unidentified products*5 listed in Table 4. The quantitative analysis of the liquid products in this experiment was performed by gas chromatography.

The gaseous products, when analyzed by gas chromatography, were found to consist of hydrogen, propane, methylacetylene, allene, ethane, ethylene, acetylene, and methane. (Columns of activated charcoal, tricresyl phosphate, dimethylsulfolane, and acetonylacetone were used.) The gaseous products could not be determined quantitatively.

Results and Discussion

The results obtained by the reaction of ethylene and hydrogen cyanide under the conditions described in Table 1 are summarized in Table 2. Further, the results obtained by running propylene with hydrogen cyanide only once in an ozonizer under the conditions listed in Table 3 are summarized in Table 4. The compositions of the reaction products given in these tables are re-

Table 1. The reaction between ethylene and hydrogen cyanide in silent electrical discharge (Experimental conditions)

Experiment No.	1	2	3	4	5	6	7	8	9	10	11
Type of discharge tube*1	A	B	B	A	B	B	A	A	A	A	Siemen*3
Packing Sort	$Hg(CN)_2$	$Hg(CN)_2$	$Hg(CN)_2$	Cu	CuCN	CuCN	Al	Al	Zn	Fe*2	—
Packing Weight (g)	80	20	10	80	20	10	50	50	80	80	—
Ethylene used (*l*)	22.75	27.41	27.78	22.01	27.63	27.49	21.90	22.56	22.05	21.28	27.63
Velocity (*l*/hr)	2.84	3.05	3.09	2.75	3.07	3.05	2.74	2.82	2.76	2.66	3.08
Discharge time (hr)	8	9	9	8	9	9	8	8	8	8	9
Second. voltage (kV)	15	15	15	15	15	15	15	15	15	15	15
Second. current (mA)	3.6	2.0	1.9	1.9	1.2	1.1	3.8	3.2	1.4	1.5	2.1
Temp. of discharge tube											
Inside (°C)	—	—	—	—	—	—	—	—	—	—	10—26
Outside (°C)	10	7	11—21	25—53	18—25	9	12	27—51	15	18	10

*1 Type A was a Pyrex tube with a glass filter which had 30 cm in length and 2 cm in diameter, and Type B was a Pyrex tube with the glass filter which had 10 cm in length and 2 cm in diameter.
*2 Reduced iron as packing material was used.
*3 This column shows the result obtained by using the Siemen tube.

Table 2. The reaction between ethylene and hydrogen cyanide in silent electrical discharge (Experimental results)

Experiment No.	1	2	3	4	5	6	7	8	9	10	11
Liquid product collected (g)	27.69	30.97	30.54	27.92	14.26	22.18	25.45	18.46	25.76	34.19	34.09
Reaction product (g)	0.92	0.62	0.37	0.66	0.04	0.02	0.70	0.79	0.40	0.45	6.47
Conversion efficiency*1 (%)	3.2	1.8	1.1	2.4	0.1	0.06	2.6	2.8	1.4	1.7	18.7
Composition of liquid reaction products*2											
Acrylonitrile (%)	72.0	84.3	95.0	71.9	76.3	83.4	71.1	57.7	57.4	68.0	45.9
Ethyl cyanide (%)	11.6	7.7	4.6	7.5	0	0	10.3	12.0	22.7	10.0	12.9
n-Butyl cyanide (%)	2.7	T	T	8.7	0	0	7.8	14.8	7.6	11.3	17.1
s-Butyl cyanide (%)	1.7	0	0	4.2	0	0	3.8	6.6	3.8	5.7	10.2
n-Propyl cyanide (%)	0.6	0	0	2.0	0	0	1.8	2.5	1.5	1.6	2.9
Isopropyl cyanide (%)	0.4	0	0	1.4	0	0	1.1	2.0	1.2	1.0	2.0
n-Hexyl cyanide (%)	0	0	0	T	0	0	T	T	T	T	T
n-Amyl cyanide (%)	0	0	0	0	0	0	0	0	0	0	T
Isoamyl cyanide (%)	0	0	0	0	0	0	0	0	0	0	T
Unidentified product (%)	11.0	8.0	0.4	4.3	23.7	16.6	4.1	4.4	5.8	2.4	9.0

*1 The conversion efficiency was given by (grams of reaction product per grams of ethylene used) $\times 100$.
*2 The yields of each compound produced were given by (grams of each compound per grams of total reaction product) $\times 100$.
T: Trace

*5 The unidentified products, when analyzed by the procedure of Soloway and Lipschitz were observed to consist of the nitriles (S. Soloway and A. Lipschitz, *Anal. Chem.*, **24**, 898 (1952).).

TABLE 3. THE REACTION BETWEEN PROPYLENE AND HYDROGEN CYANIDE IN SILENT ELECTRICAL DISCHARGE (Experimental conditions)

Experiment No.	1	2	3
Propylene used (*l*)	22.40	22.50	22.67
Velocity (*l*/hr)	2.49	2.50	2.52
Discharge time (hr)	9	9	9
Second. voltage (kV)	13.5	13.5	13.5
Second. current (mA)	1.8	2.0	2.0
Temp. of discharge tube			
Inside (°C)	24—35	20—65	50—62
Outside (°C)	24	20—59	50—53

TABLE 4. THE REACTION BETWEEN PROPYLENE AND HYDROGEN CYANIDE IN SILENT ELECTRICAL DISCHARGE (Experimental results)

Experiment No.		1	2	3
Liquid product collected	(g)	34.01	33.30	32.60
Reaction product	(g)	5.13	6.79	6.64
Conversion efficiency	(%)	12.2	16.1	15.6
Composition of liquid reaction products				
Crotononitrile	(%)	23.5	18.5	17.8
Methacrylonitrile	(%)	20.9	16.7	15.6
n-Propyl cyanide	(%)	10.0	13.4	13.1
Isopropyl cyanide	(%)	3.2	3.1	3.2
Acetonitrile	(%)	3.4	4.1	5.6
Acrylonitrile	(%)	2.6	2.4	2.7
4-Methyl-1-pentene	(%)	1.2	1.3	1.3
2,3-Dimethylbutane	(%)	0.9	1.0	1.0
1,5-Hexadiene	(%)	0.4	0.4	0.4
2-Methylpentane	(%)	0.2	0.2	0.2
1-Hexene	(%)	0.3	0.3	0.3
n-Hexane	(%)	0.2	0.2	0.3
Unidentified product	(%)	33.2	38.4	38.5

producible within 1 per cet. In both ethylene and propylene, the presence of even a small quantity of air formed a solid brown deposit on the discharge wall. Therefore, the air was completely removed from the reaction system.

Influence of the Discharge Tube on the Reaction between Ethylene and Hydrogen Cyanide. The special discharge tube shown in Fig. 1 was used for the purpose of investigating the effects of the discharge wall on the formation of acrylonitrile.

It was reported by Galvin and Pritchard[9] that, when a stream of nitrogen containing a hydrocarbon RH was passed over solid mercuric cyanide heated at 350°C, hydrogen cyanide, cyanogen, and the corresponding nitrile RCN were obtained, and that when unsaturated hydrocarbons were used the addition products were found (*i. e.*, ethylene gave ethyl cyanide and succinonitrile). Further, they also found that silver cyanide and cupric cyanide behaved analogously. Thus, in this experiment mercuric cyanide and cuprous cyanide were placed in the glass filter of the discharge tube.

As may be seen from Table 2, there are differences between the special tube and the Siemen tube. It has been found that when the Siemen tube is used the yield of the liquid product increases, and that when one side of discharge tube is replaced by a wall of the glass filter filled with mercuric cyanide, copper, cuprous cyanide, aluminum, zinc and reduced iron, the yield of the liquid products decreases, while the proportion of acrylonitrile in the liquid products increases. In the case of the special tube filled with mercuric cyanide, the yield of liquid product was at its maximum. Thus, it may be said that the use of mercuric cyanide as packing material favors the formation of acrylonitrile.

As may be seen from Experiment Nos. 1, 2, and 3 in Table 2, the yield of the reaction product depends upon the quantity of packing material used (namely, the effective length of the discharge tube); it has been found that increasing the packing material increases the yields of the liquid products and the gaseous products, while it decreases the proportion of acrylonitrile in the liquid products.

When ethylene alone was discharged in the special tube filled with mercuric cyanide, the component of the gaseous products was similar to that of the gaseous products obtained by the reaction between ethylene and hydrogen cyanide. Further, in the case of ethylene alone, a solid brown deposit was formed on the glass wall, while no liquid product was formed.

The Reaction between Propylene and Hydrogen Cyanide. When a mixture of propylene and hydrogen cyanide was allowed to react in the silent discharge, a large number of compounds (summarized in Table 4) were obtained. However, the formation of allyl cyanide, dicyano-compounds, and isocyano-compounds could not be observed by gas-chromatographic analysis.

As may be seen from Experiment Nos. 1 and 3 in Table 4, the conversion efficiency (grams of reaction product/grams of propylene used $\times$ 100) depends upon the temperature at which the discharge is carried out; it has been found that the yields of the liquid products and the gaseous products increase with a rise in the discharge temperature, and that in the case of a high-temperature discharge, the proportion of unsaturated nitriles, such as crotononitrile and methacrylonitrile, in the liquid products decreases, while the yield of the high-boiling-point compounds (the unidentified products listed in Table 4) increases. Accordingly, it may be said that a low temperature favors the formation of the directly-introduced

9) J. P. Galvin and H. O. Pritchard, *J. Phys. Chem.*, **68**, 1035 (1964).

cyano compounds.

Addition products, such as *n*-propyl cyanide and isopropyl cyanide, were also formed. In this case, the yield of *n*-propyl cyanide was higher than that of isopropyl cyanide. Therefore, the addition followed a non-Markownikoff rule. This rule was observed in both the radiation-induced addition of hydrogen sulfide to propylene[10] and the photochemical addition of hydrogen sulfide or hydrogen bromide to propylene.[11,12] The nature of the discharge-induced addition appears to be similar to that of these additions.

The Mechanism of the Formation of the Main Products Obtained by the Reaction of Propylene and Hydrogen Cyanide. The formation of the main products obtained by the reaction of propylene with hydrogen cyanide in a silent discharge may be represented as follows: The first step is the excitation of the propylene molecule and the hydrogen cyanide molecule by electron impact,*6 while the second step consists of both (1) the reaction of the excited propylene molecule with a normal propylene molecule to give 2-methylvinyl, isopropenyl, allyl, propyl, and isopropyl radicals*7 (two molecular processes*8), and (2) the decomposition of the excited propylene or hydrogen cyanide to give 2-methylvinyl, isopropenyl, allyl, and cyano radicals and the hydrogen atom.*9

The cyano compounds, such as crotononitrile, methacrylonitrile, and *n*-propyl cyanide, may be formed by the combination*10 of these radicals and the cyano radical thus obtained. Crotononitrile and methacrylonitrile were obtained in yields comparable with that of *n*-propyl cyanide. This observation indicates that 2-methylvinyl and isopropenyl radicals are fairly much involved in this reaction system. Since the yield of *n*-propyl cyanide is higher than that of isopropyl cyanide, an alternative mechanism for the formation of *n*-propyl cyanide may be the addition of a cyano radical to the terminal carbon atom of propylene, followed by the addition of a hydrogen atom to the CH_3-$\dot{C}HCH_2CN$ radical so formed.*11 The formation of allyl cyanide was not observed, presumably because of the isomerization of allyl cyanide to crotononitrile.

The dimeric products, such as 4-methyl-1-pentene, 2,3-dimethylbutane, 2-methylpentane, 1,5-hexadiene, 1-hexene, and *n*-hexane, may be formed by coupling reactions between propyl, isopropyl, and allyl radicals. For instance, the occurrence of 2,3-dimethylbutane can be explained by a combination of two isopropyl radicals.

The formation of acetonitrile and acrylonitrile may be represented as follows. The methyl radical and the vinyl radical may be formed through the bond fission of the excited propylene molecule, and acetonitrile and acrylonitrile may be obtained by combination between these radicals and the cyano radical.

The authors wish to thank Professor S. Tsutsumi of Osaka University for his kind advice.

10) K. Sugimoto, W. Ando and S. Oae, This Bulletin, **37**, 365 (1964).

11) W. E. Vaughan and F. F. Rust, *J. Org. Chem.*, **7**, 472 (1942).

12) W. E. Vaughan, F. F. Rust and T. W. Evans, *ibid.*, **7**, 477 (1942).

*6 Although ion-molecular process are possible in some electron impact reactions, in the present case this process does not seem to be a main path, judging from the results reported by Devins *et al.*, Egloff *et al.*, and Inoue. The present reaction is presumed to be mostly a radical reaction (J. C. Devins and M. Burton, *J. Am. Chem. Soc.*, **76**, 2618 (1954); C. L. Thomas, G. Egloff and J. C. Morell, *Chem. Revs.*, **28**, 1 (1941); E. Inoue, *Bull. Tokyo Inst. Technol., Series A*, **1957**, No. 2, p. 1.).

*7 $CH_2{=}CH{-}CH_3 + e^* \longrightarrow C_3H_6^* + e$

$C_3H_6^* + CH_2{=}CH{-}CH_3 \longrightarrow$

$\left\{\begin{array}{l}\dot{C}H{=}CH{-}CH_3\\ CH_2{=}\dot{C}{-}CH_3\\ CH_2{=}CH{-}CH_2\bullet\end{array}\right. + \left\{\begin{array}{l}CH_3{-}CH_2{-}CH_2\bullet\\ CH_3{-}\dot{C}H{-}CH_3\end{array}\right.$

*8 Tsutsumi reported that when ethylene was discharged, the vinyl radical and the ethyl radical were produced by two molecular processes (S. Tsutsumi, *Chem. Ind.* (*Kagaku Kogyo*), **16**, 623 (1965).).

*9 $HCN + e^* \longrightarrow HCN^* + e \longrightarrow \bullet H + \bullet CN$

$C_3H_6^* \longrightarrow \left\{\begin{array}{l}\dot{C}H{=}CH{-}CH_3\\ CH_2{=}\dot{C}{-}CH_3 + \bullet H\\ CH_2{=}CH{-}CH_2\bullet\end{array}\right.$

*10 For instance, crotononitrile and methacrylonitrile were formed as follows:

$\dot{C}H{=}CH{-}CH_3 + \bullet CN \longrightarrow CH_3CH{=}CHCN$

$CH_2{=}\dot{C}{-}CH_3 + \bullet CN \longrightarrow CH_3C(CN){=}CH_2$

*11 It was reported by Moore that when the mercury-photosensitized hydrogenation of propylene was carried out over a range of temperatures from 30 to 200°C, a hydrogen atom added preferentially to the terminal carbon atom of propylene to form the isopropyl radical (W. J. Moore, *J. Chem. Phys.*, **16**, 916 (1948).). Therefore, if a hydrogen atom is first added to propylene, the radical thus produced will yield a large quantity of isopropyl cyanide.

BULLETIN OF THE CHEMICAL SOCIETY OF JAPAN VOL. 42 1110—1112 (1969)

The α Effect. Aminolysis on a Saturated Carbon Atom*1

Shigeru OAE, Yoshihito KADOMA and Yumihiko YANO

Department of Applied Chemistry, Faculty of Engineering, Osaka City University, Sugimoto-cho, Sumiyoshi-ku, Osaka

(Received August 31, 1968)

The rates of aminolyses of methyl, isopropyl, allyl and benzyl iodides have been determined in acetonitrile. Bases used were hydrazine, morpholine, imidazole and piperidine. The rates of all the aminolysis reactions can be correlated nicely with the basicities. Hydrazine also did not show any positive deviation from the Brønsted plots. This fact suggests that the α-effect is not operative in these displacement reactions on the saturated carbon atom.

In a number of bimolecular nucleophilic reactions, various nucleophiles having unshared electron pairs adjacent to the nucleophilic center-atom show much higher reactivities than those anticipated from their basicities. These high reactivities are generally estimated from large positive deviations from the Brønsted plots and are ascribed to so called α-effect.[1] As Bruice *et al.* pointed out,[2] several possible explanations concerning the α-effect have been proposed. However, no satisfactory one has been presented; nor do we have sufficient data to draw any conclusion as to the origin of the α-effect.

One of the attractive approach to this problem is to focus the attention on the relation between the α-effect and the nature of the hybridization of the carbon atom of the reaction center, *i. e.*, sp, sp^2 and sp^3. Concerning the sp and sp^2 hybridized carbon atoms, relatively large amounts of works have been carried out and large α-effects have been observed with both nonionic[3] and ionic[1b,4] nucleophiles. But in the S_N2 reactions on the sp^3 hybridized carbon atom only two data are available, the one is the reaction of benzyl bromide with hydroperoxide anion and hydroxide anion[5] (ionic nucleophiles) and the other is the aminolysis of methyl iodide in water[3a] (nonionic nucleophiles). In either reaction, α-effects were rather small or negligible. From these investigations,[1b,3a,3c,4,5] it appears that the magnitude of the α-effect seems to depend generally on the character of the reacting site of substrate, and falls in the following order.

$$sp > sp^2 > sp^3 \text{ carbon.}$$

In general, rates of nucleophilic reaction on the sp and sp^2 carbon atoms such as nitrile[4] and carbonyl are mainly controlled by basicity rather than polarizability of the nucleophile used, while, in the case of the sp^3 carbon atom, polarizability is the more important factor than basicity. Apparently the higher the demand for stronger basicity, the larger α-effect is observed in the case with the sp and sp^2 carbon atoms whereas in the substitution reaction on the sp^3 carbon atom, the reaction requiring higher polarizable nucleophile would display a larger α-effect. Incidentally, α-effect, though small, was reported in the reaction of benzyl bromide with hydroperoxide anion in 50% acetone-water,[5] while, no α-effect was observed in the aminolysis reaction of methyl iodide in water.[3a] The former case is different from the latter one in that in the former reaction the nucleophile is ionic while π electrons of phenyl ring can delocalize to the reaction center in the transition state and hence the whole system is quite susceptible to polarizability.

The present work was initiated in order to examine the effect of the structural change of the substrates, in the aminolyses of methyl, isopropyl, allyl and benzyl iodides in acetonitrile.

Results and Discussion

The substrates examined were unfortunately very sparingly soluble in water, however, pK_a's of these

*1 Paper VIII on "Relative Reactivities of Organic Halides in Displacement Reactions."

1) a) J. O. Edwards and R. G. Pearson, *J. Am. Chem. Soc.*, **84**, 16 (1962). b) W. P. Jencks and J. Carriuolo, *ibid.*, **82**, 1778 (1960). c) S. L. Johnson in "Advances in Physical Organic Chemistry," Nol. 5, V. Gold ed., Academic Press Inc., New York, N. Y. (1967), p. 284.

2) a) T. C. Bruice, A. Donzel, R. W. Huffman and A. R. Butler, *J. Am. Chem. Soc.*, **89**, 2106 (1967). b) M. J. Gregory and T. C. Bruice, *ibid.*, **89**, 2327 (1967).

3) a) M. J. Gregory and T. C. Bruice, *ibid.*, **89**, 4400 (1967). b) T. C. Bruice and S. J. Benkovic, *ibid.*, **86**, 418 (1964). c) W. P. Jencks, *ibid.*, **80**, 4585 (1958).

4) K. B. Wiberg, *ibid.*, **77**, 2519 (1955).

5) R. G. Pearson and D. N. Edgington, *ibid.*, **84**, 4607 (1962).

Table 1. The rate constants k_2 (l mol^{-1} sec^{-1}) of aminolysis in acetonitrile

Amines	Substrates				
	CH_3I[a,c]	i-C_3H_7I[a,d]	CH_2=$CHCH_2I$[a,e]	$C_6H_5CH_2I$[b,f]	pK_a'[m]
Imidazole[g]	1.86×10^{-3}	1.17×10^{-5}	2.64×10^{-3}	3.41×10^{-3}	13.8[n]
Hydrazine[h]	4.43×10^{-2}	1.97×10^{-4}	1.33×10^{-1}	1.47×10^{-1}	16.61
Morpholine[i]	1.17×10^{-1}	1.32×10^{-4}	3.17×10^{-1}		16.61
Piperidine[j]	6.81×10^{-1}	7.73×10^{-4}	3.53	1.72	18.92
Hydroxylamine[k]				3.88×10^{-3}	
Benzylamine[l]				6.00×10^{-2}	16.76

a) Reaction was carried out at 40°C.
b) Reaction was carried out at 30°C.
c) 1.86×10^{-4}—6.08×10^{-5} mol/l.
d) 1.19×10^{-1}—1.12×10^{-2} mol/l.
e) 6.89×10^{-5} mol/l.
f) $(1.96$—$3.99)\times10^{-4}$ mol/l.
g) 3.86×10^{-1}—1.12×10^{-3} mol/l.
h) 1.35×10^{-1}—7.86×10^{-4} mol/l.
i) 9.85×10^{-2}—4.43×10^{-4} mol/l.
j) 5.80×10^{-2}—1.47×10^{-4} mol/l.
k) 1.65×10^{-3} mol/l.
l) 1.48×10^{-3} mol/l.
m) Ref. 6.
n) Ref. 3a.

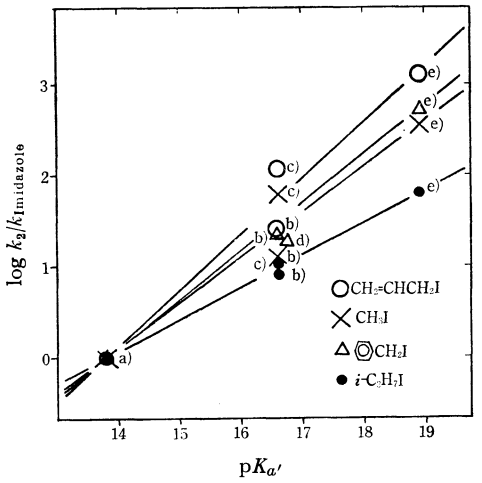

Fig. 1. Bronsted plots.
a) Imidadzole. b) Hydrazine. c) Morpholine. d) Benzylamine. e) Piperdine.

amines in acetonitrile[6] are available. Therefore we chose anhydrous acetonitrile as the solvent. The results are shown in Table 1. In all the cases fairly good correlations of logarithms of the rate constants on the pK_a's of the nucleophiles were observed, and no positive deviations from the Brϕnsted plots were observed, (Fig. 1). From the slopes, α values, the Brϕnsted parameter, were obtained and are listed in Table 2.

The α values obtained in the aminolysis reactions varied from 0.36 to 0.60. This means that the transition states of these reactions cover a certain range of spectrum from near S_N1 to S_N2.[7] The α value

Table 2. α-Values of the aminolysis reactions in acetonitrile

Substrates	α-Value	°C
Allyl iodide	0.60	40
Benzyl iodide	0.55	30
Methyl iodide	0.50	40
Isopropyl iodide	0.36	40
p-Nitrophenyl acetate[a]	0.54	30

a) See Ref. 3a.

of 0.60 in the aminolysis reaction of allyl iodide suggests that the bond forming step is the rate limiting, while α value of 0.36 of isopropyl iodide suggests the importance of bond breaking step.

It is commonly believed that the α-effect is associated with displacement reactions which are highly dependent on the basicity of the nucleophile. It would suggests then that α-effect would appear in the aminolysis reaction of allyl iodide. However, it was not the case. The aminolyses of isopropyl, methyl and benzyl iodides also showed no positive deviations from the Brϕnsted plots. As can be seen in Table 2, α values of p-nitrophenyl acetate and benzyl iodide are almost comparable and yet a large α-effect is observed in the reaction with the former compound and not with the latter.

Both benzyl and allyl iodides are considered to develop a substantial sp^2 character at the reacting center in the transition states. The lack of α-effect for these compounds may be due to the high electron delocalizations with π electrons at the transition state to kill the partial sp^2 character of the reaction center.

Experimental

Preparation of Materials. All the amines were purified according to Coetzee and Padmanabhan's

6) J. F. Coetzee and G. R. Padmanabhan, *J. Am. Chem. Soc.*, **87**, 5005 (1965).
7) R. F. Hudson and R. J. Withey, *J. Chem. Soc.*, **1964**, 3513.

method.[6] Methyl iodide was purified by fractional distillation from the commercial product, bp 42.4°C. Benzyl iodide (mp 24.1°C) and allyl iodide (bp 102.5°C) were prepared from the corresponding chlorides by halogen exchange reaction in acetone.[8] Isopropyl iodide was prepared according to Stone and Shechter's method,[9] bp 89.3°C. Commercial acetonitrile was dried over calcium chloride, and then refluxed three times over phosphorus pentoxide, then distilled into freshly fused potassium carbonate, after drying, it was finally fractionally distilled,[10] and the center-cut fraction was used, bp 81.6°C.

Kinetic Measurement. The reactions were followed by the UV spectrophotometry using the absorption of iodide ion at 246 mμ ($\varepsilon=1.38\times10^4$), except for benzyl iodide, of which the absorption band of 275 mμ was followed (no iodide ion absorption at 275 mμ). A desired amount of an organic iodide was weighed accurately in a 50 m*l* volumetric flask. After equilibration at a reaction temperature, it was made up to 50 m*l* with a desired amount of an amine solution and with the solvent at the same temperature. The flask was shaken vigorously and kept in a thermostat. Initial concentration was determined after two minutes. From time to time, 5 m*l* of the solution was pipetted out and diluted to a suitable concentration with acetonitrile. A typical run is shown below.

Table 3. Reaction of allyl iodide with piperidine in CH_3CN

Sec	O.D.[a] Observed	O.D. Corrected[b]	k_2 $l\,mol^{-1}\,sec^{-1}$	Percentage of reaction (%)
	.174			
600	.378	.242	3.57	25.4
900	.459	.338	3.67	36.1
1200	.512	.401	3.51	42.1
1800	.609	.514	3.46	54.1
2100	.658	.574	3.63	60.3
2400	.680	.600	3.45	63.2
2700	.710	.635	3.46	66.7
∞	.948			

a) Optical density at 246 mμ.
b) Observed optical density was corrected, because allyl iodide has a little absorbance at 246 mμ.

8) R. C. Fuson and H. G. Cooke, Jr., *J. Am. Chem. Soc.*, **62**, 1180 (1940).
9) H. Stone and H. Shechter, "Org. Syn.," Coll. Vol. 4, p. 323 (1963).
10) G. L. Lewis and C. P. Smyth, *J. Chem. Phys.*, **7**, 1085 (1939).

BULLETIN OF THE CHEMICAL SOCIETY OF JAPAN VOL. 42 1113—1118 (1969)

Spectrophotometric Studies of the Copolymer of L-Tryptophan and L-Glutamic Acid in an Aqueous Solution[1]

Akio OHNISHI, Katsuya HAYASHI*[1] and Junzo NOGUCHI

Department of Polymer Science, Faculty of Science, Hokkaido University, Nishi-8-chome, Kita-10-jo, Sapporo

(Received August 31, 1968)

The synthetic copolymer of L-tryptophan and L-glutamic acid exhibited two specific bands, around 292 mμ and 234 mμ, in the difference spectrum at pH 4.68 *vs.* pH 7.60 in a 0.1 M phosphate buffer. The former, that at 292 mμ, might be caused by the red shift of the ordinary absorption band around 280 mμ, and the latter, that at 234 mμ, by the red shift of the far-ultraviolet absorption band, around 220 mμ, of the tryptophanyl residue in the copolymer. This specific peak at 234 mμ in the difference spectrum of the tryptophan copolymer may be distinguished from that at 222 mμ, which is due to the hyperchromisity ($n\rightarrow\pi^*$ transition) of the amide group in the peptide bond reported with poly-L-glutamic acid. The peak at 230—235 mμ appearing in the difference spectrum between native and denaturated proteins may be due to the same red shift ($\pi\rightarrow\pi^*$ transition) of the far-ultraviolet absorption band of the tryptophanyl residue as that shown by the tryptophan copolymer. The difference in absorption at 234 mμ was five times larger than that at 292 mμ, and both of them increase proportionally with a lowering of the pH. The relation between the difference absorption and the pH was quite similar to that between the helical content and the pH. The relative fluorescence intensity of the tryptophanyl residue was also depressed with a lowering of the pH, and the profile of the pH-dependence curve on the fluorescence intensity was almost identical with the titration curve of the copolymer. Therefore, it may be said that the appearance of the difference spectrum at 234 mμ corresponds to the formation of the α-helix in polypeptide and that the protonation of the glutamyl residue induces the quenching of the fluorescence of the tryptophanyl residue.

The characteristic absorption spectrum of the tryptophanyl residue in protein has been widely used to study the structure and the biological activity of protein; *e.g.*, the enzyme-substrate complex was demonstrated spectrophotometrically by means of the concomitant change of the absorption spectrum of the tryptophanyl residue in the lysozyme molecule.[2] To elucidate the role and behavior of the tryptophanyl residue in protein, it may be instructive to ascertain spectrophotometrically basic information on the tryptophanyl residue using some simple tryptophan copolymers.

Tryptophan has two specific absorption bands in the near visible region (250—300 mμ) and the far-ultraviolet region (200—240 mμ);[3] the same absorption bands were observed in the tryptophan copolymer in these experiments. Recently, Fasman *et al.*[4] showed that the fluorescence of the tryptophanyl residue in copoly(Glu,Trp) and copoly(Lys,Trp) was strongly quenched by the unionized carboxyl group of glutamyl or the unionized amino group of the lysyl residue in these copolymers, but the fluorescence was almost independent of the conformation of α-helix in the copolymers. They suggested also that the hyperchromisity on the absorption spectrum of the tryptophanyl residue might be affected by the dissociation of the carboxyl group of the glutamyl residue from the difference spectrum between pH 4.6 and pH 7.3 in the range of 250—320 mμ, using copoly(Glu,Trp 99 : 1). However, the difference spectrum seems to be somewhat ambiguous as a basis for a further, detailed discussion of the behavior of the tryptophanyl residue, because the copolymers contained so many amide bonds in relation to the tryptophanyl residue (99 : 1 molar ratio) that the absorption band of the tryptophanyl residue in the far-ultraviolet region overlapped with that of the amide bond with a high optical density. It is interest to study the behavior of a copolymer with a higher

1) Presented at the 21st Annual Meeting of the Chemical Society of Japan, Suita, Osaka, April, 1968.

*1 Joint reseacher working on a grant from the Japan Association for the Advancement of Science (Laboratory of Biochemistry, Faculty of Agriculture, Kyushu University, Hakozaki, Fukuoka).

2) K. Hayashi, T. Imoto and M. Funatsu, *J. Biochem.*, **54**, 381 (1963).

3) D. B. Wetlaufer, "Advances in Protein Chemistry," Vol. 17, ed. by C. B. Anfinsen, Jr., Academic Press, New York and London (1962), p. 320.

4) G. D. Fasman, E. Bodenheimer and A. Pesce, *J. Biol. Chem.*, **241**, 916 (1966).

content of tryptophan, since the absorption spectrum of the tryptophanyl residue seems to be a good indicator of the molecular conformation of the tryptophan copolymer. The present work is concerned with a spectrophotometric study of copoly-(Glu,Trp 9 : 1) in an aqueous solution in relation to a study of NPA*2 hydrolysis[5] by means of the interaction between glutamyl and tryptophanyl residues.

Further, the difference spectra between the native and denaturated states of proteins containing tryptophanyl residues presented by Glazer and Smith[6,7] are discussed in comparison with the results presented in this paper.

Experimental

Preparation of the Copolymer. The copolymer of L-tryptophan and L-glutamic acid was prepared from the *N*-carboxyanhydride (NCA) of each amino acid in a molar ratio of 9 : 1 as follows; 1.34 g (0.0058 mol) of L-tryptophan NCA,[8] after having been purified in a two-layer column (charcoal-silver oxide/activated charcoal),[9] and 13.8 g (0.053 mol) of γ-benzyl-L-glutamate NCA[10,11] were dissolved in 150 m*l* of dioxane; then 0.55 g (0.0049 mol) of triethylenediamine[9] was added to the mixture as an initiator. The solution was allowed to stand for 5 days at 40°C under stirring, and then the viscous solution was poured into a large amount of water in order to precipitate the copolymer. The precipitate was washed with water and ethanol, and dried *in vacuo*. To remove the benzyl group of the glutamyl residue, the copolymer was dissolved in 90 m*l* of dioxane, and then 0.2N aqueous alcoholic sodium hydroxide (0.9 g of sodium hydroxide, 22.5 m*l* of water, and 90.0 m*l* of ethanol)[12] was added. The mixture was allowed to stand for 10 hr at 15°C to complete the debenzylation of the glutamyl residues. The debenzylation of the copolymer was confirmed by the disappearance of the 1740 cm^{-1} absorption band of the ester. The sodium salt of the copolymer was precipitated with ethanol and washed several times with ethanol. It was colorless and easily soluble in water. Yield 7.5 g (85%). The tryptophanyl residue in the copolymer was estimated from the optical density at 280 mμ,[13] while the glutamyl residue was analysed with ninhydrin[14] by paper chromatography after acid hydrolysis. The molar ratio of glutamyl and tryptophanyl residues in this copolymer was 89.7 : 10.3. The intrinsic viscosity of the copolymer was 1.84 in 0.2M sodium chloride at pH 7.6 and 25°C. The molecular weight of the copolymer was calculated to be 85000 by applying the relation between the intrinsic viscosity and the molecular weight of poly-L-glutamic acid.[15]

Poly-L-glutamic Acid. Poly-L-glutamic acid was obtained by the saponification[12] of poly-γ-benzyl-L-glutamate prepared from γ-benzyl-L-glutamate NCA.[10,11] The intrinsic viscosity was 2.13 in 0.2M sodium chloride at pH 7.6 and 25°C; the molecular weight was calculated to be 97000 by the method described above.

Fractionation of Copolymer. The copolymer was fractionated by gel filtration through a column of Sephadex G-50, using a 0.1M phosphate buffer at pH 7.0 as an eluant.

Titration. Samples were titrated with 0.1N sodium hydroxide, using a Radiometer TTT-1 titrator with a SBR2-C titrigraph. Before titration, the solution of polyamino acid was treated by passing it through a mix-bed column of Amberite IR-120 and IRA-410 to remove the sodium ions; it was then adjusted to a 0.1M so ium chloride solution by the addition of 1.0M sodium chloride.[16]

Optical Rotatory Dispersion. The optical rotatory dispersion of the copolymer in a 0.1M phosphate buffer at various pH values was measured in the 300—600 mμ range with a Yanagimoto ORD-3 spectropolarimeter using a 50-mm quartz cell at 25°C (c=0.5), and the parameter, b_0, was calculated from the Moffitt-Yang equation.[17] The helical content from b_0 was corrected by applying the results of Fasman *et al.*[18]

Absorption Spectrum and Difference Spectrum. The ultraviolet absorption spectrum and the difference spectrum were studied with a Hitachi 124 spectrophotometer, using 10-mm quartz cells at 25°C. In the measurement of the difference spectrum, a copolymer solution at pH 7.60 was used as the reference.

Fluorescence Spectrum. The fluorescence spectra of the copolymer and tryptophan in 0.1M phosphate buffer were measured with a Hitachi MPF-2 spectrofluorophotometer, using a 10-mm quartz cell at 25°C.

Results

Fractionation. The results by gel filtration on a column of Sephadex G-50 are shown in Fig. 1.

*2 *p*-Nitrophenyl acetate.

5) J. Noguchi, S. Tokura, T. Komai, H. Yamamoto and A. Ohnishi, *J. Biochem.*, in press.
6) A. N. Glazer and E. Smith, *J. Biol. Chem.*, **235**, PC43 (1960).
7) A. N. Glazer and E. Smith, *ibid.*, **236**, 2942 (1961).
8) A. Patchornik, M. Sela and E. Katchalski, *J. Am. Chem. Soc.*, **76**, 299 (1954).
9) J. Noguchi, N. Nishi, M. Itaya and S. Tokura, *Kogyo Kagaku Zasshi* (*J. Chem. Soc. Japan, Ind. Chem. Sect.*), **69**, 745 (1966).
10) H. Yuki, *Nippon Kagaku Zasshi* (*J. Chem. Soc. Japan, Pure Chem. Sect.*), **77**, 49 (1956).
11) E. R. Blout and R. H. Karlson, *J. Am. Chem. Soc.*, **78**, 941 (1956).
12) Y. Takeda, T. Okuda and S. Sakurai, Japanese Pat. 3290 (1965).
13) H. G. Beaven and E. R. Holiday, "Advances in Protein Chemistry," Vol. 7, ed. by M. L. Anson *et al.*, Academic Press, New York and London (1952), p. 320.
14) R. A. Boissonnas, *Helv. Chem. Acta*, **33**, 1975 (1950).
15) A. Wada, *Mol. Phys.*, **3**, 409 (1960).
16) K. Nitta and S. Sugai, *Nippon Kagaku Zasshi* (*J. Chem. Soc. Japan, Pure Chem. Sect.*), **88**, 412 (1967).
17) W. Moffitt and J. T. Yang, *Proc. Natl. Acad. Sci. U. S.*, **42**, 596 (1956).
18) G. D. Fasman, M. Landsberg and M. Buchwald, *Can. J. Chem.*, **43**, 1588 (1965).

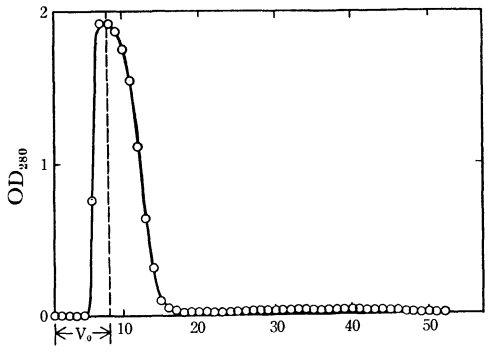

Fig. 1. Elution diagram of copoly(L-Glu, L-Trp 9 : 1) on Sephadex G-50, Fine.
Eluant: 0.1 M phosphate buffer at pH 7.0.
Bed dimensions: 2 cm×28 cm
Sample: 2 ml containing 10 mg of substance
Flow rate: 0.6 ml/min
V_0: void volume of the column which was determined with Blue Dextran 2000.

Since only one peak of the copolymer appears at the position of the void volume of the column, and since there is no other peak, the copolymer does not contain the fraction with a molecular weight less than 30000, because the effective fractionation with Sephadex G-50 for peptides is in the 1500—30000 range;*3 the molecular weight of 85000 obtained from the viscosity seems to support the above statement. It was shown also that no oxidation of the tryptophanyl residue occurred during the preparation of the copolymer, for normal absorption spectra of the tryptophanyl residue (250—300 mμ) were observed in each fraction and no absorption spectra of the oxidized tryptophanyl residue[19,20] were detected in any of the fractions.

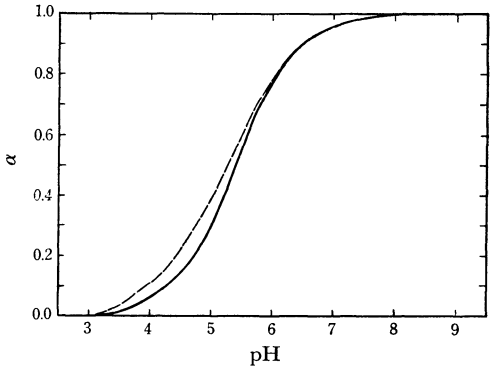

Fig. 2. Titration curve of copoly(L-Glu, L-Trp 9 : 1) (——) and poly-L-glutamic acid (------) at 20°C.
Sample: 10 ml of 0.1M NaCl aqueous solution containing 20 mg of substance
Titor: 0.1N NaOH aqueous solution

*3 The data is shown in the catalogue of Pharmacia Fine Chemicals, Uppsala, Sweden.

Titration. The titration curves of the tryptophan copolymer and poly-L-glutamic acid are shown in Fig. 2. The apparent pK values of both polymers were 5.34 and 5.26 respectively in 0.1M sodium chloride.

Optical Rotatory Dispersion. Figure 3 shows

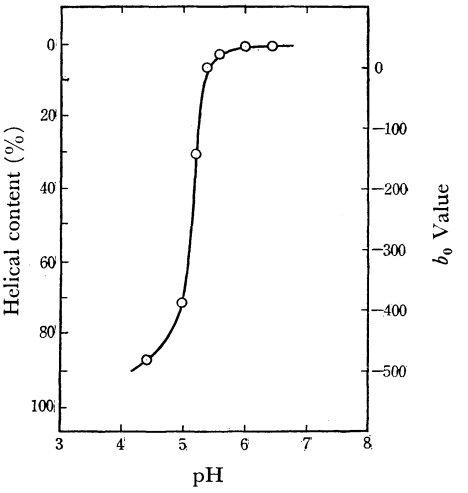

Fig. 3. Relationship between pH and helical content of copoly(L-Glu, L-Trp 9 : 1). b_0 Value are calculated from the ORD measurement in 0.1M phosphate buffer at 25°C.

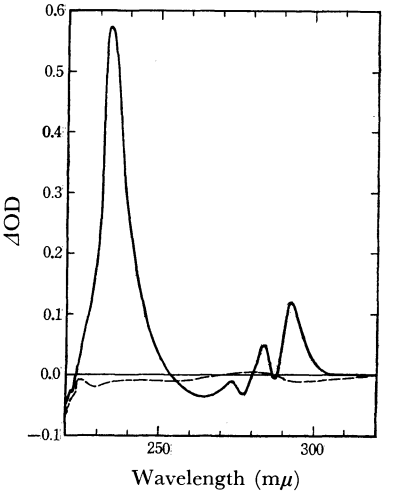

Fig. 4. Ultraviolet difference spectra of copoly(L-Glu, L-Trp 9 : 1) (——) and L-tryptophan (------) in 0.1M phosphate buffer.
Reference: pH 7.60 Sample: pH 4.68
Optical densities at 280 mμ of both substances are 1.5 at pH 7.60 and 25°C.

19) C. E. Dalgliesh, *J. Chem. Soc.*, **1952**, 137.
20) A. Previero, M.-A. Coletti-Previero and P. Jollès, *J. Mol. Biol.*, **24**, 261 (1967).

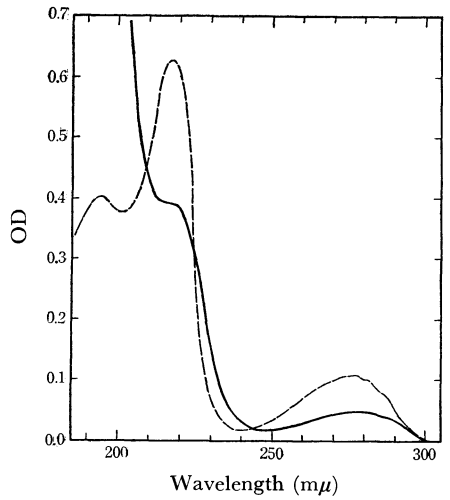

Fig. 5. Ultraviolet absorption spectra of copoly(L-Glu, L-Trp 9 : 1) (——) and L-tryptophan (------) in 0.1M phosphate buffer at pH 7.60 and 25°C.

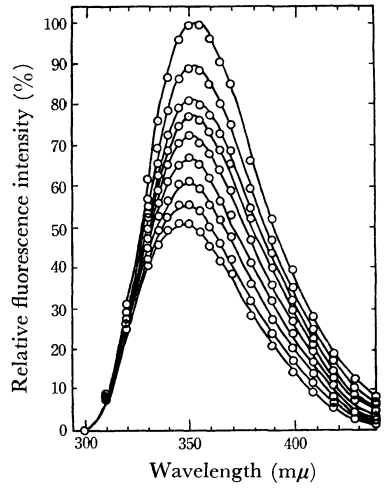

Fig. 7. Fluorescence emission spectra of copoly(L-Glu, L-Trp 9 : 1) in 0.1M phosphate buffer at various pH, pH 4.95—pH 7.40, at 25°C.
Exciting wavelength is 280 mμ.
Optical density at 280 mμ is 1.5 at pH 7.40.

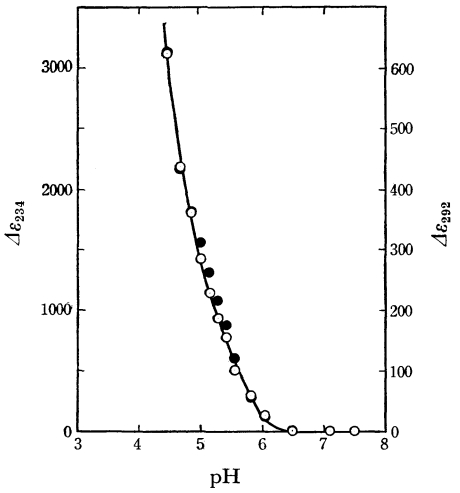

Fig. 6. Relationship between pH and difference absorption at 234 mμ (○) and 292 mμ (●) of copoly-(L-Glu, L-Trp 9 : 1).

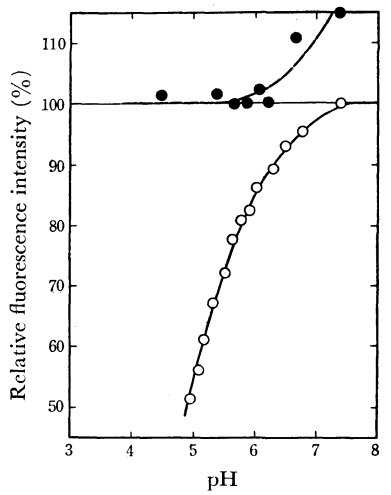

Fig. 8. Relationship between pH and the relative fluorescence intensity of copoly(L-Glu, L-Trp 9 : 1) (—○—) and L-tryptophan (--●--).

the relation between the pH and the helical content of the copolymer. The inflection point of the curve was at pH 5.2, and a helical content of 0% was shown above pH 5.5, where the copolymer was in the random state.

Difference Spectrum and Absorption Spectrum. The difference spectrum of the tryptophan copolymer and that of tryptophan itself are shown in Fig. 4. The difference spectrum of the tryptophan copolymer at pH 4.68 *vs.* pH 7.60 (shown by the solid line in Fig. 4) shows two specific bands, though that of tryptophan itself under the same conditions (shown by the dashed line) has no detectable absorption. The absorption spectrum of the tryptophan copolymer and that of tryptophan itself are shown in Fig. 5. The absorption shoulder at 220 mμ of the copolymer seems to correspond with the absorption peak at 218 mμ (ε=35000) of tryptophan.

The relationships between the pH and the difference absorption at 234 and 292 mμ respectively are shown in Fig. 6.

Fluorescence Spectrum. The fluorescence spectra of copolymers excited with a 280 mμ wavelength at various pH values are shown in Fig. 7. The fluorescence intensities of the copolymer and tryptophan at various pH values are shown in Fig. 8, in which the intensity at pH 7.40 is put as 100%. The pH-dependence of the

relative fluorescence intensity of the copolymer is quite different from that of tryptophan itself.

Discussion

The peaks at 273, 283, and 292 mμ of the difference spectrum at pH 4.68 *vs.* pH 7.60 in Fig. 4 seem to be due to the red shift ($\pi \rightarrow \pi^*$ transition) of the ordinary absorption band in the 250—300 mμ region on the tryptophanyl residue. Donovan *et al.*[21] reported that, in the difference spectrum of tryptophan at pH 1.7, 2.6, 6.4, and 8.7 *vs.* pH 1.2 at a high concentration ($OD_{280}=6$), the peak at 293 mμ decreased with a lowering of the pH; this suggested a blue shift of the absorption band around 280 mμ with a lowering of the pH. On the contrary, in the difference spectrum of the tryptophan copolymer at the low concentration of $OD_{280}=1.5$, the peak at 292 mμ increased with a lowering of the pH and showed a red shift of the absorption band around 280 mμ based on the tryptophanyl residue.

As is shown by the dashed line in Fig. 4, such a specific difference spectrum of tryptophan itself as was shown by Donovan *et al.*[21] was not observed in a dilute solution, in which tryptophan was dissolved at the same concentration as the tryptophanyl residue in the copolymer ($OD_{280}=1.5$). The difference spectrum of tryptophan itself[21] and that of the tryptophan copolymer were reversed in sign; also, the absolute value of the latter was much larger than that of the former. This might show that the behavior of the tryptophanyl residue in the copolymer is quite different from that of tryptophan itself upon a change in the pH in a solution.

The absorption peak of tryptophan itself at 218 mμ seems to correspond to the characteristic absorption shoulder in the 220 mμ region of the tryptophanyl residue in the copolymer, as is shown in Fig. 5; the red shift of the latter seems to give a peak at 234 mμ in the difference spectrum of the copolymer in Fig. 4. Therefore, from these results, it may be concluded that the sharp and large peak at 234 mμ in the difference spectrum of the copolymer was caused by the red shift ($\pi \rightarrow \pi^*$ transition) of the ultraviolet absorption band in the 220 mμ region of the tryptophanyl residue in the copolymer.

On the other hand, it has been explained that a large peak at 230—235 mμ in the difference spectrum between native and denaturated proteins, such as bovine albumin (234 mμ),[6] papain (235 mμ),[7] ovalbumin (232 mμ),[7] and lysozyme (231 mμ),[7] would be due to the hyperchromisity ($n \rightarrow \pi^*$ transition) of the amide group in the peptide bond, for in the case of poly-L-glutamic acid the hyperchromisity of the amide group was observed at 222 mμ in the difference spectrum between the α-helix and the random coil.[22] However, the difference spectrum at 230—235 mμ in proteins seems to be different from that of poly-L-glutamic acid at 222 mμ, since it is too big a shift to have the identical source ($n \rightarrow \pi^*$ transition). The hyperchromisity at 222 mμ due to the $n \rightarrow \pi^*$ transition of the amide group, as reported with poly-L-glutamic acid, was undetectable with the tryptophan copolymer (Fig. 4), for the intensity of transmitted light below 225 mμ was extremely weakened because of the high optical density of the tryptophanyl residue. The difference spectra of proteins are quite similar to that of the tryptophan copolymer (Fig. 4). Therefore, the difference absorptions at 234 mμ observed with the tryptophan copolymer and at 230—235 mμ with proteins must be due to the red shift ($\pi \rightarrow \pi^*$ transition) of the far-ultraviolet absorption band of the tryptophanyl residue, and not to the $n \rightarrow \pi^*$ transition of the amide group in peptide bond.

When we compare Fig. 6 with Fig. 3, it is obvious that the peaks of the difference absorption at both 234 mμ and 292 mμ vary proportionally to the helical content of the copolymer and that these difference absorptions are closely related to the secondary structure of polypeptides. Also, the difference absorption at 234 mμ in the tryptophan copolymer was completely proportional to that at 292 mμ; the former was five times of the latter. Therefore, it would be more accurate to confirm the conformation of a tryptophan copolymer or a tryptophan-containing protein by the difference absorption at 324 mμ instead of that at 292 mμ.

The fluorescence emission spectra of the tryptophan copolymer at various pH values (Fig. 7) are similar to that of the tyrosine copolymer, copoly-(Glu,Tyr 95 : 5), reported by Pesce and Fasman.[23]

In view of the titration curve of the tryptophan copolymer (Fig. 2), the relative intensity of fluorescence of the tryptophanyl residue at 350 mμ against the pH (Fig. 8) is in good agreement with the extent of the protonation of the carboxyl group in the copolymer against the pH. The unionized carboxyl group seems to act as a quencher of the fluorescence of the tryptophanyl residue. These results support Fasman's suggestion[4] that the fluorescence intensity of the tryptophanyl residue depends on the degree of ionization of the carboxyl group in copoly(Glu,Trp 99 : 1).

The spectrophotometric behavior of the tryptophanyl residue in polypeptide is quite different from that of tryptophan itself. The appearance of

21) J. W. Donovan, M. Laskowski, Jr., and H. A. Scheraga, *J. Am. Chem. Soc.*, **83**, 2686 (1961).

22) K. Imahori and J. Tanaka, *J. Mol. Biol.*, **1**, 359 (1959).

23) A. Pesce and G. D. Fasman, *J. Am. Chem. Soc.*, **86**, 5669 (1964).

the difference spectrum seems to correspond closely to the formation of the α-helix in the polypeptide molecule, and the protonation of carboxyl groups in polypeptide seems to induce the quenching of the fluorescence of the tryptophanyl residue. It is not yet clear whether the spectrophotometrical results are related to the catalytic activity[5] of the tryptophan copolymer.

The authors wish to thank Professor Motozo Kaneko of this Department for his help in the measurements of the fluorescence spectra; Professor Shintaro Sugai of this Department for his advice in the measurements of the optical rotatory dispersion, and Professor Masaru Funatsu of Kyushu Univeristy for his kind support of this work.

This work was supported by the Scientific Research Fund of the Ministry of Education, Japan, and of the Japan Association for the Advancement of Science.

BULLETIN OF THE CHEMICAL SOCIETY OF JAPAN VOL. 42 1118—1123 (1969)

Alkoxysilanes. II. Preparation of Tributoxysiloxychlorosilanes, Silanols, and Their Polymeric Substances

Yoshimoto ABE*1 and Ichiro KIJIMA*1

Department of Chemistry, Faculty of Science, Science University of Tokyo, Kagurazaka, Shinjuku-ku, Tokyo

(Received September 2, 1968)

Tributoxysiloxychlorosilanes $[(BuO)_3SiO]_xSiCl_{4-x}$ (Bu=*t*: $x=1, 2$; Bu=*s*: $x=1, 2, 3$ or 4) were prepared by the reaction of silicon tetrachloride with tributoxysilanol in the presence of pyridine. The hydrolysis of these compounds led to the formation of tributoxysiloxysilanols $[(BuO)_3SiO]_xSi(OH)_{4-x}$ (Bu=*t*: $x=2$; Bu=*s*: $x=2$ or 3). Tri-*t*-butoxysiloxysilanetriol was obtained from the corresponding trichlorosilane under mild hydrolytic conditions by using aniline as an hydrogen-chloride acceptor. On the other hand, the hydrolysis of the trichlorosilane with excess water in the presence of pyridine gave a resinous product. The fractional precipitation of this product gave a white powder soluble in such organic solvents as benzene, *n*-hexane, ether, and carbon tetrachloride; the powder had a molecular weight between 2500 and 4300. This resin turned into glassy solids upon being heated at 200 or 300°C under reduced pressure; these solids had molecular weights between 5500 and 12500. The possible structures for these polymeric substances were discussed on the basis of the results of the elemental analysis, the IR spectra, and the gas chromatography of volatile substances produced in the course of polymerization.

Although alkoxysilanes with functional groups have been prepared, the isolation of alkoxysilanes $(RO)_xSiX_{4-x}$ (R=Me, Et, Pr, Bu; X=OH, NH_2; $x=1, 2$ or 3) containing hydroxy or amino[1] groups as functional groups is very difficult because of the easy condensation. Tiralkoxysilanols with *s*-[2] or *t*-[3]alkoxy groups, however, are obtained, and in the latter case di-*t*-butoxysilanediol[4] is also isolated. The above facts show that the steric hindrance of alkyl groups protects the functional group from condensation. Therefore, we tried to prepare tributoxysiloxychlorosilanes in which the alkoxy group on an alkoxysilane is replaced by the tributoxysiloxy group and tried to isolate the stable silanediol and silanetriol by the hydrolysis of the corresponding chlorosilanes:

$$SiCl_4 + x(BuO)_3SiOH + xC_5H_5N = [(BuO)_3SiO]_xSiCl_{4-x} + xC_5H_5NHCl$$

$$[(BuO)_3]_xSiCl_{4-x} + xH_2O = [(BuO)_3SiO]_xSi(OH)_{4-x} + xHCl$$

In the course of our investigation into the hydrolysis of alkoxysiloxychlorosilane, our attention was called to polymeric substances produced because the structures of the polyalkyl(aryl)silsesquioxanes formed by the hydrolysis of alkyl(aryl)trichloro-

*1 Present address: Department of Industrial Chemistry, Faculty of Engineering, Science University of Tokyo, Kagurazaka, Shinjuku-ku, Tokyo.

1) R. Fessenden and T. S. Fessenden, *Chem. Revs.*, **61**, 316 (1961).

2) J. R. Wright, R. O. Bolt, A. Goldschmidt and A. D. Abbott, *J. Am. Chem. Soc.*, **80**, 1733 (1958).

3) C. R. Morgan, W. F. Olds and A. L. Rafferty, *ibid.*, **73**, 5193 (1951).

4) C. S. Miner, L. A. Bryan, R. P. Holysz and G. W. Pedlow, *Ind. Eng. Chem.*, **39**, 1368 (1947).

silane[5] or alkyltrialkoxysilanes[6,7] were discussed, but the structures of substances formed by the hydrolysis of alkoxysiloxytrichlorosilane were not. Therefore, it seemed necessary that the structures of the polymers were considered since it was thought that the polymeric substances formed by the hydrolysis of tri-*t*-butoxysiloxytrichlorosilane do not have such a simple structure constructed of silsesquioxane units as have the hydrolysis products of alkyltrichlorosilanes.

Experimental

The boilling points and melting points are uncorrected. The experiments were carried out under a dry atmosphere.

Materials. The amines and the solvents were dehydrated, and the silicon tetrachloride was purified by distillation. Tri-*s*-butoxysilanol was obtained by the method of Wright[2]; bp 89.5°C/1 mmHg, n_D^{20} 1.4135.

Tri-*t*-butoxysilanol was first prepared by Backer and Klasens[8] by the hydrolysis of sodium tri-*t*-butoxysilanolate. Wright *et al.* had described how silanol was obtained by the hydrolysis of tri-*t*-butoxychlorosilane in boilling water, but its details had not been documented. In the present work, the silanol was prepared in good yields by a modification of the procedure of Wright.

To a solution of 72.7 g of pyridine and 280 g of water, 200 g of tri-*t*-butoxychlorosilane[9] were added. Then the mixture was stirred at 70—80°C for 1 hr and left standing overnight. After the white solid thus formed was filtered and washed with water, the solid was dissolved in petroleum ether and dehydrated with anhydrous sodium sulfate. The solvent was removed, and the residue gave 130 g (70%) of a white crystalline solid, mp 65—66°C (lit. 65.5°C). Found: C, 54.67; H, 11.64; Si, 10.60%; mol wt, 268. Calcd for $C_{12}H_{28}O_4Si$: C, 54.51; H, 10.67; Si, 10.60%; mol wt, 264.

Preparation of Tri-*s*- and -*t*-butoxysiloxychlorosilanes. Into a solution of tri-*t*-butoxysilanol and pyridine in *n*-hexane, silicon tetrachloride in *n*-hexane was stirred, drop by drop, at 0——5°C. (In the preparation of *s*-derivatives the addition of the silanol was reversed, and for tris or tetrakis derivatives toluene was used as the solvent.) The mixture was refluxed for one (trichloro-derivatives) or two (the other derivatives) hours. After the filtration of pyridine hydrochloride and the removal of the solvent, the filtrate gave products by fractional distillation *in vacuo* with a 20 cm Widmer column. The results are shown in Table 1.

Preparation of Tri-*s*- and -*t*-butoxysiloxysilanols. Into a mixture of pyridine, water, and petroleum ether, tributoxysiloxychlorosilane in dry petroleum ether was vigorously stirred, drop by drop, at 0——5°C. Then the oil layer was separated and dried over anhydrous sodium sulfate. The evaporation of the solvent gave silanols by fractional distillation *in vacuo*. The results are given in Table 2.

Preparation of Tri-*t*-butoxysiloxysilanetriol. A mixture of 2.5 g of water, 13.2 g of aniline, and 300 m*l* of ether was made homogeneous by the addition of 30 m*l* of acetone.[10] To the solution, 18.7 g of tri-*t*-butoxysiloxytrichlorosilane in 200 m*l* of ether were then stirred in, drop by drop, at −10——20°C for 2 hr. Then the mixture was allowed to come to room temperature, and the aniline hydrochloride was filtered out. The white solid formed by evporation of the ether *in vacuo* was dissolved in 60 m*l* of benzene without heating. The needle crystals which formed when the solution stood for several hours were filtered out, washed with benzene, and dried *in vacuo*; yield 3 g (18.8%); mp 114—117°C. The results of the elemental analysis are given in Table 2.

Hydrolytic Polycondensation of Tri-*t*-butoxysiloxytrichlorosilane. Into a mixture of 29.8 g of pyridine, 198 g of water, and 50 m*l* of petroleum ether, a 50 g portion of the trichlorosilane in 50 m*l* of petroleum ether was stirred at 0°C. The oil layer was then separated, washed fully with water, and dried over anhydrous sodium sulfate. The evaporation of the solvent *in vacuo* gave a colorless residue (39 g). The purification of this product was carried out by fractional precipitation. Into 50 m*l* of vigorously stirred methanol there were added, drop by drop, 6 g of the product dissolved in 10 m*l* of benzene. A white precipitate was formed and separated by decantation. The precipitate was again submitted to the same treatment, giving 1.0 g (No. 1-a) of a white solid when dried *in vacuo*. The solvent was evaporated from the mother liquor under reduced pressure, and the residue was treated with 5 m*l* or 3 m*l* of benzene through the same method to give 1.2 g (No. 1-b) and 1.3 g (No. 1-c) respectively of a white solid. The results of the elemental analysis are given in Table 4.

Heat Polymerization of the Hydrolysis Product. The unpurified hydrolysis product (9.5 g) obtained in the above experiment was heated at 200 or 300°C for 2 hr under reduced pressure (1—2 mmHg). The volatile and sublimable products formed in the procedure were trapped into a vessel cooled with dry ice and acetone. The total weight loss was 1.9 g at 200°C and 4.1 g at 300°C, including 1.7 and 1.9 g, respectively, of tri-*t*-butoxysilanol as the sublimate. The colorless glassy solid (4.5 g) at 200°C was treated by the same procedure to give 1.3 g (No. 2-a; 10 m*l* of benzene), 0.6 g (No. 2-b; 5 m*l*), and 0.4 g (No. 2-c; 3 m*l*) of a white powder. The residue (1.5 g) at 300°C was extracted with 100 m*l* of benzene for 3 hr to give 1.2 g of a soluble solid and 0.3 g (20 wt%) of an insoluble one. The former (2 g) was further treated with benzene to give 1.4 g (No. 3-a; 10 m*l* of benzene) and 0.5 g (No. 3-b; 5 m*l*) of a white powder.

It was confirmed by means of gas chromatography that the volatile substance obtained in the course of

5) J. F. Brown, L. H. Vogt, A. Katchman, J. W. Eustance and K. M. Kieser, *J. Am. Chem. Soc.*, **82**, 6194 (1960).

6) M. M. Sprung and F. O. Guenther, *ibid.*, **77**, 3990, 3996 (1955).

7) M. M. Sprung and F. O. Guenther, *J. Polymer Sci.*, **28**, 17 (1958).

8) H. J. Backer and H. A. Klasens, *Rec. Trav. Chim.*, **61**, 500 (1942).

9) M. G. Voronkov, A. N. Razarev and A. K. Baigojii, *Zh. Obs. Chim.*, **26**, 3072 (1956).

10) T. Takiguchi, *J. Am. Chem. Soc.*, **81**, 2359 (1959).

the heat polymerization, which was dissolved in benzene, contained water and *t*-butyl alcohol. The results are given in Table 4.

Heat Polymerization of Tri-*t*-butoxysiloxysilanetriol. The silanetriol (2.6 g) was heated at 145—155°C for 30 min under reduced pressure (2 mmHg). The same treatment of the product with 5, 3, and 1 m*l* of benzene gave 0.3 g (No. 4-a), 0.7 g (No. 4-b), and 0.8 g (No. 4-c) of a white powder. The results are given in Table 4.

Instruments. The IR spectra were measured in a KBr disk or a liquid film with a Hitadhi EPI-S2 spectrometer. The NMR spectra were measured with a Varian A-60 spectrometer in a carbon tetrachloride solution or in dueterated chloroform, with tetramethylsilane as the internal standard. The molecular weight was determined by the cryoscopic method or the vapor-pressure method in benzene. The gas chromatography was measured under these conditions: carbowax 6000, 1-m, 136°C, 46 m*l*/min. The thermal property of the products was determined by thermogravimetric analysis and by differential thermal analysis.

Results and Discussion

Monomers. The chlorosilanes and the silanols obtained are shown in Tables 1 and 2. As is shown in Table 1, the number of the replaced chlorine atoms indicates that the tri-*t*-butoxysiloxy group has a greater steric hindrance than the tri-*s*-butoxysiloxy one. Under these experimental conditions, further substituion did not occur even when excess tri-*t*-butoxysilanol was used. The difference in this steric hindrance between the two groups greatly contributes to the stabilization of the functional group. Table 2 shows that bis(tri-*s*-

TABLE 1. TRI-*s*- AND -*t*-BUTOXYSILOXYCHLOROSILANES $[(BuO)_3SiO]_xSiCl_{4-x}$

Reactants (g)			Products						
$SiCl_4$	$(BuO)_3SiOH$		x	Yield %	Bp °C/mmHg	n_D^{20}	Mol wt Found (Calcd)	Anal, Found (Calcd) % Cl	Si
			Bu=*s*						
51.0	79.2	23.7	1	62.0	81—82/1	1.4134	402 (398)	26.86 (26.73)	13.89 (14.12)
15.0	47.0	14.0	2	67.0	165.5—166/1.5	1.4159	643 (625)	11.28 (11.34)	13.65 (13.46)
15.0	70.0	21.0	3	50.0	196—199/2	1.4196	850 (854)	4.37 (4.15)	13.29 (13.17)
6.4	40.0	15.5	4	44.1	215—217/1	n_D^{50} 1.4095	1081 (1081)	—	13.16 (12.99)
			Bu=*t*						
55.4	86.0	25.7	1	65.2	80—82/1 solid	1.4065	412 (398)	*26.62 (26.73)	14.02 (14.12)
32.2	100.0	29.9	2	82.5	151—152/2.5 Mp 47—49	n_D^{50} 1.3962	639 (625)	**11.26 (11.32)	13.47 (13.46)

* Found: C, 34.84; H, 7.37%. Calcd: C, 36.21; H, 6.84%.
** Found: C, 45.59; H, 9.16%. Calcd: C, 46.06; H, 8.70%.

TABLE 2. TRI-*s*- AND -*t*-BUTOXYSILOXYSILANOLS $[(BuO)_3SiO]_xSi(OH)_{x-4}$

Reactants (g)			Products						
*1 $(RO)_xSiCl_{4-x}$	H_2O		x	Yield %	Bp °C/mmHg	n_D^{20}	Mol wt Found (Calcd)	Anal. Found (Calcd) % Si	
			Bu=*s*						
11.4	21.2	1.3	3	67.0	221—222/1	1.4171	857 (835)	13.51 (13.45)	
37.4	47.6	12.3	2	25.2	199—201/2	1.4161	630 (589)	14.25 (14.31)	
			Bu=*t*			n_D^{60}			
25.0	42.0	7.1	2	84.9	155/1.5 Mp 49—51	1.3915	604 (589)	*3	14.35 (14.31)
18.7	2.5	13.15*2	1	18.8	Mp 114—117	—	—	*4	16.23 (16.40)

*1 R=$(BuO)_3Si$ (Chlorosilanes in Table 1). *2 Aniline
*3 Found: C, 48.58; H, 9.89%. Calcd: C, 48.95; H, 9.58%.
*4 Found: C, 44.22; H, 9.04%. Calcd: C, 42.07; H, 8.82%.

Table 3. NMR and IR spectra of tri-*s*- and -*t*-butoxysiloxysilanols

Compound	NMR Spectra : Chemical shift (τ)			IR Spectra (cm^{-1})
	t-Bu, *s*-Bu(CH_3–, $-CH_2-$) (s) (m)	–CH– (sept)	–OH (s)	ν_{OH}
$(^{t}BuO)_3SiOH$	8.67 (27.1H)	—	6.08 (1H)	3400
$(^{t}BuO)_3SiOSi(OH)_3$	8.67	—	5.85	3430
$[(^{t}BuO)_3SiO]_2Si(OH)_2$	8.68 (27.5H)	—	6.09 (1H)	3450
$(^{s}BuO)_3SiOH$	9.20—9.24 (22.1H)	6.00 (3.1H)	5.40 (1H)	3350
$[(^{s}BuO)_3SiO]_2Si(OH)_2$	8.40—9.20 (5.2H)	5.75—6.20 (1H)		3360
$[(^{s}BuO)_3SiO]_3Si(OH)$	8.40—9.25 (27.5H)	6.00 (9.3H)	6.90 (1H)	3450

butoxysiloxy)silanediol polymerizes partially during prolonged distillation at a high temperature (yield 28%), whereas bis(tri-*t*-butoxysiloxy)silanediol can be distilled quantitatively (yield 80%) without condensation. On the other hand, tri-*t*-butoxysiloxysilanetriol is unstable and easily polymerizes, like other silanetriols.

The silanetriol is slightly soluble in benzene and chloroform. The other products obtained as solids are very soluble in organic solvents and have low melting points.

The silanols were confirmed by the IR and NMR spectra given in Table 3. The IR spectra are essentially identical and exhibited characteristic peaks at 3425—3460 (OH), 1365 and 1387 (branching of the alkyl groups), and 1060—1070 (Si–O–Si) cm^{-1}. A little shift toward the lower wave numbers for the hydroxy group of going from *t*- to *s*-derivatives was observed, probably because of an increace in the hydrogen bond with a decrease in the steric effect. The relative ratio of the protons of the hydroxy to those of the alkyl group is in good accordance with each of the structures. The NMR spectra of tri-*t*-butoxysiloxysilanetriol were measured in deuterated chloroform, but an exact ratio was not given because of its low solubility. The proton signal for the hydroxy group of bis(tri-*s*-butoxysiloxy)silanediol was not detected as a singlet. Since proton signals of the *t*-derivatives have a tendency toward an up-field shift as the number of substituent increases, in this case the signal seems to overlap with that of the methine proton. The ratio of the sum of methine and hydroxy protons to that of methyl and methylene protons is in good agreement with the structure.

The signal for the hydroxy proton of the silanols has a tendency to shift up-field with a larger steric hindrance; this is parallel to that tendency observed in the IR spectra.

Polymers. The results of the hydrolytic polycondensation and the heat polymerization are given in Table 4. Although No. 3-c was insoluble and infusible, the polymers were white powders, soluble in such organic sovents as benzene, *n*-hexane, ether, and carbon tetrachloride, and insoluble in methanol and ethanol.

The structures of these polymers are thought to be similar to those of polyalkyl(aryl)silsesquioxanes.

Table 4. Polyalkoxysilsesquioxane

Product	Fused point °C	Mol wt	Analysis (Found %)			Atom ratio		
			C	H	Si	C	H	Si
No. 1-a	183—188	3180	39.03	8.31	20.89	4.4	11.2	1
No. 1-b	137—142	4300	39.31	8.36	20.05	4.6	11.7	1
No. 1-c	78—83	2550	40.68	8.48	19.20	5.0	11.8	1
No. 2-a	175—185	5500	33.86	7.05	22.50	3.5	8.7	1
No. 2-b	235—245	—	38.92	8.36	20.04	4.5	11.7	1
No. 3-a	290	12500	31.80	6.49	25.21	3.0	7.2	1
No. 3-c	infusible	—	10.50	8.99	28.51	0.9	8.9	1
No. 4-a	150—155	—	40.16	8.35	18.79	5.0	12.4	1
No. 4-b	82—87	2930	41.92	8.84	18.44	5.3	13.6	1

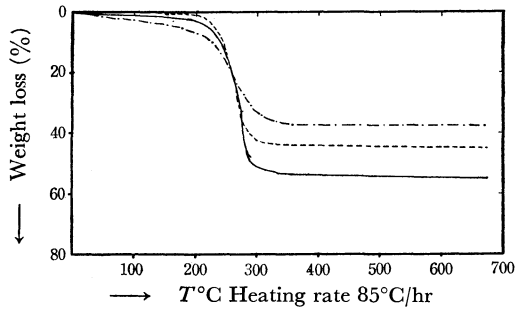

Fig. 1. Thermogravimetric analysis curve of polymer.

——— No. 1-a
---------- No. 3-a
— — — — No. 3-c

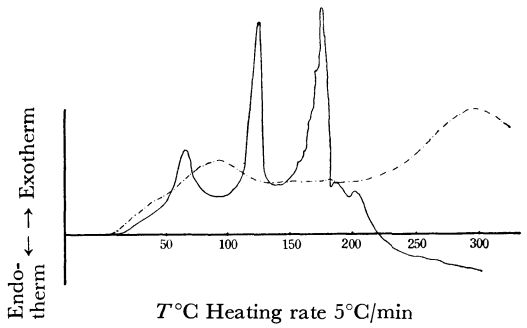

Fig. 2. Differential thermal analysis curve of tri-*t*-butoxysiloxysilanetriol (——) and No. 2-a (— — —).

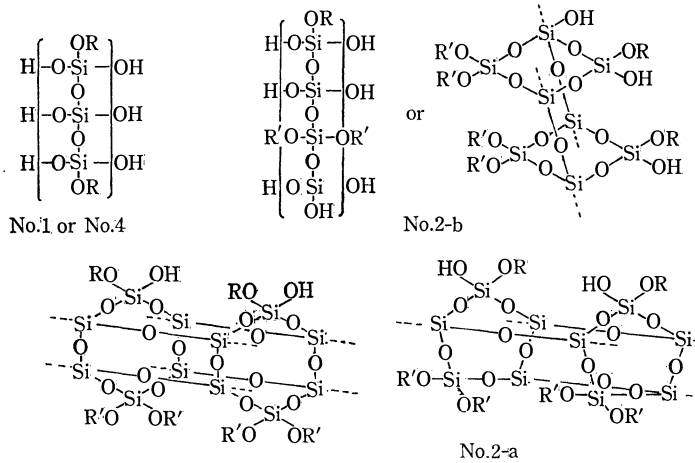

where R=Si(OBu)$_3$ and R′=Bu

Fig. 3. The possible structures of polymers.

TABLE 5. EMPIRICAL FORMULAS DERIVED FROM THE UNIT STRUCTURE

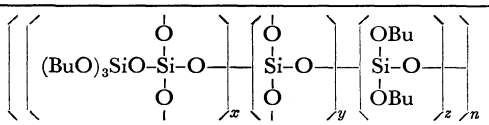

x	y	z	Atom ratio C	H	Si	Mol wt Obs	n	Corresponding polymer No. Formula	Mol wt Calcd	Anal. % (Calcd) C	H	Si
1	0	0	6	13.5	1							
1	0.4	0	5	11.3	1	4300	12.4	No. 1, No. 4 $C_{144}H_{330}O_{81}Si_{31}$	4199	41.2	7.9	20.0
1	1	0	4	9.0	1							
1	1	1	5	11.2	1							
1	2	1	4	9.0	1	5500	8.7	No. 2-b $C_{160}H_{374}O_{107}Si_{40}$	5133	37.4	7.3	21.4
1	3	1	3.3	9.5	1	5500	7.9	No. 2-a $C_{160}H_{376}O_{124}Si_{48}$	5632	34.1	6.7	23.5
1	4	1	2.9	6.4	1	12500	16.5	No. 3-a $C_{320}H_{746}O_{277}Si_{112}$	12171	31.6	6.2	25.8

It has been known that alkyl(aryl)silsesquioxanes are obtained from the corresponding trichlorosilanes or silanetriols and are composed of a ladder-type linear chain[11] or a cage-like[7,12] structure repeating a cyclosiloxane ring. In the present work, however, it is evident from the results of the elemental analysis (Table 5) that none of the polymers are constructred of a simple silsesquioxane, a so-called "T" unit. The unit structures of these polymers are the Q (tetrafunctional silicon atom: SiO_2) and the D (difunctional silicon atom $(Bu^tO)_2SiO_{0.5}$), along with the T (trifunctional silicon atom $(Bu^tO)_3SiOSiO_{1.5}$). This is confirmed from the following facts: 1. Tri-*t*-butoxysilanol was obtained as a component of the fractional precipitation and as a sublimate in the course of the heat polymerization *in vacuo*. 2. *t*-Butyl alcohol was detected as a volatile substance at from 200 to 300°C. Additional pieces of evidence are the remarkable weight loss at the temperature shown by thermogravimetric analysis curve (Fig. 1) and the three exothermic peaks at 65, 125, and 175°C observed in the differential thermal analysis of tri-*t*-butoxysiloxysilanetriol (Fig. 2). The two peaks at 90 and 295°C were also found for the No. 2-a polymer. These facts result from three different condensations in the course of the polymerization:

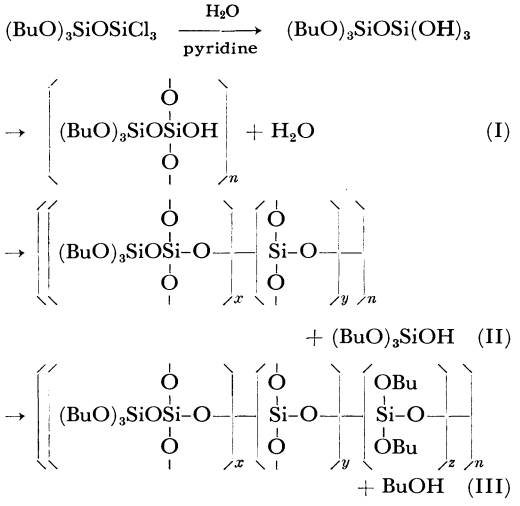

11) J. F. Brown, *J. Polymer Sci.*, **No. 1**, P-c, 83 (1963).
12) K. A. Andrianov and B. A. Izmaylov, *J. Organometal. Chem.*, **8**, 435 (1967).

The empirical formulas cited in Table 5 have been deduced by comparison with the atom ratio calculated from the experimental data (Table 4) and that obtained from the structural units, *x*, *y*, and *z*, in (II) and (III); the calculated values are also shown. The results of the elemental analysis (Tables 4 and 5) show that the polymers of No. 1 and No. 4 have no significant difference in structure except for the molecular weight and are in agreement with a (II) structure; on the other hand, the polymers of No. 2 and No. 3 are constructured of (III).

The probable structures of these polymers are shown in Fig. 3. In view of the fact that each of the polymers except for No. 3-c is very soluble in organic solvents, there appears to be no significant cross-linking. The polymers of No. 1 and No. 4 seem to have a linear sheet-like structure formed by the condensation of the three molecules of the silanetriol. As to the polymers of No. 2 and No. 3, however, it seems reasonable to assume three-dimensional polymers like a prism or cube (Fig. 4) rather than sheet-like ladder types. In this case the structural units might be eight, ten or twelve member-rings, since two or three functional silane monomers containing larger steric groups are apt to give cyclic or cage-like structures and since the stretching vibration of Si–O–Si in the cyclosiloxanes with more than eight member-rings is in the region of wave number higher than 1045 cm^{-1} (in these cases, at 1060—1070 cm^{-1}).[12,13] Besides the fact that the polymers of No. 3 contain an insoluble gel (20%) indirectly shows a three-dimensional structure in No. 2 and No. 3. The polymer of No. 3-c seems to be a network polymer.

The IR spectra of all polymers are essentially identical and show absorption peaks at 3400—3450, 2960, 1389, 1364, 1240, 1190, and 1060—1070 cm^{-1}.

The X-ray powdery diffraction pattern of No. 2-a indicates no crystallinity.

The authors wish to thank Mr. Isao Orita for his assistance in the experiments.

13) K. A. Andrianov and B. A. Izmaylov, *ibid.*, **8**, 443 (1967).

BULLETIN OF THE CHEMICAL SOCIETY OF JAPAN VOL. 42 1124—1129 (1969)

Synthesis of Carboxylic Acid from Aryl Halide and Carbon Monoxide Catalyzed by Nickel Carbonyl

Mikitake NAKAYAMA and Tsutomu MIZOROKI

Government Chemical Industrial Research Institute, Tokyo, Meguro-ku, Tokyo

(Received September 2, 1968)

In the reacion of aryl bromide with carbon monoxide in the presence of water and a catalytic amount of nickel carbonyl, it has been found that aromatic carboxylic acids (benzoic acid, polymethylbenzoic acid, α-naphthoic acid, *etc.*) are formed in very high yields when such salts of carboxylic acids as potassium acetate or sodium benzoate are added to the starting materials. The carbonylation reaction of aryl bromide is strongly inhibited by the hydrobromic acid formed, and the addition of the salt of carboxylic acid effectively decreases its concentration in the course of the reaction. When the amount of potassium acetate is larger than that of aryl bromide, the rate of the carbonylation reaction of bromobenzene to form benzoic acid is proportional to the amounts of bromobenzene, nickel tetracarbonyl, and water and to the reciprocal of the carbon monoxide pressure. From these kinetic data, the effect of the salts of carboxylic acids and the course of the reaction are discussed.

Many attempts to obtain aromatic carboxylic acids or their esters from the reactions of aryl halides with carbon monoxide using transition metal compounds as catalysts have been made. Nickel complexes have been demonstrated to be the most effective catalysts since the synthesis of benzoic acid from halobenzene with $Ni(CO)_2(Ph_3P)_2$[1] or a nickel(II) iodide catalyst[2] and that of phthalic anhydride from bromobenzene in the presence of sodium carbonate with a nickel tetracarbonyl catalyst[3] were published. The yields of aromatic carboxylic acids have, however, depended to a cansiderable degree on the nickel catalysts, the solvents, and the additives. On the other hand, it has been shown that the treatment of aryl iodide with a stoichiometric amount of nickel tetracarbonyl under milder reaction conditions results in forming an aryl carbonyl compound (carboxylic ester or diketone) in a high yield.[4] We expected that the low yields of aromatic carboxylic acids by the catalytic reactions of aryl halides with carbon monoxide would be caused by the inhibition of the hydrogen halides formed and have found that their yields really become very high when salts of carboxylic acids are added to the starting materials to decrease effectively the concentration of hydrogen halide during the reaction.[5]

This work has been undertaken to obtain substituted benzoic acids from the reactions of aryl bromides with carbon monoxide in the presence of potassium acetate and water using nickel tetracarbonyl, and to investigate their reaction rates.

Experimental

Apparatus. The same apparatus as has been described in a previous paper was used.[6] All the reactions were carried out in titanium-molybdenum alloy autoclaves (225 m*l* and 300 m*l* in volume). A titanium or a titanium-manganese alloy autoclave could not be used in these corrosive reactions. Aryl bromide, water, salt of carboxylic acid, and nickel(II) acetate were placed in the autoclave, and it was heated by a shaking-type electric furnance. The temperature of the autoclave was kept constant for about one hour before carbon monoxide was introduced from a pressure-accumulator vessel. Carbon monoxide was supplied to keep the reaction pressure constant during the reaction. After the reaction had been carried out for 90 min, both the heating and the supply of carbon monoxide were stopped and the autoclave was allowed to cool to room temperature.

Materials. 4-Bromo-*o*-xylene, 4-bromo-*m*-xylene, and 2-bromo-*p*-xylene were formed selectively from *o*-, *m*-, and *p*-xylenes respectively by the bromination of xylenes, using iodine as the catalyst according to

1) H. J. Leibu, *Chem. Abstr.*, **48**, 5214 (1954); **49**, 14807 (1955); **50**, 10775 (1956).

2) K. Yamamoto and K. Sato, This Bulletin, **27**, 389 (1954).

3) W. W. Prichard, *J. Am. Chem. Soc.*, **78**, 6137 (1956).

4) N. L. Bauld, *Tetrahedron Letters*, **1963**, 1840; E. Yoshisato, M. Ryang and S. Tsutsumi, Preprint for the 19th Annual Meeting of the Chemical Society of Japan, Yokohama (April, 1966), III, p. 321.

5) T. Mizoroki and M. Nakayama, This Bulletin, **40**, 2203 (1967).

6) T. Mizoroki, M. Nakayama and M. Furumi, *Kogyo Kagaku Zasshi* (*J. Chem. Soc. Japan, Ind. Chem. Sect.*), **65**, 1054 (1962).

Wisansky method;[7] they were purified by distillation. 5-Bromo-pseudocumene was obtained by the bromination of pseudocumene[8] and recrystallized from ethanol (mp 73°C). 2-Bromo-mesitylene was prepared from mesitylene[9] and purified by distillation. The other aryl halides and salts of carboxylic acids were commercial product; their purities were checked by gas chromatography before use. Commercially-available nickel(II) acetate and nickel tetracarbonyl (made by Alfa Inorganic, Inc.) were used without further purification. The carbon monoxide was obtained from the decomposition of formic acid; its purity was more than 98%.

Analyses. The organic products were extracted by diethyl ether, and the aqueous phase was separated from the ether phase. Carboxylic acids present in the ethereal layer were extracted with an aqueous potassium hydroxide or sodium carbonate solution (2N) from the other organic compounds. The carboxylic acids were precipitated from a given amount of the aqueous solution with an aqueous hydrochloric acid solution. Before the white precipitates were filtrated and washed well with cold water, they had been cooled well in a freezer. The amounts of carboxylic acids were determined by titration with an aqueous potassium hydroxide solution. They were identified by gas chromatographies of their methyl esters or by means of their IR absorption spectra or melting points. The amounts of Br^- and Ni^{2+} present in the aqueous phase were determined by the Volhard method and by EDTA titration respectively, and those of carbon monoxide and carbon dioxide, by absorption methods.

Results

Reaction Conditions. The reaction rates of aryl halides with carbon monoxide catalyzed by nickel tetracarbonyl depend greatly on the temperature, the pressure of carbon monoxide, and the amounts of water and of a salt of carboxylic acid to be discussed later. The effect of the temperature, for example, is shown in Fig. 1. Most of the reactions with aryl bromides were carried out under 200 kg/cm² at 250°C for 90 min. Carbon monoxide was absorbed within 40—60 min under the reaction conditions. Preliminary experiments showed that no aryl bromide was hydrolyzed under the reaction conditions, although most of the alkyl halides were hydrolyzed into alcohols and potassium halides by adding potassium acetate,

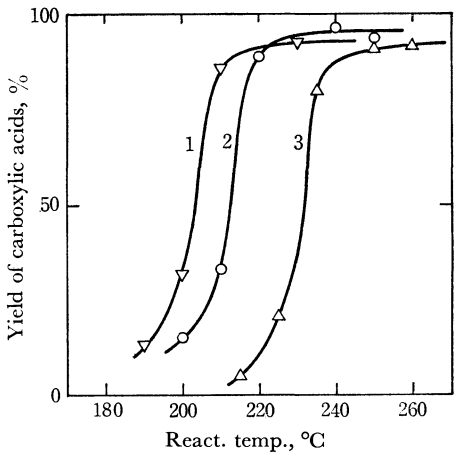

Fig. 1. Effect of temperature.
1. C_6H_5I (0.20 mol)
2. α-$C_{10}H_7Br$ (0.30 mol)
3. C_6H_5Br (0.30 mol)
Reaction conditions:
AcOK/aryl halide=1.1 mol ratio
H_2O/aryl halide=10 mol ratio
$Ni(AcO)_2 \cdot 4H_2O$/aryl halide=0.01 mol ratio
Pressure 200 kg/cm², Time 90 min.

Table 1. Synthesis of polymethylbenzoic acids

Aryl bromide 0.30 mol, H_2O 3.00 mol, potassium acetate 0.33 mol, nickel(II)acetate 0.003 mol; temp. 250°C, press. 200 kg/cm², time 90 min

Aryl bromide	Acid formed	Br^-			
		mol	%	mol	%
o-Bromotoluene	*o*-Methylbenzoic acid	0.260	86.5	0.299	99.6
m-Bromotoluene	*m*-Methylbenzoic acid	0.298	99.5	0.304	101
p-Bromotoluene	*p*-Methylbenzoic acid	0.283	94.4	0.289	96.4
4-Bromo-*o*-xylene	3,4-Dimethylbenzoic acid	0.284	94.6	0.296	98.7
4-Bromo-*m*-xylene	2,4-Dimethylbenzoic acid	0.263	84.3	0.286	95.3
2-Bromo-*p*-xylene	2,5-Dimethylbenzoic aicd	0.285	95.0	0.300	100
5-Bromopseudocumene[a]	2,4,5-Trimethylbenzoic acid	0.157	78.5	0.190	95.0
Bromomesitylene	2,4,6-Trimethylbenzoic acid	0.0923	30.8	0.202	67.3

a) 5-Bromopseudocumene used was 0.20 mol.

7) W. A. Wisansky and S. Ansbacher, "Organic Syntheses," Coll. Vol. III, p. 138, (1955).
8) J. Schramm, *Ber.*, **19**, 216 (1886).
9) L. I. Smith, "Organic Syntheses," Coll. Vol. II, p. 95 (1948).

without absorbing any carbon monoxide.

Syntheses of Substituted Benzoic Acids. The yields of polymethylbenzoic acids from the reactions with bromopolymethylbenzenes are described in Table 1. Carbon monoxide was absorbed almost quantitatively in the reactions of bromotoluenes (*o*-, *m*- and *p*-) or bromoxylenes (4-bromo-*o*-xylene, 4-bromo-*m*-xylene, and 2-bromo-*p*-xylene), and the corresponding benzoic acids were formed in very high yields. The amounts of Br^- described in Table 1 also show that bromotoluene and bromoxylene react quantitatively. In the reaction with bromobenzene, small amounts of benzene, phenol, and biphenyl were formed as by-products.*1 The corresponding hydrocarbons and phenols were also detected in the products obtained from the reactions with bromopolymethylbenzene. This is the reason why the amounts of benzoic acids formed are smaller than those of Br^-. 2,4,5-Trimethylbenzoic acid was also formed quantitatively from the reaction with 5-bromopseudocumene, while 2,4,6-trimethylbenzoic acid could not be obtained in a high yield from the reaction with bromomesitylene, probably because of the steric hindrance of two ortho methyls.

Carbonylations of *p*-bromoanisole, *p*-bromoacetophenone, and *p*-bromobenzoic acid were tested under the same conditions. *p*-Bromoanisole was very reactive, but *p*-methoxybenzoic acid was not formed selectively and a lot of by-product (*p*-methoxyphenol and anisole) were found in the product. On the other hand, *p*-bromobenzoic acid was not so reactive. Either the reaction temperature or the amount of water had to be increased in order to obtain terephthalic acid in a high yield. The reactivity of aryl bromide in the carbonylation reaction seemed to increase when methyls (electron-releasing substituents) were introduced into the benzene ring, but it was difficult to know the effects of other substituents on this reaction because of the side reactions.

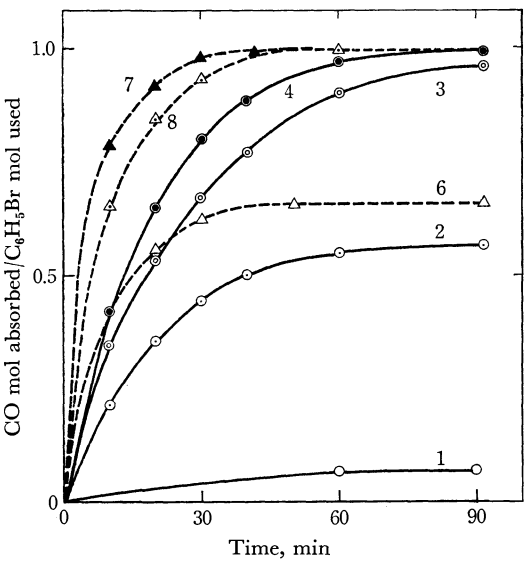

Fig. 2. Effect of potassium acetate on absorption rate of carbon monoxide.
Numbers in the figure are run No. in Table 2.

TABLE 2. EFFECT OF POTASSIUM ACETATE ADDED (at 250°C, 200 kg/cm²)

Run	Solvent	AcOK added (mol)	Convn. Acid or ester formed (%)	Convn. Br^- (%)	Ni^{2+} (%)
1	H_2O[a]	0.00	1.0	1.5	94.2
2		0.25	44.6	52.0	93.9
3		0.55	92.4	98.8	2.0
4		0.75	84.0	99.2	2.1
5	CH_3OH[b]	0.00	0.0	0.0	89.4
6		0.15	48.0	52.0	88.2
7		0.33	89.6	100	5.7
8		0.45	90.1	98.7	7.7

a) Bromobenzene used was 0.50 mol.
b) Bromobenzene used was 0.30 mol.

Effect of Salt of Carboxylic Acid. The effect of potassium acetate on the reaction of bromobenzene in the presence of either water or methanol is represented in Table 2 and Fig. 2. Figure 2 shows how effectively the addition of potassium acetate increases the absorption rate of carbon monoxide. Practically no carbonylation reaction took place when no potassium acetate was added. When the amount of potassium acetate was half of the amount of bromobenzene, that of the carbon monoxide absorbed was also nearly a half of the amount calculated from bromobenzene. Carbon monoxide was not absorbed quantitatively unless the amount of potassium acetate reached that of bromobenzene. The absorption rate of carbon monoxide was larger in methanol than in water.

Most of the nickel(II) acetate used as a catalyst was present as Ni^{2+} in the product when the amount of potassium acetate was smaller than bromobenzene. Only a small amount of Ni^{2+} was, however, detected and most of the nickel was present as nickel tetracarbonyl when enough potassium acetate was added, as is shown in Table 2. This means that the addition of potassium acetate is favorable for the formation of nickel tetracarbonyl during the reaction as well as for the carbonylation of bromobenzene. Its effect on the formation of nickel tetracarbonyl from nickel(II) bromide ($NiBr_2+5CO+H_2O\rightarrow Ni(CO)_4+CO_2+2HBr$) was,

*1 Carbon monoxide was partly consumed to form formic acid, but the amount so consumed was only 5—10% of the amount of carbon monoxide absorbed.

therefore, examined separately. Without potassium acetate, no absorption of carbon monoxide to form nickel tetracarbonyl was observed under the same conditions as for the carbonylation reaction of bromobenzene, but rapid absorption took place when twice as much potassium acetate was added as the amount of nickel(II) bromide, and most of the nickel(II) bromide (more than 95%) was reduced into either nickel tetracarbonyl or metallic nickel. Amines, such as pyridine, triethylamine, and aniline,*2 had nearly the same effect as salts of carboxylic acids, while the latter were more effective.

Kinetic Study. The rate of the carbonylation reaction of bromobenzene in the presence of enough potassium acetate ($AcOK/C_6H_5Br = 1.1$ mol ratio) was investigated on the basis of the absorption rate of carbon monoxide. $-\log(1-C_t)$ are plotted against the reaction time (min) in Fig. 3, where

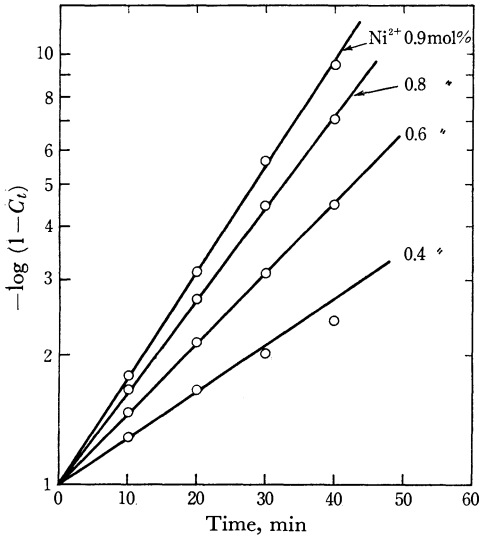

Fig. 3. Reaction rate of carbonylation of bromobenzene.
Reaction conditions: C_6H_5Br 0.50 mol, H_2O 3.00 mol, AcOK 0.55 mol, Temperature 250°C, Pressure 200 kg/cm²

C_t is the conversion of bromobenzene into benzoic acid calculated from the amount of carbon monoxide absorbed in t min. The rate was proportional to the amount of bromobenzene, and its rate constants could be obtained from the gradients of these linear plots. As is shown in Fig. 4, the rate was proportional to the amount (mol % based on bromobenzene) of nickel(II) acetate; in this figure the rate constants obtained in the case of introducing nickel tetracarbonyl*3 are also plotted. No difference between nickel(II) acetate and nickel tetra-

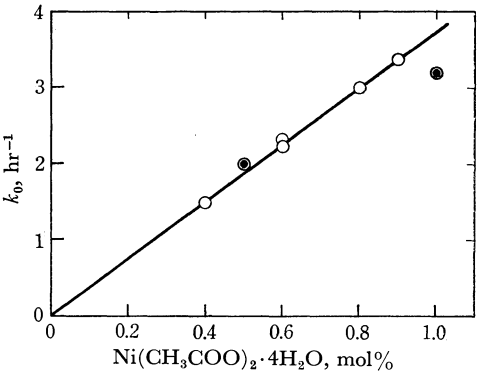

Fig. 4. Effect of nickel(II) acetate used as the catalyst on the reaction rate.
Reaction conditions: C_6H_5Br 0.50 mol, AcOK 0.55mol, H_2O 3.00 mol, Temperature 250°C, Pressure 200 kg/cm²
◉: nickel tetracarbonyl used as the catalyst

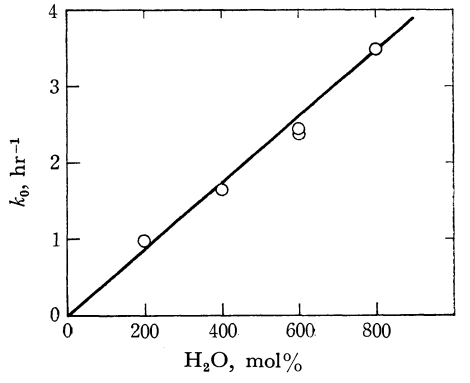

Fig. 5. Effect of water added.
Reaction conditions: C_6H_5Br 0.50 mol, AcOK 0.55 mol, $Ni(AcO)_2 \cdot 4H_2O$ 0.6 mol% (0.003 mol), Temperature 250°C, Pressure 200 kg/cm²

carbonyl was observed in their catalytic activities. The effect of water is shown in Fig. 5. The rate was also proportional to the amount of water over the range of 2—8 times as much as bromobenzene. When the amount of water added was more than 8 times, the absorption rate of carbon monoxide became too large to take its rate constant. The pressure of carbon monoxide had a strong effect, as is shown in Fig. 6 and Table 3. The maximum reaction rate was observed at 150 kg/cm² under the reaction conditions described in the figure. Under pressures of carbon monoxide higher than 150 kg/cm², the rate was nearly proportional to the reciprocal of the pressure. Somewhat different kinetic behavior was observed in the absorption

*2 Besides benzoic acid, a lot of *N*-benzoylaniline was formed.

*3 $Ni(CO)_4$ was introduced into the autoclave by carbon monoxide pressure when the temperature of the autoclave became 250°C.

TABLE 3. EFFECT OF CARBON MONOXIDE PRESSURE ON THE CARBONYLATION OF BROMOBENZENE

p_{CO} (kg/cm²)	Convn. Acid (%)	Convn. Br^- (%)	Ni^{2+} (%)	k_0 (hr^{-1})	Purge gas Vol. (l)[a]	Purge gas CO_2 (vol%)	Purge gas CO (vol%)	Purge gas Others (vol%)
400	50	60	—	0.76	22.9	9.4	75.6	15.0
300	72	80	1.7	1.42	17.1	9.6	77.2	13.2
200	92	99	2.0	2.29	11.7	9.0	78.6	12.4
170	87	101	1.3	3.04	9.5	8.9	77.5	13.6
150	79	99	3.3	3.66	8.3	16.0	70.4	13.6
140	84	101	0.0	3.52	7.8	14.0	70.9	15.1
120	65	101	5.0	2.14	6.2	27.4	54.2	18.4
100	59	94	21.7	1.39	5.2	32.2	47.7	20.1

a) at 0°C, 1 atm.

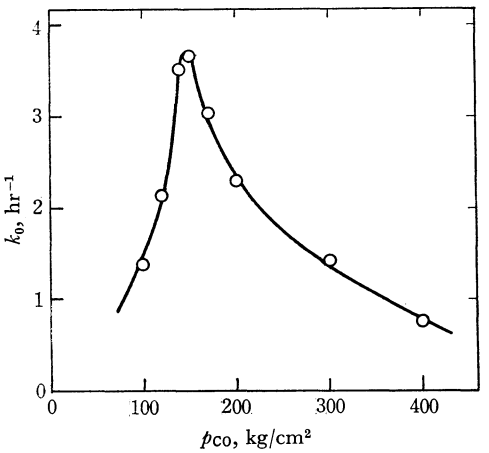

Fig. 6. Effect of carbon monoxide pressure on the reaction rate.
Reaction conditions: C_6H_5Br 0.50 mol, AcOK 0.55 mol, H_2O 3.00 mol, $Ni(AcO)_2 \cdot 4H_2O$ 0.6 mol-% (0.003 mol), Temperature 250°C

rates under lower pressures. However, it was difficult to obtain reliable data here, partly because the reaction was accompanied by side reactions (the formation of phenol and biphenyl) and benzoic acid was not selectively formed, as is shown in Table 3 (the difference between the amounts of benzoic acid and Br^- becomes large), and partly because the carbon monoxide pressure could not be assumed to be constant during the reaction as a result of the accumulations of carbon dioxide and hydrogen formed by a water-gas reaction in the autoclave.

Discussion

On the Effect of Salts of Carboxylic Acids. Figure 2 and Table 2 show that a strong protonic acid, HBr, strongly inhibits the carbonylation of bromobenzene, and that the inhibition can easily be removed by adding potassium acetate. From the facts that the equilibrium of the reaction of $RCOOK + HBr \rightleftarrows RCOOH + KBr$ ($R=CH_3-$, C_6H_5-, *etc.*) inclines much toward the right and that its reaction rate is very fast, it can be postulated that the hydrobromic acid formed from the carbonylation of bromobenzene is converted quantitatively into potassium bromide. The inhibition by hydrobromic acid can be explained as follows:

$$NiBr_2 + 5CO + H_2O \xrightarrow{r_1} Ni(CO)_4 + 2HBr + CO_2 \quad (1)$$

$$C_6H_5Br + Ni(CO)_4 \xrightarrow{r_2} (C_6H_5Br)Ni(CO)_n + (4-n)CO \quad (2)$$

$$(C_6H_5Br)Ni(CO)_n + H_2O \xrightarrow{r_2'} C_6H_5COOH + (HBr)Ni(CO)_{n-1} \quad (2')$$

$$HBr + Ni(CO)_4 \xrightarrow{r_3} (HBr)Ni(CO)_n + (4-n)CO \quad (3)$$

$$HBr + (HBr)Ni(CO)_n \xrightarrow{r_4} NiBr_2 + H_2 + nCO \quad (4)$$

The reaction rate (r_3) of $Ni(CO)_4$ with HBr would be much larger than that (r_2) of $Ni(CO)_4$ with C_6H_5Br, and the reaction rate (r_4) represented by Eq. (4) would also be very fast. Nickel tetracarbonyl is, consequently, difficult to be reformed so as to keep its concentration high, while the effective decrease in the concentration of hydrobromic acid by adding potassium acetate results in controlling the reaction of (3) and (4), and the $(HBr)Ni(CO)_{n-1}$ formed from the reaction of (2′) can be reconverted into nickel tetracarbonyl without any accompanying water-gas reaction, as is represented by Eq. (5):

$$(HBr)Ni(CO)_{n-1} \xrightarrow[-RCOOH,\ -Br^-]{+RCOO^-} Ni(CO)_{n-1} \xrightarrow{+CO} Ni(CO)_4 \quad (5)$$

The catalytic carbonylation of bromobenzene, therefore, takes place smoothly.

On the Kinetic Study. The kinetic behavior of the reaction with aryl bromide catalyzed by $Ni(CO)_4$ is similar to an oxo reaction catalyzed by $Co_2(CO)_8$. The rate of the latter is proportional to the amounts of an olefin and dicobalt octa-

carbonyl, the partial pressure of hydrogen, and the reciprocal of the partial pressure of carbon monoxide.[10] The former in the presence of enough potassium acetate is proportional also to the amounts of bromobenzene, nickel tetracarbonyl, and water, and to the reciprocal of carbon monoxide pressure, as is shown in Figs. 3, 4, 5, and 6, when the pressure is more than 150 kg/cm^2. Consequently, a reaction scheme similar to that derived from the kinetic study of the oxo reaction can be given to the carbonylation of bromobenzene catalyzed by nickel tetracarbonyl.

$$C_6H_5Br + Ni(CO)_4 \overset{K}{\rightleftarrows} (C_6H_5Br)Ni(CO)_3 + CO \quad (a)$$

$$(C_6H_5Br)Ni(CO)_3 + H_2O \xrightarrow{k} C_6H_5COOH + (HBr)Ni(CO)_2 \quad (b)$$

$$(HBr)Ni(CO)_2 + 2CO + AcOK \xrightarrow{fast} Ni(CO)_4 + AcOH + KBr \quad (c)$$

Assuming that nickel tetracarbonyl is reproduced sufficiently fast during the reaction and that the equilibrium of Eq. (a) is very small, the reaction rate, r, can be given by Eq. (d):

$$r = K \cdot k \frac{[Ni(CO)_4][C_6H_5Br][H_2O]}{p_{CO}}$$
$$k_0 = k \cdot K \frac{[Ni(CO)_4][H_2O]}{p_{CO}} \quad (d)$$

The $(k_0 \times p_{CO})$ values obtained from the k_0 of the reactions under pressures higher than 150 kg/cm^2, shown in Figs. 3, 4, 5, and 6, are plotted against $[Ni(CO)_4] \times [H_2O]$ in Fig. 7. The linear plot is in reasonable agreement with the rate Eq. (d). From these kinetic data alone, however, it was difficult to determine whether benzoic acid is formed by the attack of a water molecule or by a hydroxide ion in Eq. (b).

In the oxo reaction, hydrocobalt carbonyl was regenerated so rapidly that its concentration could be assumed to be constant during the reaction; otherwise, it is difficult to explain its kinetic behavior.[11] On the other hand, in the carbonylation of bromobenzene catalyzed by nickel tetracarbonyl, a σ-aryl nickel carbonyl could be formed by the oxidative addition of bromobenzene to nickel tetracarbonyl, as in a Grignard's reaction[12] or as in the carbonylation of aryl halide by the Rh-$(Ph_3P)_2(CO)Cl$ catalyst.[13] This σ-aryl carbonyl would also be rapidly rearranged with carbon monoxide coordinated to nickel into an acyl nickel carbonyl, which would, then, be attacked by a water molecule or a hydroxide ion to form benzoic acid; it is essential that nickel tetracarbonyl itself be regenerated rapidly for a smooth catalytic recycling. Its kinetic behavior, nevertheless, is very similar to the oxo reaction as long as enough potassium acetate is added to regenerate the nickel tetracarbonyl sufficiently fast. This means that acyl metal carbonyls are relatively stable in the catalytic carbonylation of aryl bromides as well as in oxo reactions.

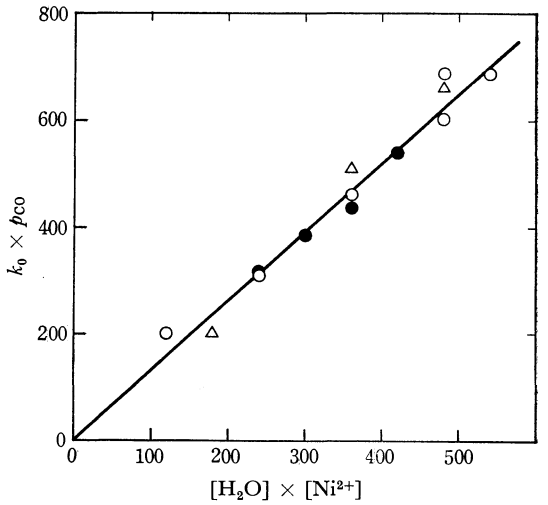

Fig. 7. Plots of k_0 according to the Eq. (d).
p_{CO}: ●, 300 kg/cm^2 ○, 200 kg/cm^2 △, 170 kg/cm^2

10) I. Wender, H. W. Sternberg and M. Orchin, "Catalysis," Vol. V, ed. by P. H. Emmett, Reinhold Publ. Co., New York (1957), p. 119.

11) A. J. Chalk and J. F. Harrod, "Advances in Organometallic Chemistry," Vol. 6, ed. by F. G. A. Stone and R. West, Academic Press, New York (1968), p. 129.

12) D. J. Cram and G. S. Hammond, "Organic Chemistry," McGraw-Hill Co., New York (1959), p. 219.

13) J. Tsuji and K. Ohno, *Tetrahedron Letters*, **1966**, 4713.

BULLETIN OF THE CHEMICAL SOCIETY OF JAPAN VOL. 42 1130—1135 (1969)

Amino-quinoid Polymeric System. The Preparation of a Polyester Containing 2,5-Diamino-*p*-benzoquinone Nuclei and Its Crosslinking

Ju KUMANOTANI, Kazuyuki SUGITA,*1 Seiji KAZAMA*2 and Toshio YOSHIKAWA*3

The Engineering Research Institute, Faculty of Engineering, The University of Tokyo, Yayoi, Bunkyo-ku, Tokyo

(Received February 20, 1968)

A polyester containing 2,5-diamino-*p*-benzoquinone nuclei was prepared by the polycondensation of 2,5-bis(ω-carboxyl-pentylamino)-*p*-benzoquinone with polyethylene glycol 400 at 160°C, 170°C and 180°C. At 160°C the esterification was brought about easily without gelation, giving an amino-quinoid polyester (prepolymer), but above 170°C an unexpected gelation was observed. The amino-quinone nuclei incorporated in the polyester thus prepared were confirmed by NMR spectroscopy. To make clear the influence of the amino-quinone nuclei upon the gelation, the thermal reactions of the model compounds, the above amino-quinoid dibasic acid, and its ethyl ester were investigated by means of IR spectroscopy and chemical analysis. It was concluded that the hydrogen atoms in the amino-groups of the quinone move to the oxygen atoms and that the resulting hydroxy groups combine with each other to form an ether bond as a result of dehydration. When the prepolymer prepared at 160°C was heated at 170°C for 4 hr with *p*-toluenesulfonic acid (5% by weight) or at 180°C for 8 hr without the acid catalyst, there was obtained an infusible and insoluble film which made crosslinkage as shown in the above mechanism.

While studying a new type of crosslinking polyamides, the present authors found that there is a possibility that the 2,5-diamino-*p*-benzoquinone nuclei introduced in the linear polymer chains will become new functional groups to undergo a crosslinking reaction upon the application of heat. Therefore, in order to elucidate the contribution of the amino-quinone nuclei linked in the polymer backbone to the crosslinking reaction, the present paper will deal with the system of a polyester prepared from 2,5-bis(ω-carboxyl-pentylamino)-*p*-benzoquinone (designated as Q-ACA) and a polyethyleneglycol. In comparison with the polyamide system, a clear interpretation can be obtained IR-spectroscopically for the change in the amino-quinone nucleus without any overlapping of its characteristic absorption bands (see Table 1) with those of the polyamides.

Thus, by using Q-ACA and a commercially-available polyethyleneglycol, PEG 400, we attempted to prepare a linear amino-quinoid polyester without gelation. The progress of the esterification was interpreted in terms of the results of the chemical and IR-spectral analyses. We also tried to reveal the mode of the crosslinking of the amino-quinone nucleus introduced into the polyester by investigating the spectral change in the amino-quinone nucleus, using model compounds of Q-ACA and its ethyl ester. The variation in the linkage of the resulting polyester was also accommodated by the mechanism shown in the scheme. (Eqs. (1), (2), and (3))

Experimental

Materials. PEG 400 of a chemically-pure grade was obtained commercially.

2,5-Bis(ω-carboxyl-pentylamino)-*p*-benzoquinone (Q-ACA) was prepared by the reaction of *p*-benzoquinone with ω-aminocaproic acid according to the method used for the preparation of 2,5-dialkylamino-*p*-benzoquinone derivatives,[1] except that methanol was used as the solvent instead of ethanol. Methanol gave a product with a higher purity than did ethanol. The blowing of air into the reacting solution, with or without cuprous acetate,[2] had no effect upon the yield. An example of the preparation of Q-ACA is the following: a solution of amino-caproic acid (12.9 g, 0.10mol) in 550 m*l* of methanol was mixed with a solution of *p*-benzoquinone (16.2 g, 0.15mol) in 200 m*l* of methanol in a one-liter, round-bottomed flask equipped with a refluxing condenser, and then the mixture was refluxed in a boiling

*1 Present address: Department of Graphic Engineering, Faculty of Engineering, Chiba University, Yayoi-cho, Chiba City.

*2 Present address: Technological Research Laboratories, Takeda Chemical Industries, Osaka.

*3 Present address: Ube Central Research Laboratories, Ube Industries, Ltd., Oguchi, Ube City.

1) a) see, *e. g.*, L. Fieser and M. Fieser, "Advanced Organic Chemistry," Reinhold, New York (1961), p. 853. b) O. Suchanek, *J. Prakt. Chem.*, **90**, 479 (1914). c) M. Martynoff and G. Tsatsas, *Bull. Soc. Chim. France*, **1947**, 52.

2) R. Baltzly and E. Lorz, *J. Am. Chem. Soc.*, **70**, 123 (1948); A. H. Crosby and R. E. Lutz, *ibid.*, **78**, 1233 (1956).

water bath for 15 min; the resulting solution was cooled to room temperature with ice. The brownish precipitates thus formed were filtered off, washed with benzene, dried *in vacuo*, and found to weigh 12.9 g (theor. 71.3%); decomposing melting point, *ca.* 204°C (measured by the capillary method).

Found: C, 58.75; H, 7.06; N, 7.49%. Calcd for $C_{18}H_{26}O_6N_2$: C, 59.00; H, 7.16; N, 7.65%.

The infrared spectrum of this compound was consistent with that of Q-ACA (see Table 1).

2,5-Bis(ω-ethoxycarbonyl-pentylamino)-*p*-benzoquinone (designated as Q-ACEt hereafter) was prepared by the reaction of *p*-benzoquinone with the ω-aminocaproic acid ethyl ester much as in the case of Q-ACA; a solution of the ω-aminocaproic acid ethyl ester (12.7 g, 0.08mol) in 50 m*l* of methanol was reacted with a solution of *p*-benzoquinone (13.0 g, 0.12mol) in 200 m*l* of methanol, and the resulting yellowish red precipitates were recrystallized from chloroform, dried *in vacuo*, and found to weigh 5.0 g (theor. 29.6%); mp 103—104°C.

Found: C, 62.40; H, 8.25; N, 6.77%. Calcd for $C_{22}H_{34}O_6N_2$: C, 62.54; H, 8.11; N, 6.63%.

The infrared spectrum of this compound was consistent with that of Q-ACEt (compare Fig. 5).

Polyesterification of Q-ACA with PEG 400. In a 50-m*l* flask equipped with an air-tight stirrer, a nitrogen inlet tube reaching to the bottom of the flask, a thermometer, and a short air-condenser for collecting water formed during the reaction, there was placed an equimolar mixture of Q-ACA (3.66 g, 0.01mol) and PEG 400 (4.00 g, 0.01mol). The mixture was heated while being stirred at 160°C, 170°C, or 180°C by means of an oil bath, while a slow stream of deoxygenated nitrogen was passed through it. In order to measure the degree of polyesterification, a sample (0.1—0.5 g) was taken out from the reacting mixture every two or three hours. This sample was dissolved in 50 m*l* of a mixed solvent (acetone-methanol-water, 10 : 5 : 1 by volume) and titrated with a 0.1N KOH ethanol solution on a Potentiograph, E336 (Methrohm Co., Ltd.). The change in the acid value *vs.* the reaction time is shown in Fig. 1.

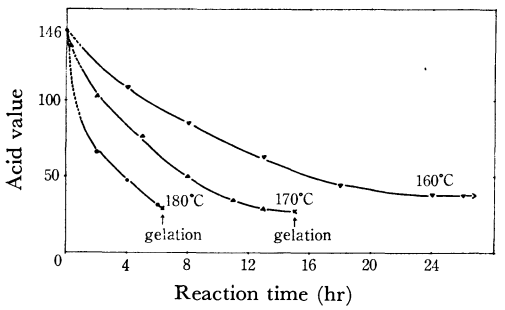

Fig. 1. Relation of the acid-value *vs.* reaction time in the polyesterification of Q-ACA with PEG 400.

Measurement of Curability of the Prepolymer. An acetone-methanol (2 : 1 by volume) solution of the prepolymer was evaporated on a glass plate (1 × 10 × 30 mm) at room temperature with or without the addition of 5% of *p*-toluenesulfonic acid as a catalyst. The thin film thus formed on the glass plate was placed into a heating apparatus *in vacuo*. In order to estimate the extent of the crosslinking of the film, the specimen on the glass plate was dipped in a mixed solvent of acetone-methanol (2 : 1 by volume) at room temperature for ten days or more to determine its solubility; the glass transition temperature was measured by the swinging-beam method.[3]

Results and Discussion

Polyesterification of Q-ACA with PEG 400. *Gelation.* On the basis of the relation between the acid value and the reaction time (see Fig. 1), the esterification of Q-ACA with PEG 400 was found to progress at 160°C, 170°C, and 180°C. In the polyesterification carried out above 170°C, gelation was found unexpectedly; it may be due to the amino-quinone nuclei, since such gelation cannot be seen in the usual polyesterification of a diol with a dibasic acid. The observed gelation time

Table 1. Characteristic absorption bands of 2,5-diamino-*p*-benzoquinone nucleus

Wave number (cm^{-1})	Assignment
3270 (s.)	νN–H
1635 (m.)	νC=C
1550 (s.)	νC=O
1500 (s.)	Amide II type band
1460 (s.)	δC–H (in plane)

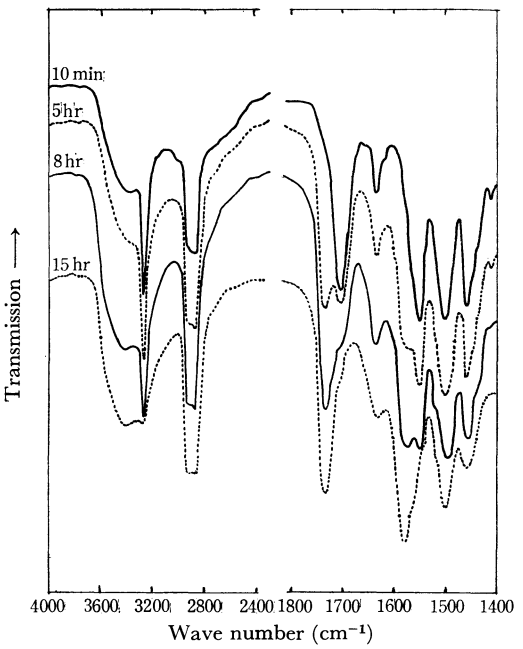

Fig. 2. IR-spectral change *vs.* reaction time in the polyesterification of Q-ACA with PEG 400 at 170°C (KBr disk).

3) K. Sato, H. Kiryu and Y. Inoue, *J. Japan Soc. Colour Material*, **31**, 81 (1958).

(the interval between the beginning of the heating of the reaction mixture and the gleation) was 15 hr at 170°C and 6.3 hr at 180°C. Accordingly, any polyesterification without such gelation should be carried out at 160°C or below.

Infrared Spectral Change. Upon an examination of the spectral change observed during the course of the polyesterification of Q-ACA with PEG 400, the characteristic absorption bands of Q-ACA could be assigned as is shown in Table 1.[4)]

As may be seen from the spectral change *vs.* the reaction time (see Fig. 2), as the polyesterification progresses, an increase in the absorption at 1730 cm^{-1} (characteristic of the carbonyl group of the ester) and a decrease in the absorption at 1705 cm^{-1} (characteristic of the carbonyl group of the carboxylic acid) may be seen.

Furthermore, remarkable spectral changes were observed for the characteristic absorption bands of the amino-quinone nucleus during the polyesterification. For example, in the polyesterification at 160°C, shown in Fig. 2, characteristic bands of the amino-quinone nucleus at 3270, 1500, and 1460 cm^{-1} decrease and the absorption band at 1550 cm^{-1} shifts to 1580 cm^{-1} as the esterification progresses. These spectral changes, nevertheless, cannot be interpreted in terms of the chemical change of the amino-quinone nucleus.

An infrared spectrum of the solution of an amino-quinoid compound differs markedly from that of a solute (*e. g.*, in a KBr disk) as a result of the strong molecular interaction of solid solute;[4)] the same is true of 2,5-bis(*n*-butylamino)-*p*-benzoquinone, as is shown in Fig. 3. This spectral difference observed for the amino-quinoid compound was used for the interpretation of the spectral change already observed in the above polyesterification. At the initial stage of the reaction, the reacting mixture, because the solubility of Q-ACA in PEG 400 was small, showed absorption bands characteristic of the solid amino-quinone, but as the esterification progressed and as the homogeneity of the reacting mixture increased, the absorptions characteristic of the amino-quinone dissolved in a solvent appeared. Moreover, the fact that the absorption shifts from 1550 cm^{-1} to 1580 cm^{-1} is in harmony with the above spectral results.

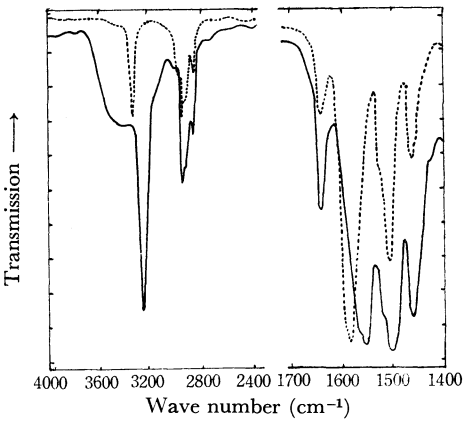

Fig. 3. IR-spectra of 2,5-bis(*n*-butylamino)-*p*-benzoquinone (—, KBr disk; ---, $CHCl_3$ solution).

NMR Spectra. A further chemical evidence for the stability of the amino-quinone nucleus was given by the NMR spectrum, measured for the polyester prepared at 160°C for 26 hr; the peak ratio between the proton (τ, 2.29) attached to nitrogen and the proton (τ, 4.81) attached to the quinone nucleus was approximately 1 : 1. Their peak intensities were comparable to the expected

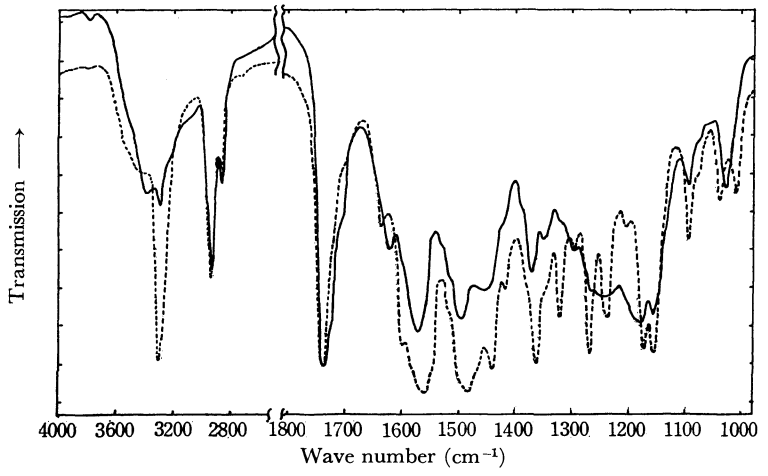

Fig. 4. IR-spectral change of Q-ACEt (---), kept at 200°C for 8 hr (—), (KBr disk).

4) Unpublished data: the spectral data of the amino-quinoid compounds will be shortly submitted for publication.

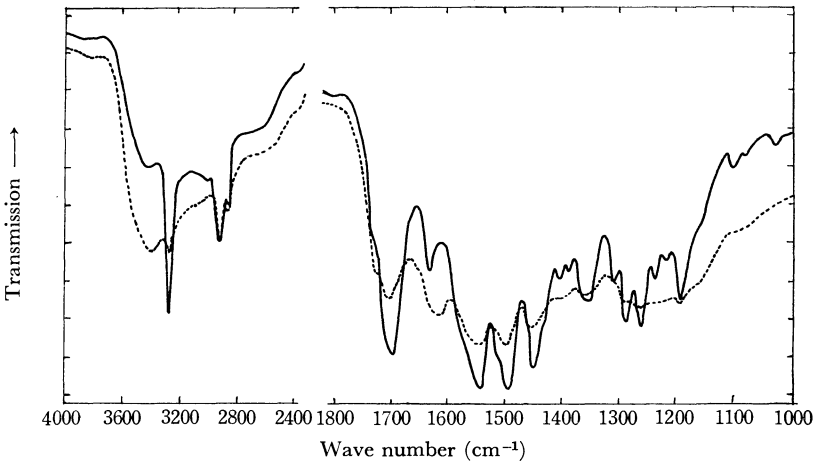

Fig. 5. IR-spectral change for Q-ACA kept at 170°C for 4 hr (—) and at 170°C for 8 hr (---), (KBr disk).

amount of the amino-quinone nuclei involved in the polyester. The assignment of the signals of protons attached to both nitrogen and the quinone nucleus was made using Q-ACEt as a standard material.

On the basis of the above results, it can readily be concluded that the polyester prepared by the reaction of Q-ACA with PEG 400 at 160°C has the expected amino-quinone nuclei.

Crosslinking Character of the 2,5-Diamino-quinone Nucleus. To avoid the trouble of interpreting the infrared spectra recorded during the course of the polyesterification, model compounds, *i. e.*, Q-ACEt and Q-ACA, were used to interpret the mode of the crosslinking of the polyesters containing amino-quinone nuclei in terms of their infrared spectra; a sample (50 mg), placed in an evacuated ampoule, was kept between 150°C and 210°C (±1°C) in an oil bath, and the spectral changes were observed in a KBr disk.

Q-ACEt. When the amino-quinone was kept at 190°C for 8 hr, the change (2—3%) of the amino-quinone was found IR-spectroscopically in a chloroform solution by measuring the intensity of the band at 3270 cm^{-1} (νN-H). As may be seen in Fig. 4, an abrupt decrease in the absorption was observed in the amino-quinone kept at 200°C for 8 hr. With this spectral change, the following absorption bands appeared: the broadened band at 3000—3600 cm^{-1}, attributable to the hydroxy groups formed according to Eq. (1); the band at 1625 cm^{-1}, attributable to the C=C group of the quinonediimine formed (Eq. (1)); the bands near 1250 cm^{-1} and 1027 cm^{-1}, attributable to the ether group of the compound formed due to Eq. (2), and understandable considering that vinyl ether homologues show the characteristic absorption bands of the ether group at 1270—1210 cm^{-1} and 1075—1020 cm^{-1} [5] and that the compound under consideration has structual units similar to those of vinyl ether compounds.

From the above spectral observations, it may be seen that hydrogen atoms in the amino-groups of the amino-quinone move to the oxygen atoms and that the resulting hydroxy groups combine with each other as a result of dehydration to form ether bonds (Eqs. (1), (2) and (3)).

Q-ACA. The amino-quinone kept at 170°C for 4 hr showed no apparent spectral change, but that kept for 8 hr showed a clear change in its nucleus. As is shown in Fig. 5:

(1) The absorption bands characteristic of the amino-quinone nucleus show a minor decrease in its intensity.

(2) The increased, broadened band at 3000—

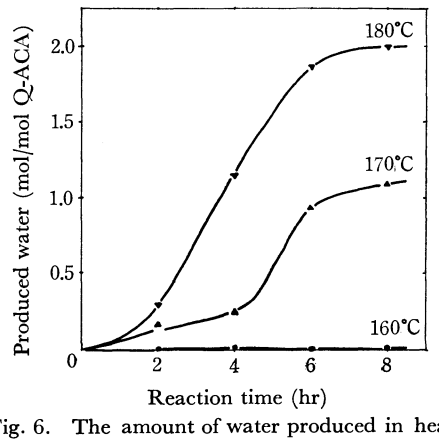

Fig. 6. The amount of water produced in heating Q-ACA at various temperatures.

5) see, *e. g.*, M. Ōki, "Sekigai Kyushu Supekutoru," (The Infrared Spectra), The Tokyo University Press, Tokyo (1968), p. 193.

3600 cm^{-1} is attributable to the hydroxy groups formed according to Eq. (1).

(3) The band attributable to the carbonyl group of the ester group occurs at 1730 cm^{-1} as a shoulder, while the absorption band of the carbonyl group at 1705 cm^{-1} decreases. This may be due to the ester group formed by the reaction between the carboxylic group present in the starting dibasic acid and the hydroxy group formed as has already been demonstrated (Eqs. (2) and (3)).

(4) In the region from 1100 cm^{-1} to 1300 cm^{-1}, near 1230 cm^{-1} and 1155 cm^{-1} there appear broadened absorption bands which may be ascribed to the ether (Eq. (2)) and ester (Eq. (3)) groups respectively. This assignment is reasonable in view of the spectral results shown already for the thermal reaction of Q-ACEt.

Further evidence supporting Eqs. (1), (2) and (3) was obtained by measuring the amount of the water formed in the thermal reaction of Q-ACA by the Karl-Fisher method: Samples (100 mg) were placed in evacuated ampoules. Several ampoules thus prepared were kept at 160°C, 170°C, or 180°C in an oil bath, and then each ampoule was taken out from the bath at intervals and cooled. The reacting mixture was taken out from the opened ampoule with 10 m*l* of methanol and submitted to titration. In order to calibrate the amount of the water formed, a blank test was carried out with the same volume of methanol as was used in the determination. The relation between the amount of the water formed and the time is plotted in Fig. 6. Figure 6 demonstrates that at 160°C and 8 hr heating, no formation of water was observed, and the amount of water per mole of Q-ACA was approximately 1 and 2 mol at 170°C-8 hr and 180°C-8 hr heating respectively, indicating that the amino-quinone nucleus was changed thermally above 170°C and that the esterification reaction (Eq. (3)) between the carboxyl groups of Q-ACA and the hydroxyl groups formed contributes predominantly to the formation of the water at 180°C.

On the basis of the results of the IR-spectral observation of the thermal reaction of Q-ACA and Q-ACEt, together with those of the above dehydration reaction of Q-ACA, the following scheme can be proposed for the thermal reaction of the 2,5-diamino-quinone nucleus; this scheme involves the isomerization of the amino-quinone nucleus and subsequent reactions:

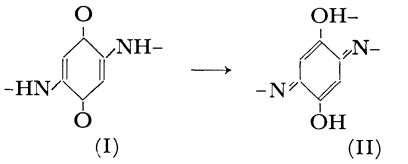

(I) (II) (1)

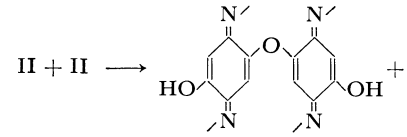

(2)

In addition, in the case of Q-ACA:

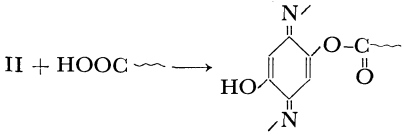

(3)

Crosslinking Character of the Quinoid Prepolymer. The mode of the crosslinkage of the prepolymer prepared by the reaction of Q-ACA with PEG 400 at 160°C for 26 hr was examined for a film baked at 180°C for 8 hr, and for that made by the addition of *p*-toluenesulfonic acid (5% by weight) to it, followed by baking at 170°C for 4 hr. For this purpose, the glass transition temperature on the cured film was measured by the swinging-beam method or the solubility of the film in a mixed

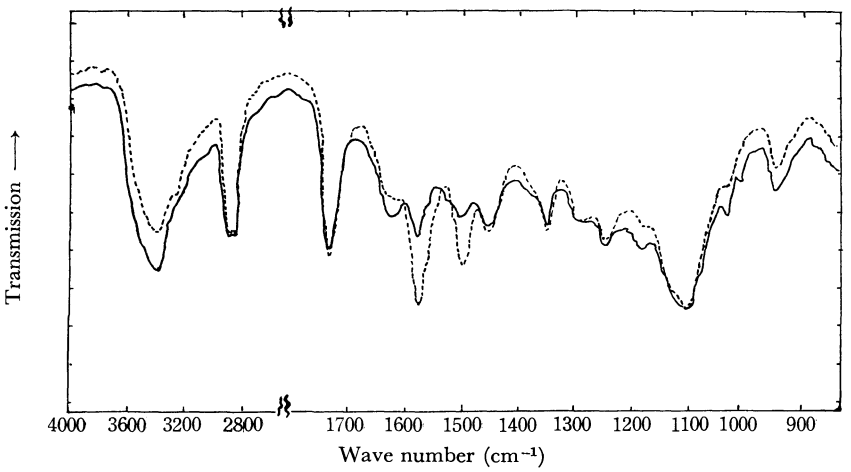

Fig. 7. IR spectra of an amino-quinoid polyester (---) and its cured film (—) at 170°C-4 hr heating with *p*-toluenesulfonic acid (5% by weight).

solvent of acetone-methanol (2 : 1 by volume) was determined. The reaction that occurred during the curing was inferred by means of an IR-spectral analysis of the cured film (see Fig. 7).

The glass-transition temperature was below 20°C for the film baked at 180°C-8 hr and 30°C for that baked at 170°C-4 hr. These facts show that the acid-catalyzed effect is predominant in giving an insoluble and infusible film, and that the glass-transition temperatures found on the cured films were not as high as had been expected from the rigid structure of the amino-quinone nucleus. This may be ascribed to the existence of flexible polyethylene ether chains introduced into the polymer chain by the PEG 400.

As may be seen in Fig. 7, a decrease in the absorption band characteristic of the amino-quinone nucleus and the appearance of the bands at 1250 cm^{-1} and 1030 cm^{-1} characteristic of the ether bond were more obvious in the film baked in the presence of *p*-toluenesulfonic acid than in that of the original polyester (prepolymer).

The thermal and acid-catalyzed baking procedures which bring about the crosslinkages to form an insoluble and infusible film are almost quite the same, since the spectra observed on the baked films formed by these two different methods are almost the same.

These results obviously indicate the contribution of the amino-quinone nuclei incorporated in the polyester to the crosslinking reaction through the steps of Eqs. (1), (2) and (3).

The authors are greatly indebted to Professor Tsutomu Kuwata, for his encouragement, help, and advice.

BULLETIN OF THE CHEMICAL SOCIETY OF JAPAN VOL. 42 1135—1141 (1969)

Electroless Nickel Plating from Acid-acetate Baths Containing Hypophosphite as a Reducing Agent

Kin'ya OGAWA

Hitachi Research Laboratory, Hitachi, Ltd., Kuji-machi, Hitachi, Ibaraki

(Received August 28, 1968)

The properties of acid-acetate baths containing hypophosphite as a reducing agent were studied in an attempt to obtain an electroless nickel deposit; further, the protective property of such deposits with phosphorus contents of 4 to 13% was investigated. The hypophosphite utilization efficiency for the deposition of electroless nickel was found to be 0.33; the deposition rate indicates a first-order dependence on hypophosphite, but it is independent of nickel concentration, within the limits specified in the range of suitable conditions. The phosphorus content of the deposits increases with a decrease in the pH value of the bath and with an increase in the initial concentration of hypophosphite, but it is independent of that of nickel. An electoless nickel with a high phosphorus content affords more protection against metallic bases.

Since the deposition of nickel containing a low percentage of phosphorus on a catalytic surface from an aqueous solution by means of the reduction of nickel salts with hypophospite was first described by Brenner and Riddell[1] in 1946, the deposit has been called electroless nickel to distinguish it from electroplated nickel. Although much research has been done on the subject, most of the work has been concerned with practical applications of the process[2-5] or with the structure[6-8] and the mechanical properties[7,9] of the deposit. It has also been

1) A. Brenner and G. E. Riddell, *J. Res. Natl. Bur. Std.*, **37**, 31 (1946); **39**, 385 (1947).

2) A. Brenner, *Metal Finishing*, **52** (11), 68; (12), 61 (1954).

3) Am. Soc. Testing Materials, Spec. Tech. Publ., No. 265, "Symposium on Electroless Nickel Plating," Philadelphia (1959).

4) G. Gutzeit, *Plating*, **46**, 1158, 1275, 1379 (1959); **47**, 63 (1960).

5) K. M. Gorbunova and A. A. Nikoforova, "Physicochemical Principles of Nickel Plating (Translated from Russian by A. J. Aladjem)," Israel Program for Scientific Translations, Ltd., Jerusalem (1963).

6) A. M. Goldenstein, W. Rostoker, W. Schossberger and G. Gutzeit, *J. Electrochem. Soc.*, **104**, 104 (1957).

7) A. H. Graham, R. W. Lindsay and H. J. Read, *ibid.*, **109**, 1200 (1962).

8) S. Urai and Y. Tanabe, *Kinzoku Hyōmen Gijutsu* (*J. Metal Finishing Soc. Japan*), **18**, 435 (1967).

9) J. P. Randin and E. H. Hintermann, *Plating*, **54**, 523 (1967).

established that the electroless nickel affords far more protection to metallic bases than does the electroplated nickel.[3,5,10] However, little attention has been paid to the phosphorus content as an important variable with regard to the protective properties of electroless nickel, except for two reports of Ishibashi, Takano and Shimizu,[11,12] and they only intimated that it should not be ignored.

The present paper will be concerned with our fundamental studies of the electroless nickel plating from an acid-acetate bath; the reaction balance, the deposition rate, and the phosphorus content of the deposit will be described, and the life of the bath will be considered. In addition, the protective properties of the deposit will be discussed as a function of its phosphorus content.

Experimental

Reagents. All the chemicals used were of the reagent grade. Sodium hypophosphite monohydrate, nickel chloride hexahydrate and sodium acetate trihydrate were used to prepare the plating baths. The pH of the bath was adjusted to the desired value by adding hydrochloric acid using a Horiba M-3 pH Meter with a glass electrode.

Plating Procedure. The equipment used in the plating tests was simple. A plating solution buffered with 0.3M acetate was placed in a covered cylindrical glass vessel; the bath temperature was kept constant within ± 0.3°C of the desired temperature by means of a water thermostat, the bath being left unagitated. A specimen, a brass or mild steel plate, which had previously been cleaned with trichloroethylene or electrocleaned, was immersed in the bath for the desired time. The deposition rate was obtained by weighing the dry specimens before and after the plating test. At each run, the nickel concentration was determined by the EDTA-titration method[13] and the phosphite and hypophosphite concentrations were determined by cerimetric procedures.[14,15]

The Determination of Phosphorus in the Deposits. The deposit on a bakelite coupon previousely sensitized with a palladium chloride solution[2] served to determine its phosphorus content. At the completion of a plating run, a calculated amount of the deposit was stripped from the base and dissolved in a small volume of hot nitric acid. The amount of phosphorus in the resulting solution was determined by spectrophotometric measurements[16] of the phosphomolybdic acid extracted with a mixed solvent composed of two parts of isobutyl alcohol and three parts of chloroform.

Estimation of the Protective Value of the Deposits. *Polarization Measurement.* Polarization curves in 1N sulfuric acid and 0.5N hydrochloric acid solutions were obtained by the galvanostatic method. Electroless nickel about 15 μ thick deposited on a brass plate, with a working area of 1 cm^2, was used as the working electrode. The potentials were measured by the direct method with a Luggin capillary using a saturated calomel electrode (SCE) as the reference electrode. A carbon plate was employed as the auxiliary electrode. All the measurements were made in 500-m*l* portions of the dilute acid solutions saturated with air, while the temperature was maintained at 30 ± 0.1°C by means of a water thermostat.

Porosity and Salt-spray Resistance. Electroless nickel for both the porosity measurements and the salt-spray test was deposited on a mild steel plate. The porosity of the deposits up to 20 μ thick was evaluated by means of a ferroxyl test. A filter paper saturated with a solution containing 10 g of potassium ferricyanide, 10 g of potassium ferrocyanide, 60 g of sodium chloride, and 5 m*l* of 28% ammonia water in 1*l* was pressed to the surface of the deposit for 5 min, and the blue spots which appeared on the filter paper were counted. The salt-spray test was performed in an Itabashi Salt-spray Chamber with a 5% sodium chloride solution at room temperature (25—30°C). Cycles of spraying for 8 hr and stopping for 16 hr were periodically repeated for five days, and then the rust spots on the surface were counted. The results of these tests are given as the average for the five samples.

Results and Discussion

Reaction Balance. According to Brenner,[1] the significant overall reaction for the deposition of electroless nickel can be writen as:

$$H_2PO_2^- + Ni^{2+} + H_2O \longrightarrow H_2PO_3^- + Ni + 2H^+ \quad (1)$$

Concurrently, more hypophosphite anions are oxidized to phosphite anions with the evolution of gaseous hydrogen according to the reaction:

$$H_2PO_2^- + H_2O \longrightarrow H_2PO_3^- + H_2 \quad (2)$$

Moreover, some of the hypophosphite anions supply the elemental phosphorus which alloys with the metallic nickel.

Table 1 lists the reaction balances for the deposition of electroless nickel from an acetate bath of pH 4.0. Attention is invited to Table 1, wherein the hypophosphite utilization efficiency, expressed as the molar ratio of the nickel deposited to the hypophosphite utilized, is always close to 0.33. Therefore, in order to examine whether this efficiency is independent of the plating conditions, a few tests were performed; the results are shown in Figs. 1 and 2. The discordance of the efficiencies in Figs. 1 and 2 must be considered as an inevitable consequence of the precision of the analytical method employed. It seems, therefore, as has been described by Gutzeit,[4] that the hypophosphite utili-

10) C. H. deMinjer and A. Brenner, *Plating* **44**, 1297 (1957).
11) S. Ishibashi, O. Takano and T. Shimizu, "The 10th Symposium on Corrosion and Prevention," Takarazuka (1963), p. 214.
12) *Idem*, *Kinzoku Hyomen Gijutsu* (*J. Metal Finishing Soc. Japan*), **16**, 236 (1965).
13) K. Ueno, "Kireto-Tekiteiho (Chelatometric Titration)," Nankodo, Tokyo (1961), p. 287.
14) D. N. Bernhart, *Anal. Chem.*, **26**, 1798 (1954).
15) K. Ogawa, This Bulletin, to be published.

TABLE 1. REACTION BALANCE FOR ELECTROLESS NICKEL DEPOSITION*

Plating time min	%P of deposit	P deposited mmol	$H_2PO_2^-$ utilized mmol	$H_2PO_3^-$ formed momol	Ni deposited mmol	Molar ratio Ni deposited / $H_2PO_2^-$ utilized
30	9.8	0.49	7.1	6.4	2.37	0.33
60	9.4	0.88	16.5	14.4	4.82	0.29
90	10.5	1.37	20.4	20.0	6.15	0.33
120	9.0	1.88	30.6	28.6	10.00	0.32

* In each run, electroless nickel was deposited on a 25 cm^2 bakelite coupon from about a 350 m*l* bath containing 44.2 mmol of nickel, 49.3 mmol of hypophosphite and 12 mmol of acetate. All the initial pH values were 4.0 and the temperatures, 90°C.

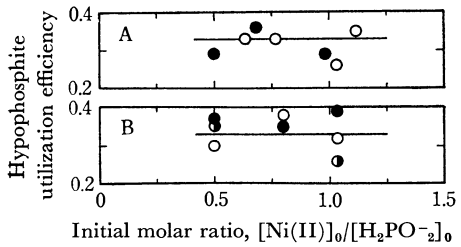

Fig. 1. Hypophosphite utilization efficiency for 30 min in electroless nickel deposition on a 25 cm^2 brass plate from a 400 m*l* bath at 90°C. The initial concentrations of baths are: (A) $[Ni(II)]_0=0.10$ M but $[H_2PO_2^-]_0$=variable, and (B) $[H_2PO_2^-]_0=0.10$ M but $[Ni(II)]_0$=variable.
○ pH 4.0; ● pH 4.5; ◑ pH 5.0

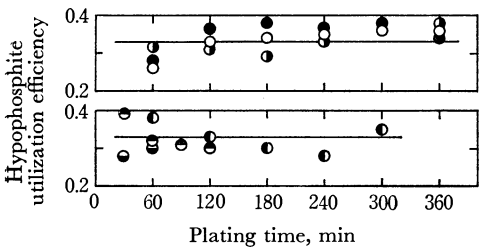

Fig. 2. Hypophosphite utilization efficiency in electroless nickel deposition on a 22.5 cm^2 mild steel plate from a 500 m*l* bath. The initial concentrations of baths are: $[Ni(II)]_0=0.10$ M, and $[H_2PO_2^-]_0=0.10$ M for pH 4.0, or 0.15 M for pH 4.5.
○ 80°C, ● 85°C, ◑ 90°C, ◐ 95°C at pH 4.0;
◒ 90°C at pH 4.5; ◓ 90°C at pH 5.0

zation efficiency is 0.33 independently of the plating conditions, within the range examined at least. This suggests that three moles of hypophosphite are consumed in order to deposit every mole of nickel, and that thus two moles of hydrogen are generated when one mole of nickel is deposited. However, we do not yet have an good explanation of why such a phenomenon occurs.

Deposition Rate. The deposition rates of electroless nickel from the baths of pH 4.0 and 4.5 are shown as the fucntions of nickel and of hypophosphite concentrations in Fig. 3. The deposition rate seems to be proportional to the hypophosphite concentration up to 0.1M at pH 4.0 or up to 0.15M at pH 4.5, but indepenent of the nickel concentration in the range of 0.05—0.2M in the pH range of 4—4.5.

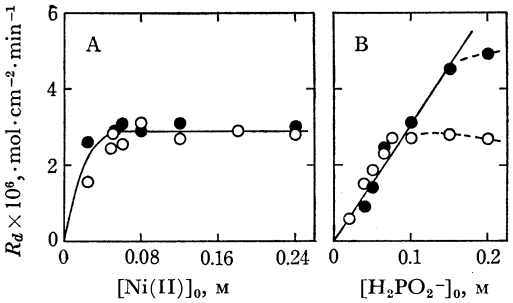

Fig. 3. The deposition rate of electroless nickel on a 25 cm^2 brass plate from a 400 m*l* bath at 90°C as the functions of nickel and of hypophosphite concentrations. The initial concentrations are:
(A) $[H_2PO_2^-]_0=0.10$ M but $[Ni(II)]_0$=variable, and
(B) $[Ni(II)]_0=0.12$ M but $[H_2PO_2^-]_0$=variable.
○ pH 4.0; ● pH 4.5

This can be verified by making the assumption, as has been described by Gutzeit[4] or by Ishibashi,[17] that the reaction undergoes an intermediate step as follows: the hypophosphite anion is converted into an active intermediate species, A^*, which is then adsorbed or loosely bonded to the catalytic surface:[18]

16) M. Ura, *Bunseki Kagaku* (*Japan Analyst*), **7**, 420 (1958).

17) S. Ishibashi *Kinzoku Hyomen Gijutsu* (*J. Metal Finishing Soc. Japan*), **12** 447 (1961).

18) Gutzeit[4] postulated that an active intermediate species is atomic hydrogen produced by the catalytic dehydrogenation of hypophosphite anion to metaphosphite anion: $H_2PO_2^- \rightarrow PO_2^- + 2H$; $PO_2^- + H_2O \rightarrow HPO_3^{2-} + H^+$. On the other hand, Ishibashi[17] departed from Gutzeit's concept and instead proposed that the hypophosphite anion converts from "normal type" into "active type" (probably adsorbed on the catalytic surface). A choice between the above explanations was not made.

$$H_2PO_2^- \underset{k_{-1}}{\overset{k_1}{\rightleftharpoons}} A^* \qquad (3)$$

thus taking part in the following simultaneous reactions:[19]

$$A^* + Ni(II) \xrightarrow{k_2} Ni \qquad (4)$$

$$A^* \xrightarrow{k_3} H_2 \qquad (5)$$

where Ni(II) represents bivalent nickel whether or not it forms complexes with acetate, and where the k's denote the rate constants of the reactions. Reaction (5) can be considered, on the basis of the aforementioned reaction balance, to take place twice as fast as Reaction (4). Therefore, by making a steady-state treatment, the deposition rate can be derived as:

$$R_d = \frac{k_1^0 k_2 [H_2PO_2^-][Ni(II)]}{k_{-1} + 3k_2[Ni(II)]} \qquad (6)$$

where R_d represents the deposition rate in mol·min^{-1}·cm^{-2}, where k_1^0 is k_1 V/A, where V is the bath volume in l, and where A is the deposited area in cm^2. By transposing Eq. (6), the following equation is derived:

$$\frac{[H_2PO_2^-]}{R_d} = \frac{3}{k_1^0} + \frac{k_{-1}}{k_1^0 k_2} \frac{1}{[Ni(II)]} \qquad (7)$$

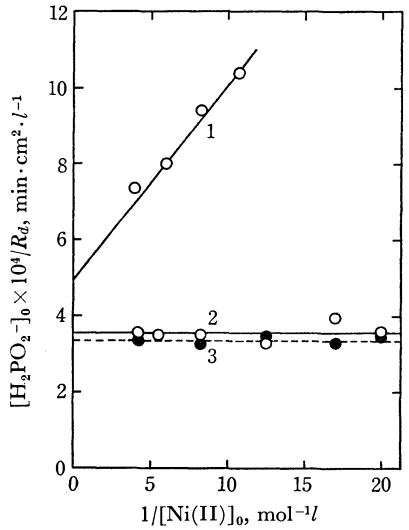

Fig. 4. Plots of $[H_2PO_2^-]_0/R_d$ *vs.* $1/[Ni(II)]_0$. The pH values of baths are: (1) 3.5, (2) 4.0, and (3) 4.5. Other plating conditions are the same as in Fig. 3(A).

19) According to West, both Reactions (4) and (5) may occur by electrochemical means: Ni(II)+2e→Ni and $2H^+ + 2e \rightarrow H_2$ for cathode reaction, $H \rightarrow H^+ + e$ for anode reaction: J. M. West, "Denseki to Fushoku (Electrodeposition and Corrosion Processes) (Translated from English by T. Ishikawa and T. Shibata)," Sangyo Tosho Publ. Co., Ltd. (1968) p. 63. A similar local cell type model for electroless nickel deposition was also suggested by Ishibashi.[17] The present author will also support West's concept.

The experimental data plotted according to Eq. (7) are shown in Fig. 4. Although the expected linearity is apparent, there are some discrepancies between the results at different pH values. A plot of pH 3.5 produces a slopig line, for instance, but the values of $[H_2PO_2^-]/R_d$ at pH 4.0 and 4.5 are almost independent of 1/[Ni(II)] in the concentration range examined. This suggests that the assumed active intermediate species, A^*, may react with Ni(II) at a much faster rate than it returns to hypophosphite anion in the pH range of 4—4.5. If this suggestion can be accepted as true, Eq. (6) takes a simpler form:

$$R_d = \frac{1}{3} k_1^0 [H_2PO_2^-] \qquad (8)$$

demonstrating that the deposition rate of electroless nickel is proportional only to the hypophosphite concentration.

The Change in the Hypophosphite Concentration of a Bath. From the aforementioned reaction balance, the hypophosphite concentration of a bath after t min can be expressed as:

$$[H_2PO_2^-]_t = [H_2PO_2^-]_0 - 3A\, x_{Ni}/V \qquad (9)$$

where x_{Ni} is the molar amounts of nickel deposited on the unit area and where the subscripts 0 and t indicate the concentrations at the initiation of the reaction and after t min respectively. By substituting Eq. (9) into Eq. (8) and by integrating, the following equation can be derived:

$$\log [H_2PO_2^-]_t = \log [H_2PO_2^-]_0 - \frac{k_1^0}{2.3} \frac{A}{V} \qquad (10)$$

The examples of plots according to Eq. (10) shown in Fig. 5 demonstrate their consistency with the

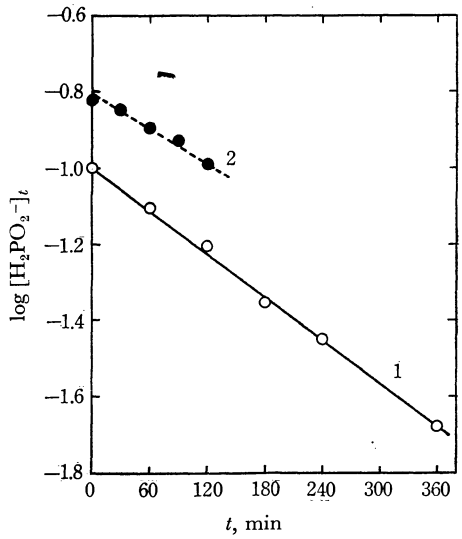

Fig. 5. Plots of $\log [H_2PO_2^-]_t$ *vs.* t at 90°C. The pH values of baths are: (1) 4.0 and (2) 4.5. Other plating conditions are the same as in Fig. 2.

Table 2. Rate constants at 90°C

pH	k_1^0 $min^{-1}\cdot cm^{-2}\cdot l$ From Fig. 4	k_1^0 $min^{-1}\cdot cm^{-2}\cdot l$ From Fig. 5	k_{-1}/k_2 From Fig. 4
3.5	(6.1×10^{-5})	—	(3.2×10^{-1})
4.0	8.4×10^{-5}	9.6×10^{-5}	Negligible
4.5	8.9×10^{-5}	8.5×10^{-5}	Negligible

Table 3. Rate constants, k_1^0, for pH 4.0 at different temperatures

Temp. °C	k_1^0 $min^{-1}\cdot cm^{-2}\cdot l$
80	5.0×10^{-5}
85	6.8×10^{-5}
90	9.6×10^{-5}
95	12.2×10^{-5}

first-order mechanism. The values of k_1^0 calculated from Fig. 5 are tabulated in Table 2, together with those obtained from Fig. 4. The two values are in reasonable agreement. Table 3 gives the values of k_1^0 obtained at different temperatures from plots according to Eq. (10). A liner relation was found between the logarithmic values of k_1^0 and the reciprocal of the absolute temperature, in which the apparent activation energy was estimated to be 15 kcal/mol.

The Life of the Bath. The only stable anion produced during the reaction is phosphite, which forms a greenish nickel phosphite precipitate.[4,10,20] This precipitate is undesirable, because it initiates the nucleation of nickel and causes the spontaneous decomposition of the bath and the eventual roughness of the deposit.

As has been indicated in connection with the reaction balance, the phosphite concentration accumulated in the bath is nearly equal to the decrease in the hypophosphite concentration, while the latter is approximately three times the decrease in the nickel concentration. Therefore, no precipitation occurs under the following conditions:

$$3x_{Ni}\frac{A}{V}\left([Ni(II)]_0 - x_{Ni}\frac{A}{V}\right) < L\left(1+\frac{[H^+]}{K_2}+\frac{[H^+]^2}{K_1K_2}\right) = L_{app} \quad (11)$$

where L and L_{app} are the absolute and the apparent solubility products of nickel phosphite, and K_1 and K_2, the first and the second acid dissociation constants of phosphorous acid; these values, determined at 90°C, are given in Table 4. The value of the left-hand of Eq. (11) cannot be above

20) S. Ishibashi, S. Orii and N. Tezuka, *Kinzoku Hyomen Gijutsu* (*J. Metal Finishing Soc. Japan*), **12**, 94 (1961).

Table 4. The acid dissociation constants of phosphorous acid and the solubility product of nickel phosphite at 90°C

H_3PO_3 *1 pK_1	H_3PO_3 *1 pK_2	$NiHPO_3$ *2 L $mol^2\cdot l^{-2}$
2.21	6.77	2.3×10^{-5}

*1 The values of pK_1 and pK_2 were determined by the pH titration method.

*2 The precipitation of $NiHPO_3$ was investigated in solutions containing 0.1 M of hypophosphite, 0.1 M of nickel and 0.3 M of acetate for various pH's and phosphite concentrations. The value of L was determined by observing whether a turbidity developed for 60 min at 90°C.

$3[Ni(II)]_0/4$. Therefore, if a set of conditions is selected where $[Ni(II)]_0 < 4L_{app}/3$, no precipitation is expected through the plating as long as no hypophosphite or nikcel salt is supplied. Calculations indicate that this limit is: $[Ni(II)]_0 < 0.13$M for pH 4.0, < 0.06M for pH 4.5, and < 0.03M for pH 5.0.

On the other hand, when the bath compositions exceed the above limit, the life can be estimated by the following equations derived from Eqs. (10) and (11):

$$life = \frac{V}{A}\frac{2.3}{k_1^0}\log\frac{[H_2PO_2^-]_0}{[H_2PO_2^-]_0 - 3\frac{A}{V}x_{Ni}} \quad 12)$$

$$\frac{A}{V}x_{Ni} = \frac{3[Ni(II)]_0 - \sqrt{9[Ni(II)]_0^2 - 12L_{app}}}{6}$$

Some examples of the estimated life are shown in Fig. 6.

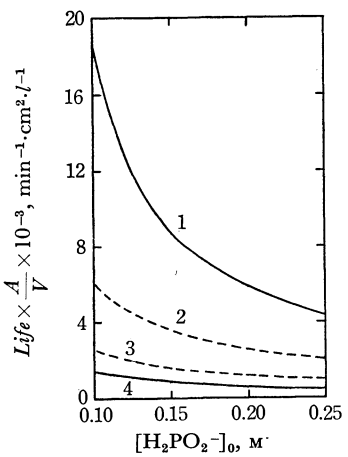

Fig. 6. The life of electroless nickel plating baths buffered with 0.3 M acetate at 90°C. (1) pH 4.0, $[Ni(II)]_0=0.2$M; (2) pH 4.5, $[Ni(II)]_0=0.1$ M; (3) pH 4.5, $[Ni(II)]_0=0.2$ M; (4) pH 5.0, $[Ni(II)]_0=0.1$ M.

The Phosphorus Content of the Deposit.

As a result of the change in the bath compositions through the plating, it is expected that a phosphorus gradient exists across a deposit. However, as may be seen in Table 1, the phosphorus content of the deposit is almost constant, independent of the plating time, up to 120 min, in spite of the fact that the bath compositions change. Therefore, a phosphorus gradient across a deposit may be not very steep.

The phosphorus content for the deposits obtained at a constant plating time of 60 min was also investigated as a function of the bath compositions. The results in Figs. 7 and 8 reveal that the phosphorus content of a deposit increases as the pH rises and with an increase in the initial concentration of hypophosphite, but that it is independent of the concentration of nickel.

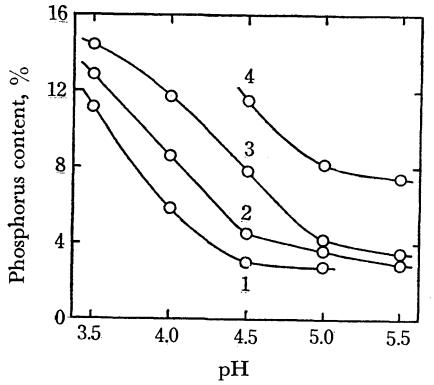

Fig. 7. The phosphorus content of electroless nickel deposit as a function of the initial pH value of bath. The initial concentrations of baths are: $[Ni(II)]_0$ =0.09 M, and $[H_2PO_2^-]_0$=(1) 0.05 M, (2) 0.10 M, (3) 0.15 M, and (4) 0.20 M.

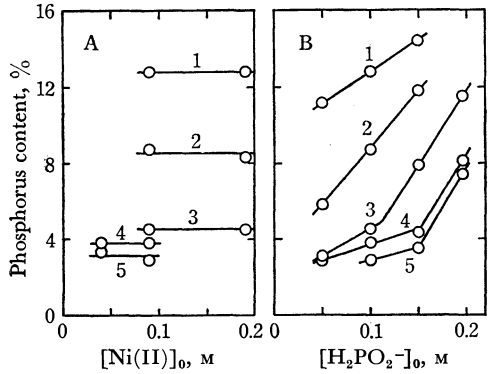

Fig. 8. The phosphorus content of electroless nickel deposit as the functions of bath compositions. The initial concentrations of baths are: (A) $[H_2PO_2^-]_0$ =0.10 M but $[Ni(II)]_0$=variable, and (B) $[Ni(II)]_0$ =0.09 M but $[H_2PO_2^-]_0$=variable. The initial pH values are: (1) 3.5, (2) 4.0, (3) 4.5, (4) 5.0, (5) 5.5.

The Protective Value of the Deposit. Examples of the polarization curves of the deposits in a 1N sulfuric acid solution are shown in Fig. 9. Similar results were obtained in a 0.5N hydrochloric acid solution. In all cases, both anodic and cathodic polarization curves exhibited Tafel-type behavior, and an increase in the phosphorus content moves the corrosion potential to a more positve value and reduces the corrosion currents. The corrosion rates calculated from the corrosion currents are given in Fig. 10, together with the minimum thickness free of pores and the salt-spray

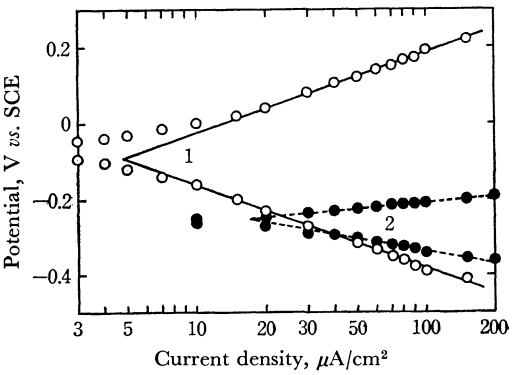

Fig. 9. The polarization curves of electroless nickel deposits in a 1 N sulfuric acid solution. The deposits contain (1) 8.7 and (2) 3.6% phosphorus.

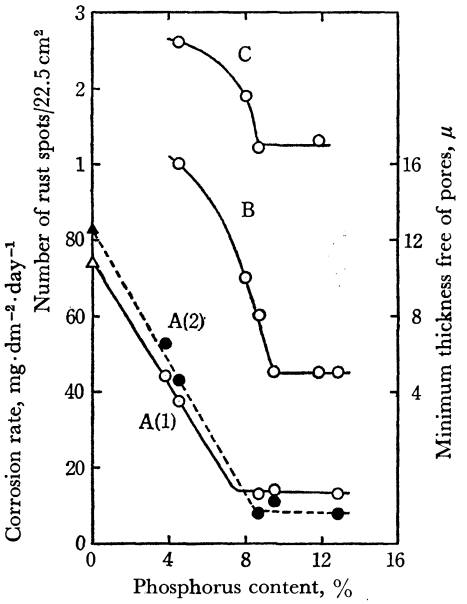

Fig. 10. The protective values of electroless nickel as the function of its phosphorus content.
(A) Corrosion rate in (1) 1 N H_2SO_4 and (2) 0.5N HCl
(B) Minimum thickness free of pores
(C) Number of rust spots by salt spray
△, ▲ Pure nickel foil

resistance as functions of the phosphorus content. Generally, an electroless nickel with a high phosphorus content affords low porosity; it also exhibits a high resistance to dilute acid media and to salt-spray. These results are in qualitative agreement with some observations of deMinjer and Brenner,[10] who reported a rise in the resistance of similar electroplated alloys to salt-spray and outdoor exprosure with an increase in the phosphorus content. In Fig. 10 it is also shown that all of the curves change in the vicinity of 9% phosphorus; the corrosion rate by dilute acid solutions, the minimum thickness free of pores, and the number of rust spots caused by salt-spray, all decrease with a rise in the phosphorus content up to about 9%, while they remain practically as constant as the phosphorus content when it increases above 9%. This behavior seems to be connected with the fact that the as-deposited electroless nickel deviates gradually from a face-centered cubic lattice condition with an increase in the phosphorus content and is converted into an amorphous state above 7.4% of phosphorus.[8]

The author wishes to express his deep gratitude to Dr. Natsuki Kawashima of the Hitachi Research Laboratory, Hitachi, Ltd., and to Dr. Takeshi Nakatogawa of the Hitachi Kasei Co., Ltd., for their guidance and encouragement throughout this work.

NOTES

BULLETIN OF THE CHEMICAL SOCIETY OF JAPAN VOL. 42 1142—1144 (1969)

Studies on Photo-polarography. II. Photo-polarographic Behavior of Dissolved Oxygen under Ultraviolet Irradiation

Hideo IMAI and Kazuo YAMASHITA

Department of Chemistry, Faculty of General Education, Hiroshima University, Hiroshima

(Received June 24, 1968)

In the past five years the photocurrents produced by the ultraviolet irradiation of the mercury electrode have been investigated and developed by several workers.[1-6]

Heyrovsky[1] has found a rapid current increase in a magnitude of about 1 microA at the irradiated dropping mercury electrode (DME) in solutions of sulfuric acid. He interpreted the experimental finding in terms of the photosensitized decomposition of water molecules adsorbed on the electrode surface. On the other hand, Barker and his co-workers[2] and Delahay and Srinivasan[3] have explained the same phenomenon by assuming a simplified model in which all the hydrated electrons*1 are deposited on a plane at a distance, δ, away from the electrode surface.

According to the radiolysis study, it is assumed that, in oxygenated aqueous solutions, the hydrated electron reacts immediately with dissolved oxygen to form the hydroperoxy radical;

$$e^-_{aq} + H^+ \rightarrow H \quad (1)^{*2}$$

$$H + O_2 \rightarrow HO_2 \quad (2)$$

$$e^-_{aq} + O_2 \rightarrow O_2^- \quad (3)^{*2}$$

The relative importance of these relevant reactions depends upon the pH and the oxygen concentration. The kinetics of the hydroperoxy radical there formed have been investigated by fast reaction techniques.[8-11]

Our present investigation is primarily concerned with anomalies of the second reduction wave of dissolved oxygen under polychromatic ultraviolet irradiation on the DME. Observations were carried out on the field dependence of the photocurrents and on the effects of surface-active substances, hydrated electron scavengers, and radical scavengers on the photocurrent. A possible reaction mechanism is proposed for the reaction of dissolved oxygen under ultraviolet irradiation.

Experimental

Reagent-grade methanol, ethanol, and acetone were redistilled. Special-grade sodium sulfate from Wako Pure Chemicals Ind., Ltd., was used without further purification. The water used was distilled twice. All the other chemicals and the apparatus used were the same as those reported in a previous paper.[12] The solutions contained 0.5 M Na_2SO_4 as the supporting electrolyte. The solutions were equilibrated with atmospheric oxygen at room temperature.

Results and Discussion

Polarograms of Dissolved Oxygen under Ultraviolet Irradiation. Oxygen develops two polarographic reduction waves in neutral aqueous salt solutions, the first wave corresponding to the two-electron reduction of oxygen to hydrogen peroxide, and the second, to the two-electron reduction of hydrogen peroxide to hydroxyl ions.

1) M. Heyrovsky, *Nature*, **200**, 880 (1963).
2) G. C. Barker, A. W. Gardner and D. C. Sammon, *J. Electrochem. Soc.*, **113**, 1132 (1966).
3) P. Delahay and V. S. Srinivasan, *J. Phys. Chem.*, **70**, 420 (1966).
4) H. Berg, *Rev. Polarog.* (Kyoto). **11**, 29 (1963).
5) For a review, see T. Kuwana in "Electroanalytical Chemistry," Vol. I, A. J. Bard ed., Marcel Dekker, New York (1966), p. 210.
6) For a review, see H. Berg, H. Schweiss, W. Stutter and K. Weller, *J. Electroanal. Chem.*, **15**, 415 (1967).
*1 Walker[7] has recently confirmed the existence of hydrated electrons at the electrode-solution interface by observing the absorption spectra during the electrolysis of water.
7) D. C. Walker, *Can. J. Chem.*, **45**, 807 (1967).
*2 The rate constants for reactions (1) and (3) are given as $2.36 \times 10^{10} M^{-1} \cdot sec^{-1}$ and $(1.88 \pm 0.2) \times 10^{10} M^{-1} \cdot sec^{-1}$ respectively.[11]
8) S. Gordon, E. J. Hart, M. S. Matheson, J. Rabani and J. K. Thomas, *J. Am. Chem. Soc.*, **85**, 1375 (1963).
9) E. Saito and B. H. J. Bielksi, *ibid.*, **83**, 4467 (1961).
10) J. H. Baxendale, *Radiation Res.*, **17**, 312 (1962).
11) G. Czapski and B. H. J. Bielsky, *J. Phys. Chem.*, **67**, 2180 (1963).
12) K. Yamashita and H. Imai, This Bulletin, **41**, 1339 (1968).

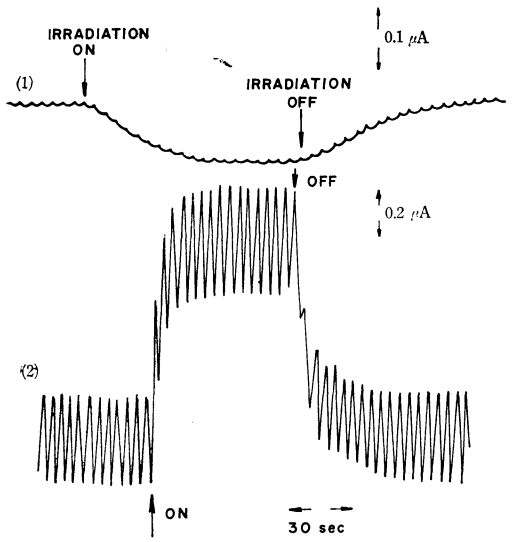

Fig. 1. Photocurrents.
(1) The negative photocurrent observed at −1.3 V *vs.* SCE in deaerated solutions of 0.5M Na_2SO_4.
(2) The positive photocurrent of the dissolved oxygen observed at −1.3 V in solutions of 0.5M Na_2SO_4.
(The photocurrent represents the difference between the currents measured with and without irradiation.)

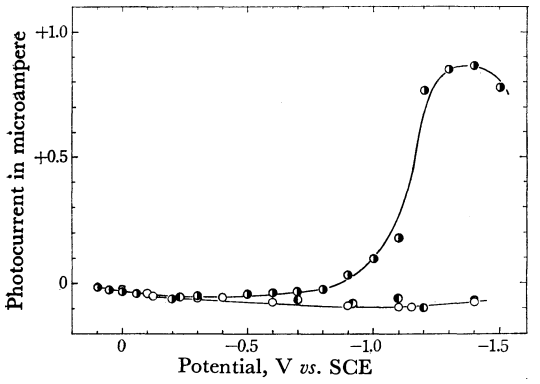

Fig. 2. Dependence of photocurrents on the electrode potentials in aqueous solutions of 0.5 M Na_2SO_4.
○ deaerated 0.5M Na_2SO_2 solutions
◑ 0.5M Na_2SO_4 solutions containing 0.25 mM oxygen
◐ 0.5M Na_2SO_4 solutions containing 0.25 mM oxygen and 0.005% gelatine

In a deaerated 0.5 M Na_2SO_4 solution, a small negative photocurrent was observed under the continuous ultraviolet irradiation of the DME. This residual photocurrent is shown in Figs. 1 and 2. The surface tension and the differential capacity of the DME and the effect of the carbon dioxide dissolved in the solution on the anodic residual photocurrent were measured with and without ultraviolet irradiation. The results, however, showed no appreciable irradiation effect. The mechanism of this negative residual photocurrent may be attributed to the presence of impurities in the solution, but the details are still unknown.

In the presence of oxygen the polarographic reduction under ultraviolet irradiation showed a different pattern from the normal wave; *i. e.*, the first wave did not show any appreciable change, while the height of the second wave was markedly increased. Figure 1 shows the positive photocurrent measured at −1.3 V *vs.* SCE. Figure 2 shows the dependence of the photocurrent on the electrode potential. The marked positive photocurrent begins to appear from the potentials at about −0.9 V when hydrogen peroxide is reduced. In this connection Silvestroni and Carelli[13] have observed anomalies in the oscillograph polarographic wave of oxygen at an irradiated mercury drop; they explain the anomalies as the effect of streaming caused by the heat absorption at the electrode-solution interface. It is noteworthy that, in our experiment, the positive photocurrent are observed at potentials more negative than −0.9 V, while the effect of irradiation was scarcely observed at potentials less negative than −0.9 V. Moreover, it was confirmed that the surface tension and differential capacity of the DME were little influenced by irradiation. Thus, the variation on the reduction wave upon exposure to light can not be interpreted in terms of a mere physical effect such as streaming. The apparent quadratic field dependence of the photocurrent (charge) has been pointed out for the scavenging of e_{aq}^- with H^+ by Delahay and Srinivasan.[3] They have cited Fowler's theory[14] on photoemission by a metal under a vacuum and monochromatic irradiation. No interpretation has, however, been worked out for their particular case, *i. e.*, emission in an aqueous electrolyte and polychromatic irradiation. In our experiment the square root of the photocurrent *versus* the potential plot was far from a linear relationship. The concave curvilinear plot seems to suggest the regeneration of H_2O_2 by a subsequent homogeneous chemical reaction, probably the bimolecular decay of O_2^- to yield H_2O_2.

Effect of Surface-active Substances on Photocurrent. The positive photocurrent was conspicuously affected by very small amounts of such surface-active substances as gelatin (*cf.* Fig. 2) and methylcellulose, and it completely disappeared in the presence of about 2×10^{-4}% gelatin or 4×10^{-4}% methylcellulose. The negative photocurrent was more pronounced with any increase in the methyl-

13) P. Silvestroni and I. Carelli, *J. Electroanal. Chem.*, **15**, 317 (1967).
14) R. H. Fowler, *Phys. Rev.*, **38**, 45 (1931).

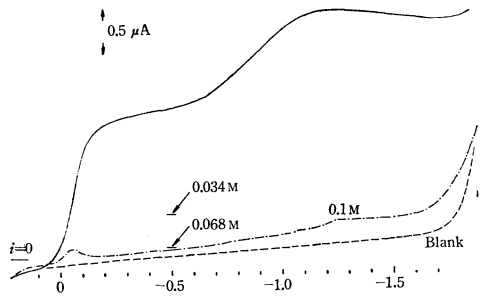

Fig. 3. Effect of acetone on the polarograms of the dissolved oxygen with the continuous irradiation in solutions of 0.5M Na_2SO_4.

cellulose concentration higher than 4×10^{-4}%. Anodic photocurrents similar to those in the case of methylcellulose have been observed in solutions of glyoxal, diacetyl, sodium oxalate, *etc.* by Heyrovsky,[15] who explained these findings by assuming that the light-absorbing species responsible for the anodic photocurrents are the complexes between the adsorbed organic molecules and the mercury electrode. In view of the photoemission of electrons and the formation of hydrated electrons, it seems that the effect of surface-active substances on the photocurrents can be interpreted on the basis of the variation in the work function due to the adsorbed molecules or/and to the scavenging of hydrated electrons by the adsorbed molecules.

Effect of Hydrated Electron Scavenger and OH Radical Scavenger on Photocurrent. The effect of acetone as a scavenger for hydrated electrons on the photocurrents was investigated. When the concentration of acetone was increased, the height of the reduction wave of the dissolved oxygen under ultraviolet irradiation was markedly decreased, and it completely disappeared upon the addition of 0.2 M acetone, as is shown in Fig. 3. This indicates that the amount of dissolved oxygen is reduced by the reduced form of acetone.*3 Reaction (3) may be followed by a slow reaction;

$$O_2^- + H_2O_2 \rightarrow O_2 + OH + OH^- \qquad (4)$$

The OH radical thus formed will pertain to the electrode process through several reaction paths such as the dimerization of OH to form H_2O_2, and the reaction of OH with H_2O_2 to form O_2^- and H^+. Methanol and ethanol are known to be effective OH radical scavengers. It was confirmed that these scavengers slightly affected the photocurrent. It

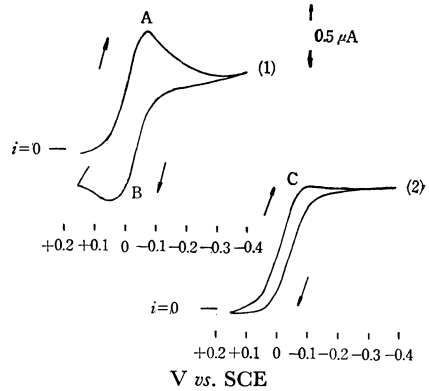

Fig. 4. Cyclic voltammetric curves of the first reduction of oxygen in aqueous solutions of 0.5 M Na_2SO_4 and 0.30 mM oxygen.
(1) without irradiation
(2) with irradiation

may be concluded that contribution of reaction (4) to the photocurrent is negligibly small.

Reaction Mechanism and Cyclic Voltammetry. From the above-mentioned results, we assumed the following reaction scheme;

$$(e^-)_{metal} + h\nu \rightarrow (e^-)^*_{metal} \qquad (5)$$

$$(e^-)^*_{metal} \xrightarrow{\text{(transfer reaction)}} e^- \qquad (6)$$

$$e^- + H_2O \rightarrow e^-_{aq} \qquad (7)$$

$$e^-_{aq} + O_2 \rightarrow O_2^- \qquad (8)$$

$$O_2^- + O_2^- + H_2O \rightarrow O_2 + H_2O_2 + 2OH^- \qquad (9)^{*4}$$

The concentration of hydrogen peroxide in the vicinity of the irradiated DME is increased through reaction (9). It is noteworthy that the cyclic regeneration of O_2 through reactions (8) and (9) results in the formation of H_2O_2. This assumption agrees well with the positive photocurrents observed in relation to the second reduction wave of dissolved oxygen.

The *i-E* curves recorded in the cyclic voltammetry of the first reduction of oxygen are shown in Fig. 4. Under continuous irradiation the anodic wave disappeared, as is shown in Fig. 4, curve (2). It seems that this results also supports the assumption of the coupled chemical reaction (possibly by reactions (8) and (9)) through which the irreversible behavior of the $O_2-H_2O_2$ redox couple is favored.

The authors wish to express their hearty gratitude to Professor Niro Matsuura of the University of Tokyo for his kind suggestions regarding this investigation.

15) M. Heyrovsky, *Nature*, **209**, 708 (1966).

*3 The reduction of methylene blue by ultraviolet irradiation was more pronounced in the presence of acetone. This inherently suggests that the reduced form of acetone was formed in the bulk of the solution.

*4 The validity of reaction (9) was confirmed by radiation chemistry reaction.

BULLETIN OF THE CHEMICAL SOCIETY OF JAPAN VOL. 42 1145—1146 (1969)

Surface Potential Study of Stearic Acid Monolayer on Mercury

Takuya YAMASHITA, Tadashi NAGAI*1 and Kozo HIROTA

Department of Chemistry, Faculty of Science, Osaka University, Toyonaka, Osaka

(Received July 4, 1968)

Numerous investigations of insoluble monolayers on aqueous surfaces have been reported. Such studies, however, are limited to materials which spread on and are insoluble in water.

Mercury is an ideal substrate to examine surface films because of the high surface tension and the insolubility of organic materials in it. The force-area properties of organic monolayers on mercury have been reported by Fahir[1] and Ellison.[2] In the present work, the surface potential of stearic acid monolayer spread on mercury surface was investigated as a function of the film area.

Experimental

Stearic acid (Merck) was of analytical grade, and used without further purification. Benzene was used as the spreading solvent. C. p. benzene was shaken with sulfuric acid until free from thiophene and then washed with alkali and water. After drying over sodium, it was distilled and kept over sodium. The solute concentration in a spreading solution was 0.04%.

Mercury was purified by the method of Nicholas *et al.*[3]; mercury was washed with a series of solutions (3N NaOH, 3N HNO_3, and 0.001N HNO_3) by bubbling air. The purified mercury was distilled *in vacuo* and stored under nitrogen.

The surface potential, ΔV, was measured by the vibrating electrode method. The potential was reproducible within ± 10 mV. Surface moment of the film, μ, was calculated by utilizing the Helmholtz formula, $\mu = \Delta V A / 4\pi$, where A is the area per molecule.

The trough measured $300 \times 100 \times 4$ mm, and was made of glass. Prior to use, the trough was washed with running water and then with distilled water. It was dried by flushing dry nitrogen.

All the experiments were carried out at room temperature under the flow of dry nitrogen.

The trough was filled with mercury. The equilibrium value of the potential was attained 20 min after formation of the surface and no appreciable change was detected after 20 hr. The potential was increased by 300 mV by replacing nitrogen with moist air (relative humidity, 80%; 22°C).

The spreading solution was applied to the mercury surface of 300 cm^2 by means of a micrometer syringe. The film area was changed by the successive injection method. The interval between injections was 10 min. When 0.01 m*l* benzene was spread on the mercury surface with 10 min interval up to the amount of 0.13 m*l*, no appreciable surface potentials were produced. Ellison[2] reported that no detectable surface pressures were developed by spreading benzene on the mercury surface in the atmosphere of nitrogen.

Results and Discussion

Figures 1 and 2 show the surface potential-area and surface moment-area curves for stearic acid on mercury, respectively. In Fig. 1, the maximal value of surface potential is 35 mV at the area of 30 $Å^2$ per molecule. Figure 2 indicates that the

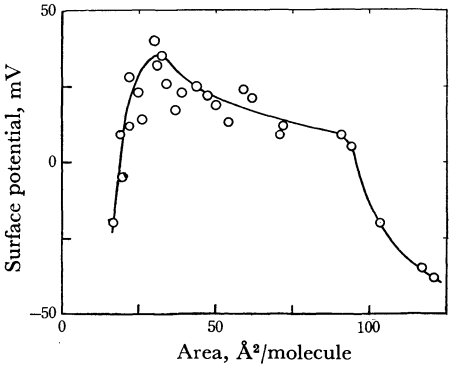

Fig. 1. Surface potential-area curve for stearic acid monolayer on mercury (23±1°C).

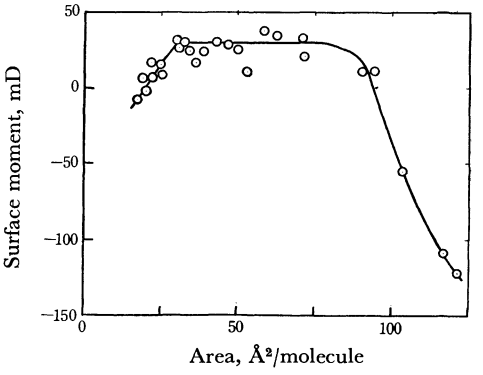

Fig. 2. Surface moment-area curve for stearic acid monolayer on mercury (23±1°C).

*1 Present address: Research Laboratories, Shionogi Pharmaceutical Company, Fukushima-ku, Osaka, Japan.

1) E. Fahir, *J. Chim. Phys.*, **27**, 587 (1930).
2) A. H. Ellison, *J. Phys. Chem.*, **66**, 1867 (1962).
3) M. E. Nicholas, P. A. Joyner, B. M. Tessem and M. D. Olson, *J. Chem. Phys.*, **65**, 1373 (1961).

surface moment is independent of the film area from 30 to 80 Å^2 per molecule with a value of 30 mD.

The results shown in Figs. 1 and 2 suggest that the monolayer of stearic acid on mercury collapses at the area of about 30 Å^2 per molecule. This area agrees well with that obtained from the surface pressure measurements.[2)]

It is to be noted that the values of surface potential and moment on mercury surface are considerably smaller than those found on acidic aqueous subphases (400 mV and 210 mD at maximum),[4)] and are comparable to the values reported on metals. Timmons and Zisman[5)] found that the values of surface potential for stearic acid monolayer ranged from a maximum of 365 mV on tungsten to −95 mV on lead. They concluded that the perpendicular component of dipole moment of the adsorbed acid molecule (surface moment) varied as a result of the specific interaction of metal substrate and the acid carboxyl group. However, they could not evaluate the values of surface moment because the surface concentration of the acid adsorbed on metals remained unknown. In the present work, the value of surface moment was found to be 30 mD for the stearic acid monolayer on mercury. The considerably small value of the moment seems to indicate a strong interaction of acid carboxyl group with liquid mercury at the interface.

Throughout the present work, no direct evidence is available regarding the chemical purity of the mercury surface. However, it should be noted that the potential value on a mercury surface without film was increased remarkably by replacing nitrogen with moist air. This fact would be caused by either oxidation of the mercury surface or adsorption of water to the surface, or by both.

4) E. D. Goddard and J. A. Ackill, *J. Colloid Sci.*, **18**, 585 (1963).

5) C. O. Timmons and W. A. Zisman, *J. Phys. Chem.*, **69**, 984 (1965).

BULLETIN OF THE CHEMICAL SOCIETY OF JAPAN VOL. 42 1146—1148 (1969)

Two-stage Polymerization of (1,3-Dioxolan-4-yl)methyl Acrylate

Hiroshi MINATO*1 and Namiko MURAMATSU

Department of Chemistry, International Christian University, Mitaka, Tokyo

(Received July 13, 1968)

A monomer containing two different polymerizable functional groups is of interest from the viewpoint of the two-stage polymerization. Monomers containing a vinyl group and an epoxy group such as glycidyl methacrylate,[1,2] and monomers containing a vinyl group and a tetrahydrofuran ring such as tetrahydrofurfuryl methacrylate[3,4] have been investigated in detail. (1,3-Dioxolan-4-yl)methyl acrylate containing a vinyl group and a dioxolane ring appears to be a very interesting monomer, but it has been mentioned only briefly in two patents.[5]

The preparation, the structure and the two-stage polymerization of this monomer have been investigated in detail, and the findings will be described in this paper.

Experimental

1,2-Methyleneglycerol. This was prepared as a mixture with 1,3-methyleneglycerol according to the method of Hibbert and Carter.[6] From 175 g of paraformaldehyde and 525 g of glycerol, 309 g of a mixture of methyleneglycols was obtained (52%).

(1,3-Dioxolan-4-yl)methyl Acrylate (DA). Into a 1-liter three-necked flask equipped with a mechanical stirrer, a condenser and a thermometer, 300 g of methylene glycerol, 122 g of acrylic acid and 258 g of benzene were added. After 1 ml of concentrated sulfuric acid and 8.6 g of copper powder were added, the mixture was placed in an oil bath at 110°C. The solution was refluxed at about 88°C, and became yellow after 12 hr of heating and stirring. The unreacted 1,3-methyleneglycerol was removed by washing with saturated sodium chloride solution. Four washings with 50 g portions of

*1 To whom correspondence should be addressed at Department of Chemistry, Tokyo Metropolitan University, Setagaya, Tokyo.

1) T. Otsu, K. Goto and M. Imoto, *Kobunshikagaku*, **21**, 198 (1964).

2) I. M. Kochnow and M. F. Sorokin, *Vyskomol Soedin.*, **6**(5), 791 (1964); *Chem. Abstr.*, **61**, 5765 (1964).

3) I. Sakurada, K. Noma and Y. Ohfuji, *Kobunshikagaku*, **21**, 295 (1964).

4) I. Sakurada, K. Noma and Y. Ohfuji, *ibid.*, **21**, 481 (1964).

5) E. Ellery, Brit. Pat. 690709 (April 29, 1953) and Brit. Pat. 695633 (Aug. 12, 1953).

6) H. Hibbert and N. M. Carter, *J. Am. Chem. Soc.*, **50**, 3120 (1928).

the salt solution removed 275 g of 1,3-methyleneglycerol. Then benzene was distilled off at 20 mmHg in a water bath at 30°C, and finally 82 g of a colorless liquid was collected by distillation at 55—57.5°C/0.2—0.3 mmHg. Its infrared spectrum shows absorptions at 1705 and 1723 cm^{-1}, which indicate that this liquid is a mixture of acrylic acid and an acrylic acid ester. The liquid was dissolved in carbon tetrachloirde, and acrylic acid was extracted with a 5% sodium hydrogen carbonate solution. Ten washings removed all the acrylic acid in the mixture. The carbon tetrachloride solution was dried by use of anhydrous sodium carbonate. The solvent was removed under reduced pressure, and 34.5 g (19%) of DA was obtained by distillation at 60—64°C/0.8 mmHg. Found: C, 53.10; 53.14; H, 6.41; 6.43%. Calcd for $C_7H_{10}O_4$: C, 53.14; H, 6.37%.

Determination of Formaldehyde from DA. About 0.1 g of DA was accurately weighed, and was added to a 20% sulfuric acid solution. The solution was refluxed for one hour, and then was steam-distilled. About 300 m*l* of a distillate was collected, which was refluxed for one hour with 20 m*l* of a 7% hydroxylamine hydrochloride solution. After cooled to room temperature, the hydrochloric acid liberated was titrated with 0.1 N sodium hydroxide solution by use of a pH meter. Because of the very dilute concentration, the titration curve was not so sharp. Eighty-three percent of formaldehyde was detected. When authentic 1,3-dioxolane was subjected to this analysis, 0.88 mol of formaldehyde per mole of dioxolane was detected.

Free Radical Polymerization of DA. *In Toluene.* One gram of DA, 0.0197 g of azoisobutyronitrile, and 3 g of toluene were heated at 80°C under nitrogen atmosphere. After 5 min of heating, viscous materials precipitated as a lower layer. After two hours of heating, the precipitated polymer was separated by decantation. The polymer was dissolved in acetone and reprecipitated by addition of petroleum ether. This purification was repeated twice. White solids obtained were soluble in acetone or chloroform, and were hygroscopic. The surface became smooth upon absorption of moisture in air.

In Benzene. DA, 0.9458 g, was refluxed in 3 g of benzene with 0.0197 g of azoisobutyronitrile for 3 hr. Though the hot solution was transparent, a transparent polymer precipitated when the solution was cooled to room temperature. The polymer was separated by decantation, and was dissolved in acetone, but a fraction of the polymer was insoluble in acetone which corresponded to 17% of the monomer used. The acetone-soluble polymer was reprecipitated by addition of petroleum ether. The dissolution-reprecipitation was repeated twice. The polymer dried under reduced pressure weighed 0.689 g (73%), and resembled to the polymer obtained in toluene.

The viscosity of the polymer was determined in acetone at 30°C, and it was found that $[\eta]$ was 0.137. The application of the equations established for poly (methyl acrylate) ($[\eta]=1.49\times10^{-3}\times P^{0.52}$, acetone, 30°C)[7] and poly (ethyl acrylate) ($[\eta]=4.19\times10^{-4}\times P^{0.66}$, acetone, 30°C)[8] gave the molecular weights of 5.14×10^5 and 3.39×10^5, respectively. Therefore, it is likely that the molecular weight of the polymer obtained is about 10^5.

Second-stage Cationic Polymerization of Poly-(1,3-dioxolan-4-yl)methyl Acrylate. The polymer obtained by azoisobutyronitrile was subjected to a ring-opening polymerization.

When the polymer was heated at 140°C with about 10 weight percent of *p*-toluenesulfonic acid, some reaction took place and the polymer became insoluble in acetone. Apparently some crosslinking occurred through opening of the dioxolane ring. The polymer was not hard solids at high temperatures, but a gummy material. Probably the crosslinking was not so extensive.

When the polymer was mixed in acetone with about 45 weight percent of boron trifluoride etherate and the mixture was evaporated under reduced pressure, the polymer became light brown in 1 hr at room temperature, and became reddish brown in 3 hr. The brown polymer was insoluble in acetone, and when heated up to 160°C it became black hard solids.

Cationic Polymerization of DA. When a mixture of 1 g of DA and 0.15 m*l* of boron trifluoride etherate was allowed to stand in a test tube protected by a calcium chloride tube at room temperature for 67 hr, a hard brown solid polymer was obtained. The polymer was not soluble in acetone, and when heated up to 180°C it was hard black solids.

Results and Discussion

(1,3-Dioxolan-4-yl)methyl acrylate (DA) was prepared from acrylic acid and a mixture of 1,2- and 1,3-methyleneglycerol. The assignment of the structure was supported by correct elemental analyses, formaldehyde determinations, infrared and NMR spectra. The NMR spectrum showed chemical shifts at 6.45 ppm(2H; H_A), 6.1 ppm (1H; H_B), 5.0 ppm (2H; H_C), 4.29 ppm (2H; H_D), 4.0 ppm (2H; H_E) and 3.8 ppm (1H; H_F).

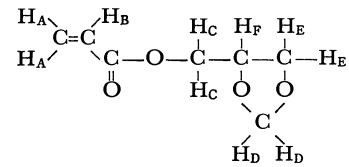

When DA was polymerized in toluene or benzene by azoisobutyronitrile at 80°C, white solid polymer was obtained. The polymer was soluble in acetone or chloroform, and its NMR spectrum showed that vinyl hydrogens (6.45 ppm and 6.1 ppm) were completely converted into aliphatic hydrogens. The evidence suggests that this polymer was formed through the polymerization of carbon-carbon double bonds without participation of dioxolane rings. When the poly DA was heated with *p*-toluenesulfonic acid or was allowed to stand at room temperature with boron trifluoride etherate, some crosslinking occurred and the polymer became insoluble in acetone.

7) H. Ito, S. Shimizu and S. Suzuki, *Kogyo Kagaku Zasshi(J. Chem. Soc. Japan, Ind. Chem. Sect.)*, **59**, 930 (1956).

8) H. Sumitomo and Y. Hachihama, *Kobunshikagaku*, **10**, 544 (1953).

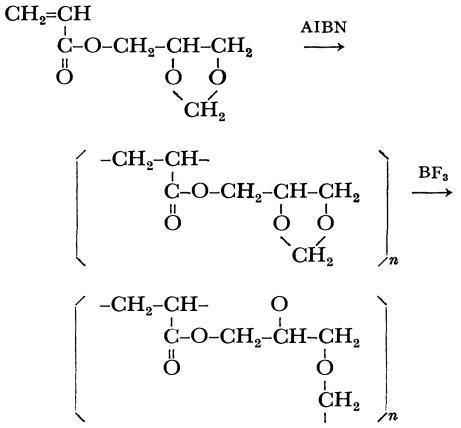

When the poly DA was heated alone to 270°C and then cooled, the polymer was insoluble in acetone. Apparently some crosslinking occurred, but much less extensively than the case with boron trifluoride, since the acetone-insoluble polymer was soft at high temperatures.

When the DA monomer was treated with boron trifluoride etherate at room temperature, a reddish brown solid polymer was obtained. It was insoluble in acetone. Its infrared spectrum resembled to that of the polymer prepared by the second-stage cationic polymerization of the poly DA obtained by azoisobutyronitrile. Therefore, it appears that the treatment of DA with boron trifluoride polymerizes not only the dioxolane rings but also vinyl bonds.

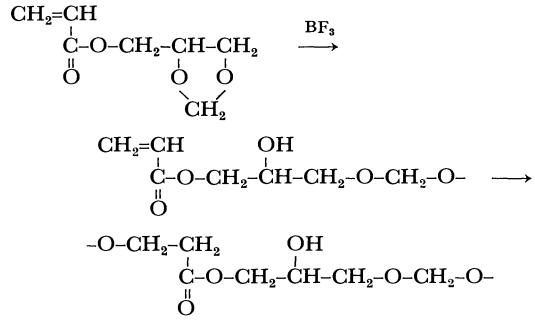

BULLETIN OF THE CHEMICAL SOCIETY OF JAPAN VOL. 42 1148—1150 (1969)

Alkoxysilanes. I. Preparation of Alkoxysiloxy Derivatives of Antimony

Yoshimoto ABE*1 and Ichiro KIJIMA*1

Department of Chemistry, Faculty of Science, Science University of Tokyo, Kagurazaka, Shinjuku-ku, Tokyo

(Received July 15, 1968)

Much work has been done concerning the preparation of alkyl or arylsiloxy derivatives of metals $(R_3SiO)_nM$ (M=Si,[1] Al,[2] Sn,[3] Ti,[4] Zr,[4]). Although the preparation of tris(triethylsilyl) antimonite by Andrianov[5] and the preparation of (trimethylsiloxy)(alkyl)antimony derivatives of the $(Me_3SiO)_nSbR_{m-n}$ ($m=3$ or 5, $n=1$ or 2, R=Me or Ph) type by Schmidbaur[6] have been reported, no other derivatives of antimony are known. Moreover, none of the alkoxysiloxyderivative of metals have been investigated.

We, therefore, attempted to prepare antimony derivatives containing a relatively stable trialkoxysiloxy group and tris(trimethyl or triphenylsilyl) antimonite.[7] The results of measurements of the relative hydrolytic stability and the infrared absorption spectra of these new compounds will also be indicated.

The preparation of tris(triorganosilyl) antimonite was carried out according to two procedures. One was a reaction between antimony trialkoxide and silanols; the other was a reaction of antimony trichloride with silanols in the presence of amine. Tris(tri-*t*-butoxysilyl) antimonite was distilled out as a white crystalline solid; it was very soluble in common organic solvents. Tris(triphenylsilyl)

*1 Present address: Department of Industrial Chemistry, Faculty of Engineering, Science University of Tokyo, Kagurazaka, Shinjuku-ku, Tokyo.

1) L. H. Sommer, L. Q. Green and F. C. Whitmore, *J. Am. Chem. Soc.*, **71**, 3253 (1947).

2) K. A. Andrianov, A. A. Zhdanov, N. A. Kurasheva and V. G. Dulova, *Dokl. Akad. Nauk S.S.S.R.*, **112**, 105 (1957).

3) H. Schmidbaur and H. Hussek. *J. Organometal. Chem.*, **1**, 244 (1965).

4) D. C. Bradley and I. M. Thomas, *J. Chem. Soc.*, **1959**, 3404.

5) K. A. Andrianov, A. A. Zhdanov and E. A. Kashtina, *Dokl. Akad. Nauk S.S.S.R.*, **126**, 1261 (1959).

6) H. Schmidbaur, H. S. Arnold and E. Beinhofer, *Chem. Ber.*, **97**, 449 (1964).

7) Methyl- and phenylsiloxy derivatives have been recently reported by Orlov and Volonkov before our work, but their details have not been fully described. N. F. Orlov and M. G. Voronkov, *J. General Chem.*, **36**, 357 (1966).

antimonite was obtained from recrystallization; it was also distilled at about 180—182°C/2 mmHg. It was soluble in THF, chloroform and hot benzene, but insoluble in ether and *n*-hexane.

The IR spectra of stibiosiloxane have been reported by Schmidbaur,[6,8] who assigned the absorption at 940—980 cm^{-1} to ν_{as}Si–O–Sb. He also observed that the absorption peaks of the Si–O–X (X=Si, Ge, Sn, Pb) bond in the structural unit of the heterosiloxanes shift systematically to lower wave numbers in the sequence; Si, Ge, Sn, Pb (1055, 990, 980, 959 cm^{-1}). Therefore, it is reasonable to assume the absorption related to ν_{as}Si–O–Sb is in the region between Ge and Sn. The absorption peaks of phenyl and methyl derivatives were observed in this region (at 990 and 995 cm^{-1} respectively), but in tris(tri-*t*-butoxysilyl) antimonite the characteristic absorption band in the vicinity of 990 cm^{-1} was not observed. It seems that the band shifts to a higher wave number (1025 cm^{-1}).

The relative hydrolytic stability of these compounds was determined by measuring the antimonous ion, Sb^{3+}, formed by hydrolysis in an acidic medium. The results are shown in Fig. 1. The results indicate that the relative stability decreases in the order; tris(triphenylsilyl) antimonite, tris(tri-*t*-butoxysilyl) antimonite, tris(trimethylsilyl) antimonite (Sb% × 10). On the other hand, when the hydrolysis was carried out using a basic solvent (THF) at 50°C, the stability decreased as follows; tris(triphenylsilyl) antimonite, tris(trimethylsilyl) antimonite, tris(tri-*t*-butoxysilyl) antimonite. The first was remarkably stable.

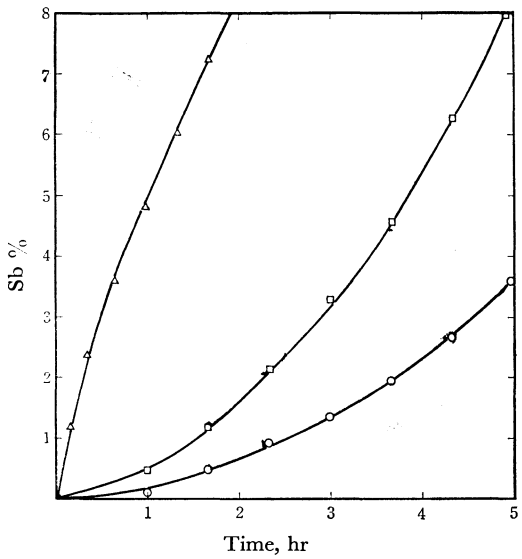

Fig. 1. The relative hydrolytic stability.
○: tris(triphenylsilyl) antimonite
□: tris(tri-*t*-butoxysilyl) antimonite
△: tris(trimethylsilyl) antimonite (Sb % × 10)

8) H. Schmidbaur, *Angew. Chem.*, **77**, 206 (1965); H. Schmidbaur, *J. Am. Chem. Soc.*, **83**, 2963 (1961).

Experimental[9]

Materials. Antimony tri-*i*-propoxide was prepared by the reaction of antimony trichloride with *i*-propyl alcohol in the presence of ammonia,[10] bp 62—63°C/1 mmHg. Trimethylsilanol was prepared by Sauer's method,[11] 99—100°C. Triphenylsilanol was prepared by the hydrolysis of triphenylchlorosilane in the presence of triethylamine, mp 149—150°C. Tri-*s*-butoxysilanol was obtained by Wright's method,[12] bp 89.5°C/1 mmHg, n_D^{20} 1.4135. Tri-*t*-butoxysilanol was first prepared by Backer and Klasens through the hydrolysis of sodium tri-*t*-butoxysilanolate.[13] Wright *et al.*[12] described how the silanol was obtained by the hydrolysis of tri-*t*-butoxychlorosilane in boilling water, but its details have not been documented. In the present work, the silanol was prepared by a modification of the procedure of Wright; tri-*t*-butoxychlorosilane[14] was hydrolyzed in the presence of pyridine, yield 69.5% mp 65—66°C (Found: Si, 10.60%; mol wt, 268).

Preparation of Tris(tri-*t*-butoxysilyl)Antimonite. *Method A.* A solution of 9.8 g (0.033 mol) of antimony tri-*i*-propoxide in 50 m*l* of *n*-hexane was added to a solution of 26.0 g (0.099 mol) of tri-*t*-butoxysilanol in 50 m*l* of *n*-hexane. Then the combined solution was refluxed for 1.5 hr, and the alcohol formed was distilled with the solvent. The residue was distilled under reduced pressure to give 22.3 g (74.5%) of a white crystalline solid, bp 200.5—201.0°C/1 mmHg, mp 102—104°C. Found: C, 47.35; H, 9.79; Si, 9.22; Sb, 13.20 %; mol wt, 900. Calcd for $C_{36}H_{81}O_{12}Si_3Sb$: C, 47.41; H, 8.94; Si, 9.24; Sb, 13.35%; mol wt, 912.

Method B. Into a solution of 26.0 g (0.099 mol) of tri-*t*-butoxysilanol, 10.0 g (0.099 mol) of triethylamine in 130 m*l* of benzene was stirred, drop by drop, at 0—5°C. At the end of the addition, the mixture was refluxed for 2.5 hr. The triethylamine hydrochloride was filtered out, and the benzene was removed. The residue was distilled under reduced pressure to give 20.0 g (66.7%) of a pale yellow solid, bp 197.0—198°C/0.5 mmHg. IR: 2975 (m), 1474(w), 1390(m), 1365(m), 1240(m), 1215(shoulder), 1190(m), 1060(s), 1025(m), 915(s), 830(m), 850(w), 705(m) cm^{-1}.

Preparation of Tris(tri-*s*-butoxysilyl) Antimonite. *Method A.* The reaction of 9.8 g of antimony tri-*i*-propoxide with 26.0 g of tri-*s*-butoxysilanol in *n*-hexane gave 10.3 g (34.4%) of a colorless liquid, bp 204—207°C/1 mmHg. Found: C, 46.80; H, 9.82; Si, 9.21; Sb, 13.79%; mol wt, 889. Calcd for $C_{36}H_{81}O_{12}$-

9) All experiments were carried out in dry atmosphere or nitrogen purge. Melting points and boilling points were uncorrected.

10) I. Kijima and N. Takahashi, *Kogyo Kagaku Zasshi* (*J. Chem. Soc. Japan, Ind. Chem. Sect.*), **67**, 1092 (1964).

11) R. O. Sauer, *J. Am. Chem. Soc.*, **66**, 1707 (1944).

12) J. R. Wright, R. O. Bolt, A. Goldshmidt and A. D. Abbott, *ibid.*, **80**, 1733 (1958).

13) H. Breederveld and H. I. Waterman, *Rec. Trav. Chim.*, **72**, 166 (1953).

14) M. Voronkov, A. N. Gazarev and A. K. Baygojii, *Zh. Obs. Khim.*, **26**, 3072 (1956).

Si_3Sb: C, 47.41; H, 8.94; Si, 9.24, Sb, 13.35%; mol wt, 912.

Method B. The reaction with the same molar ratio of reactants as the case of the tri-*t*-butoxysiloxy derivative gave 5.6 g (18.7%) of a pale yellow liquid, bp 202—204°C/0.5 mmHg.

Preparation of Tris(trimethylsilyl) Antimonite. *Method A.* The reaction of 33.3 g (0.111 mol) of antimony tri-*i*-propoxide with 34.6 g (0.388 mol) of trimethylsilanol in *n*-hexane gave 28.0 g (65.0%) of a colorless liquid, bp 108—108.2°C/21.5 mmHg, n_D^{20} 1.4368. Found: Si, 21.52; Sb, 31.24%; mol wt, 382. Calcd for $C_9H_{27}O_3Si_3Sb$: Si, 21.66 Sb, 31.28%; mol wt, 389.

Method B. The reaction of 9.0 g (0.0393 mol) of antimony trichloride with 14.0 g (0.157 mol) of trimethylsilanol in the presence of 15.9 g (0.157 mol) of triethylamine gave 8.4 g (55.0%) of a colorless liquid, bp 118—119°C/33.5 mmHg, n_D^{20} 1.4363. IR: 2900(s), 1247(s), 995(m), 900(s), 840(s), 752(m) cm^{-1}.

Preparation of Tris(triphenylsilyl) Antimonite. A solution of 6.5 g (0.0221 mol) of antimony tri-*i*-propoxide in 50 m*l* of benzene was added to a dispersed solution of 19.0 g (0.0687 mol) of triphenylsilanol in 50 m*l* of benzene. Then the clear solution was refluxed for 1.5 hr. When the solvent was removed along with the alcohol formed, a pale yellow solid appeared. After the solvent had been removed completely, the solid was recrystallized from a mixed solvent of benzene and ether(2 : 1), giving 9.7 g (94.0%) of a white, crystalline matter, mp 202—205°C. Found: C, 69.62; H, 4.75; Si, 8.41; Sb, 12.58%; mol wt, 920. Calcd for $C_{64}H_{45}O_3Si_3Sb$: C, 68.42; H, 4.78; Si, 8.98; Sb, 12.84%; mol wt, 948. IR: 3050(m), 2990(shoulder), 1585(w), 1564 (shoulder), 1480(w), 1425(m), 1380(vs), 1330(vw), 1256(vw), 1183(vw), 1155(vw), 1114(s), 1103(shoulder), 1060(vw), 1025(vw), 990(m), 905(s), 740(m), 710 and 700(s), 680(m) cm^{-1}.

Measurement of Relative Hydrolytic Stability. Weighed samples (0.5—0.8 g) of tris(triorganosilyl) antimonite were vigorously stirred at 23°C, into a mixture of 100 m*l* of a 5% aqueous hydrochloric acid solution, 30 m*l* of acetone, and 1 g of sodium potassium tartrate. After twenty minutes, 5 m*l* of the solution was neutralized with a saturated sodium bicarbonate solution and then titrated with an iodine solution, using a starch indicator. The results are shown in Fig. 1. On the other hand, samples (0.4—0.2 g) in 10 m*l* of THF were added to a solution of 1 g of sodium potassium tartrate in 20 m*l* of a 5% aqueous hydrochloric acid solution, they were titrated after having been stirred at 50°C. The results were as follows; tris(triphenylsilyl) antimonite; Sb, 72.5% (after 5 minutes), 77.0(10), 99.0(20): tris(trimethylsilyl) antimonite; 90.2(5), 100 (10): tris(tri-*t*-butoxysilyl) antimonite; 100(5).

Analysis. The antimony was determined by iodometry after a weighed sample had been hydrolyzed with a 20% alcohol solution, a few drops of concentrated hydrochloric acid, and 1 g of sodium potassium tartrate. The silicon was determined as silicon dioxide after a sample had been decomposed by concentrated sulfuric acid and a mixture of ammonium nitrate and sulfate.

BULLETIN OF THE CHEMICAL SOCIETY OF JAPAN VOL. 42 1150—1151 (1969)

Preparation of Pentacyanotriphenylphosphine- and Tetracyano-bis(triphenylphosphine)cobaltate(III)*1

Kiyokatsu WATANABE,*2 Hiroaki NISHIKAWA and Muraji SHIBATA

Department of Chemistry, Faculty of Science, Kanazawa University, Kanazawa

(Received July 27, 1968)

As far as octahedral cobalt(III) complexes containing the ligand triphenylphosphine are concerned, a few types are known. They are $[Co(DH)_2P(C_6H_5)_3X]$ (DH=dimethylglyoxime monoanion, X=halogen, alkyl and phenyl[1]; X=CN[2]), $[Co(TSB)P(C_6H_5)_3Br]$[3] (TSB=tetradendate Schiff base dianion) and $[Co(CN)_2(acac)(P(C_6H_5)_3)_2]$[4] (acac=acetylacetone anion).

We have attempted to prepare some triphenylphosphine complexes by using the so-called Werner-type complexes as the starting materials; we have now succeeded in obtaining two complexes of the cyanotriphenylphosphine series.

Experimental

Potassium Pentacyanotriphenylphosphinecobaltate(III) Trihydrate, $K_2[Co(CN)_5P(C_6H_5)_3]\cdot 3H_2O$. Potassium bromopentacyanocobaltate(III)[5] (3.8 g, 0.01

*1 Presented at the 17th Symposium on Coordination Chemistry, Hiroshima, December, 1967.

*2 Present address: Department of Chemistry, Faculty of Science, Shinshu University, Matsumoto.

1) G. N. Schrauzer and J. Kohnle, *Chem. Ber.*, **97**, 3056 (1964); G. N. Schrauzer and J. Windgassen, *ibid.*, **99**, 602 (1966).

2) T. Sasaki and F. Matsunaga, unpublished.

3) G. Costa, G. Mestroni, G. Tauzher and L. Stefani, *J. Organometal. Chem.*, **6**, 181 (1966); G. Costa, G. Mestroni and L. Stefani, *ibid.*, **7**, 493 (1967).

4) H. Nishikawa, K. Konya and M. Shibata, This Bulletin, **41**, 1492 (1968).

5) W. Adamson, *J. Am. Chem. Soc.*, **78**, 4260 (1956).

mol) was dissolved in a minimum amount of water (2 ml). On the other hand, triphenylphosphine (5.2 g, 0.02 mol) was dissolved in glacial acetic acid (70 ml). The former solution was added to the latter solution, and the mixture was stirred at 75°C for 6 hr. The resulting yellow solution was filtered and the filtrate was evaporated to dryness under reduced pressure. The residue was treated with a large amount of water (100 ml). After the filtration of the aqueous solution, the filtrate was again evaporated to dryness under reduced pressure. The residue was treated with methanol (100 ml) and the methanolic solution was concentrated to a small volume (30—40 ml). This concentrated solution was added to a cellulose column which had previously been washed with methanol. When methanol was passed through the column, a yellow band of the desired complex was eluted. This eluted solution was concentrated to a small volume under reduced pressure. When this solution was cooled a pale-yellow material separated out, this was dried over calcium chloride. Yield, 1 g. The complex was soluble in water and methanol, but not soluble in benzene.

Found: C, 47.45; H, 3.27; N, 12.65%. Calcd for $K_2[Co(CN)_5P(C_6H_5)_3]\cdot 3H_2O$: C, 47.30; H, 3.59; N, 12.00%.

The use of iodopentacyano- or chloropentacyanocobaltate(III) in place of the bromo complex gave the same product, but the yield was extremely poor in the case of the iodo complex.

Potassium Tetracyanobis(triphenylphosphine) cobaltate(III) Dihydrate, $K[Co(CN)_4(P(C_6H_5)_3)_2]\cdot 2H_2O$. To a triphenylphosphine solution in glacial acetic acid (5.2 g in 70 ml), was added an aqueous solution (a few ml) of potassium iodopentacyanocobaltate (III)[5] (4.3 g, 0.01 mol), after which the mixture was stirred at 75°C for 6 hr. The resulting yellow solution was filtered, and a large quantity of water (500 ml) was added to the filtrate; then the whole was kept in a refrigerator until a yellow solid began to appear on the surface of the solution. The solid was collected by filtration and suspended in benzene (200 ml) in oder to remove any unreacted triphenylphosphine. Finally, the remaining solid was dried over calcium chloride. Yield, 2.5 g. This complex was soluble in methanol to some extent, but it was insoluble in water and benzene.

Found: C, 63.05; H, 4.76; N, 7.48%. Calcd for $K[Co(CN)_4(P(C_6H_5)_3)_2]\cdot 2H_2O$: C, 62.99; H, 4.46; N, 7.34%.

The use of the other halogenopentacyano complexes for the preparation was also possible, but their reaction times were considerably different; the use of the chloro complex took the longest time, while the use of the iodo complex was the best.

Results and Discussion

The two complexes thus obtained were characterized by their electronic absorption spectra (Fig. 1). Each spectrum shows an absorption band as a shoulder in the longer wavelength region. Although its intensity was quite high, this band may be due to a ligand-field transition.

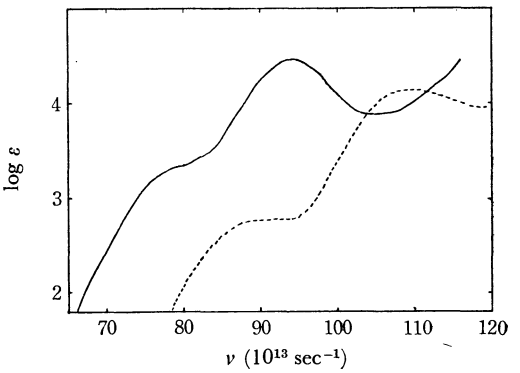

Fig. 1. Absorption spectra in methanol solution.
----- $K_2[Co(CN)_5P(C_6H_5)_3]\cdot 3H_2O$
—— $K[Co(CN)_4(P(C_6H_5)_3)_2]\cdot 2H_2O$

The existence of water of crystallization in the present complexes was established by the thermal analyses and the IR spectra. The presence of complexed CN^- was ascertained from the IR absorption peak in the neighborhood of 2100 cm^{-1} ($\nu_{C\equiv N}$); the pentacyano complex showed a well-split band (2118, 2140 cm^{-1}), and the tetracyano one, a sharp peak with a shoulder (2110, 2150_{sh} cm^{-1}). Concerning the existence of triphenylphosphine, a large number of the characteristic bands were observed for both complexes (1435, 1190, 1090, 1020, 1000 and 750 cm^{-1}). It is not certain which structure, *trans* or *cis*, is to be assigned to the present tetracyano complex.

BULLETIN OF THE CHEMICAL SOCIETY OF JAPAN VOL. 42 1152—1153 (1969)

The Reaction of 3-Chloro-benzo[*d*]isothiazole with Thiophenols

Suzuo WATANABE

Central Research Laboratories, Meiji Seika Kaisha, Ltd., Morooka-cho, Kohoku-ku, Yokohama

(Received August 5, 1968)

The condensation of 3-chloro-benzo[*d*]isothiazole 1,1-dioxide (saccharin chloride) (I) with alcohols, phenols, or mercaptans was reported to give a series of saccharin derivatives (II),[1] which have distinct melting points, so they have been used for the identification of alcohols, phenols, or mercaptans.

The present report deals with the reaction of thiophenols with 3-chloro-benzo[*d*]isothiazole (III).[2]

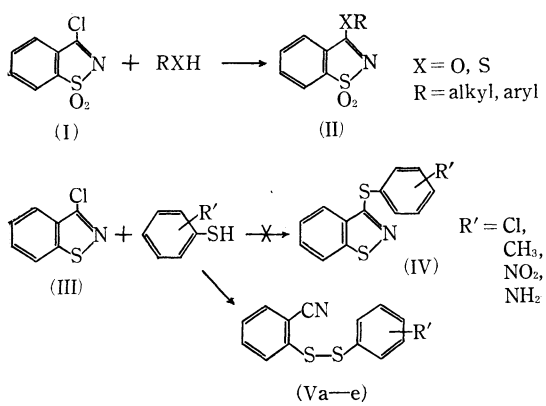

When III was treated with substituted thiophenols at 40°C, a vigorous evolution of hydrogen chloride gas occured. By adding ethanol to the reaction mixture, the crystalline product was obtained in yield of 87—28%.

This product was not the expected compound, 3-arylthio-benzo[*d*]isothiazoles (IV), but aryl *o*-cyanophenyl disulfides (V), which are listed in Table 1.

The structure of the compounds Va—e was determined by their elemental analyses and infrared spectra, which showed a characteristic band at 2210 cm^{-1} due to -CN group. To confirm the structure, Vc was reduced with lithium aluminum hydride to *p*-methylthiophenol, which was identified by its melting point and by the reaction with 2,4-dinitrochlorobenzene to *p*-tolyl 2,4-dinitrophenyl sulfide.

It was reported[3] that 2-substituted-benzo[*d*]isothiazole-3(2)-ones were reacted with aniline to afford *o*-(*N*-substituted carbamoyl)-benzenesulfenanilides. When III was treated with alcohols or aniline, no reaction occurred and starting materials were recovered.

Table 1. Disulfides by the reaction of 3-chloro-benzo[*d*]isothiazole with thiophenols

	R	Yield (%)	Mp (°C)	Anal. %	Found	Calcd
					N	S
Va	*p*-Cl	87.0	47.0—49.0	5.23	—	
				5.04	—	
Vb	*o*-CH_3	31.5	58.0—60.0	5.50	24.98	
				5.44	24.92	
Vc	*p*-CH_3	67.0	53.5—55.0	5.21	24.68	
				5.44	24.92	
Vd	*p*-NO_2	28.0	92.0—93.0	9.90	22.19	
				9.72	22.21	
Ve	*o*-NH_2	33.5	83.0—86.0	10.98	24.82	
				10.82	24.78	

The reaction mechanism of III with thiophenols was thought to be as follows.

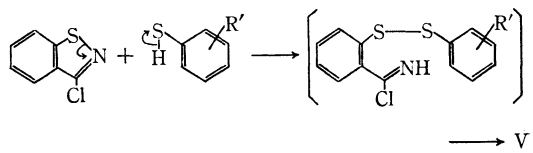

The compounds Va-e showed moderate antibacterial and antifungal activities. The minimum inhibition concentrations (MIC) are listed in Table 2.

Experimental

Two typical examples for the reaction of III with thiophenols were described below.

***p*-Chlorophenyl *o*-Cyanophenyl Disulfide (Va).** *p*-Chlorothiophenol (8.7 g) was added to 3-chloro-benzo[*d*]isothiazole (III) (10.2 g) with shaking in small portions at 40°C. The reaction mixture was thoroughly shaken until the vigorous evolution of hydrogen chloride gas stopped, and then allowed to stand in an ice box overnight. Ethanol (20 *ml*) was added to the reaction mixture, and the resulting suspension was thoroughly

1) J. R. Meadow and J. C. Cavagnol, *J. Org. Chem.*, **16**, 1582 (1951); *ibid.*, **17**, 488 (1952).

2) A. Reissert, *Ber.*, **61**, 1681 (1928).

3) R. G. Bartlett, L. E. Hart and E. W. McClelland, *J. Chem. Soc.*, **1939**, 760.

stirred over a period of 15 min, then crystals were collected, washed with ethanol and dried. Recrystallization from ethanol gave 14.5 g (87.0%) of *p*-chlorophenyl *o*-cyanophenyl disulfide, mp 47.0—49.0°C. Found: C, 56.55; H, 3.39; N, 5.23%. Calcd for $C_{13}H_8ClNS_2$: C, 56.21; H, 2.90; N, 5.04%.

o-Aminophenyl o-Cyanophenyl Disulfide (Ve). 3-Chlorobenzo[*d*]isothiazole (10.2 g) was added to *o*-aminothiophenol (14.8 g) with shaking in small portions. The reaction mixture was thoroughly shaken for an additional 15 min, and then allowed to stand in an ice box overnight. Crystalline precipitate was filtered and washed with ethanol (25 m*l*). The filtrate and the washings were combined, concentrated *in vacuo* to a half volume, and cooled, then crystals which separated were collected. Further concentration of the mother liquor to 7 m*l* yielded more crystals. The entire crystals were recrystallized from ethanol, the yield of *o*-aminophenyl *o*-cyanophenyl disulfide was 5.2 g (33.5%), mp 83.0—86.0°C. Found: C, 60.81; H, 4.37; N, 10.98; S, 24.82%. Calcd for $C_{13}H_{10}N_2S_2$: C, 60.40; H, 3.89; N, 10.82; S, 24.78%.

Table 2. Antimicrobial activities of Va—e (MIC; mcg/m*l*)

Name of test oganisms	Va	Vb	Vc	Vd	Ve
S. aureus 209P	2.0	2.0	3.9	12.5	7.8
E. coli IAM 1253	>500	>500	>500	500	>500
Mycobacterum 607	7.8	15.6	15.6	31.2	31.2
Candida albicans IAM	7.8	15.6	15.6	500	7.8
Xanthomonas oryzae	7.8	15.6	15.6	500	7.8
Asp. niger ATCC 6275	>500	>500	>500	>500	500
Pir. Sasaki	7.8	125	7.8	500	15.6

BULLETIN OF THE CHEMICAL SOCIETY OF JAPAN VOL. 42 1153—1155 (1969)

Photoreaction of Pseudoionone

Noboru SUGIYAMA, Yoshiaki SATO, Michikazu YOSHIOKA, Kazutoshi YAMADA and Hiroshi KATAOKA

Department of Chemistry, Tokyo Kyoiku University, Otsuka, Tokyo

(Received August 20, 1968)

The great majority of works on the photoreaction of conjugated dienone has been dealt extensively with cyclic compounds.[1-4] Only a few examples involving acyclic dienone have been known, *e. g.*, the photodimerization of cinnamylidene acetone[5,6] and the photoisomerization of crotonylidene acetone.[3] Büchi and Yang[3] obtained a polymeric material by the photoreaction of pseudoionone (I), an acyclic dienone. This is the only report on the photoreaction of I. As part of photochemical studies on enone systems the photoreaction of I has been studied.

First, it was confirmed that I had a structure of conjugated dienone (all trans type in diene[7]) with

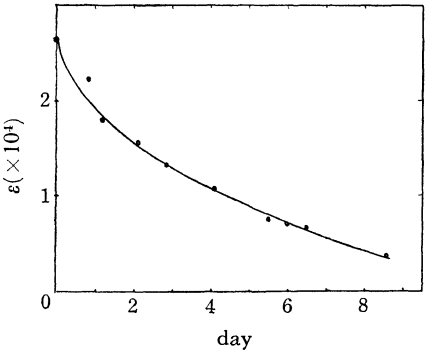

Fig. 1. The change of ε at 293 mn of pseudoionone with irradiation time.

1) W. A. Noyes, Jr., G. S. Hammond and J. N. Pitts, Jr., "Advances in Photochemistry," Vol. 4, Interscience, New York (1966), p. 81, 195.

2) P. de Mayo and S. T. Reid, *Quat. Rev.* (London), **15**, 393 (1961).

3) G. Büchi and N. C. Yang, *J. Am. Chem. Soc.*, **79**, 2318 (1957).

4) P. de Mayo, J. B. Stothers and R. W. Yip, *Can. J. Chem.*, **39**, 2135 (1961).

5) H. Stobbe and W. Simon, *J. Prakt. Chem.*, **110**, 129 (1925).

6) H. Stobbe and C. Rücker, *Ber.*, **44**, 861 (1911).

7) C. H. Chen and R. J. W. Le Fèvre, *J. Chem. Soc.*, **1965**, 5528.

one isolated double bond by UV, IR and NMR spectra as shown in experimental part. When the solution of I in *n*-hexane was irradiated with a high pressure mercury lamp, UV absorption at 293 nm gradually decreased indicating the disappearance of the conjugated double bond. (Fig. 1) The reaction mixture showed four spots of R_f values of 0.45, 0.43, 0.40 and 0.0 on a silica gel thin layer chromatogram with benzene - ethyl acetate (9 : 1). The substance of R_f 0.45 was identified with I. The substances which show the R_f values of 0.43, 0.40 and 0.0 were designated as II, III and IV, respectively. Both II and III were isolated by a silica gel chromatography. When left at room temperature, I readily, and II or III gradually polymerized. So the viscous IV would be a mixture of polymers from I, II and III.

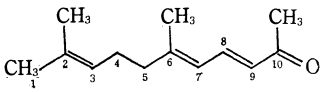

I

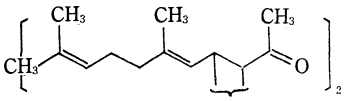

II and III

The ozonolysis of II and III, followed by decomposition with hydrogen peroxide and then by esterification with diazomethane, gave methyl levulinate as a main product. However, II and III were presumed to be cyclobutane derivatives from the following spectra and other reactions.

The UV spectra indicate that no conjugated system is contained in II and III. It is also supported by the shift of IR band at 1665 cm^{-1} of I to 1705 cm^{-1}. The NMR spectra of II and III show signals at τ 8.35 due to isopropylidene methyls. This shows that 2,3-double bond remains. The signals at τ 4.9 of II and III are assigned to 3- and 7-protons. The molecular peaks of mass spectra of (V) and (VI) (*m/e* 394 and 392 respectively), which were obtained by the catalytic reduction of II and III respectively, are consistent with the experimental facts that II absorbed five moles of hydrogen over platinum oxide and III absorbed four moles over palladium black. The above facts and A_2B_2 like multiplets at τ 7.6—6.9 of II and τ 7.1—6.3 of III also support the cyclobutane structure. The chemical shifts of 6-methyl protons and acetyl methyl protons of II and III move to a higher magnetic field, compared with I. Especially acetyl methyl protons of III show two singlets, indicating that the surrounding of two acetyl groups are slightly different. The IR spectrum of V shows strong absorption at 3450 cm^{-1} (OH) and 1700 cm^{-1} (CO). A doublet at τ 8.84 in NMR of V is due to methyl of CH_3-CH-OH and a singlet at τ 7.86 comes from acetyl methyl group. This indicates that four C=C bonds and one C=O bond were reduced in V. On the other hand, the IR spectrum of VI shows a strong absorption at 1710 cm^{-1} (CO) and no hydroxy absorption, indicating that only C=C bond were reduced in VI. Consequently it can be concluded that II and III are dimers of I, which contain cyclobutane ring at 8,9-positions.

Experimental

Pseudoionone was purified by fractional distillation *in vacuo* and column chromatography. UV: λ_{max}^{EtOH} 293 nm (ε 26000); IR: $\nu_{max}^{liq.\ film}$ cm^{-1}, 1665 (CO), 1630, 1590, 973 (diene), 825(C=C); NMR: (τ, in CCl_4), 8.36 (d, J=4.5 cps, isopropylidene methyls), 8.09 (s, 6-methyl), 7.80 (m, 4- and 5-methylenes), 7.80 (s, acetyl), 4.90 (m, 3-proton), 3.98 (d, J=12.5 cps, 7-proton), 3.93 (d, J= 15.5 cps, 9-proton) and 2.58 (q, J=12.5 and 15.5 cps, 8-proton). A Taika H-type 125W high pressure mercury lamp was used as light source. IR, UV, NMR and Mass spectra were measured by Hitachi ESI-S2 type spectrometer, Hitachi EPS-3T type spectrophotometer, Hitachi H-60 type spectrometer and Hitachi Mass spectrometer, respectively. Hitachi KGL-2A type gas chromatography apparatus (polydiethylene glycol succinate) was used for analysis.

Irradiation of Pseudoionone (I). A *n*-hexane solution of I (7.5 g/70 m*l*) was irradiated with a high pressure mercury lamp for 8 days at room temperature. The reaction was followed by UV spectra of aliquots (Fig. 1). From the reaction mixture the solvent was evaporated under reduced pressure and the residual pale yellow liquid was fractionated by column chromatography using silica gel eluted with benzene - ethyl acetate. Unreacted I (0.75 g) was recovered from the benzene elute. From the benzene - ethyl acetate (9 : 1) elute, the mixture of II and III (1.8—1.9 g), was obtained. Ratio of II by III was found to be 1 : 1 by measuring the intensity of methine proton signals in NMR spectra. Pure II and III were separated by repeating column chromatography. Photodimer II, a pale yellow liquid, Found: C, 81.49; H, 10.31%. Calcd for $C_{26}H_{40}O_2$: C, 81.20; H, 10.48%.

UV: λ_{max}^{EtOH} nm(ε), 283 (sh, 190).

IR: (cm^{-1}, liq. film) 1705, 1675, 1445, 1358, 832.

NMR: (τ, in CCl_4) 8.35 (d, J=4.5 cps, 12H), 8.34 (d, J=1.0 cps, 6H), 8.00 (s, 6H), 7.6—6.9 (m, 4H), 4.9 (m, 4H).

Photodimer III, a pale yellow liquid. Found: C, 81.79; H, 9.99%. Calcd for $C_{26}H_{40}O_2$: C, 81.20; H, 10.48%.

UV: λ_{max}^{EtOH} nm (ε), 283 (sh, 200).

IR: (cm^{-1}, liq. film) 1705, 1670, 1440, 1355, 820.

NMR: (τ, in CCl_4) 8.35 (d, J=4.5 cps, 12H), 8.36 (d, J=1.0 cps, 6H), 7.96 (s, 3H), 7.93 (s, 3H), 7.1—6.3 (m, 4H), 4.9 (m, 4H).

Catalytic Reduction of Photodimer II. In the presence of 28 mg of platinum oxide as catalyst, 205 mg of II was hydrogenated in ethanol (7.5 m*l*). The sample absorbed 59 m*l* of hydrogen. After the solvent was evaporated, 210 mg of a colorless liquid (V) was obtained.

Found: C, 79.89; H, 12.50%. Calcd for $C_{26}H_{50}O_2$: C, 79.12; H, 12.77%.

UV: λ_{max}^{EtOH} nm (ε), 282 (48).

IR: (cm^{-1}, liq. film), 3450, 1700, 1460, 1360, 1070.

NMR: (τ, in CCl_4), 9.11 (d, J=6.0 cps, 18H), 8.80 (m, 20H), 8.84 (d, J=8.0 cps, 3H), 7.86 (s, 3H), 7.8—7.3 (m, 4H), 6.4 (m, 1H), 4.7 (broad s, 1H).

Mass: (*m/e*) 394 (mol. peak), 376, 198, 197, 196, 195, 127, 113, 111, 109 (base peak), 97, 96, 85, 83, 71, 57, 43.

Catalytic Reduction of Photodimer III. In the presence of palladium black (51 mg) as catalyst, 54 mg of III was hydrogenated in ethanol (10 m*l*). The sample absorbed 12 m*l* of hydrogen. Removal of the solvent gave 55 mg of a colorless liquid (VI).

Found: C, 79.67; H, 11.86%. Calcd for $C_{26}H_{48}O_2$: C, 79.53; H, 12.32%.

UV: λ_{max}^{EtOH} nm (ε), 283 (sh, 78).

IR: (cm^{-1}, liq. film), 1710, 1460, 1360.

NMR: (τ, in CCl_4), 9.10 (d, J=6.0 cps, 18H), 8.77 (m, 20H), 7.98 (s, 3H), 7.92 (s, 3H), 7.7—6.6 (m, 4H).

Mass: (*m/e*), 392 (mol. peak), 196, 195, 127, 113, 109 (base peak), 97, 95, 85, 83, 71, 57, 43.

Ozone Oxidation of II. Ozonolysis and decomposition with hydrogen peroxide of 980 mg of II gave neutral material (260 mg) and acidic material (280 mg). Esterification of acidic material by diazomethane gave 62 mg of methyl levulinate as main product, identified with the authentic sample by NMR and gas chromatography.

Ozone Oxidation of III. By a similar procedure as described above, 800 mg of III gave 200 mg of neutral material, 220 mg of acidic material and 55 mg of methyl levulinate.

BULLETIN OF THE CHEMICAL SOCIETY OF JAPAN VOL. 42 1155—1158 (1969)

The Addition Reactions of Fluoroalkyl Ethyl Ethers to Perfluoropropene

Hiroshige MURAMATSU, Hiroshi KIMOTO and Kan INUKAI

Government Industrial Research Institute, Nagoya, Kita-ku, Nagoya

(Received September 13, 1968)

The free-radical reactions of aliphatic or alicyclic ethers to fluoroolefins under γ-irradiation[1-3] or in the presence of peroxide[4] have been reported to give the 1 : 1 adduct, the ethers with fluoroalkyl or fluorocycloalkyl group on the α-carbon, in good yields. In the addition of diethyl ether,[1-3] the 1 : 2 adduct with symmetrical structure has been produced along with the 1 : 1 adduct.

In order to investigate the scope and limitation of these addition reactions for the syntheses of fluorine-containing ethers, the reaction of various fluoroalkyl ethyl ethers and perfluoropropene was undertaken. The effects of the substitution of fluorine for hydrogen in the ethers on their reactivity in the addition reaction were also investigated by a competitive reaction.

The two types of fluoroakyl ethyl ethers with general formulas of $RCH_2OCH_2CH_3$ ($R=CH_2F$, CHF_2, CF_3, CH_2Cl, CHF_2CF_2) and $R'CF_2OCH_2CH_3$ ($R'=CHF_2$, CHFCl, $CHCl_2$) were prepared and used as addends. A mixture of perfluoropropene and an ether in an autoclave was irradiated by γ-ray ($5—20\times10^7$ R). The products were separated by distillation or by preparative gas chromatography. Their structures were established by elemental analyses, and by IR and NMR (proton and fluorine) spectra.

While the addition of ethers of the type $R'CF_2OCH_2CH_3$ gave only the 1 : 1 adduct IV, the addition of ethers of the type $RCH_2OCH_2CH_3$ resulted in a mixture of products composed of the 1 : 1 adducts, I and II, and the 1 : 2 adduct III.

$$RCH_2OCH_2CH_3 + CF_3CF{=}CF_2 \longrightarrow$$

$$\underset{\displaystyle CF_2CHFCF_3}{\underset{|}{RCH_2OCHCH_3}} + \underset{\displaystyle CF_2CHFCF_3}{\underset{|}{RCHOCH_2CH_3}} +$$

I II

$$\underset{\displaystyle CF_2CHFCF_3}{\underset{|}{RCH}}\!\!-\!\!O\!\!-\!\!\underset{\displaystyle CF_2CHFCF_3}{\underset{|}{CHCH_3}}$$

III

$$R'CF_2OCH_2CH_3 + CF_3CF{=}CF_2 \longrightarrow$$

$$\underset{\displaystyle CF_2CHFCF_3}{\underset{|}{R'CF_2OCHCH_3}}$$

IV

1) H. Muramatsu, K. Inukai and T. Ueda, *J. Org. Chem.*, **29**, 2220 (1964); *ibid.*, **30**, 544 (1965).

2) H. Muramatsu, S. Moriguchi and K. Inukai, *ibid.*, **31**, 1306 (1966).

3) H. Muramatsu, K. Inukai and T. Ueda, This Bulletin, **40**, 903 (1967).

4) W. E. Hanford, U. S. Pat. 2433844 (1948).

The reaction conditions and yields of the adducts are shown in Table 1. It is apparent that, in the case of the type $RCH_2OCH_2CH_3$, the ratio of III/I decreases with the number of fluorine on the β-carbon and that perfluoropropene adds preferentially on the α-methylene with a less electronegative group. The addition of ethers of the type $RCF_2OCH_2CH_3$ was much more difficult than that of ethers of the type $RCH_2OCH_2CH_3$.

Table 1. Reaction conditions and yields of adducts

Ether R	Molar ratio of propene/ether	Total dose MR	Yield, % I	II	III	IV
		$RCH_2OCH_2CH_3$				
CF_3	2.2	113	67	0.3	5.3	
CHF_2	2.7	60	64	1.3	19.3	
CH_2F	2.2	60	37	7.1	39	
CH_3[3]	0.3	11	43.5		56.5	
CH_2Cl	2.3	63	7.6			
CHF_2CF_2	0.9	46	35			
		$RCF_2OCH_2CH_3$				
CHF_2	0.7	143				8
CHFCl	0.8	145				10
$CHCl_2$	0.7	218				22

The 1 : 2 adduct III could be formed by two pathways. One pathway is a successive addition of two perfluoropropenes and another is an addition involving an intramolecular rearrangement.

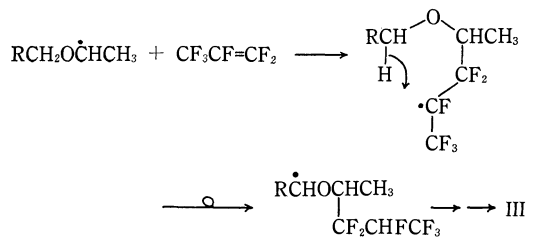

To clarify this point, we studied the addition reaction of diethyl ether to perfluoropropene under various reaction conditions. As shown in Table 2, the ratio of III/I in products was almost constant if the ratio of olefin/ether was kept constant, showing no dependence on irradiation time. Besides, the ratio of III/I increased with increasing the ratio of olefin/ether (Table 3).

The fact that the reaction of I with perfluoropropene produced only a small amount of III and that the addition reaction of a cyclic ether such as tetrahydrofuran to perfluoropropene did not give any 1 : 2 adduct,[3] also support the latter pathway involving the radical rearrangement. The rigid structure of tetrahydrofuran would prohibit the formation of six-membered cyclic structure of the intermediate radical.

Table 2. Relations between irradiation time and ratio of III to I

Propene/diethyl ether	Irradiation time, hr	Yield, % I	III	Ratio of III/I
1.0	22.9	8.0	12.2	1.52
1.0	45.6	10.8	14.7	1.36
1.0	68.6	13.2	19.1	1.44
1.0	112.0	15.3	23.2	1.52
2.0	45.6	10.9	22.8	2.08
2.0	112.0	16.2	33.6	2.08

Table 3. Relations between ratio of perfluoropropene to diethyl ether and ratio of III to I

Propene/diethyl ether	Concentration of ether, mol %	Yield, % I	III	Ratio of III/I
0.25	0.80	6.47	5.67	0.88
0.50	0.67	7.03	7.13	1.01
1.00	0.50	7.00	10.1	1.44
2.00	0.33	8.40	17.6	2.10

The relative reactivities of fluoroalkyl ethyl ethers in the addition reaction to perfluoropropene were determined by a competitive reaction. A one-to-one mixture of two substrates was irradiated with olefin in a glass ampoule. The amount of each adduct was determined by gas chromatography. The relative reactivities of the ethers are listed in Table 4, taking the reactivity of diethyl ether as 1000.

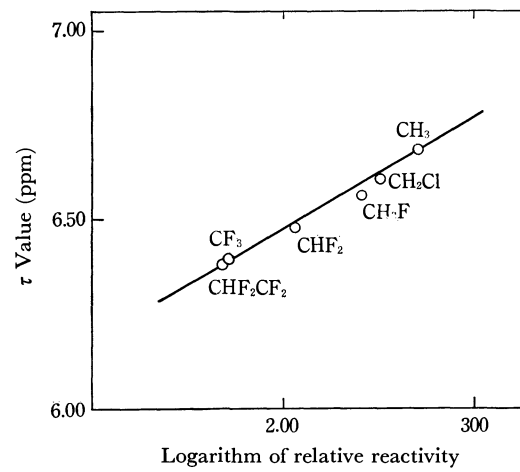

Fig. 1. Plots of the chemical shifts (τ values) of hydrogens in the methylene of $RCH_2O\underline{CH_2}CH_3$ *vs.* logarithms of its relative reactivity.

Table 4. Relative reactivity of the fluoroalkyl ethyl ethers

Ether R or R′	$RCH_2OCH_2CH_2$						$R'CF_2OCH_2CH_3$		
	CH_3	CH_2F	CHF_2	CF_3	CH_2Cl	CHF_2CF_2	CHF_2	$CHFCl$	$CHCl_2$
Relative reactivity	1000	260	110	56	320	46	0.8	1.0	0.1>

Table 5. Physical properties of the 1 : 1 adducts and 1 : 2 adducts

R	Bp °C	n_D^{20}	d_4^{20}	MR_D		C, %		H, %	
				Found	Calcd	Found	Calcd	Found	Calcd
1 : 1 Adduct, CF_3CHFCF_2R									
$CF_3CH_2OCHCH_3$	118	1.3086	1.469	35.9	36.9	30.7	30.6	2.71	2.56
$CHF_2CH_2OCHCH_3$	132	1.3233	1.441	36.1	36.8	31.7	32.3	2.92	3.10
$CH_2FCH_2OCHCH_3$	147	1.3328	1.377	36.2	36.7	34.2	34.7	3.82	3.75
$CH_2ClCH_2OCHCH_3$	165	1.3621	1.378	41.6	41.5	32.8	32.5	3.65	3.51
$CHF_2CF_2CH_2OCHCH_3$	152	1.3207	1.498	41.2	41.6	30.7	31.0	2.61	2.60
$CH_2FCHOCH_2CH_3$	116	1.3293	1.367	36.1	36.7	34.5	34.7	3.59	3.75
$CHF_2CF_2OCHCH_3$	123	1.3048	1.534	36.6	37.0	27.9	28.4	1.91	2.04
$CHFClCF_2OCHCH_3$	138	1.3307	1.532	41.7	41.8	27.3	26.9	2.01	1.93
$CHCl_2CF_2OCHCH_3$	163	1.3569	1.552	46.4	46.6	25.5	25.6	1.91	1.84
1 : 2 Adduct, $(CF_3CHFCF_2)_2R$									
$CF_3CHOCHCH_3$	164	1.3130	1.630	51.1	51.2	27.5	28.1	1.79	1.65
$CHF_2CHOCHCH_3$	168	1.3218	1.595	51.3	51.5	29.1	29.3	1.68	1.97
$CH_2FCHOCHCH_3$	176	1.3270	1.560	50.9	51.1	30.6	30.6	1.95	2.31

In the ethers of the type $RCH_2OCH_2CH_3$ (R= CH_3, CH_2F, CHF_2, CF_3), the logarithm of reactivity was found to be inversely proportional to the number of substituted fluorines in the β-methyl group, indicating that the Hammett relationship holds in the radiation-induced addition reaction. As expected, it was also observed that τ values of chemical shift of hydrogen in α-methylene of the fluoroalkyl ethyl ethers have a linear relation with the logarithms of their reactivity as shown in Fig. 1. All these facts indicate that the substituted fluorines exerted their electron-withdrawing effect remarkably through oxygen upon the α-methylene group and that the hydrogen abstraction on the α-methylene was a rate-determining step in the radiation-induced addition reaction of ethers to fluoroolefins.

The physical properties of the 1 : 1 adduct and 1 : 2 adduct are shown in Table 5. In the adducts of the type $RCH_2OCH_2CH_3$, the substitution of fluorine for hydrogen of β-methyl group of diethyl ether decreases the boiling point and refractive index of both the 1 : 1 adduct and 1 : 2 adduct, but increases their density. Similar trends were known[5] for $RCOCH_3$, $RCH_2OC_2H_5$, $RCOOC_2H_5$, and RCOCl where R is CH_2F, CHF_2 or CF_3.

5) M. Hudlicky, "Chemistry of Organic Fluorine Compound," The Macmillan Co., New York (1962), p. 298.

Experimental[6]

Preparation of Ethers of the Type $RCH_2OCH_2CH_3$. *(1) β-Fluoroethyl Ethyl Ether.* Ethylene chlorohydrin was fluorinated with potassium fluoride in ethylene glycol-diethylenel gycol solvent at 150°C to give β-fluoroethanol (60% yield). Upon heating at 130°C with ethanol in the presence of sulfuric acid, β-fluoroethanol gave β-fluoroethyl etheyl ether (30% yield). bp 75—76°C(lit.[7] 74.5—75.5°C).

(2) β,β-Difluoroethyl Ethyl Ether. $\alpha,\alpha,\beta,\beta$,-Tetrafluoroethyl ethyl ether prepared from tetrafluoroethylene and ethanol was hydrolyzed in the presence of sulfuric acid at 0°C to produce ethyl difluoroacetate (45% yield). The difluoroacetate was converted into difluoroethanol by reduction with lithium aluminum hydride in ether (65% yield). A mixture of the difluoroethanol and ethanol was heated at 130°C with sulfuric acid to give β,β-difluoroethyl ethyl ether (55% yeild). bp 66—67°C (lit.[8] 66.3—66.7°C).

(3) β,β,β-Trifluoroethyl Ethyl Ether. Reduction of trifluoroacetic acid with lithium aluminum hydride

6) All temperature readings are uncorrected. NMR spectra were taken on a JNM-C-60 NMR high resolution spectrometer with tetramethylsilane as an internal standard for ^1H and with trifluoroacetic acid as an external standard for ^{19}F.

7) E. Gryszkiewicz-Trochimowski, A. Sporzynski and J. Wnuk, *Rec. Trav. Chim.*, **66**, 413 (1947).

8) F. Swarts, *Bull. Acad. Roy. Belg.*, **1901**, 383.

was carried out in ether at 35°C to yield β,β,β-trifluoroethanol (50% yield). The trifluoroethanol was refluxed with ethanol in the presence of sulfuric acid to give trifluoroethyl ethyl ether (18% yield). bp 50—51°C (lit.[9] 49.9°C).

(4) β-Chloroethyl Ethyl Ether. β-Chloroethyl ethyl ether was prepared from ethylene chlorohydrin and ethanol as mentioned above (65% yield). bp 107—108°C (lit.[10] 108—109°C).

(5) β,β,γ,γ-Tetrafluoropropyl Ethyl Ether. A mixture of sodium β,β,γ,γ-tetrafluoropropoxide, ethyl bromide, and dioxane in a stainless steel autoclave was heated at about 190°C for 54 hr to give β,β,γ,γ-tetrafluoropropyl ethyl ether (34% yield). bp 86—88°C, n_D^{20} 1.3252, d_4^{20} 1.184.

Found: F, 47.2%; MR_D 27.2 Calcd for $C_5H_8OF_4$: F, 47.5%; MR_D 27.3.

Preparation of Ethers of the Type $RCF_2OCH_2CH_3$. α,α,β,β-Tetrafluoroethyl-, α,α,β-trifluoro-β-chloroethyl- and α,α-difluoro-β,β-dichloroethyl ethyl ether were prepared by the nucleophilic addition reaction[11] of ethanol to tetrafluoroethylene, trifluorochloroethylene, and 1,1-dichloro-2,2-difluoroethylene, respectively.

Addition Reaction of Ethers to Perfluoropropene. A mixture of 37 g (0.34 mol) of β,β-difluoroethyl ethyl ether and 137 g (0.91 mol) of perfluoropropene was placed in an autoclave (capacity, 200 m*l*) and received γ-irradiation at room temperature to a total dose 60 MR for a period of 1030 hr. After recovery of unchanged perfluoropropene (72.5 g), the content in the autoclave was distilled to give dimers of perfluoropropene (0.8 g), a mixture of 1 : 1 adducts (58.3 g), a 1 : 2 adduct (27 g, 0.066 mol, 19.3% yield) and viscous residues (8 g). From its gas chromatogram and NMR spectrum, the mixture of 1 : 1 adducts was found to consist of β,β-difluoroethyl α-methyl-β,β,γ,δ,δ,δ-hexafluorobutyl ether (57 g, 0.22 mol, 64% yield) and ethyl α-fluoromethyl-β,β,γ,δ,δ,δ-hexafluorobutyl ether (1.3 g, 0.0051 mol, 1.5% yield).

Addition reactions of other ethers were carried out under similar conditions, which are summarized in Table 1 together with the yields. Though products were mainly separated by distillation, some products were isolated by a preparative gas chromatograph. Physical properties of the 1 : 1 adducts and 1 : 2 adducts are shown in Table 5.

The authors wish to express their thanks to the Daikin Kogyo Co. for supplying perfluopropene.

9) A. L. Henne and M. A. Smook, *J. Am. Chem. Soc.*, **72**, 4378 (1950).

10) L. C. Swallen and C. E. Boord, *ibid.*, **52**, 651 (1930).

11) R. D. Chambers, "Ionic Reactions of Fluoroolefins" in "Advances in Fluorine Chemistry," Vol. 4, Butterworth & Co. (1965), p. 50.

BULLETIN OF THE CHEMICAL SOCIETY OF JAPAN VOL. 42 1158—1159 (1969)

Dipole Moments of 1,2-Dihalogeno- and 1,1,2,2-Tetrahalogenoethanes in Aromatic and Non-Aromatic Solvents

Osamu KIYOHARA and Ken-iti HIGASI[*1]

Research Institute of Applied Electricity, Hokkaido University, Sapporo

(Received September 18, 1968)

A weak interaction between 1,2-dichloroethane and aromatic solvents has been detected by studies of the dielectric relaxation times and dipole moments.[1] In the present study measurements were made of the dipole moments of 1,2-dihalogeno- and 1,1,2,2-tetrahalogenoethanes in various solvents (Table 1). The observed moment of 1,2-diiodoethane in benzene, 0.5_3D, is considerably lower than the literature value, 1.3 D,[2] which was obtained in the very early stage of dipole moment studies.

The interaction between 1,2-dichloroethane and an aromatic solvent has been believed to occur through hydrogen-bonding; the hydrogen atoms of dichloroethane have been assumed to interact with π-electrons of an aromatic solvent.[3] However, this hydrogen-bonding mechanism can not explain the "benzene effect" of 2,3-dihalogeno-2,3-dimethylbutane[4] and that of chloroacetone,[5] because this effect appears when hydrogen atoms are replaced by methyl groups.

*1 Present address: Department of Chemistry, Waseda University, Shinjuku-ku, Tokyo

1) K. Chitoku and K. Higasi, This Bulletin, **40**, 773 (1967), and papers cited therein.

2) J. W. Williams, *Z. Physik. Chem.*, **A138**, 75 (1928).

3) A. Neckel and H. Volk, *Z. Elektrochem.*, **62**, 1104 (1958); see also Ref. 1.

4) Y. Morino, I. Miyagawa, T. Haga and S. Mizushima, This Bulletin, **28**, 165 (1955).

5) A. Abadie, C. Michel and P. Mauret, *C. R. Acad. Sc. Paris*, **264**, 1433 (1967).

TABLE 1. DIPOLE MOMENTS OF 1,2-DIHALOGENO- AND 1,1,2,2-TETRAHALOGENOETHANES
(Debye unit. 20°C)

Solvent	ε	Solute				
		CH_2Cl-CH_2Cl	CH_2Br-CH_2Br	CH_2I-CH_2I	$CHCl_2-CHCl_2$	$CHBr_2-CHBr_2$
Benzene + Naphthalene (0.177 mol%)	2.360	—	—	—	1.72	—
Benzene	2.284	1.83	1.19	0.5_3	1.71	1.42
Toluene	2.385	1.71	1.09	0.5_0	1.68	1.40
p-Xylene	2.270	1.62	1.04	0.4_7	1.67	1.40
Cyclohexene	2.219	1.51	0.93	—	1.64	1.38
Amylene	2.015	1.44	0.89	—	—	—
Carbon disulfide	2.641	1.43	0.90	—	1.51	1.26
Carbon tetrachloride	2.238	1.41[a]	—	0.4_2	1.59	—
Cyclohexane	2.024	1.45	0.89	0.4_1	1.55	1.26
n-Hexane	1.898	1.39[a]	0.96(25°C)[b]	0.4_1	1.54	1.24
$P_E+P_A=1.05R_D$ (cc)		22.06	28.35	38.89	32.12	43.92

a) Recalcd. from Ref. 1.
b) Recalcd. from K. Kojima and S. Mizushiam, *Sci. Papers Inst. Phys.-Chem. Res.* (*Tokyo*), **31**, 296 (1937).

As an alternative mechanism, the chlorine atoms of 1,2-dichloroethane have been considered to play an important role in the complex formation between the solute and the aromatic solvent.[1,6] If this mechanism were true, one might expect to find some regular changes upon the replacement of Cl by Br or by I, which have smaller electronegativities than that of the chlorine atom. The results collected in Table 1 do not offer any definitive evidence for this, however.

It was pointed out by Sutton[7] to one of the present authors that the benzene effect might be due to the hyperpolarizability[8] of the aromatic solvent in the very strong field of the solute dipole. This hyperpolarizability effect is not necessarily restricted to an aromatic solvent. It is interesting to find that the dipole moments of dihalogeno- and tetrahalogenoethanes are higher in cyclohexene than those in cyclohexane and other non-aromatic solvents. However, those in amylene are not much different from the moments in cyclohexane. The effect of hyperpolarizability seems to need further study.

6) S. Kondo, E. Tagami, K. Iimura and M. Takeda, This Bulletin, **41**, 790 (1968).
7) L. E. Sutton, Private Communication.
8) C. A. Coulson, A. Maccoll and L. E. Sutton, *Trans. Faraday Soc.*, **48**, 106 (1952).

SHORT COMMUNICATIONS

Ethylene Proton Exchange in Cobalt(III) EDTA Complex as Evidenced by Nuclear Magnetic Resonance

Hayami YONEDA* and Yukiyoshi MORIMOTO**

* *Department of Chemistry, Wakayama University, Masagocho, Wakayama*
***Research Laboratories, Fujisawa Pharmaceutical Company, Kashimacho, Higashiyodogawa-ku, Osaka*

(Received January 13, 1969)

Coordinated ligands in metal complexes are under the influence of the electron-withdrawing effect of the central metal ion, and, in some complexes, some of their protons are dissociated in solution. Thus, if such complexes are dissolved in deuterium oxide, hydrogen deuterium exchange is to be observed. We noticed this kind of exchange from the finding[1] that the NMR signal of the methylene protons in malonato chelates dissolved in deuterium oxide decreased in intensity with time. We have been looking for such exchange reactions by means of the NMR technique. As a result, several other exchanges were found, *i. e.* in the methylenes in trisglycinatocobalt(III)[2] and in the palladium complex[3] of glycine and pyruvic acid and in the methyl in diammine-acetylacetone-ethylenediiminecobalt(III) complex.[4]

Here we wish to report an example of the exchange active ethylene group, *viz.* the ethylene group in the ethylenediaminetetraacetatocobaltate(III) complex.

Figure 1 shows the NMR spectra of the complex. Curve (a) represents the spectrum of the complex dissolved in neutral deuterium oxide. The spectrum shows a complicated pattern because the proton signals due to the ethylene and two kinds of methylenes (out-of-plane and in-plane) appear almost in the same region. Addition of a small amount of potassium carbonate to the solution caused a decrease in the intensity of the NMR signal as shown in curve (b) and (c). This is not surprising because Reilley[5] already reported the hydrogen-deuterium exchange in the acetato methylenes of this complex dissolved in acidified deuterium oxide solution at elevated temperature (85—105°C). However, when the solution was kept at 90°C for 20 min, all signals due to the ethylene as well as the methylene protons completely disappeared as shown in curve (d). This means that the ethylene protons are also exchanged by deuterium at elevated temperatures.

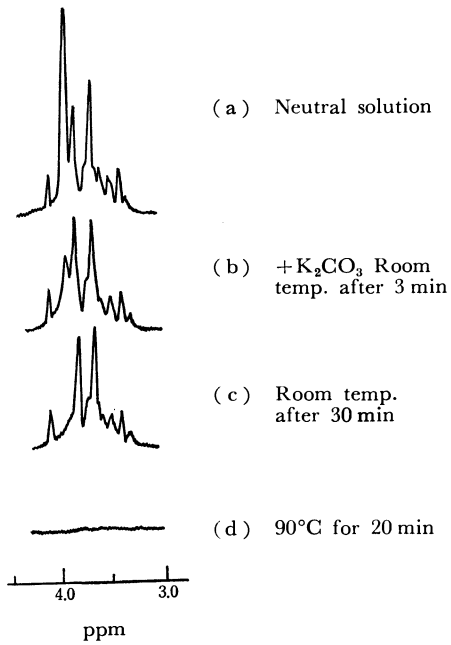

Fig. 1. The NMR spectra of Na[CoEDTA] in deuterium oxide. Sodium trimethylsilyl-propane-sulfonate was used as an internal standard.

We are now investigating the NMR spectra of other metal EDTA complexes and the results will be reported in the near future.

1) H. Yoneda and Y. Morimoto, This Bulletin, **40**, 1737 (1967); *Inorg. Chim. Acta*, **1**, 413 (1967).
2) unpublished.
3) H. Yoneda and Y. Morimoto, This Bulletin, **41**, 255 (1968).
4) H. Yoneda and Y. Morimoto, *ibid.*, **41**, 2544 (1968).
5) J. B. Terrill and C. N. Reilley, *Inorg. Chem.*, **5**, 1989 (1966).

The Adsorbed State of Oxygen on Vanadium Pentoxide Catalyst

Kimio TARAMA, Satohiro YOSHIDA, Shingo ISHIDA and Yasuo DOI

Faculty of Engineering, Kyoto University, Sakyo-ku, Kyoto

(Received December 5, 1968)

ESR studies on the adsorbed state of oxygen on metal oxides have been reported, the most extensive works being performed with the adsorbed oxygen on zinc oxide and titanium oxide.[1)]

We[2)] observed three kinds of ESR signals (α, β and γ) for oxygen adsorbed on vanadium oxide supported on silica. One of these signals, β-signal, is similar to that which was recently reported by Kasansky.[3)] The present communication is concerned with the ESR spectra of the adsorbed oxygen and their stability.

Vanadium oxide catalyst was prepared as follows. Synthetic silica which was prepared by hydrolysis of ethyl ortho silicate was impregnated with aqueous solution of ammonium meta vanadate, followed by drying at 100°C and calcination in air at 500°C. The content of vanadium oxide was 5 wt%.

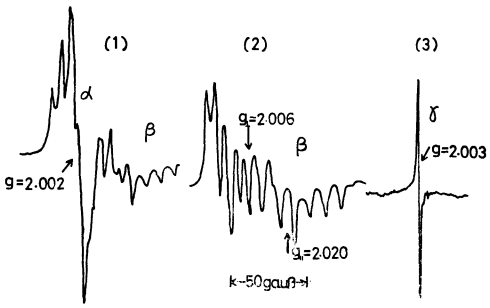

Fig. 1. ESR spectra of the oxygen adsorbed on $V_2O_{5-\delta}$-SiO_2.
(1) measured at −80°C. (P_{O_2} ; 20 Torr)
(2) measured at room temperature. (P_{O_2} ; 20 Torr)
(3) measured at room temperature. $V_2O_{5-\delta}$-SiO_2 was treated by O_2 at 200°C for 30 min and followed by evacuation at the same temperature.

Prior to the adsorption of oxygen, the catalyst was treated with hydrogen at 350°C in a glass reactor which had a quartz tube for ESR measurement as a side arm. This treated catalyst can be expressed as $V_2O_{5-\delta}$-SiO_2 ($\delta \simeq 0.1$).

ESR measurements were carried out at various temperatures by a 3BSX type spectrometer manufactured by Japan Electron Optics Co.

Some observed ESR spectra are shown in Fig. 1. Spectrum (1) is composed of two kinds of absorption signals. One (β-signal) is essentially the same as spectrum (2) which has h.f.s. due to interaction with ^{51}V ($I=7/2$),[3)] and the other (α-signal) is a singlet signal. At temperatures higher than −60°C, this α-singal is very unstable and disappears to leave β-signal. Spectrum (3) is a narrow singlet signal (γ-signal) observed for the catalyst treated with oxygen at 200°C. In Table 1, the temperature range in which each signal can be observed in spectra is shown together with characteristic parameters of signals.

By comparing these signals with those of the adsorbed oxygen on zinc oxide and titanium oxide, we tentatively assigned α-, β- and γ-signal as adsorbed $O_2^-(\alpha)$, $O_2^-(\beta)$ and O^- respectively. Preliminary studies on the reactivity of these adsorbed species reveal that $O_2^-(\beta)$ reacts with ethylene at room temperature and O^- reacts with sulfur dioxide at 200°C.

TABLE 1. CHARACTERISTICS OF SIGNALS

Signal	Observed temperature	g	A or ΔH_{msl} (gauss)
α	from −120°C to −60°C	2.002	$\Delta H=8.0$
β	from −120°C to 150°C	$g_{\parallel}=2.020$	$A_{\parallel}=9.4$
		$g_{\perp}=2.006$	$A_{\perp}=5.8$
γ	from 20°C to 350°C	2.003	$\Delta H=0.96$

1) T. Kwan *et al.*, 4th Int'l Congress on Catalysis, Preprint No. 5 (Moscow) (1968); Proc. the 21th Disc. for Catalysis, (Toyama) (1967), p. 45 ; R. Kokes, *J. Phys. Chem.*, **66**, 99 (1962) ; Proc. the 3rd Int'l Congress on Catalysis, p. 484 (Amsterdam) (1964) ; K. Sancier, *J. Catalysis*, **5**, 314 (1966) ; J. Lunsford and P. Jayne, *J. Chem. Phys.*, **44**, 1487 (1966) ; V. Kazanskii *et al.*, *Kinetika i Kataliz*, **8**, 853 (1967) ; G. Schuit *et al.*, *Discussions Faraday Soc.*, **41**, 290 (1966).

2) K. Tarama *et al.*, Proc. the 7th Disc. for ESR, (Sapporo) (1968), p. 80; Preprints for the 21th Annual Meeting of the Chem. Soc. of Japan (Osaka) (1968), No. 18115.

3) V. A. Shvets, M. E. Sarichev and V. B. Kasansky, *J. Catalysis*, **11**, 378 (1968).

The Reactions of Aroyl Peroxides with Grignard Reagents. I. On the Formation of a Stable Complex Containing Peroxide

Masao ŌKUBO,* Kazuhiro MARUYAMA** and Jirō ŌSUGI**

* *Government Industrial Research Institute, Nagoya*

** *Department of Chemistry, Faculty of Science, Kyoto University*

(Received January 30, 1969)

When a THF solution of BPO was mixed with the equimolar PhMgBr solution at 0°C under nitrogen stream and stirred for 2 hrs, 18—20% of BPO was found to remain in the solution. After the mixture was stood for 24 hr and/or even if it was heated at 50°C for 1 hr, the content of peroxide still remained unchanged. By adding ethyl ether to the concentrated reaction mixture, orange-yellow crystals were precipitated. The precipitate (ppt. 1) was filtered and dried in a vacuum-desiccator.*1 The ppt. 1 is fairly stable in air, but dissolves in water releasing bromine, finally to leave $(PhCOO)_2Mg$ and THF. The yellow color of the THF solution of ppt. 1 disappeared suddenly by the addition of a suitable amount*2 of PhMgBr solution, and the resulting mixture contained no peroxide.

On the other hand, when 50% molar excess of Grignard reagent to the peroxide was used and worked up similarly, no color change was observed during the course of the reaction, and white precipitate (ppt. 2), containing no peroxide was finally obtained. For the analysis of ppt. 2, the precipitate was dissolved in water, acidified and extracted with ether. Contents of Mg^{2+} and Br^- in the aqueous layer were analyzed by oxinechelate method[1] and $AgNO_3$-titration method, respectively. Content of THF in the ether layer was determined by v.p.c. technique. Analytical results are as follows: Mg^{2+} 7.8 (6.6)%; Br^- 21.7 (21.6)%; $PhCOO^{\ominus}$ 31.9(32.8)%; and THF 37.5(39.1)%. The values given in parentheses are calculated by assuming the formula[I] to ppt. 2. The yield of ppt. 2 based on the BPO used was quantitative. If a suitable amount of BPO was added to a THF solution of ppt. 2, an orange-yellow color appeared after a few minutes. When this solution was concentrated, orange-yellow precipitate was obtained, having the same composition as the ppt. 1. The peroxide content of ppt. 1 was determined by iodometry. A portion

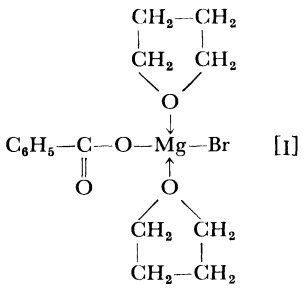

[I]

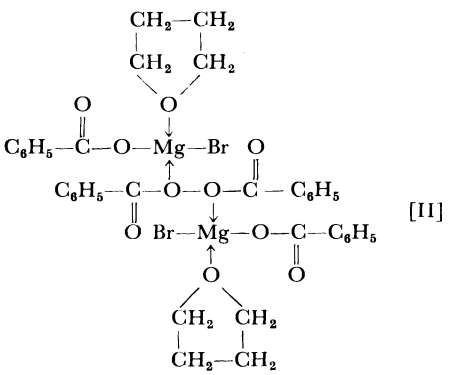

[II]

of ppt. 1 was treated with $Fe(II)SO_4$ solution, and the amounts of Br^-, PhCOOH and THF were determined. From $[PhCOO]_{total}$ and $[PhCOO]_{BPO}$, one can estimate $[PhCOO^{\ominus}]$ in ppt. 1. Another portion of ppt. 1 was submitted to the analysis of Mg^{2+} content. Analytical results are as follows: Br^- 18.0(19.1)%; Mg^{2+} 5.5(5.8)%; $PhCOO^{\ominus}$ 35.0(29.0)%; BPO 18.4(29.0)%; and THF 15.7(17.2)%. The values given in parentheses are calculated by assuming the formula[II] to ppt. 1. Moreover, the same orange-yellow colored solution was obtained, if one added BPO to the completely carbonated PhMgBr solution. Taking account of the chemical behaviors of ppt. 1 and the said reaction, formula[II] seems to be reasonable. The fact that the ppt. 1 dissolves in water releasing bromine can be nicely explained by considering the electron-transfer from the Mg–Br linkage to the peroxidic linkage through the coordination bond. The lower content of BPO and the higher content of $PhCOO^{\ominus}$, compared with the calculated values, may be due to the gradual decomposition of the ppt. 1 by moisture.

---

*1 From the filtrate, PhCOOPh was obtained.

*2 When BPO was treated with 4/3 molar equivalent of PhMgBr, the peroxide was found to be consumed completely after 2 hrs at room temperature.

1) I. M. Kolthoff and E. B. Sandell, "Textbook of Quantitative Inorganic Analysis," Macmillan Co., N. Y. (1955), pp. 362, 607.

[7](2,6)Pyridinophane and [7](2,6)Pyrylophanium Perchlorate

Hitosi NOZAKI, Shinsaku FUJITA and Takasi MORI

Department of Industrial Chemistry, Kyoto University, Sakyo-ku, Kyoto

(Received February 5, 1969)

Although preparation of [10](2,6)pyridinophane and 15-methyl[10](2,6)pyrylophanium perchlorate has been reported,[1] homologs with shorter methylene bridge still remain to be synthesized. In continuing the work on heterocyclophanes,[2] we were interested in the title compounds.

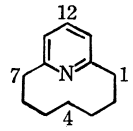

(I)

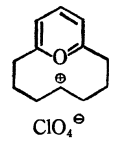

(III)

[7](2,6)Pyridinophane (I) (bp 70—73°C/3 mm Hg. Anal. Found: C, 82.5; H, 9.9; N, 7.7%) was obtained in a 44% yield by treatment of cyclododecane-1,5-dione (II) with 2.5 mol equivalents of hydroxylamine hydrochloride in an autoclave at 150—175°C. The dione II (mp 66.5—67.5°C, lit.[3] 64—65°C) was conveniently prepared by the Jones oxidation of cyclododecane-1,5-diol and/or by oxidation of *B*-acetoxy-13-borabicyclo[7.3.1]-tridecane[4] with aqueous sodium dichromate in ether.

Compound I exhibited aromatic absorptions (neat) at 3060, 1588 and 1575 cm^{-1} and a UV maximum (EtOH) at 272 nm (log ε 3.50). The bathochromic shift in the UV absorption as compared with [10](2,6)pyridinophane[5] may be ascribed to the nonplanar pyridine ring bridged by the heptamethylene group. The aromatic NMR signal (3 protons) (Fig. 1) showed a typical AB_2 pattern (ν_A δ 7.40, ν_B δ 6.87, J_{AB} 7 Hz) which resembled the splitting pattern of 2,6-lutidine very closely. The absorptions due to the heptamethylene protons were composed of three groups of multiplets. Protons of one methylene (a quintet at δ 0.16) were unexpectedly shielded in comparison with usual paraffinic methylenes. Tentatively, we assign the absorption to C_4 protons[6] locating close to the pyridine ring on inspection of the Dreiding model. Since the multiplet (centered at δ 2.84) due to C_1 and C_7 protons can be regarded as a triplet approximately, the heptamethylene chain should be flexible at room temperature.[2] Heating of I with a mixture of 30% hydrogen peroxide and acetic acid failed to give the *N*-oxide, whereas similar treatment of [10](2,6)-pyridinophane afforded the corresponding *N*-oxide.[1a] This is another point of difference introduced by the shorter polymethylene chain.

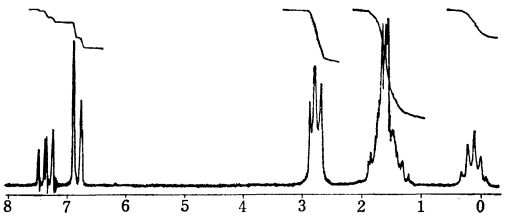

Fig. 1. NMR spectrum of I (in $CDCl_3$ at 24°, 60 MHz).

Reaction of II with trityl perchlorate in glacial acetic acid at 110—120°C afforded [7](2,6)-pyrylophanium perchlorate (III) (mp 150°C (dec.). Found: C, 52.6; H, 6.0; Cl, 12.6%) in a 65% yield. The IR spectrum (Nujol) exhibited aromatic bands at 3060, 1627 and 1498 cm^{-1} and a broad band due to the perchlorate anion at 1088 cm^{-1}. The NMR spectrum of III (in trifluoroacetic acid) consisted of an AB_2-type signal (3 aromatic protons, ν_A δ 8.85, ν_B δ 7.98, J_{AB} 8 Hz), a triplet at δ 3.42 (4 methylene protons on C_1 and C_7), a multiplet at δ 2.4—1.5 (8 methylene protons on C_2, C_3, C_5 and C_6) and a quintet at δ 0.82 (2 methylene protons on C_4). Treatment of the pyrylium salt III with ammonium acetate in glacial acetic acid yielded the pyridinophane I (66%) which was identical with the sample prepared directly from II.[7] Details of the experiments and further discussions will be presented in a paper to be published later.

1) a) K. Biemann, G. Büchi and B. H. Walder, *J. Am. Chem. Soc.*, **79**, 5558 (1957); b) A. T. Balaban, M. Gavat and C. D. Nenitzescu, *Tetrahedron*, **18**, 1079 (1962). See also A. T. Balaban, *Tetrahedron Letters*, 4643 (1968).

2) H. Nozaki, T. Koyama, T. Mori and R. Noyori, *Tetrahedron Letters*, **1968**, 2181.

3) G. S. Fonken, M. E. Merr, H. C. Murray and L. M. Reineke, *J. Am. Chem. Soc.*, **89**, 672 (1967).

4) G. W. Rotermund and R. Köster, *Liebigs Ann. Chem.*, **686**, 153 (1965).

5) [10](2,6)Pyridinophane exhibits UV maxima (EtOH) at 213 (log ε 3.82) 267 nm (3.62). See Ref. 1a.

6) For this nomenclature, see B. H. Smith, "Bridged Aromatic Compounds, Academic Press, New York, N. Y. (1964), pp. 1—23.

7) [8](2,5)Pyridinophan-1-one has recently been reported independently: H. Gerlach and E. Huber, *Helv. Chim. Acta*, **51**, 2027 (1968).

Radical Formation in the Radiolysis of Solid Isobutane as Studied by ESR Spectroscopy

Terunobu WAKAYAMA, Tetsuo MIYAZAKI, Kenji FUEKI and Zen-ichiro KURI

Department of Synthetic Chemistry, Faculty of Engineering, Nagoya University, Chikusa-ku, Nagoya

(Received February 10, 1969)

Extensive studies have been made of the mechanism of radical formation in the radiolysis of hydrocarbons in condensed phases. Generally speaking, primary radicals can be produced from the neutralization reaction between positive ions and electrons, the ion-molecule reaction, and the decomposition of directly excited molecules or ions. It is of essential importance for understanding elementary processes in radiation chemistry to elucidate the mechanism of radical formation in irradiated systems. Most of the previous studies were based on the analysis of final products and not on the direct observation of radicals.

In the present work, we have made an ESR study of radicals produced in γ-irradiated isobutane with and without additives at 77°K. Figure 1(a) shows the ESR spectrum of pure isobutane, which is assigned to the isobutyl radical.[1] Figure 1(b) shows the ESR spectrum of isobutane containing 1 mol% carbon tetrachloride.
It is seen from a comparison of Fig. 1(a) and (b) that there is a drastic change in the spectrum. The absorption line (A) in Fig. 1(b) is attributed to the CCl_3 radical.[2] Figure 2 shows the relative yields of isobutyl radical and CCl_3 radical against the concentration of carbon tetrachloride. The yield of isobutyl radical decreases and that of CCl_3 radical increases with increaseing concentration of carbon tetrachloride.

We have also investigated the radical formation in γ-irradiated isobutane containing ethyl iodide. The ESR spectrum of ethyl radical was observed in this system, while the yield of isobutyl radical did not change significantly with increasing concentration of ethyl iodide. It can be said that the ethyl radical is produced by dissociative electron attachment to ethyl iodide. The addition of electron scavengers such as nitrous oxide and sulfur hexafluoride also did not cause a change in the yield of isobutyl radical.

These results indicate that in the radiolysis of solid isobutane the isobutyl radical is not produced from the neutralization reaction, but mainly from the decomposition of directly excited isobutane molecules or ions, and that energy transfer from isobutane to carbon tetrachloride plays a role in suppressing the decomposition of isobutane.

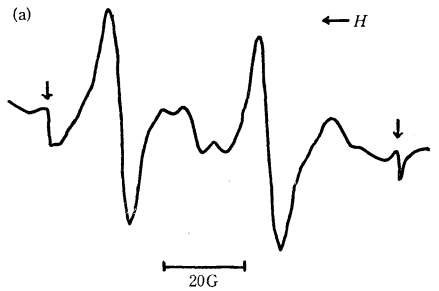

Fig. 1 (a)

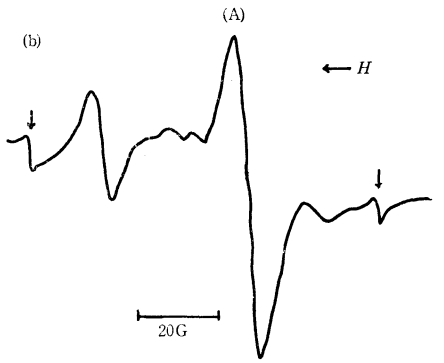

Fig. 1 (b)

Fig. 1. (a) ESR spectrum of γ-irradiated isobutane at 77°K, (b) ESR spectrum of γ-irradiated isobutane containing 1 mol% carbon tetrachloride at 77°K. Irradiation dose : 1.7×10^5 rad. The arrow indicates signal of Mn^{2+}.

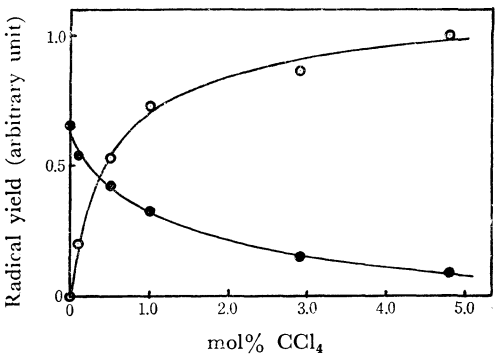

Fig. 2. Radical yields *vs.* concentration of carbon tetrachloride. —●— : isobutyl radical, —○— : CCl_3 radical. Irradiation dose : 1.7×10^5 rad. The yield of CCl_3 radical was obtained by subtracting the the contribution of solvent radical to the line (A).

1) J. Lin and F. Williams, *J. Phys. Chem.*, **72**, 3707 (1968).

2) R. F. C. Claridge and J. E. Willard, *J. Am. Chem. Soc.*, **87**, 4992 (1965).

BULLETIN OF THE CHEMICAL SOCIETY OF JAPAN VOL. 42 1165—1170 (1969)

The Surface Structure of Silica Gel Studied by Dielectric Dispersion*1

Seiichi KONDO

Osaka University of Education, Tennoji-ku, Osaka

and Masa-aki MUROYA

Osaka Electro-Communication University, Hatsu-machi, Neyagawa

(Received June 11, 1968)

The effect of water adsorption and heat treatment at various temperatures between 200 and 1100°C on the dielectric dispersions of silica gel was measured in the frequency range from 50 to 3×10^6 Hz and 9.81 GHz and in the temperature range from −196°C to 180°C. Two anomalous dispersions (Dispersion I and II) and one anomaly (Anomaly III) were found. The mechanisms of those anomalies were discussed in relation to some physical properties and silica crystal structures. Dispersion I, having activation energy ΔE equal to 11 to 14 kcal/mol, can be ascribed to the monomolecular layer of adsorbed water. Dispersion II, with activation energy of about 5 to 7 kcal/mol, can be attributed to proton diffusion through hydrogen-bond chain of surface silanol groups. Anomaly III, having activation energy of about 3 kcal/mol, may be assigned to dipolar rotation of free silanol.

Recent studies of the surface structure of silica gel by means of dielectric measurements,[1-3] infrared spectroscopy[4] and so forth have revealed many interesting aspects in detail. However, there are still some ambiguities on the nature of surface silanols and their interaction with adsorbed molecule. In this report, dielectric dispersions of silica gel were studied in respect to the effect of heat treatment and water adsorption and some interpretations of these results in combination with other physical properties are given in view of the surface structure of silica gel.

Experiment

Dielectric Measurement. The dielectric constant of silica gel in the frequency range from 50 to 3×10^6 Hz was measured with an Ando Electric Model TR-1 transformer-bridge. A dielectric cell A in Fig. 1 is composed of two coaxial cylindrical electrodes in a glass container with electric capacity of about 10 pF. The temperature of the cell can be changed from −196 to 180°C with the constancy of less than ± 1°. The dielectric constant at 9.81 GHz was measured by a transmission-line method. In this case, the sample holder was constructed so that the atmosphere and temperature of the holder could be controlled easily from −60 to 100°C within ± 1°.

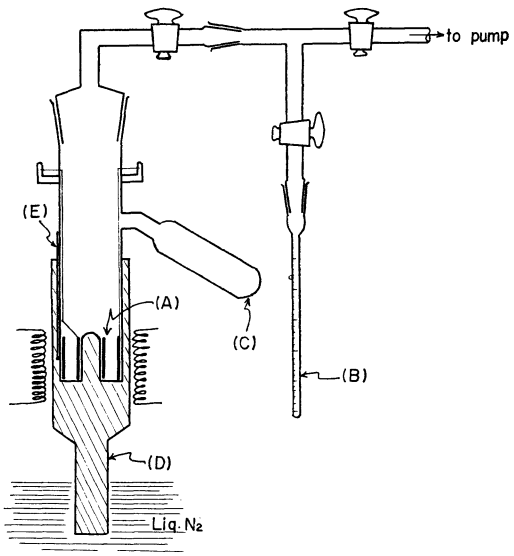

Fig. 1. Low frequency dielectric cell (A), with water burette (B), borosilicate or quartz glass tube for heat treatment (C), copper block (D), and Cu-Constantan thermocouple (E).

In order to obtain the real part of the dielectric constant ε', from the apparent value E, measured with powder sample, Pearce's equation[5] was used.

*1 Presented at the spring meeting of Japan Applied Physics Society, 1967.

1) J. Le Bot and S. Le Montagner, *Compt. Rend.*, **233**, 862 (1951).

2) K. Kamiyoshi, *Sci. Rep. Res. Inst, Tohoku Univ.*, **5**, 93 (1957).

3) K. Kamiyoshi and J. Ripoche, *ibid.*, **8**, 239 (1960).

4) J. B. Peri, *J. Phys. Chem.*, **70**, 2937 (1966); L. R. Snyder and J. W. Ward, *ibid.*, **70**, 3491 (1966).

5) C. A. R. Pearce, *Brit. J. Appl. Phys.*, **6**, 358 (1955).

$$\frac{E-1}{\varepsilon'-1} = \frac{(1-v)P}{1-vP} \quad (1)$$

Here, v is the parameter which is determined empirically and P is the volume filling factor, being equal to the ratio of bulk density of packed powder and particle density listed in Table 1. Values of the dielectric constant of powder materials of known dielectric constant obtained by this method are in good agreement with those of literature in the range under investigation.

TABLE 1. CHEMICAL COMPOSITION AND PHYSICAL PROPERTY OF SILICA GEL

Na_2O	0.01%
Fe	0.005%
Al	0.03%
Specific surface area	700 m^2/g
Pore volume (V_p)	0.35 cc/g
Particle density (d)	1.24 g/cc

Material. Silica gel was synthesized from sodium silicate and sulferic acid of analytical grade and washed carefully with dilute hydrochloric acid and distilled water. The material dried was powdered to less than 80 mesh. Some of the physical and chemical properties of the sampe thus obtained are shown in Table 1, where specific surface area, S m^2/g, was determined by BET method using nitrogen and pore volume, V_p cc/g, by liquid immersion method using ethyl alcohol. Particle density, d g/cc, of silica gel granule, which is the aggregate of primary particles having the density of 2.2 g/cc, was calculated by the following formula.

$$d = \frac{1}{V_p + 1/2.2} \quad (2)$$

The amount of water adsorbed on silica gel was obtained by drying a known amount of sample in cell A in Fig. 1 at 170°C for two hours under vacuum of 10^{-4} mmHg and then introducing to cell A a necessary amount of water in burette B which was degassed beforehand. Silica gel was heat-treated in vacuum of 10^{-4} mmHg in the quartz container C at various temperatures from 200 to 1100°C for about 2 hr and then transferred to A. There is no exposure of silica gel to the atmospheric air in the procedure.

Experimental Results

Effect of Adsorbed Water (Dispersion I). Figure 2(a) shows the curves of tan δ *versus* frequency of silica gel at 23°C having various amount of adsorbed water. The heights of tan δ maxima of these curves are roughly proportional to water content of silica gel from 0 to 10% as seen in Fig. 3. Those heights become approximately constant beyond 10% water but the accompanying increase of tan δ background level makes the measurement less accurate. Since the monomolecular layer of water is completed statistically at about 10% water, this anomaly may be interpreted as related to this statistical monomolecular layer. Tan δ maxima change with temperature as seen in Fig. 2(b), in a similar manner to tan δ *versus* frequency curves in Fig. 2(a). In this figure, we find another one at lower temperature side being discussed in

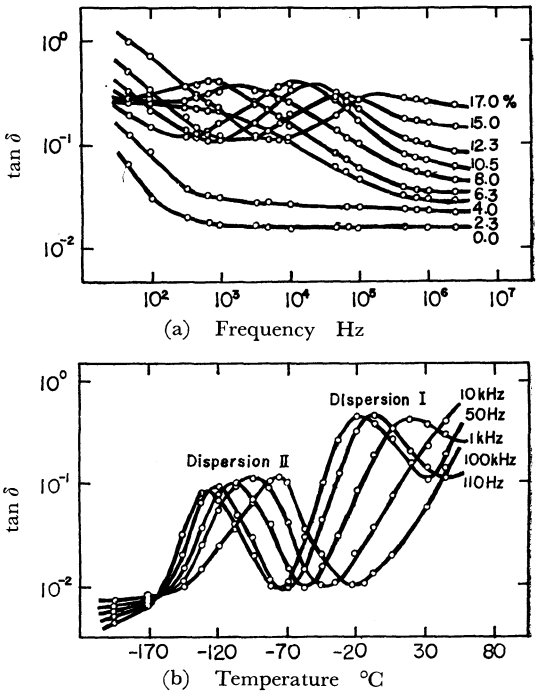

Fig. 2. Dielectric loss of silica gel with various water content.
(a) shows the frequency *versus* tan δ curves at 23°C.
(b) shows the temperature *versus* tan δ curves at 5.3% water adsorption.

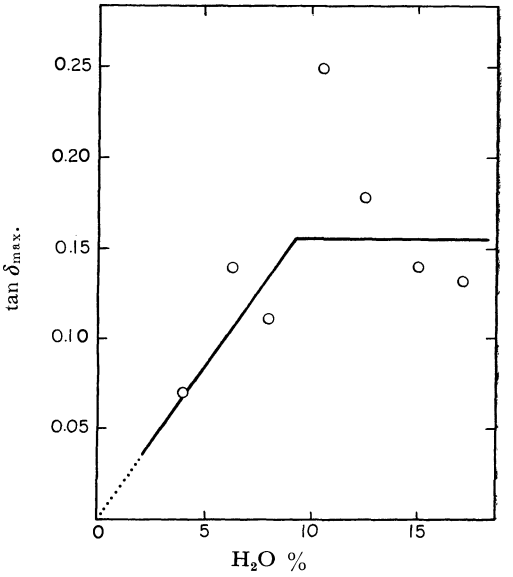

Fig. 3. Relation between the peak heights of tan δ maxima and water content of silica gel of Dispersion I at 23°C.

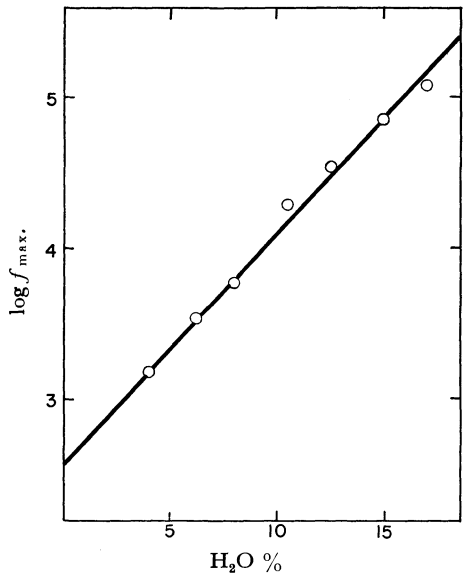

Fig. 4. Log frequency of tan δ maximum of Dispersion I *versus* water content of silica gel at 23°C.

the next section. In Fig. 4, water content is proportional to the shift of frequency of tanδ maximum at 23°C. At constant frequency, water content is proportional to the temperature of tan δ maximum.

Figure 5 shows the curves of complex dielectric constant *versus* frequency at 5.3% water adsorption

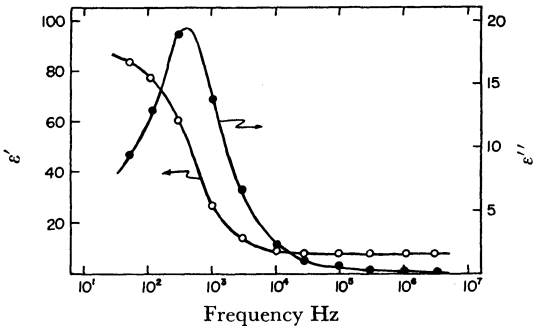

Fig. 5. Frequency *versus* complex dielectric constants, ε' and ε'', curves of Dispersion I of silica gel of 5.3% H_2O and at 23°C.

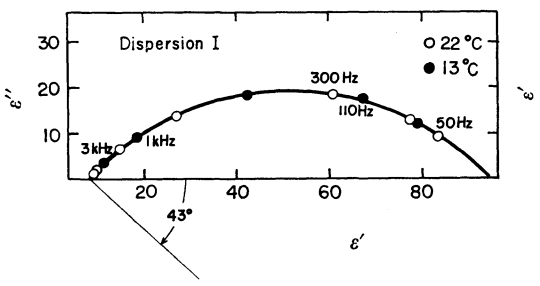

Fig. 6. Cole-Cole arc plots of Dispersion I of silica gel of 5.3% H_2O at 13 and 22°C.

and 23°C. These curves are characteristic of dielectric dispersion, so this anomaly will be called Dispersion I hereafter in this report. Cole-Cole arc plots of Dispersion I at 5.3% shown in Fig. 6 deviate largely from semi-circle law and indicate a large distribution of relaxation times. However, it is difficult to tell whether Dispersion I is the Debye or Maxwell-Wagner type from data available in this study. Figure 7 shows the curves of log relaxation time, τ, *versus* reciprocal temperature obtained from Cole-Cole arc plots, mentioned above, at various temperatures, together with the values at 11.5% water adsorption measured by Kamiyoshi.[2] Table 2 shows activation energies ΔE and constant τ_0 of Dispersion I and those by Kamiyoshi[2] and of ice measured by Auty and Cole.[6] These values of Dispersion I are close to those of ice and differ from that of water. This similarity suggests the existence of some kind of ordered configuration of

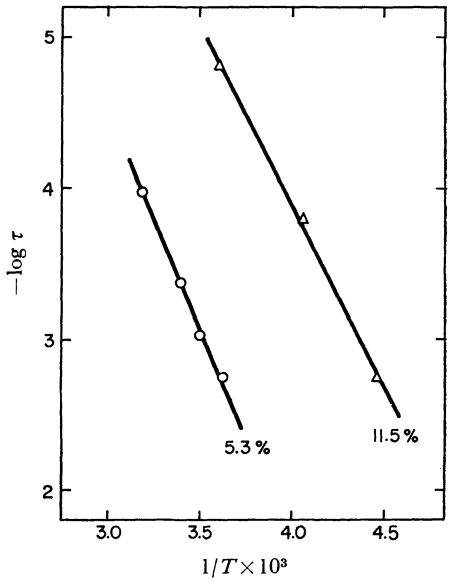

Fig. 7. Log relaxation times τ *versus* reciprocal temperature of Dispersion I by the present investigation and by Kamiyoshi[2] shown by circular and triangle plots respectively.

TABLE 2. ACTIVATION ENERGY ΔE AND RELAXATION TIME τ_0 OF DISPERSION I OF SILICA GEL CONTAINING ADSORBED WATER AND OF ICE[6]

H_2O %	ΔE (kcal/mol)	τ_0 (sec)
5.3	14.2	2.5×10^{-16}
11.5*	11.3	5.9×10^{-15}
ice	13.2	5.3×10^{-16}

* These were obtained by Kamiyoshi.[2]

6) R. P. Auty and R. H. Cole, *J. Chem. Phys.*, **20**, 1309 (1952).

adsorbed water molecule on silica gel surface, which will be discussed in section IV.

Silica Gel Without Adsorbed Water (Dispersion II). Figure 8(a) and (b) show the curves

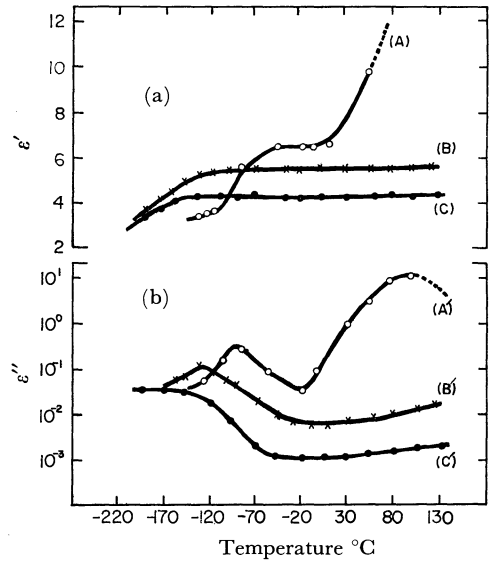

Fig. 8. Real and imaginary parts of complex dielectric constants *versus* temperature curves are shown in figures (a) and (b) respectively. Curves (A), (B) and (C) show those values at 1% H_2O, and 200 and 300°C of heat-treatment of silica gel, respectively. Note Dispersion I appearing at higher temperature.

of ε' and ε'' at 1 kHz against temperature of silica gel thermally treated at 200 and 300°C (curves B, C, B′ and C′) and those of 1% water adsorption (curves A and A′). The anomaly at 1% water adsorption of curves A and A′ is Dispersion I as described in section 1. The anomaly at −100°C can be observed not only in curves A and A′ but

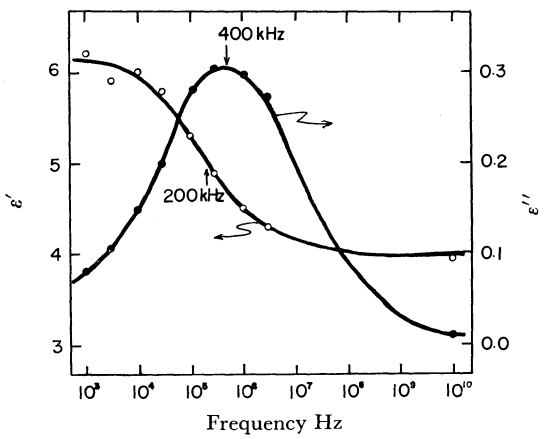

Fig. 9. Frequency *versus* complex dielectric constant curves of Dispersion II of silica gel at −58°C and 1% H_2O.

also in curves B, B′, C and C′ in which silica gels are treated at higher temperature. The curves of ε' and ε'' *versus* frequency of this anomaly at −58°C and 1% water adsorption for example, as seen in Fig. 9, suggest this anomaly to be a dielectric dispersion (Dispersion II). In this figure, the frequency of inflection point of ε' curve, about 200 kHz, differs from that of ε'' maximum, about 400 kHz, and this discrepancy suggests Dispersion II being the Maxwell-Wagner type. Cole-Cole arc plots of Dispersion II, shown in Fig. 10, indicate

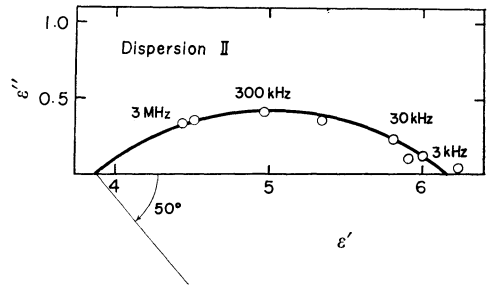

Fig. 10. Cole-Cole arc plots of Dispersion II of silica gel at −58°C and 1% H_2O.

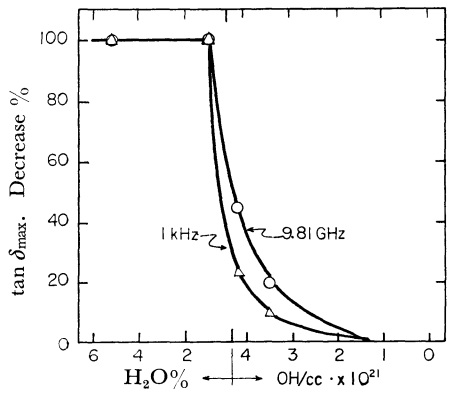

Fig. 11. Relation of decrease of the height of tan δ maxima shown by per cent of Dispersion II to water content and OH concentration per unit volume of silica gel.

the existence of large distribution of relaxation times as often seen in colloid system.[7] Figure 11 shows the height of tanδ maxima of Dispersion II at 1 kHz and 9.81 GHz against water adsorption and the concentration of silanol groups per unit volume which is equal to the weight loss by heating in the form of water divided by particle density at the temperature of heat treatment. ε'' maxima are not affected by the amount of water adsorption, become smaller by the decrease of hydroxyl concentration (or the increase of temperature) and are unobservable at about 500°C. The

7) S. Oka, "Theory of Solid Dielectrics," Iwanami Press, Tokyo (1964), p. 161.

values of ε' decrease also by elevating temperature and become almost constant and equal to that of vitrous silica above 500°C. This shows the decrease of contribution of polar silanol groups to the dielectric constant. From those results, it seems reasonable to assume Dispersion II to be caused by the diffusion of ion such as proton through hydrogen-bond chain of surface silanol groups.

The relation of log frequency of ε'' maxima of this dispersion to the reciprocal temperature is shown in Fig. 12 on silica gel treated at four different conditions; 5.3 and 1% water adsorption and 200 and 300°C of heat treatment. ε'' maxima at 2.89 GHz obtained by Le Bot and Le Montagner[1] and at low frequency by Kamiyoshi and Ripoche[3] on silica gel both dried at 110°C (about 1% water adsorption) are well on the line of 1% water of the present investigation. Table 3 shows the activation energies obtained from Fig. 12. The activation energies at 5.3% and 1% water are much larger than those without water. This may suggest the higher potential barrier for ionic diffusion by the presence of bound water. It should be added that Dispersions I and II have been found with deuterium-exchanged silica gel showing similar behavior to the ordinary silica gel.[8]

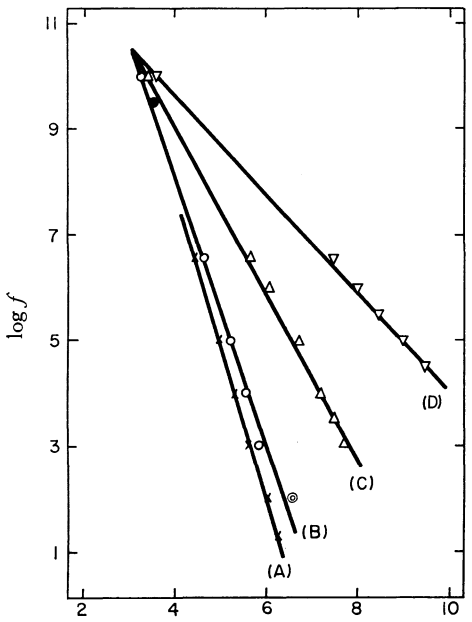

Fig. 12. Log frequency *versus* reciprocal temperature curves of Dispersion II of silica gel, in which (A), (B), (C) and (D) show those of 5.3% H_2O, 1% H_2O, and 200 and 300°C of heat treatment respectively and black and double circles show the values measured by Le Bot[1] and Kamiyoshi[2] respectively.

Table 3. Activation energy ΔE and relaxation time τ_0 of Dispersion II of silica gel containing adsorbed water and treated thermally

	ΔE (kcal/mol)	τ_0 (sec)
5.3 H_2O %	14.0	4.0×10^{-21}
1.0 H_2O %	11.4	1.9×10^{-18}
200°C	6.8	8.3×10^{-16}
300°C	5.0	1.6×10^{-14}

High Temperature Heat Treatment (Anomaly III). A very small maximum of ε'' can be observed at −178°C and at 1 kHz on silica gel treated at 500°C as seen in Fig. 13. This maximum becomes smaller by elevating the temperature of heat treatment and becomes unobservable at 1000°C. Therefore, this anomaly may be related to silanol groups existing above 500°C. Owing to the smallness of this anomaly, it is difficult to obtain the values of dielectric constant accurately and sufficiently enough to tell whether this is a dielectric relaxation. However, an approximate activation energy was obtained from the dependency of ε'' maximum frequency on temperature. ΔE and τ_0 are equal to about 3 kcal/mol and 1×10^{-10} sec respectively. The smallness of the activation energy suggests that this anomaly might be caused by the rotation of free silanol dipoles surviving after heat treatment.

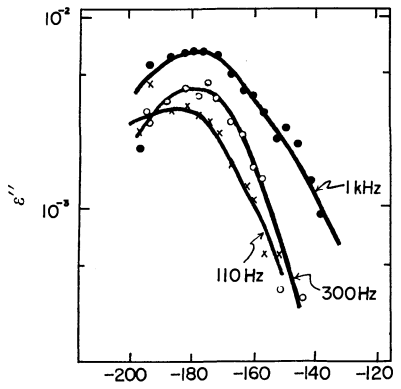

Fig. 13. Curves of imaginary part of the complex dielectric constant *versus* temperature of silica gel heat-treated at 500°C.

Discussion

The weight loss of silica gel by heating is usually considered to be caused by desorption of adsorbed water and condensational dehydration of surface

8) S. Kondo and M. Muroya, presented at the 21st Annual Meeting of The Chemical Society of Japan, 1968.

silanol groups. However, it is difficult to distinguish between each other by such means as thermogravimetric analysis and infrared spectroscopy. In the latter case, a broad and strong band at about 3500 cm^{-1} and at room temperature becomes gradually weaker by heating and almost disappears at about 600°C. On the other hand, a sharp band at 3750 cm^{-1} which is very obscure at low temperature becomes clear by heating. This latter band starts to decrease from about 600°C and disappears at 1000°C. The 3500 cm^{-1} band can be assigned to the hydrogen-bonded O–H stretching vibration of either adsorbed water or surface silanol. Since adsorbed water desorbs almost completely at 200°C as studied by the thermal behavior of Dispersion I, this band above 200°C may be assigned to the hydrogen-bonded silanol groups, in which the Dispersion II of this report originates.

Models to illustrate the structure of this type of hydrogen-bonded surface silanol have been proposed by several authors[4,9] as shown below.

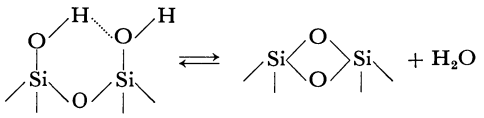

With such a model, however, it seems rather difficult to construct a reasonable siloxane skeletal structure in three dimensions and to satisfiy such physical properties of the surface as silanol surface density of about 8/100 Å^2. Moreover, the dehydration reaction according to this model requires a considerable distortion of valence angle of surface siloxane or deformation of succesive skeletal siloxane, which would cause changes of physical properties such as the decrease of surface area. This is not likely because the surface area decreases markedly only above about 500°C and drastic change of the structure starts above 700°C depending upon the nature of impurities.[10]

In this report, the model as shown in Fig. 14 (a) and (b) is taken into consideration under the assumption that primary particle of silica gel has a very short range order of siloxane structure similar to some of the silica crystals such as cristobalite, tridymite and quartz. In these crystals the silicium atom exposed on the crystal plane surface can possess one or two hydroxyl groups depending upon the index of the plane. Figure 14 (a) and (b) show the (100) and (111) planes of cristobalite as example, since the density of silica gel, 2.2 g/cc, is almost equal to that of cristobalite and silica gel changes to cristobalite most easily by heating. In Fig. 14 (a), each silicium atom on the (100) plane

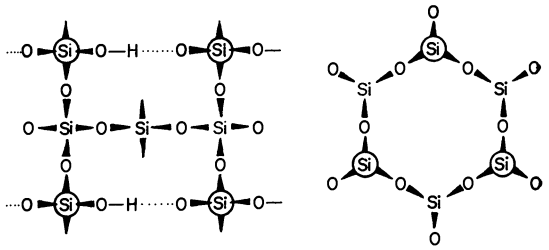

(a) (b)

Fig. 14. (a) and (b) are (100) and (111) crystal planes of cristobalite respectively. Rounded Si atoms are on the top surface.

can have two hydroxyl groups which would form hydrogen-bond chain with each other with the distance of about 2.7 Å and whose surface density is 7.85/100 Å^2. Dispersion II may be attributed to the proton diffusion through those one-dimensional chains of hydrogen-bond. Without adsorbed water, the activation energy for this diffusion may not be as large as that with the presence of adsorbed water as seen in Table 3. The dehydration reaction with this model would be as follows;

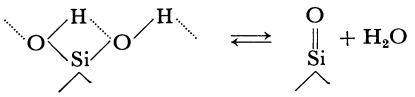

although we have no evidence for the existence of Si=O.

In such a model, the first layer, at least, of adsorbed water might have some kind of very short range order which may be three dimensional by including substrate structure, and the activation energy for the proton diffusion would be larger than that of water and close to that of ice as shown in Table 2. Considering the statistical nature of this quasi-crystalline model, the distribution of relaxation times may be large, as shown in this report.

The Anomaly III and the 3750 cm^{-1} band can both be assigned to free silanol groups. It might be interesting to see that silicium atoms on the (111) plane of cristobalite, as shown in Fig. 14 (b) for example, can have one hydroxyl group whose distance to each other is about 5 Å and is too far to form a hydrogen-bond and which has low surface silanol density of 4/100 Å^2. The dehydration reaction of such type of silanol requires some rearrangement of skeletal structure at high temperature and leads to the decrease of specific surface area and crystal growth.[10]

The authors wish to express their thanks to Messrs. Kaoru Kawabe, Toshio Tani and Hideo Kameyama of Fuji-Davison Chemical Co., Ltd., Kasugai, Japan, and Messrs. Osamu Tsukide and Shozo Uchihashi of Osaka Electro-Communication University, Neyagawa, Japan, for their help.

9) R. K. Iler, "The Colloid Chemistry of Silica and Silicates," Cornell Univ. Press, Ithaca, New York (1955), p. 243.

10) F. Matsuyama, B. S. Thesis, Osaka Univ. of Education, 1968.

BULLETIN OF THE CHEMICAL SOCIETY OF JAPAN VOL. 42 1171—1178 (1969)

Mechanism of Emulsification with Special Reference to Solid Stabilized Emulsions

S. P. JAIN and S. N. SRIVASTAVA

Chemical Laboratories, Agra College, Agra, India

(Received March 9, 1968)

Mechanism of emulsification with special reference to ferric hydroxide as emulsifier has been studied. The sol of ferric hydroxide having maximum possible stability has been prepared. Its particle size as determined by electron microscope is of 63 Å radius. The stability of the sol in presence of different amounts of electrolytes of different valencies has been studied by measuring its zeta potentials in terms of interaction energy curves. By using these different stages of partially flocculated ferric hydroxide sol as emulsifier the emulsions of toluene in water were prepared and their relative stabilities assessed by adding various electrolytes. Then the stability of the emulsions formed has been studied by the measurement of zeta potentials micro-electrophoretically in the light of the D.V.O. theory. The size of the emulsion globules as determined microphotographically is 1.1μ radius. The pH and interfacial tension measurements have also been carried out. From interfacial tensions between the disperse phase and the dispersion medium at different amounts of electrolytes, the surface charge of the emulsions has been deduced which is found to be in good agreement with the electrophoretic results. Finally a correlation has been sought between the stability of the emulsions and the corresponding partially flocculated sols used in emulsification.

A few workers[1-4] have used insoluble inorganic precipitates such as calcium and barium carbonates, basic sulphates, oxychlorides, hydrous oxide and hydroxides of various metals as emulsifiers. Pickering[5] was first to use such substances as emulsifiers for oil in water type of emulsions and was able to conclude that the size of the oil globules depends on the size of the powder. An analogous behaviour was also observed by Bechhold, Dede and Reiner[6] who concluded that smaller the grains the better is the emulsion until an optimum is reached after which smaller grains have less effect. Briggs[7] found that oil in water type emulsions could not be stabilized with colloidal ferric hydroxide or arsenious sulphide but can be obtained by the addition of some weak flocculating agents. However, emulsification was not possible by the completely flocculated sol. A similar effect was also noticed by Van der Waarden[8] for emulsions of water in mineral oil which could only be stabilized by asphaltenes if the asphaltenes were near or above the point of incipient flocculation.

In the literature the theories of stabilization of the emulsions by the solid particles generally deal with the effect of wetting and with the contact angle. Therefore, in the present work it is proposed to explain the mechanism of emulsification and subsequent stabilization on the basis of energy considerations.

Materials and Preparations

The ferric chloride and ammonium carbonate for the preparation of sol were of Analar Grade obtained from B.D.H. For the preparation of emulsion the oil phase toluene was of B.D.H. Analar Grade, which was weighted by bromoform obtained from Rhome-Poulene, France and was distilled and the fraction of 148—149°C were collected. All the other chemicals used were of B.D.H. or E. Merck (Analar Grade) and used as such. The glass apparatus used was all pyrex and the water was twice distilled.

The ferric hydroxide sol was prepared by adding concentrated ammonium carbonate solution to a solution of ferric chloride with constant stirring until the precipitate just ceased to dissolve. The precipitated ferric hydroxide was then dissolved by adding just the sufficient quantity of concentrated ferric chloride solution. The sol was then dialysed in a parchment paper bag against running distilled water, until maximum stability obtained.

The concentration of the sol was 0.002 g/m*l* of ferric hydroxide. To this sol were then added different

1) T. R. Briggs and H. F. Schimdt, *J. Phys. Chem.*, **19**, 484 (1915).
2) A. U. M. Schlaepfer, *J. Chem. Soc.*, **113**, 522 (1918); *Kolloid Z.*, **81**, 184 (1937).
3) S. N. Srivastava and L. N. Mukherjee, *Kolloid Z.*, **147**, 146 (1956).
4) F. R. Newman, *J. Phys. Chem.*, **18**, 34 (1914).
5) S. U. Pickering, *J. Chem. Soc.*, **91**, 2001 (1907).
6) H. Bechhold, L. Dede and L. Reiner, *Kolloid Z.*, **28**, 6 (1921).
7) T. R. Briggs, *Ind. Eng. Chem.*, **13**, 1008 (1921).
8) M. Van der Waarden, *Kolloid Z.*, **156**, 116 (1958).

amounts of electrolytes so as to bring about partial flocculation. Then 5 m*l* of toluene were dispersed per 100 m*l* of the partially flocculated sol, the dispersion medium. The emulsions were first well hand shaken and then homogenized well in a hand operated stainless steel homogenizer (C.W. Logenman Co., U.S.A.). The sampling was done under identical conditions.

Experimental and Theoretical

The Sol. The size of the sol particles was determined by taking the photographs (Fig. 1)

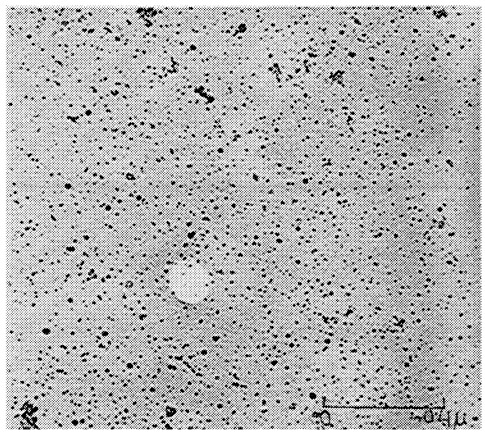

Fig. 1. Electron micrograph of $Fe(OH)_3$ sol × 77600.

by the electron microscope using 19400 x times magnification. The size of 400 particles was then measured with the help of a Cathetometer and a size frequency curve was plotted as shown in Fig. 2. The average radius was found to be 63 Å.

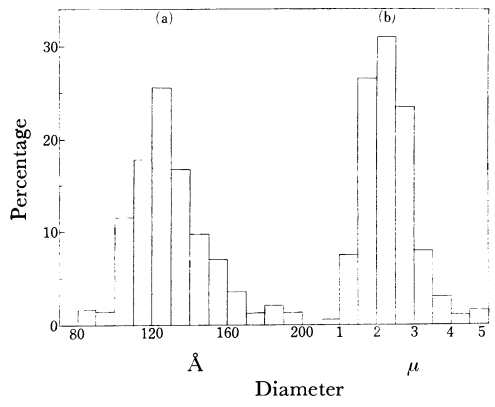

Fig. 2. Size-distribution curves.
Percentage of particles *vs.* diameter
(a) For $Fe(OH)_3$ sol (b) For Emulsion

The electrophoretic mobility of sol particles was measured by a modified form of the Burton tube method. The equiconducting solution of lithium chloride in the outer electrode vessel was used to prepare a sharp boundary, a constant current was supplied to the electrodes and the voltage across the two ends of the U tube was read off by the potentiovacuum tube voltmeter. The movement of the sol boundary per second under the applied potential gradient was measured by the Cathetometer and the electrokinetic potential ζ was calculated by the Hückel[9] equation. The correction for relaxation and the Henry effect were made using following equations given by Overbeek.[10]
For symmetrical electrolytes.

$$U = \frac{\varepsilon\zeta E}{6\pi\eta}\left[f_1(\kappa a) - Z^2\left(\frac{e\zeta}{kT}\right)^2 f_3(\kappa a) - \frac{\rho_+ + \rho_-}{2e}\frac{\varepsilon kT}{6\pi\eta e}\left(\frac{e\zeta}{kT}\right)^2 f_4(\kappa a)\right] \quad (1)$$

and for unsymmetrical electrolytes.

$$U = \frac{\varepsilon\zeta E}{6\pi\eta}\left[f_1(\kappa a) - (Z_+ - Z_-)\frac{e\zeta}{kT} f_2(\kappa a) - \frac{Z_+\rho_+ + Z_-\rho_-}{(Z_+ + Z_-)e}\frac{\varepsilon kT}{6\pi\eta e}\left(\frac{e\zeta}{kT}\right)^2 f_4(\kappa a)\right] \quad (2)$$

where U is the mobility per second per unit potential gradient, ε the dielectric constant (taken to be equal to the bulk phase *i. e.* for water at 25°C), η the viscosity of the medium, Z_+ and Z_- are the valencies, and ρ_+ and ρ_- the frictional constants of the cations and anions respectively, and f_1 is identical with the Henry function, f_2, f_3 and f_4 are the functions dependent on the values of κa which were noted from the tables.[11]

The interactions between the colloidal particles of lyophobic systems have been quantitatively treated by Derjaguin,[12] Verwey and Overbeek[13] (D.V.O. theory). On the basis of the free energy of the double layer and the London - Van der Waals' dispersion forces. According to their theory the net force on mutual approach of the particles is a resultant (V) of an attraction V_A and a repulsion V_R which increases differently as the distance apart decreases. The double layer repulsion V_R for the present system has been calculated from an approximate equation given by

$$V_R = \frac{\varepsilon a \Psi_0^2}{(U+2)} e^{-\tau U} \text{ (for small values of } \tau) \quad (3)$$

where ψ_0 is the surface potential (assumed to be eual to the electrokinetic potential for the present system), $U = H_0/a$ and $\tau = \kappa a$ and a the particle

9) E. Hückel, *Z. Physik*, **25**, 204 (1924).
10) J. Th. G. Overbeek, *Kolloid Beihefte*, **54**, 287 (1943).
11) J. Th. G. Overbeek, "Advances in colloid sciences," Vol. III, Interscience, London (1950), p. 115.
12) B. Derjaguin, *Trans. Faraday Soc.*, **36**, 203, 730 (1940); *J. Expt. Theor. Phys., USSR.*, **11**, 802 (1941); B. Derjaguin and L. B. Landau, *Acta Physico-Chim.*, **14**, 633 (1941).
13) E. J. W. Verwey and J. Th. G. Overbeek, "Theory of Stability of Lyopyobic Colloids," N. Y. Elsevier, Amsterdam (1948).

radius, H the interparticle distance and κ is the Debye-Hückel parameter. The attraction energy is calculated from the following equation.[14]

$$V_A = -\frac{Aa}{12H} \tag{4}$$

Therefore, the total interaction energies of the lyophobic systems showing the nature of flocculation and the stability can be determined by the following equation.

$$V = \frac{\varepsilon a \Psi_0^2}{(U+2)} e^{-\tau U} - \frac{Aa}{12H} \tag{5}$$

The Emulsion. The size-frequency curve of emulsion was drawn by taking the photograph (Fig. 3) microphotographically with a Olympus

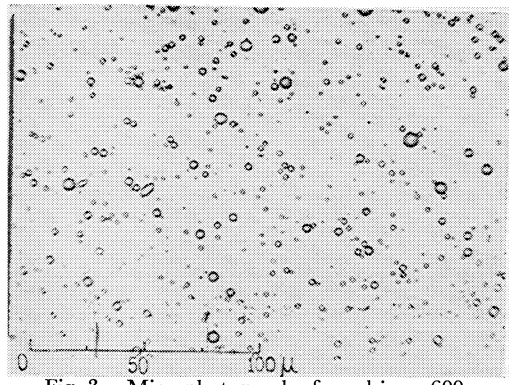

Fig. 3. Microphotograph of emulsion × 600.

Camera attached with a Olympus microscope. The radius of about 400 particles was measured by the Cathetometer and the average radius for all the emulsions was found to be 1.12μ (Fig. 2).

The electrophoretic mobility of the emulsions was determined by microelectrophoresis apparatus. The micro-electrophoresis cell used in the apparatus was of Northrup and Kunitz type, fitted in a special design apparatus and was set in a air conditioned room. The diluted emulsion was filled in the cell and the electrode vessels were filled with equiconducting potassium chloride solution to avoid diffusion. A constant d. c. voltage was applied between the two electrodes (Ag-AgCl) and the current was measured by the microammeter. From the velocity of the particles measured under the applied voltage the mobility U was calculated by the relation.

$$U = \frac{dSA}{it} \tag{6}$$

where d is the distance travelled by the particle in a time t under the influence of current i, S the specific conductance of the emulsion and A is the area of the cell.

From a knowledge of the mobility electrokinetic potential ζ can be calculated by the following equation due to Helmholtz and Smoluchowski, which is applicable to the case for spherical particles and $\kappa a \gg 1$.

$$\zeta = \frac{4\pi\eta}{\varepsilon} U \tag{7}$$

The total interaction energy between the two diffuse double layers of the emulsion globules is the summation of repulsive and attractive energies, where the repulsion energy can be calculated by the approximate equation given by Derjaguin and Kussakov.[15]

$$V_R = \frac{\varepsilon a \Psi_0^2}{2} \ln(1+e^{-\kappa H_0}) \tag{8}$$

and the attraction energy has been calculated from the following approximate equation.[16]

$$V_A = -\frac{Aa}{12H}\left\{\frac{\lambda}{\lambda+3.54H\pi}\right\} \quad \text{for } H<150\,\text{Å} \tag{9a}$$

$$V_A = -\frac{Aa}{\pi}\left\{\frac{2.45}{120H^2}\cdot\lambda - \frac{\lambda^2}{1045H^3} + \frac{\lambda^3}{5.62\times10^4\cdot H^4}\right\} \quad \text{for } H>150\,\text{Å} \tag{9b}$$

where λ is the wavelength of the London frequency (approximately equal to 10^{-5} cm) and A is the Van der Waals constant of the droplet.

Calculation of Surface Charge from Interfacial Tension. The Gibbs adsorption isotherm is

$$-d\gamma = \Gamma_S RT d\ln C_S \tag{10}$$

This permits the determination of the surface excess Γ_S of the adsorbed ions from a knowledge of change in interfacial tension γ with the concentration of the adsorbed ions C_S. The surface charge of the particle is given by the following equation.

$$\sigma = eV\Gamma_S \tag{11}$$

If no excess of electrolytes is present, Γ_S will not correspond exactly with ρ/ve, because there is a deficiency of same charge ions in the diffuse part of the double layer, though this deficiency is only a few percent of ρ.

The fraction of the counter ions present in the Stern layer can be represented by the following equation by the application of the Langmuir-Stern equation.[17]

$$\frac{\sigma_1}{eV} = \frac{N_1}{1+\frac{N}{n}e^{(ve\psi_0/kT)}} \tag{12}$$

where N_1 is the number of available positions in 1 cm^2 of the Stern layer (here assumed to be equal to 1×10^{15}), N is the number of positions available

14) H. C. Hamaker, *Physica*, **4**, 1058 (1937).

15) B. Derjaguin and M. Kussakov, *Acta Phys. Chim.*, **10**, 25, 155 (1939).

16) J. N. Schenkel and J. A. Kitchener, *Trans. Faraday Soc.*, **56**, 161 (1960).

17) H. R. Kruyt, "Colloid Science," Vol. I, N. Y. Elsevier, Amsterdam (1952), pp. 130, 133.

to the counter ions in 1 cm^3 of the homogeneous solution (which is to be equal to $6.02\times10^{23}/18$), n is the number of counter ions of valency V in 1 cm^3 of the homogeneous solution, e is the elementary charge and ψ_0 is the potential in the Stern layer with respect to a point in the aqueous phase far from the interface.

The diffuse part of the double layer has a charge σ_2 which is related to the potential at the boundary between the Stern and the Gouy Layers ψ_0 by the equation

$$\sigma_2 = \left(\sqrt{\frac{\varepsilon kT}{\pi}\sum nv^2}\right) \sinh\left(\frac{ve\psi_0}{2kT}\right) \qquad (13)$$

From the condition of electrical neutrality the total charge σ is

$$\sigma = \sigma_1 + \sigma_2 \qquad (14)$$

Thus the surface potential ψ_0 can be calculated as a function of n and σ with the help of the above equations.

The interfacial tensions between the disperse phase and the dispersion medium containing various amounts of sol and electrolytes were measured by the drop weight method. The apparatus used was as designed by Cook and Kitchener,[18] in which the drops of disperse phase were made at the edge of the capillary tube by the displacement of the mercury. A number of drops was allowed to fall into the dispersion medium, the average volume being noted from the reading of microburette. The interfacial tension was calculated by the formula

$$\gamma = \frac{v(d_2-d_1)}{rg} f \qquad (15)$$

where d_1 and d_2 are the densities of the disperse phase and the dispersion medium respectively, which were determined by the pycknometer taking water as standard, r the radius of the edge of the capillary, v the volume of the one drop of oil and f is the factor depending upon the value of v/r^3 being taken from the standard tables.[19]

Results

(a) Influence of Electrolytes on Zeta Potentials of the Sol. The ferric hydroxide sol was prepared in the excess of ferric chloride and was positively charged on account of excess of ferric ions, adsorbed to the surface of the ferric hydroxide sol particles. The flocculation was, therefore, brought about by different valent anions. The electrokinetic mobilities at different concentrations of electrolytes were measured and zeta potentials calculated by Eqs. (1) and (2). The

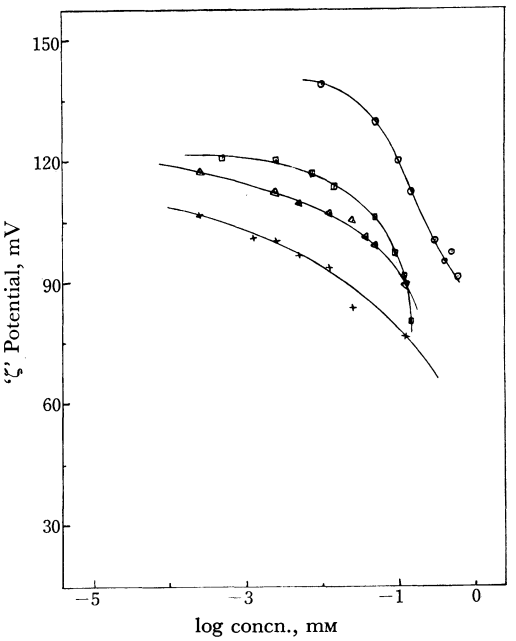

Fig. 4. Curves showing the variation in zeta potentials at various concentrations of electrolytes.
⊙ Pot. oxalate, ⊡ Pot. citrate, △ Pot. ferricyanide
× Pot. ferrocyanide

observed value of the zeta potential of the initial sol is 154.5 mV at 25°C.

The curves for the zeta potentials of ferric hydroxide sol particles as a function of log molar concentration of different electrolytes, *viz* KBr, $K_2(C_2O_4)$, $K_3Fe(CN)_6$, $K_3(C_6H_5O_7)$ and $K_4Fe(CN)_6$ are represented in (Fig. 4). In general, the zeta potential decreases as the concentration of electrolytes increases. In case of potassium bromide and potassium oxalate the fall of zeta potential is

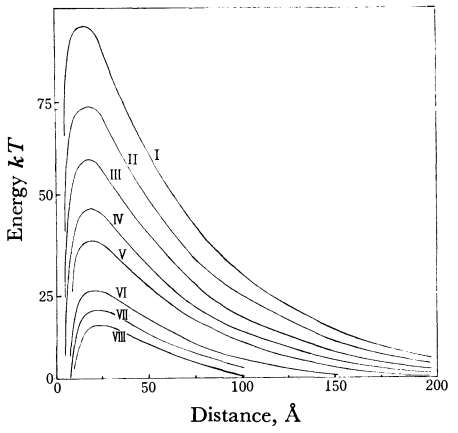

Fig. 5. Curves for potential energy of interaction in the presence of Pot. oxalate.
I Pure sol, II 0.01 mM, III 0.05 mM, IV 0.10 mM, V 0.15 mM, VI 0.40 mM, VII 0.50 mM, VIII 0.60 mM

18) J. R. Catch, A. H. Cook and J. A. Kitchener, *J. Chem. Soc.*, **1945**, 319.
19) "International Critical Tables," Vol. IV, p. 435.

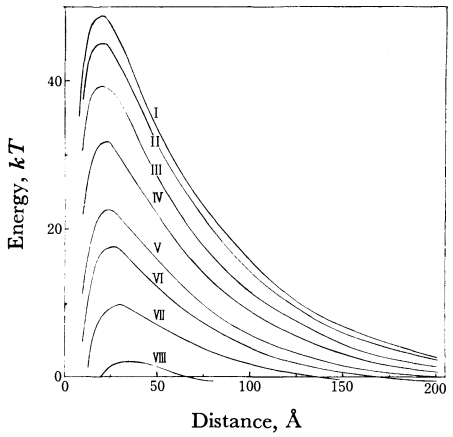

Fig. 6. Curves for potential energy of interaction in the presence of Pot. citrate.
I 5.0×10^{-4} mM, II 5.0×10^{-3} mM, III 3.0×10^{-2} mM, IV 5.0×10^{-2} mM, V 0.1 mM, VI 0.12 mM, VII 0.15 mM, VIII 0.4 mM

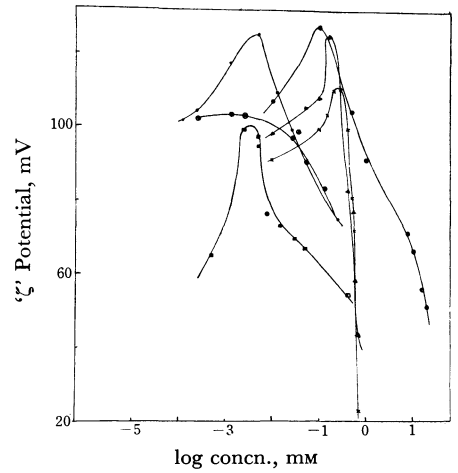

Fig. 7. Curves showing the values of zeta potentials for various concentrations of electrolytes.
⊙ KBr, △ $K_2(C_2O_4)$, × K_2SO_4, ▫ $K_2(C_6H_5O_7)$, ⊗ $K_3Fe(CN)_6$, ● $K_4Fe(CN)_6$

almost linear throughout, but in case of ferricyanide, citrate and ferrocyanide it is comparatively slow at the initial stages and then becomes sharp.

(b) Interaction Energy Curves. For the complete assessment of the stability of the sol in presence of different amounts of electrolytes the potential energies of interaction for the sol particles were calculated. Only representative energy profiles are shown in Figs. 5 and 6.

The curve I of Fig. 5 shows that the net potential energy of interaction of the ferric hydroxide sol corresponding to zeta potential 154.5 mV has the maximum energy $V_m=94.3\,kT$ which is indicative of the complete stability of the sol. In these calculations the value of the Van der Waals constant A is taken to be equal to 3.13×10^{-12} erg, the calculated value by the physico optical data which is in the range suggested by Overbeek (*loc. cit.*) for solid particles suspended in water.

In general by the addition of electrolytes the maximum energy V_m and hence the sol stability decreases with the increase in concentration of the electrolytes (Table 1).

(c) Studies of Zeta Potentials of the Emulsions. The initial emulsion with pure ferric hydroxide sol without any electrolyte had zeta potential equal to 63.5 mV (*cf.* this with the value 154.5 mV of the emulsifying sol). The corresponding emulsions were prepared by the partially flocculated sol and the zeta potentials are plotted in Fig. 7 against the log molar concentration of the electrolytes used for partial flocculation.

(d) Interaction Energy Curves and the Flocculation in the Secondary Minima. The potential energy V of the interacting emulsion droplets was calculated by Eqs. (8) and (9) and the energy curves were plotted, only a few typical curves being shown in Figs. 8 and 9 in case of potassium oxalate and potassium ferrocyanide.

From these curves it is seen that in all the emulsions globules possess a high potential energy barrier at intermediate distances, the extent of which depends upon the values of the zeta potential which invariably varies with the electrolyte concentrations. At small and larger separating distances between the particles there is net attraction which shows that at higher distances the particles are flocculated but still separated by a larger distance, called secondary minimum flocculation. The secondary minima have also been represented separately in a more elaborate form on the same graphs and are found to be 3 to 6 kT deep at 500—800Å distances (*cf.* Schenkel and Kitchener[16]). In these energy calculations the value of Van der

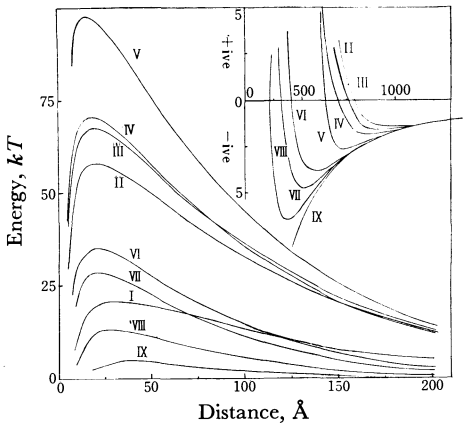

Fig. 8. Curves for potential energy of interaction in the presence of Pot. oxalate.
I Pure sol, II 0.01 mM, III 0.05 mM, IV 0.10 mM, V 0.15 mM, VI 0.40 mM, VII 0.50 mM, VIII 0.60 mM, IX 0.70 mM

TABLE 1.

Electrolyte concn. mM	Debye-Hückel parameter $\kappa \times 10^{-6}$	Potentials, mV		Max. energies V_m, kT		Depth of Sec. min. of emulsions, kT
		Sol	Emulsion	Sol	Emulsion	
Initial sol	1.043	154.5	63.5	94.3	2039	—
KBr						
0.01	1.049	149.5	106.3	85.7	7074	1.9
0.10	1.090	143.5	126.3	76.3	7718	1.45
0.25	1.160	137.3	109.1	67.0	7371	1.72
0.50	1.270	133.2	103.4	60.1	6397	2.19
1.00	1.470	121.4	90.6	43.9	4524	3.25
8.00	3.120	108.1	70.9	16.3	1645	24.58
10.00	3.440	98.1	65.9	7.9	1178	51.00
15.00	4.160	95.6	55.7	6.6	409	73.00
Pot. oxalate						
0.00	1.043	154.5	63.5	94.3	2039	—
0.01	1.060	140.4	97.5	72.9	5798	1.43
0.05	1.120	130.0	104.8	58.7	6765	1.57
0.10	1.190	119.7	107.2	45.7	7043	1.80
0.15	1.255	112.3	123.9	37.1	9621	2.65
0.40	1.540	95.2	82.3	18.6	3522	3.86
0.50	1.646	97.8	76.4	20.0	2844	4.76
0.60	1.740	91.4	58.1	14.2	1306	6.40
0.70	1.830	—	43.4	—	487	8.52
Pot. citrate						
0.00	1.043	154.5	63.5	94.3	2039	—
5.0×10^{-4}	1.044	120.7	64.9	48.8	2196	1.70
2.5×10^{-3}	1.051	120.5	98.7	48.5	5979	1.40
5.0×10^{-3}	1.059	117.6	97.0	45.1	5730	1.43
7.5×10^{-3}	1.066	116.9	76.0	43.3	3202	1.65
1.5×10^{-2}	1.088	113.7	72.9	40.5	2880	1.76
3.0×10^{-2}	1.132	112.9	69.3	39.2	2520	2.00
5.0×10^{-2}	1.180	106.1	66.9	31.6	2264	2.25
0.40	1.910	71.0	54.4	2.0	909	8.32
Pot. ferricyanide						
0.00	1.043	154.5	63.5	94.3	2039	—
2.5×10^{-4}	1.044	117.4	101.9	45.1	6431	1.40
1.25×10^{-3}	1.047	116.6	103.0	44.2	6588	1.36
2.5×10^{-3}	1.051	111.9	102.4	39.0	6492	1.38
5.0×10^{-3}	1.059	109.7	94.5	36.6	5390	1.45
2.5×10^{-2}	1.118	105.4	96.6	31.6	5642	1.64
5.0×10^{-2}	1.189	99.5	89.8	25.4	4667	1.96
0.125	1.380	89.1	82.8	15.2	3698	2.90
Pot. ferrocyanide						
0.00	1.043	154.5	63.5	94.3	2039	—
1.25×10^{-4}	1.044	99.8	101.6	27.0	6390	1.40
2.5×10^{-4}	1.045	106.8	104.1	33.8	6757	1.35
1.25×10^{-3}	1.050	101.3	116.9	28.3	8759	1.31
2.5×10^{-3}	1.056	100.6	—	27.6	—	—
5.0×10^{-3}	1.070	97.1	124.7	24.3	10057	1.30
1.25×10^{-2}	1.106	93.8	108.8	21.1	7387	1.49
2.5×10^{-2}	1.165	84.0	98.6	13.7	5839	1.78
0.125	1.560	76.4	—	6.5	—	—
0.250	1.946	—	74.5	—	2502	7.34

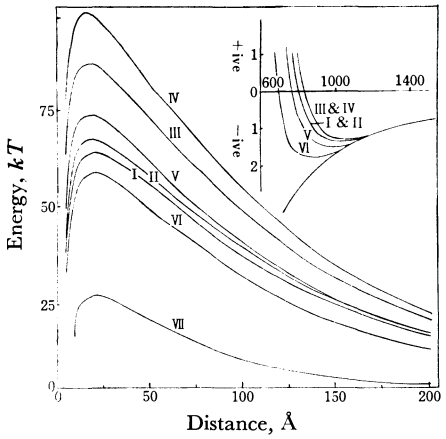

Fig. 9. Curves for potential energy of interaction in the presence of Pot. ferorcyanide.
I 1.25×10^{-4} mM, II 2.5×10^{-4} mM,
III 1.25×10^{-3} mM, IV 5.0×10^{-3} mM,
V 1.25×10^{-2} mM, VI 2.5×10^{-2} mM, VII 0.25 mM

Waals constant for the disperse globules in the dispersion medium is taken to be 1×10^{-12} erg which was obtained by physico optical data for toluene globules coated by ferric hydroxide sol and disperse in water. In case of all the electrolytes the potential energy first increases with the addition of electrolytes and after a certain maximum value it begins to decrease and the system becomes unstable.

The results obtained for ferric hydroxide sol and the corresponding emulsions for the various electrolytes are summarised in Table 1.

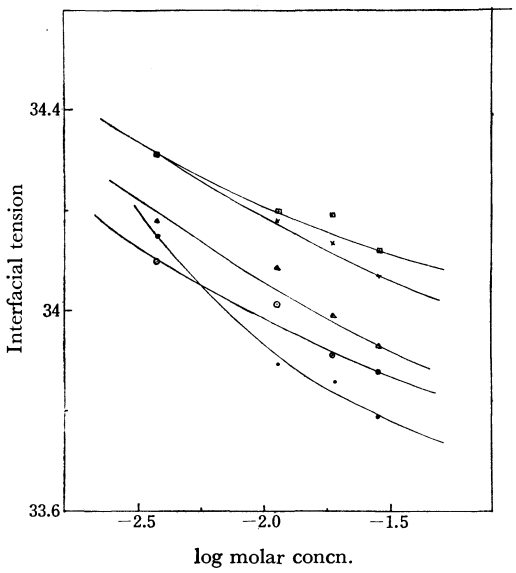

Fig. 10. Curves showing the change in interfacial tension with the concentration of $Fe(OH)_3$ sol in presence of Pot. bromide.
⊙ 0.10 mM, ⊡ 0.25 mM, × 1.0 mM, △ 8.0 mM, ● 15 mM

(e) Surface Charge by the Interfacial Tension. The change in interfacial tension with the concentration of ferric hydroxide sol in presence of different amounts of electrolytes has been also measured and a few representative curves have been shown in (Fig. 10). From these curves the surface excess of the sol particles at the particular concentration of the sol has been calculated which ultimately gives the total charge on the oil globules for that definite concentration of the sol.

The distribution of the charge between the Stern layer and diffuse double layer of the emulsion globule for the particular concentration of the sol at the same concentration of the electrolyte in the dispersion medium has been calculated from Eqs. (12), (13) and (14). A few typical curves showing the distribution of charge for the different values of $e\Psi_0/kT$ are given in (Fig. 11). From these curves the value of $e\Psi_0/kT$ has been calculated

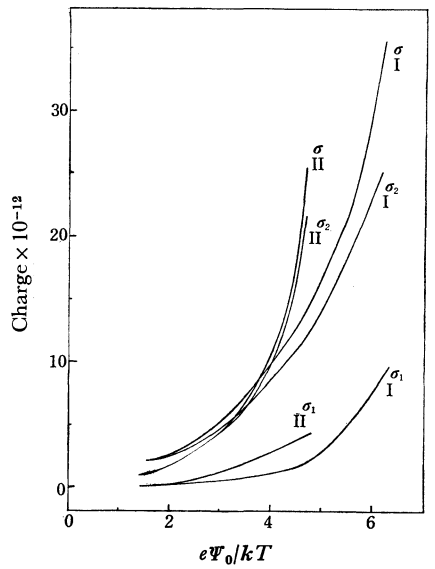

Fig. 11. Curves for the distribution of charge as a function of $e\Psi_0/kT$ in presence of I 1 mM of KBr, II 0.01 mM of Pot. oxalate.

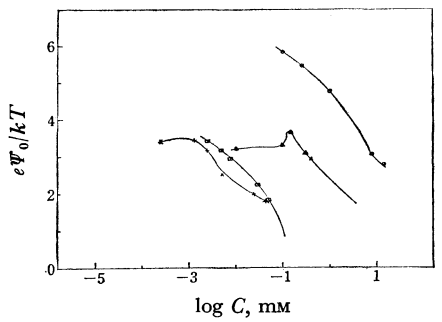

Fig. 12. Curves for the $e\Psi_0/kT$ as a function of log concentration.
⊙ KBr, △ Pot. oxalate, ⊡ Pot. citrate, × Pot. ferricyanide

corresponding to the experimentally obtained value of the total surface charge σ. The graphs in Fig. 12 have been plotted between the log molar concentrations and the value of $e\Psi_0/kT$ obtained from the interfacial tension data and the results are also given in Table 2. The results, in general, agree with those obtained electrophoretically.

TABLE 2.

Electrolyte	Concn. mmol	$\sigma/e \times 10^{-13}$	$e\Psi_0/kT$	Ψ_0 mV
Pot. bromide	8.0	1.77	3.05	78.5
Pot. oxalate	0.4	3.01	2.94	81.0
Pot. citrate	7.5×10^{-3}	2.51	2.95	79.0
Pot. ferricyanide	1.25×10^{-3}	2.60	3.46	95.0

(f) Effect of pH on the Stability of the Emulsion. This is depicted in Fig. 13 where it is found that pH of the emulsion continuously increases with the addition of the electrolyte. But zeta potentials first increase with pH, reach a maximum and then decrease regularly. The increase in pH may be due to desorption of OH^- ions from the flocculated particles which are obtained by the addition of respective anions.

Similar curves were obtained when pH is adjusted after emulsification.[20]

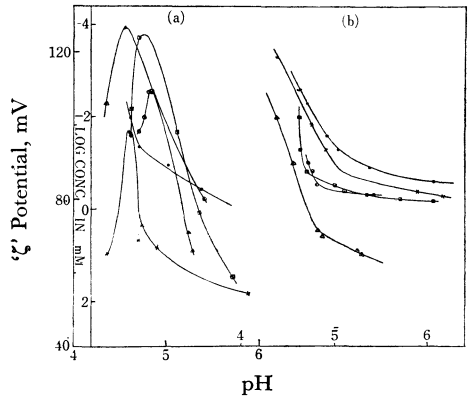

Fig. 13. (a) Curves showing the changes in zeta potential as a function of pH in presence of various electrolytes.
△ Pot. bromide, ⊡ Pot. oxalate, × Pot. citrate, ⊙ Pot. ferricyanide
(b) Curves showing the changes in pH as a function of log concentration in the presence of various electrolytes during emulsification.
△ Pot. bromide, ⊡ Pot. oxalate, × Pot. citrate, ⊙ Pot. ferricyanide

Discussion

The zeta potential of the emulsion prepared by the most stable ferric hydroxide sol (having zeta= 154.5 mV and energy barrier 94.3 kT) was 63.5 mV but by the addition of small amounts of different electrolytes the zeta potential of the emulsion first increases with the increase of electrolyte and after a certain maximum value it decreases by the further addition of electrolyte thereby indicating instability. It can be seen from Fig. 7 that the decrease is much more sharp in case of mono and bivalent anions than with tri and tetra valent.

However, when the sol is partially flocculated by the additon of electrolytes and the zeta potential is lowered to about 110 ± 10 mV and the corresponding energy barrier is reduced to nearly 40 ± 5 kT, more stable emulsions are obtained, which have zeta potentials in the range 115 ± 10 mV and the energy barrier above 7500 kT.

It is obvious that for the efficient stabilisation of an emulsion by solid particles some prevalent attraction between the sol particles is necessary. The emulsification is governed by the flocculation of the sol particles in the continuous liquid phase and the stabilizing power of solid particles as a function of their degree of flocculation thus first increases, then reaches a maximum and at still higher degrees of flocculation again decreases. Thus by the pure sol a stable emulsion cannot result on account of high potential energy barrier whereas in the case of flocculated sol by the addition of electrolytes stable emulsions can be formed when the potential energy barrier between the stabilising particles is reduced.

The authors wish to thank to Dr. S. K. Sharma, Scientist, National Physical Laboratories, N. Delhi for taking the electron microphotograph of the sol particles. They are also extremely grateful to the Ministry of Education, Government of India for the award of a research training scholarship to one of them (S.P.J.).

20) S. P. Jain and S. N. Srivastava, Under communication.

BULLETIN OF THE CHEMICAL SOCIETY OF JAPAN VOL. 42 1179—1186 (1969)

Studies in Nuclear Magnetic Resonance Spectroscopy. Long-range Shielding by Triple Bonds

J. M. JACKMAN and George Y. SARKIS

Department of Chemistry, University of Pennsylvania, Philladelphia, Pa., U.S.A.
Department of Chemistry, University of Baghdad, College of Science, Baghdad, Iraq.

(Received March 9, 1968)

The magnetic shielding of nuclei due to distant chemical groups may be calculated from the knowledge of the magnetic anisotropy of the bonds in these groups. The reverse procedure, namely, the calculation of the magnetic anisotropy of bonds from NMR relative chemical shifts has been employed here to estimate the magnetic anisotropy of $-C\equiv C$, $-C\equiv N$, and $-N\equiv C$ triple bonds. The paramagnetic contribution to the shielding of the acetylenic proton was estimated from the calculated value of $\Delta\chi^{C\equiv C}$, and from the known geometry of the molecule. The value thus obtained is compared with that calculated by quantum mechanical methods.

One of the persistent problems encountered in interpreting chemical shifts in NMR spectroscopy is of adequately taking account of effects produced by the magnetic anisotropy of neighboring atoms or groups. Unless this is done, it is difficult to decide what portion of an observed shift is indeed chemical. In certain cases, *e. g.*, acetylene and hydrogen cyanide, the occurrence of serious discrepancies between experimental shift and expectations have served to call attention to the existence of important anisotropic contributions. Unfortunately, no reliable and generally applicable methods for independently estimating such contributions have yet appeared.

The magnetic shielding ζ of a proton in a molecule can be calculated theoretically using the second-order perturbation theory of Ramsey,[1] or the variational methods.[2,3] Application of the second-order perturbation theory to this problem is possible only if the excited-state wave functions in addition to the ground-state wave functions are available for the molecule in question. Hence, very few direct theoretical calculations of ζ have been made.

McConnell,[4] have derived a quantum mechanical expression for calculating the chemical shifts due to long-range bonds or groups. For an axially symmetric bond, the expression appears in the form:

$$\zeta = \Delta\chi(1-3\cos^2\theta_z)/3L_0R^3 \qquad (1)$$

Where, R, is the radius vector for the proton, θ_z, is the angle between R and the symmetry axis of the bond (usually the bond axis itself). The scalar $\Delta\chi=\chi_L-\chi_T$, where the scalars χ_L and χ_T are the average of the susceptibility components parallel and perpendicular to the symmetry axis.

The theory has been extended by Narasimhan and Rogers,[5] to the three dimensional case, where all the three principal magnetic susceptibilities are different. These authors have also derived expressions for the case of rotating methyl groups, in which the shielding is averaged over all possible orientations.

The theory of McConnell for long-range shielding appears capable of fairly general applicability, although it is not very well suited to quantitative calculations of aromatic proton shieldings, since it has been developed only to the extent that the shielding fields are approximated by dipolar fields. Quantitative application of the shielding equation due to the magnetic anisotropy of a long-range bond in a molecule suffer from two very important difficulties. The first difficulty is that the shielding of a proton is a function of the anisotropy in the magnetic susceptibility of the distant group, and only very few data for the magnetic anisotropies of bonds are known. The second difficulty is that R, appears in the equation as R^{-3}, so that with decreasing R, the shielding becomes larger and more important, and the dipolar approximation becomes less and less accurate.[4,6,7]

For distances less than 5 Å, we have followed Pople's suggestion[7] of describing the anisotropy of the acetylenic bond in terms of the atomic

1) N. F. Ramsey, *Phys. Rev.*, **86**, 243 (1952).
2) B. R. McGarvey, *J. Chem. Phys.*, **27**, 64 (1957).
3) R. Stephen, *Proc. Roy. Soc. (London)*, **A243**, 264 (1957).
4) H. J. McConnell, *J. Chem. Phys.*, **27**, 226 (1957).
5) P. T. Narasimhan and M. T. Rogers, *J. Phys. Chem.*, **63**, 1388 (1959); *J. Chem. Phys.*, **31**, 1302 (1959).
6) J. R. Didry and J. Guy, *Compt. Rend.*, **253**, 422 (1961).
7) J. A. Pople, *Discussions Faraday Soc.*, **34**, 7 (1962).

anisotropy of the acetylenic carbons, and the shielding expression becomes,

$$\xi = \Delta\chi[\tfrac{1}{3}R_1^3(1-3\cos^2\theta_1) + \tfrac{1}{3}R_2^3(1-3\cos^2\theta_2)] \quad (2)$$

Where, R_1, R_2, θ_1, and θ_2 are shown in Fig. 1.

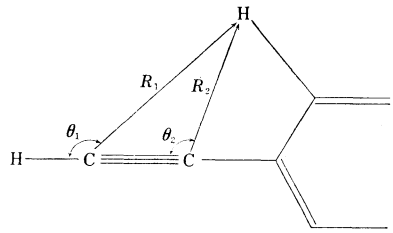

Fig. 1. Dipole approximation for the magnetic anisotropies of the acetylenic carbons in phenylacetylene.

The present work represent an attempt to investigate the role of the neighbor-anisotropy effect and to calculate the electrostatic effects due to electric fields at a particular nucleus arising from polar groups in other parts of the molecule. From the relative chemical shifts and the known molecular geometries, we determine the anisotropy in the magnetic susceptibilities of the C≡C, C≡N, and N≡C triple bonds. In doing so, we have shown experimentally that long-range shielding does exist and that it is correctly explained to lower order of accuracy by the McConnell's expression. We have also shown that the electrostatic effects in the case of –C≡N, and –N≡C triple bonds are very important in determining the chemical shift of a particular proton.

Experimental

The NMR Spectrometer. The measurements were made on a Varian Associates high-resolution spectrometer, operating at a fixed frequency of 56.45 Mc/s. The measurements of the NMR spectra of the bicyclo-compounds were made at 60 Mc/s. The frequency separation between lines were measured using the usual audiomodulation side-band technique. The chemical shifts were measured for several concentrations in carbon tetrachloride solutions containing 1% TMS, used as an internal standard, extrapolated to infinite dilution, and are quoted as τ-values. All τ-values which were employed in the calculations are the average of four determinations and are accurate to ± 0.01 ppm.

Results and Calculations

a. Diamagnetic Anisotropy. In order to simplify the problem of calculating magnetic anisotropy of a long-range bond, we have followed the general method adopted by Narasimhan and Rogers.[5] For a given proton the net shielding ζ, can be written as the sum of two quantities, namely, ζ_l and ζ_d, where ζ_l, denotes the shielding

TABLE 1. THE CHEMICAL SHIFTS OF ALL PROTONS IN I—IX

	Compound	CH_3	H-2	H-3	H-4	≡CH
I	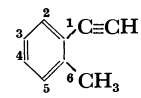	7.58				6.90
II	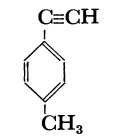	7.69	2.8	2.9		7.13
III	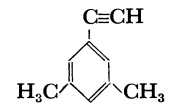	7.73	3.25		3.07	6.65
IV	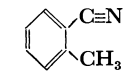	7.48				
V	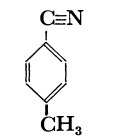	7.59	2.53	2.77		
VI	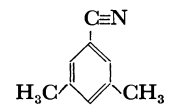	7.6	2.8		2.8	
VII	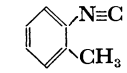	7.62	2.8	2.8	2.8	
VIII	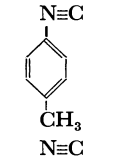	7.65	2.9	2.9		
IX	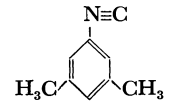	7.75	3.0		3.0	

due to the immediately surrounding electron cloud (primary shielding), and it corresponds to Pople's local diamagnetic term. The second term, ζ_d, arises from distant electron distributions within the molecule itself (secondary shielding), and corresponds to Pople's neighbor-anisotropy effect. ζ_l can be calculated by using the wave functions of the bond attached to the proton of interest.[3] ζ_d can be evaluated from a knowledge of the magnetic anisotropy $\Delta\chi$ of the various charge distributions in the molecule.[3–5] Thus we may write:

$$\zeta = \zeta_l + \zeta_d$$

A difference in the net shielding, or the internal chemical shift $\Delta\zeta$, between two protons A and B in a molecule may originate from differences in ζ_l and/or ζ_d ($\Delta\zeta_l$ and $\Delta\zeta_d$ respectively). Thus we have;

TABLE 2. THE CHEMICAL SHIFT OF ALL PROTONS IN I—VII

	Compound	α-H	β-H(CH_3)	γ-H(or CH_3)	≡CH	$(\zeta_T^{\beta}-\zeta_T^{\gamma})\times10^{-6}$
I	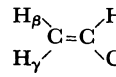	4.52	4.22_5	4.14		0.18*
II	$(CH_3)_2C{=}CH{-}C{\equiv}N$	4.89	7.63	8.06		0.43
III	$CH_2{=}CH{-}C{\equiv}CH$[8]				7.00	0.18
IV	$(CH_3)_2C{=}CH{-}C{\equiv}CH$	4.83	8.18 or 8.11	8.11 or 8.18	6.90	0.07
V	$\overset{\gamma}{C}H_3\cdot\overset{\beta}{C}H_2\cdot C{\equiv}CH$[9]		8.10	9.04	6.32	0.94
VI	$CH_3\cdot CH_2\cdot C{\equiv}N$[10]		7.00	8.04		1.04
VII	$CH_3\cdot CH_2\cdot N{\equiv}C$		7.19	8.77		1.58

* Complete analysis of the NMR spectrum of acrylonitrile and α-D-acrylonitrile are carried out by Goldstein and co-workers.[11] Several other workers have analysed the spectrum of acrylonitrile.[11-14] The results of Banwell and Sheppard[12] are different from that of Goldstein and co-workers,[11] and Bruegel,[13] in that the two protons at the β-position have been interchanged. There are some variations in the values of the chemical shifts of the three protons. The most reliable analysis is that of Castellano and Waugh.[14] In this work, the values of the chemical shifts obtained by the later authors are employed in the calculation of the magnetic anisotropy of the $-C{\equiv}N$ group.

TABLE 3. THE CHEMICAL SHIFT OF ALL PROTONS IN I—V

Compound	Olefinic	Bridgehead	H_x(exo)	H_n(endo)	C_7-H_2
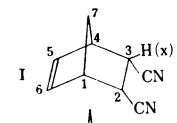 I	3.50	6.67	6.57		8.67, 8.37
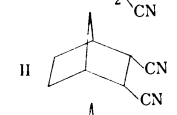 II	(C-5,6) 8.21	7.33	6.82		8.44
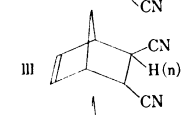 III	3.52	6.60	7.48	6.83	8.31, 8.27
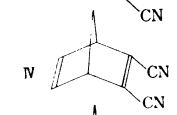 IV	3.02	5.93			7.63
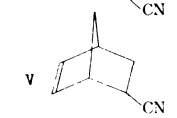 V		7.03 6.86			

$$\Delta\zeta = (\zeta^A-\zeta^B) = (\zeta_l^A-\zeta_l^B) + (\zeta_d^A-\zeta_d^B)$$
$$= \Delta\zeta_l + \Delta\zeta_d$$

Since the magnitude of the shielding contribution from distant groups depend on their diamagnetic anisotropy and on molecular geometry, we have calculated the diamagnetic anisotropy of the $-C{\equiv}C-$, $-C{\equiv}N$, and $-N{\equiv}C$ groups, using the internal chemical shift between two protons located on the same carbon atom or on two different atoms with the same electron distribution around. Hence, $\Delta\zeta_l$, for such protons will be zero, and the difference in the chemical shift $\Delta\zeta_T$, will arise from the magnetic anisotropy of the distant groups alone.

To calculate ζ_d, for cases where θ and/or R changes with internal molecular motions, one must use appropriately averaged values. The component,

$$T_z = (1-3\cos^2\theta_z)/R^3 \qquad (3)$$

was calculated numerically in the following manner:

Let us consider the case of a nucleus H, which is free to move in a circular path around the axis of the bond AC*, this axis being taken to be in

8) R. C. Hirst and D. M. Grant, *J. Am. Chem. Soc.*, **84**, 2009 (1962).
9) H. Heel and W. Zeil, *Z. Electrochem.*, **64**, 962 (1960).
10) J. R. Cavanaugh and B. P. Daily, *J. Chem. Phys.*, **34**, 1099 (1961).
11) G. S. Reddy, J. H. Goldstein and L. Mandel, *J. Am. Chem. Soc.*, **83**, 4729 (1961).
12) C. N. Banwell and N. Sheppard, *Mol. Phys.*, **3**, 351 (1960).
13) W. Bruegel, *Z. Electrochem.*, **64**, 1121 (1960).
14) S. Castellano and J. S. Waugh, *J. Chem. Phys.*, **34**, 295 (1961).

the Z–Y plane, with point dipole placed at "0" as shown in Fig. 2.

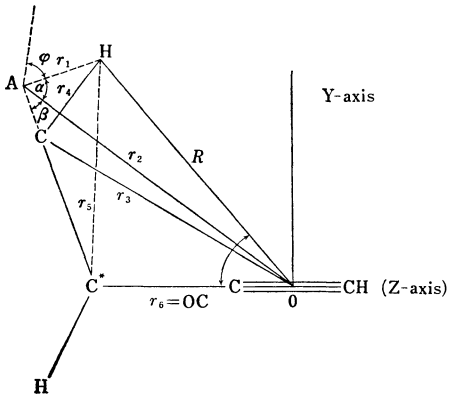

Fig. 2. Evaluation of T_z value.
The dipole is located at "0", and nucleus H free to rotate around the axis AC*.

Since r_1 and AC* are chosen to be at right angles to each other, we can express α in terms of β and φ (φ is the angle of rotation of r_1, in its plane). Thus it can be shown that,

$$\cos\alpha = \sin\beta\cdot\cos\varphi \tag{4}$$

and hence we can express R as,

$$R = (r_1^2+r_2^2-2r_1r_2\sin\beta\cdot\cos\varphi)^{1/2} \tag{5}$$

now we also have,

$$\cos\theta_z = (R^2+r_6^2-r_5^2)/2R\,r_6, \tag{6}$$

and hence we can write,

$$\begin{aligned} T_z &= (1-3\cos^2\theta_z)/R^3 \\ &= \{R^{-3}[1-3(R^2+r_6^2-r_5^2)^2/(2R\,r_6)^2]\}_{av}. \end{aligned} \tag{7}$$

Since φ varies from 0 to 2π, we can find the average value by integrating the left-hand side of Eq. (7), after substituting of Eq. (5) for R, and dividing finally by 2π. Thus after rearranging we obtain:

$$\begin{aligned} T_z = \tfrac{1}{2}H\{&J_B-\tfrac{3}{4}r_6^2[(r_6^2-r_5^2)J_C \\ &+2(r_6^2-r_5^2)J_B+J_A]\}_{av}. \end{aligned} \tag{8}$$

where,

$$J_A = \int_0^{2\pi}(a+b\cos\varphi)^{-1/2}\,d\varphi$$

$$J_B = \int_0^{2\pi}(a+b\cos\varphi)^{-3/2}\,d\varphi$$

$$J_C = \int_0^{2\pi}(a+b\cos\varphi)^{-5/2}\,d\varphi$$

with, $a = r_1^2 + r_2^2$, and
$b = -2r_1r_2\sin\beta$

The evaluation of the integrals in Eq. (8), is necessary for the calculation of T_z, for the methyl groups. These integrals are of the elleptical type and cannot be evaluated in a closed form. These were calculated numerically using the Gauss quadrature method.

b. Electrostatic Effects. In dealing with bonds which are more highly polar than the –C≡C– triple bond, account must be taken of direct electrostatic contributions to ζ_e. This problem arises in the case of the –C≡N and –N≡C triple bonds. A treatment of this problem has been given by Buckingham.[15] Buckingham has shown that molecules containing polar bonds produce an electric field at a particular nucleus, and this leads to chemical shifts proportional to the first powder of the field strength.

The electric field at any point due to a dipole can be evaluated in the usual manner.[16] In our calculations, an improved approximation for the electrostatic effect is made by replacing the point dipole by partial positive and negative charges placed at the two atoms forming the polar bond. These partial charges are derived from the dipole moment and the length of the bond.

According to Coulomb's law, the force exerted by the positive charge ($+e$) on the unit charge placed at the nucleus H in Fig. 3, is

$$E_1 = e/R_1^2$$

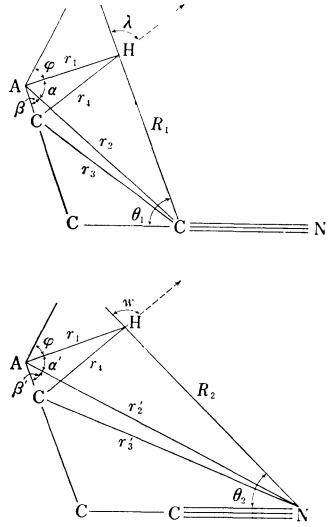

Fig. 3. Calculation of a electrical shielding for rotating methyl groups, based on the point charge approximation.

The component of this force along the C→H bond is given by,

$$E_1^{C\to H} = e/E_1^2\cdot\cos\lambda$$

Similarly,

$$E_2 = -e/R_2^2, \text{ and } E_2^{C\to H} = -e/R_2^2\cdot\cos w$$

The electrical field at the nucleus H is completely defined by the total force exerted by the two charges ($+e$) and ($-e$), and is given by:

15) A. D. Buckingham, *Can. J. Chem.*, **38**, 300 (1960).
16) V. C. A. Ferraro, "Electromagnetic Theory," The Athlone Press, London (1954), p. 70.

$$E_T = e/R_1^2 \cdot \cos\lambda - e/R_2^2 \cdot \cos w \qquad (9)$$

From the geometry of the figure, we can show,

$$\cos\lambda = (R_1^2+r_4^2-r_3^2)/2R_1r_4,$$
$$\text{and} \quad \cos w = (R_2^2+r_4^2-r_3'^2)/2R_2r_4$$

Therefore,

$$\langle E\rangle = e/R_1^2[(R_1^2+r_4^2-r_3^2)/2R_1\,r_4] - e/R_2^2[R_2^2+r_4^2-r_3'^2)/2R_2\,r_4] \qquad (10)$$

Since, $\mu=el$, therefore

$$\langle E\rangle = \mu/2lr_4[(R_1^{-1}+R_1^{-3}(r_4^2-r_3^2) - R_2^{-1} - R_2^{-3}(r_4^2-r_3'^2)]_{av}.$$

Since φ varies from 0 to 2π, we can find the average value by integrating the left-hand side of this equation after substituting the values of R_1 and R_2 given by:

$$R_1 = (r_1^2+r_2^2-2r_1r_2\sin\beta\cdot\cos\varphi)^{1/2}$$
$$R_2 = (r_1^2+r_2^2-2r_1r_2'\sin\beta'\cdot\cos\varphi)^{1/2}$$

Thus after rearranging, we obtain,

$$E = \mu/4l\pi r_4[J_{A_1}+J_{B_1}(r_4^2-r_3^2) - J_{A_2}-J_{B_2}(r_4^2-r_3'^2)]_{av}. \qquad (11)$$

Where, J_{A_1}, J_{A_2}, J_{B_1}, and J_{B_2} are the elleptical integrals referred to before.

c. Electronegativity Effects. Following the original investigation of Meyer, Saika, and Gutowsky,[17] it was found empirically by Daily and Shoolery,[18] that for a series of ethyl derivatives, a linear relation exists between the internal chemical shift of the ethyl group protons and the electronegativity of the substituent. Cavanaugh and Daily[10] have re-examined this relationship, in which they replaced the solvent (benzene) by carbon tetrachloride. These results were reviewed and measurements were made on dilute solutions of these compounds in carbon tetrachloride and extrapolated to infinite dilution. The internal chemical shifts of the ethyl derivatives as measured in carbon tetrachloride differ slightly from those measured in benzene. A revised Daily and Shoolery equation was set up using the new data.

$$\text{Electronegativity} = 0.0114\,\delta\ (\text{internal}) + 1.78$$

Where, δ is in c/s at 60 Mc/s.

Since the electronegativity of the substituent determines the electron distribution around the protons; this equation may be taken as an empirical expression for estimating $\Delta\zeta_l$, between the methyl and methylene protons in ethyl and isopropyl acetylenes, nitriles and isonitriles. The estimation of $\Delta\zeta_l$, in this manner compares favourably with the theoretical values calculated from electron density distribution.[19,20]

17) L. H. Meyer, A. Saika and H. S. Gutowsky, *J. Am. Cmem. Soc.*, **75**, 4567 (1953).
18) B. P. Daily and J. N. Shoolery, *ibid.*, **77**, 3977 (1956).
19) C. Sandorfy, *Can. J. Chem.*, **33**, 1337 (1955).
20) R. McWeeny, *J. Chem. Phys.*, **19**, 1614 (1951).

Discussion

We wish now to demonstrate experimentally the presence of long-range contributions to the shielding of a proton in a molecule. The molecules are assumed to be in the liquid state and summations in the shielding expression is over all long-range triple bonds, which are assumed to be axially symmetric with magnetic anisotropies $\Delta\chi^{X\equiv Y}$. Therefore,

$$\Delta\zeta_d^{A-B} = \Delta\chi^{X\equiv Y}\sum(T_z^A - T_z^B)/3L_0$$

Thus, from the calculated value of $\sum(T_z^A - T_z^B)/3L_0$, and the experimentally observed value of $\Delta\zeta_d^{A-B}$, we determine $\Delta\chi^{X\equiv Y}$, where, X≡Y, represents a triple bond. In Tables 4, 5, and 6, are listed the values of $\sum(T_z^A - T_z^B)/3L_0$ for specific nuclei, also are listed in the tables the appropriate experimental NMR relative chemical shifts for these nuclei, in a series of molecules containing the three different triple bonds. The values from Tables 4, 5 and 6, are plotted with $\Delta\zeta_d^{A-B}$ as abscissa and $\sum(T_z^A - T_z^B)/3L_0$ as the ordinate. A marked linear dependence of these points is found, enabling us to conclude that such long-range bonds do contribute to the shielding. Drawing the line of best fit through these points, we obtain from its slope the values of:

$$\Delta\chi^{C\equiv C} = \chi_L^{C\equiv C} - \chi_T^{C\equiv C} = -35.27\pm0.23\times10^{-6}\text{cm}^3\cdot\text{mol}^{-1} = -5.859\pm0.039\times10^{-29}\text{cm}^3\cdot\text{molecule}^{-1}$$

$$\Delta\chi^{C\equiv N} = \chi_L^{C\equiv N} - \chi_T^{C\equiv N} = -39.75\pm0.33\times10^{-6}\text{cm}^3\cdot\text{mol}^{-1} = -6.60\pm0.055\times10^{-29}\text{cm}^3\cdot\text{molecule}^{-1}$$

$$\Delta\chi^{N\equiv C} = \chi_L^{C\equiv N} - \chi_T^{N\equiv C} = -39.05\pm0.19\times10^{-6}\text{cm}^3\cdot\text{mol}^{-1} = -6.48\pm0.032\times10^{-29}\text{cm}^3\cdot\text{molecule}^{-1}$$

The fact that these points do not lie on a straight line, indicates that the assumptions we have made are not frequently valid. We feel, however, that our conclusions are justified and give every indication that other contributing effects are of high order.

The value of $\Delta\chi$ for –C≡N and –N≡C bonds depend strongly on various parameters, such as the location of the –C≡N and –N≡C dipoles. For mathematical simplification, we have idealised the dipoles by point dipoles, and such idealization is valid only when we consider the field due to these dipoles at very large distances. For actual calculations, it is customary to locate this dipole somewhere along the bond by making certain assumptions; one such assumption is to locate the dipole at the electrical centre of gravity of the electron distribution constituting the bond.

The negative sign of $\Delta\chi$ indicates that the diamagnetic susceptibility perpendicular to the axis of symmetry $|\chi_T^D|$, must be considerably smaller in magnitude than $|\chi_L^D|$. This is so because in an axially symmetric system, $\chi_L^P=0$, and only χ_T^P

TABLE 4. OBSERVED CHEMICAL SHIFT DIFFERENCES BETWEEN THE TWO PROTONS A AND B, AND THE VALUES OF $\Delta T_z^{A-B}/3L_0$, FOR THESE PROTONS, TOGETHER WITH THE VALUES OF THE MAGNETIC ANISOTROPY OF THE –C≡C– BOND ($cm^3 \cdot mol^{-1}$)

Compound	$10^6\Delta\zeta_d$	$10^6\Delta\zeta_l$	$10^6\Delta\zeta_T$	$\Delta T_z^{A-B}/3L_0$	$10^6\Delta\chi^{C\equiv C}$
$CH_3 \cdot CH_2 \cdot C\equiv CH$	− 1.268	+ 2.208	+ 0.94	+ 0.0359	− 35.26
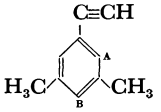	+ 0.179	assumed '0'	+ 0.179	− 0.0056	− 31.90
$(CH_3)_2 \cdot CH \cdot C\equiv CH$	− 1.267	+ 2.707	+ 1.44	+ 0.0359	− 35.26
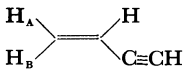	− 0.18	0	− 0.18	+ 0.0051	− 35.40

TABLE 5. OBSERVED CHEMICAL SHIFT DIFFERENCE BETWEEN THE PROTONS A AND B AND THE VALUES OF $\Delta T_z^{A-B}/3L_0$ FOR THESE PROTONS, TOGETHER WITH THE VALUES OF THE MAGNETIC ANISOTROPY OF THE –C≡N BOND ($cm^3 \cdot mol^{-1}$)

Compound	$\Delta\zeta_T$	$\Delta\zeta_e$	$\Delta\zeta_d$	$\Delta\zeta$	$\Delta T_z^{A-B}/3L_0$	$\Delta\chi^{-C\equiv N}$
$CH_3 \cdot CH_2 \cdot C\equiv N$	+ 1.033	+ 0.465	− 1.1376	+ 1.944	+ 0.0347	− 39.62
$(CH_3)_2CH \cdot C\equiv N$	+ 1.333	+ 0.465	− 1.376	+ 2.244	+ 0.0347	− 39.62
$CH_2{=}CH \cdot C\equiv N$	− 0.177	− 0.10	− 0.077		+ 0.0037	− 20.80
$CH_2{=}CH \cdot C\equiv N$	− 0.177	− 0.61	− 0.077		+ 0.0037	− 31.60
$(CH_3)_2C{=}CH \cdot C\equiv N$	− 0.433	− 0.057	+ 0.376		+ 0.0012	− 31.60
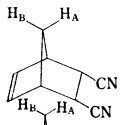	+ 0.315	+ 0.030	+ 0.285		− 0.0074	− 38.77
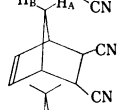	0.00	+ 0.318	− 0.318		+ 0.0085	− 37.65
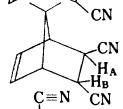	− 0.17	− 0.129	− 0.040		+ 0.001	− 40.40
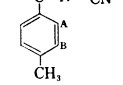	− 0.209	− 0.282	+ 0.071		− 0.0021	− 34.18

TABLE 6. OBSERVED CHEMMICAL SHIFT DIFFERENCE BETWEEN THE PROTONS A AND B AND THE VALUES OF $\Delta T_z^{A-B}/3L_0$ FOR THESE PROTONS, TOGETHER WITH THE VALUES OF THE MAGNETIC ANISOTROPY OF THE –N≡C BOND ($cm^3 \cdot mol^{-1}$)

Compound	$\Delta\zeta_T$	$\Delta\zeta_e$	$\Delta\zeta_d$	$\Delta\zeta_l$	$\Delta T_z^{A-B}/3L_0$	$\Delta\chi^{-N\equiv C}$
$CH_3 \cdot CH_2 \cdot N\equiv C$	+ 1.585	+ 0.437	− 1.352	+ 2.50	+ 0.0347	− 38.92
$(CH_3)_2 \cdot CH \cdot N\equiv C$	+ 2.420	+ 0.437	− 1.352	+ 3.33_5	+ 0.0347	− 38.92
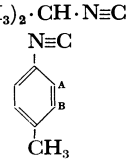	+ 0.045	− 0.209	+ 0.165		− 0.0041	− 40.45
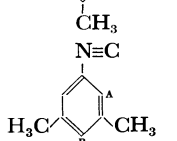	+ 0.044	− 0.234	+ 0.19		− 0.0047	− 40.75

TABLE 7. CALCULATED AND OBSERVED RESONANCE FREQUENCIES FOR C-19 METHYL PROTONS OF SOME 5-CYANO-STEROIDS IN COMPARISON WITH 5-H-STEROIDS[29]

Cyano-steroid	ζ_a^{CN} (ppm)	ζ_e^{CN} (ppm)	ζ_{Total}^{CN} (ppm)	ζ_{Total}^{CN} (c/sec) at 60 Mc/s	Parent steroid	Observed 19-H (c/sec) from TMS	Calcd 19-H (c/sec)	Obsd 19-H (5α-CN)	$\zeta_{calc}-\zeta_{obs}$ (c/sec)
5α-CN					5α-H				
Ia	+0.322	−0.125	+0.197	+11.8	IIa	49.6	37.8	60.2	−22.4
Ib	+0.322	−0.125	+0.197	+11.8	IIb	61.0	49.2	69.0	−19.8
Ic	+0.322	−0.125	+0.197	+11.8	IIc	61.5	49.7	68.5	−18.8
Id	+0.322	−0.125	+0.197	+11.8	IId	48.1	36.3	57.3	−21.0
Ie	+0.322	−0.125	+0.197	+11.8	IIe	48.8	37.0	59.6	−22.6
IIIa	+0.322	−0.125	+0.197	+11.8	IIIb	63.2	51.4	70.7	−19.3
5β-CN					5β-H				
IIIc	+0.072	−0.297	−0.225	−13.5	IIId	62.9	76.4	77.8	−1.4
IVa	+0.101	−0.297	−0.196	−11.75	Va	62.3	74.05	75.8	−1.75
IVb	+0.129	−0.297	−0.225	−10.8	Vb	57.2	70.7	70.8	−0.10

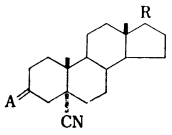

(I)

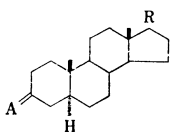

(II)

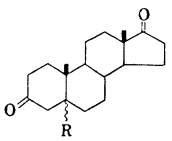

(III)

a, R=OAc, A=3β-OAc, 3α-H; b, R=OAc, A= =O; c, R=Ac, A= =O; d, R=OAc, A=3α-OAc, 3β-H; e, R=OAc, A= O-CH_2- / O-CH_2-

IVa, A= =O, R=OAc, IVb, A=3α-OAc, 3β-H

a, R=α-CN, b, R=α-H
c, R=β-CN, d, R=β-H

$(>)\neq 0$, therefore, $\Delta\chi^{X\equiv Y}=\chi_L-\chi_T=\chi_L^D-\chi_T^D-\chi_T^P<0$, therefore $|\chi_L^D|$, must be large and negative.

The measurement of $\Delta\chi$ for a triple bond by this method accomplishes what would be very difficult to do by any other method. The ideal experiment for measuring susceptibility of a triple bond in both the transverse and longitudinal directions would be to freeze acetylene, as an example, in a crystal in which all the acetylenic bonds are parallel and then performing the magnetic susceptibility measurements. By using the experimental value of $\Delta\chi$ and the quantum mechanical expression of $\Delta\chi$, the validity of different possible wave functions for the triple bond can be determined.

The present semi-quantitative treatment indicates that, in the case of ethylacetylene, ethyl cyanide, and ethyl isocyanide, the major contribution to the observed chemical shift comes from $\Delta\zeta_l$, and that the observed chemical shift cannot be satisfactorilly explained on the basis of bond magnetic anisotropy alone. It seems probable from the present work, that both bond magnetic anisotropies and electronegativity differences contribute to the chemical shift between the methyl and methylene protons in these three molecules and that both effects are of the same order of magnitude. The local shielding differences perhaps being somewhat the more important.

A review of the literature on the values of the magnetic anisotropy of the acetylenic group, calculated either from theoretical quantum mechanical treatments or from experimental data have been made by Bothner-By and Pople.[20] The theoretical values range[20,21] from -1.61 to 1.94×10^{-6} $cm^3\cdot mol^{-1}$. The experimental ones from[22] -16.5 to[23–25] -34.0×10^{-6} $cm^3\cdot mol^{-1}$. In view of the widely scattered range of values reported in the literature, our datum must be considered in good agreement with the values given by Heel and Zwil,[9,24] and that obtained by Englert and Saupe[26] in a study of some acetylenic compounds oriented

21) A. A. Bothner-By and J. A. Pople, *Ann. Rev. Phys. Chem.*, **16**, 43 (1965).
22) J. Tillieu and J. Guy, *Compt. Rend.*, **239**, 1203 (1954); *ibid.*, **241**, 382 (1955); *ibid.*, **242**, 1279, 1436 (1956); *J. Chem. Phys.*, **24**, 1117 (1956); *Ann. Phys.*, **2**, 471, 631 (1957).
23) G. S. Reddy and J. H. Goldstein, *J. Chem. Phys.*, **39**, 3509 (1963).
24) H. Heel and H. Buchert, *Z. Physk. Chem. (Frankfurt)*, **38**, 47 (1963).
25) S. Castellano and J. Lorenc, *J. Phys. Chem.*, **69**, 3554 (1965).
26) G. Englert and A. Saupe, *Mol. Crystals*, **1**, 503 (1966).

in a nematic phase.

In another attempt, Goldstein and Reddy,[27] have devised an empirical method of the estimation of diamagnetic anisotropy effects in NMR spectroscopy based upon correlations between proton chemical shift and C^{13}–H coupling constants. The anisotropy shift for the acetylenic hydrogen as obtained by this method is +4.12 ppm. This anisotropy effect for acetylene is considerably smaller than Pople's theoretical estimate of about +10 ppm. Although this result is qualitatively in the expected order with respect to ethylene and methane, the difference is considerably less than might have been anticipated.

The value of $\Delta\zeta_d^{\equiv CH}$ cantribution to the shielding of the proton in acetylene and methylacetylene could be estimated from the calculated value of $\Delta\chi^{C\equiv C}$ and the known geometry of these molecules.[28] The corresponding paramagnetic contribution to ζ is +9.03 ppm. It is interesting to compare this value with that obtained by Pople[29] in a quantum mechanical study of the proton chemical shift in acetylene. Pople found that the paramagnetic contribution to the shielding of the acetylenic proton is +10 ppm. Pople has emphasised that this value is only an order of magnitude for the effect, and is clearly large enough to account for the anomalous position of the acetylenic proton. Again, we may notice, that, both bond magnetic anisotropy and electronegativity effects of the –C≡CH group contribute to the chemical shift of the acetylenic proton.

Studies on steroids, which are available in great number, appear most promising the geometry of the steroid nucleus is well established and the effects of substituents have been shown to be nearly additive. Zürcher[30] has obtained and analysed data on a large number of steroids. He gives additive contributions for substituents and discusses the contribution of groups from equivalent positions.

Corss and Harrison[31] have studied a series of steroids with and without nitrile substituents in the 5α- or 5β-positions. In each case they observed a deshielding of the C-19 methyl protons, on substitution with –C≡N, although the dipolar formula predicts a shielding, whether the substituent is introduced α or β. The value of $\Delta\chi^{C\equiv N}$ employed in their calculations is that of Goldstein and collaborators.[11] These authors have neglected the electrostatic effect of the –C≡N group. Our calculations on these steroids, using Eqs. (2) and (11) for estimating anisotropic and electrostatic effects, shows that the C-19 methyl protons in 5α-cyano-steroids should be shifted upfields by 11.8 c/s, relative to the 5α-H-steroid, contrary to the observed shift. The explanation given by Cross and Harrison that ring A in the 5α-cyano-steroids is distorted from the chair form due to dipole-dipole interaction between substituents at the 3- and 5-positions may explain part of the observed downfield shift.

When considering 5β-cyano-steroids, our results show that the electrostatic effect of the –C≡N group is very important in determining the C-19 methyl protons shift, and explain the deshielding of these protons, relative to the parent steroid. Table 7 shows the calculated and observed shifts of these protons. The agreement between calculated and observed shifts in the 5β-cyano-steroids, where the stereochemistry of ring A is normal and repulsion between the C=O and C≡N groups is minimum, gives an indication that our value for the diamagnetic anisotropy of the –C≡N group is correct. To obtain better agreement between observed and calculated shifts in these molecules, one may take into account the electronegativity effects of the –C≡N group, as both magnetic anisotropy and electronegativity effects contribute to the proton chemical shift.

27) J. H. Goldstein and G. S. Reddy, *J. Chem. Phys.*, **36**, 2644 (1962).

28) "Tables of Interatomic Distances and Configurations in Molecules and Ions," Special Publication, No. 11, The Chemical Society, London (1958).

29) J. A. Pople, *Proc. Roy. Soc. (London)*, **A239**, 541, 550 (1957).

30) R. F. Zürcher, *Helv. Chim. Acta*, **44**, 1380 (1961); *ibid.*, **46**, 2055 (1963).

31) A. D. Cross and I. T. Harrison, *J. Am. Chem. Soc.*, **85**, 3223 (1964).

BULLETIN OF THE CHEMICAL SOCIETY OF JAPAN VOL. 42 1187—1191 (1969)

Molecular Orbital Treatment of Nitric Oxide Radicals. II. ESR Spectra of Aliphatic Nitric Oxide Radicals

Osamu KIKUCHI

Department of Chemistry, Tokyo Kyoiku University, Otsuka, Tokyo

(Received July 25, 1968)

Quantitative discussions of the ESR spectra of aliphatic nitric oxide radicals have been undertaken on the basis of the molecular orbitals of all-valence-electrons, which were evaluated by the approximate SCF method with the CNDO/2 approximation. The spin density on the methyl proton in the dimethyl nitric oxide radical is proportional to $\cos^2\theta$, where θ is the angle between the nitrogen $2p_z$ orbital and the plane containing the C–N and the C–H bonds; the small hyperfine splitting constants of β-protons appearing in some substituted nitric oxide radicals are understood as resulting from the sterically-restricted conformations of substituted groups. The deviation of the g factor of aliphatic nitric oxide from the free spin comes from the large spin densities localized on the nitrogen and the oxygen atoms, and the small excitation energy, from the non-bonding orbital of the oxygen to the odd π-orbital. The electronic structures and g factors of some other radicals are compared to those of aliphatic nitric oxide radicals.

Theoretical treatments have been made by several investigators of the β-proton coupling in free radicals.[1–4] These have mainly been carried out by the perturbation method based on the hyperconjugation model. McLachlan[2] and Lykos[3] have applied the valence bond theory to some alkyl radicals and shown that hyperconjugation takes place between methyl groups and the α-carbon atom. Symons[4] has pointed out that the theory of hyperconjugation affords the best explanation of the large hyperfine coupling of β-protons in alkyl radicals. The hyperconjugation model corresponds to the delocalization of an odd electron onto the β-protons in the molecular orbital theory. The recently-developed molecular orbital theory, in which all valence electrons are explicitly considered, will make clear the mechanism of the β-proton coupling.

Stone[5] has presented a theory which can be used to calculate the g factors of aromatic molecules and has shown that the results for hydrocarbon and semiquinone ions calculated according to the theory agree well with the experimental results. This theory has since been used for a study of the solvent effect on the g factor of the diphenyl nitric oxide radical.[6] However, there have been few theoretical investigations of the correlation between the g factor and the molecular electronic structure, perhaps because it is difficult to calculate the electronic structures for all the valence electrons of large molecules.

In the present study, the approximate self-consistent molecular orbital method of Longuet-Higgins and Pople[7] is applied to the all-valence-electron system of several nitric oxide radicals, and the hyperfine splitting constants of β-protons and the g factors for aliphatic nitric oxide radicals are discussed.

Methods

The ground configuration of the free radical is a doublet, and its antisymmetrized wave function can be described by:

$$\Psi_g = |\phi_1\bar{\phi}_1 \cdots \phi_{m-1}\bar{\phi}_{m-1}\phi_m| \quad (1)$$

where $2m-1$ is the number of the valence electrons considered. The molecular orbital, ϕ_i, is obtained using the LCAO MO approximation:

$$\phi_i = \sum_r C_{ri}\chi_r \quad (2)$$

where χ_r is the valence atomic orbital: 1s for hydrogen and 2s, $2p_x$, $2p_y$, and $2p_z$, for carbon, nitrogen, and oxygen atoms. The LCAO coefficients and the orbital energy, ε_i, are calculated by the approximate SCF method, which has been applied to the discussion of the electronic structure

1) R. Bersohn, *J. Chem. Phys.*, **24**, 1066 (1956); J. P. Colpa and E. de Boer, *Mol. Phys.*, **7**, 33 (1964); D. B. Chesnut, *J. Chem. Phys.*, **29**, 43 (1958).
2) A. D. McLachlan, *Mol. Phys.*, **1**, 233 (1958).
3) P. G. Lykos, *J. Chem. Phys.*, **32**, 625 (1960).
4) M. C. R. Symons, *Tetrahedron*, **18**, 333 (1962).
5) A. J. Stone, *Proc. Roy. Soc.*, **A271**, 424 (1963); A. J. Stone, *Mol. Phys.*, **6**, 509 (1963).
6) T. Kawamura, S. Matsunami, T. Yonezawa and K. Fukui, This Bulletin, **38**, 1935 (1965).
7) H. C. Longuet-Higgins and J. A. Pople, *Proc. Phys. Soc.*, **68**, 591 (1955).

and spectra of the H_2NO radical in a previous paper.[8]

The spin density on the valence atomic orbital, r, can be simply computed by:

$$\rho_r = C_{rm}^2 \tag{3}$$

The diagonal components of the g factor are obtained by;[5]

$$g_{aa} = 2.00232 + \Delta g_{aa} \tag{4}$$

$$\Delta g_{aa} = 2\sum_{i=1}^{m-1} \frac{\langle\phi_m|\sum_t l_a^t|\phi_i\rangle\langle\phi_i|\sum_t \zeta_t l_a^t|\phi_m\rangle}{E_{i\to m}-E_0} - 2\sum_{j=m+1}^{2m-1} \frac{\langle\phi_m|\sum_t l_a^t|\phi_j\rangle\langle\phi_j|\sum_t \zeta_t l_a^t|\phi_m\rangle}{E_{m\to j}-E_0} \tag{5}$$

where l^t is the angular momentum about the tth nucleus and where ζ_t is the spin-orbit coupling constant for the tth atom; the values of 29 cm^{-1}, 76 cm^{-1}, and 151 cm^{-1} were used for carbon, nitrogen, and oxygen atoms respectively.[9] $E_{i\to m}$ and $E_{m\to j}$ are the energies of the following antisymmetrized wave functions:

$$\Psi_{i\to m} = |\phi_1\bar{\phi}_1 \cdots \phi_i\bar{\phi}_m \cdots \phi_{m-1}\bar{\phi}_{m-1}\phi_m| \tag{6}$$

$$\Psi_{m\to j} = |\phi_1\bar{\phi}_1 \cdots \phi_i\bar{\phi}_i \cdots \phi_{m-1}\bar{\phi}_{m-1}\phi_j| \tag{7}$$

then the energy differences in Eq. (5) are computed by the following equations:

$$\left.\begin{aligned} \Delta E_{i\to m} &\equiv E_{i\to m} - E_0 = \varepsilon_m - \varepsilon_i - (mm|ii) \\ &\quad + \frac{1}{2}(mm|mm) + \frac{1}{2}(mi|im) \\ \Delta E_{m\to j} &\equiv E_{m\to j} - E_0 = \varepsilon_j - \varepsilon_m - (mm|jj) \\ &\quad + \frac{1}{2}(mm|mm) + \frac{1}{2}(mj|jm) \end{aligned}\right\} \tag{8}$$

The two-electron integrals were evaluated by the method described by Pople *et al.*[10] The g factor of the free radical in solution was estimated by:

$$g_{av} = \frac{1}{3}(g_{xx} + g_{yy} + g_{zz}) \tag{9}$$

Results and Discussion

β-Proton Coupling Constants. A simple nitric oxide radical, $(CH_3)_2NO$, was adopted for discussing the β-proton coupling; the calculations were performed using the following assumptions for bond lengths and bond angles: 1.23, 1.41, and 1.10 Å[11] for N–O, N–C, and C–H bonds respectively, and 120° for the CNO and CNC bond angles. The spin distributions have been obtained for a number of conformations of two methyl groups in the $(CH_3)_2NO$ radical. The results for a particular conformation of methyl groups (θ=90°, ϕ=90°) are presented in Table 1. In this table,

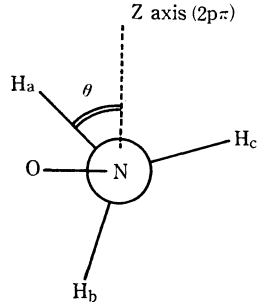

Fig. 1. CH_3–NO group in dimethyl nitric oxide radical.
The angle ϕ is defined as θ between the 2pπ orbital and the other methyl group.

Table 1. The spin distribution in the $(CH_3)_2NO$ radical*1

Atomic orbital*2	Calculated spin density	
	I	II*3
2s(C)	0.0000	−0.0019
$2p_x$(C)	0.0000	0.0002
$2p_y$(C)	0.0000	−0.0032
$2p_z$(C)	0.0000	−0.0109
2s(N)	0.0000	−0.0001
$2p_x$(N)	0.0000	−0.0002
$2p_y$(N)	0.0000	0.0000
$2p_z$(N)	0.4341	0.2284
2s(O)	0.0000	0.0000
$2p_x$(O)	0.0000	−0.0001
$2p_y$(O)	0.0000	−0.0004
$2p_z$(O)	0.4528	0.7505
$1s(H_a)$	0.0000	−0.0006
$1s(H_b)$	0.0283	0.0138
$1s(H_c)$	0.0283	0.0138

*1 Methyl groups were fixed at θ=90° and ϕ=90°.
*2 The N–O axis is taken as y axis and z axis is perpendicular to the molecular plane (CNO plane).
*3 Method II is the unrestricted SCF method.

the spin distribution calculated by the unrestricted Hartree-Fock method[10] is also presented. The odd electron is accommodated into the orbital constructed mainly by the $2p_z$ atomic orbitals of nitrogen and oxygen, and the delocalization of the odd electron onto the methyl-protons is clearly

8) O. Kikuchi, This Bulletin, **42**, 47 (1969).
9) A. Carrington and A. D. McLachlan, "Introduction to Magnetic Resonance," Harper and Row, New York (1967), p. 138.
10) J. A. Pople, D. P. Santry and G. A. Segal, *J. Chem. Phys.*, **43**, S129 (1965); J. A. Pople and G. H. Segal, *ibid.*, **44**, 3289 (1966).
11) A. W. Hanson, *Acta Cryst.*, **6**, 32 (1935).

indicated. The unrestricted SCF method shows that there are actually negative spin densities on some atomic orbitals. In the present calculation of the spin distribution on the valence atomic orbitals, the angular dependence of the spin distribution on the methyl protons is discussed on the basis of the results obtained by the I method.

The methyl groups will rotate freely in solution, and the isotropic hyperfine splitting observed will be an average one. When the methyl group is not rotating freely, the proton splitting depends on the angle, θ, between the nitrogen $2p_z$ orbital and the plane containing the C–N and C–H bonds. In the molecular orbital treatment, this angular dependence of the hyperfine splitting constants can be resolved by the direct calculation of the spin densities on the 1s orbitals of the methyl protons, which are fixed at any angle. The $(CH_3)_2NO$ radical has two methyl groups; the splitting constant (spin density) for the proton in one methyl group (CH_3(I)) depends not only on the θ angle, but also on the conformation of the other methyl group (CH_3(II)). The variation in the spin density on the methyl protons with the conformation of the other methyl group was about 0.002 (5%); this corresponds to 1 gauss of the proton hyperfine splitting constant. The spin distribution on the methyl protons fixed at the θ angle was obtained on the assumption of free rotation for the other methyl group. The results are listed in Table 2.

Table 2. Angular dependence of the spin density of the methyl-proton in $(CH_3)_2NO$

$\theta°$	ρ_H	$\rho_H/\rho_H(\theta=0)$	$\cos^2\theta$
−90	0.0000	0.000	0.000
−75	0.0026	0.068	0.067
−60	0.0097	0.255	0.250
−45	0.0193	0.506	0.500
−30	0.0288	0.754	0.750
−15	0.0356	0.933	0.933
0	0.0381	1.000	1.000
15	0.0356	0.934	0.933
30	0.0287	0.753	0.750
45	0.0192	0.504	0.500
60	0.0096	0.253	0.250
75	0.0026	0.067	0.067
90	0.0000	0.000	0.000

According to Symons,[4] if the hyperfine coupling occurs purely by hyperconjugation, it varies between zero when the β-C–H bond lies in the nodal plane of the unpaired electron and a maximum when it lies on a plane at right angles to this, while the splitting constants for intermediate positions vary according to the $\cos^2\theta$ law:

$$a_{\beta-H} = B\cos^2\theta \qquad (10)$$

The present finding regarding the angular dependence of the β-proton coupling coincides with that obtained by the hyperconjugation model, and the $\rho_{\beta-H} \propto \cos^2\theta$ relation holds strictly (Fig. 2). The spin density on the proton in the CH_3 group rotating freely can be estimated from Table 2 or Fig. 2, taking $\cos^2\theta=0.5$. The obtained value, ρ (average)$=0.019$, corresponds to the 9.5 gauss[12] β-proton splitting constant, while the experimental value of the $(CH_3)_2NO$ radical in solution is 13.4 gauss.[13]

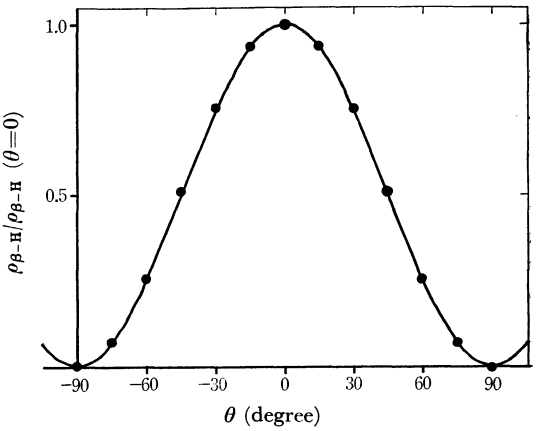

Fig. 2. Angular dependence of spin density on methyl-protons.
solid line: $\cos^2\theta$.
closed circle: calculated spin density.

From Fig. 2 or Table 2, the value of B in Eq. (10) can be estimated. The value of B is equal to $a_{\beta-H}$ at $\theta=0$. The calculated hyperfine splitting constant at $\theta=0$ was about 19 gauss; this is slightly smaller than the value of 27 gauss which was obtained from the experimental splitting constant, 13.4 gauss,[13] of the $(CH_3)_2NO$ radical in solution. From the calculated spin densities on the β-proton and on the nitrogen $2p_z$ orbital, the magnitude of McConnell's parameter, Q_{N-CH_3}, was estimated to be about 30 gauss.

The present results for the delocalization of the spin density on the β-methyl protons explain some interesting ESR experimental results for nitric oxide radicals. Some nitric oxide radicals reveal small hyperfine splitting constants of the β-protons.[13,14] For example, for di-isopropyl nitric oxide it is about 4 gauss, one third of that of β-protons in a freely-rotating methyl groups. Our results, shown in Fig. 3, indicate that the rotation of the isopropyl groups of this radical is restricted

12) Hyperfine splitting constants of hydrogen atoms are computed by $a_H=\rho$ (1s) $\times 502$ gauss.

13) G. Chapelet-Letourneux, H. Lemaire and A. Rassat, *Bull. Soc. Chim. France*, **1965**, 3283.

14) G. Coppinger and J. Swalen, *J. Am. Chem. Soc.*, **83**, 4900 (1961); J. Q. Adams, S. W. Nicksic and J. R. Thomas, *J. Chem. Phys.*, **45**, 654 (1966).

by the bulky substituents to a structure in which the β-proton oscillates through a small region ($-45°<\theta+90<45°$) close to the N–O molecular plane.

For cyclic nitric oxide radicals, the axial and equatorial β-protons show equal hyperfine splitting constants. This is due to their rapid chair-to-chair conformational interconversion, and a time-averaged splitting constant, $\frac{1}{2}(a_{ax}+a_{eq})$, was observed. For the piperidine nitric oxide radical, it is 11.3 gauss;[13] from this value and the present calculations it can be understood that the equatorial proton in cyclic nitric oxide radicals lies in the region of $\theta=90°$.

g Factors of Aliphatic Nitric Oxide Radicals. The simplest nitric oxide radical, the H_2NO radical, was used in our attempt to understand the relation between the g factor and the molecular structure for the nitric oxide radical. The electronic structure of this radical has been discussed in the previous paper,[8] while the molecular orbital scheme obtained is shown in Fig. 3. In this figure, the

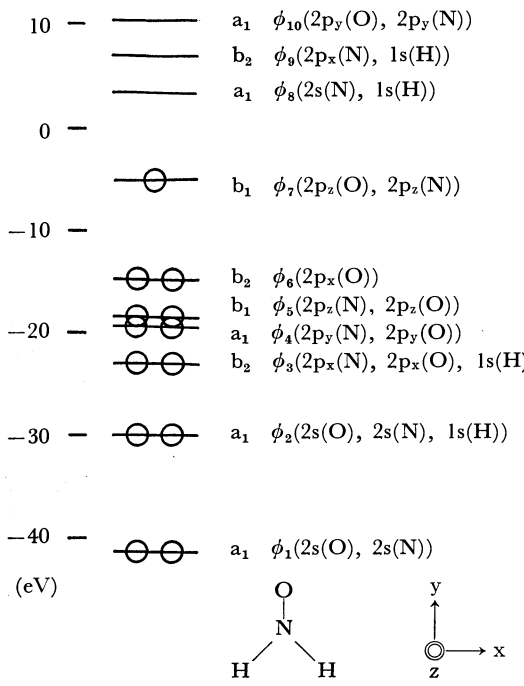

Fig. 3. Molecular orbital scheme for the H_2NO radical.

atomic orbitals contributing to each molecular orbital are also presented. The odd electron resides in the π-orbital, and since the planarity of the H_2NO radical is assumed, $\Delta g_{zz}=0$ (see Eq. (5)) and the z component of the g factor is the value for the free spin, 2.0023. The deviations, Δg_{xx} and Δg_{yy}, from the free spin can be calculated by Eq. (5). In this equation, the first term shows the contribution of the Ψ_{i-m} excited states, while the second term is the contribution of the Ψ_{m-j} excited states. The excitation energies were calculated from Eq. (8). The excitation energies and Δg_{xx} and Δg_{yy} are tabulated in Table 3. The

TABLE 3. CALCULATED EXCITATION ENERGIES AND g-FACTORS FOR THE H_2NO RADICAL*1,2

Excitation	$\Delta E_{i\to j}$ (eV)	$\Delta g_{xx}\times 10^{-5}$	$\Delta g_{yy}\times 10^{-5}$
1→ 7	28.54	6	0
2→ 7	18.31	−1	0
3→ 7	12.15	0	0
4→ 7	6.73	352	0
6→ 7	2.32	0	983
7→ 8	4.79	−72	0
7→ 9	8.08	0	−87
7→10	7.56	−13	0
Total		272	896

*1 The choice of the axis is shown in Fig. 3.
*2 $\Delta g_{zz}=0$

most important excitation for the g_{xx} is the excitation from the N–O σ-bonding orbital (ϕ_4) to the odd orbital, while for g_{yy}, it is the excitation from the lone-pair orbital of the oxygen atom (ϕ_6) to the odd π-orbital. The small contribution of the N–O anti-bonding orbital (ϕ_{10}) is due to the LCAO coefficients of the ϕ_7 and ϕ_{10} molecular orbitals; when the electrons in these orbitals are shared equally by nitrogen and oxygen atoms, the contribution of this orbital is zero. The experimental values of g_{xx}, g_{yy}, and g_{zz} for the di-*t*-butyl nitric oxide radical have been reported as 2.0061, 2.0089, and 2.0027 respectively.[15] The present results show that the large deviations of g_{xx} and g_{yy} for this nitric oxide from the free spin are due to, respectively, the N–O bonding orbital and the lone pair of the oxygen atom. The average g factor of the H_2NO radical was 2.0062; this agrees well with the g factors (2.0055—2.0061[16]) of many aliphatic nitric oxide radicals in solution.

Similar results were obtained for the dimethyl nitric oxide radical. In this radical the lone-pair orbital of the oxygen atom and the N–O σ-bonding orbital mainly contribute to Δg_{yy} and Δg_{xx} respectively, while the contribution of the N–O anti-bonding orbital was again small. $\Delta g_{xx}=167\times 10^{-5}$ and $\Delta g_{yy}=627\times 10^{-5}$. These values are smaller than those of the H_2NO radical, mainly because of the smaller electron density of the non-bonding orbital and the smaller spin density on the oxygen atom in the dimethyl nitric oxide radical.

It is important to investigate the g factors for the other radicals in order to make clear the rela-

15) O. H. Griffith, D. W. Cornell and H. M. McConnell, *J. Chem. Phys.*, **43**, 2909 (1965).
16) R. Briere, H. Lemaire and A. Rassat, *Bull. Soc. Chim. France*, **1965**, 3273; T. Kawamura, S. Matsunami and T. Yonezawa, This Bulletin, **40**, 1111 (1967).

tion between the g factor and the electronic structure of the free radical. In aromatic nitric oxide radicals such as diphenyl nitric oxide, π-electrons delocalize upon the large conjugate system. Nevertheless, some experimental results have shown that aromatic nitric oxide radicals have g factors similar to those of aliphatic nitric oxide radicals.[6,17] It would be difficult to calculate the electronic structure of the all-valence-electron system for aromatic radicals; simple method for estimating the g factor of aromatic radicals is desirable. The relation between the g factor of aromatic nitric oxide and the spin densities on the nitrogen and oxygen atoms has been obtained employing some assumptions based on the electronic structure of aliphatic nitric oxide radicals. The g factor of the diphenyl nitric oxide radical in solution has been calculated by this method to be 2.0051. The details will be reported subsequently.

Another interesting kind of radical is the amino-radical. Unlike nitric oxide radicals, only a few investigations of these radicals by the ESR technique have been presented, perhaps because of their instability. Some of the amino-radicals investigated by the ESR method have been the NH_2 radical,[18] the substituted anilino radical,[19] and substituted diphenyl aminoradicals.[20] In the present investigation, the g factor of the NH_2 radical has been calculated and compared with that for the H_2NO radical. In the NH_2 radical an odd electron occupies the $2p_z$ orbital of the nitrogen atom, and effective lone-pair electrons are on the y axis on the side away from the rest of the molecule.[21] As a result, the deviation of g_{xx} from the free spin is expected to be large; the calculated results show that $\Delta g_{xx}=347\times10^{-5}$ and that the contribution of the NH σ-bond is small. The average value was 2.0037[22]; this agrees with the experimental value.[17] The main reason for the difference between the g factor of the H_2NO radical and that of the NH_2 radical is the different spin-orbit coupling constants for oxygen and nitrogen atoms.

The author wishes to express his thanks to Professor Keizo Suzuki, Tokyo Kyoiku University, and Dr. Kazuo Someno, Government Chemical Industrial Research Institute Tokyo, for their helpful suggestions and encouragement during the course of this work.

Thanks are also due to the Matsunaga Science Foundation for financial support.

17) P. H. H. Fischer and F. A. Neugebauer, *Z. Naturforschg.*, **18a**, 1514 (1964).

18) S. Foner, E. Cochran, V. Bawers and C. Jen, *Phys. Rev. Letters*, **1**, 91 (1958).

19) E. Muller, A. Rieker and K. Scheffler, *Ann. Chem.*, **645**, 92 (1961); N. M. Atherton, E. J. Land and G. Poryer, *Trans. Faraday Soc.*, **59**, 818 (1963).

20) F. A. Neugebauer and P. H. H. Fischer, *Chem. Ber.*, **98**, 844 (1965).

21) The y axis taken as C_{2v} rotation axis; z perpendicular to the molecular plane.

22) $\Delta g_{yy}=53\times10^{-5}$ (calculated).

BULLETIN OF THE CHEMICAL SOCIETY OF JAPAN VOL. 42 1192—1196 (1969)

Decomposition of Formic Acid on Silver Catalyst —Adsorption Measurement during Surface Catalysis—

Kenzo FUKUDA, Takaharu ONISHI and Kenzi TAMARU

Department of Chemistry, The University of Tokyo, Hongo, Bunkyo-ku, Tokyo

(Received July 27, 1968)

The mechanism of the decomposition of formic acid over reduced silver catalyst has been studied by means of the adsorption measurement during surface catalysis. It was found that the decomposition of formic acid on the silver catalyst at 100°C was first order at lower pressures of formic acid, while at medium pressures it was zero order, the reaction rate being independent of the pressures of ambient formic acid; in the first region the amount of adsorbed formic acid was proportional to the pressure of formic acid, and in the second region it was constant, independent of the pressure of formic acid in the ambient gas. The second region corresponds to "saturation" in an ordinary sense. At pressures of formic acid higher than that in the "saturation" region the amount of adsorbed formic acid increases again linearly with the pressure of formic acid. The linear relation between the reaction rate and the amount of formic acid adsorbed during the reaction was observed over the whole range of the pressure of formic acid studied. It is accordingly concluded that a surface unimolecular reaction in terms of the adsorbed formic acid is the rate-determining step. The exchange reaction of surface formic acid with those in the ambient gas was studied and it was demonstrated all the formic acid in the adsorbed layer accordingly participated in the exchange reaction. The numbers of surface silver atoms occupied by one molecule of adsorbed formic acid at the saturation points at various temperatures are estimated from the number of surface silver atoms and the amount of formic acid adsorbed at the zero-order kinetics. The number of surface silver atoms occupied by one molecule of adsorbed formic acid increases linearly with temperature.

The rate of chemical reaction is generally determined by the reactivities of the reacting species of the rate-determining step. In the case of heterogeneous catalysis, the concentration of some of the reaction intermediates, as well as those of reacting species in the ambient gas, may be determined by the techniques to measure adsorption during the course of the reaction.[1] The dependence of the reaction rate upon the concentration of each of the species on the catalyst surface and those in the ambient gas would reveal the reactants of the rate-determining step or the mechanism of the overall reaction. By means of this approach, the decomposition of formic acid has been previously studied by the authors over such metal oxides as alumina and zinc oxide which are typical dehydration and dehydrogenation catalysts respectively.[2]

The decomposition of formic acid over metal catalysts has been studied extensively by many investigators. Fahrenfort, van Reijen and Sachtler[3] studied the kinetic behaviour of the formate ion on a nickel surface and concluded that the decomposition of formic acid over a nickel catalyst proceeded *via* formate ion as a key intermediate. They correlated accordingly the activities of various metals for the decomposition of formic acid with the heat of formation of their formates which gave a "volcano-shaped" curve.

On the other hand, the examination of the kinetic behaviour of surface formate layers in more detail during the decomposition of formic acid over nickel catalyst has revealed that the reaction proceeds through two different mechanisms: a part of the overall reaction proceeds between formic acid molecule and the surface not covered by the formate ion, and that *via* the surface formate ion.[4] Consequently, it is of great interest to elucidate the reaction mechanism of the dehydrogenation reaction of formic acid over a silver catalyst which is a typical metal on the left-hand side of the "volcano-shaped" curve.

The mechanism of the decomposition of formic acid over reduced silver catalyst has been previously studied by means of the adsorption measurement

1) K. Tamaru, *Advances in Catalysis*, **15**, 65 (1964).

2) Y. Noto, K. Fukuda, T. Onishi and K. Tamaru, *Trans. Faraday Soc.*, **63**, 2300, 3072, 3081 (1967).

3) T. Fahrenfort, L. L. van Reijen and W. M. H. Sachtler, "The Mechanism of Heterogeneous Catalysis," ed. by J. H. de Boer, Elsevier, Amsterdam (1963), p. 23.

4) K. Fukuda, Y. Noto, T. Onishi and K. Tamaru, *Trans. Faraday Soc.*, **64**, 522 (1968).

during surface catalysis.[5] It has been accordingly suggested to be most probable that the decomposition rate of formic acid over the silver catalyst is proportional to the amount of formic acid adsorbed. In this study, the kinetic behavior of the adsorbed species on a silver catalyst was examined in more detail by using a silver catalyst having greater specific surface area, and the dependence of the rate of the overall reaction upon the concentration of chemisorbed species was determined.

Experimental

The apparatus employed was an ordinary closed circulating system similar to that previously described.[2] The amount of adsorbed species on the catalyst surface can be calculated from the amount of the reactant introduced into the system and the pressure and composition of the circulating gas. The adsorption of formic acid by apparatus was measured spearately and was taken into consideration in estimating the adsorption on the catalyst surface during the reaction. The circulating gas was analyzed by gas chromatography, where dioctyl sebacate and molecular sieve 13X were used in the separation columns: the former for formic acid, water and carbon dioxide, and the latter for carbon monoxide and hydrogen. The silver catalyst was prepared from silver nitrate according to the method adopted by Benton and Drake.[6] The catalyst was reduced for about 160 hr at 100—120°C with circulating hydrogen gas.

The surface area of the catalyst was 7×10^5 cm^2 (61 g), which was determined by the BET method by means of nitrogen adsorption at liquid nitrogen temperature.

Results

A typical result at 100°C is given in Fig. 1, where the amount of carbon dioxide evolved, the amount of adsorbed formic acid on the silver catalyst and the partial pressure of formic acid in the gas phase are plotted against the reaction time. The composition of the adsorbed species was the same as that of formic acid as is given in Fig. 2. (It does not always follow, however, that the adsorbed species is in the form of formic acid.) The decomposition of formic acid on the silver catalyst at 100°C was first order at lower pressures of formic acid, while at medium pressures it was zero order, the reaction rate being independent of the pressures of ambient formic acid; in the first region the amount of adsorbed formic acid was proportional to the pressure of formic acid and in the second region it was constant, independent of the pressure of formic acid in the ambient gas. The second region corresponds to "saturation" in an ordinary sense.

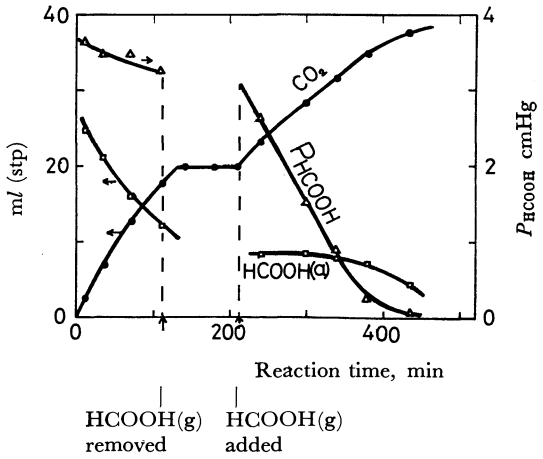

Fig. 1. Decomposition of formic acid on Ag at 100°C.

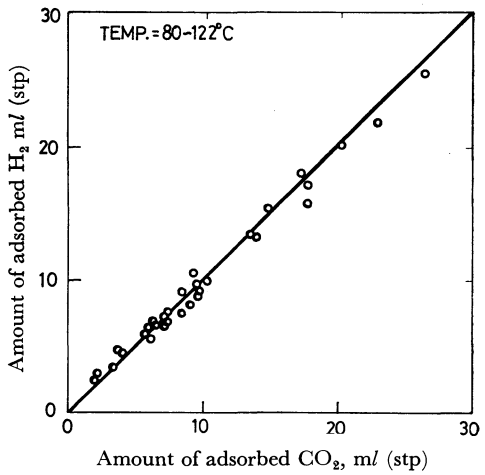

Fig. 2. Composition of adsorbed species on Ag.

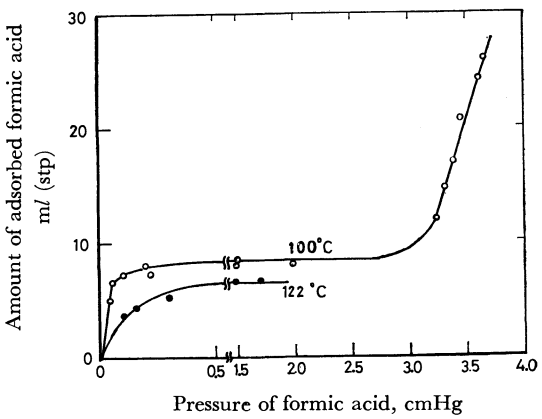

Fig. 3. Adsorption of formic acid during the decomposition on Ag.

5) K. Tamaru, *Trans. Faraday Soc.*, **55**, 824 (1959).
6) A. F. Benton and L. C. Drake, *J. Am. Chem. Soc.*, **54**, 2186 (1932).

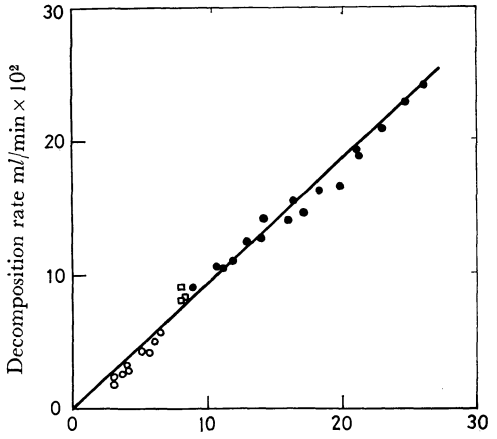

Fig. 4. Dependence of the reaction rate upon the amount of adsorbed formic acid at 100°C.

The dependence of the amount of formic acid adsorbed during the reaction upon the partial pressure of formic acid is given in Fig. 3, which shows that at lower temperatures the adsorption of formic acid reaches a "saturation" value at lower pressures, and increases again at higher pressures.

The dependence of the reaction rate upon the amount of adsorbed formic acid at 100°C is given in Fig. 4, which is obtained from three runs at 100°C. It is shown from Fig. 4 that the reaction rate is proportional to the amount of formic acid adsorbed. It should be noted here that the linear relation between the reaction rate and the amount of formic acid adsorbed during the reaction was observed over the whole range of the pressure of formic acid studied. Thus the reaction rate (r), $d(CO_2)/dt$, is expressed by the following equation;

$$r = kX_{ads.} \quad (1)$$

or

$$r = k\theta_{HCOOH} \quad (1')$$

where $X_{ads.}$ is the amount of adsorbed formic acid.

The zero order reaction rate at 80—122°C was divided by the corresponding saturation amounts of adsorbed formic acid to obtain the specific rate for the equal amount of adsorption at full coverages. The dependence of the calculated rates upon the reaction temperature gave an activation energy of 29.8 kcal/mol as shown in Fig. 5. The apparent frequency factor was 3.86×10^{15} min^{-1}. Thus the reaction rate was expressed by the following equation;

$$r = X_{ads.}(3.86 \times 10^{-15}) \exp(-29.8 \times 10^3/RT) \text{ ml/min}, \quad (2)$$

where $X_{ads.}$ is the amounts of adsorbed formic acid at zero-order kinetics at each temperature.

The exchange reaction of formic acid on the surface with that in the ambient gas was studied in the

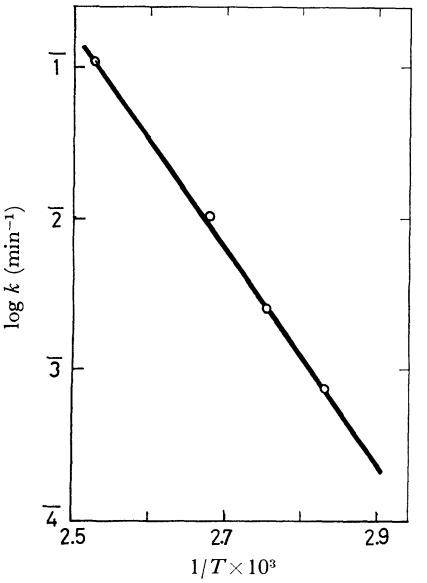

Fig. 5. Temperature dependence of the decomposition rate.

circulation system. In this experiment HCOOH was first introduced in the system and was decomposed at 100°C for a short time, then the gas phase was evacuated rapidly, the reaction vessel being cooled to about 10°C to prevent further decomposition and desorption of the formic acid remaining on the surface. Then DCOOD was introduced in the system and the change in D-content in the ambient formic acid molecule at 60°C was followed with time to study the exchange reaction. The procedure itself involved some ambiguity in its initial stage, but the exchange rate could be followed in such a manner. The ratio of HCOO/DCOO in the formic acid vapour was estimated by the infrared technique from the intensity of CH and CD stretching bands of adsorbed isotopic mixture of formic acid over fresh alumina.[2]

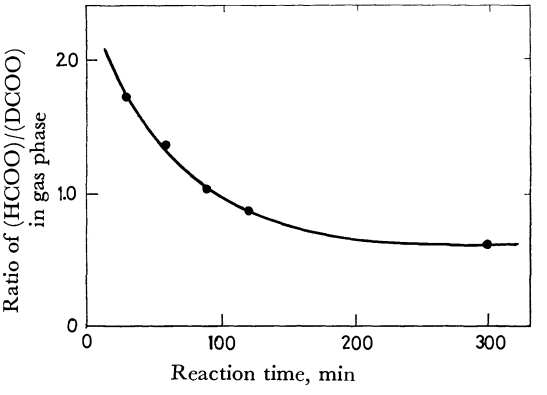

Fig. 6. Exchange reaction of surface formic acid on Ag with DCOOD at 60°C.

The exchange reaction proceeded at a comparatively slow rate as shown in Fig. 6. In this case the total amount of adsorbed formic acid was 14 m*l* (stp) at 60°C and the exchangeable formic acid on the surface was approximately estimated to be 13 m*l* (stp), which substantially corresponded to all the surface formic acid. All the formic acid in the adsorbed layer accordingly participated in the exchange reaction.

Discussion

The mechanism of the decomposition of formic acid over silver catalysts has been studied by many investigators. Otaki studied kinetic isotope effect in the decomposition of formic acid over a reduced silver catalyst.[7] He found the decomposition rate of various deuterium-substituted formic acid to be in the following decreasing order HCOOH$>$HCOOD$>$DCOOH. Schwab and Watson recently found the isotope effect in the decomposition of formic acid over a silver foil catalyst, where the order of the decomposition rate was HCOOH$>$HCOOD$>$DCOOH$>$DCOOD.[8]

Hirota, Kuwata and Asai studied the adsorption of formic acid on various metals by the infrared technique and reported that formate ion was detected on a silver surface.[9] From these observations they presumed that the primary step of the decomposition of formic acid over silver catalyst was the formation of surface formate which is subsequently followed by the processes as follows;

(1) $HCOO^-(ads.) + H^+(ads.) \rightarrow H_2 + CO_2$

(2) $2HCOO^-(ads.) \rightarrow H_2 + 2CO_2 + e$

(3) $HCOO^-(ads.) + HCOOH(ads.) \rightarrow H_2 + CO_2 + HCOO^-(ads.)$

(4) $HCOOH(ads.) \rightarrow H_2 + CO_2$

(5) $2H^+(ads.) + 2e \rightarrow H_2$

where each of these reactions was slow as compared with the formation of surface formate. Hirota and his coworkers suggested a possibility of participation of neutral formic acid molecule adsorbed on the catalyst surface.[10]

It was shown in Fig. 4 that the overall reaction rate is proportional to the total amount of adsorbed formic acid. It is accordingly concluded that a surface unimolecular reaction in terms of the adsorbed formic acid is the rate-determining step.

Block and Kral previously proposed a unimolecular mechanism for the decomposition of formic acid on a silver wire catalyst from their study on the kinetic isotope effects for various deutero-formic acids.[11] They assumed that the C–H and O–H bond in formic acid molecule cleaved at the same time in the rate-determining step, showing that the calculated kinetic isotope effects agreed with the experimental values fairly well. Eley and Leutic also proposed a unimolecular mechanism for the decomposition of formic acid on metal catalysts.[12,13] In those cases, however, any direct experimental basis for a unimolecular mechanism does not seem to be presented.

The results given in Fig. 4 and those of the exchange reaction, demonstrate that the formic acids adsorbed on the catalyst surface during the decomposition reaction behaves uniformly and the coverage of the silver surface by formic acid, which was directly measured during the decomposition, agrees with that of the active region in the surface which was estimated from the reaction kinetics, assuming that the reaction rate is proportional to the coverage of the active region. The characteristic dependences of both coverages upon pressure were quite similar as shown in Figs. 3 and 4, which strongly suggest that the coverage over the active region during the reaction agrees with that of the whole surface.

This conclusion is in marked contrast to that in the case of reduced copper catalyst obtained previously by one of the authors,[14] where the reaction rates were independent of the masured adsorption during the reaction, suggesting the heterogeneity of the adsorbed formic acid. Accordingly the adsorption measurements during surface catalysis may demonstrate the heterogeneity and/or homogeneity of the catalyst surface.

It is generally admitted that the following equation can be applied for the zero order reaction.[15]

$$\text{rate} = c_a(kT/h)\exp(-E/RT), \qquad (3)$$

where c_a is the number of adsorbed molecules on a unit surface area. Using this equation and the activation energy (E) of 29.8 kcal/mol which was obtained in this study, c_a becomes 1.8×10^{15} molecules per square centimetre at 100°C, while

7) T. Otaki, *Nippon Kagaku Zasshi* (*J. Chem. Soc. Japan, Pure Chem. Sect.*), **80**, 255 (1959).

8) G. H. Schwab and A. M. Watson, *Trans. Faraday Soc.*, **60**, 1833 (1964).

9) K. Hirota, K. Kuwata and A. Asai, *Nippon Kagaku Zasshi* (*J. Chem. Soc. Japan, Pure Chem. Sect.*), **80**, 701 (1959); *Z. Physik. Chem. N. F.*, **21**, 438 (1959).

10) K. Hirota, K. Kuwata, T. Otaki and A. Asai, Proc. 2nd. Internl. Congr. Catalysis, **1961**, 809 (Technip, Paris).

11) T. Block and H. Kral, *Z. Electrochem.*, **63**, 182 (1959).

12) D. D. Eley, *ibid.*, **60**, 797 (1956).

13) D. D. Eley and P. Leutic, *Trans. Faraday Soc.*, **53**, 1483 (1958).

14) K. Tamaru, *ibid.*, **55**, 1191 (1959).

15) S. Glasstone, K. J. Laidler and H. Eyring, "Theory of Rate Processes," McGraw-Hill Book, Co., Inc., N. Y. (1941), p. 376.

the saturation value of the adsorbed formic acid at 100°C is 3.1×10^{14} molecules per square centimetre. It suggests consequently that all of the adsorbed formic acid participates in the decomposition reaction, which is well compatiable with the results obtained from the kinetic studies.

It is of great interest that at pressures of formic acid higher than that in the "saturation" region the amount of adsorbed formic acid increases again linearly with the pressure of formic acid as shown in Fig. 3. In this region of adsorption the reaction rate was proportional to the total amount of adsorbed formic acid. This result also indicates that the adsorbed formic acids uniformly participate in the reaction over the whole range of the pressure of formic acid.

TABLE 1

Temperature °C	Number of surface silver atoms occupied by one molecule of adsorbed formic acid
80	1.7
90	2.1
100	4.4
122	5.2
134	7.2
142	8.7
160	10.8

The numbers of surface silver atoms occupied by one molecule of adsorbed formic acid at the saturation points at various temperatures are estimated from the number of surface silver atoms [1.30×10^{15} for (110) and (111) planes in average], and the amount of formic acid adsorbed at the zero-order kinetics, and are given in Table 1, where the values at 134, 142 and 160°C were obtained previously by one of the authors.[5]

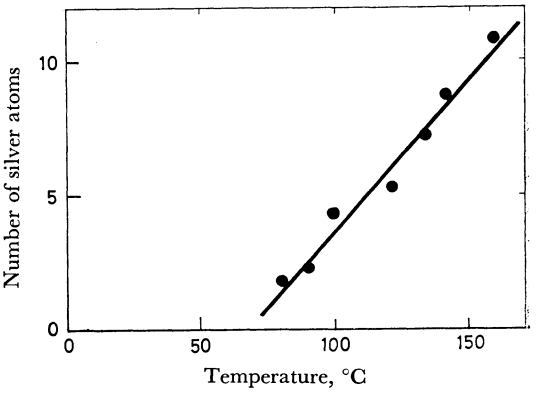

Fig. 7. Dependence of the number of silver atoms occupied by one molecule of absorbed formic acid upon temperature.

It is very interesting to note that the results in these experiments agrees reasonably well with those in the previous paper and the number of surface silver atoms occupied by one molecule of adsorbed formic acid increases linearly with temperature as shown in Fig. 7.

The area occupied by a surface formic acid at full coverage is seemingly determined by the range the surface molecule moves around at saturation, which expands with temperature.

BULLETIN OF THE CHEMICAL SOCIETY OF JAPAN VOL. 42 1197—1201 (1969)

Spectroscopic Studies on Radicals Produced from Acridine and Acridan in γ-Irradiated Rigid Solutions at −196°C

Tadamasa SHIDA and Akira KIRA

The Institute of Physical and Chemical Research, Yamatomachi, Kitaadachi-gun, Saitama

(Received August 9, 1968)

Dilute solutions of acridine in ethers and amines were frozen at −196°C to a glassy solid and were γ-irradiated. Electrons ejected by ionization are effectively scavenged by acridine to produce acridine anions which are the sole species having an electronic absorption band in the visible region. In alcohol and ester matrices the anion abstracts a proton from the matrix molecule even at −196°C and yields a semiquinone radical equivalent to the species formed by H-atom abstraction at the 9-position of acridan (dihydroacridine). Acridan in γ-irradiated butyl chloride matrix forms acridan cation which has a characteristic absorption band at 500—750 mμ. Detachment of a proton from the acridan cation produces another semiquinone radical identifiable with the species formed by H-atom abstraction at the 10-position of acridan. Both radicals have a similar yet clearly distinguishable absorption band in the visible region.

Flash photolytic studies on acridine and acridan systems have revealed that H-addition to acridine produces a C-radical (I) and that H-abstraction from acridan forms an N-radical (II).[1]

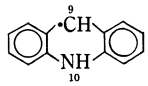

(I)

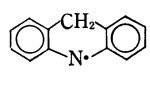

(II)

Since the spectral assignment of the N-radical in the previous work[1] was achieved by a process of elimination, it is desirable to get positive confirmation of the assignment by an independent method. Photolysis of rigid solutions at low temperatures often proves to be informative to the identification of reactive intermediates. Zanker *et al.* have shown that UV-illumination of alkylated acridans in alcoholic matrices at low temperatures yield radicals homologous to the N-radical shown above.[2]

Despite a seemingly prevailing preoccupation that γ-irradiation of organic systems leads to a chaotic mess, we have shown in a series of work[3] that γ-irradiation of rigid solutions at the liquid nitrogen temperature very frequently gives only a single species having absorption bands in the near UV through near infrared (IR) region. Applying the same radiation chemical technique we have studied acridine and acridan systems and obtained acridine anion and cation, acridan cation, the C- and N-radicals, each of which is produced exclusively from the others in a proper matrix.

Experimental

Preparations of acridine and acridan have been described in the previous paper.[1] The solvents, methyltetrahydrofuran (MTHF), diisopropyl ether, triethylamine (TEA), and *s*-butylamine were purified by vacuum distillation immediately after passing through an activated alumina column. Reagent grade *s*-butyl chloride (BuCl) and ethanol were used without further purification. Ethyl *n*-butyrate was distilled using a Vigreux column. All samples were degassed by freeze-thaw-reflux cycles, and sealed in a 1.5 mm Suprasil quartz cell which was irradiated with Co-60 γ-rays at −196°C.

A Cary 14R spectrometer and a quartz Dewar vessel with quartz windows were used for the optical measurement. Absorption spectra were obtained by plotting the difference of the absorption at the low temperature before and after irradiation.

Results

Pure MTHF forms a clear glass at −196°C which, upon γ-irradiation, yields a broad, intense absorption band with the $\lambda_{max} \cong 1.2\ \mu$. The band has been associated with the electron trapped by the matrix.[4] When 50 mM of acridine was present in the MTHF matrix, the band due to the solvent-trapped electron was replaced by a new absorption band in the visible region (Fig. 1). The spectrum

1) A. Kira and M. Koizumi, This Bulletin, **42**, 625 (1969).

2) V. Zanker, E. Erhardt and H. H. Mantsch, *Z. phys. Chem. N. F.*, **58**, 1 (1968).

3) T. Shida, *J. Phys. Chem.*, **72**, 2597 (1968).

4) P. J. Dyne and O. A. Miller, *Can. J. Chem.*, **43**, 2696 (1965).

agrees well with the reported spectrum of acridine anion which had been produced by the treatment of acridine with alkali metals.[5] Besides MTHF, glassy matrices of *s*-butylamine and diisopropyl ether, when doped with acridine, also gave a spectrum almost identical with that shown in Fig. 1.

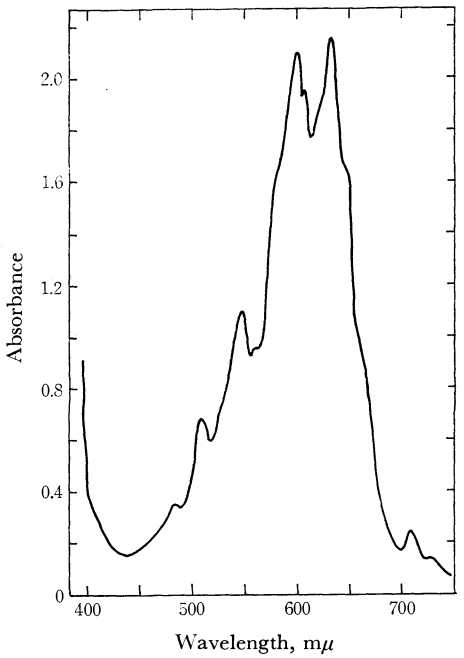

Fig. 1. Absorption spectrum of acridine anion. Acridine (50 mM) in MTHF glass γ-irradiated to the dose of 3.8×10^{19} eV/m*l*.

In contrast with ethers and amines, matrices of alcohols or esters did not yield the band of acridine anion or the band of solvent-trapped electrons; instead, a new spectrum similar to that of the C-radical in our previous paper[1] was obtained (Fig. 2). In Fig. 2 the result of acridine-ethanol system is shown. Acridine in glassy ethyl-*n*-butyrate also gave a similar spectrum.

Unlike acridine, acridan in MTHF did not affect appreciably the IR band due to the trapped electron nor did any new absorption band appear in the accessible spectral region. Apparently acridan does not scavenge electrons to form the anion. On the other hand, both acridine and acridan in BuCl matrix produced a new absorption band characteristic of the solutes (Fig. 3 and curve 1 of Fig. 4). When the irradiated acridan-BuCl solid was slightly warmed (*ca.* -170°C), the color of the sample changed from blue to purplish pink. Curve 2 of Fig. 4 demonstrates the spectrum of the pink solid measured at -196°C.

5) S. Niizuma, M. Okuda and M. Koizumi, This Bulletin, **41**, 795 (1968).

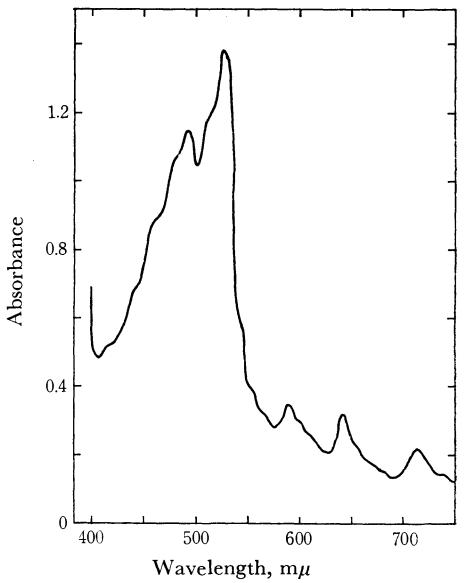

Fig. 2. Absorption spectrum of the C-radical. Acridine (50 mM) in ethanol galss γ-irradiated to the dose of 3.8×10^{19} eV/m*l*.

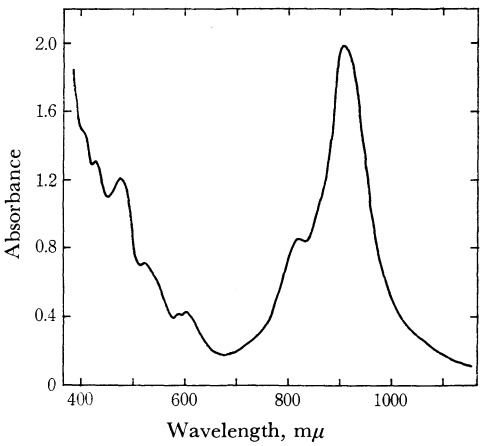

Fig. 3. Absorption spectrum of acridine cation. Acridine (50 mM) in *s*-BuCl glass γ-irradiated to the dose of 9.3×10^{19} eV/m*l*.

The spectrum of irradiated acridan in TEA matrix resembles that of the sample in curve 2 of Fig. 4. The intensity of the spectrum was markedly enhanced by the addition of a small amount of alkyl chloride, the band shape being unaltered. Curve 1 of Fig. 5 shows the spectrum in the presence of 0.1M BuCl. The curve changed to curve 4 when the sample was cautiously warmed to about -170°C. The latter spectrum is practically the same as the spectrum shown in Fig. 2. Curves 2 and 3 of Fig. 5 which are the components of curve 1 will be explained later in the discussion.

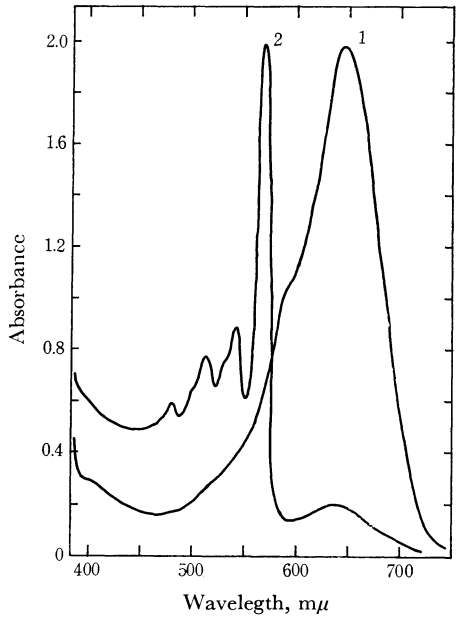

Fig. 4. Absorption spectra of acridan cation (curve 1) and the N-radical (curve 2).
Curve 1: acridan (25 mM) in *s*-BuCl glass γ-irradiated to the dose of 2.9×10^{19} eV/m*l*.
Curve 2: preceding sample after warming to *ca.* −170°C (the spectrum was recorded at −196°C).

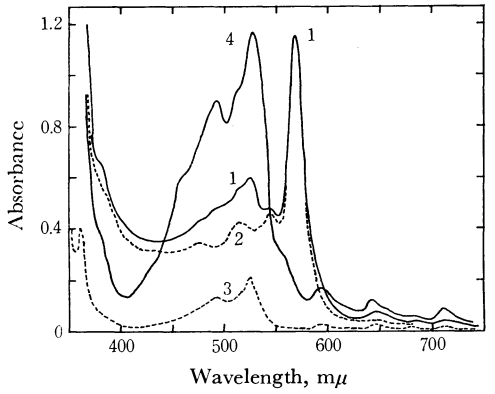

Fig. 5. Absorption spectra of the C- and N-radicals. Curve 1; acridan (50 mM) plus *s*-BuCl (100 mM) in TEA glass γ-irradiated to the dose of 9.3×10^{19} eV/m*l*. Curve 1 is divisible into two components, curves 2 and 3 where curve 2 matches with the spectrum of the N-radical shown in Fig. 4 and curve 3 is comparable with the spectrum of the C-radical in Fig. 2. Curve 4; preceding sample giving curve 1 after warming to *ca.* −170°C (the spectrum was recorded at −196°C).

Discussion

Electronic Absorption Spectra. In the low temperature rigid solution, events ensuing from ionization of the matrix molecule which is the major component of the system are "frozen" so that observation can be made at leisure. Electrons and positive holes are stabilized as intermediate products of reactions with solutes or matrix molecules. The metastable species thus formed often have strong absorption in the UV through near IR region. A proper choice of matrix enables us to produce a single species which is solely responsible for the absorption in the visible and near IR regions. Criteria for the choice have been expounded in previous papers.[3,6] A brief summary would be conducive to the following discussion; mass spectroscopic studies indicate that the parent ion of ethers, amines, alcohols and esters performs an efficient proton transfer reaction,

$$RH^+ + RH \rightarrow R\cdot + RH_2^+ \qquad (1)$$

Therefore when these substances are used as an isolating matrix for a small amount of solutes, ionization induced in the matrix molecule should result in reaction (1) while the detached electron migrates in the matrix to produce a solute anion. A typical example of this type of matrix is MTHF. Since the products of reaction (1) for MTHF do not absorb in the visible region, any absorption in the spectral region should be attributed to products of the reaction of electron with solute. Appearance of a new band in the acridine-MTHF system identifiable with acridine anion (Fig. 1) is thus accounted for in terms of electron attachment to the solute acridine.

Solute anions produced in alcoholic matrices often undergo further change by a proton addition,[7]

$$S^- + ROH \rightarrow \cdot SH + RO^- \qquad (2)$$

Acridine as the solute would yield a semiquinone radical by reaction (2). Since the band appearing in acridine-ethanol system (Fig. 2) resembles closely that of the C-radical proposed in a previous paper,[1] we regard that reaction (2) holds good for this system also. Since the electron in the acridine anion would most plausibly be populated at the nitrogen atom,[8] the alcoholic proton must have been bridged to the nitrogen of the anion before it is incorporated into the acridine ring. Thus the C-radical and not the N-radical should be favorably formed. Besides alcohols, glass-forming esters, when used as a matrix for acridine, gave the C-radical. For this system reaction (3) will take over reaction (2) to give the same radical,

$$S^- + RCH_2COOR \rightarrow \cdot SH + RCHCOOR^- \qquad (3)$$

6) T. Shida and W. H. Hamill, *J. Chem. Phys.*, **44**, 4372 (1966).
7) T. Shida and W. H. Hamill, *J. Am. Chem. Soc.*, **88**, 3689 (1966).
8) A quantitative study on the electronic state of acridine anion is currently being carried out by us.

The formation of the carbanion is assumed in numerous organic reactions.

In contrast with the matrices so far discussed, the matrix of alkyl halides provides cationic species of solute molecules.[3] This is because the electron ejected from matrix molecules is scavenged by another matrix molecule and cannot reach a solute molecule in the distance. Meanwhile the positive hole in the matrix is found to migrate quickly to the solute molecule.[3] Processes in the butyl chloride matrix will be summarized as follows,

$$BuCl \xrightarrow{\gamma} (BuCl^+)_{mobile} + e^- \quad (4)$$

$$e^- + BuCl \rightarrow Bu\cdot + Cl^- \quad (5)$$

$$(BuCl^+)_{mobile} + S \rightarrow BuCl + S^+ \quad (6)$$

Decisive evidence for reaction (5) has been obtained by ESR studies.[9] In the absence of solute S migrating holes are eventually trapped by the matrix itself giving rise to the band of the trapped hole at about 400—600 mμ.[6] The band was eliminated when acridine or acridan was present in the chloride matrix and the new bands shown in Figs. 3 and 4 appeared which is accomodated to the above scheme with the assignment of the newly appearing bands to the respective solute cations. It is noted that the spectrum of acridan cation is very much like the spectrum of diphenylamine cation,[10] and is also comparable with the spectrum of alkylated acridan cations studied by Zanker *et al.*[2] Spectral change from curve 1 to 2 in Fig. 4 is explained as follows; upon softening the sample the chloride ion produced by reaction (5) will diffuse to the acridan cation in which the positive charge would be mainly localized at the nitrogen atom. Abstraction of the proton attached to the nitrogen by chloride ion will produce the N-radical,

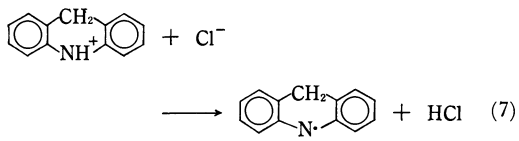

(7)

Similarity of curve 2 with both the spectra of N-radicals of alkylated acridans[2] and the spectrum of N-radical in our previous paper[1] gives credence to the previous assignment.

The formation of the N-radical was also noticed in another system. As mentioned before alkyl amines (primary and secondary) are subject to reaction (1) and are therefore used as a matrix to obtain solute anions. In tertiary amines such as TEA, however, it was found that the positive hole can migrate to some extent apparently because of the lack of protonation reaction (1).[11] Since acridan is expected to have a lower ionization potential than that of TEA,[12,13] acridan in TEA might produce acridan cation by accepting the migrating positive hole. Contrary to expectation, the spectrum obtained is very similar to that of the N-radical (curve 1 of Fig. 5). The enhancement of the signal by the addition of electron scavenger (100 mM of BuCl) suggests that the precursor of the N-radical is cationic. For the result the following scheme is proposed,

$$TEA \xrightarrow{\gamma} (TEA^+)_{mobile} + e^- \quad (8)$$

$$e^- + BuCl \longrightarrow Bu\cdot + Cl^- \quad (9)$$

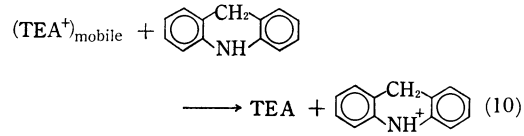

(10)

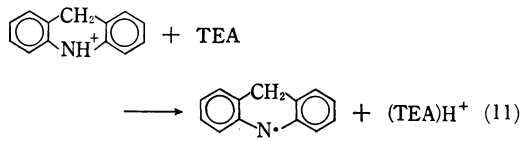

(11)

That is, although the acridan cation is once formed by reactions (8) and (10), the proton of the cation will be transferred to TEA on account of the high basicity of the amine. The spectral change from curve 1 to 4 in Fig. 5 indicates the transformation of the N-radical to the C-radical in the soft medium. In such a relaxed matrix the N-radical will be able to diffuse. On encountering an acridan molecule the radical may induce the following substitution reaction,

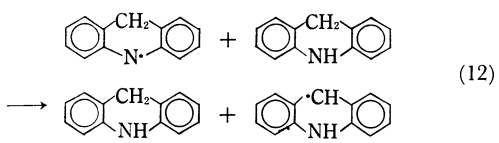

(12)

Careful comparison of curve 1 of Fig. 5 with the spectrum of the N-radical (curve 2 of Fig. 4) and of the C-radical (Fig. 2) shows that the curve in Fig. 5 comprises a small contribution of the C-

9) D. W. Skelly, R. G. Hayes and W. H. Hamill, *J. Chem. Phys.*, **43**, 2795 (1965).

10) T. Shida and W. H. Hamill, *ibid.*, **44**, 2369 (1966).

11) T. Shida and W. H. Hamill, *J. Phys. Chem.*, **72**, 723 (1968).

12) K. Watanabe, T. Nakayama and J. Mottl, *J. Quant. Spectry. Radiative Transfer*, **2**, 369 (1962).

13) A. Terenin and F. Vilessov, "Advances in Photochemistry," Vol. 2, Interscience Publishers, N. Y. (1964), p. 406.

radical. The broken curves in Fig. 5 illustrate that curve 1 is divisible into the two components. At present it is not known whether the concomitant C-radical is formed by reaction (13) which competes with reaction (11),

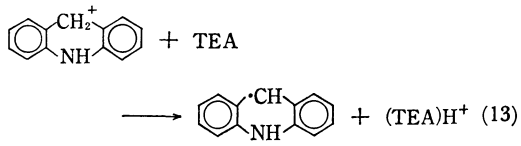

or it is subsequently formed from the N-radical by reaction (12) as a result of possible local softening of the matrix upon the formation of N-radical. The notation for acridan cation in reaction (13) implies that a fraction of positive charge may reside in the carbon atom at the 9-position.

Although conformational data are not available for the acridan molecule, most probably it has a bent form. The extraordinarily sharp peaks and well-structured spectrum of the N-radical suggest that the radical is planar or near-planar[14] and the equilibrium nuclear distances of the radical do not appreciably change upon the electronic excitation corresponding to the visible band.[14,15]

The authors wish to thank Professor Masao Koizumi for his pertinent comment on the mechanism of radical transformation (*cf.* reaction (12) in the text) and for reading the manuscript.

14) H. Suzuki, "Electronic Absorption Spectra and Geometry of Organic Molecules," Academic Press, N. Y. (1967), p. 339.

15) L. Salem, "The Molecular Orbital Theory of Conjugated Systems," W. A. Benjamin, Inc., N. Y. (1966), p. 351.

BULLETIN OF THE CHEMICAL SOCIETY OF JAPAN VOL. 42 1201—1205 (1969)

The Micellar Properties of Disodium Monoalkyl Phosphates in Aqueous Solutions

Takashi TAHARA, Iwao SATAKE and Ryohei MATUURA

Department of Chemistry, Faculty of Science, Kyushu University, Hakozaki, Fukuoka

(Received August 15, 1968)

The disodium monoalkyl phosphate with *n*-dodecyl, *n*-tetradecyl and *n*-hexadecyl radical was synthesized, and pNa and light scattering studies were performed on the micellar properties of these surfactants in aqueous solutions. The critical micelle concentrations (CMC) of these salt solutions were confirmed to be considerably higher than those of ordinary 1–1 type ionic surfactants with the same alkyl chain length. The degree of dissociation of the micelle was, however, found to be not so different from that of corresponding sodium alkyl sulfate. The fact that these salts have comparatively large aggregation number reflects one of the characteristic features of alkyl phosphate anion which has two dissociable groups.

The detailed surface chemical studies of various ionic surfactant solutions have led to the realization that the micellar properties, such as critical micelle concentration, aggregation number and the degree of dissociation of the micelle, depend on the structure of constituent detergent molecule, *e. g.*, on the valency of counter ion and on the number of ionic groups at the end of the hydrocarbon chain.

The studies with the ionic surfactants which have two dissociable groups were performed by Shinoda,[1] who determined the CMC's of potassium alkyl malonates, $RCH(COOK)_2$, and confirmed that they are much higher than those of corresponding fatty acid soaps.

The elevation of the CMC is also anticipated to be the case with the monoalkyl phosphate detergents. However, in spite of their wide industrial applications, the available informations on the basic surface chemical properties of purified alkyl phosphate detergents are extremely scanty, since the purification procedures of the reaction mixture are rather complicated. So far as we know, the only available data were presented by Cooper,[2] who synthesized the mono- and disodium alkyl phosphates with various chain length and determined the CMC's of their aqueous solutions on the basis of surface tension measurements.

1) K. Shinoda, *J. Phys. Chem.*, **59**, 432 (1955).

2) R. S. Cooper, *J. Am. Oil Chemists' Soc.*, **40**, 642 (1963).

It is, thus, desirable to investigate the micellar properties of alkyl phosphate detergents in order to make clear their characteristics which will in turn contribute to the general understanding of common features of ionic surfactants.

The present work concerns the preparation and the determination of CMC and other related micellar properties of disodium monoalkyl phosphates with alkyl chain length from n-C_{12} to n-C_{16}.

Experimental

Materials. The monoalkyl phosphoric acids {RH_2PO_4; here, R=dodecyl, tetradecyl and hexadecyl radical} were synthesized from the purified alkyl alcohols and pyrophosphoric acid by violent stirring in absolute benzene for 100 hr at 25°C.[3]

$$\begin{aligned} R\text{–}OH + H_4P_2O_7 &\rightarrow RH_2PO_4 + H_3PO_4 \\ &\rightarrow RH_3P_2O_7 + H_2O, \\ R\text{–}OH + RH_3P_2O_7 &\rightarrow R_2HPO_4 + H_3PO_4 \\ &\rightarrow R_2H_2P_2O_7 + H_2O, \ etc. \end{aligned}$$

The reaction mixture was dissolved in ether and washed twice with water to remove residual inorganic acids. The crude monoalkyl phosphoric acid in oil phase was then treated with an aqueous solution of sodium hydroxide (pH=12) to extract the water soluble disodium monoalkyl phosphate into aqueous phase. By the addition of hydrochloric acid to the aqueous phase obtained above until the pH of the solution was lowered to about 0.5, alkyl phosphoric acids were precipitated. Then the monoalkyl phosphoric acid was selectively extracted into ether at pH 0.5, since the solubility of alkyl phosphoric acids in ether is known to be in the decreasing order of mono-, di- and trialkyl substitute.[4] The purity of the monoalkyl phosphoric acid was improved by repeating above processes until a thin layer chromatographical test gave 1 spot of monoalkyl phosphoric acid.

The test plate used in the thin layer chromatography was made of silica gel mixed with 0.5N oxalic acid solution in the ratio of 7 to 10. For the purpose of activation, the plate was first heated for 1 hr at 80°C. The subsequent development was carried out by using the mixed solvent which contains five parts of benzene and one part of methanol. We used 5% ethanol solution of molybdatophosphoric acid for the detection. The value of R_f was found to be in the order of mono-$>$di-$>$ trialkyl substitute.

The evaporation of the ether solution *in vacuo* yielded white waxy solid of monoalkyl phosphoric acid. It was then recrystallized several times from hot n-hexane until the white crystalline monoalkyl ester could be obtained. The purity of the product was confirmed by elementary analysis, mp measurement and pH titration with sodium hydroxide.

The disodium monoalkyl phosphate was easily obtained by the neutralization to pH 12 with NaOH solution and the subsequent dehydration process by the successive extraction with acetone. In order to remove surface active impurities, the sodium salts were extracted with ether for 50 hr, and then dried *in vacuo* over phosphorus pentoxide. The final products are white crystalline compounds which have hygroscopicity. It was, however, confirmed by means of thermogravimetric and elementary analysis that these salts have no water of crystallization.

Apparatus and Method. The method used in the present experiment for measuring the counter ion activity in the solution was exactly the same as the technique previously used to study the solutions of sodium alkyl sulfates.[5] That is, we used a Horiba pNa meter model N-5 with the sodium sensitive glass electrode, making a cell as follows:

Na glass electrode | Detergent solution | N NH_4NO_3 | 3.33N KCl agar bridge | Calomel electrode

We used the mean activity of sodium chloride presented by Janz and Gordon[6] for calibrating the apparatus. The experimental reproducibility of the sodium ion activity was found to be within ± 0.005 pNa unit. The measurements were conducted at 35 and 45°C for C_{12} and C_{14} salts, and at 45°C for C_{16} salt, in order to prevent the formation of the precipitation of ammonium alkyl phosphate at the liquid junction.

The conductivity measurements were performed by using Yanagimoto conductivity outfit model MY-7 at the same temperature as above.

A Shimadzu photoelectric light scattering photometer model PG-21 was used for estimating the micellar molecular weights of the detergents in solution. The measurements were carried out at 436 mμ with a semi-octagonal cell. The concentration dependence of the refractive indices was estimated by a Shimadzu differential refractometer at the same wavelength. The temperature of the cell was controlled at about 48°C.

Results and Discussion

Figure 1 shows the typical plots of the logarithm of sodium ion activity *vs.* the logarithm of the molar concentration of disodium dodecyl phosphate at 35 and 45°C, and of hexadecyl phosphate at 45°C, respectively. As is clearly shown in this figure, a sharp break occurs at the CMC of each detergent. The values of CMC determined from the break points in Fig. 1 are given in Table 1, together with those obtained from the specific conductivity (κ) *vs.* concentration plots. The differences between them are found to be within an experimental error. The observed values of CMC for disodium monoalkyl phosphates are considerably higher than those of 1–1 type ionic surfactants with the same alkyl

3) K. Nelson and A. D. F. Toy, *Inorg. Chem.*, **2**, 775 (1963).

4) N. L. Gershfeld, *J. Phys. Chem.*, **66**, 1923 (1962).

5) I. Satake, T. Tahara and R. Matuura, This Bulletin, **42**, 319 (1969).

6) G. J. Janz and A. R. Gordon, *J. Am. Chem. Soc.*, **65**, 218 (1943).

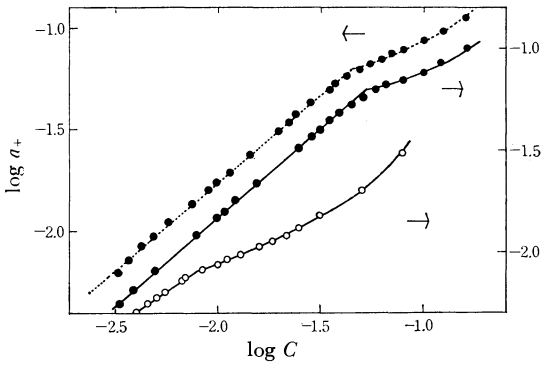

Fig. 1. The plots of log a_+ *vs.* log C for C_{12} and C_{16} salts.
●: C_{12} salt, ○: C_{16} salt, —: at 45°C, ···: at 35°C

TABLE 1. THE pNa DATA OBTAINED FOR DISODIUM MONOALKYL PHOSPHATES

Detergent	Temp. (°C)	CMC (mol/l) pNa	CMC (mol/l) κ	α	γ_+
C_{12}	35	4.46×10^{-2}	4.43×10^{-2}	0.33	0.68
	45	5.12×10^{-2}	4.92×10^{-2}	0.35	0.52
C_{14}	35	1.65×10^{-2}	1.59×10^{-2}	0.29	0.62
	45	1.84×10^{-2}	1.84×10^{-2}	0.30	0.53
C_{16}	45	7.59×10^{-3}	7.00×10^{-3}	0.28	0.54

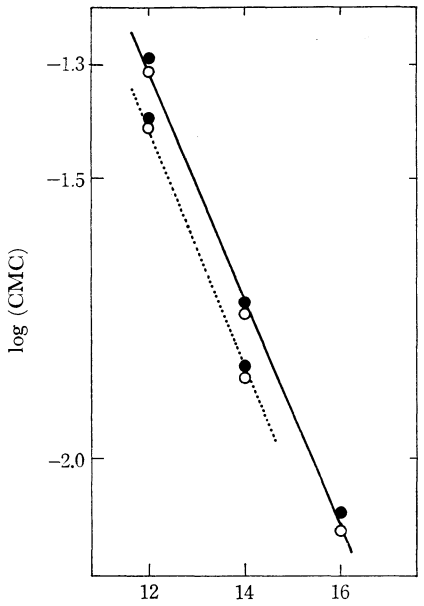

Fig. 2. The relation between log CMC and m.
●: determined from pNa data, ○: determined from conductivity data, ···: at 35°C, —: at 45°C.

chain length, suggesting the significant contribution of increased electrical repulsion between bivalent head groups to the micelle formation. The value of CMC obtained for C_{16} salt is in good agreement with that reported by Cooper.[2] A comparison of the values for C_{12} and C_{14} salts is, however, rather difficult since no exact values for these salts are given in his paper. As would be expected, the CMC's of disodium monoalkyl phosphates are nearly identical with those of potassium alkyl malonates.[1]

As is the case with ordinary 1-1 type ionic surfactants, there is a linear relationship between log CMC and the number of carbon atoms (m) in the alkyl chain. Figure 2 shows the relation between log CMC and m in the disodium monoalkyl phosphates. The slope of the straight line is determined as −0.21 at 45°C, which is considerably large compared with the value of −0.29—−0.30 observed for various types of 1-1 type surfactants.[7]

According to the theory of micelle formation of ionic surfactants,[7] the slope of the log CMC *vs.* m plot may be given as

$$\mathrm{d}\log \mathrm{CMC}/\mathrm{d}m = -\omega/2.303kT(1+iK). \quad (1)$$

Here, i is the number of ionic groups in the alkyl chain, ω the cohesive energy change transferring one methylene group from a hydrocarbon environment to an aqueous medium and K the experimental canstant for the particular surface active agent which has a meaning similar to the degree of dissociation of the micelle (α). It is thus anticipated from Eq. (1), that the values of K (or α) for the present detergents are not so different from those of 1-1 type surfactants, *e. g.*, of sodium alkyl sulfates.

The degree of dissociation of the micelle may be evaluated from the concentration dependence of the counter ion activity by using the convenient method derived by Botré *et al.*[8] and applied for various systems by subsequent authors.[9]

If we assume that the concentration of singly dispersed detergent anion is constant (C_0) over the concentration range above CMC, the sodium ion activity can be written as

$$a_+ = 2\gamma_{\pm\mathrm{app}}C = 2\gamma_+\{C_0+\alpha(C-C_0)\} \quad (2)$$

or

$$\gamma_{\mathrm{app}} = \alpha\gamma_+ + \gamma_+(1-\alpha)C_0/C, \quad (3)$$

where, C is the total analytical concentration of the detergent in mol/l, γ_{app} the apparent ionic

7) K. Shinoda, T. Nakagawa, B. Tamamushi and T. Isemura, "Colloidal Surfactants," Chap. 1, Academic Press, New York, N.Y. (1963).

8) C. Botré, V. L. Crescenzi and A. Mele, *J. Phys. Chem.*, **63**, 650 (1959).

9) L. Shedlovsky, C. W. Jakob and M. B. Epstein, *ibid.*, **67**, 2075 (1963); M. E. Feinstein and H. L. Rosano, *J. Colloid and Interface Sci.*, **24**, 73 (1967); P. Stenius and P. Ekwall, *Acta Chem. Scand.*, **21**, 1643 (1967).

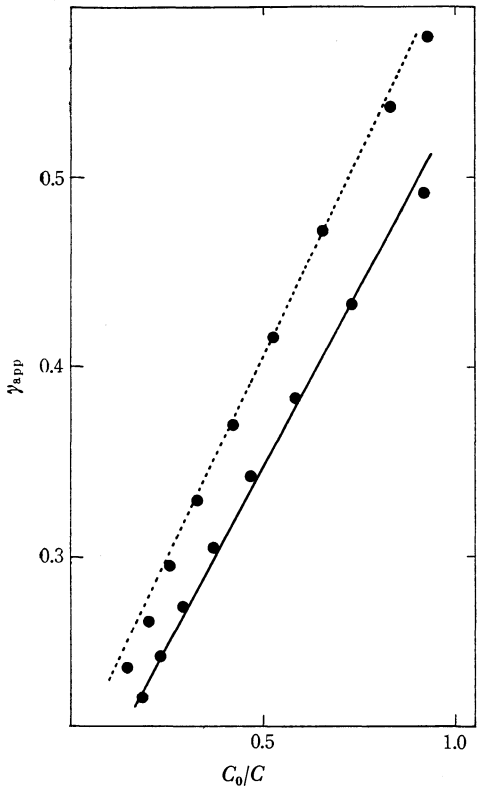

Fig. 3. The plots of γ_{app} *vs.* C_0/C for C_{14} salt at 35 (------) and 45°C (——).

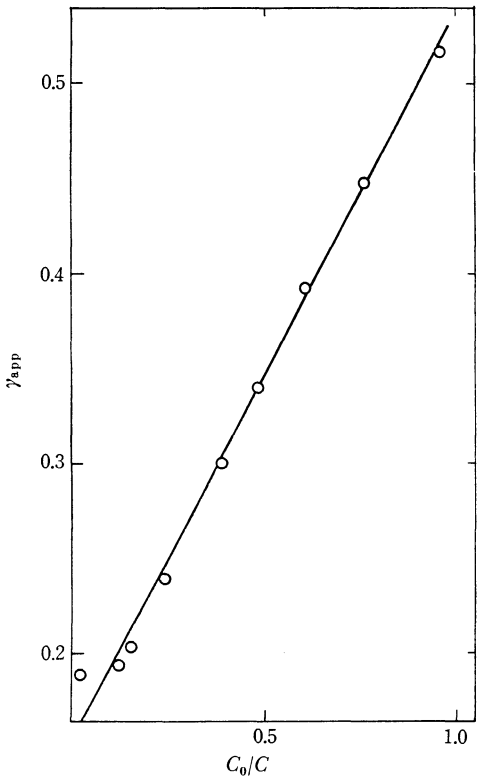

Fig. 4. The plot of γ_{app} *vs.* C_0/C for C_{16} salt at 45°C.

activity coefficient of sodium ion defined by $a_+/2C$, γ_+ the ionic activity coefficient of the sodium ion and α the degree of the dissociation of the micelle. A theoretical consideration on Eq. (3) based on lamellar micelle model was given in our previous work.[5] Equation (3) suggests that γ_{app} will vary linearly with C_0/C throughout the concentration range in which both γ_+ and α are assumed to be constant. This is the case for present experimental results. As is shown in Figs. 3 and 4, γ_{app} *vs.* C_0/C plots give straight lines over whole concentration range studied. The values of α and γ_+ estimated from the intercept and slope of γ_{app} *vs.* C_0/C plots are summarized in Table 1. In the previous pNa study with the sodium alkyl sulfates,[5] the degree of dissociation of the micelle was determined to be 0.28 for sodium dodecyl sulfate and 0.24 for sodium tetradecyl sulfate, both at 35°C. Although the values of α obtained for disodium monoalkyl phosphates are slightly larger than those of sodium alkyl sulfates it, seems reasonable to consider that the degree of dissociation of the micelle is almost unaffected by the number of ionizable groups so far as the other structural constitutions are the same.

In a crude picture of micellar solution, the activity coefficient of sodium ion may be expected to be characterized by the ionic strength of the solution. It is, therefore interesting to note that the constant

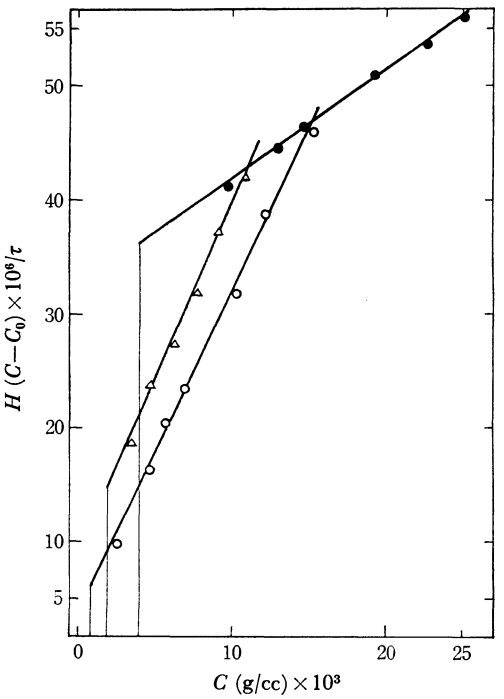

Fig. 5. $H(C-C_0)/\tau$ *vs.* C curves for disodium monoalkyl phosphates in NaCl solution at 48°C.
●: C_{12} salt, △: C_{14} salt, ○: C_{16} salt

value of γ_+ obtained for C_{14} salt at 35°C is considerably small as compared with the value of 0.83 for sodium dodecyl sulfate having the similar CMC at the same temperature. Since no difference is found between the values of α, this depression must be ascribed to the existence of more highly charged polyions in disodium tetradecyl phosphate solution than in sodium dodecyl sulfate solution. This means that the micellar aggregation number of the tetradecyl phosphate micelle is much larger than that of sodium dodecyl sulfate.

In Fig. 5 are given the scattering data for disodium monoalkyl phosphates in sodium chloride solution. The values of CMC in salt solutions were determined from turbidity curves. The micellar molecular weights estimated from the intercept at CMC are summarized in Table 2.

Table 2. The micellar molecular weights of disodium monoalkyl phosphates determined from light scattering experiment

Detergent	Solvent	CMC (mol/l)	MMW	AN
C_{12}	0.5N NaCl	1.25×10^{-2}	27800	90
C_{14}	0.2N NaCl	4.2×10^{-3}	70400	207
C_{16}	0.08N NaCl	1.73×10^{-3}	156200	426

MMW: Micellar molecular weight
AN: Aggregation number

In accordance with the consideration on the sodium ion activity coefficients above CMC, the aggregation number of 207 obtained for C_{14} salt is about twice as large as that of 101 for sodium dodecyl sulfate,[10] both in 0.2N NaCl solution. This result indicates an interesting feature of disodium monoalkyl phosphates that their micellar aggregation number is considerably large compared with that of 1-1 type surfactant which has the comparable order of CMC. It is, however, rather difficult to compare the obtained aggregation number for the present detergents with that of 1-1 type surfactants which have the same chain length, since they are found to increase with increasing concentration of added salt.[10,11]

In view of the acidic character of the phosphate radical, these detergents may be considered to be hydrolyzed in water, giving rise to the minimum in surface tension *vs.* concentration curve. It was, in fact, observed in the present experiment that the surface tension *vs.* concentration curves for these salt solutions showed a pronounced minimum. However, the fact that the minimum could be reduced with the addition of sodium chloride, explains well the hydrolyzing nature of these salts in solutions. From the pH measurements on these salt solutions, the degree of hydrolysis was estimated to be 0.12% in 0.1 mol/l, 0.14% in 5×10^{-2} mol/l and 0.55% in 1.1×10^{-2} mol/l for C_{12} salt, and 0.37% in 0.1 mol/l and 0.60% in 1.5×10^{-2} mol/l for C_{16} salt, both at 45°C, respectively. Since the values of the degree of hydrolysis of the alkyl phosphate anion are negligibly small, the effect of hydrolysis products on the bulk properties is not taken into account in this paper.

10) K. J. Mysels and L. H. Princen, *J. Phys. Chem.*, **63**, 1696 (1959).
11) D. Stigter and K. J. Mysels, *ibid.*, **59**, 45 (1955).

BULLETIN OF THE CHEMICAL SOCIETY OF JAPAN VOL. 42 1206—1212 (1969)

The Effects of Organic Additives on the Solubilities and CMC's of Potassium Alkyl Sulfates in Water. I. The Effects of Several Hydroxy Compounds

Keishiro SHIRAHAMA,* Makoto HAYASHI** and Ryohei MATUURA***

* *Department of Chemistry, Faculty of Science and Engineering, Saga University, Honjo-machi, Saga*

** *College of Foreign Students, Chiba University, Yayoi-cho, Chiba*

*** *Department of Chemistry, Faculty of Science, Kyushu University, Hakozaki, Fukuoka*

(Received August 17, 1968)

The solubilities and critical micelle concentrations (CMC) of potassium dodecyl sulfate (KDS) and hexadecyl sulfate (KHS) were measured in methanol-, ethanol-, 1-propanol-, ethylene glycol-, 1,2-propanediol-, and glycerol-water mixed solvents over the temperature range from 0 to 40°C. It was found that the higher the hydroxy group density in the solvent, the less the effects on both the solubility and the CMC, and that the presence of an alkyl group in the solvent causes a greater temperature-dependence in the solubility. The solvent effects on the CMC and on the single-ion dispersion were discussed separately. An effect of a net-work structure formed between the hydroxy compound and water on the solubility is suggested. Solvent effects on the alkyl group and the ionic group of a surfactant molecule were separated by considering the difference between the standard free-energy change for the solution process of KHS and that of KDS. The effects on the Krafft point were also discussed in term of the above suggestions.

There are many factors that govern the monomer-micelle equilibrium in the surfactant solution. The solvent effects on the CMC have been studied by many investigators; some additives raise the CMC,[1,5] while others lower it.[2,5] However, no definite conclusion has ever been drawn. These phenomena are considered to be closely related to the structure of water.[3–5] In order to make clear how the addition of an organic substance affects the solution behavior of the micelle and the single ion, which are equilibriated with each other in micellar solution, it was necessary to measure the CMC and the single-ion solubility (not equilibriated with the micelle) of the surfactant in various organic solvent–water mixtures over a wide range of temperature. The potassium alkyl sulfates used in the present work are suitable for determining the solubility and CMC separately, near room temperature, as their Krafft points are about 20°C higher than those of the sodium salt analogs, typical anionic surfactants, the micellar properties of which have been well studied.

In the present paper, we will describe the effects of added hydroxy compounds on the solution properties of the surfactant.

Experimental

Materials. The potassium alkyl sulfates were synthesized by the sulfation of the corresponding long-chain alcohols with concentrated sulfuric acid, followed by neutralization with potassium hydroxide. The crude alkyl sulfates were extracted by butanol, recrystallized from butanol and from water three times each and finally washed with ether in Soxhlet's extractor. The methanol was simply distilled. The ethanol and 1-propanol were refluxed over dried calcium oxide for hours and then distilled. The glycols were distilled under reduced pressure. Glycerol of a G.R. grade was used without further purification.

Measurements of Solubility and CMC. By using an electric conductivity meter outfit, Model CM-1 DB, of the Towa Dempa Kogyo Co., Ltd., solubility and CMC measurements were made with KDS. As the solubilities of KHS were too low to be determined by the electric conductivity method, colorimetry was employed: The supernatant of the saturated solution (a long time was necessary to reach an equilibrium, so the surfactant solution in the presence of the solid phase was shaken mechanically for more than 50 hr and then left to stand for 12 hr in a thermostat) was pipetted through a 4G sintered-glass filter and then extracted as a methylene blue-alkyl sulfate complex into a chloroform phase.[6] The optical density of the blue-colored

1) P. F. Grieger and C. A. Kraus, *J. Am. Chem. Soc.*, **70**, 3803 (1948).

2) B. D. Flockhart and A. R. Ubbelohde, *J. Colloid Sci.*, **8**, 428 (1953).

3) B. D. Flockhart, *ibid.*, **12**, 557 (1957).

4) P. Mukerjee and A. Ray, *J. Phys. Chem.*, **67**, 190 (1963).

5) M. F. Emerson and A. Holtzer, *ibid.*, **71**, 3320 (1967).

6) A simplification and modification of Longwell-Maniece's method (*Analyst*, **80**, 167 (1955)).

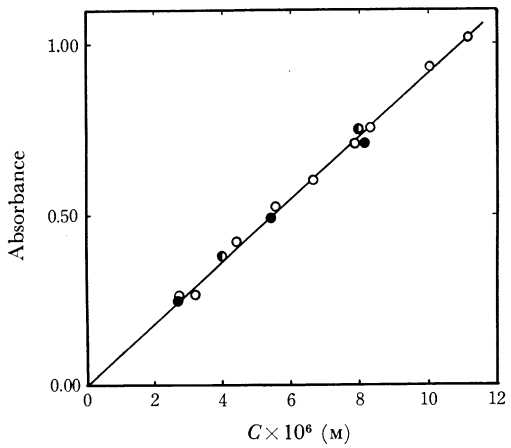

Fig. 1. Absorbance of methylene blue-alkyl sulfate at 650 mμ.
○ hexadecyl, ● tetradecyl, ◐ dodecyl
cell: 1 cm reference: chloroform with blank extraction

chloroform was measured at the wavelength of 650 mμ using a spectrophotometer, Model 139, of the Hitachi Mfg. Co., Ltd. The calibration curve is shown in Fig. 1, where it may be seen that the methylene blue-alkyl sulfate complex shows the same absorbance whatever the length of the alkyl chain.

Results and Discussion

The solubilities and CMC's of KDS are shown as a function of the temperature in Figs. 2—6. A general trend for the solubility to increase slightly in the lower temperature range and to increase markedly in the higher temperature range is apparent. The abrupt change in solubility may be understood as a change in the solution behavior of the surfactant, that is, the micelle formation.

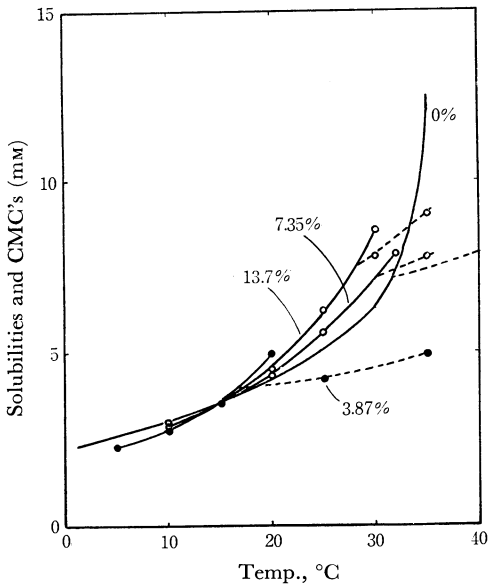

Fig. 2. Solubilities and CMC's of KDS in propanol-water mixtures ●, and in methanol-water mixtures ○.
solid line: solubility, dotted line: CMC

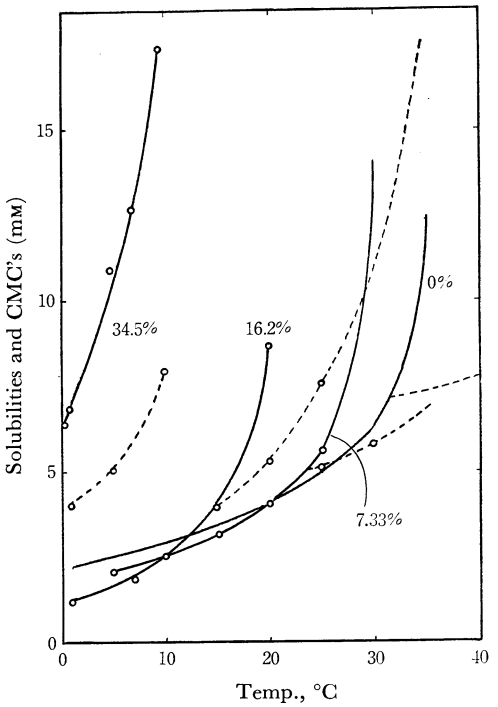

Fig. 3. Solubilities and CMC's of KDS in ethanol-water mixtures.

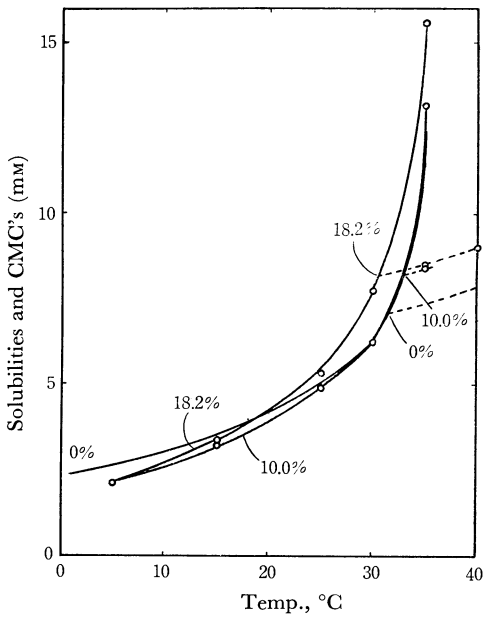

Fig. 4. Solubilities and CMC's of KDS in ethylene glycol-water mixtures.

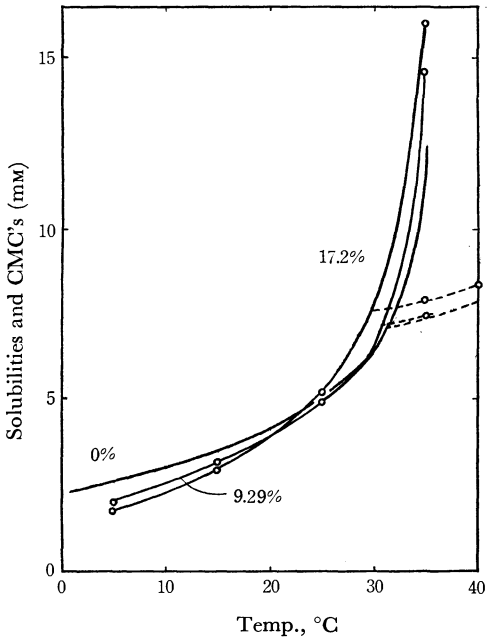

Fig. 5. Solubilities and CMC's of KDS in propylene glycol-water mixtures.

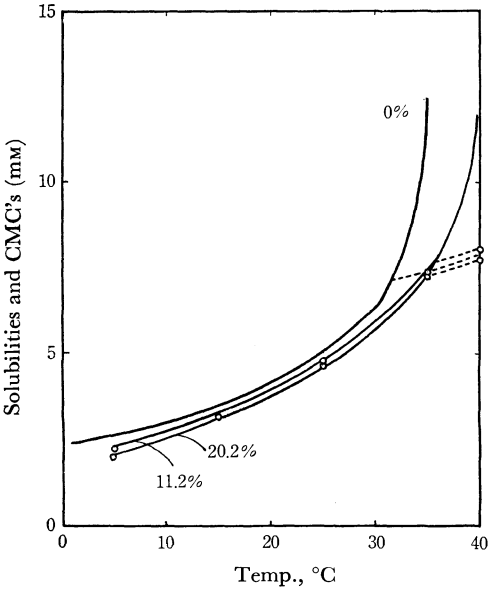

Fig. 6. Solubilities and CMC's of KDS in glycerol-water mixtures.

Thus, a temperature at which the solubility curve intersects the CMC curve is defined as the Krafft point. Therefore, it will be convenient to discuss the solvent effects on micelle formation and on single-ion dispersion separately.

Solvent Effects on Micelle Formation. The CMC's at 35°C are shown in Fig. 7, where the abscissa indicates the weight percentages of the organic

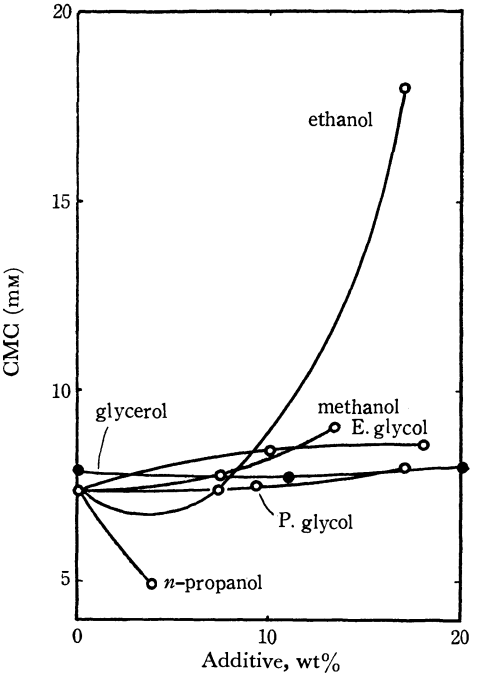

Fig. 7. CMC's of KDS in mixed solvents at 35°C (glycerol solvents at 40°C).
CMC's in ethanol-water mixtures ar extrapolated from lower temperatures to 35°C in Fig. 3.

additives. As for the effect of alcohols on the CMC, it has been known that there are both CMC-increasing and CMC-decreasing effects, depending on the chain lengths of the alcohols added.[1,3,5] The same is observed here: methanol shows a CMC-increasing effect, ethanol both, and propanol may have a CMC-decreasing effect, but the addition of much more propanol will have a CMC-increasing effect, too.[2]

In contrast, glycols have a CMC-increasing effect only. Glycerol brings about a very slight minimum in the CMC curve, but it is not clear whether or not this minimum is related to the action of sucrose, which lowers the CMC of sodium dodecyl sulfate. This is attributable to the dehydration of surfactant ions, caused by the strong hydrophile of the sucrose added.[7]

The CMC-decreasing effect found in alcohol solutions may be due to the solubilization of alcohol molecules into micelles, resulting in a decease in the free energy caused by both the entropy of mixing and the reduction of the charge density on the micelle surface.[8,9] Glycols and glycerol do not penetrate the micelle because they have fewer lipophile. Thus, solvent effects other than solubilization have to be sought in connection with

7) M. Nakagaki and S. Kawamura, *Yakugaku Zasshi* (*J. Pharm. Soc. Japan*), **84**, 246 (1964).
8) Y. Ooshika, *J. Colloid Sci.*, **9**, 254 (1954).
9) K. Shinoda, This Bulletin, **26**, 101 (1953).

these compounds.

As the CMC is the characteristic parameter of the micelle-single ion equilibrium, a solvent effect on single ions as well as on the micelle should be taken into account. For this purpose, the solubilities of the surfactants in the lower temperature range, where only single-ion dispersion is supposed, was examined.

Solvent Effects on Single Ions. It is evident from Figs. 2—6 that the addition of alcohols causes a comparatively small solubility change, but an observable increase in the temperature coefficient of the solubility. For example, the solubility of KDS in the 9.3 wt% methanol solution intersects at 16°C with that for pure water. Thus, the solubility of KDS in a methanolic solution is larger at 20°C, but becomes smaller at 10°C, than in pure water. These properties become exaggerated with increases of alcohol concentration and the chain length of alcohols.

On the other hand, in glycerol mixtures KDS is less soluble than in pure water at all temperatures lower than the Krafft point. Glycols are intermediate between glycerol and mono-alcohols, in that their solubility curves intersect at higher temperatures. In order to observe these effects more quantitatively, a standard free-energy change for the solution process, ΔF°, will now be introduced:

$$\Delta E^\circ = -2RT\ln X_s \qquad (1)$$

where X_s is a solubility in the mole fraction scale which should be replaced by an activity, but the experimental concentrations are so low (less than 5 mM) that the mole fraction can be used with a minimum loss of accuracy. The other notations have the usual meanings. The temperature coefficient of the solubility and thermodynamics also give:

$$\Delta H^\circ = -R\frac{\partial \ln X_s}{\partial\left(\frac{1}{T}\right)} \qquad (2)$$

and:

$$\Delta S^\circ = \frac{\Delta H^\circ - F\Delta^\circ}{T} \qquad (3)$$

where ΔH° and ΔS° are the standard enthalpy and entropy changes for the solution process respectively. In Fig. 8, ΔH°'s and $T\Delta S^\circ$'s are shown as functions of the weight percentages of the organic additives. It is evident that the longer the alkyl group in an alcohol molecule, the more temperature-dependent the solubility becomes, while the hydroxy group in additives surpresses the temperature dependence of the solubility. The higher hydroxy density in ethylene glycol and glycerol solutions supports the idea of a net-work structure formation which resists the thermal breaking of the structure much more than in alcohol solutions. The net-work structure also refuses to share space with dissolved solutes, *i. e.*, with surfactant molecules. This might be closely related to the smaller solvent effect seen in glycols and, above all, in glycerol solutions. On the other hand, the alkyl group in alcohol solutions interferes with the net-work formation and favors the thermal agitation. Thus, at higher temperatures, the alkyl group in a mixed solvent loosens the structure and affords space for surfactant molecules. At lower temperatures, the structure in the solvent becomes more rigid due both to hydrogen bonding and to iceberg formation about the alkyl group in the sense of Némethy-Scheraga.[10] In connection with the structure formation between the hydroxy compound and water, it may be noted that the micelle formation was found in a 34.5% ethanol solution at a lower temperature than 10°C, as may be seen in Fig. 3. As a micelle is an aggregation of "refugees" of surfactant molecules from a highly cohesive solvent, *i. e.*, water, a concentrated ethanol solution which is free from micelle formation at higher temperatures would cohesive enough to be disliked by the surfactant molecules at sufficiently low temperatures. It is also clear from Fig. 8

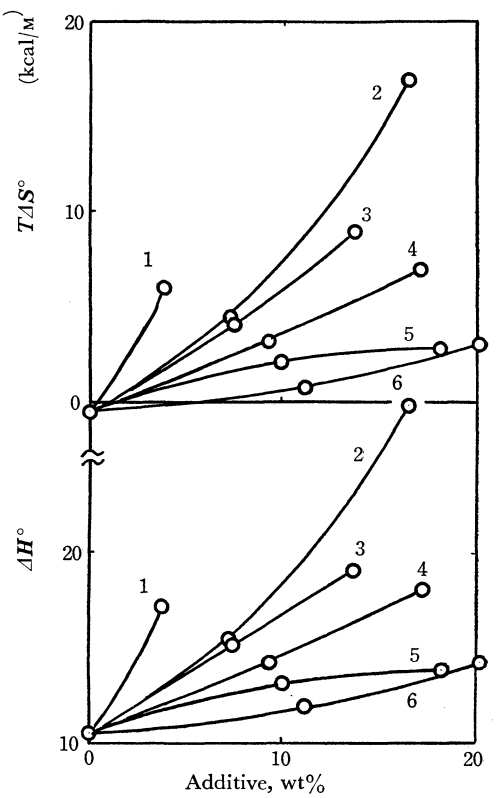

Fig. 8. ΔH°'s and $T\Delta S^\circ$'s of KDS in mixed solvents.
1: 1-propanol, 2: ethanol, 3: methanol, 4: propylene glycol, 5: ethylene glycol, and 6: glycerol.

10) G. Némethy and H. A. Scheraga, *J. Chem. Phys.*, **36**, 3401 (1962).

that propylene glycol lies between glycerol and alcohols in that it has both glycol and methyl groups in a molecule. The iceberg around the hydrocarbon entity of a surfactant molecule might be attacked by the additives, because $T\Delta S°$ increases from negative value to a positive one with the additive concentration, as may be seen in Fig. 8.

Separation of Solvent Effects. The solvent effects can be divided into two groups: the solvent effect on a nonpolar group and that on an ionic group of a surfactant molecule. On the assumption that these two effects are additive, the separation can be experimentally made by measuring the solubility of, for example, KHS in each solvent and by applying the following equation:

$$\Delta\Delta F° = \Delta F°_{KHS} - \Delta F°_{KDS} = -2RT \ln \frac{C_{KHS}}{C_{KDS}} \quad (4)$$

where $\Delta\Delta F°$ means the solvent effect on the nonpolar group (exactly on the tetramethylene group) and where the subscripts KHS and KDS refer to the surfactants used. The C's are the solubilities of the surfactants. The solubilities of KHS are shown in Figs. 9—10 except for those in propylene glycol-, and glycerol-water mixed solvents, for which measurements were made at 15°C only; the results are shown in Table 1. In Fig. 11, the $\Delta\Delta F°$'s are plotted against the weight percentages of the additives at 15°. Although the points are scattered, it is observed that all alcohols show the same inclination and that glycols and glycerol show a smaller solvent effect, as was also noted in the

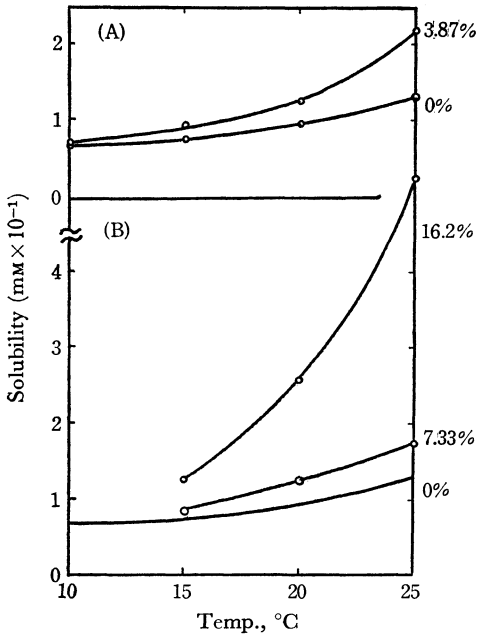

Fig. 9. Solubilities of KHS in propanol-water mixtures (A), and in ethanol-water mixtures (B).

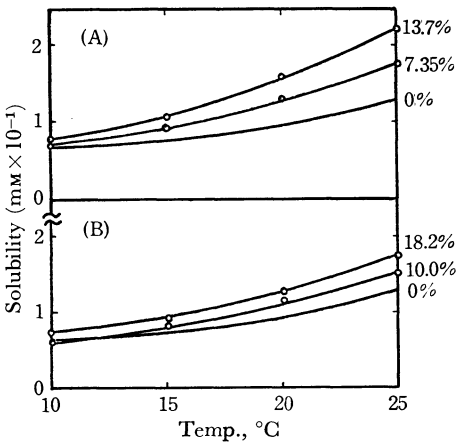

Fig. 10. Solubilities of KHS in methanol-water mixtures (A), and in ethylene glycol-water mixtures (B).

TABLE 1. SOLUBILITIES OF KHS IN MIXED SOLVENTS AT 15°C (10^{-1} mM)

Propylene glycol		Glycerol	
Add. wt %	Soly.	Add. wt %	Soly.
9.29	0.828	11.2	0.754
17.2	0.780	20.2	0.749

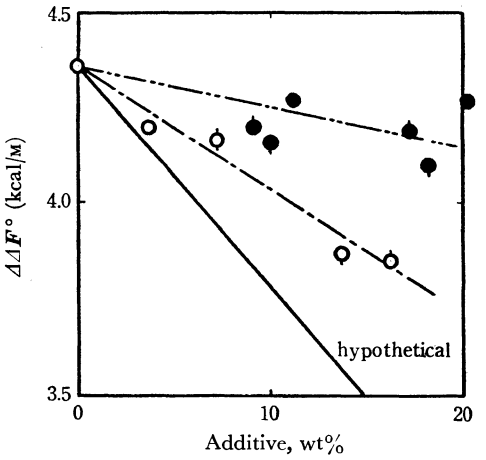

Fig. 11. Solvent effect on nonpolar group.
○: propanol, ○: ethanol, ○: methanol,
●: glycerol, ◖: propylene glycol,
◖: ethylene glycol

enthalpy change for the solution process. For comparison, a hypothetical solvent effect, defined below, may be tentatively introduced:

$$\Delta\Delta F°_{hypo} = \phi_W \Delta F°_W + \phi_H \Delta F°_H \quad (5)$$

where ϕ_W and ϕ_H are, respectively, the volume fractions of water and some hypothetical solvent such as "hexane" in a hypothetical mixed solvent where the two components are supposed to be

freely miscible without any overall change in the water structure, and where ΔF°_W and ΔF°_H are the standard free-energy changes for the nonpolar group when it is dissolved into water and into "hexane" respectively. Furthermore, $\Delta F^\circ_W > \Delta F^\circ_H \fallingdotseq 0$, because, when, for example, butane is dissolved into hexane, its free-energy change is negligibly small; therefore, Eq. (5) reduces to:

$$\Delta\Delta F^\circ_{hypo} = \Delta F^\circ_w (1-\phi_H) \qquad (6)$$

Equation (6) proves that a strongly cohesive solvent, such as water, becomes energetically void and liable to accept a hydrocarbon entity when mixed with "hexane." A formula similar to Eq. (6) can be derived from the Flory-Huggins' equation for three component system on the assumptions that: (1) the molar volumes are all alike, (2) the solution is very dilute with respect to solute, and (3) all the interaction energies except that between solute and water molecules are zero.[11] The hypothetical solvent effect is shown as a solid line in Fig. 11. A positive deviation from the hypothetical line would be due to the structure formation in alcohols-, in glycols-, and, above all, in glycerol-water mixed solvents.

The solvent effect on the ionic group can be calculated by the following equation:

$$\Delta F^\circ_{ion} = \Delta F^\circ_{KDS} - \Delta\Delta F^\circ \times 3 \qquad (7)$$

Since $\Delta\Delta F^\circ$ is a contribution from a tetramethylene group, the factor of three is introduced to obtain the contribution from a dodecyl group. The values of ΔF°_{ion}'s are plotted against the reciprocal of the dielectric constant*1 of the mixed solvents in Fig. 12. The straight line was drawn by the least-square method; the slope gives a "Born radius" of 0.3 Å. This value is smaller than the probable one (around 5 Å) deduced by the electric conductivity method for sodium dodecyl sulfate.[12] However, it may not be unacceptable taking into account the facts that the solvation energy cannot be explained by the Born mechanism alone and that, in addition, the experimental points are scattered. As a first approximation, the solvent effect on the ionic group is explained by the electrostatic theory; further mechanisms, such as selective solvation and the effect of a large hydrocarbon

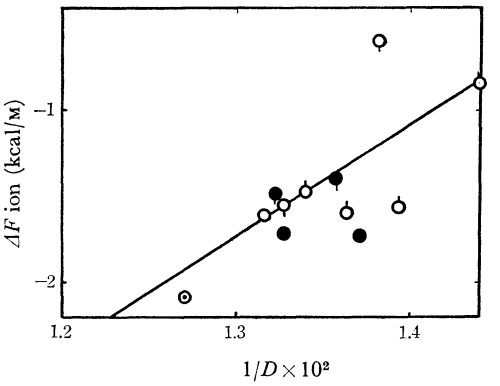

Fig. 12. Solvent effect on ionic group.
⊙: water, other indications are the same as in Fig. 11.

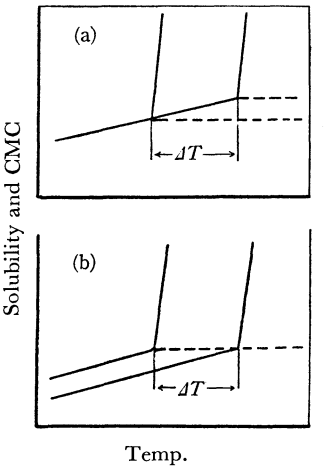

Fig. 13. Schema of the Krafft point changes.

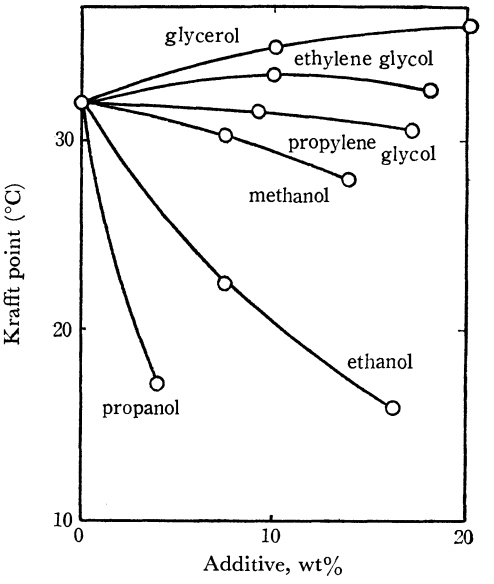

Fig. 14. The Krafft points in mixed solvents.

11) P. J. Flory, "Principles of Polymer Chemistry," Cornell Univ. Press, Ithaca, New Yrok (1953), p. 548.

*1 The dielectric constants of the mixed solvents are quoted from H. S. Harned and B. B. Owen, "The Physical Chemistry of Electrolyte Solutions," Reinhold Publ. Corp., N. Y. (1958), p. 161, except for that for aqueous propylene glycol, which was calculated by weighing the volume fractions on the dielectric constants of each component.

12) G. D. Parfitt and A. L. Smith, *Trans. Faraday Soc.*, **61**, 2736 (1965).

group adjacent to the charged center, would be important and more precise experiments and theory would be required before they could be established.

Solvent Effect on the Krafft Point. In order to clarify the solvent effects on the Krafft point, detailed knowledge of the CMC and the single-ion dispersion, and of their temperature dependence is necessary. However, for the sake of simplicity, we consider in Fig. 13 two extreme cases in which: (a) the solubility curve is unchanged, but the CMC curve is increased or decreased, and (b) the CMC curve is unchanged, but the solubility curve is altered by the addition of organic compounds. The Krafft points are shown in Fig. 14 as functions of the weight percentages of the additives. If, from (a), CMC decreases, the Krafft point also decreases. This corresponds to the effect of propanol, which lowers the CMC, as has been pointed out above. An extreme example of this type of effect has been reported by Shinoda and Nakayama, who studied the very sensitive Krafft point-decreasing power of some higher alcohols (C_6–C_8).[13] As for the (b) case, the effect of glycerol may be pointed out. The solubility-decreasing effect and the small effect on the CMC of glycerol cause an increase in the Krafft point; such an increase is rare except as an effect of added electrolytes.[14] The medium decrease in the Krafft point affected by methanol can be understood on the assumption that the mechanism (b) slightly exceeds the (a), as there is also a CMC-increasing effect, which would otherwise raise the Krafft point. The effect of ethanol is indicative of the mechanism (a), which results from the large temperature dependence of CMC. For glycols, the two mechanisms compensate each other; hence, relatively small changes in the Krafft point are observed. Propylene glycol's greater inclination to decrease may well represent the effect of the methyl group, which ethylene glycol lacks.

13) H. Nakayama and K. Shinoda, *J. Phys. Chem.*, **70**, 3502 (1965).

14) H. Nakayama and K. Shinoda, This Bulletin, **40**, 1797 (1966).

BULLETIN OF THE CHEMICAL SOCIETY OF JAPAN VOL. 42 1212—1216 (1969)

Paramagnetic Susceptibilities of Some DPPH Derivatives

Noriko OHIGASHI and Hiroo INOKUCHI

The Institute for Solid State Physics, The University of Tokyo, Roppongi, Tokyo

(Received August 22, 1968)

The static magnetic susceptibilities of polycrystalline samples of 1,1-bis(*p*-chlorophenyl)-2-picrylhydrazyl (Cl-DPPH), 1,1-bis(*p*-bromophenyl)-2-picrylhydrazyl (Br-DPPH), and 1,1-bis (*p*-methoxyphenyl)-2-picrylhydrazyl (CH_3O-DPPH) were measured in the temperature range from 10°K to 300°K. These three substances showed strong paramagnetism comparable to that of DPPH, having relatively weak interaction energies between their unpaired electrons. Of these, the paramagnetic susceptibility of CH_3O-DPPH was analysed on the basis of the singlet-triplet model with the energy separation of $2J/k=33.8$°K.

The typical neutral organic free radical, 1,1-diphenyl-2-picrylhydrazyl (DPPH), is known to have a sharp, exchange-narrowed ESR absorption line. A number of investigations have been carried out to find a transition to the magnetic ordered state on DPPH at a low temperature.[1-4] All of these measurements (except for the work of Gerritsen *et al.*[2]) agree with each other concerning the following points that the paramagnetic susceptibility of this compound obeys the Curie-Weiss law, having a Weiss constant of about −25°K between 60°K and room temperature, that it deviates at lower temperatures, and that no antiferromagnetic transition has been found, at least above liquid helium temperature.

The magnetic susceptibility of another neutral free radical, *N*-picrylaminocarbazyl (PAC), the molecular structure of which is very similar to that

1) L. S. Singer and E. G. Spencer, *J. Chem. Phys.*, **21**, 939 (1953).

2) H. J. Gerritsen, R. Okkes, H. M. Gijsman and J. Van Den Handel, *Physica*, **20**, 13 (1954).

3) W. Duffy, Jr., *J. Chem. Phys.*, **36**, 490 (1962).

4) A. Van-Itterbeek and M. Labro, *Physica*, **30**, 157 (1964).

of DPPH, behaves quite differently.[5] The magnetic susceptibility *versus* the temperature curve has a broad maximum at about 70°K. The difference in behaviour between these two compounds can mainly be attributed to the different crystal structures. However, there is another remarkable difference between them, *i. e.*, the difference in the distribution of the unpaired electron over the molecule. The electron spin resonance spectra of these compounds differ considerably from each other.[6] The spectra of DPPH and PAC apparently consist of five lines and four lines respectively; these ESR spectra can be explained in terms of almost equal hyperfine coupling constants of the two central nitrogens in the former, whereas in the latter one nitrogen should have twice as large a coupling constant as the other. This remarkable difference in the distribution of the unpaired electron is probably one of the factors distinguishing the magnetic behaviour of these compounds. The ratio of the hyperfine coupling constants of the two hydrazyl nitrogens in DPPH changes when the substituents are introduced into the para-positions of the two phenyl groups.[7] We intended to investigate the change in the magnetic properties when the distribution of the unpaired electron varied in the molecule.

In this paper we will present the results of our measurements of the temperature dependence of the static magnetic susceptibilities of several DPPH derivatives, *i. e.*, 1,1-bis(*p*-chlorophenyl)-2-picrylhydrazyl (abbreviated as Cl-DPPH), 1,1-bis(*p*-bromophenyl)-2-picrylhydrazyl (Br-DPPH), and 1,1-bis(*p*-methoxyphenyl)-2-picrylhydrazyl (CH_3O-DPPH) (Fig. 1). Among these, the paramagnetic

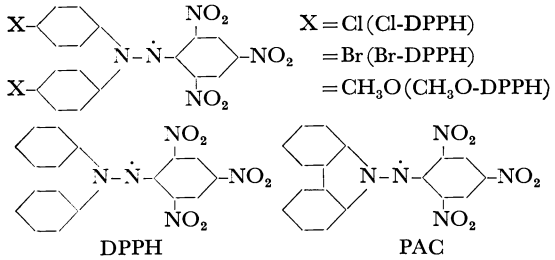

Fig. 1. Molecular structures of DPPH, derivatives of DPPH, and PAC.

susceptibility of CH_3O-DPPH is analysed on the basis of the singlet-triplet model, whereas the other two obey Curie law in the high-temperature range in spite of the appearance of the maximum in the susceptibility-*vs.*-temperature curve in Br-DPPH at 15°K.

5) R. S. Rhodes, J. H. Burgess and A. S. Edelstein, *Phys. Rev. Letters*, **6**, 462 (1961).

6) C. Kikuchi and V. W. Cohen, *Phys. Rev.*, **93**, 394 (1954).

7) M. M. Chen, K. V. Sane, R. I. Walter and J. A. Weil, *J. Phys. Chem.*, **65**, 713 (1961).

Experimental

The susceptibility measurements were made by the Faraday method. Figure 2 shows the apparatus schematically. A quartz bucket containing a powder

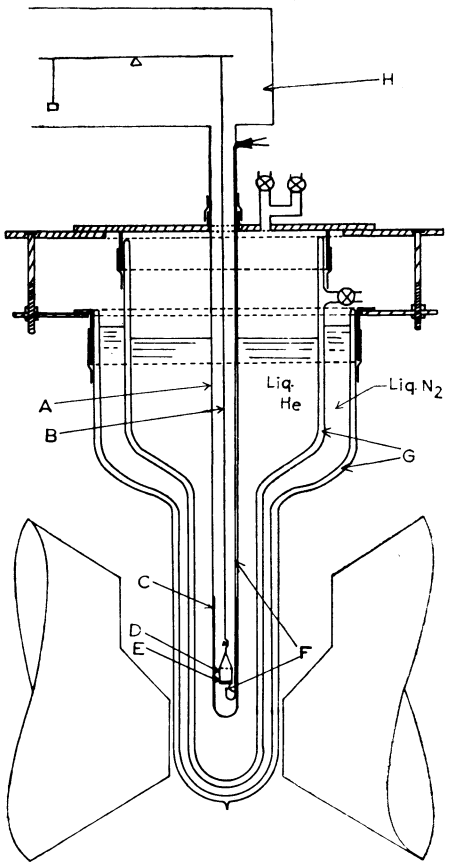

Fig. 2. Apparatus for susceptibility measurements.
A: Pyrex tube, B: Quartz string, C: Copper foil, D: Quartz bucket, E: Sample, F: Thermocouple, G: Glass Dewar, H: Vacuum balance.

sample of a few mg or more was suspended by a quartz string from the arm of a vacuum balance, a Sartorius Electrono microbalance. Helium gas (30 mmHg) which had been purified by passing it through an active charcoal at 77°K was admitted around the sample to facilitate the heat exchange. Each measurement was carried out continuously from 10°K to 300°K, the output of the microbalance being recorded on a X-Y recorder as a function of the e.m.f. of an Au : CO-Cu thermocouple. As the thermocouple was placed below the sample bucket (Fig. 2), the temperature in the sample was calibrated by measuring several times the susceptibilities of the paramagnetic salts whose susceptibilities are known, *i.e.*, Mohr's salt ($Fe(NH_4)_2(SO_4)_2 \cdot 6H_2O$) and Tutton's salt ($Mn(NH_4)_2(SO_4)_2 \cdot 6H_2O$), under the same conditions as for the usual measurements. The rate of raise of the temperature was set similarly for each run by controlling the pressure in the wall of the inner Dewar vessel. The Dewar vessel was placed between

the Sucksmith-type pole pieces with a pole gap of 5 cm, as is illustrated in Fig. 2. The sample bucket was adjusted so as to locate it at the plateau of $H\cdot\partial H/\partial x$ (usually 6.31×10^6 gauss^2/cm). At 10°K and also at room temperature while the susceptibility measurements were made the field strength was changed in order to check the field dependence. The field strength was calibrated by measuring the susceptibility of sucrose, the mass susceptibility of which was taken to be -0.566×10^{-6} emu/g.

The solvents for the recrystallization of the measured samples, Cl-DPPH, Br-DPPH, and CH_3O-DPPH, were benzene, benzene, and carbon tetrachloride respectively. All these samples were provided by R. I. Walter. Their molecular structures are illustrated in Fig. 1, along with those of DPPH and PAC.

Results and Discussion

The paramagnetic susceptibilities of all these compounds were comparable to that of DPPH; they all increased with a decrease in the temperature, as was mentioned in the previous communication.[8] In Br-DPPH and CH_3O-DPPH, however, the susceptibility reached its maximum value at 15°K and 21°K respectively, and then it decreased with the decrease in the temperature.

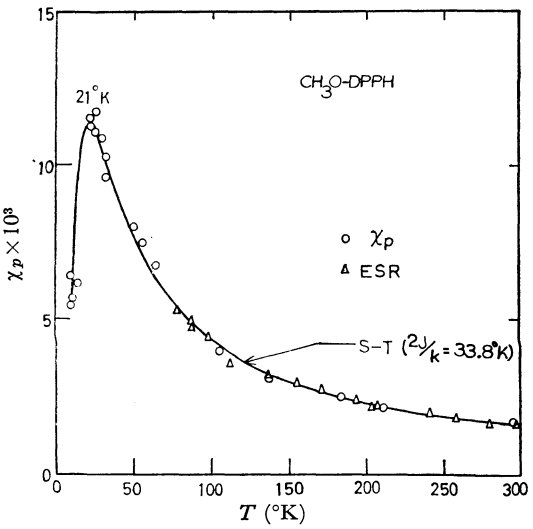

Fig. 3. Paramagnetic molar susceptibility of CH_3O-DPPH. Data are corrected for diamagnetism and an assumed impurity. The solid line is the theoretical fit based on singlet-triplet model with $2J/k$=33.8° K. The ESR data (arbitrarily normalized at 300° K) are also plotted.

The data were analysed by the formula;

$$\chi(T)=f(T)+\frac{C}{T}+D \qquad (1)$$

where $\chi(T)$ is the observed susceptibility at temperature, T; where the term C/T denotes the contribution from the assumed isolated paramagnetic "impurities"; where D is a diamagnetic term, and where $f(T)$ is a function of the temperature, which is assumed to have one of the following four forms:

1) $f(T)=Ng^2\beta^2/4kT$ (Curie law), (1-a)

2) $f(T)=Ng^2\beta^2/4k(T-\theta)$ (Curie-Weiss law), (1-b)

3) $f(T)=Ng^2\beta^2/kT\cdot(3+\exp(2J/kT))^{-1}$ (singlet-triplet model), (1-c)

4) $f(T)=Ng^2\beta^2/4kT\cdot\exp(-J/kT)$ (linear Ising model). (1-d)

In Eqs. (1-c), (1-d), we assumed the following spin exchange Hamiltonian:

$$\mathcal{H}=\sum_i^{N/2}(2JS_{2i-1}S_{2i}+2J'S_{2i}S_{2i+1}), \qquad (2)$$

and took $J\neq J'=0$ and $J=J'\neq0$, $S_iS_j=S_i^zS_j^z$, respectively.

In Eq. (1), the first term and the parameters C and D were chosen to give the best fits to the observed values. The results are shown in Figs. 3—5. Equation (1) reproduces fairly well the paramagnetic susceptibility data of CH_3O-DPPH if we take $f(T)$ as Eq. (1-c) with $2J/k$=33.8°K (the singlet-triplet energy separation) and if we assume the concentration of the impurity of spin 1/2 to be 8.7%, as is shown in Fig. 3. The maximum of χ_p was found at 21°K. The ESR measurement was

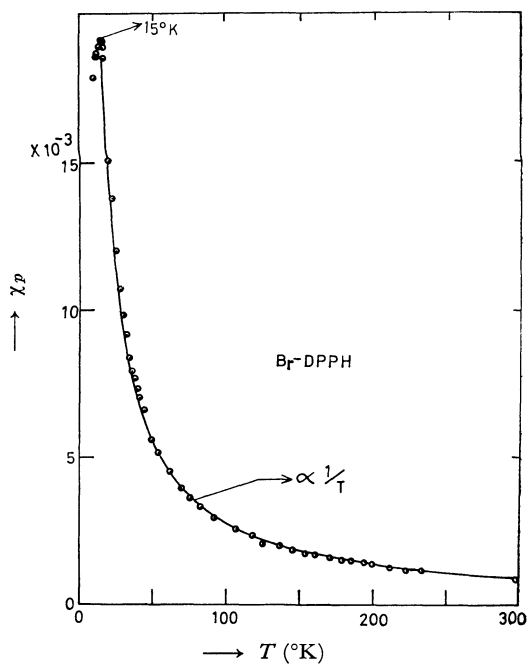

Fig. 4. Paramagnetic susceptibility of Br-DPPH.

8) N. Ohigashi and H. Inokuchi, This Bulletin, **41**, 269 (1968).

made on this powder sample between 77°K and room temperature. The absorption spectrum was very sharp, ΔH_{msl} being smaller than 1 gauss. As the absorption shape did not change with the temperature, the peak heights of the first derivative curves were thought to be proportional to the absorption intensity. These values are in good agreement with the static susceptibility data (Fig. 3), confirming that the observed strongly exchange-narrowed ESR absorption line at $g=2$ has the same origin as that giving rise to the static paramagnetic susceptibility.

The susceptibility, χ_p, of Br-DPPH had its maximum at 15°K and at higher temperatures followed a Curie law (Fig. 4), whereas that of Cl-DPPH obeyed a Curie law over the entire temperature range (Fig. 5). There is some evidence

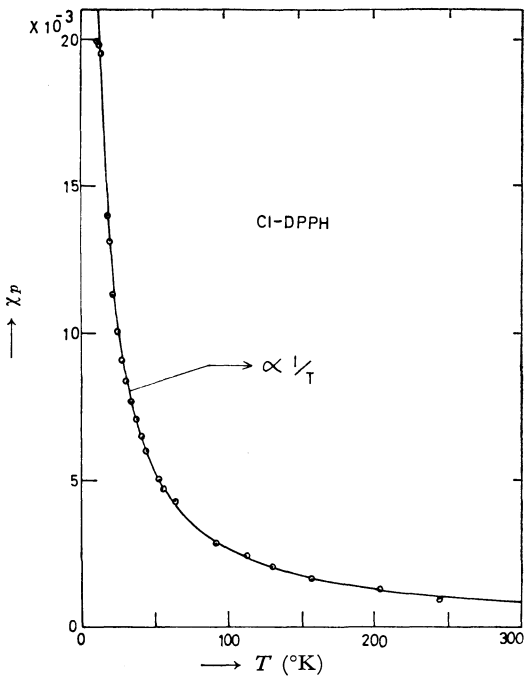

Fig. 5. Paramagnetic susceptibility of Cl-DPPH.

that the χ_p of Cl-DPPH has its maximum near 10°K, but our present apparatus can not give detailed information in this temperature region. The line widths at room temperature of the ESR absorption lines of these two compounds were about four times broader than that of CH_3O-DPPH. Further, in contrast to CH_3O-DPPH, they became narrow (about 2/3) when the temperature was lowered to 77°K. This fact probably suggests that in these two compounds, the crystal lattice spacings change with the temperature more rapidly than that of CH_3O-DPPH, and that the sudden decreases in the magnetic susceptibilities at 15°K and 10°K may be explained by the phase transitions. On the other hand, the χ_p of CH_3O-DPPH is represented by a single equation based on the singlet-triplet model from 10°K to 300°K, indicating that no phase transition occurs in this temperature range; this is consistent with the fact that no change in the line shape or width of the ESR absorption line is found from 77°K to room temperature.

As has been seen above, Cl- and Br-DPPH behave differently from CH_3O-DPPH. The crystal structures of these compounds have not yet been analysed. However, several crystal modifications of DPPH are known according to the solvents from which the crystals are grown. Our samples were crystallized from different solvents, benzene and carbon tetrachloride, but it has been inferred that their magnetic susceptibilities depend little on the solvents used for recrystallization. This is because the susceptibilities of the DPPH crystal measured by several authors seem to show small influences of solvents, whether or not the crystal contains molecules of solvation.[1-3] This suggests that the relative arrangement of the nearest neighbouring molecules is but little altered when the crystal structure changes. Similarly, in the DPPH derivatives used in this work, the arrangement of the neighbouring molecules may be determined mainly from the interaction between DPPH derivative molecules, but not from the interaction between the free radical molecule and a solvent molecule. Considering the size of the substituent, CH_3O-DPPH may fairly differ in the arrangement of molecules in the crystal from the other two radicals, Br- and Cl-DPPH.

The crystal structure of DPPH crystallized from benzene was recently determined by Williams.[9] His results show that the hydrazyl nitrogens of DPPH are surrounded sterically by the other atoms of the same molecule, indicating that the unpaired electron of DPPH is stabilized not only by conjugation with phenyl rings but also by the steric hindrance. In such circumstances, interaction among unpaired electrons in the crystal is generally small, but it may increase if the delocalization of an unpaired electron over a molecule advances upon the introduction of substituents. Of the three compounds studied, CH_3O-DPPH has the smallest hyperfine coupling constants for nitrogen nuclei,[7] suggesting that the unpaired electron in this compound delocalizes over the phenyl rings most extensively. The larger intermolecular interaction observed in CH_3O-DPPH may be attributed partly to this delocalization of the unpaired electron.

The magnetic interactions observed in DPPH-derivative crystals are smaller than those of many ion radical salts such as TCNQ anion radical salts, which crystallize with their molecular planes parallel

9) D. E. Williams, *J. Am. Chem. Soc.*, **89**, 4280 (1967).

to each other.[10] The stabilization of unpaired electrons by the steric hindrance may explain this fact.

10) D. B. Chesnut and W. D. Phillips, *J. Chem. Phys.*, **35**, 1002 (1961); R. G. Kepler, *ibid.*, **39**, 3528 (1963).

We wish to thank Professor R. I. Walter, Haverford College, for kindly providing samples.

BULLETIN OF THE CHEMICAL SOCIETY OF JAPAN VOL. 42 1216—1219 (1969)

Electrophoretic Behavior of Micelles of a Polyether-sulfate Type Surfactant

Fumikatsu Tokiwa and Kenji Ohki

Research Laboratories, Kao Soap Company, Minato-Yakushubata, Wakayama-shi

(Received August 30, 1968)

The electrophoretic properties of the micelle of sodium dodecyltrioxyethylene sulfate have been studied in the presence of various types of inorganic z_+-z_- electrolytes and in the presence of organic electrolytes (RNH_3Cl and $RCOONa$) of various sizes. The effect of the type of electrolytes on the zeta potential of the micelle, ζ, is similar in tendency to the effect to be expected on the basis of the Gouy-Chapman equation for spherical colloid particles. The valence of counter-ions has a considerable effect on ζ, but that of the co-ions has only a slight effect. With respect to the size of ions, counter-ions (RNH^+) appreciably influence the potential of the micelle, whereas co-ions ($RCOO^-$) influence the potential almost not at all. The value of ζ slightly increases, and then steeply decreases, with an increase in the size of the cations through a maximum value.

In a previous work[1] studies have been made of the effects of small electrolyte ions and long-chain alkyl ions on the surface potential of the micelle, ψ_0, of dimethyldodecylamine oxide by means of potentiometric titrations. The results have shown that the effect of small ions on ψ_0 is in accord with the effect predicted on the basis of the Gouy-Chapman equation for spherical colloid particles, while the effect of long-chain alkyl ions is directly related to their charge properties.

In the present work the zeta potential of the micelle, ζ, of sodium dodecyltrioxyethylene sulfate (SDPS-3), $C_{12}H_{25}O(CH_2CH_2O)_3SO_3Na$, has been studied by electrophoretic measurements in the presence of various electrolytes in order to learn the effect of the type of electrolytes on ζ. The reason for the choice of SDPS-3 was that the surfactant is dissolved in water in the presence of any types of electrolytes used and is, therefore, fit for the purposes of the present experiment. Further, the effect of the size of cationic and anionic ions on ζ has also been examined using a series of alkylamine hydrochlorides or sodium alkanoates.

Experimental

Materials. Sodium dodecyltrioxyethylene sulfate (SDPS-3) was synthesized by the sulfation of dodecyl trioxyethylene ether by the procedure described in a previous paper.[2] The dodecyl trioxyethylene ether, $C_{12}H_{25}O(CH_2CH_2O)_3H$, was prepared from dodecyl alcohol of a high purity by the addition of ethylene oxide and was pruified by fractional distillation to remove polyethylene glycol and higher and lower homologues. The number of oxyethylene units per molecule for the distilled ether was found, from its hydroxyl value, to be 3.05. The sample of SDPS-3 was purified by the ion-exchange method of Ginn and Church.[3] All of the inorganic electrolytes used in this experiment were of a guaranteed reagent grade. The short-chain alkylamine hydrochlorides and sodium alkanoates, which had been obtained from the Tokyo Kasei Kogyo Co., were also of a guaranteed reagent grade.

Electrophoresis. The electrophoretic measurements were carried out at 25°C with a Tiselius-type apparatus, Hitachi Model HTB-2A. The concentrations of SDPS-3 in both the upper and lower layers of the cell were taken to be higher than the critical micelle concentration in order to avoid the dissociation of the micelle into the monomers at the moving boundary;[4,5] the concentrations were taken to be 0.2 g/100 m*l* in the upper layer and 1.0 g/100 m*l* in the lower layer. An electrolyte was then added to give the solution an ionic strength of 0.10. The electrophoretic mobility of the micelle, U_M, was calculated from the velocities of the

1) F. Tokiwa and K. Ohki, *J. Colloid and Interface Sci.*, **27**, 247 (1968).

2) F. Tokiwa and K. Ohki, *J. Phys. Chem.*, **71**, 1343 (1967).

Table 1. Electrophoretic data for SDPS-3 micelles in the presence of various types of electrolytes at an ionic strength of 0.10 at 25°C

Type of electrolyte	Electrolyte	pH	$-U_M$[a] $\times 10^4$ cm²/V·sec	$-\zeta$ mV	$-\sigma_s \times 10^{-4}$ esu/cm²
1-1	NaCl	6.2	2.86	52	1.8
1-2	Na_2SO_4	6.3	2.92	53	1.6
1-3	Na_3PO_4	11.6	3.14	57	1.6
2-1	$MgCl_2$	6.2	1.62	29.6	1.15
2-2	$MgSO_4$	6.2	1.80	32.9	1.18
3-1	$AlCl_3$	3.2[b]	0.71	13.0	0.42
3-2	$Al_2(SO_4)_3$	3.4[b]	0.76	13.9	0.44[c]

a) The average value of three measurements.
b) At this pH the ion present in the solution is considered to be Al^{3+}.
c) Estimated from the σ_s *vs.* ζ curves for 3-1 and 3-3 electrolytes.

ascending and descending boundaries, V_a and V_d, by the equation[4,6]:

$$U_M = V_d\tau^\beta - \frac{V_a\tau^\alpha - V_d\tau^\beta}{(T_M{}^\beta/T_M{}^\alpha) - 1} \quad (1)$$

where T_M is the transference number of the micelle, τ is the specific conductance of the solution, and where α and β superscripts refer to the upper and lower layers respectively.

Results and Discussion

The Effect of the Type of Electrolytes. Table 1 summarizes the electrophoretic mobilities, U_M, of SDPS-3 micelles in the presence of various types of inorganic electrolytes at an ionic strength of 0.10. The zeta potential of the micelle, ζ, can be evaluated from U_M by the numerical computation developed by Wiersema *et al.*[7] on the assumptions that, for example, the interaction between micellar particles is negligible, that the micelle may be treated as a rigid sphere, and that the charge of the micelle is uniformly distributed on the surface. This numerical computation is rather elaborate. However, the relation between ζ and U_M becomes linear when the value of U_M is small; the Henry equation[8] may then be used to evaluate the zeta potential:

$$\zeta = \frac{6\pi\eta}{D \cdot f(\kappa r_0)} U_M \quad (2)$$

where $f(\kappa r_0)$ is Henry's function; κ, the Debye-Hückel parameter; r_0, the radius of the micelle, and η and D, the viscosity and dielectric constant of the medium respectively. The values of ζ obtained from U_M in terms of Eq. (2), assuming that the radius of the micelle is 25 Å in the present case, are also given in Table 1. In the solutions of $MgCl_2$, $MgSO_4$, $AlCl_3$, and $Al_2(SO_4)_3$, the ζ values obtained by Eq. (2) are reliable since the values of U_M are small. In the solutions of NaCl, Na_2SO_4, and Na_3PO_4, on the other hand, the values of U_M are relatively high. In these cases, the use of Eq. (2) will introduce errors into the calculated ζ values. For example, the errors in ζ compared with the numerical calculation are about 9%, 3%, and 1% for the values in the solutions of NaCl, Na_2SO_4, and Na_3PO_4 respectively, when $\zeta = 51$ mV and when $\kappa r_0 = 2.5$ (at a radius of 25 Å and an ionic strength of 0.10).*1 Henry's approximation (Eq. (2)) is better for 1-2 and 1-3 electrolytes than it is for the 1-1 type; it also happens to be more accurate than Overbeek's approximation.[7,9]

It may be seen in Table 1 that the difference in U_M or ζ among chlorides, sulfates, and phosphates is relatively small (*e.g.*, compare NaCl with Na_2SO_4 and Na_3PO_4), while the difference among sodium, magnesium, and aluminium salts is considerable (*e.g.*, compare NaCl with $MgCl_2$ and $AlCl_3$). Namely, the valence of anions (co-ions) has only a slight influence on U_M or ζ, but the valence of cations (counter-ions) has a considerable influence. These results are similar to those obtained in the previous work studying the effect of electrolyte ions on the surface potential of the micelle, ψ_0, of dimethyldodecylamine oxide.[1]

The surface charge density of the micelle at the plane of shear, σ_s, is given by the equation[10]:

3) M. E. Ginn and C. L. Church, *Anal. Chem.*, **31**, 551 (1955).
4) F. Tokiwa and K. Ohki, *Kolloid-Z. u. Z. Polymere*, **223**, 38 (1968).
5) T. Nakagawa and H. Inoue, *Nippon Kagaku Zasshi* (*J. Chem. Soc. Japan, Pure Chem. Sect.*), **78**, 636 (1957).
6) F. Tokiwa and K. Ohki, This Bulletin, **41**, 2828 (1968).
7) P. H. Wiersema, A. L. Loeb and J. Th. G. Overbeek, *J. Colloid and Interface Sci.*, **22**, 78 (1966).
8) D. C. Henry, *Proc. Roy. Soc.*, **A133**, 106 (1931).

*1 Estimated from Fig. 7 in Ref. 7.

9) J. Th. G. Overbeek, *Advan. Colloid Sci.*, **3**, 97 (1950).
10) A. E. Loeb, P. H. Wiersema and J. Th. G. Overbeek, "The Electrical Double Layer Around a Spherical Colloid Particle," M. I. T. Press, Cambridge, Massachusetts (1961).

$$\sigma_s = -\frac{D}{4\pi}\left(\frac{d\phi}{dr}\right)_{r=r_s} \quad (3)$$

where ϕ is the electrical potential at a certain distance, r, from the center of the particle and where the subscript s denotes values at the plane of shear. To obtain the quantity of $(d\phi/dr)_{r=r_s}$ in Eq. (3), we must solve the Poisson-Boltzmann equation for negatively-charged, spherical particles. Loeb *et al.* have solved the equation exactly under different conditions; the results are tabulated in Ref. 10. The results are given as functions of the "reduced distance" ($q_0 \equiv \kappa r_s/\lambda$, where $\lambda^2=(z_+ + z_-)/2z_+$), the "reduced potential" ($y_0 \equiv e\zeta/kT$), and the valence of positive and negative ions (z_+ and z_-). With the aid of the $I(q_0, y_0, z_+, z_-)$ tables of Loeb *et al.*, Eq. (3) may be rewritten:

$$\sigma_s = \frac{D}{4\pi} \cdot \frac{kT\kappa}{e\lambda} I(q_0, y_0, z_+, z_-) \quad (4)$$

If the values of q_0 and of z_+ and z_- are given, we can obtain the relation between σ_s and y_0, or that between σ_s and ζ, from Eq. (4). Figure 1 shows

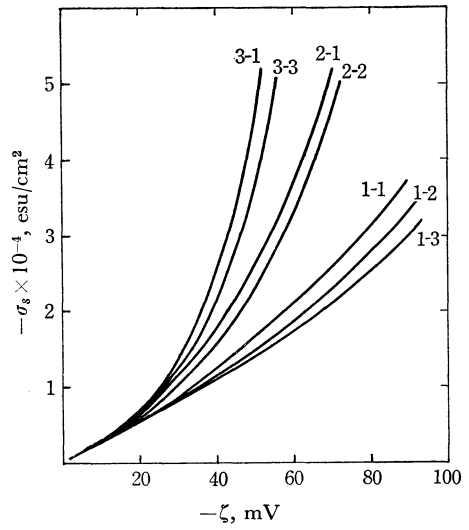

Fig. 1. The σ_s *vs.* ζ curves for a negatively charged, spherical particle with r_s of 25 Å in aqueous solutions of various z_+-z_- electrolytes at an ionic strength of 0.10.

the relation between σ_s and ζ for negatively-charged, spherical particles with r_s of 25 Å in aqueous solutions of various types of electrolytes at an ionic strength of 0.10.

As may be seen in Fig. 1, the relation of σ_s to ζ depends on the type of added electrolytes, especially on the valence of the cationic ions, which may be related to the results given in Table 1. We can now obtain the values of σ_s from ζ for the micelle of SDPS-3 using the curves shown in Fig. 1. The values of σ_s thus obtained are given in Table 1. It may be seen that the values of σ_s are also considerably influenced by the valence of the cations rather than by that of the anions. This implies that the valence of the counter-ions primarily governs the effective charge of the micelle, which must then be reflected to σ_s.

The Effect of the Size of Electrolytes. In Fig. 2 the values of U_M for SDPS-3 in the presence

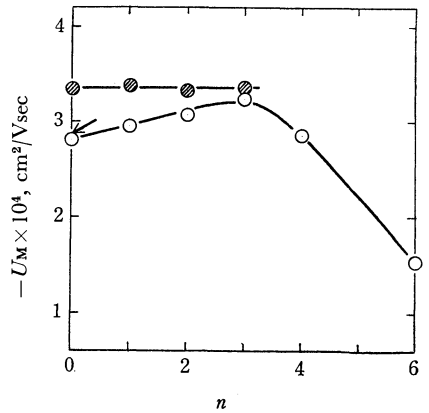

Fig. 2. The values of U_M for SDPS-3 in the presence of $C_nH_{2n+1}NH_3Cl$ (○) or $C_nH_{2n+1}COONa$ (●) at an ionic strength of 0.10 plotted against n. The arrow indicates the value in 0.10M NaCl.

of alkylamine hydrochlorides ($C_nH_{2n+1}NH_3Cl$) or sodium alkanoates ($C_nH_{2n+1}COONa$) are plotted against the alkyl chain length, n. The value of U_M is dependent on the size of the cations and is almost independent of the size of the anions. With the cations, the maximum value appears around $n=3$. It is of interest to note that the value of U_M in the presence of HCOONa is somewhat higher than the value observed in the presence of NaCl or NH_4Cl, even though the same value is to be expected for these three 1-1 electrolytes according to the Gouy-Chapman equation. The reason for this is not clear at present. However, it could be explained by the difference in steric effect between $HCOO^-$ and Cl^- anions or by the effect of the hydration of the anions.

In the general treatment of the distribution of ions in an electrical double layer based on the Boltzmann equation, electrolyte ions are assumed to be point charges instead of ions of a finite volume. A number of authors have attempted to introduce the ionic volume correction into the double-layer theory by rewriting the Boltzmann equation with some form of space restriction factor.[11] Thus, Haydon and Taylor[12] have derived relationships

11) D. A. Haydon, "Recent Progress in Surface Science," ed. by J. F. Danielli *et al.*, Academic Press, New York (1964), p. 97.

12) D. A. Haydon and F. H. Taylor, *Phil. Trans.*, **A253**, 255 (1960).

corresponding to the Gouy-Chapman equation for symmetrical electrolytes, corrected for the finite ionic volumes. According to their results, the surface potential increases with an increase in the size of the counter-ion when the surface charge density, the radius of the co-ion, and the concentration of the electrolyte are kept constant. With alkylamine hydrochlorides, the initial increase in U_M with an increase in n may be explained by the above result, although the effect is not as large as that to be expected from the calculation of Haydon and Taylor. The steep decrease in U_M after passing through a maximum value may be attributed to a direct influence of added alkylamine hydrochloride with a relatively large alkyl group. Probably, the SDPS-3 surfactant forms a complex with the alkylamine hydrochloride by the partial neutralization of the micellar charge. The fact that SDPS-3 is precipitated in the presence of octylamine hydrochloride supports this complex formation. With sodium alkanoates, the finding that the value of U_M is almost independent of n may be accounted for by the slight effect of anions on the potential of the micelle, as has been described above.

The authors wish to express their thanks to Dr. H. Kita, Director of the Research Laboratories, for his encouragement and for the permission to publish this paper.

BULLETIN OF THE CHEMICAL SOCIETY OF JAPAN VOL. 42 1219—1222 (1969)

Exo-electron Emission from Sandblasted Steel

Yasukatsu TAMAI and Yoshihiro MOMOSE

The Chemical Research Institute of Non-aqueous Solutions, Tohoku University, Sendai

(Received September 5, 1968)

The exo-electron glow curves up to about 250°C were measured for the sandblasted steel specimens, which had been kept in air for 2 min 30 sec, 2 hr 30 min or 13 hr after the sandblast. It was found that the plots of the integrated total counts against the keeping time in double-logarithmic scales gave a straight line with negative slope and that the emission peak moved to higher temperatures and at the same time the emission intensity decreased with the keeping time. It was also found that at the higher heating rate the peak intensity became larger and the peak temperature became higher than at the lower heating rate and that the remaining counts above a given temperature in the glow curve was linearly related with the temperature in semi-logarithmic scales, regardless of the heating rate. Comparing the behavior of exo-electron emission with that of the thermoluminescence of phosphors, it is supposed that electron traps are distributed on or in the deformed solid surface.

The phenomena of exo-electrons have been studied by many workers, which are emitted from solid surfaces stimulated by various treatments such as mechanical deformation and irradiation by X-rays. Some workers[1,2] have analyzed the exo-electron phenomena by means of the glow curve, which shows the characteristics of emission intensity observed at a constant rate of temperature rise, and estimated the electron trap depth. But they have not referred to the dependence of the glow curve on the time elapsed after the stimulation of the solid surface.

The reproducibility of the emission seems to be dependent on the method of surface treatment. In a previous paper[3] it was found that exo-electron glow curves were well reproducible if experimental conditions of surface treatment were properly regulated and the solid surface was uniformly deformed by suitable means such as sandblasting.

The purpose of the present work was to examine the dependence of the glow curves for sandblasted steel on the time for which the specimens, after sandblasted, were left in various atmospheres at room temperature, and to investigate the exo-electron decay mechanism.

Experimental

The details of the experimental apparatus have been

1) J. F. Young and D. J. Williams, *J. Appl. Phys.*, **34**, 3157 (1963).

2) H. Birgfellner and H. Hüller, *Acta Phys. Austriaca*, **14**, 56 (1961).

3) Y. Tamai and Y. Momose, *J. Appl. Phys.*, **39**, 5329 (1968).

described elsewhere.[4] A disk of commercial mild steel, 20 mm in diameter and 2 mm in thickness, was used. Prior to the experiments the mild steel specimens were annealed in air for 2 hr at about 400°C. Commercial standard sand (60 mesh through, the components: SiO_2 92%, Al_2O_3 4%) was used as blasting material.

A given amount (280 g) of sand was blown against the specimen by compressed air or nitrogen gas, at the gauge pressure of 1 atm, through a glass-made nozzle (2 mm, dia.) for 30 sec. The distance between the specimen and the blasting nozzle tip was 86 mm.

The counting device of the emission was a kind of open windowless Geiger-Müller counter. The working anode voltage was 1320 V and the accelerating voltage of 96 V was applied between the specimen holder and the grid (brass gauze) located at 10 mm above the holder. The counter gas was a mixture of ethanol (20 mmHg) and argon (83 mmHg). The measurements were conducted in the following way: The specimen was kept in air, argon or oxygen for a given time after sandblasting (this time is called "keeping time" hereafter) and then mounted on the specimen holder. It took about 3.5 min to evacuate the counter chamber, fill the counter gas in it for washing then repeat the same process again before the start of the counting. After one-minute counting at room temperature for steady operation of the ratemeter, the specimen was heated to about 250°C at the rate of 16°C/min or 27°C/min. Both the total counts and the count rate were recorded by a scaler and a ratemeter. The natural counting rate was approximately 0.8 counts/sec.

Results

Change of Glow Curves for Blasted Specimens Kept in Different Atmospheres. The black oxide film on the annealed specimen was removed under the present blasting conditions, and the freshly deformed metal surface was gray. Figure 1 shows the glow curves at a heating rate of 27°C/min for various keeping times in air (20°C, 50% relative humidity) after the sandblast by compressed nitrogen gas. In the glow curves, the intensity of the emission first rises, with rise of temperature, to a maximum at a definite temperature then slowly falls down to nearly the natural count rate. As seen in Fig. 1, as the keeping time becomes longer, the glow curves show a broader peak, the peak intensity and the total counts are smaller and the peak temperature is higher, but the emission intensity is almost the same in the higher temperature region in all cases.

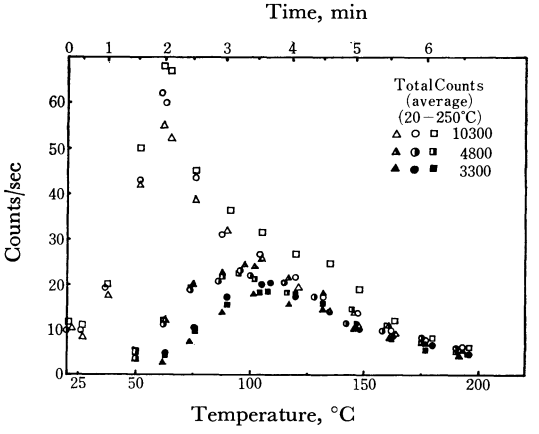

Fig. 1. Exo-electron glow curves for various keeping time in air after sandblasting.
△ ○ □: 2 min 30 sec
▲ ◑ ◨: 2 hr 30 min
▲ ● ■: 13 hr

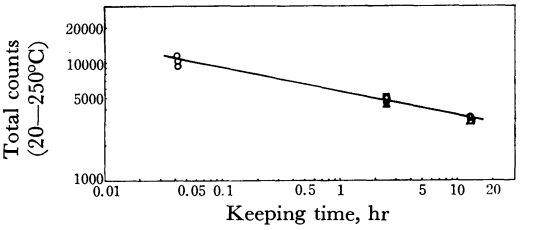

Fig. 2. Total counts of exo-electron glow curve (20—250°C) *vs.* keeping time.
○: Keeping in air (20°C, 50% relative humidity)
□: Keeping in oxygen (20°C, 1 atm)
△: Keeping in argon (20°C, 1 atm)

The plots of the total counts, N, against the keeping time, t, in double-logarithmic scales are shown in Fig. 2, which give a straight line with a negative slope. The empirical equation of the decay in air (20°C, 50% relative humidity) therefore was represented by

$$N(t) = C \cdot t^{-a}, \tag{1}$$

where a and C are constants, with $a=2.0\times10^{-1}$ and $C=2.9\times10^{4}$ (t: sec). Differentiation of Eq. (1) gives a decay of exo-electron emission in air;

$$\frac{dN}{dt} = -a \cdot C \cdot t^{-(a+1)}. \tag{2}$$

The decay equation in this form has been reported by many workers.[5,6] Lohff and Raether obtained the values of $a \cdot C$ and $(a+1)$ for various metals abraded by steel brush and for example the values of $a \cdot C$ and $(a+1)$ for aluminum were 8×10^{3} and 1.1, respectively.

On the other hand, in this experiment these values were 5.8×10^{3} and 1.2; namely the emission intensity of the sandblasted steel under the present blasting conditions had the same order as that of the abraded aluminum in their study. According

4) Y. Tamai and Y. Momose, *Kogyo Kagaku Zasshi* (*J. Chem. Soc. Japan, Ind. Chem. Sect.*), **71**, 1423 (1968).

5) J. Kramer, *Z. Physik*, **128**, 538 (1950).

6) J. Lohff and H. Raether, *ibid.*, **142**, 310 (1955).

to Eq. (2), the emission intensity at 2 hr 30 min sandblast becomes to 0.1 counts/sec. This value is the same order as the emission intensity at room temperature in the glow curve of 2 hr 30 min-keeping time in Fig. 1.

Next, the effect of keeping the blasted specimen in other atmospheres than air was examined.[3] The gases employed were oxygen and argon. It was found that the general characteristics of the peak temperature, the peak intensity and the total counts were almost the same as that obtained for the specimen kept in air after the blast. In addition, according to Eq. (1), the decay line is also applicable to the cases of argon and oxygen, as shown in Fig. 2.

Dependence of Glow Curve on Heating Rate. The effect of heating rate on the emission intensity in the glow curve was examined. The glow curves of three different specimens were obtained, which were all kept in air (25°C, 62% relative humidity) for 2.5 min after the sandblast by compressed air and were heated at a constant rate, *viz.*, 16°C/min or 27°C/min. Table 1 shows the average

Table 1. Dependence of glow curve on heating rate

Heating rate (°C/min)	Average values Peak temp. (°C)	Peak intensity (counts/sec)	Total counts (25—250°C)
16	54	32	8.1×10^3
27	62	50	8.7×10^3

values of the characteristics of three glow curves in each case. At the higher heating rate the peak intensity became larger and the peak temperature shifted to a higher potential than at the lower heating rate. The dependence of the peak temperature on the heating rate has been reported by former researchers,[2] but the increase of peak intensity at higher heating rates has not been referred to, probably because of poor reproducibility in the former studies. The total counts were nearly equal in six measurements and independent of heating rates. Concerning this problem, Haxel, Houtermans and Seeger[7] have reported the similar results that the total number of exo-electrons from abraded metals was independent of the degree of temperature rise.

The remaining counts, n, above a given temperature in the glow curve, were plotted against the temperature. The representative plots of the data of the glow curves in Table 1 are shown in semi-logarithmic scales in Fig. 3, which give almost the same straight lines independent of the heating rate in the present conditions except the initial lower temperature region. The empirical equation is represented by

$$n = S\cdot e^{-\beta T}, \tag{3}$$

where S and β are constants and T absolute temperature. The values of S and β are 4.4×10^6 and $2.0\times10^{-2}\,\mathrm{deg}^{-1}$, respectively. The value of β in the glow curve of 2 min 30 sec-keeping time in Fig. 1 is also equal to the above value.

Discussion and Conclusion

As for the source of the emission, it was found that electrons mostly originated in the deformed sand (*i. e.* SiO_2 and Al_2O_3) embedded in the metal surface by sandblasting.[3] The emission was observed from mild steel surface abraded by steel brush or by iron powder-blasting, although the intensity was rather weak. But in this experiment the emission was so strong as it was probably brought about by deformed sand.

The relation of the remaining counts *vs.* the temperature is given by Eq. (3) regardless of the heating rate. This fact suggests that the emission during temperature rise may be essentially dependent on temperature rather than time. Also, the linearity in an examined temperature range, shown in Fig. 3, suggests that the emission may

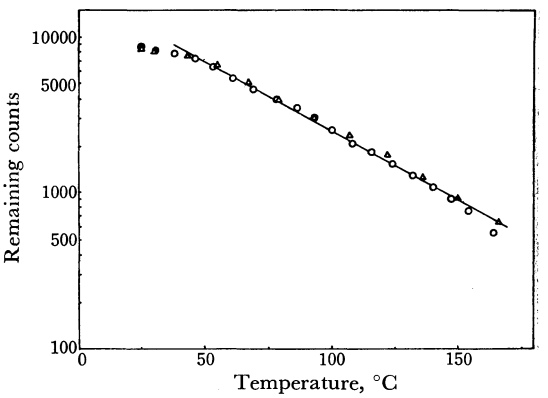

Fig. 3. Remaining counts in glow curve *vs.* temperature.
○: at the rate of 16°C/min
△: at the rate of 27°C/min

be due to the emission centers distributed in different levels of energy; this means that under the assumption that electrons are emitted by thermal energy corresponding to the depth of the electron traps in the deformed blast sand, the emission centers have the different thermal activation energies. If the emission peak in the glow curve corresponds to a single trap depth, the peak would decay as a whole and its maximum would remain at a definite temperature. However, as seen in Fig. 1, the

7) O. Haxel, F. G. Houtermans and K. Seeger, *Z. Physik*, **130**, 109 (1951).

maximum shifts to higher temperatures as the keeping time in air becomes longer; this means that a distribution of trap depth is presented and that the electrons to be emitted at lower temperatures decay more rapidly than those at higher temperatures.

Lepper[8] suggested that the behavior of exoelectron emission was very analogous to that of thermoluminescence and it has been reported by Randall and Wilkins[9] and Garlick and Gibson[10] that in the thermoluminescence glow curve of phosphors, such as KCl-Tl and ZnS-Cu, its peak shifted to higher temperatures as the phosphorescence decay proceeded.

According to Randall and Wilkins,[11] under the assumption that the distribution of the traps is exponential in form, if N_E is the number of traps between trap depth E and $E+dE$, then

$$N_E = A \cdot e^{-\alpha E} dE \tag{4}$$

and the emission intensity, I, at a given temperature is represented by

$$I \simeq f(s\boldsymbol{k}T) \cdot B \cdot t^{-(\alpha \boldsymbol{k} T+1)}, \tag{5}$$

where A, s, B and α are constants and $\boldsymbol{k}$ Boltzman constant. Also, it was shown by Randall and Wilkins[11] that if there is an equal number of electrons in all traps: the trap distribution is uniform, the emission intensity is proportional to $1/t$.

On the other hand, in the present experiments the relation of the emission intensity *vs.* time at 20°C is given by Eq. (2). The negative slope with respect to time is 1.20 and therefore it is probable that the trap distribution is exponential in form. Comparing this value with that of Eq. (5), that is $(\alpha kT+1)$, the value of α becomes 7.9 eV^{-1}.

The authors wish to thank Mr. Y. Nishiyama and Mr. T. Matsunaga for their helpful discussions.

8) J. Lepper, *Z. Naturforsch.*, **10a**, 47 (1955).
9) J. T. Randall and M. H. F. Wilkins, *Proc. Roy. Soc.* **A184**, 366 (1945).
10) G. F. J. Garlick and A. F. Gibson, *Proc. Phys. Soc.*, **60**, 574 (1948).
11) J. T. Randall and M. H. F. Wilkins, *Proc. Roy. Soc.*, **A184**, 390 (1945).

BULLETIN OF THE CHEMICAL SOCIETY OF JAPAN VOL. 42 1223—1230 (1969)

Determination of the S*–T Transition Probabilities of Some Xanthene and Thiazine Dyes on the Basis of the T-Energy Transfer. I. Experiment in Ethanol Solutions

Masae NEMOTO, Hiroshi KOKUBUN and Masao KOIZUMI

Department of Chemistry, Faclty of Science, Tohoku Univercity, Katahira-cho, Sendai

(Received September 6, 1968)

Intersystem crossing probability, φ_{ST}^{A} for fluorescein, eosine, erythrosine, methylene blue and thionine in ethanol (only for fluorescein, 30 vol% alkaline aqueous ethanol solution), has been determined by comparing the quantum yield of the direct (Φ) and sensitized photoreduction (Φ^{s}), on the basis of the following relations,

$$\Phi=\varphi_{ST}^{A}\beta \qquad \Phi^{s}=\varphi_{ST}^{D}\gamma\beta$$

where β is the fraction of triplet dye molecules that are reduced eventually, φ_{ST}^{A} and φ_{ST}^{D} are respectively for acceptor (dye) and donor (sensitizer) and γ is the energy transfer efficiency, which was assumed as 1. ATU was used as a reducing agent. 1,2,5,6-dibenzanthracene, triphenylene, anthracene and β-acetonaphthone were used as sensitizers. It has been confirmed that the above relations and assumption hold generally. Different sensitizers usually gave nearly the same φ_{ST}^{A} values (with the exception of thionine-anthracene. β-Acetonaphthone gave in general somewhat smaller values). The most probable φ_{ST}^{A} values obtained are; fluorescein (0.007), eosine 0.43 ± 0.04, erythrosine 1.1 ± 0.06, methylene blue 0.52 ± 0.03, thionine 0.62 ± 0.03. The values for xanthene dyes agree moderately well with the ones reported by Porter *et al.* for the aqueous solution of pH=9, fluorescein 0.05, eosine 0.71, erythrosine 1.07. Using the above φ_{ST}^{A} values, the ratio of the deactivation and genuine reaction between triplet dye and ATU has been evaluated. The ratio increases in the order, fluorescein$<$eosine$<$erythrosine, thionine$<$methylene blue.

One of the present authors (M. K.) with many collaborators, has long been engaged in the elucidation of the primary processes in the photochemical oxidation and reduction of some typical dyes. By means of the steady light and the flash photolytic investigations, detailed informations about many elementary processes have been obtained. But an important problem of determining the probability of S*→T transition *i. e.*, φ_{ST} still remains to be solved.

A few years ago, our group attacked this problem by Oster's method,[1] but a series of our work has revealed that the method is in general not applicable.[2-4]

Oster's method is based upon the general principle that if all the triplet dye molecules produced react with a certain substance giving a definite product, then the quantum yield of the reaction under such a condition can be taken as the value of φ_{ST}. Although the method appears simple and elegant, it often gives different φ_{ST} values depending upon the reaction adopted. For example, in the case of photoreduction, EDTA and ATU (allylthiourea) have been found to give quite different φ_{ST} values for eosine,[2] fluorescein[3] and methylene blue.[4] This fact strongly suggests that the mere deactivation of the triplet dye by the reducing agent is also occurring and that its magnitude largely depends upon the nature of the latter.

Since then our attention has been focused on the utilization of the triplet energy transfer. The principle of the method which is somewhat similar to that of Hammond,[5] is to compare the quantum yield of the direct (Φ) and sensitized photoreduction (Φ^{S}) under otherwise similar conditions. Denoting φ_{ST} for a sensitizer (donor) and a dye (acceptor) respectively as φ_{ST}^{D} and φ_{ST}^{A}, Φ and Φ^{S} will be given under favorable conditions, by

$$\Phi=\varphi_{ST}^{A}\beta^{A} \tag{1}$$

$$\Phi^{S}=\varphi_{ST}^{D}\gamma\beta^{A} \tag{2}$$

1) G. Oster and A. H. Adelman, *J. Am. Chem. Soc.*, **78**, 913 (1956).

2) T. Ohno, Y. Usui and M. Koizumi, This Bulletin, **38**, 1022 (1965).

3) Y. Momose, K. Uchida and M. Koizumi, *ibid.*, **38**, 1601 (1965).

4) N. Kosui, K. Uchida and M. Koizumi, *ibid.*, **38**, 1958 (1965).

5) A. A. Lamola and G. S. Hammond, *J. Chem. Phys.*, **43**, 2129 (1965).

where β^A is a fraction of the triplet dye that yields the product and γ is the efficiency of the triplet energy transfer. If φ_{ST}^{D} is known and if γ is unity, then the measurement of Φ^S and Φ enables us to evaluate the value of φ_{ST}^{A} from Eqs. (1) and (2). Of course some conditions must be fulfilled for the method to be applicable. In particular, it must be ascertained that β^A is really the same in value for the two reactions, and also that the only interaction between donor and acceptor is the triplet energy transfer.

For the aqueous solution, the selection of a suitable sensitizer is quite a big problem because very few work has yet been performed on the triplet energy transfer in the aqueous solution. Aromatic hydrocarbons of which the nature and the behavior of the triplet states have been investigated by many workers, cannot be used for the aqueous solution because of their very small solubility. There is of course no such obstacle for the ethanol solution; hence we have taken up the problem as a start, to decide φ_{ST} values of fluorescein, eosine, erythrosine (xanthene dyes), methylene blue and thionine (thiazine dyes) in ethanol by comparing the quantum yields of the direct and sensitized photoreduction. ATU was used as a reducing agent.

In the course of our work, some reliable data were published by Porter *et al.* on the φ_{ST} values of some xanthene dyes in aqueous solution.[6] The present results are somewhat similar to theirs in spite of a great difference in the method, supporting the reliability of their data as well as ours. In addition, our results give some interesting informations on the interaction between triplet dye and the reducing agent.

Experimental

Materials. Fluorescein and eosine of Gluber, G. R. grade, were recrystallized three times from ethanol. Erythrosine of Wako Junyaku, G. R. grade, was recrystallized three times from an ethanol-benzene mixture. Methylene blue and thionine of Merck, G. R. grade, were recrystallized three times respectively from *n*-butanol and ethanol.

1,2,5,6-Dibenzanthracene of Wako Junyaku, G. R. grade, was recrystallized from acetic acid and then from ethanol two times. Triphenylene of Tokyo Kasei, G. R. grade, was recrystallized three times from ethanol. β-Acetonaphthone of Tokyo Kasei, G. R. grade, was recrystallized three times from ligroin. Anthracene of high purity was kindly supplied by Professor Shimpachiro Kato of the Univeristy of Tokyo. Purity of these donors was checked by measuring the fluorescence and phosphorescence spectra.

Allylthiourea of Tokyo Kasei, G. R. grade, was recrystallized three times from water.

Ethanol of Wako Junyaku, G. R. grade, was fractionally distilled.

Degassing of the samples was performed by three times distillation to a trap immersed in liquid nitrogen under evacuation.

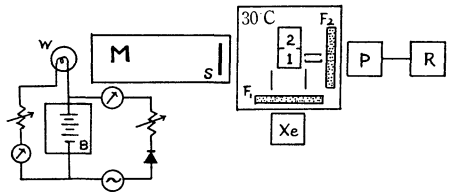

Fig. 1. Schematic diagram of the apparatus for the sensitized reaction.

B	storage battery	S	lightshuttter
F_1	Toshiba UV-D2 filter	P	photomultiplier
F_2	cut-off filter	R·	recorder
M	monochromator	W	incandescent lamp

Apparatus and Procedures. Figure 1 shows a schematic diagram of the apparatus for the sensitized reaction. As a light source, an Ushio UX-L 150D Xe-lamp was used; a Toshiba UV-D2 filter was used to excite the donor selectively.

Photobleaching of dyes was measured by a monochromatic light of the wavelength at the absorption maximum which was passed through the solution in the direction perpendicular to the exciting beam. A suitable cut-off filter was inserted to remove donor's fluorescence and scattered light. To reduce the fluctuation of light intensity, special care was taken; a storage battery employed as a power supply for monitoring light (6V-5A incandescent lamp), was kept charged during the measurement.

The measurement of the light absorption was performed as follows, using a potassium ferri-oxalate actinometer. Actinometry is made at first in cell 1 and next in cell 2 with cell 1 filled with the sample solution; the difference of the two measurements then gives the quantity of light absorbed by the sample solution.

Cells for spectrophotometry, $1\times1\times4$ cm, were used as the reaction cells. The concentration of each substance was chosen as follows; dyes 1×10^{-5}M, ATU 1×10^{-2}—5×10^{-4}M, 1,2,5,6-dibenzanthracene 5×10^{-4}M, triphenylene 1×10^{-4}M, anthracene 1.1×10^{-4}M, β-aceto naphthone 5×10^{-4}M. The reaction temperature was always 30 ± 0.5°C.

The apparatus and procedures for the direct photoreduction were similar to those described in a previous paper.[7] The quantity of light absorbed by dyes, was measured by a calibrated Kipp and Zonen thermopile having a sensitivity of 1.02×10^{-5} V/m² watt and a Shimadzu K-2 potentiometer.*1

6) P. G. Bowers and G. Porter, *Proc. Roy. Soc.*, **A299**, 348 (1967).

7) M. Nemoto, Y. Usui and M. Koizumi, This Bulletin, **40**, 1035 (1967).

*1 Some discrepancy was observed in the quantum yield of photoreduction of eosine in ethanol, as compared with the previous results.[7] This is due to the difference in the method of determining the magnitude of light absorption. In the previous paper, a relative method was employed using Imamura's Φ value on the oxydative photobleaching of eosine in the aqueous solution.[8] Reinvestigation of Φ of this reaction using the thermopile, gave about one third of the previous value.

Table 1. Quantum yield of the photoreduction of dyes in ethanol
dye concn., 10^{-5}M (30°C)

Concentration of ATU (M)	Fluorescein*1	Eosine	Erythrosine	Methylene blue	Thionine
5×10^{-4}				$0.4_5 \times 10^{-2}$	1.9×10^{-2}
1×10^{-3}				$0.7_4 \times 10^{-2}$	2.5×10^{-2}
2.5×10^{-3}		$2.7_6 \times 10^{-3}$	1.1×10^{-3}	$1.2_5 \times 10^{-2}$	
5×10^{-3}	$1.8_2 \times 10^{-4}$	3.6×10^{-3}	2.0×10^{-3}	1.3×10^{-2}	5.0×10^{-2}
7.5×10^{-3}	$1.9_8 \times 10^{-4}$	4.2×10^{-3}	3.0×10^{-3}	1.2×10^{-2}	5.4×10^{-2}
1×10^{-2}	2.3×10^{-4}	5.4×10^{-3}	3.7×10^{-3}	1.2×10^{-2}	5.4×10^{-2}

*1 30 vol% aq. alkaline (0.02N KOH) alcoholic solution.

Results

Dependence of the Quantum Yield of the Direct Photoreduction of Dye upon the Concentration of ATU. Quantum yields for five dyes in the ethanol solutions (except fluorescein) containing different concentrations of ATU are summarized in Table 1.

Some remarks will be added below on each dye.

As for eosine, the reaction has been investigated intensively in a previous paper.[7] Hence only the experiments using 1.0×10^{-5}M of dye were supplemented.

A detailed report on the photoreduction of erythrosine in ethanol will be published elsewhere. The feature of the reaction is essentially similar to eosine. Here only the results for 1×10^{-5}M of dye are listed in Table 1.

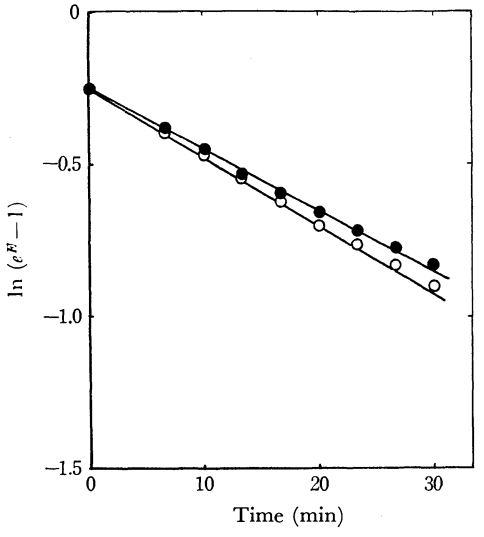

Fig. 2. Plots of $\ln(e^F - 1)$ *vs.* t for the 30 vol% aqueous alkaline (0.02N KOH) alcoholic solution of fluorescein, 1.0×10^{-5}M.
Concentration of ATU: ● 5.0×10^{-3}M
○ 7.5×10^{-3}M

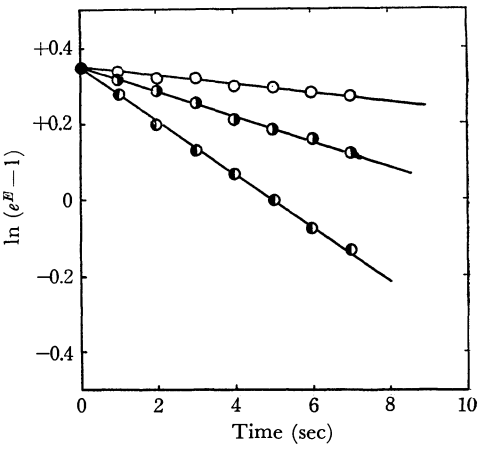

Fig. 3. Plots of $\ln(e^F - 1)$ *vs.* t for thionine, 1.0×10^{-5}M.
Concentration of ATU: ○ 5.0×10^{-4}M
◑ 1.0×10^{-3}M
◐ 5.0×10^{-3}M

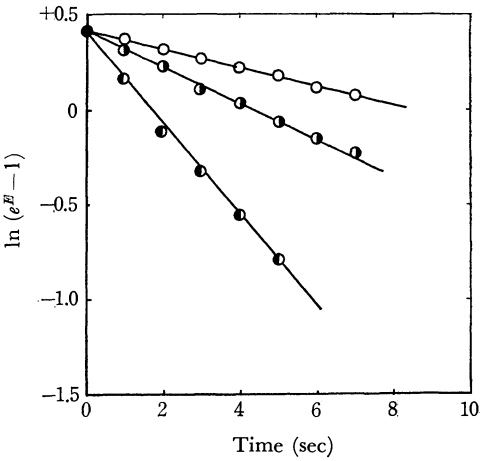

Fig. 4. Plots of $\ln(e^F - 1)$ *vs.* t for methylene blue, 1.0×10^{-5}M.
Concentration of ATU: ○ 5.0×10^{-4}M
◑ 1.0×10^{-3}M
◐ 5.0×10^{-3}M

8) M. Imamura, *J. Inst. Polytech. Osaka City Univ.*, Vol. 5, Ser. C, 85 (1956).

TABLE 2. SOME CHARACTERISTICS OF THE TRIPLET STATES OF THE SENSITIZERS AND DYES

	Triplet level (cm^{-1})	Decay constant, $1/\tau$[e] (sec^{-1})	φ_{ST}^{D}
1,2,5,6-Dibenzanthracene	18300[a]	4×10^3	0.89[g]
Triphenylene	23310[b]	2.6×10^4	0.95[g]
Anthracene	14700[a]	7×10^2	0.70[h]
β-Acetonaphthone	20746[b]	1.8×10^4	0.84[h]
Fluorescein		~50[f]	
Eosine	14900[c]	3.0×10^3	
Erythrosine	15400	6.4×10^3	
Methylene blue	— [d]	1.8×10^3	
Thionine	— [d]	1.5×10^3	

a) D. P. Craig and I. G. Ross, *J. Chem. Soc.*, **1954**, 1589.
b) W. G. Herkstroeter, A. A. Lamola and G. S. Hammond, *J. Am. Chem. Soc.*, **86**, 4537 (1964).
c) From the phosphorescence spectrum in EPA at 77°K.
d) Phosphorescence spectrum not observed in EPA at 77°K.
e) From the decay of T–T absorption at room temperature in ethanol.
f) The value for the aqueous solution. L. Lindqvist, *Arkiv Kemi.*, **16**, 79 (1960).
g) A. A. Lamola and G. S. Hammond, *J. Chem. Phys.*, **43**, 2129 (1965).
h) T. Medinger and F. W. Wilkinson, *Trans. Faraday Soc.*, **61**, 620 (1965).

As for fluorescein, it is well-known that its ethanol solution has no distinct absorption in the visible region perhaps because of the isomerization into lactonic form.[9] 30 vol% aqueous alkaline (0.02N KOH) alcoholic solution was successful for the present purpose. Figure 2 shows the $\ln(e^{E}-1)$ *vs.* t plots for the two experiments (E is the optical density).

The photoreduction of thiazine dyes by ATU in ethanol have not yet been investigated in detail. But the general feature of the reaction is believed to be similar to that of xanthene dyes. $\ln(e^{E}-1)$ *vs.* t plots for thionine and methylene blue are given in Figs. 3 and 4. They are satisfactorily linear, and it may be said that the reaction proceeds *via* D-R mechanism. No shift of the absorption maximum has been observed during the reaction, and upon introduction of air into the bleached solution, 100% recovery of the dye occurred.

Sensitized Photoreduction of Dye. In Table 2 some characteristics of the triplet states of the sensitizers and the dyes used in the present investigation, are tabulated.

The sensitizers were chosen from the following viewpoints; 1) high triplet levels compared with those of the dyes, 2) the φ_{ST} value is known and is close to unity, 3) rather small decay constant. In addition, it is desirable that a sensitizers' absorption band is located in the region where there is no appreciable absorption by dyes. For the sensitizers used in the present investigation, there was scarcely any fear of the appreciable superposition of the direct photochemical reaction over the sensitized one. From the values of τ listed in Table 2, 10^{-5}M of dye is expected to be sufficient for the energy transfer to occur as a diffusion controlled process. This was really proved in most cases by the zero order rate law as described below. It was checked by the flash experiments that the decays of the triplet sensitizers are not affected by the addition of 1×10^{-2}M of ATU. Some examples are shown in Fig. 5. The plots of optical density against

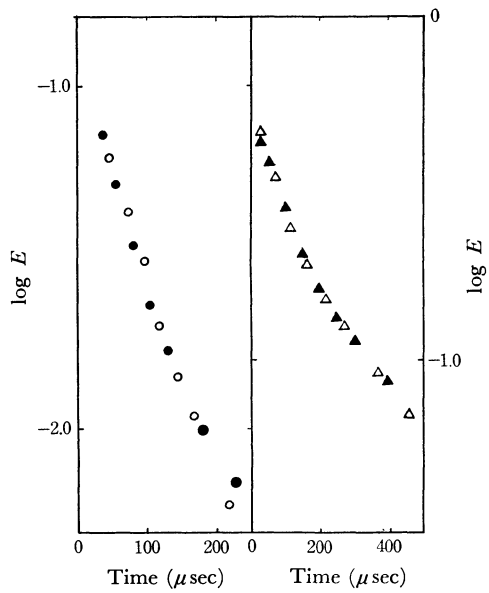

Fig. 5. Effect of the addition of ATU on the donor's triplet decay.
Triphenylene ○ [ATU]=0
● [ATU]=1.0×10^{-2}M
1,2,5,6-Dibenzanthracene
△ [ATU]=0
▲ [ATU]=1.0×10^{-2}M

9) T. Nash, *J. Am. Chem. Soc.*, **62**, 1574 (1958); V. Zanker and W. Peter, *Berichte*, **91**, 572 (1958).

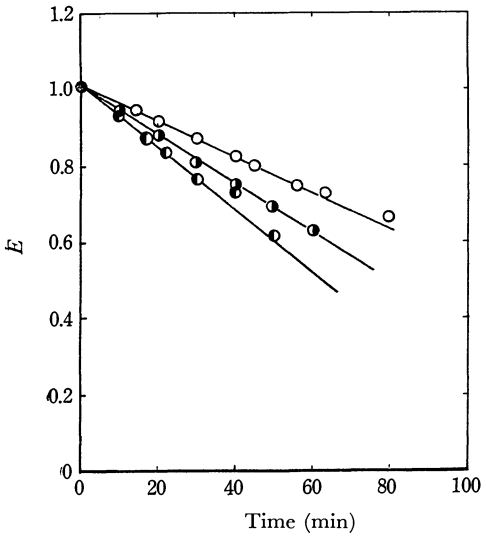

Fig. 6. An example of the plots of E *vs.* t for the sensitized reaction.
[Erythrosine] $=1.0\times10^{-5}$M
[1,2,5,6-Dibenzanthracene] $=5.0\times10^{-4}$M
Concentration of ATU: ○ 5.0×10^{-3}M
◑ 7.5×10^{-3}M
◐ 1.0×10^{-2}M

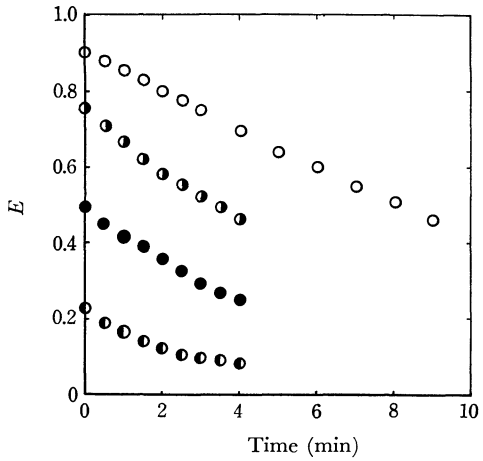

Fig. 7. Effect of dye concentration on sensitized reaction.
[1,2,5,6-Dibenzanthracene] $=5.0\times10^{-4}$M
[ATU] $=1.0\times10^{-2}$M
Concentration of eosine: ○ 9.3×10^{-6}M
◑ 7.7×10^{-6}M
● 5.3×10^{-6}M
◐ 2.4×10^{-6}M

time are always satisfactorily linear for 10^{-5}M of dye. Some examples are shown in Fig. 6.

Since the rate is expressed by the following formula,

$$-\frac{dA}{dt} = I_{ab}\varphi_{ST}^{D}\gamma\beta^{A} \qquad (3)$$

the results in Fig. 6 ensures that all the factors on the right hand side are kept constant during the reaction. On the contrary, when the concentration of dye was smaller, the rate gradually decreased which undoubtedly is due to the decrease of the energy transfer efficiency, γ. Some examples for such a case are shown in Fig. 7. In all cases there was no sign that the sensitized reaction proceeds rather in a different way than in the direct reaction.

Table 3 gives the quantum yields of the sensitized photoreduction of xanthene dyes at various ATU

Table 3. Quantum yields for the sensitized photoreduction of xanthene dyes at different ATU concentrations

	[ATU]M/donor	1,2,5,6-Dibenzanthracene	Triphenylene	β-Acetonaphthone
Fluorescein	1.0×10^{-2}	5.0×10^{-3}		2.9×10^{-2}
	7.5×10^{-3}	3.7×10^{-3}		2.6×10^{-2}
	5.0×10^{-3}	3.3×10^{-3}		1.8×10^{-2}
Eosine	1.0×10^{-2}	9.9×10^{-3}	1.3×10^{-2}	$1.3_8\times10^{-2}$
		1.0×10^{-2}	1.3×10^{-2}	
			1.2×10^{-2}	
			1.1×10^{-2}	
	7.5×10^{-3}	8.9×10^{-3}	0.9×10^{-2}	1.1×10^{-2}
		9.7×10^{-3}	1.0×10^{-2}	
		8.6×10^{-3}	$0.9_8\times10^{-2}$	
	5.0×10^{-3}	8.4×10^{-3}	$0.8_5\times10^{-2}$	9.0×10^{-3}
		6.9×10^{-3}	$0.7_2\times10^{-2}$	
		6.9×10^{-3}		
	2.5×10^{-3}			7.5×10^{-3}
Erythrosine	1.0×10^{-2}	2.8×10^{-3}	3.2×10^{-3}	3.2×10^{-3}
				$3.1_4\times10^{-3}$
	7.5×10^{-3}	$2.4_6\times10^{-3}$	2.5×10^{-3}	2.6×10^{-3}
	5.0×10^{-3}	$1.8_3\times10^{-3}$	1.7×10^{-3}	$1.8_7\times10^{-3}$

TABLE 4. QUANTUM YIELDS FOR THE SENSITIZED PHOTOREDUCTION OF THIAZINE DYES AT DIFFERENT ATU CONCENTRATIONS

	[ATU]M/donor	1,2,5,6-Dibenzanthracene	Anthracene	β-Acetonaphthone
Methylene blue	7.5×10^{-3}	2.1×10^{-2}	$2.2_4\times10^{-2}$	$2.0_9\times10^{-2}$
	5.0×10^{-3}	2.0×10^{-2}	$1.9_4\times10^{-2}$	$1.6_8\times10^{-2}$
	2.5×10^{-3}	$1.9_8\times10^{-2}$		
	1.0×10^{-3}		$1.1_8\times10^{-2}$	
	5.0×10^{-4}	0.8×10^{-2}		
Thionine	1.0×10^{-2}	7.2×10^{-2}	8.8×10^{-2}	
	7.5×10^{-3}	7.2×10^{-2}	8.7×10^{-2}	
	5.0×10^{-3}	7.2×10^{-2}	8.5×10^{-2} (10.0×10^{-2})	9.0×10^{-2}
	1.0×10^{-3}	3.8×10^{-2}	4.5×10^{-2} (6.2×10^{-2})	5.3×10^{-2}
	5.0×10^{-4}	$2.9_4\times10^{-2}$	3.7×10^{-2} (3.7×10^{-2})	4.4×10^{-2}

TABLE 5. φ^{A}_{ST} VALUES OF FIVE DYES OBTAINED BY USING DIFFERENT SENSITIZERS AND AT DIFFERENT ATU CONCENTRATIONS

	[ATU]M/donor	1,2,5,6-Dibenzanthracene	Triphenylene	β-Acetonaphthone
Fluorescein	1×10^{-2}	(0.04)		0.006_5
	7.5×10^{-3}	(0.047)		0.006_4
	5×10^{-3}	(0.04_8)		0.008_3
	average	$0.004_5\pm0.005$		$0.007_0\pm0.001$
Eosine	1×10^{-2}	0.48	0.39	0.33
		0.46	0.39	
			0.40	
			0.43	0.31
	7.5×10^{-3}	0.42	0.42	
		0.39	0.39	
		0.41	0.40	
	5.0×10^{-3}	0.3_8	0.41	
		0.4_6	0.46	
		0.4_6		
	2.5×10^{-3}			0.31
	average	0.43 ± 0.04	0.42 ± 0.04	0.31 ± 0.02
Erythrosine	1×10^{-2}	1.1	1.1	0.9_5
				0.98
	7.5×10^{-3}	1.0	1.2	0.9_8
	5×10^{-3}	0.9	1.1_4	0.9_0
	average	1.06 ± 0.01	$1.1_5\pm0.06$	0.92 ± 0.06
Methylene blue	1.0×10^{-2}			
	7.5×10^{-3}	0.51	0.47	0.41
	5.0×10^{-3}	0.57	0.57	0.54
	2.5×10^{-3}	0.56		
	1.0×10^{-3}		0.53	
	5.0×10^{-4}	0.48		
	average	0.52	0.52	0.48
Thionine	1.0×10^{-2}	0.66		0.52
	7.5×10^{-3}	0.66		0.52
	5.0×10^{-3}	0.62	0.39(0.35)	0.59
	1.0×10^{-3}	0.59	0.33(0.34)	0.49
	5.0×10^{-4}	0.58	0.30(0.30)	0.44
	average	0.62	0.34	0.51

concentrations.

In the case of fluorescein, only 1,2,5,6-dibenzanthracene and β-acetonaphthone could be used for the reason of solubility. Moreover, in the case of the former sensitizer, its absorption declined when the solution containing 1×10^{-2}M of ATU was illuminated. The reason is unknown. Such a phenomenon was not observed when the solvent was a pure ethanol.

Table 4 summarizes the similar data for thiazine dyes.

Table 5 gives the φ_{ST}^{A} values for five kinds of dye evaluated by applying Eqs. (1) and (2) respectively to Φ's and Φ^{S}'s obtained under otherwise similar conditions.

φ_{ST}^{A} values of each dye obtained by using different sensitizers, agree fairly well except the ones for fluorescein and for the thionine-anthracene system. The reason for the very low φ_{ST}^{A} value for the latter system is unknown. The value for fluorescein is somewhat doubtful on account of the scanty data. A survey of the data in Table 5 may indicate that the φ_{ST}^{A} values in the case of β-acetonaphthone are laways somewhat smaller. The value of φ_{ST}^{D} of this compound might not be correct. Apart from these points, the results are very satisfactory. It is judged that the conditions for the method to be applicable, are amply satisfied.

Discussion

In view of the results obtained, the method seems to be generally applicable. But in order to make it more confident, two further confirmations will be added below.

Firstly, according to the following reaction schemes,[2-4]

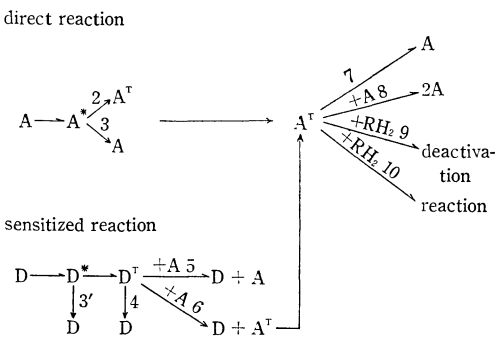

γ and β^{A} are written in general as,

$$\gamma=\frac{k_6[A]}{k_4+(k_5+k_6)[A]} \tag{4}$$

$$\beta^{A}=\frac{k_{10}[RH_2]}{k_7+k_8[A]+k_9[RH_2]+k_{10}[RH_2]} \tag{5}$$

Hence the plots $1/\Phi^{S}$ *vs.* $1/[RH_2]$ as well as $1/\Phi$ *vs.* $1/[RH_2]$ for the same dye concentration, should give, irrespective of a sensitizer, the same value of intercept/slope, which corresponds to $(k_9+k_{10})/(k_7+k_8[A])$. The comparison is made in Table 6, which shows that the above requirement is well satisfied. This assures that the steps succeeding the formation of triplet dye are quite the same in all the systems.

Secondly, the rate constant of the triplet energy transfer was estimated as follows. Under the condition $k_7>k_8$ [A], the inverse Φ^{S} is written as follows,

$$\frac{1}{\Phi^{S}}=\frac{1}{\varphi_{ST}^{D}}\left(\frac{k_9+k_{10}}{k_{10}}+\frac{k_7}{k_{10}[RH_2]}\right)\times\left(\frac{k_5+k_6}{k_6}+\frac{k_4}{k_6[A]}\right)$$

Table 6

Donor	$(k_9+k_{10})/(k_7+k_8[A])$ Fluorescein	Eosine	Erythrosine	Methylene blue	Thionine
None	~200	45—95	42	~500	1050
1,2,5,6-Dibenzanthracene	100	82	45	~750	~1000
Triphenylene		73	33		
β-Acetonaphtone	100	80	35	~750	~1000
Anthracene				~750	~1000

Table 7. Ratio of the deactivation and true reaction between triplet dye and ATU (k_9/k_{10})

Donor/Acceptor	Fluorescein	Eosine	Erythrosine	Methylene blue	Thionine
1,2,5,6-Dibenzanthracene	9	28	97	30	9
Triphenylene	—	24	81	—	—
β-Acetonaphthone	14	19	72	—	—
Anthracene	—	—	—	23	7
None	2	7	51	23	8

Thus the plot $1/\Phi^S$ *vs.* $1/[A]$ gives $k_4/(k_5+k_6)$ as the ratio, intercept/slope. The plots were drawn by using such data as given in Fig. 7. The method is of course very rough, but the values of k_5+k_6 obtained by using the k_4 values in Table 2 were 10^9—10^{10} M^{-1} sec^{-1}. This assures that the energy transfer occurs as diffusion controlled.

As seen in Table 5, the φ_{ST}^A values obtained in the present research are much larger than the tentative values already published,[2-4] and of course, the ones of Oster. They are compared with the values of Porter and Bowers[6] (in the aqueous solution of pH 9), for fluorescein (0.05), eosine (0.71), erythrosine (1.07) and Schenck's values for fluorescein (0.03), eosine (0.3) and erythrosine[10] (0.6) (in methanol at 20°C). Somewhat smaller values of Schenck may be due to the method being similar as the Oster's one. Thus it can now be concluded that the values evaluated by Oster's method are in general smaller than the real ones due to the participation of the deactivation reaction between D^T and ATU.

The φ_{ST}^A values of xanthene dyes increase in the order, fluorescein<eosine<erythrosine. This is interpreted in terms of the internal heavy atom effect.

The magnitude of the mere deactivation of triplet dye by the attack of ATU which largely influences the quantum yield can simply be evaluated as follows. Thus the values of β_{max}^A, as obtained from the intercepts of the $1/\Phi^S$ (or $1/\Phi$) *vs.* $1/[RH_2]$ plots, using the φ_{ST}^D (or φ_{ST}^A) values and assuming $\gamma=1$, give $(k_9+k_{10})/k_9$. Table 7 lists the values of k_9/k_{10}, *i. e.*, the ratio of the mere deactivation and the genuine reaction between triplet dye and ATU. It is seen that for each dye, the values are about the same for different sensitizers and also for the direct reaction. This verifies again the assumption, $\gamma=1$.

Table 7 shows that the mere deactivation of triplet dye by ATU increases in the order, fluorescein <eosine<erythrosine. Thus it has been established unequivocally that the magnitude of the photoreduction quantum yield largely depends on such a deactivation process and that the internal conversion does not matter as once Oster proposed.[1] All the values of $\Phi_F+\Phi_T$ for fluorescein (0.9_3), eosine (0.9_5) and erythrosine (~ 1.0) are close to unity.

Finally, correction will be made on the previously reported rate constants of some elementary reactions involved in the photoreduction of eosine in ethanol,*2 using the present value of φ_{ST} (0.40).*2

TABLE 8. RATE CONSTANTS OF SOME ELEMENTARY REACTIONS INVOLVED IN THE PHOTOREDUCTION OF EOSINE IN ETHANOL

From the reactions in pure ethanol

$k_7'/k_7=3.8\times10^{-3}$ (3×10^{-2})

$k_7(\approx k_7'')=2.3\times10^3$ sec^{-1}

$k_7'=\sim10$ sec^{-1} $(70$ $sec^{-1})$

$k_8'/k_8=\sim2\times10^{-3}$ $(\sim4\times10^{-3})$

$k_8=\sim2\times10^8$ M^{-1} sec^{-1}

$k_8'=\sim9\times10^4$ M^{-1} sec^{-1}

From the reactions with ATU in ethanol

$k_8'/k_8=1$—3×10^{-3} $k_8=1.3$—3.7×10^8 M^{-1} sec^{-1}

$k_8'=1$—5.5×10^5 M^{-1} sec^{-1}

$k_9'/k_9=0.7$—5×10^{-1} $k_9=1.1$—4×10^5 M^{-1} sec^{-1}

$k_9'=2.6$—5.5×10^4 M^{-1} sec^{-1}

': genuine reaction

no superscript: sum of the genuine and deactivation reaction.

The values in parentheses are the previous ones.

These values are very approximate.

10) K. Gollnick and G. O. Schenck, *Pure and Appl. Chem.*, **9**, 507 (1964).

*2 It is to be noted that some of the previous notations are changed to fit the present system.

BULLETIN OF THE CHEMICAL SOCIETY OF JAPAN VOL. 42 1231—1239 (1969)

Reactions of Singlet Oxygen and Half-reduced Oxygen which are Produced Simultaneously by the Interaction of Triplet Dye and Oxygen

Yoshiharu Usui, Chieko Iwanaga and Masao Koizumi

Department of Chemistry, Faculty of Science, Tohoku University, Katahira-cho, Sendai

(Received September 11, 1968)

Under experimental conditions in which the interaction between triplet dye and oxygen is an initiating process (D–O mechanism), the photosensitized oxidation of leucofluorescein in the aqueous solution (reaction (1)) has been found to decrease in rate with the increasing oxygen concentration and that the magnitude of the retarding effect of oxygen is almost the same independent of sensitizing dye. This is in sharp contrast to the kinetic feature of the oxidative photobleaching of dye (reaction (2)), where the rate becomes constant beyond a certain small oxygen concentration. On the basis of these findings, it has been proposed that in reaction (1), $^1O_2$ plays a dominant role and it is deactivated by process $^1O_2+{}^3O_2\rightarrow 2{}^3O_2$. As to reaction (2), strong evidence has been presented for the view that the interaction of triplet dye and oxygen in the aqueous solution produces a rather stable $D^+\cdots O_2^-$ of which only a small portion decomposes irreversibly. The principal evidence is as follows; 1) the free half-oxidized dye (produced by the reaction between triplet dye and $[Co(Ox)_3]^{3-}$ was found to oxidize FH_2 with a high rate and its decay was found to be accelerated by the addition of FH_2; 2) the decay of the half-oxidized species (first order decay!) produced in the aerated aqueous solution, on the other hand, was not affected by FH_2 under otherwise similar conditions as in (1).

It is well known that the following three mechanisms have long been proposed for the photosensitized oxidation, initiated by the interaction between triplet dye and oxygen.[1)]

a) Formation of singlet oxygen (Kautsky, Gaffron)
b) Electron transfer (Weiss, Franck)
c) Formation of molecular complex between dye and oxygen (Schenck).

At present, it seems that special interest is being focused on the first mechanism. Since the appearance of Foote and Wexler's work,[2)] a number of papers have been published in favor of the singlet oxygen theory. In spite of such a trend, the authors believe that the other two mechanisms must also be taken into account. In fact, the existence of half-oxidized and half-reduced dye found by Lindqvist,[3,4)] Grossweiner[5)] and by us[6,7)] has naturally led to the possible occurrence of photooxidation by virtue of the half-oxidized dye, *i. e.*, by the second mechanism; Lindqvist[8a)] for instance, has found such an example in the eosine-EDTA-Fe^{3+} system. Other examples have also been reported by us[19)] and by Kasche.[8b)]

The third mechanism which Schenck has long been advocating, was modified recently as a charge transfer type complex,[9)] and this mechanism is now thought to be closely related with the second one.

The first object of the present paper is to report a new kind of reaction which proceeds *via* singlet oxygen; it is the photosensitized oxidation of leucofluorescein (FH_2) initiated by D–O mechanism, some thiazine and xanthene dyes being used as sensitizer. The second object is to make it clear that the photooxidative bleaching of such dyes does not occur by singlet oxygen but *via* electron transfer reaction or alternatively *via* radical ion pair. This has been substantiated partly, by the

1) For instance, Th. Forster, *Z. Elektrochem.*, **56**, 716 (1952).
2) C. S. Foote and S. Wexler, *J. Am. Chem. Soc.*, **86**, 3879, 3880 (1964); C. S. Foote, S. Wexler and W. Ando, *Tetrahedron Letters*, **1965**, 4111.
3) L. Lindqvist, *Arkiv. for Kemi.*, **16**, 79 (1960).
4) V. Kasche and L. Lindqvist, *Photochem. Photobiol.*, **4**, 923 (1965).
5) E. F. Zwicker and L. I. Grossweiner, *J. Phys. Chem.*, **67**, 549 (1963).
6) S. Kato, M. Morita and M. Koizumi, This Bulletin, **37**, 117 (1964).
7) T. Ohno, S. Kato and M. Koizumi, *ibid.*, **39**, 232 (1966).
8) a) L. Lindqvist, *Acta Chem. Scand.*, **20**, 2967 (1966). b) V. Kasche, *Photochem. Photobiol.*, **6**, 643 (1967).
9) K. Gollnick and G. O. Schenck, *Pure and App. Chem.*, **9**, 507 (1964).

finding of a quite different dependence of the two types of reaction on the oxygen concentration. Thirdly we would like to compare the oxidative behavior of all the conceivable transient species, $D^+\cdots O_2^-$, O_2^-, $D^+\cdots D^-$ and D^+ *1 in addition to singlet oxygen $^1O_2$, choosing FH_2 as an oxidizable substance. A remarkable finding is that $D^+\cdots O_2^-$ is less reactive than singlet oxygen, whereas the free D^+ is more reactive. This may be the first chemical evidence for the formation of a rather stable complex, $D^+\cdots O_2^-$.

Experimental

Purification of materials and most of the experimental procedures are similar to those in previous papers. All the experiments were performed at 30°C. pH of the solution was fixed at 6.2 by using the buffer of acetic acid-acetate, except otherwise mentioned.

Results and Discussion

Photosensitized Oxidation of Leucofluorescein. This reaction was studied by one of the present authors (M. K.) in collaboration with Uchida and Kato.[10-12] It was found in this series of work that the oxidation of FH_2 by acridine in the presence of such a large quantity of oxygen as to make the attack of oxygen on the triplet acridine predominant (D–O mechanism), decreases in rate with the increase of the oxygen concentration. Any attempt to clarify the cause of this phenomenon, however, was not made at that time. A few years later, a similar phenomenon was found in the photooxidation of acridan by acridine in the benzene solution containing oxygen.[13] In these papers, the phenomenon was tentatively interpreted by the scheme

$$A^T + {}^3O_2 \rightarrow A + {}^1O_2$$
$$^1O_2 + AH_2 \rightarrow AH + HO_2$$
$$^1O_2 + {}^3O_2 \rightarrow 2{}^3O_2,$$

in which A^T, $^1O_2$ and AH_2 are respectively triplet acridine, singlet oxygen and acridan. If a similar scheme holds for the photooxidation of FH_2, then the ratio of the rate constants for reaction, $^1O_2+FH_2\rightarrow HO_2+FH$ and $^1O_2+{}^3O_2=2{}^3O_2$ should be constant irrespective of the sensitizing dye. To support the above scheme, it is necessary to make experiments using various sensitizers. Therefore, in the present paper, the reaction was investigated quantitatively in a somewhat modified way, using methylene blue (MB), eosine (Es), and thionine (Th), as sensitizers. Before this, some experiments were performed using MB in order to reconfirm the previous result and to find a more suitable condition for the quantitative investigation ((A) and (B)).

A) Reaction in the Degassed Solution. The photochemical oxidation of FH_2 sensitized by MB, in the degassed aqueous solution (pH, 6.2) was reconfirmed. As reported in the previous paper, MB is partially photobleached accompanied with the oxidation of FH_2. To simplify the kinetic treatment, it is desirable to keep the concentration of MB as constant; the addition of a certain quantity of H_2O_2 was attempted to reconvert the reduced MB back to the original dye. It was found that 8.8×10^{-3}M of H_2O_2 restores MB very efficiently without affecting any essential feature of the reaction.*2 In fact, the reaction was found to occur approximately as first order in FH_2 (when $[FH_2]$ is small), as expected from the following rate formula which can be derived directly from reaction scheme I.

$$\Phi_{D-F} = \varphi_{ST}\frac{k^r_L[FH_2]}{k_d^S + k_L^S[FH_2]} \qquad (I)$$

Scheme I

$$MB \xrightarrow{I_{ab}\varphi_{ST}} MB^T \xrightarrow{MB} 2MB \text{ or } MB^+ + MB^- \quad k_D^s \quad (1)$$

$$k_d \swarrow \quad \downarrow MB \qquad \downarrow FH_2 \rightarrow \begin{cases} MB + FH_2 & k_L^d \quad (2) \\ MB^- + FH_2^+ & k_L^r \quad (3) \end{cases} \Big\} k_L^s$$

$$MB \qquad k_d^s = k_d + k_D^s\,[MB]$$

φ_{ST}, k^r_L, k^S_L and k_d are respectively the probability for intersystem crossing, rate constant for the genuine reaction, the total rate constant including deactivation and the rate constant for (spontaneous) deactivation of triplet MB.

Keeping the concentration of MB as 7.8×10^{-6}M,

Table 1. Dependence of the quantum yield on the concentration of FH_2 in degassed solution

$[FH_2]\times10^5$ M	Φ	$[FH_2]\times10^5$ M	Φ
0.3	0.022	4.0	0.16_5
0.5	0.034	5.0	0.19_4
1.0	0.058	10.0	0.22
1.5	0.094		
2.5	0.105		
3.0	0.12_6		

*1 Throughout the present paper, D and D^+ denote respectively the original dye and the half-oxidized dye, irrespective of its real charge.

*2 Hence the similar quantity of H_2O_2 was added throughout the present research.

10) K. Uchida, S. Kato and M. Koizumi, This Bulletin, **35**, 16 (1962).
11) K. Uchida and M. Koizumi, *ibid.*, **35**, 1871, 1875 (1962).
12) K. Uchida, *ibid.*, **36**, 1097 (1963).
13) S. Niizuma, Y. Ikeda and M. Koizumi, *ibid.*, **40**, 2249 (1967); A. Kira and M. Koizumi, *ibid.*, **40**, 2486 (1967).

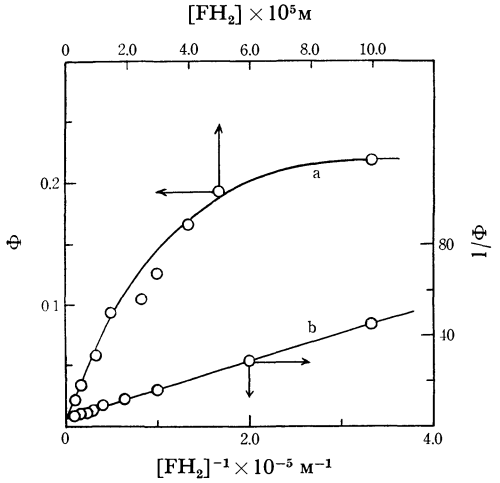

Fig. 1. Dependence of the quantum yield on the concn. of FH_2 ([MB]$=7.8\times10^{-6}$M) in degassed soln.

a ---- Φ *vs.* $[FH_2]$ plot
b ---- Φ^{-1} *vs.* $[FH_2]^{-1}$ plot

the dependence of the quantum yield on the FH_2 concentration was examined. The results are given in Table 1 and in Fig. 1.

Figure 1 shows that a linear relationship holds between $1/\Phi$ and $1/[FH_2]$, as is expected from Eq. (I). From the intercept and the slope, the values of φ_{ST} k^r_L/k^S_L and k^S_L/k^S_d were evaluated respectively as 0.30 and $2.9\times10^4M^{-1}$. The value of k^S_d reported by us is $1.5—3\times10^4$ sec^{-1}.[6] The recent value of Danziger *et al.*[14] is 2.5×10^4 sec^{-1}. Using the latter value we get k^S_L as $7.2\times10^8M^{-1}\cdot sec^{-1}$. Thus reaction $MB^T+FH_2\rightarrow MBH+FH\cdot$ occurs with a rate constant which is a little smaller than the diffusion-controlled one. The above value is more than ten times larger than the one for reaction $MB^T+EDTA\rightarrow MB^-+EDTA^+$.[14]

B) Reaction in the Aerated Solution and in the Solution Equilibrated with one Atmosphere of Oxygen (hereafter abbreviated oxygenated solution). It

Table 2. Quantum yield of FH_2 oxidation in the aerated and in the oxygenated solution

$[FH_2]\times10^5$M	Φ (air saturated)	Φ (1 atm. of oxygen)
0.3	0.011	—
0.5	0.016	0.008
1.0	0.029	0.017
2.5	0.075	—
3.0	0.083	0.052
4.0	0.104	—
5.0	0.142	0.090
6.0	0.155	0.097
10.0	0.167	0.10

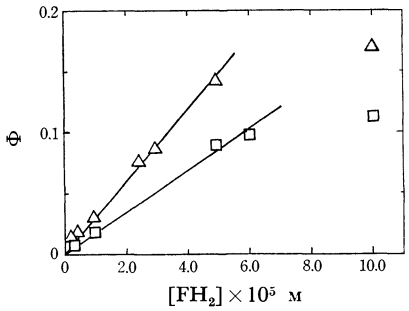

Fig. 2. Dependence of the quantum yield on the concn. of FH_2 in the aerated (△) and in the oxygenated (○) acetate buffer solution. ([MB]$=7.7\times10^{-6}$ M)

was established that the photosensitized oxidation of FH_2 by MB, occurs in the aerated solution as well as in the oxygenated solution. The results are given in Table 2 and in Fig. 2.

Figure 2 shows that the rate is proportional to $[FH_2]$ below 6×10^{-5}M of FH_2. The quantum yield in the aerated solution is about one half that of the degassed solution under otherwise similar conditions, when the FH_2 concentration is less than 1×10^{-5}M. In the oxygenated solution the rate is much smaller than in the aerated solution.

Now triplet MB is attacked by oxygen with a rate constant of $3\times10^9M^{-1}$ sec^{-1}. This value was evaluated by combining the value of $k^S_d/k^S_{O2}=7.75\times10^{-6}$ (k^S_{O2}, rate constant for the entire reaction including the mere deactivation between MB^T and O_2 reported already[15]) with the k^S_d value mentioned above. Comparison of this value with that of k^S_L ($7.2\times10^8M^{-1}$ sec^{-1}) leads to the expectation that in the aerated solution, triplet MB is mainly attacked by oxygen instead of by FH_2 as long as the latter concentration is less than 6×10^{-5}M. Accordingly there is no doubt that the above reaction is due to a certain oxidative species that is produced by the reaction between MB^T and oxygen. Moreover, the smaller Φ in the oxygenated solution suggests that this species is deactivated by the ground state oxygen. Such a possibility was investigated more quantitatively by changing the concentration of dissolved oxygen in a wider range.

C) Dependence of the Quantum Yield on the Concentration of Oxygen. Fixing the concentration of FH_2 and MB respectively at 1.0×10^{-5} and 8.0×10^{-6}M, the dependence of the quantum yield of the reaction on the oxygen concentration was examined from $[O_2]=0$ to 1.2×10^{-3}M. The results are given in Table 3 and in Fig. 3.

As Fig. 3 shows, the $1/\Phi$ *vs.* $[O_2]$ plot consists of two linear portions, which can be explained as

14) R. M. Danziger, K. H. Bar-Eli and K. Weiss, *J. Phys. Chem.*, **71**, 2633 (1967).

15) H. Obata, K. Kogasaka and M. Koizumi, This Bulletin, **32**, 125 (1959).

Table 3. Dependence of Φ on the oxygen concentration $[FH_2]=1.0\times10^{-5}$M

$[O_2]\times10^4$ M	Φ	$[O_2]\times10^4$ M	Φ
0	0.058	6.5	0.016
0.2	0.049		(0.018)
1.0	0.038	8.0	0.018
	0.036		0.019
1.7	0.032	10.0	0.015
2.4	0.027	12.0	0.014
4.0	0.025	14.0	0.011
5.0	0.021		

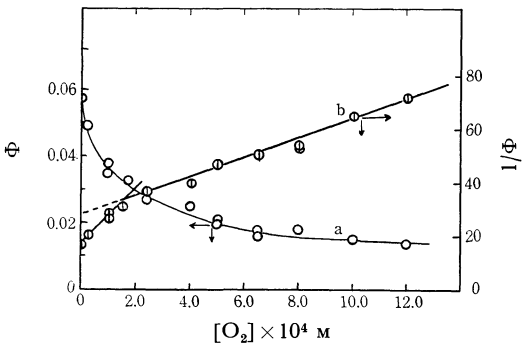

Fig. 3. Effect of oxygen concn. on the quantum yield of fluorescein formation. (Sens. ---- MB, 8.0×10^{-6}M)
a ---- Φ *vs.* $[O_2]$ plot
b ---- Φ^{-1} *vs.* $[O_2]$ plot

follows. In the low concentration region of oxygen, Φ decreases with the increase of oxygen concentration due to the competition of the reaction between MB^T and FH_2 and that between MB^T and oxygen. In the higher concentration region of oxygen where D–O mechanism prevails, the quantum yield still maintains the value of $\sim10^{-2}$ but it gradually decreases with the oxygen concentration. Thus a quite similar interpretation as in the oxidation of acridan with acridine in benzene[13] has been found to hold in the case of MB. If one assumes that Scheme II (D–O mechanism) holds for the high oxygen concentration region, one can easily derive Eq. (II).

Scheme II

$$MB \xrightarrow{I_a b\varphi_{ST}} MB^T \xrightarrow[k^s_{O_2}]{O_2} \begin{cases} {}^1O_2 + MB & k^r_{O_2} \quad (4) \\ {}^3O_2 + MB & k^d_{O_2} \quad (5) \end{cases}$$

$$^1O_2 \xrightarrow{\text{(Solvent)}} {}^3O_2 \qquad k_d' \quad (6)$$

$$^1O_2 + {}^3O_2 \rightarrow 2{}^3O_2 \qquad k'_{d,O_2} \quad (7)$$

$$^1O_2 + FH_2 \rightarrow HO_2 + FH \quad k_L' \quad (8)$$

$$\Phi_{D-O} = \varphi_{ST}\frac{k^r_{O_2}}{k^s_{O_2}}\frac{k_L'[FH_2]}{k_d'+k'_{d,O_2}[O_2]+k_L'[FH_2]} \approx \varphi_{ST}\frac{k^r_{O_2}}{k^s_{O_2}}\frac{k_L'[FH_2]}{k_d'+k'_{d,O_2}[O_2]} \qquad (II)$$

Applying Eq. (II) to the linear portion in the higher concentration region of oxygen, one can estimate the value of $k'_{d,O_2}/k'_d$ as $1.1—1.2\times10^3M^{-1}$. The linear part in the lower oxygen concentration region consists of the contribution from Φ_{D-F} and Φ_{D-O} and cannot be analysed in a simple way.

D) Comparison of the Values of $k'_{d,O_2}/k'_d$ for Several Sensitizers. If Scheme II really holds, the value of $k'_{d,O_2}/k'_d$ should be independent of a sensitizer used. To examine this, oxygen concentration effect on Φ_{D-O} in the higher concentration region of oxygen was examined using thionine

Table 4. Φ_{D-O} of the oxidation of FH_2 by using thionine and eosine as a sensitizer

a) Thionine	$[Th]=9\times10^{-6}$M	$[FH_2]=1.0\times10^{-5}$M
$[O_2]\times10^4$ M	$\Phi_{D-O}\times10^2$	
0	38.2	
2.4	3.8	
3.9	3.1	
7.0	1.6	
9.5	1.3	
12.0	1.2	
b) Eosine	$[Es]=1.0\times10^{-5}$ M	$[FH_2]=1.0\times10^{-5}$M
$[O_2]\times10^4$ M	$\Phi_{D-O}\times10^2$	
0	4.6	
2.4	~0.46	
4.0	0.38	
5.0	0.33, 0.36	
7.5	0.25, 0.28	
10.0	0.19	
12.0	0.18	

Table 5. Values of $k'_{d,O_2}/k'_d$

Sensitizer	Oxidized sub.	Solvent	E^T_{sens} (cm^{-1})†	$(k'_{d,O_2}/k'_d)\times10^{-3}$	Φ^0_{D-O}‡
MB	FH_2	water	—	1.1—1.2	0.036 0.045
Th	FH_2	water	—	1.6—2.2	0.033
Es	FH_2	water	14900	1.8—2.5	0.0067
Acridine	FH_2	water	15800ππ*	(0.6)	0.03
(Acridine	Acridan	benzene	21400nπ*	(0.4—0.6))	

† Triplet level of a sensitizer
‡ The quantum yield when reaction (7) is absent

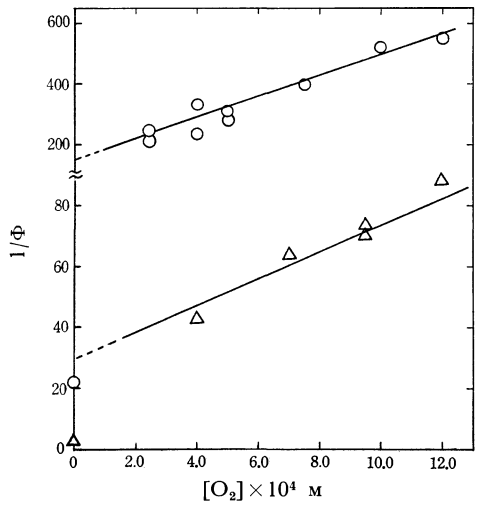

Fig. 4. Φ^{-1} *vs.* $[O_2]$ plot by using eosine (1.0×10^{-5}M, ○) and thionine (9.0×10^{-6}M, △) as a sensitizer.

and eosine as a sensitizer. The results are given in Tables 4, 5 and in Fig. 4. In Table 5 are added the values for acridine calculated from the old data.[12,13]

E) Assignment of the Oxidative Species in the Above Reaction. From the above result, one can say that in the photosensitized oxidation of FH_2 *via* D–O mechanism, the rate decreases with the increase of oxygen concentration in a quite similar way irrespective of a sensitizer used. This implies that the oxidative species reacting with FH_2 is the same one species for all the dyes. Further, one can conclude that this species does not participate in the oxidative bleaching of dye, because in contrast to the retarding effect of excess oxygen in the above reaction, the rate of oxidative bleaching of dye increases with the oxygen concentration and becomes constant when the concentration is high enough,[15,16] as shown in Fig. 5. The limiting

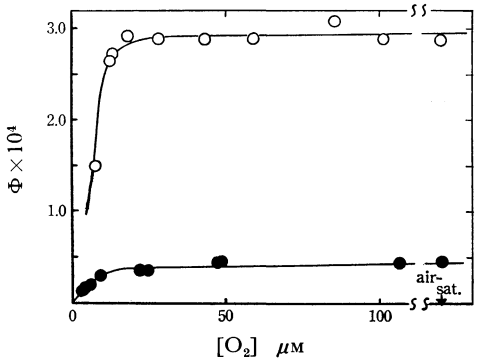

Fig. 5. Effect of the dissolved oxygen concn. on the quantum yield of photobleaching of eosine (○) and methylene blue (●).

16) M. Imamura and M. Koizumi, This Bulletin, **28**, 117 (1955).

Table 6. Quantum yield for the oxidative bleaching of dye

	$\Phi\times10^4$
Flourescein	1.3 [16]
Eosine	2.8 [16]
Erythrosine	3.7 [16]
Methylene blue	0.47[15]

quantum yields reported by our group are given in Table 6.

Table 6 shows that Φ for the oxidative photobleaching of dye is about two orders of magnitude less than that of the sensitized oxidation of FH_2.

The conceivable oxidative species produced *via* D–O mechanism are $^1O_2$, O_2^-, D^+ and $D^+\cdots O_2^-$ which are produced by the following processes.

$$D^T + {}^3O_2 \rightarrow D + {}^1O_2 \quad (9)$$

$$D^T + {}^3O_2 \rightarrow D^+\cdots O_2^- \quad (10)$$

$$\rightarrow D^+ + O_2^- \quad (11)$$

The production of half-oxidized dye has been fully established by Lindqvist,[3,17] Grossweiner[5] and by us.[6,7] To interpret the result that $k'_{d,O_2}/k'_d$ is independent of sensitizing dyes, only $^1O_2$ or O_2^- should be a reactive species. But the latter can be ruled out because D^+ which is produced accompanied by O_2^- (reaction (11)) is very reactive toward FH_2, as will be shown below. Furthermore half-oxidized dye is thought to be rather insensitive to oxygen.[6,7] Thus the most plausible interpretation is that the oxidation of FH_2 occurs *via* $^1O_2$ and the oxidative bleaching of sensitizing dyes occurs *via* electron transfer between D^T and oxygen. That acridine sensitized photooxidation of acridan, in which there is no evidence of the formation of half-oxidized form, occurs with about equal $k'_{d,O_2}/k'_d$ is also consistent with this view.

Further evidence for the electron transfer mechanism of the oxidative bleaching is supplied by our previous result that in the high concentration of dye the D–D mechanism occurs and in this case oxidative bleaching of dye as well as the rate of oxygen consumption becomes very much larger than in the D–O mechanism[18]; thus in the D–D mechanism, the reaction proceeds as follows. $D^T + D \rightarrow D^+ + D^-$ or $D^+\cdots D^-$, $D^- + O_2 \rightarrow D + O_2^-$, $D^+ \rightarrow$ destruction. If a reactive species were $^1O_2$ for the photobleaching, the larger Φ in the D–D mechanism cannot be explained.

The present results in conjunction with the results so far obtained previously lead to the conclusion that the oxidation of FH_2 and the oxidative

17) V. Kasche and L. Lindqvist, *Photochem. Photobiol.*, **4**, 923 (1965).

18) Y. Usui, K. Itoh and M. Koizumi, This Bulletin, **38**, 1015 (1965).

bleaching of sensitizing dyes occur as two different processes and that it is most likely that the former proceeds *via* $^1O_2$ while the latter *via* electron transfer.

This view will be further supported when the experimental condition is controlled in such a way that a particular species such as $D^+\cdots O_2^-$, O_2^-, $D^+\cdots D^-$ or D^+ is predominantly produced, and we compare the reactivity of these species toward FH_2. Such a comparison will, furthermore, allow us to make a more distinct discrimination of the reactive species in the oxidative bleaching of dye.

Experiments for Comparing the Reactivity of Various Transient Species to FH_2. A) $D^+\cdots O_2^-$. Strong support for the existence of such a complex has been presented already in the case of eosine.[19] Thus this dye gives the transient spectrum due to the half-oxidized dye in the aerated solution, which decays in the first order ($k=10^3$ sec^{-1}) independent of the oxygen concentration (phosphate buffer). For MB there is still no clear-cut evidence for the existence of such a complex, although this is plausible.[6,14] Hence, choosing eosine, the effect of the addition of FH_2 on the decay of $D^+\cdots O_2^-$ was examined at 458 nm (the absorption peak of the half-oxidized dye) at which the absorption due to half-reduced fluorescein is not appreciable.[3] The results are given in Table 7.

Table 7. The effect of the addition of FH_2 on the decay of $D^+\cdots O_2^-$

[Eos] $=1.0\times10^{-5}$M; aerated solution of pH=6.2 (0.1M Ac-buffer)

Concn. of FH_2 M	Decay const.* of $D^+\cdots O_2^-$ (sec^{-1}) $\times10^{-4}$
0	7
1.0×10^{-5}	5.3
4.0×10^{-5}	6.1
8.0×10^{-5}	4.9
20.0×10^{-5}	3.9—5.0

* The values have unexpectedly, been found to be more than the ones for the phosphate buffer solution. The decay constants in the 0.01M AcOH-AcONa buffer solution are nearly equal to the latter. The phenomenon is worthy of further investigation.

From Table 7, it appears that the addition of FH_2 causes a slight decrease of the decay, but this may perhaps be due to the overlap of the absorption due to F which is produced by the simultaneous oxidation of FH_2 by $^1O_2$. Thus the above experiment definitely indicates that $D^+...O_2^-$ is indifferent to FH_2, when the latter concentration is 10^{-5}—10^{-4}M.

19) Y. Usui and M. Koizumi, This Bulletin, **40**, 440 (1967).

B) O_2^-. According to Usui and Koizumi,[19] the following reaction occurs when a suitable quantity of EDTA is added to the aerated solution of eosine (phosphate buffer).

$$D^+\cdots O_2^- + EDTA \xrightarrow{k_R} D + EDTA^+ + O_2^- \quad (12)$$

Flash experiments were made in order to know the exact rate constant of the above reaction. Figure 6 gives the plot of the first order decay constant at 460 nm against the EDTA concentration. From this plot k_R was evaluated as $k_R=7.0\times10^5M^{-1}\,sec^{-1}$. This value is consistent with the results previously reported.[19] If the free O_2^- were to react with FH_2. Then the addition of a suitable quantity of EDTA is expected to increase the rate of oxidation of FH_2. The result, as shown in Table 8, is contrary to this expectation.

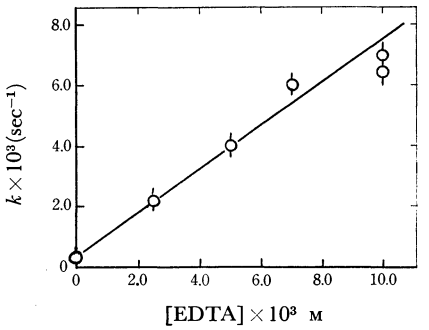

Fig. 6. Plot of the first order decay constant of $D^+\cdots O_2^-$ against [EDTA)]. (phos. buffer, pH=6.8)

Table 8. Effect of the addition of EDTA Φ_{D-0}

[Es] $=1.0\times10^{-5}$M [FH_2] $=1.0\times10^{-5}$M pH=6.2

[EDTA]M	Φ_{D-0}
0	0.0046
4×10^{-3}	0.0042
4×10^{-2}	0.0026

There is no sign of increase in Φ_{D-0} values.*3

A moderate decrease in the case of 4×10^{-2}M of EDTA may be due to the accompanied photobleaching of eosine due to reaction, $D^T+EDTA\rightarrow D^-+EDTA^+$.

C) $D^+\cdots D^-$. The formation of $D^+\cdots D^-$ has not been fully established. In the case of eosine in the aqueous solution, the formation of the free D^+ and D^- seems rather predominant, since the half-oxidized and half-reduced species decay in the

*3 We feel that the concentrations of EDTA were too low for reaction (12) to compete with the spontaneous deactivation of $D^+\cdots O_2^-$ in the present buffer solution. Further increase of EDTA may, however, change the initial process from $D^T+O_2\rightarrow D^+\cdots O_2^-$ ($k=2.5$—$3.1\times10^8M^{-1}\,sec^{-1}$ [19]) to $D^T+EDTA\rightarrow D^-+EDTA$ ($k=5\times10^5M^{-1}\,sec^{-1}$ [7]).

second order with approximately the same rate constant.[7),*4] On the other hand, according to Danziger *et al.*[14] the existence of $D^+\cdots D^-$ is likely to occur in the case of MB. Hence choosing MB, the dependence of the oxidation reaction of FH_2 on the concentration of MB was examined in the aerated solution. If the switch-over from D-O to D-D mechanism occurs with the increase in [D], it is expected that $D^+\cdots D^-$ will probably be attacked first by oxygen when $[FH_2]$ is not so large, as in the oxidative photobleaching and also as in the oxygen absorption experiment,[18] leaving D^+ as free. The free D^+ may then react with FH_2. Hence it is possible that the rate of the oxidation of FH_2 increases with the concentration of dye. Since an appreciable quantity of dimer exists in the high concentrated solution of dye, chiefly monomer was excited using a suitable cut-off filter.*5 The concentration of monomer was calculated by using the dissociation constant $K=2.8\times10^{-4}$ [21] (at 26.7°C). The results are shown in Table 9 and in Fig. 7.

As Fig. 7 shows, the quantum yield really increases with [MB] and reaches about a constant value above 2×10^{-5}M of MB. Thus the switch-over from D-O to D-D mechanism seems to occur around 2×10^{-5}M. This value is about one order smaller than the oxygen concentration, and it is suggested that the rate constant for $D^T+D\rightarrow$ is appreciably larger

Table 9. Dependence of the quantum yield of the oxidation of FH_2 on [MB]
$[O_2]=2.4\times10^{-4}$M, $[FH_2]=1.0\times10^{-5}$M

$[MB]_{total}\times10^5$M	$[MB]_{monomer}$	$I_{ab}\times10^5$mol sec^{-1}	Φ
12.0	7.7	3.5_8	0.027
10.0	6.7	3.5_2	0.025
8.0	5.8	3.4_6	0.029
7.2	5.2	3.4_0	0.025
6.0	4.5	3.2_0	0.028
4.0	3.0	2.7_6	0.030
2.0	1.8	2.1_6	0.031
1.0	0.9_5	1.3_3	0.026
0.8	0.7_6	1.1_4	0.019
0.5	0.48	2.3_2	0.0066

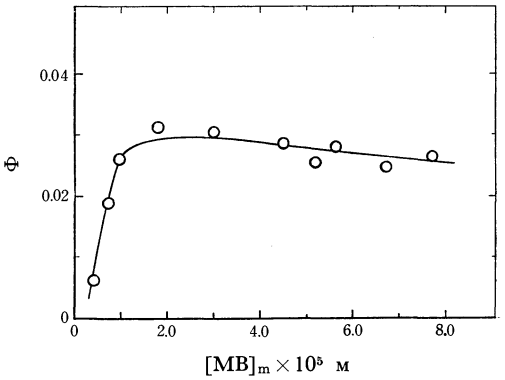

Fig. 7. Effect of the MB concn. on the quantum yield of fluorescein formation.

than that for $D^T+O_2\rightarrow$. There is, however, some possibility that the contribution of the ground state dimer still remains. In addition, it is to be noted that in the experiment described in A), D-D mechanism participates to some extent in the low concentration region of oxygen. But, for the plots drawn in Figs. 3 and 4 in the range $[O_2]>2.4\times10^{-4}$M, the contribution of D-D mechanism may be neglected. The above result indicates that a species $D^+\cdots D^-$ in the presence of oxygen is more effective than $^1O_2$.

The investigation of the influence of the oxygen concentration on the rate in the high [MB] region where D-D mechanism prevails, is thought to be interesting, because it may provide information on the reactivity of $D^+\cdots D^-$ and the free D^+ toward FH_2; the latter species may perhaps be produced by reaction $D^+\cdots D^-+O_2\rightarrow D^++D+O_2^-$. Fixing $[MB]=8.0\times10^{-5}$M ($[MB_m]=5.2\times10^{-5}$M) and $[FH_2]=1.0\times10^{-5}$M, the concentration of oxygen was changed from zero to 12.0×10^{-4}M. The results are shown in Fig. 8. It is seen that in the high concentration region of oxygen, the plot essentially coincides with that given in Fig. 3. This is natural because the D-O mechanism prevails in this region. But in the low concentration region of oxygen, the increase of Φ with the decrease in oxygen concentration is not so large as in the case of 8.0×10^{-6}M of MB. The value of $\Phi=0.041$ in the absence of oxygen is undoubtedly due to the reaction between $D^+\cdots D^-$ and FH_2, because under present experimental conditions the reaction of D^T with D prevails over that with FH_2. In the presence of a small amount of oxygen, reactions, $D^T+O_2\rightarrow D+{}^1O_2$, $D^T+O_2\rightarrow D^+\cdots O_2^-$ will compete with reaction $D^T+D\rightarrow D^+\cdots D^-$ on the one hand, and reaction $D^+\cdots D^-+FH_2\rightarrow$ and $D^+\cdots D^-+O_2\rightarrow D^++D+O_2^-$ will compete on the other hand. The last reaction may possibly increase the overall rate of FH_2-oxidation. The plot shown in Fig. 8 is consistent with this view although not conclusive, because of the scantiness of the data. At any rate,

*4 In the alcoholic solution, however, some evidence exists for the formation[20] of $D^+\cdots D^-$.

20) A. Kira and S. Kato, *Sci. Rep. of Tohoku Univ., Ser. I*, **48**, 1964 (1965).

*5 Danziger *et al.*[14] claimed that $D^+\cdots D^-$ is mainly produced by the excitation of the ground state dimer. However, we believe their result does not eliminate the possibility of $D^T+D\rightarrow D^+\cdots D^-$. The first order decay of D^T never excludes reaction $D_T+D\rightarrow2D$, as has already been domonstrated in the case of eosine.[7] Moreover, the present result cannot be explained unless reaction $D^T+D\rightarrow D^+...D^-$ occurs.

21) E. Rabinowitch and L. F. Epstein, *Ind. Eng. Chem.*, **63**, 69 (1941).

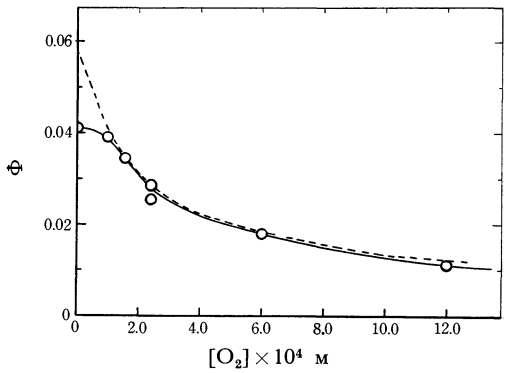

Fig. 8. Effect of oxygen concn. on the quantum yield of fluorescein formation in high MB concn. (8.0×10^{-5}M). *cf.* ---- [MB]$=8.0\times10^{-6}$M (Dotted line)

there is scarcely any doubt that in the case of MB, D–R mechanism is the most effective for the photo-oxidation of FH_2, D–D mechanism next and D–O mechanism the least effective.

D) Free D^+. In the case of the deaerated aqueous eosine solution, half-oxidized and half-reduced dye seem to exist mainly as free species.[7] But this is not yet completely conclusive. According to our result, not yet published, electron transfer reaction between triplet dye and $[Co(Ox)_3]^{3-}$ occurs very efficiently, yielding D^+ and $[Co(Ox)_3]^{4-}$. Hence the reactivity of free D^+ toward FH_2 was examined by using the system consisting eosine $\sim1\times10^{-5}$M, $K_3[Co(Ox)_3]$, 6.0×10^{-4}M and FH_2, 6.0×10^{-5}M (pH=6.2). Preliminary experiments by means of the steady light illumination has shown that the oxidation of FH_2 occurs very efficiently with $\Phi=ca.$ 0.15. This value is about the same as the quantum yield of the decomposition of eosine by $K_3[Co(Ox)_3]$ under similar conditions. It was ascertained that the bleaching of eosine never occurs in the early stage of the reaction. Thus one can conclude that the free D^+ produced by the reaction between D^T and $[Co(Ox)_3]^{3-}$ oxidizes FH_2 very quickly.

To confirm this further, the decay rate of the free D^+ was compared in the two systems, a) [Es]$=5.0\times10^{-6}$M, $K_3[Co(Ox)_3]=5.0\times10^{-4}$M, b) [Es]$=5.0\times10^{-6}$M, $K_3[Co(Ox)_3]=5.0\times10^{-4}$M, $[FH_2]=1.0\times10^{-5}$M, both in the deaerated solution. The preliminary experiment has shown that the decay for system (a) obeys rather the second order rate formula, but the apparent first order rate constant evaluated from the initial slope was $2-9\times10^2$ sec^{-1}. On the other hand, the first order rate constant for system (b) was $0.9-1.0\times10^4$ sec^{-1}, which implies that the rate constant for $D^+ + FH_2 \rightarrow D + FH + H^+$, is of the magnitude of 10^9M^{-1}·sec^{-1}.*6 Thus one can conclude that the free D^+ reacts with FH_2 very quickly.

Summary and Conclusion

In the present investigation, it has been proposed that FH_2 in the aerated solution, is oxidized by the singlet oxygen originating from the interaction of D^T with O_2 (D–O mechanism). This view was supported by the finding that the retarding effect of the excess oxygen is independent of a sensitizer. On the other hand, the oxidative photobleaching of dye occurs most (probably) *via* the electron transfer reaction. Hence the quantum yield of the two types of reaction depends on the occurrence of the following two processes.

$$D^T + {}^3O_2 \rightarrow D^+\cdots O_2^-, \quad (10)$$

$$D^T + {}^3O_2 \rightarrow D + {}^1O_2. \quad (9)$$

Table 10. Quantum yield of the oxidation of FH_2 (at 1×10^{-5}M) in the aerated solution

		MB	Th	Es	Acridine
$^1O_2$		0.035	0.038	0.006	(0.007)
	$\Phi^0_{D\text{-}O}$*	0.036—0.045	0.033—0.038	0.0067	
O_2^-				0	
$D^+\cdots O_2^-$				0	
D^+				0.15	
$D^+\cdots D^-$		0.04			
D^T	Φ_0**	0.058	0.38	0.046	
	Φ_{bleach}***	0.47×10^{-4}		2.8×10^{-4}	0

* Quantum yield when the deactivation of $^1O_2$ by $^3O_2$ is absent.
** Deaerated solution (for MB $\Phi_{0,max}=\varphi_{ST}k^r_L/k^s_L=0.3$).
*** Quantum yield for the oxidative photobleaching by oxygen.

*6 According to Ref. 7 the first order decay constant of D^+ (maybe partly exists as $D^+\cdots D^-$) is *ca.* 9×10^2 sec^{-1}. The addition of 1.0×10^{-5}M of FH_2 does not change it so much in the absence of $K_3[Co(Ox)_3]$, the observed value being 1.6×10^3 sec^{-1}. This is consistent with the view that some part of half-oxidized dye exists as $D^+\cdots D^-$.

That thiazine dyes have larger quantum yields for the oxidation of FH_2 than xanthene dyes and smaller quantum yields for the oxydative bleaching, may be attributed partly to the more favorable occurrence of (9) than (10). This seems to be well correlated with the oxidation-reduction potential of the two types of dye. In the case of acridine, the only reaction is perhaps (9), since there is no evidence of the occurrence of reaction (10).

As to the reactivity of various oxidative species toward FH_2, O_2^- and $D^+\cdots O_2^-$ have been found to be ineffective, although the evidence for the former is rather weak. Both the free D^+ and $D^+\cdots D^-$ are effective. The free D^+ is perhaps more effective than $D^+\cdots D^-$ but the quantitative comparison is a future problem and such studies will be helpful for the discrimination of the two species.

The low reactivity of $D^+\cdots O_2^-$, in sharp contrast to the free D^+, may be considered to be an unambiguous proof of the formation of such a complex by reaction $D^T+O_2\rightarrow D^+\cdots O_2^-$. This we, believe, is the first chemical evidence for the formation of transient molecular compound between dye and oxygen having the nature of ion-pair. It has now become almost certain that the half-oxidized dye produced by triplet eosine and oxygen, does not exist as free radical ion but exists as a rather stable ion pair $D^+\cdots O_2^-$. That the oxidative bleaching starts from the electron transfer process is further supported by a larger value of Φ for D–D mechanism than for D–O mechanism. In the D–O mechanism, it is most likely that most of $D^+\cdots O_2^-$ goes back to D and O_2 with only a very small portion resulting in destruction of dye. In the D–D mechanism on the other hand, oxygen will attack $D^+\cdots D^-$ or D^-, producing D and O_2^- and the remaining D^+ will give colourless product(s).

The quantitative data, some of which are still preliminary are summarized in Table 10.

The authors would like to thank Professor H. Kokubun for helpful discussions.

BULLETIN OF THE CHEMICAL SOCIETY OF JAPAN VOL. 42 1239—1247 (1969)

The Crystal and Molecular Structure of *N*-(*p*-Bromophenyl)-α-D-ribopyranosylamine 2,4-Phenylboronate

Hirotaka SHIMANOUCHI, Norio SAITO*1 and Yoshio SASADA

Laboratory of Chemistry for Natural Products, Tokyo Institute of Technology, Ookayama, Meguro-ku, Tokyo

(Received September 9, 1968)

Crystals of *N*-(*p*-bromophenyl)-α-D-ribopyranosylamine 2,4-phenylboronate, $C_{17}H_{17}O_4NBBr$, are monoclinic, with two molecules in a unit cell of the dimensions, $a=12.98$, $b=10.80$, $c=6.34$Å, and $\beta=99.4°$, and with the space group of $P2_1$. The intensity data were collected by a photographic method and the structure was solved by the heavy atom method. The final R factor is 0.100. The absolute configuration was also determined.

1,2-Diols (I) have been well known to enhance the conductivity of boric acid, suggesting that they form the borate complex of the type (II) in solution.[1] T. Sato obtained a crystalline borate complex, *N*-arylribosylamine borate, by the reaction of *N*-arylribosylamine and boric acid.[2] *N*-Arylribosylamine also forms a complex with phenylboronic acid. However, the organic chemical and spectral studies failed to reveal whether the ribose is α or β, whether it is a five- or six-membered ring, and to which oxygen atoms the boron is attached.

The present X-ray diffraction study establishes the conformation of the molecule in the crystalline state, and furthermore gives the bond lengths and angles about the boron atom.

A heavy atom derivative for the X-ray work, prepared by the reaction of D-ribose, phenylboronic acid and *p*-bromoaniline, was supplied by Y. Sato.[3]

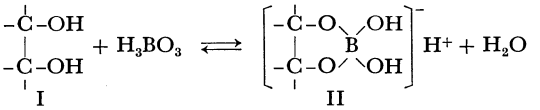

I II

*1 On leave from Chemical Laboratory, Meijigakuin University.

1) J. W. Knowlton, N. C. Schieltz and D. MacMillan, *J. Am. Chem. Soc.*, **68**, 208 (1946).

2) T. Sato, *Nippon Kagaku Zasshi* (*J. Chem. Soc. Japan, Pure Chem. Sect.*), **71**, 73 (1950).

3) Y. Sato, M. Sc. thesis submitted to Tokyo Institute of Technology in 1968 (under supervision of Professor T. Sato).

Experimental

Colorless scale-like crystals were obtained from a methanol solution, (100) plane being well developed. The unit cell dimensions were determined from zero-layer Weissenberg photographs about the b and the c axes, calibrated with superimposed aluminum powder lines.

Multiple-film equi-inclination Weissenberg photographs were taken at room temperature for the layer lines from 0 to 7 about the b axis and from 0 to 4 about c, using CuKα radiation. The crystals used were square in cross-section with rectangular dimensions of 0.03×0.10 cm and 0.06×0.03 cm for the b and c axis rotation, respectively. By visual comparison with a standard scale prepared with the same crystal, intensities were estimated, which ranged from 1 to 11900. Out of 1873 reflections recorded, about 290 were too weak to be measured. The corrections for the Lorentz and polarization factors were made in the usual way and those for spot-size variation in high layer photographs by the method of Phillips.[4] The correction for absorption was neglected.

Crystal Data

The crystallographic and physical data obtained are: N-(p-Bromophenyl)-α-D-ribopyranosylamine 2,4-phenylboronate $C_{17}H_{17}O_4NBBr$, mp 150—150.5°C. Monoclinic, $a=12.98$, $b=10.80$, $c=6.34$ Å, $\beta=99.4°$. Absent spectra, $(0k0)$ when k is odd. Space group, $P2_1$. Two molecules per unit cell. Volume of the unit cell, 876.3 Å^3. Density (by flotation), 1.461 g·cm^{-3}. Density (calculated), 1.478 g·cm^{-3}. Linear absorption coefficient for CuKα radiation, $\mu=36.9$ cm^{-1}. Total number of electrons per unit cell, $F(000)=396$.

Structure Determination

Three-dimensional sharpened Patterson function was synthesized with factors $\exp(2B\sin^2\theta/\lambda^2)$ where $B=5.0$ Å^2, and the bromine atom was located almost on the screw axis. The first three-dimensional Fourier synthesis was made with phases based on the bromine atom. In the resulting electron density distribution, a false mirror plane at $y=1/4$, in addition to that at $y=0$, appeared as a result of the special values of the bromine coordinates. In spite of a disturbance caused by additional mirrors, it was possible to pick out the atoms in the p-bromoanilino group. Minimum function, based on the Br–Br vector, also supported this interpretation.

Phases for the second Fourier synthesis were based on the eight atoms in the p-bromoanilino group. Although the false mirrors were not yet completely excluded, all the light atoms were picked out from the electron density distribution, so that a reasonable molecular model was constructed. Two successive three-dimensional Fourier syntheses with revised phases confirmed the positions of all the light atoms and considerably reduced the false details which had appeared in the earlier stages. The coordinates of all the atoms obtained from the fourth map gave a discrepancy factor, $R=\sum||F_o|-|F_c||/\sum|F_o|$, of 0.42.

TABLE 1. FINAL ATOMIC COORDINATES AND TEMPERATURE FACTORS

The anisotropic temperature factors are expressed in the form of $\exp\{-(B_{11}h^2+B_{22}k^2+B_{33}l^2+B_{12}hk+B_{13}hl+B_{23}kl)\}$.

Atom	x/a	y/b	z/c	B_{11}	B_{22}	B_{33}	B_{12}	B_{13}	B_{23}
Br	−0.0098	0.0000	−0.0202	0.00625	0.01030	0.08550	−0.00245	0.00310	−0.01084

Atom	x/a	y/b	z/c	B (Å^2)
N(1)	0.3374	0.3668	0.2678	3.24
O(2)	0.5302	0.4771	0.3647	2.56
O(3)	0.5487	0.7302	0.2846	3.78
O(4)	0.6089	0.5240	0.0517	3.10
O(5)	0.4070	0.4218	−0.0386	2.90
C(1)	0.3600	0.4683	0.1415	2.49
C(2)	0.4398	0.5512	0.2831	2.43
C(3)	0.4733	0.6609	0.1494	3.33
C(4)	0.5224	0.5994	−0.0351	2.91
C(5)	0.4392	0.5216	−0.1735	2.95
C(6)	0.1021	0.1159	0.0729	5.04
C(7)	0.1563	0.1041	0.2777	5.02
C(8)	0.2361	0.1905	0.3307	4.17
C(9)	0.2565	0.2828	0.1969	2.94
C(10)	0.1990	0.2887	−0.0162	4.45
C(11)	0.1181	0.2048	−0.0776	4.28
C(12)	0.6979	0.3729	0.3241	3.02
C(13)	0.7057	0.3122	0.5250	3.82
C(14)	0.7861	0.2289	0.5888	4.93
C(15)	0.8571	0.1985	0.4516	5.35
C(16)	0.8530	0.2594	0.2535	5.82
C(17)	0.7722	0.3430	0.1901	4.07
B	0.6094	0.4595	0.2424	2.65

To give a model with an actual absolute configuration, these positional parameters should be based on a left-handed coordinate system.

4) D. C. Phillips, *Acta Cryst.*, **7**, 746 (1954).

TABLE 2. ESTIMATED STANDARD DEVIATIONS
($\sigma(x)$, $\sigma(y)$ and $\sigma(z)$ in Å, $\sigma(B)$ in Å^2)

Atom	$\sigma(x)$	$\sigma(y)$	$\sigma(z)$	$\sigma(B_{11})$	$\sigma(B_{22})$	$\sigma(B_{33})$	$\sigma(B_{12})$	$\sigma(B_{13})$	$\sigma(B_{23})$
Br	0.0016	0.0037	0.0029	0.00009	0.00014	0.00094	0.00031	0.00046	0.00084

Atom	$\sigma(x)$	$\sigma(y)$	$\sigma(z)$	$\sigma(B)$
N(1)	0.0102	0.0110	0.0105	0.19
O(2)	0.0066	0.0077	0.0072	0.13
O(3)	0.0083	0.0103	0.0085	0.17
O(4)	0.0073	0.0086	0.0078	0.15
O(5)	0.0077	0.0085	0.0081	0.14
C(1)	0.0104	0.0108	0.0110	0.19
C(2)	0.0107	0.0115	0.0111	0.18
C(3)	0.0124	0.0138	0.0129	0.23
C(4)	0.0114	0.0126	0.0122	0.21
C(5)	0.0105	0.0127	0.0114	0.21
C(6)	0.0161	0.0173	0.0166	0.33
C(7)	0.0160	0.0178	0.0165	0.33

Atom	$\sigma(x)$	$\sigma(y)$	$\sigma(z)$	$\sigma(B)$
C(8)	0.0143	0.0149	0.0146	0.27
C(9)	0.0118	0.0121	0.0118	0.21
C(10)	0.0149	0.0152	0.0148	0.30
C(11)	0.0142	0.0148	0.0145	0.28
C(12)	0.0120	0.0131	0.0124	0.21
C(13)	0.0136	0.0143	0.0137	0.26
C(14)	0.0150	0.0186	0.0150	0.31
C(15)	0.0166	0.0174	0.0168	0.35
C(16)	0.0169	0.0223	0.0168	0.37
C(17)	0.0143	0.0150	0.0142	0.27
B	0.0128	0.0134	0.0134	0.22

Further refinement of the parameters was made by the block-diagonal matrix least-squares method. Anisotropic temperature factors in the form of $\exp\{-(B_{11}h^2+B_{22}k^2+B_{33}l^2+B_{12}hk+B_{13}hl+B_{23}kl)\}$ were applied for the bromine atom, while the light atoms were treated as undergoing isotropic thermal motions. After nine cycles of refinement, the R factor was reduced to 0.100 for the observed reflections. The atomic scattering factors used in the calculations were taken from the International Tables for X-ray Crystallography (1962). The final atomic coordinates and temperature factors are given in Table 1, and their standard deviations in Table 2. The observed and calculated structure factors are listed in Table 3. The final three-dimensional electron density distribution calculated with phases based on these parameters is shown in Fig. 1.

The computations were done on a HITAC 5020E computer in the University of Tokyo with programs written by Dr. T. Ashida.

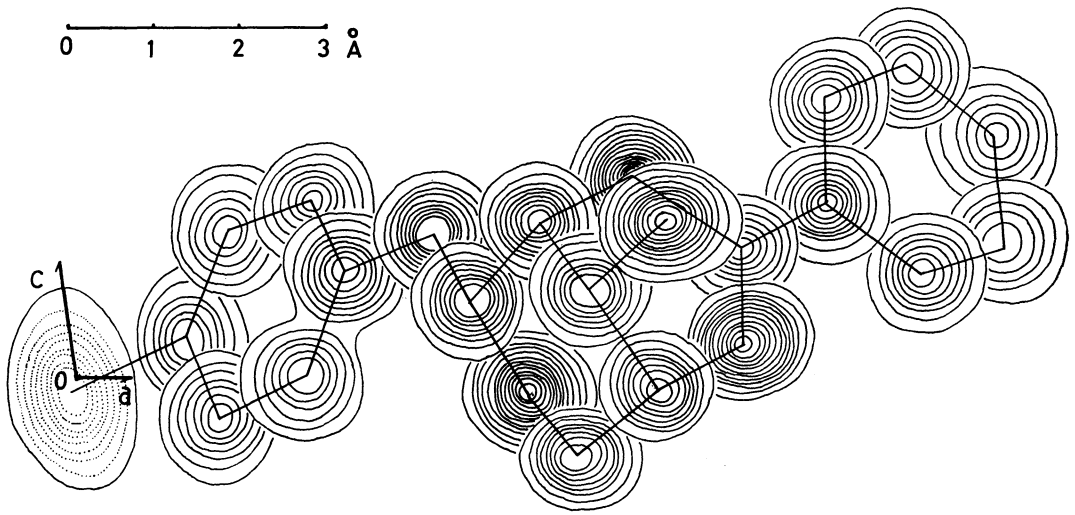

Fig. 1. Composite electron density diagram of sections parallel to (010). The contours of light atoms are at intervals of 1.0e.Å^{-3} starting with 1.0e.Å^{-3}, and those of the bromine atom are at intervals of 5.0e.Å^{-3} from 5.0e.Å^{-3} shown by dotted lines, the lowest being at 1.0e.Å^{-3}.

TABLE 3. OBSERVED AND CALCULATED STRUCTURE FACTORS

K	FO	FC	K	FO	FC	K	FO	FC	K	FO	FC	K	FO	FC	K	FO	FC	K	FO	FC	K	FO	FC
H,L= 0 0			8	10	10	H,L=-12 1			11	0	1	7	10	9	5	6	7	0	8	1	H,L= 2 2			6	6	6
2	36	47	9	7	6	0	21	21	12	6	8	8	14	11	6	4	4	1	18	17	0	44	43	7	5	6
4	71	70	10	9	9	1	13	15	13	2	4	9	9	8	7	4	5	2	26	25	1	9	8	8	4	3
6	35	36	11	8	8	2	18	20	H,L= -3	1		10	11	12	H,L= 14	1		3	11	10	2	29	29	9	5	5
8	28	26	12	3	4	3	9	11	0	19	22	11	4	3	0	0	4	4	35	34	3	28	25	10	0	3
10	16	15	H,L= 9	0		4	11	11	1	24	17	12	5	6	1	4	5	5	9	8	4	18	15	H,L= 11		2
12	5	3	0	33	31	5	10	10	2	84	80	13	4	3	2	8	7	6	20	18	5	18	18	0	0	0
H,L= 1 0			1	11	9	6	6	7	3	37	34	H,L= 5		1	3	5	5	7	4	4	6	21	20	1	12	13
1	12	14	2	14	12	7	3	4	4	24	26	0	65	63	4	3	3	8	0	2	7	23	21	2	2	3
2	17	16	3	8	6	H,L=-11		1	5	11	13	1	25	24	5	4	5	9	8	8	8	21	21	3	10	11
3	19	19	4	18	18	0	6	4	6	31	32	2	76	75	6	2	4	10	7	7	9	8	6	4	5	6
4	29	31	5	10	11	1	13	14	7	7	5	3	21	19	H,L= 15		1	11	3	1	10	12	14	5	5	5
5	7	6	6	16	18	2	10	10	8	10	20	4	36	34	0	3	3	H,L= -5		2	11	0	1	6	4	5
6	26	28	7	12	13	3	2	3	9	0	7	5	26	24	1	7	8	0	38	38	12	4	4	7	4	5
7	10	8	8	12	12	4	13	13	10	5	5	6	32	29	2	4	1	1	16	17	H,L= 3		2	8	3	3
8	21	20	9	4	3	5	6	5	11	0	3	7	7	5	3	4	6	2	36	31	0	28	25	9	1	2
9	7	5	10	5	4	6	8	11	12	6	7	8	21	21	4	2	2	3	35	34	1	21	21	H,L= 12		2
10	19	18	11	1	2	7	8	9	13	9	9	9	7	6	H,L=-16		2	4	30	29	2	48	44	0	0	3
11	6	5	12	0	2	8	6	7	H,L= -2		1	10	6	9	0	1	0	5	10	8	3	35	35	1	3	4
12	7	8	H,L= 10		0	9	0	0	0	81	92	11	4	4	1	1	3	6	15	14	4	43	40	2	9	9
13	3	3	0	18	15	H,L=-10		1	1	70	66	12	5	5	H,L=-15		2	7	3	3	5	19	19	3	7	8
H,L= 2 0			1	22	23	0	27	28	2	71	72	13	2	1	0	9	9	8	21	22	6	14	15	4	5	6
0	47	56	2	23	22	1	11	11	3	40	36	H,L= 6		1	1	6	5	9	5	3	7	14	14	5	7	7
1	23	16	3	20	21	2	25	25	4	34	31	0	5	5	2	8	10	10	7	8	8	19	16	6	2	2
2	105	123	4	11	8	3	13	11	5	21	20	1	13	16	3	5	5	11	0	0	9	8	8	7	4	5
3	19	18	5	8	8	4	19	19	6	24	24	2	35	32	4	5	5	12	5	6	10	8	9	8	1	3
4	58	58	6	12	11	5	0	3	7	16	13	3	8	8	5	4	4	H,L= -4		2	11	0	2	H,L= 13		2
5	31	30	7	7	6	6	8	8	8	20	21	4	17	16	H,L=-14		2	0	37	36	12	5	6	0	0	1
6	29	28	8	8	6	7	2	2	9	3	4	5	10	9	0	5	4	1	22	19	H,L= 4		2	1	5	7
7	6	5	9	7	7	8	7	7	10	19	20	6	22	22	1	4	4	2	46	44	0	7	7	2	6	6
8	25	23	10	6	7	9	3	5	11	0	3	7	11	10	2	5	5	3	47	41	1	0	0	3	8	8
9	5	5	11	0	2	10	5	5	12	8	9	8	7	6	3	1	2	4	27	24	2	24	23	4	2	2
10	10	11	H,L= 11		0	11	0	1	13	4	5	9	7	8	4	1	6	5	11	7	3	28	26	5	3	4
11	4	2	0	14	13	H,L= -9		1	H,L= -1		1	10	6	6	5	4	5	6	12	13	4	17	19	6	2	2
12	11	10	1	5	6	0	24	24	0	49	46	11	5	6	6	2	2	7	10	8	5	5	4	H,L= 14		2
H,L= 3 0			2	19	17	1	8	7	1	50	46	12	4	5	7	3	4	8	17	18	6	21	22	0	0	4
0	6	8	3	7	4	2	17	16	2	34	34	H,L= 7		1	H,L=-13		2	9	5	5	7	22	21	1	5	6
1	26	25	4	15	17	3	25	25	3	17	14	0	20	20	0	6	7	10	6	6	8	17	17	2	0	0
2	90	98	5	5	6	4	6	7	4	38	39	1	19	18	1	5	6	11	0	2	9	8	7	3	3	3
3	13	12	6	12	11	5	18	19	5	13	13	2	23	21	2	8	10	12	2	2	10	9	9	4	3	4
4	27	27	7	4	4	6	18	18	6	35	33	3	19	17	3	9	11	13	2	4	11	5	5	H,L= 15		2
5	11	7	8	8	8	7	12	12	7	14	13	4	38	36	4	7	9	H,L= -3		2	12	5	6	0	0	2
6	38	38	9	5	4	8	8	8	8	21	21	5	23	23	5	4	4	0	47	48	H,L= 5		2	1	0	4
7	17	16	10	3	4	9	4	2	9	6	5	6	12	11	6	6	7	1	31	29	0	25	26	H,L=-16		3
8	20	21	H,L= 12		0	10	6	8	10	17	16	7	12	11	7	3	1	2	29	29	1	20	21	0	1	0
9	13	10	0	7	4	11	0	2	11	11	13	8	15	15	H,L=-12		2	3	42	37	2	34	31	1	3	3
10	9	8	1	21	23	H,L= -8		1	12	3	4	9	7	8	0	7	7	4	41	38	3	24	22	H,L=-15		3
11	7	6	2	12	11	0	31	30	13	0	2	10	8	9	1	1	2	5	21	18	4	23	23	0	8	7
12	3	4	3	14	17	1	12	10	H,L= 0		1	11	3	0	2	13	12	6	28	26	5	15	15	1	5	3
H,L= 4 0			4	4	3	2	32	28	0	78	95	12	4	5	3	8	5	7	13	10	6	14	16	2	5	6
0	39	42	5	11	12	3	9	8	1	57	57	H,L= 8		1	4	8	10	8	16	15	7	17	19	3	2	2
1	8	10	6	5	4	4	25	27	2	80	83	0	39	39	5	0	2	9	4	2	8	9	12	4	3	7
2	23	21	7	6	7	5	17	17	3	28	23	1	22	21	6	3	3	10	7	7	9	7	7	H,L=-14		3
3	24	20	8	5	5	6	17	16	4	38	36	2	24	23	7	3	4	11	0	1	10	5	5	0	4	4
4	36	39	9	4	4	7	0	1	5	26	24	3	12	12	H,L=-11		2	12	9	10	11	0	2	1	0	1
5	8	8	H,L= 13		0	8	13	13	6	28	26	4	15	14	0	12	12	13	3	2	12	4	4	2	3	3
6	35	34	0	15	15	9	6	5	7	6	5	5	8	7	1	8	7	H,L= -2		2	H,L= 6		2	3	4	4
7	16	16	1	7	6	10	8	9	8	23	22	6	14	14	2	15	16	0	38	40	0	38	36	4	2	2
8	18	18	2	11	9	11	4	4	9	8	7	7	6	5	3	6	6	1	41	34	1	24	22	5	4	4
9	13	12	3	3	3	12	3	4	10	13	14	8	11	10	4	0	2	2	56	56	2	11	11	H,L=-13		3
10	13	13	4	8	8	H,L= -7		1	11	13	13	9	8	8	5	8	8	3	36	31	3	13	13	0	5	5
11	0	1	5	5	4	0	19	22	12	8	10	10	4	4	6	12	13	4	16	13	4	25	23	1	0	0
12	10	9	6	7	7	1	29	29	13	0	1	11	6	7	7	4	4	5	21	16	5	8	7	2	9	11
H,L= 5 0			7	6	5	2	45	43	H,L= 1		1	H,L= 9		1	8	9	9	6	17	19	6	16	16	3	8	9
0	48	49	8	6	6	3	12	13	0	32	32	0	13	9	H,L=-10		2	7	0	1	7	4	2	4	4	4
1	14	13	H,L= 14		0	4	19	17	1	70	66	1	18	17	0	21	22	8	19	19	8	8	9	5	0	1
2	56	58	0	4	3	5	17	20	2	50	46	2	13	11	1	9	8	9	5	5	9	7	7	6	1	3
3	41	39	1	6	7	6	18	18	3	20	19	3	13	13	2	11	10	10	12	12	10	6	7	H,L=-12		3
4	52	53	2	4	4	7	18	18	4	51	51	4	15	17	3	5	4	11	0	0	11	4	4	0	5	6
5	5	5	3	13	15	8	7	11	5	14	11	5	11	13	4	16	17	12	10	11	12	2	3	1	7	7
6	21	20	4	5	5	9	5	4	6	33	35	6	13	12	5	4	6	13	2	3	H,L= 7		2	2	11	11
7	14	15	5	6	6	10	5	5	7	9	7	7	10	11	6	3	3	H,L= -1		2	0	1	1	3	1	0
8	12	13	6	3	3	11	0	1	8	25	25	8	9	10	7	2	2	0	42	45	1	10	9	4	5	5
9	13	12	7	2	4	12	5	6	9	11	9	9	5	4	8	8	9	1	25	21	2	17	16	5	3	2
10	9	9	H,L= 15		0	H,L= -6		1	10	9	8	10	4	5	9	5	3	2	36	34	3	13	12	6	5	6
11	4	3	0	6	6	0	31	34	11	5	9	11	0	2	10	6	7	3	23	21	4	8	5	7	4	4
12	6	7	1	7	8	1	12	10	12	0	7	H,L= 10		1	H,L= -9		2	4	41	38	5	16	17	H,L=-11		3
13	2	3	2	5	4	2	19	18	H,L= 2		1	0	22	21	0	21	20	5	22	20	6	12	14	0	10	10
H,L= 6 0			3	7	8	3	14	12	0	71	74	1	12	12	1	12	12	6	27	26	7	4	3	1	2	4
0	28	30	4	7	6	4	44	44	1	34	31	2	14	12	2	19	20	7	6	6	8	5	4	2	6	4
1	23	22	5	5	6	5	4	4	2	25	27	3	14	16	3	16	13	8	20	20	9	12	14	3	5	4
2	34	31	H,L= 16		0	6	23	21	3	46	43	4	10	9	4	25	24	9	6	6	10	4	5	4	3	5
3	11	11	0	0	1	7	14	12	4	24	22	5	4	4	5	12	13	10	10	10	11	3	3	5	6	7
4	20	19	1	5	5	8	23	23	5	17	17	6	9	7	6	20	20	11	0	2	H,L= 8		2	6	4	3
5	11	8	2	2	2	9	5	4	6	32	30	7	10	10	7	6	5	12	6	5	0	24	28	7	3	4
6	23	25	H,L=-16		1	10	11	11	7	10	9	8	4	5	8	8	7	13	0	0	1	29	31	8	5	5
7	13	14	0	3	1	11	5	2	8	14	14	9	5	6	9	4	3	H,L= 0		2	2	32	32	H,L=-10		3
8	23	23	1	3	3	12	4	5	9	4	4	10	5	6	10	5	7	0	23	22	3	9	9	0	12	13
9	15	15	2	3	3	H,L= -5		1	10	10	11	H,L= 11		1	H,L= -8		2	1	6	5	4	12	13	1	13	13
10	12	12	3	2	3	0	53	53	11	4	3	0	21	20	0	17	17	2	44	42	5	6	5	2	13	14
11	2	3	H,L=-15		1	1	18	19	12	6	8	1	12	11	1	3	4	3	13	12	6	8	9	3	6	5
12	6	5	0	8	10	2	43	42	13	3	0	2	11	12	2	13	14	4	28	28	7	8	8	4	12	13
H,L= 7 0			1	5	5	3	16	14	H,L= 3		1	3	9	10	3	6	4	5	25	22	8	10	10	5	10	10
0	41	41	2	5	4	4	49	45	0	72	73	4	8	9	4	15	15	6	24	22	9	5	6	6	6	8
1	22	21	3	6	6	5	19	18	1	33	29	5	10	12	5	22	21	7	11	9	10	2	3	7	10	9
2	31	29	4	3	3	6	27	25	2	50	48	6	6	9	6	25	25	8	9	8	11	1	2	8	7	9
3	11	12	5	3	3	7	14	14	3	36	33	7	3	3	7	5	5	9	5	3	H,L= 9		2	H,L= -9		3
4	31	29	H,L=-14		1	8	20	19	4	87	90	8	6	7	8	9	11	10	20	20	0	5	9	0	11	12
5	19	19	0	0	0	9	7	6	5	11	12	9	3	2	9	4	3	11	3	4	1	5	4	1	2	4
6	18	14	1	6	8	10	8	10	6	26	24	H,L= 12		1	10	6	6	12	8	8	2	6	4	2	6	5
7	18	18	2	12	11	11	0	3	7	13	13	0	5	4	11	3	3	13	0	1	3	8	7	3	5	5
8	11	12	3	6	5	12	5	5	8	19	18	1	8	8	H,L= -7		2	H,L= 1		2	4	4	3	4	12	11
9	4	2	4	9	8	13	2	2	9	0	3	2	5	4	0	40	39	0	68	65	5	9	10	5	18	18
10	10	10	5	6	7	H,L= -4		1	10	13	12	3	9	12	1	9	7	1	29	27	6	4	5	6	3	3
11	4	4	6	5	5	0	44	43	11	3	2	4	6	6	2	33	30	2	20	19	7	7	7	7	11	12
12	4	4	7	3	4	1	3	2	12	6	5	5	9	9	3	10	9	3	23	22	8	6	7	8	0	2
H,L= 8 0			H,L=-13		1	2	36	29	13	0	3	6	3	4	4	28	26	4	43	41	9	0	1	H,L= -8		3
0	35	32	0	6	7	3	13	11	H,L= 4		1	7	5	6	5	12	11	5	9	8	10	6	5	0	0	0
1	18	17	1	5	4	4	38	40	0	1	1	8	3	3	6	29	28	6	33	33	H,L= 10		2	1	6	5
2	28	26	2	7	5	5	15	12	1	16	14	H,L= 13		1	7	6	6	7	6	4	0	34	38	2	18	19
3	14	15	3	4	4	6	29	28	2	34	33	0	0	0	8	6	7	8	13	11	1	9	10	3	6	4
4	28	26	4	2	5	7	7	5	3	11	9	1	7	9	9	6	5	9	9	8	2	6	7	4	13	14
5	9	8	5	5	4	8	25	23	4	17	13	2	13	14	10	5	7	10	4	5	3	12	12	5	16	16
6	22	21	6	4	7	9	9	6	5	21	20	3	9	10	11	0	2	11	5	5	4	11	13	6	11	16
7	2	3	7	4	4	10	11	10	6	19	19	4	7	6	H,L= -6		2	12	4	3	5	11	11	7	9	7

TABLE 3. (Continued)

K	FO	FC	K	FO	FC	K	FO	FC	K	FO	FC	K	FO	FC	K	FO	FC	K	FO	FC	K	FO	FC	K	FO	FC
8	5	5	0	10	13	9	2	2	6	6	8	5	8	7	5	2	2	5	8	5	8	7	8	H,L=	7	6	3	6	4
9	0	2	1	10	10	H,L= 10		3	7	2	1	6	13	14	6	2	3	6	7	7	2	5	5	0	0	0	4	3	3
10	0	4	2	20	19	0	11	12	8	8	8	7	8	6	H,L=-10		5	7	0	0	3	2	1	1	1	2	5	0	2
11	4	3	3	9	8	1	9	11	9	5	5	8	0	2	0	5	5	H,L=	3	5	4	0	1	2	0	1	H,L= -4		8
H,L= -7		3	4	9	11	2	5	7	10	3	4	9	3	3	1	1	1	0	4	5	5	0	1	3	0	3	0	0	0
0	18	20	5	15	14	3	6	5	H,L= -5		4	10	0	1	2	3	3	1	7	9	6	4	4	4	0	2	1	4	4
1	4	4	6	22	20	4	2	3	0	17	17	11	3	3	3	0	3	2	0	1	7	3	3	5	1	2	H,L= -3		8
2	14	13	7	8	6	5	7	9	1	15	14	H,L=	4	4	4	3	3	3	1	2	H,L= -5		6	H,L=	8	6	0	0	1
3	6	4	8	14	10	6	2	2	2	26	26	0	4	0	5	2	2	4	9	8	0	0	0	0	0	1	1	4	4
4	15	15	9	8	6	7	4	5	3	15	11	1	3	3	6	2	3	5	0	1	1	4	5	1	0	4	H,L= -2		8
5	13	12	10	6	7	H,L=	11	3	4	11	10	2	5	6	H,L= -9		5	6	0	1	2	4	4	H,L=	9	6	0	0	1
6	9	8	11	3	3	0	0	2	5	10	9	3	9	8	0	0	1	7	5	6	3	3	2	0	0	0	1	1	1
7	9	9	12	3	3	1	6	7	6	10	10	4	11	11	1	5	5	H,L=	4	5	4	0	1	1	1	1			
8	6	7	H,L=	2	3	2	1	1	7	7	7	5	7	7	2	8	9	0	0	4	5	0	1	H,L=-10		7			
9	0	2	0	26	23	3	4	5	8	0	2	6	6	6	3	5	5	1	0	0	6	2	2	0	8	7			
10	0	4	1	28	25	4	5	7	9	7	7	7	9	7	4	3	3	2	7	8	7	1	2	1	1	1			
11	3	2	2	13	13	5	6	7	10	0	0	8	0	2	5	4	4	3	2	1	H,L= -4		6	2	3	2			
12	1	4	3	17	17	6	2	4	11	0	3	9	3	3	6	2	4	4	8	7	0	14	16	H,L= -9		7			
H,L= -6		3	4	25	25	H,L=	12	3	H,L= -4		4	10	3	4	7	0	0	5	0	1	1	12	12	0	10	8			
0	19	18	5	22	22	0	2	2	0	3	1	11	1	0	H,L= -8		5	6	2	4	2	6	6	1	4	3			
1	6	3	6	15	16	1	4	6	1	13	11	H,L=	5	4	0	0	0	7	0	0	3	4	2	2	2	2			
2	19	20	7	21	18	2	0	1	2	3	2	0	10	12	1	8	6	H,L=	5	5	4	0	0	3	3	2			
3	11	11	8	17	15	3	4	5	3	17	16	1	8	10	2	6	4	0	1	3	5	2	2	H,L=	-8	7			
4	19	17	9	5	5	4	1	1	4	11	11	2	5	5	3	1	2	1	8	8	6	4	3	0	6	5			
5	6	5	10	7	8	5	3	3	5	8	8	3	25	26	4	1	3	2	9	9	7	1	2	1	5	4			
6	14	14	11	2	1	H,L=	13	3	6	4	4	4	11	10	5	2	3	3	1	2	H,L= -3		6	2	4	3			
7	7	6	12	4	4	0	3	6	7	6	5	5	7	7	6	3	2	4	5	6	0	8	5	3	0	2			
8	12	12	H,L=	3	3	1	4	5	8	0	5	6	6	7	7	2	3	5	7	8	1	6	7	H,L=	-7	7			
9	6	7	0	14	17	2	4	4	9	4	4	7	4	5	H,L= -7		5	6	0	2	2	9	9	0	0	0			
10	0	7	1	3	0	3	5	7	10	4	5	8	3	3	0	12	10	7	2	3	3	9	9	1	3	4			
11	7	0	2	24	22	4	3	5	11	2	3	9	0	1	1	7	5	H,L=	6	5	4	0	1	2	5	5			
12	0	0	3	14	11	H,L=	14	3	H,L= -3		4	10	2	3	2	19	17	0	7	7	5	2	2	3	0	1			
H,L= -5		3	4	6	6	0	2	4	0	8	10	11	0	1	3	10	9	1	4	5	6	2	1	4	0	1			
0	32	34	5	0	2	1	2	2	1	7	8	H,L=	6	4	4	7	7	2	10	12	7	1	3	5	1	2			
1	15	13	6	25	26	H,L=-15		4	2	12	13	0	2	4	5	4	5	3	0	2	H,L= -2		6	H,L=	-6	7			
2	8	7	7	14	11	0	5	5	3	11	11	1	6	6	6	3	4	4	4	4	0	9	8	0	0	1			
3	14	11	8	12	9	1	1	2	4	8	8	2	7	10	7	0	0	5	3	3	1	0	0	1	2	3			
4	13	12	9	3	4	H,L=-14		4	5	0	2.	3	10	10	H,L= -6		5	6	2	3	2	12	11	2	2	0			
5	12	9	10	4	4	0	5	5	6	14	12	4	7	7	0	14	11	7	0	2	3	12	13	3	2	2			
6	13	13	11	4	3	1	3	3	7	9	7	5	0	1	1	10	9	H,L=	7	5	4	6	6	4	3	2			
7	4	5	12	4	4	2	0	2	8	8	7	6	2	0	2	14	13	0	10	12	5	6	5	5	2	1			
8	7	6	H,L=	4	3	3	2	2	9	4	3	7	3	3	3	11	8	1	3	2	6	2	2	H,L=	-5	7			
9	10	10	0	13	12	4	3	2	10	4	4	8	3	4	4	4	4	2	3	3	7	4	4	0	0	4			
10	0	11	1	18	18	H,L=-13		4	11	2	0	9	5	5	5	4	5	3	5	6	H,L= -1		6	1	2	2			
11	10	1	2	4	4	0	1	2	H,L= -2		4	10	3	4	6	2	5	4	2	1	0	9	9	2	0	2			
12	0	5	3	14	12	1	0	1	0	19	20	H,L=	7	4	7	0	1	5	3	3	1	5	5	3	0	1			
H,L= -4		3	4	23	23	2	0	1	1	6	7	0	6	7	H,L= -5		5	6	2	2	2	5	4	4	0	0			
0	21	22	5	14	12	3	4	3	2	14	13	1	14	14	0	19	18	7	2	3	3	10	9	5	2	3			
1	23	23	6	4	8	4	0	2	3	4	5	2	0	1	1	10	11	H,L=	8	5	4	3	1	6	1	2			
2	45	42	7	11	10	5	0	2	4	9	8	3	6	8	2	12	8	0	6	8	5	7	8	H,L=	-4	7			
3	12	10	8	18	17	6	0	1	5	12	11	4	7	8	3	11	10	1	5	7	6	3	2	0	1	0			
4	22	22	9	4	3	7	0	2	6	5	4	5	11	12	4	11	10	2	5	6	7	4	2	1	5	4			
5	17	13	10	5	6	H,L=-12		4	7	7	6	6	4	5	5	3	1	3	0	0	H,L=	0	6	2	2	3			
6	14	15	11	4	3	0	8	8	8	4	5	7	5	5	6	3	4	4	0	1	0	2	3	3	0	1			
7	3	3	12	1	2	1	5	4	9	3	3	8	4	5	7	6	6	5	1	1	1	4	2	4	2	2			
8	7	6	H,L=	5	3	2	11	12	10	5	5	9	3	3	H,L= -4		5	6	0	2	2	1	3	5	2	2			
9	5	3	0	10	10	3	5	5	11	2	2	10	0	2	0	15	19	7	1	2	3	5	3	6	2	2			
10	8	9	1	8	8	4	3	2	H,L= -1		4	H,L=	8	4	1	9	9	H,L=	9	5	4	0	1	H,L=	-3	7			
11	2	3	2	17	16	5	0	1	0	0	1	0	2	4	2	9	7	0	0	0	5	6	7	0	4	2			
H,L= -3		3	3	11	13	6	2	4	1	2	2	1	7	7	3	9	7	1	2	2	6	5	5	1	2	3			
0	4	3	4	20	20	H,L=-11		4	2	17	17	2	7	8	4	1	0	2	0	2	7	4	2	2	4	2			
1	17	13	5	13	11	0	6	7	3	2	3	3	4	5	5	0	0	3	0	1	H,L=	1	6	3	0	2			
2	8	10	6	12	13	1	3	3	4	6	5	4	3	3	6	0	2	4	0	0	0	1	2	4	2	2			
3	26	20	7	7	8	2	4	3	5	14	12	5	0	1	7	6	4	5	2	2	1	5	6	5	1	2			
4	5	6	8	12	10	3	5	4	6	19	18	6	0	1	H,L= -3		5	H,L=	10	5	2	7	8	6	2	2			
5	21	17	9	3	5	4	4	3	7	6	5	7	0	2	0	8	7	0	0	0	3	2	3	H,L=	-2	7			
6	15	14	10	0	3	5	2	4	8	6	7	8	2	3	1	8	9	1	3	4	4	0	1	0	6	4			
7	5	6	11	4	4	6	2	3	9	3	1	9	3	3	2	12	13	2	0	1	5	3	3	1	0	1			
8	15	15	H,L=	6	3	H,L=-10		4	10	4	5	H,L=	9	4	3	8	7	3	4	6	6	0	1	2	0	0			
9	6	5	0	10	11	0	11	12	11	4	4	0	0	2	4	6	4	H,L=-12		6	7	4	4	3	0	2			
10	3	3	1	21	22	1	7	8	H,L=	0	4	1	4	4	5	4	3	0	0	0	H,L=	2	6	4	2	1			
11	2	4	2	9	7	2	12	13	0	22	23	2	0	1	6	2	0	1	1	2	0	7	8	5	2	2			
12	2	4	3	8	6	3	3	3	1	11	9	3	6	6	7	3	1	2	0	0	1	4	4	6	4	5			
H,L= -2		3	4	12	14	4	9	9	2	7	6	4	0	4	H,L= -2		5	3	2	2	2	6	5	H,L=	-1	7			
0	36	41	5	7	6	5	4	3	3	15	15	5	5	5	0	7	4	H,L=-11		6	3	0	0	0	5	4			
1	20	19	6	7	7	6	10	12	4	10	11	6	2	2	1	5	7	0	0	0	4	0	0	1	1	1			
2	40	40	7	6	4	7	2	2	5	21	21	7	0	1	2	20	22	1	4	4	5	3	1	2	1	0			
3	11	7	8	11	12	H,L=	-9	4	6	5	3	H,L=	10	4	3	0	3	2	0	3	6	0	1	3	0	2			
4	29	27	9	7	6	0	2	6	7	13	12	0	0	0	4	8	7	3	0	1	7	3	4	4	2	3			
5	6	5	10	4	5	1	0	3	8	0	3	1	4	6	5	11	9	H,L=-10		6	H,L=	3	6	5	3	3			
6	7	8	H,L=	7	3	2	5	5	9	0	3	2	3	4	6	7	7	0	4	6	6	7	6	6	4	6			
7	9	7	0	7	7	3	4	1	10	3	3	3	3	2	7	3	3	1	3	3	1	6	6	H,L=	0	7			
8	10	12	1	8	9	4	5	3	11	0	1	4	3	4	H,L= -1		5	2	0	2	2	5	5	0	3	1			
9	4	1	2	19	19	5	7	5	H,L=	1	4	5	2	3	0	0	0	3	0	1	3	2	2	1	4	4			
10	6	4	3	12	11	6	7	7	0	17	14	6	4	6	1	4	3	4	0	0	4	4	4	2	2	1			
11	4	4	4	4	4	7	4	5	1	5	3	7	2	3	2	5	5	5	4	4	5	4	4	3	0	1			
12	3	5	5	7	8	H,L=	-8	4	2	11	11	H,L=	11	4	3	6	7	H,L=	-9	6	6	2	1	4	0	0			
H,L= -1		3	6	7	7	0	6	3	3	7	8	0	3	4	4	8	10	0	0	3	7	0	1	5	0	2			
0	2	3	7	6	7	1	5	4	4	17	20	1	2	3	5	10	8	1	2	3	H,L=	4	6	6	0	2			
1	29	30	8	9	10	2	8	7	5	7	7	2	2	1	6	6	5	2	0	1	0	3	5	H,L=	1	7			
2	10	9	9	5	5	3	5	5	6	13	13	3	4	5	7	4	6	3	0	1	1	1	2	0	0	0			
3	14	11	10	5	6	4	11	12	7	7	5	4	0	2	H,L=	0	5	4	2	3	2	5	5	1	9	8			
4	21	20	11	3	3	5	4	3	8	8	8	5	2	3	0	1	1	5	3	3	3	4	3	2	6	5			
5	9	7	H,L=	8	3	6	5	4	9	0	2	H,L=	12	4	1	4	3	6	3	1	4	1	1	3	1	2			
6	24	22	0	6	8	7	2	2	10	4	6	0	0	1	2	7	7	7	1	1	5	2	3	4	0	0			
7	5	5	1	18	19	8	4	5	11	4	4	1	0	1	3	7	7	H,L=	-8	6	6	0	1	5	0	0			
8	10	10	2	13	15	H,L=	-7	4	H,L=	2	4	2	0	1	4	6	7	0	0	1	7	2	3	6	0	1			
9	7	7	3	10	12	0	22	22	0	8	8	3	3	4	5	14	12	1	0	1	H,L=	5	6	H,L=	2	7			
10	0	2	4	5	5	1	13	14	1	12	13	4	2	3	6	8	7	2	0	1	0	0	2	0	0	0			
11	3	1	5	8	10	2	15	15	2	7	7	H,L=-13		5	7	9	8	3	0	2	1	2	1	1	7	7			
12	4	5	6	3	3	3	13	12	3	11	9	0	2	0	H,L=	1	5	4	0	2	2	0	1	2	6	5			
H,L=	0	3	7	4	3	4	14	15	4	8	8	H,L=-12		5	0	8	7	5	3	3	3	2	2	3	5	4			
0	39	42	8	2	3	5	7	7	5	25	24	0	7	6	1	5	6	6	4	4	4	0	0	4	0	1			
1	20	18	9	0	2	6	3	1	6	7	7	1	0	1	2	1	0	7	2	3	5	3	4	5	0	1			
2	30	29	10	6	8	7	4	4	7	3	2	2	0	1	3	6	5	H,L=	-7	6	6	1	2	H,L=	3	7			
3	27	24	H,L=	9	3	8	3	2	8	3	4	3	0	1	4	11	13	0	0	1	7	3	5	0	0	1			
4	17	16	0	9	6	9	0	3	9	6	3	4	3	1	5	10	9	1	4	4	H,L=	6	6	1	6	5			
5	15	15	1	1	3	10	3	3	10	0	0	5	0	1	7	0	1	2	4	4	0	2	3	2	5	4			
6	5	5	2	1	1	H,L=	-6	4	11	0	1	6	1	3	7	3	4	3	0	0	1	3	3	3	6	4			
7	12	11	3	9	9	0	7	7	H,L=	3	4	H,L=-11		5	H,L=	2	5	4	3	0	2	0	1	4	2	2			
8	13	13	4	6	7	1	11	9	0	12	11	0	2	1	0	0	0	5	0	2	3	4	5	5	0	2			
9	6	4	5	4	3	2	14	11	1	11	11	1	0	1	1	1	3	6	4	5	4	2	2	H,L=	4	7			
10	9	8	6	4	5	3	16	13	2	15	14	2	0	0	2	1	2	7	3	3	5	1	1	0	0	1			
11	4	4	7	6	6	4	1	0	3	6	4	3	0	1	3	7	6	H,L=	-6	6	6	1	2	1	2	3			
H,L=	1	3	8	4	4	5	5	4	4	15	16	4	0	1	4	3	2	0	4	2	7	0	1	2	4	2			

Determination of Absolute Configuration

After the errors due to neglecting the correction for absorption were taken into account, it was observed that for seven sets of Bijvoet pair in the upper layer photographs around the c axis, intensities in each pair were significantly different. For the Bijvoet pairs, $|F(hkl)|$ and $|F(h\bar{k}\bar{l})|$ were calculated using $\Delta f'$ and $\Delta f''$ for the bromine atom on the basis of the model in a right-handed coordinate system. As shown in Table 4, inequality relation observed in each pair is opposite to that of the calculated values, so that the model used in the calculations is the mirror image of the actual molecule. Therefore, the absolute configuration of ribose has been established as indicated in Fig. 2.

TABLE 4. THE DETERMINATION OF THE ABSOLUTE CONFIGURATION

$h\ k\ l$	Calculated		Observed	
	$\|F(hkl)\|$	$\|F(h\bar{k}\bar{l})\|$	$\|I(hkl)\|$	$\|I(h\bar{k}\bar{l})\|$
12 1 1	7.8	< 8.7		>
10 4 1	9.1	< 9.4		>
12 4 1	5.9	< 6.3		>
7 1 2	9.8	> 8.1		<
7 1 3	3.4	< 4.6		>
11 1 3	7.1	< 7.9		>
7 4 3	4.0	< 5.1		>

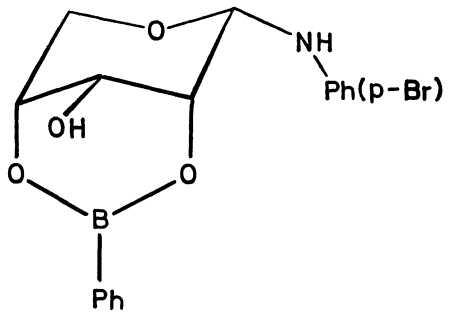

Fig. 2. Absolute configuration and conformation.

Results and Discussion

Conformation. As shown in Fig. 2 three surprising features are found in the molecular conformation. The first is that the sugar residue is pyranoid; the ribose residue so far reported is in the furanose form in crystal.[5-7] The second is that it is the α-D anomer; the free sugar customarily crystallizes as a β-D anomer. The third is that it is in a chair 1C conformation ($1e2a3e4a$); in free ribopyranose this is a very unstable form owing to strong 1,3-diaxial O(2)···O(4) interaction. These features are interrelated to each other as will be discussed below.

The conformations about the six single bonds in the pyranose ring are shown in Fig. 3[8] and the

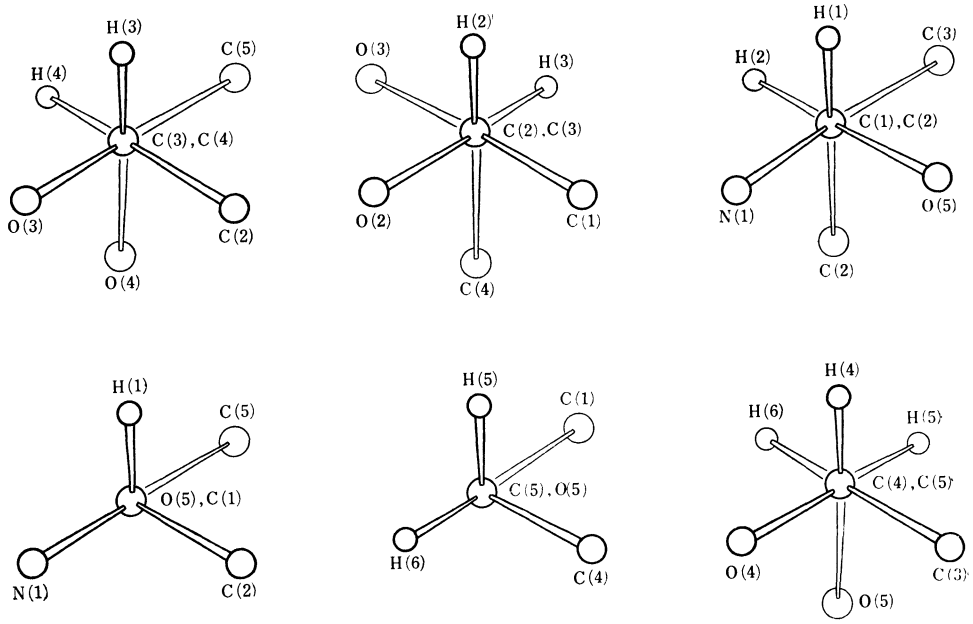

Fig. 3. Conformations about the six single bonds of the pyranose ring.

5) E. Alver and S. Furberg, *Acta Chem. Scand.*, **13**, 910 (1959).

6) S. Furberg and A. Mostad, *ibid.*, **16**, 1627 (1962).

7) J. Kraut and L. H. Jensen, *Acta Cryst.*, **16**, 79 (1963).

8) In the preparation of this figure, the positions of the hydrogen atoms were assumed.

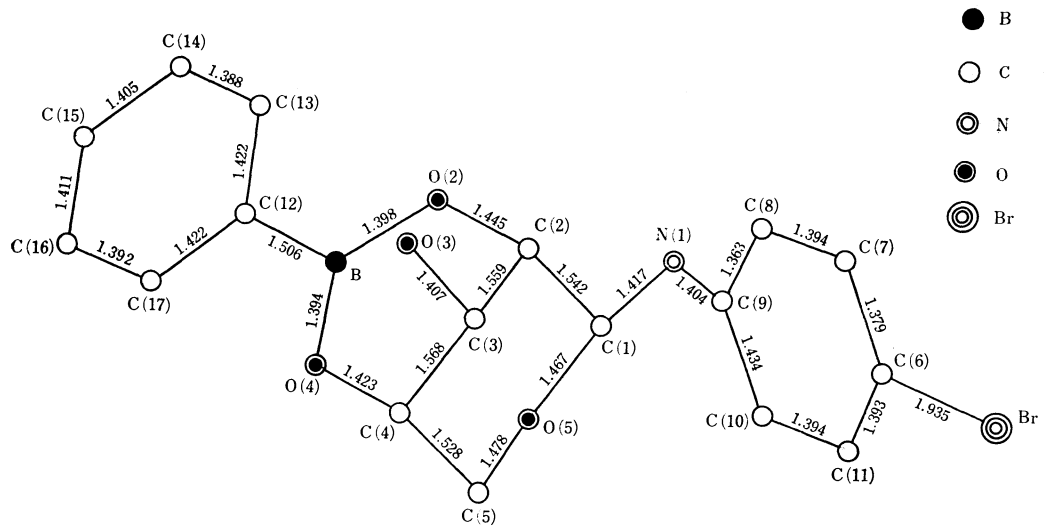

Fig. 4. Bond lengths (Å).

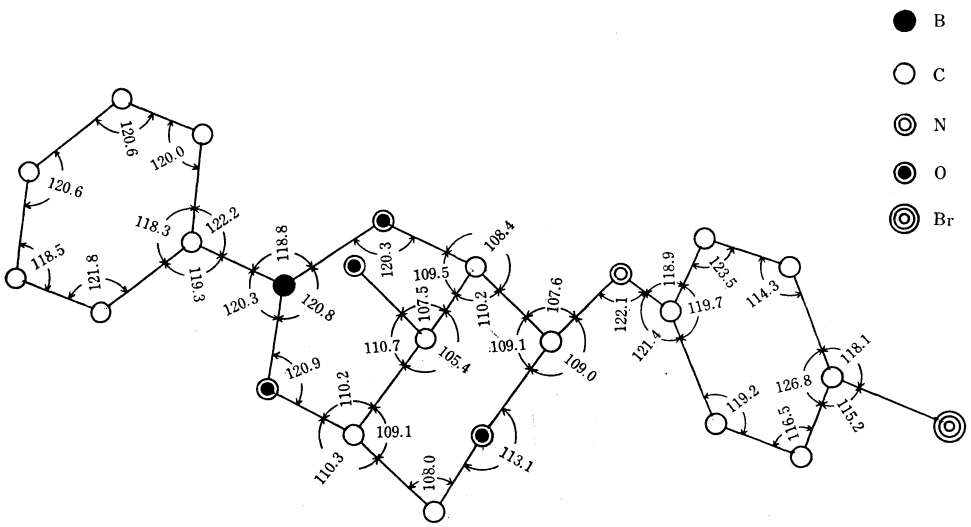

Fig. 5. Bond angles (degrees).

conformation angles range from 56.0 to 62.5°, as compared with 55.8—61.7° for an ideal pyranose ring,[9] 51.3—62.2° for glucose,[10] 54.8—56.0° for sucrose[11] and 56.2—60.5° for β-methyl maltoside.[12] The range in the present molecule is very close to that in an ideal pyranose ring indicating no evidence of strain in the ring. This suggests that the pyranose 1C conformation is most favorable to form a borate complex with ribose. In this ring conformation the present equatorial α-D anomer is more stable than the axial β-D one. It follows that the energy of the present three-dimensional structure is undoubtedly lower than any other isomer and only one isomer is predominantly formed and crystallizes as a pure form. Thus, it is reasonably interpreted that the formation of a stable borate complex is characteristic of D-ribose.[13]

Molecular Geometry. The intramolecular bond lengths and angles are shown in Figs. 4 and

9) H. M. Berman and S. H. Kim, *Acta Cryst.*, **B24**, 897 (1968).

10) G. M. Brown and H. A. Levy, *Science*, **147**, 1038 (1965).

11) G. M. Brown and H. A. Levy, *ibid.*, **141**, 920 (1963).

12) S. S. C. Chu and G. A. Jeffrey, *Acta Cryst.*, **23**, 1038 (1967).

13) T. Fujita, D. Sc. thesis submitted to Tokyo Institute of Technology in 1960 (under supervision of Professor T. Sato).

5, respectively. The mean estimated standard deviations in bond lengths of C–Br, C–O, C–N C–C, O–B and C–B, are 0.018, 0.015, 0.016, 0.021, 0.016 and 0.019 Å, respectively, and that in bond angle is about 1.2°. The C–C single bond lengths range from 1.528 to 1.568 Å and none of them differ significantly from the mean value of 1.549 Å. The C–O bond lengths range from 1.407 to 1.478 Å with the mean value of 1.444 Å. The distance of C(1)–N(1) is 1.417 Å, which is significantly shorter than the normal C(sp^3)–N< length, *i. e.* 1.463 Å in *N,N'*-dinitroethylenediamine.[14] There is no significant inequality of the ring C(1)–O(5) and C(5)–O(5) bonds. Similar shortening of the equatorial C(1)–O(1) bond, which corresponds to the present C(1)–N(1), and equality of the ring C–O bonds have been observed in pyranose sugars.[15] These phenomena have been connected with a property of the equatorial C(1)–O(1) bond,[12,15] and by the present observation this interpretation may be extended to the equatorial C(1)–X bond where X is an atom with lone pair.

The valence angles on O(2) and O(4) atoms are somewhat larger than the usual. This tendency is consistent in that the C(2)–O(2) and C(4)–O(4) distances are shorter than C(1)–O(5) and C(5)–O(5).

The two B–O bond lengths are essentially equal to the mean value of 1.396 Å. The π-bond order of these B–O bonds was found to be about 0.35 using B–O π-bond order *versus* bond length curve given by Coulson.[16] Armstrong and Perkins have predicted that in some substituted phenylboronic acids a migration of charge from the oxygen to the boron atom results in a π-bond order in the range 0.3 to 0.5.[17] The present π-bond order agrees well with their prediction. The three bond angles around the boron atom are very close to 120°. The equation for the least-squares plane of the four atoms, O(2), O(4), B and C(12) is:

$$-0.438x' - 0.751y' - 0.494z' + 7.841 = 0$$

where $x' = x + z\cos\beta$, $y' = y$ and $z' = z\sin\beta$. The deviations from this plane are shown in Fig. 6. It is apparent that the boron atom is trigonally hybridized and the C(2) and C(4) atoms also lie nearly within the plane. This seems to satisfy the most favorable condition for forming B–O π-bond. The dihedral angle between this plane and the benzene ring, C(12)–C(17), plane is only

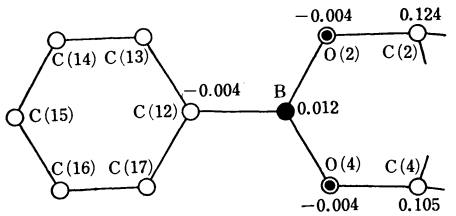

Fig. 6. The deviations (Å) of the atoms from the least-squares plane through atoms, O(2), O(4), B and C(12).

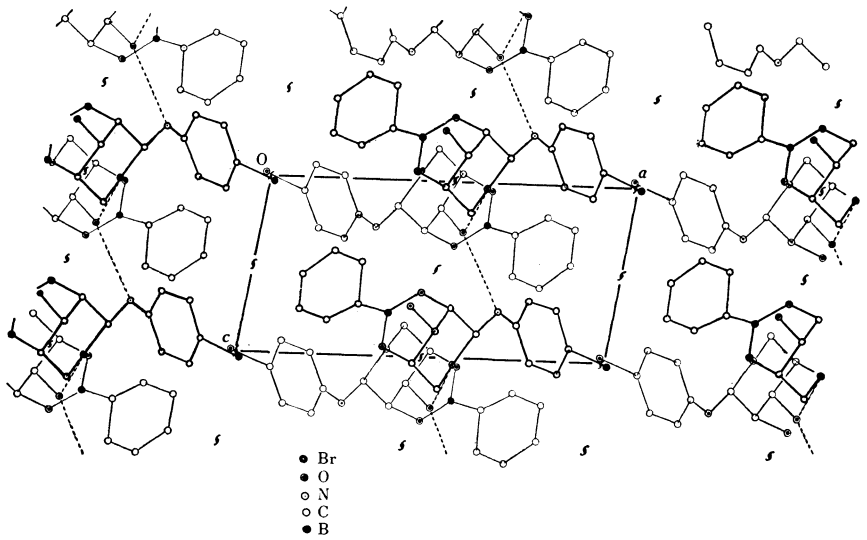

Fig. 7. The crystal structure projected along the *b* axis. The dashed lines indicate the presumed hydrogen bonds. Concerning the absolute configuration, this figure is the mirror image of the actual crystal.

14) J. W. Turley, *Acta Cryst.*, **B24**, 942 (1968).
15) S. S. C. Chu and G. A. Jeffrey, *ibid.*, **B24**, 830 (1968).
16) C. A. Coulson and T. W. Dingle, *ibid.*, **B24**, 153 (1968).
17) D. R. Armstrong and P. G. Perkins, *J. Chem. Soc.*, (*A*), **1967**, 123.

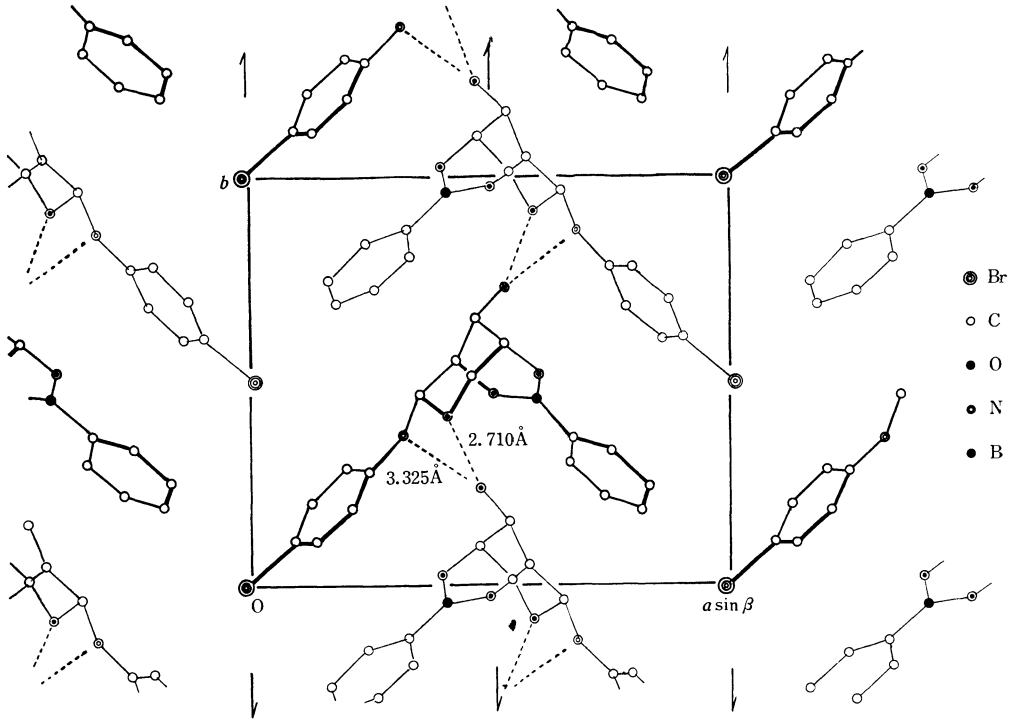

Fig. 8. The crystal structure projected along the *c* axis. The dashed lines indicate the presumed hydrogen bonds. Concerning the absolute configuration, this figure is the mirror image of the actual crystal.

TABLE 5. HYDROGEN-BOND DISTANCES AND ANGLES

Bonds		Acceptor at
O(3)···O(5)	2.710 Å	$1-x$, $\frac{1}{2}+y$, $\bar{z}$
N(1)···O(3)	3.325 Å	$1-x$, $\frac{1}{2}+y$, $1-z$

Angles	
C(3)—O(3)···O(5)	104.3°
C(9)—N(1)···O(3)	101.1°
C(1)—N(1)···O(3)	136.2°

6.8°, suggesting some π interaction between the phenyl group and the boron atom. The C(12)–B distance is 1.506 Å.

Crystal Structure. The packing arrangements of the crystal viewed along the *b* and *c* axes are shown in Figs. 7 and 8, respectively. The presumed hydrogen bonds are indicated by dashed lines. As shown in Table 5, a strong hydrogen-bond clearly exists between O(3) and O(5) atoms forming a helical chain along the b axis. Although the N(1)···O(3) distance is rather long, the angles lie within possible range to form a hydrogen-bond. There may be weak interaction between them along the *c* axis. These are compatible with the predominant shape of the crystal. There is no unusual short approach in the crystal.

The authors are indebted to Professor Tetsuo Sato for suggesting the problem and continued interest and Mr. Yoshikuni Sato for a gift of the sample.

BULLETIN OF THE CHEMICAL SOCIETY OF JAPAN VOL. 42 1248—1256 (1969)

A Theoretical Interpretation of Substituent Effects on the H-H and ^{13}C-H Spin Coupling Constants for CH_3X, $(CH_2)_2X$, and CH_2=CHX Derivatives[1]

Teijiro YONEZAWA, Isao MORISHIMA, Mutsuo FUJII and Hiroshi KATO

Department of Hydrocarbon Chemistry, Faculty of Engineering, Kyoto University, Kyoto

(Received September 27, 1968)

An attempt has been made to explain the experimental trend of H–H and ^{13}C–H nuclear spin coupling constants for CH_3X, $(CH_2)_2X$, and CH_2=CHX systems on the basis of the Pople and Santry expression for the contact term. The calculated magnitudes of the coupling constants are parallel with the observed values, but are uniformly lower by a factor of between 1.5 and 2. The variation in the calculated coupling constants with the electronegativity (E_x) of the substituent, X, follows the well-acknowledged observed tendency for directly-bonded ^{13}C–H, geminal H–H, and vicinal *cis* and *trans* H–H coupling constants. Theoretical calculations also predict the E_x dependency of the directly-bonded ^{13}C–H coupling constants for two geminal C–H bonds in the $^{13}CH_2$=CHX fragment. The difference between two geminal ^{13}C–C–H coupling constants in the CH_2=^{13}CHX system is also obtained by calculation. Discussions of the factors which dominate the couplings are also presented.

The theory of nuclear spin-coupling based on delocalized molecular orbitals presented by Pople and Santry[3] has been used, with a good deal of success, to estimate numerical values for a large number of couplings. Pople and Santry themselves applied[4] the theory to H–H, ^{13}C–H, and ^{13}C–^{13}C couplings in ethane, ethylene, and acetylene; Murrell *et al.*[5] also carried out similar calculations. Fahey *et al.*[6] calculated the H–H and ^{13}C–H coupling constants for various hydrocarbons using the extended Hückel theory. The present authors[2] also calculated the H–H couplings for saturated and unsaturated simple hydrocarbons, aldehydes, and small strained ring compounds by using a modified Hückel MO theory. In addition to these calculations of coupling constants, the couplings involving other nuclei, ^{19}F, ^{31}P, and ^{29}Si, have been investigated theoretically with fair success.[7,8]

There have, however, been only a few investigations of theoretical interpretations of the substituent effects on the signs and magnitudes of the nuclear spin coupling constants. As is well known,[9] the signs and magnitudes of geminal and vicinal H–H couplings, particularly of the geminal coupling, $J^{gem}_{H\text{-}H}$, depend sensitively on the nature of the substituent, X, for CH_3X, $(CH_2)_2X$, and CH_2=CHX systems. Pople and Bothner-By[10] gave a satisfactory interpretation of the substituent effects of geminal H–H coupling with the aid of simple MO formalism, distinguishing the electronic effects into inductive and hyperconjugative electron transfer.

However, the substituent effects on the ^{13}C–H and vicinal H–H couplings are still open to further investigation. The substituent effect on the directly-bonded ^{13}C–H couplings has been attributed to the change in the hybridization[11] of the carbon atom in the C–H bond, in the C–H bond distances,[12] or in the $1s$(H)–$2s$(C) partial bond order.[13] However, there have been no systematic studies of the substituent effect on the directly bonded ^{13}C–H and

1) Part II of "Molecular Orbital Calculations of Nuclear Spin Coupling Constants." Part I, the previous paper, Ref. 2.

2) T. Yonezawa, I. Morishima, M. Fujii and H. Kato, This Bulletin, **40**, 487 (1967).

3) J. A. Pople and D. P. Santry, *Mol. Phys.*, **8**, 1 (1964).

4) J. A. Pople and D. P. Santry, *ibid.*, **9**, 311 (1965).

5) F. B. Van Dnijnveldt, V. M. S. Gil and J. N. Murrell, *Theoret. Chim. Acta*, **4**, 85 (1966); R. Ditchfield and J. N. Murell, *Mol. Phys.*, **14**, 481 (1968).

6) R. C. Fahey, G. C. Graham and R. L. Piccioni, *J. Am. Chem. Soc.*, **88**, 193 (1966).

7) J. N. Murrell, P. E. Stevenson and G. T. Jones, *Mol. Phys.*, **12**, 265 (1967).

8) A. H. Cowley, W. D. White and S. L. Manatt, *J. Am. Chem. Soc.*, **89**, 6433 (1967).

9) J. W. Emsley, J. Feeney and L. H. Sutcliffe, "High Resolution Nuclear Magnetic Resonance Spectroscopy," Vol. 2, Pergamon Press, Oxford (1966).

10) J. A. Pople and A. A. Bothner-By, *J. Chem. Phys.*, **42**, 1339 (1965).

11) N. Müller and D. E. Pritchard, *ibid.*, **31**, 768, 1471 (1959); C. Juan and H. S. Gutowsky, *ibid.*, **37**, 2198 (1962).

12) N. Müller, *ibid.*, **36**, 359 (1962).

13) T. Yonezawa, I. Morishima and M. Fujii, This Bulletin, **38**, 1224 (1965); *ibid.*, **39**, 2110 (1966).

^{13}C–C–H couplings through the geminal two bonds, such as J_{C-H_t} and J_{C-H_c}, and vicinal J_{C-C-H_t} and J_{C-C-H_c}, specified as follows:

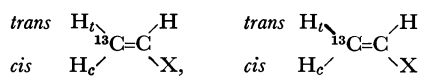

In the present study, we attempt to gain a comprehensive theoretical understanding of the substituent effect on the signs and magnitudes of directly-bonded ^{13}C–H, geminal H–H, and ^{13}C–H, and of vicinal H–H coupling constants for CH_3X, $(CH_2)_2X$, and CH_2=CHX systems.

Method of Calculation

For most of the couplings studied to date, particularly those involving only carbon and hydrogen atoms, it has been found that the Fermi contact term is most dominant.[3] All of our calculations are carried out, therefore, by neglecting the other two terms, the orbital and dipolar terms. In the LCAO approximation, the molecular orbital expression for the contact contribution to the spin-spin coupling constant between the A and B nuclei is given by:[3]

$$J_{AB} = -h\gamma_A\gamma_B\left(\frac{8\beta}{3}\right)^2 \sum_{i}^{occ}\sum_{j}^{unocc}({}^3\Delta E_{i\to j})^{-1} \times \sum_{\lambda\mu\gamma\sigma} C_{i\lambda}C_{j\mu}C_{j\gamma}C_{i\sigma}(\phi_\lambda|\delta(\gamma_A)|\phi_\mu) \times (\phi_\gamma|\delta(r_B)|\phi_\sigma) \quad (1)$$

The notations in Eq. (1) are the same as in Ref. 3. In the approximation which retains only one-center integrals involving valence s orbitals on the atoms A and B and in the one-electron independent MO approximation, Eq. (1) becomes:[3]

$$J_{AB} = \frac{16}{9}\beta^2\gamma_A\gamma_B h(S_A|\delta(r_A)|S_A)(S_B|\delta(r_B)|S_B)\pi_{S_A,S_B} = \frac{16}{9}\beta^2 h\gamma_A\gamma_B S_A^2(0)S_B^2(0)\pi_{S_A,S_B} \quad (2)$$

$S_A^2(0)$ and $S_B^2(0)$ denote the spin densities at the A and B nuclei of the valence s orbitals, and $\pi_{S_AS_B}$ is the mutual polarizability of the s valence orbital belonging to the atoms A and B. It is written as:

$$\pi_{S_A,S_B} = 4\sum_{i}^{occ}\sum_{j}^{unocc}(\varepsilon_i-\varepsilon_j)^{-1}C_{iS_A}C_{jS_A}C_{jS_B}C_{iS_A} \quad (3)$$

The values of $S_A^2(0)$ for the $1s$ and $2s$ valence orbitals for the H and C atoms were obtained using the Slater AO with an orbital exponent of 1.2 for H and using the SCF AO for the carbon atom.[14] With the appropriate constants, the H–H and ^{13}C–H spin coupling constants are given by the equations:

$$J_{H-H} = 6.235\times10^3\pi_{H-H}(\text{Hz}) \quad (4)$$

$$J_{C-H} = 7.885\times10^3\pi_{C-H}(\text{Hz}) \quad (5)$$

when π_{H-H} are π_{C-H} are given in units of $(\text{eV})^{-1}$.

In the present calculation, three types of molecular orbitals are employed for most of the molecules.

One-electron MO functions and energies were obtained by the extended Hückel method[15] (method A) and by two modified methods with a zero overlap approximation (methods B and C). The secular equations and parameters adopted in these three methods are summarized in Table 1. To construct a molecular orbital, Slater atomic orbitals were used as the basis set. The atomic coordinates for the evaluation of an overlap matrix, $S_{\mu\nu}$, were calculated from the pertienent bond distances and bond angles.[16] The valence-state ionization potentials (I_μ) used for the diagonal element of the H matrix are given in Table 2, together with the calculated values of $-0.5(I_\mu+A_\mu)$, where A_μ denotes an electron affinity. In method A, all the overlaps are included. In methods B and C, however, all the overlap integrals, $S_{\mu\nu}$, in the secular equations are replaced by $\delta_{\mu\nu}$ (=1 for $\mu=\nu$ and=0 for $\mu=\nu$). The method B was adopted in one of our previous paper,[2] where it was shown to have an advantage over method A. In the method C, the evaluation of $H_{\mu\mu}$ is slightly modified, as may be seen in Table 1. Pople and Segal[17] used this type of $H_{\mu\mu}$ parametrization for the starting

Table 1. Summary of the methods of the one-electron MO calculation

	Method A (EHMO)	Method B	Method C
$H_{\mu\nu}$	$0.5S_{\mu\nu}(H_{\mu\mu}+H_{\nu\nu})K$	$0.5S_{\mu\nu}(H_{\mu\mu}+H_{\nu\nu})K$	$0.5S_{\mu\nu}(H_{\mu\mu}+H_{\nu\nu})K$
Secular Eq.	$\lvert H_{\mu\nu}-\varepsilon S_{\mu\nu}\rvert=0$	$\lvert H_{\mu\nu}-\varepsilon\delta_{\mu\nu}\rvert=0$	$\lvert H_{\mu\nu}-\varepsilon\delta_{\mu\nu}\rvert=0$
$H_{\mu\mu}$	$-I_\mu$	$-I_\mu$	$-0.5\ (I_\mu+A_\mu)$
K	1.75	1.0	1.0

14) J. R. Morton, J. R. Rowlands and D. H. Whiffen, National Physical Laboratory Report BPR, 13 (1962).
15) R. Hoffmann, *J. Chem. Phys.*, **39**, 1397 (1963).
16) Data taken from "Tables of Interatomic Distances and Configurations in Molecules and Ions," L. E. Sutton, ed., Special Publication No. 11 and 18, The Chemical Society, London (1958 and 1965).
17) J. A. Pople and G. A. Segal, *J. Chem. Phys.*, **44**, 3289 (1966).

TABLE 2. THE VALUE OF DIAGONAL MATRIX ELEMENT $H_{\mu\mu}$ (eV)[a)]

Atom	Methods A and B Valence AO					Method C Valence AO				
	1s	2s	2p	3s	3p	1s	2s	2p	3s	3p
H	−13.60					−7.17				
C		−21.34	−11.42				−15.34	−6.00		
N		−27.50	−14.49				−20.64	−8.35		
O		−35.30	−17.76				−27.57	−11.30		
F		−38.24	−20.86				−31.30	−12.18		
Cl				−24.02	−15.03				−19.23	−9.38

a) The values of the ionization popotential and the electron affinity were taken from Pritchard and Skinner, *Chem. Revs.*, **55**, 745 (1955).

MO functions in their semi-empirical SCF MO-(CNDO) theory. Compared with method B, method C gives slightly smaller ionization potentials and coupling constants which are in better agreement with the experimental results.

Results

The calculated and observed coupling constants are compared in Tables 3 to 7. In Figs. 1 to 4, the variation in the observed and calculated H–H and ^{13}C–H coupling constants is plotted against the electronegativity, E_x, of the substituent, X. The values of E_x are tentatively taken from those of Cavanaugh and Daily,[18)] which were derived empirically from the internal chemical shifts, as is summarized in Table 8. The empirical linear correlation between the observed nuclear spin-coupling constants and their E_x values has been established by many workers.[9)] For the saturated CH_3X system, the calculation by the method A gives somewhat unfavorable*1 values of the geminal

TABLE 3. CALCULATED AND OBSERVED VALUE OF J_{HH} FOR CH_3X DERIVATIVES

Molecule	J_{AB}	Calculated J_{H-H}, Hz Method A	Method B	Method C	Observed J, Hz	Ref.
CH_4	$^2J_{HH}$ (*gem*)	−20.9	−3.9	− 4.9	−12.4	a, b
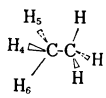	$^2J_{HH}$ (*gem*)	−24.4	−4.8	− 5.9	−12.4	a, b
	$^3J_{H_2H_4}$ (*gauche*)	+ 0.0	+0.7	+ 0.2	+ 8.3[c)]	b
	$^3J_{H_2H_6}$ (*trans*)	+ 8.0	+8.2	+19.2		
CH_3Cl	$^2J_{HH}$ (*gem*)	—	−4.2	− 3.1	−10.8	d
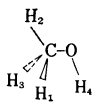	$^2J_{H_1H_2}$ (*gem*)	−28.1	−4.9	− 3.9	−10.8[c)]	d
	$^2J_{H_1H_3}$ (*gem*)	−27.8	−4.8	− 3.6		
	$^3J_{H_1H_4}$	− 1.4	−0.2	+ 0.1	—	
	$^3J_{H_2H_4}$	+ 1.4	+0.5	+ 0.5	—	
CH_3F	$^2J_{HH}$ (*gem*)	—	−4.3	− 1.6	− 9.6	d
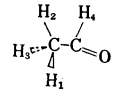	$^2J_{H_1H_2}$	—	−6.1	−11.1	−12.0[c)]	e
	$^2J_{H_2H_3}$	—	−6.4	−12.3		
	$^2J_{H_1H_3}$	—	−2.6	− 0.6		
	$^3J_{H_1H_4}$	—	+5.1	+12.3	+ 2.8[c)]	
	$^3J_{H_2H_4}$	—	+0.3	+ 2.5		
	$^3J_{H_3H_4}$	—	+0.7	− 0.6		
$CH_3C{\equiv}N$	$^2J_{HH}$	−23.7	−5.9	− 9.9	−16.9	a
$CH_3C{\equiv}CH$	$^2J_{HH}$	−24.5	−5.8	− 8.7	—	

a) M. Barfield and D. M. Grant, *J. Am. Chem. Soc.*, **82**, 4276 (1961); *J. Chem. Phys.*, **36**, 2054 (1962); *J. Am. Chem. Soc.*, **85**, 1901 (1963).
b) R. M. Lynden-Bell and N. Sheppard, *Proc. Roy. Soc. (London)*, **A269**, 385 (1962).
c) Average
d) H. J. Bernstein and N. Sheppard, *J. Chem. Phys.*, **37**, 3012 (1962).
e) E. Sackmann and H. Dreeskamp, *Spectrochim. Acta*, **21**, 2005 (1965).

18) J. R. Cavanaugh and B. P. Daily, *ibid.*, **34**, 1099 (1961).

*1 The calculated coupling constants obtained by three methods differ to some extent each other. The major concern in this work is the theoretical interpretation of the observed trend of E_x dependency and the sign of the coupling constants, with rather crude approximation. Therefore we reserve the quantitative discussion on the absolute value of the coupling constants.

TABLE 4. CALCULATED AND OBSERVED VALUES OF J_{HH} FOR $(CH_2)_2X$ DERIVATIVES

Molecule		Method A	Method B	Method C	Observed J, Hz		Ref.
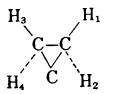	$^2J_{H_1H_2}$ (*gem*)	−30.0	−3.0	+ 2.0	−4.5		a
	$^3J_{H_1H_3}$ (*cis*)	+ 0.9	+1.8	+ 1.5	+9.2		a
	$^3J_{H_1H_4}$ (*trans*)	+ 4.2	+3.8	+10.0	+5.4		a
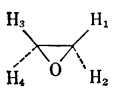	$^2J_{H_1H_2}$ (*gem*)	−35.3	−5.1	− 1.9	+5.5		b
	$^3J_{H_1H_3}$ (*cis*)	0.0	+1.6	+ 1.2	+4.5		b
	$^3J_{H_1H_4}$ (*trans*)	+ 4.3	+4.7	+12.5	+3.1		b
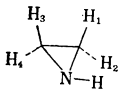	$^2J_{H_1H_2}$ (*gem*)	−32.9	−2.8	+ 5.1	+2.0		c
	$^3J_{H_1H_3}$ (*cis*)	+ 0.5	+1.7	+ 1.7	+6.3[e]	+7.2[d]	
	$^3J_{H_2H_4}$ (*cis*)	+ 1.0	+2.0	+ 2.5		+5.5[d]	
	$^3J_{H_1H_4}$ (*trans*)	+ 5.3	+5.3	+12.6	+3.8		c

a) D. J. Patel, M. E. H. Howden and J. D. Roberts, *J. Am. Chem. Soc.*, **85**, 3218 (1963).
b) N. Sheppard and J. J. Turner, *Proc. Roy. Soc. (London)*, **A252**, 506 (1959).
c) F. S. Mortimer, *J. Mol. Spectry.*, **5**, 199 (1962).
d) T. Yonezawa and I. Morishima, *ibid.*, **27**, 210 (1968).

TABLE 5. CALCULATED AND OBSERVED VALUES OF J_{HH} FOR CH_2=CHX DERIVATIVES

Molecule X	J	Calculated J, Hz Method A	Method B	Method C	Observed J, Hz	Ref.
H	$^2J_{HH}$ (*gem*)	−31.8	− 2.0	+ 5.2	+ 2.5	a, b, c
	$^3J_{HH}$ (*cis*)	+ 2.2	+ 3.8	+ 2.9	+11.6	a, c, b
	$^3J_{HH}$ (*trans*)	+13.5	+13.5	+34.0	+19.1	a, b, c
CN	$^2J_{HH}$ (*gem*)	−31.3	− 1.6	+ 1.6	+ 0.9	d
	$^3J_{HH}$ (*cis*)	+ 3.2	+ 5.1	+ 3.8	+11.8	d
	$^3J_{HH}$ (*trans*)	+13.5	+12.7	+29.6	+17.9	d
CH_3	$^2J_{HH}$ (*gem*)	—	− 2.4	+ 4.1	+ 2.1	e
	$^3J_{HH}$ (*cis*)	—	+ 2.9	+ 1.4	+10.0	e
	$^3J_{HH}$ (*trans*)	—	+12.8	+32.0	+16.8	e
CO_2H	$^2J_{HH}$ (*gem*)	−31.7	− 2.0	+ 4.0	+ 1.7	f
	$^3J_{HH}$ (*cis*)	+ 1.5	+ 2.8	− 0.4	+10.2	f
	$^3J_{HH}$ (*trans*)	+12.2	+11.6	+26.9	+17.2	f
COH	$^2J_{HH}$ (*gem*)	−31.5	− 1.6	+ 6.3	− 1.7	g
	$^3J_{HH}$ (*cis*)	+ 1.7	+ 3.1	+ 1.3	+ 6.3	g
	$^3J_{HH}$ (*trans*)	+12.7	+12.9	+32.2	+13.8	g
Cl	$^2J_{HH}$ (*gem*)	−32.2	− 3.0	+ 1.8	− 1.4	h
	$^3J_{HH}$ (*cis*)	+ 0.6	+ 1.4	− 1.1	+ 7.3	h
	$^3J_{HH}$ (*trans*)	+ 9.7	+ 9.9	+24.4	+14.6	h
OCH_3	$^2J_{HH}$ (*gem*)	—	− 3.9	− 0.7	− 2.0	i
	$^3J_{HH}$ (*cis*)	—	+ 0.4	− 1.2	+ 7.0	i
	$^3J_{HH}$ (*trans*)	—	+ 9.0	+22.2	+14.1	i
F	$^2J_{HH}$ (*gem*)	—	− 4.4	− 1.9	− 3.2	h
	$^3J_{HH}$ (*cis*)	—	0.0	− 0.8	+ 4.7	h
	$^3J_{HH}$ (*trans*)	—	+ 7.9	+20.7	+12.8	h

a) R. M. Lynden-Bell and N. Sheppard, *Proc. Roy. Soc. (London)*, **A269**, 385 (1962).
b) G. S. Reddy and J. H. Goldstein, *J. Mol. Spectry.*, **8**, 475 (1962).
c) D. M. Graham and C. E. Halloway, *Can. J. Chem.*, **41**, 2114 (1963).
d) R. T. Hobgood, Jr., R. E. Mayo and J. H. Goldstein, *J. Chem. Phys.*, **39**, 2501 (1963).
e) A. A. Bothenr-By and C. Naar-Colin, *J. Am. Chem. Soc.*, **83**, 231 (1961).
f) S. Castellano and J. S. Waugh, *J. Chem. Phys.*, **34**, 295 (1961).
g) T. Schaefer, *ibid.*, **36**, 2235 (1962).
h) C. N. Banwell and N. Sheppard, *Discussions Faraday Soc.*, **34**, 115 (1962).
i) R. T. Hobgood, Jr., G. S. Reddy and J. H. Goldstein, *J. Phys. Chem.*, **67**, 110 (1963).

TABLE 6. CALCULATED AND OBSERVED VALUES OF J_{CH} FOR CH_3X AND $(CH_2)_2X$ DERIVATIVES

Molecule	Calculated J_{CH}, Hz Method A	Method B	Method C	Observed J_{CH}, Hz	Ref.
CH_3X					
X=H	+56.8	+48.7	+ 76.0	+125	a
CH_3	+64.1	+50.9	+ 77.9	+126	a
Cl	+60.5	+50.5	+100.3	+150	a
OH	+73.3	+63.0	+103.7	+141	a
F	+68.1	+68.1	+108.5	+149	a
CHO	—	+50.4	+ 79.4	+127	a
CN	+59.3	+53.1	+ 88.1	+136	a
C≡CH	+58.6	+51.2	+ 83.4	+132	a
$(CH_2)_2X$					
X=CH_2	+91.5	+75.4	+114.5	+161	a
O	+95.0	+79.7	+125.7	+176	b
NH	+94.8	+80.3	+127.4	+168	b
	+92.3	+78.1	+125.2		

a) N. Müller and D. E. Pritchard, *J. Chem. Phys.*, **31**, 768, 1471 (1959).
b) F. S. Mortimer, *J. Mol. Spectry.*, **5**, 199 (1950).

H–H coupling; they are too negative, particularly for molecules with electronegative substituents such as X=O, N, F. The method B also gives improper results, as is depicted in Fig. 1; the substituent effect of the calculated values is opposite to that of the observed values. The results calculated by method C are the most acceptable, though the magnitudes are uniformly lower than those of the experiments by a factor of 1.5 (Fig. 1).

The linear dependence of the directly-bonded J_{CH} on E_x is also satisfactorily provided for by the method C than by the method B (Fig. 3). Thus, for the following discussion, the results obtained by method C are adopted for CH_3X systems.

For three-membered ring systems, $(CH_2)_2X$, none of the methods of calculation predict the observed trend of the H–H and C–H couplings. The most striking discrepancy between the cal-

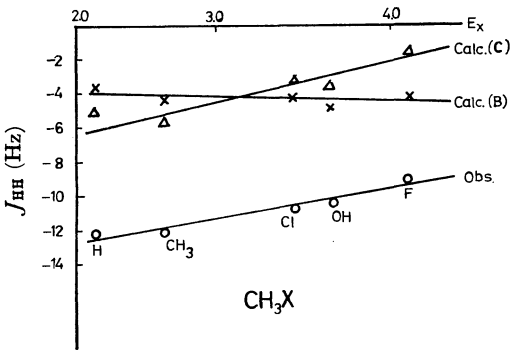

Fig. 1. The calculated and observed geminal coupling constants, J_{HH}, in CH_3X systems are ploted *versus* the electronegativity of the substituent, X (E_x).

TABLE 7. CALCULATED AND OBSERVED VALUES OF J_{CH} AND $J_{C\text{-}C\text{-}H}$ FOR CH_2=CHX DERIVATIVES

Molecule X		Calculated J_{CH} and J_{CCH}, Hz Method B	Method C	Observed J_{CH} and J_{CCH}, Hz
H	$^1J_{CH}$ (*trans*)	+72.6	+108.7	+156.4[a]
	$^1J_{CH}$ (*cis*)			
	$^2J_{CCH}$ (*trans*)	− 0.1	+ 3.5	− 2.4[a]
	$^2J_{CCH}$ (*cis*)			
CN	$^1J_{CH}$ (*trans*)	+77.9	+122.5	—
	$^1J_{CH}$ (*cis*)	+72.6	+107.9	—
	$^2J_{CCH}$ (*trans*)	+ 0.4	+ 8.1	—
	$^2J_{CCH}$ (*cis*)	− 0.4	+ 1.7	—
CH_3	$^1J_{CH}$ (*trans*)	+75.0	+113.4	+162[b]
	$^1J_{CH}$ (*cis*)	+69.7	+102.3	+156[b]
	$^2J_{CCH}$ (*trans*)	+ 0.2	+ 4.4	—
	$^2J_{CCH}$ (*cis*)	− 0.3	+ 2.2	—
CO_2H	$^1J_{CH}$ (*trans*)	+74.7	+115.3	—
	$^1J_{CH}$ (*cis*)	+73.0	+106.7	—
	$^2J_{CCH}$ (*trans*)	+ 0.2	+ 7.8	—
	$^2J_{CCH}$ (*cis*)	− 0.3	+ 1.2	—
CHO	$^1J_{CH}$ (*trans*)	+76.3	+118.9	—
	$^1J_{CH}$ (*cis*)	+71.9	+104.3	—
	$^2J_{CCH}$ (*trans*)	+ 0.1	+ 5.6	—
	$^2J_{CCH}$ (*cis*)	− 0.04	+ 2.3	—
Cl	$^1J_{CH}$ (*trans*)	+78.1	+123.0	+161[c]
	$^1J_{CH}$ (*cis*)	+69.8	+100.9	+160[c]
	$^2J_{CCH}$ (*trans*)	+ 2.5	+ 14.7	—
	$^2J_{CCH}$ (*cis*)	− 0.9	+ 0.3	—
OCH_3	$^1J_{CH}$ (*trans*)	+84.2	+135.0	—
	$^1J_{CH}$ (*cis*)	+64.2	+ 91.1	—
	$^2J_{CCH}$ (*trans*)	+ 7.2	+ 24.4	—
	$^2J_{CCH}$ (*cis*)	− 0.9	− 0.5	—
F	$^1J_{CH}$ (*trans*)	+82.6	+133.1	—
	$^1J_{CH}$ (*cis*)	+66.6	+ 96.5	—
	$^2J_{CCH}$ (*trans*)	+ 8.6	+ 25.1	—
H, Cl>C=C<Cl, H	$^1J_{CH}$(*cis*)	+88.7	+151.2	+199.1[a]
	$^2J_{CCH}$(*cis*)	− 0.6	+ 6.1	0[a]
H, Cl>C=C<H, Cl	$^1J_{CH}$(*trans*)	+96.3	+168.6	+198.3[a]
	$^2J_{CCH}$(*trans*)	+4.1	+ 21.8	+ 15.7[a]

a) N. Müller, *J. Chem. Phys.*, **37**, 2329 (1962).
b) Taken from the values for styrene.
c) E. B. Wipple, W. E. Stewart, G. S. Reddy and J. H. Goldstein, *J. Chem. Phys.*, **34**, 2136 (1961).

TABLE 8. ELECTRONEGATIVITY (E_x) OF ATOM AND FUNCTIONAL GROUP[a]

Atom and Group	E_x	Atom and Gorup	E_x
H	2.10	C_6H_5	2.75
CN	2.49	Cl	3.25
CH_3	2.50	-O-	3.31
CO_2H	2.60	OH	3.46
CHO	2.69	F	3.90

a) Taken from Ref. 18.

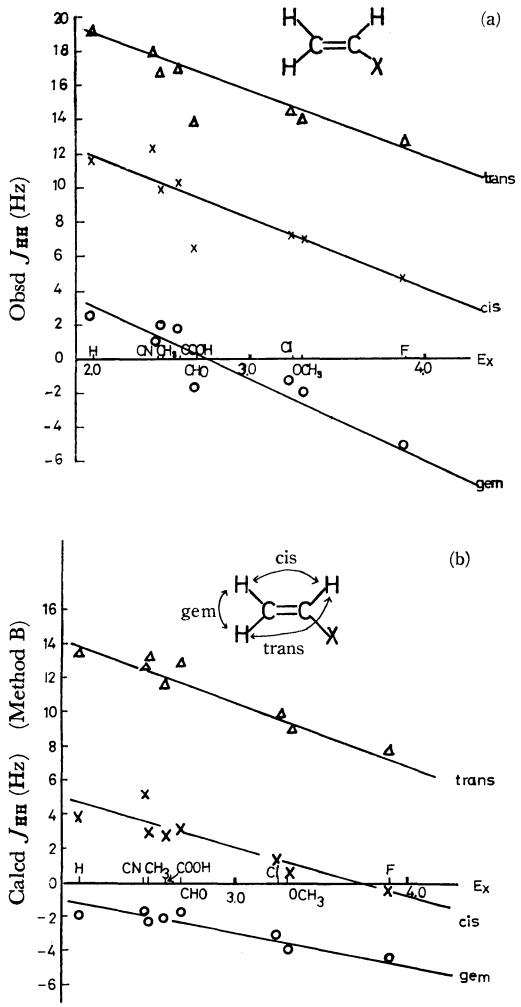

Fig. 2. The geminal, vicinal *cis*, and vicinal *trans* coupling constants in mono-substituted vinyl compounds are plotted *versus* the electronegativity of the substituent, X (E_x); (a): calculated values, (b) experimental values.

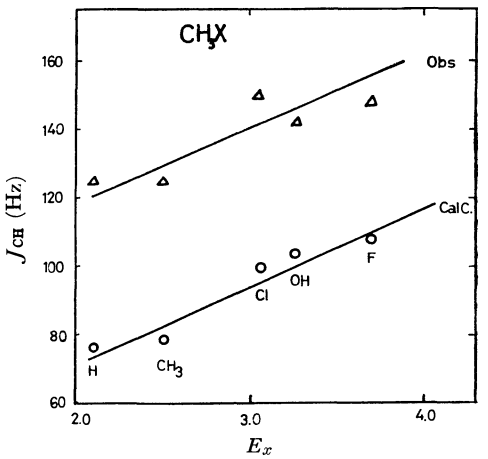

Fig. 3. The calculated and experimental ^{13}C–H coupling constants, J_{CH}, in CH_3X systems are plotted *versus* the electronegativity of the substituent, X (E_x).

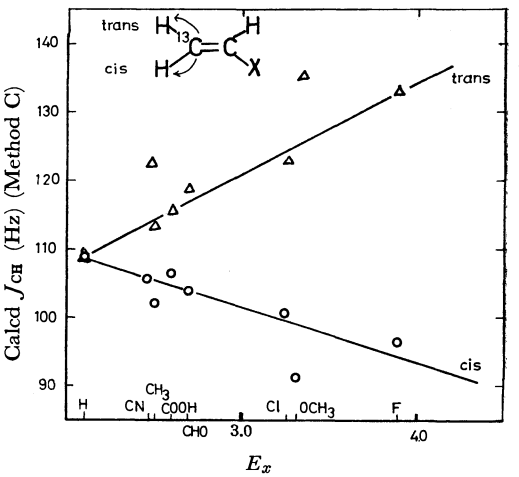

Fig. 4. The calculated ^{13}C–H coupling constants for directly bonded ^{13}C–H (*cis*) and ^{13}C–H (*trans*) in $^{13}CH_2$=CHX systems are plotted *versus* the electronegativity of the substituent, X (E_x).

culated and experimental coupling constants is in the vicinal H–H coupling constants. The greater value of the vicinal *cis* H–H coupling than that of the *trans* coupling is not reproduced by calculations.

For vinyl derivatives the geminal and vicinal *cis* and *trans* H–H coupling constants calculated by method B decrease linearly as E_x increases and are in agreement with the observed results (Fig. 2), but their magnitudes are lower than those of the experiments by a factor of about 1.5. Method C gives a poorer agreement with the experimental results in the present case because: (i) the *trans* H–H couplings are too positive, (ii) the *cis* coupling is more negative than the geminal coupling, behavior which contradicts the observed tendency, and (iii) the linear dependency of J_{H-H} on E_x disagrees with the observed feature.*2 Table 7 gives the ^{13}C–H couplings through one bond, J_{C-H}, and through two bonds, J_{C-C-H}. Because of the lack of experimental data, no comparison between calculated and observed values is yet possible. The calculated values of directly bonded ^{13}C–H coupling constants are somewhat different for ^{13}C–H_t and ^{13}C–H_c bonds, which are located respectively *cis* and *trans*, with respect to the substituent, X.

The variation in the calculated J_{C-H} values is

*2 The method C is adopted to improve the overestimated polarization due to heteroatoms in method B. However, this may cause improper sequence of σ and π orbitals in the vinyl compounds. So this may lead to a poor agreement with experiments.

plotted against E_x in Fig. 4. The J_{C-H_t} value increases as E_x increases, while the J_{C-H_c} value decreases. As may easily be seen from Table 7 and Fig. 4, the J_{C-H_c} value is generally greater than J_{C-H_t}. This definite trend of the J_{C-H} dependency on E_x has not been found experimentally. This prediction has, however, been partly confirmed experimentally by the present authors;[19] our results will be published elsewhere. However, the trend of J_{C-H_c} is also supported here by limited examples of the observed data (Table 7). Table 7 and Fig. 5 also reveal that the calculated values of

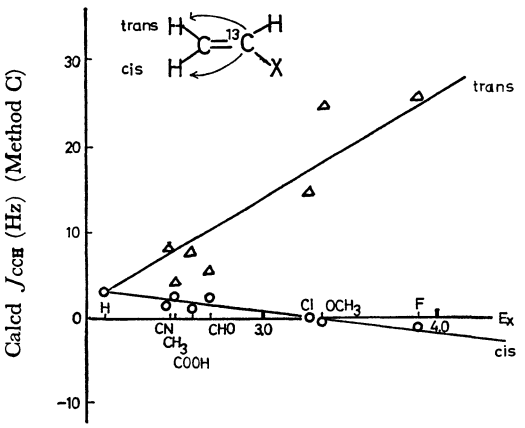

Fig. 5. The calculated ^{13}C–C–H coupling constants for *cis* and *trans* protons in CH_2=^{13}CHX systems are plotted *versus* the electronegativity of the substituent, X (E_x).

J_{C-C-H_t} are more positive than J_{C-C-H_c}. Figure 5 also reveals the opposite trend of J_{C-C-H_t} and J_{C-C-H_c}, a trend which is similar to the case with the directly-bonded ^{13}C–H coupling constants, J_{C-H_t} and J_{C-H_c}. The observed ^{13}C–C–H coupling constant for 1,2-dichloroethylene may serve as the only example of a compound with different *cis*- and *trans*-type ^{13}C–C–H coupling constants. Calculations by methods B and C reproduce the trend of the experimental value.

Discussion

Before entering into our discussion, it should be pointed out that the present calculations do not include the contributions of the π-electrons to the coupling. The neglect of σ-π-interaction in the present study fails to account for π-electron contribution. Semiempirical methods for estimating π-electron coupling have been developed by McConnell[20] and Karplus.[21] They have shown that, for ethylene, the π-contribution is 1.8 Hz for the vicinal H–H coupling. This correction, however, is insufficient to cover the difference between the calculated coupling constants and the observed values. Since a major concern of this study is to give a theoretical interpretation of the experimental trend of the nuclear spin coupling constants, apart from the magnitude and sign of the calculated coupling constants, the substituent effect on the J value will be discussed without taking any account of the π-electron contirubition.

In general, the magnitudes of the coupling constants, as calculated on the basis of the contact term, reproduce the trend of the experimental values, but they are lower by a factor of between 1.5 to 2 (Figs. 1—3). Of the three types of calculations employed here, methods B and C are generally more satisfactory for the molecules containing heteroatoms. For hydrocarbons, the extended Hückel method (method A) is promising[6,8] except for the calculation of the J_{H-H} value for geminal protons. The most unfavorable aspect of method A is the too negative values for the geminal H–H coupling constants of most compounds, particularly for a geminal coupling in the CH_2 group adjacent to the heteroatom. This shortcoming is imporved by methods B and C, as has been discussed in a previous paper.[2] For example, the geminal H–H and directly-bonded ^{13}C–H coupling constants for formaldehyde are calculated to be -39.8 Hz and $+105.6$ Hz by method A, $+2.1$ Hz and $+99.1$ Hz by method B, and $+23.7$ Hz and $+161.7$ Hz by method C. The last set is comparable with the observed values of $+40.2$ and $+172$ Hz.

Let us now discuss our theoretical predictions of a general trend of the J_{C-H} and J_{C-C-H} values in vinyl derivatives. The directly-bonded ^{13}C–H coupling constants, J_{C-H_t} and J_{C-H_c}, increase and decrease respectively, with the increase in the electronegativity, E_x, in the vinyl compound (Fig. 4):

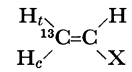

The same situation is also obtained for the geminal ^{13}C–C–H coupling constants, J_{C-C-H_t} and J_{C-C-H_c}, in:

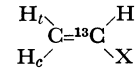

(Figs. 4 and 5). It is well accepted that a linear relationship exists between the *s* character in the bonding carbon orbital and the directly-bonded J_{C-H}. The positive trend of the geminal H–H coupling constants, J_{H-H}, with an increase in the *s* character of the C–H bond has also been observed for geminal ^{13}C–C–H coupling constants, J_{C-C-H}, in ethane (-4.5 Hz), ethylene (-2.4 Hz), and

19) T. Yonezawa and I. Morishima, unpublished work.
20) H. M. McConnell, *J. Mol. Spectry.*, **1**, 11 (1957).
21) M. Karplus, *J. Chem. Phys.*, **33**, 1842 (1960).

acetylene (+49.2 Hz).[22] Hence, an increase or decrease in the coupling constants can be expected in both cases as the *s* character of the carbon atom in the C–H bond increases or decreases. Therefore, it seems a reasonable prediction by calculation that the general trend of J_{C-H} is similar to that of J_{C-C-H}. It can also be said that the positive or negative trend of J_{C-C-H_t} and J_{C-C-H_c} depends mainly on the increase or decrease in the *s* character of the carbon atom in the C–H_t and C–H_c bonds.

In their theory of nuclear spin-coupling between geminal hydrogens, Pople and Bothner-By[10] have given elegant explanations of the general trend of J_{H-H} in terms of inductive and hyperconjugative electron withdrawal or donation of an adjacent substituent. Their theory can be qualitatively extended to the case of the ^{13}C–C–H geminal coupling in the ^{13}C–CX–H system, as has been done by McLauchlan and Shaefer.[23] However, the general features of J_{C-C-H} in H–C–^{13}C–X system can not be explained by the theory of Pople and Bothner-By.

The experimental values of J_{C-H} and J_{C-C-H} are completely lacking. The only instance of an experimental J_{C-C-H} value has been obtained for vinyl bromide,[24] $J_{C-C-H_t}=+7.5$ Hz, while $J_{C-C-H_c}=-8.5$ Hz, the calculation for which is not performed in the present study. A similar situation may hold for other substituted compounds. In fact, the values of $J_{C-C-H}=0$ in *trans*-dichloroethylene and $J_{C-C-H}=+15.7$ Hz (assumed positive) in *cis*-dichloroethylene are consistent with this assumption. Although calculation yields too positive values for J_{C-C-H_t} and J_{C-C-H_c}, the relative magnitudes of these two couplings may be reliable. The validity of the above predictions that $J_{C-H_t}>J_{C-H_c}$ and $J_{C-C-H_t}>J_{C-C-H_c}$ in the $H_2{}^{13}C{=}CHX$ and $H_2C{-}{}^{13}CHX$ systems respectively should be examined by further experiments. A similar relation, $J_{^{15}N-H_t}>J_{^{15}N-H_c}$, also holds for:

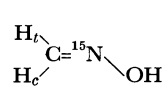

Lehn *et al.*[25] have obtained values of $J_{^{15}N-C-H_t}=-13.88$Hz and $J_{^{15}N-C-H_c}=+2.68$ Hz. Since the gyromagnetic ratio of the ^{15}N nucleus has the minus sign, the large minus coupling constant for $J_{^{15}N-C-H_t}$ is related to the large positive coupling for $J_{^{13}C-C-H_t}$ in the $H_2{}^{13}C{=}CHX$ system. Also, in this case the present calculation gives the values of −11.53 Hz and −3.09 Hz (method B) for $J_{^{15}N-C-H_t}$ and $J_{^{15}N-C-H_c}$ respectively. The large difference between these two geminal coupling constants is again reproduced by the calculation. Similar behavior is also seen in directly-bonded ^{13}C–H coupling constants of propionaldoxime:[26]

Observed:[26] $J_{C-H_c}=161$Hz $J_{C-H_t}=171$Hz

Calculated:[27] $J_{C-H_c}=131$Hz $J_{C-H_t}=141$Hz
(method C)

The ^{13}C–H coupling constant for the *trans* C–H bond with respect to the substituent OH is much larger than the *cis* one; this trend is also reproduced by the present calculation. This is also the case for formaldoxime ($J_{C-H_t}=141$ Hz and $J_{C-H_t}=129$ Hz). However, these differences in the coupling constants may possibly be considered to be due to the effect of lone-pair orientation.[26-28]

Because of the delocalized nature of the MO wave functions, and of the many different terms involved in Eq. (1), it does not seem to be easy to isolate the factors which dominate the coupling. In a previous work[2] we found a definite rule for finding the dominant contribution of the excitations which are specified by the orbital symmetry. Below we will discuss briefly the substituent effects on the coupling constant by considering how the dominant excitations vary with the substituent, X.

As we demonstrated previously,[2] a dominant contribution to the geminal H–H′ coupling constant for the CH_3X system is the excitation from the highest occupied (HO) MO, *a* (antisymmetric with respect to the two 1*s* atomic orbitals, *h* and *h*′), to the lowest or second lowest vacant (LV) MO, *a**. As the substituent, X, becomes more electronegative, the antisymmetric orbital energy is lowered, but the LV *a** orbital energy remains almost unchanged, resulting in an increase in the excitation energy ($\varepsilon_j-\varepsilon_i$). The effect of the substituent, X, on the numerator of Eq. (3) is somewhat difficult to analyse. Let us now tentatively consider the value of $2C_{i\mathrm{H}}C_{i\mathrm{H}}$, for an occupied *a* orbital which contributes dominantly to $J_{H-H'}$. This value is now designated as the "partial bond order" between *h* and *h*′ 1*s* orbitals. The partial bond order for the HO *a* orbital increases in its absolute value with an increase in the electronegativity, E_x. This enhancement of the antibonding character between H and H′ decreases the absolute value of the geminal H–H′ coupling constant. These two effects, the lowering of the HO *a* orbital energy and the increas-

22) R. M. Lynden-Bell and N. Sheppard, *Proc. Roy. Soc. London, Ser. A*, **269** 385 (1962).
23) K. A. McLauchlan and T. Schaefer, *Can. J. Chem.*, **44**, 32 (1966).
24) R. M. Lynden-Bell, *Mol. Phys.*, **6**, 537 (1963).
25) J. M. Lehn, private communication.
26) T. Yonezawa and I. Morishima, *J. Mol. Spectry.*, **27**, 210 (1968).
27) T. Yonezawa and I. Morishima, *ibid.*, in press.
28) J. P. Kintzinger and J. M. Lehn, *Chem. Commun.*, **1967**, 660.

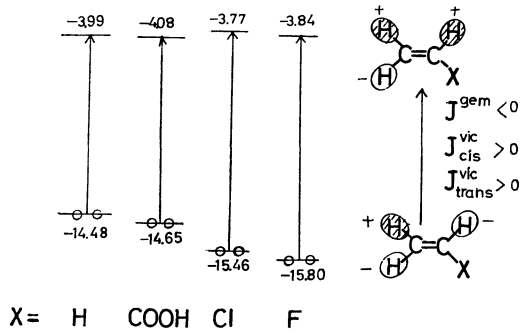

(Method B)

Fig. 6. HO and LV molecular orbital energies (eV) and signs of the orbital coefficients for monosubstituted vinyl compounds.

ing of the atomic orbital coefficient in the HO *a* orbital, contribute dominantly to the increase in the geminal H–H′ couplings in CH_3X systems.

It is well-known that the replacement of X by hyperconjugative groups, such as –C≡CH, –C≡N, and CH_3, increases the negative geminal coupling constant.[29,30] These experimental results are well reproduced by the present calculations, as may be seen in Table 3. The dominant contribution to the geminal and vicinal H–H coupling for vinyl derivatives is made by the excitation from the highest occupied to the lowest unoccupied orbitals, whose orbital symmetry are shown in Fig. 6. These electronic excitations lead to negative and positive H–H coupling constants for geminal and vicinal couplings respectively. The energy difference between these orbitals increases as the electronegative group is replaced. This is illustrated in Fig. 6. Although, of course, the atomic orbital coefficients change, the increases in the excitation energy may play a dominant role in the decrease of the geminal and vicinal coupling constants.

Further progress in the calculation of the signs and magnitudes of nuclear spin coupling constants will come from improvements in the MO energies and LCAO coefficients. Some promise in this regard is shown by the approach using a semi-empirical SCF-MO calculation developed in our laboratory.[31] We got a value of +12.3 Hz for the geminal proton-proton coupling constant of formaldehyde, for instance, by this method. The ^{13}C–H coupling constant is even more improved. The details[32] will be given in the near future.

29) M. Barfield and D. M. Grant, *J. Chem. Phys.*, **36**, 2054 (1962).

30) M. Barfield and D. M. Grant, *J. Am. Chem. Soc.*, **85**, 1899 (1963).

31) T. Yonezawa, K. Yamaguchi and H. Kato, This Bulltin, **40**, 536 (1967); H. Kato, H. Konishi and T. Yonezawa, *ibid.*, **40**, 1017 (1967).

32) T. Yonezawa, I. Morishima, H. Konishi and H. Kato, unpublished work.

BULLETIN OF THE CHEMICAL SOCIETY OF JAPAN VOL. 42 1256—1263 (1969)

An MO-Theoretical Study of the E2 Reaction of Ethyl Chloride

Hideyuki Hao,* Hiroshi Fujimoto** and Kenichi Fukui**

* *Ōe Works, Sumitomo Chemical Co., Ltd., Niihama, Ehime*

** *Department of Hydrocarbon Chemistry, Kyoto University, Kyoto*

(Received September 27, 1968)

The change in the electronic state in the course of the E2 reaction of ethyl chloride was followed by means of the extended Hückel calculation. A model is adopted in which the nucleophilic reagent approaches the *trans*-β-hydrogen atom. The valence-inactive population of the *trans*-β-hydrogen atom in the lowest unoccupied (LU) molecular orbital (MO) was employed as a theoretical reactivity index. The theoretical conclusion derived was consistent with the experimental results.

The mechanism of the base-promoted, bimolecular elimination (E2) reactions has been experimentally studied in detail.[1] In this type of reaction, the attack of bases on the β-hydrogen atom and the departure of the nucleophile, X, from the α-carbon atom are thought to occur in concert with the double-bond formation between the C_α–C_β bond, and it is accepted that the hydrogen atom *trans* coplanar with respect to the leaving group is

1) See, *e.g.*, C. K. Ingold, "Structure and Mechanism in Organic Chemistry," Cornell University Press, Ithaca, New York (1953), p. 419.

attacked dominantly.

In one of our previous papers[2] we, using MO calculations, have shown that the base should attack the *trans*-β-hydrogen atom most easily. Also, a quantitative method to interpret the reactivity in E2 reactions has been proposed.[3]

In the present paper, the change in the electronic state in the course of the E2 reaction of ethyl chloride will be discussed by the use of the extended Hückel method proposed by Hoffmann.[4] It is well established that this MO method is suitable for treating the electronic structure of sizable molecules which include unstable intermediates. Indeed, the mechanisms of various kinds of organic reactions have already been elucidated by means of this method.[2,3,5–10]

Setting-up of the Reaction Model

The β-eliminations are said to proceed by means of the following three processes[1]: one is the usual E2 mechanism (II), and the others are the two-step mechanisms, E1 (I) and E1cB (III).

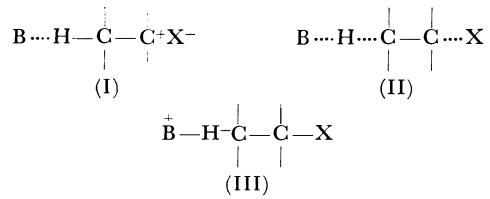

Various examples of E1 reactions are known, while the carbanion mechanism (E1cB) is observed only in the extreme case where the β-carbon atom bears strongly-electron-attracting substituents.[11] It is considered that a bimolecular E2 reaction proceeds through a transition state like the II type, with varying contributions of I and III, depending on the structure and the reaction conditions.[12–14]

An alternative E2 mechanism in which S_N2 and E2 are "merged"[15,16] has been proposed, but it applies only to very special cases.[17]

In view of this, it is appropriate to adopt the model for the bimolecular elimination in the staggered ethyl chloride molecule as occurring in normal E2 fashion, with a concerted and a nearly complete synchronous mechanism.

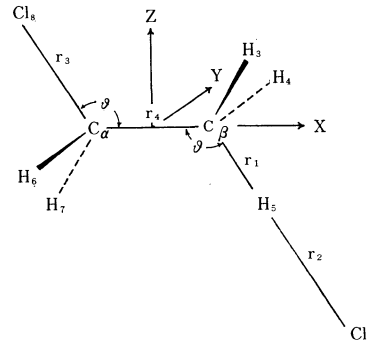

Fig. 1. The coordinates for the reacting system.

Table 1. The assumed geometries of reacting system

Model No.	ϑ (°)	r_1 (Å)	r_2 (Å)	r_3 (Å)	r_4 (Å)
Ethyl chloride	*	1.09		1.77	1.54
I	109	1.09	3.00	1.78	1.54
II	108	1.11	2.70	1.81	1.54
III	107	1.13	2.40	1.84	1.54
IV	106	1.15	2.20	1.87	1.54
V	105	1.17	2.00	1.91	1.54
V-1	105	1.17	2.00	1.91	1.51
V-2	105	1.17	2.00	1.91	1.48
V-3	105	1.17	2.00	1.91	1.45
V-4	105	1.17	2.00	1.91	1.42
VI	100	1.36	1.75	2.05	1.54
VI′	100	1.36	1.75	2.05	1.51
VII	95	2.00	1.50	2.70	1.54
VII′	95	2.00	1.50	2.70	1.51
Ethylene	90	1.09			1.34

* $\angle$CCCl=110°, $\angle$CCH=109.5°

2) K. Fukui and H. Fujimoto, *Tetrahedron Letters*, **1965**, 4303.

3) K. Fukui, H. Hao and H. Fujimoto, This Bulletin, **42**, 348 (1969).

4) R. Hoffmann, *J. Chem. Phys.*, **39**, 1397 (1963); **40**, 2474, 2480, 2745 (1964).

5) H. Kato, T. Yonezawa, K. Morokuma and K. Fukui, This Bulletin, **37**, 1710 (1964).

6) H. Kato, K. Yamaguchi, T. Yonezawa and K. Fukui, *ibid.*, **38**, 2144 (1965).

7) T. Yonezawa, O. Yamamoto, H. Kato and K. Fukui, *Nippon Kagaku Zasshi* (*J. Chem. Soc. Japan, Pure Chem. Sect.*), **87**, 26 (1966).

8) H. Fujimoto and K. Fukui, *Tetrahedron Letters*, **1966**, 5551.

9) T. Yonezawa, H. Konishi, H. Kato, K. Morokuma and K. Fukui, *Kogyo Kagaku Zasshi* (*J. Chem. Soc. Japan, Ind. Chem. Sect.*), **69**, 869 (1966).

10) T. Yonezawa, K. Shimizu and H. Kato, This Bulletin, **40**, 456, 1302 (1967).

11) J. Hine, R. Wiesböck and O. B. Ramsay, *J. Am. Chem. Soc.*, **83**, 1222 (1961); T. I. Crowell, A. A. Wall, R. T. Kemp and R. E. Lutz, *ibid.*, **85**, 2521 (1963).

12) J. F. Bunnett, *Angew. Chem.*, **74**, 731 (1962); *Angew. Chem., Intern. Ed. Engl.* **1**, 225 (1962).

13) R. F. Hudson, J. Arendt and A. Mancuso, *J. Chem. Soc.* (*B*), **1967**, 1069.

14) L. J. Steffa and E. R. Thornton, *J. Am. Chem. Soc.*, **89**, 6149 (1967).

15) G. M. Fraser and H. M. R. Hoffmann, *J. Chem. Soc.* (*B*), **1967**, 425.

16) A. J. Parker, M. Ruane, G. Biale and S. Winstein, *Tetrahedron Letters*, **1968**, 2113.

17) Compare the claims of, *e.g.*, J. F. Bunnett and E. Baciocchi, *J. Org. Chem.*, **32**, 11 (1967), and D. J. McLennan, *J. Chem. Soc.* (*B*), **1966**, 705.

For the convenience of calculation, we employ a chloride anion as the attacking base. The coordinates of this reacting system are presented in Fig. 1, where Cl_8, C_α, C_β, H_5, and Cl_9 atoms lie in the X-Z plane, the line of C_α–C_β being taken as the X-axis. The origin of the coordinates is at the middle point between C_α and C_β. The angles, H_5–C_β–H_4, H_5–C_β–H_3, H_5–C_β–C_α, Cl_8–C_α–H_6, Cl_8–C_α–H_7, and Cl_8–C_α–C_β, are all assumed to be equal to ϑ, and r_1, r_2, and r_3 refer to the distances of C_β–H_5, H_5–Cl_9, and C_α–Cl_8 respectively.

Here, we set up various combinations of r_1, r_2, r_3, and ϑ, as shown in Table 1. In these models, all the C_α–C_β and C–H bond distances, except for C_β–H_5, are fixed at 1.54 Å and 1.09 Å respectively. Of course, the C_α–C_β distance will vary with the reaction path. Therefore, in order to cover this ambiguity, we have changed the C_α–C_β ($=r_4$) distance in the models from V-1 to V-4 and in the models VI′ and VII′, as is shown in Table 1.

Method of Calculation

The numerical values used in the extended Hückel calculation are the same as those in the preceding paper.[3] For the sake of simplicity, the Coulomb integral of the attacking chloride anion is assumed to be constant throughout, equal to that of the neutral atom. The various populations calculated are defined as indicated in Table 2,[18]

Table 2. Definition of various populations

The AO population of AO r;

$$N(r) = 2\sum_{j}^{occ}\sum_{s} C_r^j C_s^j S_{rs}$$

The valence-inactive AO population of AO r;

$$p(r) = 2\sum_{j}^{occ}(C_r^j)^2$$

The valence-active AO population of AO r;

$$v(r) = 2\sum_{j}^{occ}\sum_{s\neq r} C_r^j C_s^j S_{rs}$$

The atom population of atom A;

$$M(\mathrm{A}) = \sum_{r}^{A} N(r)$$

The AO bond population between AO's r and s;

$$N(r\text{–}s) = 4\sum_{j}^{occ} C_r^j C_s^j S_{rs}$$

The atom bond population between atoms A and B;

$$M(\mathrm{A\text{–}B}) = \sum_{r}^{A}\sum_{s}^{B} N(r\text{–}s)$$

where r and s denote the rth and sth atomic orbitals respectively; C_r^j is the coefficient of the rth atomic orbital in the jth molecular orbital; $\sum_{j}^{occ}$ refers to the summation over all the occupied orbitals; $\sum_{r}^{A}$ signifies the sum over all the atomic orbitals belonging to the atom, A, and S_{rs} is the overlap integral between the rth and sth atomic orbitals as calculated by Mulliken's formula with Slater-type AO's.[19]

The geometry of an isolated ethyl chloride molecule is determined by the following interatomic distances and bond angles:[20]

C–Cl 1.77Å, C–C 1.54Å, C–H 1.09Å, ∠ClCC 110°

Also, the shape of ethylene molecule is taken as follows:

C–C 1.34Å, C–H 1.09Å, all angles 120°

Results and Discussions

1. The Electronic Structure of Ethyl Chloride. The highest occupied (HO) MO and the lowest unoccupied (LU) MO of ethyl chloride and their energies are shown in Table 3. The obtained HO energy, −12.5864 eV, is somewhat lower than is to be expected from the ionization potential value, 10.97 eV, or from the value, 11.2

Table 3. The AO coefficients and energy of HO and LU MO's of ethyl chloride

	HO	LU
Orbital energy, eV	−12.5864	1.3394
Sc_α*	0	0.140
Xc_α	0	−0.592
Yc_α	−0.343	0
Zc_α	0	0.911
Sc_β	0	0.056
Xc_β	0	−0.406
Yc_β	0.133	0
Zc_β	0	0.069
H_3	−0.117	−0.004
H_4	0.117	−0.004
H_5	0	0.281
H_6	0.258	0.099
H_7	−0.258	0.099
Sc_{l_8}	0	−0.542
Xc_{l_8}	0	−0.224
Yc_{l_8}	0.867	0
Zc_{l_8}	0	0.706

* The symbols Sc, Xc, Yc and Zc refer to the 2s, 2px, 2py and 2pz orbitals of the carbon atom and H_i denotes the 1s orbital of the ith hydrogen atom. The S_{Cl}, X_{Cl}, Y_{Cl} and Z_{Cl} signify the 3s, 3px, 3py and 3pz orbitals of the chlorine atom.

18) R. S. Mulliken, *J. Chem. Phys.*, **23**, 1841, 2338, 2343 (1955).

19) R. S. Mulliken, C. A. Rieke, D. Orloff and H. Orloff, *ibid.*, **17**, 1248 (1949).

20) J. Y. Beach and D. P. Stevenson, *J. Am. Chem. Soc.*, **61**, 2463 (1939).

eV reported by Irsa[21] and Watanabe.[22] The energy of LU MO, 1.3394 eV, is considerably lower than the value, 3.2120 eV, of ethane,[23] reflecting the reactivity toward the nucleophilic attack. The HO level shows a π-type character, with the direction of extension parallel to the Y-axis; the occupying electrons are largely localized on the Cl 3py and C_α 2py orbitals, thus contributing to the C–H bonding. The LU orbital is of a pσ-type, with a strong antibonding character on the C_α–Cl and C_α–C_β, especially on the former. These trends correspond to the fact that the C_α–Cl bond is weakened by the electron transfer from the approaching nucleophilic reagent. In this MO the coefficient of the β-hydrogen atom (H_5) situated *trans* to the chlorine atom is the largest among those of the hydrogen orbitals, as has already been pointed out.[2]

2. The Change in the Electronic Structure of Ethyl Chloride along the Reaction Path. *2-1. The Change in AO Populations.* It is, of course, not confirmed that the models adopted, indicated in Table 1, correspond to the points on the reaction path on the potential energy surface. However, they at least provide us with some qualitative information concerning the electronic process of the reaction.

The calculated values of the total energy in models I—VII are given in Table 4. The results show that the total energy increases as the reaction proceeds reaching a maximum in model VI.

The atom population, M(A), in each atom is also shown in Table 4. The $M(C_\beta)$ increases from 4.387 at the initial state (ethyl chloride) to 4.705 in model VI, and then it decreases. On the contrary, $M(C_\alpha)$ decreases from 3.958 to 3.862 in model VI and then increases to 4.234 at the final product (ethylene) through the model VII, 4.079. From these data, C_α and C_β seem to form, respectively, the cationic and anionic centers in the transition state; afterwards, however, they approach electronically the same state. The β-hydrogen atom (H_5) is attacked by the base, which possesses monotonously decreasing values of $M(H_5)$, while the atom population of the leaving nucleophilic chlorine atom, $M(Cl_8)$, increases from 7.260 to 7.926. Hence, we find that the H_5 and Cl_8 atoms are likely to depart from the molecule as a cation and an anion respectively; this is consistent with the experimental results. It should be noted that the M(H) values of the hydrogen atoms which have less direct concern with the reaction, *i.e.*, $H_3(=H_4)$ and $H_6(=H_7)$, are almost unchanged.

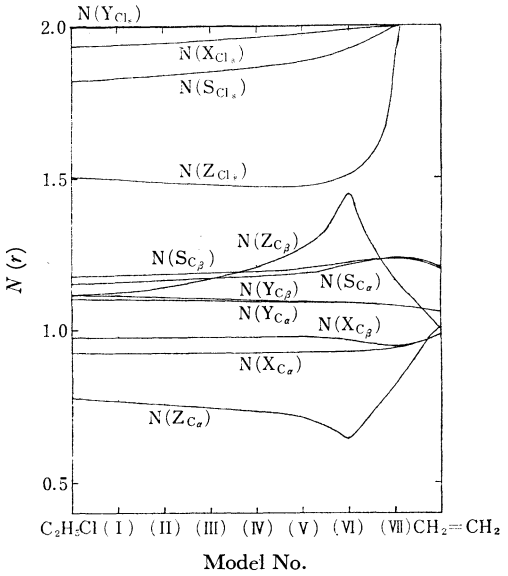

Fig. 2. The change of AO populations, $N(r)$, of the C_α, C_β and Cl_8 atoms in the reaction processes.

In order to obtain further knowledge, the AO populations of various atoms are collected in Fig. 2. The $N(Zc_\beta)$ increases remarkably from 1.114 at

TABLE 4. THE CALCULATED VALUES OF THE TOTAL ENERGY (eV) E, AND THE ATOM POPULATION, M(A), OF EACH ATOM IN ETHYL CHLORIDE, MODEL I—VII, AND ETHYLENE

	E	$M(C_\beta)$	$M(C_\alpha)$	$M(Cl_8)$	$M(Cl_9)$	$M(H_5)$	$M(H_3)$	$M(H_6)$
C_2H_5Cl		4.387	3.958	7.260		0.874	0.875	0.886
I	−474.8297	4.397	3.955	7.264	7.994	0.870	0.874	0.886
II	−474.8893	4.405	3.945	7.277	7.985	0.868	0.875	0.886
III	−474.8199	4.435	3.935	7.290	7.964	0.857	0.874	0.886
IV	−474.6652	4.476	3.925	7.304	7.938	0.840	0.874	0.885
V	−474.3657	4.545	3.912	7.324	7.896	0.810	0.872	0.884
VI	−473.9012	4.705	3.862	7.415	7.754	0.762	0.870	0.881
VII	−475.6913	4.416	4.079	7.926	7.388	0.697	0.872	0.875
$CH_2=CH_2$		4.234	4.234				0.883	0.883

21) A. P. Irsa, *J. Chem. Phys.*, **26**, 18 (1957).
22) K. Watanabe, *ibid.*, **26**, 542 (1957).
23) Kagaku Zokan, **26**, "Yuki Ryoshi Kagaku," Kagaku Dozin, Kyoto (1966), p. 257.

the ethyl chloride to 1.446 at model VI and is responsible for making C_β an anionic center, while the $N(Zc_\alpha)$ decreases prominently from 0.776 to 0.649, thus mainly contributing to the cationic character of the C_α atom in model VI. We can also see that the electrons gradually migrate from the β-carbon 2px orbital to the α-carbon 2s orbital, and from the 2py orbitals of both carbon atoms to the H_3, H_4, H_6, and H_7 atoms. The AO populations of the 2s orbitals of both carbon atoms, $N(Sc_\alpha)$ and $N(Sc_\beta)$, increase monotonously. This may correspond to the carbon hybridization change from sp^3 to sp^2, in which the valence electrons in the C_α–Cl_8 and C_β–H_5 bonds become localized at the 2s orbitals as the Cl_8 and H_5 atoms start to leave both the carbon atoms.

The changes in the AO populations of Cl_8 were found to decrease in the order of $N(Z_{Cl_8})>N(S_{Cl_8})>N(X_{Cl_8})$. The $N(Y_{Cl_8})$ is almost constant, *ca.* 2.000. Therefore, the 2py orbital of the Cl_8 atom is assigned to a lone-pair orbital.

2-2. The Change in Bond Populations. The atom bond population, $M(C_\alpha$–$C_\beta)$, increases from 0.700 (ethyl chloride) to 1.024 (Model VII), as is shown in Fig. 3.

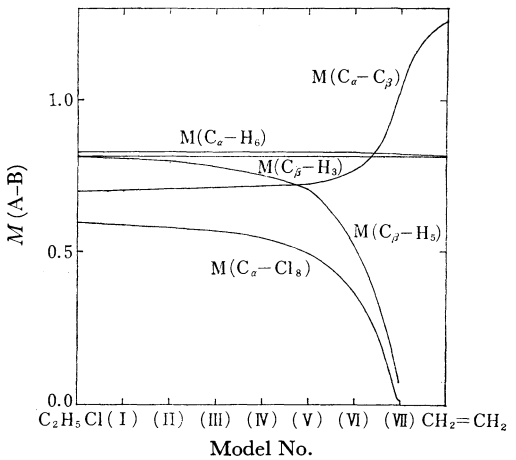

Fig. 3. The change of the atom bond populations, M (A–B), in the various models.

The values of $M(C_\alpha$–$Cl_8)$ and $M(C_\beta$–$H_5)$ decrease as their bond distances increase. The $M(C_\beta$–$H_3)$ and $M(C_\alpha$–$H_6)$ remain almost unchanged.

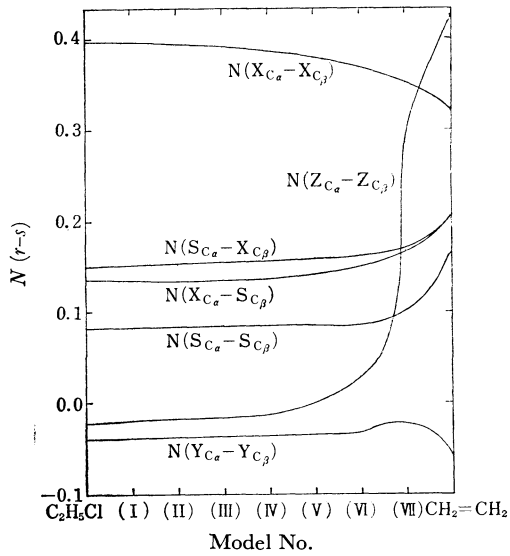

Fig. 4. The change of AO bond populations between α- and β-carbons.

For a further discussion of the C–C bond, the AO bond populations are listed in Fig. 4. The $N(Zc_\alpha$–$Zc_\beta)$ increases most remarkably from -0.022 to 0.285 (Model VII), contributing dominantly to the increase in $M(C_\alpha$–$C_\beta)$. Obviously, this reflects the progress of the double-bond formation. In models I—V, $N(Zc_\alpha$–$Zc_\beta)$ exhibits an antibonding nature, whereas models VI and VII indicate a bonding between the two 2pz orbitals. The $N(Xc_\alpha$–$Xc_\beta)$ and $N(Yc_\alpha$–$Yc_\beta)$ are larger than ethylene throughout the models from I to VII.

2-3. Influence of the Change in C–C Bond Distance upon the Electronic Structure. In the discussion above, the C–C bond distance was tentatively fixed as equal to 1.54Å. Now let us investigate the influence of the change in C–C bond distance.

Let us vary the C_α–C_β bond distance in model V as is shown in Table 1. The mode of the change in the electronic structure is given in Table 5 and in Figs. 5—7. These transient models seem to fit the states before the transition state, since the total energies are lower than the tentatively-assumed model VI. With the change from V to V-4, $M(C_\alpha)$ and $M(C_\beta)$ are reduced, showing an electron shift from the α-carbon to Cl_8, H_6, and H_7 and from the β-carbon to H_3 and H_4, while $M(H_5)$ and

Table 5. The calculated values of the total energy (eV), E, and atom population M(A) in models V-1—V-4

	E	$M(C_\beta)$	$M(C_\alpha)$	$M(Cl_8)$	$M(Cl_9)$	$M(H_5)$	$M(H_3)$	$M(H_6)$
V-1	−474.7471	4.546	3.895	7.333	7.888	0.809	0.875	0.890
V-2	−474.5721	4.542	3.891	7.338	7.887	0.809	0.876	0.891
V-3	−474.3768	4.537	3.889	7.344	7.887	0.809	0.877	0.892
V-4	−474.1588	4.533	3.883	7.349	7.886	0.809	0.878	0.893

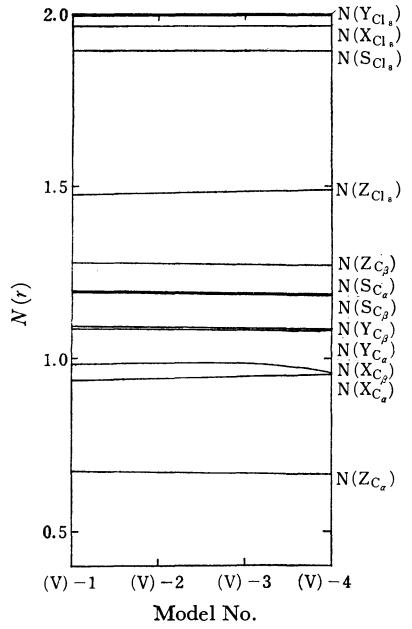

Fig. 5. The change of AO populations, $N(r)$, in the models V-1—V-4.

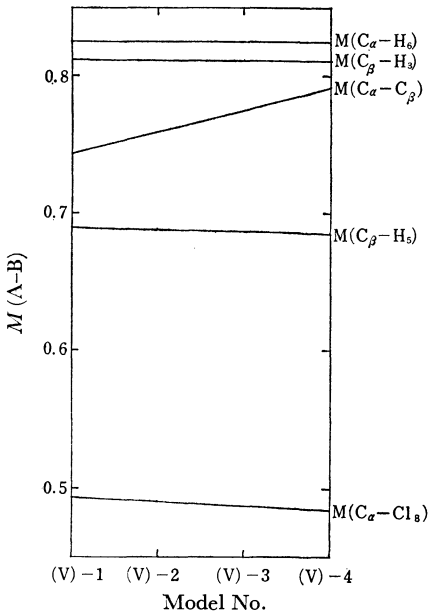

Fig. 6. The change of atom bond populations in the models V-1—V-4.

$M(Cl_9)$ remain almost unchanged. The changes in AO populations are listed in Fig. 5. The data indicate that $N(Sc_\alpha)$ and $N(Sc_\beta)$ decrease, while $N(Xc_\alpha)$ and $N(Xc_\beta)$ increase.

Figure 6 shows that $M(C_\beta-H_3)$ and $M(C_\alpha-H_6)$ remain constant. The $M(C_\beta-C_3)$ increases with a decrease in the $C_\alpha-C_\beta$ bond distance, while $M(C_\alpha-Cl_8)$ and $M(C_\beta-H_5)$ change in the reverse

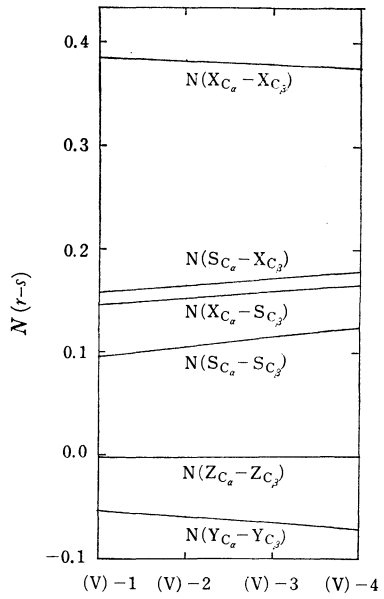

Fig. 7. The change of AO bond populations between α- and β-carbons in the models V-1—V-4.

fashion. The AO bond populations, $N(Sc_\alpha-Xc_\beta)$ and $N(Xc_\alpha-Sc_\beta)$ increase from 0.157 to 0.179 and from 0.142 to 0.166 respectively, as may be seen in Fig. 7. In this step of the reaction, the double-bond formation is not yet appreciable, as may be understood from the negative values of $N(Zc_\alpha-Zc_\beta)$.

Next, let us investigate the effect of the $C_\alpha-C_\beta$ bond distance near and after the transition state. Among the models listed in Table 1, models VI and VII seem to correspond to such states. If we change the bond distance from 1.54Å to 1.51Å, $M(C_\beta)$ decreases from 4.416 to 4.397, while $M(C_\alpha)$ increases from 4.079 to 4.090, in model VII, as may be observed from Tables 4 and 6. In this electron migration, the 2pz orbitals play a dominant role. The increase in $N(Zc_\alpha-Zc_\beta)$ expresses the double-bond formation. All the other populations, $N(r)$, $M(A)$, $N(r-s)$, and $M(A-B)$, in models VI′ and VII′, except for $M(C_\alpha)$ and $N(Zc_\alpha)$ in model VI′, come close to the corresponding ones of the ethylene molecule.

2-4. The Change in the Electronic Structure of the Leaving Chlorine Atom. In Section 2-1, it has been noted that the Cl_8 2py AO exhibits a lone-pair-like behavior. In this connection let us now attempt to discuss this point in more detail by the use of the concept of the valence atomic orbital (VAO) proposed by Ruedenberg.[24] The VAO is the orbital which makes the diagonal elements of the intra-atomic local bond order matrix reach a maximum

24) K. Ruedenberg, *Rev. Mod. Phys.*, **34**, 356 (1962).

Table 6. The calculated values of the total energy (eV) E, and the various populations in model VI′ and VII′

	E	$M(C_\beta)$	$M(C_\alpha)$	$M(Cl_8)$	$M(Cl_9)$	$M(H_5)$	$M(H_3)$	$M(H_6)$
VI′	−474.7928	4.697	3.859	7.425	7.753	0.760	0.871	0.882
VII′	−475.9340	4.397	4.090	7.928	7.385	0.698	0.874	0.878

	$N(Sc_\beta)$	$N(Xc_\beta)$	$N(Yc_\beta)$	$N(Zc_\beta)$	$N(Sc_\alpha)$	$N(Xc_\alpha)$	$N(Yc_\alpha)$	$N(Zc_\alpha)$	$N(Sc_{Cl_8})$	$N(Xc_{Cl_8})$	$N(Yc_{Cl_8})$	$N(Zc_{Cl_8})$
VI′	1.210	0.969	1.079	1.439	1.202	0.931	1.078	0.648	1.925	1.989	2.000	1.511
VII′	1.229	0.949	1.070	1.149	1.235	0.947	1.070	0.837	1.997	1.999	2.000	1.932

	$M(C_\beta$–$H_3)$	$M(C_\alpha$–$H_6)$	$M(C_\alpha$–$C_\beta)$	$M(C_\alpha$–$Cl_8)$	$M(C_\beta$–$H_5)$
VI′	0.815	0.830	0.792	0.376	0.511
VII′	0.817	0.820	1.056	0.021	0.081

	$N(Sc_\alpha$–$Sc_\beta)$	$N(Xc_\alpha$–$Xc_\beta)$	$N(Yc_\alpha$–$Yc_\beta)$	$N(Zc_\alpha$–$Zc_\beta)$	$N(Xc_\alpha$–$Sc_\beta)$	$N(Sc_\alpha$–$Xc_\beta)$
VI′	0.100	0.365	−0.035	0.034	0.158	0.170
VII′	0.101	0.351	−0.034	0.301	0.167	0.169

C_2H_5Cl

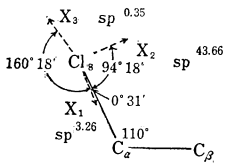

$X_1=0.485S+0.292X-0.825Z$
$X_2=0.150S+0.901X+0.407Z$
$X_3=0.862S-0.320X+0.393Z$

$p(X_1)$	$p(X_2)$	$p(X_3)$
0.999	2.022	2.029

I

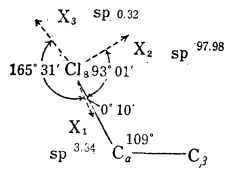

$X_1=0.480S+0.283X-0.830Z$
$X_2=0.096S+0.883X+0.357Z$
$X_3=0.871S-0.271X+0.410Z$

$p(X_1)$	$p(X_2)$	$p(X_3)$
1.004	2.022	2.029

II

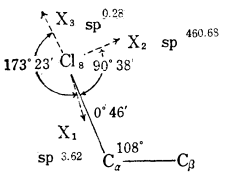

$X_1=0.465S+0.262X-0.845Z$
$X_2=0.047S+0.947X+0.319Z$
$X_3=0.884S-0.188X+0.428Z$

$p(X_1)$	$p(X_2)$	$p(X_3)$
1.026	2.022	2.030

III

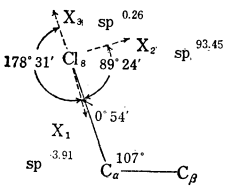

$X_1=0.451S+0.248X-0.857Z$
$X_2=0.010S+0.959X+0.282Z$
$X_3=0.892S-0.136X+0.430Z$

$p(X_1)$	$p(X_2)$	$p(X_3)$
1.048	2.022	2.031

IV

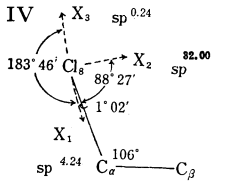

$X_1=0,437S+0.232X-0.869Z$
$X_2=-0.019S+0.968X+0.249Z$
$X_3=0.899S-0.093X+0.427Z$

$p(X_1)$	$p(X_2)$	$p(X_3)$
1.072	2.021	2.032

V

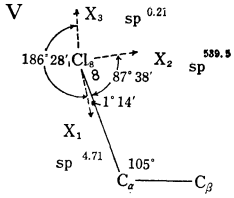

$X_1=0.418S+0.216X-0.882Z$
$X_2=-0.043S+0.975X+0.218Z$
$X_3=0.907S-0.053X+0.417Z$

$p(X_1)$	$p(X_2)$	$p(X_3)$
1.106	2.019	2.033

VI

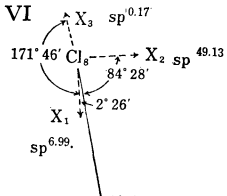

$X_1=0.354S+0.123X-0.927Z$
$X_2=-0.141S+0.987X+0.077Z$
$X_3=0.925S-0.104X+0.366Z$

$p(X_1)$	$p(X_2)$	$p(X_3)$
1.255	2.015	2.034

VII

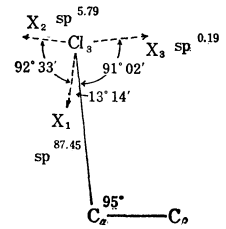

$X_1=0.106S-0.142X-0.984Z$
$X_2=0.384S-0.907X+0.173Z$
$X_3=0.917S+0.396X+0.042Z$

$p(X_1)$	$p(X_2)$	$p(X_3)$
1.928	2.001	2.011

Fig. 8. The VAO X_r, valence-inactive populations $p(X_r)$, hybrid states and bond angles of Cl_8 in the reaction processes.

or a minimum. The four VAO's belonging to the leaving chlorine atom attached to the α-carbon atom are designated as X, X_2, X_3, and X_4, among which X_4 is taken to be associated with the 3py orbital. These VAO's are obtained by using the bond-order matrix obtained by the extended Hückel calculation. The results are shown along with the hybrid states and the valence-inactive populations, in Fig. 8. The VAO X_1 is supposed to be associated with the Cl_8–C_α bond. The calculated valence angles of X_1 are well in agreement with the assumed angle, $\angle Cl_8C_\alpha C_\beta$, in models I—VI. (In Fig. 8, the discrepancy from the Cl_8–C_α bond is shown.) The hybrid of X_1 changes from $sp^{3.34}$ at the model I to $sp^{87.5}$ at the model VII. This indicates that X_1 becomes a 3p lone-pair orbital as the reaction proceeds. The X_2 and X_3 orbitals are lone-pair orbitals mainly composed of 3p and 3s AO respectively. As the reaction proceeds, the discrepancy of the obtained bond angle from the assumed angle becomes greater; *e.g.*, it is 13°14′ in model VII. This seems to be due to the decrease in the valence-active population between C_α and Cl_8 atoms.

The calculations were carried out on the HITAC 5020 computer at the computation center of the University of Tokyo.

BULLETIN OF THE CHEMICAL SOCIETY OF JAPAN VOL. 42 1263—1265 (1969)

Microwave Spectrum of Cyclohexene*1

Teruhiko OGATA and Kunio KOZIMA

Laboratory of Molecular Spectroscopy, Tokyo Institute of Technology, Ookayama, Meguro-ku, Tokyo

(Received September 30, 1968)

The microwave spectrum of cyclohexene has been investigated in the frequency region from 7.3 to 27 Gc/sec with a conventional Stark modulation spectrometer, and the spectrum in the ground vibrational state has been assigned. The dipole moment lies entirely along the *b*-principal axis; its value, as obtained from the Stark displacements, is 0.332 ± 0.012D. From the rotational constants and the orientation of the dipole moment, it can be concluded that the equilibrium conformation is a "half-chair" form. Its most probable structure has been determined.

As there are many natural compounds which have a cyclohexene ring, such as terpenes and steroids, it may be considered important to investigate the structure of cyclohexene. Cyclohexene can exist in two conformations without making very great deformations in the normal values of the bond angles, *i.e.*, in a "half-chair" form with C_2 symmetry or in a "half-boat" form with C_s symmetry,[1] as Fig. 1 shows. Beckett, Freeman,

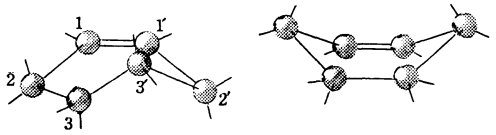

"half-chair" form "half-boat" form

Fig. 1

and Pitzer[2] concluded, by calculating its entropy and gaseous heat capacity, that the "half-chair" form was more stable than the "half-boat" form by about 2.7 kcal/mol. Sakashita[3] reported that no essential difference was observed among the infrared spectra of cyclohexene in the vapor, liquid, and solid states; that the spectrum could be assigned by assuming a single configuration, and that the value of the energy difference estimated by Beckett *et al.*, was reasonable.

X-Ray investigations of pentachlorocyclohexene[4] and naphthalenetetrachloride[5] showed that the molecules have the "half-chair" conformation. However, no detailed structural information is available on cyclohexene.

Experimental

The sample was prepared by dehydrating cyclohexanol.[6] The product was dried over calcium chloride

*1 Presented at the 21st Annual Meeting of the Chemical Society of Japan, Osaka, March, 1968.

1) W. Klyne, "Progress in Stereochemistry," Vol. 1 Butterworths, London (1954), p. 81.

2) C. W. Beckett, N. K. Freeman and K. S. Pitzer, *J. Am. Chem. Soc.*, **70**, 4227 (1948).

3) K. Sakashita, *Nippon Kagaku Zasshi* (*J. Chem. Soc. Japan, Pure Chem. Sect.*), **77**, 1094 (1956).

4) R. A. Pasternak, *Acta Cryst.*, **4**, 316 (1951).

5) M. A. Lasheen, *ibid.*, **5**, 593 (1952).

6) W. M. Dehn and K. E. Jackson, *J. Am. Chem. Soc.*, **55**, 4284 (1933).

and purified by fractional distillation. The infrared spectrum of the sample thus obtained showed no evidence of impurities.

The microwave spectrum was investigated in the frequency region from 7.3 to 27 Gc/sec by using a conventional Stark modulation spectrometer with 110 kc/sec sine- and squar-ewave modulation. All measurements were made at the temperature of dry ice. The frequency measurements were performed with a frequency standard monitored against the standard signals from Station JJY.

Results and Discussion

Microwave Spectrum. The spectrum was found to be quite rich; about 400 sharp and weak lines were observed because of its small dipole moment. No investigation of the electron or X-ray diffraction has yet been made on this molecule. Therefore, the preliminary rotational constants, which were tentatively calculated by assuming the usual values for the bond lengths and the bond angles, were not very useful for the assignments. In order to assign the spectrum, it was necessary to investigate the Stark behavior of many absorption lines.

When the Stark voltage for all the absorption lines in the frequency ranges, which differed by several hundreds Mc/sec from the tentatively-calculated frequencies for the $J=1\rightarrow2$ transitions, were changed, careful examination revealed the lines which were split in two by the Stark effect. By using the three $J=1\rightarrow2$ frequencies thus determined, the rigid-rotor rotational constants were calculated. The assignments of the other transitions, as is shown in Table 2, could be made by the use of these rotational constants. The rotational constants listed in Table 1 were determined so as to get the best fit between these observed and calculated frequencies by assuming a rigid-rotor approximation. In Table 2 the observed frequencies which are marked with * were ascertained by means of their Stark effects. Relative intensity measurements confirmed that these spectrum are due to the vibrational ground state.

The absorption line of the $0_{00}\rightarrow1_{11}$ transtion could not be observed by the spectrometer mentioned above. Therefore, the measurable frequency of the spectrometer was lowered by using 8V69 klystron of the Nippon Elec. Co. and a 6-m J-band absorption cell. As is shown in Table 2, the observed frequency of the $0_{00}\rightarrow1_{11}$ transition is in good agreement with that calculated by the rotational constants.

Table 1. Rotational constants and moment of inertia of cyclohexene in the ground vibrational state*

Rotational constant Mc/sec		Moments of inertia amu·Å²	
A	4739.148±0.01	I_a	106.6387
B	4544.406±0.02	I_b	111.2086
C	2562.402±0.02	I_c	197.2278

* Conversion factor 5.05377×10^5 amu·Å²·Mc/sec is used to caclulate moments of inertia, corresponding to $^{12}C=12$ atomic weight scale.

Table 2. Ground-state rotational transitions of cyclohexene (in Mc/sec)

Transition	Observed[a]	Calculated	$\nu_{calc}-\nu_{obs}$
$0_{00}\rightarrow1_{11}$	7301.56	7301.55	−0.01
$1_{01}\rightarrow2_{12}$	12426.36*	12426.35	−0.01
$1_{11}\rightarrow2_{02}$	12218.00*	12217.95	−0.05
$1_{10}\rightarrow2_{21}$	16779.80*	16779.84	+0.04
$2_{02}\rightarrow3_{13}$	17459.19*	17459.18	−0.01
$2_{12}\rightarrow3_{03}$	17444.86*	17444.93	+0.07
$2_{11}\rightarrow3_{22}$	21904.66*	21904.64	−0.02
$2_{21}\rightarrow3_{12}$	21252.62*	21252.58	−0.04
$2_{20}\rightarrow3_{31}$	26350.00*	26350.10	+0.10
$3_{03}\rightarrow3_{12}$	10337.85	10337.88	+0.03
$3_{13}\rightarrow3_{22}$	10405.23	10405.12	−0.11
$3_{03}\rightarrow4_{14}$	22576.76*	22576.80	+0.04
$3_{13}\rightarrow4_{04}$	22576.18*	22576.19	+0.01
$3_{12}\rightarrow4_{23}$	26771.22*	26771.32	+0.10
$3_{22}\rightarrow4_{13}$	26699.18*	26699.29	+0.11
$4_{04}\rightarrow4_{13}$	14528.38	14528.24	−0.14
$4_{13}\rightarrow4_{22}$	10224.93	10225.04	+0.11
$4_{14}\rightarrow4_{23}$	14532.39	14532.40	+0.01
$4_{04}\rightarrow5_{15}$	27701.08*	27701.22	+0.14
$4_{14}\rightarrow5_{05}$		27701.20	+0.12
$5_{14}\rightarrow5_{23}$	14505.18	14505.31	+0.13
$5_{24}\rightarrow5_{33}$	14521.72	14521.78	+0.06
$5_{23}\rightarrow5_{32}$	10073.90	10074.04	+0.14
$5_{33}\rightarrow5_{42}$	10512.43	10512.65	+0.22
$5_{42}\rightarrow5_{51}$	7745.10	7745.36	+0.26

a) ±0.1 Mc/sec

Dipole Moment. The dipole moment for the ground vibrational state was determined from the Stark displacements of the $1_{10}\rightarrow2_{21}$ and $1_{01}\rightarrow2_{12}$ transitions. The observed and calculated Stark coefficients are given in Table 3. The absorption cell was calibrated using the $J=1\rightarrow2$ transition of OCS, taking the dipole moment of OCS as 0.7124.[7]

Table 3. Stark coefficients and dipole moment

Transition	M	$\Delta\nu/E^2$ (Mc/sec)/(kV/cm)²	
		Observed	Calculated
$1_{10}\rightarrow2_{21}$	0	0.402	0.405
	1	−2.852	−2.826
$1_{01}\rightarrow2_{12}$	0	0.556	0.547
	1	3.400	3.455
$\mu=0.332\pm0.012$D			

7) S. A. Marshall and I. Weber, *Phys. Rev.*, **105**, 1502 (1957).

The value of the dipole moment of 0.332 D obtained by us is considerably lower than those of 0.75D[8] (in a hexane solution), 0.63 D[8] (in a CCl_4 solution), and 0.61 D[9] (in vapor) obtained by Debye's method. Our value supports Smyth's suggestion[10] that the value of 0.61 D is too high. Kumler *et al.*[11] obtained the value of 0.21 D (in a heptane solution) for this molecule by Debye's method. This value is a little lower than ours. However, their value of the atomic polarization, as estimated from those of analogous compounds, seems to be nearly correct.

A possible upper limit for the μ_c component of the dipole moment could be estimated from the Stark effect of the $1_{01}\rightarrow 2_{12}$ transition, since the effect of μ_c on the observed Stark effect would be to alter the Stark effect of the μ_b component. By assuming the error in the frequency measurement to be ± 0.1 Mc/sec, it could be estimated that the possible upper limit of the value of μ_c is 5.84×10^{-3}D. Therefore, it is very probable that the value of μ_c is zero within the limits of exprimental error.

Molecular Structure. The possibility of the "half-boat" form can be excluded in view of the fact that the value of μ_c is zero or nearly zero. As a possible structure, a planar cyclohexene ring might be considered, because the μ_c value of the molecule with this ring should be zero. In this case, as the molecule has C_{2v} symmetry, the quantity of $(I_c-I_a-I_b)/2$ is given approximately by $8mr^2\sin^2(\theta/2)$, where θ is the valency angle of $\angle$ H–C_i–H and where r is the bond length of the C_i–H bond ($i=2$, 2′, 3, and 3′; see Fig. 1). By assuming that θ is 109°28′ and that r is 1.10Å, we can obtain $(I_c-I_a-I_b)/2=-6.687$ amu·Å^2. Since this value is quite different from the observed value of -10.3098 amu·Å^2, the possibilities of a planar ring and of a nearly planar ring can be eliminated. Therefore, as a remaining possibility we have to check whether or not the molecule has the "half-chair" form.

As the molecule of the "half-chair" form should have C_2 symmetry, the value of μ_c is zero, in agreement with the experimental fact. Next we have to obtain a reasonable set of structural parameters so as to get the best fit between the observed and the calculated principal moments of inertia. However, as there are many structural parameters to be determined, a number of assumptions or approximations are necessary. It is reasonable to consider that the ethylene group of $\begin{matrix}H\\C\end{matrix}\!\!>\!C=C\!<\!\!\begin{matrix}H\\C\end{matrix}$ has a planar structure. Furthermore, the following assumptions may be safely made:

(1) the C–H bond of the ethylene group is located along the angle bisector of $\angle$C=C–C;

(2) the angle bisector of $\angle$H–C_i–H is that of $\angle$C–C_i–C ($i=2$, 2′, 3, and 3′);

(3) the angles of $\angle$H–C_i–H are tetrahedral;

(4) the internuclear distance, r_{2-3}, between C_2 and C_3 is equal to that, $r_{3-3'}$ between C_3 and $C_{3'}$ and

(5) all aliphatic C–H bonds are of equal length.

When taking into account the relation that only two of three $\angle$CCC bond angles are independent, there are still seven structural parameters to be determined.

By calculating the value of $\partial I_i/\partial X_j$, where I_j is the jth moment of inertia and X_i is the ith structural parameter, we can see that the angles of $\angle$C=C–C and $\angle$C–C–C and the bond length of C=C and C–C are highly sensitive to the values of the moment of inertia. By assuming the values of the aliphatic and the olefinic C–H bond lengths, r_{C-H} and $r_{=C-H}$; the double bond length, $r_{1-1'}$, and either r_{1-2} or r_{2-3}, the values of the two $\angle$CCC bond angles and either r_{1-2} or r_{2-3} were determined so as to get a good fit for the observed moments of inertia. For each set of structural parameters the value of $r_{1-1'}$ was assumed to be that of propylene.[12] For the set I, all the assumed values are those of propylene. For the set II, the assumed values of r_{2-3} and r_{C-H} are those of ethane,[13] while $r_{=C-H}$ is that of ethylene.[14] For the set III, the values of r_{2-3}, r_{C-H}, and $r_{=C-H}$ are those of propane,[15] ethane, and ethylene respectively.

The calculated values of the set III do not seem reasonable, because the r_{1-2} value is almost the same to that of r_{2-3}. The values of the sets I and II are not so different from each other. The values of both sets are very probable for the structural parameters of this molecule.

TABLE 4. STRUCTURAL PARAMETERS OF CYCLOHEXENE

	Set I	Set II	Set III
$r_{1-1'}$	1.336*	1.336*	1.336Å*
r_{1-2}	1.501*	1.495	1.523Å
$r_{2-3}=r_{3-3'}$	1.541	1.543*	1.526Å*
$r_{=C-H}$	1.090*	1.086*	1.086Å*
r_{C-H}	1.098*	1.102*	1.102Å*
$\angle C_1'C_1C_2$	123°48′	123°51′	123°22′
$\angle C_1C_2C_3$	111°32′	111°46′	111°08′
$\angle C_2C_3C_{3'}$	110°22′	110°19′	110°55′

* These values were assumed.

8) M. Puchalik, *Acta Phys. Polon.*, **4**, 145 (1935).
9) M. Kubo, *Sci. Pap. Inst. Phys. Chem. Res. Tokyo*, **32**, 26 (1937).
10) C. P. Smyth, "Dielectric Behavior and Structure," McGraw-Hill Book Co., New York (1955), p. 263.
11) W. D. Kumler, R. Boikess, P. Bruck and S. Winstein, *J. Am. Chem. Soc.*, **86**, 3126 (1964).
12) D. R. Lide, Jr., and D. Christensen, *J. Chem. Phys.*, **35**, 1374 (1961).
13) G. E. Hansen and D. M. Dennison, *ibid.*, **20**, 313 (1952).
14) H. C. Allen, Jr., and E. K. Plyler, *J. Am. Chem. Soc.*, **80**, 2673 (1958).
15) D. R. Lide, Jr., *J. Chem. Phys.*, **33**, 1514 (1960); Note added in proof–*cf. ibid.*, **49**, 2368 (1968).

BULLETIN OF THE CHEMICAL SOCIETY OF JAPAN VOL. 42 1266—1271 (1969)

On the Order of Isotopic Exchange Reactions

Tetsuo TAKAISHI

The Institute for Atomic Energy of Rikkyo (St. Paul's) University, Yokosuka

(Received October 5, 1968)

The conditions for the applicability of the McKay law were studied. It was concluded that the first order kinetics no longer holds when the concentrations of intermediates cannot be disregarded when compared with those of reactants and products and when the rate determining step cannot be specified. Some reactions were illustrated in which McKay's law cannot be applied.

In 1938, studying the kinetics of isotopic exchange reaction, McKay[1] arrived at the following conclusion. The exchange reaction is expressed by as,

$$AX^* + BX = AX + BX^*, \tag{1}$$

where X* represents a tagged X atom, and the reaction (1) is in equilibrium apart from the isotopic distribution. Let the concentration be denoted by

$$\begin{aligned} [AX] + [AX^*] &= a, & [AX^*] &= x, \\ [BX] + [BX^*] &= b, & [BX^*] &= y, \end{aligned} \tag{2}$$

and the rate of total exchange reaction by R. Then, whatever the reaction mechanism might be, the relation,

$$\frac{dx}{dt} = -\frac{dy}{dt} = R\frac{a-x}{a}\frac{y}{b} - R\frac{x}{a}\frac{b-y}{b} = -\frac{x}{a}R + \frac{y}{b}R \tag{3}$$

holds and we have

$$-\ln\left(\frac{x_\infty - x}{x_\infty}\right) = R\left(\frac{a+b}{ab}\right)t \tag{4}$$

under the condition $x+y=$const., where x_∞ designates the value for x in equilibrium. Equation (4) may be referred to as McKay's law hereafter.

Since then, many workers[2-8] have discussed the validity of McKay's law. Though some modifications must be introduced in such a case where two or more atoms in a molecule are tagged,[7,8] the main features of the law are accepted to be true. Recently, Kawaguchi[9] raised some questions as to its validity. The present author[10] briefly commented on his note, mentioning limitations to the validity of McKay's law. In the present paper, the problem is discussed in more detail and practical problems in kinetic analysis are considered, since kinetic studies today frequently involve special conditions that could not be considered in earlier days.

Conditions for the Applicability of McKay's Law

Elementary Reaction. We adopt, in what follows, the fundamental simplifying assumption that the isotopic mass effects can be ignored not only in rate processes but also in equilibrium properties. This may be appropriate to the study of the fundamental nature of McKay's law. Moreover, we assume that only an atom in a specified position in the molecule is tagged. The case where two or more atoms in some positions in the molecule with different reactivities are tagged[7,8] can be treated as an extension of the presetnt study.

Strictly speaking, McKay's law is only applicable to an elementary reaction or step. The proof of this is very simple. Let the reaction (1) be an elementary reaction. According to the theory of the absolute reaction rate, the rate in the elementary process is given by $\nu\,[Z^*]$, where Z^* denotes the activated complex and ν the frequency of vibration of the activated complexes in the degree of freedom corresponding to their decomposition. Furthermore, there exists a thermodynamic equilibrium between

1) H. A. C. McKay, *Nature*, **142**, 997 (1938).
2) N. Morita, This Bulletin, **15**, 166 (1940).
3) R. B. Duffield and M. Calvin, *J. Am. Chem. Soc.*, **68**, 557 (1946).
4) T. H. Norris, *J. Phys. Chem.*, **54**, 777 (1950).
5) O. E. Meyers and R. J. Prestwood, "Radioactivity Applied to Chemistry," A. C. Wahl and N. A. Bonner, Ed., John Wiley and Sons, Inc., New York (1951), p. 7.
6) C. P. Luehr, G. E. Challenger and B. J. Masters, *J. Am. Chem. Soc.*, **78**, 1314 (1956).
7) S. W. Benson, "The Foundation of Chemical Kinetics," McGraw-Hill Book Co., Inc., New York (1960), p. 84.
8) T. Kitayama and K. Hirota, Preprints for The 21st Annual Meeting of the Chemical Society of Japan (April, 1968), No. 23405.
9) S. Kawaguchi, *Kagaku-no-Ryoiki* (*J. Japan. Chem.*), **21**, 762 (1967), in Japanese.
10) T. Takaishi, *ibid.*, **22**, 268 (1968), in Japanese.

Z^* and the reactants. Here we consider that X-atoms at two specified positions in the activated complex are interchanged with each other in the course of the decomposition of activated complex, and that one of the exchangeable X-atoms comes from an AX-molecule and is transfered to a BX-molecule while another from a BX to an AX. These exchangeable atoms may be designated by A-site atom and B-site one, respectively. Let us consider the activated complex, Z^{**},whose A-site atom is tagged and B-site atom untagged. The ratio of the number of such tagged activated complexes to the total number of activated complexes becomes equal to $[AX^*][BX]/\{([AX]+[AX^*])([BX]+[BX^*])\}$. Consequently, for the forward reaction of (1), we have

$$\frac{(\text{rate of reaction of tagged molecules})}{(\text{total reaction rate})} = \frac{\nu[Z^{**}]}{\nu([Z^*]+[Z^{**}])} = \frac{x(b-y)}{ab},$$

irrespective of the molecularity of the reaction. Similarly, for the backward reaction of (1), we get

$$\frac{(\text{rate of reaction of tagged molecules})}{(\text{total reaction rate})} = \frac{y(a-x)}{ab}.$$

Thus, the net increase of AX^* is given by the difference of the two, *i. e.*, by Eq. (3).

Complex Reaction. When the reaction (1) is a complex reaction, the validity of Eq. (4) must carefully be examined. Even when applicable for appropirate conditions, Eq. (4) may be only approximate. As there are numerous reaction mechanisms, we cannot arrive at the necessary and sufficient conditions for general applicability of Eq. (4). Some typical cases, however, may be discussed.

Consecutive Reactions. If the reaction kinetics can well be described by assuming the existence of a rate determing step, the reaction scheme may be expressed as

$$AX+BX^* \rightleftarrows CX+DX^* \overset{R}{\rightleftarrows} CX^*+DX \rightleftarrows AX^*+BX,$$

where R designates the over-all rate and consequently that of rate determining step.
Using the notation (2), and further denoting

$$[CX] + [CX^*] = \alpha,\ [CX^*] = \xi$$

and

$$[DX] + [DX^*] = \beta,\ [DX^*] = \eta,$$

we have, irrespective of the molecularity of the reaction,

$$\frac{d(x+\xi)}{dt} = -R\frac{\xi}{\alpha} + R\frac{\eta}{\beta} = -\frac{d(y+\eta)}{dt}, \tag{6}$$

and $x+y+\xi+\eta=\text{const.}$
Since the reaction $AX+BX \rightleftarrows CX+DX$, is very rapid and in equilibrium, it becomes,

$$\frac{\xi}{\alpha} = \frac{x}{a},\ \frac{\eta}{\beta} = \frac{y}{b}.$$

Introducing these into Eq. (6), we get

$$\frac{d(x+\xi)}{dt} = R\left(\frac{y}{b} - \frac{x}{a}\right).$$

As far as the relations

$$\frac{dx}{dt} \gg \frac{d\xi}{dt} \text{ and } x, y, \gg \xi, \eta \tag{7}$$

hold the above relation reduces to

$$\frac{dx}{dt} = R\left(\frac{y}{b} - \frac{x}{a}\right),$$

i. e., Eq. (3) may be applied.

Concurrent Consecutive Reactions. When there exist parallel reaction paths, the typical reaction scheme may be expressed as

$$\begin{array}{ccccccc} & & C_1X + D_1X^* & \overset{R_1}{\rightleftarrows} & C_1X^* + D_1X & & \\ & \nearrow & & & & \searrow & \\ XA + BX^* & \rightleftarrows & C_2X + D_2X^* & \overset{R_2}{\rightleftarrows} & C_2X^* + D_2X & \rightleftarrows & AX^* + BX, \\ & \searrow & & & & \nearrow & \\ & & \cdots\cdots\cdots & & \cdots\cdots\cdots & & \\ & & \cdots\cdots\cdots & & \cdots\cdots\cdots & & \\ & & C_nX + D_nX^* & \overset{R_n}{\rightleftarrows} & C_nX^* + D_nX & & \end{array} \tag{8}$$

where the existence of rate determining step in the respective path is assumed. Then the rate equation is given by

$$\frac{d(x+\xi_1+\cdots+\xi_n)}{dt} = \sum_{i=1}^{n} R_i\left(\frac{\eta_i}{\beta_i} - \frac{\xi_i}{\alpha_i}\right),$$

where

$$\alpha_i = [C_iX] + [C_iX^*],\ \xi_i = [C_iX^*],$$

and

$$\beta_i = [D_iX] + [D_iX^*],\ \eta_i = [D_iX^*].$$

If $x, y \gg \xi_i, \eta_i$, and $dx/dt \gg d\xi_i/dt$, we have, by

virture of the relations $x/a=\xi_t/\alpha_t$ and $y/b=\eta_t/\beta_t$,

$$\frac{dx}{dt}=\left(\frac{y}{b}-\frac{x}{a}\right)\sum_{i=1}^{n}R_i=R\left(\frac{y}{b}-\frac{x}{a}\right)$$

with $$R=\sum_{i=1}^{n}R_i.$$

Since R corresponds to the over-all rate, McKay's law holds.

Rate Determining Step cannot be specified. Let us consider a more general case where the rate of reaction is controlled by several steps which occur in series; namely,

$$\left.\begin{array}{l}A_1X \overset{R_1}{\rightleftarrows} A_2X \overset{R_2}{\rightleftarrows} \cdots \overset{R_{n-1}}{\rightleftarrows} A_nX \\ \qquad\qquad\qquad\qquad + \\ B_1X^* \overset{R'_1}{\rightleftarrows} B_2X^* \rightleftarrows \cdots \overset{R_{m-1}}{\rightleftarrows} B_mX^*\end{array}\right\} \overset{R_n}{\rightleftarrows}$$

$$\left\{\begin{array}{l}A_nX^* \overset{R_{n-1}}{\rightleftarrows} \cdots \rightleftarrows A_1X^* \\ + \\ B_mX \overset{R'_{m-1}}{\rightleftarrows} \cdots \rightleftarrows B_1X.\end{array}\right.$$

Then the rate equations are

$$\frac{dx_1}{dt}=-R_1\frac{x_1}{a_1}+R_1\frac{x_2}{x_2} \tag{9}$$

$$\left.\begin{array}{l}\dfrac{dx_2}{dt}=R_1\dfrac{x_1}{a_1}-R_1\dfrac{x_2}{a_2}-R_2\dfrac{x_2}{a_2}+R_2\dfrac{x_3}{a_3} \\ \cdots\cdots\cdots\cdots \\ \cdots\cdots\cdots\cdots \\ \dfrac{dx_n}{dt}=R_{n-1}\dfrac{x_{n-1}}{a_{n-1}}-R_{n-1}\dfrac{x_n}{a_n}-R_n\dfrac{x_n}{a_n}+R_n\dfrac{y_m}{b_m} \\ \dfrac{dy_m}{dt}=R_n\dfrac{x_n}{b_n}-R_n\dfrac{y_m}{b_m}-R'_{m-1}\dfrac{y_m}{b_m}+R'_{m-1}\dfrac{y_{m-1}}{b_{m-1}} \\ \cdots\cdots\cdots\cdots \\ \cdots\cdots\cdots\cdots\end{array}\right\} \tag{10}$$

$$\frac{dy_1}{dt}=-R'_1\frac{y_1}{b_1}+R'_1\frac{y_2}{b_2}, \tag{11}$$

where

$$[A_iX]+[A_iX^*]=a_i,\quad [A_tX^*]=x_i,$$

and

$$[B_iX]+[B_iX^*]=b_i,\quad [B_iX^*]=y_i.$$

From Eqs. (9)—(11), a $(m+n)$th order differential equation for $x_1(t)$ may be obtained, and its exact solution is to have a different form from Eq. (4). Under appropriate conditions, however, this equation may be reduced approximately to Eq. (3). This is studied in the following.

If the approximation of the steady state reaction[11] is used, *i. e.*, the relations,

$$\frac{dx_2}{dt}=\frac{dx_3}{dt}=\cdots=\frac{dx_n}{dt}=\frac{dy_m}{dt}=\cdots=\frac{dy_2}{dt}=0,$$

are assumed, then Eq. (10) become

$$\left.\begin{array}{l}(R_1+R_2)\dfrac{x_2}{a_2}-R_2\dfrac{x_3}{a_3}=R_1\dfrac{x_1}{a_1}, \\ -R_2\dfrac{x_2}{a_2}+(R_2+R_3)\dfrac{x_3}{a_3}-R_3\dfrac{x_4}{a_4}=0, \\ \cdots\cdots\cdots\cdots \\ \cdots\cdots\cdots\cdots \\ -R_{n-1}\dfrac{x_{n-1}}{a_{n-1}}+(R_{n-1}+R_n)\dfrac{x_n}{a_n}-R_n\dfrac{y_m}{b_m}=0, \\ -R_n\dfrac{x_n}{a_n}+(R_n+R'_{m-1})\dfrac{y_m}{b_m}-R'_{m-1}\dfrac{y_{m-1}}{b_{m-1}}=0, \\ \cdots\cdots\cdots\cdots \\ \cdots\cdots\cdots\cdots \\ -R'_2\dfrac{y_3}{b_3}+(R'_1+R'_2)\dfrac{y_2}{b_2}=R'_1\dfrac{y_1}{b_1}.\end{array}\right\} \tag{10}'$$

Solving Eq. (10)′, we can express x_2/a_2 as a function of x_1/a_1 and y_1/b_1,

$$\frac{x_2}{a_2}=\frac{1}{\Delta}\begin{vmatrix}\dfrac{R_1}{a_1}x_1, & -R_2, & \cdots\cdots\cdots & 0 \\ 0, & R_2+R_3, & -R_3, & \vdots \\ \vdots & -R_3, & R_3+R_4, & -R_4 \\ & & -R'_3, & R'_3+R'_2 \\ \dfrac{R_1}{b_1}y_1, & \cdots\cdots\cdots, & 0, & -R'_2 \end{vmatrix}\begin{matrix} 0 \\ \vdots \\ 0 \\ -R'_2 \\ R'_1+R'_2 \end{matrix}, \tag{12}$$

11) K. J. Laidler, "Reaction Kinetics, Vol. I Homogeneous Gas Reactions," Pergamon Press, Oxford (1963).

where

$$\Delta = \begin{vmatrix} R_1+R_2, & -R_2, & 0 & \cdots\cdots & 0 \\ -R_2, & R_2+R_3, & -R_3 & & \vdots \\ 0, & \ddots & \ddots & \ddots & 0 \\ \vdots & & -R'_3, & R'_3+R'_2, & -R'_2 \\ 0 & \cdots\cdots, & 0, & -R'_2, & R'_2+R'_1 \end{vmatrix} = Q \cdot \frac{1}{R},$$

with

$$\frac{1}{R} = \frac{1}{R_1} + \cdots + \frac{1}{R_n} + \frac{1}{R'_{m-1}} + \cdots + \frac{1}{R'_1}, \tag{13}$$

and

$$Q = R_1 \cdot R_2 \cdot \cdots \cdot R_n \cdot R'_{m-1} \cdot \cdots \cdot R'_1.$$

Eq. (12) becomes

$$\frac{x_2}{a_2} = \frac{1}{\Delta}\frac{R_1}{a_1}x_1 \begin{vmatrix} R_2+R_3, & -R_3, & 0 & \cdots\cdots & 0 \\ -R_3, & R_3+R_4, & -R_4 & & \vdots \\ 0, & -R_4, & \ddots & \ddots & 0 \\ \vdots & & , -R'_3, & R'_3+R'_2, & -R'_2 \\ 0 & \cdots\cdots, & 0, & -R'_2, & R'_2+R'_1 \end{vmatrix} +$$

$$(-1)^{m+n-2}\frac{1}{\Delta}\cdot\frac{R_1}{b_1}y_1 \begin{vmatrix} -R_2, & 0, & \cdots\cdots & & 0 \\ R_2+R_3, & -R_3, & 0, & & \vdots \\ -R_3, & R_3+R_4, & -R_4, & & \\ 0, & \ddots & \ddots & \ddots & \\ \vdots & & , -R'_4, & R'_3+R'_4, & -R'_3, & 0 \\ 0 & \cdots\cdots, & 0, & -R'_3, & R'_2+R'_3, & -R'_2 \end{vmatrix}$$

$$= \frac{1}{\Delta}\frac{R_1}{a_1}x_1(R_2 \cdot R_2 \cdot \cdots \cdot R'_1)\left(\frac{1}{R_2} + \frac{1}{R_3} + \cdots + \frac{1}{R'_1}\right) + \frac{1}{\Delta}\frac{R'_1}{b_1}y_1 \cdot R_2 \cdot R_3 \cdot \cdots \cdot R'_2.$$

Introducing this relation into Eq. (9), we get

$$\frac{dx_1}{dt} = -\frac{R_1}{a_1}x_1 + \frac{R_1}{\Delta}\frac{x_1}{a_1}(R_1 \cdot R_2 \cdot \cdots \cdot R'_1)\left(\frac{1}{R_2} + \frac{1}{R_3} + \cdots + \frac{1}{R'_1}\right) + \frac{Q}{b_1 R_1}y_1$$

$$= -R_1\frac{x_1}{a} + R \cdot R_1\frac{x_1}{a_1}\left(\frac{1}{R_2} + \cdots + \frac{1}{R'_1}\right) + \frac{y_1}{b_1}R = R\left(\frac{y_1}{b_1} - \frac{x_1}{a_1}\right).$$

Thus McKay's law is proved inasmuch as R corresponds, according to Eq. (13), to the rate of the overall reaction.

It may be deduced from these examples, that McKay's law approximately holds, when concentrations of reaction intermediates are negligibly smally as compared to those of reactants and products and consequently changes of concentrations of tagged intermediates are also negligible.

Failure of McKay's Law

Now, two questions may arise: firstly, whether McKay's law necessarily breaks down in the case where concentrations of reaction intermediates cannot be disregarded, and secondly, whether such a case has a practical meaning. In the usual cases, concentrations of reaction intermediates are negligibly small as compared to those of reactants and products, but in some reactions this is not the case. Several such examples are discussed.

Excess Catalysts. The direct observation of reaction intermediates is one of current topics, especially in the field of contact catalysis. Some adsorbed species on solid catalysts constitute reaction intermediates and can be studied by ESR, NMR,

IR, isotope techniques and so on. For the convenience of measurements, in some cases, excess amounts of solid catalyst are used as compared to those of the reactants and products in gaseous phase. Such examples were reviewed by Tamaru.[12] Let us discuss one of the simplest cases.

$$\left.\begin{matrix} AX \overset{R_1}{\rightleftarrows} (AX)_a \\ + \\ BX^* \end{matrix}\right\} \overset{R_2}{\rightleftarrows} \left\{\begin{matrix} (AX^*)_a \overset{R_1}{\rightleftarrows} AX^*, \\ + \\ BX \end{matrix}\right.$$

where the subscript a designates adsorbed species. Using the notation (2), and designating

$$[(AX)_a] + [(AX^*)_a] = \alpha$$

and

$$[(AX^*)_a] = \xi,$$

we have the rate equations

$$\frac{dx}{dt} = -R_1\frac{x}{a} + R_1\frac{\xi}{\alpha},$$

$$\frac{d\xi}{dt} = R_1\frac{x}{a} - R_1\frac{\xi}{\alpha} - R_2\frac{\xi}{\alpha} + R_2\frac{y}{b},$$

and

$$\frac{dy}{dt} = -R_2\frac{y}{b} + R_2\frac{\xi}{\alpha},$$

with $x + y + \xi = \text{const.} = I.$

These equations reduce to

$$\frac{d^2x}{dt^2} + \left(\frac{R_1+R_2}{\alpha} + \frac{R_1}{a} + \frac{R_2}{b}\right)\frac{dx}{dt} + \frac{a+b+\alpha}{ab\alpha}R_1R_2x = \frac{R_1R_2}{b\alpha}I, \tag{14}$$

of which the solution becomes

$$x = x_\infty\left[1 + \frac{\rho_-}{\sqrt{D}}\exp(\rho_+t) - \frac{\rho_+}{\sqrt{D}}\exp(\rho_-t)\right], \tag{15}$$

with

$$\rho_\pm = -\frac{1}{2}\left(\frac{R_1}{a} + \frac{R_2}{b} + \frac{R_1+R_2}{\alpha}\right) \pm \frac{\sqrt{D}}{2},$$

$$D = \left(\frac{R_1}{a} + \frac{R_2}{b} + \frac{R_1+R_2}{\alpha}\right)^2 - \frac{4(a+b+\alpha)}{ab\alpha}R_1R_2,$$

and

$$x_\infty = \frac{a}{a+b+\alpha}I,$$

under the intial condition

$$x = 0,\ \xi = 0 \text{ at } t = 0.$$

Let us consider the case where R_1 is much larger than R_2, *i. e.*, the reaction $AX \rightleftarrows (AX)_a$ is in equilibrium. Then, Eq. (14) reduces approximately to

$$\left(\frac{R_1}{\alpha} + \frac{R_1}{a}\right)\frac{dx}{dt} + \frac{a+b+\alpha}{ab\alpha}R_1R_2x = \frac{R_1R_2}{b\alpha}I,$$

and hence to

$$\frac{dx}{dt} = -\frac{a+\alpha+b}{b(a+\alpha)}R_2x + \frac{a}{b(a+\alpha)}R_2I,$$

and consequently we have

$$-\ln\frac{x_\infty - x}{x_\infty} = \frac{b+a+\alpha}{b(a+\alpha)}R_2t. \tag{16}$$

This is a slight modification of Eq. (4) obtained by replacing a by $a+\alpha$.

In the case where the step $(AX)_a + BX^* \rightleftarrows (AX^*)_a + BX$ is in equilibrium, the same result is obtained. Thus, it may be concluded that in this reaction scheme McKay's law seriously breaks down only if the intermediate rate determining step cannot be specified and further the amount of intermediates cannot be disregarded in comparison with those of reactants and products.

NaCl/HCl System. Now let us show another example, to which McKay's law cannot be applied, *i. e.*, the exchange reaction between sodium chloride crystallites and hydrogen chloride gas.[13] The exchange of ^{36}Cl in this system proceeds layer by layer, and the activation energy of the reaction becomes progressively higher as the reaction proceeds from the first layer to inner layers, approaching that for self-diffusion. The exchange reaction scheme is expressed as

$$HCl + Cl^*(1) \overset{R_1}{\rightleftarrows} HCl^* + Cl(1)$$

$$Cl(1) + Cl^*(2) \overset{R_2}{\rightleftarrows} Cl^*(1) + Cl(2)$$

$$Cl(2) + Cl^*(3) \overset{R_3}{\rightleftarrows} Cl^*(2) + Cl(3)$$

and so on,

where $Cl(i)$ designates a chloride ion in the ith layer. Thus, the rate equation becomes

$$\frac{dx_g}{dt} = -R_1\frac{x_g}{a_g} + R_1\frac{x_1}{a_1},$$

$$\frac{dx_1}{dt} = R_1\frac{x_g}{a_g} - R_1\frac{x_1}{a_1} - R_2\frac{x_1}{a_1} + R_2\frac{x_2}{a_2}, \tag{17}$$

$$\frac{dx_2}{dt} = R_2\frac{x_1}{a_1} - R_2\frac{x_2}{a_2},$$

with $x_g + x_1 + x_2 = \text{const.} = I,$

and $a_1 = a_2,$

when the experiments carried out at such temperatures as that the third layer does not participate in the reaction. Solving Eq. (17) with the initial condition, which is a situation really encountered,[13]

$$x_g = 0 \text{ and } x_2 = 0 \text{ at } t = 0,$$

we get a solution quite simmilar to Eq. (15).

12) K. Tamaru, "Advances in Catalysis," XV, Academic Press Inc., New York, London (1964), p. 65.

13) L. G. Harrison, J. A. Morrison and G. S. Rose, *J. Phys. Chem.*, **66**, 1314 (1957).

Concluding Remark

We may conclude, from the above considerations, that an isotopic exchange reaction cannot be described by first order kinetics with respect to the isotopic concentration when:

the concentrations of intermediates are significant compared to those of reactants and products and no intermediate step is rate controlling

Otherwise, first order kinetics may hold. First order kinetics contains such a case as Eq. (16), and has a wider meaning than McKay's law. This conclusion cannot be proved strictly in a mathematical sense, but it may presumably be true as judged from the rather wider considerations given in the preceding sections.

As for cases where two or more atoms in the same molecule are exchanged, their reaction kinetics may have various forms[8] and may not be concerned in the present paper.

BULLETIN OF THE CHEMICAL SOCIETY OF JAPAN VOL. 42 1271—1277 (1969)

Thermodynamic Properties and Phase Transitions of Thallous Cyanide Crystal

Takasuke MATSUO, Masayasu SUGISAKI,*1 Hiroshi SUGA and Syûzô SEKI

Department of Chemistry, Faculty of Science, Osaka University, Toyonaka, Osaka

(Received October 9, 1968)

The heat capacities of TlCN crystal were measured from 15 to 300°K with an adiabatic calorimeter. Three regions of anomalously high heat capacity were discovered. Thermodynamic functions of the crystal were calculated by the graphical integration of the heat capacity data. ^{205}Tl nuclear magnetic resonance was observed as functions of temperature and applied static magnetic field. Their second moment values could be interpreted in terms of the anisotropic chemical shift tensor.

The alkali cyanides, NaCN, KCN, RbCN and CsCN all crystallize in the cubic system at room temperature and on cooling, they all transform into the less symmetric modifications. Their thermodynamic behaviors were reported in the series of our papers.[1-3] The present investigation deals with thallous cyanide crystal. Thallium belongs to the third group in the periodic table but its monovalent ion behaves much like the alkali ions. Thus, its hydroxide is strongly alkaline in aqueous solution and it forms halide crystals of similar structure. Therefore, its cyanide was expected to exhibit some properties analogous to those of the alkali cyanides.

We present here the results of low temperature heat capacity measurement carried out mainly in order to investigate the phase transition effect.

In addition to the thermodynamic method, thallous compounds can be investigated with the nuclear magnetic resonance. ^{203}Tl and ^{205}Tl nuclei involved with the natural abundance ratio; 29.5%: 70.5%, respectively, have nuclear spin 1/2 with experimentally favorable gyromagnetic ratio. Owing to the large number of electrons which Tl^+ ion has, Tl resonance shows some interesting feature which is absent from the usual proton resonance: we can expect to see the chemical shift and/or indirect nuclear spin coupling in solids.[4]

In spite of its simple composition, very little is known about the property of thallous cyanide crystal, though its chemical reactivity was studied rather extensively.[5] The only relevant works that came into our attention are two structural investigations,[5,6] both dealing with the room temperature cell constant of thallous cyanide crystal. Strada[6] showed that the crystal has the cesium chloride structure with $a=3.83$ Å while Penneman and Staritzky[5] gave $a=3.993$ Å, the latter being in good correlation with other alkali halides and

*1 Present address: Department of Physics, Faculty of Science, The University of Tokyo, Hongo, Tokyo.

1) H. Suga, T. Matsuo and S. Seki, This Bulletin, **38**, 1115 (1965).

2) T. Matsuo, H. Suga and S. Seki, *ibid.*, **41**, 583 (1968).

3) M. Sugisaki, T. Matsuo, H. Suga and S. Seki, *ibid.*, **41**, 1747 (1968).

4) N. Bloembergen and T. J. Rowland, *Phys. Rev.*, **97**, 1679 (1955).

5) R. A. Penneman and E. Staritzky, *J. Inorg. Nuclear Chem.*, **6**, 112 (1958).

6) M. Strada, *atti. acad. Lincei*, **19**, 807 (1934).

cyanides. The cesium chloride structure made up of CN^- ions is just the same situation as in the cesium cyanide crystal. That is, there must be some orientational disorder in the ionic configuration of CN^- group, which means there may be phase transitions at lower temperatures. The same line of reasoning resulted in the previous investigations on NaCN, KCN, RbCN and CsCN.

Experimental

The Sample Preparation. The thallous cyanide crystal was prepared according to the reaction

$$TlOH + HCN \rightarrow TlCN + H_2O,$$

in aqueous solution.

Thallous hydroxide was made by oxidation of metallic thallium in water[7] as follows. Metallic thallium of stated 99.9% purity supplied by Nakarai Chemicals Ltd. in a cylindrical form was machined to turnings on a lathe. 75 g of the turnings was put in a pyrex flask, furnished with a polyethylene stirrer, together with 700 cc of water purified by an ion-exchanger. It was then oxidized by bubbling cylinder oxygen gas from which carbon dioxide had been removed with aqueous solution and pellets of potassium hydroxide. No heating of the reaction vessel was employed lest the alkaline solution might react with the glass are at elevated temperatures. After 24 hr of bubbling, undissolved metal was filtered off the solution.

Hydrogen cyanide was prepared in a standard way, *i.e.*, by mixing aqueous solution of KCN with sulfuric acid and trapping the evolving gas in a glass flask chilled with an ice-salt mixture.

About 70 cc of liquid hydrogen cyanide was poured into 700 cc of aqueous solution of thallous hydroxide obtained as above. As soon as the two liquids were mixed, a white crystalline powder precipitated out. The crystal was filtered off the solution and dried in vacuum at 130°C for 4 hr. The X-ray powder photograph of the crystal taken with Cu$K\alpha$ radiation was assignable to CsCl structure with a lattice constant of $a=3.97$Å.*2 This figure may be accurate about to 1%.

The most susceptible impurity was the carbonate ion, on which we tested the sample as follows. Small amount of the sample was dissolved in water. To the solution, $Ba(OH)_2$ aqueous solution was added. If there was sufficient concentration of carbonate ion in the sample, white precipitate of $BaCO_3$ would be formed. In fact no precipitation was observed in the present case. Comparison with an independent test by using K_2CO_3 solutions of known concentration showed that the present TlCN contains less than 0.1 weight per cent of carbonate ion.

Calorimetry. The heat capacities were measured with an adiabatic calorimeter operating from 15 to 300°K. Its detail was reported elsewhere.[8] The weight of sample used for calorimetry was 29.008 g (0.12591 mol). It was packed in a gold calorimeter cell with a small amount of helium gas to facilitate thermal equilibrium.

In a preliminary run, it was found that there are three temperature regions of anomalously high heat capacity. They are around 90, 190 and 260°K. The lowest one supercools easily and causes objectionable thermal effect. In order to prepare the stable lowest temperature phase, the specimen was first cooled down to 65°K and kept at the temperature overnight. Subsequent annealing at 85°K followed by recooling to 58°K produced the stable phase. At 58°K 1st run was initiated.

Temperature step of 1—2°K was usually chosen for one measurement in the normal region. In the transition regions necessarily smaller step was used. After turning off the calorimeter heater, usually 10 min were sufficient for it to attain a thermal equilibrium. But from 79 to 87°K, more than 20 min were needed. Next anomalous region around 190°K remained unnoticed until the data were processed, for it did not cause any anomalous equilibriating behavior. Another anomalous region is around 266°K where the heat capacity becomes drastically large and also the equilibriating times were more than 1 hr. Since the high temperature (cubic) phase was found to be supercooled to 248°K, nearly 20°K below the normal transition temperature, its heat capacities were measured in this metastable region in order to facilitate determination of the "normal heat capacity."

Nuclear Magnetic Resonance. Tl nuclear magnetic resonance experiment was carried out with a Nihon-Denshi electromagnet and a locally designed spectrometer of Pound-Watkins type, followed by a phase sensitive detector and a recorder. The RF coil was housed in a copper cylinder which was suspended in a glass dewar. The specimen in a glass tube was cooled by nitrogen gas which boiled off the liquid at the bottom of the dewar flask. The sample temperature was monitored with a chromel-P constantan thermocouple attached to the specimen glass tube. The ^{205}Tl resonance signal was recorded between the liquid nitrogen and room temperatures at 10.6 MHz. The ^{203}Tl signal was also detected at room temperature but naturally with weaker intensity. On cooling both ^{205}Tl and ^{203}Tl signal broadened considerably and ^{203}Tl signal was scarcely above the noise level. Therefore, only ^{205}Tl resonance was studied in detail. In addition to the temperature dependence, static field dependence of the resonance line was studeid at 8, 10.6, 15 and 17.5 MHz for two fixed temperatures, 210°K and room temperature.

Experimental Results

Heat Capacity. The experimental molar heat capacities are given in Table 1 in the chronological order. They are the ratios of the molar enthalpy

7) F. Bahr, *Z. anorg. Chem.*, **71**, 81 (1911).

*2 Our datum, though not too accurate, favors Penneman and Staritzky's value rather than Strada's. Strada's value is definitely inconsistent when compared with the lattice parameters of alkali halides, and cyanides. Therefore, citations of Strada's value in some books should be corrected. [For instance; R. W. G. Wyckoff, "Crystal Structures" (2nd edition) Vol. 1, Interscience Publishers, New York (1963), p. 104; J. C. Slater, "Quantum theory of molecules and solids" Vol. III, McGraw-Hill, New York (1965), p. 342.]

8) H. Suga and S. Seki, This Bulletin, **38**, 1000 (1965).

TABLE 1. HEAT CAPACITIES OF THALLOUS CYANIDE CRYSTAL IN J/mol °K

T (°K)	$\Delta H/\Delta T$	ΔT (°K)	T (°K)	$\Delta H/\Delta T$	ΔT (°K)
	Series 1		77.46	52.67	1.097
58.75	41.15	2.188	78.55	53.54	1.084
60.74	43.86	1.814	79.63	54.69	1.070
62.51	44.61	1.930	80.69	56.16	1.054
64.52	45.77	1.883	81.74	58.11	1.035
66.38	46.74	1.842	82.76	61.06	1.010
68.40	47.80	2.205	83.75	66.31	0.971
70.58	48.82	2.155	84.70	72.26	0.932
72.71	49.83	2.112	85.63	72.07	0.929
74.81	50.93	2.069	86.57	67.84	0.951
76.86	52.11	2.030	87.53	63.76	0.974
			88.50	63.16	0.974
	Series 2				
93.38	59.03	1.806		Series 5	
95.18	59.20	1.794	95.83	59.05	1.972
			97.89	59.67	1.953
	Series 3		99.83	60.16	1.937
15.10	9.54	2.126	101.76	60.60	1.927
17.02	11.42	1.723	103.67	61.09	1.908
17.89	12.34	1.585	105.51	61.62	1.893
19.41	13.56	1.398	107.65	62.16	2.272
20.99	14.90	1.178	109.91	62.62	2.254
22.41	15.88	1.608	112.16	63.14	2.237
23.99	17.26	1.578	114.38	63.70	2.219
25.74	18.71	1.891	116.60	64.18	2.203
27.56	20.12	1.714	118.79	64.50	2.189
29.49	21.45	2.126	120.97	65.34	2.171
31.51	23.11	1.943	123.14	65.65	2.150
33.39	24.63	1.799	125.30	65.94	2.149
35.14	26.02	1.685	127.44	66.40	2.136
36.87	27.24	1.775	129.57	66.89	2.123
38.83	28.86	2.124	131.68	67.29	2.112
40.89	29.91	2.003	133.79	67.84	2.100
42.84	31.21	1.902	135.89	68.15	2.090
44.70	32.42	1.816	136.89	68.94	2.061
46.48	33.55	1.741	139.09	69.31	2.315
48.19	34.60	1.676	141.40	69.70	2.303
49.91	35.61	1.772	143.70	70.18	2.221
51.66	36.63	1.715	145.98	70.67	2.281
53.47	37.59	1.906	148.26	70.96	2.271
55.35	38.76	1.846	150.53	71.46	2.260
57.17	39.83	1.794	152.78	72.23	2.248
58.95	41.01	1.746	155.03	72.58	2.236
			157.26	73.04	2.226
	Series 4		159.48	73.48	2.216
76.36	51.78	1.111	161.77	73.98	2.352
164.12	74.21	2.345	261.05	86.94	2.046
166.46	75.17	2.328		Series 7	
168.78	75.39	2.321	279.93	68.02	2.394
171.10	75.93	2.310	282.36	68.20	2.384
173.40	76.47	2.299	287.11	67.86	2.476
175.30	77.32	2.279	289.58	67.69	2.471
177.57	77.77	2.270	292.04	67.83	2.463
179.84	78.35	2.259	294.50	67.86	2.457
182.09	79.04	2.248	296.95	67.79	2.452
184.33	79.77	2.237	299.40	67.77	2.447
186.56	80.55	2.225	301.84	67.83	2.443
188.78	81.40	2.212			
190.99	82.04	2.203		Series 8	
193.19	82.26	2.198	259.82	86.76	2.056
195.39	80.29	2.217	261.83	94.20	1.985
197.63	77.76	2.243	263.50	197.84	1.342
199.88	76.43	2.256	264.59	387.51	0.843
202.13	75.97	2.258	265.47	486.88	0.707
204.39	75.83	2.257	266.08	708.63	0.517
206.65	75.92	2.253	266.70	468.61	0.722
208.90	76.10	2.248	267.49	370.15	0.865
211.14	76.38	2.243	268.45	278.21	1.056
213.39	76.68	2.236	269.64	197.96	1.321
215.62	76.98	2.230	271.14	128.71	1.678
			273.05	95.23	1.938
	Series 6		274.96	82.30	2.087
218.25	77.38	2.218	277.09	74.37	2.168
220.46	77.71	2.209	279.28	69.80	2.217
222.66	78.06	2.200	281.57	69.06	2.373
224.86	78.41	2.192			
226.60	79.14	2.172	Series 9 (metastable)		
228.77	79.15	1.166	248.12	69.27	2.378
230.93	79.71	2.157	250.50	69.03	2.379
233.08	80.03	2.151	252.87	68.90	2.377
235.23	80.37	2.145	255.25	68.72	2.376
238.11	81.06	1.601	257.62	68.62	2.375
240.19	81.36	2.129	259.99	68.66	2.372
242.31	82.01	2.120	262.36	68.62	2.370
244.42	82.50	2.113	264.73	68.61	2.368
246.53	82.86	2.017	269.09	68.52	2.367
248.63	83.32	2.100	269.50	68.47	2.451
250.72	83.91	2.092	271.92	68.40	2.391
252.80	84.48	2.084	274.30	68.29	2.389
254.88	85.11	2.075	276.69	68.23	2.388
256.95	85.84	2.067			
259.01	86.67	2.057			

increment ΔH to the temperature rise ΔT. The temperature indicated is the average of the initial and the final temperatures. Also shown is the approximate temperature rises. Figure 1 is the graphical representation of the heat capacity data. There are three regions of anomalously high heat capacity. As stated above, the transitions at 85°K and 266°K are very sluggish, the intermediate one being entirely normal. As a criterion for determining the heat capacity at these temperature range, it was assumed that the temperature variation after turning off the calorimeter heater follows

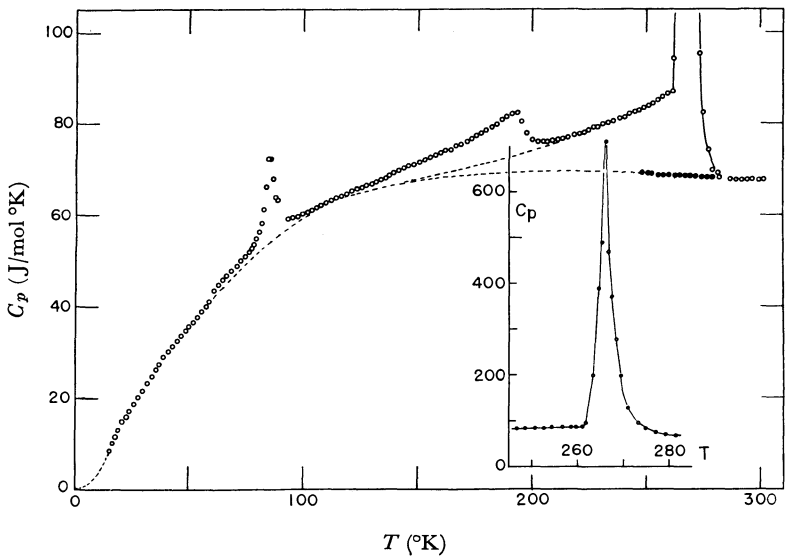

Fig. 1. Molar heat capacity *vs.* temperature of TlCN crystal.
(—○—○—○—; stable phase, —●—●—●—; the metastable cubic phase)

the exponential time dependence. That is

$$T(t) - T(\infty) = [T(0) - T(\infty)] \exp\left(-\frac{t}{\tau}\right),$$

where $T(t)$ is the temperature of the calorimeter at time t measured from the time when the heater is turned off, and τ, a time constant. Differentiation with t gives

$$\frac{dT}{dt} = -[T(0) - T(\infty)]\frac{1}{\tau}\exp\left(-\frac{t}{\tau}\right) = -\frac{1}{\tau}[T(t) - T(\infty)].$$

Therefore, if we plot $T(t)$ against $dT(t)/dt$ extrapolation of the graph to $dT(t)/dt=0$ gives $T(\infty)$. In practice, the resistance $R(t)$ of the platinum thermometer was plotted rather than the temperature.

This method rests entirely on the assumption of the exponential time dependence of the temperature, which is not always the case. Therefore, it is applied solely, for the sake of convenience, to prohibitingly long equilibriation times.

TABLE 2. ENTHALPY AND ENTROPY CHANGES OF THE TRANSITIONS

T_{tr}(°K)	ΔS_{tr}(J/mol °K)	ΔH_{tr} (J/mol)
84.7	2.242	181.3
193.2	1.458	255.7
266.1	11.481	2945.5

The enthalpy and entropy changes of the phase transitions are summarized in Table 2 together with the temperature at which the heat capacity has the peaks. These values are of the corresponding changes associated with the excess heat capacity above the dotted curves in Fig. 1. The dotted curves are assumed to represent the vibrational part of the heat capacity. They are just the extrapolation of the heat capacity of the temperature ranges where anomalous effect seems to be absent. Their significance may be rather obscure in principle, but there are many cases in practice in which the entropy of the phase transition thus obtained can be rationalized in theoretical interpretations.

^{205}Tl NMR. The typical NMR absorption derivatives are shown in Fig. 2 for the room temperature and 210°K. The room temperature absorption is narrow and symmetric in its shape, while it becomes broad and slightly but significantly asymmetric at lower temperatures. Their second moment is shown in Fig. 3 as a function of temperature. The second moment of the asymmetric spectra was approximated by the sum of the lower field and higher halves which are separated by the zero of the absorption derivative. The second moment decreases steadily to about 180 °K and remains rather constant to the upper transition point where it decreases suddenly.

Figure 4 shows the field dependence of the second moment of the absorption at the room temperature

TABLE 3. THERMODYNAMIC PROPERTIES OF THALLOUS CYANIDE CRYSTAL*

T	$C_p°$	$S°$	$\frac{(H°-H°_0)}{T}$	$-\frac{(G°-H°_0)}{T}$	T	$C_p°$	$S°$	$\frac{(H°-H°_0)}{T}$	$-\frac{(G°-H°_0)}{T}$
5	(0.900)	(0.4351)	(0.2895)	(0.146)	140	69.274	85.565	42.396	43.169
10	(4.146)	(1.902)	(1.318)	(0.584)	150	71.433	90.423	44.263	46.160
15	9.456	4.573	3.121	1.452	160	73.580	95.106	46.028	49.078
20	14.016	7.539	5.343	2.196	170	75.663	99.628	47.706	51.922
25	18.012	11.510	7.456	4.054	180	78.375	104.086	49.334	54.692
30	21.945	15.144	9.556	5.588	190	81.768	108.35	50.949	57.401
35	25.773	18.816	11.594	7.222	193.2	Phase Transition			
40	29.342	22.493	13.602	8.891	200	76.397	112.46	52.405	60.056
45	32.606	26.140	15.527	10.613	210	76.232	116.17	53.526	62.644
50	35.673	29.735	17.392	12.343	220	77.655	119.75	54.589	65.158
60	43.099	36.778	20.949	15.829	230	79.433	123.21	55.630	67.578
70	48.501	43.855	24.527	19.328	240	81.412	126.63	56.664	69.966
80	55.083	50.695	27.865	22.830	250	83.705	130.00	57.697	72.299
84.7	Phase Transition				260	86.797	133.34	58.756	74.582
90	60.388	57.561	31.221	26.340	266.1	Phase Transition			
100	60.166	63.830	33.443	30.387	280	69.551	146.82	67.697	79.123
110	62.701	69.684	36.041	33.643	290	67.881	149.20	67.726	81.474
120	64.873	75.235	38.284	36.951	298.15	67.703	151.10	67.726	83.374
130	67.070	80.514	40.413	40.101	300	67.697	151.29	67.726	83.564

* The units are °K for temperature and J/mol°K for the other quantities.

and 210°K, the latter being a temperature where the second moment retains a rather constant value. The room temperature value is field-independent; this is what is expected for the dipolar and/or exchange broadening. In the low temperature phase, the second moment is definitely larger and depends linearly on the square of the static magnetic field. Similar type of behaviors was observed in Tl_2O_3,[4] Tl,[4] UF_6,[9] XeF_4,[10] $CFCl_2 \cdot CFCl_2$[11] and $CF_2Br \cdot CF_2Br$[11] and may be attributed to the anisotropic

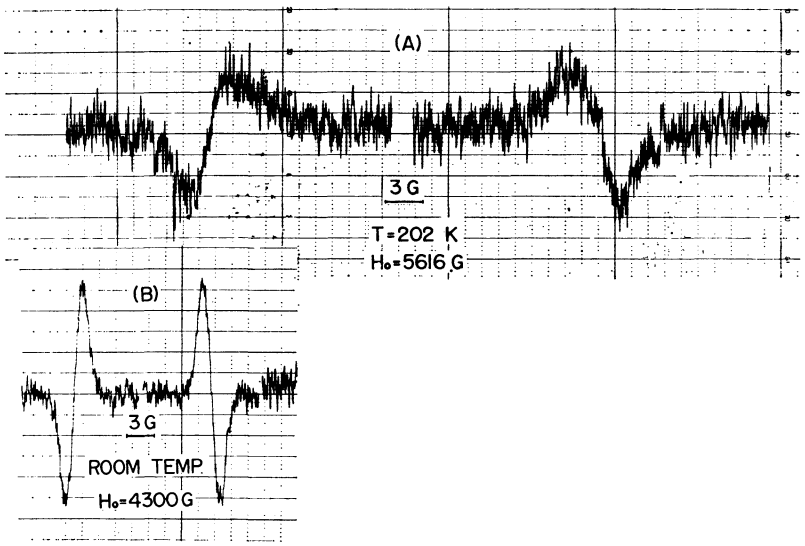

Fig. 2. ^{205}Tl NMR absorption derivatives of TlCN in the low temperature phase (A) and the cubic phase (B). In each case, the left half indicates sweeping up-field and the right half down-field.

9) R. Blinc, V. Marinkovic, E. Pirkmajer and I. Zupancic, *J. Chem. Phys.*, **38**, 2474 (1963).
10) R. Blinc, I. Zupancic, S. Maricic and Z. Vekseli, *ibid.*, **39**, 2109 (1963).
11) E. R. Andrew, D. T. Tunstall, *Proc. Phys. Soc.*, **81**, 986 (1963).

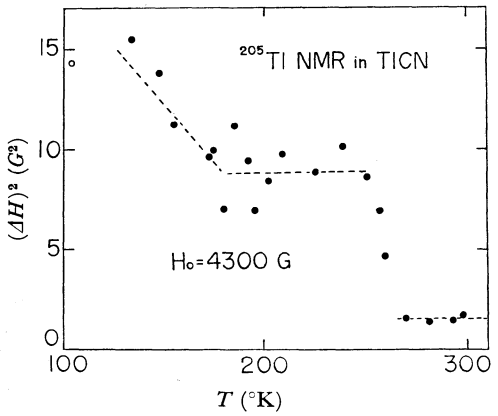

Fig. 3. Temperature dependence of apparent second moment of the ^{205}Tl NMR absorption in TlCN crystal.

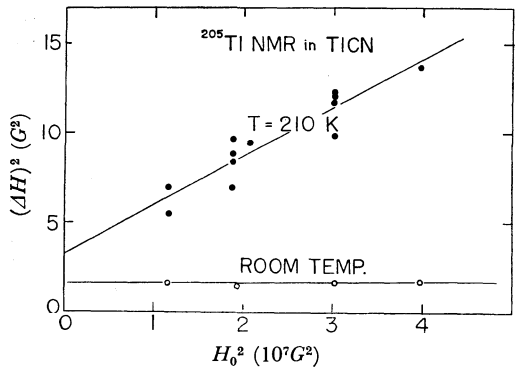

Fig. 4. Static field dependence of apparent second moment of the ^{205}Tl NMR absorption in TlCN crystal.

chemical shift.

Discussion

Phase Transitions. The total entropy associated with the three phase transitions is 15.2 J/mol°K. This value may be correlated with the possible eight directions of the cyanide ion on the four body diagonal directions in the cubic phase ($R\ln 8 = 17.2$ J/mol°K). The entropy change at the 266°K transition is approximately equal to $R\ln 4$, which implies that among the eight possible directions of the cyanide ion, two become energetically favored. This is the same situation as in the CsCN crystal. The CsCN crystal has a transition[3] at $T_{tr}=193.1$°K with $\Delta S_{tr}=15.7$ J/mol°K. Its low temperature phase has a distorted CsCl structure with one body diagonal axis elongated. If one assumes that TlCN has the same structure in the temperature region between the upper and the intermediate transitions, one can discuss the phase transition of the two salts comparatively. Among the possible molecular or ionic interactions leading to the transition, the dipole-dipole interaction between the CN^- ions is excluded on the symmetry ground. The next lower multipole is the quadrupole. The quadrupole-quadrupole interaction potential depends on the separation r as r^{-5}. The ratio of the lattice constant of TlCN to that of CsCN is equal to $a_{Tl}/a_{Cs}=3.993/4.25=0.9395$. If this value may be used also for the low temperature structures, its fifth power is expected to be approximately equal to the inverse ratio of the transition temperatures of the two salts. In fact, $(a_{Tl}/a_{Cs})^5=0.7320$ while $T_{Cs}/T_{Tl}=193.1/266.1=0.7257$. This excellent agreement may be rather fortuitous, since the change in the Madelung energy and the repulsive energy must be taken into account. However, before we are able to discuss these effects, it would be necessary to have more detailed structural informations. The scalar quadrupole moment of the CN^- ion was estimated to be $Q=0.7\times10^{-26}$cgs by equating kT_{tr} to the quadrupole-quadrupole interaction potential given by the expression[13]

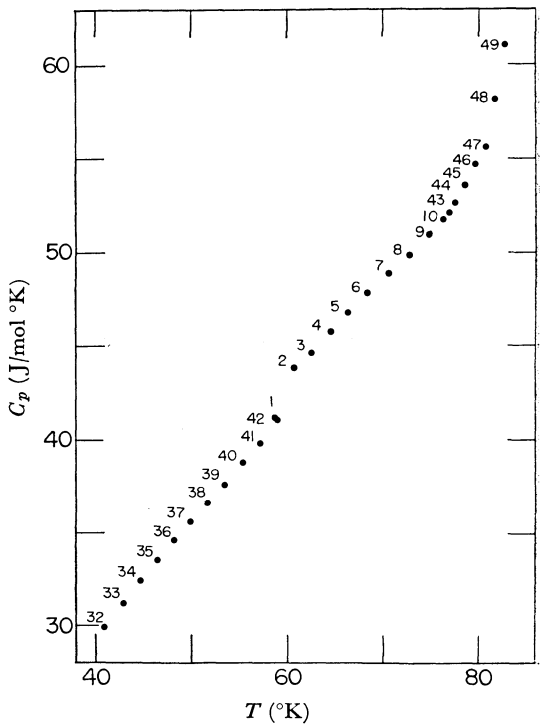

Fig. 5. The portion of the heat capacity diagram of TlCN crystal showing a small step-like anomaly. The numbers in the figure indicate the time order in which the measurements were performed.

12) J. O. Hirschfelder, C. F. Curtis, R. B. Bird, "Molecular Theory of Gases and Liquids," John Wiley & Sons, Inc., New York (1964), p. 27.

13) P. Goursot, E. F. Westrum, Jr., and J. Metzger, *Compt. Rend. Acad. Sci. Paris*, **266**, 590 (1968).

$$\Phi_{ab}^{(QQ)} = (3Q_aQ_b/16r^5)[1 - 5\cos^2\theta_a - 5\cos^2\theta_b - 15\cos^2\theta_a \cdot \cos^2\theta_b + \{2\sin\theta_a\sin\theta_b\cos(\phi_a-\phi_b) - 4\cos\theta_a\cos\theta_b\}^2],$$

where r is the intermolecular separation, θ's and ϕ's are polar and azimuthal angles measured from the intermolecular vector. Here, we used for the structural parameters their high temperature values. With regard to the other two phase transitions, no detailed interpretation seems to be possible at the present stage. In addition to these three anomalies, there is another which seems to be associated with the 85°K transition. The detailed diagram of the relevant portion of the heat capacity is shown in Fig. 5. It is not a peak but a steplike increase of the heat capacity. This type of anomaly is observed in many glass forming and other substances.[13,14] The interpretation of the detailed mechanism of this kind of transition remains for further investigations.

Hindered Rotation of the CN^- Ion. The heat capacities of the cubic phase in the stable and the metastable phases continue to each other smoothly as they should. The heat capacity value decreases with increasing temperature. This behavior is not feasible with the harmonic oscillator heat capacity. It is generally agreed that hindered rotation of molecules produces such an effect. There is wealth of literatures dealing with this phenomenon both from experimental and theoretical sides, the most recent and detailed treatment being due to Smith.[15] His investigation might be extended to apply to the present case.

The NMR Second Moment. From the NMR experiment we obtained a qualitatively interesting conclusion. The high temperature value of the second moment is comparable with the Van Vleck value for the dipolar broadening, while below the 266°K transition, it is definitely larger. The width might be due to the $I_1 \cdot I_2$ coupling through the electron and/or anisotropic chemical shift, since the lattice sum $\sum_{ij} 1/r_{ij}^6$ cannot change to this extent through the transition. Also the asymmetric shape of the spectrum suggests an anisotropic chemical shift. The slope of the line in Fig. 4 gives the anisotropy of the chemical shift, $\sigma^{\parallel} - \sigma^{\perp}$.[11] It is about 1000 ppm for the present case. If there are non-equivalent sites for the Tl ions, it may also contribute to the second moment with the similar H_0 dependence. But the asymmetric spectrum does not occur if the non-equivalent sites are same in number. Moreover, the spectrum would exhibit resolved structures if they were mere superpositions of a small number of the narrow spectra shifted from each other.*3

We can, therefore, conclude that the thallium chemical shift tensor changes on the phase transition, which in turn means that there are definite chemical bonds[16-20] among the ions which change on the phase transition. Thermodynamic consequences of such chemical bonds are still to be investigated.

Conclusion

Thallium cyanide crystal has three phase transitions below the room temperature. The uppermost one may be of the same nature as the one observed in cesium cyanide crystal. Interpretation of the other two transitions seems to be difficult at the present stage. The heat capacity of the cubic modification could be measured in the stable and the metastable temperature region and behaves as expected for a hindered rotator. ^{205}Tl NMR line widths in the low temperature phases are definitely larger than the dipolar width and may be attributed to the anisotropic chemical shift. This implies that not only the packing condition of the ions but also the electronic state changes on the phase transition to the extent to be observed in such an experiment.

The authors are grateful to Dr. Nobuo Nakamura, Osaka University, to whom they owe much in performing the NMR experiment. Also the financial support by the Toyo Rayon Co. is greatly acknowledged.

14) M. H. Brown and A. R. Taylor, Jr., private communication.

15) D. Smith, *J. Phys. Chem. Solids*, **29**, 525 (1968).

*3 The authors owe to Mr. G. Soda, Osaka University, for his pointing out these possibilities.

16) T. Kanda, *J. Phys. Soc. Japan*, **10**, 85 (1955).

17) K. Yoshida and T. Moriya, *ibid.*, **11**, 33 (1956).

18) J. Kondo and J. Yamashita, *J. Phys. Chem. Solids*, **20**, 243 (1959).

19) Y. Saito, *J. Phys. Soc. Japan*, **21**, 1072 (1966).

20) C. J. Jameson and H. S. Gutowsky, *J. Chem. Phys.*, **40**, 1714 (1964).

BULLETIN OF THE CHEMICAL SOCIETY OF JAPAN VOL. 42 1278—1281 (1969)

Gas Chromatography of Rare Earth Chelates of Pivaloyltrifluoroacetone*1

Tsunenobu SHIGEMATSU, Masakazu MATSUI and Kei UTSUNOMIYA

Institute for Chemical Research, Kyoto University, Uji, Kyoto

(Received August 15, 1968)

The gas chromatographic behavior of Sc, Y, and rare earth chelates of a new β-diketone, pivaroyltrifluoroacetone (PTA), was investigated. PTA was synthesized by a Claisen condensation from pinacolin and ethyltrifluoroacetone. Sc, Y, Nd, Sm, Eu, Gd, Tb, Dy, Er, Yb, and Lu PTA chelates were prepared. Their elemental analyses and infrared spectra indicated that they were anhydrous tris chelates, and the TGA curves of the chelates proved their good volatile characteristics, showing approximately a 100% weight loss. Gas chromatograms of all the chelates and of mixtures of Sc, Y, and several rare earth chelates were obtained. Some relationships were observed between the retention time, the volatilization temperature, and the ionic radius of the central metal: With the decrease in the ionic radius, the retention time of the chelate decreased and the volatilization temperature became lower.

Recently, it has been recognized that the volatile characteristics of a number of metal β-diketone chelates make the gas-chromatographic technique of possible use for the separation of the metals. From this point of view, the chromatographic studies have been carried out on various metal chelates with acetylacetone,[1,2] trifluoroacetylacetone,[3-5] hexafluoroacetylacetone,[6] dipivaloylmethane,[7] 1,1,1,2,2,3,3,-heptafluoro-7,7-dimethyl-4,6-octanedione[8] (FOD), *etc.* By using the latter two β-diketones, Sievers and his co-workers studied the chromatographic behavior of rare earth elements in detail; as a result, they suggested the possibility of the simple and rapid separation of the individual elements.

The present authors have been attracted by the gas chromatography of metal β-diketone chelates, and have performed a systematic investigation with several β-diketones, some of which were synthesized in our own laboratory.

In this paper, the gas-chromatographic behavior of rare earth chelates with a new β-diketone, pivaloyltrifluoroacetone (PTA), will be described. The reagent possesses a trifluoromethyl group and a *t*-butyl group, both of which enhance the volatility of the chelates. Thus, rare earth PTA chelates were eluted by the gas phase, as were the dipivaloylmethane and the FOD chelates.

Experimental

Synthesis of Pivaloyltrifluoroacetone (PTA), (1,1,1-Trifluoro-5,5-dimethyl-3,5-hexanedione). The β-diketone was synthesized by Claisen condensation from pinacolin and ethyl trifluoroacetate.[9]

Ethyl trifluoroacetate was synthesized by trifluoroacetic acid and diethyl sulfate.[10,11] One mole of trifluoroacetic acid was neutralized with a sodium hydroxide solution (1.1 mol in 100 ml of water) and was then treated with diethyl sulfate (0.6 mol). After standing at room temperature for 3 hr, the reaction mixture was refluxed on a water bath, an ester was then obtained by distillation at 55°C. The crude ester, collected in a receiver cooled in ice water, was washed with 100 ml of a cold 5% sodium carbonate solution and dried over 25 g of anhydrous calcium chloride at 0°C. The product was finally purified by distillation after having been treated with concentrated sulfuric acid. In this procedure, 68 g of a pure ester with a boiling point of 60—62°C were produced.

The Claisen condensation was carried out in the following manner. To 0.55 mol of sodium methoxide

*1 A part of the work has been briefly reported previously: T. Shigematsu, M. Matsui and K. Utsunomiya, This Bulletin, **41**, 763 (1968).

1) M. Lederer, *Nature*, **176**, 462 (1955).
2) W. J. Biermann and H. Gesser, *Anal. Chem.*, **32**, 1525 (1960).
3) R. E. Sievers, B. W. Ponder, M. L. Morris and R. W. Moshier, *Inorg. Chem.*, **2**, 693 (1963).
4) D. K. Albert, *Anal. Chem.*, **36**, 2034 (1964).
5) J. E. Schwarberg and R. W. Moshier, *Talanta*, **11**, 1213 (1964).
6) W. D. Ross, *Anal. Chem.*, **35**, 1596 (1963).
7) K. J. Eisentraut and R. E. Sievers, *J. Am. Chem. Soc.*, **87**, 5254 (1965).
8) C. S. Springer, Jr., D. W. Meek and R. E. Sievers, *Inorg. Chem.*, **6**, 1105 (1967).
9) J. C. Reid and M. Calvin, *J. Am. Chem. Soc.*, **72**, 2948 (1950).
10) J. C. Reid, *ibid.*, **69**, 2609 (1947).
11) A. L. Henne, M. S. Newman, L. L. Quill and R. A. Staniforth, *ibid.*, **69**, 1819 (1947).

suspended in 100 m*l* of dry ether, 0.5 mol of ethyl trifluoroacetate and 0.5 mol of pinacolin were added successively. The mixture was then agitated for 2 hr. After the mixture had stood overnight, the ether and the ethanol were completely removed by evaporation under reduced pressure and by heating at 90°C for 6 hr. The sodium salt of PTA was then treated with 10% sulfuric acid, and the liberated PTA was extracted with ether. The ether solution was dehydrated with anhydrous calcium chloride, and the ether was evaporated off. The PTA was then converted into copper salt, the copper salt was decomposed with 10% sulfuric acid, and finally the PTA was purified by vacuum distillation. The purified product showed a boiling point of 40—41°C/17 mmHg; the yield was about 75%.

Preparation of Rare Earth Metal (III), Sc(III), and Y(III) PTA Chelates. The rare earth chelates were prepared by the method of Sievers *et al.*[8] Rare earth oxides were converted into nitrates, which were dissolved in methanol. Into the rare earth nitrate solution, a PTA methanol solution was then stirred, while the pH of the reacting mixture was maintained between 4 and 5 with a sodium hydroxide solution. The PTA chelates thus precipitated were filtered, air-dried, and recrystallized from benzene. The chelates were finally dried in a vacuum desiccator over phosphorus pentoxide.

The gas chromatograms were obtained with a Yanagimoto GCD-5DH apparatus equipped with a thermal conductivity detector. The column, 75 cm×3 mm i. d. and of stainless steel, was packed with 5% (by weight) of Dow Corning high vacuum silicone grease on Chromosorb W (60—80 mesh). Helium was used as the carrier gas. Chelate solutions were injected with a microsyringe. The thermogravimetric analysis was made with a Shimadzu Thermano Balance. About a 20-mg portion of a sample in a platinum dish was heated at a rate of 10°C/min in a nitrogen stream at a flow rate of 50 ml/min. The infrared spectra were measured with a Perkin-Elmer Model 521 spectrophotometer.

Results and Discussion

The melting points of scandium, yttrium, and rare earth chelates are summarized in Table 1, while the results of elemental analysis for several chelates are shown in Table 2. The carbon and hydrogen contents found are in good agreement with the calculated values of the tris-PTA chelates. In Fig. 1, the infrared spectrum of the erbium chelate (as a representative tervalent rare earth chelate) does not show a band attributable to OH stretching near 3400 cm^{-1}, this fact may prove that the chelates obtained are anhydrous $M^{III}(PTA)_3$-type chelates. The NMR spectrum of $Sc(PTA)_3$ is also presented in Fig. 2.

Figures 3, 4, 5 and 6 show typical chromatograms of some multicomponent mixtures. Samples, which were prepared by dissolving the PTA chelates in

Table 1. The melting points of rare earth PTA chelates

	Mp °C	Color
Lu	160.0—163.2	White
Yb	160.2—161.0	White
Er	158.0—161.2	Pink
Dy	150.0—151.4	White
Tb	141.0—144.0	White
Gd	162.1—164.0	White
Eu	113.8—114.0	Yellow
Sm	113.1—118.0	White
Nd	126.5—128.0	Lavender
Sc	56.5— 57.0	White
Y	160.8—161.2	White

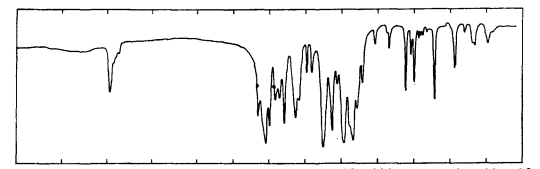

Fig. 1. IR spectrum of $Er(PTA)_3$ in KBr disk.

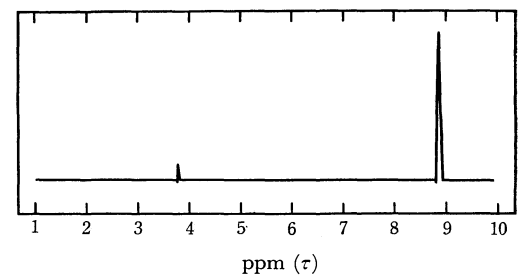

Fig. 2. NMR spectrum of $Sc(PTA)_3$. 20% $Sc(PTA)_3$ in $CDCl_3$, Standard: TMS, Temp.: 24°C

Table 2. Hydrogen and carbon contents

		% C		% H	
	PTA chelate	Calcd	Found	Calcd	Found
$Lu(PTA)_3$	$Lu(C_{24}H_{30}O_6F_9)$	37.91	37.30	3.98	4.12
$Er(PTA)_3$	$Er(C_{24}H_{30}O_6F_9)$	38.30	36.99	4.02	4.05
$Sm(PTA)_3$	$Sm(C_{24}H_{30}O_6N_9)$	39.18	39.09	4.11	4.31
$Nd(PTA)_3$	$Nd(D_{24}H_{30}O_6F_9)$	39.50	36.75	4.14	4.21
$Cu(PTA)_2$	$Cu(C_{16}H_{20}O_4F_6)$	42.34	42.49	4.44	4.55

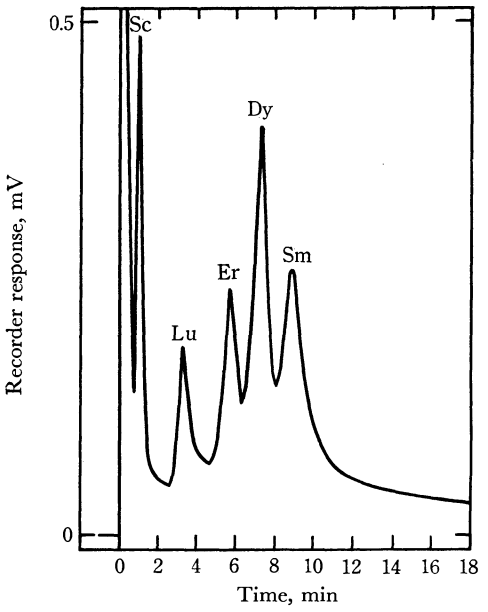

Fig. 3. The separation of $Sc(PTA)_3$, $Lu(PTA)_3$, $Er(PTA)_3$, $Dy(PTA)_3$ and $Sm(PTA)_3$. 23 μg Sc, 86 μg Lu, 83 μg Er, 123 μg Dy and 90 μg Sm in *n*-hexane (25 μl). Column temp.: programmed from 170 to 270°C at 12°C/min. Injection port temp.: 270°C. Helium flow rate: 80 ml/min.

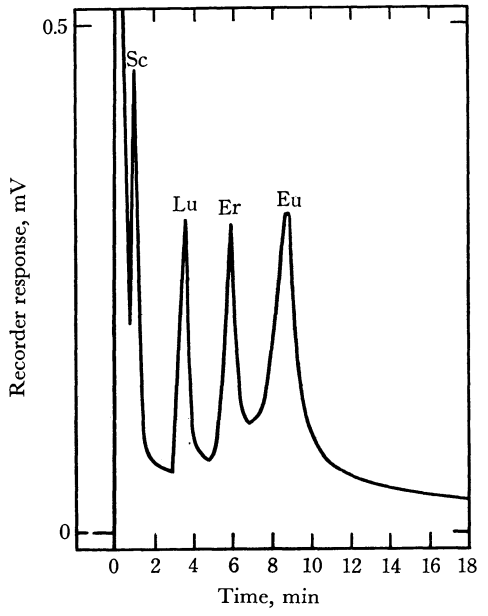

Fig. 4. The separation of $Sc(PTA)_3$, $Lu(PTA)_3$, $Er(PTA)_3$ and $Eu(PTA)_3$. 9 μg Sc, 172 μg Lu, 167 μg Er and 322 μg Eu in *n*-hexane (50 μl). Conditions: same as those in Fig. 3.

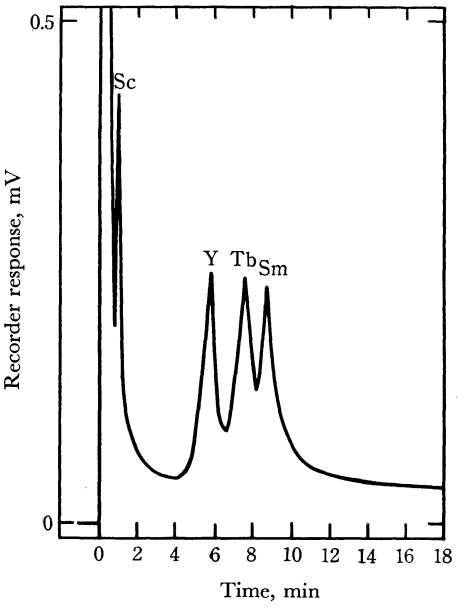

Fig. 5. The separation of $Sc(PTA)_3$, $Y(PTA)_3$, $Tb(PTA)_3$ and $Sm(PTA)_3$. 9 μg Sc, 91 μg Y, 107 μg Tb and 123 μg Sm in *n*-hexane (40 μl). Conditions: same as those in Fig. 3.

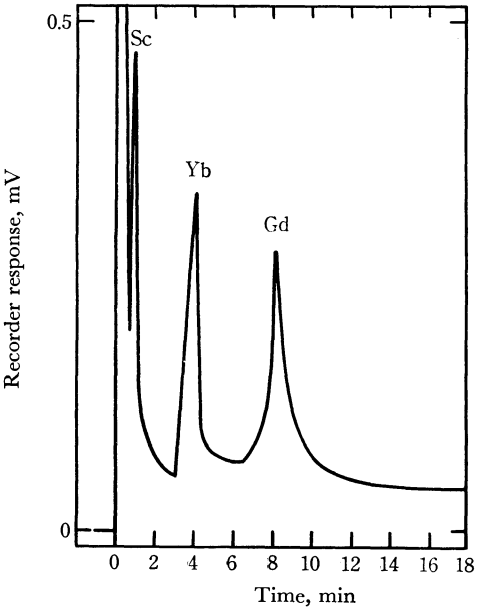

Fig. 6. The separation of $Sc(PTA)_3$, $Yb(PTA)_3$ and $Gd(PTA)_3$. 9 μg Sc, 114 μg Yb and 106 μg Gd in *n*-hexane (40 μl). Conditions: same as those in Fig. 3.

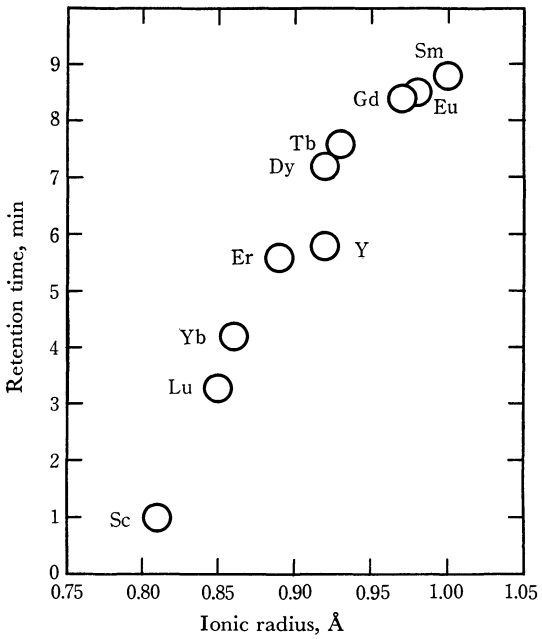

Fig. 7. Retention times for the rare earth PTA chelates as a function of ionic radius. Conditions: same as those in Fig. 3.

25—50 μl of *n*-hexane, were injected (at about 280°C), the column temperature was elevated from 170°C to 260°C at the rate of 12°C/min. For neodymium chelate, a higher injection temperature (*e.g.*, 320°C) was required.

The retention time of each PTA chelate was separately measured under similar condition (see Fig. 3), in Fig. 7, the values are plotted as a function of the ionic radii of the tervalent metal ions. The lower retention time corresponds well to the small ionic radius, as reported by Sievers *et al.* concerning the dipivaroylmethane[7] and FOD[8] chelates. As these figures indicate, it is not yet possible to separate all the rare earth metals individually at the same time. However, there may be a possibility for a group separation or for the separation of mixtures of some rare earth metals which do not contain any neighboring elements.

The thermogravimetric curves are shown in Fig. 8. The chelates of smaller metal ions, which show a shorter retention time, are volatilized at lower temperatures. The weight losses of all the chelates except the neodymium chelate approach 100%; this fact indicates that the PTA chelates are thermally stable in the volatilization process. The TGA curves of heavy rare earth metals and yttrium chelates may represent a combined sublimation-vaporization process, because the curves pass successively through the start of the weight loss, the

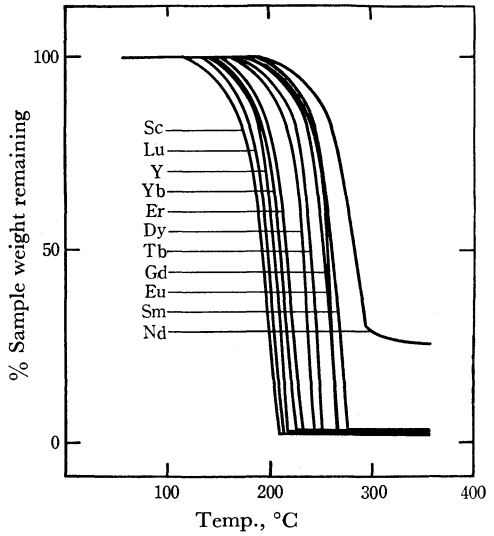

Fig. 8. Thermogravimetric curves of rare earth PTA chelates.

melting temperature of the chelate, and the end of the weight loss.

Sievers and his collaborators[8] mentioned that a fluorocarbon substituent in a ligand markedly increased the volatility of the chelates, and that the volatile ability was also enhanced by substitution with sterically-crowded alkyl groups. Berg and Acosta[12] stated that the thermal stability of β-diketone chelates is related to the hydration (of the chelate), and that anhydrous chelates were much more stable than hydrated ones in the volatilization process.

The authors had previously studied rare earth and several other metal chelates with diisobutyrylmethane,[13] but they could not obtain satisfactory chromatograms for any rare earth metals except lutetium and erbium. Even lutetium and erbium chelates seemed to be hydrated and did not show a 100% weight loss, but one of about 75%, in the TGA curves. On the contrary, dipivaroylmethane and FOD, which possessed a more bulky alkyl group or fluorocarbon group, were proposed as useful chelating reagents for the gas chromatography of rare earth metals. The PTA presented in this investigation has a similar advantage; therefore, rare earth PTA chelates were well eluted by the gas phase. The authors will deal with the participation of the terminal group of β-diketone with the volatile characteristics of the rare earth and other metal chelates in the near future.

12) E. W. Berg and J. J. C. Acosta, *Anal. Chim. Acta*, **40**, 101 (1968).

13) T. Shigematsu, M. Matsui and K. Utsunomiya, *Bull. Inst. Chem. Res., Kyoto Univ.*, **46**, (No.6) (1968).

BULLETIN OF THE CHEMICAL SOCIETY OF JAPAN VOL. 42 1282—1285 (1969)

Coulometric Titration of a Microamount of Water after Conversion to Ammonia

Takayoshi Yoshimori and Syuiti Ishiwari

Faculty of Engineering, Science University of Tokyo, Kagurazaka, Shinjuku-ku, Tokyo

(Received August 15, 1968)

Sodium amide was used to convert a microamount of water into ammonia in a carrier gas. The ammonia was then titrated with coulometrically generated hypobromite ions. The reaction between water and sodium amide was completed stoichiometrically, and the reaction rate was considerably promoted by heating sodium amide at 80°C. The sample hydrogen was oxidized with copper(II) oxide at 800°C, and the water thus produced was determined by this method. 0.096—0.665 m*l* (8.6—59.8 μg) of hydrogen and 0.055—0.465 mg of water in barium chloride crystals were determined within errors of 3.6% and 3.0% respectively. The water adsorbed on the surfaces of the weights was also determined by this method at various humidities.

Many investigations of the coulometric microdetermination of water are to be found in the literature. Meyer and Boyd[1] proposed first the use of a Karl Fischer reagent for this purpose, and several similar papers have followed theirs.[2-4] In this process, however, the location of the end point of the titration is troublesome for determining a microamount of water. The excess iodine produced after the end point usually disappeared when the reducing material was diffused from the cathode compartment.[2]

Keidel[5] proposed the phosphorous pentoxide cell, which is very useful for the continuous analysis of water in gaseous samples.[6] It was, however, recently pointed out that the cell gave relatively large residual current.[7] This current may disturb the precise determination of microamounts of water. Giegerl[8] proposed a method for the coulometric determination of hydrogen in steel. After the oxidation of the hydrogen, the water was heated with carbon at 1100°C; then the hydrogen and carbon monoxide produced were reoxidized to water and carbon dioxide respectively. The latter was then determined by the coulometric titration method. Martin, Floret, and Lemaitre[9] recommended the following process; the water in the carrier gas was converted into hydrogen chloride with phosphorus pentachloride, and then the gas was allowed to flow through a sodium bicarbonate column. The carbon dioxide thus produced was determined by coulometric titration. These circuitous processes give relatively large blank values, and also a long time is needed to make the values constant.

Sodium amide reacts with water to produce ammonia; this reaction has also been applied to the determination of water.[10] No remarkable advantage can, however, be expected when the ammonia is titrated by the ordinary volumetric method.

In this paper, the authors used the coulometric titration method to determine the ammonia produced by the above reaction; they proved that this process can be adopted to determine a microamount of water or hydrogen in the carrier gas.

Experimental

Apparatus. The apparatus for the dehydration of solid samples is shown in Fig. 1. The heating tube for the dehydration of solid samples was made of Pyrex glass. Two different U-tubes of sodium amide (15 cm × 8 mm i. d. for 20—500 μg H_2O; 10 cm × 5 mm i. d. for less than 20 μg H_2O) were used to convert water into ammonia. The U-tube used was heated in a thermostat (oil bath). In order to pack sodium amide and phosphorus pentoxide in the respective U-tubes, the authors used a moistureless glove box. The air in the U-tube was replaced with argon. Unless these precautions are taken,

1) A. S. Meyer and C. M. Boyd, *Anal. Chem.*, **31**, 215 (1959).

2) Y. Yasumori, M. Ikawa and Y. Nozawa, *Bunseki Kagaku* (*Japan Analyst*), **14**, 871 (1965).

3) M. R. Lindbeck and H. Freund, *Anal. Chem.*, **37**, 1647 (1965).

4) R. F. Swensen and D. A. Keyworth, *ibid.*, **35**, 863 (1963).

5) F. A. Keidel, *ibid.*, **31**, 2043 (1959).

6) J. J. Engelsman, A. Meyer and J. Visser, *Talanta*, **13**, 409 (1966).

7) T. Mitsui and K. Nakamura, Lecture to the 16th Analytical Conference Japan, Chiba, Japan (1967).

8) E. Giegerl, *Arch. Eisenhüttenw.*, **33**, 453 (1962).

9) F. Martin, A. Floret and J. Lemaitre, *Bull. Soc. Chim. France*, **1964**, 1836.

10) D. Klamann, *Oesterr. Chemiker Ztg.*, **54**, 165 (1953).

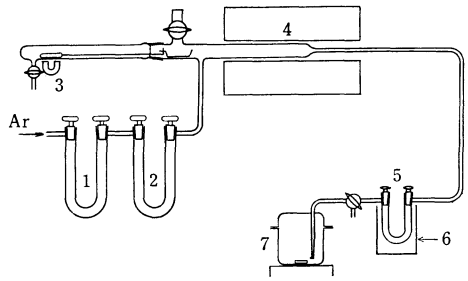

Fig. 1. Apparatus for water determination.
1. $Mg(ClO_4)_2$, 2. P_2O_5, 3. Magnet, 4. Sample heater, 5. $NaNH_2$, 6. Oil bath, 7. Titration cell

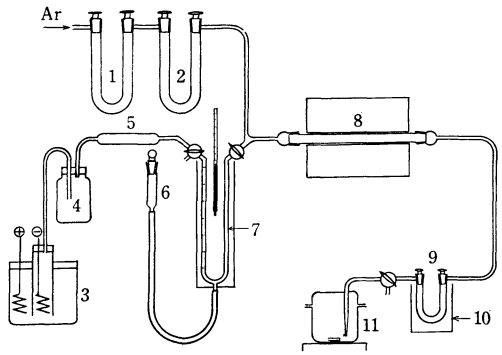

Fig. 2. Apparatus for hydrogen determination.
1. $Mg(ClO_4)_2$, 2. P_2O_5, 3. H_2 generator, 4. Alkaline pyrogallol solution, 5. $CaCl_2$, 6. Mercury reservoir, 7. Gas sampler, 8. CuO, 9. $NaNH_2$, 10. Oil bath (80°C), 11. Titration cell

their expected effectiveness are considerably shortened. The gas-sampling buret proposed by Gieger1[8] (Fig. 2) was advisable for removing the disturbance due to back-pressure of the carrier gas. Copper(II) oxide was used to oxidize the hydrogen. The temperature of the oxide was kept at 800°C.

The coulometric titration cell is shown in Fig. 3. The generator electrode was a platinum foil of 1 × 1 cm. According to the investigation by Christian, Knoblock, and Purdy,[11] the current density for the generation of hypobromite ions should be less than 9.6 mA/cm² in a solution of 1M of bromide ions. Therefore, a current of less than 19 mA was used in this investigation.

The auxiliary electrode was a platinum wire 5 cm in length and 0.5 cm in diameter. The same platinum wires, 0.5 cm in length, were used as the pair of indicator electrodes. The dead-stop method was used to detect the end point of the titration. The indicator current was measured by a microammeter (full scale: 3 μA). The potential difference between the two indicator electrodes was 0.2 V.

The electronic constant current source reported previously[12] and an electric stop clock driven by a

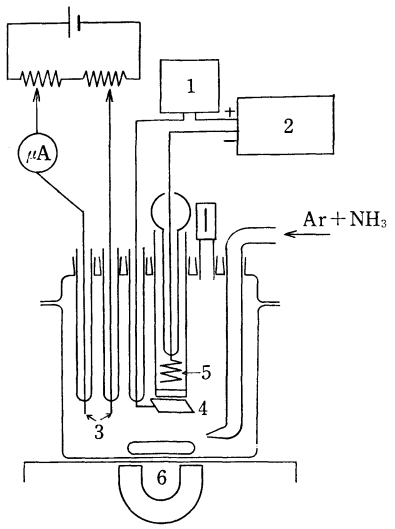

Fig. 3. Coulometric titration apparatus.
1. mA meter (full scale 10 and 30 mA), 2. Constant current source, 3. Indicator electrode pair, 4. Generator electrode, 5. Auxiliary electrode 6. Magnetic stirrer

synchronous motor were used to measure the electricity. The total error due to the measurements of the electrolytic current and of the time does not exceed 0.5%.

Reagents. *Sodium Borate Solution.* 38.1 g of sodium borate (Borax) were dissolved in 1 *l* of water; then perchloric acid was added until the pH of the solution decreased to 8.6.

The electrolyte solution was prepared by mixing 25 m*l* of a 5M sodium bromide solution and 50 m*l* of the sodium borate solution, and by then diluting the mixture to 125 m*l* with water. The above mentioned sodium borate solution was used as a catholyte. Sodium amide produced by the Daiichi Pure Chemicals Co., Ltd., could be used without any trouble. All the other reagents used were analytical grade.

Argon was dried with magnesium perchlorate and then with phosphorus pentoxide.

Procedure. *Setup of the Apparatus.* To decrease and to stabilize the blank value quickly, a column of sodium amide was heated at 110°C for half an hour; then it was cooled somewhat and kept at 80°C. During this period, argon was allowed to flow through the apparatus, but it was not introduced into the titration cell. The rate of the flow of argon was 200 or 100 ml/min. Argon was then introduced into the column and the cell by turning a three-way cock. The blank values were determined coulometrically every 5 or 10 min until the values became constant.

Introduction of Sample. The process used for sampling gaseous hydrogen was that shown by Gieger1.[8] First, U-tube buret was filled with mercury; then electrolytically generated hydrogen was introduced into the capillary buret on one side of the U-tube. After the measurement of the volume of hydrogen, a small amount of it was transferred to the tube on the other side by lowering the mercury reservoir. The transferred hydrogen was then introduced into the reaction tube containing copper(II) oxide, after which the volume of hydrogen

11) G. D. Christian, E. C. Knoblock and W. C. Purdy, *Anal. Chem.*, **35**, 2217 (1963).

12) T, Yoshimori, Y. Hino and T. Takeuchi, *Bunseki Kagaku* (*Japan Analyst*), **15**, 1234 (1966).

remaining in the buret was measured again. The difference between the two readings was the volume of hydrogen taken.

A weighed solid sample was dropped into the dried boat in the dehydration tube by the aid of a small glass funnel. The boat was then introduced into a furnace kept at 200°C by the movement of a magnet. After 10 min, the boat was removed from the furnace. Argon was allowed to flow through the apparatus continuously. The rate of the flow of argon should not exceed 200 ml/min. Lower results could be obtained at the rate of 400 ml/min with the sodium amide column mentioned above. By using a longer column, the rate of argon can perhaps be increased.

Coulometric Titration. The electrolyte prepared as above was electrolyzed with a constant current until the indicator current was raised to a definite value smaller than 1.0 μA. After recording the indicator current, argon containing ammonia was introduced into the cell. After 5 or 10 min, the titrant was generated electrolytically with a constant current until the indicator current was increased to the previous value. This titration was repeated at 5- or 10-min intervals until the electricity of the blank experiment. During the entire course of the titration, argon was allowed to flow through the apparatus and the cell continuously.

Results and Discussion

Determination of Hydrogen. Hydrogen was measured into a reaction tube containing copper-(II) oxide and heated at about 800°C using Giegerl's buret.[8] The water thus produced was determined by this method. The results obtained are shown in Table 1.

The reaction of water in a carrier gas with sodium amide is completely stoichiometric. Therefore, a standard sample or a calibration curve is not necessary. This makes it possible to obtain reliable and accurate results in the determination of micro-amounts of water.

To shorten the time required for a single determination, the heating of sodium amide is quite effective. Blank values, however, increase appreciably over 90°C. The relations obtained in the analysis of hydrogen are shown in Fig. 4. The heating of the column at 80°C is preferable.

Table 1. Determination of hydrogen

H_2 taken (ml)	H_2 found (ml)	Recovery (%)
0.096	0.092	96
0.126	0.121	96
0.209	0.207	99
0.231	0.217	94
0.241	0.245	102
0.343	0.338	99
0.351	0.348	99
0.490	0.481	98
0.508	0.542	107
0.665	0.680	102
	mean	99.2
	$\sqrt{V}$	3.6

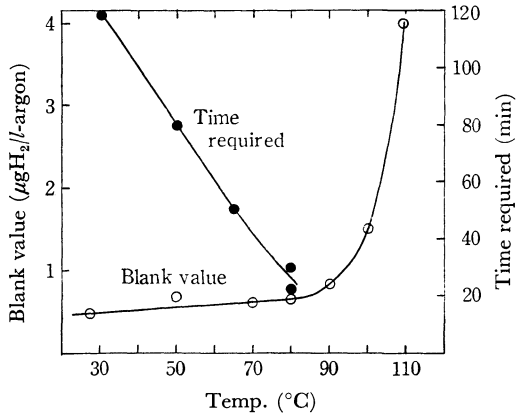

Fig. 4. Effects of heating of $NaNH_2$ column on the blank value and on the time required for single determination of hydrogen.

The increase in the blank value at a temperature higher than 90°C may be based on the some decomposition of the amide.[13] In accounting for the heating effects of the column, the authors considered the following possibility. Some of the water in argon may be adsorbed on the surface of the sodium hydroxide produced by the reaction of water and sodium amide, and the vapor pressure of water on the surface of the hydroxide may be increased at an elevated temperature.[14] These phenomena accelerate the desorption of water on the surface of sodium hydroxide and quickly complete the reaction of water and sodium amide.

In the field of gas chromatography, calcium carbide has sometimes been used for removing the tailing effect due to water in a sample. The present authors tried to use carbide to convert water into acetylene, and then the acetylene was oxidized to carbon dioxide and water. The carbon dioxide thus produced was determined by coulometric titration. This process, however, has the following disadvantages. The calcium hydroxide produced by the reaction between water and the carbide has a relatively high vapor pressure of water. Therefore, it reacts slowly with calcium carbide to produce acetylene. The reaction rate of this process is very slow even at elevated temperatures. More than 3 hr are needed for a single determination even if the carbide has previously been heated at several hundred degrees. The other problem was the purity of the carbide. Different kinds of commercially obtainable carbides and the carbide produced specially by the authors were all used.

13) Gmelin, Handbuch für anorg. Chemie, "Natrium," 8 Aufl., s. 211 (1928).
14) *Ibid.*, s. 255.

The blank values were, however, not decreased enough with these reagents.

Roth and his co-workers[15] has proposed a process to convert water into ammonia with magnesium nitride. This process was also attempted by the present authors with the aid of coulometric titration; they found the same difficulties as in the calcium carbide process.

Since sodium hydroxide does not itself set free water, it is unnecessary to consider these difficulties. By the present method, the time required for a single determination and the blank value of each determination are considerably decreased. Furthermore one mole of water is equivalent to three Faradays of electricity. This ratio is greater than in any of the other processes mentioned above. These advantages show the adaptability of this method to determine microamounts of water and hydrogen in various carrier gases which do not react with sodium amide.

Table 2. Determination of water in barium chloride dihydrate

Sample taken (mg)	H_2O calcd (mg)	H_2O found (mg)	H_2O recovery (%)
0.37	0.055	0.054	98
0.50	0.074	0.079	107
0.59	0.087	0.087	100
1.04	0.153	0.148	97
1.09	0.161	0.158	98
1.47	0.217	0.210	97
1.63	0.240	0.232	97
2.13	0.314	0.312	99
3.16	0.466	0.465	100
		mean	99.2
		$\sqrt{V}$	3.0

Determination of Water in Hydrated Barium Chloride Crystal. A weighed crystal of hydrated barium chloride was dropped into the boat in the reaction tube, and then the boat was introduced into the heating furnace by the aid of a magnet. The water content in the crystal was determined by this method. The temperature of the furnace was kept at 200°C, and the rate of flow of argon was 200 ml/min. The results obtained are shown in Table 2. In order to recover the water in the crystal completely, a somewhat longer time was needed than for the determination of hydrogen. Because of the water adsorbed on the surface of the crystal, these results were somewhat larger than their theoretical values. Considerably higher results could be obtained when the sample did not consist of a single crystal.

Table 3. Adsorbed water on the surfaces of weights (in μg)

	Kind of weight (mg)	Relative humidity (%) 55	66	76	80
Platinum	100	0.22			0.50
	200	0.49			0.62
	500	0.39			0.93
	Kind of weight (mg)	Relative humidity (%)	66	76	80
Stainless steel	100*		0.62	0.50	1.03
	200*		0.72	0.62	1.05
	500		0.16	—	0.84
	Kind of weight (mg)	Relative humidity (%) 58			
German silver	100	0.43			
	200	0.56			
	500	0.87			

* Surface is somewhat rough.

Determination of Water Adsorbed on the Surfaces of Weights. As an example of the practical use of this method, the water adsorbed on the surfaces of the weights was determined at various humidities. The appratus and the method were the same as in the case of barium chloride. The results obtained for various kinds of weights are shown in Table 3.

These results show that the water adsorbed on the weight depends greatly on the condition of the surface, and not so greatly on the relative humidity. It can be concluded that the water adsorbed on the surfaces of weights does not disturb the ordinary weighings with a microbalance.

15) F. Roth and A. Schulz, *Brennstoff Chem.*, **20**, 317 (1939); F. Roth, *ibid.*, **22**, 77 (1941); F. Roth and A. Schnoor, *ibid.*, **22**, 89 (1941).

BULLETIN OF THE CHEMICAL SOCIETY OF JAPAN VOL. 42 1286—1291 (1969)

Absorption Spectra and Circular Dichroisms of Metal Complexes. III.*1 *trans*-Dihalogeno-bis-*l*-propylenediamine Complexes of Cobalt(III), Rhodium(III), Palladium(IV) and Platinum(IV)

Haruko Ito, Junnosuke Fujita and Kazuo Saito

Department of Chemistry, Faculty of Science, Tohoku University, Katahiracho, Sendai

(Received August 21, 1968)

Absorption (AB) and circular dichroism (CD) spectra of *trans*-$[MX_2(l\text{-pn})_2]^{n+}$ (where M= Rh^{III}, Pd^{IV}- and Pt^{IV}-, and X=Cl^- and Br^-) have been discussed by comparing them with those of cobalt(III) complexes which had been studied extensively. A positive CD peak was observed at around the so called I_a band region of all the complexes studied except for *trans*-$[PtBr_2(l\text{-pn})_2]^{2+}$. A negative CD peak of this complex ion at 26000 cm^{-1} was assigned to be a split component of the I_a band. The AB peaks at 38000, 28600 and 31100 cm^{-1} for *trans*-$[PtCl_2(l\text{-pn})_2]^{2+}$, *trans*-$[PdCl_2(l\text{-pn})_2]^{2+}$ and *trans*-$[PtBr_2(l\text{-pn})_2]^{2+}$ respectively were assigned to $p_\pi \rightarrow d_{z^2}$ charge transfer transition. An ion association band was observed for *trans*-$[PtBr_2(l\text{-pn})_2]Br_2$ in 1N hydrobromic acid.

In the first paper of this series,[1] the absorption spectra of square planar platinum(II), palladium(II) and gold(III) complexes containing optically active diamines were interpreted on the basis of an analysis of their circular dichroism spectra. The present paper deals with the AB and CD spectra of octahedral platinum(IV) and palladium(IV) complexes of the type, *trans*-$[MX_2(l\text{-pn})_2]^{2+}$ (X=Cl^- and Br^-, *l*-pn=$(-)_D$-propylenediamine).

Since both platinum(IV) and palladium(IV) ions have strong tendency to form diamagnetic d^6 complexes, their AB spectra are expected to resemble those of cobalt(III) and rhodium(III) complexes.

However, assignment of their absorption bands still remains uncertain, partly because both the *d–d* transition and the charge transfer band appear in overlapping regions. The trans complexes in this paper have no optical dissymmetry around the central metal ion, but give CD peaks due to the vicinal effect coming from asymmetric ligands. Usefulness of the examination of these peaks for the band assignment has been demonstrated with various cobalt(III),[2,3] platinum(II) and palladium(II) complexes.[1]

We have attempted, therefore, to assign tentatively the absorption bands of some platinum(IV) and palladium (IV) complexes by comparing their CD spectra with those of cobalt (III) complexes which had been studied extensively.

Experimental

Preparations of the Complexes. Six new complexes were prepared by the following methods.

trans-Dichloro-bis-l-propylenediaminepla tinum(IV) Chloride monohydrate, *trans*-$[PtCl_2(l\text{-pn})_2]Cl_2\cdot H_2O$, *trans-Dichloro-bis-l-cyclohexanediaminepla tinum(IV) Chloride Monohydrate*, *trans*-$[PtCl_2(l\text{-chxn})_2]Cl_2\cdot H_2O$ and *trans-Dibromo-bis-l-propylenediaminepla tinum (IV) Bromide Monohydrate*, *trans*-$[PtBr_2(l\text{-pn})_2]Br_2\cdot H_2O$ were prepared from $[Pt(l\text{-pn})_2]Cl_2$ and $[Pt(l\text{-chxn})_2]Cl_2$ and halogens by Basolo, Bailar and Tarr's method[4] for the corresponding ethylenediamine complexes. The dichloro complexes were recrystallized from an aqueous solution by adding ethanol. The dibromo complex was converted into bromide by dissolving it in 3N hydrobromic acid and evaporating on a water bath. *trans*-$[PtCl_2(l\text{-pn})_2Cl_2$ and *trans*-$[PtBr_2(l\text{-pn})_2]Br_2$ were converted into perchlorate by dissolving them in a small amount of water and adding concentrated perchloric acid. The crystals were filtered off, dried over potassium hydroxide *in vacuo*.

trans-Dichloro-bis-l-propylenediaminepalladium(IV) Nitrate, *trans*-$[PdCl_2(l\text{-pn})_2](NO_3)_2$ was prepared by a similar method to that for *trans*-$[PdCl_2(en)_2](NO_3)_2$[5] in bright yellow crystals.

trans-Dibromo-bis-l-propylenediaminerhodium(III) Perchlorate, *trans*-$[RhBr_2(l\text{-pn})_2]ClO_4$. Seven hundred milligrams of $RhBr_3\cdot 2H_2O$, 1.13 g of *l*-pn·2HCl and 0.43 g of potassium hydroxide were dissolved in 50 ml of water, heated on a water bath with reflux, treated with a solution containing 0.43 g potassium hydroxide in 50 ml of

*1 Part II, K. Ohashi, J. Fujita, B. Shimoyama and K. Saito, This Bulletin, **41**, 2422 (1968).

1) H. Ito, J. Fujita and K. Saito, *ibid.*, **40**, 2584 (1967).

2) R. A. D. Wentworth and T. S. Piper, *Inorg. Chem.*, **4**, 202 (1965).

3) C. J. Hawkins, E. Larsen and I. Olsen, *Acta Chem. Scand.*, **19**, 1915 (1965).

4) F. Basolo, J. C. Bailar, Jr., and B. R. Tarr, *J. Am. Chem. Soc.*, **72**, 2433 (1950).

5) A. V. Babaeva and E. Ya. Khananova, *Russ. J. Inorg. Chem.*, **10**, 1441 (1965).

Table 1. Chemical analysis of the complexes

Complexes	C (%)		H (%)		N (%)	
	Calcd	Obsd	Calcd	Obsd	Calcd	Obsd
$[PtCl_2(l\text{-pn})_2]Cl_2\cdot H_2O$	14.32	14.74	4.41	4.71	11.13	10.97
$[PtCl_2(l\text{-chxn})_2]Cl_2\cdot H_2O$	24.71	24.59	5.18	5.70	9.60	9.06
$[PtBr_2(l\text{-pn})_2]Cl_2\cdot H_2O$	12.18	12.12	3.75	4.00	9.46	8.98
$[PtCl_4(l\text{-pn})]$	8.77	9.60	2.45	2.27	6.82	6.63
$[PtBr_4(l\text{-pn})]$	6.12	6.80	1.70	2.14	4.76	4.50
$[PdCl_2(l\text{-pn})_2](NO_3)_2$	16.03	16.25	4.48	4.75	18.69	18.24
$[RhCl_2(l\text{-pn})_2]ClO_4$	17.10	17.28	4.78	4.87	13.29	12.51
$[RhBr_2(l\text{-pn})_2]ClO_4$	14.12	13.80	3.95	4.09	10.98	11.22
$[CoCl_2(l\text{-pn})_2]Cl\cdot 2H_2O$	20.62	20.97	6.92	6.88	16.03	16.27
$[CoBr_2(l\text{-pn})_2]Br_2\cdot 2H_2O$	17.23	17.70	5.79	5.34	13.40	12.54
$[PtCl_2(l\text{-pn})_2](ClO_4)_2$	11.75	11.68	3.29	3.36	9.14	8.87
$[PtBr_2(l\text{-pn})_2](ClO_4)_2$	10.27	10.34	2.87	3.20	7.98	7.78

water dropwise, heated for about 2 hr and filtered. The filtrate was passed through a column containing cation exchanger Dowex 50 W in H form. The column was washed with water and the adsorbed band eluted with 3% hydrobromic acid. The eluate was evaporated to dryness *in vacuo* at 60°C. The residue was extracted with methanol and treated with ether. The precipitate was dissolved in a small amount of water and concentrated perchloric acid was added. The product was recrystallized from methanol solution by adding ether.

Tetrabromo-l-propylenediamineplatinum(IV), $[PtBr_4(l\text{-pn})]$ was obtained by oxidizing $[PtBr_2(l\text{-pn})]$ in water with bromine. Orange crystals were precipitated by concentrating the solution on a water bath.

The other complexes were prepared by the method described in the literatures.[2,3,6,7]

The results of the chemical analysis are given in Table 1.

Measurements. Visible and ultraviolet absorption spectra were obtained by using a Hitachi 124 recording spectrophotometer. The CD curves were recorded with a Model ORD/UV-5 spectrophotometer of Japan Spectroscopic Co. with its CD attachment.

To avoid the aquation of coordinated halides, cobalt and rhodium complexes, *trans*-$[PtCl_2(l\text{-pn})_2](ClO_4)_2$ and *trans*-$[PtBr_2(l\text{-pn})_2](ClO_4)_2$ were dissolved in methanol, and *trans*-$[PtCl_2(l\text{-pn})_2]Cl_2$, *trans*-$[PtCl_2(l\text{-chxn})_2]Cl_2$ and *trans*-$[PdCl_2(l\text{-pn})_2](NO_3)_2$ in 1.0N hydrochloric acid. All the measurements were made at room temperature.

Results and Discussion

The AB and CD spectra of the complexes measured are shown in Figs. 1—5. The CD spectra of *trans*-$[CoX_2(l\text{-pn})_2]^+$ (X=Cl^- and Br^-)[2,3] and *trans*-$[RhCl_2(l\text{-pn})_2]^+$ [6] had been measured only in the region of *d*→*d* transitions of these complexes.

d-d Transition. Since the complex ions, *trans*-$[MX_2(l\text{-pn})_2]^{n+}$ have a pseudo-tetragonal symmetry, the two spin-allowed *d*→*d* transitions expected for a d^6-diamagnetic system, $^1A_1\rightarrow{}^1T_1$ and $^1A_1\rightarrow{}^1T_2$, should split into two components, $^1A_1\rightarrow{}^1A_1+{}^1E^{(a)}$ and $^1A_1\rightarrow{}^1B_2+{}^1E^{(b)}$, respectively. Of these four transitions, only the $^1A_1\rightarrow{}^1B_2$ is magnetically forbidden.

Fairly strong positive CD peaks at 16600 and 15600 cm^{-1} for dichloro- and dibromo-cobalt(III)

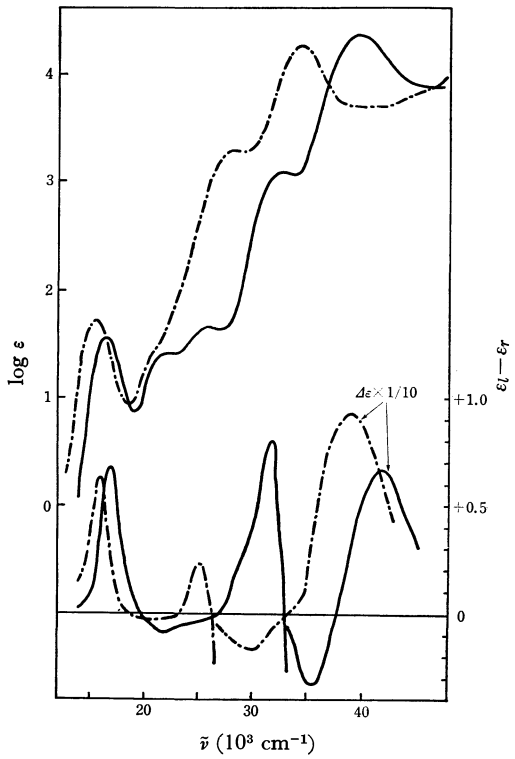

Fig. 1. AB and CD spectra of *trans*-$[CoCl_2(l\text{-pn})_2]$-Cl (——) and *trans*-$[CoBr_2(l\text{-pn})_2]$ Br (-·-·-) in methanol.

6) S. K. Hall and B. E. Douglas, *Inorg. Chem.*, **7**, 533 (1968); J. H. Dunlop and R. D. Gillard, *Mol. Phys.*, **7**, 494 (1964).

7) F. P. Dwyer and A. M. Sargeson, *J. Am. Chem. Soc.*, **81**, 5272 (1959).

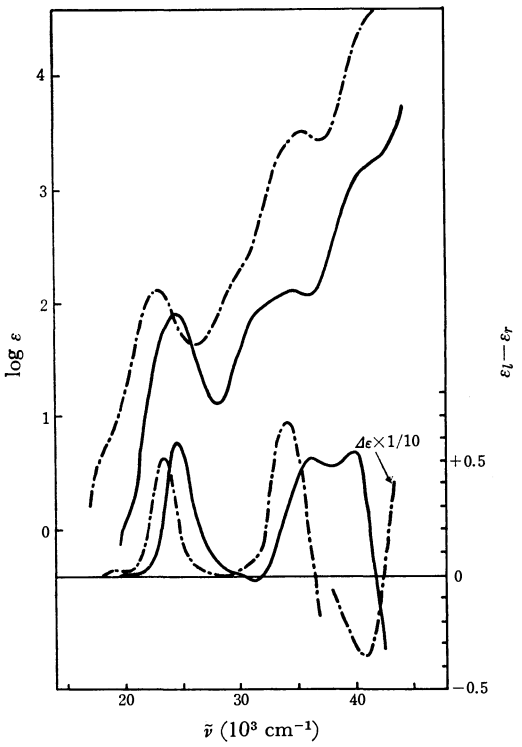

Fig. 2. AB and CD spectra of *trans*-[$RhCl_2$-(*l*-pn)$_2$]-ClO_4 (——) and *trans*-[$RhBr_2$(*l*-pn)$_2$] ClO_4 (-·-·-) in methanol.

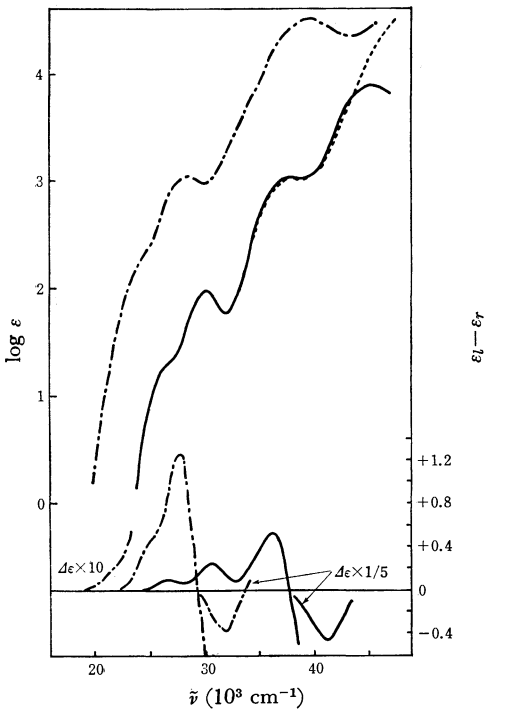

Fig. 3. AB and CD spectra of *trans*-[$PtCl_2$(*l*-pn)$_2$]-Cl_2 (-----) and *trans*-[$PdCl_2$ (*l*-pn)$_2$] $(NO_3)_2$ (-·-·-) in 1N hydrochloric acid and those of *trans*-[$PtCl_2$-(*l*-pn)] $(ClO_4)_2$ in methanol (——).

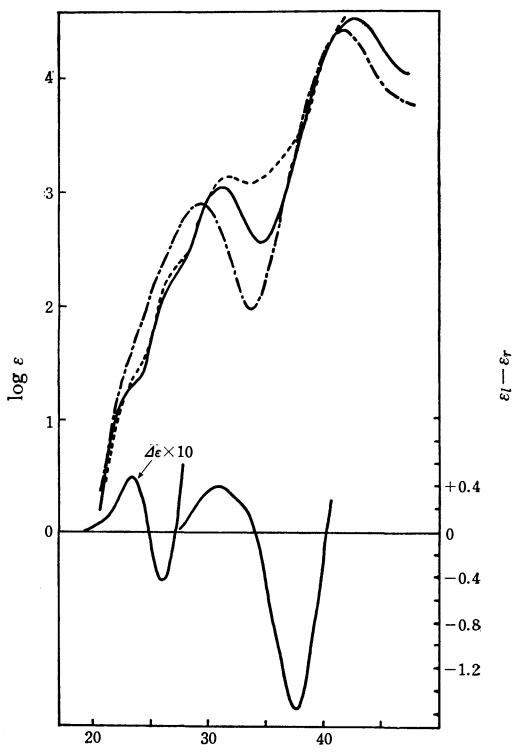

Fig. 4. AB and CD spectra of *trans*-[$PtBr_2$(*l*-pn)$_2$]-$(ClO_4)_2$ in methanol (——) and AB spectrum of *trans*-[$PtBr_2$(*l*-pn)$_2$]Br_2 in 1N hydrobromic acid (------) and that of *trans*-K_2[$PtBr_2(CN)_4$] (-·-·-).

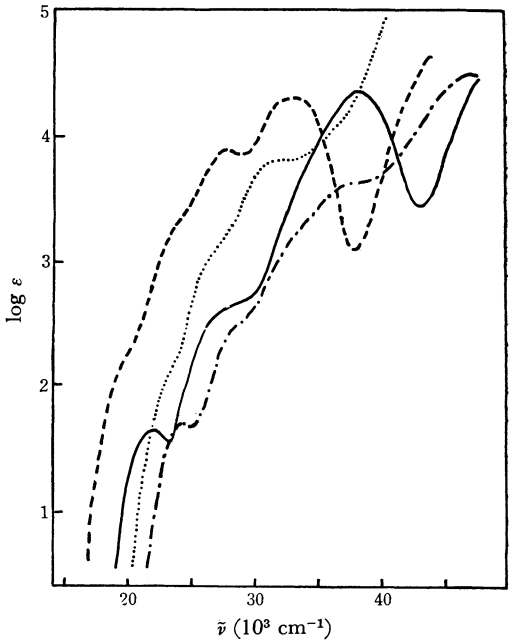

Fig. 5. AB spectra of $K_2[PtCl_6]$ (——) and [$PtCl_4$-(*l*-pn)] (-·-·-) in 1N hydrochloric acid and those of $K_2[PtBr_6]$ (------) and [$PtBr_4$(*l*-pn)] (·····) in 1N hydrobromic acid.

complexes, respectively, have been assigned to the $^1A_1 \rightarrow {}^1E^{(a)}$ transition (I_a band), a split component of the so-called first band[2,3,8] (Fig. 1).

The CD and AB spectra of rhodium(III) complexes are very similar to those of cobalt(III) complexes, except that the transition energies are higher in the former complexes (Fig. 2). Therefore, the positive CD bands at 24600 cm^{-1} for dichloro- and at 23500 cm^{-1} for dibromo complexes of rhodium(III) can reasonably be assgined to $^1A_1 \rightarrow {}^1E^{(a)}$ transition (I_a band).

The AB spectrum of *trans*-$[PdCl_2(l\text{-pn})_2]^{2+}$ exhibits no distinct ligand field bands because of the overlapping of strong charge transfer bands (Fig. 3). However, a positive CD shoulder appears at about 24500 cm^{-1} corresponding to a shoulder AB band in the same energy region. Since this frequency value is almost the same as that of I_a band of rhodium(III) complex with an isoelectronic structure, this shoulder band could be assigned to the $^1A_1 \rightarrow {}^1E^{(a)}$ transition (I_a).

Both *trans*-$[PtCl_2(l\text{-pn})_2]^{2+}$ and *trans*-$[PtCl_2(l\text{-chxn})_2]^{2+}$ show two positive CD peaks in the ligand field band region (at around 26500 and 30500 cm^{-1}) (Fig. 3). The absorption intensities of these bands indicate that the positive CD peak at the longer wavelength could correspond to the spin-forbidden transition, and the other positive peak at the shorter wavelength to the spin-allowed $^1A_1 \rightarrow {}^1E^{(a)}$ transition, although the CD intensity is relatively weak. The rhodium(III) complexes and the palladium(IV) complex show also a trace of positive CD band in the region of their spin-forbidden $d \rightarrow d$ transition (see Figs. 2 and 3).

trans-$[PtBr_2(l\text{-pn})_2]^{2+}$ gives no definite AB peak corresponding to the $d \rightarrow d$ transitions, but its CD spectrum exhibits a weak positive and a weak negative band at 23300 and 26000 cm^{-1} respectively (Fig. 4). Comparison with the data for the other complexes described above suggests that the positive CD component would be due to the spin-forbidden $d \rightarrow d$ transition.

The negative CD peak, however, should not be assigned to the I_a band, since the energy difference between this band and the I_a band of *trans*-$[PtCl_2(l\text{-pn})_2]^{2+}$ amounts to about 4500 cm^{-1}, which is somewhat too large as compared with the difference between the I_a band of dichloro- and that of dibromo complex of cobalt(III) (1000 cm^{-1}) and rhodium(III) (1100 cm^{-1}). The actual symmetry of *trans*-$[MX_2(l\text{-pn})_2]^{n+}$ ion should be lower than D_{4h}, and $^1A_1 \rightarrow {}^1E^{(a)}$ transition can split further into two components. Hawkins *et al.*[3] observed another weak negative CD band at longer wavelength side of the strong positive peak (I_a) for *trans*-$[CoCl_2(l\text{-pn})_2]^+$ ion and assigned both of them to the components resulting from the splitting of degenerate $^1A_1 \rightarrow {}^1E^{(a)}$ transition. We also observed a weak negative peak at 18600 cm^{-1} of *trans*-$[RhBr_2(l\text{-pn})_2]^+$ ion in 3N hydrobromic acid solution. Thus, the weak negative CD band of *trans*-$[PtBr_2(l\text{-pn})_2]^+$ at 26000 cm^{-1} may be considered to be a split component of this type. The positive CD component corresponding to I_a band might be hidden by the positive CD peak of charge transfer transition, which is discussed below.

The AB spectra of $[PtCl_4(l\text{-pn})]$ and $[PtBr_4(l\text{-pn})]$ are very similar to those of $K_2[PtCl_6]$ and $K_2[PtBr_6]$, respectively (Fig. 5). Thus, on the basis of the results of spectroscopic study reported by Jørgensen,[9] the positive CD peaks at 24100 cm^{-1} for tetrachloro and 21500 cm^{-1} for tetrabromo complex were assigned to spin-forbidden bands and those at 28700 cm^{-1} for tetrachloro and 26500 cm^{-1} for tetrabromo complexes were assgined to the $^1A_1 \rightarrow {}^1E^{(a)}$ transition (assumed as pseudo D_{4h} symmetry[6]).

Concerning the so-called second absorption bands, a weak negative and a positive CD were observed for *trans*-$[CoCl_2(l\text{-chxn})_2]^+$, which were assigned to be $^1A_1 \rightarrow {}^1B_2$ and $^1A_1 \rightarrow {}^1E^{(b)}$ transition, respectively.[8] On the basis of these data, the positive CD peak at 36500 cm^{-1} of *trans*-$[RhCl_2(l\text{-pn})_2]^+$ is considered to correspond to the $^1A_1 \rightarrow {}^1E^{(b)}$ transition, though its CD intensity is somewhat too large for the magnetically forbidden II band (in O_h symmetry).

Charge Transfer Transition. It is well known that complex ions, $[CoX(NH_3)_5]^{2+}$ and $[CoX_2(NH_3)_4]^+$, where X=Cl^- and Br^-, have two intense bands in the ultraviolet region of their spectra. These are interpreted on the basis of LCAO-MO theory to be charge transfer bands from p orbitals of the halide ion to mainly d_z^2 orbital of the cobalt(III) ion,[10] the one at longer wavelength involving $p_\pi \rightarrow d_z^2$ and the other at shorter wavelength $p_\sigma \rightarrow d_z^2$ transition. Two intense bands were observed for all the complexes studied in this work except for *trans*-$[RhCl_2(l\text{-pn})_2]^+$ in the ultraviolet region, which are expected to be of the same nature as those of cobalt(III) complexes. The energy of $p_\sigma \rightarrow d_z^2$ transition of *trans*-$[RhCl_2(l\text{-pn})_2]^+$ is too high to be measured, and only the $p_\pi \rightarrow d_z^2$ band was observed.

In the CD spectra, three CD peaks appear in the charge transfer band region, a relatively weak positive, a strong negative and a strong positive peak from longer to shorter wavelength. According to Treptow,[8] *trans*-$[MX_2(l\text{-chxn})_2]^{n+}$ ion (approximated as D_{4h} symmetry) can have three charge transfer transitions from halide ions to d_z^2 orbital; of these two are $p_\pi \rightarrow d_z^2$ and one is $p_\sigma \rightarrow d_z^2$.

As can be seen in Figs. 3 and 4, the CD behavior of the bands at 38000 cm^{-1} for *trans*-$[PtCl_2(l\text{-}$

8) R. S. Treptow, *Inorg. Chem.*, **5**, 1593 (1966).

9) C. K. Jørgensen, *Acta Chem. Scand.*, **10**, 518 (1956).

10) H. Yamatera, *J. Inorg. Nucl. Chem.*, **15**, 50 (1960).

Table 2. Numerical data of absorption and circular dichroism ($\tilde{\nu}$ in 10^3 cm^{-1})

	AB $\tilde{\nu}_{max}$(log ε)	CD $\tilde{\nu}_{max}(\varepsilon_l - \varepsilon_r)$	Assignment
$[CoCl_2(l\text{-pn})_2]Cl\cdot 2H_2O$[a]	16.4(1.61)	16.6(+0.76)	E[a]
	21.7(1.45)	21.6(−0.10)	A_2
	25.6(1.70)	~25 (−0.04)	B_2
	32.6(3.14)	31.3(+0.91), 35.2(−3.6)	$p_\pi \rightarrow d_{z^2}$
	39.7(4.42)	41.7(+7.6)	$p_\sigma \rightarrow d_{z^2}$
$[CoBr_2(l\text{-pn})_2]Br\cdot 2H_2O$[a]	~13 (0.4)		
	15.4(1.76)	15.6(+0.69)	E[a]
	~20.5(1.3)	20.4(−0.02)	A_2
	~23 (1.9)	~22.5(−0.02)	B_2
	28.3(3.34)	25.1(+0.27), 31.1(−1.8)	$p_\pi \rightarrow d_{z^2}$
	34.3(4.30)	38.5(+10.3)	$p_\sigma \rightarrow d_{z^2}$
$[RhCl_2(l\text{-pn})_2]ClO_4$[a]	~20	~20 (+)	Triplet
	24.7(1.92)	24.6(+0.59)	E[a]
	~31.5(1.9)	31.0(−0.03)	A_2
	34.8(2.12)	36.5(+0.51)	E[b]
	~42(~3.1)	40.0(+0.55), >44(>−3.5)	$p_\pi \rightarrow d_{z^2}$
$[RhBr_2(l\text{-pn})_2]ClO_4$[a]		~16.5(+0.006)[b]	Triplet
	23.40(2.11)	18.6(−0.010)[b], 23.5(+0.51)	E[a]
		26.7(−0.051)	A_2
	30 (2.2)		B_2
	35.7(3.50)	34.1(+0.67), ~40 (−3.6)	$p_\pi \rightarrow d_{z^2}$
	42.4(4.57)	>43.5(>+4.2)	$p_\sigma \rightarrow d_{z^2}$
$[PdCl_2(l\text{-pn})_2](NO_3)_2$[a]	~24 (2.1)	~24.5(+0.4)	E[a]
	28.6(3.03)	27.8(+1.3), 32.0(−1.8)	$p_\pi \rightarrow d_{z^2}$
	39.5(4.49)	(+)	
$[PtCl_2(l\text{-pn})_2](ClO_4)_2$[a]	~26.5(1.2)	26.6(+0.13)	Triplet
	30.2(1.99)	30.5(+0.27)	E[a]
	38.0(3.0)	36.2(+0.76), 41.7(−1.8)	$p_\pi \rightarrow d_{z^2}$
	44.8(3.89)	>44.4(>+0.8)	$p_\pi \rightarrow d_{z^2}$
$[PtCl_2(l\text{-pn})_2]Cl_2\cdot H_2O$[c]	~26.5(1.2)	26.7(+0.11)	Triplet
	30.3(1.98)	30.6(+0.25)	E[a]
	38.0(3.03)	36.4(+0.54), 41.2(−2.2)	$p_\pi \rightarrow d_{z^2}$
$[PtCl_2(l\text{-chxn})_2]Cl_2\cdot H_2O$[c]	~26.5(1.2)	26.5(+0.17)	Triplet
	30.1(2.03)	30.1(+0.35)	E[a]
	38.0(3.18)	35.7(+0.62), 39.4(−1.36)	$p_\pi \rightarrow d_{z^2}$
$[PtBr_2(l\text{-pn})_2](ClO_4)_2$[a]	~23.5(1.3)	23.3(+0.05)	Triplet
	~26.5(2.2)	26.0(−0.04)	E[a]
	31.1(3.05)	~30.5(+0.4), ~38 (−1.7)	$p_\pi \rightarrow d_{z^2}$
	42.6(4.51)	>43.5(>+5.5)	$p_\sigma \rightarrow d_{z^2}$
$[PtCl_4(l\text{-pn})]$	24.2(1.70)	24.1(+0.10)	Triplet
	~28.5(2.5)	28.7(+0.23)	
	~32.5(3.0)	~34.8(−0.2)	CT
	~37.6(3.6)	42.6(+2.34)	CT
$[PtBr_4(l\text{-pn})]$		21.5(+0.08)	Triplet
		26.5(+0.29)	
		~40.8(+3.5)	CT

a) in methanol, b) $[RhBr_2(l\text{-pn})_2]Br$ in 3N HBr, c) in 1N HCl, CT: charge transfer band.

pn)$_2$]$^{2+}$, 31100 cm^{-1} for *trans*-[$PtBr_2(l\text{-pn})_2$]$^{2+}$ and 28600 cm^{-1} for *trans*-[$PdCl_2(l\text{-pn})_2$]$^{2+}$ is quite similar to those assigned to $p_\pi \rightarrow d_{z^2}$ charge transfer for the cobalt(III) complexes. Therefore, those CD peaks could be assigned to charge transfer transitions.

The similarity of absorption spectra between $K_2[PtBr_2(CN)_4]$ and $[PtBr_2(l\text{-pn})_2](ClO_4)_2$ will support the above assignment. If the bands at 31100 cm^{-1} of the latter and 29200 cm^{-1} of the former were due to $d \rightarrow d$ transition, the order of the "spectrochemical series" of CN^- and *l*-pn should be reversed, to contradict with the usual observation. Since the d_{z^2} orbital might not be affected by coordinated ligands in the *xy* plane, the energy of charge transfer transition from *p* orbitals of halide ions to d_{z^2} orbital for *trans*-[$PtBr_2(CN)_4$]$^{2-}$ and *trans*-[$PtBr_2(l\text{-pn})_2$]$^{2+}$ should not differ largely.

Consequently, the energies of charge transfer band agree well with the general trend of ligand to metal charge transfer. That is, the energy of a charge transfer band is higher for the metal with larger atomic number, whenever the oxidation number of the central metals is the same (*e. g.* Co(III) and Rh(III) or Pd(IV) and Pt(IV)), and is also higher for the metal of smaller oxidation number with an isoelectronic structure (Rh(III) and Pd(IV)).

The AB and CD data are summarized in Table 2.

Ion Association Band. It is known that $[Pt(en)_3]^{4+}$ associates with Cl^- or $S_2O_3^{2-}$ to change

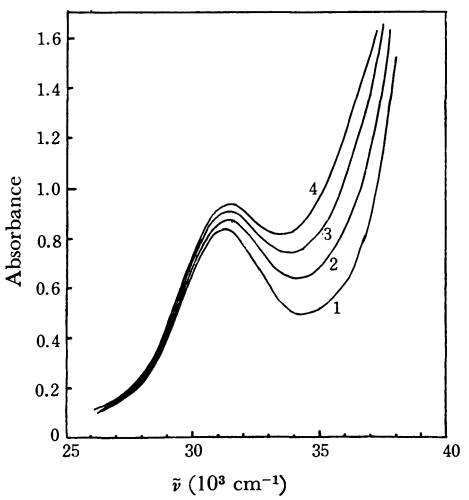

Fig. 6. AB spectra of *trans*-[$PtBr_2(l\text{-pn})_2$]Br_2 (0.664 $\times 10^{-3}$ mol/*l*) in 0.05N perchloric acid containing (1) 0.2M, (2) 0.4M, (3) 0.6M and (4) 0.8M sodium bromide.

11) R. Larsson, *Acta Chem. Scand.*, **21**, 1081 (1967).
12) A. J. Poë, *J. Chem. Soc.*, **1963**, 183.

the absorption and circular dichroism spectra.[11] Though absorption spectra of *trans*-$[PtCl_2(l\text{-pn})_2]^{2+}$ in methanol and in 1N hydrochloric acid are not very different (see Fig. 3), those of *trans*-$[PtBr_2(l\text{-pn})_2]^{2+}$ in methanol and in 1N hydrobromic acid are significantly different, *i. e.* a new band appears at about 35000 cm^{-1} in 1N hydrobromic acid (Fig. 4). Poë[12] studied the absorption spectra of *trans*-$[PtBr_2(en)_2]^{2+}$ in detail and assigned this band to an ion association band. The absorption spectra of $[PtBr_2(l\text{-pn})_2]Br_2$ in 0.05N perchloric acid (to prevent deprotonation of the coordinated amine) with varying bromide concentration are shown in Fig. 6. The intensity of this band increases with an increase in bromide concentration. The CD spectra of the solutions, however, are quite similar to one another, to indicate that the ion association is not stereoselective.

The authors wish to thank the Ministry of Education for Grand in aid.

BULLETIN OF THE CHEMICAL SOCIETY OF JAPAN VOL. 42 1291—1296 (1969)

The Separation of Hexacyanoferrate(II) and Hexacyanoferrate(III) Ions by Reversed-phase Partition Chromatography

Ikuko AKAZA, Toshiyasu KIBA and Minoru TABA

Department of Chemistry, Faculty of Science, Kanazawa University, Kanazawa

(Received September 3, 1968)

The separation of hexacyanoferrate(II) and (III) ions with a TBP-HCl extraction system has been carried out by reversed-phase partition column chromatography. TBP adsorbed on Kel-F powder was used as the stationary phase in the column. Elution was performed with hydrochloric acid of various concentrations and with water, both having been saturated with TBP. The actual separation of hexacyanoferrate(II) and (III) ions from each other was successfully achieved, even in a large volume of a sample solution, by carrying out the elution with 3N HCl. The dependencies of the distribution ratio on the acidity of the solution and on the concentration of TBP in the stationary phase were examined on the basis of the elution curves under various conditions. The liquid-liquid batch extraction was also carried out under the same conditions; it was found an identical relation of distribution between the two phases held in both column and batch extractions. The principal extracted species might be assumed to be a large ion-pair hydrated and solvated.

Reversed-phase partition column chromatography is closely related to the liquid-liquid batch extraction of the same system; the former makes possible the effective separation of each component in a mixture even when the separation factor obtained in the latter is very low, because multiple extraction is carried out in the column. Therefore, this chromatographic technique has been applied to inorganic ions difficult to separate, such as rare earths and transition metals.

In the preceding papers, one of the present authors described the liquid-liquid extraction of alkali metal ions as their poly-iodides in nitrobenzene;[1] this extraction was later developed to reversed-phase partition column chromatography, in which Kel-F powder was used to support the organic phase of nitrobenzene-iodine-iodide.[2] The liquid-liquid extraction of alkaline earth metals as their TTA-chelates in MIBK was also investigated;[3] these results were then further applied to the reversed-phase chromatography, in which the stationary phase was a MIBK solution of TTA held on Kel-F.[4] These chromatographic investigations revealed that valuable information concerning reversed-phase partition column chromatography could be given by a study of the identical liquid-liquid extraction system.

In this paper, the separation of hexacyanoferrate-(II) and hexacyanoferrate(III) ions by the reversed-phase partition chromatography will be described; a TBP-(Kel-F) column will be used. It has been reported by Kiba *et al.* that these anions can be

1) I. Akaza, This Bulletin, **39**, 465 (1966).
2) I. Akaza, *ibid.*, **39**, 585 (1966).
3) I. Akaza, *ibid.*, **39**, 971 (1966).
4) I. Akaza, *ibid.*, **39**, 980 (1966).

extracted from their hydrochloric acid solution by liquid-liquid extraction with TBP.[5] The present research aims at a more effective separation of these two ions by using reversed-phase chromatography; the relation between the chromatography and the liquid-liquid extraction will also be investigated.

It is noteworthy that reversed-phase partition chromatography has never before been applied to the separation of common anions.

Experimental

Apparatus. *Column.* A glass column, 0.92 cm in diameter and 30 cm long, and with a coarse frit at the bottom, was used during this study. A separating funnel was fitted at the top of the column as a reservoir of the eluting solution.

Fraction Collector. A fraction collector (Model SF 200A of the Toyo Roshi Co.) holding 200 tubes was employed.

Photoelectric Photometer. A photoelectric photometer, Hitachi EPW-4, was employed, along with a 1-cm cell.

Reagents and Materials. *Kel-F.* Kel-F (polytrifluorochloroethylene), a trade-name low-density 300 moulding powder, was imported from the Minnesota Mining and Manufacturing Co., U.S.A. The material was ground with a mixing grinder and sieved through screens; particles between 42 to 80 mesh were collected for use.

TBP. Commercially-available TBP was purified by washing it twice with a 5% sodium carbonate solution of an equal volume in order to remove any dibutyl- or monobutyl phosphate, and by then distilling the solvent at about 178°C and at 25 mmHg.

All the other chemicals used were of an analytical reagent grade.

Organic Solvent Useful for Both the Stationary Phase of the Column and the Organic Phase of the Batch Extraction. The TBP used in each experiment had been pre-equilibrated with hydrochloric acid of the same concentration as that for the mobile phase or the aqueous phase. No diluent such as benzene was used except when, in some experiments, it was necessary to use TBP of varying concentrations.

Eluting Solution of the Column Extraction and Aqueous Phase Solution of the Batch Extraction. Hydrochloric acid of various concentrations and water were used as the eluting solutions; both had been saturated with TBP or, in some experiments, with TBP-benzene. They were also used as the aqueous phases of the batch extraction.

Test Solution. Hydrochloric acid solutions of potassium hexacyanoferrate(II) and potassium hexacyanoferrate(III) in the range of 10^{-1}M to 10^{-4}M were prepared; the concentration of hydrochloric acid had been made up to equal that in the eluting solution of the aqueous phase solution in each case. A mixed test solution was prepared by mixing equal volumes of these solutions.

Experimental Procedure. All the experiments were performed in rooms from which sunlight was kept out and the temperature, except in the experiment of Table 2, was always about 6—10°C.

The Preparation of the Stationary Phase. Six grams of Kel-F were placed in an Erlenmyer flask fitted with a stopper, and then 6 m*l* of an organic solvent prepared as above was poured in. The volume, 6 m*l* to 6 g of Kel-F, was derived from the amount of TBP adsorbable on Kel-F, an amount which had been determined by other experiments.[2,4] The stoppered flask was shaken gently by hand until the contents became homogeneous, and then it was left for over three hours as it was. A small volume of an eluting solution was added, and the slurry was poured little by little into the chromatographic column, taking care not to include any air bubbles. Every time a small portion of slurry was added, gentle press for the column bed was done with a glass rod; the bed length eventually reached about 17.4 cm. About a 50-m*l* portion of the eluting solution was then passed through the column in order to remove any contaminant.

The volume of the mobile phase in the column was found to be 3.6 m*l*. The amount of TBP originally adsorbed on the Kel-F column was 6 m*l*; hence, the volume ratio of the stationary phase to the mobile phase was 6: 3.6.

The Elution and Separation of Hexacyanoferrate(II) and Hexacyanoferrate(III) Ions. Three milliliters of the test solution were poured onto the upper surface of the column and were then percolated through the column at the rate of about 0.25 m*l* per minute; then the inside of the glass tube above the top of the column bed was washed twice with small portions of the eluting solution, letting them flow down at the same rate. On the top of the glass tube, a separatory funnel was placed; then the elution was carried out with eluting solutions of various concentrations of hydrochloric acid supplied from the funnel at the rate of 0.5 m*l*/min. The effluent was collected in suitable fractions with a fraction collector, and the hexacyanoferrate content in each fraction was determined.

A 3-m*l* portion of the test solution was usually employed, but a larger volume, such as 50 m*l*, was also employed in some cases.

Determination of Hexacyanoferrate(II) and Hexacyanoferrate(III) Ions. The $[Fe(CN)_6]^{3-}$ content in each fraction was determined by measuring the absorbance at 420 mμ directly. On the other hand, the concentration of $[Fe(CN)_6]^{4-}$ was determined absorptiometrically after oxidizing it to $[Fe(CN)_6]^{3-}$ by the addition of hydrogen peroxide to the acidic solution. This new determination method will be described here for the first time: Hydrochloric acid and 2% H_2O_2 were added to a solution of $[Fe(CN)_6]^{4-}$, and the mixture was diluted to a definite volume; the concentrations of HCl and H_2O_2 had to be about 1.5N and 0.26% respectively. After the vessel had then been placed at 20°C for 20 min, the yellow color was measured at 420 mμ; its absorbance was invariable, even 5 hr later. The working curve of the $[Fe(CN)_6]^{4-}$ solution coincided exactly with that of $[Fe(CN)_6]^{3-}$, and in both cases the curve could be used up to 5.5×10^{-4} mmol/m*l*; when the concentration of the ions exceeded 5.5×10^{-4} mmol/m*l*, the slope of the curve became gentle.

5) T. Kiba, K. Terada and N. Kisaka, Preprints for the Annual Meeting of the Chemical Society of Japan (April, 1962), No. 16407; (April, 1963), No. 3105.

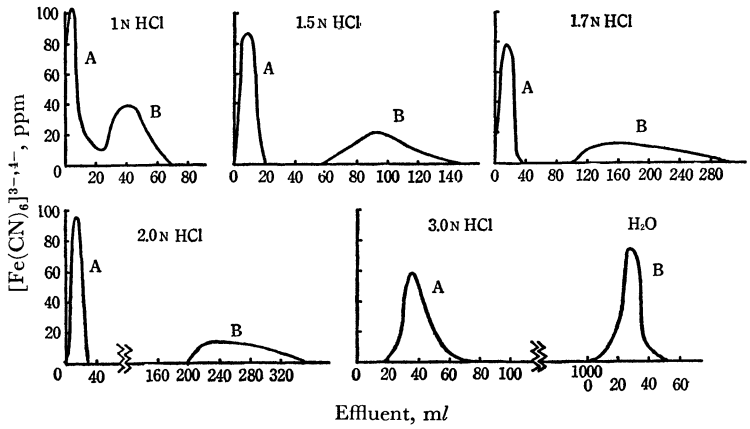

Fig. 1. The elutions at various concentration of hydrochloric acid.
Loaded: mixture of 7.5×10^{-3} mmol each ion
A: $[Fe(CN)_6]^{3-}$ B: $[Fe(CN)_6]^{4-}$

Results and Discussion

The Chromatographic Behavior of Hexacyanoferrate(II) and Hexacyanoferrate(III) Ions. The chromatographic behavior of the ion may be expected from the results of its liquid-liquid extraction. According to the results obtained in the liquid-liquid extraction of $[Fe(CN)_6]^{3-}$ and $[Fe(CN)_6]^{4-}$ by Kiba *et al.*,[5] the distribution ratios of both ions increase with the concentration of hydrochloric acid, and the difference in the distribution ratio between the two ions is large in the range from 1N to 3N of hydrochloric acid. Therefore, the authors' experiments were attempted at concentrations of hydrochloric acid within this range.

The States of the Elutions at Various Concentration of Hydrochloric Acid. Solutions of 5×10^{-3}M $[Fe(CN)_6]^{3-}$ and $[Fe(CN)_6]^{4-}$ in hydrochloric acid of various concentrations were prepared. Both of them, in the same concentration of hydrochloric acid and in equal volumes, were then mixed together. A 3-ml portion of the mixed solution was then eluted with acid of the identical concentration. The results are summarized in Fig. 1. It was found that $[Fe(CN)_6]^{3-}$ and $[Fe(CN)_6]^{4-}$ cannot be separated from each other by elution with 1N HCl, but can be easily separated with an acid of higher concentration; also, in all cases $[Fe(CN)_6]^{3-}$, which has the smaller distribution ratio, is first eluted. Moreover, the position of the peak of the elution curve shifts backward on the abscissa with an increase in the concentration of HCl—as is clearly shown in the case of $[Fe(CN)_6]^{4-}$; namely, the distribution ratio of the ion increases with the concentration of HCl. In the case of 3N HCl, all the $[Fe(CN)_6]^{4-}$ remains in the column even after an eluting solution of 1*l* has flowed down, but as soon as the 3N HCl eluting solution is replaced by a water eluting solution, $[Fe(CN)_6]^{4-}$ is eluted immediately.

Table 1. The states of the elutions at various amounts of $[Fe(CN)_6]^{3-,4-}$

Concn. of HCl N	Loaded, mmol $[Fe(CN)_6]^{3-}$	Loaded, mmol $[Fe(CN)_6]^{4-}$	Elution range, ml $[Fe(CN)_6]^{3-}$	Elution range, ml $[Fe(CN)_6]^{4-}$
2.0	1.5×10^{-2}	7.5×10^{-3}	0—34	186—395 max. at
2.0	7.5×10^{-3}	1.5×10^{-2}	0—34	167—499
1.5		15×10^{-4}		52—112 82
1.5		15×10^{-3}		43—171 93
1.5		3×10^{-2}		40—207 106

The States of the Elutions at Various Amounts of the Ions. The following two experiments were carried out, one at varying ratios of $[Fe(CN)_6]^{3-}$ to $[Fe(CN)_6]^{4-}$ in 2N HCl, and the other at varying amounts of only $[Fe(CN)_6]^{4-}$ in 1.5N HCl. The results of elution are shown in Table 1. The situation of the peak of each elution curve seems practically unchangeable, though there is a slight shift backward with an increase in the amount of the ions loaded; this is contrary to the cases of alkali polyiodides and alkaline earth-TTA chelates, in which the distribution ratios decrease with an increase in the amount of the substance loaded. This discrepancy may be attributed to the difference between the types of extraction mechanisms: in this extraction system of hexacyanoferrate ions, the extraction is not affected by the relative amounts of the ion and the reactant because the ions transfer, without any reactant, into the TBP phase as their solvated free acids.

The Separation of Hexacyanoferrate(II) and (III). Eluting solutions of from 2N to 3N hydrochloric acid may be useful in separating these two substances, as is shown in Fig. 1. Among

these solutions, the 3N solution was preferred. The sample solution of 3N HCl was loaded, and then an eluting solution with the same HCl concentration was flowed in order to elute $[Fe(CN)_6]^{3-}$. In order to elute the $[Fe(CN)_6]^{4-}$ rapidly, the eluting solution was replaced with water. A satisfactory separation was attained, as is shown in Fig. 2.

Quantitative Separation of $[Fe(CN)_6]^{3-}$ and $[Fe(CN)_6]^{4-}$ from a Mixed Test Solution of a Large Volume. To show the practical usefulness of the method and a quantitative separation of the ions, a simple process was carried out with a test solution of a 50-m*l* portion of a 3N HCl solution containing each of the two ions in 5×10^{-2} mmol (10.59 mg), and without a fraction collector.

This experiment was carried out at 20°C under a flow rate of 1 m*l*/min, faster than in the other experiments. The effluent of 3N HCl was placed successively in 100-, 50-, and 25-m*l* measuring flasks; the portions were named the first, second, and third fractions respectively. As a result of this process $[Fe(CN)_6]^{3-}$ should flow down. In order to examine if all of the $[Fe(CN)_6]^{4-}$ was left on the column, a new eluting solution of 1.5N HCl-H_2O_2*1 was supplied while about 2 m*l* of the preceding 3N HCl eluting solution still remained on the top of the column; the elution of $[Fe(CN)_6]^{4-}$ was then continued, with the fourth and fifth fractions placed in measuring flasks of 50 m*l* and 25 m*l* respectively. By this elution the $[Fe(CN)_6]^{4-}$ in the column was oxidized to $[Fe(CN)_6]^{3-}$. The absorbancy of each fraction was measured at 420 mμ. Furthermore, the absorbancy of the first and second fractions was measured again after the addition of H_2O_2. This treatment is necessary to certify the absence of $[Fe(CN)_6]^{4-}$ in the fractions of $[Fe(CN)_6]^{3-}$.

The results shown in Table 2 show that all of the $[Fe(CN)_6]^{3-}$ was eluted and recovered in the first 125-m*l* effluent, and $[Fe(CN)_6]^{4-}$ did not appear in this fraction, since the T% of the first and the second fractions after oxidation by H_2O_2 remained the same as before the oxidation. None of the ions could be detected in the next, third fraction. The results from the fourth and fifth fractions showed that $[Fe(CN)_6]^{4-}$ was left in the column quantitatively. This means that comparatively large amounts of $[Fe(CN)_6]^{4-}$ ions can be caught in the column quantitatively from the test solution of a larger volume, even at quite a fast flow rate. In this experiment the water-eluting solution was intentionally not employed for $[Fe(CN)_6]^{4-}$, unlike the ordinary elution presented in Fig. 2. A reason for this treatment is as follows. It was found in a preliminary test that $[Fe(CN)_6]^{4-}$ separated itself, as white, free acid $H_4[Fe(CN)_6]$, when a little TBP was added to a solution containing a large amount of $[Fe(CN)_6]^{4-}$ at a high concentration of hydrochloric acid. On the other hand, in the above column experiment, the concentration of $[Fe(CN)_6]^{4-}$ was be raised remarkably in a small upper part of the column, since adequate extraction conditions, such as 3N HCl, were kept; moreover, a large amount of $[Fe(CN)_6]^{4-}$ was handled here. The spontaneous separation of the free acid could be expected, as in the preliminary test. This free acid seemed unstable in water, and indeed it at once became blue when the hydrochloric acid-eluting solution was displaced with water. Hence, the water-eluting solution was omitted. The fact that $[Fe(CN)_6]^{4-}$ remained near the top of the column, has also the advantage that the separation from $[Fe(CN)_6]^{3-}$ can be achieved successfully without any consideration of the volume of the sample solution and the flow rate of elution. If one desires to take out the $[Fe(CN)_6]^{4-}$ as it is, not according to above procedure, it should be washed down to-

TABLE 2. QUANTITATIVE SEPARATION OF $[Fe(CN)_6]^{3-}$ AND $[Fe(CN)_6]^{4-}$ FROM MIXED TEST SOLUTION OF LARGE VOLUME

Fraction number	Eluant	Effluent collected m*l*	Found mg	Taken mg
1	3N HCl	100	↘10.38	10.59
2	3N HCl	25	↗($[Fe(CN)_6]^{3-}$)	
3	3N HCl	25	0.0	
4	1.5N HCl-H_2O_2	50	↘10.41	10.59
5	1.5N HCl-H_2O_2	25	↗($[Fe(CN)_6]^{4-}$)	

*1 In preparing the eluting solution of HCl-H_2O_2, 13.5 m*l* of 2% H_2O_2 were added to 50 m*l* of 3N HCl, and then the solution was made up to 100 m*l* with water.

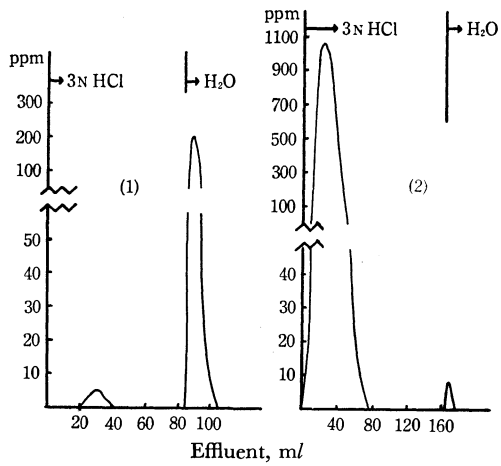

Fig. 2. The separation of $[Fe(CN)_6]^{3-}$ and $[Fe(CN)_6]^{4-}$.
Loaded: (1) 3.0×10^{-4} mmol $[Fe(CN)_6]^{3-}$
1.5×10^{-2} mmol $[Fe(CN)_6]^{4-}$
(2) 1.5×10^{-1} mmol $[Fe(CN)_6]^{3-}$
3.0×10^{-4} mmol $[Fe(CN)_6]^{4-}$

gether with the stationary phase of TBP by passing 50 m*l* of a 1N HCl-50% alcohol solution (2N HCl : C_2H_5OH=1:1) through the column.

Some Relation to the Liquid-Liquid Extraction. The mechanism of reversed-phase partition chromatography is very similar to that of the liquid-liquid extraction of the same system, has been clarified by one of the present authors. Now, the extraction of $[Fe(CN)_6]^{4-}$ with TBP was preferentially examined.

The equation for the extraction of $[Fe(CN)_6]^{4-}$ with TBP can be written simply as:

$$nH^+_{(a)} + A^{n-}_{(a)} + m\text{TBP}_{(o)} = H_nA \cdot m\text{TBP}_{(o)} \quad (1)$$

where A^{n-} is the hexacyanoferrate ion. The distribution ratio, D, for this process can be written as:

$$D = K[H^+]^n[\text{TBP}]^m \quad (2)$$

where K is the thermodynamic extraction constant. Therefore, the distribution ratio, D, depends on the activity of both TBP and hydrogen ions. These activities can, for convenience, be displaced by the concentration of an acid and TBP.

The distribution ratio in the column extraction by reversed-phase partition chromatography was calculated, by using Eq. (3), from the elution curve obtained:

$$D = (E - F)/B \quad (3)$$

where E is the volume of the effluent before the emergence of the solute in a maximal concentration; B, the volume of the stationary phase, and F, the volume of the mobile phase.

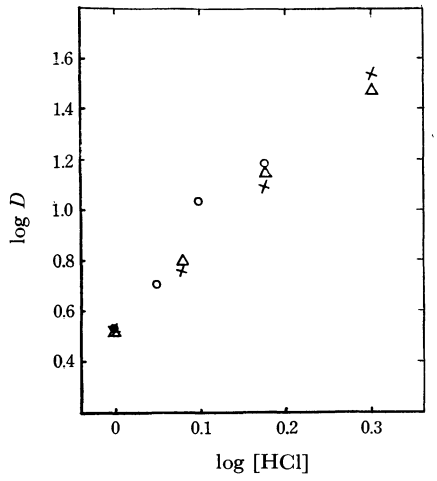

Fig. 3. Dependence of distribution ratio of $[Fe(CN)_6]^{4-}$ upon the concentration of HCl.
○ Column chromatography
△ Liq.-liq. (on Kel-F) batch extraction
× Liq.-liq. batch extraction

First, the dependence of the distribution of $[Fe(CN)_6]^{4-}$ on the concentration of hydrochloric acid was examined. Three-m*l* portions of a 5×10^{-3}M $[Fe(CN)_6]^{4-}$ solution with various concentrations of hydrochloric acid were fed into the column; elution was then carried out with a hydrochloric acid-eluting solution of the same concentration. The distribution ratio of $[Fe(CN)_6]^{4-}$ in each case was calculated by putting a value of E obtained from an elution curve into Eq. (3), and plotted on a graph of log$D$ *vs.* log[HCl] as is shown in Fig. 3.

For comparison with the above results, a series of batch extractions was carried out between (Kel-F)-TBP and an aqueous phase of the eluting solution. In a 100-m*l* glass-stoppered Erlenmyer flask, (Kel-F)-TBP was prepared with TBP pre-equilibrated with HCl of varying concentrations in the manner described above. After the solution had stood for more than three hours, 9 m*l*[*2] of each eluting solution of a definite acidity and 3 m*l*[*2] of a 5×10^{-3}M solution of $[Fe(CN)_6]^{4-}$ were introduced into the flask. The stoppered flask was gently shaken for a while and then set aside. The contents were poured on a coarse glass filter, and the aqueous phase was allowed to drain before it was submitted to photometry for $[Fe(CN)_6]^{4-}$. The results are shown in Fig. 3.

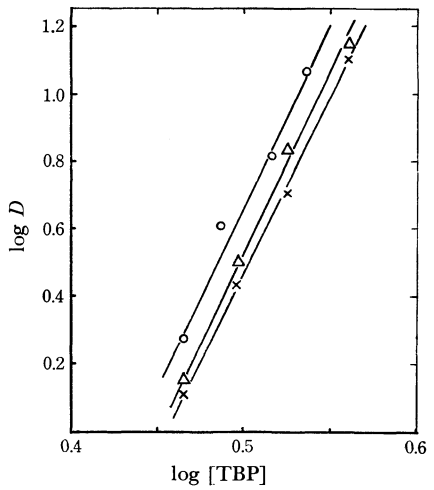

Fig. 4. Dependence of distribution ratio of $[Fe(CN)_6]^{4-}$ upon the concentration of TBP.
○ Column chromatography
△ Liq.-liq. (on Kel-F) batch extraction
× Liq.-liq. batch extraction

[*2] The reason for taking 12 m*l* as the sum of the two aqueous solutions is as follows: If the same volume ratio as in the column, organic phase: aqueous phase= 6 : 3.6, had to be kept, 3.6 m*l* of the aqueous volume would be too small to separate it from the organic solvent adsorbed on Kel-F. In this extraction system, the distribution ratio, D, did not differ upon a change in the volume ratio, so the data from the column extraction carried out at 6 : 3.6 and the batch extraction carried out at 6 : 12 are comparable.

Moreover, another series of liquid-liquid extractions, with Kel-F omitted from the system, was carried out. In this case, not only the organic solvent and the aqueous solutions, but also their volumes, were all identical to those described just above. These results are also shown in Fig. 3.

Next, the dependency of the distribution ratio on the concentration of TBP was examined by three kinds of experiments in the same manner as when the relation of log$D$ to log[HCl] was obtained. However, the concentration of hydrochloric acid was fixed at 1.5N in all these experiments, while that of TBP was varied by diluting the reagent with benzene. Organic solvents containing TBP in various concentrations were used for the stationary phase of the column chromatography, for the batch extraction with TBP-(Kel-F), and also for the liquid-liquid extraction. The data obtained are shown in Fig. 4 as a graph of log$D$ *vs.* log[TBP].

As Fig. 3 and Fig. 4, show all of the slopes showing the relation log$D$ *vs.* log[HCl] are about 3.5 and the dependency of D on the concentration of TBP is about 11 in every series of experiments. The data obtained in the column extraction chromatography and those in the liquid-liquid extraction are thus in good agreement. This shows that the extraction mechanism in the reversed-phase column chromatography is identical with that of the liquid-liquid extraction system.

In the former, however, the distribution ratio was found to be a little higher than in the liquid-liquid batch extraction; this might be caused by a small difference in temperature between the two experimental rooms,*3 not by the extraction mechanisms. Because the data obtained from the liquid-liquid batch extraction and those from the batch extraction with (Kel-F)-TBP are found to be in good agreement on the straight lines in Figs. 3 and 4, it can be said that Kel-F powder does not affect the extraction mechanism. Also, it was observed that this extraction system is readily affected by the temperature; *e.g.*, of the distribution ratios of $[Fe(CN)_6]^{4-}$ at 20°C and 10°C, the latter has a value higher than the former by about 0.5 in logarithm.

The slopes of the lines in Figs. 3 and 4 presumably do not stand directly for n and m in Eq. (2). They only indicate the average reagent-dependence of the species present; furthermore, the experimental conditions are remarkably far from ideal for an infinite dilution system. As has been shown in the papers concerning the extraction mechanism of acids by TBP by Whitney and Diamond[6] and Biddle *et al.*,[7] the principal extracted species may be assumed to be a large species which is an associate of a hexacyanoferrate ion and about four trihydrated hydronium ions, each of the hydronium ions being solvated with three TBP's.

*3 The chromatography was carried out in a room the temperature in which was kept at 6—10°C, while the extraction was done in an anteroom with a temperature slightly higher than the inner room.

Summary

The present authors have developed a liquid-liquid extraction system of hexacyanoferrate(II) and (III) with TBP to a reversed-phase column partition chromatography. In the column, TBP held on Kel-F powder was used as the stationary phase. The separation of each ion from the mixture has been successfully achieved by carrying out the elution with an eluting solution of 3N HCl; tolerable amounts could thus be treated. The relation between the method and the liquid-liquid extraction has been examined; no fundamental difference could be found between them.

6) D. C. Whitney and R. M. Diamond, *J. Phys. Chem.*, **67** 209 (1963).

7) P. Biddle, A. Coe, H. A. C. Mckay, J. H. Miles and M. J. Waterman, *J. Inorg. Nucl. Chem.*, **29**, 2615 (1967).

BULLETIN OF THE CHEMICAL SOCIETY OF JAPAN VOL. 42 1297—1300 (1969)

Reactions of Metal Chelates. III. The Reactions of Bis(salicylaldehydato)copper(II) with Amides and Esters of Glycine and Glycylglycine

Kazuko HAMADA, Hideo UEDA, Yasuo NAKAO and Akitsugu NAKAHARA

Institute of Chemistry, College of General Education, Osaka University, Toyonaka, Osaka

(Received September 5, 1968)

The reactions of bis(salicylaldehydato)copper(II) in acidic, neutral and basic media with glycinamide, glycinester, glycylglycinamide and glycylglycinester have been systematically investigated. The reaction products have, in all cases, been isolated as crystals and characterized. As a result of this investigation, six new copper(II) chelates of Schiff bases derived from salicylaldehyde and glycine- or glycylglycine-amide have been obtained. The interrelation between those chelates has also been disclosed.

In a previous paper[1] it was reported that bis(salicylaldehydato)copper(II), I, reacts readily with glycine or glycylglycine to form salicylideneglycinato- or -glycylglycinato-chelate, respectively, II, III.

We have further reported that the reaction at pH 4.5 between the same chelate, I, and tri-[2] or tetra-glycine[3] results in the hydrolytic cleavage of a peptide linkage, producing salicylideneglycylglycinatocuprate(II), III, and free glycine or glycylglycine, respectively. From biochemical interest, the investigation has been extended to reactions of the same chelate, I, with some derivatives of amino acids and peptides.

This paper describes the reactions of bis(salicylaldehydato)copper(II), I, in acidic, neutral and basic media with glycinamide, glycinester, glycylglycinamide and glycylglycinester. The preparation and properties of six new copper(II) chelates, which have been obtained as a result of this investigation, are also described.

The Reaction of Bis(salicylaldehydato)copper(II), I, with Glycinamide. The reaction between complex, I, and glycinamide varies widely with the hydrogen ion concentration in solutions. Although the reactions proceed rapidly at room temperature both in acidic and basic solutions to form the one-to-one type copper(II)-Schiff base complexes, the resulting chelate from acidic solution is green, while that from basic solution red-purple, indicating that they have different structure from each other. The structure of the green complex is easily concluded to be IV in Fig. 1 in the light of properties of acidamide found in the case of pyridine-2-carboxamide complexes,[4-6] and results of elemental analysis and electrophoretic investigation of the complex. As is clear from the structural formula, IV, the carboxamide group of the glycinamide moiety in the green complex is linked to copper(II) through the oxygen atom, and the ligand at the fourth coordination position around copper(II) is water molecule; hence the complex is a univalent cation, being isolated as chloride, bromide, perchlorate, sulfate, *etc.* On the other hand, the structure of the red-purple complex isolated from a basic solution is somewhat difficult to determine, since the complex shows a considerably subnormal magnetic moment (1.15 B. M. for copper atom). As has been established by Kishita *et al.*,[7] the subnormal magnetic moment of this kind can be elucidated in terms of binuclear structure, V, in which an interaction is expected between copper(II) atoms.

Although there is another possible binuclear structure as represented by V′, in which the bridging atoms are phenolic oxygen atoms, this structure is supposed to be less plausible from a stereochemical point of view. In other words, the steric hindrance between the benzene ring of salicylaldehyde moiety and the carboxamide nitrogen might eliminate the possibility of the structure V′. The binuclear complex, V, can be dissolved in an alkaline solution, but the structure of the complex

1) A. Nakahara, This Bulletin, **32**, 1195 (1959).

2) A. Nakahara, K. Hamada, I. Miyachi and K. Sakurai, This Bulletin, **40**, 2826 (1967).

3) A. Nakahara, K. Hamada, Y. Nakao and T. Higashiyama, *Coordin. Chem. Rev.*, **3**, 207 (1968).

4) K. Yamasaki and M. Sekizaki, This Bulletin, **38**, 2206 (1965).

5) A. Masuko, T. Nomura and Y. Saito, *ibid.*, **40**, **511** (1967).

6) Y. Nawata, H. Iwasaki and Y. Saito, *ibid.*, **40**, 515 (1967).

7) For example, M. Kishita, Y. Muto and M. Kubo, *Australian J. Chem.*, **10**, 386 (1957).

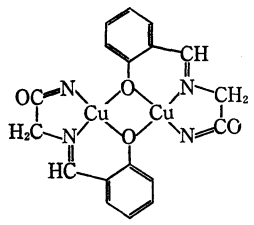

(V′)

in the solution has not been determined; hence the structure of the complex in the solution is still uncertain whether the binuclear structure is maintained or not.

In neutral solutions the chelate I reacts less rapidly than in acidic or basic solutions with glycinamide. The resulting compound is not the one-to-one but one-to-two type copper(II)-Schiff base complex, in which the carboxamide groups are free from coordination as illustrated in VI. As is understood from its structural formula, this complex is an uncharged neutral complex.

The interrelation between those chelates, IV, V and VI, has also been clarified to some extent. First, chelate IV changes to V by adjusting the pH of the solution to about 12; this isomerization is almost reversible, and accordingly, chelate IV is reproduced from V by readjusting the pH of the solution to about 4.0. However, the procedure is always accompanied by the precipitation of blue-purple crystalline powder at pH-values near 7.5. Though this precipitate is expected to have an interesting structure, the details on this particular compound is not clarified yet. Secondly, the chelate VI also changes readily to IV or V according to the pH-value of the solution, but these rearrangements are, of course, not reversible.

As has been reported previously,[3] glycylglycine-Schiff base coordinated around copper(II) in the same fashion as that depicted in the structural formula, IV, is easily hydrolyzed into the free glycine and glycine-Schiff base complex in aqueous media at low pH and especially at high temperature. However, in the present case, the hydrolysis of the carboxamide group has not been observed at least under the same condition. Though this finding seems to be inconsistent with the results of Meriwether and Westheimer,[8] who reported the metal ion-promoted-hydrolysis of glycinamide and of phenylalanylglycinamide, their experiments were made in a slightly alkaline solution, while the present datum has been obtained from an investigation on a slightly acidic solution.

Thus it can be said that carboxamide $-CO-NH_2$ linkage is difinitely more stable at low pH against the hydrolytic cleavage reaction than peptide linkage.

The Reaction of Bis(salicylaldehydato)copper(II), I, with Glycinester. This reaction is very monotonous, and always results in the formation of the one-to-two type copper(II)-Schiff base complex, (VII),[1,9] regardless of the hydrogen ion concentration in solutions. The hydrolysis of the ester groups of complex, VII, in aqueous media has not been observed under mild conditions, perhaps because of its poor solubility. At any rate, since the ester groups of glycinester moieties in chelate VII are located away from the central metal ion, the electron-withdrawing effect of metal ion would not reach the ester group to catalyze the hydrolytic reaction.

The Reaction of Bis(salicylaldehydato)copper(II), I, with Glycylglycinamide. This reaction varies also delicately with the hydrogen ion concentration in solutions. In acidic solutions, the reaction product is an olive-green Schiff base complex, in which the glycylglycinamide moiety is linked to copper(II) only through the nitrogen of the terminal amino group and the oxygen of the peptide linkage as indicated in (VIII). The structure is supported not only by the results of elemental analysis but also by the paper chromatographic identification of the glycylglycinamide after decomposing the chelate with hydrogen sulfide. Chelate VIII is easily hydrolyzed into the free glycinamide and the *N*-salicylideneglycinatoaquocopper(II), II, by heating at 70°C and at pH-value near 2.8.[3]

On the other hand, the resulting compounds from the reactions in neutral or basic solutions are copper(II) tetradentate chelates of Schiff base derived from salicylaldehyde and glycylglycinamide. However, the chelate from neutral solution is navy-blue, while that from basic solution is red-brown. The difference is apparently due to a linkage isomerism; the carboxamide group in the navy-blue chelate is considered to be linked to copper(II) through oxygen atom, and the same group in the red-brown chelate through nitrogen atom as illustrated in IX and X, respectively. This consideration is strongly supported by the fact that chelate IX is an uncharged neutral complex, whereas chelate X a univalent anion. Hydrolysis of the terminal carboxamide group has not been observed in either complexes under conditions that would be observed in case of peptide linkage. The results of experiments of paper-electrophoresis clearly indicate that the olive-green complex is a cation, the navy-blue complex an uncharged molecule, and the red-brown complex an anion. The mutual transformation between the three chelates, VIII, IX and X, is readily attained only by changing the pH of solutions.

The Reaction of Bis(salicylaldehydato)copper(II), I, with Glycylglycinester. The reaction

8) L. Meriwether and F. H. Westheimer, *J. Am. Chem. Soc.*, **78**, 5119 (1956).

9) P. Pfeiffer, W. Offermann and H. Werner, *J. prakt. Chem.*, **159**, 313 (1942).

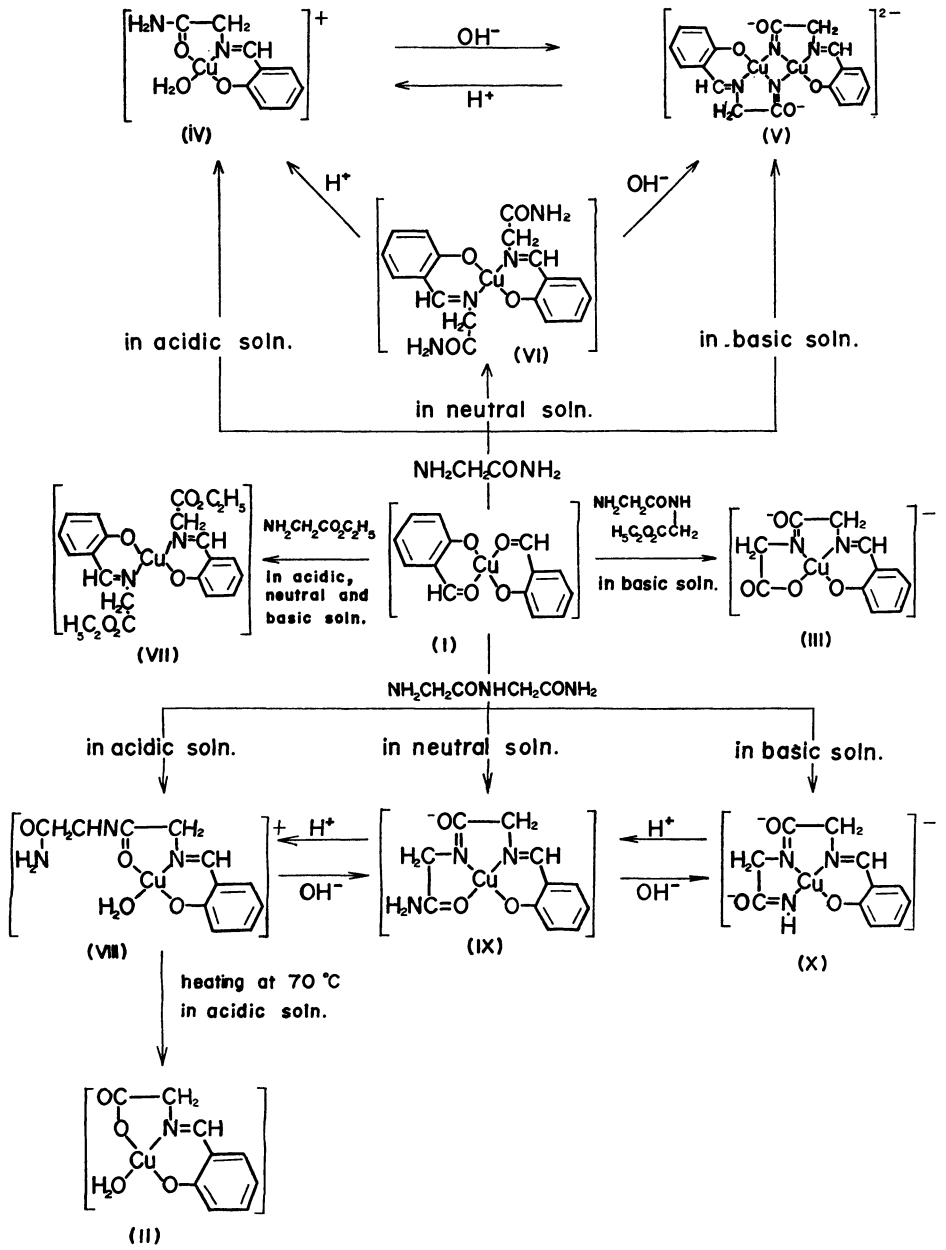

Fig. 1. The reactions of bis(salicylaldehydato)copper (II) with amides and esters of glycine and glycylglycine. The complexes, IV, V, VI, VIII, IX, and X, are new compounds.

product in basic solutions from the system containing chelate I and glycylglycinester is the *N*-salicylideneglycylglycinatocuprate(II), III,[1] indicating that hydrolysis of ester group proceeds quite readily and rapidly.

The phenomenon is understood in terms of a catalytic effect of metal ion as has very often been observed in researches on metal chelates of esters.[10]

10) For example, R. J. Angelici and D. Hopgood, *J. Am. Chem. Soc.*, **90**, 2514 (1968).

Experimental

Preparations of Amides and Esters of Glycine and Diglycine. *Glycinamide* was prepared according to directions of Bergell and Wulfing[11]

Glycylglycinamide was Prepared as acetate according to the method of Fruton and Bergmann.[12] *Glycine-*

11) P. Bergell and H. V. Wulfing, *Z. Physiol. Chem.*, **64**, 348 (1910).

12) J. S. Fruton and M. Bergmann, *J. Biol. Chem.*, **145**, 253 (1942).

and *glycylglycinethylester* were obtained from glycine and glycylglycine, respectively, by treating with absolute ethanol saturated with dried hydrogen chloride. All these amides and esters were identified through the elemental analyses. The preparation and purification of *bis(salicylaldehydato)copper(II)*, I, was performed in the same way as that described in the first paper of this series.[2)]

The Reaction of bis(salicylaldehydato)copper (II), I. *The Reaction of Complex I with Glycinamide.* A one-to-one molar mixture of complex I and glycinamide hydrochloride in aqueous ethanol was divided into three parts. The pH-values of each solution were adjusted to 3.0, 7.0 and 12.0, respectively, by using dilute solutions of sodium hydroxide and hydrochloric acid. Each reaction mixture was then stirred at room temperature for about half an hour.

From the acidic solution, a green crystalline powder was deposited, which was filtered and recrystallized from an aqueous ethanol solution to give a green prism.

The structure of this complex was easily concluded to be IV from coincidence of its decomposing temperature and infrared spectrum with those of complex IV, which can more conveniently be obtained, for the purpose of preparation, from a reaction at pH 3.0 of a system containing 1 : 1 : 1 copper(II) : salicylaldehyde : glycinamide. Mp 178—186°C (decomp.). Found: C, 37.19; H, 3.35; N, 9.44%. Calcd for $CuC_9H_{11}O_3N_2Cl$: C, 36.74; H, 3.77; N, 9.52%. The elemental analysis of sulfate of the same complex was also performed. Found: C, 33.24; H, 3.81; N, 8.43; Cu, 19.87%. Calcd for $CuC_9H_{11}O_3N_2 \cdot \frac{1}{2}SO_4 \cdot H_2O$: C, 33.30; H, 4.00; N, 8.63; Cu, 19.54%. Mp 180—200°C (decomp.). Magnetic moment, $\mu_{eff}=1.84$ B. M. (15°C).

From the reaction mixture of pH-value near 12, a red-purple crystal was isolated. The structure of this complex was concluded to be V, on the basis of the results of elemental analysis and the magnetic datum. Mp 218—220°C (decomp.). Found: C, 36.22; H, 3.73; N, 9.17; Cu, 21.59%. Calcd for $Na_2Cu_2C_{18}H_{14}O_4N_4$: C, 36.30; H, 3.70; N, 9.41; Cu, 21.34%. Magnetic moment, $\mu_{eff}=1.15$ B.M. (15°C).

The reaction mixture of pH-value near 7.0 gave an olive-green precipitate, which was recrystallized from aqueous ethanol to give a one-to-two copper(II)-Schiff base complex. Mp 255—265°C (decomp.). Found: C, 51.63; H, 4.97; N, 13.90%. Calcd for $CuC_{18}H_{18}O_4N_4$: C, 51.73; H, 4.34; N, 13.41%.

Though the two complexes, IV and V, can be prepared either through the reaction between bis(salicylaldehydato)copper(II) and glycinamide or by the direct reaction between copper (II), salicylaldehyde and glycinamide, this particular one-to-two copper(II)-Schiff base complex can be prepared only through the reaction between bis(salicylaldehydato)copper(II) and glycinamide.

The Reaction of the Complex I with Glycylglycinamide. A similar procedure to that employed for the reaction of complex I with glycinamide was adopted. In order to isolate the reaction products it was necessary, in some cases, to concentrate the solution *in vacuo*. Recrystallization was performed by using aqueous ethanol and keeping the pH-value near 3.0, 7.0 and 12.0, respectively. The resulting chelate from the acidic solution is an olive-green crystalline powder, which decomposes at 195—198°C. Found: C, 36.94; H, 3.91; N, 11.57%. Calcd for $CuC_{11}H_{12}O_3N_3Cl \cdot 1.5H_2O$: C, 36.67; H, 4.05; N, 11.66%. The product from the neutral solution is a navy-blue crystalline powder, which decomposes at 262—263°C. Found: C, 42.47; H, 3.69; N, 13.63%. Calcd for $CuC_{11}H_{11}O_3N_3 \cdot H_2O$: C, 41.96; H, 4.13; N, 13.34.% The complex obtained from the basic solution is a red-brown prism, which decomposes at 282—290°C. Found: C, 35.10; H, 4.09; N, 10.82%. Calcd for $NaCuC_{11}H_{10}O_3N_3 \cdot 3H_2O$: C, 35.44; H, 4.33; N, 11.27%.

The Reactions of the Complex I with Glycine- and Glycylglycinester. A one-to-one molar mixture of complex I and glycinester in aqueous ethanol (50% by volume) was stirred and heated at 60°C for half an hour.

The reaction product was soon deposited as an olive-green powder, and was recrystallized from ethanol. No difference in the reaction product was observed within wide range of pH and molar ratio of complex I to glycinester. The resulting complex was identified as the one-to-two type copper(II)-Schiff base chelate as illustrated in VII, from the coincidence in infrared spectrum of the complex with that obtained by Pfeiffer *et al.*[9)]

The reaction of complex I with glycylglycinester was performed only at pH value near 8.5 by a similar procedure as described above. The reaction product was, after recrystallization, a red-purple needle. The structure of this compound was easily concluded as sodium *N*-salicylideneglycylglycinatocuprate(II), III, on the basis of the coincidence of its infrared spectrum with that of the standard sample.[1)]

Magnetic Measurements. The magnetic susceptibility was determined at 15°C by using a Gouy magnetic apparatus. From susceptibilities observed, the magnetic moments were evaluated per copper atom.

Paper-electrophoretic experiments, aminoacid analyses and the measurements of *infrared spectra* were made with the use of a Yanagimoto EC-10, a Yanagimoto LC-5 and a Hitachi EPI-S2, respectively.

The authors thank the Ministry of Education for financial support granted for this research.

BULLETIN OF THE CHEMICAL SOCIETY OF JAPAN VOL. 42 1301—1304 (1969)

The Mixed Chromium(III) Complexes containing Acetylacetone and the Halogenations Thereof*1

Yuki FUJII,*2 Eishin KYUNO and Ryokichi TSUCHIYA

Department of Chemistry, Faculty of Science, Kanazawa University, Kanazawa

(Received September 9, 1968)

The following three mixed chromium(III) complexes containing acetylacetone, which had a charge of from -1 to $+1$, were prepared: $NH_4[Cr(acac)(ata)]\cdot H_2O$,*3 $[Cr(acac)(edda)]\cdot 2H_2O$*3 and $[Cr(acac)(edma)(H_2O)]Cl\cdot H_2O$.*3 The halogenations at γ-position of the acetylacetonate ring were attempted in these three mixed complexes with NCS, NBS and ICl respectively in methanol and in acetic acid solutions, where NCS, NBS and ICl are abbreviated forms of *N*-chlorosuccinimide, *N*-bromosuccinimide and iodine monochloride, respectively. From an inspection of UV-spectra of the above halogenation reaction mixtures, all the three mixed complexes were confirmed to be halogenated at the γ-position of the acetylacetonate ring. Of these complexes, $NH_4[Cr(acac\text{-}Cl)(ata)]\cdot \frac{1}{2}H_2O$ and $[Cr(acac\text{-}Br)(edda)]$ were isolated as crystals from the reaction mixtures. IR-spectra measurement was also used to certify the halogen-substitution at γ-position in the above two compounds.

Electrophilic substitution reaction (S_E reaction) at γ-position of metal acetylacetonates is of interest from the view point of the chemical reaction due to the quasi-aromaticity. Based on the experimental results recently reported,[1,2] the predominant factors governing the reactivity of 1,3-dicarbonyl chelate in S_E reaction may be focussed on the following two points: (1) the electron density at the central carbon atom (γ-position) of the chelate ring (2) the degree of the steric hindrance around the central carbon of the chelate ring. Unfortunately, however, there are still very few reports that affirm the factors described above, and most researches on the reactivity of metal acetylacetonate have been focussed only on the non-electrolyte trisacetylacetonate complexes, due to easiness for treatment in organic solvents. Furthermore, there is no report that describes the reactivity of the mixed acetylacetonate complexes, except for that of the complex ion $[Co(en)_2(acac)]^{2+}$.[1,2]

In order to obtain further information on the reactivity of the mixed complexes containing acetylacetone against halogen, such complexes having different charges of -1, 0 or $+1$ were synthesized and the halogenation reaction was investigated.

Experimental

Preparation of Mixed Complexes. *1) Ammonium Acetylacetonatoammoniatriacetatochromate(III) Monohydrate,* $NH_4[Cr(acac)(ata)]\cdot H_2O$ (I).[3] Ammonium hydroxoammoniatriacetatoaquochromate(III) dihydrate, $NH_4[Cr(OH)(ata)(H_2O)]\cdot 2H_2O$ (9.9 g, 0.03 mol), was dissolved in 40 m*l* of water and heated on a water bath. Acetylacetone (3.3 g, 0.033 mol) was added to the solution with stirring and was warmed at 80—90°C for one hour. After adjusting the pH of the solution to 5—6 by adding a small amount of ammonium carbonate, it was cooled to 0°C, when purple crystals were separated out. They were recrystallized from an aqueous solution. Yield, 10.4 g (92.0%).

Found: C, 35.09; H, 4.89; N, 7.14; Cr, 13.52; H_2O, 4.69%. Calcd for $NH_4[Cr(acac)(ata)]\cdot H_2O$: C, 35.21; H, 4.80; N, 7.47; Cr, 13.86; H_2O, 4.80%.

2) Acetylacetonato-N,N′-ethylenediaminediacetatochromium-(III) Dihydrate, $[Cr(acac)(edda)]\cdot 2H_2O$ (II). Ethylenediaminediacetic acid, $eddaH_2$,[4] (8.0 g) was added to a solution of chromium(III) chloride hexahydrate (5.3 g) in 40 m*l* of water. Heating it on a water bath, the pH of the solution was adjusted to about 3 or 4 with ammonium carbonate and then acetylacetone (2.0 g, 0.02 mol) was, with stirring, added to the solution. Adjusting the pH of the resultant solution to about 7, it was cooled to 0°C. Purple crystals were then separated out and recrystallized from 50% methanol-water solution. Yield, 1.6 g (22.2%).

*1 Presented at the 17th Symposium on Coordination Compounds of The Chemical Society of Japan, Hiroshima, Dec., 1967.

*2 Present address: Department of Chemistry, Faculty of Science, Ibaraki University, Mito.

*3 Abbreviations used are as follows: acac=anion of acetylacetone in enol form, ata=ammoniatriacetate anion, edda=ethylenediaminediacetate anion, and edma=ethylenediaminemonoacetate anion.

1) J. P. Collman, *Adv. Chem. Ser.*, No. 37, 78 (1963).

2) J. P. Collman, *Angew. Chem.*, **77**, 154 (1965).

3) A. Uehara, E. Kyuno and R. Tsuchiya, This Bulletin, **40**, 2317, 2322 (1967).

4) M. Mori, M. Shibata, E. Kyuno and F. Maruyama, *ibid.*, **35**, 75 (1962).

Found: C, 36.71; H, 5.74; N, 7.62; Cr, 14.03; H_2O, 10.0%. Calcd for $[Cr(acac)(edda)]\cdot 2H_2O$: C, 36.56; H, 5.78; N, 7.75; Cr, 14.39; H_2O, 9.98%.

3) Acetylacetonatoethylenediaminemonoacetatoaquochromium-(III) Chloride Monohydrate, $[Cr(acac)(edma)(H_2O)]Cl\cdot H_2O$ (III). Ethylenediaminemonoacetic acid dihydrochloride monohydrate, $edmaH\cdot 2HCl\cdot H_2O$*4 (4.2 g, 0.02 mol), was added to the solution of chromium(III) chloride hexahydrate (5.3 g, 0.02 mol) in 30 m*l* of water. Heating the solution on a water bath, the solution was adjusted to about pH 2 or 3 with ammonium carbonate. Acetylacetone (2.0 g, 0.02 mol) neutralized with equimolar ammonium carbonate was added to the solution, and was heated for an hour. After the pH of the solution was adjusted to about 5, it was allowed to stand for about three weeks at room temperature. Reddish purple crystals were separated out and recrystallized from an aqueous solution. Yield, 2.7 g (40%).

Found: C, 31.98; H, 5.85; N, 7.88; Cr, 14.61; H_2O, 5.02%. Calcd for $[Cr(acac)(edma)(H_2O)]Cl\cdot H_2O$: C, 31.81; H, 5.95; N, 8.25; Cr, 15.31; H_2O, 5.30%.

Isolation of Halogenated Mixed Complexes. *1) Ammonium 3-Chloroacetylacetonatoammoniatriacetatochromate(III) Hemihydrate*, $NH_4[Cr(acac\text{-}Cl)(ata)]\cdot \frac{1}{2}H_2O$ (IV). The solution of NCS (5.4 g, 0.04 mol) in 60 m*l* of glacial acetic acid was slowly added to the solution of the complex I (7.5 g, 0.02 mol) in glacial acetic acid at room temperature.[5] After being stirred for 30 min, 150 m*l* of ether was added and the resultant reddish purple precipitates were collected. Washed with ether, the powder obtained was dissolved in 70 m*l* of ethanol at 40°C. Fifty milliliters of ether were added to the solution and the reddish purple precipitates produced were collected. Washed with ether, the precipitates were recrystallized from 20% of methanol solution. Black purple crystals were separated out. Yield, 2.1 g (25.5%).

Found: C, 32.20; H, 4.49; N, 6.70; Cr, 12.36; Cl, 8.26; H_2O, 2.20%. Calcd for $NH_4[Cr(acac\text{-}Cl)(ata)]\cdot \frac{1}{2}H_2O$: C, 32.99; H, 4.28; N, 6.99; Cr, 12.96; Cl, 8.85; H_2O, 2.25%.

2) 3-Bromoacetylacetonatoethylenediaminediacetatochromium-(III), $[Cr(acac\text{-}Br)(edda)]$ (V). One gram (0.003 mol) of the complex II was dissolved in 60 m*l* of methanol and a solution of NBS (0.6 g, 0.003 mol) in methanol was added to it at room temperature. Evaporating off the solvent at room temperature, purple crystals were separated out. These were insoluble in various solvents. Yield, 0.6 g (66.0%).

Found: C, 32.81; H, 4.13; N, 6.95; Cr, 12.88; Br, 19.26%. Calcd for $[Cr(acac\text{-}Br)(edda)]$: C, 32.68; H, 4.00; N, 6.93; Cr, 12.87; Br, 19.77%.

Apparatus. The molar conductivity, the UV and visible absorption spectra and IR spectra were measured with a Yokogawa Universal Bridge BV-Z-13A, a Hitachi EPS Spectrophotometer and a Nippon Bunko DS-301 Infrared Spectrometer, respectively. The quantity of the crystalline water contained in these compounds was estimated from TGA curves measured with Derivatograph.

Results and Discussion

Visible and UV Absorption Spectra. Absorption spectra for the complexes I, II, III and IV are shown in Fig. 1 and the numerical values of the absorption bands for these complexes, including those for the other related compounds halogenated, are summarized in Table 1.

The absorption spectrum of the complex I has a band at 330 mμ which is characteristic of the coordinated acetylacetone but the maximum of the corresponding band in complex IV is shifted to 350 mμ. The spectra measured for the reaction mixtures of the complex I and NBS and those of I and ICl in methanol and in acetic acid solutions also show the shifts of the absorption maxima to 351 mμ and 357 mμ, respectively (These compounds are presumed to have the formulae, $NH_4[Cr(acac\text{-}Br)(ata)]$ and $NH_4[Cr(acac\text{-}I)(ata)]$, respectively.). Such a red shift of the maximum mentioned above which is assigned to $d_\varepsilon \rightarrow \pi_4$ transition[6] will show evidence of halogenation in

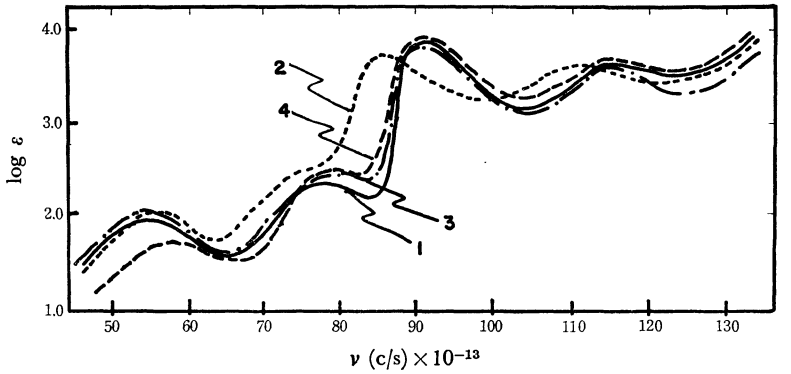

Fig. 1. The absorption spectra of the mixed complexes.
1: I (in H_2O), 2: IV (in H_2O), 3: II (in CH_3OH), 4: III (in CH_3OH)

*4 The preparation will be published elsewhere.

5) J. P. Collman, R. A. Moss, H. Maltz and C. C. Heidel, *J. Am. Chem. Soc.*, **83**, 531 (1961).

6) D. W. Barnum, *J. Inorg. Nucl. Chem.*, **21**, 221 (1961).

Table 1. UV spectra of the mixed complexes

Complex	mμ ($d_\varepsilon \rightarrow \pi_4$)	(log ε)	Solvent
$NH_4[Cr(acac)(ata)]\cdot H_2O$ I	331	(3.85)	CH_3OH, H_2O
$NH_4[Cr(acac\text{-}Cl)(ata)]\cdot \frac{1}{2}H_2O$ IV	350	(3.79)	CH_3OH, H_2O
$NH_4[Cr(acac\text{-}Br)(ata)]$*	351		CH_3OH, CH_3COOH
$NH_4[Cr(acac\text{-}I)(ata)]$*	357		CH_3OH, CH_3COOH
$[Cr(acac)(edda)]\cdot 2H_2O$ II	330	(3.80)	CH_3OH
[Cr(acac-Cl)(edda)]*	350		CH_3OH
[Cr(acac-Br)(edda)] V	351	(3.60)	CH_3OH, H_2O
[Cr(acac-I)(edda)]*	357		CH_3OH
$[Cr(acac)(edma)(H_2O)]Cl\cdot H_2O$ III	331	(3.87)	CH_3OH
$[Cr(acac\text{-}Cl)(edma)(H_2O)]Cl$*	350		CH_3COOH
$[Cr(acac\text{-}Br)(edam)(H_2O)]Cl$*	351		CH_3OH
$[Cr(acac\text{-}I)(edma)(H_2O)]Cl$*	359		CH_3OH

* Although these complexes could not be isolated, their compositions were presumed on the basis of IR spectra measurement in the respective mixed solutions.

the acetylacetonate ring[2] and this explanation can be ascertained by the fact that neither acetylacetone nor NCS (also NBS and ICl) has absorption peak near 355 mμ.

The maximum of the characteristic absorption band for the complex II appears at 330 mμ and the spectrum of the bromo-substituent V has a corresponding maximum at 351 mμ. The spectra of the chloro- and iodo-substituents (probably having the formulae, [Cr(acac-Cl)(edda)] and [Cr(acac-I)(edda)], respectively), which were measured for the reaction mixture of the complex II and NCS or ICl in methanol solution, (the reaction in acetic acid made the complex II to $[Cr(eddaH)_2]X\cdot 3H_2O$,*4 where X is halogen anion) have the maxima at 350 mμ and 357 mμ, respectively.

The maximum of the complex III appears at 331 mμ. The spectra for the complexes, which may be considered to be expressed by $[Cr(acac\text{-}X)(edma)(H_2O)]Cl$ (X=Cl, Br and I), were measured for the reaction mixtures of the complex III and halogenating reagents in acetic acid and in methanol. The band of the complex III at 331 mμ is shifted to 350 mμ by chlorination in acetic acid, but in methanol as a solvent only a small distinct shoulder appears at 350 mμ. The band at 331 mμ is also shifted to 351 mμ by bromination and to 359 mμ by iodination in methanol solvent, but in the case of acetic acid solvent, complex III decomposed very rapidly before absorption measurement.

IR Spectra. The predominant bands of IR spectra measured in the region 4000—700 cm^{-1} are listed in Table 2. The strong bands appearing between 1650 and 1670 cm^{-1} in the complexes I and IV indicate the presence of three coordinated carboxyl groups of ata. The strong bands of 1528 and 1570 cm^{-1} in the complex I are assigned to $\nu_{C=C}$ and $\nu_{C=O}$ in the coordinated acetylacetonate, respectively. In the complex IV, however, only one peak at 1560 cm^{-1} for coordinated acetylacetonate is observed in this region. This phenomenon is well known in a number of metal acetylacetonate and is commonly used to check the presence of the γ-substituted chelate ring.[1]

Table 2. IR spectra of the mixed complexes (cm^{-1})

Ccomplex	ν_{O-H}	ν_{N-H}	ν_{COO-Cr}	$\nu_{C=O(acac)}$	$\nu_{C=C}$
I	3620	3060	1650	1570	1528
		3180	1670		
		3380			
IV	3520	3040	1650	1560	
		3180			
		3390			
II	3400	3140	1635	1560	1515
	3500	3260	1675		
V		3100	1670	1550	
		3180			
		3250			
III	3410	3080	1640	1560	1530
		3140			
		3200			
		3270			

The spectra of the complexes II and III indicate the strong bands between 1630 and 1680 cm^{-1} for $\nu_{M\text{-}O\text{-}\overset{O}{\overset{\|}{C}}\text{-}}$ of coordinated edda and edma respectively and also have two strong bands characteristic of coordinated acetylacetone between 1510 and 1560 cm^{-1}. On the other hand, the spectrum of the complex V indicates only one band at 1550 cm^{-1} for acetylacetone, which suggests the substitution at γ-position.

Conductivity Measurements and Behavior toward Ion-exchangers. The values of molar conductivity of the complexes prepared in this work measured in a 1/500 mol aqueous solution at 25°C and the behavior toward ion-exchangers are summarized in Table 3, in which the symbol + indicates the possibility of the adsorption of the complexes by the resin and −, the reverse. It is found from this table that the three complexes I, II and III have the charges of −1, 0 and +1 respectively and the charges are still invariable by halogenation both in I and II.

Reactivity of the Mixed Complexes against Halogenating Agents. It may be concluded from the results obtained above that the three mixed complexes I, II and III are halogenated at

Table 3. Molar conductivity and behavior toward ion exchangers

Complex	Molar conductivity (mho cm^{-1})	Ion exchanger Na-form	Cl-form
I	104.7	−	+
IV	104.2	−	+
II	—	−	−
V	—	−	−
III	102.8	+	−

γ-position of the chelate ring irrespective of the charge in the complex ions themselves from -1 to $+1$. But the complex III which has the charge $+1$ is relatively difficult to be halogenated as compared with complex I or II. This result suggests that the positively charged complex is not as easily attacked by the electrophilic reagent, which also has positive charge, as the negatively charged or non-charged complex. This result coincides with that obtained by Collman for cobalt(III) complex and indicates that the electron density at the γ-position of acetylacetonate ring in the positively charged complex is somewhat more deficient than that of negatively charged or non-charged complexes.[1,2]

Some differences in the reactivity were observed, depending upon the solvent, and the halogenation was more vigorous in acetic acid than in methanol. NCS was milder than NBS or ICl as halogenating reagent in both solvents.

BULLETIN OF THE CHEMICAL SOCIETY OF JAPAN VOL. 42 1304—1307 (1969)

Crystal Growth of the Phosphate Coating on Iron and Steel*1

Takao UMEGAKI and Taijiro OKABE

Department of Applied Chemistry, Faculty of Engineering, Tohoku University, Sendai

and Keiichi OMORI

Institute of Mineralogy, Petrology and Economic Geology, Tohoku University, Sendai

(Received October 5, 1968)

Crystal growth of the phosphate coating on steel and pure iron was investigated by microscopic observation and X-ray diffraction. β-Hopeite was recognized as a main constituent of the phosphate coating. From the experimental results obtained in this investigation and the crystal structure of β-hopeite proposed by Gamidov and Galovachev (*Dokl. Akad. Nauk, SSSR*, **150**, 2, 381, (1963)), it was concluded that the bonding of the (010) plane of β-hopeite to the (100) plane of iron is most favorable for atomic arrangement of the phosphate coating.

Many attempts have been made to establish a theory of crystal growth since the first research by P. Curie at the end of the 19th century, and the results obtained in the course of those attempts have recently come to be applied to polymer chemistry and electronic engineering. The process of crystal growth has to be taken into account to understand the mechanism that crystals are produced on a metal surface by corrosion. The phosphate coating may be regarded as one of the most excellent utilizations of corrosion products. According to the research by Neuhaus and his coworkers,[1] phosphorus atoms in phosphate ions of the coating combine with iron atoms on the surface in such a manner that is known as Wustite bond. Notwithstanding the comprehensive investigation by Neuhaus, the detailed construction of the boundary layer between iron and phosphate coating has still remained obscure. In the present paper microscopic observation on the crystal growth of phosphates on iron surface and X-ray diffraction patterns of the phosphate coating are described and, based on our experimental results and the crystal structure of β-hopeite determined by Gamidov and Galovachev,[2] an adhesive mechanism between iron and phosphate is presented.

*1 Presented at the 21st Annual Meeting of the Chemical Society of Japan, Osaka, April, 1968.

1) A. Neuhaus and M. Gebhardt, *Dechema. Monograph*, **51**, 117 (1964).

2) R. S. Gamidov and V. P. Galovachev, *Dokl. Akad. Nauk, SSSR*, **150**, 2, 381 (1963).

Experimental

A) Microscopic Observation on Crystal Growth. The compositions of specimens of iron and steel, size of which being 3 mm×5 mm×20 mm, and that of phosphating solution are shown in Tables 1 and 2,

Table 1. Compositions of specimens (wt %)

	O	Si	Mn	F	S	Cu	Cr	Ni
iron	0.007	trace	trace	trace	0.006	0	trace	0
steel	0.20	trace	0.80	0.016	0.024	0.06	0.06	0.03

Table 2. Composition of phosphating solution

Zn^{2+} (g/l)	PO_4^{3-} (g/l)	Na_2CO_3 (g/l)	Total acidity (point)	Free acidity (point)
5.9	15.7	2.74	32.1	2.2

respectively. The specimens were polished with emery paper (0/5) and buff. When necessary, they were further etched with Nital or Picral. About 0.05 ml of the phosphating solution was dropped on the surface of the specimen placed on a deck glass. The visual field of the microscope was fixed at the same position during the observation. Most of the microscopic photographs were taken every 2 min.

B) X-Ray Diffraction. The coating obtained in the phosphating solution was scratched and stripped off with an edge of glass plate. The X-ray diffraction patterns of the powdered coating were taken with the "Geigerflex" manufactured by Rigaku Denki Co., Ltd. The diffraction data were compared with those of ASTM cards.

C) Observation on Phosphate Crystals under Polarized Light. The powdered coating used for X-ray diffraction pattern was also observed with a polarization microscope inserted with a gypsum plate. The directions of optical elasticity axes of β-hopeite were identified by comparison of the refractive indices obtained in this experiment with those in the data shown in ASTM card (9-497). The refractive indices were measured by the immersion method under the polarization microscope.

D) Calculation of the Velocity of Crystal Growth. The velocity of crystal growth of β-hopeite was calculated from the differences of the crystal length shown in microscopic photographs which were taken by the method described above.

Results and Discussion

A series of microscopic photographs from Figs. 1 to 4 shows the crystal growth of phosphate on the buff-polished carbon steel. At first, a certain number of small core crystals appeared. They grew radially, forming dendrites, and finally covered the whole surface of iron. The number of round crystals formed at the beginning remained constant during the phosphating process. A similar behavior of crystal growth was found on the buff-polished pure iron, etched carbon steel and etched pure iron. Figures 5 and 6 show the phosphate crystals which appeared on the buff-polished pure iron. The initiation of crystallization on pure iron surface was considerably delayed, compared with that on carbon steel. In Figs. 7, 8, 9 and 10, the crystals on the etched surfaces of carbon steel and of pure iron are shown. The round phosphate crystals were apt to appear in the neighborhood of grain boundaries or on the scratches of polishing.

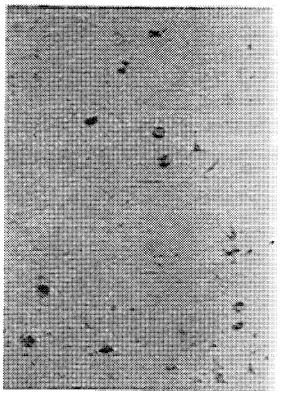

Fig. 1. Crystal growth of phosphate coating on polished carbon steel (2 min). (×180)

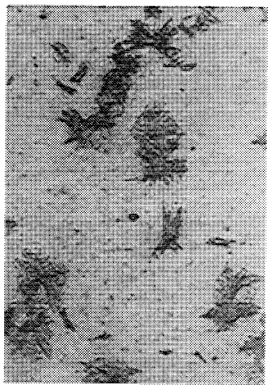

Fig. 2. Crystal growth of phosphate coating on polished carbon steel (6 min). (×180)

Fig. 3. Crystal growth of phosphate coating on polished carbon steel (10 min). (×180)

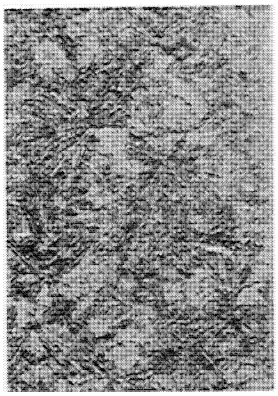

Fig. 4. Crystal growth of phosphate coating on polished carbon steel (24 min). (×180)

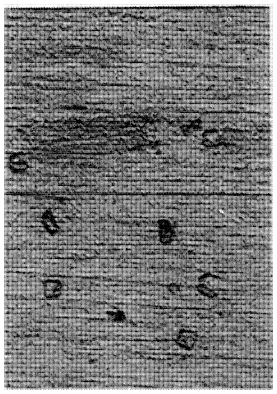

Fig. 5. Crystal growth of phosphate coating on polished pure iron (10 min). (×180)

Fig. 6. Crystal growth of phosphate coating on polished pure iron (26 min). (×180)

The order of increasing size of the phosphate crystal particles on various iron surfaces was obtained as follows: etched carbon steel, etched pure iron, buff-polished carbon steel and buff-polished pure iron. The initiation of crystallization of various iron surfaces was delayed with increasing size of the crystals. The X-ray powder diffraction pattern of the stripped coating is shown in Fig. 11. By comparison of this pattern with that in ASTM card (9-497), β-hopeite was recognized as a main constituent of the phosphate coating and a trace of vivianite was also found on it. Under the polarized microscope the direction of elongation of all β-hopeite crystals was parallel to the direction of wave motion of lower velocity, of which refractive index was 1.580. For β-hopeite two kinds of

Fig. 7. Crystal growth of phosphate coating on etched carbon steel (3 min). (×180)

Fig. 8. Crystal growth of phosphate coating on etched carbon steel (9 min). (×180)

Fig. 9. Crystal growth of phosphate coating on etched pure iron (4 min). (×180)

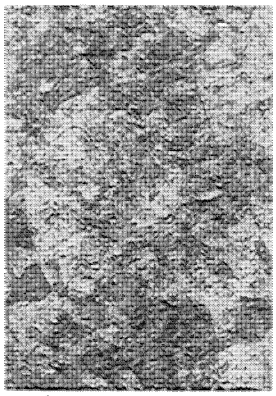

Fig. 10. Crystal growth of phosphate coating on etched pure iron (14 min). (×180)

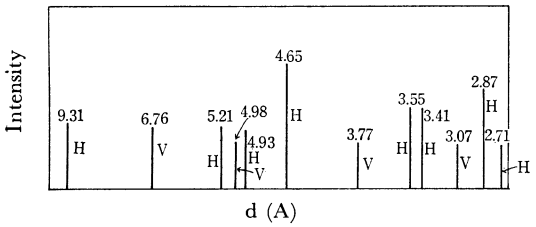

Fig. 11. X-ray diffraction pattern of stripped coating.
H: β-Hopeite V: Vivianite

optical orientation are shown in the reference:[3] $X=b$, $Y=c$, $Z=a$, or $X=b$, $Y=a$, $Z=c$. The refractive indices of β-hopeite (ASTM card 9-497) are as follows: $\alpha=1.574$, $\beta=1.582$, $\gamma=1.582$. Therefore, it is considered that the direction of elongation and also the c axis were parallel to Z axis with the minimum velocity of wave motion. The optical elasticity axes of the stripped β-hopeite were identified to be $X=b$, $Y=a$ and $Z=c$. The relations between crystal growth of β-hopeite on polished carbon steel and phosphatizing time are shown in Fig. 12. The elongation of the c axis increased linearly with time and the velocity was much greater than that in the direction perpendicular to the c axis. An overlapped projection of the (010) plane of β-hopeite and the (100) plane of iron is schematically shown in Fig. 13. In this mode of adhesion, oxygen atoms located at the apices of tetrahedra of phosphate ion can be transferred into the interstices of an iron lattice. Although some other modes of adhesion in the phosphate coating have already been presented, this mechanism may be most favorable for atomic arrangements of both iron and β-hopeite crystal.

Conclusion

The mechanism of phosphate film formation was studied with the concept that the phosphating reaction may be a kind of corrosion. Conclusions obtained from the present investigation are as follows: (a) In the phosphate coating process, small round phosphate crystals appear at the beginning as nuclei in the neighborhood of grain boundaries corroded by etching solution or on the scratches produced by polishing. (b) The nuclei of phosphate coating grow to form dendrites. The total number of nuclei does not increase during the course of phosphatization. (c) The dendritic crystals are identified as β-hopeite from a comparison of the X-ray diffraction spacings with the data of ASTM card and from the microscopic observation under polarized light. (d) Comparing the crystal structure of β-hopeite proposed by Gamidov with the results obtained in this investigation, it is concluded that the (010) plane of β-hopeite sticks on the (100) plane of iron.

This investigation was partly supported by a grant from Nippon Kokan (Japan Steel and Tube) Corp., for which the authors wish to express their sincere appreciation.

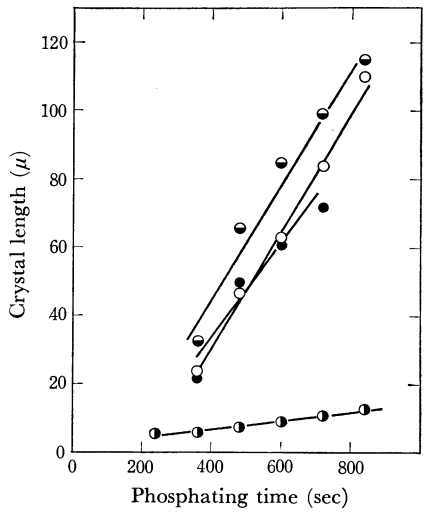

Fig. 12. Crystal growth of β-hopeite on polished carbon steel.
c-axis of various crystals
direction vertical to c-axis

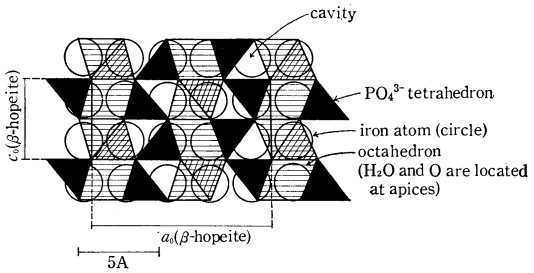

Fig. 13. Overlapped projection of the (010) plane of β-hopeite and the (100) plane of iron.
β-Hopeite: $a=10.64$A, $b=18.36$, $c=5.04$A, $Z=4$.

3) E. S. Larsen and H. Berman, "The Microscopic Determination of Nonopaque Minerals," 163, 2nd Ed. (1934).

BULLETIN OF THE CHEMICAL SOCIETY OF JAPAN VOL. 42 1308—1316 (1969)

Synthesis of Vitamin B_{12} Model Compounds

Tadashi Sasaki and Fujinao Matsunaga

Institute of Applied Organic Chemistry, Faculty of Engineering, Nagoya University, Chikusa-ku, Nagoya

(Received November 10, 1967)

Bis(dimethylglyoximato)cobalt(III) complexes with the general formula: $[CoX(DH)_2B_A]$ (X: CN^-, NO_2^-, $SeCN^-$, SCN^-, Br^-. D: dianion of dimethylglyoxime. B_A: such biologically interesting bases as imidazole, benzimidazole, 5,6-dimethylbenzimidazole, pyridine, γ-picoline, 4-vinylpyridine, nicotinic acid, isoquinoline, 5-amino-4-imidazolecarboxamide, and 6-aminopurine) were prepared from dimethylglyoxime, the base, and an adequate cobalt(III) salt. The treatment of $[CoCN(DH)_2Imd]$ (Imd: imidazole) with boron trifluoride etherate afforded $[Co(CNBF_3)(DBF_2)_2Imd]$ in an 86% yield. The reduction of $[CoCl(DH_2)Imd]$ with sodium borohydride gave a labile $[Co(I)H(DH)_2Imd]$, which was directly converted with phenylacetylene into a stable $[Co(III)(C_6H_5CH{=}CH)(DH_2)Imd]$ in a 60% yield and into $[Co(DH)_2Imd]\cdot H_2O$ in a 30% yield. These products were structurally elucidated on the basis of their spectral data.

It is known that bis(dimethylglyoximato)cobalt(III) complexes uniquely reproduce the fundamental reactions of cobalamins and are thus excellently suited for the study of the mechanisms of vitamin B_{12}-catalyzed biochemical processes.[1,2] Whereas simple alkylcobaloximes are found to be unusually stable, a surprising variation in the reactivity of the cobalt-carbon bond results from the introduction of the substituents into the cobalt-bound alkyl group.[3]

In this paper we wish to describe the preparation of new bis(dimethylglyoximato)cobalt(III) complexes containing such biologically interesting bases as imidazole, benzimidazole, 5,6-dimethylbenzimidazole, nicotinic acid, 5-amino-4-imidazolecarboxamide, and 6-aminopurine. The reactivities of some cobaloximes and the structures of these products are also discussed.

Results and Discussion

Preparation of Cobaloximes. $[CoCN(DH)_2B_A]$-*type Complexes.* Ablov[4] reported the preparation of $[CoCN(DH)_2Pyr]\cdot\frac{1}{2}H_2O$ (Pyr: pyridine) by a sequence of ligand substitution reactions:

$$[CoH_2O(DH)_2NCS] \rightarrow K[CoCN(DH)_2NCS] \rightarrow [CoCN(DH)_2Pyr]\cdot\tfrac{1}{2}H_2O.$$

On the other hand, our present preparative method is shown by:

$$4DH_2 + 2Co(OCOCH_3)_2 + 2KCN + 4B_A + \tfrac{1}{2}O_2 \rightarrow 2[CoCN(DH)_2B_A] + 2B_A\cdot CH_3COOH + 2CH_3COOK + H_2O.$$

A similar procedure has recently been reported by Varhelelyi[5] using several aromatic amines as the basic component. This report prompted us to publish this paper. The yields, compositions, colors, and results of analyses of the products using various bases are summarized in Table 1.

The yields of the products were generally lower than those of the $[CoCl(DH)_2B_A]$-type complexes described in the next paragraph. When 5-amino-4-imidazolecarboxamide or 6-aminopurine was used, the base did not coordinate to the cobalt atom, and the product was $H[Co(CN)_2(DH)_2]\cdot 2H_2O$, which was presumably formed by:

$$4DH_2 + 2Co(OCOCH_3)_2 + 2KCN + \tfrac{1}{2}O_2 \rightarrow 2H[Co(CN)_2(DH)_2] + 2CH_3COOK + H_2O.$$

$[CoCl(DH)_2B_A]$-*type Complexes.* It is well known that stable $[Co(III)Cl(DH)_2NH_3]$ can be prepared readily from DH_2, ammonia, and cobalt(II) chloride.[6] Similarly, several complexes with various bases were prepared by:

$$4DH_2 + 2CoCl_2\cdot 6H_2O + 4B_A + \tfrac{1}{2}O_2 \rightarrow 2[CoCl(DH)_2B_A] + 2B_A\cdot HCl + H_2O.$$

These results are summarized in Table 2.

$[CoX(DH)_2Imd]$-*type Complexes.* This type of

1) G. N. Schrauzer and G. Klatel, *Angew. Chem.*, **77**, 130 (1965).

2) G. N. Schrauzer and R. J. Windgassen, *J. Am. Chem. Soc.*, **88**, 3738 (1966).

3) G. N. Schrauzer and R. J. Windgassen, *bid.*, **89**, 1999 (1967), and the references cited therein.

4) A. B. Ablov and G. K. Syrtsova, *Zhur. neorg. Khim.*, **10**, 1980 (1965).

5) Cs. Varhelelyi and S. Kovendi, *J. prakt. Chem.*, **306**, 209, 341 (1967).

6) L. Tschugaeff, *Ber.*, **39**, 2694 (1906); *ibid.*, **40**, 3498 (1907).

Table 1. Preparation of $[CoCN(DH)_2B_A]$

B_A	Yield %	Composition	Found (Calcd) C%	H%	N%	Color
Imidazole	48.5	$[CoCN(DH)_2C_3H_4N_2]\cdot\frac{1}{2}H_2O$	37.43 (37.80	5.01 4.88	24.79 25.00)	orange yellow
Benzimidazole	10.1	$[CoCN(DH)_2C_7H_6N_2]\cdot H_2O$	42.57 (42.58	4.77 4.91	21.65 21.73)	yellow
5,6-Dimethyl-benzimidazole	8.5	$[CoCN(DH)_2C_9H_{10}N_2]\cdot 3/2H_2O$	44.47 (44.27	5.56 5.57	20.18 20.08)	yellow
Pyridine	25.0	$[CoCN(DH)_2C_5H_5N]\cdot\frac{1}{2}H_2O$	41.69 (41.56	5.02 5.00	20.38 20.84)	yellow
4-Vinyl pyridine	31.2	$[CoCN(DH)_2C_7H_7N]$	45.69 (45.72	5.21 5.04	19.84 19.99)	brown
Nicotinic acid	8.5	$[CoCN(DH)_2C_6H_5HNO_2]$	41.57 (41.44	4.87 4.37	16.34 15.98)	red brown
Isoquinoline	27.9	$[CoCN(DH)_2C_9H_7N]\cdot 2/3H_2O$	46.98 (47.38	4.95 4.79	19.12 18.84)	yellow
Ammonia	79.5	$[CoCN(DH)_2NH_3]\cdot 3/2H_2O$	41.57 (41.44	4.87 4.37	16.34 15.98)	orange yellow
Triphenyl-phosphine	24.5	$[CoCN(DH_2)(C_6H_5)_3P]\cdot 3/2H_2O$	54.16 (54.45	5.31 5.25	11.92 11.76)	brown
γ-Picoline	32.7	$[CoCN(DH)_2C_6H_7N]\cdot\frac{1}{2}H_2O$	43.14 (43.17	5.28 5.31	20.21 20.14)	brown yellow

Table 2. Preparation of $[CoCl(DH)_2B_A]$

B_A	Yield %	Composition	Found (Calcd) Co%	N%	Cl%	Color
Imidazole	75.6	$[CoCl(DH)_2C_3H_4N_2]\cdot H_2O$	15.0 (14.4	20.60 20.46	8.43 8.63)	yellow brown
AICA*	46.7	$[CoCl(DH)_2C_4H_6N_4O]\cdot 3/2H_2O$	12.85 (12.43	23.30 23.45	7.42 7.43)	yellow brown
Adenine	8.5	$[ClCl(DH)_2C_5H_5N_5]\cdot 4H_2O$		23.27 (23.71	7.20 6.67)	red brown
Pyridine	60.5	$[CoCl(DH)_2C_5H_5N]$	14.48 (14.58	17.19 17.34	9.14 8.78)	brown
4-Vinyl pyridine	74.5	$[CoCl(DH)_2C_7H_7N]\cdot H_2O$	14.0 (13.2	15.91 15.64	7.91 7.92)	brown
Nicotinic acid	65.5	$[CoCl(DH)_2C_6H_5NO_2]\cdot H_2O$	12.96 (12.65	15.31 15.38	7.53 7.61)	brown
Triphenyl-phosphine	57.8	$[CoCl(DH)_2(C_6H_5)_3P]$**		9.51 (9.55)		red brown

* AICA: 5-Amino-4-imidazolecarobxamide
** Found: P, 5.30%. Calcd: 5.28%.

Table 3. Preparation of $[CoX(DH)_2Imd]$ (Imd: Imidazole)

X	Yield %	Composition	Found (Calcd) C%	H%	N%	Color
NO_2	11.2	$[CoNO_2(DH)_2Imd]$	32.79 (32.60	4.62 4.48	23.80 24.20)	red brown
SeCN	8.5	$[CoSeCN(DH)_2Imd]\cdot\frac{1}{2}Imd$	32.94 (32.67	4.35 4.06	22.58 22.41)	brown
SCN	8.5	$[CoSCN(DH)_2Imd]\cdot\frac{1}{2}(Imd\cdot H_2O)$	35.93 (35.41	4.77 4.62	23.92 24.47)	red brown
NCO	8.5	$[CoNCO(DH)_2Imd]$	36.32 (36.10	5.08 4.54	24.92 24.56)	yellow
Br	32.6	$[CoBr(DH)_2Imd]$			19.40 (19.32)	yellow

complex was prepared by:

$$4DH_2+2Co(OCOCH_3)_2\cdot 4H_2O+2KX+4Imd+\tfrac{1}{2}O_2 \rightarrow 2[CoX(DH)_2Imd]+2Imd\cdot CH_3COOH+2CH_3COOK+H_2O.$$

Likewise, the preparation of $[CoBr(DH)_2Imd]$ was followed by:

$$4DH_2+2CoBr_2+2Imd+\tfrac{1}{2}O_2 \rightarrow 2[CoBr(DH)_2Imd]+2Imd\cdot HBr+H_2O.$$

The products are summarized in Table 3.

Some Reactions of Cobaloximes. The treatment of $[CoCN(DH)_2Imd].\frac{1}{2}H_2O$ with boron trifluoride etherate afforded $[Co(CNBF_3)(DBF_2)_2$-Imd] in an 86% yield. Since it is known[7] that vitamin B_{12S}, a two-electron reductant of vitamin B_{12}, shows specific reactivity with electrophilic reagents, giving complexes which are sensitive to light and air, $[CoCl(DH)_2Imd]$ was treated with sodium borohydride in a methanol-water mixture to afford a brownish-green colored, two-electron reductant. This was also unstable in air, so it was confirmed by conversion with phenylacetylene into $[Co(III)(C_6H_5CH{=}CH)(DH)_2Imd]$:

$$4[Co(III)Cl(DH)_2Imd]+NaBH_4 \rightarrow 4[Co(I)H(DH)_2Imd]+NaBCl_4.$$
$$[Co(I)H(DH)_2Imd]+C_6H_5C{\equiv}CH \rightarrow [Co(III)(C_6H_5CH{=}CH)(DH)_2Imd].$$

The side-formation of $[Co(II)(DH)_2Imd]$ in this reaction might be explained by:[2]

$$[Co(III)(C_6H_5CH{=}CH)(DH)_2Imd]+[CoCl(DH)_2Imd] \rightarrow [Co(II)(DH)_2Imd]+C_6H_5CH{=}CHCl.$$
$$[Co(I)H(DH)_2Imd]+[Co(III)(C_6H_5CH{=}CH)\text{-}(DH)_2Imd] \rightarrow [Co(II)(DH)_2Imd]+C_6H_5CH{=}CH_2.$$

These reactivities are similar to those of vitamin B_{12S}.

Structural Elucidation. The ultraviolet and visible spectra of $[CoCN(DH)_2B_A]$-type complexes showed similar absorption patterns regardless of the kind of base, except for triphenylphosphine; the absorption maxima ranged from 240 to 245 mμ ($\log\varepsilon=4.4$), from 280 to 290 (shoulder, 3.7—3.8) and from 330 to 340 (shoulder, 3.1—3.4), as is shown in Figs. 1 and 2 and in Table 4; the strongest absorption due to a coordinated dimethylglyoximate ion[8] was too strong for the other two absorptions to be obvious. Considering their similarity in the spectra of $[Co(DH)_2(NH_3)_2]Cl$, $[CoCl(DH)_2NH_3]$, $H[CoCl(DH)_2]$,[9,10] and $[Co(DH)_2A_2]Cl$[11] (A: butylamine, ammonia, pyridine), we concluded that our $[CoCN(DH)_2B_A]$-type complexes have similar structures, in which two dimethylglyoximate ions are coordinated and are coplanar with the cobalt, taking a cyano group and the base in a *trans*-configuration as is illustrated in Scheme 1. When

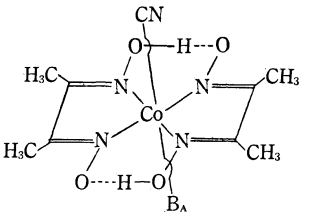

Scheme 1

triphenylphosphine was used, the UV pattern was quite different from those of the above compounds, as is shown in Fig. 3; it manifested an absorption at 374 mμ which rather resembled that of $[Co(DH)_2A']Cl$ (A′: aniline and its derivatives),[11] where an absorption at 340—380 mμ is interpreted as a charge-transfer spectrum from aniline to the cobalt atom. Therefore, we interpreted the absorption at 374 mμ as being due to a charge-transfer from triphenylphosphine to the cobalt atom. Furthermore, based on Nakahara's UV spectral data about other bis(dimethylglyoximato)cobalt-(III) complexes,[9] we concluded that the cobalt-

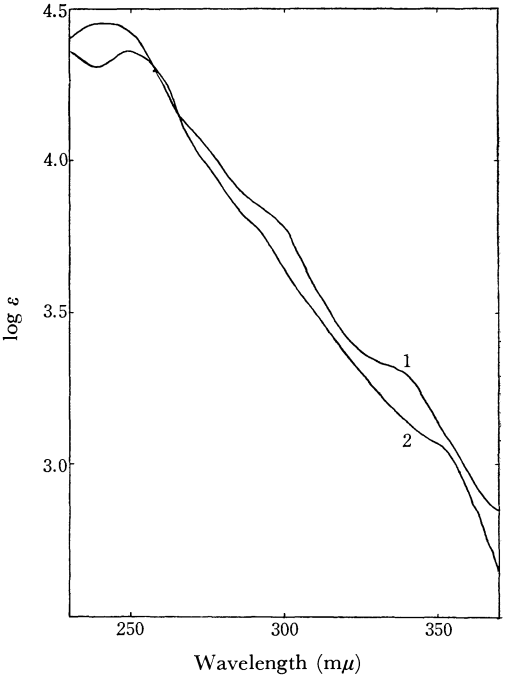

Fig. 1. UV Spectra of $[CoX(DH)_2Pyr]$ (X=CN, Cl).
Solvent: MeOH
1, $[CoCN(DH)_2Pyr]$ 2, $[CoCl(DH)_2Pyr]$

7) R. Bonnet, *Chem. Revs.*, **63**, 573 (1963).
8) A. Nakahara, This Bulletin, **27**, 560 (1954).
9) A. Nakahara, *ibid.*, **28**, 207 (1955).
10) H. Kuroya, *J. Inst. Polytechnics, Osaka City Univ.*, **1**, No. 2, Ser. C, 11 (1950).
11) C. Matsumoto, T. Kato and K. Shinra, *Nippon Kagaku Zasshi* (*J. Chem. Soc. Japan, Pure Chem. Sect.*), **86**, 1266 (1965).

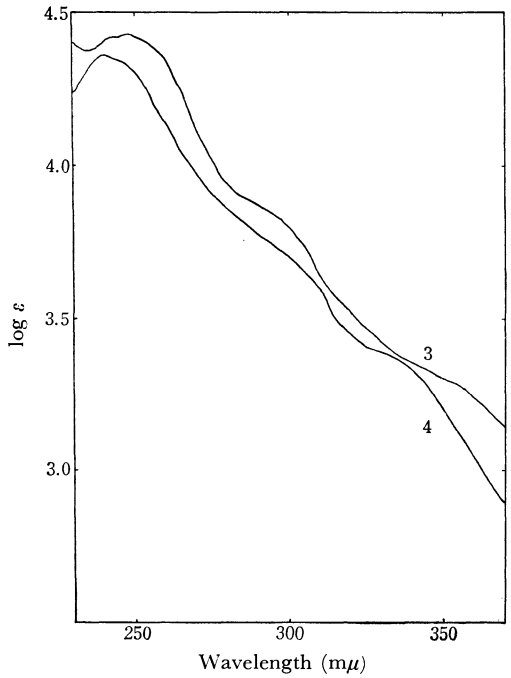

Fig. 2. UV Spectra of [CoX $(DH)_2$ Imd] (X=CN, Cl).
Solvent: MeOH
3, [CoCl$(DH)_2$Imd] 4, [CoCN$(DH)_2$Imd]

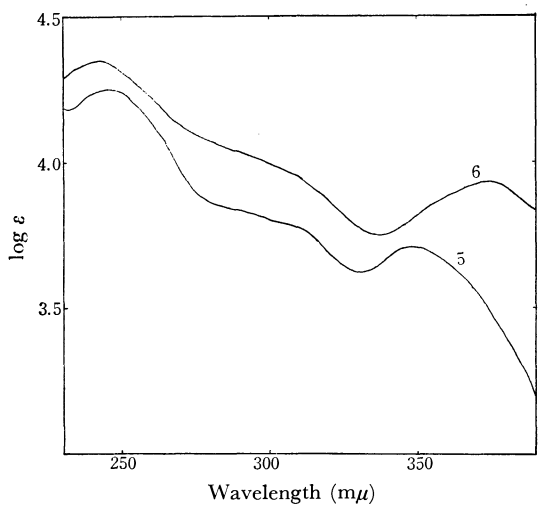

Fig. 3 UV Spectra of [CoSeCN$(DH)_2$Imd] and [CoCN$(DH)_2P(Ph)_3$].
Solvent: MeOH
5, [CoSeCN(DH_2)Imd] 6, [CoCN$(DH)_2P(Ph)_3$]

(III) formed an ionic bonding with the phosphorus atom in [CoCN$(DH)_2P(Ph)_3$].

Both [CoCl$(DH)_2B_A$]- and [CoX$(DH)_2$Imd]-type complexes showed patterns similar to [CoCN$(DH)_2$B], as Tables 5 and 6 show. These similarities demonstrate that they have similar structures.

Table 4. UV absorption maxima of [CoCN$(DH)_2B_A$] (in MeOH)

B_A	Characteristic absorption band mμ	(log ε)	Other absorption band mμ	(log ε)
Imidazole	241	(4.46)	—	
Benzimidazole	242	(4.39)	—	
5,6-Dimethyl-benzimidazole	241	(4.40)	—	
Pyridine	241	(4.45)	—	
γ-Picoline	243	(4.42)	—	
4-Vinyl pyidine	246	(4.43)	—	
Nicotinic acid	245	(4.41)	—	
Isoquinoline	245	(4.46)	—	
Triphenyl-phosphine	241	(4.35)	374	(4.10)
Ammonia	242	(4.35)	—	
Dimethyl-glyoxime	226	(4.35)	—	

The fact that the characteristic band of a dimethylglyoximate ion in [CoCl$(DH)_2B_A$] showed somewhat bathochromic shifts compared with those of [CoCN$(DH)_2B_A$] can be explained in terms of Tsuchida's spectrochemical series.[12] The same principle can be applied in explaining why the characteristic absorptions at around 250 mμ in [CoX$(DH)_2$Imd] were changed to some extent according to the species of the X ligand, as is shown in Table 6.

Table 5. UV absorption maxima of [CoCl$(DH)_2B_A$] (in MeOH)

B_A	Characteristic absorption band mμ	(log ε)	Other absorption band mμ	(log ε)
Imidazole	248	(4.43)	—	
AICA	258	(4.42)	—	
Adenine	264	(4.25)	—	
Pyridine	247	(4.38)	—	
4-Vinyl pyridine	248	(4.40)	—	
Nicotinic acid	250	(4.43)	—	
Triphenyl-phosphine	260	(4.45)	324	(4.17)
Ammonia	246	(4.38)	—	
Dimethyl-glyoxime	226	(4.35)	—	

Table 6. UV absorption maxima of [CoX$(DH)_2$Imd] (in MeOH)

X	Characteristic absorption band mμ	(log ε)	Other absorption band mμ	(log ε)
NO_2	245	(4.20)	—	
SeCN	242	(4.20)	348	(3.71)
NCO	244	(4.18)	—	
Br	250	(4.39)	—	

12) R. Tsuchida and M. Kobayashi, This Bulletin, **13**, 471 (1938); R. Tsuchida, *ibid.*, **13**, 388, 442 (1938).

The infrared spectra of the dimethylglyoximate moiety in $[CoX(DH)_2B_A]$ are shown in Tables 7, 8, and 9. As may clearly seen from these tables, the weak absorption of ν_{OH} in $[CoX(DH)_2B_A]$ at 1740—1770 cm^{-1} [13] demonstrate that these complexes take a *trans*-configuration between X and B_A; this further substantiates the conclusion from the UV data described above. This was also supported by the chemical behavior of these cobaloximes in readily forming an O–BF_2–O bonding by the interaction of two O–H–O bondings in cobaloximes with boron trifluoride etherate. The other assignments in these tables were made on the basis of Schrauzer's data.[3]

TABLE 7. IR SPECTRA OF $[CoCN(DH)_2B_A]$ (cm^{-1})

B_A	$\nu_{C\equiv N}$	$\nu_{O-H\cdots O}$	$\nu_{C=N}$	ν_{NO}	δ_{NO}
Imidazole	2155	1750	1553	1240	1095
Benzimidazole	2160	1750	1569	1240	1095
5,6-Dimethyl-benzimidazole	2155	1745	1565	1240	1097
Pyridine	2155	1745	1565	1243	1095
γ-Picoline	2160	1745	1560	1245	1094
4-Vinyl pyridine	2160	1750	1569	1240	1095
Nicotinic acid	2160	—	1568	1240	1098
Isoquinoline	2160	1750	1565	1242	1098
Triphenyl-phosphine	2155	1760	1560	1245	1090
Ammonia	2160	1760	1575	1242	1097
CN	2230	1740	1569	1248	1100

TABIE 8. IR SPECTRA OF $[CoCl(DH)_2B_A]$ (cm^{-1})

B_A	$\nu_{O-H\cdots O}$	$\nu_{C=N}$	ν_{NO}	δ_{NO}
Imidazole	1740	1555	1239	1090
AICA	1760	1565	1243	1098
Adenine	1750	1570	1230	1095
Pyridine	1740	1560	1240	1090
4-Vinyl pyridine	1740	1560	1240	1090
Nicotinic acid	—	1570	1240	1098
Triphenyl-phsophine	1770	1560	1244	1090

TABLE 9. IR SPECTRA OF $[CoX(DH_2)Imd]$ (Imd: Imidazole) (cm^{-1})

X	$\nu_{O-H\cdots O}$	$\nu_{C=N}$	ν_{NO}	δ_{NO}
CN	1750	1533	1240	1095
NO_2	1755	1568	1243	1098
SeCN	1755	1565	1245	1098
SCN	1740	1567	1241	1093
NCO	1755	1565	1245	1098
Cl	1740	1555	1239	1090
Br	1750	1560	1239	1090

13) A. Nakahara, This Bulletin, **29**, 296 (1956). He concluded that an absorption band at 1725 cm^{-1} of hydrogen dichloro-bis(dimethylglyoximato)cobalt(III) was attributable to an OH stretching frequency when intramolecular O–H···O hydrogen bonds were formed.

The multiple absorption bands due to ν_{NH} in imidazole at 2600—3110 cm^{-1} were changed into a single band at around 3150 cm^{-1} by the complex formation, as is shown in Table 10. This means that the formation of σ- or π-bonding between the nitrogen and the cobalt atom, as is shown in Scheme 2, causes any change in the electron density

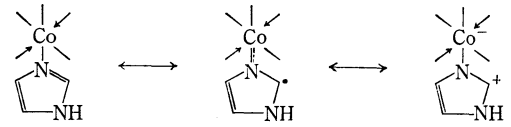

Scheme 2

of an N–H bonding or the bond distance. The simplification of ν_{NH} absorption bands by the complex formation can be explained in terms of the prohibition of the tautomerism based on the prototropy of the imidazole ring proton. George[14] has pointed out that an acid dissociation constant of an imino group of a non-coordinated imidazole is less than that of a coordinated one to an iron atom, indicating the prohibition of the ionic structures by the complex formation.

TABLE 10. NH STRETCHING VIBRATION OF IMIDAZOLE (cm^{-1})

Compound	ν_{NH}
[Imidazole]	3110—2600 (m*)
$[CoCN(DH)_2Imd]$	3150 (m)
$[CoNO_2(DH)_2Imd]$	3150 (m)
$[CoSeCN(DH)_2Imd]$	3150 (s*)
$[CoSCN(DH)_2Imd]$	3140 (s)
$[CoCl(DH)_2Imd]$	3150 (m)
$[CoNCO(DH)_2Imd]$	3150 (m)
$[CoBr(DH)_2Imd]$	3150 (m)

* Strength. m: medium and s: strong.

As for 5-amino-4-imidazolecarboxamide, a question arises regarding to which position the cobalt atom is bound. The infrared spectrum of $[CoCl(DH)_2AICA]$ (AICA: 5-amino-4-imidazolecarboxamide) gives some information on this point; it is expected[15] that if the amidocarbonyl were coordinated to a cobalt atom, as is shown in (a) of Scheme 3, the ν_{NH} absorption of the amidocarbonyl

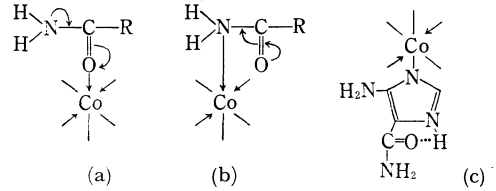

Seheme 3

14) P. George, I. H. Hanania and D. H. Irvine, *J. Chem. Soc.*, **1964**, 5689.

15) N. Gerrad, *ibid.*, **1960**, 2144.

group would shift to a lower wave number. If it were coordinated to the nitrogen atom of the amide group (b), the ν_{NH} absorption would shift to a lower, but the ν_{CO} absorption of the amide would shift to a higher wave number. Table 11 indicates that the ν_{NH} absorption shifted up by about 10 cm^{-1} and that the ν_{CO} absorption shifted down by about 17 cm^{-1}, indicating that [CoCl-$(DH)_2$AICA] has no such linkages as shown in (a) and (b). The slight shift of the ν_{CONH_2} absorption to a lower wave number can be explained in terms of the prohibition of the prototropy of an imidazole-ring proton by the complex formation, resulting in the easier formation of hydrogen bond than free AICA. This suggests that the cobalt atom is coordinated to the nitrogen atom of the imidazole ring, as is shown in (c) of Scheme 3.

Table 11. Characteristic IR absorption bands of AICA (cm^{-1})

Compound	ν_{CONH_2}	ν_{as-NH_2}	ν_{s-NH_2}	ν_{CONH_2}	δ_{NH_2}
AICA	3430	3300	3220	1680	1624
[$CoCl(DH)_2$-AICA]	3440	3300	3230	1663	1621

The same problem is encountered in 6-aminopurine. The basicity of adenine is not strong enough for the basic center to be the same as the coordination center; therefore, the basic center is not very important in this case. If the cobalt atom were coordinated to an amino group of adenine, the ν_{NH} absorption should shift to a wave number lower by 100—150 cm^{-1}, while the δ_{NH} absorption should not change at all or shift to a slightly higher wave number.[16] The fact that both the γ_{NH} and δ_{NH} absorptions shifted to lower wave numbers, as is shown in Table 12, indicates the absence of any coordination of the amino group to the cobalt atom. The 12 cm^{-1} shift of the $\nu_{C=C,C=N}$ of the purine ring to a higher wave number upon the complex formation may be explained in terms of the lowering of the resonance contribution of the purine ring. Considering that pseudo B_{12}, which is different from B_{12} in containing adenine instead of 5,6-dimethylbenzimidazole, has a coordinate bond between the nitrogen atom of the imidazole ring and the cobalt atom,[17] [$CoCl(DH)_2$Adenine] may be supposed to have the same type of coordinate bond.

Table 12. Characteristic IR absorption bands of adenine (cm^{-1})

	ν_{as-NH_2}	ν_{s-NH_2}	δ_{NH}	$\nu_{C=C,C=N}$
Adenine	3290	3110	1668	1605
[$CoCl(DH)_2$-$C_5H_5N_5$]	3310	3190	1655	1617

16) J. Chatt, L. A. Duncanson and L. M. Venanzi, *ibid.*, **1955**, 4461.

17) E. A. Kaczka, D. E. Wolf, F. A. Kuehl and K. Folkers, *J. Am. Chem. Soc.*, **73**, 3569 (1951).

Table 13 shows the characteristic infrared absorption bands of the chelates involving benzimidazole ($C_7H_6N_2$) and 5,6-dimethylbenzimidazole ($C_9H_{10}N_2$). All had a common strong band at 3120 cm^{-1} upon the complex formation; this band perhaps originated from the prohibition of the tautomerism based on the prototropy of a benzimidazole-ring proton. The fact that the absorptions due to both the ν_{NH} of the imidazole ring and the $\nu_{C=C}$ of the phenyl part did shift to higher wave numbers may be caused by the decrease in the conjugation of the benzimidazole ring, as is shown in (c) of Scheme 3.

Table 13. Characteristic IR absorption bands of chelates involving benzimidazole and 5,6-dimethylbenzimidazole (cm^{-1})

Compound	ν_{NH}	$\nu_{C=N}$	$\nu_{C=C}$
Benzimidazole	3120—2450	1621	1590
[$CoCN(DH)_2C_7H_6N_2$]	3130	1625	1598
[$CoCN(DH)_2C_9H_{10}N_2$]	3130	1630	1952

Table 14 shows the characteristic infrared absorption bands of the chelates involving pyridine derivatives in comparison with those of pyridine derivatives. If a nitrogen-cobalt linkage were formed of σ- and π-bonding, a decrease in the conjugation of the pyridine ring would be expected; such a decrease is, in fact, shown in this table by the 10—30 cm^{-1} shift to a higher wave number of the absorption due to the $\nu_{C=C}$ of the pyridine ring.

Table 14. Characteristic IR absorption bands of pyridine derivatives (cm^{-1})

Compound	$\nu_{C=C}$, ν_{CO}	$\nu_{C=C,C=N}$	$\Delta\nu_{C=C,C=N}$
4-Vinyl pyridine	1631	1598	—
[$CoCl(DH)_2C_7H_7N$]	—	1617*	$-\Delta 19$
[$CoCN(DH)_2C_7H_7N$]	—	1622*	$-\Delta 24$
Pyridine	—	1580	—
[$CoCl(DH)_2C_5H_5N$]	—	1609	$-\Delta 29$
[$CoCN(DH)_2C_5H_5N$]	—	1609	$-\Delta 29$
Nicotinic acid	1710	1600	—
[$CoCl(DH)_2C_6H_5NO_2$]	1720	1610	$-\Delta 10$
[$CoCN(DH)_2C_6H_5NO_2$]	1723	1607	$-\Delta 7$
γ-Picoline	—	1609	—
[$CoCN(DH)_2C_6H_7N$]	—	1622	$-\Delta 13$
Isoquinoline		1630	—
[$CoCN(DH)_2C_9H_7N$]		1638	$-\Delta 8$

Table 15 shows the characteristic infrared absorption bands of X in [$CoX(DH)_2Imd$] (X: NO_2, NCO). As for [$CoNO_2(DH)_2Imd$], there are possible two structures; it can be assigned either to a nitro or to a nitrito complex. Nakamoto[18] has

18) K. Nakamoto, J. Fujita and H. Haruta, *ibid.*, **80**, 4517 (1958).

provided a method of discrimination by means of infrared spectral comparison. As is shown in Table 14, the infrared spectrum of $[CoNO_2(DH)_2Imd]$ was compared with those of known nitro and nitrito complexes. From its similarity to the former, we concluded that $[CoNO_2(DH)_2Imd]$ was a nitro complex. Likewise, our $[CoNCO(DH)_2Imd]$ was concluded to be an isocyanato complex with a cobalt-nitrogen bonding.[19]

Table 15. Characteristic IR absorption bands of $[CoX(DH)_2Imd]$ (cm^{-1})

X: NO_2

Compound	ν_{as-NO_2}	ν_{s-NO_2}	δ_{NO_2}
$[Co(NH_3)_5NO_2]Cl_2$	1428	1310	824
$[Co(NH_3)_5ONO]Cl_2$	1468	1065	825
$[CoNO_2(DH)_2Imd]$	1425	1323	822

X: NCO

Compound	$\nu_{N=C=O}$
$Et_4N[Co(NCO)_4]$	2217(shoulder), 2179(very strong)
$[CoNCO(DH)_2Imd]$	2200 (very strong)

As for thiocyanato- and selenocyanatocobaloxime, these complexes are shown by their microanalyses (Table 3) to consist of 1 mol of $[CoSCN(DH)_2Imd]$ or $[CoSeCN(DH)_2Imd]$ and ½mol of Imd·H_2O. This means that the thiocyanate- and selenocyanate ions and imidazole have some specific characteristics as ligands in these complexes; concerning this subject many papers have been published.[20] As is shown in Table 16, absorptions due to $\nu_{C\equiv N}$ shifted to higher wave numbers in the following sequence:

M-CS(Se)<M-S(Se)CN<M-NCS(Se)-M,M-NCS(Se)-B

where M is the metal and where B is a base such as $PyrH^+$, NH_4^+, or Et_4N^+.

From Table 16, it can be said that:

M-NCS(Se)<2080 cm^{-1} and M-S(Se)CN>2080 cm^{-1}

It is generally believed that Co(III) forms a Co–S(Se) bonding in the thiocyanatocomplexes of B_{12}[21] and in $(NH_4)[Co(SeCN)_2(DH)_2]\cdot 3H_2O$.[22] The presence of an absorption due to ν_{CN} at 2135 cm^{-1} in $[CoSCN(DH)_2Imd]\cdot ½Imd\cdot H_2O$ and at 2120 cm^{-1} in $[CoSeCN(DH)_2Imd]\cdot ½Imd$, both located in the >2080 cm^{-1} region, demonstrates that these two complexes have a bridged structure with a

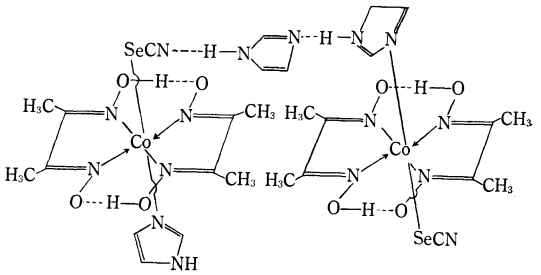

Scheme 4

Table 16. $\nu_{C\equiv N}$ of thiocyanato- and selenocyanatocomplexes (cm^{-1})

Compound	Frequency (cm^{-1})	Structure	Ref.**
KSCN	2053 s*		a
KSeCN	2070 s*		b
$K_2[Pt(SCN)_6]$	2125 s*	Pt-SCN	c
$K_2[Pt(SeCN)_6]$	2124 s*	Pt-SeCN	i
$((CH_3)_4N)_2[Co(NCS)_4]$	2075 s*		d
$((CH_3)_4N)_2[Co(NCSe)_4]$	2075 s*		d
$((C_2H_5)_4N)_2[Co(NCS)_4]$	2053 s*		i
$((C_2H_5)_4N)_2[Co(NCSe)_4]$	2053 s*		i
$(NH_4)[Cr(NCS)_4(NH_3)_2]$	2110	Cr-NCS	26
$[Co(Pyr)_2(NCS)_2]$	2088	Co-NCS-Co	e
$K_2[Co(NCS)_4]$	2058—2079	Co-NCS	f
$[(PyrH)_3Mo(NCS)_6]$	2037—2049		25
$[(PyrH)_4Mo_2O_3(NCS)_6]$	2066	Bridge suggested	25
$[Co(NH_3)_5(NCS)(NO_3)_2]$	2114		g
$[Co(en)_2(NCS)_2]Cl\cdot H_2O$	2122		g
$[HgCo(NCS)_4]$	2137	Hg-SCN-Co	h
$[(CH_3)_4N]_3[Cr(NCSe)_6]$	2067 s* 2041 sh*		26
$[Co(SCN(DH)_2Imd]\cdot ½(Imd.H_2O)$	2135	Bridge suggested	
$[CoSeCN(DH)_2Imd]\cdot ½Imd$	2120	Bridge suggested	

s*: strong. sh*: shoulder. **a) P. O. Kinell and B. Strandberg, *Acta Chem. Scand.*, **13**, 1067 (1959). b) H. W. Morgan, *J. Inorg. Nucl. Chem.*, **16**, 368 (1960). c) M. M. Chanberlain and J. C. Bailar, *J. Am. Chem. Soc.*, **81**, 6412 (1959). d) F.A. Cotton, D. M. L. Goodgame and T. E. Hass, *J. Inorg. Chem.*, **1**, 565(1962). e) P. Koshito, *Krystallografiya*, **4**, 239 (1959). f) Zhdanov, Tishchenko, and Zvanhova, *Zhur. Fis. Khim.*, **24**, (1950). g) J. Fujita, K. Nakamoto and M. Kobayashi, *J. Am. Chem. Soc.*, **78**, 3295 (1956). h) Tefferu, *Nature*, **159**, 610 (1947). i) A. Turco, C. Pecile and M. Nicolini, *J. Chem. Soc.*, **1962**, 3008.

19) The complexes thus far reported in this field all have metal-nitrogen bonding. $K_2[Co(NCO)_4]$: C. M. Blomstrand, *J. prakt. Chem.*, **3**, (2), 221 (1871); $K[M(NCO)_3]$ (M: Cu, Cd), $M[(CH_2)_6N_4]_2[(H_2O)_4M(NCO)_4]$ (M: Co, Ni, Cu): R. Ripan, *Chem. Zentr.*, **12**, (i), 967 (1930). $(NEt_4)_2[M(NCO)_4]$ (M: Mn, Fe, Co, Ni, Cu, Zn, Cd) and $(NEt_4)_2[Fe(III)(NCO_4)]$: D. Forster and D. M. L. Goodgame, *J. Chem. Soc.*, **1964**, 2790; *ibid.*, **1965**, 266.

20) S. E. Livingstone, *Quart. Revs.*, **19**, 386 (1965) and the references cited therein.

21) P. C. H. Mitchell and R. J. P. Williams, *J. Chem. Soc.*, **1960**, 1912.

22) A. V. Ablov and V. N. Safranski, *Zhur. neorg. Khim.*, **9**, 585 (1964).

Co–S(Se) bonding, while the imidazole intervenes, as is shown in Scheme 4. This is supported by the presence of a strong absorption due to the ν_{NH} of the imidazole ring; this absorption is clearly different from those of the other cobaloximes described above.

Table 17. IR absorption bands (cm^{-1})

Compound	$\nu_{C=N}$	ν_{B-O}	ν_{B-F}	δ_{B-O}
$[Ni(DBF_2)_2]$	1648	1193	1026	826
$[Co(CNBF_3)(DBF_2)_2Imd]$	1620	1203	1025	818

In Table 17 the infrared spectrum of $[Co(CNBF_3)(DBF_2)_2Imd]$ is compared with that of known $[Ni(DBF_2)_2]$, which possesses a bridged N–CN–BF_2 structure.[23] Their similar absorption patterns suggest that a bridged Co–CN–BF_2 bonding might also be involved in $[Co(CNBF_3)(DBF_2)_2Imd]$; this is further supported by the presence of an absorption due to ν_{CN} at 2240 cm^{-1}, located at a higher wave number than those of the general cobaloximes at 2155—2160 cm^{-1} described above.

Table 18. Far-infrared spectra of $[CoX(DH)_2B]$-type complexes (cm^{-1})

Compound	ν_{Co-N}
$[CoNO_2(DH)_2Imd]$	516
$[CoCN(DH)_2Imd]$	518, 519 sh*
$[CoCl(DH)_2Imd]$	518
$[CoCN(DH)_2Pyr]$	518, 529 sh*
$[CoCl(DH)_2Pyr]$	518

sh*: shoulder

Table 18 shows the far-infrared spectra due to ν_{Co-N} in $[CoX(DH)_2B_A]$-type complexes; the data are in good accordance with Schrauzer's data,[2] indicating no remarkable change upon a variation in the bases.

Experimental

Materials. Benzimidazole was prepared by the known method.[24] 5,6-Dimethylbenzimidazole was prepared from 4,5-diamino-1,2-dimethylbenzene[25] by the method of Takatori *et al.*[26] Potassium cyanate[27] and selenocyanate[28] were prepared by the usual methods. All the other reagents were commercially available and were used after purification if neccessary.

Preparation of Complexes. $[CoCN(DH)_2B_A]$, B_A: Imd. Into filtered solution*1 of 2.8 g (0.024 mol) of DH_2 and 2.6 g (0.011 mol) of $Co(OCOCH_3)_2\cdot 4H_2O$ in 100 m*l* of hot 80% ethanol, there was stirred 0.7 g (0.01 mol) of KCN*2 at room temperature. To this stirred solution there was then added 1 g (0.015 mol) of imidazole, after which the reaction mixture was aerated for 1 hr. The precipitated yellow-purple powders were collected, washed thoroughly with water, ethanol, and finally with ether, and dried in air. The yield and the results of analysis are given in Table 1.

$H[Co(CN)_2(DH)_2]$: When 5-amino-4-imidazolecarboxamide or 6-aminopurine was used as the base in the above experiments, fine, thin, yellow crystals (mp >300°C) were obtained in a yield of 31 or 43% respectively. They are quite soluble in ethanol.

Found: C, 31.38; H, 4.75; N, 22.23%. Calcd for $H[Co(CN)_2(DH)_2]\cdot 2H_2O$: C, 31.78; H, 5.07; N, 22.22%.

$[CoCl(DH)_2B_A]$: B_A: Imd. To a ho , filtered solution of 2.8 g (0.024 mol) of DH_2 and 2.5 g (0.011 mol) of $CoCl_2\cdot 6H_2O$ in 100 m*l* of 95% ethanol,*3 1 g (0.015 mol) of imidazole was added; the reaction mixture was then kept standing overnight at room temperature. The resulting brown-yellow powder was filtered and worked up as above. The results are summarized in Table 2, together with those obtained using several other bases.*4

$[CoSeCN(DH)_2Imd]\cdot \frac{1}{2}Imd$: To a hot, filtered solution of 1.4 g (0.012 mol) of DH_2 and 1.3 g (0.006 mol) of $Co(OCOCH_3)_2\cdot 4H_2O$ in 50 m*l* of hot ethanol, there was added 0.75 g (0.050 mol) of potassium selenocyanate. After it had been completely dissolved in the reaction mixture, 0.5 g (0.0075 mol) of imidazole was added. The resultant clear solution was aerated for 1 hr, after which the reaction mixture was kept standing overnight at room temperature. The crystalline precipitates were collected and worked up as above to afford a selenocyanatocomplex. Similarly, the corresponding isocyanato- and thiocyanatocomplex were prepared. These results are summarized in Table 3.

$[CoNO_2(DH)_2Imd]$: This was prepared similarly from 2.8 g (0.024 mol) of DH_2, 2.6 g (0.011 mol) of $Co(OCOCH_3)_2\cdot 4H_2O$, 1 g (0.015 mol) of potassium nitrite, and 100 m*l* of hot 80% ethanol. The results are given in Table 3.

$[CoBr(DH)_2Imd]$: To a hot, filtered solution of 1.4 g (0.012 mol) of DH_2 and 1.7 g (0.006 mol) of $CoBr_2\cdot 6H_2O$ in 50 m*l* of 95% ethanol, there was added 0.5 g (0.0075 mol) of imidazole; the reaction mixture was then kept standing overnight at room temperature, after which the precipitates were worked up as above. The results are given in Table 3.

$[Co(CNBF_2)(DBF_2)_2Imd]$: To 15 m*l* of boron trifluoride etherate there was added 0.5 g of $[CoCN(DH)_2Imd]\cdot \frac{1}{2}H_2O$, and the resulting red solution was kept standing overnight at room temperature. The precipitates were collected and worked up as above to give 0.8 g (86%) of fine, thin, yellow crystals, mp >300°C.

23) G. N. Schrauzer, *Chem. Ber.*, **95**, 1438 (1962).
24) "Organic Syntheses," Coll. Vol. II, p. 65 (1943).
25) Noelting, Braun and Thesmar, *Ber.*, **34**, 2252 (1901).
26) K. Takatori, Y. Yamada and O. Kawasima, *J. Pharm. Soc. Japan*, **75**, 881 (1955).
27) "Inorganic Syntheses," **2**, 87 (1946).
28) "Inorganic Syntheses," **2**, 186, 188 (1946).

*1 Without the filtering of the unidentified by-product, the crystallization of the produced complexes did not proceed smoothly.

*2 A desired complex could not be isolated when the base was added to the reaction mixture before potassium cyanide was added.

*3 When nicotinic acid, 5-amino-4-imidazolecarboxamide, or 6-aminopurine was used, a large amount of ethanol should be used for obtaining a clear solution because of the low solubility of these bases in ethanol.

*4 The similar treatment of 2-vinylpyridine did not afford any complex.

Found: N, 17.90%. Calcd for $[Co(CNBF_3)(DBF_2)_2\text{-}Imd]$: N, 17.93%.

$[Co(C_6H_5CH{=}CH)(DH)_2Imd]$ and $[Co(DH)_2Imd]\cdot H_2O$: Air in a suspension of 1.5 g (0.0037 mol) of $[CoCl(DH)_2Imd]$ in 10 m*l* of 80% methanol was completely removed at −70°C under a high vacuum. With strictly excluded air, a solution of 0.15 g (0.004 mol) of sodium tetrahydridoborate in a small amount of water was added to the reaction mixture. The mixture turned greenish-brown. Again, in the absence of air, 0.6 m*l* (0.0049 mol) of phenylacetylene was added to the reaction mixture and the mixture was kept standing overnight at room temperature. The resulting yellow crystals were collected and worked up as above to give 0.4 g (30%) of $[Co(DH)_2Imd]\cdot H_2O$, mp >300°C.

Found: C, 36.07; H, 5.23; N, 22.93%. Calcd for $[Co(DH)_2Imd]\cdot H_2O$: C, 35.93; H, 5.93; N, 22.53%.

The red filtrate was condensed to 30 m*l*, and the resulting orange needles were collected and recrystallized from chloroform to afford 1 g (60%) of $[Co(C_6H_5CH{=}CH)(DH)_2Imd]$, mp 232—233°C.

Found: C, 49.46; H, 5.68; N, 18.22%. Calcd for $[Co(C_6H_5CH{=}CH)(DH)_2Imd]$: C, 49.11; H, 5.52; N, 18.24%.

Measurements. The melting points were determined by a Yanagimoto micromelting-point apparatus and are uncorrected. The infrared spectra were measured in KBr pellets with a JASCO, Model IR-S infrared spectrometer, while the far-infrared were measured with a Perkin-Elmer grating infrared spectrometer, Model 337. All the ultraviolet and visible spectra were taken in methanol with a JASCO recording spectrometer, Model ORD/UV-5.

The authors would like to express their deep thanks to the Takeda Science Research Foundation for supporting this work in part.

BULLETIN OF THE CHEMICAL SOCIETY OF JAPAN VOL. 42 1316—1321 (1969)

A Mechanistic Approach to the Electrolytic Reductive Dimerization of Acrylonitrile

Teruzo ASAHARA, Manabu SENŌ and Takeshi ARAI*1

Institute of Industrial Science, The University of Tokyo, Minato-ku, Tokyo

(Received February 24, 1968)

The electrolytic reductive dimerization of acrylonitrile was investigated extensively especially in order to obtain some mechanistic information. The essential point of this reaction exists in the selective formation of adiponitrile under relatively wide conditions and this cannot be explained by a normal kinetic treatment based on the reaction scheme which has been accepted as probable. The heterogenuity in acrylonitrile concentration in the reaction system is assumed and the kinetic formulas are modified. This treatment explains the experimental results very satisfactorily. In order to confirm this mechanistic scheme, the effects of temperature, pH and solvents on the yield of reaction products were examined. All the results are consistent with the proposed mechanism.

Recently Baizer[1] *et al.* carried out extensive studies on the electro-reductive dimerization of acrylonitrile and other vinyl compounds. Their work is limited to examining the conditions for exclusive preparation of hydro-dimers and the reaction mechanism for this process is not yet clarified in detail. Therefore, the extensive studies have been designed to examine the effect of the experimental conditions on the electro-reductive dimerization of acrylonitrile to get some mechanistic information for this process. In the present paper, the effects of current densities, concentrations of acrylonitrile, temperatures, pH and solvents on the formation of adiponitrile, propionitrile and oligomers from acrylonitrile will be examined and discussed.

Experimental

Apparatus. As shown in Fig. 1, the reaction cell is a cylindrical separable flask of the area of the bottom of 0.3 dm^2, equipped with an inlet tube for N_2 gas, a thermometer, a glass electrode for the measurement of pH value, a platinum anode, a separatory funnel and a cooler with dry-ice acetone mixtures. There are a mercury pool at the bottom as the cathode, and a junction connected with a saturated calomel electrode. The separatory membrane was not used in this apparatus.

*1 Present address: Institute for Fats and Oils, Japan Fats and Oils Co., Ōhamacho, Amagasaki.

1) M. M. Baizer, *J. Electrochem. Soc.*, **111**, 215 (1964); *Tetrahedron Letters*, **1963**, 973; *J. Org. Chem.*, **29**, 1670 (1964).

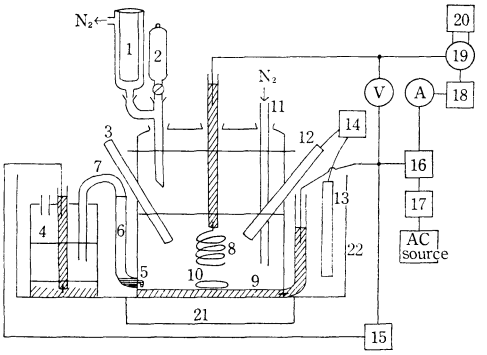

Fig. 1. Apparatus for electrolysis.
1. Dry-ice acetone cooler, 2. Dropping funnel, 3. Thermometer, 4. Saturated calomel electrode, 5. Liquid junction, 6. Sat. KCl aq. solution, 7. Sat. KCl-Agar bridge, 8. Platinum cathode, 9. Mercury anode, 10. Stirrer, 11. N_2 gas inlet, 12. Glass electrode, 13. Temp. calibrating electrode, 14. pH meter, 15. Vacuum voltmeter, 16. Constant voltage supply, 17. Stabilizer, 18. Mercury coulometer, 19. Standard resister (1 Ω), 20. Recorder, 21. Magnetic stirrer, 22. Thermostat

Chemicals. Tetraethylammonium *p*-toluenesulfonate (QAS), used as a supporting electrolyte, was prepared according to the method reported by Baizer. It was confirmed by IR spectrum to contain neither amine nor ester. Commercially available acrylonitrile was used after treatment with calcium chloride followed by distillation twice. Calcium sulfate and methylene dichloride were used without further treatments.

Electrolytic Reduction. A QAS solution was placed into the electrolytic cell and, while N_2 gas was passed through, a definite amount of acrylonitrile was added and then the electrolysis was initiated, the temperature being kept constant. The formation of precipitates in a small quantity was observed in a cathode region during electrolysis. After a definite period of electrolysis, the electrolysed soltuion was neutralized, cooled with water and transferred into a separatory funnel. The 200 m*l* of water was added and, after the precipitates were removed, the water layer was extracted four times with each 50 m*l* of methylene dichloride, and the extracts were combined to the acrylonitrile layer. The combined solution was washed with water twice, dried with calcium sulfate, and methylene dichloride was removed by distillation. The residue was analysed by gas chromatography (Shimadzu GC-1C, column Tween 80 on Chromosorb P).

The precipitates were purified twice through reprecipitation with dimethylformamide and water and analysed by IR and vapor pressure osmometer measurements.

Electrolytic Potential and Electrolytic Current. The relation of the electrode potential and the electrolytic current to the applied voltage are shown in Fig. 2 in the cases of the absence and the presence of acrylonitrile. By the addition of acrylonitrile the cathode potential decreases significantly and the electrolytic current increases. There is some difference between the reduction potentials of acrylonitrile and QAS, as shown in Fig. 3.

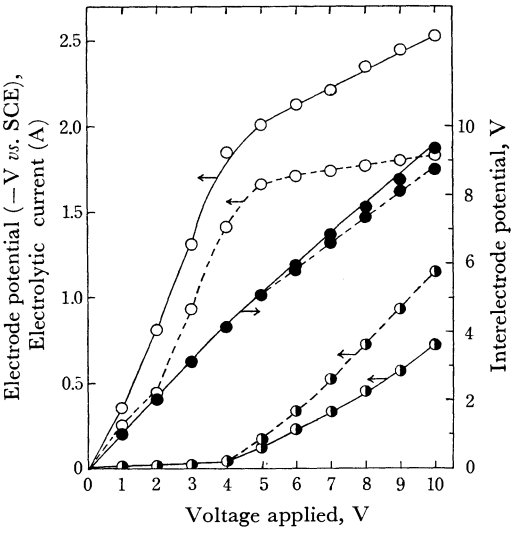

Fig. 2. Relations between electrode potential, electrolytic current and applied voltage (30°C).
○ electrode potential, ● interelectrode potential, ◑ electrolytic current
Solid line, 55.7% QAS (pH 5.5)
Dotted line, AN 30.0 g + 55.7% QAS 79.0 g (pH 5.7)

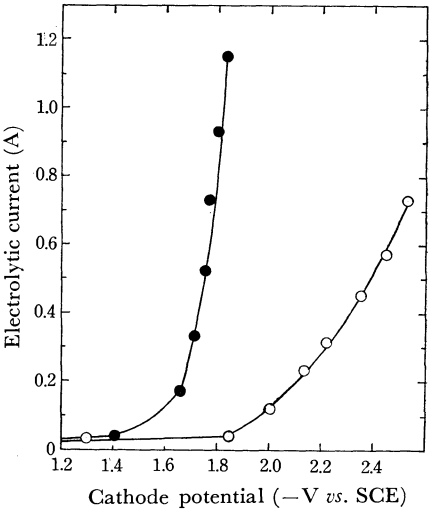

Fig. 3. Current-potential curves.
○ QAS soln. ● (QAS+acrylonitrile) soln.

Conditions of Electrolysis. In all the experiments, the total volume of the reaction solution was 100 m*l*. The current efficiency was calculated under the assumption that the theoretical electric quantity of 2 faradays is required for the formation of each 1 mol of adiponitrile.

Products of Electrolysis. The formation of propionitrile and adiponitrile was detected by GLC and IR measurements. The product precipitated from water was confirmed to be oligomers of acrylonitrile by the

Table 1. Conditions for electrolysis

No.	Acrylonitrile g	Acrylonitrile wt%	QAS soln.[1] g	Temp.[2] °C	pH	Voltage V	Cathode potential −V *vs.* SCE	Current density A/dm²	A·hr[3] ×3600 coul.
1	30.0	27.5	79.0	31.7	6—2	7.0	1.7—1.8	1.45	3.05
2	30.0	27.5	79.0	31.7	6—2	8.0	1.7—1.8	2.12	4.45
3	30.0	27.5	79.0	32.5	6—2	9.0	1.7—1.8	2.74	5.75
4	30.0	27.5	79.0	34.0	6—2	10.0	1.8—1.9	3.55	7.45
5	30.0	27.5	79.0	33.5	6—2	10.8	1.7—1.8	4.40	9.24
6	30.0	27.5	79.0	32.5	6—2	11.8	1.6—1.7	5.17	7.75
7	37.4	35.0	69.4	33.5	6—2	10.0	1.7—1.8	3.57	5.36
8	41.4	40.0	62.0	33.5	6—2	10.0	1.7—1.9	3.65	5.48
9	46.0	45.0	56.2	34.0	6—2	10.0	1.8—1.9	3.66	5.50
10	50.6	50.0	50.6	33.5	6—2	10.0	1.8—1.9	3.56	5.33
11	41.4	40.0	62.0	33.5	6—2	11.8	1.8—1.9	5.23	7.85
12	30.0	27.5	79.0	18.2	6—2	10.0	1.8—1.9	2.79	4.18
13	30.0	27.5	79.0	24.3	6—2	10.0	1.8—2.0	3.18	4.77
14	30.0	27.5	79.0	29.0	6—2	10.0	1.9—2.0	3.47	5.21
15	30.0	27.5	79.0	34.0	6—2	10.0	1.8—1.9	3.55	7.45

1) 55.7% QAS aq. solution. 2) Maximum temp., thermostat temp., 30°C (Nos. 1—11, 15), 15°C (No. 12), 20°C (No. 13), 25°C (Nos. 14, 16, 18—22), 22°C (Nos. 17, 23)
3) Time, 7 hr (Nos. 1—5, 15), 5 hr (Nos. 6—11, 12—14, 16—22), 3hr (No. 23).

IR measurement and the average degree of polymerization was estimated to be 3—5 from the vapor pressure osmometer using methyl ethyl ketone as a solvent.

Results and Discussion

Baizer[1] has established the process of electrolytic preparation of adiponitrile from acrylonitrile. The essential point of this method exists in the use of McKee's salt. Acrylonitrile dissolves or disperses into water to 4.5 wt% at room temperature in the presence of McKee's salt and McKee's salt is almost inactive to the electrode reaction even in the range of cathode potential sufficiently high for the reduction of acrylonitrile. The reaction

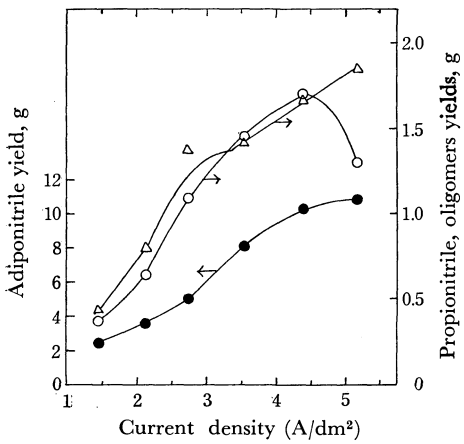

Fig. 4. Relation of yields and current density.
● Adiponitrile, ○ Propionitrile, △ Oligomers

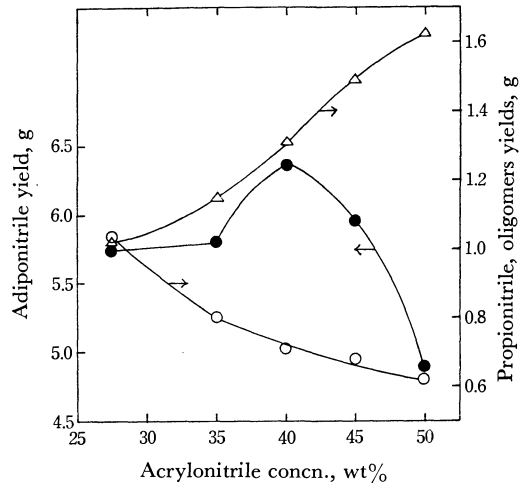

Fig. 5. Relation of yields and acrylonitrile concentration.
● Adiponitrile, ● Propionitrile, △ Oligomers

conditions, under which adiponitrile is a main product, were elucidated by Baizer as follows; the acrylonitrile concentration is in the range from 10 to 40 wt% in water and the cathode potential is about −2.0 V *vs.* SCE.

Although the principal feature of this reaction became clear by Baizer's pioneer work, further examination would be necessary to get some mechanistic information. In Figs. 4 and 5, the effect of current densities and acrylonitrile concentrations on the yields of reaction products are shown in the vicinity of optimum conditions for the adiponitrile formation.

It is considered that these results confirm the following reaction scheme which was originally suggested by Baizer and modified in part in the present work;

$$CH_2CHCN \xrightarrow[k_1]{2e} \overset{\ominus}{C}H_2\overset{\ominus}{C}HCN \longrightarrow$$

$$\begin{cases} \xrightarrow[k_2]{2H^+} CH_3CH_2CN \\ \xrightarrow[k_3]{AN} NC\overset{\ominus}{C}HCH_2CH_2\overset{\ominus}{C}HCN \longrightarrow \end{cases}$$

$$\begin{cases} \xrightarrow[k_4]{2H^+} NCCH_2CH_2CH_2CH_2CN \\ \xrightarrow[k_5]{AN} \text{oligomers} \end{cases}$$

The initial step of 2-electron reduction is confirmed by polarographic examination.[2)]

The kinetic treatment under the assumption of stationary state for the intermediate dianions leads the following formula for the formation rates of propionitrile (PN), adiponitrile (ADN) and oligomers (olig) of acrylonitrile.

$$\frac{d[PN]}{dt} = \frac{k_1k_2[AN][H^+]^2I}{k_2[H^+]^2+k_3[AN]}$$

$$\frac{d[ADN]}{dt} = \frac{k_1k_3k_4[AN]^2[H^+]^2I}{(k_2[H^+]^2+k_3[AN])(k_4[H^+]^2+k_5[AN])}$$

$$\frac{d[olig]}{dt} = \frac{k_1k_3k_5[AN]^3I}{(k_2[H^+]^2+k_3[AN])(k_4[H^+]^2+k_5[AN])}$$

where k_1, k_2,$\cdots$ are the rate constants corresponding to each step of reactions, and I denotes the current density.*2 The effect of the current density and the acrylonitrile concentration as shown in figures above are explained by these formulas. However, there is one important point that is completely inconsistent with these kinetic results, which were derived under the assumption of the uniformity through the reaction system. That is, this treatment leads to the result that the rate of formation of PN is always larger than that of ADN, if the ratio of rate constants k_2/k_3 is comparable to the ratio k_4/k_5, but Baizer's result and the present result show the reverse result; the main product in this reaction system is adiponitrile even when the AN concentration is so low as 10% as shown by Baizer.

2) T. Asahara, S. Hayano, M. Senō and H. Kaneko, *Denki Kagaku (J. Electrochem. Soc. Japan)*, **35**, 882 (1967).

*2 In these equations, the exponent 2 on the proton concentration comes from the overall reaction formula in which one dianion reacts with two protons. But the rate-determining step in this protonation reaction is not clear and, therefore, the reaction order regarding protons is not conclusive.

This experimental result is confirmed more clearly from the investigation for the rates of formation of PN and ADN, the result of which is shown in Fig. 6.

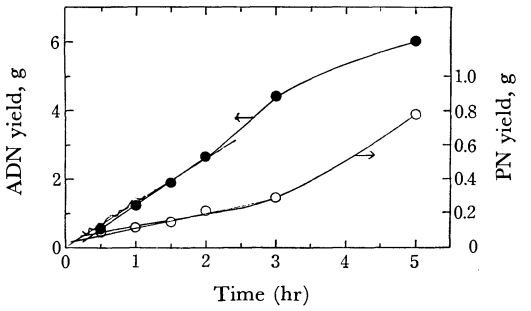

Fig. 6. Rates of formation of propionitrile and adiponitrile.

If the reaction mechanism as mentioned above would be valid, this essential behavior should be interpreted from the following reasons. Propionitrile is formed through the successive attacks of protons or proton donors to the dianion $\overset{\ominus}{C}H_2\overset{\ominus}{C}HCN$ at any positions and, on the other hand, adiponitrile is formed only through the attack of acrylonitrile to the dianion at the β-position to the nitrile group. Therefore, to explain the present result, it should be considered that the protonation ability in this system is very weak or the propionitrile dianion would be easily attacked by acrylonitrile at the β-position under the present circumstance.

In order to examine the first possibility, the effect of pH was investigated. The result is shown in Table 2. In general, the yield of propionitrile is high under the acidic condition and the yield of adiponitrile is high under the basic condition, as expected, but there is no definite quantitative correlation between pH and the product yield, and the property of each reagent used for the adjustment of pH clearly gives rise to a characteristic behavior. For example, acetic acid depresses very strongly the formation of adiponitrile, but sulfuric acid has no remarkable effect. This result reveals that the protonation ability is influenced by the physical situation of proton donors in the present system.

Moreover, it would be considered that this physical situation leads to the result that adiponitrile is formed as a main product in this reaction system. That is, taking this situation into consideration, we must modify the kinetic formula derived above under the assumption of the uniformity of the reaction system. Presumably the concentration of acrylonitrile is different in positions, *i. e.* the electrode surface and the bulk of solution, and the steps 2 and 3 of the reaction occur at the cathode surface and the steps 4 and 5 occur in the bulk. The kinetic treatment affords the following formulas;

Table 2. Effects of pH on electrolysis of acrylonitrile

No.[1]	Reagent for pH adjust	pH	Products: Adiponitrile g	Adiponitrile %[2]	Propionitrile g	Propionitrile %	Oligomers g	Oligomers Mol wt[3]	Total yield g	Yield ratio, g/g ADN/PN	Yield ratio, g/g ADN/olig
16	none	6.2	5.42	46.5	0.76	13.8	1.08	160	7.26	7.1	5.0
17	none	6.2	7.76	49.3	0.60	8.0	1.70	171	10.06	12.9	4.6
18	H_2SO_4	2.2	3.60	33.8	0.81	16.1	1.05	144	5.46	4.4	3.4
19	CH_3COOH	4.0	0.55	5.2	1.12	22.4	0.15	104	1.82	0.5	3.7
20[4]	Et_3N	8.2	6.21	53.2	0.79	14.3	1.49	147	8.47	7.9	4.2
21[4]	Et_3N	10.5	5.77	55.8	0.73	14.9	1.88	228	8.38	7.9	3.1
22	KOH	10.5	7.20	61.1	0.09	1.6	2.15	144	9.44	80.0	3.4
23	KOH	10.1	6.13	63.9	0.11	2.4	1.33	158	7.57	55.8	4.6

1) Acrylonitrile 41.4 g (40.0 wt%), QAS 55.7% aq. soln. 62.0 g. Voltage 10.0 V (Nos. 17 and 23, 11.8 V), Cathode potential 1.8—1.9 V *vs.* SCE, Time 5 hr (No. 23, 3 hr), Temp., 28—29°C.
2) Current efficiency
3) From vapor pressure osmometer
4) Trace of biscyanoethyl ether was dectected.

$$\frac{d[PN]}{dt} = \frac{k_1k_2[AN]^*[H^+]^*I}{k_2[H^+]^*+k_3[AN]^*}$$

$$\frac{d[ADN]}{dt} = \frac{k_1k_3k_4[AN]^{*2}[H^+]^2I}{(k_2[H^+]^{*2}+k_3[AN]^*)(k_4[H^+]^2+k_5[AN])}$$

$$\frac{d[olig]}{dt} = \frac{k_1k_3k_5[AN]^{*2}[AN]I}{(k_2[H^+]^{*2}+k_3[AN]^*)(k_4[H^+]^2+k_5[AN])}$$

where [ ] stands for the concentration in the bulk and [ ]* stands for that at the cathode surface.

If it is assumed from the above consideration that $[AN]^*>[AN]$ and $[H^+]^*<[H^+]$, the experimental behavior is well explained. For instance, if the concentration of acrylonitrile is larger than that of protons in the bulk, the yield ratio of adiponitrile to propionitrile is expressed from the above formulas as follows;

$$\frac{d[ADN]}{d[PN]} = \frac{k_3k_4}{k_2}\frac{[H^+]^2[AN]^*}{[H^+]^{*2}(k_4[H^+]^2+k_5[AN])} \simeq \frac{k_3k_4}{k_2k_5}\left(\frac{[H^+]}{[H^+]^*}\right)^2\left(\frac{[AN]^*}{[AN]}\right)$$

From the assumption that the ratio k_2/k_3 is in a comparable order to the ratio k_4/k_5 it could be expected that adiponitrile becomes a main product in this reaction system if the adsorption of acrylonitrile at the cathode surface takes place to a great extent.

This assumption seems to be probable from the reason that the cathode surface is active for the adsorption of polarizable organic molecules and is consistent with the concept of formation of organic layer at the electrode surface by Tomirov *et al.*[3] The direct measurement on the adsorption is now under examination.

3) L. G. Feoktistov, A. P. Tomirov and I. G. Sevastyanova, *Electrochimiya*, **1**, 1300 (1965).

The effect of the adsorption of acrylonitrile onto the cathode surface is cosidered to appear in many aspects. The effect of reagents for the pH adjustment was mentioned already and the effect of temperature should be examined. The result is shown in Fig. 7. The yield of ADN remains to be almost constant, but the yield of propionitrile increases with the increasing temperature. This result is thought to be probable from the consideration on the adsorption equilibrium; the adsorbed amount of acrylonitrile decreases relatively with the rise in temperature. The constancy in the adiponitrile yield should be attributed to the increasing reactivity of the adsorbed acrylonitrile with temperature.

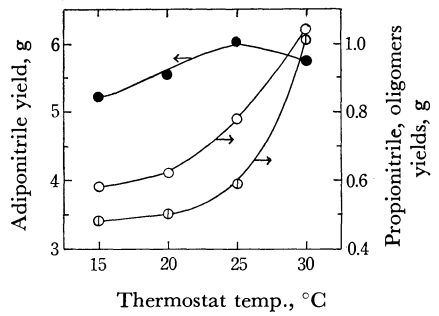

Fig. 7. Relation of yields and temperature.
○ Propionitrile, ● Adiponitrile,
◑ Oligomers

As has been discussed above, this reaction occurs through the anionic intermediates and the reactivity of those anions play an essential role in the present system and thereby the solvent effect should be anticipated. Some examinations were carried out in this respect and the result is shown in Table 3. It is clear that the higher the dielectric constants or the ionization potentials of the solvent, the less

Table 3. Solvent effects

Acrylonitrile 0.5 mol, QAS 0.1 mol, H_2O 1.0 mol, Solvent 0.5 mol, Temperature 25°C, 5 hr

Solvent	Voltage V	Electric quantity A·hr	Current density A/dm²	pH		Adiponitrile g	Adiponitrile %
1,4-Dioxane	14.0	5.04	3.36	4.7	4.6	8.05	73.3
N,*N*-Dimethylformamide	10.0	3.90	2.60	6.5	5.6	4.25	50.0
Acetonitrile	10.0	4.60	3.06	4.3	3.7	4.21	42.0
Dimethyl sulfoxide	10.0	2.82	1.88	7.5	7.7	2.29	37.3

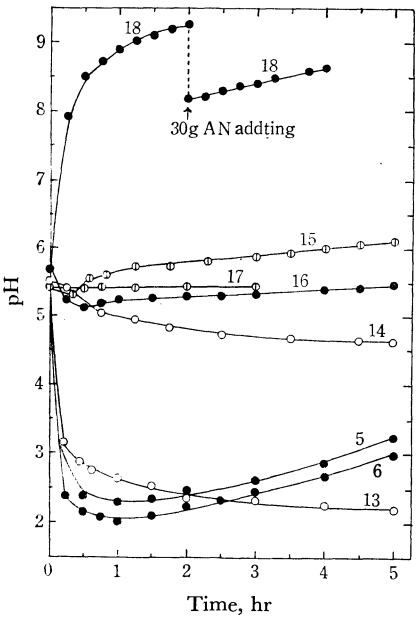

Fig. 8. Time change of pH. (Numbers in figure refer to Exp. Nos. shown in Table 1.)

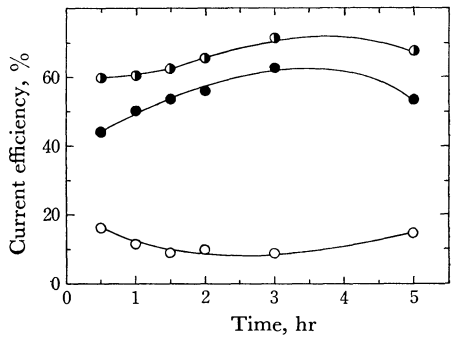

Fig. 9. Changes in current efficiencies with time.
● Adiponitrile, ○ Propionitrile,
◑ Total

the yield of adiponitrile. This shows that the extent of the solvation of ion-pairs influences the reaction. Since the free dianions react with protons more easily than the ion-pairs of the dianions and ammonium cations, this shows also that the dianions react with acrylonitrile in a near-adsorbed state at the vicinity of the cathode.

In the present experiments, the current efficiency for the production of adiponitrile does not exceed 75%. It would be considered that this is owing to the contribution of the electrolysis of QAS, for the reduction potential of QAS is close to that of acrylonitrile.

In this connection, the time change of pH and the product yields were measured and the result is shown in Figs. 8 and 9. Under normal conditions, pH of the system becomes acidic as time passes, but no remarkable changes in the yields of products were observed.

BULLETIN OF THE CHEMICAL SOCIETY OF JAPAN VOL. 42 1322—1324 (1969)

Studies of Acetothiolacetate

Shinichi Motoki and Tadao Sato

Department of Chemistry, Faculty of Science, Science University of Tokyo, Shinjuku-ku, Tokyo

(Received April 23, 1968)

Ketene dimer reacted with mercaptan to give acetothiolacetate (I) in the presence of triethylamine. The ester I underwent a thermal condensation to give dehydroacetic acid (III), with the liberation of mercaptan, merely upon heating, and the reaction was effectively promoted in the presence of triethylamine. The ester I reacted with alkyl halide and acyl halide in dioxane to give α-alkyl and α-acylacetothiolacetate (II) respectively. Ethyl acetothiolacetate, ethyl α-methylacetothiolacetate, and ethyl α-acetylacetothiolacetate reacted with mercuric oxide at a low temperature to give diacetylacetone (VI), methyl ethyl ketone, and dehydroacetic acid (III) respectively.

Although there have been some indications of the differences between esters and thiolesters, acetothiolacetate (I) has been investigated extensively by only a few workers, including Cronyn[1] and Reid.[2]

The present work was undertaken in order to establish an effective way of preparing the ester I and in order to study the chemical properties of I and the related compounds.

In the present study, mercaptans were allowed to react with ketene dimer in the presence of triethylamine; acetothiolacetates (I) were thus conveniently prepared in 30—56% yields.*1

The synthesis of I was unsuccessful when sulfuric acid or *p*-toluenesulfonic acid was used as the catalyst because of contamination by persistent impurities.*2

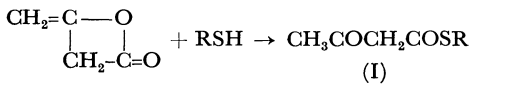

$$CH_2{=}C(-O)-CH_2-C{=}O \;+\; RSH \;\rightarrow\; CH_3COCH_2COSR \quad (I)$$

Ia) $R=C_2H_5$ Ib) $R=(CH_3)_2CH$
Ic) $R=C_2H_5(CH_3)CH$ Id) $R=(CH_3)_3C$

It has been known that 2 mol of ethyl acetoacetate lose 2 mol of ethanol when heated at about 200°C; giving dehydroacetic acid (III) in a 53% yield.[3] Similarly, it has been found that a considerable amount of Ia can be converted into III even at 100—120°C with the liberation of mercaptan. Since the anion stability of the ethylmercapto group is greater than that of the alkoxyl group, mercaptan is more readily eliminated than alcohol from the corresponding esters.

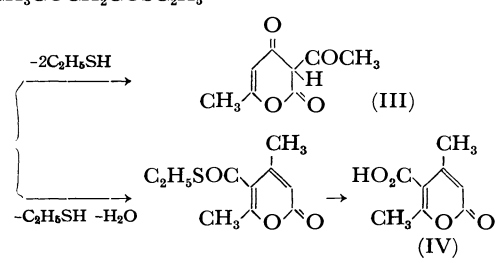

$$2\,CH_3COCH_2COSC_2H_5 \longrightarrow$$

$-2C_2H_5SH$ → (III)

$-C_2H_5SH\ -H_2O$ → C_2H_5SOC → HO_2C (IV)

The addition of a small amount of triethylamine caused a marked increase in the yield of III, whereas the reaction was not accerelated by sodium acetate. On the other hand, acetic acid rather hindered the reaction and cold concentrated sulfuric acid caused it to give isomeric isodehydroacetic acid (IV).

Table 1. Preparation of acetothiolacetate (CH_3COCH_2COSR)

R	Bp °C/mmHg	Yield %	Anal S% Calcd	Found
C_2H_5	110/30	56	21.93	21.65
$(CH_3)_2CH$	94—95/10	34	20.01	20.11
$C_2H_5(CH_3)CH$	103—104/10	30	18.40	18.71
$(CH_3)_3C$	85—86/6	31	18.40	18.31

1) M. W. Cronyn, M. P. Chang and R. A. Wall, *J. Am. Chem. Soc.*, **77**, 3031 (1955).

2) R. B. Baker and E. E. Reid, *ibid.*, **51**, 1567 (1927); *ibid.*, **59**, 1089 (1937).

*1 For the preparation of I, two methods have already been established, namely, by the Claisen condensation of thiolacetate with sodium (15% yield)[2] or isopropylmagnesium bromide (25—70% yield).[1]

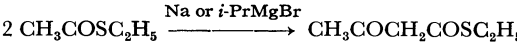

$$2\,CH_3COSC_2H_5 \xrightarrow{\text{Na or } i\text{-PrMgBr}} CH_3COCH_2COSC_2H_5$$

*2 Alkyl acetoacetate was prepared from ketene dimer and alcohols in the presence of acids (A. B. Boese, U. S. Pat. 2167168).

3) F. Arndt, "Organic Syntheses," Coll. Vol. III, p. 231 (1955).

Table 2. Thermal condensation of Ia

Catalyst	g	Product	Yield %	Recovered ester %
none	—	dehydroacetic acid	38	60
$(C_2H_5)_3N$	0.2		75	20
$NaHCO_3$	0.2		58	35
CH_3CO_2Na	0.2		35	40
CH_3CO_2H	0.2		8	80
H_2SO_4	—	isodehydroacetic acid	23	—

This thermal condensation was also extended to α-alkyl and α-acylacetothiolacetate. The alkylation and acylation of Ia were carried out by ordinary methods with the aid of sodium in dioxane, in which the sodium salt of Ia was readily dissolved. The NMR spectra of the products showed that the *C*-alkylated and *C*-acylated compounds were exclusively obtained. However, since these substituted acetothiolacetates were stable at higher temperatures even in the presence of triethylamine, the expected compounds V were not obtained.

Table 3. Preparation of α-substituted ethyl acetothiolacetate ($CH_3COCHCOSC_2H_5$, R)

R	Bp °C/mmHg	Yield %	Anal S% Calcd	Found
CH_3	114—115/30	93	20.01	19.81
C_2H_5	120—121/29	47	18.40	18.63
CH_3CO	124—125/29	58	17.04	17.27
C_2H_5CO	128—129/29	52	15.86	15.68

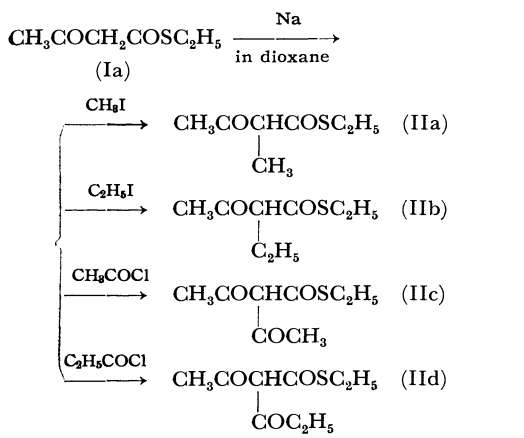

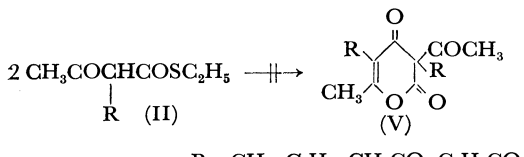

R=CH_3, C_2H_5, CH_3CO, C_2H_5CO

On the other hand, when yellow mercuric oxide was added to Ia at room temperature, a vigorous reaction took place and mercury ethylmercaptide was formed, along with carbon dioxide. At lower temperatures, the reaction proceeded slowly to give a substance melting at 44—46°C. It was not the expected dehydroacetic acid, but was identfied as diacetylacetone (VI) by elementary analysis and by conversion into its bisphenylhydrazone.

Similarly, the reaction of ethyl α-methylacetothiolacetate (IIa) with mercuric oxide gave a small amount of methyl ethyl ketone, whereas ethyl α-acetylacetothiolacetate (IIc) yielded acetylacetone and III.

$$CH_3COCH_2COSC_2H_5 + HgO \longrightarrow$$
(Ia)

$$CH_3COCH_2COCH_2COCH_3 + Hg(SC_2H_5)_2 + CO_2$$
(VI)

$$CH_3COCHCOSC_2H_5 + HgO \longrightarrow$$
$$\quad\quad|$$
$$\quad COCH_3 \quad (IIc)$$

$$CH_3COCH_2COCH_3 + III + Hg(SC_2H_5)_2 + CO_2$$

Experimental

Acetothiolacetic Acid Esters (I). To 0.35 mol of mercaptan containing 0.2 m*l* of triethylamine, 0.35 mol of the ketene dimer was added, drop by drop, over a 1-hr period at the boiling point of the mercaptan. After 1 hr, the reaction mixture was distilled and the corresponding acetothiolacetate was obtained.

In the case of the ethyl ester, the procedure had to be modified slightly to prevent the evaporation of ethylmercaptan. To 0.35 mol of ethylmercaptan containing 0.2 m*l* of triethylamine, 0.35 mol of the ketene dimer was added, drop by drop, over a 1-hr period at 0—5°C. The mixture was then stirred at room temperature until the odor of the ketene dimer was lost. Then the mixture was distilled. These results are shown in Table 1.

Ethyl α-Alkyl and α-Acylacetothiolacetate (II). To a suspension of 0.17 g atom of sodium in 60 m*l* of dioxane, 0.18 mol of Ia was added, drop by drop, at room temperature. After the sodium had dissolved, 0.18 mol of alkyl halide or acyl halide was stirred in at such a rate that the temperature did not exceed 50°C. The mixture was then stirred at the same temperature for 4 hr. After cooling, the sodium halide was filtered off and the filtrate was concentrated under reduced pressure. The residue was distilled to give ethyl α-alkyl and α-acylacetothiolacetate (II).

Dehydroacetic Acid (III). (Thermal Condensation of Ia). Ten grams of Ia containing 0.2 g of a catalyst were heated in an oil bath at 100—120°C. The evolution of ethylmercaptan was observed. After 2 hrs' heating, the reaction mixture was distilled to give III and recovered Ia. The results are summarised in Table 2.

Isodehydroacetic Acid (IV). The procedure of

the reaction of Ia with sulfuric acid was similar to that described in the preparation of IV from ethyl acetoacetate.[4] The product was recrystallised from benzene; yield, 22.5%; mp 153°C, undepressed upon admixture with an authentic sample of IV.

The Reaction of Ia with Mercuric Oxide. Ia (29 g, 0.2 mol) was added to a suspension of yellow mercuric oxide (21 g, 0.1 mol) in 60 m*l* of ether over a one-hour period between −20°C and −30°C. After the mixture had then been stirred a further 35 hr at the same temperature, mercury mercaptide (mp 85°C recrystallised from ethanol) was filtered off and the ether was evaporated. The residue was distilled to give fractions boiling at 105—118°C/8 mmHg. The distillate solidified on cooling and was recrystallised from petroleum ether to give pure diacetylacetone (VI), mp 44—46°C; yield, 5 g, and bisphenylhydrazone, mp 140—142°C, undepressed by admixture with an authentic sample.*3

Found; C, 58.99; H, 7.12%; mol wt (Cryoscopy in benzene), 140.3. Calcd for $C_7H_{10}O_3$: C, 59.14; H, 7.09%; mol wt, 142.2.

The Reaction of IIc with Mercuric Oxide. IIc (38 g, 0.2 mol) was added, drop by drop, to a suspension of yellow mercuric oxide (21 g, 0.1 mol) in 60 m*l* of ether over a 1-hr period at 0—5°C. After the mixture had then been stirred for 48 hr at the same temperature, the mercaptide thus precipitated was filtered off and the filtrate was distilled. Two fractions, boiling at 120—140°C and at 120—135°C/5 mmHg, were collected. The first fraction was redistilled to give 6 g of acetylacetone, bp 135—138°C. It was identified by the formation of the semicarbazone, mp 108—110°C, undepressed on admixture with a sample prepared from commercial acetylacetone. The second fraction immediately solidified and was recrystallised from ethanol to give 3 g of III, mp 109°C.

The authors wish to thank Professor Yojiro Tsuzuki for his helpful advice and encouragement.

4) N. R. Smith and R. H. Wiley, "Organic Syntheses," Coll. Vol. IV, p. 549 (1963).

*3 The authentic bisphenylhydrazone was obtained by the reaction of phenylhydrazine with diacetylacetone prepared from dehydroacetic acid (F. Feist, *Ann.*, **257**, 276 (1890)).

BULLETIN OF THE CHEMICAL SOCIETY OF JAPAN VOL. 42 1324—1328 (1969)

Kinetic Studies of Oxygen Exchange and Racemization Reactions of Diaryl Sulfoxides in Sulfuric Acid of Various Concentrations[1)]

Norio KUNIEDA and Shigeru OAE

Department of Applied Chemistry, Faculty of Engineering, Osaka City University, Sumiyoshi-ku, Osaka

(Received May 9, 1968)

When ^{18}O-labeled and optically active sulfoxides are dissolved in a concentrated sulfuric acid, one observes the concurrent oxygen exchange and racemization reactions of the sulfoxides, and these reactions were found to proceed through the S_N1-like path (S. Oae *et al.*, Bull. Chem. Soc. Japan, **38**, 546 (1965); **41**, 696 (1968)). We have found that the concurrent oxygen exchangeand racemization reactions also take place even in less concentrated sulfuric acid at somewhat higher temperature, *i. e.* 70% sulfuric acid at 30°C, and proceed through a different mechanistic route, very likely an S_N2-like path. Kinetic investigation on these reactions in sulfuric acid of various concentrations (66.5—96.3%) suggests there is a gradual change of mechanism of the reaction, *i. e.* from S_N2 type in 66.5% to S_N1 type in 96.3% with the increase of the concentration of sulfuric acid.

Sulfoxides, being of stable pyramidal structure, can be resolved to a pair of optically active enantiomers when two substituents on the sulfur atom are different.[2)] Meanwhile, a convenient method of synthesizing optically active sulfoxides has recently been developed.[3)] Therefore one can now study the stereochemistry of reactions of the sulfoxides very readily using these optically active compounds.[4)] The concurrent oxygen exchange and racemization reaction of sulfoxides are particularly useful for the stereochemical studies on nucleophilic reaction on the trivalent sulfur atom, because one can readily prepare both ^{18}O-labeled and optically active

1) Paper XXVI on Sulfoxides.

2) K. Mislow, "Introduction to Stereochemistry," W. A. Benjamin, Inc., New York, N. Y. (1965), p. 88.

3) K. K. Andersen, *Tetrahedron Letters*, **1962**, 93; H. Phillips, *J. Chem. Soc.*, **1925**, 2552.

4) Summarized in; K. Mislow, *Record of Chemical Progress*, **28**, 217 (1967), and our previous paper (Ref. 5b).

sulfoxides while the analysis of ^{18}O-content in sulfoxides is also quite facile. We have reported previously[5] that the rate of the oxygen exchange of ^{18}O-labeled, optically active *p*-tolyl phenyl sulfoxide was identical to that of the racemization in 95.5% sulfuric acid and the rates of the racemization were nicely correlated with $-H_0$ (slope=1.1) in the range of concentration from 96.3% to 91.8% of sulfuric acid. In the meantime, the polar effect of *p*-substituent on phenyl ring on the rates of both oxygen exchange and racemization in 95.5% or 96.2% sulfuric acid was found to be very small, while a noticeable ESR signal was detected with 96% sulfuric acid solution of a *p,p'*-disubstituted diphenyl sulfoxide.[6] From these observations we have postulated the following S_N1-like mechanism for these reactions, and favored the homolytic cleavage of the S–O bond, the route involving [B].

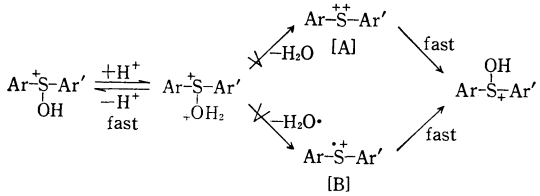

Previously, a preliminary experiment on the oxygen exchange and racemization reactions of diaryl sulfoxides was conducted in a sulfuric acid of less than 85% concentration at around 0°C[5b] and found to proceed very little. Meanwhile, we have found that these sulfoxides undergo concurrent oxygen exchange and racemization reactions with much weaker acids such as acetic, perchloroacetic acids when heated at much higher temperatures.[7] Accordingly, it was thought that the oxygen exchange reaction should take place even in dilute sulfuric acid at somewhat higher temperatures. In fact, we have found that diaryl sulfoxides undergo oxygen exchange and racemization reactions readily in a sulfuric acid of even less than 85% concentration when the reaction was carried out at considerably higher temperatures (30—50°C). We now have compiled substantial amounts of kinetic data on these reactions of diaryl sulfoxides in sulfuric acid of various concentrations (66.5—96.3%) and hence would like to report detailed accounts of the kinetic results and their implications to the mechanistic interpretations on these reactions.

5) a) S. Oae, T. Kitao, Y. Kitaoka and S. Kawamura, This Bulletin, **38**, 546 (1965). b) S. Oae and N. Kunieda, *ibid.*, **41**, 696 (1968).

6) H. J. Shine, M. Rahman, H. Seeger and G. S. Wu, *J. Org. Chem.*, **32**, 1901 (1967).

7) S. Oae, M. Yokoyama and M. Kise, This Bulletin, **41**, 1221 (1968).

Results and Discussion

At first, careful kinetic experiments were conducted on the rates of both oxygen exchange and racemization reactions of *p*-tolyl phenyl sulfoxide (0.935 atom%-^{18}O, $[\alpha]_D^{25}$ +27.8° in 96% ethanol) in sulfuric acid of various concentrations ranging between 66.5% and 96.3% at several temperatures between 0 and 60°C. The results are shown in Table 1. The sulfoxide was found to be racemized even in 66.5% sulfuric acid at a higher temparature. The mechanistic interpretation of these results will be discussed in the light of first the values of k_{ex}/k_{rac} and activation parameters, the correlation with H_0 (Zucker-Hammett hypothesis), and then the Bunnett's *w*-values.

Variation of k_{ex}/k_{rac} Values and Activation Parameters. The concurrent oxygen exchange and racemization reaction of sulfoxides in acid media may proceed through the following two extreme mechanistic routes as shown below.

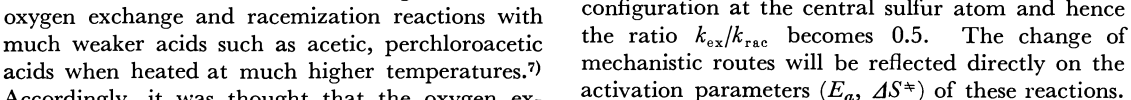

When the reaction proceeds through the S_N1-like route, each oxygen exchange will cause racemization, and the ratio k_{ex}/k_{rac} becomes unity. Whereas if it passes through the S_N2-like route each oxygen exchange will result in the inversion of configuration at the central sulfur atom and hence the ratio k_{ex}/k_{rac} becomes 0.5. The change of mechanistic routes will be reflected directly on the activation parameters (E_a, $\Delta S^{\neq}$) of these reactions. Therefore these parameters were estimated and the k_{ex}/k_{rac} values and activation parameters thus obtained in several concentrations are listed in Table 2.

As shown in our previous paper,[5] the k_{ex}/k_{rac} and $\Delta S^{\neq}$ values observed in a concentrated sulfuric acid (95.5% or 95.9%) were 1 and 11.5 *e. u.* respectively, suggesting that the reaction proceeds through a route involving the S_N1-like S–O bond cleavage at the rate determining step. However, in about 75% sulfuric acid, the k_{ex}/k_{rac} and $\Delta S^{\neq}$ values, are 0.5 and −18 *e. u.* respectively, indicating that the reaction proceeds through a different mechanistic route, *i. e.* very likely an S_N2-like process, from that in concentrated sulfuric acid. For example, the $\Delta S^{\neq}$ value of the racemization reaction of (+)-*p*-tolyl phenyl sulfoxide with acetic anhydride which show the typical S_N2-like mechanism is −28.6 *e. u.*[8] One finds in Table 2, that both

8) S. Oae and M. Kise, *Tetrahedron Letters*, **1967**, 1409.

TABLE 1. RATE CONSTANTS OF ^{18}O-EXCHANGE AND RACEMIZATION OF (+)-*p*-TOLYL PHENYL SULFOXIDE-^{18}O[a] IN SULFURIC ACID OF VARIOUS CONCENTRATIONS

H_2SO_4 %	Temp. (°C)	$10^4\ k_{rac}$ (sec^{-1})	$10^4\ k_{ex}$
96.3	5	4.48 ±0.28	
95.9	5	4.20 ±0.10	4.07 ±0.25
95.5	0	1.93 ±0.15	
	5	3.32 ±0.20	3.22 ±0.15
	10	7.25 ±0.27	
94.9	5	3.08 ±0.12	
94.4	5	2.58 ±0.06	
93.3	5	1.68 ±0.10	
91.8	5	1.26 ±0.09	
91.0	5	0.891±0.050[b]	0.705±0.012
90.8	5	0.600±0.091	
	10	1.36 ±0.03	
	15	2.22 ±0.18	
89.8	5	0.602±0.015	
	30	6.98 ±0.10	
86.9	30	2.91 ±0.07	1.89 ±0.23
85.6	15	0.458±0.020	
	25	1.35 ±0.09	
	30	2.06 ±0.08	
83.4	30	1.39 ±0.05	0.900±0.020
80.5	30	0.880±0.015	0.458±0.025
78.9	30	0.690±0.015	
75.4	30	0.419±0.011	
	40	1.17 ±0.05	0.549±0.013
	50	2.88 ±0.07	1.46 ±0.09
	60	6.95 ±0.25	3.40 ±0.15
72.5	30	0.328±0.020	
71.1	30	0.301±0.001	
66.5	30	0.198±0.005	

a) $[\alpha]_D^{25}$ +27.8° in 96% ethanol, 0.935 atom%-^{18}O. Concn. of sulfoxide; 0.1 mol/*l*.
b) Calcd from E_a.

TABLE 2. ACTIVATION PARAMETERS AND k_{ex}/k_{rac} VALUES OF (+)-*p*-TOLYL PHENYL SULFOXIDE-^{18}O

H_2SO_4 (%)	E_a (kcal)	$\Delta S^{\neq}$ (e.u.)	k_{ex}/k_{rac}
95.9	—	—	0.97
95.5	24.0±3.0	+11.5	0.97
91.0	—	—	0.75
90.8	18.5±2.7	−10.8	—
86.9	—	—	0.65
85.6	17.5±1.3	−17.5	—
83.5	—	—	0.64
80.5	—	—	0.52
75.4	18.6±0.3	−18.9	0.47[a]
			0.51[b]
			0.49[c]

a) at 40°C. b) at 50°C. c) at 60°C.

k_{ex}/k_{rac} and $\Delta S^{\neq}$ values change with the change of the concentration of sulfuric acid. The gradual increase of both k_{ex}/k_{rac} and $\Delta S^{\neq}$ values with the increase of the acid suggests that there is a gradual shift in the mechanism of the reaction from S_N2-like in about 75% sulfuric acid to S_N1-like in about 95% acid.

The Correlation with H_0-Values. The rates of many acid-catalyzed reactions are dependent on the concentrations of acid. However, the role of acid and solvent, usually water, varies depending on the reaction conditions and reactants. The Zucker - Hammett hypothesis[9] has been most widely used to gain an insight into the mechanisms of these acid-catalyzed reactions. They classified mechanisms of many acid-catalyzed reactions into the following two classes, the one (*i. e.* A-1 type) is a group of reactions which give linear plots of log *k* against $-H_0$, and belongs to a family of S_N1-like processes, and the other (*i. e.* A-2 type) is the group which give linear plots of log *k* against log-[HX], belonging to a family of S_N2-like reactions. A diagram correlating the logarithms of the rates of both oxygen exchange ($\log k_{ex}$) and racemization ($\log k_{rac}$) of *p*-tolyl phenyl sulfoxide against the $-H_0$ values of sulfuric acids of various concentrations ranging from 66.5% to 96.3% are shown in Fig. 1. In concentrated sulfuric acid (86.9% to 96.3%), both $\log k_{ex}$ and $\log k_{rac}$ values are in a

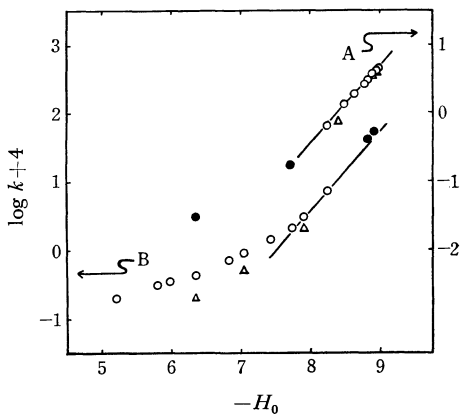

Fig. 1. The rate constants of ^{18}O-exchange and racemization of *p*-tolyl phenyl sulfoxide plotted against H_0.
○: k_{rac} (observed). ●: k_{rac} (calcd from E_a).
△: k_{ex}(observed).
A: at 5°C (the slope is 1.14, r=0.999).
B: at 30°C.

9) M. A. Paul and F. A. Long, *Chem. Revs.*, **57**, 935 (1957); L. Zucker and L. P. Hammett, *J. Am. Chem. Soc.*, **61**, 2791 (1939).

linear relationship with $-H_0$ functions[10] both at 5°C and 30°C, with the slope=1.14, r (correlation coefficient)=0.999 at 5°C. This means that a protonated species is involved in the transition state of the reaction and the reaction is of the A-1 type mechanism. However, as the concentration of sulfuric acid decreases from 86.9%, the plots of $\log k_{ex}$ and $\log k_{rac}$ starts to deviate markedly from the linear slope, suggesting that the reaction is gradually shifted from A-1 type to other with the decrease of the concentration of sulfuric acid. Although we could not find any good relationship of $\log k$ values with those of log[HX], the mechanism of the reaction in less concentrated sulfuric acids is definitely different from that with concentrated sulfuric acid as mentioned in the preceding discussion of both k_{ex}/k_{rac} and $\Delta S^{\neq}$ values.

The Correlation with Bunnett's w-Values. The w-value is an empirical function presented by Bunnett[11] and is defined by the following equation.

$$(\log k + H_0) = w \log a_{H_2O} + C$$

This parameter, w, is associated with characteristic mode of involvement of water at the rate-determining step of a reaction and according to the magnitude of the w-value many acid-catalyzed reaction can be divided into three groups. In the first group of reactions in which w is between -2.5 to 0, water does not participate in the transition state. In the second group, in which w is between $+1.2$ and $+3.3$, water acts as a nucleophile, while in the last where $w>+3.3$, water acts as a proton transfer agent. The actual diagram plotted with $(\log k+H_0)$ against $\log a_{H_2O}$ are shown in Fig. 2. Apparently, there is a gradual shift of mechanism with the change of the concentration of sulfuric acid. In fact, the w-value in the range of concentration from 75.4 to 66.5% sulfuric acid

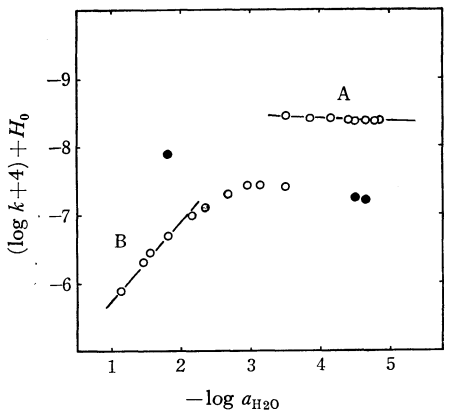

Fig. 2. Racemization of (+)-*p*-tolyl phenyl sulfoxide in sulfuric acid; plots of $(\log k_{rac}+H_0)$ against $\log a_{H_2O}$.
○: k_{rac} (observed). ●: k_{rac} (calcd from E_a).
A: at 50°C (the slope, w, is -0.06, $r=0.980$).
B: at 30°C (w is $+1.28$, $r=0.998$).

is $+1.28$ ($r=0.998$) which corresponds to the second group of reactions that belong to S_N2-like mechanism whereas in a sulfuric acid of above 86.9% concentration the w-value is -0.06 ($r=0.990$) which is in the range of S_N1-like mechanism.

Mechanistic Change from S_N1 to S_N2 Type Pathways. The k_{ex}/k_{rac} values, the activation paramaters, the correlation with Hammett's H_0 functions and that with Bunnett's w-values show that the concurrent oxygen exchange and racemization reaction of *p*-tolyl phenyl sulfoxide in the less concentrated sulfuric acids proceed through an S_N2-like pathway which is quite different from an S_N1-like route through which the oxygen exchange and racemization reactions in a cancentrated sulfuric acid proceeds. As described in the previous section the shift of the mechanism of the reaction from

Table 3. Kinetics of oxygen exchange of X-C$_6$H$_4$-S^{18}O-C$_6$H$_5$[a] in 75.4% sulfuric acid

X	$10^4 k_{ex}$ (sec^{-1}) 40°C	50°C	60°C	E_a (kcal/mol)	$\Delta H^{\neq}$ (kcal/mol)	$\Delta S^{\neq}$ (e.u.)
CH_3O[b]	3.60 ±0.05	11.1 ±0.10	—	22.7	22.1	−3.84
CH_3[c]	0.549±0.013	1.45±0.09	3.40±0.15	18.9	18.4	−19.3
H[d]	0.728±0.015	1.85±0.02	3.85±0.20	17.4	16.8	−23.5
Cl[e]	0.820±0.010	1.98±0.05	4.12±0.13	16.7	16.6	−25.8
NO_2[f]	1.03 ±0.01	2.43±0.07	—	17.3	16.7	−23.6

a) Concn. of sulfoxides: 1.0 mol/*l* b) 0.685 atom %-^{18}O
c) 0.935 atom%-^{18}O d) 0.955 atom %-^{18}O
e) 1.23 atom%-^{18}O f) 0.996 atom %-^{18}O

10) M. A. Paul and F. A. Long, *Chem. Revs.*, **57**, 1 (1957). When the H_0 values of Jorgenson and Hartter were used, the slope of this correlation was smaller slightly than 1; J. Jorgenson and D. R. Hartter, *J. Am. Chem. Soc.*, **85**, 878 (1963).

11) J. F. Bunnett, *J. Am. Chem. Soc.*, **82**, 499 (1960); **83**, 4956 (1961); **83**, 4968 (1961); **83** 4973 (1961); **83**, 4978 (1961).

S_N2-like in less concentrated sulfuric acid to S_N1-like in concentrated acid is apparently gradual. This shift of mechanism is caused by the change of the character of sulfuric acid solution, namely, the proton-donating ability of the solution diminishes steadily as acid concentration decreases while the activity of water increases. If the S_N1-like cleavage of S–O bond of the sulfoxide takes place through the diprotonated species ($R_2S^+-{}^+OH_2$) in rate-determining step as we have suggested,[5b] the formation of this diprotonated species will be decreased as the acid concentration decreases.

Polar Effect in a Less Concentrated Sulfuric Acid. The overall scheme of the oxygen exchange reaction of diaryl sulfoxides in a less concentrated sulfuric acid may be formulated as shown below:

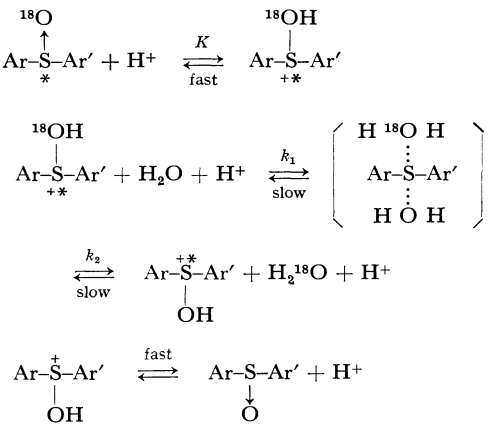

In order to comfirm the S_N2 like mechanism for this reaction, we have extended the oxygen exchange reaction on a few *p*-substituted diphenyl sulfoxides in 75.4% sulfuric acid, and the results are shown in Table 3. Except for the *p*-methoxyl compound, there is no difinite trend in the effect of these substituents and the rate varies very little (For σ^+-$\log k_{ex}$; $\rho=0.185$, $r=0.980$) like in case of S_N2 reaction of substituted alkyl halides, while the large negative $\Delta S^{\neq}$ values also suggests a S_N2-like mechanism for this reaction. The small positive value of ρ may be attributed to the fact that the polar effects on the two constants K and k in the equation for the observed rate, $k_{obs}\propto k_1K$, are canceled out considerably, since K is increased by a electron-accepting substituent while k is decreased by the same substitutent. The equilibrium constant (K) of the initial step of protonation is considered to be very large, since the pK_a values of diaryl sulfoxides are very small,[12] *i. e.* *p*-tolyl phenyl sulfoxide (−4.40) and diphenyl sulfoxide (−4.97), while H_0 function of 75.4% sulfuric acid is −6.35 and even that of 66.5% sulfuric acid is −5.20. Since the pK_a values are presumed to be the H_0 values of the half protonation of the sulfoxides, the sulfoxides are considered to be protonated nearly completely. Therefore, the second step of nucleophilic subsitution of the protonated sulfoxide by water (k_1) become the slow rate-determining step of the reaction. Only in the case of the *p*-methoxyl compound a small acceleration of rate observed, and both entropy and enthalpy of activation are off the trend of those of the other substituted sulfoxides. The mechanism of the reaction of this compound is probably different from that of the others, and similar to that of *p*-tolyl phenyl sulfoxide in a concentrated sulfuric acid, proceeding through an A-1 type route.

12) S. Oae, K. Sakai and N. Kunieda, This Bulletin, in press (1969).

Experimental

Materials. *^{18}O-Labeled p-Substituted Diaryl Sulfoxides* were prepared by the oxidation of the corresponding sulfides with bromine complex of pyridine and ^{18}O-enriched water (1.63 atom%-^{18}O) in acetic acid by the same procedure as described in our previous paper.[13] *p*-X-C_6H_4-$S^{18}O$-C_6H_5; (X, mp (°C) (lit),[14] atom%-^{18}O). H, 70—71 (71), 0.955. CH_3, 71—71.2 (71—72), 0.935. CH_3O, 60 (55—57), 0.685. Cl, 45—46 (45—46), 1.23. NO_2, 107 (106—107), 0.996 (from 3.50 atom%-^{18}O-water).

Optically Active p-Tolyl Phenyl Sulfoxide was prepared from (−)-menthyl (−)-*p*-toluenesulfinate according to the method developed by Andersen.[3] mp 91.5—92°C, $[\alpha]_D^{25}=+27.8°$ in 96% ethanol ($l=0.5$, $c=1.63$) (lit[15]; mp 92—93°C, $[\alpha]_D=+27.0°$ in 95% ethanol).

Kinetic Procedure. The rates of the oxygen exchange and racemization were measured by the same procedures as described in our previous paper[5] using Yanagimoto OR-10 type polarimeter and Hitachi-RMU-6E type mass-spectrometer.

Sulfuric Acid. Concentrations of sulfuric acid-water media were determined by titration with a standard alkali solution. The H_0 values used here is from the tables of Paul and Long,[10] and the activity of water ($\log a_{H_2O}$) of a sulfuric acid solution was tabulated by Deno and Taft.[16]

13) S. Oae, Y. Ohnishi, S. Kozuka and W. Tagaki, This Bulletin, **39**, 364 (1966).

14) G. Modena, *Gazz. Chem. Ital.*, **89**, 834 (1959).

15) K. Mislow, M. M. Green, P. Laur, J. Melillo, T. Simmons and A. L. Ternay, Jr., *J. Am. Chem. Soc.*, **87**, 1958 (1965).

16) N. C. Deno and R. W. Taft, Jr., *ibid.*, **76**, 244 (1954).

BULLETIN OF THE CHEMICAL SOCIETY OF JAPAN VOL. 42 1329—1332 (1969)

Reaction of Salicylamine with α-Dicarbonyl Compounds. I. Transamination Reaction

Hajime KANATOMI and Ichiro MURASE

College of General Education, Kyushu University, Fukuoka

(Received July 4, 1968)

The reactions of salicylamine with α-dicarbonyl compounds were examined in the hope of obtaining 2,2′-bibenzoxazine derivatives I or Schiff bases II as two-to-one condensation products; however, salicylidenesalicylamine was isolated in every case. It was found that the reaction proceeded through transamination, followed by *trans*-Schiffization between salicylamine and α-dicarbonyl compounds. The mechanism and the conditions under which the reactions take place were investigated.

It has previously been reported by one of the present authors[1] that the condensation of *o*-aminophenols with α-dicarbonyl compounds proceeded with the formation of 2,2′-bibenzoxazoline and its derivatives, and that it did not afford ordinary Schiff base derivatives. It was further noted that the oxazoline could isomerize to a Schiff base-type anion by ring opening in the presence of bivalent metal ions and formed metal chelates where the anion was coordinated as a tetradentate ligand. Therefore, the Schiff base can exist only as a ligand anion of the metal chelate in this case.

The present investigation was undertaken to study whether a similar type of condensation occurs when salicylamine (*o*-hydroxybenzylamine) reacts with α-dicarbonyl compounds. The compounds expected as the condensation products were 2,2′-bibenzoxazines of the type I or Schiff bases of the type II.

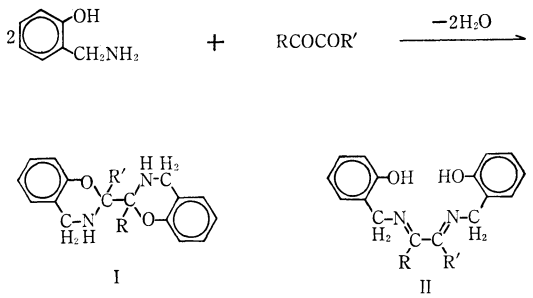

I II

The reaction of salicylamine with diacetyl was examined. When a mixture of two moles of the former and one mole of the latter was heated in methanol, yellow crystals, mp 183—184°C, were isolated. However, the compound with a molecular formula of $C_{14}H_{13}NO_2$, was neither the oxazine I nor the Schiff base II. It was easily confirmed to be salicylidenesalicylamine (III) from its infrared spectrum and by means of a mixed-melting point determination with an authentic sample.[2]

Accordingly, the mechanism of this unexpected reaction was first investigated in this paper.

Seto *et al.*,[3] have reported that salicylidenesalicylamine was isolated from an aqueous methanol solution of salicylamine by prolonged heating. The reaction was found to proceed by air oxidation, in which the amine was converted to aldimine, which was then readily hydrolized to salicylaldehyde. The aldehyde then reacted with unoxidized salicylamine to afford the Schiff base III. Although, in the present experiments, the reaction was carefully conducted under a nitrogen stream to avoid the otherwise inevitable air oxidation, the Schiff base III was always isolated in about a 40% yield.

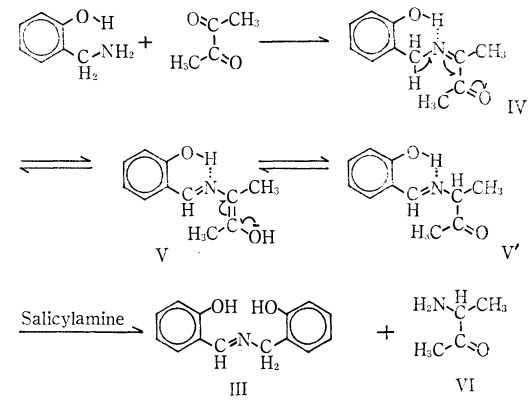

Scheme I

1) I. Murase, This Bulletin, **32**, 827 (1959); **33**, 59, 607 (1960).

2) M. Yamaguchi, *Nippon Kagaku Zasshi* (*J. Chem. Soc. Japan, Pure Chem. Sect.*), **74**, 261 (1953).

3) A. Takahashi and S. Seto, *Kogyo Kagaku Zasshi* (*J. Chem. Soc. Japan, Ind. Chem. Sect.*), **58**, 796 (1955).

Thus, the reaction did not proceed by the air oxidation of salicylamine; rather, diacetyl must have taken part in this reaction. The postulated reaction mechanisms are shown in Scheme I.

The formation of the Schiff base IV is the first step of an equimolar condensation between salicylamine and diacetyl. IV undergoes deprotonation from the methylenic group and protonation at the carbonyl oxygen, accompanied by a simultaneous electron shift, to form V, which is in equilibrium with its keto form, V'. The amine moiety of the two Schiff bases, V and/or V', is then replaced by unreacted salicylamine to give salicylidenesalicylamine (III). Thus, the overall reaction can be assumed to be transamination, followed by *trans*-Schiffization between salicylamine and diacetyl.

A similar reaction involving salicyamine has been reported by Witkop and Beiler,[4] who also isolated salicylidenesalicylalmine from the reaction mixture of salicylamine and pyridoxal. They claimed that the reaction proceeded through transamination, followed by a Schiff base exchange reaction which they termed "*trans*-Schiffization."

According to our reaction mechanism, the α-aminoketone VI should be liberated as a by-product of the *trans*-Schiffization; the determination of VI is another evidence of this mechanism. It should be noted, however, that an aliphatic α-aminoketone such as VI is, in general, very unstable and readily undergoes self-condensation to form dihydropyrazine VII, which is then readily air-oxidized to a pyrazine VIII. Thus, the formation of the α-aminoketone VI can be proven by the detection of either VII or VIII.

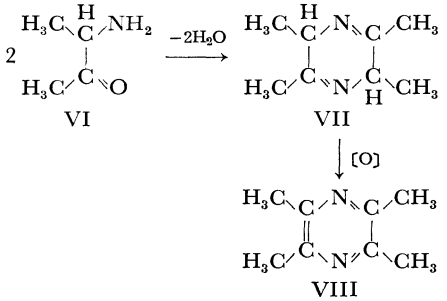

In our experiments, tetramethylpyrazine (VIII) was isolated from the reaction mixture; it was identified with an authentic sample[5] by means of the infrared spectra and by a mixed-melting point determination. The formation and isolation of VIII can be explained as resulting from the air-oxidation of VII, which has been formed from α-aminoketone VI in the reaction mixture, since the isolation and purification were unavoidable in an air atmosphere.

Different α-dicarbonyl compounds were also examined with salicylamine; the same type of reaction was found to proceed with methylglyoxal, acetylpropionyl, acetylisobutylyl, phenylglyoxal, acetylbenzoyl, and benzil, always giving rise to salicylidenesalicylamine. Among these, the reaction proceeded without a solvent for acetylbenzoyl; with the exception of acetylpropionyl and acetylisobutylyl, the others gave salicylidenesalicylamine in poor yields. Glyoxal was also examined, but no crystalline material was isolated. 5-Chlorosalicylamine as well as salicylamine reacted with diacetyl; 5-chlorosalicylidene-5'-chlorosalicylamine was thus obtained in about a 40% yield.

It was also found that the α-keto acid ester, *i. e.*, pyruvic acid ethyl ester, underwent the same type of reaction with salicylamine, and that salicylidenesalicylamine was thus obtained in a good yield. Since the amine moiety after *trans*-Schiffization should consist of the α-amino acid ester in this case, the determination was carried out by paper chromatography; α-alanine was detected in the reaction mixture from which salicylidenesalicylamine was isolated. It is clear that the reactions proceed in the same manner as in the case of the α-diketones. They are shown in Scheme II.

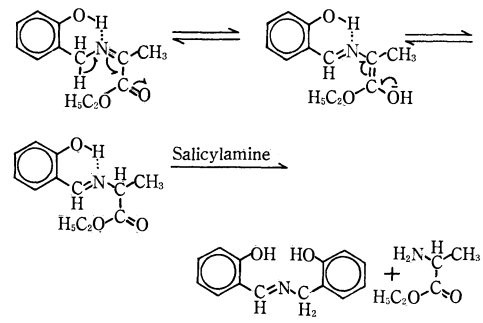

Scheme II

It is interesting with respect to this reaction to note that Nakahara *et al.*[6] have found the transamination reaction to occur from a salicylamine-pyruvic acid Schiff base to a salicylaldehyde-α-alanine Schiff base through the copper chelate. Since both Schiff bases can exist only as metal chelate ligands, the role of the metal ion may be to stabilize the azomethine linkage through the formation of a chelate ring. In the case of the ester, the Schiff base exists without any metal chelate formation; therefore, transamination could occur smoothly in the absence of metal ions.

It can be seen from these pieces of evidence that

4) B. Witkop and T. W. Beiler, *J. Am. Chem. Soc.*, **20**, 5589 (1954).

5) H. Gutknecht, *Ber.*, **12**, 2291 (1879); E. Braun, *ibid.*, **22**, 559 (1889).

6) Y. Nakao, S. Sasaki, K. Sakurai and A. Nakahara, This Bulletin, **40**, 241 (1967).

these types of transamination and *trans*-Schiffization proceed between salicylamines and α-dicarbonyl compounds except in the case of α-dialdehyde. The transamination may be due to a mesomeric effect of the carbonyl group in the Schiff base IV; this effect causes simultaneously an electron shift from the azomethine double bond to the C–C bond and deprotonation from the methylenic hydrogen. Accordingly, if there is any substituent to prevent the carbonyl group from exerting the electron-withdrawing effect, the transamination reaction will not occur. This was confirmed by the reaction of salicylamine and diacetyl monoxime, where a Schiff base IX was isolated in a good yield and where no further reactions were observed. It is clear that the electron-withdrawing effect of the carbonyl group was very much weakened by the oximino substitution and that, consequently, a further electron shift was prevented.

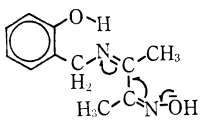

IX

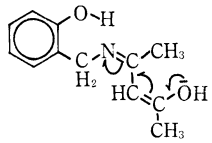

X

The significant role of the α-carbonyl group of the Schiff base IV in the transamination was further supported by the fact that transamination did not occur on a Schiff base such as X with a β-carbonyl group. The Schiff base X which was obtained by the reaction of salicylamine with acetylacetone is stable in boiling methanol; the enol structure was suggested from its infrared spectrum which exhibited strong absorptions at 1603 cm^{-1} and 1540 cm^{-1}. Since the enol group enhances the negative charge at the azomethine nitrogen atom, as is shown in the case of X, deprotonation from the methylenic hydrogen becomes difficult.

Metzler *et al.*[7] have extensively studied non-enzymatic transamination between α-amino acid and α-keto acid catalyzed by pyridoxal and by pyridoxamine. They found that the reaction was accelerated by metal chelate formation with the Schiff bases of pyridoxal-amino acid or pyridoxamine-keto acid and claimed that the significance of the nitrogen atom of the pyridine ring of pyridoxal or pyridoxamine was that it caused an electron shift from the azomethine linkage towards the pyridine ring. The role of the metal ion was explained as enhancing the electronegativity of the azomethine nitrogen; however, no mention was made concerning the role of the carboxylate group adjacent to the azomethine linkage.

The fact that the transamination could occur even between salicylamines and α-dicarbonyl compounds in the absence of metal ion may be somewhat inconsistent with their explanation. As has been stated above, the significant role of the α-carbonyl group should be taken into consideration as an electron-withdrawing source towards its own sites.

The presence of the ortho hydroxyl group in salicylamine is favorable for transamination by facilitating the formation of the Schiff base IV through intramolecular hydrogen bonding with the azomethine nitrogen. This was evidenced by the fact that benzylamine with no hydroxyl group, did not react with either the diacetyl or the pyruvic acid ester.

The effect of the metal ion, through chelate formation, on this transamination is now being investigated; the synthesis of the initially-proposed compounds, I and II, will be reported in a subsequent paper.

Experimental

Reaction of Salicylamine with Diacetyl (Transamination and *trans*-Schiffization). Under a nitrogen stream, 3.7 g (0.03 mol) of salicylamine which had been carefully purified by sublimation and by recrystallization from ethanol were dissolved in 70 m*l* of methanol, and then 1.5 g (0.018 mol) of diacetyl were added. The solution was gently refluxed under a nitrogen stream for thirty minutes and then kept in a refrigerator overnight. The resulting yellow needles were filtered, and the filtrate was concentrated to about 15 m*l*; additional crystals were thus obtained. When they were recrystallized from methanol, 1.4 g of a pure sample, mp 183—184°C, were obtained in a yield of 41.3% based on the salicylamine. The mixed-melting point with salicylidenesalicylamine was 183°C, and their infrared spectra were identical, both exhibiting a C=N absorption at 1640 cm^{-1} (KBr disk).

Found: C, 73.39: H, 5.82; N, 6.20%. Calcd for $C_{14}H_{13}NO_2$: C, 73.54: H, 5.72: N, 6.16%.

After salicylidenesalicylamine had been isolated from the reaction mixture, the mother liquor was evaporated to dryness on a water bath; the remaining resinous material was then sublimed at 80°C under reduced pressure (30 mmHg). The colorless sublimates were collected and recrystallized from water. The melting point was 81—82°C; it showed no depression upon being mixed with an authentic sample of tetramethylpyrazine, and their infrared spectra were identical.

The reaction of salicylamine with acetylpropionyl, acetylisobutylyl, methylglyoxal, phenylglyoxal, and benzil were carried out in the same manner as above; salicylidenesalicylamine was isolated in every case. The yields for acetylpropionyl and acetylisobutylyl were almost the same as those cited above; however, those of the last three substances were less than 10%.

For acetylbenzoyl, the reaction proceeded without any solvent; thus, 0.12 g (0.001 mol) of salicylamine and 0.15 g (0.001 mol) of acetylbenzoyl were mixed and heated on a water bath under a nitrogen stream. The mixture soon melted and yellow needles were gradually deposited over a ten-minute period. After the mixture

7) D. E. Metzler, M. Ikawa and E. E. Snell, *J. Am. Chem. Soc.*, **76**, 648 (1954).

had been heated for thirty minutes, the resulting salicylidenesalicylamine was isolated by treating the mixture with ethanol.

Reaction of 5-Chlorosalicylamine with Diacetyl. This reaction was carried out in the same manner as in the case of salicyalmine; 5-chlorosalicylidene-5'-chlorosalicylamine, mp 201—203°C, was isolated in a 40% yield. IR: 1665 cm^{-1} (C=N).

Found: C, 56.88; H, 3.81; N, 4.66%. Calcd for $C_{14}H_{11}NO_2Cl_2$: C, 56.79; H, 3.72; N, 4.73%.

Reaction of Salicylamine with Ethyl Pyruvate. A mixture of 0.12 g (10^{-3} mol) of pure salicylamine and 0.06 g (5×10^{-4} mol) of ethyl pyruvate in 5 m*l* of methanol was gently refluxed under a nitrogen stream for one hour. The solution turned red orange, and salicylidenesalicylamine was crystallized on cooling. The yield was 0.04 g (40% based on the salicylamine) and a mixed-melting point determination with an authentic sample showed no depression (183°C). After the filtrate of salicylidenesalicylamine had been evaporated, the resinous residue was treated with a small amount of water and filtered. To the filtrate there was added one drop of concentrated hydrochloric acid; the mixture was refluxed for one hour and then evaporated to dryness. The residue was dissolved in a small amount of water, and the solution was subjected to paper chromatography. The R_f value of the sample was 0.38, identical with that of *d,l*-alanine ($R_f=0.38$; solvent, butanol : acetic acid : water=4 : 1 : 2).

Schiff Base of Salicylamine with Diacetyl Monoxime IX. A mixture of 0.48 g (0.039 mol) of pure salicylamine and 0.4 g (0.04 mol) of diacetyl monoxime in 25 m*l* of dry benzene was refluxed for one hour under a nitrogen stream. The solution was then concentrated to 10 m*l* under reduced pressure, and the resulting precipitates were recrystallized from benzene. Colorless crystals, mp 106—108°C; yield 0.6 g (80%). IR: 3250 cm^{-1} (NOH), 1645 cm^{-1} (C=N), 1609 cm^{-1} (C=NOH).

Found: C, 63.78; H, 6.79; N, 13.67%. Calcd for $C_{11}H_{14}N_2O_2$: C, 64.06; H, 6.84; N, 13.58%.

Schiff Base of Salicylamine with Acetylacetone (X). A mixture of 1.2 g (0.01 mol) of pure salicylamine and 1 g (0.01 mol) of acetylacetone in 10 m*l* of methanol was refluxed for one hour under a nitrogen stream. On cooling, 1.7 g of an almost pure Schiff base was obtained as colorless needles in a yield of 83%; it was recrystallized from methanol; mp 141—142.5°C. IR: 1603 cm^{-1}, 1540 cm^{-1} (probably C=N and C=C of enol).

Found: C, 69.88; H, 7.27; N, 6.99%. Calcd for $C_{11}H_{13}NO_2$: C, 70.21; H, 7.37; N, 6.84%.

BULLETIN OF THE CHEMICAL SOCIETY OF JAPAN VOL. 42 1332—1336 (1969)

The Structure of Copolymers of L-Proline with γ-Benzyl-L-glutamate in Organic Solvents

Rume SAKAI, Shoichi IKEDA*1 and Toshizo ISEMURA

Institute for Protein Research, Osaka University, Kita-ku, Osaka and Faculty of Science, Osaka University, Toyonaka, Osaka

(Received July 9, 1968)

The equilibrium conformations of three copolymers of L-proline with γ-benzyl-L-glutamate were studied in 1,2-dichloroethane, *m*-cresol, and dichloroacetic acid by measuring the optical rotatory dispersion and the infrared absorption spectra. In *m*-cresol and dichloroacetic acid, the proline residues take the *trans*-configuration. In *m*-cresol their incorporation into copolymers destroys the right-handed-α-helical conformation of glutamate residues. In 1,2-dichloroethane, the proline residues assume the *cis*-configuration if the sequence of proline residues is long enough. If it is short, they are in the *trans*-configuration. The poly-L-proline-I-helix can never coexist with the α-helix.

Poly-γ-benzyl-L-glutamate (PBLG) can assume the right-handed α-helix in helicogenic solvents, such as 1,2-dichloroethane (DCE), chloroform, and *m*-cresol, while it is a random coil in dichloroacetic acid (DCA) or trifluoroacetic acid.[1] Its helix-coil transition has been extensively investigated by changing the solvent or the temperature.[2] Poly-L-proline (PLP) has two types of conformations.[3] The one, known as the form I, is a right-handed helix with all the peptide bonds in the

*1 Present address: Faculty of Science, Nagoya University, Nagoya

1) P. Urnes and P. Doty, "Advances in Protein Chemistry, XVI," Academic Press, New York (1961), p. 401.

2) B. H. Zimm, P. Doty and K. Iso, *Proc. Natl. Acad. Sci. U. S.*, **45**, 1601 (1959).

3) E. Katchalski, A. Berger and J. Kurtz, "Aspects of Protein Structure," ed. by G. N. Ramachandran, Academic Press, New York (1963), p. 205.

cis-configuration,[4] $[\alpha]_D^{25}=+50°$ [5] (immediately after the dissolution of polyproline into acetic acid). The other, the form II, takes a left-handed helix with *trans*-imide bonds,[6] $[\alpha]_D^{25}=ca.\ -500°$, and is stable in acetic acid, formic acid, DCA, and water. The mutual conversion between the forms I and II has also been elucidated in relation to the nature of the solvent. It is known that the PLP-I-helix can be readily transformed into the PLP-II-helix by dissolving it in organic acids, water, and *m*-cresol, and that it can be recovered from these solvents by the addition of aliphatic alcohols.[5]

It is of interest to study the stable conformation of the copolymers of L-proline and γ-benzyl-L-glutamate (γBLG) in various environments. DCE favors the right-handed α-helix of PBLG, it seems also to favor the right-handed PLP-I-helix, because the conformation of PLP in DCE-acetic acid (99.5—0.5%) (DCE-AA) is the form I.[7] *m*-Cresol also favors the right-handed α-helix of PBLG, but folds PLP into a left-handed PLP-II-helix. While DCA disrupts the PBLG helix into the random coil, it keeps PLP in the left-handed PLP-II-helix.[8]

We have previously reported the synthesis and some properties of the copolymers.[7] The copolymers studied were copoly-3:1-(L-proline, γBLG) (Copoly-3:1), copoly-1:1-(L-proline, γBLG) (Copoly-1:1), and copoly-1:3-(L-proline, γBLG) (Copoly-1:3).

In the present investigation, studies have been made of the conformation of these copolymers in three different solvents, DCE, *m*-cresol, and DCA, by measuring the optical rotatory dispersion and the infrared absorption spectra of films cast from those solvents.

Experimental

Materials. The *m*-cresol and DCA used in the present study were twice redistilled in a vacuum. The DCE was distilled under atmospheric pressure. The acetic acid was a JIS special grade acid from Wako Pure Chemical Industries, Ltd., and was used without further purification. All the polymers were the same as those used in the previous investigation.[7]

Optical Rotatory Dispersion (ORD). The ORD of the poly-peptides in *m*-cresol and DCA solutions was measured at room temperature with a Rudolph and Sons Model 200S photoelectric spectropolarimeter. The ORD of the DCE solutions was measured by a Perkin-Elmer Model 141 photoelectric polarimeter. The ORD results were analysed by the Moffitt-Yang equation,[9] assuming λ_0 to be 212 mμ. The a_0 and b_0 are constants. PLP and the copolymers exhibited mutarotation in a *m*-cresol solution, although less mutarotation was observed with copolymers of lower proline contents. All the ORD curves shown below were obtained at room temperature after the mutarotation had been completed. For the measurements, polymer solutions were put in a cell with a 10-cm path.

Infrared Absorption Spectra. The infrared absorption spectra of films cast from the solutions on KBr plates were measured on a Perkin-Elmer Model 221 spectrophotometer at a relative humidity of 40% and at 20°C.

Results

DCE Solutions. The ORD curves of the polymers are shown in Fig. 1, while the plots of a_0 and b_0 against the polymer composition in DCE are shown in Fig. 2.

The values of a_0 and b_0 for PBLG in DCE were found to be 202° and −630° respectively, in good agreement with the values observed by Moffitt and Yang.[9] Those values for PLP in DCE-AA were found to be −280° and +285°. For PLP in DCE-AA, the specific rotation at 589 mμ (the D-line of sodium) was almost the same value as $[\alpha]_{578}=-36°$, which lies between the $[\alpha]_D=+50°$ for the form I and $[\alpha]_D=-100°$. The form IA of PLP was discovered and thus denoted by Sasisekharan;[10] it was later identified as the form I by Traub and Shmueli.[4] Therefore, the conformation of PLP in DCE-AA seems to be the form I. This is supported by the infrared study of a film cast from the solution. A prominent

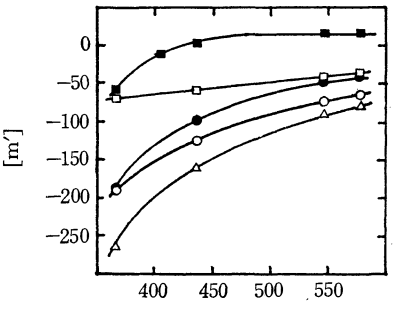

Fig. 1. The optical rotatory dispersion curves of the solutions of polymers in DCE.
□ PLP (in DCE-AA) ○ Copoly-3:1
△ Copoly-1:1 ● Copoly-1:3
■ PBLG

4) W. Traub and U. Shmueli, *ibid.*, p. 81.
5) I. Z. Steinberg, W. F. Harrington, A. Berger, M. Sela and E. Katchalski, *J. Am. Chem. Soc.*, **82**, 5263 (1960).
6) P. Cowan and S. McGain, *Nature*, **176**, 501 (1955).
7) R. Sakai, S. Ikeda and T. Isemura, This Bulletin, **39**, 2308 (1966).
8) E. R. Blout and G. D. Fasman, "Recent Advances in Gelatin and Glue Research," ed. by G. Stainby, Pergamon Press, London (1958), p. 122.
9) W. Moffitt and J. T. Yang, *Proc. Natl. Acad. Sci.*, **42**, 596 (1956).
10) V. Sasisekharan, *J. Polymer Sci.*, **47**, 373 (1960).

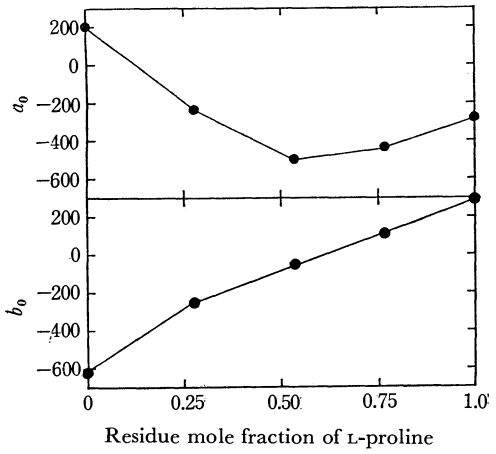

Fig. 2. The relation of a_0 and b_0 in DCE or DCE-AA to the content of proline.

feature of the copolymers is the fact that a minimum a_0 value is found at the proline content of 50%. This feature was also observed for $[m']_{546}$.[7] The inference to be drawn from this observation will be discussed below. As the residue mole fraction of proline increased from 0 to 0.25, the value of b_0 increased more sharply than it did on going from 0.25 to 1.0.

The infrared absorption spectra of polymers cast from DCE or DCE-AA are shown in Fig. 3.

In the spectrum of PLP, the CO stretching frequency of the amide (amide I) was observed at 1653 cm^{-1}, while the characteristic frequencies of the form I were observed at 960 and 1360 cm^{-1}. The last two absorptions clearly indicate that the

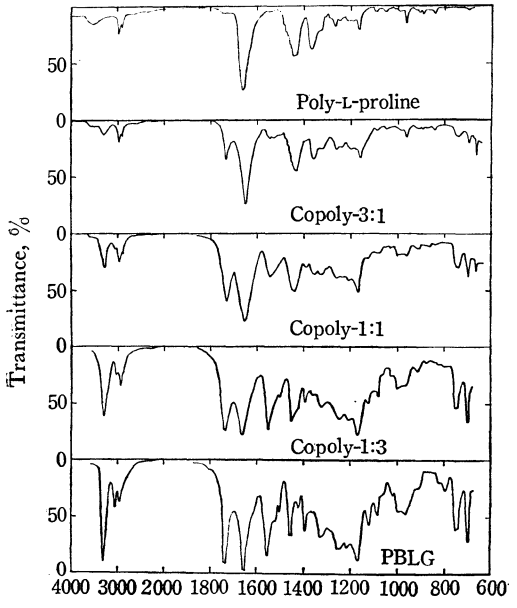

Fig. 3. Infrared absorption spectra of polymers cast from DEC of DCE-AA.

PLP-I-helix is predominant in the DCE-AA solution of PLP. An NH stretching was observed at about 3300 cm^{-1}, and a CO stretching of the γ-ester, at about 1740 cm^{-1}, together with amide I and II bands, as in the spectrum of PBLG.[11] In the neighborhood of 1360 cm^{-1}, however, no absorption was observed. For the copolymers the ratio of the intensity of the amide I to that of the absorption at 1740 cm^{-1}, defining the existence of glutamate, increased with the proline content. The absorption at 960 cm^{-1} was observed for Copoly-3:1, and the absorption at 1360 cm^{-1}, for Copoly-3:1 and Copoly-1:1. These facts suggest that the proline parts in Copoly-3:1 and Copoly-1:1 take the same conformation as in the form I of PLP. The frequencies of the amide I of the polymers are listed in Table 1.

Table 1. The amide I frequencies of polymers cast from *m*-cresol and DCE

Polymer	Solvent	
	m-Cresol cm^{-1}	DCE cm^{-1}
PLP	1637	1653
Copoly-3:1	1642	1650
Copoly-1:1	1661 1650 1642	1653
Copoly-1:3	1658	1661
PBLG	1655	1656 1650

The frequencies of Copoly-1:3 were higher than that of PBLG. The frequency of the amide I is known to be higher than that of the right-handed α-helix if ordinary polypeptides take the left-handed helix.[12–15] Therefore, Copoly-3:1 might contain some left-handed helicies.

m-Cresol Solutions. The ORD curves of the polymers in *m*-cresol are shown in Fig. 4, while the plots of a_0 and b_0 against the polymer composition in *m*-cresol are shown in Fig. 5.

The values of a_0 and b_0 for PBLG in *m*-cresol were +350° and −530° respectively. These values were not compatible with those reported by Cassim and Taylor[16] (a_0=223°, b_0=−650°). Although

11) C. H. Bamford, A. Elliott and W. E. Hanby, "Synthetic Polypeptides," Academic Press, New York (1956), p. 143.

12) K. S. Norland, G. D. Fasman, E. Katchalski and E. R. Blout, *Biopolymers*, **1**, 277 (1963).

13) E. M. Bradbury, L. Brown, A. R. Downie, A. Elliott, W. E. Hanby and T. R. R. McDonald, *Nature*, **183**, 1736 (1959).

14) M. Hashimoto and S. Arakawa, This Bulletin, **40**, 69 (1967).

15) E. M. Bradbury, B. G. Carpenter and R. M. Stephans, *Biopolymers*, **6**, 905 (1968).

16) J. Y. Cassim and E. W. Taylor, *Biophys. J.*, **5**, 553 (1965).

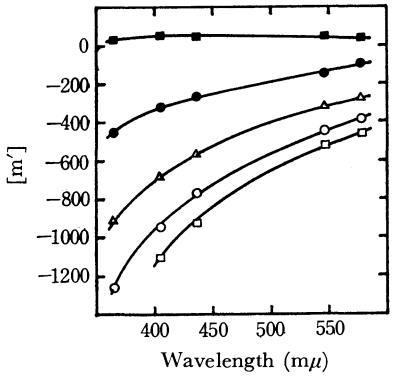

Fig. 4. The optical rotatory dispersion curves of the solutions of polymers in *m*-cresol.
The symbols are the same as in Fig. 1.

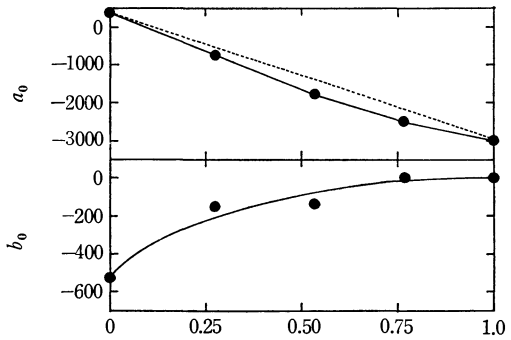

Fig. 5. The relation of a_0 and b_0 in *m*-cresol to the content of proline.

the reason for this discrepancy is not clear, the values fall in the same category as those of PBLG in helicogenic solvents. PLP had an $[\alpha]_{546}$ value of −538° in *m*-cresol, and was found to have the conformation of the form II. The values of a_0 and b_0 of PLP were −3000° and 0° respectively. The plot of a_0 was concave against the residue mole fraction of proline. The plot of b_0 was convex.

In the infrared absorption spectra of polymers cast from *m*-cresol, no absorption band near 1360 cm^{-1} was observed. This fact is to be expected for PLP, for the conformation of PLP in *m*-cresol is the form II and this conformation would be retained in a solution even after regeneration into the solid state. The frequencies of the amide I of polymers cast from *m*-cresol are listed in Table 1. The frequencies increased from PBLG to Copoly-3:1 and Copoly-1:1. This also suggests that Copoly-1:3 and Copoly-1:1 cast from *m*-cresol consist of some parts of the left-handed helices.

DCA Solutions. The ORD curves of the polymers in DCA are shown in Fig. 6, while the plots of a_0 and b_0 against the polymer composition in DCA are shown in Fig. 7.

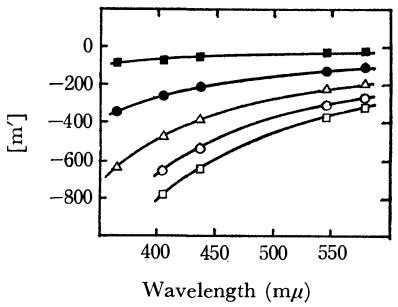

Fig. 6. The optical rotatory dispersion curves of solutions of polymers in DCA.
The symbols are the same as in Fig. 1.

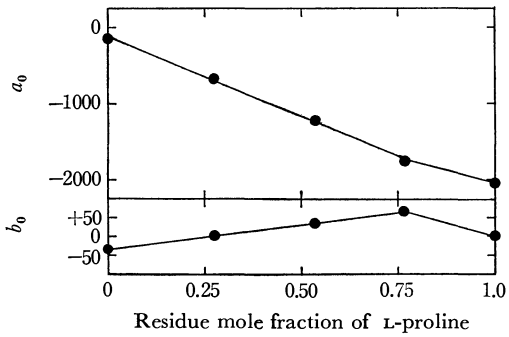

Fig. 7. The relation of a_0 and b_0 in DCA to the content of proline.

The a_0 and b_0 values of PBLG in DCA were −160° and 35°. PBLG is randomly coiled in DCA. PLP in DCA is known to be in the form II,[8] and in the present experiment it was found that $[\alpha]_{546}=-373°$. The observed value was less negative than that for PLP in formic acid or in acetic acid, but the deviation could be caused by some solvent effect or by the smaller molecular weight of our sample. The a_0 and b_0 values of PLP were −2100° and zero respectively. The b_0 value was equal to that in *m*-cresol. The plot of a_0 is concave against the increase of the residue mole fraction of proline, as is shown in Fig. 7. The b_0 value increased linearly as the proline fraction increased from zero to 0.75. However, these b_0 values are nearly zero when the ambiguity of the experiment is considered.

Discussion

The conformation of the copolymers of L-proline with γBLG will be considered as a function of the composition in different solvents, based on the following assumptions. First, the rotatory properties observed for copolymers can be reduced to those of the constituent residues. Second, the a_0 value reflects the configuration of the L-proline residue. Although it ranges from −160° for the random

coil to 400° for the α-helix in PBLG, the a_0 value of PLP changes much more, *i. e.*, from −300° for the form I to −3000° for the form II. Therefore, the second assumption is roughly justified. Third, the b_0 value depends on the conformation of the benzyl glutamate residue alone. The right-handed α-helical conformation of the glutamate residue has $b_0=-600°$, while its random coil conformation has $b_0=0$. Finally, it is assumed that the conformation of copolymers regenerated from solutions is not distinguishable from that in the original solutions when the solvent is either DCE or *m*-cresol. For DCA this assumption is not necessarily true.[17]

DCE Solutions. The observed gradual change in a_0 with the increase in proline content seems to indicate that any peptide bond associated with a proline residue assumes the *cis*-configuration if the proline content is more than 50%. This is supported by the infrared measurements, which reveal the appearance of absorption bands at 1360 and 960 cm^{-1}. In proline-rich copolymers proline residues occur consecutively more frequently, and in such sequences proline have the *cis*-configuration. On the other hand, in the copolymers with proline contents of less than 50%, the chance of finding more than two or three proline residues in a sequence is smaller and more proline residues would be isolated from the others. The change in a_0 with the proline content suggests that the proline residue tends to take the *trans*-configuration. This is consistent with the results on oligomers and low-molecular-weight polymers of proline.[18] *N*-Carbobenzoxy-di-, tri-, and tetra-L-proline had more negative specific rotations at 546 mμ in methanol or acetic acid than the monomer. Mutarotation studies of PLP dodecylamides (PPDA) of different molecular weights in organic acids have also shown that, in the initial conformation, more proline residues exist in the *trans*-configuration as the degree of polymerization decreases. Further, in a mixed solvent, benzene-alcohol, PPDA of a higher degree of polymerization existed in the PLP-I-helix. Even in this solvent, however, PPDA of a lower degree of polymerization had a higher content of *trans*-peptide bonds. Consequently, in a sequence composed of a small number of proline residues in the copolymers, the proline residues will be in the *trans*-configuration, even if they are in DCE, which stabilizes the *cis*-configuration of the peptide bond between prolines, or the form I. Proline residues take the *cis*-configuration in the PLP-I-helix-solvent only if they are included in a long sequence of proline residues.

The b_0 value increases rather markedly even if a small quantity of proline residues is incorporated into PBLG. The right-handed α-helix formed by glutamate residues is partly broken or converted into the left-handed helix by the occasional occurrence of proline residues. The latter suggestion is supported by the infrared spectra, which show a rather high amide I band frequency for the copolymer with a 27% proline content, since the high amide I frequency has thus far been attributed to the left-handed helix.[12–15]

***m*-Cresol Solutions.** All the a_0 values observed for the copolymers are more negative than those calculated from the weighted sum of the proline-II-helix and the glutamate helix. *m*-Cresol is a solvent supporting both the PLP-II-helix and α-helix. Consequently, the proline residues tend to assume the *trans*-configuration. The infrared spectra of the solid film regenerated from *m*-cresol solutions do not have any absorption around 1360 cm^{-1}. This fact also indicates that the *cis*-configuration is absent in the copolymers. The b_0 value increases rather abruptly with as the proline content increases to 27%. Considerable sections of the right-handed helix have been broken in this composition. In the same way as has been discussed in the case of DCE solution, the glutamate residues in the copolymers are considered to be folded together into a helix of the same kind as that of the proline residues, *i. e.*, into a left-handed helix.

DCA Solutions. Proline residues have the *trans*-configuration, and most benzyl glutamate residues are in random coils. The experimental curve for a_0 is lower, *i. e.*, more negative, than that expected for the simple sum of random coil glutamate residues and *trans* proline residues. This can be most adequately interpreted by assuming that the glutamate residues are folded into a PLP-II-helix or a left-handed α-helix. Since, however, b_0 does not change appreciably with the composition, the formation of a left-handed α-helix can be rejected.

In the PLP-II-solvent, proline residues take the *trans*-configuration and interrupt the formation of the right-handed α-helix conformation specific for the glutamate-rich parts in helicogenic solvents. In the PLP-I-solvent, proline residues assume a *cis*-configuration if the series of proline residues is long enough, although they take a *trans*-configuration if the number of proline residues in a sequence is small. Over the whole range of mole fractions of proline to benzyl glutamate, the right-handed α-helix of the glutamate residues and the right-handed PLP-I-helix can never coexist in the copolymers.

The authors wish thank Professor G. D. Fasman, Brandeis University, for his many helpful comments.

17) E. R. Blout and A. Asadourian, *J. Am. Chem. Soc.*, **76**, 745 (1956).

18) T. Isemura, S. Ikeda and O. Maeda, *Nippon Kagaku Zasshi* (*J. Chem. Soc. Japan, Pure Chem Sect.*), **88**, 421 (1967).

BULLETIN OF THE CHEMICAL SOCIETY OF JAPAN VOL. 42 1337—1342 (1969)

The Structure of Copolymers of L-Proline with L-Glutamic Acid in Aqueous Solutions

Rume SAKAI and Toshizo ISEMURA

Institute for Protein Research, Osaka University, Kita-ku, Osaka

(Received September 12, 1968)

Three copolymers of L-proline and L-glutamic acid were synthesized, and their equilibrium conformation in an aqueous solution was studied in relation to their composition. The molar ratios of the proline to the glutamic acid residues in the copolymers were about 1:3, 1:1, and 8:1. All the copolymers were soluble in water, as were poly-α,L-glutamic acid and poly-L-proline II. The conformational change was caused by the pH effect on proline-poor copolymers. Evidence was obtained for the possibility of the absence of such a helix as a right-handed poly-L-proline-I-helix in the copolymers examined. The conformation of Copoly-8:1 was not affected by the pH and was identified as the poly-L-proline-II-helix.

Both poly-L-proline (PLP)[1] and poly-α, L-glutamic acid[2] (PLGA) are water-soluble, and their conformations in water have been investigated in great detail. PLP exists in the PLP-I-helix[3] after being isolated from the polymerization medium, but if it is dissolved in water it changes into a left-handed PLP-II-helix[4] with a threefold screw-axis, after a gradual *trans*-conformation from PLP-I to PLP-II.[5] PLGA assumes an α-helix form at the pH of acid or at a low ionization of side-chain carboxyl groups, but is randomly coiled at a neutral or alkaline pH.[6]

The copolymers of L-proline and L-glutamic acid can be effected to be soluble in water, and can be expected to be suitable for the elucidation of the relative stabilities of those various conformations assumed by each residue in relation to its environment. The water-solubility of the copolymers permits the measurment of the circular dichroism (CD) and the optical rotatory dispersion (ORD) in the far-ultraviolet region; these measurements will give us important informations about the conformational stability. The composition of the copolymers will influence the environment of each residue and, consequently, change the conformation of each residue from that found when the residue is located in a long sequence of the same residue, *i. e.*, in a homo-polymer. Also, the change in pH will affect their conformation. These various parameters of the water-soluble copolymers can afford a greater variety of information than can those of such water-insoluble copolymers as copolymers with γ-benzyl-L-glutamate (γBLG).[7,8]

The copolymers of L-proline and L-glutamic acid have been prepared, and their ORD in the visible region and their viscosities have been measured as a function of the pH. These properties of the copolymers rich in glutamic-acid residues have shown the presence of a transition due to pH change similar to that observed for PLGA. The CD and ORD values in the far-ultraviolet region have also been measured at pH's on both sides of the copolymer transitions.

Experimental

Materials. The γBLG was synthesized from L-glutamic acid and benzyl alcohol in 60% H_2SO_4. The *N*-carboxyanhydrides (NCA's) of γBLG and L-proline were synthesized by the methods of Blout *et al.*[9] and Kurtz *et al.*[10] respectively. Polymerization was performed in nitrobenzene with a total NCA con-

1) E. Katchalski, A. Berger and J. Kurtz, "Aspects of Protein Structure," ed. by G. N. Ramachandran, Academic Press, New York (1963), p. 205.

2) G. D. Fasman, "Poly-α-amino Acids," ed. by G. D. Fasman, Marcel Dekker, Inc., New York (1967), p. 539.

3) W. Traub and U. Shmueli, "Aspects of Protein Structure," ed. by G. N. Ramachandran, Academic Press, New York (1963), p. 81.

4) P. Cowan and S. McGain, *Nature*, **176**, 501 (1955).

5) W. F. Harrington and M. Sela, *Biochim. Biophys. Acta*, **27**, 24 (1958).

6) P. Doty, A. Wada, J. T. Yang and E. R. Blout, *J. Polymer Sci.*, **23**, 851 (1957).

7) R. Sakai, S. Ikeda and T. Isemura, This Bulletin, **39**, 2308 (1966).

8) R. Sakai, S. Ikeda and T. Isemura, *ibid.*, **42**, 1332 (1969).

9) E. R. Blout, R. H. Karlson, P. Doty and B. Hargitay, *J. Am. Chem. Soc.*, **76**, 4492 (1954).

10) J. Kurtz, A. Berger and E. Katchalski, "Recent Advances in Gelatin and Glue Research," ed. by G. Stainby, Pergamon Press, London (1958), p. 131.

TABLE 1. PROPERTIES OF POLYPEPTIDES

Polypeptide	Residue mole fraction of L-proline		Intrinsic viscosity pH *ca.* 7 in 0.1M NaCl at 25°C	Molecular weight
	at polymerization	from amino acid analysis		
PLP	1	—	0.24 dl/g	6.6×10^{3}*
Copoly-8:1	0.75	0.89	0.12	3.3×10^{3}*
Copoly-1:1	0.50	0.55	0.11	—
Copoly-1:3	0.25	0.26	0.14	—
PLGA	0	—	0.46	2.0×10^{4}**

* Obtained from sedimentation equilibrium.
** Deduced from the relationship between molecular weight and intrinsic viscosity on PLGA reported by Wada.[12]

centration of 4%, and was initiated by sodium methoxide at molar ratio of the NCA's to the initiator of 100. The mixing ratios of NCA's are shown in Table 1. After the polymerization had been allowed to go on about a week, anhydrous hydrogen bromide was bubbled through all the solutions except for that of PLP. Each solution became turbid or a precipitate separated. After 24 hr standing, the excess hydrogen bromide was removed from the solutions by passing a stream of dry air through the solutions. The polymers were then isolated by the addition of ether to the solution, followed by centrifugation. They were exhaustively washed with anhydrous ether and acetone alternatively and dried *in vacuo*. All the isolated polymers except for the Copoly-8:1 were stored in a desiccator over silica gel. The compositions of the copolymers were determined by amino-acid analysis. PLP, PLGA, and three copolymers were prepared in this way; some of their properties are shown in Table 1. Copoly-8:1 has a very different proline content from that of the mixed ratio of NCA, although the other two copolymers have almost the same ratio. A polymer sample prepared in a proline to glutamate ratio of 3:1 became black and sticky within a few days after isolation. The black material (6 g) was dissolved in water, decolorized by Norit, and filtered, and then acetone was added to separate the purified polymer. It was washed with anhydrous acetone several times and designated as Copoly-8:1 (1.8 g). It seems likely that fractionation according to composition occurred during the above additional procedure.

The ORD of PLP and the copolymers changed with time after they have been dissolved in 0.1M sodium chloride or sodium fluoride. All the physical measurements described below were made on solutions after the mutarotation had ceased. The mutarotation was complete within 24 hr for the copolymers, while it took 7 days for PLP.

Amino-acid Analysis. The copolymers were hydrolysed at 110°C for 20 hr with twice-distilled hydrogen chloride. Amino-acid analysis was performed on a Beckman Spinco Model 120 amino-acid analyzer.

Molecular Weight. The molecular weights of PLP and Copoly-8:1 were determined by the method of sedimentation equilibrium performed in a Spinco E Ultracentrifuge at 26°C for PLP and at 31°C for Copoly-8:1, using a temperature control unit. To correlate the concentration with the fringe scale, a filled Epon double sector synthetic boundary cell was used. The solvent used was a 0.1M sodium chloride solution. The partial specific volume of the two polymers was assumed to be 0.758 ml/g.[11] Equilibrium patterns for both polymers showed that they were relatively homogeneous in molecular weight. The weight-average molecular weight of PLGA was determined from its intrinsic viscosity by using the molecular weight-viscosity relationship provided by the data of Wada.[12] These results are also included in Table 1.

Viscosity. The viscosity was measured using an Ubbelohde-type viscometer, with a flow time of 239 sec for a 0.1M sodium chloride solution at 25±0.01°C.

The ORD in the Visible Region. The ORD in the visible region was measured on a Perkin Elmer Model 141 spectrophotoelectric polarimeter. The measurement was made on a 0.5% solution at 25°C. The data were analyzed in the way described in previous paper.[8] The results followed the Moffitt-Yang equation.[13]

The CD and ORD in the Far Ultraviolet Region. The CD and ORD curves in the far ultraviolet region were recorded on a JASCO Model ORD/UV-5 spectropolarimeter, equipped with a circular dichroism attachment, at room temperature. For both measurements, 0.1 g/dl polymer solutions in 0.1M sodium fluoride were placed in cells of with light paths of 0.2, 1, or 2 mm, depending on the wavelength region scanned. The CD spectra are shown in terms of the residue ellipticity, $[\theta]$:

$$[\theta] = 3300(\varepsilon_L - \varepsilon_R),$$

where $(\varepsilon_L - \varepsilon_R)$ is the difference between the residue mole extinction coefficients of the left and right circularly-polarized lights. The ORD spectra are shown in terms of the residue rotation, [m]:

$$[m] = \frac{M_R}{100}[\alpha],$$

11) I. Z. Steinberg, W. F. Harrington, A. Berger, M. Sela and E. Katchalski, *J. Am. Chem. Soc.*, **82**, 5263 (1960).
12) A. Wada, *Mol. Phys.*, **3**, 409 (1960).
13) W. Moffitt and J. T. Yang, *Proc. Natl. Acad. Sci.*, **42**, 596 (1956).

where M_R is the residue weight and [α], the specific rotation. To reduced [θ] and [m] to the residue basis for copolymers, the mean residue weight calculated from the composition of the copolymer was used.

Results

The ORD of a solution of each polymer in 0.1M sodium chloride was observed at various pH's, and the parameters, a_0 and b_0, of Moffitt-Yang's equation were calculated for each solution. The pH dependence of these parameters for each polymer is shown in Fig. 1.

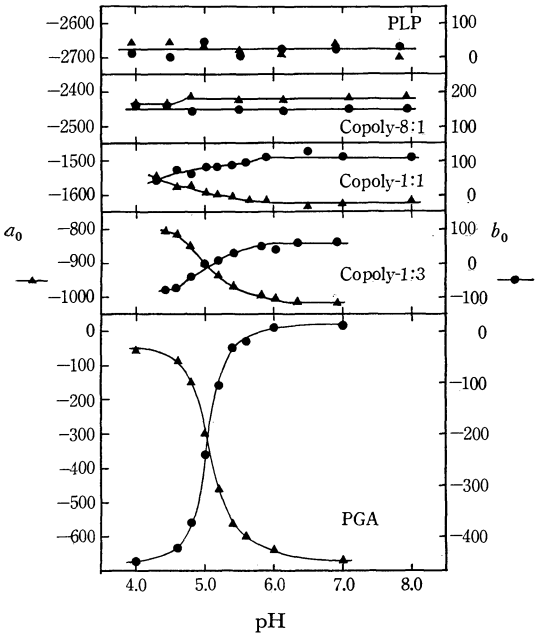

Fig. 1. The effect of pH on the a_0 and b_0 for each polymer in 0.1 M sodium chloride.

It is evident that PLP has no pH dependence of the ORD, while the largest pH dependence is observed for PLGA, which undergoes a helix-coil transition around pH 5.0, as has previously been shown by Doty *et al.*[6] Although a trivial difference in a_0 was observed for the Copoly-8 : 1, no corresponding difference in b_0 as the pH of the solution was observed. The other copolymers have a narrow pH region in which both a_0 and b_0 change with the pH. As the pH increases from 4.3 to 6, the a_0 value decreases and the b_0 value increases. As compared with that of PLGA, it is likely that the pH region observed for the copolymers represents the region where they undergo a conformational change caused by the ionization of side-chain carboxyls of the glutamic-acid residues. The differences in the two parameters, a_0 and b_0, in the two extrema are smaller as the proline content of the copolymer is higher. For example, the b_0 values of PLGA, Copoly-1:3, and Copoly-1:1 are $-450°$, $-77°$, and $44°$ at pH 4.3, while they are 10°, 60°, and 113° at a neutral pH. This is shown in Fig. 2, which clearly indicates that the differences in both a_0 and b_0, especially in the latter, decrease sharply with the proline content, more than expected.

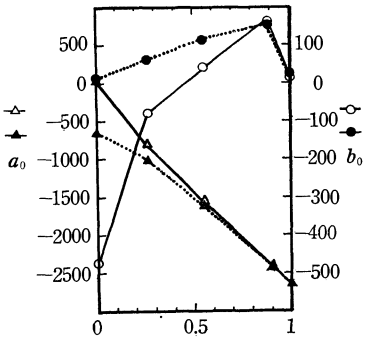

Fig. 2. The plots of a_0 and b_0 at pH 4.0—4.3 or pH 7 against residue mole fraction of L-proline.
—△— —○— pH 4.0—4.3
···▲··· ···●··· pH 7

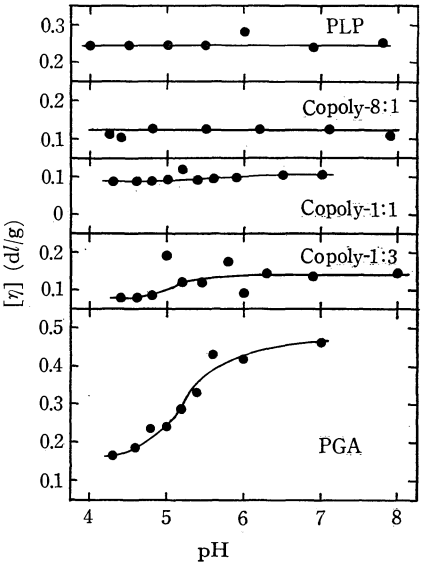

Fig. 3. The effect of pH on intrinsic viscosity.

The effect of the pH on the intrinsic viscosity of each polymer in 0.1M sodium chloride was studied as an alternative method to check the conformational change, the results are shown in Fig. 3. The results are compatible with those to be expected from ORD. The intrinsic viscosity of PLP and Copoly-8:1 are independent of the pH, while a slight pH dependence is observed for Copoly-1:1. Although the viscosity of Copoly-1:3 around the transition pH was variable, it was constant below pH 4.6 and above pH 6.3. The

intrinsic viscosity is higher at a neutral pH than at an acid pH; this finding is opposite to that reported by Doty *et al.*[6] The difference seems to come from the difference in the molecular weight or in the solvent used in the experiments. The inflection point, *i. e.*, the transition pH, on the $[\eta]$-pH curve was, at pH 5.3, slightly higher than that obtained from the ORD.

It is now generally accepted that PLP in an aqueous solution has a form-II helix after mutarotation has ceased; the present ORD and viscosity measurements of PLP at different pH values show that the same helical conformation exists in the pH region between 4 and 8. The helix-coil transition of PLGA is induced by the change in pH. PLGA is in the α-helix conformation at an acid pH, while it is randomly coiled at a neutral pH. The ORD and viscosity profiles against the pH imply that at pH 4.3 the copolymers assume definite conformations characteristic to each of them which differ from those at pH 7.

The CD and ORD, in the far ultraviolet region, of polymers at different pH's are shown in Figs. 4—7. The positions and magnitudes of the dichroic bands are given in Table 2, while the peaks and troughs of the Cotton effect are shown in Table 3.

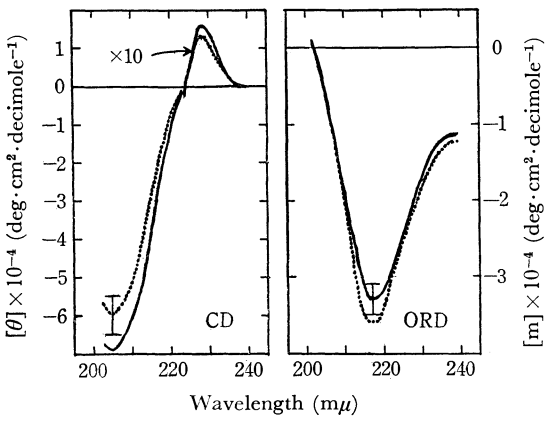

Fig. 4. The CD and ORD spectra of PLP and Copoly-8:1.
—— PLP
····· Copoly-8:1

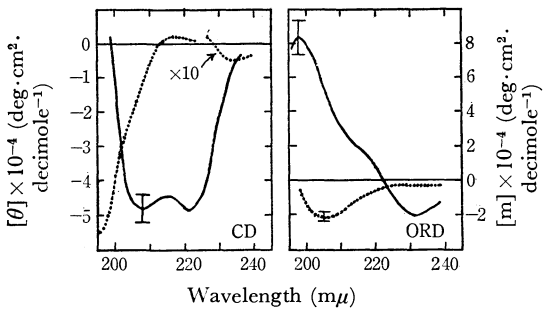

Fig. 5. The CD and ORD spectra of PLGA at acidic pH and neutral pH.
—— pH 4.5
····· pH 7

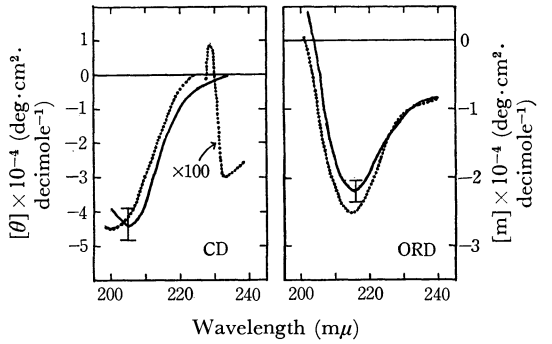

Fig. 6. The CD and ORD spectra of Copoly-1:1 at an acidic pH and a neutral pH.
—— pH 4.3
····· pH 7

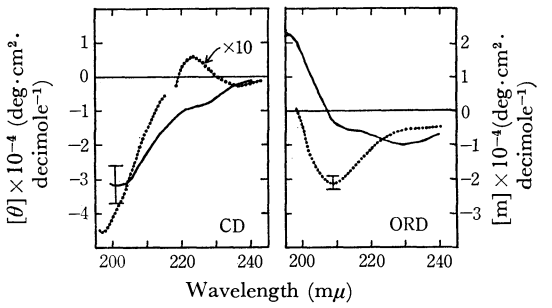

Fig. 7. The CD and ORD spectra of Copoly-1:3 at an acidic pH and a neutral pH.
—— pH 4.3
····· pH 7

TABLE 2. CD BANDS

Polypeptide	pH 4.3—4.5		pH 7	
	λ	[θ]	λ	[θ]
PLP	205	-7×10^4	205	-7×10^4
	228	1.6×10^3	228	1.6×10^3
Copoly-8:1	205	-6×10^4	205	-6×10^3
	228	1.3×10^3	228	1.3×10^3
Copoly-1:1	205	-4.4×10^4	201	-4.5×10^4
			228	90
			233	-3×10^2
Copoly-1:3	201	-3.2×10^4	~197	-4.6×10^4
			223	6×10^2
			236	-3×10^2
PLGA	208	-4.3×10^4	~196	-5.5×10^4
	221	-4.4×10^4	216	2×10^3
			234	5×10^2

λ: Wavelength (mμ)
[θ]: Residue ellipticity (deg·cm²·decimole⁻¹)

TABLE 3. THE PEAKS AND TROUGH OF COTTON EFFECTS

Polypeptide	pH 4.3—4.5		pH 7	
	λ	[m]	λ	[m]
PLP	217	-3.3×10^4	217	-3.3×10^4
Copoly-8:1	217	-3.6×10^4	217	-3.6×10^4
Copoly-1:1	216	-2.2×10^4	215	-2.5×10^4
Copoly-1:3	~196	-2.2×10^4	209	-2.1×10^4
	229	-1.0×10^4		
PLGA	198	8.4×10^4	206	-2.2×10^4
	231	-2.1×10^4		

λ: Wavelength (mμ)
[m]: Residue rotation (deg·cm^2·decimole^{-1})

The CD and ORD spectra of PLP and Copoly-8:1 in Fig. 4 are not influenced by the pH, as was to be expected from the results on ORD in the visible region and from the viscosity studies. The spectra of PLP are almost identical with those reported by Timasheff *et al.*[14] and by Bovey and Hood.[15] As is shown in Fig. 5, the CD of PLGA at pH 4.3 has two negative dichroic bands, while at a neutral pH it has a strong negative band, together with a weak positive and a trivial negative band. The spectra are almost identical with those previously reported.[16] The Cotton effects of PLGA at two pH's (shown in Fig. 5) are also similar to those already found by other workers.[17] It may be noted in Fig. 6 that Copoly-1:1 at an acid pH is associated with a single negative dichroic band similar to PLP, but it does not have any dichroic band near 228 mμ. The CD spectra of Copoly-1:1 change when the pH is raised by the shift of the negative dichroic band to a shorter wavelength and the appearance of weak dichroic bands at longer wavelengths. This change in CD is not clearly manifested in the ORD curve. The CD of Copoly-1:3 does markedly change with the pH, as is shown in Fig. 7. There are two plateau regions, around 220 and 202 mμ, at an acid pH; these regions may correspond to the negative bands of the PLGA α-helix, but the CD pattern at a neutral pH is completely different. The CD curve of Copoly-1:3 at a neutral pH is similar to that of PLGA at a neutral pH, but it is more depressed by the contribution of the proline residue. The same tendency is observed from the ORD curves in Fig. 7.

Discussion

The pH-induced conformational transitions are clearly seen in Copoly-1:3 and Copoly-1:1 as well as in PLGA in Figs. 1 and 3. It is well known that PLGA is a random coil if the side-chain carboxyl groups are highly ionized, while it assumes an α-helix if they are not. The stable form of PLP in 0.1M sodium chloride is a PLP-II-helix, a short sequence of proline residues also tends to assume the *trans*-configuration of the peptide bonds, as in the PLP-II-helix.[8] The peptide bonds of the L-proline residues in the copolymers containing a small quantity of L-proline residues would, therefore, assume the *trans*-configuration in 0.1M sodium chloride. Since the PLP-II-helix has a zero b_0 value,[5] a zero b_0 value can be assigned to a proline residue in the *trans*-configuration. Consequently, the b_0 value of the copolymers can be used as a measure of the conformation of the glutamic-acid residue. As is shown in Fig. 2, the observed difference in the b_0 value of each copolymer between acid and neutral pH values is smaller in magnitude than that to be expected if a linear relation between the difference and the glutamic-acid content is assumed. One of the reasons for the deviation is perhaps the effect of the chain length on the b_0 value. Proline residues cut up the segment composed of glutamic-acid residues. Goodman *et al.*[18] have reported that the b_0 value of the oligo-γ-methyl-L-glutamates in helicogenic solvents abruptly decreases in absolute value with a decrease in the polymerization degree. This may be because the α-helix is unstable in the oligomers or because a considerably long series of residues is necessary to produce a large negative b_0 value for the α-helix, even though oligomers can assume a perfect α-helix. The same reasons are appropriate in explaining the b_0 value of copolymers. Another reason may be that glutamic-acid residues in the copolymers take a definite conformation, *e.g.*, a left-handed helix. Even at higher pH values the copolymers can assume the same conformation as that in an acid pH, because the electric repulsion between glutamic-acid residues is more reduced than that in PLGA.

It would be interesting to ascertain whether or not these copolymers assume a definite conformation under the conditions described above. This question can be partly answered by considering the ORD and CD results in the far ultraviolet region. The results for Copoly-8:1 are very similar to those of PLP, as is shown in Fig. 4. If Copoly-8:1 contains some parts of left-handed α-helices or random coils, the CD spectra or ORD will be different from those of PLP by the inverted CD

14) S. N. Timasheff, H. R. Townend, L. Stevens, M. J. Gorbunoff and T. F. Kumonski, "Conformation of Biopolymers," Vol. 1, ed. by G. N. Ramachandran, Academic Press, London (1967).
15) F. A. Bovey and E. P. Hood, *J. Am. Chem. Soc.*, **88**, 2326 (1966).
16) G. Holzwarth and P. Doty, *ibid.*, **87**, 218 (1965).
17) E. R. Blout, I. Schmier, N. S. Simmons, *ibid.*, **84**, 3193 (1962)
18) M. Goodman, I. Listowski and E. E. Schmitt, *ibid.*, **84**, 1296 (1962).

or ORD of PLGA at an acid pH or the CD or ORD at a neutral pH. The CD and ORD of Copoly-8:1 show this tendency only a very little. Therefore, the conformation of the copolymers is probably the same as that of the PLP-II-helix.

This inference is also supported by the following facts. The axial ratio, as calculated from the intrinsic viscosity by Simha's equation[19] assuming a partial specific volume and no hydration, 11, is nearly equal to that calculated from the molecular weight on the assumption that the conformation of the copolymers is the same as that of the PLP-II-helix, 13. The CD spectra and ORD of Copoly-1:1 at an acid pH reflect those of PLP to some extent. For example, they have a negative dichroic band in the CD spectra at 205 mμ, the same wavelength as in PLP. The situation is similar in ORD. At a neutral pH, the parts rich in glutamic-acid residues in the copolymers will be in random coils, because the CD pattern is like that of PLGA at a neutral pH, although the CD band around 220 mμ shifts towards a longer wavelength, possibly because of the CD arising from proline residues.

19) R. Simha, *J. Phys. Chem.*, **44**, 25 (1940).

The CD and ORD of Copoly-1:3 at an acid or neutral pH reflect those of PLGA, as is shown in Fig. 7. Some parts in the copolymer assume the α-helix at an acid pH, but they are randomly coiled at a neutral pH.

The above discussion makes it clear that glutamic-acid residues are folded with proline residues into a PLP-II type helix when the proline residue content in the copolymers is high. The positive b_0 values of the copolymers, as is shown in Fig. 1, do not always imply the left-handed α-helix; they might come from such a helix of glutamic-acid residues as the PLP-II-helix.

The presence of no PLP-I-helix-type helix was detected in any of our experiments.

The authors wish to express their deep gratitude to Dr. S. Ikeda, Nagoya University, for his helpful discussions throughout the course of this work. The authors also wish to thank Professor G. D. Fasman, Brandeis University, for many valuable comments. One of the authors (R.S.) was a fellow of the California Foundation for Biochemistry, 1967—1968.

BULLETIN OF THE CHEMICAL SOCIETY OF JAPAN VOL. 42 1342—1344 (1969)

Graft Copolymerization onto Cellulose in Dimethyl Sulfoxide by Means of a Ceric Salt Containing Lauryl Sulfuric Ions

Kyoji KAERIYAMA

The Textile Research Institute of Japanese Government, Sawatari, Kanagawa-ku, Yokohama

(Received July 15, 1968)

Styrene was polymerized in dimethyl sulfoxide by alcohol-ceric salt containing lauryl sulfuric ions. The rate of polymerization increased with the amount of ethyl alcohol added. A deuterium isotope effect was observed when tetradeuteromethyl alcohol was used as an initiator. Accordingly, the generation of radicals by the elimination of the hydrogen atom from the alcohol molecule was concluded. When styrene was polymerized in the presence of cellulose, graft copolymer was obtained. The grafting efficiency amounted to about 70%.

Many workers have reported the graft copolymerization of vinyl monomers onto cellulose.[1] Previous investigations have, however, dealt almost exclusively with polymerizations in aqueous systems. On the other hand, some reactive monomers react with water rather than graft. No radical initiator which initiates graft copolymerization onto cellulose in an inert organic solvent is yet known.

The author has been studying the polymerization by ceric ions in an organic solvent.[2,3] Ceric salt containing lauryl sulfuric ions (hereafter refered to as CLS) was found to be an effective initiator. As our purpose is to show the effectiveness of CLS in grafting vinyl monomers onto cellulose, the present paper will deal with the polymerization of styrene.

1) For example, M. Imoto and K. Takemoto, *Kogyo Kagaku Zasshi* (*J. Chem. Soc. Japan, Ind. Chem. Sect.*), **70**, 1851 (1967).

2) K. Kaeriyama, This Bulletin, **41**, 722 (1968).

3) K. Kaeriyama, *Polymer* (*London*), **10**, 11 (1969).

Experimental

Material. The styrene, ethyl alcohol, dimethyl sulfoxide (DMSO), and dimethylformamide (DMF) were distilled under reduced pressure just prior to use. The tetradeuteromethyl alcohol was of commercial origin (E. Merck AG.).

The CLS was generally prepared according to the following procedure.[4] To a solution of 32 g of ceric ammonium nitrate in 70 m*l* of water, there was added a solution of 12 g of sodium laurylsulfate in 50 m*l* of water. The slurry was poured into 800 m*l* of water, and the precipitate thus separated was collected on a sintered filter and dried *in vacuo*. The yield was 14.8 g. The CLS thus obtained was not soluble in any of the organic solvents examined except DMSO and DMF. The ceric ion content in CLS was 23.00% by weight.

The cellulose used was 40/1 cotton cloth which had been desized and scoured according to the usual procedure.

Polymerization Procedure. In a glass tube with a capacity of 25 m*l* there was placed a 20 m*l* portion of the polymerizing mixture. After the tube had been degassed by the freeze-thaw-method, it was sealed off. After the tube had then been maintained at 60°C for a given time, the contents were poured into methyl alcohol containing a small amount of benzoquinone. The polystyrene thus precipitated was collected on a sintered filter and dried *in vacuo* to a constant weight.

The grafted cellulose was extracted with benzene until no further polymers could be extracted.

Molecular Weight. The viscometry was carried out at 30°C in a benzene solution. The molecular weight was calculated from the intrinsic viscosity based on the equation:[5]

$$\log[\eta] = -4.013 + 0.74 \log M_n$$

Definitions. In this paper, the polymer yield, the grafting, and the grafting efficiency are defined as follows:

$$\text{Polymer yield (mol/}l\text{)} = \frac{\text{weight of polymer produced per liter}}{\text{molecular weight of the polymer produced}}$$

$$\text{Grafting (\%)} = \frac{\text{weight increase of cellulose after extraction}}{\text{weight of original cellulose}} \times 100$$

$$\text{Grafting efficiency (\%)} = \frac{\text{weight increase of cellulose after extraction}}{\text{weight of polymerized styrene}} \times 100$$

Results and Discussion

Polymerization in DMF. Polymerization was carried out in DMF, in which CLS was soluble.

Table 1. Polymerization in dimethyl formamide

Ethyl alcohol (mol/*l*)	Conversion (%)
1.73	2.46
0.606	2.33
0.173	2.85
0.0346	2.69
0.00692	2.74

[Styrene]=2.18 mol/*l*; [CLS]=8.21×10^{-3} mol/*l*
Solvent: dimethyl formamide
Polymerization: at 60°C for 48 hr

The results are shown in Table 1. Polymerization is not initiated by the ethyl alcohol-CLS system in DMF. The conversion is much lower than that of similar runs in DMSO, which will be described below. In view of the above results, the polymerization was thereafter carried out in DMSO.

Polymerization in DMSO. Polymerization was carried out in DMSO. It can be seen from Table 2 that polymerization is initiated by the ethyl alcohol-CLS system in DMSO.

Table 2. Effects of the concentration of ethyl alcohol

Ethyl alcohol (mol/*l*)	Conversion (%)	$M_n \times 10^{-5}$	Polymer yield (mol/*l*) $\times 10^4$
1.73	22.5	2.4	2.1
0.606	18.9	3.4	1.3
0.173	15.8	3.7	0.97
0.0173	14.7	5.6	0.60
0.00173	10.4	5.7	0.41

[Styrene]=2.18 mol/*l*; [CLS]=8.21×10^{-3} mol/*l*
Solvent: DMSO
Polymerization: at 60°C for 48 hr

Because the polymer yield increases with the amount of ethyl alcohol added, the latter is concluded to participate in the initiation reaction of polymerization. This suggests that a graft copolymerization of styrene onto cellulose may be possible in DMSO.

Deuterium Isotope Effect. Ethyl alcohol participates in the initiation reaction, as is evident from the above results. However, it is not yet clear whether or not the radical is formed by the cleavage of the covalent bond in the alcohol molecule. In order to see how the radical is formed, styrene was polymerized by the CLS-tetradeuteromethyl alcohol system.

In the initiation step, if the reaction involves a rupture of the C–H bond, the rate of the reaction of the deuterated alcohol should be lower than that of the ordinary alcohol because of the difference in

4) S. Kaizerman, N. Plainfield and G. Mino, U. S. Pat. 2922801.

5) R. H. Ewart and H. C. Tingey, Abstracts of Papers Presented at the 111th Meeting of American Chemical Society, Atlantic City, N. J. (1947).

6) K. B. Wiberg, *Chem. Revs.*, **55**, 713 (1955).

TABLE 3. DEUTERIUM ISOTOPE EFFECT IN POLYMERIZATION CATALYZED BY METHYL ALCOHOL-CLS SYSTEM

Polymerization time (hr)	Without alcohol			CH_3OH			CD_3OD			Ratio (B−A)/(C−A)
	Conversion (%)	$M_n \times 10^{-5}$	Polymer yield $\times 10^5$ (mol/l) A	Conversion (%)	$M_n \times 10^{-5}$	Polymer yield $\times 10^5$ (mol/l) B	Conversion (%)	$M_n \times 10^{-5}$	Polymer yield $\times 10^5$ (mol/l) C	
5	2.43	1.6	3.5	3.79	1.2	7.2	3.30	1.3	5.8	1.6
10	3.61	2.2	3.7	7.34	1.4	12	6.42	1.7	8.6	1.7
15	4.91	2.9	3.8	10.2	1.7	14	8.26	1.9	9.9	1.7
20	5.41	3.3	3.7	12.3	1.9	15	11.0	2.1	12	1.4
30	7.11	3.6	4.5	16.1	1.9	19	13.3	2.4	13	1.7

[Styrene]=2.18 mol/l; [CLS]=8.21×10^{-3} mol/l; [methyl alcohol]=1.85 mol/l
Solvent: DMSO
Polymerization: at 60°C

TABLE 4. GRAFT COPOLYMERIZATION ONTO CELLULOSE

Cellulose* (g)	CLS 10^3 (mol/l)	Polymerization time (hr)	Total conversion (%)	Grafting (%)	Graft efficiency (%)
1.634	8.21	5	11.4	21.5	67.8
1.672	8.21	10	18.3	35.8	71.8
1.633	8.21	17	24.2	48.8	72.5
1.611	8.21	21	29.5	62.6	75.1
1.652	8.21	26	33.8	70.8	76.3
1.593	8.21	40	37.8	79.8	74.1
1.667	8.21	48	40.0	78.0	71.8
1.712	1.64	48	8.3	9.3	41.7
1.683	4.92	48	16.3	22.6	51.4
1.685	13.9	48	49.0	90.8	68.7
1.705	20.5	48	49.0	87.9	67.3

Styrene: 5 ml; DMSO: 15 ml
Polymerization: at 60°C
* Cotton cloth

zero-point energy and mass effect.[6] If the step is rate-determining, the difference in rates may actually be observed. In fact, the isotope effect has been observed in the radical oxidation of various alcohols.[7,8]

The results of polymerization in the presence of CH_3OH and CD_3OD and in the absence of any alcohol are shown in Table 3. Styrene was polymerized without any alcohol because of the initiation of polymerization by the CLS-DMSO system and thermal polymerization. In order to observe the effect of the methyl alcohol-CLS system, it is necessary to deduct the moles of polymer produced in the absence of alcohol from the total moles of the polymer produced. Ratios of the moles of the polymers produced by ordinary methyl alcohol to those produced by tetradeuteromethyl alcohol are shown in the last column. The mean value of the ratios is 1.6. This value suggests that a radical is formed by the elimination of a hydrogen atom from methyl alcohol in the rate-determining step; therefore, it may be concluded that it is possible to prepare graft copolymers by the initiator system.

Graft Copolymerization onto Cellulose. The results of graft copolymerization onto cellulose are shown in Table 4. The data show that styrene was graft-copolymerized onto cellulose. The grafting efficiency is high. The percentage of grafting increases with the polymerization time for 40 hr and in the range of the CLS concentration below 13.9×10^{-3} mol/l. The grafting efficiency reaches its maximum at the CLS concentration of 8.21×10^{-3} mol/l and at the polymerization time of 26 hr.

The method developed in this paper will be useful for preparing graft copolymers with functional side chains.

The author is grateful to Dr. R. Murase and Mr. K. Ishino for their interest in this work. The author also wishes to thank Dr. Y. Tanaka for his valuable discussions.

7) F. H. Westheimer and N. Nicolaides, *J. Am. Chem. Soc.*, **71**, 25 (1949).
8) L. Kaplan, *ibid.*, **76**, 4645 (1954); **77**, 5469 (1955); **80**, 2639 (1958).

BULLETIN OF THE CHEMICAL SOCIETY OF JAPAN VOL. 42 1345—1350 (1969)

Studies of the Derivatives of Epichlorohydrin. III. A New Method of Preparing γ-Alkoxy-γ-butyrolactones

Tsunehiko KUWAMURA and Hideo TAKAHASHI

Department of Synthetic Chemistry, Faculty of Engineering, Gunma University, Tenjin-cho, Kiryu

(Received July 25, 1968)

When alkyl glycidyl ethers derived from epichlorohydrin and alcohols were treated with sodium cyanide, the corresponding γ-alkoxy-β-hydroxybutyronitriles (I) were obtained. The hydrolysis of I with aqueous alkali metal hydroxide, followed by acidification and distillation, gave γ-alkoxy-γ-butyrolactones (II). The structure of II was confirmed by chemical and physical means. The reaction paths of I to II were also studied.

In previous papers,[1,2] the synthesis of alkyl glycidyl ammonium salts from epichlorohydrin and amines was described, and their properties as reactive surfactants were discussed. The purpose of this investigation is to develop the study of reactive long-alkyl-chain derivatives of epichlorohydrin. The earlier work[3] on the application of long-alkyl-chain glycidyl ethers prompted the preparation of β-hydroxynitriles, which may be convertible to lactones. Many previous workers have mentioned the lactonization of unsaturated carboxylic acids by the aid of such strong acids as polyphosphoric acid or sulfuric acid.[4] Blout and Elderfield[5] and Newman and Rosher[6] have reported the formation of γ-lactones from β-hydroxycarboxylic acids, the process involving dehydration and subsequent cyclization. Also, Campaigne and Ellis[7] have prepared highly-substituted γ-butyrolactones from unsaturated nitriles. Recently Heiba and Dessau[8] have reported a new radical synthesis of γ-lactones. Although it has been well known that γ-alkoxy-γ-butyrolactones can be prepared from esters of β-formylpropionic acid dialkylacetal, no published investigation has yet described a method of synthesizing γ-lactones directly from β-hydroxynitriles.

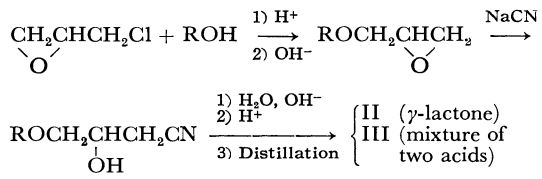

The hydrolysis of I yielded predominantly II rather than III. II and III were decided to be, respectively, γ-alkoxy-γ-butyrolactones and a mixture of γ-alkoxy-β-hydroxybutyric acid (IV) and γ-alkoxy-crotonic acid (V), as will be discussed later. From the consideration of these products, it may be predicted that the reaction involves dehydration, the hydrolysis of the cyano group, and a rearrangement of the double bond preceding cyclization. As to the sequence, it was postulated that the course of the reaction may be as is shown in the following scheme:

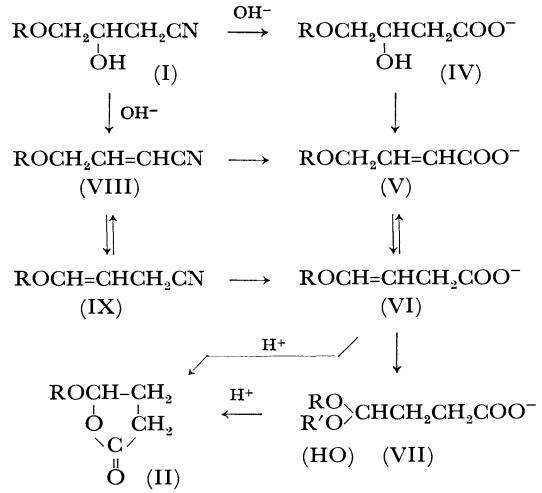

To confirm this sequence, however, we prepared several presumable intermediates (IV, V, VII, and

1) T. Kuwamura and E. Kameyama, *Kogyo Kagaku Zasshi* (*J. Chem. Soc. Japan, Ind. Chem. Sect.*), **67**, 592 (1964).

2) T. Kuwamura, E. Kameyama and H. Takahashi, *ibid.*, **68**, 2178 (1965).

3) T. Kuwamura, *ibid.*, **63**, 595 (1960).

4) M. F. Ansell and M. H. Palmer, *Quart. Rev.*, **18**, 211 (1964).

5) E. R. Blout and R. C. Elderfield, *J. Org. Chem.*, **8**, 29 (1943).

6) M. S. Newman and R. Rosher, *ibid.*, **9**, 221 (1944).

7) E. Campaigne and R. L. Ellis, *Chem. Commun.*, **1966**, 140.

8) E. I. Heiba and R. M. Dessau, *J. Am. Chem. Soc.*, **89**, 2238 (1967).

TABLE 1. PROPERTIES AND YIELDS OF ALKYL GLYCIDYL ETHERS

R	Bp °C/mmHg (lit.)[3]	n_D^{21}	[O] %* Found	[O] %* Calcd	Yield %
C_2H_5	123—128 (126.5—127.5)	1.4108	15.2	15.6	70
n-C_4H_9	72—74/25 (74—75/26)	1.4190	12.2	12.3	80
n-C_8H_{17}	120—125/20 (140.0—141.5/30)	1.4349	8.4	8.5	70

* [O]% of oxirane determined by the acetic acid-HBr method.
(Ref. Report of the F.A.C. subcommittee on oxirane oxygen, 1956, *J. Am. Oil Chemist's Soc.*, **34**, 476 (1957)).

VIII) (indicated above) and established that they did indeed exist in the reaction mixture. Furthermore, evidence was obtained that they all afford II. Then the proceeding of the reaction was followed up by measuring the nitrogen content and the hydroxyl number in the reaction mixture in order to establish the reaction path preferred. Unfortunately, however, we had only rough information because of technical difficulties.

Experimental and Results

Preparation of Alkyl Glycidyl Ethers. According to a method described in a previous report,[3] these ethers were prepared from epichlorohydrin and alcohols. Ethyl, butyl, and octyl derivatives were prepared. Their purity, as checked by gas-liquid chromatography (GLC), was satisfactory. The properties and yields are shown in Table 1.

Preparation of γ-Alkoxy-β-hydroxybutyronitriles. Alkyl glycidyl ether (1 mol) was dissolved in an equivalent volume of ethanol containing a few drops of a thymol blue solution as the indicator. Into the resulting solution, a 30% aqueous solution of sodium cyanide (1 mol) was, drop by drop, added with stirring at 30—40°C over a period of about 90 min. During the reaction, the mixture was kept at pH 7.0—7.5 by the drop-by-drop addition of a 30% aqueous solution of acetic acid. After all the sodium cyanide had been added to the reaction mixture, stirring was continued for an additional 3—6 hr at 40—50°C. When the reaction mixture no longer exhibited a color change, it was cooled. Then the separated organic layer and the ether extract of the water layer were gathered and dried over magnesium sulfate. After the ether had been removed, I was isolated by distillation and then purified using a concentric-type fractionator. Their purities were checked by GLC. Table 2 shows their properties and yields. The IR spectrum of the C-2 homologue of I is indicated in Fig. 1. The characteristic absorption band at 2240 cm^{-1} can be ascribed to the $-C\equiv N$ group.

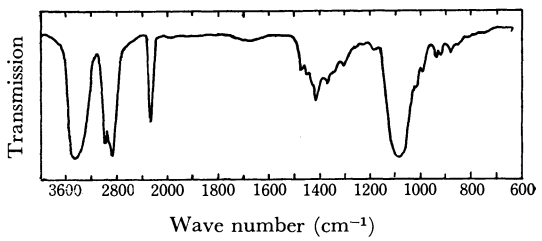

Fig. 1. IR spectrum of γ-ethoxy-β-hydroxybutyronitrile.

Preparation and Identification of II. *a) Hydrolysis of I.* A solution of I (1 mol) in an equivalent volume of ethanol was mixed with a concentrated aqueous solution of sodium hydroxide (1.1 mol). The resulting mixture was heated under reflux for 24—30 hr and then evaporated to dryness. During the first 30 min, ammonia was liberated from the reaction mixture. The residue was then made into a slurry with a small amount of water and acidified to pH 3—4 with a 50% aqueous solution of mineral acid. The separated organic layer and the ether extract from the water layer were combined and dried over magnesium sulfate. After the solvent had then been removed, the residue was distilled under reduced pressure. The substance first distilled out, II, was fractionated and its purity determined by GLC. The one distilled out next, III, was also redistilled, but it did not show a mono peak on the GLC chart. Table 3

TABLE 2. PROPERTIES AND YIELDS OF γ-ALKOXY-β-HYDROXYBUTYRONITRILE

R	Bp °C/mmHg	N% Found	N% Calcd	n_D^{18}	Yield %
C_2H_5	138.5—139.0/26.5	10.8	10.9	1.4393	87
n-C_4H_9	148.0—148.5/18	8.5	8.9	1.4455	77
n-C_8H_{17}	150—153/5	6.3	6.5	1.4490	58

Table 3. Properties and yields of II

R	Bp (°C/mmHg)	Anal. C% Found Calcd*	Anal. H% Found Calcd*	Mol wt Found Calcd*	n_D^{18}	d_4^{18}	Yield %
C_2H_5	112—113/25	55.0 55.4	7.6 7.7	115 130	1.4336	1.093	50
n-C_4H_9	93—94/2.5	60.7 60.7	8.4 8.9	156 158	1.4380	1.032	65—70
n-C_8H_{17}	102—105/1	66.9 67.2	10.5 10.4	—	1.4459***	0.969***	35
n-C_4H_9**	90—91/3	—	—	—	1.4387	—	40

* Calculated for γ-alkoxy-γ-butyrolactone.
** The authentic substance prepared by the routine method.
*** They were measured at 20°C.

shows the properties and yields of II.

b) IR Spectra. The IR spectra of II exhibit the characteristic absorption band at 1790 cm^{-1}, indicating the presence of the γ-butyrolactone carbonyl group. Its chart is given in Fig. 2.

c) Identification of II. γ-Butoxy-γ-butyrolactone, the authentic substance, was prepared by a well-known method[9] and then compared with II. β-Formylpropionitrile (1 mol) was dissolved in butyl alcohol (400 ml) containing a small amount of hydrochloric acid. The reaction mixture was heated at 110°C for 3 hr and then allowed to stand at room temperature for several hours. After neutralization with an aqueous solution of potassium carbonate, the corresponding butyl acetal was obtained by distillation; bp 104—106°C/1 mmHg (lit.,[9] 122—123°C/3.4 mmHg). β-Formylpropionitrile butyl acetal was then hydrolyzed in the presence of an alkaline catalyst. The salt thus obtained was purified and acidified. On distilling, carboxylic acid of the acetal type formed γ-butoxy-γ-butyrolactone immediately. The properties and yields are listed in Table 3. The best evidence for the identity of II with this γ-alkoxy-γ-butyrolactone is the fact that the IR spectrum and the GLC retention time of II agreed entirely with the values of the authentic sample. They are shown in Fig. 2.

d) NMR Spectra. The NMR spectra of II provided further information for the structual consideration. In Fig. 3, A and B represent the normal spectra of the C-4 and C-2 homologues of II, while C and D show the spin-spin decoupled spectra of B. As may be seen in the spectrum B, four bands are found, at τ 4.45, and 8.8 and in the regions of τ 6.1—6.6, and 7.4—7.9. The relative heights of the integrated spectrum give the number of protons as in the following ratio in the spectrum B from the low to the high field; 1:2:4:3. The band at

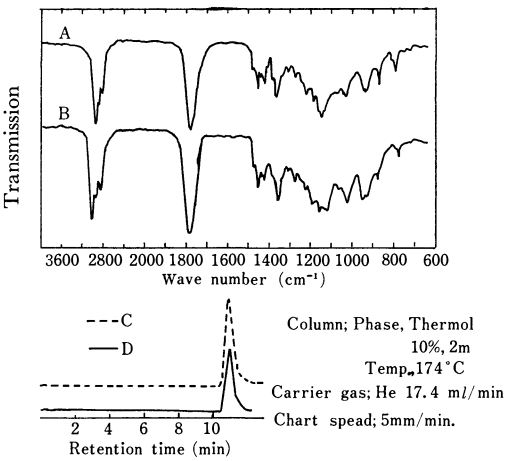

Fig. 2. IR spectra and GLC charts.
A and B; IR spectra of the authentic γ-butoxy-γ-butyrolactone and C_4-II.
C and D; GLC charts of the authentic γ-butoxy-γ-butyrolactone and C_4-II.

τ 4.45, indicating one proton, is attributable to the γ-position proton, which may be the lowest field since it is deshielded by the adjacent oxygen atoms. The two protons appearing in the region of τ 6.1—6.6 may correspond to methylene protons in the substituted ethoxy group, and their chemical shift may be lowered by the adjacent oxygen atom. The band in the region of τ 7.4—7.9 comes from the four protons at the α- and β-methylene groups. They appear as a group of bands, since they are nearly, but not exactly, equivalent protons and split each other complicatedly. The three protons of the methyl group in the side chain resonate at τ 8.8 and are split into a triplet. Spin-spin decoupling was carried out to support these assignments. In the spectrum C, decoupling the multiplet at τ 6.45 causes the triplet at τ 8.8 to collapse to a singlet and somewhat simplifies the multiplet

9) S. Motoki, S. Satsumabayashi and I. Tajima, This Bulletin, **37**, 646 (1964).

in the region of τ 7.4—7.9. On the other hand, decoupling the triplet at τ 8.8, although its spectrum is not shown here, causes a partial collapse in two regions, τ 6.1—6.6 and 7.4—7.9. As the spectrum D indicates, decoupling the multiplet at τ 4.45 partially collapses the multiplet in the region of τ 7.4—7.9, whereas the alternative decoupling in the region of τ 7.4—7.9 serves to simplify the pattern at τ 4.45. As a result, it is apparent that the relative positions of protons in the molecule deduced above are reasonable, and that the complex patterns resulted not only from a simple coupling, but also from a long-range coupling. Therefore, it was not easy to interpret them in a simple way.

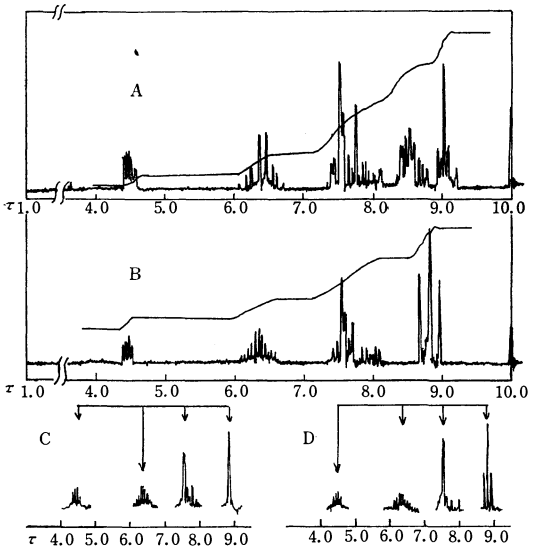

Fig. 3. NMR spectra of γ-alkoxy-γ-butyrolactone.
A: γ-Butoxy-γ-butyrolactone.
B: γ-Ethoxy-γ-butyrolactone.
C and D: Spin-spin decoupling spectra of γ-ethoxy-γ-butyrolactone.

e) *Characteristic Reaction of II.* Fife has kinetically studied the hydrolysis of γ-alkoxy-γ-butyrolactone to β-formylpropionic acid and alcohol.[10] In the present work, the C-4 homologue of II was hydrolyzed without any catalyst. The products were detected by GLC under various conditions. The acid product thus obtained was then conveniently converted to its 2,4-dinitrophenylhydrazone, mp 206—207°C. The authentic γ-alkoxy-γ-butyrolactone was treated similarly and gave a derivative with the same melting point. No depression of the melting point was observed when the two samples were mixed. The IR spectrum is shown in Fig. 4. The absorptions at 1715 cm^{-1}, at 1620 cm^{-1}, at 1530 and 1340 cm^{-1}, and at 1080 and 825 cm^{-1} are associated with -C=O, -C=N-, $-NO_2$, and 1,2,4-substituted phenyl groups respectively.

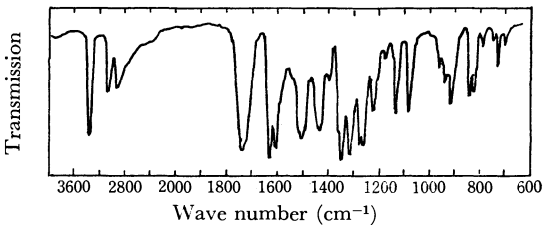

Fig. 4. IR spectrum of 2,4-dinitrophenylhydrazone of β-formylpropionic acid.

Determination of III. The determination of III, obtained as a by-product upon the hydrolysis of I, is helpful in considering the overall reaction. III was regarded as a mixture of IV and V because of its low OH number and its rather high acid value in comparison with IV alone, the separation of the two acids in III was difficult and not completed. Therefore, the mixture was esterified and fractionated effectively. The properties of the esters of IV and V thus isolated agreed with those of the authentic substances listed in Table 4.

Some Aspects of the Reaction Paths. *a*) *Preparation of Intermediates.* As has previously been pointed out, the four intermediates presumed on the reaction paths were synthesized by the following routine methods. I was manipulated with a large excess of ethanol saturated with hydrogen chloride to give the ethyl ester of IV without any significant dehydration.[11] The acetylation of the β-hydroxyl group in I and the subsequent pyrolysis of the acetate over potassium acetate yielded V.[12] According to Wohl's method,[13] the ethyl esters of VII were obtained from β-formylpropionitrile in three steps. Their properties and yields are summarized in Table 4. Their IR spectra are given in Fig. 5. All these products indicated a mono peak on the GLC chart except for the thermally unstable VII.

b) *Determination of Components in the Reaction Mixture.* The C-2 homologue of I was hydrolyzed in the same way as has been described above. The reaction mixture was neutrallized by the use of carbon dioxide and then evaporated to dryness. The residue was then recrystallized from ethanol. The sodium salt thus obtained was treated with an equivalent portion of ethyl iodide in a large amount of ethanol under reflux for 15 hr; this gave the corresponding ethyl ester. However, the esterified product distilled out at 90—120°C/20 mmHg and could not be fractionated. The GLC of this distillant indicates the presence of II and ethyl esters

10) T. H. Fife, *J. Am. Chem. Soc.*, **87**, 271 (1960).

11) C. F. Koelsh, *ibid.*, **65**, 2460 (1943).

12) L. N. Owen and M. U. S. Sultanbawa, *J. Chem. Soc.*, **1949**, 3098.

13) A. Wohl and H. Schweizer, *Ber.*, **39**, 890 (1906).

Table 4. Properties and yields of intermediates

	Bp °C/mmHg	n_D^{20}	S.V. Found	S.V. Calcd	Anal. Found	Anal. Calcd	Yield %
					OH %		
C_2-IV*	119—120/17***	1.4315	314	318	9.8	9.7	70
C_4-IV*	95—102/1.5	1.4355	271	275	8.5	8.4	85
C_2-V*	87.0—88.5/17***	1.4343	355	354	—	—	44
C_4-V*	119—120/15	1.4375	301	301	—	—	70
C_2-VII*	103—104/15***	1.4182***	276	274	—	—	54
C_4-VII*	124—127/12	1.4328	209	216	—	—	47
					N%		
C_4-VIII	102—105/13	1.4417	—	—	9.4	10.1	80
C_4-IV**	107/3	1.4357	275	275	—	—	—
C_4-V**	111.5—112.0/12	1.4373	295	301	—	—	—

* Obtained as ethyl esters.
** Ethyl esters derived from III.
*** C_2-IV,* bp 120—121°C/13mmHg: C_2-V,* bp 95—96°C/19mmHg (R. Lespieau, *Comp. rend.*, **140**, 436, 726 (1904)); C_2-VII,* bp 111—116°C/16mmHg, n_D^{20} 1.4180 (A. M. Acheson, *J. Chem. Soc.*, **1956**, 4232).

of IV, V, and VII, for their retention times correspond to those of authentic substances. A similar attempt to establish their presence was made. Thus, the C-4 homologue of I was hydrolyzed in butyl alcohol containing a suitable amount of ethanol to avoid the separation of water and was subsequently esterified to give the corresponding ethyl esters of the intermediates. The results gave evidence of the presence of C-4 homologues of IV, V, VII, and II in the reaction mixture. As is shown in Fig. 5, the IR spectrum of the ester obtained from the reaction mixture can be interpreted. Namely, it was found in the spectrum D that the four characteristic absorption bands near 3580 cm^{-1}, 1790 cm^{-1}, 1680 cm^{-1}, and 1060 cm^{-1}, referrable to the OH, γ-lactone C=O, C=C, and C–O–C–O–C groups respectively, indicate the presence of IV, II, V, and VII in the reaction mixture just before the acidification.

Table 5. Results of the preparation of γ-alkoxy-γ-butyrolactone from intermediates

	Catalyst (mol ratio)	Temp. °C	Time hr	Yield* %	Recovery** %
IV***	1.1	110—120	18	8	70
V***	1.1	110—120	15	22	65
V***	1.2	110	10	62	28
VIII	1.2	110	10	80	—
VIII	1.1	110—120	20	70	—

* Obtained as γ-alkoxy-γ-butyrolactone.
** Obtained as free carboxylic acid.
*** Ethyl ester was used as the starting material.

c) Preparation of γ-Lactone from Intermediates. The experimental procedure was analogous to that used in preparing II from I. The results are summarized in Table 5.

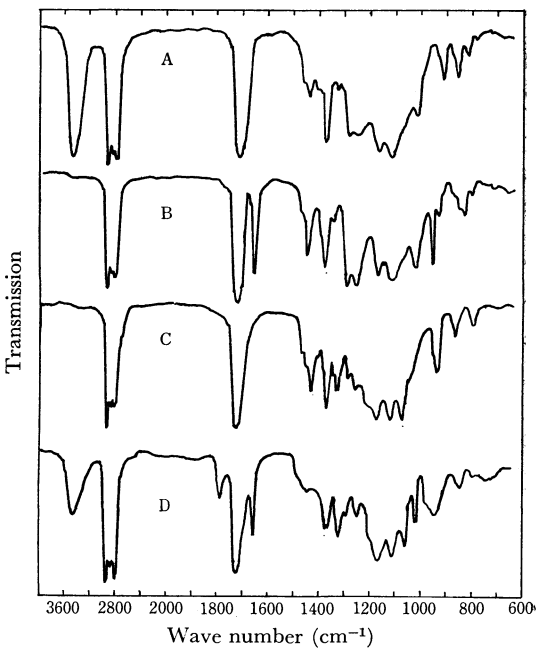

Fig. 5. IR spectra of ethyl esters of intermediates and reaction mixture.
A: γ-Ethoxy-β-hydroxybutyric acid.
B: γ-Ethoxycrotonic acid.
C: γ,γ-Diethoxybutyric acid.
D: Reaction mixture.

The products II obtained were checked by GLC, and their properties were determined. From these results, it seems likely that the predominance of VIII rather than V in the yield of γ-lactone may be attributable to its advantage in the rearrangement of the double bond, since the contribution of the resonance of the conjugate base $(-\ddot{C}H-CH=CH-CN \longleftrightarrow -CH=CH-\ddot{C}H-CN)^-$ must be larger than

that of V.

d) *Tracing of the Process of the Reaction.* The process of the reaction was followed by measuring the OH number and the N%. The sample submitted to analysis was pretreated to exclude difficulties. The neutralization of the alkaline catalyst and of the liberated ammonia with diluted hydrochloric acid, and the removal of the resulting salt and solvent, were carried out carefully. In spite of these cautions, however, there remained some doubt about the values obtained, because the loss of the species to be analyzed, which were assumed to be present, could not be avoided during the procedure. Aside from the point of whether or not the data indicates the absolute values, however, information about the estimated situation was obtained. That is, the decrease in the N% in the sample is relatively faster than that of the OH number. About 5 hr after reflux, 80—90% of the N content with respect to the theoretical amount was consumed. However, the consumption of OH was not so great. Moreover, the rate of the decrease in N% in the hydrolysis of γ-alkoxycrotonitrile is comparable to that of I. Therefore, the comparison between the consumption of OH and that of the N content gives information about the relative rates of the I to VIII and I to IV paths respectively.

Summary

The principal purpose of this investigation, the development of a new route for the synthesis of γ-alkoxy-γ-butyrolactone from epichlorohydrin, has been achieved. The identity of the products obtained with authentic substances prepared by well-known methods, and some proofs for the structure have been indicated by GLC, IR, NMR, and other appropriate procedures. In the experiments concerning the reaction paths, it was confirmed that some of the presumed intermediates indeed exist in the reaction mixture and that these intermediates, treated in the same condition to that of the hydrolysis of I, give γ-alkoxy-γ-butyrolactone. These results suggest that all the postulated paths in a scheme presented early in this paper are possible. To decide the most favorable path, however, was difficult on the basis of the results obtained in the present work. It may still be guessed that the attack on the cyano group is preferrable to the competing elimination of the hydroxyl group. As the sequence, the I→IV→V→VI→(*via* VII)→II path may eventually come to be significant, even though the rearrangement of VIII to IX is more likely than that of V to VI, as has been mentioned. The outline of the synthesis has already been published as a letter to the editor.[14]

The authors wish to thank Professor T. Mukai of Tohoku University for his providing the convenience of the NMR measurements. They are also indebted to Mr. S. Tomidokoro for his assistance in the experimental work.

14) T. Kuwamura, H. Takahashi and S. Tomidokoro, *Kogyo Kagaku Zasshi* (*J. Chem. Soc. Japan, Ind. Chem. Sect.*), **70**, 1051 (1967).

BULLETIN OF THE CHEMICAL SOCIETY OF JAPAN VOL. 42 1351—1353 (1969)

Spiro Compound Formation. III.[1] The Formation of Spiro Compounds by the Rearrangement of Bicyclo[5.4.0]-undecene(1,7) and Cyclopentylcyclohexene

Masatomo NOJIMA and Niichiro TOKURA

Department of Applied Chemistry, Faculty of Engineering, Osaka University, Suita, Osaka

(Received July 31, 1968)

The isomerizations of bicyclo[5.4.0]undecene-(1,7) (IV), spiro[5.5]undecene-1 (V), and 1-cyclopentylcyclohexene (VI) were examined with equivalent amounts of perchloric acid in acetic acid or in ethanol at 75°C. In acetic acid, IV, V, and VI all rearranged to form spiro[5.5]-undecan-1-yl acetate (VII) and spiro[5.5]undecan-2-yl acetate (VIII), together with the three olefins IV, V, and VI. No rearranged product has been obtained by the same procedure in ethanol.

The recent report by Ito[2] on the rearrangement of widdrol (I) or thujopsene (II) to chamigrene (III) under acidic conditions was very suggestive regarding the possibility of spiro-compound formation from bicyclo[5.4.0]undecane derivatives. The formation of 1-cyclopentylcyclohexene (VI) from the reaction of spiro[5.5]undecan-1-ol with zinc chloride had previously been reported by Christol, Jacquier, and Mousseron.[3]

The acetolysis of spiro[5.5]undecan-1-yl tosylate was also examined by Krapcho, McCullough, and Nahabedian[4]; they obtained spiro[5.5]undecane, cyclohexylcyclopentane, and *cis*-bicyclo[5.4.0]undecane in yields of 11, 64, and 25% respectively after the hydrogenation of the reaction mixture.

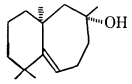

I

II

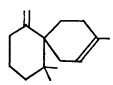

III

From these results, it is expected that bicyclo-[5.4.0]undecene(1,7) (IV), sipro[5.5]undecene-1 (V), and 1-cyclopentylcyclohexene (VI) would all rearrange under acidic conditions. Thus, the present authors attempted the isomerization reaction of IV, V, and VI in the presence of one equivalent mole of perchloric acid in both acetic acid and ethanol.

IV, V and VI all rearranged with each other and gave a mixture with VII and VIII as the major products after 24 hr.

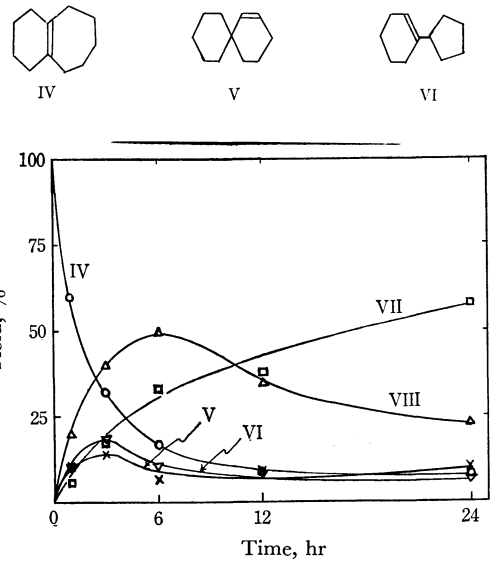

Fig. 1. The Conversion *vs.* reaction time relationship during the isomerization of IV.

The behavior of the isomerization of IV is shown in Fig. 1. At the initial stage of the reaction compound IV rearrange to V, VI, and spiro-[5.5]undecan-1-yl acetate (VII), which is then converted to spiro[5.5]undecan-2-yl acetate (VIII). This reaction probably proceeds by way of the carbonium ion B_2. After 24 hr, VIII increased to become 55.8% of the whole reaction product. Similar results were obtained by the reaction of VI in acetic acid. The fact that VIII was formed by the addition of acetic acid to V (after 24 hr an 82.8% yield of VIII was obtained) is comparable to the results in the preceding paper,[1] where V was formed by the reaction of 1-(Δ^4-pentenyl)-

1) M. Nojima, T. Nagai and N. Tokura, *J. Org. Chim.*, **33**, 1970 (1968).

2) S. Ito, K. Endo, T. Yoshida, M. Yatagai and M. Kodama, *Chem. Commun.*, **1967**, 186.

3) H. Christol, R. Jacquier and M. Mousseron, *Bull. Soc. Chim. France*, **1957**, 1027.

4) A. P. Krapcho, J. E. McCullough and K. V. Nahabedian, *J. Org. Chem.*, **30**, 139 (1965).

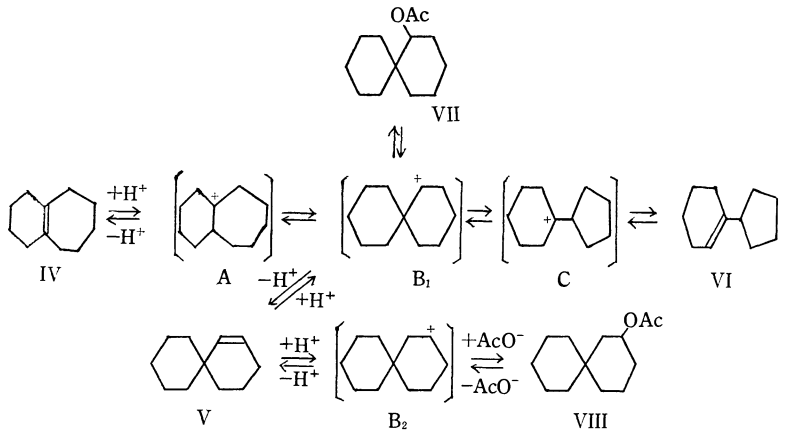

Scheme I

cyclohexanol; it is in equilibrium with VIII in acetic acid in a molar ratio of 4.5 to 95.5.

The instability of VII under these three sets of reaction conditions was confirmed by the finding that VII was converted to VIII in a high yield under the same conditions. This instability of VII may be explained from a sterical point of view.

Scheme I presents what seem to be the most plausible routes for the formation of the products.

The tertiary carbonium ions, A and C, produced by the protonation of IV and VI rearrange to a carbonium ion, B_1, which then affords VII upon the attack of the acetate anion and the compound V upon deprotonation.

The compound VII was also converted to the ion B_1 by the elimination of acetic acid after protonation; the ion was then further rearranged or deprotonated to form the three products, IV, V, and VI. Under the three sets of reaction conditions the tertiary acetate, which may be derived from A and C, is again unstable.

The reactions of IV, V, and VI in ethanol were also attempted. Contrary to the reactions in acetic acid, no rearrangement occurred after 24 hr and the original olefins used were recovered unchanged.

Experimental

Bicyclo[5.4.0]undecene-(1,7) (IV). Bicyclo[5.4.0]-undecan-2-ol was reacted with polyphosphoric acid according to the method of Christol, Jaquier, and Mousseron;[3] bp 107—108°C/25 mmHg. Found: C, 87.90; H, 12.21%. Calcd for $C_{11}H_{18}$: C, 87.92; H, 12.08%.

Spiro[5.5]undecene-1 (V). This compound was prepared from spiro[5.5]undecan-1-yl xanthate according to the procedure described by Alexander and Mudrak;[5] bp 105—106°C/25 mmHg. Found: C, 87.97; H, 11.92%. Calcd for $C_{11}H_{18}$: C, 87.92; H, 12.08%.

1-Cyclopentylcyclohexene. The reaction of cyclopentylcyclohexanol with thionyl chloride and pyridine[6] gave cyclopentylcyclohexene in a 70% yield; bp 104—105°C/25 mmHg, NMR τ=4.8 (broad 1H). Found: C, 87.88; H, 12.19%. Calcd for $C_{11}H_{18}$: C, 87.92; H, 12.08%.

Spiro[5.5]undecan-1-yl Acetate. This acetate was prepared from the corresponding alcohol with acetyl chloride and *N,N*-dimethylaniline according to the procedure of Nevitt and Hammond.[7] The yield was 55%; bp 104—105°C/7 mmHg: NMR τ=7.6 (singlet, 3H), 5.4 (broad 1H). Found: C, 74.50; H, 10.49%. Calcd for $C_{13}H_{22}O_2$: C, 74.30; H, 10.65%.

Isomerization of an Olefin, IV, V, or VI, in Acetic Acid. To 0.5 g (0.33 mmol) of the olefin in 15 m*l* of glacial acetic acid there was added a 5-m*l* portion of an acetic acid solution containing 0.4 g of 60% perchloric acid (d=1.55). The temperature was maintained at 75±2°C, and a 5-m*l* aliquot was withdrawn periodically. The aliquot was rapidly cooled, diluted with 30 m*l* of chilled water, and extracted three times with *n*-hexane. The combined organic layer was washed with saturated brine water and dried over anhydrous sodium sulfate.

The volume of the extract was kept as small as possible so that no concentration was necessary prior to vpc analysis. The products were analyzed on a Hitachi-Perkin Elmer Gas Chromatograph, Model F-6-D, equipped with a hydrogen flame-ionization detector. A 150 ft×0.01 in. column packed with Silicone DC 550 was employed, and nitrogen was used as the carrier gas. The temperature settings were at 150°C for the olefin analysis and at 200°C for the acetate analysis.

The Reaction of VII in Acetic Acid. A solution of 0.6 g of VII and 0.4 g of 60% perchloric acid (d=1.55) was heated at 75°C for 24 hr. The reaction mixture was then extracted and analyzed as above. The residue after the removal of the solvent was chromatographed over 30 g of alumina. Elution with ether (10×50 m*l*) gave 0.4 g of an oil. The infrared and NMR spectra

5) E. R. Alexander and A. Mudrak, *J. Am. Chem. Soc.*, **72**, 1810 (1950).

6) H. Heymann and L. Fieser, *ibid.*, **73**, 5252 (1951).

7) T. D. Nevitt and G. S. Hammond, *ibid.*, **72**, 1810 (1950).

were identical with those of VIII;[1] however, this product found to be 95% pure by vpc analysis on a silicone DC 550 column.

The Attempted Isomerization of Three Olfefins, IV, V, and VI, in Ethanol. To 0.5 g of the olefin and 15 m*l* of ethanol there was added a 5-m*l* portion of an ethanol solution containing 0.5 g of 60% perchloric acid ($d=1.55$). The reaction temperature was maintained at 75 ± 2°C for 24 hr. The reaction mixture was then treated and analyzed as has been described above.

BULLETIN OF THE CHEMICAL SOCIETY OF JAPAN VOL. 42 1353—1356 (1969)

The Photoreaction of β-Benzoylacrylic Acid

Noboru SUGIYAMA, Hiroshi KATAOKA, Choji KASHIMA and Kazutoshi YAMADA

Department of Chemistry, Tokyo Kyoiku University, Otsuka, Tokyo

(Received August 23, 1968)

The product of the irradiation of *trans*-β-benzoylacrylic acid (**1**) in methanol was proved to be α-methoxy-β-benzoylpropionic acid (**2**), whose methyl ester was identified with an authentic material. On the other hand, the product of the irradiation of methyl *trans*-β-benzoylacrylate (**5**) was the *cis*-isomer. The photoreaction of **1** in various solvents, including EtOH, *iso*-PrOH, *t*-BuOH, ether, and AcOH, was examined from the standpoints of the *cis-trans* isomerization and alcohol addition. The rate of the photoreaction of **1** in methanol was determined, and a reasonable mechanism for the over-all reaction was proposed.

Only a few studies of β-acyl- and β-aroyl-acrylic acids have been found in the literature.[1] Previously we ourselves reported on the structures and the reactions of these systems.[2] Also, we found three kinds of photoproducts from these systems[3]—that is, *cis-trans* isomers, angelica lactones, and alcohol adducts. Lutz[4] first reported the *cis-trans* isomerization of methyl β-benzoylacrylate under sunlight without any solvent or in benzene. Kropp[5] found that the photoaddition of alcohol to an olefinic double bond was limited to six- or seven-membered cyclic olefins; larger ring or acyclic systems capable of easily undergoing *cis-trans* photoisomerization showed no evidence of adduct formation.

Recently it has been found that methanol, when added to *trans*-β-benzoylacrylic acid (**1**) under the irradiation of UV light, gave β-benzoyl-α-methoxypropionic acid (**2**).[3,6] This is the first example of the photoaddition of methanol to acyclic olefins giving a methoxy derivative except in the case of Stoermer's work, which was reinvestigated by Kropp.[5] However, the formation of no adduct was detected. The present paper will deal with the photoreaction of *trans*-β-benzoylacrylic acid (**1**) in various solvents and will discuss the reaction mechanism.

By the external irradiation of **1** in methanol, **2** was obtained almost quantitatively. The product was methylated by diazomethane. The methyl ester was identified with the authentic methyl α-methoxy-β-benzoylpropionate (**3**)[2b] on the bases of the spectral data.

$$C_6H_5COCH_2\underset{\displaystyle R_1}{\underset{|}{C}}HCOOR_2$$

2 $R_1=OCH_3$, $R_2=H$
3 $R_1=OCH_3$, $R_2=CH_3$

It was confirmed that **2** was not obtained without light under the same conditions. Table 1 shows the results of the reactions of **1** in various solvents. Photoaddition was observed only when methanol or ethanol was used as the solvent. The alcohols with larger alkyl groups, *e.g.*, isopropanol or *t*-butanol, did not add to **1**. In ether, acetic acid, or tetrahydrofuran, or without a solvent, **1** was turned to the *cis*-isomer **4** photochemically. From these results, it is clear that the addition of alcohol becomes difficult as the alkyl group of alcohol becomes bulky.

1) For example: a) E. Shaw, *J. Am. Chem. Soc.*, **68**, 2510 (1946); b) R. Scheffold and T. Dubs, *Helv. Chim. Acta*, **50**, 798 (1967); c) N. Hellström, *Nature*, **187**, 146 (1960).

2) a) N. Sugiyama, T. Gasha, H. Kataoka and C. Kashima, This Bulletin, **41**, 971 (1968); b) N. Sugiyama, T. Gasha, H. Kataoka and C. Kashima, submitted to *J. Chem. Soc.*

3) N. Sugiyama, H. Kataoka, C. Kashima and K. Yamada, This Bulletin, **41**, 2219 (1968).

4) R. E. Lutz, *J. Org. Chem.*, **13**, 284 (1948).

5) P. J. Kropp, *ibid.*, **32**, 3222 (1967).

6) D. V. Rao, V. Lamberti and H. M. Gardner, *Tetrahedron Letters*, **1968**, 1613.

TABLE 1. PRODUCTS IN VARIOUS SOLVENTS BY THE IRRADIATION OF **1**

Solvent	Time (hr)	Product %	
		cis-isomer	alcohol adduct
none	45	12	
MeOH	12	17	12
MeOH	120		100
EtOH	72		25
i-PrOH	72	40	
t-BuOH	72	47	
Ether	45	20	
AcOH	48	30	
AcOH-MeOH (1 : 1)	48	46	
H_2O-MeOH (2 : 1)	49		20 (OMe)
Ether-MeOH*	72	40	
HCl-MeOH**	72		18
THF	72	55	

* A several drops in 1 m*l* of methanol.
** A few drops in 1 m*l* of methanol.

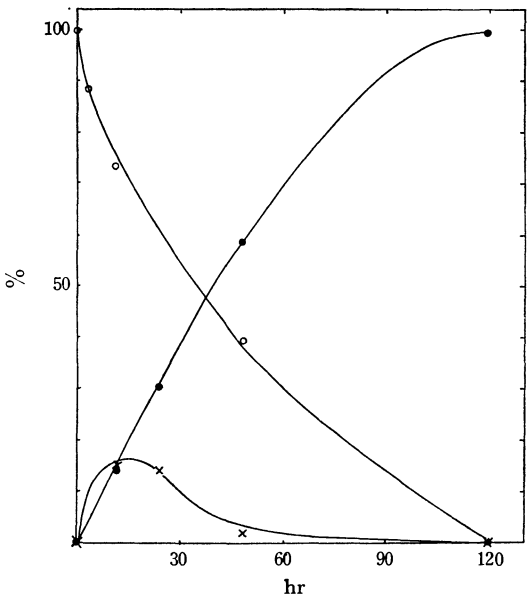

Fig. 1. The rate of the photoreaction of **1** in methanol.
○—○—○ *trans*-form
●—●—● adduct
×—×—× *cis*-form

In order to confirm the structure of the photoproduct, **4**, methyl *cis*-*β*-benzoylacrylate (**6**)[7] was prepared by the irradiation of methyl *trans*-*β*-benzoylacrylate (**5**) in methanol. As the spectral data of **6** have not yet been reported, the UV, IR, and NMR spectra of **6** were measured, as will be shown in the Experimental section. All the spectral data strongly support the structure **6**. The IR spectrum of **4** shows the characteristic *cis*-olefinic bands at 1415 cm^{-1} (CH, in-plane), 745, and 695 cm^{-1} (CH, out-of-plane).[8] The NMR spectrum shows a doublet of olefinic protons at τ 2.89 and 3.68, with a coupling constant of 12.0 Hz. These data support the *cis*-configuration of **4**.

Furthermore, in acetic acid - methanol (1 : 1) or in methanol containing a several drops of ether, methanol did not add, but the *cis*-isomer **4** was obtained. In water-methanol (2:1), the adduct **2** was obtained, indicating that methanol addition took place while water addition did not. In a methanol solution containing a few drops of hydrochloric acid, the adduct was formed, but the yield was low. These results, make it probable that the excess acidic proton disturbs the alcohol addition. Methyl *trans*-*β*-benzoylacrylate **5**, however, did not react with methanol to give the adduct in methanol under irradiation.[3] Therefore, it might be concluded that the presence of a free carboxyl group in **1** is essential for the alcohol addition.

Next, the rate of the formation of products during the irradiation of **1** in methanol was determined, as is shown in Fig. 1. The starting material, **1**, first decreased gradually and then disappeared completely after 5 days. During the course of this period, the adduct **2** gradually increased, while the *cis*-isomer first increased and then gradually decreased.

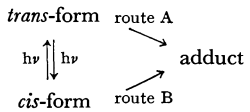

Scheme 1

From these results, it can be presumed that the adduct **2** will be produced *via* route A or B in Scheme 1. When **1** was irradiated in tetrahydrofuran (THF) for 72 hr, a mixture of *trans*- and *cis*-isomers (45:55) was obtained. When the methanol solution of this mixture was left to stand for 5 days in a dark place at room temperature, the adduct **2** and the *trans*-isomer were obtained in 37% and 63% yields respectively, and the *cis*-isomer was not found. These facts suggest that the *cis*-isomer **4**, formed by photochemical *cis*-*trans* isomerization, reacted with methanol to give the adduct **2** (route B).

Now let us presume the reaction route shown in Scheme 2. Scheme 2 explains that the free carboxylic acid is essential for the alcohol addition, and that an excess amount of acid disturbs the reaction. Considering that the *cis*-isomer **4** reacted with methanol to give the adduct **2** in a dark place,

7) G. P. Rice, *J. Am. Chem. Soc.*, **45**, 222 (1923).
8) K. Nakanishi, "Infrared Absorption Spectroscopy," Nankodo Co., Ltd., Tokyo (1962), pp. 24, 124, 125.

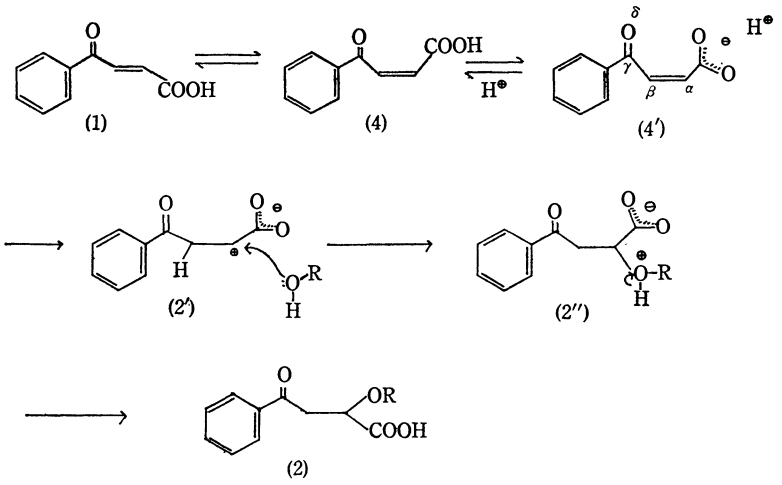

Scheme 2

the *cis*-acid **4** might be first produced by light and then dissociated to the carboxylate anion **4'**. In the presence of excess acid, the anion **4'** would change to the non-dissociated acid **4**, and the addition could not proceed. This is the reason why the adduct **2** is not obtained in acetic acid, in acetic acid - methanol (1 : 1), or in methanol containing a trace of hydrochloric acid. Moreover, isopropanol or *t*-butanol disturbed the alcohol addition and only *cis-trans* isomerization occurred. This is because the hydroxy oxygen of isopropanol or *t*-butanol is more negative than those of methanol or ethanol because of the inductive effect of the alkyl group. The dissociated proton coordinates to the hydroxy oxygen of alcohol; therefore, the alcohol cannot attack **4'**, as with **2'** or **2''**. Furthermore, the bulkiness of alcohol may also influence an alcohol attacking olefin. The fact that the *cis*-isomer was obtained in methanol containing a small amount of ether can also be explained by a consideration similar to that ether can stabilize the structure **4'**, but as for this point, more detailed experiments are needed.

Experimental

Matrials. *trans*-β-Benzoylacrylic Acid (1) was prepared by the method of Papa; yellow needles, mp 94—95.5°C (lit. 98—99°C).[9]

UV (λ_{max} nm (ε), in EtOH): 238 (11000), 272 (8900), 357 (86).

Methyl *trans*-β-Benzoylacrylate (5) was prepared by the method described in a previous paper,[2] mp 34°C.

All the solvents were commercially-available Guaranteed Reagents.

Instrumentation. The infrared and ultraviolet spectra were measured on a Hitachi EPI-2-type infrared spectrometer and a Hitachi EPS-3T-type recording spectrometer respectively.

A Taika 500 W high-pressure mercury lamp was used as the irradiation source, while a Pyrex tube was used as the filter and reaction vessel. The NMR spectra were recorded in deuterochloroform, with TMS as the internal standard, with an Hitachi H-60 high-resolution spectrometer.

For paper chromatography we used Toyo Filter Paper No. 53 and *n*-butanol (saturated with a 3% aqeuous ammonia solution).

Irradiation of *trans*-β-Benzoylacrylic Acid (1) in Methanol. One gram of **1** was dissolved in 20 m*l* of methanol, and then the solution was irradiated for 5 days. The solvent was removed under reduced pressure. It was confirmed by a study of the NMR spectrum that the starting material, **1**, did not remain, and that β-benzoyl-α-methoxypropionic acid (**2**) was formed almost quantitatively as a yellow oil.

NMR (τ, in $CDCl_3$): 1.8—2.7 (m, phenyl), 2.55 (broad s, COOH), 5.55 (t, J=6.0 Hz, α-methine), 6.42 (s, $-OCH_3$), 6.48 (d, J=6.0 Hz, β-methylene).

R_f value of paper chromatography: 0.52 (that of **1**: 0.40).

Crude **2** was methylated with diazomethane to give methyl β-benzoyl-α-methoxypropionate (**3**), which was then purified by silica-gel - column chromatography and eluted with benzene - ethyl acetate (19 : 1), as a yellow liquid.

IR (cm^{-1}, liq. film): 1750 ($COOCH_3$), 1685 (Ar–CO–) 1600 (phenyl), 1195 (C–O–C).

UV (λ_{max} nm (ε), in EtOH): 244 (11000), 280 (1100), 323 (66).

NMR (τ, in $CDCl_3$): 1.82—2.66 (m, phenyl), 5.55 (t, J=6.0 Hz, α-methine), 6.23 (s, $COOCH_3$), 6.52 (s, $-OCH_3$), 6.62 (d, J=6.0 Hz, β-methylene).

3 was identified with an authentic sample[2b] by means of its IR, UV, and NMR spectra.

Irradiation of Methyl *trans*-β-Benzoylacrylate (5) in Methanol. A methanol solution of **5** (500 mg/10 m*l*) was irradiated in a Pyrex tube for 5 days, after which the solvent was removed under reduced pressure. The NMR spectrum of this residue showed that 76% of the **5** had changed to methyl *cis*-β-benzoylacrylate

9) D. Papa, E. Schwenk, F. Villani and E. Klingsberg, *J. Am. Chem. Soc.*, **70**, 3356 (1948).

(**6**). The residue was washed with ice-cooled methanol and recrystallized from methanol. Colorless needles, mp 66°C (lit. 67°C).[7]

IR (cm^{-1}, KBr): 1725 (ester C=O), 1675 (Ar–CO–), 1640 (C=C), 1395 (*cis*-olefin, in-plane), 760, 740, 705 (*cis*-olefin, out-of-plane), 735, 690 (phenyl).

UV (λ_{max} nm (ε), in EtOH): 251 (11800), 280 (sh, 3790), 342 (152).

NMR (τ, in $CDCl_3$): 1.9—2.7 (m, phenyl), 3.13 (d, J=12.0 Hz, olefinic proton), 3.76 (d, J=12.0 Hz, olefinic proton), 6.42 (s, ester methyl).

Irradiation of 1 in Ethanol. An ethanol solution of **1** (250 mg/5 m*l*) was irradiated for 10 days. The subsequent evaporation of the solvent under reduced pressure gave β-benzoyl-α-ethoxypropionic acid (**7**), which was then purified by cellulose-powder chromatography and eluted with *n*-butanol saturated with 3% aqueous ammonia; pale yellow needles, mp *ca.* 93°C.

IR (cm^{-1}, KBr): 2800—2300 (COOH), 1715 (COOH), 1675 (Ar–CO–), 1600 (phenyl), 1260, 1210 (C–O–C), 720, 675 (phenyl).

UV (λ_{max} nm (ε), in EtOH): 244 (9300), 273 (sh, 3400), 345 (200).

NMR (τ, in $CDCl_3$): 1.2 (s, COOH), 1.8—2.7 (m, phenyl), 5.39 (t, J=6.0 Hz, methine), 6.24 (q, J=6.0 Hz, –OEt, methylene), 6.51 (d, J=6.0 Hz, methylene), 8.78 (t, J=6.0 Hz, –OEt, methyl).

β-Benzoyl-α-ethoxypropionic Acid (7). A solution of β-benzoylacrylic acid (1 g) in 30 m*l* of ethanol containing 0.1 m*l* of sulfuric acid was refluxed for 4 hr. The reaction mixture was then diluted with water and extracted with ether. The ethereal layer was washed with a sodium carbonate solution and then with water, and dried with anhydrous sodium sulfate. After the solvent had been removed, ethyl β-benzoyl-α-ethoxypropionate (**8**) was obtained; 0.4 g, yellow liquid.

IR (cm^{-1}, liq. film): 1740 (ester C=O), 1685 (Ar–CO–), 1195 (C–O–C).

UV (λ_{max} nm (ε), in EtOH): 243 (15000).

NMR (τ, in $CDCl_3$): 1.9—2.6 (m, phenyl), 5.45 (t, J=6.0 Hz, methine), 5.75 (q, J=6.0 Hz, ester methylene), 6.25 (q, J=6.0 Hz, ether methylene), 6.65 (d, J=6.0 Hz, methylene), 8.70 (t, J=6.0 Hz, ester methyl), 8.80 (t, J=6.0 Hz, ether methyl).

Found: C, 67.19; H, 7.22%. Calcd for $C_{14}H_{18}O_4$: C, 67.18; H, 7.25%.

One hundred milligrams of **8** were dissolved in 10 m*l* of 0.5% ethanolic potassium hydroxide, and then the mixture was stirred for 15 hr at room temperature. After hydrochloric acid had been added to the reaction mixture, it was extracted with ether. From the ether solution β-benzoyl-α-ethoxy-propionic acid (**7**) was obtained. This synthetic sample was found by paper chromatography and the spectral data to be identical with the photoproduct, **7**, of the preceding section.

Irradiation of 1 in Various Solvents. In 1 m*l* of a solvent, 50 mg of **1** were dissolved, and the mixture was irradiated for 2—3 days in a Pyrex tube. After irradiation, the solvent was removed under reduced pressure; the NMR spectrum of the residue was immediately measured, and the yields of the products were calculated from the integration of the spectrum.

The Solution of 1 in Methanol with Time. A solution of **1** (300 mg) in 6 m*l* of methanol was divided into six aliquots, which were then irradiated for 0, 3, 12, 24, 48, and 120 hr respectively. On each aliquot, after the removal of the solvent, the NMR spectrum of the residue was measured at τ 3.17 (d, olefinic proton of **1**), 3.65 (d, olefinic proton of **4**) and 5.55 (t, methine proton of **2**); the yields of **1**, **4** and **2** were calculated from the integration of each signal. The results are plotted in Fig. 1.

The Dark Reaction of a Methanol Solution of the Mixture of *cis*- and *trans*-Isomers of β-Benzoylacrylic Acid. Fifty milligrams of **1** were dissolved in 1 m*l* of THF, and the mixture was irradiated for 72 hr. After the solvent had been removed under reduced pressure, a 55:45 mixture of *cis*- and *trans*-β-benzoylacrylic acid was obtained. This mixture was dissolved in 1 m*l* of methanol and then left to stand for 72 hr at a dark place. The adduct **2** and the *trans*-isomer **1** were obtained in 37% and 63% yields respectively.

The authors wish to express their thanks to Mr. Kyuzaburo Furuhashi for his measurement of NMR spectra.

BULLETIN OF THE CHEMICAL SOCIETY OF JAPAN VOL. 42 1357—1359 (1969)

A Novel Method for the Synthesis of 1-Phenyl-2,3-dihydro-4-pyridones

Noboru SUGIYAMA, Makoto YAMAMOTO and Choji KASHIMA

Department of Chemistry, Tokyo Kyoiku University, Otsuka, Tokyo

(Received August 23, 1968)

The condensation of β-diketones, benzoylacetone (II), acetylacetone (III), or 6-phenyl-2,4-hexanedione (IV) with benzylidenaniline (I), in the presence of three moles of potassium amide in liquid ammonia, was found to give a dihydropyridone or an aminodiketone. Thus, the condensation of II with I afforded aminodiketone, 1-anilino-1,5-diphenyl-3,5-pentanedione (V), which cyclized to 2,3-dihydro-1,2,6-triphenyl-4-pyridone (IX) upon being treated with sulfuric acid. The condensation of III with I gave 2,3-dihydro-1,2-diphenyl-6-methyl-4-pyridone (X) without any treatment with sulfuric acid. IV and I gave 2,3-dihydro-1,2-diphenyl-6-phenethyl-4-pyridone (XI) as the main product, with 3-benzyl-2,3-dihydro-1,2-diphenyl-6-methyl-4-pyridone (XII) as a by-product.

The condensation of β-diketones with ketones or aldehydes in the presence of alkali amide in liquid ammonia has previously been reported.[1,2] It appeared of interest to investigate whether the reaction could be extended to the condensation of β-diketones with Schiff bases. Thus, the reaction of β-diketones, *e. g.*, benzoylacetone (II), acetylacetone (III), or 6-phenyl-2,4-hexanedione (IV), with benzylidenaniline (I), a Schiff base, was carried out in the presence of three moles of potassium amide in liquid ammonia. It was proved that a dihydropyridone or an aminodiketone was produced by this reaction. A few reports of dihydropyridone synthesis have appeared in the literature;[3,4] in these syntheses dihydropyridones have been prepared by the partial reduction of the corresponding pyridones. In our method, however, dihydropyridones are directly prepared from β-diketones and a Schiff base.

Results and Discussion

A β-diketone was condensed one molar equivalent of a Schiff base in the presence of three molar equivalents of potassium amide in liquid ammonia. The condensation of II with I gave 1-anilino-1,5-diphenyl-3,5-pentanedione (V). The structure of V was proved by its IR, UV, and NMR spectra and by the results of elemental analysis.

The treatment of V with sulfuric acid gave 2,3-dihydro-1,2,6-triphenyl-4-pyridone (IX), whose structure was supported by its IR, UV, and NMR spectra as well as by the results of elemental analysis. The NMR spectrum of IX showed a multiplet at τ 6.37—7.35, a triplet centered at τ 4.70 and a singlet at τ 4.42; these can be assigned to C-3 methylene, C-2 methine, and olefinic protons of the 2,3-dihydro-4-pyridone nucleus respectively. The UV maxima at 249 and 353 mμ remained unchanged in either an acidic and an alkaline solution. These facts favor the dihydropyridone structure of IX. The reaction course from V to IX is a cyclization by dehydration and seems analogous to that from an aminodiketone to a 4-pyridone.[5]

III and I were treated under the conditions similar to those described above. In this case, the expected aminodiketone (VI) was not detected, but 2,3-dihydro-1,2-diphenyl-6-methyl-4-pyridone (X) was obtained. The structure of X was supported by the spectral data and by the results of elemental analysis.

It is suggested that VI is the intermediate in the synthesis of X, as V is the intermeidate in the synthesis of IX, and that the intermediate VI is cyclized during the neutralization with ammonium chloride. Thus, the detection of VI was examined before the neutralization. However, X was the only product obtained, and no aminodiketone was detected. These facts indicate that the cyclization

1) N. Sugiyama, M. Yamamoto, T. Takano and C. Kashima, This Bulletin, **40**, 2909 (1967).

2) C. R. Hauser and T. M. Harris, *J. Am. Chem. Soc.*, **80**, 6360 (1958).

3) J. Hebky and J. Kejha, *Chem. Listy.*, **50**, 834 (1956).

4) E. Winterfeldt, *Chem. Ber.*, **97**, 2463 (1964).

5) S. Boatman, R. E. Smith, G. F. Morris, W. G. Kofron and C. R. Hauser, *J. Org. Chem.*, **32**, 3817 (1967).

of VI was already accomplished before the neutralization.

The reaction of IV and I was also carried out. Compound IV has a terminal methyl group (C-1 position) and a C-5 methylene group, which can be activated by the vicinal carbonyl group. The treatment of IV and I by the general procedure gave 2,3-dihydro-1,2-diphenyl-6-phenethyl-4-pyridone (XI) and its isomer, 3-benzyl-2,3-dihydro-1,2-diphenyl-6-methyl-4-pyridone (XII), in a molar ratio of 4:1. The structures of XI and XII were supported by the spectral data and by the results of elemental analysis. For the formation of XI and XII, it is also supposed that the VII and VIII intermediates must be formed first. Thus, it is reasonable to suppose that the reaction proceeds not only at the terminal methyl group, but also at the C-5 methylene group of IV. The yield of XI and XII supports the idea that, in IV, the terminal methyl is more reactive than the C-5 methylene group. This might be in agreement with the fact that IV and methyl iodide in the presence of sodium amide in liquid ammonia gave the corresponding methylation products at C-1 and C-5 positions in a ratio of 89:11.[6]

Furthermore, we attempted to perform experiments on the condensation of a β-diketone III with aliphatic Schiff bases, benzylidenemethylamine, and ethylidenaniline. However, neither the corresponding dihydropyridone nor the aminodiketone was obtained, probably because these Schiff bases are unstable under the conditions of the general procedure.

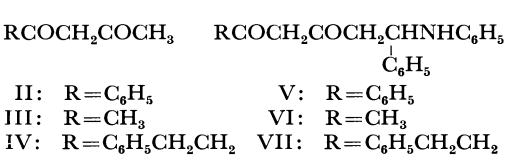

II: R=C_6H_5 V: R=C_6H_5
III: R=CH_3 VI: R=CH_3
IV: R=$C_6H_5CH_2CH_2$ VII: R=$C_6H_5CH_2CH_2$

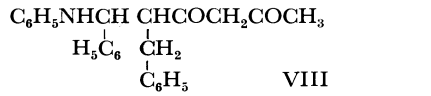

VIII

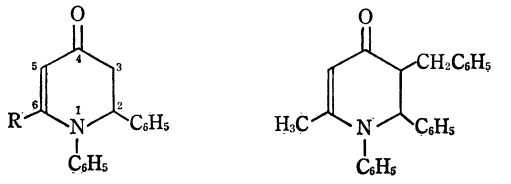

IX: R=C_6H_5 XII
X: R=CH_3
XI: R=$C_6H_5CH_2CH_2$

6) K. G. Hampton, T. M. Harris and C. R. Hauser, *J. Org. Chem.*, **31**, 663 (1966).

Experimental

General Procedure. In a 500-m*l* three-necked flask, 300 m*l* of anhydrous liquid ammonia were placed. A small amount of potassium was then added and dissolved completely. Into the blue solution there were stirred a catalytic amount of ferric chloride and then 5.85 g (0.15 mol) of potassium in small portions. The resulting blue solution turned dark gray within 90 min. To this solution there was added, in small protions, 0.05 mol of β-diketone in 30 m*l* of anhydrous ether. After stirring for 45—60 min, 0.05 mol of a Schiff base in 30 m*l* of anhydrous ether was added to the solution. After stirring for an additional hour, the reaction mixture was neutralized with ammonium chloride. The liquid ammonia was evaporated rapidly on a water bath, and 100—150 m*l* of ether were added from a dropping funnel. The ethereal layer was separated and reserved. To the remaining layer there were added 150 m*l* of dilute hydrochloric acid, and this solution was extracted with chloroform. After drying over anhydrous sodium sulfate, the ether and the chloroform were evaporated. Both residues gave a crude condensation product.

1-Anilino-1,5-diphenyl-3,5-pentanedione (V). According to the general procedure, V was prepared from 8.1 g (0.05 mol) of II and 9.05 g (0.05 mol) of I. The crude product was recrystallized from a benzene-*n*-hexane (1:1 v/v) mixture to give 7.3 g (43%) of V as colorless plates, mp 116—118°C.

Found: C, 80.05; H, 6.05; N, 4.10%. Calcd for $C_{23}H_{21}NO_2$: C, 80.44; H, 6.16; N, 4.08%.

IR (KBr): 3370 (νNH), 1600 (νC=O), 1570 (νC=C, enol) and 700 cm^{-1} (phenyl).

UV: λ_{max}^{EtOH} 249 mμ (ε 19000) and 311 mμ (ε 17200).
$\lambda_{max}^{HCl\text{-}EtOH}$ 319 mμ (ε 16600).
$\lambda_{max}^{NaOH\text{-}EtOH}$ 247 mμ (ε 22000) and 332 mμ (ε 17800).

NMR (CCl_4): τ 7.10 (doublet, 2H, $COC\underline{H}_2$–CH), τ 5.14 (triplet, 1H, CH_2–C$\underline{H}$–Ph), τ 3.92 (singlet, 1H, Ph–C=C$\underline{H}$–CO), and τ 2.08—3.50 (multiplet, 15H, phenyl).

2,3-Dihydro-1,2,6-triphenyl-4-pyridone (IX). To 2.0 g of V, 15 m*l* of concentrated sulfuric acid were added, and then the mixture was allowed to stand at room temperature for two hours. About 100 g of crushed ice were then added to the reaction mixture, and the solution was neutralized with a cold concentrated potassium hydroxide solution. This solution was extracted with chloroform, and the chloroform layer was washed with water and dried over anhydrous sodium sulfate. The solution was evaporated, and the residue was chromatographed on a silica-gel (Merck 7734) column with a benzene - ethyl acetate (2:1 v/v) mixture. The fraction, which showed a violet color in a ferric chloride test, was collected and concentrated to give crude IX, which was then recrystallized from ether to yield 0.12 g (6.3%) of IX as yellow plates; mp 149—151°C.

Found: C, 84.82; H, 5.97; N, 4.34%. Calcd for $C_{23}H_{19}NO$: C, 84.89; H, 5.89; N, 4.30%.

IR (KBr): 1645 (νC=O) and 1550 cm^{-1} (νC=C).

UV: λ_{max}^{EtOH} 249 mμ (ε 16300) and 353 mμ (ε 21500).

NMR (CCl_4): τ 6.37—7.35 (multiplet, 2H, C-3 methylene), τ 4.70 (triplet, 1H, C-2 methine), τ 4.42 (singlet, 1H, olefinic proton), and τ 2.40—3.20 (multiplet, 15H, phenyl).

2,3-Dihydro-1,2-diphenyl-6-methyl-4-pyridone(X). X was synthesized from 5.0 g (0.05 ml) of III and 9.05 g (0.05 mol) of I by the general procedure. The residue was chromatographed on a silica-gel (Merck 7734) column with a benzene-ethyl acetate (4 : 1 v/v) mixture. The fraction, which showed a brownish violet color in a ferric chloride test, was collected and evaporated to afford crude X, which was then recrystallized from carbon tetrachloride to give 6.5 g (50%) of colorless needles; mp 84—85°C.

Found: C, 81.94; 81,98; H, 6.53, 6.54; N, 5.26%. Calcd for $C_{18}H_{17}NO$: C, 82.10; H, 6.51; N, 5.32%.
IR (KBr): 1645 (νC=O) and 1560 cm^{-1} (νC=C).
UV: λ_{max}^{EtOH} 240 mμ (ε 2180) and 327 mμ (ε 10400).
$\lambda_{max}^{HCl\text{-}EtOH}$ 242 mμ (ε 1640) and 325 mμ (ε 8100).
NMR (CCl_4): τ 8.20 (singlet, 3H, CH_3–C=), τ 6.88—7.62 (ABX-type, 2H, $COCH_2$–CH), τ 5.10 (triplet, 1H, CH–Ph), τ 4.96 (singlet, 1H, olefinic proton), and τ 2.85—2.92 (multiplet, 10H, phenyl).

In order to examine for the presence of the intermediate of VI, the whole procedure was modified as follows. Two grams of V (0.02 mol) were allowed to react with 3.6 g (0.02 mol) of I, and then the liquid ammonia was evaporated without neutralization. To the residue 50 g of crushed ice and 50 g of water were added. After stirring for 10 min, the reaction mixture was extracted with chloroform. The aqueous layer was neutralized with dilute hydrochloric acid, and then again extracted with chloroform. From both solutions, only X was detected, not VI.

2,3-Dihydro-1,2-diphenyl-6-phenethyl-4-pyridone (XI). By the general procedure, XI was prepared from 9.5 g of IV and 9.05 g of I. The residue was chromatographed on a silica-gel (Merck 7729) column with a benzene-ethyl acetate (4 : 1 v/v) mixture; a fraction which showed a violet color in a ferric chloride test was collected. After the evaporation of the solvent, the residue was recrystallized from benzene-*n*-hexane (1:1 v/v) to afford 3.5 g (20%) of XI as colorless plates; mp 99—100°C.

Found: C, 84.79; H, 6.62; N, 4.10%. Calcd for $C_{25}H_{23}NO$: C, 84.95; H, 6.56; N, 3.96%.
IR (KBr): 1635 (νC=O), 1550 (νC=C) and 705 cm^{-1} (phenyl).
UV: λ_{max}^{EtOH} 238 mμ (ε 4500) and 330 mμ (ε 17500).
$\lambda_{max}^{HCl\text{-}EtOH}$ 236 mμ (ε 5200) and 326 mμ (ε 13200).
NMR (CCl_4): τ 7.72—7.10 (multiplet, 4H, Ph–CH_2–CH_2–). τ 7.28 (multiplet, 2H, C-3 methylene), τ 5.10 (triplet, 1H, C-2 methine), τ 4.66 (singlet, 1H, C=CH), and τ 2.60—3.10 (multiplet, 15H, phenyl).

3-Benzyl-2,3-dihydro-1,2-diphenyl-6-methyl-4-pyridone (XII). As in the preceding fractionating chromatography for XI, a fraction which showed a light brown color with ferric chloride was collected, concentrated, and recrystallized from benzene to yield 0.9 g (5.0%) of XII as yellow plates; mp 179—180°C.

Found: C, 84.99; H, 6.71; N, 4.09%. Calcd for $C_{25}H_{23}NO$: C, 84.95; H, 6.56; N, 3.96%.
IR (KBr): 1623 (νC=O), 1555 (νC=C) and 700 cm^{-1} (phenyl).
UV: λ_{max}^{EtOH} 240 mμ (ε 4580) and 333 mμ (ε 16900).
$\lambda_{max}^{HCl\text{-}EtOH}$ 245 mμ (ε 3620) and 331 mμ (ε 13400).
NMR ($CDCl_3$): τ 7.98 (singlet, 3H, CH_3–C=C), τ 6.62—7.23 (multiplet, 4H, C-3 methylene and Ph–CH_2–), τ 5.45 (singlet, 1H, C-2 methine), τ 4.78 (singlet, 1H, CH=C), and τ 2.60—3.10 (multiplet, 15H, phenyl).

Reaction of III with Aliphatic Schiff Bases. By the general procedure, 2.0 g (0.02 mol) of III were condensed with 2.38 g (0.02 mol) of benzylidenemethylamine or with 2.38 g (0.02 mol) of ethylideneaniline. In these reactions, neither the corresponding dihydropyridones nor the corresponding aminodiketones were detected by thin-layer chromatography.

BULLETIN OF THE CHEMICAL SOCIETY OF JAPAN VOL. 42 1360—1363 (1969)

Synthesis and Physical Properties of Long Chain Compounds. X. Studies on the X-Ray Diffraction Patterns of Normal Higher Primary Amines

Akira WATANABE,* Akio ISHIZAWA,** Masao KOSAKA* and Ryōzō GOTŌ**

* *Department of Chemistry, Faculty of Science and Engineering, Ritumeikan University, Kita-ku, Kyoto*

** *Department of Chemistry, Faculty of Science, Kyoto University, Sakyo-ku, Kyoto*

(Received August 6, 1968)

For the members of *n*-higher primary amines from C_{12} to C_{20} the crystal structure was studied by X-ray powder method. From the values of long spacings and the splitting of (110) reflections it was concluded that the structure is probably similar to that of fatty acids and that the hydrocarbon chains are tilted with respect to the plane formed by end groups. This structure seems to be stable over the temperature range between room temperature and melting points. The dependence of melting points on chain length was discussed.

X-Ray diffraction patterns of long chain compounds were first studied in detail by Müller[1] whose investigation dealt with normal paraffins with the carbon numbers from C_{18} to C_{44}. Malkin,[2] Francis,[3] and other workers also reported X-ray long spacings for the series of several long chain compounds such as alcohols, fatty acids, esters and iodides. In a previous work in this laboratory normal higher primary alcohols were studied in some detail.[4]

No X-ray study for normal higher primary amines can be found in the literature. Moreover a property of the amines in solid state has not been reported except the work of Smyth[5] who studied dielectric behavior of the amines of even carbon numbers from C_{12} to C_{18}. The present investigation was undertaken in order to study the dependence of solid structure of the amines on carbon numbers and on temperatures by X-ray powder method and to compare the results with those of higher alcohols and other compounds. The amines investigated are odd and even compounds with the carbon numbers from C_{12} to C_{20}.

Experimental

Preparation of the Amines and Their Purity.

The preparation has been reported in a preceding paper,[6] then the procedures will be described briefly. Since an extremely small amount of impurity affects the properties of long chain compounds, great care was taken throughout the preparations. Starting materials were commercial fatty acids and alcohol *e.g.*, lauric, myristic, palmitic, stearic acids and octadecyl alcohol. The acids, which had been converted to methyl esters, and the alcohol were purified by fractional distillation followed by several recrystallizations. The amines of C_{12}, C_{14}, C_{16}, C_{19} and C_{20} were synthesized by lithium aluminum hydride reduction of the corresponding acid amides in tetrahydrofuran. Most of the odd carbon numbered amines were prepared by Schmidt reaction or by Hofmann reaction from the next higher fatty acids. Melting points of the amines are given in Table 1 and Fig. 1. Data of the elemental analysis of *N*-acetylamines are recorded in Table 2. Since the melting point measurement or elementary analysis is not a reliable method to check the impurity in such long chain compounds, the efforts were exerted to find the method to establish the purity of the amines synthesized

TABLE 1. MELTING POINTS OF AMINES

Numbers of carbon atoms	Mp(°C)
12	29.0
13	28.1
14	39.9
15	39.5
16	47.1
17	47.5
18	52.0
19	53.0
20	58.0

1) A. Müller, *Proc. Roy. Soc.*, **A120**, 437 (1928); *ibid.*, **127**, 417 (1930).

2) T. Malkin, *J. Chem. Soc.*, **1931**, 2796; *ibid.*, **1930**, 3739.

3) F. Francis, S. H. Piper and T. Malkin, *Proc. Roy. Soc.*, **A128**, 214 (1930); F. Francis, F. J. E. Collins and S. H. Piper, *ibid.*, **A158**, 691 (1937).

4) A. Watanabe, This Bulletin, **34**, 1729 (1961); *ibid.*, **36**, 336 (1963).

5) J. D. Hoffman and C. P. Smyth, *J. Am. Chem. Soc.*, **71**, 3591 (1949).

6) R. Goto, A. Watanabe, K. Honjo and M. Kosaka, *Nippon Kagaku Zasshi* (*J. Chem. Soc. Japan, Pure Chem. Sect.*), **87**, 1220 (1966).

Table 2. Elemental analysis of *N*-acetylamines

$C_nH_{2n+1}NHCOCH_3$		Calcd %			Found %		
n	Formula	C	H	N	C	H	N
12	$C_{14}H_{29}ON$	73.95	12.87	6.16	73.99	13.10	6.21
13	$C_{15}H_{31}ON$	74.63	12.86	5.80	74.44	12.87	5.81
14	$C_{16}H_{33}ON$	75.32	13.02	5.48	74.97	13.00	5.50
15	$C_{17}H_{35}ON$	75.77	13.09	5.20	75.81	13.35	4.98
16	$C_{18}H_{37}ON$	76.26	13.15	4.94	76.29	13.41	4.94
17	$C_{19}H_{39}ON$	76.70	13.21	4.71	76.66	13.18	4.50
18	$C_{20}H_{41}ON$	77.10	13.27	4.50	77.23	13.50	4.24
19	$C_{21}H_{43}ON$	77.48	13.32	4.30	77.54	13.54	4.39
20	$C_{22}H_{45}ON$	77.81	13.36	4.12	78.06	13.53	4.36

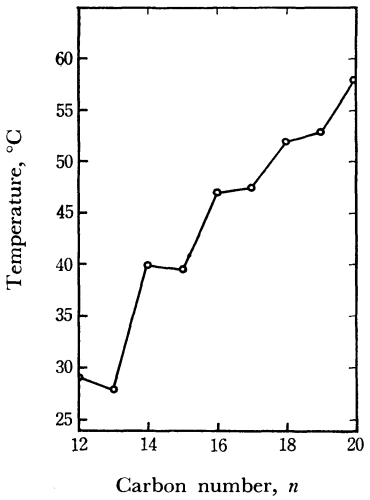

Fig. 1. Melting points of *n*-higher primary amines.

and to obtain the compounds having a suitable purity for X-ray studies.

After preliminary experiments of gas chromatographic analysis it was found that this method is quite reliable for methyl esters, alcohols as well as acetylamines to check the impurities, especially homologous compounds which have been known to cause an important effect on the properties of solid long chain compounds. Methyl esters of starting fatty acids, alcohols and intermediate methyl esters, that is, the esters of C_{19}, C_{20} acids were effectively analyzed by gas chromatography. For example, by the gas chromatography with a flame ionization detector in the best condition, 0.1 to 0.5% of C_{16} compounds in C_{18} compounds could be detected.

The hydrochlorides of the amines were purified by recrystallizing them four to six times from ether-ethanol mixture. Resulting compounds, after being acetylated with acetic acid anhydride, were referred to gas chromatography. Recrystallizations of the hydrochlorides were repeated until a purity of 99% or better was achieved. Selections of the typical chromatograms are shown in Fig. 2 and Fig. 3. Before the X-ray measurements further purifications were carried out for each material as follows. The compound free from hydrogen chloride was heated in a stream of nitrogen at the temperature slightly above its melting point in order to eliminate any carbon dioxide which had been held in the compound. After about two hours heating the compound was distilled from the vacuum system into a tube. After being filled with nitrogen gas the tube was sealed off.

Measurements of X-Ray Patterns. The X-ray photographs were all taken using Cu*K* radiation which was produced at 40 kV and 30 mA. Camera distance was 10 cm. Exposure times were 1.5 to 2.5 hr depending on the chain length of the compounds.

The samples were melted on an electric heater placed in a glove box filled with nitrogen gas, and then drawn into thin walled glass tubes of about 0.5 mm diameter.

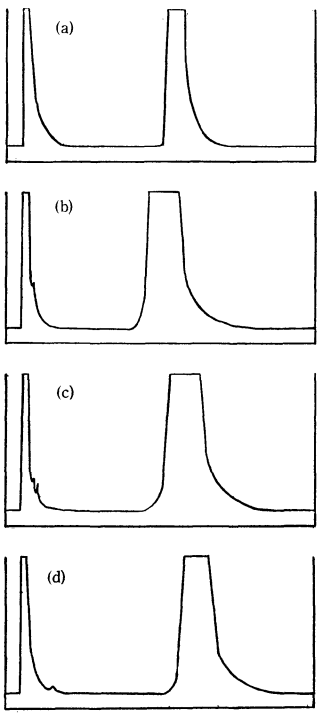

Fig. 2. Gaschromatograms of *N*-acetylamines of C_{17} (a), C_{18} (b), C_{19} (c), and C_{20} (d).
Column: 6 mm×1 m, 5% Apiezon grease L on 80—100 mesh Celite 545; temp.: 225—245°C; nitrogen flow: 48 ml/min; fuel gas: hydrogen 50—55 ml/min.

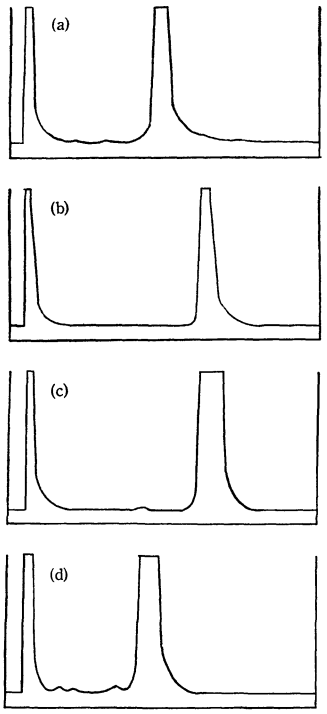

Fig. 3. Gaschromatograms of methyl esters of fatty acids of C_{18} (a), C_{19} (b), C_{20} (c), and octadecanol (d).
Column: 6 mm×2 m, 5% PEG 20 M on 60—80 mesh Celite 545 for the esters; 5% Apiezon grease L on 80—100 mesh Celite 545 for the alcohols; temp.: 155—225°C; nitrogen flow: 47 ml/min; fuel gas: hydrogen 44 ml/min.

The tubes were sealed off at their both ends. During the exposure the tubes were rotated. A brass furnace in which the tube was inserted was used for the measurements at high temperatures.

Results and Discussion

X-Ray diffraction patterns for the series of amines are presented in Fig. 4. The patterns appear to be similar throughout the series. No differences in crystal forms seem to exist between odd and even compounds nor from lower through higher members. The patterns were measured on long spacing reflections and it was found that the values of the spacings are a linerar function of carbon numbers for the series of either odd or even compounds. The data are summarized in Table 3 and illustrated in Fig. 5 together with those of normal higher alcohols quoted from previous papers.[4] The magnitude of the long spacings suggests that the molecules of the amines may be arranged in double molecules in the direction of the long axes, possibly due to the formation of hydrogen-bonding between the nitrogen atoms.

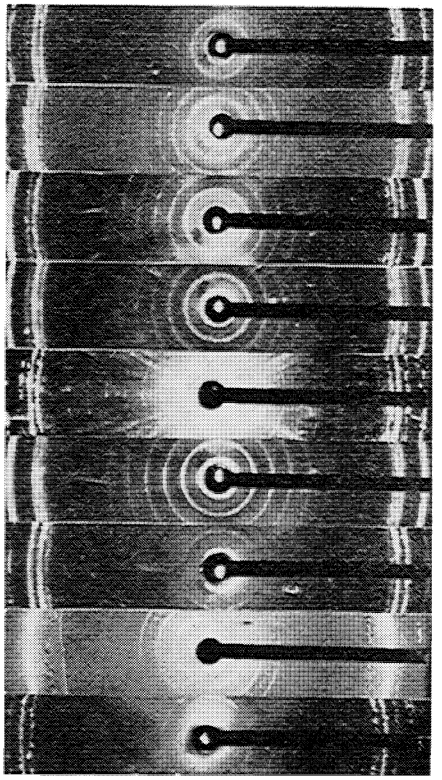

Fig. 4. X-Ray diffraction patterns of amines.
The patterns in discending order are from C_{12}, C_{13}, C_{14}, C_{15}, C_{16}, C_{17}, C_{18}, C_{19}, C_{20} amines.

By inspection of the values indicated in Table 3 it can be found that the long spacings of the amines are shorter by about 3 Å than those of the corresponding alcohols of vertical form. In view of the results of the analysis of other long chain compounds it is quite probable that the molecules of the amines extend themselves in straight zig-zag chains in the crystals, hence the shorter long spacings observed in the amines suggest that here the hydro-

TABLE 3. LONG SPACINGS OF AMINES AND ALCOHOLS

Amine		Alcohol	
Carbon number	Long spacing	Carbon number	Long spacing
12	31.01 Å	12	34.9 Å ⊥
13	34.66	13	37.3 ⊥
14	35.85	14	39.6 ⊥
15	39.42	15	42.36 ⊥
16	40.51	16	44.90 ⊥ 37.27 ∠
17	43.87	17	47.46 ⊥
18	45.13	18	41.60 ∠
19	48.40	19	52.82 ⊥
20	49.68	20	45.67 ∠

⊥ : vertical form
∠ : tilted form

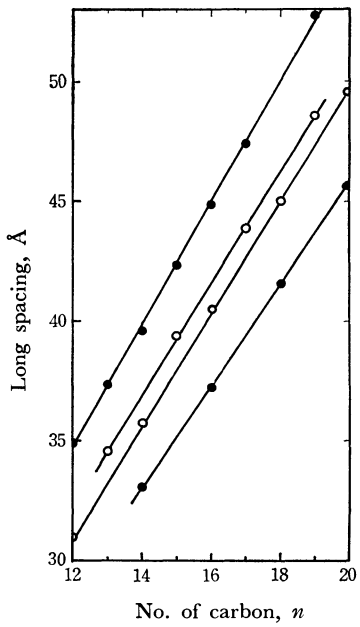

Fig. 5. Long spacings of *n*-higher primary amines and alcohols.
○ amines ● alcohols

carbon chains are inclined to the plane formed by the end groups. Additional evidence of the inclination can be obtained by the inspection of short spacing reflections. As may be seen in Fig. 4, the patterns indicate the splitting of (110) reflections in all the compounds, which is analogous to the case of tilted chain structures of higher alcohols and related compounds. If then, from the fact that the increase of the long spacings by the addition of two carbon atoms is about 4.6 Å, an approximate value of the tilt angle of the amine molecules can be estimated as 60° for both series of odd and even compounds.

Though the results obtained by powder patterns are limited to the general features of the molecular packing, some information on the conformation of the amines may be obtained by considering the intensity of the reflections with long spacings together with that of other compounds which have been analyzed previously. In the vertical form of normal higher alcohol *e. g.*, heptadecyl alcohol, the skew conformation of C–C–C–O bond has been confirmed by Seto.[7] Also it has been shown that, as a result of the existence of the skew conformations, the odd ordered long spacing reflections appear with stronger intensity as compared with those of even order. In the patterns of the amines the intensities of long spacing reflections decay gradually as the order of reflections increase. This behavior is different from that of alcohols mentioned above, and is similar to that of odd carbon numbered paraffin as heneicosane or tricosane which has been confirmed to have a straight zig-zag chain. From the intensity consideration mentioned above it seems probable that the amine molecules in the crystals consist only of transoid conformation of the C–C–C–N bonds.

Transitions in the solid state, which appear at temperatures not far from the melting or freezing points, have been found in paraffins, alcohols, bromides, and fatty acids. Therefore X-ray studies were made at various temperatures, in the hope of finding the same phenomena for the series of amines. However, no abrupt change of spacings was detected in any of the compounds studied. Accordingly, for the amine molecules tilted chain structure seems to be stable over the temperature range between room temperature and melting points.

A well known phenomenon of alternation of melting points could be observed in the series of amines investigated. As may be seen in Fig. 1, melting points of even carbon numbered amines lie on an upper curve similar to the behavior of other long chain compounds. Malkin,[8] in an earlier investigation, postulated a concept that the arrangement of tilted chain molecules makes methyl group packing less tight in odd carbon numbered compounds than in even numbered compounds. Later his concept was verified for the two forms of fatty acids by Sydow[9] with the interpretation based on the structure analysis. As mentioned above, the structure of the amine molecules, existing at the temperature just below their melting points, is the tilted one in both odd and even compounds. From the values given in Table 3 it can be found that the difference in the values of long spacings between odd and even compounds is about 1 Å. This difference will be interpreted reasonably as a result of different orientation of methyl groups, if for the odd numbered amines the C–C bond at the methyl terminal is perpendicular to the plane of methyl groups and if for the even numbered amines the bond in question is inclined at an angle. Thus the general arrangement of the molecules of the normal higher amines may be assumed to be similar to that of fatty acids, and the alternation of the melting points may be accounted for by Malkin's concept.

7) T. Seto, *Memoirs Coll. Sci. Univ. Kyoto*, **A 30**, 89 (1962).

8) T. Malkin, *Nature*, **127**, 126 (1931).

9) E. Sydow, *Arkiv Kemi*, **9**, 231 (1956).

BULLETIN OF THE CHEMICAL SOCIETY OF JAPAN VOL. 42 1364—1367 (1969)

Effects of Substituents on the Chain-transfer Reactivities of Nuclear-substituted Benzaldehydes to Polymer Radicals

Tadahiro YAMAMOTO,*1 Masaru HASEGAWA and Takayuki OTSU

Department of Applied Chemistry, Faculty of Engineering, Osaka City University, Sumiyoshi-ku, Osaka

(Received September 9, 1968)

In order to study the effect of substituents on the chain-transfer reactivities of nuclear-substituted benzaldehydes toward polymethyl methacrylate (poly-MMA) and polystyryl (poly-St) radicals, the chain transfer constants (C) of six kinds of benzaldehydes in radical polymerizations of these monomers were determined at 60°C. The C values of all the substituted benzaldehydes toward the poly-MMA radical were larger than that of unsubstituted benzaldehyde, regardless of the electron-repelling or electron-attracting nature of the substituents, while those toward the poly-St radical increased with an increase in the electron-attracting nature of the substituents. The relative reactivities toward the poly-MMA radical could not be correlated with the ordinary Hammett equation, but they could be with this modified equation: $\log(k/k_0)=\rho\sigma+\gamma E_R$, with $\rho=+0.2$ and $\gamma=0.7$. On the other hand, the relative reactivities toward the poly-St radical also fit a modified Hammett equation with $\rho=+1.4$ and $\gamma=0.65$.

One of the most interesting problems in vinyl polymerization is to clarify the relationship between the structure and the reactivity toward the attack of a polymer radical. In connection with this problem, we have investigated the effects of substituents on the chain-transfer reactions of the nuclear-substituted cumenes[1] and toluenes[2] toward various polymer radicals. From the results of these investigations, we have found that their chain-transfer reactivities are correlated not with the ordinary Hammett equation, but with a modified Hammett equation[3] including the resonance term:

$$\log(k/k_0) = \rho\sigma + \gamma E_R \quad (1)$$

where σ is the polar substituent constant; E_R, the resonance one, and ρ and γ, reaction constants giving, respectively, the degree of the polar and resonance contributions by the substituents. Clearly these results suggest that neither the resonance effect nor the polar effect of the substituents on these chain-transfer reactions should be disregarded.

The present investigation was undertaken in order to ascertain further the effect of substituents on the chain-transfer reactivities of another substrate toward a polymer radical. As substrates, six kinds of nuclear-substituted benzaldehydes were chosen. It was known that the abstraction of a hydrogen atom on the carbonyl group of benzaldehyde is easier than that on the side-chain atom of hydrocarbons.[4] Since the benzaldehyde has an oxygen atom of the carbonyl group which lies beside the reacting side-chain hydrogen atom, its substituent effect may be expected to be different from those observed in the reactions of cumenes and toluenes.[1,2]

This paper will describe the effect of substituents on the chain-transfer reactivities of nuclear-substituted benzaldehydes toward poly-MMA and poly-St radicals, as evaluated from the results of the polymerizations of methyl methacrylate and styrene in the presence of the benzaldehydes, using α,α′-azobisisobutyronitrile (AIBN) as the initiator.

Experimental

Materials. The nuclear-substituted benzaldehydes used in this study had the following substituents: *p*-methoxy, *p*-chloro, H, *p*-bromo, *m*-chloro, and *p*-cyano. The *m*-chlorobenzaldehyde and *p*-cyanobenazldehyde were synthesized as follows. The *m*-chlorobenzaldehyde was prepared from *m*-aminobenzaldehyde through a Sandmeyer reaction; bp 84—86°C/8 mmHg (lit.,[5]

*1 Present address: Himeji Institute of Technology, Idei, Himeji-shi.

1) a) T. Yamamoto, This Bulletin, **40**, 642 (1967). b) T. Yamamoto and T. Otsu, *J. Polymer Sci.*, **A-6**, 49 (1968). c) T. Yamamoto and T. Otsu, *ibid.*, **B-4**, 1039 (1966); This Bulletin, **40**, 2449 (1967); *Kogyo Kagaku Zasshi* (*J. Chem. Soc. Japan, Ind. Chem. Sect.*), **70**, 2403 (1967).

2) T. Yamamoto, S. Nakamura, M. Hasegawa and T. Otsu, *Kogyo Kagaku Zasshi* (*J. Chem. Soc. Japan, Ind. Chem. Sect.*), **72**, 727 (1969).

3) T. Otsu and T. Yamamoto, *Yuki Gosei Kagaku Kyokaishi* (*J. Soc. Org. Synth. Chem. Japan*), **23**, 643 (1965); *Chem. & Ind.*, **1967**, 787.

4) J. S. Buck and W. S. Ide, M. Szwarc, *Chem. Revs.*, **47**, 75 (1950).

5) J. S. Buck and W. S. Ide, "Organic Syntheses," Coll. Vol. II, p. 130 (1963).

84—86°C/8 mmHg). The *p*-cyanobenzaldehyde was prepared from *p*-cyanobenzyl bromide according to the procedure of Hass and Bender;[6] mp 95°C (lit.,[6] 95—96°C). The other substituted benzaldehydes were commercial materials used after purification.

All these substituted benzaldehydes except for the *p*-cyano-derivative, methyl methacrylate (MMA), and styrene were redistilled in a stream of nitrogen under reduced pressure before use.

Polymerization Procedure. The polymerizations of MMA and styrene in substituted benzaldehydes were carried out at 60°C in the presence of AIBN (3.32×10^{-3} mol/*l*) as the initiator. After a given reaction time, the resulting polymer was isolated by pouring the polymerizing mixture into an excess of methanol. Polymerization was controlled below 10% conversion.

Calculation of Number-average Degree of Polymerization ($\bar{P}_n$) and Chain-transfer Constant (C). The resulting polymer was purified by reprecipitating it from a benzene solution into a large amount of methanol. The intrinsic viscosty [η] of the polymers was determined by the viscosity measurement of its benzene solution at 30°C using an Ubbelohde viscometer. The $\bar{P}_n$ was calculated from the intrinsic viscosity obtained according to the following equations, (2) and (3):

$$\text{Poly-MMA:}^{7)}\ \log(\bar{P}_n) = 3.420 + 1.13\log[\eta] \quad (2)$$

$$\text{Poly-St:}^{8)}\ \log(\bar{P}_n) = 3.205 + 1.37\log[\eta] \quad (3)$$

The chain-transfer constants ($C=k_{tr}/k_p$) to benzaldehydes were determined by the Mayo equation (4):

$$1/\bar{P}_n = \text{Constant} + C[\text{S}]/[\text{M}] \quad (4)$$

where [S] and [M] are the initial concentrations of benzaldehydes and the monomer respectively.

Results and Discussion

The plots of the $1/\bar{P}_n$ of the polymers obtained against [S]/[M] are shown in Figs. 1 and 2. According to Eq. (4), from the slopes of the straight lines the chain-transfer constants were calculated to be as tabulated in Table 1. This table also shows the σ and E_R constants for the substituents used.

Chain-transfer Reactivities of Benzaldehydes with the Poly-MMA Radical. In Table 1 the resulting C values of substituted benzaldehydes may be seen to be larger than that of unsubstituted benzaldehyde, regardless of the electron-attracting or electron-repelling character of the substituents. The plot of the logarithms of the relative chain-transfer reactivities ($C/C_0=k/k_0$) toward the attack of the poly-MMA radical on the Hammett σ constants of the corresponding substituents is shown

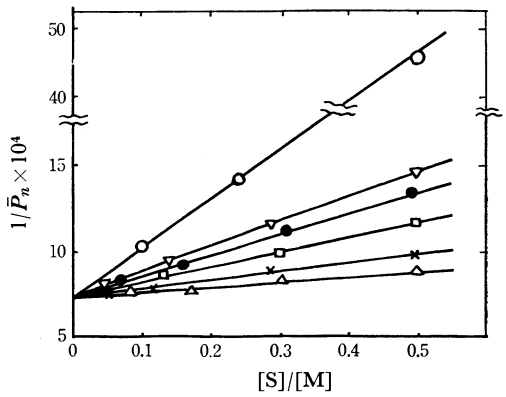

Fig. 1. The plots by Eq. (4) for the polymerization of styrene in the presence of substituted benzaldehydes at 60°C: ○ *p*-CN, ▽ *m*-Cl, ● *p*-Cl, □ H, × *p*-OCH_3, △ *p*-Br benzaldehydes.

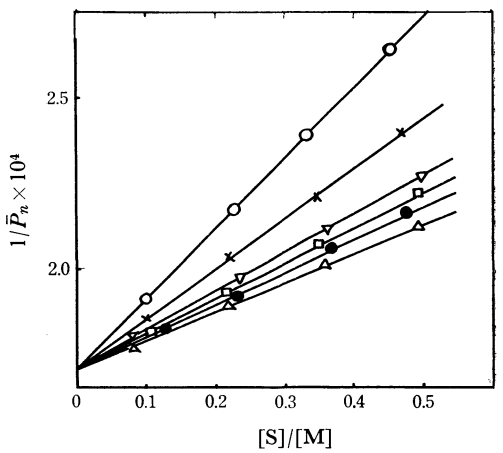

Fig. 2. The plots by Eq. (4) for the polymerization of MMA in the presence of substituted benzaldehydes at 60°C: ○ *p*-CN, × *p*-Br, ▽ *p*-OCH_3, □ *p*-Cl, ● *m*-Cl, △ H benzaldehydes.

Table 1. Chain-transfer constants (C) of substituted benzaldehydes in the radical polymerization of MMA and styrene at 60°C

Substituent in benzaldehyde	σ[9]	E_R[9]	$C\times10^4$ MMA	$C\times10^4$ Styrene
p-CH_3O	−0.268	0.11	1.11	2.86
H	0.00	0.00	0.86	4.54
p-Cl	0.227	0.10	1.03	8.63
p-Br	0.232	0.12	1.43	12.2
m-Cl	0.373	0.08	0.96	13.7
p-CN	0.660	0.24	2.06	76.7

6) H. B. Hass and M. L. Bender, *J. Am. Chem. Soc.*, **71**, 1767 (1949).

7) F. R. Mayo, R. A. Gregg and M. S. Matheson, *ibid.*, **73**, 1691 (1951).

8) B. Baysal and A. V. Tobolsky, *J. Polymer Sci.*, **9**, 171 (1952).

9) McDaniel and H. C. Brown, *J. Org. Chem.*, **23**, 425 (1958).

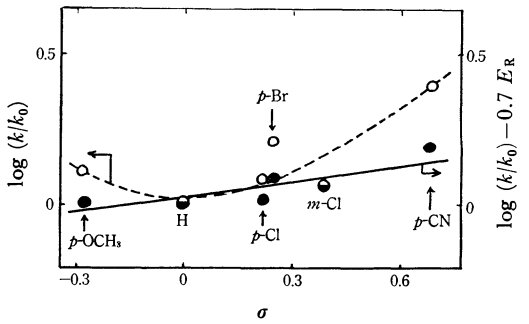

Fig. 3. The plots by the Hammett equation and Eq. (1) for the relative reactivities of benzaldehydes toward poly-MMA at 60°C.

in Fig. 3.

It may be seen that the plot of Fig. 3 gives not a straight line, but a concave curve. Such a parabola-type relation has always been observed in various chain-transfer reactions of cumenes and toluenes toward various polymer radicals[1,2] and in many radical reactions.[3a,10] Therefore, the effect of substituents on the reactivities of benzaldehydes toward the poly-MMA radical, as well as that on the other chain-transfer reactions, can not be explained by only a polar factor.

However, when Eq. (1) was applied to the present chain-transfer reaction, the straight-line relationship illustrated in Fig. 3 was obtained. From the slope of the straight line, the reaction constants, ρ and γ in Eq. (1), were found to be +0.2 and 0.7 respectively. The ρ and γ values indicated that the polar effect of substituens on the present chain-transfer reactivities was rather small, while the resonance effect was relatively important.

In previous papers, the chain-transfer reactivities of the nuclear-substituted cumenes,[1b] toluenes,[2] and acetophenones[11] toward the poly-MMA radical fit not the ordinary Hammett equation, but a modified Hammett equation (1). Tsuda and Otsu[12] reported that the chain-transfer reactivities of substituted dibenzoyl disulfides toward the poly-MMA radical were also correlated with Eq. (1).

For various chain-transfer reactions, it is interesting to compare the magnitude of the reaction constants, ρ and γ, obtained from the application of Eq. (1). Table 2 summarizes the ρ and γ values obtained for various substrates.

As can be seen in Table 2, all of the ρ values for these substrates toward the poly-MMA radical are close to zero, regardless of the substrate structure. In general, the sign and the magnitude of the ρ value are determined by both the polar character

Table 2. The ρ and γ values of the chain-transfer reactions of various substrates toward the poly-MMA radical

Substrate	ρ	γ	Ref.
Benzaldehyde	+0.2	0.7	This work
Cumene	+0.03	0.9	1a)
Toluene	+0.01	0.6	2)
Acetophenone	−0.01	2.0	11)
Diphenyl disulfide	+0.01	0.75	13)
Dibenzoyl disulfide	+0.07	0.75	12)
Phenylacetylene	0.0	1.7	14)

of the attacking radical and the electron density in the reaction center in the substrate. Accordingly, the fact that all of the ρ values in Table 2 are close to zero suggests that the poly-MMA radical has only a small polar character.

On the other hand, the γ values in Table 2 are relatively large and change with the substrate structure. Hence, it may be concluded that the polar factor of the substituents slightly affects the reactivities of these substrates toward the attack of a poly-MMA radical, while the resonance has a significant effect.

Chain-transfer Reactivities of Benzaldehydes with the Polystyryl Radical. The C values of substituted benzaldehydes toward the poly-St radical, shown in Table 1, increases gradually with an increase in the electron-attracting character of their nuclear substituents. The ordinary Hammett plots of these results, shown in Fig. 4, do not give a straight-line relationship.

However, when the σ^- canstant for the *p*-cyano substituent ($\sigma^-=1.00$)[15] was used, a fairly good

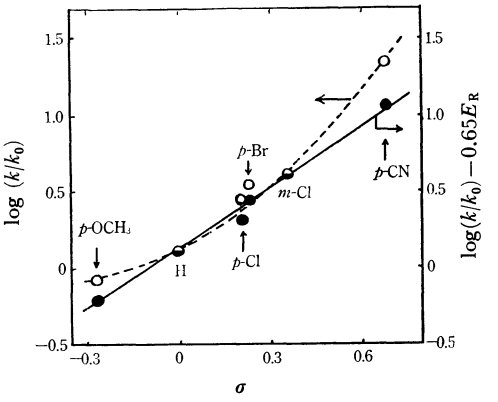

Fig. 4. The plots by the Hammett equation and Eq. (1) for the relative reactivities of benzaldehydes toward poly-St at 60°C.

10) T. Yamamoto, *Nippon Kagaku Zasshi* (*J. Chem. Soc. Japan, Pure Chem. Sect.*), **83**, 844 (1962).
11) T. Yamamoto, M. Hasegawa and T. Otsu, This Bulletin, **41**, 2788 (1968).
12) K. Tsuda and T. Otsu, *ibid.*, **39**, 2206 (1966).
13) T. Otsu, Y. Kinoshita and M. Imoto, *Makromol. Chem.*, **73**, 225 (1964).
14) H. Higashiura, Presented at the 14th Annual Meeting of High Polymer Science, Tokyo, May 1965.
15) L. P. Hammett, *J. Am. Chem. Soc.*, **59**, 96 (1937).

linear relationship was observed. This result is understandable if this reaction series is a nucleophilic reaction; the formation of the carbanion in the transition state thus becomes important.

On the other hand, when the plot was made by a modified Hammett equation (1), a much better linear relationship was obtained, as is shown in Fig. 4. From this plot, the ρ and γ values may be found to be $+1.4$ and 0.65 respectively. When we compare these ρ and γ values with those of the attack by the poly-MMA radical, it is noted that the γ values are almost the same, while the ρ values are quite different from each other.

As has been described in a previous paper,[3] the ρ values in Eq. (1) are mainly dependent on the polar natures of both the attacking radical and the substrate structure. Accordingly, the positively-large ρ value in the attack of poly-St, as compared with that of poly-MMA, is understandable, since the poly-MMA radical is less nucleophilic than the polystyryl radical because of its own α-carbomethoxy group.

BULLETIN OF THE CHEMICAL SOCIETY OF JAPAN VOL. 42 1367—1373 (1969)

An Improved Synthesis of N,β-Dimethylleucine and the Resolution Thereof*1

Hiroshi KOTAKE, Tomoo SAITO and Kazuo ŌKUBO

Department of Chemistry, Faculty of Science, Kanazawa University, Kanazawa

(Received September 10, 1968)

A diastereoisomeric mixture of racemic β-methylleucine was synthesized by the condensation of 2-benzyl-4(5*H*)-imidazolone with the methyl isopropyl ketone, followed by catalytic hydrogenation and hydrolysis. The separation of the mixture into *threo*-β-methyl-DL-leucine and *erythro*-β-methyl-DL-leucine was mainly achieved by fractional crystallization from water. The resolution of each diastereoisomer was also accomplished through salt-formation with (−)- and (+)-ephedrine alternately before or after the methylation of the amino group. The specific rotation and the NMR and IR spectra of one isomer, *threo*-N,β-dimethyl-L-leucine, corresponded closely with those reported for dimethylleucine isolated from nature.

N,β-Dimethylleucine was isolated from a hydrolysate of Ethamycin by Sheehan and his coworkers,[1] and later from Triostin C by Ōtsuka and Shōji.[2] The configuration at both centers of asymmetry of the amino acid was established as being comparable to that of L-alloisoleucine.[1,3] Although an attempt was made by Sheehan and Howell to synthesize the amino acid,[4],*2 it has not yet been done completely. In this paper, an improved synthesis of N,β-dimethyl-DL-leucine, a synthesis that might be appropriate for a method of preparation, and its favorable optical resolution using ephedrine are described.

Synthesis

2-Benzyl-4(5*H*)-imidazolone[5] (I), which can be easily produced by the condensation of ethyl phenylacetoimidinate with ethyl glycinate, may be expected to be a suitable material for the preparation of the

*1 This work was partially presented at the 20th and 21st Annual Meetings of the Chemical Society of Japan, Tokyo, April 1967 and Osaka, April 1968, and reported on *Tetrahedron Letters*, **1968**, 2015.

1) J. C. Sheehan, H. G. Zachau and W. B. Lawson, *J. Am. Chem. Soc.*, **80**, 3349 (1958).

2) H. Ōtsuka and J. Shōji, *J. Antibiotics*, **A16**, 52 (1963). More recently, the amino acid was also found in Triostin B_0 and in Quinomycin series by the same authors, *ibid.*, **A19**, 128 (1966); *Tetrahedron*, **23**, 1535 (1967).

3) J. Shōji, K. Tori and H. Ōtsuka, *J. Org. Chem.*, **30**, 2772 (1965).

4) J. C. Sheehan and M. G. Howell, *ibid.*, **28**, 2279 (1963).

*2 In the preceding work to Sheehan, the diastereomixture of β-methyl-DL-leucine was also prepared by T. Kōnotsune, *Nippon Nogei Kagaku Kaishi* (*J. Agr. Chem. Soc. Japan*), **36**, 389 (1962), from the reactios of *s*-butyl crotonate, Grignard reagent of isopropyl bromide, and bromine, followed by hydrolysis and amination. But the over-all yield was as low as about 10%.

5) H. Finger and W. Zeh, *J. prakt. Chem.*, [2] **82**, 50 (1910); H. Lehr, S. Karlan and M. W. Goldberg, *J. Am. Chem. Soc.*, **75**, 3640 (1953); A. R. Kidwai and G. M. Devasia, *J. Org. Chem.*, **27**, 4527 (1962).

titled compound because of its stability and because its reactivity with the desired ketone is sufficient. The condensation of I with methyl isopropyl ketone was successfully worked up, with the latter in a twofold excess, to give 2-benzyl-5-(α-methyl isobutylidene)-4-imidazolone (II), which was isolated as its stable hydrochloride (III) by passing dry hydrogen chloride through the solution of II in ethyl alcohol. The subsequent catalytic reduction of III over Adams' platinum oxide as a catalyst afforded 2-benzyl-5-(α-methyl isobutyl)-4-imidazolone (IV). In contrast with the favorable use of the above catalyst, palladium black did not respond when used similarly. Upon the hydrolysis of IV with aqueous barium hydroxide, the diastereoisomers of β-methylleucine (VI, VII) and *N*-phenylacetyl-β-methylleucine (V), which was considered to be a hydrolysis intermediate, were given in 52 and 44% yields respectively (Scheme 1). Since the solubility

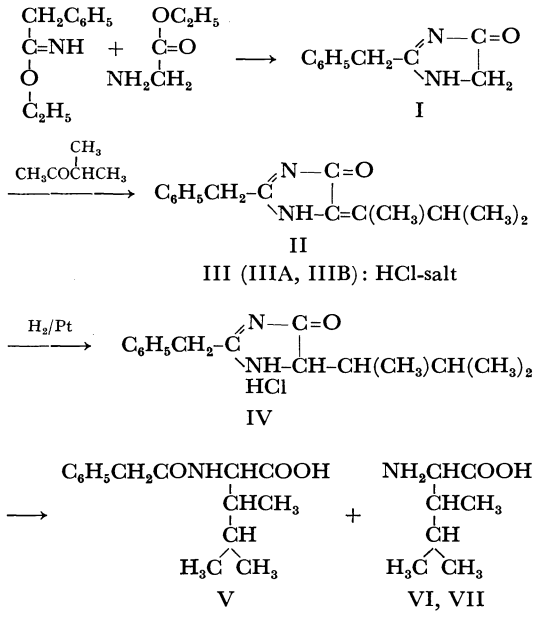

Scheme 1

of VI in water was much less than that of the other isomer, VII, the isomer VI was obtained in a pure state by repeated fractional crystallization from water. Although it was difficult to isolate the more soluble VII in the pure form, VII was separated from contaminated VI as follows: a reverse relationship in solubility was here observed between the diastereoisomeric amino acids (VI and VII) and their *N*-acetyl derivatives (VI′ and VII′), and the final purification of VII was achieved by the fractional crystallization of its *N*-acetyl derivative (VII′), followed by deacetylation. The above *N*-acetylation was carried out by using a precise equiamount of acetic anhydride in a caustic alkali solution in order to avoid any equalization of asymmetry at the α-carbon atom through the formation of azlactone, which is likely to arise through the action of acetic anhydride in glacial acetic acid.[6],*3 VI was also obtained exclusively from the intermediate V by hydrolysis either with aqueous barium hydroxide or with 6N hydrochloric acid. Thus, the ultimate ratio of fairly pure VI and VII was about 2:1 (in 57 and 28% yields respectively). The predominantly-formed diastereoisomer VI was found to be a racemate of the desired *threo*-form, thus favoring our synthetic purpose. The result is probably due to steric hindrance exerted by the carbonyl group present in the imidazolone on the isopropyl of methyl isobutylidene in the molecule II. In the route from I to IV, IIIA rather than IIIB is preferably formed, followed by the *cis*-addition of hydrogen by catalytic reduction (Scheme 2). Consideration using the Dreiding model led

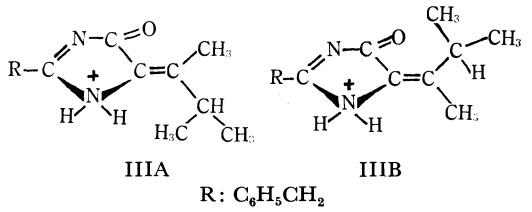

IIIA IIIB

R: $C_6H_5CH_2$

IIIA: Preferably formed structure, which expected to afford VI by *cis*-addition of hydrogen, followed by hydrolysis.

IIIB: Less prefered structure anticipated to form VII.

Scheme 2

us to understand the condensation containing the above sterically-controlled synthesis and enabled us to predict that, by subsequent catalytic hydrogenation, the preferably-formed VI would be racemic *threo*-β-methylleucine. Characteristic differences between VI and VII are observed from their IR spectra showing absorptions in the region of 1700—1600 cm^{-1}, though there was only a minor difference in the finger-print region; VI has two absorption bands at 1668 and 1628 cm^{-1}, with the former band much stronger than that of the latter, in contrast with the single band, at 1625 cm^{-1}, in VII. In addition, VI′ showed a carboxyl stretching band at 1733 cm^{-1} and a carbonyl band of amide at 1633 cm^{-1}, but the corresponding bands of VII′

6) J. P. Greenstein, S. M. Birnbaum and L. Levinton *Biochem. Prep.*, **3**, 84 (1953).

*3 When excess acetic anhydride in a warm alkali solution was used, epimerization was reported to occur at the α-carbon atom of isoleucine by W. A. H. Huffman and A. W. Ingersoll (*J. Am. Chem. Soc.*, **73**, 3366 (1951)). However, under the conditions described in this paper, VI and VII were acetylated without any considerable epimerization.

shifted to 1708 and 1615 cm^{-1} respectively.*4 There are, moreover, two characteristic bands in the 1200—1300 cm^{-1} region for VI′; one of these, at 1258 cm^{-1}, is much stronger than the other, at 1265 cm^{-1}; there is only the single band at 1418 cm^{-1} in the case of V′.

According to the method of Quitt and his coworkers,[7] the *N*-methylation of VI was accomplished through the formation of an *N*-benzyl derivative (VIII). The *N*-benzyl-*N*-methyl derivative (IX) thus formed was then hydrogenated to give *threo*-*N,β*-dimethyl-DL-leucine (X). Similarly, the other isomer, *erythro*-*N,β*-dimethyl-DL-leucine, was obtained through the isomeric intermediates, corresponding to VIII and IX, from VII. The observation that the relative configurations at the α- and β-carbon atoms of the diastereoisomers are reflected in their NMR spectra[3] was used as a basis for speculation concerning the steric structures of X and its isomer: the coupling constant at the α-proton of compound X, assumed above to be *threo*-form, was 3.9 cps, and that of the latter was 4.8 cps; these values corresponded to the values of the coupling constants (4.05 and 4.80 cps) reported in the literature for *N,γ*-dimethyl-DL-alloisoleucine and *N,γ*-dimethyl-DL-isoleucine. The IR spectra of X was, of course, distinct from that of the other isomer, and it was in good agreement with that of *N,γ*-dimethyl-DL-alloisoleucine over the whole region. The solubility behavior of both the diastereoisomers in such solvents as water, lower alcohols, and acetone was also comparable with that reported in the literature.[4]

Optical Resolution

The resolution of the *N*-benzyloxycarbonyl derivative of X is desirable for the purpose of its peptide formation; it was achieved through salt-formation alternately using (−)- and (+)-ephedrine hemihydrate.*5 *N*-Benzyloxycarbonyl-*threo*-*N,β*-dimethyl-DL-leucine (XI), prepared according to the Schotten-Baumann technique from X with benzyloxycarbonyl chloride, was combined with (−)-ephedrine hemihydrate in ethyl acetate in concentrations of 1.0 and 0.56 M respectively, thus affording exclusively a salt of the L-isomer: *N*-benzyloxycarbonyl-*threo*-*N,β*-dimethyl-L-leucine·(−)-ephedrine salt ($[\alpha]_D = -75.0°$) (XIIL) in over a 90% yield. The further addition of the antipodal base, (+)-ephedrine hemihydrate, to the mother liquor gave an optically-pure *N*-benzyloxycarbonyl-*threo*-*N,β*-dimethyl-D-leucine·(+)-ephedrine salt ($[\alpha]_D = +73.5°$) (XIID). A suspension of XIIL in ethyl acetate was treated with 2N hydrochloric acid to give *N*-benzyloxycarbonyl-*threo*-*N,β*-dimethyl-L-leucine ($[\alpha]_D = -75.9°$) (XIIIL). The XIIIL was dissolved in 30% hydrogen bromide in glacial acetic acid to afford *threo*-*N,β*-dimethyl-L-leucine ($[\alpha]_D = +38.3°$) (XIVL); this was then neutralized with triethylamine in ethyl alcohol. In a similar way, the other isomer, *threo*-*N,β*-dimethyl-D-leucine ($[\alpha]_D = -39.3°$) (XIVD), was obtained from XIID through *N*-benzyloxycarbonyl-*threo*-*N,β*-dimethyl-D-leucine ($[\alpha]_D = +75.3°$) (XIIID). The XIIID isomer, with a specific rotation of +72°, was also obtained directly from the mother liquor of XIIL, without any intermediate formation of salt, XIID. In this case, the effective washing of the solution of ethyl acetate with water to remove a small amount of contaminating salt was essential in order to increase the optical purity of the product. Unlike the case of XI, *N*-benzyloxycarbonyl-*erythro*-*N,β*-dimethylleucine did not react with ephedrine to deposit salt from a solution in such a solvent as ethyl acetate, lower alcohols, acetone, benzene, or ether. The resolution was, however, accomplished in the case of *N*-benzyloxycarbonyl-*erythro*-*β*-methyl-DL-leucine (XV). The salts, *N*-benzyloxycarbonyl-*erythro*-*β*-methyl-L-leucine·(−)-ephedrine ($[\alpha]_D = -17.6°$) (XVIL) and *N*-benzyloxycarbonyl-*erythro*-*β*-methyl-D-leucine·(+)-ephedrine ($[\alpha]_D = +17.7°$) (XVID), were obtained from the ethereal solution by a way similar to that used for the *threo*-form. They were reduced to *erythro*-*β*-methyl-L-leucine ($[\alpha]_D = +38.9°$, in 5N hydrochloric acid) (XVIIL) and its antipode, XVIID ($[\alpha]_D = -39.4°$, in 5N hydrochloric acid), and finally *N*-methylation was performed to afford *erythro*-*N,β*-dimethyl-L-leucine ($[\alpha]_D = +38.0°$) (XVIIIL) and *erythro*-*N,β*-dimethyl-D-leucine ($[\alpha]_D = -38.3°$) (XVIIID) respectively. The L-isomer without an *N*-methyl group, XVIIL, was comparable to β-methyl-L-leucine, with a

Table 1.

Compound	$[\alpha]_D^{23-25}$	Solvent	Coupling constant at the α-proton signal in NMR (cps)
XIVL	+31.5° (+33.15°)[1] (+28.4°)[3]	Water	3.9 (4.0)[3]
	+38.3° (+39.2°)[1] (+41.9°)[3]	5N HCl	
XIVD	−31.8°	Water	3.9
	−39.3°	5N HCl	
XVIIIL	+38.0°	5N HCl	4.8
XVIIID	−38.3°	5N HCl	4.8

*4 Those spectra for VI′ and VII′ are in good agreement in whole region with the corresponding those of Sheehan's.[4]

7) P. Quitt, J. Hellerbach and K. Vogler, *Helv. Chim. Acta*, **46**, 327 (1963). Further studies on the *N*-methylation of amino acids have more extensively been done in the same way by M. Ebata, Y. Takahashi and H. Ōtsuka, This Bulletin, **39**, 2535 (1966).

*5 Extensive studies on the resolution of benzyloxycarbonylamino acids by use of ephedrine will be the subject in next paper.

specific rotation of +38°, prepared by Sheehan from the racemate of the less soluble acetyl derivative in water through digestion by acylase. In this connection, the racemic acetyl derivative VI′, which afforded the desired XIV$_L$, was more soluble in water. All of the four possible optical active isomers have here been successfully prepared, as is indicated in Table 1. Among these, only XIV$_L$ has been found to be identical with natural amino acid in all respects, including optical rotation value and NMR and IR spectra.

Experimental

All melting points are uncorrected. The infrared spectra were recorded with a Koken DS-301 spectrometer using a sodium chloride prism in Nujol mulls. The NMR spectra were taken with a Nihon Denshi JNM-C-60H spectrometer on a solution in deuterium oxide, using sodium 2,2-dimethyl-2-silapentane-5-sulfonate as a reference at room temperature. The optical rotation values were measured with a Jasco DIP-SL-type polarimeter.

2-Benzyl-4(5*H*)-imidazolone (I). Prepared from ethyl phenylacetoimidinate and ethyl glycinate according to the method reported in the literature. I was obtained, in a 70% yield, as needles with a melting point of 142—143°C (lit.[5] mp 143°C).

2-Benzyl-5(*α*-methyl isobutylidene)-4-imidazolone (II). A) A mixture of finely-powdered I (25 g, 0.144 mol) and 25 g (0.288 mol) of methyl isopropyl ketone was refluxed under a nitrogen atmosphere for 6 hr at 120—130°C in an oil bath. After cooling (when the reaction mixture had solidified), the reaction mixture was triturated with 20—30 m*l* of petroleum ether and then filtered to give a crude material (mp 72—79°C) in an 89% yield (30.8 g). The material was dissolved in 300 m*l* of benzene and decolorized with active charcoal. Benzene was removed by concentration *in vacuo* to afford, in an 81% yield, colorless crystals with a melting point of 104—120°C (28.1 g). It was difficult to obtain crystals with a constant melting point, though it was possible to recrystallize them from either ether or ether-petroleum ether.

B) To the reaction mixture obtained from 68 g (0.39 mol) of I and 67 g (0.78 mol) of the ketone under conditions similar to those used in the A) procedure, 400 m*l* of ethyl alcohol were added; then dry hydrogen chloride was passed through the solution obtained above under cooling in a water bath until it was saturated. Then the mixture was sealed tightly with a stopper and stored in a refrigerator. After several hours, the deposited crystals were collected on a glass-fritted funnel and washed with much ether to give an almost pure hydrochloride of II (mp 207—210°C) in a 78% yield (85 g); this substance was designated III. It was recrystallized from ethyl alcohol-ether to afford pure crystals with a melting point of 208—210°C. Found: C, 64.52; H, 6.59; N, 9.96%. Calcd for $C_{15}H_{19}ON_2Cl$: C, 64.22; H, 6.83; N, 10.04%.

Racemic *β*-Methylleucine and Its Separation into Two Diastereoisomers (VI and VII). In a suspension of Adams' platinum oxide (200 mg) in 500 m*l* of alcohol, enough hydrogen was absorbed, and then 55 g (0.197 mol) of III were added. Hydrogenation was continued, with the aid of mechanical shaking, for 40 min, by which time about an equiamount of hydrogen (4400 m*l*) had been absorbed. After the removal of the catalyst by filtration, the filtrate was concentrated *in vacuo* to give an oily product (IV). A solution of the oil in 2000 m*l* of water containing 372 g (1.18 mol) of barium hydroxide octa-hydrate was refluxed for 40—50 hr. After cooling, 351 m*l* of 6N sulfuric acid were slowly added; the precipitate was filtered and washed several times with hot water. The combined filtrate was concentrated *in vacuo* up to about 100 m*l*, and then the solution was washed twice with 100-m*l* portions of ether. The aqueous layer was concentrated *in vacuo* to give a crystalline residue. To the solution of the dried residue in 150 m*l* of ethyl alcohol, there were added about 20 m*l* of triethylamine to afford 15 g (52.4%) of a crystalline solid. The crystals were redissolved by warming them in 70 m*l* of water and decolorized with active charcoal; then the colorless solution obtained was allowed to stand over night at room temperature. The colorless crystals thus deposited were filtered, washed with alcohol, and then recrystallized several times from water to give 3.4 g (11.9%) of fine crystals. This compound did not change over 270°C; it was designated VI. Found: C, 57.64; H, 10.68; N, 9.41%. Calcd for $C_7H_{15}O_2N$: C, 57.90; H, 10.41; N, 9.65%.

To the mother liquor obtained after the removal of VI, there was added about twice as much acetone to give the other crystals. Repeated fractional crystallization from a small amount of water and acetone afforded a somewhat sterically impure material (mp over 270°C) in a 34.2% (9.8 g) yield. The material obtained was designated VII; it differed from VI in its crystalline form. Found: C, 57.73; H, 10.24; N, 9.72%.

The previously-filtered precipitate, after hydrolysis with barium hydroxide and subsequent neutralization with sulfuric acid, was placed in a 1-*l* Erlenmeyer flask; then it was treated by effective shaking with 200 m*l* of 1N sodium hydroxide, filtered, and washed with 1N sodium hydroxide. The combined filtrate was acidified to pH 4 with concentrated hydrochloric acid. The deposited product was collected by filtration and then recrystallized from benzene to give pure *N*-phenylacetyl-*threo*-*β*-methyl-DL-leucine (V), which had a melting point of 151.5—152.5°C, in a 43.5% (21.2 g) yield. Found: C, 68.15; H, 7.69; N, 5.66%. Calcd for $C_{15}H_{21}O_3N$: C, 68.41; H, 8.04; N, 5.32%.

A suspension of 2.9 g (0.011 mol) of V in 40 m*l* of 6N hydrochloric acid was refluxed for 14 hr. After cooling, the deposited crystals were filtered off and the filtrate was concentrated *in vacuo* to give a residue. The residue was dissolved in 15 m*l* of ethyl alcohol and neutralized with 2 m*l* of triethylamine. Then the crystals were filtered and washed with ethyl alcohol to afford VI quantitatively (1.6 g). V also afforded VI exclusively upon further treatment in aqueous barium hydroxide for 31 hr at the refluxing temperature.

Acetylation of Amino Groups of VII and VI. A solution of 4.9 g (0.0337 mol) of sterically-impure VII in 8.48 m*l* of 4N sodium hydroxide was cooled to 0—5°C in an ice bath and stirred mechanically. Then, 8.48 m*l* of 4N sodium hydroxide and 3.18 m*l* (0.0337 mol) of acetic anhydride were added, at rates to maintain a

slight basicity and a temperature of about 5°C, over a 30-min period. Stirring was then continued for a further 30 min at room temperature. The solution was acidified by the addition of about 6 m*l* of 6N hydrochloric acid. White crystals deposited immediately; they were filtered to give an *N*-acetyl derivative (5.95 g, 94%). The product was repeatedly recrystallized from water to give 5.40 g of the less soluble *N*-acetyl-*erythro*-*β*-methyl-DL-leucine (VII′), which had a melting point of 169—170°C (lit.[4] 171.8—172.2°C). Found: C, 57.55; H, 9.34; N, 7.34%. Calcd for $C_9H_{17}O_3N$: C, 57.73; H, 9.15; N, 7.48%. IR: 1708, 1616, and 1553 cm^{-1}.

The combined mother liquor was concentrated to dryness to give a crystalline residue. This was repeatedly recrystallized from water and acetone to afford 0.386 g of the more soluble *N*-acetyl-*threo*-*β*-methyl-DL-leucine (VI′), which had a melting point of 159—160°C (lit.[4] 157—157.5°C). Found: C, 58.05; H, 8.91; N, 7.35%. IR: 1733, 1633, 1550, and 1418 cm^{-1}.

The VII′ and VI′ thus obtained were reduced to pure VII and VI by a usual acid hydrolysis, followed by neutralization with triethylamine. On the other hand, pure VI and VII were also acetylated in a similar way to afford VI′ and VII′ respectively; the yields were in the range of 91—95%, and no epimerization was to be seen in either case.

***N*-Benzyl-*threo*-*β*-methyl-DL-leucine (VIII).** A) According to the method of Quitt,[7] 2.9 g (0.02 mol) of VI was treated with 2.1 m*l* (0.02 mol) of freshly-distilled benzaldehyde and then with 0.23 g (0.006 mol) of sodium borohydride, while the temperature was maintained between 20 and 22°C. Then the same amounts of benzaldehyde and sodium borohydride were added to the reaction mixture; from it 4.7 g (100%) of VIII (mp 205—207°C) were then obtained. Recrystallization from an ethyl alcohol-water mixture (2:1) afforded pure crystals with a melting point of 213°C (4.0 g). Found: C, 71.48; H, 8.87; N, 5.75%. Calcd for $C_{14}H_{21}O_2N$: C, 71.45; H, 9.00; N, 5.95%.

B) When catalytic hydrogenation using palladium black as a catalyst was used instead of reduction with sodium borohydride, VIII was usually obtained in a yield relatively lower (as much as 70%) than in the case of A).

***N*-Benzyl-*erythro*-*β*-methyl-DL-leucine.** In a way similar to the procedure of VIII, A), this compound was obtained in an 87% yield; mp 225°C. The recrystallization was performed from methyl alcohol. A mixed-melting-point determination with VIII was depressed to 200—205°C. Found: C, 71.47; H, 8.76; N, 6.09%.

***N*-Benzyl-*threo*-*N*,*β*-dimethyl-DL-leucine (IX) and Its Dicyclohexylammonium Salt.** According to the method of Quitt,[7] 3 g (0.0128 mol) of finely-powdered VIII were treated with 1.8 m*l* (0.037 mol) of formic acid and 1.5 m*l* (0.018 mol) of 38% formaline. IX was thus obtained almost quantitatively as an oily product; it was often crystallized when left standing for long period of times and furnished crystals with a melting point of 56—57°C. The oil was converted to its dicyclohexylammonium salt from an acetone solution for its characterization. Recrystallization from ethyl alcohol gave a pure product in an 82% yield; mp 139°C. Found: C, 75.16; H, 10.75; N, 6.39%. Calcd for $C_{27}H_{46}O_2N_2$: C, 75.30; H, 10.77; N, 6.51%.

***N*-Benzyl-*erythro*-*N*,*β*-dimethyl-DL-leucine and Its Dicyclohexylammonium Salt.** Similarly, this compound was prepared from *N*-benzyl-*erythro*-*β*-methyl-DL-leucine as crystals with a melting point of 134—135°C in an 87% yield. Found: C, 72.68; H, 9.29; N, 5.66%. Calcd for $C_{15}H_{23}O_2N$: C, 72.25; H, 9.30; N, 5.62%. The dicyclohexylammonium salt of the material was obtained in an 81% yield; mp 127—128°C. A mixed-melting-point determination with the salt of IX was depressed to 120—122°C. Found: C, 75.38; H, 10.43; N, 6.38%.

***threo*-*N*,*β*-Dimethyl-DL-leucine (X).** The oily IX prepared from 3 g (0.0128 mol) of VIII was hydrogenated with palladium black as a catalyst in 60 m*l* of 90% acetic acid; then it was concentrated to afford crystals. Recrystallization from an ethyl alcohol-water mixture (2:1) and then a water-dioxane mixture gave pure X with a melting point of over 270°C in a 98% yield. Found: C, 60.40; H, 11.15; N, 8.89%. Calcd for $C_8H_{17}O_2N$: C, 60.34; H, 10.76; N, 8.80%.

***erythro*-*N*,*β*-Dimethyl-DL-leucine.** The same procedure as in the case of the preparation of X was used. The product was obtained from *N*-benzyl-*erythro*-*N*,*β*-dimethyl-DL-leucine in a 94% yield; mp >270°C. Found: C, 59.87; H, 10.38; N, 8.83%.

***N*-Benzyloxycarbonyl-*threo*-*N*,*β*-dimethyl-DL-leucine (XI).** To a solution of 8.8 g (0.55 mol) of X in 14 m*l* (0.055 mol) of 4N sodium hydroxide, there were added 16.7 m*l* (0.066 mol) of 4N sodium hydroxide and 10 g (0.059 mol) of benzyloxycarbonyl chloride according to the Schotten-Baumann procedure; the subsequent reaction proceeded well with concurrent stirring and cooling at 0—5°C in an ice bath. The reaction was continued for 1 hr at 0—5°C and then for an additional hour at room temperature. The reaction mixture was washed with 15 m*l* of ether, and then the aqueous layer was neutralized with 6N hydrochloric acid to pH 4. The oily product which was thus deposited was extracted twice with 30-m*l* portions of ethyl acetate, and the combined extract was washed with dilute hydrochloric acid and water. The ethyl acetate layer was dried over anhydrous sodium sulfate. The filtrate was evaporated to dryness to give 13.7 g of an oily residue. The oil was purified by redissolving it in an aqueous solution of sodium hydrogen carbonate and by washing it with ether, followed by a treatment similar to that described above. The oily product thus obtained was triturated with petroleum ether to afford a crystalline solid, which was then recrystallized from ether-petroleum ether to give 12 g (75%) of XI with a melting point of 79°C. Found: C, 65.78; H, 7.70; N, 4.94%. Calcd for $C_{16}H_{23}O_4N$: C, 65.51; H, 7.90; N, 4.78%.

***N*-Benzyloxycarbonyl-*threo*-*N*,*β*-dimethyl-L-leucine·(—)-ephedrine Salt (XIIL) and *N*-Benzyloxycarbonyl-*threo*-*N*,*β*-dimethyl-D-leucine (XIIID).** XI (8.3 g, 0.028 mol) and (—)-ephedrine hemihydrate (2.7 g, 0.0155 mol) were dissolved in 28 m*l* of warming ethyl acetate. The mixture was then allowed to stand for 24 hr at room temperature. The deposited crystals were filtered and washed with ethyl acetate to give 6.1 g (94%) of XIIL; mp 157°C. Recrystallization from an ethyl alcohol-ethyl acetate mixture (1:1) afforded 5.7 g of the pure material with a melting point of 160—161°C, $[\alpha]_D^{24} = -75.0°$ (*c* 0.40, in ethyl alcohol). Found: C, 68.26; H, 8.24; N, 6.27%. Calcd for $C_{26}H_{38}O_5N_2$: C, 68.09; H, 8.35; N, 6.11%.

The mother liquor obtained after the removal of XIIL was washed twice with a small amount of 2N hydrochloric acid and water. The organic layer was dried over anhydrous sodium sulfate. The filtrate was concentrated to dryness to give a crystalline residue in a 94% (3.9 g) yield; mp 90—91°C. Recrystallization from benzene - petroleum ether afforded 3.4 g of almost optically-pure XIIID; mp 94—95°C, $[\alpha]_D^{24}=+72°$ (*c* 1.00, in ethyl alcohol).

***N*-Benzyloxycarbonyl-*threo*-*N*,*β*-dimethyl-D-leucine•(+)-ephedrine Salt (XIID).** To a solution of 0.70 g (0.0024 mol) of XIIID ($[\alpha]_D^{24}=+72°$) in 1.5 m*l* of ethyl acetate, there was added a solution of 0.42 g (0.0024 mol) of (+)-ephedrine hemihydrate in 1.0 m*l* of ethyl acetate. The mixture was set aside for 24 hr at room temperature, and then the crystals deposited were filtered, washed with ethyl acetate, and dried to afford XIID (mp 155—157°C) in an 89% (0.975 g) yield. Recrystallization from an ethyl alcohol - ethyl acetate mixture (1 : 1) gave crystals with a melting point of 159—160°C and $[\alpha]_D^{25}=+73.5°$ (*c* 0.30, in ethyl alcohol). Found: C, 67.97; H, 8.31; N, 6.16%.

***N*-Benzyloxycarbonyl-*threo*-*N*,*β*-dimethyl-L-leucine (XIIIL).** To a suspension of 4.8 g (0.0105 mol) of the XIIL salt in 15 m*l* of ethyl acetate, there were added 7.8 m*l* (0.0156 mol) of 2N hydrochloric acid (7.8 m*l*, 0.0156 mol), and the mixture was shaken effectively in a separatory funnel. After washing further with water, the ethyl acetate layer was dried over anhydrous sodium sulfate. The ethyl acetate was evaporated to dryness to afford 3 g (98%) of crystals; mp 94—96°C. Recrystallization from benzene - petroleum ether gave 2.8 g of XIIIL with a melting point of 98—99°C, $[\alpha]_D^{26}=-75.9°$ (*c* 1.10, in ethyl alcohol). Found: C, 65.25; H, 7.99; N, 4.89%. Calcd for $C_{16}H_{23}O_4N$: C, 65.51; H, 7.90; N, 4.78%.

***N*-Benzyloxycarbonyl-*threo*-*N*,*β*-dimethyl-D-leucine (XIIID).** Following the method used for the preparation of XIIIL, from 3.2 g (0.007 mol) of XIID, 1.9 g (93%) of XIIID with a melting point of 98—99°C was obtained. $[\alpha]_D^{25}=+75.3°$ (*c* 0.7, in ethyl alcohol). Found: C, 65.72; H, 8.04; N, 4.79%.

***threo*-*N*,*β*-Dimethyl-L-leucine (XIVL).** A) To 1.0 g (0.0034 mol) of XIIIL, 3.5 g of 30% hydrogen bromide in glacial acetic acid was added. The reaction mixture was then set aside in a tight-stoppered vessel for 1 hr at room temperature. There after 30 m*l* of ether were added to complete the precipitation of the product, which was collected on a glass-fritted funnel and washedwith ether. The yield of the hydrobromide was 0.75 g (92%), and its melting point was 209—210°C. Free amino acid XIVL was obtained by treatment with triethylamine in a solution of 4 m*l* of ethyl alcohol, followed by recrystallization from a water - ethyl alcohol mixture (1 : 1). The yield was 0.43 g (86% from hydrobromide), and it had a melting point of over 270°C; $[\alpha]_D^{25}=+38.3°$ (*c* 0.90, in 5N hydrochloric acid), $[\alpha]_D^{23}=+31.5°$ (*c* 0.50, in water). Found: C, 60.39; H, 10.57; N, 8.93%. Calcd for $C_8H_{17}O_2N$: C, 60.34; H, 10.74; N, 8.80%.

B) A solution of 1.0 g (0.0034 mol) of XIIIL in 10 m*l* of glacial acetic acid was hydrogenated using 200 mg of palladium black as a catalyst under mechanical shaking for 5 hr. After the catalyst had then been removed by filtration, the filtrate was evaporated to dryness to give a crystalline residue and dried in a vacuum desiccator over concentrated sulfuric acid and solid sodium hydroxide. The residue was recrystallized from water and dioxane to give 0.47 g (87%) of XIVL with a melting point of over 270°C; $[\alpha]_D^{25}=+37.3°$ (*c* 0.70, in 5N hydrochloric acid), $[\alpha]_D^{23}=+29.1°$ (*c* 0.90, in water).

***threo*-*N*,*β*-Dimethyl-D-leucine (XIVD).** A way similar to the method A) used in the preparation of XIVL was used. From the reaction of 1.0 g (0.0034 mol) of XIIID and 3.5 g of 30% hydrogen bromide in glacial acetic acid, followed by neutralization with amine, XIVD with a melting point of over 270°C was obtained in almost the same yield. $[\alpha]_D^{25}=-39.3°$ (*c* 0.60, in 5N hydrochloric acid), $[\alpha]_D^{25}=-31.8°$ (*c* 0.40, in water). Found: C, 60.56; H, 10.63; N, 9.01%.

***N*-Benzyloxycarbonyl-*erythro*-*β*-methyl-DL-leucine (XV).** By the usual method of Schotten-Baumann, a pure product with a melting point of 62—64°C was obtained from VII in an 84% yield. The recrystallization was performed from benzene-petroleum ether. Found: C, 64.37; H, 7.42; N, 5.18%. Calcd for $C_{15}H_{21}O_4N$: C, 64.49; H, 7.58; N, 5.01%.

***N*-Benzyloxycarbonyl-*erythro*-*β*-methyl-L-leucine-(−)-ephedrine (XVIL) and *N*-Benzyloxycarbonyl-*erythro*-*β*-methyl-D-leucine•(+)-ephedrine (XVID).** To a solution of 5.58 g (0.02 mol) of XV in 6.0 m*l* of ether, there was added a solution of 1.91 g (0.011 mol) of (−)-ephedrine hemihydrate in 4.0 m*l* of ether. The reaction mixture was then allowed to stand overnight in a refrigerator to form a gelatinous material. The product was collected by filtration after it had been crushed to pieces with a glass rod and a small amount of ether had been added. A somewhat crude (−)-salt (1.6 g) (mp 120—124°C) was thus obtained. The ethereal mother liquor was washed wih 2N hydrochloric acid and then with water, and dried over anhydrous sodium sulfate. The ethereal solution was evaporated to dryness under reduced pressure; then the residue thus obtained was redissolved in 6.0 m*l* of ether. To the solution, there was added a solution of 1.91 g of (+)-ephedrine hemihydrate in 4.0 m*l* of ether. Then (+)-salt (1.4 g) (mp 124—125°C) was obtained by a way similar to that described above. The same treatment was possible again reciprocally with (−)- and (+)-ephedrine hemihydrate. Optically-active (−)-salt consisting of (−)-ephedrine was combined and recrystallized from ethyl acetate to give 2.0 g (45%) of a pure material with a melting point of 124—125°C; $[\alpha]_D^{25}=-17.6°$ (*c* 0.74 in ethyl alcohol). Found: C, 67.50; H, 8.09; N, 6.28%. Calcd for $C_{25}H_{36}O_5N_2$: C, 67.54; H, 8.16; N, 6.30%.

In the same way, optically-pure (+)-salt with a melting point of 124—125°C was obtained in a 49.5% (2.2 g) yield; $[\alpha]_D^{25}=+17.7°$ (*c* 0.95 in ethyl alcohol). Found: C, 67.60; H, 8.14; N, 6.32%. The mixed-melting-point of minus and plus salt was depressed to 101—104°C.

***erythro*-*β*-Methyl-L-leucine (XIIL) and the D-Isomer (XIID).** To a suspension of 1.9 g (0.0034 mol) of (−)-salt in 10 m*l* of ethyl acetate, there were added 3.4 m*l* of 2N hydrochloric acid; then the mixture was shaken in a separatory funnel. The organic layer was treated as usual to give 1.3 g of an oily residue. The oil was dissolved in 3.4 g of 30% hydrogen bromide in glacial acetic acid, after which the mixture was allowed to stand for 1 hr at room temperature and then

for 24 more hour in a refrigerator after the addition of 100 m*l* of ether. The deposited crystals were collected by filtration on a glass-fritted funnel and washed with ether. Recrystallization from ethyl alcohol and ether afforded a pure material with a melting point of 195—196°C in a 69% (0.66 g) yield. Similarly, from 2.18 g of (+)-salt D-isomer hydrobromide was obtained in a 73% (0.8 g) yield; mp 203—205°C. A solution of 0.6g of hydrobromide of the L-isomer in ethyl alcohol was neutralized with triethylamine. The crystals thus obtained were collected and recrystallized from water and dioxane to give 0.28 g (73% from hydrobromide) of the amino acid XVIIL; $[\alpha]_D^{24}=+38.9°$ (*c* 0.485, in 5N hydrochloric acid), $[\alpha]_D^{25}=+29.7°$ (*c* 0.37, in water). Found: C, 57.92; H, 10.38; N, 9.70%. From 0.65 g of the hydrobromide of the D-isomer, free amino acid XVIID was obtained in a 67% (0.3 g) yield; $[\alpha]_D^{25}=-39.4°$ (*c* 0.38, in 5N hydrochloric acid). Found: C, 57.82; H, 10.34; N, 9.62%.

***erythro*-*N*,*β*-Dimethyl-L-leucine (XVIIIL) and the D-Isomer (XVIIID).** The methylation of the amino groups of XVIIL and XVIID was accomplished, step by step, by *N*-benzylation, *N*-methylation, and subsequent catalytic hydrogenolysis, in a way similar to that used for the corresponding racemic *threo*-isomer. *N*-Benzyl-L-isomer: mp 218—219°C, 74% yield. Found: C, 71.62; H, 8.95; N, 5.82%. *N*-Benzyl-D-isomer: mp 218—219°C, 43% yield. Found: C, 71.70; H, 8.93; N, 6.03%. The mixed-melting-point of the two isomers was depressed to 208—210°C. *N*-Benzyl-*N*-methyl-L-isomer: mp 102—105°C, 68% yield. Found: C, 72.41; H, 9.08; N, 5.60%. *N*-Benzyl-*N*-methyl-D-isomer: mp 102—105°C, 74% yield. Found: C, 72.20; H, 9.40; N, 5.55%. The mixed-melting-point of these two isomers was depressed to 76—80°C. *erythro*-*N*,*β*-Dimethyl-L-leucine: mp>270°C, 51% yield; $[\alpha]_D^{25}=+38.0°$ (*c* 0.50, in 5N hydrochloric acid). Found: C, 60.52; H, 10.48; N, 8.91%. *erythro*-*N*,*β*-Dimethyl-D-leucine: mp >270°C, 52% yield; $[\alpha]_D^{25}=-38.3°$ (*c* 0.60, in 5N hydrochloric acid). Found: C, 60.18; H, 10.51; N, 8.76%.

BULLETIN OF THE CHEMICAL SOCIETY OF JAPAN VOL. 42 1373—1377 (1969)

Studies on Telomerization of Vinyl Chloride with Carbon Tetrabromide

Teruzo ASAHARA and M. C. CHOU

Institute of Industrial Science, The University of Tokyo, Roppongi, Minato-ku, Tokyo

(Received September 11, 1968)

The radical telomerization of vinyl chloride with carbon tetrabromide was investigated. The telomers with $n=1$ and 2 in $Br(CHClCH_2)_nCBr_3$ were isolated and identified. The molecular weight distribution of the telomers was determined by thin-layer chromatography (TLC), and it was found that the distribution varied a little with the variation of reaction conditions. From the results of the TLC, the chain transfer constants (C_n) of polylvinyl chloride radical to carbon tetrabromide were calculated, and a monotonous increase in C_n with the increasing n was found. The effects of initial ratio of vinyl chloride to carbon tetrabromide, reaction time and temperature on the conversion of vinyl chloride and the average molecular weight of the telomer were investigated. Bromoform was also used as a telogen instead of carbon tetrabromide, and the results were compared in both systems.

There are few studies on telomerization of vinyl chloride as a taxogen. Akiyoshi *et al.*[1] carried out this reaction using carbon tetrachloride as a telogen and the formation of telomers with 1:1 and 1:2 of the ratio of telogen to taxogen was confirmed. Ali *et al.*[2] investigated this reaction using carbon tetrabromide as a telogen, but liquid telomers were not obtained, probably because the amount of the chain transfer agent was low in this investigation. In order to confirm further the possibility of the preparation of oligo (vinyl chloride), the present investigation was designed under the various reaction conditions such as telogen-taxogen ratio, reaction time and temperature. Further, the separation of products by means of thin-layer chromatography was undertaken. The result will be presented in this paper.

Experimental

Materials. Vinyl chloride was purified by washing with a 30% KOH aqueous solution and drying over calcium chloride. Carbon tetrabromide was prepared from the reaction of acetone and bromine in potassium

1) S. Akiyoshi, T. Aso and S. Imoto, *Kogyo Kagaku Zasshi* (*J. Chem. Soc. Japan, Ind. Chem. Sect.*), **57**, 58 (1954).

2) D. Ali, H. F. Mark and R. B. Mesrobian, *Ind. & Eng. Chem.*, **42**, 484 (1950).

Table 1. Properties of monomer and dimer

	Monomer (n=1)				Dimer (n=2)			
Mol wt	390 (calcd 395)				460 (calcd 457)			
bp	80—87°C/2 mmHg				120—125°C/2 mmHg			
n_D^{27}	1.6490				1.6948			
	(%)				(%)			
Anal.	C	H	Cl	Br	C	H	Cl	Br
Calcd[a)]	9.14	0.76	8.99	81.1	13.15	1.32	15.53	69.99
Found	9.23	0.78	8.98	81.0	13.36	1.48	15.46	69.70

a) Calculated for $Br_3C(CH_2CHCl)Br$ and $Br_3C(CH_2CHCl)_2Br$.

hydroxide solutions and purified by recrystallization. α,α′-Azobisisobutyronitrile was purified by recrystallization from methanol before use.

Telomerizations. Into a glass ampoule with a 100 m*l* capacity, definite amounts of carbon tetrabromide and ABIN were taken and a definite amount of vinyl chloride was charged while cooling in dry ice and then sealed. Reactions were carried out in a reaction oven at a given temperature, being shut from light.

Analyses of Products. After the reaction, unreacted vinyl chloride was removed initially at room temperature under atmospheric pressure and completely under reduced pressure. The number-average molecular weights of the products (telomers) were measured cryoscopically. The lower telomers were separated with distillation and the lower and higher telomers were separated by thin-layer chromatography on silica gel.

Results and Discussions

Separation and Identification of Reaction Products. Residues of reaction mixtures after removing the unreacted vinyl chloride are colorless at lower molar ratio, vinyl chloride/carbon tetrabromide, and pale yellow or brown at higher ratios, higher temperatures and prolonged reaction time. However, it is considered that the main components of the residues are telomers of vinyl chloride and carbon tetrabromide, with a small amount of complicated products resulting from the initiator, because the measured mean molecular weights of the residues are in good agreement with those calculated from the results of quantitative analyses of telomers, as will be shown later.

Two fractions were obtained with the distillation at 2 mmHg. Properties of these products are shown in Table 1. From these results and NMR spectra (Fraction 1, 4.0 and 5.9 ppm; Fraction 2, 3.9, 5.7, 6.3 and 7.1 ppm) and IR spectra (CBr; 610; CBr_3, 630; CCl, 685 cm^{-1}), it was confirmed that these fractions are the telomers, $Br(CHClCH_2)_n$-CBr_3, with n=1 and 2 respectively.

Separation of telomers higher than n=3 was impossible by distillation, for they are unstable at elevated temperatures. Thus thin-layer chromatographic separation was carried out. Thin plates (size 20×20 cm^2, depth 0.15 mm) were prepared of Silica Gel G (Merck) and the spots of product mixtures (0.01—0.03 m*l*) were developed with cyclohexane-chloroform (8: 1.5 by volume) on the vertical plates. Detection of developed spots was made by exposure with iodine vapor or by carbonization with 50% sulfuric acid. The results of the TLC analysis are shown in Table 2, in terms of R_f

Table 2. R_f and R_m values of telomer mixture

Spot	R_f	R_m
1	0.837	−0.710
2	0.740	−0.460
3	0.641	−0.250
4	0.530	−0.052
5	0.409	0.160
6	0.287	0.359
7	0.222	0.545

(the ratio of the origin-spot distance to the origin-developing front distance) and $R_m=\log(1/R_f-1)$. It was confirmed from the development of authentic samples that the spots 1 and 2 are the telomers of n=1 and 2, respectively. Although direct identification of the other spots is impossible, it is plausible that they are the telomers with successively increasing n, for the linearity is found between R_m values and spot numbers. Thus, the spots 1, 2, 3, ··· would be assigned to be telomers

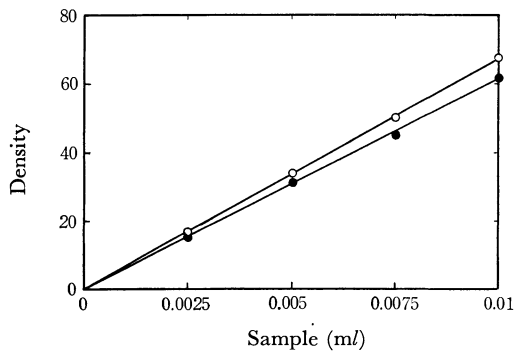

Fig. 1. Relationship between the amounts of telomers and the TLC densities.
○ n=2 telomer; ● n=3 telomer

with $n=1, 2, 3, \cdots$, respectively.

The coloration of spots carbonized with 50% sulfuric acid was measured quantitatively by a TLC densitometer (Seikyo Rika SS-7). The calibration curves for telomers with $n=2$ and 3 were obtained by using the samples separated by distillation as shown in Fig. 1. For the other telomers, it was assumed that the absorption density per mole is proportional to the carbon number in each molecule. This seems to be plausible for molecules in a homolog. The average molecular weights calculated from the results of TLC analysis agree well with the average molecular weights measured cryoscopically.

Effects of Reaction Conditions. From the analyses of the reaction product, it is considered that the telomerization of vinyl chloride with carbon tetrabromide takes place in the present reaction system. Thus, the reaction scheme would be as follows.

$$CBr_4 + R\bullet \rightarrow \bullet CBr_3 + RBr$$

$$\bullet CBr_3 + nCH_2{=}CHCl \rightarrow CBr_3(CH_2CHCl)_{n-1}CH_2\dot{C}HCl$$

$$CBr_3(CH_2CHCl)_{n-1}CH_2\dot{C}HCl + CBr_4 \rightarrow CBr_3(CH_2CHCl)_nBr + \bullet CBr_3$$

$$CBr_3(CH_2CHCl)_n\bullet + CBr_3(CH_2CHCl)_m\bullet \rightarrow CBr_3(CH_2CHCl)_{n+m}CBr_3$$

Total yields, average molecular weights and molecular weight distribution of the telomers are mainly affected by the experimental factors such as the molar ratio of vinyl chloride to carbon tetrabromide, reaction time and temperature. The results for these examinations are summarized in Table 3.

As is expected from the reaction scheme, the conversion of vinyl chloride decreases and the average n value increases with the increasing molar ratio. The increasing reaction time results in slight increases in the conversion and the average n value. Moreover, the increasing temperatures are followed by decreases in the conversion and the average n value. This might be due to the increasing reactivity in telogen molecules at higher temperatures. These results are plausible from the reaction scheme and characterize the telomerization reaction. It should be cited that Bengough *et al.*[3] investigated the telomerization reaction of vinyl chloride and bromotrichloromethane (TBr) and obtained the 1:1 adduct at the molar ratio of vinyl chloride to TBr lower than 10.

Table 3. Telomerization of vinyl chloride and carbon tetrabromide

No.	Mol ratio[a]	Time (hr)	Temp. (°C)	Conversion of V.C. (%)	Av. mol wt	$\bar{n}$
1	3	5	60	65.0	470	2.2
2	3	5	60	65.2	471	2.2
3	5	5	60	42.5	489	2.5
4	5	5	60	42.1	487	2.5
5	10	5	60	39.0	530	3.2
6	10	5	60	39.2	530	3.2
11	3	1	60	50.5	443	1.8
12	3	1	60	50.0	442	1.8
13	3	3	60	56.3	456	2.0
14	3	3	60	56.0	452	2.0
15	3	5	60	60.9	469	2.2
16	3	5	60	60.5	465	2.2
21	3	3	60	56.3	457	2.0
22	3	3	60	56.5	457	2.0
23	3	3	80	51.0	450	1.9
24	3	3	80	51.2	451	1.9
25	3	3	100	47.9	442	1.8
26	3	3	100	48.0	441	1.8

a) Molar ratio of vinyl chloride to carbon tetrabromide.

Molecular Weight Distribution. The regulation of molecular weight distribution is essentially important for practical purposes. This is difficult in the present stage but the examination was made to get the information for the effect of reaction conditions. The results at various molar ratios of vinyl chloride to carbon tetrabromide are shown in Table 4. The yield in the mole unit decreases when n increases. This is expected in general for the telomerization where the content of telogen is high. When vinyl chloride/carbon tetrabromide is 3, the telomers with $n=1$—6 are obtained and the higher telomers are formed when the molar ratio

Table 4. Distribution of degree of polymerization

Mol ratio[a]	Mol% of telomers with n mol units of V.C.							
	1	2	3	4	5	6	7	Others
3	35.34	26.15	25.44	9.54	3.20	0.33	0	0
5	41.50	28.00	25.50	8.25	2.25	1.90	—	3.10
10	30.64	20.83	17.46	10.15	5.51	4.65	3.67	7.09

a) Molar ratio of vinyl chloride to carbon tetrabomide.

3) W. I. Bengough, R. A. M. Thomson, *Trans. Faraday Soc.*, **61**, 1735 (1965).

Table 5. Distribution of degree of polymerization at low conversions

Mol ratio[a)]	Reaction time (hr)	Mol% of telomers with n mol units of V.C.					
		1	2	3	4	5	6
2	1	53.35	35.57	10.10	1.20	0	0
2.2	1	48.20	32.77	15.20	3.18	0.39	0.26
2.5	1	45.12	31.11	15.20	3.89	0.60	0.08
4	0.5	44.21	31.13	17.49	5.79	1.21	0.18
10	0.5	35.43	26.24	17.49	8.75	3.12	0.79

a) Molar ratio of vinyl chloride to carbon tetrabromide.

becomes high. However, the yield of the telomer with $n=1$ is always the largest. When the reaction time is prolonged, the distribution extends to higher telomers. The main products are the telomers with $n=1$ and 2 at the molar ratio 3, 1 hr and 60°C. When the reaction temperature is higher, the distribution shifts into lower telomers. Thus, at the molar ratio 3 and the reaction time 3 hr, he telomers with $n=1$—7, $n=1$—5 and $n=1$—3 are formed at 60, 80 and 100°C, respectively.

It was, therefore, found that the selective formation of the telomer with $n=1$, *i. e.*, Br_3CCH_2CHCl-Br, is possible in the present reaction system under the conditions of the lower mole ratio, vinyl chloride/carbon tetrabromide, shorter reaction time and higher temperature, but the selective formation of the telomers with medium adduct numbers of vinyl chloride is impossible under the reaction conditions examined in the present investigation.

Chain Transfer Constants. The chain transfer constants C_n of poly(vinyl chloride) radicals CBr_3-$(CH_2CHCl)_n^{\cdot}$ to carbon tetrabromide were calculated from the Mayo equation

$$\frac{F_n}{F_{n+1}} = C_n\frac{[S]}{[M]} + \frac{C_n}{C_{n+1}},$$

where F_n is the mole number of active species $CBr_3(CH_2CHCl)_n^{\cdot}$, [S] and [M] are molar concentrations of carbon tetrabromide and vinyl chloride respectively. The conversion must be depressed for the successful use of this relationship. In order to satisfy this requirement and get a wider distribution of molecular weight, experimental data were obtained at the higher mole ratios and the shorter reaction time, the results of which are presented in Table 5. The chain transfer coefficients thus obtained are listed in Table 6. A monotonous increase in C_n with the increasing n is found. This result is consistent with ones obtained by Lewis and Mayo,[4] in different reaction systems and may be attributed to the inductive effect

Table 6. Chain transfer constants

C_1	C_2	C_3	C_4
0.33	1.85	7.45	12.15

Table 7. Telomerization of vinyl chloride with bromoform

Mol ratio[a)]	Time (hr)	Temp. (°C)	Conversion of V.C. (%)
0.3	3	60	61.5
0.5	3	60	51.5
1.0	0.5	60	24.1
1.0	1	60	26.5
1.0	2	60	30.0
1.0	3	60	34.4
1.0	3	80	25.8
1.0	3	100	18.0
1.0	5	60	55.9
2.0	3	60	50.0

a) Molar ratio of vinyl chloride to bromoform.

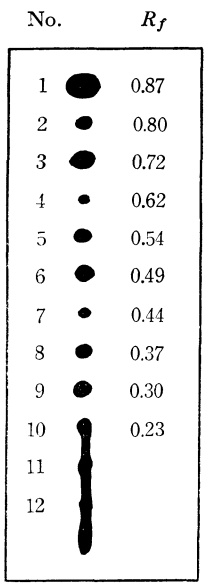

Fig. 2. Thin-layer chromatogram of the telomerization product of vinylchloride and bromoform.

4) F. M. Lewis and F. R. Mayo, *J. Am. Chem. Soc.*, **76**, 457 (1954).

of the CBr_3 group as suggested by Walling[5] and Karapetyan.[6]

Telomerization of Vinyl Chloride - Bromoform. Using bromoform instead of carbon tetrabromide as telogen, the telomerization of vinyl chloride was carried out under similar conditions and the results are compared in both systems. The experimental conditions and results are summarized in Table 7.

It was found from the results that both systems show a similar behavior when the taxogen/telogen ratio is lower than unity. That is to say, the conversion of vinyl chloride decreases when the mole ratio increases, the reaction time shortens, and temperature becomes higher. However, when the taxogen/telogen ratio increases over unity, the solid product is formed in a small amount and the conversion increases, making a minimum around unity. The solid product is confirmed to be poly(vinyl chloride). Further, a complicated pattern was found when the product mixture was developed by the thin-layer chromatography. A typical example is shown in Fig. 2. These results are interpreted from the possibilities that the chain transfer of the growing ends is not feasible to bromoform in comparison with carbon tetrabromide and the subtraction by the initiator and growing end radicals takes place at the two alternative positions of bromoform, *i. e.*, H-subtraction and Br-subtraction. For a detailed discussion, identification of products and further examinations under various conditions are necessary and are now in progress.

5) C. Walling, "Free Radicals in Solution," John Wiley and Sons, New York (1957), p. 257

6) Sh. A. Karapetyan, *Izv. Akad. Nauk*, **1963**, 1346.

BULLETIN OF THE CHEMICAL SOCIETY OF JAPAN VOL. 42 1377—1379 (1969)

Photooxidation of Anthracene*1

Noboru SUGIYAMA, Masaaki IWATA, Michikazu YOSHIOKA,*2 Kazutoshi YAMADA*3 and Hiromu AOYAMA

Department of Chemistry, Tokyo Kyoiku University, Otsuka, Bunkyo-ku, Tokyo

(Received September 12, 1968)

It was found that anthracene (I) was converted to 9,10-anthraquinone (III) and bianthrone (IV) by irradiation *via* anthracene peroxide (II). The reaction proceeded most effectively in carbon disulfide. Also IV was found to be oxidized to III by oxygen in singlet state.

Many reports on the photochemical oxidation of anthracene (I) and its derivatives have been found in literature. Among the photooxidation products of I, its dimer, anthraquinone (III), and anthracene peroxide (II)[1-8] have been reported. We have found that I afforded bianthrone (IV) beside III, the yield being 29% for IV and 21% for III. We have also found that the irradiation of II gave III and IV. This paper deals with the experiments on the formation of III and IV by the photoreaction of I or II, and the intermediacy of II, as well as the photochemical formation of III from IV.

Results and Disscution

When a solution of I in carbon disulfide was irradiated at room temperature with a 500 W high-pressure mercury lamp for 50 hr, five new spots appeared on thin-layer chromatography. These spots showed R_f values of 0.60 (A), 0.54 (B),

*1 *Chem. Commun.* (*London*), in press as short communication.

*2 Present address: Department of Chemistry, Saitama University, Urawa, Saitama.

*3 Present address: Department of Synthetic Chemistry, Chiba University, Chiba.

1) C. Dufraisse and M. Gerard, *Bull. Soc. Chim. France*, **4**, 2052 (1937).

2) C. Dufraisse and M. Gerard, *Compt. rend.*, **201** 428 (1935).

3) G. O. Schenck, *Naturwiss.*, **41**, 452 (1953): *Chem. Abstr.*, **49**, 10068e and his papers.

4) C. S. Foote and S. Wexler, *J. Am. Chem. Soc.*, **86**, 3879 (1964).

5) E. J. Corey and W. C. Taylor, *ibid.*, **86**, 3881 (1964).

6) E. J. Bowen and D. W. Tanner, *Trans. Faraday Soc.*, **51**, 475 (1955).

7) C. S. Foote, S. Wexler, W. Ando and R. Higgins, *J. Am. Chem. Soc.*, **90**, 975 (1968).

8) G. O. Schenck, *Pure Appl. Chem.*, **9**, 507 (1964).

0.43 (C), 0.33 (D), and 0.00 (E), respectively. The products A and B were isolated from the irradiation mixture by silica gel column chromatography. The product A was identified with authentic 9,10-anthraquinone (III) by IR and UV spectra, and mixture melting point. The product B, $C_{28}H_{18}O_2$, showed UV absorption maxima (ε) at 267(26700), 297(8700), and 315(5800) nm, and IR absorption bands at 1658, 1348, 1318 (one strong peak), and 690 cm^{-1}. The NMR spectrum of B showed signals in $CDCl_3$ at 4.74 (singelt), 6.80 (multiplet) and 7.90 (multiplet) at δ from TMS. The mass spectrum of B showed a parent peak at 386 *m/e* and base peak at 193 *m/e* (just half of the parent *m/e*). These physical data, elemental analysis and properties of IV described by Friend and co-worker[9] strongly suggested that B was 10,10′-bianthronyl(bianthrone) (IV).

In order to confirm the intermediacy of II in the photooxidation of I to III and IV, the authentic sample of II[7] saturated in carbon disulfide was irradiated. The reaction was followed at intervals by thin-layer chromatography. After 18 hr irradiation, III and IV were detected. The fact indicates that II is an intermediate in the photooxidation of I.

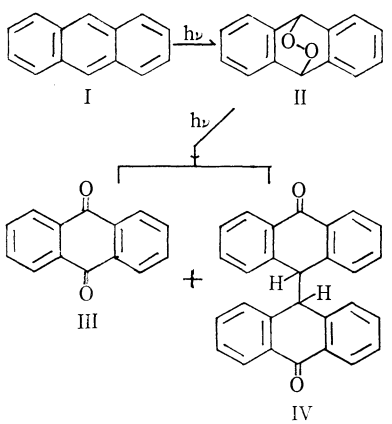

Scheme I

When an acetone solution of I was irradiated for an hour, only II was detected. The irradiation of the same solution for 50 hr gave only III. When a benzene solution of I was irradiated for an hour, II was detected. But if the irradiation period was prolonged for 50 hr, III with other products detected, but not IV.

In the case of the irradiation in ethanol solution, neither II, IIII nor IV was detected. Consequently, the photochemical reaction in an alcohol solution seems to be different from those in the other three solutions.

When a dioxane solution of IV was kept under a scattered light for 10 days, IV was quantitatively converted to III. If the solution was protected from any light with or without bubbling with oxygen, no reaction was observed.

Corey and Taylor[5] reported that I is converted to II with singlet excited O_2 produced by the method of Foner and Hudson.[10] Our experiment shows that IV is converted to III, and this conversion seems to be promoted by visible light. In fact, when IV in a dioxane solution was irradiated with 125 W high-pressure mercury lamp, III was not detected. Therefore, the formation of III from IV might be based on the photooxidation of IV with singlet excited O_2 corresponding to the excitation energy, $^1\Delta_g$ 0.977 eV (12700 Å) and $^1\Sigma_g$ 1.63 eV (7630 Å).[5] The excited oxygen might add to C_{10} and $C_{10'}$ position of IV with elimination of hydrogen to make V as intermediate, and the cleavage of O–O bond and C–C bond of V will take place between C_{10} and $C_{10'}$ position to give III.

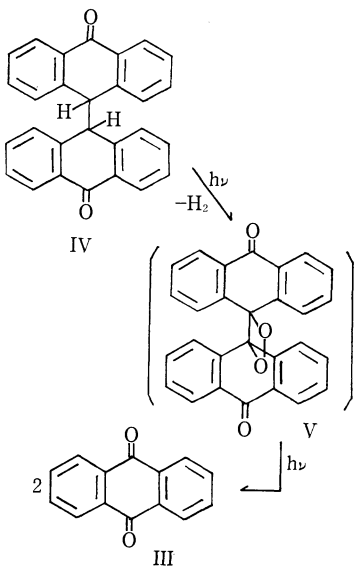

Scheme II

Charier and Crippa[11] reported that I in acetic acid containing hydrogen peroxide, as oxidant, was converted to IV accompanying other products by sun-light irradiation for 60 hr. Our result shows that I is oxidized to III and IV without oxidant in fairly good yield, 29%. The qualitative studies of the solvent effect showed that carbon disulfide promoted most effectively the formation of IV. This suggests that the CS radical produced

9) K. E. Friend and W. E. Ohnesorge, *J. Org. Chem.*, **28**, 2435 (1963).

10) S. N. Foner and R. L. Hudson, *J. Chem. Phys.*, **25**, 601 (1956); *ibid.*, **23**, 1974 (1955).

11) G. Charier and G. B. Crippa, *Gazz. Chim. Ital.*, **57**, 741 (1927).

effectively by irradiation on CS_2 with Hg-vapor lamp,[12] plays an important role for cleavage of the O-O bond of II. Without CS radical II converts solely to III, as in the case of acetone and benzene solutions. This interpretation may be supported by the fact that no formation of III or IV in alcohol solution was detected.

Experimental

As a light source, a Daika 500 W high-pressure mercury lamp was used for the irradiation experiment in carbon disulfide, benzene or ethanol, and a Toshiba 110 V 200 W lamp for the preparation of anthracene peroxide. All solvents were freshly distilled before use. Anthracene was recrystallized twice from benzene.

Anthracene Peroxide (II). The method by Foote *et al.*[7] was modified. A solution of anthracene (0.54 g, 0.003 mol) and methylene blue (50 mg) in 250 m*l* of chloroform was placed in hydrogenation apparatus filled with O_2 gas and irradiated with stirring for 3 hr. The solution temperature was kept below 15°C during the irradiation. The consumed O_2 volume was 43 m*l* (0.00244 mol). The solution was passed through the column of silica gel (Kieselgel, Merck) to remove methylene blue. The colorless solution was obtained and evaporated to dryness under reduced pressure. The residue was chromatographed over silica gel with benzene to give 0.17 g of II, mp 146—147°C, R_f 0.34 (silicagel-benzene), IR (KBr disk) 1460, 1170, 950, 770 and 720 cm^{-1}, UV λ_{max} (Dioxane) (log ε) 270 (2.9) and 278 (2.8) nm.[7,13]

Irradiation of (II) in Carbon Disulfide. A saturated solution of II in carbon disulfide (about 10^{-2} mol/*l*) was sealed in a Pyrex tube and irradiated with a high-pressure mercury lamp for 18 hr. The reaction mixture was chromatographed on silica gel. When benzene (50 m*l*) was passed through the column, 9,10-anthraquinone (III) was eluted. Then the mixture of benzene and ethyl acetate (7:3) was passed through, bianthrone (IV) was eluted. III and IV were respectively identified with an authentic sample by mp, IR, UV, and R_f.

Irradiation of Anthracene (I) in Carbon Disulfide. The saturated solution of I (about 4 g) in 150 m*l* of carbon disulfide was irradiated with the high-pressure mercury lamp for an hour. The thin-layer chromatography of an aliquot from the reaction mixture showed a new spot at R_f 0.39 (benzene), corresponding to that of II. After irradiation for 50 hr, five new spots appeared on the thin-layer chromatogram (benzene-ethyl acetate 7 : 3), while the spot of II could not be found. The reaction mixture was evaporated to dryness, *in vacuo*, and 3.5 g of the mixture was obtained. The mixture (0.3 g) was dissolved in benzene and chromatographed on 20 g of silica gel. The first elution by benzene (120 m*l*) gave 0.063 g (21%) of product A (R_f, 0.62, benzene-ethyl acetate 7:3). The second elution by benzene - ethyl acetate (9:3) gave 0.079 g (29%) of product B (R_f 0.54, benzene-ethyl acetate 7 : 3). Other products, C (R_f 0.43), D (R_f 0.33) and E (R_f 0.00), were also obtained.

The product A showed IR absorption at 1675 (>C=O), 1596 (>C=C<, aromatic), 1355, 1320, 1306, 1285 (=>C=O), and 690 (adjacent four protons of aromatic nuclei) cm^{-1}, UV absorption maxima at 252, 263, 272 and 325 nm in ethanol, and mp 272—282°C. These data were in accord with those of authentic 9,10-anthraquinone (III).[14]

The product B, recrystallized from benzene, light yellow needles, darkened at about 190°C and melted at 250—252°C (decomposition).

Found: C, 86.52; H, 4.66%. Calcd for $C_{28}H_{18}O_2$: C, 87.02; H, 4.69%. UV: λ_{max}^{EtOH} (ε) at 267 (26700), 297 (8700) and 315 (5800) nm, IR: ν_{max}^{KBr} cm^{-1} at 1658 (>C=O), 1600 (>C=C<, aromatic), 1348, 1312 (=>C=O), and 690 (adjacent four protons of aromatic nuclei). NMR: δ^{CDCl_3}, four kinds of signal at 4.74 (s, 2H, 10,10′-protons), 6.80 (m, 4H, 4,4′,5,5′-protons), 7.34 (m, 8H, 2,2′,3,3′,6,6′,7,7′-protons), and 7.90 (m, 4H, 1,1′,8,8′-protons). The mass spectrum gave parent peak at 386 *m/e* and base peak at 193 *m/e* (just half of the parent *m/e*).

Irradiation of I in Acetone. I (0.2 g) dissolved in acetone (14 m*l*), was irradiated at room temperature. In an hour, only the spot of R_f 0.34 (benzene) was detected, and after 50 hr, this spot completely disappeared and the spot of R_f 0.62 (benzene-ethyl acetate 7 : 3) appeared, indicating that II changed into III.

Irradiation of I in Benzene. I (0.2 g) dissolved in benzene (20 m*l*) was irradiated. In an hour, the spot of R_f 0.34 (benzene) was detected, and after 50 hr, five spots appeared, including a small spot of R_f 0.62 (benzene-ethyl acetate 7:3), corresponding to that of III.

Irradiation of I in Ethanol. As I was sparingly soluble in ethanol, the mixture of I and ethanol (60 m*l*) was stirred at boiling point. After the solution was placed for 24 hr at ordinary temperature, the excess of I was filtered and the filtrate was irradiated for 3 hr. II, III or IV was not detected, while the fluorescent of I disappeared.

Irradiation of Bianthrone (IV) in Dioxane. IV (1.3 mg) was dissolved in dioxane (200 m*l*) and the solution was allowed to stand. After 10 days, the UV spectrum showed that IV changed into III and the spot of R_f 0.62 (benzene-ethyl acetate 7:3) was detected. When intercepted from any light with or without oxygen, the reaction from IV to III did not take place.

12) W. Doran and A. E. Gillan, *J. Soc. Chem. Ind.*, **47**, 259T (1928), for example.

13) I. Gillet, *Bull. Soc. Chim. France*, **1950**, 1135.

14) H. Hartmann, *Z. Naturforsch.*, **7a**, 360 (1952).

BULLETIN OF THE CHEMICAL SOCIETY OF JAPAN VOL 42 1380—1382 (1969)

Reaction of Acyl Oxime with Mercaptan

Rokuro SUDO, Akira KANEDA and Nobuo FURUOYA

Laboratory of Organic Chemistry, Tokyo Institute of Technology, Meguro-ku, Tokyo

(Received September 14, 1968)

The acyl derivative of oxime, derived from a strong acid, is generally unstable. However, acyl oximes of the ethyl α-oximinoacetate derivative were prepared and were found to be more stable than ordinary acyl oxime. Acetyl, carbethoxy, benzoyl, and even tosyl ester were prepared, and their reactions with the mercaptide anion were investigated.

In general, acyl derivatives of oxime can be readily isolated as long as the acyl group is not derived from a very strong acid.[1] Recently, however, tosyl ester of α-oximinobenzylcyanide[2] and ethyl α-oximinophenylacetate[3] were found to be more stable than ordinary oxime tosylate. In our study[3] of the nucleophilic attack of the mercaptide anion on the carbon of the C=N function, some acyl esters of ethyl α-oximininopropionate (**1**) and ethyl α-oximinophenylacetate (**2**) were prepared, and their reactions with the mercaptide anion were investigated. The characteristics of these acyl oximes, prepared from the corresponding ethyl α-oximinoacetate derivative and acyl chloride, are summarized in Table 1.

TABLE 1. ACYL OXIMES $R-\underset{\underset{N-OR_1}{\|}}{C}-COOC_2H_5$

R_1	Mp (bp) °C	Yield %	Recryst. solvent	Compound number
R=CH₃				
CH_3CO	113/8 mmHg	47		**3**
C_6H_5CO	55	81	ligroin	**4**
C_2H_5-OCO	136/7 mmHg	86	isopropyl alcohol	**5**
p-$CH_3C_6H_4SO_2$	39	80		**6**
R=C₆H₅				
CH_3CO	145/1 mmHg	75		**7**
p-$CH_3C_6H_4SO_2$	96	35	ethanol	**8**

When acetyl ester (**3**) of ethyl α-oximinopropionate was treated with benzyl mercaptan in benzene, no reaction occurred, but in benzene containing an equivalent amount of triethylamine, it afforded four products: ethyl α-oximinopropionate (**1**), benzyl thioacetate (**9**), ethyl α-benzylsulfeniminopropionate (**11**), and triethylammonium acetate (**12**) (Fig. 1). **11** was characterized by elementary analysis and by a study of its IR and NMR spectra. The IR spectrum had absorptions at 1712 cm^{-1} (C=O of the ester) and at 1586 cm^{-1} (C=N), and the NMR spectrum had a CH_3-singlet at τ 7.88, indicating that the methyl group is attached to carbon, while that of the C=N-CH_3 singlet in the 2-methyliminodithiolane[4] (**13**) is at τ 6.9.

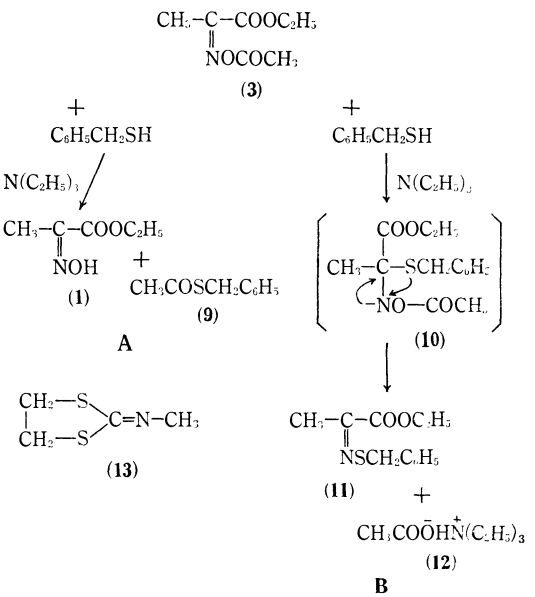

Fig. 1.

Furthermore, the fact that the reaction of this compound with hydrochloric acid in ethanol yielded dibenzyl disulfide (**14**) and ammonium chloride supported the sulfenimino structure of **11**. The presence of **14** and ammonium chloride in the

1) P. A. S. Smith, "The Chemistry of Open-Chain Organic Nitrogen Compounds," Vol. II, W. A. Benjamin, Inc., New York, (1966), p. 46.

2) T. E. Stevens, *J. Org. Chem.*, **28**, 2436 (1963).

3) A. Kaneda, M. Nagatsuka and R. Sudo, This Bulletin, **40**, 2705 (1967).

4) T. Nakai and S. Ohkawara, presented at the 21st Annual Meeting of The Chemical Society of Japan, Okaka, April 1968.

products indicates that the intermediates of the reaction are ethyl α-iminopropionate (**15**) and benzylsulfenchloride (**16**) (Fig. 2).

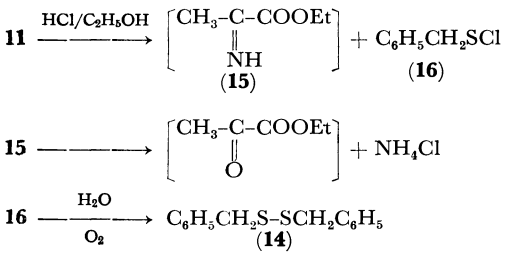

Fig. 2

Thus, acetyl ester of ethyl α-oximinopropionate can be expected to manifest its nucleophilic activity at two sites: at the carbon of the carbonyl in the acyl group, yielding **1** (A route), and at the carbon of the C=N function (B route) yielding ethyl α-benzylmercapto-α-acetoxyaminopropionate (**10**) (B route). **10** seems to have been converted to **11** through a migration of the benzylmercapto group from carbon to nitrogen, accompanied by the elimination of the acetoxy group, instead of through the Beckmann rearrangement, which usually occurs with acyl oxime. Another mechanism is possible, that in which the mercaptide anion attacks nitrogen directly, leading to a nucleophilic substitution. In a similar method, other acyl esters of the ethyl α-oximinoacetate derivative were treated with benzyl mercaptan; these results are summarized in Table 2. In the case of tosyl ester, only the

Table 2. Reaction products of acyl oximes with benzyl mercaptan

R_1 in $R-C(=N-OR_1)-COOC_2H_5$	Products: $R-C(=N-SCH_2C_6H_5)-COOC_2H_5$ %	Products: $R-C(=NOH)-COOC_2H_5$ %
R=CH₃		
H	0	no reaction
CH_3CO	8	69
C_6H_5CO	38	36
C_2H_5OCO	52	23
p-$CH_3C_6H_4SO_2$	quantitative	0
R_1=C_6H_5		
H	0	no reaction
CH_3CO	2	60
p-$CH_3C_6H_4SO_2$	quantitative	0

product from the **B** route was obtained; thus, the reaction with benzyl mercaptan gave the benzylsulfenimino compound, and also ethyl α-ethylsulfeniminopropionate (**17**) with ethyl mercaptan. On the other hand, the ethyl trichloroacetylpropionate **18** and diethyl phosphate **19** of ethyl α-oximinopropionate, which were prepared from **1** and the corresponding acid chloride, were carefully treated with benzyl mercaptan to give the original oxime **1** quantitatively (A route). Because, they appeared to undergo hydrolysis very easily and to give **1**.

It has been reported[3] that the tosyl ester of α-oximinobenzylcyanide (**20**) afforded α-benzylmercapto-α-phenylimino acetonitrile (**21**) through the Beckmann rearrangement in a similar reaction. This is erroneous, for the product was α-benzylsulfeniminobenzyl cyanide (**22**). This compound was very stable even when it was refluxed in an aqueous hydrochloric acid or sodium hydroxide solution, but it was converted to ethyl benzoate, dibenzyl disulfide(**14**), and anmmonium chloride when it was treated with hydrochloric acid in ethanol under cooling. Similarly, the tosyl ester **20′** of ethyl α-oximinophenylacetate afforded ethyl α-benzylsulfeniminophenylacetate (**22′**), which was then converted to ethyl benzoyl formate, dibenzyl disulfide, and ammonium chloride (Fig. 3).

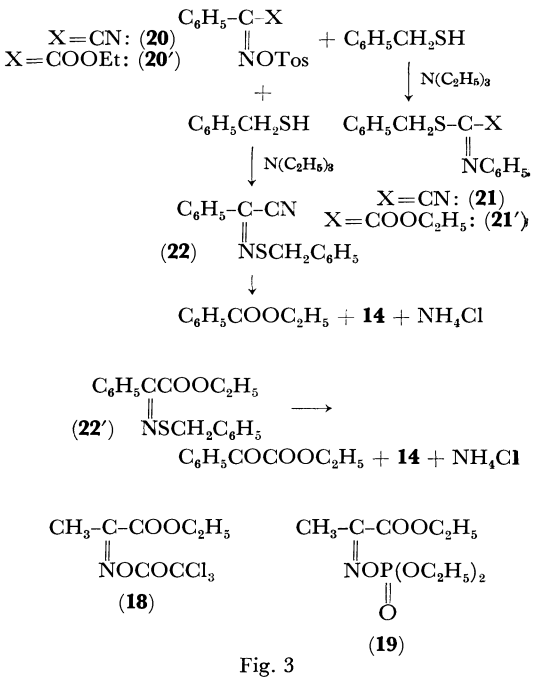

Fig. 3

Experimental

Ethyl α-oximinopropionate (**1**)[5] and ethyl α-oximinophenylacetate (**2**)[6] were prepared by the nitrosation of ethyl α-methylacetoacetate and ethyl phenylacetate; they melted at 96°C and 95—96°C respectively.

Acetylation of the Ethyl α-Oximinopropionate

5) W. Wislicenus, *Ber.*, **42**, 1934 (1909).
6) K. E. Hamlin and W. H. Hartung, *J. Biol. Chem.*, **145**, 355 (1942).

Derivatives (3, 4, 5 and 6). To a solution of 0.1 mol of **1** and 0.1 mol of triethylamine in 50 m*l* of ether there was added 0.1 mol of the corresponding acetyl chloride derivative. The mixture was then refluxed for 2 hr and, after cooling, washed with 50 m*l* of water. The ether solution was concentrated to give a crude product, which was purified by distillation or by recrystallization. The physical constants are summarized in Table 1 and Table 3.

Ethyl α-Acetoximinophenylacetate (7). Sodium salt[3] of **2** (21.5 g, 0.1 mol) was suspended in 50 m*l* of benzene. To this solution, which was stirred vigorously, there was then added, drop by drop, 8 g (0.1 mol) of acetyl chloride under cooling. After the addition had been completed, the mixture was warmed at 40°C for 30 min. After cooling, it was poured into water. The benzene layer was separated and dried over anhydrous sodium sulfate. It was concentrated to give an oil, which was distilled at 145°C/1 mmHg, giving **7**. Yield, 17.7 g (75%).

Tosyl Ester of α-Oximinophenylacetate (8). Sodium salt[3] of **2** (21.5 g, 0.1 mol) was suspended in 50 m*l* of benzene. To this solution, which was stirred vigorously, there were then added, drop by drop, 19 g of *p*-toluenesulfonyl chloride dissolved in 30 m*l* of benzene. After the addition was completed, the mixture was refluxed for 1 hr. After cooling, the mixture was washed with water and was dried over anhydrous sodium sulfate. The mixture was concentrated to give crystals which were recrystallized from ethanol. Mp 95—96°C Yield, 12.1 g (35%). The physical constants of **7** and **8** are listed in Table 1 and Table 3.

TABLE 3. ELEMENTARY ANALYSIS OF ACYL OXIMES

Compound number	Anal. %					
	Calcd			Found		
	C	H	N	C	H	N
R=CH_3						
3	48.55	6.40	8.09	48.46	6.12	8.32
4	61.27	5.57	5.96	61.44	5.68	6.17
5	47.29	6.45	6.89	47.88	6.59	6.47
6	50.52	5.30	4.91	50.63	5.29	5.01
R=C_6H_5						
7	61.27	5.57	5.96	61.45	5.43	6.09
8	58.79	4.93	4.03	58.73	4.89	3.80

Reaction of Ethyl α-Acetoximinopropionate (3) with Benzyl Mercaptan. To a solution of 17.3 g (0.1 mol) of **3** in 50 m*l* of dry benzene containing 10.1 g (0.1 mol) of triethylamine, 12.4 g (0.1 mol) of benzyl mercaptan were added. The mixture was then refluxed for 6 hr. After cooling, water was added to the mixture. The benzene layer was dried over anhydrous sodium sulfate and concentrated under reduced pressure; 50 m*l* of ligroin were then added. The precipitated crystals were collected by filtration and were found to be the original oxime (**1**) by a mixed-melting-point procedure. The ligroin filtrate was concentrated to give an oil, which was then purified by distillation and which was identified as ethyl α-benzylmercaptiminopropionate (**11**), bp 135°C/1 mmHg, mp 36—37°C. The yields of **1** and **11** are listed in Table 2. IR bands (KBr): 1712 cm^{-1} (C=O), 1586 cm^{-1} (C=N). NMR spectrum, $CDCl_3$ (TMS as internal reference): τ 8.69 (3H, triplet) for $-CH_2-C\underline{H}_3$, τ 7.88 (3H, singlet) for $-CH_3$, τ 5.74 (2H, quartet) for $-C\underline{H}_2-CH_3$, and τ 5.57 (2H singlet) for $-C\underline{H}_2-C_6H_5$. In a similar procedure, other acyl oximes, (**4**, **5** and **6**), were treated with benzyl mercaptan; the results are summarized in Table 2.

Ethyl α-Ethylsulfeniminopropionate (17). In a procedure similar to **11**, **6** was treated with ethyl mercaptan and was converted to **17**. **17** was distilled at 103°C/8 mmHg. Yield, 96%. IR bands (NaCl): 1712 cm^{-1} (C=O), 1586 cm^{-1} (C=N); NMR ($CDCl_3$, TMS as the internal reference): τ 8.67 (3H, triplet) for $-COOCH_2C\underline{H}_3$, τ 8.59 (3H, triplet) for $-S-CH_2-C\underline{H}_3$, τ 7.81 (3H, singlet) for $-CH_3$, τ 6.83 (2H, quartet) for $-S-C\underline{H}_2-CH_3$, and τ 5.72 (2H, quartet) for $-COOC\underline{H}_2-CH_3$.

Reaction of Ethyl α-Benzylsulfeniminopropionate (11) with Hydrochloric Acid in Ethanol. The propionate, **11** (11.6 g, 0.05 mol), was added under cooling to 30 m*l* of ethanol containing hydrochloric acid. The solution was then kept at room temperature overnight. The precipitated crystals were collected by filtration and found to be ammonium chloride. Yield, 1.8 g. The filtrate was concentrated to one third of the original volume and kept at room temperature. The precipitated crystals were collected by filtration and found to be dibenzyl disulfide (yield, 7 g) by a mixed-melting-point procedure. The filtrate was concentrated to an oil. The isolation of the product from this oil, by either distillation or recrystallization, was not successful.

Reaction of α-Benzylsulfeniminobenzyl Cyanide (22) with Hydrochloric Acid in Ethanol. In a procedure similar to that described above, **22**[3] was treated with hydrochloric acid. Dibenzyl disulfide and ammonium chloride were obtained, and the final oily residue was distilled to give an oil which was identified as ethyl benzoate by a study of its IR spectrum.

Reaction of Ethyl α-Benzylsulfeniminophenylacetate (22′) with Hydrochloric Acid in Ethanol. In a procedure similar to that used in the reaction of **22**, **22′** [3] was treated with hydrochloric acid to give dibenzyl disulfide, ammonium chloride, and ethyl benzoylformate, which was identified by means of the IR spectrum.

BULLETIN OF THE CHEMICAL SOCIETY OF JAPAN VOL. 42 1383—1386 (1969)

Oligomerization of Isoprene by Hafnium Catalysts

Akira MISONO, Yasuzo UCHIDA, Ken-ichi FURUHATA and Shohei YOSHIDA

Department of Industrial Chemistry, Faculty of Engineering, The University of Tokyo, Hongo, Tokyo

(Received September 17, 1968)

Oligomerization of isoprene by the catalyst system consisting of hafnium(IV) *n*-butoxide and diethylaluminum chloride was studied. Isoprene was oligomerized to a mixture of dimers, trimers and higher oligomers. The compound, 2,6-dimethyl-1-*trans*-3,6-octatriene, was the main dimer of isoprene in this reaction. The maximum yield of this dimer in the reaction at 130°C for 2 hr was accomplished when the molar ratio of diethylaluminum chloride to hafnium(IV) *n*-butoxide was 4.7. The addition of tetrahydrofuran or triphenylphosphine kept the selectivity for the dimer nearly constant. These results were compared with those obtained by the catalyst system consisting of titanium(IV) *n*-butoxide or zirconium(IV) *n*-butoxide and diethylaluminum chloride.

Many catalyst systems containing transition metals are known to oligomerize olefins. In the course of our studies on the catalytic oligomerization of conjugated dienes, we found the cyclic dimerization of isoprene into a mixture of 1,5- and 2,5-dimethyl-1,5-cyclooctadiene by iron complex catalysts.[1] Some catalyst systems containing titanium[2] or chromium[3] are reported to give a linear dimer of isoprene along with other oligomers.

In the preceding paper,[4] we reported the linear dimerization of isoprene to 2,6-dimethyl-1,*trans*-3,6-octatriene by the catalyst system consisting of zirconium(IV) *n*-butoxide, diethylaluminum chloride and with or without electron donors.

In this paper, we report on the oligomerization of isoprene by the catalyst system consisting of hafnium(IV) *n*-butoxide and diethylaluminum chloride. This catalyst system gave a mixture of oligomers of isoprene, and 2,6-dimethyl-1,*trans*-3,6-octatriene was formed predominantly among dimers of isoprene. The selectivity for this compound in the reaction at 130°C for 2 hr was 43% when the molar ratio of diethylaluminum chloride to hafnium(IV) *n*-butoxide was 4.7. The addition of triphenylphosphine or tetrahydrofuran did not raise the selectivity for the dimer. The reaction of isoprene by the catalyst system consisting of titanium(IV) *n*-butoxide and diethylaluminum chloride was also studied, but our results were different from those reported by Takahashi and Yamaguchi.[2b] These results were compared with those obtained by the catalyst system consisting of zirconium(IV) *n*-butoxide and diethylaluminum chloride.

Experimental

Reactors. A 100 m*l* stainless steel autoclave was used.

Reagents. Isoprene was dried over Drierite, distilled and was deoxygenated by the freeze-thaw method with pumping.

Benzene and tetrahydrofuran were purified by conventional methods and were distilled under a nitrogen stream.

Diethylaluminum chloride and titanium(IV) *n*-butoxide were purified by distillation and were diluted in benzene.

Hafnium(IV) *n*-butoxide was made according to the analogous method for zirconium(IV) *n*-butoxide[5] and was diluted in benzene.

Commercial triphenylphosphine was used without further purification.

Reaction Procedure. In a typical reaction, to an autoclave filled with nitrogen, 5.70 g of benzen, 50 mmol of isoprene, 0.5 mmol of hafnium (IV) *n*-butoxide (16.3 wt% benzene solution) and 2.0 mmol of diethylaluminum chloride (17.6 wt % benzene solution) were charged with injectors under a nitrogen stream. The total amount of benzene was controlled to be 8.3—8.5 g. The autoclave was then heated at 130°C for 2 hr with stirring.

Analysis. The gas chromatography was used for calculating the conversion percent of isoprene and for the quantitative analysis of products. A 2 m stainless steel column, 4 mm in diameter, packed with polydiethylene glycol succinate on Shimalite was used. Operation conditions: column temperature, 112°C and 180°C for dimers and trimers, respectively; flash evaporator, 300°C; carrier gas (helium) speed, 30 m*l*/min. Benzene

1) A. Misono, Y. Uchida, M. Hidai and Y. Ohsawa, This Bulletin, **39**, 2425 (1966).

2) a) L. I. Zakharkin, *Doklady Akad. Nauk, S.S.S.R.*, **131**, 1069 (1960); *b*) H. Takahashi and M. Yamaguchi, *Osaka Kogyo Gijutsu Shikensho Kiho*, **15**, 271 (1964).

3) G. Wilke, *J. Polymer Sci.*, **38**, 45 (1959).

4) A. Misono, Y. Uchida, K. Furuhata and S. Yoshida, This Bulletin, in press.

5) D. C. Bradley, F. M. Abd-El Halim, E. A. Sadek and W. Wardlaw, *J. Chem. Soc.*, **1952**, 2032.

was used as an internal standard.

Infrared spectra were taken using a Nihon Bunko Model DS-301.

Nuclear magnetic resonance spectra were recorded on a Nihon Denshi Model C-60.

Molecular weights were measured by the cryoscopic method in benzene.

Results and Discussion

Products obtained in the reaction of isoprene by the catalyst system consisting of hafnium(IV) *n*-butoxide and diethylaluminum chloride were dimers, trimers and higher oligomers. Two dimers were found on gas chromatography and the structure of the dimer with the relative retention time 2.8 was determined to be 2,6-dimethyl-1,*trans*-3,6-octatriene by comparing the retention time with the pure sample obtained by the zirconium catalyst.[4] A small amount of another dimer with the relative retention time 3.4 was found on gas chromatography, but this compound was not studied in detail.

The Effect of the Molar Ratio of Catalyst Components. The effect of the molar ratio of diethylaluminum chloride to hafnium(IV) *n*-butoxide on the reaction of isoprene is shown in Fig. 1. The reaction was

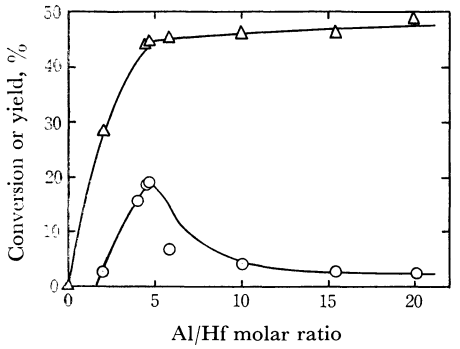

Fig. 1. Effect of the molar ratio of Et_2AlCl to $Hf(OBu)_4$.
—△—: Conversion of isoprene, %
—○—: Yield of 2,6-dimethyl-1, *trans*-3,6-octatriene, %
Reaction temp.: 130°C; reaction time: 2 hr; Isoprene/$Hf(OBu)_4$: 100

carried out at 130°C for 2 hr and the maximum yield of dimers was accomplished when the molar ratio of diethylaluminum chloride to hafnium(IV) *n*-butoxide was 4.7. At this temperature only traces of trimers were formed and the rest were higher oligomers. The infrared spectra of the mixture of these higher oligomers showed absorption bands due to a methyl group (2975, 1450 and 1375 cm^{-1}), a methylene group (2925 and 1450 cm^{-1}), a *trans* double bond (1650 and 965 cm^{-1}), a conjugated double bond (1610 cm^{-1}) and a terminal methylene group (1780 and 885 cm^{-1}). The mean polymerization degrees of liquid oligomers obtained were 6.5, 8.1 and 9.3 when the molar ratios of diethylaluminum chloride to hafnium(IV) *n*-butoxide were 4.0, 6.0 and 15.6, respectively. These data indicate that the excess of diethylaluminum chloride promoted the oligomerization of isoprene to higher oligomers. A similar result was reported in the case of oligomerization of butadiene by iron catalysts.[6,7]

The Effect of the Reaction Temperature. The effect of the reaction temperature on the formation of oligomers of isoprene was examined keeping the molar ratio of diethylaluminum chloride to hafnium(IV) *n*-butoxide constant at 4.0 and the reaction time 2 hr (Fig. 2). The maximum yield of the

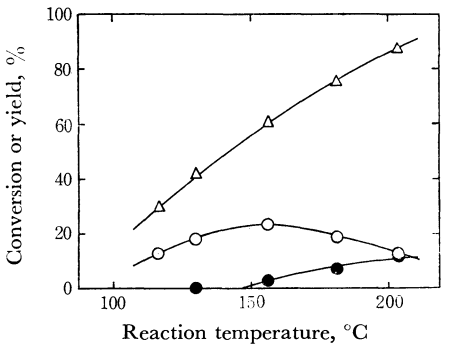

Fig. 2. Effect of the reaction temperature.
—△—: Conversion of isoprene, %
—○—: Yield of 2,6-dimethyl-1, *trans*-3,6-octatriene, %
—●—: Yield of a trimer, %
Reaction time: 2 hr; Isoprene/$Hf(OBu)_4$: 100; $Et_2AlCl/Hf(OBu)_4$: 4.0

dimer was accomplished at about 160°C. The formation of trimers was observed significantly at the temperature higher than 150°C. Four trimers were detected on gas chromatography, and one isomer was predominantly formed. Solid polymers of isoprene were precipitated from the reaction solution at higher temperature when an excess amount of methanol was added, but the higher oligomers formed in the reaction at 130°C remained in the benzene layer.

The Effect of Electron Donors. The effect of electron donors on the oligomerization of isoprene was examined using triphenylphosphine and tetrahydrofuran (Fig. 3). The reactions were carried out at 156°C for 2 hr.

The addition of triphenylphosphine to the catalyst system did not change the selectivity for 2,6-dimethyl-1,*trans*-3,6-octatriene. The same result was observed in the selectivity for the trimer.

6) M. Hidai, Y. Uchida and A. Misono, This Bulletin, **38**, 1243 (1965).

7) A. Carbonaro, A. Greco and G. Dall'Asta, *Tetrahedron Letters*, **1967**, 2037.

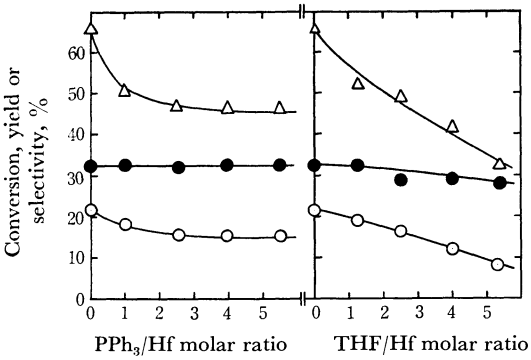

Fig. 3. Effect of electron donors.
—△—: Conversion of isoprene, %
—○—: Yield of 2,6-dimethyl-1, *trans*-3,6-octatriene, %
—●—: Selectivity for 2,6-dimethyl-1, *trans*-3,6-octatriene, %
Reaction temp.: 156°C; reaction time: 2 hr; Isoprene/Hf(OBu)$_4$: 100; Et_2AlCl/Hf(OBu)$_4$: 4.0

In the case of tetrahydrofuran, the selectivity for the dimer decreased slowly as the molar ratio of added tetrahydrofuran to hafnium(IV) *n*-butoxide increased. In this case, no trimer was found when the molar ratio exceeded five.

There was little difference between triphenylphosphine and tetrahydrofuran regarding the influence on the oligomerization of isoprene by the catalyst system consisting of hafnium(IV) *n*-butoxide and diethylaluminum chloride. These electron donors suppressed the conversion of isoprene, but the selectivity for the dimer was nearly constant in both cases, and they did not change the nature of the reaction.

In the oligomerization of olefins catalyzed by transition metals, an alkylaluminum compound acts as an alkylating reagent and the resulting alkyl-transition metal is usually reduced to a low valent state by a homolytic splitting of the transition metal-carbon bond.

In order to examine the reaction of catalyst components in the oligomerization of isoprene by this catalyst system, the nuclear magnetic resonance spectra of catalyst components were studied. Hafnium(IV) *n*-butoxide showed an absorption centered at $\tau=5.5$ ppm (triplet) due to methylene protons next to oxygen in the Hf–O–C linkage. On the other hand, ethylaluminum *n*-butoxide chloride formed by the reaction of equal amounts of diethylaluminum chloride and *n*-butanol showed an absorption centered at $\tau=6.3$ ppm (triplet), which can be assigned to methylene protons next to oxygen in Al–O–C linkage. A mixture of hafnium(IV) *n*-butoxide and diethylaluminum chloride (molar ratio: about 1:4) showed absorptions centered at $\tau=5.7$ (triplet) and 6.4 ppm (triplet) which can be assigned to methylene protons next to oxygen in the linkage of Hf–O–C and Al–O–C, respectively. From this result, it can be said that a ligand exchange reaction between hafnium(IV) *n*-butoxide and diethylaluminum chloride occurred. No significant change was observed after heating this solution at 100°C for 2.5 hr. The solution remained diamagnetic after heating at the reaction temperature and the valency of hafnium was probably four. The ligand exchange reaction could also be observed in the infrared spectra.

Brown precipitates were separated from the benzene solution of hafnium(IV) *n*-butoxide and diethylaluminum chloride after heating at 110°C for 2.5 hr, but when the solution contained a stoichiometric amount of isoprene along with hafnium(IV) *n*-butoxide and diethylaluminum chloride, it remained homogeneous for a long time after the heating. This solution was also diamagnetic before and after the heating.

From these results, it can be said that hafnium is in its four valent state in the oligomerization of isoprene by hafnium(IV) *n*-butoxide and diethylaluminum chloride, and the little difference in the effect of triphenylphosphine and tetrahydrofuran on the catalysis can be explained by the fact that there is no *d*-electron in the four-valent hafnium and thus the back donation can be of little significance in the reaction.

The Oligomerization of Isoprene by Titanium Catalysts. The oligomerization of isoprene by the catalyst system consisting of titanium(IV) *n*-butoxide and diethylaluminum chloride was studied and the results were compared with those mentioned above.

The Effect of the Molar Ratio of Catalyst Components. The effect of the molar ratio of diethylaluminum chloride to titanium(IV) *n*-butoxide is shown in Fig. 4. The reactions were carried out at 35°C for 2 hr. Takahashi and Yamaguchi reported that

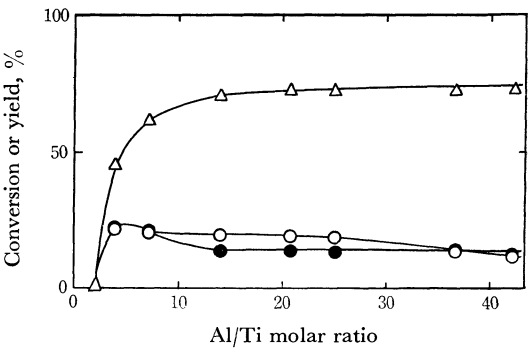

Fig. 4. Effect of the molar ratio of Et_2AlCl to Ti(OBu)$_4$.
—△—: Conversion of isoprene, %
—○—: Yield of 2,6-dimethyl-1, *trans*-3,6-octatriene, %
—●—: Yield of dimethylvinylcyclohexene, %
Reaction temp.: 35°C; reaction time: 2 hr; Isoprene/Ti(OBu)$_4$: 100

this catalyst system gave only 2,6-dimethyl-1,*trans*-3,6-octatriene as the dimer of isoprene,[2b] but in our experiment another dimer was found. This dimer was purified by preparative gas chromatography and analyzed. From the infrared and nuclear magnetic resonance spectra, this compound had two methyl groups (IR: 2975, 1450 and 1375 cm^{-1}; NMR: τ=8.37 and 9.02 ppm, 6H), three methylene groups (IR: 2925, 2850, 1440 and 1415 cm^{-1}; NMR: τ=8.02—8.63 ppm, 6H), one vinyl group (IR: 1830, 1645, 1000 and 910 cm^{-1}; NMR: τ=4.17, 4.92 and 5.22 ppm, 3H) and one three-substituted double bond (IR: 1645 and 805 cm^{-1}; NMR: τ=4.69 ppm, 1H). Therefore, this compound was 1,4- and/or 2,4-dimethyl-4-vinylcyclohexene. The boiling point (bp 48—49°C/14 mmHg) and the refractive index (n_D^{26} 1.4638) were very colse to 2,4-dimethyl-4-vinylcyclohexene reported by Zakharkin[2a] (bp 48—48.5 C/14 mmHg; n_D^{20} 1.4646).

Dimers were formed selectively when the molar ratio of diethylaluminum chloride to titanium(IV) *n*-butoxide was 3.6, and at higher molar ratio, reactions to higher oligomers were favored. The yield of dimethylvinylcyclohexene was constant at the higher molar ratio, but that of 2,6-dimethyl-1,*trans*-3,6-octatriene decreased.

The effect of electron donors on this catalyst system was shortly examined keeping the molar ratio of diethylaluminum chloride to titanium(IV) *n*-butoxide at 20. At this molar ratio, the selectivities for 2,6-dimethyl-1,*trans*-3,6-octatriene and dimethylvinylcyclohexene were 24 and 17%, respectively. When triphenylphosphine was added (molar ratio to titanium(IV) *n*-butoxide: 8.2), the selectivities for two dimers lowered to 19 and 16%, respectively. In the case of tetrahydrofuran (molar ratio to titanium(IV) *n*-butoxide: 6.7), the selectivities were 9 and 8%, respectively. An increase in the selectivity for dimers was not observed and the addition of tetrahydrofuran favored the reaction of isoprene to higher oligomers.

In the oligomerization of isoprene by the catalyst system consisting of zirconium(IV) *n*-butoxide and diethylaluminum chloride, the addition of triphenylphosphine or tetrahydrofuran raised the selectivity for 2,6-dimethyl-1,*trans*-3,6-octatriene to more than 90%.[4] The addition of these electron donors to the catalyst system consisting of titanium(IV) *n*-butoxide or hafnium(IV) *n*-butoxide and diethylaluminum chloride suppressed the conversion of isoprene but the increase of the selectivity for the linear dimer was not observed. The adidtion of triphenylphosphine kept the selectivity for the dimer nearly constant in both cases. The addition of tetrahydrofuran to the hafnium catalyst caused a faint decrease in the selectivity for the dimer. In the case of the reaction of isoprene by the catalyst system consisting of titanium(IV) *n*-butoxide and diethylaluminum chloride, the addition of tetrahydrofuran favored the reaction of isoprene to higher oligomers.

BULLETIN OF THE CHEMICAL SOCIETY OF JAPAN VOL. 42 1387—1393 (1969)

Specific Association of Riboflavin and Adenine Derivatives in Chloroform Solution and the Effect of Barbiturates on the Association

Yoshimasa KYOGOKU and Byung Sul YU

Faculty of Pharmaceutical Sciences, The University of Tokyo, Bunkyo-ku, Hongo, Tokyo

(Received September 27, 1968)

Riboflavin-2′,3′,4′,5′-tetraacetate and tetrabutyrate have been found to associate with 9-ethyladenine. They form stronger complexes with each other than with themselves and with other nucleic acid purine and pyrimidine derivatives. The association constants of the formation of the complexes were determined from the infrared spectra to be 130 and 95 M^{-1} respectively. The complex is a 1 : 1 cyclic hydrogen bonded dimer through the imino and the 2-C carbonyl groups of the isoalloxazine ring and the amino group of the adenine residue. 9-Ethyladenine is an effective quencher of the fluorescence of riboflavin tetraacetate. The quenching appears mainly due to the coplanar interaction through hydrogen bonds and partly due to the collision interaction with the purine rings. Some barbiturates were found to prevent the formation of the complex of the adenine and riboflavin derivatives by the formation of more stable complexes with ethyladenine.

The use of infrared spectroscopy has become customary for detecting the specific interaction of biologically important molecules in chloroform solutions. The method was first used for the detection of the specific association of the nucleic acid purine and pyrimidine derivatives.[1-7] It has been extended to the survey of the interaction of other kinds of molecules like drugs and coenzyme derivatives.[8-10] In a previous communication it was reported that riboflavin derivatives show fairly strong association only with an adenine compound and not with other nucleic acid base derivatives.[10] In this paper a detailed analysis of the infrared spectra of the complex will be presented and the structure of the complex will be proposed.

Previous investigators have reported that purine derivatives work as the quenchers of the fluorescence of riboflavin derivatives in aqueous solutions.[11-15] A similar phenomenon has been found in chloroform solutions. The mechanism of the quenching will be discussed in relation to the structure of flavin adenine dinucleotide (FAD).

Barbiturates were found to interact strongly with adenine derivatives.[8] In this paper it will be reported that some of barbiturates can disturb the interaction between riboflavin and adenine derivatives which might be present in the FAD molecule. Barbiturates can inhibit the respiration in mitochondria, which is thought to be related to their sedative activity in the central nervous system.[16,17] The present results might provide a basis for interpreting their mode of action.

Experimental

Materials. Riboflavin-2′,3′,4′,5′-tetraacetate (R) was prepared by the reaction of riboflavin with acetic

1) R. M. Hamlin, Jr., R. C. Lord and A. Rich, *Science*, **148**, 1734 (1965).
2) Y. Kyogoku, R. C. Lord and A. Rich, *ibid.*, **154**, 518 (1966).
3) J. Pitha, R. N. Jones and P. Pithova, *Can. J. Chem.*, **44**, 1045 (1966).
4) E. Küchler and J. Derkosch, *Z. Naturforsch.*, **21B**, 209 (1966).
5) Y. Kyogoku, R. C. Lord and A. Rich, *J. Am. Chem. Soc.*, **89**, 496 (1967).
6) Y. Kyogoku, R. C. Lord and A. Rich, *Proc. Natl. Acad. Sci. U. S.*, **57**, 250 (1967).
7) J. Miller and H. M. Sobell, *J. Mol. Biol.*, **24**, 345 (1967).
8) Y. Kyogoku, R. C. Lord and A. Rich, *Nature*, **218**, 69 (1968).
9) Y. Kyogoku, N. T. Yu, R. C. Lord and A. Rich *Biochim. Biophys. Acta*, to be published.
10) Y. Kyogoku and B. S. Yu, This Bulletin, **41**, 1742 (1968).
11) H. Weil-Marherbe, *Biochem. J.*, **40**, 363 (1946).
12) G. Weber, *ibid.*, **47**, 114 (1950).
13) L. G. Whitby, *ibid.*, **54**, 437 (1953).
14) J. C. M. Tsibris, D. B. McCormick and L. D. Wright, *Biochemistry*, **4**, 504 (1965).
15) G. Weber, "Flavins and Flavoproteins," ed. by E. Slater, Elsevier, Amsterdam (1966), p. 15.
16) S. K. Sharpless, "The Pharmacological Basis of Therapeutics," ed. by L. S. Goodman and A. Gilman, MacMillan Co., New York (1965), p. 105.
17) W. N. Aldridge, "Enzyme and Drug Action," ed. by J. L. Mongar and A. V. S. de Benck, J. & A. Churchill Ltd., London (1962), p. 155.

anhydride in pyridine. The mixture of anhydrous pyridine (35 ml) and acetic anhydride (4 ml) suspended with dried riboflavin (3 g) was stirred for fifty hours at room temperature. The solution became clear and its color changed to deep orange with green fluorescence. Pyridine was removed by the addition of ethanol and successive evaporation. The sample was recrystallized from the ethanol and chloroform mixture. A yellow flaky crystal was obtained (5 g) (mp 246°C, Found: C, 53.95; H, 5.22; N, 10.41%). 3-*N*-Methylriboflavin-2′,3′,4′,5′-tetraacetate (MeR) was obtained from 3-methylriboflavin by applying the same procedure described above (mp 185°C, Found: C, 55.62; H, 5.49; N, 10.50%). 3-*N*-Methylriboflavin and ribofiavin-2′, 3′,4′,5′-tetrabutyrate (RB) were kindly provided by Professor K. Yagi of Nagoya University and by Professor J. Okuda of Meijo University.

9-Ethyladenine (A), 1-cyclohexyluracil (U), 1-cyclohexyl-5-bromouracil (BrU), 2′,3′-benzylidene-5′-trityl-guanosine (G) and 2′,3′-benzylidene-5′-trityl-cytidine (C) were purchased from Cyclo Chemical Co., Los Angeles, U.S.A. Commercial 5-ethyl-5-phenylbarbituric acid (phenobarbital) (PB) was used after recrystallization from hot water. Crude 1-methyl-5-cyclohexenyl-5-methylbarbituric acid (CB) was obtained by the addition of hydrochloric acid to the commerical sodium salt. Resultant precipitate was recrystallized from hot water.

Procedures. For the measurement of infrared spectra the samples were dissolved in chloroform-*d* (Showa Denko Co., Kawasaki) which was purified by passing through alumina gel column. Infrared spectra were measured with a Perkin Elmer Model 621 infrared spectrophotometer. Fused quartz cells ranging from 1 to 25 mm were used for the measurement in the 3700—3000 cm^{-1} region and potassium bromide cells (including a variable thickness cell) ranging from 0.1 to 5 mm were used for the 1800—1500 cm^{-1} region. The infrared spectra shown in the figures of this paper were given in the absorbance scale, which was calculated from the observed transmission with the aid of the solvent curves as base lines.

From the concentration dependence of the intensity of the monomer bands, association constants were calculated on the theory described previously.[5,6] Six to ten spectra were recorded at different concentrations between 0.1 and 0.001M for the determination of each association constant. It is estimated that the experimental errors of measurement yield relative association constants which are accurate to ±15 per cent.

Non-deuterated chloroform was used as the solvent for the measurements of visible-ultraviolet and fluorescence spectra. The solvent was purified by distillation and by successive passage through alumina gel column. Visible-ultraviolet spectra were recorded with a Hitachi 124 spectrophotometer. The fluorescence measurements were carried out with a Hitachi MPF-2A fluorescence spectrophotometer equipped with a xenon lamp and a grating monochromator. The activating wavelength was set at 360 mμ with a slit width of 10 mμ and the fluorescence was read in the range 380—700 mμ. A fused quartz cell of 1 cm width and 1 cm length with a cap was used. To avoid self quenching at higher concentration, the solution of riboflavin derivatives should have a concentration less than 10^{-4}M.

Results and Discussion

Specific Association of Riboflavin Tetraacetate with Ethyladenine. *Infrared Spectra.* In the spectrum of the 0.02M solution of riboflavin tetraacetate a strong sharp band is observed at 3380 cm^{-1} and a broad band at 3200 cm^{-1} (Fig. 1). Since both of the bands disappear on the deuterium and methyl substitution at the 3-N position, they are associated with the NH stretching vibrations. The apparent extinction coeffecient of the 3380 cm^{-1} band increases and that of the 3200 cm^{-1} band decreases with dilution of the solution. Therefore the former band is assignable to the nonbonded NH stretching vibration and the latter is considered to be related to the bonded NH stretching vibration.

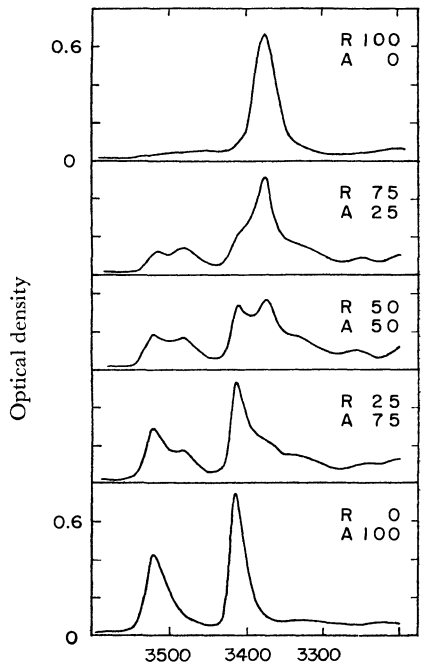

Fig. 1. Infrared spectra of various mixtures of riboflavin tetraacetate (R) and ethyladenine (A). The total concentration of the material is 0.02M and the path length is 2 mm.

The spectrum of 9-ethyladenine shows two strong bands at 3525 and 3414 cm^{-1} which are respectively due to the antisymmetric and symmetric NH stretching vibrations of the nonbonded amino group as discussed previously[5] (Fig. 1). The self-association of the ethyladenine molecules at the 0.02M solution must be negligibly small because the self-association bands at 3485, 3310, 3250 and 3200 cm^{-1} are very weak.

When both the solutions are mixed together, the nonbonded bands decrease in intensity and new

association bands appear at 3485, 3330, 3260, and 3200 cm^{-1}. The positions of some of these bands are different from those of the self-association bands of ethyladenine and riboflavin tetraacetate. It is difficult to assign each association band of the mixture to one or both components. The spectra of various mixtures of riboflavin tetraacetate and ethyladenine are given in Fig. 1. The intensity of the association bands at 3485 and 3330 cm^{-1} changes as a function of the mole ratio and reaches its maximum in the 1 : 1 region (Fig. 2). Similar

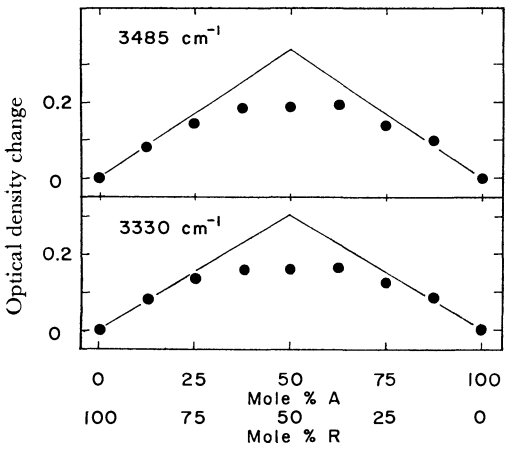

Fig. 2. Change in the optical density of the association bands found at 3485 and 3330 cm^{-1} as a function of the mole ratio of riboflavin tetraacetate and ethyladenine. The optical density of the pure solution is adjusted to zero.

phenomenon was observed for the riboflavin tetrabutyrate and ethyladenine mixture. But the spectrum of ethyladenine does not change to any observable extent by the addition of *N*-methylriboflavin tetraacetate. There is no interaction between them at this concentration.

The association constants for the formation of the R-A complex and the RB-A complex at 25°C were determined to be 130 and 95 M^{-1} respectively. The self-association constant of riboflavin tetraacetate is 4.5 and that of riboflavin tetrabutyrate is 2.3M^{-1}. The monomer band of the riboflavin derivatives at 3380 cm^{-1} and that of ethyladenine at 3525 cm^{-1} were used for the determination.

Although riboflavin tetraacetate and tetrabutyrate associate with ethyladenine fairly strongly, their interaction with other nucleic acid purine and pyrimidine derivatives are negligibly small. Figure 3 shows the infrared spectra of the equimolar mixtures of R-A, R-U, R-C and R-G at 0.008M. Except for the R-A mixture the observed spectra (solid line) are virtually identical to the sum (dotted line) of the component spectra.

In order to get further information on the structure of the R-A complex in solution the spectra in the carbonyl stretching region were studied. In the spectrum of the dilute solution of riboflavin tetraacetate a strong band is observed at 1745 cm^{-1} and two bands with medium intensity at 1710 and 1690 cm^{-1} (Fig. 4). On the deuteration of the 3-N position the strongest band remains unchanged, whereas the 1710 cm^{-1} band moves to 1713 cm^{-1} and the 1690 cm^{-1} band shifts to 1675 cm^{-1}. (The infrared spectrum of 3-*N*-methylriboflavin tetraacetate shows three bands at 1745, 1705 and 1660 cm^{-1}). The 1745 cm^{-1} band which appears at such high frequency region must be the carbonyl stretching band of the acetyl groups. The 1710 cm^{-1} band is considered to arise mainly from the

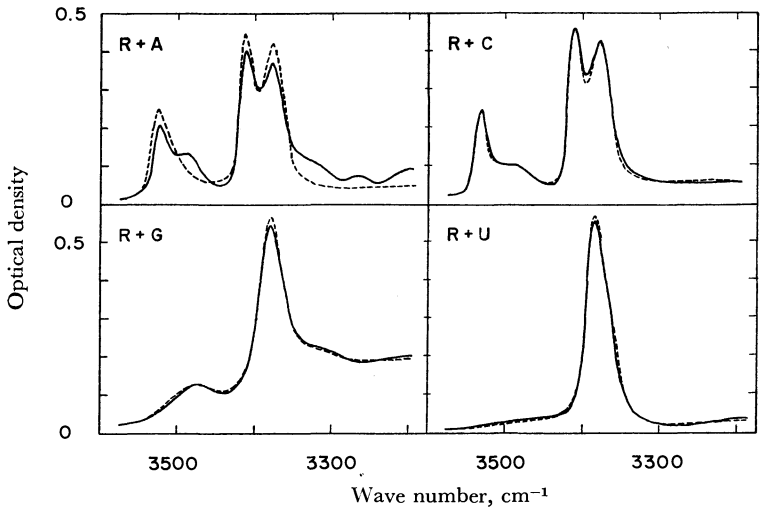

Fig. 3. Infrared spectra of the equimolar mixture solutions of riboflavin tetraacetate and one of the A, U, G and C compounds in chloroform. The total concentration is 0.008M and the path length is 5 mm. See text.

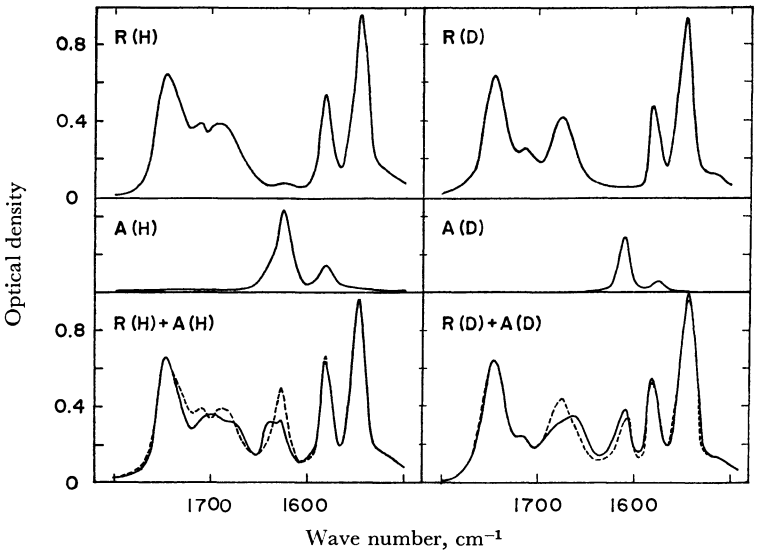

Fig. 4. Infrared spectra of the carbonyl stretching region of riboflavin tetraacetate (R) and ethyladenine (A). The concentration of each solute is 0.05M and the path length is 0.1 mm. H, nondeuterated compound; D, *N*-deuterated compound. Solid line, observed spectra; dotted line, calculated sum of the upper two spectra.

4-C carbonyl group and the 1685 cm^{-1} band from the 2-C carbonyl stretching vibrations coupled with the NH bending mode, since the 2-C carbonyl bond, being conjugated with the C=N bonds, should have lower frequency vibration than the 4-C carbonyl bond. Therefore the bands at 1713 and 1675 cm^{-1} of the *N*-deuterated compound can be assigned to the pure stretching modes of the 4-C and 2-C carbonyl groups respectively.

The spectrum of ethyladenine shows a medium band at 1625 cm^{-1} which was assigned to the coupled vibration of the NH_2 scissors vibration and the ring stretching motions.[5] On the deuteration of the amino group the band moves to 1612 cm^{-1}.

When both the solutions are mixed together, new association bands appear at 1700, 1668 and 1640 cm^{-1} and the bands at 1710, 1685 and 1625 cm^{-1} become weak. The 1745 cm^{-1} band remains unchanged. The 1710 and 1690 cm^{-1} bands of the coupled vibrations of the carbonyl stretching and the NH bending motions of riboflavin tetraacetate shift to 1700 and 1665 cm^{-1} respectively by the formation of hydrogen bonds. The NH_2 scissors vibration at 1625 cm^{-1} of ethyladenine must be moved to 1640 cm^{-1}. On the other hand in the spectrum of the mixture solution of the *N*-deuterated compounds the bands at 1745 and 1713 cm^{-1} of riboflavin tetraacetate are unaffected. Only the 1675 cm^{-1} band of the 2-C carbonyl group decreases in intensity and a new band appears at 1660 cm^{-1}. The 1612 cm^{-1} band of *N*-deuterated ethyladenine shifts to 1615 cm^{-1}.

Since only the 1675 cm^{-1} band of the *N*-deuterated compound shifts to lower frequency by the addition of ethyladenine, the 2-C carbonyl group of riboflavin tetraacetate seems to be used for the formation of the hydrogen bond with ethyladenine. Besides this it is doubtless that the imino group of the riboflavin tetraacetate and the amino group of ethyladenine are employed for the complex formation. Ethyladenine does not interact with *N*-methylriboflavin tetraacetate which is still capable of forming linear hydrogen bond with ethyladenine. This fact indicates the importance of the cyclic dimer formation for the association of riboflavin tetraacetate and ethyladenine. From the present results, however, it can not be concluded which nitrogen atom at the 1 or 7 position of ethyladenine is used for the complex formation.

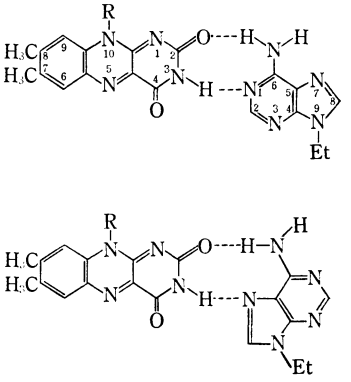

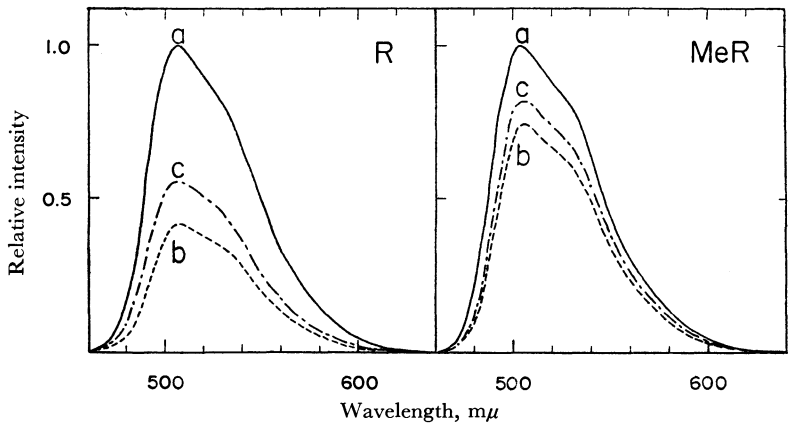

Fig. 5. Fluorescence spectra of riboflavin tetraacetate (R) and *N*-methylriboflavin tetraacetate (MeR) in chloroform solution.
a) R(2×10^{-5}M); b) R (2×10^{-5}M) and A (2×10^{-2}M);
c) R (2×10^{-5}M), A (2×10^{-2}M) and CB (2×10^{-2}M).

Recently the complex crystals of riboflavin and adenosine monophosphate[18] and of riboflavin and 8-bromoadenosine[19] have been obtained. Although their detailed structure have not yet been reported, such structure as shown above can be expected in those complex crystals.

In dilute solution of organic solvents the existence of the ring stacked complex is less possible as seen by analogy to cases of nucleic acid purine and pyrimidine complexes. The NMR study showed the absence of stacking in the chloroform solution of 9-ethyladenine and 1-cyclohexyluracil,[20] although purine derivatives in the vertical interaction caused by hydrophobic bonds are predominant in the aqueous solution at higher concentration.[21] It is generally believed that there is some kind of interaction between isoalloxazine and adenine moieties of the FAD molecule.[11–15] Not only the stacked model but also the coplanar interaction in the molecule must be taken into consideration.

Fluorescence Spectra. Fluorescence spectra of the 2×10^{-5}M chloroform solution of riboflavin tetraacetate are given in Fig. 5. When the same amount of ethyladenine was added to the solution, there was no change in the fluorescence spectrum of riboflavin tetraacetate. As the concentration of ethyladenine was increased, however, decisive quenching was detected. Sixty per cent quenching was observed for the solution containing 2×10^{-5}M riboflavin tetraacetate and 2×10^{-2}M ethyladenine. The other nucleic acid base derivatives gave smaller quenching effect than ethyladenine did (Table 1). The solubility of the C compound is less than 0.01M and the result obtained by the addition of its 0.01M solution is given in the table.

Table 1. Quenching of the fluorescence of riboflavin tetraacetate and *N*-methylriboflavin tetraacetate by some purine and pyrimidine derivatives in chloroform solution

(The figures in the table are values relative to the intensity of the fluorescence of the pure solution at 25°C. Those in parentheses are intensities relative to that of pure solution at 50°C. The error is estimated less than 2%.)

Quencher 2×10^{-2}M each	Riboflavin tetraacetate 2×10^{-5}M		*N*-Methylriboflavin tetraacetate 2×10^{-5}M	
	25°C	50°C	25°C	50°C
None	100	95 (100)	100	96 (100)
A	40	43 (45)	76	70 (73)
G	60	36 (38)	67	40 (42)
C*	92		100	
U	92		100	
BrU	93		101	
CB	99		101	
A+U	45		82	
A+BrU	50		85	
A+CB	48		83	

* 1×10^{-2}M

The quenching appears to be related to the formation of the complex with ethyladenine through hydrogen bonds, because *N*-methylriboflavin tetraacetate shows much smaller quenching effect when it is mixed together with ethyladenine. The number of the complex molecules at a given concentration can be calculated from the association

18) K. Uehara, T. Mizoguchi, S. Hosomi, T. Fujiwara and K. Tomita, *J. Biochem.*, **64**, 589 (1968).
19) D. Voet and A. Rich, private communication.
20) L. Katz and S. Penman, *J. Mol. Biol.*, **15**, 220 (1967).
21) M. V. Schweizer, S. I. Chan and P. O. P. Ts'o, *J. Am. Chem. Soc.*, **87**, 5241 (1965).

constant determined by the infrared measurements. In the binary solution of riboflavin tetraacetate (2×10^{-5}M) and ethyladenine (2×10^{-2}M) seventy two per cent of the riboflavin tetraacetate molecules are bound to ethyladenine. Since the association constant for the complex formation of R-U, R-C and R-G are estimated by the infrared measurements to be in the order of magnitude of 10M^{-1}, about ten per cent of riboflavin tetraacetate must be bound to those base derivatives. The amount of quenching is in the same order of the percentage of the riboflavin tetraacetate molecules used for the complex formation. This is another evidence showing that the quenching is mainly caused by the formation of hydrogen bonding.

However, the G compound shows greater quenching effect in both of the mixture solutions of R and MeR than those expected from the infrared measurements. Ethyladenine also shows greater quenching effect than U and C do on the fluorescence of *N*-methylriboflavin which can not form the hydrogen bonded complex. Purine compounds appear to possess a quenching ability without forming a hydrogen bond. It may be caused by a simple collision process between the isoalloxazine and purine rings. To test this idea the temperature dependency of the quenching was measured. The fluorescence of the R-A complex solution at 50°C became stronger than that at room temperature, *i.e.*, the extent of quenching decreased. This may be due to the increase of the number of the free riboflavin molecules at higher temperature. On the other hand the quenching observed for the MeR+A, R+G and MeR+G solutions increased at higher temperature. This phenomenon can be explained by the increase of the thermal collisions of the molecules at higher temperatures.[22]

The intensity of the fluorescence of FAD is about one tenth of that of riboflavin monophosphate.[15] Such big quenching could be caused not only by the vertical interaction of the isoalloxazine and adenine rings[14] but also by the coplanar interaction of the rings in the FAD molecule.

Ultraviolet and Visible Spectra. The spectra of riboflavin tetraacetate and *N*-methylriboflavin tetraacetate in chloroform are given in Fig. 6. Spectra in the same region were recorded for all of the mixture solutions that were examined by the fluorescence measurements. The absorption at 260 mμ of the purine and pyrimidine derivatives solution at 2×10^{-2}M is so strong that the spectra of the mixture solutions could not be recorded below 300 mμ. Neither position nor intensity of the absorption between 300 and 500 mμ of riboflavin tetraacetate changes by the addition of the base derivatives.

The Effects of Barbiturates on the Specific Association. In a previous paper it was reported that ethyladenine forms a stable complex with phenobarbital, the association constant of which is 1200M^{-1}.[8] The equimolar mixture of ethyladenine and phenobarbital gives precipitate, if the concentration of the solution is more than 10^{-3}M. When 10^{-3}M of phenobarbital was added to the chloroform solution containing 10^{-3}M of ethyladenine and riboflavin tetraacetate, phenobarbital-ethyladenine precipitation was still produced. The presence of riboflavin tetraacetate does not affect the formation of the phenobarbital - ethyladenine complex. In such a dilute solution as 10^{-3}M, however, the amount of the riboflavin tetraacetate-ethyladenine complex is negligibly small and most of the ethyladenine molecules exist as monomers when phenobarbital is added to the solution. Therefore 1-ethyl-5-cyclohexenyl-5-methylbarbituric acid whose complex with ethyladenine is quite soluble has been employed. The use of the compound makes it possible for us to see the effect

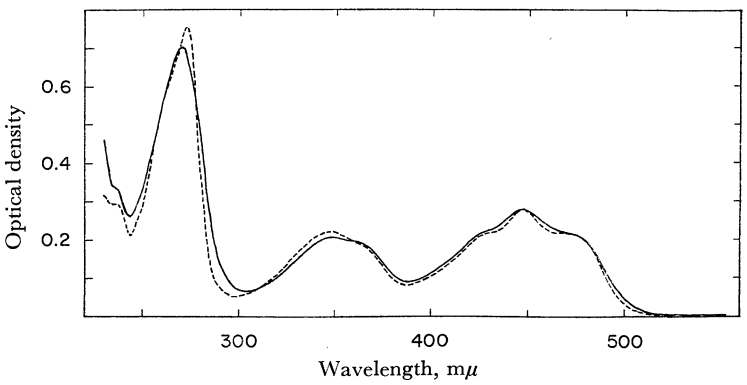

Fig. 6. Ultraviolet and visible spectra of riboflavin tetraacetate (—) and *N*-methylriboflavin tetraacetate (···) in chloroform. The concentration of the solution is 2×10^{-5}M and the path length is 1 cm.

22) K. Yagi, Z. Yoshida and R. Ohata, "Keiko (Fluorescence)," Nankodo, Tokyo (1958), p. 68.

of the addition of barbiturate at a high concentration where the R-A complex is predominant in the solution. The association constant of the CB-A complex has been determined to be $170\,M^{-1}$ which is fairly smaller than that of the PB-A complex.

An infrared spectrum was measured with the solution containing equimolar A, R and CB at 0.04M The observed spectrum is different from the calculated sum of the individual spectrum and the strong association bands are observed. But the positions of the association bands of the R-A and the CB-A complexes are almost the same. It is not possible to distinguish which complex is predominant in the mixture solution from the band position and intensity.

In the fluorescence spectrum of the R-A solution the decrease of quenching by the addition of CB was detected. Twenty per cent increase of the fluorescence of the mixture solution, *i.e.*, eight per cent recovery of the original fluorescence of riboflavin tetraacetate was observed, when $2\times10^{-2}M$ solution of CB was added to the mixture solution containing $2\times10^{-2}M$ of A and $2\times10^{-5}M$ of R. The CB-A complex is more stable than the R-A complex and the added CB releases R from the R-A complex. The binding site of A in the R-A complex appears the same as that in the CB-A complex and the triple complex like CB-(R-A) is not predominant. The enhancement of the fluorescence of the R-A solution, however, is not the special activity of CB. 1-Cyclohexyluracil and 1-cyclohexyl-5-bromouracil, which associate with ethyladenine at the constants 100 and $250\,M^{-1}$,[5,6] respectively, can also increase the fluorescence of the R-A complex. Their ability to disturb the formation of the R-A complex is not parallel with the inhibitory activity in the respiratory chain, since uracil derivatives do not have such activity. Permeability and solubility differences of these compounds in mitochondria must be taken into account.

Increase of the fluorescence of the MeR+A solution by the addition of CB or uracil derivative was also observed. Thermal motion of the ethyladenine molecule may be reduced by the formation of the complex with these compounds.

The authors wish to express their sincere thanks to Professor M. Tsuboi for his valuable discussion and encouragement. Thanks are also due to Drs. K. Nakajima and M. Watanabe for the permission to use fluorescence spectrophotometers. This work was partly supported by a grant from the U.S. Public Health Service GM 10024-05 and partly by a grant from the Ministry of Education of Japan.

BULLETIN OF THE CHEMICAL SOCIETY OF JAPAN VOL. 42 1393—1398 (1969)

Solvent Effect in a Partial Asymmetric Synthesis. II[1]

Shuji INAMASU

Research Department, Yoshitomi Pharmaceutical Ind. Ltd., Yoshitomi, Fukuoka

and Michio HORIIKE and Yuzo INOUYE

Institute for Chemical Research, Kyoto University, Uji, Kyoto

(Received September 27, 1968)

Further evidence for the unambiguous solvent polarity dependence of the stereochemistry in the base-catalyzed Michael type condensation was provided by the systems involving (−)-menthyl chloroacetate and methyl acrylate, and (−)-menthyl chloroacetate and (−)-menthyl acrylate with a modification of the work-up. The electrostatic control of the stereoselectivity was interpreted by the same theorem developed in the previous study and some novel features found for the present systems were discussed.

The first example of an olefin addition in which both the stereochemical outcome and optical yield are solvent polarity-dependent was presented in our earlier work[1a] dealing with the base-catalyzed Michael type condensation of (−)-menthyl chloroacetate with ethyl acrylate to give optically active *trans*-cyclopropane-1,2-dicarboxylic acid plus a trace of the *cis*-acid after removal of the chiral center by

1) Previous papers of this series: a) Y. Inouye, S. Inamasu, M. Ohno and H. M. Walborsky, *J. Am. Chem. Soc.*, **83**, 2962 (1961); b) Y. Inouye, S. Inamasu and M. Horiike, *Chem. Ind. (London)*, **1967**, 1293; c) Y. Inouye, S. Inamasu, M. Horiike and H. M. Walborsky, *Tetrahedron*, **24**, 2907 (1968).

alkaline hydrolysis. The stereochemistry of this asymmetric reaction depended markedly on the solvent: in toluene, the *trans*-diacid obtained was levorotatory whereas in dimethylformamide, this acid had the opposite configuration and the optical yield was higher.

In contrast to this finding, McCoy[2] argued that the actual asymmetric synthesis of the *trans*-diacid was unaffected by a change of solvent but that the change in configuration of the *trans*-acid was due to a possible asymmetric *cis*-to-*trans* isomerization of the diastereomeric (−)-menthyl ethyl *cis*-diesters which were formed in the initial kinetically controlled process. Recent results by the present authors,[1b,c] however, decidedly refuted McCoy's claim and established the solvent effect in the asymmetric synthesis of this type on a more sound basis of kinetic theory. The NaH-catalyzed condensation of (−)-menthyl α-chloropropionate with methyl methacrylate, in which the resulting *cis*- and *trans*-1,2-dimethylcyclopropane-1,2-dicarboxylic acids carry no acidic α-hydrogen and the asymmetric isomerization by alkaline hydrolysis is excluded, was conducted in a binary solvent system of continuously varied dielectric constant. The *cis*/*trans* as well as *trans*-(−)-(R:R)/(+)-(S:S) ratios of the cyclopropane products unequivocally corroborated the dependence of stereoselectivity of the reaction on solvent polarity. That is, the *trans*-isomer predominated in more polar solvents whereas the *cis* in non-polar media and the *trans*-isomer produced in non-polar media exhibited levorotation whereas those in polar media were dextrorotatory. The solvent effect was accommodated fairly well in quantitative terms by the Kirkwood-Onsager theory as shown by the fine linearity of the plots of logarithms of *cis*/*trans* and (−)-(R:R)/(+)-(S:S) ratios against the Kirkwood-Onsager parameter of the reaction media. The stereochemical outcome was nicely explicable in terms of electrostatic stabilization and non-bonded interactions in the postulated transition state conformations which were stabilized by orbital overlap and charge delocalization at the rate-, and therefore, stereochemical-determining cyclization step.

In the present work, further evidence for the unambiguous operation of solvent effect is provided by both the earlier (−)-menthyl chloroacetate-methyl acrylate and the novel (−)-menthyl chloroacetate-(−)-menthyl acrylate systems with the work-up modified so that the final product ratio can represent the kinetically controlled results of the reaction. The conventional alkaline hydrolysis of the resulting diesters was replaced by lithium aluminum hydride reduction capable of converting the diesters into the corresponding stereomeric diols without thermodynamical equilibration and jeopardization of the absolute configurations of the reaction products.

Methods and Results

(−)-Menthyl chloroacetate was condensed with equimolar methyl acrylate or (−)-menthyl acrylate by means of sodium hydride at 25°C in binary solvent system of continuously varied dielectric constant, consisting of dimethylformamide and benzene in 10 : 0 through 0 : 10 by volume and covering the polarity range of ε 37.63 through 2.28. After 2 hr's reaction period, the resulting mixture was worked up as usual[1c] and the mixture of stereomeric cyclopropane-1,2-dicarboxylate esters was reduced with an excess of lithium aluminum hydride. Addition of acetic anhydride to the reaction mixture afforded *cis*-, and *trans*-1,2-bis-(acetoxymethyl)-cyclopropane, which was purified by distillation and separated pure by means of preparative vpc.

Results of the asymmetric reactions conducted in binary solvent system of continuously varied dielectric constant are summarized in Tables 1 and 2.

Table 1. Asymmetric synthesis data in methyl acrylate-(−)-menthyl chloroacetate system

Solvent ratio DMF : benzene	Dielectric constant (ε)	% Yield glycol-diacetate	*cis* : *trans* ratio	$[\alpha]_D^{25}$(EtOH) *trans*-diacetate	% Optical yield	RR : SS ratio
10 : 0	37.65	47.8	0.14	+1.75	9.85	0.82
9 : 1	19.87	43.6	0.15	+1.40	7.89	0.85
8 : 2	13.05	44.8	0.18	+1.38	7.77	0.90
7 : 3	9.45	51.8	0.19	+0.93	5.23	0.93
6 : 4	7.26	41.5	0.28	+0.52	2.92	0.94
5 : 5	5.77	40.4	0.34	+0.44	2.47	0.95
4 : 6	4.69	41.0	0.44	+0.10	0.53	0.98
3 : 7	3.87	44.3	0.53	+0.04	0	1
2 : 8	3.22	43.5	0.60	−0.29	1.63	1.03
1 : 9	2.66	45.2	1.11	−0.73	4.11	1.09
0 : 10	2.28	41.0	4.10	−1.36	7.66	1.16

2) L. L. McCoy, *J. Org. Chem.*, **29**, 240 (1964).

TABLE 2. ASYMMETRIC SYNTHESIS DATA IN (−)-MENTHYL ACRYLATE-(−)-MENTHYL CHLOROACETATE SYSTEM

Solvent ratio DMF : benzene	Dielectric constant (ε)	% Yield glycol-diacetate	*cis* : *trans* ratio	$[\alpha]_D^{25}$ (EtOH) *trans*-diacetate	% Optical yield	RR : SS ratio
10 : 0	37.65	39.4	0.26	+0.82	4.62	0.91
9 : 1	19.87	37.8	0.31	+0.53	2.99	0.94
8 : 2	13.05	39.5	0.36	+0.27	1.52	0.97
7 : 3	9.45	36.1	0.46	0	0	1.0
6 : 4	7.26	35.8	0.48	−0.15	0.8	1.02
5 : 5	5.77	36.7	0.58	−0.54	3.04	1.06
4 : 6	4.69	35.1	0.66	−0.81	4.56	1.09
3 : 7	3.87	38.0	0.78	−1.07	6.03	1.13
2 : 8	3.22	37.2	0.88	−1.30	7.32	1.16
1 : 9	2.66	35.6	1.31	−1.63	9.18	1.19
0 : 10	2.28	34.0	6.24	−1.83	10.30	1.23

As can be seen from the data, the *cis*/*trans* ratio of the resulting glycol diacetates in these asymmetric reactions trends to increase as the solvent polarity decreases *i.e.* the *trans*-isomer predominated in more polar media rich in DMF, whereas the *cis* in less-polar media of more benzene composition.

The sign of rotation of the isolated *trans*-diacetates altered on changing the polarity of reaction media: the *trans*-diacetates obtained in less-polar media were found to be levorotatory, whereas those in more polar media were dextrorotatory. These findings, including the *cis*, *trans*-stereoselectivity, are completely consistent with those in the previous system and this fact, in the present systems where the thermodynamical equilibration of the asymmetric reaction product is excluded by the modification of work-up, furnished further cogent evidence for the unequivocal operation of solvent effect in the asymmetric cyclopropane synthesis.

Furthermore, when log (−)-(R:R)/(+)-(S:S) was plotted against the Kirkwood-Onsager parameter of the reaction media, a fine linearity was obtained in both systems (Figs. 1 and 2), as was also the case with log *cis*/*trans* *vs.* $(\varepsilon-1)/(2\varepsilon+1)$. A considerable deviation from the linearity of the regression lines of log *cis*/*trans* plots was observed also in the pure benzene runs of the present systems. This anomalous *cis*-formation in pure benzene may be accounted for by the same heterogeneity effect in this medium, as discussed in the previous paper.[1c]

The linearity of the plots obviously shows the obedience of both *cis*,*trans*-stereoselectivity and asymmetric induction to the Kirkwood equation.

The absolute configuration and maximum rotation of the final product in the present asymmetric reaction, *trans*-1,2-bis(acetoxymethyl)-cyclopropane, were determined by the conversion of (−)-*trans*-cyclopropane-1,2-dicarboxylic acid of the well-

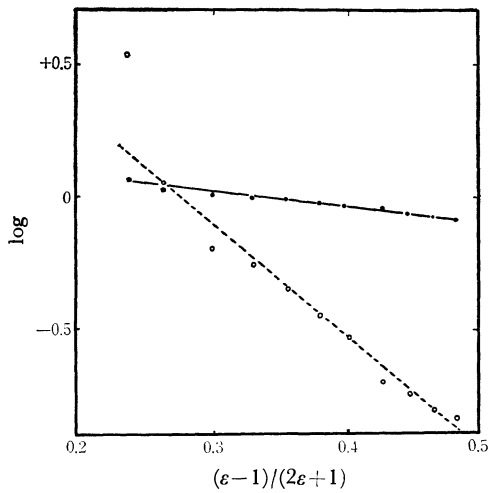

Fig. 1. The plots of log *cis*/*trans* (in dashed line) and log (−)-(R:R)/(+)-(S:S) (in solid line) *vs.* Kirkwood-Onsager parameter of media in methyl acrylate-(−)-menthyl chloroacetate system.

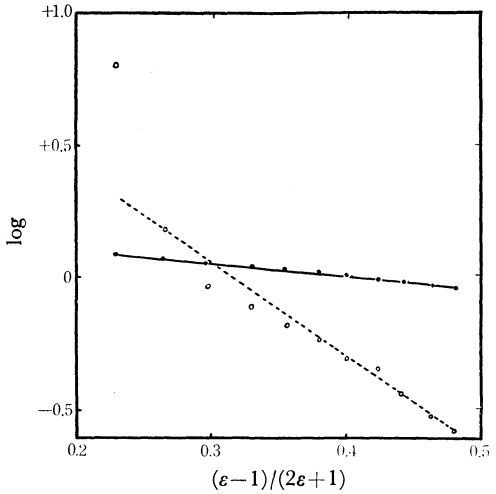

Fig. 2. The plots of log *cis*/*trans* (in dashed line) and log (−)-(R:R)/(+)-(S:S) ratio (in solid line) *vs.* Kirkwood-Onsager parameter of media in (−)-menthyl acrylate-(−)-menthyl chloroacetate system.

defined (R:R)-configuration[3] into (−)-*trans*-1,2-bis(acetoxymethyl)-cyclopropane. Since the starting (−)-(R:R)-acid, $[\alpha]_D^{25}$ −235°, was optically pure, the eventually derived (−)-diacetate, $[\alpha]_D^{25}$ −17.75°, should have the (R:R)-configuration and the rotation found should be maximal.

Discussion

The stereochemical outcome in the present systems is completely consistent with those in the previous system involving the base-catalyzed Michael type condensation of (−)-menthyl α-chloropropionate with methyl methacrylate (for convenience, designated as system A) and accordingly, can be successfully accounted for by the same theorem developed in the previous paper.[1c] Thus, the transition state of the intermediate carbanion is stabilized by orbital overlap and charge delocalization in the postulated sp^2-model conformation[1c] and, the steric factor being comparable in both competing transition state conformers as estimated by model inspection of the non-bonded interactions, then *ceteris paribus*, the electrostatic stabilization which varies depending on the solvent polarity becomes the controlling factor of the steric course of the reaction.

The carbanionic transition state *cis*-conformer with a reduced dipole moment (1.9 D) and a *cis*-compression relieved by the sodium cation chelation is electrostatically more favored in non-polar solvents than the *trans*-counterpart with a greater moment (2.75 D), and the situation is just reversed in polar and strongly solvating media. This naturally leads to the predominant formations of the *cis*-product in non-polar media, and of the *trans*-isomer in polar media. It is surprising to find that the regression line found for the log *cis*/*trans* plots in (−)-menthyl chloroacetate-(−)-menthyl acrylate system (designated as system C) is shifted towards the positive side as compared to that in (−)-menthyl chloroacetate-methyl acrylate (system B). *A priori*, the transition state *cis*-conformer in the system C may well be expected to experience a more serious *cis*-compression between two bulky carbomenthoxy groups than that between carbomenthoxy and carbomethoxy to be felt by the corresponding *cis*-conformer in the system B, and this should naturally disfavor the *cis*-formation in the system C. Despite this, the experiment actually showed that the system C is prone to produce more *cis* relative to *trans* than does the system B. A tentative interpretation of this stereochemical result is as follows. The microscopic dielectric constant (ε') of a cospherical region surrounding a carbanion is considered as being affected by the charge, steric shielding and local polarity of substituent groups of the carbanion, and is duly different from the macroscopic bulk dielectric constant (ε) outside this region. It is within this region that the reaction actually takes place. The polarization of solvent molecules within this region depends on ε' and thus, the degree and type of solvation of carbanion are also dependent on this parameter. The polarity (ε') of cybotactic region of the transition state *trans*-conformer in the system C would be lowered by the more steric shielding and the lower local polarity of the two carbomenthoxy groups than that of the corresponding *trans*-conformer in the system B which would be affected by a less bulky and more polar carbomethoxy and a carbomenthoxy group. The electrostatic stabilization of the *trans*-conformer in the system C by solvation is thus reduced by the lower polarity and steric shielding of its cybotactic region and this contributes more to the relative stability of the *cis*-counterpart with smaller moment in the unsolvated chelate form. The chemical consequence for this situation is the favored *cis*-formation in the double induction system. As a fair approximation, ε' should be a function of the bulk dielectric constant which is conveniently measured with pure solvent, so that the linearity of the log *cis*/*trans* *vs.* $(\varepsilon-1)/(2\varepsilon+1)$ plots in this case is reasonably borne out. For better understanding of this phenomenon, further investigations are needed and this will be the subject of furture publications.

A successful explanation of the solvent effect in the asymmetric synthesis of the *trans*-isomer in the present systems B and C can be made on the same theoretical basis as in the system A and/or the above-mentioned *cis*,*trans*-stereoselectivity. Of conceivable transition state conformations which fulfill the stereoelectronic requirements for orbital overlap and charge delocalization, the *trans*-conformer with a dipole moment of 2.75 D[1c] which, upon cyclization, would lead to the (R:R)-enantiomer, and the other with a slightly greater moment (3.05 D) leading to the (S:S)-product are chosen as sterically the most favored transition state conformer in each diastereomeric series, because of their minimized non-bonded repulsive interactions. Since the electrostatic stabilization of the carbanion by solvation is the controlling factor in the asymmetric induction too, the energy difference between these two transition states in solvents of varying polarity is reflected in the rate-, and consequently, the enantiomer-ratio of the *trans*-products. Reversal in sign and configuration of the *trans*-products was actually observed in the present systems B and C upon changing the solvent polarity. The fine linearity found for the log RR/SS plotted against the Kirkwood-Onsager parameter clearly shows the strict obedience of the asymmetric induction to the Kirkwood equation and provides cogent evidence based on kinetic

3) Y. Inouye, T. Sugita and H. M. Walborsky, *Tetrahedron*, **20**, 1695 (1964).

theory for the solvent effect in the asymmetric induction of this type.

By superimposing the Figs. 1 and 2, one is aware of a slight shift of the log RR/SS plots in the double induction system C towards the positive side as compared to that in the system B. This implies that the levorotatory (R:R)-enantiomer is inclined to form to a more extent relative to the (S:S)-enantiomer in the double induction system than does in the system B. This may be rationalized by the steric advantage of the (R:R)-carbanion over the (S:S)-counterpart.

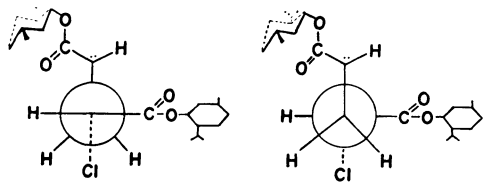

Model inspection reveals that the steric strain is comparable in the competing (R:R)- and (S:S)-transition state conformers in the system B (as was also the case in the system A), whereas in the double induction system C, the (R:R)-conformer (2.75 D) is sterically more favored than the (S:S)-counterpart (3.05 D). Upon intramolecular nucleophilic displacement, the latter carbanion has to experience more steric hindrance with the more bulky side (extended isopropyl branch) of (−)-menthyl grouping oriented towards the γ-carbon carrying the leaving chlorine atom, whilst in the former (R:R), this can be done with less hindered side of the menthyl. The (R:R)-conformer is thus sterically more favored than in the case of the system B, but this steric advantage *per se* is not great enough to control the steric course of the asymmetric induction and the electrostatic factor still remains dominant, so that the enantiomer ratio varies depending upon the solvent polarity and the sign of rotation of the products alters at ε 9.45. Although the point of the reversal of rotation was found at ε 3.87 for the system B and at ε *ca.* 2.4 for A, it is noteworthy that all the regression lines in the three asymmetric systems have nearly the same slope. In contrast to expectation, the optical yields in the double induction system C were not so high, as compared with those in the system B. This may well be understood by reasoning that the transition state in the double induction sees quite a different stereochemical environment from that in the individual asymmetric induction.

Experimental

The Asymmetric Synthesis of 1,2-Bis-(acetoxymethyl)-cyclopropane. The synthetic procedure is exemplified by a typical run of the (−)-menthyl chloroacetate-methyl acrylate system in a mixture of DMF and benzene (1 : 9 by volume). The reactions were repeated in exactly the same manner except the solvent composition. For the (−)-menthyl chloroacetate-(−)-menthyl acrylate system, the identical procedure was followed with one of the reactants changed.

Methyl acrylate (10.5 g; 0.12 mol) and (−)-menthyl chloroacetate (23.3 g; 0.1 mol) were condensed in the presence of sodium hydride (dispersed in a mineral oil from Metal Hydrides Inc., a commercial grade of 50% purity: 4.8 g; 0.1 mol) in 60 m*l* of the mixed solvent (DMF : benzene=1 : 9 by volume) at 25°C for 2 hr with stirring. The reaction temperature was maintained constant throughout the reaction by cooling with ice-water if necessary. After the duration, a small amount of methanol (*ca.* 3 g) was added dropwise to the reaction mixture with stirring and cooling to decompose any residual hydride, and then sufficient water was added to dissolve sodium chloride. The organic layer was taken up in benzene, washed with saturated sodium chloride solution and dried by means of molecular sieves. Removal of solvent *in vacuo* yielded a mixture of crude, isomeric (−)-menthyl methyl cyclopropane-1,2-dicarboxylates, which weighed *ca.* 26 g. According to the Blomquist procedure,[4] the crude diester was reduced with lithium aluminum hydride (12 g; 0.3 mol) in absolute ether (300 m*l*). Acetic anhydride (100 m*l*) was added to the reaction mixture and ether was replaced with further anhydride to facilitate stirring and refluxing. After 10 hr, acetic acid, residual anhydride and (−)-menthyl acetate were driven in steam and the residue was extracted with ether. After drying, ether was removed to give crude, isomeric 1,2-bis-(acetoxymethyl)-cyclopropanes (*ca.* 9.5 g). This was distilled on a column packed with dixone to remove (−)-menthyl acetate and a fraction boiling at 108—125°C/17 mmHg was collected (*ca.* 8.4 g). Isomeric glycol diacetates were separated by means of preparative scale vpc (Wilkins Autoprep. 700) under the following conditions*1: column 3/8 in ×10 ft, Apiezon grease 30% impregnated Diasolid L, helium gas at the flow rate 200 m*l*/min, column temp. 180°C, detector temp. 220°C, injector temp. 210°C. The retention time found for the *cis*-diacetate was 11 min; for the *trans*, 10 min. *cis*-Diacetate, bp 125—126°C/22 mmHg, n_D^{20} 1.4456, 4.43 g (23.8%). (Found: C, 58.13; H, 7.46%. Calcd for $C_9H_{14}O_4$: C, 58.05; H, 7.58%). *trans*-Diacetate, bp 130—132°C/24 mmHg, n_D^{20} 1.4406, 3.98 g (21.4%). (Found: C, 58.27; H, 7.38%. Calcd for $C_9H_{14}O_4$: C, 58.05; H, 7.58%). $[\alpha]_D^{25}$ −0.73° (*c* 4.0, EtOH). The IR- and NMR-spectra of the *cis*- and *trans*-diacetates were identical in every respect with those of the authentic specimens.[4]

Resolution of *trans*-1,2-Cyclopropanediacarboxylic Acid. The racemic *trans*-acid, mp 174—175°C. (Found:C, 46.25; H, 4.59%. Calcd for $C_5H_6O_4$: C, 46.16; H, 4.65%). (60 g; 0.46 mol) was dissolved in

4) A. T. Blomquist and D. T. Longone, *J. Am. Chem. Soc.*, **81**, 2012 (1959).

*1 McCoy described in Ref. 2 that the *cis*-isomer peak appeared as an incompletely resolved small shoulder on the long retention time side of the *trans*-peak on his qualitative VPC column, but on our column under the conditions specified above, a clear-cut separation was obtained.

boiling water (3500 ml) and cinchonidine (136 g; 0.46 mol) was added and the mixture was allowed to stand still overnight at room temperature, when the cinchonidine salt crystallized out. After fractional triangular crystallization of the salt from 20% ethanol, the salt with a constant rotation was decomposed with dilute sulfuric acid to afford the optically active (−)-acid (6.9 g). Further recrystallization of the free acid from acetonitrile gave the optically pure acid, mp 171—173°C. (Found: C, 46.21; H, 4.53%. Calcd for $C_5H_6O_4$: C, 46.16; H, 4.65%). $[\alpha]_D^{25}$ −235° (*c* 2.0, water).

Conversion of (−)-*trans*-Cyclopropane-1,2-dicarboxylic Acid into (−)-*trans*-1,2-Bis-(acetoxymethyl)-cyclopropane. The (−)-acid (2.6 g) obtained by the resolution described above was converted by the standard method with diazomethane into the corresponding dimethyl ester. According to the Blomquist procedure,[4] the (−)-diester was transformed into (−)-*trans*-1,2-bis-(acetoxymethyl)-cyclopropane, bp 130—132°C/23 mmHg, n_D^{20} 1.4408. (Found: C, 58.06; H, 7.40%. Calcd for $C_9H_{14}O_4$: C, 58.05; H, 7.58%). $[\alpha]_D^{25}$ −17.75° (*c* 2.0, EtOH). The IR- and NMR-spectra were identical in every respect with those of the authentic racemic specimen.[4] The dielectric constants of the binary solvent system consisting of DMF and benzene in continuously varied volume ratios were computed by the mixing rule and the data were given in the previous paper.[1c]

The authors are indebted to Drs. M. Ohno, M. Nakanishi and T. Mukai for their encouragement and interest in this work. Partial support of this study by grant D86547 from the Ministry of Education is gratefully acknowledged (Y. I.).

BULLETIN OF THE CHEMICAL SOCIETY OF JAPAN VOL. 42 1398—1403 (1969)

Synthetic Studies of the Flavone Derivatives. X.*1 The Synthesis of 3,4′,5-Trihydroxy-3′,6,7-trimethoxyflavone and the Structures of Chrysosplenin and Chrysosplenetin

Kenji FUKUI, Takashi MATSUMOTO and Sachihiko TANAKA

Department of Chemistry, Faculty of Science, Hiroshima University, Higashi-sendamachi, Hiroshima

(Received September 28, 1968)

The acid-catalyzed isomerization of 4-benzyloxy-2′-hydroxy-3,4′,5′,6′-tetramethoxychalcone gave 4′-benzyloxy-3′,5,6,7-tetramethoxyflavanone, which was then converted by oxidation to 4′-benzyloxy-3-hydroxy-3′,5,6,7-tetramethoxyflavone. This, after debenzylation to 3,4′-dihydroxy-3′,5,6,7-tetramethoxyflavone, was partially demethylated with aluminum chloride or aniline hydrochloride to give 3,4′,5-trihydroxy-3′,6,7-trimethoxyflavone (I) (mp 213—214°C), the structure proposed previously for the chrysosplenetin (mp 177—178°C) isolated from *Chrysosplenium japonicum* Makino. However, the synthetic flavone was found to be different from natural chrysosplenetin by a mixed melting point determination and by a comparison of the spectra. Finally, the structures of chrysosplenetin and chrysosplenin were established by the spectroscopic studies to be 4′,5-dihydroxy-3,3′,6,7-tetramethoxyflavone (XIII) and its 4′-glucoside (XIV) respectively. The revised structure for chrysosplenetin has been fully confirmed by direct comparison with an authentic sample.

Chrysosplenin, yellow glycoside, has been isolated from the dried whole herb of *Chrysosplenium japonicum* Makino by Nakaoki and Morita.[1] The hydrolysis of this glycoside with dilute sulfuric acid afforded an aglycone, chrysosplenetin. On the basis of analytical and chemical studies, those authors proposed that structures of chrysosplenetin and chrysosplenin ere 3,4′,5-trihydroxy-3′,6,7-trimethoxyflavone (I) and its 3-(or 5-)glucoside respectively.

Although Mani and Venkataraman[2] reported a synthesis of I which involved a partial demethylation of the 5-methoxyl group of 3,4′-dihydroxy-3′,5,6,7-tetramethoxyflavone (II) with anhydrous aluminum chloride in ether, a similar selective demethylation of 3-hydroxy-5,7-dimethoxyflavone

*1 Part IX: K. Fukui, M. Nakayama and T. Horie, This Bulletin, in press.

1) T. Nakaoki and N. Morita, *Yakugaku Zasshi* (*J. Pharm. Soc. Japan*), **76**, 320 (1956).

2) R. Mani and K. Venkataraman, *J. Sci. Ind. Res.* (*India*), **21B**, 477 (1962); *Chem. Abstr.*, **59**, 551g (1963).

(III) in this laboratory was unsuccessful.[3] Recently, an unsuccessful demethylation of 3,7-dihydroxy-4′,5,8-trimethoxyflavone (IV) under similar reaction conditions has also been reported by Krishnamurti *et al.*[4]

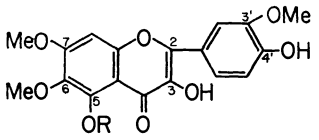

I R = H
II R = Me

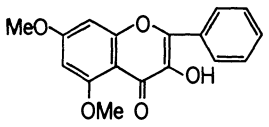

III

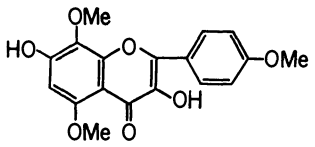

IV

For this reason, it was thought worthwhile to study further the selective demethylation of the 5-methoxyl group of II.

The present paper will describe a synthesis of I, which was found to be different from the natural pigment, and will present revised structures for chrysosplenin and chrysosplenetin.

According to the method of Hörhammer *et al*,[5] 4′-benzyloxy-3-hydroxy-3′,5,6,7-tetramethoxyflavone (V) was prepared from 2-hydroxy-4,5,6-trimethoxyacetophenone (VI) *via* 4-benzyloxy-2′-hydroxy-3,4′,5′,6′-tetramethoxychalcone (VII); it was obtained in a yield of 83% (lit.[5] 49%). The flavonol (V) was also obtained by a similar oxidation of 4′-benzyloxy-3′,5,6,7-tetramethoxyflavanone (VIII), which had been prepared by the acid-catalyzed isomerization of VII. The catalytic debenzylation of V gave II; mp 236—237°C (lit.[2] mp 235°C).

Now, an attempt at the selective demethylation of the 5-methoxyl group of II with anhydrous aluminum chloride in ether, using the method of Mani and Venkataraman[2] or a modification of it, failed, but, not unexpectedly, it did lead to the recovery of the starting material. Therefore, the other effective methods were used on II; a) leaving it with anhydrous aluminum chloride in nitrobenzene at room temperature, and b) fusion with aniline hydrochloride.

When II in nitrobenzene was treated with anhydrous aluminum chloride at room temperature for 5 hr, a demethylated flavone was isolated as yellow needles, mp 213—214°C, in a yield of 52%. The same flavone was also obtained in a yield of 19% by the fusion of II with aniline hydrochloride at 180°C for 1 hr. The mass spectrum of this demethylated flavone showed a molecular ion peak at *m/e* 360, supporting the molecular formula of $C_{18}H_{16}O_8$ (Mwt 360.31); the NMR spectrum in dimethyl sulfoxide-d_6 showed the presence of three methoxyl groups, at δ 3.74, 3.85, and 3.91 (each 3H singlet), three hydroxyl groups, at δ 9.47, 9.73, and 12.42 (each 1H singlet), and four aromatic protons, at δ 6.88 (C_8–H singlet), 6.95 ($C_{5'}$–H, doublet, J=9 cps), 7.77 ($C_{6'}$–H, double doublet, J=2 cps and 9 cps), and 7.81 ($C_{2'}$–H, doublet, J=2 cps). The demethylated flavone was also characterized as its triacetate (IX), which gave the original flavone (mp 213—214°C) (by acid hydrolysis), its dibenzyl ether (X), and its dimethyl ether, 5-hydroxy-3,3′,4′,6,7-pentamethoxyflavone (XI). The compound XI was further methylated to 3,3′,4′,5,6,7-hexamethoxyflavone (XII), which was identical with a sample prepared by the methylation of II. The structures of XI and XII were confirmed by direct comparisons with authentic sample[6]; this proved that there was no isomeric

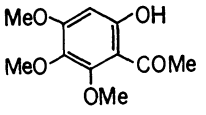

VI

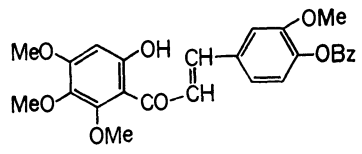

VII

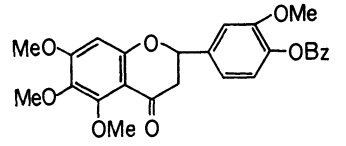

VIII

Bz = Benzyl

3) K. Fukui and T. Matsumoto, *Nippon Kagaku Zasshi* (*J. Chem. Soc. Japan, Pure Chem. Sect.*), **86**, 1079 (1965).

4) M. Krishnamurti, T. R. Seshadri and P. R. Shankaran, *Tetrahedron*, **22**, 941 (1966).

5) L. Hörhammer, H. Wagner, E. Graf and L. Farkas, *Chem. Ber.*, **98**, 548 (1965).

6) K. Fukui, T. Matsumoto, S. Nakamura, M. Nakayama and T. Horie, This Bulletin, **41**, 1413 (1968).

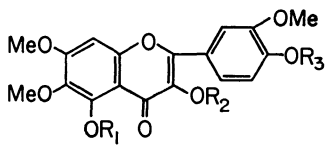

V R_1=Me, R_2=H, R_3=Bz
IX R_1=R_2=R_3= Ac
X R_1=H, R_2=R_3= Bz
XI R_1=H, R_2=R_3= Me
XII R_1=R_2=R_3= Me

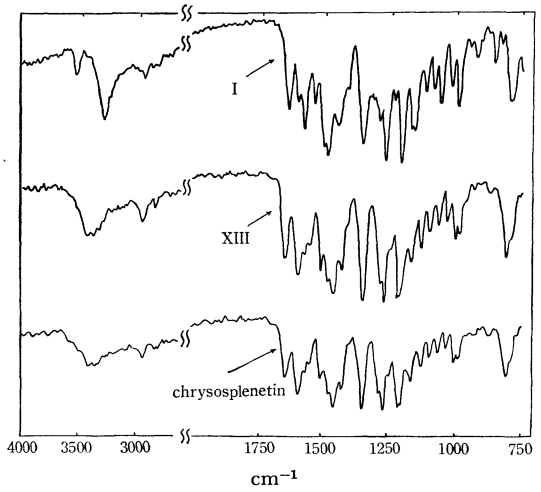

Fig. 1. Infrared spectra of I, XIII and chrysosplenetin in KBr.

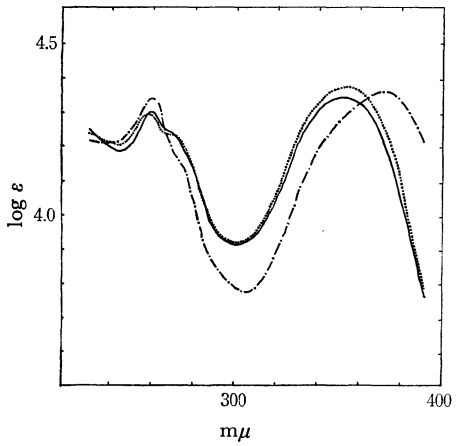

Fig. 2. Ultraviolet spectra of I (·—·—·), XIII (·····) and chrysosplenetin (——) in ethanol.

change during the demethylation of II. As is shown in Table 1, a long-wavelength band in the UV spectrum of X undergoes a bathochromic shift (29 mμ) upon the addition of aluminum chloride;[7] this shows the presence of a free 5-hydroxyl group.

From these facts, the structure of the demethylated flavone was established to be 3,4′,5-trihydroxy-3′,6,7-trimethoxyflavone (I); this identification was also supported by the UV spectra (see Table 1). The synthetic flavone (I) was found not to be identical with natural chrysosplenetin, mp 177—178°C*2 (lit.[1] mp 158—159°C) by a mixed-melting-point determination and by a comparison of their IR, UV, NMR, and mass spectra.

Consequently, the correct structures of chrysosplenetin and chrysosplenin*2 were studied further. We used spectroscopic methods because of the small amount of the natural sample available.

a) Chrysosplenetin. The NMR spectrum of chrysosplenetin in pyridine-d_5 showed the presence of four methoxyl groups, at δ 3.86 (6H singlet) and 4.01 (6H singelt), and four aromatic protons, at δ 6.87 (C_8–H, singelt), 7.37 ($C_{5'}$–H, doublet, J=9 cps), 7.93 ($C_{6'}$–H, double doublet, J=2 cps and 9 cps), and 8.00 ($C_{2'}$–H, doublet, J=2 cps). In the UV spectra (Table 1), a free 5-hydroxyl group is indicated by the bathochromic shift (31 mμ) of the long-wavelength band in the presence of aluminum chloride. The large bathochromic shift (67 mμ or 57 mμ) of the long-wavelength band in ethanol upon the addition of fused sodium acetate[8] or sodium hydroxide[7] suggests the presence of a free 4′-hydroxyl group. Chrysosplenetin is stable in an alkaline solution, for when the alkaline solution is acidified, the spectrum changes to the parent one in ethanol. This suggests the absence of a free 3,4′-dihydroxyl group. The absence of a free *o*-dihydroxyl group is also indicated by effects of the addition of boric acid and sodium acetate.[8,9] It has already been made clear that chrysosplenetin is a quercetagetin derivative.[1] Therefore, the structure of chrysosplenetin must be 4′,5-dihydroxy-3,3′,6,7-tetramethoxyflavone (XIII). In addition, the molecular ion peak in the mass spectrum of chrysosplenetin was observed at *m/e* 374, supporting the XIII structure, $C_{19}H_{18}O_8$ (Mwt 374.33). Finally, chrysosplenetin was compared with authentic XIII specimens which had previously been synthesized by Hörhammer *et al.*[5] and by Fukui *et al.*[6] by the different routes; all the samples were shown to be identical by a mixed-melting-point determination and by a comparison of their IR, UV, NMR, and mass spectra.

b) Chrysosplenin. The NMR spectrum of chrysosplenin in dimethyl sulfoxide-d_6 showed the presence of four methoxyl groups, at δ 3.75, 3.84,

7) L. Jurd, "The Chemistry of Flavonoid Compound," ed. by T. A. Geissman, Pergamon Press, Oxford (1962), Chap. 5.

*2 Natural samples were kindly supplied by Professor N. Morita; the melting points, after one crystallization, were observed in this laboratory.

8) L. Jurd and R. M. Horowitz, *J. Org. Chem.*, **22**, 1618 (1957); B. Gentili and R. M. Horowitz, *Tetrahedron*, **20**, 2313 (1964).

9) L. Jurd, *Arch. Biochem. and Biophys.*, **63**, 376 (1956).

Table 1. Ultraviolet spectra of I, X, XIII, chrysosplenin and chrysosplenetin

	λ_{max} mμ (log ε)					
	EtOH	NaOAc*3	$AlCl_3$*4	NaOH*4	NaOH-HCl*5	NaOAc-H_3BO_3*3,*4
I	259 (4.34)	259.5(4.33)	270 (4.37)	326 (4.12)	269 (4.20)	259 (4.35)
	273*6(4.17)	271*6(4.26)	304*6(3.75)		297 (4.15)	273*6(4.20)
	370 (4.36)	378 (4.27)	390*6(4.23)			373 (4.34)
		420*6(3.82)	428 (4.38)			
X	258.5(4.33)	258.5(4.32)	269 (4.32)	293.5(4.32)	259 (4.36)	
	273 (4.29)	273.5(4.28)	284 (4.31)	380*6(3.69)	272*6(4.33)	
	347 (4.34)	346 (4.32)	376 (4.33)		348 (4.32)	
Chrysosplenin	255 (4.20)	256 (4.19)	264 (4.20)	292 (4.18)	256 (4.16)	255 (4.23)
	275 (4.24)	274 (4.25)	287.5(4.26)	380 (3.73)	274 (4.21)	274 (4.27)
	344 (4.30)	342 (4.28)	367 (4.31)		342 (4.19)	342 (4.30)
Chrysosplenetin	259 (4.28)	261 (4.26)	272*6(4.27)	271 (4.19)	259 (4.26)	262 (4.30)
	271*6(4.23)	271*6(4.25)	282 (4.27)	410 (4.34)	271*6(4.20)	271*6(4.27)
	353 (4.34)	358 (4.16)	384 (4.32)		353 (4.30)	358 (4.31)
		420 (4.15)				
XIII	258 (4.28)	259 (4.27)	268.5(4.25)	270 (4.29)	258 (4.29)	
	272*6(4.23)	272*6(4.23)	282 (4.27)	410 (4.42)	270*6(4.24)	
	353 (4.37)	353 (4.33)	380 (4.36)		353 (4.42)	
		420 (3.77)				

3.90, and 3.93 (each 3H singlet), of four aromatic protons, at δ 6.96—7.85 (multiplet), and one hydrogen-bonding hydroxyl group, at δ 12.58 (1H broad singelt), which latter suggests the presence of a 5-hydroxyl group. In the UV spectra (Table 1), a free 5-hydroxyl group is also supported by the bathochromic shift (23 mμ or 36 mμ) of the long-wavelength band upon the addition of aluminum chloride or sodium hydroxide. The absence of a free 3- or 4'- or 7-hydroxyl group, a free 3,4'-dihydroxyl group, and a free *o*-dihydroxyl group is also indicated by the spectra summarized in Table 1. The above spectral evidence leads to the identification of chrysosplenin as the 4'-glucoside (XIV) of chrysosplenetin.

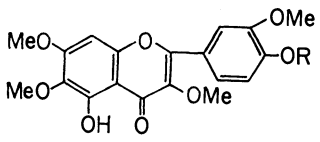

XIII R = H

XIV R = Glucosyl

*3 Saturated with fused sodium acetate.

*4 0.002 mol/*l*.

*5 The alkaline solution was acidified with dilute hydrochloric acid.

*6 Inflection.

Experimental*7

4-Benzyloxy-2'-hydroxy-3,4',5',6'-tetramethoxychalcone (VII). A mixture of 2-hydroxy-4,5,6-trimethoxyacetophenone (VI)[10] (5.5 g), 4-benzyloxy-3-methoxybenzaldehyde (13.5 g), aqueous sodium hydroxide (50%, 140 g), and ethanol (400 m*l*) was treated by a method similar to that of Hörhammer *et al.*[5] The crude product was recrystallized from a benzene-methanol mixture to give VII, mp 158—159°C, which gave a brown ferric chloride reaction in ethanol; yield 9.0 g (83%) (lit.[5] mp 158—159°C, yield 49%).

Found: C, 69.58; H, 5.61%. Calcd for $C_{26}H_{26}O_7$: C, 69.32; H, 5.82%.

4'-Benzyloxy-3', 5, 6, 7-tetramethoxyflavanone (VIII). A mixture of VII (16.0 g) and ethanolic sulfuric acid (3%: 1.6 *l*) was refluxed for 9 hr. Most of the solvent was evaporated under a vacuum, and the residue was poured into water (2 *l*). The precipitate was collected, washed with water, and then treated with methanol. From the sparingly-soluble part, the starting material (VII) (6.6 g, 41%) was recovered; the soluble part was recrystallized from methanol to give VIII as colorless needles, mp 126°C, which gave a negative

*7 All melting points are uncorrected. The NMR spectra were taken on a Hitachi Model R-20 NMR spectrometer (60 Mc/sec), using tetramethylsilane as the internal standard; their chemical shifts are presented in terms of δ values; s: singlet, bs: broad singlet, d: doublet, dd: double doublet, m: multiplet.

10) V. D. N. Sastri and T. R. Seshadri, *Proc. Indian Acad. Sci.*, **23A**, 262 (1946).

ferric chloride reaction; yield 6.4 g (40%).

Found: C, 69.47; H, 5.79%. Calcd for $C_{26}H_{26}O_7$: C, 69.32; H, 5.82%.

4'-Benzyloxy-3-hydroxy-3',5,6,7-tetramethoxyflavone (V). To a boiling solution of VIII (0.6 g) in methanol (50 ml) there were added hydrogen peroxide (30%: 3.0 ml) and then aqueous potassium hydroxide (20%: 10 ml). After the refluxing had been continued for 1.5 min, the mixture was poured onto ice (200 g), and the alkaline solution was acidified with dilute hydrochloric acid. The yellow precipitate was collected, washed with water, and then recrystallized from acetone to give V as yellow needles, mp 201—202°C, which gave a brown ferric chloride reaction in ethanol; yield 0.1 g (16%). This substance was identical with a sample (mp 201—202°C) (lit.[5] mp 202°C) prepared by the method of Hörhammer *et al.*[5] UV: λ_{max}^{EtOH} mμ (log ε); 237*[6] (4.29), 255 (4.37), 360 (4.39).

Found: C, 67.34; H, 5.25%. Calcd for $C_{26}H_{24}O_8$: C, 67.23; H, 5.21%.

Benzyl Ether of V. A mixture of V (460 mg), benzyl chloride (140 mg), anhydrous potassium carbonate (700 mg), and dimethylformamide (4.0 ml) was gently refluxed for 1 hr. After the mixture had been poured into water, the precipitate was collected, washed with water, and then recrystallized from ethanol to give colorless needles, mp 105.5—106.5°C, which gave a negative ferric chloride reaction; yield 490 mg (88%).

Found: C, 71.63; H, 5.50%. Calcd for $C_{33}H_{30}O_8$: C, 71.47; H, 5.45%.

3,4'-Dihydroxy-3',5,6,7-tetramethoxyflavone (II). A solution of V (700 mg) in ethyl acetate (700 ml) was submitted to catalytic hydrogenolysis at room temperature in the presence of Pd-C (5%; 700 mg). After the catalyst had been filtered off, the filtrate was evaporated, and then the residue was recrystallized from ethyl acetate to give II as yellow needles, mp 236—237°C (lit.[2] mp 235°C), which gave a brown ferric chloride reaction in ethanol; yield 510 mg (91%). UV: λ_{max}^{EtOH} mμ (log ε); 237*[6] (4.24), 255 (4.33), 364 (4.37). NMR in DMSO-d_6: 3.78 (s, MeO), 3.86 (s, 2MeO), 3.95 (s, MeO), 6.97 (d, J_{ortho}=9 cps, $C_{5'}$–H), 7.17 (s, C_8–H), 7.73 (dd, J_{ortho}=9 cps, J_{meta}=2 cps, $C_{6'}$–H), 7.79 (d, J_{meta}=2 cps, $C_{2'}$–H), 8.94 (bs) and 9.63 (bs) (C_3–OH and $C_{4'}$–OH). Mass spectrum: *m/e* 374 (M^+).

Found: C, 61.04; H, 4.87%. Calcd for $C_{19}H_{18}O_8$: Mwt, 374.33; C, 60.96; H, 4.85%.

Diacetate of II. Hot acetic anhydride-pyridine method; mp 169—170°C (from ethanol). NMR in $CDCl_3$: 2.35 (s, 2AcO), 3.89 (s, 2MeO), 3.98 (s, 2MeO), 6.75 (s, C_8–H), 7.15 (d, J_{ortho}=9 cps, $C_{5'}$–H), 7.41 (m, $C_{2'}$–H and $C_{6'}$–H).

Found: C, 60.13; H, 4.88%. Calcd for $C_{23}H_{22}O_{10}$: C, 60.26; H, 4.84%.

3,4',5-Trihydroxy-3',6,7-trimethoxyflavone (I). *a) With Aluminum Chloride in Nitrobenzene.* The flavone (II) (400 mg) was added to a mixture of anhydrous aluminum chloride (4.0 g) and dry nitrobenzene (40 ml). After the mixture had stood at room temperature for 5 hr, ice (25 g) and then concentrated hydrochloric acid (25 ml) were stirred into the mixture and cooled in an ice-water bath. The nitrobenzene was removed by steam distillation, and the residual precipitate was collected, washed with water, and then recrystallized from methanol to give I as yellow needles, mp 213—214°C, which gave a dark green ferric chloride reaction in ethanol; yield 200 mg (52%). The mixed melting point with natural chrysosplenetin (mp 177—178°C) was 163—174°C.

Found: C, 60.20; H, 4.41%. Calcd for $C_{18}H_{16}O_8$: C, 60.00; H, 4.48%.

b) With Aniline Hydrochloride. A mixture of II (700 mg) and aniline hydrochloride (1.50 g) was heated at 180°C for 1 hr, and then cooled. After the addition of water (40 ml), the precipitate was collected, washed with water, and recrystallized from methanol to give yellow needles, mp 213—214°C, which was shown to be identical with that of the sample of a) by a mixed-melting-point determination and by a comparison of the IR spectra; yield 130 mg (19%).

c) Hydrolysis of IX. A mixture of IX (200 mg), concentrated hydrochloric acid (20 ml), and ethanol (80 ml) was refluxed for 1.5 hr. After the evaporation of the solvent under a vacuum, the residue was poured into an ice-water mixture (*ca.* 80 ml). The precipitate was collected, washed with water, and then recrystallized from methanol to give yellow needles, mp 213—214°C, which was identical with that of the sample of a); yield 105 mg (71%).

3,4',5-Triacetoxy-3',6,7-trimethoxyflavone (IX). A mixture of I (300 mg), acetic anhydride (4.0 ml), and dry pyridine (6.0 ml) was refluxed for 1.5 hr. The crude product was then recrystallized from acetone to give the triacetate (IX) as colorless needles, mp 228—230°C, which gave a negative ferric chloride reaction; yield 320 mg (79%). UV: λ_{max}^{EtOH} mμ (log ε); 241 (4.29), 308 (4.13). NMR in $CDCl_3$: 2.30 (s, AcO), 2.33 (s, AcO), 2.46 (s, AcO), 3.84 (s, MeO), 3.87 (s, MeO), 3.97 (s, MeO), 6.88 (s, C_8–H), 7.14 (d, J_{ortho}=9 cps, $C_{5'}$–H), 7.40 (overlap, $C_{2'}$–H), 7.42 (dd, J_{ortho}=9 cps, J_{meta}=2 cps, $C_{6'}$–H). Mass spectrum: *m/e* 486 (M^+).

Found: C, 59.20; H, 4.67%. Calcd for $C_{24}H_{22}O_{11}$: Mwt., 486.42; C, 59.26; H, 4.56%.

3,4'-Dibenzyloxy-5-hydroxy-3',6,7-trimethoxyflavone (X). A mixture of I (90 mg), benzyl chloride (145 mg), anhydrous potassium carbonate (1.5 g), and dry acetone (30 ml) was refluxed for 15 hr. The crude product was then recrystallized from methanol to give the dibenzyl ether (X) as yellow needles, mp 141—142°C, which gave a green ferric chloride reaction in ethanol; yield 32 mg (24%).

Found: C, 71.05; H, 5.17%. Calcd for $C_{32}H_{28}O_8$: C, 71.10; H, 5.22%.

5-Hydroxy-3,3',4',6,7-pentamethoxyflavone (XI). To a solution of I (800 mg) in acetone (100 ml), an ethereal diazomethane solution was added; then the mixture was allowed to stand at room temperature for 3.5 hr. After the solvent had been evaporated, the residue was recrystallized from methanol to give XI as yellow needles, mp 161—162°C, which gave a green ferric chloride reaction in ethanol; yield 600 mg (70%). The melting point was undepressed on admixture with an authentic sample[6] (mp 161—162°C). UV: λ_{max}^{EtOH} mμ (log ε); 239 (4.12), 255.5 (4.27), 272.5 (4.23), 345 (4.35). NMR in $CDCl_3$: 3.85 (s, MeO), 3.90 (s, MeO), 3.95 (s, 3MeO), 6.51 (s, C_8–H), 7.00 (d, J_{ortho}=9 cps, $C_{5'}$–H), 7.75 (dd, J_{ortho}=9 cps, J_{meta}=2 cps, $C_{6'}$–H), 7.71 (d, J_{meta}=2 cps, $C_{2'}$–H), 12.60 (s, C_5–OH).

Found: C, 61.70; H, 5.33%. Calcd for $C_{20}H_{20}O_8$: C, 61.85; H, 5.19%.

3,3′,4′,5,6,7-Hexamethoxyflavone (XII). *a) From II.* A mixture of II (300 mg), dimethyl sulfate (200 mg), anhydrous potassium carbonate (2.0 g), and dry acetone (250 m*l*) was refluxed for 15 hr. After the mixture had been filtered, the filtrate was evaporated, washed successively with aqueous sodium hydroxide, and water, and then recrystallized from methanol to give XII as colorless needles; mp 142—143°C, which was identical with that of an authentic sample[6] (mp 142—143°C); yield 210 mg (65%). It gave a negative ferric chloride reaction. NMR in $CDCl_3$: 3.84 (s, MeO), 3.89 (s, MeO), 3.94 (s, 3MeO), 3.99 (s, MeO), 6.75 (s, C_8–H), 6.98 (d, J_{ortho}=9 cps, $C_{5'}$–H), 7.71 (dd, J_{ortho}=9 cps, J_{meta}=2 cps, $C_{6'}$–H), 7.70 (d, J_{meta}=2 cps, $C_{2'}$–H).

Found: C, 62.54; H, 5.37%. Calcd for $C_{21}H_{22}O_8$: C, 62.68; H, 5.51%.

b) From XI. A mixture of XI (370 mg), dimethyl sulfate (150 mg), anhydrous potassium carbonate (2.0 g), and dry acetone (150 m*l*) was refluxed for 60 hr. The reaction mixture was then treated by the method of a) to give XII; mp 142—143°C, which was identical with that of the sample of a); yield 280 mg (73%).

4′,5-Dihydroxy-3,3′,6,7-tetramethoxyflavone(XIII). The flavone (XIII: mp 181—182°C) was prepared by the method of Hörhammer *et al.*[5]; it was proved to be identical with a sample prepared by the method of Fukui *et al.*.[6] NMR in pyridine-d_5: 3.86 (s, 2MeO), 4.01 (s, 2MeO), 6.87 (s, C_8–H), 7.37 (d, J_{ortho}=9 cps, $C_{5'}$–H), 7.93 (dd, J_{ortho}=9 cps, J_{meta}=2 cps, $C_{6'}$–H), 8.00 (overlap, $C_{2'}$–H). NMR in DMSO-d_6: 3.73 (s, MeO), 3.82 (s, MeO), 3.88 (s, MeO), 3.92 (s, MeO), 6.90 (s, C_8–H), 6.99 (d, J_{ortho}=9 cps, $C_{5'}$–H), 7.65 (dd, J_{ortho}=9 cps, J_{meta}=2 cps, $C_{6'}$–H), 7.72 (overlap, $C_{2'}$–H), 9.87 (bs, $C_{4'}$–OH), 12.62 (s, C_5–OH). Mass spectrum: *m/e* 374 (M^+).

Found: C, 60.79; H, 4.76%. Calcd for $C_{19}H_{18}O_8$: Mwt., 374.33; C, 60.96; H, 4.85%.

The mixed melting point of XIII with natural chrysosplenetin (mp 177—178°C) was 178—180.5°C.

Diacetate of XIII. Mp 191—192°C, identical with that of an authentic sample[6] (mp 191—192°C). NMR in $CDCl_3$: 2.31 (s, AcO), 2.47 (s, AcO), 3.77 (s, MeO), 3.83 (s, MeO), 3.87 (s, MeO), 3.95 (s, MeO), 6.85 (s, C_8–H), 7.16 (d, J_{ortho}=9 cps, $C_{5'}$–H), 7.65 (dd, J_{ortho}=9 cps, J_{meta}=2 cps, $C_{6'}$–H), 7.74 (overlap, $C_{2'}$–H). Mass spectrum: *m/e* 458 (M^+).

Found: C, 60.03; H, 4.76%. Calcd for $C_{23}H_{22}O_{10}$: Mwt., 458.41; C, 60.26; H, 4.84%.

Chrysosplenetin. Mp 177—178°C*[2]. Mass spectrum: *m/e* 374 (M^+) ($C_{19}H_{18}O_8$: Mwt=374.33). NMR in pyridine-d_5: 3.86 (s, 2MeO), 4.01 (s, 2MeO), 6.87 (s, C_8–H), 7.37 (d, J_{ortho}=9 cps, $C_{5'}$–H), 7.93 (dd, J_{ortho}=9 cps, J_{meta}=2 cps, $C_{6'}$–H), 8.00 (d, J_{meta}=2 cps, $C_{2'}$–H). UV: λ_{max}^{EtOH} mμ (log ε); 259 (4.28), 271*[6] (4.23), 353 (4.34).

The authors are grateful to Professor N. Morita, Toyama University, for his gifts of natural chrysosplenetin and chrysosplenin. Thanks are also due to the Toyo Soda Co., Ltd., for the mass spectral measurements. This work was supported by a grant-in-aid from the Ministry of Education.

Appendix. Since this paper had been submitted, Shimizu and Morita reported on the structure of chrysosplenin in a communication form (*Chem. Pharm. Bull. Japan*, **16**, 2310 (1968)), and those authors concluded that chrysosplenin was a mixture of 4′,5-dihydroxy-3,3′,6,7-tetramethoxyflavone-4′-monoglucoside (XIV, chrysosplenoside-B) and 3′ or 4′-monoglucoside of 3′,4′,5-trihydroxy-3,6,7-trimethoxyflavone (chrysosplenoside-D) in a 68 : 32 ratio.

BULLETIN OF THE CHEMICAL SOCIETY OF JAPAN VOL. 42 1404—1407 (1969)

Reaction of Vetivazulene with Sulfur. 3,5,9-Trimethylazuleno-[1,2-*b*]thiophene

Shûichi HAYASHI, Shinji KUROKAWA*1 and Tamon MATSUURA

Department of Chemistry, Faculty of Science, Hiroshima University, Senda-machi, Hiroshima

(Received September 30, 1968)

Vetivazulene was heated with sulfur to give a new sulfur-containing azulene, 3,5,9-trimethylazuleno[1,2-*b*]thiophene. On Vilsmeier formylation, the compound normally resulted in the formation of 4-formyl derivative, while the acetylation according to the Vilsmeier procedure proceeded abnormally to produce 4-dimethylamino-3,5,9-trimethylazuleno[1,2-*b*]thiophene.

In previous papers[1,2] it has been reported that the reaction of S-guaiazulene with sulfur formed a sulfur-containing azulene, 3,5,8-trimethylazuleno-[6,5-*b*]thiophene. We will describe here how the reaction of vetivazulene with sulfur formed a new sulfur-containing azulene, whose structure was determined to be 3,5,9-trimethylazuleno[1,2-*b*]-thiophene (II). This is a condensed ring compound consisting of azulene and thiophene nuclei; an α-bond of an azulene nucleus and a *b*-bond of a thiophene nucleus were common between the two nuclei, as in the azuleno[2,1-*b*]thiophene synthesized by Matsui,[3] but the relative configurations of the two nuclei are opposite. We also attempted to compare the reactivity in the electrophilic substitution by means of Vilsmeier acylation.

Results and Discussion

The Structure of the Sulfur-containing Azulene. Vetivazulene was heated with sulfur; dark blue prisms, mp 93.5—94.0°C, with the molecular formula of $C_{15}H_{14}S$ were obtained.

When the compound was subjected to reductive desulfurization with the Raney nickel catalyst (W-2 type) and subsequent dehydrogenation by means of chloranil or 30% palladium-on-charcoal, vetivazulene, the starting material, was regenerated in a good yield. Hence, the compound is certain to retain the vetivazulene skeleton in the molecule.

In the NMR spectrum of this compound (Fig. 1-B) the isopropyl signals (methyl doublet at 1.42 ppm and methine multiplet at 3.31 ppm) which are clearly observed in that of vetivazulene (Fig. 1-A) can not be seen; the disappearnace of the isopropyl group is also observed in the IR spectrum, and the proton signals assignable to aromatic methyl groups increase from two methyl equivalents in vetivazulene to three equivalents in the compound. Such a

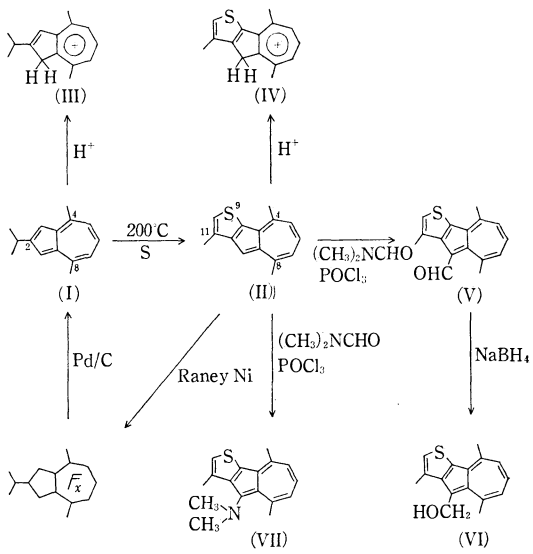

Chart 1*2

*1 Present address: Department of Chemistry, Faculty of Education, Saga University, Honjyo-cho, Saga.

1) S. Hayashi, S. Kurokawa, M. Okano and T. Matsuura, *Tetrahedron Letters*, **1967**, 3443.

2) S. Hayashi, M. Okano, S. Kurokawa and T. Matsuura, *J. Sci. Hiroshima Univ., Ser. A-II*, **31**, 79 (1967).

3) K. Matsui, *Nippon Kagaku Zasshi* (*J. Chem. Soc. Japan, Pure Chem. Sect.*), **82**, 1520, 1665, 1667 (1961).

*2 The skeleton numbering of the compound according to the IUPAC nomenclature is:

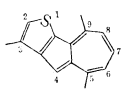

For convenience in comparing it with vetivazulene, the numbering system in the azulene compounds was adopted in this paper, though not the name of the compound.

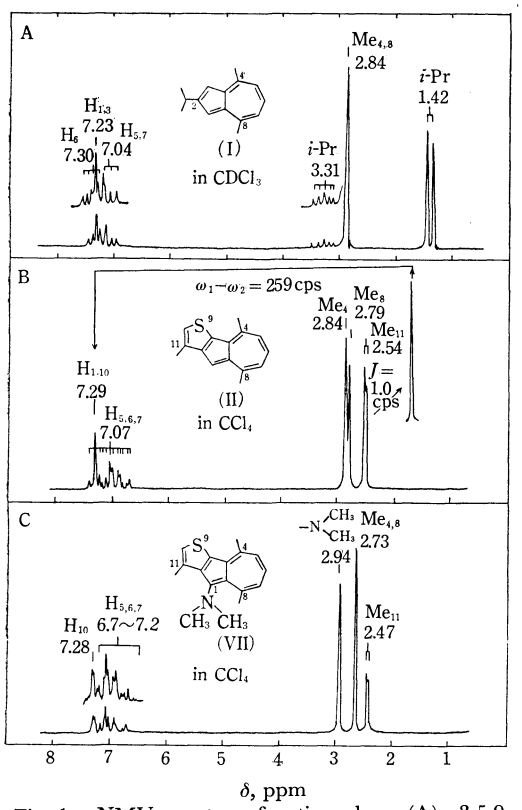

Fig. 1. NMV spectra of vetivazulene (A), 3,5,9-trimethylazuleno[1,2-*b*]thiophene (B) and 4-dimethylamino derivative (C).

change in the substituents between the starting and resulting compounds indicates that one end of the isopropyl group in vetivazulene participated in the reaction with sulfur.

The UV spectrum has an absorption maximum at 325 mμ the value of which corresponds to the bathochromic shift of 34 mμ from that of vetivazulene (291 mμ); this fact suggests that the conjugate system was elongated in the present compound. The absorption pattern of the IR spectrum in the $\nu_{C=C}$ region well resembles that of Matsui's azuleno-[2,1-*b*]thiophene.[3] The evidence of UV and IR spectroscopy thus suggests that the compound is 3,5,9-trimethylazuleno[1,2-*b*]thiophene (II).

The detailed inspection of the NMR spectrum affords reliable support for the proposed structure. An aromatic methyl doublet of 2.54 ppm (3H, J=1.0 cps) can be assigned to Me_{11} by comparison with the spectra of 3,5,8-trimethylazuleno[6,5-*b*]-thiophene,[1,2] and 3-methylbenz[*b*]thiophene,[4] and the doublet was decoupled, as expected, by irradiation upon an aromatic ring proton of 7.29 ppm (2H, singlet*3). The other two methyl singlets at 2.79 and 2.84 ppm are assigned to Me_8 and Me_4 respectively, because the groups overlapping at the same chemical shift in the spectrum of vetivazulene are considered to be resolved by the paramagnetic effect of the sulfur atom. Regarding the aromatic ring protons, one proton present in the singlet of 7.29 ppm (2H) can be assigned to H_{10} on the basis of the results of the above double-resonance experiment.

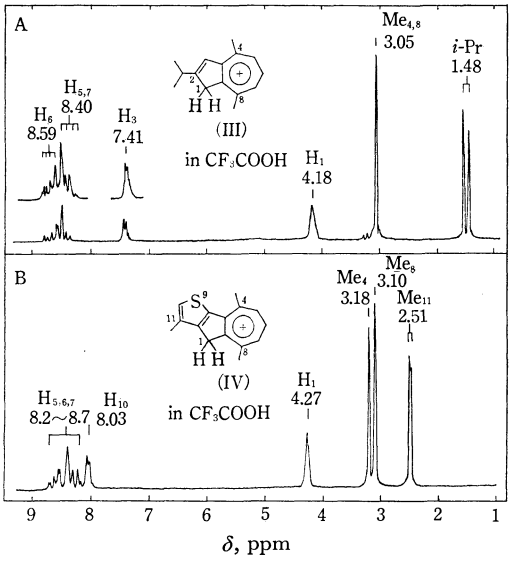

Fig. 2. NMR spectra of conjugate acids of vetivazulene (A) and 3,5,9-trimethylazuleno[1,2-*b*]thiophene (B).

If another proton of this singlet is now assigned to H_1 on the basis of comparison with the spectrum of vetivazulene, the remaining aromatic proton signals (nine lines centered at 7.07 ppm, 3H) can be assigned to H_5, H_6, and H_7 without any difficulty, for the signal pattern in nearly identical with such a spectrum of an ABC coupling system approaching an AB_2-type pattern as seen in 3-chloro-2-toluidine.[5]

The NMR spectrum (Fig. 2-B) taken in trifluoroacetic acid also supports the structure (II). A methylene singlet (2H, 4.27 ppm) which was absent in the spectrum taken in carbon tetrachloride (Fig. 1-B) can be attributed to two protons of a C_1-methylene group of the conjugate acid (IV) expected for the structure (II) on the basis of a comparison with the spectrum (Fig. 2-A) of a vetivazulenium cation. The other signals are also easily assigned as in Fig. 2-B. Regarding the conjugate acid formula (IV), the allylic coupling is expected between Me_{11} and C_{10}-ring protons, and the homoallylic coupling, between Me_8 and $2H_1$.

4) J. A. Elvidge and R. G. Foster, *J. Chem. Soc.*, **1964**, 981.

*3 Since a proton-signal of H_{10} is expected to be split into a quartet as a result of its spin-coupling with Me_{11}, this singlet may be due to the overlapping of H_{10} and H_1 signals.

5) R. E. Richards and J. Schaefer, *Mol. Phys.*, **1**, 331 (1958).

These were confirmed by double-resonance experiments; the Me_{11}-doublet at 2.51 ppm was decoupled by the saturation of H_{10}, and the half-band width (1.5 cps) of the Me_8-singlet at 3.10 ppm was reduced to two-thirds (1.0 cps) by the irradiation of H_1.

The authors have previously pointed out that Plattner's rule regarding the calculation of the visible absorption maxima of the alkylazulenes can also be applied to alkyl-substituted azulenothiophenes by replacing the standard value (17265 cm^{-1}=579 mμ) with the absorption maximum (615 mμ) of benz[*a*]azulene which has the same condensing mode.[2] The absorption maximum (592 mμ) thus calculated of the present compound*4 is in good agreement with the observed value (593 mμ). This also supports the proposed structure (II).

Electrophilic Substitution of 3,5,9-Trimethylazuleno[1,2-*b*]thiophene. Matsui has reported that azuleno[2,1-*b*]thiophene undergoes electrophilic substitution at the same position regarding the azulene nucleus, C_1 or C_3, as in the case of alkyl azulenes.[3] For confirmation of this, Vilsmeier formylation and acetylation[6] were attempted.

Formylation: Formation of 4-Formyl-3,5,9-trimethylazuleno[1,2-*b*]thiophene (V). In the presence of phosphorus oxychloride the condensation of *N*,*N*-dimethylformamide with 3,5,9-trimethylazuleno[1,2-*b*]thiophene was carried out; brown needles, mp 136—141°C, were thus obtained in a nearly theoretical yield.

The compound exhibited a strong absorption band due to an aldehyde group at 1632 cm^{-1} in the IR spectrum and formed an oxime of green needles, mp 193.0—194.5°C. The formyl derivative, upon reduction with sodium borohydride, gave dark blue crystals of a primary alcohol (VI) (ν_{OH} 3408—3584 cm^{-1}), mp 122.5—123.5°C. Although the NMR spectrum of this alcohol exhibited a hydroxyl proton signal at 3.37 ppm and methylene protons attached to the hydroxyl group at 4.97 ppm the remaining portion of the spectrum had a remarkable resemblance to that of original azulenothiophene, except that the integral strength of the signal of 7.29 ppm was reduced by half. This NMR spectrum indicates the introduction of a hydroxymethyl group into a C_1- or C_{10}-position. Of these positions, the C_1-position is adopted because the signal of Me_{11} is a doublet. Accordingly, it is certain that the formylation product has the structure of 4-formyl-3,5,9-trimethylazuleno[1,2-*b*]-thiophene (V), and that Vilsmeier formylation in the azulenothiophene takes place at the same position as in Matsui's azulenothiophene.

Acetylation: Formation of 4-Dimethylamino-3,5,9-trimethylazuleno[1,2-*b*]thiophene (VII). The acetylation of the azulenothiophene was carried out by using *N*,*N*-dimethylacetamide in the presence of phosphorus oxychloride; a green, oily substance was thus obtained. This compound, contrary to expectations, had an empirical formula of $C_{17}H_{19}NS$ containing one nitrogen atom, and its IR spectrum had no absorption band which could be assigned to a carbonyl group. The UV and visible absorption spectra are quite similar to those of the original azulenothiophene, except that their fine structures were reduced. Hence, it may be deduced that the resulting green oil is not a normal acetyl derivative.

These facts and the NMR spectrum (Fig. 1-C) can be reasonably explained when the dimethylamino group is directly introduced into an azulenothiophene nucleus. The methyl signals observed in the aromatic methyl region (2.47 ppm, doublet, 3H; 2.73 ppm, singlet, 6H; 2.94 ppm, singlet, 6H) can be assigned to three methyl groups located originally and two methyl groups of the dimethylamino group[7] newly introduced. The aromatic-ring-proton region of the spectrum shows a remarkable resemblance to that of the preceding formylated product. Accordingly, the obtained compound may be certainly said to have the structure of 4-dimethylamino-3,5,9-trimethylazuleno[1,2-*b*]thiophene(VII). Thus, the Vilsmeier acetylation of the azulenothiophene does not result in the introduction of an acetyl group, but the substituion of a dimethylamino group at the C_1-position in the azulene moiety. This is the first example of a dimethylamino derivative being produced in the Vilsmeier acetylation procedure.

Experimental

The melting points in this paper were uncorrected. The UV and visible absorption spectra were taken in cyclohexane. The gas chromatography was carried out at 170°C, using a column (1 m in length) of Diasolid-L impregnated by DEGS (10%).

Reaction of Vetivazulene (I) and Sulfur. A mixture of 2.50 g of vetivazulene and 1.25 g of powdered sulfur was heated at 200°C, for 4 hr with shaking under a nitrogen atomosphere. The reaction mixture, after being cooled at room temperature to solidify it, was crushed into small fragments. The fragments were then thoroughly ground together with petroleum ether in a mortar; 1.03 g of a dark violet, oily substance were extracted and chromatographed on a silica-gel column with petroleum ether. From a quickly-eluted fraction, 450 mg (18%) of unchanged vetivazulene were re-

*4 The contribution of the substituents held in the thiophene moiety is neglected (*cf.* Ref. 2).

Benz[*a*]azulene	16260 cm^{-1} (615 mμ)
4,8-Me	318×2 cm^{-1}
11-Me	0 cm^{-1}
Sum	16896 cm^{-1} (592 mμ)

6) K. Hafner and C. Bernhard, *Ann.*, **625**, 108 (1959).

7) Varian Associates, "High Resolution NMR Spectra Catalog," National Press, California (1962), No. 238.

covered, and from a slowly-eluted fraction, 310 mg (12.4%) of 3,5,9-trimethylazuleno[1,2-*b*]thiophene (II) were obtained as dark blue prisms, mp 93.5—94.0°C, after being purified by repeated recrystallizations from methanol.

Found: C, 79.54; H, 6.36; S, 14.16%. Calcd for $C_{15}H_{14}S$: C, 79.60; H, 6.23; S, 14.17%. Mass spectrum: $M^+=226$.

Desulfurization of 3,5,9-Trimethylazuleno[1,2-*b*]thiophene (II). A solution of 30 mg of the azulenothiophene (II) in 20 m*l* of absolute methanol was mixed with 0.6 mg of a W-2 Raney nickel catalyst freshly prepared; the mixture was then warmed at 60°C for 30 min under stirring. During this warming procedure the original blue color of the solution faded away. The reaction mixture was then filtered, and the nickel catalyst was repeatedly washed with ether. The filtrate and the washing were then combined; when the solvent was distilled off under reduced pressure, 20 mg of a colorless oily substance were obtained.

Dehydrogenation of the Desulfurized Product. *a) Dehydrogenation with Chloranil.* A solution of 20 mg of the desulfurized substance in 2 m*l* of isoamyl alcohol was mixed with 50 mg of chloranil, and then the mixture was refluxed in an oil bath for 2 hr. After the dark brown reaction mixture had been diluted by adding 30 m*l* of *n*-hexane, the solution was washed with water, dried, and the solvent distilled off under reduced pressure. The dark brown oil (60 mg) thus obtained was then eluted over silica gel with *n*-hexane to separate it into 20 mg of a colorless oil which eluted quickly and 0.7 mg of a violet oil which eluted slowly. The latter oil was confirmed through thin layer and gas chromatography to be identical with authentic vetivazulene.

b) Catalytic Dehydrogenation. The colorless oil (20 mg) eluted quickly in the preceding chromatography was sealed along with 20 mg of 50% palladized charcoal in a glass tube, and the mixture was heated at 300°C for 10 min. The dehydrogenated mixture was treated with 85% phosphoric acid in the usual manner; a violet oil (10 mg) was isolated which was found to be identical with vetivazulene by gas chromatography and by UV and visible absorption spectroscopy.

Vilsmeier Formylation of 3,5,9-Trimethylazuleno[1,2-*b*]thiophene (II). To a mixture of 30 mg of 3,5,9-trimethylazuleno[1,2-*b*]thiophene and 1 m*l* of *N,N*-dimethylformamide, 0.5 m*l* of *N,N*-dimethylformamide containing 0.1 g of phosphorus oxychloride was added, drop by drop, under ice cooling; the mixture was then allowed to stand overnight. The reaction mixture was then poured into 50 m*l* of water, kept slightly alkaline (*ca.* pH 9) by the addition of powdered potassium carbonate, and extracted with benzene. The 40 mg of a 4-formyl derivative (V) in the form of brown needles, mp 136—141°C, thus obtained showed a single brown spot ($R_f=2.5$) in thin-layer chromatography carried out using methylene chloride as the solvent. This spot turned yellow when sprayed with an acidic solution of 2,4-dinitrophenylhydrazine in alcohol.

Oxime. From 10 mg of 4-formyl-3,5,9-trimethylazuleno[1,2-*b*]thiophene, 10 mg of crude oxime was prepared using pyridine as a solvent; it was recrystallized from methanol to give green needles, mp 193.0—194.5°C.

Reduction of 4-Formyl-3,5,9-trimethylazuleno-[1,2-*b*]thiophene (V). Twenty-five milligrams of the 4-formyl derivative (V) were reduced with 50 mg of sodium borohydride in 5 m*l* of methanol by stirring at room temperature for 40 min. When the reaction mixture turned from brown to blue, a large amount of water was added; 30 mg of the 4-hydroxymethyl derivative (VI) were thus obtained as blue crystals. The crystals thus obtained were purified by recrystallization from ethanol to dark blue needles (3.0 mg), mp 122.0—123.5°C, which showed one blue-colored spot ($R_f=3.2$) in thin-layer chromatography using a *n*-hexane-ether (2 : 3) mixture.

$\delta_{TMS}^{CCl_4}$: Me_{11}, 2.65 (3H, doublet, $J=1.0$ cps); Me_4, 2.90 (3H, singlet); Me_8, 3.06 (3H, singlet); -OH, 3.37 (1H, singlet); $-CH_2(OH)$, 4.97 (2H, singlet); $H_{5,6,7}$, 6.88—7.16 (3H); H_{10}, 7.27 (1H, multiplet).

Acetylation of 3,5,9-Trimethylazuleno[1,2-*b*]thiophene (II). To 100 mg of azuleno[1,2-*b*]thiophene and 110 mg of *N,N*-dimethylacetamide dissolved in 1 m*l* of dry tetrahydrofuran, there was slowly added 1 m*l* of a dry tetrahydrofuran solution containing 200 mg of phosphorus oxychloride. The mixture was then refluxed on a water bath for 3 hr and treated in the same manner as in the formylation to afford 170 mg of a green oil, 39.3 mg of which was then chromatographed over an alumina column (Merck II-III) using an ether-*n*-hexane (1 : 9) mixture. The 4-dimethylamino derivative (VII) (19.3 mg) was thus obtained as a greenish-blue oil.

Found: N, 5.17; S, 11.80%. Calcd for $C_{17}H_{19}NS$: N, 5.20; S, 11.90%.

$\lambda_{max}^{cyclohexane}$ mμ (log ε): 240 (3.68), 288.5 (4.30), 310 sh (4.42), 318 (4.49), 330 sh (4.36), 364.5 (3.62), 382 (3.65), 398.2 (3.43). $\lambda_{max}^{cyclohexane}$ mμ (ε): 552 sh (371), 559 (460), 630 (405), 690 (189), 710 (158).

The authors are indebted to Professor Shô Itô of Tohoku University for his kind measurement of the mass spectra and to Dr. Hitoshi Minato of Shionogi Research Laboratory of Shionogi & Co., Ltd. for his measurement of the NMR spectra.

BULLETIN OF THE CHEMICAL SOCIETY OF JAPAN VOL. 42 1408—1411 (1969)

Syntheses of Pterocarpans. II.*1 The Synthesis of (±)-Pterocarpin*2

Kenji FUKUI and Mitsuru NAKAYAMA

Department of Chemistry, Faculty of Science, Hiroshima University, Higashi Sendamachi, Hiroshima

(Received September 30, 1968)

The reduction of medicagol methyl ether with lithium aluminum hydride in tetrahydrofuran yielded a diol. The dehydration of the diol in boiling diethylene glycol gave an ether (anhydropisatin, *O*-methyl anhydrosophorol). Then, the above ether was hydrogenated with 10% Pd-C to (±)-pterocarpin.

(−)-Pterocarpin was first isolated from the heartwood of the red sandalwood tree (*Pterocarpus santalinus*).[1] It was initially proposed by Robertson *et al.*[2] that in chemical structure it was a 3-methoxy-9,10-methylenedioxypterocarpan (I).*3 Lately, on the basis of NMR spectral analysis[3] and by a comparison[4] of synthetic (±)-dihydropterocarpin methyl ether ((±)-7,2′-dimethoxy-4′,5′-methylenedioxyisoflavan) (II) with the (−)-compound II derived from (−)-pterocarpin, the structure was revised and it was regarded as a 3-methoxy-8,9-methylenedioxypterocarpan (III).

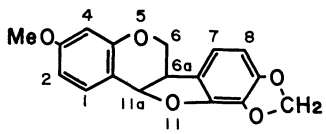

I

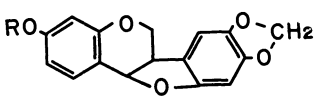

III R=Me IX R=H

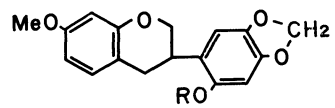

II R=Me X R=H XI R=CH_3CO

In a previous preliminary communication,[5] the present authors have already reported the total synthesis of (±)-pterocarpin*4 and confirmed the revised structure, III. The present paper will be concerned with providing a full account of the experiments. Another synthesis of (±)-pterocarpin *via* a different route has been reported.[7]

The reduction of the methyl ether (IV)[8] of medicagol (V),[9] which had been obtained by the procedure of Wanzlick's benzofurano(3′,2′ : 3,4)-coumarin synthesis,[10] with lithium aluminum hydride in tetrahydrofuran yielded 2-(2-hydroxy-4-methoxyphenyl)-3-hydroxymethyl-5,6-methylenedioxybenzo[*b*]furan (VI), with absorptions at 3350 and 3100 cm^{-1} in the infrared spectrum, in a 60% yield. This was readily transformed to a diacetate. The removal of water from the diol VI in boiling diethylene glycol gave a product (VII), $C_{17}H_{12}O_5$, which melted at 179—180°C, in a 83% yield. The

*1 Part 1: K. Fukui, M. Nakayama and T. Harano, This Bulletin, **42**, 233 (1969). Our previous paper entitled "The Synthesis of 3-Hydroxy-8,9-dimethoxypterocarpan" is included in this series.

*2 Presented at the 10th Symposium on the Chemistry of Natural Products, Tokyo, Oct., 1966. It has previously been reported in a preliminary form: K. Fukui and M. Nakayama, *Tetrahedron Letters*, **1966**, No. 16, 1805.

1) P. Cazeneuve, *Ber.*, **7**, 1789 (1874).

2) A. McGookin, A. Robertson and W. B. Whalley, *J. Chem. Soc.*, **1940**, 787.

*3 The numbering of pterocarpan is according to S. H. Harper *et al.* (*Chem. Commun.*, **14**, 309 (1965)).

3) J. B.-S. Bredenberg and J. N. Shoolery, *Tetrahedron Letters*, **1961**, No. 9, 285.

4) H. Suginome, *Experientia*, **18**, 161 (1962); This Bulletin, **39**, 1529 (1966).

5) K. Fukui and M. Nakayama, *Tetrahedron Letters*, **1966**, No. 16, 1805.

*4 (±)-Pterocarpin was derived from (±)-maackiain, a naturally-occurring pterocarpan, which had been isolated from *Sophora japonica* by Shibata and Nishikawa.

6) S. Shibata and Y. Nishikawa, *Chem. Pharm. Bull.*, **11**, 167 (1963).

7) M. Uchiyama and M. Matsui, *Agr. Biol. Chem.*, **31**, 1490 (1967).

8) K. Fukui, M. Nakayama and H. Sesita, This Bulletin, **37**, 1887 (1964).

9) a) K. Fukui, M. Nakayama, H. Tsuge and K. Tsuzuki, *Experientia*, **24**, 536 (1968); b) A. L. Livingston, S. C. Witt, R. E. Lundin and E. M. Bickoff, *J. Org. Chem.*, **30**, 2353 (1965).

10) H. W. Wanzlick, R. Gritzky and H. Heidepriem, *Chem. Ber.*, **96**, 305 (1963).

absence of a hydroxyl band in its infrared spectrum, and the close similarity of its ultraviolet spectrum (Fig. 1) of those of anhydrosophorol[11] and anhydropisatin[12] previously reported, indicated that this compound was an ether derivative. Moreover, the NMR spectrum*5 (Table 1) of VII suggested the presence of aromatic protons (5H, complex peaks from 6.5 to 7.4), methylenedioxyl protons (2H, 5.97), and methoxyl protons (3H, 3.78). The singlet peak at 5.51 (2H) is due to the ring protons. Accordingly, the structure VII is formulated: 3-methoxy-8,9-methylenedioxy-6*a*,11*a*-dehydropterocarpan (anhydropisatin,[12] *O*-methyl anhydrosophorol[13]). The identity of this product with *O*-methyl anhydrosophorol,*6 which had been obtained from sophorol (VIII)[11] by the action of acid, followed by methylation, was confirmed by a mixed-melting-point determination and by spectral comparisons. Then, VII was hydrogenated over 10% palladium-charcoal in acetic acid; this produced a product in a 60% yield. The synthetic product was found to be identical with (±)-maackiain methyl ether ((±)-pterocarpin) (III)*7 which had

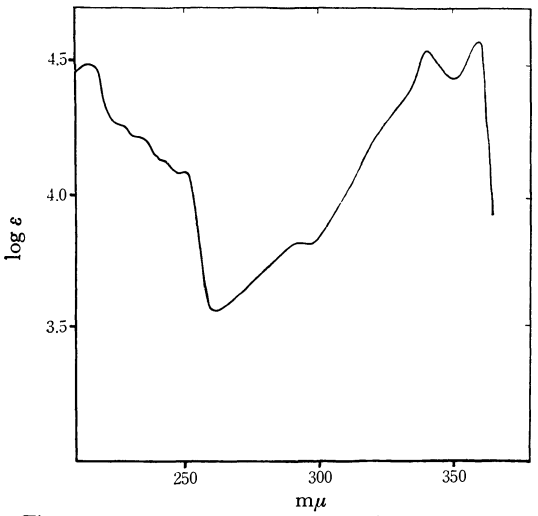

Fig. 1. UV spectrum of anhydropisatin (VII) in ethanol.

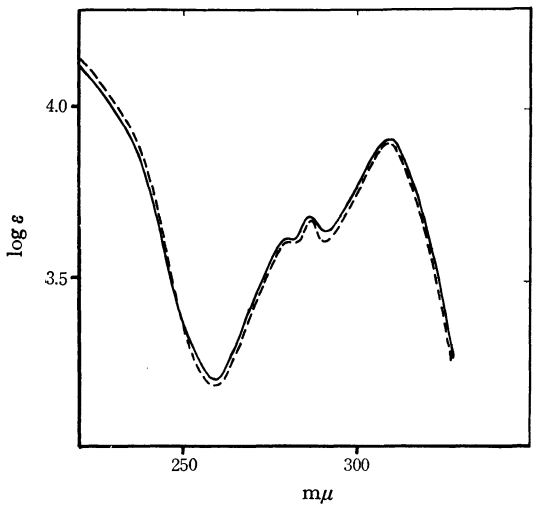

Fig. 3. UV spectra of synthetic (——) and natural (·····) (±)-pterocarpin (III) in ethanol.

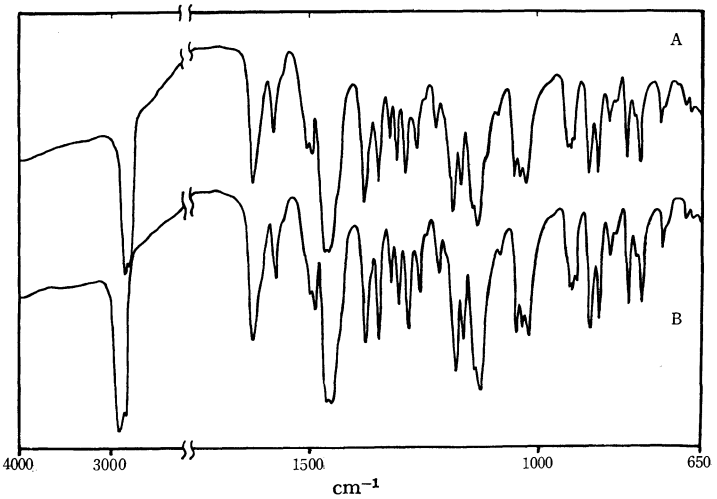

Fig. 2. IR spectra of synthetic (A) and natural (B) (±)-pterocarpin (III) in Nujol.

11) H. Suginome, *J. Org. Chem.*, **24**, 1655 (1959).

12) D. R. Perrin and W. Bottomley, *J. Am. Chem. Soc.*, **84**, 1919 (1962); D. D. Perrin and D. R. Perrin, *ibid.*, **84**, 1922 (1962).

*5 The NMR spectra were measured with Varian A-60 and Hitachi R-20 spectrometers, using tetramethylsilane as the internal standard (δ-value in $CDCl_3$).

13) H. Suginome, This Bulletin, **39**, 1525 (1966).

*6 *O*-Methyl anhydrosophorol was kindly supplied by Dr. Hiroshi Suginome, Hokkaido University.

*7 (±)-Maackiain methyl ether was kindly supplied by Professor Shoji Shibata, Tokyo University.

TABLE 1. THE NMR SPECTRAL DATA*5,*8

Protons	Compounds				
	(±)-Pterocarpin	(±)-Pterocarpin[3]	VII	(±)-II	(±)-XI
Arom.					
C-1	7.37 d	7.41 d	7.38 d	6.97 d[a]	6.97 d[a]
C-2	6.60 q	6.65 q	6.51 q	6.60 q	6.63 q
C-4	6.43 d′	6.48 d′	6.49 d′	6.41 d′	6.43 d′
C-7	6.68 s	6.72 s	6.98 s	6.64 s	6.67 s
C-10	6.40 s	6.43 s	6.70 s	6.56 s	6.59 s
Ring					
C-11*a*	5.45m	5.48m	5.51 s[b]	2.8—4.4m[c]	2.8—4.4m[c]
C-6—C-6*a*	3.35—4.20m	3.35—4.20m			
O–C$\underline{H}_2$–O	5.87 s	5.92 s	5.97 s	5.89 s	5.95 s
OC$\underline{H}_3$	3.75 s	3.78 s	3.78 s	3.78 s[d]	3.81 s
C$\underline{H}_3$CO					2.30 s

been derived from natural (±)-maackiain (IX)[6] by a mixed-melting-point determination and by infrared, ultraviolet, and NMR spectral comparisons. The infrared and ultraviolet spectra of synthetic and natural (±)-pterocarpin are superimposable, as is shown in Figs. 2 and 3. The data of the NMR spectra was in good accordance with those of (−)-pterocarpin reported by Bredenberg and Shoolery (Table 1).

The catalytic hydrogenolysis of III with either 15% palladium-charcoal or 10% palladium-charcoal at an elevated temperature in acetic acid gave (±)-2′-hydroxy-7-methoxy-4′,5′-methylenedioxyisoflavan ((±)-dihydropterocarpin (X). An acetate (XI) of X was easily prepared. Also, the methyl ether of X is identical with (±)-II reported earlier by Suginome.[4] The NMR spectra of II and XI were assigned as is shown in Table 1.

The partial synthesis of the racemate of (−)-pisatin (XII)[12] has been carried out from (−)-pterocarpin by Bevan *et al.*[14] Thus, the synthesis of (±)-XII has been now totally accomplished.

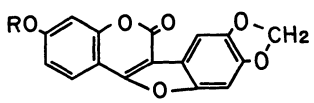

IV R=Me V R=H

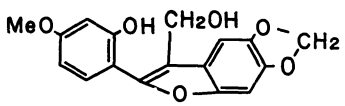

VI

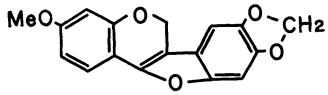

VII

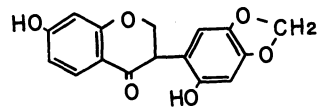

VIII

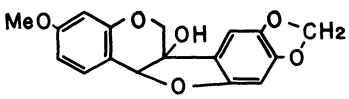

XII

Experimental*9

2-(2-Hydroxy-4-methoxyphenyl)-3-hydroxymethyl-5,6-methylenedioxybenzo[*b*]furan (VI). A suspension of medicagol methyl ether (1.0 g) (mp 269—270°C)[8] (V) in absolute tetrahydrofuran (150 m*l*) was stirred into a suspension of lithium aluminum hydride (600 mg) in absolute tetrahydrofuran (150 m*l*); the mixture was then refluxed for 3 hr. The excess lithium aluminum hydride was destroyed by the careful addition of ethyl acetate (2 m*l*) and water (50 m*l*). The cooled mixture was acidified with dilute hydrochloric acid and extracted with ether. After the removal of the solvent under diminished pressure, the resulting solid was recrystallized from benzene to give colorless prisms of VI; mp 186—187°C; yield, 600 mg (60%). IR: 3350, 3100 (OH); 1026, 941 cm^{-1} (O–CH$_2$–O). UV: λ_{max} mμ (log ε); 271 (4.11), 322 (4.36).

*8 s, singelt; d, doublet (J_{ortho}=8.5 Hz); d′, doubelt (J_{meta}=2.5 Hz); q, quartet (J_{ortho}=8.5 Hz; J_{meta}=2.5 Hz); m, multiplet.

a) The protons of C-1, 2, 4, 7 and 10 in pterocarpan is corresponding with those of C-5, 6, 8, 3′ and 6′ in isoflavan.

b) Protons (2H) of C-6.

c) Protons (5H) of C-2, 3 and 4 in isoflavan ring.

d) OCH$_3$×2=6H.

14) C. W. L. Bevan, A. J. Birch, B. Moore and S. K. Mukerjee, *J. Chem. Soc.*, **1964**, 5991.

*9 All the melting points are uncorrected; the infrared spectra were measured in Nujol, while the ultraviolet spectra were measured in an ethanol solution.

Found: C, 65.03; H, 4.64%. Calcd for $C_{17}H_{14}O_6$: C, 64.96; H, 4.49%.

The diacetate: acetic anhydride-pyridine method or hot acetic anhydride-sodium acetate method; mp 134—135°C (colorless prisms from methanol). IR: 1757, 1738 (C=O); 1025, 937 cm^{-1} (O–CH_2–O). UV: λ_{max} mμ (log ε); 274 (4.15), 320 (4.34). NMR:*5,8 7.52$_d$ (C–6′), 7.03$_s$ (C–7), 6.94$_s$ (C–4), 6.89$_q$ (C–5′), 6.73$_{d'}$ (C–3′), 5.96$_s$ (2H) (O–C$\underline{H}_2$–O), 5.23$_s$ (2H) (C$\underline{H}_2$OH), 3.87$_s$ (3H) (C$\underline{H}_3$O), 2.20$_s$ (3H) (C$\underline{H}_3$CO), 2.11$_s$ (3H) (C$\underline{H}_3$CO).

Found: C, 63.27; H, 4.60%. Calcd for $C_{21}H_{18}O_8$: C, 63.31; H, 4.55%.

3-Methoxy-8,9-methylenedioxy-6*a*,11*a*-dehydropterocarpan (Anhydropisatin, *O*-Methyl Anhydrosophorol) (VII). A solution of VI (1.2 g) in pure diethylene glycol (35 m*l*) was refluxed for 10 min. During boiling, a slow separation of the water was noted. The mixture was then cooled, diluted with water (100 m*l*), extracted with ether, and washed with a 5% aqueous sodium hydroxide solution. After the ether had been removed under diminished pressure, the resulting solid was recrystallized from ethanol to give colorless needles of VII, mp 179—180°C (lit. mp 179—180°C[12]; mp 187—188°C[13]; mp 179—180°C[14]); yield, 1.0 g (83%). IR: 1658, 1619, 1570, 1518, 1500 (C=C, aromatic); 1023, 920 cm^{-1} (O–CH_2–O). UV: λ_{max} mμ (log ε); 215 (4.49), 232$_i$ (4.22),*10 243$_i$ (4.13), 251 (4.09), 294 (3.82), 340 (4.54), 359 (4.57). (lit.[12] 215 (4.49), 234 (4.30), 244 (4.2), 257 (4.1), 291 (3.8), 339 (4.58), 358 (4.60)).

Found: C, 69.02; H, 4.14%. Calcd for $C_{17}H_{12}O_5$: C, 68.91; H, 4.08%.

This substance was found, by mixed-melting-point measurements and by ultraviolet spectral comparison, to be identical with the *O*-methyl anhydrosophorol supplied by Suginome.

(±)-Pterocarpin ((±)-Maackiain Methyl Ether) (III). A mixture of VII (500 mg) and 10% palladium-charcoal (300 mg) in acetic acid (300 m*l*) was shaken in an atmosphere of hydrogen until 1.1 mol of hydrogen had been absorbed. After the subsequent separation of the catalyst, the filtrate was evaporated under diminished pressure and the residue dissolved in ether. The ether solution was washed with a 5% aqueous sodium hydroxide solution and then with water. After the ether had been removed, the resulting solid was recrystallized from methanol to give colorless leaflets of III; mp 185—186°C (mp 185—186°C*11; lit. mp 185—186°C[6]); yield, 300 mg (60%). IR: 1634, 1585, 1503, 1493 (aromatic); 1027, 930 cm^{-1} (O–CH_2–O) (1634, 1586, 1500, 1491, 1026, 929 cm^{-1}*11; lit. 1620, 1589, 1037, 942 cm^{-1} ($CHCl_3$)[6]). UV: λ_{max} mμ (log ε); 281 (3.60), 287 (3.66), 311 (3.89) (281 (3.60), 287 (3.67), 311 (3.88)*11; lit. 280 (3.58), 286 (3.65), 310 (3.87)[6]).

Found: C, 68.55; H, 4.79%. Calcd for $C_{17}H_{14}O_5$: C, 68.45; H, 4.73%.

This substance was found, by mixed-melting-point measurements and by infrared and ultraviolet comparisons, to be identical with the natural (±)-peterocarpin supplied by Shibata.

Hydrogenolysis of (±)-III. a) A mixture of (±)-III (500 mg) and 15% palladium-charcoal (500 mg) in acetic acid (200 m*l*) was shaken in an atmosphere of hydrogen until 1.1 mol of hydrogen had been absorbed. The reaction mixture was then treated in the usual manner. The product was recrystallized from ethanol to give colorless needles of (±)-2′-hydroxy-7-methoxy-4′,5′-methylenedioxyisoflavan ((±)-dihydropterocarpin) (X); mp 177—178°C (lit. mp 176—178°C[14]); yield, 300 mg (60%). IR: 3330 (OH); 1613, 1583, 1496 (aromatic); 1025, 934 cm^{-1} (O–CH_2–O). UV: λ_{max} mμ (log ε); 287 (3.79), 297.5 (3.78).

Found: C, 68.27; H, 5.48%. Calcd for $C_{17}H_{16}O_5$: C, 67.99; H, 5.37%.

The acetate (XI): acetic anhydride-pyridine method; mp 118—119°C (colorless needles from methanol). IR: 1759 (C=O); 1036, 935 (O–CH_2–O) cm^{-1}. UV: λ_{max} mμ (log ε); 284 (3.85).

Found: C, 66.63; H, 5.23%. Calcd for $C_{19}H_{18}O_6$: C, 66.66; H, 5.30%.

b) From a mixture of (±)-III (500 mg) and 10% palladium-charcoal (500 mg) in acetic acid (200 m*l*), hydrogenolysis was carried out at 90—95°C. Recrystallization from ethanol gave (±)-X; mp 177—178°C; yield, 150 mg (30%).

(±)-7,2′-Dimethoxy-4′,5′-methylenedioxyisoflavan (II). A mixture of X (300 mg), methyl iodide (2.0 g), and anhydrous potassium carbonate (5.0 g) in anhydrous acetone (100 m*l*) was refluxed for 6 hr, and then the acetone was evaporated. The resulting solid was recrystallized from methanol to give colorless needles of (±)-II; mp 117—118°C (lit. mp 111—113°C[4]; mp 110—111°C[14]); yield, 250 mg (83%). IR: 1613, 1576, 1505 (aromatic); 1033, 939 cm^{-1} (O–CH_2–O). UV: λ_{max} mμ (log ε): 291 (3.86), 301 (3.82).

Found: C, 68.73; H, 5.89%. Calcd for $C_{18}H_{18}O_5$: C, 68.78; H, 5.77%.

The authors are grateful to Professor Shoji Shibata, Tokyo University, for supplying the (±)-maackiain methyl ether, and to Dr. Hiroshi Suginome, Hokkaido University, for supplying the *O*-methyl anhydrosophorol. They are also indebted to Professor Shô Itô, Tohoku University, for measuring the NMR spectra, and to Professor Tetsuo Mitsui, Kyoto University, for his elemental analyses. This work was supported in part by a grant-in-aid from the Ministry of Education.

*10 i=Inflection point.

*11 The natural (±)-pterocarpin was measured in this laboratory.

BULLETIN OF THE CHEMICAL SOCIETY OF JAPAN VOL. 42 1412—1416 (1969)

A Cationic Polymerization of Formaldehyde in Liquid Carbon Dioxide. V. Reaction Mechanism*1

Hisao YOKOTA*2 and Masatsune KONDO*2

Takarazuka Radiation Laboratory, Sumitomo Atomic Energy Industries Ltd., Takarazuka

and Tsutomu KAGIYA and Kenichi FUKUI

Faculty of Engineering, Kyoto University, Sakyo-ku, Kyoto

(Received October 22, 1968)

The present work was carried out in order to elucidate the reaction mechanism in the polymerization of formaldehyde in liquid carbon dioxide. Methylene glycol methylether acetate with a structure similar to that of methylene glycol monocarboxylate, which was assumed to be an initiator, exhibited a catalytic activity. On the other hand, methyl acetate terminated the polymerization. Moreover, the resulting polymer, which was terminated by the addition of methyl-$^2H_3$-acetate, contained deuterium originating from the terminator used. On the basis of these experimental results, a reaction mechanism of the elementary processes is discussed.

In our previous papers[1,2] it has been disclosed that formaldehyde, prepared by the thermal decomposition of α-polyoxymethylene, followed by no additional purification, is polymerized by a carboxylic acid catalyst in a liquid carbon dioxide solution to produce a high-molecular-weight polyoxymethylene, and that the polymerization is a cationic mechanism and belongs to a type of stationary successive polymerization with rapid initiation and no termination. Acetic anhydride added to the reaction system in advance of the polymerization reaction acetylates the endgroups of the polymer chain by means of heating the resulting polymer after the polymerization.[3] On the other hand, acetic anhydride added to a reaction system in which the polymerization was initiated by acetic acid terminates the propagation; the rate of termination was proportional to the square of the concentration of the growing polymer chain.[4]

The present paper will describe a study which was carried out in order to elucidate the role of acetic anhydride in the termination reaction and in order to discuss, in detail, the mechanism of the elementary processes in the polymerization.

Experimental

Procedure and Materials. The formaldehyde monomer was prepared and the experimental procedure of polymerization was carried out in the manner described in a previous paper.[1] The monomer concentration in each polymerization experiment was 60 wt% in liquid carbon dioxide solution, while the loading density was 10 g/30 ml.

In order to remove the contained acetic acid, acetic anhydride was purified by using the reaction with carbodiimide previously described.[3] The acetic acid content in the acetic anhydride thus prepared was less than 0.1 wt%.

Commercially-available methyl acetate and methyl formate were purified by distillation before use. Isoamyl acetate was prepared by the reaction of isoamyl alcohol with acetic acid in the presence of concentrated sulfuric acid, and was purified by distilltion under reduced pressure. Methylene glycol methylether acetate was synthesized by the reaction of potassium acetate with monochloromethyl ether[5] and was purified by distillation (bp 117—118°C). Methyl-$^2H_3$-acetate was prepared by the reaction of pure tetradeuteromethanol with acetic acid in the presence of sulfuric acid, and it was purified by distillation.

Analytical Procedures. The deuterium content in the polymer was determined by quantifying the concentration of deuterium in hydrogen gas which had been prepared from the polymer as follows.[6] The polymer was placed in a combustion tube packed with palladium

*1 A part of this work was first presented at the Meeting of International Symposium on Macromolecular Chemistry, Tokyo/Kyoto, Japan, 1966.

*2 Present address: Takarazuka Laboratory, Sumitomo Chemical Co., Ltd., Takarazuka.

1) H. Yokota, M. Kondo, T. Kagiya and K. Fukui, *J. Polymer Sci., A-1*, **6**, 425 (1968).

2) H. Yokota, M. Kondo, T. Kagiya and K. Fukui, *ibid., A-1*, **6**, 435 (1968).

3) H. Yokota, M. Kondo, T. Kagiya and K. Fukui, This Bulletin, **41**, 1668 (1968).

4) H. Yokota, M. Kondo, T. Kagiya and K. Fukui, *ibid.*, **41**, 1672 (1968).

5) L. Schreiner, *Ann.*, **197**, 8 (1879).

6) J. Graff and D. Rittenberg, *Anal. Chem.*, **24**, 878 (1952).

black and was decomposed by heating under a stream of oxygen; it was thus converted into water and carbon dioxide. The water produced was frozen out in a trap at −78°C. After evacuating the system to eliminate the carbon dioxide, the evaporated water was reduced to hydrogen gas by placing it in contact with metallic zinc heated at 400°C. The hydrogen, which was collected by the use of Toepler pump, was then analyzed by a mass spectrometer (Hitachi, Model RMU-5B).

The acetyl and hydroxyl groups of the polymer were quantified by means of a study of the infrared spectrum of the polymer film, as has already been described.[3]

Methyl acetate, acetic anhydride, and other substances were quantified by using a Perkin-Elmer Model 154D gas chromatograph equipped with a Golay column and a flame-ionization detector. The operating temperature was 80°C, and the flow rate of nitrogen as the carrier gas was 0.97 ml/min.

Results and Discussion

Endgroups of the Polymer Which Results from the Polymerization Initiated by An Acetic Acid Catalyst. When we studied the infrared spectrum of the polymer produced by the acetic-acid-initiated polymerization in a liquid carbon dioxide solution, an acetyl group was found in the polymer chain. Acetyl group in the polymer resulting from the polymerizations initiated by acetic acid both in the presence and in the absence of acetic anhydride, was quantified. The results are shown in Table 1. Here, the degree of acetylation is defined as the molar ratio of the acetyl group to the total endgroup, as has been described in a previous paper.[3] It was found that the degree of acetylation was independent of the polymer yield and the degree of polymerization in the polymerizations, both in the presence and in the absence of acetic anhydride. This fact indicates that the acetyl group in the polymer originates from acetic acid as the initiator.

Table 1. Acetyl group at chain end of the resulting polymer

Acetic anhydride mol%/ monomer	Reaction time min	Polymer yield wt%	$\bar{P}_n$	Degree of acetylation mol%
5	10	15.1	780	18
5	30	28.9	1100	12
5	60	37.2	1280	14
—	10	17.1	970	25
—	30	54.4	1750	23
—	60	70.7	2200	22

acetic acid/monomer molar ratio, 1×10^{-3}; reaction temp., 30°C

Initiation by Methylene Glycol Methylether Acetate. It has been disclosed that carboxylic acid initiates the polymerization of formaldehyde in a liquid carbon dioxide solution.[1,2] The initiator of the present polymerization was assumed to be methylene glycol monocarboxylate, produced by the following reaction between the monomer and carboxylic acid;

$$HCHO + RCOOH \rightarrow HOCH_2O\overset{O}{\overset{\|}{C}}R \qquad (1)$$

In order to verify this assumption, the catalytic activity of methylene glycol methylether acetate, $CH_3OCH_2O\overset{O}{\overset{\|}{C}}CH_3$, which has a structure similar to that of the supposed initiator, was studied in the polymerization in the absence of acetic anhydride. The effects of isoamyl acetate and methyl formate on the polymerization were also investigated for the sake of comparison. The results are shown in Table 2. Only methylene glycol methylether acetate exhibited a catalytic effect.

Table 2. Effect of esters on the polymerization[a]

Ester	Polymer yield wt%	$\bar{P}_n$	N_p[b] mol/$l\times10^2$
EA[c]	63.7	680	21
EA	42.6[d]	3400	2.8
Isoamyl acetate	7.1	370	5.5
Methyl formate	5.4	400	3.0
none	5.8	410	3.1

a) ester/monomer molar ratio, 1×10^{-3}; reaction temp., 30°C; reaction time, 10 min.
b) number of moles of polymer chain, which is defined as a ratio of the polymer yield (mol)/ the degree of polymerization.
c) methylene glycol methylether acetate
d) ester/monomer molar ratio, 1×10^{-4}

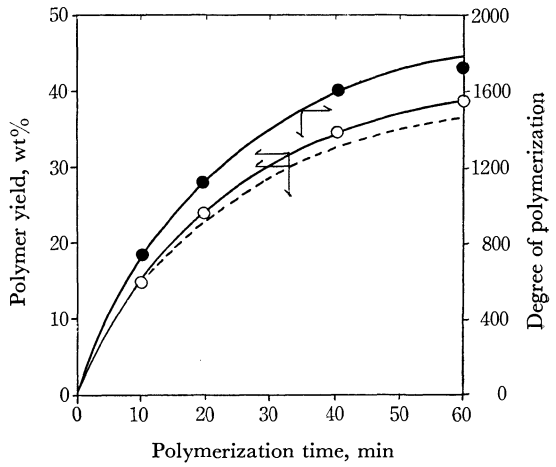

Fig. 1. Effect of methylene glycol methylether acetate on the polymerization in the presence of acetic anhydride; catalyst/monomer molar ratio, 1×10^{-3}; acetic anhydride/monomer molar ratio, 0.05; temp., 30°C; broken line, by acetic acid (quoted from the previous paper[2]).

Figure 1 shows the reaction time *versus* the polymer yield and the degree of polymerization in the polymerization which was initiated with methylene glycol methylether acetate in the presence of acetic anhydride. In the figure this polymerization is compared with the polymerization initiated by acetic acid. The results show that methylene glycol methylether acetate has almost the same catalytic activity as does acetic acid.

Formation of Methyl Acetate and the Influence of Methyl Acetate on the Polymerization. It has been already found that the termination reaction occurs only in the polymerization which is initiated with acetic acid in the presence of acetic anhydride, and that the rate of termination is proportional to the square of the concentration of the active initiating species.[4] On the other hand, the polymerization initiated with dichloroacetic acid is not terminated even in the presence of acetic anhydride.[4] Accordingly, it may be inferred that acetic acid plays an important part in the formation of a terminator. We also assumed that the methanol present in formaldehyde was another reactant in the reaction.

TABLE 3. EFFECT OF ACETIC ANHYDRIDE ON THE REACTION OF CARBOXYLIC ACIDS WITH METHANOL AT ROOM TEMPERATURE

Reactant, molar ratio			Reaction time min	Yield of ester mol%/acid	
acid	CH_3OH	$(CH_3CO)_2O$			
AA,	1	1	—	60	0 as MA
AA,	1	1	10	15	67 as MA
AA,	1	1	10	30	80 as MA
FA,	1	1	10	30	4.5 as MF
FA,	1	1	10	60	7.1 as MF
DCAA,	1	1	10	60	0 as MCA

AA, acetic acid; FA, formic acid; DCAA, dichloroacetic acid; MA, methyl acetate; MF, methyl formate; MCA, methyl dichloroacetate

In order to ascertain the above-mentioned assumptions, the influence of acetic anhydride on the esterification reaction of carboxylic acid and methanol was studied; the results are shown in Table 3. In the reaction of acetic acid with methanol, methyl acetate was not formed even after 60 min in the absence of acetic anhydride, whereas most of the acetic acid changed into methyl acetate within 30 min in the presence of acetic anhydride. The results indicate that the formation of methyl acetate is quite slow in a system in which acetic acid is absent. On the other hand, even in a reaction system in which acetic anhydride is present, formic and dichloroacetic acids, which have a stronger acidity than acetic acid, produced only a small quantity of esters. Based on the assumption that methyl acetate acts as a terminator, the above experimental results explain the extraordinary fact that the termination reaction occurred only in the polymerization initiated by acetic acid in the presence of acetic anhydride.

The reaction of methyl acetate with methylene glycol methylether acetate, which has a structure similar to that of the growing polymer chain, was studied in order to ascertain the termination reaction in which methyl acetate attacks the active chain end of the growing polymer. The results, shown in Table 4, indicate that methyl acetate reacted with methylene glycol methylether acetate to produce methylal and acetic anhydride in the following manner;

$$CH_3OCH_2O\overset{O}{\overset{\|}{C}}CH_3 + CH_3COOCH_3 \rightarrow CH_3OCH_2OCH_3 + CH_3\overset{O}{\overset{\|}{C}}O\overset{O}{\overset{\|}{C}}CH_3 \quad (2)$$

Methyl formate also produced methylal, but its yield was smaller than in the case of methyl acetate. These results support the assumption that methyl acetate terminates the propagation by means of reacting with the growing polymer chain to give a stable methoxy endgroup.

As is shown in Table 5, the addition of methyl acetate to the polymerization, which was carried out in the absence of acetic anhydride, caused the same extent of decrease in the rate of polymerization as in the polymerization which was carried out in the presence of acetic anhydride without methyl acetate, but it did not decrease the number

TABLE 4. REACTION OF ESTERS WITH METHYLENE GLYCOL METHYLETHER ACETATE AT ROOM TEMPERATURE

Reactant, molar ratio			Reaction time, min	Yield, mol%	
MGMA	Methyl acetate	Methyl formate		Methylal	Anhydride
1	1	—	30	4.5	0.21 as AH
1	1	—	100	6.2	0.65 as AH
1	1	—	200	7.8	0.68 as AH
1	—	1	180	2.1	? as MAH

MGMA, methylene glycol methylether acetate; AH, acetic anhydride; MAH, mixed anhydride of acetic and formic acids

Table 5. Effect of methyl acetate on the polymerization at 30°C

Additives, mol%/monomer			Reaction time, min	Conversion wt%	$\bar{P}_n$
CH_3COOH	$(CH_3CO)_2O$	CH_3COOCH_3			
0.1	5	—	30	25.3	980
0.1	5	—	60	36.6	1380
0.1	—	1.0	30	27.2	1260
0.1	—	1.0	60	38.0	1480
0.1	—	—	30	48.9	1730
0.1	—	—	60	53.1	1950

of moles in the resulting polymer chain. These facts lead to the conclusion that methyl acetate affects the polymerization as a terminator.

In order to confirm the terminating effect of methyl acetate, the origin of the endgroup of the polymer chain was studied by analyzing the deuterium content in the polymer which resulted from the polymerization terminated by methyl-$^2H_3$-acetate. When the amount of the deuterated methyl acetate was increased, the deuterium content increased, but both the polymer yield and the degree of polymerization decreased, as is shown in Table 6. Consequently, it was concluded that a part of the polymer chain was ended with the deuterated methyl group. This fact means that the carboxylate anion, which is a counter anion of the growing polymer chain, was replaced with a methoxy group of methyl acetate because of the termination by methyl acetate.

Table 6. Effect of methyl-D_3-acetate on the polymerization[a] and deuterium content in the resulting polymer

CH_3COOCD_3 mol%	Conversion wt%	$\bar{P}_n$	D_2/H_2 atomic %
—	48.9	1730	0.015
0.9	9.7	640	0.034
7.2	5.3	470	0.091

a) acetic acid/monomer molar ratio, 1×10^{-3}; temperature, 30°C. time, 30 min.

Mechanism of Polymerization. It has already been disclosed in the previous works of the present series[1-3] that formaldehyde is polymerized by a carboxylic acid initiator in liquid carbon dioxide solution to produce a high-molecular-weight polyoxymethylene and that the catalytic activity of carboxylic acid increases with an enhancement of the acidity of the acid used. The methanol and water present in the monomer have a chain transfer effect, but the rate of chain transfer is smaller than that of initiation or of propagation. In the polymerization which is initiated with acetic acid in the presence of acetic anhydride, acetic anhydride accelerates the formation of methyl acetate from acetic acid and methanol, and the methyl acetate thus formed attacks the active chain end of the growing polymer to terminate the propagation. Therefore, the following cationic mechanism of the polymerization in a liquid carbon dioxide solution may be presented:

Initiation: In view of the fact that methylene glycol methylether acetate showed the same catalytic activity as acetic acid, it was considered that the intiator of polymerization was methylene glycol monocarboxylate, which was formed by the loose addition reaction of formaldehyde and carboxylic acid.

$$CH_2O + RCOOH \rightarrow HOCH_2O\overset{O}{\overset{\|}{C}}R \rightarrow HOCH_2^{\oplus} \cdots {}^{\ominus}O\overset{O}{\overset{\|}{C}}R \qquad (3)$$

The ion pair formed by the dissociation of the addition compound is the initiating species. It has been reported that the rapid initiation takes place in this polymerization.[2,4] Accordingly, the dissociation of methylene glycol monocarboxylate rapidly reaches equilibrium.

Propagation: The propagation proceeds by forming a co-ordinated compound from the monomer and the initiating species as follows:

$$HOCH_2^{\oplus}\cdots{}^{\ominus}O\overset{O}{\overset{\|}{C}}R + CH_2O \longrightarrow \qquad (4)$$

$$\longrightarrow HOCH_2OCH_2^{\oplus}\cdots{}^{\ominus}O\overset{O}{\overset{\|}{C}}R \qquad (5)$$

$$\rightleftharpoons HO(CH_2O)_nCH_2^{\oplus}\cdots{}^{\ominus}O\overset{O}{\overset{\|}{C}}R \qquad (6)$$

The carboxylic acid with a larger dissociation constant gave the faster rate of propagation.[2,4] Therefore, the stability of the counter anion affects the rate of propagation.

Chain Transfer: The chain transfer reaction by methanol or water is illustrated by the following

scheme:

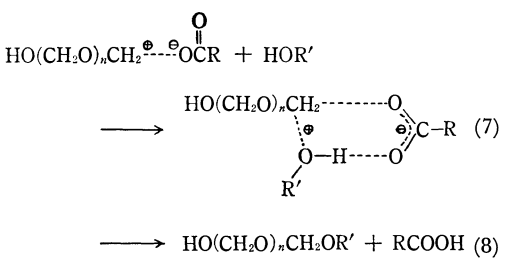

(7)

(8)

Here, R′ is the hydrogen atom or the methyl group. It has been experimentally confirmed that the rate of chain transfer caused by water or methanol is comparatively small. This fact is probably attributable to the depression in the activity of the chain transfer agent because of the solvation of liquid carbon dioxide to water and methanol, which are basic. The retardation effect of carbon dioxide on the chain transfer may be the chief reason for the high-molecular-weight polymer being produced by the cationic polymerization process at room temperature, even though the crude monomer prepared by the thermal decomposition of α-polyoxymethylene, and not additionally purified, is used as the starting material.

Termination: As has been mentioned above, the esterification of methanol and acetic acid to produce methyl acetate is remarkably accelerated in the presence of acetic anhydride. Moreover, the addition of methyl acetate terminates the propagation, with the result that the polymer produced contains methoxy endgroup originating from methyl acetate. These facts lead to the following scheme for the termination, which, extraordinarily, takes place only in the polymerization initiated with acetic acid in the presence of acetic anhydride:

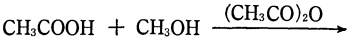

(9)

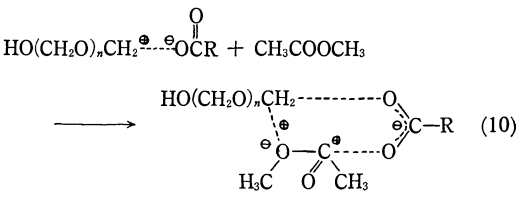

(10)

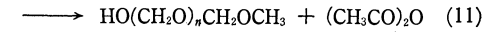

(11)

(1) The not-extremely-purified monomer, which is prepared by the thermal decomposition of α-polyoxymethylene without additional purification, can be used as the starting material to produce a high-molecular-weight polymer.

(2) The polymerization initiated by carboxylic acid proceeds by a cationic mechanism.

(3) The polymerization belongs to a successive polymerization with rapid initiation. The chain transfer caused by water or methanol present in the monomer is slower than the other elementary reactions. The rate of propagation and the number of moles of the resulting polymer chain increase with an enhancement of the acidity of the acid used as a catalyst. The termination reaction is, in general, negligible except for the polymerization to be described below.

(4) Methyl acetate, which is formed from acetic acid and methanol because of the catalytic effect of acetic anhydride, terminates the propagation only in the polymerization initiated by acetic acid in the presence of acetic anhydride.

Summary. In concluding the present series, the following summary of the characteristics of the polymerization of formaldehyde in liquid carbon dioxide and the succeeding stabilization process may be given.

The authors wish to thank Dr. K. Fujimura, Director of the Takarazuka Radiation Laboratory, for his encouragement and for permission to publish this paper. They also wish to express their gratitude to Mr. S. Nakao for his skillful measurements in the analytical procedures.

BULLETIN OF THE CHEMICAL SOCIETY OF JAPAN VOL. 42 1417—1424 (1969)

Characteristic Chemical Constitution of Pitch Materials Suitable for the MP Carbon Fiber

Sugio Ōtani and Akira Yokoyama*1

Faculty of Technology, Gunma University, Kiryu, Gunma

(Received September 16, 1968)

Pitch materials suitable for the MP carbon fiber were prepared from petroleum asphalt, coal tar pitch, and polyvinylchloride. The present investigation was undertaken to clarify the characteristic chemical constitution of each suitable pitch material and to define the significance of the special treatment required to prepare the pitch materials. The suitable pitch materials are generally composed of several structural units with aromatic fused rings and more or less alkyl side chains. The suitable pitch material finally obtained from the petroleum asphalt is characterized by a relatively high molecular weight and many quite long alkyl side chains. Special treatment is required to increase the aromaticity and the removal of the low-molecular-weight component. The suitable pitch material from the coal tar pitch is characterized by aromatic fused rings of the condensed type and only a few alkyl side chains, such as, the methyl group. The most desirable effect of the treatment is to accelerate the condensation between molecules without increasing the insoluble matter and to remove the low-molecular-weight component. The results concerning the polyvinylchloride pitch lend some support to the scheme suggested before.

In previous papers,[1-3] it has been reported that carbon fibers were prepared from polyvinylchloride (PVC), petroleum asphalt, coal tar pitch, and other pitch-like materials. We refer to the fiber so produced as the MP carbon fiber.

Pitch materials suitable for MP carbon fibers must have at least two characteristics - excellent spinnability and the ability to be easily converted into an infusible form by oxidation in the low-temperature range. The above raw materials than PVC pitch leave much to be desired. Some special treatment, therefore, is required to achieve the desirable characteristics. Up to now, only an experimental approach seems useful in discovering suitable pitch materials, because the relation between the desirable characteristics and the structures of the pitch materials is still obscure. From this point of view, it appeared of interest to investigate further the fundamental features of the pitch materials in order to improve the preparation method and the properties of the MP carbon fiber.

The present investigation was undertaken in order to clarify the following two questions the characteristic chemical constitution of the suitable materials prepared from a petroleum asphalt and coal tar pitch, and the significance of the special treatment required.

For these purposes, the pitch materials at each stage of the treatment were fractionated by extraction in turn with several solvents, and then use was made of the NMR, IR and UV spectra as well as of elemental analysis and the measurement of the mean molecular weight by the vapor-pressure osmometer method.

Experimental and Results

Raw Materials and Special Treatment. The starting raw materials and the special treatments used in this experiment are shown in Fig. 1. The PVC powder was supplied by the Kureha Chemical Ind. Co., while the PVC pitch was the pyrolyzed residue itself and was used without any further treatment. The petroleum asphalt was treated according to a procedure described previously.[2,3] In the case of the coal tar pitch, the treatment procedure was modified as is shown in Fig. 1, since the present method, in comparison with the previous method,[3] gave a better spinnability of the pitch and better mechanical properties of the carbon fiber finally obtained. The modification is characterized by the removal of the insoluble matter from the raw coal tar pitch and by heat

*1 Present address: Yokohama Plant, Nihon Carbon Co., Ltd., 1-1, Shinurashima, Kanagawa-ku, Yokohama.

1) S. Ōtani, *Carbon*, **3**, 31 (1965).

2) S. Ōtani and K. Yamada, *Kogyo Kagaku Zasshi* (*J. Chem. Soc. Japan, Ind. Chem. Sect.*), **69**, 626 (1966).

3) S. Ōtani, K. Yamada, T. Koitabashi and A. Yokoyama, *Carbon*, **4**, 425 (1966).

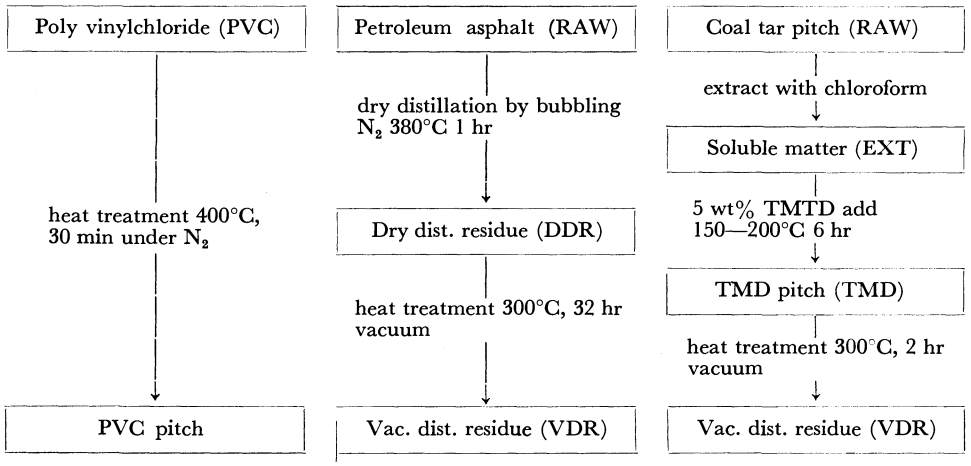

Fig. 1. Starting raw materials and the procedure of treatment.

TABLE 1. CHEMICAL COMPOSITION OF PITCH MATERIAL

Material	Stage	C%	H%	S%	N%	O% diff.	Atomic ratio H/C	Molecular weight
Petroleum asphalt	RAW	85.5	9.7	4.39	0.61	0	1.36	840
	DDR	85.3	8.3	5.27	0.73	0.4	1.16	880
	VDR	86.5	7.9	4.92	0.68	0	1.09	1530
Coal tar pitch	RAW	91.2	4.7	0.40	1.46	2.2	0.62	340
	EXT	90.9	4.7	0.24	1.46	2.7	0.62	320
	TMD	91.7	4.9	0.58	1.12	1.7	0.64	370
	VDR	92.4	4.2	0.70	0.93	1.8	0.54	990
PVC pitch		92.7	6.3	0	0	0.9	0.84	800

treatment with five percent of tetramethylthiuram disulfide (TMTD) in a low-temperature range.

The chemical composition and the mean molecular weights of the pitch materials at each stage of the above special treatments are presented in Table 1.

In Table 1, DDR is an abbreviation of the dry distilled residue, while VDR is that of the vacuum-distilled residue finally obtained. EXT is the soluble matter obtained by chloroform extraction, and TMD indicates the pitch materials heated together with TMTD. The value of the H/C atomic ratio for PVC pitch lies between those of the asphalt group and of the coal tar group. In the course of the treatment, especially during the final treatment under a vacuum. the H/C atomic ratio decreases and the mean molecular weight increases. In spite of the addition of the sulfur compound (TMTD) during the treatment, the sulfur content in the coal tai pitch material finally obtained is less than one percent. Therefore, the presence of sulfur and the other heteroatoms in the coal tar pitch material was disregarded and will not be discussed any further.

Solvent Analysis. A flow chart of the fractionation is shown in Fig. 2. The extraction was carried out at room temperature in order to prevent any possible change in quality. The bar graphs in Fig. 3 depict the results.

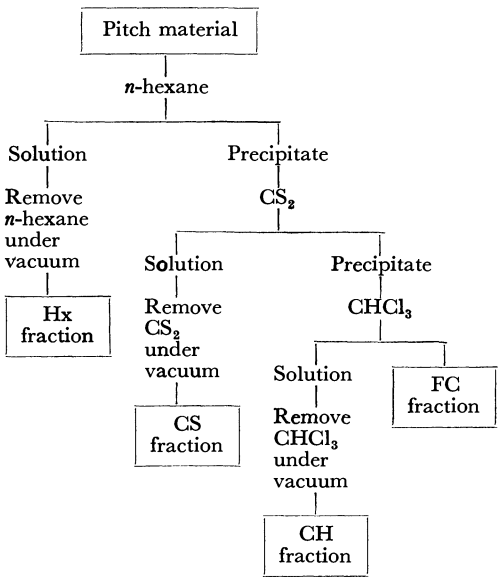

Fig. 2. Flow chart of extraction method.

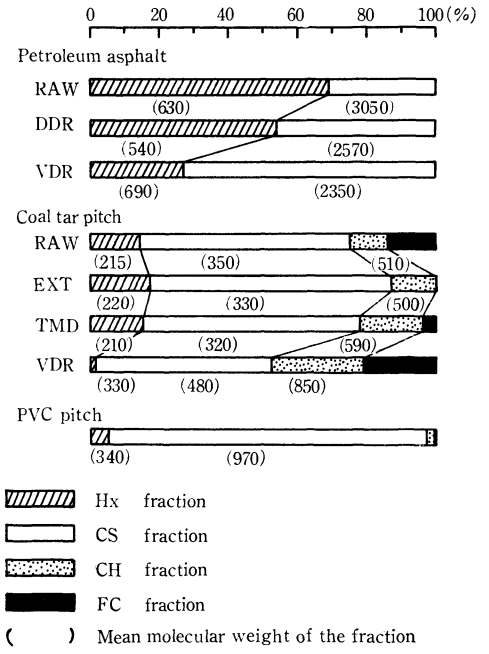

Fig. 3. Result of the solvent analysis.

The PVC pitch is characterized by a large CS fraction, and the CS fraction of the petroleum asphalt was increased to 73% by the treatment. In the case of the coal tar pitch, the mean molecular weight of each fraction increased, especially during the final treatment, and the low-molecular-weight component, the Hx fraction, vanished finally.

Chemical Composition of Each Fraction. The diagrams of the H/C atomic ratio *vs.* the stages of the treatment are shown in Figs. 4 and 5.

Figure 4 indicates that the final treatment under a vacuum for the coal tar pitch prompts a slight decrease in the atomic ratio of CH and FC. In the cases of both the fractions of the petroleum asphalt (Fig. 5), the decrease in the ratio is limited to the first step. However, the value of the entire

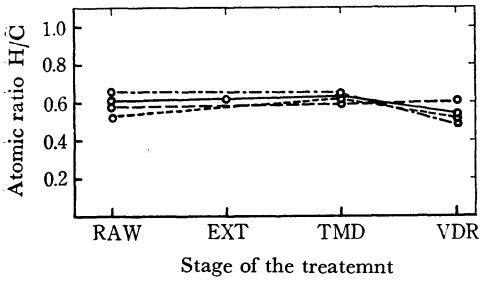

Fig. 4. The variation of atomic ratio H/C with the treatment (coal tar pitch).
—— before fractionation
—— CS
-·-·- CH
---- FC

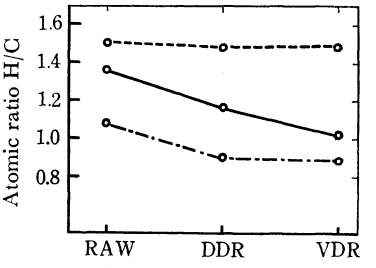

Fig. 5. The variation of atomic ratio H/C with the treatment (petroleum asphalt).
—— before fractionation
—— Hx
---- CS

sample continues to decrease during the final stage as a result of the increase in the CS content.

Spectroscopic Observations. *Infrared Spectra* Figure 6 indicates the infrared spectra of the samples before fractionation at each step of the treatments. These spectra consist of the absorption bands due to a saturated alkyl and an aromatic structure; no other band showing the presence of a hetero-atom or of unsaturated double bond is observed. Moreover, it seems that the asphalt is rich in an alkyl hydrogen, while, on the other hand, the coal tar pitch is rich in an aromatic hydrogen.

PVC pitch lies midway between the asphalt and the coal tar pitch in this case, too. Each VDR

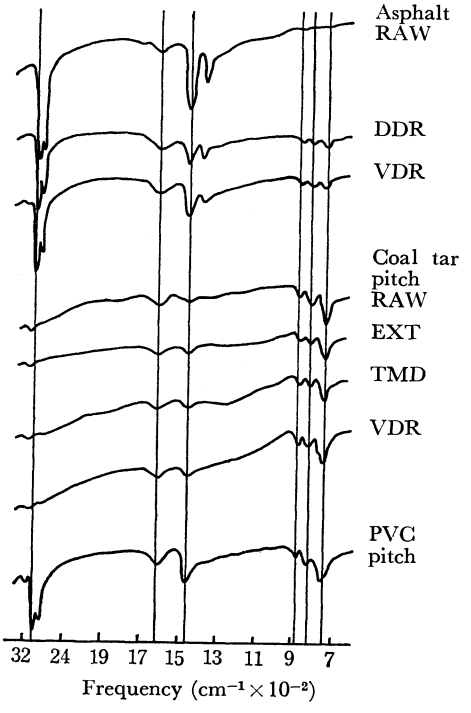

Fig. 6. Infrared spectra of the pitch materials before fractionation.

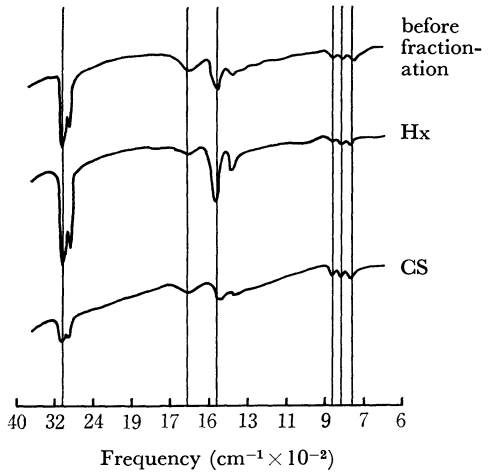

Fig. 7. Infrared spectra of petroleum asphalt (VDR).

fraction of the coal tar pitch was almost identical in infrared spectra with the sample before fractionation. In the case of the petroleum asphalt (Fig. 7), Hx exhibited a larger absorption band due to an alkyl structure than that of CS.

The Hx fraction of PVC pitch, although their content is only less than 6%, had the same tendency.

Ultraviolet Spectra. In order to get some useful information about the structure of the aromatic part, we have observed the ultraviolet and visible spectra. The spectrum of PVC pitch has been reported in our previous work,[1,4,5] in one paper,[1] we attempted to isolate the unit aromatic component by decomposition with nitric acid. On the basis of the data thus obtained and the other general information available, we concluded[1] that the spectrum of PVC pitch gives evidence of the presence of condensed aromatic nuclei composed of three or four rings, such as anthracene, chrysene, and phenanthrene. When the spectra of the two other pitch materials shown in Fig. 8 are compared with that of PVC pitch, the spectrum of coal tar pitch, VDR, is seen to be characterized by the presence of some obvious absorption bands in the range over 300 mμ.

It may be assumed that these bands are due to a sort of pyrene (250 and 340 mμ), benzpyrene (370, 380, and 390 mμ), coronene (300, 340, and 400 mμ), perylene (400 and 430 mμ), and other similar aromatic compounds. On the other hand, the spectrum of the petroleum asphalt has only one broad absorption band, that centering around 270 mμ. The two fractions (CS and Hx) of the petroleum asphalt treated at each stage were identical in ultraviolet spectra, although some general difference

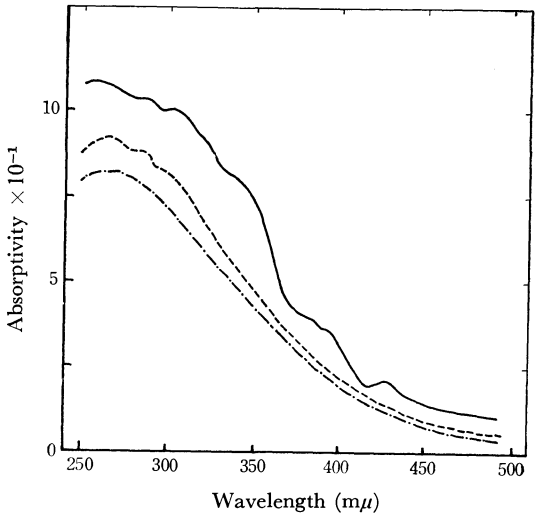

Fig. 8. UV and Vis. spectra of the pitch materials finally obtained.
----- Asphalt (VDR)
—— Coal tar piteh (VDR)
------ PVC pitch

in intensity was found throughout the wavelengths of the spectrum. When cyclohexane was used as a solvent, it was found that Hx exhibits another broad band in the range of 210—240 mμ in addition to the band at 270 mμ. The two fractions (CS and Hx) of the coal tar pitch treated at each stage were also identical in ultraviolet spectra except in intensity to that of the each entire sample before fractionation. However, the profile of the spectra changed considerably during the final treatment under a vacuum, as is shown in Fig. 9.

When the spectrum of the Hx of PVC pitch is compared with that of CS, the displacement of the wavelength of the maximum absorption is not

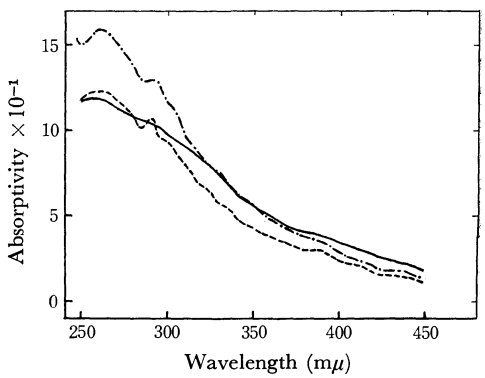

Fig. 9-a. Variation of UV and Vis. spectra of coal tar pitch with the treatment (CS fraction).
CS fraction
----- RAW
------ TMD
—— VDR

4) S. Ōtani, *Kogyo Kagaku Zasshi* (*J. Chem. Soc. Japan, Ind. Chem. Sect.*), **61,** 1324 (1958).
5) S. Ōtani, *ibid.*, **65,** 1617 (1962).

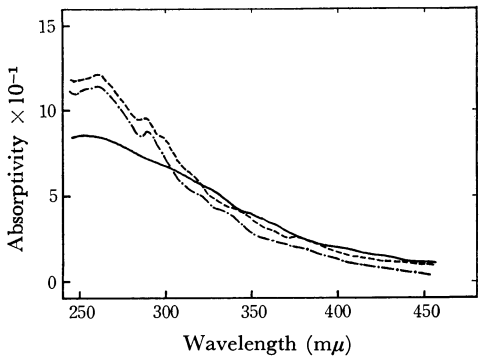

Fig. 9-b. Variation of UV and Vis. spectra of coal tar pitch with the treatment (CH fraction).
CH fraction
----- RAW
------ TMD
—— VDR

observed. However, the absorption in the range over 300 mμ apparently decreases in intensity.

Proton Magnetic Resonance Spectra. Some typical spectra are shown in Fig. 10.

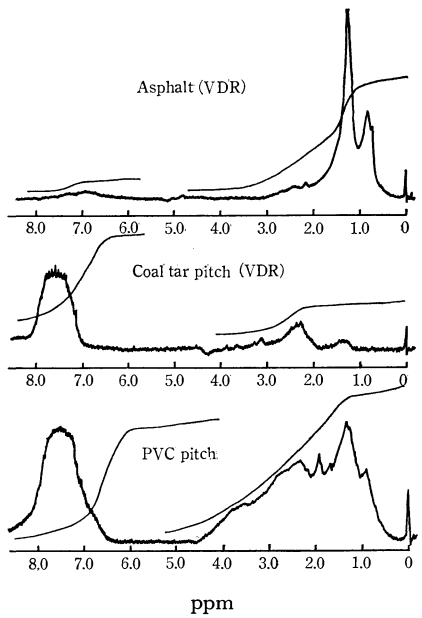

Fig. 10. Typical spectra of proton magnetic resonance.

The left-side peaks are due to an aromatic hydrogen, while the right-side peaks indicate the presence of some kinds of aliphatic hydrogen. The contents of aromatic and aliphatic hydrogen, as calculated from the peak area, are listed in Table 2.

The values in Table 2 clearly show the characteristics of each material. The treatment of the asphalt causes a slight increase in the aromatic hydrogen content. In the case of the coal tar pitch, the content remains almost constant throughout the whole process. No difference in the content is observed between the fractions of the coal tar pitch; however, in the cases of the other two materials, some difference is observed, as is shown in Table 3.

Table 2. Content of aromatic and aliphatic hydrogen of the samples before fractionation

Material	Stage	Aromatic H (%)	Aliphatic H (%)
Coal tar pitch	RAW	82	18
	EXT	81	19
	TMD	80	20
	VDR	81	19
Petroleum asphalt	RAW	5	95
	DDR	7	93
	VDR	10	90
PVC pitch		41	59

Table 3. Content of aromatic and aliphatic hydrogen of the fraction of asphalt and PVC pitch

Fraction		Aromatic H (%)	Aliphatic H (%)
Petroleum asphalt VDR	Hx	5	95
	CS	13	87
PVC pitch	Hx	35	65
	CS	40	60

A further classification of the alkyl hydrogen atoms has been attempted on the basis of the chemical shifts, and the content of each class has been calculated from the peak area. The results obtained are listed in Table 4. Some errors are, of course, unavoidable in this classification, but they are not serious, we think. In the case of the asphalt, Hx exhibits a larger content of II-type hydrogen and a smaller content of V-type hydrogen than does CS. This fact probably indicates that Hx has a longer side chain. The coal tar pitch is only 20% aliphatic hydrogen, and all the fractions are almost identical in their spectra.

Effect of the Improvement on the Procedure Used for Coal Tar Pitch. We pointed out previously[3] that the pitch material prepared from a coal tar pitch material leaves something to be desired. The procedure of the treatment has since been improved to some extent by the addition of the two steps of the extraction and TMTD treatment shown in Table 1. Table 5 shows the effect of these changes. By the removal of the insoluble residue from the raw material, the FC of the final is reduced to about half and the spinnability is doubled. The addition of TMTD results in a remarkable increase in the mean molecular weight.

Table 4. Classification of the alkyl hydrogen

Materials	Fraction	H content *vs.* total H content (%)				
		~1.0 (ppm) $CH_3-\overset{|}{C}-$ (I)	1.0—1.5 $CH_3-\overset{|}{C}-Ar$ $-\overset{|}{C}-CH_2-\overset{|}{C}-$ (II)	1.5—2.0 $Ar-\overset{|}{C}-CH_2-$ $Ar<\begin{matrix}C-CH_2\\C-CH_2\end{matrix}$ (III)	2.0—2.5 $Ar-CH_3$ (IV)	2.5~ $Ar-CH_2-$ $Ar-CH_2-Ar$ (V)
Petroleum asphalt VDR	entire*	18	42	12	8	10
	Hx	18	54	10	7	7
	CS	14	33	13	10	15
PVC pitch	entire*	7	11	9	9	22
	Hx	8	20	12	11	17
	CS	7	12	12	10	25
Coal tar pitch VDR	entire*	0	2	1	6	12

* Sample before fractionation.

Table 5. Effect of the extraction and the addition of TMTD

Procedure No.	1	2	3
Starting material	RAW	EXT	EXT
TMTD (wt%)	5	no	5
Heat treatment under N_2	180°C 1 hr	150—200°C 6 hr	150—200°C 6 hr
Heat treatment under vacuum	250°C 1 hr	300°C 2 hr	300°C 2 hr
Content of FC fraction	46.9%	22.0%	21.2%
Chemical composition C%	92.0	92.2	92.4
Chemical composition H%	4.0	4.4	4.2
Mean molecular wt.	—	670	990
Spinning speed m/min	240	470	490
Spinning temperature	250°C	270°C	300°C

Discussion

Characteristic Chemical Constitution of the Pitch Materials. Even when the pitch materials are treated by the method above described, the pitch materials are, of course, very complex mixtures composed of many kinds of molecules. The pitch materials are, indeed, too complex for their chemical structure to be determined in detail, and so the data obtained in our experiment are limited. However, the results obtained seem to lead to some significant conclusions concerning the characteristic chemical constitution of each suitable pitch material finally obtained. Moreover we feel that the presentation of the scheme of each pitch material, including most of the configurations mentioned above, will be helpful in clarifying the characteristic nature of the suitable pitch materials.

The major portion (94%) of the PVC pitch is CS, so it may be considered that this fraction represents the entire PVC pitch. On the basis of the proton magnetic resonance spectra, the atomic ratio of the aromatic hydrogen to the aliphatic hydrogen of CS is about 40/60. This value and the results presented in Table 4 are in good agreement with that calculated from the scheme (structural model) suggested previously.[1] The other results obtained in the present experiment are essentially identical with those previously reported. However, in the infrared spectra of the range from 700 cm^{-1} to 900 cm^{-1}, the absorption band at 740 cm^{-1} which is due to the four adjacent ring hydrogen atoms is the greatest in intensity. In order to ex-

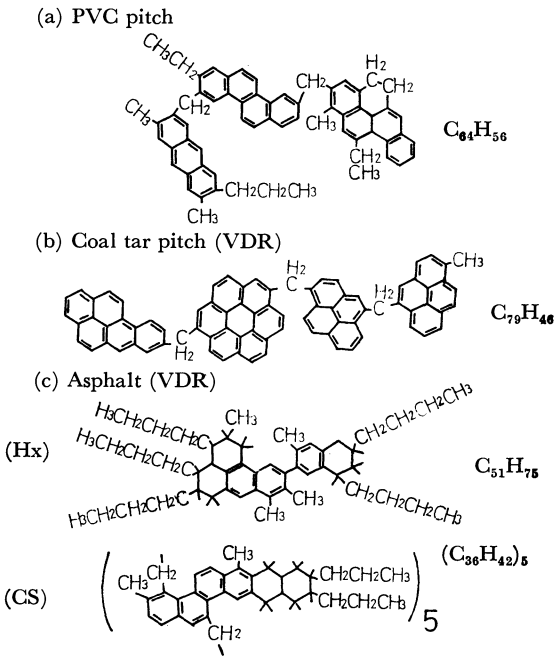

Fig. 11. Schemes including most of the characteristic configuration obtained.

plain this, it seems most reasonable to correct the model as shown in Fig. 11-a.

The pitch material finally obtained from the coal tar pitch is characterized by a small H/C atomic ratio, and its UV spectra indicates the existence of some condensed type of aromatic nuclei, such as pyrene, perylene, and coronene. The results of the proton magnetic resonance spectra (Table 4) suggest that only one methyl group is substituted in each molecule. From the results concerning the chemical composition of the entire VDR and its mean molecular weight, the experimental formula seems to correspond to $C_{79}H_{46}$. The proposed structural model is presented in Fig. 11-b. No remarkable difference has been found between fractions throughout the treatment with the exception of the mean molecular weight. Therefore, it seems reasonable to conclude that each fraction is distinguished by the number of the aromatic nuclei in a molecule. The most characteristic feature of the pitch materials prepared from the petroleum asphalt is the small value of the ratio of the aromatic hydrogen to the aliphatic hydrogen. From the UV spectra, it seems reasonable to assume that the aromatic nuclei of these materials are composed of similar aromatic fused rings to that of PVC pitch and/or some smaller aromatic fused rings such as naphthalene. When Hx is compared with CS in Table 4, it may be found that the content of II-type hydrogen of Hx is larger and the content of V-type hydrogen is smaller. These facts probably indicate that Hx has longer side chains than CS. The results of the IR spectra lend some support to this assumption. The existence of sulfur atoms in the petroleum asphalt causes some knotty problems in making up the structural model of the material. Previous investigations of sulfur in a heavy component of petroleum have given no information on its definite position in a molecule. It is said, in general, that sulfur atoms often form a C–SH (thiol) group in a side chain and/or a heterocyclic structure such as thiophene. Although the sulfur content of VDR is 3.9% corresponding to three or four atoms in a molecule, in the present spectroscopic examination, no clear characteristic information as to the presence of a sulfur atom is obtained. If the experimental formulae of CS and Hx are determined on the basis of the H/C atomic ratio and the mean molecular weight, that is, ignoring the possible presence of sulfur and other hetero-atoms, they correspond to $C_{51}H_{75}$ and $C_{180}H_{210}$ respectively. The structural models shown in Fig. 11-c are designed to satisfy the experimental formulae and the results of our spectroscopic observation. If the possible presence of sulfur atoms in taken into consideration, it seems most reasonable to correct by introducing three of four sulfur atoms into a molecule of CS in the form of thiophene and/or thiol; the atoms may then be converted to a C–S–C bond by heat treatment. In the case of Hx, one sulfur atom is introduced in the same form.

In Table 6, the values calculated from the structural models shown in Fig. 11 are listed together with those observed. As has been described above, the pitch materials are very complex mixtures and it is, of course, impossible to represent the molecules in all the pitch materials by the use of one molecular formula. However, on the basis of the results shown in Table 6 and described above, it may be concluded that these structural models express consistently the characteristic features of the pitch materials.

The Significance of the Special Treatment. *Petroleum Asphalt:* The most noticeable changes observed with the treatment are the increase in the CS content, the decrease in the H/C atomic ratio, and the variation in the mean molecular weight. The increase in CS content, of course, is mainly due to the removal of the Hx. However, the results for the fractions make it apparent that Hx and

Table 6. Comparison of the observed value with that of calculated from the structural mode shown in Fig. 11

			H/C Atomic ratio	Mean molecular weight	Arom. H / Total H (%)	Alkyl H/Total H (%)				
						CH_3–C–	CH_3–C–Ar –C–CH_2–C–	Ar–C–CH_2– Ar<C–CH_2 C–CH_2	Ar–CH_3	Ar–CH_2– Ar–CH_2–Ar
PVC pitch		Obsd	0.84	800	41	7	11	9	9	22
		Calcd	0.87	824	39	5	11	4	16	25
Coal tar pitch VDR		Obsd	0.54	900	79	0	2	1	6	12
		Calcd	0.58	994	80	0	0	0	7	13
Petroleum asphalt VDR	Hx	Obsd	1.50	690	4	18	54	10	7	7
		Calcd	1.46	687	5	20	42	9	12	11
	CS	Obsd	0.96	2350	15	14	33	13	10	15
		Calcd	1.17	2370	14	14	33	5	14	19

CS change in quality. The nature of CS changes to a much larger extent through the first distillation process at 380°C than through the vacuum-distillation process at 300°C. In the first step, for example, it has been found that the mean molecular weight, 3050 in the original, decreases to 2570; the H/C ratio, 1.57 in the original, decreases to 1.46, and the three absorption bands in the range from 700 to 900 cm^{-1} of the IR spectrum become apparent with the decrease in intensity of the bands due to an alkyl group. In view of these facts, it seems that the treatment causes, to some extent, the abscission and the aromatization of the alkyl side chains of the molecules in CS. No remarkable change in any fraction has been observed in the final step; the most important role of the step seems to be the removal of the lower-molecular-weight components which are present in the original and which are formed by the treatment.

Coal Tar Pitch: Even in the original pitch material itself, the aromaticity is satisfactory for our purposes. However, it is a great defect that the major portion of the material has a very low molecular weight and a low softening point below 80°C. It is possible to elevate the softening point and to increase the mean molecular weight by various heat treatments. However, heat treatment at higher temperatures often causes a remakable increase in FC. In general, the use of pitch materials with a large FC content results in less spinnability and in the formation of rough carbon fiber. It is desirable, therefore, to elevate the mean molecular weight without increasing the FC. In view of the results described above, the present procedure seems to fulfil the purpose quite well. Although the mechanism of the reaction with TMTD is not obvious even after the present experiments, it is certain that the addition of TMTD accelerates the condensation between the molecules. The condensation occurs more remarkably in the final treatment under a vacuum at 300°C. (Figs. 3, 4, and 9 and Table 5) The unavoidable formation of FC in this step may indicate that the treatment temperature is still too high.

Conclusion

Suitable pitch materials for MP carbon fiber are generally composed of several structural units with an aromatic fused ring and more or less alkyl side chains, as is shown in Fig. 11.

The suitable pitch finally obtained from the petroleum asphalt is characterized by a relatively high molecular weight and by many relatively long alkyl side chains.

The special treatment required promotes the increase in the aromaticity and the removal of the low-molecular-weight component.

The suitable pitch material from the coal tar pitch is characterized by aromatic fused rings of the condensed type and only a few alkyl side chains, such as, the methyl group.

The most desirable effect of the treatment is to accelerate the condensation between molecules without increasing the insoluble matter and to remove the low-molecular-weight component.

BULLETIN OF THE CHEMICAL SOCIETY OF JAPAN VOL. 42 1425—1428 (1969)

Effect of Pressure on Graphitization of Carbon. VI. Normal Pressure Heat Treatment of Soft Carbon Pre-Heat-Treated under High Pressure

Kan-ichi KAMIYA, Michio INAGAKI and Hajime SAITO

Faculty of Engineering, Nagoya University, Chikusa-ku, Nagoya

(Received September 24, 1968)

Three different samples of polyvinylchloride coke (designated as N-1, N-2, and N-3 which were pre-heat-treated at 1470, 1590, and 1620°C, respectively, under 5 kbar) were heat-treated in a flow of nitrogen under normal pressure. Process of graphitization in these samples was investigated by analyzing (004) diffraction profile. Sample N-1 has a symmetrical profile and consists only of the trubostratic component A_S. Samples N-2 and N-3 have a composite profile and are composed of the turbostratic component A_S and the graphitic component G_S. Only the profiles corresponding to the turbostratic component A_S of these samples shift gradually to higher angle together with sharpening when the heat treatment temperature under normal pressure increases. Changes in c_0-spacing and crystallite size L_C of the component A_S with heat treatment temperature follow the same course of change as in those of the original polyvinylchloride coke. However, heat treatment of the sample under normal pressure did not affect the quality and quantity of the component G_S which had been formed by the pre-heat-treatment under high pressure. These results indicate that the pre-heat-treatment of soft carbon under high pressure has no accelerating effect on the graphitization of the carbon in the subsequent heat treatment under normal pressure.

Polyvinylchloride coke PV-7, a soft carbon, has been found to be graphitized very rapidly at as relatively low a temperature as 1400—1500°C under high pressure above 3 kbar.[1-3] The process of its graphitization is divided into two stages on the basis of the change in the profile of (00*l*) diffraction line.[2,3] In the first stage, the structural component of the carbon is the turbostratic one A_S, of which the c_0-spacing is larger than 6.85 Å. In the second stage, however, two components A_S and G_S, having the turbostratic and graphitic structures, respectively, coexist in the sample and no component having an intermediate structure is observed. In this stage, the graphitization proceeds through the direct transformation from turbostratic carbon to graphite, which can be detected by the composite structure of the profile of (00*l*) diffraction line.[2,3] Such a change in the profile of (00*l*) diffraction line contrasts with that observed by the heat treatment under normal pressure.[4] It was confirmed that the composite profile observed in the sample heat-treated under pressure was not due to the temperature and pressure gradients in the specimen.[5] A similar abrupt transformation was also observed on a hard carbon PH-7 prepared from phenolformaldehyde resin.[6,7]

In the present work, in order to know whether the after-effect of high pressure heat treatment of carbon can be detected in the graphitization under normal pressure, the soft carbon PV-7 pre-heat-treated at several temperatures under 5 kbar was re-heat-treated under normal pressure. Structural changes by the re-heat-treatment were followed by X-ray diffraction.

Experimental

Pre-heat-treatment under High Pressure. A simple piston-cylinder type high pressure vessel made of tool steel was used. Its bore diameter was 30 mm. The pressure cell arrangement was similar to that previously reported,[2] except that the graphite tube heater used was larger, *i. e.* inner diameter 8 mm, outer diameter 10 mm and length 21 mm, and that the glassy carbon tube in the graphite heater was not used. The weight of the sample was about 450 mg, almost four

1) T. Noda and H. Kato, *Carbon*, **3**, 289 (1965).
2) T. Noda, K. Kamiya and M. Inagaki, This Bulletin, **41**, 485 (1968).
3) M. Inagaki, K. Kamiya and T. Noda, *Kogyo Kagaku Zasshi* (*J. Chem. Soc. Japan, Ind. Chem. Sect.*), **71**, 652 (1968).
4) M. Inagaki, K. Kamiya and H. Saito, TANSO No. 54, 84 (1968).
5) M. Inagaki, K. Kamiya and T. Noda, *Kogyo Kagaku Zasshi* (*J. Chem. Soc. Japan, Ind. Chem. Sect.*), **71**, 812 (1968).
6) K. Kamiya, M. Inagaki, M. Mizutani and T. Noda, This Bulletin, **41**, 2169 (1968).
7) K. Kamiya, S. Yugo, M. Inagaki, H. Saito and T. Tsuzuku, *ibid.*, **41**, 2782 (1968).

times the previous one. The contamination of the heat-treated samples was scarcely detected by X-ray analysis. Heat treatment temperature was estimated from the input power by using the relation between input power and temperature, which was determined especially for the present cell arrangement.

The coke PV-7 was heat-treated at three different temperatures of 1470, 1590, and 1620°C for the residence

Fig. 1-a)

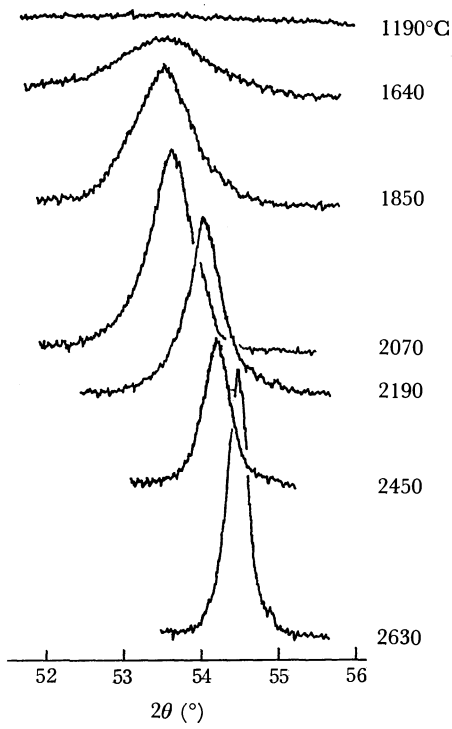

Fig. 1-b)

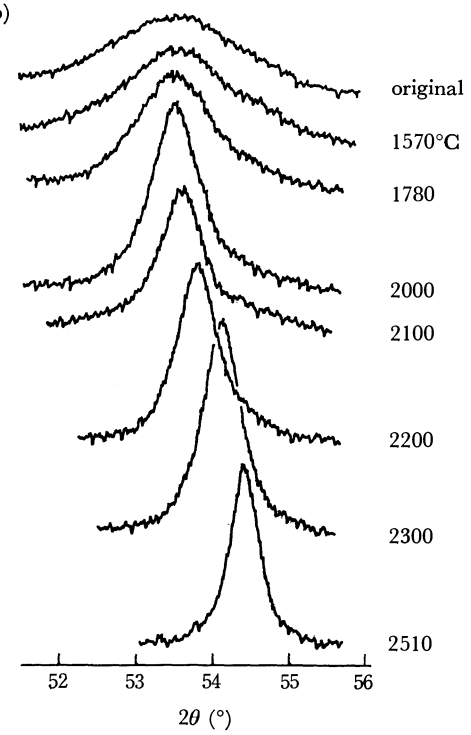

Fig. 1-c)

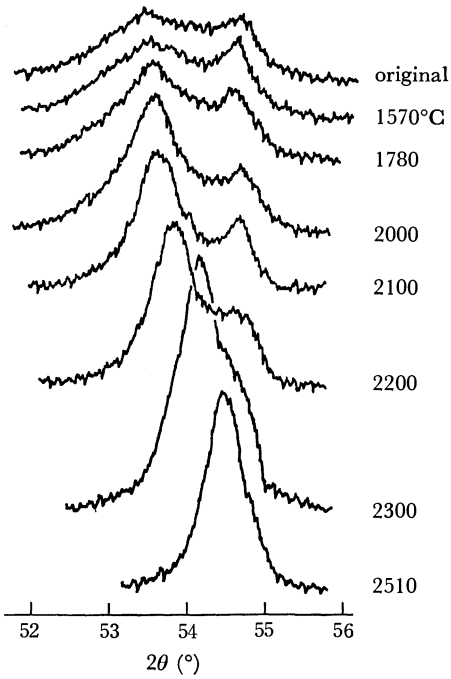

Fig. 1-d)

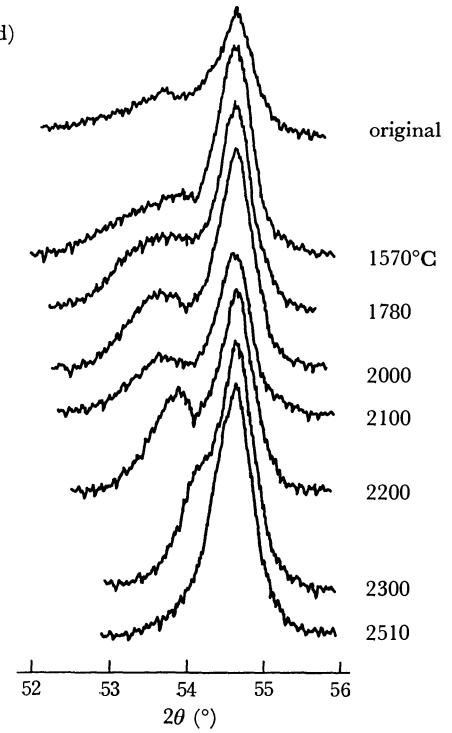

Fig. 1. Changes of the profile of (004) diffraction line with HTT.
a) Sample PV-7 b) Sample N-1
c) Sample N-2 d) Sample N-3

time of 20 min under a quasi-hydrostatic pressure of 5 kbar. The heat-treated specimens were obtained as sintered cakes *ca.* 8 mm in diameter and *ca.* 6 mm long. A tablet 8 mm in diameter and 2 mm thick was sampled from the central part of the sintered cake of each heat-treated specimen. For this central part, temperature gradient during the heat treatment under 5 kbar was scarcely observed.[5] To minimize the effect of the possible gradients of temperature and pressure along the radial direction of the tablet on the final results, each tablet of the specimen was cut into eight small pieces through the center of the tablet and these small pieces were used for the re-heat-treatment under normal pressure at different temperatures. The 1470°C-, 1590°C-, and 1620°C-treated samples were designated as N-1, N-2, and N-3, respectively, in the present work.

Re-heat-treatment under Normal Pressure. The re-heat-treatment under normal pressure was conducted at temperatures ranging from 1190 to 2630°C for the residence time of 60 min in a flow of nitrogen by using a graphite tube resistance furnace. During the heat treatment, small pieces of the samples N-1, N-2, and N-3, and the original coke PV-7 were placed in graphite crucibles separately and the crucibles were put in a large graphite container.

Heat treatment under normal pressure was performed as follows. After the central part of the graphite heater was heated to a desired temperature, the graphite container, which contained the four samples and was placed beforehand in a cold part of the heater, was pushed into the central part. It required about 10 min to heat the crucible to the desired temperature. After 60 min residence, the graphite container was pushed out to a cold part on the opposite side of the heater and then the temperature of the furnace was raised in order to perform another heat treatment. The temperature of heat treatment was determined by focusing an optical pyrometer on the surface of the graphite crucible through a hole drilled in the container wall. The optical pyrometer used was calibrated to the standard lamp for pyrometry. The temperature of the furnace was kept constant within ± 10°C by adjusting the input power manually.

X-Ray Analysis. The profiles of (004) diffraction line of all heat-treated samples were measured by using Ni-filtered Cu*Ka* radiation and a recording goniometer. The specimens for X-ray analysis were 0.2 mm thick. The heat-treated samples of PV-7 and N-1 had symmetrical profiles of (004) diffraction line, as can be seen in Fig. 1-a) and b). For the sample producing such a symmetrical profile, c_0-spacing and crystallite size L_c were measured by the usual method[8] referring to the inner standard of silicon. However, profiles of all samples derived from N-2 and N-3 had a composite structure, as can be seen in Fig. 1-c) and d). The composite profile was separated into the profiles of two components A_S and G_S, which were on low and high angle side, respectively.*1 A similar procedure to that reported previously[3] was applied to the separation of the composite profile. In the present work, the angular position of the component profile on low angle side could not be fixed at a constant value, but estimated very easily because the separation of two component profiles was relatively large. Almost all the composite profiles could be separated into two symmetrical component profiles after one or two trials. For each separated component profile, c_0-spacing and crystallite size L_c were measured by referring to the inner standard of silicon. The content of the component G_S was evaluated by measuring the ratio of area under the profile of G_S to the total area of the composite profile and correcting it for the crystallite orientation.[2,3]

Results

Changes of the profile of (004) diffraction line with temperature of heat treatment under normal pressure (HTT) for the samples PV-7, N-1, N-2, and N-3 are shown in Figs. 1-a), b), c) and d), respectively. For the sample PV-7, all the profiles are symmetrical and shift to a higher angle together with sharpening as HTT increases. Sample N-1 is found to have almost the same tendency of change in the profile as that of the sample PV-7. For samples N-2 and N-3 of which the originals have composite profiles, only the profile corresponding to the component A_S shift to a higher angle with sharpening as HTT increases, but the profile corresponding to the component G_S does not seem to change in position, relative intensity and sharpness with heat treatment.

Changes of c_0-spacing and crystallite size L_C with HTT for the samples are shown in Figs. 2-a) and b), respectively. Sample PV-7 becomes to have almost the same values of c_0 and L_C as those of the component A_S of the other samples at about 2000°C and above that temperature the changes in c_0 and L_C of A_S of the samples N-1, N-2, and N-3 as well as PV-7 follow the same course of change with HTT. On the other hand, the graphitic component G_S which has been formed by the pre-heat-treatment under high pressure has the constant c_0-spacing of 6.72 Å and the crystallite size L_C of around 300 Å during the heat treatment under normal pressure.

Changes of content of the component G_S with HTT are shown in Fig. 3. The content of the component G_S does not change by the re-heat-treatment under normal pressure. Sample N-1 does not have any amount of the component G_S originally.

Discussion

The graphitization under pressure above 3 kbar proceeds in two stages.[2,3] In the first stage the c_0-spacing of carbon decreases to *ca.* 6.85 Å and in the second stage a new component having graphitic structure develops in the original turbostratic car-

8) M. Inagaki and T. Noda, This Bulletin, **35**, 1652 (1962).

*1 In a previous work,[2] the component A_s had the c_0-spacing larger than 6.85Å. In the present work, however, the component corresponding to the separated profile on low angle side was designated as A_s, even if it has the c_0-spacing smaller than 6.85 Å.

Fig. 2-a)

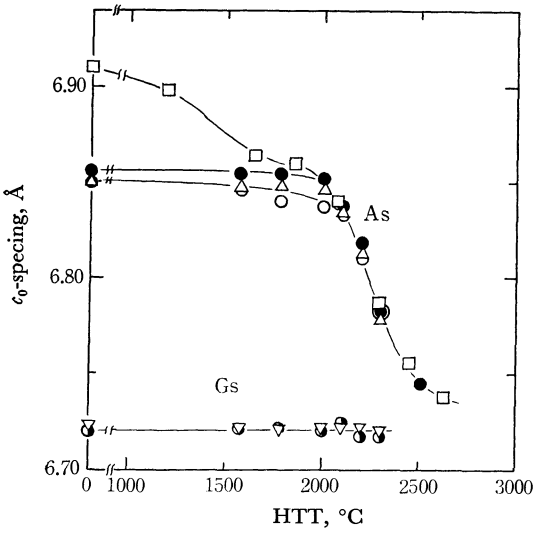

Fig. 2. b)

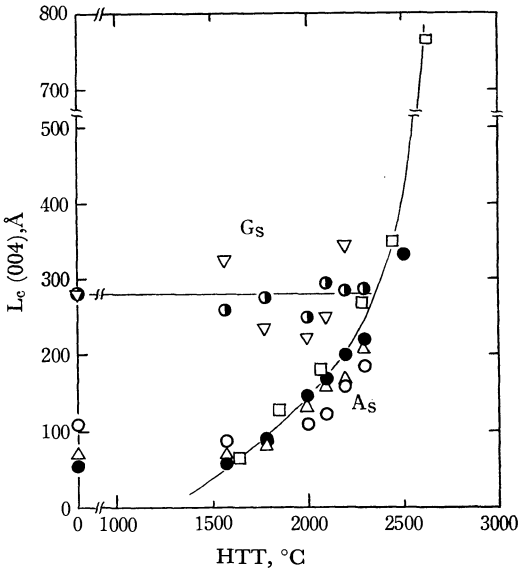

Fig. 2. Changes of the X-ray parameters of the component A_S and G_S with HTT.
a) c_0-spacing, b) crystallite size L_c
As □: PV-7, ●: N-1, △: N-2, ○: N-3
Gs ▽: N-2, ◑: N-3

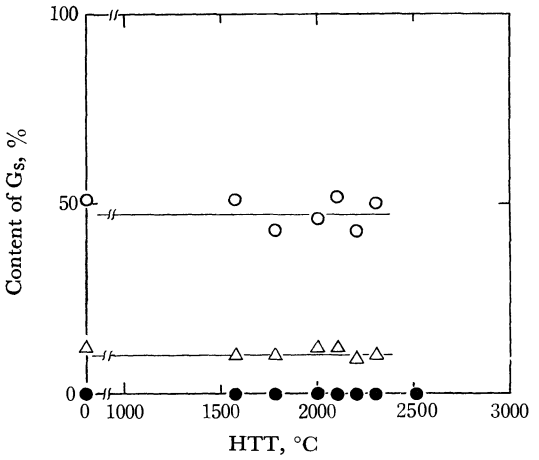

Fig. 3. Change of content of the graphitic component G_S with HTT.
●: N-1, △: N-2, ○: N-3

bon, *i.e.*, a sharp peak corresponding to c_0 of 6.72 Å develops besides the original broad peak of turbostratic carbon, making (00*l*) diffraction profile composite. This direct transformation of turbostratic carbon to graphite indicates that graphitization under high pressure proceeds heterogeneously on the scale of crystallite and can be called a heterogeneous graphitization. On the other hand, the graphitization under normal or reduced pressure proceeds homogeneously. The c_0-spacing decreases continuously to the value of graphite, and this change is detected as a continuous shift of a symmetrical profile of (00*l*) diffraction line to higher angle.

The sample N-1 has a symmetrical profile and its c_0-spacing is 6.856 Å, *i.e.*, it is on the first stage of graphitization process and consists only of turbostratic component A_S. The samples N-2 and N-3 give composite profiles and consist of turbostratic component A_S and graphitic component G_S, *i.e.*, they are on the second stage of graphitization process. The component A_S, which did not transform directly to graphitic component during the pre-heat-treatment under high pressure, was found to be graphitized homogeneously when the samples N-1, N-2 and N-3 were re-heat-treated under normal pressure. However, the re-heat-treatment of the samples under normal pressure did not affect the quality and quantity of the component G_S which has been formed by the pre-heat-treatment under high pressure.

These results indicate that the pre-heat-treatment of a soft carbon under high pressure has no accelerating effect on the graphitization of the carbon in the subsequent heat treatment under normal pressure, and that the direct transformation of the turbostratic component to graphitic component by the application of external stress causes the observed heterogeneous graphitization of soft carbon.

The authors wish to thank Dr. T. Noda, President of Mie University, for his valuable discussions and thorough review of the paper. The graphite materials used were supplied by Tokai Electrode Mfg. Co.

NOTES

BULLETIN OF THE CHEMICAL SOCIETY OF JAPAN VOL. 42 1429—1431 (1969)

Some Observations of the Water Activity in Uni-uni Valent Electrolyte Solutions

Yuko HASEGAWA

Department of Chemistry, Science University of Tokyo, Kagurazaka Shinjuku-ku, Tokyo

(Received April 24, 1968)

The association or dissociation of various ionic species has sometimes been determined in aqueous electrolyte solutions at high concentrations. In such experiments, the constant ionic medium method has usually been employed for the control of the activity coefficients. The validities and the limitations of this method have been discussed by Rossotti and Rossotti.[1]

As the association or the dissociation of ions in aqueous solutions is accompanied by hydration or dehydration, the activity of water as well as the activity coefficients of the ionic species should be controlled in order to obtain reasonable chemical constants; information about the water activity in various constant ionic media is desirable for this purpose.

For the present study, the water activity in some very common uni-uni valent electrolyte solutions has been determined by a Karl Fischer titration method based on the principle that the water concentration in a benzene phase in an equilibrium with an aqueous phase is approximately proportional to the water activity in the latter.[2] The results thus obtained were then compared with the values calculated from the previous osmotic data,[3] and some consideration was done of the validities of the constant ionic media from this point of view.

Experimental

All of the reagents used were of a reagent grade. The concentrations of thiocyanate solutions were determined by argentometry, but the other concentrations were determined by gravimetry.

All of the procedures were carried out in the manner described in a previous paper.[2]

Results and Discussion

As has been described,[2] the water activity, A_w, of an aqueous solution can be calculated from the water concentration in a benzene phase in an equilibrium with the sample solution (which will be denoted by C_w), and that in an equilibrium with pure water (which will be denoted by C_{wo}), by using the following equation:

$$A_w = C_w/C_{wo}$$

The value of C_{wo} experimentally determined at 25°C is 0.034M.[2]

Table 1 shows the water activities determined by the titration method in the present study and those calculated from the molal osmotic coefficients by using the following equation:[3]

$$\ln A_w = -\frac{mW_w\nu\phi}{1000}$$

Here, ν is the number of ions formed from one mole of electrolyte; m is the concentration of electrolytes in the molality unit; W_w is the molecular weight of water, and ϕ is the molal osmotic coefficient.

In most salt solutions, the values calculated from the osmotic coefficients on the assumption that the salts are completely dissociated in the

TABLE 1. WATER ACTIVITIES OBTAINED FROM THIS WORK AND FROM THE OSMOTIC COEFFICIENTS[3]

Solute	mol/kg water	$A_{w_{obs}}$	A_{w_ϕ}
NaSCN	1.0	0.97	0.966
	2.0	0.94	0.927
	3.0	0.91	0.889
	4.0	0.87	0.847
$NaClO_4$	1.0	0.97	0.968
	2.0	0.93	0.935
	3.0	0.90	0.901
	4.0	0.87	0.867

1) F. J. C. Rossotti and H. Rossotti, "The Determination of Stability Constants," McGraw-Hill Co., Inc., New York (1961).

2) Y. Hasegawa and T. Sekine, This Bulletin, **38**, 1713 (1965).

3) R. A. Robinson and R. H. Stokes, "Electrolyte Solutions," Butterworths, London (1959).

aqueous solutions agree with the values determined by the present titration method. However, in a few solutions (for example, in the thiocyanate solution, as we can see from Table 1), the values are rather larger than the values from the osmotic coefficient method. From these results, the following conclusions may be drawn:

As the values obtained by these two independent methods are consistent, many strong electrolytes may be considered to be dissociated completely, and both of these methods are applicable for the determination of water activities, even when the electrolyte concentration is very high. The difference between the values obtained by these two methods could be explained by that the ν in the equation is smaller than the values calculated by assuming complete dissociation; that is, sodium ions and thiocyanate ions might be associated to some extent.

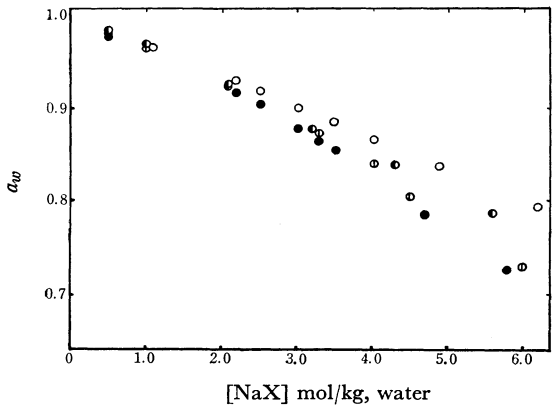

Fig. 1. Change in the water activity of four sodium salt solutions as a function of concentration of NaX.

○ Sodium perchlorate
◐ Sodium chloride
◑ Sodium bromide
● Sodium iodide

Figure 1 shows the water activities in solutions of four salts as a function of the salt concentration (molal units). We can see from Fig. 1 that, although the differences at a certain concentration are rather small, still the following decreasing order of the values of the water activity can be estimated in these sodium salt solutions:

$$A_{w_{NaClO_4}} > A_{w_{NaCl}} > A_{w_{NaBr}} > A_{w_{NaI}}$$

The water activity in aqueous salt solutions may be influenced by many factors. Robinson and Stokes[3] pointed out that the hydration of univalent anions decreases with an increase in the ionic radius. As the ionic radii of these anions decrease in the following order;

$$r_{ClO_4^-} > r_{I^-} > r_{Br^-} > r_{Cl^-}$$

the water activity in the solutions should decrease in the same order as long as we consider this problem in terms of hydration.

On the other hand, the following "*destroying-order*" of the water structure by solute anions was proposed, on the basis of IR measurements of various aqueous solutions, by Yamatera and Gordon[4] and Choppin and Buijs:[5]

$$ClO_4^- > I^- > Br^- > NO_3^- > Cl^-$$

If the water structure of these solutions is destroyed in this order, the water activity should decrease in the same order. However, the experimental observations gave just the reverse order except that the perchlorate solutions gave the largest values of water activity. Thus, factors other than the hydration or the destruction of the structure of water must be taken into account in formulating a reasonable explanation of these results.

Some more data on the water activities which will be useful in various discussions of solution chemistry are given in Table 2 by molarity and molality.

Table 2. Water activities in some electrolyte solutions

Solute	mol/l	mol/kg water	A_w
NaCl	0.50	0.51	0.98_4
	1.0	1.0	0.96_9
	2.0	2.1	0.92_6
	3.0	3.2	0.87_8
	4.0	4.4	0.83_9
	5.0	5.6	0.78_7
NaBr	0.50	0.51	0.98_4
	1.0	1.0	0.96_6
	2.0	2.1	0.92_6
	3.0	3.3	0.87_3
	4.0	4.5	0.80_6
	5.0	6.0	0.73_0
NaI	0.50	0.51	0.97_6
	1.0	1.0	0.96_4
	2.0	2.2	0.91_7
	3.0	3.3	0.86_4
	4.0	4.7	0.78_6
	4.8	5.8	0.72_6
$NaClO_4$	0.50	0.51	0.98_4
	1.0	1.1	0.96_6
	2.0	2.2	0.92_9
	3.0	3.5	0.88_6
	4.0	4.9	0.83_7
	4.8	6.2	0.79_4
	7.0	10.6	0.62_5

4) H. Yamatera and G. Gordon, The Xth Colloquium Spectroscopium Internationale (1962, Maryland, U. S. A.).

5) G. R. Choppin and K. Buijs, *J. Chem. Phys.*, **39**, 2042 (1963).

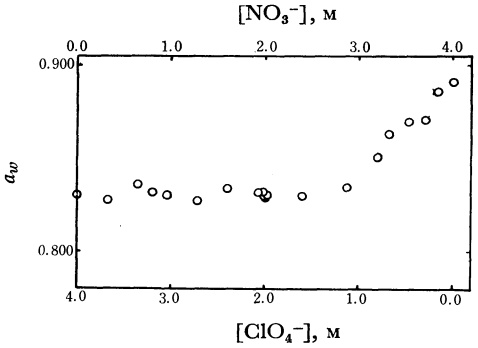

Fig. 2. Water activity in 4M Na (NO_3, ClO_4) solutions as a function of perchlorate or nitrate concentration.

Further study was carried out in mixed salt solutions in order to ascertain the ability of the constant ionic method to control the water activity. Mixtures of sodium perchlorate and nitrate were chosen as the representatives of the mixed electrolyte solutions because the difference in the water activity at 4M, for example, is largest between perchlorate and nitrate solutions.

Figure 2 shows the water activity in solutions containing sodium perchlorate and nitrate mixtures. We can seen from Fig. 2 that even when the sodium ion concentration is kept at 4M, the water activity changes continuously from 0.83 in 4M sodium perchlorate to 0.89 in 4M sodium nitrate; the water activity is almost constant until the nitrate concentration reaches 2.8M, but it increases abruptly beyond 2.8M. For the determination of very weak metal complexes, it is necessary to add a very large amount of ligand anions to the ionic media; that is, a large portion of the perchlorate ions should be replaced by the ligand anions. For example, when we examined europium(III) nitrate complexes ($K_1=1.3$ and $\beta_2=0.30$ in 4M Na(ClO_4, NO_3)),[6] it was necessary to replace almost 70% of the perchlorate ions in 4M sodium perchlorate media with nitrate ions in order to determine the second stability constants accurately. The present results indicate that even when such a large alternation of the medium is made the change in the water activity is still not very large; in view of this, the author regards the nature of the medium as still being kept constant.

The author is grateful to Dr. Tatsuya Sekine for many invaluable discussions.

6) T. Sekine, I. Sakamoto, T. Sato, T. Taira and Y. Hasegawa, This Bulletin, **40**, 251 (1967).

BULLETIN OF THE CHEMICAL SOCIETY OF JAPAN VOL. 42 1431—1432 (1969)

The Synthesis and the Properties of Some New Boroarsenites

Narayani Prasad SINGH

Radiochemistry Division, Bhabha Atomic Research Centre, Trombay, Bombay-74, India

(Received June 19, 1968)

Though heteropoly salts of boron such as borotungstates[1,2] and borotungstovanadates[3] are reported in literature, very little work has been done on boroarsenites. Lery and Curty[4] found that, borophosphoric and boroarsenic acids exist in solution provided the solutions are sufficiently concentrated, even in the presence of vigorous hydrolyzing agent such as steam. In this note the preparation of ammonium boroarsenite and there-from the boroarsenite salts of silver, lead, zinc, cadmium and iron(II) are reported. Some of the physical properties of a few of these compounds are also studied.

Experimental

Synthesis of Ammonium Boroarsenite. Boric acid (9.27 g) and arsenious oxide (9.89 g) were dissolved in aqueous ammonia separately. The solutions were mixed together and then refluxed for ten to twelve hours. The solution was then concentrated to small volume and kept in a refrigerator, when ammonium boroarsenite separated out. It was recrystallized from water two to three times and dried in a vacuum desiccator.

The other salts were prepared by adding solutions of $AgNO_3$, $Pb(CH_3COO)_2$ $Zn(CH_3COO)_2$, $Cd(CH_3COO)_2$ and $FeSO_4$ to the ammonium salts solution. The analytical results are recorded in Table 1.

Analytical. Boron was estimated by a volumetric method in the presence of mannitol using phenolphthalein as an indicator. Nitrogen was estimated by the Kjeldahl method and the percentage expressed in terms of $(NH_4)_2O$. Other metals were estimated by standard

1) H. Copaux, *Ann. Chim. Phys.*, **17**, 217 (1909).
2) D. Klein, *Bull. Soc. Chim.*, **33**, 466 (1880); **34**, 23 (1880); **37**, 202 (1882); *Ann. Chim. Phys.*, **28**, 426 (1883).
3) N. A. Polotebunova, *Uchenge. Zapiski. Kishinev*, **27**, 83 (1957).
4) G. R. Levi and R. Curty, *Gazz. Chim. Ital.*, **68**, 376 (1938).

Table 1

Compound	% of Metal oxide		% B_2O_3		% As_2O_3		% H_2O	
	Found	Calcd	Found	Calcd	Found	Calcd	Found	Calcd
$5(NH_4)_2O \cdot B_2O_3 \cdot 4As_2O_3 \cdot 25H_2O$	17.0	16.5	4.2	4.4	50.2	50.3	28.6	28.6
$5Ag_2O \cdot B_2O_3 \cdot 4As_2O_3 \cdot 21H_2O$	47.8	48.4	2.8	2.9	33.1	33.0	16.2	15.8
$5PbO \cdot B_2O_3 \cdot 4As_2O_3 \cdot 22H_2O$	46.5	47.0	2.8	2.9	34.5	33.4	16.2	16.7
$5ZnO \cdot B_2O_3 \cdot 4As_2O_3 \cdot 10H_2O$	27.3	28.0	4.6	4.8	52.9	54.7	15.2	12.4
$5CdO \cdot B_2O_3 \cdot 4As_2O_3 \cdot 6H_2O$	40.1	39.8	4.2	4.3	50.8	49.1	4.8	6.7
$5FeO \cdot B_2O_3 \cdot 4As_2O_3 \cdot 6H_2O$	27.9	27.1	5.2	5.2	57.9	59.5	8.9	8.1

methods. Water was found by difference.

Spectroscopic Studies. The infrared spectra in the range 2—15μ of ammonium boroarsenite and zinc boroarsenite were recorded on a Perkin-Elmer infrared spectrometer in KBr discs.

Discussion

It is very difficult to assign definite structures to the heteropoly acids and their salts owing to the complexity of the molecules involved. The compositions of the salts have been arrived at on the basis of analytical results. The analytical results have given the empirical formula $5(NH_4)_2O \cdot B_2O_3 \cdot 4As_2O_3 \cdot 25H_2O$ for ammonium boroarsenite. When a freshly prepared solution of this salt was subjected to ion exchange (Dowex-50 cation resin), it gave a stable free acid thus confirming the stability of boroarsenite ion in the solution. Several unsuccessful attempts were made to crystallize the acid out.

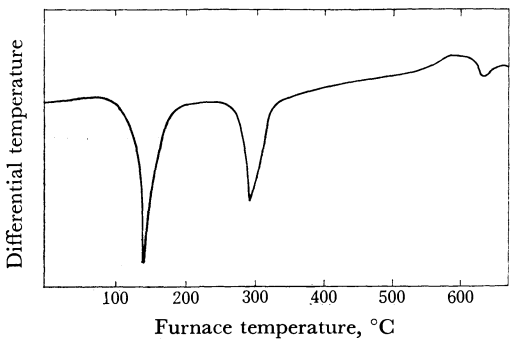

Fig. 1. Differential thermal analysis curve of ammonium boroarsenite.

The differential thermal analysis (DTA) curve reveals two endotherms one at 140°C and the other at 294°C, corresponding to the dehydration of the compound. This indicates the presence of two types of bound water molecules.

In the infrared spectra of zinc boroarsenite and ammonium boroarsenite one peak is observed in the 3μ region (3231, 3403 cm^{-1} respectively) corresponding to the –OH stretching vibrations of water molecules. The peak at 3403 cm^{-1} in case of ammonium boroasenite is broad which may due to the overlapping of –NH and –OH stretching frequencies. In the case of ammonium boroarsenite one peak is found at 1634 cm^{-1} which may be assigned as –NH bending. Peaks at 1198 cm^{-1} and 793 cm^{-1} in the case of ammonium boroarsenite and 1191 and 802 cm^{-1} in the case of zinc boroarsenite have been assigned to –BO group, though. White *et al.*[5] have reported absorption bands at 1300 and 762 cm^{-1} for –BO group in their studies on simple B_2O_3 molecule. The variation in the frequencies observed may be due to the involvement of BO group in complex formation. Bands have been observed at 1044 cm^{-1} and 1052 cm^{-1} respectively for ammonium boroarsenite and zinc boroarsenite which are attributed to As–O stretching frequency. Confirmation to this was obtained in the infrared spectrum of As_2O_3 taken by the author which showed band at 1045 cm^{-1} which can be attributed to As–O stretching frequency.

The slight differences observed in the position of the corresponding IR bands of the two salts studied may be due to the differences in their crystal structure environments.

Author's sincere thanks are due to the authorities of Banaras Hindu University for the necessary facilities provided and the C.S.I.R., New Delhi for financial assistance.

5) D. White, P. N. Walsh and D. E. Mann, *J. Chem. Phys.*, **28**, 508 (1958).

BULLETIN OF THE CHEMICAL SOCIETY OF JAPAN VOL. 42 1433—1435 (1969)

Fluorescence Spectra of Some Benzimidazoles in Acid Media

Michio KONDO and Harumitsu KUWANO

Central Research Laboratories, Sankyo Co., Ltd., Shinagawa-ku, Tokyo

(Received June 20, 1968)

Few papers have been published on the fluorescence spectra of benzimidazole in the protonated state.[1,2] For benzimidazole perchlorate, two fluorescence bands were observed in an ethanol solution at a low temperature. The weak, broad, structureless band observed at about 29000 cm^{-1} was assigned to the emission from the excited singlet state, ^1L_a, on the basis of the results of fluorescence polarization experiments.[2] This indicates the reversal of the excited energy levels, ^1L_a and ^1L_b. The present note will report on the fluorescence of some benzimidazole derivatives in acid and neutral media.

The benzimidazoles studied have pK_a values ranging from 4.9 to 6.8. The absorption spectra of these compounds show two separated absorption bands, ^1L_a and ^1L_b, in neutral and acid solutions. The protonation causes slight blue shifts in the two absorption bands for each compound.

Neutral benzimidazole molecules show an emission band at about 34500 cm^{-1}, whereas the cations give rise to a broad, structureless emission band peaking at about 27800 cm^{-1}.

Neutral molecules of 2-methylbenzimidazole give an emission band at 34250 cm^{-1}. However, two emission bands are observed in acid media where the molecules are presumed to be completely protonated. This is in marked contrast to the fact that benzimidazole cations exhibit only one emission band. One of the two emission bands of the 2-methylbenzimidazole cations is located at 34840 cm^{-1} and it has unresolved structure, whereas the other is a broad, structureless band peaking at about 27800 cm^{-1}. The former emission bands shifts 590 cm^{-1} to higher frequencies relative to the emission band observed for neutral molecules and is observed to a considerable extent even in a 10 N sulfuric acid solution. These facts suggest that this fluorescence originates not from neutral but from cationic species.

It is possible to ascribe this emission band to the neutral species which could be present in the excited state if the pK_a^* value were assumed to be much smaller than pK_a. However, it is very difficult to imagine a large difference between the pK_a^* values of benzimidazole and 2-methylbenzimidazole in the excited state, for they are very similar in physical and chemical properties.

Another derivative of benzimidazole, 5-chlorobenzimidazole, behaves quite differently from the two compounds mentioned above. Neutral molecules show an emission band at 32890 cm^{-1}. An emission band from the cations is observed at 33900 cm^{-1} with no accompanying band at lower frequencies. In this case, the protonation causes a blue shift in both absorption and emission spectra. Even in a solution of 10N sulfuric acid, no emission band was observed at about 27800 cm^{-1}. This fact suggests that the normal emission band from the protonated species should not be far apart from the absorption band, and that the broad, structureless emission observed for benzimidazole and 2-methylbenzimidazole cations is abnormal.

From the large red shift of the broad, structureless emission band of the 2-methylbenzimidazole cations, one can suspect that the emission band is attributable to the formation of a kind of excimers.[3] However, this possibility can be ruled out for the following

TABLE 1. CLASSIFICATION OF FLUORESCENCE SPECTRA OF SOME BENZIMIDAZOLES

Cation	pK_a	Emission band ~34000 cm^{-1}	Emission band 27800 cm^{-1}	Class*
Benzimidazole cation	5.5	—	+	A
2-Methyl-BI cation**	6.1	+	+	B
2-Ethyl-BI cation	6.2	+	+	B
2-Benzyl-BI cation	5.7	+	+	B
5-Methyl-BI cation	5.7	—	+	A
2,5-Dimethyl-BI cation	6.7	+	+	B
5-Chloro-BI cation	4.9	+	—	C
2-Methyl-5-chloro-BI cation	5.7	+	—	C

* Symbol A means an emission spectrum at a lower frequency. B means a fluorescence spectrum consisting of two bands. C means an emission band at a higher frequency.

** BI stands for benzimidazole.

1) T. K. Adler, *Anal. Chem.*, **34**, 685 (1962).

2) H. U. Schütt and H. Zimmerman, *Ber. Bunsenges. Physik. Chem.*, **67**, 54 (1963).

3) Th. Förster and K. Kasper, *Z. Elektrochem.*, **59**, 976 (1955).

reasons: (i) the concentration change (10^{-4} mol/l to 10^{-6} mol/l) caused no variation in the relative intensity of the two bands or in the shape of the emission spectrum, (ii) the emission spectrum was independent of the viscosity of the media, as was seen from the fact that the emission spectrum obtained in an aqueous solution was essentially the same as that obtained in aqueous glycerol (60 vol%). Furthermore, in different acids, (0.1N sulfuric, hydrochloric, perchloric, and acetic acid), the emission spectra of the two bands were essentially the same in shape and in intensity ratio. These facts suggest that the appearance of the second emission band is not due to some bimolecular or multimolecular mechanism, but to unimolecular mechanism.

The other benzimidazole derivatives studied can be classified into the three types described above on the basis of their fluorescence spectra. Table 1 presents this classification. From this table, it can be concluded definitely that there is no close relationship between the pK_a values and the appearance of the broad emission band at lower wave numbers. It is of interest to note, however, that 2-methylbenzimidazole gives an emission spectrum consisting of two components, whereas 5-methylbenzimidazole gives a single, broad, structureless fluorescence band at about 27800 cm^{-1}. This observation suggests that the introduction of a methyl group at the position 2 has a greater effect in producing the broad emission at lower frequencies than does the introduction of a methyl group at the position 5.

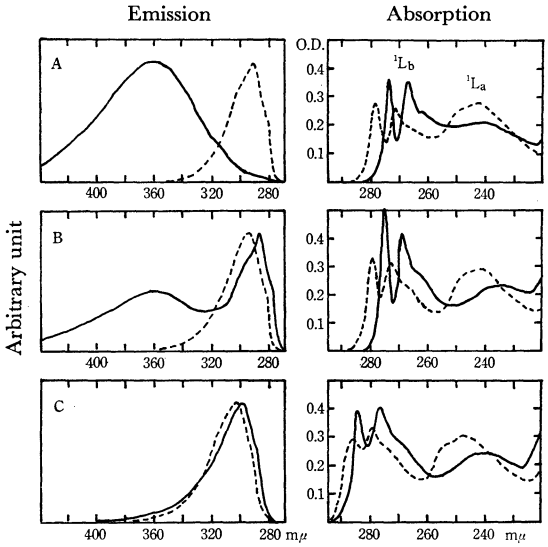

Fig. 1. Absorption and emission spectra of three benzimidazole derivatives in neutral (pH=9.3) —— and acid (0.1N H_2SO_4) —— media.
A: benzimidazole; B: 2-methylbenzimidazole; C: 5-chlorobenzimidazole.

The emission and absorption spectra are shown in Fig. 1 for the three benzimidazole derivatives in neutral and acid media. A correlation between the absorption and emission spectra in acid media can be obtained. In the case of the benzimidazole cation, the separation between the absorption bands is small and the emission is broad and is shifted to lower wave numbers. In contrast with this, two clearly-split absorption bands are observed for 5-chlorobenzimidazole cations, which show a single emission band with a small Stokes shift. For the compound with two emission bands, an intermediate splitting of the two absorption bands is observed. On the other hand, in neutral media, the two absorption bands are clearly split and only one emission band is observed for each compound. These observations suggest that the magnitude of the separation between the two excited singlet states, ^1L_a and ^1L_b, is an important factor in producing the broad emission band.

It is sure that the fluorescence originates from the equilibrium excited-state configuration, because the viscosity has no effect on the emission spectra. The relaxation process, through which the excited molecules in the Franck-Condon state change into the equilibrium-excited state, includes the reorientation of the polar solvent molecules to their equilibrium orientation in the field of the excited state of the polar solute molecules. For benzimidazole perchlorate, the emission from the ^1L_a state was observed at lower frequencies than that from the ^1L_b state.[2] This indicates that the ^1L_a state was much more stabilized than the ^1L_b state, perhaps due to the more polar character of the ^1L_a state. For the compounds, therefore, it may be possible to say that the ^1L_a states are more polar than the ^1L_b states. It is expected that the ^1L_a states are strongly stabilized by the interaction with polar solvent molecules, while the ^1L_b states are not, and that the reversal of the two excited energy levels can occur when the separation between them is small. In the case of the benzimidazole cation, the lowest vibration energy levels of the ^1L_a and ^1L_b states seem to be close to each other, and the reversal of the two energy levels could occur through the relaxation mentioned above. However, it may be difficult for the reversal to occur in the 5-chlorobenzimidazole cation because of its well-separated levels. The compounds with two excited levels intermediately split will give emission spectra consisting of two components as a result of a competitive emission from the two levels, ^1L_a and ^1L_b, which lie very close to each other after the stabilization mentioned above. Such a reversal of the two excited states has been reported for *p*-cyano-*N*,*N*-dimethylaniline,[4] for example.

4) E. Lippert, W. Lüder, F. Moll, W. Nägele, H. Boos, H. Prigge and I. Seibold-Blankenstein, *Angew. Chem.*, **73**, 695 (1961).

Experimental

Several benzimidazole derivatives were prepared by refluxing *o*-phenylenediamine and appropriate carboxylic acids in dilute hydrochloric acids.

The absorption spectra were measured with a Cary spectrophotometer Model 14. The fluorescence spectra were recorded on a Hitachi fluorescence spectrophotometer Model MPF-2.

In acid media, these compounds were stable, so the same absorption and emission spectra were obtained again on the next day. Prolonged irradiation did not cause any change in the absorption and emission spectra of benzimidazole. When the observing fluorescence was fixed at the higher-frequency band, the apparent excitation spectrum of 2-methylbenzimidazole cations was essentially the same as that obtained when the fluorescence was observed at the lower-frequency band. This is consistent with the fact that there only the protonated species are present in the solution.

BULLETIN OF THE CHEMICAL SOCIETY OF JAPAN VOL. 42 1435—1437 (1969)

The Synthetic Intermediate of Pyridoxine. I. A Novel Synthesis of 5-Alkoxy-2-carboxy-4-methyloxazole

Itsutoshi MAEDA, Masahiro TAKEHARA, Kazushi TOGO, Soichiro ASAI and Ryonosuke YOSHIDA

Central Research Laboratories, Ajinomoto Co., Inc., Suzuki-cho, Kawasaki

(Received July 2, 1968)

Recently, a few attempts have been reported to develop a new route to pyridoxine by modifying the original Harris report.[1] Most of these methods have dealt with the Diels-Alder reaction of 5-alkoxy-4-methyloxazole with various dienophiles except a few reports.[2,3] This 5-alkoxy-4-methyloxazole has been prepared from alkyl *N*-formylalaninate with phosphorus pentoxide.[4,5] However, the procedure is troublesome, for the reaction mixture forms a hard mass in the vessel.

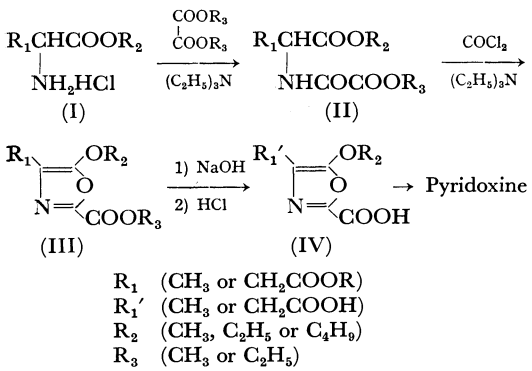

R_1 (CH_3 or CH_2COOR)
R_1' (CH_3 or CH_2COOH)
R_2 (CH_3, C_2H_5 or C_4H_9)
R_3 (CH_3 or C_2H_5)

The present authors have found an excellent method for preparing a new oxazole, 5-alkoxy-2-alkoxycarbonyl-4-methyloxazole, as an intermediate of pyridoxine. Namely, 5-alkoxy-2-alkoxycarbonyl-4-methyloxazole was prepared from alkyl *N*-alkoxalylalaninate with phosgen and triethylamine as the dehydrating agents. Other dehydrating agents

TABLE 1. THE REACTION OF METHYL *N*-METHOXALYLALANINATE[a] WITH DEHYDRATING AGENTS IN CHLOROFORM

Dehydrating agents[b]	Reaction condition		Yield[f] %
	Temp., °C	Time	
$COCl_2$[c]	20	10 min	80
$POCl_3$[d]	20	10 min	0
$POCl_3$	50	4.5 hr	23.2
$SOCl_2$[c]	20	10 min	0
$SOCl_2$	50	2 hr	18.0
$ClCOOC_2H_5$[c]	50	1 hr	25.2
P_2O_5[e]	60	3 hr	24.5

a) 0.03 mol
b) Triethylamine was used equiv. to the chlorine atom of the dehydrating agent.
c) 0.045 mol
d) 0.03 mol
e) 0.06 mol (P_2O_5) and 0.12 mol (triethylamine)
f) The yield of 5-methoxy-2-methoxycarbonyl-4-methyloxazole which was analyzed by gas chromatography (5% carbowax 20 M on chromosorb T, 4 mmϕ × 2 m; column temperature, 160°C; flow rate of He, 75 ml/min; internal standard, dimethyl terephthalate).

1) E. E. Harris and R. A. Firestone, *J. Org. Chem.*, **27**, 2705 (1962).
2) M. Murakami and M. Iwanami, This Bulletin, **41**, 726 (1968).
3) T. Miki and T. Matsuo, *Yakugaku Zasshi* (*J. Pharm. Soc. Japan*), **87**, 323 (1967).
4) Merck Co., Belg. 617499; *Chem. Abstr.*, **59**, 634 (1926).
5) F. Hoffmann-La Roche and Co., Neth. Appl. 6508673; *Chem. Abstr.*, **64**, 14193(1931).

Table 2. 5-Alkoxy-2-alkoxycarbonyl-4-substituted oxazole

	R_1	R_2	R_3	Bp °C/mmHg (Mp °C)	Found (%) C	H	N	Calcd (%) C	H	N	Yield %
IIIa	CH_3	CH_3	CH_3	113—115/5 (75—76)	49.37	5.20	8.13	49.12	5.30	8.18	75.5
IIIa	CH_3	CH_3	C_2H_5	116—118/4 (45—48)	—	—	7.88	—	—	7.56	71.0
IIIae	CH_3	C_2H_5	C_2H_5	128/4	54.54	6.89	7.13	54.26	6.58	7.03	70.0
IIIa	CH_3	C_4H_9	CH_3	134—137/3	—	—	7.10	—	—	6.57	63.7
IIIb	CH_2COOCH_3	CH_3	CH_3	156—157/3 (56—59)	47.28	4.67	6.12	47.16	4.84	6.11	50.6
IIIbe	$CH_2COOC_2H_5$	C_2H_5	C_2H_5	166—167/2	53.23	6.46	5.14	53.13	6.32	5.16	77.2

Table 3. 5-Alkoxy-2-carboxy-4-substituted oxazole

	R_1	R_2	Mp °C	Found (%) C	H	N	Calcd (%) C	H	N
IVa	CH_3	CH_3	91—92	45.58	4.65	8.86	45.86	4.49	8.92
IVae	CH_3	C_2H_5	83—84	49.50	5.23	8.24	49.12	5.30	8.18
IVa	CH_3	C_4H_9	47—49	—	—	—	—	—	—
IVbe	CH_2COOH	C_2H_5	112	44.62	4.06	6.36	44.66	4.22	6.51

gave unsatisfactory results, as is shown in Table 1. No method of synthesizing oxazole derivatives by a reaction with phosgen and triethylamine has yet been reported.

Alkyl DL-alaninate hydrochloride (Ia, $R_1=CH_3$) reacted with alkoxalylchloride to produce alkyl *N*-alkoxalylalaninate (IIa, $R_1=CH_3$),[6] but the following improved method was adopted. A mixture of 1 mol of alkyl DL-alaninate hydrochloride, 2 mol of dialkyl oxalate, and 1 mol of triethylamine was heated to give compound IIa. Compound IIa then reacted with phosgen and triethylamine to give 5-alkoxy-2-alkoxycarbonyl-4-methyloxazole (IIIa, $R_1=CH_3$). The results are summarized in Table 2. Compound IIIa was saponified with sodium hydroxide and neutralized with hydrochloric acid to crystallize 5-alkoxy-2-carboxy-4-methyloxazole (IVa, $R_1=CH_3$), as is shown in Table 3.

In a similar manner, the oxazole derivative could be obtained from dialkyl aspartate hydrochloride (Ib, $R_1=CH_2COOR$). The results are shown in Table 2 and Table 3.

Pyridine derivatives were obtained by Diels-Alder reactions with 5-alkoxy-2-carboxy-4-methyloxazole (IVa) or 5-alkoxy-2-carboxy-4-carboxymethyloxazole (IVb) and with such dienophiles as diethyl maleate, fumaronitrile, 2,5-dihydrofuran, and 4,7-dihydro-1,3-dioxepine. These pyridine derivatives were introduced to pyridoxine by the usual methods.

Experimental*1

Ethyl *N*-Ethoxalylalaninate (Iae). Ethyl DL-alaninate hydrochloride (12.3 g, 0.08 mol) was dissolved in ethanol, and then diethyl oxalate (23.4 g, 0.16 mol) and triethylamine (8.1 g, 0.08 mol) were added. After the mixture had been heated at 50°C for 5 hr, the solvent was removed by distillation and chloroform was added to the residue. The triethylamine hydrochloride was removed by washing with water. On fractional distillation, ethyl *N*-ethoxalylalaninate was obtained (bp 127°C/2 mmHg, yield, 15.7 g, 90.5%). Similarly, alkyl *N*-alkoxalylalaninate and alkyl *N*-alkoxalylaspartate were obtained.

5-Ethoxy-2-ethoxycarbonyl-4-methyloxazole (IIIae). In 100 m*l* of chloroform, ethyl *N*-ethoxalylalaninate (21.7 g, 0.1 mol) and triethylamine (30.0 g, 0.3 mol) were dissolved. Into the solution, a 100-m*l* portion of chloroform solution containing phosgen (14.8 g, 0.15 mol) was then stirred, drop by drop, at 20°C, and the mixture was heated to 50°C for 1 hr. After the reaction mixture had been washed with water to remove the triethylamine hydrochloride, the chloroform was distilled off; on fractional distillation, 5-ethoxy-2-ethoxycarbonyl-4-methyloxazole was obtained (bp 128°C/4 mmHg; yield, 13.9 g, 70.0%). Similarly, 5-alkoxy-2-alkoxycarbonyl-4-methyloxazole and 5-alkoxy-2-alkoxycarbonyl-4-alkoxycarbonylmethyloxazole were obtained from alkyl *N*-alkoxalylalaninate and alkyl *N*-alkoxalylaspartate.

2-Carboxy-5-ethoxy-4-methyloxazole (IVae). Into 9.9 g (0.05 mol) of 5-ethoxy-2-ethoxycarbonyl-4-methyloxazole, an 11.4-m*l* portion of a 5N aqueous sodium hydroxide solution (0.057 mol) was stirred. After 20 min, 9.56 m*l* of 5.95N hydrochloric acid (0.057 mol) were added to the mixture. Crystals of 2-carboxy-5-ethoxy-4-methyloxazole were filtered out and dried over phosphorus pentoxide at 30°C under reduced pressure (mp 83—84°C; yield, 7.7 g, 90%). Similarly, 5-alkoxy-2-carboxy-4-methyloxazole and 5-alkoxy-2-carboxy-4-carboxymethyloxazole were obtained.

The Diels-Alder Reaction of 2-Carboxy-5-ethoxy-4-methyloxazole. *With Diethyl Maleate.* A mixture of 2-carboxy-5-ethoxy-4-methyloxazole (IVae, 1.7 g) and

6) W. Kerp and K. Unger, *Ber.*, **30**, 579 (1897).

*1 The boiling and melting points are uncorrected.

diethyl maleate (5.2 g) was kept at 100°C for 6 hr. Upon the addition of ethanol containing hydrogen chloride and upon the further addition of ether to the reaction mixture, crystals of 4,5-diethoxycarbonyl-3-hydroxy-2-methylpyridine hydrochloride (V) were formed (mp 144—145°C; yield, 2.5 g, 86.2%).

Found: C, 49.63; H, 5.34; N, 4.88%. Calcd for $C_{12}H_{15}NO_5HCl$: C, 49.74; H, 5.57; N, 4.84%.

Similarly, a mixture of 2-carboxy-4-carboxymethyl-5-ethoxyoxazole (IVbe, 2.2 g) and diethyl maleate (5.2 g) was kept at 130°C for 4 hr. From the reaction mixture, V was obtained (mp 145—146°C; yield, 1.1 g).

With Fumaronitrile. A mixture of IVae (1.7 g), fumaronitrile (0.78 g), and methanol (20 m*l*) was refluxed for 5 hr. After the reaction mixture had then cooled, 4 m*l* of concentrated hydrochloric acid were added. The solvent was then distilled off, and the residue was dried with benzene. When recrystallized from a mixed solvent of methanol and benzene, it formed yellow crystals, 4,5-dicyano-3-hydroxy-2-methylpyridine (mp 187—188°C; yield, 0.9 g).

Found: C, 60.54; H, 3.08; N, 26.49%. Calcd for $C_8H_5N_3O$: C, 60.37; H, 3.17; N, 26.41%.

With 4,7-Dihydro-1,3-dioxepine. A mixture of 4,7-dihydro-1,3-dioxepine (20.3 g) and IVae (1.7 g) was kept at 190°C for 3 hr. After the unreacted compounds had been distilled off, a 120-m*l* portion of 2N hydrochloric acid was added to the residue and the mixture was refluxed for 2 hr. After the solvent had been distilled off, crystals of pyridoxine hydrochloride were obtained when ethanol and acetone were added to the residue (mp 202—204°C; yield, 1.0 g).

Found: C, 46.89; H, 6.15; N, 6.76%. Calcd for $C_8H_{11}NO_3HCl$: C, 46.72; H, 5.88; N, 6.81%.

BULLETIN OF THE CHEMICAL SOCIETY OF JAPAN VOL. 42 1437—1438 (1969)

Hot-Atom Chemistry of Bromine. I. Distribution of Bromine-82 Recoiled by the Bromine-82m Isomeric Transition Process in Aqueous Potassium Bromate

Chiro SHINOMIYA, Akira OYOSHI and Toshiaki KISHIKAWA

Department of Industrial Chemistry, Faculty of Engineering, Kumamoto University, Kumamoto

(Received July 4, 1968)

In spite of a number of investigations of the chemical state of recoil bromine atoms arising from radiative neutron capture in bromate,[1-3] the discovery of ^{82m}Br in independent studies[4,5] has prompted a re-evaluation of the ^{82}Br hot-atom data. Saito *et al.*,[2] in 1967, discussed isotope effects with regard to the isomeric transition-induced reaction of ^{82m}Br after (n, γ) reactions in various solid bromates.

To study the chemical state of radioactive bromine atoms after (n, γ) and (I. T.) reactions in aqueous media, the present authors irradiated an aqueous (0.1M) potassium bromate solution in a reactor for one minute (thermal neutron flux of 5×10^{12} n/cm^2/-sec and attendant γ-dose rate of 2.7×10^7 R/hr) and then investigated the distribution of ^{82}Br atoms arising from both (n, γ) and (I. T.) reactions by means of paper electrophoresis (on Toyoroshi No. 50 with a potential gradient of 50 V/cm and with 0.1M $NaClO_4$ as the electrolyte). It was found that most of the activities in the form of BrO_3^- and Br_2[6] at the end of irradiation decayed with a half-life of ^{82m}Br, while the activities in the form of Br^- grew simultaneously.

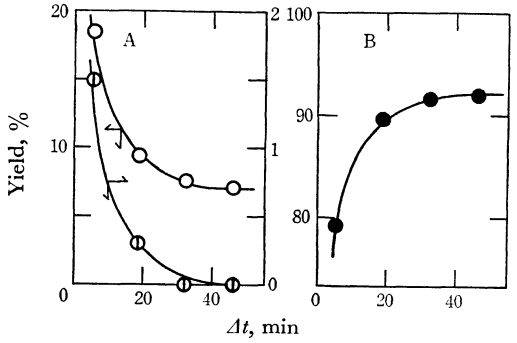

Fig. 1. Decays and growth of ^{82}Br-recoil species in irradiated aqueous BrO_3^-.
○: BrO_3^-, ◑: Br_2, ●: Br^-

Figures 1A and 1B show plots of the activities

1) The literature has been well surveyed by Saito *et al.* in Ref. 2.

2) N. Saito, F. Ambe and H. Sano, *Radiochim. Acta*, **7**, 131 (1967).

3) G. E. Boyd and Q. V. Larson, *J. Am. Chem. Soc.*, **90**, 254 (1968).

4) O. U. Anders, *Phys. Rev.*, **138**, B1 (1965).

5) J. F. Emery, *J. Inorg. Nucl. Chem.*, **27**, 903 (1965).

6) Activities remained on the point of origin on a paper strip. The neutral bromine species which could have been thought to be present in the solution after stabilization was Br_2.

of BrO_3^-, Br_2 and Br^- in percentages obtained from a neutron-irradiated aqueous potassium bromate solution which has been left to stand for various periods of time, Δt, after the end of irradiation. The curves of BrO_3^- and Br_2 decrease with an increase in the standing time, while that of Br^- increases.

About 91% of the initial radioactive bromine when the ^{81}Br atoms have been captured with neutrons is the 6.2 min ^{82m}Br isomer,[5] which decays primarily (*i.e.*, 99.8%) by means of a highly-converted transition from the 46 keV level (internal conversion coefficient $\alpha_k=268$) to the ^{82}Br ground state. This means that, in the process of the isomeric transition the ^{82}Br atom gains a highly positively-charged state as a result of the emission of a conversion electron and accompanying Auger electrons. The high positive charge results in a Coulomb repulsion. Bromine-82, which combines with oxygens to form the bromate ion, will then recoil into the aqueous medium. The chemical form in which the bromine finally remains will be the bromide ion. Early work by Libby and his co-worker[7] has shown that, if the bromate ion in solution is labeled with ^{80m}Br, the isomeric transition produces a disruption of the bromate molecule. Then the recoil ^{80}Br becomes a bromide ion.

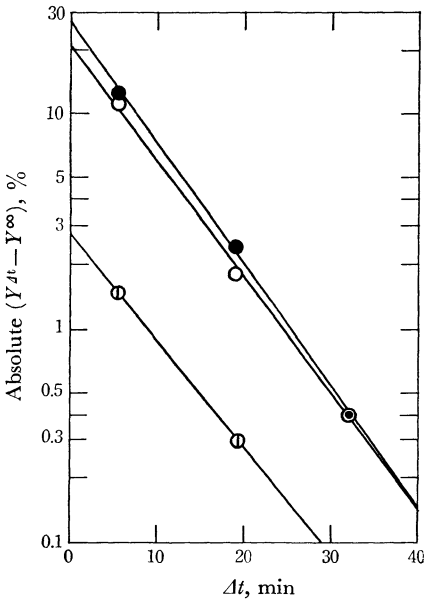

Fig. 2. ^{82}Br-recoil species as a result of isomeric transition in aqueous BrO_3^-.
○: BrO_3^-, ◑: Br_2, ●: Br^-

If the observed decrease or increase in the ^{82}Br yields of subjecting species were a result of chemical excitation by the isomeric transition alone, the rate of the decay or growth of the yield should be dependent only on the decay of ^{82m}Br and should be related to the half-life of the ^{82m}Br. Therefore, if Y^∞ represents the yield of a species reached in the solution after all the ^{82m}Br has decayed to the ^{82}Br ground state, and if Y^0 represents the yield produced at the end of neutron irradiation, the yield, $Y^{\Delta t}$, at any time before the ^{82m}Br has completely decayed minus Y^0 would be $(Y^\infty-Y^0)$ multiplied by the fraction of ^{82m}Br atoms, present when the sample was separated, which had decayed to ^{82}Br. The fraction remaining would be $\exp(-\lambda\Delta t)$, where λ is the decay constant of ^{82m}Br. The decay of ^{82m}Br in BrO_3^- or Br_2 is then given by $Y^{\Delta t}-Y^\infty=(Y^0-Y^\infty)\cdot\exp(-\lambda\Delta t)$. A plot of $Y^{\Delta t}-Y^\infty$ *vs.* Δt on a semilogarithmic scale should yield a straight line with a slope of $-0.693/2.303T_{1/2}$ (Fig. 2). The fraction which had decayed is $1-\exp(-\lambda\Delta t)$. Similarly, the growth of ^{82}Br in Br^- will be given by $Y^{\Delta t}-Y^0=(Y^\infty-Y^0)(1-\exp(-\lambda\Delta t))$. By rearranging the equation, we can see also that a plot of $Y^\infty-Y^{\Delta t}$ *vs.* Δt on the same scale should yield a straight line (Fig. 2). The ^{82m}Br half-life values were determined to be 5.53, 5.57 and 5.29 min using the yields of BrO_3^-, Br_2, and Br^- respectively. These values are in fairly close agreement with the values of 363 sec and 6.2 min reported in Refs. 4 and 5 respectively. The agreed relative rates of decrease or increase in the BrO_3^-, Br_2, or Br^- yields can be attributed to ^{82m}Br isomeric transition-excited reactions.

The Y^∞ values in BrO_3^-, Br_2, and Br^- were 7.7%, 0%, and 92.1%, and the (Y^0-Y^∞) values in them were 21.3%, 2.9%, and 27.3% respectively. By adding; $(Y^0-Y^\infty)(BrO_3^-)+Y^\infty(BrO_3^-)$; here, the latter term must be due, for the most part, to the direct formation of ^{82g}Br from the (n, γ) process; the experimentally-determined retention in BrO_3^- at the end of neutron irradiation was 29.0%, the 21.3/29.0=0.78 fraction of which was estimated to be $BrO_3^-(^{82m}Br)$. The yields of ground- and metastable-state bromine-82 in bromate at the end of irradiation arising directly from the (n, γ) reaction were distinguished.

The authors wish to express their appreciation to Dr. Shiro Iwata, Dr. Yoshiyuki Kiso, and the personnel of the Research Reactor Institute, Kyoto University, for their assistance in the irradiation. Thanks are also due to Mr. Shin'ichi Toyama for helping with the experimental work.

7) D. C. DeVault and W. F. Libby, *Phys. Rev.*, **55**, 322 (1939).

BULLETIN OF THE CHEMICAL SOCIETY OF JAPAN VOL. 42 1439—1440 (1969)

A Band Model of the Charge-Transfer Complexes

Hisanao SATO and Chisato OKAZAKI

Wireless Research Lab., Matsushita Electric Industrial Co., Ltd., Kadoma, Osaka

(Received July 13, 1968)

The purpose of this note is to propose a theoretical model to explain the high electrical conductivities of some charge-transfer complexes. The complexes of aromatic hydrocarbons with iodine are found to show low resistivities when the mole ratio deviates from 1 : 1, while those of the 1 : 1 complexes are high.[1] For example, the resistivity of the pyrene-iodine (1 : 2) complex is 75 ohm-cm at room temperature[2] and the coronene-iodine (1 : 1) complex has a resistivity of about 10^8 ohm-cm.[3] For a complex in which the ionization energy of the donor is much larger than the electron affinity of the acceptor, the ground state is mainly expressed as a non-bonding structure and the band gap may be presumed to be large. Since the ionization energy of pyrene is nearly equal to that of coronene,[1] the reason for the low resistivity of the pyrene-iodine complex must be discussed.

Since no data are available on the crystal structure of the 1 : 2 complexes, the linear chain indicated in Fig. 1 is assumed[4] in order to calculate the energy bands for the simplest case. In Fig. 1, D is a donor molecule and A is an acceptor molecule. In this arrangement two acceptors (A_1 and A_2) in a unit cell are assumed to occupy equivalent sites. Assuming that the one-electron Hamiltonian, H, has properly been chosen for the linear chain, we define the Bloch orbitals, $\phi_D(\boldsymbol{k})$, $\phi_{A_1}(\boldsymbol{k})$, and $\phi_{A_1}(\boldsymbol{k})$, as follows:

$$\phi_D(\boldsymbol{k}) = \sum_j \exp(i\boldsymbol{k}\boldsymbol{R}_{jD})\ \chi_D(r - \boldsymbol{R}_{jD}), \quad (1)$$

$$\phi_{A_1}(\boldsymbol{k}) = \sum_j \exp(i\boldsymbol{k}\boldsymbol{R}_{jA_1})\ \chi_A(r - \boldsymbol{R}_{jA_1}), \quad (2)$$

$$\phi_{A_2}(\boldsymbol{k}) = \sum_j \exp(i\boldsymbol{k}\boldsymbol{R}_{jA_2})\ \chi_A(r - \boldsymbol{R}_{jA_2}). \quad (3)$$

Here $\boldsymbol{R}_{jD}$, $\boldsymbol{R}_{jA1}$, and $\boldsymbol{R}_{jA2}$ are the coordinates of the molecules D, A_1, and A_2 respectively in the jth cell, and $\boldsymbol{k}$ is the wave vector of an electron. χ_D is the wave function for the highest occupied level of the donor, and χ_A is that for the lowest unoccupied level of the acceptor.

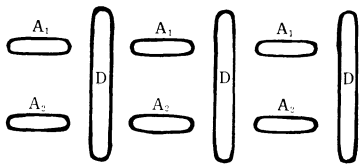

Fig. 1. Assumed structure of 1 : 2 complex. D is a donor and A is an acceptor.

It can be seen from the symmetry that the state:

$$\phi_A^- = 2^{-1/2}(\phi_{A_1} - \phi_{A_2})$$

does not combine with ϕ_D and that it is, therefore, the eigen-state. The corresponding energy, $E^{(-)}(\boldsymbol{k})$, is nearly independent of the wave vector, $\boldsymbol{k}$, since the overlap of χ_A in different cells may be neglected. The other eigen-states are obtained by taking linear combinations of ϕ_D and

$$\phi_A^+ = 2^{-1/2}(\phi_{A_1} + \phi_{A_2})$$

The energies are determined by:

$$\begin{vmatrix} H_D - E, & H_1 \\ H_1^*, & H_A - E \end{vmatrix} = 0, \quad (4)$$

where, for simplicity, the overlap integral is neglected and where:

$$H_D = \int \phi_D^* H \phi_D d\tau, \quad (5)$$

$$H_A = \int \phi_A^{+*} H \phi_A^+ d\tau, \quad (6)$$

$$H_1 = \int \phi_D^* H \phi_A^+ d\tau. \quad (7)$$

If $(H_A - H_D)^2 \gg 4|H_1|^2$, the ground state energy, $E_0(\boldsymbol{k})$, and the excited state energy, $E^{(+)}(\boldsymbol{k})$, may be written as:

$$E_0(\boldsymbol{k}) = H_D - \Delta E, \quad (8)$$

$$E^{(+)}(\boldsymbol{k}) = H_A + \Delta E, \quad (9)$$

where: $$\Delta E = |H_1|^2/(H_A - H_D). \quad (10)$$

These energies are shown in Fig. 2, where $E^{(-)}(\boldsymbol{k})$ and the magnitudes of the integrals (5), (6), and (7) are chosen arbitrarily. The band $E_0(\boldsymbol{k})$ is filled with electrons, since there are two electrons

1) Y. Matsunaga, "Yûki Handôtai" (Organic Semiconductors), ed. by H. Inokuchi, I. Nakata and M. Hatano, Kyôritsu Shuppansha, Tokyo (1966), p. 153.

2) J. Kommandeur and F. R. Hall, *J. Chem. Phys.*, **34**, 129 (1961).

3) M. M. Labes, R. Sehr and M. Bose, Internat. Conf. Semicond. Phys., Prague (1960), p. 850.

4) T. Uchida and H. Akamatu, This Bulletin, **34**, 1015 (1961).

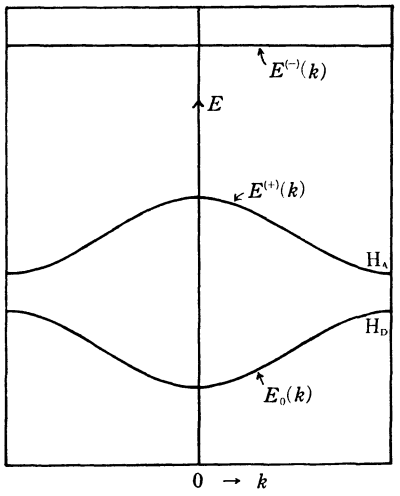

Fig. 2. Band structure of a linear 1 : 2 complex.

per molecule; hence, the smallest band gap is equal to $H_A - H_D$ at the zone boundary.

ΔE represents the part of the binding energy due to the electron transfer from D to A. This charge-transfer energy, ΔE, depends on the distance, R_A, between A_1 and A_2 through H_A. If the magnitude of $|H_1|^2$ does not decrease with R_A, R_A becomes shorter than the van der Waals distance between the two acceptors in order to lower the energy of the state $\phi_A{}^+; H_A$. Therefore, the binding energy of the lattice is expected to increase with a decrease in R_A, although the repulsive force between A_1 and A_2 causes some energy loss. Therefore, the band gap, $H_A - H_D$, may be small even if the difference between the donor ionization energy and the electron affinity of the acceptor is large. The difference between coronene and pyrene may lie in the difference between their highest occupied states, χ_D. Presumably, the χ_D of coronene spreads on a large molecular plane, so a decrease in R_A results in the reduction of the overlapping of ϕ_D and $\phi_A{}^+$.

BULLETIN OF THE CHEMICAL SOCIETY OF JAPAN VOL. 42 1440—1443 (1969)

The Nuclear Magnetic Resonance and Infrared Spectra of Aromatic Azomethines

Katsumi TABEI and Etsurou SAITOU

Tokyo College of Pharmacy, 4-600, Kashiwagi, Shinjuku-ku, Tokyo

(Received July 24, 1968)

Theoretical and experimental studies have suggested that the molecular structure of benzalaniline is not planar and that the benzene ring of the aniline part is distorted from the plane of the *trans*-benzalamino skeleton, as is shown in Fig. 1; it has

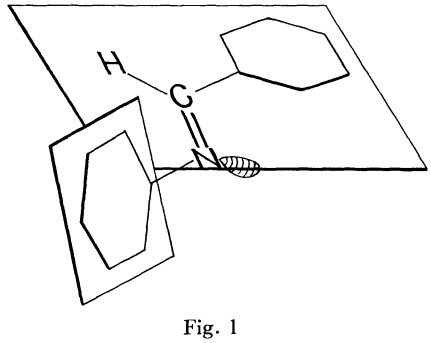

Fig. 1

also been disclosed that the substituent in the benzaldehyde ring has more effect on the electronic structure of azomethine group than that in the aniline part does.[1-7] Although a few papers suggest the above molecular geometry from the point of view of infrared spectral studies, there has been very little work on the nuclear magnetic resonance spectra of aromatic azomethines.

In the present work, the nuclear magnetic resonance spectra of more than twenty kinds of *p*-substituted benzalaniline were newly measured; the characteristic Hammett relation in the NMR and

1) V. A. Izmail'skii and E. A. Smirnov, *Zh. Obshch. Khim.*, **26**, 3042 (1956); V. A. Izmail'skii and Yu. A. Fedorov, *Zh. Fiz. Khim.*, **39**, 768 (1965).

2) N. Ebara, This Bulletin, **33**, 534, 540 (1960); **34**, 1151 (1961).

3) M. Uehara, *Nippon Kagaku Zasshi* (*J. Chem. Soc. Japan, Pure Chem. Sect.*), **86**, 901 (1961).

4) W. F. Smith, *Tetrahedron*, **19**, 445 (1963).

5) L. E. Clougherty, J. A. Sousa and G. M. Wyman, *J. Org. Chem.*, **22**, 462 (1957).

6) J. D. Margerum and J. A. Sousa, *Appl. Spectry*, **19**, 91 (1965).

7) W. Kraws and C. G. J. Wagner, *Z. Naturforsch.*, **A22**, 746 (1967).

TABLE 1. IR AND NMR SPECTRA OF BENZALANILINE AND ITS DERIVATIVES

Substituent X	Hammett's σ_p *	X-C_6H_4-CH=N-C_6H_5 (type A)				C_6H_5-CH=N-C_6H_4-X (type B)			
		mp (°C)	$\nu_{C=N}$ (cm^{-1}) in KBr	$\nu_{C=N}$ (cm^{-1}) in CCl_4**	τ in $CDCl_3$	mp (°C)	$\nu_{C=N}$ (cm^{-1}) in KBr	$\nu_{C=N}$ (cm^{-1}) in CCl_4**	τ in $CDCl_3$
$-N(CH_3)_2$	−0.83	99.5—100.5	1600	1617	1.73	101—102	1619	1630	1.51
-OH	−0.46	191—193	1616	1630**	—	182—183	1624	—	—
$-OCH_3$	−0.27	63—64	1624	1635	1.65	71—71.5	1627	1630	1.55
$-OC_2H_5$	−0.25	61—62	1621	1635	1.65	72—73	1629	1633	1.55
$-CH_3$	−0.17	146—147***	1630****	1638	1.66	158—159***	1630****	1637	1.61
-H	0.00	52—53	1629	1635	1.60				
$-C_6H_5$	+0.01					148—149	1630	1635	1.52
-Cl	+0.23	63.5—64.5	1627	1635	1.64	63—63.5	1629	1635	1.61
-Br	+0.23	73—74	1624	1634	1.64	65—66	1630	1636	1.60
-I	+0.28	90—91	1621	1629	1.64	85—86	1628	1635	1.64
-COOH	+0.27	224—225	1623	—	—	191—193	1625	—	—
-COOR*****	+0.45	125.5—126.5	1622	1632	1.53	47—48	1632	1635	1.60
$-COCH_3$	+0.52					100—101	1630	1635**	1.60
$-SO_2NH_2$	+0.57	176—179 (d.)	1619	—	—	173—174.5	1628	1634**	—
$-NO_2$	+0.78	92—93	1620	1629**	1.46				
N,N-Dibenzal-*p*-phenylenediamine						141—141.5	1618	1631**	1.51
Terephthalaldehyde dianil						161.5—163	1615	1628**	1.52
N,N-Dimethyl-*N'*-(*p*-nitrobenzal)-*p*-phenylenediamine						227—228	1619	1629**	1.42

* H. H. Jaffé, *Chem. Revs.*, **53**, 191 (1953).
** Solvent is chloroform.
*** Bp at 3 mmHg.
**** Measured in liquid film.
***** R is methyl in type A and ethyl in type B respectively.

IR spectra of the azomethine group will be discussed in order to clarify the molecular geometry.

Experimental

Materials. Twenty-nine kinds of benzalaniline were prepared by the usual condensation reaction either from aniline and *p*-substituted benzaldehydes or from *p*-substituted anilines and benzaldehyde.[8,9] The crystalline compounds were purified by repeated recrystallization from methanol or ethanol, but *N*-(*p*-methylbenzal)-aniline, *N*-benzal-*p*-toluidine, and ethyl *p*-(*N*-benzalamino)-benzoate were distilled under reduced pressure. The purity of the products was checked by thin-layer chromatography.

Nuclear Magnetic Resonance Spectra. The NMR spectra of the above compounds were measured by using a JNM-4H-100 NMR spectrometer in a deuteriochloroform solution at a 0.2—0.5 mol/*l* concentration. The spectra of the hydroxyl, carboxyl, and sulfonamido derivatives, however, could not be measured, since the compounds are not satisfactorily soluble in deuteriochloroform.

Infrared Spectra. The IR spectra of the above benzalanilines were also measured by using a JASCO DS-301 infrared spectrophotometer in a carbon tetrachloride or chloroform solution and in a disk of potassium bromide. The spectra of *p*-(*N*-benzalamino)-benzoic acid and *p*-(*N*-benzalamino)-benzenesulfonamide were not measured in the solution because of their poor solubility in the above solvents.

The τ values and the wave numbers so measured are listed in Table 1, together with the physical constants.

Results and Discussion

***N*-(*p*-Substituted-benzal)-anilines (Type-A compounds).** The NMR proton signals of the azomethine group of the *N*-(*p*-substituted-benzal)-anilines appear in the region of 1.46 τ (*p*-nitrobenzalaniline)- 1.73 τ (*p*-*N,N*-dimethylaminobenzalaniline) as a singlet peak; the introduction of an electron-donating or of an electron-withdrawing group into the para position of the benzaldehyde ring of a type-A compound brings about a small shift of the signal to a higher or to a lower field respectively.

The plot of the τ values against Hammett's σ_p constant (Fig. 2) shows a characteristic Hammett relationship between the chemical shift of an azomethine proton signal and the electronic effect of a substituent in type-A compounds.

The present NMR data permit only a qualitative discussion; however, it seems reasonable that the chemical shift of an azomethine proton signal is

8) L. Gattermann, "Die Praxis des Organischen Chemikers," 40 Aufl., 150 (1961).
9) H. Gilman, "Organic Syntheses," Coll. Vol. I, p. 80 (1956).

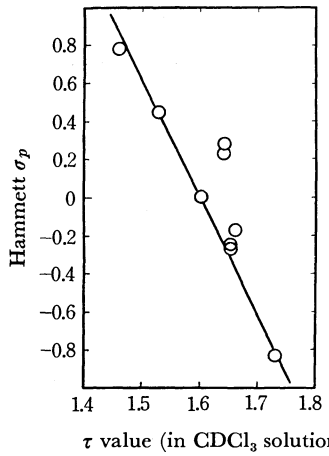

Fig. 2. τ value of azomethine proton *vs.* Hammett's σ_p in type A compounds.

mainly determined by the change in the electron density on the carbon atom in the azomethine double bond, supposing that the magnetic anisotropy of a substituent can be neglected as in the case of styrene and phenylacetylene derivatives.[10,11]

Consequently, the present chemical shift of the azomethine proton signal can be understood by taking the following resonance structures (I)—(III) into account; since an increase in the contribution of the polar structure (I) to the ground state (II) makes for an increase in the electron density of the azomethine carbon as well as in that of nitrogen,[12] the introduction of an electron-donating group to the para position of the benzaldehyde ring makes for a small shift of the azomethine proton signal to the higher-field side. The substituent effect of an electron-withdrawing group corresponding to the increase in the contribution of the polar structure (III), on the other hand, decreases the electron density at the azomethine group and, therefore, makes for a small shift of the signal to the lower-field side.

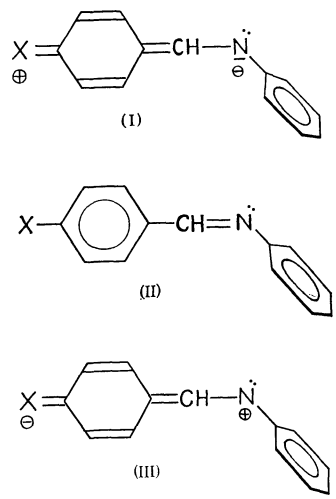

From the above discussion, it can also be expected that an increase in the contribution of either polar structure will bring about a decrease in the carbon-nitrogen bond order of the azomethine group. Previous infrared studies have not satisfactorily treated the substitution effect upon the change in the C=N bond order; therefore, the C=N stretching frequency of many kinds of type-A compounds were also measured.

When an electron-donating or electron-withdrawing group is introduced into the para position of the benzaldehyde ring, the C=N stretching band of benzalaniline, 1635 cm^{-1} in a CCl_4 solution and 1629 cm^{-1} in a KBr disk, is, as expected, shifted more or less to the longer wavelength side. The present characteristic trend is confirmed by plotting the $\nu_{C=N}$ against the Hammett's σ_p constant, as is shown in Fig. 3. The relationship obtained can also safely be explained by taking the polar structures (I) and (III) into consideration, as has been mentioned previously.

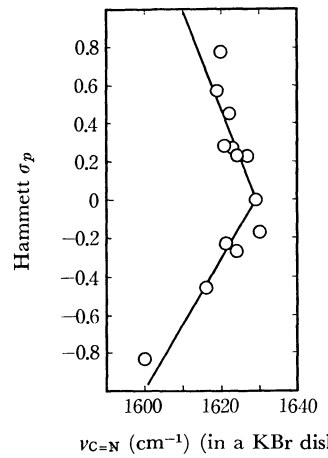

Fig. 3. $\nu_{C=N}$ *vs.* Hammett's σ_p constant in type A compounds.

***p*-Substituted *N*-benzalanilines (Type-B Compounds).** The preceding discussion does not take the effect of the aniline part into account, since the aniline ring may be distorted from the plane of the benzalamino skeleton. In order to substantiate the above description, the NMR and IR spectra of *p*-substituted *N*-benzalanilines were also studied. It was revealed that the proton signal and the C=N stretching band of the azomethine group of type-B

10) H. Kasiwagi and J. Niwa, This Bulletin, **36**, 405, 411 (1963).

11) Y. Yukawa and H. Yamada, *Nippon Kagaku Zasshi* (*J. Chem. Soc. Japan, Pure Chem. Sect.*), **85**, 501 (1964).

12) V. I. Minkin, Yu. A. Zhdanov, E. A. Medyantzeva and Yu. A. Ostroumov, *Tetrahedron*, **23**, 3651 (1967).

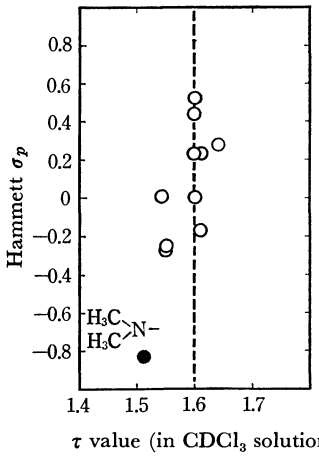

Fig. 4. τ value of azomethine proton *vs.* Hammett's σ_p in type B compounds.

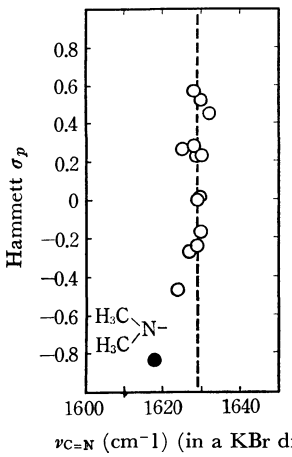

Fig. 5. $\nu_{C=N}$ *vs.* Hammett's σ_p constant in type B compounds.

compounds appear within a narrower range than those of type-A compounds do. That is, a substituent in the para position of the aniline ring can not exert any appreciable electronic effect upon the azomethine group, and the Hammett relation is not obtained, as is depicted in Figs. 4 and 5. The present results can reasonably be understood by accepting the previous non-planar structure for the benzalaniline molecule in which an aniline ring can not conjugate with a benzalamino π system.

A strong electron-donating group such as *N,N*-dimethylamino, however, shifts the proton signal considerably to the lower-field side, and at the same time shifts the C=N stretching band to the longer wavelength side. The above rather exceptional shift found in the dimethylamino derivative can be understood by considering the electron-repelling effect of the electron-rich azomethine nitrogen atom. Since an electron is concentrated on one of the sp^2 lobes, the lone-pair lobe, from the dimethylaminophenyl group, the electron-rich azomethine nitrogen atom can repel its π-electron to the benzaldehyde part inductively, as in the structure (IV), and can, therefore, increase the electron density at the azomethine carbon and at the same time decrease the bond order of the azomethine bond.

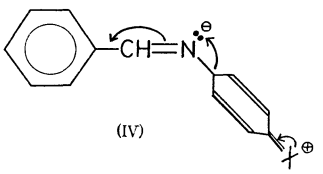

(IV)

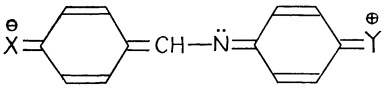

(V)

If an electron can transfer from an aniline part to a benzaldehyde one conjugatively, as is shown in the planar structure (V), the azomethine proton signal and the C=N stretching band of *N*-(*p*-nitrobenzal)-*N'*,*N'*-dimethyl-*p*-phenylenediamine can be expected to appear in a far lower-field side and in a far longer wavelength region than those of other benzalanilines. The observed values, however, are 1.42 τ in the $CDCl_3$ solution, 1629 cm^{-1} in the $CHCl_3$ solution, and 1619 cm^{-1} in the KBr disk. The present shifts are merely larger than those of *p*-nitrobenzalaniline; 1.46 τ in the $CDCl_3$ solution, 1630 cm^{-1} in the $CHCl_3$ solution, and 1621 cm^{-1} in the KBr disk.

The above results suggest that dimethylamino, a strong electron-donating group, in the para position of the aniline ring can not conjugate directly with the nitro group through the benzalaniline skeleton and that it can not greatly change the electron density and bond order of the azomethine bond. Thus, the non-planar structure of benzalaniline, the so-called Brocktehurt model, is also supported with respect to the Hammett relationship in NMR and IR spectra.

The authors wish to express their deep thanks to Mr. Toshio Ono and Mrs. Moriharu Nagase of the Tokyo College of Pharmacy for their helpful measurements of the NMR and IR spectra.

BULLETIN OF THE CHEMICAL SOCIETY OF JAPAN VOL. 42 1444—1446 (1969)

Studies on 6-Bromo-2-mercapto-3-substituted 4-(3*H*)-Quinazolinones

P. N. Bhargava and R. Lakhan

The Chemistry Department, Faculty of Science, Banaras Hindu University, Varanasi-5, India

(Received July 26, 1968)

In continuation of our earlier work on heterocyclic sulphur compounds of interest as antimalarials and ataractic agents,[1] we have extended the alkylation of the sodium salts of 6-bromo-2-mercapto-3-aryl(or alkyl)-4(3*H*)-quinazolinones in alcoholic alkali solution with typical halogen compounds (prepared by the interaction of chloroacetyl chloride and secondary amines in benzene) and also with monochloroacetic acid.

In the present communication, for example, when 6-bromo-2-mercapto-3-substituted 4(3*H*)-quinazolinone (I) was treated with aqueous alcoholic alkali, the sodium salt (Ia) was formed (soluble in aqueous ethanol) which without isolation was converted to the *S*-substituted derivative (II) by reaction with *N,N*-disubstituted chloroacetamides as shown in the reaction scheme.

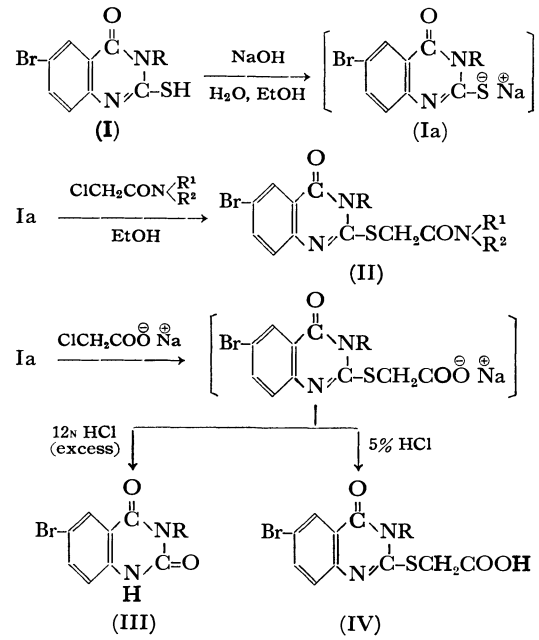

An interesting point was observed when the sodium salt (Ia) was treated in cold with sodium monochloroacetate and the precipitate obtained was kept in contact with excess of concentrated hydrochloric acid. The product was then found to be the corresponding 2-hydroxyquinazolinone (III) and not the expected 2-carboxymethylthio derivative (IV). The structure of the 2,4-diketo derivative (III) was confirmed by preparing it from 5-bromoanthranilic acid and the corresponding urea.[2]

However, the 2-carboxymethylthio derivative (IV) was obtained by a modified procedure. The solution of the sodium salt (Ia) on treatment with sodium monochloroacetate and subsequent acidification with 5% hydrochloric acid gave the desired product (IV).

Experimental

6-Bromo-2-mercapto-3-substituted 4-(3*H*)-Quinazolinones (I). These were prepared by the condensation of 5-bromoanthranilic acid and various isothiocyanates as described earlier.[1]

6-Bromo-2-(*N,N*-diethylcarbamoyl)methylthio-3-phenyl-4-(3*H*)-quinazolinone (II). 6-Bromo-2-mercapto-3-phenyl-4-(3*H*)-quinazolinone (I,R = C_6H_5 6.66 g) was dissolved in minimum amount of 10% sodium hydroxide solution (prepared in 50% ethanol). The solution was filtered and treated with 3.3 g of *N,N*-diethylchloroacetamide dissolved in 10 m*l* of ethanol. The reaction mixture was stirred at room temperature for about 4 hr when a precipitate was obtained. It was filtered, washed with water, ethanol and recrystallized from ethanol into colourless crystals.

Following the same procedure other 6-bromo-2-(*N,N*-disubstituted carbamoyl)methylthio-3-substituted 4-(3*H*)-quinazolinones have been prepared. Their yields, melting points and analytical data are recorded in Tables 1—4.

6-Bromo-3-phenyl-2,4-(1*H*, 3*H*)-quinazolindione (III). 6-Bromo-2-mercapto-3-phenyl-4-(3*H*)-quinazolinone (0.01 mol) was dissolved in 2.1 equivalents of 1N sodium hydroxide solution (in 50% ethanol) and the resulting solution was treated in cold with monochloroacetic acid (0.011 mol). The reaction mixture was stirred for 4—6 hr when a precipitate was obtained. It was filtered and the residue was kept in contact with excess of 12N hydrochloric acid at room temperature for 2 hr. The reaction mixture was then filtered and washed several times with water to remove the acid and dried. It was crystallized from acetone-ethanol mixture (1 : 1) into colourless needles to give 68% yield of 6-bromo-3-phenyl-2,4-(1*H*,3*H*)-quinazolindione.

1) P. N. Bhargava and R. Lakhan, *Current Sci. (India)*, **36**, 575 (1967), and references cited therein.

2) G. R. Dave, G. S. Mewada and G. C. Amin, *Acta Chim. Acad. Sci. Hung.*, **34**, 101 (1962).

Table 1. 6-Bromo-2-(*N*,*N*-diethylcarbamoyl)methylthio-3-substituted 4-(3*H*)-quinazolinones (II)

No.	R	Yield %	Mp °C	Formula	% Nitrogen		% Sulphur	
					Found	Calcd	Found	Calcd
1	C_6H_5	80	201	$C_{20}H_{20}BrN_3O_2S$	9.30	9.42	7.11	7.17
2	*o*-$CH_3\cdot C_6H_4$	57	169	$C_{21}H_{22}BrN_3O_2S$	9.05	9.13	7.09	6.95
3	*m*-$CH_3\cdot C_6H_4$	43	224	$C_{21}H_{22}BrN_3O_2S$	9.26	9.13	6.82	6.95
4	*p*-$CH_3\cdot C_6H_4$	85	192	$C_{21}H_{22}BrN_3O_2S$	9.18	9.13	6.78	6.95
5	*m*-$Cl\cdot C_6H_4$	45	157	$C_{20}H_{19}BrClN_3O_2S$	8.78	8.74	6.51	6.66
6	*p*-$Cl\cdot C_6H_4$	72	181	$C_{20}H_{19}BrClN_3O_2S$	8.89	8.74	6.45	6.66
7	*o*-$CH_3O\cdot C_6H_4$	49	163	$C_{21}H_{22}BrN_3O_3S$	8.65	8.82	6.62	6.72
8	*p*-$CH_3O\cdot C_6H_4$	75	171	$C_{21}H_{22}BrN_3O_3S$	8.78	8.82	6.72	6.72
9	*p*-$C_2H_5O\cdot C_6H_4$	82	165	$C_{22}H_{24}BrN_3O_3S$	8.40	8.57	6.49	6.53
10	CH_3	40	120	$C_{15}H_{18}BrN_3O_2S$	11.05	10.93	8.27	8.33
11	C_2H_5	50	135	$C_{16}H_{20}BrN_3O_2S$	10.37	10.55	7.93	8.04
12	$C_6H_5\cdot CH_2$	78	143	$C_{21}H_{22}BrN_3O_2S$	9.02	9.13	6.99	6.95

Table 2. 6-Bromo-2-(*N*-methyl-*N*-phenylcarbamoyl)methylthio-3-substituted 4-(3*H*)-quinazolinones

No.	R	Yield %	Mp °C	Formula	% Nitrogen		% Sulphur	
					Found	Calcd	Found	Calcd
1	C_6H_5	50	242	$C_{23}H_{18}BrN_3O_2S$	8.91	8.75	6.76	6.67
2	*o*-$CH_3\cdot C_6H_4$	70	209	$C_{24}H_{20}BrN_3O_2S$	8.37	8.50	6.59	6.48
3	*m*-$CH_3\cdot C_6H_4$	78	204	$C_{24}H_{20}BrN_3O_2S$	8.52	8.50	6.47	6.48
4	*p*-$CH_3\cdot C_6H_4$	65	188	$C_{24}H_{20}BrN_3O_2S$	8.49	8.50	6.65	6.48
5	*p*-$Cl\cdot C_6H_4$	52	237	$C_{23}H_{17}BrClN_3O_2S$	8.04	8.16	6.07	6.22
6	*o*-$CH_3O\cdot C_6H_4$	55	214	$C_{24}H_{20}BrN_3O_3S$	8.11	8.23	6.14	6.27
7	*p*-$CH_3O\cdot C_6H_4$	47	106	$C_{24}H_{20}BrN_3O_3S$	8.26	8.23	6.38	6.27
8	*p*-$C_2H_5O\cdot C_6H_4$	50	234	$C_{25}H_{22}BrN_2O_3S$	7.98	8.02	6.29	6.10
9	CH_3	30	115	$C_{18}H_{16}BrN_3O_2S$	10.00	10.05	7.85	7.65
10	C_2H_5	68	128	$C_{19}H_{18}BrN_3O_2S$	9.58	9.72	7.53	7.41
11	$C_6H_5\cdot CH_2$	60	142	$C_{24}H_{20}BrN_3O_2S$	8.35	8.50	6.53	6.48

Table 3. 6-Bromo-2-(*N*-ethyl-*N*-phenylcarbamoyl)methylthio-3-substituted 4-(3*H*)-quinazolinones

No.	R	Yield %	Mp °C	Formula	% Nitrogen		% Bromine	
					Found	Calcd	Found	Calcd
1	C_6H_5	62	183	$C_{24}H_{20}BrN_3O_2S$	8.59	8.50	16.06	16.19
2	*o*-$CH_3\cdot C_6H_4$	85	192	$C_{25}H_{22}BrN_3O_2S$	8.10	8.27	15.89	15.75
3	*m*-$CH_3\cdot C_6H_4$	90	206	$C_{25}H_{22}BrN_3O_2S$	8.50	8.27	15.78	15.75
4	*p*-$CH_3\cdot C_6H_4$	87	200	$C_{25}H_{22}BrN_3O_2S$	8.35	8.27	15.61	15.75
5	*m*-$Cl\cdot C_6H_4$	66	232	$C_{24}H_{19}BrClN_3O_2S$	8.13	7.95	15.00	15.14
6	*p*-$Cl\cdot C_6H_4$	43	116	$C_{24}H_{19}BrClN_3O_2S$	8.11	7.95	15.17	15.14
7	*o*-$CH_3O\cdot C_6H_4$	55	220	$C_{25}H_{22}BrN_3O_3S$	8.06	8.02	15.18	15.27
8	*p*-$CH_3O\cdot C_6H_4$	50	160	$C_{25}H_{22}BrN_3O_3S$	7.94	8.02	15.05	15.27
9	CH_3	52	146	$C_{19}H_{18}BrN_3O_2S$	9.95	9.72	18.64	18.52
10	C_2H_5	58	145	$C_{20}H_{20}BrN_3O_2S$	9.60	9.42	18.02	17.94
11	$C_6H_5\cdot CH_2$	55	173	$C_{25}H_{22}BrN_3O_2S$	8.22	8.27	15.53	15.75

TABLE 4. 6-BROMO-2-(*N*-BENZYL-*N*-PHENYLCARBAMOYL)METHYLTHIO-3-SUBSTITUTED 4-(3*H*)-QUINAZOLINONES

No.	R	Yield %	Mp °C	Formula	% Nitrogen		% Bromine	
					Found	Calcd	Found	Calcd
1	C_6H_5	51	203	$C_{29}H_{22}BrN_3O_2S$	7.47	7.55	14.30	14.39
2	*o*-$CH_3 \cdot C_6H_4$	65	215	$C_{30}H_{24}BrN_3O_2S$	7.25	7.37	14.09	14.04
3	*m*-$CH_3 \cdot C_6H_4$	48	195	$C_{30}H_{24}BrN_3O_2S$	7.16	7.37	13.81	14.04
4	*p*-$CH_3 \cdot C_6H_4$	60	244	$C_{30}H_{24}BrN_3O_2S$	7.33	7.37	14.25	14.04
5	*m*-$Cl \cdot C_6H_4$	62	206	$C_{29}H_{21}BrClN_3O_2S$	7.02	7.11	13.38	13.55
6	*p*-$Cl \cdot C_6H_4$	55	205	$C_{29}H_{21}BrClN_3O_2S$	7.18	7.11	13.41	13.55
7	*o*-$CH_3O \cdot C_6H_4$	76	237	$C_{30}H_{24}BrN_3O_3S$	7.11	7.17	13.56	13.66
8	*p*-$CH_3O \cdot C_6H_4$	45	235	$C_{30}H_{24}BrN_3O_3S$	7.32	7.17	13.78	13.66
9	*p*-$C_2H_5O \cdot C_6H_4$	57	214	$C_{31}H_{26}BrN_3O_3S$	6.84	7.00	13.27	13.33
10	CH_3	35	187	$C_{24}H_{20}BrN_3O_2S$	8.59	8.50	16.02	16.19
11	C_2H_5	50	190	$C_{25}H_{22}BrN_3O_2S$	8.30	8.27	16.00	15.75
12	$C_6H_5 \cdot CH_2$	53	185	$C_{30}H_{24}BrN_3O_2S$	7.45	7.37	13.84	14.04

TABLE 5. 6-BROMO-3-SUBSTITUTED-2,4-(1*H*,3*H*)-QUINAZOLINDIONES

No.	R	Crystallization solvent	Yield %	Mp °C	Formula	% Nitrogen		% Bromine	
						Found	Calcd	Found	Calcd
1	C_6H_5	a	68	314	$C_{14}H_9BrN_2O_2$	8.67	8.83	25.12	25.23
2	*o*-$CH_3 \cdot C_6H_4$	a	50	259	$C_{15}H_{11}BrN_2O_2$	8.35	8.46	24.11	24.17
3	*m*-$CH_3 \cdot C_6H_4$	a	70	321	$C_{15}H_{11}BrN_2O_2$	8.41	8.46	24.00	24.17
4	*p*-$CH_3 \cdot C_6H_4$	a	75	230*	$C_{15}H_{11}BrN_2O_2$	8.39	8.46	23.91	24.17
5	*m*-$Cl \cdot C_6H_4$	b	68	233[d]	$C_{14}H_8BrClN_2O_2$	7.84	7.97	23.05	22.76
6	*p*-$Cl \cdot C_6H_4$	c	55	216[d]	$C_{14}H_8BrClN_2O_2$	8.12	7.97	22.79	22.76
7	*o*-$CH_3O \cdot C_6H_4$	a	60	310	$C_{15}H_{11}BrN_2O_3$	8.02	8.07	22.85	23.05
8	*p*-$CH_3O \cdot C_6H_4$	c	62	288	$C_{15}H_{11}BrN_2O_3$	7.93	8.07	23.01	23.05
9	*p*-$C_2H_5O \cdot C_6H_4$	c	90	290	$C_{16}H_{13}BrN_2O_3$	7.58	7.76	22.03	22.16
10	CH_3	a	55	291	$C_9H_7BrN_2O_2$	11.06	10.98	31.16	31.37
11	$C_6H_5 \cdot CH_2$	a	65	264	$C_{15}H_{11}BrN_2O_2$	8.40	8.46	24.29	24.17

a Acetone and ethanol (1 : 1), b Ethanol and ethyl acetate (2 : 1),
c Acetone, ethanol and ethyl acetate mixture (1 : 2 : 1).
* Decomposition without melting, d Melting with decomposition.

Similarly, other 6-bromo-3-substituted-2,4-(1*H*,3*H*)-quinazolindiones were obtained. Their properties and analytical data are given in Table 5. The identity of these compounds was confirmed by direct comparison with authentic samples of diketoquinazolines prepared by the method of Dave *et al.*[2]

6-Bromo-2-carboxymethylthio-3-phenyl-4-(3*H*)-quinazolinone (IV). An equimolar quantity of sodium monochloroacetate was added to an alkaline solution of 6-bromo-2-mercapto-3-phenyl-4-(3*H*)-quinazolinone, and the mixture was stirred for six hours. It was then acidified with 5% hydrochloric acid to Congo red, and the precipitate obtained was dissolved in sodium bicarbonate solution and filtered. The filtrate on reprecipitation with 5% hydrochloric acid gave the required product in 50% yield. It was crystallized from 95% ethanol, mp 190°C. (Found: C, 48.92; H, 2.75; S, 8.35%. Calcd for $C_{16}H_{11}BrN_2O_3S$: C, 49.10; H, 2.81; S, 8.18%).

Authors thank the authorities of Banaras Hindu University for providing the facilities and the Council of Scientific and Industrial Research, New Delhi, India, for the award of a Junior Research Fellowship to one of them (R.L.).

BULLETIN OF THE CHEMICAL SOCIETY OF JAPAN VOL. 42 1447—1449 (1969)

Liquid-phase Selective Hydrogenation of an Aliphatic α,β-Unsaturated Aldehyde over Raney Cobalt Catalyst Modified with Ferrous Chloride

Kazuhiko HOTTA and Teruo KUBOMATSU

The Osaka Municipal Technical Research Institute, Kita-ku, Osaka

(Received August 10, 1968)

It is comparatively difficult to hydrogenate selectively an α,β-unsaturated aldehyde to an unsaturated alcohol by heterogeneous catalytic reaction. This hydrogenation can, however, be performed over the noble metal catalysts or over less active catalysts under severe conditions.[1-6] Hydrogenation under mild conditions, however, was not successful over Raney-type catalysts, except over the Raney zinc and the Raney zinc-copper catalysts.[7,8]

The present authors have studied the selectivities of Raney-type catalysts modified with various compounds. It has been found that no unsaturated alcohols can be obtained by the hydrogenation of such unsaturated aldehydes as 2-methyl-2-pentenal and cinnamaldehyde over the Raney nickel catalyst, and that the addition of such modifiers as ferrous chloride, cadmium chloride, cobalt chloride, and citric acid was not effective in producing unsaturated alcohols.[9]

On the other hand, it is interesting that unsaturated alcohols was obtained over the Raney *cobalt* catalyst under the normal hydrogen pressure at 55°C, and that the addition of ferrous chloride to the reaction mixture increased the yield of the unsaturated alcohol.

Experimental

A commercial Raney cobalt-aluminum alloy (Co: 50 wt%) was developed with a 15 % sodium hydroxide solution at 50°C, and the resulting catalyst was washed with water and then with 2-propanol. The catalyst thus prepared was stirred with ferrous chloride in 2-propanol under a hydrogen atmosphere, then the substrate was added to the solution and the mixture was stirred with a magnetic stirrer under the normal pressure of hydrogen at 55°C. 2-Methyl-2-pentenal, used as the substrate, was prepared from propionaldehyde; its purity was indicated to be more than 99% by gas chromatography. The reaction products were analyzed by gas chromatography. The amount of hydrogen adsorbed on the catalyst was estimated by methods described previously.[10,11]

Results and Discussion

The selectivity of the catalyst, which is defined as the mole percent of the unsaturated alcohol in all the products, depended on the temperature at which the development of the Raney cobalt alloy was carried out. The best selectivity was obtained with the catalyst developed at 50°C, so this catalyst was used for this hydrogenation.

The hydrogenation of 2-methyl-2-pentenal (UD) is shown in Fig. 2. 2-Methyl-2-pentene-1-ol (UA) was obtained as the main product. The rate of

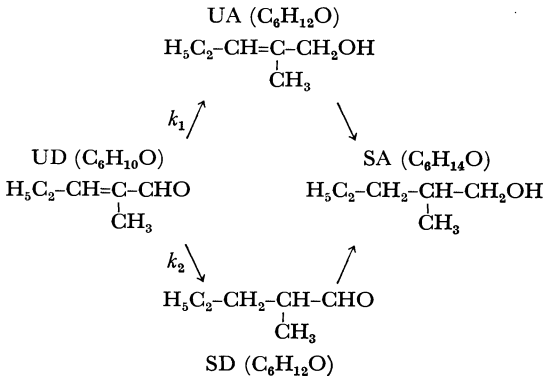

Fig. 1. Hydrogenation scheme of 2-methyl-2-pentenal.

1) H. S. Broadbent, G. C. Campbell, W. J. Bartley and J. H. Johnson, *J. Org. Chem.*, **24**, 1847 (1959).
2) W. F. Tuley and R. Adams, *J. Am. Chem. Soc.*, **47**, 3061 (1925).
3) P. N. Rylander, N. Himelstein and M. Kilroy, *Engelhard Ind. Tech. Bull.*, **4**, 49 (1963).
4) W. J. Peppel, U. S. Pat. 2448047 (1948).
5) S. Yada, T. Yamauchi and S. Kudo, *Shokubai (Catalyst)*, **5**, 2 (1963).
6) K. Yamagishi, S. Hamada, H. Arai and H. Yokoo, *Yukigosei Kagaku Kyokai-shi (J. Org. Synth. Chem. Soc.)*, **24**, 54 (1966).
7) Kh. Freidlin, A. S. Sultanov and M. F. Abidova, *Izv. Akad. Nauk SSSR, Otd. Khim. Nauk*, **1958**, 378.
8) Kh. Freidlin and V. I. Gorshkov, *ibid.*, **1959**, 2027.
9) K. Hotta and T. Kubomatsu, Preprints for the 20th Annual Meeting of the Chem. Soc. Japan (Tokyo, 1967), No. 1I303.
10) K. Tarama, T. Kubomatsu and S. Kishida, *Nippon Kagaku Zasshi (J. Chem. Soc. Japan, Pure Chem. Sect.)*, **82**, 1633 (1961).
11) K. Tarama, S. Teranishi, T. Kubomatsu and S. Kishida, *Shokubai (Catalyst)*, **7**, 289 (1965).

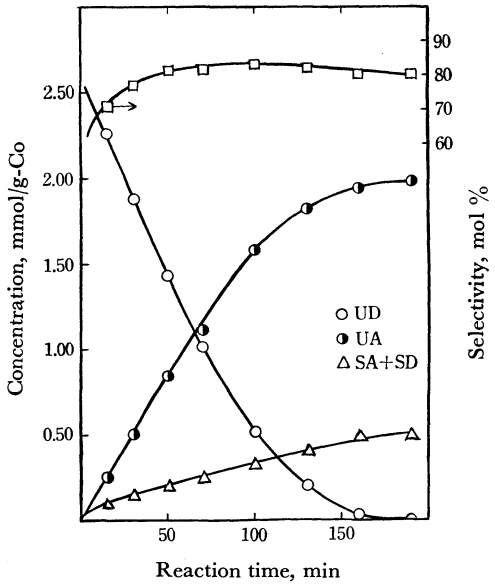

Fig. 2. Hydrogenation of 2-methyl-2-pentenal. Catalyst: 1.0 g cobalt, solvent: 2-propanol 5 m*l*, concentration of substrate: 2.60 mmol/g-Co, amount of ferrous chloride added : 0.18 mmol/g-Co.

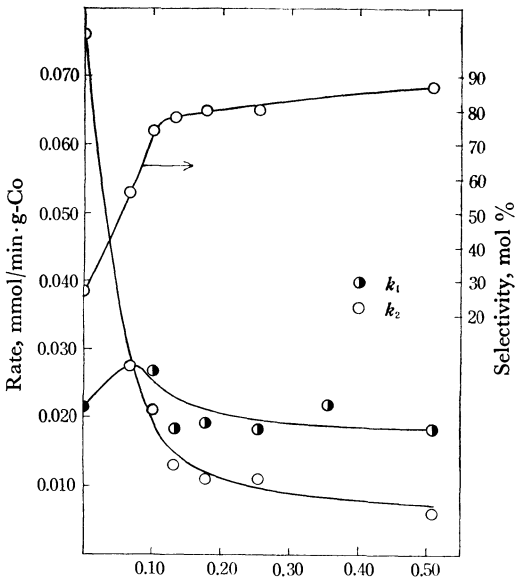

Fig. 3. Dependence of selectivity and initial rate on amount of ferrous chloride added. Catalyst: 1.0 g cobalt, solvent: 2-propanol 5 m*l*, concentration of substrate: 2.60 mmol/g-Co.

the production of UA was constant during the first period of the reaction, and the total rate of the production of the saturated compounds, 2-methylpentan-1-ol (SA) and 2-methylpentanal (SD), which were obtained as the by-products, decreased gradually. A similar situation was observed when ferrous chloride of less than 0.36 mmol/g-Co was added. The rate of the production of UA showed a progressive decrease in the course of the reaction when more than 0.51 mmol/g-Co of ferrous chloride was added.

Each hydrogenation step is supposed to be irreversible, judging from the fact that the dehydrogenation of the produced alcohols did not occur under these conditions. The isomerization of UA to SD almost did not occur at all and SD was consumed preferentially on the hydrogenation of a mixture of UA and SD. Judging from the facts mentioned above, the produced SD is readily hydrogenated to SA and the produced UA does not react further; thus, most of the SA is supposed to be produced through SD.

The yield of UA increased with an increase in the amount of ferrous chloride added, as is shown in Fig. 3. It is also shown in Fig. 3 that the rate of the hydrogenation of the carbon-carbon double bond (C=C), k_2, decreased remarkably, and that the rate of the hydrogenation of the aldehyde group, k_1, decreased only slightly, with an increase in the amount of ferrous chloride added. Thus the promotion of the selectivity of the catalyst in the hydrogenation of the unsaturated aldehyde seems to be caused by the decrease in the rate of the hydrogenation of the carbon-carbon double bond.

It was found that the color of the reaction solution changed to the blue of the cobalt(II) ion when it was stirred for about 5 min. This indicates that the cobalt of the catalyst was substituted rapidly by the iron when ferrous chloride was added. A part of the remaining ferrous chloride might be adsorbed on the catalyst surface and might react further with the Raney cobalt catalyst, judging from the fact that the concentration of ferrous chloride decreased gradually during the last period of the reaction.

It has been found that there are two types of hydrogen on the Raney nickel catalyst.[10,11] One of these is the hydrogen adsorbed weakly on the catalyst, and the other is the strongly-adsorbed hydrogen, the amount of which is termed the hydrogen content of the catalyst. These two types of adsorbed hydrogen were also found on the Raney cobalt cotalyst. The weakly-adsorbed hydrogen decreased to 40% of the original value, and the hydrogen content of the catalyst decreased to 8%, when 0.18 mmol/g-Co of ferrous chloride was added.

It seems that the selective hydrogenation could be carried out because the addition of ferrous chloride to the reaction mixture decreased the amount of the strongly-adsorbed hydrogen more than that of the weakly-adsorbed hydrogen, and thus the decrease in the rate of hydrogenation

became much greater for the carbon-carbon double bond than for the aldehyde group, assuming that the carbon-carbon double bond reactes more readily with the strongly-adsorbed hydrogen than with the weakly-adsorbed hydrogen, as has been reported by Takeuchi and Asano.[12)]

A more detailed discussion will be reserved until the results of experiments now in progress are available.

12) T. Takeuchi and T. Asano, *Z. Physik. Chem., N.F.*, **36**, (1/2) 118 (1963).

BULLETIN OF THE CHEMICAL SOCIETY OF JAPAN VOL. 42 1449—1450 (1969)

The Cerimetric Determination of Hypophosphite after Oxidation with Iron(III)

Kin'ya OGAWA

Hitachi Research Laboratory, Hitachi, Ltd., Kuji-machi, Hitachi, Ibaraki

(Received August 28, 1968)

Because hypophosphite has come to have a number of commercial applications as a reducing agent, and because phosphite is frequently an intermediate product in the oxidation of hypophosphite, it is desirable to establish an analytical procedure for the determination of hypophosphite in the presence of phosphite. For this purpose, volumetric methods with iodometric or cerimetric procedures have been described by Jones and Swift,[1] Bernhart,[2] and Rao and Rao.[3] These procedures, however, are all inapplicable to rapid analyses because of their complexity and difficulty. On the other hand, Sastri and Radhákrishnamurthi[4] found that an excess of hypophosphite reduces iron(III) quantitatively in hydrochloric acid solutions upon boiling:

$$H_3PO_2 + 2Fe^{3+} + H_2O \rightarrow H_3PO_3 + 2Fe^{2+} + 2H^+ \quad (1)$$

Sastri and Kalidas[5] later applied this reaction to the determination of hypophosphite in the presence of phosphite; their procedure consisted of boiling, for 20 min, hypophosphite with approximately twice as much iron(III) as was required for the stoichiometric reaction in a 1.0-to-2.0N hydrochloric acid medium and of titrating the iron(II) thus formed with a standard solution of cerium(IV) sulfate. This Sastri-Kalidas procedure has the advantages of simplicity and rapidity, for it requires only one standard solution which is very stable. However, it has been observed in preliminary experiments that the reaction does not reach quantitative completion, even when the Sastri-Kalidas procedure is followed completely. In this paper, therefore, the reaction between hypophosphite and iron(III) at the boiling temperature is re-examined, and the applicability of this reaction to the determination of hypophosphite in the presence of phosphite is discussed.

Experimental

Reagents. All the chemicals were of a reagent grade. The standard solutions of hypophosphite and phosphite were prepared by dissolving monosodium hypophosphite monohydrate and disodium phosphite pentahydrate respectively in distilled water. The concentrations of these solutions were determined by the Rao-Rao procedure.[3] A standard solution of cerium(IV) sulfate was prepared and standardized by the conventional method. A solution of iron(III) was prepared by dissolving ammonium iron(III) sulfate in distilled water. For the detection of the end point of titration, one drop of a 0.025M ferroin indicater solution was used.

Procedure. A solution containing hypophosphite alone or both hypophosphite and diverse salts was transferred to a 300-m*l* flask equipped with a reflux cooler. The calculated volumes of the iron(III) solution and of the hydrochloric acid were added, and then the whole was diluted to about 100 m*l*. The resulting solution was boiled on an electric heater for the required time. After cooling, the solution was titrated with the standard solution of cerium(IV) sulfate to the blue-yellow end point of the ferroin indicator.

Results and Discussion

Conditions for the Determination of Hypophosphite. The effects of the mole ratio of iron(III) to hypophosphite on the oxidation of hypo-

1) R. T. Jones and E. H. Swift, *Anal. Chem.*, **25**, 1272 (1953).
2) D. N. Bernhart, *ibid.*, **26**, 1798 (1954).
3) K. B. Rao and G. G. Rao, *Z. anal. Chem.*, **147**, 274, 279 (1955).
4) M. N. Sastri and Ch. Radhákrishnamurthi, *ibid.*, **147**, 16 (1955).
5) M. N. Sastri and Ch. Kalidas, *Rec. trav. chim.*, **75**, 1122 (1956).

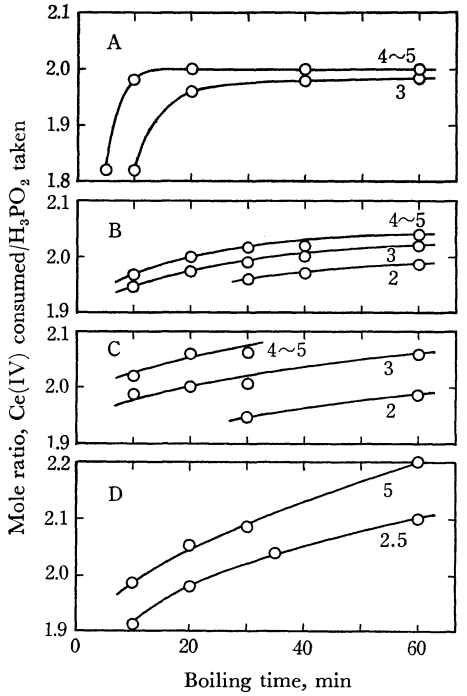

Fig. 1. Oxidation of 0.25 mmol of hypophosphite in (A) 1.6, (B) 1.2, (C) 0.8 and (D) 0.4N hydrochloric acid solutions. Numericals on curves represent amounts of iron(III) added in mmol.

phosphite at the boiling temperature were observed at different concentrations of hydrochloric acid; the results are shown in Fig. 1. When a hydrochloric acid concentration between 0.4 and 1.2N is selected, the oxidation of hypophosphite is greatly affected by the boiling time; if the solution is boiled to excess, some hypophosphites may be oxidized beyond phosphite to phosphate, while if boiling is insufficient, the oxidation to phosphite does not reach quantitative completion. In a 1.6N hydrochloric acid medium, however, 0.25 mmol of hypophosphite can be quantitatively oxidized to phosphite, without being oxidized to phosphate, with 5 mmol of iron(III) by boiling it for at least 20 min.

For the determination of hypophosphite, therefore, approximately ten times as much iron(III) as the amount required for the stoichiometric reaction was added, the final acidity was adjusted with hydrochloric acid to approximately 1.6N, and the mixture was boiled for about 20 min.

The Effects of Phosphate, Acetate, and Citrate on the Determination of Hypophosphite. Sample solutions containing about 0.2 mmol of hypophosphite and from 0.1 to 2 mmol of phosphite, acetate, or citrate were analyzed by the proposed procedure. The data in Tables 1 and 2 show an accuracy and precision of better than one percent in the presence of these anions.

The author wishes to express his deep gratitude to Dr. Takeshi Nakatogawa and Dr. Natsuki Kawashima of the Hitachi Rasearch Laboratory, Hitachi, Ltd., for thoir guidance and ercouragement throughout this work.

Table 1. Effects of phosphite on the determination of hypophosphite

Hypophosphite taken mmol	Phosphite added mmol	Cerium(IV) soln. required ml	Hypophosphite found mmol	Error %
0.273	0.103	5.60*1	0.274	+0.4
0.273	0.205	5.54*1	0.271	−0.7
0.273	0.308	5.59*1	0.274	+0.4
0.269	0.410	5.52*1	0.270	+0.4
0.269	0.513	5.56*1	0.272	+1.1
0.277	0.939	5.58*2	0.281	+1.4
0.277	1.409	5.57*2	0.280	+1.1

*1 0.0980N cerium(IV) solution.
*2 0.1007N cerium(IV) solution.

Table 2. Effects of acetate and citrate on the determination of hypophosphite*

Sodium salt added mmol	0.1073N Cerium(IV) soln. required ml	Hypophosphite found mmol	Error %
Acetate; 1	3.67	0.197	+0.5
Acetate; 2	3.63	0.195	−0.5
Citrate; 0.2	3.64	0.195	−0.5
Citrate; 1	3.66	0.196	0
Citrate; 2	3.65	0.196	0

* The amount of hypophosphite taken in each case was 0.196 mmol.

BULLETIN OF THE CHEMICAL SOCIETY OF JAPAN VOL. 42 1451—1452 (1969)

Catalytic Hydrogenation of 1,3-Diphenylpropane-1,2-dione and 2-Hydroxy-1,3-diphenylpropan-1-one

Akiko SOHMA*1 and Sekio MITSUI

Department of Applied Science, Faculty of Engineering, Tohoku University, Aoba, Sendai

(Received September 14, 1968)

In the catalytic hydrogenation of 1,3-diphenylpropane-1,2-dione (I) and 1-hydroxy-1,3-diphenylpropan-2-one (II), 1,3-diphenylpropane-1,2-diol (III), mp 65—66°C, was produced by Ruggli and Lutz.[1] Bonner and Raunio[2] considered that the diol must have been *threo*-III, and they speculated that, if I is absorbed on the catalyst surface in such a way as to orient the two polar carbonyl functions and the bulky phenyl and benzyl groups as far apart as possible, the *cis* hydrogenation of the two carbonyl groups would lead to *threo*-III. In the case of the catalytic hydrogenation of benzalacetophenone oxide (IV) over palladium-charcoal containing a small amount of sodium hydroxide, IV was isomerized to the diketone I prior to reduction. The initial main product was II, whose hydrogenation gave *erythro*-III, although it proceeded with great difficulty.

In connection with the stereochemistry of the molecules when absorbed on the catalyst surface, we have undertaken a study of the catalytic hydrogenation of 1,3-diphenylpropane-1,2-dione (I) and 2-hydroxy-1,3-diphenylpropan-1-one (V) in ethanol at an ordinary temperature and at atmospheric pressure. The reduction products were analyzed by gas chromatography and by thin-layer chromatography. The authentic samples, *erythro*- and *threo*-III, were synthesized by the procedure of Bonner and Raunio.[2]

In the catalytic hydrogenation of I over palladium-charcoal, it was found by thin-layer chromatography that two isomeric hydroxy ketones, II and V, were the primary products, in further reduction yielded 1,2-diols, but II, which was not the phenyl ketone, was not hydrogenated under our conditions. In the catalytic hydrogenation of I over palladium-charcoal containing a small amount of sodium hydroxide, II was the main product and the reduction of it did not proceed further. In the catalytic hydrogenation of I over Raney nickel and platinum oxide, the two isomeric ketones, II and V, were produced in almost equal amounts as the primary products, as analyzed by thin-layer chromatography, the 1,2-diols which were rich in the *erythro* form were further products.

The catalytic hydrogenation of V over palladium charcoal, Raney nickel, or platinum oxide, or catalysts containing a small amount of sodium hydroxide, yielded mainly *erythro*-III, which was also the main product of the catalytic hydrogenation of II.

Our results show that the catalytic hydrogenation would not proceed directly in the I→III fashion, so that the isomeric ratio of the 1,2-diols (*erythro*-III *vs.* *threo*-III) must reflect the stereochemistry of the hydroxy ketones, the primarily-desorbed products, on the catalyst surface. As there are many factors which control the orientation, we are now investigating them.

Experimental

1,3-Diphenylpropane-1,2-dione (I). I was prepared by the method of Kohler[3] by the isomerization of benzalacetophenone oxide; bp 132—138°C/1 mmHg, 40% yield.

1,3-Diphenylpropane-1,2-diol (III). *threo*-III was synthesized by the method of Bonner *et al.*[2] by the *cis* hydroxylation of *trans*-1,3-diphenylpropane[4]; mp 62°C, 80% yield, *erythro*-III was prepared by the catalytic hydrogenation of benzalacetophenone oxide

TABLE 1. CATALYTIC HYDROGENATION OF I AND V

Compd.	Catalyst	Additive	Product(III) (%)	
			erythro	*threo*
I	Raney Nickel	—	67	33
I	PtO_2	—	81	19
V	Pd-C	—	79	21
V	Pd-C	NaOH	75	25
V	Raney Nickel	—	63	37
V	Raney Nickel	NaOH	73	21
V	PtO_2	—	82	18
V	PtO_2	NaOH	91	9

*1 Present address: Department of Chemistry, Hirosaki University, Hirosaki, Aomori.

1) P. Ruggli and A. H. Lutz, *Helv. Chim. Acta*, **30**, 1070 (1947).

2) W. A. Bonner and E. K. Raunio, *J. Org. Chem.*, **31**, 291 (1966).

3) E. P. Kohler and R. P. Barnes, *J. Am. Chem. Soc.*, **56**, 211 (1934).

4) W. A. Bonner and E. K. Raunio, *J. Org. Chem.*, **31**, 397 (1966).

(IV) over palladium-charcoal; mp 82°C, 62% yield.

2-Hydroxy-1,3-diphenylpropan-1-one (V). V was prepared by the catalytic hydrogenation of benzalacetophenone oxide (IV). IV, palladium-charcoal, and ethanol were stirred with hydrogen at an ordinary temperature and at atmospheric pressure. After one mole of hydrogen had been absorbed, the catalyst was filtered and the product (V) was recrystallized from petroleum benzine containing a small amount of benzene; mp 66°C, 50% yield.

Catalytic Hydrogenation of I or V. I or V (450 mg), the catalyst, and 30 m*l* of ethanol were stirred with hydrogen at an ordinary temperature and at atmospheric pressure. After the hydrogenation was over, the catalyst the filtered, the products were acetylated with acetic anhydride in pyridine, and the acetyl derivatives were analyzed by vapor-phase chromatography. In the course of hydrogenation, the partial reduction products were analyzed by thin-layer chromatography. The results are summarized in Table 1.

BULLETIN OF THE CHEMICAL SOCIETY OF JAPAN VOL. 42 1452—1453 (1969)

Die Absolutkonfiguration des (−)-Isosakuranetins

Hisao ARAKAWA und Yukio MASUI

Science Education Institute of Osaka Prefecture, Karita-cho, Sumiyoshi-ku, Osaka

(Eingegangen am 18. September, 1968)

In der letzten Mitteilung[1] ist die Absolutkonfiguration der optisch aktiven Flavanone, (−)-Hesperetin(III), (−)-Liquiritigenin(IV) und (+)-Sakuranetin(I), bestimmt worden. Als die Flavanone wurden die Aglykone der schwer löslichen, durch fraktioniertes Umkristallisieren erhaltenen Glykoside benutzt.[2]

In dem vorliegenden Bericht sind die Bestimmung der Absolutkonfiguration des als optisch aktives Flavanon bekannten Isosakuranetins, das durch säure Hydrolyse von Poncirin zu gewinnen ist,[3]

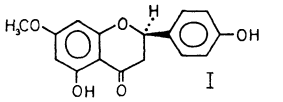

I

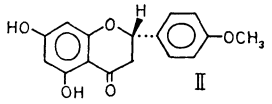

II

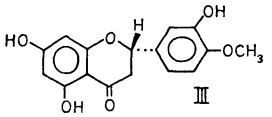

III

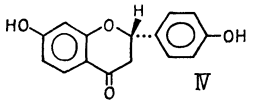

IV

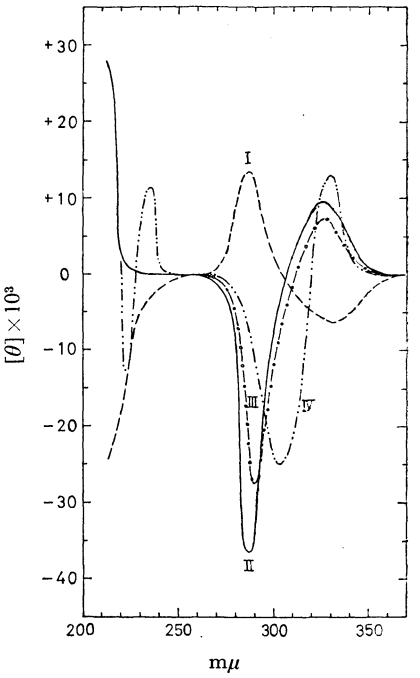

Abbild. 1. CD der optisch aktiven Flavanone in Methanol.

und das Circulardichrogramm der optisch aktiven Flavanone beschrieben.

Poncirin, Isosakuranetin-7-rhamno-glukosid, wurde mit Schwefelsäure in Methanol verseift[2] und dadurch erhaltene Nadeln von Isosakuranetin mit dem Drehwert $[\alpha]_D^{26}=-25°$ (Methanol) wurden ozonisiert und mit Persäure oxydiert. Die so erhaltene Äpfelsäure wurde dann mit Diazomethan in Äpfelsäuredimethylester von $[\alpha]_D^{20}=-5.75°$ (Me-

1) H. Arakawa und M. Nakazaki, *Ann.*, **636**, 111 (1960); *Chem. Ind.*, **1960**, 73.

2) S. Hishida, *Nippon Kagaku Zasshi* (*J. Chem. Soc. Japan, Pure Chem. Sect.*), **79**, 709 (1958).

3) S. Hattori, M. Hasegawa und M. Shimokoriyama, *ibid.*, **65**, 61 (1944).

thanol) übergeführt. Aus dem Ester wurde mit Hydrazinhydrat in Äthanol L-(−)-Äpfelsäure-dihydrazid von $[\alpha]_D^{25}=-51.3°$ (50-proz. Äthanol), Schmp. 173–174.5°C erhalten. Das Dihydrazid wurde durch $[\alpha]_D$, Misch-Schmelzpunkt und IR-Spektrum identifiziert.

Damit ist (−)-Isosakuranetin als (2S)-konfiguriert (II) bestimmt worden. Diese Tatsache zeigt, dass, wie der Verfasser schon annahm[1], alle (−)-Flavanone (S)-Konfiguration haben müssen. Das CD der (S)-(−)-Flavanone (II, III, IV) in Methanol zeigte bei 330 mμ einen positiven Cotton-Effekt und bei 280—303 mμ einen negativen Cotton-Effekt. Das CD des (+)-Sakuranetins (I) in Methanol zeigte umgekehrtes Vorzeichen. Diese Tatsache stimmt mit Gaffields u.a.[4] Kenntnissen von ORD des (+)-Naringenins überein.

Beschreibung der Versuche*1

Isolierung des Isosakuranetins. Aus 6 kg frischen Blütenblättern von *Poncinustri foliata* Refinesque wurden 4.1 g Poncirin von Schmp. 208—209°C isoliert.[3] Die erhaltene Kristalle wurden mit 1 ccm konz. Schwefelsäure/500 ccm Methanol verseift.[1,2] Man erhielt 1.9 g Isosakuranetin von Schmp. 174—175°C, $[\alpha]_D^{26}=-25.0°$ (*c* 2.2, in Äthanol).

Gef.: C, 63.08; H, 5.34%. Ber. für $C_{16}H_{14}O_5\cdot H_2O$: C, 63.05; H, 5.30%.

L-Äpfelsäuredihydrazid aus (−)-Isosakuranetin. Durch eine Lösung von 1.3 g (−)-Isosakuranetin von $[\alpha]_D=-25.0°$ in 35 ccm 95-proz. Methanol wurde bei Zimmertemperatur 3-proz. Ozon enthaltender Sauerstoff geleitet. Nach 10 Stdn. wurde das Losungsmittel fast abgedampft. Dann versetzte man mit 90-proz. Essigsäure und liess nochmals Ozon durchströmen. Nach insgesamt 28 Stdn. wurde die Lösung farblos. Man setzte 3 ccm 30-proz. Perhydrol zu und behandelte dann mit Palladium/Kohle, Calciumacetat und Ionenaustauscher.[5,6] Die so von Peressigsäure und Oxalsäure befreite wässerige Lösung wurde i. Vak. eingedampft, der Rückstand in 50 ccm Wasser gelöst und mit Äther kontinuierlich extrahiert. Durch Verdampfen des Lösungsmittels wurde ein Sirup erhalten. Verestern mit Diazomethan und Gaschromatographieren an Bernsteinsäureglykolester lieferte 40 mg L-Äpfelsäuredimethylester von $[\alpha]_D^{20}=-5.75°$ (*c* 0.957, Methanol). 30 mg Methylester wurde mit 150 mg Hydrazinhydrat in 2.5 ccm Äthanol 1 Std. gekocht. Nach dem Erkalten wurde Nadeln erhalten. Umkristallisieren aus Äthanol-Wasser lieferte farblose Nadeln vom Schmp. 173—174.5°, $[\alpha]_D^{25}=-51.3°$ (*c* 0.95, in 50-proz. Äthanol). Der Misch-Schmp. mit authentischem L-Äpfelsäuredihydrazid vom Schmp. 177—179°, $[\alpha]_D^{25}=-52.0°$ (*c* 1.50, in 50-proz. Äthanol) zeigte keine Depression. Beide IR-Spektren sind praktisch ganz identisch.

Gef.: C, 29.95; H, 6.25; N, 33.85%. Ber. für $C_4H_{10}O_3N_4$: C, 29.63; H, 6.22; N, 34.56%.

Herrn Dr. Kaoru Kuriyama, Shionogi Research Laboratories, danken wir bestens für die Aufnahme der Circulardichrogramme.

4) W. Gaffield und A. C. Waiss, Jr., *Chem. Commun.*, **1968**, 29.

*1 Für einen Teil der Versuche möchten wir Herrn Dr. Shoichi Kusumoto, Osaka City Univ., und Herrn Noboru Torimoto Dank sagen.

5) H. Arakawa, Dieses Bulletin, **33**, 200 (1960).

6) E. Hardegger, H. Gempler und A. Züst, *Helv. Chim. Acta*, **40**, 1819 (1957).

BULLETIN OF THE CHEMICAL SOCIETY OF JAPAN VOL. 42 1453—1454 (1969)

A New Synthesis of Tris(triphenylsilyl) Vanadate

Shizen SEKIGUCHI and Akira KURIHARA

Department of Chemistry, Gunma University, Kiryu, Gunma

(Received September 20, 1968)

In 1958 Orlov *et al.*[1] reported the preparation of tris(triphenylsilyl) vanadate (III) by the reaction of tri-*n*-butyl vanadate and triphenylsilanol.

Chamberlain *et al.*[2] later reported the preparation of the title compound by the reaction of triphenylsilanol and vanadium oxytrichloride in the presence of ammonia.

The present authors have now found that the title compound can be synthesized by transesterification between triphenylacetoxysilane (I) and triisopropyl vanadate (II):

$$\underset{\text{I}}{3CH_3COOSiPh_3} + \underset{\text{II}}{OV\{OCH(CH_3)_2\}_3} \rightleftarrows \underset{\text{III}}{OV(OSiPh_3)_3} + 3CH_3COOCH(CH_3)_2 \quad (1)$$

As part of our work on the preparation of metal alkoxides as polymerization catalysts, we will report

1) N. F. Orlov, B. N. Dolgov and M. G. Voronkov, *Doklady Akad. Nauk S. S. S. R.*, **122**, 246 (1958).

2) M. M. Chamberlain, G. A. Jobs and B. B. Wayland, *J. Org. Chem.*, **27**, 3321(1962).

on this new synthesis of this compound.

Experimental

Preparation of Triphenylacetoxysilane (I). Triphenylacetoxysilane was prepared by the reaction of triphenylchlorosilane and acetic anhydride.[3]

In a typical experiment, 20.0 g (0.067 mol) of triphenylchlorosilane was added to 34.2 g (0.335 mol) of acetic anhydride. After the triphenylchlorosilane had been dissolved in acetic anhydride upon heating, the mixture was refluxed for 4 hrs, then it was concentrated by distilling the excess acetic anhydride and allowed to stand at about −20°C in a dry ice-acetone bath. The crude product was precipitated, filtered, washed with cooled ether, and recrystallized from dry ether; mp 96—97°C (lit.[3] mp 97°C) The yield was 17.2 g (79%) based upon the triphenylchlorosilane.

Preparation of Triisopropyl Vanadate (II). The vanadate was prepared from 30.0 g of commercial ammonium metavanadate and isopropyl alcohol in a large excess by the procedure described by Cartan and Caughlan,[4] using the following reaction:

$$NH_4VO_3 + 3(CH_3)_2CHOH \rightleftarrows \{(CH_3)_2CHO\}_3VO + NH_3 + 2H_2O \quad (2)$$

The azeotrope was removed as it was formed. After several days, the majority of the excess alcohol was distilled. The contents in the flash were then centrifuged to remove the unreacted solids and the decomposition products. Repeated vacuum distillation gave 32.1 g (51.1%) of II; bp 75°C/2 mmHg and n_D^{25} 1.4782 (lit.[4] n_{15}^{D} 1.478).

Preparation of Tris(triphenylsilyl) Vanadate (III). This vanadate was prepared by Eq. (1). Nine grams (0.028 mol) of I and 2.1 g (0.009 mol) of II were dissolved in 100 m*l* of benzene. The mixture was refluxed for 90 hr and washed with water several times; the benzene layer was then separated and dried over anhydrous sodium sulfate overnight.

The crude product was precipitated, filtered, and recrystallized from benzene. The yield was 3.9 g (51%); mp 223—234°C (lit.[2] mp 225—226°C).

Found: C, 72.83; H, 5.29; V, 5.66; Si, 9.26%. Calcd for $C_{54}H_{45}O_4Si_3V$: C, 72.62; H, 5.08; V, 5.70; Si, 9.43%.

The NMR spectrum (60 Mc, room temperature) of this compound showed only the signals at τ near 2.75 assignable to the protons of the phenyl group and no signal characteristic for the isopropyl group.

The infrared spectrum indicated the characteristic bands of the phenyl group at 3060, 3025 (ν_{C-H}), and 1529 cm^{-1} ($\nu_{C=C}$).

In contrast, no band characteristic of the isopropyl group appeared. The strong absorption bands at 1430 and 1120 cm^{-1} are associated with the Si-phenyl group, while that at 1005 cm^{-1} can be attributed to the vanadyl group (V=O).

3) N. S. Nametkin, A. V. Topchiev and F. F. Machus, *Doklady Akad. Nauk SSSR*, **87**, 233 (1952); *Chem. Abst.*, **47**, 12281 (1953).

4) F. Cartan and C. N. Caughlan, *J. Phys. Chem.*, **64**, 1756 (1960).

BULLETIN OF THE CHEMICAL SOCIETY OF JAPAN VOL. 42 1454—1456 (1969)

Synthesis of 4,8-Diaminopyrimido[5,4-*d*]pyrimidine from Hydrogen Cyanide in Liquid Ammonia[1]

Yoshitaka YAMADA, Ichiro NODA, Izumi KUMASHIRO and Tadao TAKENISHI

Central Research Laboratories, Ajinomoto Company, Inc., Kawasaki

(Received September 25, 1968)

In a previous paper,[2] the present authors have reported that adenine and 4,5-dicyanoimidazole are formed by heating anhydrous hydrogen cyanide in excess liquid ammonia. Furthermore, a precise investigation revealed that another product, 4,8-diaminopyrimido[5,4-*d*]pyrimidine (III) is also present in the reaction mixture.

In the present paper, the identification of the compound (III) and some discussions of the course of its formation are presented. The compound (III) was not at all soluble, or only a little so, in dilute hydrochloric acid, aqueous ammonia, and most usual organic solvents. Although III was not extracted directly from the reaction mixture of hydrogen cyanide with liquidammonia, the N^4,N^8-diacetyl derivative (IV) of III was found to dissolve in hot acetic anhydride. IV was easily deacetylated by aqueous ammonia to give the free base. The structure of III was determined by elementary analysis, by a study of its ultraviolet and infrared absorption spectra, and by means of the molecular ion peak of the mass spectrum, while it was identified by comparing it with an authentic sample

1) Presented at the 21st Annual Meeting of Chemical Society of Japan, Osaka, 1968.

2) H. Wakamatsu, Y. Yamada, T. Saito, I. Kumashiro and T. Takenishi, *J. Org. Chem.*, **31**, 2035 (1966).

of 4,8-diaminopyrimido[5,4-*d*]pyrimidine.[3] By acetylation with acetic anhydride, followed by deacetylation with aqueous ammonia, III was isolated in an 11% yield (based on the hydrogen cyanide used).

In a previous paper[4] the authors presumed that III would be derived from the postulated trans-isomer of the hydrogen cyanide tetramer, diaminofumaronitrile (IIb).[5] However, when diaminomaleonitrile (IIa) and formamidine acetate were heated in liquid ammonia at 120°C, III was obtained in a 10% yield (based on the IIa). As an interpretation of the formation of III from the cis-tetramer (IIa) in the liquid ammonia system, an equilibrium between aminomalononitrile (I) and both tetramers of hydrogen cyanide, IIa and IIb, may be assumed

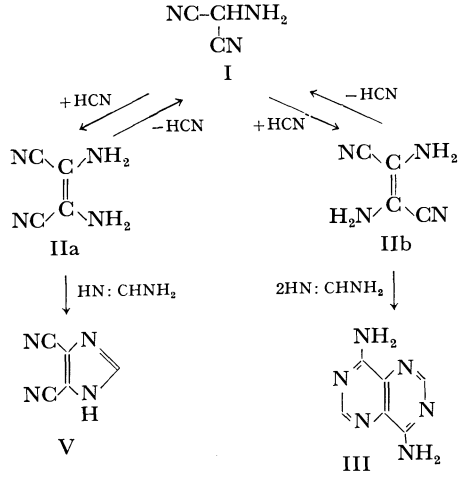

In order to demonstrate the existence of an equilibrium between I and the two tetramers, IIa and IIb, the following experiment was carried out.

When a solution of IIa in a large amount of liquid ammonia was heated in a sealed vessel, 4,5-dicyanoimidazole (V) was obtained, together with azulmic acids, but III was not isolated, probably because of its low yield. Therefore, the formation of V from IIa may be attributed to the conversion of IIa into I by dehydrocyanation prior to the cyclization to V. The hydrogen cyanide thus formed would react with ammonia to give formamidine, which may serve as a ring-closing agent.

IIa is usually obtained by the base-catalyzed oligomerization[6] of hydrogen cyanide, or as an

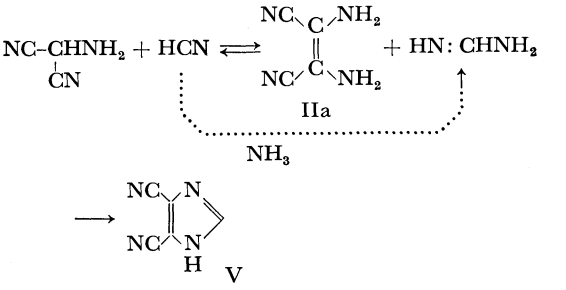

addition product[7] of I with hydrogen cyanide. However, IIb has not been found in these reaction mixtures because of its extreme lability in the presence of an acid or a base, although it has been prepared by the photochemical rearrangement of IIa.[5] Therefore, the effect of an added acid or a base on the formation of III in liquid ammonia was investigated.

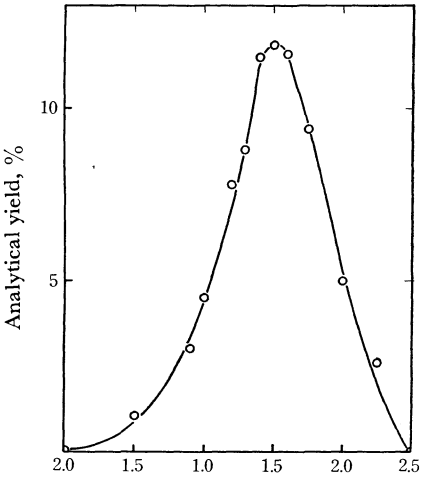

Fig. 1. The formation of III from mixtures of 20 m*l* of liquid ammonia and different amounts of sodium cyanide and ammonium chloride (120°C, 3 hr).

Although IIb is found to be most stable in a neutral medium,[5] a weakly basic region has apparently been observed to be most suitable for the formation of III.

Experimental[8]

4,8-Diacetylaminopyrimido[5,4-*d*]pyrimidine (IV). A solution of hydrogen cyanide (27 g, 1 mol) in 200

3) F. G. Fischer, *Ann.*, **631**, 147 (1960).
4) Y. Yamada, I. Kumashiro and T. Takenishi, *J. Org. Chem.*, **33**, 642 (1968).
5) Y. Yamada, N. Nagashima, Y. Iwashita, A. Nakamura and I. Kumashiro, *Tetrahedron Letters*, **1968**, 4529.
6) T. Völker, *Angew. Chem.*, **72**, 379 (1960).
7) J. P. Ferris and L. E. Orgel, *J. Am. Chem. Soc.*, **88**, 3829 (1966).
8) The melting point is uncorrected. The ultraviolet and infrared absorption spectra were measured with a Hitachi EPS-2 and a JASCO Model IR-S recording spectrophotometer respectively.

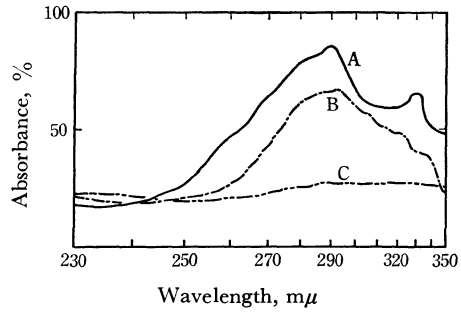

Fig. 2. UV absorption spectra of III. A, pH 1; B, pH 11; C, "hydrated" anionic molecule.

ml (at 20°C) of liquid ammonia was heated at 120°C for 8 hr in a 500-ml stainless-steel pressure vessel. After removing the ammonia and unchanged hydrogen cyanide, adenine and 4,5-dicyanoimidazole were extracted several times with hot dilute aqueous ammonia from the resulting residue. The dry extracted residue was heated under refluxing with acetic anhydride (250 g, 2.45 mol) and filtered while hot. The brown precipitate gradually formed when the filtrate stood. The crude crystals were collected by filtration and recrystallized from acetic anhydride to give 4.55 g (11%) of IV, mp 277—278°C (dec.).

Found: C, 48.75; H, 4.58; N, 34.48%. Calcd for $C_{10}H_{10}N_6O_2$: C, 48.78; H, 4.09; N, 34.14%.

4,8-Diaminopyrimido[5,4-*d*]pyrimidine (III). When IV was, at room temperature, stirred into dilute aqueous ammonia, white crystals were immediately formed. The crystals were filtered and washed with water to give III quantitatively. ν_{max}^{KBr} 3380, 3200, 1665, 1555, 1540, 1440 and 1430 cm^{-1}.

Found: C, 44.25; H, 3.95; N, 51.66%. Calcd for $C_6H_6N_6$: C, 44.44; H, 3.73; N, 51.83%.

Although a detailed study was not made, a reversible hydration phenomenon,[9] which has also been observed in some pteridines, was found from its ultraviolet absorption spectra to occur in III.

The authors wish to express their deep thanks to Dr. Toichi Yoshida, Director of these Laboratories, for his kind encouragement.

9) Y. Inoue and D. D. Perrin, *J. Chem. Soc.*, **1962**, 2600.

BULLETIN OF THE CHEMICAL SOCIETY OF JAPAN VOL. 42 1456—1458 (1969)

Manganic Acetate Oxidation of 2′-Hydroxychalcones

Kazu KUROSAWA

Department of Chemistry, Faculty of Science, Kumamoto University, Kurokami-machi, Kumamoto

(Received September 30, 1968)

Although manganic acetate has received less attention than lead tetraacetate, several oxidation reactions of phenols,[1] ketones,[2] aromatic hydrocarbons,[3] and phenyl ethers[4] by a reagent have been reported recently. During my investigation of the oxidation of various organic compounds, it was demonstrated that manganic acetate reacted with 2′-hydroxychalcones in acetic acid to give aurones in fairly good yield. Aurones have so far been prepared either by dehydrobromination of dibromochalcones or by the condensation of 3-benzofuranones with benzaldehydes. This oxidation of 2′-hydroxychalcones gave an alternative way to make aurones.

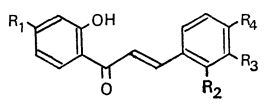

1

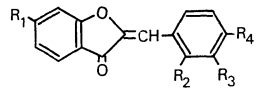

2

a $R_1=R_2=R_3=H$, $R_4=OCH_3$
b $R_1=R_2=H$, $R_3, R_4=OCH_2O$
c $R_1=R_3=H$, $R_2=R_4=OCH_3$
d $R_1=H$, $R_2=R_3=R_4=OCH_3$
e $R_1=R_4=OCH_3$, $R_2=R_3=H$
f $R_1=OCH_3$, $R_2=H$, $R_3, R_4=OCH_2O$
g $R_2=H$, $R_1=R_3=R_4=OCH_3$
h $R_3=H$, $R_1=R_2=R_4=OCH_3$
i $R_1=R_2=R_3=R_4=OCH_3$

Fig. 1

A mixture of a chalcone (1 mmol) and manganic acetate (2 mmol) was heated in acetic acid at 100°C for a period of 10 to 30 min. The reaction mixture was hydrolysed with water, extracted with chloroform, and separated on silica gel plates.

An appropriate band on the plates was scraped out and then extracted again with chloroform. Recrystallization from ethanol gave pure aurone

1) R. van Helden, A. F. Bickel and E. C. Kooyman, *Rec. Trav. Chim.*, **80**, 1237 (1961); *Chem. Abstr.*, **56**, 10026d (1961).

2) R. van Helden and E. C. Kooyman, *ibid.*, **80**, 57 (1961); *Chem. Abstr.*, **55**, 17565a (1961).

3) S. A. Zonis, *Sbornik Statei Obshchei Khim.*, **2**, 109 (1953); *Chem. Abstr.*, **49**, 5414 (1955).

4) T. Aratani and M. J. S. Dewer, *J. Am. Chem. Soc.*, **88**, 5479 (1966).

Table 1

Chalcone No.	Mp (°C)	Lit. mp	Ref.	Aurone No.	Reaction time (min)	Yield (%)	IR $\nu_{max}^{CHCl_3}$ (cm^{-1})	Mp (°C)	Lit. mp	Ref.
1a	93	93—94	5)	2a	14	29	1700, 1640, 1590	137	137—139	13)
1b	138	137—138	6)	2b	30	18	1700, 1640, 1605, 1590	190	192	6)
1c	111	107	7)	2c	20	52	1700, 1640, 1610, 1588	182	182—183	14)
1d	78	77—78	8)	2d	30	38	1700, 1640, 1584	145*	—	
1e	115	113—114	9)	2e	22	34	1700, 1644, 1600	133	134	15)
1f	148	148.5	10)	2f	10	23	1700, 1644, 1610, 1596	178	175	10)
1g	157	156—157	11)	2g	40	40	1700, 1644, 1610, 1592	186	189	16)
1h	156	157	12)	2h	8	59	1700, 1640, 1590	184*	—	
1i	147*	—		2i	30	45	1700, 1642, 1605, 1587	129*	—	

* Elemental analysis gave a satisfactory agreement with the calculated value.

which was identified with its melting point and IR spectrum (ν_{max} 1700 cm^{-1}, a characteristic carbonyl band of 3-benzofuranone), compared with those of an authentic sample. The resultes are shown in Table 1.

A chalcone having hydroxyl group other than at 2′-position was also subjected to oxidation. However, this resulted in a variety of products, none of which was isolated as a pure crystalline form.

The reaction mechanism could be written similarly to the reaction of lead tetraacetate with phenols. The first step in the reaction is the formation of Ar–O–$Mn(OAc)_2$ group.[17] Homolysis of O–Mn bond gives a radical, Ar–$\dot{O}$, and manganese diacetate as shown in Fig. 2. Heterolysis of the bond is unlikely to occur as manganic acetate is

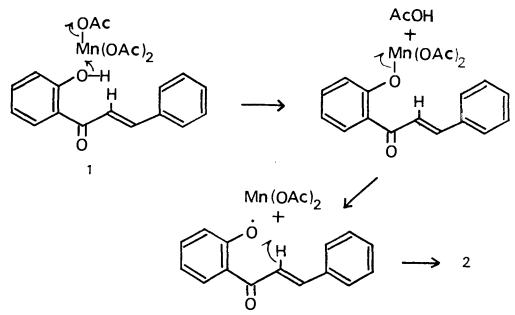

Fig. 2

one electron oxidizing reagent. Then, the radical attacks C–H bonds in suitable spatial position,[18] which is α-hydrogen in this case, to give aurone (2). Further studies on solvent effects and temperature dependence of the reaction are now in progress.

Experimental

Measurements. Melting points were determined with Mitamura Melting Point Measuring Apparatus. The IR spectra were obtained with a Shimadzu IR spectrometer in chloroform.

Chalcones. One equivalent each of 2′-hydroxyacetophenone and benzaldehyde was dissolved in a small volume of ethanol and the solution was treated with 50% aqueous potassium hydroxide with stirring. The mixture was poured into cold dilute hydrochloric acid. The precipitates were collected by filtration and recrystallized from ethanol.

Manganic Acetate. Manganic acetate was prepared according to Dewer's method.[4]

Manganic Acetate Oxidation of Chalcones. A chalcone (1 mmol), dissolved in acetic acid (15 m*l*) was heated with manganic acetate (2 mmol) at 100°C

5) F. Herstein and St. v. Kostanecki, *Ber.*, **32**, 318 (1899).
6) W. Feuerstein and St. v. Kostanecki, *ibid.*, **32**, 315 (1899).
7) S. Hattori, *Acta Phytochem. Tokyo*, **6**, 152 (1932); *Chem. Abstr.*, **26**, 4816 (1932).
8) W. D. Ollis and K. Kurosawa, unpublished result.
9) St. v. Kostanecki and F. W. Osius, *Ber.*, **32**, 322 (1899).
10) T. Emilewicz. and St.v Kostanecki, *ibid.*, **32**, 313 (1899).
11) St. v. Kostanecki and S. Nikowski, *ibid.*, **38**, 3587 (1905).
12) St. v. Kostanecki, V. Lampe and S. Triulzi, *ibid.*, **39**, 92 (1906).
13) B. I. Nurunnabi, *Pakistan J. Sci. Ind. Research*, **4**, 34 (1961).
14) J. Tambor and H. Gubler, *Helv. Chim. Acta*, **2**, 110 (1918).
15) Y. Okajima, *Yakugaku Zasshi*, **80**, 318 (1960); *Chem. Abstr.*, **54**, 18488f (1960).
16) A. Blom and J. Tambor, *Ber.*, **38**, 3590 (1905).
17) W. A. Waters and J. S. Littler, "Oxidation in Organic Chemistry," ed. by K. B. Wiberg, Academic Press Inc., New York, N. Y. and London (1965), p. 226.
18) F. F. Stephens and J. D. Bower, *J. Chem. Soc.*, **1949**, 2971.

until a dark solution turned into clear orange. After removal of the acetic acid *in vacuo*, the resulting solid was treated with water (10 m*l*) and then extracted with chloroform (20 m*l*). The chloroform layer was separated from aqueous solution and evaporated. The residue was dissolved in a small amount of chloroform and separated on silica gel plates (Wako gel B, 10 g × 5) with chloroform as an eluant. A yellow band running below the unchanged chalcone was scraped out and extracted with chloroform. The chloroform was distilled off and the crude aurone was recrystallized from ethanol.

The author wishes to thank Professor H. Matsumura of Kumamoto University for his helpful discussions and encouragement throughout the work.

BULLETIN OF THE CHEMICAL SOCIETY OF JAPAN VOL. 42 1458—1460 (1969)

Effect of the Deuterium Atom Fraction on the Stability Constant of the Main Hydrolysis Product of the Beryllium Ion

Hidetake KAKIHANA and Masunobu MAEDA

Research Laboratory of Nuclear Reactor, Tokyo Institute of Technology, Ookayama, Meguro-ku, Tokyo

(Received October 14, 1968)

It has been confirmed by several investigators that $Be_3(OH)_3^{3+}$ is the main hydrolysis product of the beryllium ion.

The present work was carried out in order to examine the variation in the stability constant of the main hydrolysis species with a variation in the deuterium atom fraction.

First, the composition and the stability constant of the main hydrolysis species were evaluated in 20% and 80% heavy water; next, the variation in the stability constant of the main species with a variation in the deuterium atom fraction(0—0.8) was studied.

Symbols

B total concentration of beryllium
L total excess concentration of lyonium ions*
l total concentration of free lyonium ions
Z average number of lyonium ions split off per beryllium
$\bar{p}$ and $\bar{q}$ average number of OL groups and beryllium atoms respectively in hydrolyzed species
$\beta_{3,3}$ stability constant of the following reaction:

$$3\,Be^{2+} + 3\,L_2O = Be_3(OL)_3^{3+} + 3\,L^+$$

* Besides, L will be used throughout to mean both H and D.

Experimental

All the reagents used were prepared and analyzed by procedures similar to those described in Ref. 1 and Ref. 2.

Heavy water was redistilled from an alkaline permanganate solution.

A Wilhelm-type half cell[3] was used for the emf measurements.

Glass electrodes of the Beckman type No. 40498 were used in combination with **a Radiometer PHM-4C(Copenhagen)**.

Silver - silver chloride electrodes were used as references.

Procedures. The hydrolysis was investigated by measurements of the total concentration of free lyonium ions using a glass electrode. $NaClO_4$ was added to all the test solutions so that they contained 3M ClO_4^-. The lyonium ion concentration was measured by the use of the cell assembly described in Ref. 3.

It was proved experimentally that the emf of the cell could be denoted as follows:

$$E = E_0 + 59.15 \log l + E_j \text{ (at 25°C)} \qquad (1)$$

where E_0 is a constant, and E_j a liquid junction potential, which was found to be approximated by $E_j = -13\,l$ for the system of 20% heavy water and by $-8\,l$ for the system of 80% heavy water.

In the present work, two kinds of experiments were carried out.

The first were "constant B titrations," the experimental details of which were similar to those presented in Ref. 1.

The second were "constant B and Z titrations," where B was maintained at 20 mM and 40 mM and where Z was adjusted to around 0.5, while only the deuterium atom fraction was varied from 0 to 0.8.

All the measurements were made in a paraffin-oil thermostat kept at 25.00±0.01°C in a room kept by a thermostat at 25±1°C.

Results and Discussion

(1) The Composition and the Stability

1) H. Kakihana and L. G. Sillén, *Acta Chem. Scand.*, **10**, 985 (1956).
2) H. Ohtaki, *Inorg. Chem.*, **6**, 808 (1967).
3) W. Forsling, S. Hietanen and L. G. Sillén, *Acta Chem. Scand.*, **6**, 901 (1952).

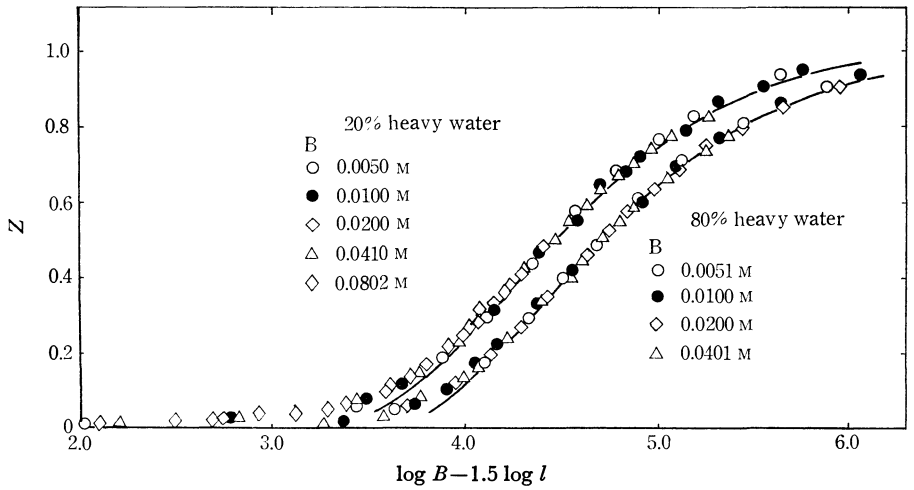

Fig. 1. Z as a function of (log B−1.5 log l).
The drawn curves for the system of 20% heavy water and 80% heavy water were calculated for $-\log \beta_{3,3}$=8.75 and 9.28 respectively.

Constant of the Main Species in 20% Heavy Water and 80% Heavy Water. From the $Z(\log l)_B$ data which were calculated from the potentiometric measurements by the use of Eq.(1), the composition of the hydrolysis species was estimated by the integration method presented by Sillén.[4]

A plot of $\bar{q}$ *vs.* $(2\bar{q}-\bar{p})$[5] suggested the presence of the (3,3) species as the main one in the region of $0.2<Z<0.8$. From this evidence, it may be said that the composition of the main species in H_2O-D_2O mixed solvents is the same as that in light water.

The values of the stability constant of the (3,3) species were calculated by the curve-fitting method described in Ref. 2.

If only the (3,3) species is present in appreciable amounts, the following equation can be derived:

$$\log X = 1/2 \log Z - 3/2 \log(1-Z)$$
$$= 1/2 \log 3 + 1/2 \log \beta_{3,3} + \log B - 3/2 \log l \quad (2)$$

A plot of Z as a function of (log B−3/2 log l) should lie on a single curve, independent of B; the experimental plots are shown in Fig. 1. The experimental plots in Fig. 1 can be fitted with a normalized curve of Z *vs.* log X.

The values of the stability constant for the system of 20% and 80% heavy water were found to be $-\log \beta_{3,3}=8.75\pm0.05$ and 9.28 ± 0.05 respectively.

(2) The Variation in the Stability Constant of the Main Species with the Deuterium Atom Fraction from 0 to 0.8. The differentiation of

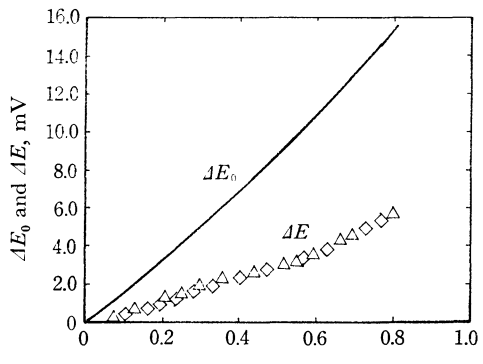

Fig. 2. The plots of ΔE_0 and ΔE *vs.* deuterium atom fraction.
△ B=0.040M, Z=0.499
◇ B=0.020M, Z=0.516

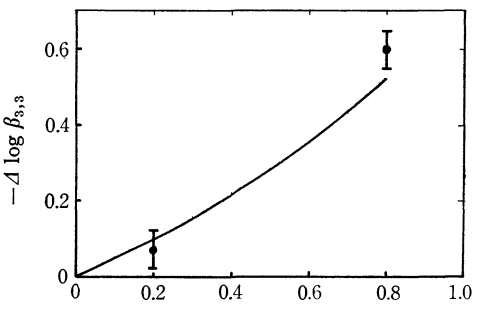

Fig. 3. The change in the stability constant with varying deuterium atom fraction.
The symbol ⊕ denotes the values calculated from Fig. 1.
The value of the stability constant of the (3,3) species in light water was assumed to be $-\log \beta_{3,3}$ =8.68, which was obtained by the authors.

4) L. G. Sillén, *ibid.*, **15**, 1981 (1961).
5) H. S. Dunsmore, S. Hietanen and L. G. Sillén *ibid.*, **17**, 2644 (1963).

Eq. (2) with respect to the deuterium atom fraction at constant B and Z values give the following equation:

$$\partial \log \beta_{3,3} = 3\, \partial \log l \qquad (3)$$

The variation in the stability constant can be calculated by the use of Eq. (3) if the change in l with the deuterium atom fraction is measured.

The variation in E_0, ΔE_0, with the deuterium atom fraction is graphed in Fig. 2. The change in E, ΔE, with a variation in the deuterium atom fraction at constant B and Z values is also shown in Fig. 2. The variation in the stability constant, $\Delta \log \beta_{3,3}$ was evaluated from Fig. 2 by the use of Eq. (3), which is shown graphically in Fig. 2.

From the above results, it may be said that the value of the stability constant of the (3,3) species decreases gradually with an increase in the deuterium atom fraction.

SHORT COMMUNICATIONS

Reductive Dehalogenation of Halobenzenes with Hydrosilanes in the Presence of Free-Radical Initiators[1]

Hideki SAKURAI, Mineo YAMAGATA, Akira HOSOMI and Makoto KUMADA

Department of Synthetic Chemistry, Kyoto University, Sakyo-ku, Kyoto

(Received January 28, 1969)

Reductive dehalogenation of unactivated aromatic halides is not easy, drastic reaction conditions being usually required.[2] In this communication, we present preliminary results of facile and mechanistically interesting reduction of halobenzenes with hydrosilanes involving free silyl radicals as intermediates.[3] To date, an example of the peroxide-catalyzed reaction of chlorobenzene with triphenylhydrosilane has been reported,[4] but no reduction product nor condensation product was detected.

In a typical experiment, 9.06 mmol of chlorobenzene, 8.94 mmol of triethylsilane, and 5.02 mmol of di-*t*-butyl peroxide were mixed and sealed in a small ampoule, and were allowed to react at 135±1°C for 15 hr. Examination of the products by GLC revealed that benzene (3.16 mmol, 35.3%), phenyltriethylsilane (0.325 mmol, 3.6%), and hexaethyldisiloxane (2.57 mmol, 57.5%) were present along with a small amount of unchanged chlorobenzene, acetone, and *t*-butyl alcohol. Bromobenzene (5.15 mmol) was also reduced to benzene (3.08 mmol, 59%) with triethylsilane (5.13 mmol), and di-*t*-butyl peroxide (2.57 mmol). The product contains also unchanged bromobenzene (1.34 mmol, 26%), acetone, and *t*-butyl alcohol. In both cases, triethylsilane was consumed completely. It is also established that no reaction took place without an initiator in otherwise the same reaction conditions.

Only a trace amount of biphenyl was detected. Therefore, intermediacy of phenyl radicals may not be excluded completely, but in the present reaction, direct abstraction of a halogen atom by free silyl radicals seems less plausible as a main reaction since no chlorobiphenyl was detected in spite of careful examination. Furthermore, recent observation in this laboratory[5] has demonstrated that silyl radicals produced by the reaction of trialkylhydrosilane with peroxide undergo successful homolytic substitution with aromatic solvents such as benzene and toluene.

These facts suggest therefore that more plausible process of reduction involves addition-elimination reactions of free silyl radicals.

(I)

$$I \longrightarrow Et_3SiPh + Cl\cdot$$

$$Cl\cdot + Et_3SiH \longrightarrow Et_3Si\cdot + HCl$$

$$Et_3SiPh + HCl \longrightarrow Et_3SiCl + PhH$$

$$I + Et_3Si\cdot \longrightarrow Et_3SiCl + Et_3SiPh$$

$$Et_3SiCl + t\text{-}BuOH \rightarrow\rightarrow Et_3SiOSiEt_3$$

It should be noted, however, that no substitution product, (chlorophenyl)triethylsilane, was obtained contrary to the cases of other aromatic solvents. This may be rationalized by the explanation that intermediate free radicals, I, could be fluxional[6] at the reaction temperature, like (trimethylsilyl)-cyclopentadiene,[7] and, moreover, elimination or abstraction of the chlorine atom from the intermediate, Ia, would be faster than hydrogen abstraction to give substitution products.

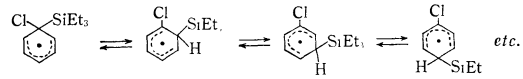

(Ia) (Ib) (Ic) (Id)

1) Silyl Radicals III. Presented in part at the 21st Annual Meeting of the Chemical Society of Japan, Osaka, April, 1968; Preprint, III, p. 1941.

2) E. Ōsawa and Z. Yoshida, This Bulletin, **40**, 1996 (1967).

3) For production of silyl radicals from hydrosilanes by hydrogen abstraction, see H. Sakurai, M. Murakami and M. Kumada, *J. Am. Chem. Soc.*, **91**, 519 (1969), and references cited therein.

4) J. Curtice, H. Gilman and G. S. Hammond, *ibid.*, **79**, 4754 (1957); however, see Y. Nagai, K. Yamazaki, N. Kobori and. M Kosugi, *Nippon Kagaku Zasshi* (*J. Chem. Soc. Japan, Pure. Chem. Sect*), **88**, 793 (1967).

5) H. Sakurai, A. Hosomi and M. Kumada, *Tetrahedron Letters*, **1969**, No. 22 in press.

6) F. A. Cotton, *Accounts Chem. Res.*, **1**, 257 (1968).

7) H. P. Fritz and C. G. Kreiter, *J. Organometal. Chem.*, **4**, 312 (1965); A. Davison and P. E. Rakita, *J. Am. Chem. Soc.*, **90**, 4479 (1968).

Infrared Spectra of BF_3-NO Mixed Solids

Shun-ichi IKAWA and Shiro MAEDA

Research Laboratory of Resources Utilization, Tokyo Institute of Technology, Ookayama, Meguro-ku, Tokyo

(Received December 13, 1968)

It has been reported that nitric oxide and boron trifluoride form an addition complex at the temperature of liquid N_2.[1] Recently we studied the infrared spectra of BF_3-NO mixed solids, which were deposited from a mixed gas onto a cold CsI window.

When a BF_3-rich mixture is deposited very slowly, the spectrum of Fig. 1 (solid line) is obtained; however, the deposit of the same sample at a higher rate gives the absorption bands of the NO dimers[2] at the same time, as is shown in Fig. 2. Such a difference seems mainly due to the blanket effect[3] in the latter case. The results for NO-rich samples are essentially the same as those of Fig. 2 except that no splitting is observed in the $(NO)_2$ absorption at 1760 cm^{-1}.

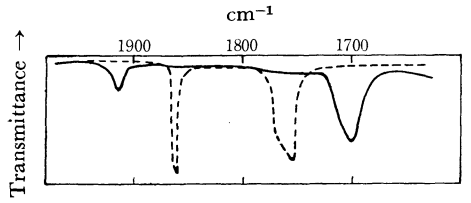

Fig. 1. Solid line; Slow deposit of a BF_3 rich (5 : 1) sample. (65°K) Dotted line; Solid NO. (65°K)

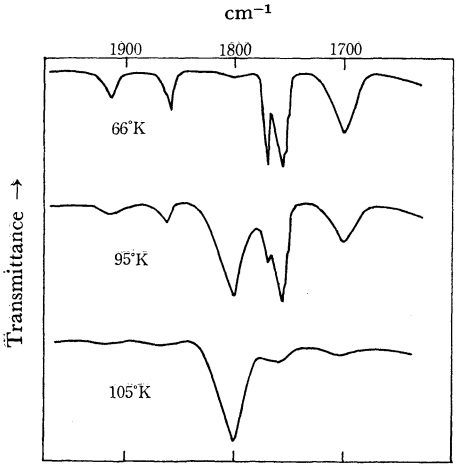

Fig. 2. Fast deposit of a BF_3 rich (5 : 1) sample, and its change by annealing.

When the sample temperature is allowed to rise slowly, an interesting spectral change occurs, as is also shown in Fig. 2. As the temperature goes up, all the bands shown at the top of Fig. 2 gradually lose their intensities, but a new absorption appears at 1800 cm^{-1} and grows up rather quickly. At about 105°K, the initially-observed bands almost disappear, but the new 1800 cm^{-1} absorption holds its maximum intensity at this temperature and is still observable at 130°K, where the individual components are never able to remain on the window. The spectral change is irreversible and common to both BF_3- and NO-rich samples.

As the transient bands at 1915 cm^{-1} and 1700 cm^{-1} are definitely different in frequency from those of gaseous or solid NO, they may be interpreted as due to the complexed states existing in the lattice of excess NO or BF_3, most likely in such a form as:

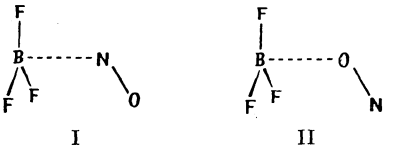

In either case, donor-acceptor interactions are conceivable between vacant orbitals of BF_3 (A_1' and A_2'') and π-electrons, as well as σ-lone pairs, of NO. Of the two principal resonance structures, $:\dot{N}::\ddot{O}:$ and $:\ddot{N}^-::\dot{O}^+:$, the former is more favorable for II, and the latter, for I, in the donation of π-electrons. This suggests that the higher frequency, 1915 cm^{-1}, should be assigned to I, and the lower, 1700 cm^{-1}, to II. The donation of σ lone pairs may be of comparable importance, so the oblique forms, as above, may be most probable.

On the other hand, the 1800 cm^{-1} band may be of a stable complex. The fact that the frequency is nearly equal to the mean value of the transient bands suggests the following n : n structure:

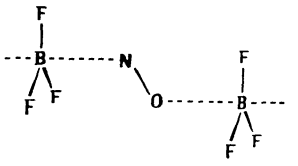

1) G. R. Finlay, *J. Chem. Educ.*, **24**, 149 (1947).

2) NO forms dimers in condensed phases. W. J. Dulmage, E. A. Meyers and W. N. Lipscomb, *Acta Cryst.*, **6**, 760 (1953); A. L. Smith, W. E. Keller and H. L. Johnston, *J. Chem. Phys.*, **19**, 189 (1951).

3) W. G. Fateley, H. A. Bent and B. Craword, Jr., *ibid.*, **31**, 204 (1959).

Chromium(III) Complexes Containing Bis(salicylaldehyde)ethylenediiminate as a Ligand

Shoichiro YAMADA and Katsumoto IWASAKI

Institute of Chemistry, College of General Education, Osaka University, Toyonaka, Osaka

(Received January 28, 1969)

Numerous metal complexes containing bis(salicylaldehyde)ethylenediiminate as a quadridentate ligand (Fig. 1)*1 have been reported in literature.[1-3] However, synthesis of the corresponding chromium(III) complexes has been unsuccessful. In general, synthesis of chromium(III) complexes with *C,N*-disubstituted salicylideneiminate ions*2 is known to be very difficult, and the complexes of the type $Cr(X\text{-}SAL.R)_3$, for example, have only recently been isolated.[4,5] A recent attempt to produce the bis(salicylaldehyde)ethylenediiminatochromium(III) complex by treating tris(salicylaldehydato)-chromium(III) with ethylenediamine was not successful, yielding only bis(*N*-α-aminoethylsalicylideneiminato)chromium(III) series.[4]

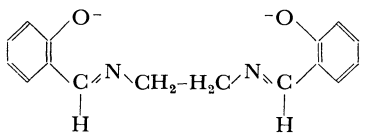

Fig. 1

By employing a method similar to that used for the synthesis of $Cr(X\text{-}SAL.R)_3$,[5] we have succeeded in preparing the chromium(III) complexes containing bis(salicylaldehyde)ethylenediiminate as a quadridentate ligand. The new chromium(III) complexes, together with analytical data, are given in Table 1. The compound $[Cr(SAL_2en)(H_2O)_2]Cl$ was prepared in the following way. To a solution of chromium(III) chloride hexahydrate (0.1 mol) in ethylene glycol-water-methanol (1:1:3, 300 m*l*) were added salicylaldehyde (0.2 mol) and ethylenediamine (0.1 mol). After the mixture was heated at about 110°C on an oil-bath for about thirty minutes, sodium carbonate (0.06 mol) was gradually added to the solution, followed by reflux of the solution for about three to four hours. Concentrating the solution yielded a reddish brown precipitate, which was recrystallized from 80% methanol to give reddish orange crystals.

The complexes II—V in Table 1 were obtained as orange crystals by reaction of $[Cr(SAL_2en)(H_2O)_2]Cl$ with an appropriate amine in methanol, followed by addition of benzene or ethyl ether. The complex VI, $K[Cr(SAL_2en)(CN)_2]\cdot H_2O$, was obtained as orange crystals by heating at about 60°C a mixture of the complex I and potassium cyanide in 80% methanol for about one hour.

All these chromium(III) complexes are soluble in methanol, ethanol and water, but insoluble in ethyl ether and benzene. The complexes at room temperature show magnetic moments of 3.80 to 3.85 B. M., which correspond to three unpaired electrons for the chromium(III) ion. Infrared spectra of these complexes are similar to those of the corresponding cobalt(III) complexes of the type $[Co(SAL_2en)\text{-}L_2]X$, where L denotes various ligands.[6]

TABLE 1. ANALYTICAL DATA OF $[Cr(SAL_2en)L_2]X\cdot nH_2O$

	L	X	*n*	Calcd, %			Found, %		
				C	H	N	C	H	N
(I)	H_2O	Cl	0	49.30	4.65	7.19	49.04	4.80	7.34
(II)	NH_3	Cl	1.5	46.31	5.59	13.43	46.47	5.53	12.84
(III)	$C_2H_5NH_2$	Cl	1.5	51.00	6.63	11.90	50.70	6.37	11.98
(IV)	$n\text{-}C_3H_7NH_2$	Cl	1	53.92	6.99	11.43	53.57	7.15	11.25
(V)	$n\text{-}C_4H_9NH_2$	Cl	2	53.77	7.52	10.45	54.02	7.42	10.29
(VI)	CN^-	K	1	50.57	3.77	13.11	49.77	3.75	12.60

*1 Abbreviated as SAL_2en in the present paper.

*2 Abbreviated as X-SAL.R, where R denotes various substituents on the nitrogen atom.

1) P. Pfeiffer, E. Breith, E. Lübbe and T. Tsumaki, *Liebigs Ann. Chem.*, **503**, 84 (1933).

2) R. H. Holm, G. W. Everett, Jr. and A. Chakravorty, "Progress in Inorganic Chemistry," Vol. VII, ed. by F. A. Cotton, Interscience Publishers, New York, N. Y. (1966), p. 83.

4) M. J. O'Connor and B. O. West, *Austral. J. Chem.*, **21**, 369 (1968).

5) S. Yamada and K. Iwasaki, This Bulletin, **41**, 1972 (1968).

6) S. Yamada, H. Nishikawa and E. Yoshida, *Proc. Japan Academy*, **40**, 211 (1964).

Acidic Cleavage of Anispinacolone. Formation of a Substituted Benzofuran *via* an Acylcarbonium Ion Intermediate

Kunio OKAMOTO, Issei NITTA and Haruo SHINGU

Department of Hydrocarbon Chemistry, Faculty of Engineering, Kyoto University, Sakyo-ku, Kyoto

(Received February 17, 1969)

The acidic cleavage of anispinacolone (ω,ω,ω-tris(*p*-methoxyphenyl)-*p*-methoxyacetophenone) in 1,2-dichloroethane has been studied by Buckles and his collaborators;[1] the major product has been identified as the tris(*p*-methoxyphenyl)methyl cation on the basis of the visible and IR spectra of the reaction mixture. Following their method, we have found that this cleavage is accelerated by the interaction of molecular oxygen and proceeds *via* a radical (presumably a cation radical) intermediate; we have ascertained this by studying the ESR spectrum of the reaction mixture.[2]

In contrast, we will now show that, under an atmosphere of nitrogen or in an evacuated system, the acidic cleavage of the titled compound proceeds in an unexpected way, affording 2,3-bis(*p*-methoxyphenyl)-6-methoxybenzofuran (I) and anisole.

A 0.1 M solution of anispinacolone in 1,2-dichloroethane was allowed to react with twenty molar equivalents of trifluoroacetic acid in a sealed tube filled with nitrogen at 50°C for 24 hr; the reaction mixture was then washed with an aqueous alkaline solution, from which a small amount of anisic acid (4.2%)[3] was later isolated. After the usual working-up of the remaining organic layer and subsequent chromatography over silica gel, we isolated anisole (40%), the substituted benzofuran I (87%), tris(*p*-methoxyphenyl)carbinol (4.5%), and small amount of unchanged anispinacolone (9.0%).

In view of the facile elimination of *m*-dimethoxybenzene from 2,6,2′,6′,2″,6″-hexamethoxytriphenylmethane in dichloromethane in the presence of trifluoroacetic acid,[4] it is most probable that an acylcarbonium ion (II) would be formed as a result of the facile elimination of anisole from anispinacolone, protonated on its *p*-methoxyphenyl group (III).

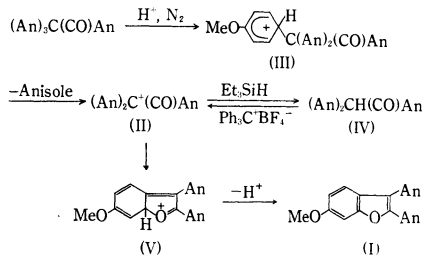

(An = *p*-methoxyphenyl)

In order to trap the supposed acylcarbonium ion II, the acidic cleavage was carried out in the presence of a hydride donor, *i. e.*, triethylsilane,[4] with the reaction conditions being otherwise the same as above; ω,ω-bis(*p*-methoxyphenyl)-*p*-methoxyacetophenone (IV) (85%) and anisole (75%) were isolated, along with a small amount of I (3.4%), by elution chromatography over silica gel. This indicates that the acylcarbonium ion II is a common precursor to IV and I.

The intramolecular cyclization of the acylcarbonium ion II to the substituted benzofuran I was confirmed by the fact that, when the ketone IV was treated with two molar equivalents of triphenylmethyl tetrafluoroborate in 1,2-dichloroethane at 50°C for 22.5 hr, I was obtained in a 3.7% yield *via* II, produced by hydride abstraction from IV. The other compounds isolated from the reaction mixture were triphenylmethane (2.2%) and unchanged ketone IV (95%); they were obtained after the usual working-up and after subsequent t.l.c. separation over silica gel. This cyclization conceivably proceeds *via* a substituted 1-oxonia-7a*H*-indene (V).[5]

Experiments with other substituted benzopinacolones are under way in order to clarify the scope of this novel reaction.

1) R. E. Buckles, R. E. Erickson, J. D. Snyder and W. B. Person, *J. Am. Chem. Soc.*, **82**, 2444 (1960).

2) The details will be reported elsewhere.

3) Satisfactory analytical data (mixed melting points, elemental analyses, NMR and IR spectra) have been secured for all the products described in this communication.

4) F. A. Carey and H. S. Tremper, *J. Am. Chem. Soc.*, **90**, 2578 (1968).

5) For a substituted 1-oxoniacyclopentene, see C. U. Pittman, Jr. and S. P. McManus, *Chem. Commun.*, **1968**, 1479; H. R. Ward and P. D. Sherman, Jr., *J. Am. Chem. Soc.*, **90**, 3812 (1968).

Synthesis of 1-Oxygenated 5β-Cholestanes

Yasuo SATOH, Tomoyoshi TAKAHASHI, Toshiji AOKI and Akira HAGITANI

Department of Chemistry, College of Science, St. Paul's University (Rikkyo Daigaku), Nishi-Ikebukuro, Toshima-ku, Tokyo

(Received February 21, 1969)

Although the synthesis of 1-oxygenated 5α-steroids has been studied by several groups,[1] little has been found in literature concerning the synthesis of 1-oxygenated 5β-steroids except for the preparation of 1-oxoetianic acid from acovenosigenin A, which has two hydroxy groups in C-1 and -3.[2]

The present communication deals with a study on the synthesis of 1-oxygenated 5β-cholestanes from 4β-bromo-3-oxo-5β-cholestane. As a key intermediate in this synthesis, we chose 3-oxo-5β-cholest-1-ene. The synthesis of this derivative in circuitous route or in the method using a special reagent has already been reported by a few groups.[3] We wish to present a more practical method for the synthesis of 3-oxo-5β-cholest-1-ene.

In a previous paper, it was reported that the substitution reaction of 4β-Br in 3-oxo-5β-steroids with AcOK/AcOH is accompanied by a new rearrangement of the substituent from C_4 to C_2 resulting in the formation of the 2β-acetoxy-3-oxo derivative in good yield.[4] In the reaction using piperidine/piperidine hydrobromide/dioxane as reagents instead of AcOK/AcOH, we have found that the 1-en- and 4-en-3-oxo derivatives were formed in the ratio of 1 : 1. Chromatographical separation and recrystallization of the product from methanol gave needles of 3-oxo-5β-cholest-1-ene, mp 103°C, in over 35% yield.

When the 4β-bromo-3-oxo derivative was refluxed with pyridine, 1-[2-(3-oxo-5β-cholestanyl)]pyridinium bromide was formed. Needles, mp 266—268°C (decomp.), ν_{max}^{KBr} cm^{-1}: 1725 (C=O), 1633, 1493 (C=C, C=N), 789, 763 (=C–H), λ_{max}^{EtOH} 261 mμ (ε 3700). On the pyrolysis of the pyridinium bromide at 480—500°C, 3-oxo-5β-cholest-1-ene was also obtained. The total yield of this α,β-unsaturated ketone from the 4β-bromo-3-oxo-5β-cholestane was 43%.

The synthesis of 1-oxygenated 5β-cholestane from this derivative was carried out using the procedure of Djerassi *et al.*[5] for the syntehsis of 1-oxygenated 5α-steroids. The physical constants of the products in this synthetic pathway are as follows:

Epoxidation of the 1-en-3-oxo derivative gave needles of 1β,2β-epoxide, mp 107—108.5°C, from methanol. ν_{max}^{KBr} cm^{-1}: 1702 (C=O), 856, 844 (C–O), ORD (*c* 0.19, Di) at 22°C: $[\alpha]_{589}$ − 5°, $[\alpha]_{333}$ −697° (trough), $[\alpha]_{329}$ −678° (peak), $[\alpha]_{325}$ −687° (trough), $[\alpha]_{280}$ +1355° (peak), NMR ($CDCl_3$) τ: 6.57 (d., J=4.5 cps, 1H), 6.72 (d., J=4.5 cps, 1H). Configuration of this product was established by analysis, IR, ORD and NMR spectra, conversion to 1β,3α-dihydroxy-5β-cholestane with lithium aluminum hydride, and conversion to the 2-halo-3-oxo-1-ene derivatives by cleavage of the epoxy ring with hydrogen halides.*1 The result of this epoxidation of 3-oxo-5β-cholest-1-ene is contrary to that reported for 5α-series which gives the α-epoxide from the 1-en-3-oxo derivative.[1]

1β-Hydroxy-5β-cholest-2-ene: mp 95—96°C, ν_{max}^{KBr} cm^{-1}: 3320 (O–H), 1655 (C=C), 740, 724 (=C–H), NMR ($CDCl_3$) τ: 4.16 (b.d., 2H), 6.16 (m., $W_{h/2}$=7 cps, 1H).

1β-Hydroxy-5β-cholestane: oil, ν_{max}^{Film} cm^{-1}: 3330 (O–H).

1β-Acetoxy-5β-cholestane: needles, mp 104—105.5°, ν_{KBr}^{max} cm^{-1}: 1720 (C=O), 1240 (C–O), $[\alpha]_D^{25}$ −10.0° (*c* 1.01, $CHCl_3$), NMR ($CDCl_3$) τ: 5.00 (b.s., $W_{h/2}$=6 cps, 1H), 7.98 (s., 3H).

1-Oxo-5β-cholestane: needles, mp 101—102°C, ν_{max}^{KBr} cm^{-1}: 1702 (C=O), ORD (*c* 0.43, Di) at 25°C: $[\alpha]_{589}$ − 69°, $[\alpha]_{322}$ −1681° (trough), $[\alpha]_{313}$ −1290° (sh.), $[\alpha]_{280}$ +1470° (peak). This derivative showed a negative Cotton effect curve having a shoulder at near 310 mμ similar to 2-oxo-5β-cholestane[6] in ORD spectrum. This 1-oxo derivative was obtained in 55% over-all yield from 3-oxo-5β-cholest-1-ene.

Further details will be published later.

1) L. F. Fieser and M. Fieser, "Steroids," Reinhold Publishing, Inc., New York (1959), p. 254; C. W. Shoppee, S. K. Roy and R. S. Goodrich, *J. Chem. Soc.*, **1961**, 1583.

2) W. Schlegel and Ch. Tamm, *Helv. Chim. Acta*, **40**, 160 (1957).

3) H. H. Inhoffen and Huang-Minlon, *Ber.*, **71**, 1720 (1938); C. Djerassi and G. Rosenkranz, *Experientia*, **7**, 93 (1951); Y. Shimizu, H. Mitsuhashi and E. Caspi, *Tetrahedron Letters*, **1966**, 4113.

4) T. Takahashi, Y. Satoh and A. Hagitani, *Nippon Kagaku Zasshi* (*J. Chem. Soc. Japan, Pure Chem. Sect.*), **89**, 974 (1968).

5) C. Dejerassi, D. H. Williams and B. Berkoz, *J. Org. Chem.*, **27**, 2205 (1962).

*1 Our report concerning these conversions has hitherto been unpublished.

6) M. Tomoeda and T. Koga, *Tetrahedron Letters*, **1965**, 3231; Y. Satoh, A. Horiuchi, T. Matsukura and A. Hagitani, This Bulletin, **41**, 3032 (1968).

Synthesis and Use of N^{im}-Tosyl-L-histidine*1

Shumpei SAKAKIBARA and Toshiyuki FUJII*2

Peptide Center, Institute for Protein Research, Osaka University, Kita-ku, Osaka

(Received March 3, 1969)

Recently, great progress has been made in peptide synthesis, but the synthesis of histidine peptides requires further improvement.[1] This paper will describe a new procedure for the protection of the imidazole residue with a tosyl group. Generally, the tosyl group in peptide derivatives is stable and can only be removed by treatment with sodium in liquid ammonia.[2] However, a tosyl group attached to a guanido group in an arginine residue can, exceptionally, be removed by treatment with anhydrous HF at 0°C for 30 min, although it is stable with HBr in acetic acid.[3] The N^{im}-tosyl group was found to be removed more easily, not only by short treatment with anhydrous HF, but also under the conditions used for ester saponification. This group was also partially decomposed with anhydrous HCl or HBr in organic solvents. Further, the N^{im}-tosyl group was found to be unaffected by treatment with trifluoroacetic acid at room temperature under the conditions used for removing Nps-, Boc-, Aoc-, or Z(OMe)-groups. These properties all suggest that this group might be used for the synthesis of histidine peptides.

The tosyl group was introduced into N^{α}-protected histidine derivatives with tosyl chloride under the conditions of the Schotten-Baumann reaction, using sodium carbonate as the base. Thus the following compounds were synthesized and obtained as crystals: Z-L-His(Tos)-OH·DCHA, yield 62%, mp 150—152°C (decomp.), $[\alpha]_D^{17}$ +19.2° (*c* 1, DMF); Aoc-L-His(Tos)-OH (I), yield 75%, mp 109—111°C (decomp.), $[\alpha]_D^{17}$ +10.0° (*c* 1, pyridine); Nps-L-His(Tos)-OH (II), yield 75%, mp 140—141°C (decomp.), $[\alpha]_D^{17}$ +39.9° (*c* 1, DMF). Elemental analyses gave correct values for these compounds within the expected limits of error. These compounds were soluble in the organic solvents for usual acylated amino acids. Compounds I and II were coupled with the glycine benzyl ester by the DCC method and by the mixed anhydride method; Aoc-L-His(Tos)-Gly-OBzl (III) and Nps-L-His(Tos)-Gly-OBzl (IV) were thus both obtained in 80% yields. III: oily compound. IV: mp 164—165°C, $[\alpha]_D^{18}$ +57.5° (*c* 1, DMF). Found: C, 55.03; H, 4.19; N, 11.24; S, 10.44%. Calcd for $C_{28}H_{27}N_5O_7S_2$: C, 55.16; H, 4.46; N, 11.48; S, 10.51%. The Aoc- or Nps-group was removed by dissolving III or IV in trifluoroacetic acid in a presence of anisole at room temperature; after 30 min, the product was coupled with Nps-L-alanine using DCC. The product, Nps-L-Ala-L-His(Tos)-Gly-OBzl, was recrystallized from ethyl acetate and *n*-hexane as needles; yield 50%, mp 88—89°C, $[\alpha]_D^{17}$ −30.0° (*c* 1, AcOEt). Better results were obtained by the *N*-hydroxysuccinimide method, in which case the yield was 75%. Found: C, 54.43; H, 4.53; N, 12.35; S, 9.43%. Calcd for $C_{31}H_{32}N_6O_8S_2$: C, 54.69; H, 4.73; N, 12.34; S, 9.42%. All the protective groups could be removed from IV by treatment with anhydrous HF[4] at 0°C for 1 hr; L-His-Gly·½H_2O was thus obtained, as expected; yield 55%, mp 190°C (decomp.), $[\alpha]_D^{17}$ +24.6° (*c* 1, water). Reported,[5] mp 190°C (decomp.), $[\alpha]_D$ +25±1° (*c* 2, water).

Thus, the procedure was demonstrated to be useful for histidine peptide syntheses. The new histidine derivatives, I and II, should be especially useful in the solid-phase method. This possibility is now being investigated in our laboratory.

*1 The abbreviations used conform with those tentatively proposed by the IUPAC-IBC: *J. Biol. Chem.*, **241**, 2491 (1966).
DCHA=dicyclohexylamine DMF=dimethylformamide
Aoc=*t*-amyloxycarbonyl

*2 Present address: Tanabe Seiyaku Co., Ltd., Higashiyodogawa-ku, Osaka.

1) E. Schröder and K. Lübke, "The Peptides," Vol. 1, Academic Press, New York (1965), p. 176.
2) V. du Vigneaud and O. K. Behrens, *J. Biol. Chem.*, **117**, 27 (1937).
3) R. H. Mazur and G. Plume, *Experientia*, **24**, 661 (1968).
4) S. Sakakibara, Y. Kishida, R. Nishizawa and Y. Shimonishi, This Bulletin, **41**, 438 (1968); S. Sakakibara, Y. Shimonishi, Y. Kishida, M. Okada and H. Sugihara, *ibid.*, **40**, 2164 (1967).
5) G. Amiard, R. Heymes and L. Velluz, *Bull. Soc. Chim. France*, **1955**, 1464.

The Electronic Structures of Base Components of Nucleic Acids and Their Tautomers Calculated by CNDO Method

Hiroko FUJITA, Akira IMAMURA and Chikayoshi NAGATA

Biophysics Division, National Cancer Center Research Institute, Tsukiji, Chuo-ku, Tokyo

(Received March 3, 1969)

The relative stability of the DNA bases and their tautomers is of interest in connection with the mechanism of mutation in which the conversion of the DNA bases into their tautomers has been supposed to be involved. By means of infrared spectra and X-ray diffraction *etc.*, the amino and the keto forms (usual forms) of the DNA bases have been confirmed to be more stable than the imino and the enol forms (rare forms) in solid state or in solution. Comparison of the energies for the usual and the rare forms obtained by the molecular orbital calculation was made by some investigators,[1,2] and the usual forms were found to be more stable than the rare forms for all bases. In these calculations, however, the electronic repulsion is not explicitly taken into account. In such circumstances, CNDO method[3] was considered to be more reliable in discussing the relative stability of molecules,[4] and it was applied to the four tautomers of purine.[5]

In the present communication, the total energies calculated by means of CNDO/2 method[3] for the usual and the rare forms of the bases of nucleic acids and a base analog, were compared and the relative stability among these compounds was discussed in relation to the mutagenesis. Bond lengths and bond angles for the usual forms of bases and a base analog were obtained from Spencer's data.[6] For the rare tautomeric forms, the geometry of the purine and pyrimidine rings was assumed to be the same as the usual form. Bond lengths for C–N and N–H bonds in the imino form were taken as 1.27 Å and 1.0 Å, respectively, and for C–O and O–H in the enol form, as 1.47 Å and 0.96 Å, respectively. The calculated total energies of the bases and the base analog in the usual and the rare forms are listed in Table 1. Except guanine,

TABLE 1. TOTAL ENERGIES FOR THE USUAL AND THE RARE FORMS OF THE BASES OF NUCLEIC ACIDS AND A BASE ANALOG (IN eV)

Bases	Usual form	Rare form	Difference
A	−2655.09	−2652.97	−2.12
G	−3156.11	−3156.68	+0.57
T	−2726.04	−2725.53	−0.51
C	−2326.68	−2325.53	−1.15
U	−2489.58	−2489.13	−0.45
FU	−3223.42	−3222.99	−0.43

the usual forms are more stable than the rare forms in agreement with the experimental results. For guanine, the rare form is found to be more stable than the usual form. But from X-ray diffraction and infrared spectra, guanine was shown to exist predominantly as the keto form in water and solid state. In connection with this, the following fact should be remarked; from the total energies calculateld by means of CNDO method for the zwitter ion and neutral form of glycine, it was predicted that the latter form was more stable than the former.[7] In fact, glycine is known to exsit as neutral molecule in gaseous state, although it exists as zwitter ion in water and solid state. Bearing this fact in mind, it may not be unreasonable to suppose that the predominant form of guanine in gaseous state is the so-called rare form, *i. e.*, the enol form. The ease of the conversion of the usual tautomeric form into the rare form decreased in the order, guanine>fluorouracil>uracil>thymine >cytosine>adenine, and this order is in accordance with Danilov's result.[2] It is interesting that fluorouracil is found to be more easily converted into the rare form than uracil and thymine in reference to the fact that fluorouracil is known to be mutagenic.

1) H. Berthod and A. Pullman, *Biopolymers*, **2**, 483 (1964); *J. chim. Phys.*, **62**, 942 (1965).

2) V. I. Danilov, *Biofisika*, **12**, 540 (1967).

3) J. A. Pople and G. A. Segel, *J. Chem. Phys.*, **44**, 3289 (1966).

4) C. Giessner-Pretler and A. Pullman, *Theoret. Chim. Acta*, **9**, 279 (1968).

5) B. Pullman, H. Berthod, E. D. Bergmann, F. Bergmann, Z. Neiman and H. Weiler-Feilchenfeid, *Compt. rend. Acad. Sci. Paris*, **267**, 1461 (1968).

6) M. Spencer, *Acta Cryst.*, **12**, 66 (1959).

7) A. Imamura, H. Fujita and C. Nagata, Preprint of the 7th Ann. Meet. Jap. Biophys. Assoc. (1968).

Natural Occurrence of α-Cadinene

Yoko NAYA and Munio KOTAKE

The Institute of Food Chemistry, 2-Chome 43, Dojimanaka, Kita-ku, Osaka

(Received March 6, 1969)

The sesquiterpene hydrocarbon, α-cadinene (I) has been isolated from Japanese hop (*Humulus lupulus* L.) for the first time.

The hydrocarbon (I) is a colorless oil, $C_{15}H_{24}$, $[\alpha]_D^{24}$ $-62.4°$ (c 0.868, $CHCl_3$). Its NMR (CCl_4) spectrum shows two vinyl protons at δ (ppm) 5.32 (1H), and 5.52 (1H). Besides the signals of isopropyl group at δ 0.78 (3H, d. $J=7$ cps), and 0.91 (3H, d. $J=7$ cps), the spectrum shows six protons at 1.65 (broad s.) corresponding to two vinyl methyl groups. The MS spectrum exhibits the molecular ion peak at m/e 204 and the base peak, at m/e 105 together with a considerably abundant peak at m/e 161 (M−43).

On partial hydrogenation with platinum oxide in a mixture of methanol and ether, a single product was provided. The IR spectrum of the product was identical with that of the dihydrocadinene prepared from γ-cadinene. The hydrocarbon (I) yielded crystalline dihydrochloride, $[\alpha]_D^{24}$ $-38.1°$ (c 1.608, $CHCl_3$), mp 115—116°C, by treating with dry hydrogen chloride in ether solution. The product showed no depression of the mixed melting point with an authentic sample of (−)-cadinene dihydrochloride[1-3] of known absolute configuration. In addition, the IR spectrum of I is different from that of β-cadinene[4,5] as shown in Fig. 1.

The above evidence leads to α-cadinene structure (I) for this hydrocarbon.

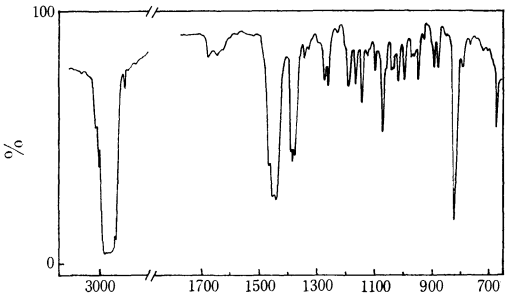

Fig. 1. IR spectrum of I.

(I)

1) M. J. Gallagher, R. P. Hildebrand and M. D. Sutherland, *Tetrahedron Letters*, **1964**, 3715.
2) F. Hanic, *Chem. Listy*, **52**, 165 (1958).
3) V. Herout and V. Sýkora, *Tetrahedron Letters*, **1958**, 130.
4) V. Herout, V. Sýkora and F. Šorm, *Coll. Czech. Chem. Commun.*, **23**, 2181 (1958).
5) V. Herout, A. Banassek and M. Romaňuk, *ibid.*, **31**, 3012 (1966).

BULLETIN OF THE CHEMICAL SOCIETY OF JAPAN VOL. 42 1469—1472 (1969)

Polarographic Studies of the Solubilization of Disperse-dyes

Shigeo HAYANO and Noriko SHINOZUKA

Institute of Industrial Science, The University of Tokyo, Roppongi, Tokyo

(Received June 20, 1968)

The apparent mean particle size of the solubilized dye in nonionic surfactant solutions is determined from the polarographic diffusion coefficient. The diffusion coefficient and the particle size obtained are in good agreement with those of the nonionic surfactant micelle reported in the literature. For the system of polyoxyethylene nonylphenyl ether (NP-$\overline{19}$) and 1,4-diaminoanthraquinone, the particle size increases with the dye concentration; however, the particle size is almost constant for the system of NP-$\overline{19}$ and 1,4,5,8-tetraaminoanthraquinone (TAA). When a certain quantity of TAA is solubilized into the 10^{-3}—10^{-2} M NP-$\overline{19}$ solution, the particle size is also constant. In the case of the polyoxyethylene lauryl ether (LA-$\overline{14}$) and TAA system, the particle size markedly decreases with the increase in the dye concentration. This tendency suggests that the numbers of micelles increase with the concentration of the solubilizate. The fact that the half-wave potential of the dye reduction is independent of the concentration of the surfactants is explained in terms of the similarity between the electrode process of the solubilized dye and that of the dissolved dye.

The solubilization of disperse-dyes has been the subject of many investigations.[1-3] Among the various methods used in the studies of solubilization, the spectroscopic method is most popular.[3-7] Few polarographic measurements have been made of the solubilization because such measurements need a large concentration of supporting electrolyte, and such a concentration has been thought to disturb the system.

To determine the CMC's, the polarographic technique was applied to anionic and nonionic surfactants,[8-10] but the polarographic CMC's sometimes did not agree with those obtained by other methods. The CMC's are found to be greatly affected by added electrolytes[11-13]: this is the reason for the above discrepancy. On the contrary, the size of the micelle is found not to change with the addition of electrolytes.[14]

Craven and Datyner[15] investigated the interaction between some acid wool dyes and nonylphenol-ethyleneoxide derivatives by means of diffusion measurements in which they calculated the apparent mean particle size of the dye-surfactant complex.

In this paper, the apparent mean particle size of the solubilized dye is determined by means of the polarographic diffusion coefficient, and the effects of the addition of nonionic surfactants are investigated. The electrode process of the solubilized-dye particle is also discussed.

Experimental

Materials. 1,4-Diaminoanthraquinone and 1,4,5,8-tetraaminoanthraquinone were used as the disperse-dyes. 1,4-Diaminoanthraquinone was recrystallized from ethyl alcohol, and 1,4,5,8-tetraaminoanthraquinone, from acetone; the melting points were 264°C and 324°C respectively.

Polyoxyethylene nonylphenyl ether (NP-$\overline{10}$,-$\overline{19}$) and polyoxyethylene lauryl ether (LA-$\overline{14}$) were received

1) K. Shinoda, T. Nakagawa, B. Tamamushi and T. Isemura, "Colloidal Surfactants," Academic Press, New York (1963), p. 139.
2) M. J. Schick Ed., "Nonionic Surfactants," Marcel Dekker, New York (1967), p. 558.
3) B. R. Craven and A. Datyner, *J. Soc. Dyners & Colourists*, **83**, 41 (1967).
4) K. Nemoto, *Kogyo Kagaku Zassi (J. Chem. Soc. Japan, Ind. Chem. Sec.)*, **62**, 542 (1959).
5) K. Nemoto, *ibid.*, **62**, 1286 (1959).
6) S. Kuroiwa and M. Kitamura, *ibid.*, **68**, 2148 (1965).
7) B. R. Craven and A. Datyer, *J. Soc. Dyers & Colourists*, **77**, 304 (1961).
8) E. L. Colichman, *J. Am. Chem. Soc.*, **72**, 4036 (1950).
9) R. Tamamushi and T. Yamanaka, This Bulletin, **28**, 673 (1955).
10) W. U. Malik and P. Chand, *J. Am. Oil Chem. Soc.*, **43**, 446 (1966).
11) M. J. Schick, S. M. Atlas and F. R. Eirich, *J. Phys. Chem.*, **66**, 1326 (1962).
12) M. J. Schick, *J. Colloid. Sci.*, **17**, 801 (1962).
13) P. Becher, *ibid.*, **17**, 325 (1962).
14) P. Becher, "Nonionic Surfactants," Marcel Dekker, New York (1967), p. 478.
15) B. R. Craven and A. Datyer, *J. Soc. Dyers & Colourists*, **79**, 515 (1963).

through the courtesy of Lion Oil and Fats Co. and the Meisei Chemical Co., and were used without further purification.

Procedure. A solution containing a nonionic surfactant, a 0.1 N acetic acid - sodium acetate buffer solution (pH=4.7), and a dye was irradiated with a 21.6 kHz surpersonic wave for 5 min, and then agitated in a water bath at 25±0.1°C for 24 hr. The solution was then stored for a week at the same temperature. The equilibrium of the solution was thus confirmed. The excess dye was removed by filtration through a G4 glass filter. The solid dye remaining on the filter was dissolved with acetone, and its quantity was determined by means of the absorption at 620 mμ.

The polarographic measurements were carried out at 25°C for a filtrate, the dye concentration of which had been corrected. Yokogawa POL-11 and POL-21 polarographs were used, and a saturated calomel electrode was used as a reference electrode. The DME had the following characteristics; $m=1.70$ mg/sec (in pure water at zero applied potential *vs.* SCE) and $t=3.9$ sec (in 10^{-2} M NP-$\overline{19}$ buffer solution at −0.64 V *vs.* SCE). The height of the mercury head was 77.5 cm.

The viscosity of the basic solution was measured with an Ostwald viscometer.

Results and Discussion

Polalographic Measurements. Dye-solubilized aqueous nonionic surfactant solutions all showed a well-defined wave corresponding to the dye reduction (Fig. 1). If the current is diffusion-controlled, the diffusion coefficient of the reductive particle can be obtained from the Ilkovic[16] equation. The relation between the current and the square root of the mercury head is shown in Fig. 2. A linear relationship was obtained in all the cases of nonionic surfactant solutions and a 50% alcoholic solution. The half-wave potentials of the dye-solubilized solutions did not change with either the concentration or the kind of surfactants.

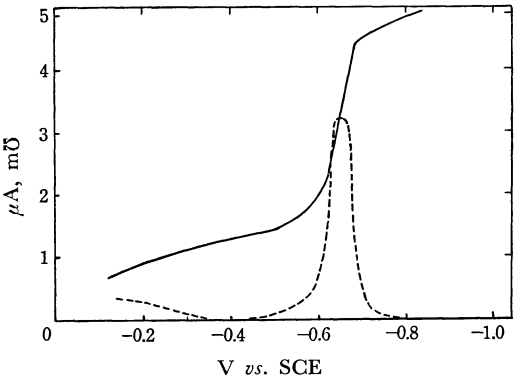

Fig. 1. DC and AC polarograms of the solubilized 1,4,5,8-TAA in NP-$\overline{19}$ solution.

16) D. Ilkovic, *Collection Czechoslov. Chem. Commun.*, **6**, 498 (1934).

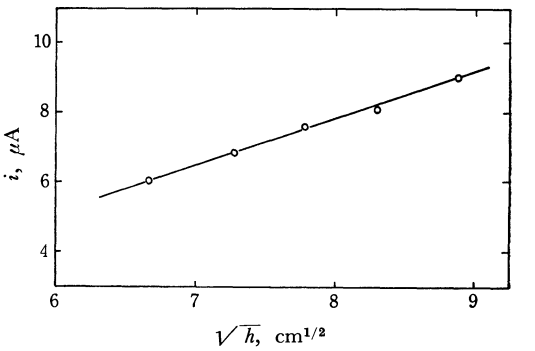

Fig. 2. Dependence of current on mercury height.

From these results, the limiting current is found to be a diffusion current, so the Ilkovic equation is applicable.

The water of hydration in the micelle has not been taken into account.

The diffusion coefficient calculated from the polalographic data is affected by the composition of the solution,[17] the ionic strength, and the species of the solvent. However, the polarographic measurement is a very convenient and simple method when the following assumptions are made: 1) the diffusion current has a linear relationship with the dye concentration; 2) the diffusing particles contain dye molecules only, and 3) the number of electrons transferred is known.

The number of electrons involved in the reduction of the dye is estimated to be 2 on the basis of the following results: 1) the AC polarograms and the cyclic voltammograms indicate a reversible dye reduction process (this makes possible the calculation of "n" from the log-plot of the currents; $n=2$ is obtained), and 2) the anthraquinone derivatives are reduced in a 2-electron step.

Concerning the diffusion coefficients from the polarographic data, an uncertainty of about ±10% usually appears, but the polarographic diffusion coefficients which are calculated in this study are in good agreement with the known values for nonionic surfactant micelles.[18]

Apparent Radii of Dye Particles in the Presence of Different Concentrations of Surfactants. By means of Stockes-Einstein's law for diffusion coefficients that the particles are spherical,[19] the apparent mean radii of dye particles at different concentrations of surfactant solutions are obtained; they are shown in Table 1. When a 0.446×10^{-4} M dye is solubilized into a 10^{-4} M surfactant solution, the particle size observed is 16 Å. This value is very small compared with

17) L. Meites, "Polarographic Techniques," 2nd Ed., John Wiley & Sons, New York (1965), p. 144.

18) H. Okuyama and K. Tyuzyo, This Bulletin, **27**, 259 (1954).

19) H. Schott, *J. Colloid & Interface Sci.*, **24**, 193 (1967).

Table 1. Apparent mean particle radii of 1,4,5,8-tetraaminoanthraquinone in NP-$\overline{19}$ solutions

Surfactant concn. (M)	Dye concn. (10^{-4} M)	Diffusion coefficient (10^{-7} cm^2/sec)	Particle radius (Å)
1×10^{-1}	1.000	2.26	38
5×10^{-2}	1.000	2.41	63
1×10^{-2}	0.922	2.45	85
5×10^{-3}	0.865	2.57	84
1×10^{-3}	0.732	3.04	73
5×10^{-4}	0.619	2.83	79
3×10^{-4}	0.451	4.41	51
1×10^{-4}	0.446	13.6	16
50% Alcoholic solution	0.718	36.5	2.5

that in a 5×10^{-4} M surfactant solution. Since the CMC of NP-$\overline{19}$ is near 10^{-4} M, small, incomplete micelles may be formed at this low surfactant concentration.[20]

As the surfactant/dye ratio increases, the apparent mean radii become constant at about 80 Å in the range of surfactant concentration of 5×10^{-4}M —10^{-2} M. The corresponding diffusion coefficient, about 3×10^{-7} cm^2/sec, is in good agreement with that of the nonionic surfactant micelle.[18]

At a surfactant concentration of 10^{-1} M, the apparent radius decreases to about 40 Å. In this case, the reproducibility of the polarographic data is improved, because of the increase in the homogeniety of the solution. The more homogeneous state than micelle formation can be regarded as the reason.[21]

The radius in a 50% alcoholic solution is 2.5 Å; the value does not change when a 10^{-2} M surfactant was added. This may be compared with the results of Becher,[22] who found that in polyoxyethylene lauryl ether solutions micelle formation does not occur when the concentration of ethanol reaches approximately 30%.

Effect of Dye Concentration on the Apparent Radii. The apparent mean radii of the particle at various dye concentrations are given in Table 2, Fig. 3, and Fig. 4. With the system of 1,4-diaminoanthraquinone and 10^{-1} M NP-$\overline{19}$, the radius of the particle increases with the dye concentration (Fig. 3). On the other hand, in the case of 1,4,5,8-tetraaminoanthraquinone solubilized in a 10^{-2} M NP-$\overline{19}$ solution, the dye particle size seems to be independent of the dye concentration. In the above NP-$\overline{19}$ systems, the diffusion coefficients are also of the same degree as those of nonionic surfactant micelles. From the polarographic diffusion coefficient, the aggregation number of NP-$\overline{19}$ can be estimated to be about 50. The above result is acceptable in comparison with the reported value of 62 for NP-$\overline{20}$.[12]

The radius of the dye particle solubilized into a polyoxyethylene lauryl ether surfactant solution markedly decreases with the dye concentration

Table 2. Apparent mean particle radii of 1,4,5,8-TAA in 10^{-2} M NP-$\overline{19}$ solution

Dye concn. (mM)	Diffusion coefficient (10^{-7} cm^2/sec)	Particle radius (Å)
0.47	3.56	60
0.92	2.45	85
1.59	3.14	67
1.91	3.22	65
3.22	3.10	69

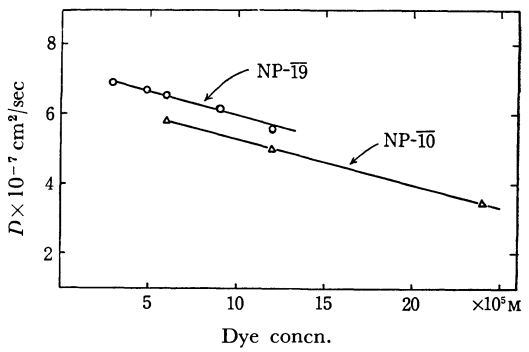

Fig. 3. Dependence of diffusion coefficient on dye concentration (1,4-DAA).

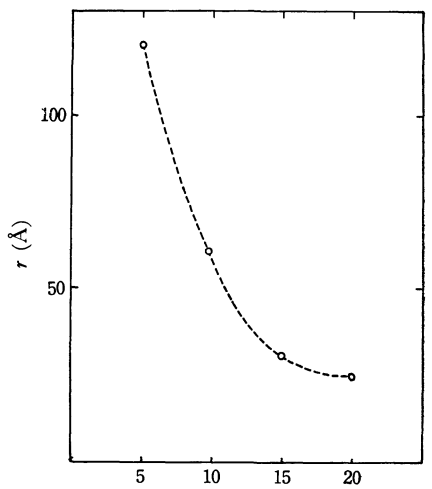

Fig. 4. Dependence of apparent mean particle radii on dye concentration (1,4,5,8-TAA in LA-$\overline{14}$ solution).

20) S. Kuroiwa, *Hyōmen (Surface)*, **3**, 690 (1965).
21) S. Kuroiwa, *Yukagaku (J. Japan Oil Chem. Soc.)*, **17**, 125 (1968).
22) P. Becher, *J. Colloid. Sci.*, **20**, 728 (1965).

(Fig. 4). The aggregation number of LA-$\overline{14}$ may be about 125; a large micelle ($r = ca.$ 40 Å) may be expected from this value. In this case, the radius of the particle falls from 60 Å to 25 Å when the 2.0×10^{-4} M dye is solubilized. This effect of the solubilizate concentration on the particle size appears to be due to the influence of the linear alkyl chain of the surfactant. The above tendency is similar to that found by Craven and Datyer,[7] but it is not ascribed to complex formation because of the constancy of the half-wave potentials. The mechanism of this phenomenone has not yet been explained.

Electrode Process of the Solubilized Dye. The fact that the half-wave potential of the dye reduction does not change when the dye is solubilized in a micellar solution indicates the similarity between the electrode process of the solubilized dye and that of the dissolved dye. It is clear that the diffusing particle is the micelle with the dye; this causes the diffusion current. The complex formation between dye and surfactant is inconceivable in this case; if it occurred, the half-wave potential might change with the concentration of the surfactant.

The rates of electron transfer are estimated by the method of Kambara-Ishii.[23] The rate constant of the solubilized dye is about 2×10^{-3} cm/sec; on the other hand, the dye dissolved into a 50% ethanolic aqueous solution has value of about 2×10^{-2} cm/sec. This difference may be attributed to the influence of the walls of the micelles near the electrode.

The authors wish to express their gratitude to Mr. O. Murakami for measuring the polarograms and to Professor S. Kuroiwa for his helpful discussions.

23) T. Kambara and T. Ishii, *Rev. Polarography*, **9**, 30 (1961).

BULLETIN OF THE CHEMICAL SOCIETY OF JAPAN VOL. 42 1472—1475 (1969)

Molecular Orbital Treatment of Nitric Oxide Radicals. III. Spin Distributions and *g* Factors of Aromatic Nitric Oxide Radicals

Osamu KIKUCHI

Department of Chemistry, Tokyo Kyoiku University, Otsuka, Tokyo

(Received July 25, 1958)

The spin distributions and *g* factors have been calculated for several aromatic nitric oxide radicals. The spin distributions calculated by the open-shell SCF method with configuration interaction, and by the unrestricted SCF method with the annihilation of the quartet component from the single determination wave function, agreed with the experimental values estimated from the ESR spectra. The contributions of the lone-pair orbital of the oxygen and of the N–O σ-bonding orbital to the *g* factor were calculated, the calculated *g* factors in solution being in the range of 2.005—2.006; these values were then discussed on the basis of the electronic structures of nitric oxide radicals.

In preceding papers,[1,2] the electronic structure and the spectrum of the H_2NO radical, and the ESR spectra of aliphatic nitric oxide radicals were discussed quantitatively on the basis of a SCF MO method in which all the valence electrons were explicitly considered. One purpose of this paper is to calculate the spin distributions for the phenyl nitric oxide, the diphenyl nitric oxide, and the carbazole *N*-oxide radicals by the open-shell SCF procedure of Longuet-Higgins and Pople[3] with configuration interaction, and also by the unrestricted Hartree-Fock method,[4] and to compare the calculated spin distributions with the experimental values estimated from the ESR spectra. The π-electrons of aromatic molecules delocalize upon a large conjugated system; nevertheless, some experimental results have shown that the aromatic nitric oxide radical reveals a *g* factor

1) O. Kikuchi, This Bulletin, **42**, 47 (1969).
2) O. Kikuchi, *ibid.*, **42**, 1187 (1969).
3) H. C. Longuet-Higgins and J. A. Pople, *Proc. Phys. Soc.*, **68**, 591 (1955).
4) J. A. Pople and R. K. Nesbet, *J. Chem. Phys.*, **22**, 571 (1954); A. Brickstock and J. A. Pople, *Trans. Faraday Soc.*, **50**, 901 (1954); A. T. Amos and L. C. Snyder, *J. Chem. Phys.*, **41**, 1773 (1964).

similar to that of the aliphatic nitric oxide radical.[5] The second purpose of this note is to estimate the g factor of the aromatic nitric oxide from the spin density on the N-O group and the orbital energy of the odd π-orbital. The results will be discussed on the basis of the electronic structures of aromatic nitric oxides.

Calculation Procedure

The calculation procedure and all the parameters except the core resonance integrals were the same as those reported elesewhere.[6] The g factor was calculated by means of the equation presented by Stone.[7] The core resonance integrals were computed by the relations:[8]

$$\left.\begin{aligned}\beta_{rs} &= -0.4172 S_{rs}(I_r+I_s) \quad (R_{rs} \leq 3\text{Å}) \\ &= 0 \qquad\qquad\qquad\quad (R_{rs} > 3\text{Å})\end{aligned}\right\} \tag{1}$$

where R_{rs} is the distance between the rth and sth atoms; S_{rs}, the overlap integral between two $2p_z$ Slater-type atomic orbitals, and I_r, the ionization potential for the valence atomic orbital, r. For all the C-C and C-N bonds, the bond lengths were assumed to be 1.40 Å, while for the N-O bonds, they were assumed to be 1.23 Å.[9] The bond angles were also assumed to be 120° and 108° for the benzene rings and the pyrol ring respectively. The overlap integrals were computed using the formula given by Mulliken, Rieke, Orloff, and Orloff[10] with the effective nuclear charges determined from the electron densities by

Table 1. Calculated and experimental[5,11] spin distributions in aromatic nitric oxide radicals

		Exp.*1	Calcd*2			
			I	II	III	IV
Phenyl nitric oxide						
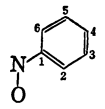	O		0.3402	0.5186	0.4792	0.4658
	N		0.2566	0.3310	0.3837	0.3751
	1		0.0155	−0.0368	−0.1472	−0.0424
	2	0.107	0.1250	0.0855	0.1725	0.0972
	3	−0.036	0.0007	−0.0336	−0.1088	−0.0348
	4	0.107	0.1293	0.0800	0.1550	0.0780
	5	−0.036	0.0000	−0.0302	−0.1072	−0.0345
	6	0.107	0.1327	0.0855	0.1728	0.0955
Diphenyl nitric oxide						
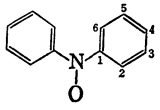	O		0.3077	0.5119	0.4771	0.4587
	N		0.2000	0.2547	0.3020	0.2958
	1		0.0099	−0.0184	−0.1157	−0.0336
	2	0.068	0.0765	0.0528	0.1362	0.0749
	3	−0.030	0.0010	−0.0061	−0.0858	−0.0276
	4	0.068	0.0756	0.0644	0.1232	0.0608
	5	−0.030	0.0002	−0.0199	−0.0853	−0.0256
	6	0.068	0.0830	0.0439	0.1378	0.0758
Carbazole *N*-oxide						
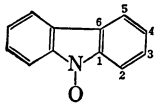	O		0.3127	0.5301	0.5066	0.4903
	N		0.1733	0.2302	0.2579	0.2606
	1		0.0202	−0.0053	−0.0717	−0.0147
	2	0.083	0.0676	0.0400	0.1076	0.0620
	3	−0.025	0.0112	0.0007	−0.0531	−0.0153
	4	0.083	0.0674	0.0592	0.0941	0.0488
	5	−0.025	0.0140	−0.0123	−0.0520	−0.0145
	6		0.0765	0.0375	0.0928	0.0584

*1 The values estimated from the relation $a_H = 27 \times \rho_C$; M. R. Das and G. K. Fraenkel, *J. Chem. Phys.*, **42**, 1350 (1965).

*2 The values calculated by the following methods;[6]

I) The open shell SCF method

II) The open shell SCF method with CI

III) The unrestricted SCF method

IV) The unrestricted SCF method with annihilation

5) Y. Deguchi, This Bulletin, **35**, 260 (1962); P. H. H. Fischer and F. A. Neugebauer, *Z. Naturforchg.*, **18a**, 1514 (1964); T. Kawamura, S. Matsunami, T. Yonezawa and K. Fukui, This Bulletin, **38**, 1935 (1965); O. Kikuchi and K. Someno, *ibid.*, **40**, 2549 (1967); G. Chapelet-Letourneux, H. Lemaire and A. Rassat, *Bull. Soc. Chim. France*, **1965**, 3283.

6) O. Kikuchi and K. Someno, This Bulletin, **40**, 2972 (1967).

7) A. J. Stone, *Proc. Roy. Soc.*, **A271**, 424 (1963); A. J. Stone, *Mol. Phys.*, **6**, 509 (1963).

8) The numerical constant was chosen so that the value of β_{rs} for benzene calculated by Eq. (1) using $R=1.39$Å and $Z=3.25$ fits the empirical value, −2.39 eV.

9) A. W. Hanson, *Acta Cryst.*, **6**, 32 (1953).

10) R. S. Mulliken, C. R. Rieke, D. Orloff and H. Orloff, *J. Chem. Phys.*, **17**, 1248 (1949).

each iteration.

Results and Discussion

The spin densities calculated for the phenyl nitric oxide, the diphenyl nitric oxide, and the carbazole *N*-oxide radicals are listed in Table 1. The spin densities of the phenyl nitric oxide agree well with the experimental values; the II and IV methods give a better agreement. From the theoretical point of view, the spin distributions calculated either by the method with configuration interaction (II) or by the annihilation of the quartet component of a single Slater-determinant (IV) are satisfactory. The ESR study of some substituted phenyl nitric oxide radicals has shown that the hyperfine splitting constants of two protons at the 2 and 4 positions differ from each other.[12] The present results (IV) show that $\rho_2 > \rho_4$; this is the relation observed in the experiment. The spin densities of the carbazole *N*-oxide radical also agree with the experimental values. The nitrogen hyperfine splitting constant (3.5—7.0 gauss[11]) of the carbazole *N*-oxide, small in comparison with that of the diphenyl nitric oxide (9.5 gauss[5]), can be explained by the calculated spin densities on the nitrogen and oxygen atoms of these two radicals.[13]

It has been shown that, in nitric oxide radicals, the deviation of the *g* factor from the value of the free spin is caused mainly by the lone-pair orbital of the oxygen atom and by the N–O σ-bonding orbital.[2] In the calculation of the *g* factor, it is necessary to estimate not only the spin distribution, but also the excitation energies from the σ-orbitals to the odd π-orbital. It is troublesome to calculate the electronic structure for the valence electron system of an aromatic radical. In the present investigations, therefore, these excitation energies were estimated by employing some assumptions based on the electronic structure of aliphatic nitric oxide radicals. The excitation energy from the σ-orbital to the odd π-orbital is given by:

$$\Delta E_{\sigma\to\pi^\circ} = \varepsilon_{\pi^\circ} - \varepsilon_\sigma - J_{\sigma\pi^\circ} + \frac{1}{2}J_{\pi^\circ\pi^\circ} + \frac{1}{2}K_{\sigma\pi^\circ} \quad (2)$$

where ε_{π° and ε_σ are the molecular orbital energies for the odd π-orbital and for the σ-orbital respectively. The LCAO approximation and the zero-differencial overlap approximation reduce the two-electron integrals in Eq. (2) to:

$$\left.\begin{aligned} J_{\sigma\pi^\circ} &= \sum_{r,s} C^2_{r\sigma} C^2_{s\pi^\circ} (r_\sigma r_\sigma \mid ss) \\ J_{\pi^\circ\pi^\circ} &= \sum_{r,s} C^2_{r\pi^\circ} C^2_{s\pi^\circ} (rr \mid ss) \\ K_{\sigma\pi^\circ} &= 0 \end{aligned}\right\} \quad (3)$$

These equations show that the integral values depend largely on the spin distribution of a radical, while for the nitric oxide radical the contribution of the spin density on the N–O group to the integral value is most important. The problem is treated as a "three-atom problem" in which the spin desnity $(1-\rho_{NO})$ is on the third atom, X, bonded to the nitrogen atom, where ρ_{NO} is the sum of the spin densities on the nitrogen and oxygen atoms. The localization of the lone-pair electrons on the oxygen atom is assumed;[14] we then obtain:

$$J_{n\pi^\circ} = \rho_O(nn \mid OO) + \rho_N(nn \mid NN) + (1-\rho_{NO})(nn \mid XX) \quad (4)$$

The one-center integral of the nitrogen, (NN|NN), is taken to be approximately equal to that of the oxygen, (OO|OO);[15] the value of the two-center integrals, γ, in this equation are taken to be approximately a half of the one-center integral.[15] Therefore,

$$J_{n\pi^\circ} = \gamma(1+\rho_O) \quad (5)$$

Similarly,*1

$$J_{\pi^\circ\pi^\circ} = \gamma(1 + \rho_O^2 + \rho_N^2) \quad (6)$$

From Eqs. (5) and (6), the excitation energy for the $n\to\pi$ excitation is given by:

$$\Delta E_{n\to\pi^\circ} = \varepsilon_{\pi^\circ} - \varepsilon_n - \frac{\gamma}{2}(1+2\rho_O - \rho_O^2 - \rho_N^2) \quad (7)$$

A simpler relation between the excitation energy and the spin density on the N–O group is obtained by setting $\rho_N = \rho_O = \frac{1}{2}\rho_{NO}$:

$$\Delta E_{n\to\pi^\circ} = \varepsilon_{\pi^\circ} - \varepsilon_n - \frac{\gamma}{4}(2+2\rho_{NO} - \rho_{NO}^2) \quad (8)$$

When the electrons in the N–O σ-bonding orbital are shared equally on the nitrogen and the oxygen atoms,[16] the same relation (8) is obtained for the excitation from the N–O σ-bonding orbital to the odd π-orbital. For the values of ε_n and $\varepsilon_{\sigma(N-O)}$, the preceding results concerning the H_2NO radical were used: $\varepsilon_n = -14.75$ eV and $\varepsilon_{\sigma(N-O)} = -19.20$ eV.[1] The value of the two-center integral, γ,

11) H. R. Falle and G. R. Luckhurst, *Mol. Phys.*, **12**, 493 (1967).

12) Th. A. J. W. Wajer, A. Mackor, Th. J. de Boer and J. D. W. van Voorst, *Tetrahedron Letters*, **20**, 1941 (1967).

13) A nitrogen hyperfine splitting constant of an aromatic nitric oxide radical can be estimated by the relation,

$$a_N = \rho_N|Q_N| - \rho_O|Q_O|.$$

14) Strictly speaking, the lone-pair electron of the oxygen atom is not completely localized on the oxygen atom (see Ref. 1.)

15) In the calculation for the H_2NO radical, the electron repulsion integrals were $\gamma_{NN}=19.3$, $\gamma_{OO}=22.5$, and $\gamma_{NO}=11.3$ eV (see Ref. 1).

*1 Equation (3) is expanded as:

$$J_{\pi\pi} = \rho_N^2(NN \mid NN) + \rho_O^2(OO \mid OO) + 2\rho_N\rho_O(NN \mid OO) + c(1-\rho_{NO}^2)$$

where the constant, *c*, corresponds to the mean value of (tt/uu) (t=C, u=C, N, O); this value is approximately equal to the two-center integral, γ.

16) For the H_2NO radical, this is correct (see Ref. (1)).

TABLE 2. CALCULATED g FACTORS FOR AROMATIC NITRIC OXIDE RADICALS

	Odd orbital energy*1 (eV)	Excitation energy (eV)		$\Delta g_{xx}\times10^{-5}$	$\Delta g_{yy}\times10^{-5}$	g, Factor*2		
		$n\rightarrow\pi^\circ$	σ(N-O)$\rightarrow\pi^\circ$			g_{xx}	g_{yy}	g_{av}*3
H_2NO radical	−3.63	2.77	7.22	388	678	2.0062	2.0091	2.0059
Phenyl nitric oxide	−4.94	1.89	6.34	265	674	2.0050	2.0091	2.0055
Diphenyl nitric oxide	−5.18	1.87	6.32	225	617	2.0046	2.0086	2.0051
Carbazole *N*-oxide	−5.64	1.47	5.92	226	798	2.0046	2.0103	2.0057

*1 Obtained from the calculation I

*2 The most important excited states correspond to the excitations from the non-bonding orbital to the odd π-orbital and from the N-O σ-bonding to the odd π-orbital and only these excitations were considered. The contributions from the other excited states are small.[2] N-O axis taken as y axis; z axis perpendicular to molecular plane.

*3 Obtained by $g_{av}=\frac{1}{3}(g_{xx}+g_{yy}+g_{zz})$ with $g_{zz}=2.0023$

is determined so that the $n\rightarrow\pi$ excitation energy of the H_2NO radical calculated from Eq. (8) agrees with the experimental $n\rightarrow\pi$ transition energy of the aliphatic nitric oxide radical (2.76 eV[17]). The relations obtained are:

$$\left.\begin{aligned}&\Delta E_{n\rightarrow\pi^\circ}(\mathrm{eV}) = \\ &\quad \varepsilon_{\pi^\circ} + 14.75 - 2.79(2+2\rho_{NO}-\rho_{NO}^2) \\ &\Delta E_{\sigma(N-O)\rightarrow\pi^\circ}(\mathrm{eV}) = \\ &\quad \varepsilon_{\pi^\circ} + 19.20 - 2.79(2+2\rho_{NO}-\rho_{NO}^2)\end{aligned}\right\} \quad (9)$$

Using the spin density on the N-O group and the orbital energy of the odd π-orbital, the excitation energies and the g factors of aromatic nitric oxide radicals were calculated; they are tabulated in Table 2. The averaged g factors for aromatic nitric oxide radicals were in the range of 2.005—2.006; they agree with the experimental values in solution.[5] It may be concluded that, in aromatic nitric oxide radicals, the spin density on the N-O group is smaller than that for the aliphatic nitric oxide radical, but the excitation energy from the σ-frame to the odd π-orbital is lower than that for the aliphatic nitric oxide, mainly because of the lower energy of the odd π-orbital. As a result, aromatic nitric oxide radicals reveal g factors similar to those of aliphatic nitric oxide radicals.

The author wishes to express his thanks to Professor Keizo Suzuki, Tokyo Kyoiku University, and to Dr. Kazuo Someno, Government Chemical Industrial Research Institute, Tokyo, for their helpful suggestions and encouragement during the course of this work. Thanks are also due to the Matsunaga Science Foundation for financial support.

17) R. Briere, H. Lemaire and A. Rassat, *Bull. Soc. Chim. France*, **1965**, 3273.

BULLETIN OF THE CHEMICAL SOCIETY OF JAPAN VOL. 42 1476—1480 (1969)

Nature of Acid Sites on the Surface of Silica-alumina. I. The Relation between the Acid Property of Sites and the Heat of Immersion

Masaji MIURA, Yukio KUBOTA,*1 Toru IWAKI, Kazuto TAKIMOTO and Yoshinori MURAOKA

Department of Chemistry, Faculty of Science, Hiroshima University, Higashisenda-machi, Hiroshima

(Received September 20, 1968)

The acidity and the acid strength of the sites of such solid catalysts as silica gel, alumina, and silica-alumina were determined by the *n*-butylamine titration method using the Hammett indicators. The distribution of the acid sites on the surfaces of these catalysts was found to vary with the outgassing temperature, and also with the alumina content in the case of silica-alumina. The heats of immersion of these catalysts in water and in an aqueous solution of *n*-butylamine were measured. The heat value corresponding to the difference between these two cases, as well as the number of acid sites, showed a maximum at contents of 10—20%. These phenomena are discussed with reference to the results of the diffuse reflection measurements.

Silica-alumina is widely used as a catalyst for such reactions as cracking, isomerization, and polymerization. Recently many studies of the nature of the catalytically-active sites[1-4] which are developed by the removal of chemisorbed water from the surface have been undertaken. The active sites thus generated possess acid properties; the Lewis-acid site can accept lone-pair electrons, and the Brönsted-acid site can donate a proton. It is thought that these acid sites play an important role in surface reactions. The distribution of these acid sites has been measured by various techniques, such as the indicator method[5,6] and the volumetric-base adsorption method.[7,8] However, no exact information on the nature of the surface of silica-alumina, has yet been obtained. In this work, the *n*-butylamine titration method using the Hammett indicators was employed to determine and characterize the acid properties of the surface of silica gel, alumina, and silica-alumina; the results will be discussed in relation to the heat of immersion caused by the interaction of water with acid sites. Furthermore, the spectra resulting from the diffuse reflection[9] of anthracene adsorbed on the samples from an *n*-hexane solution were measured in order to confirm the results obtained from the above experiments.

Experimental

Materials. The silica gel was prepared by the hydrolysis of ethyl ortho-silicate, which had been purified by distillation at 120—130°C. The product was washed with water by repeated decantation, kept standing overnight at 150°C, and then calcined at 600°C in air for 8 hr. Alumina was produced by hydrolyzing aluminum isopropoxide which had been previously purified by distillation under reduced pressure. The product was treated in the same way as in the case of silica gel. The silica-alumina was prepared by adding a suspension of aluminum isopropoxide in alcohol to the sol obtained by hydrolyzing ethyl ortho-silicate. The mixture was well

TABLE 1. SURFACE AREA OF SILICA-ALUMINAS WITH VARIOUS CONTENTS OF ALUMINA

Alumina content (wt%)	Surface area (m^2/g)
0	627
5	351
8	297
10	295
16	233
23	167
29	429
53	353
80	393
100	189

*1 Present address: Department of Chemistry, Yamaguchi University, Yamaguchi.

1) M. W. Tamele, *Discussions Faraday Soc.*, **8**, 270 (1950).
2) O. Johnson, *J. Phys. Chem.*, **59**, 827 (1955).
3) V. C. F. Holm, G. C. Bailey and A. Clark, *ibid.*, **63**, 129 (1959).
4) A. Clark, V. C. F. Holm and D. M. Blackburn, *J. Catalysis*, **1**, 244 (1962).
5) H. A. Benesi, *J. Phys. Chem.*, **61**, 970 (1957).
6) J. Kobayashi and I. Higuchi, *Shokubai (Catalysis)*, **4**, 49 (1962).
7) R. C. Richardson and S. W. Benson, *J. Phys. Chem.*, **61**, 405 (1957).
8) G. A. Mills, E. R. Boedecker and A. G. Oblad, *J. Am. Chem. Soc.*, **72**, 1554 (1950).
9) A. Terenin, V. Barachevsky, E. Kotov and V. Kolmogorov, *Spectrochimica Acta*, **19**, 1797 (1963).

stirred for 3hr at 120—130°C, and then treated as above. X-Ray analysis showed that the silica gel and silica-alumina were practically amorphous and that the alumina was of the γ-type. The specific surface areas of the samples evacuated at 300°C were determined by the B.E.T. method from the nitrogen adsorption. The results are listed in Table 1. The *n*-butylamine and benzene were purified by distillation, with several pieces of metallic sodium added to remove any moisture. The anthracene and the Hammett indicators were purified by recrystallizing them twice from a hot alcoholic solution.

Measurement of Acid Properties. The silica gel, alumina, and silica-alumina were dried at 100°C, 300°C, and 500°C for 3hr *in vacuo*. These samples were then dispersed into dry benzene, and the suspensions thus obtained were titrated with a 0.5 N benzene solution of *n*-butylamine using the Hammett indicators.[5] The treatment was made in a dry-box through which nitrogen gas flowed continuously. The amount of *n*-butylamine titrated corresponds to the number of acid sites.

Heat of Immersion. The heats of immersion of the samples were measured at 25°C in water and in an aqueous solution of *n*-butylamine by using a calorimeter equipped with a thermistor.[10]

Diffuse Reflection. An oxygen-free *n*-hexane solution of anthracene was added through a breakable joint to a sample dried at 300°C. After the adsorption equilibrium had been established, the *n*-hexane was sufficiently removed through a trap cooled with liquid nitrogen. The colored sample was then transferred into a cell used for the measurement of diffuse reflection, which was then cut off. The spectra were measured using a Hitachi-Perkin-Elemr 139 spectrophotometer, equipped with an attachment for the measurement of the diffuse reflection.

Results and Discussion

Acid Properties. The acid properties of the surfaces of silica gel, alumina, and silica-alumina show different characteristics as the evacuating temperature rises.

Figure 1 shows that silica-alumina has two acid-site groups; one group includes the strong acid sites in the range of $H_0 < -3.0$, and the other, the weak acid sites in the range of $6.8 > H_0 > 3.0$, where H_0 is the Hammett function. These are scarcely no intermediate sites between $H_0 = 3.0$ and $H_0 = -3.0$, as may be seen in the figure. The strong acid sites increase with a rise in the outgassing temperature. The acid property of alumina is quite different from that of silica-alumina, as is shown in Fig. 2. When alumina is heated at 100°C, weak acid sites alone develop. However, when the sample is treated at 300°C, strong acid sites also appear and the total number of acid sites increases. On the other hand, when heated at 500°C, all of the strong acid sites disappers. The total number of acid sites of silica gel is nearly

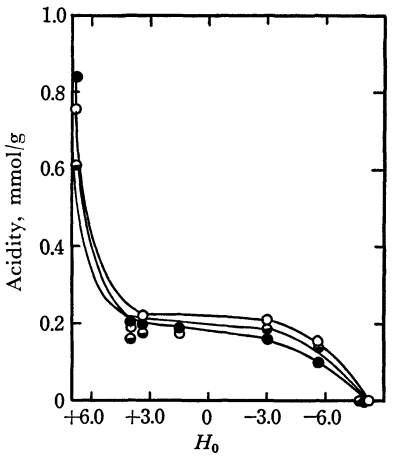

Fig. 1. Acidity *vs.* acid strength for 8.1% silica-alumina; degassing temperature: ● 100°C, ◒ 300°C, ○ 500°C.

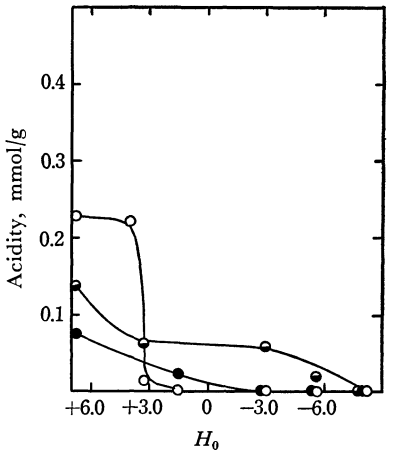

Fig. 2. Acidity *vs.* acid strength for alumina; degassing temperature: ● 100°C, ◒ 300°C, ○ 500°C.

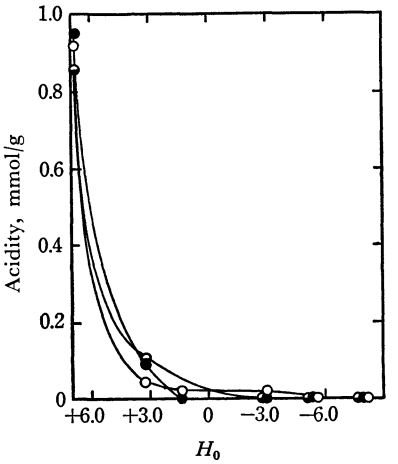

Fig. 3. Acidity *vs.* acid strength for silica gel; degassing temperature: ● 100°C, ◒ 300°C, ○ 500°C.

10) M. Miura, H. Naono, T. Iwaki, T. Kato and M. Hayashi, *Kogyo Kagaku Zasshi (J. Chem. Soc. Japan, Ind. Chem. Sect.)*, **69**, 1623 (1966).

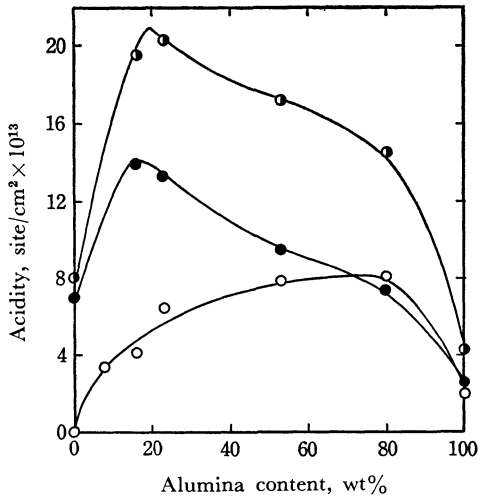

Fig. 4. Acidity of silica-alumina with various contents of alumina.
○: strong acid site, $H_0 < -3.0$
●: weak acid site, $+6.8 > H_0 > +3.0$
◑: total acid site, $H_0 < +6.8$

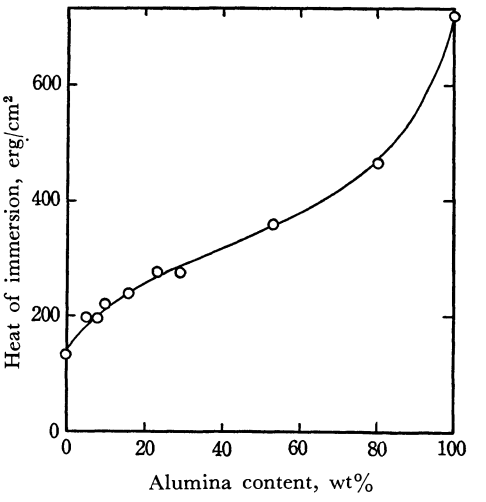

Fig. 5. Heat of immersion of silica-aluminas with various contents of alumina in water.

constant, regardless of the evacuating temperature, whereas more stronger acid sites appear with a rise in the temperature, as may be seen in Fig. 3.

The acid strength of silica-alumina also changes with the alumina content. Figure 4 shows the case of silica-aluminas evacuated at 300°C. The number of strong acid sites is almost zero for pure silica gel, but it increases with the alumina content until finally it again takes a low value for pure alumina. The maximum number of weak acid sites is at the content of 10—20%. Thus, the total number of sites is maximum at a content of about 20%. The aluminum atom originally hydrated in the surface layer of silica-alumina is dehydrated by evacuation at a high temperature. The naked aluminum atom thus produced may behave as a strong acid site, while the hydrated one may act as a weak acid site.[11] As the probability that the naked aluminum atoms will appear on the surface by evacuation increases with the alumina content, it may be generally predicted that the number of strong acid sites increases, and that of weak acid sites decreases, with an increase in the alumina content. The fact that the number of strong acid sites is less for alumina than for silica-alumina seems to be due to the difference in the mechanism of the generation of acid sites between these two materials.[12]

Heat of Immersion. The heats of immersion of silica-aluminas with various alumina contents in water are shown in Fig. 5. The heat evolved increases with the alumina content, as has been reported previously.[10] The factors responsible for the generation of the heat may be considered to be as follows: (1) the property of -OH groups on the surface, (2) the hydrogen bond between the -OH group and electronegative oxygen or the nitrogen atom in such molecules as water and *n*-butylamine, and (3) the distribution of acid sites on the surface. When the samples are immersed into water, the water molecule with non-bonding electrons generally makes a co-ordinate bond with the active acid site. The strong acid site is considered to contribute to heat generation more than the weak site does. The small amount of heat for silica gel may be due to the absence of a strong acid site on its surface and also to the weak dipole-dipole interaction of a water molecule having a large permanent dipole moment with the neutral -OH group. The gradual increase in the heat with the alumina content may be due to a slow increase in the number of strong acid sites on the surface. The large heat value for alumina may be caused mainly by the strong interaction of the negatively-charged -OH group[13] with the water molecule, since the alumina has a small number of strong acid sites.

When the samples are immersed into an aqueous solution of *n*-butylamine, more heat is generated than in the above case, as may be seen by comparing Figs. 5 and 6. The difference between the heat of immersion in water and that in the aqueous solution of *n*-butylamine is shown in Fig. 7. The amount of heat at a content of about 10% is characteristically large. The amount of *n*-butylamine adsorbed from the aqueous solution on the surface of silica-alumina is shown in Fig. 8, where the adsorbed amount was determined by means of

11) M. R. Basila, T. R. Kanter and K. H. Rhee, *J. Phys. Chem.*, **68**, 3197 (1964).
12) E. Echigoya, *Nippon Kagaku Zasshi (J. Chem. Soc. Japan, Pure Chem. Sect.)*, **79**, 430 (1958).
13) J. B. Peri, *J. Phys. Chem.*, **69**, 220 (1965).

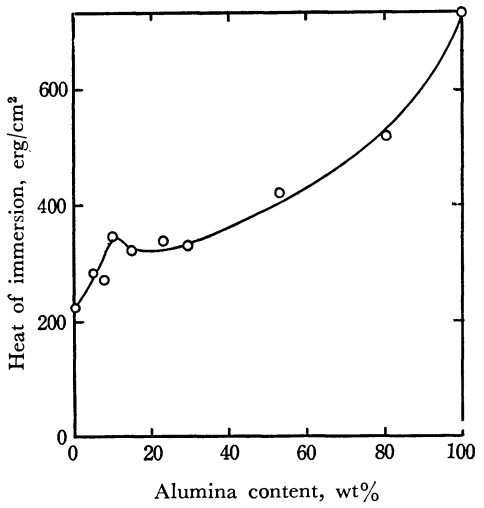

Fig. 6. Heat of immersion of silica-aluminas with various contents of alumina in the aqueous solution of *n*-butylamine.

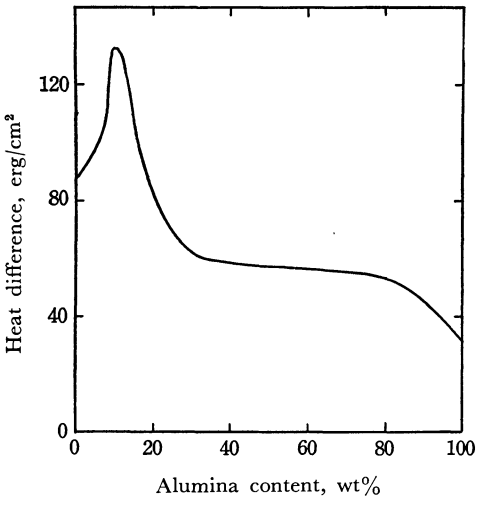

Fig. 7. Difference between the heats of immersion of silica-alumina with various contents of alumina in water and in the aqueous solution of *n*-butylamine.

an electrical conductivity method. The maximum amount of *n*-butylamine adsorbed is at a content of 10%, as may be seen in Fig. 8. Each of the curves in Figs. 7 and 8 bears a fairly good resemblance in shape to the curve of total acid sites shown in Fig. 4.

Diffuse Reflection. Anthracene was used as a molecular indicator because it is known that the spectra due to the interactions of anthracene with Lewis-acid site and with a Brönsted-acid site can be distinguished from each other.[14,15] A

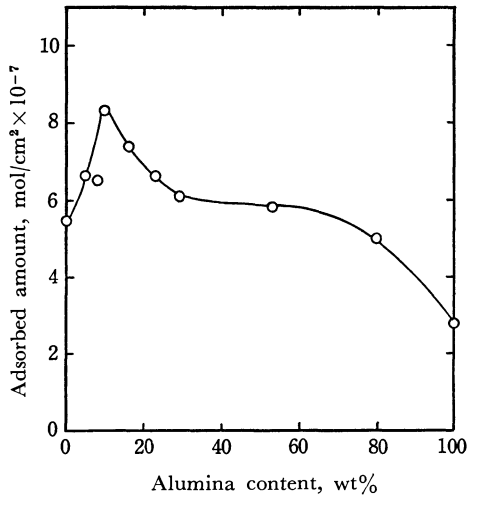

Fig. 8. Adsorbed amount of *n*-butylamine on the surface of silica-aluminas with various contents of alumina from the aqueous solution of *n*-butylamine.

degassed *n*-hexane solution of anthracene was added to a sample evacuated at 300°C through a breakable joint, the whole was allowed to stand for 1 hr, and then the *n*-hexane was removed through the other breakable joint. Upon this treatment silica-alumina turned green and alumina, palegreen, but silica gel showed no change in color. According to the observation of the color change, only the strong interaction of anthracene with the acid sites can be observed. In the measurement of diffuse reflection, alumina shows a very weak absorption at 760 mμ; this is due to the carbonium cation radical arising from electron transfer from the anthracene molecule to the Lewis-acid site. This species was confirmed by ESR measurement. Silica-alumina with a content of 80% shows an absorption at 760 mμ, stronger than in the case of alumina; this was confirmed by a study of the ESR spectra.

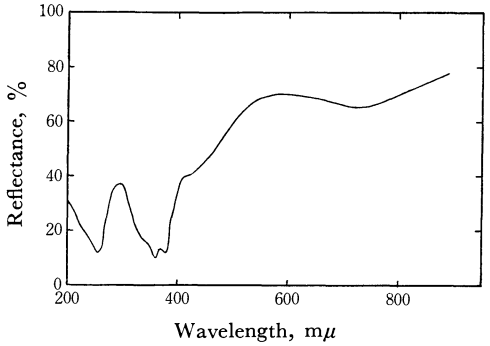

Fig. 9. Diffuse reflection spectrum of anthracene adsorbed on the surface of 10% silica-alumina.

14) W. I. Aalbergsberg, G. J. Hoijtink, E. L. Mackor and W. P. Weijland, *J. Chem. Soc.*, **1959**, 3049, 3055.

15) A. I. Kitova and J. M. Varshavsky, *Dokl. Akad. Nauk SSSR*, **135**, 1395 (1960).

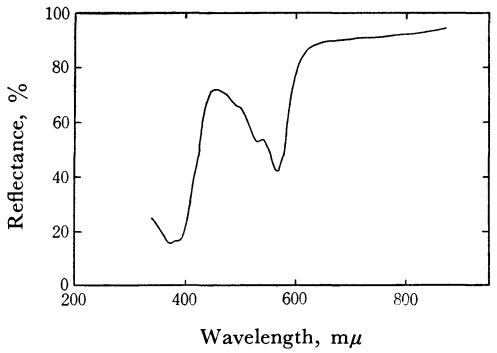

Fig. 10. Effect of water vapor on diffuse reflection spectrum of anthracene adsorbed on the surface of 10% silica-alumina.

On the other hand, silica-alumina with a content of 10% shows an absorption due to the interaction of anthracene with the Brönsted-acid site at 430 mμ in addition to that due to interaction with the Lewis-acid site at 760 mμ as Fig. 9 shows. Silica gel shows no absorption at either 760 mμ or 430 mμ.

When water molecules are adsorbed from the vapor phase through a third breakable joint, the color, the absorption bands at both 430 mμ and 760 mμ, and the ESR signal all disappear in the cases of alumina and silica-alumina, but new absorption bands at 530 mμ and 570 mμ appear in the case of silica-alumina with a content of 10%, as may be seen in Fig. 10. This new interaction is weak, since the color reverts to the original one when the system is evacuated. When anthracene is adsorbed and then water is adsorbed, it seems that water molecules squeeze themselves between the anthracene molecules and the sites on the surface. As a result, the absorption bands at 430 mμ and 760 mμ both disappear. This phenomenon suggests that the water molecule reacts with the acid sites more strongly than does anthracene, and also that the water molecule rather than *n*-butylamine is adsorbed preferentially on the sites from the aqueous solution of *n*-butylamine.

Conclusion. When silica-alumina is immersed into an aqueous solution of *n*-butylamine, the water molecule may preferentially interact with the strong acid sites and may weaken the site strength, as in the case described above. As a result, the strong acid sites may be transformed to weak ones, while the total number of the acid sites remains unchanged. If both the adsorbed amount and the heat value of *n*-butylamine depend principally on the total number of acid sites, the resemblance in shape among the curves of these three quantities (Figs. 4, 7, and 8) may be interpreted well.

BULLETIN OF THE CHEMICAL SOCIETY OF JAPAN VOL. 42 1481—1486 (1969)

Photoemission from Polycyclic Aromatic Crystals in the Vacuum Ultraviolet Region. III. Aromatic Crystals and Charge-transfer Complexes

Tomohiko HIROOKA, Masakatsu KOCHI, Jun-ichi AIHARA, Hiroo INOKUCHI and Yoshiya HARADA

The Institute for Solid State Physics, The University of Tokyo, Roppongi, Tokyo

(Received September 25, 1968)

The photoemission from various types of charge-transfer complexes, quinolinium-tetracyanoquinodimethane Q(TCNQ)$_2$ (I), dibenzophenothiazine (DBP)-dicyanodichloro-*p*-benzoquinone (DDQ)[(DBP)(DDQ)(II) and (DBP)$_2$(DDQ)(III)], trinitrobenzene (TNB)-coronene (IV), and TNB-perylene (V), and also large polycyclic aromatic hydrocarbons, violanthrene A (VI), violanthrene B (VII), coronene (VIII), pyranthrene (IX), and pyranthrone (X), was observed in the vacuum ultraviolet region. The experimental equation $Y \propto (E-E^*)^3$, where Y is the quantum yield of photoemission; E, the incident photon energy, and E^*, the threshold energy, was used to determine the ionization potential. The E^*-values, as estimated from the experimental equation, were I=4.85 eV, II 4.99, III 4.75, IV 5.62, V 5.52, VI 5.06, VII 5.13, VIII 5.58, IX 5.04, and X=5.71 eV. A band structure scheme for these organic semiconductors was introduced to analyse the emission mechanism.

In 1935, the spectral dependence of the photoemission from the naphthalene and anthracene complexes with alkali metals was observed by Suhrmann.[1] In 1963, Inokuchi and Harada[2] reported their findings on the violanthrene A complex with cesium; further, Ogino *et al.*,[3] measured the dependence of the pyrene derivatives complexes with cesium. However, the photoemission from the charge-transfer complexes, the components of which are organic substances, were not observed until recently because the wavelength region of the photoemission from them is in the vacuum ultraviolet region where measurement is difficult. On the other hand, we have already reported our findings on the current-voltage characteristics and the spectral distributions of the photoemission from polycyclic aromatic hydrocarbons.[4,5] Recently Batley and Lyons[6] reported on the photoemission from the 1,6-diaminopyrene- and the tetramethyl-*p*-phenylenediamine-complexes with various organic acceptors.

In the above previous works, two methods of determining the ionization potential of solid have been used. One was the method of obtaining the ionization potential from the threshold energy of the spectral response of the photoemission. Lyons and Morris[7] determined the threshold as the lowest detectable current. However, in this method, it is necessary for the photoemission yield to rise up abruptly at the threshold energy; this condition is not necessarily satisfied in all compounds. For instance, the bulk ionization potentials determined by Kearns and Calvin[8] by this method were too small in comparison with the values obtained by the other methods.

The second method was that of the retarding potential. Terenin and Vilessov[9] obtained the ionization potential by measuring a current-stopping potential and also a current-saturation potential. When the sample has a semiconductive character, however, it is very difficult to determine the current-stopping potential because the current becomes an asymptotic curve to the voltage axis in its neighbourhood.[10]

1) R. Suhrmann and D. Dempster, *Z. Phys.*, **94**, 742 (1935); *ibid.*, **111**, 18 (1937).

2) H. Inokuchi and Y. Harada, *Nature*, **198**, 477 (1963).

3) K. Ogino, S. Iwashima, H. Inokuchi and Y. Harada, This Bulletin, **38**, 473 (1965).

4) Y. Harada and H. Inokuchi, This Bulletin, **39**, 1443 (1966).

5) M. Kochi, Y. Harada and H. Inokuchi, *ibid.*, **40**, 531 (1967).

6) M. Batley and L. E. Lyons, *Mol. Cryst.*, **3**, 357 (1968).

7) L. E. Lyons and G. C. Morris, *J. Chem. Soc.*, **1960**, 5192.

8) D. R. Kearns and M. Calvin, *J. Chem. Phys.*, **34**, 2026 (1961).

9) A. Terenin and F. Vilessov, "Advances in Photochemistry," Vol. II, Interscience Publishers, New York (1964), p. 407.

10) See the schematic diagram of the voltage-current characteristics for an intrinsic semiconductor given by L. Apker, E. Taft and J. Dickey, *Phys. Rev.*, **74**, 1462 (1948).

This paper will give the results of the photoemission from various types of charge-transfer complexes and large polycyclic aromatic hydrocarbons. Because the voltage-current characteristic of the charge-transfer complexes used in this work is intrinsic semiconductor-like and because the photoemission yield does not rise up abruptly at the threshold energy, their ionization potentials can not be determined by the above two methods. Therefore, an experimental equation will be employed in this study to determine the ionization potential.

Experimental

Materials. The materials used in the present study are shown in Figs. 1 and 2. Figure 1 shows the structural formula of the condensed aromatic hydrocarbons—violanthrene A, violanthrene B, coronene, pyranthrene and pyanthrone. Figure 2 illustrates those of the charge-transfer complexes — quinolinium-tetracyanoquinodimethane $Q(TCNQ)_2$ and dibenzphenothiazine (DBP)-dicyanodichloro-*p*-benzoquinone (DDQ); these are two different complexes with different component ratios, (DBP)(DDQ) and $(DBP)_2(DDQ)$. The other charge-transfer complexes used are trinitrobenzene (TNB)-coronene and TNB-perylene.

Sample Preparation. Except for $Q(TCNQ)_2$, the materials were deposited on a copper disc, 10 mm in diameter, by means of sublimation *in vacuo* (10^{-5}—10^{-6} mmHg). The deposited films were several microns thick. The $Q(TCNQ)_2$ complex could not be sublimed. Therefore, as it had a high electrical conductivity in the bulk state, the complex could be used as a pressed disc stuck with silver paste onto the copper disc. The pressed sample was approximately 1 mm thick.

The formation of the complex was examined by means of the absorption spectra of the sublimed samples. We observed that (DBP)(DDQ) and $(DBP)_2(DDQ)$ have different absorption spectra, both of which possess a characteristic charge-transfer band near 7400Å.

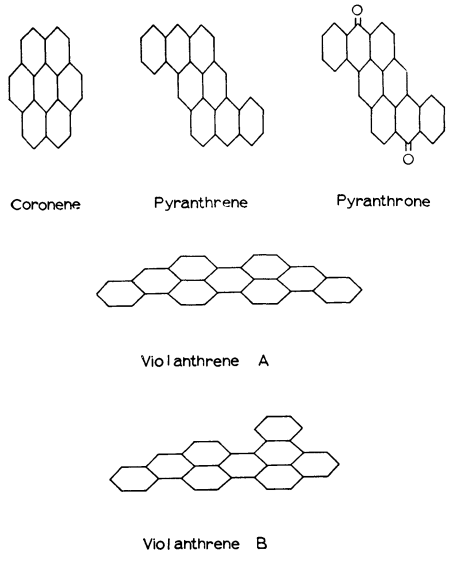

Fig. 1. The structural formulas of the condensed aromatic hydrocarbons.

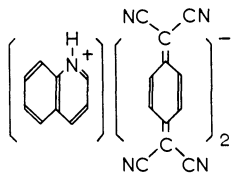

$Q(TCNQ)_2$

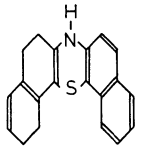

Dibenzophenothiazine (DBP)

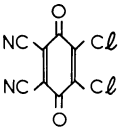

Dichlorodicyano-p-benzoquinone (DDQ)

Fig. 2. The structural formulas of the charge-transfer complexes.

To observe the photoemission, a Seya-Namioka-type vacuum ultraviolet monochromator was used. The details of the apparatus have been reported previously.[4] The collector of the photoemissive cell, a glass sphere, was about 13 cm in diameter. On the inside it was coated with a conducting layer of colloidal graphite, Aquadag. The sample was placed in the centre of the cell. In order to obtain enough intensity, the slit was made 1 mm wide at the cost of resolving power. The photoemission current was amplified and observed by a Cary 31 vibrating-reed electrometer.

The spectral dependence of the photoemission yield was measured under an applied potential of 10 V, enough to gather all of the emitting electrons, and at intervals of 20Å. The saturation of the photoemission current for $Q(TCNQ)_2$ against an applied potential was very slow, but the current observed around 50V was saturated enough for us to estimate the phtoemission yield.

The current-voltage characteristics were observed by a spherical retarding method, and the photoemission current was recorded as a function of the applied voltage with a Yokogawa X-Y recorder, PRO-12. The current saturation potential, V_s, was determined by averaging the values observed at the incident wavelength of 1600Å, 1400Å, or 1200Å. In the present study, a highly accurate saturation point was obtained because the photocell used had a good spherical geometry. This observation was carried out to a precision of less than 0.03 eV.

Results and Discussion

Figure 3 shows the photoelectric yield curves of violanthrene A and violanthrene B as functions of the incident photon energy. Figure 4 shows those of pyranthrene and pyranthrone. The threshold energy, E_{th}, can be determined by extrapolation to a quantum yield of 10^{-7} electrons per incident quantum. However, as is shown in Figs. 3 and 4,

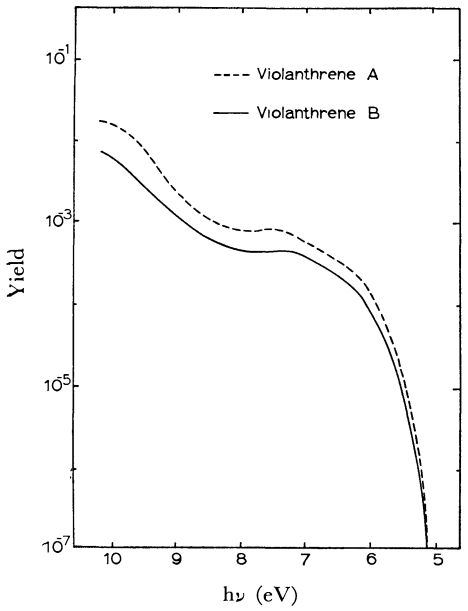

Fig. 3. The photoelectric yield curves of violanthrene A and violanthrene B.

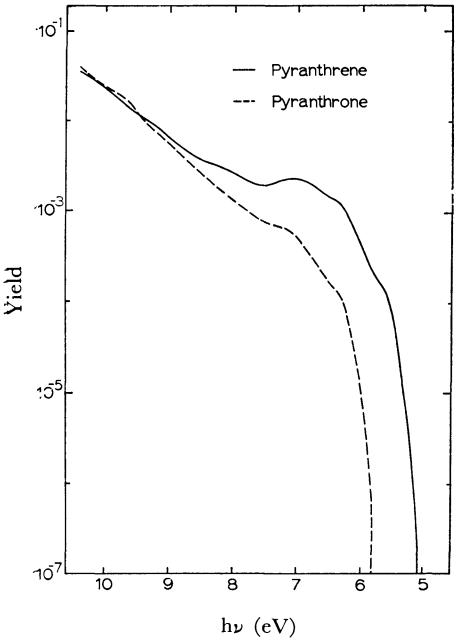

Fig. 4. The photoelectric yield curves of pyranthrene and pyranthrone.

the shapes of the rising photoemission yield curves from the threshold point are different in various compounds. For instance, violanthrene A and violanthrene B are found to have the same threshold energy by the extrapolation method described above, but the shapes of the rising photoemission yield curves are clearly different.

The spectral response patterns of the yield are very different in the two types of charge-transfer complexes used in the present study. One of them is a weak charge-transfer complex, while the other is a strong charge-transfer complex. Figure 5 shows the spectra dependence of the photoemission yield of two weak charge-transfer complexes (CT-complexes), TNB-coronene and TNB-perylene.

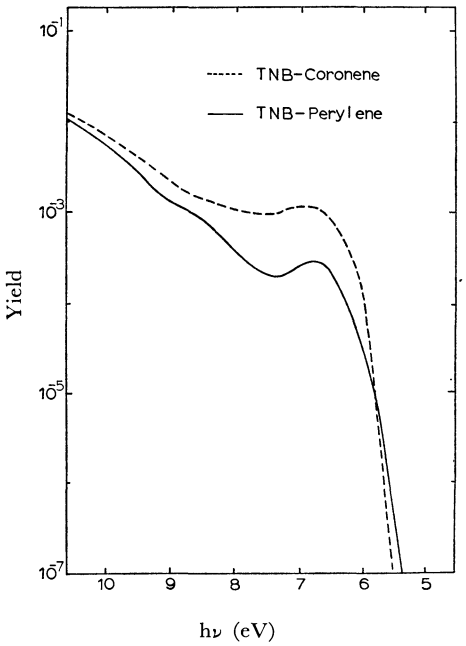

Fig. 5. The photoelectric yield curves of the weak charge-transfer complexes, TNB-coronene and TNB-perylene.

In the case of weak CT-complexes, the photoemission yield curves are almost the same as that of the donor component; for instance, the yield curve of (TNB)-coronene has a peak at about 6.7 eV corresponding to that of coronene.*1 The ionization potential of the acceptor (TNB) is estimated to be higher than that of the donor (coronene), therefore, the ionization potential of the complex can be determined by means of the threshold energy of only the donor (coronene). Figures 6 and 7 show the spectral responses of the yields of the strong charge-transfer complexes—Q(TCNQ)$_2$, (DBP)-(DDQ), and (DBP)$_2$(DDQ).

The photoemission yield curves of their separated components are shown in the same figure for comparison. In Fig. 7 the characteristic peak is observed at about 7.3 eV; this value, corresponds to

*1 This suggests that, in weak charge-transfer complexes, the two components keep their individual characteristics, so the total photoemission from complexes is almost equal to the superposition of those of the two components.

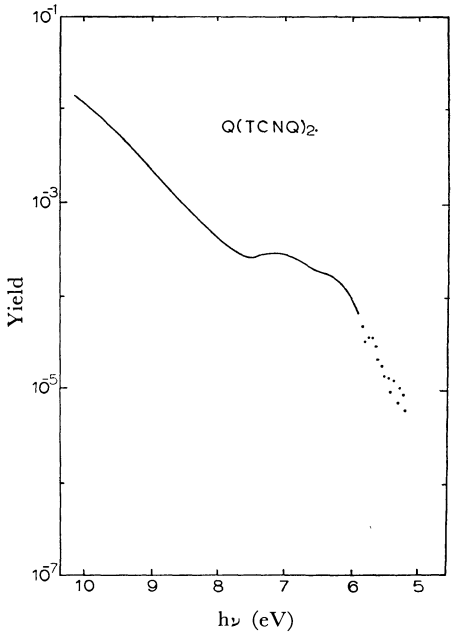

Fig. 6. The spectral response of the photoemission yield of the strong charge-transfer complex, $Q(TCNQ)_2$.

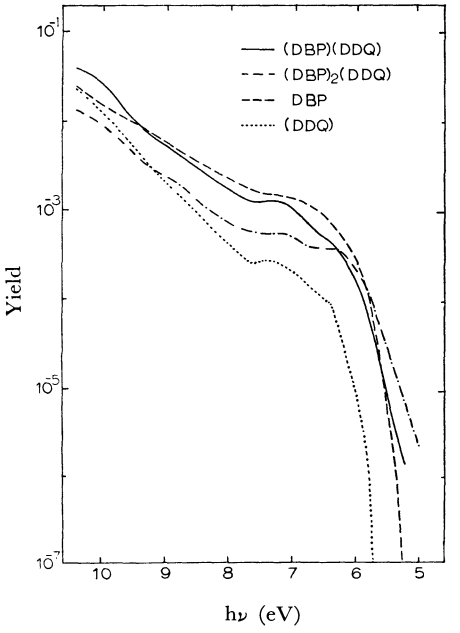

Fig. 7. The spectral response of the photoemission yield of the strong charge-transfer complexes, (DBP)(DDQ), $(DBP)_2$(DDQ) and their components.

that of the acceptor, DDQ. In $(DBP)_2$(DDQ) a new peak is observed at about 6.4 eV.

The quantum yield near the threshold energy of the strong charge-transfer complexes decreased very slowly in comparison with the other materials; therefore, the threshold energy could not be determined by the extrapolation method.

By analogy with the Fowler plot for metal, we assumed that the quantum yield in organic crystals near the threshold energy is subject to the conventional power law;*2

$$Y \propto (E-E^*)^n \qquad (1)$$

where Y is the quantum yield, E, the incident photon energy, and E^*, the threshold energy.

Figure 8 shows the spectral dependence of the photoemission yield of (DBP)(DDQ) as plotted with $n=1$, 2, and 3. This indicates that, in the lower-energy part, a cube root plot of the quantum yield becomes almost linear as a function of the incident photon energy, while in the higher-energy part the quantum yield becomes linear. The same equation, Eq. (1), was applied to the photoemission from inorganic crystals.[12] This empirical cube root law held true for all the compounds studied.

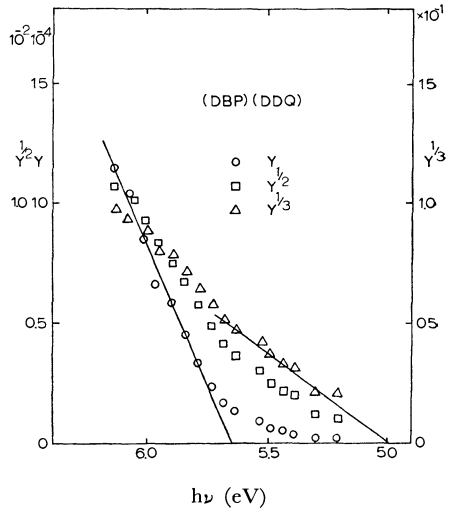

Fig. 8. The linear, square and cube root plot of the yield of (DBP)(DDQ) near the threshold energy.

*2 In inorganic semiconductors, Kane[11] proposed that the spectral yield obeys $Y \propto (E-E^*)^n$, in which $n=$ 1, 3/2, 2, and 5/2 under various conditions near the threshold energy. Gobeli and Allen[12] observed that, for an atomically-clean silicon surface, the spectral yield curve was composed of two components. One of them is the part of a linear plot of the yield which corresponds to a direct transion, while the other is the part of a cube root plot at a lower photon energy which corresponds to an indirect transition. Kane's theory was obtained assuming that the band theory can be strictly applied. However, it is doubtful whether it can be applied to organic crystals with narrow band widths.

11) E. O. Kane, *Phys. Rev.*, **127**, 131 (1962).
12) G. W. Gobeli and F. G. Allen, *ibid.*, **127**, 141 (1962).

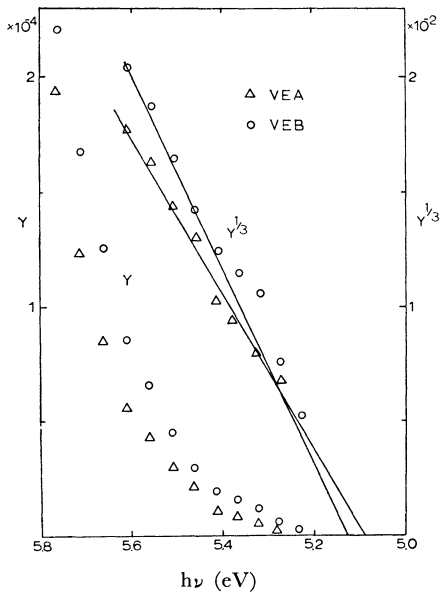

Fig. 9. The linear and cube root plot of the photoemission yield of violanthrene A and violanthrene B near the threshold energy.

Figure 9 shows the cube root plot and the linear plot of violanthrene A and violanthrene B. The difference in the photoemission yield curve near the threshold energy leads to the difference in the threshold energy, E^*.

This method can be applied to the complexes, and their threshold energy can be thus determined. For both the single component compounds and the complexes used, the cube root plot gives a straight line for the energy region of 0.3 eV—0.6 eV from the threshold energy. The E_{th} values and also the E^* values obtained by this method are given in Table 1. As this table shows, the E_{th} and E^* of single component compounds agree within the limits of 0.15 eV. Especially for the compounds which have an abrupt increase in the quantum yield near the threshold energy, the threshold energy values obtained by the extrapolation method need not be modified.

The values of the ionization potential are 0.37 eV for (DBP)(DDQ) and 0.61 eV for $(DBP)_2(DDQ)$ respectively, both values being smaller than that of the donor, DBP. If this difference is caused by any impurity which has a lower threshold energy, the quantum yield will not be subjected to the cube root law, because perhaps the impurity is only small in amount. Batley and Lyons[6] explained it as being due to the difference in polarization energy for the non-ionic complexes. For the ionic complexes they used the different explanation that the emission comes from the negative ion. The strong charge-transfer complexes in the present study have the properties between the weak charge-transfer complexes and the ionic complexes.

If we assume that the organic molecular crystals used as emitters are intrinsic semiconductors, and if a metal is used as the collector, the schematic diagram in Fig. 10 can be introduced. The Fermi level of the emitter coincides with that of the collector in thermal equilibrium. The potential difference between the vacuum level of a collector and the vacuum level of an emitter corresponds to the current saturation potential, V_s. The work function, φ, of the emitter, which corresponds to the energy difference between the vacuum level of the emitter and the Fermi level, is obtained as;

$$\varphi = \varphi_c - eV_s = 4.74 - eV_s \qquad (2)$$

where φ_c is the work function of the collector. Aquadag (colloidal graphite) is used as the collector in our study. The value of φ_c for Aquadag is 4.74 eV.[10]

Work functions can be determined independently by means of the contact potential difference method. Kotani and Akamatu[13] determined the work functions of the organic crystals using this method. Table 2 shows the work functions obtained by means of these two methods. The table indicates

Table 1. The ionization potential of the polycyclic aromatic compounds and the charge-transfer complexes

Material	E_{th} (eV)	E^*(eV)
Coronene	5.59	5.58
Violanthrene A	5.20	5.06
Violanthrene B	5.20	5.13
Pyranthrene	5.05	5.04
Pyranthrone	5.83	5.71
$Q(TCNQ)_2$	—	4.85
(DBP)(DDQ)	—	4.99
$(DBP)_2(DDQ)$	—	4.75
DBP	5.21	5.36
DDQ	5.68	5.64
TNB-coronene	—	5.62
TNB-perylene	—	5.52

Table 2. The work function (φ) of the polycyclic aromatic compounds and the charge-transfer complexes

Material	φ	φ_{CPD}*	V_s
Coronene	4.70	—	0.04
Violanthrene A	4.50	4.50	0.24
Pyranthrene	4.54	4.50	0.20
Pyranthrone	4.52	—	0.22
(DBP)(DDQ)	4.63	4.58±0.04	0.11
$(DBP)_2(DDQ)$	4.62	4.60±0.01	0.12
DDQ	4.75	—	−0.01

* The values obtained from the contact potential difference method by Kotani and Akamatsu.[13]

13) M. Kotani and H. Akamatu, private communication.

that the two work functions are in fairly good agreement.

In the case of the intrinsic semiconductor, the energy difference, δ,*3 between the top of the valence band and the Fermi level is a half of the band-gap energy, $\Delta\varepsilon/2$, based on the results of the temperature dependence of the semiconduction. If we use the work functions, φ, in Table 2, the band-gap energy, $\Delta\varepsilon$, can be estimated from the following equation:

*3 Indicated in Fig. 10.

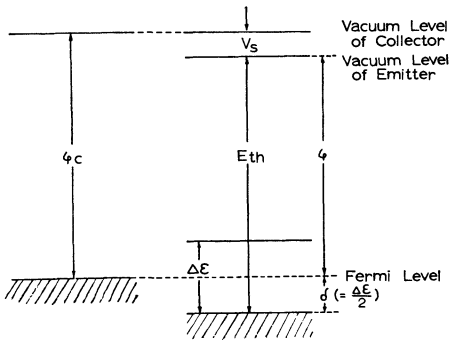

Fig. 10. The schematic diagram for the external photoelectric process of the organic molecular crystal.

*4 In previous works,[4,5] E_{th} was used as a threshold value instead of E^*.

Table 3. The energy gap ($\Delta\varepsilon$) estimated from Eq. (3)

Material	$\Delta\varepsilon$	$\Delta\varepsilon_r$*
Coronene	1.78	1.7[a]
Violanthrene A	1.12	0.9[b]
Pyranthrene	1.00	1.07[b]
(DBP)(DDQ)	0.72	0.54[c]
$(DBP)_2(DDQ)$	0.26	0.18[c]
DDQ	1.78	—

* Observerd from the temperature dependence of the electrical conductivity.

a) H. Inokuchi, H. Kuroda and H. Akamatu, This Bulletin, **34**, 749 (1961).
b) H. Inokuchi, *ibid.*, **24**, 222 (1951).
c) Y. Matsunaga, *J. Chem. Phys.*, **42**, 1982 (1965).

$$\Delta\varepsilon = 2(E^* - \varphi) = 2(E^* - \varphi_c + eV_s) \quad (3)^{*4}$$

In Table 3, the $\Delta\varepsilon$ values obtained in this way are compared with those found from the temperature dependence of the semiconduction. The two values are in fairly good agreement in spite of the rough assumption. This result suggests that the energy level diagram used is a good assumption.

We wish to thank Professors Yoshio Matsunaga and Junji Aoki, and Mr. Satoshi Iwashima for supplying us with the organic materials.

BULLETIN OF THE CHEMICAL SOCIETY OF JAPAN VOL. 42 1486—1489 (1969)

Mössbauer Effect of ^{119}Sn in Molecular Complexes of Tin(IV) Chloride with Several Aromatic Compounds

Sumio ICHIBA, Mitsuo MISHIMA*1 and Hisao NEGITA

Department of Chemistry, Faculty of Science, Hiroshima University, Hiroshima

(Received October 4, 1968)

The Mössbauer spectra of molecular complexes of tin(IV) chloride with some oxygen-containing aromatic compounds, such as hydroxybenzaldehydes and cinnamic acid, were investigated. Most of these complexes show the quadrupole splitting resulting from the addition of aromatic molecules to tin(IV) chloride, although in some cases broad absorption curves are observed. The isomer shifts of these complexes are 0.25—0.45 mm/sec, much smaller than that of tin(IV) chloride itself. These values are almost the same as those of the complexes of tin(IV) chloride with aliphatic compounds. From these results, the bond nature and structures of these complexes, which had not previously been studied, were discussed in some detail.

In a previous paper[1] dealing with the ^{119}Sn Mössbauer effect in the molecular complexes of tin (IV) chloride with some aliphatic compounds, it was shown that the spectra for most of the complexes were doublets caused by the quadrupole splitting, and that the isomer shifts of the molec-

*1 Present address: Department of Chemistry, Shimane University, Matsue.

1) S. Ichiba, M. Mishima, H. Sakai and H. Negita, This Bulletin, **41**, 49 (1968).

ular complexes with respect to SnO_2 were in the range from 0.30 to 0.45 mm/sec.

In the present work, the 1 : 2 molecular complexes of tin(IV) chloride with some aromatic compounds have been investigated by Mössbauer spectroscopy. The structures of these complexes have not been investigated. However, the preparations of most of the complexes have been reported by Pfeiffer[2,3] and by Rosenheim *et al.*[4]

In the molecular compolexes of tin(IV) chloride (electron acceptor) with oxygen-containing aromatic compounds (electron donor), there are two possibilities in the way of coordination, unlike the aliphatic compounds, because the oxygen-containing aromatic molecule has two parts serving as electron donors, *i. e.*, the benzene ring and the oxygen-containing group. In the complex of tin(IV) chloride with benzaldehyde, for example, the chlorine atom in tin(IV) chloride may be bonded to the benzene ring of benzaldehyde through its π-electron, but it is equally, or even more, likely that the oxygen atom of the aldehyde group will be coordinated to the tin atom in tin(IV) chloride directly through the lone-pair electrons of the oxygen, as in the case of aliphatic compounds reported previously. In the former case the chlorine atoms around the tin atom remain in the tetrahedron form in complexing, whereas in the latter case they change to an octahedron.

The purpose of the present study is to clarify the difference between the aliphatic and aromatic complexes and to explain, on the basis of the Mössbauer parameters, how tin(IV) chloride is bounded to the aromatic compound in the complex.

Experimental

Preparation of Molecular Complexes. The tin(IV) chloride and all the aromatic compounds were obtained commercially. All the complexes except that of tin(IV) chloride with cinnamyl alcohol were prepared by a method similar to those described by Pfeiffer[2,3] and by Rosenheim and Levy.[4] That is, the complexes were formed by dropping tin(IV) chloride (1/20 mol) into ice-cooled petroleum ether, chloroform, or a benzene solution of an aromatic compound (1/10 mol); they were then dried over silica gel in a vacuum desiccator.

The complex of tin(IV) chloride with cinnamyl alcohol was prepared by adding tin(IV) chloride (1/20 mol) to petroleum ether in which cinnamyl alcohol (1/10 mol) was suspended. Brown nonhygroscopic crystallines with a mp of 82 °C were thus obtained. All the complexes except that of tin(IV) chloride with ethyl cinnamate were purified by sublimation under a reduced pressure of 4—7 mmHg. The complexes were identified by their melting points; the results are summarized in Table 1, along with the literature values.

Table 1. Melting points of $SnCl_4$-complexes

Complex	Melting point °C	
	Obsd	Lit[a]
$SnCl_4 \cdot 2C_6H_5CHO$	177	187—189
$SnCl_4 \cdot 2C_6H_5COOH$	78—80	90
$SnCl_4 \cdot 2C_6H_4(OH)CHO(o)$	140	—
$SnCl_4 \cdot 2C_6H_4(OH)CHO(p)$	175	185
$SnCl_4 \cdot 2C_6H_4(OCH_3)CHO(p)$	178	158
$SnCl_4 \cdot 2C_6H_5CH{=}CHCH_2OH$	82	—
$SnCl_4 \cdot 2C_6H_5CH{=}CHCHO$	241	225—230
$SnCl_4 \cdot 2C_6H_5CH{=}CHCOOH$[b]	—	—
$SnCl_4 \cdot 2C_6H_5CH{=}CHCOOC_2H_5$	140	134

a) Refs. 2, 3.
b) Melting point could not be measured on account of thermal decomposition.

Measurements. The measurements were made as previously.[1] The activity at a given velocity was accumulated until it reached about 10^5 counts in order to reduce the statistical errors. The γ-ray radiation source was tin(IV) oxide containing 1 mCi ^{119m}Sn. The source was used at room temperature, whereas the absorber was cooled with liquid nitrogen. The thickness of the absorber was about 15 mg/cm^2 for Sn. X-rays were cut off by a palladium foil attached to the absorber.

Results and Discussion

The results are given in Table 2. The isomer shift, δ, and the quadrupole splitting, 2ε, of the complexes are presented in the first and second columns respectively. The third column gives the half-width, $R_{1/2}$, which was defined in the previous paper.[1] The isomer shift is referred to tin(IV) oxide at room temperature. A positive value means that the source and the absorber are approaching each other, while a negative value means that they are moving apart. When the splitting due to the quadrupole interaction was

Table 2. Mössbauer parameters for $SnCl_4$-complexes

Complex	δ[a] mm/sec	2ε[b] mm/sec	$R_{1/2}$[c] mm/sec
$SnCl_4 \cdot 2C_6H_5CHO$	0.42	0.80	2.10
$SnCl_4 \cdot 2C_6H_5COOH$	0.35	1.16	2.70
$SnCl_4 \cdot 2C_6H_4(OH)CHO(o)$	0.34	0.92	2.28
$SnCl_4 \cdot 2C_6H_4(OH)CHO(p)$	0.45	0	1.50
$SnCl_4 \cdot 2C_6H_4(OCH_3)CHO(p)$	0.35	0.64	1.90
$SnCl_4 \cdot 2C_6H_5CH{=}CHCH_2OH$	0.27	0	1.50
$SnCl_4 \cdot 2C_6H_5CH{=}CHCHO$	0.42	0.75	2.05
$SnCl_4 \cdot 2C_6H_5CH{=}CHCOOH$	0.40	0.92	2.28
$SnCl_4 \cdot 2C_6H_5CH{=}CHCOOC_2H_5$	0.25	1.20	2.80

a) δ is the isomer shift relative to the source of SnO_2 crystal. The accuracy of the measurement is $\pm 5\%$.
b) 2ε is the quadrupole splitting.
c) $R_{1/2}$ is the half-width.

2) P. Pfeiffer, *Ann.*, **376**, 285 (1910).
3) P. Pfeiffer, *Z. anorg. Chem.*, **71**, 97 (1911); *ibid.*, **112**, 81 (1920); *ibid.*, **133**, 91 (1924).
4) A. Rosenheim and W. Levy, *Ber.*, **37**, 3667 (1904).

observed, the average line position was taken as the δ-value. All the values of δ and 2ε are given in mm/sec.

Isomer Shift. In Table 2 the values of the isomer shift for all the complexes of $SnCl_4$ with oxygen-containing aromatic compounds fall in a range from 0.25 to 0.45 mm/sec. There is no appreciable difference between the δ-values for the complexes with oxygen-containing aliphatic compounds reported previously[1] and those with oxygen-containing aromatic compounds. The values are appreciably smaller than those of tin(IV) chloride, which are 0.7 ± 0.08,[5] 0.78 ± 0.1,[6] 0.8 ± 0.05,[7] and 0.9 ± 0.1[8] with respect to tin(IV) oxide. This means that tin(IV) chloride-complexes have a lower s-electron density at the tin nucleus than does tin(IV) chloride itself. In other words, the formation of the 1 : 2 complex of tin(IV) chloride with an oxygen-containing organic compound results in a decrease in the s-electron density at the tin nucleus.

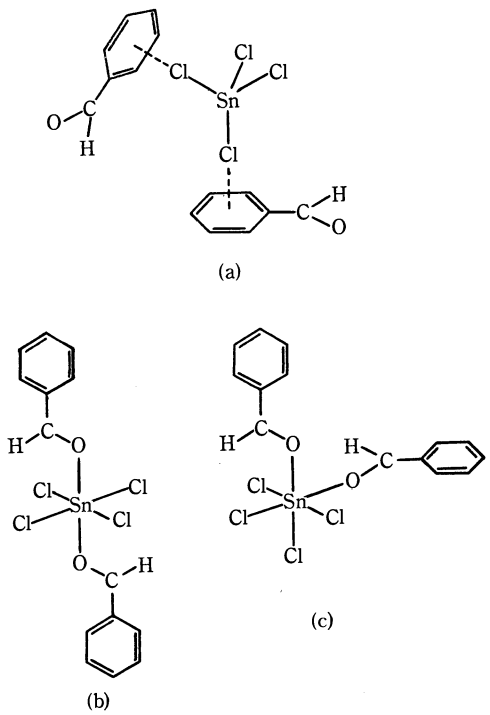

Fig. 1. Bond structures of $SnCl_4$-benzaldehyde complex.

In forming the molecular complex, it is assumed that the coordination of aromatic molecules to tin(IV) chloride permits two bond-structures, as has been mentioned above. For instance, the possible bond-structures of the complex of tin(IV) chloride with benzaldehyde are shown in Fig. 1; in (a) the π-electrons are transferred from the benzene ring to the chlorine atom of tin(IV) chloride, while in (b) and (c) the lone-pair electrons of the oxygen atom are transferred to the tin atom. In the (a) bond-structure the tetrahedral arrangement of the chlorine atoms around the tin atom is preserved, but in the structures (b) and (c) it changes to an octahedron of the *trans*- or *cis*-form.

The electron configuration outside the krypton core of a neutral tin atom is $(4d)^{10}(5s)^2(5p)^2$. In tin(IV) chloride, chlorine atoms are coordinated to the tin atom in a tetrahedral form so that the hybrid bond of the tin atom is sp^3. If the Sn–Cl bond in tin(IV) chloride is completely covalent, as has been discussed in a previous paper,[1] its s-electron character is 0.25. However, the bonds character was deduced to be approximately 40% ionic from the pure quadrupole resonance due to ^{35}Cl[9] and the Mössbauer effect of ^{119}Sn.[8,10]

If the complex has the structure (a), electrons will transfer from the benzene ring of the benzaldehyde to the chlorine atom of tin(IV) chloride. Consequently, the chlorine atom in the complex may be more ionic than that of tin(IV) chloride itself. However, the electron transferred to the chlorine atom may not influence the electron density at the tin nucleus very seriously, since it affects indirectly through the chlorine atom.

On the other hand, in the complex of the bond-structure (b) or (c) the electron-donor atom is the oxygen atom and the acceptor atom is the tin atom in tin(IV) chloride. That is to say, oxygen atoms are directly coordinated to the tin atom, and then oxygen atoms occupy a *cis*- or *trans*-position and the arrangement of atoms around the tin atom is hexacoordinated. Lone-pair electrons of the oxygen atom of the aldehyde group contribute directly to the electron core of the tin atom of tin(IV) chloride and sp^3d^2 hybrid orbitals are formed around the tin atom. If the ligand atoms are completely hexacoordinated, *i. e.*, if the Sn–O and Sn–Cl bonds are entirely equivalent and completely covalent, the s-electron character of the bonds is 0.17. Therefore, the s-electron density at the tin nucleus may be expected to be larger in the complex of the bond-structure (a) than in the complex of the bond-structure (b) or (c). Thus, the complex of the bond-structure (a) should show a larger isomer shift than the complex of the bond-structure (b) or (c). The isomer shifts of the complexes

5) R. A. Stukan, T. N. Sumarokova, V. A. Trukhatanov and V. V. Khrapov, *Dokl. Acad. Nauk. SSSR,* **156**, 400 (1964).

6) A. Yu. Aleksandrov, N. N. Delyagin, N. P. Mitrofanov, L. S. Poluk and V. S. Shpinel, *Zh. Eksperim. i Teor. Fiz.,* **43**, 1242 (1962); *Soviet Phys. JETP,* **16**, 874 (1963).

7) S. Khristrov, Tsv. Bonchev and Kl. Burin, *Compt. Rend. Acad. Bulgare Sci.,* **19**, 293 (1966).

8) M. Cordey-Hayes, *J. Inorg. Nucl. Chem.,* **16**, 915 (1963).

9) A. L. Schalow, *J. Chem. Phys.,* **22**, 1211 (1954).

10) D. A. Shirley, *Rev. Mod. Phys.,* **36**, 399 (1964).

between tin(IV) chloride and oxygen-containing aromatic compounds are 0.25 to 0.45 mm/sec, considerably smaller than that of tin(IV) chloride itself; these shifts do not differ appreciably from those of the complexes of tin(IV) chloride with aliphatic compounds, 0.31—0.45 mm/sec. Accordingly, the complex of tin(IV) chloride with aromatic compounds is considered to have the bond-structure (b) or (c). It is uncertain at this stage which of the bond-structures, (b) or (c), is the more probable, for other experimental data is lacking.

Quadrupole Splitting. With the exception of the complexes of tin(IV) chloride with *p*-hydroxybenzaldehyde and with cinnamyl alcohol, small quadrupole splittings were observed for all the complexes. A pair of clearly-split lines were observed in two complexes, those with benzoic acid and with ethyl cinnamate. The spectrum of the complex with benzoic acid is shown in Fig. 2 as an example. When the value of $R_{1/2}$ was below 2 mm/sec, only a broad absorption curve was observed. The value of the quadrupole splitting was found by analysing the curve, assuming that the component lines were of a Lorentzian type with a half-width of 1.50 mm/sec.

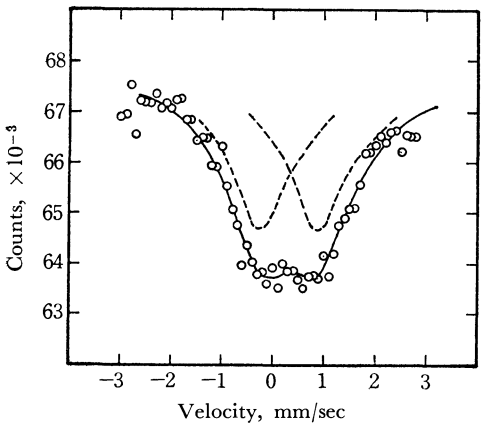

Fig. 2. Mössbauer spectrum of $SnCl_4 \cdot 2C_6H_5COOH$.

In Table 2, it is interesting to note that the complex with *p*-hydroxybenzaldehyde has no quadrupole splitting, though the complex with *o*-hydroxybenzaldehyde has. This is obviously due to the difference of the molecular structures of the ligands. However, the crystal structures of these complexes have not yet been established. Since the difference in the quadrupole splitting is caused by the relative positions of the OH- and CHO-groups, or the ortho- and para-positions, it is significant to consider how the two isomers are coordinated to the tin atom and how they give rise to the electric field gradient around the tin nucleus.

In the hexacoordinated complex of tin(IV) chloride with *p*-hydroxybenzaldehyde, the OH-groups are coordinated to the tin atom; therefore, the CHO-groups are free from the coordination, being separated from the tin atom or *vice versa*. However, it is more probable that the OH-groups are coordinated, for the complex with benzaldehyde shows splitting. On the other hand, in the complex with *o*-hydroxybenzaldehyde, the non-coordinated group at the ortho-position is very close to the tin atom and so necessarily causes an electric field gradient of some extent at the tin nucleus. Thus, the difference between the relative positions of the OH- and CHO-groups is reflected in the quadrupole splitting.

Small quadrupole splittings are also observed in the complexes with aromatic molecular ligands containing a carbonyl group with which the organic molecules are attached to the tin atom. According to Greenwood and Ruddick,[11] quadrupole interactions in tin(IV) compounds are observed only when there is an imbalance in subsidiary π-interactions.

In the spectrochemical series, carbonyl is ranked as a strong π acceptor and Cl^-, as a strong π donor. This difference in ligand ability will be enough to cause the imbalance in the π-interactions between the π orbitals of the ligands and the d_π orbitals of the central tin atom in the complex. Thus, small quadrupole splittings are observed in the complexes with benzaldehyde, benzoic acid, *etc.*, whereas no quadrupole splitting is observed in the complexes with *p*-hydroxybenzaldehyde and cinnamyl alcohol. This is because the *p*-hydroxybenzaldehyde and cinnamyl alcohol are attached to the tin atom by means of OH-groups which have little or no π-bonding abilities and which do not give rise to an electric field gradient at the tin atom. The small variation in the splitting values results from the inductive effects of the neighbouring groups of the carbonyl coordinated to the tin atom.

11) N. N. Greenwood and M. N. R. Ruddick, *J. Chem. Soc.*, **1967**, 1679.

BULLETIN OF THE CHEMICAL SOCIETY OF JAPAN VOL. 42 1490—1493 (1969)

The Heat of Immersion of Ferric Oxide in Water

Tetsuo MORIMOTO, Noriko KATAYAMA, Hiromitu NAONO and Mahiko NAGAO

Department of Chemistry, Faculty of Science, Okayama University, Tsushima, Okayama

(Received October 17, 1968)

Four kinds of ferric oxide (α-Fe_2O_3) which differ in origin and history have been used for measurements of the surface area, the water content, and the heat of immersion in water. Two cases have been discovered; in one there appears a maximum in the plot of the heat of immersion against the pretreatment temperature according to the origin of the sample, but in the other a maximum does not appear. The heavy hydration treatment carried out prior to the immersion measurements raises the value of the heat of immersion in water, but it has no serious effect on the heat of surface hydration calculated therefrom, as in the case of TiO_2. The average value of the latter was 11.3 kcal/mol H_2O.

Measurements of the heat of immersion have been made on various kinds of insoluble metal oxides in water as well as in organic liquid, and it has been brought to light that the surface hydroxyl groups on metal oxides more or less affect the wetting phenomena.[1,2] Most plots of the heat of immersion in water against the pretreatment temperature show a maximum. This heat-of-immersion anomaly has been explained in terms of the overlapped effect of the chemisorption (the formation of surface hydroxyl groups) and the physical adsorption of water. The surface hydroxyl groups can be removed gradually by heating *in vacuo*, and can be reproduced immediately after immersing the surfaces into water, when the temperature of pretreatment is relatively low. However, when the pretreatment temperature is higher than a limited degree, the rate of the reproduction of the surface hydroxyl groups is remarkably delayed. Thus, the heat treatment at elevated temperatures results in a stabilization of the surface oxide structure made by the reaction:

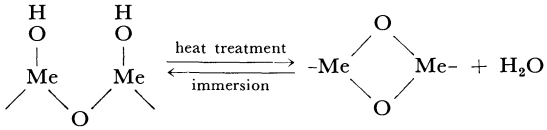

Usually the maximum in the plot of the heat of immersion *vs.* the pretreatment temperature has been reported to appear in the temperature range from 300°C to 600°C with various kinds of oxides, such as SiO_2,[3,4] Al_2O_3,[5] TiO_2,[6,7] and ZnO.[8]

It has been a question for the present authors whether or not the maximum of the heat-of-immersion curve appears with every kind of metal oxide.

This paper will report that two cases have been discovered with α-Fe_2O_3; in one a maximum appears in the plot of the heat of immersion *vs.* the pretreatment temperature, but in the other a maximum does not appear. We have also investigated the effects of hydration treatment on the heat of immersion of α-Fe_2O_3 in water, and on the heat of surface hydration calculated therefrom.

Experimental

Materials. The samples used in the present work are four kinds of α-Fe_2O_3. One of them is the α-Fe_2O_3 presented by the Nippon Bengara Co.; it was prepared by calcining $FeSO_4 \cdot 7H_2O$ at 800°C for 7 hr. This original sample was treated several times with 0.1 N nitric acid in order to remove the basic impurities, and then with 0.1 N ammonia water in order to remove the acidic impurities; then it was washed with distilled water, and finally, by means of electrodialysis, cleaned of electrolytes. The conductivity of supernatant liquid was thus brought to a limiting value. The resultant sample was dried at 110°C for 8 hr in an oven (sample C). Another kind of sample was prepared by the calcination of α-FeOOH (goethite) for 5 hr at 800°C in air; this sample had been made by the oxidation of ferrous sulfate with hydrogen peroxide. This was thoroughly washed with distilled water, and then dried at 110°C for 8 hr in an oven (sample G).

1) M. M. Egorov, V. F. Kiselev, K. G. Krasil'nikov and V. V. Murina, *Zh. Fiz. Khim.*, **33**, 65 (1959).
2) C. M. Hollabaugh and J. J. Chessick, *J. Phys. Chem.*, **65**, 109 (1961).
3) G. J. Young and T. P. Bursh, *J. Colloid Sci.*, **15**, 361 (1960).
4) J. W. Whalen, *Advan. Chem. Ser.*, **33**, 281 (1961).
5) T. Morimoto, K. Shiomi and H. Tanaka, This Bulletin, **37**, 392 (1964).
6) W. H. Wade and N. Hackerman, *J. Phys. Chem.*, **65**, 1681 (1961).
7) T. Morimoto, M. Nagao and T. Omori, This Bulletin, **42**, 943 (1969).
8) T. Morimoto, M. Nagao and M. Hirata, *Kolloid-Z. u. Z. Polymere*, **225**, 29 (1968).

A part of each sample (C and G) was immersed in hot water at 80°C for 3 days to prepare a highly-hydrated sample, which was then dried as before (samples CH and GH).

Surface-area Measurements. The specific surface areas of the samples were measured by applying the BET theory to the nitrogen adsorption data obtained at the temperature of liquid nitrogen, assuming the cross-sectional area of a nitrogen molecule to be 16.2 Å^2.

Heat-of-immersion Measurements. The calorimeter and the technique for the heat-of-immersion measurement were the same as have been described previously.[5,8] The measurement was carried out at 25°C. The sample was treated in an ampoule at a desired temperature for 4 hr in a vacuum of 10^{-5} Torr before the heat-of-immersion measurements. As the heat of breaking of the ampoule was found to be 0.28 J, this was calibrated for the heat-of-immersion data.

Water-content Measurements. The water content of α-Fe_2O_3 was measured by the successive-ignition-loss method[5,8] by using an all-glass apparatus equipped with an oil manometer. As the gases other than water vapor were found to be present in the gas phase evolved at higher temperatures, they were determined by the technique described previously.[7] For instance, the gases other than water vapor which were evolved at 300, 600, and 800°C amounted to 0.10, 0.23, and 0.27 molecules/100 Å^2 for the sample GH. The water-content values given in Fig. 2 are those free from these quantities.

Results and Discussion

The specific surface area of α-Fe_2O_3 is given in Fig. 1 as a function of the temperature of pretreatment. The data show that the surface area of these samples remains unchanged up to about 500—600°C; with a further rise in the temperature, it decreases sharply, indicating a remarkable sintering.

In Fig. 2 the water content of α-Fe_2O_3, represented in OH's/100 Å^2, is plotted against the temperature of pretreatment. Much as in the cases of the other oxides,[5,7,8] the water content of α-Fe_2O_3 decreases steeply until about 400°C, and then it does so very slowly. The hydration treatment has a considerable effect upon the water content, which becomes larger in the sample subjected to a heavy hydration procedure, as was seen in the case of TiO_2.[7]

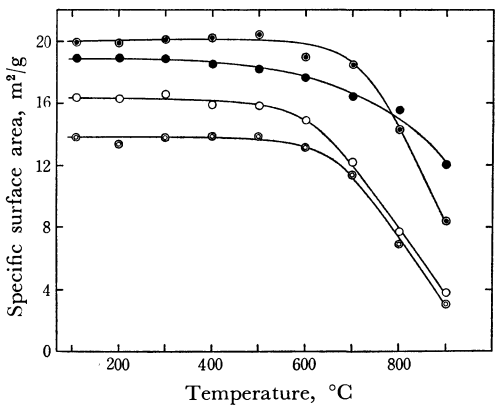

Fig. 1. Dependence of the specific surface area of α-Fe_2O_3 on pretreatment temperature.
○, Sample C; ◎, Sample CH; ●, Sample G; ⊙, Sample GH

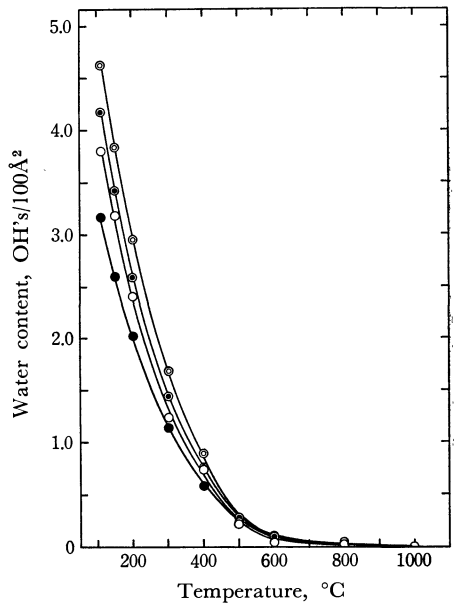

Fig. 2. Water content of α-Fe_2O_3 at various temperatures.
○, C; ◎, CH; ●, G; ⊙, GH

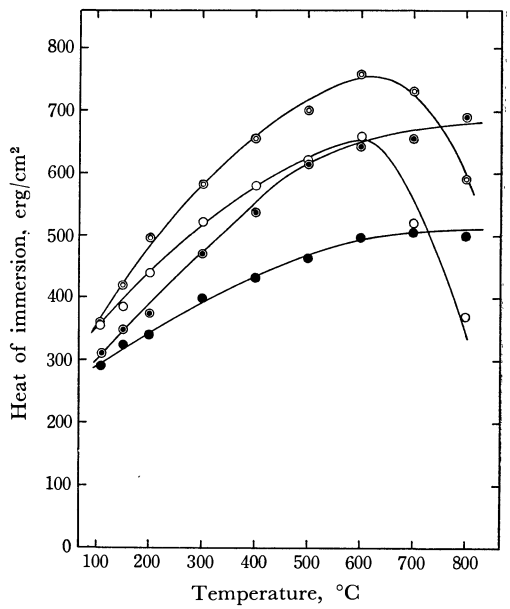

Fig. 3. Dependence of the heat of immersion of α-Fe_2O_3 in water on pretreatment temperature.
○, C; ◎, CH; ●, G; ⊙, GH

Figure 3 shows the relation between the heat of immersion of α-Fe_2O_3 in water and the temperature of pretreatment. It may be seen from Fig. 3 that the heat-of-immersion value is greater in the sample with a large water content resulting from a heavy hydration procedure.

The heat of immersion of the samples C and CH increases initially with a rise in the temperature of pretreatment; it reaches a maximum at 600°C, and then decreases slowly. Such maxima in the heat-of-immersion curve have been reported with such oxides as SiO_2,[3,4] Al_2O_3,[5] TiO_2,[6,7] and ZnO.[8]

On the other hand, the features of the heat-of-immersion curve of the samples G and GH are quite different from those of the former two samples; at first it increases to 600°C, as in the cases of the samples C and CH, but after that the heat-of-immersion value remains almost unchanged, unlike as in the latter cases, and thus no maximum appears. We have never encountered such a situation in which one sample of a substance reveals, and another one does not reveal, a maximum in the heat-of-immersion curve.

The appearance of the maximum in the plot of the heat of immersion of metal oxide in water against the temperature of pretreatment has been explained in terms of the overlapped effect of the chemisoprtion and physical adsorption of water.[3-8] As the temperature of pretreatment rises, the surface hydroxyl groups on metal oxides can be increasingly removed by condensation dehydration.[9,10] When the surfaces thus treated are immersed in water, rehydroxylation will occur on the dehydrated sites. At the same time, the additional heat of reaction will be released together with the heat evolution due to physical interaction between the solid surfaces and the water molecules. At temperatures higher than that of a maximum point, the rehydroxylation on the oxide surface is delayed by the stabilization of the surface oxide structure;[3,5] the higher the temperature, the greater the stabilization. Thus, the contribution of rehydroxylation heat decreases at extremely high temperatures, resulting in a depression of the observed heat of immersion. The fact that the heat-of-immersion curve of the samples G and GH does not reveal a maximum, but only a slow break at almost the same temperature as that of the maximum in the cases of the samples C and CH, indicates that the stabilization of the oxide structure of these samples is not remarkable. The weak stabilization of oxide structure permits a partial rehydroxylation.

Previously the water vapor adsorption isotherms have been investigated on the samples CH and GH.[11] This investigation showed that the amounts of water chemisorbed on the sample CH were 7.59 and 6.73 OH's/100 Å^2 when treated at 600°C and 800°C respectively, whereas on the sample GH it was 7.91 OH's/100 Å^2 in either case. This implies that when the sample is treated at 800°C, the rehydroxylation is incomplete with the sample CH, whereas with the sample GH it is complete; at the same time, this finding substantiates the stabilization theory accounting for the heat-of-immersion anomaly. However, the reason why it is difficult for the stabilization of surface oxide structure to occur on the sample GH has not yet been solved; it may depend on the crystal properties of the sample, which are decided by the origin and the history of the sample.

We can obtain the heat of surface hydration by assuming the complete rehydroxylation of dehydrated sites in the range of lower temperatures of pretreatment than the maximum point. Figure 4 represents the plots of the heat of immersion against the water content of α-Fe_2O_3. The same plotting can be made also for the samples G and GH, as is shown in Fig. 4. The slopes of these plots indicate the heat of formation of surface hydroxyl groups, that is, the heat of surface hydration; the results are tabulated in Table 1.

It can be seen from Table 1 that the heat of surface hydration is almost the same for every sample, being 11.3 kcal/mol H_2O on the average,

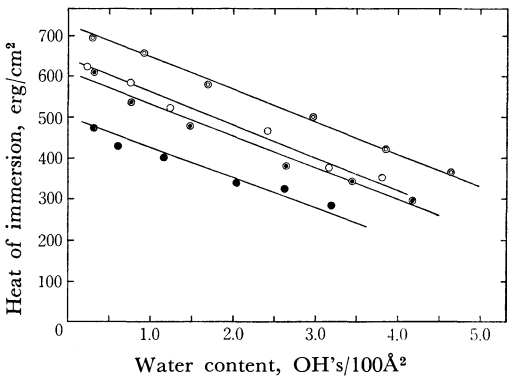

Fig. 4. Relation between the heat of immersion and the water content on α-Fe_2O_3.
○, C; ◎, CH; ●, G; ⊙, GH

TABLE 1. HEAT OF SURFACE HYDRATION OF α-Fe_2O_3 (kcal/mol H_2O)

Sample	C	CH	G	GH
Heat of surface hydration	11.8	11.4	10.3	11.6

9) T. Morimoto, M. Nagao and F. Tokuda, This Bulletin, **40**, 2723 (1967).

10) T. Morimoto, M. Nagao and F. Tokuda, *ibid.*, **41**, 1533 (1968).

11) T. Morimoto, M. Nagao and F. Tokuda, *J. Phys. Chem.*, **73**, 243 (1969).

irrespective of the origin and the history of the sample. This value of heat of surface hydration is quite small compared with the value, 24.2 kcal/mol H_2O, which was obtained for α-Fe_2O_3 by Healey *et al.*[12] by combining the heat-of-immersion data and the water adsorption data. At any rate, neither the preparation nor the hydration treatment of the sample has any serious effect on the heat-of-surface-hydration value, as was in the case with TiO_2.[7] The hydration treatment rather affects the value of the heat of immersion itself, as may be seen in Fig. 3. Thus, it is reasonable to consider that the hydration treatment causes the increased physical interaction between the surfaces of α-Fe_2O_3 and the water molecules, much as with the previous consideration in the case of TiO_2.[7]

12) F. H. Healey, J. J. Chessick and A. V. Fraioli, *ibid.*, **60**, 1001 (1956).

BULLETIN OF THE CHEMICAL SOCIETY OF JAPAN VOL. 42 1493—1497 (1969)

Nonequilibrium Thermodynamics of the Relaxing System Subject to Multinomial Distribution

Kenji ISHIDA

Department of Applied Chemistry, Ibaraki University, Hitachi, Ibaraki

(Received October 17, 1968)

It has been shown that the relaxation process in a system of noninteracting particles in contact with a heat bath, on the assumption that the system is in local equilibrium, can be described by the Markov process homogeneous in time, and that the solution of the Markov process is a multinomial distribution. The nonequilibrium thermodynamics for such a relaxing system was formulated by means of the stochastic entropy production which can be derived by the probabilistic version of classical entropy production. As a sepcial case, the stochastic nonequilibrium thermodynamics for the relaxing system of identical harmonic oscillators was discussed.

The theory of nonequilibrium thermodynamics is applicable to the description of relaxation phenomena in a physical system. As an example, there is an energy transfer between two sub-systems at different temperatures. We consider here a homogeneous system of noninteracting particles immersed in a heat bath. Although the system and the heat bath are thermally insulated as a whole, they are closed to each other so that energy is exchangeable but not so matter. The temporal behavior of the system, which has been initially prepared in a nonequilibrium state, is the relaxation to an equilibrium state through weak interaction with the heat bath. If, furthermore, the heat bath is assumed to be sufficiently large compared with the relaxing system, the former always remains in the equilibrium state characterized by a time-independent temperature $T(\infty)$ throughout the relaxation process. Both relaxing system and heat bath fill the same space with a constant volume, but they are maintained respectively at different temperatures $T(t)$ and $T(\infty)$ at any time t in the course of the relaxation process. According to the theory of nonequilibrium thermodynamic[1,2] the entropy production $\mathrm{d}_i S(t)/\mathrm{d}t$ in the whole system may be written in the form

$$\mathrm{d}_i S(t)/\mathrm{d}t = \{1/T(t) - 1/T(\infty)\}\mathrm{d}U(t)/\mathrm{d}t \qquad (1)$$

where $U(t)$ is the internal energy of the relaxing system. This thermodynamic equation is valid for the nonequilibrium system, in which the existence of local equilibrium is assumed.[3,4] The local equilibrium is one of fundamental postulates in the theory of nonequilibrium theormodynamics and will also play an important role in the present study. For the concept of local equilibrium to be applied without any justification to the stochastic version of (1), we propose that the relaxation in the system where the local equilibrium prevails at each point in the space might, in general, be expected to be a Markov process homogeneous in

1) I. Prigogine, "Introduction to Thermodynamics of Irreversible Processes," 3rd ed., Interscience Publishers, Inc., New York, N. Y. (1967), p. 20.

2) S. R. de Groot, "Thermodynamics of Irreversible Processes," North-Holland Publishing Co., Inc., Amsterdam (1952), p. 51.

3) D. D. Fitts, "Nonequilibrium Thermodynamics," McGraw-Hill Book Co., Inc., New York, N. Y. (1962), p. 21.

4) S. R. de Groot and P. Mazur, "Non-equilibrium Thermodynamics," North-Holland Publishing Co., Inc., Amsterdam (1962), p. 23.

time.[5] If, then, the transitions between energy states of particles in the relaxing system are described by a Markovian master equation with time-independent transition probabilities, the nonequilibrium thermodynamics of the relaxing system may be formulated by the procedure analogous to the stochastic theory of nonequilibrium thermodynamics of chemical kinetics discussed previously.[6]

Stochastic Entropy Production

If the relaxing system consists of N noninteracting particles and the probability for a particle to be found in an energy state ε_l at time t is denoted by $p_l(t)$, the mean energy of the relaxing system, $<E(t)>$, is given by

$$<E(t)> = N\sum_l \varepsilon_l p_l(t) = N<\varepsilon(t)> \quad (2)$$

where $<\varepsilon(t)>=\sum_l \varepsilon_l p_l(t)$ is the mean energy for one particle, because we have assumed the normalization $\sum_l p_l(t)=1$. Since the thermodynamic function $U(t)$ corresponds to $<E(t)>$, the statistical expression of $\mathrm{d}U(t)/\mathrm{d}t$ becomes

$$\mathrm{d}U(t)/\mathrm{d}t = N\sum_l \varepsilon_l \mathrm{d}p_l(t)/\mathrm{d}t \quad (3)$$

under the condition that the volume of the relaxing system is constant. Substituting Eq. (3) into Eq. (1), we obtain

$$\mathrm{d}_i S(t)/\mathrm{d}t = \boldsymbol{k}N\sum_l \{\beta(t)-\beta(\infty)\}\varepsilon_l \mathrm{d}p_l(t)/\mathrm{d}t \quad (4)$$

where $\boldsymbol{k}$ is Boltzmann's constant and the parameter $\beta(t)=1/\boldsymbol{k}T(t)$ has been introduced. In order to reform Eq. (4) into a statistical-thermodynamic expression, it is necessary to find the physical distribution law available to $p_l(t)$.

To do so, first of all, we define $P(n_0, n_1, \cdots, n_l, \cdots; t)\equiv P(\boldsymbol{n}; t)$ to be the probability that at an arbitrarily fixed time t the numbers of particles in the states of energies $\varepsilon_0, \varepsilon_1, \cdots, \varepsilon_l, \cdots$ are $n_0, n_1, \cdots, n_l, \cdots$, respectively. Since, however, the relaxing system assuming local equilibrium is governed by the Markov process homogeneous in time, we can obtain the Markovian master equation for the joint probability distribution $P(\boldsymbol{n}; t)$

$$\mathrm{d}P(\boldsymbol{n}; t)/\mathrm{d}t = \sum_{l'}{}' \sum_l{}' \lambda_{ll'}\{-n_l P(\boldsymbol{n}; t) + (n_l+1)P(\boldsymbol{n}', n_l+1, n_{l'}-1; t)\} \quad (5)$$

where $\lambda_{ll'}$ is the transition probability from ε_l to $\varepsilon_{l'}$ in unit time and the prime of $\sum'$ and $\boldsymbol{n}'$ indicates the omission of the term of $l=l'$. When the initial probability distribution is a multinomial distribution, the solution is also given by the multinomial distribution[7,8]

$$P(\boldsymbol{n}; t) = \{N!/\prod_l n_l!\}\prod_l \{p_l(t)\}^{n_l} \quad (6)$$

where $p_l(t)$, as it has been defined in regard to Eq. (2), denotes the probability for a particle to be found in the energy state ε_l at time t. It has been proved in Refs. 7 and 8 that the unique stationary solution $P(\boldsymbol{n}; \infty)$ exists independently of initial conditions. It can be concluded, therefore, that the multinomial distribution is preserved at all times throughout the Markovian relaxation process. For the system subject to such a stationary probability distribution, Nagasako has given the probabilistic proof that $p_l(\infty)$ can be expressed by the physical distribution law[9]

$$p_l(\infty) = g_l \exp[-\beta(\infty)\varepsilon_l]/\sum_l g_l \exp[-\beta(\infty)\varepsilon_l] \quad (7)$$

where g_l denotes the degeneracy.

Once local equilibrium is established, we can use the method of analysis for a nonequilibrium system with small deviations from equilibrium. We then have the Taylor series expansion of $p_l(t)$ in powers of $\beta(t)$ with only the first-order term

$$p_l(t) = p_l(\infty) + (\partial p_l/\partial\beta)_\infty\{\beta(t)-\beta(\infty)\} \quad (8)$$

because $p_l(t)$ is considered to include $\beta(t)$ as a variable. Since, however, $p_l(t)$ is differentiable with respect to $\beta(t)$, it follows that

$$(\partial p_l/\partial\beta)_\infty = \partial p_l(\infty)/\partial\beta(\infty) = -(\varepsilon_l - <\varepsilon(\infty)>)p_l(\infty)$$

where we have used Eq. (7). We thus obtain as the alternative expression of Eq. (8)

$$p_l(t) = p_l(\infty)[1-\{\beta(t)-\beta(\infty)\}(\varepsilon_l - <\varepsilon(\infty)>)] \quad (8')$$

Substituting Eq. (7) into Eq. (8') and using the approximation $1-\{\beta(t)-\beta(\infty)\}\varepsilon_l = \exp[-\{\beta(t)-\beta(\infty)\}\varepsilon_l]$, we find

$$p_l(t) = \frac{g_l \exp[-\beta(t)\varepsilon_l]}{\sum_l g_l \exp[-\beta(\infty)\varepsilon_l]} + \frac{g_l \exp[-\beta(\infty)\varepsilon_l]}{\sum_l g_l \exp[-\beta(\infty)\varepsilon_l]}\{\beta(t)-\beta(\infty)\}<\varepsilon(\infty)>$$

By using the similar approximations

$$\exp[-\beta(\infty)\varepsilon_l] = \exp[-\beta(t)\varepsilon_l]\{1+[\beta(t)-\beta(\infty)]\varepsilon_l\}$$

and

$$\sum_l g_l \exp[-\beta(\infty)\varepsilon_l] = \sum_l g_l \exp[-\beta(t)\varepsilon_l]\{1+[\beta(t)-\beta(\infty)]<\varepsilon(\infty)>\}$$

the above equation can be transformed to

$$p_l(t) = \frac{g_l \exp[-\beta(t)\varepsilon_l]}{\sum_l g_l \exp[-\beta(t)\varepsilon_l]} \times [1-\{\beta(t)-\beta(\infty)\}^2(\varepsilon_l - \langle\varepsilon(\infty)\rangle)\langle\varepsilon(\infty)\rangle]$$

5) W. Feller, "An Introduction to Probability Theory and its Applications," 2nd ed., John Wiley & Sons, Inc., New York, N. Y. (1957), p. 400.

6) K. Ishida, *J. Phys. Chem.*, **70**, 3806 (1966); **72**, 92 (1968).

7) A. J. F. Siegert, *Phys. Rev.*, **76**, 1708 (1949). See also I. M. Krieger and P. J. Gans, *J. Chem. Phys.*, **32**, 247 (1960).

8) P. M. Mathews, I. I. Shapiro and D. L. Falkoff, *Phys. Rev.*, **120**, 1 (1960).

9) N. Nagasako, This Bulletin, **35**, 179 (1962).

To the same linear approximation as Eq. (8), we finally obtain

$$p_l(t) = g_l \exp[-\beta(t)\varepsilon_l]/\sum_l g_l \exp[-\beta(t)\varepsilon_l] \quad (9)$$

For the relaxing system governed by the multinomial distribution (6), that is to say, the Maxwell-Boltzmann distribution (9) characterized by a time-dependent parameter $\beta(t)$ is also approximately preserved throughout the relaxation process. The nonequilibrium system in which the distribution law (9) is held for $0 \leq t \leq \infty$ has been called the canonically invariant system by Andersen *et al.*[10] They have investigated under what conditions a relaxing system is canonically invariant and have formulated the nonequilibrium thermodynamics for this system.

We can, however, derive the stochastic expression for the thermodynamic equation (1) on the postulate that the Markovian master equation (5) is a mathematical description of the relaxation process of the system in local equilibrium. From Eqs. (4), (7) and (9) we obtain

$$\begin{aligned} \mathrm{d}_i S(t)/\mathrm{d}t &= -\boldsymbol{k}N \sum_l \mathrm{d}p_l(t)/\mathrm{d}t \ln[p_l(t)/p_l(\infty)] \\ &= -\boldsymbol{k} \sum_l \mathrm{d}<n_l(t)>/\mathrm{d}t \ln[p_l(t)/p_l(\infty)] \end{aligned} \quad (10)$$

which is none other than the stochastic expression of Eq. (1). Of course, the non-negativity of entropy production, $\mathrm{d}_i S(t)/\mathrm{d}t \geq 0$, must also be satisfied for Eq. (10).[11] The integration of Eq. (10) becomes

$$\begin{aligned} S(t) &= -\boldsymbol{k} \sum_l <n_l(t)> \ln[p_l(t)/p_l(\infty)] + S_e \\ &= -\boldsymbol{k} <\ln \Pi_l [p_l(t)/p_l(\infty)]^{n_l}> + S_e \end{aligned} \quad (11)$$

where S_e denotes the value of the entropy at equilibrium. This equation shows that for the relaxing system the entropy is also correlated with the probability for a microscopic state of its system. If, on the contrary, we begin with Eq. (11) as the definition of the stochastic entropy for a relaxing system, we obtain the entropy production (1) through the distribution laws (7) and (9). Since the mean $<>$ in Eq. (10) is operated with respect to the probability distribution $P(\boldsymbol{n}; t)$, equation (11) may be written as

$$S(t) = -\boldsymbol{k} \sum_{\boldsymbol{n}} P(\boldsymbol{n}; t) \ln \frac{P(\boldsymbol{n}; t)}{P(\boldsymbol{n}; \infty)\Omega} \quad (12)$$

where we have set $S_e = \boldsymbol{k} \ln \Omega$. It should be noted, here, that the probability distribution is in form invariant on the assumption of local equilibrium. It is also possible to develop the nonequilibrium satatistical thermodynamics on the basis of the Eq. (12), which is called the Gibbs entropy postulate.[12]

Relaxation Equations

To obtain a better understanding of relaxation phenomena, we now return to the alternative equation of Eq. (1),

$$\mathrm{d}_i S(t)/\mathrm{d}t = 1/T(\infty)\{\beta(t)/\beta(\infty) - 1\} \mathrm{d}<E(t)>/\mathrm{d}t \quad (1')$$

Taking $1/T(\infty)\{\beta(t)/\beta(\infty) - 1\}$ as force, we see that the corresponding flux is $\mathrm{d}<E(t)>/\mathrm{d}t$. We then have, as a phenomenological relation,

$$\mathrm{d}<E(t)>/\mathrm{d}t = L/T(\infty)\{\beta(t)/\beta(\infty) - 1\} \quad (13)$$

where L is called the phenomenological coefficient. On the other hand, it follows from $\mathrm{d}<E(t)>/\mathrm{d}t = \sum_l \varepsilon_l \mathrm{d}<n_l(t)>/\mathrm{d}t$ and Eq. (A. 2) that the rate of energy change is given by

$$\mathrm{d}<E(t)>/\mathrm{d}t = N \sum_l{}' \sum_{l'}{}' \varepsilon_l \{\lambda_{l'l} p_{l'}(t) - \lambda_{ll'} p_l(t)\}$$

where $\langle n_l(t) \rangle = N p_l(t)$ has been used. We then have

10) H. C. Andersen, I. Oppenheim, K. E. Shuler and G. H. Weiss, *J. Math. Phys.*, **5**, 522 (1964); *J. Chem. Phys.*, **41**, 3012 (1964).

11) If we rewrite Eq. (10) in the form

$$\mathrm{d}_i S(t)/\mathrm{d}t = -\boldsymbol{k} \sum_l \mathrm{d}<n_l(t)>/\mathrm{d}t \ln [<n_l(t)>/<n_l(\infty)>] \quad (A.1)$$

and substitute the rate equation derived from Eq. (5)

$$\mathrm{d}\langle n_l(t)\rangle/\mathrm{d}t = \sum_{l'}{}' \{\lambda_{l'l}\langle n_{l'}(t)\rangle - \lambda_{ll'}\langle n_l(t)\rangle\} \quad (A.2)$$

into Eq. (A.l), we have

$$\mathrm{d}_i S(t)/\mathrm{d}t = -\boldsymbol{k} \sum_l{}' \sum_{l'}{}' \{\lambda_{l'l} <n_{l'}(t)> - \lambda_{ll'} <n_l(t)>\} \ln [<n_l(t)>/<n_l(\infty)>] \quad (A.3)$$

Since, however, this equation is symmetric with respect to l and l', we also have

$$\mathrm{d}_i S(t)/\mathrm{d}t = -\boldsymbol{k} \sum_{l'}{}' \sum_l{}' \{\lambda_{ll'} <n_l(t)> - \lambda_{l'l} <n_{l'}(t)>\} \ln [<n_{l'}(t)>/<n_{l'}(\infty)>] \quad (A.3')$$

The summation of Eqs. (A.3) and (A.3') leads to

$$\begin{aligned} \mathrm{d}_i S(t)/\mathrm{d}t = -\frac{1}{2} \boldsymbol{k} \sum_l{}' \sum_{l'}{}' \lambda_{ll'} <n_{l'}(t)> \{\lambda_{l'l}/\lambda_{ll'} - <n_l(t)>/<n_{l'}(t)>\} \\ \times \ln\{[<n_l(t)>/<n_{l'}(t)>]/[<n_l(\infty)>/<n_{l'}(\infty)>]\} \end{aligned} \quad (A.4)$$

Using the relation

$$\lambda_{l'l} <n_{l'}(\infty)> = \lambda_{ll'} <n_l(\infty)>$$

which is satisfied at equilibrium, we finally obtain

$$\begin{aligned} \mathrm{d}_i S(t)/\mathrm{d}t = -\frac{1}{2} \boldsymbol{k} \sum_l{}' \sum_{l'}{}' \lambda_{ll'} <n_{l'}(t)> \{<n_l(\infty)>/<n_{l'}(\infty)> - <n_l(t)>/<n_{l'}(t)>\} \\ \times \ln\{[<n_l(t)>/<n_{l'}(t)>]/[<n_l(\infty)>/<n_{l'}(\infty)>]\} \end{aligned} \quad (A.5)$$

Since $(y-x)\ln(x/y) \leq 0$ for any real numbers $x > 0$ and $y > 0$, it is concluded that $\mathrm{d}_i S(t)/\mathrm{d}t \geq 0$, where the equality holds for equilibrium state.

12) See Ref. 4, p. 126.

$$\mathrm{d}<E(t)>/\mathrm{d}t = \frac{1}{2}N\sum_{l}{}'\sum_{l'}{}'(\varepsilon_l-\varepsilon_{l'}) \times\{\lambda_{l'l}p_{l'}(t)-\lambda_{ll'}p_l(t)\}$$

The derivation is exactly analogous to that of Eq. (A.4). Substituting the linear approximation Eq. (8) into this equation and using the detailed balance $\lambda_{l'l}p_{l'}(\infty)=\lambda_{ll'}p_l(\infty)$, we obtain

$$\mathrm{d}<E(t)>/\mathrm{d}t = \frac{1}{2}N\beta(\infty)\sum_{l}{}'\sum_{l'}{}'\lambda_{l'l}(\varepsilon_l-\varepsilon_{l'})^2p_{l'}(\infty) \times\{\beta(t)/\beta(\infty)-1\}$$

We thus see by comparison of this equation with Eq. (13) that

$$L = N/2\boldsymbol{k}\sum_{l}{}'\sum_{l'}{}'\lambda_{l'l}(\varepsilon_l-\varepsilon_{l'})^2p_{l'}(\infty) \tag{14}$$

from which it follows that $L\geq 0$.

Let us now derive the relaxation equations for $<E(t)>$ and $\beta(t)$. The mean energy $<\varepsilon(t)>$ for particle is obtained through Eq. (8), namely,

$$<\varepsilon(t)> = <\varepsilon(\infty)>-\beta(\infty)\{\beta(t)/\beta(\infty)-1\} \times(<\varepsilon^2(\infty)>-<\varepsilon(\infty)>^2)$$

From this we obtain for the relaxing system

$$\beta(t)/\beta(\infty)-1 = -(1/\beta(\infty)\sigma_E{}^2)(<E(t)>-<E(\infty)>) \tag{15}$$

where the fluctuation of total energy, $\sigma_E{}^2=\langle E^2(\infty)\rangle-\langle E(\infty)\rangle^2=N(\langle\varepsilon^2(\infty)\rangle-\langle\varepsilon(\infty)\rangle^2)$, is connected with the specific heat at constant volume, C_v, by the relation $\sigma_E{}^2=\boldsymbol{k}T^2(\infty)C_v=-(\partial\langle E(t)\rangle/\partial\beta(t))_{v,\infty}$. From Eqs. (13) and (15), we find the following relaxation equations.

For energy:

$$\mathrm{d}<E(t)>/\mathrm{d}t = -(1/\tau)(<E(t)>-<E(\infty)>) \tag{16}$$

For temperature:

$$\mathrm{d}\beta(t)/\mathrm{d}t = -(1/\tau)\{\beta(t)-\beta(\infty)\} \tag{17}$$

where the relaxation time τ is given by

$$\tau = \sigma_E{}^2/L\boldsymbol{k} = T^2(\infty)C_v/L$$

System of Harmonic Oscillators

To illustrate the nonequilibrium thermodynamics of a relaxing system in weak interaction with a heat bath, we now consider the system of N independent and identical harmonic oscillators whose vibrational relaxations are described by the Markov processes with Landau-Teller transition probabilities in contact with a heat bath.[13] As it will be shown below, this system is a typical one of canonically invariant systems. Let the initial probability distribution $P(\boldsymbol{n}^0;0)$ at a temperature $T(0)$ be given by the multinomial distribution

$$P(\boldsymbol{n}^0;0) = (N!/\prod_j n_j{}^0!)\prod_j\{p_j(0)\}^{n^0j} \tag{18}$$

where $p_j(0)$ denotes the probability for an oscillator to be found on a vibrational level j at time $t=0$, $n^0{}_j$ is the number of such oscillators and $\sum_j n^0{}_j=N$. It follows then that at any time t the probability distribution $P(\boldsymbol{n};t)$ is also multinomial,

$$P(\boldsymbol{n};t) = (N!/\prod_j n_j!)\prod_j\{p_j(t)\}^{n_j} \tag{19}$$

In both Eqs. (18) and (19), the probability $p_j(t)$ for $0\leq t\leq\infty$ takes the familiar form

$$p_j(t) = \exp[-j\theta(t)](1-\exp[-\theta(t)]) \tag{20}$$

where $j=0, 1, 2,\cdots$. The time-dependent parameter $\theta(t)$ is given by

$$\theta(t) = \ln\frac{\mathrm{e}^{\theta(\infty)}(1-\mathrm{e}^{-\theta(0)})-(1-\mathrm{e}^{\theta(\infty)-\theta(0)})\mathrm{e}^{-ct}}{(1-\mathrm{e}^{-\theta(0)})-(1-\mathrm{e}^{\theta(\infty)-\theta(0)})\mathrm{e}^{-ct}} \tag{21}$$

where $T(0)$ and $T(\infty)$ in $\theta(0)=h\nu/\boldsymbol{k}T(0)$ and $\theta(\infty)=h\nu/\boldsymbol{k}T(\infty)$ are the temperature at the initial and equilibrium states, respectively, and the reciprocal of $c>0$ denotes the relaxation time (*cf.* Eq. (27)). If we introduce conventionally the relation

$$\theta(t) = \boldsymbol{h}\nu/\boldsymbol{k}T(t) \tag{22}$$

where $\boldsymbol{h}$ is Planck's constant and ν the vibrational frequency of oscillator, we can regard $T(t)$ as the effective temperature of the relaxing system at time t. Since Eq. (19), together with Eq. (20), preserves its form all the time during the relaxation process, the relaxing system is exactly of canonical invariance.

Substituting Eq. (20) into the general formula (10) of stochastic entropy production, we obtain

$$\mathrm{d}_iS(t)/\mathrm{d}t = \boldsymbol{k}N\{\theta(t)-\theta(\infty)\}\sum_j j\,\mathrm{d}p_j(t)/\mathrm{d}t \tag{23}$$

or

$$\mathrm{d}_iS(t)/\mathrm{d}t = \boldsymbol{k}\sum_j j\{\theta(t)-\theta(\infty)\}\mathrm{d}<n_j(t)>/\mathrm{d}t \tag{23'}$$

where $\langle n_j(t)\rangle=Np_j(t)$ is the mean number of oscillators on vibrational level j. Since, however, the mean energy of oscillator is given by

$$\langle\varepsilon_v(t)\rangle = \left\{\frac{1}{2}+\sum_j j\,p_j(t)\right\}\boldsymbol{h}\nu \tag{24}$$

it follows that for the total energy

$$(1/\boldsymbol{h}\nu)\mathrm{d}<E_v(t)>/\mathrm{d}t = N\sum_j j\,\mathrm{d}p_j(t)/\mathrm{d}t \tag{25}$$

Thus, the thermodynamic expression of Eq. (25) becomes

$$\mathrm{d}_iS(t)/\mathrm{d}t = \{1/T(t)-1/T(\infty)\}\mathrm{d}<E_v(t)>/\mathrm{d}t \tag{26}$$

which represents the entropy production due to the energy transfer between the system of oscillators and the heat bath. We must here point out the following. The microscopic reversibility for the transition probabilities between adjacent vibrational energy levels has been assumed in the derivation of the Markovian master equation, from which the probability distribution (19) has been obtained. From a macroscopic point of view, we may reckon for such a statement to correspond to the assumption of the existence of local equilibrium such as

13) E. W. Montroll and K. E. Shuler, *J. Chem. Phys.*, **26**, 454 (1957). See also Refs. 8 and 10.

we have already emphasized.

If we apply $\sum_j jp_j(t) = \exp[-\theta(t)](1-\exp[-\theta(t)])^{-1}$ and Eq. (21) to the right-hand side of Eq. (25), we get the relaxation equation of exponential type, after straightforward algebra,

$$d<E_v(t)>/dt = -c(<E_v(t)> - <E_v(\infty)>) \quad (27)$$

which holds rigorously for any time t. It can be easily seen from Eq. (21), however, that the relaxation process of temperature $T(t)$ is not of exponential type but so near equilibrium.[14]

On the other hand, taking the logarithm of Eq. (20), we have

$$j\{\theta(t)-\theta(\infty)\} = \ln(<n_0(t)>/<n_0(\infty)>) - \ln(<n_j(t)>/<n_j(\infty)>)$$

where $p_0(t) = 1-\exp[-\theta(t)]$ and $p_0(\infty) = 1-\exp[-\theta(\infty)]$ have been used. If we set $d\langle n_j(t)\rangle/dt = v_j$ and define the affinity A_j for the transition between two vibrational energy levels 0 and j by

$$A_j = kT(\infty)\{\ln(<n_0(t)>/<n_0(\infty)>) - \ln(<n_j(t)>/<n_j(\infty)>)\} \quad (28)$$

we obtain from Eq. (23) the entropy production in the form of the sum of products of affinities and rates

$$d_iS(t)/dt = (1/T(\infty))\sum_j A_jv_j \quad (29)$$

This may be also interpreted as the entropy production due to the irreversible processes corresponding to the changes of the internal parameter j.[15]

14) See Ref. 13.
15) See Ref. 1, p. 36.

BULLETIN OF THE CHEMICAL SOCIETY OF JAPAN VOL. 42 1497—1503 (1969)

Spectroscopic Behavior of Würster's Blue Perchlorate and *N*-Ethylphenazyl Crystals

Tadayoshi SAKATA and Saburo NAGAKURA

The Institute for Solid State Physics, The University of Tokyo, Roppongi, Minato-ku, Tokyo

(Received October 19, 1968)

The electronic absorption spectra of Würster's Blue perchlorate and *N*-ethylphenazyl in solid were measured at various temperatures ranging from 48°K to 300°K. In both cases, strong bands due to the charge-transfer between the half occupied orbitals of respective component radicals were observed in near infrared region. This assignment of these bands was supported by the polarized absorption measurement carried out with the Würster's blue perchlorate single crystal. The charge-transfer band of solid Würster's blue perchlorate was found to increase its intensity with decreasing temperatures; in particular, the increasing tendency became predominant below the phase transition point (186°K). The similar tendency was also observed for solid *N*-ethylphenazyl. The temperature dependence of the band was found to be closely related with the population of triplet excitons determined from the measurement of magnetic susceptibility or paramagnetic resonance. The separation J between the ground singlet state and the thermally accessible triplet state was determined from the analysis of the temperature dependence of the charge-transfer band to be 235 cm^{-1} and 320 cm^{-1} for Würster's blue perchlorate and *N*-ethylphenazyl, respectively.

The electronic absorption spectra of Würster's blue perchlorate (WBP) and *N*-ethylphenazyl (EP) have been studied extensively with their solutions.[1-3] In solution the spectra due to the monomers were observed at room temperature, but at low temperature new bands characteristic of the dimers were found in the near infrared region. Hausser and Murrell[2] interpreted them as the charge-transfer band between the half occupied orbitals of component radicals. From temperature and concentration dependencies of electronic absorption spectra, the enthalpy change due to the dimer formation was determined by Ooshika *et al.*[1] and by Hausser[3] to be about 5—8 kcal/mol and 2 kcal/mol for WBP and EP, respectively.

Hausser measured the static magnetic susceptibility of solid EP at three temperatures and found that the value becomes lower with decreasing

1) K. Uemura, S. Nakayama, Y. Seo, K. Suzuki and Y. Ooshika, This Bulletin, **39**, 1348 (1966); A. Kawamori, A. Honda, N. Joo, K. Suzuki and Y. Ooshika, *J. Chem. Phys.*, **44**, 4363 (1966).

2) K. Hausser and J. N. Murrell, *J. Chem. Phys.*, **27**, 500 (1957).

3) K. H. Hausser, *Z. Naturforsch.*, **11a**, 20 (1956).

temperatures.[2,3]

The paramagnetic resonance of the single crystal of WBP has been studed by McConnel *et al.*[4] They found the paramagnetic resonance signal due to triplet excitons for the WBP crystal below the orthorhombic (room temperature form) - monoclinic (low temperature form) phase transition point at 186°K. Furthermore, the sudden decrease in paramagnetic susceptibility was observed by several authors[5] with WBP at this point. These facts show that the cations form dimers in the WBP crystal of the low temperature (monoclinic) form resulting in the ground singlet state and the excited triplet state.[4] These two states may be thought to be brought about by the exchange interaction between the two cations in the monoclinic crystal. The singlet-triplet separation J was estimated to be $246\pm20\ cm^{-1}$ by McConnell *et al.* from the temperature dependence of ESR intensity.[4]

Under these circumstances, we have undertaken to study in detail the optical properties of the WBP and EP crystals at various temperatures in addition to their magnetic properties. One of our main purpose is to clarify the existence of the triplet exciton from electronic absorption measurements at various temperatures ranging from 50°K to 300°K.

Experimental

WBP and EP were prepared and purified by the same methods as described in Refs. 6 and 7, respectively. The purified sample of EP was kept at −70°C because it was fragile at room temperature.

A Cary recording spectrophotometer model 14 M was used for the measurements of electronic absorption spectra of solutions and solid samples. The solid films for absorption measurements were prepared by coating powdered samples on quartz plates by a stainless steel spatula. The solid samples prepared in this way were shown to be suitable for the measurements of absorption spectra in the near infrared and visible regions. The reliability of this method was checked by comparing the spectra of solid thin films with those observed with single crystals by the aid of a microspectrophotometer. For example, the electronic absorption spectra of tetracyanobenzene and of the naphthalene-tetracyanobenzene complex observed by the present method agree well with those observed with the respective single crystals.[8] Absorption measurements at low temperatures were made by using ordinary glass Dewar vessels containing liquid helium or liquid nitrogen as refrigerant.

A spectrophotometer attached with a microscope and a Roschen type polarizer[9] was used for the polarized absorption measurement of a single crystal.

ESR spectra were measured with a Hitachi X band spectrometer with 100kc field modulation.

Results and Discussion

Polarized Absorption Spectra of WBP. The electronic absorption spectra of the solid WBP measured at various temperatures are shown in Fig. 1. In this figure, the spectra of the ethanol solution of WBP measured at various temperatures are also shown for the purpose of comparison. Figure 1 shows that the absorption spectra of the solution and solid samples at room temperature are similar to each other[10] except for the fact that the latter exhibits a weak absorption in the near

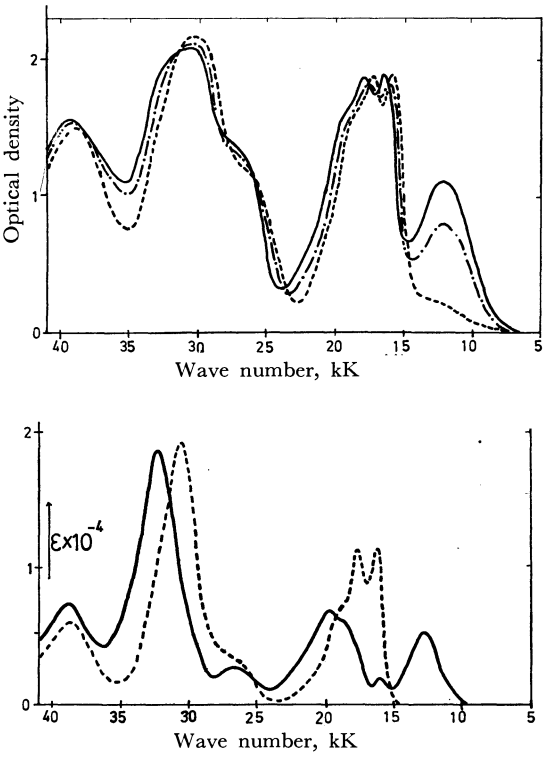

Fig. 1. Absorption spectra of WBP ($(CH_3)_2N$-⊕-$N(CH_3)_2 \cdot ClO_4^-$) at various temperatures.
upper part; in solid, —— 48°K, - - - 100°K, ---- 300°K
lower part; in ethanol solution, —— 110°K, ---- 295°K

4) D. D. Thomas, H. Keller and H. M. McConnell, *J. Chem. Phys.*, **39**, 2321 (1963).

5a) K. Okumura, *J. Phys. Soc. Japan*, **18**, 69 (1963). b) W. Duffy, Jr., *J. Chem. Phys.*, **36**, 490 (1962).

6) L. Michaelis and S. Granick, *J. Am. Chem. Soc.*, **65**, 1747 (1943).

7) H. MacIlwain, *J. Chem. Soc.*, **1937**, 1710.

8) In the ultraviolet region, the scattering of incident light was found to give some effect to the observed intensity, although the observed peak wavelengths were correct.

9) J. Tanaka, This Bulletin, **36**, 833 (1963).

10) The absorption bands in solid show the red shift of about 700 cm^{-1} compared with the corresponding bands of the solution.

infrared region longer than 700 mμ. This weak band observed for the solid sample is intensified with decreasing temperatures and its maximum wavelength corresponds well to the charge-transfer band of the radical dimer observed by Hausser[2,3] with the solution at low temperature. Therefore, it can be regarded as the band caused by the charge-transfer interaction between the WB cations in crystal.

In order to give an additional support to this interpretation, we measured the polarized absorption spectrum of the single crystal of WBP at room temperature. The results are shown in Fig. 2. The actual measurements were made by light polarized parallel to the a′ and c′ direction of the crystal shown in Fig. 3. The used crystal is a flat plate and shows the straight extinction under a polarizing microscope. This means that at least one crystal axis is on the observed plane, because the room temperature form of WBP is orthorhombic.[4] Furthermore, from the X-ray diffraction experiment,

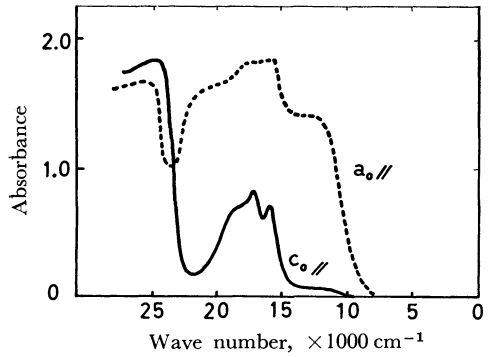

Fig. 2. Polarized absorption spectrum of the single crystal of WBP at room temperature.

the a′ c′ plane was determined to be the a_0c_0 plane.*1. On the basis of the crystal structure shown in Fig. 3, let us consider the polarization of the band near 600 mμ which can be assigned to the $^2B_{3g} \rightarrow {}^2B_{1u}$ transition of the free radical cation whose transition moment is parallel with its long molecular axis connecting the two nitrogen atoms.[11,12] This band can be expected to split into the two components parallel to a_0 and c_0 axes with the intensity ratio of $I_{//a_0} : I_{//c_0} = [\tan(90°-37.5°)]^2 : 1 = 1.7 : 1$, in the approximation of the oriented gas model. According to our measurement, this band has the maximum and minimum intensities in the directions parallel to the a′ and c′ axes, respectively, and the dichroic ratio was determined to be $I_{//a'} : I_{//c'} = 2.2 : 1$. This means that a′ and c′ axes correspond to a_0 and c_0 axes, respectively.

As is clearly seen in Fig. 2, the characteristic band which appears in the wavelength region longer than 700 mμ has the transition moment parallel to the a′ (a_0) direction. This seems to support the interpretation that the band is accompanied by the charge-transfer between the half occupied orbitals of the component radicals, in view of the fact that the line connecting their centers is parallel to a′ (a_0) axis.

Temperature Dependence of Charge-Transfer Band. *a) WBP.* In order to check the variation of the absorption spectrum above and below the phase transition point at 186°K, we measured the absorption spectrum of solid WBP at various temperatures ranging from 48°K to 300°K. The results are shown in Fig. 1. From this figure it is concluded that with lowering temperature the charge-transfer band increases its intensity and other bands due to the excitation within the radical

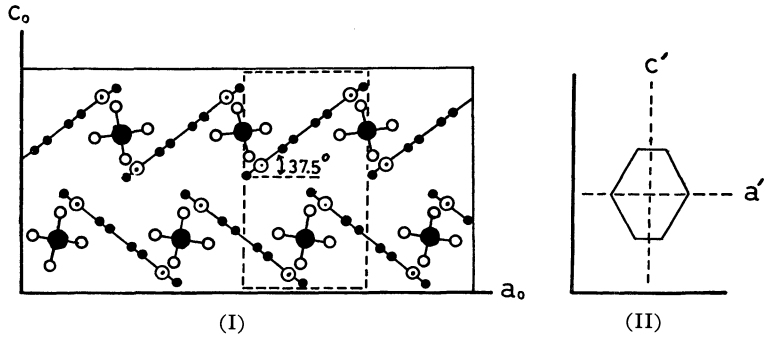

Fig. 3. I. Projection of the orthorhombic structure of WBP onto the a_0c_0 plane. ● Cl, ⊙ N, ○ O, • C
II. Rough sketch of the single crystal of WBP used for the polarized absorption spectrum measurement. a′ and c′ are extinction positions.

*1 We are indebted to Mr. Y. Oohashi of our Institute for his help in performing the X-ray diffraction experiment.

11) A. D. Albrecht and W. T. Simpson, *J. Am. Chem. Soc.*, **77**, 4461 (1955).
12) M. Goeppert-Mayer and K. J. McCallum, *Rev. Mod. Phys.*, **14**, 248 (1942).

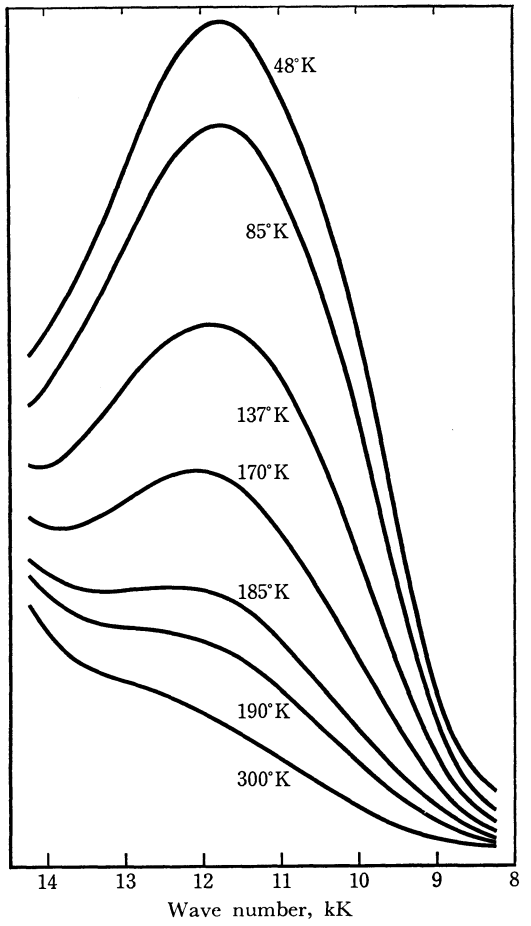

Fig. 4. The charge-transfer band of WBP at various temperatures.

cation leave their intensities almost unaltered, though their peaks shift by 700—800 cm^{-1} by changing the temperature from 300°K to 48°K.

We measured very carefully and precisely the temperature dependence of the intensity of the charge-transfer band, with the result shown in Fig. 4. This figure clearly shows that the intensity increase becomes suddenly remarkable below phase transition point. Since the dimer may be the unit in the WBP crystal below the phase transition point,[4] the observed sudden increase in absorption intensity may be thought to be due to the radical dimer formation. The details of this point are discussed in the later part in comparison with the temperature dependence of the magnetic properties.

The charge-transfer band of the WBP crystal shifts to longer wavelengths by about 1000 cm^{-1} than that of the dimer in solution. The same tendency was observed for EP. This shift may be explained qualitatively by considering the interaction between the induced transition dipoles of adjacent dimers.

b) EP. The electronic absorption spectra of EP in ethanol-ether solution and in solid are shown in Fig. 5. Concerning the solution spectrum, there appears no absorption in the near infrared region at room temperature, but at low temperature a charge-transfer band due to the dimer appears at 800 mμ.[3] The spectrum of solid EP well coincides as a whole with that of dimer in solution, although the charge-transfer band in the former appears at 900 mμ and therefore shifts by 1600cm^{-1} to lower frequencies compared with that in the latter.

The absorption spectrum of solid EP was measured at various temperatures ranging from 300°K to 55°K with the result shown in Fig. 6. The charge-transfer band of solid EP greatly increases its intensity with lowering temperature and this intensity increment becomes saturated at about 50°K. This temperature dependency is similar

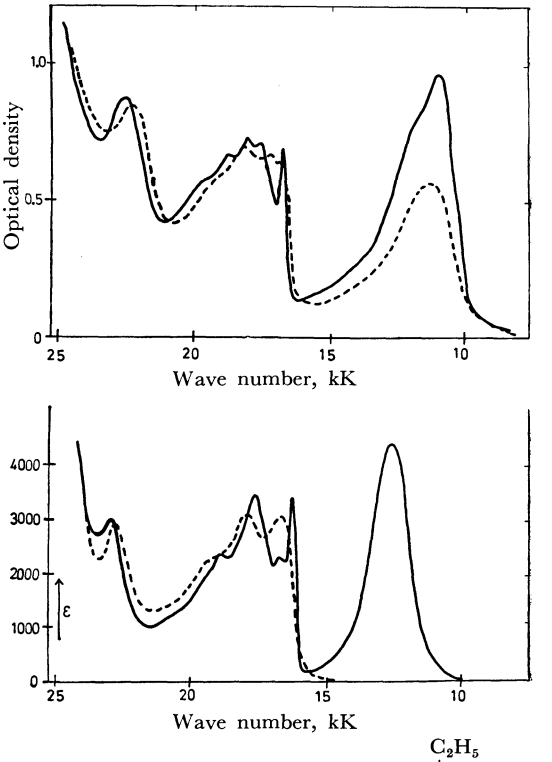

Fig. 5. Absorption spectra of EP 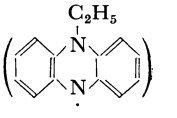

at low and high temperatures.
upper part; in solid, —— 50°K, ---- 275°K
lower part; in ethanol(2)-ether(1) solution,
—— 110°K, - - - 295°K

13) As is clearly seen in Figs. 5 and 6, the charge-transfer band is composed of two peaks in the solid sample of EP, while the solution spectrum shows only one peak. This splitting may be due to either Davydov splitting or vibrational structure.

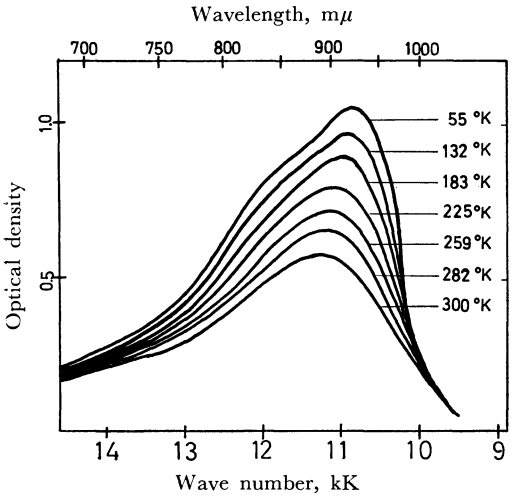

Fig. 6. The charge-transfer band of EP at various temperatures.

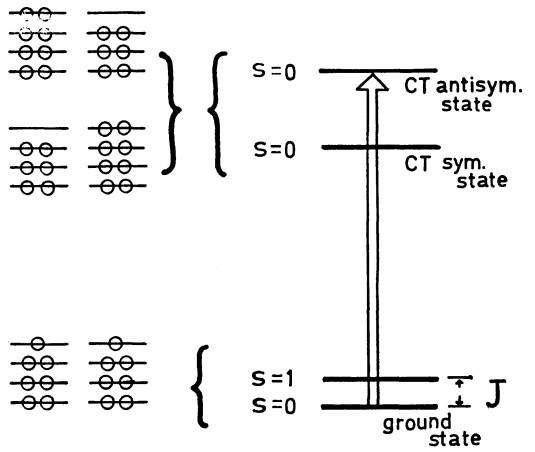

Fig. 7. Energy diagram and configurations of a radical dimer.

to that observed for the low temperature form of WBP crystal. This suggests that dimers are the unit in the EP crystal as well as in the WBP crystal below the phase transition point.[14]

The Relation Between the Temperature Dependence of Charge-Transfer Band and Magnetism. Now let us consider the reason why the charge-transfer band increases remarkably its intensity with the decreasing temperature for the WBP crystal below the phase transition point and for the EP crystal. This anomalous phenommenon can be explained by considering the existence of the thermally accessible triplet excitons in these crystals.

As described above, the radical dimer may be considered to be the unit of the structure in these crystals.[15] In the radical dimer a singlet state and a triplet state may be caused as the result of the exchange interaction between the two radical monomers of the doublet state. In the cases of WBP and EP the singlet state may conceivably be lower than the triplet state; that is to say, the ground state is singlet and the triplet excited state exists above it with the energy separation J whose magnitude is of the same order as the thermal energy kT.

The singlet triplet separation J may be considered, as in general, to be originated from the exchange interaction between two unpaired electrons in the half occupied orbitals of the component radicals. Furthermore, above the triplet state of the radical dimer, there exists the charge-transfer state which corresponds to the electron transfer between the half occupied orbitals of the component radicals. The energy diagram of this dimer is schematically shown in Fig. 7. The dimer is assumed to have a center of symmetry, as is thought to be the case in WBP and EP. When the dimer has a center of symmetry, there are two charge-transfer states, a symmetric one and an antisymmetric one; the latter is higher than the former[2] and the transition from the ground singlet state to the latter is allowed for the sandwich type dimer.

Since the charge-transfer band is observed in the near infrared region for both WBP and EP, the energy separation between the charge-transfer state and the singlet ground state may be considered to be small. From this it may be inferred that the mixing of these two states stabilizes the singlet ground state and contributes to some extent to the singlet triplet separation J.[16] However, from an analogy with the case of the hydrogen molecule the main contribution to J might be considered to be still the exchange interaction between the two unpaired electrons.[17]

On the basis of the energy level diagram shown in Fig. 7, we consider the mechanism of the temperature dependence of the absorption intensity. When a dimer is in the ground singlet state, the transition to the antisymmetric charge-transfer state is allowed, but when a dimer is in a thermally accessible triplet state the transition is forbidden from the spin multiplicity. Furthermore, as is clear from the electron configuration shown in Fig. 7, the corresponding charge-transfer triplet state does not exist. Therefore the intensity of the charge-transfer band may be considered to be propor-

14) The EP crystal has no phase transition between room temperature and 50°K.

15) The situation is the same for the solid samples with which the temperature dependence of the absorption intensity was actually measured, because they are composed of the micro crystals.

16) H. M. McConnell, "Molecular Biophysics," ed. by B. Pullman and M. Weissbluth, Academic Press, New York (1965), p. 311.

17) The authors would like to express their sincere thanks to Professor R. S. Mulliken for his valuable suggestion on this point.

tional to the number of dimers in the ground singlet state. Neglecting the interaction between dimers, the populations of the ground singlet and excited triplet states may be assumed to follow the Boltzmann distribution law. When J is of the order of magnitude of thermal energy kT, the intensity of the charge-transfer band may be expected to be strongly dependent on temperature and the change in the charge-transfer band intensity with temperature may be regarded as the measure of the number of dimers in the thermally accessible triplet state (see Fig. 8). When we consider the crystal which is an assembly of dimers, their excited states must be replaced by a exciton traveling among them. However, the preceding discussion may still be approximately applicable.

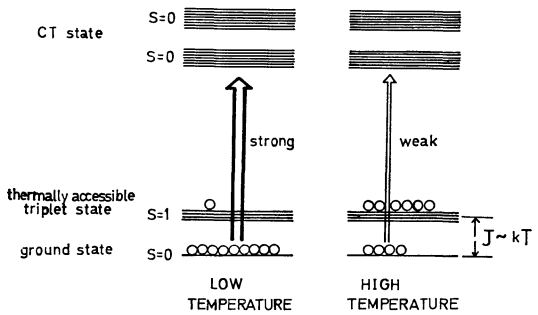

Fig. 8. A schematic explanation of the temperature dependence of charge-transfer band intensity in the solid. An arrow shows an allowed charge-transfer transition. Circles represent schematically the number of dimers of each state.

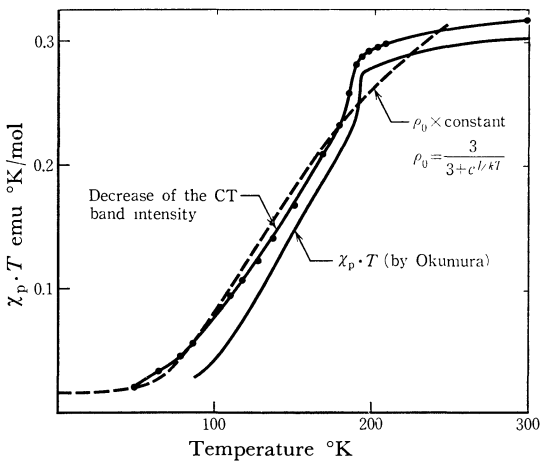

Fig. 9. Intensity of the charge-transfer band and magnetic susceptibility of WBP.

In order to make sure of the above discussion, we have undertaken to compare quantitatively the temperature dependency of the charge-transfer band intensity with that of magnetic susceptibility. The result of WBP is shown in Fig. 9. The curve showing the temperature dependence of the intensity (A) of the charge-transfer band is satisfactorily parallel with that plotting $\chi_p \cdot T$ against T measured by Okumura,[5a] where $\chi_p \cdot T$ values are known to represent the population of the dimer in the excited triplet state.[18] This means that our explanation on the temperature dependence of the charge-transfer band is correct.

The intensity of the charge-transfer band of the WBP crystal varies, though to much smaller extent than in the low temperature phase, in the room temperature phase in which WB cations are equally spaced. This seems to suggest that there exists antiferromagnetic interaction between spins on the WB cation radicals and the probability of neighboring cations having antiparallel spins decreases in higher temperatures.

Neglecting the interaction between dimers as the first approximation, the population of the triplet state ρ_0 can be represented as follows:

$$\rho_0 = 3/(3 + e^{J/kT})$$

By combining the above equation with the observed temperature dependence of the absorption intensity of the charge-transfer band, J is obtained to be $\sim 235\ \mathrm{cm}^{-1}$. This value of J agrees well with that obtained from the analysis of ESR data by McConnell ($J = 246 \pm 20\ \mathrm{cm}^{-1}$).[4]

The same consideration was applied to the solid EP and the value of J was evaluated to be $320 \pm 20\ \mathrm{cm}^{-1}$ from the temperature dependence of charge-transfer band. We also measured paramagnetic resonance spectra of the solid EP to check this value. The transition of $\Delta M = \pm 2$ was observed in addition to the ordinary transition of $\Delta M = \pm 1$.

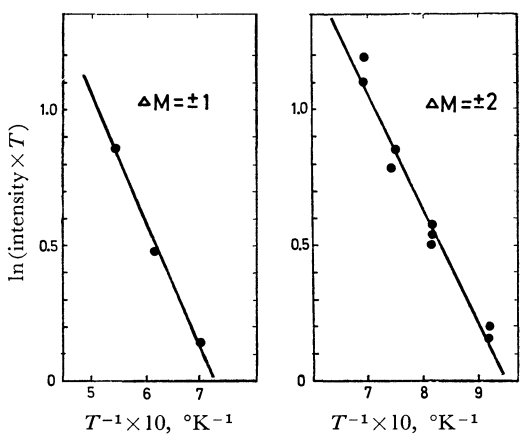

Fig. 10. Temperature dependence of paramagnetic resonance spectra of solid EP. Intensity is in arbitrary unit.

18) In connection with the above discussion, it may be added that we are not concerned with the absolute value of the population of the triplet state but only with its temperature dependence. Therefore, only the parallelism between the A-T and $\chi_p \cdot T$-T curves is important in Fig. 9. The similar parallelism can also be obtained by the use of Duffy's data[5b] instead of Okumura's data.

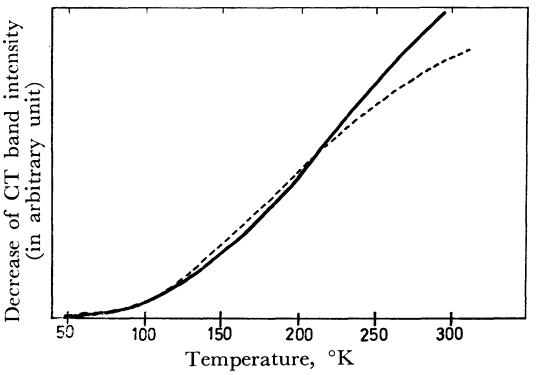

Fig. 11. Temperature dependence of the charge-transfer band intensity of solid EP. A solid line shows the decrease in the charge-transfer band intensity from the saturated value at 50°K. A dashed line represents the relation between $k\rho_0(J=320\ \mathrm{cm^{-1}})$ and T; k is a constant determined in such a way as $k\rho_0$'s fit well to the observed intensity decreases in low temperature region.

The ESR intensity I was measured at various temperatures with the results given in Fig. 10. This figure shows that a linear relationship is satisfied between $\ln IT$ and $1/T$. From the temperature dependence of paramagnetic resonance spectra, $J=330\pm20\ \mathrm{cm^{-1}}$ was obtained for $\Delta M=\pm1$, and $J=300\pm40\ \mathrm{cm^{-1}}$ for $\Delta M=\pm2$. These values agree well with the value obtained from the charge-transfer band.

As is clearly seen in Fig. 11, the experimental curve of the charge-transfer band intensity are somewhat off from the first order theoretical curve. This discrepancy becomes predominant at higher temperatures both for WBP in the low temperature phase and for EP. The reason for this discrepancy may be considered to be as follows:

1) The change in the intermolecular distance by thermal expansion.

2) The phonon induced interaction between triplet excitons.[19,20]

3) The exchange interaction between dimers.[21,22]

We also measured the temperature dependence of the other salts, especially of Würster's red perchlorate, paraphenylenediamine perchlorate and paraphenylenediamine bromide. As to these salts, such a remarkable intensity change in electronic absorption spectra as that observed with WBP and EP could not be found. This fact seems to correspond to the findings that these salts are diamagnetic at room temperature. The value of J seems to be large for these salts compared with kT.

Recently, Pott, Kommandeur *et al.*[23-26] suggested that the phase transition of WBP to be a disproportionation

$$2\ \mathrm{TMPD^+} \rightleftharpoons \mathrm{TMPD} + \mathrm{TMPD^{2+}}$$

(high temperature phase) (low temperature phase)

From our experimental results, however, this mechanism can be rejected

As is clearly seen in Fig. 1 showing the absorption spectrum of solid WBP, the 600 mμ band with vibrational structure corresponding to the $^2B_{3g}\rightarrow{}^2B_{1u}$ transition of the monopositive ion leaves its intensity and shape unaltered below the phase-transition point,[27] with the small blue shift of peak wavelengths by 700—800 $\mathrm{cm^{-1}}$ at most. This means that WB cations themselves do not suffer a large change by the phase transition and that the change in the weak interaction between WB cations is the cause of the phase transition. At least the above-mentioned observation can not be explained at all by the disproportionation mechanism by which the dipositive cation and the neutral molecule are produced below the phase-transition point.

Furthermore, the following fact may be added as a supplementary support to our opinion that the disproportionation mechanism by Pott, Kommandeur *et al.* is wrong. According to their mechanism, the singlet-triplet separation caused by the interaction between the half-occupied orbitals belonging to the neighboring WBP cations must amount to $\sim$1.5 eV (the difference between the transition energy of the charge-transfer band and the J value). This value seems to be too large judging from the distance between the two cation radicals and therefore from the magnitude of the overlap integral between the two orbitals.

The authors would like to express their sincere thanks to Professor J. Tanaka of Nagoya University for his kind advice and discussion. Their thanks are also due to Dr. H. Hasegawa and Dr. T. Maruyama of Japan Electron Optics Laboratory Co., Ltd. for the measurement of temperature dependence of the ESR signal due to $\Delta M=\pm2$ transition.

19) H. M. McConnell and Z. Soos, *J. Chem. Phys.*, **40**, 586 (1964).
20) D. B. Chesnut, *ibid.*, **41**, 472 (1964).
21) Z. G. Soos, *ibid.*, **43**, 1121 (1965).
22) Z. G. Soos, *ibid.*, **46**, 253 (1967).
23) H. J. Monkhorst and J. Kommandeur, *ibid.*, **47**, 391 (1967).
24) G. T. Pott and J. Kommandeur, *ibid.*, **47**, 395 (1967).
25) H. J. Monkhorst, G. T. Pott and J. Kommandeur, *ibid.*, **47**, 401 (1967).
26) G. T. Pott, C. F. van Bruggen and J. Kommandeur, *ibid.*, **47**, 408 (1967).
27) This finding was obtained as the repeated careful experimental works. The same conclusion was also obtained from the measurement by the KBr pellet method.

BULLETIN OF THE CHEMICAL SOCIETY OF JAPAN VOL. 42 1504—1509 (1969)

Moderator Effects on the Reactions of ^{82}Br Activated by the Isomeric Transition with Gaseous Methyl Bromide

Jiro OKAMOTO and Enzo TACHIKAWA

Division of Chemistry, Japan Atomic Energy Research Institute, Tokai-Mura, Ibaraki

(Received October 22, 1968)

^{82}Br obtained *via* the (I. T.) process has been reacted with methyl bromide. In the gaseous phase, only $CH_3{}^{82}Br$ and $CH_2{}^{82}BrBr$ are observed as major products, whereas in the solid phase other products, such as $CH^{82}BrBr_2$ and $C_2H_5{}^{82}Br$, have also been observed. Moderator experiments using He or Xe indicate that the formations of both $CH_3{}^{82}Br$ and $CH_2{}^{82}BrBr$ involve the reactions of the energetic ^{82}Br atom. This is in great contrast to the early observations of the Br_2-CH_4 system, where the ionic as well as the energetic reactions of ^{82}Br play a role in the formation of the C-^{82}Br bond. Comparisons of these results with those found in the reactions of the ^{80}Br obtained *via* the (n, γ) process suggest that the Br atom obtained *via* the (n, γ) process is more electronically excited than that from the (I. T.) process. The kinetic analysis of the present results gives the following relative α-values: α_{He}, 1.0; α_{Xe}, 8.8; α_{CH_3Br}, 10.3. It is suggested that, during the cooling-down process of ^{82}Br, a high inelasticity is involved in the collision of ^{82}Br, even with monatomic molecules.

Investigations of the recoil halogen atom reaction have included studies designed to find out more about both the primary physical state and the chemical process, and the mechanisms of chemical stabilization following these processes.[1-5]

Predominant among the subjects of interest is the relative importance of the kinetic energy and of the charge in determining the chemical reaction of the recoil atom. Definitive evidence[6] exists that the energetic reaction and also the ionic reaction sometimes play important roles in a gaseous-phase reaction of the halogen atom activated by the (n, γ) process, only part of which atom is positively charged.[7,8]

A high charge on the Br atom is developed as a consequence of the Auger process following the isomeric transition. It is postulated that this highly positive charge is partially neutralized by electron transfer from the remainder of the molecule, thus causing a repulsive force between the charged bromine atom and the remainder of the molecule.[9] The studies using a charge spectrometer indicate that free bromine atoms resulting from a molecular explosion show a charge distribution ranging up to $+14$.[10] The electron affinity of such a highly charged bromine is so high that its subsequent reaction is an electron pick-up from its surroundings.[11] Therefore, the important consideration is whether or not the Br^{+1} is reduced before reacting.

In the ^{82}Br-CH_4 system,[3] $CH_3{}^{82}Br$ is formed by the hydrogen substitution reaction of the energetic ^{82}Br atom, while $CH_2{}^{82}BrBr$ is formed *via* the ion-molecule reaction of $^{82}Br^{+1}$. The ionization potential of methyl bromide is 10.6 eV,[12] which is lower than that of bromine by 1.2 eV. This suggests the ionic reaction of ^{82}Br is less significant in an atmosphere of methyl bromide.

The present paper is concerned with a detailed study of the reaction of the ^{82}Br obtained *via* the (I. T.) process with methyl bromide. Two reactions which are conceivable for the energetic ^{82}Br atom can be written for this compound as Eqs. (1) and (2):

$$^{82}Br + CH_3Br \rightarrow CH_3{}^{82}Br + Br \quad (1)$$

$$^{82}Br + CH_3Br \rightarrow CH_2{}^{82}BrBr + H \quad (2)$$

The isolation of these hot reaction products in other reactions, such as ionic or thermal, is possible

1) J. E. Willard, "Chemical Effects of Nuclear Transformations," Vol. I, IAEA, Vienna (1965), p. 221.
2) L. D. Spicer and A. A. Gordus, *ibid.*, p. 185.
3) E. Tachikawa and J. Okamoto, submitted to *J. Phys. Chem.*
4) R. Wolfgang, *Progr. Reaction Kinetics*, **3**, 97 (1965).
5) F. Schmidt-Bleek and F. S. Rowland, *Angew. Chem. Internat. Edit.*, **3**, 769 (1964).
6) E. P. Rack and A. A. Gordus, *J. Chem. Phys.*, **34**, 1855 (1961).
7) E. P. Rack and A. A. Gordus, *ibid.*, **36**, 282 (1962).
8) S. Wexler and H. Davis, *ibid.*, **20**, 1688 (1952).
9) T. A. Carlson and M. R. White, "Chemical Effects of Nuclear Transformations," Vol. 1, IAEA, Vienna (1965), p. 23.
10) S. Wexler, *ibid.*, Vol. 1 (1961), p. 115.
11) A. R. Kazanjian and W. F. Libby, *J. Chem. Phys.*, **42**, 2779 (1965).
12) F. H. Field and J. L. Franklin, "Electron Impact Phenomena and the Properties of Gaseous Ions," Academic Press, New York (1957) Appendix.

through moderator and scavenger methods. The abstraction of the hydrogen or bromine atom in methyl bromide must also be considered as a possible reaction. However, experimental means are not available for tracing these reactions.

A series of experiments on the rigid phase,[1,13] indicative of a high yield of organically-bound ^{82}Br, have promoted a search for such a rigid phase in the present system.

Experimental

Materials. The bromine was obtained from the Kanto Chemical Company. Methyl bromide form the Tokyo Kasei Co. was purified several times by vacuum distillation techniques: gas chromatography showed no impurity greater than 0.01%. Helium and Xenon supplied by the Nihon Sanso Co. and the Takachiho Chemical Co., were used directly without additional purification (the listed purities are 99.999 and 99.995% respectively).

Sample Preparation and Irradiation. The preparation of samples followed the routine procedures used in our previous work for gas-phase bromine hot-atom chemistry.[3] A quartz capillary containing Br_2 was gas irradiated in a pneumatic tube of a Cp-5-type reactor in JAERI for 5 min. Then it was quickly inserted into a Pyrex ampoule filled with the required gases. About 10—20% of the ^{82m}Br formed during the irradiation decayed in the Pyrex ampoule, the ^{82}Br freshly formed was made to react with methyl bromide.

Radio-gas Chromatography. The organic products were separated using a dioctyl sebacate column (15% in weight) 3m long and 6mm in inside diameter. The temperature of the operation was 95°C. A short glass column containing pottasium ferrocyanide was placed before the separation column in order to isolate any inorganic bromides, such as $H^{82}Br$ or $Br^{82}Br$, formed in the reaction system. Otherwise, a gradual elution of these from the column would interfere with a precise radioactive assay of the organic bromide. Elution gas was introduced into a G-M counter in conjunction with a scaler and printer for radioactivity measurements of each product. For the determination of the absolute yields of the individual products, the total bromine activity was measured with a gamma-ray scintillation counter (a 2″+2″ well-type NaI(Tl) scintillator at 20 cm), after a complete decaying-out of the ^{80}Br (about 48 hr after irradiation).

Correction and Experimental Errors. All of the data obtained have been corrected for decays of ^{82m}Br and ^{82}Br according to the reported half-lives of 6.1 min[14,15] and 35.4hr respectively. A consideration of the kinetic energy of the ^{82}Br atom achieved by the Auger process following the isomeric transition of ^{82m}Br shows that the recoil loss of ^{82m}Br into the wall can be neglected in the pressure range studied.[11]

In most cases, the activity in $CH_3{}^{82}Br$ or $CH_2{}^{82}BrBr$ was large enough to reduce the standard deviation of counting to a small percentage. The relative short half-life of ^{82m}Br, is however, responsible for the most serious error in the absolute yields. A ninety-one percent radioactive neutron capture by ^{81}Br results in ^{82m}Br. At the end of a 5-min irradiation, 71% of the ^{82m}Br produced is still alive.

However, this is reduced to 10—20% upon the mixing of ^{82m}Br with methyl bromide, as the transit from the reactor to the laboratory and the following sample processing usually take 10—15 min. The yields of individual products constitute only a small percentage of the total ^{82m}Br produced originally. Therefore, the accuracy of these experiments is usually limited to 5%, except in a few cases in which the counting error was greater than normal.

Results

Samples were dipped into liquid nitrogen for varying periods of time (Δt) after the mixing of ^{82m}Br with methyl bromide. Such a method makes it possible to follow the reactions occurring in both the gaseous and solid phases in a series of experiments. In Table 1 the yields of the products are listed in connection with the Δt. The decrease in

Table 1. Percent yields of products as a function of Δt

Filling pressure		Δt	Products (%)			
Br_2 (cmHg)	CH_3Br (cmHg)		$CH_3{}^{82}Br$	$CH_2{}^{82}BrBr$	$CH^{82}BrBr_2$	$CH_3CH_2{}^{82}Br$
5.0	45.0	∞	4.69±0.20	1.25±0.06	0.24±0.02	—
5.0	45.0	40 min	4.40±0.20	1.80±0.09	0.35±0.02	—
5.0	45.0	25 min	3.41±0.15	1.95±0.10	0.33±0.03	—
5.0	45.0	15 min	5.12±0.25	3.15±0.15	0.50±0.03	0.10±0.02
5.0	45.0	10 min	6.89±0.30	4.54±0.20	0.60±0.04	0.17±0.03
5.0	45.9	7 min	8.27±0.40	6.30±0.30	0.97±0.05	0.37±0.03
5.0	45.9	2 min	14.14±0.70	9.19±0.40	—*	0.31±0.03
5.0	45.9	1 min	15.07±0.70	10.79±0.50	1.78±0.06	0.38±0.02
5.0	45.9	30 sec	16.93±0.80**	10.45±0.50	—*	—

* Measurement was failed by a printing trouble.
** ($CH_3{}^{82}Br+CH_3CH_2{}^{82}Br$) is listed.

13) J. A. Merrigan, W. K. Ellgren, Jr., and E. P. Rack, *J. Chem. Phys.*, **44**, 174 (1966).
14) J. E. Emery, *J. Inorg. Nucl. Chem.*, **27**, 903 (1965).
15) O. U. Anders, *Phys. Rev.*, **138**, B1 (1965).

the yields with the time is just the opposite of the increase found in the Br_2-CH_4 system.[3] This observation implies that a homogeneous mixing of the Br_2 and CH_3Br is also attained on the solidification of the mixture and the chemical reaction of the ^{82}Br from (I. T.) with methyl bromide proceeds. By contrast, in the Br_2-CH_4 system the solidification of a mixture has a clumping effect on bromine, so that bromine atoms undergoing a nuclear transformation are surrounded by an envelope of molecular bromine. Further chemical reaction of ^{82}Br with methane should thus be prevented. These two kinds of observations have also been made in solid-liquid intersystems.[7]

In the following gaseous experiments, the quantitative measurements of $CH^{82}BrBr_2$ and $C_2H_5{}^{82}Br$ were not successful, simply because of their small yields (less than 0.2%). Thus, we weighted the quantitative measurements only for the products, $CH_3{}^{82}Br$ and $CH_2{}^{82}BrBr$.

Table 2. Percent yields of $CH_3{}^{82}Br$ and $CH_2{}^{82}BrBr$ at varying pressure of methyl bromide

Filling pressure		Products (%)	
Br_2 (cmHg)	CH_3Br (cmHg)	$CH_3{}^{82}Br$	$CH_2{}^{82}BrBr$
5.0	1.8	0.32±0.02	0.21±0.02
5.0	5.7	0.85±0.04	0.43±0.03
5.0	9.5	1.32±0.07	0.59±0.04
5.0	14.2	2.01±0.10	0.65±0.05
5.0	20.1	1.87±0.10	0.79±0.05
5.0	30.6	3.78±0.19	0.58±0.03
5.0	40.6	>2.06±0.10*	>0.61±0.03*
5.0	30.9	3.08±0.15	1.23±0.06
5.0	45.9	4.68±0.24	1.25±0.06
5.0	76.6	5.89±0.29	2.29±0.12

* Part of the sample is lost during the sample processing.

Table 2 shows the dependences of the two major products on the pressure of methyl bromide, in the constant presence of 5 cmHg Br_2 as a scavenger. The observed increases in yields with the total pressure are considered to originate as follows: 1) with pressure, recoil loss into the wall is reduced; concomitantly, the amount of ^{82}Br reacted in the gaseous phase increases; 2) both products are formed *via* a ion-molecule reaction of $^{82}Br^{+1}$; 3) the primary products, $(CH_3{}^{82}Br)^*$ and $(CH_2{}^{82}BrBr)^*$, are highly excited, and their unimolecular decomposition reactions compete greatly with collisional deactivations as the pressure increases. The recoil energy of the ^{82}Br from (I. T.) is most in the range of 100 eV,[9] and the recoil loss of ^{82}Br into the wall is well below the experimental uncertainty in the pressure range studied. Thus, the first possibility above may be excluded.

One method to differentiate one possibility from the others is through the sensitivities of the reacting species to the addition of moderators. The dependency of the yields upon the mole fraction of helium or xenon added as a inert moderator has been measured. The results are shown in Figs. 1 and 2, where the yields are plotted as a function of the mole fraction of the moderator. In all the samples 5 cmHg of Br_2 is present as a scavenger, while the total pressure was always kept at 51±1 cmHg.

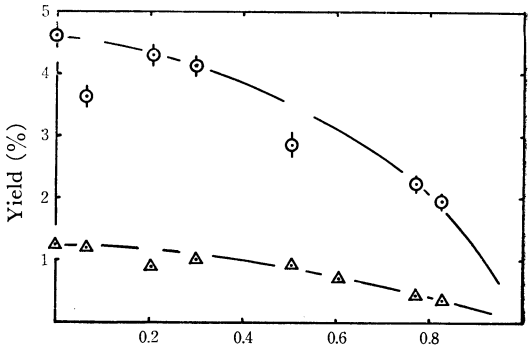

Fig. 1. Dependencies of $CH_3{}^{82}Br$ and $CH_2{}^{82}BrBr$ on the m.f. of He as a moderator.
(total pressure: 51±1 cmHg)
⊙: $CH_3{}^{82}Br$ △: $CH_2{}^{82}BrBr$

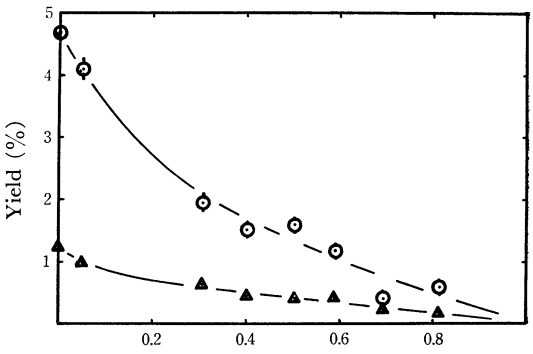

Fig. 2. Dependencies of $CH_3{}^{82}Br$ and $CH_2{}^{82}BrBr$ on the m.f. of as a moderator.
(total pressure: 51±1 cmHg)
⊙: $CH_3{}^{82}Br$ △: $CH_2{}^{82}BrBr$

Discussion

The most striking feature of the formation of the main products, $CH_3{}^{82}Br$ and $CH_2{}^{82}BrBr$, is their great sensitivity to the presence of the moderating gas. Behavior of this kind can be understood if they formed by the energetic reaction of the ^{82}Br atom, not by the thermal ionic ^{82}Br atom. The ease with which $^{82}Br^{+1}$ is neutralized to the ^{82}Br neutral atom is dependent upon the

ionization potential of the colliding partner in the system. As the ionization potential of methyl bromide is 10.6 eV, lower than that of Br (11.84 eV), the neutralization of Br^{+1} in collision with methyl bromide is energetically very much favored. Allowing this, the subsequent reaction of $^{82}Br^{+1}$ in collision with methyl bromide will be a discharging.

Although other minor products, such as $CH^{82}BrBr_2$ and $C_2H_5{}^{82}Br$, could not be measured quantitatively, their yields are so small that they can explain only a small percentage of the total organic products at most. Within this limitation, the ^{82}Br from (I. T.) reacts with methyl bromide as a hot ^{82}Br, and $CH_3{}^{82}Br$ and $CH_2{}^{82}BrBr$ are formed through the *^{82}Br for Br* and *^{82}Br for H* reactions, as has been shown in Eqs. (1) and (2).

On the other hand, previous experiments have shown that the ^{82}Br from (I. T.), in an atmosphere of methane and in the presence of Br_2 as a scavenger, reacts with methane *via* ionic as well as energetic reactions.[3,16] However, the ionization potential of methane is higher than that of Br, and the charge transfer reaction between Br^{+1} and CH_4 is calculated to be endothermic by *ca.* 1.3 eV. The different reactivities in ^{82}Br in these systems thus, leads to the following qualitative interpretations for the reaction mechanisms of ^{82}Br from (I. T.): if the ionization potential of a reactant is lower than that of Br, ^{82}Br can well be neutralized to a neutral ^{82}Br atom and reacts *via* energetic reactions. However, in a system in which the reactant has a higher ionization potential than does Br, part of the ^{82}Br may react *via* ion-molecule reactions prior to the complete neutralization. The higher the endothermicity of the neutralization reaction, $Br^{+1}+M \rightarrow Br+M^{+1}$, the more significant become the ionic reactions.

Rack and Gordus[17] have reported that the reactions of a ^{80}Br atom activated by $^{79}Br(n, \gamma)^{80}Br$ with CH_4 require only a kinetically-excited ^{80}Br atom in spite of the fact that originally at least 18% of the ^{80}Br atoms were positively charged.[18] It is, however, very likely that charge transfer will occur in a collision of Br^{+1} with CH_4 if the ion is electronically excited[18,19] in a state sufficiently high to overcome the endothermicity of the charge transfer reaction. If this is the case, the difference in the reaction mechanisms of Br atoms from different nuclear reactions can be connected with the electronic state of atoms when they are born. Thus, it may be suggested that the recoil atom resulting from the (n, γ) process is more likely to be electronically-excited than that resulting from the (I. T.) process. This discussion will have one feature in common with the results of Rack and Gordus[6,7] on the reaction of ^{128}I from $^{127}I(n, \gamma)^{128}I$ with methane, where reactions required electronically-excited ions as well as atom or ions of kinetic energy. However, the final answer to this problem must await more information concerning the physical state of the recoil atom obtained from other types of experiments.

Unimolecular Decompositions. The above discussions assist the interpretation of the results shown in Table 2 in terms of the competition between the decomposition and the collisional stabilization of the excited $(CH_3{}^{82}Br)^*$ and $(CH_2{}^{82}BrBr)^*$. These are formed by substitution reactions of hot ^{82}Br with sufficient internal excitation energy to cause secondary decomposition. Thus, the fate of the excited molecules is either stabilization by collisional deactivation with their surrounding molecules or unimolecular decomposition. The increase in the pressure serves to stabilize with an increase in the collision frequency.

Some information on the decomposition reactions of these excited molecules has been provided by studies of recoil tritium reaction. Rowland and his collaborators[20-23] have extensively studied the unimolecular decomposition reaction of internally-excited molecules formed by the substitution reaction of the recoil tritium atom. It is reasonable to assume that the chemical reaction range of the substitution reaction of the recoil T or ^{82}Br atom is not different enough to alter the decomposition paths of the resulting excited molecule.[24] Thus, very possibly the subsequent reaction of $(CH_3{}^{82}Br)^*$ or $(CH_2{}^{82}BrBr)^*$ will be:

$$(CH_3{}^{82}Br)^* \rightarrow CH_3 + {}^{82}Br$$

$$(CH_2{}^{82}BrBr)^* \rightarrow CHBr + H^{82}Br$$

$$\text{or} \quad CH^{82}Br + HBr$$

Factors Affecting the Yields. The higher yield in the solid phase is due simply to the combination of the ^{82}Br atom with the radicals formed by the radiation chemistry in the system.[11,25,26]

The present experiments were conducted in

16) E. P. Rack, Progress Report, Univ. of Nebraska, 1965.

17) E. P. Rack and A. A. Gordus, *J. Phys. Chem.*, **65**, 944 (1961).

18) C. E. Moore, "Atomic Energy Level," Natl. Bur. Standards, NO 67 (1952), p. 161.

19) J. D. Morrison, H. Hurzeler and M. G. Ingram, *J. Chem. Phys.*, **33**, 821 (1960).

20) E. K. C. Lee and F. S. Rowland, *J. Am. Chem. Soc.*, **85**, 879 (1963).

21) Y. N. Tang and F. S. Rowland, *ibid.*, **90**, 574 (1968).

22) Y. N. Tang and F. S. Rowland, *ibid.*, **90**, 570 (1968).

23) Y. N. Tang and E. K. C. Lee and F. S. Rowland, *ibid.*, **86**, 1280 (1964).

24) Y. N. Tang and F. S. Rowland, *J. Phys. Chem.*, **71**, 4576 (1967).

25) P. R. Geissler and J. E. Willard, *ibid.*, **67**, 1675 (1963).

26) P. R. Geissler and J. E. Willard, *J. Am. Chem. Soc.*, **84**, 4627 (1962).

the absence of γ-radiation from a nuclear reactor. Alternatively, electrons emitted by the ^{82}Br atom as a result of internal conversion and Auger transitions produce a high localized concentration of radicals so close to the atom that their reactions with the atom are not precluded by the Br_2 scavenger, whereas in the gas phase these radicals can easily be scavenged.

One of the most important conclusions to be drawn from the present experiments is that the total organic yield *via* a hot reaction is less than 10%. This is parallel to the observations on other recoil halogen atom reactions[27,28] and is consistent with the proposal of Rowland *et al.*[28] They ascribed the fact that these yields are lower than those in the recoil tritium reaction to the ease with which a recoil atom can change direction in response to a newly-available chemical potential. The halogen atom, heavier than the tritium atom, may very well be hindered by such bond formation; a substantially lower yield than in the corresponding tritum system will result. Although corrections for the secondary decompositions of excited molecules sholud be made in quantitative discussions, such corrections are unlikely to alter the qualitative conclusion.

Kinetic Theory. One of the assumptions involved in the Estrup-Wolfgang kinetic theory[29,30] is that the initial energy of recoil atom is sufficiently high for the atom to have made number of collisions in order to attain the statistical distribution of energies for the atoms in the reaction range. Qualitatively this assumption is plausible. In the isomeric transition of ^{80m}Br in the molecular bromine, the resulting ^{80}Br atoms show a charge spectrum ranging up to +11, with a maximum between +4 and +5.[10] The average kinetic energy of the Br arom achieved from the molecular explosion of Br_2 can thus be estimated[9] to be over 100 eV. Since precise information on the kinetic energy spectrum of ^{82}Br is not available, this could serve as a reasonable approximation.

The developed equation is given in:

$$\frac{-1}{\ln(1-P)} = \frac{\alpha_{\text{react}}}{I} - \frac{\alpha_{\text{mod}}}{I}\left(\frac{1-f}{f}\right),$$

where P is the total probability (organic yield) of a hot atom combining in any hot product and where I is the corresponding total reactivity integral. α_{react} and α_{mod} are the average logarithmic energy loss per collision for reactant and moderator respectively. f, the collision fraction, is computed using:

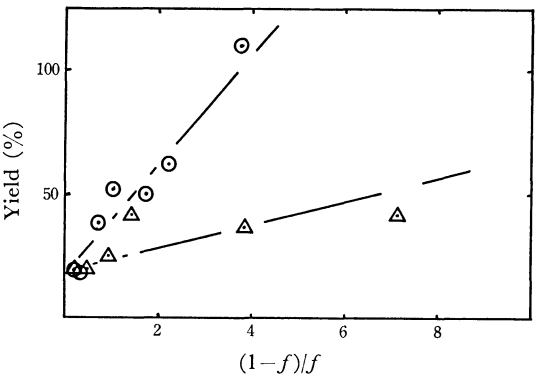

Fig. 3. Kinetic plotts of the total yields of products in moderated reactions of ^{82}Br with methyl bromide.
△: He moderator ⊙: Xe moderator

Table 3. Relative values of average logarthmic energy loss per collision, α, for collision of Br atom

system		
He-CH_3Br-Br_2	$\alpha_{He}/\alpha_{CH_3Br}$	0.27±0.03
Xe-CH_3Br-Br_2	$\alpha_{Xe}/\alpha_{CH_3Br}$	1.2±0.1
	α_{Xe}/α_{He}	4.5±0.5

$$f = \frac{X_{CH_4}S_{CH_4}}{\sum X_i S_i}.$$

Here X_i is the mole fraction of the ith molecule, and S_i is the collision cross-section for the Br-ith molecule collision. A plot of $-1/\ln(1-P)$ *versus* $(1-f)/f$ gave straight lines for the results in both He and Xe moderators as is shown in Fig. 3. The following values are obtained: (He) slope 4.8± 0.5, intercept 18±2, (Xe) slope 22±2, and intrecept 18±2. The relative values of α obtained from the intercept/slope values in Fig. 3 have been summarized in Table 3. For the calculation of S, the diameters used for individual products[31] are: He, 2.2(Å); Xe, 4.9(Å); Br, 4.2(Å), Br_2, 8.4(Å), and CH_3Br, 5.4(Å). The above graphical analysis has been carried out on the basis of the sum of the yields of $CH_3{}^{82}Br$ and $CH_2{}^{82}BrBr$. By contrast, the billiard-ball model predicts the ratio of 1.0 : 8.8 : 10.3 for $\alpha_{He} : \alpha_{Xe} : \alpha_{CH\,Br}$. This suggests a high inelasticity in the actual collisions of recoil bromine, even with monatomic molecules.

Examination of the data in Figs. 1 and 2 shows that the ratio of the two products is almost constant at any mole fraction of the moderators within the range of experimental uncertainty.

27) R. Wolfgang, *Ann. Rev. Phys. Chem.*, **16**, 15 (1965).
28) C. M. Wai and F. S. Rowland, *J. Am. Chem. Soc.*, **90**, 3638 (1968).
29) P. J. Estrup and R. Wolfgang, *ibid.*, **82**, 2661, 2665 (1960).
30) R. Wolfgang, *J. Chem. Phys.*, **39**, 2983 (1963).
31) S. Chapman and T. J. Cowling, "The Mathematical Theory of Non-uniform Gases," Vniv. Press, Cambridge (1953), p. 229.

It is thus, likely that the chemical reaction range does not change significantly in the substitution reaction of H or Br in methyl bromide by the hot Br atom. This is accord with the similar dependencies of the yields upon the pressure.

The authors are grateful to Mr. T. Ohkubo for his assistance throughout this work. They also wish to express their gratitude to Dr. K. Motojima and the members of the Reactor Chemistry Laboratory in JAERI.

BULLETIN OF THE CHEMICAL SOCIETY OF JAPAN VOL. 42 1509—1514 (1969)

The Molecular and Crystal Structure of Bis(2-hydroxyethyliminopyruvato)copper(II) Tetrahydrate

Kinya IIJIMA, Isao OONISHI, Fumio MUTO, Akitsugu NAKAHARA* and Yoshimichi KOMIYAMA*1

Department of Applied Chemistry, Faculty of Engineering, Yamanashi University, Kofu, Yamanashi
** Institute of Chemistry, College of General Education, Osaka University, Toyonaka, Osaka*

(Received October 23, 1968)

A new copper(II) chelate of the Schiff base derived from pyruvic acid and ethanolamine has been prepared. The crystal structure of this complex, $[Cu(pyv=etham)_2]\cdot 4H_2O$, has been determined from three dimensional X-ray diffraction data. The dimensions of monoclinic cell are $a=6.50$Å, $b=19.75$Å, $c=7.26$Å, $\beta=113.0°$ and $Z=2$. The space group is $P2_1/n$. The structure has been refined by three dimensional difference syntheses to $R=0.126$. It has been disclosed that copper(II) links to the 2-hydroxyethyliminopyruvate anion through the terminal carboxylate group, and the nitrogen of the Schiff base linkage. Having a center of symmetry, the complex molecule is in the *trans*-configuration and has normal bond distances and angles. The coordination around copper(II) is square planar; the Cu-O and Cu-N distances are 1.92 and 2.00Å, respectively. Two additional oxygen atoms of the water molecules at 2.57Å complete a distorted octahedron around copper(II). The complex molecules are held together in the crystal by the O-H···O hydrogen bonds, forming a three dimensional network.

The reaction of copper(II) with the Schiff base derived from salicylaldehyde and ethanolamine results in the formation of the copper(II) Schiff base complex of either one-to-one type or one-to-two type, depending upon the condition employed there.[1] On the other hand, a similar reaction of copper(II) with the Schiff base derived from pyruvic acid and ethanolamine exclusively gives the copper(II) Schiff base complex of one-to-two type, regardless of the method of preparation. The molecular structure of these one-to-two type copper(II) Schiff base complexes is not always easy to predict, in view of the fact that there are three donating groups in those Schiff base ligands, though the donating tendency of alcoholic oxygen is estimated to be comparatively weak. It is also important to know the geometrical configuration of the two 2-hydroxyethyliminopyruvate ions around the copper(II). The main purpose of the present work was to elucidate these points and determine the detailed structure of the complex.

Experimental

The preparation of bis(2-hydroxyethyliminopyruvato)-copper(II).

A mixture of copper(II), pyruvic acid and ethanolamine in 1 : 2 : 2 molar ratio was treated at about 60°C for two hours in aqueous ethanol (one-to-one by volume mixture).

A dark blue solution was gradually obtained, being accompanied by precipitation of pale blue microscopic crystals.

The precipitate was filtered by suction and recrystallized from an aqueous ethanol solution. The final pure product appears as thin pale blue needles elongated along the *c*-axis. The result of the elementary analysis nearly coincides with the calculated values for bis(2-hydroxyethyliminopyruvato)copper(II) tetrahydrate.

Found: C, 30.42; H, 5.98; N, 6.92%. Calcd: C, 30.34; H, 6.07; N, 7.08%.

Cell dimensions were calculated from measurements on rotation and Weissenberg photographs, calibrated with Cu wire ($a_0=3.6147$), using Cu$K\alpha$ radiation ($\lambda=1.5418$Å).

*1 Deceased on Aug. 1, 1968.

1) A. Nakahara, H. Matsumoto and H. Yamamoto, *Sci. Rep.*, College of General Education, Osaka Univ., **12**, 11 (1963).

The results are:

$a=6.50\pm0.01$Å, $b=19.75\pm0.02$Å, $c=7.26\pm0.01$Å

$\beta=113.0\pm0.2°$.

The cell contains two formula units of ($[Cu(HOCH_2CH_2NCCH_3COO)_2]\cdot4H_2O$); density calculated: 1.53 g·cm^{-3}; density measured: 1.52 g·cm^{-3}. Systematic absence indicates the space group to be $P2_1/n$. Relative intensities were obtained from equi-inclination Weissenberg photographs taken with Cu$K\alpha$ radiation using multiple films. The crystal was a rod of dimensions $0.1\times0.05\times2.0$ mm. Data were collected for all levels from $hk0$ through $hk6$ and $h0l$.

The intensities were estimated visually by comparison with a calibrated scale and corrected for the usual Lorentz and polarization factors. No absorption correction was made.

The range of relative intensities was 1 to 30000.

1292 reflections fell within this range, whereas 385 others were too weak to be observed.

Determination of Structure

The presence of two formula units in a unit cell of the space group $P\,2_1/n$ requires the copper atoms to occupy one of the sets of twofold positions. Without loss of generality they can be placed at 000 and ½ ½ ½.

Attempts were made to deduce the positions of the lighter atoms from a three dimensional Patterson function and Fourier synthesis of electron density, $\rho(x,y)$, of which all the phases were assumed to be positive. It was possible to locate all the atoms except one water oxygen atom.

The first three dimensional structure factor calculation on the basis of the deduced atomic positions led to an R index of 0.24. All the atomic positions were fixed by three dimensional F_o synthesis. In this calculation all those F_os were excluded for which $F_c<\frac{1}{2}F_o$. The structure was then refined by a three dimensional difference synthesis. Finally R index was reduced to 0.126. All calculations were carried out on a FACOM231 computer.

TABLE 1. FINAL COORDINATES, STANDARD DEVIATION AND TEMPERATURE FACTORS

Atom	x/a	y/b	z/c	B
Cu	0.0000	0.0000	0.0000	3.5
O(1)	−0.1885(14)	−0.0190(6)	0.1425(15)	3.0
O(2)	−0.2850(17)	0.0270(7)	0.3760(18)	3.6
O(3)	−0.0120(40)	0.2285(7)	0.0590(34)	4.6
O(4)	0.3380(22)	−0.0570(7)	0.2715(18)	3.6
O(5)	0.0805(31)	0.3195(8)	0.3615(28)	5.0
N	0.0855(17)	0.0830(4)	0.1715(15)	2.4
C(1)	−0.1785(31)	0.0275(6)	0.2720(22)	2.6
C(2)	−0.0140(22)	0.0850(7)	0.2930(18)	2.4
C(3)	0.0220(43)	0.1360(9)	0.4520(23)	3.9
C(4)	0.2490(26)	0.1320(9)	0.1705(25)	3.1
C(5)	0.1365(48)	0.1865(11)	0.0110(40)	4.0

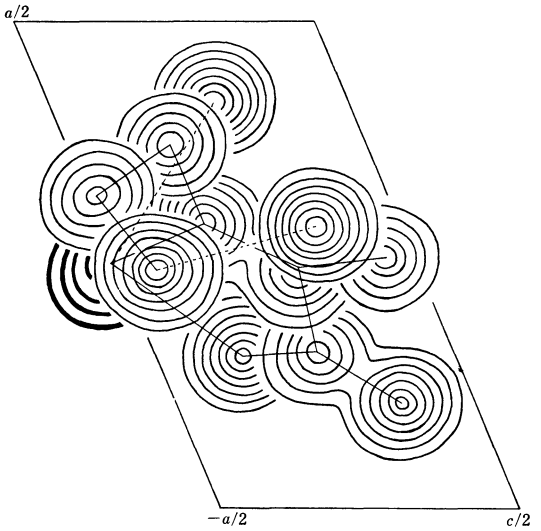

Fig. 1. Composite Fourier diagram of section parallel to (010).
Contours at intervals 1.0 e. Å^{-3}, the lowest being at 2.0 e.Å^{-3}. (Contours above 10 e. Å^{-3} are drawn at intervals of 6.0 e. Å^{-3} with thick lines).

The final atomic positions, and isotropic temperature factors and their estimated standard deviations are given in Table 1.

Table 2 gives the comparison of observed and calculated structure factors. The superimposed sections of the final electron density distribution are shown in Fig. 1.

Description and Discussion of the Structure

The structure projected upon a plane normal to the b-axis is shown in Fig. 2, and the environment of each copper atom is illustrated in Fig. 3. The interatomic distances and the bond angles calculated on the basis of the atomic parameters in Table 1 are given in Table 3.

The new complex, bis(2-hydroxyethyliminopyruvato)copper(II) is in trans-configuration. The 2-hydroxyethyliminopyruvate group is coordinated to copper(II), as a bidentate chelate, through the terminal carboxylate oxygen and the nitrogen of the Schiff base linkage, while the alcohol group is free from coordination. This is quite reasonable since the donating tendency of the alcohol oxygen has been estimated to be comparatively weak. The coordination around copper is approximately square planar. The distances from the copper(II) to the four donor atoms are 2.00 Å for Cu–N and 1.92 Å for Cu–O. The fifth and the sixth coordination positions are occupied by oxygen atoms of water molecules, being 2.57 Å distant from the copper(II) atom; hence the copper(II) has a tetragonally distorted octahedral environment, as has very often been observed in copper(II) com-

TABLE 2. CALCULATED AND OBSERVED STRUCTURE FACTORS

Columns are k, F_o, F_c. Unobserved Marked by *

Table 2. (Continued)

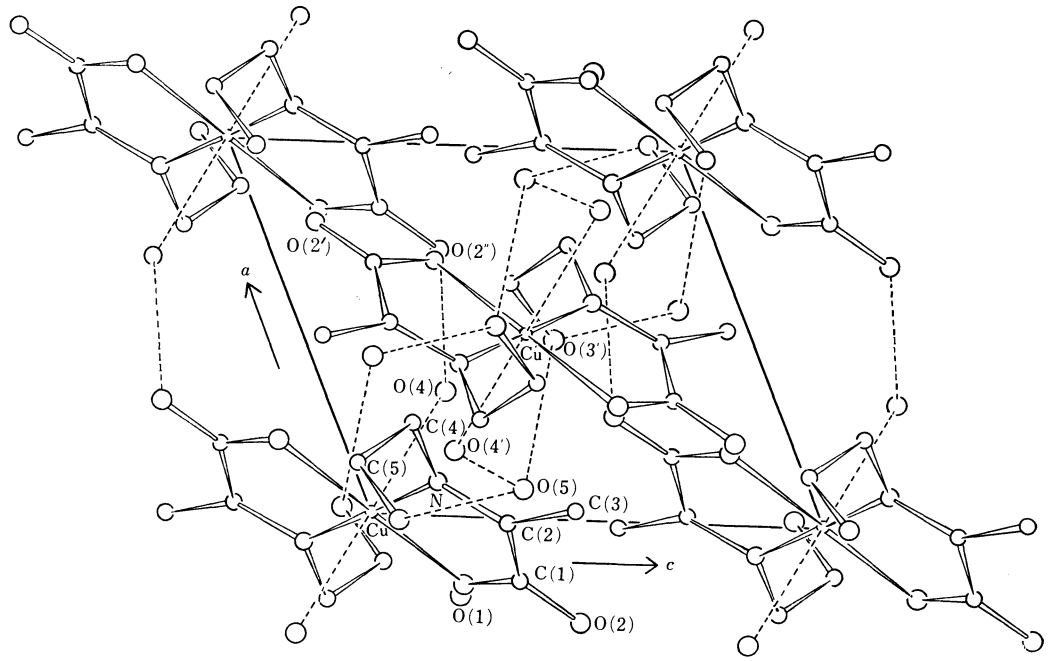

Fig. 2. Projection of the structure along the *b*-axis. Hydrogen bonds and the two long Cu···O interactions are indicated by dotted lines.

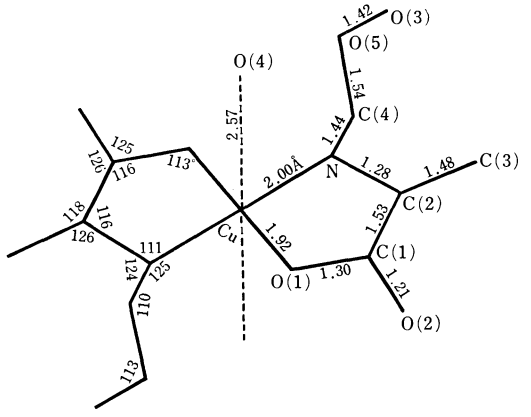

Fig. 3. The environment of the copper atom, showing bond distances and bond angles.

plexes. The N–Cu–O angle in the chelate ring is 84.6°; and the weaker Cu–OH_2 bond is inclined at an angle of 85° with respect to the plane of the copper and four ligand atoms.

These values may be compared with the corresponding values for other copper(II) complexes: Cu–O=1.95 Å, Cu-N(amino)=2.00 Å and N–Cu–O =85.2° in bis(glycinato)copper(II) monohydrate;[2] Cu–O=1.97—1.99 Å, Cu–N(amino)=2.00 Å and N–Cu–O=83.6° in copper(II) glutamate dihydrate;[3] Cu–O=1.88 Å and Cu–N(imino)= 1.99 Å in bis(*N*-phenylsalicylaldiminato)copper-(II).[4]

The bond distances in the chelate ring are: 1.30 Å for O(1)–C(1), 1.53 Å for C(1)–C(2) and 1.28 Å for O(2)–N, and are in good agreement with

Table 3. Interatomic distances and angles

I Distance			
Cu–N	2.00Å	C(1)–C(2)	1.53Å
Cu–O(1)	1.92	C(2)–C(3)	1.48
Cu–O(4)	2.57	C(4)–C(5)	1.54
O(1)–C(1)	1.30	C(3)···O(5)	2.72
O(2)–C(1)	1.21	O(3')···O(5)	2.65
O(3)–C(5)	1.42	O(4')···O(5)	2.75
N–C(2)	1.28	O(2'')···O(4)	2.81
N–C(4)	1.44		
II Angle			
N–Cu–O(1)	84.6°	N–C(4)–C(5)	110°
Cu–O(1)–C(1)	113	C(4)–C(5)–O(3)	113
O(1)–C(1)–C(2)	116	C(3)–C(2)–N	126
O(1)–C(1)–O(2)	125	C(2)–N–Cu	111
O(2)–C(1)–C(2)	120	C(2)–N–C(4)	124
C(1)–C(2)–N	116	Cu–N–C(4)	125
C(1)–C(2)–C(3)	118		
O(1)–Cu–O(4)	92		
N–Cu–O(4)	86		

2) H. C. Freeman, M. R. Snow, I. Nitta and K. Tomita, *Acta Cryst.* **19**, 1464 (1964).

3) C. M. Gramaccioli and R. E. Marsh, *Acta Cryst.* **21**, 594 (1966).

4) L. Wei, R. M. Stogsdill and E. C. Lingafelter, *Acta Cryst.* **17**, 1058 (1964).

those found in various complexes: C–O=1.28 Å and C–C=1.52 Å in bis(glcinato)copper(II) monohydrate and copper(II) glutamate dihydrate; C–O=1.31 Å and C–N(imino)=1.30 Å in bis(*N*-phenylsalicylaldiminato)copper(II) and disodium glycylglycylglycinatocuprate(II).[5]

In the carboxyl group, C(1)–O(1) bond has lengthened and C(1)–O(2) bond has shortened compared with the values found in glycine(both 1.25 Å). This fact indicates that these bonds have 20% and 80% double bond character, respectively.[6] O(2) atom of the carboxyl group, C(3) atom of the methyl group and C(4) atom of the ethanolamine group lie almost in the plane of the chelate ring, the deviation ranging from 0.04 Å to 0.09 Å. C(5) atom of the ethanolamine moiety is displaced from that plane and the angle between C(4)–C(5) bond and the plane is 62°.

The only contacts less than 3.5 Å between adjacent molecules are made by the free water oxygen O(5), the water oxygen O(4) weakly coordinated to the copper atom, the ethanolamine oxygen O(3) and the carboxyl oxygen O(2).

The distances are 2.67 Å—2.81 Å as shown in Fig. 2.

These short distances and the angles suggest hydrogen bonding between them. By these hydrogen bonds, the complexes are packed in layers parallel to the plane (101).

Stabilization within the layer is provided by hydrogenbonded bridges O(5)···O(3), O(5)···O(3′) and O(5)···O(4′).

Between adjacent layers there exists a hydrogen bond O(4)···O(2″) in the direction normal to the plane (100).

Part of the cost of this investigation has been defrayed by a Scientific Research Grant of the Ministry of Education, to which the authors' thanks are due.

Note added in proof: The crystal and molecular structures of the related complexes, pyruvidene-*β*-alaninatoaquocopper(II) dihydrate and *N*-salicylideneglycinatoaquocopper(II) hemihydrate, prepared by one of the authors (A. N.) have also been determined.[7,8]

5) H. C. Freeman and Max R. Taylor, *Acta Cryst.* **18**, 939 (1965).

6) T. Hahn, *Z. Kristallogr.*, **109**, 438 (1957).

7) T. Ueki, T. Ashida, Y. Sasada and M. Kakudo, *Acta Cryst.*, **B24**, 1361 (1968).

8) T. Ueki, T. Ashida, Y. Sasada and M. Kakudo, *ibid.*, **22**, 870 (1967).

BULLETIN OF THE CHEMICAL SOCIETY OF JAPAN VOL. 42 1515—1518 (1969)

Measurement of Negative Ions Formed by Electron Impact. III. The Ionization Efficiency Curves of Negative Ions of *m/e* 26 and 42 from Nitroalkanes

Satoru TSUDA, Akira YOKOHATA and Michihiro KAWAI

Department of Chemistry, Faculty of Engineering, University of Hiroshima, Senda-machi, Hiroshima

(Received November 8, 1968)

The studies of this series were extended to the negative ions of *m/e* 26 and 42 obtained from nitroalkanes; nitromethane, nitroethane, 1-nitropropane, and 2-nitropropane. For *m/e* 26 (probably, CN^-) ions, the contribution of three or two processes in the range from zero to ~20 eV of electron energy was observed for nitromethane or other samples. On the basis of ΔH_f values of the reactants and products, and of the value of $EA(CN)$, the plausible reactions to be assigned to each process were presented. For the first process, $CH_3NO_2+e^-\rightarrow CN^-+H_2O+OH$, $RNO_2+e^-\rightarrow CN^-+R_1OH+OH$. For the second process, $CH_3NO_2+e^-\rightarrow CN^-+H_2O+O+H$, $CH_3NO_2+e^-\rightarrow CN^-+H_2+O_2+H$, $RNO_2+e^-\rightarrow CN^-+R_1+HO_2+H$, and $C_3H_7NO_2+e^-\rightarrow CN^-+C_2H_4+H_2+O+OH$ irrespective of kind of nitropropane. For the third process, $CH_3NO_2+e^-\rightarrow CN^-+3H+O_2$. For *m/e* 42 (probably, CNO^-) ions, the contribution of two processes was observed. By taking $\Delta H_f(CNO)=x$ (eV), $EA(CNO)=y$ (eV), and also combining the observed onset values with the calculated values of appearance potential of reactions to be assigned for each process — for the first process, $CH_3NO_2+e^-\rightarrow CNO^-+H_2+OH$, $RNO_2+e^-\rightarrow CNO^-+R_1OH+H$; for the second process, $CH_3NO_2+e^-\rightarrow CNO^-+HO+2H$, $CH_3NO_2+e^-\rightarrow CNO^-+H_2+O+H$, $RNO_2+e^-\rightarrow CNO^-+R_1O+2H$ — a relation of $x-y\simeq 2$(eV) was derived.

Recently, several studies have been reported on the measurement of negative ion mass spectra by the electron impact method.[1-4] However, they were only made for limited kinds of compounds. Furthermore, data on the ionization efficiency (*IE*) curves of negative ions are very limited.[5-7] We published previously the results of measurement of *IE* curves of NO_2^-, O^- and $CH_2NO_2^-$ ions from nitroalkanes; nitromethane, nitroethane, 1-nitropropane and 2-nitropropane.[8] This work has been extended to the measurements of negative ions of *m/e* 26 and 42 and affords information on *IE* curves of these negative ions for which as far as the authors know few reports have been found.

Experimental

This investigation was carried out using a Hitachi RMU-6D mass spectrometer equipped with a T-2M ion source having a rhenium filament. The ion detection circuit consisted of a ten stage electron multiplier and of a Faraday collector. The experimental condition and the correction method of electron energy scale were identical to those previously described.[8]

The materials used were of research grade and no further purifications have been done.

Results and Discussion

Formation of *m/e* 26 Ions. In nitromethane, *m/e* 26 ions can be assigned to CN^-. Although the possibility of $C_2H_2^-$ ions in other samples might be considered, little formation[1] of $C_2H_2^-$ ions from alcohols appears to rule out this possibility. Figure 1 shows that, except for nitromethane, two processes contribute to the formation of CN^- ions. The first process appears at a considerably lower energy than 3 eV irrespective of the compounds and the second one seems to appear at ~5.2 eV in nitroethane, ~4.4 eV in 1-nitropropane

1) C. E. Melton, "Mass Spectrometry of Organic Ions," ed. by F. W. McLafferty, Academic Press, New York, N. Y. (1963), p. 163.
2) E. W. McDaniel, "Collision Phenomena in Ionized Gases," John Wiley & Sons Inc., New York (1964) p. 368.
3) R. T. Aplin, H. Budzikieweiz and C. Djerassi, *J. Am. Chem. Soc.*, **87**, 3180 (1965).
4) C. E. Melton and P. S. Rudolf, *J. Chem. Phys.*, **47**, 1771 (1967).
5) L. G. Christophorou, R. N. Compton, G. S. Hurst and P. W. Reinhardt, *J. Chem. Phys.*, **45**, 536 (1966).
6) L. G. Christophorou and R. N. Compton, *Health Phys.*, **13**, 1277 (1967).
7) T. Sugiura, T. Seguchi and K. Arakawa, This Bulletin, **40**, 2992 (1967).
8) S. Tsuda, A. Yokohata and M. Kawai, *ibid.*, **42**, 607, 614 (1969).

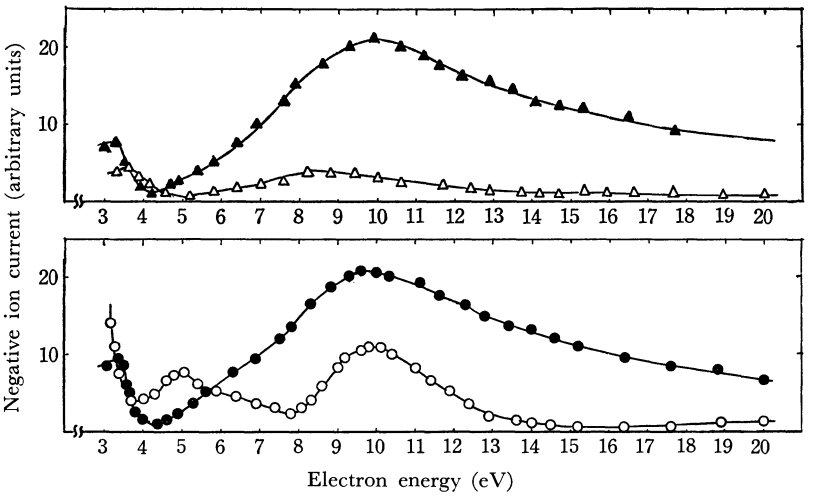

Fig. 1. Ionization efficiency curves of negative ions of *m/e* 26 from nitroalkanes.
○ CH_3NO_2 ● 1-$C_3H_7NO_2$ △ $C_2H_5NO_2$ ▲ 2-$C_3H_7NO_2$

and 2-nitropropane.*1 In nitromethane three processes can be found; the second one seems to appear at ~3.7 eV and the third at ~7.8 eV.

For the first process in nitromethane, reactions (1), (2) and (3) are expected. Their appearance potentials can be estimated to be −0.85 eV, 1.47 eV and 2.12 eV, respectively,*2 by using $\Delta H_f(CH_3NO_2) = -0.8$ eV,[9] $\Delta H_f(CN) = 3.87$ eV,[10] $\Delta H_f(H_2O) = -2.50$ eV, $\Delta H_f(OH) = 0.38$ eV, $\Delta H_f(HO)_2 = 0.2$ eV, $\Delta H_f(H_2) = 0.00$ eV, $\Delta H_f(H_2O_2) = -1.41$ eV, $\Delta H_f(H) = 2.26$ eV*3 and $EA(CN) = 3.4$ eV*4

$$CH_3NO_2 + e^- \rightarrow CN^- + H_2O + OH \quad (1)$$
$$(AP_{calc} = -0.85 \text{ eV})$$

$$CH_3NO_2 + e^- \rightarrow CN^- + HO_2 + H_2 \quad (2)$$
$$(AP_{calc} = 1.47 \text{ eV})$$

$$CH_3NO_2 + e^- \rightarrow CN^- + H_2O_2 + H \quad (3)$$
$$(AP_{calc} = 2.12 \text{ eV})$$

Among these reactions, the possibility of reaction (1) is very great, because the appearance potential of the first process has been qualitatively found to be very low. Thus, the process which appears at a considerably lower energy than 3 eV may be concluded to be due to reaction (1). A negative value of the appearance potential of this reaction means that the occurrence of this reaction is possible even with the electrons of thermal energy. The situation is quite similar to that of NO_2^- from nitromethane in which the appearance potential of dissociative electron capture shows a negative value because of $EA(NO_2) > D(CH_3\text{-}NO_2)$.

For the other samples, the occurrence of reactions (4) or (5) resulting in the formation of alcohols can be strongly expected under the analogy with reaction (1). The appearance potentials of reactions (4) and (5) can be estimated to be −0.53 eV and −0.96 eV, by using $\Delta H_f(CH_3OH) = -2.08$ eV, $\Delta H_f(C_2H_5OH) = -2.44$ eV, $\Delta H_f(C_2H_5NO_2) = -0.70$ eV and $\Delta H_f(1\text{-}C_3H_7NO_2) = -0.63$ eV.*5

*1 Since the tailing due to the first process might be overlapped with the appearance of the second process, the exact determination of appearance potential of the second process is difficult. In this work, the minimum values in *IE* curves have been taken up as the object of discussion.

*2 These values mean the lowest value of the energy needed for the appearance of the reaction.

9) R. J. Kandel, *J. Chem. Phys.*, **23**, 84 (1955).

10) V. H. Dilbeler, R. M. Reese and J. L. Franklin, *J. Am. Chem. Soc.*, **83**, 1813 (1961).

*3 For the values of ΔH_f, see the report of Bernecker. (R. R. Bernecker and F. A. Long, *J. Phys. Chem.*, **65**, 1565 (1961)).

*4 For the electron affinity (*EA*) of CN, the values of 3.2 eV and 3.6 eV have been published. In this work, 3.4 eV (the mean value) was used. (J. T. Herron and V. H. Dibeler, *J. Am. Chem. Soc.*, **82**, 1555 (1960); E. Lederle, *Z. Physik. Chem.*, **B17**, 362 (1932).

*5 The value of $\Delta H_f(C_2H_5NO_2)$ can be estimated in the following way.

$$NH \rightarrow N + H, \qquad \Delta H = 3.61 \text{ eV}$$
$$NO \rightarrow N + O, \qquad \Delta H = 6.52 \text{ eV}$$
$$NO_2 \rightarrow NO + O, \qquad \Delta H = 3.16 \text{ eV}$$

Therefore, $\Delta H_f(NO_2) = 0.32$ eV can be obtained by using the known values of $\Delta H_f(NH)$, $\Delta H_f(H)$ and $\Delta H_f(O)$. Combining the appearance potential (10.9 eV) of the reaction ($C_2H_5NO_2 + e^- \rightarrow C_2H_5^+ + NO_2 + 2e^-$) with $\Delta H_f(NO_2) = 0.32$eV, we obtain a value of −0.70 eV for $\Delta H_f(C_2H_5NO_2)$; S. Tsuda and W. H. Hamill, *Advan. Mass Spectry.*, **3**, 249 (1965).

In the same way, $\Delta H_f(1\text{-}C_3H_7NO_2) = -0.63$ eV can be also estimated; V. I. Vedeneyev, L. V. Gurvich, V. N. Kondrat'yev, V. A. Medvedev and Ye. L. Frankevich, "Bond Energies, Ionization Potentials and Electron Affinities," Edward Ltd., London (1966), p. 80.

$$C_2H_5NO_2 + e^- \rightarrow CN^- + CH_3OH + OH \quad (4)$$
$$(AP_{calc} = -0.53\ eV)$$
$$1\text{-}C_3H_7NO_2 + e^- \rightarrow CN^- + C_2H_5OH + OH \quad (5)$$
$$(AP_{calc} = -0.96\ eV)$$

For 2-nitropropane, the same interpretation would be also applied.

For the second process of nitromethane, reactions (6) and (7) might be considered. The values of their appearance potential can be estimated to be 3.53 eV and 3.59 eV which are almost consistent with the observed onset value of 3.7 eV.

$$CH_3NO_2 + e^- \rightarrow CN^- + H_2 + O_2 + H \quad (6)$$
$$(AP_{calc} = 3.53\ eV)$$
$$CH_3NO_2 + e^- \rightarrow CN^- + H_2O + O + H \quad (7)$$
$$(AP_{calc} = 3.59\ eV)$$

In other words, the second process can be interpreted with other complicated electron capture processes different from reaction (1) or resulting in a further dissociation of product of reaction (1).

For the second process of nitroethane and 1-nitropropane, the possibility of reactions (8), (9) or (10) would be pointed out. Their appearance potentials give the values of 5.02 eV, and 4.56 eV or 4.59 eV which are almost consistent with the observed onset values; 5.2 eV (for nitroethane) and ~4.4 eV (for 1-nitropropane)

$$C_2H_5NO_2 + e^- \rightarrow CN^- + CH_3 + HO_2 + H \quad (8)$$
$$(AP_{calc} = 5.02\ eV)$$
$$1\text{-}C_3H_7NO_2 + e^- \rightarrow CN^- + C_2H_5 + HO_2 + H \quad (9)$$
$$(AP_{calc} = 4.56\ eV)$$
$$1\text{-}C_3H_7NO_2 + e^- \rightarrow CN^- + C_2H_4 + H_2 + OH + O$$
$$(AP_{calc} = 4.59\ eV) \quad (10)$$

For the third process in nitromethane, reaction (11) resulting in a further dissociation of product accompanied with the rearrangement might be assigned. This reaction gives a value of 8.05 eV for the appearance potential which is almost consistent with the observed onset value, ~7.8 eV.

$$CH_3NO_2 + e^- \rightarrow CN^- + 3H + O_2 \quad (11)$$
$$(AP_{calc} = 8.05\ eV)$$

Formation of *m/e* 42 Ions. In nitromethane, the ions of *m/e* 42 can be assigned to CNO^-. In other samples, however, the possibility of $C_2H_4N^-$ ions exists. Figure 2 shows*6 that two processes contribute to the formation of these ions. The first process appears at ~3 eV in nitromethane, nitroethane and 2-nitropropane and at ~2.6 eV*7 in 1-nitropropane, and the second ones seem to appear at ~7.5 eV in nitromethane, ~7.2 eV in nitroethane and ~6.8 eV in 1-nitropropane and 2-nitropropane.

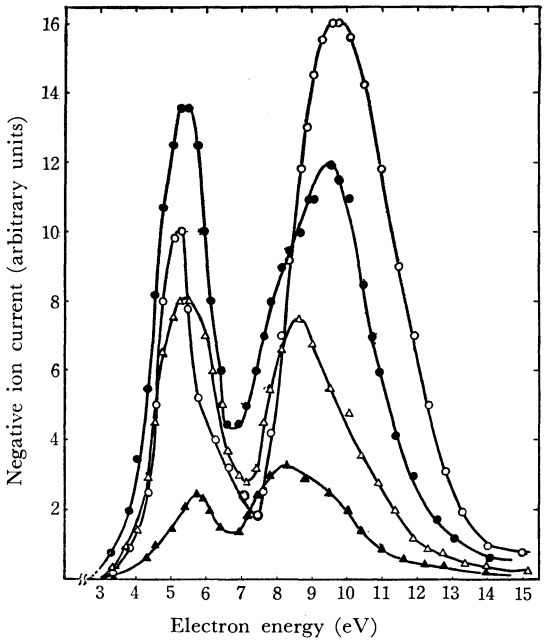

Fig. 2. Ionization efficiency curves of negative ions of *m/e* 42 from nitroalkanes.

○ CH_3NO_2 ● $1\text{-}C_3H_7NO_2$
△ $C_2H_5NO_2$ ▲ $2\text{-}C_3H_7NO_2$

In the case of CNO^- ions, the lack of knowledge of the values of $\Delta H_f(CNO)$ and $EA(CNO)$ makes difficult the assignment of reactions which correspond to each process. It is possible, however, to have some interesting discussions. Now, taking $\Delta H_f(CNO)=x(eV)$ and $EA(CNO)=y(eV)$, the appearance potentials of reactions to be expected would be estimated as follows.

For the first process;

$$CH_3NO_2 + e^- \rightarrow CNO^- + H_2O + H \quad (12)$$
$$CH_3NO_2 + e^- \rightarrow CNO^- + H_2 + OH \quad (13)$$
$$C_2H_5NO_2 + e^- \rightarrow CNO^- + CH_3OH + H \quad (14)$$
$$1\text{-}C_3H_7NO_2 + e^- \rightarrow CNO^- + C_2H_5OH + H \quad (15)$$

Then, the appearance potentials of each reaction can be estimated as follows, by using the known values of ΔH_f.

$$AP_{12} = x - y + 0.56, \quad AP_{13} = x - y + 1.18$$
$$AP_{14} = x - y + 0.88, \quad AP_{15} = x - y + 0.45$$

Combining these values with the observed onset values leads to the following results.
For nitromethane; $x-y=2.44$ or $x-y=1.82$.
For nitroethane; $x-y=2.12$, for 1-nitropropane; $x-y=2.15$.

For the second process;

*6 In general the *IE* curve of resonance type appears to correspond to the electron capture process. If so, the possibility of ion pair formation ($R^+ + NO_2^-$) discussed in the second report[8] might be required to be replaced with another mechanism (for example, $CH_3NO_2 + e^- \rightarrow NO_2^- + CH + 2H$; $AP_{calc}=7.9$ eV.

*7 estimated by extrapolation.

$$CH_3NO_2 + e^- \rightarrow CNO^- + OH + 2H \quad (16)$$

$$CH_3NO_2 + e^- \rightarrow CNO^- + H_2 + O + H \quad (17)$$

$$C_2H_5NO_2 + e^- \rightarrow CNO^- + CH_3O + 2H \quad (18)$$

$$1\text{-}C_3H_7NO_2 + e^- \rightarrow CNO^- + C_2H_5O + 2H \quad (19)$$

By the same treatment, the following results can be obtained.

For nitromethane; $x-y=1.79$ or $x-y=1.88$, for nitroethane and 1-nitropropane; $x-y=2.02$, $x-y=2.02$.

If the value of 2.44 eV is excluded,*8 a value of 1.97 ± 0.13 eV can be estimated for the mean value of $(x-y)$. Here, it should be noticed that a relatively good constancy of $(x-y)$ has been found. In other words, this suggests that the assignments above mentioned are plausible ones.

On the other hand, the appearance potential of the reactions resulting in the formation of C_2H_4N species from nitroethane (for specific example) can be approximately estimated to be 9.6 or 8.9 eV*9 by taking $D(NO\text{-}O)=3.2$ eV, $D(N\text{-}O)=6.6$ eV, $D(H\text{-}C_2H_5)=4.2$eV, $D(O\text{-}H)=4.4$eV and $D(O\text{-}O)=5.1$ eV.*10 Of course, this estimation is the approximate one in the meaning that there are assumed to be $D(H\text{-}C_2H_4NO_2)=D(H\text{-}C_2H_5)$, $D(C_2H_4NO\text{-}O)=D(NO\text{-}O)$ and $D(C_2H_4N\text{-}O)=D(N\text{-}O)$. Although the nitro group has a tendency to weaken the carbon-hydrogen bond,[9] its effect cannot be considered to be great. Now, combining the value of 9.6 or 8.9 eV with the observed value ($\sim$3 eV) of appearance potential, we can obtain the value of 6.6 or 5.9 eV for the electron affinity of C_2H_4N species. Judging from the values of electron affinity of various species published hitherto, however, this is too high. At any rate, few reports on the formation of $C_2H_4N^-$ ions and the lack of knowledges of $\Delta H_f(C_2H_4N)$ and EA (C_2H_4N) make difficult a further discussion. Thus, in this work the possibility of $C_2H_4N^-$ ions was not taken into consideration.

In the range of electron energy higher than 16—20 eV, ion pair formations might be expected. The determination of onset values, however, was difficult because of little change of ion current in addition to the weak intensity.

*8 This means that reaction (12) is to be rejected.

*9 Products to be assigned; $OH+O$ or $H+O_2$.

*10 For each D value, see the article of Vedeneyev *et al.*, in *5.

BULLETIN OF THE CHEMICAL SOCIETY OF JAPAN VOL. 42 1519—1524 (1969)

Preparation of Star-Type Graft Copolymer through the Polymerization of Methyl Methacrylate with Use of the Potassium Complexes of Polystyrene having a Benzophenone Unit

Koji NOBUTOKI and Hiroshi SUMITOMO

Faculty of Agriculture, Nagoya University, Chikusa, Nagoya

(Received November, 12, 1968)

Polystyrene ketone possessing a benzophenone structural unit in the middle part of the chain was synthesized by the coupling reaction of one-ended living polystyrene with 2,4'-dichlorobenzophenone. Polystyrene ketone potassium ketyl was prepared by the reaction of polystyrene ketone with an equivalent amount of potassium naphthalene complex in tetrahydrofuran. Polystyrene ketone potassium dianion was also formed with excess potassium in the solvent. These polystyrene ketone potassium adducts induced a quantitative polymerization of metyl methacrylate. Gross polymer from each of the reaction systems was elution-fractionated into four fractions in which a new class of star-type graft copolymer was included together with polystyrene and polymethyl methacrylate. Each fraction was characterized by means of the measurements of the yield, molecular weight and styrene content. Consideration was also made on a possible mechanism of the polymerization.

Syntheses of well defined block, graft and star-type branched copolymers by means of anionic living polymerization have been recently developed.[1-11] Polymerization and graft copolymerization initiated by the alkali metal complexes of aromatic ketone and of polyvinyl benzophenone have also been studied.[12-17] An attempt was made in a previous paper[18] to prepare a new class of star-type graft copolymers with different kinds of branches, starting from the potassium adducts of polystyrene ketone possessing one or two carbonyl groups in the middle part of the chain. Few investigations, however, have been made as to the mechanism of initiation by ketyl or dialkali metal complexes. The present paper is concerned with an attempt to obtain star-type graft copolymers with polymethyl methacrylate branches, starting from the potassium adducts of polystyrene ketone possessing a benzophenone structural unit in the middle part of the chain and with the consideration on a possible initiation mechanism of the polymerization.

Experimental

Materials. Styrene (St) and methyl methacrylate (MMA) were purified by the usual methods. Tetrahydrofuran (THF) was distilled after refluxing with sodium. Each monomer and the solvent were directly introduced into a polymerization vessel by distillation from calcium hydride and from sodium-benzophenone, respectively, after evacuation by repeating freezing and thawing in a vacuum line (10^{-6} mmHg).

2,4'-Dichlorobenzophenone (DCBP) was recrystallized from petroleum ether. Methyl phenyl isopropenyl ether was synthesized according to the method of

1) M. Morton, T. E. Helminiak, S. D. Gadkary and F. Bueche, *J. Polymer Sci.*, **57**, 471 (1962).
2) G. Finaz, Y. Gallot, J. Parrod and R. Rempp, *ibid.*, **58**, 1363 (1962).
3) T. A. Orofino and F. Wenger, *J. Phys. Chem.*, **67**, 566 (1963).
4) H. Sumitomo, K. Nobutoki and Y. Hachihama, *Kogyo Kagaku Zasshi (J. Chem. Soc. Japan, Ind. Chem. Sect.)*, **67**, 1966 (1964).
5) M. Morton, A. A. Rembaum and E. E. Bostick, *J. Appl. Polymer Sci.*, **8**, 2707 (1964).
6) R. P. Zelinski and C. F. Wofford, *J. Polymer Sci.*, **A3**, 93 (1965).
7) T. Altares, Jr., D. P. Wyman, V. R. Allen and K. Meyersen, *ibid.*, **A3**, 4131 (1965).
8) G. Kraus and J. T. Gruver, *ibid.*, **A3**, 105 (1965).
9) K. Nobutoki and H. Sumitomo, This Bulletin, **40**, 1741 (1967).
10) T. Tabuchi, K. Nobutoki and H. Sumitomo, *Kogyo Kagaku Zasshi (J. Chem. Soc. Japan, Ind. Chem. Sect.)*, **71**, 1926 (1968).
11) J. A. Gervasi, A. B. Gosnell, D. K. Woods and V. Stannett, *J. Polymer Sci.*, **A-1**, **6**, 859 (1968).
12) S. Smith, *ibid.*, **38**, 259 (1959).
13) A. Zilkha, P. Neta and M. Frankel, *Proc. Chem. Soc.*, **1960**, 364.
14) A. Zilkha, P. Neta and M. Frankel, *J. Chem. Soc.*, **1960**, 3357.
15) S. Inoue, T. Tsuruta and J. Furukawa, *Makromol. Chem.*, **36**, 77 (1959); *ibid.*, **42**, 12 (1960).
16) H. Takida and K. Noro, *Kobunshi Kagaku (Chem. High Polymers, Japan)*, **22**, 724 (1965).
17) H. Takida and T. Moriyama, *ibid.*, **24**, 57 (1967).
18) K. Nobutoki and H. Sumitomo, This Bulletin, **40**, 2725 (1967).

Ziegler and Dislich.[19]

Polymerization Procedures. General experimental techniques for a homogeneous anionic polymerization developed by Szwarc *et al.*[20] and by Morton *et al.*[21] were employed in the present investigation. Phenyl isopropyl potassium was prepared by the reaction of methyl phenyl isopropenyl ether with potassium-sodium alloy in THF *in vacuo*. This solution was filtered through a sintered glass filter to remove a small amount of potassium methoxide formed in the reaction.

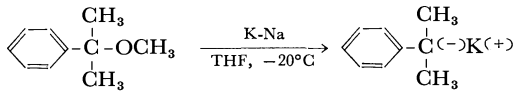

One-ended living polystyrene (PSt) prepared from the reaction of St with phenyl isopropyl potassium in THF was coupled with DCBP resulting in the formation of polystyrene ketone (PSt(CO)) having one carbonyl group in the middle part of the chain. In the coupling reaction two procedures were adopted, *i. e.* i) the solution of the coupling agent was added slowly to the solution of living polystyrene until its red color disappeared and ii) reversely, the solution of living PSt was added to the solution of the coupling agent.

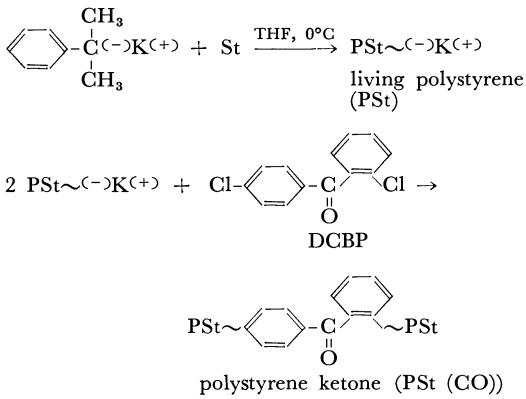

Fractional precipitation of the coupling reaction product was made using benzene as a solvent and methanol as a precipitant at room temperature.

Potassium ketyl of PSt ketone was obtained by the treatment of PSt ketone with an equivalent amount of potassium naphthalene in THF. Potassium dianion of PSt ketone was also prepared by the reaction of PSt ketone with an excess of potassium in THF and the solution was filtered through a sintered glass filter to remove excess potassium.

The polymerization of MMA initiated by these adducts was performed in a vacuum system at room temperature. The resulting gross polymer was separated into four fractions using an extraction technique. Number average molecular weights of polymers were measured in benzene at 25°C using Hewlett-Packard 302 Vapour Pressure Osmometer (VPO).

Results and Discussion

Preparation of Polystyrene Ketone. Phenyl isopropyl potassium was prepared by the reaction of methyl phenyl isopropenyl ether with potassium-sodium alloy in THF. One-ended living PSt was prepared by the polymerization of St in THF with the use of phenyl isopropyl potassium. The results are shown in Tables 1 and 2.

PSt ketone having a benzophenone structural unit in the middle part of the chain was obtained by the stoichiometric coupling reaction of the living PSt with DCBP. The results of the coupling reactions are shown in Table 3.

The number average molecular weights Mn of the products are considerably smaller than the value, 1800, for PSt ketone calculated from Mn of starting living PSt. It is likely that unreacted PSt or mono-substituted PSt may also be contained in the product because of the low rate of coupling reaction of living PSt with DCBP.

Comparing A with B there is a difference in Mn of the products. It seems probable in the coupling reaction that the substitution reaction of living PSt with two chlorine atoms is in competition with the addition reaction of living PSt to a carbonyl group in DCBP. When an excess amount of living PSt is added to DCBP, tri-chain PSt would be formed.

Fractional precipitation for the coupling reaction

Table 1. Preparation of phenyl isopropyl potassium

Methyl phenyl isopropenyl ether ml	THF ml	K : Na g	Temp. °C	Time hr
10.0	99.2	9.82 : 2.44	−20	40

Table 2. Preparation of one-ended living polystyrene

Phenyl isopropyl potassium-THF soln. ml	St g	THF ml	Temp. °C	Time hr	Concn. of living PSt mol/l	Mn of PSt[a]
74.3	21.09	305.0	0	3	7.71×10^{-2}	810

a) VPO; benzene; 25°C.

19) K. Ziegler and H. Dislich, *Chem. Ber.*, **90**, 1107 (1957).
20) M. Szwarc, M. Levy and R. Milkovich, *J. Am. Chem. Soc.*, **78**, 2656 (1956).
21) M. Morton, R. Milkovich, D. B. McIntyre and L. J. Bradley, *J. Polymer Sci.*, **A1**, 443 (1963).

Table 3. Coupling reaction of living polystyrene with 2,4'-dichlorobenzophenone

Run[a]	Living PSt-THF soln. ml	PSt g	DCBP-THF soln. ml	DCBP g	Temp. °C	Time hr	Gross polymer Yield, g	Gross polymer Mn[b]
A	278.4	17.80	110.0	2.73	25	5	20.40	1067
B	88.8	5.55	103.8	0.86	0	5	5.35	1460

a) A, The solution of living PSt in THF was added into the solution of DCBP in THF.
B, The solution of DCBP in THF was added into the solution of living PSt in THF.
b) VPO; benzene; 25°C.

Table 4. Fractionation of coupling reaction products

A) Original gross polymer, 20.25 g; benzene, 100 ml

Fr.	MeOH ml	Wt g	Mn
1	75	3.30	2310
2	90	3.56	2170
3	105	2.15	1970
4	130	1.86	1810
5	170	1.03	1740
6	MeOH insol.	4.86	960
Total		16.76[a]	

a) Methanol soluble fraction was accidentally lost.

B) Original gross polymer, 5.20 g; benzene, 25 ml

Fr.	MeOH ml	Wt g	Mn
1	25	2.66	2230
2	50	1.00	2030
3	100	0.33	1670
4	MeOH insol.	0.36	1260
5	MeOH sol.	0.64	684
Total		4.99	

product was carried out using benzene as a solvent and methanol as a precipitant at room temperature. These results are shown in Table 4.

The molecular weight of PSt ketone is calculated to be 1800 from the number average molecular weight of starting living PSt. Therefore, the values of molecular weights of Fr. 1 and Fr. 2 in both A- and B series may suggest that they contain tri-chain PSt. On the other hand, low molecular weight fractions Fr. 6 of A, Fr. 4 and 5 of B are considered to consist mainly of "mono"PSt.

Infrared-, UV- and visible absorption spectra of PSt ketone are shown in Figs. 1 and 2.

The stretching vibration of the carbonyl group in PSt ketone appears at 1660 cm^{-1} in the IR spectrum. It is known that the absorption based on the n–π^* transition of the carbonyl group of benzophenone exists at 330 mμ. PSt gives no absorption in UV- and visible absorption spectra. Therefore

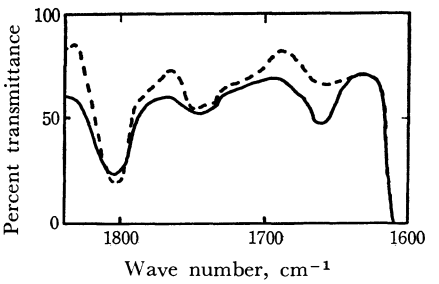

Fig. 1. Infrared spectra of polystyrene ketone and polystyrene.
——, Polystyrene ketone (A-5); ----, polystyrene

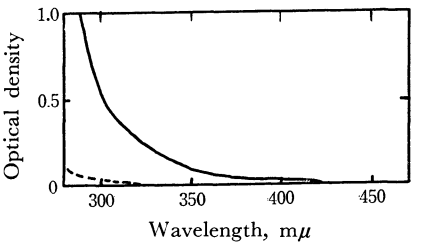

Fig. 2. UV- and visible absorption spectra of polystyrene ketone and polystyrene (in THF).
——, Polystyrene ketone (A-4) (10.0 mg/10 ml THF); ----, polystyrene (10.7 mg/10 ml THF)

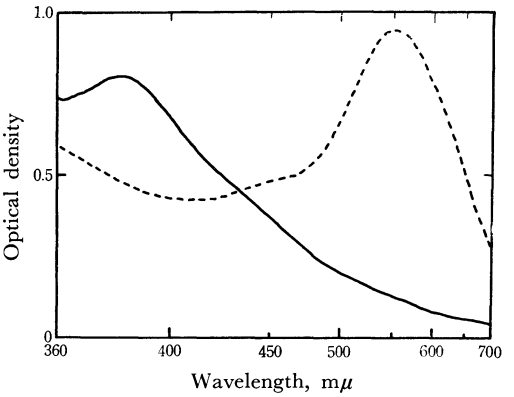

Fig. 3. Visible absorption spectra of polystyrene ketone potassium ketyl and polystyrene ketone potassium dianion (Solvent, THF).
——, PSt(CO)-K ketyl; ----, PSt(CO)-2K dianion

TABLE 5. PREPARATIONS OF POLYSTYRENE KETONE POTASSIUM ADDUCTS

PSt(CO) g	PSt(CO)-THF soln., m*l*	Potassium or potassium complex	Temp. °C	Time hr	Color	PSt(CO)-K adduct
0.920(A-5)	84.4	K-Naphthalene	r.t.[a)]	5	dark yellow	PSt(CO)-K ketyl
1.645(A-4)	120.4	K	0	2	purple	PSt(CO)-2K dianion

a) Room temperature.

TABLE 6. POLYMERIZATIONS OF METHYL METHACRYLATE WITH POLYSTYRENE KETONE POTASSIUM ADDUCTS

PSt(CO)-K adduct-THF soln.[a)] m*l*	PSt(CO) g	MMA g	THF m*l*	Temp. °C	Time hr	Yield g	Convn. of MMA %
84.4 (I)	0.92	1.53	41.6	22	1	2.34	92.8
100.9 (II)	1.38	2.06	53.1	23	1	3.15	86.0

a) I, polystyrene ketone potassium ketyl; II, polystyrene ketone potassium dianion.

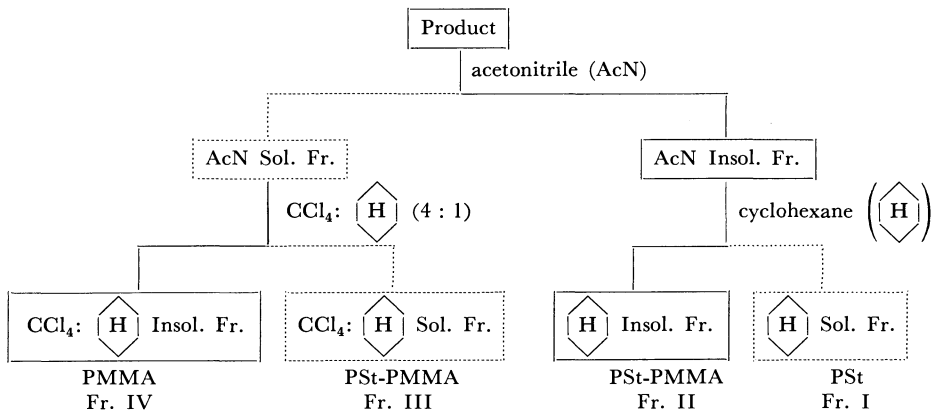

Fig. 4. An elution-fractionation scheme for the product in the system of methyl methacrylate-polystyrene ketone potassium adduct.
——, Insoluble fraction; ·····, soluble fraction

a broad absorption band in the region of 330 to 450 mμ may be considered to be characteristic of PSt ketone. It is clear from these facts that a benzophenone structural unit enters in the PSt chain.

Preparations of Polystyrene Ketone Potassium Adducts. Table 5 represents the conditions of the reactions of PSt ketone with an equivalent amount of potassium-naphthalene or excess potassium in THF.

Figure 3 illustrates visible absorption spectra of PSt ketone potassium adducts.

The maximum absorptions appear at 384 mμ for dark yellow solution of the potassium ketyl and at 545 mμ for purple solution of the potassium dianion of PSt ketone. The change of the color from dark yellow to purple is observed by the addition of the THF solution of potassium naphthalene into the THF solution of PSt ketone potassium ketyl. These maximum absorptions are respectively in accord with those of benzophenone potassium ketyl at 382 mμ and benzophenone potassium dianion at 536 mμ.

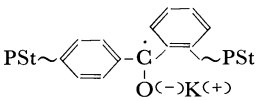

polystyrene ketone potassium ketyl

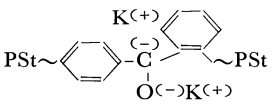

polystyrene ketone potassium dianion

Polymerization of Methyl Methacrylate with Polystyrene Ketone Potassium Adducts. The results of the polymerization of MMA with PSt ketone potassium adducts are shown in Table 6.

A gross polymer obtained in the PSt-MMA system was elution-fractionated using acetonitrile, cyclohexane and carbon tetrachloride - cyclohexane (4 : 1) as solvents into four fractions as shown in Fig. 4.

In Table 7 are presented the compositions and the molecular weights of the fractions determined by infrared analysis, elementary analysis and vapor pressure osmometry. The composition of Fr. I, as seen in the table, consists almost all of PSt. The molecular weight of Fr. I was higher than that of the parent PSt ketone. Therefore the formation of tetrachain PSt of benzpinacol type structure, to which extremely short MMA chain may attach, and its inclusion in this fraction may be considered (*cf.* reaction (5)). Fr. IV was confirmed to be polymethyl methacrylate (PMMA) from the results of infrared- and elementary analyses. The PSt-PMMA graft copolymer must be contained in

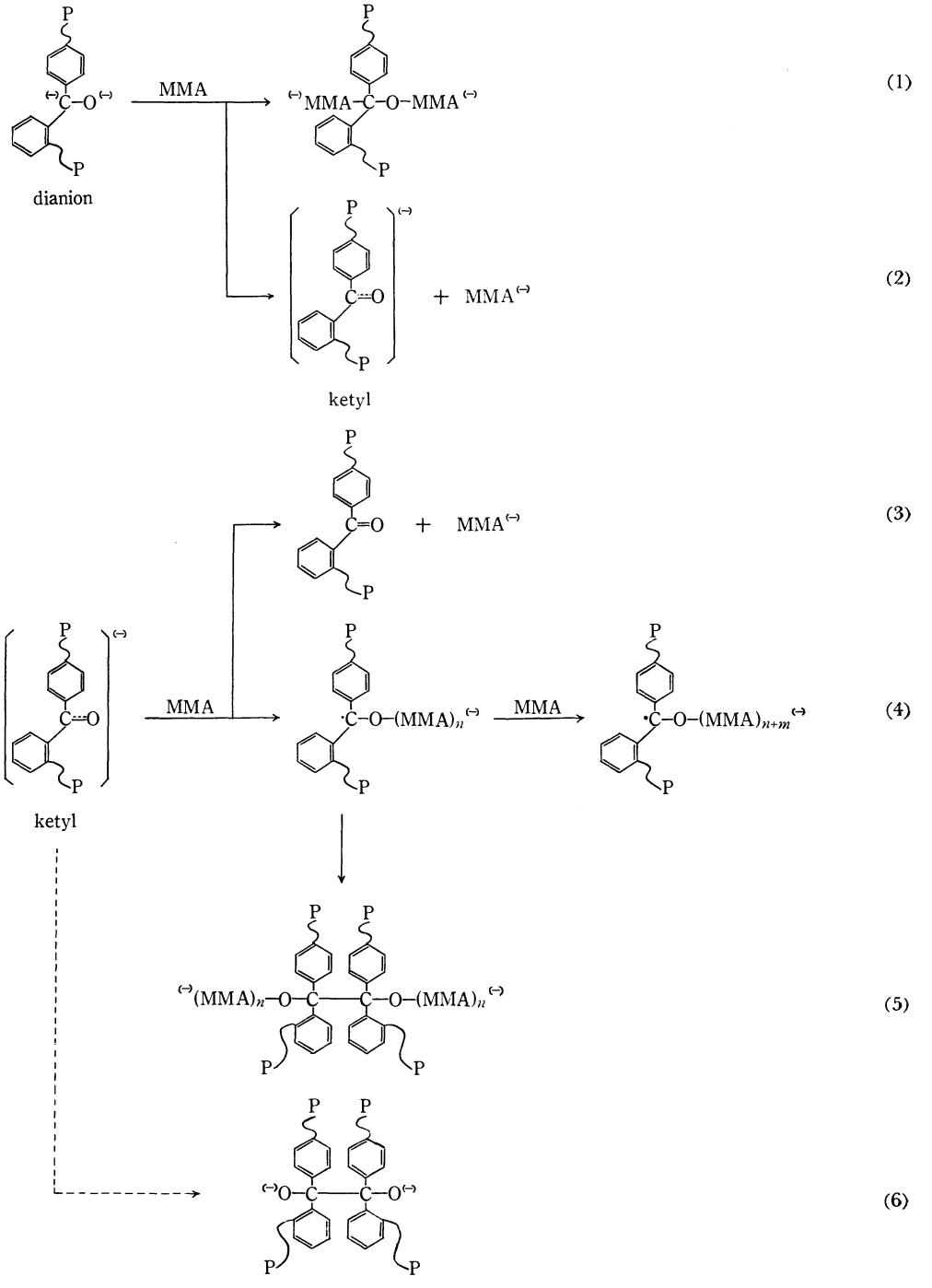

TABLE 7. COMPOSITIONS AND MOLECULAR WEIGHTS OF THE FRACTIONS

Initiator		Fr. I	Fr. II	Fr. III	Fr. IV
PSt(CO)-2K dianion	Wt, g (%)	0.60(20.8)	0.21(7.3)	1.50(51.9)	0.58(20.0)
	Mn (VPO)	2590	6010	3630	8710
	St content[a] (wt%)	87.9	39.1	19.2	0
PSt(CO)-K ketyl	Wt, g (%)	0.27(11.5)	0.02(0.9)	1.61(68.8)	0.44(18.8)
	Mn (VPO)	2500	—	2400	10000
	St content[b] (wt%)	>90	40.4	41.9	0

a) Calcd. from elementary analysis data.
b) Calcd. using calibration curve of optical density ratio (D_{700}/D_{1720}).

Fr. II and III. The fact that the molecular weight of Fr. III is much smaller than that calculated from its St content might be attributed to the intermixing of low molecular weight PMMA.

From the experimental results described above possible mechanisms of the polymerization are presumed as follows.

In the polymerizations of MMA initiated with PSt(CO)-K dianion and - ketyl, PSt and PMMA together with PSt-PMMA star-type graft copolymer were formed. PSt(CO)-K dianion would react with MMA to result in the formation of PMMA dianion through the bond-formation mechanism (1) and PSt(CO)-K ketyl and the monomer anion through the electron-transfer mechanism (2). The formation of PSt and PMMA suggests the occurrence of the electron transfer from PSt(CO)-K ketyl as shown in reaction (3).

PSt-PMMA graft copolymer may be produced by the bonding of MMA with alcoholate anion of PSt(CO)-K ketyl as represented in reaction (4).

Contrary to the case of an equilibrium between benzophenone-alkali metal ketyl and benzpinacolate, the presence of PSt substituted benzpinacolate was denied by means of the measurement of the molecular weight of killed PSt(CO)-K ketyl. The formation of PSt substituted benzpinacolate shown in reaction (6) is improbable. The molecular weight of Fr. I in Table 7 was higher than that of the parent PSt(CO). It is probable that PSt-PMMA graft copolymer formed in the reaction (5) may be partly included in Fr. I together with PSt(CO) formed in the reaction (3).

In view of so small a content, if any, of the graft copolymer with short MMA-grafts in Fr. I, it seems that the radical anion carrying extremely low molecular weight PMMA may be preferentially contributed to the further addition of MMA (reaction (4)) compared with reaction (5). The coupling reaction (5), however, may also be possible because of the decrease in the coulombic repulsion between the chain end anions. In conclusion both the electron transfer and the bond formation were ascertained to coexist in the intitations of MMA with use of PSt(CO)-K ketyl and dianion.

BULLETIN OF THE CHEMICAL SOCIETY OF JAPAN VOL. 42 1525—1530 (1969)

Thermodynamic Properties of Galvinoxyl Radical and Its Phenol Derivative; Mechanism of the Phase Transition*[1]

Akio KOSAKI, Hiroshi SUGA and Syûzô SEKI

Department of Chemistry, Faculty of Science, Osaka University, Toyonaka, Osaka

and Kazuo MUKAI and Yasuo DEGUCHI

Department of Chemistry, Faculty of Science, Kyoto University, Sakyo-ku, Kyoto

(Received November 13, 1968)

Measurements of heat capacity of Galvinoxyl radical and its phenol derivative were carried out in the temperature region from 12 to 300°K. Galvinoxyl radical exhibits a phase transition of first-order nature at 81.5°K which corresponds to the susceptibility anomaly already measured. The enthalpy and entropy of transition amount to 1504.6 J/mol and 18.67 J/(°K·mol), respectively. The entropy change, which corresponds formally to R ln 9.45, cannot be explained by taking only the magnetic contribution. On the other hand, its phenol derivative, the corresponding diamagnetic substance, has not thermal anomaly in the above temperature region. X-Ray diffraction patterns at room temperature for both substances agree well with each other in their diffraction angles. From these experimental findings, it seems to be plausible that a kind of transformation of the crystal structure of Galvinoxyl radical takes place at the transition point which may be induced by a pairing of magnetic spins between neighboring molecules.

Recently, magnetic properties of stable organic free radical crystals have attracted interest of many chemists and physicists. Among these crystals, tetracyano-quinondimethane (TCNQ salts) as anion radicals, Würster Blue (WB salts) as cation radicals and 1,3-bisdiphenylene-2-phenyl allyl (BDPA) as a neutral one would be the typical substances. As the molecular structures of these radicals are considered to be planar, the magnetic properties of crystals composed of these molecules would be similar to each other.

The present substance, Galvinoxyl radical, 2,6-di-*t*-butyl-4(3,5-di-*t*-butyl-4-oxocyclohexa-2,5-dienylidene methyl) phenoxyl (hereafter, designated as G. R., see Fig. 1) is considered to be composed of non-planar molecules due to the mutual intramolecular steric hindrance of the attached tertial butyl groups. Accordingly, it is expected that the physico-chemical properties of G. R. may be different more or less from those of the radical crystals mentioned above. The magnetic susceptibility of G. R.[1] has already been measured by two of the present authors (K. M. & Y. D.) and H. Nishiguchi. According to their results, G. R. is paramagnetic above the magnetic transition point, 82.5°K, where the susceptibility drops down very sharply on cooling. We have undertaken the measurement of heat capacity from 13 to 300°K through the transition point in order to study the mechanism of this magnetic anomaly. Furthermore, we have measured the heat capacity of its phenol derivative, 2,6-di-*t*-butyl-4 (3,5-di-*t*-butyl-4-oxocyclohexa-2,5-dienylidene methyl) phenol (see Fig. 1) for comparison, in order to elucidate the effect of the radical nature on the properties of G. R.

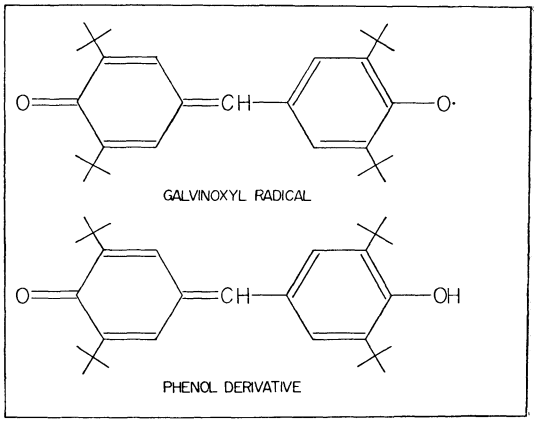

Fig. 1. Molecular Structures of galvinoxyl radical and its phenol derivative.

+: Tertial butyl group

Experimental

Samples. G. R.[2] was synthesized from 2,6-di-*t*-butyl phenol. After condensation with formaldehyde

*1 This paper was presented before the 21st Annual Meeting of the Chemical Society of Japan.

1) K. Mukai, H. Nishiguchi and Y. Deguchi, *J. Phys. Soc. Japan*, **23**, 125 (1967).

2) M. S. Kharasch and B. S. Joshi, *J. Am. Chem. Soc.*, **79**, 1439 (1957).

the product was oxidized by lead dioxide. Needle crystals of blue-black color were obtained.

Yellow needle crystal of its phenol derivative were prepared by the reaction between G. R. and di(3,5-di-*t*-butyl-4 hydroxy phenyl) methane in ether solution.

The both substances were ground, in a dry box to the fine powders for packing it into a calorimeter cell. The weight of G. R. used for measurement was 13.6159 g. The radical concentration was determined to be 106± 5% from the value of the Curie constant derived from the data of susceptibility above 82.5°K. The weight of the phenol derivative used for measurement was 18.6619 g.

Calorimeter and Cryostat. Adiabatic type calorimeter and cryostat[3] described previously were used for measurement of the heat capacity. Gold cell, provided with a platinum resistance thermometer, heater and inner platinum fins for thermal conduction, was used in order to avoid the chemical reaction with the radical. Measurements of heat capacities were performed from 11 to 300°K.

X-Ray Analysis. Taking the Debye-photographs of the samples, the identification was made at room temperature.

Results

Experimental data are listed for G. R. in Table 1 and for its phenol derivative in Table 2. These data are based on a molecular weight of 421.649 g for G. R. and 422.657 g for its phenol derivative and also on the relation 0°C=273.15°K. The heat capacities in these tables are the ratio of the increase in enthalpy to the rise in temperature and are equal to the differential heat capacity only when the correction for curvature is negligible. The temperature T listed in these tables is the arithmetic mean of the initial and the final temperature.

As are shown the experimental data of G. R.

Table 1. Heat capacities of galvinoxyl radical

T (°K)	$\Delta H/\Delta T$ (J/°K·mol)	ΔT	T (°K)	$\Delta H/\Delta T$ (J/°K·mol)	ΔT	T (°K)	$\Delta H/\Delta T$ (J/°K·mol)	ΔT
12.702	17.458	2.7800	78.259	230.68	.93011	149.494	349.42	4.0629
15.035	23.795	1.8858	79.186	254.15	.92372	153.529	358.03	4.0071
17.055	28.495	2.1549	80.089	303.88	.88380	157.512	365.63	3.9590
19.014	34.567	1.7627	80.296	370.22	2.4249	161.456	373.79	3.9285
21.079	40.109	2.3677	80.877	502.94	.69032	165.353	381.19	3.8687
23.277	46.616	2.0273	81.479	816.74	.51397	168.934	389.13	3.8320
25.505	52.665	2.4695	82.170	310.85	.86849	172.898	396.91	4.0954
28.063	60.008	2.6055	83.110	204.30	1.0121	177.249	405.65	4.6070
30.779	66.981	2.8270	84.636	204.73	2.1154	181.830	414.58	4.5549
33.443	74.917	2.5021	85.161	206.10	.99793	186.359	423.22	4.5028
36.050	81.811	2.7116	86.157	206.48	.99259	190.837	432.17	4.4536
38.651	87.800	2.4894	86.736	208.97	2.0833	195.266	441.73	4.4045
40.981	92.988	2.1708	87.147	208.53	.98680	199.650	449.45	4.3626
43.336	99.225	2.5394	88.143	209.70	1.0055	203.989	458.19	4.3165
46.028	104.43	2.8443	88.804	213.49	2.0537	208.286	466.21	4.2766
48.784	111.12	2.6689	89.135	212.39	.97842	212.541	474.66	4.2336
51.383	117.26	2.5277	90.108	216.47	.96735	216.755	482.41	4.1958
53.652	122.19	2.0112	90.843	217.67	2.0260	220.931	490.19	4.1569
56.458	129.00	3.6005	91.439	218.13	1.6940	225.070	498.08	4.1206
59.540	137.72	2.5641	93.126	221.68	1.6795	229.179	507.02	4.0969
62.056	145.52	2.4670	94.797	225.23	1.6629	233.249	514.92	4.0437
64.479	153.76	2.3794	96.490	230.32	3.6126	237.940	524.23	5.3373
66.823	159.78	2.3092	100.443	240.40	4.2938	242.868	534.57	5.3131
67.508	162.59	3.5903	104.806	250.40	4.4319	248.144	547.51	5.2444
69.097	167.18	2.2415	109.613	261.24	5.1823	253.357	558.59	5.1869
71.054	172.97	3.4842	114.620	272.30	4.8319	258.516	569.54	5.1306
71.401	174.12	2.3713	119.398	283.37	4.7248	263.620	579.59	5.0785
73.397	183.10	1.6205	123.995	293.65	4.4685	268.742	591.97	5.1618
74.415	188.50	3.2612	128.442	303.18	4.3857	274.136	603.79	5.6259
75.564	196.47	.89499	132.770	312.91	4.3102	280.470	617.18	7.0406
76.451	202.42	.87981	137.045	322.33	4.2401	287.471	631.52	6.9642
77.343	212.49	.90234	141.253	331.52	4.1766	294.145	643.55	6.3863
77.567	219.90	3.0428	145.402	340.11	4.1207	300.481	659.42	6.2880

3) T. Matsuo, H. Suga and S. Seki, Preprint of the 3rd Japanese Calorimetry Conference, B104, 40 (1967).

Table 2. Heat capacities of the phenol derivative

T (°K)	$\Delta H/\Delta T$ (J/°K·mol)	ΔT	T (°K)	$\Delta H/\Delta T$ (J/°K·mol)	ΔT	T (°K)	$\Delta H/\Delta T$ (J/°K·mol)	ΔT
12.341	16.392	2.5211	77.369	185.43	2.3275	165.554	387.15	5.0547
14.472	22.616	1.7402	79.654	191.06	2.2964	170.568	397.59	4.9738
16.069	27.313	1.4538	81.530	196.01	1.4460	175.505	407.55	4.9015
17.410	31.810	1.2280	82.897	199.18	1.2792	180.368	417.42	4.8278
17.538	32.285	3.1236	84.169	202.89	1.2642	185.162	426.94	4.7607
20.055	39.851	1.8192	85.426	205.80	1.2508	189.892	436.68	4.6959
21.747	44.891	1.5660	86.671	208.98	1.2378	194.871	446.34	5.2555
23.951	51.576	2.8426	87.902	212.36	1.2244	200.099	456.72	5.1906
26.522	59.324	2.3992	89.121	214.89	1.2140	205.255	467.11	5.1192
29.044	65.626	2.5446	90.330	217.61	1.2033	210.399	477.14	5.0515
31.586	72.920	2.5390	91.528	220.20	1.1936	215.359	486.95	4.9870
34.196	80.460	2.6808	92.716	223.77	1.1820	220.314	497.43	4.9175
36.872	87.206	2.6711	93.893	225.57	1.1739	225.203	506.49	4.8606
39.436	93.290	2.4568	95.062	228.61	1.1614	229.942	516.66	4.7989
41.709	98.817	2.0904	96.666	232.63	2.0434	234.804	525.92	4.7442
44.062	104.82	2.6150	99.030	238.41	2.6839	239.521	535.05	4.6902
46.597	110.36	2.4533	101.691	245.03	2.6376	244.351	544.33	4.9699
49.101	116.72	2.5518	104.966	252.82	3.9141	249.286	554.30	4.9048
51.715	124.29	2.6780	109.464	264.74	5.1053	254.186	564.32	4.8934
53.915	127.85	1.7229	114.508	274.24	4.9829	259.021	573.52	4.7972
56.022	132.53	2.4912	119.425	286.62	4.8522	263.800	583.64	4.7421
58.464	138.40	2.3933	124.223	297.64	4.7426	268.516	593.38	4.6897
60.922	144.95	2.5218	129.050	308.60	4.9107	273.949	604.43	6.1758
63.385	151.81	2.4614	133.908	319.48	4.8069	280.592	617.01	6.2484
65.806	157.89	2.3808	139.093	331.14	5.5653	286.262	629.05	6.1654
68.139	163.63	2.2909	144.598	343.86	5.4435	292.371	642.30	6.0724
70.402	168.56	2.2343	149.986	355.35	5.3329	298.454	652.49	6.0926
72.712	174.24	2.3859	155.269	366.19	5.2342			
75.069	179.95	2.3275	160.456	377.06	5.1399			

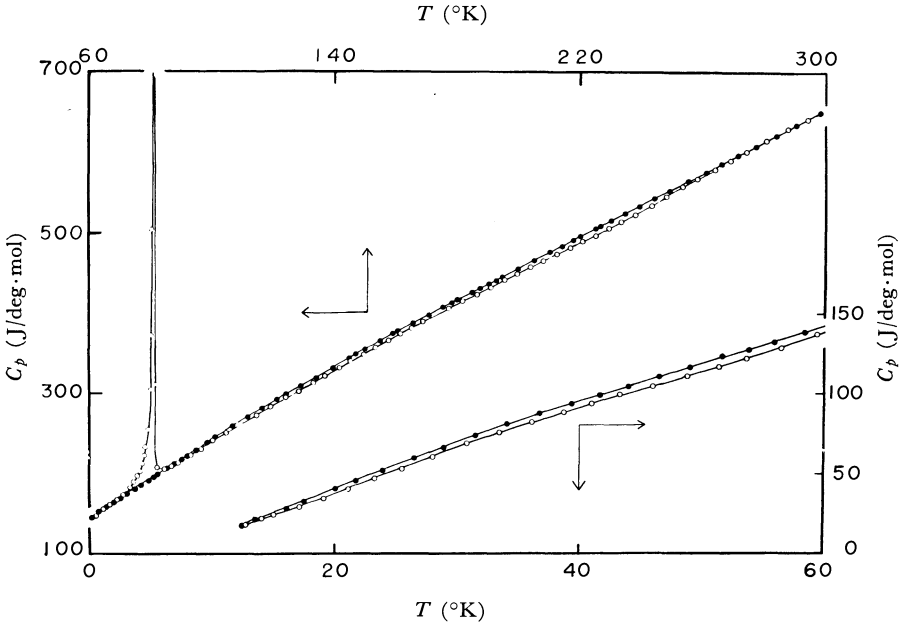

Fig. 2. Heat capacity of galvinoxyl radical and its phenol derivative.
Galvinoxyl radical: ○ Its phenol derivative: ●

Table 3. Smoothed values of heat capacity and thermodynamic functions of galvinoxyl radical

T (°K)	$C_p°$ (J/°K·mol)	$S°$ (J/°K·mol)	$(H°-H_0°)/T$ (J/°K·mol)	$-(G°-H_0°)/T$ (J/°K·mol)
15	23.60	9.543	7.040	2.503
20	37.20	18.182	12.868	5.314
30	65.68	27.927	25.666	12.907
40	91.20	61.042	38.928	22.114
50	113.65	83.839	51.656	32.183
60	139.19	106.70	64.006	42.691
70	170.59	130.54	77.003	53.351
80	292.18	157.18	92.589	64.594
90	215.03	196.32	118.67	77.646
100	239.16	220.18	129.47	90.706
120	284.91	267.82	151.55	116.26
140	328.68	315.09	173.81	141.28
160	370.57	361.78	195.89	165.93
180	411.00	407.75	217.50	190.25
200	450.18	453.08	238.80	214.27
220	488.53	497.82	259.81	238.02
240	529.46	542.07	280.55	261.52
260	572.88	586.16	301.37	284.79
280	616.15	630.20	322.31	307.89
300	658.28	671.96	343.30	328.66

Table 4. Smoothed values of heat capacity and thermodynamic functions of its phenol derivative

T (°K)	$C_p°$ (J/°K·mol)	$S°$ (J/°K·mol)	$(H°-H_0°)/T$ (J/°K·mol)	$-(G°-H_0°)/T$ (J/°K·mol)
15	25.31	9.717	7.203	2.514
20	40.00	19.054	13.604	5.450
30	68.71	40.685	27.103	13.582
40	94.80	64.151	40.874	23.277
50	118.84	87.901	54.075	33.826
60	142.56	111.51	66.779	44.731
70	167.67	135.43	79.456	55.973
80	192.04	159.39	91.992	67.402
90	216.88	183.47	104.51	78.958
100	240.91	207.54	116.93	90.613
120	287.93	255.68	141.56	114.11
140	333.29	303.48	165.72	137.76
160	376.08	350.84	189.40	161.44
180	416.85	397.49	212.41	185.09
200	456.49	443.45	234.83	208.63
220	496.02	488.81	256.79	232.03
240	536.17	533.70	278.40	255.30
260	575.46	578.17	299.74	278.43
280	616.40	622.34	320.92	301.42
300	658.35	666.29	342.01	324.29

Table 5. Thermodynamic functions of galvinoxyl radical (I) and its phenol derivative (II) at 298.15°K

Unit; (J/°K·mol)

	$C_p°$	$S°$	$(H°-H_0°)/T$	$-(G°-H_0°)/T$
I	654.28	670.10	341.36	328.74
II	654.28	662.24	340.06	322.18
I−II	000.00	7.86	1.30	6.56

Table 6. Anomalous heat capacity of galvinoxyl radical

T (°K)	$\Delta H/\Delta T$ (J/°K·mol)	ΔT	T (°K)	$\Delta H/\Delta T$ (J/°K·mol)	ΔT	T (°K)	$\Delta H/\Delta T$ (J/°K·mol)	ΔT
62.056	0.585	2.4670	74.415	11.675	3.2612	80.877	309.95	0.69032
64.479	2.233	2.3794	75.564	16.580	0.89499	81.479	622.17	0.51379
66.823	3.355	2.3092	76.451	20.331	0.87981	82.170	114.42	0.86846
67.508	4.246	3.5903	77.343	28.293	0.90234	83.110	5.794	1.0121
69.097	5.004	2.2415	79.186	64.286	0.92372	84.636	2.570	2.1154
71.045	5.710	3.4842	78.259	44.378	0.93011	85.161	2.635	0.99793
71.401	5.740	2.3713	80.089	112.77	0.88380	86.736	1.651	2.0833
73.397	8.998	1.6205	80.296	178.58	2.4249			

with the open circles in Fig. 2, an exceedingly sharp anomaly is found at 81.5°K. Around the transition temperature, it takes a long time (1—2 hr) for thermal equilibration, so that the heat capacity values in these regions are inferior in accuracy to those in the normal region where the thermal relaxation time is of the order of 2—4 min. The heat capacity peak is so sharp that 90% of the whole enthalpy change occurs in the narrow range of 3°K. Although the latent heat effect could not be observed exactly on account of the experimental difficulty, it is highly probable that the transition is of the first order. Three independent runs were performed for the determination of the enthalpy change of the transition. The average value is found to be 1504.56±5.34 J/mol. The entropy of the transition is 18.674 J/(°K·mol). This value corresponds formally to $R \ln 9.45$. The anomalous heat capacity has a tail extending down to about 60°K and sharply decreases to the normal value at the higher temperature side.

Experimental data of its phenol derivative are plotted with the filled circles in Fig. 2 with those of G. R. The result stands in contrast with that of G. R. in the point that no thermal anomaly is observed at the temperature region of G. R. Smoothed values of the heat capacity, enthalpy, entropy and Gibbs-energy functions are listed for G. R. in Table 3 and of its phenol derivative in Table 4. Values of their thermodynamic functions at 298.15 K are listed in Table 5. The detailed values of the anomalous heat capacity are listed in Table 6.

Discussions

In the present time we know only three free radical crystal whose heat capacity had been measured. Among them, for BDPA[4] and tetramethyl-2,2,6,6-piperidol-4-oxyl-1,[5] their heat capacity data show that there is no phase transition and their behaviors of the magnetic heat capacity are explained with a linear Ising and Heisenberg models with a coupling between neighboring chains. On the other hand, the heat capcacity data of Wüster Blue Perchlorate (WBP)[6] shows that there is a phase transition at 189.9 K which is corresponding to the magnetic transition temperature.[7,8] The mechanism of this magnetic transition has been discussed by Chesnut[9] and McConnell[10,11] and others. Chesnut explained the mechanism by the model of exciton-exciton interactions. McConnell *et al.* on the other hand, investigated the pressure dependence of the magnetic transition of WBP and $(C_6H_5)_3PCH_3(TCNQ)_2$ and found that this magnetic transition took place even under the low exciton density. Based on these observation, it seems to be improbable that the exciton-exciton interactions make the transition to be cooperative. Moreover the change of crystal structure of WBP[12] was observed by the X-ray analysis. According to these facts, it may be plausible to consider that the magnetic anomaly is induced by the change of the crystal structure.[13]

Now, turning to the present substances investigated, the measurement of the magnetic susceptibility of G. R.[1] shows the magnetic transition at 82.5°K and G. R. was found to be paramagnetic above the transition temperature and to be diamagnetic (weak paramgnetic[14]) below it. The sharp rise of the magnetic susceptibility from the low temperature side of the transition is considerablly

4) A. S. Edelstain and M. Mandel, *J. Chem. Phys.*, **35**, 1130 (1961); W. O. Hamilton and G. E. Pake, *ibid.*, **39**, 2694 (1963).

5) H. Lemaire, P. Rey, A. Rassat, A. D. Combarieu and J. C. Michel, *Mol. Phys.*, **14**, 207 (1968).

6) H. Chihara, M. Nakamura and S. Seki, This Bulletin, **38**, 1776 (1965).

7) K. Okumura, *J. Phys. Soc. Japan*, **18**, 69 (1963).

8) W. Duffy, Jr., *J. Chem. Phys.*, **36**, 490 (1962).

9) D. B. Chesnut, *ibid.*, **40**, 405 (1964).

10) A. W. Merkel, R. C. Hughes, L. J. Berliner and H. M. McConnell, *ibid.*, **43**, 953 (1965).

11) R. C. Hughes, A. W. Merkel and H. M. McConnell, *ibid.*, **44**, 1720 (1966).

12) D. D. Thomas, H. Keller and H. M. McConnell, *ibid.*, **39**, 2321 (1963).

13) G. T. Pott and J. Kommandour, *ibid.*, **47**, 395 (1967); H. J. Monkrost, G. T. Pott and J. Kommandour, *ibid.*, **47**, 401 (1967); G. T. Pott, C. F. van Bruggen and J. Kommandour, *ibid.*, **47**, 408 (1967).

14) K. Mukai, This Bulletin, **42** (1969), in press.

different from those of BDPA and WBP. This behavior cannot be explained only by use of a model of magnetic chains linearly interacted, but may be interpreted in such a way that a kind of pairing process of spins is assumed with, large J-value below the transition temperature and small J-value above it. If this kind of pairing state be of singlet (dimerization of spins), entropy change for this process amounts to R ln 2. The present results of the heat capacity, however, revealed that the entropy change associated with the phase transition is found to be R ln 9.45. There is a large difference, R ln 4.73 between them. In order to explain this large discrepancy, we may expect that the magnetic pairing process may be accompanied with a cooperative change of crystal structure. In this respect, it is very much desirable to study the crystal structure of the low temperature phase of this material.

We may proceed to the case of the diamagnetic phenol derivative. As is shown in Fig. 2 in the temperature above the transition points of G. R., the heat capacities of the phenol derivative are at the most 2% larger than those of G. R. While below the transition region the heat capacities of the phenol are about 5% larger than those of G. R. These facts probably mean that the crystal structure of G. R. changes at the transition temperature, whereas that of the phenol derivative does not. The results of measurements of the heat capacity and of X-ray analysis show that the crystal structure of G. R. is almost the same to that of the phenol derivative at room temperature. Therefore, we should like to consider that the phase transition of G. R. is induced by a cooperative process of pairing of magnetic spins in contrast to the case of WBP. In conection with this point of view, it may be recalled that some authors[13] attributed the phase transition of WBP to the order-disorder transition of perchlorate ion accompanied with the charge-transfer of TMPD cores. In this case perchlorate ions are in an ordered state with respect to their orientation below its transition temperature. This process results in the difference of the electrostatic potential at TMPD cores and therefore is accompanied by the charge-transfer. Here, the unpaired electrons are localized in one of the two molecules in this model. However it may be, this charge-transfer state may be called rather ionic-bonded one. On the analogy of this process, one may propose that the magnetic transition of G. R. is induced by the creation of "covalent-like" bond between two molecules. For, in contrast to the existence of perchlorate ion between WB ions, molecules of G. R. are directly in contact with each other. From this points of view, the symbol J given above means the coulomb integral rather than the exchange one.

Apart from the discussion of the phase transition of the stable free radical crystal, we may illustrate the following facts for reference.

There are known some substances which change their crystal structures accompanied with magnetic anomaly. Vanadium dioxide is one of the case. The crystal structure of the low temperature phase of this compound constitutes a deformed lattice of the rutile-type structure and that of the high temperature phase constitutes the normal rutile-type one.[15] This substance has a magnetic anomaly[16] at the corresponding transition temperature. Some authors[17] assume the appearance of metal-metal bond in its crystal, since the metal-metal distance is found to be shortened at the lower temperature phase. Our model adopted to explain the mechanism of the phase transition of G. R. may be looked upon as a similar kind one.

Summary

The heat capacities of G. R. and its phenol derivative were measured in order to study the nature of the magnetic anomaly. It was found that the heat capacity of G. R. shows an anomaly at 81.5°K which just corresponds to the magnetic transition temperature. The enthalpy and entropy of transition are 1504.6 J/mol and 18.67 J/(°K·mol) (*i. e.* R ln 9.45). The heat capacity of its phenol derivative, on the other hand, has no anomaly at the temperature region measured. The thermodynamic functions for both substances were evaluated by integrating respective heat capacity data. The values at 298.15°K are, in units of J/(°K·mol); $C_p°=654.28$, $S°=670.10$, $(H°-H_0°)/T=341.31$, $-(G°-H_0°)/T=328.74$ for Galvinoxyl radical, $C_p°=654.28$, $S°=662.24$, $(H°-H_0°)/T=340.04$, $-(G°-H_0°)/T=322.18$ for its phenol derivative.

The authors should like to express their sincere thanks to the Toyo Rayon Co., Ltd. who defrayed a part of the financial support for the present investigation.

15) S. Westman, *Acta Chem. Scand.*, **15**, 217 (1961).
16) W. Klemm and E. Hoschek, *Z. anorg. allgem. Chem.*, **226**, 359 (1936).
17) B. O. Marinder and A. Mangell, *Acta Chem. Scand.*, **11**, 1635 (1957); T. Kawakubo and T. Nagasaki, *J. Phys. Soc. Japan*, **19**, 517 (1964).

BULLETIN OF THE CHEMICAL SOCIETY OF JAPAN VOL. 42 1531—1533 (1969)

The Reactions of a Mixture of Benzene and *cis*-2-Butene Photosensitized by Cadmium

Shigeru TSUNASHIMA, Shin SATOH and Shin SATO

Department of Applied Physics, Tokyo Institute of Technology, Ookayama, Meguro-ku, Tokyo

(Received November 15, 1968)

Using the cadmium-photosensitized *cis-trans* isomerization of *cis*-2-butene, the lifetime of triplet benzene has been estimated to be of the order of 10^{-5} sec for both benzene-d_0 and -d_6. This technique provides a new method for measuring the lifetime of the triplet state of some molecules.

Recently, the efficiencies of hydrocarbons in quenching the triplet cadmium have been measured using the cadmium-photosensitized *cis-trans* isomerization of *cis*-2-butene.[1] In the cases examined previously, the activated quencher molecule formed in quenching triplet cadmium atoms did not cause the isomerization of 2-butene.[1] In the case of benzene, however, the molecule thus activated is thought to cause the isomerization, because the isomerization of 2-butene occurs effectively by means of triplet benzene.[2,3] Namely, a two-step energy-transfer-process such as cadmium→benzene →2-butene may be involved in the reactions of a mixture of benzene and 2-butene photosensitized by triplet cadmium. If this energy-transfer-process is indeed involved, it may be possible to estimate the lifetime of triplet benzene.

The lifetime of triplet benzene has already been estimated in the benzene-photosensitized *cis-trans* isomerization of 2-butene[3] and in the benzene-photosensitized phosphorescence of biacetyl.[4] In these cases, however, such complications arise as the estimation of the rate of the intersystem crossing.

With this prospect in mind, a study of the reactions of a mixture of benzene and *cis*-2-butene photosensitized by triplet cadmium was undertaken.

Experimental

Research-grade *cis*-2-butene supplied by the Takachiho Trading Co. was used after bulb-to-bulb distillation. The gas-chromatographic analysis showed that the impurities were less than 0.5%. Spectorgrade benzene supplied by the Wako Chemical Co. was used after recrystallization and bulb-to-bulb distillation. The mass-spectrometric analysis of benzene-d_6 supplied by the Merck Co. showed that the isotopic impurities were less than 2%.

The light source and the apparatus were similar to those reported on in a previous paper.[5]

A mixture of benzene and *cis*-2-butene was irradiated at 270±1°C in the presence of cadmium vapor with a cadmium lamp through a Toshiba UV-29 filter which cut off all wavelengths below 2700Å. After being separated from benzene with a cold trap at −80°C, the 2-butenes were analysed by gas chromatography using a column packed with dimethylsulforane on celite (30 m long) supplied by the Shimadzu Co.

Immediately after each run, the light intensity of the resonance line at 3261 Å was measured using the cadmium-photosensitized *cis-trans* isomerization of *cis*-2-butene assuming the quantum yield to be 0.5.[5] The initial rate of the isomerization (R) was calculated using Eq. (I):

$$R = (([C]+[T])/2t) \ln (([C]+[T])/([C]-[T])) \quad (I)$$

Here, t represents the reaction time. [C] and [T] are the amounts of *cis* and *trans*-2-butenes respectively obtained after the irradiation.[1]

Results

The rate of the *cis-trans* isomerization of 2-butene was measured at 270±1°C as a function of the benzene pressure (at constant butene pressures) and also of the butene pressure (at a constant benzene pressure and a constant pressure ratio of benzene to 2-butene).

Figure 1 shows the plots of R/R_0 as a function of the benzene pressure at 5.1 mmHg, 14.7 mmHg, and 22.2 mmHg of *cis*-2-butene. Here, R and R_0 are the rates of the isomerization of *cis*-2-butene in the presence and in the absence of benzene respectively. The rate of the isomerization decreased

1) S. Tsunashima and S. Sato, This Bulletin, **40**, 2987 (1967); S. Tsunashima, S. Satoh and S. Sato, *ibid.*, **42**, 329 (1969).

2) S. Sato, K. Kikuchi and M. Tanaka, *J. Chem. Phys.*, **39**, 239 (1963); M. Tanaka, T. Terao and S. Sato, This Bulletin, **38**, 1645 (1965); M. Tanaka, M. Kato and S. Sato, *ibid.*, **39**, 1423 (1966).

3) R. B. Cundall, F. J. Fletcher and D. G. Milne, *Trans. Faraday Soc.*, **60**, 1149 (1964); R. B. Cundall and A. S. Davis, *ibid.*, **62**, 1151 (1966).

4) C. S. Parmenter and B. L. Ring, *J. Chem. Phys.*, **46**, 1423 (1967).

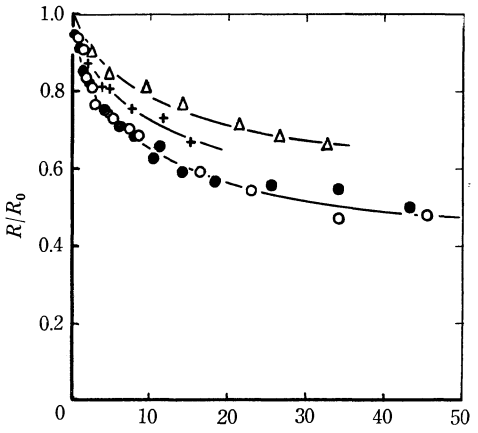

Fig. 1. The ratio of R/R_0 as a function of the benzene pressure at constant 2-butene pressures; 5.1 mmHg (○), 14.7 mmHg (+), and 22.2 mmHg (△) for for benzene-d_0; 5.1 mmHg (●) for benzene-d_6.

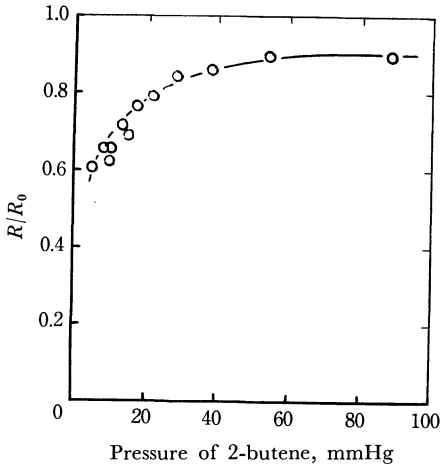

Fig. 2. The ratio of R/R_0 as a function of the 2-butene pressure at 10.9 mmHg of benzene-d_0.

with an increase in the benzene pressure. The effect of benzene-d_6 on the rate of the isomerization was almost the same as that of benzene-d_0; *i. e.*, there was no hydrogen-deuterium isotope effect on the rate of isomerization.

Figure 2 shows the plots of R/R_0 as a function of the 2-butene pressure at 10.9 mmHg of benzene. The rate of the isomerization increased with an increase in the butene pressure.

As is shown in Fig. 3, the R/R_0 values obtained with equal pressures of benzene and 2-butene increased with an increase in the total pressure. This clearly indicates that an energy transfer process such as cadmium→benzene→2-butene is involved in the mechanism.

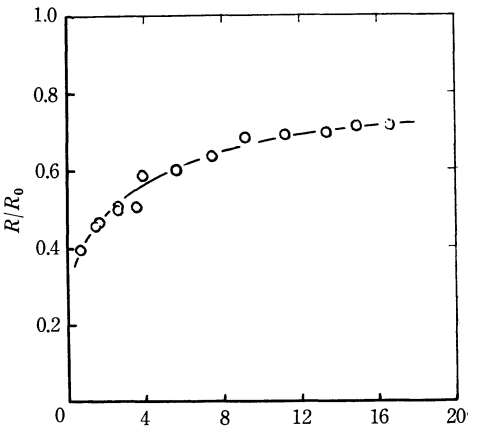

Fig. 3. The ratio of R/R_0 as a function of the total pressure at equal pressures of benzene-d_0 and 2-butene.

Discussion

If a benzene molecule quenches only the triplet cadmium atom and does not cause the *cis-trans* isomerization of 2-butene, a linear relationship should be obtained between R/R_0 and the pressure ratio, [benzene]/[2-butene].[1] As is shown in Fig. 4, this is not the case with benzene-2-butene mixtures. If an activated benzene molecule formed in quenching triplet cadmium can always cause the *cis-trans* isomerization without following the other reaction paths, the rate of the isomerization should not be affected by the pressure of benzene or 2-butene. However, the ratio R/R_0 is affected by the pressure change in both benzene and 2-butene. These facts indicate that only a part of the activated benzene formed in quenching triplet cadmium

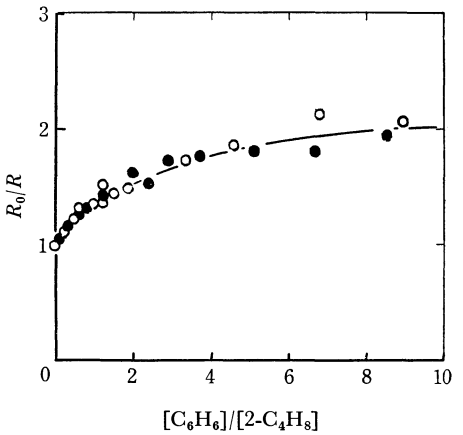

Fig. 4. The ratio of R_0/R as a function of the ratio of the pressure of benzene to that of 2-butene. ○: benzene-d_0; ●: benzene-d_6.

5) S. Tsunashima and S. Sato, This Bulletin, **41**, 284 (1968).

gives rise to the isomerization of 2-butene.

To explain these results, the following mechanism may be suggested:

$$Cd + h\nu \rightarrow Cd^*$$

$$Cd^* + 2\text{-}C_4H_8 \rightarrow Cd + 2\text{-}C_4H_8^* \quad (1)$$

$$2\text{-}C_4H_8^* + M \rightarrow \tfrac{1}{2}cis + \tfrac{1}{2}trans + M \quad (2)$$

$$Cd^* + C_6H_6 \rightarrow Cd + \alpha C_6H_6^* + (1-\alpha)C_6H_6' \quad (3)$$

$$C_6H_6^* \rightarrow C_6H_6 \quad (4)$$

$$C_6H_6^* + C_6H_6 \rightarrow 2C_6H_6 \quad (5)$$

$$C_6H_6^* + 2\text{-}C_4H_8 \rightarrow C_6H_6 + 2\text{-}C_4H_8^* \quad (6)$$

$$C_6H_6' + M \rightarrow C_6H_6 + M \quad (7)$$

where Cd* and 2-C_4H_8* are, respectively, a triplet cadmium atom and a triplet 2-butene molecule which isomerizes to *cis*- or *trans*-2-butene with an equal probability by collisional deactivation.[5] C_6H_6* may be a triplet benzene molecule in the state of $^3B_{1u}$, because its excitation energy is close to that of triplet cadmium. C_6H_6' denotes an activated quencher molecule which can not cause the isomerization of 2-butene and which is probably the vibrationally-excited ground state of benzene. α is the fraction of C_6H_6* formed by the reaction (3).

The steady-state treatment of the above mechanism gives the following equation:

$$(1-\beta)/(R/R_0-\beta) = 1/\alpha(1+k_4/k_6[C_4H_8] + (k_5/k_6)([C_6H_6]/[C_4H_8])) \quad (II)$$

where

$$1/\beta = 1 + (k_3/k_1)([C_6H_6]/[C_4H_8])$$

The left-hand side of Eq. (II) involves k_3/k_1, which is the relative efficiency of benzene against 2-butene in quenching triplet cadmium.

Using the data obtained with a constant pressure ratio, the left-hand side of Eq. (II) is in Fig. 5 plotted against the reciprocal of the 2-butene pressure, assuming various values for k_3/k_1. As the figure shows, the relation in Eq. (II) holds when the value of k_3/k_1 is assumed to be in the range of 2.5—1.5. This value is slightly larger than that calculated from the quenching cross-section of benzene obtained by Steacie and LeRoy by a physical method.[6] The value also is a little larger than those of olefins.[1] This is not unreasonable because benzene has six π-electrons and the excitation energy of triplet benzene is close to that of triplet cadmium.

Using the data obtained at a constant benzene pressure (Fig. 2), the α ratios are estimated to be 0.77±0.18 (2.5), 0.71±0.20 (2.0), and 0.66±0.23 (1.67), where the values in parentheses indicate the assumed values of k_3/k_1. That is, triplet benzene is about 70% formed through the reaction (3), although the ratio depends slightly on the estimation of k_3/k_1.

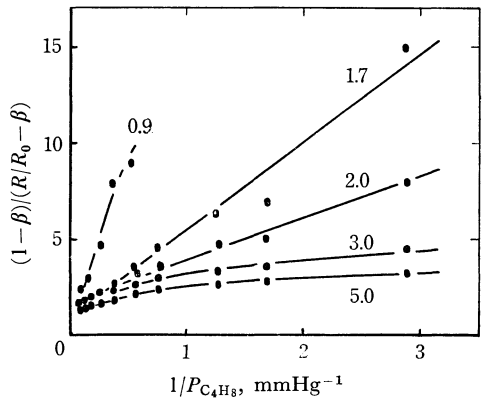

Fig. 5. The plots of Eq. (II) at various values of k_3/k_1 as a function of the reciprocal of the 2-butene pressure.

The rate constant ratios of k_5/k_6 and k_4/k_6 are estimated to be 0.05 and in the order of 10^{-4} mol/l using Eq. (II), k_5/k_6, which is the ratio of the rate constant of the self-quenching of triplet benzene against that of the energy-transfer process to 2-butene, is very small. This is consistent with the results obtained in the benzene-photosensitization of 2-butene.[2]

The lifetime of triplet benzene ($1/k_4$) is estimated to be in the order of 10^{-5} sec assuming the value of k_6 to be 10^9 l/mol sec (*cf.* 0.96×10^9 l/mol sec[4] and 2.0×10^9 l/mol sec[3,7]). The value of the lifetime is correct, however, in terms of the order because of a large experimental error and because of the uncertainty of the values used for the calculations, such as k_3/k_1, α, and k_6. In the benzene-photosensitization, the lifetime of triplet benzene has been estimated to be 12 μsec[3] and 26 μsec[4] at room temperature. In spite of a higher temperature and a different source of triplet benzene, the lifetime estimated here agrees well with the literature values.[3,4]

In conclusion, it may be said that the lifetime of the triplet state of some molecules can be estimated using the cadmium-photosensitized *cis-trans* isomerization of 2-butene, although this method contains a few parameters.

6) E. W. R. Steacie and D. J. LeRoy, *J. Chem. Phys.*, **11**, 164 (1943).

7) A. Morikawa and R. J. Cvetanović, *Can. J. Chem.*, **46**, 1813 (1968).

BULLETIN OF THE CHEMICAL SOCIETY OF JAPAN VOL. 42 1534—1538 (1969)

Electrodeposition of Water-soluble Resin by a Constant Voltage or by Pulses*1

Yoshio NAKAMURA, Fumio OKI and Hiroshi NOZAKI

Institute of Industrial Science, The University of Tokyo, Roppongi, Minato-ku, Tokyo

(Received November 20, 1968)

The mechanism of deposition was investigated using maleic-linseed oil as a sample. The deposition was made by a constant voltage or by continuous pulses with high voltages, and the initial current-time relations were observed by means of a synchroscope. When we applied pulses with α/β values which were smaller than a value, the current decreased gradually after some time and a deposited film was found on the anode, but the decreases in the current was not found for a long time when the value of β was much larger than the value of α. The induction time was found from the current-time curve observed during a constant voltage deposition. These results were discussed from the standpoint that the deposited film is formed by coagulation resulted from ionic combination with hydrogen ions.

Detailed knowledge of the mechanism of the electrodeposition of water-soluble resin would be useful in enabling the coating method to be satisfactorily applied in varying circumstances.

Finn and Mell[1] pointed out that local ionic precipitation or coagulation may be important factor in the film formation. From the results of the analyses of the deposited film, it has been made clear that the role of metal ions in deposition is minor,[2-4] this is clear from the fact that we can obtain the deposited film on platinum plates. Tawn and Berry[5] suggested a mechanism in which the coagulation of organic anions results from an increase in the concentration of hydrogen ions generated at the anode, but they could not support the mechanism with specific experimental results. Maeda *et al.*[3] found that $I \cdot \tau^{1/2}$ is nearly constant and explained $I \cdot \tau^{1/2}$ as a parameter which gives a critical concentration of hydrogen ions at the anode, where I=current density and τ is the induction time on the anode potential *vs.* the time curve which is observed during a constant current deposition. Moreover, they found that the period of the induction time increases with an increase in the acid value of the sample.

From the results of many analyses of the gases given off at the anode,[6-9] it has been clarified that the Kolbe reaction of organic anions in deposition is minor and that the principal electrode reaction during deposition is the oxygen evolution reaction.

Up to the present, many fundamental investigation related to the mechanism of the deposition have been performed at a constant current. In the case of the deposition of water-soluble resin, the current density is low, so that the anode potential for the period of induction time is of the order 1 to 2 V (*vs.* SCE). On the other hand, the practical application of the deposition of water-soluble resin to painting has been performed at a constant voltage, the values of the applied voltages ranging 50 to 200 V. It is questionable whether or not there is any essential difference in the electrode reaction between the cases of a constant current deposition and those of a constant voltage deposition.

In this report, we will describe the results observed by the use of a synchroscope in observing the electrode phenomena at a constant voltage deposition or at a continuous pulse deposition.

Experimental

Samples. The maleic-linseed oil used as the water-soluble resin was obtained by the additive reaction of maleic anhydride to linseed-oil. The reaction was performed for three hours at 200°C and for an hour at

*1 Electrodeposition of Water-soluble Resin. V.

1) S. R. Finn and C. C. Mell, *J. O. C. C. A.*, **41**, 219 (1964).
2) M. R. Sullivan, *J. Paint Tech.*, **38**, 424 (1966).
3) S. Maeda, N. Hirai, H. Okada and K. Inoue, *Denki-Kagaku*, **34**, 705 (1966).
4) T. Nakamura, M. Nagasawa and I. Kagawa, *J. Ind. Chem. Japan*, **70**, 2(1967).
5) A. R. H. Tawn and J. R. Berry, *J. O. C. C. A.*, **28**, 790 (1965).
6) L. R. L. Brass, *J. Paint Tech.*, **38**, 493 (1966).
7) S. Yoshizawa, N. Watanabe, I. Tari and I. Totake, 34th Conference of Electrochem. Soc. Japan.
8) Y. Nakamura, N. Higashiyama and H. Nozaki, *Denki-Kagaku*, **36**, 278 (1968).
9) Y. Nakamura, S. Ando and H. Nozaki, *J. Electrochem. Soc. Japan*, to be published.

230°C. During the reaction, the mixed solution was stirred mildly and kept in a nitrogen atmosphere. The mole ratio of maleic anhydride to linseed oil was 2.4 : 1. The crude maleic-linseed oil was neutralized by a potassium hydroxide solution in order to make it soluble in water after which the solution was kept in a separating funnel for a few days. After removing the unsoluble substances, we added sulfuric acid to the solution in order to coagulate the maleic-linseed oil. Then the coagulated maleic-linseed oil was dissolved in an ethylcellosolve-water solution and stirred for about ten hours.

A small quantity of carbon tetrachloride was then added to the solution. The solution was shaken for about an hour and then kept in a separating funnel for a day. The maleic-linseed oil was recovered in the carbon tetrachloride layer and the carbon tetrachloride was removed by vaporization. Finnally, maleic-linseed oil was kept for several hours at 50°C and 5 mmHg. The purification procedure after the coagulation by sulfuric acid was performed two times. The purified maleic-linseed oil was then dissolved into a potassium hydroxide solution and the solution used as a sample. The pH of the solution was adjusted only by a potassium hydroxide solution and by the maleic-linseed oil.

Apparatus. The cell was of a beaker type with two platinum plates as the cathodes. The distance between the cathodes was 5 cm, and the surface area of each cathode was 6 cm^2. The platinum anode was placed at the center of the cathodes. A bright platinum plate and wire were used as the anodes; the apparent surface areas of the platinum plate and wire were 2 and 0.31 cm^2 respectively. The platinum plate and wire were rinsed with a concentrated potassium hydroxide solution and dipped in a nitric acid solution for several minutes before each run.

A Takasago Regulated DC Power Supply GPO-50-2 was used as the potentiostat. The pulse generator used in this experiment was an Iwasaki Power Supply PS-201. The potential-time or current-time curves were observed by means of a National Synchroscope SS-5302 B.

The deposition (electrolysis) circuit is shown in Fig. 1. The bath solution was kept at 25±0.5°C.

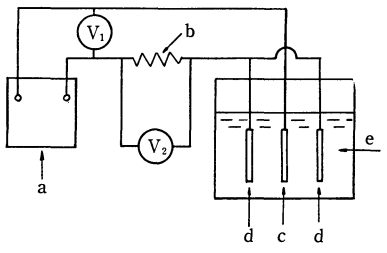

Fig. 1. Deposition circuit.

a: D.C. source, b: resistance, c: anode, d: cathode, e: bath solution, V_1, V_2 are observed by synchroscope.

Results

Deposition by Continuous Pulses. When we applied continuous pulses to the deposition cirucit, the figure shown in Fig. 2 was obtaind.

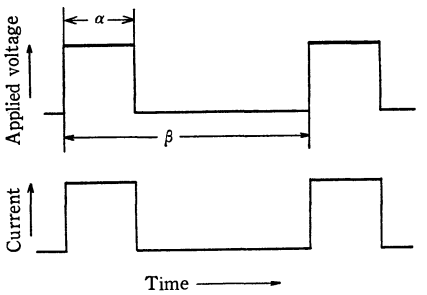

Fig. 2. Applied voltage and current curves against to time before deposited film is formed.

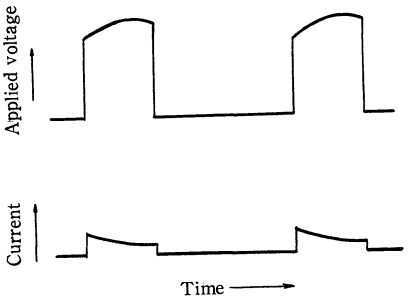

Fig. 3. Applied voltage and current curves against to time after deposited film was formed.

On the other hand, when we decreased only the value of β (see Fig. 2) while keeping the pulse width, α (see Fig. 2), constant, the figure gradually changed to the figure shown in Fig. 3.

The current decreased and the applied voltage increased. These phenomena were caused by the resistance of the deposited film on the anode. Actually, the film was found to have been deposited on the anode after the current decreased.

On the other hand, when the value of β was much larger than the value of α, the current has never been observed to decrease over a long period. These phenomena show that the film formation is not made by the direct discharge of organic anions. If the film formation is made by the direct discharge of organic anions, the current will decrease in spite of the value of β.

In order to make these phenomena clear, we investigated the effects of the current density, the pH of the bath solution, and the rate of the rotation of the electrode on the value of α/β_0, where β_0 is a value of β such that the current begins to decrease one minute after the value of β has been set at a constant value of α. The relation α and α/β_0 are shown in Table 1 at several applied potentials. The values of the applied potential and the current in Table 1. were measured before the deposited film was formed, that is, before the current decreased. The resin concentration was 5% in weight and the pH of the bath solution was 7.6. As may be seen in Table 1, the value of

α/β_0 is nearly constant in spite of the value of α at a constant applied voltage.

Using a platinum wire as the anode, we measured the relation between I and α/β_0 at various applied voltages at pH 7.5 and 8.6, where I is the current density. The results at pH 7.5 are shown in Table 2.

Table 1. Relation between α and α/β_0

Applied voltage (V)	Current density (mA/cm²)	α (μsec)	β_0 (μsec)	α/β_0
		5	19	0.26
		20	76	0.26
5	33	50	185	0.27
		100	390	0.26
		500	1900	0.26
		2000	7600	0.26
		1.2	8.2	0.12
8.5	55	10	80	0.13
		50	400	0.13
		200	1600	0.13

Resin concentration 5% in weight, pH 7.7

Table 2. Relation between current densities and α/β_0

Applied voltage (V)	Current density (mA/cm²)	α (μsec)	β_0 (μsec)	α/β_0
10	68	35	420	0.073
8	50	25	210	0.11
5	32	25	90	0.22
2.8	18	25	50	0.34

Resin concentration 5% in weight, pH 7.5

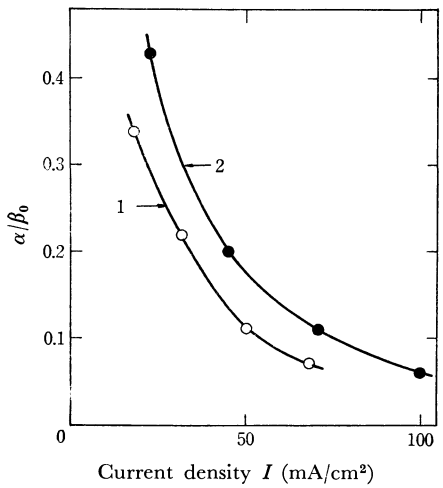

Fig. 4. α/β_0 against to current density.
pH, 1: 7.5, 2: 8.6
Resin concentration 5% in weight

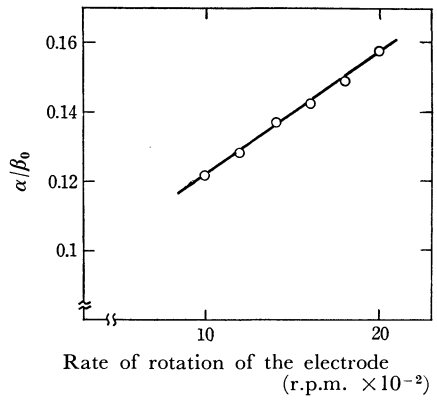

Fig. 5. Relation between α/β_0 and rate of rotation of the electrode. Resin concentration 5% in weight, pH 8.8.

Figure 4 shows the relation between I and α/β_0. α/β_0 decreases with an increase in the current densities.

Using a rotative electrode, we established the effects of the rate of the rotation of the electrode on the α/β_0 value at a constant applied voltage. The results are shown in Fig. 5. The resin concentration was 5% in weight, and the pH of the bath solution was 8.8. The observed current density was not affected by the rate of the rotation.

Constant Voltage Deposition. An induction time has been observed on the potential-time curve when the deposition was performed by a constant current density. It has been found that the values of $I \cdot \tau^{1/2}$ are nearly constant.[3,10] On the other hand, when the deposition was performed by a constant voltage with a high applied voltage, we found no induction time on the current-time curve recorded by means of an XY recorder. These findings show that the direct discharge of organic anions may occur at a constant voltage deposition. However, when the deposition is performed by a constant voltage, the initial current density is much higher than a current density at a constant current deposition. Therefore, the induction time may be considered to be very short at the constant-voltage deposition according to the relation that $I \cdot \tau^{1/2} =$ constant.

Then we observed an initial current-time relation by means of a synchroscope during a constant voltage deposition.

When the bath solution was a buffer solution composed of a 1/15 M Na_2HPO_4 solution (160 cc) and a 1/15 M KH_2PO_4 solution (10 cc), we obtained the current-time curve shown in Fig. 6. When the bath solution was a buffer solution including 5% (by weight) of maleic-linseed oil, the results shown in Fig. 6 were obtained. Curve 2 decreases with time more rapidly than Curve 1 and has some

10) Y. Nakamura, H. Kaneko, N. Higashiyama and H. Nozaki, *Denki-Kagaku*, **36**, 217 (1968).

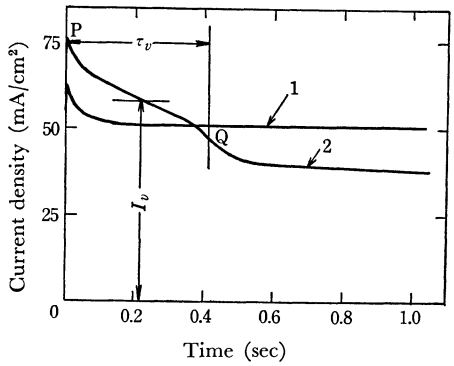

Fig. 6. Current density-time curves.
1: buffer solution (1/15 M Na_2HPO_4 solution 160 cc and 1/15 M KH_2PO_4 solution 10 cc)
2: buffer solution including 5% in weight of maleic-linseed oil.

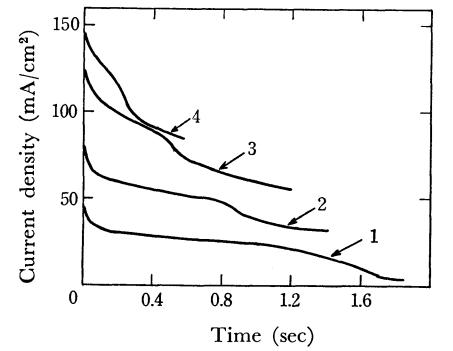

Fig. 7. Current density-time curves at various applied voltages.
Applied voltage, 1 : 5, 2 : 8, 3 : 12 4 : 15 (v)
Resin concentration 5% in weight, pH 7.7.

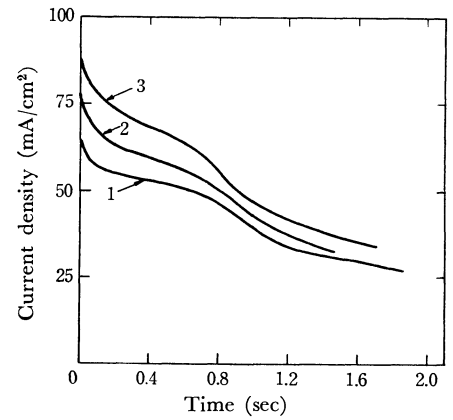

Fig. 8. Current density-time curves at various pHs.
pH, 1: 7.7, 2: 8.4, 3: 8.8
Resin concentration 5% in weight
Applied voltage 8 (V)

induction time. The period of time from P to Q is the induction time; we named that time τ_v. τ_v corresponds to the induction time τ (see Fig. 10) in the constant-current deposition.

Current-time curves observed at various applied voltages are shown in Fig. 7, where the resin concentration was 5% (by weight) and where the pH of the solution was kept at 7.7. The current densities for the induction time increase weight an increase in the applied voltages, but the length of the induction time decreases with an increase in the applied voltages.

The current-time curves observed at various pHs of the solution are shown in Fig. 8. The applied voltage was kept at 8 V, and the resin concentration was kept at 5% (by weight). The current densities for the induction time increase with an increase in the pHs of the solution.

Discussion

Deposition by Continuous Pulses. We consider that the decrease in the current, *i. e.*, the deposition of organic anions, was affected by only the value of β when α was constant. The anode reaction during the current flow must be the electrolysis of water as follows:

$$4H_2O = 4H^+ + 2O_2 + 4e \quad (1)$$

$$4OH^- = 2H_2O + O_2 + 4e \quad (2)$$

Hydroxide ions are in equilibrium as follows:

$$H^+ + OH^- = H_2O \quad (3)$$

Thus, the concentration of hydrogen ions will increase near the anode surface. However, hydrogen ions will decrease upon diffusion and the chemical reaction shown in Eq (4):

$$R(COO^-)_n + H^+ = R(COO^-)_{n-1}COOH \quad (4)$$

This reaction leads to the coagulation of organic anions, *i.e.*, deposition.

The schematic representation of the change in the concentration of hydrogen ions against the time at the anode is given in Fig. 9 (a) and (b). Figure 9(a) shows current *vs.* time curves, while Fig. 9(b) shows a speculative representation of the concentration of hydrogen ions *vs.* time curves at the anode surface. If the current is like Curve 1, that is to say, if β is sufficiently long in comparison

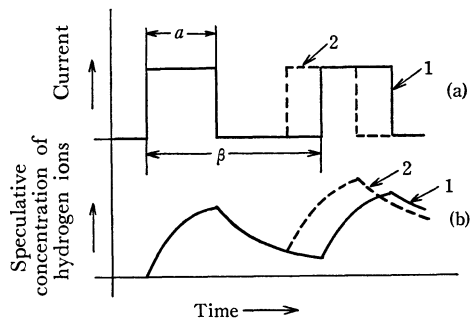

Fig. 9. Current and speculative concentration of hydrogen ions curves against to time.

with α, the diffusion time of the hydrogen ions is so long compared with the generation time of hydrogen ions that the increase in hydrogen ions at the anode surface remains very small.

However, if the β value is decreased while the value of α is kept constant, the decrease in the number of hydrogen ions by diffusion is restrained compared with the generation of the ions, so that the hydrogen ion concentration will increase rapidly at the anode. Thus, when the β value is decreased while the value of α is kept constant, the current may decrease as a result of the coagulation of organic anions.

When the applied voltages are increased, the current densities increase. If the value of α is kept constant, the rate of the generation of hydrogen ions at the anode increases with an increase in the current densities, in accordance with Faraday's law. Therefore, the period of time until hydrogen ion concentration increases to a certain critical concentration will decrease with an increase in the current densities. Thus, the value of α/β_0 decreases with an increase in the applied voltages, *i. e.*, the current densities.

As the sample became soluble in water at about pH 7 and as the pH of the neutralization point was about 9 to 10, carboxyls of this sample are not neutralized completely below pH 9. Therefore, as the number of dissociated organic anions per molecule increases with an increase in the pHs, the number of hydrogen ions required to neutralize dissociated anions will increase with an increase in the pHs of the bath solution. Consequently, if the value of α and the current density are kept constant, the value of β_0 must decrease with an increase in the pHs of the solution.

If the solution is stirred, the diffusion layer of the hydrogen ions will decrease. As a result, the diffusion rate of hydrogen ions from the anode to the bulk solution increases upon an increase in the rate of the rotation of the electrode. Therefore, the increase rate of the hydrogen ion concentration at the anode during electrolysis will decrease with an increase in the rate of the rotation of the electrode when the other conditions are kept constant. Thus, if the value of α and the current density are kept constant, the value of β_0 must decrease, *i. e.*, α/β_0 increases with an increase in the rate of the rotation of the electrode.

Constant Current Deposition. In order to compare these findings with the results on constant-current deposition, we measured the relation between I and $I\cdot\tau^{1/2}$ in the constant-current deposition using the same sample as we used in studying the constant-voltage deposition: the results are shown in Fig. 10. $I\cdot\tau^{1/2}$ increases with an increase in the current densities. We calculated the values of $I_v\cdot\tau_v{}^{1/2}$ from the results of the constant-voltage deposition (see Fig. 7): they are shown in Fig. 10, where I_v is the arithmetic mean value of the current density at induction time τ_v (see Fig. 6). As is shown in Fig. 10, the values of $I_v\cdot\tau_v{}^{1/2}$ are comparable to the values of $I\cdot\tau^{1/2}$. The values of $I_v\cdot\tau_v{}^{1/2}$, calculated from Fig. 8, are shown against the pHs of the bath solution in Fig. 11. $I_v\cdot\tau_v{}^{1/2}$ increases with an increase in the pHs of the bath solution. These results can be explained by the same consideration as we used to describe the effects of the pHs of the solution on the α/β_0 in continuous-pulse deposition. Thus, the film formation in constant-voltage deposition can also be explained in terms of the coagulation of organic anions.

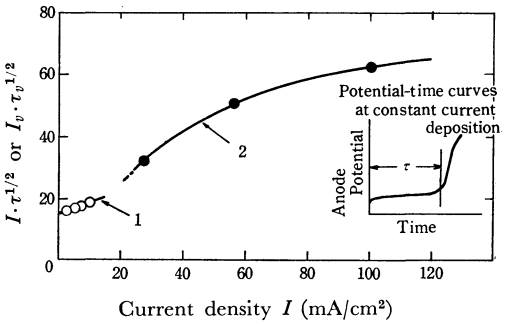

Fig. 10. Relation between $I\cdot\tau^{1/2}$ or $I_v\cdot\tau_v{}^{1/2}$ and current density.

1: $I\cdot\tau^{1/2}$, 2: $I_v\tau_v{}^{1/2}$, resin concentration 5% in weight, pH 7.7.

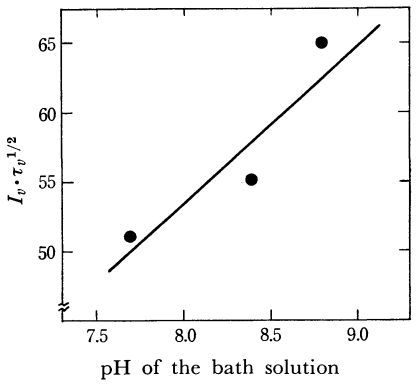

Fig. 11. Relation between $I_v\cdot\tau_v{}^{1/2}$ and pH.

BULLETIN OF THE CHEMICAL SOCIETY OF JAPAN VOL. 42 1539—1545 (1969)

Infrared Spectra of Biuret-hydrate and Its Deuterated Compound

Toyozo UNO, Katsunosuke MACHIDA and Yutaka SAITO

Faculty of Pharmaceutical Sciences, Kyoto University, Sakyo-ku, Kyoto

(Received December 2, 1968)

The infrared spectra between 4000 and 33 cm^{-1} of biuret-hydrate and between 4000 and 250 cm^{-1} of its deuterated compound have been recorded. The vibrational assignments have been made by referring to the infrared spectra of the related compounds and the isotopic frequency shift. Normal coordinate analysis of the in-plane vibrations of biuret and biuret-d_5 as twelve-body problem has been carried out by using the molecular model of the planar *trans-cis* conformation. A simple Urey-Bradley force field has been employed and the force constants have been refined by the least squares method. The calculation of potential energy distributions has shown that the NH in-plane deformation and the CN stretching vibrations couple appreciably with each other and give the imide II and III bands at 1515 and 1365 cm^{-1}, respectively, just as in the case of diacetamide.

In the infrared spectra for the condensed phase, aliphatic imides[1] and monosubstituted amides[2] show the imide II band and the amide II band, respectively, in the region between 1550 and 1500 cm^{-1}. These bands are fairly strong and quite characteristic of the –CONH– group in which the C=O and the NH bonds take the *trans* conformation with each other.[3] It has been proved by the normal coordinate analysis of *N*-methylacetamide[4] and diacetamide[5] that both the amide II and the imide II bands arise from the coupling between the NH in-plane deformation and the CN stretching vibrations of the *trans* –CONH– group. According to the X-ray analysis, a molecule of biuret ($NH_2CONHCONH_2$) has the *trans-cis* –CONHCO– group[6] in the biuret-hydrate crystal. It is interesting to examine the infrared spectra of this crystal and to see if there exists the coupling analogous to the case of amides and imides.

Besides the hydrate crystal, biuret has also the anhydrate crystal. The infrared spectra of both crystals have been recorded in the region between 4000 and 650 cm^{-1} and several bands have already been assigned.[7-9] In the present paper, we report the infrared spectra of biuret-hydrate between 4000 and 33 cm^{-1} and the assignment of the fundamental frequencies of biuret given on the basis of the spectral change on deuteration and a comparison with related compounds such as urea,[10] diacetamide[5] and acylureas.[11] This paper includes also the normal coordinate analysis of the in-plane vibrations of biuret and biuret-d_5 in the *trans-cis* conformation.

Experimental

Commercially available biuret was purified several times by recrystallization from water and ethanol. The hydrate was prepared by crystallization from water.[12] Deuterated biuret-hydrate was prepared by the usual exchange reaction with heavy water, and was left in the atmosphere saturated with heavy water for three weeks in order to avoid the contamination of the anhydrate crystal in the sample.

The infrared spectra were recorded on a Koken DS 301 infrared spectrophotometer equipped with sodium chloride and potassium bromide prisms (4000—450 cm^{-1}), on a Perkin Elmer model 521 grating spectrophotometer (900—250 cm^{-1}) and on a Hitachi FIS-3 grating spectrophotometer (400—33 cm^{-1}). The samples were subjected to the measurement in the form of a solid dispersed in Nujol and hexachlorobutadiene (H.C.B.). The absorption frequencies are listed in Tables 1 and 2 together with the assignment.

1) T. Uno and K. Machida, This Bulletin, **34**, 551 (1961).
2) L. J. Bellamy, "The Infrared Spectra of Complex Molecules," 2nd ed., Methuen & Co., Ltd., London, John Wiley & Sons, Inc., New York (1958), p. 203.
3) T. Miyazawa, T. Shimanouchi and S. Mizushima, *J. Chem. Phys.*, **24**, 408 (1956).
4) T. Miyazawa, T. Shimanouchi and S. Mizushima, *ibid.*, **29**, 611 (1958).
5) T. Uno and K. Machida, This Bulletin, **36**, 427 (1963).
6) E. W. Hughes, H. L. Yakel and H. C. Freeman, *Acta Cryst.*, **14**, 345 (1961).
7) B. I. Sukhorukov and A. I. Finkei'shtein, *Optics and Spectroscopy*, **6**, 414 (1959).
8) K. Aida, *J. Inorg. & Nuclear Chem.*, **23**, 155 (1960).
9) M. Takimoto, *Nippon Kagaku Zasshi (J. Chem. Soc. Japan, Pure Chem. Sect.)*, **85**, 168 (1964).
10) A. Yamaguchi, *ibid.*, **78**, 1467 (1957).
11) T. Uno, K. Machida, K. Hanai and Y. Saito, This Bulletin, **42**, 619 (1969).
12) R. Behrend and R. Schultz, *Liebigs. Ann.*, **365**, 21 (1909).

Results and Discussion

The Region above 1800 cm^{-1}. Biuret-hydrate shows four bands at 3487, 3438, 3214 and 3010 cm^{-1}. These bands are obviously due to the stretching vibrations of the NH and the NH_2 group as well as of the crystal water, but it is rather difficult to assign them to the specific vibrations of individual groups. These bands are replaced by the bands at 2585, 2412, 2321 and 2272 cm^{-1} on deuteration.

The Region between 1800 and 900 cm^{-1}. Figure 1 shows the infrared spectra between 1800 and 800 cm^{-1} of biuret-hydrate and its deuterated compound. The undeuterated compound shows only three bands between 1750 and 1550 cm^{-1}, although two C=O stretching and two NH_2 bending bands are expected in this region. On deuteration, the two bands at 1749 and 1718 cm^{-1} shift slightly to lower frequencies and the band at 1608 cm^{-1} disappears completely as seen in Fig. 1. It is obvious therefore that the former bands are due to the C=O stretching vibrations and the latter to the NH_2 bending vibrations. By referring to biuret-anhydrate which shows two peaks at 1620 and 1588 cm^{-1},[8,6] it is conceivable that the two NH_2 bending absorptions of hydrate crystal overlap to give one band at 1608 cm^{-1}. The corresponding ND_2 bending absorptions of deuterated biuret-hydrate were identified as the weak bands at 1168 and 1130 cm^{-1} from analogy with urea-d_4.[10] The band at 1130 cm^{-1} of biuret-hydrate may be assigned to the NH_2 rocking vibrations and the band at 915 cm^{-1} of deuterated biuret-hydrate to the ND_2 rocking vibrations. These frequencies are comparable to the corresponding frequencies of urea and urea-d_4.[10]

Takimoto assigned the bands of biuret-anhydrate at 1420, 1326 and 950 cm^{-1} to the CN stretching vibrations.[9] The bands of biuret-hydrate corresponding to these bands are observed at 1420, 1365 and 958 cm^{-1}. Among these bands, the bands at 1420 and 958 cm^{-1} hardly shift on deuteration as seen in Fig. 1, and are assigned undoubtedly to the CN stretching vibrations. The 1365 cm^{-1} band cannot be assigned to a simple CN stretching vibration since this band disappears on deuteration as seen in Fig. 1. Uno and Machida concluded in consequence of the normal coordinate analysis of diacetamide that the imide II and III bands arise from the coupling between the NH in-plane deformation and the CN stretching vibrations of the –CONHCO– group. Analogously the deuteration sensitive band at 1365 cm^{-1} of biuret-hydrate may be assigned to the imide III band arising from the coupling between the NH in-plane deformation and the CN stretching vibrations of the –CONHCO– group. To the imide II absorption of biuret-hydrate expected from this coupling, we assigned the weak band at 1515 cm^{-1} which disappears on deuteration. Such a weak imide II band has also been found around 1480 cm^{-1} for acylureas.[11] The 1096 cm^{-1} band is assigned to the remaining CN stretching vibration. For deuterated biuret-hydrate, the bands at 1462, 1435, 1273 and 935 cm^{-1} can be assigned to the four CN stretching vibrations. According to the normal coordinate analysis, however, the band at 1273 cm^{-1} is due to a complicated vibration concerned with the CN stretching, the ND in-plane deformation (imide III') and the ND_2 rocking vibrations.

The Region between 900 and 33 cm^{-1}. Figure 2 shows the infrared spectra between 900 and 33 cm^{-1} of biuret-hydrate and between 900 and 250 cm^{-1} of deuterated biuret-hydrate. Referring to the C=O out-of-plane deformation frequency of urea (785 cm^{-1}) and urea-d_4 (776 cm^{-1}),[10] we assigned the bands at 801 and 765 cm^{-1}

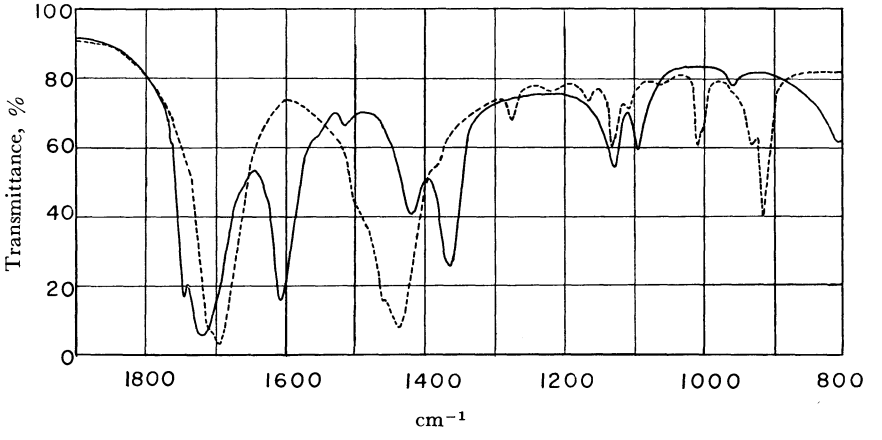

Fig. 1. Infrared spectra of biuret-hydrate (——) and its deuterated compound (----) in the region between 1900 and 800 cm^{-1}.

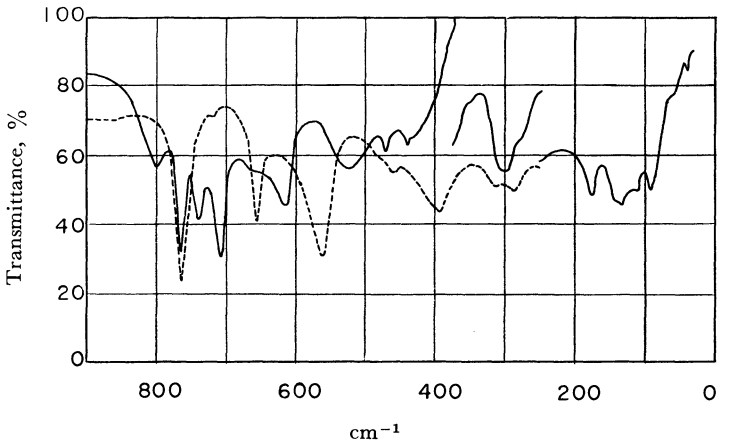

Fig. 2. Infrared spectra biuret-hydrate (——) and its deuterated compound (----) in the region between 900 and 33 cm^{-1}.

of biuret-hydrate and the band at 764 cm^{-1} of deuterated biuret-hydrate to the corresponding vibrations. The band at 712 cm^{-1} is assigned to the NH_2 wagging or the NH out-of-plane deformation (imide V) vibrations and the band at 520 cm^{-1} to the NH_2 torsional vibration from analogy with urea[10] and diacetamide.[5] The counterparts of these bands for deuterated biuret-hydrate are found at 558 and 392 cm^{-1}. Throughout this region the spectral change on deuteration is so complicated that the assignment of the bands due to the in-plane deformation vibrations is quite difficult. From the large separation between the in-plane NH and ND deformation and the in-plane skeletal deformation frequencies, it is expected at first sight that the shift of the latter frequencies on deuteration may not be appreciable. Normal coordinate analysis revealed, however, fairly big effects of the deuteration on the in-plane skeletal deformation frequencies. We assigned the bands at 741, 618, 471, 439 and 178 cm^{-1} for biuret-hydrate and the bands at 653, 558, 450 and 392 cm^{-1} for deuterated biuret-hydrate to the skeletal in-plane deformation vibrations by referring to the calculated frequencies.

Normal Coordinate Analysis

Since it is almost impossible to give a complete assignment of all fundamental frequencies of such a big molecule as biuret on the purely empirical basis, we have carried out the normal coordinate analysis according to Wilson's method.[13] The **G** matrices were set up by using the *trans-cis* conformation and the structural parameters based on Hughes *et al.*'s X-ray study[6] as shown in Fig. 3. The

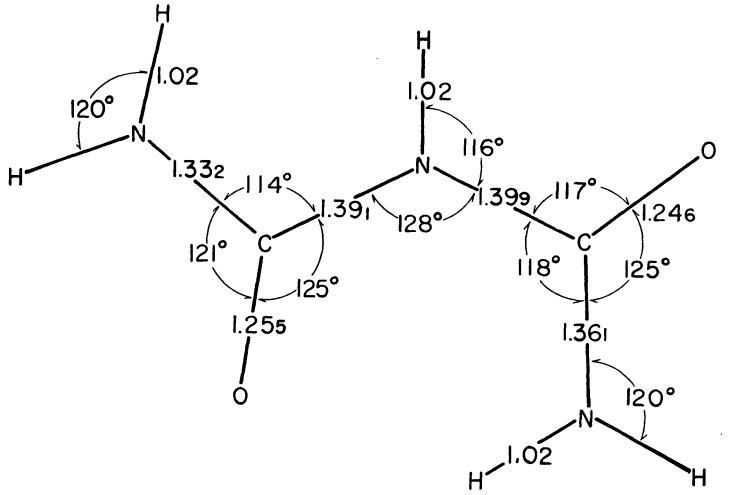

Fig. 3. Structural parameters.

13) E. B. Wilson, Jr., *J. Chem. Phys.*, **7**, 1047 (1939); **9**, 76 (1941).

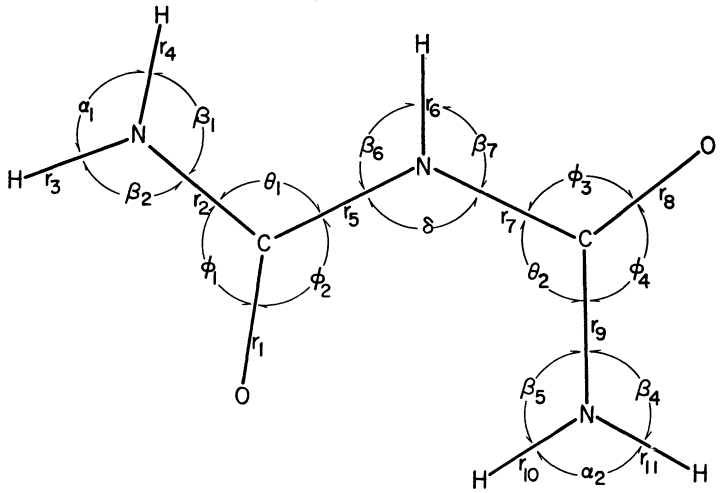

Fig. 4. Internal coordinates.

Table 1. Infrared frequencies of biuret-hydrate

	Assignment
3487 s, 3438 s, 3214 sb, 3010 m	NH_2 asym. and sym. stretching; NH stretching; OH stretching
1745 s	C=O stretching
1718 vs	C=O stretching
1608 s	NH_2 bending
1515 w	Imide II band
1420 m	CN stretching
1365 s	Imide III band
1130 m	NH_2 rocking
1096 m	CN stretching
958 w	CN stretching
801 w	C=O out-of-plane deformation
765 m	C=O out-of-plane deformation
741 m	skeletal in-plane deformation
712 m	NH_2 wagging or NH out-of-plane deformation
618 m	skeletal in-plane deformation
520 w	NH_2 torsion
471 w	skeletal in-plane deformation
439 w	skeletal in-plane deformation
300 mb	skeletal out-of-plane deformation
280 sh	skeletal out-of-plane deformation
178 w	skeletal in-plane deformation

Table 2. Infrared frequencies of deuterated biuret-hydrate

	Assignment
2585 s, 2412 s, 2321 s, 2272 sh	ND_2 asym. and sym. stretching; ND stretching; OD stretching
1710 sh	C=O stretching
1695 vs	C=O stretching
1462 sh	CN stretching
1435 vs	CN stretching
1273 m	CN stretching
1168 vw, 1130 w	ND_2 bending
1011 w	ND deformation and skeletal stretching
935 w	CN stretching
915 m	ND_2 rocking
764 m	C=O out-of-plane vibration
653 m	skeletal in-plane deformation
558 s	skeletal in-plane deformation; ND_2 wagging or ND out-of-plane deformation
450 w	skeletal in-plane deformation
392 m	skeletal in-plane deformation; ND_2 torsion
307 mb	skeletal out-of-plane deformation
280 mb	skeletal out-of-plane deformation

NH_2 and the NH stretching vibrations were separated from the other vibrations.[13,14] A description of the internal coordinates is shown in Fig. 4 and the internal symmetry coordinates were constructed as shown in Table 3. A simple Urey-Bradley force field was employed, and the fifteen force constants shown as the set A of Table 4 were used first. In a trial calculation we transferred the bending constant H(CNC) and the repulsion constant F(CNC) from diacetamide[5] and the other force constants from urea,[15] but the calculated frequencies were

14) E. B. Wilson, J. C. Decius and P. C. Cross, "Molecular Vibrations," McGrow Hill, New York (1955), p. 74.

15) A. Yamaguchi, *Nippon Kagaku Zasshi (J. Chem. Soc. Japan, Pure Chem. Sect.)*, **78**, 1319 (1957); A. Yamaguchi, T. Miyazawa, T. Shimanouchi and S. Mizushima, *Spectrochim. Acta*, **10**, 1319 (1957).

TABLE 3. INTERNAL SYMMETRY COORDINATES

Symmetry coordinates	Description of modes	Abbr.
$S_1=\Delta r_1$	C=O stretching	νC=O
$S_2=\Delta r_8$	C=O stretching	νC=O
$S_3=\Delta r_2$	CN stretching	νCN
$S_4=\Delta r_5$	CN stretching	νCN
$S_5=\Delta r_7$	CN stretching	νCN
$S_6=\Delta r_9$	CN stretching	νCN
$S_7=(2\Delta\alpha_1-\Delta\beta_1-\Delta\beta_2)/\sqrt{6}$	NH_2 bending	βNH_2
$S_8=(\Delta\beta_1-\Delta\beta_2)/\sqrt{2}$	NH_2 rocking	ρNH_2
$S_9=(2\Delta\alpha_1-\Delta\beta_4-\Delta\beta_5)/\sqrt{6}$	NH_2 bending	βNH_2
$S_{10}=(\Delta\beta_4-\Delta\beta_5)/\sqrt{2}$	NH_2 rocking	ρNH_2
$S_{11}=(2\Delta\delta-\Delta\beta_6-\Delta\beta_7)/\sqrt{6}$	CNC deformation	δCNC
$S_{12}=(\Delta\beta_7-\Delta\beta_6)/\sqrt{2}$	NH deformation	δNH
$S_{13}=(2\Delta\theta_1-\Delta\phi_1-\Delta\phi_2)/\sqrt{6}$	NCN deformation	δNCN
$S_{14}=(\Delta\phi_2-\Delta\phi_1)/\sqrt{2}$	CO deformation	δCO
$S_{15}=(2\Delta\theta_2-\Delta\phi_3-\Delta\phi_4)/\sqrt{6}$	NCN deformation	δNCN
$S_{16}=(\Delta\phi_4-\Delta\phi_3)/\sqrt{2}$	CO deformation	δCO

TABLE 4. FORCE CONSTANTS

Set A		Set B		Dispersion
K(CO)	7.83	$K(CO)_T$	8.00_0	0.41
		$K(CO)_C$	8.05_6	0.32
$K(CN)_U$	6.07	$K(CN)_{UT}$	6.04_7	0.19
		$K(CN)_{UC}$	5.49_5	0.33
$K(CN)_I$	3.56	$K(CN)_I$	3.73_6	0.18
H(HNH)	0.35	H(HNH)	0.35_1	0.00
$H(CNH)_I$	0.26	$H(CNH)_I$	0.19_0	0.01
$H(CNH)_U$	0.42	$H(CNH)_U$	0.42_3	0.00
H(NCN)	0.63	H(NCN)	0.77_6	0.07
H(CNC)	0.50*	H(CNC)	0.13_5	0.04
H(NCO)	0.27	H(NCO)	0.22_8	0.01
F(HNH)	0.0*	F(HNH)	0.0*	—
$F(CNH)_I$	0.61	$F(CNH)_I$	0.83_8	0.07
$F(CNH)_U$	0.22	$F(CNH)_U$	0.16_8	0.02
F(NCN)	0.89	F(NCN)	0.77_7	0.09
F(CNC)	0.54	F(CNC)	0.98_5	0.28
F(NCO)	1.28	F(NCO)	1.34_3	0.03

* assumed

so deviated from the observed ones that we could not enter the refinement process. Then we took the values of the $K(CN)_I$, $H(CNH)_I$, H(CNC), $F(CNH)_I$ and F(CNC) from diacetamide[5] (the subscript I specifies the force constant concerned with the –CONHCO– group) and the other force constants from urea.[15] In the first step of the force constant refinement, only the frequencies higher than 900 cm^{-1} of biuret and deuterated biuret were taken into account, and the values of the stretching constants and the bending constants concerned with hydrogen atoms were adjusted several times by referring to the Jacobian matrix elements and were further refined by the least squares method. After this refinement the absorption frequencies below 900 cm^{-1} were assigned to the vibrational modes by referring to the calculated frequencies. This assignment was checked by the product rule[16] by assuming that the two unobserved frequencies of deuterated biuret were the same as the calculated frequencies. The observed product ratio (7.21) agrees well with the theoretical ratio (7.06) obtained from calculated frequencies. In the next step, we fixed the values of the repulsion constant F(HNH) and the bending constant H(CNC) to zero and 0.50, respectively, since they showed large dispersions, and refined all the other force constants to obtain a converged set (see the set A in Table 4). The value of the stretching constant $K(CN)_I$ obtained in this step is smaller than that of the CN stretching constant for the $-CONH_2$ groups, $K(CN)_U$. This result is comparable with the case of bis(biuret) copper(II) chloride[17] and is consistent with the expectation from the difference in the CN bond lengths between the –CONHCO– and the $-CONH_2$ groups. Since the two $-CONH_2$ groups are not equivalent to each other in the *trans-cis* conformation of biuret, it seems too crude to fix the two constants appearing pairwise for the two $-CONH_2$ groups to the same value. On the other hand, the increase in the number of independent force constants is not favorable to obtain any converged set of force constants uniquely. Accordingly, in the final step of the force constant refinement, we tried to refine only the stretching constants for the C=O and the CN bonds of each $-CONH_2$ group independently. Their values were initially taken from the set A, and the sixteen force constants except the repulsion constant F(NHH) were refined by the least squares method to obtain a converged set. The force constants used in the final calculation are shown as the set B of Table 4

16) O. Redlich, *Z. Phys. Chem. Abstr.*, **B28**, 371 (1935).
17) B. B. Kedzia, P. X. Armendarez and K. Nakamoto, *J. Inorg. & Nuclear Chem.*, **30**, 849 (1968).

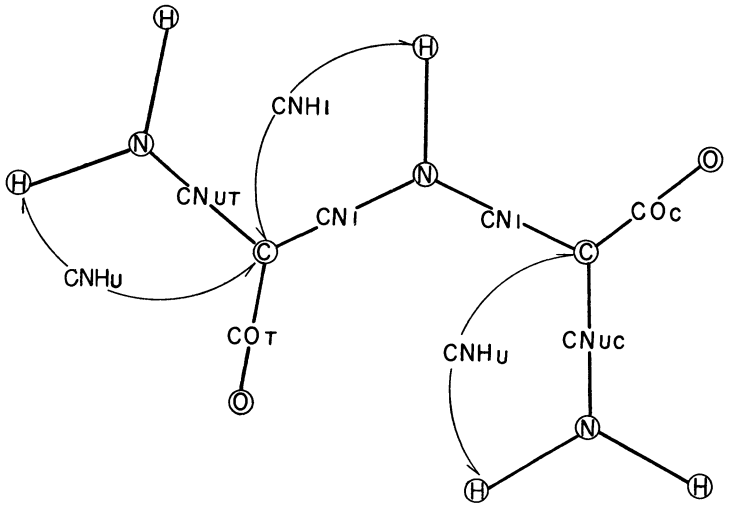

Fig. 5. The bonds and angles specified by the subscripted notation for the force constants.

Table 5. Fundamental frequencies and main potential energy distributions for biuret

	Obsd	Calcd	Δ(%)	P. E. D. (%)	Abbr.
ν_1	1745	1743	0.1	$S_1(53)$, $S_3(17)$, $S_{12}(16)$, $S_{13}(15)$	νC=O
ν_2	1718	1722	0.3	$S_2(56)$, $S_6(21)$, $S_{15}(15)$	νC=O
ν_3	1608	1611	0.2	$S_7(68)$, $S_3(11)$, $S_8(10)$	βNH_2
ν_4	1608	1604	0.1	$S_9(70)$	βNH_2
ν_5	1515	1522	0.4	$S_{12}(71)$, $S_4(13)$	Imide II
ν_6	1420	1419	0.1	$S_5(35)$, $S_4(30)$, $S_3(17)$, $S_6(15)$	νCN
ν_7	1365	1368	0.3	$S_3(29)$, $S_5(20)$, $S_6(20)$, $S_{12}(10)$	Imide III
ν_8	1130	1133	0.3	$S_8(40)$, $S_{10}(33)$, $S_1(10)$	ρNH_2
ν_9	1130	1125	0.5	$S_{10}(36)$, $S_8(31)$, $S_2(13)$	ρNH_2
ν_{10}	1096	1097	0.1	$S_4(20)$, $S_3(15)$, $S_1(14)$	νCN
ν_{11}	958	964	0.4	$S_6(25)$, $S_5(18)$, $S_{13}(10)_5$	νCN
ν_{12}	741	732	0.9	$S_{14}(25)$, $S_{15}(24)$, $S_{11}(10)$	skel.
ν_{13}	618	617	0.1	$S_{16}(46)$, $S_{14}(22)$, $S_{13}(21)$	skel.
ν_{14}	471	471	0.0	$S_{15}(37)$, $S_{14}(28)$, $S_{13}(12)$	skel.
ν_{15}	439	427	2.7	$S_{16}(30)$, $S_{13}(29)$	skel.
ν_{16}	178	172	4.4	$S_{11}(73)$, $S_{15}(12)$	skel.

$\Delta = (|\nu_{obsd} - \nu_{calcd}|/\nu_{obsd}) \times 100$

together with their dispersions. The bonds and angles specified by the subscripted notation for the force constants are indicated in Fig. 5. Tables 5 and 6 show the frequencies calculated from these force constants, the corresponding observed frequencies and the potential energy distributions. The agreement between the calculated and the observed frequencies is excellent throughout both isotopic species.

It is seen from Table 5 that the coupling of the NH in-plane deformation vibration with the CN stretching vibrations does occur for the imide II and III frequencies empirically assigned, although it is not so appreciable as in the case of diacetamide.[5] As seen in Tables 5 and 6, the skeletal in-plane deformation vibrations couple appreciably with one another for the frequencies below 700 cm^{-1}, and it is difficult to assign each fundamental frequency to the vibration of a particular group. The vibrational mode of 1011 cm^{-1} band of deuterated biuret is quite complicated by the mixing of the C=O stretching, the CN stretching, the ND in-plane deformation, the ND_2 bending and the CNC deformation vibrations as seen in Table 6. This situation may be comparable with the cases for the 1035 cm^{-1} band of diacetamide-d_1 contributed by the skeletal stretching and deformation vibrations[5] and for the 1005 cm^{-1} band of urea-d_4 contributed by the C=O stretching and the ND_2 bending vibrations.[15] As seen in Table 4, the values of the stretching constant $K(CO)_T$ and $K(CO)_C$ obtained in the final calculation are not

TABLE 6. FUNDAMENTAL FREQUENCIES AND MAIN POTENTIAL ENERGY DISTRIBUTIONS FOR DEUTERATED BIURET

	Obsd	Calcd	Δ(%)	P. E. D. (%)	Abbr.
ν_1'	1710	1713	0.2	$S_1(52)$, $S_2(17)$, $S_3(15)$, $S_{13}(13)$	νC=O
ν_2'	1695	1692	0.2	$S_2(56)$, $S_1(18)$, $S_6(14)$, $S_{15}(12)$	νC=O
ν_3'	1462	1462	0.0	$S_3(51)$, $S_4(45)$, $S_{14}(13)$	νCN
ν_4'	1435	1431	0.3	$S_6(50)$, $S_5(45)$, $S_{16}(14)$, $S_9(11)$	νCN
ν_5'	1273	1270	0.3	$S_4(19)$, $S_5(14)$, $S_{12}(28)$, $S_7(20)$	νCN+δND+βND$_2$
ν_6'	1168	1181	1.4	$S_9(56)$, $S_5(12)$	βND$_2$
ν_7'	1130	1112	1.8	$S_7(39)$, $S_{13}(35)$	βND$_2$+δND
ν_8'	1011	1007	0.4	$S_1(19)$, $S_7(15)$, $S_{12}(9)$, $S_{13}(7)$	νC=O+βND$_2$+δND
ν_9'	935	937	0.2	$S_3(19)$, $S_6(15)$, $S_{10}(14)$, $S_9(13)$	νCN+ρND$_2$
ν_{10}'	915	909	0.6	$S_{10}(45)$	ρND$_2$
ν_{11}'	—	853	—	$S_8(39)$, $S_6(14)$	ρND$_2$
ν_{12}'	653	664	1.9	$S_{14}(25)$, $S_{10}(18)$, $S_{15}(12)$	skel.
ν_{13}'	558	560	0.4	$S_{16}(50)$, $S_{13}(15)$, $S_{14}(13)$, $S_8(11)$	skel.
ν_{14}'	450	451	0.2	$S_{14}(34)$, $S_{15}(32)$	skel.
ν_{15}'	392	397	1.1	$S_{13}(39)$, $S_{16}(19)$	skel.
ν_{16}'	—	163	—	$S_{11}(72)$, $S_{15}(14)$	skel.

$\Delta=(|\nu_{obsd}-\nu_{calcd}|/\nu_{obsd})\times 100$

much different from each other, reflecting rather small difference between the two C=O bond lengths. These values correspond nearly to the average of the K(CO)'s for urea (6.49) and diacetamide (9.80). The values of the stretching constants for the CN bonds increase in the order $CN_I < CN_{UC} < CN_{UT}$ as expected from the difference in the bond lengths. The $K(CN)_I$ is similar to the $K(CN)_I$ of diacetamide,[5] and the $K(CN)_{UC}$ to the K(CN) of urea(5.24) and close to the K(CN) of acetamide(5.53).[18,19] The $K(CN)_{UT}$ is close to that of *N*-methylformamide(6.15).[20] The values of H(NCN), F(NCN) and F(NCO) are comparable with those of urea. These results may be taken as indicating an excellent transferability of the Urey-Bradley force constants throughout a variety of urea and amide derivatives.

The authors would like to express their thanks to Professor Toru Takenaka and Miss Kazuko Nogami of Kyoto University for the measurement of the infrared spectra between 900 and 250 cm^{-1} and the staff of Central Research Laboratory, Hitachi, Ltd. for the measurement between 400 and 33 cm^{-1}. Thanks are due to the staff of the Kyoto University Computer Center for the use of the KDC II computer.

18) T. Uno, K. Machida and Y. Saito, This Bulletin, **42**, 897 (1969).
19) I. Suzuki, *ibid.*, **35**, 1279 (1962).
20) I. Suzuki, *ibid.*, **35**, 540 (1962).

BULLETIN OF THE CHEMICAL SOCIETY OF JAPAN VOL. 42 1546—1554 (1969)

The Crystal Structure of Riboflavin Hydrobromide Monohydrate

Nobuo TANAKA,*1 Tamaichi ASHIDA, Yoshio SASADA*2 and Masao KAKUDO

Institute for Protein Research, Osaka University Joan-cho, Kita-ku, Osaka

(Received December 5, 1968)

The crystal structure of riboflavin hydrobromide monohydrate has been determined by a three-dimensional X-ray analysis. The space group is $P2_12_12_1$ with four formula units in the unit cell of dimensions $a=18.28$, $b=6.99$ and $c=14.77$ Å. The structural parameters were refined by means of a block-diagonal least-squares method, the final R factor being 0.07. The ribitol does not form a furanose ring but a chain. The protonation of the isoalloxazine ring occurs at the N(1) atom, and the C(4a)-N(10) bond is found to be a double bond. The bromide ion is situated midway between two isoalloxazine rings separated by a period along the b axis.

Riboflavin, in the form of the mono- and dinucleotide, is a prosthetic group of several enzymes concerning biochemical oxidation-reduction. These enzymes act as hydrogen carriers from a substrate to an acceptor molecule, when riboflavin alternatively accepts and releases two hydrogen atoms.

The electronic structure of riboflavin has been investigated in order to elucidate the mechanism of the transfer of the hydrogen atom. Guzzo and Tollin[1] have suggested from the study of EPR spectra that it is reduced into semiquinone by strong acid. On the other hand, Pullman and Pullman have proposed the keto form to the reduced riboflavin from the theoretical calculation.[2]

The present study has been undertaken to establish the relationship between the structural characteristics of mono-protonated riboflavin and its biological function.

Experimental

The crystals were obtained from 6 N HBr solution of riboflavin. They are yellow rods elongated along the b axis. Unit cell dimensions were determined from the equatorial Weissenberg photographs about the b and c axes, on which the powder pattern of aluminum were superposed for calibration. The crystal data are shown in Table 1.

The equi-inclination Weissenberg photographs were taken for layer lines 0 to 5 about the b axis and 0 to 10 about c with Cu$K\alpha$ radiation. The number of independent reflections recorded was 2261, but the intensities of 225 of these were too weak to be measured. The relative intensities were measured visually and the range was 1 to 4000. They were corrected for Lorentz and polarization factors and spot-size factors for the equi-inclination Weissenberg photographs, but the corrections for absorption and secondary extinction were neglected. A rod-shaped crystal having a cross section of 0.5 mm × 0.3 mm was used for the b axis photographs. A crystal for the c axis photographs, cut perpendicularly to the b axis, has a dimension of 0.2 mm × 0.2 mm × 0.3 mm.

Table 1. Crystal data

Unit cell dimensions	$a=18.28\pm0.04$ Å $b=6.99\pm0.02$ $c=14.77\pm0.03$
Absent spectra	$(h00)$; $h=2n+1$ $(0k0)$; $k=2n+1$ $(00l)$; $l=2n+1$
Space group	$P2_12_12_1$
Density	$D_m=1.68$ g/cm^3 $D_c=1.67$ g/cm^3, when $Z=4$
Molecular weight	475.3
Linear absorption coefficient for Cu$K\alpha$ radiation	30.4
$F(000)$	976

Structure Determination and Refinement

From a three-dimensional Patterson function the bromide ion was easily located at $x=0.205$, $y=0.250$ and $z=0.119$. Fourier synthesis with the phases based on the bromide ion has an additional mirror plane because the y parameter of the heavy atom was a special value. The atoms in the isoalloxazine ring and C(1') in the ribityl group were located near the planes of $y=0.25$, while the as-

*1 Present address: Faculty of Technology, Tottori University, Koyama-cho, Tottori.

*2 Present address: Faculty of Science, Tokyo Institute of Technology, Ookayama, Meguro-ku, Tokyo.

1) A. V. Guzzo and G. Tollin, *Arch. Biochem. Biophys.*, **103**, 231 (1963).

2) B. Pullman and A. Pullman, *Proc. Natl. Acad. Sci. U. S.*, **45**, 136 (1959).

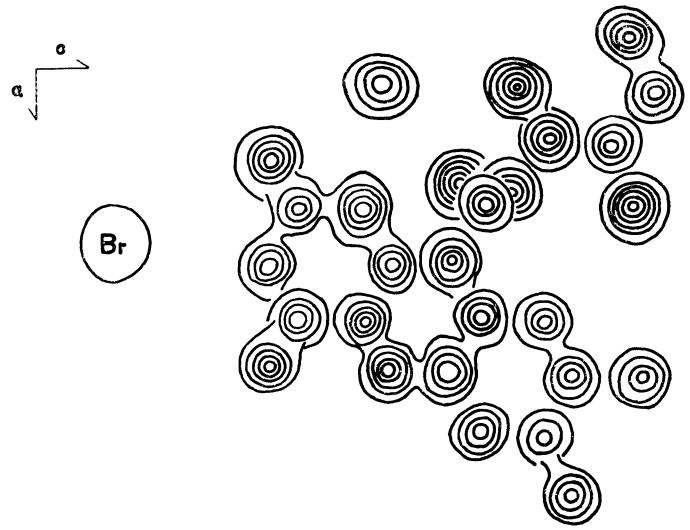

Fig. 1. Composite drawing of the final electron density map viewed along the *b* axis. Contours are drawn at intervals of 2.0 e·Å^{-3}; those for the bromide ion are not drawn. The lowest is 1.5 e·Å^{-3}.

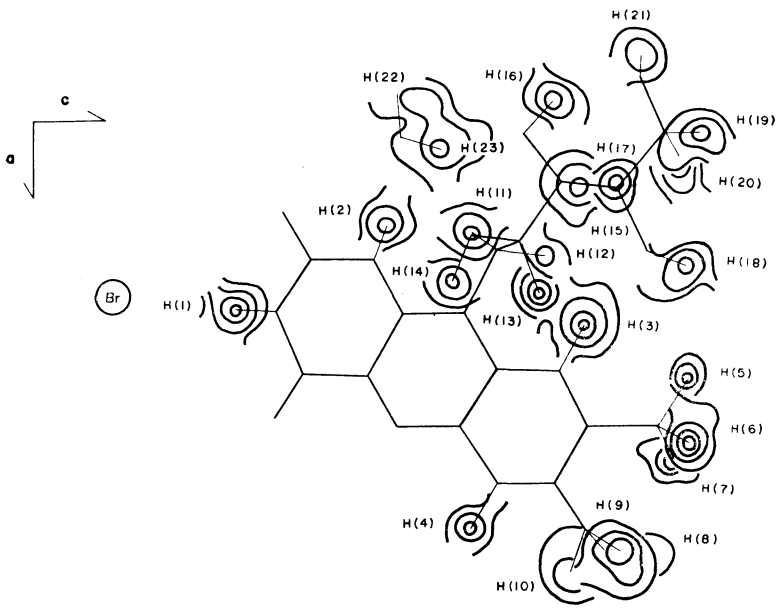

Fig. 2. Location of hydrogen atoms from a three-dimensional difference Fourier map. First contour 0.1 e·Å^{-3}; interval 0.2 e·Å^{-3}.

signment of the peaks to the other light atoms was somewhat puzzling because of the presence of the additional mirror plane. Successive Fourier summations were able to give well resolved peaks for all twenty-nine non-hydrogen atoms.

Atomic positions and anisotropic temperature factors were refined by a block-diagonal least-squares method. A difference Fourier map, calculated after several cycles of least-squares refinement, gave a fair indication of the positions of the hydrogen atoms. Further refinement, including hydrogen atoms, was proceeded with anisotropic temperature factors for all the non-hydrogen atoms and with isotropic ones for hydrogen atoms. Atomic scattering factors were taken from the "International Tables for X-Ray Crystallography." Anomalous scattering effect was corrected for the bromide ion ($\Delta f' = -0.9$, $\Delta f'' = 1.4$). Weighting scheme was as follows;

$$w = 1.0 \quad \text{if } |F_o| > 0$$
$$w = 0.5 \quad \text{if } |F_o| = 0$$

TABLE 2(a). ATOMIC PARAMETERS AND THEIR ESTIMATED STANDARD DEVIATIONS

Atom	x	y	z	β_{11}	β_{22}	β_{33}	β_{12}	β_{13}	β_{23}
Br	0.2062(1)	0.2367(2)	0.1173(1)	234(3)	1960(26)	365(5)	382(21)	−52(8)	−11(28)
C(2)	0.1642(6)	0.2414(20)	0.3988(9)	212(31)	1705(239)	348(54)	2(190)	−51(70)	162(266)
C(4)	0.2953(6)	0.3106(15)	0.3945(8)	171(29)	939(197)	291(50)	152(144)	113(76)	122(179)
C(5)	0.4261(6)	0.2966(19)	0.6746(9)	179(32)	1111(305)	334(51)	5(170)	105(69)	−344(222)
C(6)	0.4294(6)	0.2904(19)	0.7664(9)	187(32)	1362(288)	337(51)	−16(173)	−2(70)	−5(226)
C(7)	0.3617(6)	0.2770(19)	0.8158(8)	210(33)	1205(249)	279(45)	35(188)	67(66)	−24(225)
C(8)	0.2964(6)	0.2714(17)	0.7740(7)	170(27)	1467(229)	273(42)	−170(197)	33(63)	209(212)
C(4a)	0.2966(6)	0.2916(15)	0.4950(7)	177(29)	979(231)	236(41)	−82(161)	47(65)	97(172)
C(8a)	0.2937(6)	0.2781(15)	0.6795(7)	175(27)	874(198)	232(39)	85(169)	6(62)	−299(178)
C(9a)	0.2287(5)	0.2651(17)	0.5400(8)	181(28)	1026(195)	277(43)	35(153)	7(57)	47(214)
C(10a)	0.3592(5)	0.2911(16)	0.6287(9)	140(27)	709(233)	370(52)	−111(141)	62(67)	174(221)
C(6m)	0.5009(6)	0.3012(24)	0.8182(9)	203(33)	2929(446)	334(55)	−198(214)	88(75)	25(283)
C(7m)	0.3632(6)	0.2697(20)	0.9200(8)	243(35)	1600(255)	293(47)	−268(208)	0(69)	−116(246)
N(1)	0.1659(5)	0.2370(16)	0.4921(6)	197(25)	1481(192)	238(36)	−125(149)	−35(51)	211(183)
N(3)	0.2281(5)	0.2744(15)	0.3533(6)	198(27)	1764(203)	241(36)	99(140)	25(51)	−92(173)
N(9)	0.2278(4)	0.2663(13)	0.6305(6)	142(21)	841(152)	284(37)	227(114)	46(47)	324(177)
N(10)	0.3584(5)	0.3028(14)	0.5360(6)	163(26)	972(230)	229(37)	−214(133)	58(54)	−105(161)
O(2)	0.1081(4)	0.2118(19)	0.3582(6)	206(24)	3889(361)	324(39)	−259(179)	−151(54)	552(234)
O(4)	0.3480(5)	0.3588(14)	0.3498(6)	224(26)	1872(227)	322(37)	−33(139)	167(51)	52(165)
C(1′)	0.1573(5)	0.2585(19)	0.6838(7)	116(24)	1729(220)	257(41)	436(167)	20(54)	−375(228)
C(2′)	0.1439(6)	0.0554(17)	0.7179(8)	135(29)	1411(254)	254(48)	158(152)	5(64)	−156(203)
C(3′)	0.0775(6)	0.0442(17)	0.7774(8)	143(31)	1452(242)	285(49)	3(153)	29(67)	80(203)
C(4′)	0.0844(6)	0.1629(18)	0.8607(9)	194(33)	1696(280)	303(55)	−116(169)	134(72)	4(209)
C(5′)	0.0242(7)	0.1130(21)	0.9305(9)	250(40)	1857(327)	396(64)	25(207)	161(86)	376(263)
O(2′)	0.1347(4)	−0.0664(12)	0.6397(6)	187(23)	1359(173)	311(38)	45(113)	−4(49)	−241(143)
O(3′)	0.0168(4)	0.1002(14)	0.7258(6)	171(25)	2155(231)	277(37)	−6(135)	44(50)	96(173)
O(4′)	0.1545(5)	0.1279(15)	0.9028(6)	204(24)	3052(276)	343(43)	102(150)	−18(56)	−200(193)
O(5′)	−0.0462(4)	0.1137(13)	0.8916(8)	213(26)	1878(207)	588(55)	235(129)	245(70)	−53(217)
OW	0.0149(5)	0.1111(16)	0.5370(7)	240(30)	2700(277)	353(41)	113(161)	−49(61)	92(197)

Anisotropic temperature factors in the expression, $\exp\{-(h^2\beta_{11}+k^2\beta_{22}+l^2\beta_{33}+hk\beta_{12}+hl\beta_{13}+kl\beta_{23})\}$, are multiplied by 10^5. The estimated standard deviations given in parentheses refer to the last decimal positions at respective values.

TABLE 2(b). THE FINAL PARAMETERS OF HYDROGEN ATOMS

Atom	**	x	y	y
H(1)	N(3)	0.2173	0.2480	0.2791
H(2)	N(1)	0.1158	0.1801	0.5204
H(3)	C(8)	0.2422	0.2827	0.8004
H(4)	C(5)	0.4729	0.3214	0.6363
H(5)	C(7m)	0.3013	0.2675	0.9622
H(6)	C(7m)	0.3752	0.3626	0.9610
H(7)	C(7m)	0.3992	0.1286	0.9410
H(8)	C(6m)	0.5145	0.1450	0.8551
H(9)	C(6m)	0.5069	0.4366	0.8548
H(10)	C(6m)	0.5324	0.3291	0.7826
H(11)	C(1′)	0.1140	0.3097	0.6552
H(12)	C(1′)	0.1672	0.3218	0.7495
H(13)	C(2′)	0.1886	0.0001	0.7500
H(14)	O(2′)	0.1840	−0.1250	0.6200
H(15)	C(3′)	0.0858	−0.0581	0.7855
H(16)	O(3′)	−0.0216	0.1003	0.7556
H(17)	C(4′)	0.0808	0.2741	0.8508
H(18)	O(4′)	0.1475	0.1694	0.9846
H(19)	C(5′)	0.0439	0.1447	0.9967
H(20)	C(5′)	0.0496	−0.0077	0.9629
H(21)	C(5′)	−0.0652	0.1770	0.8858
H(22)	OW	−0.0285	0.0707	0.5273
H(23)	OW	0.0258	0.0774	0.5868

* The mean value of the e.s.d. of the parameters are $\sigma(x)=0.13$ Å, $\sigma(y)=0.15$ Å and $\sigma(z)=0.14$ Å.
** The heavy atoms bonded to each hydrogen atom.

TABLE 3. OBSERVED AND CALCULATED STRUCTURE FACTORS ($\times 2.5$)

Table 3. (continued)

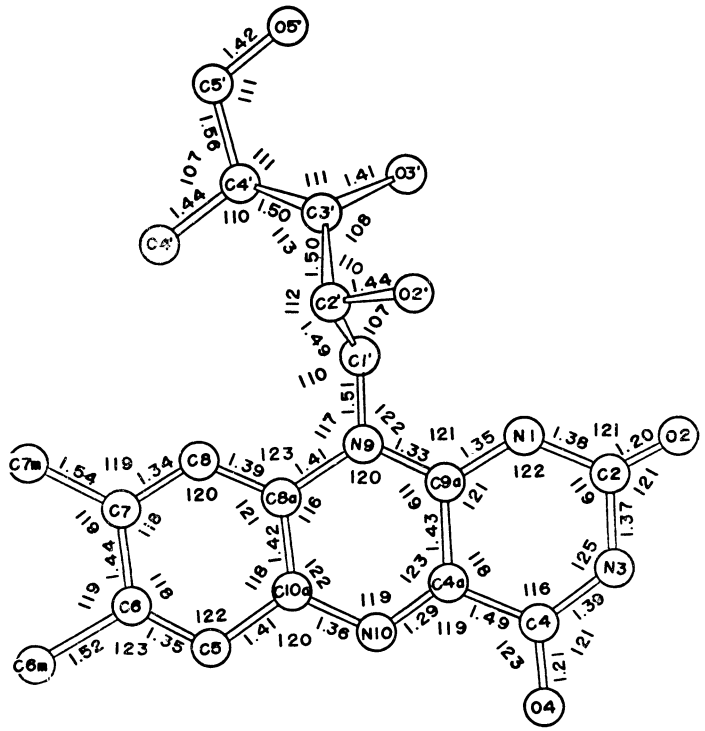

Fig. 3. Bond lengths (Å) and angles (degree).

the R factor was reduced to 0.07 after the refinement. Final atomic parameters are listed in Table 2, and $|F_o|$ and $|F_c|$ are tabulated in Table 3.

Discussion

The bond lengths and angles are shown in Fig. 3. The mean value of the estimated standard deviations for the bond lengths between non-hydrogen atoms except the bromide ion is 0.02 Å and that for the bond angles is 1.0°.

The difference Fourier synthesis (Fig. 2) shows that the addition of proton does not occur at the O(2) atom but at N(1) by hydrogen bromide. This is also supported by the fact that both exocyclic C–O lengths correspond to that of the double bond. The present result agrees with the location of the proton suggested by theoretical calculation,[2,3] and suggests that the pathway 1 in the reduction of riboflavin shown in Fig. 4 is reasonable, contrary to Guzzo and Tollin's expectation.[1]

The C(4)–C(4a) bond in the isoalloxazine ring is 1.49 Å, which corresponds to the single bond length, and the C(4a)–N(10) bond is shorter than the mean value of the other C–N lengths. Therefore, it is presumed that π-electrons are localized at the C(4a)-N(10) bond.

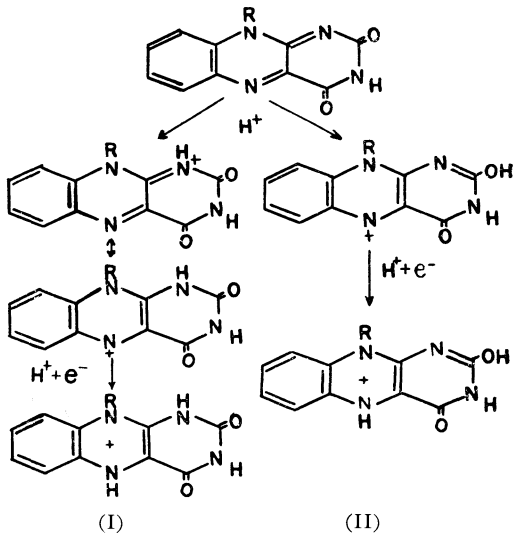

Fig. 4. Alternative pathways for the reduction of isoalloxazine.

On the theoretical calculation of the bond orders in the ring, the Hückel approximation was applied to a system of 16 conjugated π-electrons and 4 mobile electrons due to the hyperconjugation of the two methyl groups, where the Coulomb and exchange integrals were taken from the Ladik's[4]. There are several relations proposed

3) B. Grabe, *Biopolymer symposia*, **No. 1**, 289 (1964).

Table 4. Bond orders and bond lengths

Bond	Bond order	Bond length	
		Theoretical	Experimental
N(1)—C(2)	1.34	1.38 Å	1.38 Å
N(1)—C(9a)	1.39	1.38	1.35
N(3)—C(2)	1.43	1.36	1.37
N(3)—C(4)	1.45	1.35	1.39
N(9)—C(8a)	1.54	1.33	1.41
N(9)—C(9a)	1.65	1.31	1.33
N(10)—C(4a)	1.70	1.30	1.29
N(10)—C(10a)	1.56	1.33	1.36
C(4a)—C(9a)	1.52	1.42	1.43
C(8a)—C(10a)	1.50	1.42	1.42
C(4)—C(4a)	1.30	1.47	1.49
C(5)—C(6)	1.73	1.38	1.35
C(5)—C(10a)	1.55	1.41	1.41
C(6)—C(7)	1.59	1.40	1.44
C(7)—C(8)	1.72	1.38	1.34
C(8)—C(8a)	1.56	1.41	1.39

for converting the bond order into length.[5-10] For C–C bonds, approximately the same values were obtained by all the relations, and the converted bond lengths by, say, Coulson's[5] are in good agreement with those observed, as shown in Table 4. On the other hand, the converted C–N lengths show somewhat wider variations with the relations, and agreement between the theoretical and observed lengths is not so good. But if experimental errors are taken into account, significant disagreement is only for N(9)–C(8a). This may suggest that this approximation is not necessarily satisfactory in the present molecule.

The valence angles at the N(1) and N(3) atoms with an extra-annular hydrogen atom are 125° and 122°, respectively, and that at N(10) without hydrogen is 119°. They are consistent with the nitrogen valence angle in heterocyclic compounds discussed by Singh.[11] There are some small valence angles at the C(8a) and C(4) atoms which are bonded to the nitrogen atoms with an extra-annular hydrogen atom, whereas slightly large ones are found at the C(4a) and C(10a) atoms bonded to the N(10) atom. These facts have been reported in alloxane,[12] anhydrous alloxane,[13] anhydrous barbituric acid,[14] barbituric acid dihydrate,[15] pyridimine,[16] and 2-amino-4,6-dichloropyridine.[17]

The best planes of the isoalloxazine ring and the six-membered rings are listed in Table 5 together with the deviations of the atoms from them, where the nomenclatures of the rings are as follows:

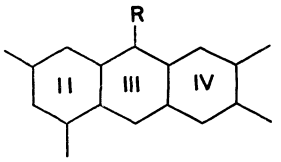

Table 5. The best plane of the rings

Atom	Plane I	Plane II	Plane III	Plane IV
N(1)	0.097	−0.014	0.153*	
C(2)	0.119	0.014		
N(3)	0.039	0.019		
C(4)	−0.109	−0.038	−0.100*	
C(4a)	−0.035	0.037	−0.015	
N(10)	−0.020	0.135*	−0.012	−0.033*
C(10a)	0.007		0.025	−0.001
C(5)	0.068		0.073*	0.001
C(6)	0.063			0.001
C(7)	−0.002			0.001
C(8)	−0.062		−0.011*	−0.001
C(8a)	−0.057		−0.016	0.000
N(9)	−0.071	−0.089*	−0.017	0.045*
C(9a)	−0.007	−0.025	0.037	
C(6m)	0.092*			
C(7m)	−0.012*			
O(2)	0.242*			
O(4)	−0.315*			
C(1′)	−0.185*			

Plane I** $0.104X-0.994Y-0.041Z=-1.717$
Plane II $0.175X-0.984Y-0.040Z=-1.375$
Plane III $0.089X-0.995Y-0.033Z=-1.765$
Plane IV $0.053X-0.998Y-0.036Z=-2.010$

Dihedral angles between the planes

Plane I—Plane II	4.1 (degree)
Plane I—Plane III	1.0
Plane I—Plane IV	3.0
Plane II—Plane III	5.0
Plane II—Plane IV	7.1
Plane III—Plane IV	2.1

* Not included in the calculation of the equation of the plane.
** X, Y and Z in the Å unit.

4) T. A. Hoffman and J. Ladik, *Adv. Chem. Phys.*, **7**, 84 (1964).
5) C. A. Coulson, *Proc. Roy. Soc.*, **A169**, 413 (1939).
6) L. Pauling, "The Nature of the Chemical Bond," 3rd ed., Cornell University Press, Ithaca, New York (1960).
7) E. Cox and G. A. Jeffrey, *Proc. Roy. Soc.*, **A207**, 110 (1951).
8) T. H. Goodwin and A. L. Porte, *J. Chem. Soc.*, **1956**, 3595.
9) T. Anno, M. Ito, R. Shimada, A. Sado and W. Mizushima, This Bulletin, **30**, 638 (1957).
10) M. J. S. Dewar and H. N. Schmeising, *Tetrahedron letters*, **5**, 166 (1959).
11) C. Singh, *Acta Cryst.*, **19**, 861 (1965).
12) C. Singh, *ibid.*, **19**, 759 (1965).
13) W. Bolton, *ibid.*, **17**, 147 (1964).
14) W. Bolton, *ibid.*, **16**, 166 (1963).
15) G. A. Heffrey, S. Ghose and J. O. Warwicker, *ibid.*, **14**, 881 (1961).
16) P. J. Wheatley, *ibid*, **13**, 80 (1960).
17) C. J. B. Clews and W. Cochran, *ibid.*, **1**, 4 (1948).

and the I represents the isoalloxazine ring. The dihedral angles between the planes are also given in this table. Though the ring IV is strictly planar, the other two rings are puckered; the deviations of the atoms from their best planes are significant. The dihedral angles between the planes indicate that the isoalloxazine ring takes, though slightly, a boat form. However, the isoalloxazine ring in

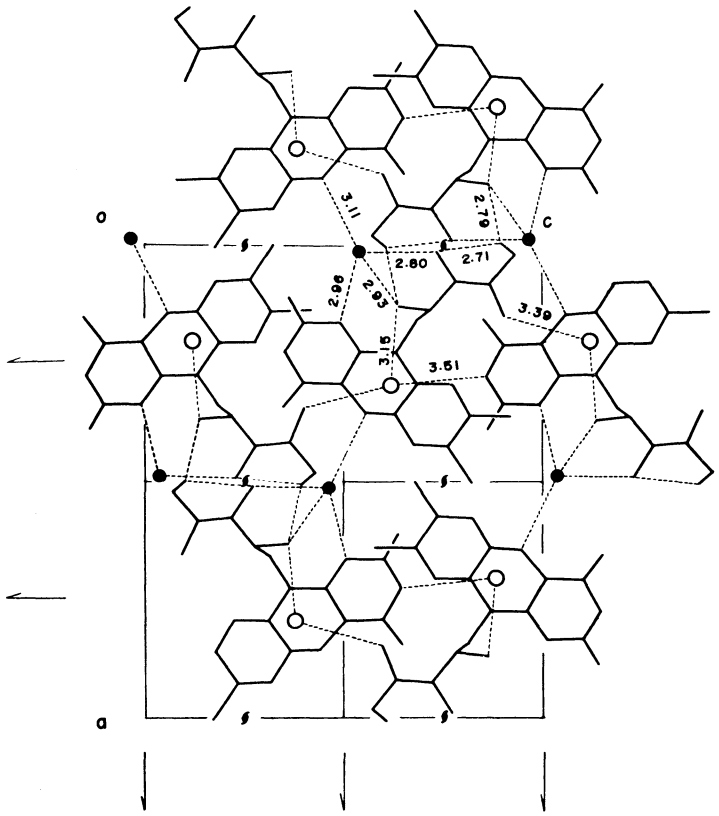

Fig. 5. The packing of the molecules viewed along the *b* axis. The dotted lines show the possible hydrogen bonds.
Medium circle: bromide ion, black circle: water molecule

Table 6. List of possible hydrogen bonds

X—HY	X—Y	X—H	∠XHY
Br(i)—H(14, v)O(2', v)	3.15 Å	2.52 Å	151 degree
Br(i)—H(1, i)N(3, i)	3.51	2.40	171
Br(i)—H(18, ii)O(4', ii)	3.39	2.28	146
OW(i)—H(2, i)N(1, i)	2.96	1.92	162
O(2', i)—H(23, i)OW(i)	2.93	2.36	130*
O(3', i)—H(23, i)OW(i)	2.80	2.06	151*
N(10, iii)—H(22, i)OW(i)	3.11	2.43	162
O(5', i)—H(16, i)O(3', i)	2.71	2.06	135**
O(2, iv)—H(21, i)O(5', i)	2.79	2.22	177

Key for molecules

i: x, y, z
ii: $x, y, 1+z$
iii: $-1/2+x, 1/2-y, 1-z$
iv: $-x, 1/2+y, 3/2-z$
v: $1/2-x, -y, -1/2+z$

* May be a bifurcated hydrogen bond
** The intramolecular hydrogen bond

1,3,10-trimethyl isoalloxazine iodide[18] has been reported to be nearly coplanar.

In the ribityl group, the C(1')–C(2'), C(2')–C(3') and C(3')–C(4') bonds are a little shorter than the normal C–C length of sp^3 hybridization, whereas the C(4')–C(5') does not differ significantly from the normal one. The C–O lengths in this group are between 1.41 Å and 1.44 Å, and their mean value, 1.428 Å, corresponds to the usual single C–O length. The valence angles C–C–C and C–C–O in this group do not differ significantly from their mean value, 107° and 110°, respectively.

The ribitol does not form a furanose ring but a chain, which has not been found in cases of nucleoside, nucleotide and nucleic acid. The conformation angles defined by Sundarlingam[19] are; $\phi_{C_2'-C_3'}=62°$ and $\phi_{C_3'-C_4'}=167°$, whereas they are 34° and −37° in the furanose ring of 5'-AMP.[20]

The molecular packing viewed along the *b* axis is shown in Fig. 5. The hydrogen bonds are shown by the dotted lines, where each figure represents a distance between the non-hydrogen atoms. Table 6 tabulates the X-H distances and X–H–Y angles related to the hydrogen bond. The H(2,i)-OW(i), 1.92 Å, is the normal hydrogen bond. The H(23,i) is located near both O(2',i) and O(3',i) atoms; the distances are 2.36 Å and 2.06 Å, respectively. Thus, the two contacts, OW-H(23)-O(2') and OW-H(23)-O(3'), seem to consist a bifurcated hydrogen bond. Another hydrogen atom of water molecule makes *a* weak hydrogen bond with the N(10) atom related by the screw axis along the *a*. This hydrogen bond may suggest the subsequent transfer of the hydrogen atom from the substrate.

The bromide ion contributes to the three hydrogen bonds with the N(3), O(2') and O(4') atoms. Though the Br(i)-N(3,i) distance, 3.51 Å, seems a little longer, the Br(i)-H(1,i) is 2.40 Å, which shows that it is a normal hydrogen bond. The bromide ion is situated midway between two isoalloxazine rings separated by a period along the *b* axis, and nearly above the center of the ring III which is indicated to have positive charge from the theoretical calculation of the bond orders.

TABLE 7. CLOSE INTERMOLECULAR CONTACTS

Atom	Nearest atom	Molecular position	Distance
Br	C(6m)	iii	3.87
O(2)	C(5)	iii	3.35
O(2)	C(6m)	iii	3.26
O(3')	O(4)	iii	3.29
OW	O(4)	iii	3.48
C(1')	O(5')	iv	3.39
Br	C(8a)	v	3.70
Br	C(9a)	v	3.86
Br	C(10a)	v	3.87
Br	N(9)	v	3.71
Br	C(2')	v	3.72
C(4)	O(4')	v	3.19
C(4a)	O(4')	v	3.34
O(2)	C(7)	v	3.50
O(4')	C(2')	v	3.48
O(4)	C(3')	v	3.30
O(4)	O(4')	v	3.48
Br	C(4a)	vi	3.75
Br	C(8a)	vi	3.50
Br	C(9a)	vi	3.84
Br	C(10a)	vi	3.50
Br	N(9)	vi	3.67
Br	N(10)	vi	3.62
C(2)	C(7m)	vi	3.45
N(3)	C(8)	vi	3.40
O(5')	C(7m)	vii	3.34

Key for molecules

iii: $-1/2+x$, $1/2-y$, $1-z$
iv: $-x$, $1/2+y$, $3/2-z$
v: $1/2-x$, $-y$, $-1/2+z$
vi: $1/2-x$, $1-y$, $-1/2+z$
vii: $-1/2+x$, $1/2-y$, $2-z$

This table shows the contacts shorter than 4.0 Å between the bromide ion and the other heavy atom, and those shorter than 3.5 Å in the other cases.

The authors wish to express their appreciation to Professor T. Miyazawa for his valuable discussion. They are also indebted to Dr T. Takano and Dr T. Ueki in this laboratory for their kind cooperation. They thank 'UNICON' for making an IBM 7090 computer available to them.

18) P. Kierkegaard, R. Norrestam and P. E. Werner, *Chem. Commun.*, **1967**, 288.

19) M. Sundaralingam, *Acta Cryst.*, **21**, 495 (1966).

20) J. Kraut and L. H. Jensen, *ibid.*, **16**, 79 (1963).

BULLETIN OF THE CHEMICAL SOCIETY OF JAPAN VOL. 42 1555—1558 (1969)

Influence of Impurities on Phosphate Coating Formation*1

Takao UMEGAKI, Hiroshi ITO*2 and Taijiro OKABE

Department of Applied Chemistry, Faculty of Engineering, Tohoku University, Sendai

(Received October 5, 1968)

The applicability of wet-process phosphoric acid containing such impurities as Al^{3+}, Ca^{2+}, Fe^{3+} and SO_4^{2-} was examined. From the viewpoint of the corrosion resistivity of the phosphate coating, Al^{3+} ion was found to be the most undesirable contaminator. NaF was recognized as the most effective masking reagent for an elimination of Al^{3+} hindrance. SO_4^{2-} also affected the phosphate coating formation, but the presence of less than 1% SO_4^{2-} did not disturb the coating formation when an appropriate amount of accelerator was added to the phosphatizing solution.

This investigation was initiated for the purpose of examining whether phosphoric acid manufactured by wet-process was applicable to a process of phosphate coating or not. Recently, a wet-process phosphoric acid has come to be available at cheap cost in Japan. In ordinary methods, however, it is impossible to use phosphoric acid as raw material for the phosphatizing solution because of the presence of such impurities as Al^{3+}, Ca^{2+}, SO_4^{2-} and so on. Khain[1-4] has already investigated the formation of the phosphate coating, using the phosphatizing solution containing nitrates of metals with mono-, bi- and trivalency as reaction accelerators. As the pH lowering occured in their solutions, characteristic effect of nitrates could not be examined individually. The qualitative study of undesirable influences of SO_4^{2-}, AsO_4^{3-}, Cr^{3+} and Al^{3+} in the ordinary acidic bath of zinc phosphate was also reported by Nagai.[5] In the present paper influences of Al^{3+}, Fe^{3+}, Ca^{2+} and SO_4^{2-} on $Zn_3(PO_4)_2$ phosphatizing solutions were described, and an effective chemical procedure was proposed to eliminate the hindrance of Al^{3+}.

Experimental

A) Stock Solution for Phosphatization. A solution was prepared by dissolving 17 g of zinc oxide in 34 g of boiling 85% phosphoric acid, cooled to room temperature, and then adding 6 g of 60% nitric acid, diluted finally to 100 m*l* with distilled water. All chemicals used were reagent-grade materials. Table 1 shows the composition of the solution thus prepared.

Table 1. Composition of stock solution for phosphating (wt%)

Zn^{2+}	PO_4^{3-}	NO_3^-
10.3	24.8	4.34

B) Phosphatizing Solution. Various kinds of phosphatizing solutions were prepared by adding 1.7 g of Na_2CO_3 and a certain amount of 18% $NaNO_2$ solution as an accelerator to 95 g of the above-mentioned stock solution, and diluting to 1 *l* with distilled water. At this stage, free acidity and total acidity of the solution were 1.98 and 30.56 in point,*3 respectively. Furthermore, SO_4^{2-}, NO_3^-, Al^{3+}, Ca^{2+} and Fe^{3+} were added to the above solutions for experiments on the effects of these materials.

C) Procedure. Specimens of commercial mild steel, 3 mm × 5 mm × 20 mm, were used for the phosphate coating. The elemental composition of the mild steel is given in Table 2. The specimens were polished with emery paper (No. 400), degreased with benzene, dried, and dipped into the phosphatizing solution. After phosphatization at 25°C, the amount of iron dissolved from the specimen in the solution was determined by colorimetric analysis with Nitroso R salt. The corrosion resistance of phosphate coating was tested by dipping the specimen in a 100 m*l* of air-bubbled 3% NaCl solution for 10 hr at 25°C and then determining the amount of iron dissolved in the solution. A relative resistivity of phosphate coating may be indicated by this test, although it has not been officially approved yet.

Table 2. Composition of mild steel used (wt%)

C	Si	Mn	P	S	Cu	Cr	Ni
0.13	trace	0.53	0.03	0.026	0.05	trace	trace

*1 Presented at the 21st Annual Meeting of the Chemical Society of Japan, Osaka, April, 1968.

*2 Present address: Fukushima Technical College, Taira, Iwaki, Fukushima.

*3 Point is equal to m*l* of 0.1 N NaOH which is required to titrate 10 m*l* of a phosphatizing solution. Total acidity represents the the titer of 0.1 N NaOH when phenolphthalein is used as an indicator. Free acidity is equal to the titer of 0.1 N NaOH in case of bromophenol blue.

1) I. I. Khain, *J. Appl. Chem. USSR.*, **32**, 2531 (1959).

2) I. I. Khain, *ibid.*, **32**, 2542 (1959).

3) I. I. Khain, *ibid.*, **32**, 2662 (1959).

4) I. I. Khain, *ibid.*, **32**, 1481 (1959).

5) Y. Nagai, *Kinzoku Hyomen Gijutsu (J. Metal Finishing Soc. Japan)*, **12**, 7, 253 (1961).

Results and Discussion

The experimental results at various concentrations of accelerators are shown in Figs. 1 and 2. The amount of dissolved iron increased linearly with phosphatizing time, in the case of the solution containing 1 g/*l* of the accelerator concentration as shown in Fig. 1, whereas, at 2g/*l* and 3 g/*l* of the accelerator concentration, the amount of dissolved iron reached saturation after 20 min. Figure 2 shows that, with respect to the corrosion resistance of phosphate coating, the most favorable concentration of accelerator was 4 g/*l*. The influences of sulfate addition to the phosphatizing solution are shown in Figs. 3 and 4. Sulfate ion caused an increase in amounts of dissolved iron and a decrease of resistivity. The presence of more than 1% sulfate was undesirable in the process of the phosphate coating. Figures 5 and 6 show that the amount of dissolved iron and the corrosion resistance were dependent on the concentration of accelerator when the phosphatizing solution contained 1% of sulfate ion. From the results shown in Fig. 6, it was concluded that the presence of 1% sulfate ion did not disturb the film formation

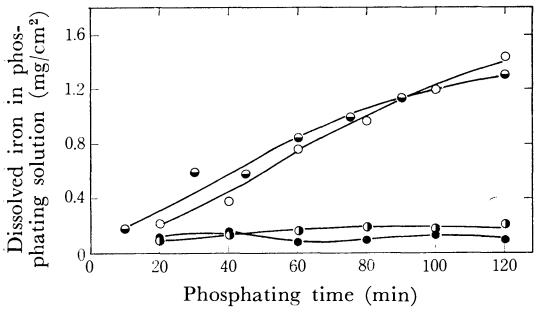

Fig. 1. Variation of amount of dissolved iron in phosphatizing solution with phosphatizing time at various concentrations of accelerator.
Accelerator concn. —◒—: 1 g/*l*, —○—: 2 g/*l*, —◑—: 4 g/*l*, —●—: 8 g/*l*

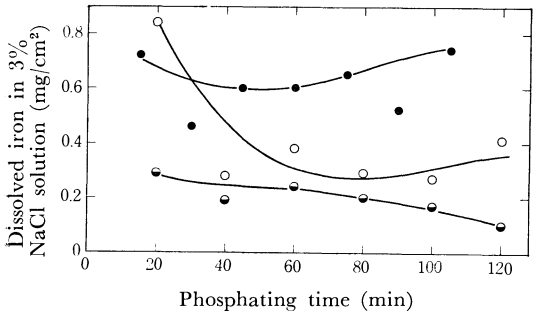

Fig. 2. Variation of relative resistivity with phosphating time at various concentrations of accelerator.
accelerator concn. —●—: 1 g/*l*, —○—: 2 g/*l*, —◒—: 4 g/*l*

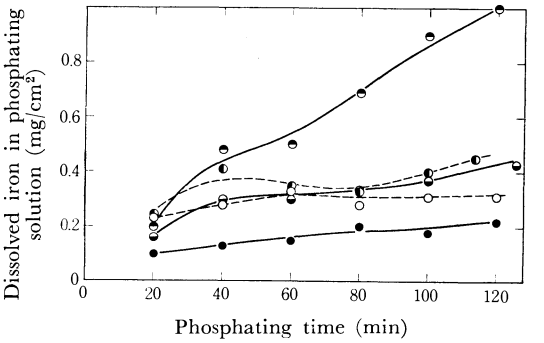

Fig. 3. Variation of amount of dissolved iron in phosphating solution with phosphating time at various concentrations of SO_4^{2-} ion.
SO_4^{2-} concn. —◒—: 3%, - -◐- -: 1.0%, —◒—: 0.6%, - -○- -: 0.3%, - -●—: 0%.

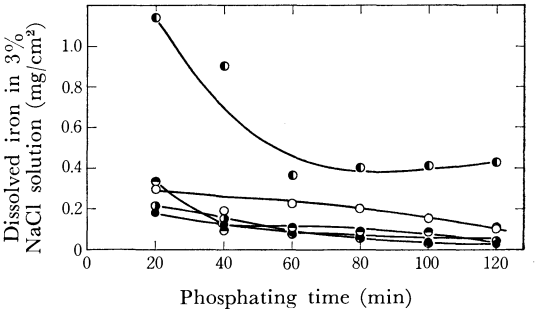

Fig. 4. Variation of relative resistivity with phosphating time at various concentrations of SO_4^{2-} ion.
concn. SO_4^{2-} —◐—: 3.0%, —○—: 1.0%, —●—: 0.6%, —◒—: 0.3%, —◑—: 0%

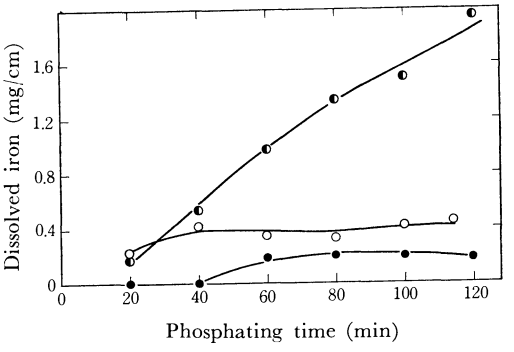

Fig. 5. Variation of amount of dissolved iron in phosphating solution containing 1% SO_4^{2-} with time and accelerator concentration
accelerator concn. —◐—: 1 g/*l*, —○—: 4 g/*l*, —●—: 8 g/*l*

if more than 4 g/*l* of the accelerator was added to the phosphatizing solution. As shown in Fig. 7, the lessening of corrosion resistivity was caused by addition of $Al(NO_3)_3$ and $Fe(NO_3)_3$, whereas the phosphatizing solution containing 3—5 g/*l* of

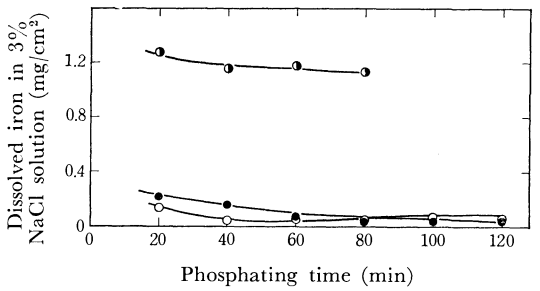

Fig. 6. Variation of relative resistivity with phosphating time at various concentrations of accelerator in case of the addition of 1% SO_4^{2-}.
accelerator concn. —◑—: 1 g/*l*, —●—: 4 g/*l*, —○—: 8 g/*l*

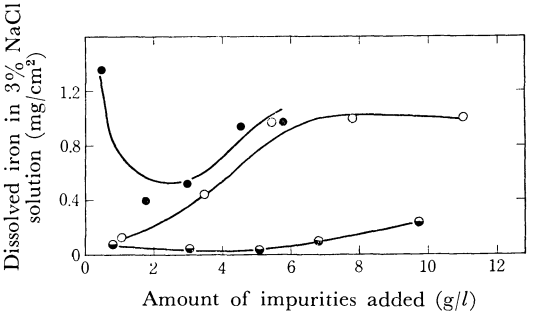

Fig. 7. Variation of relative resistivity with concentration of various impurities.
●: Al^{3+}, ○: Fe^{3+}, ◒: Ca^{2+}

$Ca(NO_3)_2$ gave more sturdy film. Fe^{3+} ion does not exist in the phosphatizing solution with high pH, and therefore the influence of Fe^{3+} ion could be easily eliminated by adding alkaline to enhance the pH of the phosphatizing solution. On the other hand, Al^{3+} was recognized as one of the most undesirable contaminators on the phosphatizing solution, because a milky-white amorphous coating lacking in adhesive ability to iron surface appeared by the addition of only 0.585 g/*l* of Al^{3+} and the solution containing 1.76 g/*l* of Al^{3+} gave neither amorphous coating nor oxide film. The maximum allowable concentration of Al^{3+} in the phosphatizing solution was estimated to be less than 0.01 g/*l*. Therefore, various kinds of Al^{3+} masking reagents were examined in order to avoid the Al^{3+} hindrance. Table 3 and Table 4. shown that the corrosion resistivity of the phosphate coating was improved by an addition of NaF, and that the masking effect of NaF was most remarkable. A sturdy coating was obtained by the addition of more than 2 g/*l* of NaF, even though the phosphatizing solution contained 2.93 g/*l* of Al^{3+}. In the case of the presence of 0.23 g/*l* of Al^{3+}, the addition of more than 1.3 g/*l* of NaF to the phosphatizing solution was necessitated. The sturdiness of phosphate coating thus obtained was comparable with that obtained from an ordinary phosphatizing solution without Al^{3+}.

Table 3. Effect of Al^{3+} masking reagents

Masking reagents	Reagent concn. g/*l*	Al^{3+} concn. g/*l*	Dissolved iron in 30% NaCl soln. (mg/cm²)
NaF	2.50	2.93	0.578
$(NaPO_3)_6$	2.59	2.93	0.699
$Na_4P_2O_7 \cdot 10H_2O$	2.45	2.93	1.49
$KNaC_4H_4O_6 \cdot 4H_2O$	2.75	2.93	1.05
$Na_2C_4H_4O_6 \cdot 6H_2O$	2.79	2.93	0.867
$Na_2C_6H_5O_7 \cdot 2H_2O$	2.60	2.93	0.691
$(NaPO_3)_6$	2.50	0.23	0.850
$Na_4P_2O_7 \cdot 10H_2O$	2.50	0.23	0.831
$KNaC_4H_4O_6 \cdot 4H_2O$	2.50	0.23	1.02
$Na_2C_4H_4O_6 \cdot 6H_2O$	2.50	0.23	0.197
$Na_2C_6H_5O_7 \cdot 2H_2O$	2.50	0.23	0.732

Table 4. Masking effect of NaF

NaF concn. g/*l*	Al^{3+} concn. g/*l*	Dissolved iron in 3% NaCl soln. (mg/cm²)
0.42	2.93	0.920
1.26	2.93	0.976
1.68	2.93	0.125
2.10	2.93	0.123
2.94	2.93	0.075
4.62	2.93	0.031
0.43	0.23	0.933
1.28	0.23	0.058
2.13	0.23	0.043
3.05	0.23	0.074
3.83	0.23	0.010
4.68	0.23	0.023

Conclusion

The reaction mechanism of phosphate coating formation is commonly accepted as follows:

(1) $Fe + 2H_3PO_4 = Fe(H_2PO_4)_2 + H_2$

(2) $Zn(H_2PO_4)_2 = ZnHPO_4 + H_3PO_4$

(3) $ZnHPO_4 = Zn_3(PO_4)_2 + H_3PO_4$

Corrosion reaction represented by Eq. (1) begins when the iron specimen is dipped in the phosphatizing solution. As a result, both equilibriums of Eq. (2) and (3) are shifted to the right hand by the decrease of H_3PO_4 concentration and then an insoluble $Zn_3(PO_4)_2$ crystallized on the iron surface. Recently, composition and crystal structure of the phosphate coating have been classified by many investigators. Therefore, in addition to the above-mentioned qualitative explanation, the rate-determining factors of the coating formation can be

discussed, taking the precise crystal structure into consideration. Later, the hindrance of Al^{3+} and the reaction mechanism will be reported, from a viewpoint of electrochemistry. Although a theoretical explanation of the influence of each impurity has not been established yet, the following conclusions have been made: (a) Al^{3+} is the most undesirable contaminator for the phosphatizing solution, and the addition of NaF is effective in eliminating the hindrance of Al^{3+}. (b) The interference of Fe^{3+} can be avoided by the addition of alkali to the phosphatizing solution. (c) The addition of an appropriate amount of the accelerator makes it possible to use the wet-process phosphoric acid containing Ca^{2+} and SO_4^{2-} as raw material for the phosphatizing solution.

This investigation was supported by a grant from Nippon Kokan (Japan Steel and Tube) Corp., for which the authors wish to express their sincere appreciation.

BULLETIN OF THE CHEMICAL SOCIETY OF JAPAN VOL. 42 1558—1561 (1969)

Determination of Traces of Constituents with Schiff Bases. III.[1] Extraction-Spectrophotometric Determination of Nickel with Salicylidene-*o*-aminophenol

Hajime Ishii and Hisahiko Einaga

National Institute for Researches in Inorganic Materials, Science and Technology Agency, Hon-komagome, Bunkyo-ku, Tokyo

(Received October 7, 1968)

A method was established for the spectrophotometric determination of microgram amounts of nickel after the extraction of nickel(II) as a salicylidene-*o*-aminophenol (SAP) complex from an alkaline aqueous solution into chloroform. Nickel(II) reacts with SAP to form a complex which can be extracted into organic solvents such as benzene, chloroform, methyl isobutyl ketone, *etc.*, in the presence of ammonium ions. The extraction of nickel was almost quantitative, and a maximum and constant absorbance was obtained in the pH range from 8.5 to 9.8. The complex extracted was very stable and had an absorption maximum at 418 mμ. The composition of the complex was confirmed to be 1 to 1 (metal to ligand). A linear relationship was maintained between the concentration of nickel and the absorbance. The molar extinction coefficient and the sensitivity for $\log(I_0/I)=0.001$ at 418 mμ were 17000 and 3.5×10^{-3} μg Ni/cm^2, respectively. Several ions such as cobalt(II), copper(I and II), chromium(III), lead(II), manganese(II) and citrate interfered with the determination.

Recently, salicylidene-*o*-aminophenol (SAP), a Schiff base obtained by the condensation of salicylaldehyde with *o*-aminophenol, has been used for the spectrofluorimetric determination of aluminum[2-7] and gallium[7] and for the separation and indirect spectrophotometric determination of copper.[8] The authors have previously reported the direct spectrophotometric determination of copper using the complex formation of SAP with copper(II).[1] This reagent was found to react also with nickel(II) in an alkaline aqueous medium to form a complex which could be extracted in the presence of ammonium ions into organic solvents such as benzene, chloroform, carbon tetrachloride, methyl isobutylketone (MIBK), *etc.* This paper will describe a direct spectrophotometric method for the determination of traces of nickel after extraction of it as a SAP complex into chloroform.

1) Part II of this series: H. Ishii and H. Einaga, *Bunseki Kagaku (Japan Analyst)*, **18**, 230 (1969).

2) R. M. Dagnall, R. Smith and T. S. West, *Talanta*, **13**, 609 (1966).

3) V. V. Klimov, O. S. Didkovskaya and V. N. Kozachenko, *Zav. Lab.*, **28**, 652 (1962); *Anal. Abstr.*, **10**, 91 (1963).

4) E. A. Bozhevol'nov, G. B. Serebryakova, V. M. Yanishevskaya and S. U. Kreingol'd, *Acta Chim. Acad. Sci. Hung.*, **32**, 199 (1962); *Anal. Abstr.*, **10**, 1308 (1963).

5) N. B. Lebed' and R. P. Pantaler, *Zav. Lab.*, **31**, 163 (1965); *Anal. Abstr.*, **13**, 2874 (1966).

6) I. I. Kurbatova, *Zav. Lab.*, **32**, 1064 (1966); *Anal. Abstr.*, **14**, 7501 (1967).

7) R. M. Dagnal, R. Smith and T. S. West, *Chem. Ind.*, **34**, 1499 (1965); *Anal. Abstr.*, **13**, 6769 (1966).

8) K. Isagai, *Nippon Kagaku Zasshi (J. Chem. Soc. Japan, Pure Chem. Sect.)*, **82**, 1172 (1961).

Experimental

Apparatus. The recording of absorption spectra and all the other spectrophotometric measurements were made with a Hitachi Model EPS-3T automatic recording spectrophotometer and a Hitachi Model 139 spectrophotometer, respectively, using 10 mm matched cells. The pH measurements were made with a Toa Dempa glass-electrode Model HM-5A pH meter. The shaking was done with an Iwaki Model KM shaker.

Reagents. *Standard Nickel(II) Solution.* A stock solution containing about 1000 μg of nickel per m*l* was prepared by dissolving nickel chloride in water, followed by adding a small amount of hydrochloric acid enough to give approximately 0.1 N hydrochloric acid solution. Standardization was made by titration with a 0.01 M EDTA solution. The stock solution was appropriately diluted to make working solutions of nickel(II).

SAP Solution. A 0.01% solution was prepared by dissolving 25 mg of SAP in 250 m*l* of chloroform. SAP used in this work was synthesized and purified by the method proposed by Dagnall *et al.*[2]

Buffer Solutions. Buffer solutions were prepared by mixing a 1 M ammonium chloride solution and a 1 M aqueous ammonia solution in the ratios required.

Extracting Solvent. Commercial chloroform of analytical reagent grade was used without further purification.

Recommended Procedure. In a 50 m*l* separatory funnel, an aliquot of the sample solution containing less than 30 μg of nickel(II) is taken. Add 1 m*l* of the buffer solution (pH 9), and dilute to 30 m*l* with distilled water. Add 10.0 m*l* of a 0.01% SAP solution in chloroform, and shake vigorously for 10 min. After the phase separation, transfer the organic phase into a 50 m*l* flask containing about 1 g of anhydrous sodium sulfate. Then transfer the organic solution into a cell and measure the absorbance at 418 mμ using a reagent blank as a reference. The amount of nickel can be obtained from the calibration curve.

Results and Discussion

Selection of Extracting Solvent. Nickel(II) is extracted as its SAP complex from an alkaline aqueous solution into organic solvents such as benzene, chloroform, carbon tetrachloride, MIBK, *etc.* in the presence of ammonium ions. Among them, chloroform seemed to be the best for the present purpose, because of the relatively high extractability of the complex and the good separability of two phases; an aqueous and an organic phases. For this reason, chloroform was used as the extracting solvent in this work.

Absorption Spectra. Figure 1 shows the absorption spectra of SAP and its nickel(II) complex extracted in chloroform at pH 9. The absorption maximum of the complex appears at 418 mμ, while that of SAP, at 354 mμ. This maximum absorption wavelength of 418 mμ, which was used for the determination of nickel, did not shift in either case, when pH value of the aqueous phase was varied from 7 to 10.5 or when the molar ratio

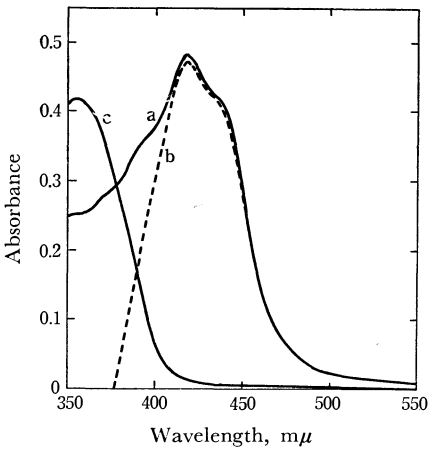

Fig. 1. Absorption spectra of SAP and its nickel-(II) complex.
Ni: 16.5 μg, SAP: 4.3×10^{-7} mol/10 m*l* of chloroform, pH : 9, $V_{aq}/V_{org}=1$, Shaking time: 30 min.
a : Ni(II)-SAP complex measured against chloroform
b : Ni(II)-SAP complex measured against a reagent blank
c : SAP alone (reagent blank) measured against chloroform

of nickel to SAP was varied 1 : 5 to 5 : 1. Taking this fact and those described in the subsequent paragraph into account, it was considered that only one species of the complex was extracted into chloroform under the conditions studied. The absorption spectra of the complex in benzene and in MIBK were essentially similar to that in chloroform, except that the absorbancepeak occurred at 424 mμ in benzene and 420 mμ in MIBK, respectively.

The Effect of pH Value. The effect of pH value on the absorbance at 418 mμ was examined over a pH range from 6.8 to 10.3. As shown in Fig. 2, it can be seen that a maximum and constant absorbance is obtained in the pH range from 8.5

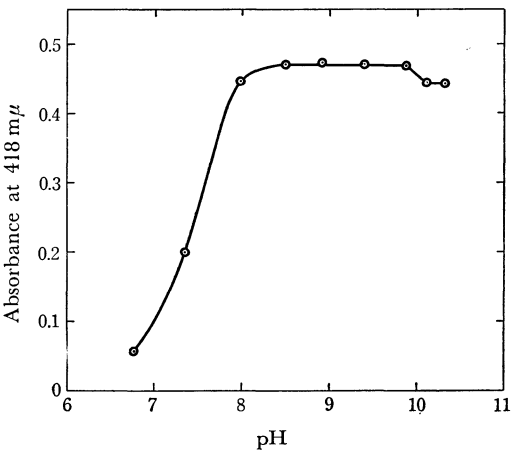

Fig. 2. Effect of pH.
Ni: 16.5 μg, $V_{aq}/V_{org}=1$

to 9.8. In subsequent experiments, therefore, the extraction of nickel was carried out at about pH 9.

The Effect of the Amount of SAP. Figure 3 shows the effect of the amount of SAP on the absorbance. About an 8-fold molar excess of the reagent over the amount of nickel is necessary to obtain a maximum and constant absorbance. Therefore, 10 m*l* of a 0.01% solution of the reagent in chloroform was used. This corresponds to 4.7×10^{-6} mol, and it is about an 8-fold molar excess over the highest point on the calibration curve in Fig. 4, *i. e.*, 33 μg of nickel.

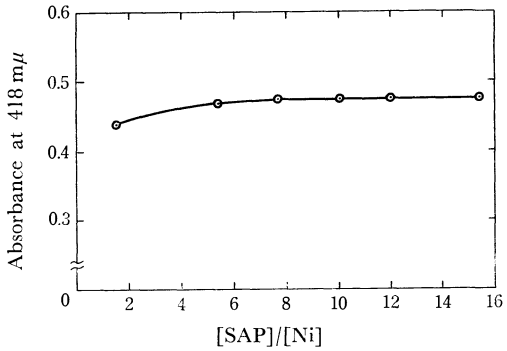

Fig. 3. Effect of amount of SAP.
Ni: 16.5 μg, $V_{aq}/V_{org}=1$

The Effect of the Shaking Time. The variation of shaking time from 1 to 30 min revealed that a 5-min shaking was enough to attain a good extraction under the recommended conditions, although the shaking time must be increased with the decrease of the ratio of SAP to nickel. The extraction of nickel was reproducible and 93.1% of it present in an aqueous phase were extracted by a single extraction. Therefore, one extraction seems to be sufficient for the determination of nickel.

The Effect of Volume of the Aqueous Phase. The absorbance of the extract was decreased with increasing the volume of the aqueous phase to that of organic phase. Considering this fact and the application of the method to the analysis of practical sample, the volume ratio of the aqueous to the organic phase was kept 3 in the recommended procedure.

The Stability of the Color. The absorbance of the extract did not change at all for at least 12 hr. The complex, therefore, seems to be very stable in chloroform.

Adherence to Beer's Law. As is seen in Fig. 4, a linear relationship was maintained between the concentration of nickel and the absorbance up to at least 33 μg of nickel per 10 m*l* of the extract. The molar extinction coefficient was about 17000, and the sensitivity was 3.5×10^{-3} μg Ni/cm^2, which corresponds to $\log(I_0/I)=0.001$.

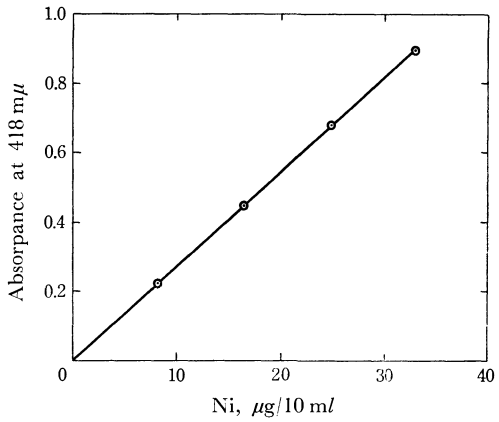

Fig. 4. Calibration curve for nickel.
pH: 9, $V_{aq}/V_{org}=3$

The Effect of Diverse Ions. The effect of diverse ions on the determination of nickel was examined at pH 9 and the results are summarised in Table 1. Cobalt(II), copper(I and II), chromium(III), lead(II), manganese(II) and citrate interfered with the determination. The interferences by these cations and citrate may be due to the complex formation with SAP and with nickel, respectively.

The Composition of the Complex. Although the composition of the complex has been already reported to be 1 to 1 (metal to ligand) from the analytical results of the isolated complex,[7] the authors also examined the composition in chloroform by means of the continuous variation and the molar ratio methods. Extraction was performed at pH 9, and the absorbance was measured at three wavelengths between 400 and 440 mμ. Both methods revealed that nickel(II) forms a 1-to-1 complex with SAP. As an example, the result of the continuous variation method is shown in Fig. 5.

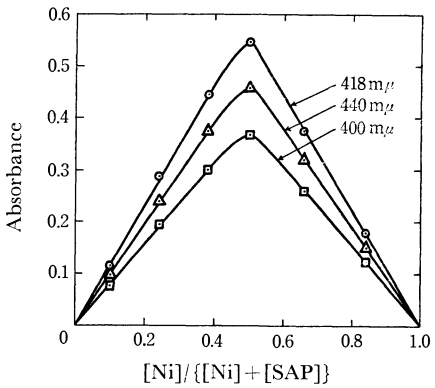

Fig. 5. Continuous variation method.
$[Ni]+[SAP]=7.0\times10^{-5}$ M, pH: 9,
$V_{aq}/V_{org}=1$, Shaking time: 30 min

TABLE 1. EFFECT OF DIVERSE IONS (Ni taken: 16.5 μg)

Ion	Added μg	Ni found μg	Relative error %	Ion	Added μg	Ni found μg	Relative error %
Al(III)	27.0	16.3	−1.2	Si(IV)	18.3	16.7	1.2
Ca(II)	40.1	16.7	1.2	Ti(IV)	16.5	16.5	0
Cd(II)	50.0	16.7	1.2	V(IV)	20.0	16.6	0.6
Co(II)	20.6	17.9	8.5	V(V)	20.0	16.6	0.6
Cr(III)	50.0	5.9	−64.2	W(VI)	52.6	16.7	1.2
Cr(VI)	25.0	16.6	0.6	Zn(II)	32.8	16.7	1.2
Cu(I)	5.0	30.0	81.8	Zr(IV)	18.2	16.8	1.8
Cu(II)	12.4	27.0	63.6	ClO_4^-	49.7*	16.6	0.6
Fe(II)	20.0	16.4	−0.6	NO_3^-	31.0*	16.5	0
Fe(III)	20.1	16.5	0	SO_4^{2-}	48.0*	16.5	0
Hg(II)	57.7	16.6	0.6	PO_4^{3-}	47.0*	16.7	1.2
Mg(II)	24.3	16.7	1.2	Acetate	29.5*	16.6	0.6
Mn(II)	3.6	36.0	118.2	Tartrate	37.0*	16.7	1.2
Mo(VI)	47.6	16.7	1.2	Citrate	31.5*	10.8	−34.5
Pb(II)	50.0	17.5	6.1				

*: In mg unit

Comparison with Other Methods. The proposed method has the following advantages: A relatively broad pH range is tolerable, the color of the extract is very stable, and the sensitivity is superior to that of other methods, *e. g.*, the dimethylglyoxime-oxidizing agent method (sensitivity: 4.2×10^{-3} μg Ni/cm^2).[9]

9) E. B. Sandell, "Colorimetric Determination of Traces of Metals," Interscience Publishers, Inc., New York (1965), p. 669.

BULLETIN OF THE CHEMICAL SOCIETY OF JAPAN VOL. 42 1561—1569 (1969)

Scandium Content of Igneous Rocks and Some Oceanic Sediments

Tsuneo SHIMIZU

Department of Chemistry, Faculty of Education, Gunma University, Maebashi, Gunma

(Received October 23, 1968)

Based on the analyses of 105 individual samples and 5 composites, totaling 158 rock samples, the following averages of scandium for various types of Japanese igneous rocks have been obtained (in ppm): granites 5.6, granodiorites 7.4, liparites 6.1, quartz diorites and diorites 11.4, dacites 14.1, andesites 21.8, gabbros 26.9, basalts 27.2 and ultramafic rocks 9.5. Scandium is determined by a combined ion-exchange-spectrophotometric method. Using Poldervaart's suggested ratio of rock types, an abundance figure of 17 ppm Sc for the crust is suggested. The results on the abundance values for scandium in various types of igneous rocks confirm generally the figures given by Norman and Haskin in 1968. Analyses are also performed on Pacific oceanic sediments, giving as averages 18.7 ppm Sc for 4 red clays, 12.1 ppm Sc for 2 volcanic muds and 13.1 ppm Sc for 2 globigerina oozes. Brief discussion on the geochemistry of scandium is given.

A considerable amount of data has been reported for the abundance of scandium in igneous rocks, mostly based on spectrochemical methods. However, data on the abundance of scandium in granitic rocks is rather unreliable because of lack of sensitivity in usual spectrochemical methods. Fryklund and Fleischer[1] have reviewed the previous works involving the geochemistry of scandium prior to 1962, and presented the abundance figures for various igneous rock clans and for the earth's crust as a whole. Currently, averages and concentration ranges for scandium as well as many other elements have been reported

1) V. C. Fryklund, Jr. and M. Fleisher, *Geochim. Cosmochim. Acta*, **27**, 643 (1963).

by Kolbe and Taylor[2] for granites and granodiorites from Australia and South Africa using an improved spectrographic technique. Detailed geochemistry of scandium was not discussed.

Recent development in neutron activation analysis has facilitated the accurate determination of scandium in rocks and minerals, yielding and accumulating reliable data for scandium in materials of geochemical interest. Thus, Stueber and Goles[3] have analyzed 113 ultramafic rocks for sodium, manganese, chromium, scandium, and cobalt by a neutron activation method. Discussing the effect of serpentinization on the abundances of the elements, these authors revealed that scandium abundance is highly dependent on mineral composition and also that the pre-serpentinization mineral composition determines the scandium abundance in the serpentine. Norman and Haskin[4] have reported the results of neutron activation analyses for scandium and iron in 76 samples of igneous and sedimentary rocks, including 9 composites. The highest scandium contents (average, 30 to 40 ppm) were found in basalts and gabbros and the lowest in nepheline syenites and limestones (−1 ppm). Despite increasing amount of data for scandium in igneous rocks, there is still much controversy among the authors as to a possible geochemical relationship between Sc^{3+} and Fe^{2+}, Mg^{2+}, or other major elements or ions in igneous rocks. Taylor[5] gives a general review of the geochemistry of elements including scandium as well as a survey of the analytical data published previously.

In order to develop a routine analytical method for scandium, which is comparable in accuracy to neutron activation analysis, a combined ion-exchange-spectrophotometric method has been worked out for scandium in rocks.[6] Furthermore, 158 igneous rock samples including 5 composites and 8 pelagic sediments from the Pacific Ocean have been analyzed for scandium in order to define the occurrence and abundance of scandium in the igneous rocks and sediments of Japan. It is also intended to summarize the geochemical behavior of scandium. Average abundance figures are suggested for various types of igneous rocks and for the earth's crust as a whole. The results on the abundance values for scandium in various types of igneous rocks confirm generally the figures given by Norman and Haskin.[4]

Analytical Method

The procedure has been described in detail elsewhere.[6] In brief, after 0.5 to 1.5 g of a powdered rock sample is decomposed by means of perchloric-hydrofluoric acid digestion, the resulting residue is dissolved in dilute hydrochloric acid. When any undissolved residue is found, it is put into solution by fusion with sodium carbonate. Traces of scandium in the solution are separated from all interferences by successive cation- and anion-exchange chromatographic techniques in acid ammonium sulfate media. Scandium in the effluent then is coprecipitated together with ferric hydroxide and separated from the ferric ion by an anion-exchange in hydrochloric acid medium. Finally, scandium is determined spectrophoto-

TABLE 1. SCANDIUM IN THE ROCK STANDARDS (in ppm)

Author	Method*	G-1	G-2	GSP-1	AGV-1	W-1	BCR-1	PCC-1	DTS-1
Brunfelt and Steinnes[a]	NA	2.8	3.4	5.6	11.5	33.3	31.0	7.4	3.0
Flanagan[b]	S	—	2—6	6—15	9—25	—	29—53	8—11	2—7
Gordon *et al.*[a]	NA	—	3.5±0.2	6.0±0.3	11.7±0.4	34.8±0.8	32.5±0.5	—	—
Fleischer[d]	R	3	—	—	—	34	—	—	—
This work		2.8	4.1	6.4	13	34	35	6.1	2.9
			3.7	5.9	10	33	32	5.6	2.6
			3.4	5.8	10	33	29	5.5	2.3
			av. 3.7	av. 6.0	av. 11	av. 33	av. 32	av. 5.7	av. 2.6

a) A. O. Brunfelt and E. Steinnes, *Geochim. Cosmochim. Acta*, **30**, 921 (1966).
b) F. J. Flanagan, *ibid.*, **31**, 289 (1967).
c) G. E. Gordon, K. Randle, G. G. Goles, J. B. Corliss, M. H. Beeson and S. S. Oxley, *ibid.*, **32**, 369 (1968).
d) M. Fleischer, *ibid.*, **29**, 1263 (1965).
* NA=neutron activation; S=spectrographic; R=recommended value; —=not determined.

2) P. Kolbe and S. R. Taylor, *Contr. Mineral. Petrol.*, **12**, 202 (1966).
3) A. M. Stueber and G. G. Goles, *Geochim. Cosmochim. Acta*, **31**, 75 (1967).
4) J. C. Norman and L. A. Haskin, *ibid.*, **32**, 93 (1968).
5) S. R. Taylor, "The Application of Trace Element Data to Problems in Petrology." Physics and Chemistry of The Earth, Vol. VI, p. 135. Pergamon Press, London (1965).
6) T. Shimizu, *Talanta*, **14**, 473 (1967).

metrically with bromopyrogallol red as a color reagent.

In order to obtain information about the accuracy and precision of the procedure, 8 standard rock samples, G-1 (granite), G-2 (granite), GSP-1 (granodiorite), AGV-1 (andesite), W-1 (diabase), BCR-1 (basalt), PCC-1 (peridotite) and DTS-1 (dunite), were analyzed for scandium. The results are quoted in Table 1. For comparison, earlier literature values for scandium in the rock standards are also listed in Table 1. Generally agreement with previous values is excellent. The following standard deviations (in ppm) indicated by ± sign for three types of igneous rocks also give a general idea of precision of the present method: av. 34.7± 1.2 for basalt (8 detens.), av. 20.7±1.3 for andesite (13 detens.), av. 11.9±1.2 for quartz diorite (8 detens.).

Analytical Results

Analytical results are presented in Tables 2 to 6 along with necessary descriptions. Marine sediments of the Pacific Ocean were collected in 1925—1928 through the deep sea expedition carried out by the Hydrographical Department of the former Japanese Navy.

Discussion

Abundance of Scandium. From the values listed in Table 2 the following averages for ultramafic rocks are obtained:

	Sc, ppm	Range
7 Peridotites	10.0	5.5—13.5
Dunite	8.5	
Cortlandite	6.9	
All ultramafic rocks (9 samples)	9.5	5.5—13.5

For an average abundance figure of scandium in ultramafic rocks, Turekian and Wedepohl[7] give 15 ppm on the basis of the data of Pinson, Ahrens and Frank.[8] Vinogradov[9] gives 10 ppm Sc. Vinogradov[10] also gives a value of 5 ppm Sc, deriving this figure from Borisenko,[11] who estimated the average scandium contents of ultramafic rocks of the Soviet Union to be 5 ppm for peridotites, 3 ppm for dunites, and 52 ppm for pyroxenites. Compiling the determinations of Pinson, Ahrens and Frank,[8] Liebenberg,[12] and Borisenko and Rodionov,[13] Fryklund and Fleischer[1] give an average scandium abundance of 9 ppm for peridotites, of 30 ppm for perknites and of less than 5 ppm for olivine dunites. Stueber and Goles[3] give an average of 5.4 ppm Sc for 14 dunites, of 42 ppm Sc for 9 pyroxenites, and of 15.7 ppm Sc for all ultramafic rocks studied. Norman and Haskin[4] have reported measurement for scandium in 3 peridotites (all about 12 ppm Sc), 2 pyroxenites (8 and 56 ppm Sc), 2 dunites (9.1 and 3.6 ppm Sc) and 3 perknites (3.4, 3.7 and 17.1 ppm Sc) from various locations. The values found in this work all fall within the range for individual samples analyzed by the above authors. Because of the large number of determinations involved, the overall average given by Stueber and Goles[3] may at the present time provide a sound representation of ultramafic rocks of variable mineralogical composition. However, the striking preference of scandium for pyroxene is now well established so that the compiled averages given by Fryklund and Fleischer[1] for dunites, peridotites and perknites may provide a better basis for comparison between averages for the individual rock classes. An average for scandium obtained in this work (9.5 ppm) is in good agreement with their average (9 ppm) for peridotites.

Table 2. Scandium in ultramafic rocks

Rock mark	Sample	Sc (ppm)
HOK	Orthopyroxene peridotite Horoman, Hokkaido	13.5
HK56081904	Peridotite, Besshi, Ehime	13.3
YN64010907	Peridotite, Toba, Mie	12.5
HK56081902	Enstatite bearing peridotite, Besshi, Ehime	11.7
HK51031101	Peridotite, Kamogawa, Chiba	7.3
10127	Peridotite, Ogawa, Saitama	6.2
Tamura 95	Peridotite, Miharu, Fukushima	5.5
49IIO-189	Dunite, Oshika, Nagano	8.5
TA-4	Cortlandite, Miharu, Fukushima	6.9

Averages for mafic rocks are computed from Table 3 as follows:

	Sc, ppm	Range
15 Basalts	27.2	15.5—42.5
10 Gabbros	26.9	16.6—32.3
9 Diabases	18.1	17.7—18.5
All mafic rocks (34 samples)	25.4	15.5—42.5

For average abundance figures of scandium for "basaltic rocks" Vinogradov[9,10] gives 24 ppm,

7) K. K. Turekian and K. H. Wedepohl, *Geol. Soc. Am. Bull.*, **72**, 175 (1961).
8) W. H. Pinson, L. H. Ahrens and M. L. Frank, *Geochim. Cosmochim. Acta.*, **4**, 251 (1953).
9) A. P. Vinogradov, *Geokhimiya*, **1**, 6 (1956).
10) A. P. Vinogradov, *ibid.*, **7**, 555 (1962).
11) L. F. Borisenko, *ibid.*, **No. 7**, 623 (1959).
12) C. J. Liebenberg, *Publ. Univ. Pretoria*, **12**, 79 (1960).
13) L. F. Borisenko and D. A. Rodionov, *Geokhimiya*, **No. 9**, 765 (1961).

TABLE 3. SCANDIUM IN MAFIC ROCKS

Rock mark	Sample	Sc (ppm)
200714	Basalt, Tateyama, Toyama	42.5
KB-1	Basalt, Toyooka, Hyogo	35.8
NB-2	Basalt, Mt. Mihara, Izu-oshima Island	32.8
OB-2	Basalt, Hata, Shizuoka	31.9
NB-1	Basalt, Ajiro, Shizuoka	28.0
OB-1	Basalt, Fudo, Shizuoka	21.3
OB-3	Basalt, Karatsu, Saga	16.3
OB-4	Basalt, Karatsu, Saga	15.5
HG-1	Gabbro, Shisaka Island, Ehime	32.3
3302	Olivine gabbro, Kamioka, Gifu	29.7
KG-1	Gabbro, Miharu, Fukushima	26.7
SH135	Picrite gabbro, Hidaka Hokkaido	16.6
65081902	Diabase, Katashina Gunma	18.5
	Basalt, composite of 7, Japan	21.5
	Gabbro, composite of 6, Japan	19.4
	Diabase, composite of 8, Japan	17.7
OB-5	Basalt, Hawaii, U.S.A.	17.0
666-SC-11	Gabbro, South California U.S.A.	17.0

and Turekian and Wedepohl[7] give 30 ppm. Borisenko[11] gives 20 ppm Sc for gabbros, and Hamaguchi and his collaborators[14] give a neutron activation value of 32 ppm Sc for a composite of 7 Japanese basaltic rocks. Fryklund and Fleischer[1] give a figure of 38 ppm Sc for 99 basalts. Norman and Haskin[4] have recently reported that 8 oceanic sub-alkaline basalts have more than 35 ppm Sc, ranging 35 to 50 ppm; five of 8 continental and island alkali basalts contain less than 30 ppm Sc, ranging from 10 to 55 ppm; a composite of 282 continental (alkali and tholeiitic) basalts contains 30 ppm Sc.

With 36 mafic rocks scandium contents obtained here range from 16 to 42 ppm, the difference involved being a factor of approximately three. The average 24 ppm for 36 mafic rocks is somewhat lower than those given by Fryklund and Fleischer,[1] and Norman and Haskin.[4] This average is also considerably lower than the activation value for the composite of 7 basaltic rocks given by Hamaguchi and his collaborators.[14] The scandium contents of two American mafic rocks are somewhat lower than the average reported here.

14) H. Hamaguchi, R. Kuroda, K. Tomura, M. Osawa, K. Watanabe, N. Onuma, T. Yasunaga, K. Hosohara and T. Endo, *Geochim. Cosmochim. Acta*, **23**, 296 (1961).

It is of interest to see how the scandium distribute among rock-forming minerals in a basaltic rock. Based on radioactivation analysis, Onuma[15] revealed that an alkali olivine basalt from Takashima, Kyushu, shows a scandium content of 18.1 ppm, while values for scandium in its constituent minerals are:

51.2 ppm	for augite (clinopyroxene)
21.4 ppm	for bronzite (orthopyroxene)
not detected	for plagioclase

The striking preference of scandium for pyroxene, particularly clinopyroxene, is well illustrated. With Skaergaard rocks Wager and Mitchell[16] found scandium in the clinopyroxenes of all basic rocks and in apatites of the later basic differentiates, but not in plagioclase or in olivine or opaque iron minerals.

The following averages are obtained from the data listed in Table 4 for intermediate rocks.

	Sc, ppm	Range
32 Andesites	21.8	12.4—28.6
5 Dacites	14.1	10.0—19.1
7 Quartz diorites and diorites	11.4	5.7—21.6
5 Obsidians	29.9	26.5—34.9
2 Pitchstones	7.6	6.0— 9.2
All intermediate rocks (51 samples)	19.1	5.7—34.9

For average abundance figures of scandium in intermediate rocks, Vinogradov gives values of 15 ppm in 1956[9] and of 2.5 ppm in 1962[10] for "neutral rocks" (diorites+andesites). Borisenko[11] gives 3 ppm Sc for diorites. There is no basis for comparison with Turekian and Wedepohl,[7] as they listed no figure for andesites. Fryklund and Fleischer[1] report averages of 34 ppm Sc for 72 andesites, 21 ppm Sc for 68 dacites, and 14 ppm Sc for 32 rhyodacites. Norman and Haskin[4] give 15 ppm Sc for a composite of 85 intermediate rocks of many localities, consistent with the average obtained in this work for intermediate rocks.

Scandium does not distribute uniformly even in the same province as can be seen from its abundance in the rocks of Mt. Asama, Nagano (Table 4). In andesites of Mt. Asama, scandium content ranges 10 to 35 ppm, the difference involved being a factor of more than three.

There is comparatively little reliable information about the abundance figure of scandium in silicic rocks. As can be seen in Table 5 scandium content in 61 silicic rocks ranges from 2.9 to 13 ppm, and average scandium values are:

15) N. Onuma, private communication.

16) L. R. Wager and R. L. Mitchell, *Geochim. Cosmochim. Acta*, **1**, 129 (1951).

TABLE 4. SCANDIUM IN INTERMEDIATE ROCKS

Rock mark	Sample	Sc (ppm)
972705	Andesite, Mt. Asama, Nagano	28.6
KA-3	Andesite, Suwa, Nagano	27.8
AS-214	Andesite, Mt. Asama, Nagano	26.3
EM9822	Andesite, Mt. Asama, Nagano	25.0
7X2204B	Andesite, Mt. Asama, Nagano	24.5
KA-2	Andesite, Tanashita, Gunma	24.5
AS-358	Andesite, Mt. Asama, Nagano	24.0
HA-4	Andesite, Sakurajima, Kagoshima	23.9
EM7701	Andesite, Mt. Asama, Nagano	23.7
770210	Andesite, Mt. Asama, Nagano	23.1
HA-3	Andesite, Mt. Ishizuchi Ehime	22.3
HA-1	Andesite, Shimabara, Nagasaki	21.6
AS-336	Andesite, Mt. Asama, Nagano	20.3
AS-375-3	Andesite, Mt. Asama, Nagano	17.1
KA-1	Andesite, Mt. Haruna, Gunma	17.1
NI44	Garnet-biotite-andesite, Mt. Nijo, Nara	15.8
OA-15	Quartz andesite, Amagi, Izu, Shizuoka	15.2
EM9121	Andesite, Mt. Asama, Nagano	12.4
7X2101	Dacite, Mt. Asama, Nagano	19.1
770204	Dacite, Mt. Asama, Nagano	17.3
47121401a	Garnet-biotite-dacite, Mt. Nijo, Nara	12.9
G1061	Dacite, Mizunami, Gifu	11.2
213	Dacite, Mt. Asama, Nagano	10.0
HI-1	Diorite, Tsushima, Ehime	21.6
7820	Biotite-hornblende-gabbro-diorite Kamioka, Gifu	10.7
TK57	Diorite, Tanakura, Fukushima	9.3
OQ-1	Quartz diorite, Kinkazan, Miyagi	12.4
KQ-1	Quartz diorite, Yubiso, Gunma	11.6
NQ-1	Quartz diorite, Sanriku, Iwate	8.6
55080112	Quartz diorite, Yamakita Kanagawa	5.7
7X2204A	Obsidian, Mt. Asama, Nagano	34.9
7X2205	Obsidian, Mt. Asama, Nagano	32.6
882102A	Obsidian, Mt. Asama, Nagano	28.7
241	Obsidian, Mt. Asama, Nagano	27.0
882102B	Obsidian, Mt. Asama, Nagano	26.5
MT132	Pitchstone, Uchimura, Nagano	9.2
15249	Pitchstone, Izu-shikine Island	6.0
	Andesite, composite of 14, Japan	14.3

TABLE 5. SCANDIUM IN SILICIC ROCKS

Rock mark	Sample	Sc (ppm)
NR-11	Granite, Agematsu, Nagano	10.5
OR-2	Granite, Kofu, Yamanashi	9.9
KR-3	Granite, Sudagai, Gunma	9.8
NR-6	Granite, Ishikawa Fukushima	7.7
HR-2	Granite, Kashiwa Island, Kochi	7.1
NR-15	Granite, Makabe, Ibaragi	6.5
NR-7	Granite, Chiyoda, Ibaragi	6.4
HR-7	Granite, Mt. Okue, Miyazaki	5.9
NR-16	Granite, Kasama, Ibaragi	5.9
HR-10	Granite, Tsushima, Ehime	5.8
HR-8	Granite, Odaira, Oita	5.6
KR-2	Granite, Mt. Tsukuba, Ibaragi	5.5
NR-2	Granite, Oyama Toyama	5.5
NR-9	Granite, Tateyama, Toyama	5.3
NR-13	Granite, Iwase, Ibaragi	5.3
NR-1	Granite, Omachi, Nagano	5.3
HR-9	Granite, porphyry, Mt. Osuzu, Miyazaki	5.3
NR-8	Granite, Niihari Ibaragi	5.2
NR-10	Granite geniss, Tateyama, Toyama	5.1
HR-5	Granite, Omogokei, Ehime	4.8
TK41	Granite, Tanakura, Fukushima	4.7
NR-14	Granite, Kasama, Ibaragi	3.9
KR-1	Granite, Abukuma district	3.9
NR-4	Granite, Kawamata, Fukushima	3.6
NR-12	Granite, Agematsu, Nagano	3.1
NR-3	Granite, Ashio, Tochigi	3.0
KR-4	Granite, Kawaba, Gunma	2.8
NR-5	Granodiorite, Ono, Fukushima	12.8
OR-1	Granodiorite, Tono, Iwate	11.5
OR-3	Granodiorite, Enzan, Yamanashi	11.3
OR-5	Granodiorite, Kamaishi, Iwate	11.3
KR-5	Granodiorite, Sori, Gunma	7.8
ON-2	Granodiorite, Ono, Fukushima	7.4
HR-6	Granodiorite, Omogokei, Ehime	7.1
HR-11	Granodiorite, Namikata, Ehime	6.9
OR-4	Granodiorite, Iwaizumi, Iwate	5.4
OR-7	Granodiorite, Kinkazan, Miyagi	5.0
OR-6	Granodiorite, Mt. Minakami, Iwate	4.0
OR-9	Granodiorite, Sumita, Iwate	3.0
OR-8	Granodiorite, Ofunato, Iwate	2.9
HR-12	Liparite, Tsuzuragawaguchi, Ehime	7.2
G1034	Liparite, Tobi Island, Yamagata	6.7
G1256	Liparite, Naruko, Miyagi	4.3
	Granite and granodiorite, composite of 18, Japan	6.4
666-SC-12	Granodiorite, South California, U.S.A.	4.6

27 granites	5.6 ppm
13 granodiorites	7.4 ppm
composite of 7 granites and 11 granodiorites	6.4 ppm
3 liparites	6.1 ppm

An average for all silicic rocks is 6.3 ppm. Acidic igneous rocks have much less scandium than intermediate and mafic rocks. Hamaguchi and his collaborators[14] give a neutron activation value of 2.3 ppm for scandium in a composite of 20 Japanese granitic rocks, so there is a difference of a factor of almost three in an average scandium between the composite and 61 silicic rocks reported here.

Borisenko[11] gives 1 ppm Sc for granites. Turekian and Wedepohl[7] give 14 ppm Sc for high-calcium granites and 7 ppm Sc for low-calcium granites. Vinogradov gives 7 ppm Sc[9] and 3 ppm Sc[10] as the average for scandium in silicic rocks. Fryklund and Fleischer[1] obtain average scandium values of 11 ppm for 14 quartz latites and 5 ppm for 24 rhyolites. Kolbe and Taylor[2] have recently given averages and ranges for 32 elements including scandium for granitic rocks of the Snowy Mountains, Australia and South-Western Cape Province, South Africa. Their scandium averages are 13 ppm for 4 gneissic rocks, 13 ppm for 20 granodiorites, and 5 ppm for 8 leucogranites, all from the Snowy Mountains. For Cape granites, they give 6.6 ppm Sc for 17 coarsely porphyritic granites, 4.1 ppm Sc for 6 medium-grained granites, and 2.3 ppm Sc for 8 fine-grained granites. Norman and Haskin[4] suggest an average value of 5 ppm Sc for granites, based principally on the analyses of the composites. Scandium averages obtained in the present work are well in line with such recent estimates as given by Kolbe and Taylor,[2] and Norman and Haskin.[4]

Scandium values for sedimentary rocks and oceanic sediments are listed in Table 6. Scandium content of oceanic clays ranges from 11 to 20 ppm, averaging 19 ppm. Red clays tend to have a little higher value of scandium than volcanic muds. Judging from scandium contents of both igneous rocks and oceanic sediments there seems to be no prominent tendency for scandium to become enriched, relative to average igneous rocks, at the oceanic bottom by some mechanism. Plotting the scandium contents *vs.* iron or manganese for the oceanic clays listed in Table 6 has revealed no positive correlations. As far as the scandium is concerned, coprecipitation along with hydrated oxide of iron or manganese or adsorption (ion-exchange) mechanisms caused by submarine ferro-manganese minerals are unlikely to play an important role in accumulating scandium into oceanic sediments.

Turekian and Wedepohl[7] summarize scandium figures of 13 ppm for shales, 1 ppm for sandstones, and 1 ppm for carbonates, estimating also 2 and 19 ppm for deep sea carbonates and clays, respectively. Horn and Adams[17] have currently made a new approach to geochemical balancing and to estimation of element abundances using a high speed digital computer. Their computer-derived abundance figures for scandium are 10.1 ppm for shale, 0.733 ppm for sandstone, 0.683 ppm for carbonate, 22.8 ppm for oceanic clay, and 2.09 ppm for oceanic carbonate. Norman and Haskin[4] took a value of 12 ppm Sc found in the composite of 40 North American shales as a representative value for that rock type. They also found 20 ppm Sc for a composite of 55 North American metamorphosed shales. Their values for scandium in 4 carbonate sediments and 2 carbonate metasediments were quite low, ranging 0.40 to 1.57 ppm. Scandium estimates (14.4 and 11.5 ppm) in the present work for 2 globigerina oozes are markedly higher than the averages just mentioned for oceanic carbonates. High contents of scandium in globigerina ooze can partly be accounted for as due to the con-

TABLE 6. SCANDIUM IN MARINE SEDIMENTS AND SEDIMENTARY ROCKS

Sample record number	Sample	Location	Depth (m)	Sc (ppm)
1666	Red clay	11°19'N, 151°57'E	5893	20.3
1539	Red clay	27°42'N, 147°46'E	5948	19.9
1623	Red clay	10°11'N, 128°12'E	5395	19.0
1620	Red clay	12°26'N, 132°54'E	5640	15.7
712	Volcanic mud	29°45'N, 140°36'E	3181	13.0
709	Volcanic mud	25°49'N, 141°24'E	3191	11.2
1618	Globigerina ooze	8°15'N, 134°27'E	3656	14.4
1654	Globigerina ooze	5°29'N, 146°47'E	4032	11.5
KS-1	Slate	Iwamuro, Gunma		9.1
KS-2	Mudstone	Numata, Gunma		1.8
KS-3	Limestone	Kawaba, Gunma		trace
KS-4	Limestone	Nagatoro, Saitama		trace

17) M. K. Horn and J. A. S. Adams, *ibid.*, **30**, 279 (1966).

tribution of red clays included in globigerina ooze.

Computations are carried out to obtain an approximate figure for the crustal bundance of scandium. Assuming the average crust to be composed of equal portions of the continental crust consisting of one part of basaltic and five parts of granitic rocks and the oceanic crust consisting of basaltic rocks only (Hamaguchi and Kuroda[18]), a value has been estimated to be 17.3 ppm for the crustal abundance of scandium. Using Poldervaart's suggested ratio of rock types in the crust (basalt+tholeiite 48.9%; diorite-andesite 10.3%; granodiorite 40.8%),[19] a value of 17.1 ppm for the crustal abundance of scandium has been estimated. The two estimates are in excellent agreement.

The classic abundance values usually given for the crust are 5 to 6 ppm Sc (*e. g.*, Fleischer[20]). Vinogradov[10] gives 10 ppm Sc. These figures refer to the abundance of scandium in the continental crust, based on a 2 : 1 weight ratio of felsic to basic rock abundances. Fryklund and Fleischer[1] suggest a figure of 30 ppm Sc for the crust, using Poldervaart's estimate.[19] Abundances in the continental crust, based on a mixture of equal portions of basaltic and granitic rocks, have been given by Taylor,[21] who gives a value of 22 ppm for scandium. Horn and Adams[17] give 15.1 ppm as the abundance for scandium in igneous rocks. Matsuo and Onuma[22] suggest 22 ppm Sc using Poldervaart's ratio.[19]

Geochemical Behavior of Scandium. Judging from the distribution of scandium in magmatic rocks, it may be reasonably stated that scandium concentrates preferentially into early crystallization products. This behavior of scandium is consistent with the previous knowledge about the geochemical behavior of scandium during magmatic differentiation. However, there is still considerable controversy about the geochemical coherence between scandium and other major elements or ions in igneous rock. Rankama and Sahama[23] state that during magmatic crystallization scandium preferentially enters the early ferro-magnesian minerals, occupyring the Mg-Fe positions, thereby becoming impoverished in residual magma. Because the radius of Sc^{3+} (0.81 Å) is considerably larger than that of Mg^{2+} (0.66 Å) and its electronegativity is also greater ($E_{Sc}=1.3$, $E_{Mg}=1.2$), scandium would be retarded from entering crystals compared to Mg^{2+}. On the other hand, the radius of Fe^{2+} (0.74 Å) is much closer to that of Sc^{3+}, and the electronegativity of Sc^{3+} is much smaller than that of Fe^{2+} ($E_{Fe}=1.65$). Based on these observations Ringwood[24] postulated that scandium should exhibit a far greater tendency to enter a suitable lattice site than iron, and this tendency dominates its behavior.

Reviewing the previous knowledge about the diadochy of scandium with other metal ions, Fryklund and Fleischer[1] indicated that plots of scandium content against total iron actually show a better correlation than those against FeO alone, although they believe the geochemical correlation can be best expressed by saying that Sc^{3+} is in diadochy with Fe^{2+}.

Norman and Haskin[4] stated that the presently available evidence does not support predictions for a close geochemical relationship between Sc^{3+} and Fe^{2+}, Mg^{2+}, or any other major element or ion in igneous rocks. According to these authors there should be obvious correlation between scandium and iron within a single class of rocks, say all basic rocks, or all basalts, as well as over the broader range of rock acidities, if a coherence of scandium with iron is really being observed. In view of the possibility of scandium provinces and the absolute lack of observed correlation between iron and scandium for individual rock types, they concluded that the correlation diagrams such as Fe^{2+} *vs.* Sc, $Fe^{2+}+Fe^{3+}$ vs. Sc are not adequate to establish or to refute the existence of any close geochemical relationship between scandium and iron.

It is true that an ordinary coefficient of correlation, which is computed to obtain a quantitative measure of the strength of a relationship such as Fe^{2+} *vs.* Sc, can lead to extremely misleading conclusions unless it is interpreted carefully. Essentially, we have to deal primarily with many geochemical relations as problems of partial correlation. Therefore, observed geochemical correlations (measured by the coefficient of correlation) should be corrected by converting the ordinary coefficient to the coefficient of partial correlation, which does a fair job of eliminating the disturbing effects of other variables. However, this is not always an easy task in geochemical works. It may be thought that the close geochemical correlation of scandium against Fe^{2+} or total iron revealed by many workers does not exclude the possibility that Fe^{2+} or Fe^{2+} plus Fe^{3+} ions are the cause of enrichment of scandium in mafic rocks by diadochy, although it can imply that high contents of both iron and scandium in mafic rocks are

18) H. Hamaguchi and R. Kuroda, *ibid.*, **17**, 44 (1959).

19) A. Poldervaart, *Geol. Soc. Am. Special Paper*, **62**, 119 (1955).

20) M. Fleischer, *U. S. Geol. Surv. Circular*, **285**, (1953).

21) S. R. Taylor, *Geochim. Cosmochim. Acta*, **28**, 1273 (1964).

22) T. Matsuo and N. Onuma, *Kagaku (Science)*, **37**, 554 (1967).

23) K. Rankama and T. G. Sahama, "Geochemistry," Chicago Univ. Press, Chicago (1950).

24) A. E. Ringwood, *Geochim. Cosmochim. Acta*, **7**, 189 (1955).

merely the effects of some other common cause. This cause is not established at the present time. and if present it is not thought so decisive as to change the sign of the coefficient of correlation usually found in diagrams of Fe^{2+} *vs.* Sc^{3+}.

The anthor does not expect that the whole behavior of scandium is governed strictly by the geochemical behavior of iron. There may be some contribution of other major or minor elements like Mn^{2+} (Taylor,[5] Liebenberg[12]), which may in part affect the behavior of scandium during magmatic crystallization. Also, even though not appreciable, a certain amount of scandium becomes concentrated in residual magmas, because it acts as network former in magmas rich in volatiles, thus forming big tetrahedral complexes (ScO_4^{5-}), which is not accepted into silicate minerals and is therefore concentrated in residual magmas (Ringwood[25]).

Although the behavior of scandium is complex, we have no positive reason at the present time to reject the close geochemical coherence between Fe^{2+} (or Fe^{2+} plus Fe^{3+}) and Sc^{3+} ions. Substitution of scandium for iron may dominate its behavior during magmatic crystallization. Norman and Haskin[4] noted that Goldschmidt's rules, even with corrections, should not be applied to group III transition elements, and a successful theory can not be based solely or mostly on comparison of the general properties of the Sc^{3+} cation with those for major elements in melts. Curtis[26] has already drawn attention to the fact that the behavior of certain cations of the transition elements, involving d electrons, is dependent largely on their stabilization energy in six-fold and in four-fold co-ordination. However, with no deposition of its d orbitals in four- or six-fold co-ordination, scandium ion (Sc^{3+}) should not acquire any additional stabilization energy, so that the effects of such stabilization may be negligible.

Recently, Nockolds[27] has attempted to estimate bonding energies for metal-oxygen bonds, in which charge, radius, and electronegativity would be involved in a single function, and to use the results to account for behavior of elements during magmatic crystallization. As far as scandium is concerned, a coupled substitution like $X^{3+}Al \rightleftharpoons X^{2+}Si$ or $2X^{3+} \rightleftharpoons 3X^{2+}$ + vacant octahedral site must be considered. According to Nockolds,[27] when two cations of different valency involving the coupled substitution are capable of substitution in a crystal lattice, that substitution will take place preferentially whose sum of relative total bonding energies is the greater. Accepting Goldschmidt's fifteen per cent tolerance in ionic radius for easy substitution, we may expect that major elements Mg^{2+} and Fe^{2+} in six-fold co-ordination should be replaced by Sc^{3+}. For coupled substitutions of the type $X^{3+}Al \rightleftharpoons X^{2+}Si$, the sums of the relative bonding energies are:

$$ScAl = 600$$
$$MgSi = 580$$
$$Fe^{2+}Si = 560$$
$$Fe^{3+}Al = 545$$

Therefore, scandium should exhibit a markedly preferential entry and would be incorporated preferentially with respect to Mg^{2+} as well as with respect to Fe^{2+}. This kind of substitution must depend on the presence of available aluminum, thus perhaps playing a major role in controlling the behavior of scandium during magmatic differentiation.

It is well established that scandium becomes concentrated in early pyroxenes. Although scandium is substituting for Fe^{2+} in this mineral, it is of interest to see that scandium does not favor the coexisting olivines at levels above the analytical detection limit. This is usually accounted for as due to the difficulty of balancing charges (Taylor[5]). However, if we assume the substitution of the type $2X^{3+} \rightleftharpoons 3X^{2+}$ + vacant octahedral site, we might have substitutions involving $3Mg^{2+}$, 606; $2Sc^{3+}$, 600; $3Fe^{2+}$, 534, where numerical values stand for the relative bonding energies. If this substitution could occur in olivine-rich ultramafic rocks, scandium should not show any preferential incorporation with respect to Mg^{2+}. This may account for low abundance of scandium in olivine-rich ultramafic rocks.

Favorable evidence supporting the idea that scandium is replacing Ca^{2+} rather than Mg^{2+} or Fe^{2+} have also been offered by Snyder.[28] Based on many available determinations of scandium and calcium in rocks and related minerals, Norman and Haskin[4] pointed out that scandium contents closely paralleled calcium contents. If scandium substitutes for calcium, the coupled substitution of the type Sc Al=Ca Si must be assumed, the sums of the relative total bonding energies being:

Sc Al, 600 and Ca Si, 580

Therefore, scandium may enter into early fractions in excess of calcium, thus becoming impoverished in the magma. However, this substitution suffers from the embarrassment that scandium is not observed in feldspars, not even in the most calcic plagioclases. This is presumably due to the fact that the effective ionic radius range for substitution of calcium is 0.96 to 1.30 Å, far removed from the radius of scandium (0.81 Å). The substitution Sc Al=Ca Si is not thought to proceed as readily as does the coupled substitution Sc Al=Fe^{2+} Si

25) A. E. Ringwood, *Geochim. Cosmochim. Acta.*, **7**, 242 (1955).
26) C. D. Curtis, *ibid.*, **28**, 389 (1964).
27) S. R. Nockolds, *ibid.*, **30**, 267 (1966).
28) J. L. Snyder, *ibid.*, **16**, 243 (1959).

under normal conditions. The apparent correlation between scandium and calcium is thought to be due to some other common cause.

The author is indebted to Professor H. Hamaguchi, The University of Tokyo, and Professor R. Kuroda, University of Chiba, for their helpful discussion, and to Professor Y. Kizaki, Gunma University, Professor K. Horikoshi, Ehime University, Dr. D. Gottfried, U. S. Geological Survey, Dr. H. Ishikawa, Kagoshima University, and Dr. H. Onishi, Japan Atomic Energy Research Institute, for placing numerous rock samples. Thanks are also due to Dr. F. J. Flanagan, U. S. Geological Survey, Washington, D. C., for providing the rock standards, and to Dr. N. Onuma, The University of Tokyo, for permission to use his unpublished data.

BULLETIN OF THE CHEMICAL SOCIETY OF JAPAN VOL. 42 1569—1572 (1969)

Chromium(III) Complexes with *N,N'*-Ethylenediaminediacetic Acid*[1]

Yuki FUJII,*[2] Eishin KYUNO and Ryokichi TSUCHIYA

Department of Chemistry, Faculty of Science, Kanazawa University, Kanazawa

(Received October 23, 1968)

The following chromium(III) complexes containing *N,N'*-ethylenediaminediacetic acid (EDDA) were newly prepared: $[Cr(Hedda)_2]Cl\cdot 3H_2O$ (red) (I), $[Cr_2(OH)_2(edda)_2]\cdot 6H_2O$ (purple) (II), $H[Cr(edda)(ox)]\cdot 2H_2O$ (purple) (III), $[Cr(edda)(dip)]I\cdot 5H_2O$ (orange) (IV), $K[Cr(NCS)_2(edda)]\cdot H_2O$ (reddish purple) (V) and $[Cr(Cl)(edda)(H_2O)]\cdot 3H_2O$ (bluish purple) (VI), where edda, ox and dip are the abbreviations of the *N,N'*-ethylenediaminediacetate and oxalate anions, and α,α'-dipyridyl respectively. On the basis of the experimental results, it was concluded that EDDA is coordinated as a terdentate ligand in complex I and as a quadridentate in the other complexes prepared in the present work. Furthermore, it was also suggested that complex II has a dimer structure and complex V has *trans* configuration (with respect to the coordinated carboxylate oxygen).

The preparation and properties of the cobalt(III) complexes with *N,N'*-ethylenediaminediacetic acid (EDDA) have already been reported;[1-3] here EDDA behaves only as a quadridentate ligand, not as a terdentate toward a cobalt(III) ion. In the case of the platinum(II) and platinum(IV) complexes with EDDA, however, it has been pointed out that the ligand behaves as a bidentate or quadridentate toward a platinum(II) ion, whereas it behaves as a terdentate or a quadridentate toward platinum(IV) ion.[4]

The purpose of this study was to find how EDDA could behave toward a chromium(III) ion by attempting to prepare various complexes containing EDDA as a quadridentate or a terdentate ligand and to investigate the structure of these complexes.

Experimental

Preparation of the Complexes. *1) Bis-(hydrogen-N,N'-ethylenediaminediacetato)chromium(III) Chloride Trihydrate,* $[Cr(Hedda)_2]Cl\cdot 3H_2O$ (I). To the aqueous solution of chromium(III) chloride hexahydrate (5g, 0.019 mol), about 10g (0.056 mol) of EDDA were added and the mixture was heated on a water bath. After adjusting the pH of the solution to 2—3, it was cooled to 0°C. Pink crystals were separated out and recrystallized from aqueous solution. Yield, 2.5g (27.1%). Found: Cr, 10.27; C, 29.46; H, 5.41; N, 11.31; Cl, 7.35%. Calcd for $[Cr(Hedda)_2]Cl\cdot 3H_2O$: Cr, 10.57; C, 29.30; H, 5.75; N, 11.39; Cl, 7.24%.

Bromide of the complex I, $[Cr(Hedda)_2]Br\cdot 3H_2O$, was obtained by treating the mixed acetylacetone complex, $[Cr(acac)(edda)]\cdot 2H_2O$,[5] with *N*-bromosuccinimide in glacial acetic acid. Found: C, 27.14; H, 5.33; N, 10.57%. Calcd for $[Cr(Hedda)_2]Br\cdot 3H_2O$: C, 26.97; H, 4.91; N, 10.49%.

2) Bis-(ethylenediaminediacetato)-μ-dihydroxodichromium(III) Hexahydrate, $[Cr_2(OH)_2(edda)_2]\cdot 6H_2O$ (II). Five

*1 Presented in part at the 21st Annual Meeting of the Chemical Society of Japan, Osaka, March, 1968.

*2 Present address: Department of Chemistry, Faculty of Science, Ibaraki University, Mito.

1) M. Mori, M. Shibata, E. Kyuno and F. Maruyama, This Bulletin, **35**, 75 (1962).

2) J. I. Legg and D. W. Cooke, *Inorg. Chem.*, **4**, 1576 (1965).

3) J. I. Legg, D. W. Cooke and B. E. Douglas, *ibid.*, **6**, 700 (1967).

4) C. F. Liu, *ibid.*, **3**, 680 (1964).

5) Y. Fujii, E. Kyuno and R. Tsuchiya, This Bulletin, **42** 1301 (1969).

grams (0.01 mol) of complex I were suspended in 50ml of water and the mixture was heated on a water bath. The complex I was gradually dissolved as a small amount of ammonium carbonate was added and then the color of the solution turned from red to purple. After adjusting the pH of the solution to about 7, it was cooled to 0°C. Reddish purple crystals were separated out and recrystallized from aqueous solution. Yield, 2.5g (84.2 %). Found: Cr. 17.73; H_2O, 17.20%. Calcd for $[Cr_2(OH)_2(edda)_2]\cdot 6H_2O$: Cr, 17.50; H_2O, 18.19%.

The thermal decomposition for this complex was carried out and the complexes which contain various amount of water of crystallization were obtained by successive dehydration. The dehydrated products at several desined temperatures were as follows: $[Cr_2(OH)_2(edda)_2]$ $4H_2O$ (at 46°C) (Found: C, 26.42; H, 5.32; N, 10.27%. Calcd: C, 25.81; H, 5.09; N, 10.03%), $[Cr_2(OH)_2(edda)_2]\cdot 2H_2O$ (at 80°C) (Found: C, 27.52; H, 5.09; N, 10.44%. Calcd: C, 27.59; H, 5.04; N, 10.73%), and $[Cr_2(OH)_2(edda)_2]$ (at 110°C) (Found: Cr, 20.80; C, 29.84; H, 4.65; N, 11.12%. Calcd: Cr, 21.38; C, 29.63; H, 4.57; N, 11.52%.).

3) Hydrogen Ethylenediaminediacetatooxalatochromate(III) Dihydrate, H[Cr(edda)(ox)]·$2H_2O$(III). To the aqueous solution of the complex II (2.8g, 0.005 mol), 1.3g (0.01 mol) of oxalic acid dihydrate was added and the solution was heated on a water bath. After adjusting the pH the solution to 1—2 with a small amount of oxalic acid dihydrate, it was cooled to 0°C. Purple crystals were separated out. Yield, about 2.7g (83.6%). Found: Cr, 13.74; C, 27.01; H, 4.45; N, 7.89%. Calcd for H[Cr(edda)(ox)]·$2H_2O$: Cr, 14.81; C, 27.35; H, 4.02; N, 7.98%.

4) Ethylenediaminediacetato- α,α'-dipyridylchromium(III) Iodide Pentahydrate, [Cr(edda)(dipy)]I·$5H_2O$ (IV). To the aqueous solution of the complex II (2.8)g, 1.6g (0.01 mol) of α, α'-dipyridyl was added and the mixture was heated on a water bath. After adjusting the pH of the solution to 3—4, about 5 g of sodium iodide, ethanol and ether were added. When it was cooled to 0°C, orange crystals were separated out and recrystallized from the mixed solution of water, ethanol and ether. Yield, about 2.6g (43.3%). Found: C, 32.32; H, 4.35; N, 8.50%. Calcd for [Cr(edda)(dipy)]I·$5H_2O$: C, 32.06; H, 4.72; N, 9.31%.

5) Potassium Diisothiocyanatoethylenediaminediacetatochromate(III) Monohydrate, K[Cr(NCS)$_2$(edda)]·H_2O (V). To the aqueous solution of the complex II (2.8g), 4g (0.04 mol) of potassium thiocyanate was added and the solution was heated on a water bath. After adjusting the pH of the solution to 4—5, it was cooled to 0°C. Reddish purple crystals were separated out and recrystallized from aqueous solution. Yield, about 2.4g (60.0%). Found: Cr, 13.19; C, 23.68; H, 3.12; N, 13.71%. Calcd for K[Cr(NCS)$_2$(edda)]·H_2O: Cr, 13.02; C, 24.06; H, 3.03; N, 14.03%.

6) Chloroethylenediaminediacetatoaquochromium(III) Trihydrate, [Cr(Cl)(edda)(H_2O)]·$3H_2O$ (VI). To the aqueous solution of the complex II (2.8g,) 4g (0.03 mol) of ethylenediamine dihydrochloride was added and the solution was heated on a water bath. When it was cooled to 0°C, blusidh purple crystals were separated out. Yield, about 0.5g (15.0%). Found: Cr, 15.09; C, 22.15; H, 4.95; N, 8.48%. Calcd for [Cr(Ci)(edda)(H_2O)]·$3H_2O$: Cr, 15.58; C, 21.59; H, 4.84; N, 8.39%.

Apparatus. The absorption spectra, reflecting absorption spectra and infrared absorption spectra were measured with a Hitachi EPS Spectrophotometer, a Hitachi EPU-2A Spectrophotometer equipped with the standard Hitachi Reflection Attachment, and a Nippon Bunko DS-301 Infrared Spectrometer. The quantity of the water of crystallization contained in the complex II was estimated from TGA curves measured with Derivatograph. The magnetic susceptibility was measured with a Gouy balance at room temperature.

Results and Discussion

Electronic Absorption Spectra. The visible absorption spectra for the complexes I, II, IV, V and VI and those by the diffusc-reflectance method for the complexes II and III are shown in Fig. 1, Fig. 2 and Fig. 3, respectively, and the numerical values of the absorption maxima are summarized in Table 1 together with those of the related compounds.

The first absorption peak of the complex I is in good agreement with that of *trans*-K[Cr(ida)$_2$]·$3H_2O$,*3 differing from that of the complexes II, III, and that of NH_4[Cr(edta)]·$2H_2O$[6] and [Cr(acac)(edda)]·$2H_2O$. From these results, it may be presumed that the complex I belongs to N_2O_4-type complex which has a *trans* structure

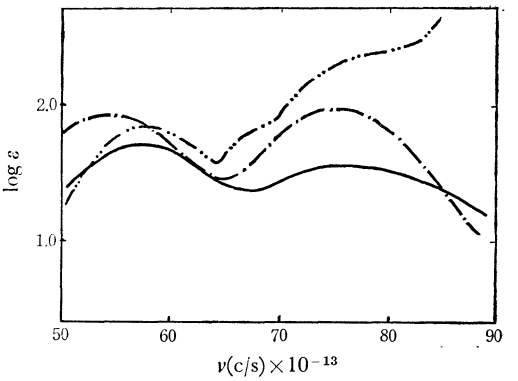

Fig. 1. Electronic spectra: I (——), II (—·—), IV (—··—).

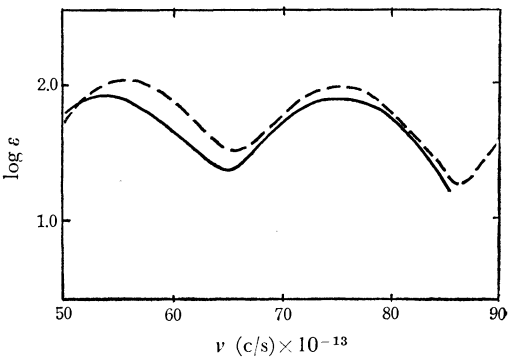

Fig. 2. Electronic spectra: V (----), VI (——).

*3 It will be published elsewhere.

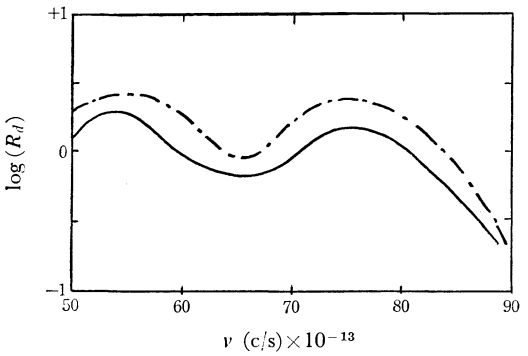

Fig. 3. Absorption spectra by the diffuse-reflectance method: II (—·—), III (——).

with respect to coordinated nitrogen atoms.

Since the spectrum of the complex II in an aqueous solution nearly agrees with the reflecting absorption spectrum of II, it may be suggested that the structure of the complex II in the solid state is also hold in the aqueous solution.

The spectra of the complexes II and III are very close to that of the edta complex, $NH_4[Cr(edta)]\cdot 2H_2O$, and they are also similar to the spectrum of the complex, $[Cr(acac)(edda)]\cdot 2H_2O$. Therefore, it may be suggested that the complexes II and III belong to N_2O_4-type.

The spectrum for the complex IV gives a complicated curve, showing two shoulders at 67.5×10^{13}/sec and at 79.0×10^{13}/sec, probably due to the α,α'-dipyridyl.

The complex V shows a specific absorption band at 100×10^{13} sec ($\log\varepsilon=2.99$) and the presence of this band indicates that the NCS^- coordinates with the chromium(III) ion.[7]

Since the spectrum of the complex VI in an aqueous solution was slowly turned to the spectrum of the complex II, it may suggest that the complex VI gradually undergoes dechlorination to form the dimer structure with respect to chromium(III) ion in an aqueous solution.

Derivatogram and Magnetic Moment. The derivatogram of the complex II is shown in Fig. 4. From the TGA curve, the formula of II may be $[Cr_2(OH)_2(edda)_2]\cdot 6H_2O$ and the composition of the thermal decomposition product between 100 and 180°C must be $[Cr_2(OH)_2(edda)_2]$.

The values of the effective magnetic moment of complex II and of the thermal decomposition products are remarkably lower than that of complex I which corresponds to the spin only value for tervalent chromium, as seen in Table 2. These facts may suggest that complex II and the thermal

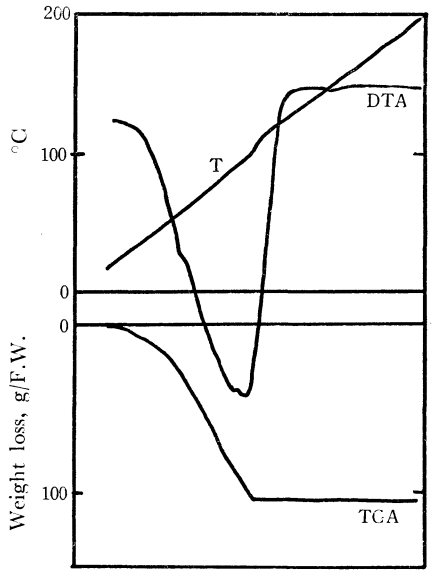

Fig. 4. Derivatogram of the complex II.

Table 1. Absorption spectra for the complexes

Complex	ν_1 (log ε)	ν_2 (log ε)	ν_3 (log ε)
I	57.5 (1.70)	75.0 (1.55)	
II	54.4 (1.93)	75.4 (1.96)	105.5 (sh)
	54.6 (+0.43)*	75.0 (+0.39)*	
III	54.2 (+0.31)*	75.8 (+0.18)*	
IV	57.5 (1.85)	67.5 (sh)	79.0 (sh) 97.1 (4.35)
V	56.3 (2.06)	60.6 (1.99)	100.0 (2.99)
VI	54.1 (1.91)	75.0 (1.87)	
$K[Cr(ida)_2]\cdot 3H_2O$	57.5 (1.85)	77.1 (1.87)	
$NH_4[Cr(edta)]\cdot 2H_2O$	55.2 (2.30)	76.5 (2.06)	
$[Cr(acac)(edda)]\cdot 2H_2O$	55.7 (2.00)	78.7 (2.33)	90.9 (3.80)
cis-$K[Cr(NCS)_2(ox)(en)]$	57.3 (2.07)	76.3 (1.99)	102.4 (3.70)

The frequencies are given in 10^{13} sec^{-1}.
* Data by the diffuse-reflectance method.

6) E. Kyuno, Read at the 14th Annual Meeting of the Chemical Society of Japan, Tokyo, April, 1961.

7) R. Tsuchida and M. Kobayashi, This Bulletin, **13**, 471 (1938).

Table 2. Magnetic moments

Complex	B. M.
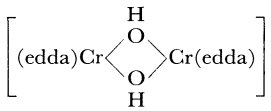	3.61
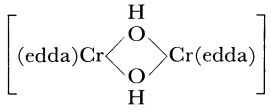	3.52
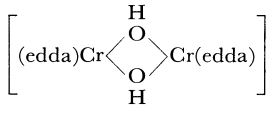	3.52
$[Cr(eddaH)_2]Cl\cdot 3H_2O$	3.89
spin only value	3.88

decomposition products have a dimer structure bridged by OH^- groups.[8]

IR Spectra. Infrared absorption spectra of the six new complexes were measured to confirm whether carboxylate groups were coordinated or not and to obtain the configurational informations on the coordinated edda. It is well known that the carboxylate group, in general, exhibits the absorption band in the region between 1700 and 1750 cm^{-1} for the free acids.[9]

All the spectra of the complexes studied show bands at 1620 and 1675 cm^{-1}, as seen in Table 3. Therefore, it will be obvious that these bands are due to coordinated carboxylate groups.

The complex V shows the strong $\nu_{C\equiv N}$ band at 2095 cm^{-1}, and *cis*-$K[Cr(NCS)_2(ox)(en)]$[10] shows three strong $\nu_{C\equiv N}$ bands at 2120, 2080 and 2062 cm^{-1}. These suggest that the complex V has a higher symmetry than *cis*-$K[Cr(NCS)_2(ox)(en)]$, and then, α-form may be considered as the configuration of edda in the complex V.

Table 3. IR data (cm^{-1})

Complex	-COO-Cr(III)
$eddaH_2$	1736 (-COOH)
$[Cr(edda\ H)_2]Cl\cdot 3H_2O$	1670, 1635
$[Cr_2(edda)_2(OH)_2]\cdot 6H_2O$	1635
$[Cr(edda)(dipy)]I\cdot 5H_2O$	1656
$H[Cr(edda)(ox)]\cdot 2H_2O$	1655
$K[Cr(NCS)_2(edda)]\cdot H_2O$	1670, 1622
$[Cr(Cl)(edda)(H_2O)]\cdot 3H_2O$	1675(sh), 1640, 1620
$[Cr(edda)(acac))]\cdot 2H_2O$	1675(sh), 1630

On the other hand, the complex $[Cr(acac)(edda)]\cdot 2H_2O$ shows the splitted bands of ν_{N-H} at 3260 and 3140 cm^{-1} and this suggests that the configuration of the edda in the complex may be β-form (*cis* with respect to coordinated carboxylate oxygens).

Properties of the Complexes. Complex II was prepared from complex I with the appropriate pH adjustment in an aqueous solution, but the conversed attempt to prepare complex I from complex II was successful only in the case when both the pH adjustment and the addition of $eddaH_2$ were achieved. This fact supports that the complex I is 1 : 2 complex, as mentioned in the term of the absorption spectra.

The structure of complex I is very interesting because it has two eight membered-rings in the complex and the edda coordinates to the metal ion as a terdentate ligand, with one nitrogen and two oxygen atoms.

Since it is very easy to expel the water of crystallization from complex II, it is dehydrated to $[Cr_2(OH)_2(edda)_2]\cdot 4H_2O$ not only from hot aqueous solution but also often even at room temperature.

Though complex VI is easily decomposed to complex II in an aqueous solution, it is certain that Cl^- coordinates to Cr(III) ion in the fresh solution of VI, because it is adsorbed by neither Na nor Cl form ion exchangers.

8) T. Morishita, K. Hori, E. Kyuno, and R. Tsuchiya, This Bulletin, **38**, 1276 (1965).

9) D. H. Busch and J. C. Bailar, Jr., *J. Am. Chem. Soc.*, **75**, 4574 (1953).

10) E. Kyuno, M. Kamada and N. Tanaka, Read at 15th Annual Meeting of the Chemical Society of Japan, Kyoto, April, 1962.

BULLETIN OF THE CHEMICAL SOCIETY OF JAPAN VOL. 42 1573—1578 (1969)

Ionic Equilibria in Mixed Solvents. IV.*[1] Solvent Effect on Dissociation Constants of Acids

Hitoshi OHTAKI

The Laboratory of Analytical Chemistry, Faculty of Science, Nagoya University, Chikusa, Nagoya

(Received October 25, 1968)

Equilibrium of hydronium ions with alkoxonium ions in water-alcohol mixtures being taken into account, solvent effects on dissociation constants of acids were quantitatively interpreted by the following: free energy changes on transferring ions from an aqueous solution to a mixed solvent and difference in standard states in different solvent compositions. Choosing suitable values for "effective ionic radii" for ions involved, satisfactory agreements were found between experimental and calculated values of ΔpK, the difference of pK in water and in an aqueous mixture, for positively charged acids (*e. g.*, ammonium, anilinium, *etc.*) as well as neutral acids yielding a negatively charged conjugate base (*e. g.*, acetic acid, benzoic acid, *p*-nitrophenol, *etc.*).

Numerous investigations have been made on dissociation equilibria in aqueous mixed solvents. Variation of a dissociation constant of an acid, HA (*e. g.*, acetic acid), was qualitatively interpreted in terms of the variation of activity coefficients of component ions in different media applying the Born solvation energy equation. Taking into consideration the variation of the concentration of water in the solution, the behavior of the dissociation constant was better expressed as a function of dielectric constant of bulk solutions.[1] However, the above treatment was not successful for positively charged acids, which dissociate as follows:

$$BH^+ \rightleftarrows H^+ + B$$

A dissociation constant of the acid, BH^+, usually *increases* and then sharply *decreases* passing through a maximum with decreasing water concentration in the solvent. Paabo, Bates and Robinson[2] introduced a quantity not clearly defined which they called the "basicity effect" in their study of dissociation equilibria of ammonium ion in aqueous methanol solutions. Glover's assumptions[3] of formation of polymerized methanol molecules or somewhat unusual complexes of organic solvent molecules with water have not been confirmed.

Previous authors have paid little attention to the equilibrium between hydronium ion and an organic solvent molecule in their studies on the solvent effects on dissociation constants of acids. Equilibrium constants of a hydronium ion with a series of alcohol molecules have been determined by Conway, Bockris and Linton.[4] Equilibrium constants of the reaction

$$H_3O^+ + ROH \rightleftarrows H_2O + ROH_2^+ \qquad (1)$$

were found to be 0.23, 0.059 and 0.037 for R= $-CH_3$, $-CH_2CH_3$ and $-CH_2CH_2CH_3$, respectively.[4]

The present paper attempts a quantitative interpretation for the variation of dissociation constants of acids in aqueous methanol and ethanol solutions on the basis of the knowldege of hydronium-alkoxonium ion equilibria and of a suitable model for solvated ions in solution.

Standard Chemical Potential of Hydrogen Ion in an Aqueous Mixture. A chemical potential of hydrogen ion in a solution is formally described as:

$$\mu_H = \mu^\circ_H + \boldsymbol{R}T \ln(H^+) \qquad (2)$$

where μ_H and μ°_H denote the chemical potential and the standard chemical potential of hydrogen ion, respectively. ( ) represents activity. The standard state is defined so that the activity coefficient of hydrogen ion, as well as those of any other ions present in the solution, tends to unity as the composition of the solution approaches the given solvent composition.

In an aqueous solution all protons exist as hydrated ones so that Eq. (2) may be described as:

$$\mu_H(w) = \mu^\circ_H(w) + \boldsymbol{R}T \ln(H_3O^+(w)) \qquad (3)$$

the hydronium ion, H_3O^+, being assumed to be a unique entity of hydrated proton. Symbol (w) stands for water.

As seen in Eq. (1), however, in aqueous mixtures both hydronium and alkoxonium ions are considered to be thermodynamic entities which determine the chemical potential of hydrogen ion. Therefore, μ_H in aqueous alcohol mixtures must be

* Part III, *Inorg. Chem.*, **7**, 1205 (1968).

1) M. Yasuda, This Bulletin, **32**, 429 (1959).

2) M. Paabo, R. G. Bates and R. A. Robinson, *J. Phys. Chem.*, **70**, 247 (1966).

3) D. Glover, *J. Am. Chem. Soc.*, **87**, 5275, 5279 (1965).

4) B. E. Conway, J. O'M. Bockris and H. Linton, *J. Chem. Phys.*, **24**, 834 (1956).

described as:

$$\mu_{H}(s) \equiv (1-x)\mu_{H_3O}(s) + x\mu_{ROH_2}(s)$$
$$= (1-x)\mu^{\circ}_{H_3O}(s) + x\mu^{\circ}_{ROH_2}(s) + \boldsymbol{R}T\ln(H_3O^{+}(s))^{1-x}(ROH_2^{+}(s))^{x} \quad (4)$$

when one mole of hydrogen ion produces fractions of $1-x$ of hydronium ion and of x of alkoxonium ion. The symbol (s) denotes the solvent of an aqueous alcohol mixture. Thus, the standard chemical potential of hydrogen ion in the aqueous alcoholic solution is defined as:

$$\mu^{\circ}_{H}(s) \equiv (1-x)\mu^{\circ}_{H_3O}(s) + x\mu^{\circ}_{ROH_2}(s) \quad (5)$$

and hence, the activity of hydrogen ion, (H^{+}), is denfied as:

$$(H^{+}(s)) \equiv (H_3O^{+}(s))^{1-x}(ROH_2^{+}(s))^{x} \quad (6)$$

Dissociation Constants of Ammonium Ion in Water-Methanol Solutions. One mole of proton liberated from a mole of ammonium ion is shared to both H_2O and ROH according to the equilibrium given in Eq. (1). Thus, the dissociation equilibrium of ammonium ion in a water-methanol mixture is described as:

$$NH_4^{+}(s) + (1-x)H_2O(s) + x\mathrm{ROH}(s) \rightleftarrows NH_3(s) + (1-x)H_3O^{+}(s) + x\mathrm{ROH}_2^{+}(s) \quad (7)$$

Here x denotes a fraction of alkoxonium ion formed and is given by the following equation through the equilibrium constant, κ, of Eq. (1):

$$x = \frac{\kappa y}{1 - y + \kappa y} \quad (8)$$

activities of water and methanol being approximated to be equal to their mole fractions. y represents the mole fraction of methanol in the solvent.

The free energy change given as $(pK(s) - pK(w))\boldsymbol{R}T\ln 10$ corresponds to the free energy change of the transfer reaction:

$$NH_4^{+}(s) + (1-x)H_2O(s) + x\mathrm{ROH}(s) + H_3O^{+}(w) + NH_3(w) \rightarrow NH_4^{+}(w) + (1-x)H_3O^{+}(s) + x\mathrm{ROH}_2^{+}(s) + H_2O(w) + NH_3(s) \quad (9)$$

Thus, the difference of dissociation constants in an aqueous solution and in an aqueous methanol solution, $\Delta pK = pK(s) - pK(w)$, is given as:

$$\Delta pK = [(\mu^{\circ}_{NH_4}(w) - \mu^{\circ}_{NH_4}(s)) + (\mu^{\circ}_{H_2O}(w) - (1-x)\mu^{\circ}_{H_2O}(s) - x\mu^{\circ}_{ROH}(s)) + (\mu^{\circ}_{NH_3}(s) - \mu^{\circ}_{NH_3}(w)) + ((1-x)\mu^{\circ}_{H_3O}(s) + x\mu^{\circ}_{ROH_2}(s) - \mu^{\circ}_{H_3O}(w))]/\boldsymbol{R}T\ln 10 \quad (10)$$

Estimation of the Variation of the Standard Chemical Potentials. The variation of the standard chemical potential corresponds to the variation of the free energy on transferring one mole of the relevant species from one medium to another. We estimate the variation of the standard chemical potentials of ions from an aqueous solution to an aqueous methanol solution on the basis of a model which is essentially similar to that proposed by Stokes[5] with a slight modification for hydronium ion: The hydronium ion, H_3O^{+}, is a sphere with a "crystal radius" of $r = 1.4$ Å and is surrounded by a layer of 2.8 Å (the diameter of a water molecule) thickness of the first hydration shell. This layer has a minimum dielectric constant of about 5[5-7] (ε_1). The first hydration shell is covered with the second hydration shell whose thickness is 2.8 Å. The dielectric constant in the second hydration shell (ε_2) is given as:[5]

$$\frac{1}{\varepsilon_2} = \frac{1}{2}\left(\frac{1}{\varepsilon_1} - \frac{1}{\varepsilon_0}\right) \quad (11)$$

For values of dielectric constant of bulk solution, ε_0, a monograph by Harned and Owen[8] is referred to.

According to this model, the variation of the standard chemical potentials, or the free energy change of the transfer, of a hydronium ion, $\Delta\mu^{\circ}_{H_3O}$ is evaluated from an aqueous solution to an aqueous methanol solution.

$$\Delta\mu^{\circ}_{H_3O} = \mu^{\circ}_{H_3O}(s) - \mu^{\circ}_{H_3O}(s)(w) = \frac{Ne^2}{2}\left[\frac{2.8}{r(r+2.8)\varepsilon_1(s)} + \frac{2.8}{(r+2.8)(r+5.6)\varepsilon_2(s)} + \frac{1}{(r+5.6)\varepsilon_0(s)}\right] - \left[\frac{2.8}{r(r+2.8)\varepsilon_1(w)} + \frac{2.8}{(r+2.8)(r+5.6)\varepsilon_2(w)} + \frac{1}{(r+5.6)\varepsilon_0(w)}\right] = \frac{Ne^2}{2}\left[\left(\frac{0.0952}{\varepsilon_2(s)} + \frac{0.143}{\varepsilon_0(s)}\right) - 0.0112\right] \quad (12)$$

where N denotes the Avogadro number and e the charge unit.

For an alkoxonium ion, ROH_2^{+}, the corresponding radius of the ion is assumed to be the same as that of the hydronium ion, while it is assumed that the alkoxonium ion is not solvated. In the course of the transfer of ROH_2^{+} ion from pure water to an aqueous methanol solution, the values of $\Delta\mu^{\circ}_{ROH_2}$ are given as:

$$\Delta\mu^{\circ}_{ROH_2} = \mu^{\circ}_{ROH_2}(s) - \mu^{\circ}_{ROH_2}(w) = \frac{Ne^2}{2}\left(\frac{1}{1.4\varepsilon_0(s)} - 0.00910\right) \quad (13)$$

The crystal radius of ammonium ion is reported to be 1.48 Å.[2,9] An assumption of unsolvated ammonium ion leads to the value of $\Delta\mu^{\circ}_{NH_4}$ calculated by the following equation:

5) R. H. Stokes, *J. Am. Chem. Soc.*, **86**, 979 (1964).
6) J. B. Hasted, D. M. Riston and C. H. Collie, *J. Chem. Phys.*, **16**, 1 (1948).
7) G. H. Haggis, J. B. Hasted and T. J. Buchanan, *ibid.*, **20**, 1452 (1952).
8) H. S. Harned and B. B. Owen, "The Physical Chemistry of the Electrolytic Solutions," 3rd ed., Reinhold Publ. Corp., New York (1964), p. 161.
9) R. A. Robinson and R. H. Stokes, "Electrolyte Solutions," 2nd ed., Butterworths, London (1959), p. 461.

$$\Delta\mu^\circ_{NH_4} = \mu^\circ_{NH_4}(s) - \mu^\circ_{NH_4}(w) = \frac{Ne^2}{2}\left(\frac{1}{1.48\varepsilon_0(s)} - 0.00861\right) \quad (14)$$

A neutral ammonia molecule is expected to be subjected to the smallest change in free energy in the course of the transfer of the molecule from an aqueous solution to an aqueous methanol solution.

The free energy change caused by the variation of the standard state in each solution, which is given in terms of $\mu^\circ_{H_2O}(w) - (1-x)\mu^\circ_{H_2O}(s) - x\mu^\circ_{ROH}(s)$ in Eq. (10), is given as:

$$\mu^\circ_{H_2O}(w) - (1-x)\mu^\circ_{H_2O}(s) - x\mu^\circ_{ROH}(s) = RT\ln(H_2O(s))^{1-x}(ROH(s))^x/(H_2O(w)) = RT\ln(1-y)^{1-x}\cdot y^x \quad (15)$$

since the activity of water in aqueous solution is defined to be unity.

Table 1. Variation of dissociation constant of ammonium ion in water-methanol solutions at 25°C

Methanol, wt%	ΔpK(calcd)	ΔpK(obsd)[2]
0	—	—
10	−0.10	−0.099
20	−0.19	−0.201
33.4	−0.32	−0.352
50	−0.51	−0.558
60	−0.63	−0.654
70	−0.75	−0.674
80	−0.84	—
90	−0.71	—
100	+0.10	—

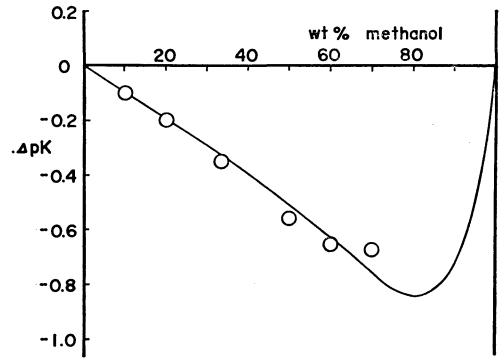

Fig. 1. Variation of ΔpK of ammonium ion as a function of the concentration of methanol. —— calculated; ○ experimental values by Paabo *et al.*[2]

In Table 1 are listed values of ΔpK of ammonium ion thus calculated by Eq. (10) and are compared with values of ΔpK reported by Paabo *et al.*[2] and the results are visualized in Fig. 1.

Dissociation Constants of Other Acids in Water-Methanol Solutions. Similar treatments were applied to systems of some acids in water-methanol solutions.

For an acid of BH^+ type, ΔpK is described in a form similar to Eq. (10); thus,

$$\Delta pK = [(\mu^\circ_{BH}(w) - \mu^\circ_{BH}(s)) + (\mu^\circ_{H_2O}(w) - (1-x)\mu^\circ_{H_2O}(s) - x\mu^\circ_{ROH}(s)) + (\mu^\circ_B(s) + \mu^\circ_B(w)) + ((1-x)\mu^\circ_{H_3O}(s) + x\mu^\circ_{ROH_2}(s) - \mu^\circ_{H_3O}(w))]/RT\ln 10 \quad (16)$$

and $\Delta\mu^\circ_{BH}$ is given as:

$$\Delta\mu^\circ_{BH} = \mu^\circ_{BH}(s) - \mu^\circ_{BH}(w) = \frac{Ne^2}{2r}\left(\frac{1}{\varepsilon_0(s)} - \frac{1}{\varepsilon_0(w)}\right) \quad (17)$$

the acid, BH^+, being assumed to be unsolvated. For terms of $\Delta\mu^\circ_{H_3O}$, $\Delta\mu^\circ_{ROH_2}$, $\Delta\mu^\circ_{H_2O}$, $\Delta\mu^\circ_{ROH}$ and $\Delta\mu^\circ_B$, the same values as calculated in the preceding section were used.

For an acid of HA type, ΔpK is given as:

$$\Delta pK = [(\mu^\circ_{HA}(w) - \mu^\circ_{HA}(s)) + (\mu^\circ_{H_2O}(w) - (1-x)\mu^\circ_{H_2O}(s) - x\mu^\circ_{ROH}(s)) + ((1-x)\mu^\circ_{H_3O}(s) + x\mu^\circ_{ROH_2}(s) - \mu^\circ_{H_3O}(w)) + (\mu^\circ_A(s) - \mu^\circ_A(w))]/RT\ln 10 \quad (18)$$

In Eq. (18) we put $\mu^\circ_{HA}(s) - \mu^\circ_{HA}(w) \simeq 0$, because HA is neutral. For the ion A^-

$$\Delta\mu^\circ_A = \mu^\circ_A(s) - \mu^\circ_A(w) = \frac{Ne^2}{2r}\left(\frac{1}{\varepsilon_0(s)} - \frac{1}{\varepsilon_0(w)}\right) \quad (19)$$

Since "crystal radius" of any ion of these acids has not been evaluated, r of the ion was used as a parameter of calculation so that calculated results would best fit the experimental data. In this sense we shall call r the "effective ionic radius".

Table 2. Effective ionic radii of ions in water-methanol solutions

Ion	r (Å)	Ref.
Ammonium	1.48	2
Diethylethanolammonium	1.4	10
Anilinium	1.8	11, 12
Diethanolammonium	2.3	10
Piperidinium	1.1	10
Trimethylpyridinium	0.9	10
Pyridinium	0.9	10
Acetate	0.8	10, 11, 15
Mandelate	0.8 (0.7—0.9)*	10
p-Nitrophenolate	1.3	10
o-Nitrophenolate	1.1 (1.0—1.2)*	10
m-Nitrophenolate	1.1 (1.0—1.2)*	10
3,4-Dinitrophenolate	1.4	10
2,5-Dinitrophenolate	1.4	10
2,4-Dinitrophenolate	1.3	10

* Values in brackets show the range of r spread.

Comparison of ΔpK values thus calculated with those observed are demonstrated for some aliphatic and aromatic amines, heterocyclic nitrogen compounds, aliphatic and aromatic carboxylic acids and phenols, and some examples are graphically represented in Fig. 2. The values of the "effective ionic radii" adopted are summarized in Table 2.

Dissociation Constants of Acids in Water-Ethanol Solutions. The validity of the present treatment was tested for dissociation equilibria of some acids in water-ethanol solutions. Resulting values of ΔpK in some examples are shown in Fig. 3 and values of r examined are tabulated in Table 3.

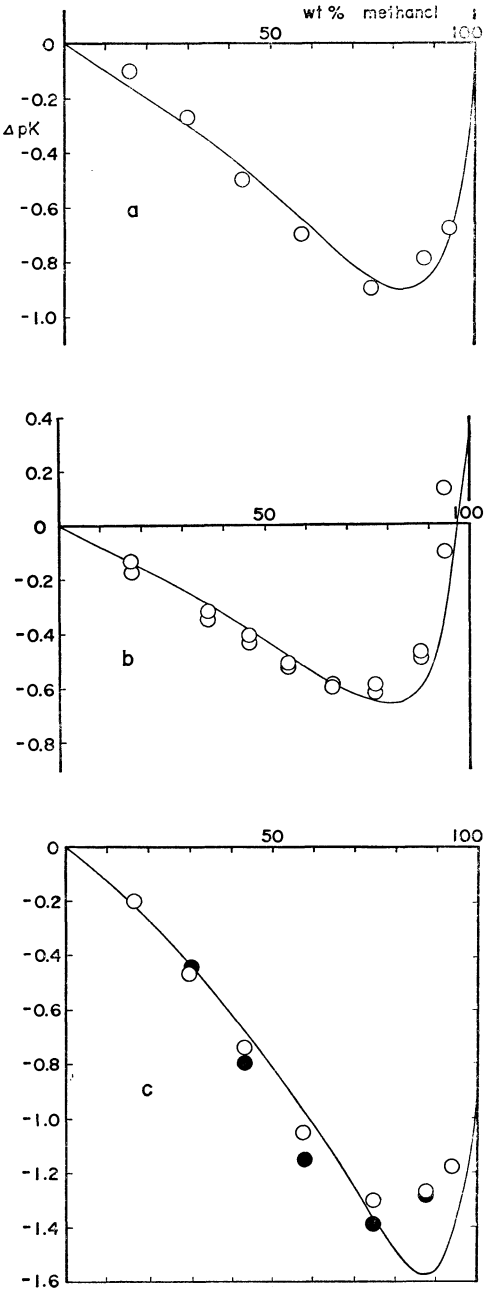

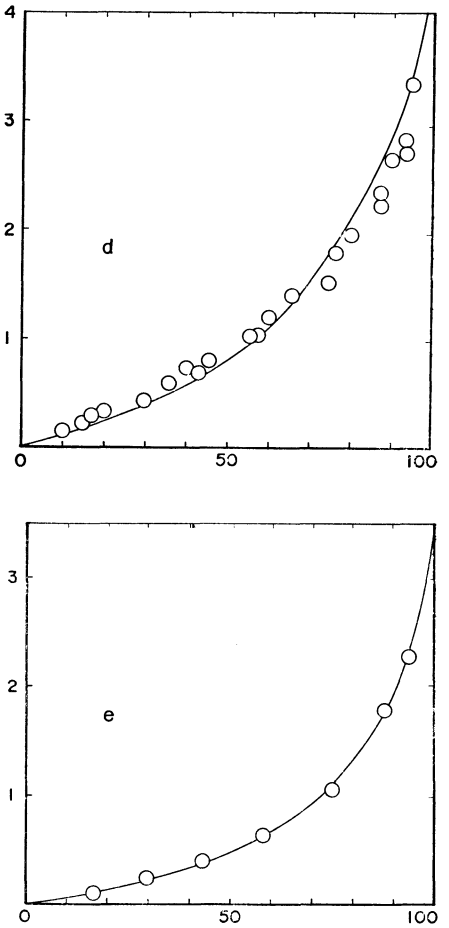

Fig. 2. Variation of ΔpK of various acids as a function of the concentration of methanol. Lines drawn show calculated values of ΔpK's using corresponding values of r in Table 2.
a, diethylethanolammonium
b, anilinium
c, pyridinium (○) and trimethylpyridinium (●)
d, acetic acid
e, *p*-nitrophenol

Discussion

From Tables 2 and 3 it is seen that ammonium, diethylethanolammonium and anilinium ions have similar values of the effective ionic radius despite the fact that their pK values are widely spread (pK(ammonium)=9.245,[2] pK(diethylethanolammonium)=9.90[10] and pK(anilinium)=4.60[11]

10) R. Gaboriaud, *Compt. Rend.*, **263**, 911 (1966).
11) G. Douheret, *Bull. Soc. Chim. France*, **1967**, 1412.

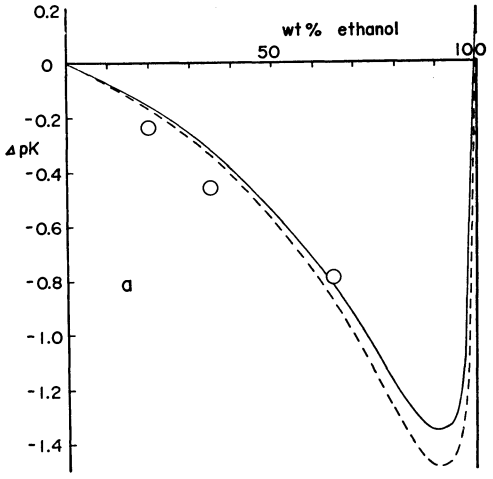

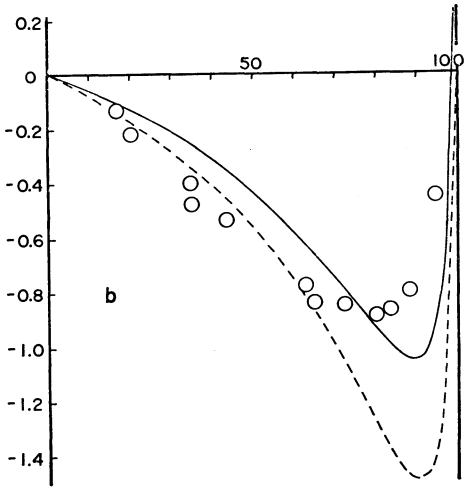

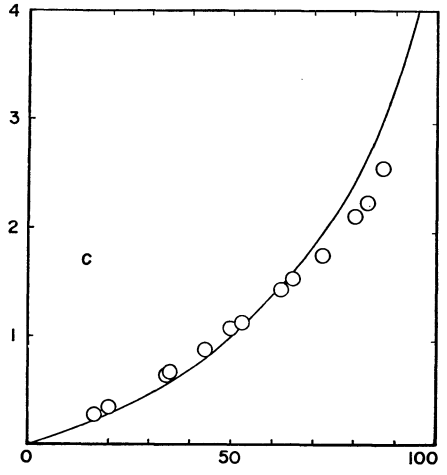

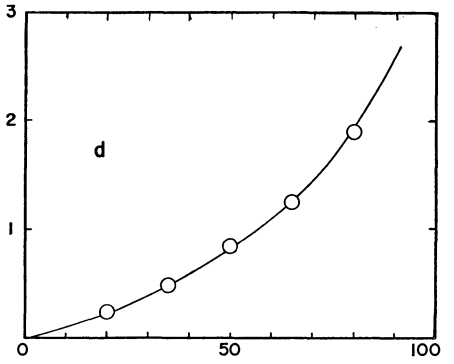

Fig. 3. Variation of ΔpK of various acids as a function of the concentration of ethanol. Lines drawn show calculated values of ΔpK's using corresponding values of r in Table 3.
a, ammonium (——, $r=1.4$ Å; ----, $r=1.5$ Å);
b, anilinium (——, $r=1.4$ Å; ----, $r=1.8$ Å);
c, acetic acid; d, formic acid.

Table 3. Effective ionic radii of ions in water-ethanol solutions

Ion	r (Å)	Ref.
Ammonium	1.4—1.5	13
Anilinium	1.4—1.8	11, 13
Acetate	0.8 (0.7—0.9)*	11, 13, 14
Formate	1.3	13, 14
Propionate	0.9 (0.8—1.0)*	13, 14
Benzoate	0.8 (0.7—0.9)*	13, 14

* Values in brackets show the range of r spread.

or 4.62[12]) in aqueous solution at 25°). Similar phenomena may be found in systems of acetic acid ($pK=4.76$[10-12]) in aqueous solution at 25°), propionic acid ($pK=4.87$,[13,14]) benzoic acid ($pK=4.20$[13,14]) and mandelic acid ($pK=3.45$[10]). Thus the variation of pK may mainly be caused by the energy change of electrostatic interactions of charged atom with solvent moleculeus.

The effective ionic radius is found to remain unchanged when the solvent is changed from water-methanol to water-ethanol mixtures.

The fact that the effective ionic radius scarcely changes for various ions with the same functional group but with different molecular volumes may indicate that the effective ionic radius may not give the size of the whole molecule but that of a charged site such as oxygen in a carboxylate group and a phenolate or nitrogen in an ammonium group and a heterocyclic compound. A charge in

12) A. Bacarella, E. Grunwald, H. P. Marshall and E. L. Purlee, *J. Org. Chem.*, **20**, 747 (1955).
13) R. G. Bates, "Determination of pH," John Wiley and Sons, Inc., New York (1964), p. 195.
14) E. Grunwald and B. J. Berkowitz, *J. Am. Chem. Soc.*, **73**, 4939 (1951).

an ion may be located on a specific site such as oxygen or nitrogen atom, and the electrostatic interaction of the ion with the surrounding medium may be described as a function of the distance from the charged atom in question. A hydrophobic group which occupies the major part of the volume of an ion may contribute to a lesser extent to the electrostatic interaction between the charged site in the molecule and the surrounding medium. Solvation of ions having hydrophobic groups may be smallest so that the relationships of Eqs. (17) and (19) may hold with a good approximation.

Similarly the assumption that the alkoxonium ion, $R\text{-}OH^{2+}$, has the same effective ionic radius as that of hydronium ion may be supported in spite of their different molecular volumes.

From results in Tables 2 and 3, the effective ionic radii are estimated as follows: 1.4—1.5 Å for $-NH_3^+$ in ammonium and aliphatic ammonium ions, 0.9—1.1 Å for $>NH^+$ in hererocyclic compounds, 0.7—0.9 Å for $-O^-$ in carboxylic acids, 1.1—1.4 Å for $-O^-$ in phenols. Values of the effective ionic radii of diethanolammonium and formate ions are large as compared with the related compounds. This may be attributed to easier hydration of these ions: relatively hydrophilic ethanol groups in the former may allow water molecules to approach a charged nitrogen atom with electrostatic interactions, and the latter, formate ion, has no aliphatic radicals.

Some discrepancies observed in water-ethanol systems seem to be due to a more or less crude approximation that activities of water and ethanol are put equel to their mole fractions. Vapor pressure data show that water-methanol mixtures[16] are better approximated to the ideal mixtures than water-ethanol mixtures.[17]

The author wishes to thank Professors Motoharu Tanaka and Yutaka Miyahara for their helpful advice. The financial support given by the Ministry of Education is gratefully acknowledged.

15) T. Shedlovsky and R. L. Kay, *J. Phys. Chem.*, **60**, 151 (1956).

16) J. Timmermans, ed., "The Physico-chemical Constants of Binary Systems in Concentrated Solutions," Vol. 4, Interscience Publ., Inc., New York (1960), p. 154.

17) E. A. Guggenheim, "Thermodynamics," 2nd Ed., North-Holland Publ. Co., Amsterdam (1950), p. 187.

BULLETIN OF THE CHEMICAL SOCIETY OF JAPAN VOL. 42 1578—1583 (1969)

The Kinetics of Substitution Reactions Involving Metal Complexes. XIII. Reactions of Zinc(II) with *meso*-Butylenediaminetetraacetatocobaltate(II) and with Propylenediaminetetraacetatocobaltate(II)

Hiroshi OGINO, Toshiyuki BABA*1 and Nobuyuki TANAKA

Department of Chemistry, Faculty of Science, Tohoku University, Katahira-cho, Sendai

(Received October 31, 1968)

Kinetics of the substitution reactions of zinc(II) with *meso*-butylenediaminetetraacetatocobaltate(II) (cobalt(II)-*meso*-BDTA) and propylenediaminetetraacetatocobaltate(II) (cobalt(II)-PDTA) have been studied. The reaction of zinc(II) with cobalt(II)-*meso*-BDTA complex proceeds through two simultaneous reaction paths involving the acid dissociation reactions of the cobalt(II) complex. On the other hand, the reaction of zinc(II) with cobalt(II)-PDTA proceeds through four simultaneous reaction paths, of which two involve electrophilic substitution reactions and the others, the acid dissociation reactions of the cobalt(II) complex. This kinetic behavior is discussed on the basis of the natures of the ligands.

Kinetic studies of the reactions of zinc(II) with ethylenediaminetetraacetatocobaltate(II) (cobalt(II)-EDTA) and trimethylenediaminetetraacetatocobaltate(II) (cobalt(II)-TRDTA) have been reported.[1] According to the results, the variation of ligands affects the rates of both the electrophilic substitution (S_E) reactions and the acid dissociation reactions of the cobalt(II) complexes. As it seems important to know of the effects of other ligands on both the mechanisms and the rates of the reactions, substitution reactions of zinc(II) with cobalt(II) complexes containing *meso*-butylene-

*1 Present address: Nitsuko Ltd., Kawasaki.

1) H. Ogino and N. Tanaka, This Bulletin, **40**, 857 (1967).

diaminetetraacetate (*meso*-BDTA)*2 and propylenediaminetetraacetate (PDTA)*3 are investigated at ionic strength 0.2 and 25°C in this study.

Experimental

The preparations and standardizations of the solutions of zinc(II) nitrate, cobalt(II) nitrate and disodium dihydrogen propylenediaminetetraacetate (Na_2H_2pdta) were made by the same method as reported previously.[2,3]

meso-Butylenediaminetetraacetic acid was prepared by the following procedures: *meso*-Butylenediamine was prepared by the method of Dickey *et al.*,[4] and this diamine was converted to the *meso*-BDTA by the method of Dwyer and Garvan.[5] Crude *meso*-BDTA was recrystallized from hot water. Found: C, 40.19; H, 7.00; N, 8.03%. Calcd for $C_{12}H_{20}N_{20}O_8 \cdot 2H_2O$; C, 40.38; H, 6.78; N, 7.83%.

By measuring NMR spectra of *meso*-butylenediamine,[6] *meso*-BDTA[6] and cobalt(III)-*meso*-BDTA complex[7] in aqueous solutions, it was confirmed that *meso*-BDTA thus obtained did not contain *dl*-BDTA as impurity.

The stock solution of disodium dihydrogen *meso*-butylenediaminetetraacetate (Na_2H_2*meso*-bdta) was prepared from equimolar sodium carbonate and H_4*meso*-bdta. The concentration of *meso*-BDTA was determined by amperometric titration with the above-mentioned solutions of metal nitrates. All other chemicals used were analytical reagent grade.

It was reported that cobalt(II)-EDTA, cobalt(II)-TRDTA and cobalt(II)-PDTA give polarographic one-electron oxidation waves in acetate buffer-potassium nitrate media.[8] In this study, it was found that cobalt(II)-*meso*-BDTA gives a similar polarographic one-electron anodic wave with the half-wave potential at +0.099 V *vs.* SCE. The rates of the reactions of zinc(II) with cobalt(II)-*meso*-BDTA and cobalt(II)-PDTA were followed by the measurements of the decrease of the polarographic anodic diffusion current with time.

The measurements of both current-voltage and current-time curves were made with a Yanagimoto GR-103 Galvarecorder and a Yanagimoto AP-1 applying potentiometer. The dropping mercury electrode had an m value of 1.84 mg/sec and a drop time t_d of 4.26 sec at 55 cm of the mercury height in an air-free solution containing 0.1 M acetate buffer and 0.1 M potassium nitrate at 25°C and −0.50 V *vs.* SCE.

The ionic strength was adjusted to be 0.2 with potassium nitrate. Gelatin was added as a maximum suppressor by 0.005% in concentration. The pH of the solution was measured with a Hitachi-Horiba F-5 pH meter.

Results

It is known that zinc(II) and cobalt(II) ions form monoacetato complexes in acetate buffer solutions at ionic strength of 0.2.[9,10] Therefore, the overall reactions of zinc(II) with cobalt(II)-*meso*-BDTA or cobalt(II)-PDTA are expressed by

$$\left\{\begin{matrix}Zn^{2+}\\ \rightleftarrows\\ ZnOAc^{+}\end{matrix}\right\} + \left\{\begin{matrix}CoY^{2-}\\ \rightleftarrows\\ CoHY^{-}\\ \rightleftarrows\\ \vdots\end{matrix}\right\} \underset{k^-}{\overset{k^+}{\rightleftharpoons}} \left\{\begin{matrix}ZnY^{2-}\\ \rightleftarrows\\ ZnHY^{-}\\ \rightleftarrows\\ \vdots\end{matrix}\right\} + \left\{\begin{matrix}Co^{2+}\\ \rightleftarrows\\ CoOAc^{+}\end{matrix}\right\} \quad (1)$$

where Y^{4-} means a quadrivalent *meso*-BDTA or PDTA anion. The reactions were initiated by adding a known amount of cobalt(II)-*meso*-BDTA or cobalt(II)-PDTA solution into an acetate buffer-potassium nitrate solution containing zinc(II) ions in a large excess. Considering the anodic current, $\bar{i}$, given by cobalt(II)-*meso*-BDTA or cobalt(II)-PDTA complex, the forward rate constant of Eq. (1), k^+, is written as follows:[10]

$$2.303 \log \frac{\bar{i}_0^2 - \bar{i}_e\bar{i}}{\bar{i}_0(\bar{i} - \bar{i}_e)} = \frac{\bar{i}_0 + \bar{i}_e}{\bar{i}_0 - \bar{i}_e} k^+ t \quad (2)$$

where subscripts e and 0 denote equilibrium and initial conditions, respectively.

It was found that the changes in the initial concentration of cobalt(II) complex did not affect the values of k^+.

Figure 1 shows the values of k^+ which were obtained from the reactions between zinc(II) and cobalt(II)-*meso*-BDTA as a function of the hydrogen ion concentration. The change in concentrations of zinc(II) ions does not affect the values of k^+ as shown in Fig. 1. The plots fit the equation in which the rate is dependent on the

*2 *meso*-Butylenediaminetetraacetic acid:

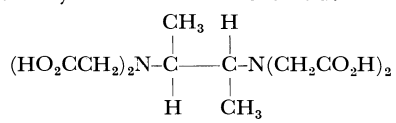

*3 Propylenediaminetetraacetic acid:

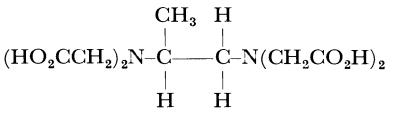

2) N. Tanaka and H. Ogino, This Bulletin, **38**, 439 (1965).

3) H. Ogino, *ibid.*, **38**, 771 (1965).

4) F. P. Dickey, W. Fickett and H. J. Lucus, *J. Am. Chem. Soc.*, **74**, 944 (1952).

5) F. P. Dwyer and F. L. Garvan, *ibid.*, **81**, 2955 (1959).

6) J. L. Sudmeier and C. N. Reilley, *Anal. Chem.*, **36**, 1707 (1964).

7) R. J. Day and C. N. Reilley, *ibid.*, **37**, 1326 (1965).

8) N. Tanaka and H. Ogino, This Bulletin, **38**, 1054 (1965).

9) N. Tanaka and K. Kato, *ibid*, **33**, 417 (1960).

10) N. Tanaka, M. Kamada, H. Osawa and G. Sato, *ibid.*, **33**, 1412 (1960).

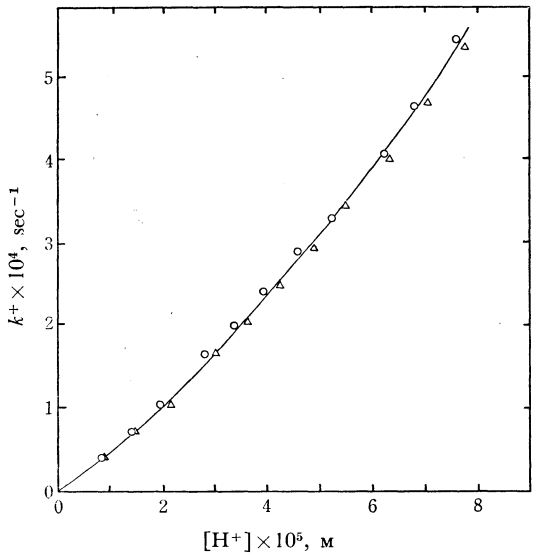

Fig. 1. k^+ for the reaction between zinc(II) and cobalt(II)-*meso*-BDTA as a function of hydrogen ion concentration. $[Zn^{2+}]_{0,app}$'s are 10.3 mM for ○ and 20.6 mM for △. Acetate ion concentrations are 0.096_8 M for ○ and 0.093_8 M for △.

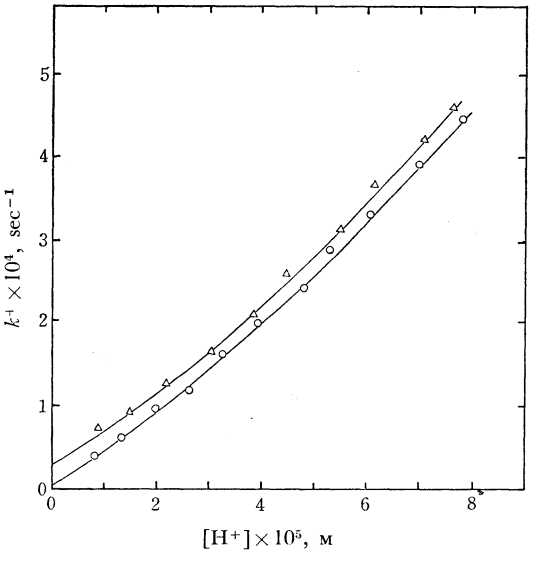

Fig. 2. k^+ for the reaction between zinc(II) and cobalt(II)-PDTA as a function of hydrogen ion concentration. $[Zn^{2+}]_{0,app}$'s are 5.15 mM for ○ and 25.8 mM for △. Acetate ion concentrations are 0.098_4 M for ○ and 0.092_4 M for △.

second power of the hydrogen ion concentration. From Fig. 1, the equation,

$$k^+ = 0.51_0 \times 10[H^+] + 0.02_7 \times 10^6[H^+]^2 \quad (3)$$

was obtained at $[Zn^{2+}]_{0,app}$ equal to both 10.3 mM and 20.6 mM.

In Fig. 2, the values of k^+ which were obtained from the reactions between zinc(II) and cobalt(II)-PDTA are plotted against the hydrogen ion concentration. In this case, the values of k^+ increase with the concentration of zinc(II) ions. From Fig. 2, the following equations were obtained:

$$\text{At } [Zn^{2+}]_{0,app} = 5.15 \text{ mM},$$
$$k^+ = 0.05 \times 10^{-4} + 0.40_8 \times 10[H^+] + 0.02_0 \times 10^6[H^+]^2 \quad (4)$$
$$\text{At } [Zn^{2+}]_{0,app} = 25.8 \text{ mM},$$
$$k^+ = 0.33 \times 10^{-4} + 0.43_3 \times 10[H^+] + 0.01_7 \times 10^6[H^+]^2 \quad (5)$$

From the results mentioned above and those reported in the previous paper,[1] the reaction of zinc(II) with cobalt(II)-*meso*-BDTA and that of zinc(II) with cobalt(II)-PDTA are considered to proceed through the following reaction paths:

$$\text{(i)} \quad Zn^{2+} + CoY^{2-} \overset{k_{Zn}^{CoY}}{\rightleftharpoons} ZnY^{2-} + Co^{2+} \quad (6)$$

$$\text{(ii)} \quad CoY^{2-} + H^+ \rightleftharpoons CoHY^- \quad (7a)$$
$$Zn^{2+} + CoHY^- \overset{k_{Zn}^{CoHY}}{\rightleftharpoons} ZnHY^- + Co^{2+} \quad (7b)$$

$$\text{(iii)} \quad CoY^{2-} + H^+ \overset{k_{H}^{CoY}}{\rightleftharpoons} Co^{2+} + HY^{3-} \quad (8a)$$
$$Zn^{2+} + HY^{3-} \rightleftharpoons ZnY^{2-} + H^+ \quad (8b)$$

$$\text{(iv)} \quad CoY^{2-} + 2H^+ \overset{k_{2H}^{CoY}}{\rightleftharpoons} Co^{2+} + H_2Y^{2-} \quad (9a)$$
$$Zn^{2+} + H_2Y^{2-} \rightleftharpoons ZnY^{2-} + 2H^+ \quad (9b)$$

Equation (10) was obtained on the basis of these reaction mechanisms.

$$k^+\alpha_{CoY(H)} = k_{Zn}^{CoY}\frac{[Zn^{2+}]_{0,app}}{\alpha_{Zn(OAc)}} + (k_{Zn}^{CoHY}K_{CoHY}^{H}\frac{[Zn^{2+}]_{0,app}}{\alpha_{Zn(OAc)}} + k_{H}^{CoY})[H^+] + k_{2H}^{CoY}[H^+]^2 \quad (10)$$

where

$$\alpha_{CoY(H)} = 1 + K_{CoHY}^{H}[H^+]$$
$$\alpha_{Zn(OAc)} = 1 + \beta_{ZnOAc}[OAc^-]$$
$$[Zn^{2+}]_{0,app} = [Zn^{2+}]_0 + [ZnOAc^+]_0$$
$$K_{CoHY}^{H} = [CoHY^-]/[CoY^{2-}][H^+]$$

β_{ZnOAc} represents the formation constant of acetatozinc(II) complex reported in the previous paper.[9] It has been shown that the values of K_{CoHY}^{H} are $10^{3.0}$ and $10^{2.4}$ for cobalt(II)-EDTA and cobalt(II)-TRDTA complexes, respectively.[11] Since it is unlikely that the values of K_{CoHY}^{H} for cobalt(II)-*meso*-BDTA and cobalt(II)-PDTA complexes are very different in magnitude from those for Co(II)-EDTA and cobalt(II)-TRDTA complexes and all measurements were carried out

11) G. Anderegg, *Helv. Chim. Acta*, **47**, 1801 (1964).

at pH range from 4.2 to 5.0, it is reasonable to assume that the values of $\alpha_{CoY(H)}$ do not differ significantly from unity.

The rate constants for the reaction between zinc(II) and cobalt(II)-*meso*-BDTA were obtained from the analysis of Eq. (3) with the aid of Eq. (10), and are given in Table 1. It should be noted that reaction paths (i) and (ii) were not observed in this reaction.

The rate constants for the reaction between zinc(II) and cobalt(II)-PDTA were obtained from the analysis of Eqs. (4), (5) and (10), and are also given in Table 1.

Table 1. Rate constants at ionic strength 0.2 and 25°C

Rate constant	*meso*-BDTA	PDTA
k_{Zn}^{CoY} ($l\,mol^{-1}\,sec^{-1}$)	$<7\times10^{-4}$	2×10^{-3}
k_{Zn}^{CoHY} ($l\,mol^{-1}\,sec^{-1}$)	—	$\sim2\times10^{-2}$
k_{H}^{CoY} ($l\,mol^{-1}\,sec^{-1}$)	5.1	4.3
k_{2H}^{CoY} ($l^2\,mol^{-2}\,sec^{-1}$)	3×10^{4}	2×10^{4}

Discussion

By the application of the treatment of Bydalek *et al.*,[12-14] it was proposed previously[1] that the binuclear intermediate,

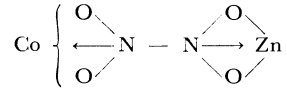

(A)

was formed for the acid-independent electrophilic substitution (S_E) reaction,

$$Zn^{2+} + CoY^{2-} \xrightarrow{k_{Zn}^{CoY}} ZnY^{2-} + Co^{2+} \qquad (11)$$

where Y^{4-} denotes a quadrivalent EDTA or TRDTA anion. Furthermore, it was shown that the change of the rate constants of reaction (11) can be related to the equation,[1]

$$\frac{k_{Zn}^{Cotrdta}}{k_{Zn}^{Coedta}} = \frac{K_{Coedta}}{K_{Cotrdta}} \qquad (12)$$

It is shown in Table 2 that the order of the observed rates of S_E reactions is given as

$$TRDTA > EDTA > PDTA > meso\text{-}BDTA \approx 0$$

Table 2 gives also the comparisons of the observed rate constant ratios of various S_E reactions, $k_{Zn}^{CoY'}/k_{Zn}^{CoY}$, and the stability constant ratios, $K_{CoY}/K_{CoY'}$. The observed values of PDTA system and especially *meso*-BDTA system are not in agreement with the calculated values. These disagreements are considered to be due to the following reasons: The formation of binuclear intermediate (A) is accompanied necessarily by the rotation about the ethylenic carbon-carbon bond. PDTA and *meso*-BDTA complexes contain one and two methyl groups on the ethylenic carbon-carbon bond, respectively. Hence, the rotational barrier about the ethylenic bond increases with the order,

$$EDTA < PDTA < meso\text{-}BDTA$$

This steric hindrance of methyl groups leads to the decrease in the rate of reaction (11), so that the acid-independent S_E reaction of zinc(II) with cobalt(II)-*meso*-BDTA could not be observed. In addition, the inductive effect of the methyl groups increases the basicity of nitrogen in ligands and strengthens the cobalt-nitrogen bonds. This effect may assist also the decrease of reaction rate because the S_E reaction is accompanied by breaking of a cobalt-nitrogen bond.

In the previous paper,[1] the value of k_H^{CoY}/k_{Zn}^{CoY} for both EDTA and TRDTA matched best with the calculated intermediate stability constant ratio of $K_{Himda}\times K_{el}/K_{Znimda}$, where imda denotes iminodiacetate segment and K_{el} implies a correction for an electrostatic attraction. This fact suggests that the intermediate formed in the reac-

Table 2. Comparisons of ratios of observed rate constants with those of stability constants

Obsd*		Calcd**
$k_{Zn}^{Cotrdta}/k_{Zn}^{Coedta}$	1.1×10	$K_{Coedta}/K_{Cotrdta} = 1.7\times10$
$k_{H}^{Cotrdta}/k_{H}^{Coedta}$	1.7×10	
$k_{Zn}^{Copdta}/k_{Zn}^{Coedta}$	9×10^{-3}	$K_{Coedta}/K_{Copdta} = 4.4\times10^{-2}$
$k_{H}^{Copdta}/k_{H}^{Coedta}$	1.4×10^{-1}	
$k_{Zn}^{Comeso\text{-}bdta}/k_{Zn}^{Coedta}$	$<3\times10^{-3}$	$K_{Coedta}/K_{Comeso\text{-}bdta} = 3.8\times10^{-2}$
$k_{H}^{Comeso\text{-}bdta}/k_{H}^{Coedta}$	1.7×10^{-1}	

* The values[1] ($l\,mol^{-1}\,sec^{-1}$) used in this calculation are: 0.23 for k_{Zn}^{Coedta}, 3×10 for k_{H}^{Coedta}, 2.5 for $k_{Zn}^{Cotrdta}$ and 5×10^{2} for $k_{H}^{Cotrdta}$.

** Stability constants used in this calculation are: 15.71[3] for log K_{Coedta}, 14.48[3] for log $K_{Cotrdta}$, 17.07[3] for log K_{Copdta} and 17.13[15] for log $K_{Comeso\text{-}bdta}$.

12) T. J. Bydalek and D. W. Margerum, *Inorg. Chem.*, **2**, 678 (1963).

13) T. J. Bydalek and M. L. Blomster, *ibid.*, **3**, 667 (1964).

14) T. J. Bydalek and A. H. Constant, *ibid.*, **4**, 833 (1965).

15) H. Ogino, T. Baba and N. Tanaka, unpublished results.

tion between CoY^{2-} ion and hydrogen ion corresponds to the structure,

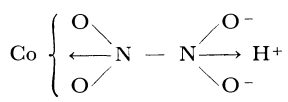

(B)

If the basicities and steric environments of ligands are similar, it is expected that the rate constant of the reaction of CoY^{2-} with a hydrogen ion, k_H^{CoY}, can be related to Eq. (13), which is analogous to Eq. (12):

$$\frac{k_H^{CoY'}}{k_H^{CoY}} \fallingdotseq \frac{K_{CoY}}{K_{CoY'}} \tag{13}$$

In Table 2, are also given the comparison of the ratios of observed rate constants, $k_H^{CoY}/k_H^{CoY'}$, and those of the stability constants, $K_{CoY}/K_{CoY'}$. Although the value of $k_H^{Cotrdta}/k_H^{Coedta}$ is in good agreement with the value of $K_{Coedta}/K_{Cotrdta}$, the observed values of $k_H^{Copdta}/k_H^{Coedta}$ and $k_H^{Co\,meso\text{-}bdta}/k_H^{Coedta}$ do not agree with the ratios of the stability constant. However, these disagreements are not so marked as those in the values of $k_{Zn}^{CoY'}/k_{Zn}^{Coedta}$. This seems to be attributable to the fact that the complete rotation about the ethylenic carbon-carbon bond is not required for the reaction between CoY^{2-} and a hydrogen ion taking place. In fact, molecular models show that both hydrogen and cobalt ions can coordinate simultaneously to each nitrogen atom in a ligand without complete rotation about the ethylenic bond. An extreme case is the reaction between cyclohexanediaminetetraacetato complex (CyDTA complex) ions and hydrogen ions. Although cyclohexane ring in CyDTA forbids the rotation of the two iminodiacetate groups, the reaction of CyDTA complex ions with hydrogen ions proceeds.[16,17]

Table 3. Values of k_H^{CoY} and k_{Co}^{HY} at ionic strength 0.2 and 25°C

Ligand	k_H^{CoY} $l\,mol^{-1}\,sec^{-1}$	k_{Co}^{HY} $l\,mol^{-1}\,sec^{-1}$	Ref.
TRDTA	5×10^2	8×10^6	1
EDTA	3×10	8×10^6	1
meso-BDTA	5.1	4×10^6	This work
PDTA	4.3	7×10^6	This work

In Table 3, are shown the values of k_H^{CoY} for various ligands. The values of k_H^{CoY} can be related to the rate constants, k_{Co}^{HY} of the complex-forming reactions,

$$Co^{2+} + HY^{3-} \underset{k_H^{CoY}}{\overset{k_{Co}^{HY}}{\rightleftharpoons}} CoY^{2-} + H^+ \tag{14}$$

with the equation,

$$k_H^{CoY} = \frac{k_{Co}^{HY}}{K_{CoY}K_{HY}} \tag{15}$$

where K_{HY} denotes the fourth dissociation constant of H_4Y. The values of k_{Co}^{HY} calculated by Eq. (15) are also given in Table 3. In accord with the previous conclusion that the second-order rate constants of the complex-forming reactions of a metal ion with related ligands (with the same charge and a similar size) are almost the same,[1,18] the values of k_{Co}^{HY} given in Table 3 are essentially identical for various ligands. Hence, the nature of ligands may reflect predominantly to the values of k_H^{CoY}.

It may be seen in Table 3 that the order of the values of k_H^{CoY} is as follows:

$$TRDTA > EDTA > meso\text{-}BDTA > PDTA$$

The increase in basicities of PDTA and *meso*-BDTA by the presence of methyl groups may cause the decrease in the value of k_H^{CoY} with the following order:

$$k_H^{Coedta} > k_H^{Copdta} > k_H^{Co\,meso\text{-}bdta}$$

However, as is seen in Table 3, the value of $k_H^{Co\,meso\text{-}bdta}$ is larger than the value of k_H^{Copdta} in spite of the increase of the number of methyl groups in the ligand. This can be understood by considering the conformation of methyl groups in the coordinated ligands. There are two possibilities of the orientation of a methyl group on the N–C–C–N chelate ring of the coordinated PDTA; that is, an equatorial and an axial orientations. The complex with a methyl group of equatorial orientation is strainless as in the EDTA complex, while the complex with a methyl group of axial orientation is more crowded on the chelate and is strained. In fact, it is known that the orientation of a methyl group of the coordinated PDTA is equatorial.[19-22] In the *meso*-BDTA complex, there are two methyl groups on the N–C–C–N chelate ring. Molecular models reveal that the orientation of one methyl group in the coordinated *meso*-

16) D. W. Margerum and T. J. Bydalek, *Inorg. Chem.*, **2**, 683 (1963).
17) D. W. Margerum, P. J. Menardi and D. L. Janes, *ibid.*, **6**, 283 (1967).
18) H. Ogino and N. Tanaka, This Bulletin, **40**, 852 (1967).
19) D. H. Busch and D. W. Cooke, *J. Inorg. Nucl. Chem.*, **23**, 145 (1961).
20) F. P. Dwyer and F. L. Garvan, *J. Am. Chem. Soc.*, **83**, 2610 (1961).
21) F. P. Dwyer and T. E. MacDermatt, *ibid.*, **85**, 2916 (1963).
22) R. J. Day and C. N. Reilley, *Anal. Chem.*, **37**, 1326 (1965).

BDTA is equatorial and the orientation of another methyl group is necessarily axial. Therefore, it is considered that the *meso*-BDTA complex is not more stable than the PDTA complex due to the presence of axial methyl group.

The authors thank the Ministry of Education for the financial support granted for this research.

BULLETIN OF THE CHEMICAL SOCIETY OF JAPAN VOL. 42 1583—1588 (1969)

Preparation and Circular Dichroism of *trans(N)*- and *cis(N)*-Isomers of (Ammoniatriacetato)(amino-acidato)cobalt(III) Complexes

Norio KOINE and Naokazu SAKOTA

Department of Industrial Chemistry, Faculty of Engineering, Ehime University, Bunkyo-cho, Matsuyama

and Jinsai HIDAKA and Yoichi SHIMURA

Department of Chemistry, Faculty of Science, Osaka University, Toyonaka, Osaka

(Received November 1, 1968)

Eleven new complexes, *trans(N)*- or *cis(N)*-isomers of (ammoniatriacetato)(amino-acidato)-cobalt(III) ions, have been synthesized as their potassium salts, where the amino acids are glycine, β-alanine, γ-aminobutyric acid, sarcosine, L-alanine, L-serine, L-valine and L-proline. The geometrical isomers have been separated by ion-exchange column chromatography and their structures determined on the basis of their absorption spectra and proton magnetic resonance spectra. Stereoselectivity about the formation of the *trans* and *cis* isomers was found. The circular dichroism of the complexes containing optically active amino acidato ligands has been measured and discussed in relation to so-called vicinal contribution by the optically active ligands.

It has been recognized that the transition metal complexes, in which the configuration around the central metal ion is not chiral but the ligand coordinated has a kind of chiral configuration, show markedly the cotton effect in the d→d absorption bands of the central metal ion by so-called vicinal effect.[1] It has been pointed out that the CD curve due to the vicinal effect shows the split components of the d→d absorption bands more clearly than that of the configurational effect which arises from a chiral configuration near around the central metal ion.[2] These investigations have been achieved on the basis of the fact that the vicinal and the configurational contributions to the CD are separable and additive.[3,4] In these circumstances, it is thought to be desirable to study more in detail the vicinal contribution for various kinds of metal complexes. Two geometrical isomers, *trans(N)* and *cis(N)*, are possible for the (ammoniatriacetato)(L-amino-acidato)cobalt(III) ion, $[Co(ata)(L\text{-}am)]^-$, where the ata and the L-am are coordinated as a tetradentate and a bidentate ligand respectively.*1 Both the isomers of this complex have no chiral configuration near around the central cobalt(III) ion in a first approximation but have the vicinal CD contribution mainly due to an asymmetric carbon atom of the ligand amino acid ion.

The present study is concerned with the preparation, the d→d absorption spectra and CD spectra of the *trans(N)*- and *cis(N)*-K[Co(ata)(am)] complexes including both optically active and non-active amino acid ions as the bidentate ligand am. Only one complex, *cis(N)*-K[Co(ata)(gly)]·$2H_2O$,

1) For the octahedral cobalt(III) complexes: Y. Shimura, This Bulletin, **31**, 315 (1958); J. Fujita, T. Yasui and Y. Shimura, *ibid.*, **38**, 654 (1965); T. Yasui, J. Hidaka and Y. Shimura, *ibid.*, **39**, 2417 (1966).

2) C. T. Liu and B. E. Douglas, *Inorg. Chem.*, **3**, 1356 (1964).

3) B. E. Douglas and S. Yamada, *ibid.*, **4**, 1561 (1965). B. E. Douglas, *ibid.*, **4**, 1813 (1965); J. I. Legg, D. W. Cooke and B. E. Douglas, *ibid.*, **6**, 700 (1967); M. Shibata, H. Nishikawa and Y. Nishida, *ibid.*, **7**, 9 (1968); K. Yamasaki, J. Hidaka and Y. Shimura, This Bulletin, **42**, 119 (1969).

4) D. A. Buckingham, S. F. Mason, A. M. Sargeson and K. R. Turnbull, *Inorg. Chem.*, **5**, 1649 (1966).

*1 The abbreviation "ata" represents a tervalent ammoniatriacetate ion, $N(CH_2COO)_3^{3-}$ and "am" a univalent amino acid ion in general, and "gly" glycinate, "β-ala" β-alaninate, "γ-ambut" γ-aminobutyrate, "sar" sarcosinate, "L-ala" L-alaninate, "L-ser" L-serinate, "L-val" L-valinate, and "L-pro" L-prolinate ion.

has been known[5] in this group.

Experimental

Preparation of Potassium (Ammoniatriacetato)-(amino-acidato)cobaltate(III): K[Co(ata)(am)]·n-H_2O. A solution of 10.2 g of cobalt(II) acetate tetrahydrate in 20 m*l* of water was added to a solution containing 8.0 g of ataH_3 in 15 m*l* of 2 N potassium hydroxide. To this 6.0 g of lead dioxide was added and the resulting mixture was mechanically stirred at 60°C for about 30 min. The color of the solution changed from dark red to blue violet. After the mixture had been cooled to room temperature, an excess of lead dioxide was filtered off. To the filtrate a calculated amount of the amino acid concerned was added and the solution was mechanically stirred at 60°C until its color changed to reddish violet. The solution was cooled in an ice bath for one hour and a small quantity of insoluble material precipitated was filtered off. The reddish violet filtrate was treated as follows; as in (1) for the glycinato, sarcosinato and L-serinato complexes and as in (2) for the other amino acidato complexes. (1): A large amount of ethanol was added to the filtrate. The reddish violet deposit was filtered and washed with methanol and ether, and then dried in a vacuum desiccator. The yield was approximately 14 g. (2): In order to remove the lead(II) ion, 3.7 g of potassium sulfate was added to the filtrate and the mixed solution was thoroughly stirred at 60°C. After the resulting solution had been cooled to room temperature, the lead sulfate precipitated was filtered off. The filtrate was concentrated to the syrup on a vacuum evaporator. This syrup was diluted by adding an appropriate amount of methanol and then the insoluble by-products were filtered off. It was confirmed, by the column chromatographic method, that the by-products were not the complex desired. A large amount of ethanol-ether mixture (1 : 1) was added to the filtrate. The reddish violet product deposited was filtered and washed with methanol-ether mixture and ether, and then dried in a vacuum desiccator. The yield was approximately 7 g.

Separation of *trans*(*N*)- and *cis*(*N*)-K[Co(ata)·(am)]·$n$$H_2O$. Each of the products obtained in (1) or (2) was separated into the *trans*(*N*) and *cis*(*N*) isomers by the column chromatographic method. Namely, about 7 g of the crude product was dissolved in water and passed through a column (30 mm×500 mm) containing strong anion exchange resin(Dowex 1X-8, 100—200 mesh, chloride form). After the column had been swept with water, the adsorbed band was eluted with 0.07 N aqueous solution of potassium chloride at a rate of about 2.5 m*l* per min. By elution with 0.07 N potassium chloride, two colored bands, a reddish purple one and a violet one, were eluted in this order and completely separated from each other. The earlier fraction was confirmed to be the *trans*(*N*) isomer and the one eluted later to be the *cis*(*N*) isomer by the measurement of their absorption spectra.[5,6]

Each of the eluates was concentrated to dryness on a vacuum evaporator. The resulting crude complexes, which were contaminated with a small amount of potassium chloride, were treated as follows. In the case of the *trans*(*N*) isomers of the glycinato, sarcosinato and L-serinato complexes and of all the *cis* isomers, the crude complex was dissolved in a least amount of water as possible and less soluble potassium chloride was filtered off. The complex desired was obtained by adding methanol, little by little, to the filtrate. It was then recrystallized from water by adding methanol, washed with a water-methanol, methanol and then ether, and dried in air.

On the other hand, each of the *trans*(*N*) complexes other than the glycinato, sarcosinato and L-serinato ones was dissolved in methanol at 50°C. After the potassium chloride remaining in solid had been filtered off, the filtrate was kept in a refrigerator overnight. The complex deposited was gathered by filtration and washed with a small amount of methanol and ether, and then dried in air. The complex was recrystallized from hot methanol containing a small amount of water.

The *cis* isomers of the β-alaninato, γ-aminobutyrato and sarcosinato complexes could not be isolated because of their negligible yields. In the elution of L-prolinato

Table 1. Analytical results (amounts in %)

Complex	C		H		N	
	Found	Calcd	Found	Calcd	Found	Calcd
trans(*N*)-K[Co(ata)(gly)]·$2H_2O$	24.45	24.25	3.10	3.57	7.04	7.07
cis(*N*)-K[Co(ata)(gly)]·$2H_2O$	24.35	24.25	3.36	3.57	7.12	7.07
trans(*N*)-K[Co(ata)(β-ala)]·$2H_2O$	26.01	26.34	3.98	3.94	6.79	6.83
trans(*N*)-K[Co(ata)(γ-ambut)]·$3H_2O$	27.22	27.15	4.31	4.57	6.22	6.33
trans(*N*)-K[Co(ata)(sar)]·H_2O	27.83	27.55	3.44	3.61	7.05	7.14
trans(*N*)-K[Co(ata)(L-ala)]·$2.5H_2O$	25.77	25.78	4.05	4.09	6.59	6.68
cis(*N*)-K[Co(ata)(L-ala)]·$3H_2O$	25.41	25.24	3.91	4.24	6.46	6.54
trans(*N*)-K[Co(ata)(L-ser)]·H_2O	26.40	26.48	3.41	3.46	6.84	6.86
cis(*N*)-K[Co(ata)(L-ser)]·$2H_2O$	25.09	25.36	3.81	3.79	6.54	6.57
trans(*N*)-K[Co(ata)(L-val)]·$3H_2O$	28.80	28.95	4.70	4.87	6.08	6.14
cis(*N*)-K[Co(ata)(L-val)]·$4H_2O$	28.02	27.85	4.63	5.11	5.91	5.91
trans(*N*)-K[Co(ata)(L-pro)]·$3H_2O$	29.21	29.08	4.27	4.45	6.10	6.17

5) J. Hidaka, Y. Shimura and R. Tsuchida, This Bulletin, **35**, 567 (1962).

6) N. Matsuoka, J. Hidaka and Y. Shimura, This Bulletin, **40**, 1868 (1967).

complex, the violet band (*cis* isomer) was not observed; only the *trans*(*N*) isomer (reddish purple band) was isolated.

All of the complexes reported here are soluble in water. Of these complexes the *trans* isomers are soluble in methanol except those of the glycinato, sarcosinato and L-serinato complexes, which are sparingly soluble, while all the *cis* isomers are insoluble in methanol.

The results of the chemical analyses for all the complexes prepared are shown in Table 1.

Measurements. The electronic absorption spectra of the complexes were measured by a Beckman DU spectrophotometer. The CD spectra were recorded with a Roussel-Jouan dichrograph and the RD curves with a Yanagimoto recording spectropolarimeter model-185. All the measurements were made in aqueous solutions at room temperature.

The proton magnetic resonance (PMR) spectra of the complexes were obtained on a Japan Electron Optics JNM-4H-100 spectrometer operating at 100 Mc/sec, in deuterium oxide with NaTMS (sodium trimethylsilylpropanesulfonate) as an internal standard. The acidic solution (pH: about 0.6) was prepared by adding concentrated hydrochloric acid to the deuterium oxide solution.

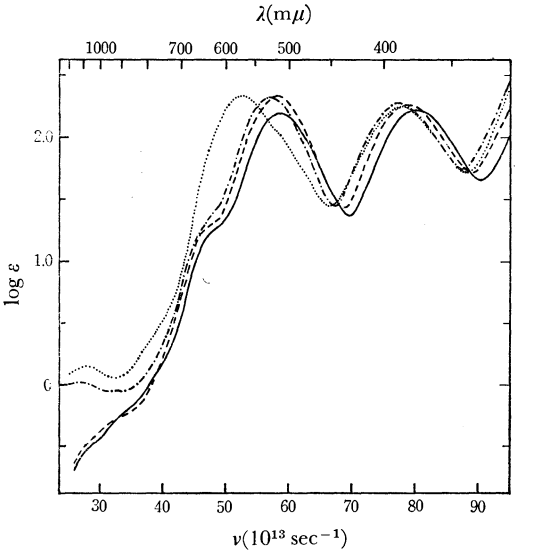

Fig. 1. Absorption curves of *trans*(*N*)-K[Co(ata)(am)]: (——) gly, (----) β-ala and (-·-·-) γ-ambut, and (·····) *cis*(*N*)-K[Co(ata)(L-ala)].

Results and Discussion

Stereoselectivity. As described in Experimental section, the column chromatographic investigation shows that the *trans*(*N*) isomer of L-prolinato complex is stereospecifically formed. This coincides with the consideration derived from the construction of molecular models. Namely, the stereospecificity of L-prolinato complex is attributed to the fact that the steric hindrance is remarkable between a pyrrolidine ring of the coordinated L-prolinate and one of the three acetate groups of ata in the *cis*(*N*) isomer. This consideration is also available in the case of *cis*(*N*) sarcosinato complex. A similar unbalanced formation is also observed in the case of β-alaninato or γ-aminobutyrato complex. Considering the formation of a trace amount of the *cis* isomer, it seems likely that the unbalance depends on the crowding of $-NH_2$ protons of the amino acid ion with the protons of the two acetate groups of ata in the *cis* isomers. This kind of crowding is expected to exist also in the *cis* isomers of glycinato or other L-aminoacidato complexes: so the pronounced unbalance in the case of the β-alaninato and γ-aminobutyrato complexes is mainly due to the instability of the six or seven membered chelate ring as compared with the five membered chelate ring.

Absorption Spectra. The absorption data of $[Co(ata)(am)]^-$ complex ions are summarized in Table 2 and their representative curves are shown in Fig. 1. It has been well known that *trans*-$[Co(O)_4(N)_2]$-type complexes show more remarkable splitting than *cis* isomers in their first absorption bands.[6-8] The first absorption bands of the reddish purple complexes obtained in the present study show quite similar splitting patterns, and this absorption behavior points out that the reddish purple complexes have the *trans*(*N*) structure (Fig. 1). In the first band of *trans*-$[Co(O)_4(N)_2]$-type complexes, it may be of interest that the ratio, $\{\log \varepsilon_{max}(\text{sub.})/\log \varepsilon_{max}(\text{major})\}$, of a sub- and a major-band for the complexes with tridentate ligand is smaller than those for the complexes with bidentate ligand.[5,9,10] This situation also stands for the present *trans*(*N*) complexes.

In the absorption curves of the violet complexes, a vague shoulder is observed at the shorter wavelength side of the major peak of the first absorption band (at *ca.* 570 mμ). This pattern shows that the violet complex is the *cis*(*N*) isomer.[6]

Proton Magnetic Resonance Spectra. In order to confirm the structure of the complexes, the PMR spectra of *cis*(*N*)-$[Co(ata)(gly)]^-$ and *trans*(*N*)-$[Co(ata)(L\text{-}ala)]^-$ ions were measured in deuterium oxide (Fig. 2) and in acidic deuterium oxide solution. Recently, Smith and Sawyer[10] discussed the PMR spectra of the ata complexes, $[Co(ata)(OH)(OH_2)]^-$ and *trans*(*N*)-$[Co(ataH)_2]^-$ and it has been shown that the methylene protons of the acetate groups of the complexes exhibit one symmetrical AB pattern and one singlet in the region of 4.6—3.7 ppm from NaTMS and that the chemical shift on the singlet, which was assigned to

7) J. Hidaka and Y. Shimura, This Bulletin, **40**, 2312 (1967).

8) H. Yamatera, *ibid.*, **31**, 95 (1958).

9) Unpublished results concerning bis(L-aspartato)-cobalt(III) complex.

10) B. B. Smith and D. T. Sawyer, *Inorg. Chem.*, **7**, 922 (1968).

TABLE 2. ABSORPTION MAXIMA OF [Co(ata)(am)]$^-$ IONS

Complex ion	I Band		II Band	
	ν_{max}	(log ε_{max})	ν_{max}	(log ε_{max})
trans(*N*)-[Co(ata)(gly)]$^-$	*ca.* 48	(1.3)	80.1	(2.22)
	58.7	(2.20)		
trans(*N*)-[Co(ata)(β-ala)]$^-$	*ca.* 48	(1.3)	79.0	(2.26)
	58.2	(2.33)		
trans(*N*)-[Co(ata)(γ-ambut)]$^-$	*ca.* 47	(1.3)	77.9	(2.26)
	57.0	(2.31)		
trans(*N*)-[Co(ata)(sar)]$^-$	*ca.* 48	(1.3)	80.2	(2.27)
	58.5	(2.23)		
trans(*N*)-[Co(ata)(L-ala)]$^-$	*ca.* 48	(1.3)	80.5	(2.24)
	58.7	(2.21)		
trans(*N*)-[Co(ata)(L-ser)]$^-$	*ca.* 48	(1.3)	80.4	(2.24)
	58.6	(2.23)		
trans(*N*)-[Co(ata)(L-val)]$^-$	*ca.* 48	(1.3)	80.7	(2.24)
	58.6	(2.21)		
trans(*N*)-[Co(ata)(L-pro)]$^-$	*ca.* 48	(1.3)	80.0	(2.28)
	58.5	(2.23)		
cis(*N*)-[Co(ata)(gly)]$^-$	52.8	(2.34)	78.0	(2.23)
cis(*N*)-[Co(ata)(L-ala)]$^-$	52.6	(2.33)	78.1	(2.23)
cis(*N*)-[Co(ata)(L-ser)]$^-$	52.4	(2.32)	78.1	(2.22)
cis(*N*)-[Co(ata)(L-val)]$^-$	52.3	(2.32)	77.9	(2.22)

The frequencies are given in 10^{13} sec^{-1}.

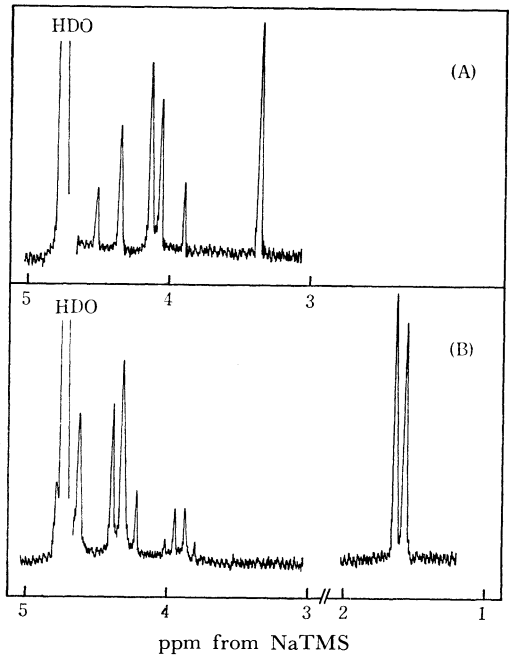

Fig. 2. PMR spectra in deuterium oxide: (A) *cis*(*N*)-K[Co(ata)(gly)] and (B) *trans*(*N*)-K[Co(ata)(L-ala)].

the protons of the uncoordinated acetate group of the latter complex, is much affected by the pH variation of the solution.

In the corresponding field, the spectra for the acetate protons of ata of the present complexes are quite similar to those reported by Smith and Sawyer, and all the peaks can be assigned as follows. For the glycinato complex (Fig. 2A), the AB pattern with centers at 4.41 and 3.99 ppm (J_{AB}= 17 cps) is assigned to the nonequivalent coupled acetate protons of two chelate rings of the ata, which are not co-planar with the glycinate ring, and the singlet at 4.12 ppm to the acetate protons of the third chelate ring of the ata, which is co-planar with the glycinate ring. The spectra of glycinato and L-alaninato complexes resemble each other, though a more complicated spectrum may be expected for the L-alaninato complex because all the acetate protons of ata have different environments. The AB pattern at 4.68 and 4.30 ppm (J_{AB}=17 cps) and the singlet at 4.30 ppm are assigned to the coordinated ata (Fig. 2B).

In acidic deuterium oxide solution (pH: about 0.6), no variation is observed in chemical shifts for all the peaks except the lowest field peak of AB pattern of the L-alaninato complex, which is overlapped by the HDO peak and shifts to down-field in acidic solution. These observations confirm that the ata functions as a tetradentate ligand.

The singlet at 3.35 ppm for the glycinato complex is assigned to the methylene protons of the glycinate chelate ring. For the L-alaninato complex, the AX_3 quartet at 3.90 ppm and the AX_3 doublet at 1.59 ppm, each with a coupling constant of 7 cps, are assigned to the methine proton and methyl protons of the L-alaninate chelate ring respectively.

These results agree with those reported by Buckingham and co-workers for several glycinato and L-alaninato complexes.[4,11]

Circular Dichroism. The CD or RD curves of the *trans*(*N*) ata complexes are quite similar to each other (Fig. 3), and the same relationship is also true for the CD or RD curves of the *cis*(*N*) ata complexes (Fig. 4).

As mentioned above, Liu and Douglas[2] pointed out that the existence of absorption components of the visible d→d transition band is shown more clearly through the CD due to the vicinal contribution than that due to the configurational one. Considering the symmetry of the *trans*(*N*) ata

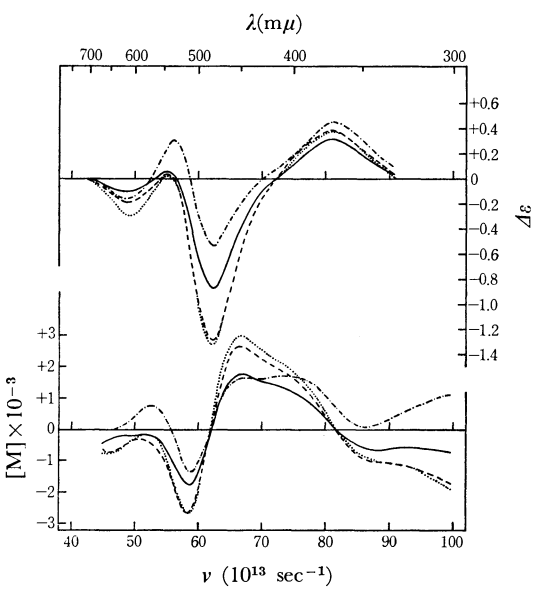

Fig. 3. CD (upper) and RD (lower) curves of *trans*(*N*)-K[Co(ata)(L-am)]: (——) L-ala, (----) L-ser, (·····) L-val and (-·-·-) L-pro.

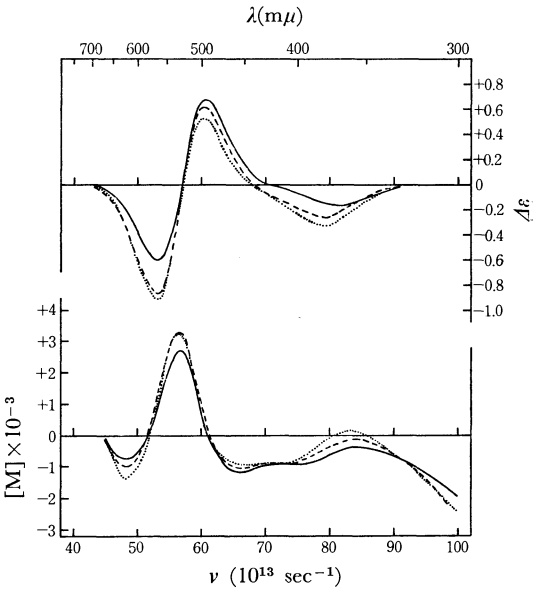

Fig. 4. CD (upper) and RD (lower) curves of *cis*(*N*)-K[Co(ata)(L-am)]: (——) L-ala, (----) L-ser and (·····) L-val.

TABLE 3. CD DATA OF [Co(ata)(L-am)]⁻ IONS

Complex ion	I Band		II Band	
	ν_{ext}	$(\Delta\varepsilon_{ext})$	ν_{ext}	$(\Delta\varepsilon_{ext})$
trans(*N*)-[Co(ata)(L-ala)]⁻	48.2	(−0.10)	81.5	(+0.30)
	55.3	(+0.06)		
	62.4	(−0.87)		
trans(*N*)-[Co(ata)(L-ser)]⁻	48.6	(−0.19)	81.1	(+0.38)
	55.2	(+0.04)		
	62.1	(−1.29)		
trans(*N*)-[Co(ata)(L-val)]⁻	48.8	(−0.29)	81.3	(+0.37)
	55.5	(+0.02)		
	62.1	(−1.32)		
trans(*N*)-[Co(ata)(L-pro)]⁻	48.5	(−0.16)	81.7	(+0.45)
	56.3	(+0.31)		
	62.2	(−0.54)		
cis(*N*)-[Co(ata)(L-ala)]⁻	53.1	(−0.60)	81.5	(−0.17)
	60.6	(+0.68)		
cis(*N*)-[Co(ata)(L-ser)]⁻	52.9	(−0.87)	79.7	(−0.26)
	60.4	(+0.61)		
cis(*N*)-[Co(ata)(L-val)]⁻	53.2	(−0.91)	78.9	(−0.33)
	60.2	(+0.53)		

The frequencies are given in 10^{13} sec^{-1}.

11) D. A. Buckingham, L. Durham and A. M. Sargeson, *Australian J. Chem.*, **20**, 257 (1967).

complex ion, the CD curves of the *trans*(N) complexes may be expected to split into three components.[2,7] In fact, the CD curves show the three components, a negative, a positive and a negative ones, listing from the longer wavelength side; on the contrary the absorption band splits into only two components in appearance (Figs. 1 and 3). This behavior resembles that of $[Co(ox)(\beta\text{-ala})_2]^-$ ion rather than that of $[Co(ox)(gly)_2]^-$ ion.[7]

The first absorption bands of *cis*(N) ata complexes split into two components as mentioned before. In the corresponding region, their CD curves show two components (a negative one and a positive one), as may be seen in Fig. 4.

From these facts, it may be concluded that the CD curve due to only the vicinal effect points out more clearly the absorption components than that due to the configurational chirality.

As shown in Table 3, the CD peaks are more intense for the ata complexes than those of the other optically active complexes which have only the so-called vicinal effect due to the optically active ligand.[1] Similar behavior was observed between the CD curves of triethylenetetramine and ethylenediamine complexes, and it was assumed that the fixed conformation of triethylenetetramine causes a greater effect than the rather mobile conformation of ethylenediamine.[12] Similar consideration may also be available for the present case.

12) C.-Y. Lin and B. E. Douglas, *Inorg. Nucl. Chem. Letters*, **4**, 15 (1968).

BULLETIN OF THE CHEMICAL SOCIETY OF JAPAN VOL. 42 1588—1595 (1969)

Spectroscopic Studies of the Structures of the Dimer of Diethylaluminum 2-Aminoethoxide $(AlEt_2OCH_2CH_2NH_2)_2$ and Related Compounds*[1]

Hideo SATO, Ryokichi TARAO and Hiromi HIGASHI

The Central Research Laboratories, Chisso Co., Ltd., Kamariya, Kanazawa-ku, Yokohama

(Received December 14, 1968)

The infrared and proton nuclear magnetic resonance spectra of the solutions of diethylaluminum 2-aminoethoxide $(AlEt_2OCH_2CH_2NH_2)_2$ and related compounds were measured. The infrared frequencies and intensities of the NH_2 stretching, scissors, and rocking vibration bands, and the NMR internal chemical shifts of the ethyl groups attached to the aluminum atom were compared with the corresponding data of suitable model compounds. It was concluded by taking the results of these experiments into consideration that $(AlEt_2OCH_2CH_2NH_2)_2$ was represented by the structural formula I with two Al←NH_2 coordination bonds. Similarly, most of the related compounds studied were reasonably represented by the formulas with two Al←NRR′ coordination bonds, while $(AlEt_2OCH_2CH_2N(C_6H_{11})_2)_2$ was assumed to be represented by formula III with two Al←O coordination bonds, exceptionally.

It has been reported by one of the authors and by Hurley and his coworkers that the reactions of triethylaluminum $(AlEt_3)_2$ with several aminoethanols ($HOCH_2CH_2NRR'$; R,R′=H, alkyl, cycloalkyl, and/or aryl groups) in the 1 : 1 molar ratio give the crystals of the dimers of diethylaluminum 2-aminoethoxides formulated as $(AlEt_2OCH_2CH_2NRR')_2$ quantitatively.[1-3] There are three possible structural formulas, I, II, and III, for these dimeric substances, $(AlEt_2OCH_2CH_2NRR')_2$:

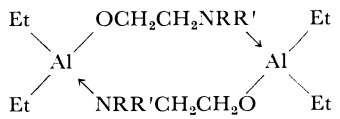

[I]

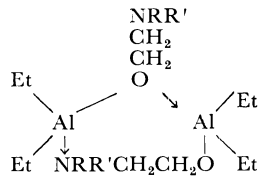

[II]

*1 Presented at the Symposium on Organometallic Compounds, Tokyo, October, 1968.

1) H. Higashi and S. Namikawa, *Kogyo Kagaku Zasshi (J. Chem. Soc. Japan, Ind. Chem. Sect.)*, **70**, 93, 368 (1967).

2) H. Higashi and K. Watabe, *ibid.*, **70**, 1800 (1967).

3) T. J. Hurley, M. A. Robinson, J. A. Scruggs and S. I. Trotz, *Chem. Abstr.*, **67**, 7582h (1967).

Table 1. Diethylaluminum 2-aminoalkoxides (new compounds)

Compound	Yield (%)	Al(%)		Mol wt		Mp, °C*1
		Found	Calcd	Found*2	Calcd	
$(AlEt_2OCH_2C(CH_3)_2NH_2)_2$	75.7	15.57	15.57	340.1	346.5	119—121.5
$(AlEt_2OCH_2CH(CH_3)NH_2)_2$	47.7	16.80	16.95	311.6	318.4	110.5—112.5
$(AlEt_2OCH_2CH(C_2H_5)NH_2)_2$	82.2	15.58	15.57	343.7	346.5	90—92.5

*1 Uncorrected.
*2 Determined by measuring the freezing point depression of benzene solution.

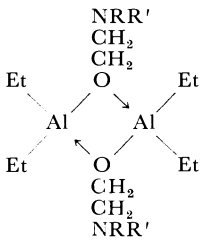

[III]

Formula I with a 10-membered ring has two Al←NRR' coordination bonds, formula II with a 7-membered ring has one Al←NRR' and one Al←O bond, and formula III with a 4-membered ring has two Al←O bonds. Several attempts were made by Higashi and by Hurley to assign the most probable formula on the basis of several experimental facts but no decisive evidence was obtained.[2,3] In this paper this problem will be investigated by the infrared (IR) and proton nuclear magnetic resonance (NMR) spectra of the solution of diethylaluminum 2-aminoethoxide $(AlEt_2OCH_2CH_2NH_2)_2$. At first, the IR and NMR spectra of ethylaluminum chloride-*n*-propyl amine coordination compounds—$AlEt_{3-m}Cl_m \cdot n\text{-}PrNH_2$ (m=0, 1, 2, 3)—will be studied and the results will be used to discuss the problem mentioned above.

Experimental

Preparation of the Samples. $(AlEt_2OCH_2CH_2NH_2)_2$, $(AlEt_2OCH_2CH_2NMeH)_2$, $(AlEt_2OCH_2CH_2NMe_2)_2$, $(AlEt_2OCH_2CH_2NEtH)_2$, $(AlEt_2OCH_2CH_2NEt_2)_2$, $(AlEt_2OCH_2CH_2NPhH)_2$, $(AlEt_2OCH_2CH_2NPh_2)_2$, $(AlEt_2OCH_2CH_2N_2(C_6H_{11})_2)_2$, $(AlEt_2OCH_2CH_2CH_2CH_2NH_2)_2$, and $(AlEt_2OCH(CH_3)CH_2NH_2)_2$ were prepared by the reactions of $(AlEt_3)_2$ with the corresponding alkanolamine, following the synthetic methods described in Refs. 1 and 2. $(Ali\text{-}Bu_2OCH_2CH_2NH_2)_2$ was prepared by the reaction of $Ali\text{-}Bu_3$ with monoethanolamine, following the method given in Ref. 3. $(AlEt_2OCH_2C(CH_3)_2NH_2)_2$, $(AlEt_2OCH_2CH(CH_3)NH_2)_2$, and $(AlEt_2OCH_2CH(C_2H_5)NH_2)_2$ were obtained by the reaction of $(AlEt_3)_2$ with the corresponding alkanolamine as transparent prismatic crystals. Since the last three substances are new compounds, their yields in syntheses, aluminum contents, measured molecular weights and melting points are summarized in Table 1.

Measurements of IR and NMR Spectra. The IR spectra of the dilute solutions of the samples (in general, the concentrations of the solutions were fixed to either 5.26 g/100 m*l* soln for the measurements using the cell of thickness of 0.1 mm or 1.10 g/100 m*l* soln for the measurements using the cell of thickness of 0.5 mm) were measured in the 4000—420 cm^{-1} region by using KRS-5 liquid fixed cell (thickness: 0.1 mm and/or 0.5 mm). Another cell of the same thickness filled with the solvent was put in the reference optical path to compensate the absorption of the solvent. A Japan Spectroscopic Co. Model DS-402G infrared spectrophotometer was used. In general, benzene was used as solvent except for the measurement in the 720—620 cm^{-1} region, in which the absorption of benzene was very intense. In the 720—620 cm^{-1} region, *p*-xylene was used because it was transparent in this region.

The NMR spectra were measured by Varian A-60 A high resolution NMR spectrometer at 60 Mc, 14092 gauss, and at room temperature. About 0.5 m*l* of the benzene solution of the sample (5% weight/volume solution) was injected into the sample tube by a hypodermic syringe under nitroegen atmosphere and sealed. The values of chemical shifts were represented by ppm units (standard: benzene, the field higher than benzene signal was taken as positive).

Results and Discussion

The Spectra of $AlEt_{3-m}Cl_m \cdot n\text{-}PrNH_2$ (m= 0, 1, 2, 3). The NMR spectra of the equimolar mixtures of $(AlEt_{3-m}Cl_m)_2$ (m=0, 1, 2) and $n\text{-}PrNH_2$ in benzene were measured. The internal

Table 2. NMR spectra of $AlEt_{3-m}Cl_m \cdot n\text{-}PrNH_2$ (m=0, 1, 2); the internal chemical shifts (δ) of al-Et groups

	δ (ppm)
$AlEt_3 \cdot n\text{-}PrNH_2$	−1.30
$AlEt_2Cl \cdot n\text{-}PrNH_2$	−1.16
$AlEtCl_2 \cdot n\text{-}PrNH_2$	−1.04

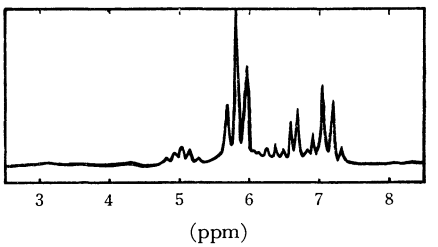

Fig. 1. The NMR spectrum of $AlEt_3 \cdot n\text{-}PrNH_2$.

Table 3. Observed IR frequencies of $AlEt_{3-m}Cl_m \cdot n\text{-}PrNH_2$ ($m=0$, 1, 2, 3)*1,*2

$AlEt_3 \cdot n\text{-}PrNH_2$	$AlEt_2Cl \cdot n\text{-}PrNH_2$	$AlEtCl_2 \cdot n\text{-}PrNH_2$	$AlCl_3 \cdot n\text{-}PrNH_2$	$n\text{-}PrNH_2$	Assignment
			3319 w		
3320 m	3298 m	3274 m	3262 m	3390 w	NH_2 antisym. str.
3268 m	3252 m	3234 m	3224 m	3330 vw	NH_2 sym. str.
	3133 vw	3126 vw			
2959 sh	2966 w	2967 m	2966 m	2959 vs	CH str.
2936 vs	2938 s	2941 m	2935 w	2928 s	
2895 s	2899 s	2902 m	2895 vw	2872 m	
2855 vs	2861 vs	2867 m	2876 w	2859 sh	
2789 w	2791 w	2791 vw		2752 vw	
2718 vw					
1578 m	1576 m	1571 m	1571 m	1626 w	NH_2 scissors
1449 w	1457 m	1455 m	1448 w	1451 m	
1411 m	1410 w	1407 w			
	1387 w	1388 w			
1374 w	1376 w	1377 vw	1383 vw	1381 w	
1314 vw	1317 w	1319 w	1318 w	1295 vw	
1275 vw	1274 vw	1276 vw	1275 w	1260 vw	
	1221 vw		1206 sh		
1184 m	1192 m	1201 m	1186 m		
1160 m					
1074 s	1084 m	1091 m	1080 m	1094 vw	
	1046 w	1040 w		1071 m	
982 s	988 s	986 m	990 w		
			974 w	975 w	
946 m	952 m	946 w	956 w		
			941 vw		
916 w	918 w	920 vw			
	888 w	887 w	888 w	897 s	
	877 vw	878 vw	879 sh		
	847 vw	845 vw	849 vw		
				810 s	NH_2 wag
663 vs	673 s	673 s	673 m		NH_2 rock,
651 vs	668 s		662 m		AlC str.
	636 sb	626 s	601 w		CH_2 rock (AlC_2H_5)
		575 w			
	541 w	537 w	532 s		
		525 m	526 s		
492 vw	483 vw	491 s	499 w		
			467 s		

*1 m, medium; s, strong; w, weak; v, very; b, broad.
*2 4000—720 cm^{-1} and 620—420 cm^{-1}; benzene solution.
720—620 cm^{-1}; *p*-xylene solution.

chemical shifts (δ) of the ethyl group attached to the Al atom (hereafter abbreviated as the al-Et group) are shown in Table 2. The NMR spectrum of $AlEt_3 \cdot n\text{-}PrNH_2$ is shown in Fig. 1. Although in benzene solution the solvent effect on the chemical shift values of the NMR signals of the solute is very large, such an effect can be neglected so far as the internal chemical shift value ($\delta = \delta_{CH_3} - \delta_{CH_2}$) of the compounds of CH_3CH_2X type is concerned.[4] It has been known that in ethylaluminum compounds the magnetic anisotropy of the atom in the β-position relative to the methylene group affects the δ value of the al-Et group.[5] The δ value of the al-Et group of $AlEt_3 \cdot n\text{-}PrNH_2$ is -1.30 ppm, which is almost equal to the δ value of the al-Et group in $AlEt_3 \cdot NEt_3$ (-1.29 ppm).

The IR spectra of the equimolar mixtures of $(AlEt_{3-m}Cl_m)_2$ ($m=0$, 1, 2, 3) and $n\text{-}PrNH_2$ in benzene and in *p*-xylene were measured. The spectra in the 4000—2700 cm^{-1} region are shown in Fig. 2. The frequencies and the intensities (qualitative) are shown in Table 3, and these data for the NH_2 stretchings and NH_2 scissors are summarized in Table 4. The bands at 3390 and 3330 cm^{-1} of $n\text{-}PrNH_2$ correspond to the bands at 3389 and 3323 cm^{-1} found by Wolff and Schmidt in carbon tetrachloride solution and assigned to the NH_2 antisymmetric and symmetric stretching vibrations, respectively, by them.[6] The band at 1626 cm^{-1} is assigned to the NH_2 scissors. All of these three bands—the NH_2 antisymmetric and symmetric stretchings and the NH_2 scissors—shift to lower frequencies and their intensities increase when $n\text{-}PrNH_2$ forms coordination compounds with $AlEt_{3-m}Cl_m$. As regards the magnitudes of the shifts and the intensities of these three bands caused by the coordination bond formation with

4) P. T. Narasimhan and M. T. Rogers, *J. Am. Chem. Soc.*, **82**, 34 (1960).
5) O. Yamamoto, This Bulletin, **36**, 1463 (1963).
6) H. Wolff and U. Schmidt, *Ber. Bunsenges. Physik. Chem.*, **68**, 579 (1964).

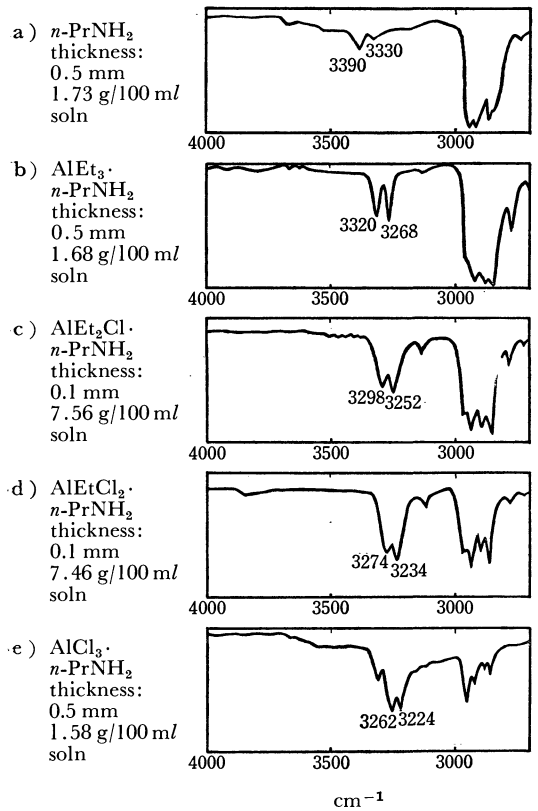

Fig. 2. The IR spectra of $AlEt_{3-m}Cl_m \cdot n\text{-}PrNH_2$ ($m=0$, 1, 2, 3).

Table 4. The frequencies and intensities (molar extinction coefficients: l/cm·mol—shown in parentheses) of the NH_2 vibration bands of $AlEt_{3-m}Cl_m \cdot n\text{-}PrNH_2$ ($m=0$, 1, 2, 3)

	$\gamma_{as}(NH_2)$ cm^{-1}	$\gamma_s(NH_2)$ cm^{-1}	$\delta(NH_2)$ cm^{-1}
$n\text{-}PrNH_2$	3390 (8.7)	3330 (4.9)	1626 (10)
$AlEt_3 \cdot n\text{-}PrNH_2$	3320 (44)	3268 (50)	1578 (68)
$AlEt_2Cl \cdot n\text{-}PrNH_2$	3298 (70)	3252 (80)	1576 (100)
$AlEtCl_2 \cdot n\text{-}PrNH_2$	3274 (94)	3234 (113)	1571 (93)
$AlCl_3 \cdot n\text{-}PrNH_2$	3262 (121)	3224 (113)	1571 (98)

$(AlEt_3)_2$, $(AlEt_2Cl)_2$, $(AlEtCl_2)_2$, and $(AlCl_3)_2$, the shifts and the intensities (molar extinction coefficients) increase in this order. This observation can be explained by the well-known fact that the electron-accepting tendency of $AlEt_{3-m}Cl_m$ becomes larger in the order of $m=0$, 1, 2, 3, and corresponds with the fact that the lower frequency shifts of the COC stretching absorption bands of diethyl ether (Et_2O) in the coordination compound $AlEt_{3-m}Cl_m \cdot Et_2O$ become larger in the order of $m=0$, 1, 2, 3.[7]

The IR Spectrum of $(AlEt_2OCH_2CH_2NH_2)_2$. The IR spectrum of the solution of $(AlEt_2OCH_2CH_2NH_2)_2$ is shown in Figs. 3a and 3b, together with the spectrum of the solution of $(AlEt_2OCH_2CH_2NMe_2)_2$ in Fig. 3c. The tentative assignments of the principal absorption bands given in Table 5 are made by taking the assignments of $(AlEt_2OEt)_2$,[8] ethanol,[9] ethylamine,[10] and $n\text{-}PrNH_2$,[6] into consideration.

Two sharp bands at 3375 and 3309 cm^{-1} are assigned to the NH_2 antisymmetric and symmetric

Table 5. Observed IR frequencies of $(AlEt_2OCH_2CH_2NH_2)_2$—benzene solution—and assignment*1

	Assignment
3375 w	NH_2 antisymmetric str.
3309 vw	NH_2 symmetric str.
2935 s	CH_3 degenerate str. (AlC_2H_5), overtone of CH_3 deform. (AlC_2H_5)
2892 s	CH_2 antisymmetric str. (AlC_2H_5, $OC_2H_4NH_2$)
2858 vs	CH_3 symmetric str. (AlC_2H_5),
2793 w	CH_2 symmetric str. (AlC_2H_5, $OC_2H_4NH_2$)
2718 vw	
1590 m	NH_2 scissors
1454 w	CH_3 degenerate deform., CH_3 symmetric deform. (AlC_2H_5), CH_2 scissors (OCH_2)
1414 w	CH_2 scissors (AlC_2H_5), CH_2 scissors (CH_2NH_2)
1368 w	CH_2 wag (CH_2NH_2)
1281 w	CH_2 wag (OCH_2), CH_2 twist ($OC_2H_4NH_2$)
1256 w	
1228 vw	
1190 m, 1108 s	CH_2 wag, CH_2 twist (AlC_2H_5); CH_3 rock (AlC_2H_5), NH_2 twist
1051 vw, 1016 s	CCN anti-phase str.; CCO anti-phase str.
974 s	CC str.
950 w	
902 m, 868 w	CCO in-phase str.; CCN in-phase str., NH_2 wag
664 vs*2, 639 vs*2	AlC_2 antisymmetric str. B_{1u}, NH_2 rock; CH_2 rock (AlC_2H_5)
565 vw	
478 w	AlC_2 symmetric str. B_{3u}

*1 m, medium; s, strong; w, weak; v, very.
*2 *p*-xylene solution.

7) S. Takeda and R. Tarao, This Bulletin, **33**, 1567 (1965).
8) R. Tarao, *ibid.*, **39**, 2126 (1966).
9) C. Tanaka, *Nippon Kagaku Zasshi (J. Chem. Soc. Japan, Pure Chem. Sect.)*, **81**, 1042 (1960); **83**, 398, 521, 657, 661, 792 (1962).
10) C. Matsuoka, A. Hirakawa, K. Tamagake and M. Tsuboi, Preprints for the 19th Annual Meeting of the Chemical Society of Japan (April, 1966), 1C 204.

a) $(AlEt_2OCH_2CH_2NH_2)_2$, 4000—420 cm^{-1}

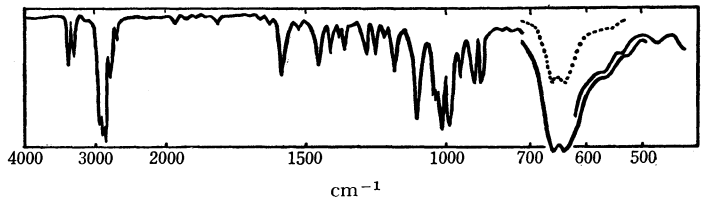

b) $(AlEt_2OCH_2CH_2NH_2)_2$, 4000—2700 cm^{-1}

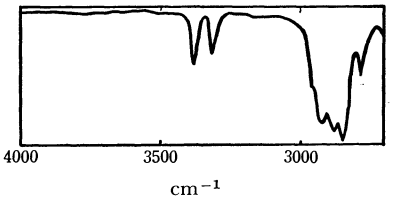

c) $(AlEt_2OCH_2CH_2NMe_2)_2$, 4000—420 cm^{-1}

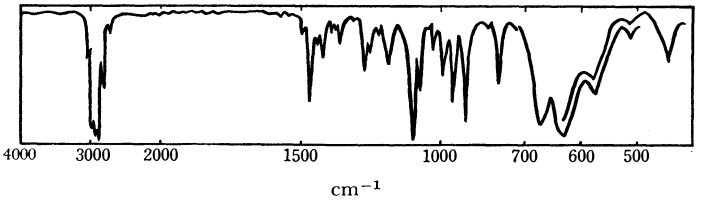

Fig. 3. The IR spectra of $(AlEt_2OCH_2CH_2NH_2)_2$ and $(AlEt_2OCH_2CH_2NMe_2)_2$.
Cell thickness: 0.1 mm
Concentration: a) Real Line: 5.26 g/100 m*l* soln.
Dotted Line: 1.10 g/100 m*l* soln.
b) 5.26 g/100 m*l* soln.
c) 6.22 g/100 m*l* soln.

stretching vibrations respectively. These assignments are consistent with the fact that these two bands disappear in the spectrum of $(AlEt_2OCH_2CH_2NMe_2)_2$.

A sharp band at 1590 cm^{-1} is assigned to the NH_2 scissors. $(HgNH_2)^+$ has a sharp band due to the NH_2 scissors at 1543 cm^{-1}.[11] This band disappears in the spectra of $(AlEt_2OCH_2CH_2NMeH)_2$ and $(AlEt_2OCH_2CH_2NMe_2)_2$.

The broad and strong band at 664 cm^{-1} is assigned to the NH_2 rocking band overlapped by the AlC_2 antisymmetric stretching band. As shown in Fig. 4, this band (AlC_2 antisymmetric stretching) is much narrower in $(AlEt_2OEt)_2$, $(AlEt_2OCH_2CH_2NMeH)_2$, and $(AlEt_2OCH_2CH_2NMe_2)_2$, in which no NH_2 group exists. In each spectrum of $AlEt_{3-m}Cl_m \cdot n\text{-}PrNH_2$ ($m=0$, 1, 2, 3), there is a band of considerable intensity at about 670—660 cm^{-1}, which can be assigned to the NH_2 rocking, as shown in Table 3. In $(HgNH_2)^+$, the NH_2 rocking band appears at 668 cm^{-1}. These facts support this assignment.

Next, the problem to assign the most probable formula from among I, II, and III as the structural formula of the dimer $(AlEt_2OCH_2CH_2NH_2)_2$ will be discussed by taking the IR spectroscopic observations described above into consideration. The frequencies and intensities of the NH_2 stretchings, scissors, and rocking of $(AlEt_2OCH_2CH_2NH_2)_2$ will be compared with the frequencies and intensities of these bands of $AlEt_3 \cdot n\text{-}PrNH_2$, in which the NH_2 group coordinates with Al atom, and of $n\text{-}PrNH_2$ in dilute solution, in which the NH_2 group does not coordinate with any atom. The detailed discussion will be given below.

As described previously the NH_2 antisymmetric and symmetric stretching bands of $(AlEt_2OCH_2CH_2NH_2)_2$ exist at 3375 cm^{-1} (molar extinction coefficient, $\kappa=58$ *l*/cm·mol) and 3309 cm^{-1} ($\kappa=42$), respectively. In $n\text{-}PrNH_2$, these appear at 3390 cm^{-1} ($\kappa=8.7$) and 3330 cm^{-1} ($\kappa=4.9$) respectively. On the other hand, in $AlEt_3 \cdot n\text{-}PrNH_2$, these appear at 3320 cm^{-1} ($\kappa=44$) and 3268 cm^{-1} ($\kappa=50$) respectively. The data of frequencies do not make clear the problem whether the NH_2 group coordinates to the Al atom or not. The values of molar extinction coefficients of $(AlEt_2OCH_2CH_2NH_2)_2$, however, are almost equal to the values of $AlEt_3 \cdot n\text{-}PrNH_2$, and too large for the NH_2 group not to be coordinated with the Al atom. The lower frequency shift and the increase of

11) S. Mizushima, I. Nakagawa and D. M. Sweeny, *J. Chem. Phys.*, **25**, 1006 (1956).

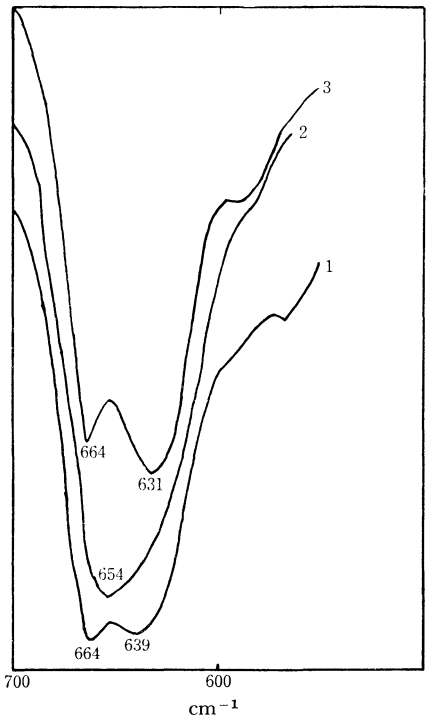

Fig. 4. The IR bands containing the NH_2 rocking band (superposed by the AlC_2 antisymmetric stretching and the CH_2 rocking band of al-Et group). Cell thickness: 0.1 mm, *p*-xylene solution.
1. $(AlEt_2OCH_2CH_2NH_2)_2$ 5.26 g/100 m*l* soln.
2. $(AlEt_2OEt)_2$ 5.26 g/100 m*l* soln.
3. $(AlEt_2OCH_2CH_2NMeH)_2$ 5.75 g/100 m*l* soln.

the intensity of the NH_2 antisymmetric and symmetric stretching vibration bands caused by the coordination of the NH_2 group are generally interpreted by the increase of the polar character of the N–H bond owing to the coordination bond formation.[12]

The NH_2 scissors band of $(AlEt_2OCH_2CH_2NH_2)_2$ exists at 1590 cm^{-1} (κ=69). The frequency and the intensity of this band are almost equal to the values of the corresponding bands of $AlEt_3$·*n*-$PrNH_2$ (1578 cm^{-1}, κ=68), and different from the values of the corresponding bands of *n*-$PrNH_2$ (1626 cm^{-1}, κ=10).

The NH_2 rocking band of $(AlEt_2OCH_2CH_2NH_2)_2$ exists at 664 cm^{-1}; this frequency coincides with the frequencies of the NH_2 rocking bands of $AlEt_{3-m}Cl_m$·*n*-$PrNH_2$ (m=0, 1, 2, 3), though the intensity is uncertain owing to the superposition of the band with the AlC_2 antisymmetric stretching band.

These observations apparently support formula I; they cannot be interpreted reasonably by assuming either formula II or III.

The relative intensities and frequencies of all bands (including the NH_2 stretching and the NH_2 scissors) remained unchanged when the concentration of $(AlEt_2OCH_2CH_2NH_2)_2$ in the solution was changed from 1.10 g/100 m*l* to 10.0 g/100 m*l*; this implies that intermolecular hydrogen bondings are not present. The relation between the concentrations and the molar extinction coefficients are shown in Table 6.

In Table 7, the frequencies and the molar extinction coefficients of the NH_2 stretching and scissors bands are shown for $(AlEt_2OCH_2CH_2NH_2)_2$ and six related compounds. It is apparent from these data that the dimers of these six related compounds also take the structures with two Al←NH_2 coordination bonds, in other words the structures corresponding to formula I.

The NMR Spectrum of $(AlEt_2OCH_2CH_2NH_2)_2$. The NMR spectrum of the solution of $(AlEt_2OCH_2CH_2NH_2)_2$ is shown in Fig. 5. For the sake of comparison, the spectrum of $(AlEt_2OCH_2CH_2NMe_2)_2$ is shown in Fig. 6. The broad signal at 6.3 ppm present in Fig. 5 is assigned to the NH_2 protons because it disappears in Fig. 6. The quintet at 5.17 ppm present in Fig. 5 turns to a triplet in Fig. 6. This quintet can be assigned to the NCH_2 protons because this change (quintet→triplet) is interpreted as due to the presence or the absence of the spin-spin coupling with the NH_2 protons. The assignments of the rest of the signals can also be easily made as shown in these figures by considering the signal intensities and the spin-spin couplings. In Fig. 7, the chemical shifts of methyl and methylene protons of the al-Et groups of $(AlEt_2OCH_2CH_2NH_2)_2$ and twelve related compounds are shown. For the sake of comparison, the corresponding chemical shifts of $(AlEt_3)_2$ and $(AlEt_2OEt)_2$ are also shown in this figure.

Table 6. The concentration dependence of the intensities (molar extinction coefficients: l/cm·mol) of the NH_2 vibration bands of $(AlEt_2OCH_2CH_2NH_2)_2$

Concentration		$\gamma_{as}(NH_2)$ 3375 cm^{-1}	$\gamma_s(NH_2)$ 3309 cm^{-1}	$\delta(NH_2)$ 1590 cm^{-1}
g/100 m*l*	(mol/cm^3)×10^3			
1.10	0.0759	57	41	61
5.26	0.3623	58	42	69
10.0	0.6887	60	43	69

12) I. Nakagawa, *Kagaku no Ryoiki (J. Japanese Chem.)*, **22**, 281 (1968).

Table 7. The frequencies and intensities (molar extinction coefficients: l/cm·mol— shown in parentheses) of the NH_2 vibration bands of $(AlEt_2OCH_2CH_2NH_2)_2$ and related compounds

	$\gamma_{as}(NH_2)$ cm^{-1}	$\gamma_s(NH_2)$ cm^{-1}	$\delta(NH_2)$ cm^{-1}
$(AlEt_2OCH_2CH_2NH_2)_2$	3375 (58)	3309 (42)	1590 (69)
$(AlEt_2OCH_2CH_2CH_2NH_2)_2$	3354 (28)	3296 (19)	1586 (57)
$(AlEt_2OCH(CH_3)CH_2NH_2)_2$	3380 (47)	3319 (31)	1589 (59)
$(Al\text{-}i\text{-}Bu_2OCH_2CH_2NH_2)_2$	3374 (54)	3309 (35)	1589 (70)
$(AlEt_2OCH_2C(CH_3)_2NH_2)_2$	3359 (43)	3298 (28)	1584 (84)
$(AlEt_2OCH_2CH(CH_3)NH_2)_2$	3364 (53)	3296 (28)	1587 (73)
$(AlEt_2OCH_2CH(C_2H_5)NH_2)_2$	3369 (43)	3294 (23)	1583 (70)

As mentioned previously, in ethylaluminum compounds the magnetic anisotropy of the atom in the β-position relative to the methylene group affects the δ value of the al-Et group. For this reason, it seems quite possible to choose the most probable formula among I, II, and III as the formula of $(AlEt_2OCH_2CH_2NH_2)_2$ by considering the δ value of the al-Et group, independent of the assumption based on the IR spectroscopic observations.

The δ value of the al-Et group of $(AlEt_2OEt)_2$, which can be regarded as a model compound of the formula III, is -1.14 ppm, as shown in Fig. 7. The corresponding δ values of $(AlEt_2OCH_2CH_2NH_2)_2$ and related compounds are, except for the following three compounds, $(AlEt_2OCH_2CH_2NPhH)_2$, $(AlEt_2OCH_2CH_2NPh_2)_2$, and $(AlEt_2OCH_2CH_2N(C_6H_{11})_2)_2$, always -1.31——-1.38 ppm; these values differ from the δ value of $(AlEt_2OEt)_2$ by about 0.2 ppm.

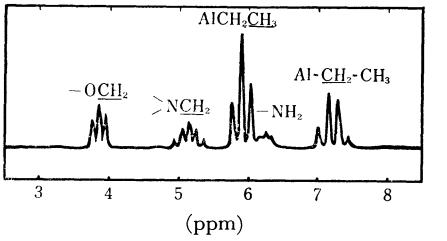

Fig. 5. The NMR Spectrum of $(AlEt_2OCH_2CH_2NH_2)_2$.

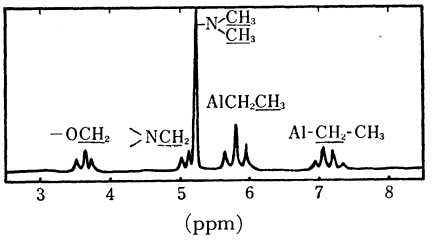

Fig. 6. The NMR spectrum of $(AlEt_2OCH_2CH_2NMe_2)_2$.

If formula III is assumed, this difference of the δ value should be interpreted as the effect of the N atom exerted through two methylene groups. The fact that the δ value of $(AlEt_2OCH_2CH_2CH_2NH_2)_2$ is -1.37 ppm is, however, the strong evidence against this interpretation. The δ value of the ethyl group of $HOCH_2CH_2NEt_2$ is 1.47

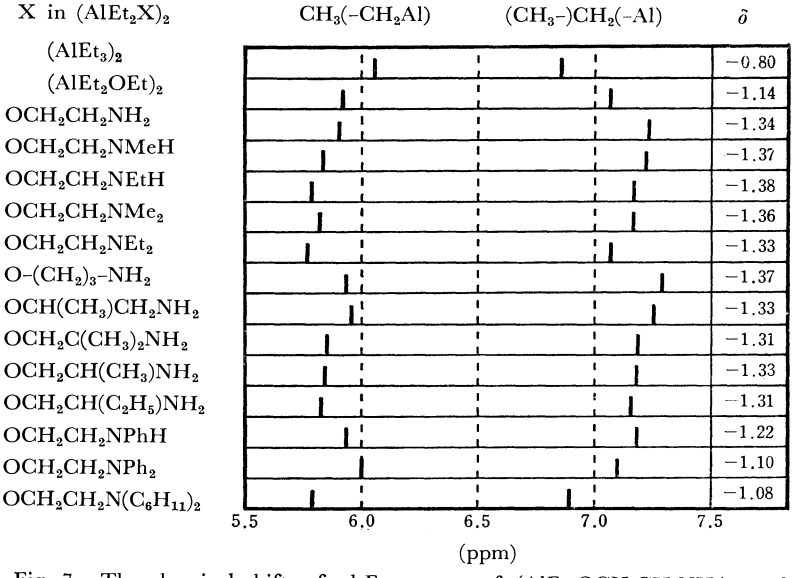

Fig. 7. The chemical shifts of al-Et groups of $(AlEt_2OCH_2CH_2NH_2)_2$ and related compounds.

ppm in benzene, and the δ value of the ethyl group of $(AlEt_2OCH_2CH_2NEt_2)_2$ attached to the N atom is 1.80 ppm. This difference of the δ value is reasonably interpreted by the decrease of the electron density of the N atom caused by the coordination of unshared electron pair of the N atom with the Al atom.

Next, if formula II is assumed, there should be two aminoethoxyl groups, one coordinating with Al atom and the other possessing an unshared electron pair. The facts that the NH_2 signal appears as a broad signal and that the NCH_2 and the OCH_2 signals do not suggest the presence of two kinds of the $-CH_2CH_2NH_2$ groups, do not support formula II.

These considerations lead to the conclusion that the dimers of $(AlEt_2OCH_2CH_2NH_2)_2$ and related compounds, whose δ values of the al-Et groups are about -1.34 ppm, are represented by the structural formula I with two Al←NRR′ coordination bonds. This conclusion is consistent with the result of considerations based on IR spectroscopic data described previously. $(AlEt_2OCH_2CH_2N(C_6H_{11})_2)_2$ has the δ value of -1.08 ppm, which is nearly equal to the δ value of the al-Et group of $(AlEt_2OEt)_2$. This anomalous value may be interpreted by the assumption that this compound exceptionally takes the structural formula III, since the unshared electron pair of the N atom could not coordinate with the Al atom owing to the steric hindrance of two cyclohexyl groups The δ values of the al-Et groups of $(AlEt_2OCH_2CH_2NPhH)_2$ and $(AlEt_2OCH_2CH_2NPh_2)_2$, -1.22 and -1.10 ppm respectively, may be due to the magnetic anisotropy of the phenyl rings, although the possibility of formula III could not be excluded.

Still another support of the formula I is obtained from the NMR spectra of the system $(AlMe_2OCH_2CH_2NMe_2)_2+(AlEt_3)_2$. In this system, the redistribution of the al-Me groups and al-Et groups take place, and the species $(AlRR'OCH_2CH_2NMe_2)_2$—R, R′=methyl or ethyl—is produced. There are fine structures corresponding to $NMe_2\rightarrow AlEt_2O-$, $NMe_2\rightarrow AlEtMeO-$, and $NMe_2\rightarrow AlMe_2O-$ in the signal of the methyl group of $(AlRR'OCH_2CH_2NMe_2)_2$ attached to the N atom. Although this observation no doubt supports formula I for $(AlRR'OCH_2CH_2NMe_2)_2$, the details will be described in the forthcoming publication.

The authors are indebted to Professors Takehiko Shimanouchi and Ichiro Nakagawa of the University of Tokyo and to Dr. Osamu Yamamoto of the Government Chemical Industrial Research Institute, Tokyo, for valuable discussions. They are also grateful to Dr. Go Hata of Toyo Rayon Co. for his advice on the measurement of IR spectra, and to Dr. Akiko Hirakawa of the University of Tokyo for her advice on the IR spectrum of n-$PrNH_2$ in solution.

BULLETIN OF THE CHEMICAL SOCIETY OF JAPAN VOL. 42 1596—1600 (1969)

Spectrophotometric Study of Solution Equilibria between Ammonia and Copper(II) and Nickel(II) Chelates of Aminopolycarboxylic Acids

Mutsuo KODAMA and Katsumi MIYAMOTO

Department of Chemistry, Ibaraki University, Mito, Ibaraki

(Received November 20, 1968)

The addition of ammonia produces a remarkable change in the visible absorption spectra of copper(II)- and nickel(II)-aminopolycarboxylate chelates. This can be ascribed to the formation of a mixed ligand chelate involving ammonia and the aminopolycarboxylate anion. On the basis of the change in the absorbance of copper(II)- and nickel(II)-aminopolycarboxylate chelates, the solution equilibria between ammonia and these aminopolycarboxylate chelates were investigated. Copper(II) and nickel(II) chelates of ethylenediaminetetraacetic acid (EDTA), *N*-(2-hydroxyethyl)-ethylenediamine-*N*,*N'*,*N'*-triacetic acid (EDTA-OH), ethylenediaminetetrapropionic acid (EDTP), cyclohexanediaminetetraacetic acid (CyDTA), and diethylenetriaminepentaacetic acid (DTPA) were found to form mixed ligand chelates with a composition of $M(NH_3)Z^{2-n}$. From the intercept of the linear relation between $\log (A_Y-A)/(A-A_M)$ and $\log [NH_3]_f$, the equilibrium constant, K^{NH_3}, defined as $K^{NH_3}=[M(NH_3)Z^{2-n}]/[MZ^{2-n}]\cdot[NH_3]_f$, was determined.

In a previous paper,[1] we studied the effects of ammonia and the thiocyanate ion on the substitution reaction of the nickel(II)-EDTA chelate with Eriochrom Black T (BT). The addition of ammonia or the thiocyanate ion brought about a considerable change in the absorption spectrum of the nickel(II)-EDTA chelate in the visible-light region, and made the substitution reaction of nickel(II)-EDTA chelate more sluggish. This was ascribed to the formation of a mixed ligand chelate involving ammonia or the thiocyanate ion, which is non-reactive in the substitution reaction between the nickel(II)-EDTA chelate and BT.

Ammonia was also found to exert a strong effect on the visible absorption spectra of copper(II) and nickel(II) chelates of EDTA and its related compounds. This also can be attributed to the formation of a mixed ligand chelate involving ammonia. In this paper, a spectrophotometric study of the solution equilibria between ammonia and copper(II) and nickel(II) chelates of aminopolycarboxylic acids will be presented.

Experimental

Reagents. The purification of ethylenediaminetetraacetic acid (EDTA), *N*-(2-hydroxyethyl)-ethylenediamine-*N*,*N'*,*N'*-triacetic acid (EDTA-OH), ethylenediaminetetrapropionic acid (EDTP), cyclohexanediaminetetraacetic acid (CyDTA), and diethylenetriaminepentaacetic acid (DTPA) and the preparation of their solutions have been described previously.[2-5] The methods of preparing and standardizing metal(II) perchlorate solutions have also been given in previous papers.[2,4] The concentration of the ammonia solution was standardized against a standard hydrochloric acid solution, using Methyl Organge as an indicator. All the other chemicals were of an analytical reagent grade and were used without further purification. The ionic strength of the sample solution was adjusted to 0.30 by adding an appropriate volume of a 1.0 M sodium perchlorate solution.

Apparatus and Experimental Procedures. All the absorption measurements were conducted at 25°C using a Hitachi EPS-3 pen-recording spectrophotometer. The experimental procedures employed were the same as before.[2]

Results and Discussion

The visible spectra of copper(II) and nickel(II) chelates of EDTA, EDTA-OH, EDTP, CyDTA, and DTPA in solutions ($\mu=0.30$) containing an excess amount of un-complexed aminopolycarboxylate are reproduced in Figs. 1 and 2. Copper(II)- and nickel(II)-aminopolycarboxylate chelates showed absorption maxima at about 700 and 370 mμ respectively. When ammonia was added to the metal(II)-aminopolycarboxylate chelate solution, as has previously been observed in the absorption curve of the nickel(II)-EDTA chelate,[1] a remarkable change in the absorbance of these metal(II)-aminopolycarboxylate chelates was also observed. However, the shape of the absorption

1) M. Kodama and K. Miyamoto, This Bulletin, **42**, 833 (1969).
2) M. Kodama and H. Ebine, *ibid.*, **40**, 1857 (1967).
3) M. Kodama and A. Kimura, *ibid.*, **40**, 1639 (1967).
4) M. Kodama, *ibid.*, **40**, 2575 (1967).
5) M. Kodama and C. Sasaki, *ibid.*, **41**, 127 (1968).

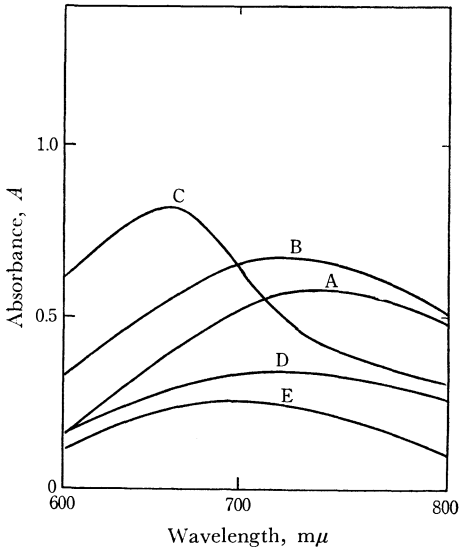

Fig. 1. Absorption spectra of copper(II)-aminopolycarboxylate chelates.
μ=0.30, pH=9.30
Concentration of un-complexed aminopolycarboxylate=10.0 mM
Concentration of copper(II)-aminopolycarboxylate chelate=5.0 mM
A: EDTA, B: EDTA-OH, C: EDTP,
D: CyDTA, E: DTPA

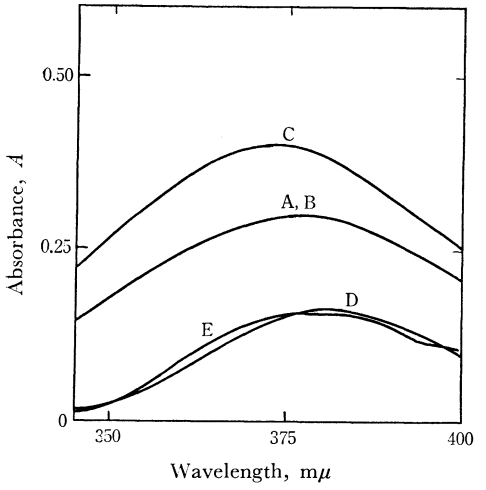

Fig. 2. Absorption spectra of nickel(II)-aminopolycarboxylate chelates.
μ=0.30, pH=9.30
Concentration of un-complexed aminopolycarboxylate=10.0 mM
Concentration of nickel(II)-aminopolycarboxylate chelate=10.0 mM
A: EDTA, B: EDTA-OH, C: EDTP,
D: CyDTA, E: DTPA

spectra was little affected by the addition of ammonia. Typical results obtained in an EDTA-OH system are shown in Figs. 3 and 4. Although the results are not shown here, similar results were also obtained in other systems. In the copper(II)-EDTA-OH system, as is illustrated by the absorption curves in Fig. 3, the absorbance decreased with an increase in the concentration of ammonia until

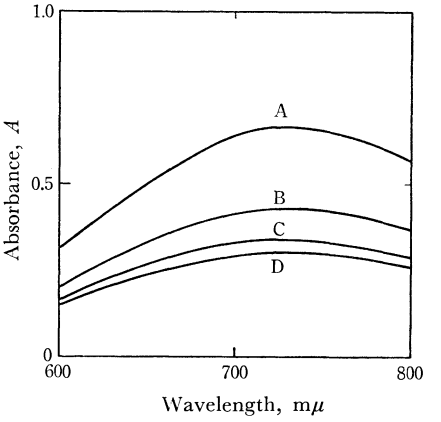

Fig. 3. Effect of ammonia on the absorption spectra of copper(II)-EDTA-OH chelate.
μ=0.30, pH=9.30
Concentration of un-complexed EDTA-OH=10.0 mM
Concentration of copper(II)-EDTA-OH chelate=5.0 mM
Concentration of ammonia
A: no ammonia, B: 15.0 mM, C: 50.0 mM,
D: 100.0 mM

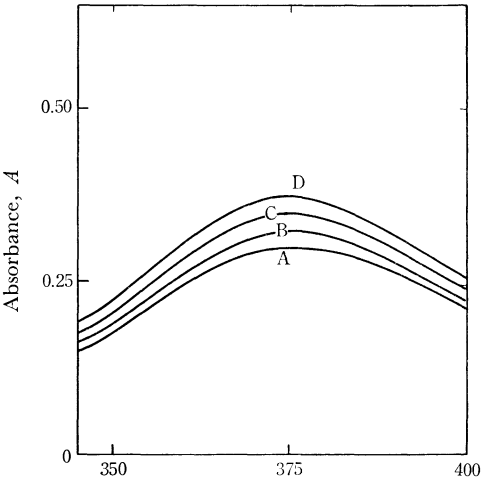

Fig. 4. Effect of ammonia on the absorption spectra of nickel(II)-EDTA-OH chelate.
μ=0.30, pH=9.30
Concentration of un-complexed EDTA-OH=10.0 mM
Concentration of nickel(II)-EDTA-OH chelate=10.0 mM
Concentration of ammonia
A: no ammonia, B: 16.0 mM, C: 30.6 mM,
D: 52.8 mM

it reached its minimum value. On the other hand, in the nickel(II) system, the absorbance in the region from 300 to 450 mμ was found to increase with an increase in the concentration of ammonia until it reached its maximum value (Fig. 4). The above change in the absorbance of metal(II)-aminopolycarboxylate chelates upon the addition of ammonia may be attributed to the formation of a mixed ligand chelate involving ammonia.

As has been discussed previously,[1,2] if the mixed ligand chelate $M(NH_3)Z^{2-n}$ is formed, the following relation can be expected thermodynamically:

$$\log \frac{A_Y - A}{A - A_M} = \log K^{NH_3} + \log [NH_3]_f \qquad (1)$$

where A_Y, A, A_M, K^{NH_3}, and $[NH_3]_f$ have the same meanings as before.[1] Here, $(A_Y - A)/(A - A_M)$ can be equated with $[M(NH_3)Z^{2-n}]/[MZ^{2-n}]$.

When $M(NH_3)_2Z^{2-n}$ and $M(NH_3)Z^{2-n}$ are both formed, the following relation can be derived in place of Eq. (1), provided that the molar extinction coefficients of $M(NH_3)Z^{2-n}$ and $M(NH_3)_2Z^{2-n}$ are the same:

$$K^{NH_3}(1 + K^{2NH_3}[NH_3]_f) = \frac{A_Y - A}{A - A_M} \times \frac{1}{[NH_3]_f} \qquad (2)$$

where $K^{2NH_3} = [M(NH_3)_2Z^{2-n}]/[M(NH_3)Z^{2-n}] \cdot [NH_3]_f$ and $(A_Y - A)/(A - A_M)$ can be equated with $[M(NH_3)_iZ^{2-n}]_t/[MZ^{2-n}]$. Here, $[M(NH_3)_iZ^{2-n}]_t$ means the total concentration of mixed ligand chelates.

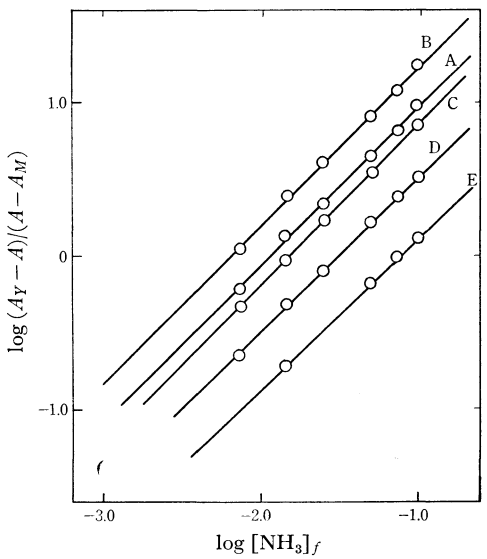

Fig. 5. The plot of $\log (A_Y - A)/(A - A_M)$ against $\log [NH_3]_f$.
$\mu = 0.30$, pH = 9.30
Concentration of copper(II)-aminopolycarboxylate chelate = 5.0 mM
Concentration of un-complexed aminopolycarboxylate = 10.0 mM
A: EDTA, B: EDTA-OH, C: EDTP,
D: CyDTA, E: DTPA

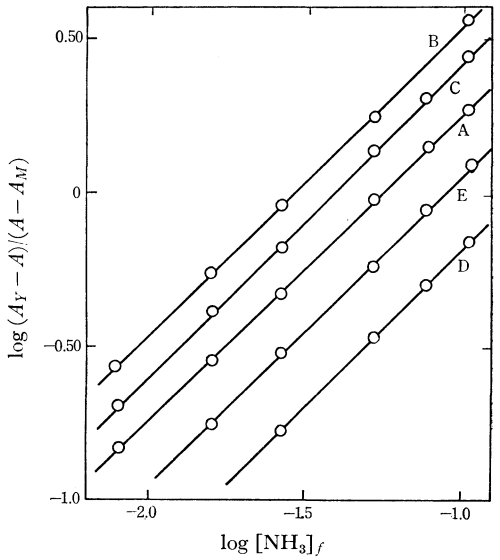

Fig. 6. The plot of $\log (A_Y - A)/(A - A_M)$ against $\log [NH_3]_f$.
$\mu = 0.30$, pH = 9.30
Concentration of nickel(II)-aminopolycarboxylate chelate = 10.0 mM
Concentration of un-complexed aminopolycarboxylate = 10.0 mM
A: EDTA, B: EDTA-OH, C: EDTP,
D: CyDTA, E: DTPA

The effect of ammonia on the absorption curves of copper(II)- and nickel(II)-aminopolycarboxylate chelates was studied in the ammonia concentration range from 15 to 200 mM. The experimental data were then analyzed with the aid of Eqs. (1) and (2). In both cases, only the plot of $\log (A_Y - A)/(A - A_M)$ against $\log [NH_3]_f$ gave a straight line with a slope of unity. The results are shown in Figs. 5 and 6. This clearly indicates that, under the present experimental conditions, only the mixed ligand chelate $M(NH_3)Z^{2-n}$ is formed.

$\log K^{NH_3}$ values were evaluated from the $\log (A_Y - A)/(A - A_M)$ values at $\log [NH_3]_f = 0$; they are listed in Table 1. At lower ammonia concentrations, the decrease in the concentration of un-complexed ammonia due to the formation of the mixed ligand chelate should be taken into consideration. Hence, the correct concentration of un-complexed ammonia at lower ammonia concentrations was calculated by using successive approximations with the aid of the following relations:

$$\frac{[NH_3]_i - X}{(\alpha)_{HNH_3}} = [NH_3]_f \qquad (3a)$$

$$\frac{K^{NH_3}}{(\alpha_H)_{NH_3}} \cdot X^2 - \left[\frac{K^{NH_3}}{(\alpha_H)_{NH_3}}([NH_3]_i + MZ^{2-n}]) - 1\right] \cdot X + \frac{K^{NH_3}}{(\alpha_H)_{NH_3}}([NH_3]_i \times [MZ^{2-n}]) = 0 \qquad (3b)$$

TABLE 1. EQUILIBRIUM CONSTANTS AND $(k)_{NH_3}/(k)_{Ac}$ OR $(k)_{NH_3}/(k)_{prop}$

i) $\log K^{NH_3}$ values

	EDTA	EDTA-OH	EDTP	CyDTA	DTPA
Cu(II)	1.96	2.23	1.85	1.55	1.10
Ni(II)	1.25	1.53	1.41	0.82	1.05

ii) $\log (k_i)_{NH_3}$ values

	$\log k_1$	$\log k_2$	$\log k_3$	$\log k_4$	$\log k_5$	$\log k_6$
Cu(II)[6]	3.97	3.32	2.71	1.95	−0.61[7]	−2.66[8]
Ni(II)[6]	2.59	2.04	1.53	0.99	0.55	−0.26

iii) $\log (k_i)_{Ac}$ values

	$\log k_1$	$\log k_2$
Cu(II)[9]	1.67	0.23
Ni(II)[10]	1.07	0.67

iv) $\log (k_i)_{prop}$ values

	$\log k_1$	$\log k_2$
Cu(II)[11]	1.80	1.24

v) $\log (k_1)_{NH_3}/(k_1)_{Ac}$ and $\log (k_1)_{NH_3}/(k_1)_{prop}$

	$\log (k_1)_{NH_3}/(k_1)_{Ac}$	$\log (k_1)_{NH_3}/(k_1)_{prop}$
Cu(II)	2.30	2.11
Ni(II)	1.52	—

where $(\alpha_H)_{NH_3}$ is the (α_H) value of ammonia; $[NH_3]_i$, the initial concentration of ammonia, and $[MZ^{2-n}]$, the concentration of the metal(II)-aminopolycarboxylate chelate.

In EDTA, EDTP, and CyDTA system, if these aminopolycarboxylates act as hexadentate ligands and if metal(II)-aminopolycarboxylate chelates have octahedral configurations, the formation of the mixed ligand chelate with ammonia will always involve the breakage of one metal(II)-oxygen (carboxylate) bond and the subsequent formation of one metal(II)-nitrogen (ammonia) bond. Therefore, the mixed ligand chelate would have one of the two structures shown in Fig. 7.

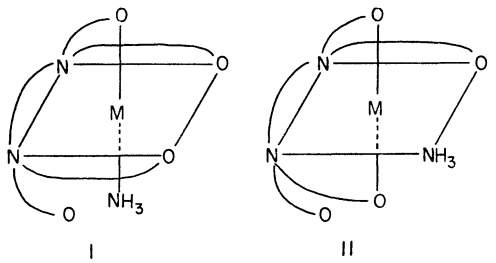

Fig. 7. The structure of a mixed ligand chelate.

As is illustrated by the successive formation constants of copper(II)-ammine complexes,[6] if the structure I is assumed for the copper(II) chelate, the equilibrium constant, K^{NH}, must be very small because of the expected Jahn-Teller distortion of the copper(II) chelate. On the other hand, if the structure II fits, the equilibrium constant is expected to have a value nearly identical with $(k_1)_{NH_3}/(k_1)_{Ac}$. Here, $(k_1)_{NH_3}=[Cu(NH_3)^{2+}]/[Cu^{2+}]\cdot[NH_3]_f$, $(k_1)_{Ac}=[Cu(Ac)^+]/[Cu^{2+}]\cdot[Ac^-]_f$ and $[Ac^-]_f$ denotes the concentration of un-complexed acetate ions. From the thermodynamic point of view, $(k_1)_{NH_3}/(k_1)_{Ac}$ corresponds to the following chemical equilibrium, where an acetate ion replaced by ammonia gains its complete translational, rotational, and conformational freedom:

$$CuZ(Ac)^{1-n} + NH_3 = Cu(NH_3)Z^{2-n} + Ac^- \qquad (4)$$

In the formation of the mixed ligand chelate between metal(II)-aminopolycarboxylate chelate and ammonia, however, the $-CH_2-COO^-$ group of the aminopolycarboxylate anion replaced by ammonia obtains in part its freedom of translation, rotation, and conformation. Therefore, in the above discussion, the instability due to the fact that the $-CH_2-COO^-$ group gains less translational, rotational and conformational freedom should be taken into consideration. Because of the lack of knowledge on the entropy effect described above, we can not estimate the instability due to the entropy loss quantiatively or even semi-quantitatively. At least, however, from the thermodynamic point of view, K^{NH_3} can safely be expected to be smaller than the $(k_1)_{NH_3}/(k_1)_{Ac}$ value. In spite of the rather rough approximation, however, the agree-

6) A. Ringbom, "Complexation in Analytical Chemistry," Insterscience Publishers, New York (1963), p. 301.

7) J. Bjerrum, *Kgl. danske Vindenskab Selskab, mat-fys. Medd.*, **12**, No. 15 (1934).

8) J. Bjerrum, C. J. Ballhausen and C. K. Jørgensen, *Acta Chem. Scand.*, **8**, 1276 (1954).

9) N. Tanaka and K. Kato, This Bulletin, **33**, 417, 1412 (1960).

10) S. K. Siddhanta and S. N. Baberjee, *J. Indian Chem. Soc.*, **35**, 423, 427 (1958).

11) D. L. Marten and F. J. C. Rossotti, unpublished results.

ment between the observed K^{NH_3} value and the calculated $(k_1)_{NH_3}/(k_1)_{Ac}$ value was satisfactory (Table 1). This agreement may confirm the latter structure, II, for the copper(II) chelate. In the EDTP system, $(k_1)_{prop}$, defined as $[Cu(prop)^+]/[Cu^{2+}]\cdot[prop^-]_f$, was used in place of $(k_1)_{Ac}$. Here, the smaller K^{NH} values for the CyDTA and DTPA systems can be ascribed to the steric effect due to the cyclohexane ring of CyDTA and the $-CH_2-CH_2-N(CH_2-COO^-)-CH_2-CH_2-N(CH_2-COO^-)_2$ group of DTPA. It is also interesting to note that the K^{NH_3} value of the EDTA-OH chelate is approximately twice that of the EDTA chelate. This may be attributed to the fact that, statistically, ammonia is expected to form a mixed ligand chelate more easily with the EDTA-OH chelate than the EDTA chelate.

In the nickel(II) system, as nickel(II)-aminopolycarboxylate and ammine complexes are essentially octahedral, no definite conclusion about the location of coordinated ammonia in the mixed ligand chelate can be drawn on the basis of a comparison of the observed K^{NH_3} value with the $(k_1)_{NH_3}/(k_1)_{Ac}$ value.

BULLETIN OF THE CHEMICAL SOCIETY OF JAPAN VOL. 42 1600—1603 (1969)

Determination of Kinetic Parameters of the Electrode Reaction of Ethylenediaminetetraacetatoaquochromate(III) Ions by the Potentiostatic Method

Akifumi YAMADA and Nobuyuki TANAKA

Department of Chemistry, Faculty of Science, Tohoku University, Katahira-cho Sendai

(Received November 22, 1968)

Kinetic parameters of the electrode reaction of ethylenediaminetetraacetatoaquochromate-(III)/ethylenediaminetetraacetatoaquochromate(II) at the dropping mercury electrode have been determined by the potentiostatic method in sodium chloride solutions of ionic strength 0.5 containing 0.1 M acetate buffer. The measured standard rate constant $(k_s)_{ms}$ is 2.1×10^{-1} cm sec^{-1} and the measured transfer coefficients $(\alpha_c)_{ms}$ and $(\alpha_a)_{ms}$ are 0.58 for the cathodic and 0.39 for the anodic process. The correction for the effect of the electrical double layer has been made on these parameters. The values obtained are: $(k_s)^{\xi}_{corr}=1._7\times10$ cm sec^{-1}, $(\alpha_c)_{corr}=0.54$ and $(\alpha_a)_{corr}=0.43$. The standard potential -1.220 V *vs.* SCE determined by the potentiostatic method is compared with -1.218 V *vs.* SCE obtained by the measurement of the equilibrium potential. These values are in good agreement within the experimental error.

The reduction of ethylenediaminetetraacetatoaquochromate(III) (Cr(III)-EDTA) ions at the dropping mercury electrode was studied by Pecsok and co-workers[1] over a wide range of pH. These authors showed that the electrode reaction of Cr(III)-EDTA proceeds reversibly at the dropping mercury electrode and they reported the values of the polarographic half-wave potential at various pH's. Kinetic parameters of the electrode reaction, however, have not been reported yet for either Cr(III)-EDTA or Cr(II)-EDTA complexes.

In this study, the theoretical treatment of the potentiostatic method for the study of fast electrode reactions, which was reported previously,[2] has been applied to the electrode reaction of Cr(III)-EDTA ions on the dropping mercury electrode and the kinetic parameters have been determined.

Experimental

Hydrogen ethylenediaminetetraacetatoaquochromate-(III) was prepared according to the method of Hamm.[3] Cr(II)-EDTA was prepared with Cr(III)-EDTA by electrolytic reduction. Redistilled water was used to prepare the solution of a desired concentration. The potentiostat was constructed in this laboratory[4] with an operational amplifier. The rise time and the input impedance are 3 μsec and 100 MΩ, respectively. A dropping mercury electrode of a long drop time (about 60 sec) was used for a cathode. The resistance of this capillary was 2.00 Ω at room temperature. The potential of the working electrode was measured against a saturated calomel electrode (SCE) with a Luggin

1) R. L. Pecsok, L. D. Shields and W. P. Schaefer, *Inorg. Chem.*, **3**, 114 (1964).

2) N. Tanaka and A. Yamada, *Electrochim. Acta*, in press.

3) R. E. Hamm, *J. Am. Chem. Soc.*, **75**, 5670 (1953).

4) unpublished.

capillary. A platinum wire electrode served as an auxiliary electrode. Electrolytic solutions were deaerated by bubbling purified nitrogen gas through the solution. Measurements were made at 25°C in solutions of ionic strength 0.5 (NaCl) containing 0.1 M acetate buffer. The pH of the solution was kept at 5.0 in order to avoid the formation of acid complexes.[1,5] Correction was made for the charging current, although the charging current decreased to zero within 30 to 40 μsec in most cases.

Results

Some preliminary measurements of current-potential behavior following the application of potential step were made with Cr(III)-EDTA ions at the slowly dropping mercury electrode. Figure 1 shows a typical example of a cathodic current-potential curve of Cr(III)-EDTA ions which was obtained in an acetate buffer solution of pH 5.0. The current was measured at 0.5 msec after the beginning of the electrolysis. Figure 2 shows plots of the logarithmic function of the current against the electrode potential. Plots of $\log\{I/(I_d-I)\}$ *vs.* E, where I is the current density, I_d, the limiting diffusion current density, and E, the electrode potential, yielded a straight line with a reciprocal slope of 60 mV and a half-wave potential of -1.222 V *vs.* SCE.

From the relation given by the equation,

$$E_e = (E_0)_{eq} + 0.0591 \times \log\{[\text{Cr(III)-EDTA}]/[\text{Cr(II)-EDTA}]\} \quad \text{at } 25°\text{C} \qquad (1)$$

the standard oxidation-reduction potential $(E_0)_{eq}$ of the reaction

$$\text{Cr(III)-EDTA} + e \rightleftharpoons \text{Cr(II)-EDTA}$$

is obtained by plotting $\log\{[\text{Cr(III)-EDTA}]/[\text{Cr(II)-EDTA}]\}$ against equilibrium potential E_e. The results are shown in Fig. 3. The value of $(E_0)_{eq}$ and the reciprocal slope of the plots were calculated to be -1.218 V *vs.* SCE and 57.8 mV, respectively. The concentration of each complex was determined by the potentiostatic or the polarographic method.

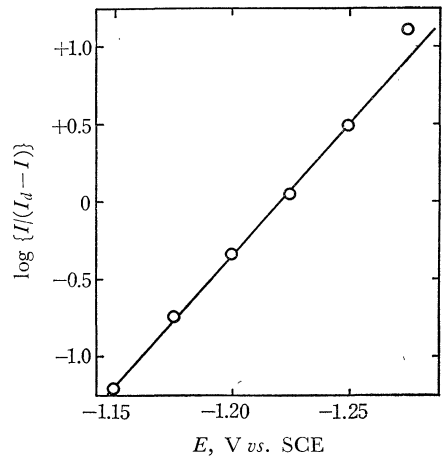

Fig. 2. Log-plots for the reduction of 2 mM Cr(III)-EDTA which were obtained by the potentiostatic method in the solutions containing 0.1 M acetate buffer and 0.4 M NaCl (pH 5.0) at 25°C. The currents were measured at 0.5 msec after the beginning of electrolysis.

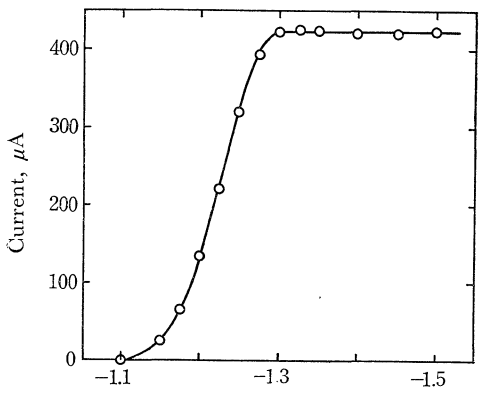

Fig. 1. Current-potential relations for the reduction of 2 mM Cr(III)-EDTA which were obtained by the potentiostatic method in the solutions containing 0.1 M acetate buffer and 0.4 M NaCl (pH 5.0) at 25°C. Surface area of the electrode is 0.0346 cm². The currents were measured at 0.5 msec after the beginning of electrolysis.

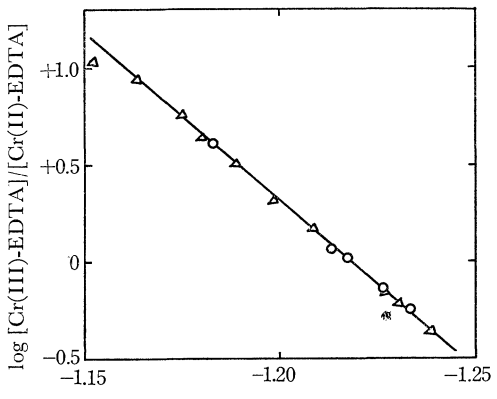

Fig. 3. Reaction of $\log[\text{Cr(III)-EDTA}]/[\text{Cr(II)-EDTA}]$ in Eq. (1) *vs.* equilibrium potential E_e which was obtained in the solutions containing 0.1 M acetate buffer and 0.4 M NaCl (pH 5.0) at 25°C. The concentration of each complex was determined by the potentiostatic method (indicated with ○) or by the polarographic method (indicated with △). In the case of polarographic measurement, the solution contains 2×10^{-6} M LEO as a maximum suppressor.

5) G. Schwarzenbach, R. Gut and G. Anderegg, *Helv. Chim. Acta*, **37**, 937 (1954).

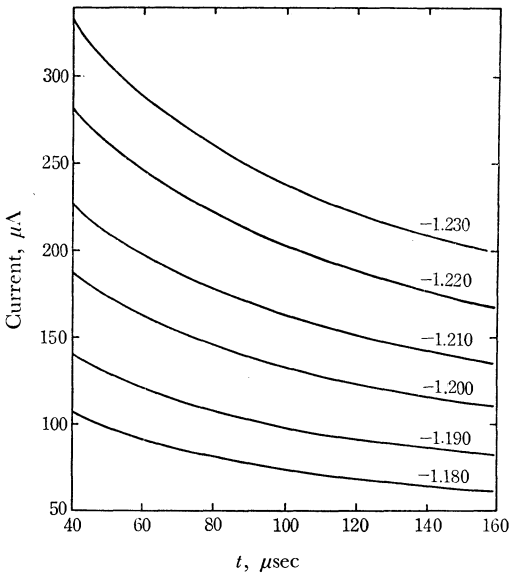

Fig. 4. Current-time relations for the reduction of 1 mM Cr(III)-EDTA which were obtained by the potentiostatic method in the solutions containing 0.1 M acetate buffer and 0.4 M NaCl (pH 5.0) at 25°C. Surface area of the electrode is 0.0346 cm². The figure on each curve indicates the controlled electrode potential (V *vs.* SCE).

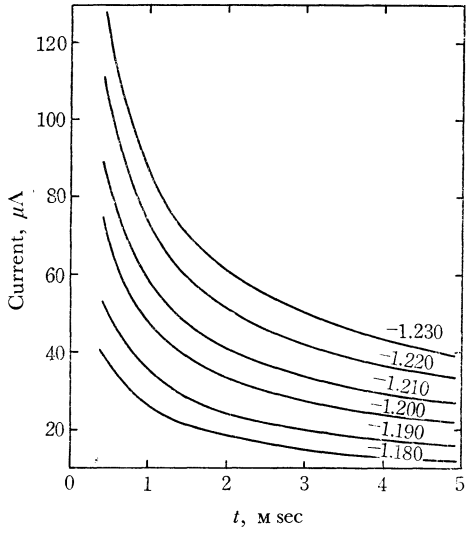

Fig. 5. Current-time relations for the reduction of 1 mM Cr(III)-EDTA which were obtained by the potentiostatic method in the solutions containing 0.1 M acetate buffer and 0.4 M NaCl (pH 5.0) at 25°C. Surface area of the electrode is 0.0346 cm². The figure on each curve indicates the controlled electrode potential (V *vs.* SCE).

Examples of current-time curves obtained at various electrode potentials are given in Figs. 4 and 5. Charging currents were immediately decreased to zero within 30 to 40 μsec.

If only the oxidant O is present initially in the solution and the reductant R is generated *in situ*, the relation between current and time on the potentiostatic method can be represented by the equations,[2]

$$I\sqrt{t}/I_\tau\sqrt{\tau} = \sqrt{\pi}\lambda_{ms}\sqrt{t}\exp(\lambda^2_{ms}\sqrt{t})\mathrm{erfc}(\lambda_{ms}\sqrt{t}) \quad (\tau \gg t) \tag{2}$$

$$(k_c)_{ms} = I_\tau\sqrt{\pi}\lambda_{ms}\sqrt{\tau}/n\boldsymbol{F}C_0^\circ \tag{3}$$

$$(k_a)_{ms} = \lambda_{ms}\sqrt{D_\mathrm{R}} - \sqrt{D_\mathrm{R}/D_\mathrm{O}}\,(k_c)_{ms} \tag{4}$$

In Eqs. (2) to (4), I means the current density at time t, τ the sufficiently long time (*e.g.*, $\lambda_{ms}\sqrt{\tau} > 5$), I_τ the current density at time τ, D the diffusion coefficient, and $(k_a)_{ms}$ and $(k_c)_{ms}$ are the measured anodic and the measured cathodic rate constant at a given potential.

Since the left-hand side of Eq. (2) and t are measurable, the values of λ_{ms} at various potentials can be determined. With these λ_{ms} values the rate constant $(k_c)_{ms}$ and $(k_a)_{ms}$ are determined provided the diffusion coefficients are known. The current-time relations shown in Figs. 4 and 5 were analyzed by means of these equations for the potentiostatic method with the results given in Table 1. The diffusion coefficients were calculated from the measurements of limiting current density following the application of potential step. They are 6.3×10^{-6} cm² sec^{-1} for Cr(III)-EDTA and 5.6×10^{-6} cm² sec^{-1} for Cr(II)-EDTA.

Table 1. Kinetic parameters of the electrode reaction of Cr(III)-EDTA/Cr(II)-EDTA in 0.1 M acetate buffer + 0.4 M NaCl (pH 5.0) 25°C

E V *vs.* SCE	$(k_c)_{ms}$ cm sec^{-1}	$(k_a)_{ms}$ cm sec^{-1}	$(k_c)_{corr}$* cm sec^{-1}	$(k_a)_{corr}$* cm sec^{-1}
−1.180	0.085_2	0.37_8	0.098_8	0.43_8
−1.190	0.10_5	0.32_1	0.11_9	0.36_4
−1.200	0.13_7	0.27_4	0.15_3	0.30_5
−1.210	0.16_6	0.24_2	0.18_3	0.26_7
−1.220	0.20_8	0.20_5	0.22_6	0.22_3
−1.230	0.23_5	0.16_0	0.25_2	0.17_1

* Calculated with the assumption that no specific adsorption takes place and ϕ_0 is constant over the potential region under investigation.

Kinetic parameters of the electrode reaction are calculated from the relations,*1,2

$$(k_c)_{ms} = (k_s)_{ms}\exp\left[-\frac{(\alpha_c)_{ms}n\boldsymbol{F}}{\boldsymbol{RT}}(E-(E_0)_{ms})\right] \tag{5}$$

$$(k_a)_{ms} = (k_s)_{ms}\exp\left[+\frac{(\alpha_a)_{ms}n\boldsymbol{F}}{\boldsymbol{RT}}(E-(E_0)_{ms})\right] \tag{6}$$

where $(k_s)_{ms}$ is the measured standard rate constant, $(E_0)_{ms}$ the measured standard potential, $(\alpha_c)_{ms}$

*1 $(\alpha_c)_{ms}$ and $(\alpha_a)_{ms}$ are denoted as α_{ms} and β_{ms}, respectively, in Ref. 2.

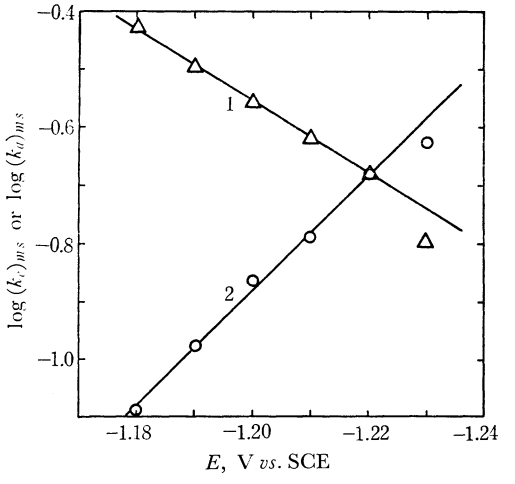

Fig. 6. Relations of (1) $\log(k_a)_{ms}$ *vs.* E and (2) $\log(k_c)_{ms}$ *vs.* E obtained with 1 mM Cr(III)-EDTA in the solutions containing 0.1 M acetate buffer and 0.4 M NaCl (pH 5.0) at 25°C

and $(\alpha_a)_{ms}$ are the measured cathodic and the measured anodic transfer coefficient, respectively, and $\boldsymbol{F}$, $\boldsymbol{R}$ and T have their usual meanings. The relation of $\log(k_a)_{ms}$ *vs.* E and that of $\log(k_c)_{ms}$ *vs.* E are shown in Fig. 6. Using the values given in Table 1 the following kinetic parameters were obtained:

$$(E_0)_{ms} = -1.220 \text{ V } vs. \text{ SCE}$$
$$(k_s)_{ms} = 2.1\times10^{-1} \text{ cm sec}^{-1}$$
$$(\alpha_c)_{ms} = 0.58,\ (\alpha_a)_{ms} = 0.39$$

Discussion

Since the measured rate constants $(k_c)_{ms}$ and $(k_a)_{ms}$, which were determined by the above-mentioned method, involve the influence of the electrical double layer, the correction for the effect of the double layer is necessary. The Levich and the Frumkin correction[2] were made on the assumption that no specific adsorption took place and that the value of ϕ_0 was constant in the potential region under investigation:*2

$$(k_c)_{corr} = (k_c)_{ms}\left[1-\frac{\zeta_O}{\kappa D_O}(k_c)_{ms}-\frac{\zeta_R}{\kappa D_R}(k_a)_{ms}\right]^{-1} \quad (7)$$

$$(k_a)_{corr} = (k_a)_{ms}\left[1-\frac{\zeta_O}{\kappa D_O}(k_c)_{ms}-\frac{\zeta_R}{\kappa D_R}(k_a)_{ms}\right]^{-1} \quad (8)$$

with

$$\zeta_j = \frac{\exp[(|z_j|-|z|/2)\boldsymbol{F}\phi_0/\boldsymbol{RT}]-1}{+|z_j/z|-1/2} \quad (9)$$

$$1/\kappa = \sqrt{\boldsymbol{RT}\varepsilon/8\pi z^2\boldsymbol{F}^2C_t} \quad (10)$$

where z_j is the ionic charge of the jth species, z the charge of the symmetrical indifferent electrolyte, ϕ_0 the difference of potential across the diffuse double layer from the plane of closest approach to the bulk of solution, ε the dielectric constant, C_t the total concentration of a z-z indifferent electrolyte.

Corrected kinetic parameters are determined by the relation,*3,2)

$$(k_c)_{corr} = (k_s)_{corr}\exp\left[-\frac{(\alpha_c)_{corr}n\boldsymbol{F}}{\boldsymbol{RT}}(E-(E_0)_{corr})\right] \quad (11)$$

$$(k_a)_{corr} = (k_s)_{corr}\exp\left[+\frac{(\alpha_a)_{corr}n\boldsymbol{F}}{\boldsymbol{RT}}(E-(E_0)_{corr})\right] \quad (12)$$

$$(k_s)_{corr} \fallingdotseq (k_s)^c_{corr}\exp[((\alpha_c)_{corr}n-z_O)\boldsymbol{F}\phi_0)/\boldsymbol{RT}] \quad (13)$$

where $(k_s)_{corr}$ is the corrected rate constant at $E=(E_0)_{corr}$ and $(k_s)^c_{corr}$ is the corrected standard rate constant expressed in terms of concentration for the cathodic process.

In order to estimate the potential ϕ_0, the differential capacity and the electrocapillary curve of the supporting electrolyte were measured by the conventional method. The equipment for these measurements was previously described.[6] The value of ϕ_0 was calculated to be −0.073 V at −1.220 V *vs.* SCE by the Gouy-Chapman theory.[7]

The rate constants at various potentials which were determined by this procedure are also given in Table 1. The corrected kinetic parameters were as follows:

$$(E_0)_{corr} = -1.220 \text{ V } vs. \text{ SCE}$$
$$(k_s)_{corr} = 2.2\times10^{-1} \text{ cm sec}^{-1}$$
$$(\alpha_c)_{corr} = 0.54$$
$$(\alpha_a)_{corr} = 0.43$$
$$(k_s)^c_{corr} = 1._7\times10 \text{ cm sec}^{-1}$$

The standard potential $(E_0)_{corr}$ was found to be the same, within the experimental error, with $(E_0)_{eq}$ which was obtained by the measurement of the equilibrium potential.

The authors are grateful to Dr. Reita Tamamushi, the Institute of Physical and Chemical Research, for his valuable suggestion on this study. They also thank the Ministry of Education for the financial support granted for this research.

*2 $(k_c)_{corr}$ and $(k_a)_{corr}$ are denoted as $(k_c)_{app}$ and $(k_a)_{app}$, respectively, in Ref. 2.

*3 $(k_s)_{corr}$, $(k_s)^c_{corr}$, $(E_0)_{corr}$, $(\alpha_c)_{corr}$ and $(\alpha_a)_{corr}$ are denoted as $(k_s)_{app}$, $(k_s)^c_{app}$, $(E_0)_{app}$, α_{app} and β_{app}, respectively, in Ref. 2.

6) R. Tamamushi and N. Tanaka, *Z. physik. Chem., Neue Folge*, **28**, 158 (1961).

7) M. Breiter, M. Kleinerman and P. Delahay, *J. Am. Chem. Soc.*, **80**, 51 (1958).

BULLETIN OF THE CHEMICAL SOCIETY OF JAPAN VOL. 42 1604—1608 (1969)

Epoxidation of Eight- and Twelve-Membered Cyclic Olefins with Hydrogen Peroxide in the Presence of Metal Oxide Catalysts*[1]

Jo ITAKURA, Hisao TANAKA and Hiroo ITO

Research Laboratory, Toa Gosei Chemical Industry Co., Funami-cho, Minato-ku, Nagoya

(Received April 25, 1968)

The oxidation of eight- and twelve-membered cyclic olefins by H_2O_2 was carried out in various alcohols using some metal oxides as catalysts. In contrast to the case of cyclohexene and norbornene, which can be hydroxylated, the oxidation of 1,5,9-cyclododecatriene, cyclododecene, 1,3- and 1,5-cyclooctadiene and cyclooctene with H_2O_2 in the presence of selenium dioxide resulted in selective formation of the corresponding monoepoxides. The following rate equation was obtained with cyclooctene (COE) in isopropanol:

$$-d[H_2O_2]/dt = k_3'[SeO_2][H_2O_2] + k_3''[SeO_2][H_2O_2][COE].$$

It is well known that the oxygen compounds of some heavy metals, such as tungsten, selenium, vanadium, osmium, molybdenum and chromium, catalyze the H_2O_2 oxidation in characteristic fashion. The oxidation of olefins yields α-diols as the main product.[1-4] Epoxide formation as intermediate was suggested for WO_3 and SeO_2 catalyzed reactions.[3,4] The present paper describes some results obtained on the H_2O_2 oxidation of eight- and twelve- membered cyclic olefins in the presence of metal oxides, especially selenium dioxide.

Experimental

Materials. Commercial cycloolefins were distilled to remove antioxidants before use. *trans, cis*-1,5-Cyclodecadiene was prepared by the cooligomerization of butadiene with ethylene using a catalyst composed of nickel acetylacetonate, triphenyl phosphite and triethylaluminum. Hydrogen peroxide and selenium dioxide (G. R. grade) were used without further purification. Alcohols of G. R. grade were distilled and used as solvents in the preparation, but for the kinetic purposes, they were dried by refluxing over magnesium or calcium metal.

Preparative Experiments. SeO_2 was dissolved in alcohol, olefin was then added, and the alcoholic solution of H_2O_2 was added dropwise with agitation and cooling within 2 hr. After agitation for further several hours, the reaction mixture was washed with aqueous solutions of sodium bisulfite and sodium carbonate. The ether extract of aqueous washings and other organic layers were brought together and dried over sodium sulfate. The product was distilled under reduced pressure. The determination of the amount of epoxide formed was carried out with the hydrogen chloride-dioxane-method,[5] in which the optimal reaction time of epoxide with H_2O_2 was pre-determined for each epoxide.

Kinetic Procedure. The reaction was carried out in alcoholic media at 25—50°C with the following initial concentration ranges of reagents: $[SeO_2]_0$=3.33—26.67 mmol/*l*, $[Olefin]_0$=0.300—1.333 mol/*l*, $[H_2O_2]_0$=0.147—0.294 mol/*l*, $[H_2O]_0$=29.8 mmol/*l*. Aliquots were taken out at intervals, the reaction was stopped by addition of an alcoholic potassium hydroxide solution, and the peroxide content was determined iodometrically.

Results and Discussion

Oxidation of Several Cylcoolefins. The results of oxidation of *trans,trans,cis*-1,5,9-cyclododecatriene (*t,t,c*-CDT) under various reaction conditions are shown in Table 1.

In contrast to the oxidation of cyclohexene,[4] epoxide was produced selectively regardless of solvents. The content of water exhibited little effect on the selectivity of epoxide. 9,10-Epoxy-1,5-cyclododecadiene was obtained by distillation of the product: bp 102°C/2.5 mmHg, n_D^{20} 1.5017. Found: C, 80.72; H, 10.03%. Calcd for $C_{12}H_{18}O$: C, 80.85; H, 10.18%. The infrared spectrum, which was identical with that reported,[6] showed strong absorption bands of *trans* and *cis* double bonds at 972cm^{-1} and 700 cm^{-1}, respectively. Meanwhile, gas chromatography indicated the presence of two isomers in a molar ratio of 97 to 3,

*1 A part of this paper was presented at the 6th Meeting of the Oil Chemical Society of Japan, Nagoya, Oct. 1967.

1) M. Mugdan and D. P. Young, *J. Chem. Soc.*, **1949**, 2988.

2) N. Sonoda and S. Tsutsumi, *Kogyo Kagaku Zasshi (J. Chem. Soc. Japan, Ind. Chem. Sect.)*, **63**, 110 (1960).

3) G. B. Payne and C. W. Smith, *J. Org. Chem.*, **22**, 1682 (1957).

4) N. Sonoda and S. Tsutsumi, This Bulletin, **38**, 958 (1965).

5) G. Wilke, Japanese Pat. 7822 (1961).

6) W. Stumpf and K. Rombusch, *Ann. Chem.*, **687**, 136 (1965).

Table 1. Oxidation of *t,t,c*-CDT

Solvent[a]	SeO_2 mol	CDT mol	H_2O_2 %	H_2O_2 mol	H_2O_2/CDT mol/mol	Temp. °C	Time hr	ECDD[b] formed mol	ECDD[b] yield, % vs. reacted CDT	ECDD[b] yield, % vs. H_2O_2
t-BuOH	0.054	0.36	90	0.44	1.24	25—30	16	0.16	54	37
	0.045	0.71	90	0.44	0.62	25—30	16	0.21	81	49
	0.036	0.75	90	0.30	0.32	25—30	16	0.19	77	63
i-PrOH	0.045	0.60	90	0.30	0.50	25—30	40	0.21	92	70
	0.045	0.60	90	0.60	1.00	25—30	40	0.28	65	46
	0.045	0.60	90	1.60	2.67	25—30	40	0	0	0[c]
	0.045	0.60	90	0.30	0.50	45—50	40	0.15	83	49
	0.090	0.60	60	0.30	0.50	25—30	40	0.22	84	74
	0.045	0.60	30	0.30	0.50	25—30	40	0.12	87	40
n-PrOH	0.045	0.60	90	0.30	0.50	25—30	40	0.10	92	35
EtOH	0.045	0.60	90	0.30	0.50	25—30	40	0.08	83	26

a) 300 m*l* was used.
b) ECDD=9,10-epoxy-1,5-cyclododecadiene.
c) Mono- and diepoxides could not be isolated by distillation.

Table 2. Oxidation of CDE (150 m*l* solvent, 25—30°C, 16 hr)

Solvent	SeO_2 mol	CDE mol	H_2O_2 %	H_2O_2 mol	H_2O_2/CDE mol/mol	ECDA[a] formed mol	ECDA[a] yield, % vs. consumed CDE	ECDA[a] yield, % vs. H_2O_2	ECDA[a] isomer ratio[b]
t-BuOH	0.023	0.30	90	0.27	0.90	0.167	89	62	75/25
i-PrOH	0.023	0.30	90	0.15	0.50	0.135	96	90	73/27
	0.023	0.30	90	0.30	1.00	0.212	95	71	73/27
	0.023	0.30	90	0.45	1.50	0.283	96	63	74/26
	0.023	0.30	60	0.15	0.50	0.132	95	88	71/29
n-PrOH	0.023	0.30	90	0.15	0.50	0.170	91	82	73/27
EtOH	0.023	0.30	90	0.30	1.00	0.253	—	84	—

a) ECDA=epoxycyclododecane.
b) Determined by gas chromatography.

Table 3. Oxidation of eight-membered cyclic olefins
(35—40°C, 4 hr, in 300 m*l* isopropanol)

	Olefin mol	SeO_2 mol	H_2O_2 %	H_2O_2 mol	H_2O_2/Olef. mol/mol	Epox. formed mol	Unreacted olefin mol	Epox. yield, % vs. consumed olefin	Epox. yield, % vs. H_2O_2
COE	1.00	0.10	90	0.77	0.77	0.68	0.30	97	68
1,3-COD	1.20	0.12	90	0.60	0.50	0.43	0.68	83	72
1,5-COD	1.20	0.12	90	0.60	0.50	0.45	0.63	79	75

suggesting that *trans* double bond of *t,t,c*-CDT is oxidized more easily than *cis*. This could be attributed to the larger internal strain of the former. Similar results have also been reported recently for the organic peracid oxidation of the same olefin.[7]

Table 2 shows the oxidation results of cyclododecene (CDE).

A mixture of *trans* and *cis* CDE in a molar ratio of 68 to 32 was oxidized to give two isomeric epoxides in an approximately constant ratio. Epoxycyclododecane (a *trans-cis*-mixture with 72 : 28) was isolated by distillation: bp 116—117°C/4.7mmHg, n_D^{20} 1.4763. Found: C, 79.05; H, 12.08%. Calcd for $C_{12}H_{24}O$: C, 79.06; H, 12.17%.

The epoxidation of eight-membered cyclic olefins is summarized in Table 3. An excellent yield was attained with cyclooctene (COE), while lower yields were observed with 1,3- and 1,5-cyclooctadiene (COD).

7) J. L. Jungnickel, E. D. Peters, A. Polgar and F. T. Weiss, "Organic Analysis," Vol. I, ed. by J. Mitchel, Jr., I. M. Kolthoff, E. S. Proskauer and A. Weissberger, Interscience Publishers, New York, N. Y. (1953), p. 135.

TABLE 4. H_2O_2 OXIDATION WITH METAL OXIDE CATALYSTS

Olefin		Catalyst		Solvent	H_2O_2		Reacn. condn.	Epox. formed	Epox. yield, %	
	mmol		mol	ml	%	mol	°C/hr	mol	*vs.* consumed olefin	*vs.* H_2O_2
CDT	0.60	WO_3	13	*i*-PrOH 250	90	0.30	35—40/16	0	—	—
	0.60	$H_2WO_4 \cdot H_2O$[a]	11	*i*-PrOH 200	90	0.40	30—35/16	0.16	89	40
	0.60	$H_2WO_4 \cdot H_2O$	19	*i*-PrOH 205 $+H_2O$ 5	90	0.40	30—35/16	0.21	83	53
	0.60	$H_2WO_4 \cdot H_2O$	19	*i*-PrOH 180 $+H_2O$ 30	90	0.40	30—35/16	0.21	76	53
	0.60	$H_2WO_4 \cdot H_2O$	11	*t*-BuOH 200	90	0.40	30—35/16	0.23	82	57
	0.60	H_2MoO_4	31	*i*-PrOH 200 $+H_2O$ 30	90	0.40	30—35/16	0.18	91	44
	0.60	V_2O_5	17	*i*-PrOH 200 $+H_2O$ 10	90	0.40	30—35/16	0.19	90	49
CDE	0.60	$H_2WO_4 \cdot H_2O$[a]	8	*i*-PrOH 200	90	0.40	30—35/16	0.24	88	61
1,5-COD	0.60	$H_2WO_4 \cdot H_2O$[a]	8	*i*-PrOH 200	90	0.40	30—35/4	0.09	23	14
COE	0.60	$H_2WO_4 \cdot H_2O$[a]	8	*i*-PrOH 200	90	0.40	30—35/3	0.31		78

a) In these runs the catalyst was added to a hydrogen peroxide solution and agitated for 30 min at room temperature.

TABLE 5. RATE DATA OF OXIDATION OF COE

Solvent	$[SeO_2]$ mmol/*l*	$[H_2O_2]_0$ mol/*l*	$[H_2O]_0$ mmol/*l*	$[COE]_0$ mol/*l*	Temp. °C	$(pH)_0$	$(k_1)_0 \times 10^3$ min^{-1}	$(k_2)_0 \times 10^1$ $l \cdot mol^{-1} \cdot min^{-1}$
i-PrOH	13.33	0.147	29.8	1.333	25		2.68	2.01
	13.33	0.147	29.8	0.900	25		1.84	1.38
	13.33	0.147	29.8	0.533	25		1.21	0.91
	26.67	0.147	29.8	1.333	30	3.7	7.02	2.63
	20.00	0.147	29.8	1.333	30	4.0	5.24	2.62
	13.33	0.147	29.8	1.333	30	4.1	3.51	2.63
	6.67	0.147	29.8	1.333	30	4.3	1.65	2.46
	3.33	0.147	29.8	1.333	30	4.4	0.68	2.04
	13.33	0.147	29.8	0.900	30	4.2	2.46	1.83
	13.33	0.294	59.6	0.533	30	4.3	1.56	1.17
	26.67	0.147	29.8	0.300	30	4.1	1.84	0.73
	13.33	0.147	740	1.333	30		2.64	1.98
	13.33	0.147	1850	1.333	30		1.93	1.45
	13.33	0.147	3700	1.333	30		1.35	1.02
	13.33	0.147	29.8	1.333	40		5.74	4.30
	13.33	0.147	29.8	0.900	40		3.95	2.96
	13.33	0.147	29.8	0.533	40		2.47	1.85
	13.33	0.147	29.8	0.300	40		1.48	1.11
	13.33	0.147	29.8	0.900	50		6.47	4.85
	13.33	0.147	29.8	0.533	50		4.05	3.04
	13.33	0.147	29.8	0.300	50		2.51	1.88
t-BuOH	13.33	0.147	29.8	1.333	30		9.05	6.78
EtOH	13.33	0.147	29.8	1.333	30		1.61	1.21

Physical properties of the isolated epoxides were as follows: epoxycyclooctane, mp 56—57°C; 3,4-epoxy-1-cyclooctene, bp 74—75°C/13 mmHg, n_D^{20} 1.4832; 5,6-epoxy-1-cyclooctene, bp 80—81°C/18 mmHg, n_D^{20} 1.4890.

The SeO_2 catalyzed H_2O_2 oxidation of *trans, cis*-1,5-cyclodecadiene, however, resulted in the formation of several products including small amounts of epoxides which could not be identified. No examination was made on the possibility of double bond isomerization, though the olefin is known to be a relatively unstable compound, which can easily be isomerized either to *cis,cis*-1,6-cyclodecadiene,[8] or to 1,2-divinylcyclohexane.[9]

The oxidation results with several metal oxides

8) P. Heimbach, *Angew. Chem.*, **78**, 604 (1966).
9) G. Wilke and P. Heimbach, *ibid.*, **75**, 10 (1963).

other than SeO_2 are summarized in Table 4. Epoxides were also obtained in good selectivities with the oxides of tungsten, molybdenum and vanadium as catalysts. All the systems given in Table 4 were heterogeneous because of the poor solubilities of catalysts. With $H_2WO_4 \cdot H_2O$, the amount of distillation residue increased, as did the water content in the reaction medium.

Kinetics on Oxidation of Cyclooctene. The only example of kinetic investigation on H_2O_2 oxidation in the presence of SeO_2 so far seems to be that reported by Ogata and Tabushi,[10] who employed dimethylaniline as substrate. No information has been available on the kinetic behavior of the oxidizing system on olefinic double bond. The fact that the oxidation of cycloolefin was essentially an epoxidation prompted us to the kinetic study. Cyclooctene was chosen as the substrate.

No reaction occurred on treatment of cyclooctene with 90% H_2O_2 alone or SeO_2 alone. The system SeO_2-H_2O_2 in isopropanol shows a very slight decrease in the H_2O_2 concentration only after a long period with agitation.

Effects of the Concentration of Reaction Components. The results of oxidation of COE are summarized in Table 5. In every run, plots of H_2O_2 consumption against reaction time indicated that the rate $-d[H_2O_2]/dt$ was directly proportional to H_2O_2. Water, which was formed by the reaction, did not seem to influence the rate at all, while the apparent value of pH varied slightly (in the range of 0.1 to 0.2) during the course of reaction. Hence the following equation is obtained:

$$-\frac{d[H_2O_2]}{dt} = k_1[H_2O_2] \quad (1)$$

To determine the effect of SeO_2, rates of H_2O_2 consumption were measured at various initial concentrations of SeO_2, while keeping initial concentration of H_2O_2 and COE constant. The results are given in Fig. 1, which suggests a first order relationship between the rate and $[SeO_2]$. A slight deviation from the direct proportionality as observed for low concentrations of SeO_2 might be ascribed to the decrease in acidity. Combining the result with Eq. (1), we have the following equation:

$$-\frac{d[H_2O_2]}{dt} = k_2[H_2O_2][SeO_2] \quad (2)$$

In order to determine the effect of cyclooctene concentration, rates were measured varying its initial concentration, and the extrapolated values of $(-d[H_2O_2]/dt)/[H_2O_2]$ at $t=0$, or $(k_1)_0$, were calculated (see Table 5). Although a linear relationship exists between $(k_1)_0/[SeO_2]$ and $[COE]_0$, as shown in Fig. 2, they are not directly proportional to each other. This was proved to be valid for different temperatures applied. Figure 2 gives the

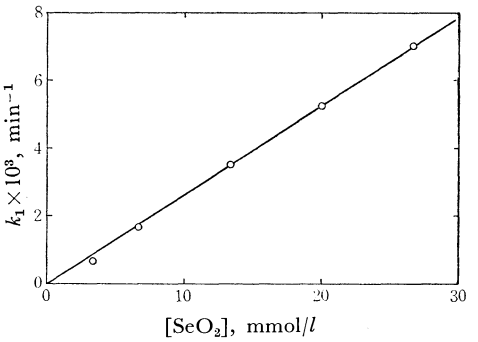

Fig. 1. Effect of concentration of SeO_2 on the rate.
($[COE]_0=1.333$ mol/l, $[H_2O_2]_0=0.147$ mol/l, $[H_2O]_0=29.8$ mmol/l, 30°C, in isopropanol)

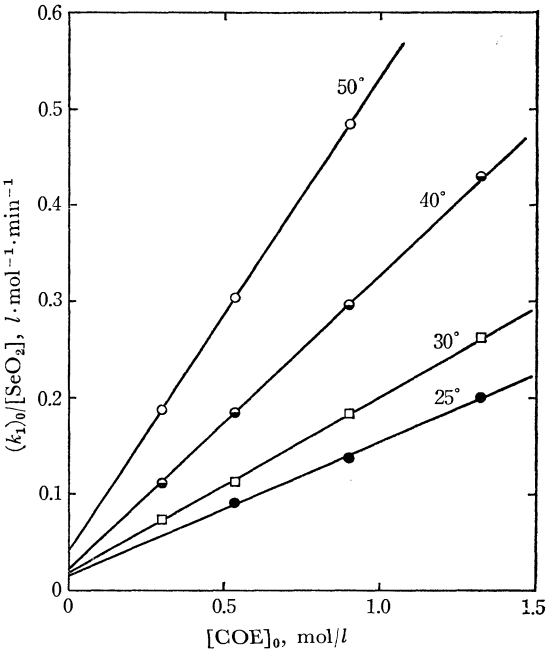

Fig. 2. Effect of initial concentration of COE on the rate.
($[H_2O_2]_0=0.147$ mol/l, $[H_2O]_0=29.8$ mmol/l, in isopropanol)

equation:

$$-\frac{d[H_2O_2]}{dt} = k_3'[SeO_2][H_2O_2] + k_3''[SeO_2][H_2O_2][COE] \quad (3)$$

Table 6 summarizes the values of k_3' and k_3''. For k_3'', the Arrhenius plot gives a straight line, from which apparent activation energy and activation entropy are calculated:

$$\Delta H^{\ddagger} = 9.67 \text{ kcal} \cdot \text{mol}^{-1},$$
$$\Delta S^{\ddagger} = -38.2 \text{ cal} \cdot \text{mol}^{-1} \cdot {}^{\circ}\text{C}^{-1} \ (40^{\circ}\text{C}).$$

The first term of the right side in Eq. (3) expresses the rate of H_2O_2 consumption, which is of

10) Y. Ogata and I. Tabushi, This Bulletin, **32**, 215 (1959).

Table 6. Values of k_3' and k_3''

Temp. °C	k_3' $l\cdot mol^{-1}\cdot min^{-1}$	k_3'' $l^2\cdot mol^{-2}\cdot min^{-1}$
25	0.0155	0.138
30	0.017	0.184
40	0.021	0.306
50	0.038	0.495

zeroth order with respect to COE concentration. On the other hand, the rate of H_2O_2 consumption in the system SeO_2–H_2O_2–*i*PrOH (in the absence of COE) was shown to be much smaller than the corresponding value of the term $k_3'[SeO_2][H_2O_2]$. This fact means that the term expresses mainly reactions of H_2O_2 in which both SeO_2 and COE actually participate. The k_3' values do not satisfy the Arrhenius equation, so that the activation energy is not obtainable. The term may therefore include several reactions, in which COE does and does not participate. Ogata and Tabushi[10] have previously obtained comparable results on the oxidation of dimethylaniline with SeO_2-H_2O_2, and proposed two independent routes for amine oxide formation. Considering our results, this concept is now extended for oxidation of olefinic double bonds as follows:

$$H_2O_2 + SeO_2 \rightleftarrows \text{Peracid } A_1 \xrightarrow{+\text{Olefin}} H_2SeO_3 + \text{Epoxide} \quad (4)$$

$$H_2O_2 + SeO_2 \rightleftarrows \text{Peracid } A_2 \xrightarrow{+\text{Olefin}} H_2SeO_3 + \text{Epoxide} \quad (5)$$

A highly active peracid A_1 in Eq. (4) would be formed by a slow reaction of H_2O_2 with SeO_2, which then reacts with COE rapidly, whereas a more stable peracid A_2, formed through a fast reaction, would oxidize the olefin slowly. No attempts, however, were made by us to obtain information on the structures of these active peracids.

Effect of Solvents. As Table 5 indicates, less-polar alcohols favor the oxidation.

The effect of water content in the reaction medium is also given in Table 5. It is apparent that an increase in water concentration causes a marked reduction of the rate. As already discussed in the previous report on oxidation of dimethylaniline in methanol-water medium,[10] this effect could be attributed mainly to a hindering action of water in regenerating SeO_2 dehydration of H_2SeO_3, that is formed through the oxidation reaction (see Eqs. 4 and 5). If SeO_2 is not smoothly regenerated, the effective concentration of the oxide is lowered, and then, according to Eqs. (4) and (5), the formation of active peracids may also be hindered.

Hydroxylation and Epoxidation. On studying the hydroxylation of cyclohexene with H_2WO_4-H_2O_2, Payne and Smith[3] proposed a reaction scheme including formation of epoxide as the intermediate. A similar conclusion was also obtained by Sonoda and Tsutsumi for SeO_2-catalyzed hydroxylation of the cycloolefin on the basis of the product analysis.[4] Our results have now provided examples, in which the epoxides can actually be isolated by treating cycloolefins with SeO_2- of H_2WO_4-H_2O_2. It is evident, that the reaction of H_2O_2 with the olefinic double bond in the presence of oxides of W, Se, Mo and V is essentially an epoxidation, and it is also hardly doubtable that the hydroxylation occurs with many olefins as the successive hydrolysis of the epoxide formed. In fact, there seem to exist certain differences between epoxides of cyclohexene and higher-membered cyclic olefins in the ease of ring opening in acidic media.[11] Such differences can not simply be explained through the electronic effect, as is known for epoxides of substituted aliphatic olefins, since we have here no branched chains. Some steric effects such as steric hindrance or internal strain should be considered to play a part.

The authors wish to thank Toa Gosei Chemical Industry Co. for permission to publish these results.

11) J. Itakura and H. Tanaka, unpublished results.

BULLETIN OF THE CHEMICAL SOCIETY OF JAPAN VOL. 42 1609—1617 (1969)

Studies on Fluorene Derivatives. XXV.[1] Abnormal Products, Tribiphenylenepropanes, of the Michael Addition of 9,9'-Bifluorenylidenes and Fluorenes, and Syntheses of Related Compounds

Kazuo SUZUKI, Masahiro MINABE, Minoru FUJIMOTO* and Noboru NOHARA*[1]

Department of Industrial Chemistry, Faculty of Engineering, Utsunomiya University, Ishii-cho, Utsunomiya

** Department of Industrial Chemistry, Faculty of Engineering, Yamaguchi University, Tokiwadai, Ube*

(Received July 27, 1968)

A normal compound, 2',7'-dibromotribiphenylenepropane (IV), and an abnormal compound, 2',7',2'',7''-tetrabromotribiphenylenepropane (VI), were obtained by the Michael addition of 9,9'-bifluorenylidene (I) and 2,7-dibromofluorene (III). In addition, another normal compound, 2,7,2',7'-tetrabromotribiphenylenepropane (VIII) and three abnormal compounds, IV, VI, and tribiphenylenepropane (VII), were isolated by the Michael addition of 2,7,2',7'-tetrabromo-9,9'-bifluorenylidene (IX) and fluorene (II). In both cases, the normal compounds were obtained in the presence of sodium ethoxide in ethanol. The abnormal compounds might be formed by the further condensation of 2,7-dibromo-9,9'-bifluorenylidene (V) and III or II in the presence of alkali. The related compounds, 2,7-dibromotribiphenylenepropane (X), IV, VI, VIII, and 2,7,2',7',2'',7''-hexabromotribiphenylenepropane, were synthesized by the reaction of substituted 9-fluorenyllithium and substituted 9-bromo-9,9'-bifluorenyl in an absolute xylene solution. The thermal decomposition of X and VIII afforded bromosubstituted or non-bromosubstituted-9,9'-bifluorenylidenes, 9,9'-bifluorenyls, fluorenones, and fluorenes. The ethanolysis of 2,7-dibromo-9'-hydroxy-9,9'-bifluorenyl gave fluorenone and III.

The formation of an abnormal addition product, 2',7',2'',7''-tetrabromotribiphenylenepropane(VI), together with a normal addition product, 2',7'-dibromotribiphenylenepropane (IV), by a Michael addition reaction between 2, 7-dibromofluorene (III) and 9,9'-bifluorenylidene (I) has been previously reported in this series.[2] The reactions of 2,7,2',7'-tertabromo-9,9'-bifluorenylidene (IX) and fluorene (II) have also been investigated by Pinck and Hilbert,[3] but they isolated no specific compound except tribiphenylenepropane (VII).

In view of the interest in the formation of abnormal addition products, we have sought to clarify the mechanism of this addition reaction.

The present study has been primarily concerned with a re-examination of the formation of several compounds, including IV, VI, and VII,[3,4] by reactions between I and III, IX and II under various base conditions.

A Michael addition between I[5] and III was carried out in ethanol using sodium ethoxide (15%) as the catalyst; it gave a good yield of IV. In the case of potassium hydroxide (1%) in a pyridine solution, VI was obtained as the major product, while II, IV, VII, fluorenone, and 2,7-dibromofluorenone were the minor products. These results are summarized in Table 1.

In other observations of the Michael addition between IX and II, the normal compound VIII was obtained exclusively with sodium carbonate (5%) in a pyridine solution, or VIII and 2,7-dibromo-α, δ-dibiphenylenebutadiene were obtained with sodium ethoxide (5.8%) in an alcoholic solution. A compound (mp 303—304°C (dec)), three abnormal products, IV, VI and VII, and two elimination products, III and 2,7-dibromofluorenone, were also isolated using potassium hydroxide (0.5—5%) in a pyridine solution. These results are summarized in Table 2.

A transitory carbanion (A) is formed in the initial step by an attack of the 2,7-dibromo-9-fluorenyl carbanion (III') on the highly-polarized acceptor

---

*1 Present address: Department of Synthetic Chemistry, Faculty of Engineering, Gunma University, Tenjin-cho, Kiryu.

1) Part XXIV: K. Suzuki, M. Fujimoto, M. Murakami and M. Minabe, This Bulletin, **40**, 1259 (1967).

2) K. Suzuki, *Nippon Kagaku Zasshi (J. Chem. Soc. Japan, Pure Chem. Sect.)*, **72**, 825 (1951).

3) L. A. Pinck and G. E. Hilbert, *J. Am. Chem. Soc.*, **68**, 2014 (1946).

4) K. Suzuki, *Nippon Kakagu Zasshi (J. Chem. Soc. Japan, Pure Chem. Sect.)*, **70**, 189 (1949).

5) R. C. Fuson and H. D. Porter, *J. Am. Chem. Soc.*, **70**, 895 (1948); J. Thiele and A. Wansheidt, *Ann.*, **376**, 278 (1910).

Table 1. Reaction products of I and III under varied conditions

Run	Starting materials			Reaction conditions			Reaction products						Recvd.	
	I g	III g	Mol ratio of I/III	Solvent m*l*	Catalyst (base concn.) %	Time hr	IV g (%)	VI g	VII g	II g	Fluorenone g	2,7-Dibromo-fluorenone	I g	III g
1	3.3	3.2	1/1	Py 30	KOH 0.05	12	3.6 (55)	0.8	0.01		0.07	0.3	0.3	0.2
2	3.3	3.2	1/1	Py 30	KOH 0.1	2	1.0	3.5	0.2	0.25	0.18	0.25	0.01	
3	3.3	3.2	1/1	Py 30	KOH 1	2	0.6	4.0	0.25	0.2	0.2	0.3		0.03
4	3.3	3.9	1/1.2	Py 30	KOH 1	2	0.47	4.3	0.18	0.28	0.1	0.35		0.2
5	3.3	6.4	1/2	Py 30	KOH 1	2	0.3	6.55	0.05	0.35	0.08	0.4		0.85
6	6.6	3.2	2/1	Py 30	KOH 1	12	0.6	4.0	1.25	0.52	2.4	0.1	0.1	
7	3.3	3.2	1/1	EtOH 30	NaOEt 2.5	2.5	4.0 (61)	Trace					0.4	0.9
8	3.3	3.2	1/1	EtOH 30	NaOEt 15	2.5	5.72 (89)	0.08			0.02			

a) Py=Pyridine, EtOH=Ethanol, NaOEt=Sodium ethoxide.

b) Run 8: 9,9'-Bifluorenyl (0.06 g) and 2,7-dibromo-α, δ-dibiphenylenebutadiene (0.09 g) were also isolated.

Table 2. Reaction products of IX and II under varied conditions

Run	Substrates			Reaction conditions			Products							Recvd.	
	IX	II	Mol ratio of IX/II	Solvent ml	Catalyst (base conc.) %	Time hr	VIII g	VI g	IV g	VII g	III g	2,7-Dibromo-fluorenone g	Fluorenone g	IX g	II g
1	2.00	1.55	1/3	Py 20	—	200							trace	1.95	1.46
2	2.00	1.55	1/3	EtOH 30	NaOEt 5.8	13	1.31						0.43	0.30	0.26
3	2.00	1.55	1/3	EtOH 30	NaOEt 15	19.5	0.16*	0.54	0.33		0.08	0.01	0.08		0.73
4	2.00	1.55	1/3	Py 30	Na_2CO_3 5	100	1.85		0.02		trace	0.02	0.08	0.05	0.85
5	2.00	1.55	1/3	Py 30	KOH 0.5	10	0.58*	0.64	0.57	0.10	0.40	0.05	trace	trace	0.64
6	2.00	1.55	1/3	Py 30	KOH 3	5.7	0.20*	0.86	0.55	0.04	0.40	0.15	trace	trace	0.59
7	2.00	1.55	1/3	Py 30	KOH 5	4.3	0.34*	0.55	0.69	0.04	0.28	0.19	trace	trace	0.35
8	2.00	1.55	1/3	Py 30	KOH 5	12	0.06*	0.94	0.61	0.03	0.19	0.51	0.04		0.48
9	2.00	0.52	1/1	Py 30	KOH 3	5.7		1.04	0.08		0.06	0.30	0.06	0.65	trace
10	1.50 (V)	1.55	1/3	Py 30	KOH 3	1/6			1.57			trace			0.99
11	1.50 (V)	3.03 (III)	1/3	Py 30	KOH 3	1/6		2.42			1.44 (recvd.)				

a) Py=Pyridine, EtOH=Ethanol, NaOEt=Sodium ethoxide.
b) *=mp 303—304°C.
c) Reactions were carried out in sealed tube at 93—95°C (Runs 1—9) or 97—98°C (Runs 10, 11).
d) Run 2: The reaction was carried out in nitrogen medium at boiling point. 2,7-Dibromo-α,δ-dibiphenylenebutadiene was also obtained (0.56 g).
e) Run 3: 2,7-Dibromo-α,δ-dibiphenylenebutadiene (0.46 g) was also isolated.
f) Run 10: X (0.46 g) was also isolated.

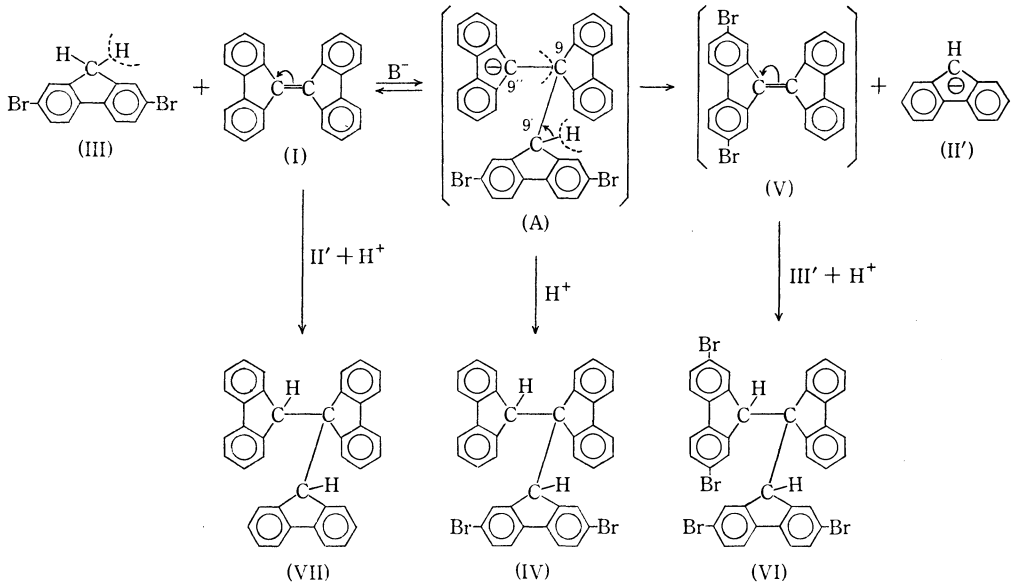

Scheme I

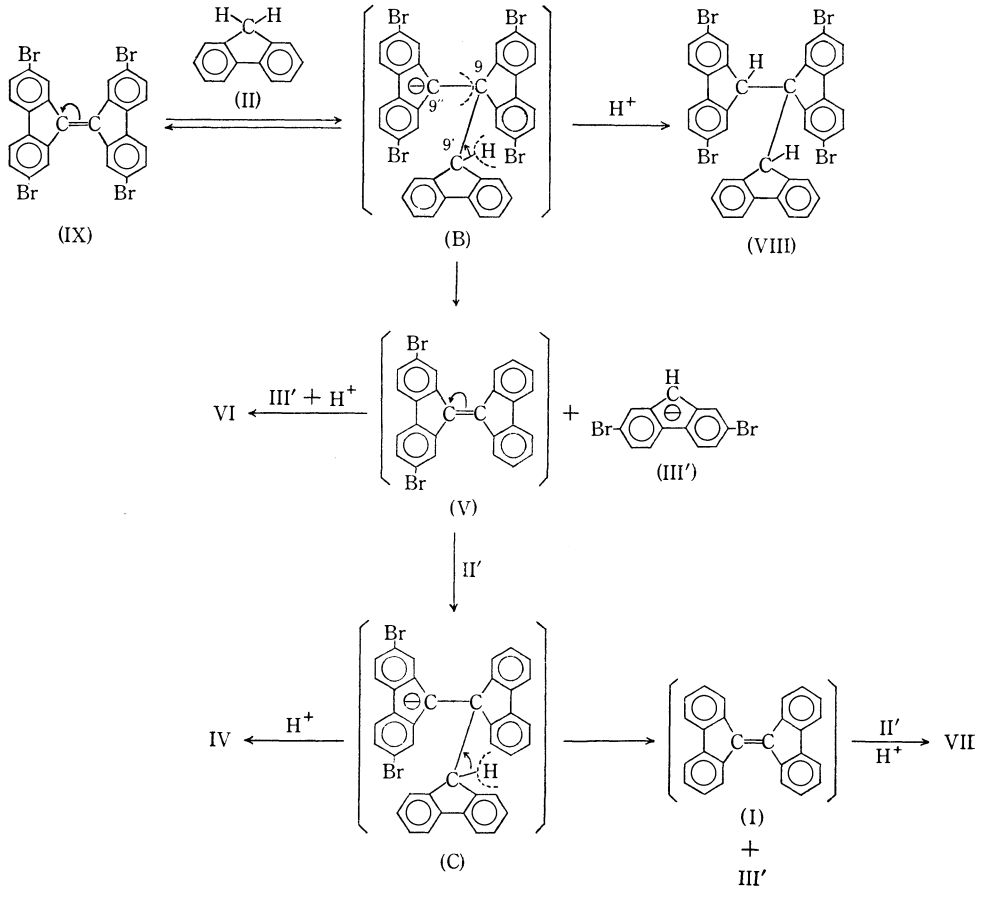

Scheme II

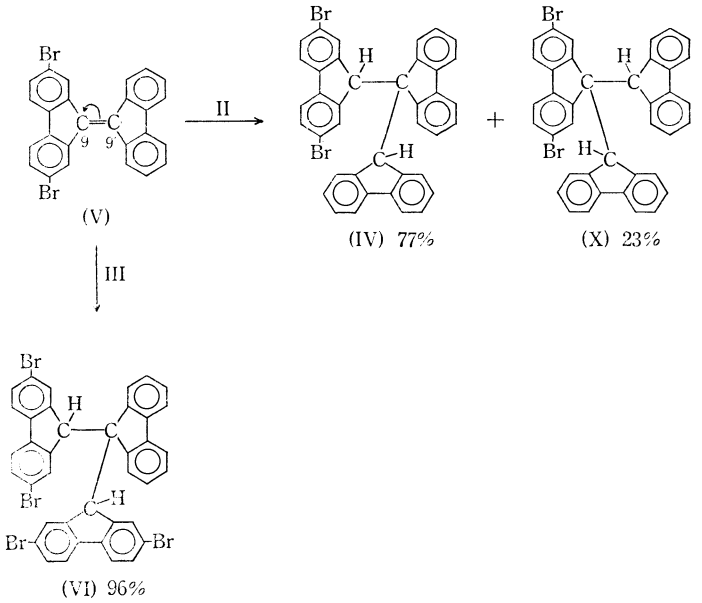

Scheme III

I in the presence of the base. (A) may then be transformed to the normal compound IV by protonation. The 9'-methine proton in (A) is reactive, and the fission of the 9—9'' carbon-carbon bond is accelerated when 2,7-dibromo-9,9'-bifluorenylidene (V) and 9-fluorenyl carbanion (II') are formed upon an increase in the alkali concentration. The abnormal VI is formed by a second Michael addition of III' and V. In this case, the yield of the secondary product, VI, is also increased if the amount of the donor, III, is raised (see Table 1, Run 5). The isomeric VIII was not formed. The unexpected formation of VII can be explained in terms of the interaction of I with II' which was eliminated from (A). The sequence of steps is shown in Scheme I.

A second transitory carbanion (B) is also formed by the interaction of IX with II. The formation of normal, abnormal, and elimination products is also conceivable as in the case of Scheme I. This sequence of steps is shown in Scheme II.

(A) and (B) are very crowded ions, and so the formation of II', III', or the stable V by an elimination reaction is perhaps favored over the protonation of (A) or (B) because there is sufficient space to release steric compression upon an increase in the alkali concentration.

The reactions of V and II or III were also carried out separately (see Table 2, Scheme III). The former reaction gave the two isomers in the ratio of 77% (IV) to 23% (X). The latter afforded a 96% yield of VI.

The 9'-carbon is more electro-positive than the 9-carbon for such highly-polarized acceptors as V because of the inductive effect of the two bromines. Also, the active methylene in the 9-position of III is greatly activated by the same means. Thus, IV and VI were formed exclusively in both reactions through, respectively, addition and protonation.

Thus, the yield of VI was higher than that of IV, while X was not isolated from the reaction products *via* the intermediate V during the interaction between IX and II. The tertiary product VII might be formed by the reaction of II and the I is eliminated from the carbanion (C).

Five related bromosubstituted tribiphenylenepropanes, IV, VI, VIII, X, and 2,7,2',7',2'',7''-hexabromotribiphenylenepropane,[6] were synthesized in order to confirm the reaction products from the interaction between substituted-9-bromo-9,9'-bifluorenyl and 9-lithiofluorenes by the halogen-lithium interconversion reaction shown in Table 3.

The thermal decomposition products of bromosubstituted tribiphenylenepropanes are interesting from the standpoint of free radical reaction. The thermal decomposition of X at 320°C led to 2, 7-dibromo-9,9'-bifluorenyl,[7] IX, V, 9,9'-bifluorenyl,[8] II, fluorenone, and 2,7-dibromofluorenone. Also, the thermal decomposition of VIII at 320—330°C led to IX, 2,7,2',7'-tetrabromo-9,9'-bifluorenyl,[6] V, 2,7-dibromo-9,9'-bifluorenyl, I, 9,9'-bifluorenyl, 2,7-dibromofluorenone, fluorenone, III, and II. These compounds were probably obtained by means of the formation and interaction of substituted

6) K. Suzuki, *Nippon Kagaku Zasshi (J. Chem. Soc. Japan, Pure Chem. Sect.)*, **75**, 795 (1954).

7) A. Sieglitz, *Ber.*, **53**, 2249 (1920); K. Suzuki, *Nippon Kagaku Zasshi (J. Chem. Soc. Japan, Pure Chem. Sect.)*, **72**, 828 (1951).

8) R. Weissgerber, *Ber.*, **46**, 2913 (1908).

Table 3. Syntheses of related bromosubstituted tribiphenylenepropanes by halogen-lithium interconversion reaction

Run	n-C_4H_9Br g	Li g	Fluorenes g	9,9'-Bifluorenyls g	Tribiphenyl-enepropanes	mp °C	g (%)	Anal Found C(%)	Found H(%)	Calcd C(%)	Calcd H(%)
1	4.2	0.4	2,7-Dibromo- 10.0	9-Bromo-[d] 6.3	2',7'-Dibromo- (IV)	284—285	3.45 (34.4)				
2	2.8	0.28	Fluorene 5.0	2,7,9'-Tribromo-[5] 5.7	2',7'-Dibromo- (IV)	285—287	3.85 (58.7)		Mixture mp test		
3	2.8	0.28	2,7-Dibromo- 3.5	2,7,9'-Tribromo-[5] 7.3	2',7',2'',7''-Tetrabromo- (VI)	313—314	5.75 (55.2)				
4	2.8	0.28	Fluorene 3.8	2,7,9-Tribromo-[5] 5.8	2,7-Dibromo- (X)	303—303.5	4.6 (70.1)	71.84	3.83	$C_{39}H_{24}Br_2$ 71.79	3.68
5	2.8	0.28	2,7-Dibromo- 10.0	2,7,9-Tribromo-[5] 5.8	2,7,2',7'-Tetrabromo- (VIII)	293—294	3.14 (7.9)	58.05	2.88	$C_{39}H_{22}Br_4$ 57.79	2.74
6	1.0	0.1	2,7-Dibromo- 2.3	2,7,2',7',9-Pentabromo- 5.1	2,7,2',7'2'',7''-Hexabromo-	332	1.45 (1.3)	48.82	2.39	$C_{39}H_{20}Br_6$ 48.39	2.08

a) All reactions were carried out in dry xylene medium.

b) Run 1: I (0.3 g), 9-hydroxy-9,9'-bifluorenyl (1.1 g) and III (1.55 g) were also isolated.

c) Run 6: 2,7,2',7',9-Pentabromo-9,9'-bifluorenyl (mp 420°C, 0.34 g), IX (0.04 g), 2,7,2',7'-tetrabromo-9-hydroxy-9,9'-bifluorenyl (0.5 g), 2,7,2',7'-tetrabromo-9,9'-bifluorenyl (0.26 g), III (0.6 g), and 2,7-dibromofluorenone (0.9 g) were also isolated.
2,7,2',7'-Tetrabromo-9-hydroxy-9,9'-bifluorenyl (mp 255—256°C, Found: C, 47.41; H, 2.39%. Calcd for $C_{26}H_{14}OBr_4$: C, 47.17; H, 2.13%). 2,7,2',7',9-Pentabromo-9,9'-bifluorenyl (mp>416°C, 79%) was obtained from the corresponding hydroxy compound by the action of hydrogen bromide in acetic acid.

d) cf). S. Kajigaeshi, *Nippon Kagaku Zasshi (J. Chem. Soc. Japan, Pure Chem. Sect.)*, **82**, 1712 (1961).

9-fluorenyl free radical species.

When 2,7-dibromo-9'-hydroxy-9,9'-bifluorenyl[9], one of the intermediates in the preparation of 2,7,9'-tribromo-9,9'-bifluorenyl,[9] was refluxed in ethyl alcohol for 25 min, fluorenone (89%) and III (78%) were formed. However, no reaction occured under the same conditions in a benzene solution. In two similar compounds, 9-hydroxy-9,9'-bifluorenyl[10] and 2,7-dibromo-9-hydroxy-9,9'-bifluorenyl[9], the same reaction did not occur in an ethyl alcohol solution.

In such a case, the reaction is presumably affected by an electron-attracting group, which makes the elimination of the two bromines easier. Ethanolysis can proceed through the hydrogen-bonded complex by means of the interaction of the substrate and a molecule of ethanol, as is indicated in Scheme IV.

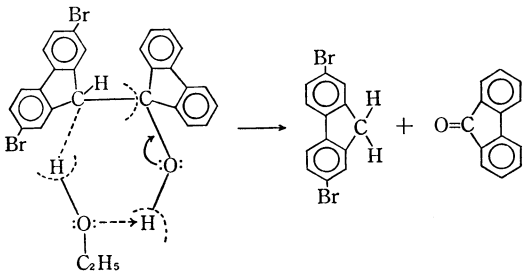

Scheme IV

Experimental[11]

The Michael Reaction of 9,9'-Bifluorenylidene (I) with 2,7-Dibromofluorene (III). *General Procedure.* A mixture of 3.3g (0.01mol) of I, 3.2g (0.01 mol) of III, and 3m*l* of a 10% aqueous potassium hydroxide solution in 30m*l* of pyridine was heated in a sealed tube for 2hr. The mixture turned dark after 1.5hr, and precipitates were formed. Upon the filtration of the hot solution, a light yellow product was obtained.

The resulting product was extracted several times with ethyl acetate; the evaporation of the solvent from this extract afforded 0.1g of colorless fluffy crystals of IV; mp 285—287°C (dec). Found: C, 71.92; H, 3.68%. Calcd for $C_{39}H_{24}Br_2$: C, 71.78; H, 3.68%. The residue was recrystallized from benzene to yield 3.1g of colorless VI; mp 312—314°C (dec). Found: C, 57.86; H, 22.7%. Calcd for $C_{39}H_{22}Br_4$: C, 57.79; H, 2.74%.

After the orange yellow pyridine mother liquor had been allowed to cool, a light yellow deposit was collected and extracted with hot cyclohexane. Upon the cooling of the cyclohexane extract, 0.05g of 2, 7-dibromofluorenone, mp 198—200°C, was isolated. The residue was extracted by refluxing it with ethyl acetate to afford 0.4g of IV, mp 286°C (dec). The last residual part was recrystallized from benzene to yield 0.2g of VI, mp 313—314°C (dec).

The original pyridine mother liquor was poured into water; the yellowish-orange material thus precipitated was collected by filtration, dried, and purified by fractional vacuum sublimation at 100—160°C to afford 0.15g of fluorenone, mp 82—84°C, 0.2g of II, mp 112—114°C, and 0.1g of 2, 7-dibromofluorenone, mp 197—200°C. The work-up of the residual part by column chromatography (benzene) and fractional recrystallization from ethyl acetate gave 0.15g of 2,7-dibromofluorenone, mp 198—200°C, 0.05g of fluorenone, mp 83°C, 0.25g of VII, mp 291—293°C (dec), (no halogen), 0.7g of VI, mp 313—314°C (dec), 0.1g of IV, mp 286°C (dec), and 0.03 g of III, mp 163—164°C

The Michael Reaction of 2,7,2',7'-Tetrabromo-9,9'-bifluorenylidene (IX) with Fluorene (II). *Materials.* IX was prepared according to a method in the literature,[12] but the product remained impure. Found: C, 51.20; H, 1.79%. Calcd for $C_{26}H_{12}Br_4$: C, 48.49; H, 1.88%. IX was then oxidized by means of sodium bichromate in acetic acid; the oxidation products, 2,7-dibromofluorenone and a small amount of 2-bromo-7-chlorofluorenone[13] as an impurity, were confirmed by gas chromatography. Pure IX, mp 429°C (dec), (Found: C, 48.55; H, 1.79%) was prepared by the reaction of 2,7,9-tribromofluorene[9] with methanolic potassium hydroxide in acetone under conditions similar to those used in the preparation of I.[5]

General Procedure. A mixture of 2.00g (0.0031 mol) of IX, 1.55g (0.0093 mol) of II, 0.9g of potassium hydroxide in 5m*l* of water, and 25m*l* of pyridine was heated in a sealed tube at 93—95°C for 5.7hr. During this period, the mixture turned from red to dark, and colorless crystals were formed.

Upon cooling, the deposited crystals were filtered, to this filtrate was added 25m*l* of methanol with stirring and the precipitated material was filtered again. The pyridine-methanol mother liquor was poured into water, and the precipitate was filtered, washed with water, dried, and sublimed *in vacuo* at 80—200°C.

The crops of the first and second portions were combined, washed with water, and dried, and then the residue of the sublimation was added. There were subsequently isolated 0.55g of IV, mp 285—286°C (dec), 0.86g of Vl, mp 313—314°C (dec), 0.04g of VII, mp 292—293°C (dec), (no halogen), 0.20g of a material with a mp of 303—304°C (dec) (Found: C, 57.78; H, 2.53%. Calcd for $C_{39}H_{22}Br_4$: C, 57.79; H, 2.74%), and a trace of recovered IX, mp 429°C (dec) by means of fractional recrystallization from ethanol, ethyl acetate, and benzene. The material with a mp of 303—304°C (dec) (see Table 2) contained a small percentage VI in VIII. This contamination with VI could not be removed. It seems to be the reason for these solubilities lying close together; the IR and UV absorption spectra and the R_f-values obtained by thin layer chromatography are also similar. A phase diagram plotting the melting points *versus* the compositions of synthetic mixtures of authentic VIII and VI indicates that a material with a melting point o 303—304°C (dec) would correspond to about 4—5% VI in 96—95% VIII. The small amount of VI causes only a small elevation in the melting point of VIII.

9) K. Suzuki and M. Fujimoto, This Bulletin, **36**, 1654 (1963).

10) V. Grignard and C. Courtot, *Compt. rend.*, **152**, 1493 (1911); C. Courtot, *Ann. Chem.*, **4**, 84 (1915).

11) All melting points are uncorrected.

12) J. Schmidt and H. Wagner, *Ann.*, **387**, 147 (1912).

13) K. Suzuki, *Nippon Kagaku Zasshi (J. Chem. Soc. Japan, Pure Chem. Sect.)*, **75**, 714 (1954).

The cyclohexane solution of the sublimed product was chromatographed on alumina. Further fractional recrystallization from ethanol gave 0.40g of III, mp 162—164°C, 0.15g of 2,7-dibromofluorenone, mp 200—202°C, and a trace of fluorenone, mp 82—84°C, while 0.59g of the II of the starting material, mp 112°C was also separated.

When sodium ethoxide was the catalyst, an unknown compound, mp 364°C (dec) was isolated as red needles (Table 2, Runs 2 and 3 or Table 1, Run 8). On oxidation with sodium bichromate in acetic acid, this material gave 73% of 2,7-dibromofluorenone and 41% of fluorenone, while the analytical results agreed with the value calculated for $C_{28}H_{16}Br_2$. The IR and UV absorption spectra of the compound with a mp of 364°C (dec) were very similar to those of α,δ-dibiphenylenebutadiene[14] and 2,7,2',7'-tetrabromo-α,δ-dibiphenylenebutadiene[15] respectively. Thus, the structure of the unknown compound is presumably 2,7-dibromo-α,δ-dibiphenylenebutadiene, which has not been described hitherto.

All the compounds in this reaction series were identified by mixed-melting-point determinations and by comparing their IR and UV absorption spectra with those of authentic samples.

The Michael Reactions of 2,7-Dibromo-9,-9-'bifluorenylidene (V) with Fluorene (II) or 2,7-Dibromofluorene (III). The reaction was performed in a similar manner, 1.5g (0.0031 mol) of V,[7] mp 242-243°C, 1.55g (0.0093 mol) of II, 0.9g of potassium hydroxide in 5m*l* of water, and 25m*l* of pyridine in a sealed tube were heated at 97—98°C for 10min.

The precipitate which formed upon cooling was fractionally recrystallized from ethyl acetate and benzene to afford 1.57g (77%) of IV, mp 285—286°C (dec) and 0.46g (23%) of X, mp 303°C (dec). Found (for X): C, 71.55; H, 3.59%. Calcd for $C_{39}H_{24}Br_2$: C, 71.78; H, 3.68%. In addition, 0.99g of II, mp 112—115°C, and a trace of 2,7-dibromofluorenone, mp 198°C, were isolated from the mother liquor and were purified by a combination of vacuum sublimation and column chromatography.

The product, 2.42 g of VI, mp 314°C (dec), was obtained in a good yield (96%) from 1.50 g of V and 3.03 g (0.0093 mol) of III under the reaction conditions described above.

The identities were confirmed by mixed-melting-point determinations and by a comparison of the IR and UV absorption spectra with those of authentic samples.

The Synthesis of 2',7'-Dibromotribiphenylenepropane (IV). *1) General Procedure.* The reaction of *n*-butyllithium and III in xylene led to 2,7-dibromo-9-fluorenyllithium, which then, upon treatment with carbon dioxide, gave 2,7-dibromofluorene-9-carboxylic acid, mp 208—209°C. Found: C, 45.49; H, 2.23%. Calcd for $C_{14}H_8O_2Br_2$: C, 45.69; H, 2.19%. IR: 1705 cm^{-1} (ν C–O) (KBr-disk).

2) *n*-Butyllithium was prepared from 2.8g (0.04 mol) of *n*-butyl bromide in 25 m*l* of anhydrous ether and 0.28g (0.04g atom) of lithium in 20m*l* of anhydrous ether. Then 9-fluorenyllithium was formed by adding 5g (0.03 mol) of fluorene in 50m*l* of anhydrous xylene to the *n*-butyllithium solution. To this mixture was added slowly 130m*l* of anhydrous xylene containing 5.7g (0.01 mol) of 2,7,9'-tribromo-9,9'-bifluorenyl with stirring.

After the reaction mixture had been allowed to stand overnight at room temperature, the precipitate was filtered, hydrolyzed with a dilute ammonium chloride solution, and recrystallized from ethyl acetate to give 3.8g (58.7%) of IV, mp 285—286°C (dec). mol wt: 658. Calcd for $C_{39}H_{24}Br_2$: 652.

Thermal Decomposition of 2,7-Dibromotribiphenylenepropane (X). Powdered X (5.0g; 0.0077 mol) was placed in a 100m*l* Erlenmeyer flask and then decomposed at 320°C in a preheated salt bath.

The red molten product was ground and extracted with boiling benzene, which had been filtered while hot. The orange colored residue was recrystallized form a large volume of benzene to yield 0.04g (2%) of IX, mp 430°C (dec).

The mother solution from this recrystallization was evaporated to dryness under reduced pressure. The fractional recrystallization of the residue from a mixture (1 : 1) of benzene and ethyl acetate gave 1.3g (35%) of 2,7-dibromo-9,9'-bifluorenyl, mp 268—270°C, 0.1g (4%) of 9,9'-bifluorenyl, mp 242—244°C, and 0.3g (6%) of of the starting material X, mp 303°C (dec).

When the product of the first benzene extraction was left to stand, red crystals (0.7g) of V, mp 240—242°C, separated out. This mother liquor was then evaporated to dryness under reduced pressure, and the residue was dissolved in benzene and chromatographed on alumina. A 0.7-g portion (27%) of 2,7-dibromofluorenone, mp 198—200°C, and 0.2g (7%) of fluorenone, mp 83°C, were isolated from the yellow band on the column. The colorless benzene eluate, upon evaporation and vacuum sublimation at 100°C, gave 0.05g (2%) of fluorene, mp 114°C. The residue from the sublimation was recrystallized from ethyl acetate to yield 0.15g of V, mp 240—242 °C (total; 0.85g, 23%).

Thermal Decomposition of 2,7,2',7'-Tetrabromotribiphenylenepropane (VIII). Finely powdered VIII (3.24g; 0.004 mol) was decomposed at 320—330°C in a preheated metal bath. The red molten product was then ground and extracted with boiling benzene. The insoluble red part was recrystallized from pyridine to yield 0.35g (14%) of IX (mp 429—430°C (dec)).

After the benzene mother liquor had been evaporated to a small volume, 0.59g (23%) of 2,7,2',7'-tetrabromo-9,9'-bifluorenyl,[3,5,7] mp 317—318°C, 0.68g (35%) of 2,7-dibromo-9,9'-bifluorenyl, mp 269—270°C, 0.25g (13%) of V, mp 241—242°C and the recovered VIII (0.02g; 1%) were separated by fractional recrystallization from ethyl acetate or benzene.

When the residual benzene solution was chromatographed on alumina, 0.03g (5%) of I, mp 182—184°C, 0.02g (3%) of 9.9'-bifluorenyl, mp 241—243°C, 0.01g (2%) of II (mp 114°C), and a trace of III were isolated. Moreover, 0.15g (6%) of 2,7-dibromofluorenone, mp 197—198°C, and 0.07g (10%) of fluorenone, mp 78—80°C, were separated from the two yellow bands.

The Reaction of 2,7-Dibromo-9'-hydroxy-9,9'-bifluorenyl in Ethanol. A mixture of 1.0g (0.002 mol) of 2,7-dibromo-9'-hydroxy-9,9'-bifluorenyl and 25m*l* of absolute ethanol was refluxed for 25min; the mixture turned yellow during this period. After half the volume

14) a) K. Suzuki, *Nippon Kagaku Zasshi (J. Chem. Soc. Japan, Pure Chem. Sect.)*, **75**, 711 (1954); W. Wislicenus, *Ber.*, **48**, 617 (1915); R. Kuhn and A. Weinterstein, *Helv. Chim. Acta*, **11**, 119 (1928). b) M. K. Starfass, *Bull. Soc. Chim.*, [4] **29**, 145 (1921).

15) See Refs. 2 and 14 b; E. Bergmann, H. Hoffman and D. Winter, *Ber.*, **66**, 46 (1933).

of the original alcohol had then been removed, pure crystals (0.5g;78%) of III, mp 165°C, were deposited.

The mother liquor was evaporated to dryness under reduced pressure, and the benzene solution of the residual part was chromatographed on alumina. Moreover, 0.32g (89%) of fluorenone, mp 81°C, was isolated from the yellow band and recrystallized from alcohol.

On the other hand, when 1.0g (0.002 mol) of 2,7-dibromo-9-hydroxy-9,9′-bifluorenyl was refluxed in absolute ethanol (45m*l*) for 3hr, 0.89g (89%) of the starting material was recovered.

The authors wish to express their gratitude to Drs. John and Elizabeth Weisburger of the National Institutes of Health, U.S.A., for supplying valuable information.

BULLETIN OF THE CHEMICAL SOCIETY OF JAPAN VOL. 42 1617—1621 (1969)

Synthesis of Adamantane Derivatives. III.[1] Synthesis of Adamantane Heterocycles

Tadashi SASAKI, Shoji EGUCHI and Takeshi TORU

Institute of Applied Organic Chemistry, Faculty of Engineering, Nagoya University, Chikusa-ku, Nagoya

(Received July 29, 1968)

Preparation of 1-adamantyl and adamantane-1-carbonyl derivatives having benzimidazole, 1,3,5-oxadiazole, oxazoline-2, quinoxaline, 2-aminothiazole, thiazolone, 2-methylthiazole, 1,2,3-thiadiazole, pyrazole or pyrazoline ring is described.

The unique structure of adamantane and the pharmaceutical effects of 1-adamantylamine hydrochloride on virus[2] have attracted many chemists and pharmacologists to do considerable work on the syntheses of adamantane derivatives,[3] although the biological activities of adamantane-containing agents are known in general to be quite reduced as the result of seemingly minor structural changes in the adamantane moiety.[4]

However, only a few 1-adamantyl heterocycles have been reported,[5] in which interesting interactions between adamantane and heterocyclic moiety could be anticipated from the pharmacological and also chemical viewpoints. Our present paper is concerned with the preparation of some 1-adamantane derivatives having a five- or six-membered heterocyclic ring.

Results and Discussion

Adamantane-1-carboxylic acid (I) was heated with *o*-phenylenediamine in the presence of hydrochloric acid or polyphosphoric acid, according to the general procedure for the preparation of benzimidazoles from aliphatic acids and *o*-phenylenediamine,[6] but these attempts were unsuccessful; in the former reaction, only the starting materials were recovered, and in the latter, adamantane was formed. The imidazole was obtained by the following stepwise method: *N*-(adamantane-1-carbonyl)-*o*-phenylenediamine (III) was prepared from adamantane-1-carbonyl chloride (II, Ad= adamantyl)[7,8] and *o*-phenylendiamine and III were refluxed with polyphosphoric acid ester (ppe) in chloroform to yield a benzimidazole derivative (IV).

1) Part II of this series; T. Sasaki, S. Eguchi and T. Toru, This Bulletin, **41**, 238 (1968).

2) W. L. Davis, R. R. Grunert, R. F. Hoff, J. W. McGahen, E. M. Neumayer, M. Paulschock, J. W. Watts, T. R. Wood, E. C. Herman and C. E. Hoffmann, *Science*, **144**, 862 (1964).

3) R. C. Fort, Jr., and P. von R. Schleyer, *Chem. Revs.*, **64**, 277 (1964).

4) K. Gerzon, D. J. Tobias, Jr., R. E. Hilmes, R. E. Rathbun and R. W. Kattau, *J. Med. Chem.*, **10**, 603 (1967), and references cited therein.

5) H. Stetter and E. Rauscher, *Chem. Ber.*, **93**, 2054 (1960).

6) J. B. Wright, *Chem. Revs.*, **48**, 397 (1951).

7) H. Stetter, M. Schwartz and A. Hirschhorn, *Angew. Chem.*, **71**, 429 (1959); *Chem. Ber.*, **92**, 1629 (1959); H. Stetter and E. Rauscher, *ibid.*, **93**, 1161 (1960).

8) The crude acid, obtained from 1-adamantyl bromide and formic acid, should be purified by the alkaline extraction, followed by acidification with hydrochloric acid. The purified I was dissolved in a mixture of dry benzene and thionyl chloride and the reaction mixture was kept standing at around 50°C for 2 hr. If the crude acid was used for the preparation of the acid chloride II, a large amount of 1-adamantyl chloride was formed besides the desired acid chloride, as was pointed out by a recent report: L. F. Fieser, M. Z. Nazer, S. Archer, D. A. Berberian and R. G. Slighter, *J. Med. Chem.*, **10**, 517 (1967).

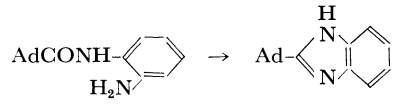

III IV

N,N'-Bis(adamantane-1-carbonyl)hydrazine (V), prepared from II, was treated with perchloric acid in acetic anhydride[9] to afford 2,5-di(1-adamantyl)-1,3,4-oxadiazole (VI) in 50% yield. VI was also prepared in a 40% yield from the reaction between V and ppe in chloroform, but treatment of V with concd. sulfuric acid was unsuccessful and gave only adamantane-1-carboxylic acid I. Acylaziridine is known to be rearranged by heating with sodium iodide to oxazoline derivative.[10] Thus, 2-(1-adamantyl)-2-oxazoline (VIII), isolated as its picrate, was prepared from adamantane-1-carbonylaziridine (VII) which was obtained from II and ethyleneimine.

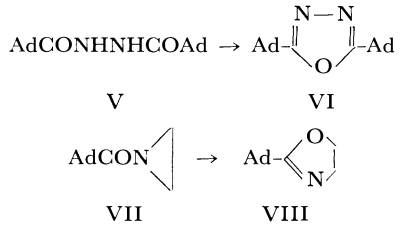

V VI

VII VIII

Adamantane-1-carbonyldizaomethane (IX)[11] could be an excellent precursor for the preparation of adamantane heterocycles. Treatment of II with excess diazomethane in ether gave the diazoketone IX in a good yield. Although reaction of IX with triphenylphosphine proceeded rather slowly (1 day) at room temperature, the triphenylphosphazine (X)[11] was obtained in a good yield of 88%. Phosphazine X was decomposed with nitrous acid to give 1-adamantylglyoxal (XI)[11-12] which, without isolation, was condensed with *o*-phenylenediamine to afford a quinoxaline derivative (XII) in 35% yield. Condensation of IX with thiourea in refluxing ethanol for 5 days afforded 4-(1-adamantyl)-2-aminothiazole (XIII) only in 8% yield after purification on a silica gel column, while heating a mixture of an ethanolic solution of IX and thiourea in a sealed tube at 100°C for 5 days afforded XIII in 20% yield, accompanied by a large amount of untractable decomposition products. The yield was improved up to 65% by using condensation reaction of thiourea with the haloketone (XIV)[11-12] which was easily prepared from IX and concd. hydrochloric or hydrobromic acid.

Reaction of the chloroketone (XIVa) with potassium thiocyanate gave oily adamantane-1-carbonylmethyl thiocyanate (XV) which was hydrolyzed to afford 4-(1-adamantyl)thiazol-2-one (XVI), whereas attempts to cyclize IX with potassium cyanide to the triazine in an aqueous medium were unsuccessful. A thiazole derivative (XVII) was also prepared by the cyclization of the haloketone (XIV) with thioacetamide.

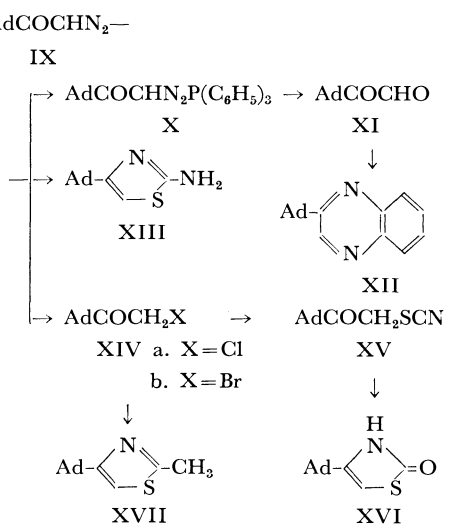

IX X XI XIII XII XIV a. X=Cl b. X=Br XV XVII XVI

Though 1,3-dipolar cycloaddition reaction of diazoalkanes is well known to afford some heterocycles, the reactivity of most diazoketones in the cycloaddition reaction has been pointed out to be low.[13] Compound IX was also not expected to be very reactive, so drastic conditions were applied to the 1,3-dipolar cycloaddition of IX. Treatment of IX with cyanoacetylene in dioxane at 100°C gave 3(5)-(adamantane-1-carbonyl)-5(3)-cyanopyrazole (XVIII) in 92% yield, while IX did not react with it at room temperature. The structure of XVIII was confirmed from analytical and spectral data; the NMR spectrum of XVIII showed a singlet at 2.72 τ due to a ring proton and a broad singlet at -4.2 τ due to an NH proton which disappeared on deuteration. Cycloaddition of IX with acrylamide gave 3-(adamantane-1-carbonyl)-5-carbamoyl-2-pyrazoline (XIX), the structure of which was confirmed from analytical and spectral data.[14] The cycloaddition of diazoalkane with isocyanate has been reported by

9) G. V. Boyd, *Chem. Commun.*, **1967**, 954.

10) H. W. Heine and M. S. Kaplan, *J. Org. Chem.*, **32**, 3069 (1967), and references cited therein.

11) H. Stetter, M. Schwartz and A. Hirschhorn, *Chem. Ber.*, **92**, 1629 (1959); *Neth. Appl.*, **6**, 404, 856 (1965); *Chem. Abstr.*, **64**, 12569f (1966).

12) M. Kuchar, *Collection Czech. Chem. Commun.*, **33**, 880 (1968).

13) See the excellent review, R. Huisgen, R. Grashey and J. Sauer, "Cycloaddition Reactions of Alkene" in "The Chemistry of Alkene," ed. by S. Patai, Interscience Publishers, New York, N. Y. (1964), p. 806—878.

14) R. Sustmann, R. Huisgen and H. Huber, *Chem. Ber.*, **100**, 1802 (1967).

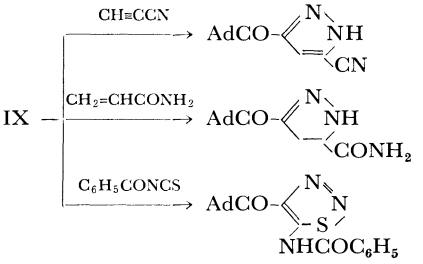

several workers.[15] The reaction of IX with benzoylisothiocyanate in dioxane at 100°C gave a thiadiazole derivative (XX) in 47% yield. This structure was confirmed from infrared and ultraviolet spectrum[16] which had the maxima at 238 mμ (ε 18200) and 299 mμ (ε 15700) in ethanol.

The infrared, NMR and ultraviolet spectral data of the reaction products are summarized in Table 1.

Table 1. Spectroscopic data of the reaction products

Compound	Infrared spectrum cm^{-1} (KBr)	NMR spectrum[a] τ ($CDCl_3$)	Ultraviolet spectrum $\lambda_{max}^{ethanol}$, mμ (ε)
III	3500, 3400, 3300, 3040, 1645, 1615, 1520, 740		
IV	3040, 1620, 1590, 1530, 740		281(10450), 275(9400), 243(7150)
VI	1590, 1560, 1050		250(23)
VIII[b]	1625, 1610	8.28(6H, s), 8.06(6H, s), 8.00(3H, br. s), 6.00(2H, m), 5.09(2H, m), 5.0(1H, br. s), 1.44(2H, s)	
IX	2110, 1620	8.29, 8.25, 8.20(12H, os), 7.98(3H, br. s) 4.61(1H, s)	340(320), 250(7310)
X	3060, 1627, 1590, 1530		
XII	3020, 1610, 1553, 762	8.16(6H, s), 7.85(9H, s), 2.08(4H, m), 1.00(1H, s)	319(7450), 309(6670) 235(2980)
XIII	3480, 3310, 3180, 1640, 1625, 1607, 1530, 1520[c]	8.25, 8.22(6H, os), 8.13, 8.09(6H, os), 7.99(3H, br. s) 3.98(1H, s), 4.95(2H, br. s)	253(5790)
XVIa	1710		
XIVb	1702		
XVI	3000, 1650, 1600	8.27, 8.20, 8.15(12H, os), 7.97(3H, br. s), 4.45(1H, d, J=2.1 Hz)[f]	217(6580)
XVII	3100, 1513[d]	8.18(6H, s), 7.98(9H, s), 7.33(3H, s), 3.38(1H, s)	242(4050)
XVIII	3250, 3140, 2270, 1655, 1575, 1537	8.20(6H, s), 7.96(6H, s) 7.88(3H, br. s), 2.72(1H, s), −4.2(1H, br. s)[g]	237(8710)
XIX	3350, 3250, 3220, 1685, 1670, 1640, 1605[e]	8.22(6H, s), 7.94(9H, s), 6.9(2H, m), 5.8(1H, m), 3.25(2H, br. s), 2.37(1H, s)[h,g]	209(16400), 234(7710)
XX	3250, 3050, 1665, 1630, 1600, 1580, 1510		299(15700), 238(18200)

a) br.=broad, s=singlet, d=doublet, m=multiplet, os=overlapped singlet.
b) 2-(1-adamantyl)-2-oxazoline picrate
c) 3480, 3310(ν_{NH}), 3180($\nu_{ring\ CH}$), 1640, 1625, 1607, 1530 (ring vibration), 1520 (δ_{NH}); P. J. Chouteau, G. Davidovics, J. Metzger, M. Azzaro and M. Poite, *Bull. Soc. Chim. France*, **1962**, 1794.
d) 3100 ($\nu_{ring\ CH}$), 1513 (ring vibration).
e) 3350, 3250, 3220 (ν_{NH}), 1685, 1670, 1605 (amide I and II), 1640 ($\nu_{C=N}$).
f) The doublet is due to the interaction with NH proton.
g) The NMR measurement was carried out in deuterated chloroform-deuterated dimethylsulfoxide.
h) The coupling constants could not be ascertained, see R. Sustmann, R. Huisgen and H. Huber, *Chem. Ber.*, **100**, 1802 (1967).

15) W. Ried and B. M. Beck, *Ann.*, **673**, 128 (1964); D. Martin and W. Mucke, *ibid.*, **682**, 90 (1965); J. C. Sheehan and P. T. Izzo, *J. Am. Chem. Soc.*, **71**, 4059 (1949).

16) 4-Nitrofuryl-5-benzoylamino-1,2,3-thiadiazole had the ultraviolet absorptions at 233 mμ (ε 29700), 306 mμ (ε 17800) and 374 mμ (ε 17800) and the infrared absorptions at 3430, 3340, 1675, 1630, 1603 and 1585 cm^{-1}; unpublished data of our laboratory.

Experimental

The microanalyses were performed on a Yanagimoto C. H. N. Corder, Model MT-1, while the IR spectra and the UV spectra were obtained on a JASCO Model IR-S infrared spectrophotometer and a JASCO Model ORD/UV-5 ultraviolet spectrophotometer, respectively. All the melting points were measured on a Yanagimoto micromeltingpoint apparatus and are uncorrected.

***N*-(Adamantane-1-carbonyl)-*o*-phenylenediamine (III).** To a solution of *o*-phenylenediamine (0.3 g) and triethylamine (0.3 g) in dry ether was added a solution of II, obtained from 0.5 g of I, in the same solvent. The reaction mixture was stirred overnight at room temperature and filtered. The precipitates were washed with water and recrystallized from aqueous methanol to give 470 mg (63%) of III as colorless plates, mp 229—231°C.

Found: C, 74.99; H, 8.53; N, 10.42%. Calcd for $C_{17}H_{22}ON_2$: C, 75.52; H, 8.20; N, 10.36%.

2-(1-Adamantyl)benzimidazole (IV). The compound III (200 mg) was refluxed in chloroform added with 5 drops of ppe. The mixture was poured into water and the organic layer was washed with aqueous sodium bicarbonate, dried over sodium sulfate and evaporated to dryness. Recrystallization of the residue from chloroform afforded 180 mg (96%) of IV as colorless needles, mp>300°C.

Found: C, 80.82; H, 8.06; N, 11.20%. Calcd for $C_{17}H_{20}N_2$: C, 80.91; H, 7.99; N, 11.10%.

2,5-Di(1-adamantyl)-1,3,4-oxadiazole (VI). *N,N'*-Bis(adamantane-1-carbonyl)hydrazine (V)[6] (400 mg) was dissolved in hot acetic anhydride (15 m*l*), added with 4 drops of 60% perchloric acid. After 10 min, the mixture was cooled and filtered. Water was added to the filtrate and the separated crystals were collected. The combined crystals were washed with water and recrystallized from aqueous acetone affording the oxadiazole (VI) (190 mg, 50%) as colorless plates, mp >300°C in a sealed tube.

Found: C, 78.26; H, 9.21; N, 8.38%. Calcd for $C_{22}H_{30}ON_2$: C, 78.06; H, 8.93; N, 8.28%.

2-(1-Adamantyl)-2-oxazoline (VIII). A mixture of ethyleneimine (0.13 g) and triethylamine (0.3 g) in dry ether was added dropwise to a solution of II, obtained from 0.5 g of I, in dry ether. The reaction mixture was stirred for 30 min under ice-cooling and then for 10 min at room temperature. The solution was filtered and the precipitates were washed with dry ether. The filtrate was dried over sodium sulfate and evaporated *in vacuo* affording a brownish oil (VII); the infrared spectrum showed absorptions at 3050 (ν_{CH}) and 1680 (ν_{CO}) cm^{-1}. The oil VII was refluxed in acetone (15 m*l*) with sodium iodide (0.2 g) for 26 hr. The solution was concentrated *in vacuo* and the residual oil was extracted with ether. The ether extracts were washed with water, dried and condensed *in vacuo*. The residue gave the picrate on treatment with picric acid, which was recrystallized from ethanol to afford yellow needles (0.52 g, 43% based on I), mp 216—218°C.

Found: C, 52.75; H, 5.20; N, 13.24%. Calcd for $C_{19}H_{22}O_8N_4$: C, 52.53; H, 5.10; N, 12.90%.

Adamantane-1-carbonyldiazomethane (IX). A solution of II, obtained from 1.0 g of I, in ether was added to a solution of diazomethane in ether under cooling. After standing for 2 days at room temperature, the solvent and excess diazomethane were removed *in vacuo* and residual yellow solid was recrystallized from methanol to give 0.82 g (72% based on I) of IX as yellow plates, mp 69—71°C.

Found: C, 70.85; H, 8.00; N, 13.34%. Calcd for $C_{12}H_{16}ON_2$: C, 70.56; H, 7.90; N, 13.72%.

α-(Adamantane-1-carbonyl)triphenylphosphazine (X). A mixture of the diazoketone IX (200 mg) and triphenylphosphine (330 mg) in dry ether was stirred for 1 day, cooled and the resulting precipitates were filtered. The precipitates were washed with dry ether and recrystallized from benzene affording 410 mg (88%) of the triphenylphosphazine X as yellow crystals, mp 125—127°C.

Found: C, 76.81; H, 6.20; N, 5.56%. Calcd for $C_{30}H_{31}ON_2P$: C, 77.23; H, 6.70; N, 6.00%.

2-(1-Adamantyl)quinoxaline (XII). An aqueous solution of sodium nitrite (60 mg) was added to a suspension of X (410 mg) in acetone (2 m*l*) and then 20% hydrochloric acid was added to the mixture under ice-cooling. The reaction mixture was stirred for 30 min under ice-cooling and then for 30 min at room temperature. The mixture was extracted with ether and the ether extracts were washed, dried and evaporated *in vacuo* leaving an oil of XI whose infrared spectrum showed absorptions at 2730 (ν_{CHO}), 1700 (ν_{CO}) and 1660 (ν_{CO}) cm^{-1}. A mixture of XI, *o*-phenylenediamine (100 mg) and anhydrous acetic acid (1 drop) was refluxed in ethanol for 4 days. The solvent was evaporated leaving a brownish oil which was dissolved in a small amount of methanol and solidified on cooling. Recrystallization from methanol gave 80 mg (35% from X) of a quinoxaline XII as dark brown plates, mp 119—120°C.

Found: C, 82.04; H, 7.58; N, 10.57%. Calcd for $C_{18}H_{19}N_2$: C, 81.78; H, 7.68; N, 10.60%.

1-Adamantyl chloromethyl ketone (XIVa). Concentrated hydrochloric acid was added to a solution of IX (0.8 g) in dioxane (4 m*l*) under ice-cooling. The reaction mixture was heated at 70°C for 5 min until evolution of nitrogen had ceased completely. The reaction mixture was allowed to cool to room temperature and then water was added to it. The resulting precipitates were collected by filtration, and recrystallized from a mixture of acetone and petroleum ether (bp 40—60°C) to give 0.7 g (84%) of XIVa as colorless plates, mp 106—107°C, which showed a positive Beilstein test.

Found: C, 67.47; H, 8.05%. Calcd for $C_{12}H_{17}OCl$: C, 67.76; H, 8.06%.

1-Adamantyl bromomethyl ketone (XIVb). The work-up as above except using hydrobromic acid instead of hydrochloric acid afforded the precipitates which were recrystallized from methanol giving 220 mg (87.5%) of XIVb as colorless powder, mp 78—79°C, from 200 mg of IX. XIVb showed a positive Beilstein test.

Found: C, 56.17; H, 6.93%. Calcd for $C_{12}H_{17}OBr$: C, 56.04; H, 6.67%.

4-(1-Adamantyl)-2-aminothiazole (XIII). *a) from IX.* A mixture of IX (300 mg) and thiourea (400 mg) was heated at 100°C in ethanol (10 m*l*) in a sealed tube for 5 days. Ethanol was removed and the residue was dissolved in chloroform. The solution was washed with water, dried and chromatographed on a silica gel column, using chloroform as an eluent. Recrystalliza-

tion from acetone gave 70 mg (20%) of XIII as colorless needles.

b) from XIVa. XIVa (80 mg) and thiourea (150 mg) were refluxed in ethanol for 12 hr. The solvent was removed *in vacuo* and the residue was recrystallized from acetone to give 70 mg (65%) of XIII, mp 224—226°C.

Found: C, 66.91; H, 7.82; N, 11.73%. Calcd for $C_{13}H_{18}N_2S$: C, 66.60; H, 7.74; N, 11.95%.

4-(1-Adamantyl)thiazolone (XVI). An acetone solution (15 m*l*) of XIVa (170 mg) and potassium thiocyanate (78 mg) was refluxed for 5 hr. After cooling, the solution was filtered and the filtrate was evaporated *in vacuo*. The residue was dissolved in a mixture of methanol (1 m*l*), water (3 m*l*) and concd. hydrochloric acid (0.5 m*l*) and the mixture was maintained at 70°C for 15 hr. After cooling, the precipitates were collected and recrystallized from a mixture of chloroform and *n*-hexane to give 80 mg (42.5%) of XVI as colorless plates, mp 293.5—295.5°C.

Found: C, 65.95; H, 7.24; N, 5.80%. Calcd for $C_{13}H_{17}ONS$: C, 66.36; H, 7.28; N, 5.95%.

4-(1-Adamantyl)-2-methylthiazole (XVII). A solution of thioacetamide (120 mg) in dry benzene (2 m*l*) was added in small portions to a solution of XIVa (200 mg) in the same solvent (2 m*l*). After refluxing for 24 hr, benzene was removed *in vacuo* and the residue was recrystallized from methanol affording 100 mg (45.5%) of XVII as colorless plates, mp 97—98°C.

Found: C, 72.17; H, 8.19; N, 6.00%. Calcd for $C_{14}H_{19}NS$: C, 72.16; H, 8.22; N, 6.01%.

4-(Adamantane-1-carbonyl)-5-benzoylamino-1,2,-3-thiadiazole (XX). A mixture of IX (100 mg) and benzoyl isothiocyanate (0.5 m*l*) was kept at 100°C for 1 day. On addition of *n*-hexane to the cooled reaction mixture, yellowish white crystals were separated and further crops were obtained from the mother liquor giving an overall yield of 85 mg (47%) of XX. Recrystallization from a mixture of acetone and *n*-hexane gave yellowish white needles, mp 225—226°C.

Found: C, 65.46; H, 5.68; N, 11.48%. Calcd for $C_{20}H_{21}O_2N_3S$: C, 65.36; H, 5.76; N, 11.44%.

3(5)-(Adamantane-1-carbonyl)-5(3)-cyanopyrazole (XVIII). IX (200 mg) and cyanoacetylene (100 mg) was heated at 100°C in anhydrous dioxane for 1 day. Water was added to the cooled solution to give colorless crystals. Recrystallization from a mixture of methanol and *n*-hexane afforded 230 mg (92%) of XVII as colorless needles, mp 224.5—225.5°C.

Found: C, 70.53; H, 6.43; N, 16.45%. Calcd for $C_{15}H_{17}ON_3$: C, 70.56; H, 6.71; N, 16.46%.

3-(Adamantane-1-carbonyl)-5-carbamoyl-2-pyrazoline (XIX). IX (270 mg) and acrylamide (120 mg) were heated at 100°C in dioxane in the presence of triethylamine (1 drop) for 1.5 days. Addition of water to the cooled reaction mixture afforded solids which were recrystallized from methanol giving 50 mg (14%) of XIX as yellow needles, mp 275—277.5.5°C.

Found: C, 65.63; H, 7.37; N, 15.25%. Calcd for $C_{15}H_{21}O_2N_2$: C, 65.43; H, 7.69; N, 15.26%.

The authors wish to express their thanks to Takeda Chemical Industries, Ltd., for running the NMR spectra, and especially to Mr. Akiho Ishihara of their laboratories who carried out the microanalyses.

BULLETIN OF THE CHEMICAL SOCIETY OF JAPAN VOL. 42 1622—1627 (1969)

The Alkaline Ethanolyses of Chlorophenyldiphenylsulfonium Halides, Chlorophenyl Phenyl Sulfones and Chloronitrobenzene in Aqueous Ethanol[1)]

Shigeru OAE and Yong He KHIM

Department of Applied Chemistry, Faculty of Engineering, Osaka City University, Sugimoto-cho, Sumiyoshi-ku, Osaka

(Received September 5, 1968)

o-, *m*-, and *p*-Chlorophenyldiphenylsulfonium halides were prepared and subjected to the alkaline ethanolysis in order to compare the activating effects of *o*-, *m*-, and *p*-diphenylsulfonio groups with those of *o*-, *m*-, and *p*-phenylsulfonyl and nitro-groups. The diarylsulfonio group at either ortho or para position was found to facilitate the nucleophilic substitution of aryl chloride powerfully. While the effect of diarylsulfonio group was not only substantially larger than that of phenylsulfonyl group, but also exceeding even that of nitro group. Meanwhile, with ethoxide ion in ethanol the alkaline decomposition reaction, presumed to be initiated by the attack of ethoxide on the sulfur atom of chlorophenyldiphenylsulfonium halide, occurred competitively along with the S_N reaction, but the rate of the S_N reaction of *p*-chlorophenyldiphenylsulfonium perchlorate was found to be about 9 times larger than that of the decomposition reaction. Substitution of a methyl group at ortho to diphenylsulfonio, phenylsulfonyl and -sulfinyl groups did change very little the rates of the ethanolyses of the corresponding *p*-substituted chlorobenzenes, suggesting that essentially there is no or little steric inhibition for the 3d-orbital resonance with either sulfonio, sulfinyl, or sulfonyl group in the S_N reaction of these compounds.

In the previous paper,[1)] dealing with the alkaline hydrolyses of chlorophenyl phenyl sulfones and sulfoxides in aqueous dimethyl sulfoxide, we have shown that both phenylsulfonyl and -sulfinyl groups at either *o*- or *p*-positions markedly accelerate the aromatic S_N reaction of hydrolysis.

This reaction is presumed to involve the initial formation of an addition intermediate (I or I') which is undoubtedly stabilized by the 3d-orbital conjugative effect of phenylsulfonyl or phenylsulfinyl group.

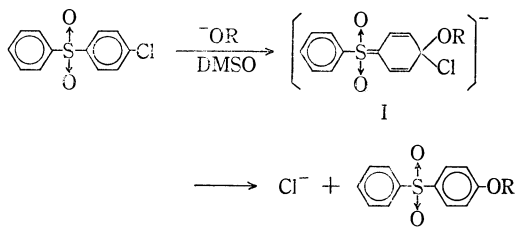

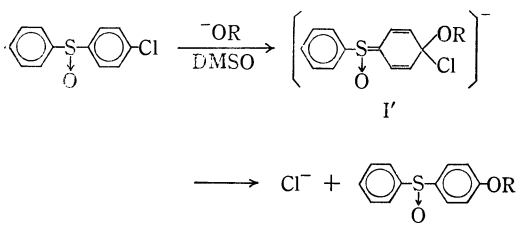

In the nucleophilic substitution of aromatic halides, an electron-accepting group such as sulfonyl or nitro group, is known to accelerate the rate especially when the group is located at either ortho or para to the halogen group.[2)] Meanwhile the acidity constants[3)] of *m*- and *p*-methylsulfinyl, sulfonyl and dimethylsulfonio-phenols reveal that the sulfonio group at *p*-position can display a relatively strong electron-accepting 3d-orbital resonance effect, and its effect is even larger than that of the corresponding sulfonyl group. Therefore, the sulfonio group when substituted at either ortho or para-position is expected to facilitate the alkaline hydrolysis substantially more than when substituted at meta-position, while the ethanolysis of the sulfonio-substituted chlorobenzene will be much faster than the corresponding sulfonyl compound. In fact, *p*-dimethylsulfonic group is known to increase the reactivity of 2-nitrochlorobenzene more than *p*-trimethylammonio

1) For previous work see: S. Oae and Y. H. Khim, This Bulletin, **40**, 1716 (1967).

2) H. R. Todd and R. L. Shriner, *J. Am. Chem. Soc.*, **56**, 1382 (1934).

3) a) S. Oae and C. C. Price, *ibid.*, **80**, 3482 (1958). b) C. C. Price and S. Oae, "Sulfur Bonding," Donald Press, New York, N. Y. (1962), Chapter 3. c) F. G. Bordwell and P. S. Bountan, *J. Am. Chem. Soc.*, **78**, 87 (1956).

group in the alkaline methanolysis.[4] However there is no quantitative data to compare the activating effects of sulfonio group with other corresponding sulfur groups. In order to examine the effect of sulfonio group in the aromatic S_N reaction we have synthesized comparatively more stable sulfonium salts, *i. e.*, *o*-, *m*- and *p*-chlorophenyldiphenylsulfonium perchlorate from diphenylethoxysulfonium tetrafluoroborate and chlorophenyl Grignard reagents and subjected to the alkaline S_N reactions in aqueous ethanol in order to compare the relative activating effect of diphenylsulfonio group with those of phenylsulfonyl and nitro groups.

Meanwhile, in view of the formation of the various products in the treatment of triarylsulfonium salt with bases, the alkaline decomposition is expected to give different products dependent on the nature of the bases. In fact, we have found that the reaction of triphenylsulfonium bromide with dimsyl anion in dimethyl sulfoxide gives diphenyl sulfide, benzene, thioanisole and *o*-methylmercaptophenol, while the treatment with piperidide anion gives diphenyl sulfide and phenylpiperidine; meanwhile the reaction with *p*-methylthiophenoxide ion also gave diphenyl sulfide and phenyl tolyl sulfide. In the case with ethoxide anion, diphenyl sulfide, benzene and aldol resins were obtained as main products together with a small amount of phenetole. The detailed mechanisms of these alkaline decompositions of triarylsulfonium halides will be reported in another paper.[5]

For the kinetic experiments of S_N and alkaline decomposition reactions, the ethoxide anion in aqueous ethanol was selected as the base. In this case the attack could occur at both the carbon atom bearing chlorine atom and the sulfur atom of the sulfonium salt. However, when *o*- and *p*-chlorophenyldiphenylsulfonium perchlorate were treated with potassium hydroxide in 70% (vol%) aqueous ethanol, both *o*- and *p*-ethoxyphenyldiphenylsulfonium perchlorate were the major isolable products, indicating that the reaction appears to proceed through a typical aromatic S_N path like in the cases of the sulfones and the sulfoxides[1] as reported in our previous paper.

The products obtained after the treatment with ethoxide in aqueous ethanol were carefully recrystallized and subjected to the IR, NMR, UV and elemental analyses. Since both hydroxide and ethoxide ion can exist in an equilibrium, one would expect to obtain both *p*-ethoxyphenyl- and *p*-hydroxyphenyl-diphenylsulfonium compounds, however, the *p*-hydroxyphenyl compound could not be detected among the products. This means that ethoxide ion being more nucleophilic than hydroxide ion, attacks preferentially the aromatic carbon undergoing the S_N reaction. While the alkaline decomposition reaction was expected to take place competitively with the aromatic S_N reaction, only under a prolonged heating diphenyl sulfide and benzene were obtained as the main products from the reaction of triphenylsulfonium bromide with ethoxide ion. Undoubtedly, this decomposition is initiated by the attack of ethoxide ion on the sulfur atom of the sulfonium salt.

Recently, Bunnett and Happer[6] demonstrated that *o*-chlorophenyl-triphenylphosphonium iodide reacts with sodium methoxide in methanol to afford triphenylphosphin oxide and chlorobenzene suggesting the reaction to proceed through a nucleophilic attack of methoxide ion on the phosphorus atom with the elimination of chlorobenzene.

The mode of the alkaline decomposition (or the nucleophilic attack on the sulfur atom) of triphenylsulfonium and *p*-chloro- or *p*-ethoxyphenyldiphenylsulfonium halides would be identical, and the ease of their alkaline decompositions would not be much different each other, since the effect of only one chloro group from para-position would be very small. Therefore, the rates of the aromatic S_N reaction of chlorophenyldiphenylsulfonium halides by ethoxide ion can be estimated by measuring the amounts of both the aromatic S_N reaction and the alkaline decomposition and correcting the amount of the alkaline decomposition into the aromatic S_N reaction of chlorophenyldiphenylsulfonium halides. Thus we have compared the relative magnitudes of the activating effect of diphenylsulfonio group with those of phenylsulfonyl, -sulfinyl and nitro groups in the aromatic S_N reaction of alkaline ethanolysis.

Results and Discussion

The alkaline decomposition of triarylsulfonium bromide was found to obey the second order kinetic rate law; first order with respect to both the sulfonium concentration and potassium hydroxide concentration as shown in Figs. 1 and 2. The results of the alkaline decompositions of triarylsulfonium halides are shown in Table 1.

The rates of the aromatic S_N ethanolyses of *o*- and *p*-chlorophenyldiphenylsulfonium perchlorate which are corrected with that of the alkaline decomposition of triphenylsulfonium perchlorate are shown in Table 2 along with those of similar aromatic S_N reactions of chloronitrobenzenes and chlorophenyl phenyl sulfones. The rates of the sulfones at 105°C are calculated by extrapolating the values at 155°C using their activation

4) N. J. Daly, G. Durger and J. Miller, *Aust. J. Chem.*, **11**, 290 (1958).

5) The details of this study will be reported later.

6) J. F. Bunnett and D. A. R. Happer, *J. Org. Chem.*, **32**, 2701 (1967).

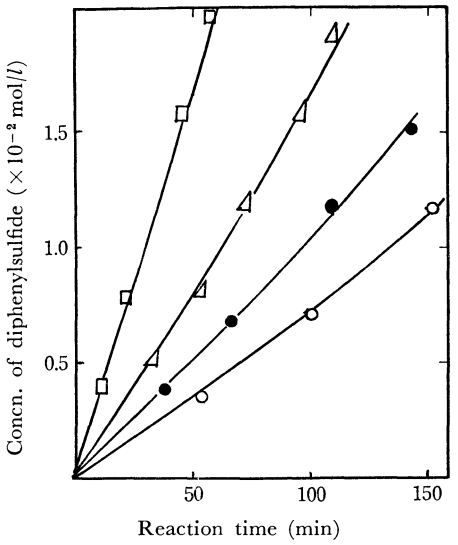

Fig. 1. The dependence of the mole of diphenyl sulfide on the sulfonium salt concentration.
[KOH]: 2.69×10^{-1} mol/l: constant
□, Salt/KOH=1/2 △, Salt/KOH=3/8
●, Salt/KOH=1/4 ○, Salt/KOH=1/8

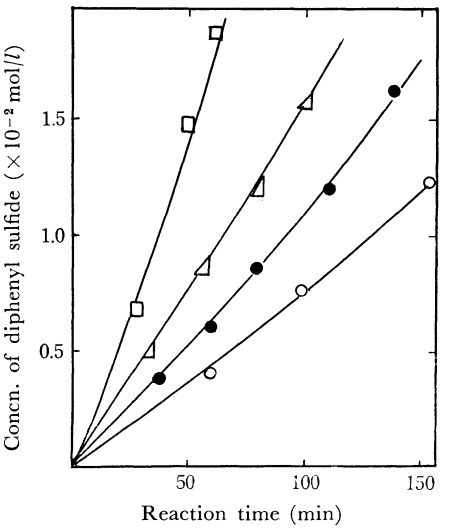

Fig. 2. The dependence of the mole of diphenyl sulfide on the potassium hydroxide concentration.
[Salt]: 7.806×10^{-2} mol/l: constant
□, KOH/Salt=8 △, KOH/Salt=4
●, KOH/Salt=3 ○, KOH/Salt=2

parameters.

All the values of $\Delta H^{\neq}$ and $\Delta S^{\neq}$ are also shown in Table 2. When the relative rates of the sulfonium perchlorates are compared with those of the sulfones and the nitrobenzenes, one finds that the activating effects of diphenylsulfonio group are markedly larger than those of the corresponding phenylsulfonyl and even exceed those of nitro groups.

Unfortunately, the rate of the aromatic S_N reaction of the *m*-isomer of the sulfonium perchlorate cannot be obtained directly because the aromatic S_N reaction is apparently so slow that the alkaline decomposition takes place faster than the S_N reaction, leading to the preferential decomposition. This means, however, that the S_N reaction of both the *o*- and *p*-sulfonium perchlorates are markedly faster than that of the *m*-isomer, since the S_N reaction of the *p*-isomer is nearly ten times faster than the decomposition of triphenylsulfonium perchlorate.

Our previous assumption that the reactivity of the alkaline decomposition of chlorophenyldiphenylsulfonium perchlorate is nearly the same as that of triphenylsulfonium perchlorate, would be quite valid because there is little or negligible difference in the rates of the decomposition of triphenyl- and tritolyl-sulfonium bromides. Thus, the markedly increased reactivities of the ortho- and para-isomers over that of the *m*-isomer is undoubtedly associated with the 3d-orbital conjugative effect of the diphenylsulfonio groups to stabilize the intermediate complex (III and IV) rather than their

Table 1. Alkaline decomposition of triarylsulfonium bromide with potassium hydroxide in 70% aqueous ethanol at 105±0.1°C

Compound	Sulfonium halide (concentration) mol l^{-1}	KOH mol l^{-1}	k_2 l mol^{-1} sec^{-1}
$(C_6H_5)_3\overset{+}{S}ClO_4^-$	7.93×10^{-2}	27.6×10^{-2}	1.21×10^{-4}
$(C_6H_5)_3\overset{+}{S}Br^-$	7.78×10^{-2}	22.0×10^{-2}	1.42×10^{-4}
$(C_6H_5)_3\overset{+}{S}Br^-$	7.81×10^{-2}	26.7×10^{-2}	1.53×10^{-4}
$(C_6H_5)_3\overset{+}{S}Br^-$	5.96×10^{-2}	22.47×10^{-2}	1.62×10^{-4}
$(H_3C\text{-}C_6H_4)_3\overset{+}{S}Br^-$	7.6×10^{-2}	15.8×10^{-2}	1.33×10^{-4}

TABLE 2. THE S_N2 REACTIONS OF CHLOROPHENYLSULFONIUM PERCHLORATES, CHLOROPHENYL SULFONES AND CHLORONITROBENZENES WITH ETHOXIDE ION IN AQUEOUS ETHANOL* AT 105±0.1°C

Compounds R-C$_6$H$_4$-Cl		k_2 $l\,mol^{-1}\,sec^{-1}$	rel. rate (total)	rel. rate (with in the isomers)	$\Delta H^{\neq}$ kcal	$\Delta S^{\neq}$ (eq)
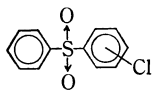	*m*-Cl	1.40×10^{-7}	1	1	22	−38
	p-Cl	3.30×10^{-6}	24	24	20	−26
	o-Cl	1.41×10^{-6}	10	10	20	−34.9
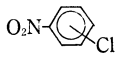	*m*-Cl	5.80×10^{-6}	41	1		
	p-Cl	3.63×10^{-4}	2600	65	21	−20
	o-Cl	1.52×10^{-4}	1010	45	19	−24
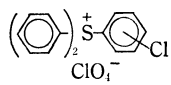	*m*-Cl	**	—	—	—	—
	p-Cl	1.15×10^{-3}	8215	1.54	22.9	−11.4
	o-Cl	7.50×10^{-4}	5300	1.0	21.2	−17.1

* The volume ratio of ethanol and water in the reaction is 7 : 3.
** The decomposition of sulfonium halide is much faster than the S_N2 reaction of *m*-isomer.

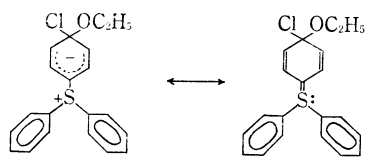

(III)

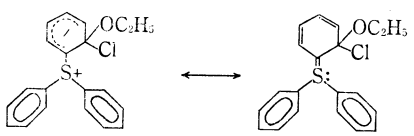

(IV)

inductive effect, like in the similar cases of the sulfoxide and the sulfones reported previously.[1]

In the previous cases of the aromatic S_N reactions of chlorophenyl phenyl sulfones and chloronitrobenzenes, the *p*-isomers are the most reactive in both cases and the relative rate of the *p*-sulfone is 24 times as that of the *m*-isomer.

Earlier, the theoretical considerations[7] and the studies of dissociation constants[8] of various sulfoxides, sulfones and sulfonium halides have revealed that the 3d-orbital resonance effect is quite stereo-insensitive. In seeking further supporting evidence for the stereo-insensitivity of the 3d-orbital resonance, we have synthesized sterically crowded sulfoxide, sulfone and sulfonium perchlorate which have one methyl group at ortho position and subjected them to the kinetic experiments of the alkaline ethanolysis in aqueous ethanol for both the sulfone and the sulfonium compound and the hydrolysis in aqueous dimethyl sulfoxide for the sulfoxide. The kinetic results are shown in Table 3.

Inspection of the data reveals clearly that the electron-accepting conjugative effects of diphenylsulfonio, phenylsulfonyl and sulfinyl groups are not much inhibited by the bulky ortho methyl group at the *o*-position. The small reductions of the rates by the substitution of *o*-methyl group are undoubtedly due to the electron-releasing inductive effect of methyl group.

This may serve another evidence to support that there is little or almost no steric hindrance in the electron-accepting type conjugation involving 3d-orbital resonance of the sulfur atom.

Experimental

***o*-, *m*- and *p*-Chlorophenyldiphenylsulfonium Perchlorate.** The titled compounds were prepared by the method of Andersen.[9] Diphenyl sulfoxide (8 g) was dissolved in 15 m*l* of anhydrous methylene chloride containing triethyloxonium tetrafluoroborate[10] (8.6 g). After the solution was stirred for about 30 min at room temperature, 50 m*l* of anhydrous ethyl ether was added to this solution and then the methylene chloride - ethyl ether mixture was replaced by tetrahydrofuran by decantation. This solution of ethoxydiphenylsulfonium tetrafluoroborate[11] was slowly added to the Grignard reagent prepared from *p*-chlorobromobenzene (20.4 g) and magnesium (2.7 g) in anhydrous

7) a) G. E. Kimball, *J. Chem. Phys.*, **8**, 188 (1940). b) H. P. Koch and W. E. Moffitt, *Trans. Faraday Soc.*, **47**, 7 (1951).

8) a) H. Kloosterziel and H. von J. Basper, *Rec. Trav. Chim.*, **72**, 185 (1953). b) W. E. Doering and L. K. Levy, *J. Am. Chem. Soc.*, **77**, 509 (1955). c) E. A. Fehnel and M. Carmack, *ibid.*, **79**, 1291 (1950).

9) K. K. Andersen and N. E. Papanikolaov, *Tetrahedron Letters*, **1966**, 5445.

10) a) H. Meerwein, V. Hederich and K. Wunderlich, *Arch. Pharm.*, **291**, 552 (1958). b) H. Meerwein, E. Bettercherg, H. Gold, E. Pfeil and G. Willfang, *J. Prakt. Chem.*, (2) **154**, 83 (1940).

11) C. R. Johnson and D. Macants, Jr., *J. Am. Chem. Soc.*, **87**, 5406 (1965).

Table 3. The rates of S_N2 reaction of chlorophenylsulfonium perchlorates, sulfones and sulfoxides with ethoxide ion in aqueous ethanol and hydroxide ion in aqueous dimethyl sulfoxide

Compound	Solvent	Temp (°C)	(mol/sec l) k_2	rel. rate
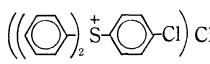	EtOH-H_2O[a)]	115±0.1	1.01×10^{-3}	1.85
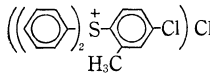	EtOH-H_2O[a)]	115±0.1	5.49×10^{-4}	1
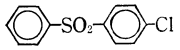	EtOH-H_2O[b)]	148±0.1	7.02×10^{-5}	1.9
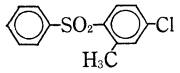	EtOH-H_2O[b)]	148±0.1	3.68×10^{-5}	1
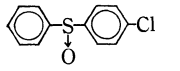	DMSO-H_2O[c)]	161±0.1	4.82×10^{-5}	1.2
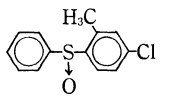	DMSO-H_2O[c)]	161±0.1	4.0×10^{-5}	1

a) The volume ratio of ethanol and water in the reaction is 4 : 3.
b) The volume ratio of ethanol and water in the reaction is 7 : 3.
c) The volume ratio of DMSO and water in the reaction is 7 : 3.

tetrahydrofuran (60 ml) below −5°C with vigorous stirring. After the addition was over, the solution was stirred further for 30 min and then allowed to stand at room temperature overnight. The mixture was hydrolyzed with 0.5 N hydrobromic acid solution, extracted with chloroform four times, and then dried over calcium chloride. Evaporation of chloroform followed by recrystallization of the residue from acetone-chloroform mixture gave 8.7 g (59%) of colorless *p*-chlorophenyldiphenylsulfonium bromide. Mp 221—222°C. Found: C, 57.63; H, 4.10%. Calcd for $C_{18}H_{14}ClBrS$: C, 57.4: H, 3.72%. When a sodium perchlorate solution was added to a hot solution of *p*-chlorophenyldiphenylsulfonium bromide, colorless crystals of the corresponding sulfonium perchlorate salt appeared immediately, which was collected and recrystallized from ethylene chloride-ether, Mp 160—161°C. Found: C, 54.71; H, 3.65%. Calcd for $C_{18}H_{14}Cl_2O_4S$: C, 54.5; H, 3.52%.

The *o*- and *m*-isomers were similarly prepared from the corresponding *o*- and *m*-chlorophenylphenylethoxysulfonium tetrafluoroborate which were obtained from the corresponding sulfoxides, the Meerwein salt and phenylmagnesium bromide. Both *o*- and *m*-isomers were recrystallized from chloroform-acetone-ether.

o-Isomer: Mp 147—148°C. Found: C, 54.8; H, 3.70%. Calcd for $C_{18}H_{14}Cl_2O_4S$: C, 54.5; H, 3.52%.

m-Isomer: Mp 118—120°C. Found: C, 55.01; H, 3.80%. Calcd for $C_{18}H_{14}Cl_2O_4S$: C, 54.5; H, 3.52%.

Triphenylsulfonium and Tritolylsulfonium Halide. Diphenylethoxysulfonium tetrafluoroborate prepared from diphenyl sulfoxide (9.4 g) and triethyloxonium tetrafluoroborate (10 g) was added to phenylmagnesium bromide in tetrahydrofuran below −5°C, then the reaction mixture was treated similarly to that described above, and 8 g (50%) of colorless triphenylsulfonium bromide was obtained. Mp 292—293°C (Ref.[12]) Mp 291—292°C); perchlorate; Mp 212—213°C.

Tritolylsulfonium bromide was similarly prepared from ditolylethoxysulfonium tetrafluoroborate and tolyl magnesium bromide. Mp 244—245°C.

2-Methyl-4-Chlorophenyldiphenylsulfonium Perchlorate. The titled bromide compound was prepared from 2-methyl-4-chloro-phenylphenylethoxysulfonium tetrafluoroborate obtained by reacting the corresponding sulfoxide (6 g, 0.024 mol) with triethyloxonium tetrafluoroborate (5.25 g, 0.028 mol), with the phenylmagnesium bromide (0.072 mol) as described above. The bromide salt was purified by recrystallization from acetone-ethylene chloride mixture, mp 222—223°C, yield 4.0 g (33%): 2-methyl-4-chlorophenyl-diphenylsulfonium perchlorate was quantitatively obtained by treating the corresponding sulfonium bromide with a sodium perchlorate solution. mp 193—194°C. Found: C, 55.07; H, 4.09%. Calcd for $C_{19}H_{16}O_4Cl_2S$: C, 55.5; H, 3.94%.

2-Methyl-4-Chlorophenylphenylsulfoxide and Sulfone. 2-Methyl-4-chlorophenyl phenyl sulfide, prepared by the reaction of 2-methyl-4-chlorobenzenediazonium salt with thiophenolate, was oxidized as usual with hydrogen peroxide in glacial acetic acid containing a few drops of concentrated sulfuric acid to the corresponding sulfoxide and sulfone in nearly quantitative yields and both sulfoxide and sulfone were recrystallized from benzene-petroleum ether mixture: sulfoxide, mp 39—40°C, sulfone, mp 82—83°C. Found: C, 58.70; H, 4.18%. Calcd for $C_{13}H_{11}O_2ClS$: C, 58.50; H, 4.33%.

2-Methyl-4-Chloroaniline. *o*-Methylacetoanilide

12) a) W. A. Bammer, *J. Am. Chem. Soc.*, **74**, 5078 (1952). b) B. S. Wildi, S. W. Taylar and H. A. Potratz, *ibid.*, **73**, 1965 (1951).

(47 g) obtained from the reaction of *o*-toluidine with acetic acid was dissolved in 70 m*l* of glacial acetic acid in a three necked flask and then liquid chlorine (14.5 g) was introduced into the flask in a sealed system which is connected with rubber tubes with vigorous stirring. After the reaction was over, the mixture was poured into a large amount of cold water, filtered, washed with cold water, recrystallized from ethanol, and 55 g of colorless crystals of 2-methyl-4-chloroacetoanilide was obtained. The amide (55 g) was hydrolyzed with hydrochloric acid in aqueous ethanol and then the salt (20 g) was treated with sodium hydroxide solution to give 2-methyl-4-chloroaniline (11 g). Bp 103—104°C/2 mmHg.

Chlorodiphenyl Sulfones and Chloronitrobenzenes. *o*-, *m*- and *p*-Chlorophenylphenyl sulfones were obtained by the oxidation of corresponding sulfide with hydrogen peroxide in glacial actic acid; the *o*-isomer, mp 108—109°C, the *m*-isomer, mp 113—114°C, the *p*-isomer, mp 90—91°C. Freshly distilled *o*-, *m*- and *p*-chloronitrobenzenes were used in the kinetic experiments.

Alkaline Ethanolyses of Chlorophenyldiphenylsulfonium Perchlorate. *p*-Chlorophenyldiphenylsulfonium perchlorate (1.7 g) was reacted with potassium hydroxide (0.75 g) in 6.3 m*l* of aqueous ethanol (3.6 m*l* ethanol +2.7 m*l* H_2O) at 90°C for 8 hr in an ampoule and then the mixture was poured into cold water, acidified with hydrochloric acid, extracted with chloroform 5 times and the chloroform extract was dried over calcium chloride. After chloroform was evaporated, the crystalline residue (1.2 g) was found to be the mixture of the starting sulfonium and *p*-ethoxyphenylsulfonium salt. The *p*-ethoxysubstituted sulfonium perchlorate (0.8 g) was separated by careful recrystallization with alcohol-acetone-methylene chloride mixture and finally with methylene chloride-acetone-ether. Mp 109—110°C. Found: C, 59.00; H, 4.71%. Calcd for $C_{20}H_{19}ClO_5S$: C, 58.98; H, 4.78%. The NMR charts of both *p*-chlorophenyldiphenylsulfonium perchlorate and *p*-ethoxyphenyldiphenylsulfonium perchlorate were shown in Fig. 3.

The kinetic Experiment. Ethanol was purified first by distillation after refluxing with sodium hydroxide for 10 hr, then with magnesium ethoxide for 3 hr and again distilled. Kinetic measurements and the rate

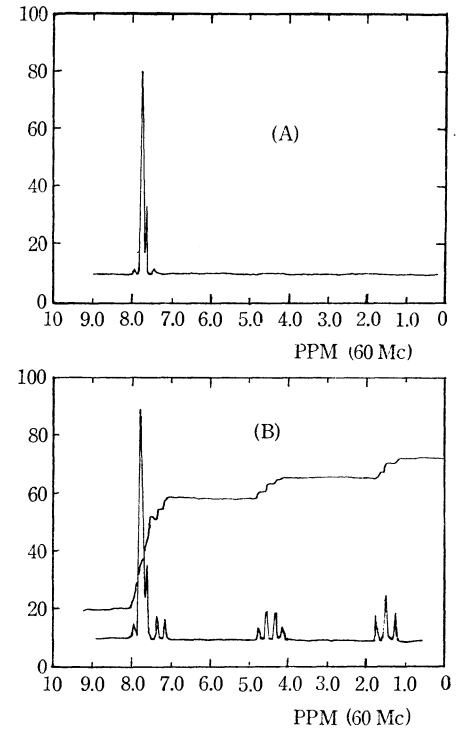

Fig. 3. NMR spectra of *p*-chlorophenyldiphenylsulfonium perchlorate (A) and *p*-ethoxyphenylsulfonium perchlorate (B).

calculations of alkaline ethanolyses were carried out using the same method described in our previous work[1] by the usual Volhard method. Each run was carried out in ampoules. The concentrations of both an aryl chloride and potassium hydroxide were at around 1.3×10^{-1} N and 2.8×10^{-1} N, respectively. Kinetic measurement and the rate calculations of alkaline decomposition of the triarylsulfonium salt were performed under the same condition as in the ethanolyses, but by the use of the ultraviolet spectra of the diaryl sulfides (at $\lambda=285$ mμ).

BULLETIN OF THE CHEMICAL SOCIETY OF JAPAN VOL. 42 1628—1633 (1969)

A Study of the Solvent Effect in the Copolymerization of *N*-Phenylethylenimine with β-Propiolactone

Tsutomu KAGIYA, Tomizo KONDO and Kenichi FUKUI

Faculty of Engineering, Kyoto University, Sakyo-ku, Kyoto

(Received September 9, 1968)

The effect of the solvent on the copolymerization of *N*-phenylethylenimine with β-propiolactone has been studied quantitatively. The copolymerization rates for the various solvents used increase in the order: diethyl ether < toluene < carbon tetrachloride < methyl acetate < *N,N*-dimethylacetamide < anisole < dioxane < acetone < ethylene dichloride < acetonitrile < acetophenone < nitrobenzene < dimethyl sulfoxide < nitroethane. The rates in solvents with high dielectric constants are much larger than those in solvents with low dielectric constants. However, in the case of solvents with similar dielectric constants, the rates decrease with an increase in the nucleophilicity of the solvent; moreover, the dependency of the copolymerization rate on the nucleophilicity of the solvents is much larger in the solvents with high dielectric constants than in those with low dielectric constants. The rate of the consumption of *N*-phenylethylenimine is markedly affected by the nucleophilicity of the solvents in solvents with high dielectric constants, but it is little affected in solvents with low dielectric constants. Although there is no effect of the nucleophilicity of the solvents on the consumption rate of β-propiolactone, the rate of the consumption of β-propiolactone varies with the electrophilicity of the solvent in solvents with high dielectric constants. On the other hand, the β-propiolactone content in the copolymer increases in proportion to the nucleophilicity of the solvents with high dielectric constants, whereas the β-propiolactone content in solvents with low dielectric constants is almost constant regardless of the electric nature of the solvents.

We have studied the copolymerization of *N*-phenylethylenimine with β-propiolactone. As has been mentioned in a previous paper, *N*-phenylethylenimine and β-propiolactone copolymerized with the acid present in the β-propiolactone without the addition of any catalyst,[1] while in the copolymerization with various Brönsted acids, the composition of the copolymer varied with the kind of acid.[2] On the other hand, it has been reported that, in the polymerization of *N*-phenylethylenimine with formic acid, the polymerization rates were markedly affected by the nucleophilicity and the dielectric constant of the solvents.[3]

In the ionic copolymerization, a number of instances have been reported in which the rate and the composition of the copolymer were markedly influenced by the solvents. No quantitative study of the solvent effect on the polymerization has, however, yet been reported.

The purpose of this paper is to investigate quantitatively the solvent effect on the rate and the composition of the copolymer in the copolymerization of *N*-phenylethylenimine with β-propiolactone.

Experimental

Materials. The method of the preparation and purification of *N*-phenylethylenimine and purification of β-propiolactone were described in a previous paper.[1] The acetonitrile, anisole, diethyl ether, methyl acetate, *N,N*-dimethylacetamide, carbon tetrachloride, toluene, ethylene dichloride, acetone, nitrobenzene, nitroethane, and acetophenone were purified by the usual methods.[4] Dimethyl sulfoxide of a guaranteed reagent grade was used without further purification.

Copolymerization Procedure. Measured amounts of β-propiolactone (0.005 mol) and a solvent (5 *ml*) were placed into a glass ampule under nitrogen atmosphere, and then *N*-phenylethylenimine (0.005 mol) was added to this system at −78°C. After the ampule had been sealed and maintained at 0—1°C for a definite period of time, the products were washed with chloroform and diethyl ether, separated by a centrifuge, and dried *in vacuo*. The method of the determination of the copolymer composition has already been described.[1]

Results and Discussion

The copolymerization was carried out without the addition of any catalyst in various kinds of

1) T. Kagiya, T. Kondo, S. Narisawa and K. Fukui, This Bulletin, **41**, 172 (1968).

2) T. Kagiya, T. Kondo and K. Fukui, *ibid.*, **41**, 1682 (1968).

3) T. Kagiya, T. Kondo, K. Nakao and K. Fukui, *ibid.*, **42**, 1094 (1969).

4) A. Weissberger *et al.*, "Technique of Organic Chemistry, Vol VII, Organic Solvents," Interscience Publishers, Inc., New York (1955).

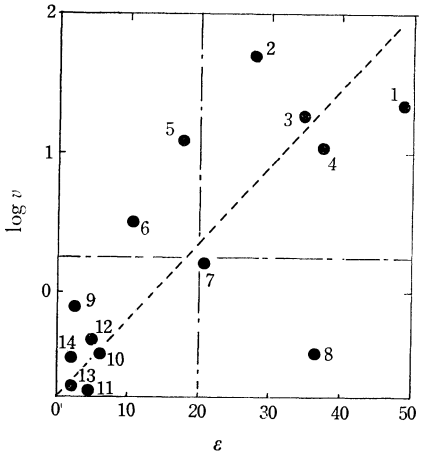

Fig. 1. The plots of the copolymerization rate against the dielectric constant of the solvents.
1, dimethyl sulfoxide; 2, nitroethane;
3, nitrobenzene; 4, acetonitrile;
5, acetophenone; 6, ethylene dichloride;
7, acetone; 8, *N,N*-dimethylacetamide;
9, dioxane; 10, methyl acetate;
11, diethyl ether; 12, anisole; 13, toluene;
14, carbon tetrachloride.

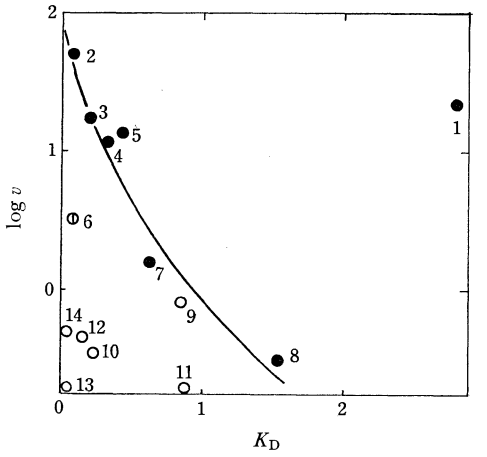

Fig. 2. The plots of the copolymerization rate against the K_D value of the solvents.
●, high dielectric constant ($\varepsilon>10$)
⊕, ethylene dichloride ($\varepsilon\fallingdotseq10$)
○, low dielectric constant ($\varepsilon<10$)
The number of a solvent is same as Fig. 1.

solvents. The plots of the copolymerization rate against the dielectric constant of the solvent (ε) are shown in Fig. 1. Although the rates tend to increase with an increase in the dielectric constant of the solvent, there are great differences in the rate, even in the solvents with similar dielectric constants, *i. e.*, nitrobenzene, acetonitrile, and *N,N*-dimethylacetamide.

In order to investigate the effect of the electric nature of the solvent, the rate was plotted against K_D, where K_D is the nucleophilic equilibrium constant of a solvent in the nucleophilic solvation to a deuterium atom of a methanol-d molecule[5] (Fig. 2). It was found that the effects of the solvents on the copolymerization rate may be classified into two large groups, that is, solvents with high dielectric constants ($\varepsilon>10$) and those with low dielectric constants ($\varepsilon<10$).

In solvents with high dielectric constants, the rates decrease markedly with an increase in the nucleophilicity of the solvent, while in solvents with low dielectric constants the rates are almost constant, regardless of the nucleophilicity of the solvent. Ethylene dichloride ($\varepsilon\fallingdotseq10$) shows the intermediate behavior in these groups. The cause of the great deviation of dimethyl sulfoxide from the other solvents with high dielectric constants may be due to its much larger electrophilicity.

The relation between the consumption rates of the monomers and the K_D values is shown in Fig. 3. The consumption rate of *N*-phenylethylenimine in

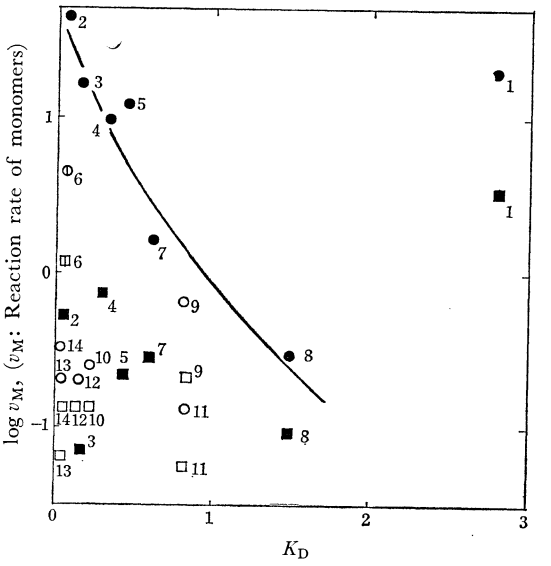

Fig. 3. The relations between the reaction rates of the monomers and the K_D value of the solvents.
Reaction rate of *N*-phenylethylenimine
●, high dielectric constant ($\varepsilon>10$)
⊕, ethylene dichloride ($\varepsilon\fallingdotseq10$)
○, low dielectric constant ($\varepsilon<10$)
Reaction rate of *β*-propiolactone
■, high dielectric constant ($\varepsilon>10$)
⊞, ethylene dichloride ($\varepsilon\fallingdotseq10$)
□, low dielectric constant ($\varepsilon<10$)
The number of a solvent is same as Fig. 1.

the solvents with high dielectric constants decreased markedly with an increase in the nucleophilicity of the solvents, while in the solvents with low dielectric constants the consumption rate was almost

5) T. Kagiya, Y. Sumida and T. Inoue, This Bulletin, **41**, 767 (1968).

constant, regardless of the nucleophilicity of the solvents. On the other hand, the consumption rate of β-propiolactone is much smaller than that of *N*-phenylethylenimine, and the effect of the nucleophilicity of the solvent on the rate of the consumption of β-propiolactone was small. These facts show that, in the solvents with high dielectric constants, the consumption rate of *N*-phenylethylenimine is more affected by the nucleophilicity of the solvents than is the consumption rate of β-propiolactone.

Moreover, in order to investigate the effect of the electrophilicity of the solvent on the consumption rates of each monomer, the rates were plotted against the $\Delta\nu_{C=O}$ values of the solvents (Fig. 4), where $\Delta\nu_{C=O}$ was defined as the relative difference between the C=O absorption band of acetophenone observed in solution and the C=O absorption band of acetophenone in benzene.[5] As is shown in Fig. 4, although the effect of the electrophilicity of the solvent on the consumption rate of *N*-phenylethylenimine is small, the consumption rate of β-propiolactone decreased markedly with an increase in the $\Delta\nu_{C=O}$ value of the solvents in the case of the solvents with high dielectric constants. On the other hand, in the solvents with low dielectric constants, the rate consumption of β-propiolactone is not affected by the $\Delta\nu_{C=O}$ value of the solvents.

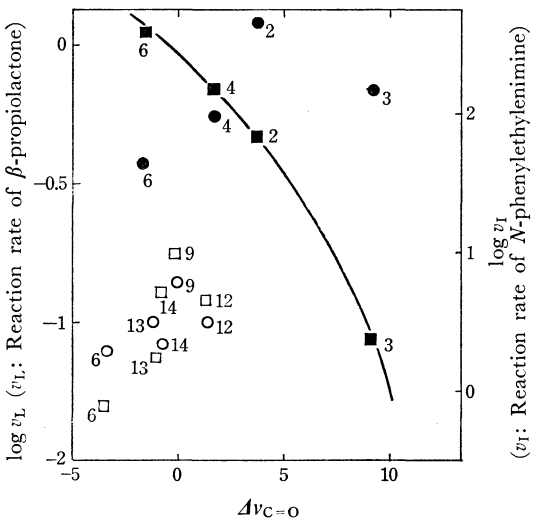

Fig. 4. The relations between the reaction rates of the monomers and $\Delta\nu_{C=O}$ value of the solvents.
The notes are the same as Fig. 3.
The number of a solvent is same as Fig. 1.

In view of these facts, it may be assumed that, although the solvents with low dielectric constants have no effect on the propagation reaction, in the solvent with high dielectric constants, the propagation reaction of *N*-phenylethylenimine is much affected by the nucleophilicity of the solvent, and that of β-propiolactone, by the electrophilicity. These results may lead to the explanation that *N*-phenylethylenimine (large nucleophilicity) directly attacks the cationic end group of the polymer, whereas β-propiolactone (large electrophilicity) coordinates electrophilically with the counter-anion and then reacts with the cationic end group. Therefore, in the solvents with high dielectric constants the competitive coordination of the solvents with the cationic end group (or the counter-anion) may depress the reaction of *N*-phenylethylenimine (or β-propiolactone).

The relation between the β-propiolactone content in the copolymer and the K_D values of the solvents is shown in Fig. 5. In the solvent with high dielectric constants the β-propiolactone content is much smaller than in the solvents with low dielectric constants, and it increases in proportion to the K_D value of the solvent. On the other hand, in the solvents with low dielectric constants, the β-propiolactone content is almost constant (32%). The variation in the copolymer composition with the kind of solvent also indicates that the effect of the solvent on the reaction of *N*-phenylethylenimine differs from that of β-propiolactone.

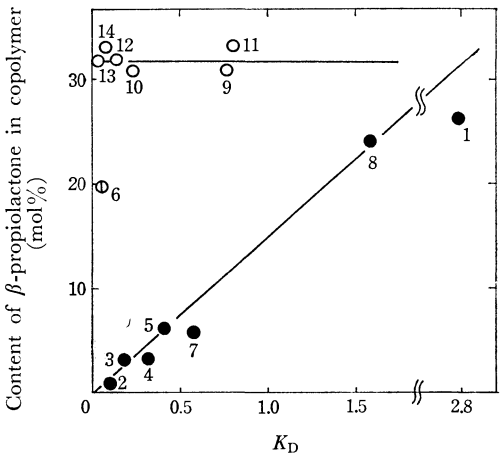

Fig. 5. The relations between the composition of the copolymer and K_D value of the solvents.
The notes are the same as Fig. 2.
The number of a solvent is same as Fig. 1.

Mechanism of the Copolymerization. From these experimental facts, the mechanism of the copolymerization may be postulated as follows:

Initiation

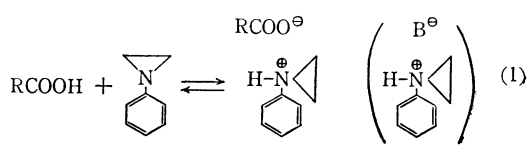

Propagation

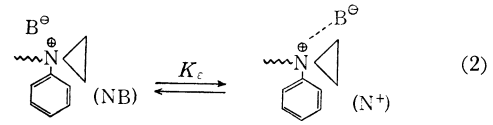

(2)

Nucleophilic solvation

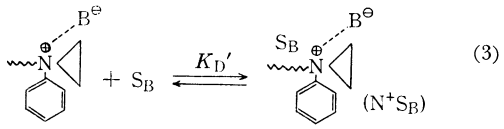

(3)

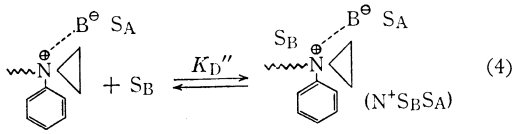

(4)

Electrophilic solvation

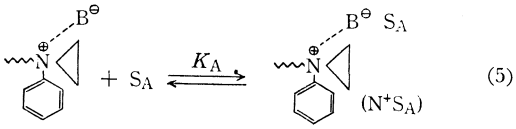

(5)

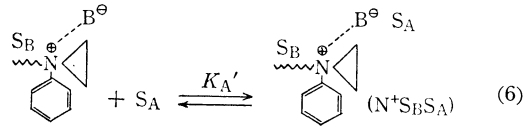

(6)

S_B; nucleophilic solvent, S_A: electrophilic solvent.

Reaction of N-phenylenimine in propagation

Reaction with dissociated immonium ion:
Nonsolvated

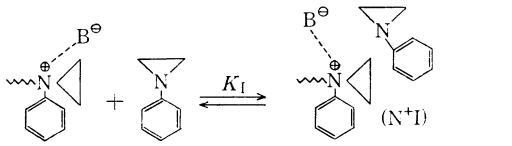

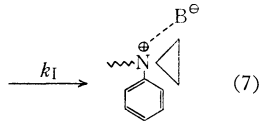

(7)

Solvated

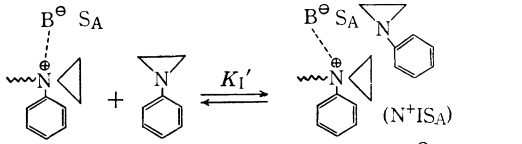

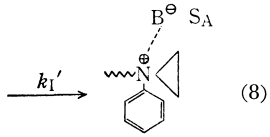

(8)

Reaction with undissociated immonium ion:

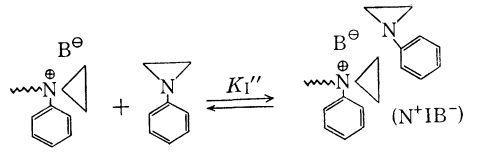

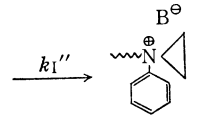

(9)

Reaction of β-propiolactone in propagation

Reaction with dissociated immonium ion:
Nonsolvated

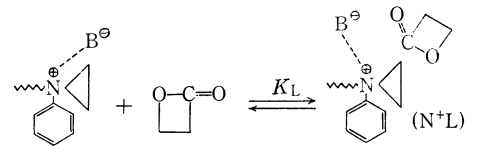

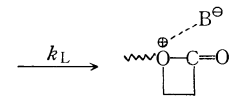

(10)

Solvated

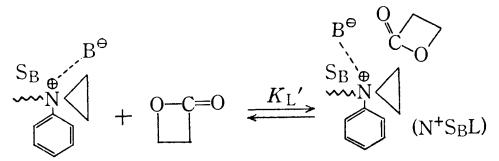

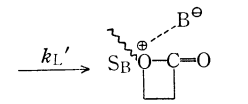

(11)

Reaction with undissociated immonium ion:

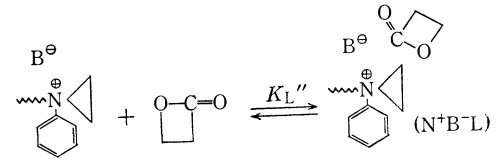

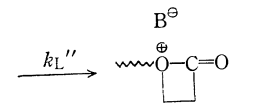

(12)

The initiation reaction is considered to be the reaction of the acid present in β-propiolactone with *N*-phenylethylenimine to produce compound I as has been described in a previous paper.[2] This compound dissociates partially from the immonium ion, and the reaction is in equilibrium. The equilibrium constant (K_ε) is considered to increase with an increase in the dielectric constant of the solvent. Equations (3) and (4) show the nucleophilic solvation of the solvent to the immonium ion. Since the coordinations of the solvents with both propagating species and methanol-d are nucleophilic reac-

tions, the equilibrium constants (K_D' and K_D'') are considered to increase with an increase in K_D. Equations (5) and (6) show the electrophilic solvation of the solvent to the counter-anion of the polymer end. The coordination of the solvent with both the counter-anion and acetophenone are considered to be electrophilic reactions. Therefore it seems reasonable to assume that K_A and K_A' are larger in the solvents with larger $\Delta\nu_{C=O}$ values. On the other hand, on the basis of the fact that there is no effect on the propagation reaction in the solvents with low dielectric constants, it is considered that the coordination of the solvent with the undissociated immonium ion is small.

In the propagation reaction, immonium and oxonium ions are considered to react with the monomers by the same mechanism. Therefore, the propagation reactions of immonium ions with monomers are shown as an example. The reaction rate of *N*-phenylethylenimine decreases with an increase in the nucleophilicity of the solvent; *i. e.*, in a low-nucleophilic solvent such as the nitro compound, the reaction rate of *N*-phenylethylenimine is much larger than in a nucleophilic solvent such as dimethylacetamide. Since these facts may indicate that the competitive coordination of the nucleophilic solvent with the cationic end group depresses the coordination of *N*-phenylethylenimine, the reaction of *N*-phenylethylenimine is considered to occur by means of a nonsolvated immonium ion, as is shown by Eqs. (7) and (8). From the fact that the reaction rate of *β*-propiolactone decreases with an increase in the electrophilicity of the solvent in the solvents with high dielectric constants, the reaction of *β*-propiolactone may proceed by means of a dissociated immonium ion whose counter ion is not solvated by the solvent, as is shown by Eqs. (10) and (11). On the other hand, the propagation in the solvents with low dielectric constants is assumed to occur by means of the reaction of the undissociated immonium ion with monomers (Eqs. (9) and (12)).

Kinetics. On the basis of the mechanism postulated, the effect of the solvent on the copolymerization rate and the copolymer composition was kinetically investigated. From the fact that the amount of *β*-propiolactone consumed is much less than that of *N*-phenylethylenimine, the quantity of immonium ions is considered to be much larger than that of oxonium ions. Therefore, the concentration of the compound I, $\alpha[C]_0$, may be approximately expressed by Eq. (13), where $[C]_0$ is the initial concentration of the catalyst and where α is a constant ($0<\alpha<1$):

$$\alpha[C]_0 = [N^+] + [N^+B^-] + [N^+S_B] + [N^+S_A] + [N^+I] + [N^+L] + [N^+S_BL] + [N^+IS_A] + [N^+B^-I] + [N^+B^-L] + [N^+S_AS_B] \quad (13)$$

On the other hand, according to Eqs. (2), (3), ⋯, (11) and (12), the equilibrium equations will be:

$$[N^+]/[N^+B^-] = K_\varepsilon \quad (14)$$

$$[N^+S_B]/([N^+][S]) = K_D' \quad (15)$$

$$[N^+S_A]/([N^+][S]) = K_A \quad (16)$$

$$[N^+S_AS_B]/([N^+S_A][S]) = K_D'' \quad (17)$$

$$[N^+S_AS_B]/([N^+S_B][S]) = K_A' \quad (18)$$

$$[N^+I]/([N^+][I]) = K_I \quad (19)$$

$$[N^+IS_A]/([N^+S_A][I]) = K_I' \quad (20)$$

$$[N^+B^-I]/([N^+B^-][I]) = K_I'' \quad (21)$$

$$[N^+L]/([N^+][L]) = K_L \quad (22)$$

$$[N^+S_BL]/([N^+S_B][L]) = K_L' \quad (23)$$

$$[N^+B^-L]/([N^+B^-][L]) = K_L'' \quad (24)$$

where [I] and [L] are the concentrations of *N*-phenylethylenimine and *β*-propiolactone respectively. By combining Eqs. (13), (14), ⋯, (23) and (24), the concentrations of N^+I, N^+L, N^+S_BL, N^+IS_A, N^+B^-I, and N^+B^-L are represented by Eqs. (25), (26), (27), (28), (29) and (30) respectively:

$$[N^+I] = K_\varepsilon K_I\alpha[C]_0[I]/f(K,M,S) \quad (25)$$

$$[N^+L] = K_\varepsilon K_L\alpha[C]_0[L]/f(K,M,S) \quad (26)$$

$$[N^+S_BL] = K_\varepsilon K_L'K_D'\alpha[C]_0[L][S]/f(K,M,S) \quad (27)$$

$$[N^+IS_A] = K_\varepsilon K_I'K_A\alpha[C]_0[I][S]/f(K,M,S) \quad (28)$$

$$[N^+B^-I] = K_I''\alpha[C]_0[I]/f(K,M,S) \quad (29)$$

$$[N^+B^-L] = K_L''\alpha[C]_0[L]/f(K,M,S) \quad (30)$$

where $f(K,M,S) = 1+K_I''[I]+K_L''[L]+K_\varepsilon(1+K_I[I]+K_L[L]+K_D'[S]+K_A[S]+K_L'K_D'[S][L]+K_AK_I'[S][I]+K_A'K_D'[S]^2)$.

The reaction rates of *N*-phenylethylenimine and *β*-propiolactone are represented by Eqs. (31) and (32) respectively:

$$-d[I]/dt = k_I[N^+I] + k_I'[N^+IS_A] + k_I''[N^+B^-I] \quad (31)$$

$$-d[L]/dt = k_L[N^+L] + k_L'[N^+S_BL] + k_L''[N^+B^-L] \quad (32)$$

By substituting Eqs. (25), ⋯, (29) and (30) into Eqs. (31) and (32), Eqs. (33) and (34) are derived:

$$-\frac{d[I]}{dt} = \frac{(K_\varepsilon K_Ik_I+K_\varepsilon K_I'K_Ak_I'[S]+K_I''k_I'')\alpha[C]_0}{f(K,M,S)}[I] \quad (33)$$

$$-\frac{d[L]}{dt} = \frac{(K_\varepsilon K_Ik_L+K_\varepsilon K_L'K_D'k_L'[S]+K_L''k_L'')\alpha[C]_0}{f(K,M,S)}[L] \quad (34)$$

Since the propagations in the solvents with high dielectric constants occur mainly by the reaction of the dissociated immonium ion and the monomers, Eqs. (33) and (34) may be expressed approximately by Eqs. (35) and (36):

$$-\frac{d[I]}{dt} = \frac{K_\varepsilon(K_I k_I + K_A K_I k_I'[S])\alpha[C]_0}{f(K,M,S)}[I] \quad (35)$$

$$-\frac{d[L]}{dt} = \frac{K_\varepsilon(K_L k_L + K_D K_L' k_L'[S])\alpha[C]_0}{f(K,M,S)}[L] \quad (36)$$

Because $[S] \gg 1$, $K_A K_I' k_I'[S]$ and $K_D' K_L' k_L'[S]$ are considered to be much larger than $K_I k_I$ and $K_L k_L$ respectively. Therefore, Eqs. (35) and (36) may be approximately expressed by Eqs. (37) and (38) respectively:

$$-d[I]/dt = (K_\varepsilon K_A K_I' k_I'[S]\alpha[C]_0[I])/f(K,M,S) \quad (37)$$

$$-d[L]/dt = (K_\varepsilon K_D' K_L' k_L'[S]\alpha[C]_0[L])/f(K,M,S) \quad (38)$$

Taking the reciprocal of Eqs. (37) and (38), and considering that the concentration of the solvent is much larger than unity, two approximate equations, Eqs. (39) and (40), may be obtained:

$$1/(-d[I]/dt) \fallingdotseq \frac{K_D'(1+K_L'[L])}{K_A K_I' k_I'\alpha[C]_0[I]} + \frac{(1+K_I'[I]+K_D''[S])}{K_I' k_I'\alpha[C]_0[I]} \quad (39)$$

$$1/(-d[L]/dt) \fallingdotseq \frac{K_A(1+K_I'[I])}{K_D' K_L' k_L'\alpha[C]_0[L]} + \frac{(1+K_L'[L]+K_A'[S])}{K_L' k_L'\alpha[C]_0[L]} \quad (40)$$

Equations (39) and (40) explain the experimental results that, in the polar solvents with similar dielectric constants, the reaction rate of *N*-phenylethylenimine (or *β*-propiolactone) decreases with an increase in the K_D' (or K_A). On the other hand, considering that the terms containing K_ε in Eqs. (33) and (34) are negligible in the solvents with low dielectric constants, the rate equations of the monomers may be approximately expressed by Eqs. (41) and (42) respectively:

$$-d[I]/dt = K_I'' k_I''\alpha[C]_0[I] \quad (41)$$

$$-d[L]/dt = K_L'' k_L''\alpha[C]_0[L] \quad (42)$$

According to Eqs. (41) and (42), we can explain the experimental finding that, in the solvents with low dielectric constants, there was no effect of the electric nature of the solvent on the reaction rates of the monomers.

Since the scale of the reaction of *N*-phenylethylenimine is much larger than that of *β*-propiolactone in the solvents with high dielectric constants, the copolymerization rate may be almost equal to the reaction rate of *N*-phenylethylenimine. Therefore the copolymerization rate (R_p) in the solvents with high dielectric constants is:

$$R_p \fallingdotseq K_\varepsilon(K_I k_I + K_A K_I' k_I'[S])\alpha[C]_0[I]/\{1+K_I''[I]+K_L''[L]+K_\varepsilon(1+K_I[I]+K_L[L]+K_D'[S]+K_A[S]+K_L' K_D'[S][L]+K_A K_I'[S][I]+K_A' K_D'[S]^2)\} \quad (43)$$

By assuming $0 < K_\varepsilon < 1$, Eq. (43) explains the experimental facts that, in solvents with high dielectric constants, the copolymerization rate increased with an increase of the K_ε value, while in solvents with similar dielectric constant the rate decreased with an increase in the K_D'. The copolymerization rate in solvents with low dielectric constants is represented by the sum of Eqs. (41) and (42);

$$R_p \fallingdotseq -d[I]/dt + -d[L]/dt = (K_I'' k_I''[I]+K_L'' k_L''[L])\alpha[C]_0 \quad (44)$$

This equation shows that there is no effect of the solvents with low dielectric constants on the copolymerization rate.

The *β*-propiolactone content in the copolymer (C_L) is given by Eq. (45):

$$C_L = [Y]_L/([Y]_I + [Y]_L) \quad (45)$$

where $[Y]_I$ and $[Y]_L$ are the amounts of *N*-phenylethylenimine and *β*-propiolactone respectively present in the copolymer. In the solvents with high dielectric constants, by considering that $[Y]_I \gg [Y]_L$ because the *β*-propiolactone content in the copolymer is smaller than 26%, as is shown in Fig. 5, the *β*-propiolactone content may be approximately expressed by Eq. (46):

$$C_L \fallingdotseq [Y]_L/[Y]_I \quad (46)$$

By combining Eqs. (35), (36) and (46), and by assuming that $[I] \fallingdotseq [L]$ in the early stage of the copolymerization, Eq. (47) is derived:

$$C_L \fallingdotseq (K_L k_L + K_D' K_L' k_L'[S])/(K_I k_I + K_A K_I' k_I'[S]) \quad (47)$$

This approximate equation can explain the experimental fact that the *β*-propiolactone content increases in proportion to the K_D' value of the solvent. On the other hand, in the solvents with low dielectric constants, *β*-propiolactone content is approximately expressed by Eq. (48), which is derived from Eqs. (41), (42) and (45):

$$C_L \fallingdotseq K_L'' k_L''/(K_L'' k_L'' + K_I'' k_I'') \quad (48)$$

Equation (48) explains the fact that, in the solvents with low dielectric constants, the *β*-propiolactone content is almost constant, independent of the characteristic nature of the solvents.

BULLETIN OF THE CHEMICAL SOCIETY OF JAPAN VOL. 42 1634—1640 (1969)

Effect of the Binary Solvent System on the Copolymerization of *N*-Phenylethylenimine with β-Propiolactone

Tsutomu KAGIYA, Tomizo KONDO and Kenichi FUKUI

Fuculty of Engineering, Kyoto University, Sakyo-ku, Kyoto

(Received October 17, 1968)

The effect of the binary solvent system on the copolymerization of *N*-phenylethylenimine with β-propiolactone has been studied quantitatively. The copolymerization was carried out in three kinds of binary solvent systems, each consisting of components with similar dielectric constants (ε) and with very different nucleophilicities: (1) the nitrobenzene - *N,N*-dimethylacetamide system, $\varepsilon \fallingdotseq 36$, (2) the ethylene dichloric'e - tetrahydrofuran system, $\varepsilon \fallingdotseq 10$, (3) the toluene-anisole system, $\varepsilon \fallingdotseq 3$. In the binary solvent system with the highest dielectric constant, the copolymerization rate decreased with an increase in the content of the nucleophilic solvent. In the nitrobenzene - *N,N*-dimethylacetamide system, the copolymerization rate markedly decreased upon the addition of a small amount of *N,N*-dimethylacetamide in nitrobenzene. On the other hand, in the ethylene dichloride - tetrahydrofuran binary solvent system, with a lower dielectric constant than the nitrobenzene and *N,N*-dimethylacetamide system, the rates decreased in proportion to the tetrahydrofuran content. The β-propiolactone content in the copolymer increased with the amount of the larger nucleophilic solvents, and the dependency of the copolymer composition on the nucleophilicity of the solvents was much larger in the binary solvents with high dielectric constants than in the binary solvents with low dielectric constants. In the toluene - anisole system, which has a very low dielectric constant, the copolymerization rate and the composition of the copolymer were almost constant, independent of the composition of the solvents.

We have studied the solvent effect in the copolymerization of *N*-phenylethylenimine with β-propiolactone. It has been reported[1] that, in the copolymerization of *N*-phenylethylenimine with β-propiolactone in various solvents, the copolymerization rate and the composition of the copolymer were much affected by the nucleophilicity, the electrophilicity, and the dielectric constant of the solvents. The dependency of the rate and the composition of the copolymer on the nucleophilicity and electrophilicity of the solvent increased with an increase in the dielectric constant of the solvent. On the basis of the kinetic study, the roles of the solvent in the copolymerization could be quantitatively explained.

In this paper, the effect of the binary solvent system on the copolymerization of the *N*-phenylethylenimine with β-propiolactone will be quantitatively investigated.

Experimental

Material. The methods of the purification of the materials were described in a previous paper.[1]

Copolymerization Procedure. Measured amounts of β-propiolactone (0.005 mol) and the binary solvents (total volume: 2 ml) were placed in a glass ampule under a nitrogen atmosphere, and then *N*-phenylethylenimine (0.005 mol) was added to this system at −78°C. After the ampule had been sealed and maintained at 0—1°C for a definite period of time, the solid products were washed with chloroform and diethyl ether, separated by a centrifuge, and dried *in vacuo*.

The method of the determination of the copolymer composition was described in a previous paper.[2]

Results and Discussion

The copolymerization of *N*-phenylethylenimine with β-propiolactone was carried out in the binary solvent system without the addition of any catalyst. Three binary solvent systems, each consisting of components with similar dielectric constants and very different nucleophilicities, were used, as is shown in Table 1.

The Effect of the Solvent on the Copolymerization Rate. The relations between the copolymerization rate and the mole fraction of the solvents are show in Fig. 1 (A, B, C). In the binary solvent system A, with the highest dielectric constant, the copolymerization rate in nitrobenzene was much larger than that in *N,N*-dimethylacetamide, and the rate was markedly depressed by the addition of small amounts of *N,N*-dimethylacetamide. According to

1) T. Kagiya, T. Kondo and K. Fukui, This Bulletin, **42**, 1628 (1969).

2) T. Kagiya, T. Kondo, S. Narisawa and K. Fukui, *ibid.*, **41**, 172 (1968).

TABLE 1. THE PHYSICAL PROPERTIES OF THE SOLVENT IN THE BINARY SOLVENT SYSTEMS

	Solvent	Dielectric constant ε	Nucleophilicity[3] $\Delta\nu_{O-D}$	Electrophilicity[3] $\Delta\nu_{C=O}$
Binary solvent system (A)	Nitrobenzene	34.8	21	8.0
	N,N-Dimethylacetamide	36.7	113	—
Binary solvent system (B)	Ethylene dichloride	10.4	2	−1.5
	Tetrahydrofuran	7.4	90	0.2
Binary solvent system (C)	Toluene	2.38	2	−0.9
	Anisole	4.33	26	1.4

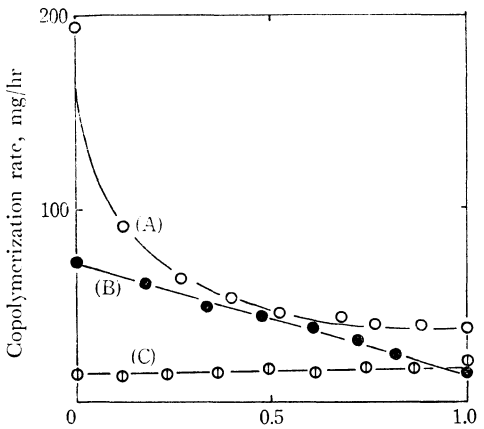

Fig. 1. Relations between copolymerization rates and mole fraction of the solvents in the binary solvent systems.
○: (A) Nitrobenzene ↔ *N,N*-Dimethylacetamide
●: (B) Ethylene dichloride ↔ Tetrahydrofuran
◑: (C) Toluene ↔ Anisole
Abscissa is mole fraction of *N,N*-dimethylacetamide, tetrahydrofuran and anisole.

the mechanism postulated in the previous paper, that the competitive coordination of the nucleophilic solvent to the cationic growing end of the polymer depresses the reaction of the monomers, this fact indicates that *N, N*-dimethylacetamide, with a larger nucleophilicity, coordinates selectively to the cationic growing end of the polymer.

On the other hand, in the ethylene dichloride-tetrahydrofuran binary solvent system B, with a lower dielectric constant than A, the copolymerization rate decreased in proportion to the amount of tetrahydrofuran. In view of this fact, the coordination of the solvent to the cationic polymer end may be considered to increase proportionally with the amount of tetrahydrofuran. The effect of the nucleophilicity of the solvent on the copolymerization rate in A is larger than that in B. This finding is in accord with the finding that the dependency of the rate on the nucleophilicity of the solvent increased with the dielectric constant of the solvent.

In the binary solvent system C, consisting of components with low dielectric constants, the effect of the solvents on the copolymerization rate is small compared with that of the solvent with a high dielectric constant. This fact may lead to a consideration that the propagation mechanism in the solvent with a low dielectric constant differs from that in the solvents with high dielectric constants. It is considered that, in the solvent with a low dielectric constant, the propagation proceeds mainly by means of undissociated ions, whereas that in the solvents with high dielectric constants proceeds by means of dissociated ions, and that coordination of the solvent to the undissociated ions is small.

The Effect of the Solvent on the Copolymer Composition. The plots of the β-propiolactone content (mol%) in the copolymer (conversion 6.5—17.8%) against the mole fraction of the solvent are shown in Fig. 2. It may be seen that, in the solvents with high dielectric constants, A and B, the β-propiolactone content increased with an incerase in the amounts of nucleophilic solvents. Moreover, Fig. 2

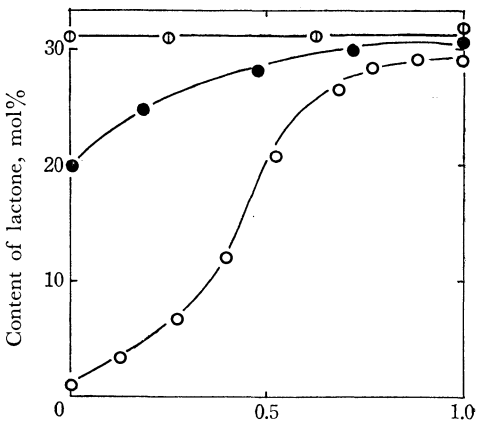

Fig. 2. Relations between contents of β-propiolactone and mole fraction of the solvent in the binary solvent systems.
○: (A) Nitrobenzene ↔ *N,N*-Dimethylacetamide
●: (B) Ethylene dichloride ↔ Tetrahydrofuran
◑: (C) Toluene ↔ Anisole
Abscissa is mole fraction of *N,N*-dimethylacetamide, tetrahydrofuran and anisole.

shows that the dependency of the copolymer composition on the nucleophilicity of the solvent in A is larger than that in B. In view of this fact and the results obtained previously, it may be considered that the degree of the effect of the nucleophilic solvent on the copolymer composition increases with the dielectric constant of the solvent. On the other hand, in the solvent with a low dielectric constant (the toluene - anisole system), the solvent has no effect on the copolymer composition.

The Effect of the Solvent on the Reaction Rates of Monomers. The reaction rates of the monomers were obtained from the copolymerization rate and the composition of the copolymer as shown in Fig. 1 and Fig. 2. The relations between the reaction rate of *N*-phenylethylenimine and the mole fraction of the solvent are shown in Fig. 3. In A, with the highest dielectric constant, the effect of the nucleophilic solvent on the reaction rate of *N*-phenylethylenimine is larger than that in the ethylene dichloride - tetrahydrofuran system.

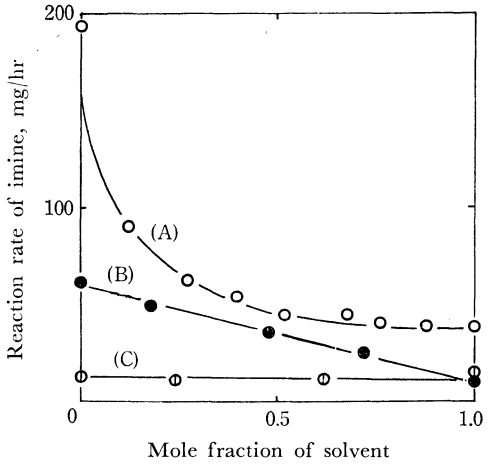

Fig. 3. Relations between reaction rate of *N*-phenylethylenimine and mole fraction of solvent in the binary solvent systems.
○: (A) Nitrobenzene ↔ *N*,*N*-Dimethylacetamide
●: (B) Ethylene dichloride ↔ Tetrahydrofuran
⦶: (C) Toluene ↔ Anisole
Abscissa is mole fraction of *N*,*N*-dimethylacetamide, tetrahydrofuran and anisole.

In C, with its low dielectric constant, the reaction rate of *N*-phenylethylenimine remains almost constant, independent of the mole fraction of the solvent. In comparison with Fig. 1, it is found that the relations of the apparent copolymerization rate and the reaction rate of *N*-phenylethylenimine to the mole fraction of the solvent resemble each other, whereas the plots of the reaction rate of *β*-propiolactone against the mole fraction (Fig. 4) differ, in Fig. 1 and Fig. 3. These facts may indicate that the copolymerization rate is much more affected by the reaction rate of *N*-phenylethylenimine with the propagating species than by that of *β*-propiolactone, considering that the reaction rate of *β*-propiolactone is very small. Therefore, it may be suggested that the propagating species consist mainly of immonium ions and a few oxonium ions.

The relations between the reaction rate of *β*-propiolactone and the mole fraction of the solvent are shown in Fig. 4. In A and B, the reaction rate of *β*-

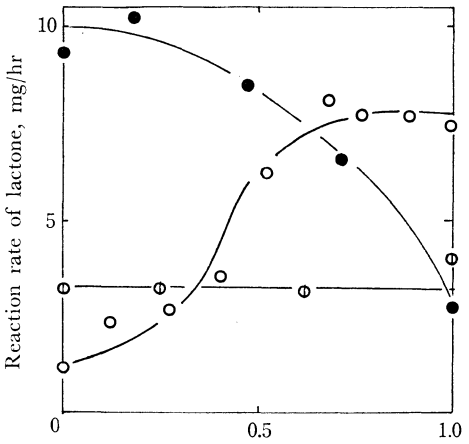

Fig. 4. Relations between reaction rate of *β*-propiolactone and mole fraction of solvents in the binary solvent systems.
○: (A) Nitrobenzene ↔ *N*,*N*-Dimethylacetamide
●: (B) Ethylene dichloride ↔ Tetrahydrofuran
⦶: (C) Toluene ↔ Anisole
Abscissa is mole fraction of *N*,*N*-dimethylacetamide, tetrahydrofuran and anisole.

propiolactone decreases with an increases in the amounts of nitrobenzene and tetrahydrofuran respectively. Considering that, in a solvent with a high dielectric constant, the reaction of *β*-propiolactone is much depressed by the electrophilic solvent, as has been described in a previous paper, this fact may be due to the larger electrophilicities, of nitrobenzene and tetrahydrofuran than of *N*,*N*-dimethylacetamide and ethylene dichloride respectively. In the nonpolar solvent, C, there is no effect of the solvent on the reaction rate of *β*-propiolactone.

Mechanism of the Copolymerization. From these experimental facts, the following mechanism of the copolymerization was postulated:
Initiation

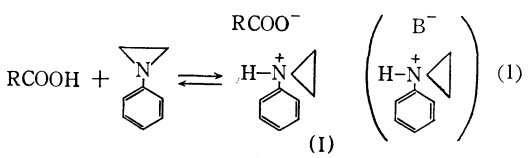

Propagation

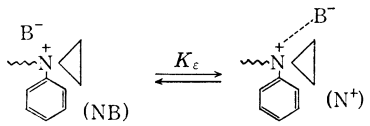

(2)

Nucleophilic solvation

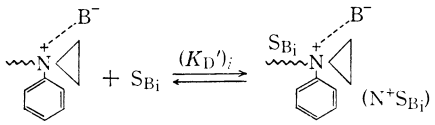

(3)

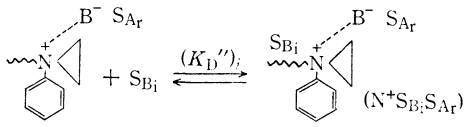

(4)

Electrophilic solvation

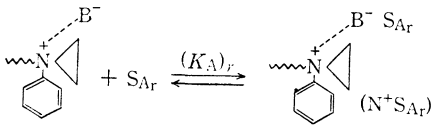

(5)

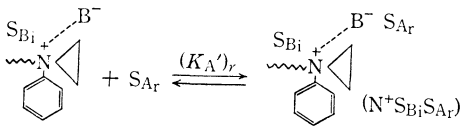

(6)

S_B; nucleophilic solvent, S_A; electrophilic solvent, i; 1, 2. r; 1, 2.

Reaction of N-Phenylethylenimine in propagation

Reaction with dissociated immonium ion;
Nonsolvated

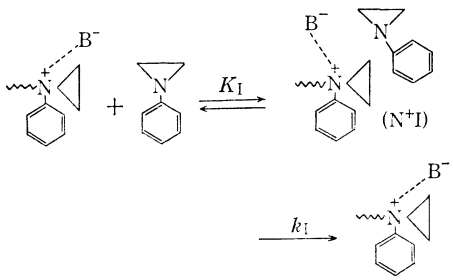

(7)

Solvated

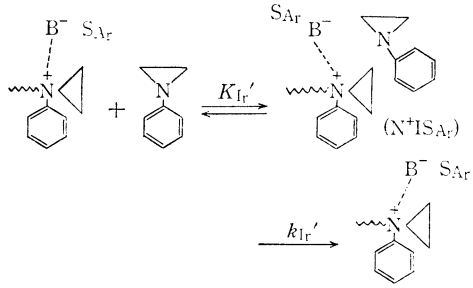

(8)

Reaction with undissociated immonium ion;

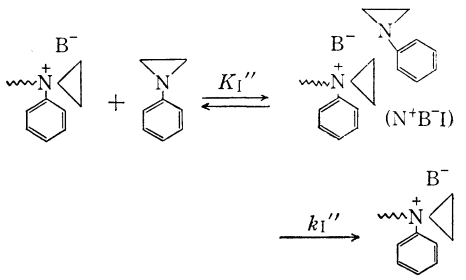

(9)

Reaction of β-propiolactone in propagation

Reaction with dissociated immonium ion;
Nonsolvated

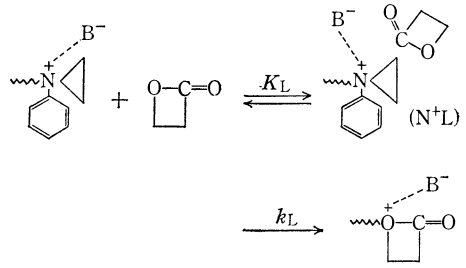

(10)

Solvated

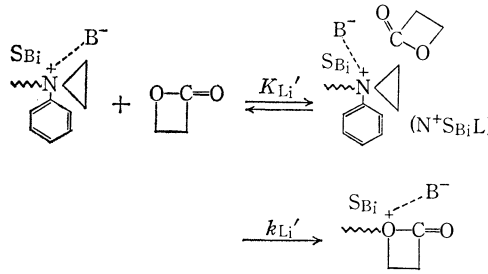

(11)

Reaction with undissociated immonium ions;

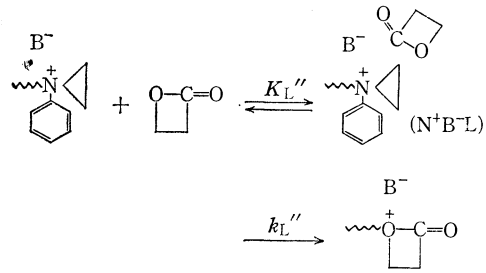

(12)

The initiation reaction is considered to be the reaction of the acid present in β-propiolactone with *N*-phenylethylenimine to produce compound (I), as has been described in a previous paper. This compound dissociates partially to the immonium ion, and the reaction is in equilibrium. The equilibrium constant (K_ε) is considered to increase with an increase in the dielectric constant of the

solvent. Equations (3) and (4) show the nucleophilic solvation of the solvents to the immonium ion. Since the coordinations of the solvent to both the propagating species and methanol-d are nucleophilic reactions, the equilibrium constants (K_D' and K_D'') are considered to increase with an increase in the $\Delta\nu_{O-D}$ (or K_D) value.[3] Equations (5) and (6) show the electrophilic solvation of the solvent to the polymer end. Since the coordination of the solvent to both the counter-anion and acetophenone are electrophilic reactions, it seems reasonable to assume that K_A and K_A' are larger in the solvents with larger $\Delta\nu_{C=O}$ values.[3] On the other hand, on the basis of the fact that there is no effect on the propagation reaction in the solvents with low dielectric constants, it may be considered that the coordination of the solvent to the undissociated immonium ion is small.

In the propagation reaction, both immonium ions and oxonium ions are considered to react with the monomers by the same mechanism. Therefore, the propagation reactions of immonium ions with monomers are shown as an example. From the fact that, in the solvent with high dielectric constants, the reaction rate of *N*-phenylethylenimine was depressed with an increase in the nucleophilicity of the solvent, the reaction of *N*-phenylethylenimine is considered to occur by means of nonsolvated immonium ions, as is shown in Eqs. (7) and (8). Since, in the solvents with high dielectric constants, the reaction rate of β-propiolactone decreased with an increase in the electrophilicity of the solvent, the reaction of β-propiolactone may proceed by means of dissociated immonium ions whose counter ions are not solvated by the solvent, as is shown by Eqs. (10) and (11). On the other hand, the propagation can proceed in a solvents with a low dielectric constant; therefore, it is assumed to occur by means of the reaction of the undissociated immonium ions with monomers (Eqs. (9) and (12)).

Kinetics. On the basis of the mechanism postulated, the effects of the solvent on the copolymerization rate and the copolymer composition were quantitatively investigated. From the fact that the amount of β-propiolactone consumed is less than that of *N*-phenylethylenimine, the quantity of immonium ions is considered to be much larger than that of oxonium ions. Therefore, the concentration of compound I, $\alpha[C]_0$, may be approximately expressed by Eq. (13), where $[C]_0$ is the initial concentration of the catalyst and where α is the constant $(0<\alpha<1)$:

$$\alpha[C]_0 = [N^+] + [N^+B^-] + \sum_{i=1}^{2}[N^+S_{Bi}] + \sum_{r=1}^{2}[N^+S_{Ar}] + \sum_{i=1}^{2}\sum_{r=1}^{2}[N^+S_{Bi}S_{Ar}] + [N^+I] + [N^+L] + \sum_{r=1}^{2}[N^+IS_{Ar}] + \sum_{i=1}^{2}[N^+S_{Bi}L] + [N^+B^-I] + [N^+B^-L] \quad (13)$$

On the other hand, according to Eqs. (2), (3),⋯, (11) and (12), the equilibrium equations will be:

$$[N^+]/[N^+B^-] = K_\varepsilon \quad (14)$$

$$[N^+S_{Bi}]/([N^+][S_i]) = (K_D')_i \quad (15)$$

$$[N^+S_{Ar}]/([N^+][S_r]) = (K_A)_r \quad (16)$$

$$[N^+S_{Ar}S_{Bi}]/([N^+S_{Ar}][S_i]) = (K_D'')_i \quad (17)$$

$$[N^+S_{Ar}S_{Bi}]/([N^+S_{Bi}][S_r]) = (K_A')_r \quad (18)$$

$$[N^+I]/([N^+][I]) = K_I \quad (19)$$

$$[N^+L]/([N^+][L]) = K_L \quad (20)$$

$$[N^+IS_{Ar}]/([N^+S_{Ar}][I]) = (K_I')_r \quad (21)$$

$$[N^+S_{Bi}L]/([N^+S_{Bi}][L]) = (K_D')_i \quad (22)$$

$$[N^+B^-I]/([N^+B^-][I]) = K_I'' \quad (23)$$

$$[N^+B^-L]/([N^+B^-][L]) = K_L'' \quad (24)$$

where [I] and [L] are the concentrations of *N*-phenylethylenimine and β-propiolactone respectively. By combining Eqs. (13), (14),⋯, (23) and (24), the concentrations of N^+I, N^+L, N^+IS_{Ar}, N^+S_{Bi}, N^+B^-I, and N^+B^-L may be represented as in Eqs. (25), (26), (27), (28), (29), and (30) respectively:

$$[N^+I] = K_\varepsilon K_I\alpha[C]_0[I]/f(K,M,S) \quad (25)$$

$$[N^+L] = K_\varepsilon K_L\alpha[C]_0[L]/f(K,M,S) \quad (26)$$

$$[N^+IS_{Ar}] = K_\varepsilon(K_I')_r(K_A)_r\alpha[C]_0[I][S_r]/f(K,M,S) \quad (27)$$

$$[N^+S_{Bi}L] = K_\varepsilon(K_L')_i(K_D')_i\alpha[C]_0[L][S_i]/f(K,M,S) \quad (28)$$

$$[N^+B^-I] = K_I''\alpha[C]_0[I]/f(K,M,S) \quad (29)$$

$$[N^+B^-L] = K_L''\alpha[C]_0[L]/f(K,M,S) \quad (30)$$

where $f(K,M,S) = 1 + K_I''[I] + K_L''[L] + K_\varepsilon(1 + K_I[I] + K_L[L] + \sum_{i=1}^{2}(K_D')_i[S_i] + \sum_{r=1}^{2}(K_A)_r[S_r] + \sum_{r=1}^{2}\sum_{i=1}^{2}(K_D')_i(K_A')[S_i][S_r])$.

The reaction rates of *N*-phenylethylenimine and β-propiolactone are represented by Eqs. (31) and (32) respectively:

$$-d[I]/dt = k_I[N^+I] + \sum_{r=1}^{2}k_{Ir}'[N^+IS_{Ar}] + k_I''[N^+B^-I] \quad (31)$$

$$-d[L]/dt = k_L[N^+L] + \sum_{i=1}^{2}k_{Li}'[N^+S_{Bi}L] + k_L''[N^+B^-L] \quad (32)$$

By substituting Eqs. (25),⋯, (29) and (30) into Eqs. (31) and (32), Eqs. (33) and (34) are derived:

3) T. Kagiya, Y. Sumida and T. Inoue, This Bulletin, **41**, 767 (1968).

$$-\mathrm{d[I]}/\mathrm{d}t = (K_\varepsilon K_\mathrm{I} k_\mathrm{I} + K_\varepsilon \sum_{r=1}^{2} (K_\mathrm{I}')_r (K_\mathrm{A})_r k_{\mathrm{I}r}' [\mathrm{S}_r] + K_\mathrm{I}'' k_\mathrm{I}'') \alpha [\mathrm{C}]_0 [\mathrm{I}] / f(\mathrm{K,M,S}) \tag{33}$$

$$-\mathrm{d[L]}/\mathrm{d}t = (K_\varepsilon K_\mathrm{L} k_\mathrm{L} + K_\varepsilon \sum_{i=1}^{2} (K_\mathrm{L}')_i (K_\mathrm{D}')_i k_{\mathrm{L}i}' [\mathrm{S}_i] + K_\mathrm{L}'' k_\mathrm{L}) \alpha [\mathrm{C}]_0 [\mathrm{L}] / f(\mathrm{K,M,S}) \tag{34}$$

Since the propagation in the solvents with high dielectric constants is considered to occur mainly with the dissociated immonium ions, Eqs. (33) and (34) may be approximately expressed by Eqs. (35) and (36):

$$-\frac{\mathrm{d[I]}}{\mathrm{d}t} = \frac{K_\varepsilon (K_\mathrm{I} k_\mathrm{I} + \sum_{r=1}^{2} (K_\mathrm{I}')_r (K_\mathrm{A})_r k_{\mathrm{I}r}' [\mathrm{S}_r]) \alpha [\mathrm{C}]_0 [\mathrm{I}]}{\mathrm{C}_1 + K_\varepsilon (\mathrm{C}_2 + \sum_{i=1}^{2} (K_\mathrm{D}')_i [\mathrm{S}_i] + \sum_{r=1}^{2} (K_\mathrm{A})_r [\mathrm{S}_r] + \sum_{i=1}^{2} \sum_{r=1}^{2} (K_\mathrm{D}'')_i (K_\mathrm{A}')_r [\mathrm{S}_i][\mathrm{S}_r])} \tag{35}$$

$$-\frac{\mathrm{d[L]}}{\mathrm{d}t} = \frac{K_\varepsilon (K_\mathrm{L} k_\mathrm{L} + \sum_{i=1}^{2} (K_\mathrm{L}')_i (K_\mathrm{D}')_i k_{\mathrm{L}i}' [\mathrm{S}_i]) \alpha [\mathrm{C}]_0 [\mathrm{L}]}{C_1 + K_\varepsilon (C_2 + \sum_{i=1}^{2} (K_\mathrm{D}')_i [\mathrm{S}_i] + \sum_{r=1}^{2} (K_\mathrm{A})_r [\mathrm{S}_r] + \sum_{i=1}^{2} \sum_{r=1}^{2} (K_\mathrm{D}'')_i (K_\mathrm{A}')_r [\mathrm{S}_i][\mathrm{S}_r])} \tag{36}$$

where $C_1 = 1 + K_\mathrm{I}''[\mathrm{I}] + K_\mathrm{L}''[\mathrm{L}]$, $C_2 = 1 + K_\mathrm{I}[\mathrm{I}] + K_\mathrm{L}[\mathrm{L}]$.

Considering that the nucleophilic equilibrium constants of *N,N*-dimethylacetamide ($(K_\mathrm{D}')_\mathrm{DMA}$ and $(K_\mathrm{D}'')_\mathrm{DMA}$) are much larger than those of nitrobenzene ($(K_\mathrm{D}')_\mathrm{NB}$ and $(K_\mathrm{D}'')_\mathrm{NB}$), the following relationships may be obtained, even in the case of $[\mathrm{S}]_\mathrm{DMA} \gg [\mathrm{S}]_\mathrm{NB}$: $(K_\mathrm{D}')_\mathrm{DMA}[\mathrm{S}]_\mathrm{DMA} \gg (K_\mathrm{D}')_\mathrm{NB}[\mathrm{S}]_\mathrm{NB}$, $(K_\mathrm{D}'')_\mathrm{DMA}[\mathrm{S}]_\mathrm{DMA} \gg (K_\mathrm{D}'')_\mathrm{NB}[\mathrm{S}]_\mathrm{NB}$. Therefore, since the selective solvation of *N,N*-dimethylacetamide to the cationic end of the polymer brings on an increase in the terms containing K_D' and K_D'' in a denominator of Eq. (35), the reaction rate of *N*-phenylethylenimine may markedly decrease upon the addition of *N,N*-dimethylacetamide. On the other hand, in the ethylene dichloride - tetrahydrofuran system, considering that the equilibrium constants of tetrahydrofuran ($(K_\mathrm{D}')_\mathrm{THF}$ and $(K_\mathrm{D}'')_\mathrm{THF}$) are much larger than those of ethylene dichloride ($(K_\mathrm{D}')_\mathrm{EDC}$ and $(K_\mathrm{D}'')_\mathrm{EDC}$), the terms containing K_D' and K_D'' in a denominator of Eq. (35) may be approximately expressed by Eqs. (37) and (38):

$$\sum_{i=1}^{2} (K_\mathrm{D}')_i [\mathrm{S}_i] = (K_\mathrm{D}')_\mathrm{THF} [\mathrm{S}]_\mathrm{THF} \tag{37}$$

$$\sum_{i=1}^{2} \sum_{r=1}^{2} (K_\mathrm{D}'')_i (K_\mathrm{A})_r [\mathrm{S}_i][\mathrm{S}_r] = \sum_{r=1}^{2} (K_\mathrm{D}'')_\mathrm{THF} [\mathrm{S}]_\mathrm{THF} (K_\mathrm{A})_r [\mathrm{S}_r] \tag{38}$$

Equations (37) and (38) indicate that the terms containing $(K_\mathrm{D}')_\mathrm{THF}$ and $(K_\mathrm{D}'')_\mathrm{THF}$ increase in proportion to the amounts of tetrahydrofuran. Therefore, considering that these terms are larger than the other terms in the denominator of Eq. (35), the experimental finding that the reaction rate of *N*-phenylethylenimine decreased in proportion to the amount of tetrahydrofuran can be explained.

Equation (36) explains the fact that, in the solvents with high dielectric constants, the reaction rate of *β*-propiolactone decreased with an increase in the amounts of the electrophilic solvents, such as nitrobenzene and tetrahydrofuran.

On the other hand, in the solvents with low dielectric constants, the terms containing K_ε in Eqs. (33) and (34) are considered to be negligible. Therefore, the rate equations of monomers may be approximately expressed by Eqs. (39) and (40):

$$-\mathrm{d[I]}\mathrm{d}t = K_\mathrm{I}'' k_\mathrm{I}'' \alpha [\mathrm{C}]_0 [\mathrm{I}] \tag{39}$$

$$-\mathrm{d[L]}/\mathrm{d}t = K_\mathrm{L}'' k_\mathrm{L}'' \alpha [\mathrm{C}]_0 [\mathrm{L}] \tag{40}$$

According to Eqs. (39) and (40), we can explain the experimental finding that, in the solvent with low dielectric constants, the nucleophilicity and electrophilcity of the solvent has no effect on the reaction rates of the monomers.

Since the *N*-phenylethylenimine content is much larger than that of *β*-propiolactone in the solvents with high dielectric constants, the copolymerization rate may be almost equal to the reaction rate of *N*-phenylethylenimine. Therefore, the copolymerization rate (R_p) in the solvents with high dielectric constants will be:

$$R_p = \frac{K_\varepsilon (K_\mathrm{I} k_\mathrm{I} + \sum_{r=1}^{2} (K_\mathrm{I}')_r (K_\mathrm{A})_r k_{\mathrm{I}r}' [\mathrm{S}_r]) \alpha [\mathrm{C}]_0 [\mathrm{I}]}{C_1 + K_\varepsilon (C_2 + \sum_{i=1}^{2} (K_\mathrm{D}')_i [\mathrm{S}_i] + \sum_{r=1}^{2} (K_\mathrm{A})_r [\mathrm{S}_r] + \sum_{i=1}^{2} \sum_{r=1}^{2} (K_\mathrm{D}'')_i (K_\mathrm{A}')_r [\mathrm{S}_i][\mathrm{S}_r])} \tag{41}$$

Considering that $C_1 > C_2 + \sum_{i=1}^{2} (K_\mathrm{D}')_i [\mathrm{S}_i] + \sum_{r=1}^{2} (K_\mathrm{A})_r [\mathrm{S}_r] + \sum_{i=1}^{2} \sum_{r=1}^{2} (K_\mathrm{D}'')_i (K_\mathrm{A}')_r [\mathrm{S}_i][\mathrm{S}_r]$, Eq. (41) explains the following experimental facts: in the solvents with high dielectric constants, the copolymerization rate increased with the K_ε value, while in the solvents with similar dielectric constants, the rate decreased with an increase in the amounts of the nucleophilic solvents.

In the solvents with low dielectric constants, the β-propiolactone content in the copolymer is larger than in the solvents with high dielectric constants. Therefore, the copolymerization rate in a solvent with a low dielectric constant should be represented by the sum of Eqs. (39) and (40):

$$R_p = -\mathrm{d[I]}/\mathrm{d}t + -\mathrm{d[L]}/\mathrm{d}t$$
$$= (K_I''k_I''[\mathrm{I}] + K_L''k_L''[\mathrm{L}])\alpha[\mathrm{C}]_0 \quad (42)$$

This equation shows no effect of the solvents with low dielectric constants on the copolymerization rate.

The β-propiolactone content in the copolymer (C_L) is given by Eq. (43):

$$C_L = [\mathrm{Y}]_L/([\mathrm{Y}]_I + [\mathrm{Y}]_L) \quad (43)$$

where $[\mathrm{Y}]_I$ and $[\mathrm{Y}]_L$ are the amounts of *N*-phenylethylenimine and β-propiolactone respectively present in the copolymer. In the solvents with high dielectric constants, by considering the fact $[\mathrm{Y}]_I \gg [\mathrm{Y}]_L$, the β-propiolactone content may be approximately expressed by Eq. (44):

$$C_L \fallingdotseq [\mathrm{Y}]_L/[\mathrm{Y}]_I \quad (44)$$

By combining Eqs. (35), (36) and (44), and by assuming $[\mathrm{I}] \fallingdotseq [\mathrm{L}]$ in the early stages of the copolymerization, Eq. (45) is derived:

$$C_L \fallingdotseq \frac{K_L k_L + \sum_{i=1}^{2} (K_L')_i (K_D')_i k_{Li}'[\mathrm{S}_i]}{K_I k_I + \sum_{r=1}^{2} (K_I')_r (K_A)_r k_{Ir}'[\mathrm{S}_r]} \quad (45)$$

This approximate equation can explain the experimental fact that the β-propiolactone content increased with an increase in the amounts of the nucleophilic solvents. On the other hand, in the solvents with low dielectric constants, the β-propiolactone content can be approximately expressed by Eq. (46), which is derived from Eqs. (39), (40), and (43):

$$C_L = K_L''k_L''/(K_L''k_L'' + K_I''k_I'') \quad (46)$$

This equation (46) explains the fact that, in the solvents with low dielectric constants, the β-propiolactone content is almost constant, regardless of both the electric natures and the dielectric constants of the solvents.

BULLETIN OF THE CHEMICAL SOCIETY OF JAPAN VOL. 42 1640—1643 (1969)

Studies on Stable Free Radicals. II.*[1] Reactivity of Stable Nitroxide Radicals and NMR Spectra of Reaction Products

Keisuke MURAYAMA, Syoji MORIMURA and Takao YOSHIOKA

Central Research Laboratoies Sankyo Co., Ltd., Shinagawa-ku, Tokyo

(Received September 9, 1968)

We have isolated coupled products of such stable free radicals as 2,2,6,6-tetramethyl-4-oxopiperidine-1-oxyl (II), cyclohexane-1-spiro-2'-(4'-oxoimidazolidine-1'-oxyl)-5'-spiro-1''-cyclohexane (IV) and 2,2,6,6-tetramethyl-4-oxopiperidine-1-thiyl derived from bis-[2,2,6,6-tetramethyl-4-oxopiperidyl-(1)]disulfide (VII) with a *C*-radical derived from α,α'-azo-bis(isobutyronitrile). The reactive site in these stable free radicals was studied from the structure of the coupled products. The homolysis of the disulfide (VII) appeared to be accelerated by an attack of the *C*-radical, 1-methyl-1-cyanoethyl. The NMR spectra of the products suggested a slow inversion of the nitrogen atom in piperidine derivatives.

Extremely stable free radicals, such as 2,2,6,6-tetramethylpiperidine-1-oxyl (I), 2,2,6,6-tetramethyl-4-oxopiperidine-1-oxyl (II) and 2,2,6,6-tetramethyl-4-hydroxypiperidine-1-oxyl (III), have

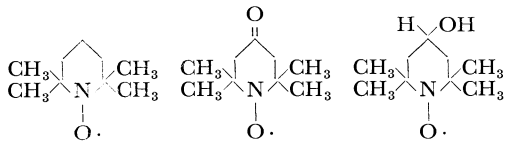

(I) (II) (III)

recently been prepared[1] by the oxidation of corresponding hindered amines. These radicals, which are considered to exist in an *O*-radical form (A)

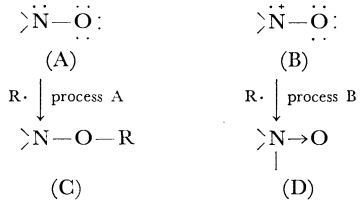

*1 Part I: K. Murayama, S. Morimura, O. Amakasu, T. Toda and E. Yamao, *Nippon Kagaku Zasshi (J. Chem. Soc. Japan, Pure Chem. Sect.)*, **90**, 296 (1969).

1) M. B. Neiman, Yu. G. Madedova and E. G. Rozantzev, *Azerb. Khim. Zh.*, **1962**, 37.

and/or another *N*-radical form (B),[2-4] can be preserved for long periods in air under normal conditions without undergoing any significant changes. It has further been found that these radicals were stable even under ionic reaction conditions.[2]

Reactions of the stable free radicals with *C*-radicals[5,6] have also been found; Neiman *et al.* deduced that the stable free radicals, I, II, and III, reacted only with an active *C*-radical (R·) derived from ethylbenzene,[5] while they did not react with a peroxy radical (ROO·). However, they did not isolate coupled products of the *C*-radical with the stable radicals. Therefore, the reactive site in the stable radicals has not been firmly established as being either an *O*-radical (A) or an *N*-radical (B). Depending upon the radical present either an N-O-R compound (C) (process A) or an *N*-oxide (D) (process B) would be expected when the radicals having Form A and Form B respectively are treated with a reactive radical, R·.

The present authors sought to confirm the reactive site of stable *N*-oxide radicals with another radical by isolating coupled products of the radicals with a typical *C*-radical derived from α,α'-azobisisobutyronitrile (ABIN). From the structure of these coupled products, we have then determined the reactive site in these radicals.

Results and Discussion

The reaction of II or a new stable free radical, cyclohexane-1-spiro-2'-(4'-oxoimidazolidine-1'-oxyl)-5'-spiro-1''-cyclohexane (IV) with ABIN, was carried out in a 2:1 molar ratio in a solution

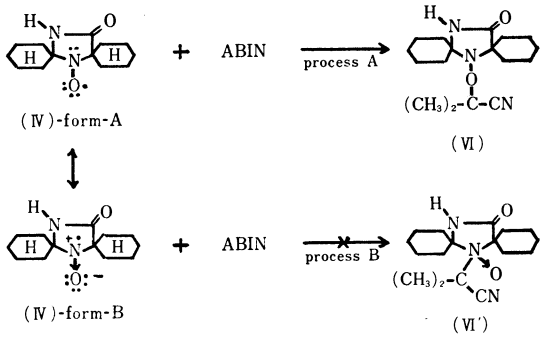

of anhydrous methanol at 63°C for 30 hr. Subsequently the coupled reaction product, prepared from the 1-methyl-1-cyanoethyl radical (derived from ABIN) and a stable radical, II or IV, was obtained, accompanied by 2,3-dimethyl-2,3-dicyanobutane. As is shown below, the structures of these products were deduced to be 1-(1-methyl-1-cyanoethoxy)-2,2,6,6-tetramethyl-4-oxopiperidine (V) or 1-(1-methyl-1-cyanoethyl)-2,2,6,6-tetramethyl-4-oxopiperidine-1-oxide (V') and cyclohexane-1-spiro-2'-[1'-(1-methyl-1-cyanoethoxy)-4'-oxoimidazolidine]-5'-spiro-1''-cyclohexane (VI) or cyclohexane-1-spiro-2'-[1'-(1-methyl-1-cyanoethyl)-4'-imidazolidine-1'-oxide]-5'-spiro-1''-cyclohexane (VI') respectively, on the basis of the results of elemental analyses, the molecular weight measurements, and the molecular peaks in the mass spectra. The structures V' and VI' were, however, doubtful, since no deoxy products were obtained in the reactions of the above coupled products with triphenylphosphine (or triethylphosphite) in an acetic acid solution at 110°C for 5 hr.[7] Strong support

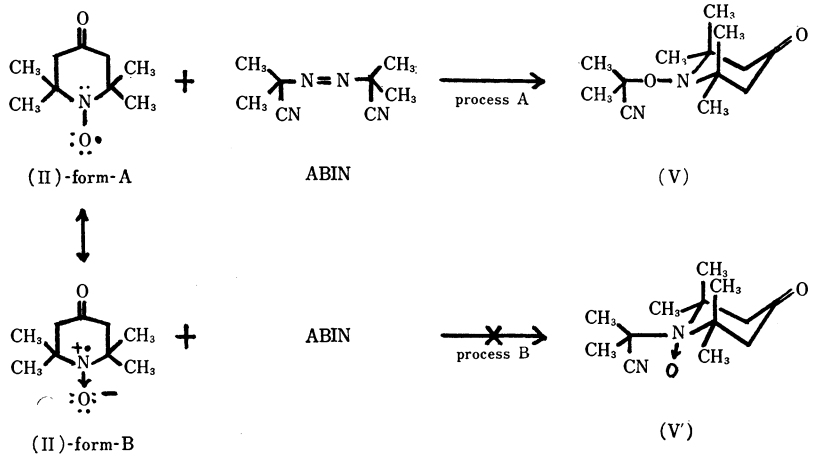

2) E. G. Rozantzev and M. B. Neiman, *Tetrahedron*, **20**, 131 (1964).

3) H. Lemaire, Y. Marechal, R. Ramasseul and A. Rassat, *Bull. Soc. Chim. France*, **1965**, 372.

4) E. G. Rozantzev and E. G. Gintsberg, *Izv. Akad. Nauk SSSR, Ser. Khim.*, **1966**, 571.

5) a) M. B. Neiman and E. G. Rozatnzev, *ibid.*, **1964**, 1178. b) M. S. Khloplyankina, A. L. Buchachenko, M. B. Neiman and A. G. Vasil, eva, *Kinetikai Kataliz.*, **6**, 394 (1965).

6) E. G. Rozantzev and V. A. Golubev, *Izv. Akad. Nauk SSSR, Ser. Khim.*, **1966**, 891.

7) L. Horner and H. Hoffmann, *Angew. Chem.*, **68**, 480 (1956).

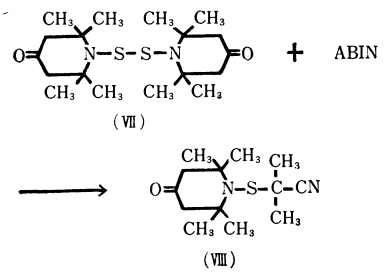

for the two molecular structures V and VI was given by the high-resolution double-focusing mass spectra. The expected molecular ion peaks at *m/e* 238.169 and 305.211, corresponding to $C_{13}H_{22}N_2O_2$ and $C_{17}H_{27}N_3O_2$ respectively, were found by the measurement of the millimass units. Since no fragment ion peak $(M-16)^+$ [8] or $(M-17)^+$ [9] was found, the V′ and VI′ structures were eliminated.

In order to investigate the behavior of stable free radicals other than *N*-oxyl radicals, a reaction of ABIN was carried out with a stable *N*-thiyl radical such as 2,2,6,6-tetramethyl-4-oxopiperidine-1- thiyl, which had been established by Bennett *et al.* using an ESR technique.[10] The precursor, bis-[2,2,6,6-tetramethyl-4-oxopiperidyl-(1)] disulfide (VII),[10] reacted with ABIN in a 1 : 2 molar ratio to give 1-(1-methyl-1-cyanoethylthio)-2,2,6,6-tetramethyl-4-oxopiperidine (VIII) in a benzene solution under gentle reflux for 7 hr. The product VIII could be characterized as the corresponding 2,4-dinitrophenylhydrazone and semicarbazone. The structure of VIII was deduced from the results of elemental analyses and the IR and NMR spectra, especially from the absence of the fragment ion peaks, $(M-32)^+$ and $(M-33)^+$.

This finding that the disulfide VII reacted with ABIN at 80°C to give VIII as the product in a good yield is instructive; over the limited range of 140—200°C, the homolytic fission of the S–S bond into the *N*-thiyl radical has been confirmed by ESR techniques,[10] while we observed no homolytic fission of the S–S bond at 80°C (ESR). Therefore, the homolytic cleavage of the disulfide bond appeared to be accelerated by the action of the 1-methyl-1-cyanoethyl radical at 80°C. Similar cleavages of various disulfides by the 1-methyl-1-cyanoethyl radical have been observed by Schmidt *et al.* when they examined the effect of substituents on the homolysis of the S–S bond.[11]

The NMR spectra of *N*-substituted 2,2,6,6-tetramethyl-4-oxopiperidines (V) and VIII showed interesting features. In the NMR spectra of 2,2,6,6-tetramethyl-4-oxopiperidine (IX),[12] 1,2,2,6,6-pentamethyl-4-oxopiperidine (X)[12] and 1-benzenesulfonyl-2,2,6,6-tetramethyl-4-oxopiperidine (XI),[13] the C-3 and C-5 methylene protons, and the

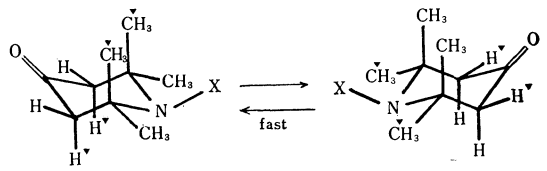

[X=-H,(IX), -CH_3 (X), -SO_2-⟨○⟩ (XI)][14]

C-2 and C-6 methyl protons have been found to give single sharp lines in a carbon tetrachloride and in a benzene solution. These facts suggest that the nitrogen inversion and/or the ring inversion is rapid at room temperature, as is shown above. It was, however, found that four methyl groups of *N*-substituted piperidines (V) and (VIII) (Fig. 1) gave rise to two sharp lines, indicative of two kinds of methyl protons. A_2B_2 quartets ($J_{gem}=13.5$ cps), indicative of two methylene protons, were further observed as well as in the case of 1-benzenesulfenyl-2,2,6,6-tetramethyl-4-oxopiperidines (XII).[13] Hence, the inversion rates of the nitrogen atom and of the piperi-

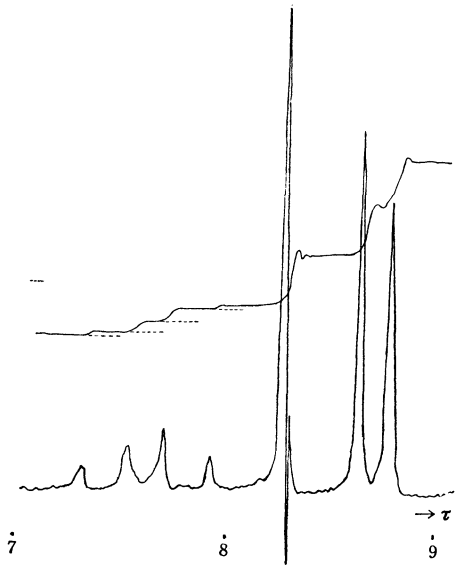

Fig. 1. Methyl and methylene protons (NMR) of 2,2,6,6-tetramethyl-4-oxo-1-(1-methyl-1-cyanoethoxy)piperidine (V) in CCl_4 at 32°, (60 Mc).

8) a) T. A. Bryce and J. R. Maxwell, *Chem. Commun.*, **1965**, 206. b) R. E. Banks, R. N. Haszeldine and M. J. Stevenson, *J. Chem. Soc., C*, **1966**, 901.

9) R. Grigg and B. G. Odell, *ibid., B*, **1966**, 218.

10) J. E. Bennett, H. Sieper and P. Tavs, *Tetrahedron*, **23**, 1697 (1967).

11) U. Schmidt and A. Müller, *Liebigs Ann. Chem.*, **672**, 90 (1964).

12) M. J. Aroney, C.-Y. Chen, R. J. W. Le Fèvre and A. N. Singh, *J. Chem. Soc., B*, **1966**, 98.

13) K. Murayama and T. Yoshioka, *Tetrahedron Letters*, **1968**, 1363.

dine ring may be considered to be slower in V and VIII than in IX, X, and XI.

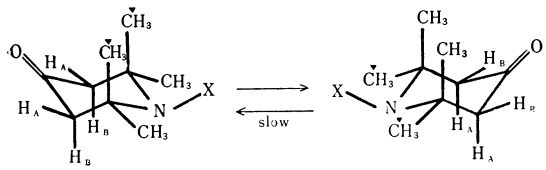

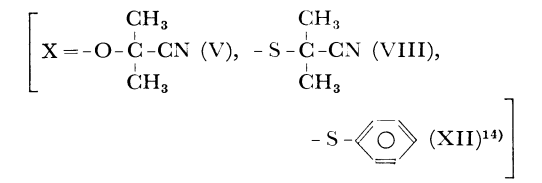

Thus, we confirmed that the *N*-oxyl and *N*-thiyl radicals could react with the *C*-radical derived from ABIN, and that the reaction apparently proceeded through process A, since no *N*-oxides V′ and VI′ were obtained even by careful separation techniques.

Experimental

All melting points are uncorrected.

The IR spectra were determined by means of Nujol mull and liquid films.

The NMR spectra were obtained using a Varian A-60 NMR spectrometer, using tetramethylsilane as the internal standard at 32°C.

The mass spectra were obtained using a JEOL-JMS-OIS mass spectrometer with an ionizing voltage of 70eV.

2,2,6,6-Tetramethyl-4-oxo-1-(1-methyl-1-cyanoethoxy)-piperidine (V). A mixture of 2,2,6,6-tetramethyl-4-oxopiperidine-1-oxyl (II) (11.7 g, 0.069 mol) and α,α'-azo-bis(isobutyronitrile)(ABIN) (5.0g, 0.0305 mol) was gently refluxed in a methanol solution for 30hr. After the solvent had then been evaporated under diminished pressure at 30°C, 2,3-dimethyl-2,3-dicyanobutane was excluded by sublimation under diminished pressure (0.060 mmHg) at 90°C. Then the oily residue was chromatographed on 100 g of Brockmann aluminum oxide and eluted with anhydrous petroleum ether to give 7.3 g (50.4 %)[14] of crude V. The crude crystals, V, were recrystallized from petroleum ether to give an analytically pure sample; mp 72.5—73.5°C.

Found: C, 65.48; H, 9.27; N, 11.74%; MW, 226.9 (V. O. P. method in $CHCl_3$). Calcd for $C_{13}H_{22}N_2O_2$: C, 65.55; H, 9.33; N, 11.76%; MW, 238.2.

IR cm^{-1}: $\nu_{C=O}$ 1725; ν_{N-O} 1460 and ν_{C-O} 1145.

NMR (τ)(in CCl_4): 8.78 (6H)(ax CH_3–); 8.63 (6H)(eq CH_3–); 8.28(6H)[$(CH_3)_2$–C–C≡N]. A_2B_2 quartet (J=13.5 cps); 7.92, 7.70, 7.53 and 7.32(4H).

Mass spectrum: M^+, *m/e* 238.169.

Cyclohexane-1-spiro-2′-(4′-oxoimidazolidine-1′-oxyl)-5′-spiro-1″-cyclohexane (IV). To a suspension of cyclohexane-1-spiro-2′-(4′-oxoimidazolidine)-5′-spiro-1″-cyclohexane[15] (corresponding amine) (22.2 g, 0.10 mol) in acetic acid (200 m*l*) were slowly added a solution of EDTA (0.5 g) and sodium tungstate (0.45 g) in water (3 m*l*) and then a 30 % aqueous solution of hydrogen peroxide (25 m*l*) with stirring at room temperature. Stirring was continued for an additional 50 hr at room temperature. After the solvent had been evaporated *in vacuo*, a 50 m*l* portion of water was added to the residue. The suspension of the crude product the (residue) was treated with potassium carbonate, and additional stirring was continued for 3 hr. The separated crystalline substance was filtered and washed with water. By recrystallization from benzene, IV was obtained as faintly reddish crystals, mp 227—228°C, in a good yield of 20.6 g (86.8%).

Found: C, 65.84; H, 8.93; N, 11.87%. Calcd for $C_{13}H_{21}N_2O_2$: C, 65.79; H, 8.92; N, 11.87%.

IR cm^{-1}: $\nu_{C=O}$ 1708; ν_{N-H} 3180 and 3070.

Cyclohexane-1-spiro-2′-[1′-(1-methyl-1-cyanoethoxy)-4′-oxoimidazolidine]-5′-spiro-1″-cyclohexane (VI). A mixture of cyclohexane-1-spiro-2′-(4′-oxoimidazolidine-1′-oxyl)-5′-spiro-1″-cyclohexane (IV) (10.0 g, 0.0422 mol) and ABIN (3.5 g, 0.0214 mol) was refluxed in a methanol solution. After 30hr, 10.3 g (79.8 %) of crude VI were separated out as crystals. These crystals were filtered and washed with ether. The crude material was recrystallized from glacial acetic acid to give an analytically pure sample; 7.8g, mp 190—191°C.

Found: C, 66.64; H, 8.99; N, 13.61%. Calcd for $C_{17}H_{27}N_3O_2$: C, 66.84; H, 8.91; N, 13.76%.

IR cm^{-1}: $\nu_{C=O}$ 1695, ν_{N-O} 1450 and ν_{C-O} 1150.

NMR: only a broad signal of cyclohexane-protons.

Mass spectrum: M^+, *m/e* 305.211.

2,2,6,6-Tetramethyl-4-oxo-1-(1-methyl-1-cyanoethylthio)piperidine (VIII). A mixture of bis-[2,2,6,6-tetramethyl-4-oxopiperidyl-(1)] disulfide (VII) (3.7 g, 0.00995 mol) and ABIN (3.2 g, 0.0195 mol) was refluxed in a benzene solution for 7 hr. After the solvent had then been evaporated under diminished pressure, 2,3-dimethyl-2,3-dicyanobutane was removed by sublimation under diminished pressure (0.1 mmHg) at 110—113°C. The oily residue was distilled to give an analytically pure oil, bp 139—141°C/0.05 mmHg, 4.1 g (81.2 %).

Found: C, 61.46; H, 8.65; N, 10.93%. Calcd for $C_{13}H_{22}N_2OS$: C, 61.39; H, 8.72; N, 11.02%.

IR cm^{-1}: $\nu_{C=O}$ 1725 and $\nu_{C\equiv N}$ 2220.

NMR(τ)(in CCl_4): 8.75 (6H)(ax CH_3–); 8.55 (6H)(eq CH_3–); 8.39 (6H)[$(CH_3)_2$–C–C≡N]; A_2B_2 quartet (J=13.5 cps) 7.79, 7.56, 7.39 and 7.16(4H).

Mass spectrum: M^+, *m/e* 254.

2,4-Dinitrophenylhydrazone, mp 155—156°C.

Found: C, 52.46; H, 6.00; N, 19.24%. Calcd for $C_{19}H_{26}N_6O_4S$: C, 52.52; H, 6.03; N, 19.35%.

Semicarbazone, mp 191—192°C.

Found: C, 54.21; H, 7.97; N, 22.32%. Calcd for $C_{14}H_{25}N_5OS$: C, 54.00; H, 8.09; N, 22.49%.

The authors wish to thank Professor Makoto Okawara of the Tokyo Institute of Technology for his valuable comments, Dr. Issei Iwai of these laboratories for his helpful guidance during the course of this work, and Mr. Susumu Higashida for his technical assistance.

14) From the reaction mixture, 2,2,6,6-tetramethyl-1-hydroxy-4-oxopiperidine (XIII) (38.4% yield) was isolated. Detailed mechanism of the formation of XIII will be reported in a forthcoming paper.

15) W. E. Noland, R. J. Sundberg and M. L. Michaelson, *J. Org. Chem.*, **28**, 3576 (1963).

BULLETIN OF THE CHEMICAL SOCIETY OF JAPAN VOL. 42 1644—1649 (1969)

Anionic Copolymerization of Isoprene and 1,1-Diphenylethylene

Heimei YUKI and Yoshio OKAMOTO

Department of Chemistry, Faculty of Engineering Science, Osaka University, Toyonaka, Osaka

(Received September 19, 1968)

Anionic copolymerization of isoprene (M_1) and 1,1-diphenylethylene (M_2) was carried out in tetrahydrofuran (THF), dioxane, benzene, and *n*-heptane by using *n*-butyllithium (*n*-BuLi), Na-naphthalene, Na- and K-dispersions as initiators. An alternating copolymer was obtained in the copolymerization in THF, which proceeded without a chain transfer and a termination. Monomer reactivity ratios, r_1, obtained by assuming the rate constant $k_{22}=0$, were 0.12 (Li^+), 0.11 (Na^+), and 0.11 (K^+) in THF at 0°C. The r_1 value in benzene at 40°C, however, was affected by the counter ion as follows: 37 (Li^+), 0.38 (Na^+), and 0.05 (K^+). With Li^+ counter ion the values were 0.50 in dioxane at 30°C and 29 in *n*-heptane at 40°C. The order of rate constants in the copolymerization in THF with *n*-BuLi at 0°C, was $k_{12}>k_{11}>k_{21}$, the last of which was 2.64×10^{-3} *l*/mol sec.

Among the anionic copolymerizations of the monomer pairs which copolymerize alternatingly,[1] the results of detailed studies were reported previously on the copolymerizations of 1,1-diphenylethylene and styrene,[2] of 1,1-diphenylethylene and 2,3-dimethylbutadiene,[3] and of *trans*-stilbene and styrene.[4]

In the present study, the copolymerization of isoprene (M_1) and 1,1-diphenylethylene (M_2) will be investigated under various reaction conditions. The results will be correlated with those of the copolymerization reported previously.

Experimental

Materials. *Isoprene.* The purified monomer (Phillips polymerization grade) was redistilled *in vacuo* from lithium aluminum hydride before use.

1,1-Diphenylethylene. This was first stirred with Na-K alloy under dry nitrogen, and then *n*-butyllithium (*n*-BuLi) in heptane was added to the mixture until a red color due to 1,1-diphenylhexyllithium appeared. The colored solution was carefully distilled *in vacuo* to obtain the pure monomer.

Tetrahydrofuran (THF) and Dioxane. Each of these solvents was refluxed over metallic sodium and then over lithium aluminum hydride, from where it was distilled onto Na-K alloy and naphthalene. From the green solution the solvent was transferred to a reaction vessel on a vacuum system before use.

Benzene and n-Heptane. Each of these solvents purified in the usual manner was distilled under high vacuum in the presence of *n*-BuLi.

n-BuLi. *n*-BuLi was prepared in *n*-heptane and the concentration was determined by double titration.[5]

Na-Naphthalene (Na-Naph.). The concentration of the solution was determined by the titration of a sample solution after hydrolysis by water.[6]

n-Butyl Alcohol. A small amount of metallic sodium was added to the alcohol (spectro grade). The alcohol containing sodium butoxide was then distilled under high vacuum to prepare a standard *n*-butyl alcohol solution in *n*-heptane. The solution was used for the colorimetric titration of a carbanion solution.

Polymerization. The polymerization was carried out in a glass ampoule under dry argon. To the ampoule, isoprene and a solvent were distilled by means of a vacuum line, and then 1,1-diphenylethylene and an initiator were added with hypodermic syringes. The polymerization was terminated after the manner of titration with the *n*-butyl alcohol solution in *n*-heptane to estimate the concentration of living ends.

Electronic Spectrum. The electronic spectrum of a reaction mixture was measured with a Hitachi 124 Spectrophotometer. The sample solution was prepared in a high vacuum system.

NMR Spectrum. The spectrum of the polymer was taken in a carbon tetrachloride solution with a JNM-4H-100 Spectrometer (Japan Electron Optics Laboratory Co., Ltd.) at 60°C.

Molecular Weight. The molecular weight of the polymer was measured on a Mechrolab Vapor Pressure Osmometer, Model 301A, using benzene as a solvent.

Viscosity. The solution viscosity of the polymer in toluene was measured at 30.0°C.

1) H. Yuki, K. Kosai, S. Murahashi and J. Hotta, *J. Polymer Sci. B*, **2**, 1121 (1964).

2) H. Yuki, J. Hotta, Y. Okamoto and S. Murahashi, This Bulletin, **40**, 2659 (1967).

3) H. Yuki, K. Hatada and T. Inoue, *J. Polymer Sci. A-1*, **6**, 3333 (1968); H. Yuki, Y. Okamoto and K. Sadamoto, This Bulletin, **42**, (1969).

4) H. Yuki, M. Kato and Y. Okamoto, This Bulletin, **41**, 1940 (1968).

5) H. Gilman and A. H. Haubein, *J. Am. Chem. Soc.*, **66**, 1515 (1944).

6) G. M. Burnett and R. N. Young, *Europ. Polym. J.*, **2**, 329 (1966).

Results

The copolymerization of isoprene (M_1) and 1,1-diphenylethylene (M_2) in THF at 0°C was carried out with *n*-BuLi as an initiator, the initial molar ratio of monomers, $[M_1]_0/[M_2]_0$, being 0.650. The results are shown in Fig. 1. The reaction

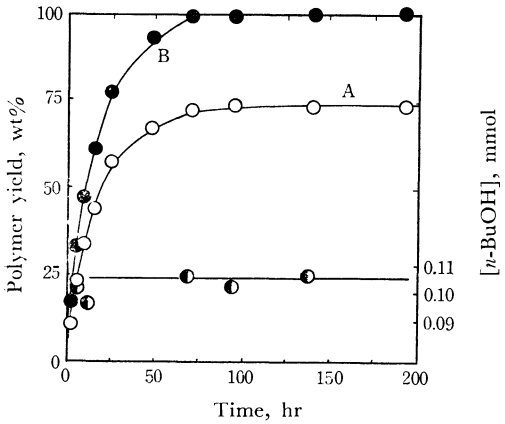

Fig. 1. Anionic copolymerization of isoprene and 1,1-diphenylethylene. —— Time *vs.* polymer yield (THF)

A: Polymer yield against total monomers
B: Polymer yield as alternating copolymerization
◐: *n*-Butyl alcohol required for terminating copolymerization
$[M_1]_0$: 6.48 mmol, $[M_2]_0$: 9.97 mmol,
[*n*-BuLi]: 0.107 mmol, THF: 15 m*l*, temp.: 0°C

proceeded so slowly that it took 80 hr to be completed, when unchanged 1,1-diphenylethylene remained in the system, but isoprene was completely consumed. Since 1,1-diphenylethylene can not be homopolymerized, the yield of the copolymer is maximum when the two monomers copolymerize alternatingly, if $[M_1]_0/[M_2]_0<1$. In Fig. 1, the yield against the theoretical amount of the alternating copolymer is also shown. It reaches 100%, indicating the formation of the alternating copolymer in the system. It was observed that the concentration of the living ends titrated by *n*-butyl alcohol was constant regardless of the reaction time and was nearly equal to the concentration of the initiator used.

The relationship between the polymer yield (curve B in Fig. 1) and the polymer molecular weight is shown in Fig. 2. A linear relationship was found between the two and the line almost agreed with the theoretical line for the living polymer produced by alternating copolymerization. There was also a linearity between log Yield and log [η].

The material balance after the prolonged copolymerization reaction was examined. A part of the results is listed in Table 1. As isoprene was com-

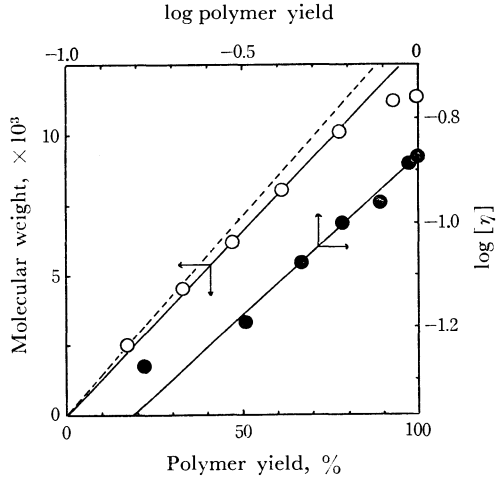

Fig. 2. Anionic copolymerization of isoprene and 1,1-diphenylethylene. —— Relationship between polymer yield and molecular weight
Dotted line: Molecular weight calculated as living polymer
$[M_1]_0$: 6.48 mmol, $[M_2]_0$: 9.97 mmol,
[*n*-BuLi]: 0.107 mmol, THF: 15.0 m*l*,
temp.: 0°C

pletely incorporated into the copolymer, the copolymer composition, $[m_1]/[m_2]$, was calculated from the polymer yield and the initial monomer concentrations.[3,4] The $[m_1]/[m_2]$ ratio in the copolymer obtained in THF slightly exceeded unity with increasing the $[M_1]_0/[M_2]_0$ ratio from 0.6 to 0.9. The alternating copolymer was powder. On the other hand, the copolymer obtained in benzene was viscous and contained a great deal of isoprene, even at $[M_1]_0/[M_2]_0=0.6$.

The copolymer composition was also examined by other methods as shown in Table 2. The elementary analyses of the copolymer are well consistent with the calculations based on the copolymer compositions derived from the polymer yields. The copolymer compositions obtained from the ratios of aromatic to aliphatic protons in their NMR spectra are also in accord with the above compositions within analytical errors.

The monomer reactivity ratio, r_1, was obtained from the integrated Mayo-Lewis copolymer composition equation, assuming $k_{22}=0$.[2] The r_1 values thus obtained are listed in Tables 3—5. In the copolymerizations in THF at 0°C using *n*-BuLi, Na-naphthalene, and K-dispersion as initiators, the r_1 values were almost constant (0.11—0.12). In benzene at 40°C, however, the values were 37, 0.38, and 0.05 with *n*-BuLi, Na-dispersion, and K-dispersion respectively. With *n*-BuLi in dioxane at 30°C and in *n*-heptane at 40°C, the values were 0.50 and 29 respectively. The r_1 value at 25°C in THF seemed to be smaller than that at 0°C. The copolymerization carried out in benzene without an initiator gave no polymer even after 216 hr at 40°C

TABLE 1. ANIONIC COPOLYMERIZATION OF ISOPRENE (M_1) AND 1,1-DIPHENYLETHYLENE (M_2)
MATERIAL BALANCE

M_1: 0.442 g, initiator: *n*-BuLi 0.11 mmol, temp.: 0°C in THF, 40°C in benzene

Solvent 15.0 ml	Time hr	M_2 g	$[M_1]_0/[M_2]_0$ mol/mol	Polymer g	Unchanged[a] M_2, g	$[m_1]/[m_2]$[b] mol/mol
THF	96	1.293	0.904	1.544	0.187	1.06
THF	96	1.522	0.770	1.589	0.370	1.02
THF	96	1.797	0.607	1.625	0.630	1.00
Benzene	120	0.506	2.32	0.494	0.440	24.8
Benzene	120	1.162	1.01	0.562	1.042	9.87
Benzene	120	1.733	0.653	0.600	1.554	7.47

a) Contained *ca.* 7 mg of Li-compounds.
b) Molar ratio of monomers in copolymer.

TABLE 2. ANIONIC COPOLYMERIZATION OF ISOPRENE (M_1) AND 1,1-DIPHENYLETHYLENE (M_2)
COPOLYMER COMPOSITION

Initiator: *n*-BuLi

Solvent 15.0 ml	Yield wt%	$[m_1]/[m_2]$[a]	Elementary analysis				NMR $[m_1]/[m_2]$[c]
			Calcd[b]		Found		
			C%	H%	C%	H%	
THF	11.1	1.00	91.76	8.24	91.95	8.20	—
THF	23.4	1.00	91.86	8.14	91.86	8.07	—
THF	72.6	1.00	91.88	8.12	92.00	8.11	0.96
Dioxane	78.7	1.23	91.56	8.44	91.23	8.23	1.27
Dioxane	97.4	2.34	90.88	9.12	90.98	8.98	2.40
Benzene	27.9	7.47	89.16	10.50	89.16	10.41	7.10
Benzene	43.6	13.9	88.98	11.02	88.93	10.89	—

a) Copolymer composition calculated from polymer yield.
b) Based on the copolymer composition. Correction was done for end group of low molecular weight polymer.
c) Copolymer composition obtained from NMR spectrum.

TABLE 3. ANIONIC COPOLYMERIZATION OF ISOPRENE (M_1) AND 1,1-DIPHENYLETHYLENE (M_2)
MONOMER REACTIVITY RATIO, r_1 (THF)

$[M_1]_0$: 6.53—6.62 mmol, solvent: 15.0 ml, temp.: 0°C

Initiator 0.11 mmol	$[M_1]_0/[M_2]_0$	Time hr	Yield mol%	$[m_1]/[m_2]$[a]	η_{sp}/C dl/g	r_1
Na-Naph.	1.07	96	96.9	1.15	0.190	0.16
Na-Naph.	1.00	96	94.7	1.11	0.211	0.15
Na-Naph.	0.962	96	94.3	1.09	0.200	0.11
Na-Naph.	0.852	96	90.8	1.03	0.204	0.05
Na-Naph.[b]	0.997	96	95.2	1.10	0.213	0.13
					<Average	0.12>
K-disp.	1.00	96	94.0	1.14	—	0.17
K-disp.	0.906	123	86.5	1.11	—	0.15
K-disp.	0.830	144	85.4	1.03	—	0.05
K-disp.	0.781	144	81.3	1.03	—	0.06
					<Average	0.11>

a) Molar ratio of monomers in copolymer.
b) Contained 0.50 mmol of $NaB(Ph)_4$.

Table 4. Anionic copolymerization of isoprene (M_1) and 1,1-diphenylethylene (M_2)
Monomer reactivity ratio, r_1 (benzene, *n*-BuLi)
$[M_1]_0$: 6.51—6.57 mmol, solvent: 15.0 ml, initiator: 0.12 mmol, temp.: 40°C

$[M_1]_0/[M_2]_0$	Time hr	Yield mol%	$[m_1]/[m_2]$[a]	η_{sp}/C dl/g	r_1
2.32	120	72.8	24.8	0.122	47.4
1.53	120	64.8	13.9	0.120	34.7
1.01	120	55.3	9.87	0.122	33.5
1.00	72	54.7	10.7	0.115	37.5
0.654	120	45.8	7.47	0.123	31.7
				<Average	36.8>
1.00[b]	216	0	—	—	—

a) Molar ratio of monomers in copolymer.
b) Without initiator.

Table 5. Anionic copolymerization of isoprene (M_1) and 1,1-diphenylethylene (M_2)
Monomer reactivity ratio, r_1

Solvent	Initiator	Temp. °C	Number of experiment	r_1
THF	*n*-BuLi	0	5	0.11
THF	*n*-BuLi	25	2	0.04
THF	Na-Naph.	0	4	0.12
THF	K-disp.	0	4	0.11
Dioxane	*n*-BuLi	30	6	0.50
Benzene	*n*-BuLi	40	5	37
Benzene	Na-disp.	40	5	0.38
Benzene	K-disp.	40	4	0.05
n-Heptane	*n*-BuLi	40	4	29

(Table 5), suggesting that no polymerization occurred by free radical mechanism under the reaction conditions employed.

The NMR spectrum of the alternating copolymer obtained with *n*-BuLi in THF is shown in Fig. 3. The homopolymerization of isoprene by *n*-BuLi in the same solvent yielded a polymer with 29% 1,2-, 71% 3,4- and ~0% 1,4-structures. The analysis was done with NMR spectrum according to the method of Chen.[7] The alternating copolymer showed no peak in its NMR spectrum at the same position as that of the polyisoprene. On the other hand, in the IR spectrum of the copolymer, an absorption due to the vinyl group was found at 910 cm^{-1}, but very weak suggesting that there was little 1,2-structure in the copolymer. Therefore, assuming that the isoprene was incorporated in the copolymer through 3,4- and 1,4-additions, the ratio of 3,4- to 1,4-addition was 17:83, on the basis of the NMR spectrum.

At $[M_1]_0/[M_2]_0=0.650$, the copolymerization by *n*-BuLi carried out in THF at 0°C was followed spectrophotometrically. As soon as *n*-BuLi was added, the reaction mixture showed an absorption maximum at 496 mμ due to the diphenylethylene anion; its optical density had been constant during 150 hr at least. The molar extinction coefficient*1 was 1.7×10^4, which agrees closely with 1.8×10^4 of 1,1-diphenylhexyllithium anion.[8] These results apparently indicate that the most of the living ends present in the system were 1,1-diphenylethylene anion.

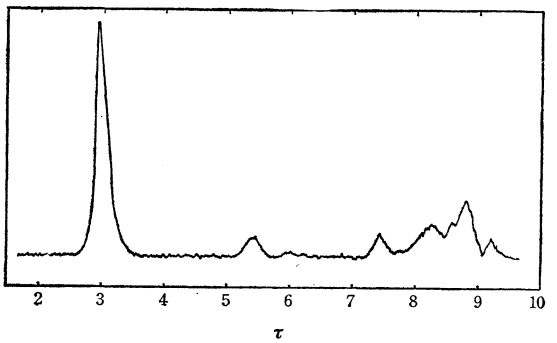

Fig. 3. NMR spectrum of the alternating copolymer of isoprene and 1,1-diphenylethylene in carbon tetrachloride at 60°C.

Discussion

The copolymerization of isoprene (M_1) and 1,1-diphenylethylene (M_2) initiated by *n*-BuLi in THF under a condition of $[M_1]_0/[M_2]_0<1$ proceeded without a termination and a chain transfer to give an alternating copolymer. Among the rate constants of the propagation reactions, k_{22} must be zero and k_{12} must be greater than k_{11} in such a copolymerization reaction.

$$\sim\sim M_1^- + M_1 \xrightarrow{k_{11}} \sim\sim M_1^- \quad (1)$$

$$\sim\sim M_1^- + M_2 \xrightarrow{k_{12}} \sim\sim M_2^- \quad (2)$$

$$\sim\sim M_2^- + M_1 \xrightarrow{k_{21}} \sim\sim M_1^- \quad (3)$$

*1 Calculated for the initiator concentration assuming the living polymer system.

7) H. Y. Chen, *Anal. Chem.*, **34**, 1793 (1962).

8) R. Waack and M. A. Doran, *J. Am. Chem. Soc.*, **85**, 1651 (1963).

$$\sim\sim M_2^- + M_2 \xrightarrow{k_{22}} \sim\sim M_2^- \quad (4)$$

The sum of the concentrations of the living ends, $[M_1^-]+[M_2^-]$, should be equal to that of the initiator, $[C]_0$.

$$[M_1^-] + [M_2^-] = [C]_0 \quad (5)$$

In Eq. (5), $[M_1^-]$ is negligible because the anion existing in the system was mostly M_2^-, which must be far more stable than the M_1 anion owing to the conjugation with its two benzene rings. So we can assume $k_{12} \gg k_{21}$ and get[3]

$$-\frac{d[M_1]}{dt} = k_{21}[C]_0[M_1] \quad (6)$$

The equation shows that process (3) is the rate determining step in the copolymerization.

Recently, Ureta *et al.*[9] have reported the anionic copolymerization of styrene (M_1) and 1,1-diphenylethylene (M_2), in which they found that process (3) was a reversible reaction as follows:

$$\sim\sim M_2^- + M_1 \underset{k_{-21}}{\overset{k_{21}}{\rightleftarrows}} \sim\sim M_2M_1^- \quad (7)$$

If so in the present copolymerization, Eq. (6) must be rewritten as

$$-\frac{d[M_1]}{dt} = k_{21}[M_2^-][M_1] \times \frac{k_{12}[M_2]}{k_{-21}+k_{12}[M_2]} \quad (8)$$

The analysis of the results in Fig. 1 gave a linear relationship between log $[M_1]$ and t as is shown in Fig. 4, indicating that the rate of the consumption of isoprene is first order with respect to its own concentration as represented by Eq. (6). Consequently, there must be $k_{12}[M_2] \gg k_{-21}$ in Eq. (8) and the reversible reaction (7) may be neglected. From Fig. 4, we can get $k_{21}=2.64\times10^{-3}$ *l*/mol sec in THF at 0°C. Taking into account the difference of the reaction temperature, the above value seems to be greater than $k_{21}=1.3$—1.8×10^{-3} *l*/mol sec found in the copolymerization of 2,3-dimethylbutadiene (M_1) and 1,1-diphenylethylene (M_2) by means of *n*-BuLi at 22°C. The values indicate that isoprene is sterically and electronically more reactive than 2,3-dimethylbutadiene because the latter has one more methyl group.

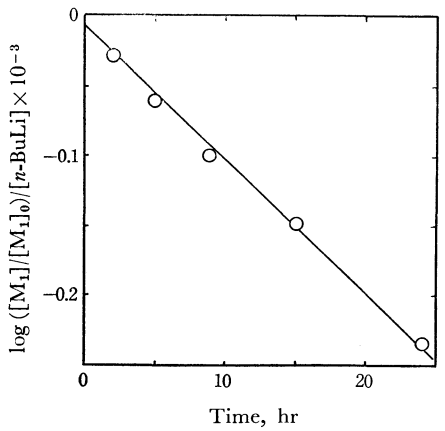

Fig. 4. Anionic copolymerization of isoprene (M_1) and 1,1-diphenylethylene (M_2).—First order plot
$[M_1]_0$: 6.48 mmol, $[M_2]_0$: 9.97 mmol,
[*n*-BuLi]: 0.107 mmol, THF: 15.0 m*l*,
temp.: 0°C.

The monomer reactivity ratios, r_1, obtained in the copolymerizations of 1,1-diphenylethylene (M_2) with three comonomers (M_1) by *n*-BuLi are summarized in Table 6. 1,1-Diphenylethylene was always more reactive to the M_1 anion than the corresponding M_1 monomer in THF. In benzene, 1,1-diphenylethylene was more reactive when the comonomer was styrene or 2,3-dimethylbutadiene, while less reactive when isoprene was the comonomer. In the copolymerization of isoprene and 1,1-diphenylethylene with *n*-BuLi, the monomer reactivity ratio was strongly influenced by the solvent (Table 5). The r_1 value in hydrocarbon solvent was larger than unity, while in dioxane and THF, the value approached zero with the increasing polarity of the solvent. No effect of the initiator on the r_1 value was observed in the copolymerization in THF, but in benzene the value varied in the order of $Li^+ \gg Na^+ > K^+$. When the counter ion was either Na^+ or K^+, a small influence of the solvent was observed on the r_1 value. These tendencies suggest that the r_1 value may decrease with an increase in the ionic character of the carbon - metal bond. Similar results have been reported in the anionic copolymerizations of butadiene and styrene,[10] and of isoprene and styrene.[11] The high reactivity of the dienes observed in these copolymerizations was explained by preferential absorption of the dienes at the active center.*2 Such an absorption may be excluded for 2,3-dimethylbutadiene because of its steric hindrance.

TABLE 6. MONOMER REACTIVITY RATIO, r_1, IN ANIONIC COPOLYMERIZATION OF 1,1-DIPHENYLETHYLENE AND OTHER MONOMERS BY *n*-BuLi

M_1 monomer	M_2 monomer 1,1-Diphenylethylene	
	in THF	in Benzene
Isoprene	0.11	37
2,3-Dimethylbutadiene	0	0.23
Styrene	0.13	0.71

9) E. Ureta, J. Smid and M. Szwarc, *J. Polymer Sci. A-1*, **4**, 2216 (1966).

10) I. Kuntz, *J. Polymer Sci.*, **54**, 569 (1961).

11) A. V. Tobolsky and C. E. Rogers, *ibid.*, **38**, 205 (1959).

*2 Worsfold denied the above explanation from the result of the kinetic study of the copolymerization of styrene and isoprene. D. J. Worsfold, *J. Polymer Sci. A-1*, **5**, 2783 (1967).

It is well known that $NaB(Ph)_4$ depresses the dissociation of an ion pair to free ions in the anionic polymerization of styrene.[12] The presence of $NaB(Ph)_4$ of the present copolymerization with Na^+ counter ion in THF had no influence on the r_1 value as is shown in Table 3. The fact demonstrates that, if the copolymerization may involve two kinds of propagating species, a free ion and an ion pair, the r_1 values for these two species will be very similar.

The alternating copolymer consisted of isoprene unit having 83% of 1,4-structure, in comparison with ~0% in the polyisoprene polymerized under the same conditions. In the copolymerization isoprene adds to the bulky 1,1-diphenylethylene anion at the sterically less hindered 4-position, and then the resulting isoprenyl anion adds to 1,1-diphenylethylene at the less hindered 1-position than the 3-position. A similar result was observed in the alternating copolymer of 2,3-dimethylbutadiene and 1,1-diphenylethylene,[3] in which the microstructure of 2,3-dimethylbutadiene was only 1,4 addition. A small portion of the 3,4-addition appeared in the copolymer of isoprene and 1,1-diphenylethylene may be attributed to the less steric hindrance than that of 2,3-dimethylbutadiene.

12) D. N. Bhattacharyya, C. L. Lee, J. Smid and M. Szwarc, *J. Phys. Chem.*, **69**, 612 (1965); H. Hostalka and G. V. Schulz, *J. Polymer Sci. B*, **3**, 175 (1965).

BULLETIN OF THE CHEMICAL SOCIETY OF JAPAN VOL. 42 1649—1652 (1969)

Synthetic Studies of the Flavone Derivatives. IX.*1 The Syntheses of Axillarin and Its Related Compounds*2

Kenji FUKUI and Mitsuru NAKAYAMA

Department of Chemistry, Faculty of Science, Hiroshima University, Higashi Sendamachi, Hiroshima

and Tokunaru HORIE

Department of Applied Chemistry, Faculty of Engineering, University of Tokushima, Tokushima

(Received September 26, 1968)

By using the method of Allan-Robinson's flavone synthesis, the condensation of 3,ω-dimethoxy-2,4,6-trihydroxyacetophenone with 3,4-dibenzyloxybenzoic anhydride gave a mixture of 3,6- and 3,8-dimethoxy-3',4'-dibenzyloxy-5,7-dihydroxyflavone (X and XI). The catalytic debenzylation of the above flavones then gave axillarin (I) and 3,8-dimethoxy-5,7,3',4'-tetrahydroxyflavone (IV) respectively. Axillarin 7-*O*-methyl ether(III) was prepared by the partial methylation of X, followed by catalytic debenzylation.

Axillarin (quercetagetin 3,6-dimethyl ether) was first isolated from the leaves of cocklebur (*Xanthium pensylvanicum*)[1] and later from the flowers and leaves of *Iva axillaris* Pursh. ssp. *robustor*.[2] Its structure was identified as 3,6-dimethoxy-5,7,3',4'-tetrahydroxyflavone (I) (quercetagetin type) on the basis of spectral data[1] and by a comparison of the tetraethyl ether (II) of I with a synthetic sample.[2] 5,3',4'-Trihydroxy-3,6,7-trimethoxyflavone (III) (7-*O*-methyl ether of I) was also isolated from the leaves of *Cyanostegia microphylla*.[3] On the other hand, 3,8-dimethoxy-5,7,3',4'-tetrahydroxyflavone (IV) (gossypetin type), an isomer of I, was isolated from *Ricinocarpus muricatus* Muell. Arg.[4] Recently, a synthesis of IV starting from 4-benzyloxy-2-hydroxy-3,6,ω-trimethoxyacetophenone (V) has been reported.[5]

In previous papers,[6,7] the authors reported the

*1 Part VIII of this series: K. Fukui, T. Matsumoto, M. Nakayama and T. Horie, This Bulletin, **41**, 2805 (1968).

*2 This has previously been reported in a preliminary form: K. Fukui, M. Nakayama and T. Horie, *Experientia*, **24**, 769 (1968).

1) A. O. Taylor and E. Wong, *Tetrahedron Letters*, **1965**, 3675.

2) W. Herz, L. Farkas, V. Sudarsanam, H. Wagner, L. Hörhammer and R. Rüger, *Chem. Ber.*, **99**, 3539 (1966).

3) E. L. Ghisalberti, P. R. Jefferies and C. I. Stacey, *Australian J. Chem.*, **20**, 1049 (1967).

4) C. A. Henrick and P. R. Jefferies, *Tetrahedron*, **21**, 3219 (1965).

5) L. Farkas and M. Nogradi, *Tetrahedron Letters*, **1966**, 3759.

6) K. Fukui, T. Matsumoto, S. Nakamura, M. Nakayama and T. Horie, *Experientia*, **24**, 108 (1968); This Bulletin, **41**, 1413 (1968).

7) K. Fukui, M. Nakayama and T. Horie, *Experientia*, **24**, 417 (1968); K. Fukui, T. Matsumoto, M. Nakayama and T. Horie, This Bulletin, **41**, 2805 (1968).

syntheses of jaceidin (VI) and 5,7,4'-trihydroxy-3,8,3'-trimethoxyflavone (VII) from 3,ω-dimethoxy-2,4,6-trihydroxyacetophenone (VIII). The present paper will describe the total syntheses of I and III, and a new synthesis of IV from the ketone VIII in a manner similar to that previously described.[6,7]

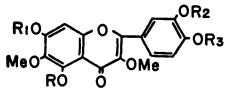

I R=R1=R2=R3=H
II R=R1=R2=R3=Et
III R=R2=R3=H, R1=Me
VI R=R1=R3=H, R2=Me
XII R=R1=R2=R3=Ac
XV R=R2=R3=Ac, R1=Me

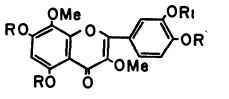

IV R=R1=H
VII R=H, R1=Me
XVI R=R1=Ac
XVII R=R1=Et
XVIII R=Ac, R1=Me
XIX R=Et, R1=Me

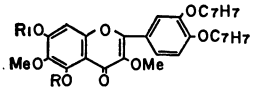

IX R=R1=Ac
X R=R1=H
XIV R=H, R1=Me

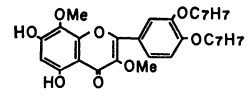

XI

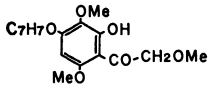

V

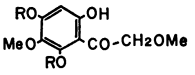

VIII R=H
XIII R=Et

By using the method of Allan-Robinson's flavone synthesis, the reaction of the ketone VIII with 3,4-dibenzyloxybenzoic anhydride and potassium 3,4-dibenzyloxybenzoate, followed by treatment with alcoholic potassium hydroxide, yielded a mixture of flavones. The mixture was then acetylated without further purification. After repeated recrystallizations of the acetylated product from methanol, 5,7-diacetoxy-3',4'-dibenzyloxy-3,6-dimethoxyflavone (IX), $C_{35}H_{30}O_{10}$, mp 135—136.5°C, was obtained as colorless needles. The NMR spectrum*3 of IX showed a singlet at δ 7.19 (1H) which could be attributed to the C-8 proton (not the C-6 proton) on the basis of a comparison with the spectra data of some of the flavones reported on in the literature (Table 1).[4,8] The treatment of IX with dilute alkali gave 3',4'-dibenzyloxy-5,7-dihydroxy-3,6-dimethoxyflavone (X), mp 147.5—148.5°C. From the mother-liquor of the recrystallization of IX, 3',4'-dibenzyloxy-5,7-dihydroxy-3,8-dimethoxyflavone (XI), mp 180—181.5°C (from ethyl acetate), was obtained after treatment with aqueous potassium hydroxide.

The catalytic debenzylation of X gave the desired flavone I, which was shown to be identical with natural axillarin*4 by a mixed-melting-point determination and by a comparison of their ultraviolet spectra. Moreover, the IR-spectra of natural quercetagetin 3,6-dimethyl ether,*5 natural axillarin,*4 and the synthetic axillarin were superimposable upon one another. I was also obtained from IX by debenzylation and subsequent hydrolysis.

The synthetic axillarin (I) was converted to tetraacetate XII and tetraethyl ether II by the usual methods. The tetraethyl ether II was also synthesized by the Allan-Robinson reaction of

Table 1. The NMR spectral data of flavones*3

Proton	Compound					
	IX	XII	II	XV	XVI	XVII
Arom. *H*						
C-8	7.19_s	7.33_s	6.78_s	6.90_s		
C-6					6.81_s	6.47_s
C-2'	$7.77_{d'}$	7.99_{bs}	7.71_{bs}	8.08_{bs}	$8.06_{d'}$	$7.89_{d'}$
C-5'	7.08_d	7.41_d	7.02_d	7.39_d	7.38_d	7.03_d
C-6'	7.64_q	8.07_q	7.74_q	8.01_q	8.09_q	7.88_q

s, singlet; bs, broader singlet; d, doublet (J_{ortho}=9.0 Hz); d', doublet (J_{meta}=2.5 Hz); q, quartet (J_{ortho}=9.0 Hz; J_{meta}=2.5 Hz).

*3 The NMR spectra were measured with a Hitachi R-20 spectrometer, using tetramethylsilane as the internal standard (δ-value in $CDCl_3$).

8) a) C. A. Henrick and P. R. Jefferies, *Australian J. Chem.*, **17**, 934 (1962); b) J. Massicot and J-P. Marthe, *Bull. Soc. Chim. France*, **1962**, 1962; c) J. Massicot, J-P. Marthe and S. Heitz, *ibid.*, **1963**, 2712.

*4 The natural axillarin and its tetraethyl ether were kindly supplied by Professor W. Herz, Florida State University.

*5 The IR-spectrum of natural quercetagetin 3,6-dimethyl ether was kindly supplied by Dr. E. Wong, Plant Chemistry Division, Department of Science and Industrial Research, New Zealand.

4,6-diethoxy-5,ω-dimethoxy-2-hydroxyacetophenone (XIII)[6] with 3,4-diethoxybenzoic anhydride.

The partial methylation of X gave 3',4'-dibenzyloxy-5-hydroxy-3,6,7-trimethoxyflavone (XIV). The debenzylation of XIV yielded axillarin 7-*O*-methyl ether (III). Its triacetate (XV) was prepared by acetylation. The properties of these compounds were identical with those described by Ghisalberti *et al.*[3]

On the other hand, the debenzylation of XI afforded a tetrahydroxyflavone (IV) whose identity with the natural substance*[6] was confirmed by a mixed-melting-point determination and by a comparison of their ultraviolet spectra. Its tetraacetate (XVI) and tetraethyl ether (XVII) were prepared by the usual methods. The NMR spectra of these compounds (XVI and XVII) show one proton signal corresponding to the C-6 proton at δ 6.81 and 6.47 respectively; these values are in accordance with those observed for the triacetate (XVIII) and triethyl ether (XIX) of VII.[3,7]

Experimental*[7]

3,6-Dimethoxy- (X) and 3,8-dimethoxy-3',4'-dibenzyloxy-5,7-dihydroxyflavone (XI). A mixture of the ketone (VIII)[6] (3.1 g), 3,4-dibenzyloxybenzoic anhydride (29 g), and potassium 3,4-dibenzyloxybenzoate (13 g) was heated at 170°C for 5 hr and then at 180°C for 8 hr under reduced pressure. The reaction mixture was then cooled and refluxed for 20 min with a solution of potassium hydroxide (15 g) in aqueous ethanol (80%; 350 m*l*). After the evaporation of the solvent under a vacuum, the residue was dissolved in water and saturated with carbon dioxide. The resulting precipitate was extracted with ethyl acetate. The extract was washed with water, dried, and evaporated to 25 m*l*. The separating crystals (3,4-dibenzyloxybenzoic acid) were then filtered off and washed with ethyl acetate. The combined filtrate was evaporated, and the residue was recrystallized from methanol to give a crude flavone mixture (about 4.7 g).

A mixture of the crude flavones, acetic anhydride (12 g), and pyridine (1.0 m*l*) was heated at 120°C for 2 hr and then poured into water. The resulting mixture was extracted with ether, and the extract was washed with dilute hydrochloric acid and a dilute sodium carbonate solution and then allowed to stand in a refrigerator for one day. The separating crystals were collected and recrystallized from methanol and then ethanol to give 5,7-diacetoxy-3',4'-dibenzyloxy-3,6-dimethoxyflavone (IX) in the form of colorless needles, mp 135—136.5°C; yield, 2.13 g (26% from VIII). IR: 1764, 1641, 1609, 1601 cm^{-1}. UV: λ_{max}^{EtOH} mμ (log ε); 252 (4.32), 350 (4.21).

Found: C, 69.08; H, 4.80%. Calcd for $C_{35}H_{30}O_{10}$: C, 68.84; H, 4.95%.

A solution of IX (1.47 g) in ethanol (200 m*l*) was gently refluxed with aqueous potassium hydroxide (10%; 10 m*l*) for 3 min. The resulting solution was acidified with dilute hydrochloric acid, and the solvent was evaporated under a vacuum. The resulting precipitate was collected and recrystallized from methanol to give X in the form of pale yellow needles, mp 147.5—148.5°C; yield, 1.2 g (95%). It gave a green color with an alcoholic ferric chloride solution. IR: 3430, 1653, 1613, 1593 cm^{-1}. UV: λ_{max} mμ (log ε); (EtOH) 255 (4.27), 273 (4.23), 347 (4.35); (EtOH-AcONa) 276 (4.36), 322 (4.38), 364 (4.23); (EtOH-EtONa) 277 (4.47), 298 (4.18), 312 (4.18), 384 (4.27); (EtOH-$AlCl_3$) 262, 285, 368.

Found: C, 70.66; H, 4.76%. Calcd for $C_{31}H_{26}O_8$: C, 70.71; H, 4.98%.

The concentration of the methanolic filtrate which was obtained in the case of recrystallization of IX, followed by hydrolysis with aqueous potassium hydroxide (a 2% potassium hydroxide solution (25 m*l*) and methanol (75 m*l*)), yielded yellow crystals. On repeated crystallizations from ethyl acetate, XI was obtained in the form of yellow needles, mp 180—181.5°C; yield, 1.32 g (18% from VIII). It gave a green color with an alcoholic ferric chloride solution. IR: 3155 (broad), 1653, 1604, 1592, 1577 cm^{-1}. UV: λ_{max} mμ (log ε); (EtOH) 258 (4.28), 277 (4.32), 339 (4.21), 355 (4.20); (EtOH-AcONa) 257.5 (4.04), 284 (4.38), 320 (4.18), 366 (4.08); (EtOH-NaOEt) 233 (4.21), 286.5 (4.40), 316 (4.11), 390 (3.98); (EtOH-$AlCl_3$) 263, 287, 306i,*[8] 360, 420.

Found: C, 70.99; H, 4.97%. Calcd for $C_{31}H_{26}O_8$: C, 70.71; H, 4.98%.

Axillarin (3,6-Dimethoxy-5,7,3',4'-tetrahydroxyflavone) (I). *a) From the dihydroxyflavone X.* A mixture of X (560 mg) and Pd-C (5%; 1.0 g) in methanol-ethyl acetate (2:1; 150 m*l*) was shaken in an atmosphere of hydrogen until 2.1 mol of hydrogen had been absorbed. After the catalyst had been filtered, the filtrate was evaporated under a vacuum; the residue was recrystallized from acetonitrile to give I in the form of yellow needles, mp 207—208°C (192—193°C sinter); yield 292 mg (80%). It gave a green color with an alcoholic ferric chloride solution.

Found: C, 56.11; H, 4.26%. Calcd for $C_{17}H_{14}O_8 \cdot H_2O$: C, 56.04; H, 4.43%.

After drying at 120—130°C/0.2 mmHg for 3 hr, this substance had a mp of 207—208°C or 217—218°C (207—209°C sinter). It was identified with natural axillarin by a mixed-melting-point determination and by a comparison of their infrared and ultraviolet sepctra. IR: 3380, 3130, 1652, 1602 cm^{-1}. UV: λ_{max} mμ (log ε); (EtOH) 259 (4.25), 295 (3.91), 358 (4.32); (EtOH-AcONa) 272 (4.27), 300 (3.95), 367 (4.24); (EtOH-EtONa) 273 (4.32), 410 (4.35); (EtOH-$AlCl_3$) 278, 410. Natural axillarin:*[4] mp 207.5—209°C. IR: 3390, 3130, 1653, 1604 cm^{-1}. UV: λ_{max} mμ (log ε); (EtOH) 259 (4.26), 296 (3.92), 355 (4.33); (EtOH-AcONa) 273 (4.27), 299 (3.94), 369 (4.25). (lit mp 207—209°C,[1] mp 211—213°C,[2] mp 199—200°C.[9] UV:[2] λ_{max}^{EtOH} mμ (log ε); 260 (4.37), 270i

*6 The natural pigment and its tetraacetate were kindly supplied by Professor P. R. Jefferies, University of Western Australia.

*7 All the melting points are uncorrected; the infrared spectra were measured in Nujol.

*8 i=Inflection.

9) D. K. Bhadwaj, S. Neelakantan and T. R. Seshadri, *Indian J. Chem.*, **4**, 417 (1966).

(4.33), 295_i (4.04), 358 (4.42)).

Found: C, 58.86; H, 3.96%. Calcd for $C_{17}H_{14}O_8$: C, 58.96; H, 4.08%.

Axillarin Tetraacetate (XII): hot acetic anhydride - pyridine method; mp 161—161.5°C (colorless needles from methanol). IR: 1769, 1758, 1639, 1616 cm^{-1}. UV: λ_{max}^{EtOH} mμ (log ε); 256 (4.16), 320 (4.06), 340_{sh} (4.03).*9

Found: C, 58.29; H, 4.34%. Calcd for $C_{25}H_{22}O_{12}$: C, 58.37; H, 4.31%.

b) From the diacetoxyflavone IX. A mixture of IX (450 mg), Pd-C (5%: 1.0 g), and methanol - ethyl acetate (2 : 1 : 150 m*l*) was treated by a method similar to that used for a). Then, the crude product was hydrolyzed with 20% sulfuric acid (5 m*l*) in methanol (25 m*l*) for 2 hr. After the addition of water (10 m*l*), the solvent was evaporated under a vacuum. The resulting precipitate was recrystallized from acetonitrile, mp 207—208°C (192—193°C sinter); yield, 180 mg (71%). It was identical with the sample described in a).

Axillarin Tetraethyl Ether (3,6-Dimethoxy-5,7,3',4'-tetraethoxyflavone) (II). *a) From Axillarin (I).* A mixture of synthetic axillarin (I) (80 mg), anhydrous potassium carbonate (2.0 g), and diethyl sulfate (1.0 m*l*) in dry acetone (20 m*l*) was refluxed for 24 hr, and then the reaction mixture was treated in the usual manner. Recrystallization from *n*-hexane give II in the form of colorless needles, mp 99.5—100.5°C; yield, 100 mg (89%). After drying at 80°C/0.1 mmHg for 1 hr, it had a mp of 110—111.5°C. It was identified with natural axillarin tetraethyl ether by a mixed-melting-point determination and by a comparison of their ultraviolet spectra. IR: 1641, 1623, 1607 cm^{-1}. UV: λ_{max}^{EtOH} mμ (log ε); 240 (4.31), 335 (4.36). Natural one:*4 mp 109.5—111°C. UV: λ_{max}^{EtOH} mμ (log ε); 240 (4.29), 335 (4.33). (lit mp 109°C,[2] mp 108—110 °C[2]).

Found: C, 65.25; H, 6.56%. Calcd for $C_{25}H_{30}O_8$: C, 65.49; H, 6.60%.

b) From the ketone XIII. A mixture of XIII[6] (1.0 g), 3,4-diethoxybenzoic anhydride (3.0 g), and potassium 3,4-diethoxybenzoate (1.0 g) was treated by a method similar to that used for X and XI. The crude product was recrystallized from *n*-hexane to give II, mp 99.5—100.5°C (after drying; mp 110—111.5°C; yield, 200 mg (13%). It was identical with the sample described in a).

Found: C, 65.30; H, 6.61%. Calcd for $C_{25}H_{30}O_8$: C, 65.49; H, 6.60%.

3',4'-Dibenzyloxy -5- hydroxy - 3,6,7 - trimethoxyflavone (XIV). To a solution of X (400 mg) in ethyl acetate (30 m*l*), an ethereal diazomethane solution was added; then the solution was allowed to stand in a refrigerator for 24 hr. After the evaporation of the solvent, the residue was recrystallized from ethanol to give XIV in the form of pale yellow needles, mp 151.5—153°C; yield, 380 mg (93%). It gave a green color with an alcoholic ferric chloride solution. IR: 1652, 1640, 1615, 1599 cm^{-1}. UV: λ_{max} mμ (log ε); (EtOH) 239 (4.28), 256 (4.31), 274 (4.26), 345 (4.39); (EtOH-$AlCl_3$) 265, 286, 366.

Found: C, 70.78; H, 5.25%. Calcd for $C_{32}H_{28}O_8$: C, 71.10; H, 5.22%.

Axillarin 7-*O*-Methyl Ether (3',4',5-Trihydroxy-3,6,7-trimethoxyflavone) (III). A mixture of XIV (300 mg), Pd-C (5%; 450 mg), and methanol - ethyl acetate (1:1; 150 m*l*) was treated by a method similar to that used for I. The crude product was recrystallized from methanol to give III in the form of pale yellow prisms, mp 237—238°C; yield, 160 mg (80%). It gave a green color with an alcoholic ferric chloride solution. IR: 3380, 1651, 1603, 1593 cm^{-1}. UV: λ_{max} mμ (log ε); (EtOH) 260 (4.32), 356 (4.37); (EtOH-$AlCl_3$) 279, 415. (lit[3] mp 235—236°C. UV: λ_{max}^{EtOH} mμ (log ε); 271 (4.29), 360 (4.31)).

Found: C, 60.21; H, 4.47%. Calcd for $C_{18}H_{16}O_8$: C, 60.00; H, 4.48%.

The Triacetate (XV); hot acetic anhydride - pyridine method; mp 158—159°C (colorless needles from methanol). IR: 1764, 1636_{sh}, 1622 cm^{-1}. UV: λ_{max}^{EtOH} mμ (log ε); 262_{sh} (4.19), 326 (4.25). (lit[3] mp 159—160°C. UV: λ_{max}^{EtOH} mμ (log ε); 262 (4.25), 317 (4.37)).

3,8-Dimethoxy-5,7,3',4'-tetrahydroxyflavone (IV). A mixture of XI (590 mg), Pd-C (5%; 1.0 g) and methanol - ethyl acetate (1:1; 200 m*l*) was treated by a method similar to that used for I. The crude product was recrystallized from methanol - water to give IV in the form of yellow needles, mp 297—299°C; yield, 300 mg (77%). It gave a green color with an alcoholic ferric chloride solution. It was identified with the natural pigment by a mixed-melting-point determination and by a comparison of their ultraviolet spectra. IR: 3440, 3360, 3290, 1657, 1616 cm^{-1}. UV: λ_{max} mμ (log ε); (EtOH) 262 (4.34), 275 (4.31), 298 (3.98), 368 (4.27); (EtOH-AcONa) 266_i (4.27), 277 (4.34), 374 (4.17); (EtOH-$AlCl_3$) 283, 380_i, 440. Natural pigment:*6 mp 296—298°C. UV: λ_{max} mμ (log ε); (EtOH) 261 (4.33), 274 (4.32), 298 (3.99), 366 (4.27); (EtOH-AcONa) 266_i (4.29), 276.5 (4.33), 370 (4.19); (EtOH-$AlCl_3$) 283, 380_i, 435. (lit mp 301—303°C,[4] mp 300—301°C.[5] UV:[4] λ_{max}^{EtOH} mμ (log ε); 267_{sh} (4.35), 276 (4.40), 338_{sh} (4.15), 373 (4.21)).

Found: C, 58.87; H, 3.83%. Calcd for $C_{17}H_{14}O_8$: C, 58.96; H, 4.08%.

The Tetraacetate (XVI): hot acetic anhydride - pyridine method; mp 157—158°C (colorless needles from methanol). IR: 1765 (broad), 1641, 1611 cm^{-1}. UV: λ_{max}^{EtOH} mμ (log ε); 249_i (4.23), 255 (4.24), 311 (3.93), 354 (4.05). (lit mp 149—150°C,[4] mp 158—160°C,[5] mp 150—151°C[5]). This was identified with the natural derivative by a mixed-melting-point determination.

Found: C, 58.67; H, 4.18%. Calcd for $C_{25}H_{22}O_{12}$: C, 58.37; H, 4.31%.

The Tetraethyl Ether (XVII): mp 124.5—125.5°C (colorless needles from aqueous methanol) (lit.[4] mp 125—126°C).

Found: C, 65.62; H, 6.44%. Calcd for $C_{25}H_{30}O_8$: C, 65.49; H, 6.60%.

The authors are grateful to Professor W. Herz, the Florida State University, for samples of axillarin and its tetraethyl ether, to Professor P. R. Jefferies, the University of Western Australia, for samples of natural pigment and its acetate, and to Dr. E. Wong, Department of Science and Industrial Research, New Zealand, for supplying IR spectrum of quercetagetin 3,6-dimethyl ether. This work was supported in part by a grant-in-aid from the Ministry of Education.

*9 sh=shoulder.

BULLETIN OF THE CHEMICAL SOCIETY OF JAPAN VOL. 42 1653—1659 (1969)

Reactions of α-Cyano-β-methoxy-β-alkylacrylic Esters with Hydrazine and Hydroxylamine

Hideo BABA, Isaburo HORI, Toshio HAYASHI and Hiroshi MIDORIKAWA

The Institute of the Physical and Chemical Research, Yamato-machi, Saitama

(Received September 27, 1968)

α-Cyano-β-methoxy-β-alkyl (Me, Et, *n*-Pr, *n*-Bu, *n*-Am, and *i*-Bu)-acrylic esters (I) react with hydrazine to give β-hydrazino intermediates. The hydrazino group of these intermediates is cyclized preferentially between its terminal NH_2 and the cyano group in a neutral or acidic medium to give 5-aminopyrazole derivatives, and preferentially between the terminal NH_2 and the ester group in the presence of a base to give 5-pyrazolone derivatives. When the β-alkyl of I is isopropyl, *t*-butyl, *etc.*, I affords only the 5-pyrazolone derivatives in the reaction with hydrazine. The reactions of I with hydroxylamine gave 5-aminoisoxazole derivatives, but in the case of the β-*t*-butyl derivative of I they gave 5-aminoisoxazole accompanied by the 5-isoxazolone derivative.

It has recently been found that the alkoxyl group of α-cyano-β-methoxycrotonic esters is easily displaced with such simple amines as ammonia, alkylamine, and benzylamine to give α-cyano-β-aminocrotonic esters, which exist in the enamine form, with an intramolecular hydrogen-bond between the amino and the ester carbonyl group.[1)]

The reaction has now been extended to use with hydrazine and hydroxylamine as the amine in view of the formation of two possible cyclized compounds, as is illustrated in Charts 1 and 2.

Both geometric isomers of methyl α-cyano-β-methoxycrotonate (Ia) reacted rapidly with one mole of hydrazine hydrate in water at room temperature to form the same methyl α-cyano-β-hydrazinocrotonate (IIa) in a 90% yield. Similarly, from Ib—g the corresponding intermediates (IIb—g) were obtained.

The cyclization of II took place preferentially

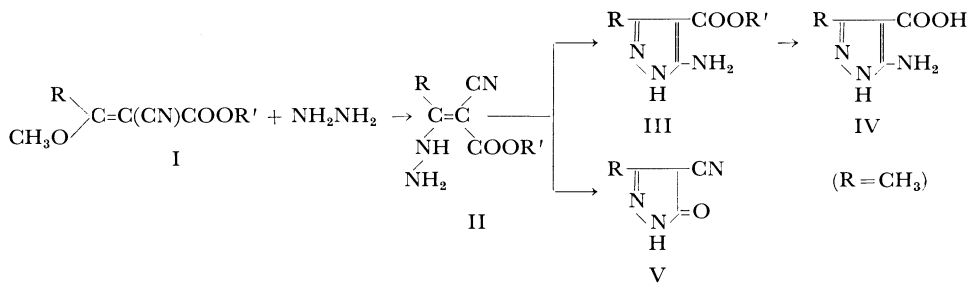

I, II, III	R	R'
a	Me	Me
b	Me	Et
c	Et	Me
d	*n*-Pr	Me
e	*n*-Bu	Me
f	*n*-Am	Me
g	*i*-Bu	Me

V	R
a	Me
b	Et
c	*n*-Pr
d	*n*-Bu
e	*n*-Am
f	*i*-Bu
g	*i*-Pr
h	*t*-Bu
i	Ph

Chart 1

1) T. Hayashi, I. Hori, H. Baba and H. Midorikawa, This Bulletin, **40**, 2160 (1967).

between the hydrazino and the cyano group to afford only the corresponding 3-alkyl-4-alkoxycarbonyl-5-aminopyrazole (III) in a neutral or acidic medium. That is, II cyclized to III slowly when left standing at room temperature for prolonged periods, when heated over the melting point, when refluxed in ethanol - water (4:1), or immediately after being dissolved in 15% hydrochloric acid. However, in the presence of a base such as hydrazine, ammonia or potassium carbonate, II cyclized preferentially between the hydrazino and the ester group to give only the corresponding 3-alkyl-4-cyano-5-pyrazolone (Va—f), while II was recovered in abundance.

V was also isolated along with a large amount of II when I was reacted with an excess of hydrazine. That this reaction perhaps proceeds through II can be seen by the experimental results shown in Table 1. Namely, the variations in the amounts of IIb and Va with the variety of the reaction time in Reactions (1) and (2) were approximately equal. Furthermore, this result indicetes that the cyclization of II to V is significantly slower than the formation of II from I.

Table 1. The results of the reactions of Ib or IIb with hydrazine by varing the reaction time

(1) Ib + 2 NH_2NH_2 —
(2) IIb + NH_2NH_2 — → IIb + Va

Reaction time hr	Yield in (1), %		Yield in (2), %	
	IIb	Va	IIb	Va
0.25	87	2	90	trace
1	79	9.7	78	8.3
2	72	13.9	73	12.5
5	50	26.4	56	26.4

The infrared spectra of II exhibited an intense cyano band due to conjugation with an unsaturated bond in the 2198—2210 cm^{-1} region similar to that of β-aminoacrylonitriles.[2] The NMR spectra of II and ethyl α-cyano-β-(2,2-dimethylhydrazino)-crotonate (VI) prepared from Ib and 1,1-dimethylhydrazine indicated broad signals in the highly deshielded region (10.63—10.79 ppm). These signals were assigned to the NH proton hydrogen-bonded with the ester carbonyl group, much as with the simple β-amino derivatives described in a previous report.[1] Therefore, these spectral observations reveal that II has a hydrazino-ethylene structure rather than a tautomeric hydrazone structure; moreover, there is a *cis*-relation between the hydrazino and the ester group. Consequently, the following courses (Schema 1—3) for the cyclizations of II to III and V are possible.

On the other hand, I with a bulky β-alkyl group such as isopropyl or *t*-butyl, or with a β-aryl group instead of β-alkyl, on a similar reaction with one mole of hydrazine hydrate, gave merely the corresponding 3-alkyl(aryl)-4-cyano-5-pyrazolone (Vg—i) as the cyclized product, plus a fairly large amount of the unchanged material (I); no open-chain intermediate was isolated. In order to obtain a high yield of V, an excessive use of hydrazine was necessary because hydrazine was consumed to form its salt of the acidic V. For example, one hour's treatment of I (R = *i*-Pr, R' = Me) with one mole of hydrazine gave 41.4% of the pyrazolone (Vg), whereas a similar treatment with two moles of hydrazine gave almost a two-fold yield. In these reactions, the formation of Vg—i was distinctly faster than that of Va from Ib or IIb, as is shown in Table

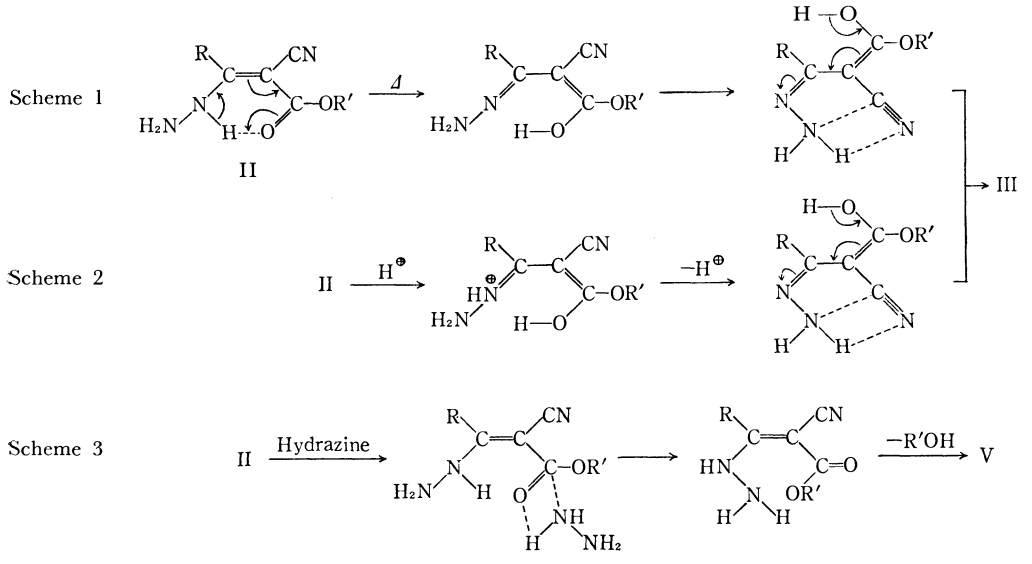

2) F. Scotti and E. J. Frazza, *J. Org. Chem.*, **29**, 1800 (1964).

1, although this primary nucleophilic attack by hydrazine on the β-carbon atom was expected to be probably more restricted by the steric hindrance than that in the case of I (R=*n*-alkyl and *i*-Bu).

It is evident that no hydrazine attaches to the ester group of I to form the acid hydrazide, for the reaction of I (R=*i*-Pr, R'=Et) with ammonia gave only the normal enamine (VII) instead of the acid amide expected.

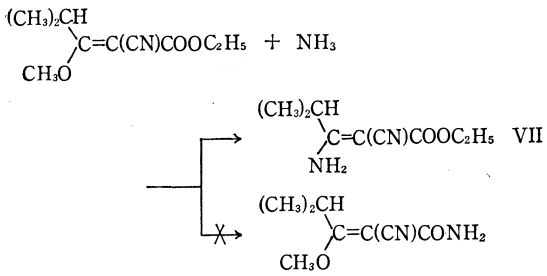

For the intermediate (II) in the formation of Vg—i, a strong steric compression is expected between the bulky β-alkyl (or aryl) and the hydrazino group on the β-carbon atom. Presumably the bulky alkyl groups push against the ester guoup to strengthen the hydrogen-bonding between the hydrazino and the ester group and follow the cyclization between them, as is illustrated below:

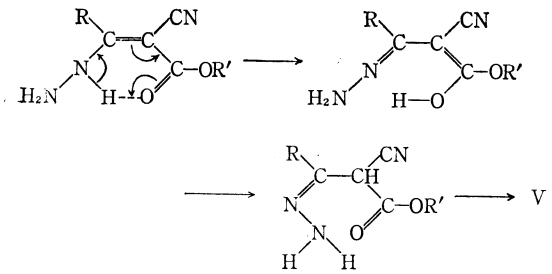

(R=*i*-Pr, *t*-Bu, Ph)

On the other hand, under conditions similar to those in the reaction with hydrazine, the starting materials (I, except for R=*t*-Bu) and hydroxylamine reacted readily to give only the 3-alkyl(aryl)-4-alkoxycarbonyl-5-aminoisoxazoles (VIII) in better yields. I (R=*t*-Bu) afforded approximately equivalent amounts of 5-aminoisoxazole (VIIIi) and 3-*t*-butyl-4-cyano-5-isoxazolone (IX) in poor total yields. However, in all cases, no open-chain intermediate was isolated.

Dornow and Teckenburg[3] have reported that I (R=Ph, R'=Et) reacted with hydroxylamine to form the 5-aminoisoxazole (VIIIj) in a neutral medium and the 5-isoxazolone (IX, R=Ph) in an alkaline medium, presumably by means of the cyclization of the intermediate α-cyano-β-oximino ester (X).

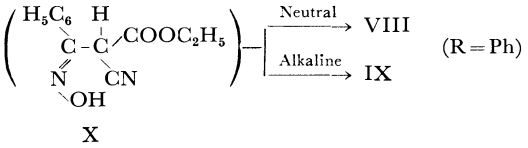

(R=Ph)

X

However, the similar reaction of diethyl 1-ethoxyethylidenemalonate with hydroxylamine in a neutral medium easily gave the cyclized product, 3-methyl-4-ethoxycarbonyl-5-isoxazolone (XI), no intermediate being isolated. Therefore, if the reaction

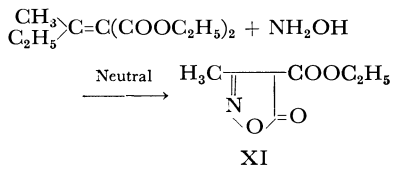

XI

reported proceeds *via* the β-oximino ester (X), the VIII yielded in the neutral medium will be contaminated by the IX cyclized on the ester group. Furthermore, ethyl α-cyano-β-methoxy-aminocrotonate (XII), which can not be cyclized, was prepared from the reaction of Ib with *O*-methylhydroxylamine. The broad NH signal in the highly deshielded region (11.64 ppm) observed

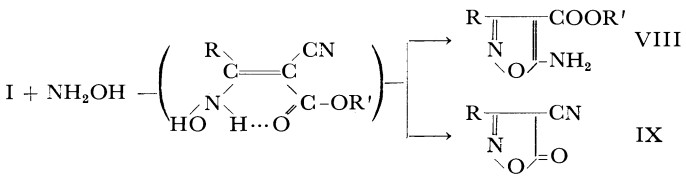

VIII	R	R'	VIII	R	R'
a	Me	Me	f	*n*-Am	Me
b	Me	Et	g	*i*-Bu	Me
c	Et	Me	h	*i*-Pr	Me
d	*n*-Pr	Me	i	*t*-Bu	Me
e	*n*-Bu	Me	j	Ph	Et

Chart 2

3) A. Dornow and H. Teckenburg, *Chem. Ber.*, **93**, 1103 (1960).

Table 2. Methyl acylcyanoacetate R-CO-CH(CN)COOCH$_3$

R	Bp, °C 10 mmHg	Yield %	Formula	Calcd, % C	H	N	Found, % C	H	N
n-Pr	111—113[a)]	30.1	$C_8H_{11}O_3N$	56.79	6.55	8.28	56.75	6.58	8.82
n-Bu	123—124	24.5	$C_9H_{13}O_3N$	59.00	7.15	7.65	58.98	6.58	7.72
n-Am	128—130	27.4	$C_{10}H_{15}O_3N$	60.89	7.67	7.10	60.51	7.88	7.22
i-Bu	118—120	26.3	$C_9H_{13}O_3N$	59.00	7.15	7.65	58.78	6.95	7.73

a) Lit, mp 135.3°C/25 mmHg, J. Guinchant, *Compt. Rend.*, **121**, 72 (1895).

Table 3. Methyl α-cyano-β-methoxy-β-alkylacrylate

$$CH_3O\diagdown\!\!\diagup\!\!\diagup\!\!\diagdown R \diagdown C{=}C(CN)COOCH_3$$

R	Bp, °C 10 mmHg	Yield %	Formula	Calcd, % C	H	N	Found, % C	H	N
Id *n*-Pr	151—152	51.8	$C_9H_{13}O_3N$	59.00	7.15	7.65	58.69	7.47	7.52
Ie *n*-Bu	171—172	66.0	$C_{10}H_{15}O_3N$	60.89	7.67	7.10	60.88	7.55	6.97
If *n*-Am	160—162	32.7	$C_{11}H_{17}O_3N$	62.54	8.11	6.63	62.40	7.96	6.31
Ig *i*-Bu	151—152	29.5	$C_{10}H_{15}O_3N$	60.89	7.67	7.10	60.82	7.32	7.17

in its NMR spectrum showed that it has the structure of the enamine with hydrogen-bonding:

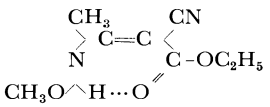

XII

From these observations, it seems likely that the formations of VIII and IX proceed *via* the β-hydroxyamino analog (II′) of II and follow the mode of the cyclization represented in Schema 1 and 3 respectively.

Experimental[4)]

Materials. Methyl α-cyano-β-methoxy-β-alkylacrylates (Id—g, Table 3) were synthesized, by the use of a method described in a previous paper[5)], from the corresponding acylcyanoacetic esters (Table 2), which had themselves been prepared from a modification of the Hori and Midorikawa method[6)] using acid chloride instead of acid anhydride.

The Reaction of Ia—g with Hydrazine (The Formation of II). To a solution of 80% hydrazine hydrate (5 mmol) in water (4 ml), there was added I (5 mmol) all at once; the mixture was then stirred at room temperature for 15—30 min. The resulting precipitate was collected by filtration, washed with a small quantity of ice water, and recrystallized from methanol (IIa and IIb), ethanol (IIe and IIg, or benzene (IIc, IId, and IIf).

In the reaction of both Ia and Ic, two geometric isomers[5)] were used as the starting material, but both the isomers gave the same product (IIa and IIc, respectively) in approximately equal yields. Therefore, only a stable isomer or an equilibrium mixture was used as the starting material (I) in all the reactions to be described below.

Methyl α-cyano-β-hydrazinocrotonate (IIa): colorless needles, mp 133—134°C, yield 90% from either of the geometric isomers. IR (νcm^{-1}): 2198 (νC≡N), 1667 (νC=O). NMR: 10.68 (NH).

Found: C, 46.75; H, 5.57; N, 26.84%. Calcd for $C_6H_9O_2N_3$: C, 46.44; H, 5.58; N, 27.08%.

Ethyl α-cyano-β-hydrazinocrotonate (IIb): colorless plates, mp 116—117°C, yield 90.5%. IR (cm^{-1}): 2201 (νC≡N), 1664 (νC=O). NMR: 10.73 (NH).

Found: C, 50.09; H, 6.44; N, 24.54%. Calcd for $C_7H_{11}O_2N_3$: C, 49.69; H, 6.55; N, 24.84%.

Methyl α-cyano-β-hydrazino-β-ethylacrylate (IIc): colorless needles, mp 100—101°C, yields 86% from a stable isomer, and 85% from a labile isomer. IR(cm^{-1}): 2208 (νC≡N), 1664 (νC=O). NMR: 10.63(NH).

Found: C, 49.49; H, 6.68; N, 24.49%. Calcd for $C_7H_{11}O_2N_3$: C, 49.69; H, 6.55; N, 24.84%.

Methyl α-cyano-β-hydrazino-β-*n*-propylacrylate (IId)-colorless needles, mp 114.5—115.5°C, yield 83%. IR (cm^{-1}): 2198 (νC≡N), 1667 (νC=O). NMR: 10.70(NH).

Found: C, 52.74; H, 7.15; N, 22.85%. Calcd for $C_8H_{13}O_2N_3$: C, 52.44; H, 7.15; N, 22.94%.

Methyl α-cyano-β-hydrazino-β-*n*-butylacrylate (IIe): colorless prisms, mp 109—110°C, yield 90%. IR (cm^{-1}): 2208(νC≡N), 1664 (νC=O). NMR: 10.68 (NH).

Found: C, 54.97; H, 7.43; N, 21.49%. Calcd for $C_9H_{15}O_2N_3$: C, 54.80; H, 7.67; N, 21.31%.

4) All melting points and boiling points were uncorrected. The infrared absorption spectra were measured with a Shimadzu Model IR-27A infrared spectrophotometer in Nujol solid state. The NMR spectra were recorded with a JNM-C-60 high-resolution NMR spectrometer operating at 60 Mc. The chemical shift values for imino group of IIa—g, VI and XII were reported in ppm downfield from tetramethylsilane as an internal standard, in deuteriochloroform (carbon tetrachloride for VI) as solvent.

5) T. Hayashi, I. Hori, H. Baba and H. Midorikawa, *J. Org. Chem.*, **30**, 695 (1965).

6) I. Hori and H. Midorikawa, *Sci. Papers Inst. Phys. Chem. Res. (Tokyo)*, **56**, 216 (1962).

Methyl α-cyano-β-hydrazino-β-*n*-amylacrylate (IIf): colorless plates, mp 117—118°C, yield 85.3%. IR (cm^{-1}): 2208 (νC≡N), 1664 (νC=O). NMR: 10.74 (NH).

Found: C, 57.15; H, 7.19; N, 19.85%. Calcd for $C_{10}H_{17}O_2N_3$: C, 56.85; H, 8.11; N, 19.89%.

Methyl α-cyano-β-hydrazino-β-isobutylacrylate (IIg): colorless needles, mp 97—98°C, yield 86.8%. IR (cm^{-1}): 2210 (νC≡N), 1667 (νC=O). NMR: 10.79 (NH).

Found: C, 55.13; H, 7.59; N, 21.63%. Calcd for $C_9H_{15}O_2N_3$: C, 54.80; H, 7.67; N, 21.31%.

The Formation of 3-Alkyl-4-alkoxycarbonyl-5-aminopyrazoles (III) from II. (i) The foregoing β-hydrazino compound (IIa, IIb, or IIc) was heated to 130—140°C for 3 hr. After cooling, the resinous product was triturated in ether to give a precipitate. Recrystallization from benzene afforded IIIa and IIIb in yields of over 80%.

(ii) A mixture of II (6 mmol) and ethanol (4 m*l*) containing water (1 m*l*) was refluxed for 4—8 hr on a steam bath. The resulting clear solution was evaporated under reduced pressure. The resinous residue was cooled in an ice-box for 2—3 days; the crystallization was induced by scratching the inside wall of the vessel with a glass rod. It was purified by recrystallization from benzene to obtain III in yields of 75—90%.

(iii) To a suspended mixture of 2 mmol of the β-hydrazino compound (IIa, IIb, or IIc) in water (4 m*l*) there was added 15% hydrochloric acid (2 m*l*); the mixture was then warmed on a steam bath until it became a clear solution. After cooling to room temperature, the mixture was neutralized with an aqueous potassium carbonate solution. The crystalline substance thus formed was recrystallized from benzene, affording III in yields over 75.5%.

The same product (IIIa, IIIb, or IIIc) was obtained from all three reactions. For the formation of IIId—g only the method (ii) was used; IIId was obtained as a hydrate. Also, IIIg afforded a benzene-addition product (determined by a study of the IR and the NMR spectra). The benzene-free product of IIIg was obtained by triturating it with ether instead of by recrystallization from benzene. IIIb and IIIc easily took the water of crystallization when they were allowed to stand in moist air or were recrystallized from water. These crystal waters (IIIb, IIIc, and the forgoing IIId) were driven off by heating the substances under reduced pressure or by leaving them standing in a desiccator ($CaCl_2$).

3-Methyl-4-methoxycarbonyl-5-aminopyrazole (IIIa): colorless microcrystals, mp 145—146.5°C.

Found: C, 46.83; H, 5.43; N, 27.36%. Calcd for $C_6H_9O_2N_3$: C, 46.44; H, 5.85; N, 27.08%.

3-Methyl-4-ethoxycarbonyl-5-aminopyrazole (IIIb): colorless prisms, mp 109—110°C (lit[7] 113°C).

Found: C, 49.83; H, 6.48; N, 25.07%. Calcd for $C_7H_{11}O_2N_3$: C, 49.69; H, 6.55; N, 24.84%.

Hydrate: colorless needles (from water), mp 66—67°C (lit[7] 69°C).

Found: C, 44.77; H, 7.01; N, 22.63%. Calcd for $C_7H_{11}O_2N_3 \cdot H_2O$: C, 44.91; H, 7.00; N, 22.45%.

3-Ethyl-4-methoxycarbonyl-5-aminopyrazole (IIIc): colorless needles, mp 102—103°C.

Found: C, 49.94; H, 6.37; N, 24.34%. Calcd for $C_7H_{11}O_2N_3$: C, 49.69; H, 6.55; N, 24.84%.

Hydrate: colorless needles (from water), mp 81—82°C.

Found: C, 47.24; H, 6.64; N, 23.38%. Calcd for $C_7H_{11}O_2N_3 \cdot \frac{1}{2}H_2O$: C, 47.18; H, 6.79; N, 23.58%.

3-*n*-Propyl-4-methoxycarbonyl-5-aminopyrazole(IIId): colorless prisms, mp 80—81°C

Found: C, 52.70; H, 6.80; N, 23.61%. Calcd for $C_8H_{13}O_2N_3$: C, 52.44; H, 7.15; N, 22.94%.

Hydrate: colorless needles (from water) or colorless prisms (from benzene), mp 70—71°C.

Found: C, 50.22; H, 7.12; N, 22. 20%. Calcd for $C_8H_{13}O_2N_3 \cdot \frac{1}{2}H_2O$: C, 49.99; H, 7.34; N, 21.86%.

3-*n*-Butyl-4-methoxycarbonyl-5-aminopyrazole(IIIe): colorless capillaries, mp 72—73°C.

Found: C, 54.88; H, 7.59; N, 21. 71%. Calcd for $C_9H_{15}O_2N_3$: C, 54.80; H, 7.67; N, 21.31%.

3-*n*-Amyl-4-methoxycarbonyl-5-amipopyrazole(IIIf): colorless capillaries, mp 73—74°C.

Found: C, 56.58; H, 7.84; N, 19.88%. Calcd for $C_{10}H_{17}O_2N_3$: C, 56.85; H, 8.11; N, 19.89%.

3-Isobutyl-4-methoxycarbonyl-5-aminopyrazole(IIIg): colorless microcrystals, mp 104—106°C.

Found: C, 55.27; H, 7.57; N, 21.25%. Calcd for $C_9H_{15}O_2N_3$: C, 54.80; H, 7.67; N, 21.31%.

Benzene-addition compound: colorless microcrystals, mp 109—110°C. IR (cm^{-1}): 684 (benzene, -CH, out of plane). NMR: 7.36 (benzene).

Found: C, 59.17; H, 7.32; N, 19.07%. Calcd for $C_9H_{15}O_2N_3 \cdot \frac{1}{3}C_6H_6$: C, 59.17; H, 7.68; N, 18.82%.

The formation of III was proved by the absence of the cyano group in the infrared spectra and by the reaction to be described below.

The Hydrolysis of IIIa or IIIb. A mixture of IIIa or IIIb (3 mmol) and 4N sodium hydroxide (6 m*l*) was gently refluxed for 2 hr. After this mixture had been cooled, the resulting clear solution was adjusted to pH 5 with hydrochloric acid under cooling in ice water. The crystals which separated were collected and washed with water and ethanol.

3-Methyl-5-aminopyrazole-4-carboxylic acid (IV): colorless needles, mp 124—125°C, yields 87—95%.

Found: C, 42.76; H, 4.90; N, 29.71%. Calcd for $C_5H_7O_2N_3$: C, 42.55; H, 5.00; N, 29.78%.

Both IIIa and IIIb gave the same product.

The Decarboxylation of IV. A mixture of 2.5 g of the foregoing carboxylic acid (IV) in water (20 m*l*) was boiled for 2 hr, and then the solvent was evaporated under reduced pressure. In order to remove a trace of water, benzene (3 m*l*) was added to it and again evaporated. The distillation of the residue gave 1.5 g (87.5%) of a fraction distilling at 146.5—147°C/4 mmHg; it became a crystalline mass on cooling.

3-Methyl-5-aminopyrazole: hygroscopic colorless needles, mp 47—48°C (lit 47°C,[8] 94°C[9]).

Found: C,48.61; H, 7.15; N, 40.71%. Calcd for $C_4H_7N_3$: C, 49.46; H, 7.27; N, 43.27%.

Picrate: yellow needles, mp 206—207°C (lit 213—214°C,[7] 205—209°C[9]).

Found: C, 36.79; H, 2.81; N, 25.79%. Calcd for $C_{10}H_{10}O_7N_6$: C, 36.81; H, 3.09; N, 25.76%.

7) H. Beyer and G. Wolter, *Chem. Ber.*, **89**, 1658 (1956).

8) P. Kurtz, H. Gold and H. Disselnkötter, *Ann.*, **624**, I (1959).

9) M. J. S. Dewar and F. E. King, *J. Chem. Soc.*, **1945**, 114.

The Formation of 3-Alkyl-4-cyano-5-pyrazolones (V). A. By the Base Treatment of II. (i) A suspension of powdered IIa—g (6 mmol) and 80% hydrazine hydrate (6 mmol) in water (8 m*l*) was stirred at room temperature for 1 hr. The reaction mixture was filtered to give a large amount of unchanged material (the melting point was not depressed on admixture with II). After the filtrate had been acidified with hydrochloric acid, the resulting precipitate was collected by filtration, washed with a small amount of ice water, and recrystallized from water to give Va—f.

Both IIa and IIb gave the same product (Va); the yields were 6.3% and 8.3% respectively. Vb was obtained in a yield of 12.8%. The results of this reaction (for IIb) obtained by varying the reaction period are shown in Table 1 (Reaction 2). In the case of IId—g, the reaction period was extended to 5 hr, giving the corresponding yields of 50% (Vc), 6.06% (Vd), 20% (Ve), and 78.2% (Vf).

(ii) To a solution of 28% ammonia water (3 m*l*) and water (3 m*l*), 3.3 mmol of powdered IIa or IIb were added; the mixture was then stirred at room temperature for 4 hr. Filtration gave the unchanged material. The filtrate was worked up as before to afford Va in a yield of 76%.

(iii) A mixture of IIa or IIb (0.2 g) and a 10% aqueous potassium carbonate solution (4 m*l*) was stirred at room temperature for 1 hr. After the resulting clear solution had been acidified with hydrochloric acid, the separated crystals were purified as before to obtain 43.6—50% of Va.

In the reaction of IIa and IIb, the same product (as shown by the melting point and the infrared spectrum) was obtained from all three reactions (A(i)—(iii)).

3-Methyl-4-cyano-5-pyrazolone (Va): colorless prisms, mp 275—277°C (dec). IR (cm^{-1}): 2242 ($\nu C{\equiv}N$).

Found: C, 48.68; H, 4.30; N, 34.08%. Calcd for $C_5H_5ON_3$: C, 48.78; H, 4.09; N, 34.14%.

3-Ethyl-4-cyano-5-pyrazolone (Vb): colorless prisms, mp 232—234°C. IR (cm^{-1}): 2242 ($\nu C{\equiv}N$).

Found: C, 52.63; H, 4.93; N, 30.70%. Calcd for $C_6H_7ON_3$: C, 52.54; H, 5.15; N, 30.64%.

3-*n*-Propyl-4-cyano-5-pyrazolone (Vc): colorless plates, mp 215—216°C. IR (cm^{-1}): 2232 ($\nu C{\equiv}N$).

Found: C, 55.87; H, 6.30; N, 28.05%. Calcd for $C_7H_9ON_3$: C, 55.61; H, 6.00; N, 27.80%.

3-*n*-Butyl-4-cyano-5-pyrazolone (Vd): colorless plates, mp 174—175°C. IR (cm^{-1}): 2237 ($\nu C{\equiv}N$).

Found: C, 58.28; H, 6.54; N, 25.64%. Calcd for $C_8H_{11}ON_3$: C, 58.16; H, 6.71; N, 25.44%.

3-*n*-Amyl-4-cyano-5-pyrazolone (Ve): colorless plates, mp 168—169°C. IR (cm^{-1}): 2237 ($\nu C{\equiv}N$).

Found: C, 60.45; H, 7.40; N, 23.23%. Calcd for $C_9H_{13}ON_3$: C, 60.31; H, 7.31; N, 23.45%.

3-Isobutyl-4-cyano-5-pyrazolone (Vf): colorless plates, mp 220—221°C. IR (cm^{-1}): 2232 ($\nu C{\equiv}N$).

Found: C, 58.09; H, 6.31; N, 25.92%. Calcd for $C_8H_{11}ON_3$: C, 58.16; H, 6.71; N, 25.44%.

B. By the Reaction of Ia and Ib with an Excess of Hydrazine. Into a solution of 80% hydrazine hydrate (12 mmol) in water (8 m*l*), I (6 mmol) was stirred at room temperature, and then the mixture was stirred for an additional hour. Filtration gave a large amount of II (mp and mixed mp 131°C (IIa) or 115°C (IIb)). The treatment of the filtrate as A(i) gave Va in yields of 6.3—9.7%; mp 275—276°C. The product was identified with the Va obtained by Procedure A by a mixed-melting-point determination and by a study of the infrared spectra. The results of this reaction (for Ib) are shown in Table 1 (Reaction 1).

C. By the Reaction of I (R=*i*-Pr, *t*-Bu and Ph, R'=Me) with Hydrazine. I (3.3 mmol) was stirred into a solution of 80% hydrazine hydrate (3.3 mmol) and water (4 m*l*) at room temperature, and then the mixture was stirred for 1 hr. After the same work-up as in A(i), the separated V was recrystallized from water, benzene-methanol (Vg), or methanol-water (Vh and Vi). The use of more hydrazine resulted in an increase in the yield. Thus, the use of two equivalent moles of hydrazine nearly doubled the yield. In the case of I (R=Ph), a large amount of the starting material was recovered.

3-Isopropyl-4-cyano-5-pyrazolone (Vg): colorless microcrystals, mp 222—223°C, yield 41.4% and 80% (with two equivalent moles of hydrazine). IR (cm^{-1}): 2227 ($\nu C{\equiv}N$).

Found: C, 55.80; H, 5.72; N, 27.90%. Calcd for $C_7H_9ON_3$: C, 55.61; H, 6.00; N, 27.80%.

3-*t*-Butyl-4-cyano-5-pyrazolone (Vh): colorless prisms, mp 254—255°C, yields 30% and 73% (with two equivalent moles of hydrazine). IR (cm^{-1}): 2232 ($\nu C{\equiv}N$).

Found: C, 57.94; H, 6.44; N, 25.91%. Calcd for $C_8H_{11}ON_3$: C, 58.16; H, 6.71; N, 25.44%.

3-Phenyl-4-cyano-5-pyrazolone (Vi): colorless microcrystals, mp 254—255°C, yields 3.5% and 7.5% (with two equivalent moles of hydrazine). IR (cm^{-1}): 2237 ($\nu C{\equiv}N$).

Found: C, 64.79; H, 3.63; N, 22.60%. Calcd for $C_{10}H_7ON_3$: C, 64.86; H, 3.81; N, 22.69%.

All the compounds of V obtained by all the procedures (A, B, and C) gave a positive color reaction with ferric chloride, and their infrared spectra all indicated the presence of the cyano group and the disappearance of the ester-carbonyl group.

The Preparation of Ethyl α-Cyano-(2,2-dimethylhydrazino)crotonate (VI). A mixture of 1,1-dimethylhydrazine (0.36 g) in water (8 m*l*) and 1 g of powdered Ib was stirred at room temperature for 1 hr. The resulting precipitate was collected by filtration, washed thoroughly with water, and recrystallized from acetone-water to give 0.75 g (63.5%) of VI. Colorless needles, mp 83—85°C. IR (cm^{-1}): 2203($\nu C{\equiv}N$), 1668 ($\nu C{=}O$). NMR: 10.26 (NH).

Found: C, 54.75; H, 7.63; N, 21.38%. Calcd for $C_9H_{15}O_2N_3$: C, 54.80; H, 7.67; N, 21.31%.

The Reaction of I (R=*i*-Pr, R'=Et) with Ammonia. A mixture of 28% ammonia water (1 m*l*) in water (2 m*l*) and I (3.3 mmol) was stirred at room temperature for 1 hr. The resulting precipitate was collected by filtration, washed with water, and recrystallized from benzene to give 0.4 g (74.2%) of ethyl α-cyano-β-amino-β-isopropylacrylate (VII). Colorless columns, mp 119—120°C. IR(cm^{-1}): 2203($\nu C{\equiv}N$), 1686($\nu C{=}O$).

Found: C, 59.65; H, 7.47; N, 15.37%. Calcd for $C_9H_{14}O_2N_2$: C, 59.32; H, 7.74; N, 15.37%.

The Reaction of Ia—g and I (R=*i*-Pr and Ph) with Hydroxylamine. A solution of hydroxylamine hydrochloride (5 mmol) in water (3 m*l*) was neutralized with a solution of potassium carbonate (2.5 mmol) in water (3 m*l*). Into this I (5 mmol) was stirred at

room temperature. (In the reactions of Id—g, methanol was added to the mixture until it became a clear solution.) After it had been stirred for 1 hr, the precipitate which separated was recrystallized from ethanol (VIIIa, b, c, f, and VIIIj), ethanol - water (VIIIe,d, and VIIIg), or benzene (VIIIh). All the infrared spectra showed the disappearance of the cyano group.

3 - Methyl - 4 - methoxycarbonyl - 5 - aminoisoxazole (VIIIa): colorless prisms, mp 140—141°C, yield 78%.

Found: C, 46.20; H, 4.93; N, 17.81%. Calcd for $C_6H_8ON_2$: C, 46.15; H, 5.16; N, 17.94%.

3-Methyl-4-ethoxycarbonyl-5-aminoisoxazole (VIIIb): colorless needles, mp 133—134°C (lit[10] 133—134°C), yield 88.2%.

Found: C, 49.80; H, 5.91; N, 16.59%. Calcd for $C_7H_{10}O_3N_2$: C, 49.40; H, 5.92; N, 16.46%.

3-Ethyl-4-methoxycarbonyl-5-aminoisoxazole (VIIIc): colorless prisms, mp 151—152°C, yield 97%.

Found: C, 49.40; H, 5.71; N, 16.70%. Calcd for $C_7H_{10}O_3N_2$: C, 49.40; H, 5.92; N, 16.46%.

3 - *n* - Propyl - 4 - methoxycarbonyl -5- aminoisoxazole (VIIId): colorless prisms, mp 116—117°C, yield 56.5%.

Found: C, 52.06; H, 6.40; N, 15.36%. Calcd for $C_8H_{12}O_3N_2$: C, 52.16; H, 6.57; N, 15.21%.

3 - *n* - Butyl - 4 - methoxycarbonyl - 5 - aminoisoxazole (VIIIe): colorless needles, mp 97—98°C, yield 75.8%.

Found: C, 54.48; H, 6.86; N, 14.24%. Calcd for $C_9H_{14}O_3N_2$: C, 54.53; H, 7.12; N, 14.13%.

3 - *n* - Amyl - 4 - methoxycarbonyl - 5 - aminoisoxazole (VIIIf): colorless needles, mp 129—130°C, yield 84.5%.

Found: C, 56.75; H, 7.25; N, 13.20%. Calcd for $C_{10}H_{16}O_3N_2$: C, 56.59; H, 7.60; N, 13.20%.

3 - Isobutyl - 4 - methoxycarbonyl - 5 - aminoisoxazole (VIIIg): colorless prisms, mp 99—100°C, yield 50%.

Found: C, 54.54; H, 6.99; N, 14.08%. Calcd for $C_9H_{14}O_3N_2$: C, 54.53; H, 7.12; N, 14.13%.

3 - Isopropyl - 4 - methoxycarbonyl - 5 - aminoisoxazole (VIIIh): colorless prisms, mp 121—122°C, yield 54.5%.

Found: C, 52.50; H, 6.61; N, 14.92%. Calcd for $C_8H_{12}O_3N_2$: C, 52.16; H, 6.57; N, 15.21%.

3-Phenyl-4-ethoxycarbonyl-5-aminoisoxazole (VIIIj): colorless needles, mp 123°C (lit[3] 123°C), yield 85%.

Found: C, 62.23; H, 5.14; N, 12.11%. Calcd for $C_{12}H_{12}O_3N_2$: C, 62.06; H, 5.21; N, 12.06%.

In the case of the reaction of I (R = *t*-Bu) with hydroxylamine, an excess of hydroxylamine (10 mmol) was used, and to the mixture ethanol was added until it became a clear solution. The mixture was then stirred for 30 hr at room temperature and subsequently concentrated to about 2 m*l*. Upon the cooling of the mixture in an ice-chest, the product was obtained. Recrystallization from ethanol - water gave VIIIi, whose infrared spectrum indicated the absence of the cyano group.

3 - *t* - Butyl - 4 - methoxycarbonyl - 5 - aminoisoxazole (VIIIi): colorless needles, mp 112—113°C, yield 16.7%.

Found: C, 54.59; H, 7.22; N, 14.50%. Calcd for $C_9H_{14}O_3N_2$: C, 54.53; H, 7.12; N, 14.13%.

Furthermore, the filtrate was acidified with hydrochloric acid to give a precipitate whose recrystallization from ethanol yielded IX. Its ferric chloride test was positive.

3 - *t* - Butyl - 4 - cyano -5- isoxazolone (IX): colorless prisms, mp 217—218°C, yield 12.7%. IR (cm^{-1}): 2237($\nu C{\equiv}N$).

Found: C, 57.82; H, 5.89; N, 17.11%. Calcd for $C_8H_{10}O_2N_2$: C, 57.82; H, 6.07; N, 16.86%.

The Reaction of Diethyl 1-Ethoxyethylidenemalonate with Hydroxylamine. To a neutralized solution of hydroxylamine hydrochloride (0.18 g) with potassium carbonate, diethyl 1-ethoxyethylidenemalonate (0.6 g) was added at room temperature, and then the mixture was stirred for 1 hr. After the reaction mixture had been acidified with hydrochloric acid, the crystallization of the resulting product from methanol afforded 0.31 g (69.5%) of 3-methyl-4-ethoxycarbonyl-5-isoxazolone (XI), whose ferric chloride test was positive. Colorless needles, mp 167—168°C (lit 170—171°C,[11] 166°C[12]).

Found: C, 49.37; H, 5.20; N, 8.09%. Calcd for $C_7H_9O_4N$: C, 49.12; H, 5.30; N, 8.18%.

The Preparation of Ethyl α-Cyano-β-methoxyaminocrotonate (XII). *O*-Methylhydroxylamine hydrochloride (0.85 g) was neutralized with a solution of potassium carbonate (0.7 g) in water (10 m*l*). To the solution there was added Ib (1.6 g), and then the mixture was stirred at room temperature for 3 hr. After the usual work-up, the recrystallization of the resulting precipitate from methanol - water gave 1.6 g (87%) of XII. Colorless needles, mp 60—62°C. IR (cm^{-1}): 2198 ($\nu C{\equiv}N$), 1667 ($\nu C{=}O$). NMR: 11.64 (NH).

Found: C, 52.27; H, 6.72; N, 14.98%. Calcd for $C_{18}H_{12}O_3N_2$: C, 52.16; H, 6.57; N, 15.21%.

The authors wish to express their hearty thanks to Professors Taro Hayashi and Tatsuo Takeshima for their kind advice and encouragement and to Professor Toshiro Miwa of Osaka City University for his suggestions about the reaction mechanism. Thanks are also due to Dr. Haruo Homma and his staff for their microanalyses.

10) G. Shaw and G. Sugowdz, *J. Chem. Soc.*, **1954**, 668.

11) A. R. Katritzky, S. Oksne and A. J. Boulton, *Tetrahedron*, **18**, 790 (1962).

12) F. C. Pallazzo, *Gazz. Chim. Ital.*, **36**, II, 596 (1906).

BULLETIN OF THE CHEMICAL SOCIETY OF JAPAN VOL. 42 1660—1663 (1969)

Solvent Effect under High Pressure. III.[1] The Application of the Electrostriction Model to the Activation Entropy

Yasuhiko KONDO and Niichiro TOKURA

Department of Applied Chemistry, Faculty of Engineering, Osaka University, Suita, Osaka

(Received September 30, 1968)

The expression which relates the activation entropies of the reactions measured in various solvents with the products of the coefficients of thermal expansion and the molar volumes of the respective solvents has been derived based on the concepts of the electrostriction theory. For three Menschutkin reactions and one acylation reaction linear correlations to be expected from the above expression have been found between the activation entropies and the products of the coefficients of thermal expansion and the molar volumes of the solvents. Moreover, the interrelation between the activation volumes and the activation entropies has been discussed based on this model.

Various attempts have been made to clarify the mechanism of how the solvent influences the rate of the reaction in solution. These attempts have used two alternative methods. One of which seeks out the quantitative relation between the experimental results and the various characteristics of the solvents.[2-6] The other is the method of applying empirically-determined solvent parameters.[7]

In a previous paper[1] the present authors have used an analytical expression which combined the activation volumes measured in various solvents with compressibilities of those solvents based on an electrostriction model.

As that relation has been proved to hold for two Menschutkin reactions,[1] the present authors have now tried to extend this model to an analysis of the dependence of an activation entropy of a reaction in a solution on the nature of the solvent.

In this paper the analytical expression proposed by the present authors will be compared with the experimental results of the various workers.

Discussion

In the previous paper[1] the following expression has been derived to describe the dependence of an activation volume on the compressibility of the solvent;

$$\Delta V_0^{\neq} = \{V_{\neq} - (\overline{V}_A^\circ + \overline{V}_B^\circ)\} - Z\Delta PKV^\circ \qquad (1)$$

where $V_{\neq}$, $\overline{V}_A^\circ$, $\overline{V}_B^\circ$ and V° denote the molar volumes of an activated complex, the reactant A, the reactant B, and a solvent in its pure state and where Z, ΔP, and K denote the solvation number of an activated complex, an average pressure within a solvation shell of an activated complex, and the compressibility of the solvent, respectively.

As one example of the above relationship, the experimental results of $\Delta V_0^{\neq}$ measured by Hartmann *et al.*[8] are plotted against the value of KV° in Fig. 1.

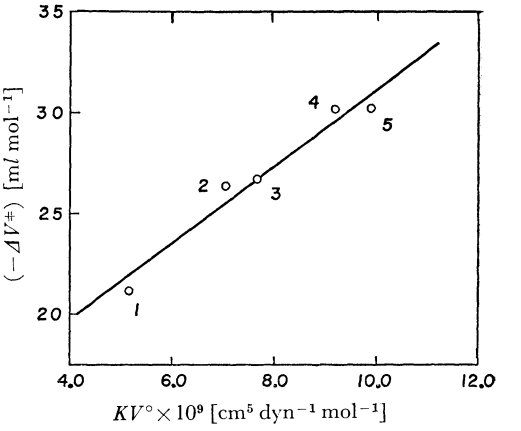

Fig. 1. Plot of $(-\Delta V^{\neq})$ measured in various solvents by Hartmann *et al.*[8] *vs.* KV°.
Reaction: ω-Bromoacetophenone+α-Picoline
Solvent 1: $PhNO_2$, 2: PhBr, 3: PhCl,
4: Acetone, 5: $PhCH_3$

1) Part II, Y. Kondo, M. Uchida and N. Tokura, This Bulletin, **41**, 992 (1968).

2) A. Streitwieser, "Solvolytic Displacement Reactions," McGraw-Hill, New York (1962).

3) J. D. Reinheimer, J. D. Harley and W. W. Meyers, *J. Org. Chem.*, **28**, 1575 (1963).

4) H. G. Grim, H. Ruf and H. Wolf, *Z. Physik. Chem.*, **13B**, 301 (1931).

5) S. Glasstone, K. J. Laidler and H. Eyring, "The Theory of Rate Processes," McGraw-Hill, New York (1941).

6) J. B. Rossel, *J. Chem. Soc.*, **1963**, 5183.

7) C. Reichardt, *Angew. Chem.*, **77**, 30 (1965).

8) H. Heytmann, A. P. Schmidt and H. Hartmann, *Ber. Bunsen Ges. Physik. Chem.*, **70**, 444 (1966).

In order to derive the expression for the activation entropy, it would be suitable to adopt a procedure similar to that used in the preceding paper for deriving the activation volume.

We assume that in the vicinity of an ionic species in the solution the entropy of a solvent, S_{solv}°, is changed to S_{solv}' by the electrostatic influence caused by the ionic charge of the solute.

Then the total entropy, S_t, of the solution composed of N moles of a solvent and n moles of a solute may approximately be expressed, as follows;

$$S_t = (N-nZ)S_{solv}^{\circ} + nS_s^{\circ} + nZS_{solv}' + \Delta S_{cratic} \quad (2)$$

where S_{solv}°, S_s°, S_{solv}', ΔS_{cratic} and Z are the molar entropies of a free solvent, a pure solute and a solvated solvent, and a cratic entropy change on dilution and a solvation number, respectively.

Therefore, the partial molar entropy of a solute, $\bar{s}_s$, is given by;

$$\bar{s}_s = \left(\frac{\partial S_t}{\partial n}\right) = s_s^{\circ} + Z(S_{solv}' - S_{solv}^{\circ}) + \Delta s_{cratic} \quad (3)$$

In Eq. (3) the term $(S_{solv}' - S_{solv}^{\circ})$ indicates the entropy change which accompanies the transfer of a solvent molecule from the pure state under an atmospheric perssure into the ionic cosphere of a solute.

Practically, the change is produced by the electrostriction of a solvent molecule resulting from the electrostatic interaction of a solvent molecule with the ionic charge of a solute. However, at present we will estimate the value assuming that the entropy change is produced by exerting an external pressure on a solvent molecule.

Making use of the thermodynamical relation,[9] Eq. (4);

$$\left(\frac{\partial S}{\partial P}\right)_T = -\left(\frac{\partial V}{\partial T}\right)_P \quad (4)$$

and the coefficient of a thermal expansion, α, as defined by:

$$\frac{1}{V}\left(\frac{\partial V}{\partial T}\right) = \alpha \quad (5)$$

the entropy change caused by applying external pressure on a solvent molecule may be approximately given by;

$$\Delta S = -\alpha V^{\circ}(P-1) = -\alpha V^{\circ}\Delta P \quad (6)$$

where V° and P denote the molar volume of a pure solvent and the average pressure within the cosphere of an ionic solute.

The partial molar entropy of a solute can be obtained approximately by substituting Eq. (6) into Eq. (3):

$$\bar{s}_s = s_s^{\circ} - Z\Delta P\alpha V^{\circ} + \Delta s_{cratic} \quad (7)$$

In the discussion of an activation entropy we have only to treat the entropy at an appropriately chosen standard state. Since the cratic entropy term is dependent only on the composition of the solution, not on the characteristics of the solvent, it makes an equal contribution to all the activation entropies based on the same standard state.

If we assume that the activated complex is of an ionic nature while the reactants are nonpolar, we would be able to use Eq. (7) as the entropy of the activated complex. Then the activation entropy for the bimolecular reaction is given by:

$$A + B \longrightarrow M^{\ddagger} \longrightarrow \text{Product}$$

$$\Delta S^{\ddagger} = \{\overline{S_{\ddagger}}^{\circ} - (\overline{S_A}^{\circ} - (\overline{S_A}^{\circ} + \overline{S_B}^{\circ})\}$$

$$= S_{\ddagger}^{\circ} - (\overline{S_A}^{\circ} + \overline{S_B}^{\circ}) + C - Z\Delta P\alpha V^{\circ} \quad (8)$$

where C denotes the constant characteristic of the chosen standard state.

As the activation entropies measured in various solvents should be affected by the second term on the right hand side of Eq. (8), the linear relation may be expected to hold in the plotting of the activation entropies against the αV° values of the solvents. These plots are given in Figs. 2, 3, 4 and 5.*1,*2

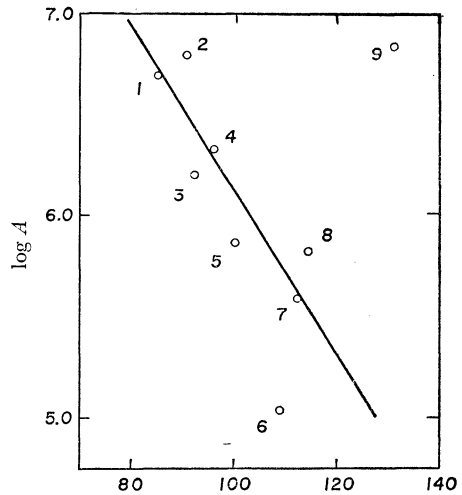

$\alpha V^{\circ} \times 10^3$ [ml mol^{-1} deg^{-1}]

Fig. 2. Plot of log$A$ measured in various solvents by Grim *et al.*[4] *vs.* αV°.
Reaction: EtI + Et_3N
Solvent 1: $PhNO_2$, 2: PhCN, 3: PhI, 4: PhBr, 5: PhCl, 6: Bz, 7: PhF, 8: $PhCH_3$, 9: Cyclohexane

9) G. N. Lewis and M. Randall, "Thermodynamics and the Free Energy of Chemical Substances," McGraw-Hill, New York (1923); 2nd Ed., Revised by K. S. Pitzer and L. Brewer (1961).

*1 The values of the density and the coefficient of the thermal expansion were calculated at 25°C by means of the polynominal equation in "The International Critical Tables" and by means of the differentiation of these with respect to the temperature.

*2 In Figs. 2, 3, and 5, log A is used in place of an activation entropy where A was calculated by this equation:

$$k = A\exp(\Delta E^{\ddagger}/\boldsymbol{R}T)$$

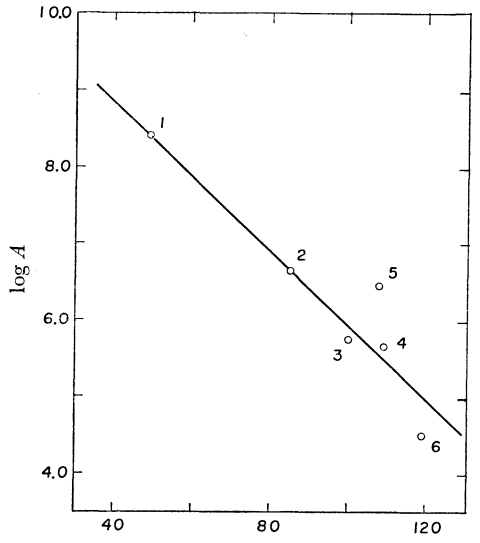

Fig. 3. Plot of log A measured in various solvents by Hartmann *et al.*[10] *vs.* $\alpha V°$.
Reaction: MeI + Pyridine
Solvent 1: MeOH, 2: $PhNO_2$, 3: PhCl, 4: Bz, 5: Acetone, 6: CCl_4

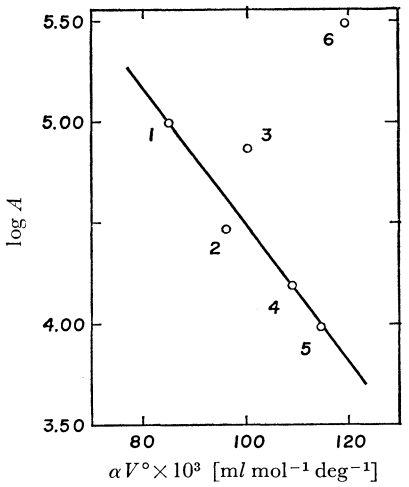

Fig. 5. Plot of log A measured in various solvent by Hinshelwood *et al.*[11] *vs.* $\alpha V°$.
Reaction: *m*-Nitroaniline + Benzoyl chloride
Solvent 1: $PhNO_2$, 2: PhBr, 3: PhCl, 4: Bz, 5: $PhCH_3$, 7: CCl_4

As is shown in these figures, approximately linear correlations have been found in all these examples in spite of the varieties of the solvent used. Moreover, the signs of the solpes of these plots are those to be expected from Eq. (8).

When we compare Eq. (8) with Eq. (1), we can see that the solpes of both these plots represent the values of $Z\Delta P$.

If the assumed model describes the reaction in a solution precisely, the values of $Z\Delta P$ obtained by the two methods should be equal to each other (Table 1).

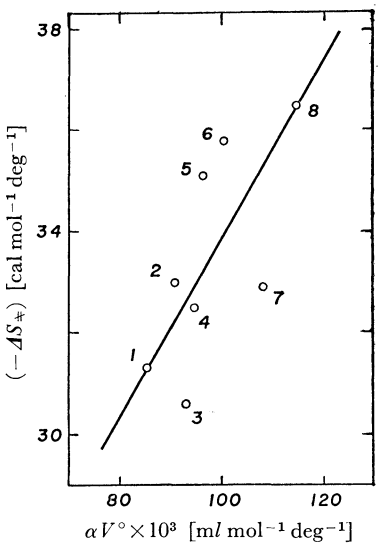

Fig. 4. Plot of $(-\Delta S^{\neq})$ measured in various solvents by Hartmann *et al.*[8] *vs.* $\alpha V°$.
Reaction: ω-Bromoacetophenone + α-Picoline
Solvent 1: $PhNO_2$, 2: PhCN, 3: Propionitrile 4: Cyclohexanone, 5: PhBr, 6: PhCl, 7: Acetone, 8: $PhCH_3$

TABLE 1. THE VALUES OF $Z\Delta P$ DERIVED BY THE TWO METHODS

	Reaction		
	EtI + Et_3N	MeI + Pyridine	MeI + α-Picoline
$Z\Delta P$ from $\Delta V_0^{\neq}$ (kg·cm^{-2})	2.6×10^3	2.6×10^3	1.9×10^3
$Z\Delta P$ from $\Delta S^{\neq}$ (kg·cm^{-2})	7.9×10^3	9.4×10^3	7.6×10^3

Though this equality does not hold accurately in these cases as is shown in Table 1, these values are of the same order for each example.

Previously Laidler and Chen[12] reported a linear correlation between the activation volumes and the activation entropies for the alkaline hydrolysis of esters in an aqueous solution. Recently Hepler[13] found a similar relation between the volume changes

10) H. Hartmann, H. Kelm and G. Rinck, *Z. Physik. Chem. N. F.*, **44**, 335 (1965).
11) N. J. T. Pickles and C. N. Hinshelwood, *J. Chem. Soc.*, **1936**, 1353.
12) K. J. Laidler and D. Chen, *Trans. Faraday Soc.*, **54**, 1026 (1958).
13) L. G. Hepler, *J. Phys. Chem.*, **69**, 965 (1965). In the original formula Hepler considered the above relation to be based on the Maxwell equation: $(\partial S/\partial V)_T = (\partial P/\partial T)_v$. Thermodynamically, the following equation can be proved easily: $(\partial P/\partial T)_v = (\alpha/K)$ where K indicates the coefficient of an isothermal compressibility. Therefore Eq. (11) agrees with his opinion.

and the entropy changes for the acid dissociation reaction in a water solvent.

For the reaction in the single solvent the effect of changing reactants reveals itself in the activation entropy change upon the variation in $Z\Delta P$, for in our model the values of $Z\Delta P$ function as the measure of the development and the redistribution of the charge accompanying the formation of an activated complex.

Then, from Eq. (7) the following equation may be obtained:

$$\Delta\Delta S^{\ddagger} = -\alpha V^{\circ} \cdot \Delta(Z\Delta P) \tag{9}$$

Similarly, for the activation volume:

$$\Delta\Delta V_0^{\ddagger} = -KV^{\circ} \cdot \Delta(Z\Delta P) \tag{10}$$

By combining Eqs. (9) and (10), we obtain:

$$\Delta\Delta S^{\ddagger} = (\alpha/K)\Delta\Delta V^{\circ\ddagger} \tag{11}$$

This relation is similar not only that derived thermodynamically be Hepler,[13] but also to the alternative form of the observation by Laidler and Chen.[12] Thus, it may be concluded that this model, based on the electrostriction theory, is applicable to the analysis of the activation volume and entropy for a reaction in a solution.

BULLETIN OF THE CHEMICAL SOCIETY OF JAPAN VOL. 42 1663—1667 (1969)

The Hydrogenation Catalysts Prepared from Transition Metal Chloride and Triethylaluminum*1

Yoshinobu TAKEGAMI, Toru UENO and Takao FUJII

Department of Hydrocarbon Chemistry, Faculty of Engineering, Kyoto University, Sakyo-ku, Kyoto

(Received October 4, 1968)

Catalysts composed of anhydrous iron(III) chloride, cobalt(II) chloride, or nickel(II) chloride plus triethylaluminum have been used for the hydrogenation of olefin. The catalytic activity has changed with the $Al(C_2H_5)_3/MCl_n$ ratio. The optimum ratios for the hydrogenation of styrene have been found to be 1—7 for the iron catalyst, 0.2—1 for the cobalt catalyst, and 0.3—2 for the nickel catalyst. Cyclohexane has been used satisfactorily as a solvent. Tetrahydrofuran could be used for the nickel catalyst, but its presence was unfavorable for the iron and cobalt catalysts. The gas evolved in the reaction of the transition metal chlorides with triethylaluminum has been found to be essentially ethane, and sluggish gas absorption was observed when the atmosphere was switched to hydrogen. Ethylbenzene was formed in the treatment of the catalyst with styrene under nitrogen; the amount increased considerably if the catalyst was pre-treated with hydrogen. Ethane was formed in the hydrogen-treatment of the reaction mixture of nickel chloride and triethylaluminum. On the basis of these results, it has been assumed that metal hydride has been formed by the hydrogenolysis of metal - ethyl bonds.

Breslow and his co-workers[1] have reported Ziegler-type soluble catalysts composed of acetylacetonates or alkoxides of transition metals plus triethyl- or tri-isobutylaluminum. They hydrogenated various olefins at 30—50°C and at 3.7 atm. They postulated that the active sites for the hydrogenation are transition metal - hydrogen bonds. Lapporte and Schuett[2] have reported the hydrogenation of aromatic hydrocarbons with catalysts composed of nickel(II) 2-ethylhexanoate plus triethylaluminum at 150—210°C and at 1000 psi, and they assumed that finely-divided transition metal is responsible for the hydrogenation. Analogous catalyst systems have also been patented.[3,4]

As part of their investigation of the synthesis and the catalysis of transition metal hydrides prepared by the use of Grignard reagents[5-8] or lithium aluminum hydride,[9-12] the present authors have

*1 The Preparation of Heavy Metal Hydride and Its Catalystic Activity. XI. Part X: Ref. 11.

1) M. F. Sloan, A. S. Matlack and D. S. Breslow, *J. Am. Chem. Soc.*, **85**, 4014 (1963).

2) S. J. Lapporte and W. R. Schuett, *J. Org. Chem.*, **28**, 1947 (1963).

3) California Reserch Corp., French Pat. 1390570 (1965).

4) W. R. Kroll, U. S. Pat. 3329502 (1967).

5) Y. Takegami, T. Ueno and K. Kawajiri, *Kogyo Kagaku Zasshi (J. Chem. Soc. Japan, Ind. Chem. Sect.)*, **64**, 1068 (1963).

6) Y. Takegami, T. Ueno, K. Shinoki and T. Sakata, *ibid.*, **67**, 316 (1964).

7) Takegami, T. Ueno and K. Kawajiri, *Shokubai (Catalyst)*, **4**, 13 (1962).

8) Y. Takegami, T. Ueno and K. Kawajiri, This Bulletin, **39**, 1 (1966).

studied the activity of the catalysis prepared by the reaction of iron(III) chloride, cobalt(II) chloride, or nickel(II) chloride with triethylaluminum. In this paper, some novel aspects of the natures of these catalysts and of the mechanism of catalyst formation will be reported.

Experimental

Materials. Triethylaluminum was obtained from the Ethyl Co. Anhydrous iron(III) chloride was prepared by the dehydration of a hexa-hydrate (from Merck) with thionyl chloride.[13] The solvent, tetrahydrofuran and cyclohexane, were dried over sodium and distilled just before use. The other reagents used were the purest among the available commercial materials.

The Preparation of the Catalysts and the Hydrogenation. The apparatus consisted of a four-necked flask (100 m*l*) equipped with a stirrer, a dropping funnel, and a thermometer; it was jointed to a gas buret through a silica gel tube. To a solution of 40 m*l* of cyclohexane containing 0.003 — 0.005 mol of transition metal chloride, a desired amount of triethylaluminum solution in cyclohexane was added through the dropping funnel. The solution immediately turned black or brown-black, and there was an accompanying gas evolution. The mixture was then stirred for an additional hour until the gas evolution ceased.

The hydrogenation of olefin was carried out by introducing 2 m*l* of olefin into the catalyst solution prepared above. The speed of stirring was kept constant (900 rpm) during the hydrogenation. After the hydrogenation, the reaction mixture was poured into cold aqueous hydrochloric acid in order to destroy the catalyst. The hydrogenation product was extracted with ethyl ether, washed with water, concentrated by the evaporation of ether, and gas-chromatographed.

Determination of Ethane. Anhydrous nickel(II) chloride (0.005 mol) was placed in a 300 m*l* two-necked flask equipped with a magnetic stirrer, and the flask was flushed with nitrogen. The triethylaluminum solution was added slowly. When the gas evolution ceased, the reaction mixture was degassed completely by evacuating the flask until a half of the solvent had been distilled. Then, the atmosphere was switched to hydrogen. Gas samples (2—5 m*l*) were removed periodically by the use of a syringe and subjected to gas chromatography. The amount of ethane was determined by the use of the absolute calibration curve prepared for a hydrogen - ethane mixture.

Results and Discussion

The Reaction of Transition Metal Chlorides with Triethylaluminum. The reaction of anhydrous transition metal chlorides with triethylaluminum was carried out under a nitrogen atmosphere and at 0°C. A black-colored substance (suspended in the solvent)was formed immediately, and there was an accompanying gas evolution. The amount and composition of the gas are represented in Table 1. A great portion of the evolved gas was ethane, but its amount was relatively small. When the atmosphere was switched from nitrogen to hydrogen after the reaction, a diminution in the gas volume was observed. However, the rate was quite sluggish; the gas-volume diminutions represented in the last columm of Table 1 are those observed during reaction periods of 5—15 hr.

Hydrogenation of Olefin. Using a black-colored suspension as a catalyst, the hydrogenation of styrene was carried out at 0 or 35°C. For most of the experiments, about 0.003 mol of transition metal chlorides and 3 m*l* of styrene were used. Cyclohexane was used as the solvent. Figures 1—3 show the hydrogen absorption curves for the hydrogenation with iron, cobalt, and nickel catalysts respectively. The numerals attached to

TABLE 1. PREPARATION OF THE MCl_n-$Al(C_2H_5)_3$ CATALYSTS[a]

Run	MCl_n	Solvent	$AlEt_3/MCl_n$	Amt. of gas evolved[b]	Ethane %	Gas vol. dimin. on H_2-treatment[c]
1	$NiCl_2$	C_6H_{12}-THF	1.08	0	—	0
2[d]	$NiCl_2$	C_6H_{12}-THF	2.08	0.02	100	0.14
3	$NiCl_2$	C_6H_{12}-THF	2.00	0.34	97.3	0.03
4	$NiCl_2$	C_6H_{12}	2.06	0.34	96.3	0.43
5	$FeCl_3$	C_6H_{12}	2.13	0.29	94.5	—
6	$FeCl_3$	C_6H_{12}	2.11	0.22	93.4	0.35
7	$CoCl_2$	C_6H_{12}	2.08	0.52	98.3	0.31

a) MCl_n: 0.005 mol; reaction temp.: 35°C. b) Represented by mol/mol MCl_n.
c) Gas volume diminution observed during the hydrogen-treatment of the catalyst component (mol/mol MCl_n).
d) Reaction temp., 0°C.

9) Y. Takegami and T. Ueno, *Kogyo Kagaku Zasshi (J. Chem. Soc. Japan, Ind. Chem. Sect.)*, **67**, 246 (1964).
10) Y. Takegami, T. Ueno and T. Fujii, *ibid.*, **67**, 1009 (1964).
11) Y. Takegami, T. Ueno and T. Fujii, *ibid.*, **69**, 1467 (1966).
12) Y. Takegami, T. Ueno and T. Fujii, This Bulletin, **39**, 1279 (1965).
13) "Inorganic Synthesis," Vol. V, p. 153 (1957)

each curve represent the $Al(C_2H_5)/MCl_n$ ratios (abbreviated as "molar ratio" below further description). As may be seen in Figs. 1—3, the catalytic activity of these catalysts is dependent on the molar ratio; the optimum molar ratios for iron, cobalt, and nickel catalysts are 1—7, 0.2—1, and 0.3—2 respectively.

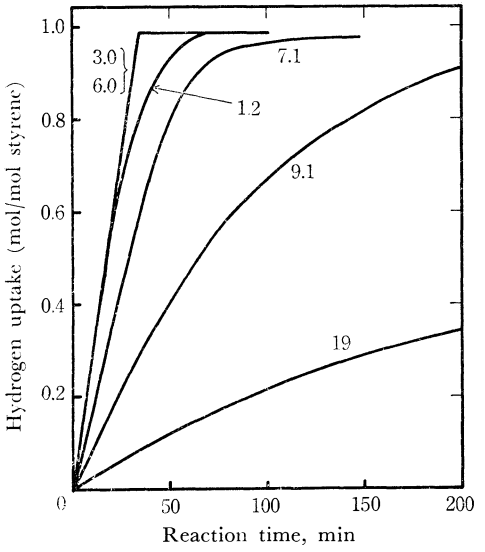

Fig. 1. Hydrogenation of styrene with the $FeCl_3$-$AlEt_3$ catalyst.
At 35°C and in cyclohexane solvent.
Numerals attached to the curves represent the $AlEt_3/FeCl_3$ ratios.

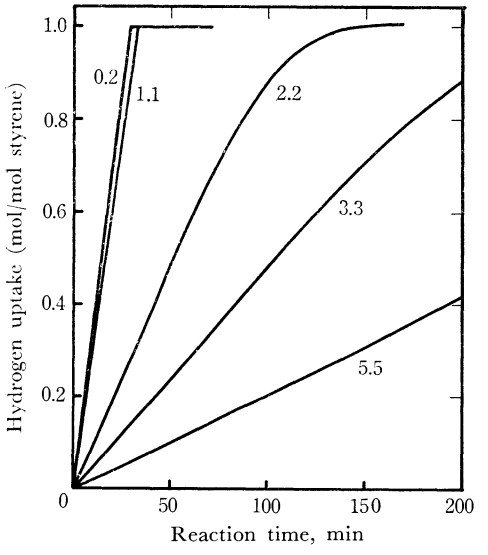

Fig. 2. Hydrogenation of styrene with the $CoCl_2$-$AlEt_3$ catalyst.
At 35°C and in cyclohexane solvent.
Numerals attached to the curves represent the $AlEt_3/CoCl_2$ ratios.

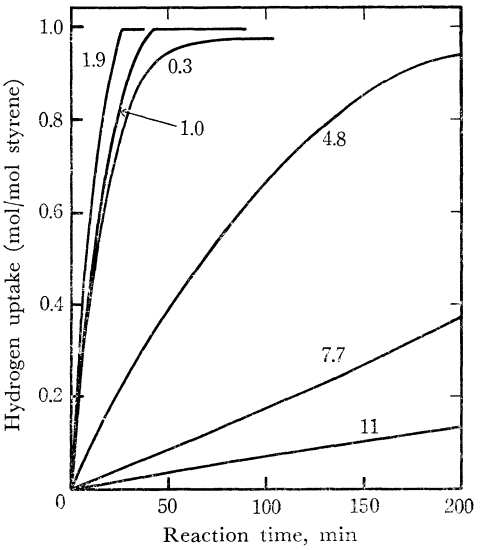

Fig. 3. Hydrogenation of styrene with the $NiCl_2$-$AlEt_3$ catalyst.
At 35°C and in cyclohexane solvent.
Numerals attached to the curves represent the $AlEt_3/NiCl_2$ ratios.

Several other olefins were tentatively hydrogenated using the iron catalyst (the molar ratio was 3); the ease of hydrogenation was found to vary in the order; styrene > indene > cyclohexene > safrole > *d*-limonene > isosafrole. Actually, the rate of the hydrogenation of isosafrole was nearly zero. Acetophenone and ethyl vinyl ether could not be hydrogenated with this catalyst; furthermore, in the presence of the ketone or ether, the hydrogenation of styrene was considerably depressed.

In the runs shown in Figs. 1—3, cyclohexane was used as the solvent. When a cyclohexane-tetrahydrofuran (1 : 3—10) mixture was used as the solvent, the catalysts was quite different in nature from those observed in the cyclohexane solvent. In the cases of the iron and cobalt catalysts, no active catalyst for the hydrogenation of styrene could be obtained at any molar ratio of 1—12. Furthermore, when a small amount of tetrahydrofuran was added the halfway through the rapid hydrogenation carried out in the cyaclohexane solvent, the rate of hydrogenation was considerably lowered, showing the presence of tetrahydrofuran to be unfavorable for the iron and cobalt catalysts. In the case of the nickel catalyst, on the other hand, an active catalyst was prepared in the cyclohexane-tetrahydrofuran solvent. As may be seen in Fig. 4, the optimum molar ratio for the hydrogenation of styrene was 1—12; this was a very much wider range than the optimum ratio of 0.3—2 observed in the cyclohexane solvent (Fig. 3).

Centrifugation of the Catalyst. Breslow and his co-workers[1b] have pointed out that the use of halogen derivatives of transition metals leads,

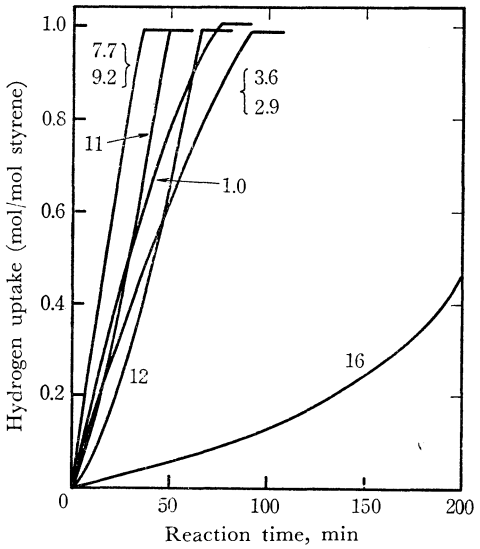

Fig. 4. Hydrogenation of styrene with the $NiCl_2$-$AlEt_3$ catalyst.
As 0°C and in cyclohexane/tetrahydrofuran solvent.
Numerals attached to the curves represent the $AlEt_3/NiCl_2$ ratios.

in general, to insoluble catalyst systems. In our experiments, the black-colored substance suspended well in a solvent and the black-colored substance did not separate from the solvent even when the mixture stood for several days. When the catalyst system was centrifuged (2800 rpm), a black-colored precipitate was isolated, while the solvent was still black-colored. The precipitate and the solution were assumed to constitute the soluble and insoluble parts of the catalyst system respectively. The precipitate and the solution were then tested for the hydrogenation of styrene. The rates were taken as the reaction periods for 50% hydrogen uptake and are listed in Table 2. In general, both the solution and the precipitate were active in the hydrogenation, while there was a trend for the activity of the former or the latter to be predominant in the case of the nickel or the cobalt catalyst respectively. In the case of the nickel catalyst prepared in the cyclohexane - tetrahydrofuran solvent, only the solution was active, as may be seen in run 7. Since, in these experiments, the amount of the precipitate decreased with an increase in the molar ratio, and since only a small amount of the precipitate was isolated in runs 2, 4, and 6, the rate of the hydrogenation catalyzed by precipitates may depend on both the catalytic activity and the amount of the precipitate. However, the rate of the hydrogenation seems to be affected by the catalytic activity, rather than the amount, of the precipitate, since it was found in a preliminary experiment that the rate of the hydrogenation was very slightly affected by changing the amount of catalyst (1—0.1 times), and since a rapid hydrogenation occurred with a very small amount of the precipitate in runs 2 and 4.

TABLE 2. ACTIVITIES OF THE SOLUTION AND THE PRECIPITATE[a)]

Run	Catalyst	Molar ratio[b)]	Solution[c)]	Precipitate[c)]
1	Fe	1.00	29	51
2	Fe	3.60	51	10
3	Co	1.01	63	15
4	Co	3.58	(585)	34
5	Ni	1.02	18	24
6	Ni	5.99	240	(3900)
7	Ni[d)]	4.63	124	e)

a) For the hydrogenation of styrene. MCl_n: 0.003 mol; Reaction temp.: 35°C
b) $Al(C_2H_5)_3/MCl_n$
c) Activities are represented by reaction periods (min) for 50% hydrogen uptake.
d) In cyclohexane-tetrahydrofuran solvent.
e) Only 1% of hydrogen was absorbed during the reaction period of 300 min.

Styrene-treatment of the Nickel Catalyst. In the previous publications,[8,10)] it has been reported that, when the catalyst prepared by the use of a Grignard reagent or lithium aluminum hydride was treated with styrene under a nitrogen atmosphere, ethyl benzene was formed by the hydrogen migration from the catalyst to styrene. We applied this styrene-treatment to the nickel catalysts prepared in the cyclohexane - tetrahydrofuran solvent at the molar ratio of 6.0. 1) One of the catalysts was treated with styrene under nitrogen (at 35°C, for 8 hr) immediately after the preparation of the catalyst; 0.08 mol of ethylbenzene was formed per mol of nickel chloride. 2) The other catalyst was stirred under hydrogen for 20 min*[2] after the preparation of the catalyst. Thereafter, the atmosphere was switched to nitrogen and the catalyst was treated with styrene; 0.35 mol of ethylbenzene was thus formed per mole of nickel chloride.

Formation of the Catalyst. It is felt that the strict dependence of the catalytic activity on the molar ratio is strong evidence that metallic component does not furnish an active sites. If the catalysts are finely-divided metal, as Lapporte reported,[2)] the fact that a higher molar ratio lowers the catalytic activity can not be explained. In fact, however, Lapporte operated under conditions which were not as mild as ours. The agreement in the molar ratio dependence between the present catalysts and the transition metal hydride catalysts prepared by the use of a Grignard reagent or lithium aluminum hydride suggests that the active sites of the present catalysts are, at least in part, transition-metal-hydride in character.

*[2] No gas absorption was observed during the treatment.

Three processes for the transition metal hydride formation are possible: (a) the elimination of ethylene from the transition metal - ethyl bonds; (b) the absorption of hydrogen on the transition metal, and (c) the hydrogenolysis of the transition metal - ethyl bonds. However, the elimination of ethylene to give transition metal hydride is improbable, since the greater part of the gas evolved during the preparation of the catalyst was ethane, as may be seen in Table 1. Ethylene might not be observed if it polymerized immediately, but the catalyst was found to be inactive in the polymerization of ethylene under the conditions employed. When the reaction of transition metal chloride with triethylaluminum was carried out under nitrogen and the atmosphere was switched to hydrogen, a sluggish gas absorption was observed if cyclohexane was used as the solvent, while no gas absorption occurred if a cyclohexane - tetrahydrofuran mixture was used as the solvent. The gas absorption might result from the reaction of the transition metal with hydrogen to form transition-metal-hydride sites, but in view of the sluggishness of the gas absorption, it appears improbable that the hydride sites thus formed can be intermeditaes in the relatively rapid hydrogenation of olefin which we observed.

The hydrogenolysis of metal - ethyl bonds to give transition-metal hydride and ethane seems to offer the most probable explanation for the formation of transition-metal-hydride sites without any apparent gas absorption, and for the fact that the amount of ethylbenzene formed in the styrene-treatment of the nickel catalyst increased considerably if the catalyst was pre-treated with hydrogen.

$$M\text{-}Cl \xrightarrow{Al(C_2H_5)_3} M\text{-}C_2H_5 \xrightarrow{H_2} M\text{-}H + C_2H_6 \uparrow$$

In order to establish the hydrogenolysis process, the ethane which was formed in the hydrogen-treatment of the catalyst component was determined. As may be seen in Fig. 5, ethane was formed rapidly.

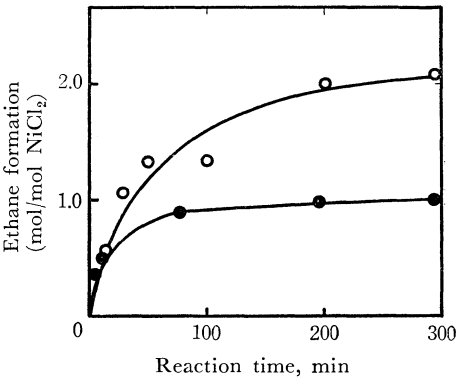

Fig. 5. Ethane formation in the hydrogen-treatment of the $NiCl_2$-$AlEt_3$.
○: molar ratio=2.2, at 35°C, in cyclohexane solvent.
●: molar ratio=2.2, at 35°C, in cyclohexane-tetrahydrofuran solvent.

Although no gas absorption was observed during the hydrogen-treatment of the nickel catalyst in the cyclohexane - tetrahydrofuran solvent (Expt. 1 in Table 1), about 2 mol of ethane was formed per mole of nickel chloride, confirming the hydrogenolysis process described above.

BULLETIN OF THE CHEMICAL SOCIETY OF JAPAN VOL. 42 1668—1678 (1969)

Benzylidenation of L-Sorbose[1—3]

Takashi MAEDA, Mitsuru KIMOTO (née KATSUHARA), Shigeru WAKAHARA and Kanji TOKUYAMA

Shionogi Research Laboratory, Shionogi & Co., Ltd., Fukushima-ku, Osaka

(Received September 15, 1968)

The acid-catalyzed benzylidenation of L-sorbose (I) was studied. The reaction by Reichstein's procedure gave a mixture of two diastereomeric 2,3:4,6-di-*O*-benzylidene-α-L-sorbofuranoses (III and IV), which were then successfully separated by preparative thin-layer chromatography. The use of slightly acidic conditions yielded 1,3:4,6-di-*O*-benzylidene-β-L-sorbofuranose (XI), 1,2:4,6-di-*O*-benzylidene-α- (XVII and XVIII) and -β-L-sorbofuranoses (XIX and XX), 1,2-*O*-benzylidene-α-L-sorbopyranoses (XXI and XXII), and 1,3-*O*-benzylidene-L-sorbose (XXIII). The absolute configurations at the acetal center of the five-membered benzylidene rings were assigned. A reaction sequence (I→(XXI, XXII⇄XXIII)→XI→IV→III) comparable with that of the ethylidenation of I was established.

1,2-*O*-Isopropylidene-α-L-sorbopyranose has been proposed as a key intermediate in the acetonation of L-sorbose(I)yielding 2,3:4,6-di-*O*-isopro-pylidene-α-L-sorbofuranose.[4] However, in the course of recent studies of the acetonation of I using weakly acidic conditions, we have isolated for the first time several types of isomers such as 1,3:4,6-di-*O*-isopropylidene-β-L-sorbofuranose,[5] and 1,3:4,6-di-*O*-isopropylidene-α-[6] and -β-L-sorbofuranoses.[5] The presence of these isomers suggests the complicated nature of the acetalation of I. More recently, ethylidenated L-sorboses corresponding to the acetonated ones have also been isolated from the ethylidenation of I under weakly acidic conditions, and a reaction sequence of the ethylidenation has been established as follows: I→[1,2-*O*-ethylidene-α-L-sorbopyranose ⇄ 1,3-*O*-ethylidene-α-L-sorbopyranose (1,3-*O*-acetal)] → 1,3:4,6-di-*O*-ethylidene-β-L-sorbofuranose(1,3:4,6-di-acetal) → 2,3:4,6-di-*O*-ethylidene-α-L-sorbofuranose.[2]

An important difference between the acetonation and the ethylidenation is that, with the former, a compound corresponding to the 1,3-*O*-acetal was not isolated, a fact probably explainable in terms of the Brown-Brewster-Schechter rule.[7] A pathway from the 1,3-*O*-acetal to the 1,3:4,6-di-*O*-acetal seemed to be required in the acetalations of I. The idea of the existence of this important pathway from a pyranose to a furanose would receive strong support if compounds of the 1,3-*O*-acetal type could be found in other acetalation reactions. From this point of view, we have described the benzylidenation of I with benzaldehyde. The structures of the products were determined by proton magnetic resonance (PMR) spectroscopic and chemical evidence. The PMR data are reported in Tables 1 and 2, and some of the spectra are shown in Figs. 1—4, which also indicate a clue to the elucidation of the diastereomeric configurations at the acetal centers of the products.

Reichstein and Grüssner[8] reported that the reaction of I with benzaldehyde in the presence of an acid gave a brown syrup. We could separate this syrup into two dibenzylidene-L-sorboses, III and IV, by preparative thin-layer chromatography. As the oxidation of the syrup mixture of III and IV afforded L-xylo-hexulosonic acid in good yield,[8] III and IV can be said to be diastereomeric 2,3:4,6-di-*O*-benzylidene-α-L-sorbofuranoses. The facts that III and IV reacted with trityl chloride-pyridine to yield tritylates (V and VI respectively) and with acetic anhydride-pyridine to give acetates (IIIa and IVa respectively) (see Figs. 1 and 2) supported their structures. The general characteristics of the PMR data of III and IV, especially the small coupling constants of $J_{3,4}$ (0.5 Hz),[5,9,10] leave no doubt that they have a furanose ring. As the phenyl group is equatorial in the chair con-

1) Sorboses XIV. For Part XIII, See Ref. 2.

2) T. Maeda, M. Kiyokawa and K. Tokuyama, This Bulletin, **42**, 492 (1969).

3) Some of the results of this paper have appeared in a preliminary form in T. Maeda and K. Tokuyama, *Tetrahedron Letters*, **1968**, 3079.

4) K. Tokuyama, E. Honda and N. Hōki, *J. Org. Chem.*, **29**, 133 (1964).

5) T. Maeda, This Bulletin, **40**, 2122 (1967).

6) K. Tokuyama and E. Honda, *ibid.*, **37**, 591 (1964).

7) H. C. Brown, J. H. Brewster and H. Schechter, *J. Am. Chem. Soc.*, **76**, 467 (1954).

8) T. Reichstein and A. Grüssner, *Helv. Chim. Acta*, **17**, 311 (1934).

9) T. Maeda, K. Tori, S. Satoh and K. Tokuyama, This Bulletin, **41**, 2495 (1968).

10) J. D. Stevens and H. G. Fletcher, Jr., *J. Org. Chem.*, **33**, 1799 (1968).

Table 1. Chemical shifts in $CDCl_3$ (τ)[a]

Compound	H_1, H_1'	H_3	H_4	H_5	H_6, H_6'	Benzylic H of 1,3-dioxolane	Benzylic H of 1,3-dioxane	OAc	Aromatic H	Other H
III	~6.07[b]	5.27	5.41	~5.76[b]	~5.53,[b] ~5.97[b]	3.80	4.55		2.4—2.8	OH, 7.83
IIIa	5.34, 5.64 (5.15, 5.47)	5.32 (5.23)	5.40 (5.87)	5.75 (6.32)	5.52, 5.95 (5.79, 6.58)	3.80 (3.86)	4.55 (4.89)	8.12 (8.49)	2.5—2.7 (2.3—3.0)	
IV	~6.03[b]	5.30	5.50	5.77	5.57, 5.98	4.07	4.58		2.5—2.8	OH, 7.67
IVa	5.33, 5.61 (5.21, 5.46)	5.37 (5.34)	5.50 (5.88)	5.73 (6.07)	5.70, 5.97 (5.82, 6,59)	4.07 (4.09)	4.58 (4.91)	8.02 (8.40)	2.5—2.7 (2.3—2.9)	
V	6.26, 6.55	5.13	5.47	~5.78[b]	~5.63,[b] ~6.03[b]	3.80	4.67		2.3—2.9	
VIII	~6.12[b]	5.38	5.58	5.5	6.1[b]		4.56			OH, 7.93
IX	~5.61[b]	5.43	4.53	5.31	5.65, 5.87	3.77		7.89, 7.92, 8.00	2.62	
X	~5.58[b]	5.48	4.63	5.33	5.62, 5.88	4.07		7.87, 7.88, 7.95	2.5—2.6	
XI	5.71, 6.01	5.3			6.1[b]		4.47 4.53		2.5—2.8	OH, 5.98
XV	5.56, 6.09	5.67	4.62	5.15	5.7— 5.8[b]		4.53	7.92(6H)	2.5—2.8	OMe, 6.68
XVIIa	5.45, 5.78 (5.47, 5.77)	4.61 (4.50)	5.5 (5.97)	(6.17)	5.8,[b] 5.95 (5.80, 6.55)	4.04 (3.93)	4.55 (4.88)	8.01 (8.30)	2.5—2.7 (2.3—3.0)	
XVIIIa	5.53, 5.77 (5.50, 5.80)	4.76 (4.70)	5.5 (6.01)	(6.16)	5.8,[b] 5.92 (5.87, 6.63)	4.21 (4.07)	4.54 (4.90)	7.89 (8.23)	2.4—2.7 (2.2—3.0)	
XIXa	5.73, 5.90 (5.73, 5.85)	4.60 (4.42)	5.5 (5.93)	6.38	6.1[b] (5.73, 6.49)	3.80 (3.68)	4.60 (4.80)	7.94 (8.43)	2.6—2.8 (2.2—3.0)	
XXa	5.77, 5.95 (5.78, 6.15)	4.50 (4.40)	5.5 (6.00)	(6.43)	6.1[b] (5.74, 6.51)	3.97 (4.07)	4.56 (4.80)	7.89 (8.38)	2.2—2.8 (2.1—3.0)	
XXIa	5.82, 6.15 (5.92, 6.19)	4.87 (4.73)	4.47 (4.18)	4.98 (4.86)	6.1— 6.3[b] (6.2— 6.4)[b]	3.95 (3.96)		7.87, 7.98, 8.02 (8.25(6H), 8.42)	2.5—2.7 (2.4—3.0)	
XXIIa	5.95, 6.02 (5.88, 6.19)	4.82 (4.68)	4.45 (4.21)	4.95 (4.83)	6.0— 6.2[b] (6.1— 6.3)[b]	4.00 (4.08)		7.95, 7.98(6H) (8.27, 8.33, 8.35)	2.4—2.7 (2.3—3.0)	
XXIV	5.73, 6.07 (5.73, 6.25)	5.67 (5.82)	4.57 (4.58)	~5.2[b] (~5.3)[b]	5.5—5.8[b] (5.5—5.8)[b]		4.50 (4.73)	7.88, 7.95 (8.28, 8.31)	2.5—2.8 (2.3—2.9)	OH [c] OH [c]
XXV	5.9 — 6.5[b] (5.9 — 6.9)[b]		4.43 (4.58)	4.96 (~4.75)[b]	5.9— 6.5[b] (5.9— 6.9)[b]		4.43 (4.81)	7.95, 7.97 (8.27, 8.37)	2.5—2.8 (2.4—3.0)	OH [c] OH [c]
XXVI	5.31, 5.67 (5.15, 5.85)	5.17 5.29	4.57 (4.61)	~5.1[b] (~5.2)[b]	5.6— 5.8[b] (5.6— 5.8)[b]		4.37 (4.58)	7.92, 7.94(6H) (8.32(6H), 8.36)	2.5—2.7 (2.4—3.0)	
XXVII	5.62, 6.42	6.30	4.36	4.97	6.13, 6.40		4.45	7.97(6H)	2.5—2.8	OMe 6.64

a) Values in parentheses are those observed in C_6D_6.
b) Unresolved.
c) Obscured.

TABLE 2. COUPLING CONSTANTS (J, Hz)

Compound	$J_{1,1'}$	$J_{3,4}$	$J_{4,5}$	$J_{5,6}$	$J_{5,6'}$	$J_{6,6'}$	Other J
III	a)	0.5	2.5	~2	~2	a)	
IIIa	(−)12.0	0.5	2.5	~2	2.0	(−)13.0	
IV	a)	0.5	2.5	~2	2.0	(−)13.0	
IVa	(−)12.0	0.5	2.5	~2	2.0	(−)13.0	
V	9.8	0.5	2.5	a)	a)	a)	
VIII	a)	0.5	2.5	a)	a)	a)	
IX	a)	0.5	3.6	5.0	7.0	(−)11.5	
X	a)	0.5	3.0	5.0	7.0	(−)11.5	
XI	(−)12.0	a)	a)	a)	a)	a)	
XV	(−)12.0	0.5	6.0	a)	a)	a)	$J_{1,3}\leq 0.5$
XVIIa	(−) 9.0	0.5	3.0	~2	2.0	(−)13.0	
XVIIIa	(−) 9.0	0.5	3.0	~2	2.0	(−)13.0	
XIXa	(−) 9.0	0.5	3.0	~2	2.0	(−)13.0	
XXa	(−) 9.0	0.5	3.0	~2	2.0	(−)13.0	
XXIa	(−) 9.2	9.6	9.6	a)	a)	a)	
XXIIa	(−) 9.3	9.6	9.3	a)	a)	a)	
XXIV	(−)12.0	0.5	4.5	a)	a)	a)	$J_{1,3}\leq 0.5$
XXV	a)	~9.5	~9.5	a)	a)	a)	
XXVI	(−)12.0	0.5	5.5	a)	a)	a)	$J_{1,3}\leq 0.5$
XXVII	(−)12.0	10.0	9.3	6.3	10.7	(−)10.7	

a) Not determinable.

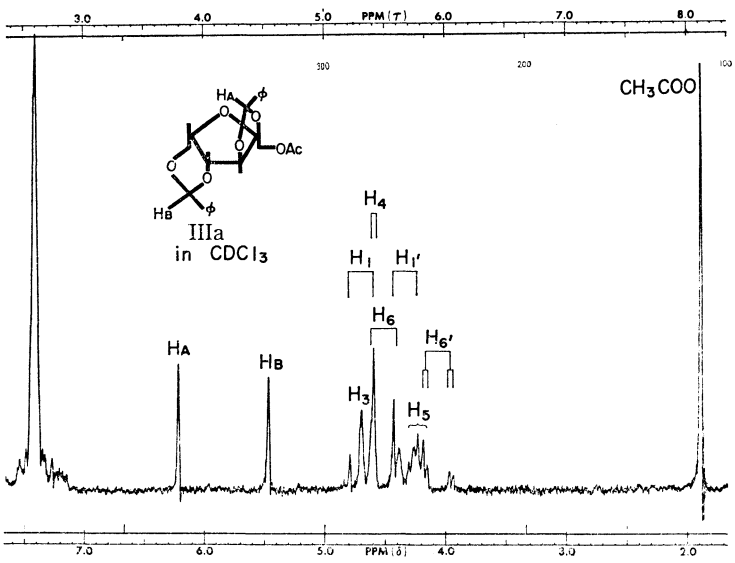

Fig. 1. PMR spectrum of IIIa in $CDCl_3$ at 60 MHz.

formation of the six-membered 4,6-*O*-benzylidene group, the diastereomerism between III and IV must be caused by the five-membered 2,3-*O*-benzylidene ring. The benzylic proton signals of III and IV in $CDCl_3$ appear at τ 3.80 and 4.55 and at τ 4.07 and 4.58 respectively. It is well known that a benzylic proton of 1,3-dioxolane resonates at a lower field than that of 1,3-dioxane.[11] The signals observed at τ 3.80 and 4.07 can be assigned to the benzylic protons of 2,3-*O*-benzylidenacetals. This assignment was supported by the benzylic proton signal (τ 4.56) of 4,6-*O*-benzylidene - 2,3 - *O* - isopropylidene - α - L - sorbofuranose (VIII), which was derived from 2,3-*O*-isopropylidene-α-L-sorbofuranose (VII)[12] and which was hydrolyzed to the starting material quantitatively.

11) N. A. Baggett, K. W. Buck, A. B. Foster and J. M. Webber, *J. Chem. Soc.*, **1965**, 3401, and earlier papers in this series.

12) T. I. Temnikova and V. V. Sklyarava, *Zh. Prikl. Khim.*, **21**, 1131 (1954); *Chem. Abstr.*, **49**, 2952 (1955).

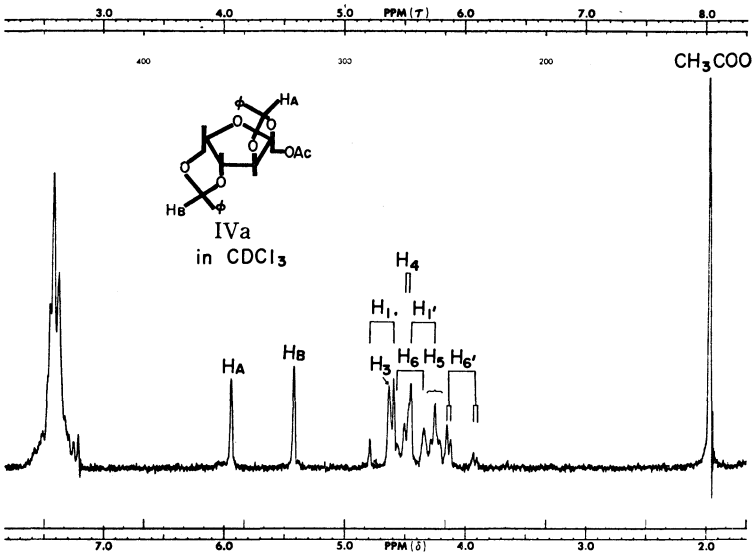

Fig. 2. PMR spectrum of IVa in $CDCl_3$ at 60 MHz.

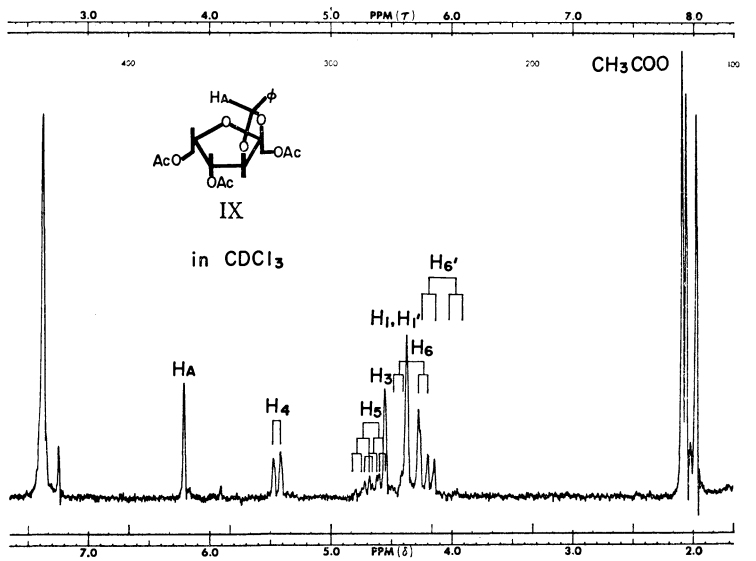

Fig. 3. PMR spectrum of IX in $CDCl_3$.

The selective removal of the 4,6-*O*-benzylidene rings of III and IV, followed by acetylation, yielded two 1,4,6-tri-*O*-acetyl-2,3-*O*-benzylidene-α-L-sorbofuranoses, IX and X respectively; in them the spectra of the lower-field benzylic protons of the parent compounds, III and IV, remained unchanged (see Figs. 3 and 4). Thus, it was unequivocally established that III and IV are, respectively, H-*endo* and H-*exo*[11,13] diastereomers at the acetal center of the 2,3-*O*-benzylidene ring. Since benzylic protons on dioxolane rings fused directly to five-membered cyclic systems are deshielded when in the *endo* position,[2,11,14] III and IV are assigned the H-*endo* and H-*exo* configurations respectively. Recently, Ferrier and Hatton[13] reported the assignment of diastereomeric 1,2 : 3,5-di-*O*-benzylidene-α-D-xylofuranoses on the basis of the difference in benzylic protons in the chemical shifts at τ 3.83 (H-*endo*) and 4.10 (H-*exo*); these values are in good agreement with our findings for sorbose derivatives (see Chart I).

13) R. J. Ferrier and L. R. Hatton, *Carbohyd. Res.*, **5**, 132 (1967).

14) F. Kametani and Y. Minoura, paper presented at the Annual Meeting of the Pharmaceutical Society of Japan, Tokyo, April, 1968.

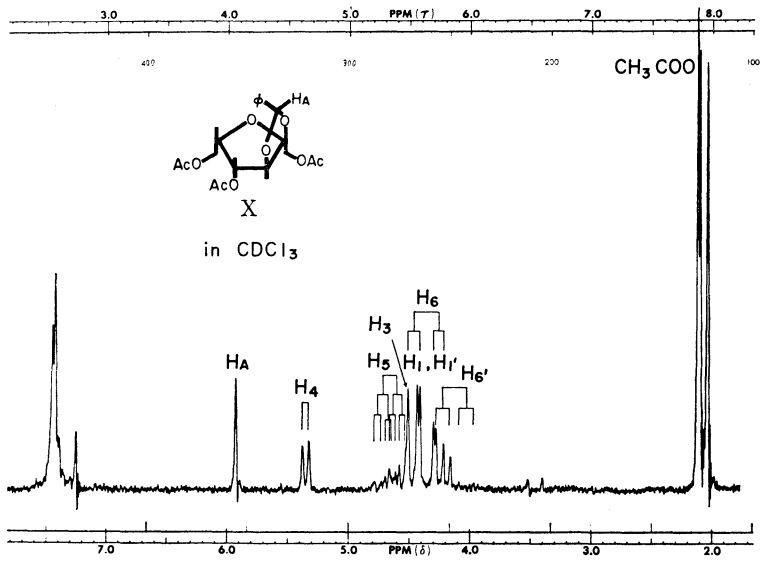

Fig. 4. PMR spectrum of X in $CDCl_3$ at 60 MHz.

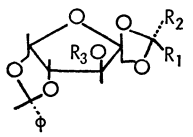

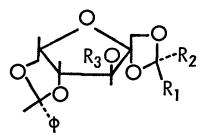

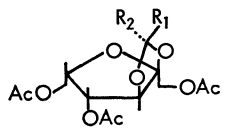

XVII $R_1 = \phi$, $R_2 = R_3 = H$

XVIIa $R_1 = \phi$, $R_2 = H$, $R_3 = Ac$

XVIII $R_1 = H$, $R_2 = \phi$, $R_3 = H$

XVIIIa $R_1 = H$, $R_2 = \phi$, $R_3 = Ac$

XIX $R_1 = \phi$, $R_2 = R_3 = H$

XIXa $R_1 = \phi$, $R_2 = H$, $R_3 = OAc$

XX $R_1 = H$, $R_2 = \phi$, $R_3 = H$

XXa $R_1 = H$, $R_2 = \phi$, $R_3 = Ac$

IX $R_1 = \phi$, $R_2 = H$

X $R_1 = H$, $R_2 = \phi$

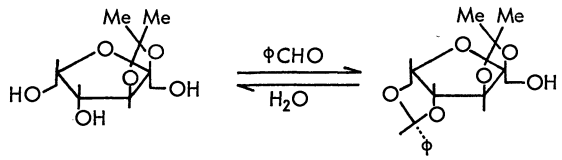

VII VIII

Chart I

The use of a trace of *p*-toluenesulfonic acid as a catalyst afforded mainly another dibenzylidene derivative (XI), which reduces a Fehling solution. The methylation of XI with methyl iodide in the presence of silver oxide yielded methyl glycoside (XII), which was also obtainable by the acetal interchange reaction of methyl 1,3:4,6-di-*O*-isopropylidene-*β*-L-sorbofuranoside (XIII)[5] with a large excess of benzaldehyde. The debenzylidenation of XII with 60% acetic acid, followed by acetylation, afforded methyl 1,3,4,6-tetra-*O*-acetyl-*β*-L-sorbofuranoside (XIV)[9] and partially debenzylidenated sorbofuranoside (XV). The PMR spectra of XV, showing a pattern closely related to that of the methyl 4,6-di-*O*-acetyl-1,3-*O*-isopropylidene-*β*-L-sorbofuranoside (XVI)[9] obtained from XIII by a similar procedure, suggest that the structure of XV is methyl 4,6-di-*O*-acetyl-1,3-*O*-benzylidene-*β*-L-sorbofuranoside. Therefore, the structure of XI was determined to be 1,3:4,6-*O*-benzylidene-*β*-L-sorbofuranose. The benzylic proton singlets at τ 4.47 and 4.53 in $CDCl_3$, showing the presence of two 1,3-dioxanes, also supported the proposed structure. The absence of diastereomers in XI is quite natural, since it has only 1,3-dioxanes (see Chart II).

TABLE 3. THE ASSIGNMENT OF THE ANOMERIC AND DIASTEREOMERIC CONFIGURATIONS OF 1,2:4,6-DI-*O*-BENZYLIDENE-L-SORBOFURANOSES

Compound	$[\alpha]_D$	IR spectra OH (in CCl_4)	PMR spectra Benzylic H of 1,2-*O*-ring (in $CDCl_3$)	Configuration	
				Anomeric	Diastereomeric
XVII	−31.0	3558 cm^{-1}	τ 4.04	α	H-*endo*
XVIII	+34.7	3556	4.21	α	H-*exo*
XIX	+22.7	3629	3.80	β	H-*endo*
XX	+166.6	3630	3.97	β	H-*exo*

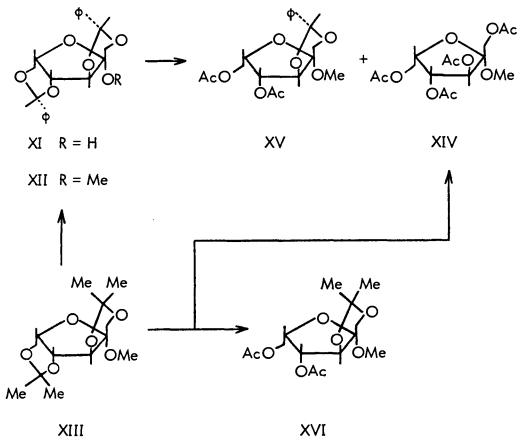

Chart II

When the benzylidenation reaction was carried out in dimethyl sulfoxide (DMSO), four non-reducing dibenzylidenated sorboses (XVII, XVIII, XIX, and XX) (see Table 3) and three mono-benzylidenated sorboses (the reducing XXIII and the non-reducing XXI and XXII) were isolated. The PMR spectra of their respective actates of XVII, XVIII, XIX, and XX, XVIIa, XVIIIa, XIXa, and XXa in C_6D_6[15] gave H_3 signals appearing at τ 4.40—4.73 in the AcO–CH region as somewhat broad singlets. The coupling constants of $J_{3,4}$ (0.5 Hz) furnished obvious evidence for their furanose structures.[9,10,13] Furthermore, two benzylic protons were observed at τ 3.80—4.21 (1,3-dioxolane) and τ 4.54—4.60 (1,3-dioxane) in each case. These results firmly established that XVII, XVIII, XIX, and XX are the anomeric and diastereomeric 1,2:4,6-di-*O*-benzylidene-L-sorbofuranoses.

Their anomeric configurations were substantiated by the use of the infrared spectra, where characteristic bands due to intramolecular hydrogen bonding between C_3–OH and C_2–O are sometimes present in α-anomers, but are always, absent in β-ones. Strong bands due to hydrogen bonding were observed in infinite dilute carbon tetrachloride solutions of XVII (3558 cm^{-1}) and XVIII (3556 cm^{-1}), but not in the cases of XIX (3629 cm^{-1}) and XX (3630 cm^{-1}). Therefore, XVII and XVIII were identified as α-anomers, and XIX and XX, as β-anomers. These identifications were in accord with the results of the optical rotation of the respective acetates XVIIa—XXa; the α-anomers (XVIIa and XVIIIa) showed negative signs of rotations, while the β-anomers (XIXa and XXa) showed positive signs, as was to be expected from the signs of the corresponding acetonated derivatives. The two α-anomers and β-anomers should differ only in stereochemistry at the acetal center of the 1,2-*O*-benzylidene ring. Model experiments indicated, for the H-*endo* configuration, the nearness of the benzylic proton of the 1,2-*O*-benzylidene ring to the ring oxygen of furanose and that of the acetoxy group of the α-anomer or H_3 of the β-anomer to the phenyl group of 1,2-*O*-benzylidene ring. Therefore, in the PMR spectra, benzylic proton signals should be deshielded,[11] and the acetoxy signal of the α-anomer,

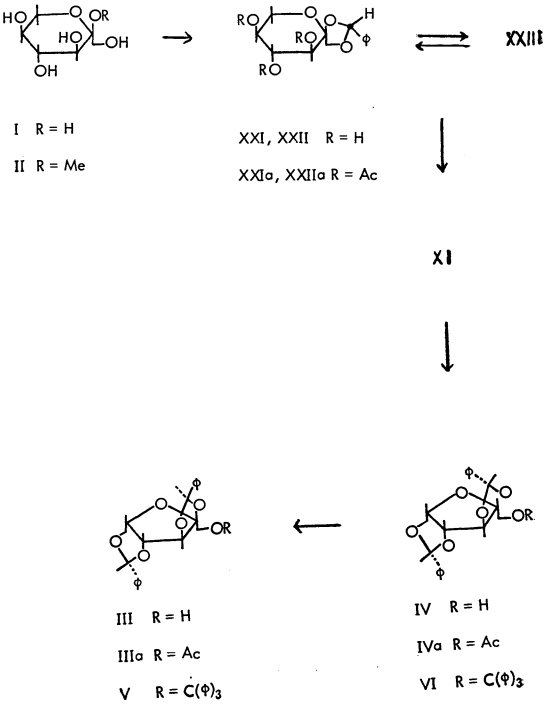

Chart III

15) The signals in C_6D_6 are more resolved than in $CDCl_3$.

and the H_3 signal of the β-anomer should be shielded,[16] when the position is H-*endo*. Table 1 obviously shows that, in each case, benzylic protons of the 1, 2-*O*-benzylidene rings of XVIIa and XIXa resonate at a field lower by 0.17 ppm than those of the corresponding anomers, XVIIIa and XXa respectively, while the acetoxyl of XVIIa and the H_3 of XIXa appear at a higher field than those of XVIIIa of XIXa appear at a higher field than those of XVIIIa and of XXa. Accordingly, XVIIa and XIXa were assigned the H-*endo* configuration, and XVIIIa and XXa, the H-*exo* (see Chart III).

The triacetates, XXIa and XXIIa, were very similar in IR and PMR spectra. The benzylic proton signals at τ 3.95 (XXIa) and 4.00 (XXIIa) (in $CDCl_3$)[16] fall into the range of 1,3-dioxolanes.[11,13,14] The coupling constants obtained, $J_{3,4}$, $J_{4,5}$, and $J_{5,6}$ are evidently the values of $J_{a,a}$, of pyranose in the 1C conformation.[17] Signals due to H_3, H_4, and H_5 appeared in the range of AcO–$\underset{|}{\overset{|}{C}}$H. The structures of XXI and XXII are, then, consistent with diastereomeric 1, 2-*O*-benzylidene-α-L-sorbopyranoses. They correspond to that of 1,2-*O*-isopyropylidene-α-L-sorbopyranose, which has been concluded to be the initial intermediate in the acetonation reaction of I.[4]

The acetylation of reducing monobenzylidene sorbose (XXIII) at an ordinary temperature gave three acetylated compounds, two reducing diacetates (XXIV and XXV) and one non-reducing triacetate (XXVI). These diacetates were methylated with methyl iodide in the presence of silver oxide to yield glycosides. The glycoside derived from XXIV was identified with XV, and the glycoside from XXV was identified with methyl 4,5-di-*O*-acetyl-1,3-*O*-benzylidene-α-L-sorbopyranoside (XXVII), which had been prepared by the benzylidenation[18] of methyl α-L-sorbopyranoside (II),[19] followed by acetylation. Therefore, the structure of XXIV and XXV were determined to be 4,6-di-*O*-acetyl-1,3-*O*-benzylidene-β-L-sorbofuranose and 4,5-di-*O*-acetyl-1,3-*O*-benzylidene-α-L-sorbopyranose respectively. These products showed that XXIII is 1,3-*O*-benzylidene-L-sorbose, an equilibrium mixture of 1,3-*O*-benzylidene-β-L-sorbofuranose (XXIIIf) and α-L-sorbopyranose (XXIIIp). The results of the optical rotationary dispersion (ORD) showing the absence of any carbonyl group (see Fig. 5), a value of optical rotation similar to those of XV and XXIV, and a small coupling constant of $J_{3,4}$ suggest that the structure of XXVI is 2,4,6-tri-*O*-acetyl-1,3-*O*-benzylidene-β-L-sorbofuranose.

The behavior of XXIII is very interesting. It may be considered to exist as the furanose (XXIIIf) in a crystalline state from its sharp melting point and its positive optical rotation in chloroform; however, it may be considered to be in an eqilibrium with the furanose (XXIIIf), a keto-form (XXIIIk) and the pyranose (XXIIIp) in solutions since the optical rotation, in pyridine, for instance, changes slowly with the time (see Chart IV).

During the course of these structure studies, an

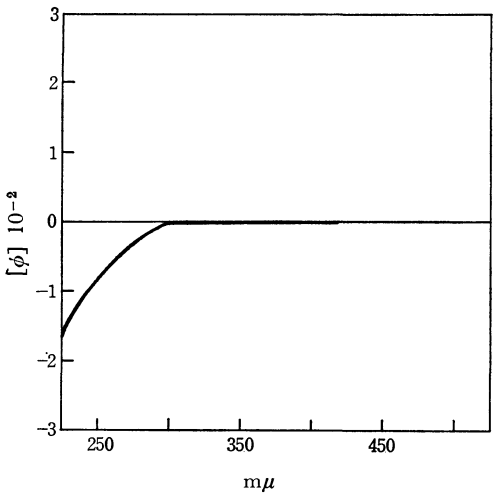

Fig. 5. The ORD curve for XXVI.

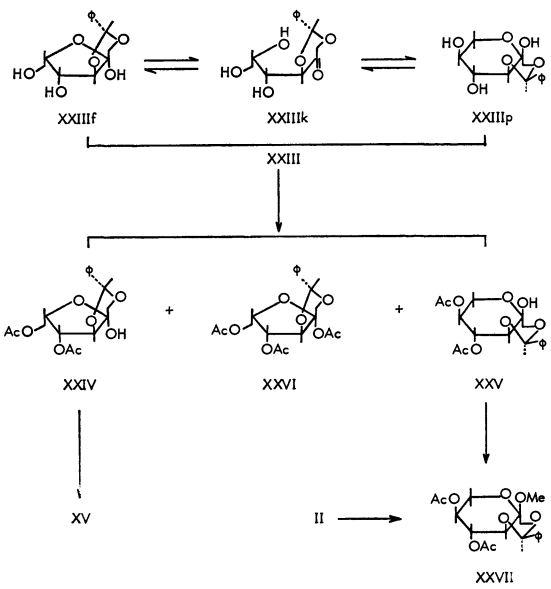

Chart IV

16) For example, see R. H. Bible, Jr., "Interpretation of NMR Spectra," Plenum Press, New York, N. Y. (1965).

17) a) F. W. Lichtenthaler and H. K. Yahya, *Tetrahedron Letters*, **1965**, 1805. b) F. W. Lichtenthaler and H. K. Yahya, *Chem. Ber.*, **100**, 2389 (1967). c) H. Paulsen, H. Köster and K. Heyns, *ibid.*, **100**, 2669 (1967).

18) D. Murphy, *J. Chem. Soc., C*, **1967**, 1732.

19) a) G. Arragon, *Compt. Rend.*, **199**, 1231 (1943). b) H. H. Schlubach and G. Graefe, *Ann.*, **532**, 211 (1937).

interesting transformation between III, IV and XI was observed. Under usual benzylidenation conditions, III and IV were the major products and the amounts of the others were negligibly small. The relative yields were checked by means of the PMR spectra using the benzylic proton singlets at τ 3.80 (III), 4.07 (IV), and 4.47 (XI) as the key signals; the results are reported in Table 4. Table 4 shows clearly that the reaction proceeds in the sequence of XI→IV→III. It has been suggested that the H-*exo* isomer is produced in a kinetic phase and that the H-*endo* isomer is preponderant at an equilibrium,[11,13] in the benzylidention of I, the H-*exo* isomer (IV) was also found as a kinetic product, indicating that the reaction occurred with the retention of the diastereomeric configuration at the acetal center in the step XI→IV.

As the monobenzylidenated compounds (XXI, XXII, and XXIII) were obtained under slightly acidic conditions, the benzylidenation of I can be said to proceed *via* a pathway, I→(XXI, XXII⇄XXIII)→XI→IV(H-*exo*)→III(H-*endo*), similar to that in the ethylidenation of I.[2] Since these types of ethylidenated and benzylidenated compounds correspond to the acetonated ones, the reaction pathway of the acetonation should be concluded to be the same as that above. A detailed discussion of this mechanism of the acetalation of I will be presented in following papers.

Experimental

All the melting points were recorded on a Kofler micro-stage apparatus and have been corrected.

The solvents used were removed under reduced pressure.

Thin-layer chromatography was carried out on a silica gel plate with benzene - ether (3:1 v/v, solvent A), ether - petroleum ether (5:1 v/v, solvent B; 2:1 v/v, solvent C; 1:1 v/v, solvent D; 1:2, solvent E), and chloroform - acetone (9:1 v/v, solvent F; 1:1, solvent G). Seliwanoff reagent[20] spray was used for detection; the R_f values are listed in Table 5. Preparative thin-layer chromatography was performed on silica gel with the same solvent systems as were used for detection, while the spots located with iodine vapor were extracted with either acetone or chloroform - methanol (9:1 v/v).

Table 4. Product-ratio (±5%) from the reaction of L-sorbose (I) (1.6 g) and benzaldehyde (40 ml) at 25°C for 6 hr in the presence of TsOH

Product	The acid concentration		
	0.1%	1.0%	10.0%
III	15.0	22.5	42.5
IV	35.0	55.0	52.5
XI	50.0	22.5	5.0

20) A. Anno and N. Seno, "Jikken Kagaku Kōza," Bd. 23, ed. by Chem. Soc. Japan, Maruzen, Tokyo (1957), p. 374.

The evaporation of the solvents gave the materials.

The optical rotations were determined in chloroform containing 1% ethanol unless otherwise stated, and the concentrations have been recorded in percentages. The ORD curve of XXVI was obtained for the methanol solution on a Nippon-Bunko ORD/UV 5 spectrometer.

The PMR spectra were measured on a Varian A-60A spectrometer using 5% solutions of the samples in either $CDCl_3$ or C_6D_6, with TMS used as the internal standard. The results obtained from the analysis of the spectra of the compounds examined are listed in Tables 1 and 2. Some of the spectra are shown in Figs. 1—4.

The IR spectra measurements of XVII, XVIII, XIX, and XX were made using a Nippon-Bunko DS402G infrared spectrometer and a 3.5±0.5 mg/8 m*l* solution in a carbon tetrachloride solution (in a 20 mm cell).

Benzylidenation of L-Sorbose (I). a) Dry hydrogen chloride (0.75 g) was introduced into a mixture of L-sorbose (I) (2.0 g) and benzaldehyde (48 m*l*). The mixture was stirred at room temperature for 6 hr and then stored in a refrigerator overnight. The clear solution was diluted with ether and the solution was washed with aqueous sodium bicarbonate, and then with water, dried, and the solvent removed. The syrup thus obtained was dissolved in chloroform, and the chloroform solution was washed with a sodium hydrogen sulfite solution, and then with water, and dried. The evaporation of the solvent gave a syrup (3.4 g) whose thin-layer chromatogram showed the presence of III and IV. From the syrup, III (0.28 g) and IV (0.11 g) were separated in pure states by repeated PTC (first with the solvent A and then two times with the solvent C).

III: plates (174 mg), mp 129—131°C (recrystallized from benzene - petroleum ether), $[\alpha]_D^{24}$ −8.7° (*c* 0.722). Found: C, 67.46; H, 5.59%; mol wt, 341. Calcd for $C_{20}H_{20}O_6$: C, 67.40; H, 5.66%; mol wt, 356.

IV: Amorphous powder, mp <51°C, $[\alpha]_D^{23}$ −10.6° (*c* 0.993). Found: C, 67.14; H, 5.52%; mol wt, 366. Calcd for $C_{20}H_{20}O_6$: C, 67.40; H, 5.66%; mol wt, 356.

b) A mixture of L-sorbose (I) (1.00 g), benzaldehyde (24m*l*), and TsOH (0.24 g) was stirred at room temperature. After 20 hr, the solution was worked up by the above-described procedure. A syrup (1.86 g) containing III, IV and XI was thus obtained. XI (9.5 mg) was isolated as plates by PTC with the solvent C followed by recrystallization from ethanol, mp 164.6—167°C, $[\alpha]_D^{22}$ +48.8° (*c* 0.934). Found: C, 67.48; H, 5.79%; mol wt, 363. Calcd for $C_{20}H_{20}O_6$: C, 67.40; H, 5.66%; mol wt, 356.

c) To a solution of L-sorbose (I) (10 g) in DMSO (60 m*l*), there were added benzaldehyde (100 m*l*) and conc. sulfulic acid (0.5 g). After stirring at room temperature for 3 days, the solution was neutralized with 2N sodium bicarbonate, dried, and evaporated. A crystalline syrup (8.47 g) was obtained by the same work-up as above. (i) The addition of ethanol to the syrupy crystals thus obtained gave XI (2.9g). The evaporation of the ethanol from the mother liquor yielded a syrup (4.91g). From the syrup, XVII, XVIII, XIX and XX were isolated by PTC (first with the solvent A and then with the solvent D). The isolated materials were further purified by recrystallization.

XVII: Cubics, mp 113.7—114.7°C (recrystallized from ether - petroleum ether; yield, 12 mg), $[\alpha]_D^{22}$ −31.0° (*c* 0.813). Found: C, 67.56; H, 5.72%; mol wt, 350.

TABLE 5. R_f VALUES OF THE BENZYLIDENATED COMPOUNDS ON A SILICA GEL PLATE

Compound	Solvent system						
	A	B	C	D	E	F	G
III	0.43	—	0.57	0.34	0.19	—	—
IIIa	—	—	—	0.43	0.17	—	—
IV	0.48	—	0.65	0.38	—	—	—
IVa	—	—	—	0.59	—	—	—
V	—	—	—	0.51	0.37	—	—
VI	—	—	—	0.74	0.56	—	—
IX	—	—	0.60	—	—	—	—
X	—	—	—	0.26	—	—	—
XI	0.78	—	0.82	0.60	—	—	—
XII	—	—	—	0.73	0.60	—	—
XIV	—	—	0.46	—	—	—	—
XV	—	—	0.59	—	—	—	—
XVII	0.54	—	0.45	—	—	—	—
XVIIa	—	—	0.65	—	—	—	—
XVIII	0.41	—	0.36	—	—	—	—
XVIIIa	—	—	0.64	—	—	—	—
XIX	0.27	—	0.28	—	—	—	—
XIXa	—	—	0.38	—	—	—	—
XX	0.20	—	0.20	—	—	—	—
XXa	—	—	0.39	—	—	—	—
XXI, XXII	—	—	—	—	—	—	0.15—0.43
XXIa	—	—	—	0.45	—	—	—
XXIIa	—	—	—	0.55	—	—	—
XXIII	—	—	—	—	—	—	0.43—0.65
XXIV	—	0.38	—	—	—	0.36	—
XXV	—	0.60	—	—	—	0.36	—
XXVI	—	0.60	—	—	—	0.70	—

Calcd for $C_{20}H_{20}O_6$: C, 67.40; H, 5.66%; mol wt, 356.

XVIII: Needles, mp 121.5—125°C (recrystallized from ethanol), $[\alpha]_D^{22}$ +34.7° (*c* 0.864). Found: C, 67.61; H, 5.81%; mol wt, 357. Calcd for $C_{20}H_{20}O_6$: C, 67.40; H, 5.66%; mol wt, 356.

XIX: Needles, mp 186—196°C (recrystallized from chloroform), $[\alpha]_D^{24}$ +22.7° (*c* 0.343). Found: C, 67.22; H, 5.76%; mol wt, 353. Calcd for $C_{20}H_{20}O_6$: C, 67.40; H, 5.66%; mol wt, 356.

XX: Needles, mp 148—154°C (recrystallized from ethanolpetroleum ether), $[\alpha]_D^{24}$ +166.6° (*c* 0.393). Found: C, 67.30; H, 5.66%; mol wt, 337. Calcd for $C_{20}H_{20}O_6$: C, 67.40; H, 5.66%; mol wt, 356.

(ii) The syrup (6.15 g was used) was separated into XXIII (1.38 g) and a mixture syrup of XXI and XXII (1.27 g) by PTC with the solvent G.

XXIII: Cubics, mp 183.5—184.6°C (recrystallized from methanol; yield, 342 mg), $[\alpha]_D^{23}$ +30.5° (*c* 0.387, methanol); $[\alpha]_D^{23}$ +36.0→+20.2° after 24 hr (*c* 0.962, pyridine); $[\alpha]_D^{23}$ +20.4° (*c* 0.984, DMSO). Found: C, 58.13; H, 6.03%; mol wt, 244. Calcd for $C_{13}H_{16}O_6$: C, 58.20; H, 6.01%; mol wt, 268.

The latter mixture, a syrup (1.27 g), was treated with acetic anhydride (13 m*l*) in pyridine (13 m*l*) in the usual way, and the reaction mixture was poured into ice water. From the resulting syrup, the triacetates XXIa and XXIIa were isolated by PTC with the solvent C. The isolated materials were then further purified by recrystallization.

XXIa: Needles, mp 126—131.5°C (recrystallized from ether; yield, 487 mg), $[\alpha]_D^{22}$ −125.2° (*c* 0.956). Found: C, 57.53; H, 5.62%; mol wt, 405. Calcd for $C_{19}H_{22}O_9$: C, 57.86; H, 5.62%; mol wt, 394.

XXIIa: Needles, mp 111—115°C (recrystallized from ether; yield, 118 mg), $[\alpha]_D^{23}$ −89.2° (*c* 0.937). Found: C, 57.94; H, 5.53%; mol wt, 396. Calcd for $C_{19}H_{22}O_9$: C, 57.86; H, 5.62%; mol wt, 394.

d) A mixture of L-sorbose (I) (1.6 g), and benzaldehyde (40m*l*) containing 0.1, 1.0 and 10.0% (w/v%) TsOH respectively was stirred at 25°C in a thermostat for 6 hr. The solution was then worked up much as in a). The PMR spectra of the resulting syrup was measured without further purification. The values are listed in the Table 4.

Tritylation of III and IV. a) A solution of III (139 mg) in pyridine (0.4 m*l*) was treated with trityl chloride (115 mg) at room temperature. After 2 days, the product was poured onto ice water, and the resulting syrup, separated from water by decantation, was taken up with chloroform. The chloroform solution was then washed with 1N HCl and water. The concentration of the dried solution and the purification of the residue by PTC with the solvent E and by recrystallization from ether gave V (122 mg) as cubics, mp 166—168°C, $[\alpha]_D^{23}$ −8.6° (*c* 0.985). Found: C, 78.20; H, 5.73%; mol wt, 601. Calcd for $C_{39}H_{34}O_9$: C, 78.24; H, 5.72%; mol wt, 599.

b) Needles of VI (40 mg) were obtained from IV

(118 mg) by the same procedure as that above. It had a mp of 195—197°C; $[\alpha]_D^{24}$ −20.4° (*c* 0.992). Found: C, 78.51; H, 5.83%; mol wt, 623. Calcd for $C_{39}H_{34}O_6$: C, 78.24; H, 5.72%; mol wt 599.

Acetylations of III and IV. a) A sample of III (122 mg) was acetylated in a mixture of acetic anhydride (3.0 m*l*) and pyridine (3.0 m*l*) in a refrigerator for 6 hr. The mixture was then poured onto crushed ice and neutralized with an excess of sodium hydrogen carbonate. The solution was extracted with chloroform; the chloroform solution was washed with water, 2N HCl, and water, dried with anhydrous magnesium sulfate and evaporated to a syrup. IIIa (93 mg) was then isolated by PTC with the solvent C; $[\alpha]_D^{24}$ −17.9° (*c* 1.617). Found: C, 66.23; H, 5.75%; mol wt, 411. Calcd for $C_{22}H_{22}O_7$: C, 66.32; H, 5.57%; mol wt, 398.

b) IV (218mg) gave IVa (217mg) as a syrup, $[\alpha]_D^{24}$ −12.1° (*c* 0.810). Found: C, 64.58; H, 5.43%; mol wt, 410.[21] Calcd for $C_{22}H_{22}O_7$: C, 66.32; H, 5.57%; mol wt, 398.

Hydrolysis of III and IV. a) A sample of III (150 mg) was hydrolyzed with 60% acetic acid (15m*l*) at 70°C. After 1.5 hr, the solvent was removed by the addition of an excess of ethanol and by subsequent evaporation. The residual syrup (112 mg) was acetylated with acetic anhydride (1.5 m*l*) and pyridine (1.5 m*l*) in a manner similar to that used for IIIa. The purification of the product by PTC with the solvent C gave IX (83mg) as a syrup; $[\alpha]_D^{23}$ −1.6° (*c* 0.973). Found: C, 57.96; H, 5.68%; mol wt, 401. Calcd for $C_{19}H_{22}O_9$: C, 57.86; H, 5.62%; mol wt, 394.

b) X (152 mg) was obtained from IV (600 mg) by the same work-up as that used for IX. It was a syrup, $[\alpha]_D^{22}$ −15.6° (*c* 0.286). Found: C, 56.17; H, 5.71%; mol wt, 434.[21] Calcd for $C_{19}H_{22}O_9$: C, 57.86; H, 5.62%; mol wt, 394.

Preparation of VIII from VII. A solution of VII (1.10 g) and benzaldehyde (0.55 g) in dioxane (10 m*l*) containing TsOH (0.50 g) was allowed to stand overnight at room temperature. The crystals thus deposited were then fitered. Recrystallization from acetone gave needles (1.2 g) of VIII; mp 207—208°C; $[\alpha]_D^{24}$ −8.0° (*c* 0.747, acetone). Found: C, 62.46; H, 6.74%. Calcd for $C_{16}H_{20}O_6$: C, 62.32; H, 6.64%.

Hydrolysis of VIII. VIII (0.5 g) was treated with 60% acetic acid (5 m*l*) at 70°C for 1.5 hr to yield VII quantitatively.

Acetylation of XI. XI (0.10 g) was not acetylated with acetic anhydride - pyridine or acetic anhydride-sodium acetate at 60°C; XI was thus recovered almost quantitatively.

Methylation of XI. XI (0.78 g) in methyl iodide (50 g) was refluxed for 24 hr in the presence of silver oxide (3.75 g). The cooled solution was filtered, and the filtrate evaporated. The recrystallization of the residue (1.02 g) from ethanol - petroleum ether gave XII (0.55 g) as needles mp 114—116°C, $[\alpha]_D^{23}$ +56.3° (*c* 0.959). Found: C, 68.13; H, 6.03; OCH_3, 8.40%; mol wt, 367. Calcd for $C_{21}H_{22}O_6$: C, 68.09; H, 5.99; OCH_3, 8.40%; mol wt, 370.

Preparation of XII from XIII. A mixture of XIII (98.5 mg),[5] benzaldehyde (10 g), and TsOH (10 mg) was stirred at room temperature. After 7.0 hr, a 2N sodium bicarbonate solution (1 m*l*) was added to the solution, which was then extracted with benzene. The benzene solution was evaporated to give a syrup, which was then purified by PTC using the solvent E. Recrystallization from ethanol gave XII as needles (20.6 mg), mp 114—115.5°C, this substance was found to be identical with XII by a study of the IR spectra, and by thin-layer chromatograms and admixture tests.

Hydrolysis of XII. XII (660 mg) was treated with 60% acetic acid at 50°C for 50 min. The mixture was then diluted with ethanol and evaporated. The resulting syrup (0.55 g) was acetylated in a way similar to that used for IIIa. The syrup (638mg) thus produced was separated into XIV (51 mg) and XV (245 mg) by PTC with the solvent C. The isolated materials were then further purified by recrystallization.

XIV: Needles (15 mg), recrystallized from ether-*n*-hexane; this substance was identified with an authentic sample.[9]

XV: Needles, mp 87.5°C (recrystallized from ethanol; yield, 42mg); $[\alpha]_D^{21}$ +23.5° (*c* 0.970). Found: C, 58.58; H, 5.97%; mol wt, 364. Calcd for $C_{18}H_{22}O_8$: C, 59.01; H, 6.05%; mol wt, 366.

Acetylations of XVII, XVIII, XIX and XX. The acetates, XVIIa, XVIIIa, XIXa and XXa were obtained from XVII, XVIII, XIX and XX, respectively in the same manner as has been described for the preparation of IIIa.

XVIIa: Syrup; $[\alpha]_D^{22}$ −38.6° (*c* 1.083). Found: C, 66.44; H, 5.56%; mol wt, 411. Calcd for $C_{22}H_{22}O_7$: C, 66.32; H, 5.57%; mol wt, 398.

XVIIIa: Needles, mp 144.5−146°C (recrystallized from ethanol); $[\alpha]_D^{22}$ −28.6° (*c* 0.979). Found: C, 66.29; H, 5.55%; mol wt, 412. Calcd for $C_{22}H_{22}O_7$: C, 66.32; H, 5.57%; mol wt, 398.

XIXa: Syrup; $[\alpha]_D^{22}$ +34.4° (*c* 0.987). Found: C, 66.79; H, 5.40%; mol wt, 392. Calcd for $C_{22}H_{22}O_7$: C, 66.32; H, 5.57%; mol wt, 398.

XXa: Needles, mp 136.5—139°C (recrystallized from ether-petroleum ether); $[\alpha]_D^{22}$ +147.1° (*c* 0.961). Found: C, 66.34; H, 5.67%; mol wt, 410. Calcd for $C_{22}H_{22}O_7$: C, 66.32; H, 5.57%; mol wt, 398.

Acetylation of XXIII. a) To a cooled solution (−5—−6°C) of XXIII (387 mg) in pyridine (4 m*l*), acetic anhydride (4 m*l*) was added. After storage in a refrigerator for 16 hr, the mixture was worked up much as IIIa had been to give a syrup (530 mg). From the syrup, XXIV (107 mg) was isolated in a pure state by PTC with the solvent B. Another syrup (160 mg) was obtained which contained mixture of XXVI major and XXV minor.

XXIV: Syrup, $[\alpha]_D^{23}$ −3.3° (*c* 0.859). Found: C, 57.96; H, 5.77%; mol wt, 363. Calcd for $C_{17}H_{20}O_8$: C, 57.95; H, 5.72%; mol wt, 352.

b) XXIII (351mg) was acetylated at room temperature for 16 hr. The resulting syrup (686 mg) was then separated into XXV (39 mg) and XXVI (349 mg) by repeated PTC (first with the solvent B and then with the solvent F.).

XXV: Needles, mp 181—183.5°C (recrystallized from chloroform - petroleum ether; yield, 19 mg), $[\alpha]_D^{23}$ −47.6° (*c* 0.550). Found: C, 57.77; H, 5.76%; mol wt, 373. Calcd for $C_{17}H_{20}O_8$: C, 57.95; H, 5.72%; mol wt, 352.

XXVI: Cubics, mp 75—77°C (recrystallized from

21) It was difficult to analyze correctly, because of its hygroscopic nature. However, the interpretation of the PMR spectrum supported the formula given.

aqueous ethanol; yield, 290 mg); $[\alpha]_D^{24}$ −10.5° (*c* 0.703). Found: C, 58.02; H, 5.64%; mol wt, 402. Calcd for $C_{19}H_{22}O_9$: C, 57.86; H, 5.62%; mol wt, 394. The ORD curve is shown in Fig. 5.

Methylation of XXIV. XXIV (44 mg) was methylated in a way similar to that used for XI. The recrystallization of a crude products (46 mg) gave cubics (9 mg) of XV; mp 87—88°C.

Methylation of XXV. XXV (92.5 mg) was methylated by the same procedure as was used for XI. The recrystallization of the residue (81 mg) gave XXVII (62 mg) as needles, mp 185—186°C; $[\alpha]_D^{23}$ −74.0° (*c* 0.995). Found: C, 59.09; H, 6.02%; mol wt, 364. Calcd for $C_{18}H_{22}O_8$: C, 59.01; H, 6.05%; mol wt, 366.

Preparation of XXVII from II. A mixture of II[19] (3.0 g), benzaldehyde (30 m*l*), and conc. sulfuric acid (0.15 g) was stirred at room temperature for 4 hr. The solution was then neutralized with a 2N K_2CO_3 solution and evaporated to a thick syrup. Methyl 1,3-*O*-benzylidene-α-L-sorbopyranoside[18] (202 mg) isolated as needles by PTC with the solvent *G* (R_f 0.47—0.58), followed by recrystallization from chloroform-ether. It had a mp of 187—188°C, and $[\alpha]_D^{23}$ −55.0° (*c* 0.936); Murphy[18] reported the values of mp 183—184°C and $[\alpha]_D$ −54.6° (*c* 1.06). The crystals (151 mg) were acetylated in the usual manner with acetic anhydride - pyridine. Needles (*c* 161 mg) of XXVII were obtained by recrystallization from ethanol; mp 186—186.5°C.

The authors express their deep gratitude to professor Toshihiko Okamoto, The University of Tokyo, and Dr. Ken'ichi Takeda, Director of this laboratory, for their encouragement. They are also indebted to Drs. Kazuo Tori, Shiroh Satoh and Kaoru Kuriyama for their useful discussions.

BULLETIN OF THE CHEMICAL SOCIETY OF JAPAN VOL. 42 1678—1683 (1969)

Mass Spectrometry of Tautomeric Compounds. I. Absence of Keto-Enol Tautomerism in Fragment Ions

Hisao NAKATA

Department of Chemistry, Aichi Kyoiku University, Daiko-cho, Higashi-ku, Nagoya

and Akira TATEMATSU

Faculty of Pharmacy, Meijo University, Showa-ku, Nagoya

(Received October 18, 1968)

In order to examine a possibility of keto-enol tautomerism in molecular and fragment ions, diethyl di-*n*-butylmalonate (Ia), methyl 2-*n*-butylhexanoate (IIa), and 2,2-di-*n*-propyl-5,5-dimethyl-1,3-cyclohexanedione (IIIa) were synthesized and their mass spectra were compared with those of respective mono-alkyl derivatives, Ib, IIb, and IIIb. The first step of the fragmentation of each dialkyl compounds is the cleavage of one of the alkyl side chains by McLafferty rearrangement to give an enol fragment ion (E). Comparisons of the behavior of this enol fragment ion with that of the corresponding molecular ion (K) of mono-alkyl derivatives indicate that the keto and enol forms of these compounds exhibited entirely different fragmentation patterns. Thus, the enol fragment ion of *m/e* 216 from Ia loses $C_3H_7\cdot$ through the allylic cleavage of an enol double bond to give an abundant *m/e* 173 peak, while the keto ion of *m/e* 216 from Ib loses C_4H_8 to afford a strong *m/e* 160 peak. In a similar manner, the enol fragment ion of *m/e* 130 from IIa gives an intense peak at *m/e* 87, and the keto ion of *m/e* 130 from IIb yields an ion at *m/e* 74. In the spectrum of IIIa, a peak at *m/e* 140 that is observed in the IIIb spectrum did not appear. These results clearly suggest that no keto-enol tautomerism takes place in these ions in a mass spectrometer.

During the course of an investigation of mass spectrometry of barbituric acid derivatives[1] we have found that the keto and enol forms of ethylbarbituric acid showed different fragmentation patterns, and therefore, a suggestion has been made[1] that no keto-enol tautomerism of this compound occurred in a mass spectrometer. We now extended the work to other tautomeric systems to clarify the correlation between mass spectrometry and prototropic rearrangement.

It is possible to produce unstable enol intermediates in a mass spectrometer by utilizing the well-

1) H. Nakata, A. Tatematsu, H. Tsuyama and H. Doi, *Shitsuryo Bunseki (Mass Spectroscopy)*, **5**, 112 (1967).

defined McLafferty rearrangement[2-4] of suitably chosen compounds. We have synthesized diethyl di-*n*-butylmalonate (Ia), methyl 2-*n*-butylhexanoate (methyl di-*n*-butylacetate) (IIa), and 2, 2-di-*n*-propyl-5,5-dimethyl-1,3-cyclohexanedione (IIIa), and their corresponding mono-alkyl derivatives (Ib, IIb, and IIIb). The mass spectra of these compounds are shown in Figs. 1—6.

The first step of the fragmentation of these dialkyl compounds is the cleavage of one of the alkyl side chains by the McLafferty rearrangement to give an enol fragment ion, *e.g.*, E. The corresponding ion of the keto form, *e.g.*, K, is identical with the molecular ion of mono-alkyl derivatives. Therefore, if we compare the mass spectral behavior of these enol fragment ions with that of respective mono-alkyl derivatives, it can be seen whether or not the keto-enol tautomerism, E⇌K, takes place in a mass spectrometer.

From spectra shown in Figs. 1 and 2, it is clear that the keto and enol forms of mono-*n*-butylmalo-

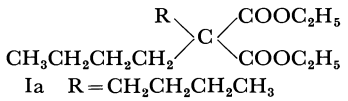

Ia R=$CH_2CH_2CH_2CH_3$
Ib R=H

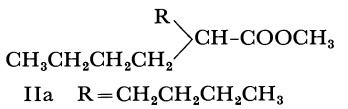

IIa R=$CH_2CH_2CH_2CH_3$
IIb R=H

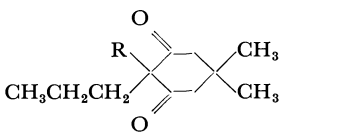

IIIa R=$CH_2CH_2CH_3$
IIIb R=H

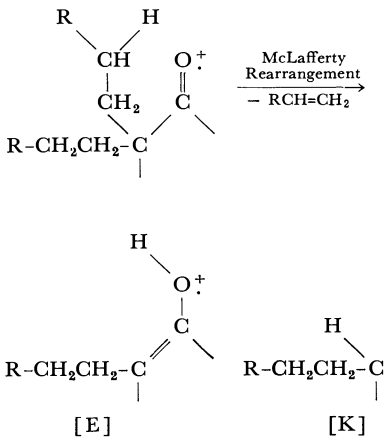

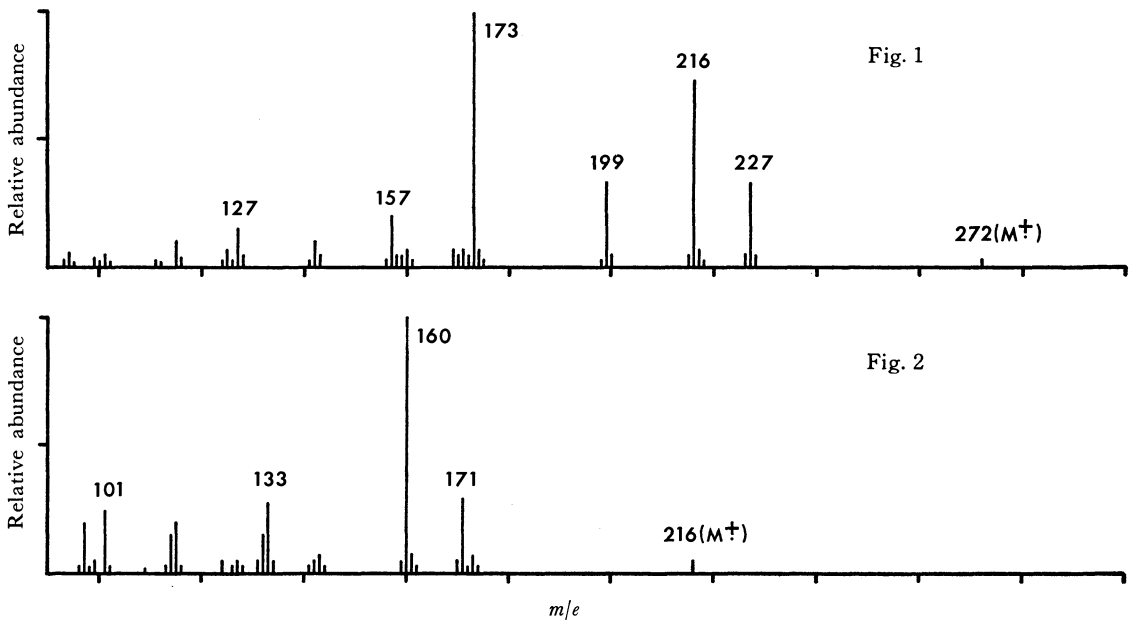

Fig. 1

Fig. 2

Fig. 1. Mass spectrum of diethyl di-*n*-butylmalonate (Ia).
Fig. 2. Mass spectrum of diethyl *n*-butylmalonate (Ib).

2) F. W. McLafferty, *Anal. Chem.*, **31**, 82 (1959).
3) S. Meyerson and J. D. McCollum, "Advances in Analytical Chemistry and Instrumentation," ed. by C. N. Reilley, Vol. II, Interscience, New York (1963), p. 184.
4) H. Budzikiewicz, C. Djerassi and D. H. Williams, "Mass Spectrometry of Organic Compounds," Holden-Day, San Francisco (1967), p. 155.

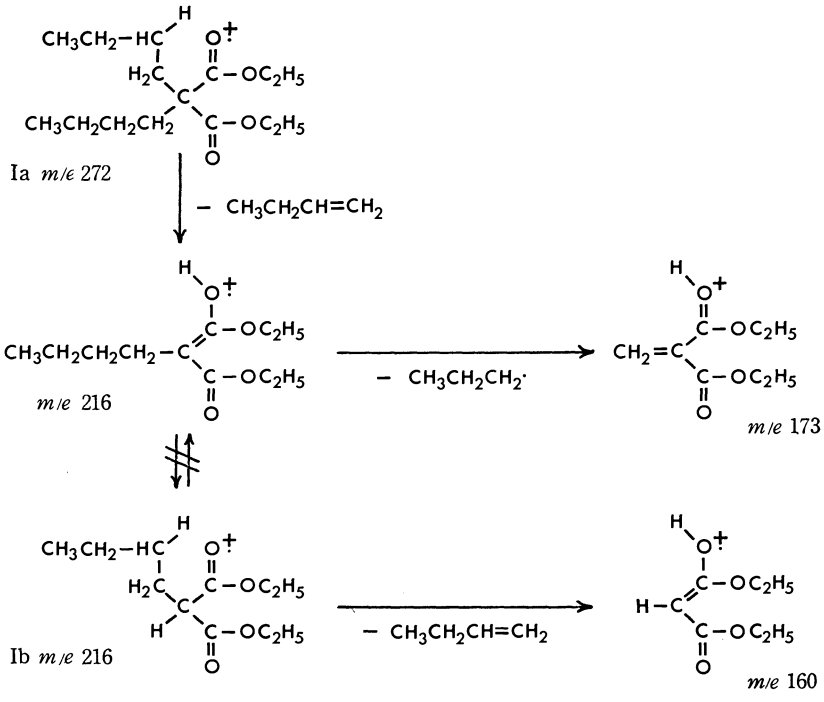

Scheme I

nate exhibited entirely different fragmentation patterns. Thus, the enol fragment ion of *m/e* 216 from di-*n*-butylmalonate (Ia) loses $C_3H_7\cdot$ through the allylic cleavage of an enol double bond to give an abundant *m/e* 173 peak (observed metastable ion peak at *m/e* 138.6), while the keto ion of *m/e* 216 from mono-*n*-butylmalonate (Ib) loses C_4H_8 by the McLafferty rearrangement to afford a strong *m/e* 160 peak. These fragmentations are summarized in Scheme I. Because no common peak of appreciable intensity was observed in these two spectra, it is concluded that the keto-enol tautomerism in these *m/e* 216 ions did not occur in a mass spectrometer.

Moreover, the *m/e* 160 ion from mono-*n*-butylmalonate (Ib) (Scheme I) corresponds to the enol form of diethyl malonate itself. It has already been known that the latter compound shows a very strong peak at *m/e* 115.[5] In Fig. 2, however, no intense peak at *m/e* 115 appeared, and this is consistent with the conclusion for the absence of the keto-enol tautomerism in this case also.

Essentially the same results were obtained with other two pairs of compounds. In the spectrum of methyl 2-*n*-butylhexanoate (IIa) (Fig. 3), the McLafferty rearrangement of the molecular ion gives an enol fragment ion at *m/e* 130, which then affords an intense peak at *m/e* 87 with elimination of $C_3H_7\cdot$ through the allylic cleavage. On the other hand, methyl hexanoate (IIb) (keto form) yields a strong *m/e* 74 peak (Scheme II). A moderately intense peak at *m/e* 87 in IIb probably arises from a fragmentation that is often encountered in long-chain methyl esters,[6] and not from the allylic cleavage of an enol double bond of the ester. From the bond energy considerations[7] the enol form of the ester is very unstable and should rearrange very rapidly to the ordinary ester (keto form), if other factors are not operative. The absence of the *m/e* 74 peak in the IIa spectrum (Fig. 3), therefore, showed that apparently very facile enol→keto tautomerism did not take place at all in fragment ions.

The general features of fragmentation of 2-*n*-propyl-5,5-dimethyl-1,3-cyclohexanedione (IIIb) are in good agreement with those observed for the corresponding 2-ethyl derivative, the fragmentation of which has been discussed in detail on the basis of double focusing technique[8] and deuterium labeling experiments.[9] The only difference in the IIIb spectrum is the appearance of an intense peak at *m/e* 140 (Fig. 6). This peak corresponds to M−42 and should originate from the McLafferty rearrangement of the molecular ion. The 2,2-di-*n*-propyl deriva-

5) J. H. Bowie, D. H. Williams, S.-O. Lawesson and G. Schroll, *J. Org. Chem.*, **31**, 1792 (1966).

6) Ref. 4, p. 179.

7) G. W. Wheland, "Advanced Organic Chemistry," 3rd Ed., John Wiley, New York (1960), p. 695.

8) T. Goto, A, Tatematsu, Y. Nakajima and H. Tsuyama, *Tetrahedron Letters*, **1965**, 757.

9) A. Maquestiau and P. Lejeune, *Bull. Soc. Chim. Belges*, **76**, 133 (1967).

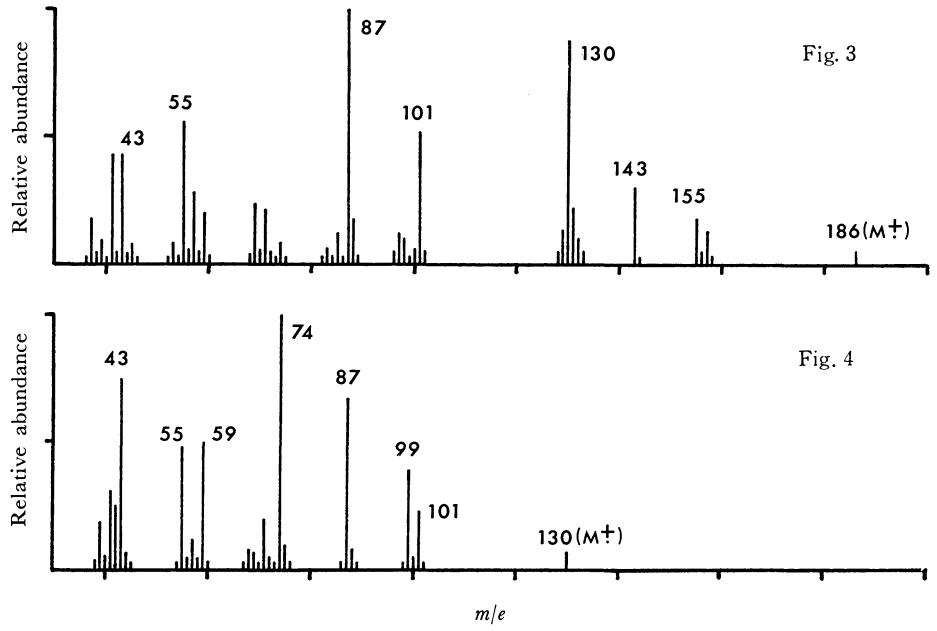

Fig. 3. Mass spectrum of methyl 2-*n*-butylhexanoate (IIa).
Fig. 4. Mass spectrum of methyl hexanoate (IIb).

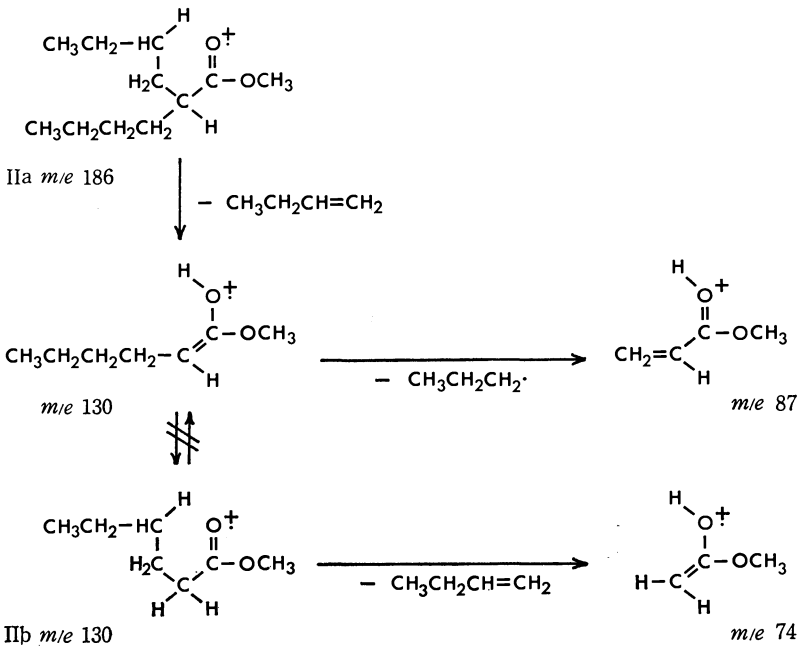

Scheme II

tive (IIIa) also exhibited an M−42 peak at *m/e* 182. This ion must be represented as an enol structure because its formation is ascribable to the similar McLafferty rearrangement. If enol→keto tautomerism took place in this *m/e* 182 ion, the 2,2-di-*n*-propyl derivative (IIIa) would have afforded the intense *m/e* 140 peak. Although there are several common peaks in the spectra of IIIa and IIIb, the absence of this double McLafferty rearrangement peak at *m/e* 140 in the IIIa spectrum (Fig. 5) clearly excludes the possibility of keto-enol tautomerism in the *m/e* 182 ions.

In conclusion, we have no evidence for tautomeric changes in the molecular and fragment ions in a

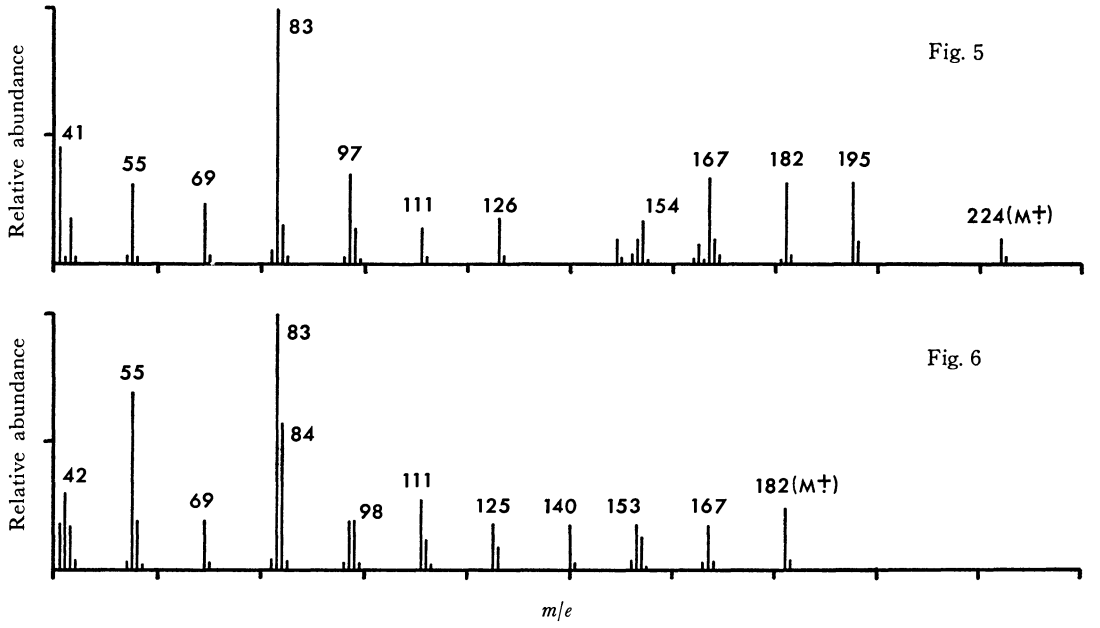

Fig. 5. Mass spectrum of 2,2-di-*n*-propyl-5,5-dimethyl-1,3-cyclohexanedione (IIIa).
Fig. 6. Mass spectrum of 2-*n*-propyl-5,5-dimethyl-1,3-cyclohexanedione (IIIb).

mass spectrometer.[10] From the viewpoint of the quasi-equilibrium theory of mass spectra[11] these results are not unexpected, for the production of ions in a mass spectrometer is usually considered to be a very rapid process and the average life time of ordinary ions is roughly in the range of 10^{-12}—10^{-5} sec.

One corollary from the present results is the argument against the arbitrary postulation for the structure of the molecular ion of tautomeric compounds. The fact that keto and enol forms of a given compound show different fragmentaion patterns should be noted in the formulation of the molecular ion. For the compounds we have examined, the molecular ion seems to have the structure of the most stable form that predominates in solution and in solid state. For other compounds, however, the molecular ion may not necessarily be the same as the most stable structure in solution, because several environmental factors such as hydrogen-bonding and solvation would affect the tautomeric equilibrium in solution. Conversely, the stability of each tautomeric form in gas phase may well be studied by applying the technique of mass spectrometry.

Experimental

The mass spectra were measured with a Hitachi RMU-7 mass spectrometer by using an all-glass inlet system heated at 200°C. The ionizing energy was maintained at 70 eV and the total ionizing current 80 μA. The infrared spectra were recorded with a JASCO model IR-G spectrophotometer. All melting points and boiling points are uncorrected.

Diethyl *n*-Butylmalonate (Ib). Diethyl *n*-butylmalonate (Ib) was prepared from diethyl malonate and *n*-butyl bromide.[12] Bp 128—129°C/20 mmHg. $\nu_{C=O}^{neat}$ 1755, 1736 cm^{-1}.

Found: C, 60.72; H, 9.66%. Calcd for $C_{11}H_{20}O_4$: C, 61.09; H, 9.32%.

Diethyl Di-*n*-butylmalonate (Ia). Diethyl di-*n*-butylmalonate (Ia) was synthesized from 38 g of Ib and 34 g of *n*-butyl bromide in the presence of sodium ethoxide (6 g of sodium in 130 m*l* of ethanol). The procedure was essentially the same as described for alkylation of diethyl methylmalonate with *n*-decyl bromide.[13] The material boiling at 155°C/23 mmHg[14] was collected. Yield 26 g. $\nu_{C=O}^{neat}$ 1730 cm^{-1} (broad).

Found: C, 65.96; H, 10.63%. Calcd for $C_{15}H_{28}O_4$: C, 66.14; H, 10.36%.

Methyl 2-*n*-Butylhexanoate (IIa). Alkaline hydrolysis and subsequent decarboxylation of Ia were carried out in a similar manner as described for the synthesis of 2-methyldodecanoic acid.[13] Re-esterification of the product with methanol afforded IIa. Thus, 38 g of diethyl di-*n*-butylmalonate (Ia) was treated with a solution of 40 g of potassium hydroxide in 200 m*l* of 95% ethanol and the mixture heated at reflux, with

10) A recent report by Djerassi and co-workers also indicated the absence of keto-enol tautomerism in fragment ions. See, J. K. MacLeod, J. B. Thomson and C. Djerassi, *Tetrahedron*, **23**, 2095 (1967).

11) H. M. Rosenstock and M. Krauss, "Mass Spectrometry of Organic Ions," ed. by F. W. McLafferty, Academic Press, New York (1963), p. 1.

12) R. Adams and R. M. Kamm, "Organic Syntheses," Coll. Vol. I, p. 250 (1941).

13) C. F. Allen and M. J. Kalm, "Organic Syntheses," Coll. Vol. IV, p. 616 (1963).

14) R. Dolique, *Ann. Chim.*, [10] **15**, 425 (1931); *Chem. Abstr.*, **26**, 2971 (1932).

stirring, for 3 hr. About 10 m*l* of water was added to the refluxed mixture when a white jelly solid appeared during the hydrolysis. About two-thirds of the solvent was removed by distillation, 100 m*l* of water was added, and the solution was acidified, under cooling, with 6 N sulfuric acid to bring the pH of the solution to 1—2. A white, precipitated solid was collected and dissolved in ether, and the aqueous layer was extracted with ether. Combined ether solutions were washed with water and with saturated sodium chloride solution, and dried over anhydrous sodium sulfate. Evaporation of the solvent afforded crystalline di-*n*-butylmalonic acid. This material was carefully heated over its melting point under reflux for 3 hr to perform decarboxylation.

The crude 2-*n*-butylhexanoic acid, after checked by its IR spectrum,[15] was dissolved in 150 m*l* of methanol containing 5 m*l* of concentrated sulfuric acid. The mixture was refluxed for 3 hr, and then 50 m*l* of benzene was added and about 50 m*l* of azeotropic mixture was distilled, and the residue was again refluxed for 1 hr. The esterification was effected by repeating the above procedure three times to remove water produced. Finally the mixture was cooled and poured onto ice-water. The organic phase was separated and aqueous phase was extracted with ether. The organic phase and the ether extracts were combined, washed with sodium bicarbonate solution, and dried over anhydrous sodium sulfate. The solvent was removed and the residue was distilled under reduced pressure. The material boiling at 112—116°C/32 mmHg was collected. Redistillation gave 13 g of pure methyl 2-*n*-butylhexanoate (IIa), bp 108—109°C/25 mmHg.[16] $\nu_{C=O}^{CHCl_3}$ 1739 cm^{-1}.

Found: C, 71.06; H, 11.84%. Calcd for $C_{11}H_{22}O_2$: C, 70.92; H, 11.90%.

Methyl Hexanoate (IIb). The commercially available methyl hexanoate (IIb) was purified by repeated distillation. Bp 148.5°C.

2,2-Di-*n*-propyl-5,5-dimethyl-1,3-cyclohexanedione (IIIa). About 9 g of 5,5-dimethyl-1,3-cyclohexanedione[17] was dissolved in a solution of 5 g of sodium bicarbonate in 200 m*l* of water and 10 m*l* of ethanol. To this solution was added 50 m*l* of allyl bromide and the mixture was refluxed for 5 hr. A sufficient amount of crystalline sodium bicarbonate was added to the reaction mixture for every 30 min during this period in order to maintain the water layer neutral or slightly basic. After cooling, the mixture was extracted with ether and the ether extracts were washed with sodium bicarbonate solution and dried over anhydrous sodium sulfate. Removal of the solvent gave a yellow oil. This material was chromatographed on 150 g of silica gel (40×400 mm column). Elution of the first band with chloroform afforded 12.6 g of 2,2-diallyl-5,5-dimethyl-1,3-cyclohexanedione as colorless needles, mp 65—75°C.[18] $\nu_{C=O}^{CHCl_3}$ 1724, 1693 cm^{-1}. Catalytic hydrogenation of 6.5 g of this 2,2-diallyl derivative in ethanol under atmospheric hydrogen over platinum oxide yielded 6.8 g of a colorless oil. After chromatographed on 150 g of silica gel (40×400 mm column), pure 2,2-di-*n*-propyl-5,5-dimethyl-1,3-cyclohexanedione (IIIa) was obtained. The pure material solidified on cooling, mp 42—43°C. $\nu_{C=O}^{CHCl_3}$ 1721, 1690 cm^{-1}.

Found: C, 74.95; H, 10.96%. Calcd for $C_{14}H_{24}O_2$: C, 74.95; H, 10.78%.

2-*n*-Propyl-5,5-dimethyl-1,3-cyclohexanedione (IIIb). Mono-allylation of 5,5-dimethyl-1,3-cyclohexanedione was conveniently carried out according to the directions of Lukeš and Hofman.[19] 2-Allyl-5,5-dimethyl-1,3-cyclohexanedione was obtained as colorless plates, mp 152—154°C.[18,19] $\nu_{C=O}^{CHCl_3}$ 1739, 1707 cm^{-1}. Catalytic hydrogenation of this 2-allyl derivative and recrystallization of the product from aqueous ethanol gave pure 2-*n*-propyl-5,5-dimethyl-1,3-cyclohexanedione (IIIb) as colorless, flattened needles, mp 167—168°C.[18,20] $\nu_{C=O}^{CHCl_3}$ 1741, 1709 cm^{-1}.

Found: C, 72.28; H, 10.06%. Calcd for $C_{11}H_{18}O_2$: C, 72.49; H, 9.96%.

The authors wish to express their gratitude to Mr. Hideo Yoshizumi of Meijo University for his measurements of mass spectra. This work was supported in part by a grant from the Ministry of Education.

15) D. L. Guertin, S. E. Wiberley and W. H. Bauer, *Anal. Chem.*, **28**, 1194 (1956).
16) V. Franzen, *Chem. Ber.*, **87**, 1219 (1954).
17) R. L. Shriner and H. R. Todd, "Organic Syntheses," Coll. Vol. II, p. 200 (1943).
18) R. D. Desai, *J. Chem. Soc.*, **1932**, 1079.
19) R. Lukeš and J. Hofman, *Chem. Listy*, **51**, 2309 (1957); *Chem. Abstr.*, **52**, 6172 (1958).
20) W. E. Silbermann and T. Henshall, *J. Am. Chem. Soc.*, **79**, 4107 (1957).

BULLETIN OF THE CHEMICAL SOCIETY OF JAPAN VOL. 42 1684—1687 (1969)

The Addition Reactions of Dialkyl Phosphites to Polyfluorocyclobutenes

Teruo UEDA, Kan INUKAI and Hiroshige MURAMATSU

Government Industrial Research Institute, Nagoya, Kita-ku, Nagoya

(Received October 23, 1968)

The radiation-induced addition reactions of dialkyl phosphites to polyfluorocyclobutenes, such as perfluoro-, 1,2-dichlorotetrafluoro-, 1-chloro-2,3,3,4,4-pentafluoro-, 1,3,3,4,4-pentafluoro- and 1-chloro-3,3,4,4-tetrafluorocyclobutenes were carried out. In general, the corresponding dehydrohalogenated 1 : 1 adducts, polyfluorocyclobutenylphosphonates, were obtained as the main products instead of the expected 1 : 1 adducts. The direction of attack of the phosphonyl radical on the unsymmetrical double bond and reaction mechanism were discussed.

The syntheses of the polyfluorocycloalkenylphosphonates *via* ionic process have been investigated rather extensively. Knunyants and co-workers[1,2] prepared diethyl perfluorocyclobutenylphosphonate by the Arbuzov rearrangement of the phosphorane, which was obtained in the reaction between perfluorocyclobutene and triethyl phosphite. In the reactions between 1,2-dichloroperfluorocycloalkenes and trialkyl phosphites,[3] only the corresponding diphosphonates were obtained and no monophosphonates could be detected, regardless of the order of addition or the ratio of reactants.

No paper has appeared so far on the syntheses of polyfluorocycloalkenylphosphonates by a free radical-induced addition reaction. As dialkyl chlorofluoroethylphosphonates were found to be produced in moderate yields by the radiation-induced addition reaction of dialkyl phosphites to chlorofluoroethylenes,[4] we extended the addition reaction under γ-ray irradiation to polyfluorocyclobutenes for syntheses of the polyfluorocyclobutyl- or polyfluorocyclobutenylphosphonates.

Results and Discussion

Perfluorocyclobutene (Ia), 1,2-dichlorotetrafluorocyclobutene (Ib), 1-chloro-2,3,3,4,4-pentafluorocyclobutene (Ic), 1,3,3,4,4-pentafluorocyclobutene (Id) and 1-chloro-3,3,4,4-tetrafluorocyclobutene (Ie) were prepared by conventional methods (see Experimental).

A mixture of polyfluorocyclobutene and dialkyl phosphite in a molar ratio of about 1 : 2 in a glass ampoule was irradiated at room temperature for a month. After unchanged reactants were recovered, products were separated by distillation and/or by preparative gas chromatography. The structure of the products was determined by elemental analysis, IR, NMR and mass spectroscopy. The reaction conditions and yields of products are shown in Table 1.

As a whole dehydrohalogenated 1:1 adducts were obtained as the main products instead of the expected simple 1:1 adducts. Addition of the dialkyl phosphites to Ia gave a mixture of dialkyl 2,3,3,4,4-pentafluoro - 1 - cyclobutenylphosphonate (II) and 2 - alkoxy-3, 3, 4, 4-tetrafluoro -1- cyclobutenylphosphonate (III) in total yields of 23—27%. Addition to Ib, however, resulted in only trace amounts of diethyl 2-chloro-3,3,4,4-tetrafluoro-1-cyclobutenylphosphonate (IV), probably due to a steric interaction between the attacking phosphonyl radical and chlorine atoms on the double bond.

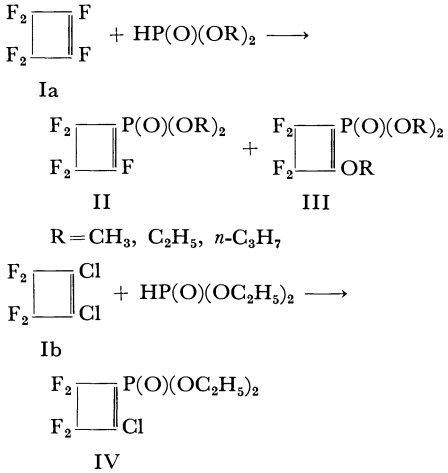

In an addition to Ic, IV was also obtained along with III. The absence of II in the products in this case indicates that a phosphonyl radical attacked exclusively on the carbon bearing fluorine. Preferential attack of the phosphonyl radical on the

1) I. L. Knunyants, E. Ya. Pervova and V. V. Tyuleneva, *Dokl. Akad. Nauk SSSR*, **129**, 576 (1959).
2) I. L. Knunyants, V. V. Tyuleneva, E. Ya. Pervova and R. N. Sterlin, *Izv. Akad. Nauk SSSR, Ser. Khim.*, **1964**, 1797.
3) A. W. Frank, *J. Org. Chem.*, **30**, 3663 (1965).
4) K. Inukai, T. Ueda and H. Muramatsu, *ibid.*, **29**, 2224 (1964).

Table 1. Irradiation conditions and yields in addition reactions

Polyfluoro-cyclobutene	$HP(O)(OR)_2$ R	Molar ratio of $HP(O)(OR)_2$ to cyclobutene	Total dosage MR	Yield, %* II	III	IV	VII	VIII
Ia	CH_3	3.0	31	16.8	11.5	—	—	—
	C_2H_5	2.0	31	14.8	14.0	—	—	—
	n-C_3H_7	2.0	31	19.5	7.2	—	—	—
Ib	C_2H_5	2.0	41	—	—	1.6	—	—
Ic	C_2H_5	2.0	40	—	10.5	9.3	—	—
Id	C_2H_5	2.0	40	—	—	—	8.1	9.5
Ie	C_2H_5	2.0	41	—	—	—	9.7	11.9

* Based on the amount of the polyfluorocyclobutenes added.

carbon bearing fluorine over on the carbon bearing chlorine of a double bond was observed in the addition to chlorofluoroethylenes.[4] The direction of the radical attack may be explained both by the steric effect and by the stability of an intermediate radical.

The structure of III was confirmed by comparing its IR spectrum with that of an authentic sample, prepared by a reaction of II or IV with alcohol in the presence of potassium hydroxide. Since the dialkyl phosphites produced the corresponding alcohols even at room temperature in the presence of hydrochloric acid or hydrofluoric acid, which was always formed in γ-irradiation of a mixture of the polyfluorocyclobutene and the dialkyl phosphite, III seems to be formed by the reaction of the 1 : 1 adducts, II or IV, with the alcohols. The carbon to carbon double bond of dialkyl polyfluorocyclobutenylphosphonates are known[3] to be reactive toward nucleophiles due to the electron-withdrawing effect of the P=O group.

The reasons why only the dehydrohalogenated 1 : 1 adducts were obtained in the addition to polyfluorocyclobutenes whereas the addition to chlorofluoroethylenes[4] produced the simple 1:1 adducts, may be the steric interaction between the substituted halogens and phosphorus atom, the conjugation of the P=O group with C=C group in the cyclobutenylphosphonates formed, and the instability of the 1 : 1 adducts.

Since a mixture of polyfluorocyclobutene and dialkyl phosphite gave no products upon standing in the dark at room temperature for a month, the reactions under radiation seem to proceed through a free radical mechanism. For formation of II or IV from Ia—c, two routes are conceivable. One of them (a) involves a radical elimination of fluorine from an intermediate radical (V). The other (b) is through formation of an unstable 1:1 adduct (VI), which is supposed to be readily dehydrofluorinated.

There are seveal papers[5] on the chlorine elimination from an intermediate radical in addition reactions, but no example of fluorine elimination has been reported so far except one, in which removal of fluorine by a radical was assumed in a reaction of

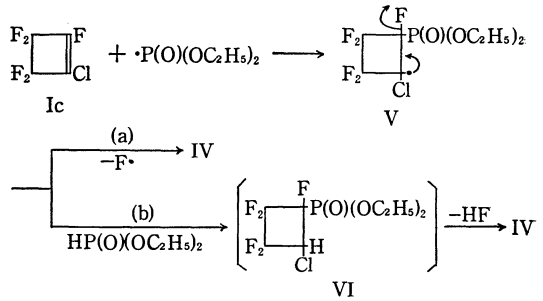

perfluorobenzene with trimethylsilane under UV irradiation to explain the formation of pentafluorophenyltrimethylsilane.[6] Although it is difficult to obtain unambiguous evidence, the ionic elimination of hydrogen fluoride from VI seems to be the more probable route for the formation of IV.

Both Id and Ie gave diethyl 3,3,4,4-tetrafluoro-1-cyclobutenylphosphonate (VII) together with the diphosphonate (VIII) in the addition reaction with diethyl phosphite.

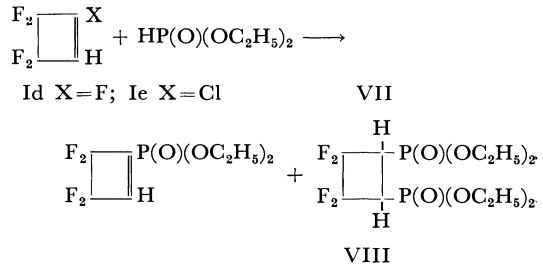

Though the directions of phosphonyl radical attack are not clear in these cases, in the addition reaction to 1,1-difluoroethylene the phosphonyl radical was found to attack exclusively on the $=CH_2$ side, yielding diethyl 2,2-difluoroethylphosphonate (IX) and

5) C. Walling, "Free Radical Rearrangements," in "Molecular Rearrangements," Vol I, ed. by P. de Mayo, Interscience Publishers, New York (1963), p. 423; H. Muramatsu, K. Inukai and T. Ueda, *J. Org. Chem.*, **30**, 544, 2546 (1965).

6) J. M. Birchall, W. M. Daniewski, R. N. Haszeldine and L. S. Holden, *J. Chem. Soc.*, **1965**, 6702.

TABLE 2. DIALKYL POLYFLUOROCYCLOBUTENYLPHOSPHONATES,

X	R	Bp °C(mmHg)	n_D^{20}	d_4^{20}	MR_D Found	MR_D Calcd	P, % Found	P, % Calcd	MW Found	MW Calcd	$\nu_{C=C}$ cm^{-1}	$\nu_{P=O}$ cm^{-1}
F	CH_3	80—81 (5)	1.3773	1.476	39.3	39.0	12.0	12.3	260	252	1645	1280
F	C_2H_5	73—74 (1)	1.3829	1.359	48.1	48.2	10.5	11.1	284	280	1643	1276
F	n-C_3H_7	82—83 (1)	1.3910	1.298	56.4	57.4	9.5	10.1	308	308	1640	1278
CH_3O	CH_3	100—101 (5)	1.4058	1.441	45.0	45.2	11.7	11.7	264	264	1658	1295
C_2H_5O	C_2H_5	92—95 (1)	1.4057	1.282	58.6	59.0	9.3	10.0	306	306	1647	1294
n-C_3H_7O	n-C_3H_7	106—107 (1)	1.4139	1.204	72.2	72.9	8.7	8.9	348	348	1646	1292
Cl	C_2H_5	77—80 (1)	1.4098	1.337	54.9	53.0	10.0	10.4	297	297	1603	1280
H	C_2H_5	60—63 (1)	1.3957	1.291	48.7	48.1	11.2	11.8	263	262	1583	1277
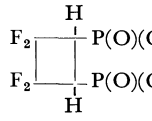		122—125 (1)	1.4162	1.341	75.0	78.0	14.8	15.5	400	400		1262

2,2,4,4-tetrafluorobutylphosphonate (X).

$$CF_2{=}CH_2 + HP(O)(OC_2H_5)_2 \longrightarrow CHF_2CH_2P(O)(OC_2H_5)_2 \quad \text{IX}$$

$$+ H(CF_2CH_2)_2P(O)(OC_2H_5)_2 \quad \text{X}$$

Furthermore, in the addition of tetrahydrofuran and 2-propanol to Id (X=F) and Ie (X=Cl) under similar conditions,[7] the 1 : 1 adduct formed was exclusively XI in the case of Ie and a mixture of two isomers, XI and XII, was obtained in a ratio of about 80 : 20 in the case of Id.

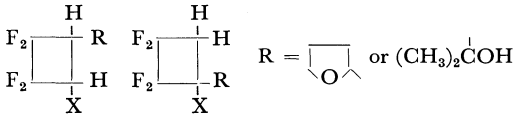

XI XII

From these observations, it may be reasonable to assume that the phosphonyl radical attacked preferentially on the double bond carbon bearing a hydrogen atom and the 1 : 1 adduct (XIII) formed by hydrogen abstraction from diethyl phosphite evolved readily hydrogen halide to give VII. Further addition of diethyl phosphite to VII would produce VIII. This was confirmed by the irradiation of a mixture of VII and diethyl phosphite, which yielded VIII. Dehydrofluorination of VIII with powdered potassium hydoxide gave tetraethyl 2,3,3-trifluoro-1-cyclobutenyl-1,4-diphosphonate (XIV).

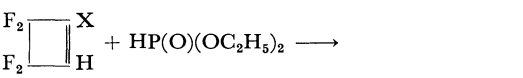

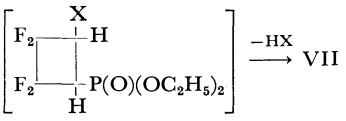

XIII

The physical properties and results of analyses of new dialkyl polyfluorocyclobutenylphosphonates prepared are listed in Table 2.

Experimental[8]

Materials. 1,2-Dichlorotetrafluorocyclobutene (Ib) was obtained from the Peninsular ChemResearch, Inc., and used without further purification. Perfluorocyclobutene (Ia)[9] and 1-chloro-2,3,3,4,4-pentafluorocyclobutene (Ic)[10] were prepared by dechlorination with zinc dust from 1,2-dichlorohexafluoro- and 1,1,2-trichloropentafluorocyclobutenes, respectively. 1,3,3,4,4-Pentafluorocyclobutene (Id)[11] was synthesized from 1,2-dichlorohexafluorocyclobutane by reduction with lithium aluminum hydride in dibutyl ether, followed by dehydrofluorination with aqueous potassium hydroxide. 1-Chloro-3,3,4,4-tetrafluorocyclobutene (Ie)[12] was prepared from Ib by reduction with sodium borohydride in diglyme.

Addition Reactions of Dialkyl Phosphites to Perfluorocyclobutene (Ia). A mixture of 85 g (0.62 mol) of diethyl phosphite and 50 g (0.31 mol) of Ia was sealed in a glass tube and irradiated from ^{60}Co to a total dosage of 30.5 MR for a period of 480 hr. Distillation of the irradiation products under reduced pressure and nitrogen atmosphere, after removal of

7) H. Muramatsu, K. Inukai and T. Ueda, unpublished.

8) All temperature readings are uncorrected.

9) A. L. Henne and R. P. Ruh, *J. Am. Chem. Soc.*, **69**, 279 (1947).

10) E. L. Kropa and J. J. Padbury, U. S. Pat. 2590019 (1952).

11) R. N. Haszeldine and J. E. Osborne, *J. Chem. Soc.*, **1956**, 61.

12) D. J. Burton and R. L. Johnson, *J. Am. Chem. Soc.*, **86**, 5361 (1964).

the unchanged diethyl phosphite and cyclobutene, gave 12.8 g (0.045 mol, 14.8% yield) of diethyl perfluoro-1-cyclobutenylphosphonate (II), bp 73—74°C/1 mmHg, 13.2 g (0.043 mol, 14.0% yield) of diethyl 2-ethoxy-3,3,4,4-tetrafluoro-1-cyclobutenylphosphonate (III), bp 92—95°C/1 mmHg, and 5 g of a tarry material.

Using the same procedures, the addition reactions of other dialkyl phosphites to perfluorocyclobutene were carried out. The irradiation conditions and yields based on the amounts of the cyclobutene charged for each run are shown in Table 1.

Addition Reaction of Diethyl Phosphite to 1-Chloro-2,3,3,4,4-pentafluorocyclobutene (Ic). In a glass tube were sealed 135 g (0.98 mol) of diethyl phosphite and 88 g (0.49 mol) of Ic. After the content in the tube was irradiated to a total dosage 40 MR at room temperature, it was washed with aqueous sodium carbonate to remove the unchanged diethyl phosphite and extracted with ether. Distillation of the extract under reduced pressure and a nitrogen atmosphere gave 12.5 g of diethyl fluorophosphate, bp 75—77°C/45 mmHg,[13] 13.6 g (0.046 mol, 9.3% yield) of diethyl 2-chloro-3,3,4,4-tetrafluoro-1-cyclobutenylphosphonate (IV), bp 77—80°C/1 mmHg, and 15.9 g (0.052 mol, 10.5% yield) of III, bp 92—95°C/1 mmHg.

In a similar way, diethyl phosphite was added to the other polyfluorocyclobutenes, Ib, Id and Ie.

Dialkyl 2-Alkoxy-3,3,4,4-tetrafluoro-1-cyclobutenylphosphonate (III). To 0.7 g (0.013 mol) of potassium hydroxide in 1-propanol in a flask, 3.7 g (0.012 mol) of di-*n*-propyl perfluoro-1-cyclobutenylphosphonate was added. The reaction mixture was stirred at 40°C for 3 hr and, after addition of 50 m*l* of ether, poured into water. The organic layer was separated and distilled to give 2.0 g (0.005 mol, 48% yield) of di-*n*-propyl 2-propoxy-3,3,4,4-tetrafluoro-1-cyclobutenylphosphonate, bp 106—107°C/1 mmHg, whose IR spectrum and retention time of gas chromatogram were identical with those of III ($R=n\text{-}C_3H_7$) obtained in the addition of di-*n*-propyl phosphite to Ia.

Tetraethyl 3,3,4,4-Tetrafluorocyclobutenyl-1,2-diphosphonate (VIII). A mixture of 1.0 g (6 mmol) of diethyl phosphite and 0.5 g (1.9 mmol) of VII was irradiated to a total dosage of 40 MR. After treatment with aqueous sodium carbonate, the irradiation product was extracted with ether and dried. Upon evaporation of ether, there remained 0.65 g (1.5 mmol, 81% yield) of crude tetraethyl 3,3,4,4-tetrafluorocyclobutyl-1,2-diphosphonate, whose IR spectrum was identical with that of VIII produced in the addition of diethyl phosphite to Id or Ie.

Dehydrofluorination of VIII. To 0.5 g (12.5 mmol) of VIII, 0.7 g (12.5 mmol) of potassium hydroxide was added and stirred at room temperature for 2 hr. After addition of 50 m*l* of ether, the reaction mixture was poured into water and the organic layer was separated and dried. Distillation gave 2.7 g (7.1 mmol, 57% yield) of tetraethyl 2,3,3-trifluoro-1-cyclobutenyl-1,4-diphosphonate (XIV), bp 122—125°C/1 mmHg, n_D^{20} 1.4173, d_4^{20} 1.333, $\nu_{C=C}$ 1683 cm^{-1}, $\nu_{P=O}$ 1265 cm^{-1}.

Found: P, 16.4%; mol wt, 380. Calcd for $C_{12}H_{21}F_3O_6P_2$: P, 16.3%; mol wt, 380.

Addition Reaction of Diethyl Phosphite to 1,1-Difluoroethylene. To 138 g (0.1 mol) of diethyl phosphite in an autoclave cooled in a dry ice - acetone bath, 3.2 g (0.05 mol) of 1,1-difluoroethylene was condensed. The mixture was irradiated to a total dosage of 35 MR. Distillation of the irradiation products under reduced pressure and a nitrogen atmosphere gave 6.4 g (0.032 mol, 63.4% yield) of diethyl 2,2-difluoroethylphosphonate (IX), bp 73—76°C/5 mmHg, and 2.0 g (0.008 mol, 15% yield) of diethyl 2,2,4,4-tetrafluorobutylphosphonate (X), bp 100—103°C/1 mmHg. The orientation of the addition was established by means of the NMR spectra[14] of IX and X, which are presented below. The splitting pattern and coupling constants of the protons clearly indicated that the phosphonyl radical attacked the CH_2 group of 1,1-difluoroethylene.

IX: n_D^{20} 1.3990, d_4^{20} 1.194, τ_{CH_3} 8.69 ppm (triplet), J_{CH_3,CH_2} 7.2 cps, $\tau_{\underline{CH_2}CF_2H}$ 7.46 ppm (doublet of triplet), J_{CH_2,CF_2} 19.5 cps, $J_{CH_2,P}$ 4.9 cps, $\tau_{\underline{CH_2}CH_3}$ 5.86 ppm (doublet of quartet), $J_{CH_2,P}$ 8.2 cps, τ_{CHF_2} 3.78 ppm (triplet of quartet), $J_{H,F}^{gem}$ 56.1 cps.

Found: P, 14.9%. MR_D 41.0. Calcd for $C_6H_{13}F_2O_3P$: P, 15.3%; MR_D 40.9.

X: n_D^{20} 1.4002, d_4^{20} 1.287, τ_{CH_3} 8.65 ppm, $\tau_{\underline{CH_2}CF_2H}$ 7.20 ppm, $\tau_{\underline{CH_2}CH_3}$ 5.80 ppm, τ_{CHF_2} 3.72 ppm, $J_{H,F}^{gem}$ 54.3 cps.

Found: P, 11.0%; MR_D 50.2. Calcd for $C_8H_{15}F_4O_3P$: P, 11.6%; MR_D 50.3.

13) The structure was determined by comparing its IR spectrum with that of an authentic sample reported in the literature: L. W. Daasch and D. C. Smith, *Anal. Chem.*, **23**, 853 (1951).

14) The NMR spectra were obtained using a JNM-C-60 high resolution spectrometer (60 Mc for ^1H and 56.4 Mc for ^{19}F).

BULLETIN OF THE CHEMICAL SOCIETY OF JAPAN VOL. 42 1688—1693 (1969)

Polymerization of Formaldehyde in Liquid Carbon Dioxide. I. The Cause of the Polymerizability of the Monomer

Tsutomu KAGIYA, Masatsune KONDO,*1 Kōzō NARITA and Kenichi FUKUI

Faculty of Engineering, Kyoto University, Sakyo-ku, Kyoto

(Received November 4, 1968)

The cause of the polymerizability of formaldehyde in liquid carbon dioxide was studied in connection with the preparation conditions of the monomer. A liquid carbon dioxide solution of the monomer was prepared by two different methods, by means of the pyrolysis of α-polyoxymethylene and by means of that of the hemiformal of polyethylene glycol, under a carbon dioxide stream. By adding various sodium salts to the pyrolysis system of α-polyoxymethylene, the polymerization rate, without the addition of any catalyst, of the monomer thus obtained was found to decrease with an increase in the pK_a value of the conjugated acid of the salt. The polymerization rate also decreased with the amount of sodium carbonate added. The hemiformal of polyethylene glycol was prepared by bubbling the gas evolved by the pyrolysis of paraformaldehyde into polyethylene glycol. The amount of acid present in the hemiformal thus obtained increased linearly with the pyrolysis time. The polymerization rate of the monomer obtained by the pyrolysis of the hemiformal increased in proportion to the acid content in the hemiformal. On the basis of these results, the initiation mechanism in the polymerization of formaldehyde without any additional initiator in a liquid carbon dioxide solution was discussed.

In respect to the polymerization of formaldehyde, many papers have been reported. It is well known that formaldehyde is so reactive that it can be polymerized easily by the initiating action of an impurity in a monomer solution, even at the temperature of −78°C.[1] For this reason, little reproducibility of experimental results is observed in the polymerization. Little attention has, however, been paid to the cause of this phenomenon.

The present authors have already reported that the polymerization rate of formaldehyde is remarkably retarded by the addition of carbon dioxide,[2] and that reproducible results can be obtained in a formaldehyde polymerization in a liquid carbon dioxide solution.[3,4]

As has previously been reported, a liquid carbon dioxide solution containing 60 wt% of monomer is obtained when α-polyoxymethylene is pyrolyzed under a carbon dioxide stream and the mixed gas thus obtained is cooled at −78°C.[3]

In the present paper, the cause of the polymerizability of formaldehyde in this solution will be studied quantitatively in connection with the preparation conditions of the monomer solution; the initiation mechanism in the polymerization of formaldehyde without any additional initiator will also be discussed.

Experimental

Materials. Commercially available α-polyoxy methylene (α-POM; the degree of polymerization *ca.* 100) and paraformaldehyde (paraform; the degree of polymerization is from 10 to 100) are used without further treatment. The calcium carbonate, sodium carbonate, sodium hydroxide, sodium acetate, sodium sulfate, sodium cyanide, and sodium chloride were commercially obtained. Commercial polyethylene glycol (PEG; average molecular weight is 380 to 420) was used after removing a volatile fraction of PEG by heating it at 200°C for one hour under normal pressure. Commercial carbon dioxide was dried by passing it through two drying tubes packed with phosphorus pentoxide.

Preparation of Monomer. *Direct Method by the Pyrolysis of α-POM.* The monomer was prepared directly by the pyrolysis of α-POM. 100 g of α-POM or a mixture of 100 g of α-POM and a measured amount of various sodium salts was put into a 300 ml decomposer (A) and then decomposed by heating at 150 to 180°C under a carbon dioxide stream (flow rate: 160 ml/min) (Fig. 1.1). The resulting mixture of formaldehyde and carbon dioxide was condensed in the monomer reservoir (B) at −78°C. The solution thus obtained was homogeneous and contained 59 to 61 wt% of the monomer and 39 to 41 wt% of carbon dioxide.

Two-steps Method by Pyrolysis of the Hemiformal of PEG. The hemiformal was prepared by the reaction of PEG with the monomer produced by pyrolyzing paraform

*1 Present address: Sumitomo Chemical Co., Ltd., Takatsuki.

1) J. F. Walker, "Formaldehyde", 3rd Ed., Reinhold, New York (1964), pp. 46, 52.

2) H. Yokota, M. Kondo, T. Kagiya and K. Fukui, *J. Polymer Sci., A-1*, **5**, 3129 (1967).

3) H. Yokota, M. Kondo, T. Kagiya and K. Fukui, *ibid.*, **6**, 425 (1968).

4) H. Yokota, M. Kondo, T. Kagiya and K. Fukui, *ibid.*, **6**, 435 (1968).

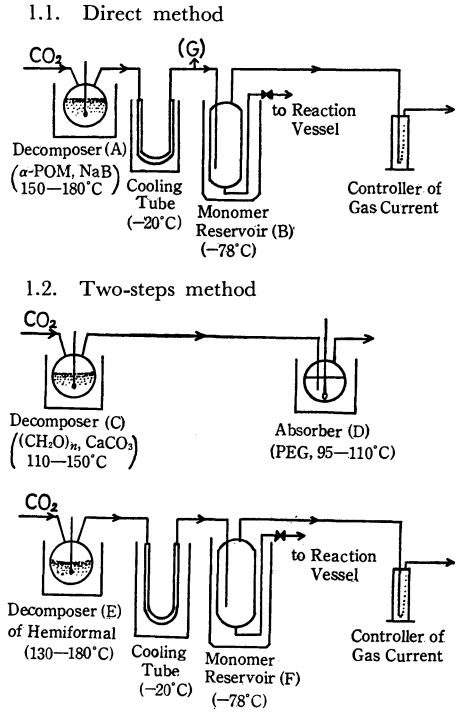

Fig. 1. Preparation apparatus of the carbon dioxide solution of formaldehyde.

(Fig. 1.2). 500 g of the paraform and a measured amount of the additive were placed in a 1000 m*l* decomposer (C) and decomposed by heating at 110 to 150°C under a carbon dioxide stream (flow rate: 160 m*l*/min). The mixed gas thus obtained was then introduced into a 1000 m*l* absorber (D) (95—110°C) containing 500 g of PEG to give the hemiformal. The formaldehyde content in the hemiformal was found to be *ca.* 25 wt%.

The monomer was prepared by the pyrolysis of the hemiformal (Fig. 1.2). 500 g of the hemiformal were put into a 1000 m*l* decomposer (E) and pyrolyzed at 130 to 180°C under a carbon dioxide stream (flow rate: 160 m*l*/min). The resulting mixture of formaldehyde and carbon dioxide was passed through a tube cooled at −20°C and then liquefied in the monomer reservoir (F) at −78°C.

Polymerization Procedure. A stainless-steel autoclave with a capacity of 30 m*l* (16 mmϕ × 150 mm) was used as the reaction vessel. Into the vessel, which has been degassed *in vacuo* and cooled with liquid nitrogen, 10 m*l* of a carbon dioxide solution of formaldehyde was charged; this solution was maintained at 20±1°C for one hour. After the polymerization, the unreacted monomer and carbon dioxide gas were purged out. The white powdery polymer thus obtained was washed sufficiently with cooled diethyl ether, dried *in vacuo* at room temperature, and weighed.

Analysis. *Measurement of the Acid Content in the Hemiformal of PEG.* 10 m*l* of a 0.1 N NaOH aqueous solution was added to 10 m*l* of the hemiformal, and the excess of sodium hydroxide was titrated with a 0.1 N HCl aqueous solution using phenolphthalein as the indicator.

Measurement of the Number-average Degree of polymerization of the Polymer. The inherent viscosity measurement of a solution containing 0.5 g of the polymer in 100 m*l* of *p*-chlorophenol containing 2% of α-pinene was carried out with the use of an Ostwald viscometer at 60°C. The number-average degree of polymerization of the polymer was calculated by the following equation.[3]

$$\eta_i = 2.14 \times 10^{-2} \bar{P}_n^{0.61} \quad (1)$$

Measurement of the Adsorption of Acid by Sodium Salts. A measured amount of sodium salt was added to a PEG solution containing a measured amount of formic acid. After the solution had been kept standing for one hour at room temperature, 10 m*l* of this PEG solution was titrated back with a 0.1 N HCl aqueous solution.

Gas Chromatographic Analysis of the Impurities Involved in the Monomer. The impurity content in the gas produced by the pyrolysis of α-POM was determined by gas chromatography (Yanagimoto, Type GCG-3D) using a diglycerol column. The gas sample was collected in a micro-syringe from a side arm (G) (*cf.* Fig. 1.1) through a rubber stopper.

Results and Discussion

Polymerizability of the Monomer Obtained by the Pyrolysis of α-POM with the Addition of Various Sodium Salts. The polymerizability of the monomer obtained by the pyrolysis of a mixture containing 0.1 mol of sodium salts of various Brönsted acids in 100 g of α-POM was studied without any additional initiator. As shown in Fig. 2, the

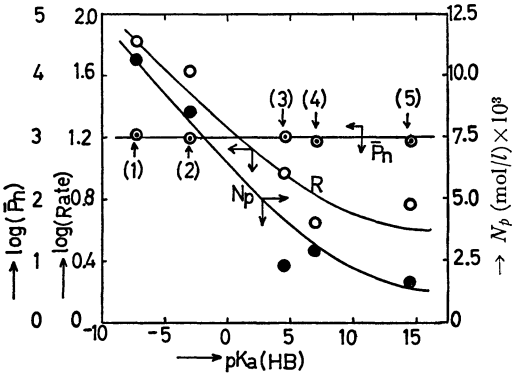

Fig. 2. Influence of pK_a of conjugated acid of sodium salts on the polymerization rate (R), the degree of polymerization ($\bar{P}_n$) and the number of moles of polymer chain (N_p). Pyrolysis condition: temperature, 150—180°C; time, 90 min; sodium salt/α-POM, 0.1 mol/100 g; Polymerization condition: temperature, 20°C; time, 60 min; monomer content, 60 wt-%; (1) NaCl, (2) Na_2SO_4, (3) $NaOCOCH_3$, (4) Na_2CO_3, (5) NaOH.

polymerization rate of the monomer thus obtained edcreased rapidly with an increase in the pK_a of the conjugated acid (HB) of sodium salt (NaB); the rate was almost constant above a pK_a of *ca.* 7. On the other hand, the degree of polymerization of the

polymer was not affected by the addition of sodium salts. The number of moles of the polymer chain of the resulting polymer, which was defined as the ratio of the polymer yield (polymerized monomer mol/unit volume of reaction vessel) to the number-average degree of polymerization, was plotted against the pK_a, as shown in the same figure. The number of moles of the polymer chain also decreased with an increase in the pK_a of acid, almost reaching a constant above a pK_a of *ca.* 7. These results suggest that the quantity of initiating species decreases with an increase in the pK_a. Therefore, the decrease in the polymerizability of the monomer may be ascribed to the decrease in the amount of the initiator. These results lead to the conclusion that the polymerization is initiated by an acidic substance present in the monomer. In order to confirm the role of sodium salt, the adsorption of acids, such as formic acid, by sodium salt was examined. The amount of the acid adsorbed by sodium salt increased with an increase in the pK_a of the conjugated acid of the salt, as is shown in Fig. 3.

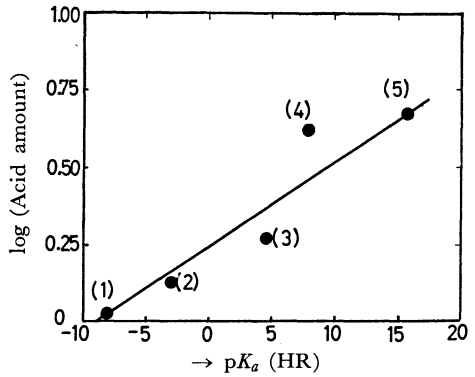

Fig. 3. Relationship between the amount of acid adsorbed by the salt and pK_a of conjugated acid of sodium salt. Formic acid content, 1.18 mol/*l* in PEG solution; reaction time, 1 hr; temperature, 20°C; (1) NaCl, (2) Na_2SO_4, (3) $NaOCOCH_3$, (4) Na_2CO_3, (5) NaOH.

From these results, it may be concluded that the sodium salt catches the Brönsted acid in the monomer, the polymerizability of the monomer was ascribed to the acid content of the monomer solution.

Effect of the Addition of Sodium Carbonate on the Pyrolysis of α-POM. As has been described above, the polymerizability of the monomer obtained by the pyrolysis of α-POM in the presence of sodium salts varied with the kind of sodium salts, and a remarkably depressing effect of the polymerizability was observed in the case of the addition of sodium carbonate. When the monomer was prepared by the pyrolysis of α-POM containing 0 to 10 wt% of sodium carbonate, the effect of the sodium carbonate content on the polymerizability of the monomer was examined.

As is shown in Fig. 4, both the polymerization rate and the number of moles of the polymer chain of the resulting polymer decrease with an increase in the amount of sodium carbonate, while the degree of polymerization is hardly affected by sodium carbonate. These findings indicate that the quantity of initiating species in the monomer decreases upon the addition of sodium salts.

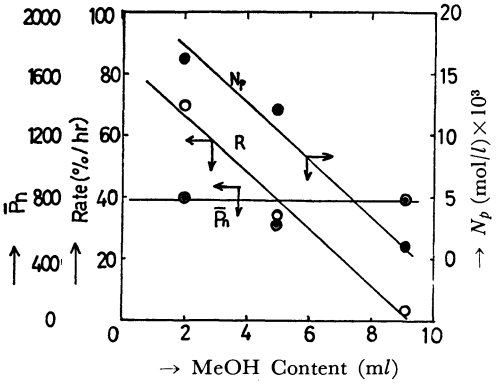

Fig. 4. Influence of the amount of sodium carbonate in decomposer (A) on the polymerization rate (R), the degree of polymerization ($\bar{P}_n$) and the number of moles of polymer chain (N_p). Pyrolysis and polymerization condition: the same condition as in case of Fig. 2.

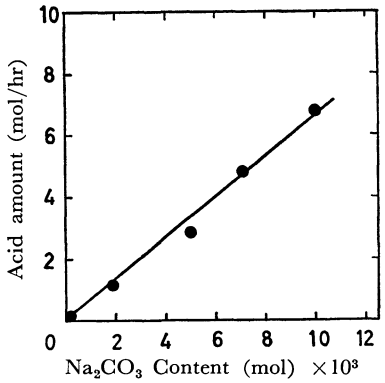

Fig. 5. Relationship between the amount of acid adsorbed by the salt and the amount of sodium carbonate. Formic acid content, 0.25 mol/*l*; reaction time, 1 hr; temperature, 20°C.

In order to make sure of the role of sodium salt, the ability of sodium carbonate to adsorb formic acid was also examined. As Fig. 5 shows, the amount of formic acid adsorbed by sodium carbonate increases proportionally with the amount of sodium carbonate.

These results are in accordance with the above finding that the polymerization caused by Brönsted acid is retarded by the adsorption of acid upon the addition of sodium salt.

Effect of the Impurities Present in the Monomer Gas on the Monomer Polymerizability. Gas chromatographic analysis of the pyrolyzed gas in the absence of sodium salts showed that the monomer contained methanol (0.45 mol%), water (0.35 mol%), and methyl formate (0.01 mol%) as impurities. In order to determine the influence of these impurities on the polymerization, the polymerizability of the monomer was examined in the presence of such additives as formic acid, methanol, water and methyl formate.

The results are shown in Table 1. Methyl formate had no influence on the polymerization, while water or methanol depressed the degree of polymerization but had no influence on the polymerization rate. On the other hand, both the polymerization rate and the degree of polymerization increased upon the addition of formic acid. These results show that formic acid acts as an initiator, while water and methanol act as chain transfer agents in the polymerization.

Table 1. Influence of substances contained in the gas obtained by the pyrolysis of α-POM on the monomer polymerizability

Substance	Rate (%/hr)	$R-R_0$ (%/hr)	$\bar{P}_n \times 10^2$	$N_p \times 10^3$ (mol/l)
Formic acid	21.9	18.4	20.0	3.8
Methanol	5.9	2.4	3.5	4.1
Methyl formate	5.2	1.7	5.9	1.8
Water	3.5	0	2.8	3.2
No additive	3.5	0	5.1	1.5

Polymerization condition: temperature 20°C, time 1 hr, substance/monomer (mole ratio) = 1/1000, R_0 is polymerization rate without any additive.

Formation of Acid. In order to clarify the acid formation quantitatively, the influence of the pyrolysis time and that of the addition of water on the acid formation in the pyrolysis of paraform were investigated.

As Fig. 6 shows, the amount of acid in the hemiformal thus prepared increased linearly with the pyrolysis time of the paraform. This indicates that the acid is not contained in paraform as an impurity, but is produced by a side reaction in the course of pyrolysis. In addition, the amount of acid also increased linearly with the amount of water added. From these results, it may be considered that formaldehyde reacts with water as in Eq. (2) and produces the equivalent mole of formic acid and methanol;

$$2CH_2O + H_2O \rightarrow HCOOH + CH_3OH \qquad (2)$$

According to these results, it may be concluded that the polymerization is initiated mainly by the formic acid produced by the reaction of formaldehyde with the water which is originally present in the paraform used.

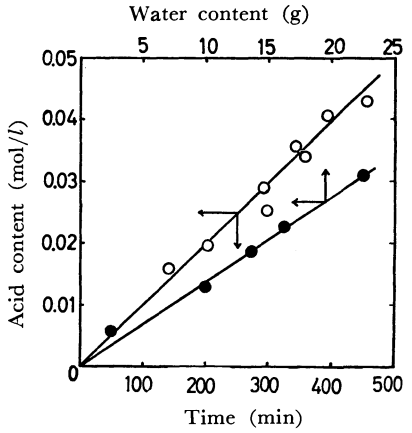

Fig. 6. Influence of the pyrolysis time and of the addition of water on the acid content of the hemiformal. Preparation condition: temperature, 95—115°C; PEG/paraform (weight ratio) = 1; $CaCO_3$/paraform (weight ratio) = 1; pyrolysis time, 110—150 min. (●).

Influence of the Acid Content in the Hemiformal on the Monomer Polymeizability. The monomer polymerizability was studied in connection with the acid content in the hemiformal. Hemiformals containing different amounts of acid were prepared by varying the pyrolysis time of the paraform or by adding different amounts of calcium carbonate to the paraform.

It was found that the polymerization rate increased linearly with the acid content in the hemiformal (Fig. 7). From this, it may be concluded that the polymerization is initiated by formic acid as in Eq. (3) and that the monomer polymerizability depends on the amount of acid in the monomer.

$$HCOOH + CH_2O \rightarrow HOCH_2{}^{\delta+}\cdots{}^{\delta-}OCH \qquad (3)$$
$$\qquad\qquad\qquad\qquad\qquad\qquad\qquad\qquad\qquad\quad \| \; O$$

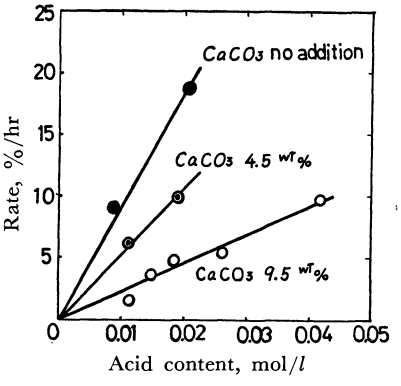

Fig. 7. Influence of the acid content of the hemiformal on the polymerization rate. Hemiformal preparation condition: the same condition as in case of Fig. 6; polymerization condition: the same condition as in case of Fig. 2.

On the other hand, straight lines with slopes differing with the amount of calcium carbonate were observed. That is, when a large amount of calcium carbonate was added to the paraform in the hemiformal preparation step, a great decrease in the polymerization rate was observed in spite of the higher acid content in the hemiformal.

In order to study the cause of this, hemiformals containing almost the same acid content (0.01 mol/*l*) were prepared by adding different amounts of calcium carbonate; the monomer polymerizability was then examined by the use of the monomer obtained by the pyrolysis of these hemiformals. As is shown in Fig. 8, both the polymerization rate and the

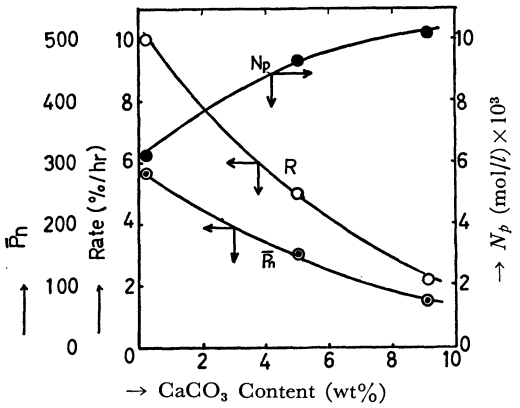

Fig. 8. Influence of the amount of calcium carbonate in the hemiformal preparation step on the polymerizability of monomer obtained by the pyrolysis of the hemiformals of the same acid content (0.01 mol/*l*).

degree of the polymerization of the resulting polymer decrease with an increase in the calcium carbonate content in the hemiformal preparation step, while the number of moles of the polymer chain increases.

This indicates that when hemiformals with the same acid content are prepared, the amount of a substance which acts as both a retarding and a chain transfer agent in the hemiformal may increase with the calcium carbonate content in the hemiformal preparation step. On the other hand, methanol content in the hemiformal may increase with the calcium carbonate content, because the pyrolysis time must be long when the calcium carbonate content is large.

Influence of the Addition of Methanol to the Hemiformal on the Monomer Polymerizability. Methanol may be considered to react with formic acid in the hemiformal pyrolysis step. From this, it may be supposed that methanol acts as both a retarding and a chain transfer agent.

In order to determine the influence of the methanol in the hemiformal pyrolysis step on the monomer polymerizability, methanol was added to a hemiformal containing 0.13 mol/*l* of the acid; the

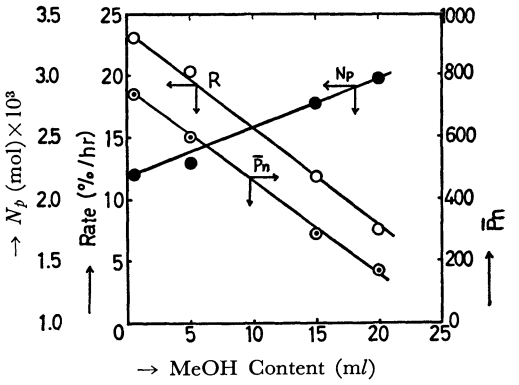

Fig. 9. Influence of the amount of methanol contained in the hemiformal on the rate of polymerization, the degree of polymerization and the number of moles of polymer chain. The hemiformal preparation condition: temperature, 100–115°C; time, 70 min; $CaCO_3$/paraform (weight ratio) = 0.1; acid content of the hemiformal, 0.3 mol/*l*.

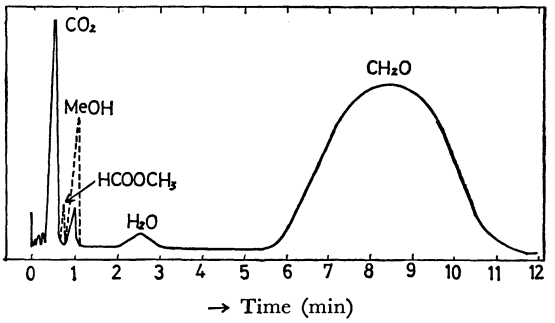

Fig. 10. Gas chromatography of the gas obtained by pyrolyzing the hemiformal. Pyrolysis condition: temperature, 135°C; measurement condition of gas chromatography: temperature, 120°C; carrier gas, He (74 ml/min); column, diglycerol.

polymerizability of the monomer obtained by the pyrolysis of these hemiformals was then examined. As Fig. 9 shows, both the polymerization rate and the degree of polymerization of the resulting polymer decreased proportionally with the amount of methanol added to the hemiformal, while the number of moles of the polymer chain increased.

On the other hand, from the results of the gas chromatographic analysis of the gas obtained by the pyrolysis of the hemiformal (Fig. 10), it was found that the amount of methyl formate formed increased with the amount of methanol in the hemiformal.

From these results, it may be concluded that methyl formate is produced by the reaction of methanol with formic acid present in the hemiformal during the course of the pyrolysis, and that the monomer polymerzability decreases in consequence of the decrease in the acid content of the monomer.

This is in accordance with the facts that both the polymerization rate and the degree of polymerization decrease, while the number of moles of the polymer chain of the polymer increases, with the amount of methanol in the hemiformal.

On the basis of these results, it may be concluded that, in the hemiformal preparation step, the addition of calcium salt to the paraform causes a decrease in the amount of an initiator (acid) in the hemiformal because of adsorption with the salt, and that then, in the hemiformal pyrolysis step, the addition of methanol to the hemiformal causes a decrease in the acid content of the monomer by means of a reaction with the alcohol.

BULLETIN OF THE CHEMICAL SOCIETY OF JAPAN VOL. 42 1693—1697 (1969)

Syntheses of Pterocarpans. III.*1 Synthetic Analogues of Neodulin*2

Kenji FUKUI, Mitsuru NAKAYAMA and Teruo HARANO

Department of Chemistry, Faculty of Science, Hiroshima University, Higashi Sendamachi, Hiroshima

(Received November 4, 1968)

4',5'-Dimethoxy-2'-hydroxyfurano[3'',2'':6,7]isoflavone was obtained from isoelliptol isoflavone by selective demethylation with boron tribromide. The treatment of the 2'-hydroxyisoflavone with sodium borohydride in absolute alcohol - tetrahydrofuran afforded 8,9-dimethoxyfurano[3',2':2,3]pterocarpan. 8,9-Dimethoxyfurano[2',3':3,4]pterocarpan was prepared from elliptol isoflavone by a similar procedure.

(−)-Neodulin was isolated from *Neorautanenia edulis* C. A. Sm. by Van Duuren.[1] Its structure was identified as 8,9-methylenedioxyfurano[3',2':2, 3]pterocarpan (I) on the basis of degradative studies and the results of spectral analyses. Recently, I was derived from dehydroneotenone (II), a naturally-occurring furano[3'',2'':6,7]isoflavone, by Brink *et al.*;[2] further the present authors achieved the total syntesis of II.[3] These facts confirmed the chemical structure of neodulin to be I. An analogue of I containing *ortho*-dimethoxyl groups instead of a methylenedioxy group, 8,9-dimethoxyfurano[3',2':2,3]pterocarpan (III), is a commonly-occurring type in coumestans and rotenoids. The present paper will describe the synthesis of III by a modification of the procedure reported earlier.[4,5]

The selective demethylation of dihydroisoelliptol isoflavone (2',4',5'-trimethoxy-4'',5''-dihydrofurano[3'',2'':6,7]isoflavone (IV)[6] with either boron tribromide or anhydrous aluminum chloride in acetonitrile[4,7] afforded 4',5'-dimethoxy-2'-hydroxy-4'',5'' - dihydrofurano[3'',2'':6,7] isoflavone (V), which then gave a mono-acetate by the usual method. The reduction of the 2'-hydroxydihydroisoflavone V with sodium borohydride in absolute alcohol - tetrahydrofuran, followed by cyclization with hydrochloric acid, gave 8,9-dimethoxy-4',5'-dihydrofurano[3',2':2,3]pterocarpan (VI). The dehydrogenation of the dihydrofuranoisoflavone IV with 2,3-dichloro-5,6-dicyano-1,4-benzoquinone (D. D.Q.) or with 10% Pd-C gave isoelliptol isoflavone (2', 4', 5' - trimethoxyfurano[3'', 2'':6,7]isoflavone) (VII), which had been previously obtained from IV with *N*-bromosuccinimide.[6] By a procedure similar to that used for IV, VII gave the desired furanopterocarpan III *via* 4',5'-dimethoxy-2'-hydroxyfurano[3'',2'':6,7]isoflavone (VIII). The catalytic hydrogenation of III afforded dihydrofuranopterocarpan VI.

8, 9 - Dimethoxyfurano[2', 3', : 3, 4] pterocarpan (IX), an isomer of III, was also obtained from elliptol isoflavone (X)[8] *via* 2'-hydroxy-4',5'-di-

*1 Part II: K. Fukui and M. Nakayama, This Bulletin, **42**, 1408 (1969).

*2 Presented at the Ube Local Meeting (November, 1966) and the 21st Annual Meeting (Osaka, April, 1968) of the Chemical Society of Japan.

1) B. L. Van Duuren, *J. Org. Chem.*, **26**, 5013 (1961).

2) C. v. d. M. Brink, J. J. Dekker, E. C. Hanekom, D. H. Meiring and G. J. H. Rall, *J. S. African Chem. Inst.*, **18**, 21 (1965); *Chem. Abstr.*, **63**, 14834h (1965).

3) K. Fukui and M. Nakayama, *Experientia*, **20**, 668 (1964); This Bulletin, **41**, 2733 (1968).

4) K. Fukui, M. Nakayama and T. Harano, *ibid.*, **42**, 233 (1969).

5) V. K. Kalra, A. S. Kukla and T. R. Seshadri, *Indian J. Chem.*, **5**, 607 (1967).

6) K. Fukui, M. Nakayama, A. Tanaka and S. Sasatani, This Bulletin, **38**, 845 (1965).

7) a) K. Aghoimurthy, A. S. Kukla and T. R. Seshadri, *J. Indian Chem. Soc.*, **38**, 914 (1961); b) V. K. Kalra, A. S. Kukla and T. R. Seshadri, *Indian J. Chem.*, **5**, 287 (1967); c) K. Fukui, M. Nakayama and T. Harano, *Experientia*, **23**, 613 (1967).

8) K. Fukui, M. Nakayama and M. Hatanaka, This Bulletin, **36**, 872 (1963).

methoxyfurano[2'',3'':7,8]isoflavone (XI).[9]

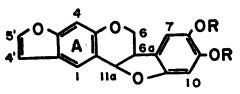

I R-R=CH_2

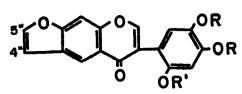

II R-R=CH_2, R'=Me

III R=Me

VII R=R'=Me

VIII R=Me, R'=H

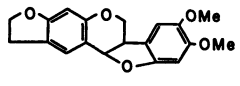

VI

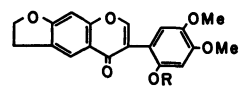

IV R=Me

V R=H

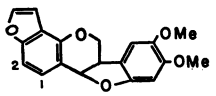

IX

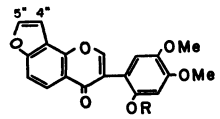

X R=Me

XI R=H

The NMR spectra of the two isomeric furanopterocarpans, III and IX, and the dihydrocompound VI are shown in Figs. 1—3 and Table 1.*3 In the spectra of these compounds the signals at δ 3.2—4.5 (3H, complex multiplets) and at δ 5.3—5.7 (1H, multiplet) can be assigned to the C-6 and C-6a, and the C-11a protons, respectively; the signals are fully consistent with the formulation of the pterocarpan system on the basis of the analyses previously reported.[4] Furthermore, a set of one-proton signals at δ 6.80 and 6.48 (each, 1H, singlet) in the spectrum of III (Fig. 1), which closely resemble those in the spectra of VI and IX, can be assigned to the aromatic protons at C-7 and C-10 respectively. The remaining two signals, those of aromatic protons at δ 7.70 (1H, singlet) and 7.07 (1H, doublet, J=1 Hz), can be attributed to the protons at C-1 and C-4 respectively in view of their small coupling constants.[10] However, in the spectrum of IX, the corresponding signals were found at δ 7.43 (1H, doublet) and 7.16 (1H, broad doublet) and formed an AB-type (J_{AB}=8.5 Hz), indicating that the two protons are oriented in *ortho* positions (C-1 and C-2) to one another. These facts show that the structures

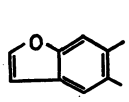

(A)

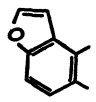

(B)

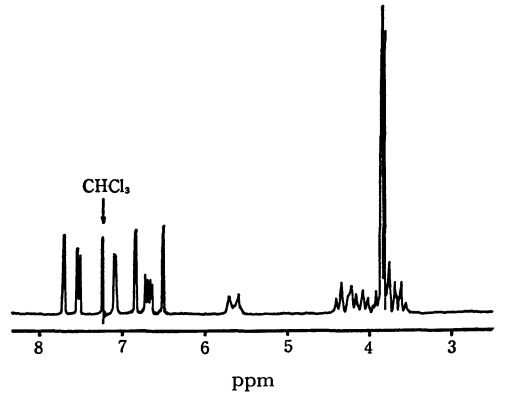

Fig. 1. NMR spectrum of III.

of III and IX belong to the linear ring system (A) and the angular ring system (B) respectively. From these results, it is apparent that the linear or angular pattern of furanopterocarpans can be determined easily by analyzing the NMR pattern of the aromatic protons of the A-ring. A long-range coupling is observed between the aromatic proton at C-4 or C-2 (broad singlet) and the β-furano-proton at C-4' (double doublet or broad singlet) in the

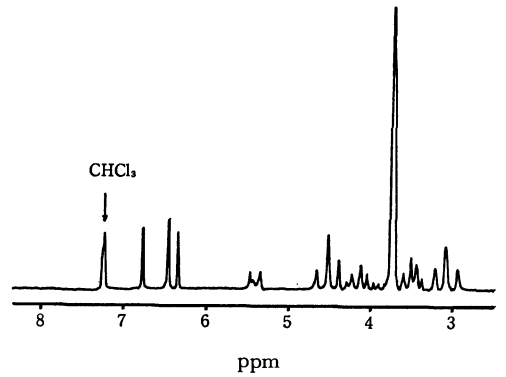

Fig. 2. NMR spectrum of VI.

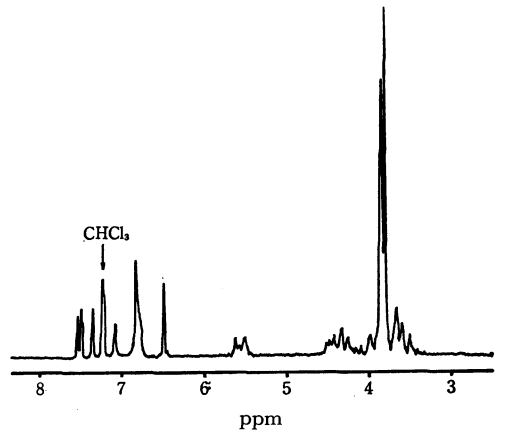

Fig. 3. NMR spectrum of IX.

9) V. Chandrashekar, M. Krishnamurti and T. R. Seshadri, *Tetrahedron*, **23**, 2505 (1967).

*3 The NMR spectra were measured with a Varian A-60 spectrometer and a Hitachi R-20 spectrometer, using tetramethylsilane as the internal standard (δ-value in $CDCl_3$).

10) H. S. Gutowsky, C. H. Holm, A. Saika and G. A. Williams, *J. Am. Chem. Soc.*, **79**, 4596 (1957).

Table 1. NMR data of pterocarpans*3,4

Proton		Compound III	VI	IX
Arom.	C-1	7.70_s	7.27_s	7.43_d (J=8.5)
	C-2			7.16_{bd} (J=8.5)
	C-4	7.07_d (J=1.0)	6.47_s	
	C-7	6.80_s	6.79_s	6.82_s
	C-10	6.48_s	6.35_s	6.50_s
Furan	C-4′	6.68_{dd} (J=2.0, 1.0)	3.13_t (J=8.0)	6.82_{bs}
	C-5′	7.52_d (J=2.0)	4.55_t (J=8.0)	7.52_d (J=2.0)
Ring	C-11a	5.63_m	5.45_m	5.57_m
	C-6—C-6a	$3.3—4.5_m$	$3.2—4.3_m$	$3.3—4.5_m$
OCH_3		3.78_s	3.80_s	3.80_s
		3.81_s	3.83_s	3.83_s

*4 s=singlet; bs=broad singlet; d=doublet; bd=broad doublet; t=triplet; m=multiplet

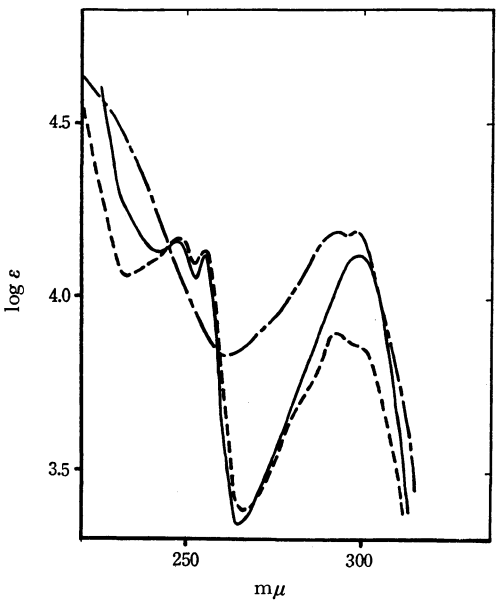

Fig. 4. UV spectra of III (——), VI (– – –) and IX (----) in ethanol solution.

furanopterocarpans, III and IX. Similar observations have been reported in several earlier reports.[11] This phenomenon also appears as a double doublet at the C-4″ proton of acetyl derivatives of the furanoisoflavones, VIII and XI.

The ultraviolet spectra of the furanopterocarpan, III, and its dihydro compound, VI, are shown in Fig. 4. The former contains two absorption maxima, at *ca.* 25 mμ and at *ca.* 300 mμ, while the latter contains only one maximum, at *ca.* 300 mμ. The strong absorption in the region *ca.* 250 mμ is characteristic of the benzofuran grouping, as has previously been noted by the present authors and by others.[3,12]

Experimental*5

4′,5′-Dimethoxy-2′-hydroxy-4″,5″-dihydrofurano-[3″,2″:6,7]-isoflavone (V). *a) With Boron Tribromide.* A solution of boron tribromide in anhydrous methylene chloride (5 ml) was added, at room temperature, to a solution of the isoflavone IV[6] (1.0 g) in the same solvent (200 ml), and then allowed to stand overnight in the dark. After the solution had been poured into water, the separated solid was collected and washed with water. The product was recrystallized from ethanol to give V as light yellow needles; mp 204—205°C; yield, 0.8 g. It showed a negative ferric chloride reaction. IR: 1623 cm^{-1} (C=O). UV: λ_{max} mμ (log ε); 264 (3.92), 306 (4.10).

Found: C, 66.96; H, 4.81%. Calcd for $C_{19}H_{16}O_6$: C, 67.07; H, 4.75%.

b) With Aluminum Chloride. A mixture of IV (1.2 g) and anhydrous aluminum chloride (4.0 g) in anhydrous acetonitrile (30 ml) was refluxed for 12 hr. The solvent was removed as far as possible, and then the residue was treated with 10% hydrochloric acid. The separated solid was collected, washed with water, and recrystallized from ethanol to give V, mp 203—204°C, which was identical with the sample obtained in a); yield, 1.05 g.

The acetate: hot acetic anhydride - anhydrous sodium acetate method; mp 196—197°C (colorless needles from ethanol). IR: 1752, 1643 cm^{-1} (C=O). UV: λ_{max}

11) a) J. A. Elvidge and R. G. Foster, *J. Chem. Soc.*, **1963**, 590; b) E. A. Abu-Mustafa and M. B. E. Fayez, *Can. J. Chem.*, **45**, 325 (1967); c) K. Fukui, M. Nakayama and S. Tanaka, This Bulletin, **42**, No. 7 (1969), in press.

12) a) K. Fukui, M. Nakayama and K. Okazaki, *Nippon Kagaku Zasshi (J. Chem. Soc. Japan, Pure Chem. Sect.)*, **87**, 1096 (1966); b) D. K. Chatterjee, R. M. Chatterje and K. Sen, *J. Org. Chem.*, **29**, 2467 (1964).

*5 All the melting points are uncorrected. The infrared spectra were measured in Nujol, while the ultraviolet spectra were measured in ethanol, unless otherwise stated.

mμ (log ε); 276 (4.17), 307 (4.17). NMR:*3,4 δ 8.06$_s$ (C-5); 7.80$_s$ (C-2); 6.83$_s$, 6.73$_s$, 6.68$_s$ (C-8,3',6'); 4.79$_t$ (J=8.0, C-5''); 3.91$_s$ (6H, OC$\underline{H}_3$), 3.33$_t$ (J=8.0, C-4''); 2.15$_s$ (3H, OCOC$\underline{H}_3$).

Found: C, 65.99; H, 4.73%. Calcd for $C_{21}H_{18}O_7$: C, 65.96; H, 4.75%.

8,9-Dimethoxy-4',5'-dihydrofurano[3',2':2,3]-pterocarpan (VI). A solution of sodium borohydride (600 mg) in absolute ethanol (15 m*l*) was added, drop by drop, to a solution of the above isoflavone V (500 mg) in anhydrous tetrahydrofuran (80 m*l*). The reaction mixture was then kept for 60 hr at room temperature while being stirred. After acetone (20 m*l*) had been added to decompose the excess reducing agent, the solvent was removed under reduced pressure. The residue was treated with 10% hydrochloric acid, and then the separated solid was collected, washed with water and recrystallized from ethanol to give VI as colorless plates; mp 174—175°C; yield, 400 mg. IR: 1624, 1598, 1498 cm^{-1} (phenyl). UV: λ_{max} mμ (log ε); 294 (4.19), 298 (4.19); ($CHCl_3$) 299.5 (4.08).

Found: C, 69.92; H, 5.51%. Calcd for $C_{19}H_{18}O_5$: C, 69.92; H, 5.56%.

Isoelliptol Isoflavone (2',4',5'-Trimethoxyfurano-[3'',2'':6,7]isoflavone) (VII). *A) With* 10% *Pd-C.* A mixture of IV (1.7 g) 10% palladium-charcoal (300 mg), and diphenyl ether (30 m*l*) was refluxed for 12 hr. The catalyst was then filtered off, and the solvent removed by steam distillation. The resulting precipitate was collected and recrystallized from ethanol to give VII as colorless needles; mp 191—192°C (lit. mp 190—190.5°C[6]; mp 191°C[13]); yield, 1.0 g. This was identical with an authentic sample obtained from IV by the *N*-bromosuccinimide method.[6]

b) With D.D.Q. A mixture of IV (1.0 g), 2,3-dichloro-5,6-dicyano-1,4-benzoquinone (700 mg), and absolute benzene (70 m*l*) was refluxed for 20 hr. After the solution had then been cooled, the precipitated hydroquinone derivative was filtered off and the solvent was removed as far as possible. The residual solid was recrystallized from ethanol to give a mixture of two compounds as colorless needles; mp 190—199°C; yield, 700 mg. The mixture (500 mg) was chromatographed on a silica gel column (12 g); subsequent elution with chloroform - *n*-hexane gave the desired isoflavone, VII (mp 190—191°C), which was identical with the sample derived by the above-described method; yield, 100 mg. Further elution with the same solvent gave the starting isoflavone, IV (mp 200—201°C; 400 mg).

3',4'-Dimethoxy-2'-hydroxyfurano[3'',2'':6,7]isoflavone (VIII). A mixture of VII (500 mg), boron tribromide (130 mg), and methylene chloride (20 m*l*) was treated by a method similar to that used for IV. The crude product was recrystallized from ethanol to give VIII as light yellow needles; mp 212—213°C (lit,[13] mp 200—201°C); yield, 400 mg. This was identical with an authentic sample obtained from VII by the aluminum chloride - acetonitrile method.[13] IR: 1620 cm^{-1} (C=O). UV: λ_{max} mμ (log ε); 239 (4.56), 260$_{sh}$*6 (4.36), 304 (4.15).

Found: C, 67.50; H, 4.44%. Calcd for $C_{19}H_{14}O_6$: C, 67.45; H, 4.17%.

The acetate: hot acetic anhydride - anhydrous sodium acetate method; mp 216—217°C (colorless needles from ethanol). IR: 1745, 1643cm^{-1} (C=O). UV: λ_{max} mμ (log ε); 239 (4.53), 306 (4.02). NMR:*3,4 δ 8.55$_s$ (C-5); 7.94$_s$ (C-2); 7.59$_{bs}$ (C-8); 7.75$_d$ (J=2.5, C-5''); 6.90$_{dd}$ (J=2.5, 1.0, C-4''); 6.89$_s$ (C-6'); 6.73$_s$ (C-3'); 3.90$_s$ (6H, OC$\underline{H}_3$); 2.13$_s$ (3H, OCOC$\underline{H}_3$).

Found: C, 66.41; H, 4.33%. Calcd for $C_{21}H_{16}O_7$: C, 66.31; H, 4.24%.

8,9-Dimethoxyfurano[3',2':2,3]pterocarpan (III). A mixture of VIII (350mg), sodium borohydride (400mg), and absolute tetrahydrofuran - ethanol (4 : 1, 50m*l*) was treated by a method similar to that used for V. The crude product was recrystallized from ethanol to give III as colorless needles; mp 172—173°C; yield, 200mg. IR: 1617, 1586, 1535, 1510, 1500cm^{-1} (phenyl); ($CHCl_3$) 1620, 1590, 1520, 1493cm^{-1} (phenyl). UV: λ_{max} mμ (log ε); 247 (4.24), 255 (4.12), 299 (4.12); ($CHCl_3$) 250 (4.05), 256.5 (4.06), 302 (4.10).

Found: C, 70.28; H, 5.01%. Calcd for $C_{19}H_{16}O_5$: C, 70.36; H, 4.98%.

Hydrogenation of III. Furanopterocarpan III (300 mg) was hydrogenated in ethyl acetate (40 m*l*) over 10% Pd-C (600 mg) at atmospheric pressure and at room temperature. The catalyst was then filtered off, and the solvent was removed under reduced pressure. The residue was dissolved in benzene. The benzene solution was washed with a 5% aqueous sodium hydroxide solution and then with water. The evaporation of the dried solution and the chromatography of the resulting solid on silica gel with chloroform - *n*-hexane (1 : 1) gave colorless crystals, which were then recrystallized from ethanol to give VI; mp 174—175°C; yield, 150 mg. This was identical with the sample derived by the method described above.

4',5'-Dimethoxy-2'-hydroxyfurano[2'',3'':3,4]isoflavone (XI). 2'-Hydroxyisoflavone XI was prepared, according to the directions of Seshadri,[9] from elliptol isoflavone, X.[8] Recrystallization from ethanol gave XI; mp 207—208°C (lit.[9] mp 204—205°C).

Found: C, 67.57; H, 4.27%. Calcd for $C_{19}H_{14}O_6$: C, 67.45; H, 4.17%.

The acetate: hot acetic anhydride - anhydrous sodium acetate method; mp 205—206°C (colorless needles from ethanol). IR: 1770, 1744, 1637 cm^{-1} (C=O). UV: λ_{max} mμ (log ε); 230 (4.53), 247$_i$*7 (4.48), 312$_{sh}$*6 (3.81). NMR:*3,4 8.12$_d$ (J=9.0, C-5); 7.97$_s$ (C-2); 7.73$_d$ (J=2.0, C-5''); 7.55$_d$ (J=9.0, C-6); 7.13$_{bs}$ (C-4'') 6.87$_s$ (C-6'); 6.72$_s$ (C-3'); 3.90$_s$ (6H, OC$\underline{H}_3$); 2.13$_s$ (OCOC$\underline{H}_3$, 3H).

Found: C, 66.27; H, 4.40%. Calcd for $C_{21}H_{16}O_7$: C, 66.31; H, 4.24%.

8,9-Dimethoxyfurano[2',3':3,4]pterocarpan (IX). A mixture of XI (150 mg), sodium borohydride (200 mg), and absolute tetrahydrofuran - ethanol (6 : 1, 35 m*l*) was treated by a method similar to that used for V. The crude product was recrystallized from ethanol to give IX as colorless prisms; mp 180—181°C; yield, 70 mg. IR: 1613, 1596, 1492 cm^{-1} (phenyl). UV: λ_{max} mμ (log ε); 247.5 (4.17), 255.5 (4.13), 292.5 (3.90); ($CHCl_3$) 251 (4.12), 256 (4.12), 292.5 (3.89), 300$_i$*7 (3.86).

13) V. Chandrashekar, M. Krishnamurti and T. R. Seshadri, *Curr. Sci. (India)*, **36**, 623 (1967); *Chem. Abstr.*, **68**, 59402q (1968).

*6 sh=shoulder.

*7 i=inflection point.

Found: C, 70.19; H, 5.08%. Calcd for $C_{19}H_{16}O_5$: C, 70.36; H, 4.98%.

The authors wish to express their thanks to Professor Shô Itô, Tohoku University, for his NMR measurements, and to Miss Toshiko Hiwaki, of this laboratory, for her microanalyses and her measurements of the ultraviolet spectra.

BULLETIN OF THE CHEMICAL SOCIETY OF JAPAN VOL. 42 1697—1702 (1969)

Thermal Decomposition of 1,1-Disubstituted-3-aryl-3-(aryloxythiocarbonyl)-2-thioureas*[1)]

Koshin MIYAZAKI

Research Department of the Takaoka Plant, Nippon Soda Co., Ltd., Mukaino-honmachi, Takaoka-shi, Toyama

(Received November 8, 1968)

1,1-Disubstituted-3-(4-chlorophenyl)-3-(phenoxythiocarbonyl)-2-thioureas of the formula R,R'N-C^1(=S)-N(*p*-Cl-C_6H_4-)-C'(=S)-OC_6H_5 (II), when kept at an elevated temperature without any solvent, decomposed into the corresponding thionocarbamates of the formula R,R'N-C(=S)-OC_6H_5 (III), while *p*-chlorophenyl isothiocyanate was eliminated. A carbon-14-labeling experiment showed that the decomposition proceeded only through the following path:

$$\text{II} \longrightarrow \text{R,R'N-C}^2\text{(=S)-OC}_6\text{H}_5 + p\text{-Cl-C}_6\text{H}_4\text{-N=C}^1\text{=S}$$

Kinetic studies of the various II showed that the decompositions were strictly first order. The rate constant at 175°C increased in the order: R,R'=$(CH_3)_2$>$(C_2H_5)_2$>CH_3,4-methylbenzyl≳(n-$C_3H_7)_2$>CH_3, benzyl>CH_3, 4-chlorobenzyl. Neither the products nor the rate of the decomposition reaction was influenced by the presence of a radical scavenger. Furthermore, a crossover decomposition reaction did not give any crossover products. On the basis of these results, a possible intramolecular mechanism of the decomposition involving a four-membered cyclic intermediate structure was proposed.

In an earlier paper,[1)] it was shown that *O*-aryl-*S*-(*N*,*N*-dimethylthiocarbamoyl)-*N*-(aryl)thiolimido carbonates with the formula I, when kept at a temperature higher than their melting points, rearranged within a few minutes into the corresponding 1, 1-dimethyl-3-aryl-3-(aryloxythiocarbonyl)-2-thioureas with the formula II (Eq. (1)).

$$(CH_3)_2N\text{-}\underset{\underset{S}{\|}}{C}\text{-}S\text{-}\underset{\underset{N\text{-}Ar'}{\|}}{C}\text{-}OAr \longrightarrow (CH_3)_2N\text{-}\underset{\underset{S}{\|}}{C}\text{-}\underset{\underset{Ar'}{|}}{N}\text{-}\underset{\underset{S}{\|}}{C}\text{-}OAr \qquad (1)$$

During the course of a continuous investigation of the rearrangement of I to II, it has been found that II gradually decomposed, when the reaction time was prolonged, into the aryl *N*,*N*-dimethylthionocarbamate (III), while aryl isothiocyanate (IV) was eliminated. It can easily be considered, however, that IV can be split off in the two ways shown in Eq. (2):

$$(CH_3)_2N\text{-}\underset{\underset{S}{\|}}{C^1}\text{-}\underset{\underset{Ar'}{|}}{N}\text{-}\underset{\underset{S}{\|}}{C^2}\text{-}OAr \xrightarrow{A} (CH_3)_2N\text{-}\underset{\underset{S}{\|}}{C^1}\text{-}OAr + Ar'\text{-}N{=}C^2{=}S$$
$$\text{(III)} \qquad \text{(IV)}$$
$$(CH_3)_2N\text{-}\underset{\underset{S}{\|}}{C^1}\text{-}\underset{\underset{Ar'}{|}}{N}\text{-}\underset{\underset{S}{\|}}{C^2}\text{-}OAr \xrightarrow{B} (CH_3)_2N\text{-}\underset{\underset{S}{\|}}{C^2}\text{-}OAr + Ar'\text{-}N{=}C^1{=}S \qquad (2)$$

In the present paper, a carbon-14-labeling experiment and the kinetics of the decomposition have been studied for a series of 1,1-disubstituted-3-(4-chlorophenyl)-3-(phenoxythiocarbonyl)-2-thioureas in order to clarify the decomposition mechanism.

Results and Discussion

The compounds II studied here were prepared by the reaction of an appropriate 1,1-disubstituted-3-(4-chlorophenyl)-2-thiourea with a proper aryl chlorothionoformate, as has been reported previously.[1)] The data are shown in Table 1. On being heated at 175°C without any solvent and under a slow stream of nitrogen, the compounds II underwent a gradual decomposition, with the elimination

*1 Presented in part at the 19th Annual Meeting of the Chemical Society of Japan, Yokohama, April, 1966.

1) A. Kaji and K. Miyazaki, *Nippon Kagaku Zasshi (J. Chem. Soc. Japan, Pure Chem. Sect.)*, **87**, 727 (1966).

TABLE 1. 1,1-DISUBSTITUTED-3-(4-CHLOROPHENYL)-3-ARYLOXYTHIOCARBONYL-2-THIOUREAS

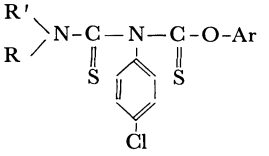

Compd. No	R R′	Ar	Appearance	Mp[a] °C	Yield[b] %	Formula	Anal. C(%) Found (Calcd)	Anal. H(%) Found (Calcd)	Anal. N(%) Found (Calcd)
II-1	CH_3 CH_3	phenyl	Colorless prisms[c]	169—170	74.5	$C_{16}H_{15}ClNO_2S_2$[e]	—	—	—
II-2	C_2H_5 C_2H_5	phenyl	Colorless needles[c]	112—113	71	$C_{18}H_{19}ClN_2OS_2$	56.70 (56.70)	5.07 (9.02)	7.42 (7.40)
II-3	n-C_3H_7 n-C_3H_7	phenyl	Colorless prisms[d]	90— 91	71	$C_{20}H_{23}ClN_2OS_2$	59.00 (59.05)	5.42 (5.66)	7.09 (6.90)
II-4	C_2H_5 C_2H_5	4-tolyl	Colorless needles[c]	157—158	68	$C_{19}H_{21}ClN_2OS_2$	57.70 (58.09)	5.55 (5.35)	6.97 (7.15)
II-5	CH_3 4-Methylbenzyl	phenyl	Colorless needles[c]	110—111.5	66	$C_{23}H_{21}ClN_2OS_2$	62.30 (62.66)	4.93 (4.77)	6.11 (6.36)
II-6	CH_3 Benzyl	phenyl	Colorless needles[c]	121.5—122.5	65	$C_{22}H_{19}ClN_2OS_2$	61.70 (61.90)	4.52 (4.45)	6.43 (6.57)
II-7	CH_3 4-Chlorobenzyl	phenyl	Colorless needles[c]	131—132	68	$C_{22}H_{18}Cl_2N_2OS_2$	57.20 (57.27)	4.03 (3.90)	6.33 (6.07)

a) All melting points are uncorrected. b) Yields recorded are those of recrystallized products. c) From ethanol - acetone.
d) From methanol. e) Reported previously (lit. 1).

of *p*-chlorophenyl isothiocyanate (IVa); the corresponding aryl *N,N*-disubstituted-thionocarbamates could be detected as the other major decomposition products. The compounds IVa and the thionocarbamates isolated by a chromatograph were identified by a mixed-melting-point test and/or by the agreement of the IR spectra with those of the corresponding authentic samples. It will easily be seen that there are two possible ways to split off the compound IVa, as has been expressed in Eq. (2). In order to ascertain which way was preferable, the thermal decomposition of II-1, but with the C^2 atom (in Eq. (2)) labeled with a radioactive carbon, was studied; the radioactive II-1 was prepared by the method shown in the following scheme.

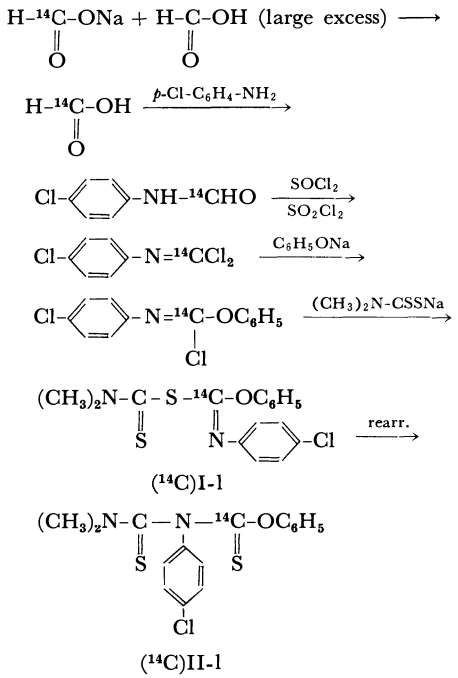

As a result of the experiment, it was found that the compound, IVa, formed by the decomposition of (14C)II-1 did not have any radioactivity, while phenyl *N,N*-dimethylthionocarbamate (IIIa) still retained its radioactivity, with almost the same specific activity as that of the starting material, (14C) II-1. These results show that the decomposition proceeds exclusively through the path B in Eq. (2).

In order to investigate the influence of the substituent (R, R') on the rate of decomposition, the kinetics of the decomposition were investigated on three compounds (II-1—II-3). The decomposition rates were determined by measuring the amount of the product IVa by spectrophotometry. As a result, it was found that the decomposition reactions followed good first-order kinetics (Fig. 1). The first-order rate constants, which were derived from the slopes of the straight lines in Fig. 1, are listed in Table 2.

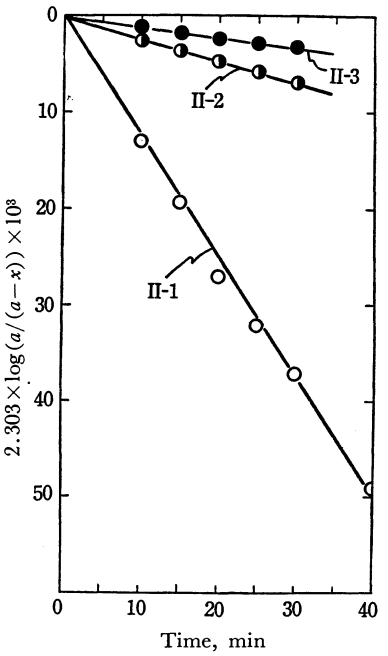

Fig. 1. First-order plots of kinetic data for II-1—II-3 at 175±0.5°C.

TABLE 2. FIRST-ORDER RATE CONSTANTS (k_1) OF THE DECOMPOSITION REACTIONS AT 175±0.5°C FOR II-1—II-3

Compd. No.	$k_1 \times 10^3$ (min^{-1})	Relative rate
II-1	12.80	(1)
II-2	2.32	0.18
II-3	1.04	0.08

In order to examine whether the decomposition, which followed the path B in Eq. (2), proceeded by an intermolecular route or by an intramolecular route, a crossover experiment was performed with two compounds of II. That is, an equimolecular mixture of II-1 and II-4 was heated without any solvent at 175°C for 1.5 hr under a slow stream of nitrogen. If the compounds II decomposed according to an ionic intermolecular mechanism involving the heterolytic cleavage of the (R, R')N–C^1 bond and the Ar'N–C^2 bond, crossover products, such as 4-tolyl *N,N*-dimethylthionocarbamate (IIId) and phenyl *N, N*-diethylthionocarbamate (IIIb), should be detected in the crossover reaction mixture. The thin-layer chromatograms of that reaction mixture, however, showed no detectable amounts of IIIb or IIIb. This result suggests that the decomposition involves an intramolecular mechanism rather than an intermolecular mechanism.

Another possible mechanism for the decomposition of II is homolytic cleavages of the above-mentioned two bonds. In order to investigate this possibility, the decomposition reaction of the compound

II-1, mixed with a small amount (*ca.* 2 wt%) of a radical scavenger such as *p*-quinone or 1,1-diphenyl-2-picrylhydrazyl (DPPH), was studied at 175°C. As a result, the decomposition products were found to be the same as in the absence of the scavenger, while the rate was scarcely affected by the presence of the scavenger. In view of the above facts, one may presume that the decomposition did not involve a radical route.

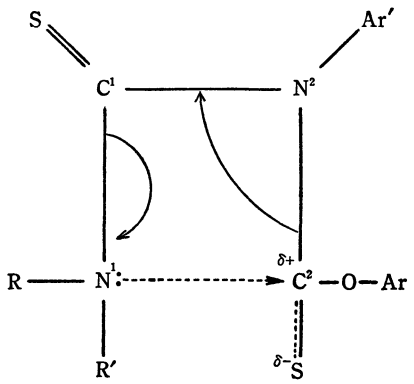

Fig. 2. Four-membered cyclic mechanism.

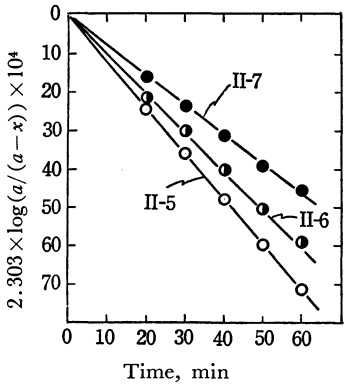

Fig. 3. First-order plots of kinetic data for II-5—II-7 at 175±0.5°C.

Taking the above results into consideration, it has been presumed that the decomposition of the compound II took place through an intramolecular mechanism involving a four-memberd cyclic intermediate structure, as in Fig. 2.

Since the decomposition reaction should be caused by a nucleophilic attack of the N^1 atom on the C^2 atom, it was expected that a stronger electron-donating inductive effect of the substituent (R, R'), which might promote the nucleophilic character of the N^1 atom, would result in a larger rate of decomposition. However, the results obtained concerning II-1—II-3 betrayed this expectation; the rate constants increased in the order of $R=CH_3>C_2H_5>n\text{-}C_3H_7$ (Table 2). This finding that the rate constants diminish regularly with an increase in the bulkiness of the alkyl groups indicates that the steric effect of R much outweighs the electronic effect. In an effort to determine the inductive effect of the substituent (R, R') upon the decomposition, further kinetic studies were carried out on a series of N^1-(4-substituted-benzyl)-N^1-methyl- analogues (II-5—II-7). Since the steric effects in three compounds should be virtually the same, the substituent effect caused by the inductive effect upon the rate of the decomposition can be demonstrated clearly. The kinetic results obtained are shown in Fig. 3, while the rate constants are listed in Table 3.

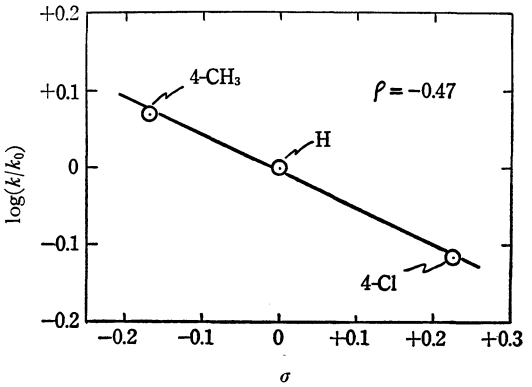

Fig. 4. Hammett plots for the thermal decompositions of II-5—II-7 at 175±0.5°C.

TABLE 3. FIRST-ORDER RATE CONSTANTS (k_1) OF THE DECOMPOSITION REACTION AT 175±0.5°C FOR II-5—II-7

Compd. No.	$k_1\times10^4$ (min^{-1})	Relative rate
II-5	12.0	1.18
II-6	10.2	(1)
II-7	7.8	0.77

Hammett plots of $\log(k/k_0)$ *vs.* σ gave a straight line, with $\rho=-0.47$ (Fig. 4). This fact indicates that the decomposition should be essentially accelerated by a stronger electron-donating inductive effect of the substituent on the N^1 atom.

The results of the carbon-14 labeling experiment, the crossover experiment, the scavenger experiment, and the Hammett correlation lend some support to the presumption of an internal four-membered cyclic mechanism such as that expressed in Fig. 2.

Experimental*2

Materials. *p*-Chlorophenyl Isothiocyanate (IVa). This was obtained by the usual method. Mp 44—45°C.[2]

1,1-Disubstituted-3-(4-chlorophenyl)-2-thioureas. These were prepared by the reaction of *p*-chlorophenyl

*2 All boiling and melting points are uncorrected.

2) G. M. Dyson, "Org. Synth.," Coll. Vol. I, p. 165 (1948).

isothiocyanate with a proper secondary amine: 1,1-dimethyl- mp 168—169°C,[3] 1,1-diethyl- mp 89—90°C. Found: C, 54.22; H, 5.87%. Calcd for $C_{11}H_{15}ClN_2S$: C, 54.43; H, 6.19%. 1,1-Di-*n*-propyl- mp 108—109°C. Found: C, 57.40; H, 6.80%. Calcd for $C_{13}H_{19}ClN_2S$: C, 57.67; H, 7.02%. 1-Benzyl-1-methyl- mp 157—158°C. Found: C, 61.78; H, 4.88%. Calcd for $C_{15}H_{15}ClN_2S$: C, 61.96; H, 5.16%. 1-(4-Chlorobenzyl)-1-methyl- mp 136—137°C. Found: C, 55.20; H, 4.15%. Calcd for $C_{15}H_{14}Cl_2N_2S$: C, 55.38; H, 4.31%. 1-(4-Methylbenzyl)-1-methyl- mp 126—127°C. Found: C, 62.80; H, 5.61%. Calcd for $C_{16}H_{17}ClN_2S$: C, 63.05; H, 5.58%.

Aryl Chlorothionoformates. These were prepared by the reaction of a corresponding phenol with thiophosgene according to a procedure described earier;[1] phenyl- bp 101—103°C/18 mmHg, 4-tolyl- bp 102—103°C/8 mmHg.

1,1-Disubstituted-3-(4-chlorophenyl)-3-(aryloxythiocarbonyl)-2-thioureas (II-1—II-7). These compounds were pepared from an appropriate 1,1-disubstituted-3-(4-chlorophenyl)-2-thiourea and a proper aryl chlorothionoformate, as has been reported previously.[1] The data are shown in Table 1.

Aryl *N,N*-Disubstituted-thionocarbamates (III). These compounds were prepared from a corresponding secondary amine and an aryl chlorothionoformate following the general procedure given in the literature:[4] phenyl *N,N*-dimethyl- (IIIa) bp 118—120°C/3 mmHg mp 29.5—30°C,[5] phenyl *N,N*-diethyl- (IIIb) bp 125—126°C/3 mmHg mp 34—35°C. Found: C, 62.88; H, 7.05; N, 6.70%. Calcd for $C_{11}H_{15}NOS$: C, 63.16; H, 7.18; N, 6.70%. Phenyl *N,N*-di-*n*-propyl- (IIIc) bp 131—132°C/0.6 mmHg. Found: C, 66.10; H, 7.68; N, 5.70%. Calcd for $C_{13}H_{19}NOS$: C, 65.83; H, 7.68; N, 5.71%. 4-Tolyl *N,N*-dimethyl- (IIId) mp 96—97°C.[6] 4-Tolyl *N,N*-diethyl- (IIIe) mp 67.5—68.5°C. Found: C, 64.70; H, 7.35; N, 6.22%. Calcd for $C_{13}H_{17}NOS$: C, 64.57; H, 7.62; N, 6.28%. Phenyl *N*-benzyl-*N*-methyl- (IIIf) colorless oil*3 n_D^{23}: 1.6137. Found: C, 69.90; H, 5.88; N, 5.21%. Calcd for $C_{15}H_{15}NOS$: C, 70.04; H, 5.84; N, 5.45%. Phenyl *N*-(4-chlorobenzyl)-*N*-methyl- (IIIg) colorless oil*3 n_D^{23}: 1.6173. Found: C, 61.70; H, 4.88; N, 4.98%. Calcd for $C_{15}H_{14}ClNOS$: C, 61.75; H, 4.80; N, 4.80%. Phenyl *N*-(4-methylbenzyl)-*N*-methyl- (IIIh) colorless needles (from methanol) mp 57—58°C. Found: C. 70.70; H, 6.27; N, 5.15%. Calcd for $C_{16}H_{17}NOS$: C, 70.85; H, 6.28; N, 5.17%.

Carbon-14 Labeling Experiments. The sodium formate-^{14}C (specific activity: 10.8 mCi/mmol) was obtained from the Radiochemical Centre in England; it was dissolved into nonradioactive formic acid in order to obtain a moderate radioactive formic acid-^{14}C.

Labeled 4-Chloroformanilide. This was prepared in a 96% yield from 4-chloroaniline and the above formic acid-^{14}C.

Labeled (4-Chlorophenyl)imidocarbonyl Chloride. This was prepared in a 77% yield using the above labeled anilide and according to a procedure described in the literature.[7] Bp 132—135°C/29 mmHg.

Labeled Phenyl *N*-(4-Chlorophenyl)chloroformimidate. This was prepared in a 57% yield from the above labeled chloride and phenol, as has been described earlier.[1] Bp 157—159°C/4 mmHg.

Lableld *O*-Phenyl-*S*-(*N,N*-dimethylthiocarbamoyl) *N*-(4-Chlorophenyl)thiolimidocarbonate (^{14}C)I-1). This was prepared from sodium *N,N*-dimethyldithiocarbamate and the above labeled chloroformimidate by a method reported previously.[1] The crude reaction product was recrystallized several times from ethanol-acetone to give colorless prisms in a 58% yield. Specific activity: 1.40 μCi/mol.

Labeled 1,1-Dimethyl-3-(4-chlorophenyl)-3-(phenoxythiocarbonyl)-2-thiourea (^{14}C)II-1). This was prepared by the thermal rearrangement of (^{14}C)I-1, as has been reported previously.[1] In order to obtain the pure product, the crude product was chromatographed on silica gel twice and then recrystallized several times from ethanol-acetone to give colorless prisms in a 28% yield. A thin-layer chromatographic analysis of that refined product showed that it contained no impurities. Specific activity: 1.51 μCi/mol.

Thermal Decomposition of II. The apparatus used for the decomposition consisted of a 5-m*l*, pear-shaped flask fitted with an air condenser. Thin-layer chromatography was conducted by the use of silica gel (WAKO GEL B5-F); the prepared plate was activated at 110°C for 1hr and then stored in a deciccator. Silica-gel-column chromatography was carried out by the use of silica gel (WAKO GEL C-200) activated at 110°C for 1hr before use.

In a run, a weighed amount (*ca.* 100 mg) of II was placed in the reaction flask. The flask was flushed with nitrogen for 10 min at room temperature and then heated to 175±0.5°C in a constant-temperature bath for the desired length of time, nitrogen being passed into the flask at a slow rate throughout the decomposition. The reaction mixture, which showed two main spots besides the unchanged II upon thin-layer chromatography with a solvent mixture of *n*-hexane and chloroform (2/1), was chromatographed on a silica-gel column (15×250 mm) with the same solvent as was used above. After about 200 m*l* of the solution had been eluted, fractions (5 m*l* each) were tested by thin-layer chromatography in order to separate the newly-formed products. The two main products thus separated were identified by means of IR and melting-point comparisons with authentic samples.

Decomposition of (^{14}C)II-1. (^{14}C)II-1 (200 mg) was decomposed for 1.5hr in the same manner as above. IIIa and IVa, which had been carefully separated by cloumn chromatography, were each recrystallized several times from ligroin. Thus 15 mg of IIIa (specific activity: 1.44 μCi/mol) and 18 mg of IVa (specific activity: 0) were obtained.

Crossover Experiment. An equimolar mixture of II-1 and II-4 was heated at 175°C for 1.5 hr under a slow stream of nitrogen. The reaction mixture was then submitted to thin-layer chromatography on silica gel, using a solvent mixture of *n*-hexane - chloroform - acetic acid

3) R. H. Hunter and E. S. Styles, *J. Chem. Soc.*, **1927**, 1211.

4) R. P. Mull, *J. Am. Chem. Soc.*, **77**, 581 (1955).

5) H. Rivier, *Bull. Soc. Chim. France*, (3) **35**, 837 (1906).

6) A. Kaji, This Bulletin **34**, 254 (1961).

*3 These compounds were obtained as a viscous oil and were purified by chromatography.

7) German Pat. 1094737; *Chem. Abstr.*, **55**, 25860 (1961).

Table 4. Decomposition rates of II-1 with a scavenger

	t(min)	10	20	30	40
$\ln(a/(a-x))$	(quinone)	0.128	0.267	0.368	0.490
	(DPPH)	0.125	0.261	0.372	0.480
	(neat)	0.130	0.270	0.370	0.493

(30 : 1 : 1) as the developer. After repeated attempts at chromatography, five major products: (R_f=0.31 (unchanged II-1), 0.45 (unchanged II-4), 0.47 (IIIa), 0.66 (IIIe) and 0.93 (IVa)) were obtained. However, neither IIIb (R_f: 0.61) nor IIId (R_f: 0.51) was detected.

Decomposition with a Scavenger. II-1, mixed with a small amount (*ca.* 2 wt% of II-1) of a scavenger, was heated at 175±0.5°C under a slow stream of nitrogen. The decomposition rates at each interval were as follows:

Decomposition Rate Measurement. In the above-described decomposition procedure, five or six runs for Compound II were started at the same time. Each one of these was taken out from a bath at every appropriate interval and cooled to room temterature by immersion in cold water. Each run thus obtained was then submitted to column chromatography in order to separate the IVa. The absorbance of the elute containing IVa was then measured at 275 mμ, which is the characteristic absorption for IVa. Since the change in the absorbance with the concentration of IVa in the solvent followed Beer's law well, the amount of IVa could be determined from the calibration line, which was decided in advance. Good first-order straight lines were obtained in this way (Figs. 1 and 3). From these data, the rate constants were calculated (Tables 2 and 3). The absorbance was measured on a Shimadzu MPS-50L spectrophotometer.

Radioactivity Counting. The radioactivity was measured by a liquid scintillation spectrometer (Nuclear Chicago Corp., Model 6801) using the following scintillator: naphthalene, 120 g; PPO, 7g; POPOP, 0.05 g; dioxane, 1000 m*l*.

The author wishes to express his deep gratitude to Professor Ryōzō Gotō of Kyoto Universiy for his kind direction, to Professor Aritsune Kaji of same University for his valuable suggestions and continuous encouragement, and to Dr. Jun-ichi Hayami of the same University for his helpful advice. Thanks are also due to Dr. Teruhisa Noguchi of the Biological Research Laboratory of Nippon Soda Co., Ltd., for his eager interest throughout the course of this investigation.

BULLETIN OF THE CHEMICAL SOCIETY OF JAPAN VOL. 42 1702—1704 (1969)

A New σ-Bonded Complex Formation between 2-Vinylpyridine and Palladium(II) or Platinum(II) Chloride

Akira KASAHARA, Keiko TANAKA[1] and Taeko IZUMI[2]

Department of Chemistry, College of General Education, Yamagata University, Yamagata

(Received November 11, 1968)

Sodium tetrachloropalladate(II) reacts with 2-vinylpyridine in methanol, ethanol, or isopropyl alcohol, to give, respectively, di-μ-chloro-bis[2-methoxy-2-(α-pyridyl)ethyl]dipalladium(II), di-μ-chloro-bis[2-ethoxy-2-(α-pyridyl)-ethyl]dipalladium(II), and di-μ-chloro-bis[2-isopropoxy-2-(α-pyridyl)ethyl]-dipalladium(II). The reaction of potassium tetrachloroplatinate(II) with 2-vinylpyridine in methanol or ethanol affords, respectively, di-μ-chloro-bis[2-methoxy-2-(α-pyridyl)ethyl]diplatinum(II) and di-μ-chloro-bis[2-ethoxy-2-(α-pyridyl)ethyl]diplatinum(II). The structures of these complexes containing the covalent metal - carbon bonding have been confirmed by a study of their absorptions and of the NMR spectra.

Recently, Cope and his co-workers reported that azobenzenes and *N*,*N*-dimethylbenzylamines react with palladium(II) halides or platinum(II) halides in an alcoholic solution to give complexes, **1**[3] and **2**[4], with carbon - methal σ-bonds.

1) Present address: Research Laboratory, Japan Electron Optics Laboratory Co., Akishima, Tokyo.

2) Present address: Department of Chemical Engineering, Faculty of Engineering, Yamagata University, Yonezawa, Yamagata.

3) A. C. Cope and R. W. Sieman, *J. Am. Chem. Soc.*, **87**, 3272 (1965).

4) A. C. Cope and E. C. Friedrich, *ibid.*, **90**, 909 (1968).

Furthermore, they found palladium(II) halides to react with allylic amines in an alcoholic solution to give complexes **3** containing an alkoxy group.[5] Yukawa and Tsutsumi[6] have also reported propagylamines which react with palladium(II) chloride in the presence of lithium chloride to give chlorovinylated products 4. Here we wish to report that, in alcoholic media, 2-vinylpyridine undergoes a similar electrophilic substitution by palladium(II) or platinum(II) chloride, producing a new σ-bonded complex.

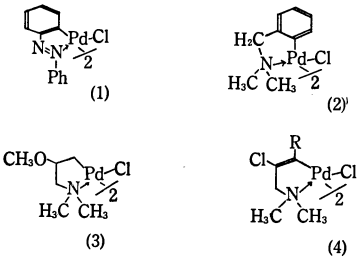

(1) (2) (3) (4)

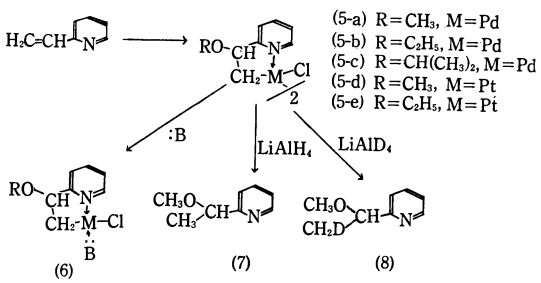

(6) (7) (8)

Experimental

All melting points and boiling points are uncorrected. Molecular weights were determined with an osmometer (benzene: at 45°C). The NMR spectra were recorded on a Hitachi H-60 spectrometer in deuteriochloroform, using tetramethylsilane as the internal reference.

Di-μ-chloro-bis[2-methoxy-2-(α-pyridyl)ethyl]-dipalladium(II) (5-a). To a solution containing 6.96 g (0.02 mol) of sodium tetrachloropalladate(II) in 70 m*l* of methanol, a solution of 2-vinylpyridine (2.10 g, 0.02 mol) in 20 m*l* of methanol was added. After standing at room temperature for 10 hr, the reaction mixture was evaporated *in vacuo* to dryness and extracted with chloroform. The chloroform layer was washed with water and dried over anhydrous magnesium sulfate. After the removal of the solvent, the residue was chromatographed on alumina using dichloromethane. Recrystallization from benzene afforded yellow crystals (**5-a**); mp 157—159°C, (1.2 g, 11%). IR spectrum (KBr): 3018, 2950, 2830, 1608, 1580, 1495,1450, 1115, 842, and 765 cm^{-1}. NMR spectrum: 6.58 (singlet, $-OCH_3$), 5.82 (multiplet, $-CH_2-$), 4.55 (multiplet, –CH–), and 2.90—0.96 τ (multiplet, pyridyl protons).

Found: C, 34.68; H, 3.75; N, 5.11%; mol wt, 548. Calcd for $C_{16}H_{20}N_2O_2Pd_2Cl_2$: C, 34.56; H, 3.62; N, 5.03%; mol wt, 556.

Di-μ-chloro-bis[2-ethoxy-2-(α-pyridyl)ethyl]-dipalladium(II) (5-b). The ethoxy complex (**5-b**) was obtained similarly from sodium tetrachloropalladate(II) and 2-vinylpyridine in ethanol (100 m*l*). The yellow crystals were recrystallized from benzene-cyclohexane; mp 153—155°C. IR spectrum (KBr): 3020, 2970, 1602, 1580, 1490, 1450, 830, and 772 cm^{-1}. NMR spectrum: 8.77 and 6.38 (ethoxy protons), 5.80 (multiplet, $-CH_2-$), 4.50 (multiplet, –CH–), and 2.92—0.92 τ (multiplet, pyridyl protons).

Found: C, 37.22; H, 4.08; N, 4.89%; mol wt, 568. Calcd for $C_{18}H_{24}N_2O_2Pd_2Cl_2$: C, 37.04; H, 4.14; N, 4.79%; mol wt, 584.1.

Di-μ-chloro-bis[2-isopropoxy-2-(α-pyridyl)-ethyl]dipalladium(II) (5-c). The reaction between sodium tetrachloropalladate(II) and 2-vinylpyridine in isopropyl alcohol afforded the isopropoxy complex (**5-c**) (23% yield). The yellow crystals were recrystallized from benzene; mp 165—167°C. IR spectrum (KBr): 3020, 2980, 1608, 1580, 1490, 1450, 1385, 1377, 830, and 772 cm^{-1}. NMR spectrum: 8.87, 8.78, and 6.21 (isopropoxy protons), 5.86 (multiplet, $-CH_2-$), 4.38 (multiplet, –CH–), and 2.95—0.98 τ (multiplet, pyridyl (protons).

Found: C, 39.67; H, 4.63; N, 4.45%; mol wt, 601. Calcd for $C_{20}H_{28}N_2O_2Pd_2Cl_2$: C, 39.24; H, 4.61; N, 4.57%; mol wt, 612.1.

Di-μ-chloro-bis[2-methoxy-2-(α-pyridyl)ethyl]-diplatinum(II) (5-d). To a solution of 1.0 g (0.0024 mol) of potassium tetrachloroplatinate(II) in 20 m*l* of water and 5 m*l* of methanol, 0.25 g (0.0024 mol) of 2-vinylpyridine in 30 m*l* of methanol was added at room temperature. After the mixture had then stood for 2 days, a yellow-orange precipitate was filtered out and washed well with methanol (0.55 g, 62%); mp 240—243°C (dec). This yellow-orange solid was insoluble in all common solvents. IR spectrum (KBr): 3020, 2940, 2820, 1608, 1590, 1488, 1450, 1120, 790, and 758 cm^{-1}.

Found: C, 25.95; H, 2.62; N, 3.36%. Calcd for $C_{16}H_{20}N_2O_2Pt_2Cl_2$: C, 26.18; H, 2.74; N, 3.54%.

Di-μ-chloro-bis[2-ethoxy-2-(α-pyridyl)ethyl]diplatinum(II) (5-e). A yellow-orange product (**5-e**) was obtained similarly from potassium tetrachloroplatinate(II) and 2-vinylpyridine in ethanol-water (55% yield); mp 237—240°C (dec). IR spectrum (KBr): 3020, 2940, 1606, 1581, 1480, 1445, 1390, 830, 798, and 770 cm^{-1}.

Found: C, 28.04; H, 2.96; N, 3.43%. Calcd for $C_{18}H_{28}N_2O_2Pt_2Cl_2$: C, 28.27; H, 3.14; N, 3.67%.

The Preparation of 2-Alkoxy-2-(α-pyridyl)ethylpalladium(or platinum) Chloride *p*-Toluidine (6). A mixture of 0.10 g of Complex **5** and *p*-toluidine (5% excess) in benzene (30 m*l*) was heated to reflux for 30 min. After the solvent had then been removed under reduced pressure, the residue was recrystallized from a benzene-cyclohexane mixture to give the following complexes.

2-Methoxy-2-(α-pyridyl)-ethylpalladium(II) Chloride *p*-Toluidine (6, B:=*p*-Toluidine, R=CH_3, M=Pd). Yellow crystals, mp 215—218°C (dec).

Found: C, 48.45; H, 4.79; N, 7.16%. Calcd for $C_{16}H_{19}N_2OPdCl$: C, 48.38; H, 4.82; N, 7.02%.

5) A. C. Cope, J. M. Kliegman and E. C. Friedrich, *ibid.*, **89**, 287 (1967).

6) T. Yukawa and S. Tsutsumi, *Inorg. Chem.*, **7**, 1458 (1968).

2-Ethoxy-2-(α-pyridyl)ethylpalladium(II) Chloride *p*-Toluidine (6, B:=*p*-Toluidine, R=CH_2CH_3, M=Pd). Yellow crystals, mp 231—233°C (dec).

Found: C, 49.77; H, 5.26; N, 6.84%. Calcd for $C_{17}H_{21}N_2OPdCl$: C, 49.65; H, 5.14; N, 6.81%.

2-Isopropyoxy-2-(α-pyridyl)ethylpalladium(II) Chloride *p*-Toluidine (6, B:=*p*-Toluidine, R=$CH(CH_3)_2$, M=Pd). Yellow crystals, mp 175—178°C (dec).

Found: C, 51.04; H, 5.01; N, 6.63%. Calcd for $C_{18}H_{23}N_2OPdCl$: C, 50.86; H, 4.97; N, 6.58%.

2-Methoxy-2-(α-pyridyl)-ethylplatinum(II) Chloride *p*-Toludine (6, B:=*p*-Toluidine, R=CH_3, M=Pt). Yellow crystals, mp 198—200°C (dec).

Found: C, 39.71; H, 4.07; N, 5.66%. Calcd for $C_{16}H_{19}N_2OPtCl$: C, 39.54; H, 3.94; N, 5.74%.

2-Ethoxy-2-(α-pyridyl)ethylplatinum(II) Chloride *p*-Toluidine (6, B:=*p*-Toluidine, R=CH_2CH_3, M=Pt). Yellow crystals, mp 195—198°C (dec).

Found: C, 41.26; H, 4.25: N, 5.55%. Calcd for $C_{17}H_{21}N_2OPtCl$: C, 41.01; H, 4.23; N, 5.63%.

Reduction of Complex. General Procedure. To the complex (3.3 g) in absolute ether (200 m*l*), there was slowly added a mixture containing 1.0 g of lithium aluminum hydride or deuteride in 100 m*l* of absolute ether. The resulting black mixture was stirred at room temperature for 3 hr, then water or deuterium oxide (5 m*l*) was added with cooling. The ether layer was washed with water and dried over anhydrous magnesium sulfate. After the removal of the solvent, the product was isolated by distillation.

Reduction of Complex 5-a with Lithium Aluminum Hydride. This reduction gave a product, bp 205—208°C, which can be identified as 1-(α-pyridyl)-1-methoxyethane (**7**) on the basis of the following evidence. IR spectrum: 2820 cm^{-1} ($-OCH_3$). NMR spectrum: 8.71 (doublet, J=6.0 cps, $-CH_3$); 6.67 (singlet, $-OCH_3$); 6.37 (quartet, J=6.0 cps, –CH–), and 3.03—1.35 τ (multiplet, pyridyl protons).

Found: C, 69.85; H, 8.01; N, 10.09%, mol wt, 135. Calcd for $C_8H_{11}NO$: C, 70.03; H, 8.08; N, 10.21%, mol wt, 137.

Reduction of Complex 5-a with Lithium Aluminum Deuteride. This reduction gave 1-(α-pyridyl)-1-methoxyethane-2-d_1, bp 205—208°C. IR spectrum: 2820 cm^{-1} ($-OCH_3$). NMR spectrum: 8.70 (doublet, J=6.0 cps, $-CH_2D$), 6.67 (singlet, $-OCH_3$), 6.36 (triplet, J=6.0 cps, –CH–), and 3.02—1.32 τ (multiplet, pyridyl protons).

Found: C, 69.77; H, 8.69; N, 10.32%; mol wt, 136. Calcd for $C_8H_{10}DNO$: C, 69.54; H, 8.74; N, 10.13%, mol wt, 138.

Reduction of Complex 5-d with Lithium Aluminum Hydride. This reduction gave 1-(α-pyridyl)-1-methoxyethane (**7**), bp 205—208°C, which can be identified by means of its IR and NMR spectra.

Reduction of Complex 5-d with Lithium Aluminum Deuteride. This reduction gave 1-(α-pyridyl)-1-methoxyethane-2-d_1 (10), bp 205—208°C, which can be identified by means of its IR and NMR spectra.

Results and Discussion

The reaction of 2-vinylpyridine with sodium tetrachloropalladate(II) in alcohol produced di-μ-chloro-bis[2-alkoxy-2-(α-pyridyl) ethyl]dipalladium(II) (**5-a—c**). The dimeric structures for these complexes were supported by the molecular-weight determinations and by their reactions with *p*-toluidine, which give readily-soluble, monomeric derivatives. The structure of complex **5-a** was established by the following data.

The infrared spectrum of complex **5-a** shows new bands at 2830 and 1115 cm^{-1} which can be assigned to the CH_3O- stretching mode. In agreement with the proposed structure, the NMR spectrum of complex **5-a** shows four bands, at 6.58 (singlet), 5.82 (multiplet), 4.55 (multiplet), and 2.90—0.96 τ (multiplet), in the ratio 3 : 2 : 1 : 4. They are assigned to *O*-methyl protons, methylene protons, methine protons, and pyridyl protons respectively. The lithium-aluminum-hydride reduction of complex **5-a** gives 1-(α-pyridyl)-1-methoxy-ethane (**9**), whose structure can be established by means of its IR and NMR spectra. The lithium-aluminum-deuteride reduction of complex **5-a** gives deuterated amine (**10**), which was identified as 1-(α-pyridyl)-1-methoxy-ethane-2-d_1. The position of the deuterium and, therefore, the site of the carbon-to-palladium σ-bond, was established by a comparison of the NMR spectrum of **10** with that of the undeuterated **9**. The spectrum of **9** consists of a doublet at 8.71 τ (methyl protons, wt 3), a singlet at 6.67 τ (methoxy protons, wt 3), a quartet at 6.37 τ (methine proton, wt 1), and a multiplet at 3.03—1.35 τ (pyridyl protons, wt 4), whereas **10** shows the corresponding signals at 8.70 (doublet), 6.67 (singlet), 6.36 (triplet), and 3.02—1.32 τ (multiplet) in the ratio 2 : 3 : 1 : 4. The above evidence establishes that a σ-bond has been formed between the metal and the terminal methylene group of the vinyl moiety. The structures of complexes **5-b** and **5-c** are also proved by their NMR spectra.

The reactions of 2-vinylpyridine with potassium tetrachloroplatinate(II) in aqueous methanol or in aqueous ethanol give di-μ-chloro-bis[2-alkoxy-2-(α-pyridyl)ethyl]diplatinum(II) (**5-d,e**). The insolubility of these complexes in common solvents made impossible any NMR-spectra or molecular-weight measurements. However, the reactions with *p*-toluidine and with lithium aluminum hydride or deuteride indicate that they have a dimeric structure of the same type as that obtained from 2-vinylpyridine and sodium tetrachloropalladate(II). The reduction of complex **5-d** with lithium aluminum hydride gives 1-(α-pyridyl)-1-methoxyethane (**7**), while that with lithium aluminum deuteride gives 1-(α-pyridyl)-1-methoxy-ethane-2-d_1 (**10**).

The authors wish to thank the Ministry of Education for the financial support granted this research.

BULLETIN OF THE CHEMICAL SOCIETY OF JAPAN VOL. 42 1705—1708 (1969)

The Solvent Effects in the Acylation of Alcohol. The Effects of Liquid Sulfur Dioxide on the Dissociation of Hydrogen-bonded Alcohol

Toshikazu NAGAI, Hironobu ABE and Niichiro TOKURA

Department of Applied Chemistry, Faculty of Engineering, Osaka University, Suita, Osaka

(Received November, 21, 1968)

The reason for the rate-enhancing effect of liquid sulfur dioxide on the rate of the benzoylation of methanol has been studied. The observation of the NMR spectra revealed that the amount of the hydrogen-bonded methanol is decreased (but not completely eliminated) by sulfur dioxide in the liquid SO_2-CCl_4 system. The existence of a correlation between the rates of esterification and the dissociation of the associated alcohol accounts for the role of the sulfur dioxide as the agent for the dissociation of the methanol-hydrogen bonding during the esterification.

In continuation of our work on the solvent effect of the acylation of alcohol, the obvious effect of liquid sulfur dioxide has aroused the interest of the present authors since the reaction proceeds very rapidly in both first- and second-order-rate reactions.[1)]

Liquid sulfur dioxide is an electrophilic solvent, the reaction in which the ρ value in the Hammett's equation is negative, *viz.*, in which a cation plays a predominant role, being favored in this solvent.[2)]

The first-order acylation where the reaction rate is described as: Rate=k[RCOCl] can be well elucidated by the above interpretation because the rate-determining formation of the RCO^+ cation should be favored in liquid sulfur dioxide. However, the enhanced acylation by the second-order-rate law, first order both in alcohol and in acyl halide, is difficult to understand. An alternative explanation is that the association of alcohol by the hydrogen bonding may be disrupted in the presence of liquid sulfur dioxide, as was indicated by Hoyer,[3)] and the alcohol may be increased when the solvent is replaced by liquid sulfur dioxide.

In the present communication the effect of the sulfur dioxide concentration on the hydrogen bonding of methanol and the effect of that solvent on the reaction rate of the acylation have been compared with each other. The correlation between the two effects may be useful as evidence for the role of sulfur dioxide.

As for the effect of hydrogen-bonding on the rate of a reaction, the inhibition of phenol alkylation by ethers has been reported on by Hart *et al.*;[4)] they accounted for the quantitative decrease in the rate by assuming the formation of a 2 : 1 phenol-dioxane complex.

The dissociation of the hydrogen bonding which may be brought about by sulfur dioxide has been measured by means of the proton magnetic resonance spectra in liquid sulfur dioxide-carbon tetrachloride systems. The reaction rates of the esterification of benzoyl chloride with methanol, which follow the second-order rate law, have been followed by GLC analysis.

Experimental

Apparatus. The chemical shift data were determined from the proton magnetic resonance spectra obtained on a Nihondenshi spectrometer at 60 Mc. The reaction rates were measured by pressure vessels equipped with needle valves.

Materials. The methanol was dehydrated over magnesium and distilled. The liquid sulfur dioxide was purified by distillation over phosphorus pentoxide. The carbon tetrachloride was purified by washing it with alkali and sulfuric acid; it was distilled after dehydration over calcium chloride. The benzoyl chloride was purified by an ordinary method.

Procedure. *Proton Magnetic Resonance.* The solutions to be studied were prepared in NMR tubes as follows. After weighing the reagents in the tube and after adding methylsilane, the tube was connected with a pressure vessel containing liquid sulfur dioxide; then there was added a definite amount of sulfur dioxide by distillation under cooling in a liquid nitrogen bath. Finally, the tube was sealed and submitted to NMR analysis. The chemical shifts were all determined relative to the internal standard, tetramethylsilane. A dilution study of methanol in carbon tetrachloride was undertaken in order to determine the chemical shift associated with

1) a) N. Tokura and F. Akiyama, This Bulletin, **37**, 1723 (1964). b) F. Akiyama and N. Tokura, *ibid.*, **39**, 131 (1966). c) F. Akiyama and N. Tokura, *ibid.*, **41**, 2690 (1968).

2) a) N. Tokura, T. Kawahara and S. Ikeda, *ibid.*, **37**, 138 (1964). b) N. Tokura, M. Matsuda and M. Iino, *ibid.*, **36**, 278 (1963). c) R. Asami and N. Tokura, *J. Polymer Sci.*, **42**, 545 (1963).

3) H. Hoyer, *Angew. Chem.*, **72**, 269 (1960).

4) H. Hart, F. A. Cassis and J. J. Bordeaux, *J. Am. Chem. Soc.*, **76**, 1639 (1954).

monomeric methanol. This study covered the concentration range of 1.193—0.019 wt% methanol and was done at a constant temperature of 20°C. To establish complete hydrogen bonding, a measurement was carried out at around the melting point of methanol. For the purpose of detecting the dissociation of the hydrogen bonding, the molar ratios of the SO_2-CCl_4 mixtures were varied from 0 to 100%, while the methanol concentration was kept constant at about 6 mol/*l*.

Kinetic Procedure. The procedure used to follow the kinetics was as follows. Into a pressure vessel there were introduced 0.6164 mol/*l* of benzoyl chloride and 2.8829 mol/*l* of methanol in a liquid SO_2-CCl_4 mixture (SO_2: 0—92 mol%); then, after a definite period of time at 0°C, the reaction mixtures were added to a large amount of water. The solution was then introduced into a separatory funnel including a definite amount of nitrobenzene in CCl_4 and then washed seven times with pure water in order to remove any unreacted methanol and benzoyl chloride. The solvent of the CCl_4 solution thus obtained was distilled out under reduced pressure after drying over $MgSO_4$. The residual solution was submitted to GLC analysis. The concentration of methyl benzoate formed was determined by measuring the area of the gas chromatograms and by applying a previously-determined calibration factor, which was obtained from the area of methyl benzoate relative to that of a definite amount of nitrobenzene added as a standard. GLC was carried out under the following conditions: column; P.E.G. 6000, 4 m, 132°C; carrier; H_2 70 ml/min. The retention times were 9.5 min for methyl benzoate and 16.5 min for nitrobenzene.

Results and Discussion

The Hydrogen Bonding of the Methanol Molecules Themselves. The results of the dilution study of methanol in carbon tetrachloride are presented in Fig. 1. This study suggests that, below a concentration of 0.117 wt%, the methanol in carbon tetrachloride exists in only one state, probably the monomeric form. Assuming this to be the case, the value of δ_1, the chemical shift of monomeric methanol relative to tetramethylsilane, is 2.08 ppm.

The value of δ_A, the chemical shift of associated methanol, was determined to be δ 5.84 ppm by measuring the value for pure methanol around its melting point, −93°C.

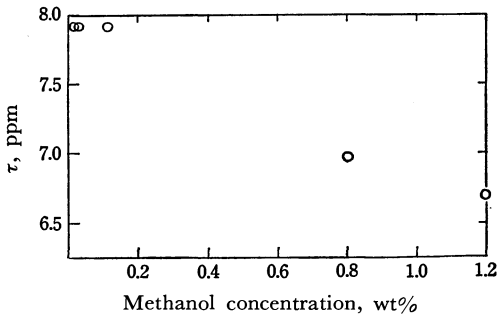

Fig. 1. Dilution study of methanol in carbon tetrachloride.

The chemical shift data, δ_{obs}, for the hydroxylic hydrogen atom of methanol measured at 20, 0, and −20°C at a definite concentration of about 6 mol/*l* in the SO_2-CCl_4 solvent mixture, together with those for the methyl, δ_{CH_3}, are listed in Table 1.

As may be seen in Table 1, upon an increase in the relative amount of SO_2, the hydroxylic hydrogen atom shifts to a higher magnetic field. This could be attributed to the change in the molecular complexation of alcohol, possibly owing to a weak interaction of the oxygen atoms of methanol with the sulfur atoms of sulfur dioxide, as is shown in Fig. 2, I, rather than that visualized in Fig. 2, II, which would result in a shift to a lower field, a shift contrary to the facts.

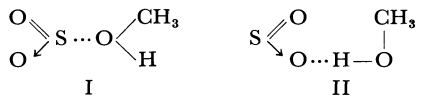

Fig. 2

The neighbor anisotropy effect of SO_2 on the shift will be omitted here since the shifts of the methyl protons remain constant throughout the various compositions of the solvent mixtures used.

TABLE 1. THE VALUES (ppm) OF δ_{CH_3} AND δ_{obs} OF THE HYDROXYLIC HYDROGEN ATOM RELATIVE TO TMS FOR METHANOL

Methanol (mol/*l*)	Solvent (molar ratio) SO_2 : CCl_4	20°C		0°C		−20°C	
		δ_{CH_3}	δ_{obs}	δ_{CH_3}	δ_{obs}	δ_{CH_3}	δ_{obs}
5.98	0 : 100	3.36	4.77	3.40	5.25	3.34	5.32
5.93	15.64 : 84.36	3.43	4.70	3.40	5.17	3.25	5.28
5.69	38.83 : 61.17	3.36	4.30	3.39	4.71	3.37	4.98
6.68	59.77 : 40.23	3.36	4.15	3.39	4.67	3.37	4.93
7.45	72.36 : 27.64	3.38	4.08	3.38	4.56	3.40	4.82
6.47	79.53 : 20.47	3.35	3.88	3.39	4.43	3.38	4.70
6.37	90.77 : 9.23	3.36	3.63	3.38	4.20	3.37	4.52
5.98	100 : 0	3.38	3.70	3.38	3.96	3.40	4.47

Comprehensive studies[5-7] have been made of the nuclear magnetic resonance on the molecular complexation of alcohol or on hydrogen bonding between proton-donating acids and bases. In these studies, the shifts of the NMR signals have been considered from the standpoint of dilution or enthalpy change upon the formation of a hydrogen bond. Meanwhile, Hoyer[3] has observed in his IR studies that sulfur dioxide molecule can neither permit a hydrogen bond among alcohol molecules themselves nor make hydrogen bridges with the hydrogen atoms of the alcohols by using oxygen atoms of the sulfur dioxide molecule.

Saunders and Hyne[6] have interpreted their data by making the simplifying assumption that the methanol molecule exists in carbon tetrachloride in equilibrium with the monomer and the tetramer as follows:

$$4CH_3OH \overset{K_4}{\rightleftharpoons} (CH_3OH)_4 \qquad (1)$$

Assuming this to be the case in the present system, the following value, K_4, will be a parameter of the complexation in this system:

$$K_4 = \frac{M_4}{M_1^4} = \frac{C - M_1}{4M_1^4} \qquad (2)$$

$$C = M_1 + 4M_4 \qquad (3)$$

where M_1 and M_4 are the molar concentrations of the monomer and the tetramer respectively.

On the other hand, the observed chemical shift, δ_{obs}, follows Eq. (4):

$$\delta_{obs} = \frac{\delta_1 M_1 + \delta_A (C - M_1)}{C} \qquad (4)$$

where δ_1 and δ_A are the chemical shifts of the hydroxylic protons of the noncomplexed and complexed states respectively.

The K_4 values derived from Eqs. (2) and (4), together with the values of M_1/C, are listed in Table 2.

These results indicate that the association of methanol is possible in an appreciable amount in liquid SO_2 alone; this is somewhat different from the observation made by IR.[3]

When a smaller concentration of methanol (1.8 mol/l) was used, the hydroxylic hydrogen atom shifted to a higher field, δ 2.67 ppm relative to the TMS in liquid SO_2 at 20°C, thus affording larger M_1/C value; this is further evidence of the presence of the complexation of methanol in liquid SO_2.

Rate of S_N2-type Esterification. Benzoyl chloride was submitted to reaction with methanol in liquid sulfur dioxide-carbon tetrachloride mixtures. The reaction obeyed the second-order-rate law at the initial stage of the reaction, indicating that methanol acts in the rate-determining step of

Table 2. The values of M_1/C and K_4 at 0°C

Methanol (mol/l)	SO_2 (mol%)	M_1/C	K_4 (l^3mol^{-3})
5.98	0	0.157	1.630
5.93	15.64	0.178	0.980
5.69	38.83	0.301	0.120
6.68	59.77	0.311	0.061
7.45	72.36	0.341	0.030
6.47	79.53	0.376	0.029
6.37	90.77	0.436	0.015
5.98	100	0.500	0.0094

Table 3. The second-order-rate constants (k_2, min^{-1} mol^{-1} l) of the benzoylation of methanol in various liq. SO_2-CCl_4 mixtures at 0°C

SO_2 (mol%)	$k_2 \times 10^4$
0	5.31
51.02	6.10
70.37	8.60
81.37	11.86
91.68	16.30

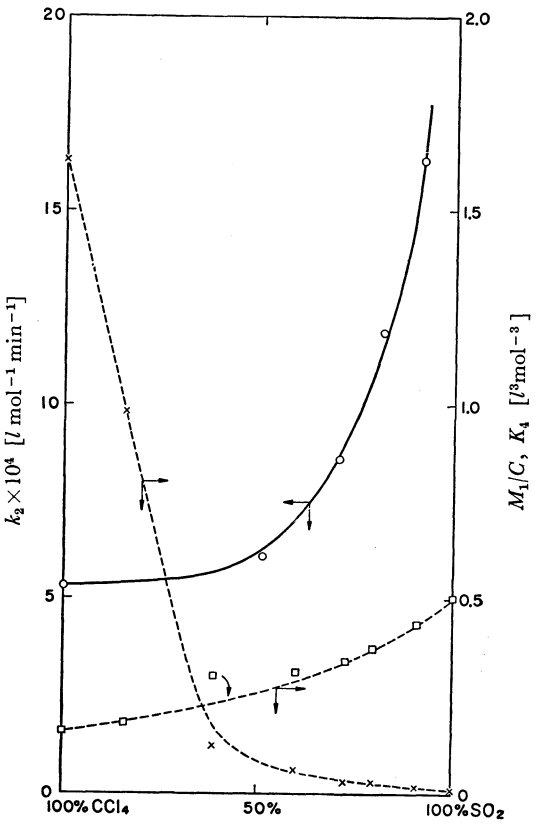

Fig. 3. Effect of added SO_2 on the values of the k_2, K_4, and M_1/C.

5) C. M. Huggins, G. C. Pimental and J. N. Shoolery, *J. Phys. Chem.*, **60**, 1311 (1956).

6) M. Saunders and J. B. Hyne, *J. Chem. Phys.*, **29**, 1319 (1958).

7) D. P. Eyman and R. S. Drago, *J. Am. Chem. Soc.*, **88**, 1617 (1966).

Table 4. The rate constants, k'_2 derived using the monomeric methanol concentration as the methanol concentration

SO_2 mol %	K_4* l^3 mol^{-3}	C mol l^{-1}	M** mol l^{-1}	k'_2 l mol^{-1} min^{-1} $\times 10^3$
0	1.630	2.8829	0.76	2.02
51.02	0.080	2.8829	1.46	1.36
70.37	0.038	2.8829	1.68	1.48
81.37	0.028	2.8829	1.78	1.92
91.68	0.014	2.8829	2.00	2.35
				Mean=1.83

* K_4: obtained from the K_4 *vs.* SO_2 % curve in Fig. 3.
** M_1: the unassociated monomer concentration derived from the equation: $4[M_1]^4K_4+[M_1]=C$.

the reaction. Another support for this was given by the fact that a small isotope effect was observed when CH_3OD was used in this esterification reaction. Consequently, the rate constant, k_2, should afford some information regarding the effect of the complexation of methanol on the S_N2-type reaction.

The k_2 values, together with the M_1/C and K_1 values, are visualized in Fig. 3.

The k_2 values increase as the amount of sulfur dioxide added is greater; however, the k_2' values, defined as is indicated in Eq. (5), were nearly constant, as is shown in Table 4.

$$\text{Rate} = k_2[\text{benzoyl chloride}][C] = k'_2[\text{benzoyl chloride}][M_1] \quad (5)$$

$$k'_2 = k_2\frac{[C]}{[M_1]} \quad (6)$$

The increase in the reaction rate of the esterification of benzoyl chloride by methanol, brought about by the addition of sulfur dioxide, may adequately be accounted for by assuming that the dissociated methanol monomer rather than the associated methanol participates in the esterification reaction and also by assuming that sulfur dioxide acts as the hydrogen bond-disrupting agent in the reaction.

The authors are grateful to Seitetsu Kagaku K. K. for its donation of liquid sulfur dioxide.

BULLETIN OF THE CHEMICAL SOCIETY OF JAPAN VOL. 42 1708—1712 (1969)

Reaction Rates in Binary Mixed Solvents. V[1)]

Yasuhiko KONDO, Toshiharu KUSAKA and Niichiro TOKURA

Department of Applied Chemistry, Faculty of Engineering, Osaka University, Suita, Osaka

(Received November 22, 1968)

The rate constants of the Menschutkin reaction between methyl iodide and pyridine, *N,N*-dimethylaniline, 2,6-dimethylpyridine, and *N,N*-dimethyl-*o*-toluidine have been measured in a liq. SO_2-nitrobenzene mixture. These results have then been analyzed by the procedure described in a previous paper. The findings regarding the reactions of unsubstituted amines with methyl iodide have been explained theoretically by taking into account the specific solvation of amines by liq. SO_2 and that of an activated complex by a nitrobenzene solvent, whereas the behavior of the rate constants in the reactions of *o*-substituted amines in mixed solvents can be explained by assuming the specific solvation of an activated complex by liq. SO_2 only. In conformity with the above results and the difference in the effect of an *o*-methyl group on the reaction rates between liq. SO_2 and a nitrobenzene solvent, the mutual relation of the activation free energies of these reactions has been discussed.

In a previous paper of this series the present authors have discussed the theoretical procedure for analyzing the reaction rates measured in solvent mixtures. The additional possibility has been suggested that knowledge about the solvation phenomena of the solute could be drawn from an

1) Y. Kondo, Y. Honjo and N. Tokura, This Bulletin, **41**, 987 (1968).

analysis of the rate constants measured in mixed solvents which could not be drawn from an analysis of the reaction rates measured in pure solvents.

For a complete understanding of the reaction in solution it is necessary to summarize various informations originating from different sources.

One of the most useful methods of detecting the behavior of the solvent molecules near the reaction center is to examine the effect of the *o*-substitutent on the reaction rates in solution.[2-4] Accordingly, the effects of the *o*-methyl group on the rates of the Menschutkin reaction in liq. SO_2 have been compared with those in a methanol solvent,[3] and the difference in the behavior of the *o*-methyl group between these two solvents has been attributed to the specific solvation of the amines in liq. SO_2.[3]

In this paper the procedure for considering the mutual relation among activation free energies for the reactions in solution will be discussed by combining experimental results of different kinds obtained from different sources regarding the effects of an *o*-methyl group and the reaction rates in mixed solvents.

Experimental

Materials. The materials used in this experiment have been purified by methods described elsewhere.[3]

Kinetic Procedure. In most of all the kinetic runs given amounts of stock solutions of methyl iodide in liq. SO_2 were introduced into a reaction vessel containing given amounts of an amine solution in a nitrobenzene solvent, the mixture held at about −70°C by means of a pressure buret described elsewhere.[5a,5b] The reaction was started by placing the vessel into a thermostat bath held at the reaction temperature. The method of detecting the iodide ions produced during the reaction is almost the same as those described earlier.[3]

Typical results are shown in Table 1.

Table 1. Rate constants of the reaction between pyridine and methyl iodide in the liq. SO_2-nitrobenzene mixture

	50.0°C	40.0°C	30.0°C
$k\times10^4$	5.16	2.37	0.966
x	0	0	0
$k\times10^4$	7.39	3.05	1.15
x	0.190	0.228	0.190
$k\times10^4$	8.47	3.72	1.34
x	0.380	0.384	0.380
$k\times10^4$	9.24	4.08	1.61
x	0.598	0.604	0.598
$k\times10^4$	10.3	4.64	1.76
x	0.790	0.790	0.790
$k\times10^4$	21.3	11.1	5.52
x	1.0	1.0	1.0

k: $l\,mol^{-1}sec^{-1}$, x: mole fraction of nitrobenzene in a nitrobenzene - liq. SO_2 mixture.

Results

According to the theory developed in a previous paper[5] the logarithm of the rate constant has been plotted against the mole fraction of a nitrobenzene solvent (Figs. 1 and 2), the shapes of these curves

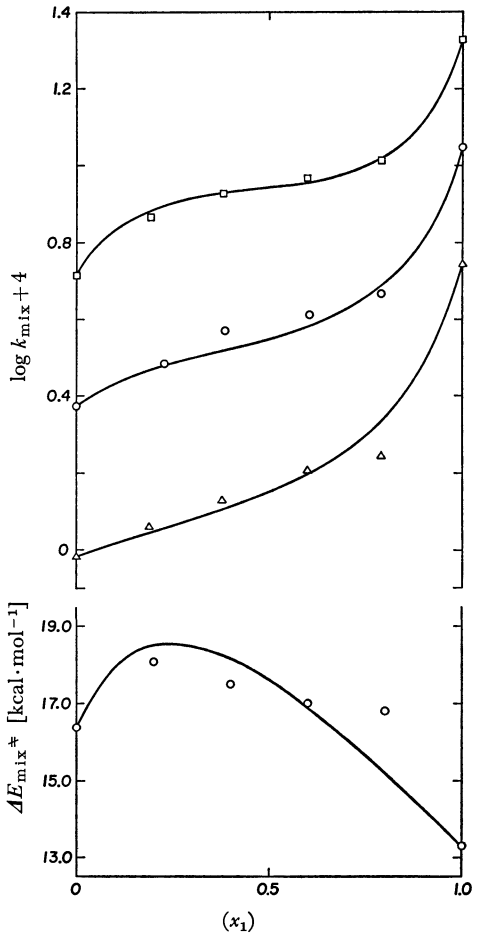

Fig. 1. Dependence of log k_{mix} and $\Delta E_{mix}^{\neq}$ for the reactions of pyridine with methyl iodide in liq. SO_2-nitrobenzene mixture upon mole fraction of nitrobenzene (x_1).
□ (50°C), ○ (40°C), △ (30°C): experimental results, —: calculated results

2) J. B. Hyne and R. Wills, *J. Am. Chem. Soc.*, **85**, 3650 (1963).

3) Y. Kondo and N. Tokura, This Bulletin, **37**, 133 (1964).

4) M. Hojo, M. Utaka and Z. Yoshida, *Yuki Gosei Kagaku Kyokai Shi (J. Syn. Org. Chem. Japan)*, **23**, 1034, 1040 (1965).

5) a) N. Tokura, M. Matsuda and F. Yazaki, *Makromol. Chem.*, **42**, 108 (1960). b) N. Tokura, R. Asami, M. Matsuda and H. Negishi, *Kogyo Kagaku Zasshi (J. Chem. Soc., Japan, Ind. Chem. Sec.)*, **64**, 717 (1961).

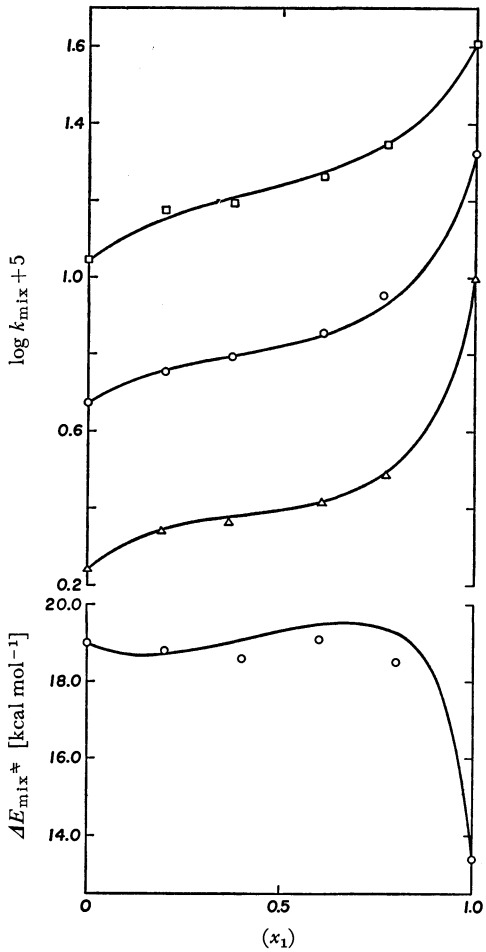

Fig. 2. Dependence of log k_{mix} and ΔE_{mix}^{*} for the reaction of *N,N*-dimethylanilne with methyl iodide in liq. SO_2-nitrobenzene mixture upon mole fraction of nitrobenzene (x_1).
□ (50°C), ○ (40°C), △ (30°C): experimental results, —: calculated results

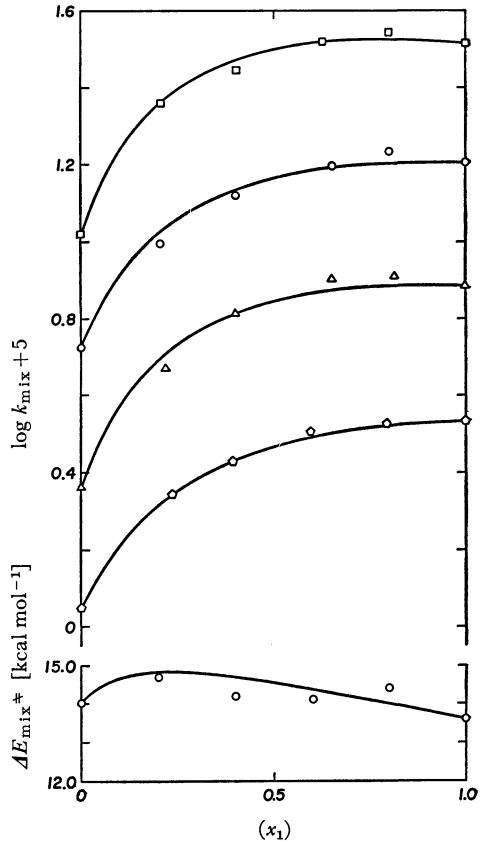

Fig. 3. Dependence of log k_{mix} and ΔE_{mix}^{*} for reaction of 2,6-dimethylpyridine with methyl iodide in nitrobenzene - liq. SO_2 mixture upon mole fraction of liq. SO_2 (x_1).
□ (50°C), ○ (40°C), △ (30°C), ⬠ (20°C): experimental results, —: calculated results

are obviously similar to that of curve 8 of model II in the previous paper.[1] The calculations were then made by taking the specific solvation of amines by liq. SO_2 and that of an activated complex by a nitrobenzene solvent into consideration. The interaction term, $\alpha_{14}x_1x_4$ and the molar volumes of the solvents which had been included in the original formula have been neglected in these calculations in order to make the computation easier.

$$\ln k_{mix} = x_1 \ln k_1 + x_4 \ln k_4 + \{x_4 \ln(K_R+1) - \ln(x_4K_R+1) - x_1 \ln(K_A+1) + \ln(x_1K_A+1) - x_1x_4\alpha_{14}\} \quad (1)$$

$$\Delta E_{mix}^{*} = x_1\Delta E_1^{*} + x_4\Delta E_4^{*} + x_1x_4\left\{\frac{\Delta H_A^{\circ}}{(1+1/K_A)(x_1+1/K_A)} - \frac{\Delta H_R^{\circ}}{(1+1/K_R)(x_4+1/K_R)}\right\} \quad (2)$$

The procedure of the calculation was as follows. (1) The calculated value of log k_{mix} have been best-fitted to the experimental values of log k_{mix} by searching for suitable values of both K_A and K_R. (2) The enthalpy changes, $\Delta H_A^{\circ} - \Delta H_R^{\circ}$, have been computed from the rates of the variation in K_A and in K_R thus obtained with respect to the temperature. (3) The theoretical values of ΔE_{mix}^{*} have been calculated from Eq. (2) by substituting into Eq.(2) the numerical values of ΔH_A° and ΔH_R° and of K_A and K_R obtained above.

These theoretical values are shown as smooth curves in Figs. 1, 2, 3 and 4.

As for the reactions of *o*-substituted amines, the results were analyzed by similar procedures except that only the specific solvation of an activated complex by liq. SO_2 has been taken into account. The parameters used in these calculations are summarized in Table 2.

Discussion

In these calculations the best values of K_A and K_R have been chosen without considering the boundary conditions, *i. e.*, Eqs. (3) and (4), which should

TABLE 2. THE PARAMETERS USED IN THESE CALCULATIONS

Reactions		Temperature 20°C	30°C	40°C	50°C	60°C	
Pyridine+MeI	K_A		1.5	3.0	6.0		$H_A^\circ=12.2$ (kcal mol^{-1})
	K_R		10	10	10		$H_R^\circ=0$ (kcal mol^{-1})
N,*N*-Dimethylaniline +MeI	K_A		4.0	3.0	3.0		$H_A^\circ=-3.8$ (kcal mol^{-1})
	K_R		17	11	6.0		$H_R^\circ=-10.2$ (kcal mol^{-1})
2,6-Dimethylpyridine +MeI	K_A	6.0	8.0	7.0	8.5		$H_A^\circ=2.2$ (kcal mol^{-1})
	K_R	0	0	0	0		$H_R^\circ=0$ (kcal mol^{-1})
N,*N*-Dimethyl-*o*-toluidine+MeI	K_A		7.5	7.0	6.5	6.0	$H_A^\circ=-1.5$ (kcal mol^{-1})
	K_R		0	0	0	0	$H_R^\circ=0$ (kcal mol^{-1})

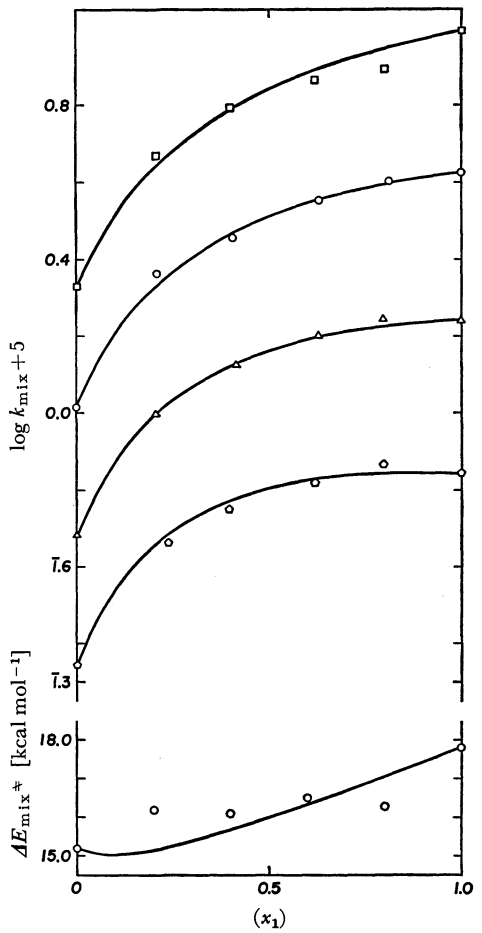

Fig. 4. Dependence of log k_{mix} and E_{mix}^* for the reaction of *N*,*N*-dimethyl-*o*-toluidine with methyl iodide in nitrobenzene - liq. SO_2 mixture upon mole fraction of liq. SO_2 (x_1).
□ (60°C), ○ (50°C), △ (40°C), ⬠ (30°C): experimental results, —: calculated results

be satisfied whenever the model is self-consistent.

$$(k_1/k_4) = \exp(\alpha_{A1}-\alpha_{A4}) \times \exp(\alpha_{B1}+\alpha_{M4}^*) \times (K_A+1)(K_R+1)(V_1/V_4) \quad (3)$$

$$(\Delta E_1^*-\Delta E_4^*) = \left\{\frac{\Delta H_A^\circ}{(1+1/K_A)} + \frac{\Delta H_R^\circ}{(1+1/K_R)}\right\} \quad (4)$$

However, if we try to describe an S-shaped curve like those in Figs. (1), and (2) by this model, values of both K_A and K_R must be chosen larger than those required by the boundary condition, Eq. (3).

One example of these situations is shown in Fig. 5, where the deviations from linearity, *i. e.*, $\Delta\log k_{mix}$, are calculated for various values of $(k_1/k_4)/(K_A+1)(K_R+1)$, which stand for the degree of consistancy.

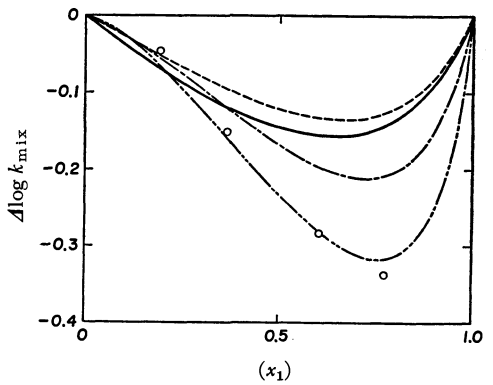

Fig. 5. Plots of the deviation from linearity, $\Delta\log k_{mix}$ *vs.* x_1 for the reaction of *N*,*N*-dimethylaniline with methyl iodide at 30°C, $(k_1/k_4)=5.69$.
experimental results: ○, calculated results: —— ($K_R=4.69$, $K_A=0$), ---- ($K_R=4.7$, $K_A=1$), —·— ($K_R=8.5$, $K_A=2$), —··— ($K_R=15$, $K_A=2.9$)

Judging from the above inconsistency, our model would be better applicable to the reaction rates of *o*-substituted amines than to those of unsubstituted amines; for unsubstituted amines the values of $(k_1/k_4)/(K_A+1)(K_R+1)$ are within the factor of three.

Though ΔE_{mix} could be fitted by this procedure to a considerable extent, the boundary condition, Eq. (4), could not be satisfied. The reason is the inconsistency described above. Therefore, the estimations of the theoretical values of ΔE_{mix}^* may be concluded to be richer in errors since, for these calculations, we have to rely only on the variation

TABLE 3. THE EFFECT OF *o*-METHYL GROUP IN LIQ. SO_2 AND IN A NITROBENZENE SOLVENT AT 40°C

Reaction	Solvent		
N,N-Dimethylaniline+MeI	$PhNO_2$	$k_H=21.0\times10^{-5}$, $k_{o-Me}=0.480\times10^{-5}$	$k_H/k_{o-Me}=43.7$
	Liq. SO_2	$k_H=4.69\times10^{-5}$, $k_{o-Me}=1.74\times10^{-5}$	$k_H/k_{o-Me}=2.69$
Pyridine+MeI	$PhNO_2$	$k_H=11.1\times10^{-4}$, $k_{o-Me}=5.31\times10^{-5}$	$k_H/k_{o-Me}=20.9$
	Liq. SO_2	$k_H=2.37\times10^{-4}$, $k_{o-Me}=1.60\times10^{-4}$	$k_H/k_{o-Me}=1.48$

k: $l\,mol^{-1}\,sec^{-1}$, k_H/k_{o-Me}; the ratio of the rate constants of the substituted and *o*-methyl substituted amines

in K_A and in K_R with a change in the temperature.

Although the above inconsistencies must be kept in mind, for the cases of unsubstituted amines the values of K_R are always larger than those of K_A, while for substituted amines only the values of K_A are needed for these calculations. In addition to these facts regarding the reactions of unsubstituted amines, the rate constants in a nitrobenzene solvent are larger than those in liq. SO_2. From these facts we can determine the positions of the activation free energies in liq. SO_2 relative to those in a nitrobenzene solvent.

As is shown in Table 3, the retarding effect by an *o*-substituted methyl group is more remarkable in a nitrobenzene solvent than in liq. SO_2. Consequently, the rate constants for the reactions of *o*-substituted amines become larger in liq. SO_2 than in a nitrobenzene solvent.

The difference in the effect of an *o*-methyl substituent between a methanol and a liq. SO_2 solvent has been attributed to the effect of the solvation of amines by liq. SO_2[3]. The addition compound formed from 2-methylpyridine and trimethyl boron has been reported to be less stable than that of 3- or 4-methylpyridine and trimethyl boron because of the *o*-methyl group.[6]

Therefore, if we assume that *o*-substituted amines are solvated to a lesser extent in liq. SO_2 than are unsubstituted amines, but that there is not much difference between the two in the solvation energy in a nitrobenzene solvent, we can determine the positions of the activation free energies of the former amines relative to those of the latter amines.

Summing up these conclusions, the following figure (Fig. 6) describes the mutual relations of the activation energies.

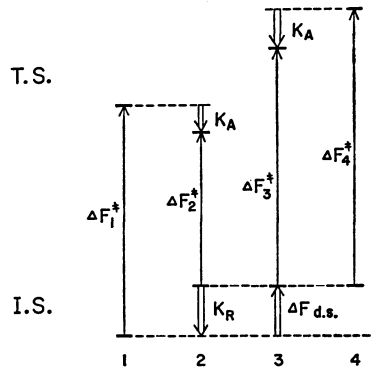

Fig. 6. The mutual relation of the activation free energies.
1: Unsubstituted amine+MeI in liq. SO_2
2: Unsubstituted amine+MeI in nitrobenzene
3: *o*-Substituted amine+MeI in liq. SO_2
4: *o*-Substituted amine+MeI in nitrobenzene
$\Delta F_{d.s.}$: desolvation free energy by the existence of *o*-methyl group

6) H. C. Brown and G. K. Barbaras, *J. Am. Chem. Soc.*, **69**, 1137 (1947).

BULLETIN OF THE CHEMICAL SOCIETY OF JAPAN VOL. 42 1713—1718 (1969)

Phosphorus-proton Spin-spin Coupling in the P–O–C–H Group. A Comparison of Cyclic and Acyclic Systems

Masatsune KAINOSHO,* ASAO NAKAMURA* and Masamichi TSUBOI**

* *Central Research Laboratory, Ajinomoto Co., Inc., Kawasaki, Kanagawa*

** *Faculty of Pharmaceutical Sciences, The University of Tokyo, Bunkyo-ku, Tokyo*

(Received December 4, 1968)

Proton magnetic resonance spectra for eleven compounds with the POCH system have been examined. They are three 4-phenyl-2,2-disubstituted(X,Y)-1,3,2-dioxaphosphorinanes where X=Cl, Y=O (I); X=Cl, Y=S (II); and X=O$^-$K$^+$, Y=O (III); four 5,5-dimethyl-2,2-disubstituted (X,Y)-1,3,2-dioxaphosphorinanes where X=Cl, Y=O (IV); X=Br, Y=O (V); X=Cl, Y=S (VI); and X=OH, Y=O (VII); and four dimethyl phosphates, Y=P(-X)-(-OCH_3)$_2$, where X=Cl, Y=O (VIII); X=Br, Y=O (IX); X=Cl, Y=S(X); and X=O$^-$ ½Ba^{2+}, Y=O (XI). It has been found that the *1,3,2-dioxaphosphorinane* ring in each of I—VIII is virtually fixed in a chair form in the solution, and there is no appreciable ring inversion as confirmed by NMR spectra. The phosphorus-proton coupling constant of the POCH system with the *gauche* relation (J_g) and that with the *trans* relation (J_t) were determined in each of these compounds (I—VII). The $\frac{2}{3}J_g+\frac{1}{3}J_t$ values calculated from the determined J_g and J_t values are always smaller than the $\frac{2}{3}J_g+\frac{1}{3}J_t$ values observed for the corresponding acyclic compounds (VIII—XI). This difference was explained in terms of a slight flattening of *1,3,2-dioxaphosphorinane* ring from the ideal chair conformation.

In our previous papers,[1,2] it has been shown that the phosphorus-proton coupling constants in the POCH group show a marked stereospecificity; *i. e.*, 1.5—2.3 Hz for J_g and 22—28 Hz for J_t.

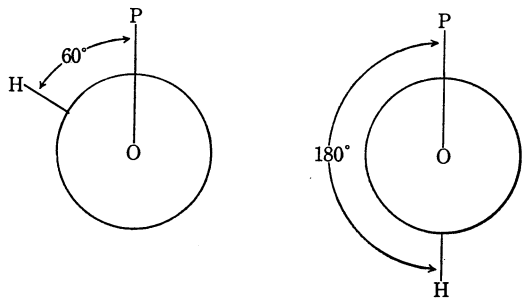

gauche *trans*

Fig. 1. The POCH system with *gauche* and *trans* conformations. Projected along the C–O axis.

The values of J_g and J_t, so far given, have rather large range of ambiguity. Nevertheless, they were very useful in determining the approximate conformation of a few phosphoric acid esters[1] and nucleotides.[2] A few other reports about the dihedral angular dependence of J_{POCH} have been made.[3,4] In this paper we present more precise knowledge of the J_g and J_t values on the basis of the NMR spectra of seven 1,3,2-dioxaphosphorinanes and four dimethyl phosphate derivatives.

Two series of the cyclic compounds were examined; they are 4-phenyl-2,2-disubstituted-1,3,2-dioxaphosphorinanes (I, II, III) and 5,5-dimethyl-2, 2-disubstituted-1,3,2-dioxaphosphorinanes (IV, V, VI, and VII):

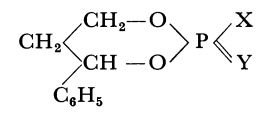

I: X=Cl, Y=O
II: X=Cl, Y=S
III: X=O$^-$K$^+$, Y=O

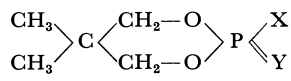

IV: X=Cl, Y=O
V: X=Br, Y=O
VI: X=Cl, Y=S
VII: X=OH, Y=O

As will be detailed below, each of these cyclic compounds has been found to have a virtually frozen conformation, which is similar to the chair form of the cyclohexane ring as shown in Fig. 2. Therefore, J_g should be approximately equal to J_{AP} (or $J_{B'P}$) and J_t should be equal to J_{BP} (or $J_{A'P}$). The J_t and J_g values thus determined for various compounds will then be compared with

1) M. Tsuboi, F. Kuriyagawa, K. Matsuo and Y. Kyogoku, This Bulletin, **40**, 1813 (1967).

2) M. Tsuboi, M. Kainosho and A. Nakamura, "Recent Developments of Magnetic Resonance in Biological System," ed. by S. Fujiwara and L. H. Piette, Hirokawa Publishing Co., Tokyo (1968), p. 43.

3) J. G. Verkade and R. W. King, *Inorg. Chem.*, **1**, 948 (1962).

4) L. D. Hall and R. B. Malcolm, *Chem. & Ind.*, **1968**, 92.

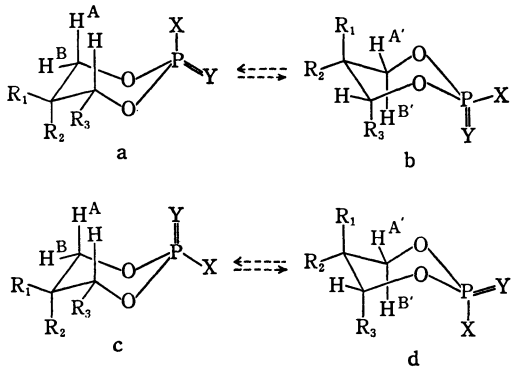

I—III $R_1,R_2=$; $R_3=C_6H_5$-
IV—VII $R_1,R_2=CH_3$-; $R_3=H$ (in this case a≡d, b≡c)

Fig. 2. Possible chair conformations of substituted 1,3,2-dioxaphosphorinanes.

one another. A question next arises: Are these values of J_t and J_g applicable to the acyclic system? For an answer to this question, we examined the NMR spectra of the following four acyclic dimethyl phosphate derivatives:

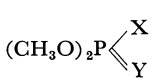

VIII: X=Br, Y=O
IX: X=Br, Y=O
X: X=Cl, Y=S
XI: X=O$^-$½Ba, Y=O

In each of these acyclic compounds, the observed POCH coupling constant should be considered as the mean of the values of equally populated three rotamers; *i. e.*, $J_{obs}=\frac{2}{3}J_g+\frac{1}{3}J_t$. A comparison will be made for the values of $\frac{2}{3}J_g+\frac{1}{3}J_t$ of cyclic (I—VII) and acyclic (VIII—XI) systems, and a discussion will be given to the differences found in these values.

Conformations of the 1,3,2-Dioxaphosphorinanes (I—VII). The NMR spectrum of I is shown in Fig. 3, a. As is seen here, the spectrum is too complicated to be analyzed on itself. The analysis was made by adopting two techniques. One of them is a triple resonance. On irradiating C and D protons simultaneously, the complex signals of E, A, and B protons become simpler (see Fig. 3, b), while on irradiating A and B signals simultaneously, the signals of C and D protons become simpler (see Fig. 3, c). The other method for the simplification of the spectra is to substitute C and D protons with deuterium. The NMR spectrum of the deuterated I is shown in Fig. 4. The signals of A, B, and E are now simpler patterns which can be readily analyzed. As an example, the parameters thus determined with II by a first order approximation are given in Table 1.

The observed values of the proton-proton coupling constants (Table 1) are in good agreement with what is expected when the *1,3,2-dioxaphosphorinane* ring is fixed to a chair form carrying the bulky phenyl group on the equatorial bond (Fig. 2, a, c). Thus, the coupling constants J_{AD} and J_{DE} are 11.3—11.9 Hz, and these values are expected when A, D and D, E are nearly in the *trans* relations[5] (see Table 1). On the other hand J_{AC}, J_{BC}, J_{BD} and J_{CE} are all small (2.4—5.0 Hz), and they are just what is expected for *gauche* coupling.[5]

The NMR spectrum of IV is given in Fig. 5, a. There are two methyl signals observed corresponding to the two methyl groups on C_5. When the lower-field methyl signal is irradiated strongly, the lower-field transitions of the ring methylene protons become sharper (see Fig. 5, b). This

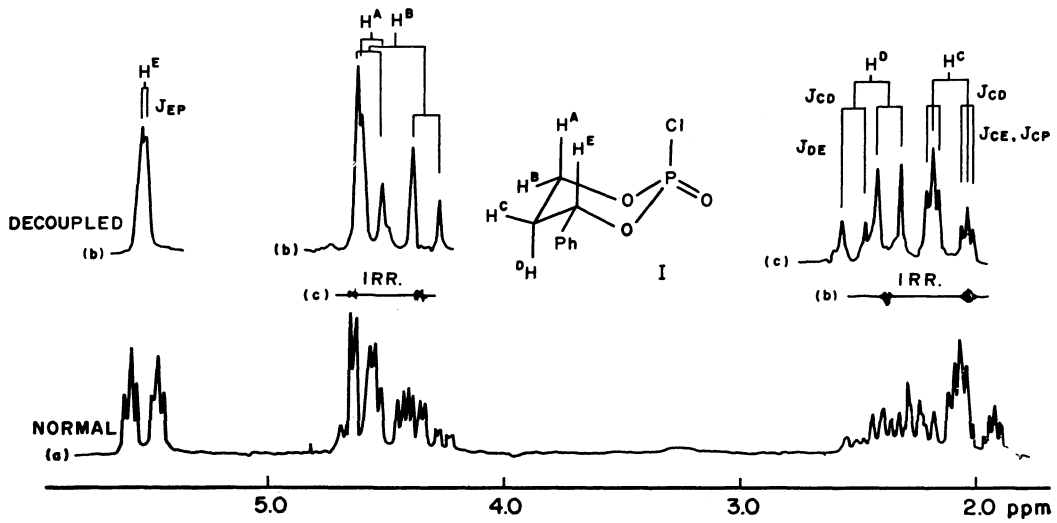

Fig. 3. 100 MHz spectrum of 2-oxo-2-chloro-4-phenyl-1,3,2-dioxaphosphorinane (I). Solvent $CDCl_3$ with ~5% C_6H_6.

5) M. Karplus, *J. Chem. Phys.*, **30**, 11 (1959); *J. Am. Chem. Soc.*, **85**, 2870 (1963).

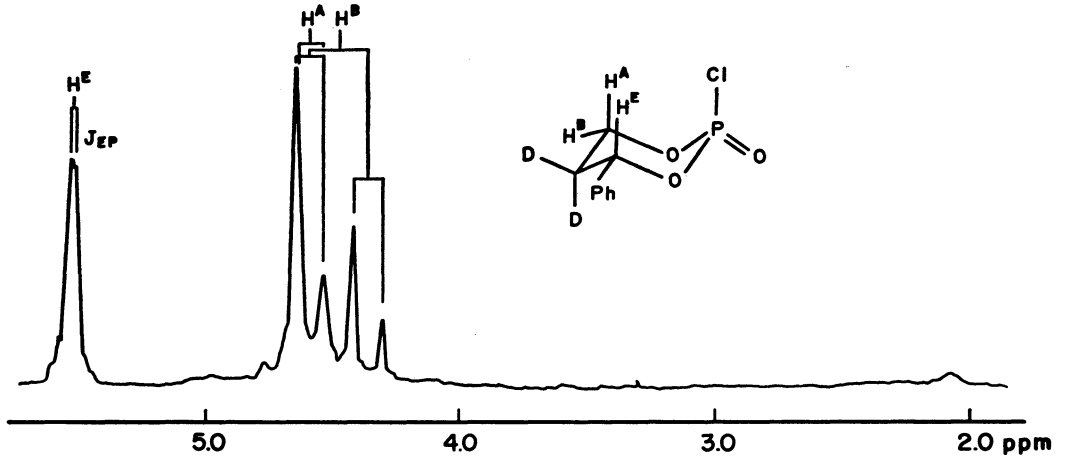

Fig. 4. 100 MHz spectrum of 5,5-dideuterio-2-oxo-2-chloro-1,3,2-dioxaphosphorinane. Solvent $CDCl_3$ with ~5% C_6D_6.

Table 1. NMR Parameters of II (benzene solution; 100 MHz)

Proton[a)]	Chemical shift[b)] (Multiplicity[c)])	Coupling constant[d)]				
		P	A	B	C	D
A	4.98(d,d,d,d)	5.4				
B	4.68(d,d,d,d)	29.2	11.7			
C	2.11(d,d,d,d,d)	2.5	2.4	1.9		
D	2.76(d,d,d,d)	—	11.9	5.0	14.8	
E	6.12(d,d,d)	3.6	—	—	3.6	11.3

a) 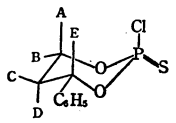 II

b) ppm from internal TMS.
c) d,d···indicates doublet of doublets···and so on.
d) each element of this table corresponds to the coupling constant; *i.e.* J_{AP} is 5.4 Hz.

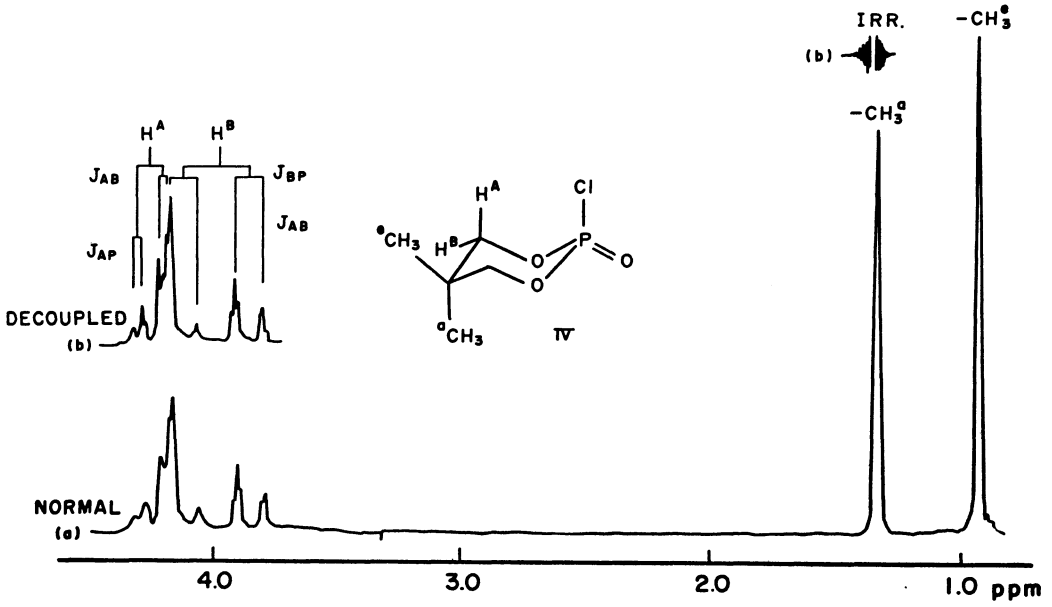

Fig. 5. 100 MHz spectrum of 5,5-dimethyl-2-oxo-2-chloro-1,3,2-dioxaphosphorinane (IV). Solvent $CDCl_3$.

observation indicates that there is a long range coupling existing between these protons.[6] Such an appreciable long range coupling through four bonds is known to take place only when the interacting nuclei are arranged so as to have the coplanar zigzag orientation ("W" letter orientation) with each other.[7,8] Therefore, the lower-field methyl signal must be assigned to the axial one. This implies that IV should have a nearly fixed conformation, either (a) or (b) in Fig. 2. If these two conformers were mixed with each other to a considerable amount, both two methyl groups would have a chance to experience the zigzag orientation with ring protons. Actually, however, no effect was observed in the methylene signals on irradiating at the upper-field methyl signal.

J_t and J_g Values in the Cyclic Systems (I —VII). Now that the conformation of *1,3,2-dioxaphosphorinane* systems is found to be fixed at one of the possible chair structures (Fig. 2), the J_g and J_t values are readily obtained. Those values, obtained by the ABX treatments of the simplified methylene spectra, are given in Table 2.

It has been shown that the J_t value (ranging, 22.3—32.2 Hz) is much greater than the J_g value (1.5—4.3 Hz). Thus the spin-spin coupling in the POCH system has a similar stereospecificity to that of the HCCH system.[5] It is interesting to point out that the substituent effect on the J_t value seems to be greater than that on the J_g value (see Table 2).

TABLE 2. PHOSPHORUS-PROTON COUPLING CONSTANTS (J_{POCH}) OF 1,3,2-DIOXAPHOSPHORINANES[a]

Compound	Solvent	J_g	J_t	J_g+J_t	X	Y
I[b]	$CDCl_3$	−(2.2)[c]	—	33.2	Cl	O
IV	$CDCl_3$	2.9	27.5	30.4		
V	$CDCl_3$	3.6	30.0	33.6	Br	O
II	$CDCl_3$	3.6(3.6)	32.2	35.8	Cl	S
VI	$CDCl_3$	4.3	28.6	32.9		
III	D_2O	1.9(1.5)	22.3	24.2	O^-K^+	O
VII	D_2O	12.2[d]			OH	O

a) Coupling constants are obtained by ABX treatment for the ring methylene protons.
b) Spectrum of I seems to be unsuitable for ABX treatment because of the line overlapping (see Fig. 3, 4).
c) Values in the parentheses show the coupling constant between phosphorus and E proton as defined in Table 1.
d) Estimated by the spacing of the doublet; equal to $\frac{1}{2}(J_g+J_t)$.

J_{POCH} Values in the Acyclic Systems (VIII —XI). In an acyclic system the J_t and J_g are not obtained separately. The observed J_{POCH} in a CH_3OP system, however, is considered to be exactly equal to $\frac{2}{3}J_g+\frac{1}{3}J_t$. The $\frac{2}{3}J_g+\frac{1}{3}J_t$ values, listed in Table 3, have been observed for VIII, IX, X and XI.

TABLE 3. PHOSPHORUS-PROTON COUPLING CONSTANTS IN VARIOUS DIMETHYL PHOSPHATES; $(CH_3O)_2P(=Y)X$[a]

Compound	Solvent	J_{obs}[b]	J_{calcd}[c]	ΔJ[d]	X	Y
VIII	$CDCl_3$	13.6	11.1	2.5	Cl	O
IX	$CDCl_3$	14.3	12.4	1.9	Br	O
X	$CDCl_3$	18.9	13.1 12.4	5.8 6.5	Cl	S
XI	D_2O	10.8	8.7	2.1	$O^-\frac{1}{2}Ba^{2+}$	O

a) Preparation of these compounds were carried out by conventional methods.
b) Obtained directly from the spacing of doublets.
c) Estimated using the corresponding J_g and J_t valuses in Table 2, by $J_{calcd}=\frac{1}{3}J_t+\frac{2}{3}J_g$.
d) $\Delta J=J_{obs}-J_{calcd}$

Discussion

As may be seen in Table 3, the $\frac{2}{3}J_g+\frac{1}{3}J_t$ value is always greater in an acyclic system than that in the corresponding cyclic system (the difference is 1.9—6.5 Hz). One might attribute this difference to an inversion of the *1,3,2-dioxaphosphorinane ring*. As was already shown, the six-membered ring is almost frozen to (a) or (c) given in Fig. 2. But the possibility that the ring experiences other conformations, such as (b) or (d), in a small fraction (α) of time has never been completely excluded. This would give slightly different coupling constants (J'_t and J'_g) from the strict J_t and J_g. The situation might make the $\frac{2}{3}J'_g+\frac{1}{3}J'_t$ value always greater than the $\frac{2}{3}J_g+\frac{1}{3}J_t$ value.
Thus,

$$\begin{aligned}\tfrac{1}{3}J'_t+\tfrac{2}{3}J'_g &= \tfrac{1}{3}[(1-\alpha)J_t+\alpha J_g]\\ &\quad+\tfrac{2}{3}[(1-\alpha)J_g+\alpha J_t]\\ &= (\tfrac{1}{3}J_t+\tfrac{2}{3}J_g)+\alpha/3(J_t-J_g)\\ &> \tfrac{1}{3}J_t+\tfrac{2}{3}J_g,\end{aligned}$$

as far as $J_t>J_g$. Therefore, the possible inversion of the ring, if any, does not explain the fact that the apparent $\frac{1}{3}J_t+\frac{2}{3}J_g$ value of the cyclic system is smaller than that of the acyclic system.

Instead, this fact can be explained by considering a slight deviation of the dihedral angle from 60° or 180°. X-ray studies of three 1,3,2-dioxaphosphorinanes, as are listed in Table 4, show that there is actually a ring flattening in each of the compounds examined. As may be seen in the table, the dihedral angle for the "*gauche*" and "*trans*" POCH group is 65° and 185°, respectively. It is

6) K. D. Bartle, R. S. Edmundson and D. W. Jones, *Tetrahedron*, **23**, 1701 (1967).
7) M. Barfield, *J. Chem. Phys.*, **41**, 3825 (1964).
8) S. Sternhell, *Rev. Pure Appl. Chem.*, **14**, 15 (1964).

Table 4. Dihedral angles of P-O-C-H system in 1,3,2-dioxaphosphorinanes[a)]

Compound	∠P-O-C-H_A[b)]	∠P-O-C-H_B[b)]
2-Oxo-2-phenoxy[9)]	67°	187°
5-Methyl-5-bromomethyl-2-oxo-2-bromo-[10)]	64	184
VII[11)]	65	185

a) All angles are estimated by the assumption of tetrahedral carbon atom, using X-ray crystallographc data.
b) See Fig. 2.

probable that these dihedral angles are kept not only in the crystals but also in solutions. If the curve for J_{POCH} *versus* dihedral angle is similar to the curve for J_{HCCH} *versus* dihedral angle given by Karplus[5)], these greater dihedral angles should cause smaller values of apparent J_g and J_t than what would be observed when the dihedral angles were exactly 60° and 180°, respectively. Therefore, a correction should be made of each of the observed values of J_g and J_t, so as to bring it to the value corresponding to 60° or 180°.

As was already shown in a previous paper,[2)] ^{31}P spectra in D_2O solution of inosine-5'-monophosphate (IMP) and guanosine-5'-monophosphate (GMP) give a triplet whose spacings are considered to correspond to two approximately equal J_{POCH}'s where J_{POCH}=4.5 Hz. The fact that two equal J_{POCH}'s are observed means that the two dihedral angles $POC_5'H$ are both 60° in IMP or in GMP. Therefore, let us assume that J_g equals 4.5 Hz when the dihedral angle POCH equals exactly 60° (instead of 65°). The correction of the J_{POCH} value from that of the dihedral angle 185° to that of 180°C is considered to be about +5%, on the basis of the curve presented by Karplus[5)] for J_{HCCH}. This leads the J_t value to about 23.5 Hz for H-C-O-P(=O)O$^-$ system. With these values of J_g and J_t, the $\frac{2}{3}J_g+\frac{1}{3}J_t$ value (10.8 Hz) of the cyclic system is in an exact agreement with that of the acyclic system.

In summarizing, what has so far been observed can be explained by postulating the following items:

1) The *1,3,2-dioxaphosphorinane* ring of each of I—VII is fixed in a chair form in solution, and there is no appreciable inversion taking place.

2) In the fixed chair form, the dihedral angle of $POCH_A$ (see Fig. 2, a) is about 65° (instead of 60°) and that of $POCH_B$ (see Fig. 2, a) about 185° (instead of 180°).

3) The ^{31}POCH coupling constant depends upon the dihedral angle in a similar way to that of HCCH.

4) We do not need to assign different values of the coupling constant to cyclic and acyclic systems, as far as the same set of atoms (X and Y) are placed on P.

5) The nuclear spin coupling constant in the 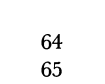 group is 4.5 Hz if the dihedral angle is 60°, and 23.5 Hz if the dihedral angle is 180°.

Experimental

NMR Measurements. All spectra were recorded with a Varian A-60 and a HA-100 spectrometer. The 100 MHz frequency sweep decoupling experiments were achieved with two Hewlett-Puckard 200 ABR oscilators at the field-frequency controlled mode.

Lithium Aluminum Hydride Reduction of Ethyl Benzoylacetate. A solution of ethyl benzoylacetate (7.69 g, a mixture of 58% *keto* and 42% *enol* forms, determined by NMR analysis) in dry ether (50 m*l*) was added to an ice-cold solution of $LiAlH_4$ (24 g) in ether (100 m*l*), over a period of an hour. Stirring was continued for an additional 1 hr, then the mixture was treated with a small amount of water, dried ($MgSO_4$) and was fractionally distilled. The diol was distilled at 125°C/1.5 mmHg and the yield was 85% from *keto* form of ethyl benzoylacetate.

Found: C, 70.88; H, 7.66%. Calcd for $C_9H_{12}O_2$: C, 71.02; H, 7.95%.

Ethyl(*α,α*-dideuterio) benzoylacetate. The deuteration was achieved by the deuterium-hydrogen exchange reactions between ethyl benzoylacetate and *O*-deuterioethanol. The process of the reaction was followed by the NMR measurement.

2,2-Dideuterio-1-phenyl-1,3-propanediol. Lithium aluminum hydride reduction of ethyl (α,α-dideuterio)-benzoylacetate afforded the dideuterio diol. Its NMR spectrum showed that deuterium-hydrogen exchange was negligible during the course of preparation.

2-Oxo-2-chloro-4-phenyl - 1, 3,2 - dioxaphosphorinane (I). The cyclic phosphorochloridate was prepared by a similar method to that of Lanham.[12)] The yield was 29%.

Found: C, 46.55; H, 4.53; Cl, 15.32%. Calcd for $C_9H_{10}ClO_3P$: C, 46.47; H, 4.33; Cl, 15.24%.

2- Thiono -2- chloro - 4 - phenyl - 1,3,2 - dioxaphosphorinane (II). This compound was synthesized by following the procedure given in Lanham's patent,[12)] and was obtained as light yellow oil, which partly changed to colorless needles while it was kept in a refrigerator in a vacuum dessicator. Purification through vacuum distillation was not successful because a decomposition of the oil took place. Its purity was judged only by the NMR measurement.

Potassium 2-Oxo-2-hydroxy-4-phenyl-1,3,2-dioxaphosphorinane (III). To a solution of II (1.02 g) in a mixture of dioxane-water (17 : 3) was added 2 N KOH solution (5 m*l*). After stirring for a few minutes, the solvent was distilled off, and the residue was extracted.

9) H. J. Geise, *Res. Trav. Chim. Pays-Bas*, **86**, 362 (1967).
10) T. A. Beineke, *Chem. Commun.*, **1966**, 860; *Acta Crystal.*, in press. The preprint of this paper was kindly sent from Dr. Beineke before the publication.
11) W. Murayama and M. Kainosho, to be published.
12) W. Lanham, U. S. Pat. 2894016 (1959).

with ethanol. After removal of ethanol the product was deposited as colorless solid, which was washed with acetone, and dried in air. The yield was 1.04 g (94%). The structure was characterized by NMR.

5,5-Dideuterated Compounds of I, II, and III. These compounds were prepared from 1-phenyl-1,3-(2,2-dideuterio)-propanediol by similar methods to those described for I, II, and III, above. The products were identified by their NMR spectra.

5,5-Dimethyl-2-thiono-2-chloro-1,3,2-dioxaphosphorinane (IV). To a solution of neopentylglycol (0.3 mol) in 150 m*l* of dichloroethane, was added gradually thiophosphoryl chloride (0.3 mol) in 50 m*l* of dichloroethane, with continuous stirring, while the reaction mixture was kept below 26°C by ice-water cooling. After the addition of thiophosphoryl chloride was completed, hydrogen chloride was removed by the vigorous bubbling of dry nitrogen. Removing the solvent under the reduced pressure, colorless crystals were obtained. Recrystallization from *n*-hexane gave colorless needles. Yield, 69%. Mp 92—93.5°C.

Found: C, 29.72; H, 5.11%. Calcd for $C_5H_{10}O_2$·SClP: C, 29.93; H, 5.02%.

5, 5-Dimethyl-2-oxo-2-bromo-1,3,2-dioxaphosphorinane (V). To a solution of neopentylglycol (5.2 g) in 30 m*l* dichloroethane was added slowly phosphoryl bromide in 20 m*l* dichloroethane. The orange colored product was obtained by a similar procedure to that for IV. The product was crystallized as colorless needles from *n*-hexane solution and they turned gradually to yellow with moisture. Mp 98—99°C.

Found: C, 27.06; H, 4.71%. Calcd for $C_5H_{10}O_3$-BrP: C, 26.22; H, 4.40%.

V was also prepared by the Michaelis-Arbuzov reaction between 5,5-dimethyl-2-methoxy-1,3,2-dioxaphosphorinane and bromine.

5,5-Dimethyl-2-oxo-2-chloro-1,3,2-dioxaphosphorinane (VI). VI was prepared by a known procedure[13] with 68% Yield. Mp 107—108°C.

Found: C, 32.83; H, 5.54%. Calcd for $C_5H_{10}O_3$-ClP: C, 32.54; H, 16.46%.

5, 5-Dimethyl-2-oxo-2-hydroxy-1,3,2-dioxaphosphorinane (VII). VII was prepared by the hydrolysis of VI in aqueous acetone. Recrystallization from hot aqueous solution gave colorless needles. A *thermogravimetric* analysis showed the product contained one water molecule.

Found: C, 33.16; H, 7.06%. Calcd for $C_5H_{11}O_4P \cdot H_2O$: C, 32.51; H, 7.12%.

The authors wish to express their gratitude to Miss Masako Kaneko for her help throughout this study, and to Dr. M. C. Woods and Mr. Iwao Miura of the Tohoku University for their help in the NMR measurements at an early stage of this work.

Note Added in Proof. After the completion of this work, the authors have extensively studied the conformation of 2,2-disubstituted-1,3,2-dioxaphosphorinanes by dipole moment measurements[14], infra-red[15] and NMR spectra.[16] The results thus far obtained strongly indicates a-conformation of Fig. 2 is the preferred one.

13) R. L. McConnel and H. W. Coover, Jr., *J. Org. Chem.*, **24**, 630 (1967).

14) M. Kainosho and T. Shimozawa, *Tetrahedron Letters*, **1969**, 865.

15) M. Kainosho, T. Morofushi and A. Nakamura, This Bulletin, **42**, 845 (1969).

16) M. Kainosho, to be published.

BULLETIN OF THE CHEMICAL SOCIETY OF JAPAN VOL. 42 1719—1725 (1969)

The Synthesis of Cyclic α-Amino Acids. III. The Synthesis of Methyl (+)- and (−)-3-Amino-3-*C*-carboxy-3-deoxypentopyranosides

Hiroaki YANAGISAWA, Mitsuhiro KINOSHITA and Sumio UMEZAWA

Department of Applied Chemistry, Faculty of Engineering, Keio University, Koganei-shi, Tokyo

(Received December 14, 1968)

Cyclization of D'-methoxy-diglycolaldehyde, prepared by periodate cleavage of methyl β-L-arabinopyranoside, with ethyl nitroacetate gave a mixture of stereoisomers of cyclic α-nitro ester, *i.e.* methyl (+)-3-deoxy-3-*C*-ethoxycarbonyl-3-nitropentopyranoside. Catalytic reduction of the cyclic α-nitro ester afforded an isomeric mixture of cyclic α-amino esters, from which, on column chromatography, there could be isolated four diastereoisomers of methyl (+)-3-amino-3-deoxy-3-*C*-ethoxycarbonylpentopyranoside. Hydrolysis of each diastereoisomer gave the corresponding cyclic (+)-α-amino acid having a skeleton of pentopyranoside. The stereochemistry of the isomeric amino acids was studied by NMR spectroscopy and chemical degradation. On the other hand, three enantiomeric cyclic (−)-α-amino acids were also obtained from methyl β-D-xylopyranoside by the analogous route as that from methyl β-L-arabinopyranoside.

In a previous paper[1] one of the authors and others reported the synthesis of a cyclic amino acid, *i. e.* 1-amino-2,6-dihydroxycyclohexane-1-carboxylic acid by condensation of glutardialdehyde with ethyl nitroacetate, followed by reduction and hydrolysis. The present paper is concerned with an extension of this work and presents the synthesis of methyl (+)- and (−)-3-amino-3-*C*-carboxy-3-deoxypentopyranosides (VI-d, VI-1) which are the first synthetic examples of cyclic α-amino acid having a pyranoside-skeleton.

Details of the synthesis are summarized in Scheme 1. The starting materials, D'- and L'-diglycolaldehyde (III-d. III-1) were prepared from methyl β-L-arabinopyranoside (I) and β-D-xylopyranoside (II) respectively, by periodate oxidation as was reported by Bear and Fischer[2].

The condensation reaction of III-d with ethyl nitroacetate was carried out in the presence of potassium acetate and potassium carbonate to give a dextrorotatory methyl (+)-3-deoxy-3-*C*-ethoxycarbonyl-3-nitropentopyranoside (IV-d) in 81% yield. The purification of IV-d was accomplished by silica gel chromatography, although the diastereoisomeric separation of IV-d was unsuccessful in this step. The acetylation of IV-d with acetic anhydride in pyridine gave a diacetyl derivative of IV-d, the NMR spectrum (in $CDCl_3$) of which showed the presence of two *O*-acetyl groups at about τ 7.84 and 7.92.

The condensation reaction of III-1 with ethyl nitroacetate gave a levorotatory nitro ester (IV-1).

The catalytic hydrogenation of the nitro esters IV-d and IV-1 with Raney Ni T-4 gave methyl (+)- and (−)-3-amino-3-deoxy-3-*C*-ethoxycarbonylpentopyranosides (V-d and V-1) as a syrup, respectively.

The amino ester V-d was shown by thin-layer chromatography to contain four ninhydrin positive components, VA-d (R_f 0.73), VB-d (R_f 0.55), VC-d (R_f 0.36) and VD-d (R_f 0.23). These components were separated from each other by silica gel column chromatography. The major component VB-d and minor one VD-d were obtained in crystalline states. The components, VA-d, VB-d, VC-d and VD-d were acetylated to give dextrorotatory crystalline triacetates, VIIA-d, VIIB-d, VIIC-d and VIID-d, respectively. These acetates were characterized as the fully acetylated diasteroisomeric amino esters on the basis of elemental and NMR analysis (Tables 1, 3 and 4).

By analogous chromatography four diastereoisomers of levorotatory amino esters, VA-1 (R_f 0.73), VB-1 (R_f 0.55), VC-1 (R_f 0.36) and VD-1 (R_f 0.23) were obtained from the mixed amino ester V-1. The crystalline major and minor isomers, VB-1 and VD-1 were characterized as the enantiomers of VB-d and VD-d, respectively (Table 1). Furthermore, the crystalline triacetates, VIIA-1, VIIB-1, and VIID-1 were also obtained from VA-1, VB-1 and VD-1, respectively (Table 1). The IR and NMR spectra of VIIA-1, VIIB-1 and VIID-1 were completely identical with those of VIIA-d, VIIB-d and VIID-d, respectively.

The hydrolysis of VA-d, VB-d, VC-d and VD-d afforded the isomeric methyl (+)-3-amino-3-*C*-carboxy-3-deoxypentopyranosides, VIA-d, VIB-d, VIC-d and VID-d, respectively, in good yields. Analogously, the enatiomeric (−)-amino acids,

1) S. Zen, Y. Takeda, A. Yasuda and S. Umezawa, This Bulletin, **40**, 431 (1967).

2) H. H. Bear and H. O. Fischer, *J. Am. Chem. Soc.*, **81**, 5184 (1959).

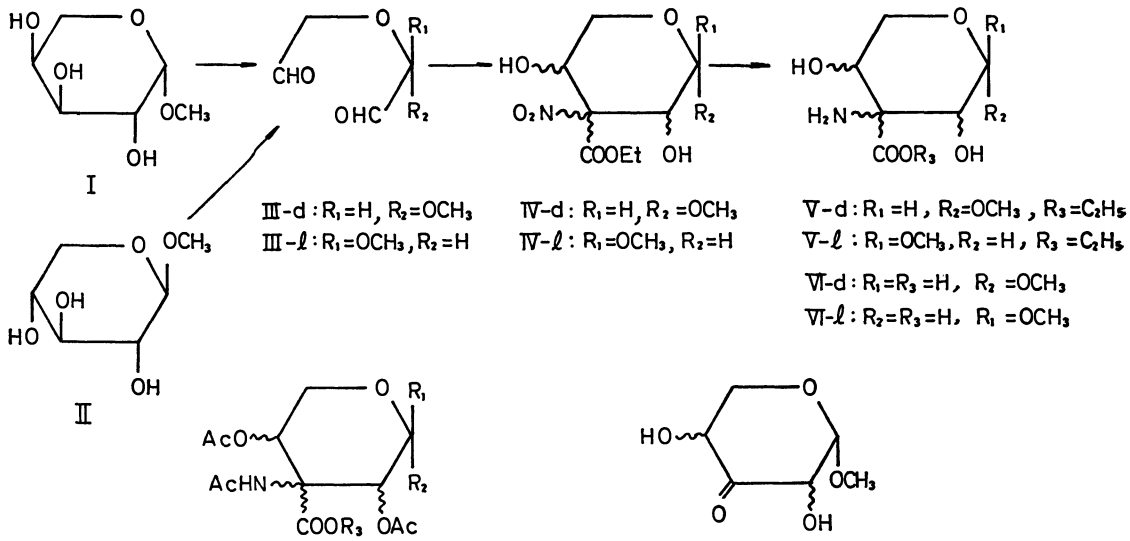

Scheme 1

TABLE 1. ISOMERIC AMINO ESTERS AND THEIR ACETYL DERIVATIVES

Compound	Mp °C	$[\alpha]_D^\circ$ (Temp. °C, Concn. %, Solv.*)	Formula	Calcd C, %	Calcd H, %	Calcd N, %	Found C, %	Found H, %	Found N, %
VB-d	133—4	+135 (23, 0.7, A)	$C_9H_{17}NO_6$	45.95	7.28	5.96	46.28	7.54	5.64
VD-d	161—2	+ 39 (23, 0.7, A)					46.44	7.39	5.70
VB-l	132—3	−133 (21, 0.5, A)					46.20	7.40	6.03
VD-l	161—2	− 37 (21, 0.5, A)					46.24	7.37	5.96
VIIA-d	174—5	+ 98 (22, 0.7, E)	$C_{15}H_{23}NO_9$	49.86	6.42	3.88	50.26	6.60	3.88
VIIB-d	118—20	+166 (22, 0.7, E)					50.06	6.63	3.69
VIIC-d	151—2	+ 55 (22, 0.7, B)					50.21	6.62	3.65
VIID-d	115—6	+ 49 (22, 0.7, E)					50.13	6.45	3.74
VIIA-l	174—5	−100 (29, 1.0, B)					50.16	6.62	3.89
VIIB-l	118—20	−171 (29, 1.0, E)					49.99	6.58	3.97
VIID-l	116—6.5	− 43 (18, 0.7, E)					50.08	6.46	3.89

* A=ethanol; E=ethyl acetate

TABLE 2. ISOMERIC AMINO ACIDS

Compound	Mp[a] °C (Dec.)	$[\alpha]_D^{21}$ (Conc. %) in water		R_f[b]	Formula	Calcd C, %	Calcd H, %	Calcd N, %	Found C, %	Found H, %	Found N, %
VIA-d	250	+ 51	(0.4)	0.13	$C_7H_{13}NO_6$	40.58	6.32	6.76	41.09	6.50	6.37
VIB-d	230	+193	(0.4)	0.18					41.07	6.47	6.28
VIC-d	180	+121	(0.3)	0.27					40.72	6.50	6.69
VID-d	160	+ 28*	(0.4)	0.16					40.41	6.58	6.43
VIA-l	250	− 41	(0.9)	0.13					40.44	6.97	6.34
VIB-l	230	−204**	(0.9)	0.18					40.92	6.79	6.67
VID-l	160	− 30	(0.7)	0.16					40.77	6.87	6.51

a) Determined on a Yanagimoto micro hot stage.
b) Solvent system; *n*-butanol - acetic acid - water (4 : 1 : 1).
* At 16°C, ** At 26°C

VIA-1, VIB-1 and VID-1 were also obtained from the amino esters, VA-1,VB-1 and VD-1, respectively (Table 2).

Stereochemical Considerations. The anomeric carbon atom C-1 in each of the isomers of the (+)-amino acid (VI-d) apparently has the same configuration as that of the anomeric carbon atom in the methyl β-L-arabinopyranoside (I) used as a starting substance. The other asymmetric carbon atoms (C-2, C-3 and C-4), however, have unknown configurations, because they are new asymmetric centers which have been formed by the condensation reaction of the dialdehyde (II-d) with ethyl nitroacetate. The steric configurations

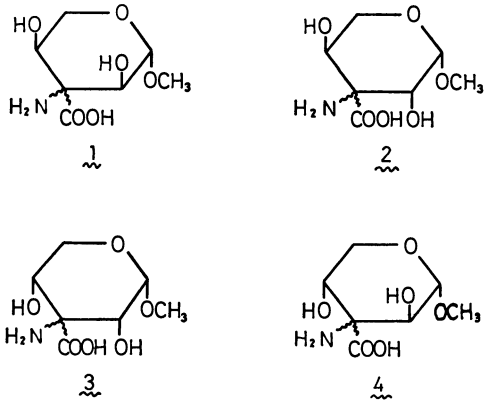

Fig. 1

of the isomeric (+)-amino acids, VIA-d, VIB-d, VIC-d and VID-d, therefore, must be assigned to any of the eight possible configurations. When the configuration at C-3 is let aside, the four formulas shown in Fig. 1 are possible for the isomeric (+)-amino acids.

Conformational and configurational studies based on the NMR (in $CDCl_3$) analysis[3] of the fully acetylated amino esters, VIIA-d, VIIB-d, VIIC-d and VIID-d, served to deduce the configurations at the two carbon atoms (C-2 and C-4) of the above-mentioned three unknown asymmetric carbon atoms in the amino acid isomers. The spectral features were assigned on the basis of chemical shifts, integrated area, magnitudes of splittings and decoupling splitting patterns (Fig. 2). The assigned chemical shifts and coupling constants are listed in the Tables 3 and 4. From the following results partial conformations for VIIA-d, VIIB-d, VIIC-d and VIID-d could be deduced on the assumption that most pyranoside sugars and their derivatives may exist in the chair conformations (*C1*, *1C*)[4].

The ring proton coupling constants ($J_{1,2}=1.8$, $J_{4,5e}=J_{4,5a}=2.0$ Hz) observed in the spectrum (Fig. 2, A) of VII-d indicate that the pair of H-1 and H-2 protons is in equatorial-axial or equatorial-equatorial orientation and H-4 proton is not antiparallel to H-5 axial proton. Decoupling reveals that the long range coupling of 1.5 Hz is found between H-2 proton and H-4 proton. Therefore, H-2 proton may be located on equatorial as well as

Table 3. Chemical shifts (τ) in $CDCl_3$ at 100 MHz

Compound	NH	H-1	H-2	H-4	H-5a	H-5e	O-Ac	NAc	CH_2	CH_3	OCH_3
VIIA-d	3.96	5.26	4.92	4.28	5.65 or 6.20		7.79, 7.88	8.08	5.75	8.71	6.68
VIIB-d	3.21	5.29	4.72	4.18	5.52 or 6.27		7.78, 7.87	8.12	5.75	8.71	6.63
VIIC-d	3.22	5.10	4.17	4.07	5.79	6.24	7.93, 8.00	8.04	5.69	8.68	6.62
VIID-d	3.27	5.18	4.33	4.09	6.22	5.91	7.96, 7.96	8.03	5.68	8.67	6.52
VIIID-d	—*	4.88 or 5.14		4.88	5.9 — 6.2		8.01, 8.03	7.83	—	—	6.55

* Not observed.

Table 4. Coupling constants (*J*, Hz)

Compound	$J_{1,2}$	$J_{4,5a}$	$J_{4,5e}$	$J_{5a,5e}$	$J_{2,4}$	J_{CH_2,CH_3}
VIIA-d	1.8	2.0	2.0	13.2	1.5	7.2
VIIB-d	3.1	2.0 or 1.4		13.2	0	7.2
VIIC-d	4.7	10.1	6.2	11.5	0	7.5
VIID-d	5.7	7.3	5.0	12.5	0	7.1
VIIID-d	8.3	10	3	12	0	—

3) R. U. Lemieux and J. D. Stevens, *Can. J. Chem.*, **43**, 2059 (1965).

4) N. S. Bhacca and D. Horton, *J. Am. Chem. Soc.*, **89**, 5993 (1967); L. D. Hall, *Advan. Carbohydrate Chem.*, **19**, 51 (1964).

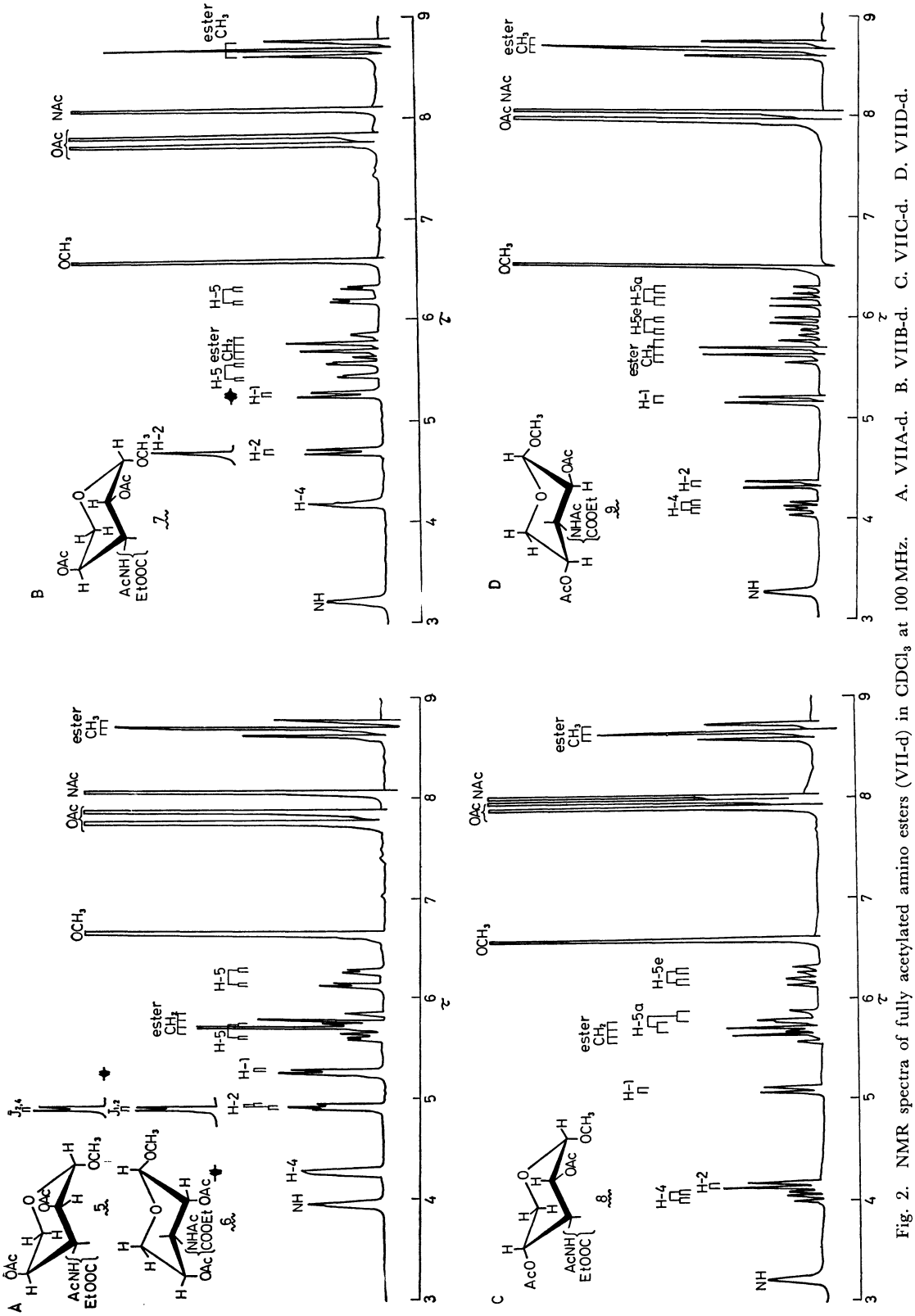

Fig. 2. NMR spectra of fully acetylated amino esters (VII-d) in $CDCl_3$ at 100 MHz. A. VIIA-d. B. VIIB-d. C. VIIC-d. D. VIID-d.

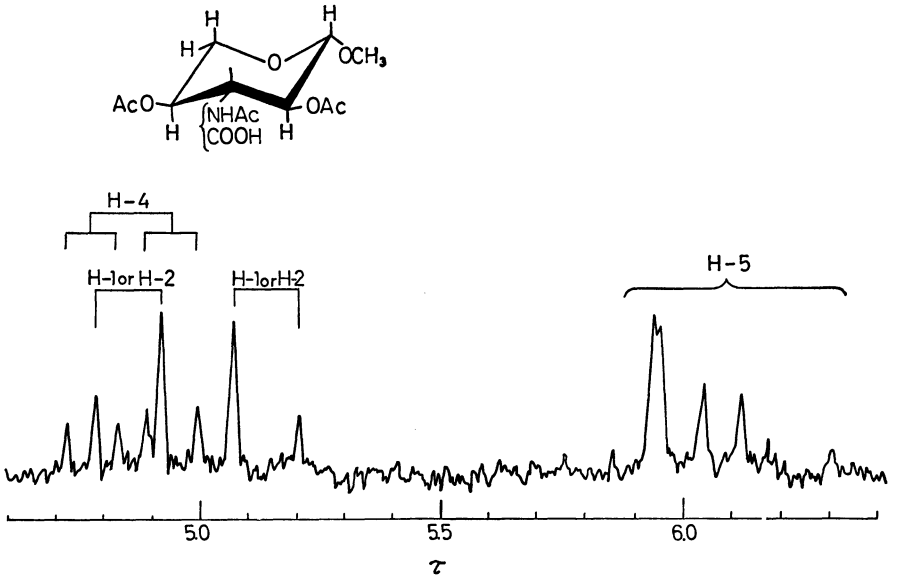

Fig. 3. NMR spectrum of VIIID-d in $CDCl_3$ at 60 MHz.

H-4 proton according to stereospecificity of the long-range coupling ("W"-conformation[5]). The chemical shifts (τ 7.79 and 7.88) for the ring-acetoxy protons at C-2 and C-4 also support this conformation, because they fall in the range of the chemical shifts (τ 7.80—7.90) reported for the axial orientation.[6] There must be then considered two possible partial conformations, **5** and **6** for VIIA-d (Fig. 2, A). The former is a *C1* conformation corresponding to the configuration **1** and the later is a *1C* conformation corresponding to the configuration **3**.

In the NMR spectrum (Fig. 2, B) of VIIB-d, the ring proton coupling constants ($J_{4,5a}=J_{4,5e}=1.4$—2.0 Hz) show that H-4 proton is not antiparallel to H-5 axial proton, therefore, H-4 proton is equatorial. The H-2 proton may be in axial orientation, because decoupling experiment shows no long-range coupling between H-2 and H-4 protons. The small coupling constant ($J_{1,2}=3.1$ Hz) shows that H-1 proron is gauche to the H-2 proton. Consequently, the H-1 proton thus may be located on equatorial orientation. The acetoxy signal at τ 7.78 indicates that one axial acetoxy group exists in VIIB-d. Conformation **7** is deduced as a possible partial conformation for VIIB-d and this is *C1* conformation corresponding to the configuration **2**.

The NMR spectrum (Fig. 2, C) of VIIC-d shows that the pair of H-1 and H-2 protons is in equatorial-axial or equatorial-equatorial orientation($J_{1,2}=4.7$ Hz), while H-4 proton is located on axial orientation ($J_{4,5e}=10.1$ Hz). The acetoxy signals at τ 7.93 and 8.00 indicate that VIIC-d has two equatorial ring-acetoxy groups.[6] Consequently, H-2 proton is located on axial orientation and H-1 proton is to be regarded as equatorial. A possible partial conformation for VIIC-d is deduced as **8** which is a *C1* conformation corresponding to the configuration **3**.

In the NMR spectrum (Fig. 2, D) of the last isomer VIID-d, the observed ring-proton coupling constants ($J_{1,2}=5.7$ and $J_{4,5a}=7.3$ Hz) reveal that H-1, H-2 and H-4 protons are all in axial orientation. The existence of two equatorial acetoxy groups is shown by the sharp singlet at τ 7.96, which is caused by overlapping of the two acetoxy signals. These results are confirmed by the NMR analysis for the triacetate (VIIID-d) of the free amino acid VID-d, which affords a spectrum of the AB and ABX type arising from the protons at the 1,2- and 4,5,5-positions, respectively (Fig. 3). Treating these protons as an isolated AB and ABX system, the following coupling constants are obtained; $J_{1,2}=8.3$, $J_{5a,5e}=12$, $J_{4,5e}=3.0$ and $J_{4,5a}=10.0$ Hz. From these results a possible partial conformation for VIID-d is to be considered as **9** which is a *1C* conformation corresponding to configuration **1**.

It is not possible to distinguish between the conformations **5** and **6** by the study of the ring proton resonances as described above. In other words, it remains unknown which of the configurations **1** and **3** is to be assigned for VIA-d. On the other hand, oxidation of the isomeric amino acids (VI-d) with chloramine-T yielded the corresponding methyl pentopyranosid-3-uloses (IX-d). They were isolated by preparative layer chromatography in the forms

5) L. D. Hall and L. Hough, *Proc. Chem. Soc.*, **1962**, 382; K. Heyns, J. Weyer and H. Paulsen, *Chem. Ber.*, **98**, 327 (1965); C. V. Holland, D. Horton and J. S. Jewell, *J. Org. Chem.*, **32**, 1818 (1967).

6) R. U. Lemieux, R. K. Kulling, H. J. Berstein and W. G. Schneider, *J. Am. Chem. Soc.*, **80**, 6098 (1958); F. W. Lichtenthaler and P. Emig, *Tetrahedron Letters*, **1967**, 577.

of their *p*-nitrophenylhydrazone derivatives which were characterized by IR spectra and mixed melting point determinations. The two same kinds of *p*-nitrophenylhydrazones, A_1 (mp 172°C dec., R_f 0.32) and A_2 (mp 174.5°C dec., R_f 0.43) were obtained from each of the oxidation products of VIA-d and VID-d. This indicates that the amino acids, VIA-d and VID-d are converted to a same methyl pentopyranosid-3-ulose by the chloramine-T oxidation and that VIA-d is the C-3 epimer of VID-d. The structures of the above-mentioned *p*-nitrophenylhydrazones can not be stated clearly at the present stage, because there must be considered the prototropy phenomenon which may be caused in the α-hydroxycarbonyl grouping[–(C=O)–CH(OH)–] of the oxidation products. However, the configuration **1** is to be assigned to VIA-d as well as to VID-d. The oxidation products of VIB-d and VIC-d afforded the *p*-nitrophenylhydrazones, B (mp 162—164°C dec., R_f 0.26) and C (mp 168°C dec., R_f 0.42), respectively, each of which was completely different from A_1 and A_2.

In conclusion, the above-mentioned experimental findings permit the assignment of the structural formulas **2** and **3** to VIB-d (major component)and VIC-d, respectively, and the formula **1** to VIA-d and VID-d, which are in epimeric relation with each other at C-3. The compound corresponding to the configuration **4** was not obtained.

Experimental

Paper chromatograms of amino acids were run with *n*-butanol - acetic acid - water (4 : 1 : 1) on Toyo Roshi No. 50 paper using an ascending technique, and spots were detected by means of a spray of a 0.5% pyridine solution of ninhydrin. Thin layer chromatography (TLC) and preparative layer chromatography (PLC) were conducted by the use of silica gel (Daiichi Pure Chemicals Co., Inc.). The prepared plates were activated at 110°C and the spray reagents used were 10% sulfuric acid and 0.5% pyridine solution of ninhydrin. Silica gel column chromatography was carried out by the use of silica gel (Kanto Chemical Co., Inc.) activated at 110°C before use. NMR spectra were taken with Japan Electron Optics JNM-4H-100 spectrometer and Varian A-60D spectometer at a frequency of 100 and 60 MHz by using about 10—20% solution of the sample in deuteriochloroform with tetramethylsilane as an internal standard.

Methyl (+)-3-Deoxy-3-*C*-ethoxycarbonyl-3-nitropentopyranoside (IV-d). Methyl β-L-arabinopyranoside[7] (I) (10.0 g, 0.061 mmol) was added in small portions to a stirred solution of periodic acid (27.8 g, 0.122 mmol based on H_5IO_6) in 500 m*l* of water at 20°C. The reaction mixture was allowed to stand for 20 hr at room temperature and was neutralized (pH 5) with hot 0.244 M strontium hydroxide solution (250 m*l*, 0.061 mol). The precipitate was removed by filtration and was washed with ethanol. The filtrate and washings were evaporated to afford the syrupy D'-methoxy-diglycolaldehyde (III-d), which was dissolved in ethanol (100 m*l*) and was filtered to remove a small amount of undissolved matter. The ethanolic solution of III-d was stirred under ice-cooling, while ethyl nitroacetate (8.1 g, 0.061 mol), 40% aqueous potassium acetate solution (14.2 m*l*) and 40% aqueous potassium carbonate solution (8.8 m*l*) were added successively. After the mixture was stirred in an ice bath for 3 hr, Amberlite IR-120 (100 m*l*) was added and was stirred for an additional one hour. The resin was removed by filtration and the filtrate (pH 4) was evaporated in a vacuum to afford a yellow syrup (14.6 g) of the title compound (IV-d). The product was purified through a silica gel (123 g) column. Elution with benzene-acetone (6 : 1) afforded 13.1 g (81%) of the pure nitro ester IV-d, $[\alpha]_D^{23}$ +157° (*c* 0.58, water), ν_{max}^{Film} 3455(OH), 1750 (ester C=O) and 1564 cm^{-1} (NO_2).

Found: C, 41.08; H, 5.91; N, 5.30%. Calcd for $C_9H_{15}NO_8$: C, 40.75; H, 5.70; N, 5.28%.

Di-*O*-acetyl Derivative of IV-d. A mixture of the nitro ester (IV-d) (136 mg), pyridine (6 m*l*) and acetic anhydride (2 m*l*) was allowed to stand overnight at room temperature. The reaction mixture was poured into ice-water and the liberated oil was extracted with four 10 m*l* portions of chloroform. The extracts were evaporated and the last trace of pyridine was removed by co-distillation with toluene. The residue was purified through a silica gel (20 g) column. Elution with benzene-acetone (10 : 1) afforded the title compound as a yellow syrup, yield 151 mg (84.5%), $[\alpha]_D^{32}$ +164° (*c* 0.9, ethyl acetate). The acetate was shown to be a mixture of diastereoisomers by its NMR spectrum. The NMR signals for the main isomer were observed at τ ($CDCl_3$): 7.84 and 7.92 (singlets, acetoxy protons); 6.62 (singlet, glycoside methyl protons); 5.60 (quartet, J=7.5 Hz, ester methylene protons); 8.67 (triplet, ester methyl protons); 6.06 and 5.62 (doublets, J=3.5 Hz, H-1 and H-2 proton); 6.19 (quartet, J=2.0 and 2.5 Hz, H-4 proton); 5.58 (quartet J=2.5 and 14.0 Hz, H-5 proton) and 6.12 (quartet J=2.0 and 14.0 Hz, H-5 proton).

Found: C, 44.95; H, 5.83; N, 4.13%. Calcd for $C_{13}H_{19}NO_{10}$: C, 44.69; H, 5.49; N, 4.01%.

Methyl (−)-3-Deoxy-3-*C*-ethoxycarbonyl-3-nitropentopyranoside (IV-1). Methyl β-D-xylopyranoside[8] (II) (9.0 g, 0.055 mol) was oxidized with a solution of periodic acid (25 g, 0.11 mol) in 300 m*l* of water by the same procedure as described for the preparation of III-d. A solution of the resulting L'-methoxy-diglycolaldehyde (III-l) in ethanol (120 m*l*) was stirred under ice-cooling, while ethyl nitroacetate (7.3 g, 0.055 mol), 40% aqueous potassium acetate solution (15 m*l*) and 40% aqueous potassium carbonate solution (10 m*l*) were added successively. The mixture was then worked up by the same procedure as described for the preparation of the nitro ester IV-d. The purified title compound IV-1 was obtained as a syrup, yield 13.7 g (94%), $[\alpha]_D^{20}$ −123° (*c* 1.14, water), ν_{max}^{Film} 3455 (OH), 1750 (ester C=O) and 1564 cm^{-1} (NO_2).

7) F. Smith and J. W. Cleve, *J. Am. Chem. Soc.*, **77**, 3159 (1955).

8) M. L. Wolfrom, J. W. Spoors and R. A. Gibbons, *J. Org. Chem.*, **22**, 1513 (1957).

Methyl (+)-3-Amino-3-deoxy-3-*C*-ethoxycarbonylpentopyranoside (V-d). A solution of methyl (+)-3-deoxy-3-*C*-ethoxycarbonyl-3-nitropentopyranoside (IV-d) (9.79 g) was hydrogenated in ethanol (45 m*l*) with Raney Ni T-4 (30 m*l*) for 4.5 hr under 120 kg/cm² of an initial hydrogen pressure at 20—25°C. The contents were then filtered to remove the catalyst and the filtrate was evaporated in a vacuum to afford the crude V-d (6.93 g) as a brown syrup. The sample was shown by TLC using ethyl acetate to contain four diastereoisomeric amino esters, each of which was ninhydrin positive.

Separation of Diastereoisomers of V-d. The brown syrup (6.92 g) in a small amount of ethyl acetate was placed on a silica gel column (300 g, 5×43 cm) and eluted with ethyl acetate - ethanol (6 : 1). Fractions (*ca.* 10 m*l*) were collected and examined by TLC. Fractions, 113—123, 127—135, 138—157 and 163—185 gave the isomers, VA-d (syrup, 0.92 g, R_f 0.73), VB-d (crystalline solid, 2.76 g, R_f 0.55), VC-d (syrup, 0.64 g, R_f 0.36) and VD-d (crystalline solid, 0.56 g, R_f 0.23), respectively. Total yield was 47.5% based on the original nitro ester IV-d. The analytical sample of VB-d was obtained by two recrystallizations from ethyl acetate, followed by sublimation (90—110°C/1.5 mmHg), while the analytical sample of VD-d was given by only two recrystallizations from ethyl acetate (Table 1).

Methyl (−)-3-Amino-3-deoxy-3-*C*-ethoxycarbonylpentopyranoside (V-l) and Its Diastereoisomeric Separation. The nitro ester (IV-l) (9.95 g) was hydrogenated with Raney Ni T-4 (30 m*l*) as described on the preparation of the antipode V-d. The obtained brown syrup (7.75 g) of the crude V-1 was chromatographed on a silica gel column (250 g, 4.5×40 cm). Elution with ethyl acetate - ethanol (6 : 1) afforded four isomers, VA-1 (syrup, 1.39 g, R_f 0.73), VB-1 (crystalline solid, 2.45 g, R_f 0.55), VC-1 (syrup, 1.30 g, R_f 0.36) and VD-1 (crystalline solid, 1.19 g, R_f 0.23). The analytical sample of VB-1 was obtained by two recrystallizations from ethyl acetate, followed by sublimation (110—120°C/3 mmHg), while the pure sample of VD-1 was given by two recrystallizations from ethyl acetate (Table 1).

Methyl (+)-3-Acetamido-2,4-di-*O*-acetyl-3-deoxy-3-*C*-ethoxycarbonylpentopyranoside (VIIB-d). *(A Typical Example of the General Method for the Preparation of Isomeric Amino Ester Triacetate).* A mixture of the amino ester (VB-d) (297 mg), acetic anhydride (4 m*l*) and pyridine (12 m*l*) was allowed to stand for 2 days at room temperature. The mixture was evaporated in a vacuum. The semi-crystalline residue (498 mg) was purified through a silica gel (10 g) column. Elution with methyl ethyl ketone - *n*-hexane (1 : 1) afforded crystalline title compound (VIIB-d), yield 379 mg (83%), mp 115—117°C. Recrystallization from diisopropyl ether-acetone (20 : 1) yielded an analytically pure sample of VIIB-d, mp 118—120°C.

The other triacetates of the isomeric amino esters, VIIA-d, VIIC-d, VIID-d, VIIA-l, VIIB-l and VIID-l were prepared from the corresponding amino esters by the general procedure (Table 1).

Methyl (+)-3-Amino-3-*C*-carboxy-3-deoxypentopyranoside (VIB-d) *(A Typical Example of the General Procedure for the Preparation of the Isomeric Free Amino Acids).* The amino ester (VB-d) (230 mg, 0.98 mmol) was dissolved in a 0.457N barium hydroxide solution (2.32 m*l*, 0.53 mmol). After the solution had been allowed to stand for 20hr at 37°C in an incubator, the reaction mixture was treated with 1N sulfuric acid. The supernatant layer which was separated from barium sulfate by centrifuging was evaporated in a vacuum. The residual colorless powder was recrystallized from water-acetone to afford crystalline amino acid VIB-d (180 mg, 87.3%), from which an analytical sample was obtained by two recrystallizations from water-acetone, followed by drying over phosphorus pentoxide for 5 hr at 105—110°C/3 mmHg. (Table 2).

The other amino acid isomers, VIA-d, VIC-d and VID-d and their enantiomeric amino acids VIA-1, VIB-1 and VID-1 were prepared from the corresponding amino esters by the general procedure (Table 2).

Methyl (+)-3-Acetamido-2,4-di-*O*-acetyl-3-*C*-carboxy-3-deoxypentopyranoside (VIIID-d). The amino acid (VID-d) (40 mg) was acetylated with acetic anhydride (0.5 m*l*) and pyridine (1.5 m*l*) at room temperature overnight. After the mixture was evaporated in a vacuum, the crystalline residue was recrystallized from acetone - diisopropyl ether to afford a pure sample of VIIID-d, yield 25 mg (38.8%), mp 203—204°C, $[\alpha]_D^{26}$ +44° (*c* 0.7, Ethyl acetate).

Found: C, 46.85; H, 6.11; N, 4.11%, Calcd for $C_{13}H_{19}NO_9$: C, 46.83; H, 5.76; N, 4.20%.

Chloramine-T Oxidation *Oxidation of VIA-d.* To a solution of the amino acid (VIA-d) (80 mg 0.39 mmol) in water (1 m*l*) was added chloramine-T (109 mg, 0.39 mmol), and the mixture was shaken for 1 hr. The reaction mixture was filtered to remove an insoluble material. The filtrate was mixed with a solution of *p*-nitrophenylhydrazine hydrochloride (80 mg, 0.43 mmol) in methanol (1 m*l*) and was allowed to stand overnight. The orange-yellow precipitate was separated by centrifuging and was subjected to PLC [1 plate (20 cm×20 cm×0.8 mm), benzene - ethyl acetate (2 : 1)] and two kinds of *p*-nitrophenylhydrazones, A_1 (R_f 0.32) and A_2 (R_f 0.42) were obtained as crystals. They were recrystallized from ethyl acetate-ether: A_1, mp 172°C dec., ν_{max}^{KBr} 1593, 1538, 1501, 1470 and 1415 cm^{-2}; A_2 mp 174.5°C dec., ν_{max}^{KBr} 1595, 1504, and 1487 cm^{-1}.

Oxidation of VID-d was worked up by the same procedure as mentioned above. The oxidation product afforded the two kinds of crystalline *p*-nitrophenylhydrazone, which were identical with the above-mentioned *p*-nitrophenylhydrazones, A_1 and A_2 on the basis of melting points and IR spectra.

Oxidation of VIB-d and VIC-d were also carried out by the same procedure as described above to give crystalline *p*-nitrophenylhydrazones, B and C, respectively: B, mp 162—164°C dec. (from ethyl acetate), R_f 0.26, ν_{max}^{KBr} 1602, 1520, 1500, 1472, 1448 and 1407 cm^{-1}; Found: C, 49.26; 5.47; N, 13.71%. Calcd for $C_{12}H_{15}N_3O_6$: C, 48.48; H, 5.09; N, 14.14%; mp 168°C dec. (from ethyl acetate-ether), R_f 0.42, ν_{max}^{KBr} 1597, 1517, 1495 and 1468 cm^{-1}.

The authors thank Mr. Saburo Nakada for his elementary analysis, and Mr. Akihiro Takahashi and Mr. Tatsumi Kawakami for their technical assistance.

BULLETIN OF THE CHEMICAL SOCIETY OF JAPAN VOL. 42 1726—1729 (1969)

Photoreversible Photographic Systems. V. Reverse Photochromism of (Photospiran/Acid) System in Acetone

Isamu SHIMIZU, Hiroshi KOKADO and Eiichi INOUE

Imaging Science and Engineering Laboratory, Tokyo Institute of Technology, Ookayama, Meguro-ku, Tokyo

(Received June 17, 1968)

1,3,3-Trimethylindolino-6'-nitro-benzopyrylspiran (**1**) exhibits a photoreversible color change which is called "photochromism". However, it is transformed from a colorless form (A) into a colored form (C) which has a salt-like structure when acid such as malonic acid is added into acetone without irradiation with light. The color is bleached by irradiation with light. The color reappears thermally as the light source is removed. This photoreversible color change is termed "reverse photochromism". Another colored form (B) of compound (1) which has a merocyanine dye-like structure is converted into (C) as acid is added into the solution (B). The quantum yield of the photoconversion from C to A by irradiation with visible light depends on the solvent polarity. The quantum yield of the photoconversion from A to B also depends on the solvent polarity.

A photospiran 1,3,3-trimethylindolino-6'-nitro-benzopyrylspiran (**1**) is converted into a colored form (B) from the stable colorless one (A) by irradiation with ultraviolet light in organic solvents. The colored species (B) which is assumed to have a merocyanine dye-like structure is further transformed into another kind of colored species (C) as acid such as malonic acid (Brönsted acid) or $SnCl_4$ (Lewis acid) is added into the solution of B. The photospiran of the form (A) is directly transformed into the colored species (C) which is assumed to have a salt-like structure in the dark at room temperature, when acid is added in acetone. The colored species (C) is converted back into the colorless form (A) by irradiation with visible light. Therefore, the (photospiran(**1**)/acid) system in acetone exhibits a photoinduced reversible color change which is called reverse photochromism.

In this paper, the thermal or photochemical interconversion of the two isomers A and C is discussed. The molecular structures of A and C are given in Fig. 1.

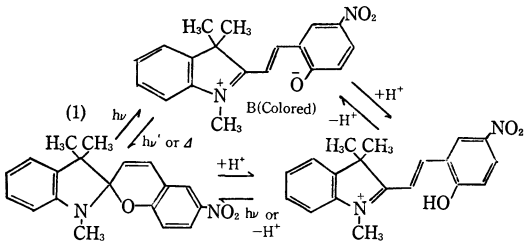

A (Colorless) C (Colored)

Fig. 1. Reaction mechanism of reverse photochromism.
hν : ultraviolet light
hν' : visible light
Δ : thermal

Experimental

Experimental procedures were the same as described in a previous paper,[1] expcept for filters. The visible

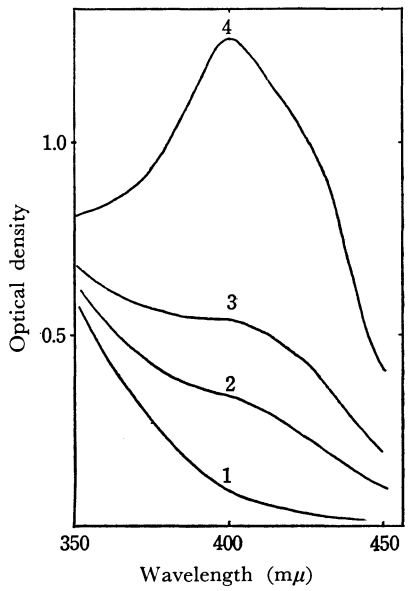

Fig. 2. Absorption spectra of (photospiran(**1**)/acid) system in acetone.
Photospiran (**1**) 6.9×10^{-5} mol/*l*.
Malonic acid 1) 9.9×10^{-4} mol/*l* 2) 5.0×10^{-3} mol/*l* 3) 9.9×10^{-3} mol/*l* 4) 8.9×10^{-2} mol/*l*

1) I. Shimizu, H. Kokado and E. Inoue, *Kogyo Kagaku Zasshi (J. Chem. Soc. Japan, Ind. Chem. Sect.)*, **70**, 2344 (1967).

light was obtained with a high pressure mercury lamp fitted with the Toshiba glass filters (V-V40×2)×V-Y43. The light intensity entering the cell was determined by the potassium ferrioxalate actinometry.

Results and Discussion

A colored species (B) was transformed into another colored form (C) by the addition of acid in the organic solvent. The colorless species, however, did not undergo any change by the addition of acid at room temperature in the organic solvents except for acetone and methyl ethyl ketone. In acetone the colorless form (A) was converted into the colored form (C) in the dark by addition of malonic acid. A thermal equilibrium was established between A and C. The absorption spectral change of the system (photospiran/acid) in acetone is shown in Fig. 2. In the system, the equilibrium constant of the reaction Eq. (1) can be formulated as

$$\mathrm{A} + \text{acid} \rightleftarrows \mathrm{C}, \tag{1}$$

$$K = \frac{[\mathrm{C}]}{[\mathrm{A}][\text{acid}]} \tag{2}$$

$$[\mathrm{C}] = [\mathrm{A}_0] - [\mathrm{A}], \tag{2}$$

where [A], [acid] and [C] are the concentrations of A, (acid), and C, and $[A_0]$ is the initial concentration of A.

Since the experiments are carried out with an excessive acid, we have

$$[\text{acid}] \gg [\mathrm{C}].$$

Thus we obtain from **2** and **3**

$$\frac{1}{[\text{acid}]} = \frac{K[\mathrm{A}_0]}{[\mathrm{C}]} - K. \tag{4}$$

Equation (4) can be converted into Eq. (5) in terms of the optical density (D_λ) and the molar extinction coefficient (ε_λ) at the absorption maximum ($\lambda m\mu$) of the colored species.

$$\frac{1}{[\text{acid}]} = \frac{K\varepsilon_\lambda[\mathrm{A}_0]}{D_\lambda} - K. \tag{5}$$

Figure 3 shows the plots of 1/[acid] against $1/D_\lambda$ for the systems photospiran/malonic acid and photospiran/maleic acid. The values of K and ε_λ were obtained from Fig. 3 and are shown in Table 1. The equilibrium constant increases as the dissociation constant of acid in water increases.

The colored species (C) was transformed into the colorless one (A) by irradiation with visible light, but color reappeared when irradiation was stopped. This *reversible* color change could be repeated as many times as desired. The absorption spectral change of the reverse photochromic system which is induced by irradiation with light

Table 1. Equilibrium constant of the reaction Eq. (1) and molar extinction coefficient of (C) at the absorption maximum wavelength in visible region

Acid	K	ε_{405}	K_1
Malonic acid	58.5	2.2×10^4	1.40×10^{-3}
Maleic acid	201	2.2×10^4	1.42×10^{-2}

K_1 : dissociation constant of acid in water at room temperature

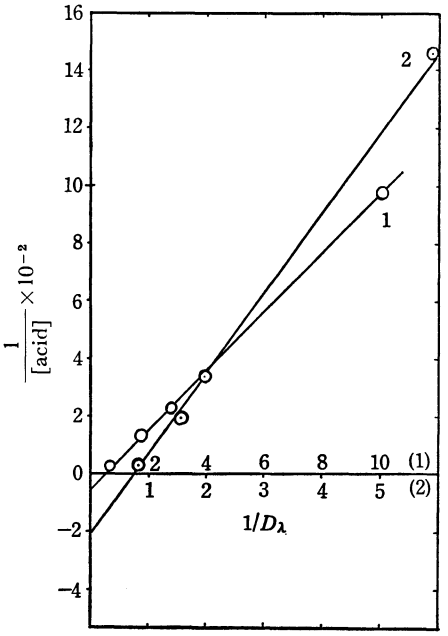

Fig. 3. Plots of $1/[\text{acid}]-1/D_\lambda$
1) Malonic acid
2) Maleic acid

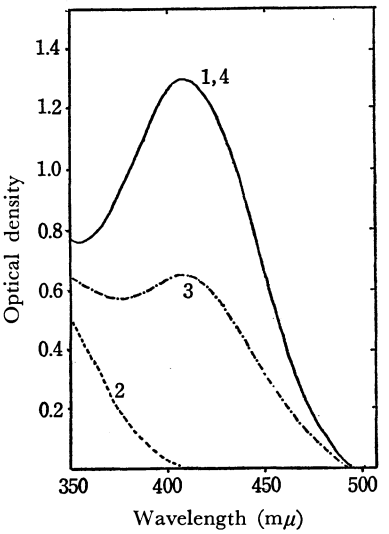

Fig. 4. Absorption spectral changes of the reverse photochromic system (photospiran (**1**) 1.1×10^{-4} mol/l + excess malonic acid).
1) Absorption spectrum of the system
2) After irradiation with visible light
3), 4) After standing the irradiated sample in the dark

is given in Fig. 4. The thermal reaction from A to C followed first order reaction kinetics. The activation energy for the thermal reaction from A to C was calculated as 31.9 kcal/mol. The Arrhenius plot is shown in Fig. 5.

The colored species (B) of the photospiran (**1**) could be isolated in a stable form and was converted into C by dissolving into various solvents containing malonic acid in excess. The absorption spectra and their change by irradiation with visible light in methanol are shown in Fig. 6. The thermal reaction from A to C in each solvent was so slow that it could be neglected. The quantum yield of photoconversion from C to A in acetone and the other various solvents by irradiation with visible light (4358Å) are given in Table 2. The quantum yield of photoconversion from C to A in acetone by irradiation with ultraviolet light (3650Å) changed with irradiation time. The quantum yield of decoloration *versus* irradiation time (irradiation with either 4358Å or 3650Å light) is shown in Fig. 7. In the case of interconversion of two isomers (C) and (A) under the action of ultraviolet light, a photoequilibrium was established by light (3650Å). It changes with the molar extinction coefficients of the two isomers and also with the quantum yields $\phi_{C\to A}$ and $\phi_{A\to C}$ of photoconversion in both directions C to A and A to C *via* B. In other words, the colorless species (A) absorbed ultraviolet light and the transformation to B took place. The colored species (B) was transformed

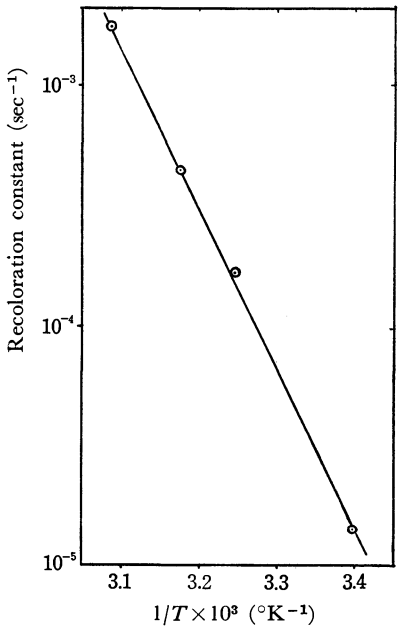

Fig. 5. Arrhenius plot for recoloration rate of the system (photospiran (**1**)/acid) in acetone.

ΔE : 31.9 kcal/mol

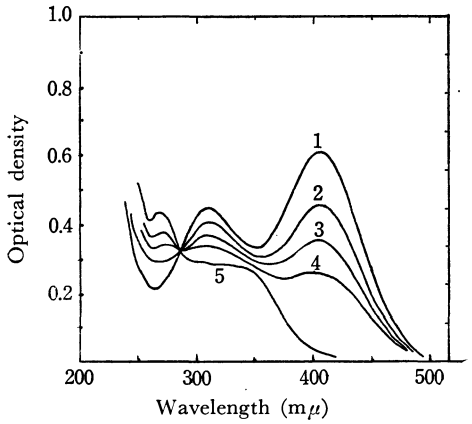

Fig. 6. The effect of irradiation with visible light on (photospiran (**1**)/malonic acid) system in methanol.

1) Absorption spectrum of the system ((**1**): 2.0×10^{-5} mol/l + malonic acid ; 7.9×10^{-3} mol/l) in methanol.
2), 3), 4), 5) The progressive change of the spectrum of the system by irradiation with light.

TABLE 2. QUANTUM YIELD OF PHOTOCONVERSION FROM C TO A IN VARIOUS SOLVENTS BY 4358 Å LIGHT

Solvent	$\varepsilon_\lambda\times\phi_{C\to A}$	Quantum yield
H_2O	$(3.5\ 0.1)\times10^3$	0.16
CH_3OH	$(7.3\ 0.2)\times10^3$	0.33
C_2H_5OH	$(8.0\ 0.3)\times10^3$	0.36
i-C_3H_7OH	$(1.2\ 0.2)\times10^3$	0.55
n-C_3H_7OH	$(1.0\ 0.1)\times10^3$	0.46
Acetone	$(1.6\ 0.1)\times10^3$	0.73

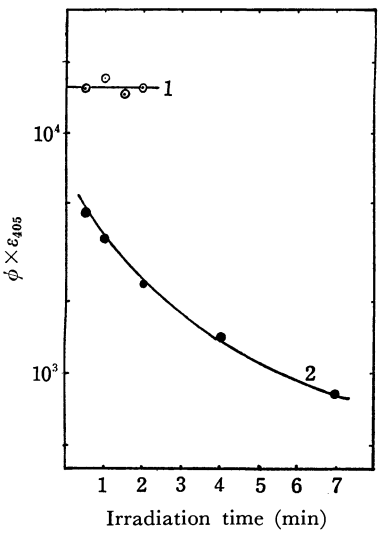

Fig. 7. Quantum yield of photoconversion from C to A in acetone *versus* irradiation time.

1) Irradiated with 4358 Å
2) Irradiated with 3650 Å

instantly into C by the reaction with excess acid in the solution. These reactions are

$$C + h\nu\ (3650\,Å) \xrightarrow{\phi_{C\to A}} A \quad (6)$$

$$A + h\nu\ (3650\,Å) \xrightarrow{\phi_{A\to C}} B \quad (7)$$

$$B + \text{excess acid} \xrightarrow{\text{fast}} C \quad (8)$$

The quantum yield $\phi_{C\to A}$ was claculated as described below.

The rate of the photoconversion is represented by Eq. (8).

$$\frac{d[A]}{dt} = -\frac{d[C]}{dt}$$
$$= I_\lambda\{\varepsilon_C\phi_{C\to A}([C_0]-[A]) - \varepsilon_A\phi_{A\to C}[A]\} \quad (9)$$

I_λ: intensity of the irradiation light at λ mμ

$\phi_{C\to A}$, $\phi_{A\to C}$: quantum yield of the photoconversion from C to A, or from A to C

$[C_0]$: initial concentration of C

t: irradiation time.

Since the reaction rates for both directions are equal at the photoequilibrium

$$\varepsilon_C\phi_{C\to A}\{[C_0] - [A_\infty]\} - \varepsilon_A\phi_{A\to C}[A_\infty] = 0 \quad (10)$$

$$[A_\infty] + [C_\infty] = [C_0] \quad (11)$$

we have

$$\frac{\phi_{C\to A}}{\phi_{A\to C}} = \frac{\varepsilon_A}{\varepsilon_C}\left(\frac{[C_0]}{[C_\infty]} - 1\right) \quad (12)$$

The solution of Eq. (9) is given as

$$I_\lambda t = \frac{1}{\varepsilon_C\phi_{C\to A}+\varepsilon_A\phi_{A\to C}} \ln\left\{\frac{[C]-[C_\infty]}{[C_0]-[C_\infty]}\right\} \quad (13)$$

$[A_\infty]$, $[C_\infty]$; concentrations of A and C at photoequilibrium. Plots of $\log\{[C]-[C_\infty]\}/\{[C_0]-[C_\infty]\}$ *versus* irradiation time at 3650Å in various solutions are given in Fig. 8. The observed linearity of the curves in Fig. 8 provides a support for the proposed reaction scheme represented by Eqs. (6), (7) and (8). The quantum yield of photoconversion from A to C *via* B is calculated from Eq. (12) using values of $\phi_{C\to A}$ in Table 2 and is shown in Table 3.

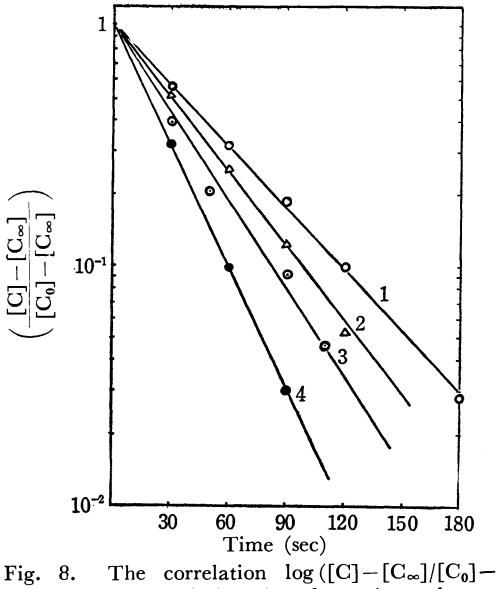

Fig. 8. The correlation $\log([C]-[C_\infty]/[C_0]-[C_\infty])$ with irradiation time for various solvents.
1) Methanol 2) Ethanol, 3) Isopropanol, 4) Acetone

Table 3. Quantum yield of rhotoconversion from A to C

Solvent	Quantum yield ($\phi_{A\to C}$)
CH_3OH	0.07
C_2H_5OH	0.15
i-C_3H_7OH	0.23
n-C_3H_7OH	0.23
Acetone	0.27

Irradiation light : 3650 Å

The quantum yield of photoconversion from (C) to (A) decreases as the solvent polarity increases. On the other hand, the quantum yield of photoconversion from B to A increases as the solvent polarity increases. In a previous paper,[1] we presented evidence for the existence of the different colored species (B) and (C) from absorption spectra. The colored species (B) is assumed to have a mercyanine dye-like structure and C a salt-like structure. The difference in the solvent effect on the decoloration efficiencies $\phi_{C\to A}$ and $\phi_{B\to A}$ gives another evidence for the existence of B and C. The quantum yield of photoconversion from A to C *via* B as shown in Table 3 decreases as the solvent polarity increases. The absorption spectrum of A, especially its longest wavelength absorption band is shifted to the longer wavelength as the solvent polarity increases. In polar solvents, the excited state of the colorless species (A) interacts with the solvent, and also the efficiency of radiationless deactivation may increase, thus the quantum yield of the photoconversion from A to C through B decreases.

Conclusion

The photospiran (**1**) in acetone is converted into a colored form as acid is added, and the colored form C is bleached by irradiation with visible light. Thus, the (photospiran/acid) system in acetone exhibits a reverse photochromism. The photoconversion efficiency from colored to colorless form is controlled by external factors such as the solvent polarity. The reverse photochromism of the system is shown in a polymer film such as styrene - maleic acid copolymer. The color image can be printed out directly on the reverse photochromic film by irradiation with visible light through the transparent original picture, and the image can be erased by heating.

The reverse photochromic system described above is promising for use as reusable photobleaching type photosensitive material which has photosensitivity in visible regions.

BULLETIN OF THE CHEMICAL SOCIETY OF JAPAN VOL. 42 1730—1734 (1969)

Photoreversible Photographic Systems. VI. Reverse Photochromism of 1,3,3-Trimethylspiro[indoline-2,2′-benzopyran]-8′-carboxylic Acid

Isamu SHIMIZU, Hiroshi KOKADO and Eiichi INOUE

Imaging Science and Engineering Laboratory, Tokyo Institute of Technology, Ookayama, Meguro-ku, Tokyo

(Received June 17, 1968)

Many derivatives of 1,3,3-trimethylspiro[indoline-2,2′-benzopyran] (**1**) exhibit photoreversible color changes in organic solvents. One of the derivatives 1,3,3-trimethylspiro[indoline-2,2′-benzopyran]-8′-carboxylic acid (**2**) shows "reverse photochromism" in polar solvents. The compound **2** exhibits a deep color in the polar solvent and the color is bleached by irradiation with either visible or ultraviolet light. The color reappears thermally as the irradiation is ceased. The thermal conversion rate from the colorless form to the colored one depends on the solvents. On the other hand, the isomer 1,3,3-trimethylspiro[indoline-2,2′-benzopyran]-6′-carboxylic acid shows neither normal nor reverse photochromism under usual conditions, but exhibits reverse photochromism when acid such as malonic acid is added into the solution. The compound **2** is assumed to have a merocyanine dye-like structure due to the intramolecular proton transfer.

The photochromism of some derivatives of 1,3,3-trimethylspiro[indoline-2,2′-benzopyran] have been investigated by Fisher,[1] Lashkov,[2] Balny,[3] and the present authors.[4] It has also attracted the interest of workers in technological field photomemory, masking materials, optical switches and optical displays.

The ordinary photochromism of the spiran has been known for the conversion of a stable colorless state into a colored metastable state with ultraviolet light. The colorless modification is transformed from the colored one either spontaneously when the solution is stored in the dark, or by irradiation with visible light. The process that takes place in the photochromic system is presented as

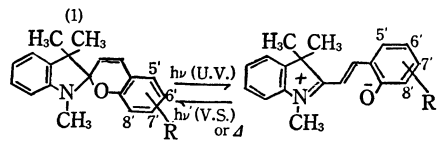

A (colorless) B (colored)

R (**2**) -8′-COOH
(**3**) -6′-COOH
(**4**) -6′-NO_2
Δ heat

Some of these colorless photospirans are converted into colored forms when they are adsorbed on the solid surface such as silica gel or alumina, and the color can be bleached with visible light. This type of reversible photo-color change is called "reverse photochromism." The authors have found that 1,3,3-trimethylspiro[indoline-2,2′-benzopyran]-8′-carboxylic acid (**2**) shows a reverse photochromism without adsorbents. The substance **2** exhibited intense color when it was dissolved in organic solvents. The color of the solution was diminished by irradiation with either visible or ultraviolet light. The colorless species was converted into the original colored one as the irradiation was ceased.

In this paper, the properties of the compound **2** are described in comparison with a colorless isomer 1,3,3-trimethylspiro[indoline-2, 2′-benzopyran]-6′-carboxylic acid (**3**). The effects of added acid or alkali on the solution of the compound **2** or **3** are also described.

Experimental

Absorption spectra with short life were obtained with a Hitachi Rapidscan Spectrophotometer SPR-2 which scanned from 200 mμ to 700 mμ within 0.15 sec. The other experimental procedures were given in other reports.[4,5]

Results and Discussn

The compound **2** is soluble in polar solvents, but not in non-polar solvents. The isomer **3**, however, is not soluble in polar solvents but soluble in non-

1) R. Heiligmen-Rim, Y. Hirshberg and E. Fisher, *J. Phys. Chem.*, **66**, 2465 (1962).

2) G. I. Lashkov and A. V. Shablye, *Opt. Spect*, **19**, 455 (1965).

3) C. Balny and P. Douzou, *Compt. Rend.*, **262C**, 1235 (1966).

4) I. Shimizu, H. Kokado and E. Inoue, *Kogyo Kagaku Zasshi (J. Chem. Soc. Japan, Ind. Chem. Sect.)*, **70**, 2344 (1967).

5) I. Shimizu, H. Kokado and E. Inoue, *Nippon Kagaku Zasshi (J. Chem. Soc. Japan, Pure Chem Sect.)*, **89**, 755 (1968).

polar solvents. The absorption spectra of the compound **2** and **3** in ethanol are shown in Fig. 1. The compound **2** exhibits an intense color which depends on the solvent, while the isomer **3** does not have any absorption band in visible region. The shape and the strength of the absorption band of the compound **2** in visible region is similar to that of the colored state of photospiran **4**. From the absorption spectrum and solubility, the compound **2** is assumed to have a merocyanine dye-like structure which is homologue of the colored state of the photospiran **4**.

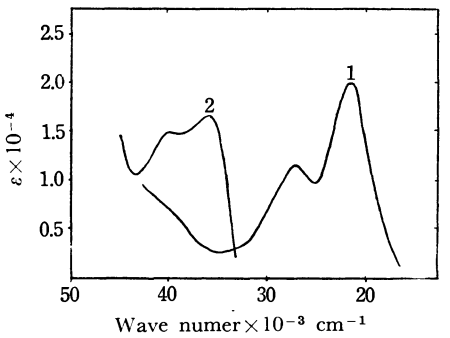

Fig. 1. Absorption spectra of **2** and **3** in ethanol.

1 Compound **2**
2 Compound **3**

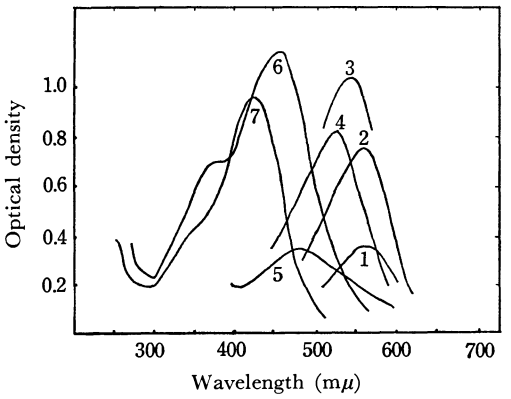

Fig. 2. Absorption spectra of **2** in various solvents.

1) ethyl acetate, 2) pyridine, 3) acetone, 4) acetonitrile, 5) *n*-butanol, 6) methanol, 7) water

The absorption spectrum of **2** in visible region is shifted towards shorter wavelength with the increase in a solvent polarity. Dependence of the spectral shift on the solvent as shown in Fig. 2 was elucidated by considering the dipole moment of the colored species. The ground state of the colored species **2** would be stabilized by interaction with the solvent dipole, but the first excited state would not be

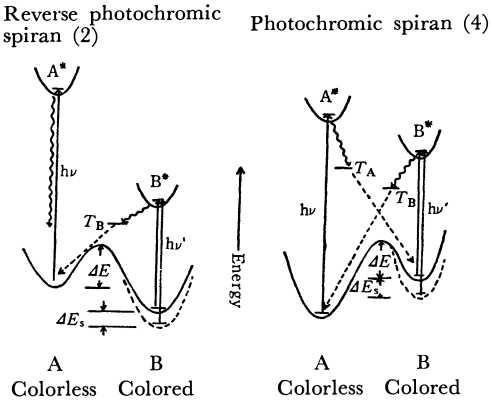

Fig. 3. Energy schemes which illustrate normal or reverse photochromism.

A*B*; excited state of A (B)
ΔE; activation energy for the reaction A→B or B→A
ΔE_S; stabilization energy
T_A,T_B; triplet state of A (B)

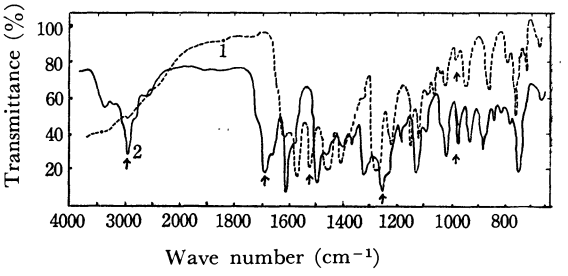

Fig. 4. IR spectra of **2** and **3** in KBr.

1) ····· compound **2**
2) —— compound **3**

stabilized. The energy difference between ground and first excited state would then increase with increasing stabilization energy. This process is shown in Fig. 3 schematically.

The absorption spectra of **2** and **3** in infrared region are shown in Fig. 4. The ν(C=O) band of COOH in 1720 cm^{-1} was observed in **3** but not in **2**. An absorption band in 1525 cm^{-1} was, however, found in **2** and it was assigned to $\nu(CO_2^-)$. The spiran band at 954 cm^{-1} that had been reported by Schiele[6] was found to be much weaker for **3** than for **2**. The 1237 cm^{-1} band of **2** that had been assigned to be ν(C=C–O)[6] was shifted towards a longer wave number. It could be the electron transfer from C to O atom of the pyran ring which increased the charge density of the O atom.[6] This fact on IR spectra gives good support to the previous assumption that the colored species of **2** has a structure like a merocyanine dye in which the pyran ring is ruptured due to the internal proton transfer.

6) C. Schiele and G. Arnold, *Tetrahedron Letters*, **1967**, 1191.

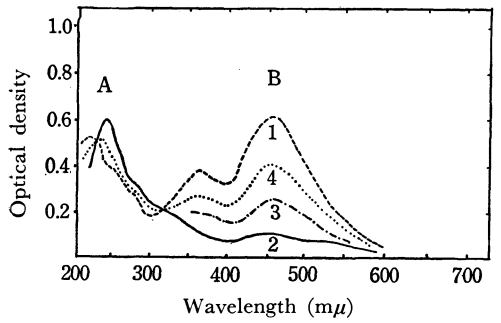

Fig. 5. The effect of irradiation on the ethanol solution **2** at room temperature.

1) Absorption spectrum of **2** in ethanol
2) After irradiation with light
3), 4) After standing the photo-bleached solution in the dark

It would be quite plausible to consider that the proton transferred structure is more favored because of energy.

The compound **2** in ethanol exhibited a deep color. The color was bleached with UV or visible light and the absorption band near the ultraviolet region was intensified. After the irradiation was stopped the color reappeared thermally. The absorption spectral changes are shown in Fig. 5. From the fact that the absorption spectrum of **2** in ethanol did not show any change at low temperature (−120 °C), the color change in the solution does not seem to be thermochromic. The photo-bleaching was performed utilizing visible light at −30°C. At this temperature, the thermal recovery to the colored one was not observed under the same condition. This behavior of the photo-bleached spiran (**2**) is quite the same as observed in the colorless spiran (**3**).

The thermal back reaction of **2** from the colorless state to the colored state followed the first order

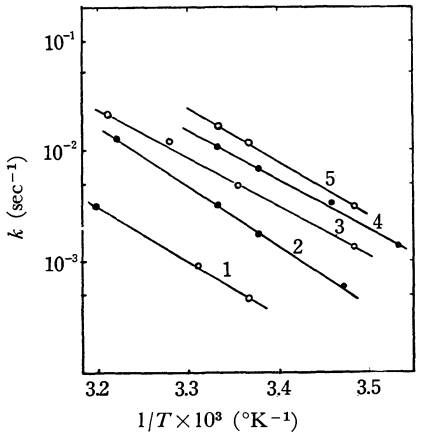

Fig. 6. Arrhenius plots for the recoloration rates of **2** in various solvents.

1) water, 2) pyridine, 3) ethanol, 4) acetone, 5) acetonitrile

TABLE 1. ACTIVATION ENERGIES FOR THE RECOLORATION OF THE COMPOUND **2**

Solvent	Activation energy kcal/mol
Water	22.6
Pyridine	25.4
Ethanol	20.2
Acetone	17.7
Acetonitrile	22.5

rate equation. The reaction rate depended on the solvent and the temperature. The temperature dependence of the rate constant in various solvents is shown in Fig. 6. The activation energies for the back reaction are presented in Table 1. The rate of thermal back reaction from colored to colorless state of photospiran (**4**) was determined in different solvents. The activation energy increased with the increasing solvent polarity. This results from the stabilization of meta-stable colored state of **4** by large polarity of the solvent. Thus, the higher the solvent polarity, the slower the thermal decoloration rate of compound **4**. On the other hand, the thermal recoloration rate of the compound **2** did not show any direct relationship with solvent polarity. This is understandable if we take into account the fact that the meta-stable form (colorless) of **2** is not sensitive. The energy scheme of the reactions are shown in Fig. 3. The colored state of spiran is assumed to have a zwitter ionic structure that is sensitive to added acid or alkali.

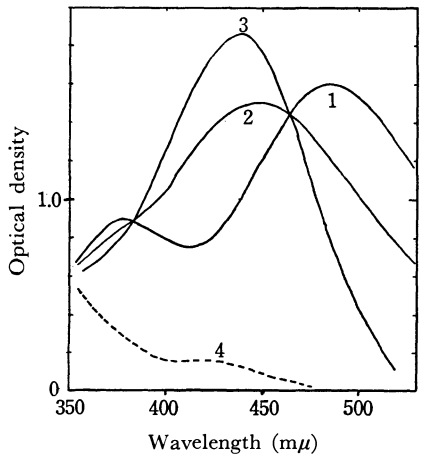

Fig. 7. Absorption spectra of **2** and malonic acid systems, and effect of irradiation with light on the systems.

1) Absorption spectrum of **2**; 7.0×10^{-5} mol/l
2) **2**; 7.0×10^{-5} mol/l + malonic acid; 1.0×10^{-3} mol/l
3) **2**; 7.0×10^{-5} mol/l + malonic acid; 9.4×10^{-2} mol/l
4) after irradiation 3) with light.

On addition of acid into the solution of **2** the absorption spectrum of the solution shifted to the shorter wavelength. The shift was proportional to the amount of added acid. The new colored species (C) produced by adding acid into the solution **2** was bleached by irradiation with UV or visible light. The color reappeared as the irradiation was stopped. The absorption spectral change in the reverse photochromic reaction is shown in Fig. 7. In ethanol solution of **2** the absorption band in visible region diminished quickly on addition of alkali. On the other hand, in aqueous solution the absorption band at longer wavelength (560 mμ) appeared as soon as the aqueous alkaline solution was added. The absorption band at 560 mμ decreased gradually at room temperature. The shape

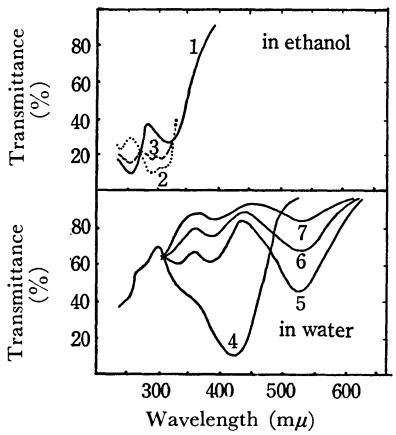

Fig. 8. The effect of added alkali on the absorption spectra of **2** in ethanol and water.

1) Absorption spectrum of **2** in ethanol just after ethanolic alkali was added
2), 3) After the solution 1) had been allowed to stand for 2 or 3 min
4) Absorption spectrum of **2** in aqueous solution
5) After aqueous alkali solution was added into 4)
6), 7) After the solution 5) had been allowed to stand in the dark for few minutes

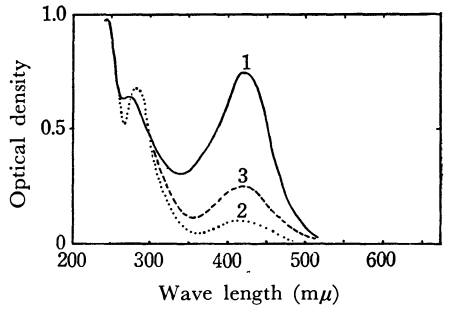

Fig. 9. The effect of irradiation with visible light on **2**: 6.7×10^{-5} mol/*l*, malonic acid; 1.0×10^{-2} mol/*l*, in ethanol.

1) Absorption spectrum of the system
2) After irradiation with visible light
3) After standing 2) in the dark for 5 min.

of the band was similar to that of the colored species of **2** in alcoholic solution. The absorption spectral changes with addition of alkali are shown in Fig. 8. The intermediate colored species was believed to have a merocyanine dye-like structure.

The solution of **3** in ethanol had an absorption band only near the ultraviolet region, and did not show any color change by irradiation with light even at a low temperature. As acid was added in the solution of **3** an absorption band in visible region appeared. The color was bleached by irradiation with visible light, but recovered thermally. The absorption spectrum of this colored species was

Table 2. Quantum yield of the photoconversion from colored species to colorless one

Compound	Quantum yield (ϕ)×ε	
	4358 Å	3650 Å
2	1.7×10^{-3}	1.3×10^{-3}
2 Malonic acid	9.0×10^{-3}	
3 Maleic acid	1.1×10^{-4}	1.1×10^{-4}

Solvent: ethanol
4358 Å, 3650 Å; irradiation light
ε; molar extinction coefficient of the colored species

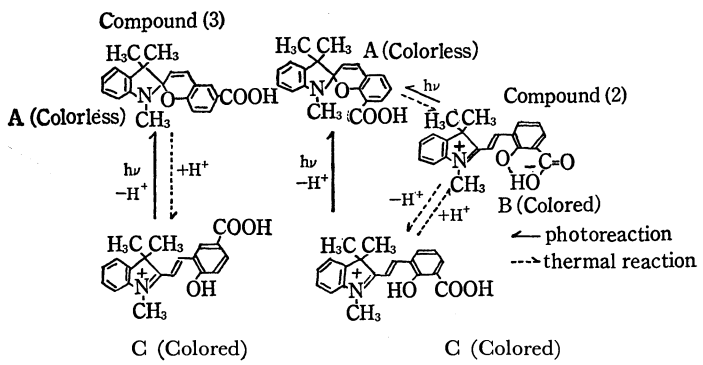

Fig. 10. Reaction mechanisms of the reverse photochromic systems.

similar to the colored species (C) of the compound **2**. The spectral change described above is shown in Fig. 9. The reaction mechanism of the reverse photochromism about the compound **2** and the system (compound **3**/acid) are shown in Fig. 10.

The photo-bleaching efficiencies of the compound **2** and the systems (compound **2**, or **3**/maleic acid) in ethanol are given in Table 2.

Conclusion

Depending on the nature and the position of substituted groups, the derivatives of 1,3,3-trimethylspiro[indoline-2,2-benzopyran] (**1**) differ from each other to a great extent in photochromic property. 1,3,3-Trimethylspiro[indoline-2,2'-benzopyran]-8'-carboxylic acid (**2**), shows a reverse photochromism. On the other hand, the isomer **3** which is substituted at 6'-position with COOH does not exhibit either the normal or reverse photochromism. As acid is added into the solution of the compound **3**, however, the system (compound **3**/acid) shows a reverse photochromism.

BULLETIN OF THE CHEMICAL SOCIETY OF JAPAN VOL. 42 1734—1738 (1969)

Properties of Butyl Acrylate Copolymer with Metal Ionic Crosslinkage

Jun-ichi HAKOZAKI,*1 Einosuke HIGASHIMURA and Yūji HAYASHIBARA

Research and Development Department, Mitsubishi Rayon Co., Ltd., Kyobashi, Chuo-ku, Tokyo

(Received July 31, 1968)

Some properties of the butyl acrylate-acrylic acid copolymer, which has ionic crosslinkage with a mono- or divalent cation, were observed. The organic solvent resistance tends to increase with an increase in the degree of neutralization with metal ions at room temperature and at 50°C. The tensile and flow properties exhibit a linear increase with the amounts of metal ions incorporated. The activation energies of the melt viscosity were 7.5, 10.5, and 22.0 kcal/mol for 1, 1/4, and 1/2 of metal-ion equivalents respectively. The stress relaxation behavior was observed at the temperature of 92°C; it was found that relaxation at the highest rate takes place at the initial stage of the relaxation process.

As the linear polymers showing a rubbery elasticity generally have a small cohesive energy density between the molecules, there are some deficiencies of their mechanical, thermal, and chemical properties. Therefore with an eye to practical application, some attempts have been made here to improve the above-mentioned properties by crosslinking reaction. A number of ways for crosslinking reaction have been reported, such as by radiation, a chemical reaction incorporating some functional groups, vulcanization with sulfur or peroxide, and introduction of metal ions.

In recent years, many types of ionic polymers containing covalent and ionic bonds have been introduced. For example, butadiene - acrylic acid[1] and butadiene - acrylonitrile - acrylic acid copolymers[2] were vulcanized with zinc oxide. They are called carboxyl rubber. Styrene-acrylic acid[3] and α-olefin-unsaturated carboxylic acid copolymers[5] were crosslinked with monovalent and sometimes divalent cations, and so they were called "Ionomers."

This paper will deal with some properties of the butyl acrylate - acrylic acid copolymers, which has an ionic crosslinkage with a mono- or divalent cation. The properties investigated here include the temperature dependence of the organic solvent resistance, the mechanical, and viscous flow properties, and the stress relaxation behavior.

Experimental

Samples. The butyl acrylate (BA)-acrylic acid (AA) copolymer used in this study was prepared by emulsion polymerization; the BA/AA composition in this copolymer was 89/11 by mol%. The intrinsic viscosity was

*1 Present address: Nippon Unicar Co., Ltd., Kawasaki Plant, Ukishima-cho, Kawasaki-shi.

1) H. P. Brown, *Ind. Eng. Chem.*, **47**, 1006 (1955).
2) H. B. Brown, *Rubber Chem. Technol*, **30**, 1347 (1957).
3) M. Morawetz, *J. Polymer Sci.*, **29**, 307 (1958).
4) W. Cooper, *ibid.*, **28**, 195 (1958).
5) Goodrich, Brit. Pat. 707425 (1954).

around 1.0 in dioxane.

The ionic crosslinking reaction of this copolymer with a mono- or divalent cation such as sodium hydroxide or zinc acetate was performed in a solvent medium; these samples, purified with an excess of the solvent at room temperature, were dried under a vacuum at 50°C. The test specimens were prepared by compression-molding into the various types desired. Some of the properties of these samples are summarized in Table 1.

Table 1. Samples

Code	Metal	Neutralized equivalent	Molding temp. (°C)
BAA	—	0	100
BAA-Zn-1/4	Zn	1/4	150
BAA-Zn-1/2	Zn	1/2	200
BAA-Na-1/4	Na	1/4	120
BAA-Na-1/2	Na	1/2	150
BAA-Na-1	Na	1	200

Tensile Properties. The tensile properties were measured by an Instron-type tensile tester. The cross-head travel speed was 50 mm/min. The test specimens were a modified type 25 mm long, 4 mm wide, and 0.5 mm thick. A conditioning chamber was used for high-temperature tests.

Viscous Flow Properties. For the purpose of investigating the temperature dependence of the characteristics of these ionic linkages, the viscous flow deformation was measured by means of a Williams parallel-plate plastometer at various temperatures. Test specimens were compression-molded into a standard disk 4 mm diameter and 2 mm thick. The temperature range investigated was 120 to 220°C, especially 180°C, while the compression load was varied between 2 and 50 kg. Assuming a Newtonian flow, the melt viscosity, η_m(poise), was calculated by using the following equation:

$$1/h^4 = (8F/3\eta_m V^2)t + C \qquad (1)$$

where h is the thickness (cm) at time t (min) under a load of F (dyn), V is the volume of the specimen, and C is a constant.

Stress-relaxation. In oder to investigate the ionic crosslinking behavior under stress at high temperatures, the tensile stress relaxation was measured. The apparatus used was the tensile tester described above, and the temperature of the controlling chamber was 70—90°C. The stress decay with time was analysed by means of an auto-recording chart.

Results and Discussion

Organic-solvent Resistance. The organic-solvent resistance of these polymers has been observed in various solvents at room temperature and at 56°C, 6 hr after immersion in the solvents. The results are illustrated in Table 2, along with the cohesive energy density (CED) of these solvents.

Table 2. Organic solvent resistance

Solvent	CED	BAA		BAA-Zn-1/4		BAA-Zn-1/2	
		23	56	23	56	23	56(°C)
Ethanol	12.7	d	d	g	d	s	g
Butanol	11.4	d	d	g	d	s	s
Acetone	10.0	d	d	g	g	s	s
Dioxane	9.9	d	d	g	d	s	g
MEK	9.2	d	d	g	g	s	s
Butyl Acetate	8.5	d	d	s	g	s	s
Benzene	9.2	d	d	s	g	s	s
Cyclo-hexane	8.2	d	d	s	s	s	s

d: dissolved, g: gel-like solution, s: swelling

It has been found that the parent BA-AA copolymer can be dissolved easily in all the solvents investigated, but the solubility of ionically-crosslinked copolymers tends to decrease as the degree of neutralization with metal ions increases. Judging from the above observation, ionic crosslinkage with a divalent metal has quite a strong network structure and can not be broken at about 50°C in these solvents. In the case of small amounts of metal ions, however, they can be dissolved at high temperatures in ethanol or butanol, either of which is a hydrogen-bond-scission reagent with a cohesive energy density of about 12.

Table 3. Tensile prorerties

Temp. (°C)	Sample	Tensile strength (kg/cm²)	Modulus at 75% (kg/cm²)	Elongation (%)	Breaking energy (kg-cm/cm²)	App. deg. of crosslinking (mol/cm³)
23	BAA	1.5	0.1	5300	2.4	1.6×10^{-6}
	BAA-Zn-1/4	4.2	0.5	1500	55	7.0×10^{-6}
	BAA-Zn-1/2	15	4.4	500	56	4.5×10^{-5}
	BAA-Na-1/4	3.9	0.3	6900	92	4.7×10^{-6}
	BAA-Na-1/2	20	0.8	600	64	1.2×10^{-5}
	BAA-Na-1	37	8.1	400	55	1.2×10^{-4}
93	BAA	0.5	3.1[a]	1000	0.2	—
	BAA-Zn-1/4	3.4	3.4[a]	1850	2.2	—
	BAA-Zn-1/2	8.5	3.2	1500	12	—

[a] 10% modulus

6) P. J. Flory, *Chem. Revs.*, **35**, 51 (1944).

Tensile Properties. It is generally well known that the tensile propetries of elastomers change remarkably with the increase in the density of crosslinking. Table 3 shows these values measured at 23 and 93°C. The apparent density of crosslinking (ν_a) was calculated by using Eq. (2), which is based on the kinetic theory of rubber elasticity:[6]

$$f=\nu_a \boldsymbol{R} T(\alpha-1/\alpha^2) \qquad (2)$$

where f is the tensile stress; $\boldsymbol{R}$, the gas constant; T, the absolute temperature, and α, the extension ratio defined as the ratio of extended to unstrained length.

It is obvious that, at low temperatures, the tensile strength, the modulus, and the breaking energy increase, but the elongation decreases with an increase in the metal present. Therefore, these properties depend on the equivalent of metal used, *i. e.*, the degree of the neutralization of carboxylic acid. However, it seems that the values tested here are mostly somewhat lower than those of other practical rubbers. Figure 1 illustrates the variation in the tensile strength with a neutralized equivalent for both Na and Zn at room temperature. Figure 2 shows the density of crosslinking calculated from Eq. (2) against, the neutralized equivalent. It was observed that the density of crosslinking by metal ions increases exponentially with the neutralization amount for an acidic group and that there is a considerable difference between the monovalent Na and the divalent Zn. At the high temperature of 93°C, deformation by viscous flow and by a fall in tensile properties were generally observed. However in a copolymer with a large amount of metal, the retention of tensile strength is large at a high temperature, and so this type of linkage is fairly strong. The above facts suggest the following structures of the crosslinkage of these copolymers. For Zn^{2+}, it may be $-COO^-\ Zn^{2+}\ OOC^-$. For Na^+, the structure may be:

$$\begin{array}{l} -CO-O^- \cdots Na^+ \\ \quad\vdots\quad\ \vdots \\ \quad Na^+ \cdots O^- - CO- \end{array}$$

as has been suggested by Morawetz,[3] where ion-dipole interaction between two ion pairs forms a quadrupole ion. Moreover, these structures may be the cause of a higher level of tensile strength and modulus compared to those of the parent copolymer.

Viscous-flow Properties. In order to investigate the properties of the crosslinkage by metal ions introduced between the parent backbone of BA-AA copolymer, deformation under a load was measured at high temperatures by means

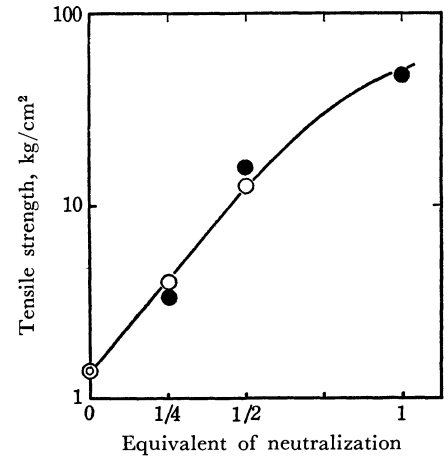

Fig. 1. Dependence of tensile strength on equivalent of neutralization.
◎ BAA ○ BAA-Zn ● BAA-Na

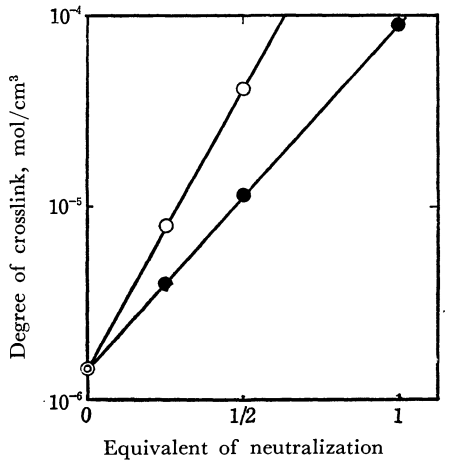

Fig. 2. Dependence of degree of crosslinking on equivalent of neutralization.
◎ BAA ○ BAA-Zn ● BAA-Na

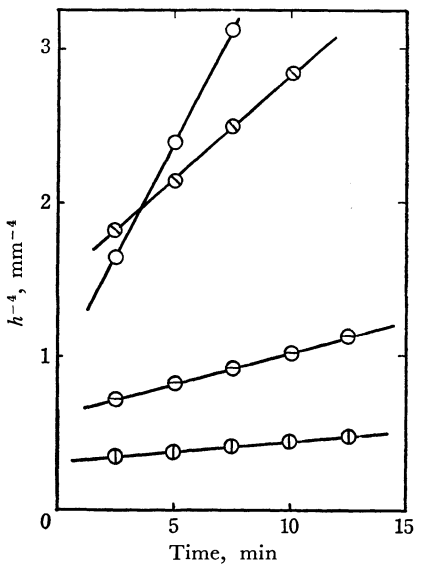

Fig. 3. Relationship between h^{-4} and t.
○ BAA, 150°C. ◑ 120°C of, ⊖ 150°C of, ⊘ 180°C of BAA-Zn-1/4

of a Williams parallel-plate plastometer. In the measurement of the melt viscosity using various samples with different quantities of metal ions, the load and temperature were varied between 1.9—51.5 kg and 118—250°C respectively. The linear relationship between h^{-4} and t, according to Eq. (1), is shown in Fig. 3. Assuming this flow deformation to be Newtonian from the relationship shown in Fig. 3, η_m was calculated by Eq. (2); the results are listed in Table 4. η_m apparently exhibits a sharp increase with the quantity of metal ions at the same temperature. The temperature dependence of the η_m of various samples is illustrated in Figure 4. The apparent activation

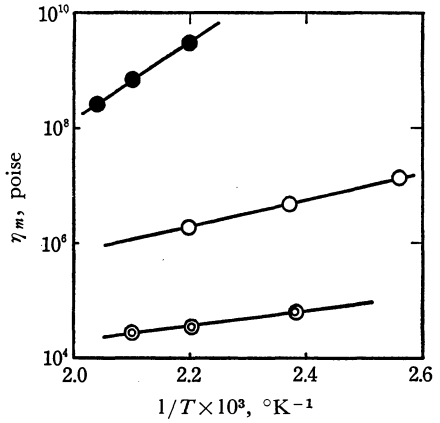

Fig. 4. Temperature dependency of melt viscosity.
◎ BAA ○ BAA-Zn-1/4 ● BAA-Zn-1/2

TABLE 4. MELT FLOW PROPERTIES

Sample	Temp. (°C)	Load (kg)	η_m (poise)	E_{vis} (kcal/mol)
BAA	150	5	8.8×10^4	7.5
	180	3	5.2×10^4	
	200	1.9	3.3×10^4	
BAA-Zn-1/4	150	51.5	1.4×10^7	10.9
	180	51.5	5.3×10^6	
	200	51.5	2.3×10^6	
BAA-Zn-1/2	180	51.5	1.5×10^9	22.0
	200	51.5	6.1×10^8	
	220	51.5	2.2×10^8	

energies were calculated from the gradient of these curves according to Arrhenius' equation and are shown in the last column of Table 4.

Stress-relaxation Behavior. The stress-relaxation behavior is also a good method for determining the properties of crosslinkage.

If we assume that stress relaxation at high temperatures is due to random network scission, the following relation holds between the stress decay ratio (relative stress) at a constant extension and at a constant number of crosslinking:

$$f(t)/f(0)=n(t)/n(0)=e^{-kt} \quad (3)$$

where $f(0)$ and $n(0)$ are the stress and number of

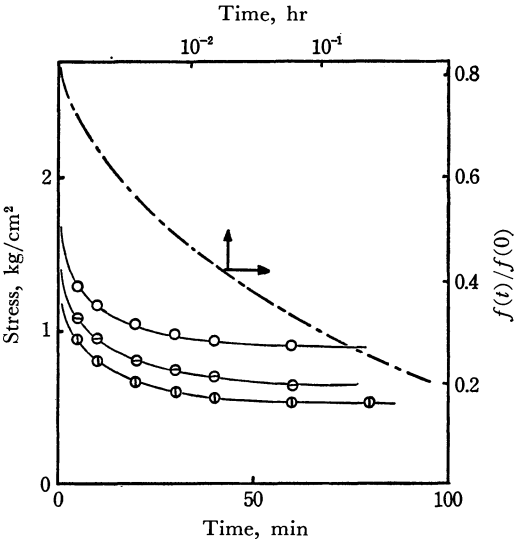

Fig. 5. Typical stress decay curve of BAA-Zn-1/2.
○ 70°C ⊖ 82°C ◐ 92°C

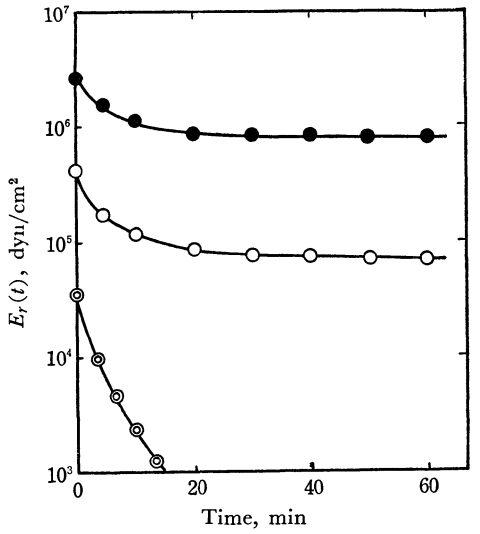

Fig. 6. Relaxation modulus *vs.* time.
◎ BAA ○ BAA-Zn-1/4 ● BAA-Zn-12

crosslinking, respectively, at the initial stage, and where $f(t)$ and $n(t)$ are those at time t. Figure 5 illustrates a typical stress decay curve with BAA-Zn-1/2 as the sample. From this figure, it can be seen that the highest rate of stress relaxation takes place at the initial stage of the relaxation process, and that this rate decreases with an increase in the metal-ion content. Figure 6 shows the change in the relaxation modulus with the time. At 92°C, the viscous flow was observed with the parent BAA copolymer, which does not contain any metal, whereas the equilibria, E_r were 10^5 and 10^6 with the copolymers containing Zn-1/4 and Zn-1/2 respectively.

We have observed that some types of relaxation take place at the initial stage of the relaxation process. These higher rate-relaxation phenomena can be considered to be due to a partial loosening of the chain entanglement or to a slippage of labile crosslinkage caused by sufficient residual interaction of acrylic acid side groups. Network linkage by divalent metal ions is relatively stable even at high temperatures. For most of the properties tested in this study, the ionically-crosslinked butyl acrylate copolymer exhibits a lower level than do other practical rubbers. However, it is considered that the above deficiencies can be improved by investigating the parent copolymer, vulcanization, the molecular size, the chemical composition of the comonomer, the carboxylate content, the vulcanizate recipe, and the types and quantities of cations.

BULLETIN OF THE CHEMICAL SOCIETY OF JAPAN VOL. 42 1738—1740 (1969)

Effect of Coexisting Minerals on Graphitization of Carbon under Pressure. III. Accelerating Effect of Calcium Hydroxide

Tokiti NODA,*1 Michio INAGAKI, Shin-ichi HIRANO and Hajime SAITO

Faculty of Engineering, Nagoya University Furo-cho, Chikusa-ku, Nagoya

(Received October 18, 1968)

The polyvinyl chloride coke was heat-treated under the pressure of 3.2 kbar at 600—850°C for 20—240 min in a simple piston-cylinder type vessel, being sandwiched between two disks of calcium hydroxide. By electron microscopic observations, particles having the six-fold symmetry diffraction pattern of graphite single crystal were found besides particles of amorphous carbon even in the specimen heat-treated at temperature as low as 600°C. Above 800°C, the sharp peak corresponding to the graphitic component appeared on (002) diffraction profiles, overlapping with the broad band of the turbostratic component. The formation of the graphitic component seems to be related to the recrystallization of coexisting calcium hydroxide, as in the case of limestone and calcium carbonate. However, the fact that a small amount of free calcium oxide formed by the decomposition of calcium hydroxide was detected in the heat-treated carbon specimens suggests a chemical theory for the accelerating effect of calcium compounds on the graphitization of carbon under pressure.

It has been found in the previous works[1,2] that the graphitization of carbon is accelerated by the heat treatments under pressure in the presence of limestone or calcium carbonate. The beginning of graphitization, that is the appearance of the component having the graphitic structure, was found to be closely related to the recrystallization of coexisting minerals.[2]

According to Wyllie and Tuttle,[3] the melting point of calcium carbonate is lowered by the addition of water. For example, the melting point of calcium carbonate, 1310°C at 1 kbar, is depressed to 1130°C by the addition of only 8 wt% of water. In our preliminary experiment, a soft carbon was heat-treated under pressure in the presence of calcium carbonate disks, which absorbed about 8 wt% of water. The graphitization of carbon was found to start at about 1000°C, about 100°C lower than that in the case of dry calcium carbonate.[2] However, we could not draw any conclusion at that time, because the exact control of the water content of calcium carbonate disks was experimentally difficult and also it was not known whether water vapor affects the graphitization of carbon or not.

In the present work, heat treatments of carbon were performed under pressure by using disks of calcium hydroxide, whose melting point is 840°C at 3 kbar,[3] in order to confirm the relation between the graphitization of carbon and recrystallization of coexisting minerals.

Experimental and Results

The carbon sample used was the polyvinyl chloride coke (PV-7) which was used in the previous works.[1,2] Disks of calcium hydroxide, 8.0 mm in

*1 Present address: Mie University, Tsu, Mie-ken.

1) T. Noda, M. Inagaki, S. Hirano and K. Amanuma, This Bulletin, **41**, 1245 (1968).

2) T. Noda, M. Inagaki, S. Hirano and H. Saito, *Kogyo Kagaku Zasshi (J. Chem. Soc. Japan, Ind. Chem. Sect.)*, **72**, 643 (1969).

3) P. J. Wyllie and O. F. Tuttle, *J. Petrology*, **1**, 1 (1960).

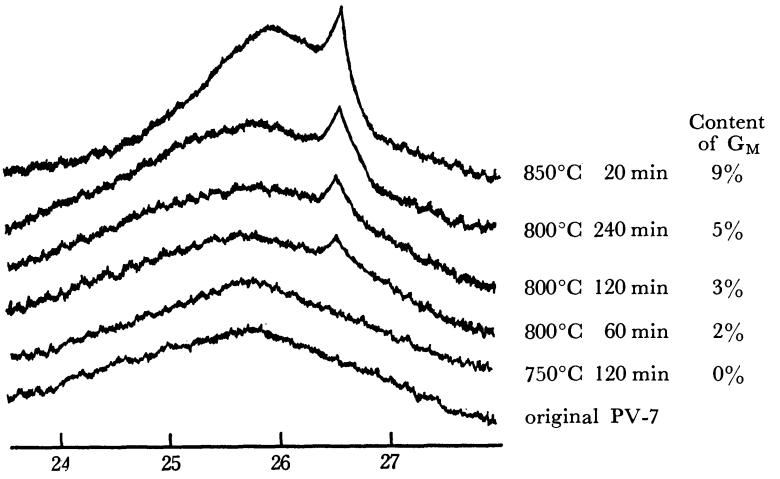

Fig. 1. Change of observed profile of (002) diffraction line with heat treatment

diameter and 3.5 mm thick, were made by compressing calcium hydroxide powder (chemical reagent grade) under 3.5 kbar. The bulk density of the disks was about 2.2 g/cm^3 (*ca.* 15% porosity). The disks and powder of calcium hydroxide were kept in an evacuated desiccator to avoid the absorption of carbon dioxide during the stroage. The heat treatments were performed at temperatures between 600 and 850°C for residence times of 20—240 min under the quasi-hydrostatic pressure of 3.2 kbar in a simple piston-cylinder type vessel. The arrangement of the pressure cell and the procedure for the heat treatments were exactly the same as used previously.[1,2] Temperature of heat treatment (HTT) was determined from input power by using the relation between temperature and input power. Pressure was calibrated by using the transition points of KNO_3 and AgI.[4]

The profile of (002) diffraction line of the central part of the heat-treated specimens was measured by using Ni-filtered Cu$K\alpha$ radiation. The same part of the specimen was dispersed in trichloroethylene by ultrasonic vibration, then supported by an evaporated carbon film, and observed by transmission electron microscope.

The carbon specimens heat-treated above 600°C were obtained as sintered cakes. In the cakes, calcium hydroxide was detected by X-ray diffraction method. The disks of calcium hydroxide recrystallized above 600°C, and were found to melt above 800°C at the part in contact with carbon specimen. Above 800°C, a small amount of calcium oxide was detected by X-ray diffraction method not only in the disks of calcium hydroxide but in the carbon specimen.

Figure 1 shows the change of observed profile of (002) diffraction line with heat treatment. Above

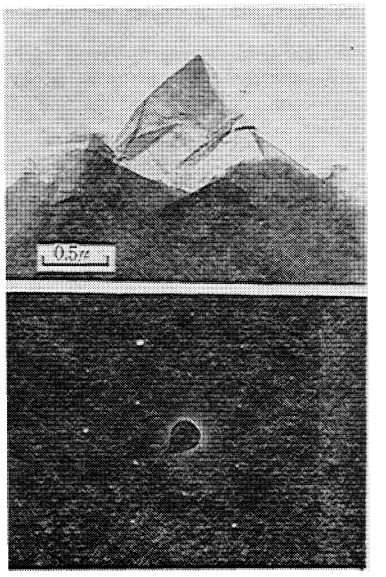

Fig. 2. Bright-field micrograph and selected area diffraction pattern of graphitic particle in carbon specimen heat-treated at 600°C for 60 min under 3.2 kbar.

800°C, a sharp peak is observed on a broad band. According to the same procedure reported previously,[1] the composite profile was separated graphically into two profiles for the graphitic component G_M and the turbostratic component A_M. The component G_M had almost constant c_0-spacing of 6.72 Å, and the component A_M of 6.90Å which was not so different from the original value. The content of the graphitic component G_M was obtained from the ratio of the area under the profile of G_M to the total area under the composite profile after the correction for the preferred orientation of crystallites in the specimen used for the X-ray measurement. The measured content of the component G_M is given for each profile in Fig. 1.

4) M. Inagaki, S. Hirano and H. Saito, *Yogyo Kyokai Shi*, **76**, 264 (1968).

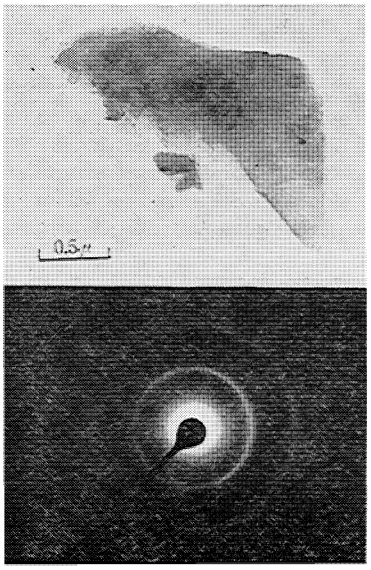

Fig. 3. Bright-field micrograph and selected area diffraction pattern of turbostratic particle in carbon specimen heat-treated at 600°C for 60 min under 3.2 kbar.

By electron microscopic observation, particles having the diffraction pattern of six-fold symmetry of graphite single crystal, were found besides particles having the turbostratic structure even in the specimen heat-treated at 600°C for 60 min. Bright-field micrographs and selected area diffraction patterns of graphitic and turbostratic particles are shown in Figs. 2 and 3, respectively.

The heat treatment above 900°C was difficult to carry out because the calcium hydroxide melts and reacts with graphite heater.

Discussion and Summary

The accelarating effect of coexisting calcium hydroxide on graphitization of carbon is more remarkable than that of calcium carbonate.[2] Even at HTT as low as 600°C, particles having the graphitic structure were found with electron microscopy. The temperature of the beginning of formation of the graphitic component is much lower than those found in the heat treatments of the same coke in the presence of limestone and calcium carbonate,[2] as well as without any minerals.[2,5] The content of the component G_M increases slightly with the increase in residence time. However, the increase in HTT seems to be more effective than the increase in residence time, when the result at 850°C for 20 min is compared with that at 800°C for 60 min.

A close relation seems to be present between the graphitization of carbon under pressure in the presence of foreign minerals and the recrystallization of the coexisting minerals, when a conclusion can be drawn from the present result together with the results of the works on the effect of calcium carbonate previously reported.[1,2] However, the fact that a small amount of free calcium oxide was found in the heat-treated specimens suggests a chemical theory of acceleration of graphitization. Active calcium oxide formed by the decomposition of calcium hydroxide can react at relatively low temperatures, *vis.*, 600°C, with amorphous carbon to form an intermediate compound, probably calcium carbide, which decomposes inversely to form stable graphite and calcium oxide. In order to verify this theory, more detailed and extensive experiments will be needed.

5) T. Noda, K. Kamiya and M. Inagaki, This Bulletin, **41**, 485 (1968).

NOTES

BULLETIN OF THE CHEMICAL SOCIETY OF JAPAN VOL. 42 1741—1743 (1969)

3-[8′-Quinolinol-(5′)-yl]alanine and Related Compounds

Konomu MATSUMURA, Takamasa KASAI and Hisako TASHIRO

Department of Chemistry, Kitasato University, Minato-ku, Tokyo

(Received February 22, 1968)

An improved method of preparing the two known compounds[1] 5-chloralyl-8-quinolinol (I) and 5-formyl-8-quinolinol (II) and preparation of 3-[8′-quinolinol-(5′)-yl]alanine (V) which, to our knowledge, has not heretofore been reported are presented in this paper. On heating a mixture of 8-quinolinol and chloral at 65°C I was formed in 93% yield. A mixture of I and a solution of sodium in cold acetone after 3 days standing at room temperature yielded the hydrolyzed product II in 67% yield. After the hydrolysis was finished the reaction mixture was filtered [the solid (A) on the filter was worked up to isolate II.]. The chloroform residing in the acetone filtrate (B) was quantitatively estimated as the following by the Cole method[2] with minor modifications. The filtrate (B) was subjected to distillation. To the distillate pyridine and concentrated sodium hydroxide solution were added. On heating, the color of the solution became red, the extinction at wavelength 490 mμ was determined and the concentration of chloroform was quantitatively estimated. In parallel to this, the following control experiment was carried out. A known amount of chloroform was mixed with a solution of sodium in acetone and the resulting solution was treated in the same manner as in the case of hydrolysis of I and the remaining chloroform was estimated by the Cole method. By this control experiment, it was found that about 91% of the chloroform initially added had been destroyed by hydrolytic fission during the treatment under the conditions specified. For interpretation of the mechanism of hydrolysis of I this percentage of chloroform was taken into account. It was indicated that the amount of produced chloroform during the hydrolysis of I was nearly equal to the calculated one from the following scheme

$$Q\text{-}CH(OH)\text{-}CCl_3 \rightarrow Q\text{-}CH(OH)^+ + -CCl_3^-$$

Q = 8-Quinolinol-(5)-yl

From this, it may be postulated that the hydrolysis of I with sodium acetonate would involve an ionic cleavage affording CCl_3^-, whose mechanism is different from that postulated for the hydrolysis of I in ethanolic potassium hydroxide solution.[1]

On condensation with hippuric acid or hydantoin, followed by treatment with hydroiodic acid and phosphorus, the compound II yielded 3-[8′-quinolinol-(5′)-yl]alanine (V).[3]

Results of Biological Study.[*1] The compound V has been found inactive in antifungal test *in vitro* (50 μg/ml of V indicated inactive against *candida albicans*) and contrary to expectation, it was toxic (tolerated dosis: 500 mg per kg body weight of a mouse either subcutaneously or intra peritoneally).

Experimental

5-Chloralyl-8-quinolinol (I). On adding chloral (22.2 g, 0.15 mol) to 8-quinolinol (14.5 g, 0.1 mol) an orange solid was formed. After standing for 3 days at room temperature until it turned to a light yellow solid, it was heated at 65°C in a water bath for 35 hr. The reaction mixture was treated with 3 N hydrochloric acid (250 ml) at 80°C until the orange reaction mass completely turned to yellow crystalline hydrochloride which was filtered after cooling. It was suspended in hot water (200 ml) and sodium acetate hydrate (40 g) was added to the suspension. The mixture was heated on a water bath (80°C) for 0.5 hr, the resulting orange yellow free base was filtered on cooling, and it was repeatedly washed

1) a) K. Matsumura and M. Ito, *J. Am. Chem. Soc.*, **77**, 6671 (1955). b) R. Hull, *J. Chem. Soc.*, **1957**, 4845; G. R. Clemo and R. Howe, *ibid.*, **1955**, 3552; J. P. Phillips, E. M. Barrall and R. Breese, *Transact. Kentucky Acad. Science*, **17**, 135 (1956); H. Fujikawa, K. Hirai, T. Toyoda, T. Tamata, K. Sai, M. Naito and T. Tsukuma, *Yakugaku Zasshi (J. Pharmaceut. Soc. Japan)*, **87**, 844 (1967).

2) K. Fujiwara, *Sitzungsb. U. Abhandl. naturfors. Ges. Rostock*, **1914**, vi, i; *Chem. Abstr.*, **1917**, xi. 3201; J. H. Ross, *J. Biol. Chem.*, **58**, 641 (1923—1924); W. H. Cole, *J. Biol. Chem.*, **71**, 173 (1927).

3) a) A. P. Phillips, *J. Am. Chem. Soc.*, **67**, 744 (1945); E. Dyer and W. Yokoyama, *J. Org. Chem.*, **26**, 2124 (1961); W. Ried and H. Schiller, *Ber.*, **86**, 730 (1935). b) H. B. Gillepsie and H. R. Snyder, "Organic Syntheses," Coll. Vol. II, p. 489 (1943).

*1 We are indebted to Dr. Katsuhiko Tago of Kitasato Institute who kindly performed the biological testing and reported the results.

Table 1. Derivatives of 3-[8'-quinolinol-(5')-yl]alanine

Compound	Formula	C, % {Calcd {Found	H, % {Calcd {Found	N, % {Calcd {Found	Mp °C[f]	Description	Solvent
Dihydrochloride[a]	$C_{12}H_{12}O_3N_2 \cdot 2HCl$	{47.21 {47.84	{4.59 {3.95	{ 9.18 { 9.23	295	Yellow plates	6N HCl
Monopicrate[b]	$C_{12}H_{12}O_3N_2 \cdot C_6H_3N_3O_7$	{46.85 {46.84	{3.23 {3.17	{15.18 {14.85	240	Needles	EtOH(30%)
Dipicrate[c]	$C_{12}H_{12}O_3N_2 \cdot 2C_6H_3N_3O_7 \cdot 2.5H_2O$	{39.18 {38.78	{3.13 {3.13	{15.24 {14.97	218	Prisms	EtOH(30%)
Diacetyl[d]	$C_{16}H_{16}O_5N_2$	{60.77 {60.52	{5.06 {5.12	{ 8.86 { 8.78	211.5	Colorless needles	Acetone
7-Iodo-[e]	$C_{12}H_{11}O_3N_2I \cdot 1.5H_2O$	{37.40 {37.43	{3.64 {4.11	{ 7.27 { 6.93	200	Tan colored columns	H_2O

a) Dried at 115°C *in vacuo*. b) The quinolinolylalanine (V) (0.116 g, 0.005 mol) was reacted with picric acid (0.23 g, 0.001 mol) in hot water. The crude product when twice recrystallized from dilute ethanol (30%) yielded monopicrate. The mother liquor of the recrystallizations separated dipicrate on concentration. c) Vacuum-dried over potassium hydroxide at room temperature. d) Made by heating a mixture of quinolinolylalanine (V) (0.116 g, 0.0005 mol) acetic anhydride (0.5 g, 0.005 mol) and glacial acetic acid (0.5 m*l*) for 7 min at 100°C. It gave no color reaction with ferric chloride. e) Made in 66%yield by applying the Harington method of iodinating tyrosine to this compound C. R. Harington and R. V. Pitt-Rivers, *Biochem. J.*, **39**, 157 (1945). The compound is soluble in one hundred and sixty times its weight of boiling water. f) All substances melted with decomposition.

with hot water and dried on a water bath, yield 29.7 g (93%). It was pure enough for use in the next step of synthesis. For comparison a portion was recrystallized from acetone. Its identity with that obtained by the known method[1] was ascertained by IR spectra and thin layer chromatography.

5-Formyl-8-quinolinol (II). Chipped sodium (3.6 g, 0.157 mol) was added to the cooled (0°C) acetone (dried with calcium chloride and distilled, 180 m*l*). The mixture was frequently shaken until a homogeneous suspension resulted, whereupon 5-chloralyl-8-quinolinol (9.6 g, 0.03 mol) was added and the resulting mixture was stirred for a few minutes until a homogeneous paste resulted. After standing for 3 days at room temperature the resulting precipitates (A) were filtered, repeatedly washed with acetone [the combined filtrate and washings (B) were stored for the estimation of chloroform] and were dissolved in water (100 m*l*) (charcoal). On acidifying with acetic acid (50%) the filtered aqueous solution afforded a straw yellow solid (4.6 g), mp 160—173°C. A mixture of this solid product, sodium bisulfite (15 g) and water (30 m*l*) was well triturated at about 60°C. After cooling, the mixture was filtered (charcoal) and washed with water. Concentrated hydrochloric acid was added to the combined filtrate and washings (50 m*l*) and the solution was concentrated on a water bath until the odor of sulfur dioxide became faintly discernible. After standing overnight the separated solid was filtered, dissolved in hot water (100 m*l*) and the solution (charcoal) was filtered. On addition of sodium acetate (6 g) to the filtrate the free base separated, which was filtered and washed with water, yield, 3.5 g (67%); mp 176—178°C. It was recrystallized from benzene to form almost colorless prisms, mp 177—178°C. It was identified with the authentic sample of 5-formyl-8-quinolinol[1] by IR spectra and thin layer chromatography.

Estimation of Chloroform in Acetone Solution

(a) Preparation of the Standard Curve. The procedure which has been standardized for measuring the amount of chloroform is essentially similar to that of Cole[2] and the extinction at the wavelength of 490 mμ was determined by spectrophotometer.

From this, the standard curve

$E = 0.281\ C$

E: Extinction

C: g/100 m*l*

Width of the solution = 1 cm

was obtained.

(b) Estimation of Chloroform. The filtrate (B), which was originated from 0.03 mol of chloralylquinolinol (I) was acidified with dilute sulfuric acid, and distilled on a water bath. When no more distillate came out a small amount of acetone was added to the residue and the distillation was continued. The chloroform content in the total distillate was measured by Cole method using the standard curve. Found: $CHCl_3$, 0.28 g (7.8% of the theoretical). Calcd (from the reaction formula) $CHCl_3$, $119 \times 0.03 = 3.58$ g.

(c) Control Test. Chloroform (3.582 g, 0.03 mol) was added to the cooled solution of sodium (3.6 g, 0.157 mol) in acetone (180 m*l*). After 3 days standing at room temperature, the mixture was treated in the same manner as that in the hydrolysis of I. Found: $CHCl_3$, 0.31 g (8.7% of the theoretical).

2-Phenyl-4-[8'-acetoxyquinol-(5')-ylmethylene]-5-oxazolone (III). A mixture of 5-formyl-8-quinolinol

(1.73 g, 0.01 mol), hippuric acid (1.88 g, 0.0105 mol), acetic anhydride (4.6 g, 0.045 mol) and fused sodium acetate (0.8 g, 0.01 mol) was heated at 100°C for 2 hr. After cooling the reaction mixture was treated with ice water (200 m*l*). The separated yellow solid (3.6 g, mp 138—173°C) after being dried at room temperature over potassium hydroxide *in vacuo* was recrystallized from benzene (50 m*l*) to give azlactone (III). Yield, 2.9 g (80%), mp 160—188°C. It gave no color reaction with ferric chloride and can be used without further purification for the next step of synthesis. For analytical purpose, it was recrystallized from benzene. Garnet colored prisms or yellow needles melting at 192°C. Found: C, 70.26; H, 4.41; N, 7.76%. Calcd for $C_{21}H_{14}O_4N_2$: C, 70.39; H, 3.91; N, 7.81%.

2-Phenyl-4-[8′-quinolinol-(5′)-ylmethylene]-5-oxazolone. A solution of the acetoxyazlactone (III) (100 mg) in dilute ethanol (33%, 20 m*l*) was heated in a boiling water bath for one half hour. After cooling, the separated solid was filtered and crystallized from benzene to give brownish orange rods, mp 240—248°C (decomp). The solution in ethanol gives a violet brown color with ferric chloride. Found: C, 72.08; H, 3.85; N, 8.83%. Calcd for $C_{19}H_{12}O_3N_2$: C, 72.15; H, 3.80; N, 8.96%.

β-[8-Quinolinol-(5)-yl]-α-benzoylaminoacrylic Acid. A mixture of the azlactone (III) (120 mg) and 3 N hydrochloric acid (3 m*l*) was gently boiled over a free flame for 6 min until complete dissolution of the material into an orange red solution was effected. After cooling the reaction mixture was made alkaline with sodium carbonate solution, the resulting solution was acidified with acetic acid and the separated solid was recrystallized from hot ethanol to give prismatic needles of intense yellow color, mp 208—209°C (decomp). It exhibited a deep brown color with ferric chloride. Found: C, 67.45; H, 4.27; N, 8.18%. Calcd for $C_{19}H_{14}O_4N_2$: C, 68.26; H, 4.19; N, 8.38%.

5-[8′-Quinolinol-(5′-)ylmethylene]hydantoin (IV). A mixture of 5-formyl-8-quinolinol (1.73 g, 0.01 mol), hydantoin (1 g, 0.01 mol), acetic anhydride (5 g, 0.05 mol) and fused sodium acetate (0.85 g, 0.01 mol) was heated at 100°C for 5 hr. After evaporation under reduced pressure and cooling, the residue was treated with ice water. The separated solid (A) was converted to the hydrochloride by treating with hot dilute hydrochloric acid. The hydrochloride was dissolved in dilute sodium hydroxide solution and the solution was acidified with acetic acid to give the deacetylated product (1.5 g, 59%); mp 285—295°C (decomp). Without any further purification, it was used for the next step of synthesis. When crystallized from hot dioxane, it formed yellow prismatic needles, mp 198°C (decomp). It gave a violet brown color reaction with ferric chloride. Found: C, 61.54; H, 3.69; N, 16.14%. Calcd for $C_{18}H_9O_3N_3$: C, 61.18; H, 3.53; N, 16.47%.

The Hydrochloride of IV formed yellow needles and was hydrolysed in water, mp 296—300°C (decomp). Found: C, 50.41; H, 4.18; N, 13.22%. Calcd for $C_{13}H_9O_3N_3 \cdot HCl \cdot H_2O$: C, 50.40; H, 3.88; N, 13.57%.

5-[8′-Acetoxyquinol-(5′)-ylmethylene]hydantoin. The solid (A) in the preceding experiment after being dried at room temperature was treated with warm benzene. Recrystallization of the benzene insoluble solid from acetone afforded yellowish leaflets, mp 261—263°C, giving no color reaction with ferric chloride. Found: C, 60.58; H, 3.37; N, 13.95%. Calcd for $C_{15}H_{11}O_4N_3$: C, 60.61; H, 3.70; N, 14.14%.

3-[8′-Quinolinol-(5′)-yl]alanine (V).[3] A mixture of hydroiodic acid (52%, 9.8 g, 0.044 mol), red phosphorus (1 g), acetic anhydride (6.8 g) and the azlactone (III) (1.79 g, 0.005 mol) or the hydantoin (IV) (1.49 g, 0.005 mol) was gently refluxed in an oil bath for 6 hr. The subsequent treatment was almost similar to that stated in the standard procedure.[3b] The yield of the amino acid as monohydrate was 1.2 g (96%) starting from the azlactone and 1.05 g (84%) from the hydantoin. On recrystallization in five hundred times its weight of boiling water, the amino acid afforded colorless elongated plates, mp 287°C (decomp). It exhibited a violet red color with ninhydrin and a green color with ferric chloride.

The pK_2, 4.5; pK_3, 10.5, isoelectric point. 7.5, IR spectra $\nu_{cm^{-1}}^{KBr}$ 3480, 2920, 1630, 1575; 1520; 1435, 1410, 1350 and 1170. Paper chromatogram by descending technique R_f 0.3 (Solvent: Butanol-acetic acid-water, 4 : 1 : 2).

Found: C, 57.63; H, 5.54; N, 11.24%. Calcd for $C_{12}H_{12}O_3N_2 \cdot H_2O$*[2]: C, 57.60; H, 5.60; N, 11.20%.

The authors are grateful to Dr. Yoshio Matsumoto for help and advice in quantitative analysis of chloroform and measurements of pK and R_f values of the amino acid.

*[2] Vacuum dried at room temperature over potassium hydroxide.

BULLETIN OF THE CHEMICAL SOCIETY OF JAPAN VOL. 42 1744—1747 (1969)

The Surface Rearrangement*1 of Adsorbed Hydrogen on Platinum Electrodes

Kazuo SASAKI and Shigeyuki YOSHIDA

Department of Applied Chemistry, Faculty of Engineering, Hiroshima University, Senda-machi, Hiroshima

(Received April 24, 1968)

It is an accepted fact that the adsorbed hydrogen waves (ahw) which appear in a current-potential curve obtained by a linear potential sweep experiment with a noble metal electrode are depressed by the competitive adsorption of foreign substances in the solution. This character of the ahw has been utilized to determine the surface coverage of various organic substances[1-4] as well as the carbon monoxide[3,5,6] adsorbed on platinum electrodes. The method employed in these experiment is very useful in determining the relative surface coverage of adsorbent under given conditions. However, because of the competitive adsorption of unavoidable impurities in the solution and also the spontaneous structural change in the ahw itself, it seems inadequate as a basis for discussing in detail either the kinetics of adsorption or the absolute determination of adsorbent.

In the present paper, some basic characteristics of the ahw observed in sulfuric acid solutions containing no additional substance will be described.

Experimental

Super Special Grade sulfuric acid of Wako Pure Chemicals, Ltd., was used as the electrolyte. The tap water was first purified by means of an ion-exchange column and then distilled twice in glass vessels. In order to avoid contamination by foreign anions, a mercury-mercurous sulfate electrode was used as the reference electrode. The potential values in this paper are referred to this electrode. A platinized platinum wire with an apparent area of 0.19 cm^2 was used as the test electrode. Similar results were obtained in comparative experiments with a smooth platinum electrode. Nitrogen gas was bubbled into the solution to remove any dissolved gases. The rate of potential sweep was mainly kept at 0.2 V/sec. Current-potential curves were recorded by means of an XY-recorder, Model XYR-1A, of Toa Electronic Co., Ltd.

Results and Discussion

The curve in Fig. 1 respresents the current-potential curve at the steady state of the potential sweep. The steady-state curve is obtained after repeating the cyclic potential sweep several times, but the curve deforms more or less during the first few cycles of the potential sweep depending on the conditions under which the electrode was stored before use. Once the steady state is attained, the curve form remains unchanged during further repetitions of the sweep. When the sweep is stopped at a given constant potential for a short period of time, the ahw again is deformed during several succeeding cycles of the potential sweep. Some actual observations are shown in Fig. 2. This sort of phenomenon seems to have drawn the attention of several workers,[7-9] and the simultaneous adsorption of contaminants has been held

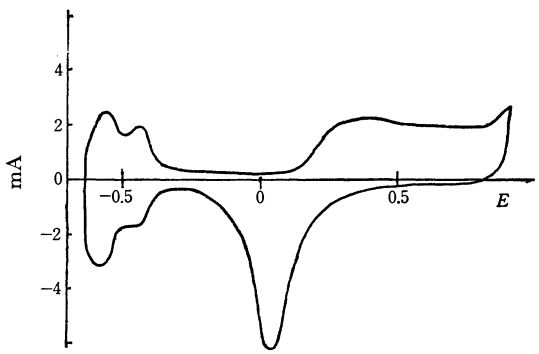

Fig. 1. Steady state current-potential curve in 1 N sulfuric acid solution. Platinized platinum electrode, Sweep rate: 0.1 V/sec, Reference electrode: mercury - mercurous sulfate

*1 The authors prefer to use the term "rearrangement" rather than "migration," since it is questionable whether or not the geometric migration actually takes place in the phenomenon reported in this paper.

1) M. W. Breiter *et al.*, *J. Electrochem. Soc.*, **109**, 622, 1099 (1962); **110**, 449 (1963); *J. Electroanal. Chem.*, **14**, 407 (1967).

2) V. S. Bagotzkii *et al.*, *Electrochim. Acta*, **9**, 869 (1964); *Russ. J. Electrochem.*, **1**, 70, 916 (1966).

3) S. B. Brummer *et al.*, *J. Phys. Chem.*, **68**, 1448 (1964); **69**, 562 (1965); **71**, 3494 (1967).

4) S. Gilman, *J. Electrochem. Soc.*, **113**, 1036 (1966).

5) S. Gilman, *J. Phys. Chem.*, **66**, 2657 (1962); **67**, 78 (1963); **71**, 2424 (1967).

6) S. B. Brummer and J. I. Ford, *ibid.*, **69**, 1366 (1965).

7) S. Trasatti, *Electrochim. Metallorum* (Milan), **3**, 1 (1966).

8) W. G. French and T. Kuwana, *J. Phys. Chem.*, **68**, 1279 (1964).

9) S. D. James, *J. Electrochem. Soc.*, **114**, 1113 (1967).

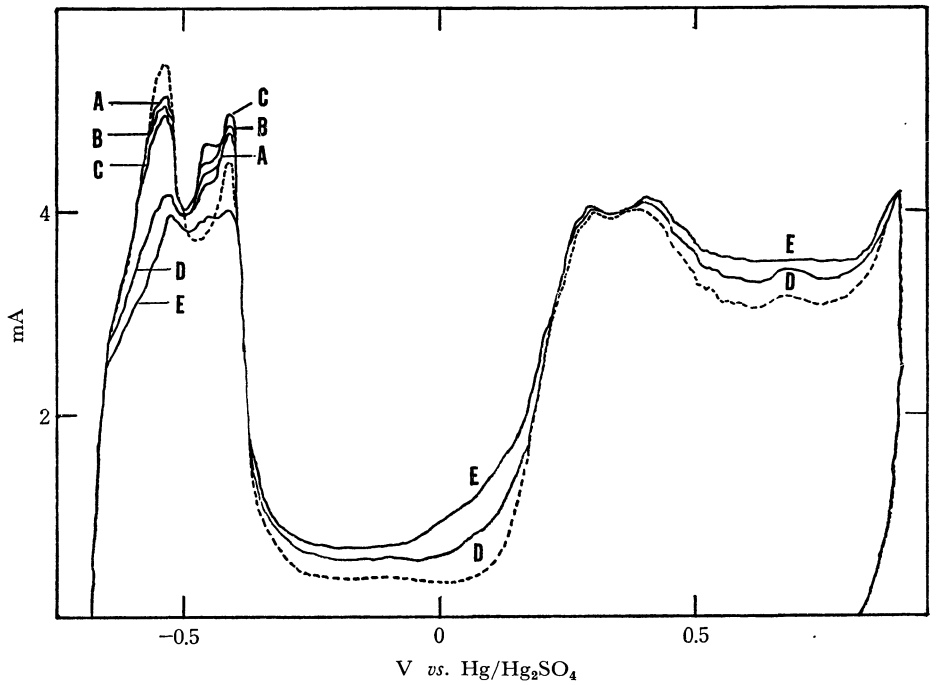

Fig. 2. Effect of the constant potential treatment.
Dashed curve indicates the steady state curve. Curve A was obtained after 5 sec. B, 10 sec; C, 20 sec; D, 25 min; E, 60 min. Curves for 5, 10 and 20 sec merge in the steady state curve at higher potential range. The potential sweep was paused at −0.68 V.

to account for the depression of ahw.[7,9] *2) A close inspection of Fig. 2 indicates, however, that there is another source of the depression of the ahw. In obtaining the curves in Fig. 2, after the steady state curve(dashed line) had been attained, the potential sweep was stopped at a desired potential (−0.68 V in this case) for various periods of time ("waiting time" will be used hereafter); then the potential sweep was carried out in order to record the full lines of the curves.

It may be seen in Fig. 2 that the left half of the double peak (peak I) diminishes monotonously with the time, while the right half (peak II) first increases and then gradually decreases. After a prolonged treatment at −0.68 V, the ahw becomes a hump-like single peak. Although the depression of the ahw can be attributed to the adsorption of contaminants, the transient increase in peak II requires explanation. Two reasons can be cited for this transient increase: 1) the steady state curve does not represent the saturation coverage of

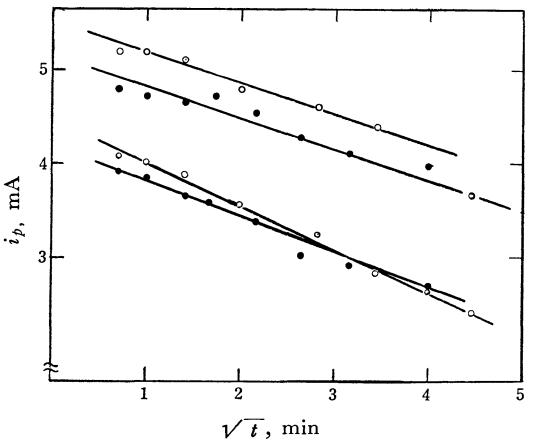

Fig. 3. Decrease in peak current with time.
Full circle: Potential sweep was paused at −0.45 V.
Empty circle: Potential sweep was paused at −0.25 V.
After the constant potential treatment, the electrode was first polarized cathodically and then reversed at −0.68 V to anodic direction. Upper two curves stand for peak I and lower two for peak II.

*2 French and Kuwana[8] found an essentially similar effect. They attributed the depression of the ahw to the deactivation of platinum atoms at the electrode surface. In the present case, however, the deactivation of the electrode surface does not seem to be the main reason. This was concluded from the fact the decrease in the ahw resulted in an increase in the quantity of electricity at the potential regions of both the double-layer charging and the surface oxide formation. The quantity of electricity recovered at these two potential regions always exceeded that at the ahw (see Fig. 2). This point will be discussed in a later paper.

hydrogen, but rather the adsorption continues during the waiting time, and 2) some of the hydrogen adsorbed at peak I migrates or rearranges*1 to a more stable form at peak II. The former explanation seems unlikely, because the transient increase only appeared in peak II, not at all in peak I.

The transient increase in peak II was not found when the sweep was paused at a potential more negative than the saddle point of the double peak. At these potentials, peak II decreased monotonously with the time. This is illustrated in Fig. 3, where the decrease in the peak current is plotted against the square root of the waiting time. Since the transient increase was found only when the potential sweep was paused at a potential range covered by peak I, it is reasonable to assume that some of the hydrogen adsorbed at peak I migrates to peak II. The following facts support this assumption. The decrease at peak I roughly holds a linear relationship with the square root of the waiting time. The square-root dependence does not, however, hold exactly, and a small deviation arises at a shorter time, as may be seen in Fig. 4.

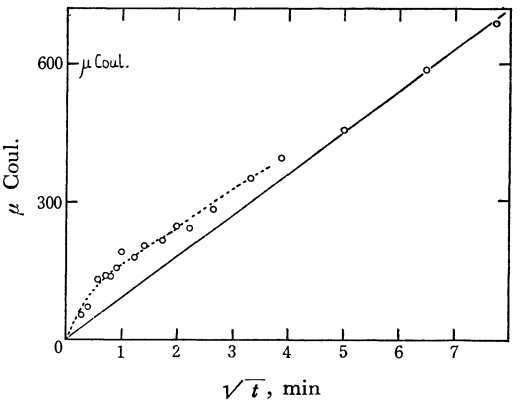

Fig. 4. Decrease of peak I with time.
Potential sweep was paused at −0.68 V.

This indicates that the decrease at peak I is caused not only by the diffusion-controlled adsorption of contaminants, but also by something else. It must be noted that the points deviating from linearity in Fig. 4 fit on a straight line when the abscissa is drawn on a logarithmic scale instead of on the basis of the square root (curve A in Fig. 5). Accordingly, the depression of peak I can be approximated by the equation:

$$\Delta q_{\mathrm{I}} = -kt^{1/2} + k' \log t \qquad (1)$$

where Δq_{I} represents the difference in the quantities of electricity between the steady state curve and the curve obtained after the waiting time, t. The negative signs in the right-hand side terms were given to express the decrease at the ahw. k should be the sum of the diffusion coefficients (not the diffusion constants) of the contaminants, and k', the rate constant of the rearrangement of the adsorbed hydrogen. The behavior of peak II in Fig. 2 suggests that there might be two counteracting processes. The curve B in Fig. 5 shows this in more detail. Of course, it is reasonable to assume the counteracting processes to be the contaminant adsorption and the surface rearrangement of the adsorbed hydrogen. Thus, the rate of change at peak II can be expressed as:

$$\Delta q_{\mathrm{II}} = -kt^{1/2} + k' \log t \qquad (2)$$

By combining Eqs. (1) and (2), the effect of the contaminant adsorption can be cancelled:

$$q_R = \Delta q_{\mathrm{II}} - \Delta q_{\mathrm{I}} = 2k' \log t \qquad (3)^{*3}$$

where one half of q_{R} represents the amount of hydrogen rearranged from peak I to peak II.

Curve C in Fig. 5 shows the difference between Δq_{II} and Δq_{I}. In accord with the expectation from Eq. (3), the curve shows a linear relationship with log t when t does not exceed twenty to thirty minutes. At a longer waiting time, the curve become flat (although this part is not seen in Fig. 5), thus indicating the equlibrium of the rearrangement. The total amount of hydrogen which takes part in the rearrangement was found to be less than 10% of the adsorbed hydrogen at saturation.

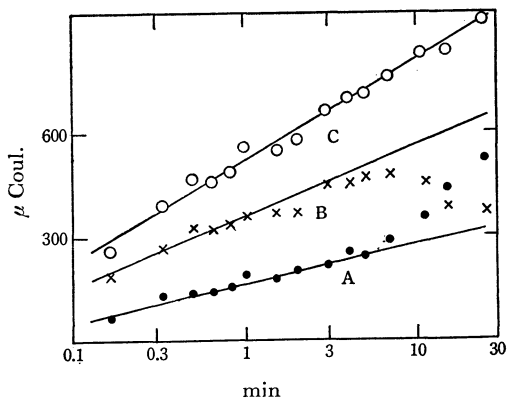

Fig. 5. Curve A: Decrease of peak I, B: Incerase of peak II C: Corrected change at peak II.

*3 In the above discussion, k' was taken to be common to both Δq_{I} and Δq_{II}. The treatment is, therefore, equivalent to assuming that no hydrogen adsorbs on vacant sites produced after the rearrangement. Actually, this is not true, since it was found that the increase in the charge at peak II (Δq_{II}) was greater than the decrease at peak I (Δq_{I}) unless the waiting time exceeded thirty seconds or so. Accordingly, Eq. (1) will require an additional term to express the adsorption on vacant sites produced after the rearrangement. Because of the present lack of experimental accuracy, however, it seems meaningless to attempt to discuss the mechanism in such detail.

In order to find the activation energy of the process, experiments were carried out at three different temperatures, 5, 25, and 40°C. The results indicated that the activation energy, if it existed, was less than 1 kcal/mol.

BULLETIN OF THE CHEMICAL SOCIETY OF JAPAN VOL. 42 1747—1749 (1969)

β-Diketone Involving Fluorine. V.[1] NMR Studies of Pivaloyltrifluoroacetone in Various Alcohols

Kimitaka SATO, Hisao OCHI[2] and Kiichi ARAKAWA[2]

Tokyo Research Institute, Yawata Iron and Steel Co., Ltd., Kawasaki, Kanagawa

(Received May 17, 1968)

It was noted, in our previous papers,[1,3-5]— that an equilibrium existed between β-diketones involving fluorine and alcohols by the activation of the carbonyl carbon adjacent to a trifluoromethyl (CF_3-) group due to the *I* effect exerted by the fluorine atom. Such a phenomenon has already been described with β-diketones like trifluoroacetylacetone (TFA),[1,3] benzoyltrifluoroacetone (BTA), 2-furoyltrifluoroacetone (FTA), 2-thenoyltrifluoroacetone (TTA)[4] or hexafluoroacetylacetone (HFA),[1] and with alcohols like methanol, ethanol, 1-propanol, 2-propanol, allyl alcohol, propargyl alcohol, benzyl alcohol, ethylene glycol or some halohydrins. The equilibrium is affected by the steric effect and the nucleophilicity of alcoholic oxygen, therefore some changes in property are expected to be found by changing not only the variety of alcohols but also that of β-diketones. For these reasons, pivaloyltrifluoroacetone (PTA) with a bulky functional group was newly synthesized, and the behavior of that β-diketone (PTA) in alcohols and water has been studied by means of high resolution NMR spectroscopy.

Results and Discussion

The proton magnetic resonance signals of PTA appeared at 8.77 ppm due to the pivaloyl proton and at 4.01 ppm due to methine proton, but any signals which should be attributed to methylene proton did not appear. Thus PTA exists as 100% enolized structure of either Ia or Ib.

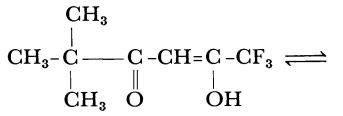

(Ia)

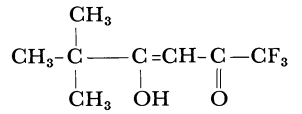

(Ib)

As (Ia) was probably regarded as the preferred enol form in the equilibrium (Ia) and (Ib),[6] the following discussions were carried out assuming that the structure of PTA was (Ia).

Table 1 lists the values of chemical shifts in the fluorine magnetic resonance spectra of various kinds of β-diketone-alcohol solutions mixed at the volume ratio, 1 : 1. Two signals appeared at about 76 ppm

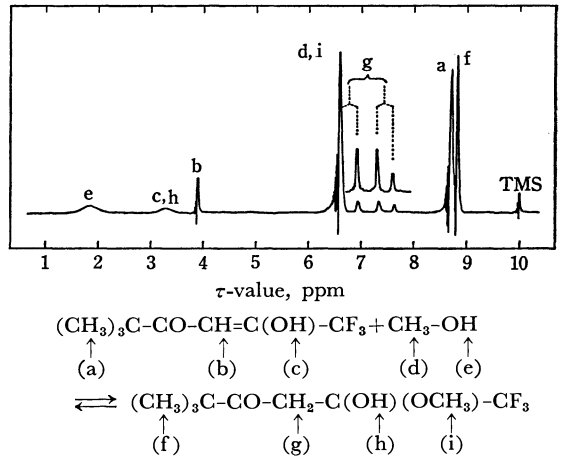

$(CH_3)_3C$-CO-CH=C(OH)-CF_3 + CH_3-OH
(a) (b) (c) (d) (e)
⇌ $(CH_3)_3C$-CO-CH_2-C(OH)(OCH_3)-CF_3
(f) (g) (h) (i)

Fig. 1. PMR spectrum of a mixture of pivaloyltrifluoroacetone (PTA) and methanol in CCl_4 at 60 Mc.

1) Part IV of this series: K. Sato, Y. Kodama and K. Arakawa, *Nippon Kagaku Zasshi (J. Chem. Soc. Japan, Pure Chem. Sect.)*, **88**, 968 (1967).

2) Present address: School of Pharmaceutical Sciences, Showa University, Hatanodai, Shinagawa-ku, Tokyo.

3) K. Sato, Y. Kodama and K. Arakawa, *Nippon Kagaku Zasshi (J. Chem. Soc. Japan, Pure Chem. Sect.)*, **87**, 821 (1966).

4) Y. Kodama, K. Sato and K. Arakawa, *ibid.*, **87**, 1092 (1966).

5) K. Sato and K. Arakawa, *ibid.*, **88**, 470 (1967).

6) K. Sato and K. Arakawa, *ibid.*, **89**, 1110 (1968).

Table 1. The values of chemical shift in fluorine magnetic resonance spectra of solutions

Alcohol	R	$(CH_3)_3CCOCH=C(OH)C\underline{F}_3$ (ppm)	$(CH_3)_3CCOCH_2C(OH)(OR)C\underline{F}_3$ (ppm)	II / Ia+II
(PTA)		76.0	—	—
CH_3OH	CH_3-	75.1	80.7	0.50
CH_3CH_2OH	CH_3CH_2-	75.4	81.1	0.21
$CH_3(CH_2)_2OH$	$CH_3(CH_2)_2$-	75.5	80.8	0.15
$(CH_3)_2CHOH$	—	75.5	—	—
$BrCH_2CH_2OH$	$BrCH_2CH_2$-	75.2	81.2	0.19
$CNCH_2CH_2OH$	$CNCH_2CH_2$-	74.3	80.9	0.50
$ClCH_2CH_2OH$	$ClCH_2CH_2$-	75.4	81.5	0.18
$CH_2=CHCH_2OH$	—	75.4	—	—
$PhCH_2OH$	$PhCH_2$-	75.3	80.7	0.18
H_2O	H-	74.9	84.8	0.18

and 81 ppm in the spectra of these solutions: the signal at 76 ppm was equal to PTA, $(CH_3)_3CCOCH C(OH)CF_3$, and that at 81 ppm may be due to the new reaction product(II). Figure 1 shows the case of PTA-methanol solution as an example in the PMR spectra of those solutions. Of the two signals at 8.74 and 8.84 ppm, the down-field one was apparently due to the pivaloyl proton of PTA because of having a definite intensity in spite of the values of II/(Ia+II), and the up-field one might be due to the pivaloyl proton of the new product (II). It was easily estimated that the AB-type signal at 7.11 ppm was based on methylene proton in comparison with the case of TFA[4] and the integrated ratios between the signal at 7.11 ppm and at 8.84 ppm were about 2 : 9. The signal at 6.61 ppm might be due to not only methyl proton of methanol but also methoxy proton, since that intensity was much stronger than that due to only methanol. It was thought that the broad signals at about 2 and 3 ppm must be based on some hydroxyl protons. Therefore, it was expected that the new reaction product consisted of such functional groups as pivaloyl,methoxyl, hydroxyl, methylene and trifluoromethyl in this equilibrium.

From these results, it has been deduced that the following equilibrium exists also in PTA similar to TFA, TTA, *etc.*:

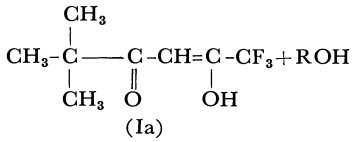

(Ia)

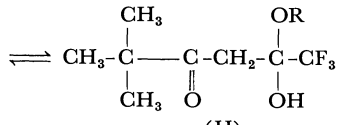

(II)

R=H-, CH_3-, CH_3CH_2-, $CH_3(CH_2)_2$-, $BrCH_2CH_2$-, $CNCH_2CH_2$-, $ClCH_2CH_2$-, $PhCH_2$-.

It was found, however, that PTA hardly reacted with isopropyl alcohol, allyl alcohol and propargyl alcohol in such equilibrium. This is probably due to the steric hindrance or the less nucleophile nature of alcoholic oxygen effective in such alcohols.

Such exceptions found in isopropyl, allyl and propargyl alcohol solutions have never been found with β-diketones like TFA, HFA, TTA, BTA and FTA reported in the previous papers.[1,3,5] This may be due to the fact that the steric hindrance of pivaloyl group mainly contributes to these phenomena. The carbon atom adjacent to the trifluoromethyl group is optically active in the new reaction product (II), which is consequently possible to take conformations IIIa, IIIb and IIIc.

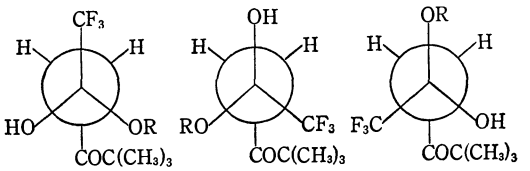

(IIIa) (IIIb) (IIIc)

It seems reasonable to conclude that IIIa is the most preferred of three conformations and is major conformation in the sample solution. It was estimated that PTA hardly reacted with isopropyl, allyl and propargyl alcohols because of the considerable contribution of steric hindrance even in IIIc conformation together with nucleophilicity of alcoholic oxygen. Above-mentioned characteristics of PTA are apparently different from that of TFA, TTA and HFA.

Experimental

Measurements. A JNM C-60 high-resolution nuclear magnetic resonance spectrometer was used. Proton resonance spectra and fluorine resonance spectra were run at 60 Mc and 56.45 Mc, respectively. Each sample was dissolved in carbon tetrachloride at a concentration of 25 vol%. The temperature was maintained at 23±1°C. Tetramethylsilane (TMS: proton) and monofluorotrichloromethane ($CFCl_3$:

fluorine) were employed as the internal standards.

Materials. *Commercial alcohols and halohydrins* were used without further purification. Water was purified by passing it through an ion exchange resin.

Pivaloyltrifluoroacetone (PTA) used in this investigation was prepared in the following method, a modification of Henne's[7]: Sodium ethylate freshly prepared by treating 14 g of absolute ethanol with 7.6 g of finely dispersed sodium was dissolved in ether. To the resulting suspension was added slowly 42.6 g of ethyl trifluoroacetate in 40 m*l* of ether. Privaloylmethane, 30 g, in 30 m*l* of ether was then added, and the mixture refluxed for about six hours. On account of the avidity of the condensates for moisture, the following procedure of isolation was adopted. The reaction mixture was treated with a 50% solution of sodium bisulfide in a very slight excess over neutralization requirements, then with a saturated aqueous solution of cupric aectate (180 m*l*). The organic layer was distilled off, then 43.6 g of crystalline copper derivative, mp 85—87°C, was extracted with ether. The dry copper derivative was suspended in 500 m*l* of dry ether, in which it was partly dissolved, and was subjected to a stream of hydrogen sulfide. After removal of the cupric sulfide, the condensed compound was separated from the ether by fractional distillation, with rigorous precautions to avoid loss by volatility, to give 23.5 g of a light yellow oil, bp 129.5—130.5°C.

UV: λ_{max}^{MeOH} mμ (ε); 288 (8700).

Found: C, 49.51; H, 5.99%. Calcd for $C_8H_{11}O_2F_3$: C, 48.98; H, 5.64%.

The authors wish to express their thanks to Professor Yojiro Tsuzuki of Science University of Tokyo for his valuable discussion.

7) A. L. Henne, M. S. Newman, L. L. Quill and R. A. Staniforth, *J. Am. Chem. Soc.*, **69**, 1819 (1957).

BULLETIN OF THE CHEMICAL SOCIETY OF JAPAN VOL. 42 1749—1751 (1969)

Studies on Polymorphism of Glutathione

Muneji MIYOSHI, Keishi KOTERA, Hiroyasu SEKO, Kenji MASUKAWA, Sataro IMADO and Kentaro OKUMURA

Chemical Research Laboratory, Tanabe Seiyaku Co., Ltd., Higashiyodogawa-ku, Osaka

(Received July 25, 1968)

Glutathione is known as an important constituent of all living cells, and has recently been used in clinical fields. Various synthetic routes have been reported by many investigators since Harington and Mead[1] first synthesized the tripeptide in 1935.

The crystal of glutathione is well known as a colorless needle which is easily soluble in water, and its structure has also been discussed.

However, studies on the crystallization conditions of glutathione have scarcely been reported, although some preparative methods are shown.[2-6]

In the present paper, both nuclei formation and the conditions of crystal growth of glutathione were investigated in water and ethanol-water (1 : 2), with varying supersaturated concentration and temperature respectively.

Results

Crystallization in Water System. The glutathione used in this study was repeatedly purified through Cu-salt. Paper electrophoresis did not show any spots of impurities.

Condition of nuclei formation was examined in water without seeding.

The different crystalline nuclei of the glutathione (named type B) were formed when 100% supersaturated solution (100g glutathione/100g water) was maintained above 50°C for 30 min where the crystallization conditions were quite different from those used in the previous reports.

The selective crystal growth of this new type B as well as that of the other one formed under the usual conditions (named type A) may be carried out by seeding the crystalline nuclei of each type to the supersaturated solution under usual crystallization conditions.

In the supersaturated concentrations from 27 to 50%, type A was selectively grown at 10°C after 72 hr, with or without seeding type A. If crystalline nuclei of type B were seeded to the same supersaturated solution at 10°C, only crystal of type B was grown selectively.

In the 100% supersaturated concentration, type

1) C. A. Harington, T. H. Mead, *Biol. J.*, **29**, 1602 (1935).

2) F. E. King, S. W. Clark-Lewis and R. Wade, *J. Chem. Soc.*, **1957**, 880.

3) F. Weygand and R. Geiger, *Chem. Ber.*, **90**, 634 (1957).

4) C. Berse, R. Boucher and L. Piche, *Can. J. Chem.*, **37**, 1733 (1959).

5) S. Goldschmidt, W. Lautenschlager, B. Kolb and G. Zumach, *Chem. Ber.*, **97**, 2424 (1964).

6) St. Guttmann, *Helv. Chim. Acta*, **49**, 83 (1966).

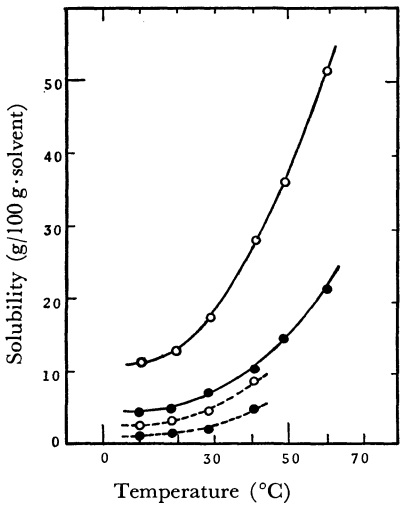

Fig. 1. Solubility curves of type A and B.

— type A
--- type B
○ H_2O
● EtOH-H_2O (2:1)

B was selectively formed with or without seeding type B, when the solution was kept for 30 min at 50°C and then for 72 hr at 30°C. However, if type A was seeded under the same condition, only type A was found in the grown crystal.

The final concentrations in the mother liquor showed 14.0% with A and 5.1% with B respectively after 72 hr at 10°C, and these results suggested that considerable differences of solubilities in water would exist between both types. In fact, these data approximately agreed with those of the solubility curves at 10°C shown below. (Fig. 1)

Crystallization in Ethanol-Water (1 : 2) System. Preparative crystallization of glutathione has been usually carried out by adding suitable amount of ethanol to the aqueous solution. Therefore the crystallization condition was also investigated in ethanol-water (1 : 2) system to check which nuclei of type A or B would be formed.

Remarkable decrease in solubilities of the glutathione (Fig. 1) was found in comparison with those in water system. In this solvent system, only the crystalline nuclei of type A were obtained under conditions in this study.

Chemical and Physicochemical Properties. The new crystalline form named type B was found to be a colorless rigid and fine crystal, while that of type A was a colorless needle.

The solubilities of both types in water were remarkably different as shown in Fig. 1.

Type B was proved to be more stable on storage at 40°C in 100% relative humidity. Thus, the amount remaining unchanged was as much as 75% for B and was only 15% for A after 17 days.

Elemental analysis, paper electrophoresis, $[\alpha]_D$, and mp of type B quite agreed with those of type A.

Both types gave completely the same patterns of NMR (in D_2O, d_6-DMSO, CF_3COOD), ORD (in H_2O) and IR (in D_2O) except IR in KBr tablets. In the pattern of IR spectra, the difference between both types was observed at absorption bands assigned to both amide and carboxyl groups. (Fig. 2)

X-ray diffraction patterns were also measured. It was found that type A showed a very strong peak at d=4.00Å while type B at d=4.19Å, and the spacing of the latter was a little longer than the former.

Discussion

On the Crystallization Conditions. From Fig. 1, the range in which the nuclei of type B were

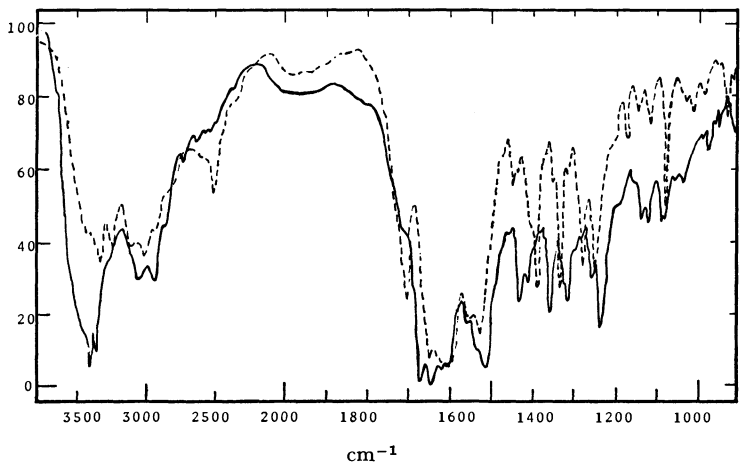

Fig. 2. Infrared spectra in KBr tablets.
---- type A —— type B

formed might exist at higher temperatures or higher concentrations, as the difference between solubility curves of type A and B was much greater. However it was practically difficult to obtain the crystal above 60°C because partial decomposition of glutathione was observed more than an hour later. It is interesting to note that the condition to form nuclei of type B must be restricted within a very small range of temperature and concentration as mentioned above.

It should also be noted that only the selective crystallization of one type took place, with seeding, even in the supersaturated solution where the other type of crystal should be formed without seeding. This fact suggests that the work of nucleus formation of both types would be unusually greater than that of crystal growing. Therefore by seeding one type of nuclei, the same type of crystal would be selectively grown, while nucleus formation of the other type might be disturbed.

Estimation of the Structural Configuration. Many papers about the polymorphism of peptides, in which two different forms are proposed, have been reported. Both of them are "the folded form" with intramolecular hydrogen bonds, and "the extended form" with intermolecular hydrogen bonds. In this connection, IR alternations due to the structural configurations of peptides have also been studied.[7-8] In IR spectra of KBr tablets obtained in this experiment, type B of the glutathione showed a lowering of absorption frequencies at amide ν_{NH} ($\Delta 116\ cm^{-1}$), amide I ($\Delta 25\ cm^{-1}$) and amide II ($\Delta 20\ cm^{-1}$) in comparison with those of type A, respectively. These results would be in satisfactory agreement with those previously reported.

As to the X-ray analysis, Wright[9] reported that the structure of glutathione was held together by a three dimensional network with intramolecular hydrogen bonds. The spacings were calculated as the orthorhombic system, using the unit cell dimensions found by Wright ($a=28.05\pm0.02$Å, $b=8.802\pm0.002$Å, $c=5.630\pm0.002$Å). The calculated value for type A agreed with the observed value in type A.

From these data, the structure of type A must be "the folded form" with intramolecular hydrogen bonds, which is well known previously, and that of the new type B would be "the extended form" with intermolecular hydrogen bonds.

Experimental

Crystallization of Type B. a) Glutathione (10 g) dissolved in water (20 ml) was concentrated to total weight 20 g *in vacuo* at 40°C. This supersaturated solution was maintained at 50°C for 30 min with mild stirring, and the solution was allowed to stand for 72 hr at 30°C. Crystal was filtered and washed with a small amount of water and dried in a desiccator under reduced pressure. Colorless, rigid and fine crystal was obtained, yield, 6.5 g. Mp 195°C (dec.), $[\alpha]_D^{20}$ −17.3° (*c* 2, H_2O). Solubility in water at 10°C, 3.67%. Elemental analysis agreed with the starting glutathione.

b) Nuclei of type B (0.2 g) were seeded to the solution of glutathione (10 g) in water (20 g), and allowed to stand for 72 hr at 10°C. The crystal formed was treated in the same way as above. Yield, 8.9 g. Mp 195°C (dec.), $[\alpha]_D^{20}$ −17.4° (*c* 2, H_2O). Solubility in water at 10°C, 3.70%.

Apparatus. IR spectra were recorded on a Hitachi IR-G Spectrometer (0.025 mm thickness. KRS-5 sample cell) in D_2O solution and in KBr tablets.

NMR spectra were obtained with an internal standard TMS, JEOL c-60 spectrometer (60 Mc) in D_2O, d_6-DMSO, and CF_3COOD.

X-Ray diffraction patterns were measured with the apparatus of D-3F type made by Rigakudenki, Ltd., in the region of $2\theta=5-40°$ with the use of Cu$K\alpha$ radiation ($\lambda=1.5418$ Å).

7) C. N. R. Rao, "Chemical Applications of Infrared Spectroscopy," Academic press, N. Y. (1963), pp. 485—488.
8) C. C. Cannon, *J. Chem. Phys.*, **24**, 491 (1956).
9) W. B. Wright, *Acta Cryst.*, **11**, 632 (1958).

BULLETIN OF THE CHEMICAL SOCIETY OF JAPAN VOL. 42 1752—1754 (1969)

Synthesis and Melanogenesis of the DOPA Dimer

Yoshimori OMOTE, Yoshimori FUJINUMA and Noboru SUGIYAMA

Department of Chemistry, Tokyo Kyoiku University, Otsuka, Tokyo

(Received August 19, 1968)

It is generally accepted that, in the presence of tyrosinase, β-(3,4-dihydroxyphenyl)alanine (DOPA) yields melanin *via* cyclization to 5,6-dihydroxyindole.[1] Molecular orbital calculation[2-4] suggests that 5, 6-dihydroxyindole will polymerize oxidatively at the 4 and 7 positions, which correspond to the positions 2 and 5 of DOPA. Recently the presence of uncyclized units in DOPA melanin has been suggested by several groups of investigators,[5-7] This suggests the possibility that DOPA will polymerize at the position 2, 5, or 6 without any cyclization to 5,6-dihydroxyindole. Therefore, it is of interest to examine whether or not the dimer at the position 2, 5, or 6 of DOPA can be an intermediate of the melanogenesis of DOPA. One DOPA dimer, a novel bi-(amino acid), 5,5'-bi-[β-(3,4-dihydroxyphenyl)alanine](V), has thus been synthesized, and its melanogenesis has been examined.[8]

Elbs prepared 2,2'-diacetoxy-5,5'-diformyl-3,3'-dimethoxybiphenyl (I)[9,10] from dehydrodivanillin. The treatment of I and hippuric acid under reflux with fused sodium acetate in acetic anhydride yielded 5,5'-bi-[4-(4-acetoxy-3-methoxybenzylidene)-2-phenyloxazolone](II). Heating the oxazolone II under reflux with fused sodium acetate in methanol gave the unsaturated ester, 5,5'-bi-(methyl 4-acetoxy-α-benzamido-3-methoxycinnamate)(III). The oxazolone II showed IR absorptions at 1790 (oxazolone C=O) and 1766 (enol acetate C=O) cm^{-1}, while the unsaturated ester III showed absorptions at 1766 (enol acetate C=O) and 1720 (unsaturated ester C=O) cm^{-1}.

The catalytic hydrogenation of III with platinum oxide in acetic acid at atmospheric pressure and at room temperature afforded a saturated ester, 5,5'-bi-(methyl 4-acetoxy-α-benzamido-3-methoxydihydrocinnamate)(IV). When IV was hydrolyzed with hydrobromic acid and neutralized with ammonium hydroxide, the DOPA dimer(V) was produced as a colorless powder. Both the UV and the IR spectra, as well as the elemental analyses, favor the structure V for the DOPA dimer. Considering that the UV absorption spectrum of V is similar to that of monomeric DOPA (Fig. 1), it is probable that the two phenyl nuclei of V are almost perpendicular to one another.

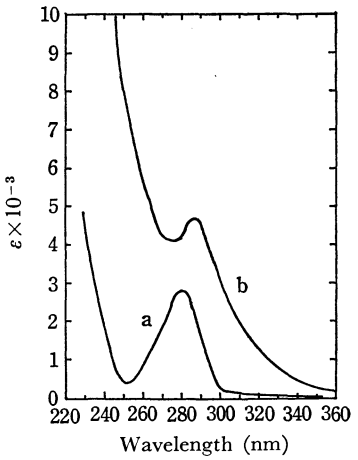

Fig. 1. Ultraviolet absorption spectra of DOPA and the DOPA dimer (V) in water.

a: DOPA b: DOPA dimer

Also, we succeeded in the direct synthesis of the DOPA dimer V from the unsaturated ester III by boiling them with hydroiodic acid and red phosphorus in acetic anhydride, as will be described in the Experimental section.

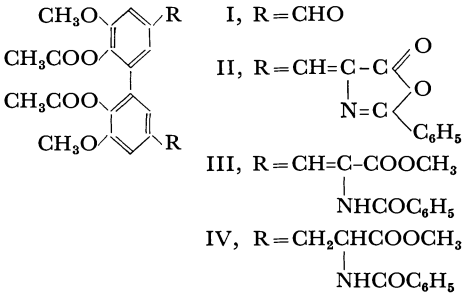

1) H. S. Raper, *Biochem. J.*, **21**, 89 (1927).
2) B. Pullman, *Biochem. Biophys. Acta*, **66**, 164 (1963).
3) A. Pullman and B. Pullman, *ibid.*, **54**, 384 (1961).
4) H. Chang, *Acta Phys. Sinica*, **20**, 1289 (1964).
5) S. N. Mishra and G. A. Swan, *J. Chem. Soc. (C)*, **1967**, 1424.
6) M. Piattelli, E. Fattorusso, S. Magno and R. A. Nicholaus, *Tetrahedron*, **18**, 941 (1962).
7) G. W. Kirby and L. Ogunkoya, *Chem. Commun.*, **1965**, 546.
8) Preliminary report appeared in the following communication. Y. Omote, Y. Fujinuma and N. Sugiyama, *ibid.*, **1968**, 190.
9) K. Elbs and H. Lerch, *J. Prakt. Chem.*, **93**, 1 (1916).
10) H. Booth and B. C. Saunders, *J. Chem. Soc.*, **1956**, 910.

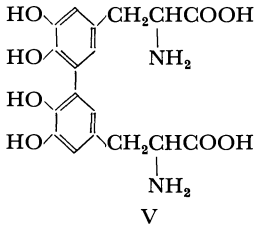

V

In the presence of atmospheric oxygen, it has been shown that DOPA and the DOPA dimer polymerized at about the same rate. In the presence of tyrosinase and atmospheric oxygen, however, the melanogenesis of DOPA was very much accelerated, while that of the DOPA dimer was accelerated only slightly. This suggests that the role of the DOPA dimer as an intermediate of enzymatic melanogenesis is rather improbable, though the possibility of a role in non-enzymatic melanogenesis can not be eliminated.

Experimental

All the melting points are uncorrected.

5,5'-Bi-[4-(4-acetoxy-3-methoxybenzylidene)-2-phenyloxazolone] (II). A mixture of 2,2'-diacetoxy-5,5'-diformyl-3,3'-dimethoxybiphenyl (I) (46 g), hippuric acid (46 g), and fused sodium acetate (24 g) in acetic anhydride (200 m*l*) was heated at 100°C for 2 hr with stirring. Into the reaction mixture ethanol (50 m*l*) was then gradually stirred, after which the mixture was kept overnight in an refrigerator. The solid substance which thus separated was filtered, and washed with a small portion of cold ethanol and then with boiling water. Treatment with chloroform-benzene gave the oxazolone II as a yellow powder (40 g); mp 287°C. Found: C, 66.13; H, 4.23; N, 4.33%. Calcd for $C_{38}H_{28}O_{10}N_2$: C, 67.85; H, 4.20; N, 4.17%. UV $\lambda_{max}^{CHCl_3}$ nm (ε) 380 (75000) and 402 (76000). IR ν^{KBr} cm^{-1} 1790, 1766, 1653 and 1593.

5,5'-Bi-(methyl 4-acetoxy-α-benzamido-3-methoxycinnamate) (III). The oxazolone II (20 g) and fused sodium acetate (9 g) in absolute methanol (250 m*l*) were refluxed for 3 hr, by which time the solid had dissolved completely. Then the solution was condensed to about one third of its initial volume; after cooling, it was poured into ice water (300 m*l*) and kept overnight in a refrigerator. The treatment of the precipitates with benzene gave III as a colorless amorphous powder (17.3 g); mp 141—145°C. Found: C, 65.62; H, 5.09; N, 3.81%. Calcd for $C_{40}H_{36}O_{12}N_2$: C, 65.21, H, 4.93; N, 3.80%. UV: λ_{max}^{EtOH} nm (ε) 225 (46600) and 295 (31000). IR ν^{KBr} cm^{-1} 3320, 1766, 1720, 1655 and 1585.

5,5'-Bi-(methyl 4-acetoxy-α-benzamido-3-methoxydihydrocinnamate) (IV). A mixture of III (2 g) in acetic acid (10 m*l*) and platinum oxide (0.05 g) was stirred with hydrogen at atmospheric pressure and room temperature for 8 hr. After the catalyst had then been filtered off, the solution was treated with active charcoal and evaporated under reduced pressure. There was thus obtained an amorphous powder of IV; mp 65—75°C. It was pure enough for the next step. Found: C, 63.32; H, 5.91; N, 3.53%. Calcd for $C_{40}H_{40}O_{12}N_2$: C, 64.85; H, 5.44; N, 3.78%. UV λ_{max}^{EtOH} nm (ε) 281 (4500). IR ν^{KBr} cm^{-1} 3400, 1770, 1753, 1653 and 1600.

5,5'-Bi-[β-(3,4-dihydroxyphenyl)alanine] (V). A solution of IV (20 g) in hydrobromic acid (47%, 100 m*l*) was refluxed for 3 hr. Then toluene (250 m*l*) was added, a Dean-Stark trap equipped with a stopcock outlet for the removal of water was inserted between the flask and the reflux condenser, and the mixture was refluxed until no more water was collected in the trap (about 8 hr). Then the hydrogen bromide salt of V, which had separated, was filtered off. It was brown and decomposed at 132°C. The salt dissolved in water (40 m*l*) was neutralized with ammonium hydroxide. The solution was evaporated to dryness. The crude DOPA dimer was boiled in water containing a little sulfur dioxide and was filtered while still hot. The filtrate was then allowed to evaporate slowly under reduced pressure to separate the pure DOPA dimer V as a colorless powder (yield 7.1 g); mp above 300°C. The color became brown and changed gradually at about 230°C from brown to black. Found: C, 55.06; H, 5.12; N, 7.08%. Calcd for $C_{18}H_{20}O_8N_2$: C, 55.10; H, 5.14; N, 7.14%. UV $\lambda_{max}^{H_2O}$ nm (ε) 287 (4700). IR ν^{KBr} cm^{-1} 3200 (broad), 1628 and 1598. The elemental analysis was carried out just after the sample had been dried at 100°C/10^{-3}—10^{-4} mmHg for 3 hr.

The DOPA dimer V was also obtained directly from III by the following reductive hydrolysis. A mixture of III (5 g), hydroiodic acid (d=1.7, 35 m*l*) and red phosphorus (3.5 g) was refluxed for 3 hr. After cooling, the unreacted phosphorus was filtered off, the solution was evaporated to dryness under reduced pressure, and water (50 m*l*) was added. The solution was extracted five times with ether (50 m*l*) in order to remove any benzoic acid and iodine, and then the aqueous solution was evaporated to dryness under reduced pressure. The residual solid was dissolved in water (10 m*l*), neutralized with ammonium hydroxide, and purified as has been described above. Yield, 1.2 g.

DOPA Melanin and DOPA Dimer Melanin. *(a) Melanogenesis by Autoxidation.* A solution of DOPA (250 mg) or the DOPA dimer (100 mg) dissolved in, respectively, 100 m*l* or 200 m*l* of a M/30 phosphate buffer at pH 6.9 was stirred in the presence of atmospheric oxygen at 25°C. Both the DOPA and DOPA dimer solutions became faint orange after one hour and then gradually turned dark over an 8-hr period. The relative rates of melanogenesis, based on the absorbancy of the solution (C=10^{-3} mol/*l*) at 550 nm (shoulder), were as follows: DOPA, 1.0 : 1.5 : 6.4 : 14.0, and the DOPA dimer, 1.0 : 1.9 : 6.6 : 13.4, after 1, 4, 8 and 16 hr respectively. Both the DOPA solution and the DOPA dimer solution produced melanin after 24 hr. Each solution was acidified, and black pigments were collected by centrifugation. The melanin thus produced was treated with concentrated hydrochloric acid at room temperature for 4 days, collected by centrifugation, washed with dilute hydrochloric acid, ethanol and finally acetone, and dried. DOPA melanin (yield, 100 mg). Found: C, 58.05; H, 3.14; N, 8.41%. DOPA dimer melanin (yield, 40 mg). Found: C, 55.00; H, 3.73; N, 7.23%.

(b) Enzymatic Melanogenesis. To a solution of DOPA (200 mg) or the DOPA dimer (200 mg) dissolved in, respectively, 100 m*l* or 500 m*l* of a M/30

phosphate buffer at pH 6.9, there was added mushroom tyrosinase (Nutritional Biochemicals Corp., 500 units/mg) (10 mg); a stream of air was then passed through for 24 hr at 35°C. The DOPA solution immediately turned red and then changed to purple within 10 min; black precipitates appeared soon after. The DOPA dimer solution changed gradually from brown to dark over an 8-hr period. After 24 hr each solution was treated as has been described above. DOPA melanin (yield, 150 mg). Found: C, 57.15; H, 3.03; N, 8.61.% DOPA dimer melanin (yield, 110 mg). Found: C, 55.16; H, 3.61; N, 7.71%.

BULLETIN OF THE CHEMICAL SOCIETY OF JAPAN VOL. 42 1754—1755 (1969)

Anionic Copolymerization of 2,3-Dimethylbutadiene and 1,1-Diphenylethylene with *n*-Butyllithium in Benzene

Heimei YUKI, Yoshio OKAMOTO and Katsutoshi SADAMOTO

Department of Chemistry, Faculty of Engineering Science, Osaka University, Toyonaka, Osaka

(Received September 19, 1968)

Anionic copolymerization of 2,3-dimethylbutadiene (M_1) and 1,1-diphenylethylene (M_2) by *n*-butyllithium (*n*-BuLi) in tetrahydrofuran (THF) has been studied by means of NMR spectroscopy,[1] in which the rates of consumptions of the two monomers were followed. The copolymerization proceeded alternately, when the initial molar ratio of the monomers, $[M_1]_0/[M_2]_0$, was less than unity. In the present study, the copolymerization of the same monomer pair is investigated in benzene at 40°C with *n*-BuLi as an initiator.

Experimental

Meterials. 2,3-Dimethylbutadiene was synthesized by the dehydration of pinacol.[2] The monomer purified by fractional distillation was redistilled *in vacuo* from lithium aluminum hydride. Bp 69°C/760 mmHg, n_D^{20} 1.4360.

1,1-Diphenylethylene prepared from diphenylmethyl carbinol[3] was first treated with a small amount of Na-K alloy and distilled. Bp 115°C/3 mmHg, n_D^{20} 1.6085. Then *n*-BuLi was added to the monomer until the red color of its anion appeared. The monomer was redistilled from the colored mixture *in vacuo*.

Benzene purified by the usual method was redistilled in the presence of a small amount of *n*-BuLi under high vacuum before use.

n-BuLi was prepared in *n*-heptane according to the method of Ziegler.[4]

Polymerization. Copolymerization was carried out in a glass ampoule which had been previously heated with a gas burner *in vacuo*. Benzene and 2,3-dimethylbutadiene were transferred to the ampoule on a vacuum line, and then 1,1-diphenylethylene and *n*-BuLi were added with hypodermic syringes under dry nitrogen. The copolymerization was terminated by adding methanol. The polymer precipitated in methanol was filtrated, washed with methanol, and dried.

Viscosity. The viscosity of the copolymer was measured in toluene solution at 30.0°C.

Results and Discussion

The copolymerization of 2,3-dimethylbutadiene (M_1) and 1,1-diphenylethylene (M_2) by *n*-BuLi was followed in benzene at 40°C, the initial molar ratio of M_1 to M_2 being 0.683. The results are shown in Fig. 1. The copolymerization proceeded slowly to reach a constant polymer yield in about 50hr. In this period 2,3-dimethylbutadiene was completely consumed and only unchanged 1,1-diphenylethylene remained in the system. The softening point of the copolymer was about 135°C.

In Fig. 2 the plot of $\log[\eta]$ *vs.* log yield of polymer is shown. The linear relationship suggests that the

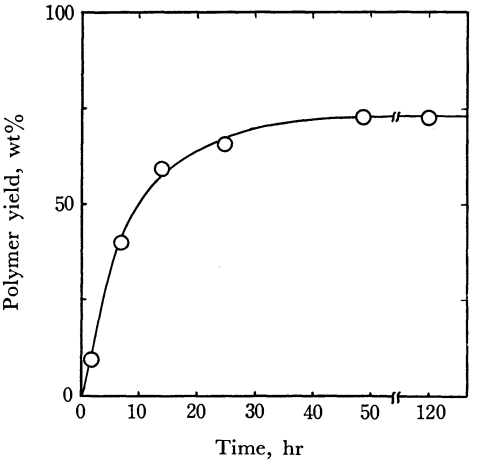

Fig. 1. Anionic copolymerization of 2,3-dimethylbutadiene (M_1) and 1,1-diphenylethylene (M_2) in benzene by *n*-BuLi.——Time *vs.* polymer yield. Total monomer: 9.89 mmol, $[M_1]_0/[M_2]_0$: 0.683, benzene: 15.0 ml, *n*-BuLi: 0.090 mmol, temp.: 40°C

1) H. Yuki, K. Hatada and T. Inoue, *J. Polymer Sci. A-1*, **6**, 3333 (1968).

2) C. F. H. Allen and A. Bell, "Organic Syntheses," Coll. Vol. III, p. 312 (1955).

3) C. F. H. Allen and S. Converse, *ibid.*, Coll. Vol. I, p. 226 (1956).

4) K. Ziegler and A. Colonius, *Ann.*, **479**, 135 (1930).

TABLE 1. ANIONIC COPOLYMERIZATION OF 2,3-DIMETHYLBUTADIENE (M_1) AND 1,1-DIPHENYLETHYLENE (M_2) IN BENZENE BY *n*-BuLi

Benzene: 15.0 ml, *n*-BuLi: *ca.* 1 mol% against total monomers, temp., 40°C, time: 96—140 hr.

M_1 g	M_2 g	$[M_1]_0/[M_2]_0$ mol/mol	Polymer g	Yield mol%	Unchanged M_2, g	$[m_1]/[m_2]$[a] mol/mol	r_1
0.405	0.873	1.017	1.150	92.7	0.127	1.19	0.25
0.335	0.776	0.960	0.978	91.8	0.210	1.14	0.21
0.405	0.960	0.925	1.081	90.0	0.284	1.18	0.27
0.405	0.976	0.910	1.099	89.3	0.189	1.14	0.22
0.405	1.057	0.840	1.190	85.8	0.265	1.14	0.23
0.269	0.848	0.694	0.810	76.1	0.178	1.09	0.18

a) Molar ratio of monomers in the copolymer. Average 0.23

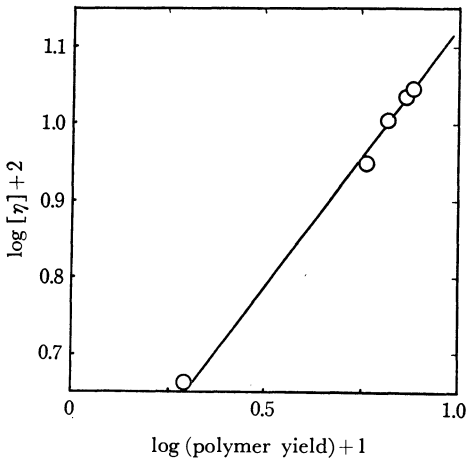

Fig. 2. Anionic copolymerization of 2,3-dimethylbutadiene (M_1) and 1,1-diphenylethylene (M_2) in benzene by *n*-BuLi.——Relationship between polymer yield and viscosity of polymer.

copolymerization proceeded without a termination and a chain transfer, probably to give a living polymer.

The copolymerization was carried out for a prolonged time and the material balance was checked in order to confirm the complete consumption of the M_1 monomer. The results are listed in Table 1. It was found that the total amount of the monomers charged, M_1+M_2 (g), was substantially equal to the sum of the polymer obtained and the unchanged M_2 monomer recovered from the mother liquor of the polymer precipitation. This fact means that 2,3-dimethylbutadiene was completely incorporated into the copolymer. The molar ratio of the monomers in the copolymer, $[m_1]/[m_2]$, can then be calculated from the polymer yield. The $[m_1]/[m_2]$ ratio decreased with a decrease in the ratio of the charged monomers, $[M_1]_0/[M_2]_0$.

The monomer reactivity ratio, r_1, is obtained by means of the integrated copolymer composition equation, assuming that the M_2 monomer does not homopolymerize and the M_1 monomer has been completely consumed.[5] The r_1 values are shown in Table 1. As a mean value, 0.23 was obtained. This indicated that 1,1-diphenylethylene is more reactive to 2, 3-dimethylbutadienyl anion than 2,3-dimethylbutadiene. In the copolymerization in THF, the r_1 value was almost zero and an alternating copolymer was obtained, when the $[M_1]_0/[M_2]_0$ ratio was less than unity.

In the copolymerizations of styrene and butadiene,[6] styrene and isoprene,[7] and 1,1-diphenylethylene (M_2) and isoprene (M_1)[8] by lithium catalysts, greater relative reactivities of conjugated dienes than the comonomers have been found in a nonpolar solvent, contrary to the less reactivities in a polar solvent. In the last pair of monomers, the r_1 values were 0.13 in THF and 37 in benzene. The relative reactivities of the two monomers against isoprene anion reversed in these two solvents. In the copolymerization of 2,3-dimethylbutadiene and 1, 1-diphenylethylene, the latter was always more reactive in both THF and benzene.

5) H. Yuki, J. Hotta, Y. Okamoto and S. Murahashi, This Bulletin, **40**, 2659 (1967).
6) I. Kuntz, *J. Polymer Sci.*, **54**, 569 (1961).
7) A. V. Tobolsky and C. E. Rogers, *ibid.*, **38**, 205 (1959).
8) H. Yuki and Y. Okamoto, This Bulletin, **42**, 1644 (1969).

BULLETIN OF THE CHEMICAL SOCIETY OF JAPAN VOL. 42 1756—1757 (1969)

The Schotten-Baumann Reaction of Dimethylaminobenzyl Alcohols[1)]

Makoto TSUCHIYA,*[1] Hiroshi YOSHIDA, Tsuyoshi OGATA and Saburo INOKAWA

Department of Synthetic Chemistry, Faculty of Engineering, Shizuoka University, Johoku, Hamamatsu

(Received September 28, 1968)

As an extension of our previous work on the benzoylation of aliphatic *t*-aminoalcohols, we have carried out the benzoylation of such aromatic *t*-aminoalcohols as *ortho*-〔1〕, *meta*-〔2〕, and *para*-dimethylaminobenzyl alcohol 〔3〕. When the reaction mechanism proposed in a previous paper[2)] is applied to dimethylaminobenzyl alcohols, it should be written as follows:

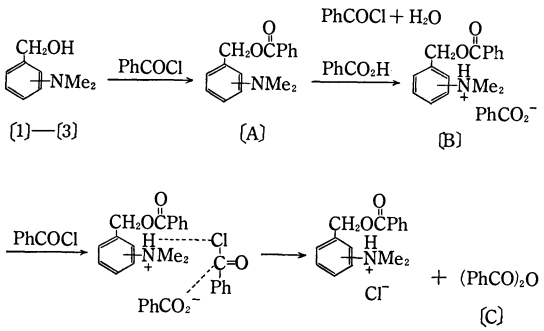

The *t*-aminoalcohols and the *t*-amines used in this experiment are as follows: *o*-dimethylaminobenzyl alcohol 〔1〕, *m*-dimethylaminobenzyl alcohol 〔2〕, *p*-dimethylaminobenzyl alcohol 〔3〕, 2-dimethylaminocyclohexylmethanol 〔4〕, *N,N*-dimethylaniline 〔5〕, *N,N*-dimethyl-*o*-toluidine 〔6〕, *N,N*-dimethyl-*p*-toluidine 〔7〕, *N,N*-dimethyl-*o*-cumidine 〔8〕, and *N,N*-dimethyl-*p*-cumidine 〔9〕.

Results and Discussion

The Schotten-Baumann reactions of 〔1〕—〔3〕 were carried out under the same conditions as those described in a previous paper[2)] and also under other conditions using different amounts of sodium hydroxide (0.35 mol)*[2]. The results are summarized in Table 1. The yields of 〔A〕 from 〔1〕—〔3〕 were almost all the same, but the yields of 〔C〕 increased in the order of 〔1〕, 〔2〕, and 〔3〕. According to previous works,[2,3)] the yield of 〔C〕 seems to depend mainly on the basicity of 〔A〕 because of the facility of the formation of 〔B〕. In the cases of 〔1〕—〔3〕, however, the observed pK_a-values of 〔A〕[4)] decreased slightly in the order of 〔1〕, 〔2〕, and 〔3〕, as is shown in Table 1. Therefore, the yields of 〔C〕 can not simply be correlated with the basicity.

TABLE 1. BENZOYLATION OF AMINOALCOHOLS

Method	Aminoalcohol	〔A〕 (g)	Yield[a)] (%)	〔C〕 (g)	pK_a of 〔A〕
I	*o*-〔1〕	11.6	(91)	0	
	m-〔2〕	11.8	(93)	2.3	
	p-〔3〕	11.2	(88)	4.2	
II	*o*-〔1〕	11.3	(89)	7.6	2.6
	m-〔2〕	11.2	(88)	10.5	2.5
	p-〔3〕	11.4	(90)	12.1	2.4
	〔4〕	12.2	(94)	18.8	7.4

Method I : aminoalcohols 0.05 mol, benzoyl chloride 0.25 mol, sodium hydroxide 0.525 mol 10% aqueous solution.

Method II : aminoalcohol and benzoyl chloride: the same as the above, sodium hydroxide: 0.35 mol 10% aqueous solution.

a) Yield shows a crude one.

*1 Present address: Hoya Glass Works, Ltd., Akishima, Tokyo.

1) Partly presented at the 20th Annual Meeting of the Chemical Society of Japan, Tokyo, April, 1967.

2) T. Ogata, T. Asano, H. Yoshida, and S. Inokawa, This Bulletin, **40**, 997 (1967).

3) K. Oshiro, T. Ogata, H. Yoshida and S. Inokawa, *Nippon Kagaku Zasshi (J. Chem. Soc. Japan, Pure Chem. Sect.)*, **89**, 211 (1968).

*2 In the reaction of benzoyl chloride with different amounts of a 10% aqueous sodium hydroxide solution in the presence of 〔5〕, the yield of 〔C〕 increased as the amount of sodium hydroxide decreased, reaching a maximum at the concentration of an equimolar amount of the benzoyl chloride used.

4) S. Nakamura, *Yuki Gosei Kagaku Kyokaishi (J. Synth. Org. Chem., Japan)*, **24**, 923 (1966).

Table 2. Relation between yield of [C] and twist-angle

Dimethylaniline	λ_{max} (mμ)	ε_{max}	φ°C	[C] g[b]
[5]	250	14700	0	16.3
2-Me [6]	249	6160	50	12.0
4-Me [7]	252	14300	10	18.3
2-*i*-Pr [8]	248	4180	58	7.3
4-*i*-Pr [9]	252	14300	10	17.0
2-CH_2OCOPh [1A]	248	5960	51	7.6
3-CH_2OCOPh [2A]	255	13200	19	10.5
4-CH_2OCOPh [3A]	250[a]	14700[a]	0	12.1

a) There is no λ_{max} near 250 mμ. The value is one at 250 mμ.
b) amine 0.05 mol, benzoyl chloride 0.25 mol, sodium hydroxide 0.35 mol 10% aq. soln.

In order to obtain further knowledge on the yields of [C] in the case of weak bases, the aromatic *t*-amines of [5]—[9] were treated with benzoyl chloride under the same conditions (0.35 mol of 10% sodium hydroxide solution) as in the cases of [1]—[3]. The results are shown in Table 2. Though [6] and [8] are stronger bases[5] than [7] and [9] respectively, the *ortho* isomers, [6] and [8], gave smaller amounts of [C] than do the *para* isomers, [7] and [9], undoubtedly due to the steric hindrance in the former compounds. The degree to which the ester-group in [A] hinders the front of the nitrogen therein from the formation of [B] is possibly related to the twist-angle (φ)[6] between the *t*-amino group and the benzene ring. Just as is shown in Table 2, the yields of [C] are found to decrease as the φ values increase. This consideration was also supported by the fact that the titration curve of benzoic acid in the presence of [A] with sodium hydroxide coincided more closely with the blank titration curve without [A] in the order of [3], [2], and [1].

Finally, though there may be little difference in steric hindrance between [1] and [4], the yield of [C] from [4] was found to be more than twice that from [3].

In conclusion, the yield of [C] depends mainly on the basicity of [B], but in the case of weak bases of a similar basicity, steric hindrance has a great effect on the yield of [C].

Experimental

o-Dimethylaminobenzyl Alcohol [1]. [1] was prepared by the method of Willstätter.[7]

m-Dimethylaminobenzyl Alcohol [2]. *m*-Dimethylaminobenzaldehyde[8] was reduced with lithium aluminum hydride. Bp 127—130°C/3 mmHg, n_D^{12} 1.5710, Found: N, 9.11%. Calcd for $C_9H_{13}NO$: N, 9.27%.

p-Dimethylaminobenzyl Alcohol [3]. [3] was prepared by the method of Hass and Bender.[9]

2-Dimethylaminocyclohexylmethanol [4]. [1] was reduced in the presence of Adams platinum oxide catalyst[10] under atmospheric pressure in an ethanol solution. Bp 125—127°C/17 mmHg, n_D^{17} 1.4990, Found: N, 8.50%. Calcd for $C_9H_{19}NO$: N, 8.92%.

***N,N*-Dimethyl-*o*-toluidine [6] and *N,N*-Dimethyl-*p*-toluidine [7].** [6] and [7] were prepared by the method of Hunig.[11]

***N,N*-Dimethyl-*o*-cumidine [8] and *N,N*-dimethyl-*p*-cumidine [9].** [8] and [9] were prepared by the nitration of cumene,[12] the reduction of the *o*- and *p*-nitrocumenes thus obtained[13] and the methylation of the *o*- and *p*-aminocumenes.[11]

[9]: bp 123—125°C/21 mmHg, n_D^{20} 1.5255, Found: N, 8.37%. Calcd for $C_{11}H_{18}N$: N, 8.54%.

The Schotten-Baumann Reaction. The general procedure was carried out as has been described in a previous paper,[2] and [A] and [C] were separated from the reaction mixtures by an extraction method using ether. The characteristics of [A] are summarized in Table 3.

Table 3. Characters of esters [A]

Ester	Bp °C/mmHg	n_D (°C)	Analysis, N% Found	Calcd
[1A]	176—177/3	1.5700 (22.5)	5.45	5.49
[2A]	196—197/3	1.5852 (20)	5.44	5.49
[3A]	86— 87[a]	—	5.81	5.49
[4A]	155—157/2	1.5401 (15)	5.37	5.36

a) melting point

Reaction of Tertiary Amines [5]—[9] with Benzoyl Chloride. Benzoyl chloride (0.25 mol) was added to the *t*-amine in a 10% aqueous sodium hydroxide (0.35 mol) solution under the same conditions as in the above-mentioned Schotten-Baumann reaction.

The Measurement of the Twist-angle (φ) between the Planes of the Benzene Ring and the *t*-Amino Group. φ was calculated[6] from ε_{max} near 250 mμ (K-band) in the UV spectrum in isooctane.

Measurement of pK_a. The pk_a values of the amines were measured in methanol by the back-titration method described in a preceeding paper.[3]

This work was partly supported by a grant of the Ministry of Education, to which the authors' thanks are due.

5) H. C. Brown and A. Kahn, *J. Am. Chem. Soc.*, **72**, 2939 (1950).
6) B. M. Wepster "Progress in Stereochemistry," Vol. II, ed. by W. Klyne and P. B. D. de la Mare, Butterworths Scientific Publications, London (1958), Chapter 4.
7) R. Willstätter and W. Kahn, *Ber.*, **37**, 401 (1904).
8) W. Cocker, J. O. Harris and J. V. Loach, *J. Chem. Soc.*, **1938**, 751.
9) H. B. Hass and M. L. Bender, *J. Am. Chem. Soc.*, **71**, 1767 (1949).
10) G. S. Hiers and R. Adams, *Ber.*, **59**, 162 (1926).
11) S. Hunig, *Chem. Ber.*, **85**, 1059 (1952).
12) C. Hansch and G. Helmkamp, *J. Am. Chem. Soc.*, **73**, 3080 (1951).
13) M. Osowiecki, C. Tamm and T. Reichstein, *Helv. Chim. Acta*, **41**, 1606 (1958).

BULLETIN OF THE CHEMICAL SOCIETY OF JAPAN VOL. 42 1758—1759 (1969)

A Simple Treatment for the Kinetics of Radical Polymerization with Primary Radical Termination

Katsukiyo Ito and Tatsuo Matsuda

Government Industrial Research Institute, Nagoya, Kita-ku, Nagoya

(Received October 2, 1968)

Several workers have reported on the importance of primary radical termination.[1-6] Bamford, Jenkins and Johnston[7] devised a simple treatment for the kinetics of radical polymerization with primary radical termination in the following.

$$C \rightarrow 2R\cdot \qquad k_d \qquad (1a)$$

$$R\cdot + M \rightarrow X_1\cdot \qquad k_i \qquad (1b)$$

$$X_r\cdot + M \rightarrow X_{r+1}\cdot \qquad k_p \qquad (1c)$$

$$X_r\cdot + X_s\cdot \rightarrow P_r + P_s \text{ or } P_{r+s} \qquad k_t \qquad (1d)$$

$$X_r\cdot + R\cdot \rightarrow P_r \qquad k_{ti} \qquad (1e)$$

$$2R\cdot \rightarrow \text{Products} \qquad k_{tii} \qquad (1f)$$

Decomposition of the initiator C gives primary radicals R· which react with monomer M to form chain radicals X·. $X_r\cdot$ and P_r respectively denote radicals and polymer molecules containing r monomer units. In this treatment for the kinetics of radical polymerization with primary radical termination, they derived the cubic Eq. (2)

$$\frac{x^2(1+x)}{(1-x)} = \frac{2fk_dk_{ti}^2[C]}{k_sk_i^2[M]^2} = a^2 (a \geq 0), \qquad (2)$$

where

$$x = \frac{k_{ti}[X\cdot]}{k_i[M]} ([X\cdot] = \Sigma[X_r\cdot])$$

and f is initiator efficiency. Because of Eq. (2) being inconvenient for calculating the polymerization rate R_p for given values $2fk_d[C]$, the reverse procedure of calculating $2fk_d[C]$ for R_p was mainly used for simple treatment. According to this treatment, polymerizations for styrene and acrylonitrile were analyzed. On the modification of this treatment for very low monomer concentrations, Baldwin[8] analyzed radical polymerization with primary radical termination for methyl methacrylate. But this treatment is very sensitive to experimental errors at very low monomer concentrations. Furthermore, Baldwin's treatment and Bamford, Jenkins and Johnston's treatment are more complex than our treatment in the following.

In this paper, the treatment for the kinetics o radical polymerization with primary radical termination given by Bamford, Jenkins and Johnston was simplified. Using Baldwin's results,[6] Bamford, Jenkins and Johnston's results[7] and Mayo, Gregg and Matheson's results,[9] this simplified treatment was confirmed.

A Simplification for the Kinetics of Radical Polymerization with Primary Radical Termination. From Eq. (2), we obtain

$$a = x\left(\frac{1+x}{1-x}\right)^{1/2} \geq x$$

Accordingly, by the two approximations

$$\frac{1}{1-x} \cong 1 + x$$

and

$$(1 + 4a)^{1/2} \cong 1 + 2a - 2a^2$$

under the condition $x \leq a \ll 1$, Eq. (2) becomes

$$x(1+x) = a \qquad (3)$$

The solution of Eq. (3) is

$$x = \frac{1}{2}[(1+4a)^{1/2} - 1] \cong a - a^2 \qquad (4)$$

Under a condition $a \ll 1$, [X·] is given by

$$[X\cdot] = \left(\frac{2fk_d}{k_t}\right)^{1/2}[C]^{1/2}\left[1 - \frac{k_{ti}}{k_i}\left(\frac{2fk_d}{k_t}\right)^{1/2}\frac{[C]^{1/2}}{[M]}\right] \qquad (5)$$

Using Eq. (5), R_p is given by

$$R_p = k_i[R\cdot][M] + k_p[X\cdot][M] \cong k_p[X\cdot][M] = A[M][C]^{1/2}\left(1 - B\frac{[C]^{1/2}}{[M]}\right) \qquad (6)$$

where

$$A = k_p\left(\frac{2fk_d}{k_t}\right)^{1/2} \quad \text{and} \quad B = \frac{k_{ti}}{k_i}\left(\frac{2fk_d}{k_t}\right)^{1/2}$$

1) A. Chapiro, M. Magat, J. Sebban and P. Whal, *Ric. Sci.*, **25A**, 73 (1955).

2) G. Henrici-Olive and S. Olivé, *Makromol. Chem.*, **37**, 71 (1960).

3) J. C. Bevington and J. K. Allen, *Trans. Faraday Soc.*, **56**, 1762 (1960).

4) P. Hyden and H. Melville, *J. Polymer Sci.*, **43**, 201 (1960).

5) P. E. M. Allen and C. R. Patrick, *Makromol. Chem.*, **48**, 89 (1961).

6) G. M. Brunett and L. D. Loan, *Trans. Faraday Soc.*, **51**, 219 (1955).

7) C. H. Bamford, A. D. Jenkins and R. Johnston, *Trans. Faraday Soc.*, **55**, 1451 (1959).

8) M. G. Baldwin, *J. Polymer Sci.*, **A1**, 3209 (1963).

9) F. R. Mayo, R. A. Gregg and M. S. Matheson, *J. Am. Chem. Soc.*, **73**, 1691 (1951).

Eq. (6) yield a convenient linear relationship

$$\frac{R_p}{[M][C]^{1/2}} = A - AB\frac{[C]^{1/2}}{[M]} \quad (7)$$

Eq. (7) indicates that $R_p/[M][C]^{1/2}$ is constant at the low value of $[C]^{1/2}/[M]$ (a familiar relationship) and the increase of $[C]^{1/2}/[M]$ increases deviation from this familiar relationship. This conclusion is equivalent to Bamford, Jenkins and Johnston's conclusion.[7] Furthermore, using A and B in Eq. (7), $k_{ti}/k_t k_p$ is directly calculated without the knowledge of the value fk_d or k_t/k_p^2 by Eq. (8)

$$\frac{B}{A} = \frac{k_{ti}}{k_i k_p} \quad (8)$$

Applications

On the application of Eq. (7) to Baldwin's results[8] in the polymerization of methyl methacrylate (MMA) initiated by 2,2'-azobisisobutyronitrile (AIBN), a linear relationship between $R_p/[M][C]^{1/2}$ and $[C]^{1/2}/[M]$ comes into existence in the range 0 to 0.3 $(l/mol)^{1/2}$ (Fig. 1). Using A and B in this linear relationship and Eq. (8), $k_{ti}/k_i k_p$ is

$$\frac{k_{ti}}{k_i k_p} = 3.09\times10^3 \text{ mol}\cdot\text{sec}/l$$

On the application of Eq. (7) to Bamford,

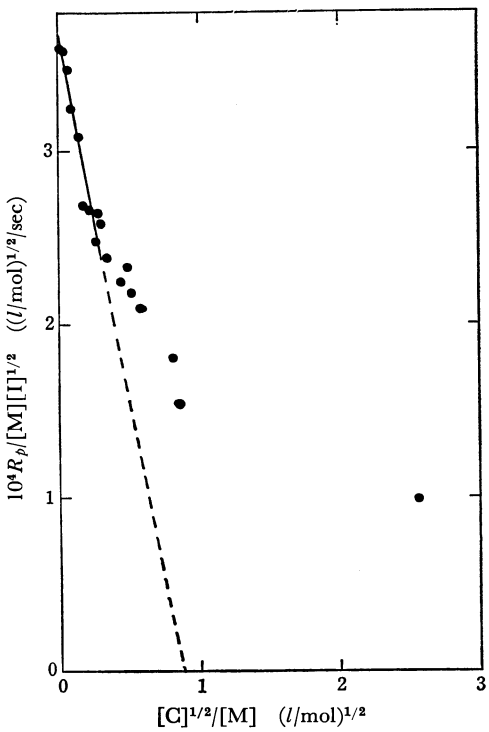

Fig. 1. Relationship between $R_p/[M][C]^{1/2}$ and $[C]^{1/2}/[M]$ for radical polymerization of MMA initiated by AIBN at 60°C.[8]

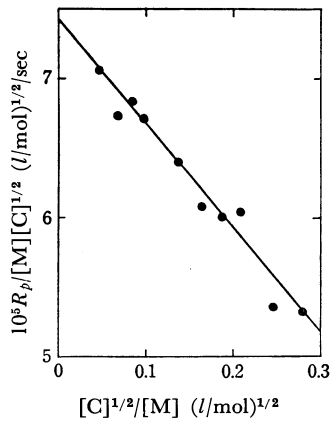

Fig. 2. Relationship between $R_p/[M][C]^{1/2}$ and $[C]^{1/2}/[M]$ for radical polymerization of styrene initiated by AIBN at 60°C.[7]

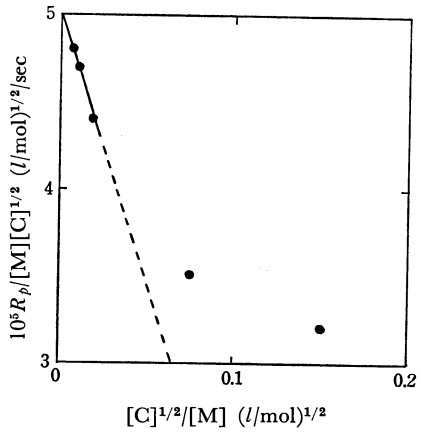

Fig. 3. Relationship between $R_p/[M][C]^{1/2}$ and $[C]^{1/2}/[M]$ for radical polymerization of styrene initiated by BPO at 60°C.[9]

Jenkins and Jonston's results[7] in the polymerization of styrene initiated by AIBN, a linear relationship between $R_p/[M][C]^{1/2}$ and $[C]^{1/2}/[M]$ comes into existence in the all experimental range (Fig. 2). $k_{ti}/k_i k_p$ for this polymerization system is

$$\frac{k_{ti}}{k_i k_p} = 1.36\times10^4 \text{ mol}\cdot\text{sec}/l$$

On the application of Eq. (7) to Mayo, Gregg and Matheson's results[9] in the polymerization of styrene initiated by benzoyl peroxide (BPO), a linear relationship between $R_p/[M][C]^{1/2}$ and $[C]^{1/2}/[M]$ comes into existence in the range 0 to 0.02 $(l/mol)^{1/2}$ (Fig. 3). $k_{ti}/k_i k_p$ for this polymerization system is

$$\frac{k_{ti}}{k_i k_p} = 1.23\times10^5 \text{ mol}\cdot\text{sec}/l$$

In conclusion, these applications indicate that a simple treatment based on Eq. (7) is very useful for discussion or calculation of $k_{ti}/k_i k_p$ for the kinetics of radical polymerization with primary radical termination.

BULLETIN OF THE CHEMICAL SOCIETY OF JAPAN VOL. 42 1760—1761 (1969)

The Mössbauer Spectrum of Iron Adsorbed on an Anion Exchange Resin

Yoshimasa TAKASHIMA, Yonezo MAEDA and Shunji UMEMOTO

Department of Chemistry, Faculty of Science, Kyushu University, Fukuoka

(Received October 2, 1968)

It is well known that iron(III) is strongly taken up on an anion exchange resin from relatively concentrated hydrochloric acid solutions. This fact can be interpreted on the basis of the results of chemical analysis, as indicating formation of negatively-charged complex ions, $FeCl_4^-$. Because of the opacity of resins, most spectroscopic techniques are not applicable to the direct investigation of chemical species sorbed on ion exchange resins. However, Mössbauer spectroscopy can be applied to such a study because penetrating γ rays are used in this technique. Several studies along this line have already been reported,[2,3] and interesting results have been obtained concerning the nature of individual species sorbed on ion exchangers.

The present paper is concerned with Mössbauer spectroscopic study of iron(III) sorbed on an anion exchange resin; the study was undertaken in order to confirm the symmetry and coordination of ligands surrounding the iron atom.

Experimental

Materials. The resin sample was prepared by passing a solution containing 27 g of $FeCl_3 \cdot 6H_2O$ in 100 m*l* of 7M hydrochloric acid through a column of Dowex 1-X4 (100—200 mesh); the excess solution was removed by washing the sample with 7M hydrochloric acid. Two types of samples, wet and dry, were used for the measurements. The dry sample was prepared by drying the resin obtained above in a vacuum dessiccator.

The selected reference samples, $KFeCl_4$, NH_4FeCl_4, *etc.*, were prepared according to the procedure used by Friedman and Taube.[4]

Mössbauer Spectrometer.[5] A multichannel pulse-height analyser coupled with an instantaneous velocity measurement of the γ ray source was used. The source of radiation was ^{57}Co diffused onto metallic copper. The spectrometer was calibrated by sodium nitroprusside, and the isomer shift was expressed in mm/sec relative to the center of the nitroprusside spectrum. The measurements were performed both at room temperature and at the temperature of liquid nitrogen.

Results and Discussion

No discernible Mössbauer effect was observed for the resin samples at room temperature, but one was observed at the temperature of liquid nitrogen. Unlike the resin samples, all the reference samples showed a measurable effect, even at room temperature. All of the spectra obtained showed a fairly sharp single absorption, which is responsible for the symmetrical charge distribution around the iron atom. Table 1 summarizes the results obtained by the Mössbauer measurements of the resins and the other reference samples. The errors involved in Table 1 showing the estimation of the isomer shifts were about ± 0.02 mm/sec; the variation in the isomer shift, depending on the temperature, was estimated to be small (probably less than 0.05 mm/sec).

TABLE 1. ISOMER SHIFT

Sample	Temperature	Isomer shift* (mm/sec)	Coordination
Wet resins	liq.-N_2 temp.	0.57	
Dry resins	liq.-N_2 temp.	0.54	
$KFeCl_4$	liq.-N_2 temp.	0.54	tetrahedral, $4Cl^-$
$KFeCl_4$	room temp.	0.54	tetrahedral, $4Cl^-$
NH_4FeCl_4	room temp.	0.50	tetrahedral, $4Cl^-$
$FeCl_3$	liq.-N_2 temp.	0.73	octahedral, $6Cl^-$
$FeCl_3$	room temp.	0.70	octahedral, $6Cl^-$
$FeCl_3 \cdot 6H_2O$	room temp.	1.12 0.12	octahedral

* Relative to the center of sodium nitroprusside.

Between the values of the isomer shift for typical tetrahedral and octahedral compounds, a remarkable difference was found. Since the isomer shift reflects the degree of covalency, we may conclude from this observation that the tetrahedral compounds have more covalent bonds than the octahedral compounds.

The strong similarities between the isomer shift of the resin samples and that of the tetrahedral

1) G. E. Moore and K. A. Kraus, *J. Am. Chem. Soc.*, **72**, 5792 (1950).

2) S. Y. Wang, A. H. Lu and P. G. Tseng, *Chinese J. Phys.*, **2**, 50 (1964).

3) J. L. Mackey and R. L. Collins, *J. Inorg. Nucl. Chem.*, **29**, 655 (1967).

4) H. L. Friedman and H. Taube, *J. Am. Chem. Soc.*, **72**, 2236 (1950).

5) Y. Takashima and S. Ohashi, Presented at the 20th Annual Meeting of the Chemical Society of Japan, Tokyo, March, 1967; Abstract II, p. 212.

compounds suggest that the iron sorbed on the anion exchange resin is in a tetrahedral environment.

It is also noticed that there is very little difference in the isomer shift between wet and dry resin samples.

This indicates that the water molecules play only a minor role in the coordination sphere of the iron sorbed on the resins.

It may be reasoned from the data on $FeCl_3$ and $FeCl_3 \cdot 6H_2O$ that the isomer shift distinctly increases as chloride ligands bound to central iron(III) ion are replaced by the less polarizable water ligands. In view of the above results, it may be concluded that the iron(III) sorbed on an anion exchanger under these experimental conditions in the undistorted tetrahedral coordination sphere which arises from chloride ligands. There are two peaks in the absorption of $FeCl_3 \cdot 6H_2O$. However, we do not yet know their exact origins.[6]

6) W. Kerler, *Z. Physik*, **167**, 194 (1962); H. Bernas and M. Langevin, *J. Phys.*, **24**, 1034 (1963).

BULLETIN OF THE CHEMICAL SOCIETY OF JAPAN VOL. 42 1761—1762 (1969)

Synthetic Reactions of Aliphatic Nitro-Compounds. III. The Synthesis and Configurational Analysis of 2-Hydroxymethyl-2-aminocyclohexanediol

Shonosuke ZEN and Akiko NISHIKAI (née YASUDA)

Kitasato University, College of Pharmaceutical Sciences, Shirokane, Minato-ku, Tokyo

(Received October 8, 1968)

In a previous communication,[1] the synthesis of a cyclic amino acid, 1-amino-2,6-dihydroxycyclohexane-1-carboxylic acid (**1**), by the base-catalyzed cyclization of glutaraldehyde with ethyl nitroacetate was described. The structure of **1**, as determined by interpreting the NMR spectrum of its derivative, was designated as 2β-carboxyl-2α-aminocyclohexane-1β,3β-diol.

In order to obtain further evidence to support the above configuration, we have now synthesized the tetraacetyl derivative (**4**), mp 149—150.5°C, of 2-hydroxymethyl-2-aminocyclohexanediol-1,3 (**3**), mp 150.5—151.5°C. We prepared in the steps shown in Chart 1, and then established its configuration by means of NMR spectroscopy. The NMR spectrum*2 of **4** shown in Fig. 1, shows three sharp singlets (3 : 6 : 3 in relative intensity) resulting from one equatorial acetamido group[2] (τ 8.06), one axial acetoxy group (τ 7.92) of a acetoxymethyl*1 at the C-2 position, and two equatorial acetoxy groups[2] (τ 7.96), suggesting that these two *O*-acetyl groups have the same orientation, a *cis*-configuration. The two axial ring protons on C-1 and C-3 appear as a broad signal at about τ 4.36, while the methylene protons on C-2 appear as a singlet at τ 5.36. The proton on nitrogen in the amide group shows its signal at 4.19 τ.

As a result of the consideration of the NMR spectrum of **4**, it can be concluded that the structure of **1** takes the same configuration as that described in our previous studies.

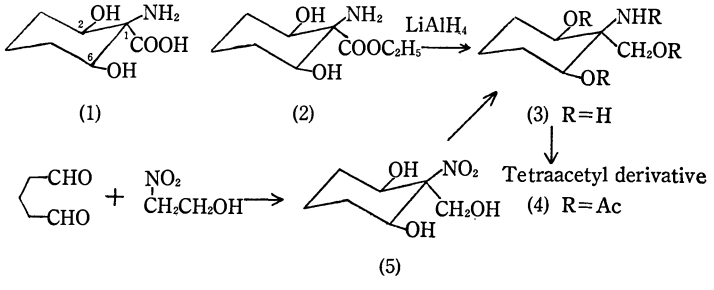

Chart. 1

1) S. Zen, Y. Takeda, A. Yasuda and S. Umezawa, This Bulletin, **40**, 431 (1967).

2) F. W. Lichtenthaler and P. Emig, *Tetrahedron Letters*, **1967**, 557.

*1 This group corresponds to the carboxyl group of **1**.

*2 These data agree well with those of F. W. Lichtenthaler (private communication).

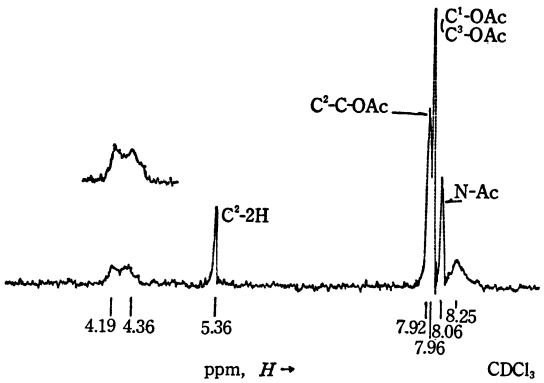

Fig. 1. NMR spectrum of tetraacetyl derivative (**4**).

Furthermore, we obtained the identical compounds, (**3** and **4**), through different steps; *i. e.*, we prepared then from 2-hydroxymethyl-2-nitrocyclo hexane-1,3-diol (**5**), mp 167—169°C, which had itself been synthesized by a cyclization of glutaraldehyde with nitroethanol under non-aqueous conditions. This fact leads to the conclusion that this cyclization proceeds in fashion analogous to Lichtenthaler's nitromethane-dialdehyde cyclization, in which the corresponding product has the *trans*-configuration.[3-5]

Experimental

2 - Hydroxymethyl - 2 - aminocyclohexanediol-1,3 (3).—Procedure-A *Prepared from 2-Ethoxycarbonyl-2-aminocyclohexanediol-1,3* (***2***). To a mixture of lithium aluminium hydride (333 mg) and dioxane (60 m*l*), 600 mg of **2**[1] was added; then the mixture was heated for 9 hr with occasional shaking under reflux, guarded by a tube containing calcium chloride, and subsequently allowed to stand overnight. Then 30 m*l* of water was added slowly, and the mixture was stirred for one hour. The precipitate thus formed was collected by filtration, and the filtrate was concentrated to dryness *in vacuo*. A yellow solid, 384 mg, was obtained in a yield of about 80%; it was crystallized from ethanol to give colorless needles, mp 150.5—151.5°C: ν(KBr), 3500, 3220 (OH) 1540 (NH), 1093 and 1050 cm^{-1} (OH). Found: C, 52.19; H, 9.35; N, 8.49%. Calcd. for $C_7H_{15}O_3N$: C, 52.17; H, 9.31; N, 8.69%.

Procedure-B *Prepared by the Reduction of 2-Hydroxymethyl-2-nitrocyclohexanediol-1,3* (***5***). 500 mg of the nitro-alcohol (**5**) was hydrogenated for 1 hr with 3m*l* of the Raney Nickel T-1[6] catalyst in 30 m*l* of ethanol at about 40°C under 55 psi of hydrogen*[3]. The filtrate from the nickel was evaporated *in vacuo* to dryness to give the crude product, light green-yellow crystals (377 mg), mp 144—146°C in a 90% yield. The sample, consisting of colorless needles for analysis obtained from ethanol, had a mp of 150—151°C.

This product was found to be identical with the above sample prepared from **2** (by procedure A) by a mixed-melting-point determination and by a comparison of their infrared spectra.

Tetraacetyl Derivative (***4***) *of* ***3***. To a solution of 50mg of **3** (prepared by Procedure A), in acetic anhydride (5 m*l*), 5 m*l* of pyridine was added, and then the mixture was allowed to stand overnight at room temperature. After the mixture was then treated as usual, an amorphous powder was obtained in a yield of 96%; it was then recrystallized from ethyl acetate-ligroin as colorless needles (mp 149—150.5°C), ν(KBr): 1740 (CO), 1640, 1560, 1250 and 1225 cm^{-1}(amide). The NMR spectrum*[4] of this compound is shown in Fig. 1.

Found: C, 54.81; H, 7.11; N, 4.34%. Calcd for $C_{15}H_{23}O_7N$: C, 54.71; H, 6.99; N, 4.25%.

The tetraacetyl derivative obtained by "procedure B" was found to be the same product (**4**) by an examination of its mp, the results of its elementary analysis, and its IR and NMR spectra.

2 - Hydroxymethyl - 2 - nitrocyclohexanediol - 1,3 (5). Freshly-distilled glutaraldehyde (3.0 g) and equimolar nitroethanol[7] (2.73 g) were dissolved in 10 m*l* of methanol. 1.5 m*l* of 3 N potassium hydroxide in methanol was then added to the mixture, which was agitated continuously at room temperature. The reaction mixture was made alkaline (pH 8.0—8.2). After two hours, it was acidified to pH 4 using a sulfuric acid. The salt thus precipitated was separated by filtration and then the filtrate was evaporated to dryness under reduced pressure.

The crystalline residue was washed with ethyl acetate to yield 1.40 g of the crude product, mp 150—160°C. After recrystallization from acetone, the analytical sample, mp 167—169°C was obtained as colorless needles. ν(KBr): 3260 (OH), 1542, 1355 cm^{-1} (C–NO_2).

Found: C, 43.79; H, 7.17; N, 7.16%. Calcd for $C_7H_{13}O_5N$: C, 43.98; H, 6.85; N, 7.33%.

The authors are indebted to Dr. Hamao Umezawa, the head of Institute of Microbial Chemistry, for his kindness for the measurements of NMR spectra.

3) F. W. Lichtenthaler, *Angew. Chem.*, **76**, 84 (1964).
4) F. W. Lichtenthaler, *Chem. Ber.*, **96**, 845 (1963).
5) T. Suami and S. Ogawa, This Bulletin, **37**, 194 (1964).
6) X. A. Dominguez, I. C. Lopez and P. Franco, *J. Org. Chem.*, **26**, 1625 (1961).
*3 Parr low-pressure hydrogenator (Parr Instrument Co.).
*4 The NMR spectrum (in $CDCl_3$) was determined by means of a Varian A-60 spectrometer. Tetramethylsilane was used as the internal reference.
7) W. E. Noland, "Organic Syntheses," Vol. 41, p. 67 (1961).

BULLETIN OF THE CHEMICAL SOCIETY OF JAPAN VOL. 42 1763—1765 (1969)

Radiolysis of Methanol Containing Cyanogen Iodide

Hajime OGURA, Tsutomu MIYAGAWA and Masaharu KONDO

Department of Chemistry, Faculty of Science, Tokyo Metropolitan University, Setagaya-ku, Tokyo

(Received October 24, 1968)

The use of cyanogen iodide as a scavenger of some intermediates formed in the radiolysis of several organic solvents has been reported by Hughes *et al.*[1,2] The present paper, in addition to reporting on the formation of iodine, which has also been studied by previous investigators, reports on the effect of cyanogen iodide on the radiolytic yield of hydrogen and formaldehyde, which are known to be the main products from irradiated methanol. The reactivity of solvated electron towards cyanogen iodide has also been determined by using nitrous oxide as a competing solute.

Experimental

Methanol was purified according to the procedure proposed by Lichtin *et al.*[3] Cyanogen iodide was prepared by the method of Goy *et al.*[4] and sublimated in a vacuum several times before use. ^{60}Co γ-irradiation was carried out at a dose rate of 1.56×10^{18} eV·ml^{-1} hr^{-1}. A deaerated solution of 5 ml prepared by the conventional vacuum technique with freeze-and-thaw cycles was sealed in a cylindrical glass cell (20 ml). Nitous oxide was taken in a calibrated volume to a definite pressure and then transferred to the irradiation vessel by using liquid nitrogen. The concentration of the gas in the solution was calculated from the solubility data.[5] The iodine was determined spectrophotometrically at 450 mμ. The formaldehyde was determined by means of chromotropic acid; however, this method could not be applied to the solutions above 10 mM ICN because of the inhibition of iodine produced by the decomposition of ICN. The amounts of hydrogen and nitrogen were determined by gas chromatography using a molecular sieve 5A column and argon as the carrier gas.

Results

Figure 1 shows the yields of hydrogen and iodine as a function of the concentration of cyanogen iodide in deaerated methanol. The radiolytic yields of these products were obtained from the initial slopes of the product-dose plots and are expressed as G-values. $G(I_2)$ appears to increase with an increase in the concentration of cyanogen iodide, but it tends to reach a limiting value of 3.2 at 5 mM ICN. The value for $G(I_2)$ reported by Hughes was slightly higher than our result. The addition of cyanogen iodide decreases the $G(H_2)$ considerably. One can obtain 5.4 for $G(H_2)$ when the solute concentration is extrapolated to zero; this is the same value as the $G(H_2)$ value for pure methanol determined by several investigators.[6-8] The yield of formaldehyde is considerably

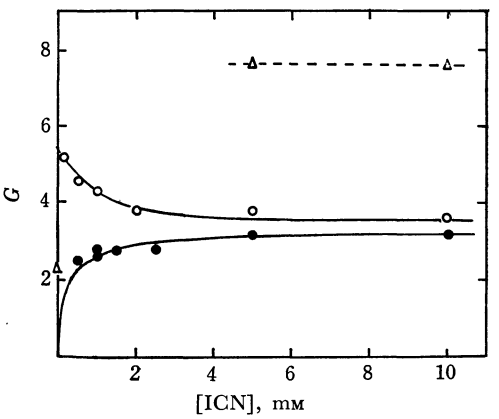

Fig. 1. The radiolytic yield as a function of ICN concentration in deaerated methanol.
●; $G(I_2)$, ○; $G(H_2)$, △; $G(CH_2O)$

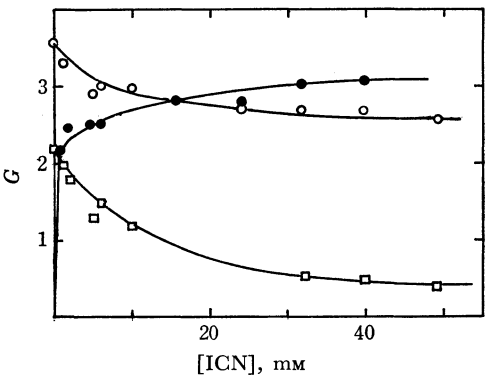

Fig. 2. The radiolytic yield as a function of ICN concentration in deaerated methanol containing 5 mM N_2O.
●, $G(I_2)$; ○, $G(H_2)$; □, $G(N_2)$

1) G. Hughes and W. M. Garisson, *J. Phys. Chem.*, **64**, 695 (1960).
2) G. Hughes, *ibid.*, **65**, 2160 (1961).
3) M. Imamura, S. U. Choi and N. N. Lichtin, *J. Am. Chem. Soc.*, **85**, 3565 (1963).
4) C. A. Goy, D. H. Shaw and H. O. Pritchard, *J. Phys. Chem.*, **69**, 1504 (1965).
5) Inetern. Critical Tables, **3**, 264 (1928).
6) G. Meshitsuka and M. Burton, *Red. Res.*, **8**, 285 (1958).
7) J. H. Baxendale and F. W. Mellows, *J. Am. Chem. Soc.*, **83**, 4720 (1961).
8) K. N. Jha and G. R. Freeman, *J. Chem. Phys.*, **48**, 5480 (1968).

increased by the addition of cyanogen iodide, even at a low concentration; over the concentration range investigated the yield is seen to be almost steady at about 7.6, a value which is very high compared with the value (2.3) for pure methanol.

The radiolytic yield curves for hydrogen, nitrogen, and iodine as a function of the cyanogen iodide concentration in deaerated methanol containing 5 mM N_2O are presented in Fig. 2.

A competition between cyanogen iodide and nitrous oxide for solvated electrons in methanol is obvious in Fig. 3.

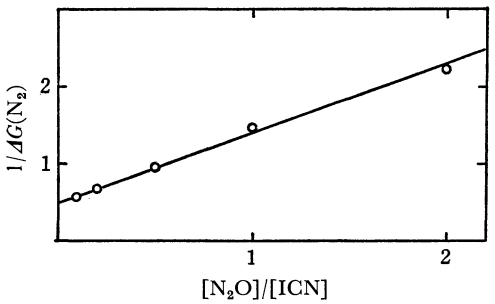

Fig. 3. $1/\Delta G(N_2)$ *vs.* $[N_2O]/[ICN]$ plotted according to Eq. (III).

Discussion

The chemical species initially produced during the absorption of ionizing radiation in methanol are usually represented as follows:

$$CH_3OH \rightsquigarrow e^-_{sol},\ H,\ CH_2OH,\ CH_3OH_2^+ \text{ and molecular products} \quad (0)$$

According to the well-established mechanism for hydrogen formation from methanol radiolysis, the following reactions are taken into consideration:

$$e^-_{sol} + CH_3OH_2^+ \rightarrow H_2 + CH_2OH \quad (1)$$

$$H + CH_3OH \rightarrow H_2 + CH_2OH \quad (2)$$

The solvated electron can react with cyanogen iodide as follows:

$$e^-_{sol} + ICN \rightarrow I + CN^- \quad (3)$$

Hughes *et al.*[1] have proposed the following reactions:

$$H + ICN \rightarrow I + HCN \quad (4)$$

$$CH_2OH + ICN \rightarrow I + HCHO + HCN \quad (5)$$

$$2I \rightarrow I_2 \quad (6)$$

The addition of cyanogen iodide decreases $G(H_2)$ effectively, as is shown in Fig. 1; this indicates that the precursor of hydrogen will react with the solute as in reactions (3) and (4). The observed increase in the yield of formaldehyde upon the addition of cyanogen iodide may be attributed to reaction (5). This reaction scheme, together with what is presented by Hughes *et al.*,[1] can afford the following meterial balance:

$$2G(I_2) = G_{e^-_{sol}} + G_H + G_{CH_2OH} = G(R) \quad (I)$$

where $G(R)$ denotes the total radical yield from methanol.*1 One can obtain 6.4 for $G(R)$ from the observed $G(I_2)$ value; this is in good agreement with the values reported by Baxendale[9] and by Lichtin.[10] As to the yield of formaldehyde, the following expression can be derived from our present reaction scheme:

$$G(CH_2O) = G_0(CH_2O) + G(R) - \Delta G(H_2) \quad (II)$$

where $G_0(CH_2O)$ denotes the molecular yield of formaldehyde and where $\Delta G(H_2)$ is the decrease in hydrogen yield due to the addition of cyanogen iodide in methanol. Taking $G_0(CH_2O)$, $G(R)$, and $\Delta G(H_2)$ to be 2.05,[9] 6.4, and 1.6—1.8 respectively, one can obtain the $G(CH_2O)$ value from (II) to be 6.7—6.9 over the concentration range of 5 to 10 mM ICN; this is nearly the same as our present data, as is shown in Fig. 1.

As may be seen in Fig. 2, $G(H_2)$ decreases gradually with an increase in the concentration of cyanogen iodide in methanol containing nitrous oxide at 5 mM. Since all the solvated electrons are scavenged by nitrous oxide at this concentration or by cyanogen iodide, the observed decrease in $G(H_2)$ may be attributed to reaction (4). It may be seen that $G(H_2)$ continues to decrease very gradually with an increase in the concentration of cyanogen iodide. This finding suggests that reaction (4) proceeds very slowly as compared with reaction (3) and that it is not so important to reduce $G(H_2)$ at the concentration of cyanogen iodide below 10 mM. When nitrous oxide is present in the system, reaction (7) will compete with reaction (3):

$$e^-_{sol} + N_2O \rightarrow N_2 + O^- \quad (7)$$

Based on simple competition kinetics, one can formulate:

$$\frac{1}{\Delta G(N_2)} = \frac{1}{G_{e^-_{sol}}}\left\{1 + \frac{k_7[N_2O]}{k_6[ICN]}\right\} \quad (III)$$

where $\Delta G(N_2)$ denotes the decrease in nitrogen yield due to the added cyanogen iodide in the presence of nitrous oxide. A plot of $1/\Delta G(N_2)$ *vs.* $[N_2O]/[ICN]$ is seen to give a straight line, as in Fig. 3. From the intercept in the ordinate, one can obtain 2.2 for Ge^-_{sol}, and from the slope

*1 In addition to these major radical products, CH_3 and OH radicals are considered to be present in very low yields, but these may be converted to CH_2OH radicals by the reaction with methanol. Therefore, these are equivalent to other radicals with regard to the formation of iodine.

9) G. E. Adams and J. H. Baxendale, *J. Am. Chem. Soc.*, **80**, 4215 (1958).

10) S. V. Choi and N. N. Lichtin, *ibid.*, **86**, 3948 (1964).

of line, one can obtain k_7/k_3 for 1.9. Taking 1.3×10^{10} M^{-1}sec^{-1} for k_7,[11] k_3 is estimated to be 6.8×10^{9} M^{-1}sec^{-1}. Reactions (4) and (5) indicate that hydrogen cyanide should be produced. However, it is detected only qualitatively at the present stage because of the interference of cyanogen iodide.

11) H. Seki and M. Imamura, *J. Phys. Chem.*, **71**, 870 (1967).

BULLETIN OF THE CHEMICAL SOCIETY OF JAPAN VOL. 42 1765—1766 (1969)

σ-Bonded Arylpalladium(II) Complex: Bis-[*N*,*N*-dimethylbenzylamine-2-*C*,*N*]-palladium

Akira KASAHARA and Taeko IZUMI*1

Department of Chemistry, College of General Education, Yamagata University, Yamagata

(Received October 23, 1968)

Recently the preparations of σ-bonded arylpalladium complexes have been investigated by several workers.[1-4] For example, Calvin and Coates[1] have prepared palladium complexes of the type of $Ar_2Pd(PEt_3)_2$ which were stabilized by π-bonding phosphine donors. Cope and Sieman[2] have found palladium(II) halides to react with azobenzenes to give the chloro-2-(phenylazo)-phenylpalladium dimer (1) as a surprisingly stable product. Furthermore, *N*,*N*-dimethylbenzylamine,[3] α-*N*,*N*-dimethylaminonaphthalene,[3] and 2-phenylpyridine[4] reacted with palladium chloride to form similar

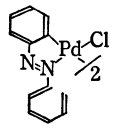

(1)

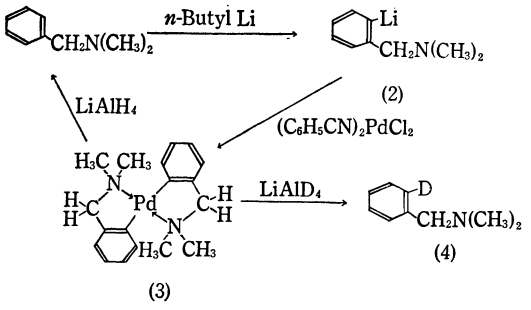

Fig. 1.

σ-bonded aryl derivatives of palladium. Recent observations[5] that *o*-lithio-*N*,*N*-dimethylbenzylamine reacts with chromium(III) chloride or cobalt(II) chloride to give complexes with carbon-to-metal σ-bonds have led us to examine a similar reaction between dibenzonitrile-dichloropalladium and *o*-lithio-*N*,*N*-dimethylbenzylamine.

Experimental[6]

Materials. *N*,*N*-Dimethylbenzylamine was obtained commercially, while dibenzonitrile-dichloropalladium was prepared by a literature method.[7] The NMR spectra were recorded with a Hitachi H-60 instrument in deuterochloroform, using tetramethylsilane as the internal standard; the peak positions were expressed in terms of τ values. The mass spectra were obtained on a Hitachi RMU-6 mass spectrophotometer. The molecular weight was determined in benzene using a Hitachi vapor-pressure osmometer.

Bis-[*N*,*N*-dimethylbenzylamine-2-*C*,*N*]-palladium(II) (3). A mixture of *N*,*N*-dimethylbenzylamine (2.70 g, 0.02 mol), *n*-butyl lithium in ether (28 m*l* containing 0.024 mol), and ether (60 m*l*) was stirred in a nitrogen atmosphere for 24 hr. The resulting mixture of *o*-lithio-*N*,*N*-dimethylbenzylamine was cooled in an ice-salt bath and then reacted with dibenzonitrile-dichloropalladium(II) (3.83 g, 0.01 mol) under a stream of nitrogen. After stirring for 6 hr at room temperature, the mixture was treated with water (50 m*l*) and extracted with methylene chloride. The extract was washed with water, dried over anhydrous magnesium sulfate, and concentrated on a rotary evaporator. The resultant red oil was triturated with petroleum ether; the yellow crystals were filtered off and recrystallized from benzene. The yield was 0.46 g (12%); mp 209—210°C (dec.). Infrared spectrum (KBr pellet): 3020, 1590, 1465, 1440, 1000, 844 and 750 cm^{-1}. NMR spectrum: 7.52 (singlet, $N-CH_3$), 7.04 (doublet, $J=10$ cps, benzylic

*1 Present address: Department of Chemical Engineering, Faculty of Engineering, Yamagata University, Yonezawa, Yamagata.

1) G. Calvin and G. E. Coates, *J. Chem. Soc.*, **1960**, 2008.

2) A. C. Cope and R. W. Sieman, *J. Am. Chem. Soc.*, **87**, 3272 (1965).

3) A. C. Cope and E. C. Friedrich, *ibid.*, **90**, 909 (1968).

4) A. Kasahara, This Bulletin, **41**, 1272 (1968).

5) a) G. Bähr and H. Zohm, *Angew. Chem.*, **75**, 94 (1963). b) A. C. Cope and R. W. Gourly, *J. Organometal. Chem.*, **8**, 527 (1967).

6) The melting points are uncorrected.

7) M. S. Kharasch, R. C. Seyler and F. R. Mayo, *J. Am. Chem. Soc.*, **60**, 882 (1938).

protons), 6.56 (singlet, N-CH_3), 6.20 (doublet, J=10 cps, benzylic protons) and 2.88—2.17 τ (multiplet, aromatic protons).

Found: C, 57.81; H, 6.62; N, 7.57%; mol wt, 368. Calcd for $C_{18}H_{24}N_2Pd$: C, 57.68; H, 6.45; N, 7.46%; mol wt, 374.8.

Reduction of Complex. General Procedure. The complex (0.2 g) to be reduced was slowly added to a stirred mixture containing 0.1 g of lithium aluminum hydride or deuteride in 30 m*l* of absolute tetrahydrofuran. The resulting black mixture was stirred at room temperature for 30 min; then water or deuterium oxide was added with cooling. The mixture was made acid with dilute hydrochloric acid, and the tetrahydrofuran was removed by evaporation under reduced pressure. After having been made alkaline with sodium carbonate, the mixture was extracted with ether. The ether solution was dried ($MgSO_4$) and concentrated by evaporation, and the product was isolated by preparative gas chromatography.

Reduction of 3 with Lithium Aluminum Hydride. This gave *N,N*-dimethylbenzylamine. The treatment of the product with methyl iodide gave the methodide as white crystals: mp 177—178°C.

Reduction of 3 with Lithium Aluminum Deuteride. This gave *N,N*-dimethyl-benzylamine-d_1. Methiodide derivative was made in the usual manner; mp 177—178°C. The mass spectrometric analysis showed that the product consisted of 92% d_1 and 8% d_0 species.

Results and Discussion

The *o*-metalation of *N,N*-dimethylbenzylamine with *n*-butyl lithium has previously been reported by Jones and his co-workers.[8] We reacted *o*-lithioamine (**2**) with dibenzonitrile-dichloropalladium in ether to give a yellow crystalline complex (**3**). The structure of **3** was assigned as follows. The elemental analysis is satisfactory, and the molecular weight measurement agrees with the assigned structure. In the infrared spectrum of **3**, the characteristic C–H out-of-plane deformation modes of a mono-substituted benzene at 770—730 and 690 cm^{-1} are absent; they are replaced by one at 750 cm^{-1} which can be assigned to a C–H deformation mode of an *ortho*-disubstituted benzene.[9] The lithium aluminum hydride reduction of **3** gave *N,N*-dimethylbenzylamine, whose mass spectrum and methiodide were identical with those of an authentic sample. On the other hand, the lithium aluminum deuteride reduction of **3** gave *N,N*-dimethylbenzylamine-d_1 (**4**). The gas-chromatographic analysis of **4** showed it to have the same retention time as an authentic sample of non-deuterated *N,N*-dimethylbenzylamine. The location of the deuterium in the *ortho*-position of the aromatic ring and, therefore the site of the carbon-to-palladium σ-bond, were indicated by the infrared spectrum of **4**, in which the characteristic absorption of an *ortho*-substituted benzene at 738 cm^{-1} was observed. Furthermore, the NMR spectrum of **3** is consistent with the proposed structure. We think that the complex **3** probably has a tetrahedral structure because the two *N*-methyl protons in the *N,N*-dimethylamino group are non-equivalent and appear as two singlets, at 7.52 and 656 τ. Moreover, the two protons in each pair of benzylic protons are also non-equivalent and appear as two doublets, at 7.04 and 6.20 τ. If the complex (**3**) were square-planar, a simple singlet pattern for the *N*-methyl protons of the *N,N*-dimethylamino group and also for the benzylic protons would be expected.

8) E. N. Jones, M. E. Zinn and C. R. Hauser, *J. Org. Chem.*, **28**, 663 (1963).

9) L. J. Bellamy, "The Infrared Spectra of Complex Molecules," 2nd ed., John Wiley and Sons, Inc., New York, N. Y. (1958).

BULLETIN OF THE CHEMICAL SOCIETY OF JAPAN VOL. 42 1767—1768 (1969)

An Application of Mulliken's Theory of the Charge-transfer Complex to the Hydrogen-bonding Mechanism

Koichi TOYODA

Department of Chemistry, Faculty of Science, Kumamoto University, Kurokami-machi, Kumamoto

(Received October 28, 1968)

Recently several authors[1-4] have emphasized the importance of the charge-transfer mechanism of hydrogen bonding. Therefore, we may expect the appearance of charge-transfer bands in hydrogen-bonding systems as well as in molecular complexes. However, the present author could not find any certified charge-transfer bands for hydrogen-bonding systems except for the C. T. band of the hydrogen maleate anion found by Nagakura and his co-workers.[3] Regarding hydrogen-bonding systems, the relations between the shift of the X–H stretching vibration; the enthalpy of formation of the complex, ΔH; the excess dipole moment for the complex over the sum of the ingredients, $\Delta\mu$; the equilibrium constant of the complex, K, and the coefficients of Mulliken's theory, a and b, will be discussed here, and the C. T. band of the formic acid dimer will be estimated.

Mulliken[5] has written the wave functions for the ground and first excited states of the complex as:

$$\Psi_N = a\phi_0 + b\phi_1, \qquad \Psi_E = a^*\phi_1 - b^*\phi_0$$

In the approximation of the variation method, the following relation[6] holds:

$$aW_0 + bH_{01} = W_N(a + bS). \tag{1}$$

Here,

$$W_0 \equiv H_{00} = \int\phi_0 H\phi_0 d\tau,\ H_{01} = \int\phi_0 H\phi_1 d\tau,$$

$$S = \int\phi_0\phi_1 d\tau,$$

$$\Delta H \approx W_N = \int\phi_N H\phi_N d\tau / \phi_N{}^2 d\tau.$$

H is the exact Hamiltonian operator for the entire set of nuclei and electrons. In weak complexes, $a\approx 1$, and bS is a sufficiently small number compared with a. Therefore, Eq. (1) may be reduced to:

$$W_0 + b\beta_0 = \Delta H.$$

Here, $\beta_{01}=H_{01}-W_0S$; then, for weak complexes, $\beta_0\approx H_{01}$ will hold. If we suppose W_0 and β_0 to be approximately constant for given complexes, there is a direct relation between b and ΔH. However, there is no theoretical reason to expect W_0 and β_0 to remain constant for weak complexes, even with the same donor. On the other hand, as is well known, ΔH is given by:

$$\Delta H = -\boldsymbol{R}T \ln K + \text{constant}$$

Here $\boldsymbol{R}$ and T are the gas constant and the absolute temperature respectively. According to Mulliken,[5] for weak complexes the excess dipole moment for the complex over the sum of the acceptor and the donor, $\Delta\mu$, is given approximately by:

$$\Delta\mu \equiv \mu_M = \mu_1(b^2 + abS) \approx b^2\mu_1 \tag{2}$$

The value of μ_1, the dipole moment of the dative structure, will be quite large due to the high charge separation in the dative structure, and it will be approximately constant for weak complexes. Therefore, the following direct relation will hold:

$$\sqrt{\Delta\mu} \propto \log K$$

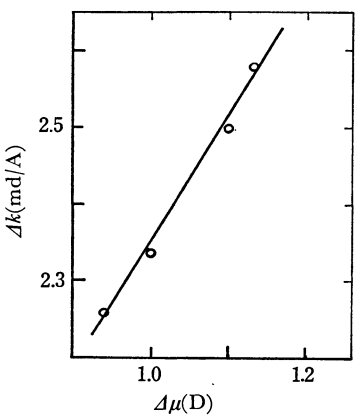

Fig. 1

1) R. S. Mulliken, *J. chim. phys.*, **1963**, 20.
2) H. B. Friedrich and W. B. Person, *J. Chem. Phys.*, **44**, 2161 (1966).
3) S. Nagakura, *J. chim. phys.*, **1964**, 217.
4) S. Bratož, "Advance in Quantum Chemistry," Vol. III, ed. by P. O. Löwdin, Academic Press, New York, N. Y. (1967), p. 221.
5) R. S. Mulliken, *J. Am. Chem. Soc.*, **74**, 811 (1952).
6) G. Briegleb, "Elektronen-Donator-Acceptor-Komplexe," Springer-Verlag, Berlin (1961), p. 11, Eq. (II, 16).
7) G. C. Pimental and A. L. McClellan, "The Hydrogen Bond," W. H. Freeman and Company, San Francisco (1960), p. 25.

Table 1

	Free OH str. (cm^{-1})	k_0* (md/A)	Bonded OH str.[a] (cm^{-1})	k_n* (md/A)	Δk (md/A)	$\Delta\mu$ (D)
HCOOH	3700	7.59	3077	5.25	2.34	1.00[b]
CH_3COOH	3700	7.59	3100	5.33	2.26	0.94[c]
C_6H_5COOH	3700	7.59	3007	5.01	2.58	1.13[c]
CCl_3COOH	3700	7.59	3030	5.09	2.50	1.1[d]

* Force constants are estimated approximately for OH molecule.

a) S. Bratož, D. Hadži and N. Sheppard, *Spectrochim. Acta*, **8**, 249 (1956).

b) C. T. Zahn, *Phys. Rev.*, **37**, 1516 (1931). See also McClellan, "Tables of Experimental Dipole Moments," W. H. Freeman and Company (1963), p. 41.

c) H. A. Pohl, M. E. Hobbs and P. M. Gross, *J. Chem. Phys.*, **9**, 408 (1941). See also Ref. 7, p. 24.

d) R. J. W. Le Févre and H. Vine, *J. Chem. Soc.*, **1938**, 1795. See also McClellan's Tables, p. 52.

Pimental and McClellan[7] find a proportionality between $\sqrt{\Delta\mu}$ and $\log K$ in the triethylamine-phenols and carboxylic acid dimers.

Person and Friedrich[2] have given the following equation:

$$(k_0-k_n)/k_0 \equiv \Delta k/k_0 = (1-k_1/k_0)(b^2+abS) \qquad (3)$$

If Eq. (2) is inserted into Eq. (3), the relation between Δk and $\Delta\mu$ is found to be:

$$\Delta k = [(k_0-k_1)/\mu_1]\Delta\mu$$

Here k_n, k_0, and k_1 are the X–H stretching force constants in the bonded X–H, free X–H, and $(X–H)^-$ molecules respectively. If k_0, k_1, and μ_1 are supposed to be approximately constant, there is a proportionality between Δk and $\Delta\mu$. Empirically there is a direct relation, as is shown in Fig. 1, between Δk and $\Delta\mu$ in a series of carboxylic acid dimers. The k_0, k_1, and $\Delta\mu$ values of carboxylic acid dimers are summarized in Table 1. Nakamoto *et al.*[8] have selected a constant frequency for each type of X–H stretching band; they concluded that each type of hydrogen bond shows a distinct relationship between the shift of the X–H band and the distance of the hydrogen bond. They selected 3700 cm^{-1} as the value of the free OH stretching band, so it seems reasonable to suppose that k_0 and k_1 are approximately constant.

Thereby, Mulliken's theory for the C.T. complex can be applied to hydrogen bonding systems. We may estimate 150 mμ as the approximate value for the charge transfer band characteristic of the interaction between the electron donor and acceptor in a formic acid dimer by using the following equation[9]:

$$\Delta H \approx h\nu_{CT}(b^2/a^2)$$

8) K. Nakamoto, M. Margoshes and R. E. Rundle, *J. Am. Chem. Soc.*, **77**, 6480 (1955).

9) See Ref. 7, p. 22, Eq. (IV, 10).

BULLETIN OF THE CHEMICAL SOCIETY OF JAPAN VOL. 42 1769—1770 (1969)

Kinetic Studies of the Acid-catalyzed Etherification of Ethyl Acetoacetate with Ethanol

Yoshiaki FURUYA, Iwao URASAKI, Kazuo ITOHO and Shin'ichi MIYAZAKI

Department of Industrial Chemistry, Faculty of Engineering, Kumamoto University, Kumamoto

(Received November 1, 1968)

It has been reported that the facility of the acid-catalyzed etherification of the allelotrope of *p*-nitrosophenol and *p*-benzoquinoneoxime may depend upon a special kind of keto-enol tautomerism.[1] It seemed that another system of keto-enol tautomerism could, therefore, be etherified easily with alcohols in the presence of acid as well. Actually, the acid-catalyzed etherification of ethyl acetoacetate with ethanol took place when well-dried hydrochloric acid was passed through the ethanolic solution for 10 min at −10°C; only the ethyl β-ethoxycrotonate was formed.[2]

Experimental

Materials. The ethyl β-ethoxycrotonate was prepared by refluxing a mixture of ethyl acetoacetate, acetyl chloride, and ethyl orthoformate;[3] it was recrystallized from petroleum ether after the crude product had been obtained by the removal of the other ingredients; yield 40%; mp 31°C (lit., 30°C,[2] 31°C[3]). Ethanol containing 0.16 M water was used as the reactant and solvent. The ethanolic solution of sulfuric acid was prepared from guaranteed sulfuric acid and the ethanol mentioned above.

Ultraviolet Spectrophotometry and Chemical Analysis. The reactions were followed by a Hitachi Perkin-Elmer UV-VIS spectrophotometer, model 139. The reaction product, ethyl β-ethoxycrotonate, has a broad absorption maximum at 235 mμ, while the reactant, ethyl acetoacetate, has only a small absorption in this UV region, as is illustrated in Fig. 1. Mixtures of ethyl acetoacetate, ethyl β-ethoxycrotonate, and sulfuric acid of known concentrations corresponding to 0, 20, 40, 60, 80, and 100% conversions were prepared; a plot of the difference in extinctions, $(E_{235}-E_{270})$ *vs.* $(E_{235}-E_{255})$, gave a straight line, and the calculated conversion from the values of $(E_{235}-E_{255})$ at 0 and 100% conversion agreed well, within about a 1% error, with the conversions calculated from the composition of the mixture.

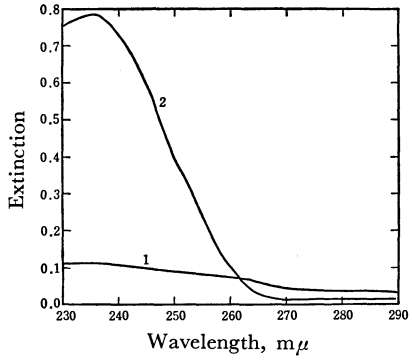

Fig. 1. Ultraviolet spectra of reactant and product in 5×10^{-5} M methanolic solution.
1, ethyl acetoacetate; 2, ethyl β-ethoxycrotonate.

Criterion of the Reaction. As the $(E_{235}-E_{270})$ *vs.* $(E_{235}-E_{255})$ plots of the actual reactions did not deviate at all from the calibration curve, it can be considered that the reaction forming ethyl β-ethoxycrotonate proceeds without any side reaction.

A Typical Run for the Rate Measurements. A solution of 2.5 m*l* of 1 N sulfuric acid in ethanol was poured into a 2.5 m*l* portion of a 1 M ethanolic solution of ethyl acetoacetate to start the reaction after both solutions had attained temperature equilibrium. Aliquots (0.1 m*l* each) were taken out at appropriate time intervals; each one was diluted with methanol to a 5×10^{-5} M total concentration of ethyl acetoacetate and ethyl β-ethoxycrotonate. The conversion percentage was calculated from the observed value of $(E_{235}-E_{255})$, and then the value of the apparent first-order rate constant, k, was calculated graphically.

Determination of the Water in the Reaction System. The water present in the reaction system was determined to be 0.20 M by the Karl Fischer method.

Results and Discussion

As the forward and reverse reactions are regarded as pseudo first-order reactions, the reaction will follow the pseudo first-order kinetics for a reversible reaction:

$$\ln [z/(z-x)] = kt, \quad (1)$$

where x and z are the concentrations of the consumed reactant at time t and at the equilibrium stage respectively. In these studies, the plots of $\log[z/(z-x)]$ *vs.* t gave a straight line, and the value of the apparent rate constant, k, was obtained graphically. Assuming the pseudo first-order rate constants for the forward and reverse reactions to be k_1 and k_{-1} respectively, the forward rate constant, k_1, can be

1) Y. Furuya, D. Morikawa and K. Itoho, This Bulletin, **40**, 1425 (1967).
2) R. S. Curtiss, *Am. Chem. J.*, **17**, 435 (1895).
3) F. Arndt, L. Loewe and M. Ozansoy, *Ber.*, **73** 779 (1940).

Table 1. The rate data for the reversible reaction of ethyl acetoacetate with ethanol

$[EAA]_0$ M	$[H_2SO_4]$ N	Temp. °C	$-\log (C_{BH^+}/C_B)$	H_0	$10^5 k_1$ sec^{-1}
0.1	0.5	20	−0.3045	0.996	1.63
0.5	0.5	20	−0.3045	0.996	1.62
1.0	0.5	20	−0.3045	0.996	1.66
0.5	0.1	20	0.4991	1.799	1.45
0.5	1.0	20	−0·6572	0.643	1.79
0.5	0.5	30	−0.3045	0.996	2.84
0.5	0.5	40	−0·3045	0.996	7.20

E_a, 6.53 kcal mol^{-1} $\Delta S^{\neq}$, −21.8 e.u.

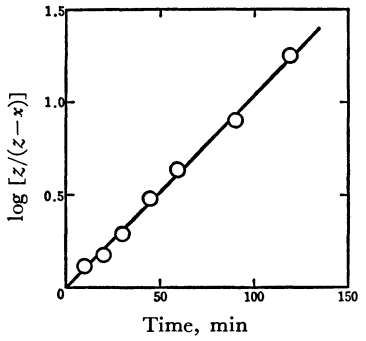

Fig. 2. The rate plots for the reversible first-order reaction at 20°C.
$[EAA]_0$: 0.5 M, $[H_2SO_4]$: 1 N z: 4.34%

obtained from the following equations[4]:

$$\ln [z/(z-x)] = (k_1+k_{-1})t = kt$$
$$z/(a-z) = k_1/k_{-1}$$

where a is the initial concentration of ethyl acetoacetate. The rate data are shown in the table.

The rate was not affected by the acidity, though the reaction does not occur without acid. The plots of log k_1 *vs.* H_0[5] gave a straight line with a slope of −0.07, as is illustrated in Fig. 3. Therefore, a proton may participate after the rate-determining step.

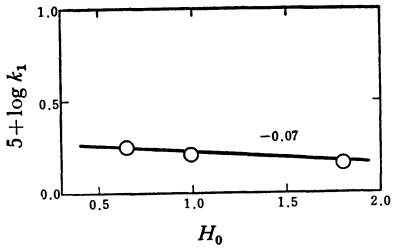

Fig. 3. The plots of log k_1 *vs.* H_0 for the etherification at 20°C.

It is well known that only β-ethoxycrotonic acid is obtained by the reaction of ethanol containing sodium ethoxide with potassium β-chlorocrotonate and/or β-chloroisocrotonate[6] and also with ethyl β-chloroisocrotonate.[7] In the title reaction as well, only ethyl β-ethoxycrotonate was obtained; no ethyl β-ethoxyisocrotonate formed at all, as has been described above. Therefore, a mechanism which involves the rate-determining formation of the hydrogen-bonding complex, I, can be considered.

From these findings, the following over-all mechanism can be suggested:

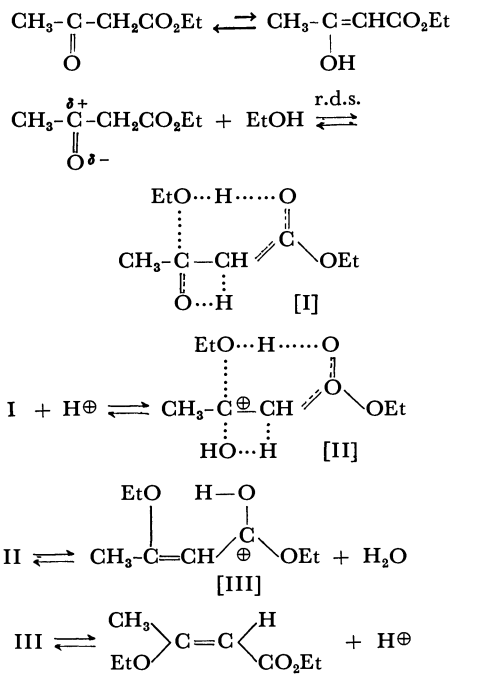

The autors are grateful to Mr. T. Sonobe for his aid in performing these experiments.

4) Y. Ogata, Y. Furuya and K. Aoki, This Bulletin, **38**, 838 (1965).

5) *p*-Nitroaniline was used as the indicator; its pK_{BH^+} value in ethanol was 1.3. M. A. Paul and F. A. Long, *Chem. Revs.*, **57**, 1 (1957).

6) R. Friedrich, *Ann.*, **219**, 322 (1883).

7) A. Koll, *ibid.*, **249**, 303 (1888).

BULLETIN OF THE CHEMICAL SOCIETY OF JAPAN VOL. 42 1771—1772 (1969)

Nuclear Quadrupole Resonance of Nitrogen-14 in Some Aliphatic Nitriles[1]

Shinzaburo ONDA, Ryuichi IKEDA, Daiyu NAKAMURA and Masaji KUBO

Department of Chemistry, Nagoya University, Chikusa, Nagoya

(Received November 9, 1968)

The pure quadrupole resonance of nitrogen-14 in some aliphatic nitriles was observed by means of a modified Pound-Watkins type spectrometer previously described.[2] Frequency modulation was used for the determination of resonance frequencies, while Zeeman modulation was employed for the assignment of observed resonance absorptions to ν^{I} and ν^{II}. The samples were procured from commercial sources and purified by repeated distillation. All the compounds investigated are liquids at room temperature. Therefore, they were solidified slowly in glass tubes and cooled gradually to liquid nitrogen temperature.

Since nitrogen-14 has a nuclear spin equal to unity, one can usually observe a pair of resonance lines, ν^{I} and ν^{II}, for equivalent nitrogen nuclei when the asymmetry parameter η is finite.

$$\nu^{I} = \frac{1}{4} eQq(3+\eta)$$

$$\nu^{II} = \frac{1}{4} eQq(3-\eta)$$

Here eQq denotes the quadrupole coupling constant in frequency units. From the observed resonance frequencies, the quadrupole coupling constant and the asymmetry parameter were calculated with the use of these equations as shown in Table 1.

Two sets of weak ν^{I} and ν^{II} resonance lines were observed for succinonitrile. For other compounds investigated, a single set of resonance lines was observed, indicating that all atomic sites of nitrogen are equivalent in each crystal. Accordingly, quadrupole coupling constants and asymmetry parameters can be evaluated in a straightforward manner.

Quite recently, Colligiani *et al.*[3] published the results of their comprehensive study on the ^{14}N nuclear quadrupole resonance of organic nitriles. Some of their results (propio-, butyro-, amylo-, isopropio-, glutaro-, adipo- and sebaco-nitriles) are in good agreement with ours. However, resonance frequencies ($\nu^{I}=2881.4$ and $\nu^{II}=2824.6$ kHz) observed by them for pimelonitrile do not agree with ours ($\nu^{I}=2907.7$ and $\nu^{II}=2793.3$ kHz) within experimental errors. Colligiani *et al.*[3] detected only one set of resonance lines for succinonitrile at practically the same temperature, the frequencies ($\nu^{I}=2995.7$ and $\nu^{II}=2844.7$ kHz) being in good agreement with those (2995.2 and 2844.1 kHz) of a set observed in the present investigation.

The appearance of the two sets of ν^{I} and ν^{II} lines indicates that there are two kinds of crystallographically nonequivalent nitrogen atoms in the crystals at liquid nitrogen temperature, although the two nitrogen atoms are chemically equivalent in the molecule. Unfortunately, no X-ray crystal data are available. For this compound, one-to-one correspondence cannot be made between ν^{I} and ν^{II} owing to the proximity of doublet lines. Therefore, the frequencies of the doublet lines were averaged to evaluate eQq and η.

One is tempted to consider the existence of the trans and the gauche forms in the crystals of succinonitrile. However, we could observe only a single set of ν^{I} and ν^{II} frequencies for tetramethylsuccinonitrile having a chemical formula analogous to that of succinonitrile. On the other hand, malononitrile[4] having no rotational isomers show two sets of ν^{I} and ν^{II} at liquid nitrogen temperature. These facts suggest that the nonequivalence of nitrogen atoms is due to the difference in the crystal

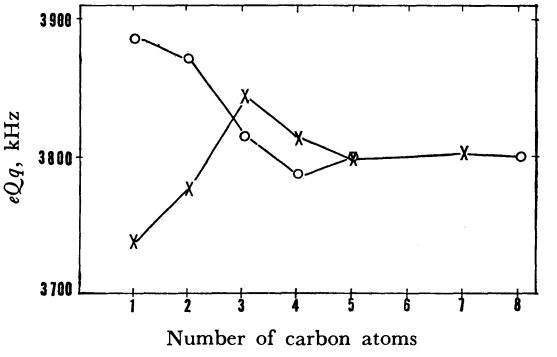

Fig. 1. The quadrupole coupling constants of ^{14}N in nitriles (cross) and dinitriles (circle).

1) Presented at the 21st Annual Meeting of the Chemical Society of Japan, Osaka, April 1968.

2) R. Ikeda, D. Nakamura and M. Kubo, *J. Phys. Chem.*, **70**, 3626 (1966).

3) A. Colligiani, L. Guibé, P. J. Haigh and E. A. C. Lucken, *Mol. Phys.*, **14**, 89 (1968).

4) A. Sussman and S. Alexander, *Solid State Communications*, **5**, 259 (1967).

Table 1. Nuclear quadrupole resonance frequencies, ν^{I} and ν^{II}, quadrupole coupling constants, eQq, and asymmetry parameters, η, of ^{14}N in some aliphatic nitriles at liquid nitrogen temperature

Compound	ν^{I}, kHz	ν^{II}, kHz	eQq, kHz	η, %
$CH_3(CH_2)_2CN$	2935.5±0.1	2832.1±0.1	3845.0±0.1	5.38±0.01
$CH_3(CH_2)_3CN$	2911.5±0.1	2808.6±0.2	3813.5±0.1	5.40±0.01
$CH_3(CH_2)_4CN$	2894.8±0.1	2804.2±0.1	3799.4±0.1	4.77±0.01
$CH_3(CH_2)_6CN$	2897.2±0.2	2806.9±0.2	3802.7±0.3	4.75±0.02
$(CH_3)_2CHCN$	2879.9±0.1	2830.1±0.4	3806.7±0.3	2.62±0.02
$NC(CH_2)_2CN$	{2995.2±0.2 2962.5±0.2}	{2844.1±0.3) 2816.9±0.2}	3872.9	7.66
$NC(CH_2)_3CN$	2923.1±0.1	2799.5±0.1	3815.0±0.1	6.48±0.01
$NC(CH_2)_4CN$	2861.4±0.1	2818.7±0.1	3786.7±0.1	2.26±0.01
$NC(CH_2)_5CN$	2907.7±0.2	2793.3±0.2	3800.6±0.3	6.02±0.02
$NC(CH_2)_8CN$	2895.8±0.1	2805.8±0.2	3801.1±0.2	4.74±0.01
$NCC(CH_3)_2C(CH_3)_2CN$	2976.1±0.1	2903.8±0.1	3919.9±0.1	3.69±0.01

field rather than to the existence of different kinds of isomeric molecules.

As pointed out by Colligiani *et al.*,[3] long-chain nitriles and dinitriles show essentially the same quadrupole coupling constant and asymmetry parameter. The asymptotic value of eQq for large number of carbon atoms in a nitrile molecule is 3.80 rather than 3.81 MHz[3] as shown in Fig. 1. It is noteworthy that the asymmetry parameter is considerably large and varies over a fairly wide range in spite of the cylindrical symmetry of a single $-C\equiv N$ group. It is presumed that both the intramolecular charge distribution and the crystal field are responsible for this effect.

BULLETIN OF THE CHEMICAL SOCIETY OF JAPAN VOL. 42 1772—1773 (1969)

Simple HMO Calculation of the Substituent Effects in Tropolone Derivatives*[1]

Kimiaki IMAFUKU and Hisashi MATSUMURA

Department of Chemistry, Faculty of Science, Kumamoto University, Kurokami-machi, Kumamoto

(Received November 25, 1968)

It is well known that the observations concerning the effects of substituents on the rates and equilibrium data for the reaction of benzene derivatives are correlated by the Hammett equation.[1] Further, this equation was found to be applicable to some heterocyclic aromatic compounds, such as pyridines,[2] furans,[3] thiophenes,[4] *etc.*

For tropolone derivatives, which have a seven-membered ring structure, their dissociation constants have been reported to be linearly correlated with Hammett's substituent constants.[5] The chemical shifts of their acidic protons measured in the binary systems of tropolones-pyridine in infinite dilutions were found to be linear with their dissociation constants.[6]

On the other hand, the Hammett equation has been studied with molecular orbital theory in recent years, and it has been found that substituent constants are related to π-electron density[7] as well as localization energy[8] pertinent to reactions.

In order to explain the linearity of pK_a values

*1 Presented at the 20 th Annual Meeting of the Chimical Society of Japan, Tokyo, April, 1967.

1) L. P. Hammett, *J, Am. Chem. Soc.*, **59**, 96 (1937); "Physical Organic Chemistry," McGrow-Hill Book Co., New York (1940), Chap. 7.

2) H. H. Jaffé and G. O. Doak, *J. Am. Chem. Soc.*, **77**, 4441 (1955).

3) W. E. Catlin, *Iowa State Coll. J. Sci.*, **10**, 65 (1935); *Chem. Abstr.*, **30**, 935[5] (1936).

4) E. Imoto, Y. Otsuji and T. Hirai, *Nippon Kagaku Zasshi (J. Chem. Soc. Japan, Pure Chem. Sect.)*, **77**, 804 (1956).

5) N. Yui, *Sci. Repts. Tohoku Univ., I*, **40**, 102 (1956); *Chem. Abstr.*, **51**, 17354[c] (1957); *Sci. Repts. Tohoku Univ., I*, **40**, 114 (1956); *Chem. Abstr.*, **51**, 17354[e] (1957).

6) Y. Ikegami, T. Ikenoue and S. Seto, *Kogyo Kagaku Zasshi (J. Chem. Soc. Japan, Ind. Chem. Sect.)*, **68**, 105 (1965).

7) H. H. Jaffé, *J. Chem. Phys.*, **20**, 279, 285, 1554 (1952); **21**, 415 (1953).

8) F. L. J. Sixma, *Rec. trav. chim.*, **72**, 673, (1953); *Chem. Abstr.*, **47**, 11935[f] (1953); *Rec. trav. chim.*, **73**, 243 (1954); *Chem., Abstr.*, **49**, 6893[g] (1955).

in the dissociation of tropolone derivatives with σ constants, we calculated the π-electron densities of some of 4- and 5-substituted tropolones by using the simple Hückel molecular orbital method, and examined whether or not these calculated values may be correlated with the substituent constants. The substituent constants of *m*- and *p*-positions of benzenes were used for 4- and 5-positions in tropolone derivatives, respectively.

Calculation

Treatment of Oxygen Atoms. The oxygen atoms of tropolones were treated according to Kubo *et al.*[9] The numbering of each atom is shown in Fig. 1. Although the two oxygen atoms are not

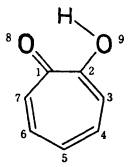

Fig. 1. The numbering for each atom.

identical, they are almost equivalent, owing to the hydrogen bonding and resonance. The molecule is assumed to be symmetrical with respect to a plane which involves the C_5-atom and the middle point of C_1- and C_2-atoms and is perpendicular to the ring. Molecular orbitals are constructed from the π-orbitals of the seven carbon atoms and of the two oxygen atoms. The number of the π-electrons which occupy these orbitals is ten.

The Coulomb integral for the oxygen atoms and the resonance integral for the oxygen-carbon bonds were obtained by repeating calculations until the dipole moment calculated for tropolone agreed reasonably with its observed value. Thus, the finally calculated dipole moment was 3.96 Debyes (observed, 3.53 Debyes[10]). The Coulomb integral for oxygen atoms and the resonance integral for the oxygen-carbon bonds were $\alpha+1.31\beta$ and 1.27β, respectively. The parameter of the Coulomb integral for the carbon atoms attached to the oxygen atoms was assumed to be one-tenth of the value of the latter atoms.

Integral Parameters for Substituents. The integral parameters for substituents were exactly those adopted by Fueno *et al.*[11] in the calculations of the molecular orbitals of benzene derivatives.

Results and Discussion

The π-electron densities q_C and q_O of C_1- or C_2-atoms and O_8- or O_9-atoms, respectively, were calculated and listed in Table 1. When these values are plotted against the Hammett substituent constants σ, linearity among them is obtained as shown in Fig. 2.

Table 1. π-Electron densities

No.	Substituent	σ	q_C	q_O
1	5-OCH_3	−0.268	0.9022	1.7196
2	5-CH_3	−0.170	0.8821	1.7065
3	4-CH_3	−0.069	0.8780	1.7031
4	H	0.000	0.8691	1.6954
5	5-Cl	0.227	0.8459	1.6696
6	5-Br	0.232	0.8431	1.6675
7	5-NO_2	0.778	0.7955	1.5970

No. of substituents are referred to Fig. 2.

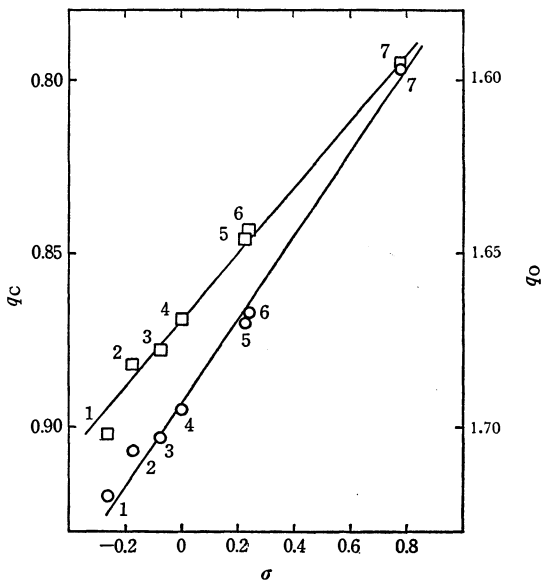

Fig. 2. The relation of π-electron densities of oxygen atoms (○) and adjacent carbon atoms (□) to substituent constants.

The linear correlations of q_C and q_O with σ are compatible with the experimental results that the pK_a values fit the Hammett plot. The linearity of q_O also illustrates the correlation of the chemical shifts of the acidic protons to the substituent constants, since their chemical shifts are influenced by the screening effect of the electrons around the oxygen atom.

Thus, it may be concluded that, for molecular orbital calculations of the seven-membered tropolone derivatives, the integral parameters for substituents obtained in benzene derivatives can be used as they are.

The authors wish to thank Dr. Koichi Toyoda of Kumamoto University for his helpful suggestions and discussions.

The authors' thanks are also due to the Ministry of Education for financial support.

9) Y. Kurita and M. Kubo, This Bulletin, **24**, 13 (1951).

10) Y. Kurita, T. Nozoe and M. Kubo, *ibid.*, **24**, 10 (1951).

11) T. Fueno, T. Okuyama and J. Furukawa, *ibid.*, **39**, 569 (1966).

BULLETIN OF THE CHEMICAL SOCIETY OF JAPAN VOL. 42 1774—1775 (1969)

The Spectrophotometric Determination of Anions by Solvent Extraction with Metal Chelate Cations. XLI.*1 Indirect Determination of β-Hydroxynaphthoic Acid by Atomic Absorption Spectrophotometry

Yuroku YAMAMOTO, Takahiro KUMAMARU, Yasuhisa HAYASHI and Susumu MATSUSHITA

Department of Chemistry, Faculty of Science, Hiroshima University, Higashisenda-machi, Hiroshima

(Received December 2, 1968)

In atomic absorption spectrophotometry, a hollow cathode lamp which emits the bright spectral lines of the element to be determined is generally used as a light source. Hence, organic compounds do not lend themselves directly to determination by conventional atomic absorption methods.

The indirect determination of some organic compounds can, however, be readily performed with this analytical tool. In our previous papers, such applications have been reported in the determination of phthalic acid[1,2] and pentachlorophenol[3]; these methods were based on the solvent extraction of ion-pairs stoichiometrically formed between the anion of the organic acid and the cationic metal chelate, such as bis(neocuproine)copper(I) or tris-(1,10-phenanthroline)iron(II), and on the subsequent determination of the metal concentration in the extracts by atomic absorption spectrophotometry, the results being related quantitatively to the associated organic compound. In connection with these investigations, this study was undertaken to establish a method for the determination of β-hydroxynaphthoic acid (3-hydroxy-2-naphthoic acid), which has until now been produced through Kolbe's reaction of β-naphthol, for industrial use, mainly as an intermediate of dyestuffs. The present procedure involves the selective extraction of tris(1,10-phenanthroline)nickel(II) β-hydroxynaphthoate into nitrobenzene, followed by the measurement of the nickel concentration in the extract by atomic absorption spectrophotometry as a function of the amount of β-hydroxynaphthoic acid initially present in the aqueous phase. The presence of β-naphthol, which has been well known as a main contaminative substance in the process of manufacturing β-hydroxynaphthoic acid, did not interfere with the determination.

Experimental

Apparatus. The atomic absorption was measured with a Hitachi Model EPU-2 spectrophotometer and a Hitachi Model 0420 atomic absorption attachment equipped with a nickel hollow cathode lamp. An air-acetylene flame was burned with a water-cooled 9-cm slot burner. The shaking for the extraction was carried out by means of an Iwaki Model KM shaker.

Reagents. All the solutions were prepared from analytical reagent-grade chemicals. A stock solution of β-hydroxynaphthoic acid (1.0×10^{-2} M) or β-naphthol (1.0×10^{-2} M) was prepared by dissolving 0.941 g of β-hydroxynaphthoic acid or 0.721 g of β-naphthol in 2 m*l* of a 6N sodium hydroxide solution and a small volume of water, and then by diluting the mixture to 500 m*l* with water. These solutions were diluted to an appropriate concentration for the experiment. A phenanthroline-nickel(II) sulfate solution (1.0×10^{-2} M) was prepared by dissolving 6.343 g of 1,10-phenanthroline ($C_{10}H_8N_2\cdot H_2O$) and 0.281 g of refined nickel sulfate ($NiSO_4\cdot7H_2O$) to a volume of 1000 m*l* with water.

Procedure. Ten milliliters of the phenanthroline-nickel(II) sulfate solution, 5m*l* of a phosphate buffer solution (1/15 M, pH 6—7), and 4 m*l* of the β-hydroxynaphthoic acid solution (2.0×10^{-3} M) were placed in a 100-m*l* separatory funnel, and then the aqueous-phase volume was adjusted to 25 m*l* with water. After 10 m*l* of nitrobenzene had been poured in, the funnel was shaken for 1 min. It was left still for about 20 min after the extraction, and then the organic phase was taken out and dried with 1 g of anhydrous sodium sulfate. The absorption due to nickel in the organic phase was then determined by the use of the atomic absorption spectrophotometer against a reagent blank used as a reference, and expressed as the initial concentration of β-hydroxynaphthoic acid in the aqueous phase. The instrument-operating conditions were as follows: a wavelength of 2320Å, slit-width of 0.20 mm, and a lamp current of 15 mA (nickel lamp). The flow rates of gases for the air-acetylene flame were 8.0 *l*/min of air and 1.5 *l*/min of acetylene. The burner height was adjusted to make the light beam pass 6 mm above the tip of the burner.

Results and Discussion

Atomic Absorption of Nickel. The effects of the variation in the composition of the air-acetylene mixture on the nickel absorption in the organic extract were studied. The absorption was nearly constant when the air-flow rate was set at a constant value, although the sensitivity was enhanc-

*1 Part XL: Y. Yamamoto, N. Okamoto, and E. Tao, *Anal. Chim. Acta*, **69** (1969), in press.

1) T. Kumamaru, Y. Hayashi, N. Okamoto, E, Tao and Y. Yamamoto, *Anal. Chim. Acta*, **35**, 525 (1966).

2) T. Kumamaru, *ibid.*, **43**, 19 (1968).

3) Y. Yamamoto, T. Kumamaru and Y. Hayashi, *Talanta*, **14**, 611 (1967).

ed with an increase in the air-flow rate. For convenience, the gas-flow rates were adjusted to 8.0 *l*/min of air and 1.5 *l*/min of acetylene in subsequent work. Under these flame conditions, the highest sensitivity was obtained when the burner was so positioned that the radiation from the light source passed through the base of the flame 5—6 mm above the tip of the burner.

Extraction of β-Hydroxynaphthoic Acid with Phenanthroline-Nickel(II) Chelate. Among various commercially-available organic solvents tested for the extraction, nitrobenzene was found to be the most effective extractant for phenanthroline-nickel(II) β-hydroxynaphthoate. Moreover, nitrobenzene is a suitable solvent for atomic absorption spectrophotometry because it provides a stable flame during the combustion and a higher sensitivity of measurement. The extraction efficiency was estimated by extracting the ion-pair with successive 10 m*l* portions of nitrobenzene. It was found that 92% of β-hydroxynaphthoate was extracted in a single pass according to the procedure. Variations in the shaking time showed that shaking for longer than 0.5 min did not improve the extraction. The effect of the pH on the extraction is shown in Fig. 1.

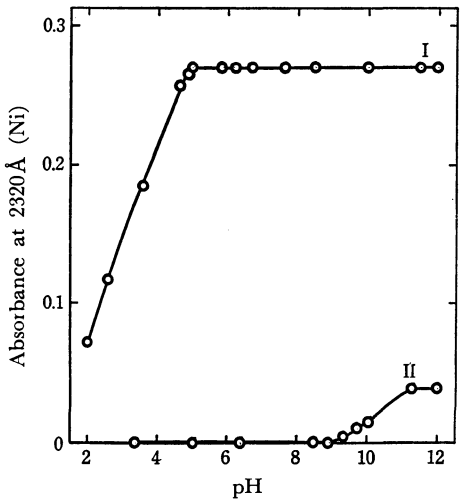

Fig. 1. Effect of pH on the extraction.
Concentration of aqueous phase: 3.2×10^{-4} M
I β-Hydroxynaphthoic acid, II β-Naphthol

The degree of the extraction of β-hydroxynaphthoate is at its maximum and is constant when the pH is held greater than 5, while β-naphtholate is only slightly extracted above pH 9. Therefore, when the method is, for instance, applied to the determination of β-hydroxynaphthoic acid in the industrial process, the pH should be in the 5—9 range in order to suppress the extraction of β-naphthol, which might contaminate the sample.

The effect of the concentration of phenanthroline-nickel(II) sulfate on the extraction of β-hydroxynaphthoate was also investigated. The absorbance of the nitrobenzene phase approached a limit when the chelate concentration was more than 1.6×10^{-3} M and when the β-hydroxynaphthoic acid concentration was kept at 3.2×10^{-4} M in the aqueous phase. Since at least a 5-fold excess (molar) of the phenanthroline chelate over β-hydroxynaphthoic acid was necessary for quantitative extractions, we decided for the sake of convenience to keep the chelate concentration at 4.0×10^{-3} M.

Calibration Curve. A plot of the absorbance due to nickel *vs.* the concentration of β-hydroxynaphthoic acid was obtained according to the procedure using varying amounts (1—5 m*l*) of the standard β-hydroxynaphthoic acid solution (2.0×10^{-3} M). As is shown in Fig. 2, this plot gives a linear relationship in the range from 8×10^{-5} to 4×10^{-4} M of β-hydroxynaphthoic acid initially present in the aqueous phase.

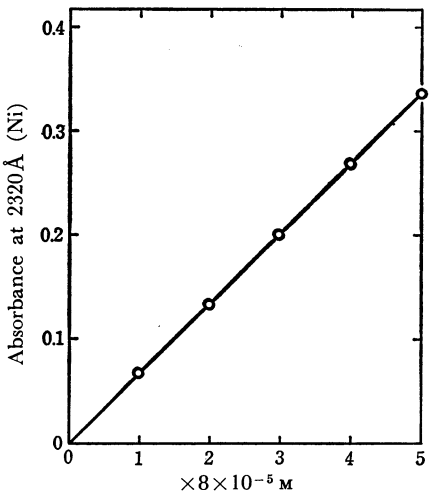

Fig. 2. Calibration curve.

Composition of Extracted Species. The continuous variation plots obtained by the atomic absorption spectrophotometric method were made in order to confirm the composition of tris (1,10-phenanthroline)nickel(II) β-hydroxynaphthoate. These plots suggested that a 1 : 2 associated ion-pair formed between the tris (1,10-phenanthroline)nickel(II) cation and the univalent anion of β-hydroxynaphthoic acid is extracted into nitrobenzene.

BULLETIN OF THE CHEMICAL SOCIETY OF JAPAN VOL. 42 1776 (1969)

A Convenient Synthesis of 3,4-Dialkyl-5-carbomethoxy-2-pyrone

Shosuke YAMAMURA, Shuichi IWADARE, Shusi UEDA and Yoshimasa HIRATA

Chemical Institute, Nagoya University, Chikusa, Nagoya

(Received December 3, 1968)

In general, it is difficult to make 3,4-dialkyl-2-pyrone derivatives. We here describe a three-step synthesis of 3,4-dialkyl-5-carbomethoxy-2-pyrone from the β-keto ester.[1]

When heated with carbomethoxymethylene-triphenyl-phosphorane at 100—110°C for 15 hr under nitrogen, and then submitted to silica gel chromatography (Mallinckrodt, 100 Mesh), 2-carbomethoxycyclopentanone did not afford a condensation product (I), but it did afford, in a 62% yield, an isomer (II), bp 101—102°C/4 mmHg; ν_{max}^{film} 1748, 1713 and 1650 cm^{-1}; NMR spectrum (in benzene): 1.65 (2H, near q, J=7.5 cps), 2.1—2.8 (4H, br), 3.37 (3H, s), 3.40 (3H, s) and 3.73 ppm (2H, s).*1 In the presence of sodium methoxide,*2 II was treated with methyl formate at room temperature for 40 hr to afford a brown solution;[2] this solution was then cooled at 0°C and reacted with hydrogen chloride gas at 0°C for 30 min. The reaction mixture was then allowed to stand at room temperature overnight to afford, in a 41% yield, the desired pyrone (III), mp 95—96°C, the structure of which was supported by the following physical data: ν_{max}^{KBr} 1726 br, 1624 and 1548 cm^{-1}; λ_{max}^{MeOH} 291 and 265 mμ (ε, 4550 and 8025 respectively); NMR spectrum: 2.10 (2H, near q, J=7.5 cps), 2.83 (2H, t, J=7.5 cps), 3.21 (2H, t, J=7.5 cps), 3.87 (3H, s) and 8.25 ppm (1H, s).

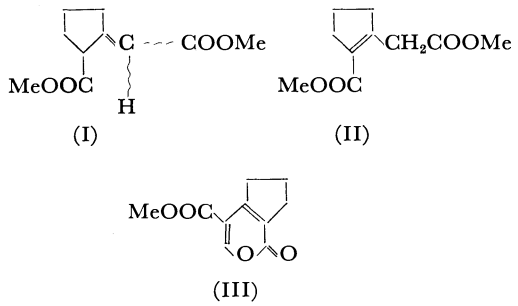

(I) (II) (III)

Experimental

The melting point was uncorrected. The IR and UV spectra were recorded with JASCO IR-S and Hitachi-124 spectrometers respectively. The NMR spectra were obtained on a Varian Associates A-60 spectrometer. Chemical shifts for all the NMR spectra are given in ppm from an internal TMS standard, with $CDCl_3$ used as the solvent unless otherwise stated. The mass spectra were measured with a Hitachi RMU-6D mass spectrometer with an ionization energy of 70 eV.

Condensation of 2-Carbomethoxy-cyclopentanone with Carbomethoxymethylene - triphenyl - phosphorane. A mixture of the keto ester (20 g) and carbomethoxymethylene - triphenyl - phosphorane (26 g) was stirred at 100—110°C for 15 hr under nitrogen, and then cooled at room temperature to give a brown solid which was extracted with a large amount of carbon tetrachloride. The solvent was removed under reduced pressure to give a brown oil, which was then chromatographed on silica gel (200 g) and eluted with CCl_4-$CHCl_3$ (4 : 1) to afford 9.6 g of a colourless liquid (II), bp 101—102°C/4 mmHg; *m/e* 198 (M^+); NMR spectrum: 1.95 (2H, near q, J=7.5 cps), 2.4—2.9 (4H, br), 3.71 (3H, s) 3.74 ppm (5H, s) (Found: C, 60.00; H, 7.11%. Calcd for $C_{10}H_{14}O_4$: C, 60.59; H, 7.12%).

Formation of 3,4 - Dialkyl-5-carbomethoxy - 2 - pyrone. A mixture of II (14 g) and methyl formate (14 g) was slowly stirred into 400 ml of dry ether containing fresh sodium methoxide (7.0 g) at 0°C. After having been kept at 0°C for 3 hr, the reaction mixture was allowed to stand at room temperature for 40 hr with stirring; then it was cooled at 0°C and saturated with hydrogen chloride gas at 0°C for 30 min. The reaction mixture was allowed to stand again at room temperature overnight, and then extracted with a large amount of ether. The ethereal solution was successively washed with water, 5% $NaHCO_3$, and water saturated with NaCl. Finally, the solution was dried over Na_2SO_4 and the solvent was removed under reduced pressure to afford a brown solid, which was chromatographed on silica gel (100 g) and eluted with CCl_4-$CHCl_3$ (4 : 1) to give pale yellow crystals. Recrystallization from methanol afforded 5.6 g of white crystals, mp 95—96°C; *m/e* 194 (M^+) (Found: C, 62.05; H, 5.11%. Calcd for $C_{10}H_{10}O_4$: C, 61.85; H, 5.19%).

The authors are indebted to Mr. Yoshihiko Deguchi, Meijo University, for microanalyses.

1) S. Iwadare, S. Ueda, Y. Hirata and S. Yamamura, Preprints for the 21st Annual Meeting of the Chemical Society of Japan (march 31, 1968), p. 1726.

*1 An exocyclic double bond of I migrated to a more stable position, as is shown in II.

*2 Sodium methoxide should be used immediately after preparation.

2) G. H. Coleman and D. Craig, "Organic Syntheses," Coll. Vol. II, p. 179 (1943).

SHORT COMMUNICATIONS

Cyclopropenones. III. The Reaction of Diphenylcyclopropenone and Ammonia to Afford *cis*- and *trans*-3,4-Diphenylazetidinones

Fumio TODA, Tamio MITOTE and Katsuhiko AKAGI

Department of Industrial Chemistry, Faculty of Engineering, Ehime University, Matsuyama

(Received March, 22, 1969)

In a previous paper[1] of this series, we have reported a novel substitution reaction of diphenylcyclopropenone (I) with ammonia at −78°C to afford α-phenyl-β-amino-*trans*-cinnamaldehyde (III). When, however, the reaction was carried out at room temperature, *cis* (VIc) and *trans*-3,4-diphenylazetidinone (VIt) were obtained. This is the first instance in which azetidinone has been found to be formed from I, even though the ring-expansions of I by the reactions with hydroxylamine,[2] diazomethane,[2,3] enamine[4] and with azomethine ylid[5] to yield isoxazolone, pyridazone, cycloheptatrienone, and oxazoline respectively have been reported.

The treatment of an ether-tetrahydrofuran solution of I with ammonia at room temperature for 2 hr, followed by chromatographic separation on alumina, afforded VIc as colorless prisms (30%); mp 153°C; $\nu_{max}^{CHCl_3}$, 3410 (NH) and 1760 cm^{-1} (CO); NMR ($CDCl_3$), 2.94 (d, C_6H_5, 10H), 4.88 (d, J_{AB}= 6 Hz, H_A, 1H) and 5.13τ (d, J_{AB}=6 Hz, H_B, 1H) and (Vt) as colorless needles (30%), mp 124°C; $\nu_{max}^{CHCl_3}$, 3410(NH) and 1760 cm^{-1} (CO); NMR ($CDCl_3$), 2.62 (d, C_6H_5, 10 H), 5.34 (d, J_{AB}=3 Hz, H_A, 1H) and 5.71τ(d, J_{AB}=3 Hz, H_B, 1H). The above data were identical with those reported[6] for VIc and VIt, which were prepared in 13 and 3% yields respectively by the photochemical reaction of α-phenylcinnamamide for 70 hr.

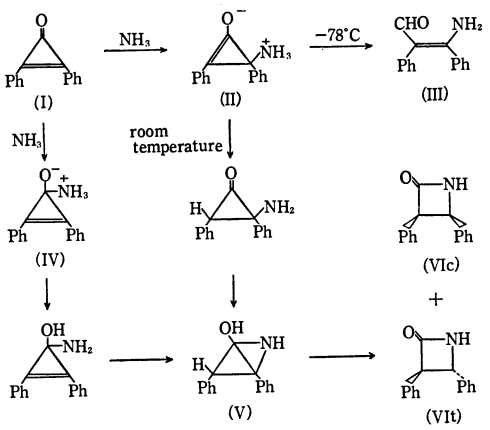

Scheme 1

Since the treatment of an ether-tetrahydrofuran solution of III with ammonia at room temperature gave no product, and since III was recovered quantitatively, the reaction yielding VI and the reaction yielding III may be independent of each other. The reaction path leading to VI can be interpreted as is shown in Scheme 1. Of two possible reaction paths, one is the initial formation of the same intermediate (II) as in the case of the substitution reaction leading to III followed by ketonization and ring-expansion *via* the bicyclic intermediate (V). The other possible reaction path is the formation of IV by the reaction of ammonia with carbonyl carbon of I, followed by ring-expansion *via* the bicyclic intermediate (V).

On the other hand, the reactions of both I and methylamine at −78°C and at room temperature afforded the *N*-methyl derivative of VI (VII) as colorless needles (68% in both cases); mp 132°C; $\nu_{max}^{CHCl_3}$, 1750 cm^{-1} (CO); NMR($CDCl_3$), 2.94(d, C_6H_5, 10 H), 5.05 (d, J_{AB}=6 Hz, H_A, 1 H), 5.15 (d, J_{AB}=6 Hz, H_B, 1 H) and 7.09τ (d, CH_3, 3 H). Found: C, 80.85; H, 6.20%; mol wt (benzene), 246. Calcd for $C_{16}H_{15}ON$: C, 80.98; H, 6.37%; mol wt, 237. By comparing its NMR data, especially the coupling constant of the vicinal protons (J_{AB}) and the shielding effect against the phenyl protons, with those of VIc and VIt, VII was identified as the *cis*-isomer. It is not clear, however, why the *cis*-isomer was produced exclusively in this case.

The production of the *cis*-azetidinones in this series in good yields is of particular importance since these compounds are not easily obtainable by other procedures.

1) F. Toda, T. Mitote and K. Akagi, *Chem. Commun.*, **1969**, 228.

2) R. Berslow, T. Eicher, A. Krebs, R. A. Peterson and J. Posner, *J. Am. Chem. Soc.*, **87**, 1320 (1965).

3) P. T. Izzo and A. S. Kende, *Chem. Ind.*, **1964**, 839.

4) J. Ciabattoni and G. A. Berchtold, *J. Am. Chem. Soc.*, **87**, 1404 (1965).

5) J. W. Lown, R. K. Smalley and G. Dallas, *Chem. Commun.*, **1968**, 1543.

6) O. L. Chapman and W. R. Adams, *J. Am. Chem. Soc.*, **89**, 4243 (1967).

The Two Bitter Principles of *Isodon shikokianus* Kudo

Takashi KUBOTA and Isao KUBO

Faculty of Science, Osaka City University, Sugimoto-cho, Sumiyoshi-ku, Osaka

(Received March 24, 1969)

Chromatography of the ether extract of *Isodon shikokianus* Kudo yielded two crystalline bitter diterpenoid compounds, (I) $C_{20}H_{28}O_6$, mp 258—262 °C(decomp.), $[\alpha]_D^{18°}$ −45.0° (pyridine), λ_{max}^{EtOH} 238 mμ (log ε 4.04) and (II) $C_{24}H_{32}O_8$ (*m/e* 448), mp 286—288°C (decomp.), $[\alpha]_D^{22°}$ −38.6° (pyridine).

Compound I, according to its physical constants and spectral properties, is identical with the known oridonin[1] which is present in *I. trichocarpus* Kudo and *I. japonicus* Hara.

Compound II, which is found to be new and designated as shikokianin, exhibits in UV and IR spectra λ_{max}^{EtOH} 237 mμ (log ε 3.98) and ν_{max} 1720 and 1645 cm^{-1}. The IR spectrum indicated also the presence of hydroxyl groups (ν_{max}^{Nujol} 3600 and 3350 cm^{-1}, $\nu_{max}^{CHCl_3}$ 3600 and 3350 cm^{-1}) and chelated five membered ketone (1720 cm^{-1}).*1 The NMR spectrum in $CDCl_3$ showed the presence of two acetoxyl groups (8.10 and 7.90 τ, each 3H, s.), an exocyclic methylene group (4.02 and 4.54 τ, each 1H, s.), an ether type methylene group (5.60 and 6.10 τ, AB-type J=12 cps, $-CH_2-O-$), two tertiary methyl groups (8.84 τ, 6H, s., $(CH_3)_2C<$) and two hydroxyl groups (4.02 and 4.21 τ, disappeared on addition of D_2O). Catalytic hydrogenation of II on Pd-C yielded dihydroshikokianin (III), $C_{24}H_{35}O_8$, mp 266—267°C (decomp.), $[\alpha]_D^{20°}$ −61.2° (pyridine), which exhibits no UV and IR band due to double bond or NMR signal due to a secondary methyl group. Although II and III could not be acetylated with acetic anhydride and pyridine,*1 on treatment with acetic anhydride and BF_3-etherate III gave tetraacetate (IV), $C_{28}H_{38}O_{10}$, mp 187—192°C (decomp.) which exhibits no IR band due to hydroxyl group. In NMR spectrum

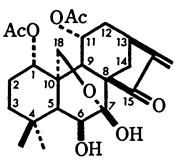

(II)

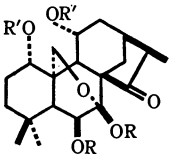

(III) R′=H, R=Ac
(IV) R=R′=Ac
(V) R=R′=H

IV shows four acetoxyl groups (7.86, 7.95, 7.96 and 7.99 τ, each 3H, s.) and this suggests the presence of two hydroxyl groups in III and also II itself. Dihydroshikokianin III was hydrolysed with 0.05N 50% methanolic potassium hydroxide or 1N 50% ethanolic hydrochloric acid to give the tetraol (V), $C_{20}H_{30}O_6$, mp 256—261°C (decomp.) which exhibits no signal in NMR spectrum due to acetoxyl group and reverted to III on treatment with acetic anhydride and pyridine. This indicated that the change of carbon skeleton did not take place during hydrolysis with alkali or acid. Finally, tetraol V on oxidation with periodic acid gave dihydronodosin, $C_{20}H_{28}O_6$, mp 250—252°C (decomp.) which was obtained from nodosin[2] by catalytic hydrogenation on Pd-C.

As the results of the foregoing experiments, the structural formula II including its absolute configuration is proposed for shikokianin. The assignment of α-configuration of C(11) in II was also supported by an observation that the signal of the proton attached to C(11) appeared as double doublet at 6.20 τ (J_{ax}=9 cps and J_{bx}=18 cps), as in the case of isodonal[3] (6.27 τ, d. d. J_{ax}=7 cps and J_{bx}=15 cps).

*1 These results indicated the presence of a chelated five membered ketone. Therefore the 6-hydroxyl group must be of β-configuration as oridonin.[1]

1) E. Fujita, T. Fujita, H. Katayama and M. Shibuya *Chem. Commun.*, **1967**, 252.

2) E. Fujita, T. Fujita and M. Shibuya, *Chem. Pharm. Bull.*, **16**, 509 (1968).

3) T. Kubota and I. Kubo, *Tetrahedron Letters*, **1967**, 3781.

Additivity of Vicinal Circular Dichroism Contributions from Different Ligands in a Cobalt(III) Complex without Configurational Chirality

Norio KOINE and Naokazu SAKOTA

Department of Industrial Chemistry, Faculty of Engineering, Ehime University, Bunkyo-cho, Matsuyama

and Jinsai HIDAKA and Yoichi SHIMURA

Department of Chemistry, Faculty of Science, Osaka University, Toyonaka, Osaka

(Received April 10, 1969)

The present communication is concerned with the additivity of the vicinal CD contributions of *trans*(*N*)-[Co(L- or D-alada)(L-ala)]$^-$, which have no chiral configuration around the central cobalt(III) ion in the first approximation. Three new complexes, *trans* (*N*)-K[Co(L-alada)(gly)]·H_2O, *trans*(*N*)-K[Co·(L-alada)(L-ala)]·$2H_2O$ and *trans*(N)-K[Co(D-alada)(L-ala)]·$2H_2O$, were prepared and separated by the method similar to that of *trans*(*N*)-K[Co(ata)(L-ala)]·$2.5H_2O$.[1],*1

The geometrical structure of these complexes was confirmed to be *trans*(*N*) one on the basis of their visible absorption spectra and from the ion-exchange column chromatographic behavior. Three geometrical isomers concerning the position or orientation of a methyl group of the coordinated L- or D-alada are possible for each of the present complexes. The NMR spectra confirmed that the complexes obtained here commonly have only one type of geometrical structure and no indication was obtained for the isolation of the other two isomers.

The good agreement of the observed CD curves (3 and 4) with the calculated ones (5 and 6) substantiates the additivity of the two vicinal contributions from the quadridentate ligand, L- or D-alada, and from the L-alaninate ligand. This result indicates that each of the asymmetric carbon atoms of the two optically active ligands independently contribute to the optical activity of the complex ion.

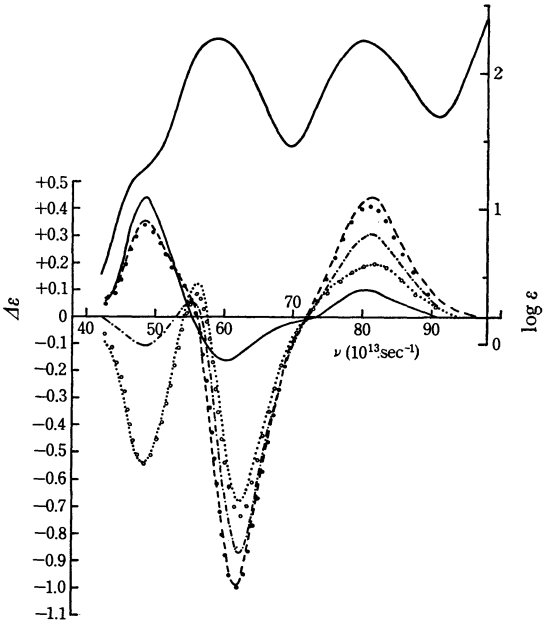

Fig. 1. Absorption and CD curves of *trans*(*N*)-[$Co(O)_4(N)_2$] type complexes.
Absorption curve: ——, [Co(L-alada)(gly)]$^-$, CD curves: (1) -·-·-, [Co(ata)(L-ala)]$^-$; (2) —— [Co(L-alada)(gly)]$^-$; (3) ----, [Co(L-alada)(L-ala)]; (4) ·····, [Co(D-alada)(L-ala)]$^-$; (5) ····, calculated curve, (1)+(2); (6) ∘∘∘∘∘∘, calculated curve, (1)—(2).

1) N. Koine, N. Sakota, J. Hidaka and Y. Shimura, This Bulletin, **42**, 1583 (1969).

*1 The following abbreviations are used for the ligands. gly: glycinate ion, L-ala: L-alaninate ion, ata: ammoniatriacetate ion, L- or D-alada: L- or D-alaninate-*N*,*N*-diacetate ion.

Interaction of Stannic Chloride with Polymethylbenzenes

Masahiro HATANO and Osamu ITO

The Chemical Research Institute of Non-Aqueous Solutions, Tohoku University, Sendai

(Received April 21, 1969)

In a number of papers, it has been found that inorganic acceptors, such as $SnCl_4$, $TiCl_4$, $VOCl_3$, and VCl_4, form charge-transfer (CT) complexes with various organic donors including aromatics.[1-5] The formation of these CT complexes has been confirmed using spectroscopic and other physicochemical methods. Since these inorganic acceptors are also a group of Lewis acids, it may be expected that the electron affinities of these inorganic acceptors, E_A, which are estimated from transition energies of CT absorption ($h\nu_{CT}$), will be of importance as effective measures of the strength of Lewis acids.

Although there have been some investigations of the CT interaction between $SnCl_4$ and aromatics as donors,[1,2,5] no CT absorption maximum has been separated; hence, the E_A of $SnCl_4$ has not yet been estimated. In the present communication we report that, in the systems of $SnCl_4$ and some polymethylbenzenes, new absorption bands were successfully separated from the absorption of the components and that these new bands were assigned and the E_A of $SnCl_4$ estimated.

Mixtures of $SnCl_4$ and hexamethylbenzene (HMB), pentamethylbenzene (PMB), durene, or mesitylene in a cyclohexane solution absorb significantly in the UV and visible region, where solutions of the individual components show negligible absorption. All the absorption spectra are summarized in Fig. 1.

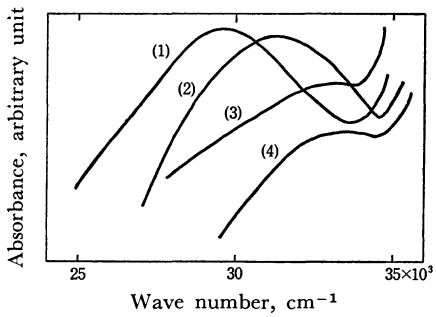

Fig. 1. Spectra of various donors with $SnCl_4$ in cyclohexane; (1), HMB (2), PMB; (3), durene; (4), mesitylene: (at 24.5°C)

The transition energies which were estimated from new absorption bands appearing in the systems of $SnCl_4$-polymethylbenzenes are also plotted against the ionization potentials (I_P) of the corresponding aromatic hydrocarbons in Fig. 2-I, where a linear relationship can be seen. The similar linear relationship of $h\nu_{CT}$ *vs.* I_P has been estsblished in the system of I_2-aromatics, as may be seen in Fig. 2-II. The transition energies of absorption bands due to σ-complexes or protonated carbonium ions of polymethylbenzenes are also plotted in Fig. 2-III against I_P.[6]

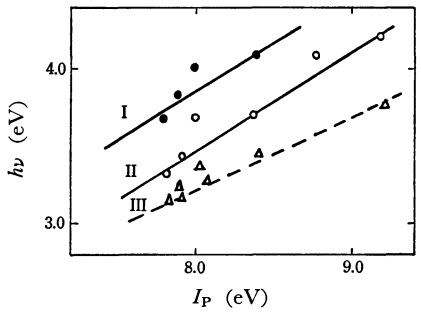

Fig. 2. Relationships between transition energies and I_P of aromatics; I, $SnCl_4$-aromatics; II, I_2-aromatics; III, σ-complexes or protonated carbonium ions of aromatics.

From the comparison of I with II and III in Fig. 2, it could be confirmed that the new absorption bands appearing in the systems of $SnCl_4$-polymethylbenzenes are due not to σ-complexes or protonated carbonium ions, but to the CT complexes of $SnCl_4$ with aromatics, as in the case of I_2-aromatics.

Using the same donor, the E_A value of any given acceptor or can be estimated by means of the following approximate equation;

$$(h\nu_{CT})_0 - (h\nu_{CT})_i = (E_A)_i - (E_A)_0$$

where the suffixes 0 and i indicate those for the standard and for any given acceptor respectively. Here, I_2 and mesitylene were chosen as the standard acceptor and donor, and the E_A of I_2 was assumed to be 1.8_0 eV; hence the E_A of $SnCl_4$ could be estimated to be 1.4_6 eV.

1) H. Tsubomura, This Bulletin, **27**, 1 (1954).
2) J. J. Myher and K. E. Russell, *Can. J. Chem.*, **42**, 1555 (1964).
3) C. Dijkgraaf, *J. Phys. Chem.*, **69**, 660 (1965).
4) H. L. Krauss and H. Huttmann, *Z. Naturforsch.*, **21b**, 490 (1966).
5) Z. Kecki and B. Izdebska, *Roczniki Chem.*, **40**, 1529 (1966).
6) G. Dallinga, E. L. Mackor and A. A. V. Stuart, *Mol. Phys.*, **1**, 123 (1958).

Determination of Volume Magnetic Susceptibility (χ_v) by NMR

Koichi HATADA, Yoshio TERAWAKI and Hiroshi OKUDA

Department of Chemistry, Faculty of Engineering Science, Osaka University, Toyonaka, Osaka

(Received April 23, 1969)

The evaluation of χ_v by NMR has been done using a precision coaxial tubing by Zimmerman[1] or using the method devised by Bernstein and Frei.[2] The former procedure, however, is liable to be affected by the setting of the sample tube in the magnetic field, thereby introducing ambiguity into the measurement.[3,4] The latter involves a difficult arrangement of the noncoaxial tubing. In the present work we have rapidly and easily carried out an accurate determination of the χ_v value by NMR measurements using the microcell devised by Flath[5] (Fig. 1).

The measurements were done on a JNM-4H-100 spectrometer at 22.5±0.2°C, and using an internal lock system at 100 MHz. The chemical shifts were calibrated by means of the built-in frequency counter. The precision of the measurements was ±0.1 Hz. All the reagents were obtained commercially and were purified and dried by usual methods. The microcell was obtained from the Wilmad Glass Co. The sample bulb was filled with hexamethyldisilane (HMDS') up to its neck, and the space around the bulb was filled with the sample liquid or solution. At first the chemical shifts of the sample (δ_1) were measured with the spherical part of the bulb at the center of the receiver coil, using the HMDS' signal from the sphere as the lock signal. Then the bulb was put down to the bottom of the cell and the chemical shifts of the sample (δ_2) were measured by using the HMDS' signal from the cylindrical part of the microbulb as the lock signal. A good linear relation was obtained by plotting the $\delta_1-\delta_2$ value in ppm against the known values of χ_v[6] for bromoform, chloroform, benzene, and acetone.

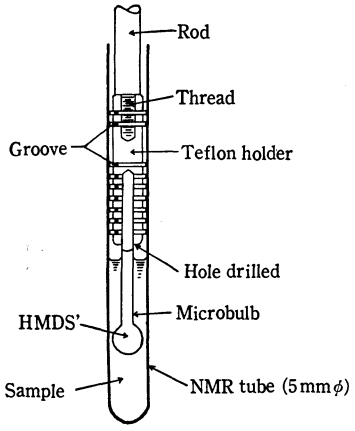

Fig. 1. Illustration of Flath's microcell.[5]

$$\delta_1 - \delta_2 = k[\chi_v(\text{sample}) - \chi_v(\text{HMDS'})] \quad (1)$$

In Eq. (1) k is the difference between the geometrical constants, $g_{cyl}-g_{sph}$, it would be $[2\pi/3-0]=2.094$ for an ideal geometry, but in practice it needs to be determined by calibration.[2,7] In the present case k was shown to be 2.245 from the slope of the linear relation described above. This value was dependent on the shape of the inner bulb, but it was independent of the outer cell and also of the time of measurement if the magnetic field homogeneity had been properly adjusted.

Using Eq. (1) the χ_v values were determined for several organic compounds. The results ($-\chi_v\times 10^6$) are: isobutyl alcohol, 0.623; acetonitrile, 0.527; toluene, 0.620; methanol, 0.523. These values are in good agreement with the results recorded in the literature[6] (0.623, 0.531, 0.620 and 0.527 respectively). The interpolation of the above plots to $\delta_1-\delta_2=0$ shows that χ_v is -0.585×10^{-6} cgs unit for HMDS'; this value has not previously been known, though it can be evaluated to be -0.568×10^{-6} using the gross estimate from Pascal's constant. The relative standard deviation in this technique is about 1.5%.

1) J. R. Zimmerman and M. R. Foster *J. Phys. Chem.* **61**, 282 (1957).
2) H. J. Bernstein and K. Frei, *J. Chem. Phys.*, **37**, 1891(1962).
3) D. C. Douglass and A. Fratiello, *ibid.*, **39**, 3161 (1963).
4) N. C. Li, R. L. Scruggs and E. D. Becker, *J. Am. Chem. Soc.*, **84**, 4650 (1962).
5) R. A. Flath, N. Henderson, R. E. Lundin and R. Teranishi, *Appl. Spectry.*, **21**, 183 (1967).
6) J. W. Emsley, J. Feeney and L. H. Sutcliffe, "High Resolution Nuclear Magnetic Resonance Spectroscopy," Pergamon Press (1965), p. 605.
7) *Ibid.*, p. 260.

Circular Dichroism of the Square Planar Nickel(II) Complexes of [Ni(N)$_4$] Type with L-Amino Acid Amides

Takashi KOMORITA, Jinsai HIDAKA and Yoichi SHIMURA

Department of Chemistry, Faculty of Science, Osaka University, Toyonaka, Osaka

(Received April 30, 1969)

In spite of its fundamental importance, the electronic spectral study has not been made enough on the ligand field bands of square planar nickel(II) complexes of [Ni(N)$_4$] type. This communication is concerned with the confirmation of the spectral correspondence between the bis(L-α-amino-acid-amidato)-nickel(II) and -palladium(II) complexes on the basis of solvent effect on the complexes. The latter has been spectroscopically determined to be the *trans* form.[1]

Bis(L-leucinemethylamidato)nickel(II) and *trans*-bis(L-leucinemethylamidato)palladium(II) were newly isolated as [Ni(L-leuma)$_2$]·H_2O[2] (Found: C, 46.58; H, 8.72; N, 15.45%. Calcd for $C_{14}H_{32}N_4O_3Ni$: C, 46.30; H, 8.88; N, 15.43%.) and [Pd(L-leuma)$_2$] (Found: C, 42.53; H, 7.78; N, 14.08%. Calcd for $C_{14}H_{30}N_4O_2Pd$: C, 42.81; H, 7.70; N, 14.26%). As is seen in Figs. 1 and 2, the negative CD bands at *ca.* 19000 cm^{-1} for then ickel-(II) and at 27100—28100 cm^{-1} for the palladium-(II) complexes change their sign to positive as the solvent changes from water or ethanol to *N,N*-dimethylformamide (DMF). The same spectral behavior was also observed for the nickel(II) and *trans* palladium(II) complexes with L-valinamidate or L- phenylalaninamidate. Furthermore, the higher wave number CD bands of the nickel(II) complexes (*ca.* 24000 cm^{-1})were affected parallel with those of the palladium(II) complexes (*ca.* 36000 cm^{-1}) by the solvents employed.

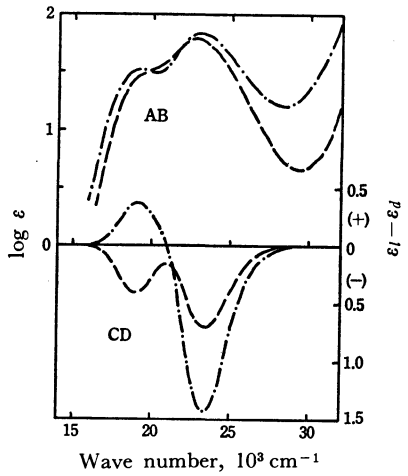

Fig. 1. Absorption (AB) and circular dichroism (CD) spectra of *trans*-[Ni(L-leuma)$_2$].
--- in ethanol, -·-· in DMF

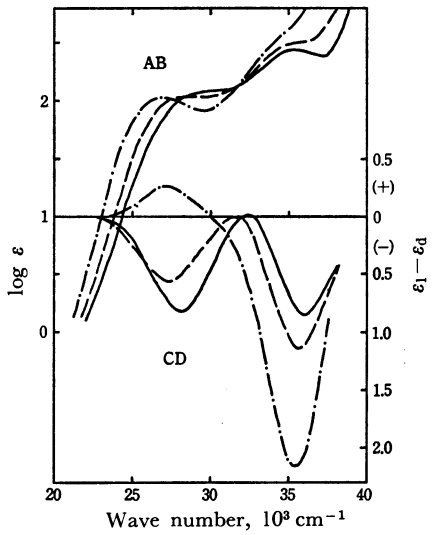

Fig. 2. AB and CD spectra of *trans*-[Ni(L-leuma$_2$].
—— in water, --- in ethanol, -·-· in DMF

The effect of the solvents on the CD of the *cis* palladium(II) complexes is distinctly different from that in the case of the *trans* complexes, especially in the higher wave number CD band (*ca.* 36000 cm^{-1}): the negative intensity of this band is lowered in the *cis* complex with L-leucinamidate or L-valinamidate as the solvent changes from water or ethanol to DMF.

These facts point out that the three nickel(II) complexes cited have the *trans* form in the solutions, and that their CD (or absorption) bands at *ca.* 19000 and *ca.* 24000 cm^{-1} correspond in electronic nature to the bands at *ca.* 28000 and *ca.* 36000 cm^{-1}, respectively, in the corresponding palladium(II) complexes.

1) T. Komorita, J. Hidaka and Y. Shimura, This Bulletin, **41**, 854 (1968).

2) Abbreviation: leuma^{-1}=leucinemethylamidate anion.

BULLETIN OF THE CHEMICAL SOCIETY OF JAPAN VOL. 42 1783—1786 (1969)

The Yield of Hydrogen Atoms in the Vapor Phase Radiolysis of Ammonia

Masaru NISHIKAWA, Kazufumi KURODA and Niro MATSUURA

Department of Pure and Applied Sciences, The University of Tokyo, Komaba, Meguro-ku, Tokyo

(Received June 17, 1968)

γ-Radiolysis of $NH_3+C_3H_8$ mixtures was investigated at 22 ± 1°C and total pressure $\sim$50 cmHg. From the observed yield of hydrogen, H atom yield of ammonia radiolysis of $G_H=5.1$—5.8 was obtained after subtraction of contribution from the propane fraction. The value is significantly lower than that determined from the study of NH_3+D_2 and $NH_3+N_2H_4$ systems, and also that from the study of $NH_3+C_3H_8$ system reported previously. A variety of possibilities is discussed with respect to the cause of the disagreement. The effect of addition of N_2O or SF_6, which acts as an electron scavenger, was also studied. The yield of hydrogen from $NH_3+C_3H_8$ mixtures decreased appreciably, and $\Delta G(H_2)$ in the absence and presence of electron scavengers was related to the change in the neutralization process.

Similarity in the primary processes of radiation chemistry of ammonia and water has often been recognized although the observed yields of products suggest that the subsequent reactions are different. In the radiolysis of water vapor, there exists a controversy over the primary yield of hydrogen atoms. From the study of isotopic exchange in H_2O+D_2 system Firestone[1] obtained $G_H=11.7\pm0.6$, but using organic compounds as H atom scavengers Baxendale and Gilbert[2] determined $G_H=8.0\pm0.7$. To add another factor to the similarity, two different values were recently reported for the hydrogen atom yield in the radiolysis of ammonia, namely $G_H=12.5\pm1$ by Jones and Sworski[3] from the study on NH_3+D_2 and $NH_3+N_2H_4$ systems, and $G_H\gtrsim7.2$ from that on $NH_3+C_3H_8$ system by Johnson and Smic.[4] Again, the value estimated from isotopic exchange is larger than that with the use of organic scavenger. We have also been investigating the radiolysis of ammonia vapor in an attempt to determine G_H using propane as a scavenger for H atoms. The results we observed are similar to those of Johnson *et al.* However, our interpretation involving the estimation of contribution of propane fraction to the total hydrogen production indicated still another value of G_H which is lower than their value.

Experimental

Ammonia (Matheson, 99.9%), propane (>99.8%), nitrous oxide (99.9%), and sulfur hexafluoride (Matheson, >98%) were purified as described previously.[5] Gas chromatographic analysis using squalane on alumina (4.5 m) of propane thus purified indicated that no organic impurities were present at levels exceeding 10^{-3} mol%.

Irradiations were carried out in glass vessels (about 50 ml) fitted with break-seals, baked both in air and at $<10^{-6}$ mmHg before use, in a source of approximately 1000 Ci of ^{60}Co at ammonia pressure of about 50 cmHg and 22 ± 1°C.

Nitrous oxide was used for dosimetry, assuming $G(N_2)=10.0$.[6] The energy absorbed in ammonia (E_a) and in propane (E_p) were calculated using the ratio of stopping powers per molecule obtained by Meisels.[7] The dose rate used was 1.5×10^{16} eV mol^{-1}sec^{-1} in ammonia.

The non-condensable products, hydrogen and nitrogen, were analyzed by combustion in a cupric oxide furnace heated at $\gtrsim$350°C.

Results

Product yields are expressed in terms of G-values calculated for energy absorbed by ammonia, unless otherwise stated. Effect of additives on the product yields are as follows.

Propane. Hydrogen yield steadily increased from $G(H_2)=4.1$ of pure ammonia to 7.8 at 8.6 mol% of propane, while nitrogen yield was markedly depressed (Fig. 1). The increase of hydrogen yield with propane concentration suggests hydrogen production from the direct radiolysis of propane fraction in addition to scavenging H atom from

1) R. F. Firestone, *J. Am. Chem. Soc.*, **79**, 5593 (1957).
2) J. H. Baxendale and G. P. Gilbert, *Discussions Faraday Soc.*, **36**, 186 (1963).
3) F. T. Jones and T. J. Sworski, *Trans. Faraday Soc.*, **63**, 2411 (1967).
4) G. R. A. Johnson and M. Simic, *Nature*, **216**, 479 (1967).
5) M. Nishikawa and N. Shinohara, *Radiation Res.*, **33**, 194 (1968).
6) F. T. Jones and T. J. Sworski, *J. Phys. Chem.*, **70**, 1546 (1966).
7) G. G. Misels, *J. Chem. Phys.*, **41**, 51 (1964).

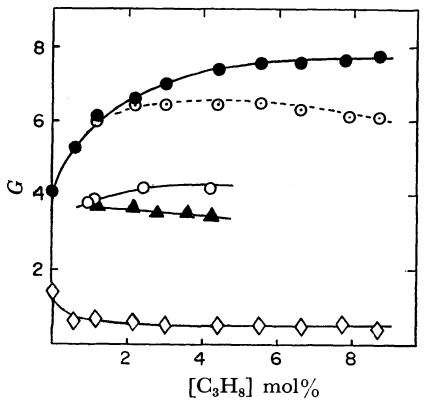

Fig. 1. G-Values of products from $NH_3+C_3H_8$ mixtures.
●, total H_2 from $NH_3+C_3H_8$; ○, H_2 corrected for contribution of C_3H_8 fraction; ○, total H_2 with N_2O ($p_{N_2O}/p_{NH_3}\cong 0.05$); ▲, total H_2 with SF_6 ($p_{SF_6}/p_{NH_3}\cong 0.005$); ◇, N_2 from $NH_3+C_3H_8$

ammonia, so that correction is necessary. The amount of hydrogen produced from propane fraction was estimated from the energy absorbed in propane taking $G(H_2)=7.5$[8] and assuming absence of energy transfer. The yield of hydrogen corrected in this manner, which is a measure of hydrogen produced in ammonia fraction, is also plotted in Fig. 1. The contribution of propane fraction to the total hydrogen can also be estimated by plotting G-values of total yield (G_t) calculated for the total energy absorbed by the mixture ($E_t=E_a+E_p$) against the fraction of energy absorbed in propane ($f_p=E_p/E_t$). The plot was utilized by Johnson and Simic,[9] and by Jones and Sworski.[3] A good straight-line relationship is demonstrated for lower f_p region where energy transfer between ammonia and propane is negligible, but at f_p higher than 0.15, $G(H_2)_t$ is seen to deviate from the straight line in Fig. 2. Extrapolation of straight portion to $f_p=0$ yields $G(H_2)^\circ=5.84\pm0.05$.

Hydrazine. At the concentration of 5.3 mol%, $G(H_2)=10.0$ and $G(N_2)=7.8$; at 7.4 mol%, $G(H_2)=9.9$ and $G(N_2)=7.6$. They are in fair agreement with the values reported by Jones and Sworski,[3] if converted into $G(H_2)_t$/fraction of stopping power of $NH_3(f_a)$ for comparison.

Sulfur Hexafluoride. $G(H_2)$ decreased from 0.91 at 0.6 mol% to 0.84 at 1.1 mol%, while $G(N_2)$ increased from 2.1 to 2.2.

Propane + Nitrous Oxide or Sulfur Hexafluoride. The effect of addition of N_2O ($p_{N_2O}/p_{NH_3}=0.05$) or SF_6 ($p_{SF_6}/p_{NH_3}=0.005$) to $NH_3+C_3H_8$ mixtures is shown in Figs. 1 and 2. The previous study indicates the concentration of N_2O

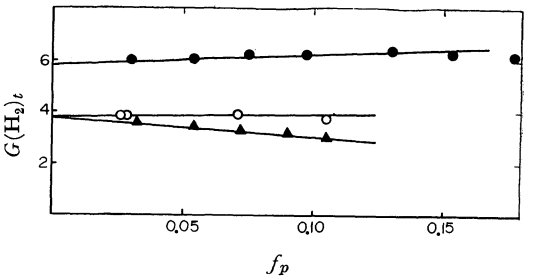

Fig. 2. Dependence of $G(H_2)_t$ on the fraction of energy absorbed by C_3H_8 ($f_p=E_p/E_t$).
●, from $NH_3+C_3H_8$; ○, with N_2O($p_{N_2O}/p_{NH_3}\cong 0.05$); ▲, with SF_6 ($p_{SF_6}/p_{NH_3}\cong 0.005$)

to be sufficient to scavenge all the electrons produced at the dose rate employed. In Fig. 2, a straight line relationship is demonstrated between $G(H_2)_t$ and f_p in both cases, extrapolation of which leads to approximately the same value, $G(H_2)^\circ\cong 3.8$. In order to see if the energy absorbed in the SF_6 in the mixture contributes to the formation of hydrogen, the concentration of SF_6 was varied to $p_{SF_6}/p_{NH_3}=0.016$ at the propane concentration of 3.6 mol%, and to 0.012 at 4.2 mol%. At both concentrations $G(H_2)_t$ increased by about 10%, indicating the presence of small contribution. It is tentatively assumed that the contribution is negligible at $p_{SF_6}/p_{NH_3}=0.005$. $G(N_2)$ is depressed from 9.8 of NH_3+N_2O (100 : 5) to 3.5 by the addition of C_3H_8 (1—3 mol%) to NH_3+N_2O mixtures.

Discussion

Hydrogen atoms react with propane by

$$H + C_3H_8 \rightarrow H_2 + C_3H_7 \quad (k\sim 2\times 10^6 M^{-1}\cdot sec^{-1})[10] \qquad (1)$$

Charge and proton transfer from NH_4^+, which is the principal ionic species in the radiolysis of ammonia,[11] to propane can be excluded on the energetic grounds because of the low ionization potential for NH_4,[12] and the high proton affinity of NH_3,[13] while on the same ground transfer from $C_3H_8^+$ to NH_3 can occur. The hydrogen yield from the radiolysis of $NH_3+C_3H_8$ mixtures may be composed of the "molecular" hydrogen from ammonia (A), that produced through reaction (1) by H atoms formed in ammonia (B), and that produced in propane fraction (C). In order to estimate the contribution of propane fraction to the hydrogen yield, it is necessary to determine the extent of energy transfer between propane and ammonia. Since this cannot be accomplished from the product analysis without the use of isotopically

8) G. R. A. Johnson and J. M. Warman, *Trans. Faraday Soc.*, **61**, 1709 (1965).
9) G. R. A. Johnson and M. Simic, *J. Phys. Chem.*, **71**, 1118 (1967).
10) H. A. Kazmi, R. J. Diefendorf and D. J. Le Roy, *Can. J. Chem.*, **41**, 690 (1963).
11) C. E. Melton, *J. Chem. Phys.*, **45**, 4414 (1966).
12) C.E. Melton and H. W. Joy, *ibid.*, **46**, 4275 (1967).
13) A. P. Altschuller, *J. Am. Chem. Soc.*, **77**, 3480 (1955).

labeled additives, two methods were used as the zeroth approximation, both assuming energy transfer being negligible at lower concentration range of propane. One of the methods is simply to subtract the yield of hydrogen calculated for energy absorption in propane from the total yield. A narrow range of plateau in $G(H_2)$ is seen in Fig. 1, which should be a measure of (A)+(B), *i. e.*, $G_H+G_{H_2}=6.5$. The other method is based on the equation

$$G(H_2)_t = G(H_2)_a^\circ \cdot f_a + G(H_2)_p^\circ \cdot f_p = G(H_2)_a^\circ + [G(H_2)_p^\circ - G(H_2)_a^\circ] \cdot f_p \quad (1)$$

where G_a° and G_p° are those due to energy deposited in ammonia and in propane, respectively, and f_a and f_p are the fraction of energy absorbed by ammonia and by propane in the mixture, which is given by $f_a = s_a[NH_3]/(s_a \cdot [NH_3] + s_p \cdot [C_3H_8])$ where s is the relative stopping power per unit concentration.[7] At the lower f_p region the plot of $G(H_2)_t$ *versus* f_p demonstrates a sufficiently straight line in Fig. 2, which, according to Eq. (1), indicates that the assumption may be justified. The intercept, $G(H_2)_a^\circ = 5.84 \pm 0.05$, should then be another measure of $G_H+G_{H_2}$ of ammonia. The slope of the straight line gives $G(H_2)_p^\circ = 10.4$; the value determined by Johnson and Warman is 7.5.[8] $G_{H_2}=0.74$ of ammonia radiolysis determined earlier[5] is in excellent agreement with 0.75 reported by Jones and Sworski[3] and with <0.8 by Johnson and Simic.[4] It follows that the value of G_H lies in the range of 5.1 to 5.8, which is significantly lower than those reported by Jones and Sworski and by Johnson and Simic. It is not obvious whether due corrections were made to the contribution of propane fraction to hydrogen yield by Johnson and Simic. If not, the neglect of (C), could account for most of the disagreement with their value. It is also possible that the disagreement is due to difference in the dose rate used (their dose rate is higher by a factor of 100), although it is not altogether clear how it should affect the yield in ammonia-propane system. The more serious disagreement with Sworski's value might be, at least in part, inherent in the system they used. For example, with the NH_3+D_2 system they observed G_H as high as 90 ± 66 at the ammonia pressure of 600 Torr by a fairly complicated kinetic analysis using a variety of parameters. High G-values are usually attributed to some kind of chain mechanism. In fact, very high G(HD) observed at 200°C is explained in terms of a chain mechanism involving D atoms. Since $G_H=90$ was determined at 24°C, the mechanism would probably include ionic species, if chain reactions are to be invoked. Some ambiguity, therefore, still remains in $G_H = 12.5 \pm 3.0$ at 200 Torr.

In $NH_3+N_2H_4$ system, H_2 is considered to be formed from H atoms as precursors mainly by the reaction $H+N_2H_4 \rightarrow H_2+N_2H_3$,[3] as well as a minor fraction of "molecular" H_2. Johnson and Simic observed that $G(H_2)$ of $NH_3+C_3H_8$ system is independent of temperature over the range 20—200°C at around 8.0, while that of pure ammonia increases to $G(H_2) \cong 15$ at 200°C. Similar results in the pure ammonia were observed by Jones and Sworski. Our results on the $NH_3+C_3H_8$ system at high densities ($d \sim 0.1$ g/ml) and 140°C also indicate a constant $G(H_2)$ independent of temperature and density.[14] Since the marked depression of $G(N_2)$ by propane, observed by Johnson and also in the present work, suggests scavenging of precursors of nitrogen,

$$NH_2 + C_3H_8 \rightarrow NH_3 + C_3H_7 \qquad \Delta H = -9\text{—}11 \text{ kcal/mol} \quad (2)$$

the difference in the hydrogen yield between pure ammonia and $NH_3+C_3H_8$ at elevated temperatures could be accounted for by hydrogen formation from intermediates other than H atoms which is favored at higher temperatures. At low temperatures reactions conceivable for H and NH_2 include:

$$H + H \rightarrow H_2 \quad (3)$$
$$H + NH_2 \rightarrow NH_3 \quad (4)$$
$$H + NH_3 \rightarrow NH_2 + H_2 \quad (5)$$
$$NH_2 + NH_2 \rightarrow N_2H_4 \quad (6)$$
$$H + N_2H_4 \rightarrow H_2 + N_2H_3 \quad (7)$$
$$NH_2 + N_2H_4 \rightarrow NH_3 + N_2H_3 \quad (8)$$

Reaction (5) is unimportant at $\sim$20°C because of the activation energy of 10—15 kcal/mol,[15] while it certainly is favored at elevated temperatures, resulting in the enhancecment of NH_2 concentration, hence the importance of reactions (6) and (8) over that of reaction (4). It appears, therefore, that the reactions involving NH_2 and/or species whose precursor is NH_2 might not be excluded as a source of hydrogen. One such example is seen in the reaction included by Dainton *et al.*[16] in the mechanism of radiolysis of liquid ammonia.

$$NH_2 + N_2H_3 \rightarrow NH_3 + N_2 + H_2 \qquad \Delta H = -99 \text{ kcal/mol} \quad (9)$$

Addition of hydrazine to ammonia as the scavenger for hydrogen atoms would, at the same time, increase such possibilities even at $\sim$20°C, while with propane as additive the main reaction paths are (1) and (2), which do not lead to such possibilities.

Explanation of $G_H=12.5$ analogous to what has been advanced to account for $G_H=11.7$ of water vapor in terms of the neutralization $H_3O^+ + e^- \rightarrow 2H + OH$[17] is not feasible, since if $NH_4^+ + e^- \rightarrow NH_2 + 2H$ occurs in ammonia at a higher tempera-

14) M. Nishikawa, K. Kuroda and N. Matsuura, This Bulletin, **42**, 116 (1969).

15) M. Schiavello and G. G. Volpi, *J. Chem. Phys.*, **37**, 1510 (1962).

16) F. S. Dainton, T. Skwarski, D. Smithies and E. Wezranowski, *Trans. Faraday Soc.*, **60**, 1068 (1964).

17) E. J. Hart and R. L. Platzman, "Mechanisms in Radiobiology," Vol. 1, Academic Press, New York (1961), p. 176.

ture where the extent of clustering would be less than that at 20°C, hydrogen yield from $NH_3+C_3H_8$ mixtures should increase in controversy to the observation. Futhermore, the reaction

$$NH_4^+\cdot(NH_3)_2 + e^- \rightarrow 2NH_3 + NH_2 + 2H$$

is endothermic by 40 kcal/mol[18] and $NH_4^+\cdot(NH_3)_2$ is the most abundant ions observed at 1 Torr and 100°C.[19]

Sulfur hexafluoride does seem to react with H atoms as well as electrons in the radiolysis of NH_3+SF_6 mixtures, as is indicated by the marked decrease in $G(H_2)$ which approaches the value obtained using olefins as additives, although the reaction of H atoms with SF_6 is reported to be slow.[20] It is not unreasonable, since the reaction $H+NH_3\rightarrow NH_2+H_2$ does not proceed at room temperature. Other possibilities such as quenching of precursor for H atoms by SF_6 cannot be ruled out.

The reactions of SF_6 and N_2O may be considered to be solely the scavenging of electrons in the $NH_3+C_3H_8$ system, since the molar ratio N_2O/C_3H_8 and SF_6/C_3H_8 in the present work are well below those reported by Johnson and Simic[9] where the reaction of H atoms with N_2O and with SF_6 can be excluded. The decrease in the yield of hydrogen by these additives may, therefore, be assumed to be due to the change in the neutralization process of ammonium ions from ion-electron to ion-ion. The depression of the hydrogen yield, $\Delta G(H_2)=3$—4, shown in Fig. 1 (the difference was taken from the uncorrected values of $G(H_2)$ as an approximation), is of the order of $100/W$ and is consistent with the change of the neutralization process from $NH_4^++e^-\rightarrow NH_2+H$, to the ion-ion recombination, where no hydrogen is produced. On the other hand, in Fig. 2, the plot of $G(H_2)_t$ with SF_6 and with N_2O *vs.* f_p both extrapolate to $G(H_2)^\circ=3.8$. The difference in $G(H_2)^\circ$ in the presence and absence of electron scavengers in this case is only ~2, which is significantly lower than the value estimated from W-value, if it really represents the contribution of ionic processes. The increase in the $\Delta G(H_2)$ with propane concentration in Fig. 2 may suggest that these electron scavengers influence hydrogen formation in the propane fraction more strongly. In ammonia+propane system all the ions are supposed to be rapidly converted into NH_4^+ by the ion-molecule reactions before neutralization.

$$NH_3^+ + NH_3 \rightarrow NH_4^+ + NH_2 \quad (10)$$

$$NH_2^+ + NH_3 \rightarrow NH_3^+ + NH_2 \quad (11)$$

$$RH^+ + NH_3 \rightarrow NH_4^+ + R \quad (12)$$

where RH^+ represents hydrocarbon ions. The dose rate employed in the present work might be in the region where electrons can diffuse to the wall and the neutralization at wall can compete with that in the gas phase. In fact, $\sim5\times10^{11}$ eV/m*l*·sec of the present work lines in the range where Woodward and Back[21] observed the depression of hydrogen yield for a variety of hydrocarbons which was explained in terms of the stabilization of species formed by the wall neutralization. If the neutralization of NH_4^+ takes place at the wall, hydrogen is bound to be produced, although some stability was shown for the species NH_4.[12] The lower value of $G(H_2)^\circ$ estimated in Fig. 2 may be ascribed to the competition between neutralization of ammonium ions in the gas phase and at the wall. At the present stage, the experimental data are still by far insufficient to decide which of the $\Delta G(H_2)$ by electron scavengers is the true measure of the importance of ionic processes.

The slope of the straight line for $NH_3+C_3H_8+N_2O$ system gives $G(H_2)_p{}^\circ=4.5\pm0.4$ in comparison to $G(H_2)=4.9$ of the propane radiolysis in the presence of N_2O determined by Johnson and Warman.[8] The slope of the line with SF_6 as electron scavenger and the difference from the line with N_2O are still puzzling. The effect of impurities in SF_6 may be ruled out, because the discrepancy becomes larger with propane concentration if SF_6 concentration is kept constant to that of ammonia. The trend may suggest the presence of some kind of interactions between SF_6 and propane. Another possibility is the production of hydrogen by the reaction of N_2O, for example, with NH_2. $G(N_2)=9.8$ at $N_2O/NH_3=0.05$ is markedly depressed by the addition of propane to $G(N_2)=3.5$ over the concentration range of 1 to 3 mol%, suggesting the principal mode of reaction between NH_2 and N_2O is to produce nitrogen, however, reactions such as

$$NH_2 + N_2O \rightarrow N_3 + H_2O$$

$$N_3 + NH_3 \rightarrow 2N_2 + H_2 + H$$

cannot be ruled out. In any case, the study using isotopically labeled additives together with the electron scavengers is definitely necessary to obtain informations for the elucidation of the discrepancy.

We should like to acknowledge valuable discussion with Dr. K. Fueki of Nagoya University and with Dr. N. Shinohara of Yokohama City University.

18) Thermochemical data used in the calculation are: Ionization potential; NH_4=5.9 eV,[12] H=13.6 eV; Proton affinity; NH_3=202 kcal/mol,[13] Heat of clustering of NH_4^+; $\Delta H_{0,2}=-46.3$ kcal/mol,[19] $D(H_2N\text{–}H)$ =104 kcal/mol.

19) A. M. Hogg, R. M. Haynes and P. Kebarle, *J. Am. Chem. Soc.*, **88**, 28 (1966).

20) C. P. Fenimore and G. W. Jones, *Combust. Flame*, **8**, 231 (1964).

21) T. W. Woodward and R. A. Back, *Can. J. Chem.*, **41**, 1463 (1963).

BULLETIN OF THE CHEMICAL SOCIETY OF JAPAN VOL. 42 1787—1795 (1969)

Effect of Some Cationic Detergents on Macromolecularly Stabilised Emulsions with Special Reference to Sodium Alginate and Gum Arabic as Emulsifiers

Chandra PRAKASH and S. N. SRIVASTAVA

Chemical Laboratories, Agra College, Agra, India

(Received August 21, 1968)

The effect of some cationic detergents *viz.* cetyl pyridinium bromide, lauryl pyridinium chloride and phenyl trimethyl ammonium chloride has been studied on stabilised by sodium alginate and gum arabic emulsions. Zeta potentials were measured at different concentrations of cationic detergents microelectrophoretically. The particle size was determined microphotographically. With the help of zeta potential and particle size the interaction energies were calculated by summing up attraction and repulsion energies in the light of D.V.O. theory. For attraction energy the van der Waals constant was computed theoretically from the optical data and was obtained to be 6.7×10^{-14} erg. The interaction energies thus obtained gave very high energy barriers which completely obviated the occurrence of flocculation in primary minima, causing flocculation to occur in secondary minima. The theoretical degrees of aggregation were calculated and plotted at different values of A. The flocculation occurring in the system was observed haemocytometrically by counting the number of singlets and doublets and the degrees of aggregation were calculated. With the help of observed degrees of aggregation the operating value of van der Waals constant has been estimated by interpolating them into the theoretical curves, which is an indirect approach to ascertain the value of van der Waals constant. The values of A obtained are 3.0×10^{-13} and 2.6×10^{-13} erg for sodium alginate and gum arabic systems respectively. The binding parameters, number of binding sites available and free energy of adsorption have also been calculated.

Cationic detergents are the substances, generally, of high formula weight and are very specific in their surface active effects. These substances ionize in water giving positively charged long chain groups as well as anion. This positively charged part behaves as a typical polyvalent cation and hence is more efficient in flocculating negatively charged sols and emulsions. Cationic detergents produce hydrophobic surfaces, thus they have got much importance in industry. The hydrophobic groups bearing cationic polar heads are adsorbed on the surface of either negatively charged oil globules of an emulsion or solid sol particles.

A number of references on detergents are available in the literature of colloid science. Neogy and Ghosh[1] have made an exhaustive investigation of xylene-in-water emulsions stabilised by cationic detergents *viz.* cetyl dimethyl benzyl ammonium chloride, cetyl pyridinium bromide and cetyl trimethyl ammonium bromide. Recently Haydon and Phillips[2] have published some papers dealing, in general, with cationic and anionic detergents. They dealt with Gibbs equation and the surface equation of state for soluble ionized monolayers in absence of added electrolyte at the oil-water interface. They[3] studied the influence of trace of electrolytes on interfacial tension at the oil/water interface for dodecyl trimethyl ammonium bromide and sodium dodecyl sulphate systems. Haydon and Taylor[4] investigated the influence of ionic size on double layer potentials at the oil-water interface. They tested the systems for adsorbed long chain alkyl sulphates in water and of sodium dodecyl sulphate and dodecyl trimethyl ammonium bromide. Biswas and Haydon[5] studied the effect of tetradecyl trimethyl ammonium bromide on the stability of petroleum ether drops at flat surface in 0.1% bovine serum albumin solution and also compared the stability of petroleum ether drops stabilized by 0.1% bovine

1) R. K. Neogy and B. N. Ghosh, *J. Indian Chem. Soc.*, **29**, 573 (1952); **30**, 113 (1953).

2) D. A. Haydon and J. N. Phillips, *Trans. Faraday Soc.*, **54**, 698 (1958).

3) D. A. Haydon and J. N. Phillips, *Nature*, **178**, 813 (1956).

4) D. A. Haydon and F. H. Taylor, III Intern. Congress of Surface Activity Cologne, Vol. 2 (1960).

5) B. Biswas and D. A. Haydon, *Kolloid-Z.*, **185**, 32 (1962).

serum albumin in presence of tetradecyl trimethyl ammonium bromide, with the shear moduli of elasticity of the adsorbed films. Lyklema[6] recieved the factors governing the stability of thin detergent films.

From the survey of the above literature it is concluded that a number of studies have been made covering different aspects of cationic detergents but still there is lack of quantitative data in the light of D.V.O. theory. Therefore, under the present investigation an attempt has been made to study the effect of some cationic detergents *viz.* phenyl trimethyl ammonium chloride (Ammonyx-200), lauryl pyridinium chloride and cetyl pyridinium bromide on emulsion stability in the light of D.V.O. theory and to evaluate van der Waals constant with the help of flocculation data. These studies were made in detail with sodium alginate system only and partially with gum arabic emulsion also.

Experimental

Sodium alginate and gum arabic samples were obtained from B.D.H. A pure sample (99.5%) of phenyl trimethyl ammonium chloride was obtained with the courtesy of Onyx Corporation, U.S.A. A pure sample of lauryl pyridinium chloride (LPC) was supplied by Industrial Products, Bombay, which was further crystallised with acetone. An I.C.I. sample of cetyl pyridinium bromide was used which was recrystallised with acetone.

The emulsion was prepared by dispersing 4% of petroleum ether in aqueous solution of sodium alginate or gum arabic containing 0.01% KCl initially. The counting of the drops for flocculation studies was carried out haemocytometrically as mentioned elsewhere.[7] The electrophoretic measurements were carried out in a rectangular Northrup and Kunitz flat type microcataphoretic cell mounted on the base of the Carl Zeiss Zena microscope. To minimise polarization Ag-AgCl electrodes were used, which were fitted in electrode chambers, filled with electrolyte solution of equiconducting to that of emulsion. A D.C. microammeter of Cambridge Industrial Co., Ltd., England, No. L 32132 was used for measuring the current. The microscope was focussed at stationary level which was obtained by studying the mobilities of particles at different depths which in trun gave a parabolic curve. The mobilities of the particles were measured in direct as well as reverse direction and the mean was taken. The accuracy of the apparatus was 1.0 mV.

From the mobility data, the zeta potentials were calculated by using the Overbeek[8] equation for symmetrical electrolytes, where the relaxation correction has been applied.

$$U = \frac{\epsilon\zeta E}{\sigma\pi\eta}\left[f_1(\kappa a) - Z^2\left(\frac{e\zeta}{kT}\right)^2 f_3(\kappa a) - \frac{\rho_+ + \rho_-}{\sigma\pi\eta e}\left(\frac{e\zeta}{kT}\right)^2 f_4(\kappa a)\right]$$

where U, velocity of the particle, ρ_+ and ρ_- the friction constants, η the viscosity of the dispersion medium, k the Boltzmann constant, e the electronic charge. $f_1(\kappa a)$, $f_2(\kappa a)$, $f_3(\kappa a)$, $f_4(\kappa a)$, the Henry functions taken from elsewhere (Overbeek *loc. cit.*).

The interfacial tension measurements were carried out with Du Nouy tensiometer No. 70535 (Central Scientific Co., Chicago, U.S.A.) having an accuracy of 0.1 dyne.

Theory of the Particle Interaction

In the frame work of D.V.O. theory the interaction energy of the colloidal particles is given by $V = V_R + V_A$, where V_A, the attraction energy, V_R, the repuslvie energy and V, the sum of the repulsive and attraction energies. The repulsive energy calculations were carried out by using an approximate expression by Derjaguin and Kussakov.[9]

$$V_R = \frac{\varepsilon a \psi^{\circ 2}}{2} \ln(1 + e^{-\kappa H}) \qquad (1)$$

where ψ° the surface potential (assumed equal to the electro-kinetic potential for the present system having ($\kappa a \gg 1$), ε is the dielectric constant in the double layer, a the particle radius, H the interparticle distance and κ the Debye-Hückel parameter.

The attraction energies were calculated, keeping in view the retardation correction, by equation due to Schenkel and Kitchener.[10]

$$\left.\begin{aligned} V_A &\approx \frac{-Aa}{\pi}\left(\frac{2.45\lambda}{120H^2} - \frac{\lambda^2}{1045H^3} + \frac{\lambda^3}{5.62\times 10^4 H^4}\right) && \text{Valid for } H > 150\text{Å} \\ V_A &\approx \frac{-Aa}{12H}\left(\frac{\lambda}{\lambda + 3.54H\pi}\right) && \text{Valid for } H < 150\text{Å} \end{aligned}\right\} \qquad (2)$$

where λ is the wavelength of the London frequency and is taken as 1000 Å, and A is the van der Waals constant.

Thus the interaction energy V can be evaluated. Therefore, knowing V, the number of particles in a shell ds around a central particle and consequently degree of aggregation or the total number of particles associated with a given central particle can be calculated[7] theoretically from the following equation.

$$D = \int 4\pi n_0 a^3 S^2 e^{-V/kT} ds \qquad (3)$$

6) J. Lyklema, *Rec. Trav. Chim.*, **81**, 890 (1962).
7) C. Prakash and S. N. Srivastava, This Bulletin, **40**, 1765 (1967).
8) J. Th. G. Overbeek, "Advances in Colloid Science," Vol. III, p. 115.
9) B. Derjaguin and M. Kussakov, *Acta. Phys. Chim., URSS*, **10**, 25 (1939).
10) J. N. Schenkel and J. A. Kitchener, *Trans. Faraday Soc.*, **56**, 161 (1960).

where n_0 is the number of droplets per unit volume of the emulsion and $s=2+H/a$. The intergrand of the above expression is evaluated graphically and the integration limits are arbitrarily selected. The lower limit is readily chosen keeping in view that at sufficiently small values of s, V becomes strongly positive. Again as $s\rightarrow\infty$, $V\rightarrow 0$ and the integral tends to infinity. Therefore, the choice of the upper limit is not straightforward. In the present systems, however, V becomes strongly negative in a narrow range of s, and the value of the integral is, for any reasonable choice of the upper limit, approximately constant.

In case of the reversible or secondary minimum flocculation, as in the present system, a singlet-doublet equilibrium temporarily exists in the system and the extent of flocculation in the system can be determined from the formula.

Calculation of Binding Parameters

Binding parameters were calculated from the treatment mentioned earlier[7] and the important equations are presented below

$$\sigma_s = \frac{N_1 ev}{1+\frac{55.6}{C}\exp\left(\frac{\Delta G}{kT}\right)} \tag{4}$$

where σ_s, the charge density of the Stern layer, e the electronic charge, v valency of the cation, c the molar concentration of the added electrolyte, N_1 the binding sites per cm^2 and $-\Delta G$ is the free energy of adsorption per molecule.

This can be put in the form

$$\left.\begin{aligned} \sigma_s &= \frac{k_1 c}{1+k_2 c} \\ \text{where}\quad k_2 &= \frac{\exp\left(\frac{-\Delta G}{kT}\right)}{55.6} \\ k_1 &= N_1 k_2 ev \end{aligned}\right\} \tag{5}$$

These k_1 and k_2 are the adsorption constants which can be calculated from the following equations at the zero point of charge, which finally yields the following equations

$$\frac{1}{c} = \left(\frac{4\pi ev N_1 k_2}{\kappa\varepsilon\psi_\delta^\circ} - k_2\right) \tag{5}$$

$$\left(\frac{d\psi_\delta^\circ}{d\ln c}\right)_{\psi_{\delta=0}^\circ} = \left(\frac{\kappa\varepsilon\psi_\delta^\circ}{4\pi ev k_1} - 1\right)\psi_\delta^\circ \tag{7}$$

where v is the valency and $\left(\frac{d\psi_\delta}{d\ln c}\right)\psi^\circ_{\delta=0}$ is the slope of the log C-zeta potential curve (assuming $\psi_s^\circ=\zeta^\circ$), c is the concentration of the electrolyte at the zero point charge.

Computation of van der Waals Constant

Hamaker[11] suggested that van der Waals constant can be calculated from the following equation

$$A_{ii} = \pi^2 q_i^2 B_i \tag{8}$$

where q_i is the number of atoms of kind i contained in 1 ml of the matter. B_i is the London constant relative to the same substance, which is to be computed separately. But in the present system since the petroleum ether (p.e.), instead of being separated by a vacuum, is immersed in an aqueous medium, the net constant is given by following equation.[12]

$$A = (A_{\text{p.e.-p.e.}}^{1/2} - A_{\text{H}_2\text{O-H}_2\text{O}}^{1/2}) \tag{9}$$

The London constant, B can be calculated by four approximate formulae (a) The London equation[13]

$$B_L = \frac{3}{4}\alpha^2 h\nu_0 \tag{10}$$

Where ν_0 is the characteristic London frequency corresponding to the rotation of peripheral electrons and α is the polarisability.

(b) The Slater-Kirkwood equation[14]

$$B_{S-K} = 11.25\times 10^{-24}\cdot n^{1/2}\cdot\alpha^{3/2} \tag{11}$$

where n, number of valency electrons.

(c) The Slater-Kirkwood equation modified by Moelwyn-Hughes[15]

This new equation takes into account the effective number of dispersion electrons, S_1, thereby leading to

$$B_{S-K-M} = \frac{3}{4}\sqrt{S_1 n}\cdot h\nu_e\alpha^2$$

where ν_e, the electronic vibration frequency is given by

$$\nu_e = \frac{2532}{\sqrt{\alpha}}$$

and S_1, is given by an empirical equation,

$$S_1 = 0.39n$$

$$B_{S-K-M} = 7.8\times 10^{-24}\times n\cdot\alpha^{3/2} \tag{12}$$

(d) The Neugebaur, equation[16]

11) H. C. Hamaker, cited in "Theory of Stability of Lyophobic Colloids," Elsevier Publishing Co., Amsterdam (1948).
12) H. C. Hamaker, *Physics*, **4**, 1058 (1937).
13) F. London, *Z. Physik*, **63**, 245 (1930).
14) J. C. Slater and J. C. Kirkwood, *Phys. Rev.*, **37**, 682 (1931).
15) Moelwyn-Hughes, "Physical Chemistry," Pergamon Press, London, pp. 383, 1957.
16) Th. Neugebaur, *Z. Physik*, **167**, 785 (1937).

$$B_N = -1.62\times10^{-6}\cdot\alpha\chi \qquad (13)$$

where χ being the diamagnetic susceptibility.

As mentioned before, the calculation of van der Waals constant from Eqs. (10)—(13) requires the polarisability which has been calculated from the Clausius-Mosotti equation[17] modified by Moelwyn-Hughes (*loc. cit.*),

$$\alpha = \frac{3M}{4\pi Nd}\cdot\frac{\rho^2-1}{\rho^2+1}\cdot\frac{v_0^2-v^2}{v_0^2} \qquad (14)$$

where M, the molecular weight, N the Avogadro number and ρ is the index of refraction at the London wavelength. Since the refractive index is not directly available at the London wavelength, the quantity, $\frac{v_o^2-v^2}{v_o^2}$ is the extrapolation factor for ρ determined at the frequency. The latter quantity in its turn is also determined indirectly from the dispersion equation of Sellmeier[18] *viz.*

$$\rho^2 - 1 = \frac{C\lambda_1^2}{\lambda_1^2-\lambda_0^2}$$

where λ_1 and λ_0 are respectively the wavelengths of light and of the characteristic absorption bands and C is a constant. It is obvious that to solve such equation, refractive indices at least for two wavelengths are required. For this the refractive index of petroleum ether was measured spectrometrically at 4047 Å, 4358 Å, 5461 Å and 5770 Å and corresponding indices were found to be 1.419, 1.4155, 1.408 and 1.405 respectively. Feeding these values into the above equation λ_0 can be evaluated. The value of v_0 obtained from λ_0 is 2.50×10^{15} cm/sec. This leads to a value of the extrapolation factor to be 0.957 at 5770 Å. Thus the value of ρ for the calculation of α has been taken as 1.4056 at 5770 Å.

The molecular weight of petroleum ether has been taken as 100 which agrees with the observed value (98.5) of molecular weight determined cryoscopically. The observed value of density (d) is 0.72 at 25°C. The value of α found in this manner is 1.635×10^{-23} cm^3/mol.

For calculating the London constant α, h and v_0 are available and with the proper choice of units the London constant is

$$B_{L_{p.e.}} = \frac{3}{4}(1.635\times10^{-23})^2\times6588\times10^{-27}\times2.5\times10^{15}$$
$$= 3.277\times10^{-57}\ \text{erg}\cdot\text{cm}^6$$

$$B_{S-K_{p.e.}} = 11.25\times10^{-24}\times(8)^{1/2}\times(1.635\times10^{-23})^{3/2}$$
$$= 2.10\times10^{-57}\ \text{erg}\cdot\text{cm}^6$$

where n, the number of electrons is 8, assuming that the petroleum ether molecule is composed of CH_4. Further

$$B_{S-K-M_{p.e.}} = 7.8\times10^{-24}\times8\times(1.635\times10^{-23})^{3/2}$$
$$= 4.12\times10^{-6}\times1.635\times10^{-23}$$
$$\times(-0.88\times10^{-6})\times\frac{100}{6\times10^{23}}$$
$$= 3.73\times10^{-57}\ \text{erg}\cdot\text{cm}^6$$

where the value of the specific susceptibility is -0.88×10^{-6} cgs units.[19]

The corresponding values of these constant for water with $=1.43\times10^{-24}$ cm^3/mol, $n=8$, $\chi=0.72\times10^{-6}$ cgs units as given by Verwey and Overbeek[20]

$$B_L^{H_2O} = 3.30\times10^{-59}$$
$$B_{S-K}^{H_2O} = 5.40\times10^{-59}$$
$$B_{S-K-M}^{H_2O} = 7.28\times10^{-59}$$
$$B_N^{H_2O} = 5.10\times10^{-59}$$

now by finding q (4.34×10^{21}), the number of molecules of petroleum ether contained per ml from the knowledge of its molecular weight and density with the help of Eq. (8), the van der Waals constant for petroleum ether and corresponding constants for water can be calculated and hence net attraction constant for petroleum ether drops can be estimated from Eq. (9). The results are summarised in Table 1, where in the last column a correction has been made for the reduction of London force due to its transmission through a medium whose dielectric constant is not equal to unity. This is done by dividing the constant A by 1.8, the square of the refractive index of water, 1.36. The mean of the first three readings was taken because fourth is very low.

The mean value of van der Waals constant thus obtained is 6.7×10^{-14} erg, which will be taken for calculation of interaction profiles.

Results and Discussion

(a) Particle Size. For particle size of the drops the microphotographs were taken with Olympus camera at 15×40 magnification. These were further enlarged four times. From the each photograph the size frequency curves were plotted by measuring the size of about 500 drops. The average size for sodium alginate is 1.0 μ and for gum arabic is 1.2 μ. The size frequency curve of

17) Ref. 15.

18) W. Sellmeier, *Pogg. Ann.*, **143**, 272 (1871); "The Science and Petroleum," A. E. Dunsten *et al.*, Oxford University, London, **2**, 1141 (1938).

19) International Critical Table, **6**, 362 (1929).

20) E. J. W. Verwey and J. Th. G. Overbeek, "Theory of Stability of Lyophobic Colloids," Elsevier Publishir.g Co., Amsterdam (1948).

TABLE 1

Equation used	$A_{p.e.-p.e.}$ in vacuum $\times 10^{13}$ erg	$A_{H_2O-H_2O}$ $\times 10^{13}$ erg	A in H_2O $\times 10^{14}$ erg	A (corrected) $\times 10^{14}$ erg
S-K	1.34	5.95	16.5	9.16
S-K-M	2.64	7.70	13.2	7.33
N	2.39	5.61	6.2	3.44
L	2.10	3.66	2.2	1.22
			Mean of the first three values=6.7	

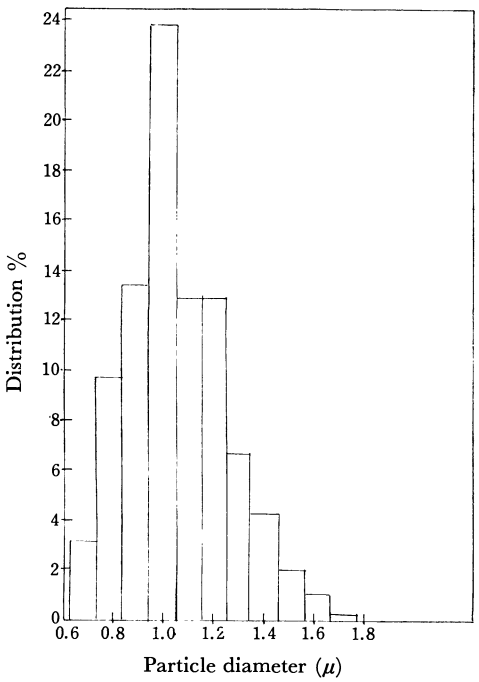

Fig. 1. Particle size distribution of sodium alginate emulsion.
mean diameter=1.0 μ

sodium alginate is shown in Fig. 1.

(b) Effect of Cationic Detergents on Zeta Potential. The zeta potentials of stabilised emulsions by sodium alginate and gum arabic were measured in the presence of cetyl pyridinium bromide (CPB, $C_{16}H_{33}C_6H_5NBr$), lauryl pyridinium chloride (LPC, $C_{12}H_{25}C_6H_5NCl$) and phenyl trimethyl ammonium chloride (Ammonyx-200, $C_6H_5N(CH_3)_3Cl$). In Fig. 2 the plots of zeta potential against log molar concentration are given for sodium alginate and gum arabic systems.

The curves obtained, in general, are of inverted S-shape. It can be seen that only LPC and CPB could reverse the charge of sodium alginate system. The effect of LPC on gum arabic emulsion was studied only. An appreciable change in zeta potential could not be observed even upto 1 mM of it. The relevant data are presented in Table 3. Ammonyx-200 could not reverse the charge even

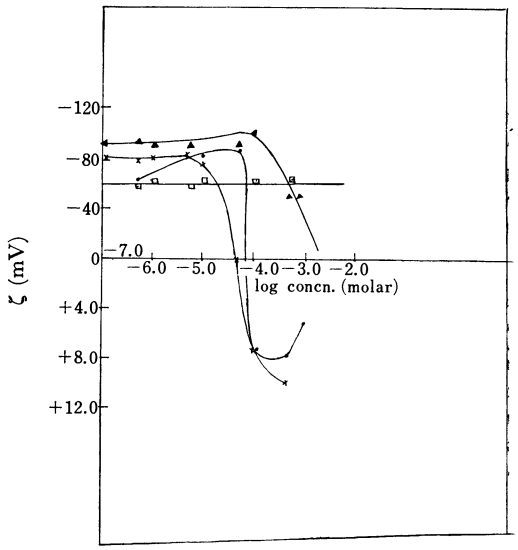

Fig. 2. Zeta potentials as a function of log concentration (molar) of cationic detergents.
Sodium alginate
(•) Lauryl Pyridinium chloride
(×) Cetyl Pyridinium bromide
(▲) Phenyl trimethyl ammonium chloride
Gum arabic
(⊡) Lauryl Pyridinium chloride

upto 10^{-2}M, exhibiting thereby its weak efficacy. With increasing concentration of LPC and CPB, the zeta potential decreases continuously but at higher concentrations the charge of the system is reversed. After reversal of charge the absolute value of the zeta potential again increases with increasing concentration and the system again acquires stability, though the emulsion globules are now positively charged. During this the critical micelle concentrations of the surfactants are also reached. These variations in stability can be explained as follows. It is likely that during the addition and mixing concentrated solution of detergent to the system conditions could occur in which the micellar solution of the detergent became submicellar. The breaking down of micelles to submicelles is a very fast reaction.[21] The time required during mixing the detergent to the system is of the same order as required for breaking down of the micelles, mutual coagulation would occur between the micelles and the stabilised emulsion drops resulting in an artificial decrease in stability.

Ammonyx-200 seems to have a very weak cationic efficacy. The ζ-potential increased with increasing concentration of the detergent and then a continuous decrease is obtained. This behaviour has got close analogy with 1 : 1 electrolytes.

21) R. H. Ottwill and M. C. Rastogi, *Trans. Faraday Soc.*, **56**, 866 (1960).

(c) Determination of Flocculation Concentration and Calculation of Some Binding Constants. The flocculating concentrations obtained at the zero point of charge are presented in respective Table 2. From the flocculating concentrations it is obvious that the capacity for reversing the charge is CPB, LPC, Ammonyx-200 because the carbon chain lengths are in decreasing order and hence their CMC values are expected to be in increasing order. Therefore, the concentrations required for flocculation should be in increasing order as the carbon chain decreases.

The low flocculating concentrations are in accordance with the idea that coagulation under these conditions is due to the adsorption of the cationic surface active agent on the negatively charged drops. At low detergent concentrations adsorption appears to occur by interaction of the positively charged head group of the molecules. Thus increasing chain length decreases the available area for adsorption and hence decreases the flocculation concentration. Therefore, CPB with larger chain length is more effective than LPC. Bromide and chloride ions have little influence on the process.[21] The same interpretation can be given for Ammonyx-200 also.

The binding constant k_1, k_2, number of binding sites available N_1, and free energy of adsorption $-\Delta G$ were calculated with the help of flocculating concentration and the slope of the log concentration-zeta potential curve. The calculated values are presented in the Table 2.

From the values of the number of binding sites, in case of these detergents, it is evident that LPC and CPB are having fewer number than Ammonyx-200 which clearly shows that number of sites available would depend upon its capacity for charge reversal. Thus Ammonyx-200 could not reverse the charge in spite of adding upto 1×10^{-3}M concentration while in the case of others of the order of 10^{-5}M is quite sufficient. The low value of the free energy is in conformity with the value that Ammonyx-200 is a weak cationic detergent. The greater number of cations is required to reverse the charge if cations have got low free energy of adsorption.

(d) Interfacial Tension Measurements in Presence of Cationic Detergents. Since interfacial tension has some bearing on the stability of emulsion, it was thought of interest to make some interfacial tension measurements also in the presence of cationic detergents on sodium alginate system. The interfacial tension studies were carried out in the presence of 0.01% KCl and 0.01% sodium alginate in aqueous phase. The cationic detergents used were LPC and CPB. The interfacial tension in dynes/cm is plotted against log molar concentration in Fig. 3.

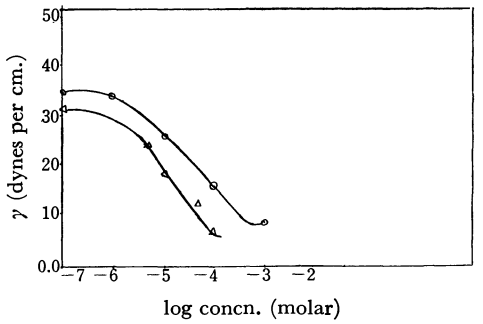

Fig. 3. Interfacial tension of sodium alginate emulsions as a function of cationic detergents.
(⊙) Lauryl pyridinium chloride
(△) Cetyl pyridinium bromide

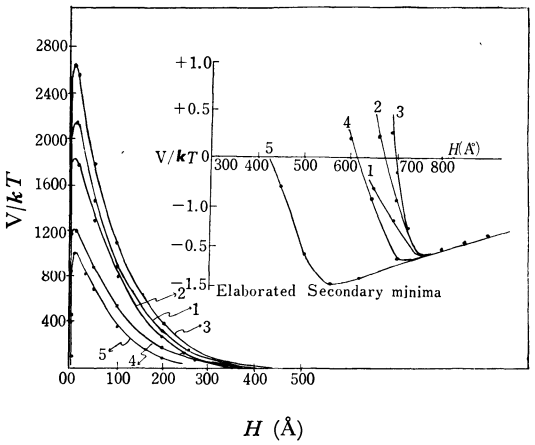

Fig. 4. Plot of interaction energy *versus* interparticle distance for sodium alginate emulsions flocculated by lauryl pyridinium chloride.
(1) 1×10^{-7}M (4) 1×10^{-4}M
(2) 1×10^{-6}M (5) 1×10^{-3}M
(3) 1×10^{-5}M

TABLE 2

Detergent	Flocculating concentration	k_1	k_2	N_1 groups/cm^2	$-\Delta G$ kcal/mol
Sodium alginate system					
LPC	8.1×10^{-5}M	2.84×10^{7}	3.70×10^{4}	1.60×10^{12}	7.92
CPB	5.0×10^{-5}M	2.26×10^{6}	1.24×10^{4}	3.80×10^{11}	8.58
Gum arabic system					
LPC	Charge reversal is not obtained up to the concentration of 5.0×10^{-4}M.				

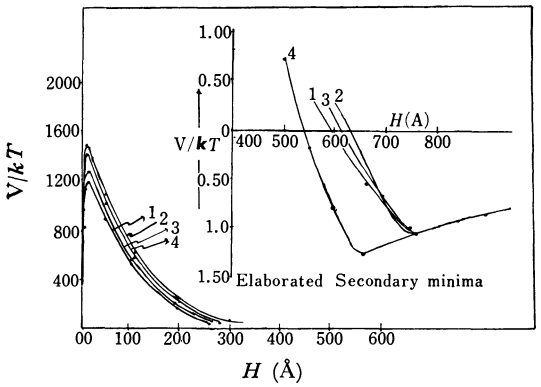

Fig. 5. Plot of interaction energy *versus* interparticle distance for gum arabic emulsions flocculated by lauryl pyridinium chloride.
(1) 5×10^{-7}M (3) 1×10^{-4}M
(2) 1×10^{-5}M (4) 5×10^{-4}M

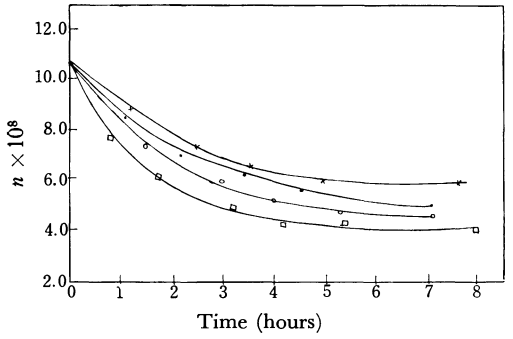

Fig. 6. Plot of number of individual drops against time for sodium alginate emulsions flocculated by lauryl pyridinium chloride.
(•) Zero, (□) 1×10^{-6}M, (○) 1×10^{-5}M,
(×) 1×10^{-3}M

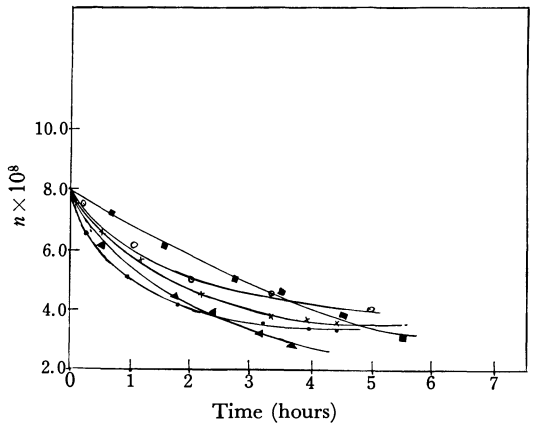

Fig. 7. Plot of number of individual drops against time for gum arabic emulsions flocculated by lauryl pyridinium chloride.
(•) Zero, (■) 1×10^{-7}M, (▲) 1×10^{-6}M,
(×) 1×10^{-5}M, (⊙) 5×10^{-5}M

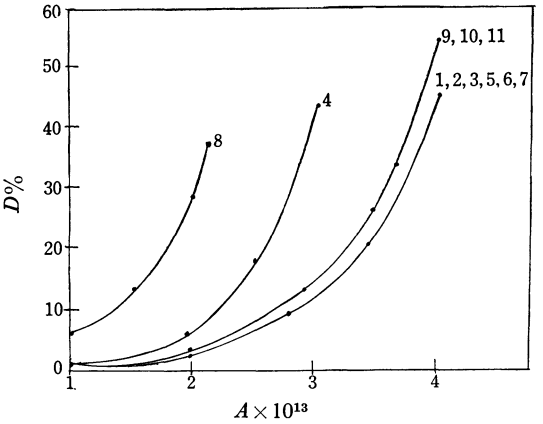

Fig. 8. Degrees of flocculation as a function of van der Waals constant for sodium alginate system.
1, 2, 3 for 10^{-7}M, 10^{-6}M, 10^{-5}M Lauryl pyridinium chloride.
4 for 10^{-3}M Lauryl pyridinium chloride.
5, 6, 7 for 10^{-7}M, 10^{-6}M, 10^{-5}M of cetyl pyridinium bromide
8 for 10^{-4}M of cetyl pyridinium bromide
9, 10, 11 for 10^{-7}M, 10^{-6}M, 10^{-5}M of Ammonyx-200

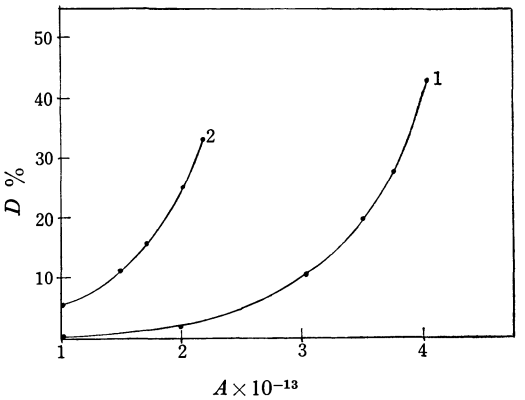

Fig. 9. Degrees of flocculation as a function of van der Waals constant for gum arabic emulsions.
1 for 10^{-5}M Lauryl pyridinium chloride
2 for 5×10^{-5}M Lauryl pyridinium chloride

From the figure it is obvious that the interfacial tension, at lower concentrations, does not change much but at higher concentrations the fall is rapid.

(e) Interaction Energy Curves, the Degrees of Aggregation and the van der Waals Constant of the Emulsion Droplets. The interaction energies between two drops at different concentrations of Ammonyx-200, LPC and CPB have been calculated with the help of corresponding zeta potentials. These energies, for $La(NO_3)_3$, are plotted against distance in Figs. 4 and 5 choosing as representative curves for sodium alginate and gum arabic systems. The relevant data for all the curves are presented in Table 3. From the table it is obvious that the energy barrier in each

TABLE 3

Detergent concentration molar	Zeta potential mV	Height of maxima kT	Interparticle distance at $V=0$ (graphically) Å
For sodium alginate emulsion			
Cetyl pyridinium bromide			
1×10^{-7}	−81.0	2481.5	670
1×10^{-6}	−80.3	2401.5	670
1×10^{-5}	−75.8	2146.5	620
1×10^{-4}	+75.0	2134.5	625
Lauryl pyridiniym chloride			
1×10^{-7}	−57.0	1163.5	570
1×10^{-6}	−69.3	1788.0	650
1×10^{-5}	−82.7	2585.0	670
1×10^{-4}	+76.0	2134.5	620
Ammonyx-200			
1×10^{-7}	−90.0	2469.0	670
1×10^{-6}	−92.0	3236.0	720
1×10^{-5}	−60.0	1296.5	630
1×10^{-3}	−57.9	2361.5	625
For gum arabic emulsion			
Lauryl pyridinium chloride			
1×10^{-5}	−64.0	1444.5	650
1×10^{-4}	−61.1	1241.5	580
1×10^{-4}	−63.0	1391.5	610

TABLE 4

Concentration of the detergent	D% observed	Value of A corresponding to D% observed $A\times10^{13}$ erg	Mean value
Sodium alignate emulsion			
Ammonyx-200			
1×10^{-7}M	18.7	3.16	
1×10^{-6}M	18.0	3.30	
1×10^{-5}M	16.4	3.07	
CPB			
1×10^{-7}M	13.1	3.05	3.03×10^{-13} erg
1×10^{-6}M	16.0	3.20	3.0×10^{-13} erg
1×10^{-5}M	13.5	3.10	
1×10^{-4}M	12.4	3.05	
LPC			
1×10^{-7}M	13.0	3.05	
1×10^{-6}M	14.1	3.10	
1×10^{-5}M	10.9	2.95	
1×10^{-3}M	12.1	2.30	
Gum arabic emulsion			
LPC			
1×10^{-5}M	15.9	3.30	2.6×10^{-13} erg
5×10^{-5}M	17.9	1.80	

case is very high, which obviated the possibility of occurrence of flocculation in the primary minima. The observed flocculation occuring in the system is only possible in secondary minimum. All the curves are levelled off after certain time indicating the flocculation in secondary minima. To indicate the nature of flocculation occurring in the systems, the monomers and dimers were counted at different intervals. The number of monomers are plotted against time and two representative set of curves for both the systems are shown in Figs. 6 and 7. Therefore, these secondary minima, which are of main importance, are depicted separately. These secondary minima are a few kT deep. These depths though sufficient for the occurrence of secondary minima flocculation are rather insufficient to explain the observed degrees of aggregation. This apparent discrepancy may be due to not choosing the correct (operating value) of A. Therefore, an indirect method of estimating A has been adopted. To estimate van der Waals constant of the system, the theoretical degrees of aggregation were calculated at dirrerent values of A at different concentration of the detergents. These observed degrees of aggregation were interpolated in the theoretical curves, as shown in Figs. 8 and 9, and

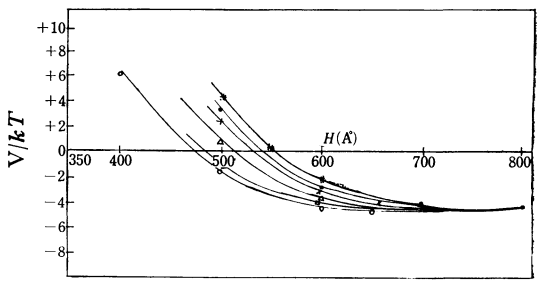

Fig. 10. Plot of secondary minima with observed value of van der Waals constant for sodium alginate.
(●) 1×10^{-7}M Cetyl pyridinium bromide
(×) 1×10^{-5}M Cetyl pyridinium bromide
(○) 1×10^{-7}M Lauryl pyridinium chloride
(△) 1×10^{-6}M Lauryl pyridinium chloride
(※) 1×10^{-7}M Ammonyx-200
(□) 1×10^{-5}M Ammonyx-200

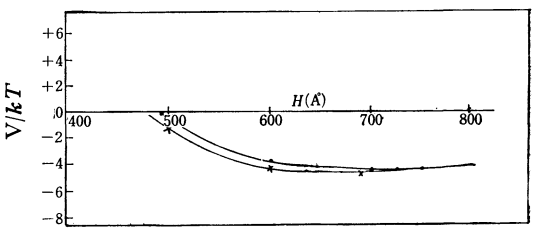

Fig. 11. Plot of secondary minima with observed value of van der Waals constant for gum arabic.
(•) 1×10^{-5}M Lauryl pyridinium chloride
(×) 1×10^{-4}M Lauryl pyridinium chloride

the corresponding values of A obtained are tabulated in Table 4.

The theoretical and experimental degrees of aggregation were calculated similarly as mentioned before. The van der Waals constants for sodium alginate and gum arabic systems are 3.0×10^{-13} erg and 2.6×10^{-13} erg respectively. The van der Waals constant of petroleum ether differs from the theoretical value (6.7×10^{-14} erg) of A, probably because of the difference between adsorption of an emulsifier and that of detergent.[22] The secondary minima are plotted with the revised value of A, which are sufficiently deep to warrant reversible flocculation (Figs. 10 and 11).

The authors wish to express the thanks to Professor B. N. Ghosh, Calcutta University for kindly allowing one of them to carry out microelectrophoresis and also to the authorities of C.S.I.R., New Delhi for kindly granting a fellowship to one of them (C.P.).

22) M. J. Vold, *J. Coll. Sci.*, **11**, 575 (1956).

BULLETIN OF THE CHEMICAL SOCIETY OF JAPAN VOL. 42 1795—1799 (1969)

Role of Doped Lithium in Nickel Monoxide in the Formation of Higher Valency Nickel Oxides by Anodic Oxidation

Hiroshi YONEYAMA and Hideo TAMURA

Department of Chemical Technology, Faculty of Engineering, Osaka University, Yamadakami, Suita, Osaka

(Received September 27, 1968)

The anodic oxidation and cathodic reduction behavior of a sintered body of lithiated nickel oxide were studied. The electrode with the higher Li content was more active than that with the lower Li content with regard to the electrochemical oxidation and reduction in the potential range between oxygen and hydrogen evolution. The quantity of the higher-valency nickel oxide having an apparent valence state of nickel ions from +8/3 to +4 formed by the anodic oxidation was estimated by measuring the quantity of electricity required for reducing it to −0.14V *vs.* SCE. This quantity is proportional to the Li content for electrodes containing more than 0.04 atom% of Li.

Lithium ions in the electrolyte have significant effects on the charge-discharge behavior of the nickel electrode in the Ni–Cd battery system;[1] for example, they increase the capacity and decrease the self-discharge. In battery systems the nickel electrode is usually prepared by "forming" nickel hydroxide, and the composition of this active mass is changed complicatedly by charge-discharge cycles.[2,3] Therefore, the role of the lithium in the behavior of the electrode during charge-discharge cycles has not yet been determined quantitatively. As, however, it has been proved that lithium ion enters into the active mass by repeated charge-discharge cycles,[3] the increase in the capacity of the electrode may be attributed to this phenomena. We have studied the oxidation and reduction behavior of a nickel monoxide electrode containing a fixed amount of lithium ions in order to clarify the relation between the lithium content and the quantity of the higher valency nickel oxides formed by anodic oxidation.

1) E. J. Casey, A. R. Dubois, P. E. Lake and W. J. Moroz, *J. Electrochem. Soc.*, **112**, 371 (1965).

2) G. W. Briggio and W. F. K. Wynne-Jones, *Trans. Faraday Soc.*, **52**, 1272 (1956).

3) D. Tuomi, *J. Electrochem. Soc.*, **112**, 1 (1965).

Experimental

Chemicals. All the chemicals used in this study were of a guaranteed reagent grade.

Preparation of Samples. Nickel monoxide was prepared from $Ni(NO_3)\cdot 6H_2O$ by heating it at 600°C for 4 hr in the air. NiO powder thus prepared contained the following impurities; Zn: 140, Ca: 330, Mg: 2750, Pb: 80, Cu: 920, Cr: 60, Mn: 190, Al, Si, Fe, trace (the contents are represented in ppm). This powder was mixed with a known amount of a Li_2CO_3 solution in acetic acid. After having been mixed for about 30 min with a magnetic stirrer, they were evaporated to dryness and then heated again at 600°C for a few hour in the air. The powder was formed into a tablet at 1.5 t/cm^2 (10 mm dia. 3—5 mm thick) and this tablet was sintered at 1200°C for 4 hr covered with a

thick-layer of the same powder to prevent the Li from evaporating. After sintering, platinum contacts on the end faces of the tablet were made by firing platinum powder pasted on them at 1250°C by the procedure used in the sintering.

Specific Resistivity of the Sample. The specific resistivity of the sample pieces ρ was estimated from the voltage drop V between the platinum contacts, the surface area S and the thickness L of the sample, according to the $V/I=\rho \cdot S/L$ relation, where I is the current passed through the contacts.

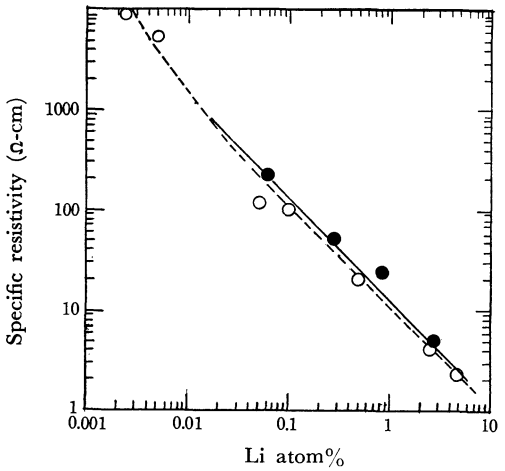

Fig. 1. Relation between Li content and resistivity at 25°C.
-●- this studies, --○-- by Verway *et al.*[4]

Li Content. The samples which were not used in the following experiments were dissolved in hot concentrated HNO_3 and the Ni was removed as nickel dimethyl glyoxim. The quantity of Li in the filtrate was measured by spectrophotometry. The relations between the resistivity and Li content in the samples were very similar to the results obtained by Verway *et al.*,[4] as is shown in Fig. 1. From these results, the Li contents of the samples used in this study were estimated from the results of the measurement of the resistivity. The resistivities and Li contents of the test electrodes are shown in Table 1.

TABLE 1. THE SAMPLES USED AS TEST ELECTRODE

Notation of electrode	A	B	C	D	E
Resistivity at 25°C (Ω-cm)	5.6	40	66	400	1800
Li content (atom %)	2.6	0.30	0.21	0.04	0.009

Cell Equipment. Before carrying out the experiment in a cell equipment, one side of the platinum contacts was erased and polished with emery papers. As these samples had a porosity of 3—10%, they were impregnated with a benzene solution of polystylene under a vacuum and then evaporated to dryness. This procedure was repeated a few times, and then the surface of the sample was slightly polished with 1000-mesh emery paper. The sample was then mounted in a glass tube with epoxy resin and used as the test electrode. Before the electrode behavior was examined, the resistance of this electrode was measured in 6N KOH by means of the impedance bridge and the effective electrode area was estimated, by the same procedure as was used in estimating the specific resistivity, assuming that the thickness of the sample piece used as the electrode was equal to an unmounted one. After being dipped in concentrated HNO_3 and then washed with de-ionized water, the electrode was placed in a conventional cell. The cell was sealed with a rubber stopper with a gas inlet and outlet. The counter electrode was a platinized platinum plate. All the measurements were carried out at 25°C in a nitrogen atmosphere and with the light shielded. The electrolyte was 0.1N NaOH.

Measurement of the Anodic-cathodic Behavior. The electrode potential was measured against the SCE. In the cathodic reduction 100 μA/cm^2 was usually chosen, while in anodic oxidation various current densities, ranging from 100 μA/cm^2 to 10 mA/cm^2 were chosen. The oxidation-reduction cycles at each electrode did not exceed 10 in this study.

Result

Figure 2 shows the electrode potential behavior of the A and the C electrodes when they were anodically oxidized immediately after the cathodic reduction in which their potential had attained that of hydrogen evolution. On the other hand, when they were cathodically reduced immediatly after the anodic oxidation for 5 min under a fixed current density, the electrode potential was gradually changed, as is shown in Fig. 3. The phase-transition potential calculated thermodynamically is also shown in these figures (the phase transition from Ni_3O_4 to $Ni(OH)_2$ or the inverse is indicated Ni_3O_4-$Ni(OH)_2$, while another transition is also indicated in a similar fashion). As these results show, if the electrode was oxidized until its potential

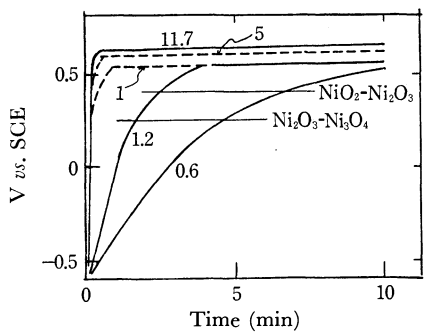

Fig. 2. Electrode potential behavior during anodic oxidation.
Solid line: 5.6 Ω-cm. Dotted line: 66 Ω-cm. The numbers in the figure represent current density (mA/cm^2).

4) E. J. W. Verway, P. W. Haaijman, F. C. Romeijn and G. W. van Osterhout, *Philips Res. Rept.*, **5**, 173 (1950).

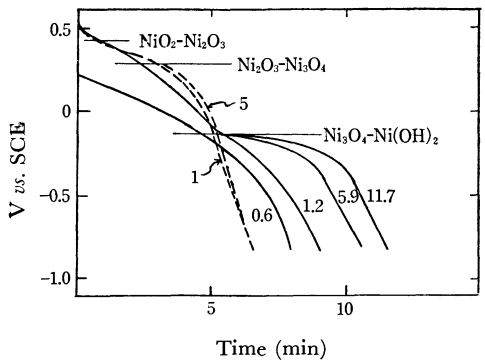

Fig. 3. Electrode potential during reduction of constant current immediatly after anodic oxidation for 5 min.
Solid line: 5.6 Ω-cm, reduction current density 590 μA/cm^2. Dotted line: 66 Ω-cm, reduction current density 200 μA/cm^2. The numbers in the figure represent current density of anodic oxidation (mA/cm^2).

was reached in the flat region, the behavior of the electrode potential during the cathodic reduction to −0.14 V was not influenced by the current density of anodic oxidation. At the A electrode (5.6Ω-cm), however, a stagnation of the potential change, indicating transformation from Ni_3O_4 to $Ni(OH)_2$[5] was observed, and its length was influenced by the anodic-oxidation-current density. This was not observed in the C electrode (66Ω-cm). These facts show that the nickel monoxide electrode, which contains a large amount of Li, has a tendency to undergo composition change more easily. The length of the stagnation of the potential change above mentioned was also influenced by the repeating cycles especially when a high current density was used in the oxidation. Therefore, in the following experiments, we studied the electrode behavior in the potential region above −0.14 V.

Figure 4 shows the potential behavior of four electrode, A (5.6Ω-cm), B (40Ω-cm), D (400Ω-cm), and E (1800Ω-cm), when they were oxidized at 100 μA/cm^2 and 1 mA/cm^2 after they had been reduced to −0.14 V. The potential rise is much faster in the electrode containing less Li, and at current densities above 1 mA/cm^2 the electrode potential reaches the flat region within 5 min. When the electrode whose potential lay in the flat region as a result of anodic oxidation was reduced mainly at 100 μA/cm^2, the quantity of electricity Q required for reduction to −0.14 V was constant for each electrode, regardless of the current density of the anodic oxidation and oxidation-reduction cycles. For example, the results obtained at the A (5.6 Ω-cm) and D (400 Ω-cm) electrodes are as shown in Table 2 while the potential

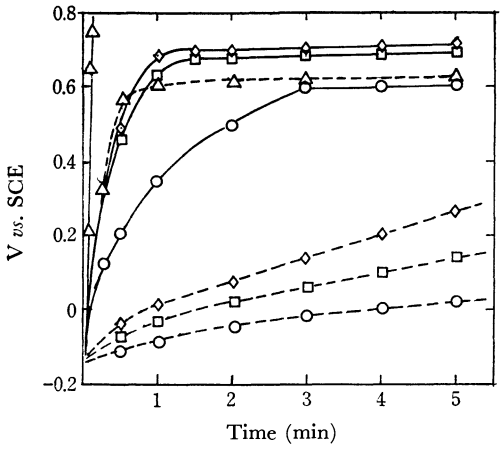

Fig. 4. Electrode potential behavior during oxidation.
Solid line: current density 1 mA/cm^2. Dotted line: current density 100 μA/cm^2.
○ 5.6 Ω-cm, □ 40 Ω-cm, ◇ 400 Ω-cm, △ 1800 Ω-cm

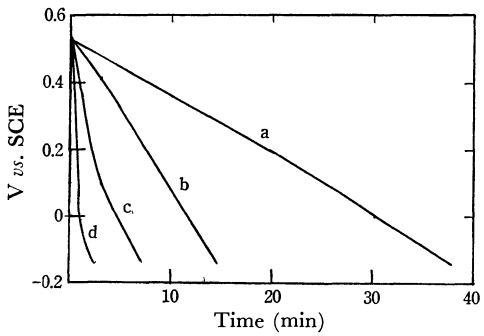

Fig. 5. Electrode potential behavior during cathodic reduction immediately after anodic oxidation.
a: 5.6 Ω-cm, b: 40 Ω-cm, c: 400 Ω-cm, d: 1800 Ω-cm

Table 2. Quantity of electricity required in reduction to −0.14V of the oxides formed under the various oxidation conditions

Electrode	Oxidation current density × time (mA/cm^2) (min)	Quantity of electricity required in reduction to −0.14 V (mC/cm^2)
A	10 × 5	188*
(5.6Ω-cm)	10.4× 5	203**
	1 × 5.05	206
	1 ×10	207**
D	1 × 5	38.8
(400Ω-cm)	0.1×20.9	37.5
	0.5×2.2	37.6
	0.5×5	39.3
	1 ×4.8	38.7

Reduction current density was 100 μA/cm^2, except for * 50 μA/cm^2, ** 1 mA/cm^2.

5) The value calculated thermodynamically is −0.119 V *vs.* SCE.

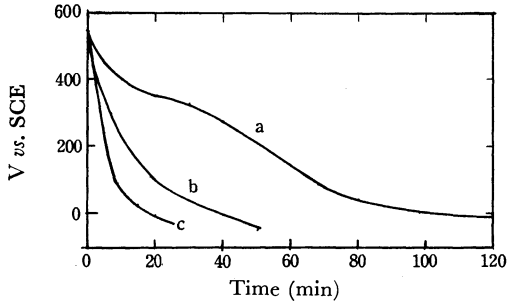

Fig. 6. Behavior of open circuit potential after oxidation up to oxygen evolution under the oxidation condition (mA/cm^2×min).
a: 5.6 Ω-cm (1×16), b: 40 Ω-cm (0.1×23)
c: 400 Ω-cm (1×3)

behavior of each electrode during reduction to −0.14 V is as shown in Fig. 5. When the electrodes were open-circuited after oxidation up to the oxygen evolution, the potentials of these electrode gradually fell, as Fig. 6 shows. On the other hand, when the electrodes were reduced to −0.14 V at 100 μA/cm^2, a build-up of the potential was observed after the reduction current had been interrupted at various potentials between that of oxygen evolution and −0.14 V, though at the A electrode it did not appear clearly. Even with this electrode, however, this phenomenon was observed distinctly when the reduction-current density was 10 mA/cm^2. When the reduction current was interrupted at a potential below −0.14 V, the build-up of potential was observed distinctly and the potential of the electrode easily reached −0.14 V or more, as is shown in Fig. 7.

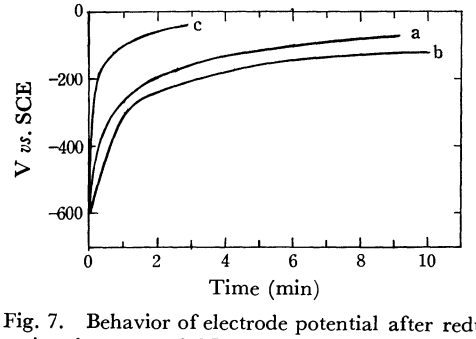

Fig. 7. Behavior of electrode potential after reduction down to −0.6 V *vs.* SCE under the reduction current density (mA/cm^2).
a: 5.6 Ω-cm (1 mA/cm^2), b: 40 Ω-cm (0.1 mA/cm^2), c: 400 Ω-cm (0.1 mA/cm^2)

Discussion

The quantity of electricity Q obtained by reducing the electrode to −0.14 V is calculated to be 10—200 mC/cm^2, depending on the Li content in the electrode. Q is nearly equivalent to the quantity of the higher-valency nickel oxides, with the apparent valence state of nickel ions ranging from +8/3 to +4.

Taking the specific gravity of NiO as 6.66, the number of Ni ions per sq. cm of the NiO electrode surface is calculated to be 1.4×10^{15}/cm^2. Although the specific gravity may be changed by doping the Li, it could not be changed greatly in this study because the electrode in this study contained only 2.6 atom% Li at most. Therefore, if it is supposed that 1.4×10^{15}/cm^2 divalent nickel ions exist on the electrode surface and that all of these ions are oxidized to the tetravalent, Q is calculated to be 0.3 mC/cm^2. By comparing this calculated Q value with the experimental Q value, the nickel ions participating in the electrochemical reaction amount to 30—600 times the value calculated, depending on the Li content. This suggests the depth of the NiO ion layer from the surface participating in the reaction at potentials above −0.14 V. However, by considering the error introduced in the estimation of the specific resistivity, the true electrode area must be much larger than the apparent area, hence, the reaction is limited in the thinner surface layer of the electrode.

When NiO is oxidized electrochemically, oxygen ions enter into the NiO lattice. As the NiO electrode was confirmed to be well crystallized by X-ray diffraction, the transfer of oxygen ions into the interior of the NiO crystal may be difficult. Considering the fact that Q is constant regardless of the oxidation conditions, the formation of higher-valency oxides with apparent valence states from +8/3 to +4 is limited by some factor related to the crystal structure rather than with the rate of the diffusion of oxygen ions. This is also suggested by the results shown in Fig 3. In this figure the plateau showing a transition from Ni_3O_4 to $Ni(OH)_2$ appears at the A electrode in proportion to the current density of anodic oxidation, though the potential behavior is coincident at higher potentials. This phenomenon may indicate that oxygen ions are transfered into the NiO lattice in proportion to the electric field across the electrode in such a way that one oxygen ion is arranged into three ion pairs of Ni^{2+} and O^{2-} after the formation of the higher-valency oxides with apparent valence states of nickel ions from +8/3 to +4. Probably this structure would be energetically most stable.

Nickel hydrate is probably formed at potentials above −0.14 V, and $Ni(OH)_2$ is formed below this potential while reducing the electrode. The former can not be produced in a quantity more than the equivalent of Q, the formation of the latter is also considered to be poor, for the potential of the electrode easily fell to that of the hydrogen evolution and the recovery of the electrode potential after interrupting the reduction current at potentials lower than −0.14 V was quick as is shown in

Fig. 7. The difficulty of the formation of $Ni(OH)_2$ may be due to the same reason as in the formation of the higher-valency oxides; that is, in this case the transfer of H_2O into the NiO lattice is apparently necessary to convert NiO to $Ni(OH)_2$, and this is probably difficult. Therefore, it is probable that Ni_3O_4 was reduced to NiO on the plateau of the potential showing the conversion of Ni_3O_4 to $Ni(OH)_2$ in Fig. 3.[6]

On the basis of the finding that Q was constant on each electrode, almost all of the protons in nickel hydrate or $Ni(OH)_2$ were considered to be possibly transferred into the electrolyte when the electrode was oxidized under the experimental conditions. This is probable because the hydrate or hydroxide layer was very thin, if it was present at all.

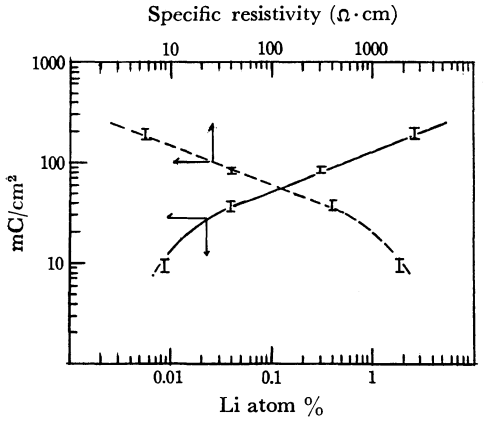

Fig. 8. Plot of Q against Li content and resistivity of the electrode.

The Q values at each electrode are plotted against the resistivity of the electrode and the Li content in Fig. 8. In the case of Li contents more than 0.04 atom%, the following relationship exists between Q and the Li content C in NiO, if allowance is made for the accuracy of Q being within ±5%.

$$\log Q = 0.40 \log C + 2.14$$

where Q is shown in mC/cm^2 and C, in atom%.

In the reduction period, diffusion of ions in the electrode-surface region is slow, especially at low Li contents, hence, Q does not indicate correctly the quantity of the higher-valency oxides with the apparent valence states of nickel ions from +8/3 to +4, especially at electrodes of low Li contents. In order to make Q exactly equivalent to the quantity of the higher valency oxides in question, the lower current density must be adopted, but if this is done the error based on self-discharge, shown in Fig. 6 will be introduced. The departure of Q at the E electrode from the above relation may be related to the error introduced by the slowness of the diffusion of ions.[7]

When Li is doped in NiO, the divalent nickel ions equal to the amount of doped Li are converted to the trivalent state. Therefore, whether Q is large or small supposedly depends on the amount of trivalent nickel ions in monoxide.

6) The potential of the transition from Ni_3O_4 to NiO is −0.142 V *vs.* SCE.

7) S. Yoshizawa, Z. Takehara, M. Kato and K. Kumazaki, *Denki Kagaku (J. Electrochem. Soc. Japan)*, **34**, 661 (1966).

BULLETIN OF THE CHEMICAL SOCIETY OF JAPAN VOL. 42 1800—1806 (1969)

A Kinetic Study on the Homogeneous Liquid-phase Oxidation of Cumene in the Presence of Triphenylsulfonium Chloride

Katsutoshi OHKUBO, Tokio YAMABE and Kenichi FUKUI

Faculty of Engineering, Kyoto University, Sakyo-ku, Kyoto

(Received September 28, 1968)

A kinetic study of the homogeneous liquid-phase oxidation of cumene was carried out in order to clarify the characteristic behavior of triphenylsulfonium chloride as an autoxidation catalyst. The reaction proceeded with no incubation period. The experimental dependence of the rate upon catalyst and hydrocarbon concentrations and also upon the oxygen pressure was reproduced with a good analytic fit by the following equation:

$$r=k'(\mathrm{RH})^{1.27}(\mathrm{O_2})^{0.68}(\mathrm{Cat.})_0\ (e^{-at}-e^{-bt})$$ (a, b, and k' are constants).

A reaction mechanism was proposed to derive the rate equation. It seems likely from this scheme that sulfonium chloride activates molecular oxygen by means of a reversible molecular association with it.

It is well known that some transition metal compounds and some halogen compounds are effective catalysts for the liquid-phase reactions of hydrocarbons with molecular oxygen. Recently, several onium compounds, in particular sulfonium and phosphonium salts, have been found to accelerate this type of oxidation. In view of the distinguishing character[1] of the behavior of these compounds as autoxidation catalysts, a kinetic study appeared significant. In the present paper, a kinetic study of cumene oxidation catalyzed by triphenylsulfonium chloride will be reported.

The kinetic study was carried out with particular reference to the initial short reaction time. In this initial range, the decomposition of cumene hydroperoxide, which would give free radicals, was disregarded since the concentration of hydroperoxide was very low, and the product was accumulated as hydroperoxide. The dependency of the initial rate upon the catalyst and hydrocarbon concentrations, and also upon the oxygen pressure, was determined. A tentative reaction mechanism will be proposed. The stationary-state method was employed to solve kinetic equations describing the mechanism. The experimental results can be well interpreted by the proposed mechanism, in which the behavior of the sulfonium catalyst is characterized in terms of forming a complex with molecular oxygen.

Experimental

Measurement of Oxygen Absorption. The course of oxidation reaction was followed by measuring the volume changes of the oxygen absorbed; the volume was observed every minute in the initial stage of the reaction and every ten minutes thereafter.

The reaction apparatus used the one described in an earlier report.[2]

The reaction vessel was thermostatically controlled in an oil bath; the temperature range was kept constant within ± 0.05°C, and the speed of stirring was regulated at more than 500 rpm/min. The rate of oxygen absorption was found to be independent of the stirring frequency in the above range.

Preparation of Catalyst. Equimolar quantities of phenylmagnesium bromide and diphenylsulfoxide were refluxed in benzene for 48 hr to form a precipitate of triphenylsulfoxymagnesium bromide. The precipitate was triturated with 20% tetrafluoroboric acid, and the resulting crystal of triphenylsulfonium tetrafluoroborate was recrystallized from chloroform and ether to give pure colorless crystals which melted at 192—193°C. An equimolar mixture of triphenylsulfonium tetrafluoroborate and potassium chloride was kept standing for a day in ethyl alcohol. The potassium tetrafluoroborate was then filtered off and the filtrate was removed to afford colorless needles of triphenylsulfonium chloride melting at 297—298°C (recrystallized from chloroform and ether).

Found: Cl, 11.6%. Calcd for $C_{18}H_{15}SCl$: Cl, 11.9%.

Oxidation Procedure. Homogeneous solutions of triphenylsulfonium chloride in cumene were prepared in a nitrogen atmosphere. Each ten-milliliter portion of the solution contained 3.35×10^{-4}, 1.68×10^{-4}, and 0.84×10^{-4} mol/l of the catalyst; these solutions were taken as the samples of the oxidation reaction. Oxidation was carried out at the temperatures of 50, 65, 70, and 80°C, and the rates of oxygen absorption were studied by graphical differentiation of the absorption curves of oxygen. The reaction rate was regarded as

1) K. Fukui, K. Ohkubo and T. Yamabe, This Bulletin, **42**, 312 (1969).

2) K. Fukui, K. Kanai, T. Takezono and H. Kitano, *Kogyo Kagaku Zasshi* (*J. Chem. Soc. Japan, Ind. Chem. Sect.*), **67**, 1131 (1964).

corresponding to that of the formation of cumene hydroperoxide, since the moles of oxygen absorbed were equal to those of the hydroperoxide formed in the initial step of the oxidation.

Result

Oxygen Absorption and Reaction Rate. The oxygen absorption of cumene was remarkably accelerated with a sulfonium catalyst. The reaction rate reached a maximum soon after the start of the reaction, without any appreciable incubation period, and then it gradually decreased. The lowering of the temperature decreased the maximum rate and delayed the time of reaching it. A typical curve of oxygen absorption is indicated in Fig. 1, while that of the initial range in particular is shown in Fig. 2. Figure 3 shows the rate curves indicating the characteristic feature[1] of sulfonium catalysts in accelerating the oxygen absorption at the initial step. The variation of the rate (r: $mol^{-1}l^{-1}\,sec^{-1}$) with the reaction time was analyzed from these curves; it can apparently be represented by the equation:

$$r = k(e^{-at} - e^{-bt}),\ (b>a) \qquad (1)$$

where k ($mol\,l^{-1}\,sec^{-1}$), a (sec^{-1}), and b (sec^{-1}) are constants and where t (sec) is the reaction time. In Fig. 4 the curves calculated from Eq. (1) by the use of the most fitting values of a, b, and k are presented by broken lines. The values of a, b and k are summarized in Table 1. From Table 1 it can be found that the a and b constants are not much influenced by the catalyst concentration, while k is linearly dependent upon the catalyst

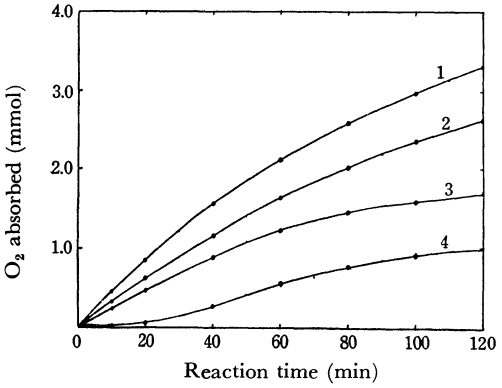

Fig. 1. Absorption curves of oxygen at 70°C.
1: 3.35×10^{-4} mol/l of $(C_6H_5)_3SCl$
2: 1.68×10^{-4} mol/l of $(C_6H_5)_3SCl$
3: 0.84×10^{-4} mol/l of $(C_6H_5)_3SCl$
4: none

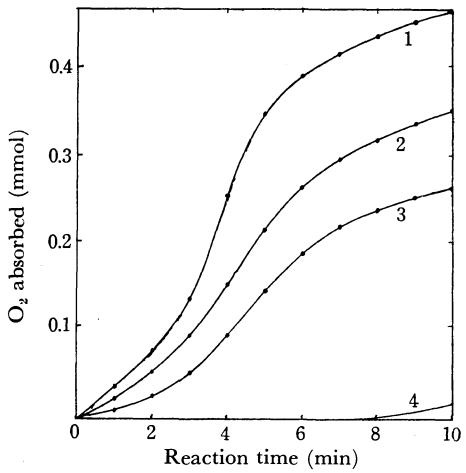

Fig. 2. Absorption curves of oxygen in the initial range at 70°C.
1: 3.35×10^{-4} mol/l of $(C_6H_5)_3SCl$
2: 1.68×10^{-4} mol/l of $(C_6H_5)_3SCl$
3: 0.84×10^{-4} mol/l of $(C_6H_5)_3SCl$
4: none

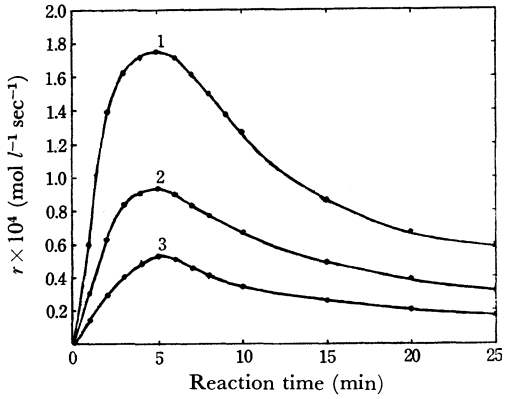

Fig. 3. Rate curves of oxygen absorption at 70°C.
1: 3.35×10^{-4} mol/l of $(C_6H_5)_3SCl$
2: 1.68×10^{-4} mol/l of $(C_6H_5)_3SCl$
3: 0.84×10^{-4} mol/l of $(C_6H_5)_3SCl$

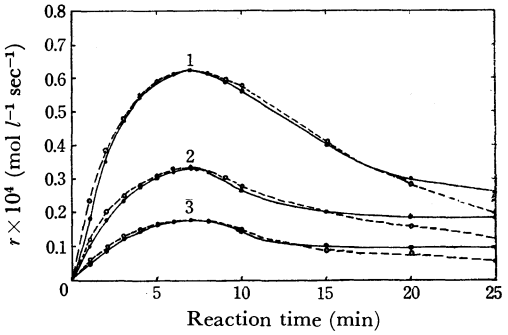

Fig. 4. Rate curves of oxygen absorption at 50°C.
1: 3.35×10^{-4} mol/l of $(C_6H_5)_3SCl$
2: 1.68×10^{-4} mol/l of $(C_6H_5)_3SCl$
3: 0.84×10^{-4} mol/l of $(C_6H_5)_3SCl$
Broken lines represent the rates derived from Eq. (1) with specific values of a, b and k (in Table 1).

TABLE 1. THE VARIATION IN a, b AND k VALUES WITH THE REACTION TEMPERATURE AND THE CATALYST CONCENTRATION

Reaction temperature (°C)	Initial catalyst concentration (mol/l)	$a\times10^3$ (sec^{-1})	$b\times10^3$ (sec^{-1})	$k\times10^4$ (mol l^{-1}. sec^{-1})
50	3.35×10^{-4}	1.38	3.90	1.37
	1.68×10^{-4}	1.10	4.40	0.685
	0.84×10^{-4}	0.96	4.80	0.360
70	3.35×10^{-4}	0.840	8.40	2.62
	1.68×10^{-4}	0.643	9.65	1.34
	0.84×10^{-4}	1.34	6.70	0.700
80	3.35×10^{-4}	2.38	6.67	4.78
	1.68×10^{-4}	2.29	6.86	2.50
	0.84×10^{-4}	2.20	7.04	1.55

concentration, as will be discussed in the next paragraph.

The Variation in the Rate with the Catalyst Concentration. The effect of the catalyst on the rate of oxygen absorption was studied by the varying catalyst concentrations to 3.35×10^{-4}, 1.68×10^{-4}, and 0.84×10^{-4} mol/l. Figure 5 shows the log k *versus* log (Cat.)$_0$ plot, where (Cat.)$_0$ denotes the initial concentration of the catalyst; the plot is a straight line with a slope equal to about 1.0. The linear relation is expressed as follows: $k\propto(\text{Cat.})_0^{0.940}$ at 50°C, $k\propto(\text{Cat.})_0^{0.952}$ at 70°C, and $k\propto(\text{Cat.})_0^{0.803}$ at 80°C. From these results, the dependency of k upon (Cat.)$_0$ can be represented, at least at lower temperatures, as follows:

$$k\propto(\text{Cat.})_0 \qquad (2)$$

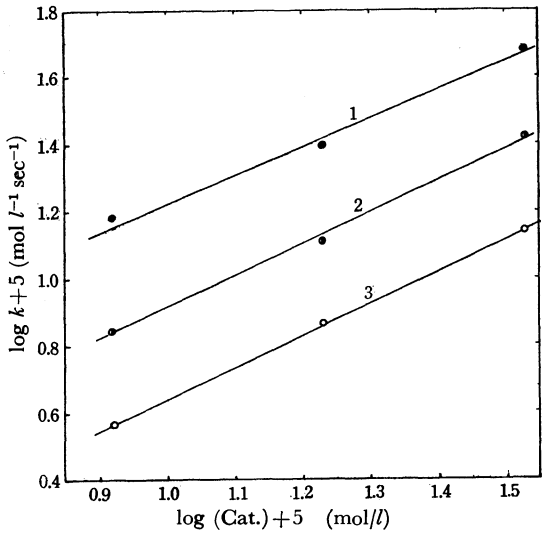

Fig. 5. The dependency of the constant, k, upon (Cat.).
-●- : at 80°C, -◑- : at 70°C, -○- : at 50°C

The Variation in the Rate with the Hydrocarbon Concentration. In order to investigate the rate dependency upon the hydrocarbon concentration, (RH), the oxidation of cumene (6.75, 6.31, 6.12, 5.03, and 3.80 mol/l) using chlorobenzene as the diluent was carried out under atmospheric pressure at 65°C in the presence of 3.35×10^{-4} mol/l of the catalyst. Figure 6 indicates the oxygen

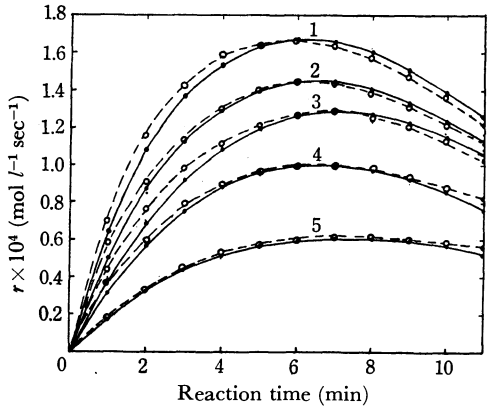

Fig. 6. Rate curves of oxygen absorption with varing concentration of cumene.
1: 6.75 mol/l 2: 6.31 mol/l 3: 6.12 mol/l
4: 5.03 mol/l 5: 3.80 mol/l
Broken lines are derived from Eq. (1) with specific values of a, b and k (in Table 2).

absorption rate at various hydrocarbon concentrations and shows a plot of the oxygen absorption rate against the reaction time. The most suitable values of a, b and k are listed in Table 2. Table 2

TABLE 2. THE VARIATION IN a, b AND k VALUES WITH THE HYDROCARBON CONCENTRATION

Initial hydrocarbon concentration (mol/l)	$a\times10^3$ (sec^{-1})	$b\times10^3$ (sec^{-1})	$k\times10^4$ (mol l^{-1} sec^{-1})
6.75	1.24	5.06	3.31
6.31	1.23	4.81	3.05
6.12	1.21	4.65	2.80
5.03	1.17	4.05	2.30
3.80	1.12	3.40	1.59

suggests that the a and b constants, are slightly affected by the initial value of (RH). Figure 7 shows the plot of log k against log (RH). The slope of the straight line obtained is 1.27, giving the relationship:

$$k\propto(\text{RH})^{1.27} \qquad (3)$$

The Variation in the Rate with the Oxygen Pressure. Since the liquid phase concentration of dissolved oxygen is proportional to the oxygen concentration in the gas phase, designated as (O_2),

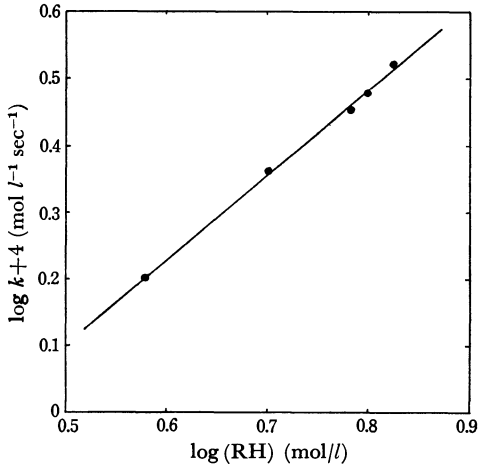

Fig. 7. The dependency of the constant, k, upon (RH) at 65°C.

the latter variable was adopted in place of the former. At a fixed cumene concentration (6.75 mol/l) and a constant temperature (65°C) in the presence of 3.35×10^{-4} mol/l of the catalyst, mixtures of oxygen and nitrogen were used for examining the effect of the oxygen concentration. Figure 8 indicates the influence of the oxygen concentration upon the rate of oxygen absorption in the initial stage of the reaction. The values of the constants (a, b and k) fitting the initial rates are listed in

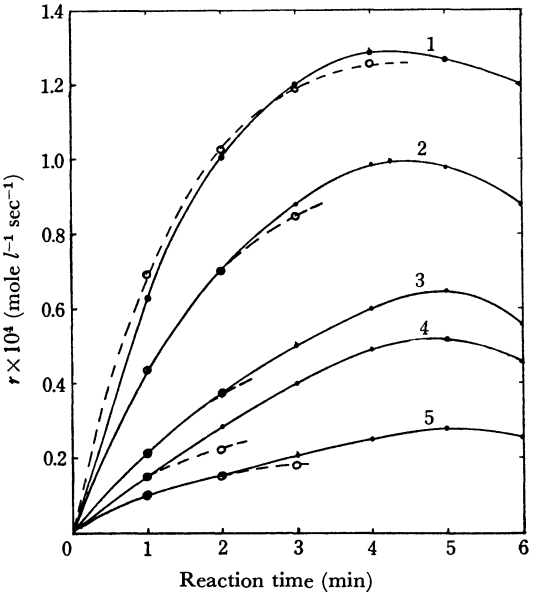

Fig. 8. Rate curves of oxygen absorption in variation with oxygen concentration
1: 4.22×10^{-2} mol/l 2: 2.11×10^{-2} mol/l
3: 0.603×10^{-2} mol/l 4: 0.422×10^{-2} mol/l
5: 0.211×10^{-2} mol/l
Broken lines at initial step are derived from Eq. (1) with specific values of a, b and k (in Table 3).

Table 3. The variation in a, b and k values with the oxygen concentration

Initial oxygen concentration (mol/l)	$a\times10^3$ (sec^{-1})	$b\times10^3$ (sec^{-1})	$k\times10^4$ (mol l^{-1} sec^{-1})
4.22×10^{-2}	1.25	10.0	1.89
2.11×10^{-2}	1.34	7.75	1.53
0.603×10^{-2}	1.36	6.60	0.793
0.422×10^{-2}	1.38	6.62	0.565
0.211×10^{-2}	1.47	6.33	0.388

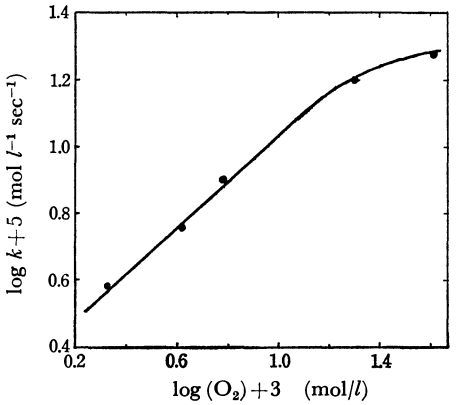

Fig. 9. The dependency of the constant, k, upon (O_2) at 65°C.

Table 3; a and b are influenced by the initial value of (O_2). Figure 9 shows the shape of the log k *versus* log (O_2) curve. The initial part of the curve is a straight line with a slope of 0.68, so that we have:

$$k\propto(O_2)^{0.68} \tag{4}$$

From Eq., (2), (3) and (4), the dependency of k upon $(Cat.)_0$, (RH) and (O_2) can be represented by:

$$k\propto(RH)^{1.27}(O_2)^{0.68}(Cat.)_0 \tag{5}$$

The rate shown in Eq. (1) may then be rewritten by the following expression:

$$r=k'(RH)^{1.27}(O_2)^{0.68}(Cat.)_0(e^{-at}-e^{-bt}) \tag{6}$$

where k' is a constant which is dependent upon neither the hydrocarbon nor oxygen concentrations, nor upon the catalyst concentration.

The Variation in the Rate with the Reaction Temperature. The reaction was studied in the temperature range from 50 to 80°C by the use of catalysts in the amounts of 3.35×10^{-4}, 1.68×10^{-4}, and 0.84×10^{-4} mol/l. Figure 10 shows the Arrhenius plots. The overall energy of activation of this process comes out to be $E_{overall}$=5.25—6.15 kcal/mol from the temperature dependence of the overall velocity constant (k).

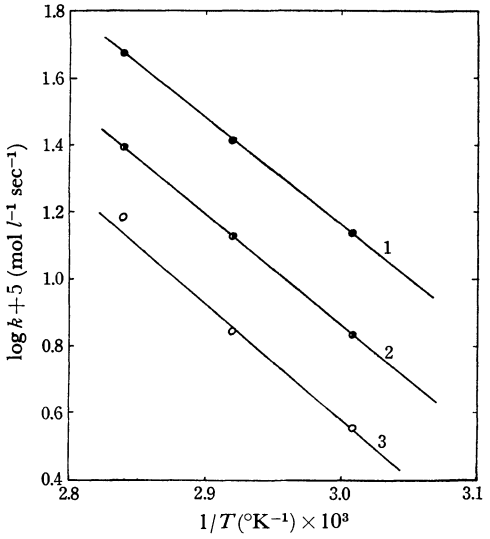

Fig. 10. Arrhenius plots of $\log k$ against $1/T$.
(1): 3.35×10^{-4} mol/l of $(C_6H_5)_3SCl$
(2): 1.68×10^{-4} mol/l of $(C_6H_5)_3SCl$
(3): 0.84×10^{-4} mol/l of $(C_6H_5)_3SCl$

It should be stressed here that, in this kinetic study, triphenylsulfonium chloride could not act as a radical source, as was discussed in a previous report.[1] Neither chloride compounds, such as alkyl chloride and hydrogen chloride, nor decomposed fragments of such catalysts as benzene, chlorobenzene, sulfide, and sulfoxide were detected.

In addition, the catalytic action of sulfonium chloride was not based mainly upon the chloride anion. This will be discussed in detail in a subsequent paper.

Discussion

The main purpose of this kinetic study was to clarify the features of the catalytic action of the sulfonium compounds. The analysis of the experimental results so far obtained would make it possible to build a tentative reaction mechanism. The nature of the reaction is most probably radical and not ionic, for the reaction is stopped by a radical inhibitor such as phenol. A "complex" formation between the catalyst and the oxygen molecule has been suggested in a previous paper;[1] such a formation would be capable of hydrogen abstraction from hydrocarbon molecules. It is worth summing up here the important experimental results:

a) The activity of the catalyst is characterized in the initial stage, in which the oxygen absorption occurs essentially with no incubation period. b) The shape of the rate curves expressed in Figs. 3, 4 and 5 suggests the involvement of a catalyst deactivation. c) The value of the overall energy of activation is relatively small. This may indicate radical reaction caused by catalytic hydrogen abstraction by the "complex."

The experimental results, then, lead to the following reaction scheme. The first step consists of the formation of a complex between the catalyst $(Cat.)_0$ and the oxygen molecule (discussed in detail in a previous report[1]):

$$Cat. + O_2 \underset{k'_c}{\overset{k_c}{\rightleftarrows}} Cat.\cdots O_2 \qquad (7a)$$

Such a complex then abstracts an active hydrogen from hydrocarbon (RH) to produce an alkyl radical (R·):

$$Cat.\cdots O_2 + RH \xrightarrow{k_1} R\cdot + Cat. + \cdot O_2H \qquad (7b)$$

followed by the usual propagation steps:

$$R\cdot + O_2 \xrightarrow{k_p} RO_2\cdot \qquad (7c)$$

$$RO_2\cdot + RH \xrightarrow{k_2} ROOH + R\cdot \qquad (7d)$$

The termination step may be described by the following scheme:

$$RO_2\cdot \xrightarrow{k_t} \text{inactive products} \qquad (7e)$$

$$Cat. \xrightarrow{k_d} \text{inactive form} \qquad (7f)$$

Terminations of other types (R·+R· or R·+RO_2·) are negligible compared to the process of (7e) at oxygen pressures above 200 mm of mercury. The disappearance of RO_2· may be a first or second-order process. Here the first-order termination is assumed for mathematical convenience. The deactivation of the sulfonium catalyst (7f) is considered to be another important process in retarding the reaction. It may be caused partly by interaction with oxidation products such as hydroperoxide. In view of the fact that more than 70% of the catalyst is recovered from the reaction mixture by the use of larger amounts of catalyst, as was reported in the previous paper,[1] it is very likely that the "deactivation" is due to the masking action*1 of some reaction products.

According to the reaction scheme discussed above, the following differential equations are obtained:

$$d(Cat.)/dt = (k_1(RH) + k_c')(Cat.\cdots O_2) - (k_c(O_2) + k_d)(Cat.) \qquad (8a)$$

$$d(Cat.\cdots O_2)/dt = k_c(O_2)(Cat.) - (k_1(RH) + k_c')(Cat.\cdots O_2) \qquad (8b)$$

$$d(R\cdot)/dt = k_1(RH)(Cat.\cdots O_2) + k_2(RH)(RO_2\cdot) - k_p(O_2)(R\cdot) \qquad (8c)$$

$$d(RO_2\cdot)/dt = k_p(O_2)(R\cdot) - (k_2(RH) + k_t)(RO_2\cdot) \qquad (8d)$$

*1 This subject will be discussed in a subsequent paper.

$$d(ROOH)/dt = k_2(RH)(RO_2\cdot) \quad (8e)$$

Assuming the stationary-state for the concentrations of R· and RO_2·, the overall rate of oxygen absorption (r) can be represented by the equation:

$$r = \frac{k_1 k_2 (RH)^2}{k_t} (Cat.\cdots O_2) \quad (8f)$$

The time change of $(Cat.\cdots O_2)$ is controlled by Eqs. (8a) and (8b), which are solved simultaneously. The solution of $(Cat.\cdots O_2)$ is introduced into Eq. (8f), giving;

$$r = \frac{k_1 k_2 k_c (RH)^2 (O_2)(Cat.)_0}{k_t(\lambda_2 - \lambda_1)} (e^{-\lambda_1 t} - e^{-\lambda_2 t}) \quad (9)$$

where:

$$\lambda_1 = \frac{1}{2}\left\{k_c(O_2) + k_c' + k_1(RH) + k_d\right\} \times \left[1 - \sqrt{1 - \frac{4k_d(k_c' + k_1(RH))}{(k_c(O_2) + k_c' + k_1(RH) + k_d)^2}}\right] \quad (9a)$$

$$\lambda_2 = \frac{1}{2}\left\{k_c(O_2) + k_c' + k_1(RH) + k_d\right\} \times \left[1 + \sqrt{1 - \frac{4k_d(k_c' + k_1(RH))}{(k_c(O_2) + k_c' + k_1(RH) + k_d)^2}}\right] \quad (9b)$$

Here the oxygen and the hydrocarbon concentrations can be assumed to be unchanged, namely, to be equal to the initial value. Equation (9) is in accordance with Eq. (1), which is obtained experimentally, and is in qualitative agreement with the rate dependency upon (RH), (O_2) and $(Cat.)_0$ shown by Eq. (6). Therefore, the a, b and k constants are correspondingly represented by;

$$a = \lambda_1 \quad (10a)$$

$$b = \lambda_2 \quad (10b)$$

$$k = \frac{k_1 k_2 k_c (RH)^2 (O_2)(Cat.)_0}{k_t(\lambda_2 - \lambda_1)} \quad (10c)$$

From Eqs. (9a) and (9b) we obtain:

$$(\lambda_1)_{(RH)=0} = \frac{1}{2}\left\{k_c(O_2) + k_c' + k_d\right\} \times \left[1 - \sqrt{1 - \frac{4k_d k_c'}{(k_c(O_2) + k_c' + k_d)^2}}\right] \quad (11a)$$

$$(\lambda_2)_{(RH)=0} = \frac{1}{2}\left\{k_c(O_2) + k_c' + k_d\right\} \times \left[1 + \sqrt{1 - \frac{4k_d k_c'}{(k_c(O)_2 + k_c' + k_d)^2}}\right] \quad (11b)$$

where $(\lambda_1)_{(RH)=0}$ and $(\lambda_2)_{(RH)=0}$ are extreme values of λ_1 and λ_2 respectively when (RH) is extrapolated to zero.

From Eqs. (11a) and (11b), it follows that;

$$(\lambda_1)_{(RH)=0} + (\lambda_2)_{(RH)=0} = k_c(O_2) + k_c' + k_d \quad (12a)$$

$$(\lambda_2)_{(RH)=0} - (\lambda_1)_{(RH)=0} = \sqrt{(k_c(O_2) + k_c' + k_d)^2 - 4k_d k_c'} \quad (12b)$$

Similarly, we get;

$$(\lambda_1)_{(O_2)=0} = k_d \quad (12c)$$

$$(\lambda_2)_{(O_2)=0} = k_c' + k_1(RH) \quad (12d)$$

Figures 11 and 12 show the plots of the values of a and b against (RH) and (O_2) respectively, giving the following extrapolated values:

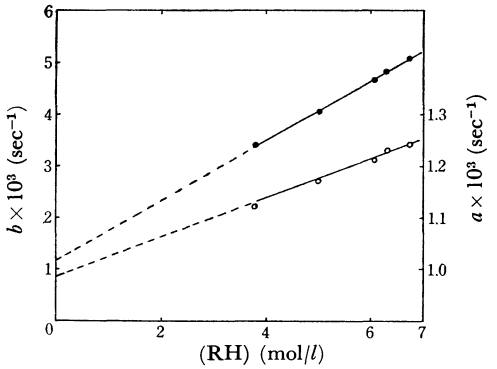

Fig. 11. The dependency of the constants, a and b upon (RH) at 65°C.
-●- : The plots of b against (RH)
-○- : The plots of a against (RH)

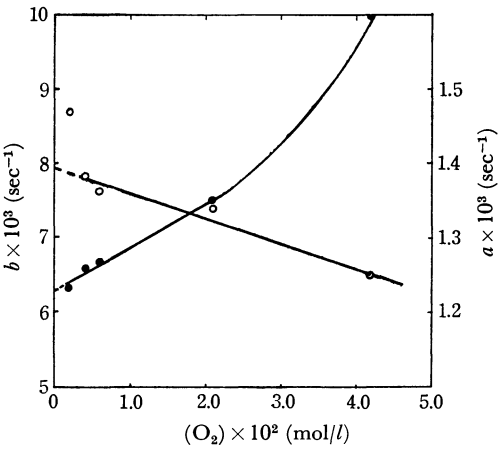

Fig. 12. The dependency of the constants, a and b, upon (O_2) at 65°C.
-●- : The plots of b against (O_2)
-○- : The plots of a against (O_2)

$$(\lambda_1)_{(RH)=0} = 0.95 \times 10^{-3}\ sec^{-1} \quad (13a)$$

$$(\lambda_2)_{(RH)=0} = 1.195 \times 10^{-3}\ sec^{-1} \quad (13b)$$

$$(\lambda_1)_{(O_2)=0} = 1.392 \times 10^{-3}\ sec^{-1} \quad (13c)$$

$$(\lambda_2)_{(O_2)=0} = 6.18 \times 10^{-3}\ sec^{-1} \quad (13d)$$

from Eqs. (12a—12d) and (13a—13d), the rate constants at 65°C can be determined to be as follows:

$k_c = 2.23 \times 10^{-2}$ mol^{-1}l sec^{-1}

$k_c(O_2) = 0.94 \times 10^{-3}$ sec^{-1}

$k_c' = 0.82 \times 10^{-3}$ sec^{-1}

$k_1 = 0.794 \times 10^{-3}$ mol^{-1}l sec^{-1}

$k_1(RH) = 5.36 \times 10^{-3}$ sec^{-1}

$k_d = 1.39 \times 10^{-3}$ sec^{-1}

From these rate constants and from the experimental values of k (shown in Table 2) under the conditions of $(O_2)=4.42 \times 10^{-2}$ mol/l and $(Cat.)_0=3.35 \times 10^{-4}$ mol/l, the value of k_2/k_t can be calculated by the use of Eq. (10c) as follows:

$$k_2/k_t = 1.79 \times 10^2 \text{ mol}^{-1}\, l$$

When this value is applied to Eq. (10c), the calculated values of k are consistent with the experimental values, as is shown in Fig. 13. These values

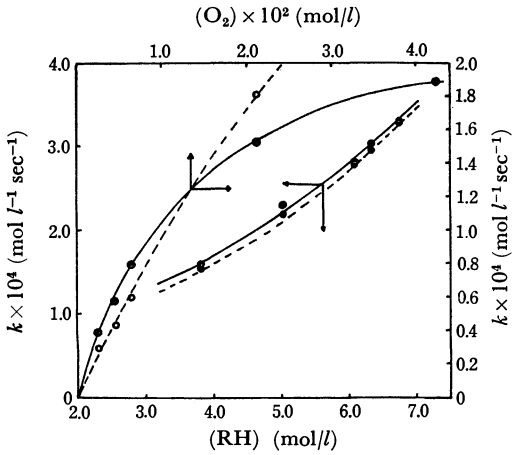

Fig. 13. The dependency of k upon (RH) and (O_2).
-◓- : k against (RH) from experimental result
-⊙- : k against (O_2) from experimental result
-●- : k against (RH) from Eq. (14a)
-○- : k against (O_2) from Eq. (14b)

of rate constants may supply the following information concerning the elementary processes involved:

a) In the case of atmospheric oxygen pressure, $k_c(O_2)$ and k_c' become comparable, so that the conversion is essentially reversible. Accordingly, the complex formations is more favored by a higher oxygen pressure.

b) The small value of k_1 implies that the hydrogen abstraction by the "complex" is a step limitting the overall rate.

c) Traylor reported[3] that the value of k_2 was nearly equal to 5.35×10^{-3} *2 mol^{-1} l sec^{-1} in cumene oxidation in the presence of t-butyl hydroperoxide at 60°C. If this value is applied to the present case, the value of k_t can be calculated to be 2.98×10^{-5} sec^{-1}. This value, small compared with k_d, indicates that the termination of peroxy-radical may not play an important role in retarding the rate. The deactivation of the catalyst may be caused by the oxidation products, such as hydroperoxide. This point will be discussed in detail in a subsequent paper.

Next, let us discuss the influence of (RH) and (O_2) upon the rate by the direct use of the values obtained above. The dependency of k upon (RH) is represented by;

$$k = \frac{4.47 \times 10^{-5}(RH)^2}{\sqrt{0.630(RH)^2 + 0.58(RH) + 5.39}} \qquad (14a)$$

under the conditions of $(Cat.)_0=3.35 \times 10^{-4}$ mol/l and $(O_2)=4.22 \times 10^{-2}$ mol/l. From a graphical fit of this expression, we also get the approximate representation;

$$k \simeq 4.47 \times 10^{-5}\,(RH)^{1.21} \text{ mol } l^{-1} \text{ sec}^{-1} \qquad (14a')$$

which reflects the experimental result of Eq. (3). Similarly, the dependency of k upon (O_2) at fixed concentrations of $(RH)=6.75$ mol/l and $(Cat.)_0=3.35 \times 10^{-4}$ mol/l can be shown as follows:

$$k = \frac{4.83 \times 10^{-3}(O_2)}{\sqrt{4.98(O_2)^2 + 3.37(O_2) + 0.229}} \qquad (14b)$$

It is obvious that such an equation can be a rough approximation of Eq. (4).

The present kinetic study afforded very favorable support to the idea, partly suggested in our previous report,[1] that the distinguishing feature of the catalyst behavior might involve a direct association with molecular oxygen, although the "complex" has not yet been isolated.

3) T. G. Traylor and C. A. Russell, *J. Am. Chem. Soc.*, **87**, 3698 (1965).

*2 The value of k_2 was converted in terms of above dimensions from the original value.

BULLETIN OF THE CHEMICAL SOCIETY OF JAPAN VOL. 42 1807—1812 (1969)

Freezing of the Droplets of Aqueous Solution Aerosols

Yuhei Uzu and Isamu Sano

Department of Chemistry, Nagoya University, Nagoya

(Received October 4, 1968)

By atomizing aqueous solutions both of electrolytes and non-electrolytes, fog droplets of 8μ in diameter were prepared, and their freezing temperatures were measured in a thermostat-like cold chamber fitted with an electrically heated platinum wire. The results were compared with that obtained with fog droplets of pure water of the same size. It was found that non-electrolytes hardly influence the freezing, whereas electrolytes do a great deal. The freezing temperature rises in the presence of an electrolyte and varies with its concentration, the highest temperatures being observed at the concentrations around 1×10^{-4}M for 1-1 type electrolytes and at lower concentrations for 1-2 and 1-3 type electrolytes. K^+ is the most effective of the alkali metal cations having the same species of anion in common, and I^- of the halide anions having the same species of cation in common. Applying the theory of nucleation, the sizes of the hydrated K^+ and the critical nucleus developed from it for ice-nucleation were estimated to be about 6 and 21 Å in radius, respectively.

The formation of ice in supercooled water is a phenomenon of great interest from the physicochemical point of view. Although some sort of coherent picture about it is now beginning to emerge, the theory seems to be far from complete and, in addition, experimental evidence is confusing. Since an investigation of the phenomenon of ice-formation provides information on the nucleation mechanism in supercooled liquids and in supersaturated solutions, much work has been done concerning the roles of insoluble and soluble substances in promoting ice-nucleation in water. It has been found for the former[1] that they would act as a catalyst. Their surface concentrates water molecules to accelerate the phase transition, mainly because of the similarity of the crystallographic structure to that of ice, and partly through the electric force fields that are ionic or non-ionic according to the nature of the constituent of surface, imperfections such as growth steps, re-entrant corners or screw dislocations.

It is questionable, however, whether soluble substances promote ice-nucleation; few reliable data are available and many of the conclusions reached are contradictory to one another. This might be attributed to the difference in the purity of the water and aqueous solutions and the characteristics of the experimental procedures.

This report deals with the effects of soluble substances, electrolytes and non-electrolytes, upon the freezing temperature of a droplet of water, and shows, in the case of electrolytes, that the concentration and valence definitely affect the freezing temperature. Additional information is given about the functions of electrolyte ions in ice-nucleation in water.

Experimental Procedure and Results

The technique has been described in detail.[2,3] The fog droplets of water or aqueous solutions whose size is 8 μ in diameter were introduced into a thermostat-like cold chamber to be supercooled and the freezing temperature was determined by making use of a heated platinum wire as a detector

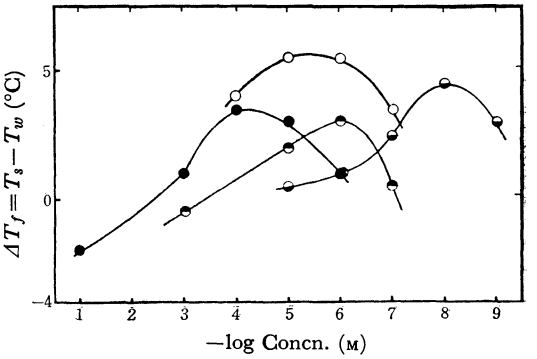

Fig. 1. Relation between the relative freezing temperature and the concentraion of electrolyte.
-●- KCl -○- K_2SO_4 -◓- Na_2SO_4
-◒- K_3PO_4

1) N. H. Fletcher, *Austral. J. Phys.*, **13**, 408 (1960); *Discussions Faraday Soc.*, No. 30, 39 (1960).

2) Y. Uzu, I. Sano and Y. Fujitani, *J. Colloid Sci.*, **18**, 697 (1963).

3) Y. Fujitani, Y. Uzu and I. Sano, *J. Meteor. Soc. Japan*, **39**, 249 (1961); Y. Uzu and I. Sano, *ibid.*, **43**, 290 (1965).

of the droplets frozen.

The principal features of the results, also mentioned in our reports,[2,3] are as follows. It was found for electrolytes that a maximum appears in the change in relative freezing temperature with concentration. Some of the results are given in Fig. 1, where $\Delta T_f = T_s - T_w$ is the threshold freezing temperature of solution droplets relative to that of water droplets. The subscript symbols s and w refer to solution and water, respectively. Similar results have been obtained with other electrolytes such as $MgSO_4$, $CuSO_4$, $ZnSO_4$, $(NH_4)_2SO_4$. The results for non-electrolytes are illustrated in Fig. 2. ΔT_f takes a small negative value or zero in the concentration range studied, only becoming appreciable at higher concentrations.

Comparison of the results shown in Figs. 1 and 2 suggests that the change in relative freezing temperature found in electrolyte solution droplets might be due to the presence of ions. For a detailed study, we made measurements for 1×10^{-4} molar aqueous solutions of various electrolytes. The results are summarized in Fig. 3, in which almost all points represent the average of several measurements. It is clear that, for the 1-1 type electrolytes having the same type of cation, the relative freezing temperature rises with the size of the anion, the highest being observed for I^- and the lowest for Cl^-. For those having the same type of anion, the highest is found for K^+ among all the halides studied.

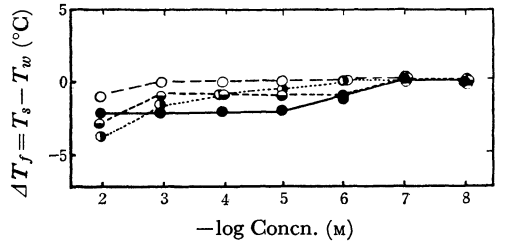

Fig. 2. Relation between the relative freezing temperature and the concentration of non-electrolyte.
-○- saccharose -◒- ethanol -◑- urea
-●- thiourea

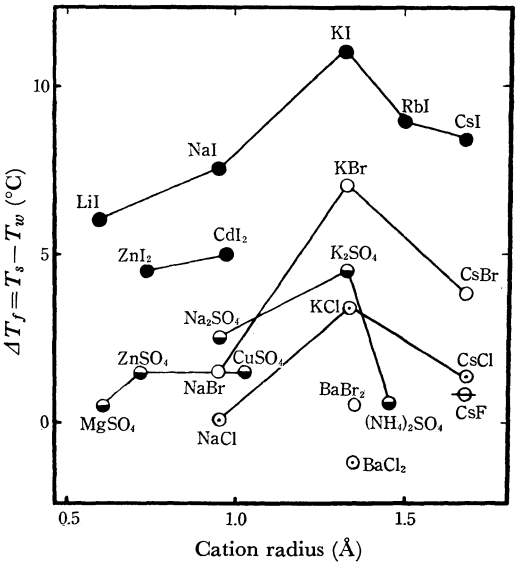

Fig. 3. Relation between the relative freezing temperature and the radius of cation.

Discussion

Two models as to the mechanism of freezing of the droplets of electrolyte solutions have been advanced lately.

1) Critical nuclei for ice-formation would be formed as the consequence of water molecules being attracted to electrolyte ions owing to their electric forces to be arranged around them in a fashion more or less similar to that in ice.

2) Critical nuclei would be insoluble particles which might have been either held tenaciously in water or introduced together with solute, and, in some cases those which might have been activated through reaction with solute.[4]

The results seem to be in line with model 1. Firstly, from the observation $\Delta T_f > 0$ for electrolytes, electrolyte ions could promote either the freezing of droplets by themselves or in cooperation with insoluble particles. Secondly, the finding that ΔT_f is nought in the case of non-electrolytes is evidence that ions alone can be active to effect ice-nucleation. This is supported by the fact that there is regularity, as shown in Fig. 3, in the relation between the relative freezing temperature and the cation radius. It should be added that insoluble particles, if present in water, might have little influence upon ice-nucleation. The reasons are: (1) ΔT_f might be positive in the case of non-electrolytes, if insoluble particles accelerated ice-nucleation. (2) Fogs were prepared with purified materials, such as water subjected to redistillation[2,3] and solutions filtered through 0.1 μ pore size millipore filter. (3) For the purpose of lessening the possibility of a droplet containing insoluble particles, droplets having the mean size as small as 8 μ in diameter were used. (4) To investigate the effect of insoluble particles, some measurements were conducted of the filtered water and 1×10^{-4} molar CdI_2 solutions, and also unfiltered ones. The freezing temperatures were found to be −29.0°C and −24.3°C for the former, and −28.5°C and −24.5°C for the latter.*1

From these considerations, we are led to the conclusion that the rise in relative freezing temperature is caused by electrolyte ions and not by insoluble

4) H. R. Pruppacher, *J. Chem. Phys.*, **39**, 1586 (1963).

*1 *Cf.* the Ph. D. thesis presented by Y. Uzu to the Nagoya University (1966).

particles which may be present in the droplets. Assuming that the nuclei are electrolyte ions more or less hydrated to build a layer of ice structure, we shall apply the theory of nucleation to our findings.

Macroscopic quantities such as interfacial energy have been used in the theory. Their use in assemblies containing molecules numbering from a few score to several hundreds is questionable. However, the theory is in good accord with experiment.

Application of the Nucleation Theory. According to the theory,[5] J, the rate of ice-nucleation or the rate at which the critical nuclei acquire an additional molecule to reach a size from which they grow directly toward ice particles, is given by

$$J = (kT_s/h)n \cdot 4\pi r^{*2} \exp\{-(\Delta G^* + \Delta g)/kT_s\}, \quad (1)$$

where ΔG^* is the free energy of formation of the critical nuclei or the maximum free energy necessary for their creation, Δg the free energy of activation of water molecules for self-diffusion in water or across the water-ice boundary, n the number of water molecules in contact with unit area of the surface of critical nuclei whose radius is r^*, k Boltzmann's constant and h Planck's constant.

It is apparent in Eq. (1) that the rate J is much more sensitive to the magnitudes of ΔG^* and Δg in the exponential term as compared to the pre-exponential kinetic term, the magnitude of which is of the order of 10^{28} r^{*2} $\sec^{-1}$ in the case of supercooled water as n is approximately equal to 3×10^{-8} n_0, where n_0 represents the density of water expressed in number of molecules per cm^3.

ΔG^* may be expressed as

$$\Delta G^* = (4\pi/3)(r^{*3} - r_h^3)\Delta G_v + \Delta E_{st} + 4\pi(r^{*2} - r_h^2)\sigma + \Delta E_{el}, \quad (2)$$

r_h being the radius of ions in hydrated state. ΔG_v means the change in free energy per unit volume of ice accompanying the phase transition from water to ice, ΔE_{st} the change in strain energy coming from water molecules fixed to form ice around the hydrated ions, σ the interfacial energy per unit area between the two phases, and ΔE_{el} the change in electrical energy of water molecules when they are subjected to phase transition.

Little is known about the strain energy ΔE_{st}. However, according to the structural models of liquid water, proposed theoretically by Bernal and Fowler,[6] Frenkel[7] and Frank and Wen-Yang Wen,[8] and confirmed experimentally by Dorsch and Boyd,[9] liquid water supercooled to temperatures below 4°C consists, with increasing degree of supercooling, of increasing number of molecules which constitute a structure closely resembling the structure of tridymite type ice, it follows that ΔE_{st} could be neglected.

Realizing that the hydration number of ion is 6 for K^+ and for I^-, it is difficult to imagine a surface for hydration layer. Thus the interfacial energy term, $4\pi r_h^2\sigma$ might be neglected.

For monovalent ion, the electrical energy change ΔE_{el} is calculated to be

$$\Delta E_{el} = (e^2/2D_s)(1/r_h - 1/r^*) + (e^2/2D_l) \times (1/r^* - 1/R) - (e^2/2D_l)(1/r_h - 1/R). \quad (3)$$

It is assumed herewith that there are two successive layers of water molecules around a hydrated ion. Regarding the inner layer as ice and the outer as liquid, the electrical energy which would be held by a single layer of water molecules if it were wholly in liquid state, is subtracted from the electrical energy of two layers. In this equation, D_s is the dielectric constant of the inner layer having a thickness, $r^* - r_h$, D_l the dielectric constant of the outer layer extending to the surface of the droplet with radius R and the electronic charge e. Since $R \gg r^* > r_h$, ΔE_{el} can be written in a simplified form

$$\Delta E_{el} = (e^2/2)(1/D_s - 1/D_l)(1/r_h - 1/r^*). \quad (4)$$

It is thus possible to transform Eq. (2), to a first approximation, into

$$\Delta G^* = (4\pi/3)(r^{*3} - r_h^3)\Delta G_v + 4\pi r^{*2}\sigma + (e^2/2)(1/D_s - 1/D_l)(1/r_h - 1/r^*). \quad (5)$$

Δg was estimated by McDonald[10] to be nearly constant, the value being as small as about 4×10^{-13} erg/molecule in a limited range of temperature below 0°C.

We have found that potassium iodide is most active. Thus for K^+, both r^* the size as critical nucleus and r_h the size in hydrated state were estimated by virtue of Eqs. (1) and (5).

Calculation of r^* and r_h of K^+. For this purpose, we require the relations

5) R. Becker and W. Döring, *Ann. Phys.*, **24**, 719 (1935); **32**, 128 (1938); J. Frenkel, "Kinetic Theory of Liquids," Oxford Univ. Press, Oxford (1946), p. 366; D. Turnbull and J. C. Fischer, *J. Chem. Phys.*, **17**, 71 (1949); B. J. Mason, "The Physics of Cloud," Oxford Univ. Press, Oxford (1957), p. 129; N. H. Fletcher, "The Physics of Rainclouds," Cambridge Univ. Press, Cambridge (1962), p. 214.

6) J. D. Bernal and R. H. Fowler, *J. Chem. Phys.*, **1**, 515 (1933).

7) J. Frenkel, "Kinetic Theory of Liquids," Oxford Univ. Press, Oxford (1946), p. 366.

8) H. S. Frank and Wen-Yang Wen, *Discussions Faraday Soc.*, No. 24, 133 (1957).

9) R. G. Dorsch and B. Boyd, *U. S. Nat. Adv. Comm. Aero. Washington, Tech. Note*, No. 2532 (1951).

10) J. E. McDonald, *J. Meteor.*, **10**, 416 (1953).

$$\partial \ln J/\partial r^* = 0, \qquad \partial \ln J/\partial r_h = 0. \tag{6}$$

Denoting by ΔS_v the entropy of fusion per unit volume of ice at 273°K and by $\Delta T_s(=273-T_s)$ the degree of supercooling, it follows through thermodynamical arguments that $\Delta G_v = -\Delta S_v \cdot \Delta T_s$. ΔS_v is evaluated to be approximately 1.22×10^7 erg/°K·cm^3. Denoting by ΔH_∞ the heat of fusion per unit mass of bulk ice and by ΔH_r that corresponding to the nucleus ice of radius r^*, we have thermodynamically[10] $\Delta H_r = \Delta H_\infty - (2\sigma/\rho r^*)$, where ρ is the density of ice that could be regarded to be practically independent of temperature and size. It follows that

$$\Delta G_v = -\rho/273(\Delta H_\infty - 2\sigma/\rho r^*)\Delta T_s. \tag{7}$$

By substituting Eq. (7) into Eq. (5) and carrying out differentiation, regarding T_s and Δ_g as constant, we obtain

$$2kT_s/r^* + (4\pi/3)(\rho/273)\Delta T_s\{3r^{*2}(\Delta H_\infty - 2\sigma/\rho r^*) + (r^{*3} - r_h^3)(2\sigma/\rho r^{*2})\} - 8\pi r^*\sigma - (e^2/2)\,(1/D_s - 1/D_l)1/r^{*2} = 0, \tag{8}$$

$$(4\pi/3)(\rho/273)\Delta T_s(\Delta H_\infty - 2\sigma/\rho r^*)3r_h^2 - (e^2/2)\,(1/D_s - 1/D_l)1/r_h^2 = 0 \tag{9}$$

In order to calculate r^* and r_h of K^+ from Eqs. (8) and (9), we use the following data

$T_s = 253$°K,*2 $\Delta T_s = 20$°K, $\rho = 0.92$ g/cm^3, $\Delta H_\infty = 79.7$ cal/g, $\sigma = 22$ erg/cm^2,[11] $D_s = 3$, $D_l = 96$.

As has been stated, the concentration of the solution is of the order as low as 10^{-4} mol/l, so all the above values except those for ΔT_s and consequently T_s could be approximated by the characteristics of water. It should be mentioned that the value of D_l, 96, is obtained by extrapolation of the values at room temperature down to −20°C. The result is

$$r^* = 20.6 \text{ Å}, \qquad r_h = 6.1 \text{ Å}.$$

It is of interest examine how r^* and r_h vary with σ and D_l. Using the following approximate equations instead of Eqs. (8) and (9),

$$\partial \ln J/\partial r^* \simeq \partial \ln \Delta G^*/\partial r^* \simeq (4\pi/3)(\rho/273)\Delta T_s \times \{3r^{*2}\Delta H_\infty - (2\sigma/\rho)2r^*\} - 8r^*\pi\sigma - (e^2/2)\,(1/D_s - 1/D_l)1/r^{*2} = 0, \tag{10}$$

$$\partial \ln J/\partial r_h \simeq \partial \ln \Delta G^*/\partial r_h \simeq (4\pi/3)(\rho/273)\Delta T_s \times \Delta H_\infty 3r_h^2 - (e^2/2)(1/D_s - 1/D_l)1/r_h^2 = 0, \tag{11}$$

11) L. Dufour and R. Defay, "Thermodynamics of Clouds," Academic Press, New York (1963), p. 226.

*2 The freezing temperatures actually observed for the potassium iodide solution droplets were around −20°C.

Table 1. Variation of r^* and r_h as functions of D_l and σ

D_l	D_s	σ (dyne/cm)	r^* (Å)	r_h (Å)
96	3	24	22.6	6.0
4			22.5	4.3
96	3	22	20.7	6.0
4			20.6	4.3
96	3	20	18.9	6.0
4			18.7	4.3
96	3	18	17.1	6.0
4			16.9	4.3
96	3	22	20.6	6.1

we find the results as shown in Table 1. The values given in the lowest line are obtained by Eqs. (8) and (9). They are recorded in order to confirm the accuracy of Eqs. (10) and (11).

It is seen from the table that, while the value of r^* hardly changes with D_l, it is largely dependent upon σ, being in the range of 17 to 23 Å for all the probable magnitudes of σ and in close agreement with that for supercooled water at −20°C which is shown in Table 2[12] together with those at other temperatures. As regards r_h, it remains effectively constant irrespective of the variation in σ, changing with D_l within the range of 6 Å which is usually admitted as plausible.

Table 2. Radius of the critical nucleus for ice formation in a drop of pure water

Temperature (°C)	Radius of water drop (cm)	σ (dyne/cm)	Radius of critical nucleus (cm)
0	∞	23.8	∞
−10	∞	22.8	4.20×10^7
	10^{-6}	22.8	4.88
−20	∞	21.8	2.08
	10^{-6}	21.8	2.26
−30	∞	20.7$_5$	1.38
	10^{-6}	20.7$_5$	1.46
−40	∞	19.7	1.03
	10^{-6}	19.7	1.08

The calculated values of r^* and r_h are found to be of the right order of magnitude. Further, it is known that the thickness of the ionic atmosphere around K^+ in a solution of the concentration 1×10^{-4} mol/l is approximately 300 Å. This is much larger than the radius of the critical nucleus, 21 Å. Hence we might regard K^+ alone as the center of the ice nucleus. Thus, we have ignored the presence of I^- in the solution.

12) L. Dufour and R. Defay, "Thermodynamics of Clouds," Academic Press, New York (1963), p. 150, 176.

The Influence of K^+ on the Structure of Water. There are some factors of interest. One is that a potassium iodide containing water droplet freezes, as shown in Fig. 3, at a temperature about 10°C higher than that at which a potassium iodide not containing droplet of the same size freezes. This means that the critical nucleus in water which is supposed to be only of 14 Å in radius (Table 2) might make rapid development to 21 Å if potassium iodide is present at a concentration of the order of 10^{-4} mol/*l*. It has been observed that all the cations other than K^+ freeze at temperatures lower than that for K^+ (Fig. 3). This suggests their higher ΔG^* values.

In spite of many publications on the structure of liquid water as well as electrolyte solutions, no definite conclusion has been reached. However, utilizing the information obtained herewith, we are able to give additional interpretation.

It is certain that an electrolyte ion could, owing to its ability of fixing water molecules oriented around itself through its electric forces, exhibit a function to break the structure of water. The structure breaking function should depend, firstly, on the size of ion, and secondly, on the extent of misfit. Here we have introduced the misfit as a measure of the disparity between the water structure contiguous to an ion and the ice structure to be formed from it. This might help interpret the finding that T_s for cations smaller than K^+ falls down in the same way as for those larger than K^+ (Fig. 3), the misfit being taken to be greater for an ion differing more largely in size from a water molecule. Addtional reference must be made to the finding,[13] provided by the studies of electrolyte solutions using X-ray diffraction technique, that ions such as K^+, NH_4^+ and OH^- which are close in size to water molecules have virtually no influence upon the structure of water, whereas those such as Li^+, Na^+ and Cl^- the sizes of which are decisively different from water molecules exert a more or less positive disturbance to the water structure owing to their structure breaking function. Moreover, according to the studies[14] of the self-diffusion of water in electrolyte solutions, both Cs^+ and Li^+ are the structure breakers, and this is particularly the case with Cs^+. Water molecules in the vicinity of Cs^+ display a mobility higher than that characteristic of those in pure water, indicating that the water structure has been made unstable by the presence of an ion. In the case of Li^+, water molecules are bound to the ion, yielding hydration members which are in strained state and hardly display mobility.

We conclude that an ion, which could be included in the water structure with least influence upon it and which could attract water molecules by electric forces to arrange them at least in an ice-like structure, can establish a certain extent of order in supercooled water so that it serves as a critical nucleus in ice formation. As a matter of fact, we observed that the most effective ion is K^+.

The Role of I^- in Ice-nucleation. Hitherto, we have discussed the rise in freezing temperature of water droplets in the presence of electrolytes, taking the behavior of cations alone into consideration. It might now be asked what about anions. It has been shown in Fig. 3 that, for anions having a common cation, their ice nucleability increases with the size of anion in such a way as $I^- > Br^- > Cl^-$. These anions should possess weaker electric fields around them because of their larger size as compared to cations. This might imply that it is next to impossible for anions to fix water molecules so as to form a critical nucleus. The water molecules around anions are supposed to be in situations similar to those of the water molecules around Cs^+, the size of which is large enough to impart them large mobilities. It is therefore possible for an anion to make contribution to the function of a cation in that the former allows water molecules to be taken away by the latter.

Concerning the roles of anions, there are views[15,16] worthy of mention. Anions are mostly of considerable polarizability on account of their large size, so that they might affect the structure of the surface of a water droplet as well as the structure of the interface between solid ice and liquid water. Once favored with these positions, they would act to reduce the strain there, thus facilitating ice formation. The polarizability was taken to be in the order $I^- > Br^- > Cl^-$, which is in line with that for the nucleability.

Concluding Remarks

We have examined the influence of the electrolyte concentration upon the freezing temperature of water droplets, and have indicated some of the results in Fig. 1. On the basis of these results, we conclude that there exists an optimum in electrolyte concentration, at which the droplets freeze most readily to give the highest freezing temperature. The optimums have been determined to be 1×10^{-4} mol/*l* or thereabout for 1-1 type electrolytes and to be at lower concentrations for 1-2 and 1-3 type electrolytes, though it would be necessary to make more exact determinations by future measurements for the latter two. Similar reports have been presented by some investigators[15] with a number of electrolytes, in which little account has been taken of the function of ions, and the greater part of

13) G. W. Brady, *J. Chem. Phys.*, **33**, 1079 (1960).
14) J. H. Wang, *J. Phys. Chem.*, **58**, 686 (1954).
15) C. L. Hosler and C. R. Hosler, *Trans. Am. Geophys. Union*, **36**, 126 (1955); R. G. Pena, J. V. Iribarne and E. M. Achaval, *J. Atmos. Sci.*, **19**, 302 (1962).
16) W. A. Weyl, *J. Colloid Sci.*, **6**, 389 (1951).

discussion has been given assuming the presence of insoluble particles in water.

It would be significant to search for reasons for the occurrence of the optimum in freezing temperature. It seems to us that the decrease in freezing temperature on the higher concentration side arises from the structure of water being broken down by a large number of cations so that the nuclei could grow with considerable difficulty. The finding that the optimums for 1-2 and 1-3 type electrolytes appear at lower concentrations might be attributed to the presence of more cations in water as compared with the case of 1-1 type electrolytes having the same concentration.

BULLETIN OF THE CHEMICAL SOCIETY OF JAPAN VOL. 42 1812—1819 (1969)

Evaluation of the Activation Energies of Radical Substitution Reactions in the Gaseous Phase. I. An Empirical Method Employing the Morse Function

Tsutomu KAGIYA, Yūzō SUMIDA, Tokuji INOUE and Fridrich S. DYACHKOVSKII*1

Faculty of Engineering, Kyoto University, Sakyo-ku, Kyoto

(Received October 11, 1968)

An empirical evaluation of the activation energy has been carried out for the radical substitution reaction involving polyatomic molecules. The potential energy along the reaction path is assumed to be expressed for the initial and the final systems by the two Morse functions with the coefficient "a'," which is different from the "a" in the usual Morse function of the bond. The difference between the $a'\Delta r^*$ values in the Morse functions of the initial and the final systems in the transition state is empirically determined as a function, $a_f'\Delta r_f^* - a_i'\Delta r_i^* = \beta Q$, of the reaction heat, Q. From the Morse function with "a'" and the above relation, the activation energy is calculated by using the bond dissociation energies of the initial and the final molecules. The treatment proposed is useful for the evaluation of the activation energies of many types of radical substitution reactions.

Quantitative studies aimed at evaluating the activation energy of the radical substitution reaction in the gaseous phase have been carried out from the latter half of the 1930's. Since Polanyi[1] and Horiuchi[2] found that the difference in the activation energies in a homologous reaction decreased with an increase in the difference in the reaction heats, the activation energy has been considered in relation to the reaction heat. Bagdasaryan,[3] Tikhomirova-Voevodskii,[4] and Semenov[5] have accumulated a number of the experimental data; they have indicated that the activation energies are in regular correlation with the reaction heats. It has also been found[6] that, for the homologous reactions with a similar reaction heat, the activation energy is proportional to the bond dissociation energy of the initial bond.

On the other hand, the theoretical study of the evaluation of the activation energy of the radical reaction has been started by Eyring[7] and followed by Evans and Polanyi.[1]

In the reaction involving a polyatomic molecule, however, the Evans-Polanyi treatment is so complicated that it is very difficult to evaluate theoretically each energetic term along the reaction path.

We have extended the Morse bond-energy function to a polyatomic molecule, as reported by Ogg-Polanyi.[8] The potential energy along the reaction path has been assumed to be approximately expressed by the two functions of the initial and

*1 Present address: Institute of Chemical Physics, Academy of Sciences of the USSR, Moscow.

1) M. G. Evans and M. Polanyi, *Trans. Faraday Soc.*, **34**, 11 (1938).

2) J. Horiuchi and M. Polanyi, *Acta Physicochim. U.R.S.S.*, **2**, 505 (1935).

3) Kh. S. Bagdasaryan, *Zh. Fiz. Khim.*, **23**, 1375 (1949).

4) N. N. Tikhomirova and V. V. Voevodskii, *Dokl. Akad. Nauk, U.S.S.R.*, **79**, 993 (1951).

5) N. N. Semenov, "Some Problems in Chemical Kinetics and Reactivity" English Ed., Princeton Univ. Press, Princeton, New Jersey (1958).

6) F. S. Dyachkovskii and A. E. Shilov, *Kinetika i Kataliz*, **4**, 919 (1963).

7) H. Eyring and M. Polanyi, *Z. physik. Chem.*, **B**, **12**, 279 (1931).

8) R. A. Ogg, Jr., and M. Polanyi, *Trans. Faraday Soc.*, **31**, 604 (1935).

the final systems. The coefficient "a'" is different from the "a" in the Morse function[9] of a bond in which the presence of a radical is disregarded. Moreover, the difference between the $a'\Delta r^*$ values in the Morse functions of the initial and the final systems in the transition state was found to be proportional to the reaction heat, where Δr^* is an expansion of a bond between the ground state and the transition state.

From the Morse function with the "a'" coefficient, the $a_f'\Delta r_f^* - a_i'\Delta r_i^* = \beta Q$ relation, and the bond dissociation energies of the initial and the final bonds, an equation for the evaluation of the activation energies of radical substitution reactions is derived, and its propriety is discussed in connection with the observed values.

General Considerations

In the evaluation of the activation energy of the radical substitution reaction, we consider such reactions of the three-center type as:

$$A + BC \rightarrow AB + C \qquad (1)$$

where A, B, and C are reacting atoms or groups. As has been proposed by Evans and Polanyi,[1] the energy changes involved in the reaction can be divided into: (i) the repulsion forces between A and BC, (ii) the attraction forces of the BC molecule, (iii) the repulsion forces between C and AB, (iv) the attraction forces of the AB molecule, and (v) the perturbation energy between the states. The quantitative evaluation of each term in the reaction involving a polyatomic molecule is, however, very difficult.

In this paper, the following picture is assumed to give an approximate method for evaluating the activation energy of the reaction (1):

$$\underset{}{A + B\text{–}C} \xrightarrow{D_i^0} \underset{(a)}{(A\ B\cdots C)} \longleftrightarrow \underset{(b)}{(A\cdots B\ C)} \xrightarrow{D_f^0} A\text{–}B + C \qquad (2)$$

where (a) or (b) represents the transition state in which the potential energy of the system along the reaction path is localized on the initial B–C bond or on the final A–B bond.

Considering the above speculation in connection with the reaction process, the reaction (1) can be explained by the following three steps. (i) Until the transition state, the A radical approaches from infinity to the initial BC molecule, the BC molecule absorbs the energy of the A radical, and the B–C bond is stretched as the A–B distance decreases. (ii) In the transition state, the energy localized on the B–C bond migrates on the A–B bond. (iii) After the transition state, the energy is concentrated on the A–B bond, and the AB molecule is formed.

9) P. M. Morse, *Phys. Rev.*, **34**, 57 (1929).

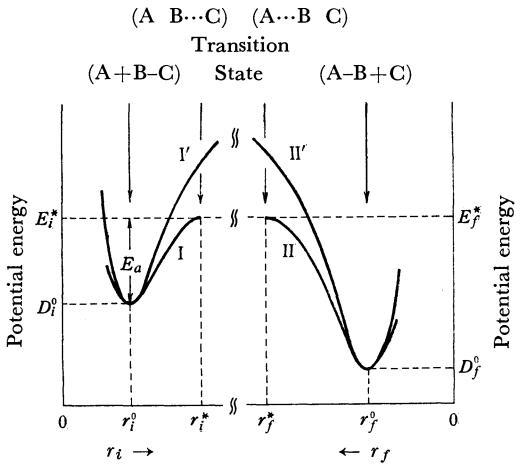

Fig. 1. The potential energy curves of the initial and the final systems along the reaction path.

We may explain the above reaction process with Fig. 1. The potential energy along the reaction path is expressed by the two curves (I and II) of the initial and the final systems, while I′ and II′ are the bond-energy curves neglecting the presence of the A and C radicals, respectively. Then, the curve I can be understood to include not only the curve I′, but also the attraction of the final bond, AB, and the repulsion between A and C.

In order to evaluate the activation energy on the basis of the above scheme, the function of the potential energy curve (I, II) along the reaction path must be determined and the conditions in the transition state must be established.

The Function of the Potential Energy Curve along the Reaction Path. As has been described before, the curve I is mainly determined by three energetic terms of the partial dissociation (the attraction) of BC, the partial formation (the attraction) of AB, and the repulsion between A and C. In consideration of these interaction energies, we assumed that the potential energy of the system along the reaction path is expressed by the two Morse functions, (3) for the initial system (curve I) and (4) for the final one (curve II):

$$E_i = D_i^0 - D_i^0(1 - e^{-a_i'(r_i - r_i^0)})^2 \qquad (3)$$

$$E_f = D_f^0 - D_f^0(1 - e^{-a_f'(r_f - r_f^0)})^2 \qquad (4)$$

where the subscripts i and f represent the initial and the final systems; E, the potential energy along the reaction path; r, the distance between the reacting components, B···C or A···B; D^0, the sum of the zero-point energy and the bond dissociation energy; r^0, the equilibrium distance of the bond, and a', the Morse constant, depending on the energetic terms described above.

Neglecting the zero-point energy in comparison with the bond dissociation energy, we can obtain, from Eqs. (3) and (4), Eqs. (5) and (6):

$$a_i'\Delta r_i^* = -\ln\left(1-\sqrt{1-\frac{E_i^*}{D_i}}\right) \quad (5)$$

$$a_f'\Delta r_f^* = -\ln\left(1-\sqrt{1-\frac{E_f^*}{D_f}}\right) \quad (6)$$

where E^* is a potential energy in the transition state and $E_i^*=E_f^*=E^*$. Equations (5) and (6) show that the activation energy can be evaluated on the basis of the "a'" coefficient and the Δr^* values.

In order to evaluate the "a'" values in Eqs. (3) and (4), we will consider the reaction (1) as a model of the radical substitution reactions. When the A radical approaches from infinity to the initial BC molecule, the Morse constant, "a_i'", of the initial system should change from the original "a_i" value to the new "a_i'" value. It is considered that this change in the "a_i'" value depends on both the attraction of AB and the repulsion between A and C. Taking into account the fact that these energetic terms are expressed as functions of a distance between the components, we postulate the new "a'" value by the following formulas:

$$a_i' = a_i(1-e^{-\gamma\cdot r_f^0}) \quad (7)$$

$$a_f' = a_f(1-e^{-\gamma\cdot r_i^0}) \quad (8)$$

where "a" is a Morse constant in the bond dissociation neglecting the presence of a radical and where γ is assumed to be a constant, regardless of the kind of reaction. The Morse constant, "a", is equal to $0.1227\omega_0\sqrt{\mu/D}$, where ω_0 is the fundamental vibrational frequency (cm^{-1}); μ, the reduced mass, and D, the bond dissociation energy (cm^{-1}), depending on both terms of the electronic energy and the energy of the repulsion between two nuclei.

In this study, it is assumed that the dissociation energy curve of a bond in a polyatomic molecule is essentially expressed by the Morse function as well as that in a diatomic molecule. For example, in computing the Morse functions of methyl halides, the methyl group is treated as a rigid unit with a mass of 15. The totally symmetric stretching vibrational frequency is used as a fundamental vibrational frequency, ω_0. The Morse constants, "a", of a bond in a polyatomic molecule, as calculated with the above characteristic values, are summarized in Table 1.

On the other hand, we can empirically evaluate the "a'" value of the exchange reaction of a hydrogen atom with a hydrogen molecule. It is known in this reaction that the activation energy is 6.7 kcal/mol; the normal distance between hydrogen atoms, 0.74 Å; the distance between hydrogen atoms in the transition state, 1.01 Å, and the bond dissociation energy of the hydrogen molecule, 103.0 kcal/mol. By substituting these values into Eq. (5) or (6), the new "a'" value along the reaction path is obtained as 1.10 $Å^{-1}$, *i. e.*, $a_i'=a_f'=a'=1.10$ $Å^{-1}$.

Table 1. The "a" constants in the Morse function

Bonds	ω_0 (cm^{-1})	D (kcal/mol)	μ (amu)	a ($Å^{-1}$)
HO–H	3657	117	0.945	2.16
HS–H	2611	90.2	0.971	1.78
BF_2–F	888	151	13.7	1.87
NH_2–H	3336	102	0.941	2.10
CH_3–H	2915	101	0.938	1.84
C_2H_5–H	2915	98	0.967	1.90
CH_2Cl–H	2968	97	0.980	1.96
$CHCl_2$–H	2990	93	0.989	2.02
CCl_3–H	3021	89	0.991	2.09
CH_2Br–H	2972	95.2	0.990	1.99
$CHBr_2$–H	2988	87.7	0.994	2.09
CF_3–H	3062	103	0.986	1.96
CCl_3–Cl	458	68.4	27.3	1.90
CH_3–F	1049	108(126)†	8.38	1.92(1.97)†
CH_3–Cl	733(712)†	83.5(73)†	10.5	1.74(1.77)†
CH_3–Br	611(603)†	68.0(59)†	12.6	1.73(1.83)†
CH_3–I	534	55.0(44)†	13.4	1.73(1.95)†
H–Cl	2990	102	0.973	1.91†
H–H	—	103	0.500	(1.85)††
				Av. 1.92±0.24

† Reported in Ref. 8.
†† Reported in Ref. 9.

With the use of the above data, *i. e.*, $a=1.85$ $Å^{-1}$, $a'=1.10$ $Å^{-1}$, and $r^0=0.74$ Å, the coefficient, γ, is determined to be 1.19 from Eqs. (7) and (8).

The Conditions in the Transition State. Taking the difference between Eqs. (5) and (6) and using the relations (7) and (8), we can derive the following equation:

$$a_f'\Delta r_f^* - a_i'\Delta r_i^* = -\ln\left(1-\sqrt{1-\frac{E_f^*}{D_f}}\right)\Big/\left(1-\sqrt{1-\frac{E_i^*}{D_i}}\right) \quad (9)$$

$$= a_f(1-e^{-\gamma\cdot r_i^0})\Delta r_f^* - a_i(1-e^{-\gamma\cdot r_f^0})\Delta r_i^* \quad (10)$$

As may be seen from Table 1, the "a" value turns out to be approximately constant; thus we may put $a_i=a_f=a_m=1.92$ $Å^{-1}$ (the average value of "a"). Moreover, since r_i^0 is nearly equal to r_f^0 in many reactions, the average value, $r_m^0=1/2(r_i^0+r_f^0)$, is employed for the value of r_i^0 and r_f^0.

$$a_f'\Delta r_f^* - a_i'\Delta r_i^* = a_m(1-e^{-\gamma\cdot r_m^0})(\Delta r_f^* - \Delta r_i^*) \quad (11)$$

When the following type of reactions is chosen as the standard reactions in computing; $R+HR'\rightarrow RH+R'$, the value of $a_m(1-e^{-\gamma\cdot r_m^0})$ is calculated to be approximately 1.40 $Å^{-1}$.

In the transition state, it is considered that the expansion of the initial bond is equal to that of the final bond in the reaction with the heat $Q=0$,

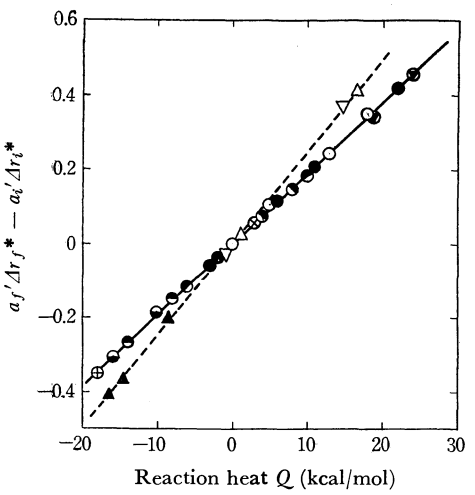

Fig. 2. Plot of the differences, $a_f'\Delta r_f^* - a_i'\Delta r_i^*$, *versus* the reaction heats.

○ H+RH→H_2+R, ⊗ D+RH→HD+R, ● CH_3+RH→CH_4+R, ◔ C_2H_5+RH→C_2H_6+R, ◐ *n*-C_3H_7+RH→*n*-C_3H_8+R, ◓ *i*-C_3H_7+RH→*i*-C_3H_8+R, ◒ *t*-C_4H_9+RH→*t*-C_4H_{10}+R, ⊕ CH_3CO+RH→CH_3CHO+R, ▼ H+RCl→HCl+R, △ H+HX→H_2+X, ▽ CH_3+HX→CH_4+X, ▲ Br+RH→HBr+R.

that it is smaller in the exothermic reaction $Q>0$, and that it is larger in the endothermic reaction $Q<0$.

On the basis of these considerations, the right side in Eq. (9) is evaluated from the experimental data and is plotted against the heat of reaction (Fig. 2). The linear relation in Fig. 2 can be expressed by the following formula for the standard reactions:

$$a_f'\Delta r_f^* - a_i'\Delta r_i^* = \beta Q = 0.0190Q \quad (Q\text{: kcal/mol}) \tag{12}$$

Therefore, $(\Delta r_f^* - \Delta r_i^*)$ is equal to $0.0136Q$.

The Evaluation of the Activation Energy. As has been described above, the potential energies along the reaction path are expressed by the two following Morse functions:

$$E_i = D_i(2e^{-a_i'\Delta r_i} - e^{-2a_i'\Delta r_i}) \tag{13}$$

$$E_f = D_f(2e^{-a_f'\Delta r_f} - e^{-2a_f'\Delta r_f}) \tag{14}$$

By substituting the conditions in the transition state, *i. e.*, $E_i^* = E_f^* = E^*$ and $a_f'\Delta r_f^* - a_i'\Delta r_i^* = 0.0190Q$, into Eqs. (13) and (14), we can derive the formulas expressing the expansions of the bond lengths and the potential energy of the bond in the transition state:

$$\Delta r_i^* = -\frac{1}{a_i'} \ln \frac{2\alpha(D_f - \alpha D_i)}{D_f - \alpha^2 D_i} \tag{15}$$

$$\Delta r_f^* = -\frac{1}{a_f'} \ln \frac{2(D_f - \alpha D_i)}{D_f - \alpha^2 D_i} \tag{16}$$

$$E^* = \frac{4\alpha(1-\alpha)D_iD_f(D_f - \alpha D_i)}{(D_f - \alpha^2 D_i)^2} \tag{17}$$

where α is equal to $\exp(0.0190Q)$. The activation energy can then be expressed by the following equation:

$$E_a = D_i - E^* = \frac{D_i((1-2\alpha)D_f + \alpha^2 D_i)^2}{(D_f - \alpha^2 D_i)^2} \tag{18}$$

Equation (18) shows that the activation energy can be calculated by using the bond dissociation energies of the initial and the final molecules. In the reaction with the heat $Q=0$, both the denominator and the numerator are zero in Eq. (18). Therefore, the activation energy of this type of reaction can be estimated by interpolating the activation energies of the reactions with $Q\neq 0$.

Results and Discussion

The expansions (Δr_i^*, Δr_f^*) of the bond lengths and the activation energies as calculated by Eqs. (15)—(18), are listed in Table 2, where they are shown in comparison with the observed values.[5,10,11]

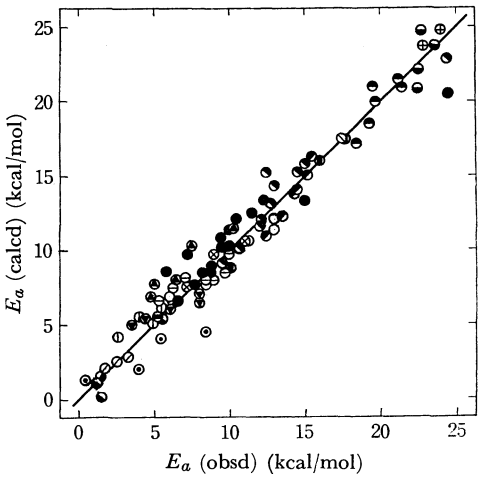

Fig. 3. Comparison of the calculated values with the observed values of the activation energies of the radical substitution reactions.

○ H+RH→H_2+R, ⊗ D+RH→HD+R, ⊙ OH+RH→H_2O+R, ● CH_3+RH→CH_4+R, ◔ C_2H_5+RH→C_2H_6+R, ◐ *n*-C_3H_7+RH→*n*-C_3H_8+R, ◓ *i*-C_3H_7+RH→*i*-C_3H_8+R, ◒ *t*-C_4H_9+RH→*t*-C_4H_{10}+R, ◭ CF_3+RH→CF_3H+R, ⊕ CH_3CO+RH→CH_3CHO+R, ▼ H+RCl→HCl+R, ⊖ Na+RCl→NaCl+R, ⓘ Na+RBr→NaBr+R, ⊘ Na+RI→NaI+I, ⊘ Na+RF→NaF+R, ◔ H+HX→H_2+X, ◕ CH_3+HX→CH_4+X, ⊖ Cl+RH→HCl+R, ◖ Br+RH→HBr+R.

10) E. W. R. Steacie, "Atomic and Free Radical Reactions," Reinhold Co., New York (1946); *ibid.*, Second Ed. Vol. II (1954).

11) N. N. Tikhomirova and V. V. Voevodskii, *Chem. Abstr.*, **45**, 9940 (1951).

TABLE 2. THE ACTIVATION ENERGIES OF VARIOUS RADICAL SUBSTITUTION REACTIONS†

RH or RX	D_i (kcal/mol)	Δr_i^* (Å)	Δr_f^* (Å)	E^* (kcal/mol)	E_a(calcd) (kcal/mol)	E_a(obsd)[5,10,11] (kcal/mol)
$H + RH \longrightarrow H_2 + R$						
H_2	103	(0.27)††	(0.27)††	(96.3)††	(6.7)††	6.7
CH_4	101	0.291	0.318	89.71	11.3	13.0
C_2H_6	98.0	0.279	0.347	87.76	10.2	9.5
$C(CH_3)_4$	98.0	0.279	0.347	87.76	10.2	9.3
i-C_3H_8	90.0	0.250	0.427	82.11	7.9	8.5
CH_3CHO	85.0	0.236	0.481	78.24	6.8	6.0
$D + RH \longrightarrow HD + R$						
CH_4	101	0.280	0.321	90.39	10.6	11.0
C_2H_6	98.0	0.269	0.351	88.31	9.7	9.0
i-C_3H_8	90.0	0.243	0.433	82.54	7.5	7.2
$OH + RH \longrightarrow H_2O + R$						
CH_4	101	0.170	0.388	96.45	4.5	8.5
C_2H_6	98.0	0.159	0.417	94.12	3.9	5.5
CH_3CHO	85.0	0.118	0.553	83.04	2.0	4.0
$HCHO$	79.0	0.104	0.621	77.55	1.4	0.5
$CF_3 + RH \longrightarrow CF_3H + R$						
CH_4	101	0.291	0.318	89.71	11.3	10.3
C_2H_6	98.0	0.279	0.347	87.76	10.2	7.5
i-C_3H_8	90.0	0.250	0.427	82.11	7.9	6.5
i-C_4H_{10}	89.0	0.247	0.439	81.30	7.7	5.1
t-C_4H_{10}	85.0	0.236	0.481	78.24	6.8	4.7
$CH_3 + RH \longrightarrow CH_4 + R$						
H_2O	117	0.388	0.170	96.45	20.5	24.5
H_2	103	0.318	0.291	89.71	13.3	15.0
CF_3H	103	0.318	0.291	89.71	13.3	12.3
CH_4	101	—	—	—	(12.4)†††	11.5
CH_3OH	100	0.306	0.320	87.87	12.1	10.4
C_2H_6	98.0	0.297	0.338	86.65	11.3	10.0
$C(CH_3)_4$	98.0	0.297	0.338	86.65	11.3	10.0
CH_3Cl	97.0	0.293	0.348	85.99	11.0	9.4
n-C_3H_8	95.0	0.286	0.367	84.67	10.3	9.5
CH_3Br	95.0	0.286	0.367	84.67	10.3	10.1
n-C_4H_{10}	94.0	0.282	0.377	84.00	10.0	9.3
CH_2Cl_2	93.0	0.279	0.388	83.29	9.7	7.2
i-C_3H_8	90.0	0.269	0.419	81.14	8.9	8.7
i-C_4H_{10}	89.0	0.266	0.429	80.40	8.6	8.2
$CHCl_3$	89.0	0.266	0.429	80.40	8.6	5.8
CH_2Br_2	88.0	0.263	0.440	79.64	8.4	8.7
t-C_4H_{10}	85.0	0.255	0.473	77.33	7.7	7.7
CH_3CHO	85.0	0.255	0.473	77.33	7.7	7.5
C_2H_5CHO	85.0	0.255	0.473	77.33	7.7	7.5
$HCHO$	79.0	0.243	0.542	72.43	6.6	6.6
$C_2H_5 + RH \longrightarrow C_2H_6 + R$						
H_2O	117	0.417	0.159	94.12	22.9	24.5
HD	104	0.351	0.269	88.31	15.7	15.0
H_2	103	0.347	0.279	87.76	15.2	14.5
CF_3H	103	0.347	0.279	87.76	15.2	12.5
CH_4	101	0.338	0.297	86.65	14.3	13.0
C_2H_6	98.0	—	—	—	(13.1)†††	12.8
n-C_3H_8	95.0	0.314	0.355	82.97	12.0	12.2

TABLE 2. Continued

RH or RX	D_i (kcal/mol)	Δr_i^* (Å)	Δr_f^* (Å)	E^* (kcal/mol)	E_a(calcd) (kcal/mol)	E_a(obsd)[5,10,11] (kcal/mol)
n-C_4H_{10}	94.0	0.310	0.364	82.38	11.6	11.9
i-C_3H_8	90.0	0.298	0.407	79.53	10.5	11.3
i-C_4H_{10}	89.0	0.295	0.417	78.85	10.1	10.7
t-C_4H_{10}	85.0	0.284	0.461	75.85	9.1	9.6
n-C_3H_7 + RH ⟶ n-C_3H_8 + R						
CH_4	101	0.367	0.286	84.67	16.3	15.5
C_2H_6	98.0	0.355	0.314	82.97	15.0	15.2
n-C_3H_8	95.0	—	—	—	(14.1)†††	14.5
n-C_4H_{10}	94.0	0.343	0.357	80.29	13.7	14.3
i-C_3H_8	90.0	0.327	0.395	77.83	12.2	13.5
i-C_4H_{10}	89.0	0.324	0.406	77.13	11.9	13.1
t-C_4H_{10}	85.0	0.314	0.450	74.25	10.8	12.4
i-C_3H_7 + RH ⟶ i-C_3H_8 + R						
HD	104	0.433	0.243	82.54	21.5	21.2
H_2	103	0.427	0.250	82.11	20.9	21.5
CF_3H	103	0.427	0.250	82.11	20.9	19.5
CH_4	101	0.419	0.269	81.14	19.9	19.7
C_2H_6	98.0	0.407	0.298	79.53	18.5	19.3
n-C_3H_8	95.0	0.395	0.327	77.83	17.2	18.5
t-C_4H_9 + RH ⟶ t-C_4H_{10} + R						
CF_3H	103	0.481	0.236	78.24	24.8	22.7
CH_4	101	0.473	0.255	77.33	23.7	23.7
C_2H_6	98.0	0.461	0.284	75.85	22.1	22.6
n-C_3H_8	95.0	0.450	0.314	74.25	20.7	22.4
CH_3CO + RH ⟶ CH_3CHO + R						
H_2O	117	0.553	0.118	83.04	34.0	36.0
H_2	103	0.481	0.236	78.24	24.8	24.0
CH_4	101	0.473	0.255	77.33	23.7	22.8
H + RCl ⟶ HCl + R						
CH_3Cl	83.5	0.242	0.494	76.57	6.9	8.0
C_2H_5Cl	80.5	0.236	0.528	74.13	6.4	8.0
CH_2Cl_2	78.0	0.232	0.558	72.03	6.0	6.0
$CHCl_3$	73.5	0.226	0.614	68.08	5.4	4.5
CCl_4	68.4	0.225	0.682	63.41	5.0	3.5

† Calculated by Eq. (18) with β=0.0190
†† An experimental value
††† Evaluated by interpolation

The calculated values of the activation energies are in good accordance with the observed values for many, though not all, types of reactions within ±2.0 kcal/mol. It should be noted that Eq. (18) holds not only in the homopolar reactions, but also in the reactions with some ionic character.

In the reaction, R+HR′→RH+R′, with the same reaction heat and the same β value (0.0190), it is also found that the activation energy decreases with an increase in the value of D_i (or D_f). This relation may be due to the increase in the expansion, Δr_i^*, with a decrease in the dissociation energy of the initial molecule.

On the other hand, in the following reaction, in which the hydrogen atom pulls the hydrogen of hydrogen halides:

$$H + HX \rightarrow H_2 + X \qquad (19)$$

the values calculated by Eq. (18) with the standard β value are considerably larger than the observed values. This disagreement may be explained as follows. On the basis of the facts that r^0_{H-X} (1.22—1.47 Å) and r^0_{H-H} (0.74 Å) are not equal to each other and both differ from r^0_{R-H} (1.09 Å), Eqs. (11) and (12) do not hold for the reaction (19).

In our treatment, the difference in the equilibrium distances results in changes in both the Morse constant "a" and the β value. We assume that the value of $(a_f'\Delta r_f^* - a_i'\Delta r_i^*)$ is expressed by Eq. (12), which has a new β (β') value which is different from 0.0190 (Fig. 2):

$$a_f'\Delta r_f^* - a_i'\Delta r_i^* = \beta' Q \quad (Q\text{: kcal/mol}) \qquad (20)$$

The β' value is calculated with the use of the experimental data, *i. e.*, $\beta' = 0.0260$ for the reaction (19).

Moreover, in the following reaction, it is well known that the activation energy generally decreases in the order RF > RCl > RBr > RI and cannot be evaluated by Eq. (18) using the standard β value:

TABLE 3. THE ACTIVATION ENERGIES OF VARIOUS RADICAL SUBSTITUTION REACTIONS

RH or RF	D_i (kcal/mol)	Q (kcal/mol)	β'	E_a(calcd) (kcal/mol)	E_a(obsd)[5,10] (kcal/mol)
Na + RF ⟶ NaF + R					
CH_3F	108	1.0	0.0133	29.7	>25.0
Na + RCl ⟶ NaCl + R					
C_6H_5Cl	87.0	10.5	0.0190	10.0	10.2
CH_2=CHCl	86.5	11.0	0.0190	9.8	10.0
CH_3Cl	83.5	14.0	0.0190	9.0	9.7
C_2H_5Cl	80.5	17.0	0.0190	8.4	9.7
n-$C_5H_{11}Cl$	80.0	17.5	0.0190	8.4	8.4
n-C_4H_9Cl	79.5	18.0	0.0190	8.4	8.8
i-$C_5H_{11}Cl$	79.0	18.5	0.0190	8.3	8.3
CH_2Cl_2	78.0	19.5	0.0190	8.1	8.2
CH_3CHCl_2	77.9	19.6	0.0190	8.1	7.2
n-C_3H_7Cl	77.5	20.0	0.0190	8.0	9.0
t-C_4H_9Cl	75.0	22.5	0.0190	7.7	8.0
$CHCl_3$	73.5	24.0	0.0190	7.4	6.2
CCl_4	68.4	29.1	0.0190	6.9	5.0
CH_2=$CHCH_2Cl$	58.0	39.5	0.0190	6.6	5.3
Na + RBr ⟶ NaBr + R					
CH_2=CHBr	73.4	14.3	0.0224	5.9	5.4
C_6H_5Br	71.0	16.7	0.0224	5.4	4.0
CH_3Br	68.0	19.7	0.0224	4.9	5.0
C_2H_5Br	67.0	20.7	0.0224	4.8	4.9
CH_2Br_2	61.0	26.7	0.0224	4.1	2.6
Na + RI ⟶ NaI + R					
CH_2=CHI	58.0	12.7	0.0301	2.7	3.2
CH_3I	56.3	14.4	0.0301	2.5	2.5
C_2H_5I	53.0	17.7	0.0301	2.1	1.7
H + HX ⟶ H_2 + X					
HCl	102	1.0	0.0260	5.4	5.6
HBr	86.5	16.5	0.0260	1.0	1.2
HI	70.0	33.0	0.0260	0.0	1.5
CH_3 + HX ⟶ CH_4 + X					
HCl	102	− 1.0	0.0260	6.5	6.2
HBr	86.5	14.5	0.0260	1.5	1.4
Cl + RH ⟶ HCl + R					
H_2	103	− 1.0	0.0260	6.4	6.6
CH_4	101	1.0	0.0260	5.5	5.2
Br + RH ⟶ HBr + R					
H_2	103	−16.5	0.0260	17.5	17.7
CH_4	101	−14.5	0.0260	16.0	15.9
CH_3Br	95.0	− 8.5	0.0260	12.0	13.4
$CHCl_3$	89.0	− 2.5	0.0260	8.7	10.0

$$Na + XR \rightarrow NaX + R \quad (X=\text{a halogen atom}) \quad (21)$$

On the basis of the similar considerations described above, the new β values can be empirically evaluated. The following empirical relation can be obtained between β'_{R-X} and r^0_{R-X}:

$$\beta'_{R-X} = \beta'_{R-F} + 5.0 \times 10^{-5}((r^0_{R-X})^6 - (r^0_{R-F})^6) \quad (22)$$

where $\beta'_{R-F}=0.0133$ and $r^0_{R-F}=1.96$ Å. The activation energies of the reaction (21), calculated with the new β value obtained from Eq. (22), are listed in Table 3. It may also be found in Table 3 that, in the reaction (21) with the same reaction heat and a different β value, the acitvation energy decreases with a decrease in the dissociation energy of the initial bond. If the relation, $\Delta r_f^* - \Delta r_i^* = \text{constant} \times Q$, holds for the reaction (21) as well as for the standard reaction, a decrease in the dissociation energy may result in a remarkable decrease in the slope of the Morse function curve and, consequently, in that of the activation energy.

These results lead to the following conclusions. The activation energy of the radical substitution reactions can be evaluated by the method based on the Morse function. In reactions of the R+HR′→RH+R′ type, with the same reaction heat, the activation energy depends on the expansion of the bond, while in reactions of the Na+XR→NaX+R type, with the same reaction heat, the change in the activation energy depends mostly on the difference in the slope of the Morse function curve.

The authors would like to express their gratitude to Professor Kenichi Fukui for his valuable suggestions throughout this work and to Mr. Keisuke Makino and Mr. Toshihiro Tachi for their assistance in computing and in gathering of the experimental data.

BULLETIN OF THE CHEMICAL SOCIETY OF JAPAN VOL. 42 1819—1824 (1969)

The Crystal Structure of 5,5-Dimethyl-2-oxo-2-hydroxy-1,3,2-dioxaphosphorinane Monohydrate

Wataru MURAYAMA and Masatsune KAINOSHO

Central Research Laboratories, Ajinomoto Co., Inc., Suzukicho, Kawasaki

(Received November 4, 1968)

The crystal structure of 5,5-dimethyl-2-oxo-2-hydroxy-1,3,2-dioxaphosphorinane monohydrate (I) has been determined by the three dimensional X-ray diffraction method. The crystals belong to monoclinic system, with space group $P2_1$. The unit cell dimensions are; $a=9.50$, $b=5.86$, $c=8.31$ Å, $\beta=106°8'$, and two molecules per unit cell. The six-membered dioxaphosphorinane ring has a chair conformation, with P=O bond in equatorial position. The bond angles and distances of the phosphate group are similar to those found in the corresponding acyclic phosphates.

One of the most interesting roles of the molecular structure of nucleotide is the conformation around the phosphate linkage. Recently, the conformation of two naturally occurring nucleotides, inosine-5′-monophosphate and guanosine-5′-monophosphate, have been studied both in aqueous solution and in crystalline state by ^{31}P NMR measurements[1] and X-ray diffraction method,[2,3] respectively. The results, so far obtained, suggest that quite similar conformations of the phosphate fragment are preferred both in aqueous solution and in crystalline state.

Determination of the dihedral angle in P–O–C–H system by NMR method is based upon the dihedral angular sensitive nature of J_{POCH} (phosphorus-proton spin-spin coupling constant).[1,4-6] Thus, in order to determine the values of "*gauche*" and "*trans*" P–H coupling (Fig. 1) a variety of the conformationally fixed 1,3,2-dioxaphosphorinanes

1) M. Tsuboi, M. Kainosho and A. Nakamura, "Recent Development of Magnetic Resonance in Biological System," ed. by S. Fujiwara and L. H. Piette, Hirokawa Publishing Co., Tokyo (1968), p. 43.

2) N. Nagashima and Y. Iitaka, *Acta Cryst.*, **B 24**, 1136 (1968).

3) W. Murayama and N. Nagashima, to be published.

4) M. Tsuboi, F. Kuriyagawa, K. Matsuo and Y. Kyogoku, This Bulletin, **40**, 1813 (1967).

5) M. Kainosho, A. Nakamura and M. Tsuboi, *ibid.*, **42**, 1713 (1969).

6) L. D. Hall and R. B. Malcolm, *Chem. & Ind.*, **1968**, 92.

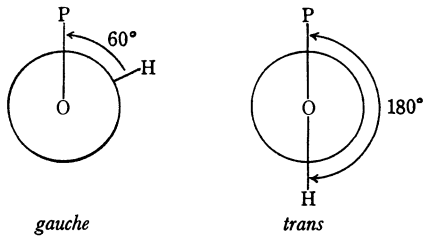

gauche *trans*

Fig. 1. Newman projection formulae (along O–C axis) for "gauche" and "trans" P–O–C–H group.

were studied by NMR.[1,4–6]

During the course of our NMR studies, we realized the necessity of knowing the actual dihedral angles and bond distances in 1,3,2-dioxaphosphorinanes.[5]

The present study gives further structural information about the six-membered cyclic phosphates, for only two of the derivatives (II[7] and III[8]) were studied by X-ray diffraction method. I is a particularly informative molecule for comparison with acyclic phosphoric acid esters and for the examination of preference of P=O bond at the equatorial bond.[7,8]

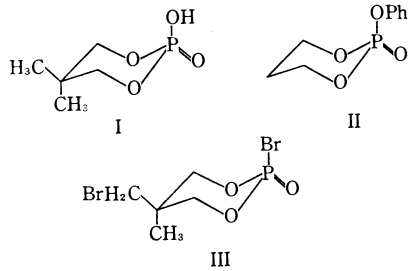

I II III

Fig. 2

Experimental

5,5-Dimethyl-2-oxo-2-hydroxy-1,3,2-dioxaphosphorinane (I) can be obtained as either orthorhombic (α-form) or monoclinic crystals (β-form), when I is crystallized out from an aqueous solution. Crystal data of these two forms are given below.

α-form (orthorhombic; $P2_12_12_1$)
$a = 9.05$, $b = 6.08$, $c = 16.06$ Å,
$D_x = 1.38$, $Z = 4$.

β-form (monoclinic; $P2_1$)
$a = 9.50$, $b = 5.86$, $c = 8.31$ Å, $\beta = 106°8'$,
$D_x = 1.38$, $Z = 2$.

The structure determination by X-ray diffraction method was carried out with a crystal of the β-form. A needle-shaped crystal (elongated along the monoclinic b-axis) was mounted on a Weissenberg camera and rotated around its axis. Equi-inclination Weissenberg photographs for the five layer $0 \leq k \leq 4$ were recorded by multi-film technique with Cu$K\alpha$ radiation. The intensities were estimated visually. No corrections were made for absorption. The x and z coordinates of the phosphorus atom were determined readily from (u, 1/2, w) Harker section. The y parameter of the phosphorus atom was taken as zero. Three dimensional Fourier syntheses, based on the phase angles calculated from the position of phosphorus atom, revealed all the other peaks due to lighter atoms together with their mirror images. One set of the peaks could be picked out as real. The R-index at this stage was 0.33. Several cycles of block-matrix least squares refinements with isotropic temperature factors reduced R-index to 0.16, and following full-matrix least-squares refinements with isotropic temperature factors reduced R to 0.151. Finally, anisotropic temperature factors were introduced and several cycles of block-matrix least squares refinements were carried out. The weighting schemes at this step were $F_{max}/|F_0|$ for $|F_0| > F_{max}$, 1.0 for $F_{min} < |F_0| < F_{max}$ and 0.5 for $|F_0| < F_{min}$, where $F_{max}=20.0$ and $F_{min}=7.0$. The final R-index was 0.127.

TABLE 1. THE FINAL POSITIONAL PARAMETERS AND THEIR STANDARD DEVIATIONS (Å)

	x/c	$\sigma(x)$	y/b	$\sigma(y)$	z/c	$\sigma(z)$
P	0.1927	0.0027	0.0000	0.0000	0.3233	0.0030
O(1)	0.0889	0.0118	−0.1494	0.0176	0.2077	0.0112
O(2)	0.2824	0.0093	0.1679	0.0126	0.2474	0.0098
O(3)	0.3138	0.0102	−0.1394	0.0153	0.4574	0.0101
O(4)	0.1097	0.0087	0.1475	0.0145	0.4283	0.0097
O(5)	0.1540	0.0102	0.4652	0.0149	0.0512	0.0093
C(1)	0.4036	0.0115	0.0045	0.0253	0.6034	0.0141
C(2)	0.3055	0.0167	0.1211	0.0293	0.6964	0.0156
C(3)	0.2042	0.0163	0.2766	0.0250	0.5773	0.0158
C(4)	0.2213	0.0179	−0.0626	0.0260	0.7745	0.0173
C(5)	0.4109	0.0191	0.2549	0.0266	0.8312	0.0169

7) H. J. Geise, *Rec. Trav. Chim. Pays-Bas*, **86**, 362 (1967).

8) T. A. Beineke, *Chem. Commun.*, **1966**, 860.

Table 2. The final anisotropic temperature factors

	B_{11}	B_{22}	B_{33}	B_{12}	B_{13}	B_{23}
P	0.0061	0.0089	0.0095	0.0008	0.0008	−0.0010
O(1)	0.0128	0.0369	0.0139	−0.0072	−0.0013	−0.0054
O(2)	0.0084	0.0172	0.0138	−0.0017	0.0029	0.0032
O(3)	0.0086	0.0274	0.0142	0.0019	0.0006	−0.0018
O(4)	0.0068	0.0256	0.0136	0.0027	0.0027	−0.0020
O(5)	0.0137	0.0070	0.0130	0.0035	0.0008	0.0021
C(1)	0.0055	0.0340	0.0156	0.0097	0.0009	−0.0011
C(2)	0.0123	0.0387	0.0128	−0.0032	0.0014	−0.0025
C(3)	0.0113	0.0304	0.0141	0.0046	−0.0008	−0.0088
C(4)	0.0135	0.0427	0.0162	0.0016	0.0073	0.0098
C(5)	0.0164	0.0309	0.0126	−0.0077	−0.0010	−0.0038

The temperature factors are in the form

$$T = \exp(-B_{11}h^2 - B_{22}k^2 - B_{33}l^2 - 2B_{12}hk - 2B_{13}hl - 2B_{23}kl)$$

Table 3. Description of thermal ellipsoids

$B_i = 8\pi^2 U_i^2$, where U_i is the root mean square displacement corresponding to i axis of the ellipsoid.

C_{ia}, C_{ib}, C_{ic} are the direction cosines of the i axis with respect to the crystal axis.

Atom	Axis	B_i	U_i	C_{ia}	C_{ib}	C_{ic}	Atom	Axis	B_i	U_i	C_{ia}	C_{ib}	C_{ic}
P	1	1.25	0.13	−0.1871	0.9780	0.0921		3	5.44	0.26	0.9453	0.1287	−0.2996
	2	1.93	0.16	0.7593	0.0845	0.6452	C(1)	1	0.75	0.10	−0.8617	0.4586	−0.2172
	3	2.93	0.19	−0.6232	−0.1906	0.7584		2	3.92	0.22	0.0741	−0.3098	−0.9479
O(1)	1	2.07	0.16	0.5009	0.4520	0.7381		3	6.37	0.28	−0.5021	−0.8329	0.2329
	2	5.30	0.26	−0.3648	−0.6630	0.6536	C(2)	1	1.83	0.15	0.7075	0.5850	0.3965
	3	6.35	0.28	0.7848	−0.5967	−0.1672		2	3.59	0.21	−0.2949	−0.2654	0.9179
O(2)	1	2.03	0.16	0.4673	0.8482	−0.2493		3	7.54	0.31	0.6423	−0.7663	−0.0153
	2	2.92	0.19	0.8103	−0.2980	0.5046	C(3)	1	2.24	0.17	0.0775	−0.6854	−0.7240
	3	3.96	0.22	−0.3537	0.4379	0.8265		2	3.04	0.20	−0.7857	0.4050	−0.4676
O(3)	1	2.62	0.18	0.8220	−0.2580	0.5077		3	6.91	0.30	−0.6137	−0.6051	0.5072
	2	3.43	0.21	−0.0689	0.8399	0.5384	C(4)	1	2.43	0.18	0.5672	0.3708	−0.7354
	3	4.75	0.25	−0.5653	−0.4776	0.6726		2	4.55	0.24	−0.8194	0.3445	−0.4582
O(4)	1	1.98	0.16	0.9298	−0.3641	0.0537		3	7.62	0.31	−0.0834	−0.8624	−0.4992
	2	3.27	0.20	0.1199	0.4378	0.8911	C(5)	1	2.17	0.17	0.4103	0.5343	0.7390
	3	4.16	0.23	0.3495	0.8221	−0.4507		2	4.37	0.24	−0.2089	−0.7338	0.6465
O(5)	1	0.82	0.10	−0.1877	0.9661	−0.1771		3	7.26	0.30	0.8877	−0.4196	−0.1895
	2	3.25	0.20	0.2667	0.2236	0.9375							

Table 4. Bond distances and angles

P–O(1)	1.457±0.014 Å	C(1)–C(2)	1.522±0.028 Å
P–O(2)	1.542±0.011	C(2)–C(4)	1.580±0.030
P–O(3)	1.582±0.012	C(2)–C(5)	1.494±0.016
P–O(4)	1.579±0.012	C(2)–O(5)	2.483±0.016
O(3)–C(1)	1.523±0.022	O(1)–O(5)	2.766±0.018
O(4)–C(3)	1.510±0.023		
O(1)–P–O(2)	117.8±0.8°	O(3)–C(1)–C(2)	112.3±2.0°
O(1)–P–O(3)	112.4±0.8	O(4)–C(3)–C(2)	112.3±2.0
O(1)–P–O(4)	110.1±0.8	C(1)–C(2)–C(3)	108.1±3.0
O(2)–P–O(3)	103.0±0.8	C(1)–C(2)–C(4)	109.9±3.0
O(2)–P–O(4)	106.5±0.8	C(1)–C(2)–C(5)	104.3±3.0
O(3)–P–O(4)	106.1±0.8	C(3)–C(2)–C(4)	111.5±3.0
P–O(3)–C(1)	114.2±1.2	C(3)–C(2)–C(5)	111.4±3.0
P–O(4)–C(3)	117.5±1.2	C(4)–C(2)–C(5)	111.4±3.0
		O(1)–O(5)–C(2′)	103.0±2.0

Results and Discussion

The crystal structure projected on *bc*-plane is shown in Fig. 3. The oxygen atom of the water molecule is located in the middle of the two phosphorinane molecules, which are separated from each other by one period along the *b*-axis and a hydrogen bond system is formed along this direction. The closest intermolecular distance is 3.42 Å between C(3)-atom of the one molecule and O(3)-atom of the neighboring molecule along the *b*-axis.

The bond distances and angles in the phosphate group are generally in good agreement with the corresponding values reported for some acyclic organic phosphates. For the sake of comparison, some reported values of P–O bond distances and O–P–O angles are listed in Table 5. It should be noted that the observed values of P–OR bond distance (1.58 Å) in I coincide with calculated values based on Cruickshank's rule for P–OR bonds in RPO_4^{2-} or $R_2PO_4^-$ groups.[9] Thus, it can be concluded that the six-membered cyclic phosphate forms an ordinal ester linkage similar to that in the acyclic phosphate.

The conformation of the molecule is a chair form carrying the P–OH in axial and P=O bond in equatorial position, respectively. In the previously reported two phosphorinanes (II and III), the P=O bonds are also in equatorial and P–OPh and –Br are in axial positions.[7,8] The P–O–C angles in

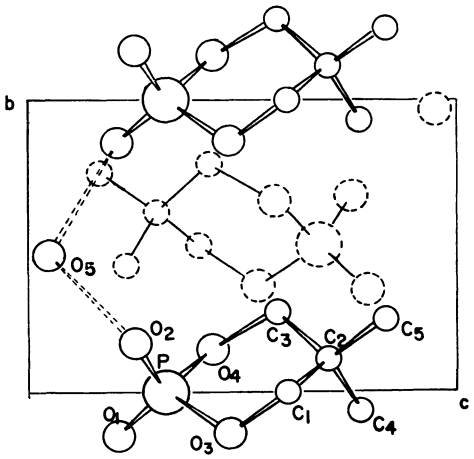

Fig. 3. Crystal structure of 5,5-dimethyl-2-oxo-2-hydroxy-1,3,2-dioxaphosphorinane monohydrate. Projected along the *a*-axis.

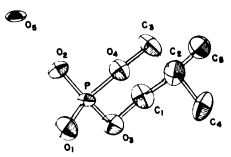

Fig. 4. Thermal vibrations of 5,5-dimethyl-2-oxo-2-hydroxy-1,3,2-dioxaphosphorinane monohydrate. The figure indicates that the atoms lie within the ellipsoids with 50% probability.

TABLE 5. BOND DISTANCES AND ANGLES OF ACYCLIC AND CYCLIC PHOSPHATES

Compound	Bond lengths (Å)				Bond angles (Å)				Ref.
	P=O	P–O⁻	P–OH	P–OR	O=P–OH	O=P–OR	OH–P–OR	OR–P–OR	
Dibenzyl phosphate	1.48		1.56	1.56, 1.57				103.8	a)
Di-*p*-chlorophenyl phosphate	1.497		1.49	1.579		106.5	109.7	108.1	b)
Barium diethyl phosphate		1.51		1.59, 1.62				103.5	c)
L-Serin phosphate	1.479	1.517	1.560	1.680					d)
2-Aminoethyl phosphate	1.493	1.503	1.557	1.591	109.8	103.9	106.2		e)
Cytidylic acid (orthorhombic)	1.483	1.504	1.551	1.611	113.6	10.1	101.5		f)
Cytidylic acid (monoclinic)	1.480	1.493	1.588	1.610	112.6	105.5	104.3		g)
Adenylic acid	1.495	1.514	1.566	1.610	106.4	105.7	106.5		h)
II	1.48			1.56, 1.57 1.59(–POh)		115.3 111.8(ring)		106.6 (ring)	7)
III	1.46			1.58 1.54		112.6 111.4		105.5	8)
I	1.465		1.546	1.597 1.597	117.8	112.4 110.1	106.5 106.1	106.1	

a) J. D. Dunitz, *Acta Cryst.*, **9**, 327 (1964).
b) M. Calleri and J. C. Speakman, *ibid.*, **17**, 1097 (1964).
c) Y. Kyogoku and Y. Iitaka, *ibid.*, **21**, 49 (1966).
d) H. G. McCallgm, J. M. Robertson and G. A. Sim, *Nature*, **184**, 1863 (1959).
e) J. Kraut, *Acta Cryst.*, **14**, 1146 (1961).
f) M. Sundaralingam and L. H. Jensen, *J. Mol. Biol.*, **13**, 914 (1965).
g) C. E. Bugg and R. E. Marsh, *ibid.*, **25**, 67 (1967).
h) J. Kraut and L. H. Jensen, *Acta Cryst.*, **16**, 79 (1963).

9) D. W. J. Cruickshank, *J. Chem. Soc.*, **1961**, 5486.

TABLE 6. THE OBSERVED AND CALCULATED STRUCTURE FACTORS

L	FO	FC	L	FO	FC	L	FO	FC	L	FO	FC	L	FO	FC	L	FO	FC	L	FO	FC
H,K= 0 0			-2 134	103		7* 83	78		-1 121	79		0 110	112		-1 149	151		1* 38	52		4* 60	79
1*294	366		-3* 45	79		8* 0	9		-2 255	262		1*101	88		-2* 0	15		H,K= 0 3			H,K= 5 4	
2 223	226		-4* 36	21		9* 49	61		-3*303	336		2* 95	88		-3* 83	71		-1 116	104		0 225	253
3* 43	56		-5* 64	45		H,K= 3 1			-4* 39	43		3* 64	66		-4* 86	80		-2 112	103		1* 75	62
4* 87	79		-6* 43	42		0 104	69		-5* 89	77		4* 45	34		-5* 45	36		-3 144	116		2* 47	43
5* 61	36		-7* 92	95		1 191	167		-6 121	132		5* 0	17		-6* 55	42		+4 245	248		3* 47	57
6* 0	2		-8* 74	72		2*321	338		H,K= 5 1			6* 98	83		-7* 51	40		-5 187	219		6* 43	64
7* 0	16		-9 123	116		3 116	91		-1 127	96		H,K= 7 2			-9* 43	63		+6* 79	88		H,K= 6 4	
8 149	132		+10* 48	40		4 154	156		-2 112	86		0* 99	90		H,K= 8 2			+7* 77	78		0* 63	53
9* 66	54		H,K= 3 0			5 195	224		-3* 85	66		1* 91	79		-1* 0	33		H,K= 1 3			1* 76	85
H,K= 1 0			-1 120	84		6* 50	57		+4 201	194		2 161	200		-2 143	147		+1 103	96		2* 0	35
0 143	166		+2* 69	40		H,K= 4 1			-5 189	193		3* 63	50		-3 135	128		+2 111	93		3* 63	69
1 161	194		-3 164	155		0 119	85		+6* 0	26		4* 64	51		-4* 0	14		-3 163	169		H,K= 7 4	
2 106	90		-4* 30	33		1 143	128		-7 129	145		5* 63	66		-5* 75	79		+4 179	173		0* 81	59
3* 65	35		-5 116	109		2 125	104		-8* 59	57		6* 48	63		H,K= 9 2			-5 114	107		1* 46	47
4* 96	80		-6* 0	3		3 129	112		H,K= 6 1			H,K= 8 2			-1* 53	54		-6 131	156		2* 92	86
5* 66	46		-7* 0	10		4 153	159		-1* 0	29		0* 79	85		-2* 0	31		H,K= 2 3			3* 54	52
6* 0	14		-8* 83	80		5 110	99		+2* 60	46		1* 71	68		-3* 0	18		+1* 60	58		4* 50	45
7 150	138		-9* 66	66		6* 75	72		-3 139	125		2* 0	11		-4* 39	58		+2*359	228		H,K= 8 4	
H,K= 2 0			H,K= 4 0			H,K= 5 1			+4* 89	77		3* 73	68		-5* 42	41		+3* 86	67		0* 75	65
0*451	534		-1* 92	68		0* 72	47		+5* 59	54		4* 0	21		-6* 36	33		-4 144	132		1* 70	65
1 218	202		-2 119	117		1 145	132		+6* 104	110		5* 41	41		-7* 65	67		+5*387	255		2* 0	13
2 176	171		-3* 75	87		2* 92	66		H,K= 7 1			H,K= 9 2			-8* 30	46		+6* 93	81		3* 66	76
3 236	221		-4*310	324		3*100	91		+1* 0	26		0* 39	22		H,K= 10 2			+7* 60	81		H,K= 9 4	
4 179	167		-5 127	104		4 182	203		+2 138	126		1 103	82		-1* 76	70		H,K= 3 3			0* 34	45
5 195	168		-6* 66	49		5*100	66		+3 128	134		2* 93	83		+2* 0	8		+1 141	137		1* 46	53
6* 73	55		-7 130	136		6 103	61		-4 102	88		3* 36	30		-3* 82	59		+2 129	128		2* 48	59
7 105	103		-8* 52	51		7* 67	58		+5 159	163		4* 49	57		-4* 61	49		+3 122	113		H,K= 0 4	
H,K= 3 0			H,K= 5 0			H,K= 6 1			+6* 98	84		H,K= 10 2			-5* 0	24		+4 116	99		+1* 83	58
0 232	193		-1* 31	36		0* 87	86		-7* 59	72		0* 48	45		-6* 45	51		+5 106	104		-2* 52	49
1* 0	29		+2* 44	33		1* 47	46		H,K= 8 1			1* 0	9		H,K= 11 2			-6 126	120		+3 154	169
2* 88	55		-3* 57	56		2 175	191		+1* 61	68		2* 57	64		H,K= 0 2			-7* 63	58		+4 108	100
3 194	188		-4 158	163		3 116	123		+2* 79	71		H,K= 0 2			-5* 79	74		H,K= 4 3			+5* 59	58
4 172	167		-5* 95	81		4* 27	26		+3* 67	63		-1* 83	72		H,K= 1 3			+1 132	120		+6* 88	91
5* 58	70		-6 109	109		5* 94	87		+4 107	108		+2 104	81		0 109	91		-2 170	178		H,K= 1 4	
6* 84	83		-7* 71	79		6* 53	48		+5* 41	44		-3 279	302		1* 93	80		+3 171	173		+1* 86	20
7* 35	42		H,K= 6 0			H,K= 7 1			+6* 48	40		-4* 75	50		2 188	164		+4* 0	9		-2* 83	66
8* 73	71		-1* 53	47		0* 76	58		+7* 89	85		+5 137	125		3 166	163		+5* 53	46		-3* 54	60
H,K= 4 0			-2* 35	32		1 124	123		H,K= 9 1			+6 104	100		4* 84	84		+6* 61	60		+4 210	240
0 141	132		-3* 73	47		2* 57	46		+1* 70	62		-7* 72	80		5 116	118		+7* 39	53		-5 183	157
1* 95	43		-4 219	214		3* 55	49		+2* 86	70		-8* 50	65		6* 76	81		+8* 33	51		+6* 0	6
2 187	190		-5 263	316		4* 77	60		+3 153	159		+9* 34	38		H,K= 2 3			H,K= 5 3			+7* 68	65
3* 0	10		-6* 42	19		5* 64	61		H,K= 10 1			H,K= 1 2			0* 77	60		-1 171	189		H,K= 2 4	
4*328	362		-7 114	97		6* 77	65		+1* 54	65		-1 273	246		1 145	138		-2 176	193		+1 134	119
5 167	178		+8* 86	72		H,K= 8 1			+2* 76	72		+2 183	176		2* 80	64		+3* 35	25		+2* 51	53
6* 30	31		H,K= 7 0			0* 62	67		+7* 51	56		+3 157	153		3 107	95		+4* 45	49		+3 149	127
7* 93	83		+1* 96	109		1 119	122		H,K= 11 1			+4 203	215		4 105	95		+5* 39	26		+4 149	144
H,K= 5 0			+2* 0	3		2 123	109		+1 105	94		+5 159	156		5* 0	22		+7* 67	67		+5* 0	5
0* 0	14		-3* 0	18		4* 67	64		+3* 67	56		+6* 49	36		6 124	97		H,K= 6 3			+6* 60	69
1* 69	45		-4 118	124		H,K= 9 1			+4* 35	41		+7 110	119		7* 45	45		+1 178	201		+7* 85	84
2* 89	65		+5* 52	44		0 146	142		H,K= 1 2			+8* 39	37		H,K= 3 3			+2* 33	15		H,K= 3 4	
3 215	230		-6* 43	69		H,K= 10 1			0 111	98		H,K= 2 2			0 108	90		-3 122	116		+1* 91	69
4* 95	90		+7* 81	84		0* 0	9		1 191	173		+1 142	120		1 157	147		+9* 43	69		-2 127	117
5* 0	24		-9* 38	44		1* 55	55		2 161	153		+2* 79	59		2 157	141		H,K= 7 3			+3 134	122
6* 86	76		H,K= 8 0			H,K= 11 1			3* 87	77		+3 112	66		3* 32	53		+1* 56	58		+4* 27	14
H,K= 6 0			+1* 42	36		0* 77	72		4 153	163		+4 208	213		4* 43	46		+2 133	142		+5 136	125
0* 0	11		-2 127	126		H,K= 0 1			5* 49	42		+5* 96	97		5* 61	79		+3* 76	62		+6* 56	40
1* 0	0		-3 125	133		+1 205	217		6 108	105		+6 138	154		6* 0	44		H,K= 8 3			+7* 45	47
2* 97	91		+4* 0	32		+2 248	225		7 172	157		+7 102	87		8* 66	84		+1* 69	59		+8* 46	66
3 174	177		-5 159	150		+3 137	88		H,K= 2 2			+8* 44	51		H,K= 4 3			+2* 56	39		H,K= 4 4	
4 165	151		-6* 62	52		+4 143	112		0 141	126		+9* 44	57		0 253	288		+3* 39	47		+1 171	169
5* 0	16		-7* 34	40		+5* 90	88		1 180	177		H,K= 3 2			1 210	212		+4* 52	39		+2 131	117
6* 86	69		-8* 38	44		+6* 97	109		2*324	402		-1 113	94		2 103	97		+7* 49	64		+3* 98	87
7* 61	54		H,K= 9 0			+7 119	121		3 220	223		-2*369	381		3* 38	27		H,K= 9 3			+4 105	96
H,K= 7 0			+1 117	109		+8* 60	70		4 153	134		+3*285	331		H,K= 5 3			+3* 63	64		+5* 0	4
0* 0	3		-2 105	87		H,K= 1 1			5* 82	64		+4 107	85		0* 55	48		+6* 52	68		+6* 0	38
1* 29	23		-3* 0	1		+1*386	534		6 115	126		+5 154	153		1 160	165		H,K= 10 3			+7* 67	82
2* 99	97		-4* 56	51		+2 159	136		7* 0	15		+6* 98	100		2* 0	19		+4* 81	71		+8* 32	42
3* 43	40		-5* 41	52		+3 126	103		8* 51	60		+6* 55	70		3* 48	61		+5* 74	67		H,K= 5 4	
4* 41	51		H,K= 10 0			+4* 91	65		H,K= 3 2			H,K= 4 2			4* 39	57		H,K= 1 4			+1 174	153
5* 69	54		-1 173	148		+5* 0	12		0 196	211		+1 211	225		5* 0	6		0* 27	36		+2 82	74
6* 33	14		+2* 49	42		+6* 93	85		1 196	211		+2* 76	62		6* 57	50		1* 84	67		+3* 91	88
H,K= 8 0			+3 114	104		+7* 0	28		2 115	104		+3* 78	59		7* 44	55		2*100	77		+4* 71	70
0 128	126		+4* 67	59		+8* 55	60		3* 98	91		+4 149	158		H,K= 6 3			3 141	135		+8* 66	68
1* 96	91		H,K= 11 0			+9 105	111		4* 30	33		+5* 38	43		0 211	243		4 183	199		H,K= 6 4	
2* 0	6		+1* 34	37		H,K= 2 1			5* 71	68		+6 105	99		1* 0	17		5* 42	37		+1* 76	83
3* 40	47		+2* 80	87		+1 127	114		6 115	103		+7 120	128		2 107	118		6* 51	43		+2* 84	99
H,K= 9 0			+3* 32	31		+2*479	642		7* 72	58		+8* 39	32		3* 0	29		7* 70	80		+3* 55	44
0* 0	2		+5* 36	40		+3 206	195		8* 38	38		+9* 48	56		4* 0	17		H,K= 2 4			+4* 47	45
3* 65	67		H,K= 1 1			+4* 81	49		H,K= 4 2			H,K= 5 2			5* 61	65		0*100	99		+5* 22	48
4* 32	43		0*493	607		+5* 90	78		0* 60	40		+1 156	160		H,K= 7 3			1* 67	74		+8* 46	71
H,K= 10 0			1 187	167		+6* 0	13		1 267	226		+2 146	135		0* 63	69		2 152	108		H,K= 7 4	
0 161	137		2*420	462		+7* 44	51		2 164	156		+3 177	161		1* 79	99		3 142	145		+2* 0	20
2* 36	41		3 209	197		+8* 66	73		3* 39	47		+4* 98	56		2* 0	21		4* 65	73		+3* 70	49
H,K= 1 0			4* 58	43		+9* 61	65		4 105	95		+5 109	102		3* 25	50		5* 65	69		+4* 66	70
+1 246	269		5 119	118		H,K= 3 1			5* 40	38		+6* 55	54		4* 45	60		H,K= 3 4			H,K= 8 4	
+2* 99	94		6 117	103		+1* 56	61		6* 0	7		+7* 63	49		H,K= 8 3			0 188	203		+1* 0	13
+3 118	86		7* 79	85		+2 174	158		7* 97	84		H,K= 6 2			0* 0	28		1 183	156		H,K= 7 4	
+4 167	155		8* 57	61		+3 194	166		H,K= 5 2			+1 150	161		1* 99	104		2* 41	36		+1 130	141
+5 118	109		H,K= 2 1			+4 109	91		0 202	211		+2 174	178		2* 92	87		3 105	114		H,K= 8 4	
+6* 39	43		0* 45	12		+5* 89	64		1* 38	29		+3* 66	46		3* 0	22		4* 0	12		+2* 79	62
+7* 83	80		1*310	340		+6 148	136		2 107	90		+4* 66	64		4* 74	80		5* 0	24		+3* 59	57
+8 127	123		2 124	130		+7 117	118		3 117	135		+5* 96	96		H,K= 9 3			6* 54	58		+4* 0	18
+9* 41	43		3 202	192		+8* 0	22		4* 49	51		+6* 0	17		0* 49	63		H,K= 4 4			+5* 48	71
+10* 29	42		4 109	99		+9* 92	87		5* 28	40		+7* 54	48		2* 39	41		1* 87	76		H,K= 9 4	
H,K= 2 0			5* 38	35		+10* 54	57		6* 77	71		+8* 60	58		3* 65	83		2 111	109		+4* 76	75
+1*465	592		6 161	171		H,K= 4 1			H,K= 6 2			H,K= 7 2			H,K= 10 3			3* 42	34		+5* 56	50

the phosphorinane ring are fairly large compared with the C–C–C angle of 111° in cyclohexane.[10] Beineke[7] also pointed out that the phosphorinane rings are somewhat more flattened than the cyclohexane ring, and suggested such ring-deformation causes the reduction of the steric repulsion between the axial substituent at the phosphorus atom and the hydrogen atom at 1,3-diaxial position.

It is of interest that the S=O bond in the cyclic sulfite of 1,3-propanediol tends to favor the axial position.[11] The dihedral angle in P–O–C–C system in I is about 55°, which is considerably smaller than the dihedral angle in a strict *gauche* conformation (60°).

All of the crystallographic computations were carried out on a CDC 3600 computor with the UNICS crystallographic system programs.[12]

10) M. Davis and O. Hassel, *Acta Chem. Scand.*, **17**, 1181 (1963).

11) H. F. Van Woerden and E. Havinga, *Rec. Trav. Chim. Pays-Bas*, **86**, 341 (1967) and references cited therein.

12) *UNICS* program system, edited by T. Sakurai, Crystallographic Association of Japan (1967).

BULLETIN OF THE CHEMICAL SOCIETY OF JAPAN VOL. 42 1824—1830 (1969)

Solvent Effects of Charge-transfer Complexes

Jun-ichi AIHARA, Motoyuki TSUDA and Hiroo INOKUCHI

The Institute for Solid State Physics, The University of Tokyo, Roppongi, Tokyo

(Received November 7, 1968)

The solvent effects of charge-transfer complexes were examined in various solvents. During the course of investigations pertaining to aromatic-TCNE complexes, Brownstein's and McRae's formulae were found to be valid. The gas-phase spectra of these charge-transfer complexes may be regarded as the origin of the solvent effects. The anomalous behaviour of carbonyl solvent molecules was also discussed.

It has been easily assumed that increasing the solvating power of a medium for a charge-transfer (CT) complex should shift the CT-band of the absorption spectra to a lower energy region.[1] Contrary to this prediction, however, it is often found that an increase in solvent polarity results in the shift of the CT-band to higher energy region.[2] Specific interaction between the charge-transfer complex and the surrounding solvent causing these blue shifts should thus also be considered as significant in these systems.[3]

Several explanations have been proposed for these solvent effects: some of them emphasized the small heat of formation, ΔH, of the complex, which implies that the complex-binding can be looser with little change in the surroundings.[4]

Davis and Symons believed a charge redistribution in the ground state of the complex to be responsible for the blue shift in polar solvents.[3] Therefore, they concluded that the commonly-accepted concept regarding solvent shifts on the absorption spectra of charge-transfer complexes has to be abandoned. Weiss proposed that a donor-acceptor complex can be considered as an electron-hole pair in correlation with the theory of Wannier exciton, but his theory also seems to be unsuccessful.[5] One of the purposes of the present work is to reexamine the solvent effects of the charge-transfer complexes; another is to locate the absorption spectra of the gaseous complexes in the solvent diagrams for various relationships.

Experimental

Naphthalene, durene, diphenyl and pyrene used in this work were recrystallized and zone-refined materials. Stilbene was twice recrystallized from ethanol. Tetracyanoethylene (TCNE) was synthesized according to the method of Ref. 6 and purified by recrystallization

1) N. S. Bayliss and E. G. McRae, *J. Phys. Chem.*, **58**, 1002 (1954).

2) H. W. Offen and M. S. F. A. Abidi, *J. Chem. Phys.*, **44**, 4642 (1966).

3) K. M. C. Davis and M. C. R. Symons, *J. Chem. Soc.*, **1965**, 2079.

4) J. Czekalla and K. O. Meyer, *Z. Physik. Chem. (Frankfurt)*, **27**, 185 (1961).

5) J. J. Weiss, *Phil. Mag.*, **8**, 1169 (1963).

6) "Organic Syntheses," Coll. Vol. IV, p. 877 (1963).

from chlorobenzene and by sublimation.

The solutions of charge-transfer complexes were prepared by mixing the respective components to appropriate concentrations. The absorption spectra were measured using a Cary Model 14 spectrophotometer.

The optical data for the charge-transfer complexes in the gas phase were obtained with an Aminco 4-8401 monochromator. TCNE and equimolecular aromatic hydrocarbon were placed in a quartz cell 7 cm or 40 cm long, which was then sealed after evacuation. The cell was heated to an appropriate temperature in a large, 50-kW electric furnace, and the absorption spectra were measured rapidly, as Fig. 1 shows schematically. The light source was a 200-W Wolfram lamp.

Survey of Gas-phase Spectra. In a previous paper, we have already reported some of the general features of the absorption spectra in the gas phase.[7] In this article, we will describe the individual characteristics in detail, as Figs. 2—7 show, in comparison with those of the carbon tetrachloride solution. The CCl_4 solvent is the most popular non-polar solvent. In general, gas-phase spectra are very similar to those in the solution in respect to shape and width. Moreover, the gaseous spectra of the complexes have no vibrational structures, such as are often found in the gaseous spectra of simple molecules. Exceptionally, the durene-TCNE complex (Fig. 3) has an asymmetric spectrum in solution.

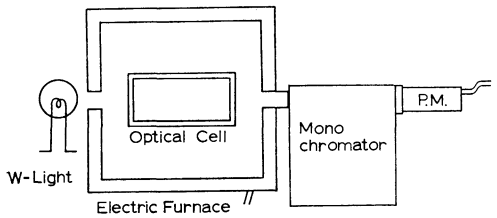

Apparatus for Spectrophotometry

Fig. 1. The apparatus for spectrophotometry of gaseous charge transfer complexes.

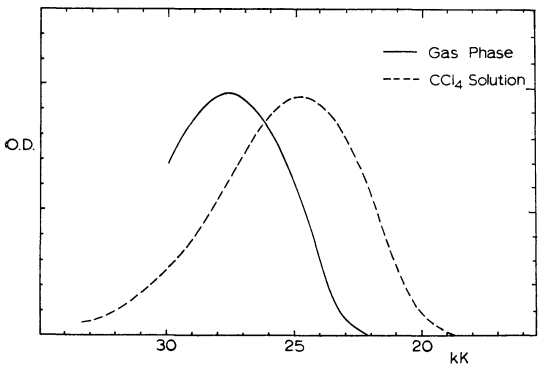

Fig. 2. The gaseous spectrum of toluene-TCNE.

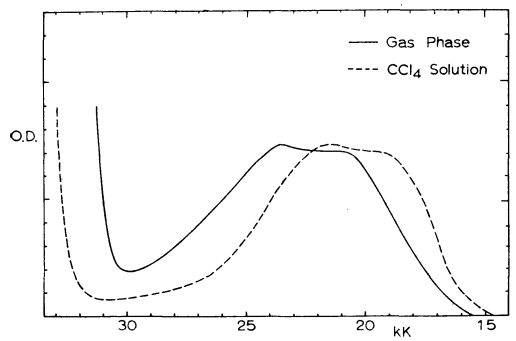

Fig. 3. The gaseous spectrum of durene-TCNE.

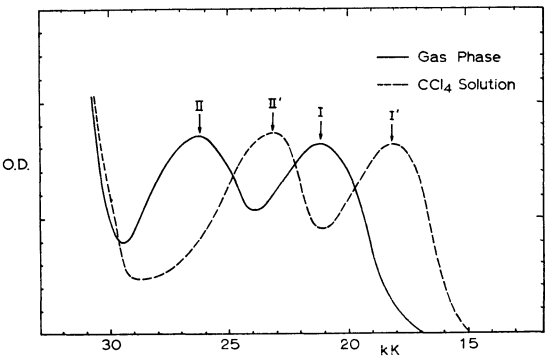

Fig. 4. The gaseous spectrum of naphthalene-TCNE.

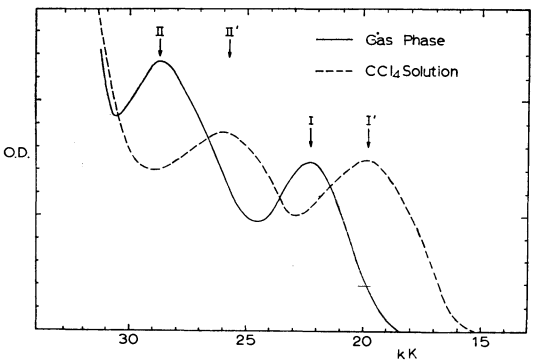

Fig. 5. The gaseous spectrum of diphenyl-TCNE.

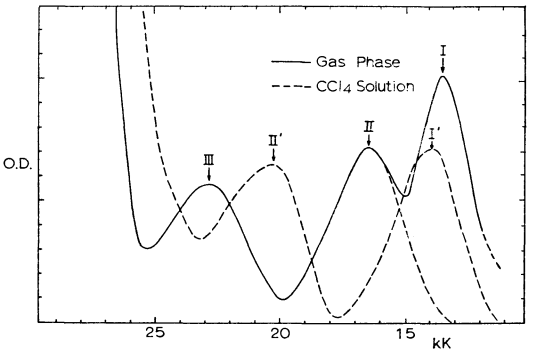

Fig. 6. The gaseous spectrum of pyrene-TCNE.

7) J. Aihara, M. Tsuda and H. Inokuchi, This Bulletin, **40**, 2460 (1967).

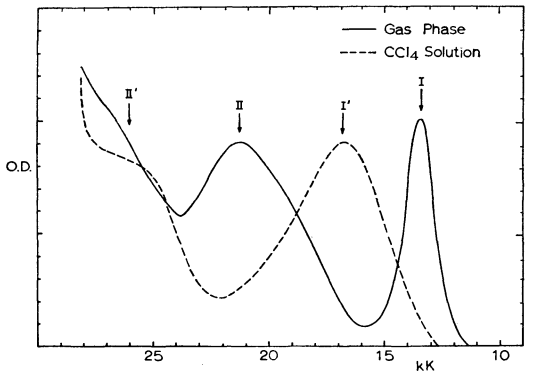

Fig. 7. The gaseous spectrum of stilbene-TCNE.

However, in the gas phase it is reproduced within the range of the structures in the solution. This suggests that the location of the 0–0 band in the gaseous spectrum is at the same position as in the solution specturm.

Therefore, the following conventional method was adopted to treat the data: the absorption maxima were taken as the position for the 0–0 band, and the peaks were assigned by comparing the spectra in carbon tetrachloride with those in the gas phase.

The absorption spectra of the naphthalene-TCNE complex are shown in Fig. 4. This complex has two charge-transfer bands, which may be interpreted as transitions from the highest occupied orbital of naphthalene to the lowest and the second lowest vacant orbitals of TCNE. The complexes of diphenyl (Fig. 5), pyrene (Fig. 6), and stilbene (Fig. 7) with TCNE are the same. The intensity ratio of the two bands is kept nearly constant between gas and solution.

Pyrene-TCNE complex has obviously different features. In the gas phase, the absorption spectra has three bands in the visible region, while in the solution only two bands are observed. In the pyrene-TCNE complex, we may except the lowest energy band for the following reasons. In the first place, the location of this band has a fairly good reproducibility, but it is poor in its intensity ratio in relation to other bands. The shapes of the first and the second bands in the solution are apparently comparable respectively to those of the second and the third bands in the gas phase. Moreover, the solvent effect to be described in the next section supports this interpretation. It is probable that the first gaseous band may be ascribed to that produced by the reaction or decomposition of the complex. An anomaly is also found in the stilbene-TCNE complex, so the first band is ommitted for the same reasons. In these two cases these phenomena appeared in nearly the same wavelength region. All the gaseous data are summarized in Table 1. Each shows a red gas-to-solution shift.

TABLE 1. THE LIST OF CT-BANDS OF TCNE CHARGE-TRANSFER COMPLEXES

Donor	CT-band (kK) in gas phase	CT-band (kK) in CCl_4 solution	Gas-to-solution shift (kK)
Toluene	27.6	24.7	−2.9
Durene	20.8	19.2	−1.6
Naphthalene	21.1	18.0	−3.1
	26.3	23.0	−3.3
Diphenyl	22.2	20.0	−2.2
	28.6	25.7	−2.9
	13.5	—	—
Pyrene	16.5	14.0	−2.5
	23.0	20.5	−2.5
	13.4	—	—
Stilbene	21.1	16.8	−4.3
	—	26.0	—

Discussion

It is very interesting to ascertain where the gaseous data are located in the solvent diagrams. As has been mentioned before, if the solvent effect is substantially abnormal, solvation itself is a theme of importance.

Several authors have attempted to relate the solvent shift of absorption spectra to the rate of the solvolysis reaction.[8] Following Kosower's idea, Brownstein developed an empirical relationship which obviously resembles the so-called Hammett rule.[9] He estimated an S-value for each solvent comparable to Hammett's σ value.

Brownstein's rule is expressed as follows.

$$SR = \frac{\nu_0 - \nu_E}{\nu_0} \tag{1}$$

where R is a constant characteristic of the system, where ν_E is the value in a given solution, and where ν_0 is the value obtained for ethanol as a standard.

To survey the general behaviour of the solvent effect of the charge-transfer bands, we adopted this rule for the naphthalene-TCNE complex. Figure 8 shows Brownstein's relation; a general correlation is found between the spectral shift and the S-value. From this validity to the complex, R is determined to be −0.433, a value which is fairly large in comparison with ordinary π–π^* or n–π^* transitions. The spectra from a gaseous specimen deviates much to the higher energy region, and so do those in ethyl-acetate and acetone. Some of these data were first cited in Refs. 2 and 10.

Next, we applied these data to the McRae relation, one of the most popular formulae of the solvent effect, expression of which is:[11]

$$\Delta h\nu \cong (AL_0 + B)\frac{n^2 - 1}{2n^2 + 1} + C\left(\frac{\varepsilon - 1}{\varepsilon + 2} - \frac{n^2 - 1}{n^2 + 2}\right) \tag{2}$$

8) E. M. Kosower, *J. Am. Chem. Soc.*, **80**, 3253 (1958).
9) S. Brownstein, *Can. J. Chem.*, **38**, 1590 (1960).
10) G. Briegleb, J. Czekalla and G. Reuss, *Z. Physik. Chem. (Frankfurt)*, **30**, 316 (1961).
11) E. G. McRae, *J. Phys. Chem.*, **61**, 562 (1957).

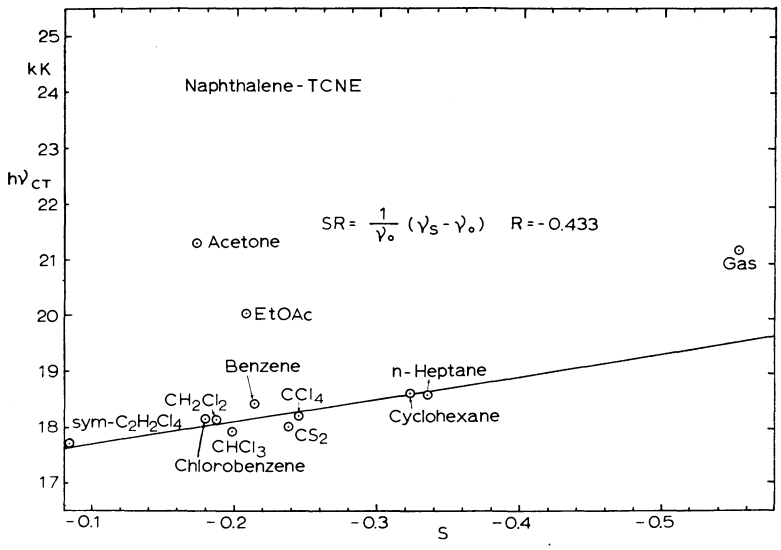

Fig. 8. The Brownstein's plots for naphthalene-TCNE.

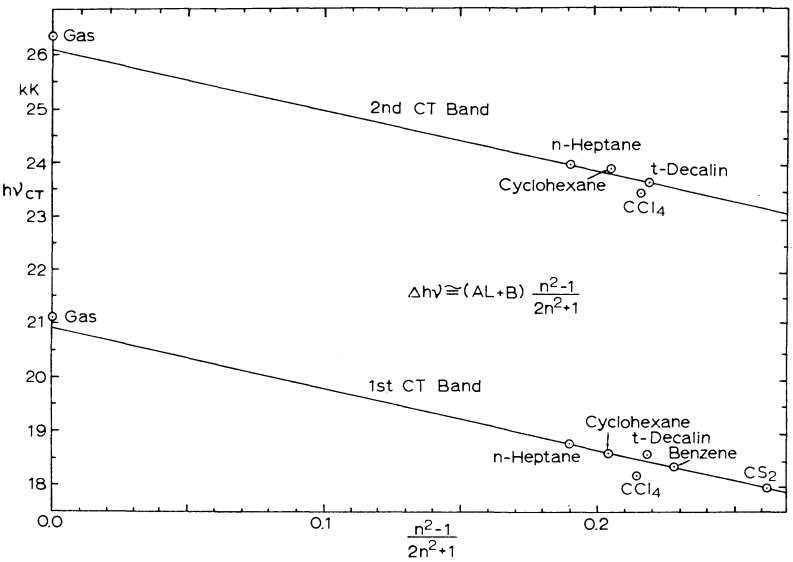

Fig. 9. The non-polar solvent effect of naphthalene-TCNE.

where n is the refractive index and where ε is the dielectric constant of the solvent. (AL_0+B) and C are constants characteristic of the solute. We plotted the absorption maxima in non-polar solvents, in which case the second term can be disregarded because $n^2 \cong \varepsilon$. The n and ε values were taken from Refs. 12 and 13. In Fig. 9 we found a fairly complete linearity between spectral shifts and $n^2-1/2n^2+1$ and obtained 11.00 kK as the (AL_0+B) value.

This means that, in these complexes, interaction between the solute-induced dipole and the solvent-induced dipole and/or between the solute dipole and the solvent-induced dipole is very large, compared to the general trend of solvent shifts. The wave numbers extrapolated to zero agree with the gaseous data.

Offen and Abidi suggested that there is no correlation between the magnitude of the shift and the refractive index or dielectric constant,[2] but this complex seems to behave normally, at least in non-polar solvents. Accordingly the nature of the complex is substantially the same in the gaseous state and in solution. Probably the large (AL_0+B)

12) A. D. E. Pullin, *Spectrochim. Acta*, **16**, 12 (1960).
13) "Organic Solvents," 2nd Ed., Interscience Publishers, New York (1955).

value reflects the abnormal blue shift of the gas phase in Brownstein's relation.

Using this value, we tried to obtain the C-value of McRae's formula; therefore $h\nu_{CT}-(AL_0+B)\frac{n^2-1}{2n^2+1}$ is plotted against $\frac{\varepsilon-1}{\varepsilon+2}-\frac{n^2-1}{n^2+2}$ in Fig. 10. Several

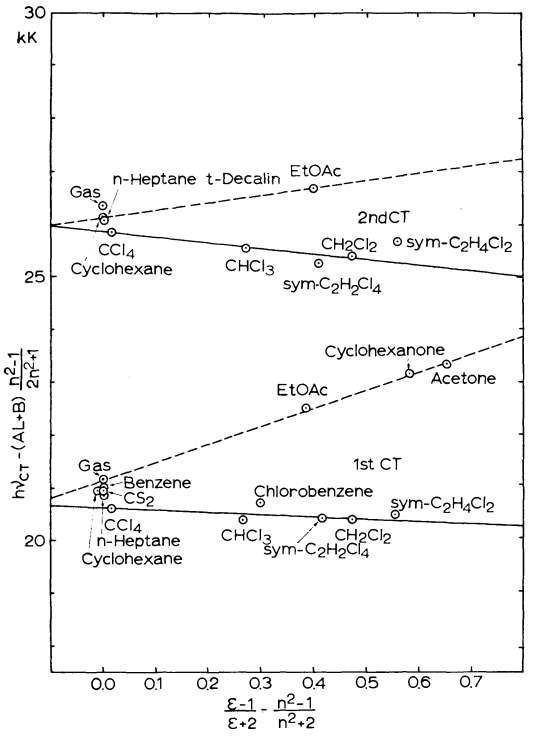

Fig. 10. The polar solvent effect of naphthalene-TCNE.

disordered solvents appeared among the polar solvents. This term indicates part of the solute dipole-solvent dipole interaction; explicitly, C is expressed as $2\mu_g(\mu_g-\mu_a)/a^3$, where μ_g and μ_a are the dipole moments of the ground state and the excited state respectively, and where a is the cavity radius of the solvent. As to the naphthalene-TCNE complex, the dipole moment of the ground state is reported to be 1.28 D, while that of the excited state can be assumed to be 10—15 D on the basis of the data of the excited hexamethylbenzene-TCNE complex.[4,14] Accordingly, the value of C must be negative in a normal case. Figure 10 shows a group of solvents which exhibit a good linear correlation between those whose gradient is -490 cm^{-1}. This group consists mainly of haloalkanes and alkenes.

For these solvents, we can estimate the charge distribution of the complex to be nearly constant.

14) G. Briegleb, J. Czekalla and G. Reuss, *Z. Physik. Chem. (Frankfurt)*, **30**, 333 (1961).

Now let us estimate the Coulomb term contributing to the charge-transfer transition. $h\nu_{CT}$ is frequently approximated by the expression;[15]

$$h\nu_{CT} = I_D - E_A - \frac{e^2}{R_{DA}} - P \qquad (3)$$

where I_D is an ionization potential of the donor, where E_A is the electron affinity of the acceptor, and where P is the polarization energy due to solvent molecules. R_{DA} indicates the distance between donor and acceptor molecules. When we apply this formula to the heptane solution, we can deduce P directly from Fig. 9 as the value of the spectral shift, 0.50 eV. The electron affinity of TCNE is 2.60 eV if we take as the standard *p*-benzoquinone, whose value, 1.40 eV, was recently determined by a magnetron method.[16] Therefore, the Coulombic ion-pair attraction term results in 2.38 eV.

Ikemoto calculated the molecular orbitals of this complex in the crystalline phase.[17] According to him, the Coulomb energy of the first band may be estimated to be 3.32 eV. The decrease in the Coulombic interaction suggests that there exists a looser complex in both the gas and the solution with a larger intermolecular distance. However, the charge distribution in the complex may be considerably different from that in the solid state, so the displacement between the two components can not be estimated straightforwardly.

From the above results, the spectral shifts may all be ascribed to a simplification of McRae's formula. The possibility of some orientational isomers in the gas phase or in the various solvents is not very important.[18] If a different form of charge-transfer isomers exists, those isomers may be expected to produce a secondary shift compared to the usual dipole-polarization shifts. The only questionable point is that the plots for the non-polar solvents in Fig. 9 are slightly displaced upward from the linearity of the regular solvents.

On the other hand, the plots for the oxygen-containing solvents are mainly dispersed to the blue side. This irregularity is in good accord with the trend in Brownstein's relationship. Generally the values found in ethyl acetate, acetone, and cyclohexanone are far remove from those in methylene chloride.[2,19] Therefore, we can conclude that these groups behave abnormally, so special theoretical attention should be given to them.

15) H. McConnell, J. S. Ham and J. R. Platt, *J. Chem. Phys.*, **21**, 66 (1953).

16) L. Farragher and F. M. Page, *Trans. Faraday Soc.*, **62**, 3072 (1966).

17) I. Ikemoto, private communication.

18) J. R. Gott and W. G. Maisch, *J. Chem. Phys.*, **39**, 2229 (1963).

19) H. W. Offen and A. H. Kadhim, *ibid.*, **45**, 269 (1966).

How can we examine this phenomenon? As Bayliss pointed out, this point-dipole model, in a uniform medium, is not the best approximation.[1] In the case of the charge-transfer complex especially, these solvents may change the nature of the complex.

Using the above data of the normal solvation, the cavity radius of the solvent is calculated to be 6.60±0.30 Å. This radius is quite large. In this connection the typical solvents have molecular radii in the range of from 2.0 to 4.0 Å. Therefore, a solvent which does not have a very marked partial moment may be regarded as a continuous medium.

Table 2. The results of solvent effect for the charge-transfer complexes

Species	Band	AL_0+B (kK)	C (kK)	C'** (kK)	a (Å)
Naphthalene-TCNE					
	1st CT	−11.07	−0.49	~3.44	6.60
	2nd CT	−10.72	−1.08	~1.50	
Azulene*	^1L_b	− 0.131	0.286	—	3—4
	^1L_a	− 2.734	0.209	—	
	^1B_b	− 7.154	0.000	—	

* Cited from W. W. Robertson, A. D. King, Jr., and O. E. Weiganger, Jr., *J. Chem. Phys.*, **35**, 464(1961).
** Determined from the dotted line in Fig. 10.

However, some polar solvent molecules will tend to become oriented so as to stabilize these partially-charged complexes through stereospecific solvation; that is, the solvent molecules around the complex may take such orientations that maximum attractions between the solvent and the solute molecules are obtained. In forming such a local field, the proper geometrical conditions of solvent molecules as well as proper polarities are necessary.[20]

Moreover, a new interaction of carbonyl compounds was reported a few years ago.[21] An oxygen atom in the carbonyl group is closely attached to the carbon atom of the same group in the neighbouring molecule. The usual van der Waals distance between them is expected to be at least 3.1 Å, according to Pauling's list of van der Waals radii.[22] However, those of chloranil, parabanic acid, and aloxan are 2.85, 2.77, and 2.79 Å respectively. Such an effect may be expected also in acetone, ethyl acetate, cyclohexanone, and so on. Carbonyl group has an ionic character of several tens per cent, too.

If we proceed to develop such an idea, the concept of a local field formed by the surroundings acting on the complex in the direction from the acceptor molecules to the donor molecules, the ground state of the complex is further polarized.[23] This explanation is somewhat related to those by Davis and Symons, and Offen and Abidi, who also suggested the enhancement of the mixing of the dative bond.[2,3] In the present case, the carbonyl solvent molecules around the complex may take such orientations as described above. It is probable that these interactions are large enough to invert the direction of the solvent shifts.[22] The dotted

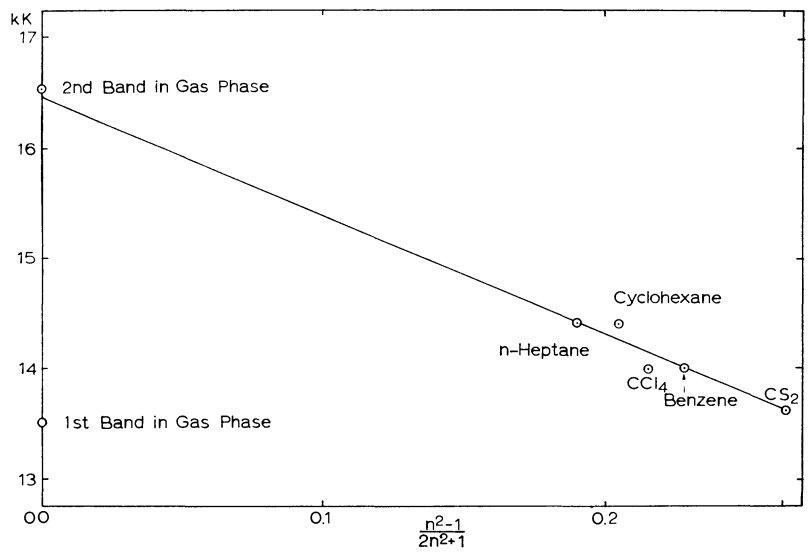

Fig. 11. The non-polar solvent effect of pyrene-TCNE.

20) G. Briegleb and T. Schachowskoy, *Z. Physik. Chem.*, **B19**, 255 (1932).
21) W. Bolton, *Acta Cryst.*, **16**, 166 (1963).
22) L. Pauling, "The Nature of the Chemical Bond," 3rd Ed. Cornell Univ. Press, New York (1960).
23) S. Yomosa, *Progr. Theor. Phys. Supplement.*, No. 40, 249 (1967).

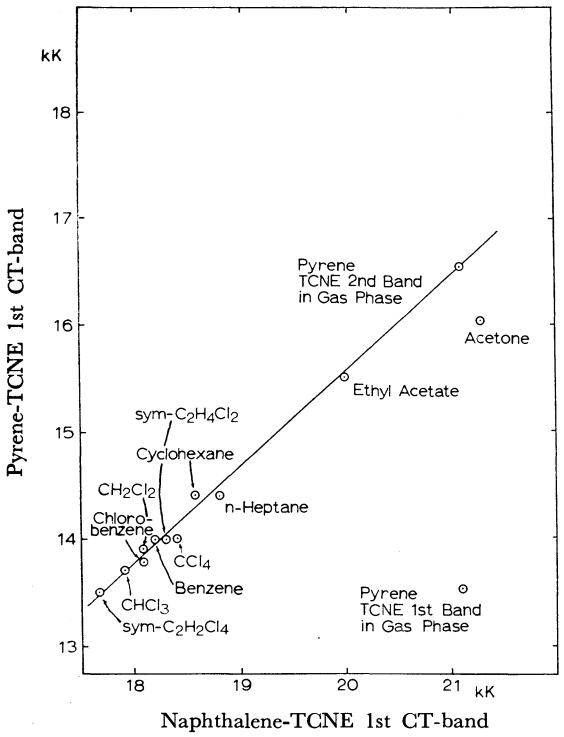

Fig. 12. The correlation between naphthalene-TCNE and pyrene-TCNE.

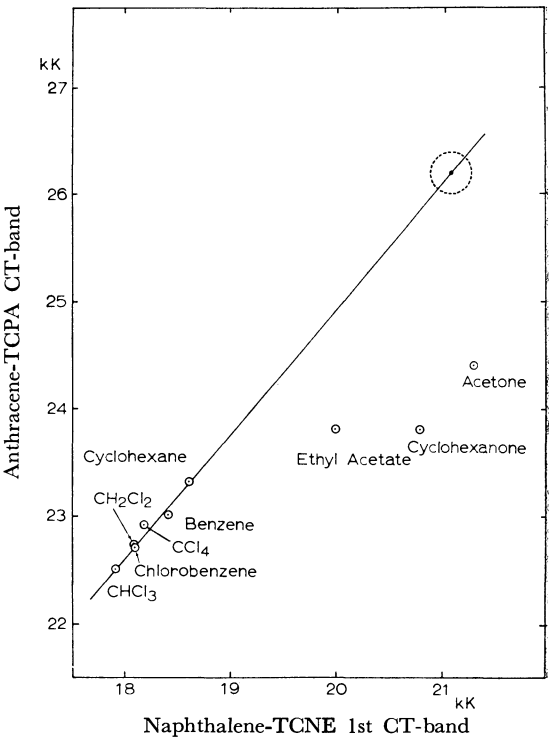

Fig. 13. The correlation between naphthalene-TCNE and anthracene-TCPA.

line in Fig. 10 suggests the possibility of such a case.

So far we have discussed mainly the naphthalene-TCNE complex, but the parallelism of solvation is widely valid among a variety of complexes.[2] In Fig. 11 another example is shown, here the first band of the gaseous pyrene-TCNE complex can be omitted as a band originating for a different reason.

We can ascertain another correlation between the spectral shifts of naphthalene-TCNE and pyrene-TCNE complexes. The results shown in Fig. 12 also give support to the above reasoning as to the first band of the gaseous pyrene-TCNE complex. The first band of the gaseous stilbene-TCNE complex is omitted for the same reason.

In Fig. 13 the correlation with a different type of complex, that is, the anthracene-TCPA (tetrachlorophthalic anhydride) complex, is examined. The gaseous spectrum of this complex could not be observed because of overlapping with that of component molecules as a result of the blue shift. However, the location of the peak is assumed to be around the dotted circle.

In both these diagrams, the carbonyl solvent behaves independently as before. We must leave further investigation of this problem to later. In this step, however, we should stress the regularity of the solvent effect and the location of gaseous spectra as a standard of that effect.

BULLETIN OF THE CHEMICAL SOCIETY OF JAPAN VOL. 42 1831—1836 (1969)

The Photochemical Rearrangement of Phenyl Acetate

Haruo SHIZUKA and Toshifumi MORITA

Department of Chemistry, Gunma University, Tenjin-cho, Kiryu, Gunma

and Yuji MORI and Ikuzo TANAKA

Department of Chemistry, Tokyo Institute of Technology, Ookayama, Meguro-ku, Tokyo

(Received November 20, 1968)

The photochemical rearrangements of phenyl acetate and *p*-substituted phenyl acetates have been studied. The quantum yields of the rearrangements of phenyl acetate in cyclohexane were independent of the irradiation time, the concentration of phenyl acetate ($<2\times10^{-2}$ mol/*l*), the temperature (20—70°C), and the presence of piperylene (a triplet quencher) or oxygen. The quantum yields for the formations of *o*- and *p*-hydroxyl acetophenones and of phenol were 0.17, 0.15, and 0.06 respectively in cyclohexane. Comparing the quantum yields for phenyl acetate rearrangements with those for *p*-methylphenyl acetate, the quantum yields for the predissociation of the O–CO bond and the back reaction, and the recombination ratio were estimated to be 0.61, 0.23, and 0.9 respectively in cyclohexane. The relative rate constants of the back reaction and the *o*- and *p*-rearrangements were parallel to the odd π electron densities of the phenoxy radical. These results have shown that the reaction scheme of phenyl acetate in the liquid phase at 2537 Å is similar to that of acetanilide.

The photochemical reactions of phenyl esters in a solution yield products of rearrangement similar to those of the Fries reaction. Anderson and Reese[1] have reported that phenyl esters rearrange to yield *o*- and *p*-hydroxyl-aryl ketones by UV irradiation. Kobsa,[2] Finnegan and Hagen,[3] and Elad *et al.*[4] have reported similar findings on the photo-Fries-rearrangement.

In the study of the photochemical reactions of acetanilide,[5-7] it has been shown that, in the liquid phase, the photochemical rearrnagement occurs *via* the predissociation by the intersystem crossing $^3\sigma_0(\text{N–C})\leftarrow S_1(\pi\pi^*)$, forming anilino and acetyl radicals which recombine efficiently in a solvent cage into the original substance, *o*- and *p*- isomers. The photochemical reactions have been examined in the vapor phase and in a rigid matrix, but no photochemical rearrangement was observed in either case.[8]

The photochemical reaction of phenyl acetate has been investigated and discussed on the basis of the mechanism of the photo-Fries-rearrangement, which was established in the study of the photochemical rearrangement of acetanilide.

Experimental

The experimental procedure and solvents were similar to those previously described.[5-7] The phenyl acetate, phenol, *p*-cresol, *p*-chlorophenol, *p*-nitrophenol and *p*-hydroxyacetophenone were Tokyo Kasei Co. G. R.-grade products. The *p*-methyl, *p*-chloro, and *p*-nitrophenyl acetates were prepared by treating the corresponding *p*-substituted phenols with acetic anhydride and were purified by distillation or by recrystallization. The 2-hydroxy-5-methyl- and 2-hydroxy-5-chloroacetophenones were produced from the corresponding phenyl acetates by means of Fries reactions and were purified by repeated recrystallization.

A low-pressure mercury lamp with a Vycor glass filter was used as the 2537 Å radiation source. Actinometry was carried out in the same way as has been described in a previous paper.[5] The light intensity at 2537 Å was 9.7×10^{14} photons $\text{sec}^{-1}\,\text{cm}^{-2}$.

The flash apparatus was an ordinary one and has previously been described.[7] The fluorescence and phosphorescence were measured by Hitachi MPF-2 and Aminco Bowman Spectrophotofluorometers respectively. In these measurements, the concentrations of the solutions were so adjusted that the values of optical density were 0.600 at 2537 Å.

1) J. C. Anderson and C. B. Reese, *Proc. Chem. Soc. (London)*, **1960**, 217; *J. Chem. Soc.*, **1963**, 1781.
2) H. Kobsa, *J. Org. Chem.*, **27**, 2293 (1962).
3) R. A. Finnegan and A. W. Hagen, *Tetrahedron Letters*, **1963**, 369.
4) D. Elad, *ibid.*, **1963**, 873; D. Elad, D. V. Rao and V. I. Stenberg, *J. Org. Chem.*, **30**, 3252(1965).
5) H. Shizuka and I. Tanaka, This Bulletin, **41**, 2343 (1968).
6) H. Shizuka, *ibid.*, **42**, 52 (1969).
7) H. Shizuka, *ibid.*, **42**, 57 (1969).
8) H. Shizuka and I. Tanaka, *ibid.*, **42**, 909 (1969).

Results and Discussion

Electronic Structures of Phenyl Acetate. Table 1 shows the near UV absorption band of para-substituted phenyl acetates, which are related to the $^1B_{2u}\leftarrow{}^1A_{1g}$ transition of benzene at 255 mμ and which resemble the absorption bands in the corresponding phenols (See Table 2, Figs. 2 (a), 3(a), and 4).

TABLE 1. NEAR UV ABSORPTION BANDS OF *p*-X-SUBSTITUTED PHENYL ACETATES

Substance X	λ_{max} mμ	ε_{max}
H	259	290
CH_3	266	540
Cl	269	500

Baba and Suzuki have shown that acetylation causes a blue shift and a decrease in intensity for the Band I ($^1B_2\leftarrow{}^1A_1$) of aniline, while for Band II ($^1A_1\leftarrow{}^1A_1$) it causes a red shift and an increase in intensity.[9] For the longest wavelength band ($^1B_2\leftarrow{}^1A_1$) of phenol, the acetylation also causes a blue shift and a decrease in intensity. It is believed that the acetylation to the electron-donating atom (oxygen atom) surpresses the electron migration from the oxygen atom to the phenyl group, and that the electron migration to the carbonyl group results in a shift of the n–π^* band in phenyl acetate to a shorter wavelength (blue shift), as in the case of acetanilide.[6] Therefore, the n–π^* level in phenyl acetate may lie above the lowest singlet excited state, $S_1(\pi\pi^*)$; this possibility is supported by the observation of the fluorescence (Fig. 1(a)). That is, it is reasonable to assume that the fluorescence is the emission from $S_1(\pi\pi^*)$ to S_0 because of its red shift in a polar solvent. On the other

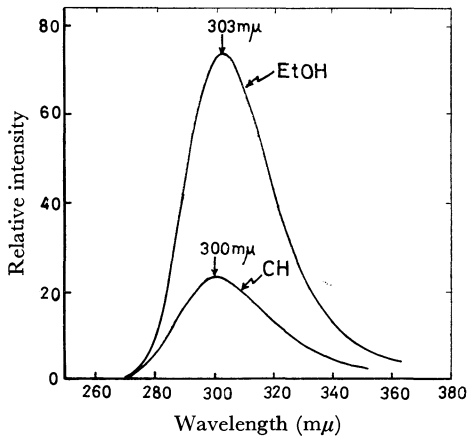

Fig. 1(a). Fluorescence spectra of phenyl acetate by the excitation at 2537 Å at room temperature.

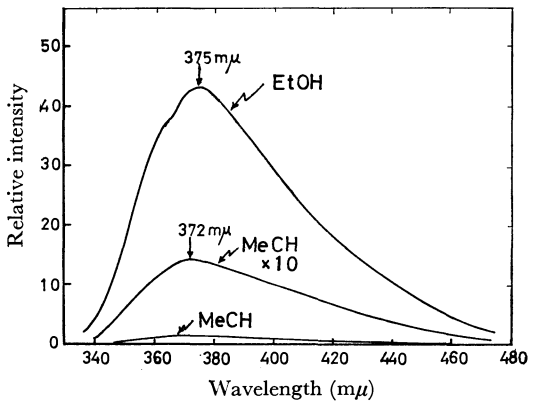

Fig. 1(b). Phosphorescence spectra of phenyl acetate by the excitation at 2537 Å at 77°K.

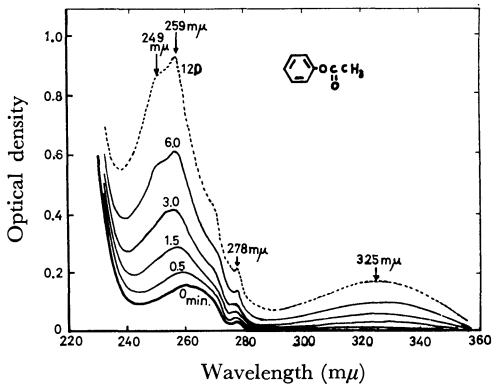

Fig. 2(a). Spectral change of cyclohexane solution of phenyl acetate with lapse of time at 2537 Å. Numbers refer to time at measurement in minutes.

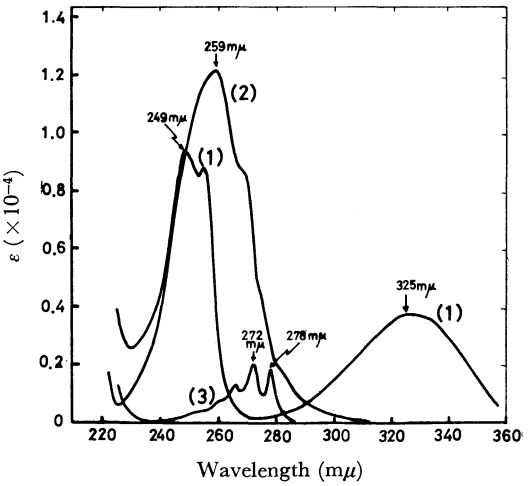

Fig. 2(b). UV absorption spectra of *o*-hydroxyacetophenone (1), *p*-hydroxyacetophenone (2), and phenol (3).

9) H. Baba and S. Suzuki, *J. Chem. Phys.*, **32**, 1706 (1960).

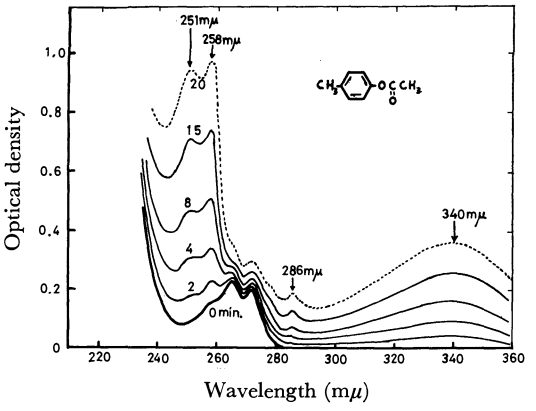

Fig. 3(a). Spectral change of cyclohexane solution of *p*-methylphenyl acetate at 2537 Å.

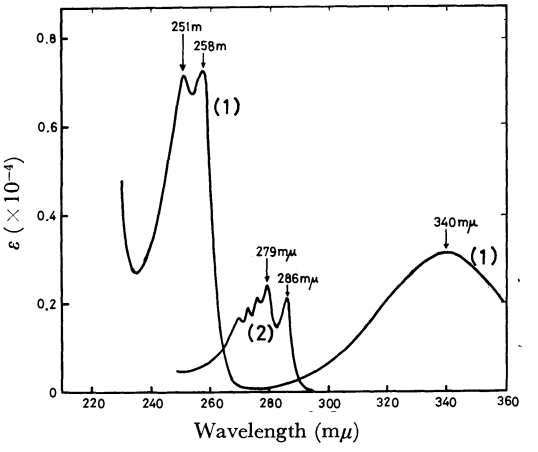

Fig. 3(b). UV absorption spectra of 2-hydroxy-5-methylacetophenone (1) and *p*-cresol (2).

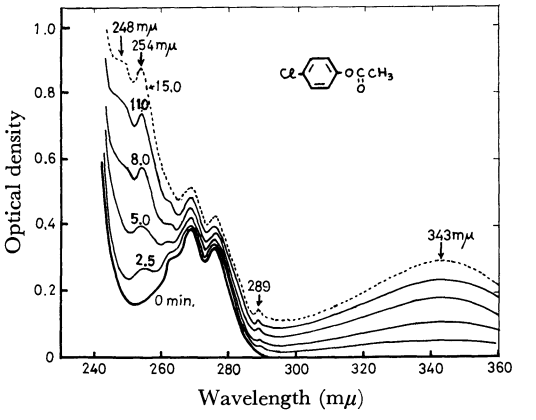

Fig. 4. Spectral change of cyclohexane solution of *p*-chlorophenyl acetate at 2537 Å.

hand, the phosphorescence which is shown in Fig. 1(b) can be assigned to the emission from the triplet state $T_1(\pi\pi^*)$ to S_0, since the phosphorescence has a long lifetime (several seconds) at 77°K.

Reaction Products. Figures 2(a), 3(a), and (4) show, respectively, the spectral changes of cyclohexane solutions of phenyl acetate, *p*-methylphenyl acetate, and *p*-chlorophenyl acetate during photolysis at 2537 Å.

The spectral change in phenyl acetate upon the irradiation at 2537 Å (Fig. 2(a)) indicates that the reaction products are *o*-hydroxyacetophenone, *p*-hydroxyacetophenone, and phenol, the absorption spectra of all of which have been measured (Fig. 2(b)). The spectral change in *p*-methylphenyl acetate indicates that not a *p*-rearrangement but an *o*-rearrangement product is obtained, plus *p*-cresol, as is shown in Fig. 3(a); Fig. 3(b) shows the absorption spectrum of each of the reaction products. The photochemical reaction of *p*-chlorophenyl acetate is similar to that of *p*-methylphenyl acetate (Fig. 4). Scarcely no spectral change was observed in an ethanol solution of *p*-nitrophenyl acetate. The substituted nitro group has an intramolecular quenching action.[7,10,11] The quantum yields for the formation of these photochemical products were measured spectrophotometrically. The molar extinction coefficients of the photochemical products are summarized in Table 2.

Table 2. Molar extinction coefficients[a]

Substance	λ mμ	ε(×10⁻⁴)
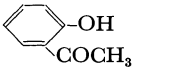	249 325	0.927 0.374
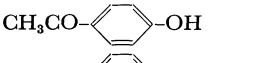	259	1.22
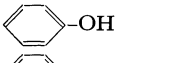	272 278	0.199 0.189
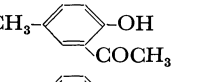	258 340	0.731 0.308
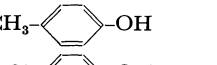	286	0.211
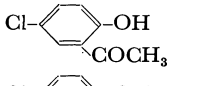	254 343	0.429 0.235
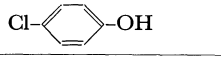	289	0.178

a) In a cyclohexane solution.

Effect of Irradiation Time, Concentration, Oxygen, Temperature, Solvent, and Triplet Quencher on Quantum Yields. The quantum yields were measured under various conditions; the results are shown in Fig. 5 and in Table 3. The quantum yields for the product formations from phenyl acetate in cyclohexane at 2537 Å did not

10) I. Tanaka, Y. Mori, *et al.*, presented at the Symposium on Electronic State, Osaka, Oct., 1966.
11) H. Kokubun and M. Kobayashi, presented at the 20th Annual Meeting of the Chemical Society of Japan, Tokyo, April, 1967.

Table 3. Quantum yields for the product formations of *p*-X-substituted phenyl acetates at 2537 Å

X	Solvent	Quantum yield (Φ) Φ_o	Φ_p	Φ_{OH}
H	Cyclohexane (aerated)	0.17	0.15	0.06
	Cyclohexane (degassed)	0.17	0.15	0.06
	Ethanol (aerated)	0.14	0.13	*
	Ethanol (degassed)	0.14	0.13	*
	Water (aerated)	0.09	0.08	*
CH_3	Cyclohexane (aerated)	0.23	0	0.07
	Ethanol (aerated)	0.20	0	*
Cl	Cyclohexnae (aerated)	0.26	0	0.08
	Ethanol (aerated)	0.22	0	*

Φ_o, Φ_p, and Φ_{OH} are the quantum yields for the formation of *o*- and *p*-rearrangements and *p*-X-phenol respectively.

* denotes that the quantum yield for the formation of *p*-X-phenol could not be observed spectrophotometrically because of the overlapping of the absorption spectra.

change with the variation in the irradiation time and the concentration of phenyl acetate ($<2\times10^{-2}$ mol/*l*), as is shown in Figs. 5(a) and (b). Dissolved oxygen had no effect on the quantum yields, as is shown in Table 3. The addition of piperylene as a triplet quencher (E_T=2.48 eV)[5,12,13] did not affect the quantum yields of this isomerization in concentration from 10^{-4} up to 10^{-2} mol/*l*, as is shown in Fig. 5(d). There was scarcely no effect of the temperature (20—70°C) on the quantum yields of phenyl acetate photoisomerization (Fig. 5(c)), though a small temperature effect has been observed in the case of acetanilide.[7] This difference may be due to the fact that the intersystem crossing, $^3\sigma_0(O\leftarrow CO)\leftarrow S_1(\pi\pi^*)$, in phenyl acetate is quite rapid in comparison with that in acetanilide. The very small effect of the temperature on the quantum yields for phenyl acetate rearrangements is due to the high quantum yield for the predissociation of phenyl acetate, as will be described later. Of course, the effect of the temperature on the quantum yield at low temperatures (*e. g.*, at the temperature of liquid nitrogen) may be expected because of the increasing stiffness of the solvent cage at low temperatures, as has been described in a previous paper.[8]

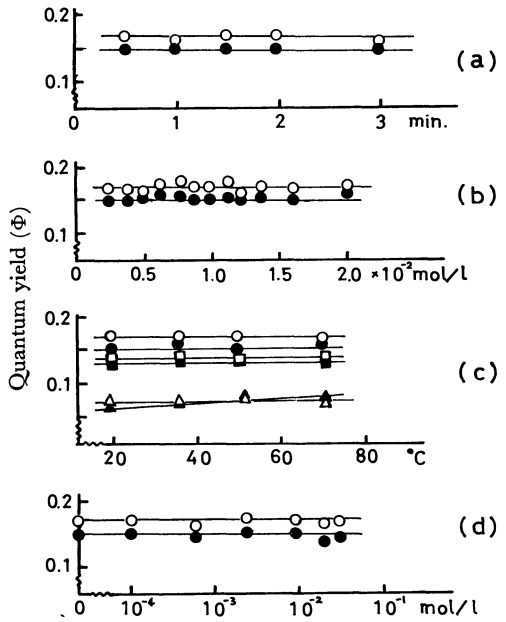

Fig. 5. Dependence of quantum yeield.

(a) on irradiation time at 20°C with initial concentration of 8.5×10^{-3} mol/*l*.
(b) on concentration at 20°C
(c) on temperature
(d) on addition of piperylene
Φ of *o*-hydroxyacetophenone;
○ in cyclohexane, □ in EtOH, △ in water
Φ of *p*-hydroxyacetophenone;
● in cyclohexane, ■ in EtOH, ▲ in water

The quantum yields decreased in polar solvents, as is shown in Table 3. However, the variation in the rearrangement quantum yields on solvents were smaller than that of acetanilide.[6] This may be due to the fact that phenyl acetate has no hydrogen atom to form a hydrogen-bond with a proton acceptor.

The features of the lowest excited singlet state and of the photochemical reaction of phenyl acetate are very close to those of acetanilide.[5-7] Its reaction mechanism involves the predissociation to phenoxy and acetyl radicals and subsequent recombination reactions between the pair radicals in a solvent cage.

Estimations of Back Reaction and Predissociation Quantum Yields. The recombination reaction between pair radicals consists of a back reaction and of *o*- and *p*-rearrangements in a solvent cage. These reactions have been shown in the photochemical rearrangement of acetanilide.[7] The quantum yield for the back reaction (Φ_B) and the predissociation (Φ_{dis}) were estimated by the method described in a previous paper.[7]

In the first approximation, the photochemical primary process in *p*-methylphenyl acetate is the same as that in phenyl acetate, because the UV absorption spectrum of *p*-methylphenyl acetate is similar to that of phenyl acetate. Therefore, Eq. (1) is given on the basis of the same assumption as was presented in a previous paper;[7]

$$\Phi^{H}_{dis} \approx \Phi^{CH_3}_{dis} \quad (1)$$

Blocked by a methyl group at the *p*-position of the phenoxyl radical, *p*-rearrangement can not occur.

12) P. E. Eaton and W. S. Hurt, *J. Am. Chem. Soc.*, **88**, 5038 (1966).
13) E. Y. Y. Lam, D. Valentine and G. S. Hammond, *ibid.*, **89**, 3482 (1967).

Thus, the values of quantum yields for the back reaction (Φ_B), the *o*-rearrangement (Φ_o), and the *p*-methylphenol formation increase.

$$\Delta\Phi_o = \Phi_o^{CH_3} - \Phi_o^{H} = 0.06 \quad (2)$$

$$\Delta\Phi_B = \Phi_\Sigma^{H} - \Phi_\Sigma^{CH_3} = 0.08 \quad (3)$$

$$\Delta\Phi_{OH} = \Phi_{OH}^{CH_3} - \Phi_{OH}^{H} = 0.01 \quad (4)$$

where:

$$\Phi_\Sigma^{H} = \Phi_o^{H} + \Phi_p^{H} + \Phi_{OH}^{H},\ \Phi_\Sigma^{CH_3} = \Phi_o^{CH_3} + \Phi_p^{CH_3} + \Phi_{OH}^{CH_3}$$

The ratio of Φ_B to 1/2 Φ_o is given approximately by:

$$\frac{\Phi_B}{\frac{1}{2}\Phi_o} \approx \frac{\Delta\Phi_B}{\frac{1}{2}\Delta\Phi_o} = 2.7 \quad (5)$$

Therefore, the values of Φ_B and Φ_{dis} may be evaluated as follows:

$$\left.\begin{aligned} \Phi_B^{H} &= \frac{1}{2}\Phi_o^{H} \times 2.7 \approx 0.23 \\ \Phi_{dis}^{H} &= \Phi_B^{H} + \Phi_\Sigma^{H} \approx 0.61 \end{aligned}\right\} \quad (6)$$

and:

$$\left.\begin{aligned} \Phi_B^{CH_3} &= \frac{1}{2}\Phi_o^{CH_3} \times 2.7 \approx 0.31 \\ \Phi_{dis}^{CH_3} &= \Phi_B^{CH_3} + \Phi_\Sigma^{CH_3} \approx 0.61 \end{aligned}\right\} \quad (7)$$

Also, the values of Φ_B^{Cl} and Φ_{dis}^{Cl} are estimated to be 0.35 and 0.69 respectively. The quantum yields for the back reaction and the predissociation are summarized in Table 4.

Table 4. Quantum yields for the back reaction (Φ_B) and the predissociation (Φ_{dis}) of *p*-X-substituted phenyl acetate at 2537 Å

Substance X	Quantum yield (Φ) Φ_Σ	Φ_B	Φ_{dis}
H	0.38	0.23	0.61
CH_3	0.30	0.31	0.61
Cl	0.34	0.35	0.69

The quantum yield for the predissociation of phenyl acetate is quite large in comparison with that of acetanilide (~0.25).[7] This means that the intersystem crossing probability for the predissociation of phenyl acetate is larger than that of acetanilide.

The recombination ratios (β) are obtained from Eq. (8):

$$\left.\begin{aligned} \beta_H &= \frac{\Phi_o^{H} + \Phi_p^{H} + \Phi_B^{H}}{\Phi_{dis}^{H}} = 0.90 \\ \beta_{CH_3} &= \frac{\Phi_o^{CH_3} + \Phi_B^{CH_3}}{\Phi_{dis}^{CH_3}} = 0.89 \\ \beta_{Cl} &= \frac{\Phi_o^{Cl} + \Phi_B^{Cl}}{\Phi_{dis}^{Cl}} = 0.88 \end{aligned}\right\} \quad (8)$$

These high recombination ratios ($\beta = \sim 0.9$) indicate that the recombination reactions between phenoxy and acetyl radicals occur efficiently in a solvent cage, as do those in the photochemical rearrangement of acetanilide.[7]

No intermediate absorption was observed by means of the flash technique. The absorptions of the products appeared immediately after the flash.

From these results, the photochemical secondary processes of phenyl acetate can be given as follows:

1) Recombination reaction (Main reaction)

a) Back reaction

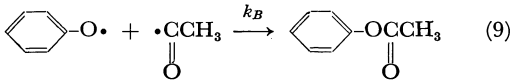

(9)

b) *o*-rearrangement

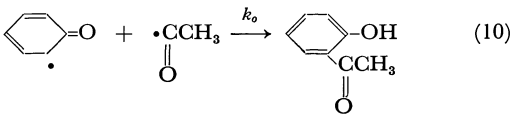

(10)

c) *p*-rearrangement

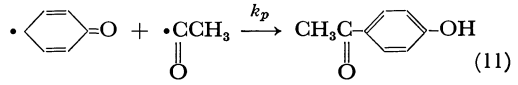

(11)

2) Hydrogen atom abstraction reaction

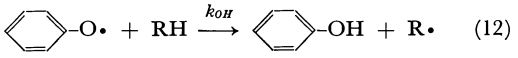

(12)

where k_B, k_o, and k_p are the rate constants of the back reaction, the *o*-rearrangement, and the *p*-rearrangement respectively, and where RH is a solvent molecule.

The rate constants (k_B, k_o, and k_p) for the recombination reactions between the pair radicals in a solvent cage will be proportional to the odd π electron distributions (δ) of the phenoxy radical which were obtained by Müller *et al.*[14] (Fig. 6).

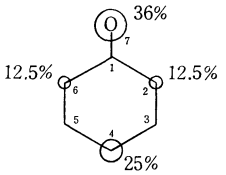

Fig. 6. Odd π electron distributions of the phenoxy radical.

$$k_B : k_o : k_p = \Phi_B : \frac{1}{2}\Phi_o : \Phi_p \quad (13)$$

$$= 1 : 0.37 : 0.65$$

$$\delta_7 : \delta_2 : \delta_4 = 1 : 0.35 : 0.69 \quad (14)$$

$$k_B : k_o : k_p \approx \delta_7 : \delta_2 : \delta_4 \quad (15)$$

14) E. Müller, A. Rieker and K. Scheffer, *Liebigs Ann.*, **645**, 92 (1961).

From these results, it can be said that the photochemical reaction of phenyl acetate can be explained by a mechanism similar to that for acetanilide presented in previous papers.[5-7]

In conclusion, the reaction scheme of phenyl acetate at 2537 Å in the liquid phase is as follows:

$$S_0 + h\nu \longrightarrow S_1(\pi\pi^*)(^1B_2) \tag{16}$$

$$S_1(\pi\pi^*) \xrightarrow{k_s} S_0 \tag{17}$$

$$S_1(\pi\pi^*) \xrightarrow{k_F} S_0 + h\nu' \tag{18}$$

$$S_1(\pi\pi^*) \xrightarrow{k_c} T_1(\pi\pi^*) \tag{19}$$

$$S_1(\pi\pi)^* \xrightarrow{k_{dis}} \phi\text{-O}\cdot + \cdot\text{CCH}_3 \quad (\text{O}) \tag{20}$$

ϕ-O· + ·CCH$_3$ (O) → k_B → S_0; k_o → o-hydroxyacetophenone; k_p → p-hydroxyacetophenone; k_{OH} → phenol (21)

BULLETIN OF THE CHEMICAL SOCIETY OF JAPAN VOL. 42 1836—1840 (1969)

Electron Spin Resonance Studies of the Formation of Anion Radicals on γ-Irradiated Silica Gel

Yoshio YAMADA, Akinori HASEGAWA and Masaji MIURA

Department of Chemistry, Faculty of Science, Hiroshima University, Higashisenda-machi, Hiroshima

(Received November 22, 1968)

The ESR spectra assigned to the anion radicals of SO_2^-, $(TCNE)^-$ (tetracyanoethylene), and O_2^- were obtained for, respectively, sulfur dioxide, TCNE, and oxygen when these gases were adsorbed on γ-irradiated silica gel. As regards sulfur dioxide, a characteristic change in the concentration of the SO_2^- radical was observed during the post-irradiation with high-energy UV light. In the case of carbon dioxide, the CO_2^- radical was produced only when UV post-irradiation was added to γ-irradiation. The assignments were principally made in comparison with the reported g-values. Especially, the identification of the CO_2^- radical was ascertained by using ^{13}C. The analyses of the g-factor for the O_2^- radical and of ^{13}C hyperfine constants for the CO_2^- radical gave information on the interaction of the radicals on a solid surface with the cations in the adsorption center. In view of the fact that each of these molecules possesses a different degree of electron affinity, the results described above indicate that the electrons trapped in the defects of the silica gel surface transfer to the adsorbed molecules and that UV light promotes the electron transfer.

The application of ESR spectroscopy to the study of the state of molecules adsorbed on solid surfaces has been of considerable interest since it permits an analysis of the radical species produced from the molecules. The radicals detected by this method are generally classified into two types by taking the properties of adsorbents into account: (1) neutral radicals adsorbed on insulators[1,2] and (2) anion radicals on n-type semiconductors.[3-5] In respect to the radicals of the first type, the adsorbent contributes mainly to the stabilization rather than to the formation of radicals. Those of the second type are produced as a result of electron transfer from the adsorbent to the adsorbate with a high electron affinity. However, Lunsford and Jayne[6,7] have recently found that such anion radicals as CO_2^- or O_2^- are produced even on UV-irradiated magnesium oxide, an insulator. They have concluded from their studies that the trapped electrons created by UV irradiation take part in the formation of the anion radicals. All the investigations using silica gel, which is also an insulator, have, however, dealt only with neutral radicals

1) C. L. Gardner, *J. Chem. Phys.*, **46**, 2991 (1967).

2) V. B. Kazanskii, G. B. Pariiskii, I. V. Aleksandrov and G. M. Zhidomirov, *Fiz. Tverdogo Tela*, **5**, 649 (1963).

3) A. I. Mashchenko, G. B. Pariiskii and V. B. Kazanskii, *Kinet. Katal.*, **8**, 704 (1967).

4) A. I. Mashchenko, V. B. Kazanskii, G. B. Pariiskii and V. M. Sharapov, *ibid.*, **8**, 853 (1967).

5) I. D. Mikheikin, A. I. Mashchenko and V. B. Kazanskii, *ibid.*, **8**, 1363 (1967).

6) J. H. Lunsford and J. P. Jayne, *J. Phys. Chem.*, **69**, 2182 (1965).

7) J. H. Lunsford and J. P. Jayne, *J. Chem. Phys.*, **44**, 1487 (1966).

produced from the adsorbed-state molecules by γ- or UV-irradiation.[1,2]

In the present study, such anion radicals as SO_2^-, $(TCNE)^-$, and O_2^- were obtained from, respectively, sulfur dioxide, TCNE, and oxygen adsorbed on γ-irradiated silica gel. As for carbon dioxide, the CO_2^- radical was formed when UV post-irradiation was added to γ-irradiation.

Experimental

Materials. The method of the preparation of silica gel was described in the preceding paper.[8] Sulfur dioxide, oxygen, and carbon dioxide were purified by distillation under a vacuum. TCNE from the Wako Pure Chemical Co. was purified by sublimation.

Measurements. The silica gel was placed in a quartz tube fitted with a breakable seal and was outgassed in a vacuum of 10^{-5} Torr for 5 hr at 450—500°C. The tube was sealed off under a vacuum and then was irradiated at room temperature for *ca.* 15 hr with a ^{60}Co γ-source at a dose rate of 10^6 rad/hr. After the irradiation, the silica gel in a tube was exposed to sulfur dioxide, oxygen, carbon dioxide, or the vapor of TCNE through the breakable seal in a vacuum system. The ESR spectra were measured by a Japan Electron Optics Laboratory JES-3BS-X type ESR spectrometer operating at a cavity resonance frequency of 9400 Mc/sec with 100 kc modulation. The *g*-value was obtained by comparison with the value for DPPH. The error in *g*-value was estimated to be ±0.0002.

A high-pressure mercury lamp equipped with a Toshiba UV-D25 or VY-42 filter and also a low-pressure mercury lamp were employed in order to examine the effects of UV irradiation. UV-D25 and VY-42 filters transmit the light between 2400 Å and 4000 Å, and that between 4200 Å and 6000 Å, respectively. Carbon dioxide containing 60.8 atom% $^{13}CO_2$ which had been obtained from the Ateledyne Co., was used to identify the radical species. The TCNE anion radical was confirmed by a study of the diffuse reflectance spectra in addition to ESR spectra.

Results and Discussion

The spectrum of silica gel irradiated at room temperature is shown in Fig. 1. It was previously identified as being due to the electrons trapped in the defects.[9,10] The *g*-value (2.0009) of the spectral line is smaller than that of the free spin, and this spectrum is apt to be saturated with microwave power. These results support the above assignment.

In view of the facts that the silica gel used here has a high surface area (S=790 m²/g) and that the introduction of such a gas as sulfur dioxide results in the destruction of the defects, it seems reasonable that the electrons are trapped in the defects at the surface or its vicinity.

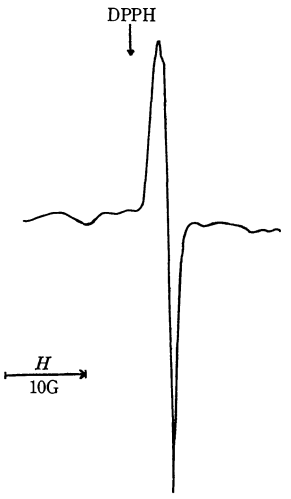

Fig. 1. ESR spectrum of γ-irradiated silica gel at room temperature.

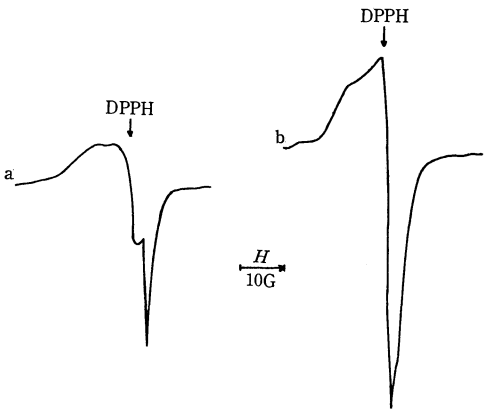

Fig. 2. (a) Spectrum recorded after sulfur dioxide was introduced at a pressure of 5 Torr to pre-irradiated silica gel, (b) spectrum recorded after sample (a) was irradiated with UV light for 5 min.

Sulfur Dioxide Adsorbed on Silica Gel. When sulfur dioxide was introduced into the silica gel at a pressure of 5 Torr, the gel, which had taken a faint violet color upon γ-irradiation, became colorless and a new ESR spectral line appeared, as is shown in Fig. 2a. This spectral line, however, did not appear on unirradiated silica gel. The values of $g_\perp$=2.0018 and $g_{//}$=2.0079 can be compared with those of the SO_2^- radical adsorbed on reduced titanium dioxide or zinc oxide.[3] On the basis of these results, the spectrum exhibited in Fig. 2a may be considered to be due to the SO_2^- radical. The formation of the SO_2^- radical on such semiconductors as titanium dioxide and zinc oxide has been interpreted as being due to the fact that the sulfur dioxide molecule, having a

8) M. Miura, A. Hasegawa and Y. Yamada, This Bulletin, **41**, 1320 (1968).

9) H. W. Kohn, *J. Chem. Phys.*, **33**, 1588 (1960).

10) V. B. Kazanskii, G. B. Pariiskii and V. V. Voevodskii, *Discussions Faraday Soc.*, **31**, 203 (1961).

high electron affinity, easily accepts an electron from the adsorbents because of the narrow energy gap between the valence and conduction bands.[11] In the case of silica gel, therefore, it is probably the trapped electrons that transfer to the adsorbed sulfur dioxide molecules, since silica gel is a typical insulator.

The signal (g=2.0009) corresponding to the electron trapped in the defect still remains, though faintly, after the adsorption. However, post-irradiation with UV light leads to the disappearance of this signal and, at the same time, to an increase in the intensity of the ESR signal due to the SO_2^- radicals. The increment in SO_2^- radicals by UV light in two different ranges of wavelengths are presented in Fig. 3 as a function of the irradiation time.

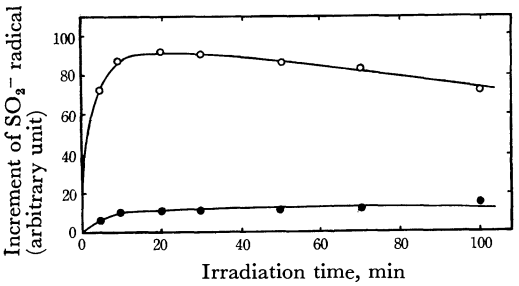

Fig. 3. The increment of SO_2^- radical by UV irradiation.

○: 2400—4000 Å (transmittance 60%)
●: 4200—6000 Å (transmittance 95%)

The illumination with light of wavelengths from 4200 Å to 6000 Å resulted in little increase in the radical. On the other hand, when light from 2400 Å to 4000 Å was used, the amount of the radical increased remarkably, though the short-wavelength light is more scattered than that of long wavelengths. Moreover, the increase in the radical reached a maximum after *ca.* 20 min and then decreased with the irradiation time. These results indicate that an energy higher than *ca.* 3 eV, which is equivalent to 4000 Å, is effective for the electron transfer. It has previously been reported that absorption spectra with peaks at 2.3, 4.1, and 5.6 eV appear on X-irradiated fused quartz,[12] the chemical composition of which is similar to that of silica gel. If these absorption bands are available to γ-irradiated silica gel, it should be mentioned, in view of the electron affinity of sulfur dioxide (2.8 eV), that even deeply-trapped electrons equivalent to 4.1 and 5.6 eV can migrate to the sulfur dioxide molecules on the surface upon UV illumination, supposing that the activation energy for the formation of the SO_2^- radical is overestimated.

The diminution in the radical concentration with the irradiation time can be interpreted if the following reactions are taken into consideration:

$$SO_2 + e^- \rightarrow SO_2^- \quad (1)$$

$$SO_2^- \rightarrow SO_2 + e^- \quad (2)$$

where e^- in Reaction (1) corresponds to an electron trapped in the defect, while that in Reaction (2) denotes an electron bleached. Namely, Reaction (2) should bring about a decrease in the radical concentration. Upon the illumination with the light from 4200 Å to 6000 Å, an appreciable increase in the radical amount was observed in the first stage, but it showed no change after *ca.* 20 min. It may be concluded from these facts that an energy less than *ca.* 3 eV contributes slightly to Reaction (1) through the transfer of the electrons trapped in the shallow potential at the first stage, but that it is inactive for Reaction (2).

TCNE Adsorbed on Silica Gel. When γ-irradiated silica gel was exposed to the vapor (10^{-2}—10^{-3} Torr) of TCNE for 10 hr, an ESR spectrum was obtained, as is shown in Fig. 4. On the other hand, no ESR signal was detected for unirradiated silica gel. The spectrum given in Fig. 4 is in good agreement with that of the TCNE anion radical formed when TCNE was adsorbed on alumina.[13] In order to identify the radical species further the reflectance spectrum of adsorbed TCNE was measured. The absorption band at *ca.* 420 mμ nearly corresponds to that of the TCNE anion radical in solution.[14] These results lead to the conclusion that the radical formed on silica gel is the TCNE anion. This is further supported by the characteristic features that TCNE has a high electron affinity and that the TCNE anion radical, as is well known, is stable even at room temperature. It seems reasonable that electron transfer is involved in the formation of the TCNE anion radical as in the case of the SO_2^- radical on silica gel. The spectral lines of the TCNE anion radical on silica gel are ill-resolved in contrast with those in solution, where four equivalent nitrogen atoms give nine lines as a result of interaction with the unpaired electron. This is explained by the fact that the anisotropy of the hyperfine structure arises from the lack of motional degrees of freedom. The signal due to the electrons trapped in the defects can scarcely be seen in Fig. 4, and the UV irradiation has no remarkable effect, different from the case of the SO_2^- radical.

Oxygen Adsorbed on Silica Gel. Oxygen was introduced at a pressure of 100 Torr to silica gel which had been irradiated by γ-ray at room temper-

11) V. B. Kazanskii and G. B. Pariiskii, 3rd International Congress on Catalysis, Amsterdam, 1964.
12) R. Yokota, *J. Phys. Soc. Japan*, **7**, 316 (1952).
13) K. Hirota, K. Kuwata and Y. Akagi, This Bulletin, **38**, 2209 (1965).
14) W. D. Phillips, J. C. Rowell and S. I. Weissman, *J. Chem. Phys.*, **33**, 626 (1960).

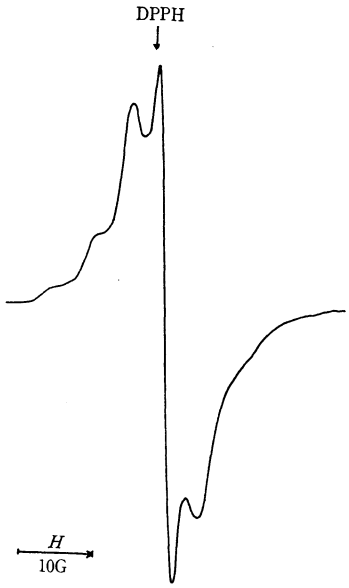

Fig. 4. Spectrum recorded after TCNE was introduced at a vapor pressure of 10^{-2}—10^{-3} Torr to pre-irradiated silica gel.

ature. A broad asymmetric spectrum appeared in addition to the signal responsible for the electrons trapped in the defects (Fig. 5a). The g-values of the new spectral line are $g_1=2.0250$, $g_2=2.0095$, and $g_3=2.0031$. Similar experiments have already been carried out by several investigators. Kazanskii *et al.*[10] showed that, for the sample outgassed at 200—300°C, the radicals formed by the cleavage of surface hydroxyl groups react with oxygens to produce the surface peroxide radicals ($g_1=2.025$, $g_2=2.002$, and $g_3=2.002$). In the case of the sample pre-treated at 500°C, however, they did not discuss the weak, different ESR spectrum formed by the introduction of oxygen to γ-irradiated silica gel. Since the present sample was outgassed at 450—500°C, the signal obtained here is considered not to be due to the surface peroxide radicals. As the matter of fact, the signal exhibited in Fig. 5a is identical with that observed under outgassing at 500°C by Kazanskii *et al.* Haul *et al.*[15] studied the effect of oxygen, nitrogen oxide, and a number of other gases on the ESR signal of irradiated silica under static and dynamic flow conditions. However, they did not find the new spectrum obtained here.

In order to elucidate the radical species corresponding to the asymmetric spectrum, a sample containing oxygen is irradiated by UV light for 30 min (Fig. 5b). The intensity of the spectral line is clearly enhanced. From these experiments and the assignment mentioned above for SO_2^- and $(TCNE)^-$, it may be concluded that the broad asymmetric spectrum is due to the O_2^- radical formed by the electron transfer from the solid to the adsorbed oxygen. This assignment is not necessarily inconsistent with the conclusions described above. The O^- radical may also be considered as a radical species. However, the g-values observed here are not suitable for the O^- radical reported,[16] and the energy required for the dissociation of O_2^- into

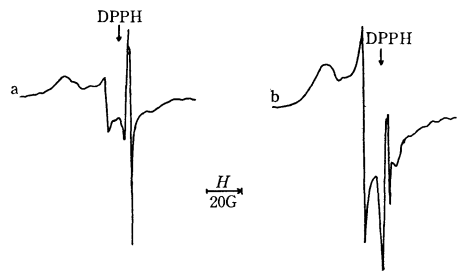

Fig. 5. (a) Spectrum recorded after oxygen was introduced at a pressure of 100 Torr to pre-irradiated silica gel, (b) spectrum recorded after sample (a) was irradiated with UV light for 30 min.

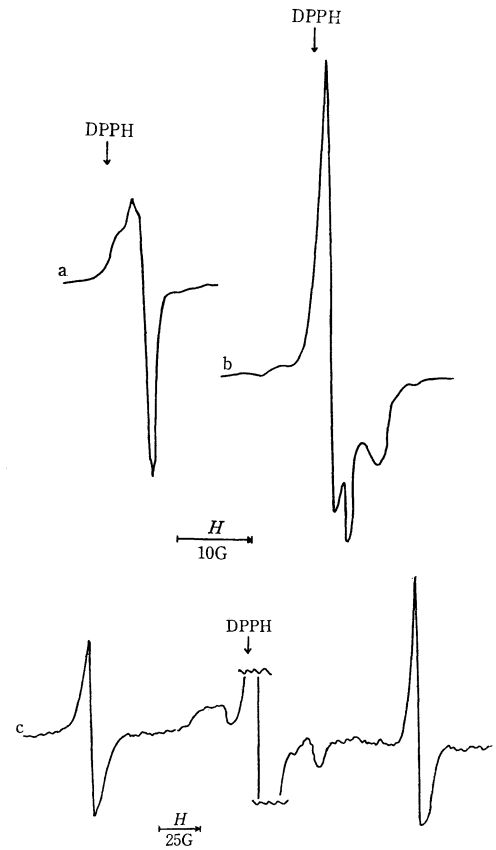

Fig. 6. (a) Spectrum recorded after $^{12}CO_2$ was introduced at a pressure of 100 Torr to the pre-irradiated silica gel, (b) spectrum recorded after sample (a) was irradiated with UV light for 30 min, (c) spectrum recorded at the similar condition to (b) with the exception of using the mixture of $^{13}CO_2$ 60.8 atom% and $^{12}CO_2$ 39.2 atom%.

15) R. Haul, J. Karra and J. Turkevich, *J. Am. Chem. Soc.*, **87**, 2092 (1965).

$O+O^-$ is 4.1 eV,[17] an energy which is impracticable under the present experimental conditions. Therefore, the formation of the O^- radical should be excluded. After all, then, these discussions give strong evidence for our tentative identification.

Kazanskii *et al.*[5] pointed out, from their analysis of *g*-values, that the most probable state of the peroxide radical on silica gel and of O_2^- radicals on various solid surfaces is such that the O–O axis of these radicals is parallel to the surface. The analysis of the *g*-values obtained in the present case suggests that the O_2^- radical on silica gel is also adsorbed in such a situation.

Carbon Dioxide Adsorbed on Silica Gel. On the exposure of pre-irradiated silica gel to $^{12}CO_2$ gas at 100 Torr, the spectrum illustrated in Fig. 6a was observed. It is similar in shape to that of irradiated silica gel itself. With the UV irradiation, the shoulder grew, whereas the signal due to the electrons trapped in the defects was weakened (Fig. 6b). The *g*-values of the new spectral line ($g_1=g_2=2.0024$ and $g_3=1.9975$) are in complete agreement with those of the CO_2^- radical reported in a preceding paper.[8] In this case, the UV light may contribute to the electron transfer since the electron affinity of carbon dioxide is much less than those of sulfur dioxide, TCNE, and oxygen. The spectrum, which was measured under the same conditions by using a mixture of 60.8 atom% $^{13}CO_2$ and 39.2 atom% $^{12}CO_2$, is illustrated in Fig. 6c. The ^{13}C hyperfine coupling constants evaluated from this spectrum are presented in Table 1, along with the values in the literatures. At the same time the experiment of Lunsford and Jayne[6] on the CO_2^- radical on magnesium oxide was repeated. The isotropic and anisotropic hyperfine constants obtained are almost identical with their results shown in Table 1, within the limits of experimental error. The values of a_s^2 and a_p^2, which give the unpaired electron density in the 2*s* and 2*p* orbitals respectively of the carbon atom, were calculated by analogy with Ovenall and Whiffen's article.[18] These values correspond to the isotropic and anisotropic parts of ^{13}C coupling.

Coulson[19] introduced the following formula for the bond angle of such molecules as CO_2^- and NO_2:

$$\cos\theta = -\lambda^2/(2+\lambda^2) \qquad (3)$$

where θ denotes the OCO bond angle and λ, the ratio of a_s to a_p. The bond angle of the CO_2^- radical on γ-irradiated silica gel was determined by the use of Eq. (3). The value of the hyperfine splitting constant introduces some error ($\pm$8G) because of the overlapping of the anisotropies of *g*-factors and hyperfine constants. The bond angle of the CO_2^- radical on silica gel is much less than that on magnesium oxide, as is obvious from Table 1. The narrowing of the OCO bond angle of the CO_2^- radical on silica gel may be attributed to the characteristic adsorption: the separation of silicon atoms on the silica gel surface is smaller than that of magnesium atoms on the magnesium oxide surface. The narrowing of the OCO angle should also have an influence upon the molecular orbitals of the CO_2^- radical. The OCO angle of the CO_2^- radical may be expected to become narrow as the energy gaps between $3b_2$ and $4a_1$ and between $2b_1$ and $3b_2$ in the energy levels of the CO_2^- radical molecular orbital become large. Accordingly, the $4a_1 \leftarrow 3b_2$ and $2b_1 \leftarrow 3b_2$ promotions are reduced. The $4a_1 \leftarrow 3b_2$ and $2b_1 \leftarrow 3b_2$ contribute to the deviation of the values of g_1 and g_2 respectively from the value of free spin. Thus, the narrowing of the OCO angle results in the approach of g_1 and g_2 to the value of the free spin. The experimental result ($g_1=g_2=2.0024$) is consistent with these considerations.

In conclusion, it was found that the anion radicals are formed by introducing such gases as sulfur dioxide, TCNE, and oxygen to γ-irradiated silica gel. As for the CO_2^- radical, it was formed by UV irradiation in addition to γ-irradiation because carbon dioxide has a low electron affinity. The O_2^- radical seems to be adsorbed in such a state that the O–O axis is parallel to the gel surface. In addition, the analysis of the ^{13}C hyperfine constants for the CO_2^- radical gave a closer OCO angle than that of the CO_2^- radical on magnesium oxide. This finding may be ascribed to the difference in the crystal radii of the cations on the solid surface.

TABLE 1. HYPERFINE COUPLING CONSTANTS AND PARAMETERS FOR CO_2^- RADICAL

	Hyperfine coupling constants (gauss)				Parameters			
	A_x	A_y	A_z	A_{iso}	a_s^2	a_p^2	λ^2	θ
$^{13}CO_2^-$ in NaCOOH[a]	156	151	195	167	0.14	0.66	4.71	134°
$^{13}CO_2^-$ on MgO[b]	184[c]	···	230	199	0.17	0.73	5.21	132°
$^{13}CO_2^-$ on SiO_2	199[c]	···	215	204 (Estd. error $\pm$8)	0.17	0.26	1.53	116°

a) Ref. 18
b) Ref. 6
c) It is impossible to distinguish between A_x and A_y.

16) M. J. Blandmer, L. Shields and M. C. R. Symons, *J. Chem. Soc.*, **1964**, 4352.
17) E. R. S. Winter, *Advan. Catalysis*, **10**, 196 (1958).
18) D. W. Ovenall and D. H. Whiffen, *Mol. Phys.*, **4**, 135 (1961).
19) C. A. Coulson, Victor Henri Volume Commemoratif, Contribution à l'étude de la Structure Moléculaire (1948), p. 15.

BULLETIN OF THE CHEMICAL SOCIETY OF JAPAN VOL. 42 1841—1852 (1969)

The Electronic Spectra and the Intermolecular Interaction of Würster's Ions in Crystals

Jiro TANAKA and Masagi MIZUNO*1

Department of Chemistry, Faculty of Science, Nagoya University, Chikusa-ku, Nagoya

(Received November 30, 1968)

The electronic spectra and the intermolecular interaction of Würster's radical have been studied for the dimer state and for the crystalline states. The polarization properties of the excited states have been investigated in detail, and the longest wavelength absorption band of the dimer has been established as having a charge-transfer character. The strength of the charge-transfer band and the shift of the monomer band in the dimer or in the crystalline states are shown to be intimately correlated with the strength of the intermolecular interactions between the stacked radicals. A theoretical analysis of the excited state of the dimer and the crystals is presented; the results are in good agreement with the experimental findings.

Würster's ions are well known to dimerize at lower temperatures in a solution. Hausser and Murrell[1] first pointed out that the origin of the longest-wavelength absorption band of the dimer is charge-transfer in nature and suggested that the ions might be stacked on each other in a solution. Suzuki, Ooshika, and their coworkers[2] extended the earlier work and found the equilibrium constant for dimerization. A similar line of experiment was carried out by Kimura, Yamada, and Tsubomura[3] recently. Kommandeur and Pott[4] discussed the nature of the electronic transition from a different viewpoint and suggested that a doubly-charged cation and a neutral molecule might be involved in the appearance of the longest-wavelength band. On the other hand, McConnell and his group,[5] however, insisted on the charge-transfer mechanism and a recent experiment by Sakata and Nagakura[6] has also supported this interpretation.

In this laboratory an X-ray structure analysis has been carried out on several Würster's salts,[7] and a combined investigation of the spectra and structure of the crystals has been attempted. The measurement of the absorption spectra with a single crystal by means of polarized light is the most reliable method for confirming the symmetry properties of the excited state if the crystal structure has already been established. In this paper we will present: (1) a theoretical treatment of the dimer interaction, (2) the findings on the crystalline absorption spectra of various Würster's salts, and (3) a discussion of the nature of the electronic transition in the crystalline state.

The longest-wavelength absorption bands of the crystals have definitely been determined to be an intermolecular charge-transfer between the stacked radicals. The appearance of the charge-transfer band in the crystalline spectra is intimately correlated with the magnitude of the intermolecular electron exchange interaction, which can be estimated by means of the overlap integrals between the molecular orbitals of the radicals. The polarization properties of the radical excited states have been determined; the findings are supported by the theoretical analysis[8] of the radical spectra. The configurational mixing between the charge-transfer state with the local excited state shifts the visible band of the radical to a shorter wavelength. It may be concluded that the electron-exchange effect between the radicals is most important in determining the optical and other electronic properties of organic free-radical crystals.

Theory of the Dimer Interaction

According to results of the X-ray crystal structure analysis, the interplanar distances between the

*1 Present address: The Government Chemical Industrial Research Institute, Tokyo.

1) K. H. Hausser and J. N. Murrell, *J. Chem. Phys.*, **27**, 500 (1957).

2) K. Uemura, S. Nakayama, Y. Seo, K. Suzuki and Y. Ooshika, This Bulletin, **39**, 1348 (1966).

3) K. Kimura, H. Yamada and H. Tsubomura, *J. Chem. Phys.*, **48**, 440 (1968).

4) J. Kommandeur and G. T. Pott, *ibid.*, **47**, 395 (1967).

5) P. L. Nordio, Z. G. Soos and H. M. McConnell, *Ann. Rev. Phys. Chem.*, **17**, 237 (1966).

6) T. Sakata and S. Nagakura, *Technical Report of Institute for Solid State Physics, The University of Tokyo, Ser. A*, No. 244 (1967).

7) J. Tanaka and N. Sakabe; *Acta Cryst*, **B24**, 1345 (1968).

8) To be published elsewhere.

stacked radicals are in the range of 3.1—3.7 Å. In the region of these intermolecular distances, covalent bondings between the radicals may be expected; their strength can be estimated by the electron overlap between the half-filled molecular orbitals of the radicals. The Heitler-London approach is most appropriate for the treatment of the inter-radical interaction at these distances, since the molecular orbital method would emphasize the electron delocalization effect too much. In the following treatment we will consider only the highest singly-occupied orbital as a one-electron problem and will neglect the effects of all the other occupied orbitals. The singly-occupied highest molecular orbitals of a and bth radicals are denoted by $\psi_a{}^m$ and $\psi_b{}^m$, and vacant orbitals, by $\psi_a{}^e$ and $\psi_b{}^e$.

The orbital wave function of the singlet state may be given as follows:

Ground Configuration:

$$\Psi_G = \frac{1}{\sqrt{2(1+S_{mm}^2)}}[\psi_a{}^m(1)\psi_b{}^m(2) + \psi_b{}^m(1)\psi_a{}^m(2)]$$

Charge-transfer Configuration:

$$\Psi_{CT\pm} = \frac{1}{\sqrt{2(1\pm S_{mm}^2)}}[\psi_a{}^m(1)\psi_a{}^m(2) \pm \psi_b{}^m(1)\psi_b{}^m(2)]$$

Molecular Excited Configuration:

$$\Psi_{M\pm} = \frac{1}{\sqrt{4+2S_{me}^2+2S_{mm}S_{ee}}}[\psi_a{}^e(1)\psi_b{}^m(2) + \psi_b{}^m(1)\psi_a{}^e(2) \pm \psi_a{}^m(1)\psi_b{}^e(2) \pm \psi_a{}^m(2)\psi_b{}^e(1)]$$

where the upper sign corresponds to the symmetric state and the lower one to the antisymmetric state.

The total Hamiltonian for the system is given by;

$$H = H_a + H_b + V_{ab}$$

$$H_a = -\frac{1}{2}\nabla_1{}^2 - \sum_i \delta_i/R_{a_i 1}$$

$$H_b = -\frac{1}{2}\nabla_2{}^2 - \sum_j \delta_j/R_{b_j 2}$$

$$V_{ab} = -\sum_j \delta_j/R_{b_j 1} - \sum_i \delta_i/R_{a_i 2} + 1/r_{12} + \sum_{i,j} \delta_i\delta_j/R_{a_i,b_j}$$

where $\sum_i \delta_i R_{a_i 1}$ indicates the core attraction potentials for the first electron by the ith atomic core of the ath radical with a δ_i effective charge, which is produced by stripping off one electron from the complete radical. The molecular orbital of the radical is given by the LCAO form while the orbital energies for the isolated system are given by:

$$\psi_a{}^m = \sum_i C_i{}^m \chi_{a_j}$$

$$H_a\psi_a{}^m = \varepsilon_a{}^m\psi_a{}^m$$

$$H_b\psi_b{}^m = \varepsilon_b{}^m\psi_b{}^m$$

The overlap integral and other integrals between radicals are described by:

$$S_{mm} = \sum_i\sum_j C_i{}^m C_j{}^m \langle \chi_{a_i}|\chi_{b_j}\rangle$$

$$\langle \psi_a{}^m|1/R_b|\psi_b{}^m\rangle = \sum_i\sum_j C_i{}^m C_j{}^m \langle \chi_{a_i}|\delta_j/R_{b_j}|\chi_{b_j}\rangle$$

$$(\psi_a{}^m\psi_a{}^m|\psi_b{}^m\psi_b{}^m) = \sum_i\sum_j C_i{}^{m2} C_j{}^{m2} \langle \chi_{a_i}(1)\chi_{a_i}(1)|1/r_{12}|\chi_{b_j}(2)\chi_{b_j}(2)\rangle$$

$$S_{mm}\langle \psi_a{}^m|1/R_b|\psi_b{}^m\rangle = \sum_i\sum_j C_i{}^{m2} C_j{}^{m2} \langle \chi_{a_i}|\chi_{b_j}\rangle\langle \chi_{a_i}|\delta_j/R_{b_j}|\chi_{b_j}\rangle$$

By the use of these notations, the diagonal energy for the ground state may be given by:

$$E_{G,G} = 2\varepsilon_a{}^m - 2\langle \psi_a{}^m|1/R_b|\psi_a{}^m\rangle + (\psi_a{}^m\psi_a{}^m|\psi_b{}^m\psi_b{}^m)(1-S_{mm}^2) + \sum_i\sum_j \frac{\delta_i\delta_j}{R_{a_i,b_j}}$$
$$-2S_{mm}\langle \psi_a{}^m|1/R_b|\psi_b{}^m\rangle + 2S_{mm}^2\langle \psi_a{}^m|1/R_b|\psi_a{}^m\rangle + (\psi_a{}^m\psi_b{}^m|\psi_a{}^m\psi_b{}^m) \quad (4)$$

The diagonal energy for the molecular excited state relative to the ground state is calculated as:

$$E_{E,E\pm} - E_{G,G} = \varepsilon_a{}^e - \varepsilon_b{}^m - \langle \psi_a{}^e|1/R_b|\psi_a{}^e\rangle + \langle \psi_a{}^m|1/R_b|\psi_a{}^m\rangle + (\psi_a{}^e\psi_a{}^e|\psi_b{}^e\psi_b{}^e)(1-S_{ee}S_{mm})$$
$$-(\psi_a{}^m\psi_a{}^m|\psi_b{}^m\psi_b{}^m)(1-S_{mm}^2) - 2S_{me}\langle \psi_a{}^e|1/R_b|\psi_b{}^m\rangle + 2S_{mm}\langle \psi_a{}^m|1/R_b|\psi_b{}^m\rangle$$
$$\pm(\psi_a{}^m\psi_a{}^e|\psi_b{}^m\psi_b{}^e)(1-S_{ee}S_{mm}) \pm (\psi_a{}^e\psi_b{}^m|\psi_a{}^e\psi_b{}^m) \quad (5)$$

If we use the following approximations, which are valid for a rough calculation:

$$C_i{}^m{}^2 = C_i{}^e{}^2, \qquad S_{mm}\psi_a{}^m = S_{me}\psi_a{}^e$$
$$\langle\psi_a{}^e|1/R_b|\psi_a{}^e\rangle = \langle\psi_a{}^m|1/R_b|\psi_a{}^m\rangle \tag{6}$$

Equation (5) is reduced to:

$$E_{M,M_\pm} - E_{G,G} = \varepsilon_a{}^e - \varepsilon_b{}^m \pm (\psi_a{}^m\psi_a{}^e|\psi_b{}^m\psi_b{}^e)(1-S_{ee}S_{mm}) \pm (\psi_a{}^e\psi_b{}^m|\psi_a{}^e\psi_b{}^m)$$
$$\simeq \varepsilon_a{}^e - \varepsilon_b{}^m \pm (\psi_a{}^m\psi_a{}^e|\psi_b{}^m\psi_b{}^e) \tag{7}$$

The diagonal energy of the charge-transfer state relative to the ground state is evaluated as;

$$E_{CT,CT} - E_{G,G} = [(\psi_a{}^m\psi_a{}^m|\psi_a{}^m\psi_a{}^m) - (\psi_a{}^m\psi_a{}^m|\psi_b{}^m\psi_b{}^m)](1-S_{mm}^2) \tag{8}$$

The off-diagonal matrix element between the charge-transfer and molecular excited configurations and the ground configuration have been calculated, The results are:

$$E_{G,CT_+} = \sqrt{2}\,[S_{mm}\varepsilon_a - S_{mm}\langle\psi_a{}^m|1/R_b|\psi_a{}^m\rangle - \langle\psi_a{}^m|1/R_b|\psi_b{}^m\rangle$$
$$+ (\psi_a{}^m\psi_a{}^m|\psi_a{}^m\psi_b{}^m) + S_{mm}/R_{a,b}] \tag{9}$$
$$E_{M_\pm,CT_\pm} = \sqrt{2}\,[\pm S_{me}\varepsilon_a \mp S_{me}\langle\psi_a{}^m|1/R_b|\psi_a{}^m\rangle \mp \langle\psi_a{}^m|1/R_b|\psi_b{}^e\rangle$$
$$+ (\psi_a{}^m\psi_a{}^e|\psi_a{}^m\psi_b{}^m) \pm (\psi_a{}^m\psi_a{}^m|\psi_a{}^m\psi_b{}^e) \pm S_{me}/R_{a,b}]$$

The off-diagonal element between the molecular excited and the ground state is set equal to zero since this term has already been diagonalized.

With a view to interpretating the spectra of the dimer and the crystal, we have performed semi-empirical calculations. Three configurations, the ground, the charge-transfer, and the molecular excited state, of the lowest energy of the y axis polarization have been taken into account, where the x and y axes have been chosen to be as shown in Fig. 1.

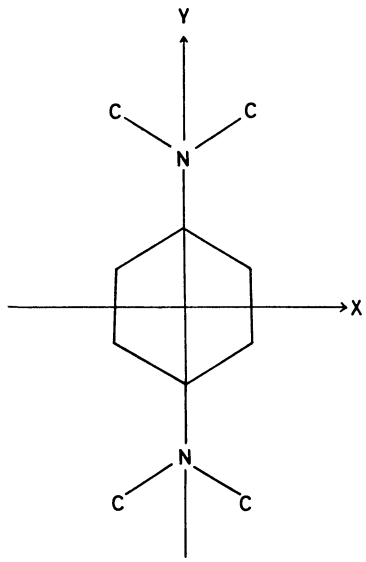

Fig. 1. The molecular axis of p-phenylenediamine.

The matrices for the symmetric (3×3) and the antisymmetric (2×2) states have been solved:

$$\begin{vmatrix} E_G & \beta & 0 \\ \beta & E_{CT_+} & \beta' \\ 0 & \beta' & E_{M_+} \end{vmatrix} = 0 \tag{10}$$

$$\begin{vmatrix} E_{CT_-} & \beta'' \\ \beta'' & E_{M_-} \end{vmatrix} = 0$$

Here the terms $S_{G,CT}\,E$, $S_{CT_+,M_+}\,E$, and $S_{CT-M_-}\,E$ are neglected in order to simplify the calculation. The actual calculation of the matrix elements is rather complicated; therefore, we have used semi-empirical values for the diagonal and off-diagonal elements. The diagonal element for the molecular excited state is taken from the peak of the absorption spectra in a solution. The energy of the charge-transfer state can be calculated by Eq. (8); however, the value is about 1 eV larger than the value envisaged from the dimer spectra in a solution. Therefore, we have used values which will fit the observed dimer spectra, 1.9 eV for the p-phenylenediamine cation dimer, 1.7 or 1.8 eV for Würster's red and 1.6 eV for Würster's blue dimers. The off-diagonal elements have been examined in detail; it is found that they are related to the overlap intergrals between the relevant molecular orbitals. In order to make a spectral assignment and an interpretation, we have used several sets of tentative matrix elements, β, β', and β''; the numerical values are tabulated in Table 1.

The results of the calculation are presented in

Table 1. Matrix elements for Eq (10)
The units are in eV.

	E_{CT}	E_M	β	β'	β''
I	1.9	2.5	0.9	0.5	0.5
II	1.7	2.2	0.9	0.7	0.5
III	1.8	2.2	0.6	0.4	0.4
IV	1.6	2.1	0.25	0.1	0.05
V	1.6	2.1	0.23	0.1	0.1
VI	1.6	2.1	0.22	0.1	0.1
VII	1.6	2.1	0.11	0.05	0.05
VIII	1.6	2.1	0.10	0.05	0.04
IX	1.6	2.1	0.08	0.05	0.04

TABLE 2. ENERGY LEVELS AND WAVE FUNCTIONS

	Energy (eV)	G	CT_+	M_+	Energy (eV)	CT_-	M_-
I	−0.376	0.9225	−0.3802	0.0662			
	1.905	−0.3401	−0.7199	0.6050	1.617	0.8702	−0.4927
	2.866	0.1823	0.5806	0.7935	2.783	0.4927	0.8702
II	−0.419	0.9008	−0.4196	0.1121			
	1.517	−0.3829	−0.6452	0.6611	1.392	0.8520	−0.5241
	2.804	0.2050	0.6384	0.7419	2.508	0.5241	0.8520
III	−0.187	0.9533	−0.2978	0.0499			
	1.695	−0.2673	−0.7552	0.5985	1.553	0.8507	−0.5257
	2.492	0.1406	0.5839	0.7995	2.447	0.5257	0.8507
IV	−0.038	0.9885	−0.1513	0.0071	1.595	0.9951	−0.0985
	1.618	−0.1496	−0.9681	0.2008			
	2.120	0.0235	0.1996	0.9796	2.105	0.0985	0.9951
V	−0.0298	0.9909	−0.1342	0.0063			
	1.610	−0.1327	−0.9712	0.1981	1.595	0.9951	−0.0985
	2.120	0.0205	0.1971	0.9802	2.105	0.0985	0.9951
VI	−0.0247	0.9924	0.1225	0.0058	1.595	0.9951	−0.0985
	1.605	−0.1213	−0.9730	0.1965	2.105	0.0985	0.9951
	2.120	0.0185					
VII	−0.0075	0.9977	−0.0683	0.0016	1.597	0.9969	−0.0792
	1.6025	0.0681	0.9927	−0.0998	2.103	0.0792	0.9969
	2.1050	0.0052	0.0996	0.9950			
VIII	−0.006	0.9981	−0.0622	0.0148	1.597	0.9969	−0.0792
	1.601	0.0620	0.9931	0.0996	2.103	0.0792	0.9969
	2.105	0.0047	0.0994	0.9950			
IX	−0.0040	0.9988	−0.0498	0.0118	1.597	0.9969	−0.0792
	1.599	0.0497	0.9938	0.0992	2.103	0.0792	0.9969
	2.105	0.0038	0.0991	0.9951			

Tables 2 and 3. In Table 2 the wave functions are presented; by the use of these functions we can estimate the oscillator strength for each transition; their components are as shown in Table 3. Here the structure of the dimer is taken from the results of the crystal structure analysis.

The electronic absorption spectra of the Würster's dimer have been studied by several people; the results of Suzuki *et al.*[2] are shown in Fig. 2. In this figure the spectra of *p*-phenylenediamine and Würster's blue cation are presented; the monomer band (curve 1) consists of R, X, and Y bands, while the dimer spectra (curve 2) show a new longer wavelength charge-transfer (CT) band and shifted R′, X′, and Y′ bands. The splitting between the CT and R′ bands and the intensities are greatly dependent on the magnitude of the intermolecular interaction. In Table 3 the calculated oscillator strengths are presented; it is there shown that the intensity ratio for the CT and R band is so sensitively dependent on the magnitudes of the matrix elements that we might be able to estimate the strength of the interaction accurately by comparing the observed and calculated values. In Fig. 3 the results of the calculation are illustrated; the appearance of

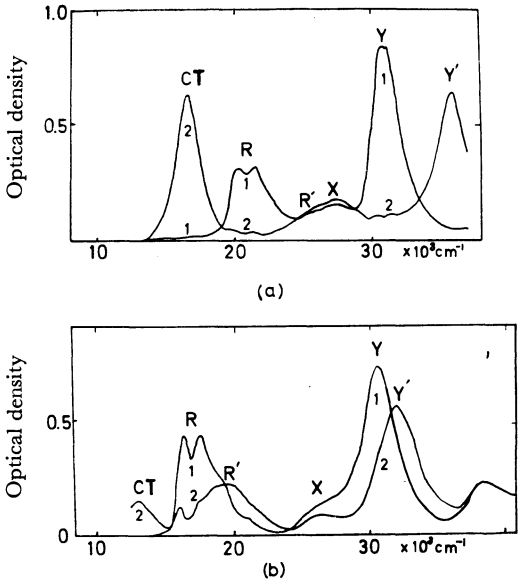

Fig. 2. Absorption spectra of (a) *p*-phenylenediamine cation and (b) Würster's blue perchlorate in solution. Curve 1 for the monomer and curve 2 for the dimer band. The data are taken from Uemura, Suzuki *et al.*[2]

TABLE 3. TRANSITION ENERGIES AND ABSORPTION INTENSITIES

	Transition energies (eV)		Calculated intensities: Transition moments (Å)			Calculated intensities: f (ocsillator-strength)	The intensity ratio of the CT and the R′ bands of the dimer	
	Calcd	Obsd	μ (total)	μ ($\perp$)	μ (//)		Calcd	Obsd
I	1.99	2.04(a)	1.42	1.02	0.97	0.36	3.6 : 1	3.6 : 1[a]
	3.15	3.22	0.60	0.45	0.40	0.10		
II	1.81	1.85(b)	1.60	1.15	1.10	0.41	2.8 : 1	
	2.93	3.06	0.75	0.70	0.13	0.15		
III	1.74		1.18	0.78	0.88	0.22	2.4 : 1	1.6 : 1[b]
	2.63		0.58	0.50	0.31	9.09		
IV	1.63	1.61	0.62	0.53	0.40	0.055	0.5 : 1	0.59 : 1[c]
	2.14	2.36	0.73	0.05	0.73	0.11		
V	1.63		0.50	0.44	0.36	0.044	0.44 : 1	0.46 : 1[d]
	2.14		0.73	0.04	0.73	0.10		
VI	1.62		0.50	0.38	0.35	0.035	0.35 : 1	0.44 : 1[e]
	2.13		0.73	0.04	0.73	0.10		
VII	1.60		0.30	0.22	0.20	0.013	0.12 : 1	0.052 : 1[f]
	2.11		0.77	—	0.77	0.11		
VIII	1.60		0.27	0.20	0.19	0.01	0.09 : 1	
	2.11		0.77	—	0.77	0.11		
IX	1.60		0.23	0.16	0.17	0.007	0.06 : 1	0.063 : 1[g]
	2.11		0.77	—	0.77	0.11		

a) p-Phenylenediamine cation dimer in solution. Refs. 2 and 3.
b) Würster's red bromide in solution. Ref. 3.
c) Würster's blue bromide in crystal at room temprature. This work.
d) Würster's blue perchlorate in crystal at low temperature. Ref. 6.
e) Würster's blue perchlorate in solution. Refs. 2 and 6.
f) Würster's blue iodide in crystal at room temperature. This work.
g) Würster's blue perchlorate in crystal at room temperature. This work.

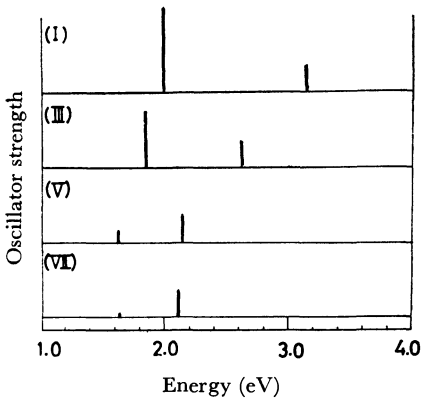

Fig. 3. The calculated energies and oscillator strength of the dimer spectra.
The results shown in Tables 2 and 3 are presented; the numbers I, III, V and VII correspond to numbers in the tables.

the strong CT band and the large blue shift of the R band are intimately correlated with the intermolecular interaction. In Table 3 it may be seen that the case I corresponds to the p-phenylenediamine cation dimer in a solution, while the case II explains the Würster's red dimer and the case IV or V agrees well with Würster's blue dimer in a solution. The selected values of the off-diagonal matrix elements are quite reasonable from the point of view of steric repulsion, since the dimethyl group will hinder the stacking of the radicals.

In the next section several examples of crystal absorption will be presented, in which the change in the components of transition moments is exemplified by the intensity of the polarization spectra.

The ground-state stabilization energies, calculated as in Table 2, are intimately correlated with the singlet-triplet separation energies of the radical crystals. The experimental results on the magnetic susceptibilities of these crystals will be discussed in a separate paper.

Crystalline Absorption Spectra

The crystals of Würster's blue perchlorate, blue iodide, blue bromide, and red bromide were synthesized by the method of Michaelis and Granick.[9] Small crystals of microscopic size were selected under a polarization microscope for the spectral measurements, and the orientation of the crystalline axis was determined by taking X-ray photographs. The spectra were measured using a microspectrophotometer consisting of a Carl Zeiss monochromator and an Olympus microscope. Some of these crystals are unstable at room temperature; therefore, the measurements were carried out as soon as possible after preparation.

i) Würster's Blue Perchlorate. The crystals of Würster's blue perchlorate show a brownish metallic reflection, hexagonal or square in rhomb shape. The crystalline structure has been analysed by Turner and Albrecht;[10] their results, as yet unpublished, have been confirmed in this laboratory. The crystal belongs to the orthorhombic system of the P_n2_n space group with lattice constants of $a=5.98$, $b=10.21$, and $c=10.23$ Å. It includes two molecules in a unit cell; the projection of molecules onto the *ac* plane is depicted in Fig. 4. There were two crystalline types, the developing *ac* plane and the developing *ab* plane. The crystalline absorption measured on the *ac* plane is shown in Fig. 5; it is remarkable that the charge-transfer band is very weak in crystals. It appears at 11500 cm^{-1} with its polarization along the *a* axis. In Fig. 6 another spectra with an *ab* plane developing is presented; the band has no component along the *b* axis. These two results have shown that the charge transfer band is polarized along the direction of the *a* axis; in this direction the lines connecting the centers of the stacked radicals are parallel. In view of the theoretical results, the charge-transfer transition should have a polarization parallel to the line connecting the center of the donor and the acceptor molecules. In the present system the Würster's ion acts as both the electron donor and the acceptor by itself; therefore, the polarization of the charge transfer band may be expected to be found only along the *a* axis. Therefore the weak 11500 cm^{-1} band is confirmed to be predominantly charge-transfer in character. It is very interesting that, in a solution at a lower temperature, the intensity of the charge-transfer band of the dimer was larger than in a crystal. The fact that the intensity of the charge-transfer band is greatly dependent on the overlapping of pi-electrons suggests that the stacking of radicals might be more effective for the dimer in a solution than in a crystal. Recent experiments by Anderson[11] and Sakata and Nagakura[6] have shown that the intensity of the charge transfer band increases

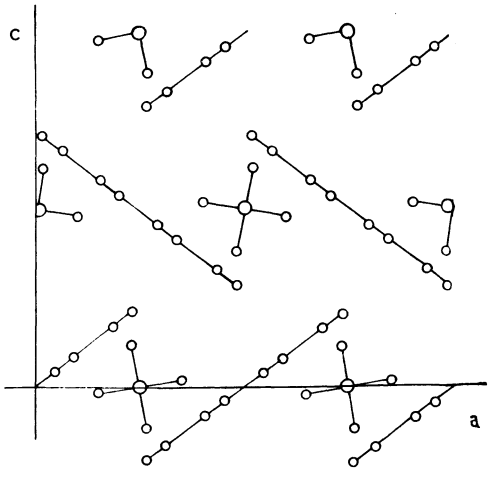

Fig. 4. Projection of Würster's blue perchlorate crystal onto the *ac* plane.

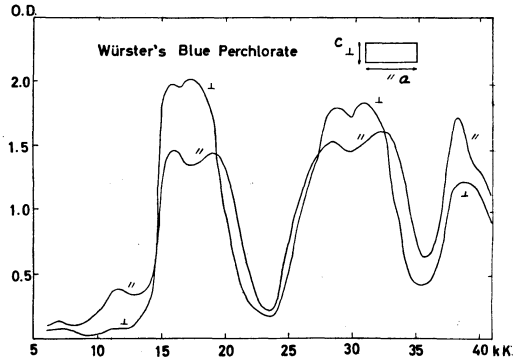

Fig. 5. The crystalline absorption spectra of Würster's blue perchlorate on the *ac* plane.

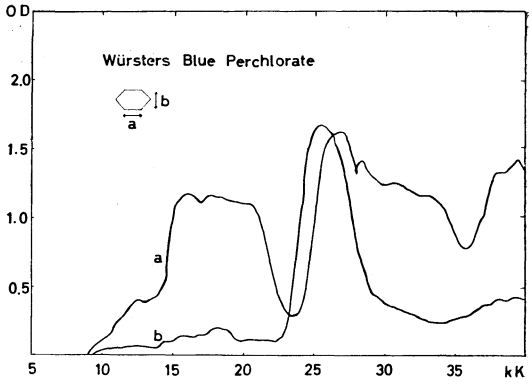

Fig. 6. The crystalline absorption spectra of Würster's blue perchlorate on *ab* plane.

9) L. Michaelis and S. Granick, *J. Am. Chem. Soc.*, **65**, 1747 (1943).

10) J. D. Turner and A. C. Albrecht, unpublished results (1955); see *J. Chem. Phys.*, **39**, 2321 (1963). We are grateful to Professor Albrecht for his communication on his unpublished result.

11) G. R. Anderson, *J. Chem. Phys.*, **47**, 3853 (1967).

markedly below the transition point of the crystal. However, at room temperature, the crystalline spectrum is much like the spectrum of the radical monomer in a solution; therefore, the succeeding band may be regarded as representing the polarization characteristics of the radical excited states. In the 15000—20000 cm^{-1} region, the R-band is not observed along the *b* axis on the *ab* plane. If the polarization of this band is the short axis of the radical (the *x* axis in Fig. 1), it should be very strong along the *b* axis. The observed result is contrary to this prediction; therefore, the transition moment must be on the long axis (*y* axis). This is in harmony with our theoretical results presented in a separated paper.[8] The observed dichroic ratio, $I_a : I_c$ was 0.7 : 1.0, while the calculated value, assuming the long-axis polarization, is 1.3 : 1.0. The agreement is not perfect; however, the last choice of a polarization vertical to the benzene ring is not acceptable since the R-band is undoubtedly a pi-pi transition and so its transition moment must be on the plane of the benzene ring. The deviation of the dichroic ratio might result from a mixing with other excited states. In the calculation presented in Table 3, the intensity ratio for the CT and R band is evaluated. The observed value is 0.063 : 1, while the value calculated by means of the parameter (IX) is 0.06 : 1. This agreement suggests that interaction parameters as small as $\beta=0.08$ eV are valid for this crystal.

In the *b* axis spectrum a peak is observed at 25500 cm^{-1}, it corresponds to the X-band in the monomer spectrum. This band is not observed along either the *a* axis or the *c* axis; therefore, its polarization is confirmed to be the short axis of the radical. This result is also consistent with our prediction of the sequence of the excited state energy levels. In the range of 26000—34000 cm^{-1} a very broad band is observed along the spectra of both the *a* and *c* axes. This is correlated to the Y-band in a solution, and the polarization may safely be regarded as being to the long axis of the radical. In a higher energy region at about 38000 cm^{-1} another peak is observed; it is the W-band, and its polarization is also the long axis of the radical. Summarizing these results, it may be concluded that the polarizations of the radical excited states for R, Y, and W bands are *y* axis, while that for the X-band is *x* axis. Although the longest wavelength charge-transfer band is not as prominent in crystals, its polarization is perfectly on the line connecting the radicals, consistent with the theoretical results, shown in Table 3.

ii) Würster's Blue Iodide. The crystal structure of Würster's blue iodide is very much like that of blue perchlorate; the structure has recently been determined by De Boer, Vos, and Huml.[12] The crystal belongs to the orthorhombic system; the space group is *Pnnm* with $Z=2$. The unit cell dimensions are $a=5.919$, $b=9.855$, and $c=9.901$ Å. The projection of molecules onto the *ab* plane is shown in Fig. 7.

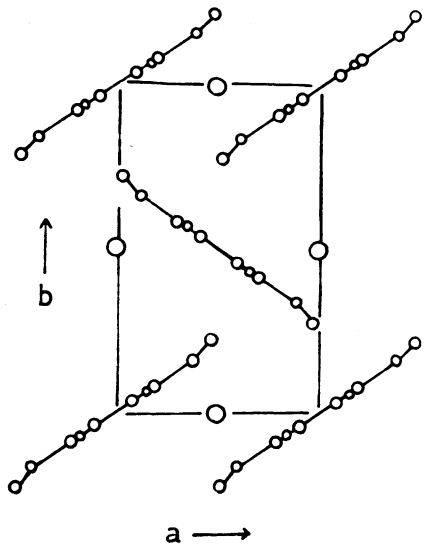

Fig. 7. Projection of Würster's blue iodide crystal onto the *ab* plane.

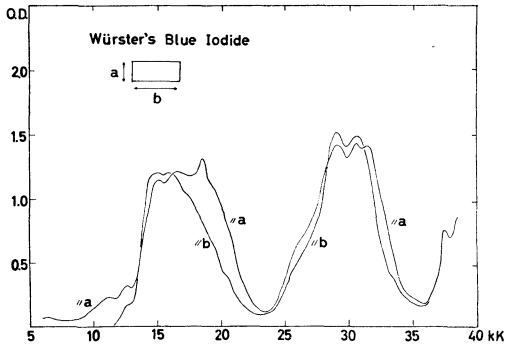

Fig. 8. The crystalline absorption spectra of Würster's blue iodide on the *ab* plane.

The crystalline absorption spectrum has been measured on the *ab* plane (Fig. 8). Although the inclination of the long axis to the *a* axis is decreased by 2.5° as compared to Würster's blue perchlorate, the spectrum is very close to the *ac* plane spectrum of perchlorate. The charge-transfer band is found at 11200 and 12500 cm^{-1}. The theoretical analysis presented above showed that the transition moment for this band is on the *a* axis of the crystal. The broad R-band is observed around the 14000—21000 cm^{-1} region and it showed several peaks which may be supposed to be due to the vibrational progressions. The X band is not obvious on this plane, but a little shoulder was found at 26000 cm^{-1}. The Y band is observed in the 28000—33000 cm^{-1}

12) J. L. De Boer, A. Vos and K. Huml, *Acta Cryst.*, **B24**, 542 (1968).

range; the polarization results are consistent with the previous conclusions drawn from the perchlorate crystalline spectrum.

In the iodide crystal the intensity ratio for the CT and R bands is found to be 0.052 : 1. This result suggests that the weakest interaction parameters will be valid for this crystal; however, the magnetic results show that the interaction might be slightly larger than in the perchlorate crystal. The overlap integral between the highest occupied orbitals will be discussed in the last section; it supports the idea of rather bigger parameters for this crystal.

Different crystalline modifications of Würster's blue iodide have been reported by Hughes and Hush.[13] In this experiment it has also been found that the other crystalline form is sometimes found in crystals obtained from a methanol solution. However, these crystals are rather unstable and rare; therefore, this form is not reported on in this paper.

iii) Würster's Blue Bromide. The crystal of Würster's blue bromide was obtained as brown-black needles, and a small, thin crystal was dark blue in light polarized parallel to the elongation axis and pale reddish in light polarized in the perpendicular direction. The crystal structure is now under investigation in this laboratory, while the space group and the cell constants have been determined to be as follows:

Crystal Data: Orthorhombic, Cmcm, $a=9.54$, $b=19.27$, $c=7.03$ Å, $z=4$.

The preliminary crystal structure results show that the elongation axis is the c axis, the benzene ring is perpendicular to the c axis, and the y-axis of the radical is parallel to the b axis. The projection of molecules onto the ab plane is shown in Fig. 9, and the projection onto the bc plane, in Fig. 10. The crystalline absorption spectra have been measured on the ac and bc planes by a polarized light; the results are shown in Figs. 11 and 12. In the range of 8000—15000 cm^{-1}, where a charge-transfer transition is expected, a broad peak is observed along both the b and c axes, but not along the a axis, where a weak absorption tail is observed. The transition moment of the charge-transfer transition is on the line connecting the stacked radicals; therefore, it has components along the c and b axes, but not along the a axis. The observed intensity ratio for the CT and R bands is about 0.55 : 1, while the calculated values are 0.35 : 1—0.5 : 1. The values of the intensity ratio for the perpendicular (c axis) and parallel (b axis) directions are 1.35 : 1 for the CT band and the calculated values are 1.2 : 1—1.7 : 1, in fairly good agreement with the observed values.

The next strong band is observed particularly along the b axis in the 15000—23000 cm^{-1} region;

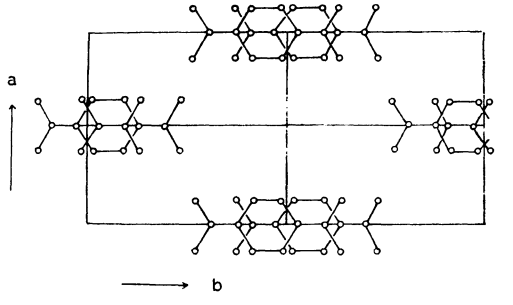

Fig. 9. Projection of Würster's blue bromide crystal onto the ab plane by the preliminary X-ray results.

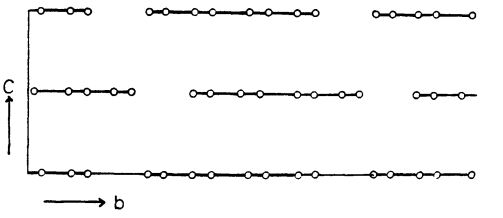

Fig. 10. Projection of Würster's blue bromide crystal onto the bc plane by the preliminary X-ray results.

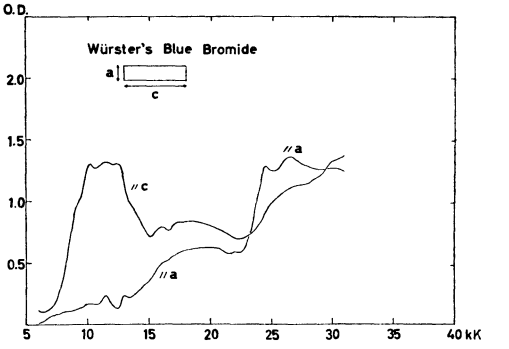

Fig. 11. The crystalline absorption spectra of Würster's blue bromide on the ac plane.

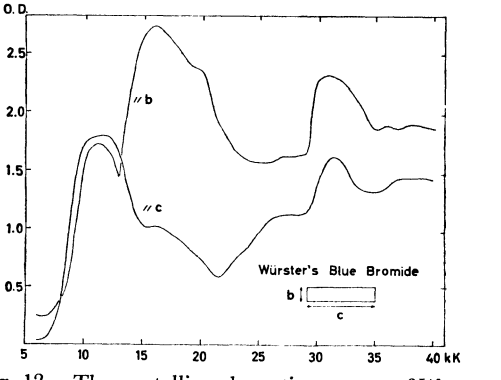

Fig. 12. The crystalline absorption spectra of Würster's blue bromide on the bc plane.

13) G. K. Hughes and N. S. Hush, *J. Proc. Roy. Soc. N.S.W.*, **81**, 48 (1947).

it may be regarded as an R-band mixed to some extent with the CT band. The R-band originally has its own polarization parallel to the long axis of the radical; however, the mixing with the charge-transfer configuration will result in some component along the out-of-plane of the benzene ring. The observed weak peak at 18000 cm^{-1} in the *c* axis direction may be explained on this basis. The intensity ratio observed is 0.02 : 1 for the *c* axis-to-*b* axis polarization, while the value calculated by the model IV is 0.005.

In the 26000 cm^{-1} region the next peak is found for the *a* axis spectrum; it may safely be assigned to the short-axis polarized X band.

As has been discussed above, if we increase the intermolecular interaction, the intensity of the charge-transfer band will be increased and the splitting between the CT and R bands will be enlarged. Judging by this criterion, the strength of the interaction in the Würster's blue bromide crystal is an intermediate case compared to the blue perchlorate and red bromide.

Another crystalline form of Würster's blue bromide has been obtained by rare chance. It was transparent when observed along the elongation axis and dark black in the perpendicular direction. The spectra have been recorded, but the crystalline data have not yet been obtained; therefore, we will not here discuss the spectral results in detail.

iv) Würster's Red Bromide. The crystals of Würster's red bromide (*N,N*-dimethyl-*p*-phenylenediamine bromide) have been prepared as dark green needles. The thin crystals are dark green in light polarized parallel to the elongation axis, and pale green in light polarized in the perpendicular direction. The crystalline structure has been analyzed in this laboratory[7]; it has been found that the radicals are stacked at equal distances from each other, with unusually short interplanar spacing in the one-dimensional column. The intermolecular interaction is extraordinary large in this crystal, and the spectra are quite different from that of other types of Würster's salt.

The thin crystal develops the *ac* plane; its absorption spectra have been measured by a polarized light. The spectra are presented in Fig. 13, while the projection of radicals on the *ac* plane is shown in Fig. 14. The projection on the *ab* plane is also

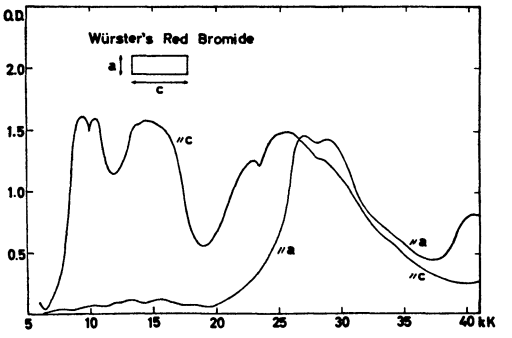

Fig. 13. The crystalline absortion spectra of Würster's red bromide on the *ac* plane.

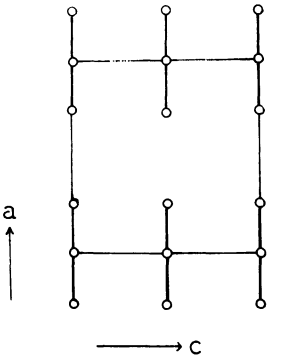

Fig. 14. Projection of Würster's red bromide crystal onto the *ac* plane.

depicted in Fig. 15. The broad strong bands are observed along the *c* axis in the 7000—18000 cm^{-1} region, which consists of two prominent peaks. The polarization of this band is definitely in the direction of the out-of-plane of the benzene ring; therefore, this band must be charge-transfer in origin. The next broad band observed along the *c* axis starts at 18000 cm^{-1} and extends to the 40000 cm^{-1} region. The polarization characteristic of this band may be understood if we assume that extensive mixing occurs between the charge transfer and the R-excited configurations. Since the long axis of the radical is parallel to the crystalline *b* axis, the R′ band can not be observed along the *c* axis unless the configurational interaction with the charge transfer state takes place. The calcula-

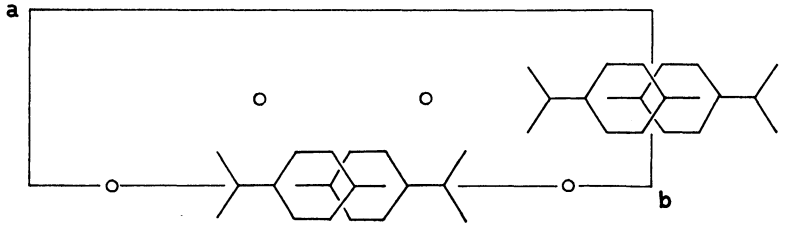

Fig. 15. Projection of Würster's red bromide crystal onto the *ab* plane.

tions of the previous section showed that the R′ band has a fairly strong component in out-of-plane direction as a result of the large mixing of the CT and R states. The intensity ratio for the out-of-plane direction of the CT and R′ bands is calculated to be 1.5 : 1, while the observed value is 0.9 : 1.

Although the first charge-transfer band might be accompanied by several vibrational progressions, it is quite noteworthy that it shows two peaks, one in the 9500 cm^{-1} region and another in the 13500 cm^{-1} region. The splitting of this band is an indication of the strong radical-radical interaction in the one-dimensional column in the crystal. A possible explanation of this band splitting will be given in the last section.

The short-axis polarized band is observed along the *a* axis, and it appears in the 25000—33000 cm^{-1} region. It is assigned to the X band; this is in conformity with the previous findings on other Würster's salts.

v) *p*-Phenylenediamine Bromide. The crystals of *p*-phenylenediamine bromide have been obtained as dark brown microcrystals. The crystalline data could not be obtained with this crystal, however, since it is not large enough for X-ray examination. The crystalline absorption spectra have been measured by a polarized light for the elongation axis and in the perpendicular direction (Fig. 16).

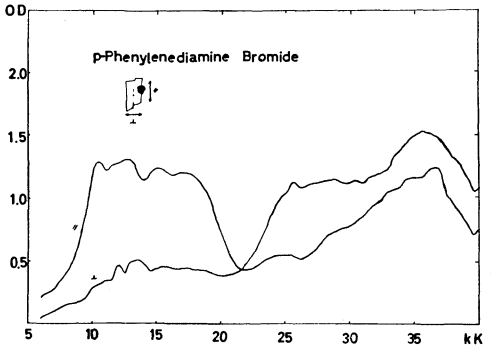

Fig. 16. The crystalline absorption spectra of *p*-phenylenediamine bromide.

The crystalline absorption bands are similar to that of Würster's red bromide, but it is remarkable that the absorption bands are broader than those of any other Würster's crystals. This means that the intermolecular interaction is the largest in this series of radical salts. This finding is supported by the experimental results[2,3] on the solution and by the calculation, and it is consistent with the steric considerations. The crystal structure is not yet known; therefore, our results will not be discussed further.

Interaction between Radicals and Crystalline Spectra. The effects of the intermolecular interaction are most significant in radical salt crystals than in any other type of molecular crystals since the unpaired electron on each radical will make a bonding between the radicals. The covalent force bind the radicals close to each other, while the exchange repulsion of the closed-shell electrons, including the so-called steric repulsions, increase the radical-radical distances. The positive charge carried on each ion is also repulsive in the present system. The analysis of these intermolecular forces might be difficult, however, the actual crystal structure represents a counterbalance of these several composite forces.

However, the tendency toward binding is shown by the formation of the radical dimer in a solution. It has been observed in Würster's radical, the ethylphenazyl radical,[1-3] the tetracyanoquinodimethane anion,[14] and pyridinium radicals[15] to form dimers in solutions, particularly at low temperatures. Characteristic of the aromatic radical dimer system is the appearance of a new absorption band in the longer-wavelength region. This band appears regardless of the charges on the radical; therefore, interaction between the unpaired electrons must be essential for the appearance of the new band. The interaction with the singly-occupied orbital is greatly dependent on the relative interatomic distances and orientations. Therefore, the present system of Würster's radicals will provide typical cases to be investigated, cases where the interplanar spacings are somewhat different from crystal to crystal: spectral and crystallographic data have accordingly been assembled.

The origin of the new band has been explained above in terms of the charge-transfer mechanism. Although we believe that the Heitler-London approach is most valid for discussions of the inter-radical electronic interactions, for the stronger dimers at shorter intermolecular distances the molecular orbital method is also illuminating. The appearance of the longer-wavelength absorption band can be explained simply in terms of a transition from the bonding to the antibonding orbital (*cf.* Fig. 17).[3] The inclusion of the ionic structures and

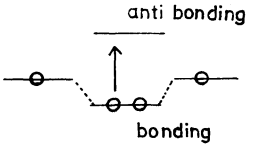

Fig. 17. Molecular orbital description of the radical-radical interaction.

the appearance of the new band which is polarized in the out-of-plane direction are naturally predicted by this method. However, the defect of this

14) R. H. Boyd and W. D. Phillips, *J. Chem. Phys.*, **43**, 2927 (1965).

15) M. Itoh and S. Nagakura, *J. Am. Chem. Soc.*, **89**, 3959 (1967).

TABLE 4. OVERLAP INTEGRALS BETWEEN RADICALS

	Würster's red bromide	Würster's blue bromide	Würster's blue perchlorate	Würster's blue iodide
S_{mm}	0.205×10^{-1}	0.344×10^{-2}	0.121×10^{-2}	0.247×10^{-2}
S_{ee}	-0.166×10^{-2}	-0.69×10^{-4}	0.297×10^{-2}	-0.266×10^{-2}
S_{me}	0.404×10^{-2}	-0.325×10^{-2}	0.195×10^{-2}	0.268×10^{-2}
Positions of radicals	(0, 0, 0) and (0, 0, ½)	(0, 0, 0) and (0, 0, ½)	(0, 0, 0) and (1, 0, 0)	(0, 0, 0) and (1, 0, 0)

TABLE 5. THE INTERACTION MATRIX ELEMENTS AND THE OVERLAP INTEGRALS

	Würster's blue perchlorate	Blue iodide	Blue bromide	Red bromide
β (eV)	0.08 (IX)	0.11 (VII)	0.22 (IV)	0.9 (II), 0.6 (III)
S_{mm}	0.0012	0.0025	0.0034	0.021

approach is its incapability of explaining the appearance of a weak charge-transfer band in nearly the same energy region. Therefore, the molecular orbital method is limited only for cases of the stronger interaction.

According to both theories the strength of the electronic interaction can be roughly estimated by means of the magnitude of the overlap integrals. The overlap integrals of the radical pair evaluated for several crystals are shown in Table 4. The atomic orbitals used are those of the Hartree-Fock AO of Clementi[16] and the calculations were carried out at the Computation Center of the University of Tokyo. The results of the calculation have also been compared with the parametrs of the interaction estimated in the previous sections. They are listed in Table 5 where it is found that a rough correlation exists between these values.

The intensities of the CT band and the R band are mostly determined by the extent of the mixing of the CT configuration with other configurations. Each state can be described as a mixture of three configurations, Ψ_G, Ψ_{CT}, and Ψ_M, as Table 2 shows. The transition moments consist of terms proportional to $\langle\Psi_{CT}|\boldsymbol{r}|\Psi_{CT}\rangle$ and $\langle\Psi_G|\boldsymbol{r}|\Psi_M\rangle$; therefore, the directions of the transition moments are determined by the extent of the mixing of these configurations. In Würster's blue perchlorate, where the overlap integral is the smallest, the intensity of the charge-transfer band is the weakest. Würster's blue bromide shows an intermediate case in both absorption intensity and calculated overlap integral. In Würster's red bromide the charge-transfer band is extraordinarily large and the overlap integral is the largest.

The appearance of the broad and doublet structure of the CT band of the red bromide and *p*-phenylenediamine bromide crystals is puzzling; it must be intimately connected with the large electron overlap between the radicals. These absorption band are, of course, associated with the vibrational structures; however, we believe that the large breadth might be due to an electronic effect. Now let us discuss this effect by considering only the unpaired electrons on each radicals, as is shown in Fig. 18. There are two sites in the one-dimensional radical column in a unit cell; we will denote the unpaired orbitals in the ith cell by φ_i and θ_i. The wave function for the ground configuration (no charge-transfer structure) is:

$$\Phi_0 = \frac{1}{\sqrt{2N!}}\mathcal{A}\prod_{i=0}\varphi_i(i)\theta_i(2i)$$

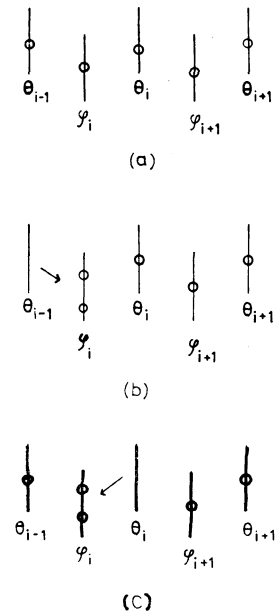

Fig. 18. Unpaired electrons on radicals in the one-dimesional crystal.

(a) ground configuration (b) left to right charge transfer state (b) right to left charge transfer state.

16) E. Clementi, *IBM Journal*, **9**, 2 (1965).

where N is the number of unit cells considered and where $\mathfrak{a}$ is the antisymmetrizer. There are two kinds of charge-transfer states; one is from the left site to the right site, and the other is from right to left. The crystalline charge-transfer states which satisfy the requirements of translational symmetry are given by:

$$\Psi_{CT}(\rightarrow, \pm) = \frac{1}{\sqrt{2}} \sum_i \left(\frac{\Phi_0}{\theta_{i-1}} \varphi_i \pm \frac{\Phi_0}{\varphi_i} \theta_i \right)$$

$$\Psi_{CT}(\leftarrow, \pm) = \frac{1}{\sqrt{2}} \sum_i \left(\frac{\Phi_0}{\theta_i} \varphi_i \pm \frac{\Phi_0}{\varphi_i} \theta_{i-1} \right)$$

There are also symmetric and antisymmetric combinations; therefore, four different kinds of excited states altogether must be considered. The plus combinations are optically active along the *c* axis in Fig. 18, while minus combinations are active along the *b* axis. The right- and left-directed charge-transfer states which have degeneracy will combine again; only the two states shown below are optically active, being active along the *b* and *c* axes respectively.

$$\Phi_{CT}(a, \perp) = \frac{1}{\sqrt{2}} [\Psi_{CT}(\rightarrow, -) + \Psi_{CT}(\rightarrow, -)]$$

$$\Phi_{CT}(a, //) = \frac{1}{\sqrt{2}} [\Psi_{CT}(\rightarrow, +) - \Psi_{CT}(\leftarrow, +)]$$

The inactive excited states are obtained by the following combinations;

$$\Phi_{CT}(i, \perp) = \frac{1}{\sqrt{2}} [\Psi_{CT}(\rightarrow, -) - \Psi_{CT}(\leftarrow, -)]$$

$$\Phi_{CT}(i, //) = \frac{1}{\sqrt{2}} [\Psi_{CT}(\rightarrow, +) + \Psi_{CT}(\leftarrow, +)]$$

Now let us concern ourselves with the *c* axis polarized spectrum. Here, there are two relevant states, $\Phi_{CT}(a,//)$ and $\Phi_{CT}(i, //)$. The splitting of these two states is given by the off-diagonal element, $\langle \Psi_{CT}(\rightarrow,+)|H|\Psi_{CT}(\leftarrow,+) \rangle$. This element has not terms proportional to the first order in the nearest neighbor electron overlap. However, the electron-electron interaction of a dipolar type appears and the splitting is given by:

$$\langle \varphi_i(1)\theta_{i-1}(1)|1/r_{12}|\varphi_i(2)\theta_i(2) \rangle.$$

The numerical estimation of this value gives a stabilization of the active state amounting to 0.75 eV (6000 cm^{-1}) relative to the inactive state. The splitting of the band observed in the crystalline spectra is of just the same order of magnitude; therefore, it is conceivable that the inactive state appears by means of the intensity borrowing through the vibrational or other kinds of perturbations.

The alternative approach to the understanding of the spectral characteristics is by the band theory, which is an extension of the molecular orbital method. We believe, however, that it will be inadequate for the present system of crystals, and so it will not be discussed further.

The authors acknowledge to the Ministry of Education for the research grant.

BULLETIN OF THE CHEMICAL SOCIETY OF JAPAN VOL. 42 1853—1857 (1969)

Kinetics of the Transition of Titanium Dioxide Prepared by Sulfate Process and Chloride Process

Akira SUZUKI* and Ritushi TUKUDA**

* *Government Chemical Industrial Research Institute, Tokyo, Shibuya-ku, Tokyo*
** *Shonan Sekisui Stock Company, Mutsuzaki Kumanodo, Sakura-shi, Chiba*

(Received December 3, 1968)

The kinetics of the phase transformation of anatase to rutile was studied by means of X-ray diffraction. Samples of anatase were prepared by sulfate and chloride processes. The kinetic data could well be expressed by the equation

$$\alpha = 1 - e^{-bt^n},$$

where α is the fraction of anatase transformed in time t, and b and n constants. The activation energy of the phase transformation is 105 kcal/mol for the sample prepared by the sulfate process, and 107 kcal/mol for the sample prepared by the chloride process. These values of activation energy are compared with those previously obtained.

The kinetics of the transition of polymorphic compounds such as silicon dioxide,[1] titanium dioxide,[2-7] germanium dioxide,[8] zirconium dioxide,[9] ferric oxide[10] or calcium carbonate[11] has been previously investigated. The rate of the transition of these compounds is complicated by the variable processes of the preparation of samples, the size of sample particles, the surrounding atmosphere and the presence of impurity, *etc.*

Titanium dioxide is prepared by the sulfate process or by the chloride process on an industrial scale. In the present study the rate of the transition of anatase to rutile has been measured using samples prepared by both processes. It might be interesting to compare the kinetic data of the two samples and to compare them with the data obtained by previous investigators.

Experimental

Samples. The samples of anatase were prepared by the two following processes.

(1) Sulfate Process. Sulfuric acid solution of titanium was prepared from purified titanium tetrachloride and extra pure grade sulfuric acid by the method previously reported.[5] Concentrations of total sulfuric acid and titanium were 670 g/*l* and 100 g/*l* respectively. The sulfuric acid solution of titanium was poured into a beaker, which was set in an autoclave. The solution was hydrolyzed at 160—170°C for 2hr in the closed autoclave. The precipitated gel was washed several times with sulfurous acid and deioned water, and the product thus obtained was heated at 100°C for 12hr and then at 700°C for 2hr.

(2) Chloride Process. Pure titanium dioxide (anatase) can be prepared by the following reaction between pure titanium tetrachloride and oxygen at 650°C.

$$TiCl_4 + O_2 = TiO_2 + 2Cl_2$$

The method of preparing the sample was as follows. Pure titanium tetrachloride was brought into the silica tube, nitrogen being used as a carrier gas. Nitrogen was passed through the liquid of pur titanium tetrachloride in a reservoir and brought into the silica tube. Oxygen preheated at 500°C was added to titanium tetrachloride-nitrogen mixture at the entrance of the silica tube. The temperature of the reservoir was controlled to 100—120°C, and that of the silica tube at 650±2°C. Titanium dioxide (anatase) formed was collected.

Properties of Sameples. Physical properties of anatase prepared by the two processes were examined by means of electron microscopy, the B.E.T. and picnometric method. The results are shown in Table 1 with those of rutile described below. A small number of crystals (~0.5 μ) with tetragonal habit were observed among the particles prepared by the chloride process. X-ray diffraction lines of rutile were not observed in the

1) R. W. Grimshaw, J. Hargreaues and A. L. Roberts, *Trans. Brit. Ceram. Soc.*, **55**, 36 (1956).
2) W. F. Sullivan and S. S. Cole, *J. Am. Ceram. Soc.*, **42**, 127 (1959).
3) A. W. Czanderna, C. N. R. Rao and J. M. Honig, *Trans. Faraday Soc.*, **54**, 1069 (1958).
4) C. N. R. Rao, *Can. J. Chem.*, **39**, 498 (1961).
5) A. Suzuki and Y. Kotera, This Bulletin, **35**, 1353 (1962).
6) S. R. Yaganarasimhan and C. N. R. Rao, *Trans. Faraday Soc.*, **58**, 1579 (1962).
7) R. D. Shannon and J. A. Pask, *J. Am. Ceram. Soc.*, **48**, 391 (1965).
8) Y. Kotera and M. Yonemura, *Trans. Faraday Soc.*, **59**, 147 (1963).
9) E. D. Whitney, *ibid.*, **61**, 1911 (1965).
10) F. E. DeBoer and P. W. Selwood, *J. Am. Chem. Soc.*, **76**, 3365 (1954).
11) G. Chaudron, Proceeding International Symposium on the Reactivity of Solids, Gotteburg, 9 (1952).

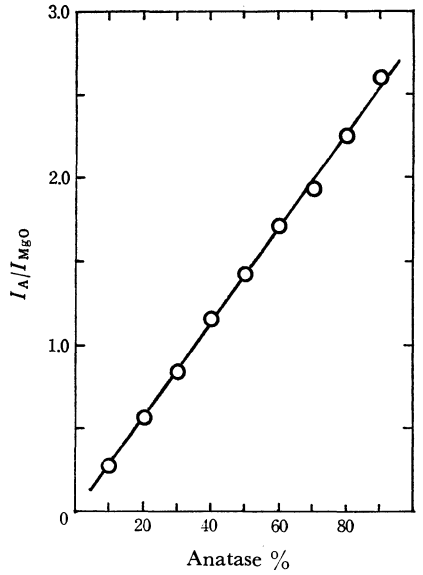

Fig. 1. Calibration curve for the determination of anatase content.
Internal standard: Magnesium oxide. I_A and I_{MgO} are integrated intensity of diffraction line of anatase (d=3.521 Å) and magnesium oxide (d=2.106 Å) respectively.

diffraction patterns of the samples. The relative intensities of all peaks of anatase agree well with those of an A.S.T.M. card.

Procedures of the Determination of the Kinetic Data. For the kinetic runs, samples were set in the sintered alumina boats and heated in a tube electric furnace. The heating procedure was the same as that already described.[5]

The composition of anatase-rutile mixtures was analyzed by the X-ray diffraction method using the Geiger Counter X-ray Diffractometer. Magnesium oxide was used as an internal standard. The weight ratio of magnesium oxide and the anatase-rutile mixture was 1 : 4. The d values of the peak used to compare the intensity were 3.521 Å and 2.106 Å, for anatase and magnesium oxide respectively. Figure 1 shows the calibration curve determined as follows: The I_A/I_{MgO} ratio was measured for a series of ten samples of anatase-rutile magnesium oxide mixture with a definite mixing ratio and the average value of this ratio was plotted against the anatase % in the anatase-rutile mixture. A series of five determinations of the I_A/I_{MgO} ratio for each sample-magnesium oxide mixture was made in the case of the determination of anatase content in the samples after partial transformation.

Results and Discussion

The two samples prepared by the sulfate process and by the chloride process were transformed to rutile after heating at 1050°C for 3 hr, and anatase was not detected in these samples. The properties of these two kinds of rutile are shown in Table 1, and their particle sizes, specific surface areas and

Table 1. Physical properties of anatase and rutile types of titanium dioxide

Process of the preparation of sample	Sulfate process		Chloride process	
	Anatase	Rutile	Anatase	Rutile
Particle form	round	round	angular, round, tetragonal habit	round
Particle size (μ)	0.2—0.3	0.5—0.7	0.05—0.3	0.5—0.7
Specific surface area (m^2/g)	16	1.6	34	1.6
Specific gravity	3.77*	4.14	3.63*	4.10

Each rutile type sample was prepared from respective anatase type sample by heating at 1050°C for 3 hr.
* The difference in the specific gravities of the two kinds of anatase is difficult to explain, and seems to be attributed to the difference in the crystal growth during preparation.

specific gravities were almost the same. A small number of crystals with tetragonal habit were detected when the sample prepared by the chloride process was heated at 830°C for the longer time. It may indicate that transformation in these crystals begins later than that in other crystals.

The diffraction lines of anatase decreased and those of rutile increased monotonously in their intensities during the transformation and the relative intensities of all peaks of anatase or rutile agreed well with those of A.S.T.M. card.

The experimental results of the transformation rate studied over the temperature range between 800 and 880°C are shown in Figs. 2 and 3. From Figs. 2 and 3, it can be seen that in the early stage of the reaction carried out at the same temperature the transformed amount of the samples prepared by the sulfate process is lower than that of the samples prepared by the chloride process. These

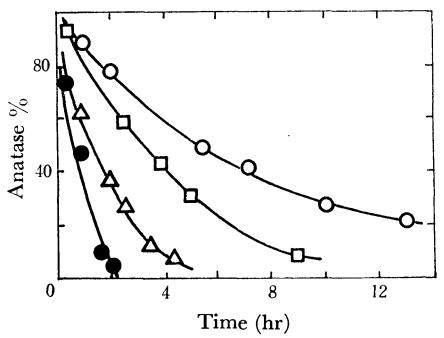

Fig. 2. Plots of anatase % as a function of time at different temperatures (Sulfate process).
-○- 820°C -□- 840°C
-△- 860°C -●- 880°C

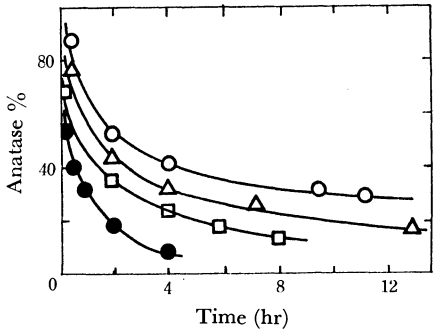

Fig. 3. Plots of anatase % as a function of time at different temperatures (Chloride process).
-○- 800°C -△- 820°C
-□- 840°C -●- 860°C

results would be explained by the fact that particles with small size are contained in the sample prepared by the chloride process. Experimental results in which the transformation rate of the sample with small particle size is larger than that of the sample with large particle size were published previously.[1,5]

It is well known that the following kinetic equation describes the process of the reaction proceeding through nucleation and crystal growth.[12,13]

$$\alpha = 1 - e^{-bt^n}, \tag{1}$$

where α is the fraction of material transformed in time t, and b and n constants. Differentiating Eq. (1), we get

$$\frac{d\alpha}{dt} = nbt^{(n-1)}(1-\alpha). \tag{2}$$

This is a first-order equation for $n=1$.
From Eq. (1), we get

$$\ln(1-\alpha) = -bt^n, \tag{3}$$

or

$$t = \left\{\frac{-\ln(1-\alpha)}{b}\right\}^{1/n}. \tag{4}$$

From Eqs. (2) and (4), we have

$$\frac{d\alpha}{dt} = nb^{1/n}\{-\ln(1-\alpha)\}^{(n-1)/n}(1-\alpha)$$
$$= k\{-\ln(1-\alpha)\}^{(n-1)/n}(1-\alpha), \tag{5}$$

where $k=nb^{1/n}$.
k is a constant, and may be defined as the rate constant of kinetic equation (5).
From Eq. (3) we have

$$\ln\{-\ln(1-\alpha)\} = \ln b + n\ln t. \tag{6}$$

12) M. Avrami, *J. Chem. Phys.*, **7**, 1103 (1939); *ibid.*, **8**, 212 (1940).
13) B. V. Erofeev, *Doklady Akad. Nauk S. S. S. R.*, **52**, 515 (1946).

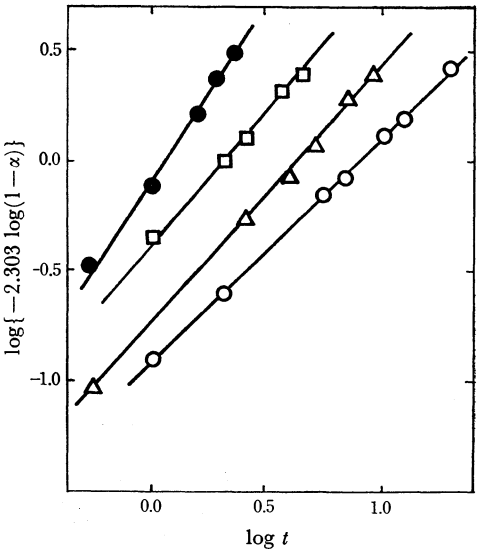

Fig. 4. Plots of $\log\{-2.303\log(1-\alpha)\}$ as a function of $\log t$ at different temperatures (Sulfate process).
-○- 820°C -△- 840°C
-□- 860°C -●- 880°C

Thus, b and n can be obtained from the curves of the figure in which data are plotted with the coordinates $\ln\{-\ln(1-\alpha)\}$ and $\ln t$. As shown in Figs. 4 and 5, experimental data fit the relationship of Eq. (6) reasonably well except for the data of the early stage in the reaction for the sample prepared by the chloride process.

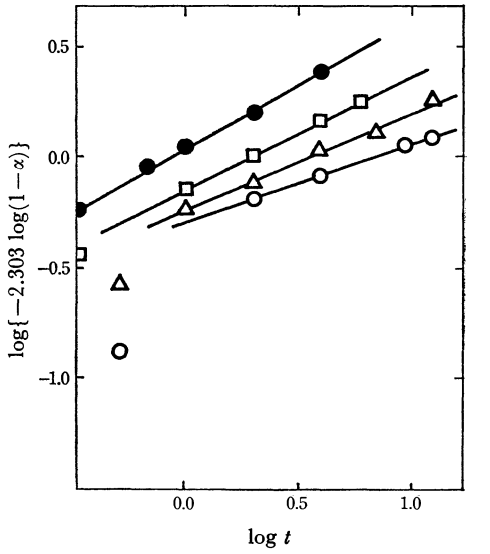

Fig. 5. Plots of $\log\{-2.303\log(1-\alpha)\}$ as a function of $\log t$ at different temperatures (Chloride process).
-○- 800°C -△- 820°C
-□- 840°C -●- 860°C

Table 2. Values of n, b and k at different temperatures

Preparation process of anatase	Constant	Temperature (°C) 800	820	840	860	880
Sulfate process	n	—	0.961	1.16	1.21	1.61
	b	—	0.135	0.189	0.440	0.811
	k (t^{-1})	—	1.20×10^{-1}	2.75×10^{-1}	6.14×10^{-1}	1.41
Chloride process	n	0.344	0.432	0.492	0.621	—
	b	0.522	0.580	0.733	1.10	—
	k (t^{-1})	5.21×10^{-2}	1.20×10^{-1}	2.62×10^{-1}	7.40×10^{-1}	—

Values of n, b and k calculated from the curves of Figs. 4 and 5 are shown in Table 2. Table 2 indicates that there is not a large difference between k of the sample prepared by the sulfate process and that of the sample prepared by the chloride process at the same temperature. Attention should be paid to the fact that the data in the early stage of the transition for the sample prepared by the chloride process do not fit the relationship of Eq. (6). This fact may be related to a wide distribution of particle size in the sample prepared by the chloride process as shown in Table 1.

In the model presented by Avrami,[12] b depends on temperature, shape and growth rate of the new phase and nucleation frequency, and n has a value from 1 to 4 according to the variety of habit of the new phase.

In the present study the values of n varied in the vicinity of unity over the temperature range between 820 and 860°C among the samples prepared by the sulfate process as shown in Table 2. It is interesting to consider that the kinetic data followed the first-order law fairly well, when the sample prepared by the hydrolysis of sulfuric acid solution of titanium at 90—100°C was used.[5]

The values of n were all below unity for the samples prepared by the chloride process as shown in Table 2. Deviation from the values of n in the Avrami expression was observed.[9,14,15] Such a deviation might be related to the following facts.

1) The small number of nuclei occur and/or the samples with small particle size are used.[14]

2) The edgewise impingement of new phase occurs.[15]

Such situations may exist in the transition of anatase to rutile for the samples prepared by the chloride process.

Arrhenius plots of log k against $1/T$ are shown in Fig. 6. The activation energies estimated from Fig. 6 are 107 and 105 kcal/mol for the samples prepared by the sulfate process and by the chloride process respectively. Thus, both values of activation energies in this work are almost the same.

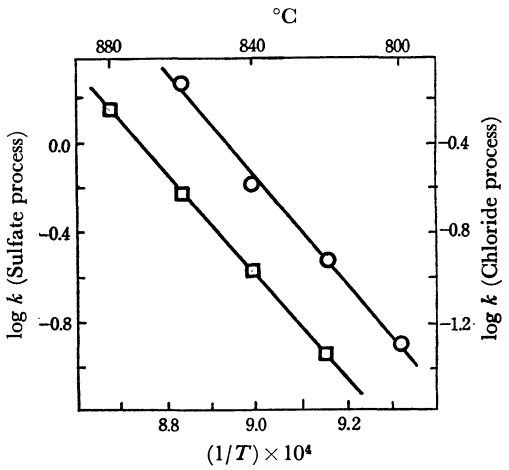

Fig. 6. Arrhenius plots of log k against $1/T$.
-□- Sulfate process
-○- Chloride process

Several values of the activation energy for the anatase-rutile transformation were reported, and are listed in Table 3 with those in the present study. Sullivan and Cole[2] investigated the relation between the kinetics of the anatase-rutile transformation and the preparing conditions of anatase for the first time. They used four hydrated titanium dioxide samples obtained by the hydrolysis of industrial titanium sulfate. Though the details of preparing conditions, *e. g.* drying temperature, were not described, the values of activation energy obtained in their investigation are almost the same as those obtained in the present study. Yaganarasimhan and Rao pointed out that the activation energy of the transition of anatase prepared by sulphate hydrolysis (No. 5 in Table 3) is considerably higher than that of pure anatase (No. 2, 3, 6 in Table 3). It seems certain that the activation energy of the transition of anatase prepared by the sulfate process differs from that of pure anatase. However, attention should be paid to the effect of the drying temperature of the sample (anatase) on the activation energy of the transition. It is shown

14) W. G. Burgers and L. I. Groen, *Discussions Faraday Soc.*, **23**, 183 (1957).

15) D. Turnbull, "Solid State Physics," Vol. 3, Academic Press, Inc., New York (1956), p. 225.

TABLE 3. ACTIVATION ENERGIES FOR ANATASE-RUTILE TRANSITION

No.	Investigator	Process of the preparation of anatase	E kcal/mol
1	W. F. Sullivan S. S. Cole	Hydrolysis from sulfuric acid solution of titanium by heating	100, 103 105, 111
2	A. W. Czanderna C. N. R. Rao J. M. Honig	Oxidation of titanium metal in ammoniacal solution of 90% H_2O_2 Drying at 160°C	110± 10 90± 10
3	C. N. R. Rao	Same as No. 2	80± 10
4	A. Suzuki Y. Kotera	Hydrolysis from sulfuric acid solution of titanium by heating at 90—100°C Drying at 700°C	110 116
5	S. R. Yaganarasimhan C. N. R. Rao	Hydrolysis from sulfuric acid solution of titanium with ag. ammonia Drying at 100°C	120± 10
6	S. R. Yaganarasimhan C. N. R. Rao	Same as No. 2 Drying at 400°C	102—114
7	R. Shannon J. A. Pask	Three commercial anatase samples	94—204
8	A. Suzuki R. Tukuda	Oxidation of titanium tetrachloride at 650°C	107
9	A. Suzuki R. Tukuda	Hydrolysis from sulfuric acid solution of titanium by heating at 160—170°C Drying at 700°C	105

by Suzuki and Kotera[5] that it is difficult to dehydrate completely the titania gel prepared by the hydrolysis of an aqueous solution of titanium salt and the crystal growth of anatase is incomplete, if titania gel is dried at a relatively low temperature. The precipitated titania gel prepared by hydrolysis of the sulfuric acid solution of titanium contains sulfate ion probably as sulfuric acid adsorbed on the surface of the gel. To remove the adsorbed sulfuric acid completely, it is necessary to heat the gel at considerably high temperature. The assumption that the adsorbed sulfuric acid could be removed with difficulty only by means of washing is partly supported by our preliminary experiments where pH of the suspensions prepared by mixing an equal amount of deioned water with two kinds of anatase dehydrated at 100°C and 700°C were 2.5 and 5.5 respectively. Meanwhile, it is interesting to note that the activation energies of the transition of anatase to rutile are not so different if the drying temperature of anatase is considerably high (No. 4, 6, 8, 9 in Table 3). These results suggest that the rate-determining reaction in transformation of anatase to rutile would be independent of the sample preparation. Shannon and Pask[7] also investigated the transition of the three commercial anatase powders to rutile and obtained various activation energies from 94 to 204 kcal/mol (Table 3). These results suggest that commercial anatase contains various impurities, thus causing variation in activation energies.

The authors wish to thank Dr. Y. Kotera of this Institute for his valuable discussions.

BULLETIN OF THE CHEMICAL SOCIETY OF JAPAN VOL. 42 1858—1861 (1969)

Electronic Absorption Spectra of Unstable Species Formed by the Ultraviolet Irradiation of *N,N*-Dimethylaniline at 77°K

Satoshi ARIMITSU, Katsumi KIMURA*1 and Hiroshi TSUBOMURA

Department of Chemistry, Faculty of Engineering Science, Osaka University, Toyonaka, Osaka

(Received December 3, 1968)

Electronic absorption spectra of unstable species formed by the ultraviolet irradiation of *N,N*-dimethylaniline (DMA) were studied in various rigid matrices at 77°K. It was concluded that there are two unstable species which exhibit similar absorption spectra in the visible and the near ultraviolet regions. These species were identified with the cation radical $\left(\left[\bigcirc\!\!\rangle\text{-}N(CH_3)_2\right]\right)^+$ and the neutral radical $\left(\bigcirc\!\!\rangle\text{-}\dot{N}(CH_3)\right)$, based on various experimental results concerning solvent effect, electron attachment, stimulated emission by the infrared light, *etc.* The molar extinction coefficient of the cation at 470 mμ was found to be about 1200 (l/cm·mol).

Studies on the primary photochemical processes of aromatic compounds have been made by use of electronic absorption spectroscopy and ESR technique.[1-9] It has been concluded that there are mainly two different types of processes.[10] One is photoionization and the other is photodissociation. Photoionization occurs predominantly for compounds having relatively low ionization potentials such as *p*-phenylenediamine and its methyl-derivatives.[11,12] On the other hand, photodissociation occurs prevalently for compounds having relatively high ionization potentials such as toluene and *p*-hydroquinone derivatives.[6,13]

Ultraviolet irradiation of *N,N*-dimethylaniline (DMA) in EPA (a mixture of ether, isopentane and ethanol) rigid matrix was investigated previously by Lewis *et al.*[3] and by Porter and co-workers.[4-6] They reported two absorption maxima at 3166 and 4590 Å, which they assigned to the *N*-methylanilino radical and the DMA^+ cation, respectively. Porter and his collaborators made flash-photolytic experiments on DMA in liquid paraffin solution at room temperature, and obtained absorption bands at 3140 and 4000 Å which were assigned tentatively to the *N*-methylanilino radical.[8]

Recently we have studied the triplet-triplet absorption spectrum of DMA using the flash technique at room temperature.[14] The studies reported here were made to identify the carriers of the absorption bands arising from the ultraviolet irradiation of DMA in the low temperature matrix.

Experimental

Materials. Commercial G. R. grade DMA and *N*-methylaniline (NMA) were purified by distillation from zinc powder under reduced pressure, and kept in a deoxygenated condition. Solvents used as transparent organic matrices were ethanol, MP (1 part methylcyclohexane, 1 part isopentane) and liquid paraffin. Ethanol was purified by fractional distillation. Ether and isopentane were dried with sodium for a day and purified by distillation. Methylcyclohexane and liquid paraffin were purified by passing through a 100 cm column of activated silica gel. About 10^{-3} molar solutions were used in most experiments. All samples examined were deaerated by the freeze-pump-thaw technique.

Apparatus. Absorption spectra were measured with

*1 Present address: Chemistry Laboratory, Institute of Applied Electricity, Hokkaido University, Sapporo.

1) G. N. Lewis and D. Lipkin, *J. Am. Chem. Soc.*, **64**, 2801 (1942).
2) G. N. Lewis and J. Bigeleisen, *ibid.*, **65**, 520 (1943).
3) G. N. Lewis and J. Bigeleisen, *ibid.*, **65**, 2419, 2424 (1943).
4) I. Norman and G. Porter, *Proc. Roy. Soc.*, **A230**, 339 (1955).
5) G. Porter and F. J. Wright, *Trans. Faraday Soc.*, **51**, 1469 (1955).
6) G. Porter and E. Strachan, *ibid.*, **54**, 2027 (1958).
7) E. J. Land, G. Porter and E. Strachan, *ibid.*, **57**, 1885 (1961).
8) E. J. Land and G. Porter, *ibid.*, **59**, 2027 (1963).
9) N. M. Atherton, E. J. Land and G. Porter, *ibid.*, **59**, 818 (1963).
10) H. Tsubomura, *Nippon Kagaku Zasshi (J. Chem. Soc. Japan, Pure Chem. Sect.)*, **89**, 1 (1968).
11) H. Tsubomura, K. Kimura, H. Yamada and M. Kato, *Tetrahedron Letters*, **47**, 4217 (1965).
12) N. Yamamoto, Y. Nakato and H. Tsubomura, This Bulletin, **40**, 451 (1967).
13) K. Kimura, K. Yoshinaga and H. Tsubomura, *J. Phys. Chem.*, **71**, 4485 (1967).
14) K. Kimura, S. Arimitsu, N. Yamamoto and H. Tsubomura, This Bulletin, **41**, 1274 (1968).

a Cary Spectrophotometer, Model 15. The solution in a cylindrical quartz cell 1.3 cm in diameter was immersed in liquid nitrogen contained in a quartz dewar. Photolysis was carried out with a 250-W Ushio high pressure mercury lamp through a Toshiba UV-D25 filter transparent in the wavelength from 250 to 400 mμ. A 500-W Xe-lamp was used as an infrared light source together with a Toshiba IR-D1A filter transparent in the infrared region. Emission spectra and emission decay were measured with an Aminco-Bowman Spectrofluorimeter or a Nalumi RM-23 spectrometer.

Results

Absorption Spectra of Irradiated DMA. When DMA was illuminated in the ultraviolet region at the temperature of liquid nitrogen, the matrix colored yellow. It showed sharp bands in the near ultraviolet region and relatively broad absorption bands in the visible region as shown in Fig. 1. These absorption bands disappeared when the matrix was warmed and did not reappear by refreezing at 77°K. Figure 1 shows the absorption spectra obtained for DMA irradiated in ethanol, MP and liquid paraffin at 77°K.

In the case of non-polar matrices such as MP, illumination of the irradiated DMA in the infrared region diminished the C_1 (~470 mμ) and C_2 (~334 mμ) bands as shown by curves 3) and 3') in Fig. 1 and at the same time the sample emitted blue light.

When a mixture of DMA and diphenyl in a rigid

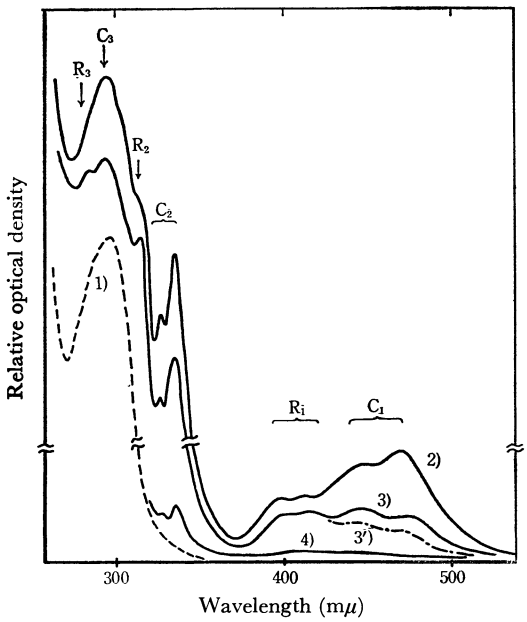

Fig. 1. Electronic absortion spectra of DMA irradiated in various matrices at 77°K. 1: before irradiation; 2, 3, 4: after irradiation in ethanol, MP and liquid paraffin, respectively; 3': same as 3, after photobleaching by infrared light.

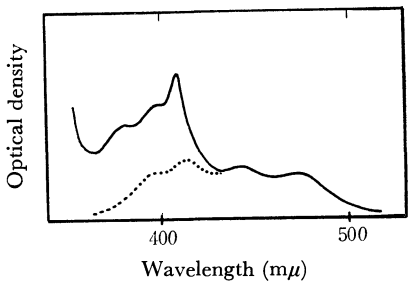

Fig. 2. Electronic absorption spectrum of a mixture of DMA and diphenyl in MP solution irradiated by UV-light at 77°K.

MP matrix was illuminated in the ultraviolet region, a spectrum shown in Fig. 2 was obtained. The absorption band near 400 mμ is identical with that of diphenyl anion.[15,16] When the UV-irradiated sample was treated with infrared light, it was found that the absorption band of the diphenyl anion decreased in intensity slightly, together with C_1 and C_2 bands.

Emission Spectra of Irradiated DMA. A

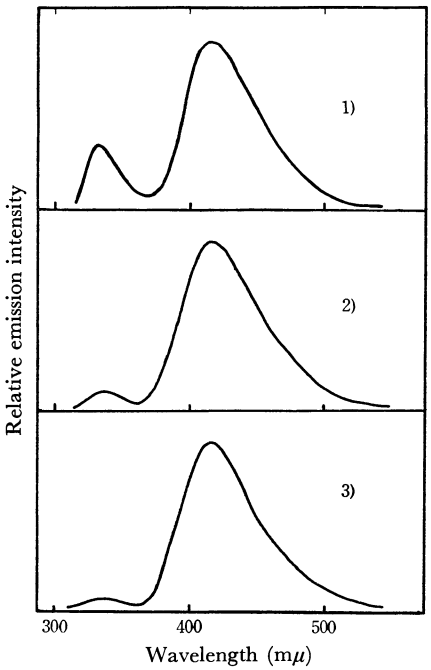

Fig. 3. Luminescence spectra of DMA in MP matrix irradiated in the ultraviolet region.
1, normal fluorescence and phosphorescence spectrum of DMA excited at 300 mμ at 77°K; 2, thermoluminescence; 3, delayed luminescence at 77°K after irradiation.

15) P. Balk, G. J. Hoijink and J. W. H. Schreurs, *Rec. Trav. Chim.*, **76**, 815 (1957).

16) M. R. Ronayne, J. P. Guariro and W. H. Hamill, *J. Am. Chem. Soc.*, **84**, 4230 (1962).

weak emission was observed from DMA irradiated in the non-polar MP matrix even after irradiation was terminated. The emission was stimulated either by illuminating the irradiated matrix in the infrared region or by warming. These luminescence spectra are given in Fig. 3, together with the ordinary emission spectrum of DMA excited by ultraviolet light at 77°K. From Fig. 3, it may be seen that these luminescence spectra are fluorescence and phosphorescence of DMA. The decay of the delayed luminescence at 410 mμ was found to fit in approximately with the first order kinetics with a half-life, $\tau_e = 23$ min.

Absorption Spectra of Irradiated NMA. For the purpose of identifying the absorption bands obtained in the case of DMA, we studied the ultraviolet irradiation of *N*-methylaniline (NMA) by a similar procedure. Figure 4 shows the absorption spectra obtained in the case of NMA irradiated in ethanol and MP matrices at 77°K. New absorption bands in the visible and the near ultraviolet regions faded out by warming the matrices. In the case of non-polar matrices such as MP, illumination of the irradiated NMA in the infrared region diminished C_1' (~450 mμ) band and the spectrum changed from 3) to 3') as shown in Fig. 4. At the same time, the sample emitted light. Thermoluminescence and delayed luminescence are observed also in the case of the irradiated NMA.

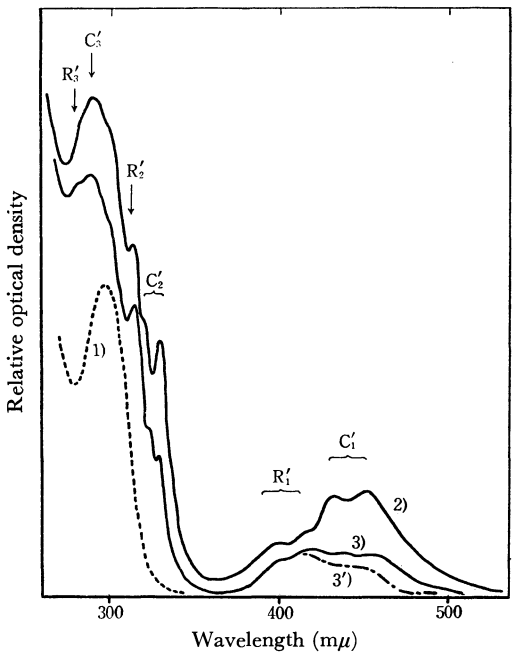

Fig. 4. Electronic absorption spectra of NMA irradiated in various materices at 77°K.
1: before irradiation; 2,3: after irradiation in ethanol and MP matrices; 3′: same as 3, after photobleaching by infrared light.

Discussion

From inspection of the spectra 2) and 3) in Fig. 1, it may be seen that the absorption spectrum changed with solvents; namely band C_1 is as strong as band R_1 in the non-polar solvents, but much stronger in the polar ones. This shows that there are at least two different species showing absorption in the wavelength region 400—500 mμ. Band C_2 is also stronger in polar medium than in non-polar ones and the ratio of the intensity of the C_2 band to that of the C_1 band is nearly constant. Considering the fact that photoionization occurs more easily in polar solvents than in non-polar ones as observed in the case of *N,N,N′,N′*-tetramethyl-*p*-phenylenediamine (TMPD),[10] absorption bands C_1 and C_2 may be ascribed to the DMA^+ cation.

When the DMA irradiated in MP matrix was illuminated in the infrared region, bands C_1 and C_2 decreased in intensity, while the intensity of band R_1 remained the same. This result is quite reasonable, because the action of the infrared light is supposed to excite the electrons trapped in the matrix, to make them mobile till some of them recombine with their parent molecular cations. The diphenyl anion formed in the MP matrix also provides a conclusive proof for the formation of the DMA^+ cation. The luminescence stimulated by the infrared light, together with the thermoluminescence, of the irradiated DMA is much stronger in the phosphorescence component compared with the emission of the same sample excited by ultraviolet light. A similar phenomenon is observed for the luminescence of photoionized TMPD.[17,18]

As a results of the experimental analaysis mentioned above, it may be concluded that the absorption bands C_1 and C_2 are assigned to the DMA^+ cation.

Similarly, from the experimental results on the absorption and emission spectra of the UV-irradiated NMA, the absorption bands C_1' and C_2' shown in Fig. 4 may be assigned to the NMA^+ cation.

It is a little bit more difficult to provide enough evidence for establishing the assignment of the bands which we call R_1 and R_2 for the species formed from DMA and R_1' and R_2' for the species formed from NMA. From the extensive work done by Porter and his group, it has been concluded that fission of the β-bond in the side chain is the main consequence of the photolysis of aromatic compounds. It has also been empirically noticed that a hydrogen atom in the substituent is more easily

17) E. Dolan and A. C. Albrecht, *J. Chem. Phys.*, **38**, 567 (1963); N. Yamamoto, Y. Nakato and H. Tsubomura, This Bulletin, **39**, 2603 (1966).

18) W. M. McClain and A. C. Albrecht, *J. Chem. Phys.*, **43**, 465 (1965).

photodissociated than a methyl group. Thus, photolysis of 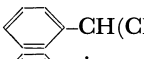 –$CH(CH_3)_2$ and 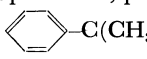 –$C(CH_3)_3$ both yield 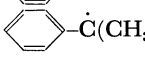 –$\dot{C}(CH_3)_2$.[19] By applying these results to our case, we see that the most probable species formed from the irradiated DMA, except DMA^+ cation, must be 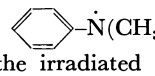 –$\dot{N}(CH_3)$, and the radical expected from the irradiated NMA must also be 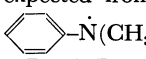 –$\dot{N}(CH_3)$.

Bands R_1 and R_1' were not affected by illumination in the infrared light after ultraviolet irradiation at 77°K and their intensities are mostly indifferent to the change of the solvents. It can be seen from our results that bands R_1 and R_2 for DMA is in good agreement with bands R_1' and R_2' for NMA. Thus, it seems quite probable that the species relevant to these bands is *N*-methylanilino radical 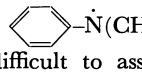 –$\dot{N}(CH_3)$.

It is also difficult to assign bands C_3 and R_3 shown in Fig. 1. Band C_3 is observed both in ethanol and MP, but band R_3 is observed only in MP. Therefore, we may tentatively assign bands C_3 and R_3 to the DMA^+ cation and *N*-methylanilino radical, respectively. As a result of a similar reasoning, the absorption bands C_3' and R_3' shown in Fig. 4 may be assigned to the NMA^+ cation and *N*-methylanilino radical, respectively.

N-methylanilino radical and DMA^+ cation are π-isoelectronic species and hence they should have very similar electronic spectra. Similarities in the electronic spectra between radicals and cations have been demonstrated in our previous work on *p*-disubstituted aromatics.[12] Therefore, with respect to this view, our conclusion that the C_1, C_2, C_3 bands are for the cation and the R_1, R_2, R_3 bands are for the radical is more reasonable than the assignment of previous authors.

We have found that the weak delayed luminescence emitted from the UV-illuminated DMA shows exponential decay at 77°K. If electrons trapped in the matrix were to migrate in the medium and combine with any of the positive ions distributed at random, the decay of the emission would be of the second order. On the other hand, if the electron returns mostly to its parent positive ion, the decay curve of the emission would be of the first order, in agreement with the experimental results mentioned above.

We also tried to estimate the molar extinction coefficient of DMA^+ cation. In the case where a dilute ethanol solution of DMA was irradiated at 77°K, it was observed that only the absorption bands assigned to the DMA^+ cation appeared noticeably at the initial stage of irradiation, and the ratio of radical to cation gradually increased as the irradiation was continued. It was also observed that, for a short time of irradiation, the decrease of DMA absorption at 300 mμ was nearly propotional to the increase of DMA^+ absorption at 470 mμ. If radical formation is neglected for this short UV-irradiation time, the molar extinction coefficient of DMA^+ cation at 470 mμ is found to be about 1200 (l/cm·mol).

19) G. Porter and E. Strachan, *Trans. Faraday Soc.*, **54**, 1595 (1958).

BULLETIN OF THE CHEMICAL SOCIETY OF JAPAN VOL. 42 1862—1870 (1969)

A Theory of the Gel-forming Polymerization of Polyvinyl Compounds

Kenichi FUKUI and Tokio YAMABE

Faculty of Engineering, Kyoto University, Sakyo-ku, Kyoto

(Received December 9, 1968)

A theory of the molecular-size distribution of the cross-linked polymers to be formed from a mixture of vinyl monomers with a distribution of functionalities by radical polymerization is presented. It is assumed that all the unconverted vinyl groups are equireactive to the propagation, which proceeds without cyclization. The distribution is obtained by applying the statistical theory of gel formation with multifunctional interunit junctions, which are, in this case, equivalent to cross-linking chains. The general theory is applied to three practical cases; the curing reaction of unsaturated polyesters, the polymerization of polyvinyl compounds, and the copolymerization of vinyl and divinyl compounds.

A theory of gel formation by the radical copolymerization of divinyl compounds with monovinyl compounds was originally presented by Flory[1] and subsequently by Stockmayer[2] under principal assumptions which will be presented at the outset of the next section. In the first place, Flory[1] tried to explain the gel point of the polymerization. In his theory, he regarded every doubly-converted divinyl monomer as a single tetrafunctional monomer, each functional group of which was able to react independently with the vinyl groups of other monomers. According to this concept, a polymerization of this type is equivalent to the condensation reaction of tetrafunctional and bifunctional monomers.

Then he applied the results obtained in the case of the condensation to the case of this polymerization only in order to obtain the gel point. This interpretation, however, disregards the fact that the mechanism differs essentially from the condensation reaction in that polymerization and cross-linking are concomitant rather than consecutive. (This type of polymerization is usually called "cross-polymerization.") Hence, he hesitated to adopt, in the case of cross-polymerization, the molecular-size distribution of the copolymers obtained by the condensation. Subsequently, Stockmayer[2] treated this case with the following concept: every cross-link of the copolymers is equivalent to the cross-link between chains which would be obtained by cutting the middle of every doubly-reacted divinyl monomer of the copolymers. Thus he also reduced the polymerization to the cross-linking of primary-chain molecules, in any arbitrary size distribution, where the gel point was as presented by Eq. (1). Then he concluded that Eq. (1) was also valid in this case if another assumption was made.*1

$$\rho_c = \frac{1}{w_2 (P_w - 1)} \tag{1}$$

where ρ_c is the fraction of converted vinyl groups at the gel point, where P_w is the weight-average size of the cross-linking chains, and where w_2 is the weight fraction of the divinyl monomers. In the same paper, he demonstrated that, according to the same interpretation, the distribution for the cross-linking of primary chains might be also employed in the present case. Stockmayer's concept is, however, not only based on the unnatural interpretation mentioned above, but is also quite invalid for such simple cases as the cross-polymerization of trivinyl compounds.

By the use of another method, not by statistical methods, but by solving kinetic equations, Ohiwa[3] first obtained a reasonable size distribution of polymers obtained by the cross-polymerization of f-vinyl monomers. In his theory, the critical value is presented by Eq. (2) under the same assumptions as ours:

$$\rho_c = \frac{1}{(f-1)(P_w - 1)} \tag{2}$$

Thus, in the cross-polymerization or copolymerization of primary polyvinyl compounds, the gel

1) P. J. Flory, "Principles of Polymer Chemistry," Cornell University Press, Ithaca, New York (1953), Chap. 9.

2) W. H. Stockmayer, *J. Chem. Phys.*, **12**, 125 (1944).

*1 This assumption was that, at any instant, the fraction of material involved in active growing chains is negligible compared to the amounts of stable polymers and residual monomers.

3) M. Ohiwa, *Nippoin Kagaku Zassi (J. Chem. Soc. Japan, Pure Chem. Sect.)*, **76**, 508, 684 (1955).

point can at any rate be predicted by the Flory method[1] of the expectation value or by the other methods described above. However, the molecular-size distribution of the polymers and the post-gelation relationships have not been presented except for a few special cases treated by Ohiwa.[3]

On the other hand, a number of experiments[4] have qualitatively supported these theories with respect only to the critical value, ρ_c. Some remarkable quantitative deviations from the theoretical value which had been attributed to the effect of cyclization reactions were fairly well explained by modified theories including this effect.[4,5]

The present paper will present an exact and reasonable size distribution and the post-gelation relationships in the cross-polymerization of polyvinyl compounds, in any arbitrary distribution of their vinyl groups. Help was not sought from unnatural explanations nor by solving complicated kinetic equations. Only the statistical theory of gel formation with multifunctional interunit junctions developed by the present authors[6] was applied to the case. The basic concept is that a cross-linking chain is to be regarded as an interunit junction. This general theory is employed in three practical cases; the curing reaction of unsaturated polyesters, the polymerization of polyvinyl compounds, and the copolymerization of vinyl and divinyl compounds.

The Size Distribution and the Gel Point

The present treatment is based on the following usual assumptions in the first approximation: (1) all of the vinyl groups in polymers and primary molecules are equally reactive, and (2) no kind of intramolecular reaction leading to a cyclic structure occurs. Also, it is assumed that: (3) the distribution of cross-linking chains follows the Flory distribution[1] during the entire course of the polymerization. The last assumption is, however, not essential. Other distributions are also applicalbe, if desired.

The initial system treated here is generally composed of primary molecules with any arbitrary distribution of their vinyl groups, say, N_1 mono-, N_2 di-,$\cdots$, N_s s-vinyl compounds. The weight fraction, w_s, of the s-vinyl compounds is, then:

$$w_s = \frac{sN_s}{F}, \quad F = \sum_s sN_s$$

Now, to speak of a single polymeric molecule, it is constructed of chains (called "cross-linking chains" in this paper) formed by the polymerization of some vinyl groups, each in different primary molecules. A simple case can be visualized thus:

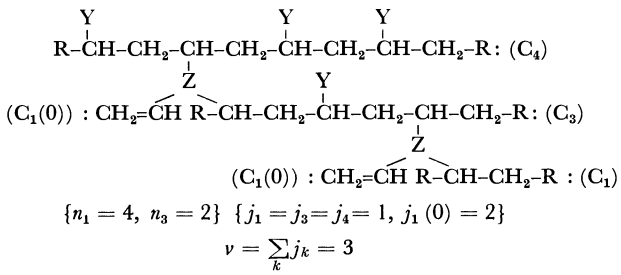

The cross-polymerization of vinyl compounds (CH_2=CHY) and trivinyl compounds ($[CH_2=CH]_3Z$) is illustrated in the above scheme, where C_k represents a cross-linking chain formed by the polymerization of k vinyl groups, where $C_1(0)$ is an unconverted vinyl group, and where R stands for one of the terminators or initiators produced from, for example, the catalysts. The description of any single polymer requires, therefore, the specification of the number of primary molecules of each kind and the number of crosslinking chains of each size. We denote the numbers of primary molecules by n_1, n_2, n_3,$\cdots$, n_s, and the numbers of cross-linking chains by j_1, j_2, j_3,$\cdots$, j_k, *etc.* For brevity, any particular set of these numbers is represented by the symbols $\{n_s\}$ and $\{j_k\}$. The number of unconverted vinyl groups, $j_1(0)$, can be obtained from the $\{n_s\}$ and $\{j_k\}$ as presented by Eq. (7). The symbol $m(\{n_s\}; \{j_k\})$ will be used for the mole fraction of polymers described by a particular set $\{n_s\}$ and $\{j_k\}$.

In this paper, the results obtained by the use of our previous general theory[6] are directly employed to derive the distribution of the molecular size. The essential point of the present paper is based on the reasonable concept that any cross-linking chain is to be regarded as a kind of interunit junc-

4) T. Holt and W. Simpson, *Proc. Roy. Soc.*, **A238**, 154 (1954); M. Gordon and R-J. Roe, *J. Polymer Sci.*, **21**, 27, 39, 57, 75 (1956); L. Minnema and A. J. Stavermann, *ibid.*, **29**, 281 (1958); B. T. Storey, *ibid.*, **A3**, 265 (1965).

5) M. Gordon, *J. Chem. Phys.*, **22**, 610 (1954); R. N. Haward, *J. Polymer Sci.*, **14**, 535 (1954); C. A. J. Hoeve, *ibid.*, **21**, 1, 11 (1956).

6) K. Fukui and T. Yamabe, This Bulletin, **40**, 2052 (1967).

tion as defined in the previous paper.[6] Therefore, a C_k-chain corresponds to a k-functional interunit junction. Unconverted vinyl groups should be distinguished from C_1-chains, although, according to the definitions, both are monofunctional interunit junctions; they are treated here as different monofunctional interunit junctions.

According to the third assumption, the total number of C_k-chains, J_k, in the system is presented as follows:

$$J_k = F\rho\alpha^{k-1}(1-\alpha)^2$$

where ρ is the fraction of converted vinyl groups and where α is the probability of chain propagation. The probability of the formation of a C_k-chain, p_k, is then given from the definition of Eq. (8) in Ref. 6 as follows:

$$p_k = \frac{kJ_k}{F} = k\alpha^{k-1}(1-\alpha)^2\rho \quad (k = 1, 2, 3, \cdots) \tag{3}$$

Hence, ρ can be rewritten as:

$$\rho = \sum_k p_k$$

The fraction of unconverted vinyl groups, $p_1(0)$, can then be simply expressed as:

$$p_1(0) = 1 - \sum_k p_k = 1 - \rho \tag{4}$$

From Eq. (48) in Ref. 6 and Eqs. (3) and (4), the distribution of the molecular size of the polymeric species can readily be obtained as follows:

$$m(\{n_s\};\{j_k\}) = \frac{(\sum_s (s-1)n_s)!\,(\sum_s n_s - 1)!}{(\sum_s (s-1)n_s - \sum_k j_k + 1)!} \times \rho^{\sum_k j_k}(1-\rho)^{\sum_s (s-1)n_s - \sum_k j_k + 1} \times \alpha^{\sum_s n_s - 1}(1-\alpha)^{2\sum_k j_k} \prod_k \frac{k^{j_k}}{j_k!} \prod_s \frac{w_s{}^{n_s}}{n_s!} \tag{5}$$

where $\{j_k\}$, $j_1(0)$, and $\{n_s\}$ satisfy the following relations:

$$\sum_k (k-1)j_k = \sum_s n_s - 1 \tag{6}$$

$$j_1(0) = \sum_s (s-1)n_s - \sum_k j_k + 1 \tag{7}$$

From this distribution, we can easily obtain the mol fraction, $m(\{n_s\};\nu)$, of polymers containing $\sum_k j_k = \nu$ cross-linking chains;

$$m(\{n_s\};\nu) = \sum_{\sum_k j_k = \nu} m(\{n_s\};\{j_k\}) = \frac{(\sum_s (s-1)n_s)!\,(\sum_s n_s + 2\nu - 1)!}{(\sum_s (s-1)n_s - \nu + 1)!\,(2\nu-1)!\,\nu!} \times \rho^{\nu}(1-\rho)^{\sum_s (s-1)n_s - \nu + 1} \times \alpha^{\sum_s n_s - 1}(1-\alpha)^{2\nu} \prod_s \frac{w_s{}^{n_s}}{n_s!} \tag{8}$$

The gel point is characterized by the following equation (see Eq. (19) in Ref. 6):

$$1 = (\lambda_w - 1)(\mu_w - 1)$$

where:

$$\lambda_w = \sum_s s w_s$$

$$\mu_w - 1 = \sum_k (k-1)p_k$$

or by the use of the weight-average chain length, P_w:

$$\mu_w - 1 = \rho(P_w - 1)$$

Hence, the fraction, ρ_c, of converted vinyl groups at the gel point is represented by:

$$\rho_c = \frac{1}{(\lambda_w - 1)(P_w - 1)} \tag{9}$$

This expression can be used for any arbitrary distributions of chain length and includes the previous results (Eqs. (2) and (3)) in their most simple case. In the present case, P_w is equal to $(1+\alpha)/(1-\alpha)$; hence, Eq. (9) is reduced to:

$$\rho_c = \frac{1-\alpha}{2\alpha(\lambda_w - 1)} \tag{9'}$$

The number- and weight-average molecular sizes can immediately be obtained from the results of the previous paper as follows respectively:

$$\langle \sum_s s n_s \rangle = \frac{\sum (\sum_s s n_s)\, m(\{n_s\};\nu)}{\sum m(\{n_s\};\nu)} = \frac{\lambda_n}{1-\alpha\rho\lambda_n} \tag{10}$$

$$\langle (\sum_s s n_s)^2 \rangle = \frac{\sum (\sum_s s n_s)^2 m(\{n_s\};\nu)}{\sum (\sum_s s n_s)\, m(\{n_s\};\nu)} = \frac{(1-\alpha+2\alpha\rho)\lambda_w}{1-\alpha-2\alpha\rho(\lambda_w - 1)} \tag{11}$$

or, more generally:

$$\langle (\sum_s s n_s)^2 \rangle = \frac{\lambda_w [1+\rho(P_w - 1)]}{1-\rho(\lambda_w - 1)(P_w - 1)} \tag{11'}$$

where $\lambda_n = 1/\sum_s (w_s/s)$

Likewise, the number- and weight-average degrees of polymerization are, respectively:

$$\langle (\sum_s n_s) \rangle = \frac{1}{1-\alpha\rho\lambda_n} = \frac{\langle (\sum_s s n_s) \rangle}{\lambda_n} \tag{12}$$

and:

$$\langle (\sum_s n_s)^2 \rangle = \frac{1-\alpha+2\alpha\rho}{1-\alpha-2\alpha\rho(\lambda_w - 1)} = \frac{\langle (\sum_s s n_s)^2 \rangle}{\lambda_w} \tag{13}$$

These average numbers are, of course, only valid until the gel point is reached.

Relationships after the Gel Point

The relative abundances of cross-linking chains and of various primary species in the sol and in the gel fractions may be easily determined by applying

our previous general theory[6] to the present case. The results of the previous theory will be used here after without further remark. The characteristic equation defined by Eq. (26′) in Ref. 6 is presented in this case as:

$$x = \sum_s w_s u^{s-1} \tag{14}$$

$$u(x) = p_1(0) + \sum_k p_k x^{k-1} \tag{15}$$

which, on substituting the expression given by Eq. (3) for p_k, reduces to:

$$u(x) = 1 - \rho + \rho\left(\frac{1-\alpha}{1-\alpha x}\right)^2 \tag{15′}$$

where ρ is the over-all fraction of polymerized vinyl groups beyond the gel point. It is proved that the lowest real positive root, x_1, of this equation is equal to unity before the gel point, and less than unity after that point. With x_1 or $u_1 = u(x_1)$, the sol fraction $w_s^{(sol)}$ of s-vinyl compounds is given by:

$$w_s^{(sol)} = w_s u_1^s \quad (s = 1, 2, \cdots) \tag{16}$$

Hence, the total fraction, W_{sol}, of the sol is:

$$W_{sol} = \sum_s w_s u_1^s \tag{17}$$

which, by the use of Eq. (14), reduces to:

$$W_{sol} = x_1 u_1 \tag{17′}$$

Finally,

$$W_{sol} = x_1\left[1-\rho\left(1-\left(\frac{1-\alpha}{1-\alpha x_1}\right)^2\right)\right] \tag{17″}$$

The weight fraction, $w_s'^{(sol)}$, of the sol consisting of s-vinyl primary compounds is:

$$w_s'^{(sol)} = w_s^{(sol)}/W_{sol} = w_s u_1^s/W_{sol} \tag{18}$$

The number- and weight-average values of s in the sol fraction are then, respectively:

$$\lambda'_n = 1/\sum_s (w_s'^{(sol)}/s) \tag{19}$$

and:

$$\lambda'_w = \sum_s s w_s'^{(sol)} \tag{20}$$

Similarly, the fraction of C_k-chains in the sol is given by:

$$p_k^{(sol)} = p_k x_1^k \tag{21}$$

Hence, the fraction of the sol consisting of C_k-chains, $p_k'^{(sol)}$ is expressed by:

$$p_k'^{(sol)} = p_k^{(sol)}/W_{sol} = p_k x_1^k/W_{sol} \tag{22}$$

The number- and weight-average lengths of the chains in the sol are, then, respectively:

$$\langle k_n\rangle^{(sol)} = 1/(\sum p_k'^{(sol)}/k) = \frac{1}{1-\alpha x_1} \tag{23}$$

and:

$$\langle k_w\rangle^{(sol)} = \sum_k k p_k'^{(sol)} = \frac{1+\alpha x_1}{1-\alpha x_1} \tag{24}$$

The fraction of polymerized vinyl groups in the sol, ρ', is obtained from the definition as follows:

$$\rho' = \sum_k p_k'^{(sol)} = 1 - \frac{(1-\rho)}{1-\rho+\rho\left(\frac{1-\alpha}{1-\alpha x_1}\right)^2} \tag{25}$$

or:

$$\rho' = 1 - \frac{(1-\rho)}{u_1} \tag{25′}$$

which shows, on the contrary, the fraction of unconverted vinyl groups of the sol $p'^{(sol)}_{1(0)}$ to be $1-\rho'$.

Furthermore, from these equations, the number- and weight-average molecular sizes in the sol are, respectively:

$$\langle(\sum_s s n_s)\rangle^{(sol)} = \frac{\lambda'_n}{1-\alpha\rho'\lambda'_n} \tag{26}$$

and:

$$\langle(\sum_s s n_s)^2\rangle^{(sol)} = \frac{(1-\alpha+2\alpha\rho')\lambda'_w}{1-\alpha-2\alpha\rho'(\lambda'_w-1)} \tag{27}$$

Likewise, the number- and weight-average degrees of polymerization are, respectively:

$$\langle(\sum_s n_s)\rangle = \frac{1}{1-\alpha\rho'\lambda'_n} \tag{28}$$

and:

$$\langle(\sum_s n_s)^2\rangle = \frac{1-\alpha+2\alpha\rho'}{1-\alpha-2\alpha\rho'(\lambda'_w-1)} \tag{29}$$

It is noteworthy that these equations (Eqs. (26) and (29)) possess the same forms as Eqs. (10) and (12) after the replacement of λ_n, λ_w, and ρ in Eqs. (10) and (13) by λ'_n, λ'_w, and ρ' respectively.

The weight fraction of s-vinyl compounds in the gel, $w_s^{(gel)}$, is then obtained by the difference:

$$w_s^{(gel)} = w_s - w_s^{(sol)} = w_s(1-u^s) \tag{30}$$

Hence,

$$W_{gel} = 1 - W_{sol} \tag{31}$$

Likewise, the weight fraction, $p_k^{(gel)}$, of C_k-chains in the gel is:

$$p_k^{(gel)} = p_k - p_k^{(sol)} = p_k(1-x_1^k) \tag{32}$$

The fraction of vinyl groups in the gel which have polymerized, ρ'', is:

$$\rho'' = \frac{\sum_k p_k^{(gel)}}{W_{gel}} = \frac{1-\left(\frac{1-\alpha}{1-\alpha x_1}\right)^2}{1-x_1\left[1-\rho+\rho\left(\frac{1-\alpha}{1-\alpha x_1}\right)^2\right]}\cdot\rho \tag{33}$$

Namely,

$$\rho'' = \frac{2\alpha-(1+x_1)\alpha^2}{(1-\rho)\alpha^2 x_1^2+\alpha(2-2\rho+\alpha\rho)x_1+1}\cdot\rho \tag{33′}$$

Similarly, the number- and weight-average lengths of the cross-linking chains with which the gel is constructed are, respectively:

$$\langle k_n\rangle^{(\mathrm{gel})} = \frac{\sum_k p_k^{(\mathrm{gel})}}{(\sum_k p_k^{(\mathrm{gel})}/k)} = \frac{1-\alpha^2 x_1}{(1-\alpha)(1-\alpha x_1)} \tag{34}$$

$$\langle k_w\rangle^{(\mathrm{gel})} = \frac{\sum_k k p_k^{(\mathrm{gel})}}{\sum_k p_k^{(\mathrm{gel})}} = \frac{1+(1+x_1)\alpha-6x_1\alpha^2+x_1(1+x_1)\alpha^3+x_1{}^2\alpha^4}{(1-\alpha)(1-\alpha x_1)(1-\alpha^2 x_1)} \tag{35}$$

These relationships for the gel may afford some information to make clear the structure of the gelled network polymers, which we will discuss in detail elsewhere. It should be noticed here however that, before the gel point, the number-average length of the cross-linking chains maintains a constant value:

$$\langle k_n\rangle = \frac{1}{1-\alpha}$$

and that even beyond the gel point the same value remains as an average over the whole system containing the sol and the gel, while the average length in the sol and in the gel are different from each other, as Eqs. (23) and (34), respectively, indicate. This is a consequence of the preferential acquisition of larger molecules by the gel.

Near the gel point, both x_1 and u_1 may be slightly smaller than unity; these can then be written as:

$$x_1 = 1-\varepsilon \qquad 1 \gg \varepsilon > 0 \tag{36}$$

$$u_1 = 1-\delta \qquad 1 \gg \delta > 0 \tag{37}$$

By substituting the x_1 of Eq. (36) into Eqs. (14) and (15) and by neglecting the terms of a higher order than ε and δ, these factors may be approximated by:

$$\varepsilon \cong \frac{[2\alpha\rho(\lambda_w-1)+\alpha-1](1-\alpha)}{\alpha^2\rho[2\rho\lambda_z+3(\lambda_w-1)]} \tag{38}$$

$$\delta \cong \frac{[2\alpha\rho(\lambda_w-1)+\alpha-1](1-\alpha)}{\alpha\rho[(1-\alpha)\lambda_z+3\alpha(\lambda_w-1)^2]} \tag{39}$$

where $\lambda_z=\sum_s (s-1)(s-2)w_s$. Furthermore, if ρ is expressed by the following equation, which may be employed to define Δ,

$$\rho = \rho_c(1+\Delta) \qquad 1 \gg \Delta > 0 \tag{40}$$

ε and δ can then be rewritten in other expressions:

$$\varepsilon \cong \frac{2(1-\alpha)(\lambda_w-1)^2}{(1-\alpha)\lambda_z+3\alpha(\lambda_w-1)^2}\cdot\Delta \tag{38'}$$

$$\delta \cong \frac{2(1-\alpha)(\lambda_w-1)}{(1-\alpha)\lambda_z+3\alpha(\lambda_w-1)^2}\cdot\Delta \tag{39'}$$

By the use of ε and δ, we can obtain the relationships available near the gel point as follows:

$$\rho' \cong \rho_c\left[1-\frac{\alpha(\lambda_w-1)^2-(1-\alpha)[2(\lambda_w-1)+\lambda_z}{(1-\alpha)\lambda_z+3\alpha(\lambda_w-1)^2}\cdot\Delta\right] \tag{41}$$

$$\rho'' \cong \frac{1}{\lambda_w}+\frac{\lambda_w-1}{\lambda_w{}^2}\left\{1-\frac{(\lambda_w-1)(3\alpha\lambda_w-\alpha-2)}{(1-\alpha)(\lambda_z+3\alpha(\lambda_w-1)^2}\right\}\Delta \tag{42}$$

$$\lambda_n' = \lambda_n[1-(\lambda_w-\lambda_n)\delta] \tag{43}$$

$$\lambda_w' = \lambda_w\left[1-\left(\lambda_w-\frac{\lambda_z}{\lambda_w}\right)\delta\right] \tag{44}$$

$$W_{\mathrm{sol}} = 1-\lambda_w\delta \tag{45}$$

$$\langle k_n\rangle^{(\mathrm{sol})} = \frac{1}{1-\alpha}\left(1-\frac{\alpha}{1-\alpha}\varepsilon\right) \tag{46}$$

$$\langle k_w\rangle^{(\mathrm{sol})} = \frac{1+\alpha}{1-\alpha}-\frac{2\alpha}{(1-\alpha)^2}\varepsilon \tag{47}$$

$$\langle k_n\rangle^{(\mathrm{gel})} = \frac{1+\alpha}{1-\alpha}-\frac{\alpha}{(1-\alpha)^2}\varepsilon \tag{48}$$

At incipient gelation, it holds that $\rho''=1/\lambda_w$ and $\rho'=\rho_c$; that is, the converted fraction of the vinyl groups of the first increment of gel is $[(\lambda_w-1)/\lambda_w]\cdot(P_w-1)$ times as large as that of the sol. Similarly, $\langle k_n\rangle^{(\mathrm{sol})}=P_n$, $\langle k_n\rangle^{(\mathrm{gel})}=\langle k_w\rangle^{(\mathrm{sol})}=P_w$, and, in addition:

$$\langle k_w\rangle^{(\mathrm{gel})} = P_z \tag{49}$$

where $P_n=1/(1-\alpha)$, and $P_z=(1+4\alpha+\alpha^2)/(1-\alpha)^2$.

It is noticeable that, at incipient gelation, the number-average chain length of the gel is equal to the weight-average chain length of the sol.

These general relationships has thus been obtained for the partitioning of the components between the sol and the gel obtained by the cross-polymerization of primary molecules with any arbitrary distribution. Tractable expressions are also, of course, obtained for certain specified primary distributions. Three special cases will be discussed below.

Curing Reaction of Unsaturated Polyesters

As the first example of the specified distribution of the vinyl groups of primary molecules, let us consider the curing reaction of unsaturated polyesters. In this case we may employ the Flory distribution for the distribution of primary chains (linear unsaturated polyesters):

$$w_s = s(1-\gamma)^2\gamma^{s-1} \tag{50}$$

where γ is the fraction of converted functional groups in condensation reaction, such as, for instance, between glycol and maleic anhydride. Once the distribution has been determined thus, all the relationships obtained in the previous section can be expressed with observable quantities, such as α, γ, and ρ.

In the first place, we will try to obtain the mole fraction $m(n, p; \nu)$ of polymers constructed by ν

cross-linking chains connecting the n primary chians which had p vinyl groups at all in the initial state. From the definition,

$$m(n, p; \nu) = \sum m(\{n_s\}; \nu) \tag{51}$$

where the summation should cover all non-negative integers, $\{n_s\}$, satisfying the conditions; $\sum_s n_s = n$ and $\sum_s s n_s = p$. Simple manipulations lead to the following distribution:

$$m(n,p;\nu) = \frac{1}{(p+n-\nu)} \binom{n+\nu-1}{n} \binom{p+n-1}{\nu} \binom{p+n-\nu}{2n-1} \times \rho^{\nu}(1-\rho)^{p-n-\nu+1}\alpha^{n-1}(1-\alpha)^2(1-\gamma)^{2n}\gamma^{p-n} \tag{51'}$$

If the number of converted vinyl groups, $i=\nu+n-1$, and the number of cross-links in the polymer, $j=n-1$, are employed instead in the above distribution, it is consistent with the distribution obtained by Ohiwa[3] with the aid of the kinetic method. He demonstrated that it is different from that of the case of cross-linking by the condensation reactions of primary chins.

By substituting the relationships available for the present case into Eqs. (9′) and (13),

$$\lambda_n = \frac{1}{1-\gamma}, \quad \lambda_w = \frac{1+\gamma}{1-\gamma} \tag{52}$$

we obtain:

$$\rho_c = \frac{(1-\alpha)(1-\gamma)}{4\alpha\gamma} \tag{53}$$

$$\langle p \rangle = \frac{1}{1-\gamma-\alpha\rho} \tag{54}$$

$$\langle p^2 \rangle = \frac{(1+\gamma)(1-\alpha+2\alpha\rho)}{(1-\alpha)(1-\gamma)-4\alpha\gamma\rho} \tag{55}$$

$$\langle n \rangle = \frac{1-\gamma}{1-\gamma-\alpha\rho} \tag{56}$$

$$\langle n^2 \rangle = \frac{(1-\gamma)(1-\alpha+2\alpha\rho)}{[(1-\alpha)(1-\gamma)-4\alpha\gamma\rho](1+\gamma)} \tag{57}$$

which are, of course, valid only before the gel point.

The characteristic equation (Eq. (14)) is now simply:

$$x = \left(\frac{1-\gamma}{1-\gamma u}\right)^2 \tag{58}$$

or, alternatively:

$$u = \frac{1}{\gamma}\left[1 - \frac{(1-\gamma)}{\sqrt{x}}\right] \tag{58'}$$

From Eqs. (15′) and (58), it follows that:

$$\rho = \frac{1-\gamma}{\alpha\gamma} \frac{(1-\alpha x_1)^2}{(x_1+\sqrt{x_1})(2-\alpha-\alpha x_1)} \qquad (\rho \geqq \rho_c) \tag{59}$$

from which x_1 or u_1 can be obtained for a given value of ρ as well as α and γ, even if numerically. To get the sol fraction or other fractions presented in the previous section one need, then, do nothing but do the numerical calculations using this x_1.

The sol fraction is now simply:

$$W_{\text{sol}} = \frac{x_1 - (1-\gamma)\sqrt{x_1}}{\gamma} \tag{60}$$

In this case, the number- and weight-average sizes of the primary chains in the sol decrease as the reaction proceeds beyond the gel point, following the relations:

$$\lambda_n' = \frac{1}{1-\gamma u_1}, \quad \lambda_w' = \frac{1+\gamma u_1}{1-\gamma u_1} \tag{61}$$

These are, however, constant until the gel point, as is shown in Eq. (52). From Eqs. (28) and (29), the number- and weight-average degrees of polymerization are presented with $\gamma' = \gamma u_1$ and ρ', or, equivalently, u_1 and ρ (since, from Eq. (25′),

$$\langle n \rangle^{(\text{sol})} = \frac{1-\gamma'}{1-\gamma'-\alpha\rho'} \tag{62}$$

and

$$\langle n^2 \rangle^{(\text{sol})} = \frac{(1-\alpha+2\alpha\rho')(1-\gamma')}{[(1-\alpha)(1-\gamma')-4\alpha\gamma'\rho'](1+\gamma')} \tag{63}$$

At incipient gelation, ε and δ can now be obtained from Eq. (28′) and Eq. (39′) respectively:

$$\varepsilon \cong \frac{2(1-\alpha)}{6(1-\alpha)(\gamma/[1+\gamma]^2+3\alpha} \cdot \Delta \tag{64}$$

and:

$$\delta \cong \frac{(1-\alpha)}{6(1-\alpha)(\gamma/[1+\gamma])^2+3\alpha} \cdot \frac{(1-\gamma)}{\gamma} \cdot \Delta \tag{65}$$

Hence, from Eq. (45):

$$W_{\text{sol}} \cong 1 - \frac{(1-\alpha)}{6(1-\alpha(\gamma/[1+\gamma])^2+3\alpha} \cdot \frac{1+\gamma}{\gamma} \cdot \Delta \tag{66}$$

The approximation used in deriving these equations is, of course, based on the condition that the Δ defined by Eq. (40) is sufficiently small compared to unity and, hence, valid only very near the gel point. In curing reactions, however, ρ is usually small since ρ_c is sufficiently small; the primary chain length is, therefore, great (*cf.* Eq. (9)). This situation leads Eq. (66) to another approximation:

$$x_1 \cong W_{\text{sol}} \tag{67}$$

When we apply this approximation to Eq. (25), ρ' nearly becomes:

$$\rho' \cong \rho\left(\frac{1-\alpha}{1-\alpha W_{\text{sol}}}\right)^2 \tag{68}$$

which is useful apart from the gel point as long as ρ is small.

Similarly, from Eq. (33), ρ'' is:

$$\rho'' \cong \rho \frac{\alpha[2-\alpha(1+W_{\text{sol}})]}{(1-\alpha W_{\text{sol}})^2} \tag{69}$$

At incipient gelation $\rho'' \cong (P_w - 1)\rho'$, as has been pointed out at the end of the preceding section.

Polymerization of Polyvinyl Compounds

In this section, the case of the polymerization of f-vinyl monomers will be treated as the second example of the general case. Polyallyl compounds as well as polyvinyl compounds are also valid for the monomer, since allyl groups polymerize much like vinyl groups. In fact, some kinds of diallyl or triallyl esters are used to produce some thermosetting resins.

Now, from Eq. (8), the mole fraction $m(n; \nu)$ of polymers composed of n monomers connected by ν cross-linking chains can be immediately presented by:

$$m(n;\nu) = \frac{(fn-n)!(n+2\nu-1)!}{(fn-n-\nu+1)!(2\nu-1)!\nu!n!} \times \rho^{\nu}(1-\rho)^{fn-n-\nu+1}\alpha^{n-1}(1-\alpha)^{2\nu} \quad (70)$$

The gel point is simply:

$$\rho_c = \frac{(1-\alpha)}{2\alpha(f-1)} \quad (71)$$

The number-average degree of polymerization is given by:

$$\langle n \rangle = \frac{1}{1-f\alpha\rho} \quad (72)$$

Its weight-average degree of polymerization is:

$$\langle n^2 \rangle = \frac{1-\alpha+2\alpha\rho}{1-\alpha-2(f-1)\alpha\rho} \quad (73)$$

These equations (Eqs. (70) and (73)) agree with that obtained by the kinetical method.[3] Formulas derived in quite a different manner have proved to be a special case of the present general theory.

The sol fraction or the composition of the gel can be calculated by means of the root of the characteristic equation, x_1, which, for this case, is presented by:

$$x = \left[1-\rho+\rho\left(\frac{1-\alpha}{1-\alpha x}\right)^2\right]^{f-1} \quad (74)$$

This root, x_1, is usually obtained by numerical calculations. For the simplest case (f=2), it is obtained explicitly as follows:

$$x_1 = \frac{(2-\alpha\rho) - \sqrt{[\alpha\rho+4(1-\alpha)]\alpha\rho}}{2\alpha} \quad (\rho \geqq \rho_c) \quad (75)$$

The relation between x_1 and ρ is shown in Fig. 1 for the cases of f=2 and 3, and α=0.8.

The sol fraction, W_{sol}, is simply:

$$W_{sol} = x_1^{\frac{f}{f-1}} \quad (76)$$

which is shown in Fig. 2 for the case of f=2 and 3.

Likewise, the relationships of the number-average lengths of the cross-linking chains in the sol and in the gel are drawn in Fig. 3 according to Eqs. (23) and (34). This figure may afford information about the structure of the gel and about the difference between the sol and the gel.

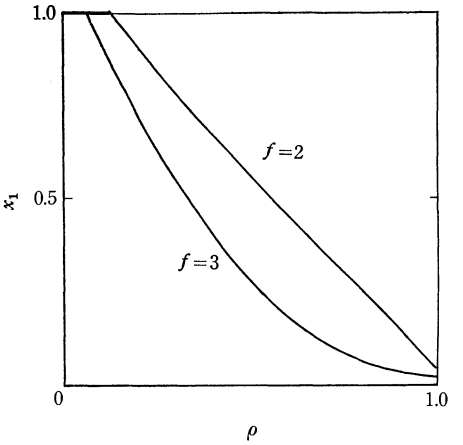

Fig. 1. The relationships between x_1 and ρ (α=0.8).

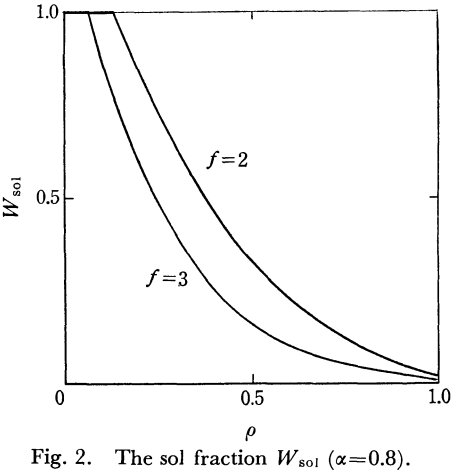

Fig. 2. The sol fraction W_{sol} (α=0.8).

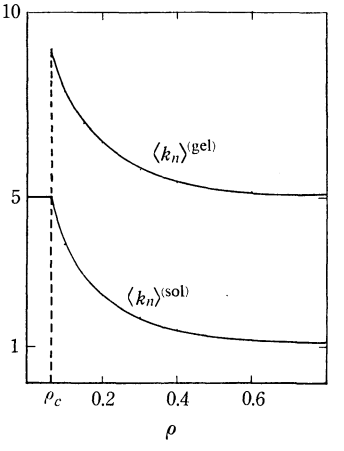

Fig. 3. The number average lengths of crosslinking chains in the sol and in the gel.

Copolymerization of Vinyl and Divinyl Monomers

Lastly, let us treat the case of the copolymerization of vinyl and divinyl monomers, which we discussed in the introduction of this article. The general relationships for calculating the distribution obtained by cross-polymerizing primary molecules of any arbitrary distribution have been derived in the first section. Then, in the present case, the molecularsize distribution of Eq. (8) reduces to:

$$m(n_1,n_2;\nu) = \frac{(n_1+n_2+2\nu-1)!}{n_1!(n_2-\nu+1)!(2\nu-1)!\nu!} \times \rho^{\nu}\cdot(1-\rho)^{n_2-\nu+1}\alpha^{n_1+n_2-1}(1-\alpha)^{2\nu} \times w_1^{n_1}\cdot w_2^{n_2} \quad (77)$$

This is, therefore, the exact and reasonable distribution first obtained by the present authors.

The number- and weight-average molecular sizes are, respectively:

$$\langle(n_1+2n_2)\rangle = \frac{2}{2-w_2-2\alpha\rho} \quad (78)$$

and:

$$\langle(n_1+2n_2)^2\rangle = \frac{(1-\alpha+2\alpha\rho)(1+w_2)}{1-\alpha-2\alpha\rho\cdot w_2} \quad (79)$$

The gel point is now given from Eq.(9′) by:

$$\rho_c = \frac{1-\alpha}{2\alpha w_2} = \frac{1}{w_2(P_w-1)} \quad (80)$$

which coincides with Eq. (1) obtained by Flory[1] and by Stockmayer.[2] It is of interest to see that this Eq. (1) derived from quite different considerations, is also obtained as a special case of the more general theory. This equation shows that, since $\rho_c \leqq 1$, w_2 should be larger than $(1-\alpha)/2\alpha = 1/(P_w-1)$ for the attainment of the gel point (even if intramolecular reactions are excluded); otherwise the gelation does not occur at any extent of polymerization reaction. Such a situation is fully discussed in another paper.*

The polymer conversion, W_p, is given by:

$$W_p = 1 - [w_1(1-\rho) + w_2(1-\rho)^2] \quad (81)$$

since the monomers should be excluded from the polymers. Hence, the fraction of the unconverted vinyl groups in polymers, $R_{u.s.}$, is:

$$R_{u.s.} = \frac{W_p-\rho}{W_p} = \frac{w_2(1-\rho)}{1+w_2(1-\rho)} \quad (82)$$

At the initial stage of the reaction, Eq. (81) reduces to:

$$R_{u.s.} \cong \frac{w_2}{1+w_2} \quad (83)$$

The charactristic equation can now be rewritten in the following form:

$$x = w_1 + w_2\left[1-\rho+\rho\left(\frac{1-\alpha}{1-\alpha x}\right)^2\right] \quad (84)$$

which, after simple manipulation, gives:

$$x_1 = \frac{(2-\alpha w_2\rho) - \sqrt{[4(1-\alpha)+\alpha w_2\rho]\alpha w_2\rho}}{2\alpha} \quad (85)$$

Hence:

$$u_1 = \frac{(2-\alpha w_2\rho) - \sqrt{[4(1-\alpha)+\alpha w_2\rho]\alpha w_2\rho}}{2\alpha w_2} \quad (86)$$

where the relation $(1-x_1)=w_2(1-u_1)$ is used to obtain the u_1 from the x_1.

At incipient gelation, from Eqs. (38′) and (29′):

$$x_1 = 1 - \frac{2(1-\alpha)}{3\alpha}\cdot\Delta \quad (85')$$

$$u_1 = 1 - \frac{2(1-\alpha)}{3\alpha w_2}\cdot\Delta \quad (86')$$

On the other hand, near complete conversion ($\rho\cong 1$), these may be approximated as follows:

$$x_1 = 1 - w_2\rho + \frac{(1-\alpha)^2}{w_2\rho} \quad (85'')$$

$$u_1 = 1 - \rho + \frac{(1-\alpha)^2}{w_2^2\rho} \quad (86'')$$

where it is supposed that $w_2 \gg (1-\alpha)$. It should be remarked that, in Eqs. (85″) and (86″) near the full conversion, $x_1\cong 1-w_2=w_1$, whereas $u_1\cong 0$. The latter value means that both monomers are almost entirely changed into gel near the full conversion since $W_{sol}=w_1u_1+w_2u_1^2$. On the other hand, the former indicate that in the gel the monovinyl monomers do not take part in the unit of branches extending to infinity as it ought to. These situa-

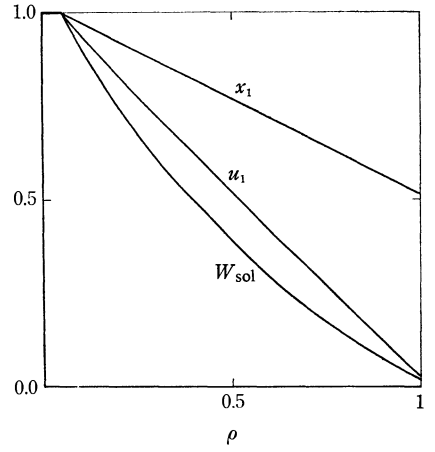

Fig. 4. The relationships between x_1, u_1, W_{sol} and ρ (W_2=0.5, α=0.95).

*2 T. Yamabe and K. Fukui, This Bulletin, to be submitted.

tions, visualized in Fig. 4, may reflect the difference between the meanings of x_1 and u_1, as will be discussed in the Appendix.

Appendix

Recently, Dobson and Gordon[7] presented a theory of branching processes and of the statistics of rubber elasticity by adopting the stochastic theory of cascade processes. As an example, they treated vulcanization by cross polymerization and obtained the same equation (see Eq. (4) in Ref. 7) as Eq. (14) in this paper:

$$x = \sum_s w_s u^{s-1} \tag{A-1}$$

where u was as presented by the following equation (translated into our notations (see Eq. (43) in Ref. 7):

$$u = 1 - \rho + \rho(1 - \alpha + \alpha x)^2 \tag{A-2}$$

This is, however, in disagreement with the corresponding equation (Eq. (15)) of the present paper; namely,

$$u = 1 - \rho + \rho\left(\frac{1-\alpha}{1-\alpha x}\right)^2 \tag{A-3}$$

Apparently, Eq. (A-2) was derived on the basis of the same concept as Flory's with regard to the cross-linking chain; hence, as has been discussed above, it is not reasonable and does not represent the characteristic features of the polymerization. Figure A-1 indicates the remarkable difference between $1-\alpha+\alpha x$ and $(1-\alpha)/(1-\alpha x)$, a difference equivalent to the difference between Eq. (A-2) and Eq. (A-3).

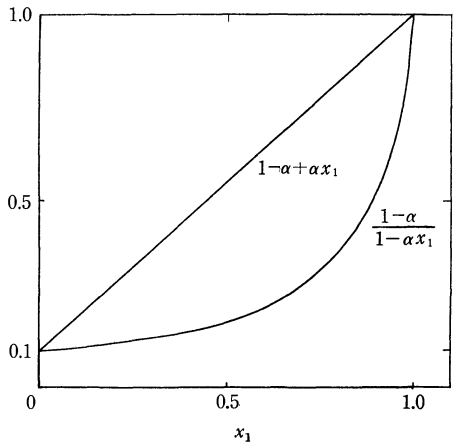

Fig. A-1. Functions $1-\alpha+\alpha x_1$ and $(1-\alpha)/(1-\alpha x_1)$ ($\alpha=0.9$).

Equation (A-2) is, however, approximated by Eq. (A-1) for $\alpha x \ll 1$, since:

$$\frac{1-\alpha}{1-\alpha x} \approx 1 - \alpha + \alpha x$$

Such an approximation is valid only for $x \ll 1$. The other case, that $\alpha \ll 1$, is almost meaningless since no polymer is obtained in this case. Therefore, the theory presented by Dobson and Gordon should be reformulated by our treatment. A paper on this subject will be presented elsewhere.

7) G. R. Dobson and M. Gordon, *J. Chem. Phys.*, **43**, 705 (1965).

BULLETIN OF THE CHEMICAL SOCIETY OF JAPAN VOL. 42 1871—1874 (1969)

Raman Effect in Ferroelectric Sodium Nitrite Crystal. II. Dependence of B_2 Type Phonon Spectrum on Propagation Direction

Masamichi TSUBOI,* Minoru TERADA** and Teruo KAJIURA***

* *Faculty of Pharmaceutical Sciences, The University of Tokyo, Hongo, Bunkyo-ku, Tokyo*

** *Mitsubishi Atomic Power Industries, Inc., Omiya, Saitama*

*** *Japan Electron Optics Laboratory, Company, Nakagami, Akishima, Tokyo*

(Received December 16, 1968)

The Raman spectra corresponding to the (bc) component (B_2 type vibrations) of the polarizability tensor in the ferroelectric sodium nitrite crystal (C_{2v}^{20}) have been observed with various directions of the phonon propagation. It has been found that one of the B_2 Raman lines at 160 cm^{-1} splits into two components when the phonon propagates in a direction 45° from the c axis in the ac plane. This splitting has been ascribed to an interaction of a B_2 and B_1 type lattice-vibrations whose frequencies are accidentally equal to each other in the phonon propagation direction now in question.

A great improvement has been made in the Raman spectroscopy of crystals by the introduction of laser light sources. We can now easily distinguish Raman lines corresponding to different components of the polarizability tensor of a crystal, if its single crystal with a size greater than or comparable to the diameter of the laser beam is available. In addition, we can now examine whether each of the Raman frequencies changes depending upon the direction of the phonon propagation. In an ionic crystal, an appreciable frequency difference is often observed between the transverse and longitudinal waves of the same mode of vibration.[1,2] Such a frequency difference is observed only for an optical mode and is considered to be caused by a long-range electric field.[3,4]

We have been examining the Raman effect of ferroelectric sodium nitrite crystal (C_{2v}^{20}—*Im2m*) by use of helium-neon and argon ion lasers. In our previous paper,[5] we reported Raman frequencies observed with the orientations of the incident and scattered beams which allow the frequencies of the transverse waves to appear. In a further experiment, different frequencies have been found in general for different orientations. As was once reported by Tramer,[6] a marked shift (from 1230 to 1360 cm^{-1}) in one of the B_2 frequencies has been observed on changing the direction of the phonon propagation from a axis to c axis in the ac plane. One of the other two B_2-type Raman lines, on the other hand, shows a peculiar behavior in a similar change of the phonon propagation direction. This peculiar behavior will be described below with an interpretation for it.

Experimental

The single crystals of sodium nitrite ($NaNO_2$) used in our experiment were kindly provided by Dr. S. Hirotsu and Mr. K. Suzuki, Tokyo Institute of Technology. Final data were taken on two $NaNO_2$ crystals. One of the crystals was cut so that each of the a, b, and c axes is parallel to a sample edge. The other was cut so that the b axis is parallel to a sample edge and the a and c axes are parallel to a sample face and at 45°C to the sample edges.

Each Raman spectrum was recorded a number of times by use of three different setups: (1) a Perkin-Elmer LR-1 Raman Spectrometer with a 10 milliwatt He-Ne laser, (2) a Spex 1400-II Double-monochromator in combination with a 30 milliwatt He-Ne laser made by Japan Electron Optics Laboratory, Company, and (3) a Spex 1400-II Double-monochromator in combination with a 50 milliwatt argon ion laser made by Japan Electron Optics Laboraty, Company. Each laser beam is completely polarized along a certain direction. The scattered beam from the crystal was sent to the monochromator slit through a polarizer so that only a particular component of the scattered beam can be observed.

1) T. C. Damen, S. P. S. Porto and B. Tell, *Phys. Rev.*, **142**, 570 (1966).

2) B. Tell, T. C. Damen and S. P. S. Porto, *ibid.*, **144**, 771 (1966).

3) R. H. Lyddane, R. G. Sachs and E. Teller, *ibid.*, **59**, 673 (1941).

4) M. Tsuboi and A. Wada, *J. Chem. Phys.*, **48**, 2615 (1968).

5) M. Tsuboi, M. Terada and T. Kajiura, This Bulletin, **41**, 2545 (1968).

6) A. Tramer, *Compt. rend.*, **248**, 3546 (1959).

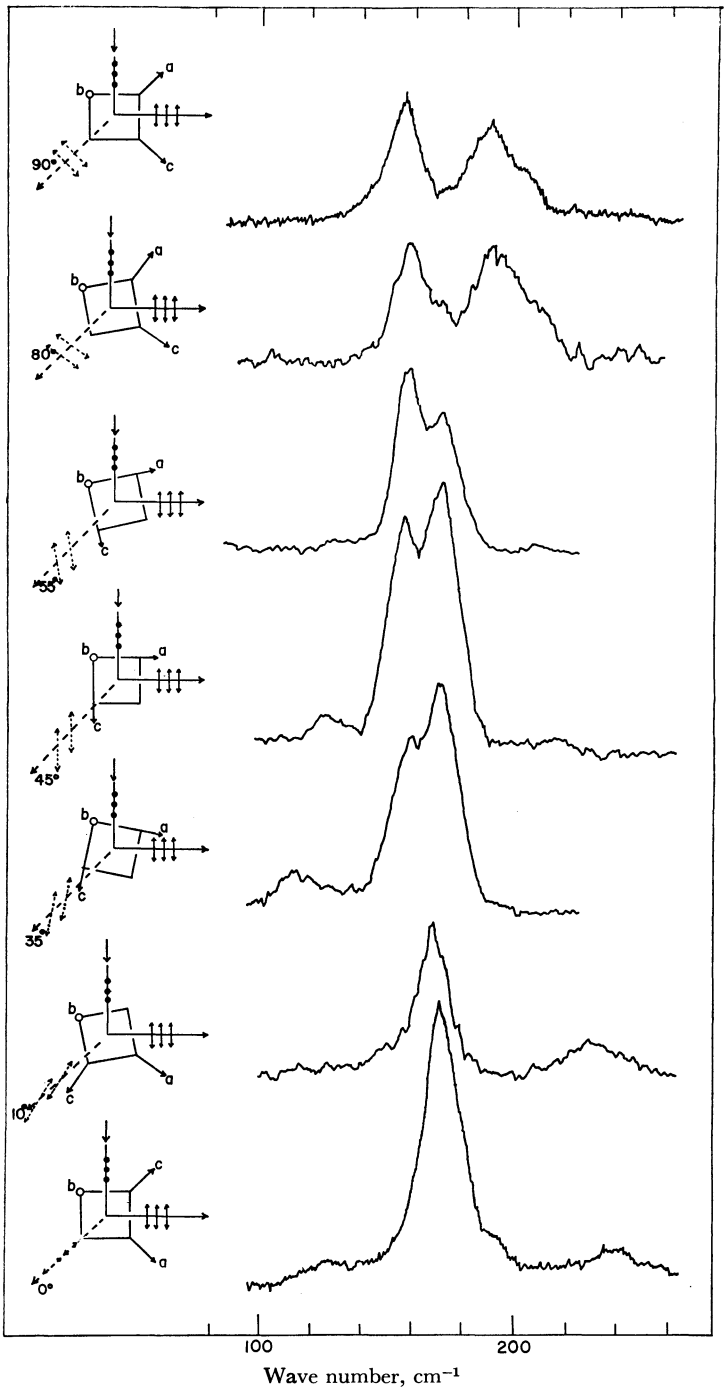

Fig. 1. Raman spectra of $NaNO_2$ crystal (C_{2v}^{20}) observed at room temperature. Orientations of the incident and scattered beams and their electric vectors are given in the left side of each spectrum. The broken lines indicate the direction of the phonon propagation and the direction of its electric polarization.

Result and Interpretation

Figure 1 shows the Raman spectra of the $NaNO_2$ crystal (C_{2v}^{20}) with various orientations in the 100—260 cm^{-1} region recorded at room temperature. Here, the incident and scattered beams are always set so that the Raman lines corresponding to the (bc) component in the polarizability tensor should appear. In this setting there should appear only the B_2-type vibrations, in which the dipole oscillation takes place along the c axis. The single crystal was placed so that the phonon propagation direction is in the ac plane and makes an angle θ indicated in the figure with the c axis. When θ is 90° (transverse wave) the B_2 Raman lines are at 157 and 190 cm^{-1}, while when θ is 0° (longitudinal wave) they are at 172 and 236 cm^{-1}. When θ is 55—35° the first Raman line splits into two at 157 and 171 cm^{-1}.

The splitting just stated is considered to be caused by B_1 vibration whose frequency comes accidentally in the vicinity of 165 cm^{-1}. In fact, there is a B_1 vibration whose frequency was located by Axe[7] at 149 cm^{-1} for the transverse wave and at 193 cm^{-1} for the longitudinal wave. It is true that any vibration belonging to the B_2 species cannot interact with a vibration belonging to the B_1 species as far as

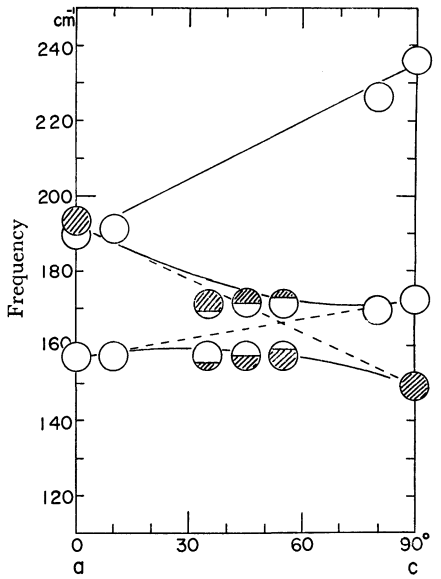

Fig. 2. Frequencies of a few Raman-active vibrations of $NaNO_2$ crystal plotted against the phonon propagation direction.

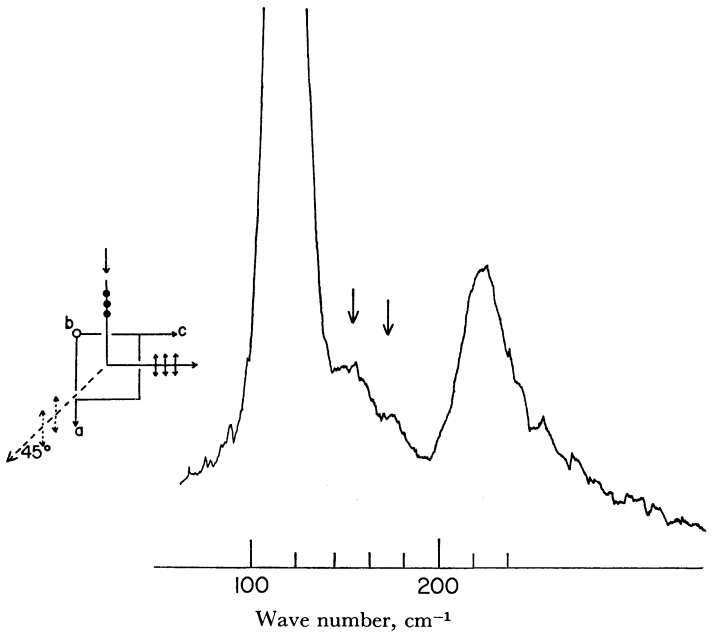

Fig. 3. Raman spectrum of $NaNO_2$ crystal (C_{2v}^{20}) observed at room temperature. Orientations of the incident and scattered beams and their electric vectors are shown in the left side of the figure. The broken lines indicate the direction of the phonon propagation and the direction of its electric polarization. A strong Raman line observed at 120 cm^{-1} is assigned to the A_2 type vibration.

7) J. D. Axe, *Phys. Rev.*, **167**, 573 (1968).

these symmetry classifications are strictly valid. Actually, however, these are so only for vibrations whose wavevectors are exactly zero. What we are observing in the Raman spectra are vibrations with small but appreciable amounts of phase difference between the adjacent two unit cells, and therefore, an approximate "B_1" vibration may interact with an approximate "B_2" vibration through, for example, a long-range electric field. Figure 2 shows a relation of the frequencies of the Raman-active lattice vibrations with the direction of its phonon propagation direction in the ac plane. The broken lines indicate the frequencies expected when there were no interaction between the "B_1" and "B_2" vibrations, and the solid lines are what are expected when there is an interaction. The circles indicate the observed frequencies; white circles are those corresponding to the (bc) component (B_2-type vibration) and black circles to the (ba) component (B_1-type vibration) of the polarizability tensor. The partly-white, partly-black circles indicate Raman lines which are considered to have partly B_2 and partly B_1 character. The relative intensities observed of the doublet Raman lines in Fig. 1 may be taken as indicating the relative amount of the B_2 character, becuase the incident and scattered beams are set here so that almost only B_2 vibrations should appear.

On the basis that both of the 157 and 171 cm^{-1} Raman lines are due to lattice vibrations which have halfway B_2 and halfway B_1 character, these Raman lines should appear not only in a B_2 type phonon spectrum but also in a B_1 type phonon spectrum. This has been found to be actually the case as shown in Fig. 3. Here, the incident and scattered beams are set so that only Raman lines corresponding to the (ba) component (B_1 type vibrations) of the polarizability tensor should appear. The propagation direction of the phonon should be 45° with the a axis in the ac plane. Besides the Raman lines at 225 cm^{-1} (assigned to a B_1 vibration), there are two weak Raman lines observed at nearly 157 and 171 cm^{-1}, which are indicated by two arrows in Fig. 3. This result supports our interpretation of the splitting of the Raman line.

This work was supported partly by a grant from the Ministry of Education.

BULLETIN OF THE CHEMICAL SOCIETY OF JAPAN VOL. 42 1874—1878 (1969)

Solution Properties of Poly-*m*-chlorostyrene

Kimiyoshi MATSUMURA

Department of Chemistry, Aichi Kyoiku University, Nagoya

(Received December 19, 1969)

The solution properties of poly-*m*-chlorostyrene in toluene and butanone were measured by the light-scattering and viscosity methods. The dependencies of the second virial coefficients, the end-to-end distances, and the intrinsic viscosities on the molecular weights were not very different from those of the other polystyrene derivatives. It was made clear that the unperturbed dimension of poly-*m*-chlorostyrene was larger than that of poly-*p*-chlorostyrene, and similar to that of poly-*o*-chlorostyrene. The relationships between poly-*m*-chlorostyrene and solvents (toluene and butanone) were similar to those between polystyrene and poly-*o*-chlorostyrene and the solvents, but the reverse of that between poly-*p*-chlorostyrene and the latter; that is, compared with butanone, toluene was a "good" solvent for poly-*m*-chlorostyrene.

A number of reports on the solution properties of polystyrene and its derivatives, mainly *p*-substituted polymers, have been made.

In this paper, by light-scattering and viscosity measurements of poly-*m*-chlorostyrene solutions, the effects of the substituted position of the chlorine atom on the polymer chain are compared with the findings concerning poly-*o*-chlorostyrene and poly-*p*-chlorostyrene.

Experimenta

Sample. *m-Chlorostyrene.* *m*-Chlorostyene was prepared from *m*-chlorophenylmethylcarbinol, which had been obtained by the Grignard reaction of *m*-chlorobenzaldehyde and methylbromide,[1] by dehydration with potassium bisulfate; bp 56—58°C/7 mmHg.

1) L. A. Brooks, *J. Am. Chem. Soc.*, **66**, 1295 (1944).

Polymer. The monomer was polymerized by heating it in a sealed tube at 90°C for 60 hr without any initiator. The conversion rate was about 85%.

The polymer was dissolved in benzene (*ca.* 20 g/*l*), and the solution was fractionated at 35°C by successive precipitation with methanol. Thirteen fractions were obtained from 25 g of the polymer. Each fraction was redissolved in benzene, reprecipitated with methanol, and dried under reduced pressure.

Solvents. The toluene was washed successively with sulfuric acid, water, a solution of sodium hydroxide, and water. The purified toluene was refluxed with metallic sodium and distilled; bp 110.4—110.6°C.

The butanone was boiled with potassium permanganate for a day, dried with magnesium sulfate, and distilled; bp 79.2—79.5°C.

Measurements. For the measurements of the light-scattering of the solutions, a Shimadzu photometer was used. The measurements were performed at 35°C with toluene solutions and at 30°C with butanone solutions, by the use of the 436 mμ wavelength and the angular range covering 40—135°. The increments of the refractive index of the solution with the concentration, dn/dc, were measured at each temperature with the wavelength of 436 mμ.

For the viscosity measurements of the solutions with both solvents, a modified Ubbelohde viscometer was used. At 30°C the flow time of toluene was 270.1 sec in this viscometer. The measurements were performed at 30°C.

Results and Discussion

Results. By the light-scattering measurements, the weight average molecular weight, M_w, the second virial coefficient, A_2, and the root-mean-square end-to-end distance of the polymer chain, $\langle L^2\rangle^{1/2}$, were obtained by the Zimm plot for each fraction according to the ordinary method.

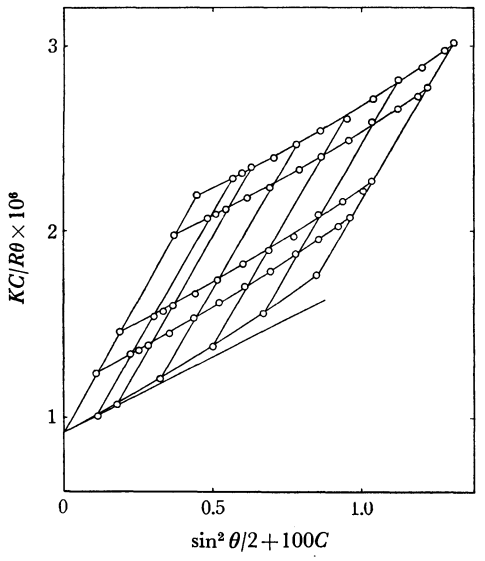

Fit. 1. Zimm plot for poly-*m*-chlorostyrene fraction 2 in butanone at 30°C.

An example of the Zimm plot for Fraction 2 of poly-*m*-chlorostyrene in butanone at 30°C is shown in Fig. 1. The observed values of dn/dc were 0.118 ml/g in a toluene solution at 35°C and 0.211 ml/g in a butanone solution at 30°C for the wavelength of 436 mμ.

As Figs. 2 and 3 show, the intrinsic viscosity,

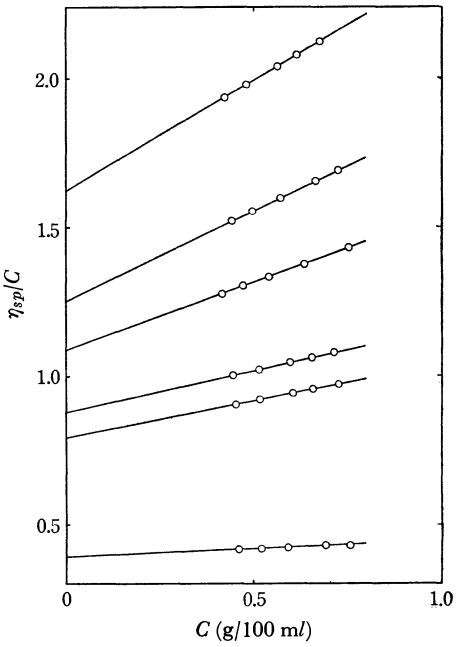

Fig. 2. Relation between reduced viscosity and concentration of poly-*m*-chlorostyrene in toluene at 30°C.

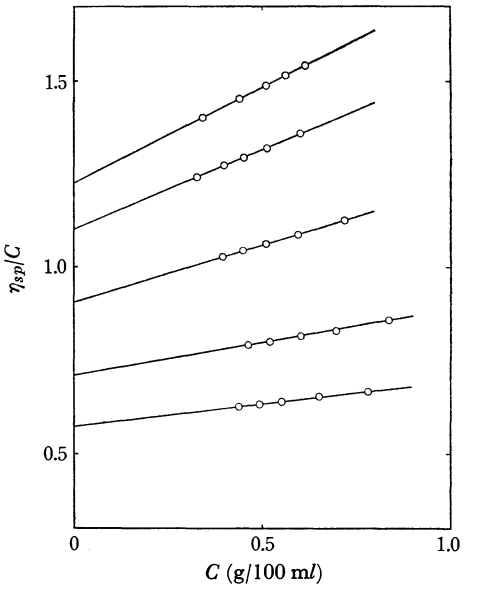

Fig. 3. Relation between reduced viscosity and concentration of poly-*m*-chlorostyrene in butanone at 30°C.

$[\eta]$, and the Huggins constant, k', are obtained through the viscosity measurements.

These results are shown in Tables 1 and 2.

The molecular-weight dependencies of $[\eta]$, A_2, and $\langle L^2\rangle^{1/2}$ are calculated by the log-log relations of M_w to these values; they are shown in Figs. 4, 5, and 6. By the least-squares method, these relations are found to be as follows:

$$[\eta] = 1.19\times10^{-4}\cdot M_w^{0.68} \text{ (dl/g)}$$
in toluene at 30°C,
$$= 1.71\times10^{-4}\cdot M_w^{0.64}$$ in butanone at 30°C,
$$A_2 = 26.5\times10^{-3}\cdot M_w^{-0.33} \text{ (mol·cc/g}^2\text{)}$$
in toluene at 35°C,
$$= 1.54\times10^{-3}\cdot M_w^{-0.17}$$ in butanone at 30°C,
$$\langle L^2\rangle^{1/2} = 0.60\times M_w^{0.54}(\text{Å})$$ in toluene at 35°C,
$$= 0.31\times M_w^{0.58}$$ in butanone at 30°C.

TABLE 1. THE EXPERIMENTAL RESULTS OF THE LIGHT-SCATTERING MEASUREMENTS AT 35°C FOR THE WAVELENGTH 436 mμ, AND OF THE VISCOSITY MEASUREMENTS AT 30°C, FOR POLY-*m*-CHLOROSTYRENE IN TOLUENE

Fraction	$M_w\times10^{-4}$	$A_2\times10^4$ $\left(\frac{\text{mol·cc}}{\text{g}^2}\right)$	$\langle L^2\rangle^{1/2}$ (Å)	$[\eta]$ (dl/g)	k'	$\Phi\times10^{-21}$
2	107.5	2.42	1080	1.515	0.37	1.3
3-1	84.8	2.90	955	1.245	0.40	1.2
3-2	64.5	3.40	830	1.080	0.39	1.2
4-1	47.6	3.50	715	0.867	0.39	1.1
4-2	41.7	4.11	645	0.788	0.40	1.2
6	14.5	5.08	370	0.387	0.36	1.1

TABLE 2. THE EXPERIMENTAL RESULTS OF THE LIGHT-SCATTERING MEASUREMENTS FOR THE WAVELENGTH 436 mμ, AND OF THE VISCOSITY MEASUREMENTS AT 30°C, FOR POLY-*m*-CHLOROSTYRENE IN BUTANONE

Fraction	$M_w\times10^{-4}$	$A_2\times10^4$ $\left(\frac{\text{mol·cc}}{\text{g}^2}\right)$	$\langle L^2\rangle^{1/2}$ (Å)	$[\eta]$ (dl/g)	k'	$\Phi\times10^{-21}$
2	106.4	1.44	992	1.224	0.35	1.4
3-1	87.7	1.52	876	1.099	0.36	1.5
3-2	67.3	1.57	721	0.904	0.38	1.6
3-3	44.1	1.68	592	0.706	0.35	1.5
4-3	32.2	1.78	493	0.571	0.37	1.5

Discussion. The relations of M_w to $[\eta]$, A_2, and $\langle L^2\rangle^{1/2}$ for poly-*m*-chlorostyrene in toluene and butanone are not very different from those for the other polystyrene derivatives.

Stockmayer and Fixman[2] proposed the following equation, by which the unperturbed dimension of the polymer chain could be deduced from the experimental values of the intrinsic viscosities and the molecular weights of the polymer in a good solvent:

$$[\eta]/M^{1/2} = K_\theta + 0.51B_0\Phi\cdot M^{1/2},$$

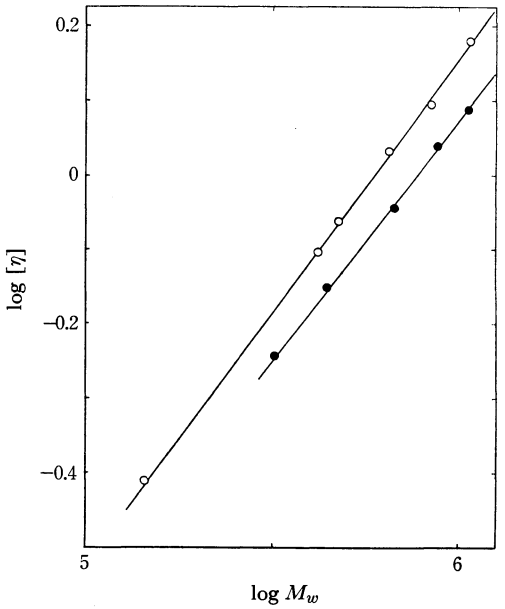

Fig. 4. Molecular weight dependencies of the intrinsic viscosities for poly-*m*-chlorostyrene at 30°C: open circle, toluene solution; colsed circle, butanone solution.

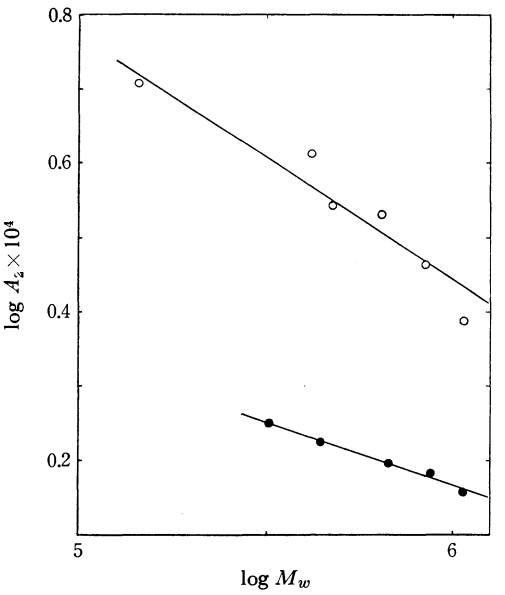

Fig. 5. Molecular weight dependencies of the second virial coefficients for poly-*m*-chlorostyrene: open circule, toluene solution at 35°C; closed circle, butanone solution at 30°C.

2) W. H. Stockmayer and M. Fixman, *J. Polymer Sci.*, **C1**, 137 (1963).

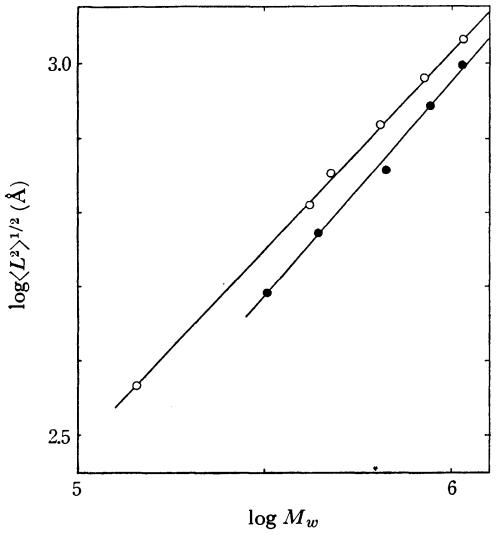

Fig. 6. Molecular weight dependencies of the end-to-end distances for poly-*m*-chlorostyrene: open circle, toluene solution at 35°C; closed circle, butanone solution at 30°C.

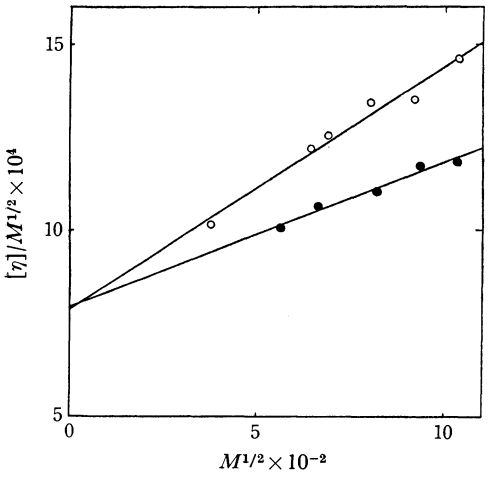

Fig. 7. Viscosity plots for poly-*m*-chlorostyrene in toluene (open circle) and in butanone (closed circle) at 30°C, by the Stockmayer-Fixman equation.

where $K_\theta=[\eta]_\theta/M^{1/2}=\Phi_0(\langle L^2\rangle_0/M)^{3/2}$, where $[\eta]_\theta$ is the intrinsic viscosity at the theta state, where $\langle L^2\rangle_0$ is the unperturbed dimension of the polymer chain, and where Φ_0 is the Flory parameter at the theta state, for which the value of 2.87×10^{21} is assumed in this paper.

As is shown in Fig. 7, the K_θ values for poly-*m*-chlorostyrene in toluene and butanone calculated by the above equation are 7.89×10^{-4} and 7.93×10^{-4} respectively; the least-squares method was used for the extrapolation to obtain the K_θ values. These values show an excellent agreement with each other and give $(7.91\pm 0.02)\times 10^{-4}$ (dl/g) as the average value.

On the basis of the K_θ value, the value of $(\langle L^2\rangle_0/M)^{1/2}$ was found to be 0.651 (Å), and the value of σ, $(\langle L^2\rangle_0/\langle L^2\rangle_f)^{1/2}$, in which $\langle L^2\rangle_f$ is the mean-square end-to-end distance, assuming a fixed valence angle of 109.5°, but a completely free internal rotation for the polymer chain; this value is obtained as 2.48.

The σ value for poly-*m*-chlorostyrene, 2.48, is slightly larger than that obtained for poly-*p*-chlorostyrene by the light-scattering measurement, 2.23,[3] and by the osmotic pressure measurements, 2.15[4] and 2.30.[5] This result shows that the chain of poly-*m*-chlorostyrene is considered to be more extended than that of poly-*p*-chlorostyrene. As the σ value for poly-*m*-chlorostyrene is also slightly larger than that for poly-*o*-chlorostyrene, 2.41,[6] the chain of the former polymer seems to be more extended than that of the latter. However, as the difference between both σ values is exceedingly small, the extension of the poly-*m*-chlorostyrene chain may be considered to be similar to that of poly-*o*-chlorostyrene.

The large σ value of poly-*m*-chlorostyrene shows that either the steric repulsion or the electrostatic repulsion, or both the repulsions, exist between the neighboring side groups, unlike the case of poly-*p*-chlorostyrene, for which no electrostatic repulsion is seen in the findings on various *p*-substituted polystyrenes.[7] The difference in σ value between these two polymers is surely caused by the difference in the substituted positions of the chlorine atoms on the phenyl group. Of course, at present, it is impossible to decide which of the two types of repulsions has the more effect on the dimensions of poly-*m*-chlorostyrene. For this purpose, it becomes necessary to measure the solution properties of *m*-substituted polystyrene, in which no electrostatic interaction occurs between the substituents. In addition, experiments under the theta conditions are necessary.

The effect of the solvent on the polymer-chain dimensions is measured by the $(\langle L^2\rangle/\langle L^2\rangle_0)^{1/2}$ ratio. A solvent which has a large value of the ratio has a strong interaction with the polymer segment; as a result of this, the polymer chain is considered to be extended greatly compared with the unperturbed state. That is, such a solvent is one of the "good" solvents. Table 3 shows the $(\langle L^2\rangle/\langle L^2\rangle_0)^{1/2}$ ratios for polychlorostyrene and polystyrene with the same degree of polymerization,

3) T. Saito, This Bulletin, **35**, 1580 (1962).
4) N. Kuwahara, K. Ogino, A. Kasai, S. Ueno and M. Kaneko, *J. Polymer Sci.*, **A3**, 985 (1965).
5) K. Takamizawa, This Bulletin, **39**, 1186 (1966).
6) K. Matsumura, *Makromol. Chem.*, in press.
7) N. Kuwahara, K. Ogino, M. Konuma, N. Iida and M. Kaneko, *J. Polymer Sci.*, **A2**, 614 (1966).

Table 3. The effects of solvents on the expansion of polychlorostyrene and polystyrene at the same degree of polymerization $P_w=7220$

Polymer	Solvent	Temp. (°C)	$\left(\frac{\langle L^2\rangle}{\langle L^2\rangle_0}\right)^{1/2}$
Poly-*m*-chlorostyrene	Toluene	35	1.61
	Butanone	30	1.45
Poly-*o*-chlorostyrene	Toluene	35	1.48
Poly-*p*-chlorostyrene	Toluene	room temp.	1.57
	Butanone	room temp.	2.05
Polystyrene	Toluene	room temp.	1.36
	Butanone	room temp.	1.04

$P_w=7220$, which corresponds to the molecular weight of 10^6 for polychlorostyrene, in toluene and butanone at about 30°C. The ratio, 1.61, for poly-*m*-chlorostyrene in a toluene solution; this is similar to that of poly-*p*-chlorostyrene in toluene, but larger than that for a butanone solution, 1.45, which is itself similar to that of poly-*o*-chlorostyrene in toluene. From a comparison of these values, it is considered that toluene is a "good" solvent for poly-*m*-chlorostyrene compared with butanone. These relationships between poly-*m*-chlorostyrene and solvents (toluene and butanone) are similar to those of polystyrene and poly-*o*-chlorostyrene*1 and the reverse to that of poly-*p*-chlorostyrene.

The relations between M_w and $[\eta]$, A_2, and $\langle L^2\rangle^{1/2}$ also give a means by which to know whether or not a solvent is a "good" solvent for a polymer. As Figs. 3, 4, and 5 shows, the observed values of $[\eta]$, A_2, and $\langle L^2\rangle^{1/2}$ of the toluene solution are larger than those of a butanone solution at the same molecular weight of poly-*m*-chlorostyrene. These relationships between poly-*m*-chlorostyrene and solvents support the above conclusion when compared with the $(\langle L^2\rangle/\langle L^2\rangle_0)^{1/2}$ ratio.

The author wishes to express his thanks to Professor Akira Kotera for his helpful discussions, and to Dr. Takahide Saito for his encouragement. The author is also indebted to Professor Tomoji Inoue for the use of the instrument for the experiments.

*1 It has been observed by the author that butanone is a theta solvent for poly-*o*-chlorostyrene.

BULLETIN OF THE CHEMICAL SOCIETY OF JAPAN VOL. 42 1878—1881 (1969)

The Dipole Moments of Diphenyl Sulfide, Sulfoxide, Sulfone, and Their Derivatives

Yoshio TOSHIYASU,*1 Yoshio TANIGUCHI, Ko KIMURA, Ryoichi FUJISHIRO, Masakuni YOSHIHARA,*2 Waichiro TAGAKI*2 and Shigeru OAE*2

Department of Chemistry, Faculty of Science, Osaka City University, Sumiyoshi-ku, Osaka

(Received December 27, 1968)

The electric dipole moments of diphenyl sulfide, sulfoxide, and sulfone and their derivatives were determined in benzene solutions at 25°C. The observed moments are used to estimate the mesomeric moments on the assumption of the vector addition of group moments. The mesomeric moments of the phenylmercapto, phenylsulfinyl, and phenylsulfonyl groups are estimated to be −0.12, 0.10, and 0.44 D, respectively. The steric effect of ortho-substituents is also discussed on the basis of the dipole moment data.

Quantum chemical considerations[1] and spectral investigations[2] both lead to the conclusion that the delocalization of π-electrons from benzene ring to the vacant 3d-π orbitals of a sulfur atom is important for aryl sulfoxides and sulfones. The chemical evidence[3] is in conformity with this prediction.

*1 Present address: Science Education Institute of Osaka Prefecture, Sumiyoshi-ku, Osaka.

*2 Permanent address: Department of Applied Chemistry, Faculty of Engineering, Osaka City University, Sumiyoshi-ku, Osaka.

1) W. E. Moffitt, *Proc. Roy. Soc. (London)*, **A200**, 409 (1950); H. P. Koch and W. E. Moffitt, *Trans. Faraday Soc.*, **47**, 7 (1951).

2) H. H. Jaffe and M. Orchin, "Theory and Application of Ultraviolet Spectroscopy," John Wiley and Sons, New York, N. Y. (1963).

3) C. C. Price and S. Oae, "Sulfur Bonding," Ronald Press, New York (1962); E. L. Wehry, *J. Am. Chem. Soc.*, **89**, 41 (1967).

Contrary to the cases of sulfoxides and sulfones, the chemical behavior of diphenyl sulfides[4] was interpreted in terms of the electron-donating conjugation of the sulfur atom, just like that of diphenyl ethers. Craig and others,[5] however, concluded that both the sulfur 3p and 3d orbitals are utilized in the sulfur-carbon bonding of aryl sulfides. The electric dipole moments of diphenyl sulfide, sulfoxide, and sulfone, and some of their derivatives were already reported,[6] but the available data are not sufficient to discuss the nature of sulfur-carbon bonding in aryl sulfides, sulfoxides, and sulfones. This paper will describe the observed dipole moments of diphenyl sulfide, sulfoxide, sulfone, and their derivatives, such as:

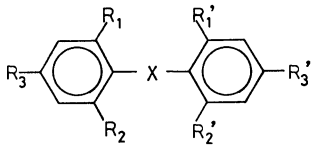

X: S, SO, SO_2

$R_1=R_1'$, $R_2=R_2'$: H, CH_3

$R_3=R_3'$: H, CH_3, OCH_3

The mesomeric moments of these compounds are estimated by comparing the present data with the observed moments of relevant aliphatic sulfides, sulfoxides, and sulfones. The contribution of the vacant 3d orbitals of sulfur atoms to conjugation will be discussed, together with the steric effect of substituents.

Experimental

The preparation of all the materials used in this work was described elsewhere.[7] Benzene was used as a solvent throughout this work, and purified by fractional distillation through a 100-cm column packed with stainless-steel helices after being shaken with concentrated sulfuric acid.[8]

The measurements of the dielectric constants, ε, the specific volumes, v, and the square of the refractive indices, n^2, were carried out by the same apparatus and method as in a previous work.[9] All the data were obtained at 25 ± 0.02°C. In the present investigation, the weight fraction, w, of solutes covers up to about 0.02.

Results and Discussion

The observed values of ε's, v's, and n^2's are, fairly well within the range of experimental errors, expressed by the linear equations of w's. The results are summarized in Table 1. The molecular polarizations, P's, were obtained from these experimental data according to the Halverstadt-Kumler's method.[10] The molecular refractions, R_D's, for the sodium D line were used to estimate the total distortion polarizations. They were assumed to be

Table 1. Dielectric constants, specific volumes, and refractive indices

	R_1,	R_2,	R_3			
X=S						
AI	H	H	H	$\varepsilon=2.2725+1.65w$	$v=1.1445-0.255w$	$n_D^2=2.244+0.326w$
AII	H	H	OCH_3	$\varepsilon=2.2725+3.38w$	$v=1.1442-0.306w$	$n_D^2=2.245+0.281w$
AIII	CH_3	CH_3	OCH_3	$\varepsilon=2.2725+1.96w$	$v=1.1444-0.244w$	$n_D^2=2.245+0.242w$
AIV	CH_3	CH_3	CH_3	$\varepsilon=2.2725+1.01w$	$v=1.1441-0.197w$	
X=SO						
BI	H	H	H	$\varepsilon=2.2725+9.36w$	$v=1.1444-0.325w$	$n_D^2=2.243+0.316w$
BII	H	H	OCH_3	$\varepsilon=2.2725+9.63w$	$v=1.1442-0.348w$	$n_D^2=2.245+0.253w$
BIII	CH_3	CH_3	OCH_3	$\varepsilon=2.2725+6.71w$	$v=1.1442-0.321w$	$n_D^2=2.244+0.302w$
BIV	CH_3	CH_3	CH_3	$\varepsilon=2.2725+6.45w$	$v=1.1442-0.246w$	
X=SO_2						
CI	H	H	H	$\varepsilon=2.2725+13.1w$	$v=1.1443-0.362w$	$n_D^2=2.243+0.232w$
CII	H	H	OCH_3	$\varepsilon=2.2725+13.7w$	$v=1.1441-0.383w$	$n_D^2=2.244+0.260w$
CIII	CH_3	CH_3	OCH_3	$\varepsilon=2.2725+9.26w$	$v=1.1441-0.334w$	$n_D^2=2.244+0.174w$
CIV	CH_3	CH_3	CH_3	$\varepsilon=2.2725+9.10w$	$v=1.1441-0.278w$	

4) A. Mangini and R. Passerini, *J. Chem. Soc.*, **1956**, 4954; G. Bergson, *Arkiv. Kemi.*, **19**, 181, 265 (1962).

5) D. P. Craig and C. Zauli, *Gazz. Chim. Ital.*, **90**, 1700 (1960); L. Goodman and R. W. Taft, *J. Am. Chem. Soc.*, **87**, 4386 (1965).

6) C. W. N. Cumper and S. Walker, *Trans. Faraday Soc.*, **52**, 193 (1956); M. J. Aroney, L. R. Fischer and R. J. W. LeFevre, *J. Chem. Soc.*, **1963**, 4450; C. W. N. Cumper, J. F. Read and A. I. Vogel, *ibid.*, **1965**, 5323, 5860.

7) S. Oae, M. Yoshihara and W. Tagaki, This Bulletin, **40**, 951 (1967).

8) A. Weissberger *et al.*, "Organic Solvents," Interscience Publishers, New York (1955).

9) K. Kimura, Y. Toshiyasu and R. Fujishiro, This Bulletin, **39**, 1681 (1966).

10) I. F. Halverstadt and W. D. Kumler, *J. Am. Chem. Soc.*, **64**, 2988 (1942).

Table 2. Polarization data and dipole moments

	P (cc)	R_D (cc)	μ (D)
AI	107.2	63.8	1.46
AII	217.9	77.5	2.62
AIII	195.8	98.4	2.18
AIV	138.0	93.1	1.48
BI	405.5	63.8	4.09
BII	537.3	77.7	4.79
BIII	480.0	100.0	4.31
BIV	423.9	93.1	4.02
CI	587.4	62.7	5.07
CII	782.2	79.7	5.87
CIII	662.9	94.9	5.27
CIV	595.5	92.0	4.96
R	SR_2*	OSR_2*	O_2SR_2*
Methyl	(1.45D)	(3.89D)	(4.26D)
Ethyl	1.61	4.02	4.50
n-Propyl	1.60	3.97	4.48
n-Butyl	1.60	4.04	4.53
n-Amyl	1.60	3.98	4.53
Average	1.60	4.00	4.50

* These data were taken from Ref. 6.

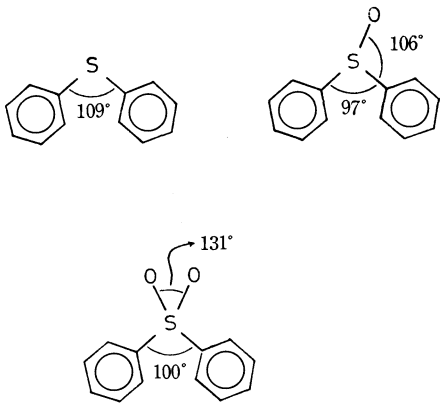

Fig. 1. The valence angles of diphenyl sulfide, sulfoxide, and sulfone.

equal to 1.05 R_D. The polarization values and dipole moments, μ's, are tabulated in Table 2, together with the dipole moments of the relevant alkyl sulfur compounds. The mesomeric moments of diphenyl sulfides, sulfoxides, and sulfones were calculated on the basis of the following two assumptions: (1) the difference in dipole moments between diphenyl sulfur compounds and the relevant dialkyl ones is due to delocalization, and the vector subtraction of the latter dipole moments from the former gives the mesomeric moments, and (2) the valence angles[11] of the aryl sulfur compounds

11) S. C. Abrahams, *Quart. Rev.*, **5**, 407 (1956).

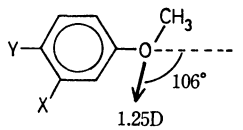

*1 X : H
Y : Cl, Br, CH_3
*2 X : Cl
Y : H

Fig. 2. The group moments of anisole.

*1 Data found in the following tables: A. L. McClellan, "Tables of Experimental Dipole Moments," W. H. Freeman and Company, San-Francisco (1963).
*2 Y. Toshiyasu, unpublished work.

Table 3. Mesomeric moments*

AI	−0.12D
AII	−0.03
BI	0.10
BII	0.14
CI	0.44
CII	0.52
Thioanisole**	−0.51
2,4,6-Trimethyl thioanisole**	−0.16

* The sense of moments is directed in such a way as C^+–S^- is positive.
** These moments were calculated by the use of data found in "Tables of Experimental Dipole Moments."

depicted in Fig. 1 are used to calculate the mesomeric moments per carbon-sulfur bonding.

It is not a reasonable assumption to divide the conjugation of bis-*p*-methoxyphenyl sulfur compounds in two methoxyphenyl and one diphenyl sulfur part. However, the approximate mesomeric moments of carbon-sulfur bonding are determined by taking the vector subtraction of the group moment of anisole, which is shown in Fig. 2. In order to calculate the mesomeric moment of BI (or BII), it is necessary to estimate the S–O bond moment. This was done by the use of the dipole moment of dialkyl sulfide, that of BI (or BII), and that of dialkyl sulfoxide. The mesomeric moments thus calculated are tabulated in Table 3, together with those of anisole and one of its derivatives.

Table 3 clearly shows that the conjugative effect operative in AI or AII is the same as that of thioanisole, although the mesomeric moment of AI or AII is considerably smaller than that of thioanisole. The conformation[12] of diphenyl sulfide is similar to that of diphenyl ether.[13] It may be inferred that the maximum conjugation of diphenyl sulfide is inhibited by the twisting of two benzene rings. On

12) J. Toussaint, *Bull. Soc. Chim. Belges*, **54**, 319 (1945).

13) K. Higasi, "Dielectric Relaxation and Molecular Structure," Res. Inst. App. Elect., Hokkaido Univ., No. 9, 1961.

the other hand, the mesomeric moments of BI and CI are directed in the opposite sense of those of A's.

As Moffitt[1] and others[2] pointed out, the 3d vacant orbitals of sulfur atoms contribute to the conjugative effect, which is enhanced by methoxy substituents at the para positions. There is a possibility of this type of conjugation in aryl sulfides,[5] also. As far as the ground state is concerned, the increase in the effective positive charge of sulfur atoms[2] is a necessary condition for this type of conjugation. This condition is fulfilled for aryl sulfoxides and sulfones. Any conclusion about the contribution of the vacant 3d orbitals of aryl sulfides to the conjugative effect, however, can not be drawn from the dipole moment measurements alone, but it is evident that the electron-withdrawing conjugation of the sulfur atoms of aryl sulfides is negligible or at least much less than the electron-donating one.

As already stated, the two benzene rings of diphenyl sulfide are twisted about 40° out of the C–S–C plane.[14] This may be due to the steric effect. Hence, the steric hindrance by methyl substituents at the ortho positions may not be observed appreciably. The dipole moment of dimesityl sulfide is not so much different from that of diphenyl sulfide. This is true for aryl sulfoxides and sulfones, although the decrease in the dipole moment of dimesityl sulfone relative to that of diphenyl sulfone amounts to 0.11 D. The change in the valence angle is probably, at least in part, responsible for this decrease in the dipole moment.

14) M. J. Aroney, R. J. W. LeFevre and J. Saxby, *J. Chem. Soc.*, **1963**, 1167.

BULLETIN OF THE CHEMICAL SOCIETY OF JAPAN VOL. 42 1881—1885 (1969)

Derivatographic Studies on Transition Metal Complexes. I. Deaquation-Anation Reaction of Aquopentaammine-chromium(III) Complexes*1

Ryokichi TSUCHIYA, Yoriko KAJI, Akira UEHARA and Eishin KYUNO

Department of Chemistry, Faculty of Science, Kanazawa University, Kanazawa

(Received August 13, 1968)

By using a Derivatograph, the simultaneous analyses in TGA, DTA and DTG on the several aquopentaamminechromium(III) complexes were attempted. The enthalpy changes, ΔH, in the deaquation-anation processes of aquopentaamminechromium(III) nitrate, chloride, bromide, iodide, sulfate and sulfite were calculated as 11.9, 6.1, 9.0, 10.8, 13.8 and 12.8 kcal/mol, respectively, the activation energies, $E^{\neq}$, in the corresponding processes of the nitrate, chloride, bromide, sulfate and sulfite were obtained by the DTG curve analysis as 18, 28, 38, 36 and 33 kcal/mol, and those in the nitrate, chloride, bromide, iodide, sulfate and sulfite were obtained by the DTA curve analysis as 14, 25, 36, 19, 39 and 32 kcal/mol, respectively.

A number of thermochemical studies on the metal complexes by means of thermogravimetric analysis (TGA) with a thermobalance[1] or by means of the dissociation pressure method[2] have been reported. Since the application of the differential thermal analysis (DTA) alone to the solid phase reaction of the metal complexes in the field of thermochemical studies can not give satisfactory information on the reactions, owing to the ambiguity of the stoichiometric relation in it, simultaneous measurements of DTA, TGA and derivative thermogravimetric analysis (DTG) are indispensable for obtaining a consistent interpretation for the reactions. Nevertheless, such a technique for the simultaneous measurements of TGA and DTA was never applied until several years ago.[3]

The simultaneous measurements of TGA and DTA with a Derivatograph on the transition metal complexes with a single sample was undertaken.

*1 Presented at the 17th Symposium on Coordination Compounds of the Chemical Society of Japan, Hiroshima, December, 1967.

1) M. Mori and R. Tsuchiya, This Bulletin, **33**, 841 (1960); N. Tanaka and M. Nanjo, *ibid.*, **37**, 1330 (1964).

2) M. Mori and R. Tsuchiya, *ibid.*, **32**, 467 (1959).

3) W. W. Wendlandt and J. L. Bear, *J. Inorg. Nucl. Chem.*, **22**, 77 (1961).

As the first series of derivatographic studies, the deaquation-anation reaction of aquopentaamminechromium(III) complexes was investigated with the above equipment and a comparison of the thermal properties between them and the corresponding cobalt(III) complexes was also made.

Experimental

Materials. The aquopentaamminechromium(III) nitrate (I) was prepared by the methods proposed by one of the authors.[4] The corresponding chloride (II), bromide (III), iodide (IV), sulfate (V) and sulfite (VI) were prepared by adding ammonium chloride and hydrochloric acid, potassium bromide and hydrobromic acid, potassium iodide, sodium sulfate and potassium hydrogen sulfite to aquopentaamminechromium(III) nitrate I as a starting material, respectively;[4] they were identified by the chemical analysis and the infrared absorption spectra.

Measurements. The TGA, DTA and DTG curves were automatic-photographically recorded with a single sample in a constant nitrogen stream with a Metrimpex Derivatograph Typ-OD-102 made in Hungary,[5] which is a most useful equipment for the simultaneous measurements of the above three curves. Five hundred milligrams of samples were used in each measurement unless otherwise stated. The particle size of the samples was within the range between 100 and 200 mesh. The heating rate was about 1°C per minute. IR and far-IR spectra of the samples, both before and after the deaquation-anation reactions, were measured with a JASCO Model IR-E IR Spectrophotometer and a Hitachi EPI Far-IR Spectrophotometer, respectively.

Results and Discussion

The derivatograms, containing T, TGA, DTA and DTG curves, recorded for the complexes, II, III and IV, are shown in Fig. 1, and those for I, V and VI are shown in Fig. 2. In these figures, TGA curves are recorded in the lower part of the chart and the other T, DTA and DTG curves are in the upper part. Recordings of DTA and DTG were operated so as to be approximately expanded within the upper part of the chart by adjusting the sensitivity of the galvanometer.

That the aquopentaamminechromium(III) complexes, $[Cr(H_2O)(NH_3)_5]X_3$ (X=halogenide, nitrate, sulfate or sulfite anion), give rise to the deaquation-anation reaction, that is, they lose the coordinated water to yield acidopentaamminechromium(III) complexes, $[CrX(NH_3)_5]X_2$, is well known.[6] The first dropping of the TGA curves and the simultaneous appearance of the endothermic peaks in DTA curves for the complexes concerned shown in Figs. 1 and 2 suggest the occurrence of such deaquation-anation processes in the solid phase.

The temperatures at which the deaquation of the aquopentaamminechromium(III) complexes begins, appearing in TGA curves, T, and the temperatures at which endothermic peaks show the maximum in DTA curves, T_m, for the respective reactions, shown in Figs. 1 and 2 are summarized in Table 1.

It is found from this table that the temperature at which the deaquation starts becomes higher in the order of I<II<III<IV<V<VI. This order is not in good agreement with that proposed by Wendlandt *et al.*[3] for the complexes, I, II, III and IV, but it is approximately in agreement with that reported by Tanaka *et al.*[7] for hexaamminenickel(II) complexes, so far as the nitrate, chloride, bromide and iodide are concerned. The sequence obtained in this work is approximately parallel to the increasing order of the ionic radii of the counter-anions entering into the coordination sphere after

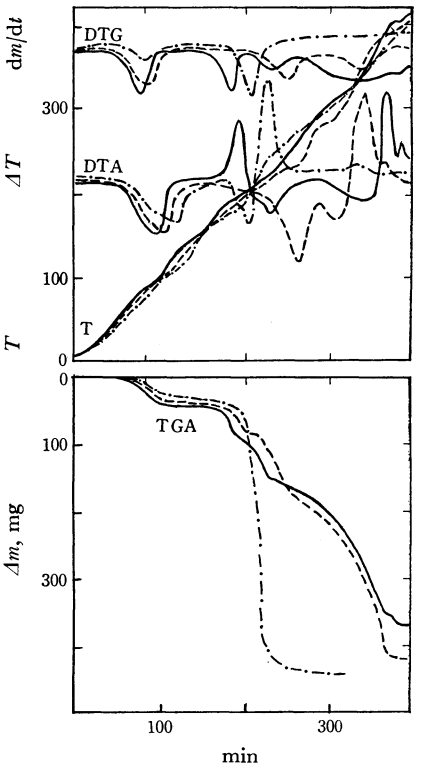

Fig. 1. Derivatograms for aquopentaamminechromium(III) chloride (——), bromide (------) and iodide (-----).

4) E. Kyuno, M. Kamada and N. Tanaka, This Bulletin, **40**, 1848 (1967).

5) F. Paulik, J. Paulik and L. Erdey, Hung. Patent No. 144, 548 (1954); No. 145, 469 (1955); No. 146, 461 (1956).

6) S. M. Jφrgensen, *J. Prakt. Chem.*, **18**, 209 (1878).

7) N. Tanaka, M. Kagawa and M. Kamada, Presented at the 16th Symposium on Coordination Compounds of the Chemical Society of Japan, Tokyo, December, 1966.

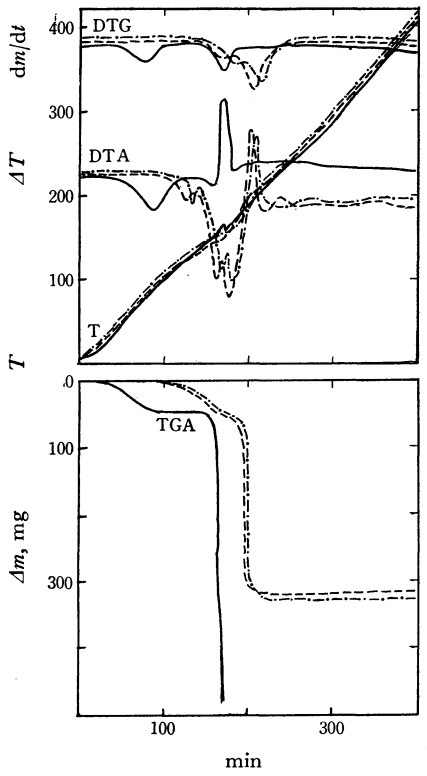

Fig. 2. Derivatograms for aquopentaaminechromium(III) nitrate (——), sulfate (------) and sulfite (-----).

Table 1. The temperatures, T, at which the complexes begin to be deaquated and the peak temperatures, T_m (°C)

Complex	T	T_m
I	40	85
II	60	82
III	68	95
IV	70	125
V	100	134
IV	120	140

the deaquation. It may suggest the apparent increasing order of the thermal stability against the deaquation-anation reaction among the above aquopentaammine complexes concerned.

The enthalpy change, ΔH, in the deaquation-anation reaction per mole of sample is expressed as below in terms of the peak area, A, formed by DTA curves.

$$\Delta H = \frac{K}{N} A, \qquad (1)$$

where K is a constant containing the conductivity of the sample and depending upon the structure of the equipment and the heating conditions, and N is the numbers of moles of sample, *i. e.*, the value of the mass divided by the molecular weight of the sample. The ratio, $\Delta H/A$, should be, therefore, the function of the dehydration temperature of the materials.

In order to confirm these relationships, the values of $\Delta H/A$ were plotted against the peak temperatures of DTA curves in the dehydration reactions in Fig. 3 for barium chloride dihydrate, cobalt(II) sulfate heptahydrate, copper(II) sulfate pentahydrate, nickel(II) sulfate heptahydrate, ammonium aluminum alum, potassium chromium(III) alum, copper(II) sulfate monohydrate and cobalt(II) sulfate pentahydrate. Since these plottings lie approximately on a smoothed curve, it may be appropriate to select copper(II) sulfate pentahydrate as a standard sample to determine the constant K in Eq. (1).

By comparing the peak area in the DTA curves in the deaquation-anation reaction of aquopentaamminechromium(III) complexes concerned with that appearing in DTA in the dehydration of copper(II) sulfate pentahydrate, and applying ΔH= 13.6 kcal/molH_2O as the mean value of the enthalpy change per one mole of water calculated from the total enthalpy change[8] in the liberation of the first four moles of water from copper(II) sulfate pentahydrate, the enthalpy change in the deaquation-anation reaction desired can be determined.

These values, ΔH, for the aquopentaamminechromium(III) complexes obtained by the above method are listed in Table 2, together with those for the aquopentaamminecobalt(III) complexes cited from reference.[9]

It is seen in this table that the values of ΔH for the complexes, I, II and III, are in remarkably good agreement with those for the corresponding

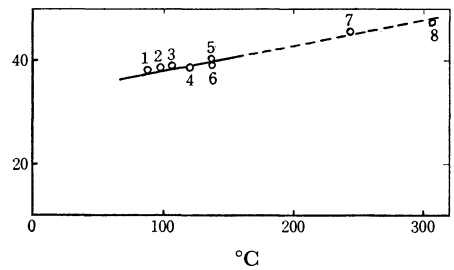

Fig. 3. Correlation of the ratio, $\Delta H/A$, *vs.* temperature.

1, $BaCl_2 \cdot 2H_2O$ 2, $CoSO_4 \cdot 7H_2O$
3, $CuSO_4 \cdot 5H_2O$ 4, $NiSO_4 \cdot 7H_2O$
5, NH_4-Al-Alum 6, K-Cr-Alum
7, $CuSO_4 \cdot H_2O$ 8, $CoSO_4 \cdot 5H_2O$

8) K. Sano, *Sci. Rep. Tohoku Imp. Univ., Ser. I*, **24**, 719 (1936).

9) F. D. Rossini, D. D. Wagman, W. H. Evans, S. Levine and I. Jaffe, "Selected Values of Chemical Thermodynamic Properties," United States Government Printing Office, Washington, D. C. (1952).

Table 2. Enthalpy changes, ΔH, in the deaquation-anation reactions of aquopentaammine-chromium(III) and the corresponding cobalt-(III) complexes

Complxe	ΔH kcal/mol	Complex	ΔH kcal/mol
I	11.9	$[CoH_2O(NH_3)_5](NO_3)_3$	11.6
II	6.1	$[CoH_2O(NH_3)_5]Cl_3$	6.7
III	9.0	$[CoH_2O(NH_3)_5]Br_3$	8.7
IV	10.8		
V	13.8		
VI	12.8		

cobalt(III) complexes, respectively, and the increasing order of the values, ΔH, such as in II$<$III$<$IV$<$I$<$VI$\lesssim$V, is approximately parallel, except for the nitrate, I, to the order of their increasing thermal stability presumed by the deaquation-anation temperatures, T or T_m, listed in Table 1.

Up to date, the kinetic analysis has, in general, been performed by the isothermal method, but it is very troublesome, though accurate, owing to the necessity of, at least, several measurements of the quantity concerning the reactants or products at various temperatures. On the contrary, the kinetic analysis in the thermal decomposition processes became very advantageous, if the DTG curve is applied, because it will be possible by using only one curve obtained by the temperature-elevating method.

The rate constant, k, is given by the equation[10]

$$k = \frac{(A/N_0)^{n-1}(-\mathrm{d}x/\mathrm{d}t)}{(A-a)^n}, \qquad (2)$$

where N_0 is the number of mole of the sample at the time at which the DTG peak appears, A and a are the total peak area and the area swept up till the time, t, respectively, $\mathrm{d}x/\mathrm{d}t$ is the displacement of the DTG curve from the base line at time t, that is, parallel to the rate of the weight change,

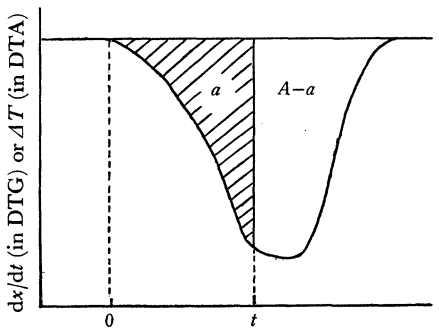

Fig. 4. Kinetic analyses on the basis of DTG and DTA curves.

and n is the reaction order, as shown in Fig. 4.

If the reaction proceeds in the first order, Eq. (2) is simplified as

$$k = \frac{-\mathrm{d}x/\mathrm{d}t}{A-a}. \qquad (3)$$

The logarithm values of the rate constant for the deaquation-anation reaction in the aquopenta-ammine complexes, I, II, III, V and VI, are calculated by using Eq. (3) and they are plotted against the reciprocal of the absolute temperature, which are shown in Fig. 5.

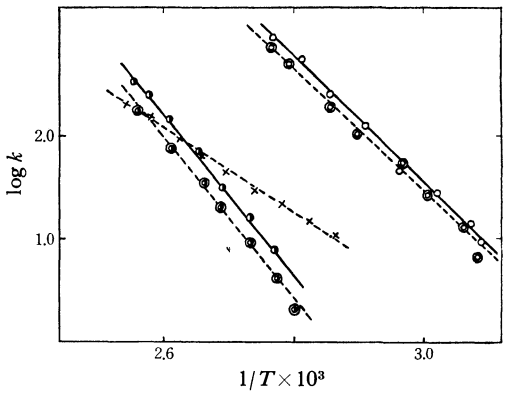

Fig. 5. Arrhenius plots, $\log k - 1/T$, for the deaquation-anation reactions of aquopentaamminechromium(III) chloride (○◎), bomide (◐◑) and iodide (×), from DTG (——) and from DTA (------).

Another available method of kinetic analysis is the use of the DTA curve. The rate constant is given by the equation[11]

$$k = \left(\frac{KAV}{N_0}\right)^{n-1} \frac{C_p(\mathrm{d}\Delta T/\mathrm{d}t) + K\Delta T}{\{K(A-a) - C_p\Delta T\}^n}, \qquad (4)$$

where V is a volume of a sample, ΔT is the temperature difference between the sample and the inert material, $\mathrm{d}\Delta T/\mathrm{d}t$ expresses the slope of DTA curve at time t, and C_p is the molecular heat of the sample. ΔT is corresponding to $\mathrm{d}x/\mathrm{d}t$ in the case of DTG curve shown in Fig. 4, and other terms are identical to the corresponding ones noted in Eq. (2).

It will be difficult to find the value of the rate constant from Eq. (4), since the molecular heat is not generally known. However, when the terms containing the molecular heat in Eq. (4) are negligibly small and the reaction is assumed to proceed in the first order, Eq. (4) is simplified as

$$k = \frac{\Delta T}{A-a}. \qquad (5)$$

Equation (5) can be formerly obtained by replacing $-\mathrm{d}x/\mathrm{d}t$ in Eq. (3) by ΔT, and the analytical

10) N. G. Dave and S. K. Chopra, *Z. Physik. Chem.*, **48**, 257 (1966).

11) H. J. Borchardt and F. Daniels, *J. Am. Chem. Soc.*, **79**, 41 (1957).

processes are quite the same in both DTG and DTA curves.

Arrhenius plots obtained for the chloride, bromide and iodide as the representatives by using Eq. (5) are also shown in Fig. 5, together with the plots by DTG analysis. The activation energies, $E^{\neq}$, obtained from the Arrhenius plots in the case of DTG and DTA analyses are summarized in Table 3.

Table 3. Activation energies, $E^{\neq}$, in the deaquation-anation reactions of aquopentaamminechromium(III) and that of one of the cobalt(III) complexes

Complex	$E^{\neq}$ kcal (from DTG)	$E^{\neq}$ kcal (from DTA)	$E^{\neq}$ by Wendlandt[3]
I	18	14	16
II	28	25	18
III	38	36	31
IV	—	19	18
V	36	39	—
VI	33	32	—
$[CoH_2O(NH_3)_5]Cl_3$			22[12]

In this table, the activation energies in the deaquation-anation reactions of aquopentaamminechromium(III) halides and nitrate reported by Wendlandt *et al.*[8] and that of the corresponding aquopentaamminecobalt(III) chloride reported by one of the authors[12] are also included, which was, however, obtained by the isothermal kinetic measurement different from those in the present work by the dynamic temperature-elevating method.

That nitrate has the smallest value of activation energy supports the fact that nitrate has the lowest dissociation temperature of all the complexes treated in this paper and undergoes deaquation most easily.

Although the methods to obtain the activation energy employed by authors in this study and by Wendlandt *et al.*, so far as the nitrate and the halides are concerned, are different from each other, the data by two groups of workers are in satisfactory agreement with one another except for those of the chloride.

12) M. Mori, R. Tsuchiya and Y. Okano, This Bulletin, **32**, 1029 (1959).

If these deaquation-anation reactions belong to S_N1 reaction, *i. e.*, the rate-determining step in these reactions consists in the deaquation process such as

$$N_5Cr\text{–}OH_2 \longrightarrow N_5Cr + OH_2\,, \qquad (a)$$

where N_5Cr expresses $Cr(NH_3)_5$ group, the activation energies in these reactions should be approximately close to each other. But it is not always the case as shown in Table 3. When the rate of the anation process such as,

$$N_5Cr + X \longrightarrow N_5CrX\,, \qquad (b)$$

where X expresses halide ions, nitrate, sulfate or sulfite anions, is larger than that of the deaquation process, (a), the deaquation-anation reaction will belong to S_N1 reaction owing to the rate-determining step of (a) as described above, whereas the rate of the process (b) is smaller than that of the process (a), the reaction will belong to S_N2 reaction due to the rate-determining step of (b).

The fact given in Table 3 that the activation energies in the deaquation-anation reactions of the bromide, sulfate and sulfite are, above all, larger than those of the chloride, iodide and nitrate, suggests that the deaquation-anation reactions in the former complexes, the bromide, sulfate and sulfite, include, to some extent, the tendency of S_N2 reaction, at least, at the earlier step of these reactions, differing from those in the latter complexes. The reason for this may be attributed to the larger ionic radii of the bromide, sulfate and sulfite anions, but a more decisive reason is not clear.

That the activation energy for the aquopentaamminechromium(III) chloride is slightly larger than that for the corresponding cobalt(III) chloride as shown in the table may be due to a somewhat larger force constant in $Cr\text{–}OH_2$ in the former complex than that in $Co\text{–}OH_2$ in the latter one.[13]

The authors wish to express their appreciation to the Ministry of Education for the financial support granted for this research.

13) T. Shimanouchi, I. Nakagawa and J. Shiraishi, Presented at the 12th Symposium on Coordination Compounds of the Chemical Society of Japan, Tokyo, December, 1962.

BULLETIN OF THE CHEMICAL SOCIETY OF JAPAN VOL. 42 1886—1891 (1969)

Derivatographic Studies on Transition Metal Complexes. II.*1 Thermal Reaction in the Solid State of Chromium(III) and Cobalt(III) Aquo-EDTA-like Complexes*2

Ryokichi Tsuchiya, Akira Uehara and Eishin Kyuno

Department of Chemistry, Faculty of Science, Kanazawa University, Kanazawa

(Received August 13, 1968)

The thermal reaction processes in the solid state of the following chromium(III) and cobalt(III) aquo complexes with EDTA or the related aminopolycarboxylic acids were investigated by means of derivatography: [CrHedta(H_2O)] (I), [CrHpdta(H_2O)]·H_2O (II), [CrHtmta(H_2O)]·H_2O (III), [Cr(OH)Hapda(H_2O)$_2$] (IV) and [Co(OH)Hapda(H_2O)$_2$] (V) (edta, pdta, tmta and apda are the abbreviated forms of ethylenediaminetetraacetate, propylenediaminetetraacetate, trimethylenediaminetetraacetate and ammoniapropionicdiacetate anions, respectively.). With complex I, the carboxylate anion free from coordination to metal coordinated when the dehydration took place at *ca.* 280°C. It resulted in the change of the coordination number of EDTA from quinquedentate to sexadentate. In the case of complexes II and III, the transition appeared below *ca.* 100°C where the coordinated water molecule in the coordination sphere is thermally expelled to the outer sphere as the protonated form due to the coordination of a carboxylate anion. PDTA and TMTA (conjugated acids of pdta and tmta respectively) also changed from quinquedentate to sexadentate ligands in this step. Of complexes IV and V, the coordinated hydroxo group was excluded as a water molecule together with the hydrogen in a free carboxylate anion at *ca.* 140°C to make the coordination number of APDA(conjugated acid of apda) change from terdentate to quadridentate. The activation energies and the enthalpy changes in each thermal reaction process were determined by the analysis of their derivatograms.

The thermal behaviors in the deaquation-anation reaction of a series of the aquopentaamminechromium(III) complexes in the solid phase have been discussed on the basis of the data obtained from "Derivatograms" in the preceeding paper.*1 One merit in the simultaneous measurements of TGA and DTA curves by "Derivatograph" is being able to deduce whether the enthalpy change appearing in the DTA curve is due to the weight loss of the sample or due to only the phase change. The combination of the IR data concerning the samples before and after the thermal reactions with the results obtained by Derivatograph may give detailed information about the structural transformations in the reactions.

Several aquo complexes of chromium(III) and cobalt(III) with EDTA or the related ligands, PDTA, APDA or TMTA were prepared. Investigations were carried out (1) to obtain information on the structural change in the successive, thermal reaction processes for these complexes and (2) to determine, if possible, the enthalpy changes and the energies of activation concerning the respective reactions. The ligands used in this study are given in Fig. 1.

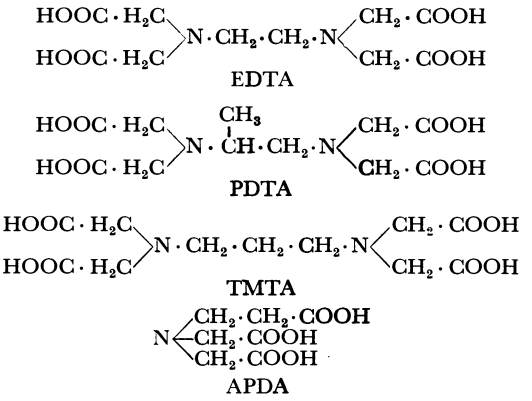

Fig. 1. Rational formulas of the ligand.

Experimental

Preparation of Starting Materials. *Hydrogenethylenediaminetetraacetatoaquochromium(III)*: [CrHedta(H_2O)] (I). This was prepared by a method given in literature[1] and was identified by elemental analysis

*1 Part I of this series: R. Tsuchiya, Y. Kaji, A. Uehara and E. Kyuno, This Bulletin, **42**, 1881 (1969).

*2 Presented at the 21st Annual Meeting of the Chemical Society of Japan, Osaka, March, 1968.

1) D. T. Sawyer and J. M. Mckinnie, *J. Am. Chem. Soc.*, **82**, 4191 (1960).

and IR spectral measurement.

Hydrogen propylenediamine tetraacetato aquo chromium(III) Monohydrate: [CrHpdta(H_2O)]·H_2O (II). The preparation was carried out by the same method[1] and the chemical formula was checked by elemental analysis and IR spectra.

Hydrogen trimethylenediaminetetraacetatoaquochromium(III) Monohydrate: [CrHtmta(H_2O)]·H_2O (III). Thirteen grams of chromium(III) chloride hexahydrate were dissolved in 100 m*l* of water and then 15 g of TMTA were added. After the solution was heated on a water bath at about 80°C for a while, 25 g of potassium hydrogencarbonate was added little by little. After being evaporated to half the volume by aeration, the solution was when necessary, quickly filtered and the filtrate was kept to stand for a while. When red crystals were deposited, they were filtered and washed with a small amount of ethanol-water (1:1) mixture and then with ethanol-ether (1:1) mixture and air-dried. Yield about 18 g. The product was recrystallized in water.

Found: C, 33.77; N, 6.95; H, 4.69%. Calcd for [CrHtmta(H_2O)]·H_2O: C, 33.75; N, 7.16; H, 4.61%.

Hydroxohydrogenammoniapropionicdiacetatodiaquochromium-(III): [Cr(OH)Hapda(H_2O)$_2$] (IV). This was prepared by the method reported previously[2] and the identification was carried out in a way similar to that described above.

Hydroxohydrogenammoniapropionicdiacetatodiaquocobalt(III): [Co(OH)Hapda(H_2O)$_2$] (V). Twelve grams of cobalt-(II) chloride hexahydrate were dissolved into 100 m*l* of water and another 100 m*l* of water containing 10 g of APDA neutralized with 10 g of potassium hydrogencarbonate was added, and then the mixture was heated on a water bath for about one hour. The clear pink solution obtained was oxidized by 10 m*l* of 10% hydrogen peroxide solution to produce the cobalt(III) complex. After the pH of the solution was adjusted to 2—3, the solution was stood for a few hours. Purple crystals were obtained. The products were recrystallized from its concentrated aqueous solution. Yield about 5 g.

Found: C, 26.49; N, 4.72; H, 4.65%. Calcd for [Co(OH)Hapda(H_2O)$_2$]: C, 26.65; N, 4.44; H, 4.47%.

Derivatographic Measurement. The derivatograms of these complexes expressing simultaneously the results of thermogravimetric analysis (TGA), differential thermal analysis (DTA) and derivative thermogravimetric analysis (DTG) were obtained with a Metrimpex Derivatograph Typ-OD-102 made in Hungary. All the experiments were carried out in a nitrogen stream under the heating rate of 1°C/min, and 500 mg of the sample was used in each run. The analyses of derivatograms for each reaction process were carried out in a manner similar to that explained in a previous paper.*[1]

IR Measurement. The IR spectra were measured with a JASCO Model IR-E Spectrophotometer in Nujol mull state for the samples in the successive, appropriate heating steps appointed from the derivatograms.

Conductivity Measurement. The conductivities of the samples were determined with a Yokogawa Universal Bridge BV-Z-13A.

Result and Discussion

Dehydration Mechanisms in Aquo-EDTA-Like Complexes. Some chemical properties of the samples, I—V, including their IR data are shown in Table 1. Their IR spectra show two characteristic bands near at 1730 and 1640 cm^{-1} which correspond to those assigned by Busch and Bailar[3] in cobalt(III) EDTA complex to the stretching vibration concerning the non-coordinated and coordinated carboxylate anions, respectively. In complexes III, IV and V, above all, the band at 1730 cm^{-1} is shifted to about 1690 cm^{-1} probably due to the stronger interaction between the non-coordinated carboxylate and the neighboring, coordinated H_2O or OH group.[2]

Table I. Some chemical properties of complexes

Complex	IR ($\nu_{C=O}$)(cm^{-1})		Molar conductivity* (mho cm^{-1})	pH**
	-COOH	-COO-M		
I	1738 (s)	1640 (vs)	211.6	2.5
II	1728 (s)	1635 (vs)	278.1	2.6
III	1685 (s)	1630 (vs)	153.8	4.2
IV	1690 (s)	1640 (vs)	2.8	6.4
V	1689 (s)	1640 (vs)	3.2	6.2

* 1.0×10^{-3} mol/*l* aqueous solution was used.
** 1.0×10^{-2} mol/*l* aqueous solution was used.

The lower values of pH and the higher values of the conductivities in complexes, I, II and III, show that they dissociate, to a great extent, into the hydrogen ion and complex anion. But complexes IV and V are all non-electrolytic species in aqueous solution.

The derivatograms for each complex, I—V, are shown in Figs. 2 and 3. The IR spectra of the samples taken at the appropriate step of the thermal reaction processes appearing in the derivatograms were measured. They are shown in Fig. 4.

Complex I loses one mole of the coordinated water about 280°C as seen in Fig. 2, and Fig. 4-a shows that the absorption peak at 1738 cm^{-1} assigned to the non-coordinated carboxylate disappears after the heating at 280°C. It may suggest that, in complex I, the non-coordinated carboxylate comes into the coordination to metal as soon as one water molecule is liberated at the temperature.

In the case of complex II, a small but distinct endothermic change is observed in the DTA curve just before the TGA curve begins to show any weight decrease of the sample as seen in Fig. 2. Fig. 4-b shows that the band assigned to the non-coordinated carboxylate also disappears but the band assigned to the coordinated one remains

2) A. Uehara, E. Kyuno and R. Tsuchiya, This Bulletin, **41**, 2385 (1968).

3) D. H. Busch and J. C. Bailar, Jr., *J. Am. Chem. Soc.*, **75**, 4574 (1953).

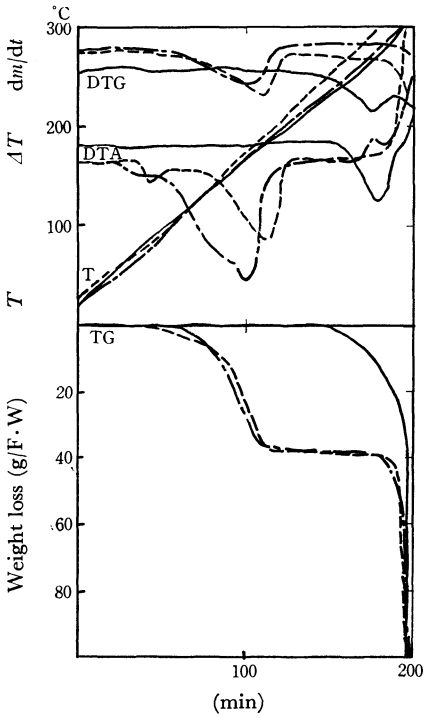

Fig. 2. Derivatogrammes for I (——), II (------) and III (———).

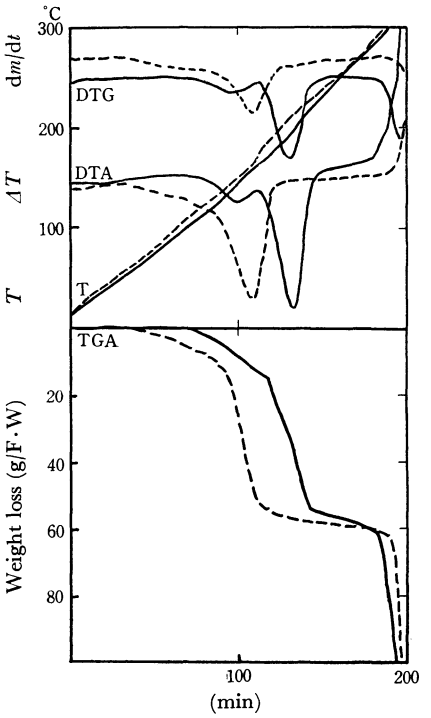

Fig. 3. Derivatogrammes for IV (——) and V (------).

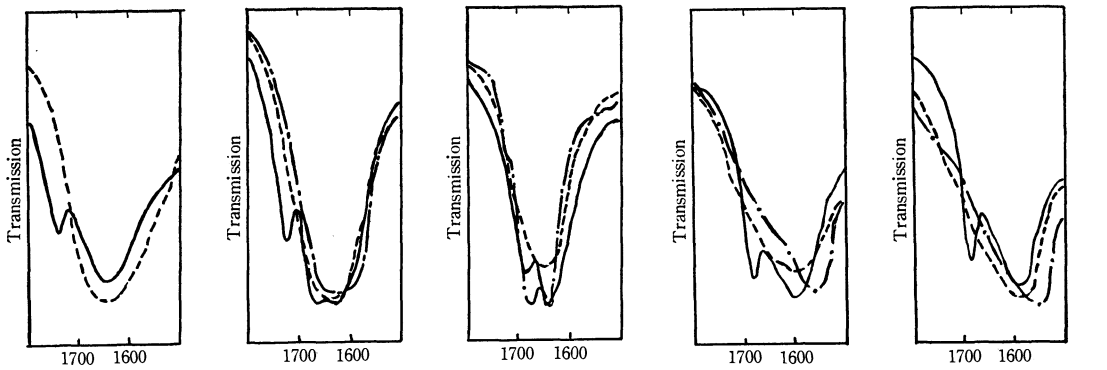

Fig. 4. Infrared spectra.

upon heating at *ca.* 95°C. In this step, PDTA anion behaving as a quinquedentate ligand may turn to a sexadentate ligand in the same way as EDTA in complex I. However, differing from I, the change occurring in the coordination number in complex II is due not to the complete liberation of water molecule from the complex, but probably to the separation of water molecule from coordination sphere in the complex itself, without any weight loss.

Above 95°C, the weight loss of the sample begins, and two moles of water are successively liberated up to 220°C, which are shown by TGA and DTA curves in Fig. 2. The IR spectrum concerning the carboxylate stretching vibration at 200°C is shown to be similar to that at 95°C as seen in Fig. 4-b,

which may indicate no structural change in the coordinated PDTA molecule.

As shown in Fig. 2, in the case of complex III, a small change on the DTA curve also appears at relatively low temperature region, 60—80°C, without giving any weight loss in TGA curve, where the complex shows only a slight color change from red to reddish-violet. The sharp band at 1685 cm^{-1} in IR spectra at room temperature could not be detected in the sample at 80°C as seen in Fig. 4-c, giving the verification that a coordinated carboxylate may come out from the coordination sphere as H_3O^+ in this step, resulting in the coordination of the carboxylate ion, where TMTA molecule turns from a quinquedentate ligand to a sexadentate one. At 90—220°C the DTA curve shows a split peak, probably due to the stepwise liberation of two moles of water from the intermediate, H_3O-[Crtmta]·H_2O. Further decomposition begins to proceed at about 280°C and a small exothermic peak appears immediately before decomposition, its significance not being so clear. The reappearance of the peak assigned to the non-coordinated carboxylate in IR spectra in Fig. 4-c may suggest the formation of the ionic intermediate, but its structure is unknown.

The derivatogram for complex IV in Fig. 3 shows the relatively small, distinct changes in both DTA and DTG curves at 130—160°C corresponding to the weight loss for just one mole of water, and they are accompanied by the great sharp peaks in DTA and DTG at 160—210°C corresponding to the liberation of two moles of water. The IR spectra of IV at 160°C and 210°C, as shown in Fig. 4-d, do not give the band assigned to the non-coordinated carboxylate which was presented at 1690 cm^{-1} at room temperature. These results may suggest that APDA which acted as a terdentate ligand keeping one of the carboxylate group non-coordinated behaves as a quadridentate at 160—210°C owing to the liberation of the first one mole of water which comes from the coordinated OH^- and H^+ of the free carboxylate group.

With complex V, it is found in Fig. 3 that one mole and another two moles of water are gradually liberated, successively. The IR spectra of V at 150°C and 180°C in Fig. 4-c also give no band assigned to non-coordinated carboxylate group

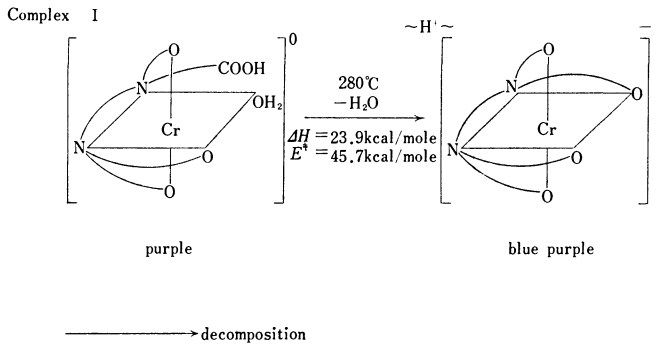

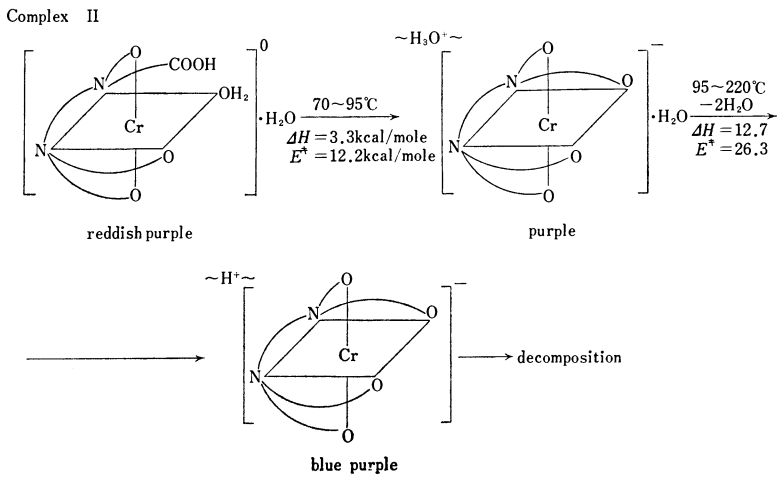

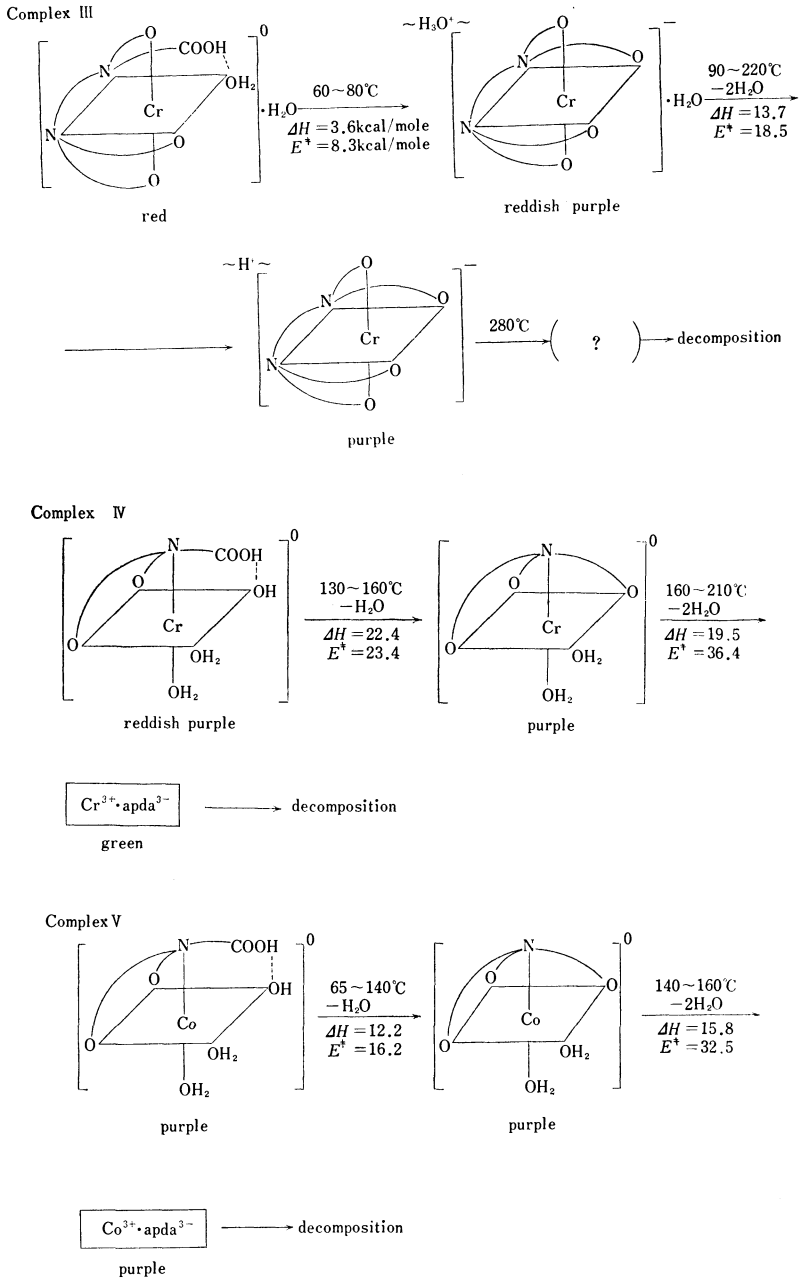

Fig. 5. Possible thermal reaction schemes.

which appeared at room temperature in the same way as those of complex IV. It may suggest that, in complex V also, APDA turns to a quadridentate ligand from a terdentate one at 150°C. The possible thermal reaction schemes for complexes, I—V, are proposed in Fig. 5.

Enthalpy Change and Activation Energy. The enthalpy changes, ΔH, for each step of the thermal decomposition of these complexes were estimated from DTA in the same way as described previously.*1 The activation energies, E^*, for the corresponding steps were calculated by using DTA[4] or DTG[5] curves and by applying the Arrhenius plots to this calculation. The representative Arrhenius plots, $\log k$ *vs.* $1/T$, where k is the rate constant for complexes III and IV are shown in Fig. 6-a, b and Fig. 7-a, b, respectively. The values

4) H. J. Borchardt and F. Daniels, *J. Am. Chem. Soc.*, **79**, 41 (1957).

5) N. G. Dave and S. K. Chopra, *Z. Phys. Chem.*, **48**, 257 (1966).

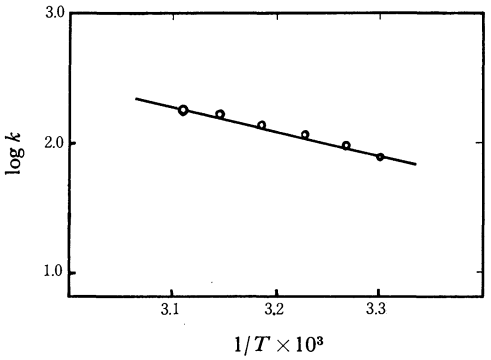

Fig. 6-a. Arrhenius plots for the endothermic reaction at 60—80°C of [CrHtmta (H_2O)]·H_2O from DTA.

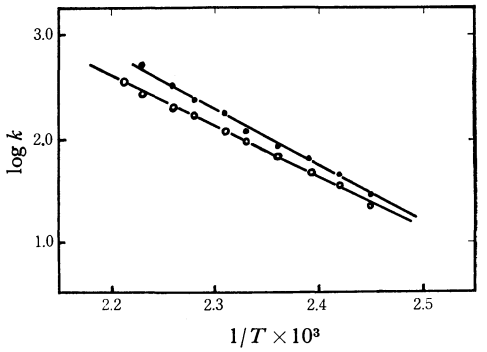

Fig. 7-a. Arrhenius plots for the dehydration reaction at 130—160°C of [Cr(OH)(Hapda)(H_2O)$_2$].
○—○ : from DTA ●—●: fromDTG

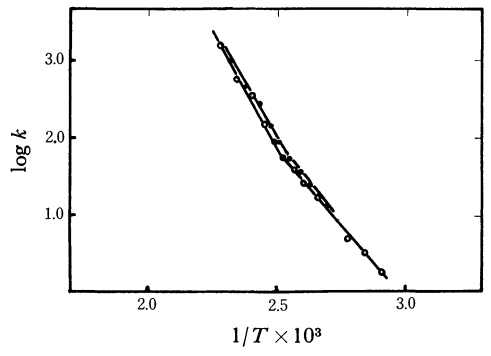

Fig. 6-b. Arrhenius plots for the dehydration reaction at 90—220°C of [CrHtmta (H_2O)]·H_2O.
○—○: from DTA ●—●: from DTG

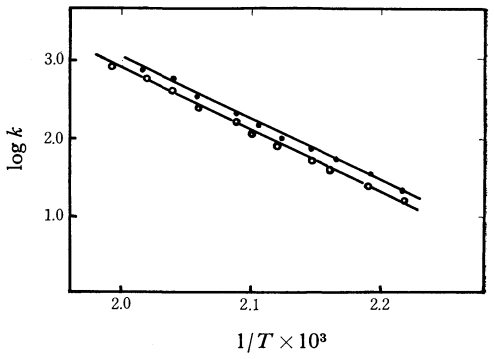

Fig. 7-b. Arrhenius plots for the dehydration reaction of 160—210°C of [Cr(OH)(Hapda)(H_2O)$_2$].
○—○: from DTA ●—●: from DTG

of ΔH and E^* obtained above are given in the corresponding processes in Fig. 5.

The enthalpy changes in the first step of the thermal reaction of complexes II and III, where the coordinated water came out from the coordination sphere to the outer sphere without the liberation of water molecules from the solid phase of the complexes, are obtained in the range of ΔH=3.3—3.6 kcal/mol. On the other hand, those in the second step, where one mole of water was expelled, are estimated within the range of ΔH=12.7—13.7 kcal/mol. Complex III in particular indicates a small exothermic change as ΔH=5.6 kcal/mol at about 280°C. The activation energy for III in the first dehydration process including the transition, 26.8 kcal/mol, is smaller than that in the corresponding process in complex I, 45.7 kcal/mol. It is likely due to the fact that TMTA can coordinate to metal as a sexadentate ligand with less strain than EDTA, owing to a six-membered ring in it.

The activation energies in the first dehydration process for complexes IV and V are approximately close to the respective enthalpy changes. The lower temperature at which the dehydration beings, the smaller enthalpy changes and the lower activation energies in the first and second dehydration processes on cobalt(III) complex V than those on chromium(III) complex IV may indicate that the former is thermally less stable than the latter.

The authors wish to express their appreciation to the Ministry of Education for financial support granted for this research.

BULLETIN OF THE CHEMICAL SOCIETY OF JAPAN VOL. 42 1892—1897 (1969)

Mixed Conduction in Stabilized Zirconia at a Low Oxygen Partial Pressure*1

Kazushi HIROTA

Department of Chemistry, Tokyo Institute of Technology, Ookayama, Meguro-ku, Tokyo

(Received October 11, 1968)

The electromotive force of the oxygen concentration cell, O_2 gas|stabilized zirconia|Fe(+C)-melt+COgas, was measured at 1900°K as a function of the carbon concentration in iron melt, and the transference number of the stabilized zirconia was calculated. The transference number of the ions in the stabilized zirconia partition is less than unity over the whole range of carbon concentration. When the results are compared with the equations derived from plausible models, a reasonable coincidence is obtained.

In the stabilized zirconia crystals, the mobility or the diffusion coefficient of the oxygen ion is exceptionally large at temperatures far from the melting point,[1,2] while those of the metal ions are negligibly small.[3] The stabilized zirconia, therefore, has practically only one kind of charge carrier at an elevated temperature.[4,5]

This ideal character as an ionic conductor disappears at very low oxygen partial pressures due to the partial reduction of zirconia. Kiukkola and Wagner[4] first showed that the electronic conduction is negligible in comparison with the oxygen ion conduction at oxygen partial pressures as low as $10^{-21.5}$ atm at 870°C.

Vest and Tallan[6] have since reported on the transference number of the oxygen ion in calcia-stabilized zirconia, determined by their polarization method, as a function of the oxygen partial pressure at 1000°C, and have reported a transference number of less than 0.5 at 10^{-16} atm, for example.

Schmalzried[7] has measured the electromotive force of the cell, air|ZrO_2(+CaO)|Ca+CaO, at temperatures from 700 to 1000°C and has shown that, at 1000°C for example, the average transference number of oxygen ions in the zirconia electrolyte is about 0.5 when the oxygen partial pressure is 10^{-35} atm at one side of the electrolyte, while the other side is air.

Baker and West[8] have measured the electromotive force of the cell, H_2+H_2O|solid electrolyte|H_2+H_2O, over the range of temperatures from 1000 to 1600°C. They thought that their results for calcia-stabilized zirconia were consistent with those of Schmalzried. However, the numerical coincidence in their transference number for the zirconia electrolyte is only apparent, because the difference in oxygen partial pressure between air and a hydrogen-steam mixture at the reference electrodes must result in a difference in the transference number in the zirconia for the same oxygen partial pressures at the other side of the electrodes.

Tretyakov[9] has measured the electromotive force of the cell, air|ZrO_2(+CaO)|Cr+Cr_2O_3, or Mn+MnO, at temperatures from 600 to 1600°C and has given the relation;

$$\log P_{O_2}^* = -60.5 \cdot 10^3/T + 19.5$$

where $P_{O_2}^*$ (in atm) is the partial pressure of oxygen gas at which the transference number of the ion in the zirconia becomes 0.5.

As one can see, these findings on the transference number cited above do not coincide with each other.

In these investigations, the measurements were done at several fixed oxygen partial pressures, or under several sets of limited conditions; the results were then extended to more general expressions by

*1 Presented at the 73rd I. S. I. J. Meeting, Tokyo, April, 1967.

1) L. A. Simpson and R. E. Carter, *J. Am. Ceram. Soc.*, **49**, 139 (1967).

2) W. D. Kingery, J. Pappis, M. E. Doty and D. C. Hill, *ibid.*, **42**, 393 (1959).

3) W. H. Rhodes and R. E. Carter, *ibid.*, **49**, 244 (1966).

4) K. Kiukkola and C. Wagner, *J. Electrochem. Soc.*, **104**, 379 (1959).

5) The literature was cited in detail by M. F. Lasker and R. A. Rapp, *Z. phys. Chem. Neue Folge*, **49**, 198 (1966).

6) R. W. Vest and V. M. Tallan, *J. Appl. Phys.*, **36**, 543 (1965); *cf.* also R. W. Vest and V. M. Tallan, *J. Am. Ceram. Soc.*, **48**, 472 (1965).

7) H. Schmalzried, *Z. Elektrochem., Ber. Bunsenges. physik. Chem.*, **66**, 572 (1962).

8) R. Baker and J. M. West, *J. Iron Steel Inst.*, **1966**, 212.

9) Yu. D. Tret'yakov, *Izv. Akad. Nauk SSSR Neorgan. Materialy*, **2**, 501 (1966) [*Chem. Abstr.*, **65**, 1759c (1966)]; *cf.* also A. A. Vecher and D. A. Vecher, *Zh. Fiz. Khim.*, **41**, 1288 (1967).

adopting plausible, but not decisive, models for mixed conduction.

For the use of zirconia as a solid electrolyte, it is necessary to establish facts on the transference number over a wide range of oxygen partial pressure; such facts will make it possible to calculate the region of oxygen partial pressure in which the electronic conduction can be neglected.

Richardson and Dennis[10] and Rist and Chipman[11] have given a reliable value for the activity coefficient of carbon in liquid iron. In this system, the equilibrium:

$$C(\text{in Fe melt}) + O(\text{in Fe melt}) = CO(\text{in gas phase}) \quad (1)$$

can be expected. Therefore, one may calculate the activity of oxygen from the carbon concentration in the iron melt and the partial pressure of CO in the gas phase in equilibrium with the iron melt. This system can cover a wide range of oxygen partial pressures at low oxygen partial pressures, and has a relatively large buffer action in reaction to the leak of oxygen. Therefore, this system was used in the following experiment.

Similar cells, iron melt|stabilized zirconia|reference oxygen activity, have been reported by many investigators. They have given the relation between the electromotive force of their cells and the O in the iron melt, in the region where the average transference number of the stabilized zirconia was assumed to be unity.[12] In their measurments, the iron melts were in contact with such inert gases as argon gas; this may result in the serious scattering of the observed values.

Experimental

The electromotive force of the cell; O_2 gas|stabilized zirconia|Fe(+C), CO gas, was measured at 1900±2°K. Commercial zirconia tubes, Zr-23 of the Degussa Co., Ltd., were used in the cell as the stabilized zirconia partition. The results of the wet analysis of the tubes used are listed in Table 1, together with their change in chemical composition with use in the measurements. The arrangement of the cell is shown in Fig. 1. The cell was hung in a vertical-tube furnace, and then CO gas, mixed with from 0% to 3% of CO_2 gas, was made to flow upwards through the furnace at the flow rate of 2 cm/sec.

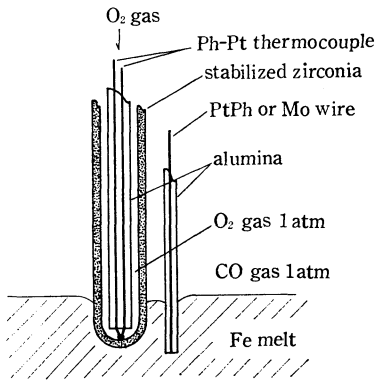

Fig. 1. Schematic illustration of cell arrangement.

The furnace used was a resistance-type furnace. A wire of 60%Pt-40%Rh alloy was wound round an alumina tube (40 mm in diameter, Al-23, of the Degussa Co., Ltd.), coated with fine powder of pure alumina (99.9% pure, Alcoa Co., Ltd.) and surrounded with the same powder about 15 cm thick for thermal insulation. The thermocouple for temperature control was fixed close to the wire. The temperature controllers used were the EC-51 type of the Ohkura Electric Co., Ltd. The center of the furnace, about 18 cm wide, was kept at 1900±2°K during operation.

The electromotive force was measured between a Pt-Rh wire of the thermocouple at the inside of the zirconia tube and a Pt-Rh wire or Mo wire immersed in the iron melt outside the zirconia tube. Because of the use of molybdenum wire, a correction of the electromotive force of the cell, corresponding to the thermoelectromotive force, was made. The dissolution rates of these wires in the iron melt were so high that the time available for the measurement of the electromotive force was about ten seconds for each measurement. The contamination of the iron melts from these wires was about 0.3% in atm ratio; this contamination was assumed to be negligible.

The 6%Rh94%Pt-30%Rh70%Pt thermocouple used in the cell was checked with the gold point, the diopside point, and the palladium point both before and after the experiment. No change in electromotive force was found.

Table 1. Chemical compositions of stabilized zirconia tubes used in the measurement

Tube No.		ZrO_2(in wt%)	MgO	Fe_2O_3	TiO_2	Al_2O_3, CaO
Tube 1	before use	94.7 (±0.3)	5.0 (±0.1)	0.18 (±0.02)	0.20 (±0.1)	<0.1
	after use*	—	5.0	0.46	0.25	—
Tube 2	before use	94.5	5.0	0.16	0.20	<0.1
	after use**	—	5.1	0.32	0.20	—

* The part immersed in iron melt at the measurement condition for about 30 hr.
** For about 10 hr.

10) F. D. Richardson and V. E. Dennis, *Trans. Faraday Soc.*, **49**, 171 (1953).

11) A. Rist and J. Chipman, "The Physical Chemistry of Steelmaking," ed. by J. F. Elliott, John Wiley and Sons, New York (1958), p. 3.

12) For example, W. A. Fischer and W. Ackermann, *Arch. Eisenhüttenwes.*, **36**, 643 (1965); Y. Matsushita and K. Gotō, *Transactions, I. S. I. J.*, **6**, 131 (1966).

Each iron sample was prepared by mixing 99.9% pure iron powder with graphite powder of a spectroscopic grade. The iron sample was placed in an alumina crucible, and was elevated slowly in the furnace. Then, the zirconia tube was immersed in the iron melt thus obtained and kept at 1900±2°K for ten minutes or more, after which the electromotive force was measured.

After the measurement, the sample was quenched immediately by lowering the crucible in the gas flow. A half of each sample pellet (about 30 g in weight) thus obtained was made into chips by a shaper or a diamond cutter and a hammer. The carbon concentration was measured by the method prescribed in JIS G-1211-2.3 (1963), *i. e.* the volume metric method. A standard sample of U. S. National Bureau of Standards, Cat. No. 12h (0.41 wt% carbon) was analyzed to check the carbon analysis; the value of 0.43 wt% carbon was thus obtained.

The immersion of the zirconia tube in a high-carbon iron melt results in numerous fine cracks on the zirconia surface. The cracks enlarge upon repeated exposure to the heating, immersing, and cooling cycle. Thus, the gas-tightness of the zirconia tube was lost in the work on high-carbon specinens. The effect of cracks on electromotive force was also examined; it was found that immediately after the stirring of the iron melt, the electromotive force of the cell was independent of the cracks, even if the cracks were not small.

The exposure of zirconia tubes to air at a high temperature results in a reaction between the zirconia and the iron drops retained on the surface of the zirconia tube; it also results in a decrease in the electromotive force. When this reaction is avoided, no detectable change in the appearance of the zirconia tube results from repeated coolings, heatings, and immersions in low-carbon iron.

Results and Discussion

1) Average Transference Number in Zirconia Partition. The relation between the carbon concentration of the iron melt and the electromotive force of the cell is plotted in Fig. 2. The values scatter about ±5 mV in electromotive force and about 10% in carbon concentration from the calculated line, shown as a solid line in Fig. 2.

The important part of this scattering, perhaps, results from the fact that the iron melt is not homogeneous, a condition which itself results partly from the transfer of carbon from or to gas phase, and partly from the permeation of oxygen through the zirconia partition. It was found that the stirring of the iron melt produced, sometimes, a fluctuation in the magnitude of the electromotive force. The contamination of the zirconia by the iron oxide during the measurements was negligible in comparison with the iron oxide originally present. The error resulting from the presence of iron oxide may be smaller than the other errors, since the correlation between the iron concentration and the electromotive force was not observable in contamination of this magnitude.

From the results shown in Fig. 2, the average

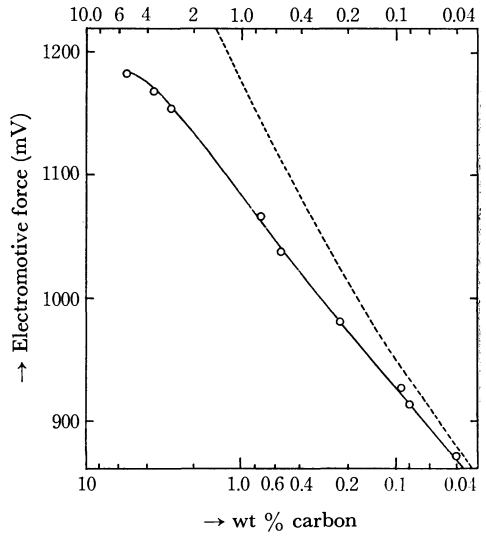

Fig. 2. Electromotive force of the cell as a function of carbon concentration in iron melt at 1900±2°K.

----- calculated from Eq. (6) when $\bar{t}_{ion}=1$,
○○ measured electromotive force,
—— calculated from Eqs. (6), and (10) or (11) giving $A=1$ and $B=1.7\cdot10^3$.

transference number of the oxygen ion in the zirconia partition, $\bar{t}_{ion}$, was calculated as follows. The electromotive force of the cell, E, may be expressed by the use of $\bar{t}_{ion}$:

$$E = \bar{t}_{ion}\cdot E_{cal},$$

$$E_{cal} = -(RT/4F)\int_0^{\ln P} d(\ln f_{O_2}) \qquad (2)$$

where P is the fugacity of molecular oxygen, which is in equilibrium with the oxygen in the iron melt, where R, T, and F are the gas constant, the absolute temperature, and the Faraday constant respectively, and where f_{O_2} is the fugacity of O_2.

Rist and Chipman[11] have given the carbon concentration in the carbon-iron system as a function of the partial pressures of CO and CO_2, P_{CO} and P_{CO_2} as follows;

$$\log \gamma_c = 4450(1-N_{Fe}^2)/T$$
$$\log K = -7280/T + 7.98$$
$$\log K' = \log K + \log \gamma_c$$
$$K' = P_{CO}^2/P_{CO_2}\cdot N_C, \qquad (3)$$

where N_C and N_{Fe} are the mole fractions of carbon and iron in the iron melt and where γ_C is the activity coefficient of carbon.

The standard free energy change of the reaction,

$$CO + (1/2)O_2 = CO_2 \qquad (4)$$

has previously been given as −28220 cal/mol at

1900°K.[13] The fugacity of molecular oxygen can, then, be given as a function of P_{CO} and P_{CO_2} when the system is in equilibrium.

$$-\ln P = 2\cdot\ln(P_{CO}/P_{CO_2}) + 14.95 \qquad (5)$$

From Eqs. (2), (3), and (5) and from the fact that $P_{CO}=1$, one may give the electromotive force of the cell as a function of the carbon concentration in the iron melt:

$$E = \bar{t}_{ion}[(\log N_C - 2.34\,N_{Fe}^2)/5.305 + 1.835] \qquad (6)$$

When $\bar{t}_{ion}=1$, Eq. (6) gives the broken line shown in Fig. 2. The average transference number, $\bar{t}_{ion}$, was calculated on the basis of Eq. (6) from the measured electromotive force of the cell; it is given in Fig. 3 as a function of the carbon concentration.

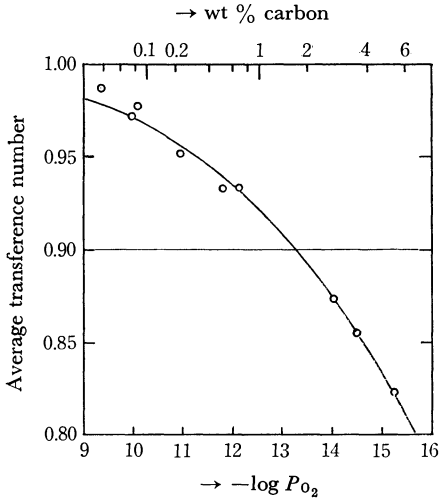

Fig. 3. Average transference number, $\bar{t}_{ion}$, of zirconia partition at 1900°K.

○○ measured values,
—— calculated with Eq. (10) or (11) giving $A=1$ and $B=1.7\cdot10^3$.

2) Oxygen Permeation Resulting from Electronic Conduction. In Fig. 3 the depression in the transference number of the oxygen ion is shown over the whole range of carbon concentration. Such a depression in transference number must, theoretically, restrict the application of Eq. (6). In the experiment, the electromotive force is measured when the external current of the cell is zero. However, this does not mean that the ionic current in the zirconia partition is zero. The electronic current and the ionic current might be equal in absolute value and opposite in current direction. The consequent leakage or permeation of oxygen may result in the disturbance of the equilibrium of the system. Therefore, Eq. (6) can be applied only when the equilibration rate within the iron melt is sufficiently large in comparison with the transport of oxygen through the zirconia partition.

The electrical resistance of the stabilized zirconia partition per square centimeter was about 10 ohm. Therefore, the leakage rate, corresponding to the carbon concentration from 10^{-4} to 10^{-2} mol/cm^3, may be from 10^{-8} to 10^{-7} mol/sec·cm^2. The temperature of the system is so high that the distrubance of this magnitude was ignored in these measurements.

3) Transference Number of the Oxygen Ion in the Zirconia Electrolyte. It is well recognized that, in a sufficiently low oxygen partial pressure region, the zirconia becomes dark in color, diminishes in weight, and changes in volume as the partial reduction proceeds. It is reasonable, therefore, to doubt whether the partial reduction of zirconia has any effect on the ionic conductivity under the present experimental conditions. Two models, as examples, were compared with the experimental results from this point of view:

$$\text{Model 1:}\quad \sigma_I = C_1 + C_2 f_{O_2}^{-1/4},\quad \sigma_e = C_3 f_{O_2}^{-1/4}$$
$$\text{Model 2:}\quad \sigma_I = C_1 + C_2 f_{O_2}^{-1/4},\quad \sigma_e = C_3 f_{O_2}^{-1/4}$$

where C_1, C_2, and C_3 are the constants and where σ_I and σ_e are the ionic and electronic conductances respectively. Model 1 corresponds to the case where the loss of an oxygen ion results in two additional defects in the electrolyte; *i. e.*, each electron remained needs to be trapped in the defect of the crystal lattice near the oxygen-deficient zirconium ion. Model 2 means that the loss of an oxygen ion results in one additional defect in the crystal lattice.

From the relation:

$$E = \int[\sigma_I/(\sigma_I + \sigma_e)]\mathrm{d}E_{cal} \qquad (9)$$

one may obtain the following relations for these models:

Model 1:

$$(1 - \bar{t}_{ion}) = A_1\ln[(P^{-1/4} + B_1)/(1 + B_1)]/\ln P^{-1/4},$$
$$A_1 = C_3/(C_3 + C_2),\ B_1 = C_1/(C_3 + C_2) \qquad (10)$$

Model 2:

$$(1-\bar{t}_{ion}) = A_2\ln[(P^{-1/4}+B_2)(1+D)/(P^{-1/4}+D) \times (1+B_2)]/\ln P^{-1/4},$$
$$A_2 = (C_3/2C_2)/[(C_3/2C_2)^2 - C_1/C_2]^{1/2},$$
$$B_2 = C_3/2C_2 - [(C_3/2C_2)^2 - C_1/C_2]^{1/2},$$
$$D = C_3/2C_2 + [(C_3/2C_2)^2 - C_1/C_2]^{1/2} \qquad (11')$$

or, in a good approximation:

$$(1 - \bar{t}_{ion}) = A_2\ln[(P^{-1/4} + B_2)/(1 + B_2)]/\ln P^{-1/4} \qquad (11)$$

13) Natl. Bur. Standards Series. III. March, 1949, and June, 1948 or "Thermochemistry for Steelmaking," Vol. 1, ed. by J. F. Elliott and M. Gleiser, Addison-Wesley Pub. Co., Reading, Mass. (1960).

Equation (10) or (11) may be rewritten in this form:

$$\frac{(1-\bar{t}_{\mathrm{ion},1})\log P_1^{-1/4}}{(1-\bar{t}_{\mathrm{ion},2})\log P_2^{-1/4}} = \frac{\log[(P_1^{-1/4}+B)/(1+B)]}{\log[(P_2^{-1/4}+B)/(1+B)]} \tag{12}$$

where B is B_1 or B_2, corresponding to Model 1 or 2, and where $\bar{t}_{\mathrm{ion},1}$ and $\bar{t}_{\mathrm{ion},2}$ are the transference numbers when $P=P_1$ and $P=P_2$ respectively. The left side of Eq. (12) is an observable quantity; it is plotted against log P_1 in Fig. 4, where P_2 is the

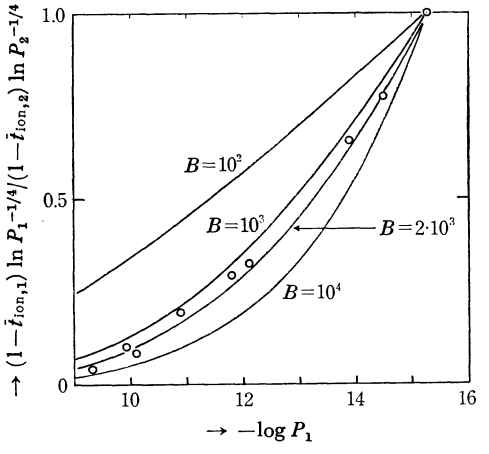

Fig. 4. Evaluation of B in Eq. (12).
○○ calculated with left side of Eq. (12)
—— calculated with right side of Eq. (12)

fugacity of oxygen in carbon-saturated iron. The right side of Eq. (12) gives the lines in Fig. 4, corresponding to the values of B. Judging from Fig. 4, B must be about 2.10^3, perhaps in the range:

$$1.7\cdot10^3 \leqq B \leqq 2\cdot10^3 \tag{13}$$

One may, then, estimate the probable value of A:

$$1.0 \leqq A \leqq 1.1 \tag{14}$$

It is obvious from their definitions that $A_1 \leqq 1 \leqq A_2$. If A_1, $A_2=1$, then $C_2/C_1=0$. Since A is very close to unity, C_2/C_1 is not larger than $1.3\cdot10^{-8}$ when Model 2 holds true, which means that the ionic conductivity, σ_I, is constant within the range of experimental error under the present experimental conditions. Therefore, we cannot choose between Models 1 and 2 on the basis of only the present results. This means that the concentration of additional defects resulting from the loss of oxygen is rather negligible in comparison with the concentration of magnesium oxide. This finding may consistent with the fact that the stabilized zirconia is doped deeply and has a large concentration of lattice defects.

The transference number was reproduced from these constants when $B=1.7\cdot10^3$ and $A=1$, for example; it is given by a solid line in Fig. 3. The electromotive force of the cell, E, was calculated from the same constants; it is given by a solid line in Fig. 2. The coincidence between the calculated and measured values seems to be satisfactory.

From these constants, the "true" transference number, $\sigma_I/(\sigma_I+\sigma_e)$, can also be calculated as a function of the oxygen fugacity; it is shown in Fig. 5. According to Tretyakov's empirical equation, which is the only finding available at this temperature, $-\log P_{O_2}^*$ is 12.3 for calcia-stabilized zirconia at 1900°K. The corresponding value, $-\log f_{O_2}$ at $\sigma_I/(\sigma_I+\sigma_e)=0.5$, is about 12.8 for magnesia-stabilized zirconia in Fig. 5. It seems that these two values coincide very well with each other in spite of the difference in the chemical composition of the electrolytes.

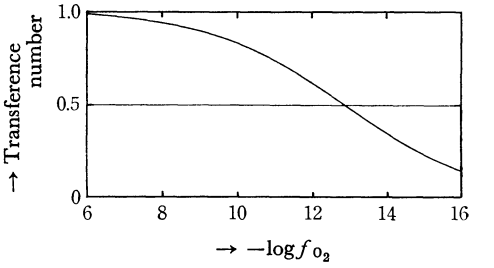

Fig. 5. Transference number, $\sigma_I/(\sigma_I+\sigma_e)$, of stabilized zirconia as a function of oxygen fugacity at 1900°K, when $C_2/C_1=0$ and $C_1/C_3=1.7\cdot10^3$, *i.e.* $B=1.7\cdot10^3$ and $A=1$.

The partial reduction of zirconia may result not only in electronic conduction but also in a volume change or in a response-time increase in electromotive force. The penetration of partial reduction in the zirconia partition can be calculated as follows. It is obvious that:

$$\mathrm{d}E = (1/\sigma_e)\, i\, \mathrm{d}l, \tag{15}$$

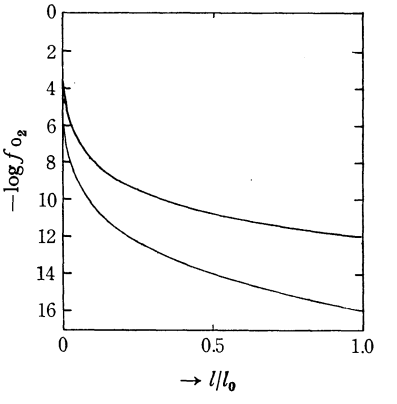

Fig. 6. Oxygen fugacity in zirconia partition calculated with $C_1/C_3=1.7\cdot10^3$ and $C_2/C_1=0$. l_0 is the thickness of the partition, and l is the length vertical to the partition.

where i is the electronic current in zirconia and where l is the length parallel with the electronic current. At the steady state, i is independent of l. From Eqs. (2), (9), and (15), the following equation can be derived:

$$-idl = \frac{\sigma_I\sigma_e}{\sigma_I + \sigma_e} \cdot \frac{RT}{4F} \cdot d(\ln f_{O_2}) \qquad (16)$$

The result calculated from Eq. (16) is shown in Fig. 6. The result shows that the partial reduction penetrates deeply into the partition.

This experiment was supported by the Central Research Laboratory of Hitach, Co. Ltd. The writer wishes to express his thanks to Dr. N. Ono, Mr. A. Kurabayashi, Dr. S. Abe and Professor T. Katsura for their valuable discussions and encouragement during this investigation.

The writer also wishes to express his thanks to Professor A. Muan and Professor Yu. D. Tret'yakov for their kindness in reading the manuscript and in making kind suggestion.

BULLETIN OF THE CHEMICAL SOCIETY OF JAPAN VOL. 42 1897—1900 (1969)

Synthetic Hydrogen-containing Ultramarine Phases

Yasushi KUBO and Goro YAMAGUCHI

Institute of Industrial Science, The University of Tokyo, Roppongi, Tokyo
Department of Industrial Chemistry, The University of Tokyo, Hongo, Tokyo

(Received October 15, 1968)

Hydrogen was analyzed on synthetic sulfur-containing sodalite-type sodium aluminosilicates. Specimens synthesized from the $NaAlSiO_4$-Na_2S system in a H_2 or N_2 atomsphere or in a N_2-S_2 atmosphere contained hydrogens which were introduced by ion-exchange during water-washing. Specimens synthesized from the same system in H_2S-containing atmospheres also contained hydrogens introduced from the synthetic atmosphere. The latter specimens had the formula: $Na_8Al_6Si_6O_{24}S \cdot xH_2S \cdot yS$, which was characterized by a constant number of sodium ions (eight per unit cell), whereas the former contained variable numbers of sodium ions according to the duration of water-washing. A difference in correlation between the sulfur content and the lattice constant was observed between these two series of specimens, indicating different manners of existence of the hydrogen.

In previous papers,[1,2] two sorts of sulfur-containing sodalite-type sodium aluminosilicates, designated sulfosodalite and leuco-ultramarine, were reported on. The former was synthesized by heating a $NaAlSiO_4$-Na_2S mixture at temperatures of from 850 to 950°C in a H_2 or N_2 atmosphere with no sulfur vapor pressure, while the latter was synthesized in a N_2 atmosphere with a sulfur partial pressure of from 0.75 to 1.0 atm. Almost all of the sulfur was contained in a sodalite-type aluminosilicic framework as the monosulfidic ion S^{2-} in the former compound, and in the latter, as the disulfidic ion S_2^{2-}. The nomenclature was based on this fact. According to the results of these papers, the formulae for these compounds were $6NaAlSiO_4 \cdot xNa_2S$ and $6NaAlSiO_4 \cdot xNa_2S_2$ respectively, and solid solutions were formed continuously between these phases.

The present paper has two objects. First, a fact overlooked in the previous papers[1,2] is reported —that the specimens previously analysed contained some hydrogen. Second, the syntheses of new sorts of sulfur-containing sodalite-type sodium aluminosilicates which also contain hydrogens but which are different from the compounds mentioned above will be reported. These new compounds will be reported. These new compounds will be synthesized by heating the $NaAlSiO_4$-Na_2S system in atmospheres containing H_2S. The composition and lattice constant will be determined, and a comparison made between these two series of synthetic hydrogen containing ultramarine phases.

Experimental

Specimens. The sulfosodalite and leuco-ultramarine specimens to be examined here are those which have been prepared in the previous investigations.[1,2] They were synthesized from the starting mixture of

1) G. Yamaguchi and Y. Kubo, This Bulletin, **41**, 2641 (1968).
2) G. Yamaguchi and Y. Kubo, *ibid.*, **41**, 2645 (1968).

the $NaAlSiO_4$-Na_2S system. The details of the method of preparation were given in those papers. The former specimens were obtained by heating the mixture in a H_2 or N_2 atomosphere at temperatures of from 850 to 950°C. The latter specimens were prepared by heating the mixture in a N_2-S_2 atmosphere at various sulfur partial pressures, from 0.25 to 1.00 atm. To indicate these specimens, the system of specimen symbols used in the previous papers will be employed in this paper.

It was found that, when the starting mixture was heated in a H_2-H_2S or H_2S-S_2 atmosphere, sodalite-type phases were also obtained. Specimens of these new phases were prepared by almost the same method as that used for the above-described specimens, except that the atmosphere system was changed. Details of these specimens will be given in a subsequent paper, which will also treat the relationship between the synthetic conditions and the compositions of these phases.

Analyses. After they had been synthesized, all the specimens were immersed in water as soon as they had cooled and were taken out of the furnace of the synthetic apparatus. They were fully washed with water until no alkali could be detected by a phenolphthalein indicator, and then dried at 110°C. Subsequently, a carbon disulfide extraction was made in order to remove completely the free sulfur condensed on the specimen.

The procedure for the determination of the chemical composition of the sodalite-type phase involves two processes; chemical analysis for every component and the determination of the yield of the sodalite-type phase by the X-ray diffraction method. The details of these processes were given in a previous paper.[1)]

The amount of hydrogen present in the specimen was determined by measuring the amount of water which was liberated when the specimen was heated in an O_2 gas stream at about 800°C. For this purpose, an element-analysis apparatus, Shimadzu UM-3, was employed. About an 80-mg portion of the specimen was placed in the combusting system of the apparatus. Prior to oxidation, the specimen was heated at about 170°C in a N_2 gas stream for 1 hr in order to fully remove the water absorbed on the surface of the specimen. The gas stream was then changed to that of O_2 gas, and the temperature was raised to about 800°C. Any SO_3 gas which may have been produced by this treatment was trapped by Ag meshes, and the water was absorbed with magnesium perchlorate. The results obtained were found to be sufficiently reproducible.

X-Ray Diffraction Measurements. The lattice constant was determined by a diffractometer measurement using Cu-$K\alpha$ radiation. MgO powder was added as an internal standard. The diffraction (444), (710, 550, 543), or (721, 633, 552) of the sodalite-type phase, at 2θ values of about 73°, 74° and 77.5° respectively, was measured at the scanning speed of 0.25°/min; calibration was made using the diffraction, (311) or (222), of MgO, at 2θ values of 74°41.52′ and 78°38.52′ respectively on the same diffractometer trace.

Results and Discussion

Specimens Synthesized in a H_2 or N_2 Atmosphere. The results of the analyses of several typical specimens are given in Table 1. The content of every component is represented by the number per unit cell. Lattice constants are also given in the last column of the same table.

Although there must not have been any water in the reaction system, $NaAlSiO_4$-Na_2S, in either the H_2 or N_2 atmosphere, the sulfosodalite specimens liberated considerable amounts of water (about 1 to 1.3%) when heated in O_2 gas. In a previous paper,[1)] it was remarked that, in these specimens, the sodium content determined from the residual Na_2SO_4 was always less than that expected from the charge balance with anions. Thus, in that paper, the content given by the latter method, *i. e.*, that determined indirectly from the ionic charge balance, was adopted as more reliable. The liberation of water as revealed in the present experiment strongly indicates that hydrogen is another constituent of the cations in these specimens. It may be seen that, by taking the hydrogen content into account, the balance of ionic charges between the cations, $Na^+ + H^+$, and the S^{2-} anion is greatly improved. (The sign of the "Charge Balance," + or −, in Table 1 indicates an overbalance of cations or anions respectively). Thus, the inconsistency observed in the sodium analysis can be attributed to the presence of hydrogen. Here the values given as the Na^+ content and the total Na content in Table 2 of a previous paper[1)] are cor-

TABLE 1. MOLAR COMPOSITIONS OF SODALITE-TYPE SPECIMENS SYNTHESIZED IN H_2, N_2 AND (N_2, S_2) ATMOSPHERES

Sample	Yield (%)	SiO_2	$AlO_{1.5}$	$NaO_{1.5}$	Ionic S	Non-ionic S	Na^+	H^+	Charge balance	Total Na	a (Å)
H-C	95.5	6.23	5.77	5.77	1.47	0.01	1.56	1.42	+0.04	7.33	8.948
H-F	94	6.11	5.89	5.89	1.60	0.08	2.54	0.85	+0.20	8.43	8.959
H-M	91	6.21	5.79	5.79	1.49	0	2.19	1.29	+0.53	7.99	8.951
H-T	98	5.96	6.04	6.04	1.65	0.08	2.50	1.36	+0.56	8.54	8.906
N-E	81	6.11	5.89	5.89	1.76	0.22	2.70	1.61	+0.79	8.59	8.976
N-I	84	6.11	5.89	5.89	1.80	0.14	2.88	1.21	+0.48	8.78	8.972
U-H	100	6.12	5.88	5.88	1.50	0.61	2.11	0.87	−0.02	7.99	9.058
U-O	97	6.19	5.81	5.81	1.51	1.58	2.34	0.49	−0.19	8.15	9.064

TABLE 2. MOLAR COMPOSITIONS OF SODALITE-TYPE SPECIMENS SYNTHESIZED IN (H_2S, H_2) AND (H_2S, S_2) ATMOSPHERES

Sample	Temp. (°C)	Mixing Ratio of Gases H_2S	H_2	S_2	Yield (%)	SiO_2	$AlO_{1.5}$	$NaO_{1.5}$	Ionic S	Non-ionic S	Na^+	H^+	Charge balance	Total Na	a (Å)
HS1-A3	855	0.33	0.66		96.5	6.14	5.86	5.86	1.80	0.09	2.11	1.87	+0.37	7.97	8.940
HS2-A3	860	0.66	0.33		94	6.16	5.84	5.84	1.88	0.22	2.22	1.98	+0.44	8.06	8.950
HS3-A3	850	1.00	0		90	6.19	5.81	5.81	1.84	0.27	2.21	2.06	+0.59	8.01	8.960
HS1.5-B3	900	0.50	0.50		100	6.08	5.92	5.92	2.03	0.15	2.09	2.00	+0.04	8.01	8.939
HS3-B3	935	1.00	0		97	6.22	5.78	5.78	2.04	0.56	2.12	2.01	+0.04	7.90	8.964
SH4-A3	863	0.75		0.25	91	6.19	5.81	5.81	1.86	1.14	2.13	1.57	−0.03	7.94	8.998
SH5-A2	860	0.50		0.50	71	6.25	5.75	5.75	1.66	1.45	2.46	1.23	+0.37	8.21	9.001
SH6-A3	857	0.25		0.75	73	6.20	5.80	5.80	1.67	1.28	2.35	1.41	+0.42	8.15	8.996

rected to those given in Table 1 of the present paper.

The hydrogen seems to have originated from the process of washing with water after synthesis. Just after having been synthesized and cooled, the sulfosodalite phase may have contained more than eight Na^+ ions per unit cell. It is rather natural that the excess sodium ions should be easily ion-exchanged in water. This may have occurred to various extents according to the duration of water-washing; the sodium content, which apparently varies at random in Table 1, seems to indicate such conditions. As can also be seen in the table, the content of the cations, $Na^+ + H^+$, usually overbalances that of the anion, S^{2-}. This may indicate that some hydration has also occurred in these specimens.

Specimens Synthesized in a (N_2, S_2) Atmosphere. The results of analyses for two other specimens, U-H (950°C, $P_{S_2}=0.50$ atm) and U-O (950°C, $P_{S_2}=1.00$ atm), are also given in Table 1. These specimens are characterized by a low hydrogen content, indicating that these specimens are more stable than sulfosodalite when washed in water.

Specimens Synthesized in a (H_2S, H_2) or (H_2S, S_2) Atmosphere. For specimens synthesized in atmospheres of various gas compositions, the analytical results are given in Table 2 in the same manner of representation as in Table 1. The second and the third columns of the table give, respectively, the synthetic temperature and the mixing ratio of two gases in atmosphere. The relation between the synthetic conditions and the composition is not treated here, but will be discussed in a separate paper. Lattice constants are also given in the last column.

The hydrogen content in these specimens is much larger than in the sulfosodalite and leuco-ultramarine of the preceding section. Furthermore, it must be pointed out that the number of Na^+ ions per unit cell is almost constant at eight, corresponding to the ideal number of cation sites per unit cell of the sodalite-type structure. The rather large deviations from eight in the SH5-A2 and SH6-A3 specimens may be attributed to an enlarged experimental error due to lower yields of the sodalite-type phase in these specimens. The same phenomenon as in sulfosodalite, that the content of cations, $Na^+ + H^+$, exceeds that of the anion, S^{2-}, is also observed in these specimens, indicating the possibility of some hydration in the water-washing process. However, if the secondary effect by water-washing is elim-

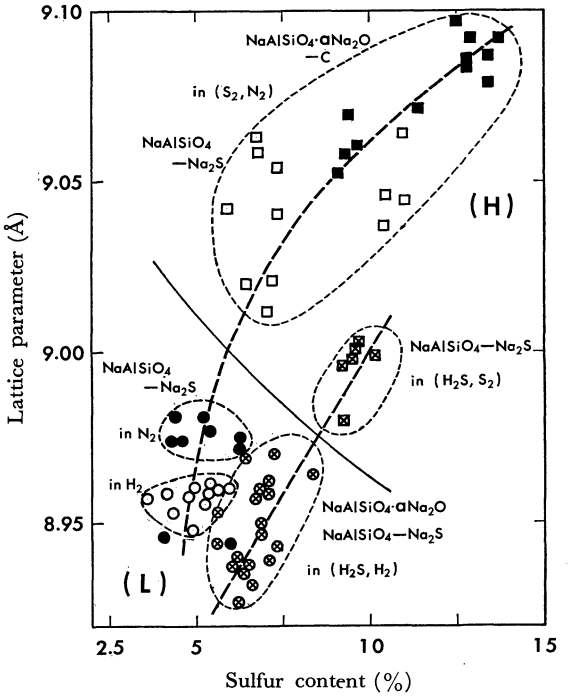

Fig. 1. Simultaneous plot of lattice parameter and sulfur content for sulfur-containing sodalite-type sodium aluminosilicates formed in every system. Two series of correlations are recognizable as shown by two broken line curves. Difference in chemical and physical characteristics are somewhat remarkable between two regions (L) and (H).

inated, the formula of the sodalite-type phase may be expressed by; $6NaAlSiO_4 \cdot Na_2S \cdot xH_2S \cdot yS$ or $Na_8Al_6Si_6O_{24}S \cdot xH_2S \cdot yS$. Thus, the composition of this compound can be represented by two characteristic values, x and y.

In the end case of $x=1$ and $y=0$, the formula becomes $Na_8Al_6Si_6O_{24}(SH)_2$, corresponding exactly to the homostructure of sodalite $Na_8Al_6Si_6O_{24}Cl_2$. In fact, in the specimen with a composition near this, the intensity distribution of the power X-ray diffraction was almost the same as that of sodalite. Thus, this compound may be named hydrosulfosodalite.

Relationship between the Total Sulfur Content and the Lattice Constant. On numbers of sulfur-containing sodalite-type phases, synthesized in various reaction systems and under various conditions by the method described above, the lattice constant (in A) was plotted against the total sulfur content (in percentages). The resulting diagram is given in Fig. 1. Since the lattice constant is not determined by the single factor of the total sulfur content, the plotted points scatter over a certain range even at the same total sulfur content. A separated region, however, proper to specimens of every atmosphere system is formed in the diagram. Furthermore, two series of correlations are clearly recognizable; they are shown by two broken lines. In these correlations, it is seen that specimens synthesized in atmospheres containing H_2S have a lattice constant smaller by about 0.8% at the same total sulfur content than that of specimens synthesized in atmospheres not containing H_2S.

Since the lattice constant was measured on specimens washed fully with water, the ion-exchange of excess Na^+ ions in the latter specimens with protons of water must have proceeded to a considerable extent; some of the specimens had almost the same Na^+ ion content as the former specimens, as can be seen in Table 1. Nevertheless, there is a difference in lattice constant between these two series of specimens. This indicates that there is some essential difference in the manner of existence between the hydrogen introduced into the former specimens from the synthetic atmospheres containing H_2S and that introduced by ion-exchange into the latter specimens, which were formed originally as alkali-rich phases in synthetic atmospheres not containing H_2S. Further details, however, have not yet been made clear.

The authors wish to thank Mr. M. Yuyama and Mr. K. Ohara of our laboratory for their aid in this investigation, and Mr. A. Miyashita, Japan Chemical Co., for his help with the hydrogen analysis.

BULLETIN OF THE CHEMICAL SOCIETY OF JAPAN VOL. 42 1901—1908 (1969)

Polarographic Reduction of Cobalt(II) in Acetonitrile in the Presence of Acetate Ions

Eiki ITABASHI and Shigero IKEDA

Department of Chemistry, Faculty of Science, Osaka University, Toyonaka, Osaka

(Received October 28, 1968)

The effect of the nature and the concentration of the supporting electrolyte on the polarographic reduction of cobalt(II) acetate in acetonitrile has been investigated. An acetonitrile solution of cobalt(II) acetate yields a two-step and a three-step reduction wave in 0.05M $LiClO_4$ and in 0.05M $NaClO_4$ solution, respectively. The same solution gives ill-defined reduction waves in the presence of quaternary ammonium perchlorates, such as $(CH_3)_4NClO_4$, $(C_2H_5)_4NClO_4$, or $(n\text{-}C_4H_9)_4NClO_4$. The $Co(CH_3CN)_n^{2+}$, $Co(OAc)^+$, and $Co(OAc)_3^-$ species are present in a solution containing alkali metal perchlorate electrolyte. $Co(OAc)^+$ and $Co(OAc)_3^-$ are the predominant species in a quaternary ammonium perchlorate solution. The reduction potential becomes more negative with increase in the number of acetate ions coordinated to cobalt(II). The reduction potential of cobalt(II) acetate becomes less negative upon the addition of alkali metal perchlorate to the quaternary ammonium perchlorate supporting electrolyte. This effect is caused by the dissociation reaction of cobalt(II) acetate, in which an acetate ligand is transferred to the alkali metal ion.

The supporting electrolyte effects on the non-aqueous inorganic polarography have been reported by several investigators, especially Murray and Hiller,[1] who have done extensive work on the polarography of a number of metal acetylacetonates in acetonitrile and have found that the reduction potentials were shifted to less negative potentials by the addition of lithium perchlorate to the tetraethylammonium perchlorate supporting electrolyte. They concluded that this effect was due to the chemical reaction of the electrode reduction product, in which an acetylacetonate ligand was transferred to the lithium ion.

The present authors have previously reported on the supporting electrolyte effects on the polarographic reduction of nickel(II) in acetonitrile containing small amounts of glacial acetic acid.[2] The reduction potentials of nickel(II) acetate become less negative and the limiting current decreases with an increase in the radius of the cation of the supporting electrolyte. These effects have been explained by taking into consideration of the dissociation reaction of nickel(II) acetate. Nickel(II) acetate is dissociated into $Ni(CH_3CN)_n^{2+}$ or $Ni(OAc)^+$ by the addition of a supporting electrolyte.

Such a dissociation reaction upon the addition of a supporting electrolyte may also be expected in other acetato metal complexes.

The present paper is concerned with the supporting electrolyte effect on the polarographic behavior of cobalt(II) acetate in acetonitrile.

Experimental

Reagents. Acetonitrile and glacial acetic acid were purified by procedures which have been described previously.[2] Hexaaquocobalt(II) perchlorate, $Co(H_2O)_6(ClO_4)_2$, was prepared and recrystallized by the procedure given in the literature.[3] The analysis of $Co(H_2O)_6(ClO_4)_2$ gave the following results: Found: Co, 17.2±1.8; ClO_4, 52.6±1.3%. Calcd for $Co(H_2O)_6(ClO_4)_2$: Co, 16.11; ClO_4, 54.36%. A guaranteed reagent cobalt(II) acetate, $Co(CH_3COO)_2\cdot 4H_2O$, was recrystallized from an aqueous solution containing 5M acetic acid. The analysis of the salt gave the following results: Found: Co, 22.0±1.0; C, 19.21; H, 5.83%. Calcd for $Co(CH_3COO)_2\cdot 4H_2O$: Co, 23.66; C, 19.29; H, 5.67%.

A tetra-*n*-butylammonium acetate, $n\text{-}Bu_4NOAc$, was prepared by neutralizing an alcoholic solution of tetra-*n*-butylammonium hydroxide with acetic acid, after which the salt was recrystallized from benzene. The analysis of the salt gave the following results: Found: C, 71.48; H, 13.63; N, 4.48%. Calcd for $(n\text{-}C_4H_9)_4NCH_3COO$: C, 71.71; H, 13.03: N, 4.65%.

A dried tetramethylammonium perchlorate (Me_4NClO_4), tetraethylammonium perchlorate (Et_4NClO_4) and tetra-*n*-butylammonium perchlorate ($n\text{-}Bu_4NClO_4$) were prepared by the same procedure as has been described previously.[2] The water content of the polarographic solution containing supporting electrolyte and the depolarizer was determined by Karl Fisher titration to be *ca.* 20 mM.

1) R. W. Murray and L. K. Hiller, Jr., *Anal. Chem.*, **39**, 1221 (1967).

2) S. Ikeda and E. Itabashi, This Bulletin, **41**, 1844 (1968).

3) N. A. Matwiyoff and S. V. Hooker, *Inorg. Chem.*, **6**, 1127 (1967).

Procedures. The polarograms and current-time (*i-t*) curves of an individual drop at the constant potential were recorded with the circuit which has previously been described.[2]

The alternating current (*a. c.*) polarograms were recorded with a Yanagimoto PA-102 polarograph.

The dropping mercury electrode had an *m* value of 1.33_4 mg/sec and a drop time of 4.98 sec in a deaerated 0.1M sodium perchlorate acetonitrile solution at −0.80 V *vs.* SCE and at a mercury height of 60 cm.

The potential of the DME was measured against a saturated calomel electrode (SCE).

The cell equipment was the same as has been reported on previously.[2] The dissolved oxygen in the solution was removed by bubbling pure nitrogen gas through the solution. Measurements were made at 25±0.1°C. In the following section, "current" (denoted *i* in the figures) means the maximum current observed just before the mercury drops.

Results

Cobalt(II) acetate $Co(OAc)_2 \cdot 4H_2O$ does not dissolve in an acetonitrile solvent alone, but it dissolves easily in the same solvent containing small amounts of glacial acetic acid.*1 Typical polarograms for an acetonitrile solution of cobalt(II) acetate containing 0.4% glacial acetic acid and various supporting electrolytes are given in Fig. 1.

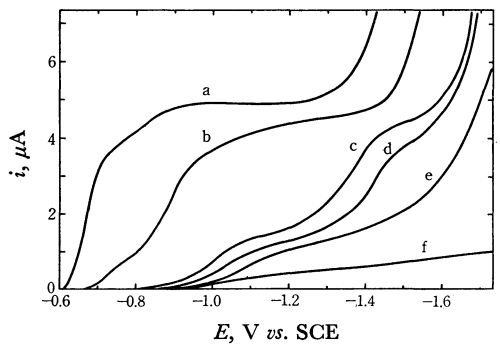

Fig. 1. Effect of supporting electrolyte on the polarograms of Co (II).
$[Co(OAc)_2 \cdot 4H_2O]$=0.5 mM, [HOAc]=0.4%
(a) 0.05M $LiClO_4$; (b) 0.05M $NaClO_4$;
(c) 0.05M Me_4NClO_4; (d) 0.05M Et_4NClO_4;
(e) 0.05M *n*-Bu_4NClO_4; (f) no electrolyte

The polarographic data on cobalt(II) acetate in various supporting electrolyte solutions are summarized in Table 1. An acetonitrile solution of cobalt(II) perchlorate in the same solvent containing 0.4% glacial acetic acid gives a reversible reduction wave, as is shown in Table 2. The polarographic behavior of cobalt(II) perchlorate in acetonitrile has been studied by several investigators. Their results are also listed in Table 2.

Table 1. Summary of polarographic data of $Co(OAc)_2 \cdot 4H_2O$ in 0.05M perchlorate solutions containing 0.4% glacial acetic acid

Elecctrolyte	Co(II) mM	$E_{1/2}$ V *vs.* SCE	*x* value[a]	$E_{a.c.}$ V *vs.* SCE
$LiClO_4$	0.5	−0.66[c]	0.25	−0.75
		−0.80[d]	0.18	−0.88
$NaClO_4$	0.5	−0.72[c]	0.39	−0.76
		−0.88[d]	0.24	−0.97
		−1.15[e]	0.17	−1.26
Me_4NClO_4	0.2	−1.01[c]	0.45	−1.03
		−1.35[d]	0.67	—
Et_4NClO_4	0.2	−1.04[c]	0.44	−1.09
		−1.42[d]	0.71	—
n-Bu_4NClO_4	0.2	−1.08[c]	0.48	−1.15
	0.5	−1.10[c]	0.41	−1.15

a) The slope of the plot of log *i* *vs.* log *t* for the *i-t* curve at the potential region giving the limiting current.
b) The peak potential of a.c. polarogram, which is not corrected for the ohmic drop across the electrolysis cell.
c) 1st reduction step.
d) 2nd reduction step.
e) 3rd reduction step.

Table 2. Summary of polarographic data of cobalt(II) perchlorate in acetonitrile

Electrolyte	$E_{1/2}$ V *vs.* SCE	Reciprocal slope of log-plot mV	$E_{a.c.}$ V *vs.* SCE
0.05M $LiClO_4$[a]	-0.63_5	30	−0.75
0.05M $NaClO_4$[a]	-0.64_0	29	−0.76
0.05M Me_4NClO_4[a]	-0.62_0	31	−0.71
0.05M Et_4NClO_4[a]	-0.62_0	30	−0.72
0.05M *n*-Bu_4NClO_4[a]	-0.61_7	31	−0.70
0.1M $NaClO_4$[b]	−0.65	37	—
0.1M *n*-Bu_4NClO_4[c]	−0.67	41	—

a) This work. Acetonitrile solution contains 0.4% glacial acetic acid.
b) From Ref. 4
c) From Ref. 5
d) The peak potential of a.c. polarogram, which is not corrected for the ohmic drop across the electrolysis cell.

*1 When cobalt(II) acetate was dissolved in acetonitrile containing small amounts of glacial acetic acid, cobalt(II) was present in the solution almost as $Co(OAc)_2(HOAc)_n(H_2O)_{4-n}$. The potentiometric titration of an acetonitrile solution of cobalt(II) acetate with anhydrous perchloric acid indicated that two moles of acetato ions are coordinated to cobalt(II), as in the previously-reported case of $Ni(OAc)_2 \cdot 4H_2O$.[2]

4) I. M. Kolthoff and J. F. Coetzee, *J. Am. Chem. Soc.*, **79**, 1852 (1957).
5) A. I. Popov and D. H. Geske, *ibid.*, **79**, 2047 (1957).

Alkali Metal Perchlorate Systems. In a 0.05M lithium perchlorate electrolyte solution, cobalt(II) acetate is reduced in two steps.

Cobalt(II) acetate in a 0.05M sodium perchlorate electrolyte solution gives three ill-defined steps.

A. c. polarograms of cobalt(II) acetate in the same solution show three peaks which correspond to the above-mentioned three steps of the d. c. polarograms. The limiting current of the first (at −0.82 V) and the second (at −1.16 V) steps, named from positive to negative potentials, are found to be partially kinetic-controlled, but that of the third step (at −1.30 V) is diffusion-controlled.

The total wave height of the three steps is proportional to the concentration of cobalt(II) acetate up to 2.5 mM. In both lithium and sodium perchlorate electrolyte solutions, the reduction current increases at potentials more negative than −1.35 V and −1.45 V *vs.* SCE, respectively, as is shown in Fig. 1.

The rising potential of the hydrogen ion reduction wave obtained in a 0.05M lithium perchlorate containing 0.4% glacial acetic acid is observed at −1.76 V *vs.* SCE. The reduction potential of hydrogen ion becomes less negative with an increase in the concentration of cobalt(II) acetate. As a result, the increase in the reduction current obtained at potentials more negative than −1.35 V *vs.* SCE may be caused by the catalytic reduction of the hydrogen ion.

Quaternary Ammonium Perchlorate Systems. Cobalt(II) acetate in tetramethyl- and tetraethyl-ammonium perchlorate electrolyte solutions gives a double step in a d.c. polarogram, but an a.c. polarogram shows a single peak, one which corresponds to the first step of a double wave.

The exponent of the *i-t* curve for the first step has a value of 0.45. On the other hand, that for the second step obtained at relatively low concentrations of cobalt(II) acetate has values of 0.67 and 0.71 in 0.05M tetramethyl- and tetraethyl-ammonium perchlorate electrolyte solutions, respectively, as is shown in Table 1. The exponent value of the *i-t* curve of the second step is close to that of 0.67 to be expected for a pure kinetic-controlled electrode mechanism.[6]

The *i-t* curve for the second step obtained at the concentrations of cobalt(II) acetate higher than 0.5 mM, shows an irregular shape (*cf.* Fig. 2).

When the concentrations of cobalt(II) acetate are greater than 1.0 mM, the second step shows a peak current. The residual current in a quaternary ammonium perchlorate electrolyte solution containing 0.4% glacial acetic acid begins to rise at about −1.7 V *vs.* SCE. These findings indicate that the second step in tetramethyl- and tetraethylammonium perchlorate electrolyte solutions does not correspond to the reduction of cobalt(II) acetate, but to the catalytic reduction of hydrogen ion.

The effect of the concentration of glacial acetic acid on the polarograms was investigated. No appreciable change in the reduction wave was observed up to 4% in volume. In the experiments described in the following section, the concentration of glacial acetic acid was maintained at 0.4% in volume unless otherwise stated.

Effect of Mixed Electrolytes. The step-by-step addition of lithium perchlorate to quaternary ammonium perchlorate electrolyte solutions containing cobalt(II) acetate causes the reduction potential to become less negative, a single wave to split into a double wave and the wave height of both waves to increase. Figure 3 shows polarograms of an acetonitrile solutions of cobalt(II) acetate containing various concentrations of lithium perchlorate and tetramethylammonium perchlorate at the ionic strength of 0.05.

Table 3 shows the exponent of *i-t* curve of the limiting current plateau for the double wave observed in the presence of various concentrations of lithium perchlorate. The exponent of the *i-t*

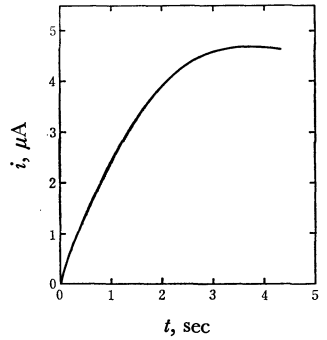

Fig. 2. Current-time curve of 0.5 mM cobalt(II) acetate measured at −1.50 V *vs.* SCE in 0.05M $LiClO_4$ electrolyte solution containing 0.4% glacial acetic acid.

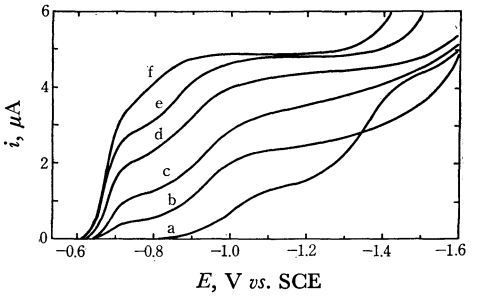

Fig. 3. Effect on concn. of $LiClO_4$ on the polarograms of Co(II) in Me_4NClO_4 solution (μ=0.05). $[Co(OACc)_2 \cdot 4H_2O]$=0.5 mM, [HOAc]=0.4% $[LiClO_4]$: (a) 0; (b) 0.5 mM; (c) 2 mM; (d) 10 mM; (e) 25 mM; (f) 50 mM

6) P. Delahay, "New Instrumentation in Electrochemistry," Interscience Publishers, New York (1954), pp. 87—144.

Table 3. Effect of $LiClO_4$ on the exponent of *i-t* curve for the reduction of 0.5 mM $Co(OAc)_2 \cdot 4H_2O$ in Me_4NClO_4 electrolyte solution containing 0.4% glacial acetic acid at ionic strength 0.05

Concn. of $LiClO_4$ mM	x at $i_l = kt^x$	
	1st wave	2nd wave
0	—	0.45
1.0	0.42	0.25
2.0	0.37	0.22
5.0	0.33	0.23
10.0	0.31	0.21
50	0.25	0.18

curve decreases with an increase in the concentration of lithium perchlorate up to about 10 mM.

There is no appreciable change in the wave height and in the exponent of the *i-t* curve upon the further addition of lithium perchlorate.

Effect of the Concentration of the Supporting Electrolyte. The d.c. and a.c. polarograms for an acetonitrile solution of cobalt(II) acetate in the presence of various concentrations of sodium perchlorate are shown in Figs. 4-a and -b, respectively.

Ill-defined reduction waves change to well-defined waves with increase in the concentration of sodium perchlorate. The a.c. polarogram obtained in 0.05M sodium perchlorate exhibits three peaks. The increase in the concentration of sodium perchlorate causes the height of the first peak to increase and that of the third one to decrease. The height of the peak is almost independent on the concentration of sodium perchlorate up to 0.5M, but the peak disappears upon further increases in the concentrations of the electrolyte. In the 1M sodium perchlorate electrolyte solution, a single peak is observed at the potential of −0.80 V *vs.* SCE.

When lithium perchlorate was employed as the supporting electrolyte, an a. c. polarogram with two peaks was observed at concentrations of lithium perchlorate lower than 0.2M.

With an increase in the concentration of lithium perchlorate, the height of the first peak increases and that of the second decreases.

A single peak corresponding to the first peak is observed when the concentration of lithium perchlorate is greater than 0.5M.

The d. c. and a. c. polarograms obtained in quaternary ammonium perchlorate electrolyte solutions, on the other hand, are not greatly influenced by the concentration of electrolytes. An increase in the concentration of the electrolyte causes the reduction potentials to become more negative and reduces the wave height, however.

Effect of Acetate Ions. Figure 5 shows polarograms of cobalt(II) perchlorate in a 0.05M tetra-*n*-butylammonium perchlorate solution containing 0.4% glacial acetic acid and various concentrations of tetra-*n*-butylammonium acetate.

An acetonitrile solution of cobalt(II) perchlorate, in the absence of tetra-*n*-butylammonium acetate, gives a reversible reduction wave with the half-wave potential of −0.62 V *vs.* SCE in 0.05M tetra-*n*-butylammonium perchlorate. The addition of tetra-*n*-butylammonium acetate causes the single wave to split into a double wave and the wave

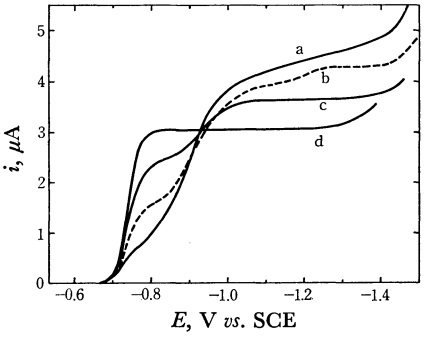

Fig. 4-a. Effect of concn. of $NaClO_4$ on the polarograms of Co(II).
$[Co(OAc)_2 \cdot 4H_2O] = 0.5$ mM, [HOAc] = 0.4%
$[NaClO_4]$: (a) 0.05M; (b) 0.2M; (c) 0.5M; (d) 1.0M

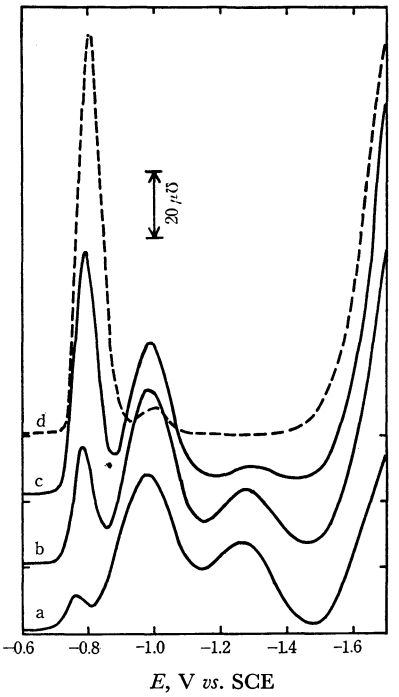

Fig. 4-b. Effect of concn. of $NaClO_4$ on the a. c. polarograms of Co(II).
$[Co(OAc)_2 \cdot 4H_2O] = 0.5$ mM, [HOAc] = 0.4%
$[NaClO_4]$: (a) 0.05M; (b) 0.2M; (c) 0.5M; (d) 1.0M

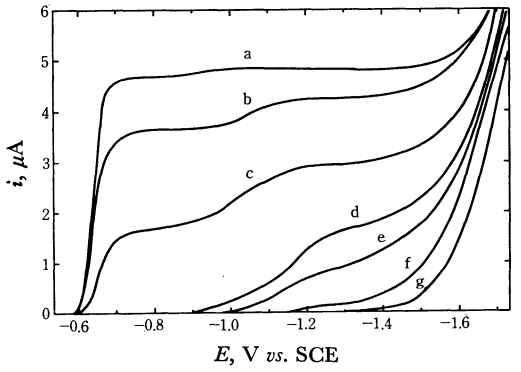

Fig. 5. Effect of concn. of n-Bu_4NOAc on the polarograms of Co(II).
$[Co(H_2O)_6(ClO_4)_2]$=0.5 mM, [HOAc]=0.4%, $[n\text{-}Bu_4NClO_4]$=0.05M
[n-Bu_4NOAc]: (a) 0; (b) 0.2 mM; (c) 0.6 mM; (d) 1.0 mM; (e) 1.4 mM; (f) 2.0 mM; (g) 3.0 mM

height of both steps to decrease.

When the concentration of tetra-*n*-butylammonium acetate is greater than 1 mM, the first step ceases to exist and an irreversible wave corresponding to the second step is observed. The irreversible wave also vanishes at concentrations of tetra-*n*-butylammonium acetate higher than about 2 mM.

In the presence of glacial acetic acid, the polarographic behavior of cobalt(II) at potentials more negative than −1.7 V *vs.* SCE is not clear because of the discharge of hydrogen ions produced by the dissociation of acetic acid.

The effect of acetate ion on the polarograms of cobalt(II) perchlorate in the absence of glacial acetic acid was also investigated. The results are reproduced in Fig. 6.

When the $[OAc^-]/[Co(II)]$ ratio is less than 2,

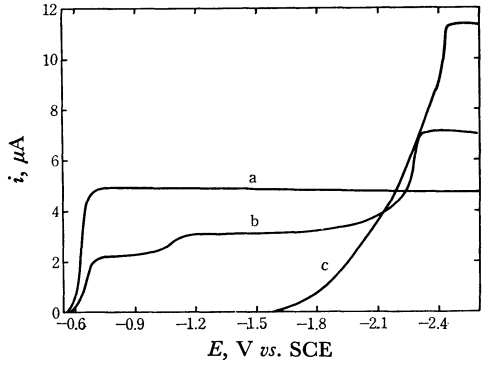

Fig. 6. Effect of concn. of n-Bu_4NOAc on the polarograms of Co(II) in the absence of glacial acetic acid.
$[Co(H_2O)_6(ClO_4)_2]$=0.5 mM,
$[n\text{-}Bu_4NClO_4]$=0.05M
[n-Bu_4NOAc]: (a), 0; (b), 0.5 mM; (c), 1.6 mM

Table 4. Effect of n-Bu_4NOAc on the exponent of i-t curve for the reduction of 0.5 mM cobalt(II) perchlorate in a 0.05 M n-Bu_4NClO_4 electrolyte solution in the absence (a) and the presence (b) of 0.4% glacial acetic acid

Concn. of n-Bu_4NOAc mM	x at $i_l=kt^x$		
	1st wave	2nd wave	3rd wave
0.20[a]	0.19	0.23	0.25
0.50[a]	0.18	0.23	0.24
0.75[a]	0.18	0.25	0.33
1.50[a]	—	—	0.65
2.0[a]	—	—	0.65
2.5[a]	—	—	0.67
3.0[a]	—	—	0.66
0[b]	0.19	—	
0.20[b]	0.19	0.23	
0.40[b]	0.18	0.23	
0.60[b]	0.18	0.25	
0.80[b]	0.19	0.32	
1.00[b]	—	0.40	
1.20[b]	—	0.44	
1.40[b]	—	0.56	

three waves are observed. The first two waves are similar to those observed in the presence of glacial acetic acid. The reduction potential of the third step observed at potentials more negative than −2.2 V *vs.* SCE becomes more negative values and the wave height increases with an increase in the concentration of tetra-*n*-butylammonium acetate. When the $[OAc^-]/[Co(II)]$ ratio is greater than 2, but less than 3, cobalt(II) is precipitated.

When the $[OAc^-]/[Co(II)]$ ratio is greater than 3, an ill-defined reduction wave is observed. The nature of the limiting current for the three steps is shown in Table 4.

The limiting current of the first step is diffusion-controlled. The exponent of the i-t curve for the second and third steps, on the other hand, increases with an increase in the concentration of tetra-*n*-butylammonium acetate. This indicates that the process has an appreciable contribution from a kinetic controlled electrode mechanism.[7]

Plots of the wave height against the $[OAc^-]/[Co(II)]$ ratio and the concentration of tetra-*n*-butylammonium acetate are given in Fig. 7.

The wave height of the first step decreases linearly with the increase of the concentrations of tetra-*n*-butylammonium acetate, becoming zero at the point where the $[OAc^-]/[Co(II)]$ ratio is equal to 2. The total wave height of the first two steps

7) J. Kůta and I. Smolor, "Progress in Polarography," ed. by P. Zuman and I. M. Kolthoff, Vol. 1, Interscience Publishers, New York (1962), pp. 43—63.

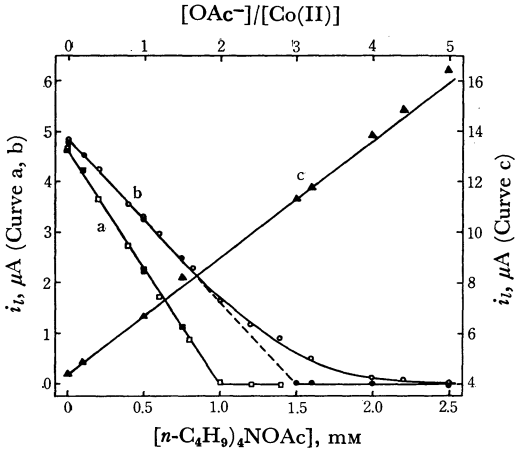

Fig. 7. Variation of limiting current with concn. of n-Bu_4NOAc in the absence (closed mark) and the presence (open mark) of 0.4% glacial acetic acid.
(a), 1st wave; (b), (a)+2nd wave; (c), (b)+3rd wave.

(curve b in Fig. 7) also decreases almost linearly with the concentration of tetra-n-butylammonium acetate to about 1 mM, but it deviates from the line at higher concentrations of tetra-n-butylammonium acetate containing 0.4% glacial acetic acid. In the absence of glacial acetic acid, the limiting current of the second step becomes zero at concentrations of tetra-n-butylammonium acetate higher than 1.5 mM. If curve b in Fig. 7 extrapolated to the point where the current is zero, the extrapolated point corresponds to [OAc⁻]/[Co(II)]= 3.0. The wave height at the potential where the third step is observed in the absence of glacial acetic acid (curve c in Fig. 7), on the other hand, is nearly proportional to the concentrations of tetra-n-butylammonium acetate to about 2 mM.

Discussion

The polarographic reduction of cobalt(II) perchlorate in acetonitrile containing acetate ions is dependent on the concentration of acetate ions. When the [OAc⁻]/[Co(II)] ratio is less than 2, the plots of the limiting current in relation to the acetate ion concentration indicate that the first step (wave I) involves the reduction of uncomplexed cobalt(II), while the second step (wave II) involves that of $Co(OAc)^+$. When the $Co(H_2O)_6(ClO_4)_2$ compound is dissolved in acetonitrile in the absence of acetate ions, cobalt(II) is present in the solution almost as $Co(CH_3CN)_6^{2+}$ ions.[8]

An acetonitrile solution of cobalt(II) perchlorate reacts with acetate ions to form $Co(OAc)_2$, which then dissociates into $Co(OAc)^+$ and $Co(OAc)_3^-$. $Co(OAc)_2$ is an electroinactive species; an acetonitrile solution of cobalt(II) acetate, in the absence of any supporting electrolyte, gives no apparent reduction wave, as Fig. 1 shows.

$$Co^{2+} + 2OAc^- \rightleftarrows Co(OAc)_2 \quad (1)$$

$$2Co(OAc)_2 \rightleftarrows Co(OAc)^+ + Co(OAc)_3^- \quad (2)$$

$$\text{Wave I: } Co^{2+} + 2e + Hg \rightleftarrows Co(Hg) \quad (3)$$

$$\text{Wave II: } Co(OAc)^+ + 2e + Hg \longrightarrow Co(Hg) + OAc^- \quad (4)$$

where the coordinated acetonitrile molecules were omitted for the sake of simplicity.

The third step (wave III) observed in the absence of glacial acetic acid can be attributed to the reduction of $Co(OAc)_3^-$ produced by reaction (2):

$$\text{Wave III: } Co(OAc)_3^- + 2e + Hg \longrightarrow Co(Hg) + 3OAc^- \quad (5)$$

When the [OAc⁻]/[Co(II)] ratio is greater than 2, but less than 3, an acetonitrile solution of cobalt(II) in the presence of 0.4% glacial acetic acid gives a single irreversible wave corresponding to the wave II.

The over-all reaction can be represented by the equilibrium reaction (6) and the electrode reaction (4):

$$Co(OAc)^+ + 2OAc^- \rightleftarrows Co(OAc)_3^- \quad (6)$$

The reduction wave of $Co(OAc)_3^-$ is not observed because of the discharge of hydrogen ions. The kinetic nature of the limiting current may be due to the equilibrium reaction (6).

When the [OAc⁻]/[Co(II)] ratio is greater than 3, an ill-defined reduction wave corresponding to the wave III is observed in the absence of glacial acetic acid. The limiting current of wave III receives an appreciable contribution from the kinetic-controlled electrode mechanism, judging from the results of the measurement of the i-t curve, shown in Table 4.

Although this kinetic mechanism is uncertain, wave III, under the proposed conditions, involves the reduction of $Co(OAc)_3^-$ but not of $Co(OAc)_4^{2-}$; wave III is also observed when the [OAc⁻]/[Co(II)] ratio is less than 2. The partial electrochemical reactions may be written as in the reactions (7) and (5):

$$Co(OAc)_3^- + OAc^- \rightleftarrows Co(OAc)_4^{2-} \quad (7)$$

The $Co(OAc)_4^{2-}$ species may be unstable in the solution, if present at all.

Acetate ion yields a double anodic dissolution wave of mercury, as is shown in Fig. 8. The total limiting current is diffusion-controlled and is proportional to the concentration of acetate ions. In the presence of cobalt(II) perchlorate, the dissolution wave is not observed until the [OAc⁻]/[Co(II)] ratio exceeds 3, as is shown in Fig. 9. The curves a and b in Fig. 9 show the plots of the wave height

8) B. J. Hathaway, D. G. Holah and A. E. Underhill, *J. Chem. Soc.*, **1962**, 2444.

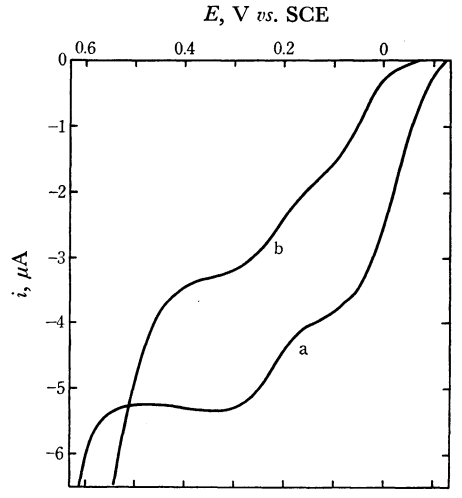

Fig. 8. Anodic dissolution waves of mercury for acetate ion in 0.05M n-Bu_4NClO_4 solution in the absence (a) and the presence (b) of 0.5 mM $Co(H_2O)_6(ClO_4)_2$.
[n-Bu_4NOAc]: (a), 1.0 mM; (b), 2.0 mM

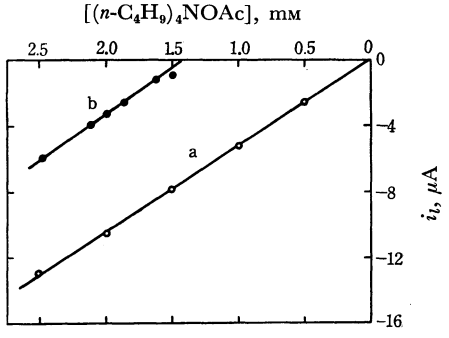

Fig. 9. Variation of total height of the anodic wave with concn. of n-Bu_4NOAc in the absence (a) and the presence (b) of 0.5 mM $Co(H_2O)_6(ClO_4)_2$.

against acetate ion concentrations in the absence and in the presence of cobalt(II), respectively. These results indicate that $Co(OAc)_4^{2-}$ is unstable and dissociates easily into $Co(OAc)_3^-$.

From the above arguments, the change in the reduction wave for an acetonitrile solution of cobalt(II) acetate in the presence of small amounts of glacial acetic acid can be said to be due to the variety of electroactive species of cobalt(II) in the solution.

The reduction wave for an acetonitrile solution of cobalt(II) acetate in the presence of quaternary ammonium perchlorate corresponds to the reduction of the $Co(OAc)^+$ which is produced by the dissociation reaction (2).

An acetonitrile solution of cobalt(II) acetate in the absence of any supporting electrolyte does not show any apparent reduction wave. This indicates that cobalt(II) acetate, in the absence of any supporting electrolyte, is only slightly dissociated in acetonitrile and that the dissociation reaction is accelerated by the presence of a supporting electrolyte; also, neutral cobalt(II) acetate $Co(OAc)_2$ is electroinactive at the DME.

The reduction waves of cobalt(II) acetate in alkali metal perchlorate supporting electrolyte solutions are dependent on the concentration of the electrolyte.

When the concentration of lithium perchlorate is less than 0.2M, a double wave corresponding to the reduction of $Co(CH_3CN)_n^{2+}$ and $Co(OAc)^+$ is observed, while a single wave corresponding to the reduction of $Co(CH_3CN)_n^{2+}$ is observed at concentrations of lithium perchlorate higher than 0.5M. The a.c. polarogram also suggests that two electroactive species are present in the solution containing 0.05M lithium perchlorate. The solution equilibria in a lithium perchlorate electrolyte solution can probably be represented by the following sequence:

$$2Co(OAc)_2 \rightleftarrows Co(OAc)^+ + Co(OAc)_3^- \quad (2)$$

$$Co(OAc)_3^- + 2Li^+ \rightleftarrows Co(OAc)^+ + 2LiOAc \quad (8)$$

$$Co(OAc)^+ + Li^+ \rightleftarrows Co^{2+} + LiOAc \quad (9)$$

The wave height of a double wave observed at relatively low concentrations of lithium perchlorate or that of a single wave at concentrations of electrolyte higher than 0.5M is proportional to the concentration of cobalt(II) acetate.

These findings indicate that $Co(OAc)_2$ and $Co(OAc)_3^-$ are only slightly present in lithium perchlorate electrolyte solutions. As a result, the predominant reaction participating in the electrode process of cobalt(II) acetate in lithium perchlorate electrolyte solutions may be presented by the reaction (9).

Three ill-defined steps are observed in a 0.05M sodium perchlorate electrolyte solution. The a.c. polarograms obtained in the same solution also show three peaks. These results show that three electroactive species of cobalt(II) are present in the solution. The solution equilibria of cobalt(II) acetate in a 0.05M sodium perchlorate electrolyte solution may be described by the following sequence:

$$2Co(OAc)_2 \rightleftarrows Co(OAc)^+ + Co(OAc)_3^- \quad (2)$$

$$Co(OAc)_3^- + 2Na^+ \rightleftarrows Co(OAc)^+ + 2NaOAc \quad (10)$$

$$Co(OAc)^+ + Na^+ \rightleftarrows Co^{2+} + NaOAc \quad (11)$$

Three steps are responsible for the reductions of $Co(CH_3CN)_n^{2+}$, $Co(OAc)^+$, and $Co(OAc)_3^-$, and the reduction potential becomes more negative with an increase in the number of coordinated acetate ions.

When the concentration of sodium perchlorate exceeds about 0.5M, the predominant species is $Co(CH_3CN)_n^{2+}$. When the concentration of sodium perchlorate is less than 0.2M, $Co(OAc)^+$ and $Co(OAc)_3^-$ are the predominant species.

The reduction potential of cobalt(II) acetate becomes less negative upon the addition of alkali metal perchlorate to the quaternary ammonium perchlorate supporting electrolyte solutions, and the wave height also increases, as is shown in Fig. 3. This effect may be attributed to the increases in the concentrations of $Co(CH_3CN)_n^{2+}$ and $Co(OAc)^+$, presented by reactions (8) and (9).

The authors wish to thank the Ministry of Education for the financial support granted for this research.

BULLETIN OF THE CHEMICAL SOCIETY OF JAPAN VOL. 42 1908—1915 (1969)

New Methods of Preparing the Mixed Cyano Cobalt(III) Complexes*1

Nobufumi MAKI and Shukichi SAKURABA

Department of Chemistry, Faculty of Engineering, Shizuoka University, Johoku, Hamamatsu

(Received November 1, 1968)

The following new cyano cobalt(III) complexes have been prepared by treating the corresponding chloro complexes with silver cyanide: *cis*-$[Co(CN)_2dip_2]NO_3 \cdot 7H_2O$, *cis*-$[Co(CN)_2dip_2]_2SO_4 \cdot 12H_2O$, *cis*-$[Co(CN)_2en(NH_3)_2]NO_3$, $[Co(CN)_3en(NH_3)] \cdot H_2O$, and *trans*-$[Co(CN)dg_2(NH_3)] \cdot \frac{1}{2}H_2O$. This method has also been used in the preparation of the following compounds: *cis*-$[Co(CN)(NO_2)en_2]NO_3 \cdot H_2O$,*2 *cis*-$[Co(CN)(SO_3)en_2]$, *trans*-$[Co(CN)(SO_3)en_2]$, *cis*-$[Co(CN)(OH_2)en_2]SO_4 \cdot 2H_2O$,*2 *cis*-$[Co(CN)_2en_2]NO_3$,*2 *cis*-$[Co(CN)_2pn_2]NO_3$,*2 *cis*-$[Co(CN)_2phen_2]NO_3 \cdot 6H_2O$,*2 and *cis*-$[Co(CN)_2phen_2]Cl \cdot 4H_2O$. Another new method has been attempted in dimethyl sulfoxide or an acetonitrile-water solution by the step-by-step substitution of a chloro ligand with a CN^- ion *via* the monocyanomonochloro complex of the $[Co(CN)Cl\ N_4]$-type; we thus succeeded in obtaining these dicyano-ammine complexes, *trans*-$[Co(CN)_2(NH_3)_4]NO_3 \cdot H_2O$, *trans*-$[Co(CN)_2en(NH_3)_2]Cl \cdot H_2O$, and *cis*-$[Co(CN)_2(NH_3)_4]NO_3 \cdot H_2O$. The methods of preparing the following new complexes are also described: *trans*-$Na[Co(CN)_2dg_2] \cdot 2H_2O$, *trans*-$K[Co(CN)_2dg_2] \cdot \frac{3}{2}H_2O$, *trans*-$(NH_4)_2[Co(CN)dg_2(SO_3)] \cdot 4H_2O$, and *trans*-$H[Co(CN)dg_2Cl] \cdot 4H_2O$. The absorption spectra in the visible, ultraviolet, and infrared regions have been measured.

The direct substitution of diacido-cobalt(III) complexes, $[CoX_2N_4]$, with CN^- ions has heretofore been considered to be difficult. For example, the $[Co(CN)_2en_2]^+$ ion could be obtained only *via* the $[Co(S_2O_3)_2en_2]^-$ ion.[1] When the dichloro complex is treated with potassium cyanide, a disproportionation occurs to produce such precipitates as $[Co\ en_3][Co(CN)_5OH]$. One of the reasons for this is certainly the hydrolysis of potassium cyanide in solution, and another, the difference in bonding character between Co–Cl and Co=C=N$^-$. The method of Rây and Sarma[1] is based on the similarity in coordinate bond character between Co–S_2O_3 and Co=C=N$^-$ in the sphere of the bis(ethylenediamine)cobalt(III) complex. Their method, however, is invalid for the preparation of dicyano-bis(2,2′-dipyridyl) and dicyanobis(1,10-phenanthroline)cobalt(III) complexes.

Recently, Yoneda *et al.*[2] have succeeded in obtaining the *trans*-$[Co(CN)_2en_2]Cl$ complex in dimethyl sulfoxide. In such a non-aqueous solution, the substitution occurs only gently and is not accompanied by the disruption of the complex, since the dissociation and hydrolysis of potassium cyanide are depressed to some extent.

Regarding the cobalt(III) complexes of the cyano-ammine series, Konya *et al.*[3] have reported the preparation of *cis*- and *trans*-$[Co(CN)_2(NH_3)_4]Cl$. Independently of their work, other methods of preparing the nitrates of these isomers have been attempted and will be described in the present

*1 Presented at the 18th Symposium on Coordination Chemistry, Kyoto, October 18, 1968.

*2 The complex cation is known, but has not yet been reported as a compound.

1) P. R. Rây and B. Sarma, *J. Indian Chem. Soc.*, **28**, 59 (1951).

2) H. Yoneda, T. Baba and M. Muto, This Bulletin, **40**, 1736 (1967); M. Muto, T. Baba and H. Yoneda, *ibid.*, **41**, 2918 (1968).

3) K. Konya, H. Nishikawa and M. Shibata, *Inorg. Chem.*, **7**, 1165 (1968).

report. On the other hand, Shibata *et al.*[4] reported the syntheses of $[Co(CN)(NH_3)_5]Cl_2$ and $[Co(CN)_3(NH_3)_3]$, while Siebert[5] independently described the preparation of the former, $[Co(CN)(NH_3)_5]X_2$ (X=Cl, Br, NO_3, ClO_4 or $\frac{1}{2}SO_4$). By the successive substitution method of the tricarbonatocobaltate(III) complex developed by Shibata *et al.*[4] an odd number of CN^- ligands is introduced into the coordination sphere of the ammine cobalt(III) complex in the presence of active charcoal. Recently, Kuroda[6] reported a similar method of preparing the dicyano complex, *cis*-$[Co(CN)_2en_2]ClO_4$, *via* the carbonato complex, $[Co(CO_3)en_2]ClO_4$. Several years ago, Cambi and Daglia[7] reported the isolation of $K_2[Co(CN)_5(NH_3)]$. The complexes of *cis*- and *trans*-$M[Co(CN)_4(NH_3)_2]$, however, are now still missing members in this series.

Several other papers dealing with the mixed cyano cobalt complexes are listed as Ref. 8—10.

In the present work, the direct substitution of chloro ligands has been found to be possible in water provided that the cyanide ions are present in a very dilute concentration. For this purpose, we have adopted the silver cyanide, the solubility of which in water is $2.2\cdot10^{-5}$ g/100 g water at 20°C, and have succeeded in obtaining directly the mixed ligand complexes of cyano-cobalt(III), as listed in the synopsis.

On the other hand, the syntheses of ammine complexes with a *trans*-configuration have been carried out in dimethyl sulfoxide with potassium cyanide. The following complexes were obtained: *trans*-$[Co(CN)_2(NH_3)_4]NO_3\cdot H_2O$ and *trans*-$[Co(CN)_2en(NH_3)_2]Cl\cdot H_2O$.

The present paper will deal with the preparation methods and the absorption spectra of these cyano cobalt(III) complexes.

Experimental

Preparation of *cis*-$[Co(CN)_2en_2]NO_3$ (anhydrous). Twenty grams of *trans*-$[CoCl_2en_2]NO_3$ were suspended in 700 m*l* of distilled water, mixed with 20 g of AgCN, and heated on a water bath (90°C) for three hours. The color of the solution changed from green to yellow. The solution was then filtered, concentrated by evaporation, and allowed to stand. On cooling, yellow crystals separated from the solution; they were recrystallized once from hot water. Found: Co, 19.98; C, 24.49; N, 33.49; H, 5.63%. Calcd for $[Co(CN)_2en_2]NO_3$: Co, 20.10; C, 24.58; N, 33.44; H, 5.50%.

The dicyanobis(propylenediamine)cobalt(III) nitrate was analogously prepared by treating *trans*-$[CoCl_2pn_2]NO_3$ (20 g) with AgCN (20 g) in 500 m*l* of water below 60°C for half an hour. The orange-yellow filtrate was concentrated *in vacuo* below 50°C with a rotatory evaporator. Finally the complex was precipitated from the concentrated solution with the addition of ethanol. Found: Co, 18.22; C, 30.04; N, 30.21; H, 6.26%. Calcd for $[Co(CN)_2pn_2]NO_3$: Co, 18.35; C, 29.91; N, 30.52; H, 6.28%.

The perchlorate, *cis*-$[Co(CN)_2en_2]ClO_4$, was analogously prepared: 20 g of *trans*-$[CoCl_2en_2]ClO_4$ were treated with 20 g of AgCN in 600 m*l* of water at 90°C for three hours. The complex has no crystallization water. Found: Co, 17.90; C, 21.78; N, 25.34; H, 4.90%. Calcd for $[Co(CN)_2en_2]ClO_4$: Co, 17.83; C, 21.80; N, 25.42; H, 4.88%.

Preparation of *cis*-$[Co(CN)_2(NH_3)_4]NO_3\cdot H_2O$. Forty grams of *trans*-$[Co(CN)Cl(NH_3)_4]NO_3$[11] were mixed with 29 g of AgCN in 400 m*l* of acetonitrile containing 5% of water at room temperature and then heated on a water bath (50—60°C) for three hours. The temperature of the solution was kept below 60°C during the reaction. No smell of ammonia was recognized. The suspension was then filtered, and the residue was repeatedly washed with water. The orange-yellow water solution was concentrated *in vacuo* below 50°C with a rotatory evaporator. Orange-yellow crystals separated from the solution when it was allowed to stand overnight. The crude complex was recrystallized from hot water containing a trace of acetic acid. Found: Co, 22.65; C, 9.11; N, 37.69; H, 5.70%. Calcd for $[Co(CN)_2(NH_3)_4]NO_3\cdot H_2O$: Co, 22.74; C, 9.27; N, 37.84; H, 5.45%.

Preparation of $[$*cis*-$Co(CN)_2en(NH_3)_2]NO_3$. This complex was quite analogously prepared. That is, 60 g of *trans*-$[CoCl_2en(NH_3)_2]NO_3$[12] were treated with 80 g of AgCN in 500 m*l* of acetonitrile containing 5% of water at 80°C for three hours. Found: Co, 21.97; C, 18.04; N, 36.88; H, 5.31%. Calcd for $[Co(CN)_2en(NH_3)_2]NO_3$: Co, 22.06; C, 17.99; N, 36.70; H, 5.28%.

Preparation of *cis*-$[Co(CN)_3en(NH_3)]\cdot H_2O$. Sixty grams of *trans*-$[CoCl_2en(NH_3)_2]Cl\cdot H_2O$[12] were treated with 100 g of AgCN in 500 m*l* of acetonitrile containing 10% of water at 90°C for ten hours. Large yellow crystals were obtained. Found: Co, 25.41; C, 25.92; N, 36.15; H, 5.66%. Calcd for $[Co(CN)_3en(NH_3)]\cdot H_2O$: Co, 25.39; C, 25.87; N, 36.21; H, 5.65%.

Preparation of *cis*-$[Co(CN)_2dip_2]NO_3\cdot 7H_2O$.[13] Fifteen grams of *trans*-$[CoCl_2dip_2]NO_3$[14],*3 were treated with 10 g of AgCN in 500 m*l* of water on a water bath

4) M. Shibata, M. Mori and E. Kyuno, *ibid.*, **3**, 1573 (1964).

5) H. Siebert, *Z. anorg. u. allgem. Chem.*, **327**, 63 (1964).

6) K. Kuroda, *Nippon Kagaku Zasshi (J. Chem. Soc. Japan, Pure Chem. Sect.)*, **89**, 720 (1968).

7) L. Cambi and E. Daglia, *Gazz. chim. ital.*, **88**, 691 (1964).

8) K. Ohkawa, J. Hidaka and Y. Shimura, This Bulletin, **40**, 2830 (1967).

9) S. C. Chan and M. L. Tobe, *J. Chem. Soc.*, **1963**, 966.

10) G. Favini and E. Paglia, *J. Inorg. Nucl. Chem.*, **8**, 155 (1958).

11) K. Ohkawa, J. Hidaka and Y. Shimura, This Bulletin, **39**, 1715 (1966).

12) N. Maki and K. Okawa, *J. Electroanal. Chem.*, **8**, 262 (1964).

13) N. Maki, This Bulletin, **42**, No. 9 (1969) in the press: N. Maki, T. Hamazaki and S. Sakuraba, *ibid.*, **41**, 1735 (1968).

14) F. M. Jaeger and J. A. van Dijk, *Z. anorg. u. allgem. Chem.*, **227**, 273 (1936).

*3 dip=2,2′-dipyridyl; $C_{10}H_8N_2$.

(80°C) for three hours. Lustrous, needle-shaped yellow crystals were obtained from the filtrate. The crude complex was recrystallized from hot water. Found: Co, 9.51; C, 43.15; N, 15.97; H, 5.03%. Calcd for $[Co(CN)_2dip_2]NO_3 \cdot 7H_2O$: Co, 9.64; C, 43.22; N, 16.04; H, 4.95%.

The solubility of the complex in water was 1.0904 g/100 g water (25°C). The corresponding sulfate was obtained by using *trans*-$[CoCl_2dip_2]_2SO_4$ (anhydrous) instead of *trans*-$[CoCl_2dip_2]NO_3$ as the starting complex. Found: Co, 10.12; C, 45.54; N, 14.45; H, 5.01%. Calcd for $[Co(CN)_2dip_2]_2SO_4 \cdot 12H_2O$: Co, 10.17; C, 45.60; N, 14.50; H, 4.88%.

Preparation of *cis*-$[Co(CN)_2phen_2]NO_3 \cdot 6H_2O$.[13],*4 Twenty grams of *trans*-$[CoCl_2phen_2]NO_3$[15] were treated with 15 g of AgCN in 500 m*l* of water at 70—80°C for three hours. The suspension was then filtered and concentrated by evaporation. When the solution was allowed to stand, silky yellow crystals deposited on the wall of the beaker. Found: Co, 9.11; C, 48.39; N, 15.17; H, 4.67%. Calcd for $[Co(CN)_2phen_2]NO_3 \cdot 6H_2O$: Co, 9.19; C, 48.68; N, 15.29; H, 4.40%.

The solubility of the complex in water was 0.6736 g/100 g water; in absolute methanol, 0.1952 g/100 g methanol; and in absolute ethanol, 0.0111 g/100 g ethanol at 25°C.

The chloride of the complex was obtained by treating the nitrate with a solution of potassium chloride, for the chloride of the complex is less soluble in water than the nitrate. Found: Co, 10.08; C, 54.07; N, 14.66; H, 4.52%. Calcd for $[Co(CN)_2phen_2]Cl \cdot 4H_2O$: Co, 10.18; C, 53.95; N, 14.52; H, 4.18%.

Preparation of *cis*-$[Co(CN)(NO_2)en_2]NO_3 \cdot H_2O$. The orange-red crystals of *cis*-$[CoCl(NO_2)en_2]NO_3$[16] (60 g) were treated with 30 g of AgCN in 500 m*l* of water at 80—90°C for an hour. The color of the solution changed from red to yellow. The solution was then filtered, concentrated by evaporation, and allowed to stand. Bright yellow crystals deposited. The yield was 84% of theory. Found: Co, 17.69; C, 18.03; N, 29.65; H, 5.67%. Calcd for $[Co(CN)(NO_2)en_2]NO_3 \cdot H_2O$:[17] Co, 17.80; C, 18.13; N, 29.61; H, 5.48%.

Preparation of *trans*-$[Co(CN)(SO_3)en_2]$. Twenty grams of *trans*-$[CoCl(SO_3)en_2] \cdot H_2O$[18] were treated with 10 g of AgCN in 500 m*l* of water at 90°C for three hours. Brownish-yellow crystals were thus obtained. Found: Co, 20.53; C, 20.89; N, 24.77; H, 5.78%. Calcd for $[Co(CN)(SO_3)en_2]$: Co, 20.66; C, 21.06; N, 24.56; H, 5.66%.

Preparation of *cis*-$[Co(CN)(SO_3)en_2]$ (anhydrous). The complex was prepared by the following two methods: (1) To a solution in which *trans*-$[Co(CN)(SO_3)(NH_3)_4] \cdot 2H_2O$[6] (30 g) had been completely dissolved there were added 135 m*l* of 10% ethylenediamine under continuous stirring; the solution was then heated and evaporated on a water bath for three hours. The reaction took place, evolving ammonia. The yield was 54% of theory. Found: Co, 20.37; C, 21.22; N, 24.56; H, 5.71%. Calcd for $[Co(CN)(SO_3)en_2]$: Co, 20.66; C, 21.06; N, 24.56; H, 5.66%.

(2) Analogously, 20 g of *cis*-$[CoCl(SO_3)en_2] \cdot 3H_2O$ were treated with 10 g of AgCN in 500 m*l* of water at 90°C for three hours. The *cis*-$[Co(CN)(SO_3)en_2]$ complex (anhydrous) was obtained from the filtrate. Found: Co, 20.68; C, 20.97; N, 24.83; H, 5.91%. Calcd for $[Co(CN)(SO_3)en_2]$: Co, 20.66; C, 21.06; N, 24.56; H, 5.66%.

Preparation of *trans*-$[Co(CN)dg_2(NH_3)] \cdot {}^1/_2H_2O$.[*5] The complex was prepared by the following three methods:

(1) Thirty-four grams of *trans*-$[CoCldg_2(NH_3)] \cdot H_2O$[19] were treated with 20 g of AgCN in 500 m*l* of water at 90°C for three hours. Bright brownish-yellow crystals were obtained from the filtrate. The crude product was recrystallized from hot water containing acetic acid. Found: Co, 17.33; C, 32.00; N, 24.51; H, 5.38%. Calcd for $[Co(CN)dg_2(NH_3)] \cdot \frac{1}{2}H_2O$: Co, 17.27; C, 31.68; N, 24.63; H, 5.32%.

(2) To 15.0 g of *trans*-$[Co(CN)(OH_2)(NH_3)_4]Cl_2$[6] in 150 m*l* of water there were added 14.4 g of dimethylglyoxime. The mixture was heated on a water bath for three hours. The reaction proceeded, evolving ammonia, according to the following scheme:[20]

$$[Co(CN)(OH_2)(NH_3)_4]^{2+} + 2dgH \rightarrow [Co(CN)dg_2(NH_3)] + 3NH_3.$$

Every half hour during the reaction, 5—7 g of ammonium acetate were added to the solution. A total of 20 g of ammonium acetate was used. Lustrous orange-yellow crystals separated from solution when it was allowed to stand. The product was filtered and washed with 80% ethanol to eliminate traces of unreacted dimethylglyoxime. The yield was more than 82% of theory. Found: Co, 17.21; C, 31.44; N, 24.89; H, 5.45%. Calcd for $[Co(CN)dg_2(NH_3)] \cdot \frac{1}{2}H_2O$: Co, 17.27; C, 31.68; N, 24.63; H, 5.32%.

(3) A solution of 400 m*l* containing 27 g of potassium cyanide was mixed with a solution of 100 g of $[Codg_2(NH_3)_2]Cl \cdot 5H_2O$[21] dissolved in 400 m*l* of water and heated on a water bath for an hour at 90°C. The insoluble orange-yellow crystals which were deposited from the solution were filtered and washed with cold water several times and then with ethanol. The crude complex was recrystallized from hot water containing acetic acid. Found: Co, 17.22; C, 31.43; N, 24.78; H, 5.40%. Calcd for $[Co(CN)dg_2(NH_3)] \cdot \frac{1}{2}H_2O$: Co, 17.27; C, 31.68; N, 24.63; H, 5.32%.

Preparation of *trans*-$K[Co(CN)_2dg_2] \cdot {}^3/_2H_2O$.[22] The complex was prepared by the following two methods:

(1) A solution (200 m*l*) containing 13.7 g of potassium cyanide was mixed with a solution of 50 g of

*4 phen=1,10-phenanthroline; $C_{12}H_8N_2$.

15) P. Pfeiffer and Br. Werdelmann, *Z. anorg. u. allgem. Chem.*, **236**, 31 (1950).

16) A. Werner and L. Gerb, *Ber.*, **34**, 1740 (1901).

17) Independent of this work, the preparation of the nitrite of the complex, *cis*-$[Co(CN)(NO_2)en_2]NO_2$, has been reported; *cf.*, Ref. 8.

18) A. Werner and M. Pokrowska, *Liebig. Ann.*, **386**, 81 (1912).

*5 dg_2=a pair of dimethylglyoximes: $2CH_3 \cdot C(NO) \cdot C(NOH) \cdot CH_3$.

19) L. Tschugaeff, *Ber.*, **39**, 2694 (1906); *ibid.*, **40**, 3499 (1907).

20) N. Maki, T. Itoh and S. Sakuraba, This Bulletin, **41**, 529 (1968).

21) L. Tschugaeff, *Z. anorg. u. allgem. Chem.*, **46**, 160 (1905).

22) N. Maki, This Bulletin, **38**, 2013 (1965).

$[Codg_2(NH_3)_2]Cl\cdot 5H_2O$[21] dissolved in 300 m*l* of water under stirring and then heated on a water bath until the reaction mixture had been evaporated to one-third of its former volume. From the smell of ammonia evolved, it could be discerned that the following reaction was in progress:

$$[Codg_2(NH_3)_2]Cl\cdot 5H_2O + 2KCN \rightarrow K[Co(CN)_2dg_2]\cdot \tfrac{3}{2}H_2O + 2NH_3 + 2KCl.$$

During the course of the reaction, insoluble orange-yellow crystals deposited. These crystals were ascertained to be the *trans*-$[Co(CN)dg_2(NH_3)]\cdot \tfrac{1}{2}H_2O$[19] complex by the elementary analyses and by the study of the absorption spectra in the IR, UV, and visible regions.[23] These crystals of the cyano-ammine complex were filtered off during the reaction, and the filtrate was further concentrated by evaporation. On cooling, large needle-shaped yellow crystals were obtained. Found: Co, 14.41; C, 29.63; N, 20.55; H, 4.32; K, 9.50%. Calcd for $K[Co(CN)_2dg_2]\cdot \tfrac{3}{2}H_2O$: Co, 14.47; C, 29.49; N, 20.63; H, 4.21; K, 9.60%.

Sodium salt of the complex was obtained by using sodium cyanide instead of potassium cyanide. Found: Co, 14.63; C, 29.97; N, 20.14; H, 4.49%. Calcd for $Na[Co(CN)_2dg_2]\cdot 2H_2O$: Co, 14.73; C, 30.01; N, 20.00; H, 4.53%.

(2) Seventy-eight grams of *trans*-$[Co(CN)dg_2(NH_3)]\cdot \tfrac{1}{2}H_2O$[19] were suspended in 800 m*l* of water containing 16 g of potassium cyanide. To the suspension there were stirred 25 g of active charcoal. Then the suspension was warmed on a water bath for ten hours at 40—50°C. The substitution occurred gently and slowly, evolving ammonia, below 50°C. The charcoal was filtered off, and the filtrate was concentrated by evaporation at 60—70°C until needle-shaped yellow crystals were deposited. Found: Co, 14.39; C, 29.61; N, 20.40; H, 4.10%. Calcd for $K[Co(CN)_2dg_2]\cdot \tfrac{3}{2}H_2O$: Co, 14.47; C, 29.49; N, 20.63; H, 4.21%. The aiming dicyano complex was very soluble in water, while the starting of the monocyanoammine complex was insoluble. Therefore, the isolation was easy and complete.

Preparation of *trans*-$(NH_4)_2[Co(CN)dg_2(SO_3)]\cdot 4H_2O$. To a solution (1.2 *l*) containing 40 g of *trans*-$[Co(CN)(SO_3)(NH_3)_4]\cdot 2H_2O$[6] there were added 50 g of dimethylglyoxime (dgH). The mixture was then boiled at 100°C for three hours. The reaction took place, evolving ammonia. No deposition of metallic cobalt was observed. After cooling, the solution was filtered to eliminate the unreacted dimethylglyoxime, and then the filtrate was further concentrated by evaporation on a water bath at 80°C. When it was allowed to stand, orange-yellow crystals separated from the solution; they were filtered and washed with ethanol and ether. The crude product was recrystallized from hot water. Found: Co, 11.50; C, 21.33; N, 19.07; H, 6.32%. Calcd for $(NH_4)_2[Co(CN)dg_2(SO_3)]\cdot 4H_2O$: Co, 11.71; C, 21.47; N, 19.48; H, 6.01%.

Preparation of *trans*-$H[Co(CN)dg_2Cl]\cdot 4H_2O$. Thirty grams of *trans*-$(NH_4)_2[Co(CN)dg_2(SO_3)]\cdot 4H_2O$ were dissolved in 500 m*l* of water. To this solution there were added 300 m*l* of concentrated HCl. The temperature of the solution was maintained at 50—60°C for ten hours under continuous stirring. The reaction proceeded, evolving sulfur dioxide. The yellow precipitates were separated from the solution when the reaction was over. The mixture was filtered and washed several times with ethanol and ether. The crude complex was purified by treating it again with 200 m*l* of concentrated HCl at 60°C. Above 90°C, it could be seen that the CN-ligands were partly replaced with Cl^- ions to produce the $H[CoCl_2dg_2]$ complex. The residue was filtered and washed with concentrated HCl, ethanol and ether. Found: Co, 13.69; C, 25.69; N, 16.73; H, 5.50%. Calcd for $H[Co(CN)dg_2Cl]\cdot 4H_2O$: Co, 13.91; C, 25.51; N, 16.53; H, 5.47%.

Preparation of *cis*-$[Co(CN)(OH_2)en_2]SO_4\cdot 2H_2O$. Into 150 g of the *trans*-$[Co(CN)(SO_3)en_2]$ obtained previously there were stirred, drop by drop, 150 m*l* of concentrated H_2SO_4 in ice. The reaction occurred immediately, evolving SO_2 and yielding a viscous liquid of $[Co(CN)(SO_4)en_2]$, which tends to aquate in water. The aimed-at aquo complex was precipitated from the solution with the addition of methanol. The yield was 38%. Found: Co, 16.48; C, 17.01; N, 19.83; H, 6.40%. Calcd for $[Co(CN)(OH_2)en_2]SO_4\cdot 2H_2O$: Co, 16.59; C, 16.90; N, 19.71; H, 6.24%.

Preparation of *trans*-$[Co(CN)_2(NH_3)_4]NO_3\cdot H_2O$. Dried crystals of potassium cyanide were ground into fine powder in a porcelain mortar, and 3.00 g of them were dissolved in 500 m*l* of dimethyl sulfoxide at 60°C. Then the solution was transferred into a three-necked flask equipped with a reflux condenser and a mechanical stirrer. To this solution there were added 11.66 g of *trans*-$[Co(CN)Cl(NH_3)_4]NO_3$.[11] The suspension was heated on a water bath at 70—85°C for three hours. When the solution was then allowed to stand overnight, orange-yellow crystals were deposited from the solution; they were filtered and washed with acetone several times. The crude complex was recrystallized from hot water below 50°C. The yield was 53.4% of theory. Found: Co, 22.51; C, 9.08; N, 37.72; H, 5.60%. Calcd for $[Co(CN)_2(NH_3)_4]NO_3\cdot H_2O$: Co, 22.74; C, 9.27; N, 37.84; H, 5.45%.

Preparation of *trans*-$[Co(CN)_2en(NH_3)_2]Cl\cdot H_2O$. This complex was prepared according to the following reaction steps:

$$\textit{trans}\text{-}[Co(CN)(SO_3)(NH_3)_4]\cdot 2H_2O \xrightarrow{en} \textit{cis}\text{-}[Co(CN)(SO_3)en(NH_3)_2] \xrightarrow{HCl} \textit{cis}\text{-}[Co(CN)Clen(NH_3)_2]Cl \xrightarrow[\text{in DMSO}]{KCN} \textit{trans}\text{-}[Co(CN)_2en(NH_3)_2]Cl\cdot H_2O.$$

(1) Thirty grams of *trans*-$[Co(CN)(SO_3)(NH_3)_4]\cdot 2H_2O$[5] were dissolved in 100 m*l* of a water solution containing 8.6 g of ethylenediamine, and then the mixture was heated on a water bath (80°C) for two hours. The complex was once dissolved completely in solution, and then again deeper-colored yellow or brown crystals separated from the solution as a result of the reaction. The reaction mixture was further heated on a water bath for three or four hours, filtered while in a hot state, and washed several times with hot water, ethanol, and ether. The *cis*-$[Co(CN)(SO_3)en(NH_3)_2]$ complex (12 g) was thus obtained; it was used for the next reaction without further purification, since it was insoluble in water.

23) Previously, it was speculated that these crystals were the $[Co(dgH)_3]\cdot 2.5H_2O$ complex, but this speculation should be corrected; *cf.*, Ref. 22.

(2) Thirty grams of *cis*-$[Co(CN)(SO_3)en(NH_3)_2]$ (anhydrous) were dissolved in 300 m*l* of concentrated HCl and heated on a water bath at 80—85°C for five hours. The color of the solution changed from orange-yellow to red. At last, the solution became a half of its former volume. The solution was once filtered. To the filtrate there were added, drop by drop, 200 m*l* of absolute ethanol under ice cooling. Then, fine red crystals were separated from the solution. The *cis*-$[Co(CN)Cl\,en(NH_3)_2]Cl$ complex is pure enough to be used for the next procedure without further recrystallizations.

(3) Dried powder of potassium cyanide (2.30 g) was completely dissolved in 300 m*l* of dimethyl sulfoxide at 70—80°C in a flask which equipped with a reflux condenser and a mechanical stirrer. Then, 6.0 g of *cis*-$[Co(CN)Cl\,en(NH_3)_2]Cl$ were added in small portions to the solution and the mixture was heated at 80°C for an hour. The yellow solution soon became muddy as the reaction proceeded. The reaction mixture was allowed to stand overnight, filtered and washed with acetone several times. The crude complex was recrystallized from hot water below 60°C. Found: Co, 22.63; C, 18.50; N, 32.61; H, 6.39%. Calcd for $[Co(CN)_2en(NH_3)_2]Cl\cdot H_2O$: Co, 22.79; C, 18.58; N, 32.49; H, 6.24%.

Preparation of *trans*-$[Co(CN)_2en_2]NO_3$. This complex was prepared by the method of Muto *et al.*[2] That is, 4.68 g of *trans*-$[CoCl_2en_2]NO_3$ were treated with 3.00 g of KCN in 500 m*l* of dimethyl sulfoxide for three hours at 70°C. The crude complex was recrystallized from hot water below 60°C. Found: Co, 20.22; C, 24.39; N, 33.43; H, 5.69%. Calcd for $[Co(CN)_2en_2]NO_3$: Co, 20.10; C, 24.58; N, 33.44; H, 5.73%.

Measurements. The absorption spectra in the visible and ultraviolet regions were determined with a Beckmann DU spectrophotometer. The IR spectra were recorded on a Perkin-Elmer grating infrared spectrophotometer, model 337, with a KBr-pellet. The proton spectra were recorded on a Hitachi-Perkin-Elmer high resolution NMR spectrometer, model R-20. As a solvent for the NMR measurements we used 99.75% D_2O at 35°C.

Results and Discussion

The Method of Syntheses. The CN^- ion is located at the end position of the spectrochemical series and has the strongest coordinating ability among the cobalt(III) complexes of the Werner type. Hence, the attack on the acido-cobalt(III) complexes by the cyanide ions causes the ligands with lesser coordination ability to be expelled totally or partly from the coordination sphere and results in an overall rearrangement of the ligands; *i. e.*, a disproportionation occurs, since the ligands in general tend to surround a cobalt with bonds of the same nature or similar covalent character as far as possible.

The results of the preparations, however, suggest that the substitution of chloro ligands is possible even in a water solution by the use of silver cyanide. When the cyanide ions are present in a very dilute concentration, the substitution can take place only without any accompanying disproportionation, because the silver ion leaves the reaction system as a precipitate of AgCl and the equilibrium of silver cyanide moves in the direction of dissociation to supply Ag^+ or CN^- ions.

For the preparation of dicyano-ammine complexes, the attempts to let the dichloro-ammine complexes cited below react with AgCN have failed due to the disruption of the complex used: *cis*-$[CoCl_2(NH_3)_4]NO_3$, *trans*-$[CoCl_2(NH_3)_4]NO_3$, and *trans*-$[CoCl_2tn_2]NO_3$.*6

TABLE 1. THE ABSORPTION MAXIMA OF THE MIXED CYANO COBALT(III) COMPLEXES

Compound	I-band	II-band	C.T.-band
cis-$[Co(CN)_2(NH_3)_4]NO_3\cdot H_2O$	25.23(1.86)	31.28(2.03)	47.26(4.31)
trans-$[Co(CN)_2(NH_3)_4]NO_3\cdot H_2O$	*ca.* 22(1.81) 24.02(1.95)	31.60(2.05)	47.80(4.14)
cis-$[Co(CN)_2en(NH_3)_2]NO_3$	24.63(1.91)	32.46(1.96)	47.31(4.41)
trans-$[Co(CN)_2en(NH_3)_2]Cl\cdot H_2O$	*ca.* 22.4(1.55) 24.40(1.77)	32.10(1.78)	47.60(3.89)
cis-$[Co(CN)_2en_2]NO_3$	24.73(1.91)	32.37(1.93)	47.37(4.32)
trans-$[Co(CN)_2en_2]NO_3$	*ca.* 22(1.38) 24.33(1.90)	32.38(1.93)	47.62(4.44)
trans-$Na[Co(CN)_2dg_2]\cdot 2H_2O$	*ca.* 26(2.3)	*ca.* 30.7(3.24)	*ca.* 36.7(3.90) 41.40(4.45)
cis-$[Co(CN)(SO_3)en_2]$	24.39(2.13)	——*	36.76(4.20)
trans-$[Co(CN)(SO_3)en_2]$	22.99(1.97)	*ca.* 30(2.4)	36.23(4.19)
cis-$[Co(CN)(OH_2)en_2]SO_4\cdot 2H_2O$	22.37(2.11)	*ca.* 30(2.4)	36.23(4.22)
cis-$[Co(CN)(NO_2)en_2]NO_3\cdot H_2O$	23.42(2.12)	31.45(3.36)	42.02(4.22)
trans-$[Co(CN)dg_2(NH_3)]\cdot \frac{1}{2}H_2O$	——*	——*	——* 42.30(4.52)
trans-$[Co(CN)(SO_3)(NH_3)_4]\cdot 2H_2O$	23.50(2.16)	30.70(1.73)	42.41(3.41)
cis-$[Co(CN)(OH_2)(NH_3)_4]Cl_2$	21.91(1.90)	30.00(1.81)	42.20(3.48)
$[Co(CN)(NH_3)_5](ClO_4)_2\cdot \frac{1}{2}H_2O$	22.72(1.77)	30.71(1.73)	42.40(3.40)
$[Co(CN)_3en(NH_3)]\cdot H_2O$	25.51(1.90)	32.36(1.92)	48.31(4.45)
$[Co(CN)_3dien]$	26.45(2.45)	33.33(2.39)	48.54(4.11)

Unit: wave number, 10^3/cm; absorbance (log ε); dien=diethylenetriamine; * shoulder band

*6 tn=trimethylenediamine; $NH_2CH_2CH_2CH_2NH_2$.

In addition to these complexes, the substitution of the following complexes with KCN in a dimethyl sulfoxide has been attempted, but all attempts have failed, and for the same reason: *trans*-$[CoCl_2pn_2]NO_3$,*7 *trans*-$[CoCl_2dip_2]NO_3$, *trans*-$[CoCl_2phen_2]NO_3$, and *trans*-$[CoCl_2(NH_3)_4]NO_3$.

Accordingly, for obtaining dicyano-ammine complexes the step-by-step substitution method *via* the monocyano-monochloro complex of the $[Co(CN)ClN_4]$-type has been adopted and found to be suitable for replacing a chloro ligand with a CN^- ion without disrupting the complex, as has been described previously.

In connection with this, the method using silver cyanide always gave rise to the *cis*-isomer rather than the *trans*-isomer, even if a *trans*-isomer was used as the starting complex, except in the case of the preparation of *trans*-$[Co(CN)(SO_3)en_2]$, in which the method using silver cyanide carried out in a water solution gave a *trans*-isomer. On the other hand, the method using KCN in dimethyl sulfoxide always gave a *trans*-isomer.

The dimethylglyoximato-cobaltate(III) complex, $H[CoCl_2dg_2]$, did not react with AgCN because the aquation of the complex was too rapid to allow the replacement of the Cl-ligands with CN^- ions within the sphere of coordination. The disruption of the complex used is ascribed to the formation of diaquocobalt(III) cyanide, $[Co(OH_2)_2dg_2]CN$. Thus, the substitution with CN^- ions has to take place within the sphere of coordination.

Absorption Spectra in the Visible and Ultraviolet Regions. Table 1 shows the numerical data of the absorption maxima of the cobalt(III) complexes measured.

In the table, the first two absorption bands are assigned to ligand-field bands. The third, or last, strong band can be attributed to a charge-transfer caused by the ligands, such as CN and SO_3.

Figures 1 and 2 show that the first spin-allowed band of dicyano cobalt(III) complexes of the

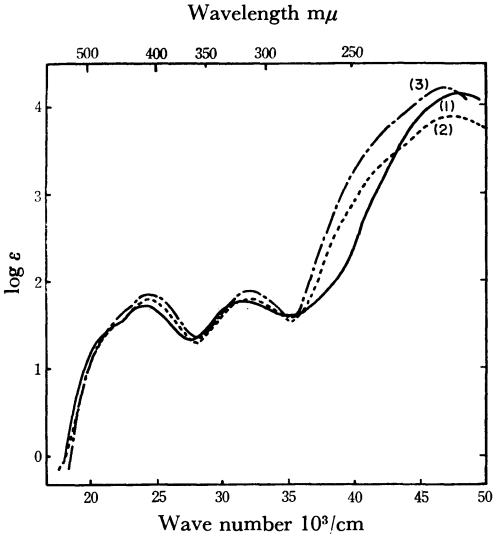

Fig. 1. The absorption spectra of the cyano cobalt(III) complexes with a *trans*-configuration: (1) —— *trans*-$[Co(CN)_2(NH_3)_4]NO_3\cdot H_2O$; (2) ------ *trans*-$[Co(CN)_2en(NH_3)_2]Cl\cdot H_2O$; (3) —·—·— *trans*-$[Co(CN)_2en_2]NO_3$.

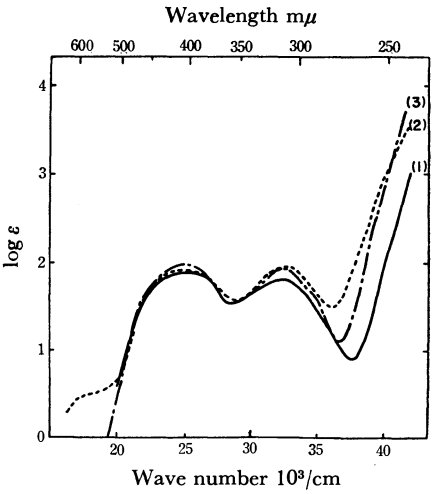

Fig. 2. The absorption spectra of the cyano cobalt(III) complexes with a *cis*-configuration: (1) —— *cis*-$[Co(CN)_2(NH_3)_4]NO_3\cdot H_2O$; (2) ------ *cis*-$[Co(CN)_2en(NH_3)_2]NO_3$; (3) —·—·— *cis*-$[Co(CN)_2en_2]NO_3$.

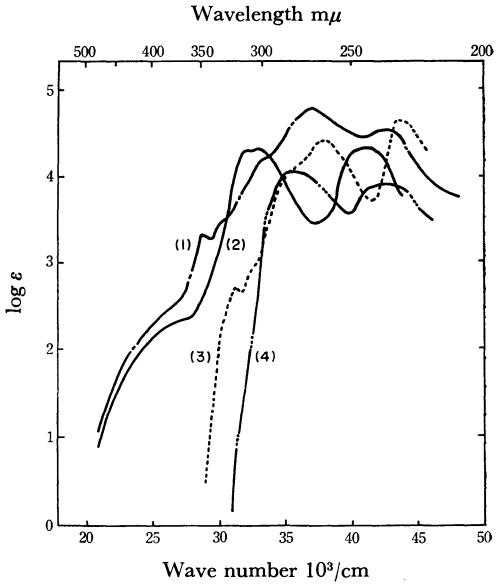

Fig. 3. The absorption spectra of the dicyano cobalt(III) complexes with 2,2′-dipyridyl and 1,10-phenanthroline, and of their ligands only: (1) —·—·— *cis*-$[Co(CN_2)phen_2]NO_3\cdot 6H_2O$; (2) —— *cis*-$[Co(CN)_2dip_2]NO_3\cdot 7H_2O$; (3) ------ 1,10-phenanthroline; (4) —·—·—·— 2,2′-dipyridyl in ethanol.

*7 pn=propylenediamine; $NH_2CH(CH_3)CH_2NH_2$.

ethylenediamine-ammine series for *cis*- and *trans*-isomers shifts towards a shorter wavelength according to the order of the spectrochemical series, except in the case of the *cis*-$[Co(CN)_2(NH_3)_4]^+$ ion.[3]

In agreement with the spectra obtained by Konya *et al.*[3] and Muto *et al.*,[2] all the first bands of *trans*-isomers split into two components, while those of *cis*-ones do not show any splitting.

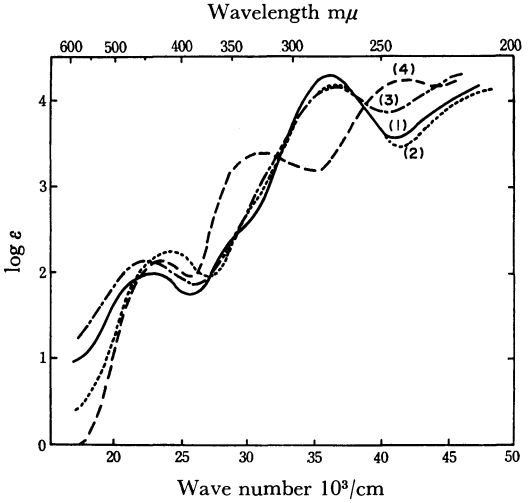

Fig. 4. The absorption spectra of the monocyano cobalt(III) complexes: (1) —— *trans*-[Co(CN)-$(SO_3)en_2$]; (2) ------ *cis*-[Co(CN)$(SO_3)en_2$]; (3) – – – – *cis*-[Co(CN)$(OH_2)en_2]SO_4\cdot 2H_2O$; (4) – – – – *cis*-[Co(CN)$(NO_2)en)_2]NO_3\cdot H_2O$.

Table 2. Frequencies (cm^{-1}) of the C≡N stretching vibration for the mixed cyano cobalt(III) complexes in solid state

Compound	Frequency (cm^{-1})	
cis-$[Co(CN)_2(NH_3)_4]NO_3\cdot H_2O$	2190 s	2140 s
trans-$[Co(CN)_2(NH_3)_4]NO_3\cdot H_2O$	2130 s	
cis-$[Co(CN)_2en(NH_3)_2]NO_3$	2150 s	2130 s
trans-$[Co(CN)_2en(NH_3)_2]Cl\cdot H_2O$	2145 s	2080w
cis-$[Co(CN)_2en_2]NO_3$	2150 s	2130 s
trans-$[Co(CN)_2en_2]NO_3$	2150 s	
cis-$[Co(CN)_2dip_2]NO_3\cdot 7H_2O$	2150 s	2130 s
cis-$[Co(CN)_2phen_2]NO_3\cdot 6H_2O$	2140 s	2130 s
trans-$Na[Co(CN)_2dg_2]\cdot 2H_2O$	2150 s	2130 s
trans-$K[Co(CN)_2dg_2]\cdot \frac{3}{2}H_2O$	2140 s	
trans-$(NH_4)_2[Co(CN)dg_2(SO_3)]\cdot 4H_2O$	2170 s	2140m
trans-$[Co(CN)dg_2(NH_3)]\cdot \frac{1}{2}H_2O$	2140 s	
cis-$[Co(CN)(NO_2)en_2]NO_3\cdot H_2O$	2145 s	
cis-$[Co(CN)(NO_2)en_2]ClO_4$	2175w	2128m
cis-$[Co(CN)(SO_3)en_2]$	2173m	2152m
trans-$[Co(CN)(SO_3)en_2]$	2150 s	
$[Co(CN)(NH_3)_5](ClO_4)_2\cdot \frac{1}{2}H_2O$	2140 s	
cis-$[Co(CN)(OH_2)(NH_3)_4]Cl_2$	2170w	2140 s
cis-$[Co(CN)_3en(NH_3)]\cdot H_2O$	2140 s	
$[Co(CN)_3dien]$	2140 s	2090m
trans-$[Co(CN)dg_2(OH_2)]$	2176 s	

s=strong; m=medium; w=weak

Figure 3 shows the spectra of *cis*-dicyano-bis(2,2′-dipyridyl) and -bis(1,10-phenanthroline)cobalt(III) complexes, and of their ligands, respectively. The absorption spectrum of the latter complex agreed above all with that reported by Favini and Paglia[10] as a whole, but it did not necessarily coincide in detail, especially with regard to the presence of a small peak at around 27—29 kK.

Figure 4 shows the absorption spectra of the monocyano-cobalt(III) complexes prepared by the method using silver cyanide in water. The spectra quite agreed with those obtained by Ohkawa *et al.*[8] and by Chan and Tobe.[9]

Infrared Absorption Spectra. Table 2 lists the frequencies of the C≡N stretching vibrations measured for the mixed cyano cobalt(III) complexes.

Generally, a complex with a *trans*-configuration exhibits only one C≡N stretching band, while some of the complexes with a *cis*-configuration show two or more of their C≡N stretching bands split by the lowering of the symmetry, although there are some exceptions.

The differentiation between *cis*- and *trans*-isomers for bis(ethylenediamine)cobalt(III) complexes has been made in the infrared spectra of the CH_2-rocking vibrations in the region of 870—900 cm^{-1}. According to Baldwin,[24] the complexes with a *cis*-configuration show two bands, while those with a *trans*-structure exhibit one. Table 3 shows the frequencies of the CH_2-rocking vibrations in the regions measured.

Hughes and McWhinnie[25] suggested there is a correlation between the structure of the steric isomers and the complexity of that part of the

Table 3. Frequencies (cm^{-1}) of absorption bands in the regions of 870—900 cm^{-1} of the complexes of $[Coen_2XY]$-type

Compound	Frequency (cm^{-1})	
cis-$[Co(CN)_2en_2]NO_3$	893m	887 sh
trans-$[Co(CN)_2en_2]NO_3$	896 s	
cis-$[Co(CN)_2en_2]Cl$	889 s	878 s
trans-$[Co(CN)_2en_2]Cl$	889 s	
cis-$[Co(CN)(SO_3)en_2]$	894m	886m
trans-$[Co(CN)(SO_3)en_2]$	892m	
cis-$[Co(CN)Cl\ en_2]Cl\cdot H_2O$	889 s	877 s
cis-$[Co(CN)Br\ en_2]NO_3\cdot H_2O$	894m	884 sh
cis-$[Co(CN)(NO_2)en_2]NO_3\cdot H_2O$	890m	874 sh
trans-$[Co(SO_3)Cl\ en_2]$	883m	

s=strong; m=medium; sh=shoulder band.

24) M. E. Baldwin, *J. Chem. Soc.*, **1960**, 4369.
25) M. N. Hughes and W. R. McWhinnie, *J. Inorg. Nucl. Chem.*, **28**, 1659 (1966).

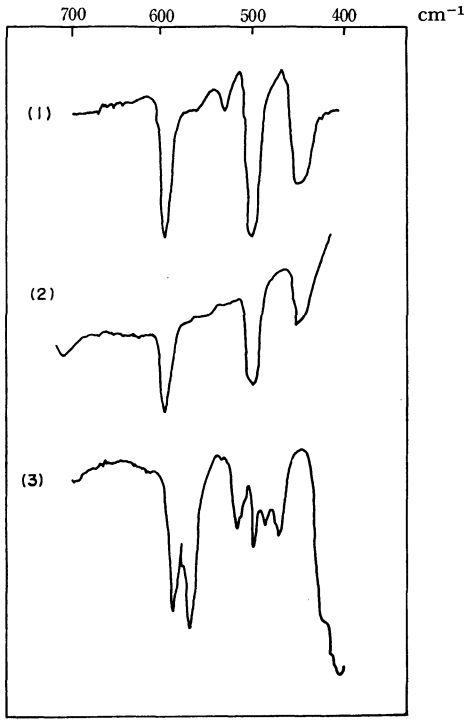

Fig. 5. Far-infrared spectra of dicyano cobalt(III) complexes in the region 400—700 cm^{-1}: (1) *trans*-$[Co(CN)_2en(NH_3)_2]Cl \cdot H_2O$; (2) *trans*-$[Co(CN)_2en_2]NO_3$; (3) *cis*-$[Co(CN)_2en_2]NO_3$.

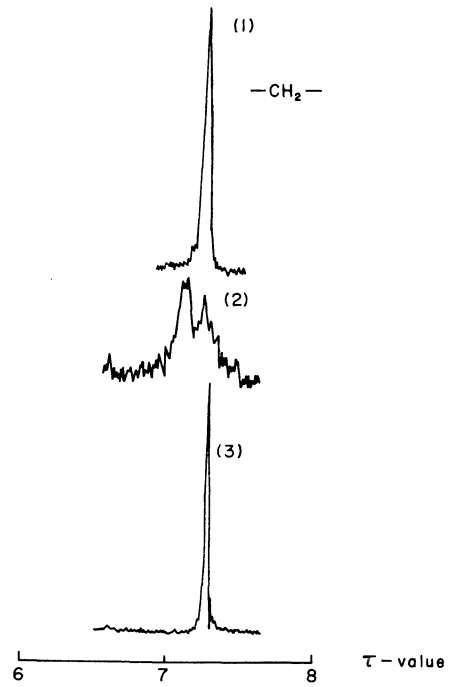

Fig. 6. The NMR spectra of dicyano cobalt(III) complexes obtained in 99.75% D_2O: (1) *trans*-$[Co(CN)_2en_2]NO_3$; (2) *cis*-$[Co(CN)_2en_2]NO_3$; (3) *trans*-$[Co(CN)_2en(NH_3)_2]Cl \cdot H_2O$.

spectrum, in which most bands are assigned to some "metal-ligand" stretching vibrations, *i. e.*, in the far-infrared region of 620—450 cm^{-1}. According to them, no *trans*-complex of the bis(ethylenediamine)-type has more than three strong bands between 604 and 510 cm^{-1}, while all the *cis*-complexes have more than three strong bands between 608 and 503 cm^{-1}.

Figure 5 shows the IR pattern of *trans*-$[Co(CN)_2en(NH_3)_2]Cl \cdot H_2O$ (a new complex) in comparison with those of the *cis*- and *trans*-dicyanobis(ethylenediamine)cobalt(III) complexes.

Nuclear Magnetic Resonance Spectra. Figure 6 indicates the proton spectra of some dicyano complexes obtained in D_2O. The complex with a *trans*-configuration exhibits only one band, while those of *cis*-isomers show two or more bands. This result might be used for the differentiation of the *cis*- and *trans*-pair of ethylenediamine complexes.

The authors wish to thank Mr. Taihei Hamazaki, Mr. Masaharu Mochizuki, Mr. Kouei Yamamoto, and Mr. Setsuro Ito for their assistance in the experiments. They also wish to express their thanks to the Ministry of Education for the financial support granted for this research.

BULLETIN OF THE CHEMICAL SOCIETY OF JAPAN VOL. 42 1916—1921 (1969)

The Chemistry of Protactinium. VII. The Stability of Protactinium(V) in Perchloric Acid and TTA-Benzene Solutions

Shin Suzuki and Yasushi Inoue

The Research Institute for Iron, Steel and Other Metals, Tohoku University, Katahira-cho, Sendai

(Received December 17, 1968)

With a view to understand the reasons for the confusion in published works as to the chemical behavior of protactinium(V) in a perchloric acid solution, the effect of the contact time and the stability of the perchloric acid solution of the pentavalent protactinium in the TTA-benzene extraction have been investigated in relation to the methods of preparing the solution. Four sample solutions, prepared by various methods, were used, and definite differences among them were observed. Two of them have been confirmed to be very stable and not to suffer a change in their distribution ratios with the time of standing, while the others are unstable-that is, their distribution ratios decrease with standing, thereby reaching a constant value which agrees with that of the former two. However, the value consistent with that obtained from backward extraction is not this constant value but the value obtained from fresh solutions of the latter type. Protactinium species in the TTA-benzene solution are also not stable, and their distribution ratios increase with standing. This increase in the distribution ratio is mainly due to the formation of unstrippable species. The mechanism of this irreversible change is assumed, from the indirect evidence of extraction experiments and absorption spectroscopy, to be the irreversible dehydration of $Pa(OH)_2T_3 \cdot HT$ to form $PaOT_3 \cdot HT$ in the organic phase. These unfavorable features of the extraction equilibrium should be taken into account in interpreting the results obtained by TTA extraction experiments.

As a result of an investigation by TTA-benzene extraction and by the ion exchange and filtration methods, of the chemical behavior of protactinium in a perchloric acid solution, it was concluded that $PaO_m(OH)_n^{5-2m-n}$ (where $2m+n=3$ and 4) was the predominant species present in a perchloric acid solution of 0.3—2.0M when the concentration of protactinium was lower than 10^{-6}M.[1] When the protactinium concentration was higher than 10^{-5}M, however, quite different behavior was observed. For example, when a perchloric acid solution which was made 10^{-7}M in protactinium by diluting a 10^{-5}M solution which had been prepared in advance was subjected to TTA extraction, the log-log plot of the distribution ratio and the TTA activity in the organic phase were different from those obtained with a solution which was directly made 10^{-7}M in protactinium concentration. In the former case, the distribution ratio decreased remarkably with the time. In the filtration experiments, the percentage of the removal of protactinium from a perchloric acid solution by membrane filters increased with a decrease in the pore sizes. However, this effect was especially noticeable when the protactinium concentration was as high as 10^{-5}M. In the same kind of experiments with Tōyō Roshi No. 5C filter paper (the finest filter for quantitative use), virtually no effect of aging was observed in the case of either carrier-free or 10^{-7}M protactinium solutions, while in the case of a 10^{-5}M solution the removal increased with the aging time, attaining a value of 45% after 80 days. The results can be understood in terms of the formation of colloidal aggregates to a great extent. These observations suggest that the method of preparation and the concentration of protactinium both affect the nature of protactinium in a perchloric acid solution. Much of the confusion in published works which has been pointed out previously[1] may be attributed to these facts. Furthermore, the contact time required to attain a constant distribution ratio in the TTA-benzene extraction system was different with different authors; that is, in a previous experiment by the present authors, only 30 min was long enough to attain a constant distribution ratio,[1] while Kolarich and his co-workers reported that a one-day contact was necessary to reach an extraction equilibrium.[2] This also constitutes one of the very important keys to solve the reasons for the discrepancies among the results obtained by various experimenters.[1]

The purpose of the present study is to investigate the effect on the TTA extraction behavior of the method of the preparation of the perchloric acid

1) S. Suzuki and Y. Inoue, This Bulletin, **39**, 1705 (1966).

2) R. T. Kolarich, V. A. Ryan and R. P. Schuman, *J. Inorg. Nucl. Chem.*, **29**, 783 (1967).

solution of protactinium. In the course of the investigation, interesting results regarding the stability of the protactinium species in the TTA-benzene solution have been obtained.

Experimental

Reagents and Apparatus. *^{231}Pa and ^{233}Pa.* Stock solutions of these isotopes in hydrochloric-acid and hydrofluoric-acid mixtures were prepared by the methods reported previously.[3] The concentration of protactinium in the ^{231}Pa solution was determined by gravimetry by using protactinium pentoxide as a weighing form.

Benzene was purified by distillation, and doubly-distilled water was used throughout this experiment. The acidity of the solution was determined by titration with a standard sodium hydroxide solution. The other chemicals, such as the thenoyl trifluoroacetone (TTA), perchloric acid, hydrofluoric acid, and aluminum perchlorate, were of the highest purity. For the solvent extraction procedure, a Iwaki universal mechanical shaker, Model V-S was used. A Kōbe Kōgyō Model PS-400 well-type scintillation probe coupled with a Kōbe Kōgyō Model SA-400 scaler was used for the gamma-ray assay.

Procedures. All the experiments were carried out at room temperature. Ordinary separatory funnels made of glass were used for the solvent extraction. To eliminate distortions of the experimental results related to the adsorption on glass, the walls of the funnels were preliminarily saturated with protactinium by shaking the test solution for a time sufficient for adsorption equilibrium to be reached. Care was taken to ascertain the material balance in each experiment; each value given is the average of the results of at least two determinations. For all the solvent extractions except for Fomin's method,[4] 5-m*l* portions of the aqueous and organic phases were used, and after the separation of the two phases, a 2-m*l* aliquot of each phase was placed in a polyethylene test tube and its γ radioactivity counted; the distribution ratio was calculated by means of the usual relationship.

$$D = \frac{\gamma \text{ activity per ml of the organic phase}}{\gamma \text{ activity per ml of the aqueous phase}}$$

Forward Extraction. Four perchloric acid solutions of protactinium prepared by the various methods to be described below, were used. Examinations of the effect of contact time and of the stability of the solution, and analysis by Fomin's method, were carried out for each of the solutions.

No. 1: Aliquots of ^{231}Pa and ^{233}Pa stock solutions (total, 5 m*l*) and 30 m*l* of concentrated perchloric acid were transferred into a platinum dish and heated on a hot plate until the white fumes of perchloric acid appeared. Then the mixture was violently heated directly on a gas burner for five minutes. After cooling, 13 m*l* of concentrated perchloric acid were added. This solution was then diluted to 250 m*l* with distilled water. The concentrations of protactinium and of perchloric acid in this solution were 10^{-7} and 1.38 M respectively.

No. 2: Aliquots of ^{231}Pa and ^{233}Pa stock solutions (total, 5 m*l*) and a small amount of concentrated hydrofluoric acid were transferred into a platinum dish and evaporated almost to dryness, initially on a hot plate and finally on a water bath. The residue was then dissolved by heating it with 2.31 m*l* of 1.17M hydrofluoric acid. Then 95 m*l* of a 5.28M perchloric acid solution and 2.5 m*l* of a 3M aluminium perchlorate solution were added, in this order, and the mixture was diluted with distilled water to 500 m*l*. The concentrations of protactinium, perchloric acid, fluoride ions, and aluminum ions in this solution were 5×10^{-8}, 1.05, 0.005, and 0.015M respectively.

No. 3: Aliquots of ^{231}Pa and ^{233}Pa stock solutions (total, 5 m*l*), a few milliliters of concentrated hydrofluoric acid, and 2 m*l* of concentrated perchloric acid were placed in a platinum crucible, and the mixture was heated until the white fumes of perchloric acid appeared. Heating was then continued until the volume of the solution was reduced to about 1 m*l*. The residual solution was transferred to a polyethylene bottle, and 1 m*l* of concentrated perchloric acid was added to the crucible. The solution was then reduced to 0.5 m*l* by heating it on a hot plate; the residual solution was combined with the solution in the same bottle. The procedure was repeated until all the activity was removed from the crucible. The concentrations of protactinium and of perchloric acid in this solution were 8.7×10^{-6} and 8.48M respectively. Before use, this solution was diluted to 10^{-7}M with respect to protactinium with perchloric acid of a suitable concentration, to make 1.00M in acidity.

No. 4: Aliquots of ^{231}Pa and ^{233}Pa stock solutions (total, 5 m*l*) and a small amount of hydrofluoric acid were transferred into a platinum dish and evaporated almost to dryness, initially on a hot plate and finally on a water bath. The residue was dissolved out of the dish by heating it with concentrated perchloric acid until all the activity on the dish had been removed. The solution was then diluted to 250 m*l* with distilled water. The concentrations of protactinium and of perchloric acid in this solution were 10^{-7} and 0.998M respectively.

Backward Extraction. Aliquots of ^{231}Pa and ^{233}Pa stock solutions were transferred into a platinum dish and heated to dryness on a hot plate. The residue was dissolved in 0.64 m*l* of 1.17M hydrofluoric acid, and then 0.948 m*l* of a 5.28M perchloric acid solution and 1.7 m*l* of a 1.33M aluminum perchlorate solution were added, in this order. The solution was diluted to 50 m*l* with distilled water. A protactinium solution in TTA-benzene was then prepared by extracting protactinium from 25 m*l* of this solution with 75 m*l* of a 0.1M TTA-benzene solution for 25 min. The concentration of protactinium in the TTA-benzene solution thus prepared was 0.98×10^{-7}M. The backward extraction was performed by bringing into contact 5-m*l* portions of this solution and of the perchloric acid solution of definite concentration which had been pre-equilibrated with the 0.1M TTA-benzene solution.

Fomin's Method.[4] The percentage of inextractable forms (P) which were not in rapid equilibrium with extractable forms, and the distribution ratio of extractable forms, D_t, were determined by Fomin's method. The essence of this method consists of the measurement of

3) S. Suzuki and Y. Inoue, This Bulletin, **39**, 490 (1966).

4) V. V. Fomin, E. P. Mairova, M. I. Krapivin and V. G. Yudina, *Zh. Neorg. Khimiya*, **3**, 2113 (1958).

two or more distribution ratios in successive extractions:

$$D_t = \frac{D_n}{VD_{n+1}} + D_n - \frac{1}{V} \quad (1)$$

$$P = \frac{D_t - D_n}{(1+VD_n)D_t} \quad (2)$$

where D_n is the distribution ratio which is obtained in the nth extraction and where V is the ratio of the volumes of the organic and aqueous phases.

In practice 15-m*l* portions of both phases were first brought into contact. The $D_1(1/D_1)$ ratio was calculated, and then a 10-m*l* portion of the aqueous (organic) phase was placed in contact with 10-m*l* portion of the new organic (aqueous) phase to determine the $D_2(1/D_2)$ ratio. Finally, a 5-m*l* portion of the aqueous (organic) phase was shaken with a 5-m*l* portion of the new organic (aqueous) phase to determine the $D_3(1/D_3)$ ratio. From Eqs. (1) and (2), two sets of $D_t(1/D_t)$ and P values, one by using $D_1(1/D_1)$ and $D_2(1/D_2)$ and the other by using $D_2(1/D_2)$ and $D_3(1/D_3)$, were calculated. As an example, Table 1 shows one of these sets of results. The last column on the table (P_c) shows the P values, which should be in a $1/D_2-1/D_3$ couple, as calculated from the results of the $1/D_1-1/D_2$ couple. The experimental and calculated values agree within experimental error.

Table 1. Fomin's method
Org. phase: C. F. ^{233}Pa in 0.1M TTA-benzene
Aq. phase: 1M $HClO_4$
12 days after the preparation

$1/D_1$	$1/D_2$	$1/D_3$	$1/K_t$	P (%)	P_c(%)
0.215	0.128		0.894	62.5	
	0.128	0.074	0.863	75.5	75.9
0.244	0.133		1.08	62.2	
	0.133	0.066	1.14	77.9	77.4

Results

The Results from Forward Extraction. *The Relation between the Method of Preparation and the Rate of Extraction.* The effect of the contact time on the distribution ratio is shown in Figs. 1 and 2. No significant difference in the curves with different methods of preparation is observed. In the case of No. 3, however, a contact time of only 1 min is sufficient to achieve a constant distribution ratio, while about 10 min is necessary in the cases of No. 1 and No. 4. As is clearly shown in Fig. 2, in the case of No. 2 the trend is slightly different: D reaches a maximum after a short contact time and then decreases with an increase in the contact time, finally reaching a constant. These tendencies hold irrespective of the aging time of the solution; Fig. 2 shows an example. From the above results, it can be said that 20 min of contact is sufficient to attain a constant distribution ratio in a forward extraction, regardless of the method of preparation.

The Effect of Aging Time on the Distribution Ratio. As is shown in Fig. 3, for some time after preparation Nos. 1 and 3 show constant distribution ratios which coincide with the values obtained from the backward distribution of a fresh solution of protactinium in TTA-benzene. The value from No. 1 begins to decrease 20 days after preparation and reaches a constant after 40 days of standing. The value from No. 3 begins to decrease 10 days after preparation and reaches a constant after 20 or 30

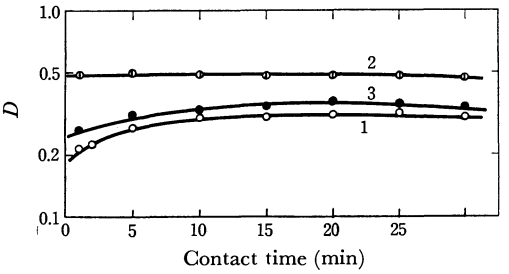

Fig. 1. The effect of contact time on the extraction of Pa. I.
Org. phase: 0.1M TTA-benzene
1: Sample No. 1
2: Sample No. 3
3: Sample No. 4

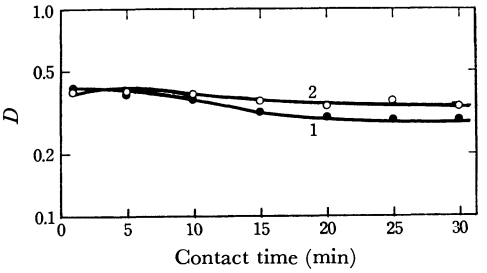

Fig. 2. The effect of contact time on the extraction of Pa. II.
Aq. phase: sample No. 2, Org. phase : 0.1M TTA-benzene
1: Immediately after the preparation
2: Aged for 48 days

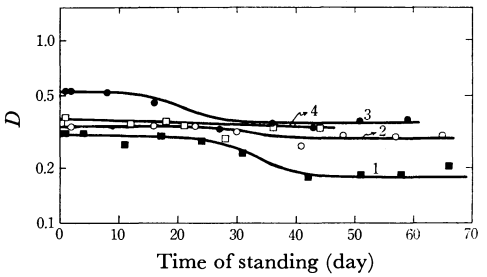

Fig. 3. The stability of Pa in perchloric acid solutions.
Org. phase: 0.1M TTA-benzene
1: Sample No. 1
2: Sample No. 2
3: Sample No. 3
4: Sample No. 4

days of standing. On the other hand, the Nos. 2 and 4 samples are stable for about 2 months and no change in distribution ratios beyond the limits of the experimental error are observed. Interestingly enough, these constant distribution ratios are nearly the same as those obtained from No. 3 and No. 1 after a long period of standing (if normalized to the value which will be obtained in 1M perchloric acid).

The Results from Backward Extraction. *The Effect of the Contact Time.* The effect of the contact time on the distribution ratio from the backward extraction which was carried out by using a freshly-prepared protactinium solution in 0.1M TTA-benzene was investigated; the results are shown in Fig. 4. The stripping solution was 1M perchloric acid. It is apparent from Fig. 4 that the distribution ratio reaches a constant after 5 minutes' contact. The value of the distribution ratio coincides fairly well with that obtained by the forward extraction of a freshly-prepared No. 1 sample.

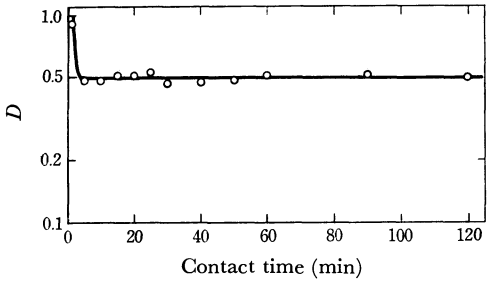

Fig. 4. The effect of contact time on the stripping of Pa.
Org. phase: 10^{-7}M Pa, 0.1M TTA-benzene
Aq. phase: 1M $HClO_4$

The Effect of Aging Time on the Distribution Ratio. A TTA-benzene solution of protactinium was stored in a brown bottle in the dark, and the change in the distribution ratio during standing was followed. The protactinium in a 0.1M TTA-benzene solution was stripped by a 1M perchloric acid solution. It is apparent from Fig. 5 that at first the distribution ratio decreases remarkably with standing; it shows a minimum at 30 min and then increases a little before reaching a constant. This constant value continues for about five hours. Then the distribution ratio increases continuously. After 2 weeks of standing, nearly all the protactinium becomes unstrippable. Essentially the same phenomenon is observed when carrier-free ^{233}Pa is used. When hydrochloric or sulfuric acid is used as the stripping reagent, virtually the same phenomenon is observed, as is shown in Fig. 6.

Fomin's Method. As one of the methods for understanding the rather peculiar behavior observed in the stripping, Fomin's method was applied. The relation between the standing time and the percentage of unstrippable species (P) is shown in

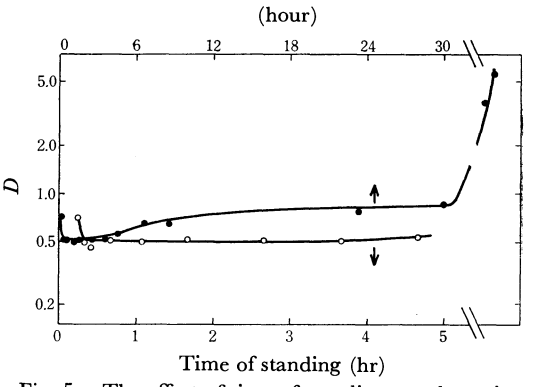

Fig. 5. The effect of time of standing on the stripping of Pa. I.
Org. phase: 10^{-7}M Pa, 0.1M TTA-benzene
Aq. phase: 1M $HClO_4$

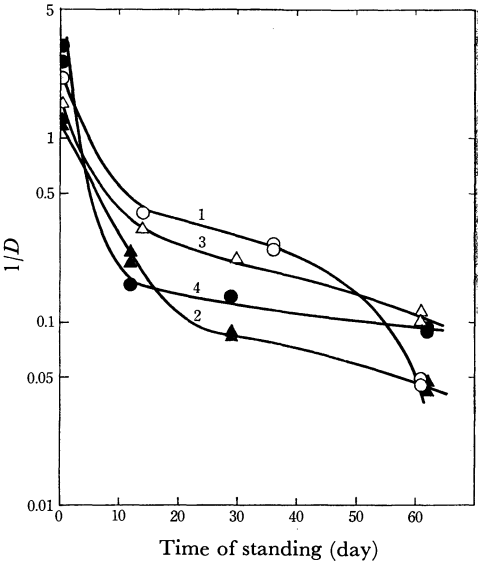

Fig. 6. The effect of time of standing on the stripping of Pa. II.
1: Aq. phase, 1M $HClO_4$; Org. phase, 10^{-7}M Pa in 0.1M TTA-benzene
2: Aq. phase, 1M $HClO_4$; Org. phase, C.F. ^{233}Pa in 0.1M TTA-benzene
3: Aq. phase, 0.4N H_2SO_4; Org. phase, 10^{-7}M Pa in 0.1M TTA-benzene
4: Aq. phase, 1M HCl; Org. phase, 10^{-7}M Pa in 0.1M TTA-benzene

Fig. 7. The P value for a fresh Pa-TTA-benzene solution is only 2—3%. It increases remarkably with standing and reaches 80 or 90% after 2 months of standing, irrespective of the protactinium concentration or the kind of stripping reagent. The $1/K_t$ value decreases slowly with the time of standing, as is shown in Fig. 8. It is clear from these results that the reason for the decrease in stripping is mainly the formation of unstrippable species, but also partly the increase in the distribution ratio (K_t) of the strippable species.

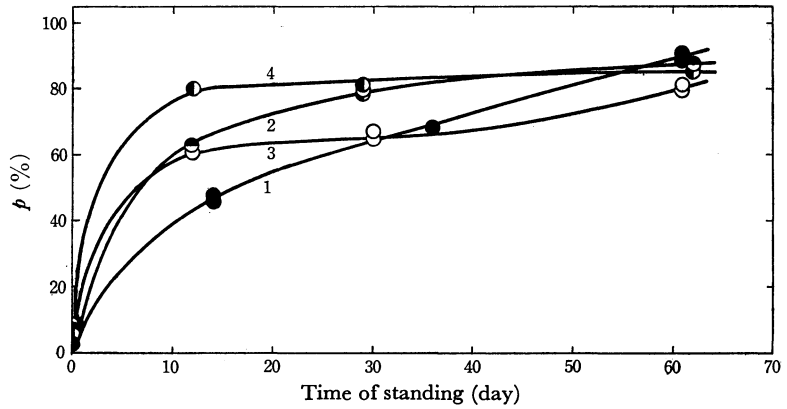

Fig. 7. The growth of unstrippable species of Pa in 0.1M TTA-benzene.
1: Aq. phase, 1M $HClO_4$; Org. pahse, 10^{-7}M Pa
2: Aq. phase, 1M $HClO_4$; Org. phase, C.F. ^{233}Pa
3: Aq. phase, 0.4N H_2SO_4; Org. phase, 10^{-7}M Pa
4: Aq. phase, 1M HCl; Org. phase, 10^{-7}M Pa

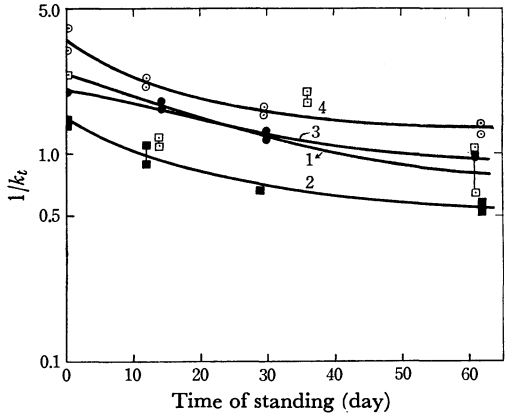

Fig. 8. The true distribution ratio of strippable species in 0.1M TTA-benzene.
1: Aq. phase, 1M $HClO_4$; Org. phase, 10^{-7}M Pa
2: Aq. phase, 1M $HClO_4$; Org. phase, C.F. ^{233}Pa
3: Aq. phase, 0.4N H_2SO_4; Org. phase, 10^{-7}M Pa
4: Aq. phase, 1M HCl; Org. phase, 10^{-7}M Pa

The Relation between the Distribution Ratio and the Perchloric Acid Concentration as Determined by Backward Extraction. The distribution ratio was determined as a function of the perchloric acid concentration by using a fresh solution of protactinium in 0.1M TTA-benzene. As is clearly shown in Fig. 9, the curve obtained was nearly the same as that shown in Fig. 6 of the second report of this series.[1] As has been described earlier, the values of the distribution ratio agree with those from the forward extraction which is made by using either a No. 1 or No. 3 solution.

Absorption Spectra of the Pa-TTA Complex. As another way to understand the peculiar behavior in stripping, the change in the absorption spectrum with standing was traced. The protactinium concentration was about 3×10^{-5}M. An absorption

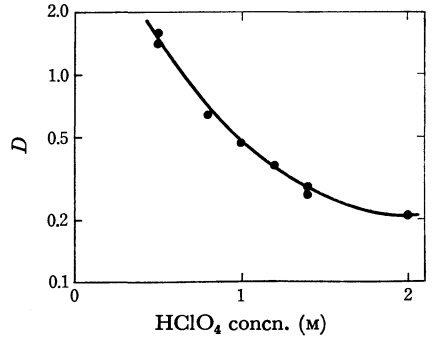

Fig. 9. Distribution ratios determined by stripping as a function of $HClO_4$ concentration.
TTA concn.: 10^{-1}M, Pa concn.: 10^{-7}M

maximum was observed at 410 mμ. The spectrum did not change except for a slight decrease in absorbance with standing. As is shown in Table 2, the absorbance at 410 mμ decreases by 10% after 51 days of standing.

Table 2. The effect time of standing on the absorbance of Pa in TTA-benzene solution
TTA: 0.1M Pa: *ca.* 3×10^{-5}M

Time (day)	Absorbance at 410 mμ
0	0.705
3	0.697
5	0.683
12	0.691
20	0.688
51	0.630

Discussion

In the equilibration experiment, it is obvious that a contact time of longer than half an hour makes no sense for the following reasons. In the forward

extraction, the distribution ratio reaches a constant value within 20 min of contact time, irrespective of the method used to prepare the perchloric acid solution of protactinium. Five minutes' contact is long enough to get a constant value from backward extraction. Another important thing is the peculiar behavior of the stripping, which makes it impossible to establish a true equilibrium because of the unfavorable formation of unstrippable species.

The method of preparing No. 3 corresponds in protactinium concentration to that shown in Fig. 5b of the second report of this series,[1] but the method used to prepare the stock solution is different. From this comparison it may be concluded that a protactinium solution with a concentration as high as 10^{-5}M is unstable. Besides, the solution prepared by such method as No. 1 is unstable regardless of the protactinium concentration.

The change in the absorption spectrum of protactinium(V) in a hydrochloric acid solution has been ascribed to the onset of hydrolysis, which is accompanied by the disappearance of solvent extractability.[5] The extractability of protactinium from a nitric acid solution decreases with standing, a fact which has been ascribed to the formation of inextractable species.[6,7] Even in the case of a fresh solution, the amount of protactinium in inextractable forms comprises 3%.[7] These phenomena have been ascribed to the formation of colloidal aggregates in the aqueous phase, which is not in rapid equilibrium with monomeric forms. Similar behavior was observed in our previous experiment in perchloric acid solution. About 17% and 44% of protactinium in 0.5 and 3.1M perchloric acid solutions respectively were unadsorbable species on cation exchange resin, and consistent results were obtained in the filtration experiments. No such phenomenon could, however, be observed in the TTA extraction.[1]

The same kind of investigation was undertaken in this experiment with relation to both the methods of preparing the protactinium solutions and their aging. It is evident that, in all the cases examined, the distribution coefficient remains unchanged in successive extraction. Therefore, the change in the distribution ratio with the time of standing is directly related to the change in K_t value. This difference between TTA extraction and other methods can be explained by the existence of a dynamic equilibrium in the TTA extraction; this in turn destroys the colloidal aggregates to some degree by means of the strong chelating action of TTA. It is obvious from these results that the extraction behavior differs greatly with the method of preparation, even in such a dilute solution as 10^{-7}M; nearly the same distribution ratio is obtained regardless of the method of preparation when the solution has been aged for longer than a month. However, the value consistent with that obtained from back extraction is not this value but the value obtained from fresh No. 1 and No. 3 samples. These observations suggest that the method of preparing either No. 1 or No. 3 is suitable from the standpoint of extraction equilibrium; however, No. 3 can not be considered to be very appropriate because of its unique behavior, discussed in a previous report. From the above considerations, about a 30-min contact of a fresh No. 1 sample with a TTA-benzene solution is most suitable for the investigation. It should be noted, however, that this statement of experimental conditions takes no cognizance of the thermodynamically-stable state of protactinium in a perchloric acid solution.

In any case these difficulties should be taken into account in interpreting the results.

There are many possibilities for interpreting the interesting behavior observed in stripping. One possibility is the polymerization of the extracted Pa-TTA chelate in the organic phase. However, this may be rejected on the basis of the fact that this phenomenon is observed irrespective of the protactinium concentration. Besides, the rate of the formation of the unstrippable species is faster in carrier-free ^{233}Pa than in 10^{-7}M protactinium. This obviously mitigates against this possibility. Another possibility is the decomposition of the chelate by some such means as thermal or radiation decomposition. This possibility is not warranted either because the rate of decrease in absorbance is too slow to interpret the rather drastic increase of unstrippable species. The last possibility is a minor and irreversible change of the extracted compounds in the organic phase. If the TTA chelate of protactinium is assumed to be absent in the aqueous phase, the extracted species should be $Pa(OH)T_4$, according to the second report of this series.[1] Strictly speaking, though, this form is not general enough; as alternate forms species like $Pa(OH)_2T_3 \cdot HT$ and $PaOT_3 \cdot HT$ are possible. If we consider that the first form participates in the extraction equilibrium and irreversibly undergoes dehydration to form the second form, which is naturally assumed to be more hydrophobic than the first form, the peculiar stripping behavior may be understood. Of course, there is no direct evidence for this hypothesis. Further study to support this hypothesis is being undertaken and will be reported on in the near future.

5) D. Brown, A. J. Smith and R. C. Wilkins, *J. Chem. Soc.*, 1463 (1959).

6) C. J. Hardy, D. Scargill and J. M. Fletcher, *J. Inorg. Nucl. Chem.*, **7**, 257 (1958).

7) V. I. Spitsyn, R. A. D'yachkova and V. P. Khlebnikov, *Radiokhimiya*, **7**, 257 (1965).

Part of the expenses for this investigation have been defrayed by a grant-in-aid from the Ministry of Education.

BULLETIN OF THE CHEMICAL SOCIETY OF JAPAN VOL. 42 1922—1926 (1969)

The Kinetic Studies of the Acid-catalyzed Etherification of the Tautomers of *p*-Nitrosophenol and *p*-Benzoquinoneoxime with Ethanol in Dioxane

Yoshiaki FURUYA, Iwao URASAKI, Kazuo ITOHO and Akiyoshi TAKASHIMA

Department of Industrial Chemistry, Faculty of Engineering, Kumamoto University, Kumamoto

(Received April 17, 1968)

The rates of the acid-catalyzed reversible etherification of the allelotrope of *p*-nitrosophenol and *p*-benzoquinoneoxime with ethanol in dioxane-forming *p*-nitrosophenetole have been measured by ultraviolet spectrophotometry. The rate of the forward reaction was expressed as the sum of the second- and the third-orders over a fairly large concentration region of the allelotrope and of ethanol. The plots of the logarithm of the apparent forward second-order rate constant against $-\log(C_{BH^+}/C_B)$ gave a straight line with a slope of -0.95. A probable mechanism involving the rate-determining formation of a σ-complex by the nucleophilic attack of the hydroxyl O-atom of ethanol on the α-carbon of the hydroxyl group of protonated *p*-nitrosophenol, and also the rate-determining deprotonation from the oxime group of the σ-complex by the allelotrope of *p*-nitrosophenol, was postulated.

The introduction of a nitroso group at the para position of phenol facilitates the etherification of the phenolic hydroxyl group.[1] The investigation of the optimum reaction conditions for the formation of *p*-nitrosophenetole has previously been reported by one of the present authors.[2] It has been considered, on the basis of synthetic results, that the facile equilibrium between the allelotrope of *p*-nitrosophenol and its ether presumably depends on the powerful activating effect of the protonated nitroso group.[3] However, the kinetics of this reaction was expressed as the sum of the second and third-orders under the conditions of these studies. It is interesting to investigate the reaction mechanism expressed by two terms.

Experimental

Materials. The allelotrope of *p*-nitrosophenol was prepared according to Bridge's method[4] and then recrystallized from benzene; yield 67%, mp 134°C (decomp). The ethanol was refluxed over calcium oxide for several hours and then rectified; bp 78.3°C. The dioxane was boiled under reflux for 7 hr with 10% of its volume of 1N aqueous hydrochloric acid, a slow stream of air being passed in through the condenser in order to remove the acetaldehyde formed. The organic layer was separated after treatment with potassium hydroxide and then distilled from the sodium; bp 101°C. The dioxane solution of sulfuric acid was prepared from guaranteed sulfuric acid and the anhydrous dioxane obtained as above.

Ultraviolet Spectrophotometry and Chemical Analysis. The reactions were followed by means of a Hitachi Perkin-Elmer UV-VIS spectrophotometer, model 139. The absorption maxima of the allelotrope and *p*-nitrosophenetole were 300 and 343 mμ respectively. Dioxane solutions of the allelotrope, *p*-nitrosophenetole, sulfuric acid, and ethanol of known concentrations (corresponding to 0, 20, 40, 60, 80 and 100% conversion) were prepared; a plot of the difference of extinction, $(E_{370}-E_{315})$ *vs.* $(E_{343}-E_{315})$, gave a straight line, and the conversion calculated from the values of $(E_{343}-E_{315})$ at 0 and 100% conversion agreed well (within a 1% error) with the conversions obtained from the composition of the solution.

Criterion of the Reaction. As the $(E_{370}-E_{315})$ *vs.* $(E_{343}-E_{315})$ plots of the actual reaction did not deviate at all from the calibration curve obtained above, it can be considered that the reaction forming *p*-nitrosophenetole occurs without any side reaction.

The reaction mixtures obtained using ethyl mercaptan and/or ethanol were extracted with ether; they were washed with water in order to eliminate the acid and then dried. The solutions were examined by means of gas chromatography employing a Yanagimoto gas chromatograph, model GCG-550FTP, operated with an F.I.D. and a 1.5-m column packed with 1.5% SE-30 coating Celite 545, using nitrogen with a flow rate of 45 ml/min from 50 to 150°C and with a programing rate of 12°C/min and a chart speed of 1 cm/min. The retention times of the authentic samples in ether and the two ethereal solutions prepared as described above are as follows:

1) A. Schoro, A. Kraaijeveld and E. Havinga, *Rec. trav. chim.*, **74**, 1256 (1955).
2) Y. Furuya and R. Oda, *Kogyo Kagaku Zasshi* (*J. Chem. Soc. Japan, Ind. Chem. Sect.*), **65**, 214 (1962).
3) J. T. Hays, E. H. de Butts and H. L. Young, *J. Org. Chem.*, **32**, 153 (1967).
4) J. L. Bridge, *Ann.*, **277**, 85 (1893).

TABLE 1. THE RETENTION TIMES OF AUTHENTIC SAMPLES AND THE PRODUCTS OBTAINED FROM THE ETHERIFICATION OF THE ALLELOTROPE WITH ETHYL MERCAPTAN AND/OR ETHANOL

	Authentic samples and unknown products						
	EtSH	PhSH	PhOEt	PhOH	PhSEt	*p*-EtO–C_6H_4–NO	The Allelo.
Retention time (min)	1.20	1.35	1.50	1.85	2.95	4.55	6.75
	Reaction mixture treated with EtSH						
	1.10	—	—	—	2.30	—	—	6.50
	Reaction mixture treated with EtOH						
	—	—	—	—	—	—	4.55	6.55

A Typical Run for the Rate Measurements. A solution of 0.25 m*l* of 2N sulfuric acid in dioxane was poured into a solution of 4.75-m*l* portions of both 0.211M allelotrope and ethanol in dioxane in order to start the reaction after both solutions had attained temperature equilibrium. Aliquots (each 0.1 m*l*) were taken out at appropriate time intervals; each one was diluted with methanol to a 5×10^{-5}M total concentration of the allelotrope and *p*-nitrosophenetole. The conversion percentage was calculated from the observed value of $(E_{343}-E_{315})$, while the values of the apparent forward second-order rate constant, k_2', were calculated graphically.

Determination of the Water in the Reaction System. The remaining water in the reaction system was determined to be 0.2M by the Karl Fischer method.

Measurement of the Isotope Effect. The preparation of the dioxane containing heavy water was carried out as follows: the water present in dioxane as a reaction solvent was removed by distillation after the solvent had been heated under reflux with metal sodium. Heavy water, D_2O, was added, and then removed as above. These procedures were repeated three times. The dioxane containing the usual water was treated in the same manner.

The mobile hydrogen in the allelotrope of *p*-nitrosophenol was exchanged with deuterium as follows: the allelotrope (1.01 g, 0.0082 mol) was dissolved in a mixture of absolute methanol (11.2 g, 0.35 mol) and deuterium oxide (0.94 g, 0.047 mol), after which the mixture was allowed to stand for 4 hr at room temperature. Then the medium was removed under reduced pressure. These procedures were repeated three times. It was determined by infrared analysis*1 that some of the mobile hydrogen in the allelotrope was exchanged with deuterium by the above treatment.

As alcohol, the usual alcohol and tetradeuteriomethanol were used for the usual reactions and for the reactions of the deuterio-compounds respectively. *p*-Nitrosoanisole, as an authentic sample, was prepared by the acid-catalyzed reaction of *p*-nitrosophenol with methanol and was recrystallized 3 times from petroleum ether; mp 24°C.

The rate constants, k_2 and k_3, were expressed as k_{2H} and k_{3H} for the usual reactions of the allelotrope with methanol and as k_{2D} and k_{3D} for the reactions of the deuterio-allelotrope with tetradeuteriomethanol in the presence of dideuteriosulfuric acid in dioxane containing deuterium oxide only.

*1 For this analysis, the potassium bromide tablet method was used. The intermolecular hydrogen bonding band in 3450 cm^{-1} was decreased and the hydroxyl stretching band in 2780 cm^{-1} was increased in the case of this sample.

Results and Discussion

A typical rate plot of the reaction at 60°C is shown in Fig. 1. The reaction follows the second-order reversible kinetics:

$$dx/dt = k_2'(a-x)(b-x) - k'_{-2}(c+x)x, \qquad (1)$$

where *a*, *b*, and *c* are the initial concentrations of the allelotrope, ethanol, and water respectively, and where *x* is the concentration of the consumed reactant at time *t*. The following equation is obtained by integrating Eq. (1):

$$\log\frac{x+m}{z-x} = \frac{ab(c+2z)-(a+b+c)z^2}{2.303z(c+z)}k_2't + \log\frac{m}{z} \qquad (2)$$

where:

$$m = \frac{ab(c+z)}{ab-(a+b+c)z}$$

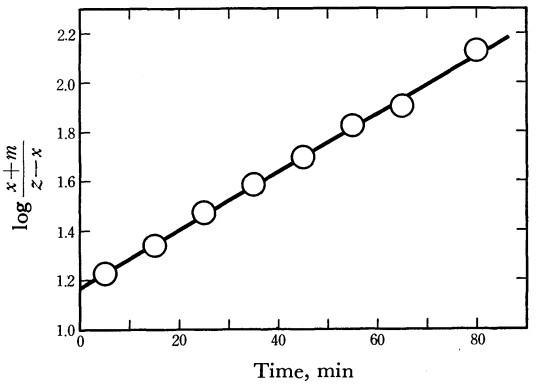

Fig. 1. The reversible second-order rate plot for the acid-catalyzed etherification of the allelotrope in dioxane at 60°C.
Concn. of H_2SO_4: 0.1N
Initial concn. of the allelotrope: 0.2M
Initial concn. of H_2O: 0.2M
Initial concn. of C_2H_5OH: 0.3M

and where z is the concentration of the consumed reactant at equilibrium. The plots of $\log(x+m)/(z-x)$ *vs.* t gave a straight line, and the value of the forward rate constant, k_2', was calculated from the slope. Here, the plots for the reversible second-order reaction, $\log(x+m)/(z-x)$ *vs.* t, bear a close resemblance to that for the reversible first-order reaction, $\log z/(z-x)$ *vs.* t. Therefore, we have misapprehended the reaction order in a previous report.[5] During repeated measurements, the first-order rate constant, k_d', has scarcely ever been found.

On the variation of the initial concentration of the ethanol, the apparent forward second-order rate constant, k_2', holds constant, as is obvious in Fig. 2. The plots of the k_2' rate constant against the initial concentration of the allelotrope gave a straight line with a definite slope, a line which did not pass through the point of origin, as is shown in Fig. 3. Thus, the forward rate equation may be given by:

$$v_{\text{forward}} = k_2'[\text{Allelo.}][\text{Ethanol}]$$
$$= \{k_2 + k_3[\text{Allelo.}]\}[\text{Allelo.}][\text{Ethanol}] \quad (3)$$

The rate was also affected by the acidity of the reaction medium. The indicator ratio, C_{BH^+}/C_B, at 373 mμ for each medium was determined spectrophotometrically using *p*-nitroaniline. The values of $\log k_2'$ were plotted against $-\log(C_{BH^+}/C_B)$ instead of H_0. As is illustrated in Fig. 4, a straight line with a slope of -0.95 was obtained. Therefore, both the k_2 and k_3 rate constants should involve the term of h_0.

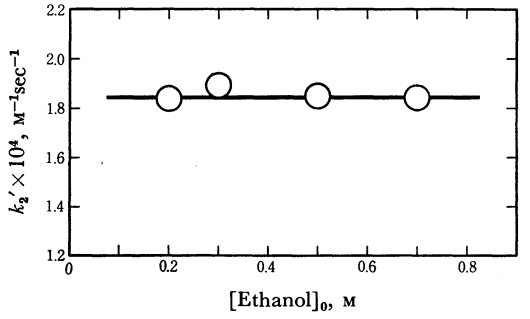

Fig. 2. The plots of $\log k_2'$ *vs.* initial concentration of ethanol for the etherification of the allelotrope in dixoane at 60°C.
Concn. of H_2SO_4: 0.1N
Initial concn. of the allelotrope: 0.2M
Initial concn. of H_2O: 0.2M

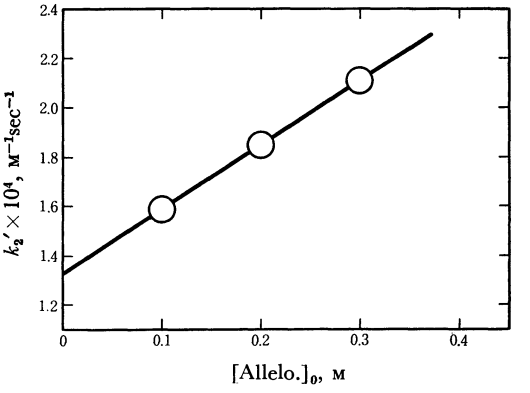

Fig. 3. The plots of $\log k_2'$ *vs.* initial concentration of the allelotrope for the etherification of the allelotrope in dioxane at 60°C.
Concn. of H_2SO_4: 0.1N
Initial concn. of C_2H_5OH: 0.5M
Initial concn. of H_2O: 0.2M

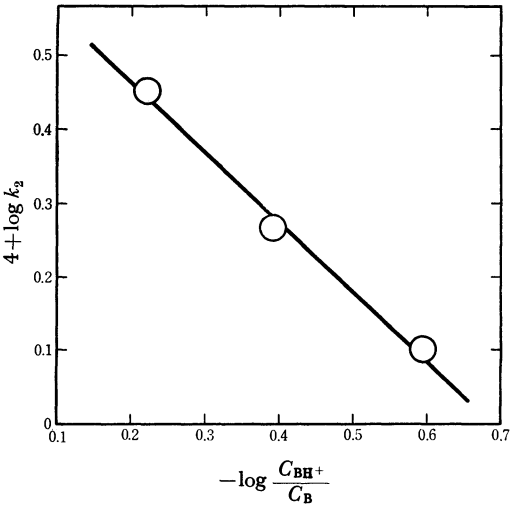

Fig. 4. The plots of $\log k_2'$ *vs.* $-\log(C_{BH^+}/C_B)$ for the etherification of the allelotrope in dixoane at 60°C.
Initial concn. of the allelotrope: 0.2M
Initial concn. of C_2H_5OH: 0.5M
Initial concn. of H_2O: 0.2M

It has been reported that the ratio of quinoidal (keto) and benzenoid (enol) forms in an equilibrium was determined by the difference in hydrogen-bond fission in the aggregated molecules.[6] The present authors have thought that the promoting forces are protonation and/or deprotonation. As the tendency of protonation to the nitroso group on the benzenoid form, I, is larger than that to the carbonyl group in the quinoidal form, II,[5] the rate of the formation of II is larger than that of I. An analogous situation holds in a protic solvent such as alcohols. In the case of an aprotic solvent such as dioxane, deprotonation is probably the promoting force. As deprotonation from the O-atom of the oxime group in II may be more difficult than that from the hydroxyl group in I, and as protonation to the

5) Y. Furuya, D. Morikawa and K. Itoho, This Bulletin, **40**, 1425 (1967).

6) E. Havinga and A. Schors, *Rec. trav. chim.*, **69**, 457 (1950).

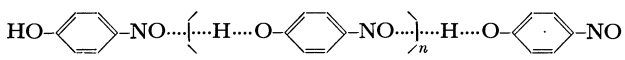

[I]

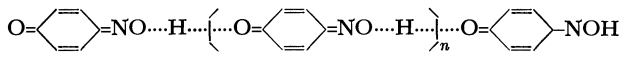

[II]

nitroso group in **I** is easier than that to the carbonyl group in II,[5] the allelotrope probably exists largely in the quinoldal form. These presumptions agree well with the experimental results.[6]

The allelotrope seems to be in the monomolecular state, mostly in dioxane ranging from 0.1 to 0.3M.[7] Therefore, the intermediate of tautomerism is the protonated *p*-nitrosophenol in an acidic and/or protic solvent and the deprotonated *p*-nitrosophenol anion, IV, in an aprotic solvent:

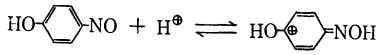

[III]

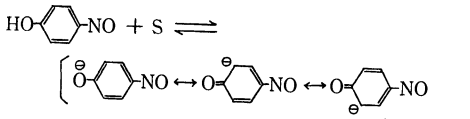

[IV]

The participation of the proton in this reaction system can be considered to be as follows:

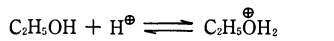

(4)

(5)

(6)

When two equilibria, (4) and (5), occur in a reaction mixture, the slope of the straight line obtained from the plots of $\log k_2'$ *vs.* H_0 should be -1. Considering the relationship of H_0 and J_0,[8] the value of the slope should be smaller than -1 when the (5) and (6) equilibria take place. As has been described above, the plots of $\log k_2'$ against H_0 gave a straight line with a slope of -0.95. Thus, the protonation to ethanol will give a protonated ethanol, not an ethyl cation.

Now, the pK_{BH^+} values of ethanol, dioxane, and the allelotrope are -2.5,[9] -4.4,[10] and -3.4[11] respectively. Thus, the order of the ease of the protonation is as follows: ethanol > the allelotrope > dioxane.

The ethyl cation, $C_2H_5^+$, is not formed under the reaction conditions described above. Hence, we may conclude the attack of protonated *p*-nitrosophenol on the hydroxyl O-atom of ethanol. This can be assumed also from the fact that a new peak, which is probably due to *p*-nitrosothiophenetole, is found by gas chromatography in the reaction mixture using ethyl mercaptan. If the ethereal O-atom of *p*-nitrosophenetole is derived from *p*-nitrosophenol, *p*-nitrosothiophenetole should not be formed by the reaction of *p*-nitrosophenol with ethyl mercaptan whose C–S bond is firm. Therefore, the promoting force of the reversible reaction forming *p*-nitrosophenetole from the allelotrope does not depend on the protonated ethanol, but on protonated *p*-nitrosophenol. Thus, the reaction will be promoted by a nucleophilic attack of the hydroxyl O-atom of ethanol on the α-C of the hydroxyl group of protonated *p*-nitrosophenol.

In constructing the second term of Eq. (3), the following three cases can be considered: (1) the formation of a π-complex between a molecule of protonated ethanol and the allelotrope, (2) the existence of the dimer of the allelotrope, and (3) the behavior of the allelotrope as a base in the deprotonation step. The formation of π-complex was scarcely observed at all under these reaction conditions. Also, the molecular association of the allelotrope was not found by the freezing-point-depression method, as has been mentioned above. Thus, the allelotrope can be expected to behave as a base in the deprotonation step from the σ-complex, V. For caution's sake, the kinetic isotope effects of hydrogen were also examined. The ratios of k_{2H}/k_{2D} and k_{3H}/k_{3D} were 0.83 and 2.58 respectively.

Therefore, we may consider that the first and second terms correspond to Steps (7) and (8) respectively. The value of k_2 is comparable to that of k_3. When the proton is abstracted by strong

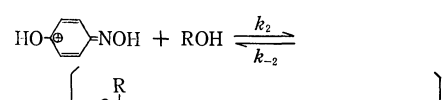

[V]

(7)

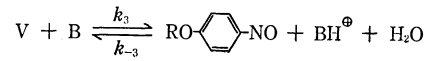

(8)

7) From the molecular weight of the allelotrope obtained by the freezing-point-depression method, scarcely no molecular association was found.

8) M. A. Paul and F. A. Long, *Chem. Revs.*, **57**, 1 (1957).

9) It was presumed that the pK_{BH^+} value of ethanol was nearly equal to that of methanol; *cf.* N. C. Deno and J. O. Turner, *J. Org. Chem.*, **31**, 1969 (1966).

10) H. Lemaire and H. J. Lucas, *J. Am. Chem. Soc.*, **73**, 5198 (1951).

11) According to our measurements using the UV method.

bases, such as water and alcohol, the value of k_3 in Step (8) becomes very large. Thus, Step (7) controls the rate in a pathway participated in by a strong base; this step is expressed as the first term in Eq. (3). This is demonstrated also by the fact that the k_2' rate constant does not contain the concentration of ethanol; moreover, the isotope effect was not observed. On the other hand, in the case of the deprotonation by a weak base such as the allelotrope of *p*-nitrosophenol, it is obvious, from the kinetics and isotope effect, that Step 8 determines the rate.

From these findings the following probable mechanism may be suggested (Scheme I).

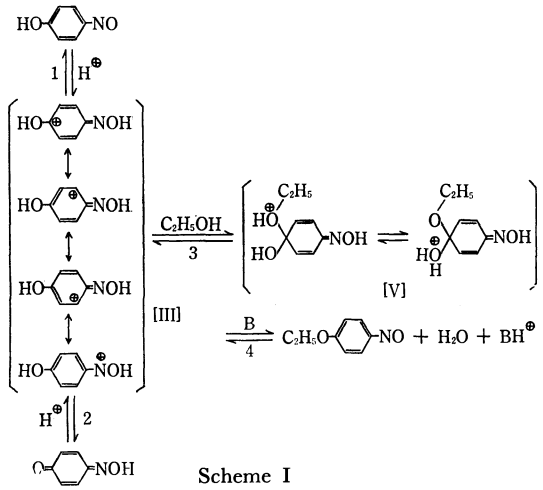

Scheme I

B: H_2O, C_2H_5OH, the allelotrope, dioxane and HSO_4^-, *etc.*

The authors wish to thank to Mr. S. Miyazaki and R. Ueoka for their aids in performing the work. We also acknowledge with pleasure the support of this work by the Scientific Research Foundation of the Ministry of Education.

BULLETIN OF THE CHEMICAL SOCIETY OF JAPAN VOL. 42 1926—1934 (1969)

Proton NMR Studies of Substituent Effects. The Hammett-type Relationship in *meta*- and *para*-Substituted Formanilides*1

Jun NIWA

Chemical Laboratory, Department of General Education, Nagoya University, Chikusa-ku, Nagoya

(Received July 20, 1968; in revised form December 25, 1968)

The spectral analyses of 23 *meta*- and *para*-substituted formanilides in dimethyl sulfoxide have proved that they exist in an equilibrium of *cis*- and *trans*-forms of restricted rotational isomers in the solvent. The chemical shifts of the protons on the formanilides are strongly dependent on the polar nature of the substituent. In the *cis*-form, the chemical shifts of both the imino and the formyl protons correlate with the Hammett σ^0. In the *trans*-form, a plot of the chemical shifts of the formyl protons against the σ^0-constants reveals a good correlation in the case of *meta*-derivatives, but serious deivations for the *para*-substituents, both for the electron-releasing conjugative substituents and for the electron-withdrawing conjugative substituents. The deviations for both types of substituents are in the direction to be anticipated for any important extra conjugative interaction between the *para*-substituent and the side-chain. The Yukawa-Tsuno equation is precisely applicable to these shifts when we assume that this system has the same *r*-value for both types of substituents; the relation is expressed as:

$$\Delta\delta = -12.0(\sigma^0 + 1.12\Delta\bar{\sigma}_R) + 0.5.$$

where $\Delta\bar{\sigma}_R=\sigma^+-\sigma^0$ for the electron-releasing conjugative substituents and where $\Delta\bar{\sigma}_R=\sigma^--\sigma^0$ for the electron-withdrawing conjugative substituents ($r=0.993$, $s=0.8$). From the solvent effect on the substituents, such as NH_2, OH, and COOH, their σ^0-values in dimethyl sulfoxide are proposed. It is also deduced that this solvent effect affects principally the part of the inductive contribution in the overall substituent effect.

It has been extensively verified that the respective Yukawa-Tsuno equation, either (1) or (2), can be applied to the electrophilic or the nucleophilic reaction of the side-chain derivatives of benzene whenever the opportunity arises for a strong conjugative interaction between the substituent

*1 Presented in part at the 21th Annual Meeting of the Chemical Society of Japan, Osaka, March, 1968.

and the reaction site:[1]

$$\log k/k_0 = \rho(\sigma^0 + r\Delta\bar{\sigma}_R^+) \quad (1)$$

where $\Delta\bar{\sigma}_R^+ = \sigma^+ - \sigma^0$, or:

$$\log k/k_0 = \rho(\sigma^0 + r\Delta\bar{\sigma}_R^-) \quad (2)$$

where $\Delta\bar{\sigma}_R^- = \sigma^- - \sigma^0$. Yukawa and Tsuno[1] have also suggested that if the σ^+- and σ^--values[2,3] are used as a common reference of the substituent constants in a series of side-chain derivatives, Eqs. (1) and (2) will turn to:

$$\log k/k_0 = \rho(\sigma^0 + r\Delta\bar{\sigma}_R) \quad (3)$$

where $\Delta\bar{\sigma}_R = \sigma^+ - \sigma^0$ and $\sigma^- - \sigma^0$.

Meanwhile, in NMR studies, a number of correlations have been noted between the reactivity parameters and the chemical shifts of the protons on benzene derivatives. In such a situation, it has been reported that Eq. (1) or (2) can be precisely applied to the side-chain derivatives.[4],*2 However, no work has been reported on the series of compounds in which Eq. (3) commonly holds both for the electron-releasing conjugative substituent and for the electron-withdrawing conjugative substituent.

In the present study, we have measured the chemical shifts of protons on the side-chain of 23 *meta*- and *para*- substituted formanilides dissolved in dimethyl sufoxide, where they exist in an equilibrium of *cis*- and *trans*-forms of restricted rotational isomers. This paper will describe how the substituent effect on the chemical shifts of protons on each isomer has been investigated from the viewpoint of the Hammett-type relationship. Especially, we will reveal that the Yukawa-Tsuno equation (3) is commonly applicable to the chemical shifts of the formyl proton of the *trans*-form for both types of substituents mentioned above when we assume that this system has the same *r*-value for the above substituents, and we adopt the σ^+- and σ^--values as a common reference of the substituent constants.

Moreover, from the investigation of the solvent effect on the substituents, such as NH_2, OH, and COOH, which form a strong hydrogen bonding with dimethyl sulfoxide, their σ^0-values in this solvent will be proposed. We will also discuss which part of the inductive and mesomeric contributions of the overall substituent effect this solvent effect has an influence on.

Experimental

Materials. *The substituted and the unsubstituted formanilides* used in the present study were prepared from formic acid*3 and the appropriate substituted anilines*4 according to the literature methods. The *p*-aminoformanilide was prepared by reducing *p*-nitroformanilide by iron dust in diluted formic acid. All the melting points or the boiling points of the formanilides, except for the compounds described below, agreed with the value described in the literature. *m*-Hydroxy derivative, mp: 112.7—113.2°C; *m*-Fluoro derivative, mp: 61.0—62.0°C; *p*-Fluoro derivative, mp: 66.0—66.5°C; *m*-Acetyl derivative, mp: 98.5—99.5°C; *p*-Acetyl derivative,

TABLE 1. VALUES OF THE CHEMICAL SHIFTS OF THE PROTONS OF *meta*- AND *para*-SUBSTITUTED FORMANILIDES (in cps relative to the unsubstituted compound)

	Substituent	*cis*-Form		*trans*-Form
		-NH-	-CHO	CHO[a]
1	*p*-NH_2	29.2	9.1	22.7
2	*p*-$N(CH_3)_2$	18.6	5.1	15.2
3	*p*-OH	18.5	5.0	16.3
4	*m*-OH	8.6	2.2	1.8
5	*p*-CH_3O	8.4	3.5	12.0
6	*m*-CH_3O	0.6	−1.0	−1.6
7	*p*-CH_3	5.1	1.9	4.8
8	*m*-CH_3	4.5	0.3	1.5
9	H	0.0	0.0	0.0
10	*p*-F	−5.1	−0.4	4.6
11	*m*-F	−13.7	−2.7	−3.5
12	*p*-Cl	−7.2	−1.4	−0.6
13	*m*-Cl	−11.8	−2.5	−2.8
14	*p*-Br	−8.9	−1.3	−1.0
15	*m*-Br	−10.0	−1.9	−3.4
16	*p*-$COCH_3$	−16.9	−3.9	−9.4
17	*m*-$COCH_3$	−11.5	−3.0	−4.0
18	*p*-COOH	−18.0	−5.0	−8.7
19	*m*-COOH	−8.4	−0.8	−2.6
20	*p*-CN	−26.6	−6.7	−12.6
21	*m*-CN	−22.0	−5.1	−6.4
22	*p*-NO_2	−34.7	−6.8	−13.9
23	*m*-NO_2	−26.9	−6.3	−9.4

a) The chemical shift of this proton was calculated according to the typical AB-system.

b) The values of the coupling constants in the case of all the formanilides were 2.1 ± 0.5 cps for the *cis*-proton and 11.0 ± 0.5 cps for the *trans*-proton respectively, the substituent effect on which was not detected.

1) Y. Yukawa and Y. Tsuno, *Nippon Kagaku Zasshi* (*J. Chem. Soc. Japan, Pure Chem. Sect.*), **86**, 873 (1965); Y. Yukawa, Y. Tsuno and M. Sawada, This Bulletin, **39**, 2274 (1966).

2) H. C. Brown and Y. Okamoto *J. Am. Chem. Soc.*, **79**, 1913 (1957).

3) H. H. Jaffé, *Chem. Revs.*, **53**, 191 (1953).

4) Y. Yukawa and H. Yamada, *Nippon Kagaku Zasshi* (*J. Chem. Soc. Japan, Pure Chem. Sect.*), **85**, 501 (1964).

*2 For example the unpublished data by the present author : $\Delta\delta = -17.2(\sigma^0 + 0.32\Delta\bar{\sigma}_R^+)$ for the chemical shifts of the formyl protons of *m*- and *p*-substituted benzaldehydes in dimethyl sulfoxide.

*3 Product of the Katayama Kagaku Kogyo Co., Ltd.

*4 Products o 1the Tokyo Kasei Kogyo Co., Ltd.

TABLE 2. THE SUBSTITUENT CONSTANTS

Substituent	σ^0	$\Delta\bar{\sigma}_R^+$ and $\Delta\bar{\sigma}_R^{-}$ [a]	σ_i [a]	σ_π^+ and σ_π^- [a]
1 *p*-NH_2	−0.36[e]	−1.00	0.06	−0.42
2 *p*-$N(CH_3)_2$	−0.48[a]	−1.30	0.06	−0.54
3 *p*-OH	−0.16[a]	−0.82	0.19	−0.34
4 *m*-OH	0.121[b]	—	—	—
5 *p*-CH_3O	−0.100[a]	−0.678	0.185	−0.281
6 *m*-CH_3O	0.115[b]	—	—	—
7 *p*-CH_3	−0.124[a]	−0.187	−0.045	−0.078
8 *m*-CH_3	−0.069[b]	—	—	—
9 H	0.00	0.00	0.00	0.00
10 *p*-F	0.212[a]	−0.285	0.363	−0.118
11 *m*-F	0.337[b]	—	—	—
12 *p*-Cl	0.28[a]	−0.167	0.348	−0.070
13 *m*-Cl	0.37[b]	—	—	—
14 *p*-Br	0.30[a]	−0.15	0.337	−0.054
15 *m*-Br	0.39[b]	—	—	—
16 *p*-$COCH_3$	0.46[c]	0.41[e]	0.21	0.29
17 *m*-$COCH_3$	0.376[b]	—	—	—
18 *p*-COOH	—	(0.28)[d]	—	—
19 *m*-COOH	—	—	—	—
20 *p*-CN	0.66[b]	0.34[c]	0.41	0.25
21 *m*-CN	0.62[c]	—	—	—
22 *p*-NO_2	0.82[c]	0.45[c]	0.47	0.34
23 *m*-NO_2	0.71[b]	—	—	—

a) Cited from the paper by Yukawa and Tsuno.[1]
b) Cited from the paper by McDaniel and Brown. D. H. McDaniel and H. C. Brown, *J. Org. Chem.*, **23**, 420 (1958).
c) Cited from the paper by Taft. R. W. Taft, Jr., *J. Phys. Chem.*, **64**, 1805 (1960).
d) The $\Delta\bar{\sigma}_R^-$-value for *p*-COOR.
e) $\Delta\bar{\sigma}_R^- = \sigma^- - \sigma^0$. The σ^--value are cited from Ref. 3.

mp: 106.0—107.0°C. These compounds were confirmed by elemental analysis and by a study of the IR spectra.

*Dimethyl Sulfoxide.**4 This was distilled under reduced pressure after having been refluxed with calcium hydride for a few hours, avoiding any uptake of atmospheric moisture, and was stored over Linde-3A molecular sieves[5] (bp: 61°C/3 mmHg).

All the sample solutions were left standing for about 48 hr at room temperature after the sample tube had been sealed, so as to reach equilibrium completely.

Measurement of NMR Spectra. All the spectra were obtained on a JNM C-60 spectrometer. The prove temperature was maintained at 20.0±0.5°C. The chemical shift was measured by relating it to the resonance peak of 0.5 mol% benzene added as an internal reference by the side-band technique. Since, in every case, the signal of benzene appeared 159.7±0.5 cps down field from the low-field ^{13}C–H satellite of dimethyl sulfoxide, it was confirmed that benzene could be utilized as an internal reference. The proton signals were independent of the concentration, ranging from 5 to 0.5 mol%, and of addition of a small amount of water. In Table 1 the chemical shifts of the protons of 23 *meta*- and *para*-substituted formanilides at a 5 mol% concentration are given relative to formanilide itself. The precision of the measurement was within about ±0.5 cps for the chemical shifts of the formyl protons, while, within about ±0.8 cps for the imino protons.

5) R. J. Ouellette, *Can. J. Chem.*, **43**, 707 (1963).

Results and Discussion

Analyses of Spectra of *meta*- and *para*-Substituted Formanilides. From the observation of near-infra-red absorption spectrum and the measurement of apparent dipole moment of formanilide in carbon tetrachloride solution, Mizushima *et al.*[6] have indicated that it exists in two forms—*cis*- and *trans*-forms of restricted rotational isomers, which are caused by a partial double-bond character of the C-N bond. Recently, inspecting the NMR spectra of formtoluidides in carbon tetrachloride, measured at 60 Mc and 100 Mc, Nishiyama and Yamada[7] proved that the *cis*- and *trans*-forms of the formtoluidide existed in an equilibrium:

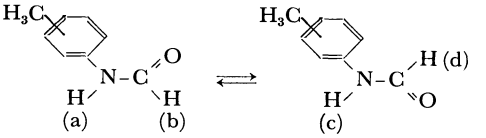

(I) *cis*-Form (II) *trans*-Form

On the basis of the above informations, we analysed the spectra of *meta*- and *para*-substituted formanilides at several concentrations in carbon tetrachloride, benzene, acetone, and dimethyl sulfoxide. The formanilides, except for the formtoluidides and the unsubstituted formanilide, were too sparingly soluble in such non-polar solvents as carbon tetrachloride and benzene for the spectra to be examined. As an example, the spectra of form-*p*-toluidide at 5 mol% in carbon tetrachloride and dimethyl sulfoxide are shown in Figs. 1 and 2.

The spectrum of Fig. 1 shows the same pattern as that obtained by Nishiyama and Yamada,[7] and it reveals that the formtoluidide exists in the *cis*- and *trans*-forms in carbon tetrachloride. They were assigned by comparing, with each other, the coupling constants between the imino and the formyl protons of them. The resonance signals, (a) and (c), were assigned to the imino protons of the two forms, because their line width may be broadened due to a relaxation phenomenon involving the ^{14}N

6) I. Suzuki, M. Tsuboi, T. Shimanouchi and S. Mizushima, *Spectrochim. Acta*, **16**, 471 (1960).
7) T. Nishiyama and F. Yamada, *Nippon Kagaku Zasshi (J. Chem. Soc. Japan, Pure Chem. Sect.)*, **89**, 979 (1968).

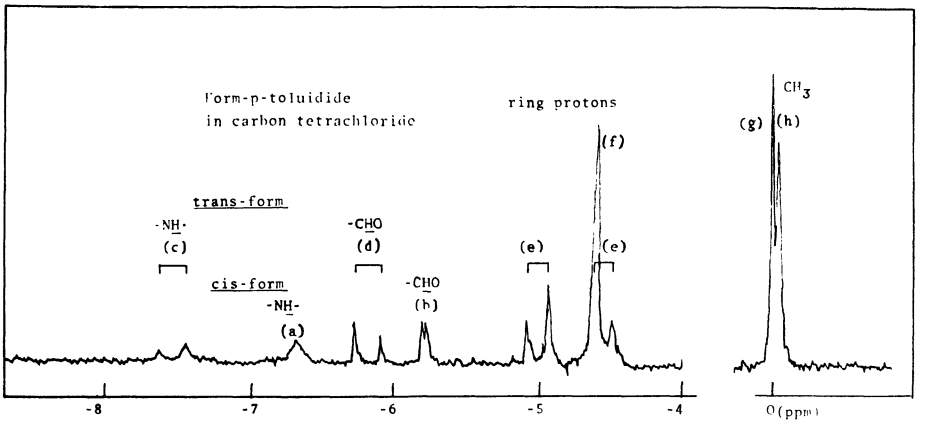

Fig. 1. Proton resonance spectrum (60 Mc/sec) of form-*p*-toluidide at 5 mol% in carbon tetrachloride at 20.0±0.5°C. The chemical shifts shown are relative to the methyl group of the *cis*-form.

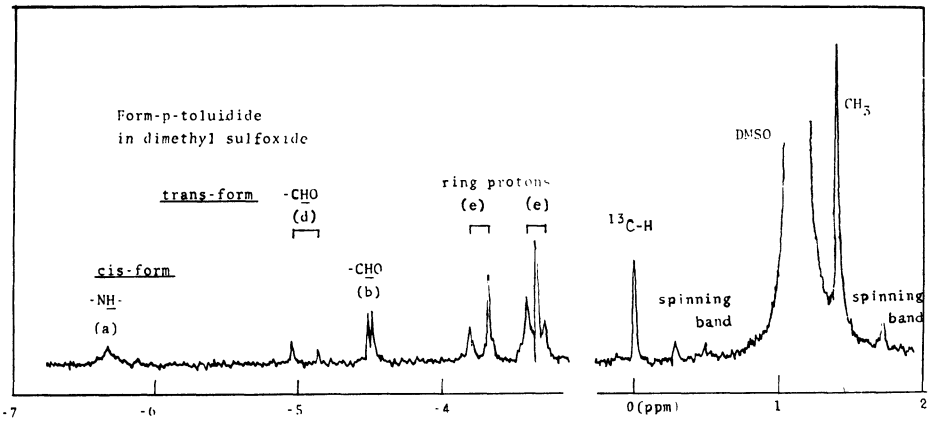

Fig. 2. Proton resonance spectrum (60 Mc/sec) of form-*p*-toluidide at 5 mol% in dimethyl sulfoxide at 20.0±5°C. The chemical shifts are shown relative to the low-field ^{13}C–H satellite of dimethyl sulfoxide.

quadrupole.[8] The signal (a) also shifted variably depending on the kind of solvents. The resonance signals, (b) and (d), were assigned to the formyl protons of the two forms, because they gave sharp resonance lines and the shift by variation of solvents little occured. The signal (a) of the imino proton was ascribed to belong to the *cis*-form, and the signal (b), to arise from the proton of the formyl group in the *cis*-form, which was a doublet due to the spin-spin coupling with the imino hydrogen. The value of the coupling constant was 2.2 cps, which was consistent with that obtained for the *cis*-proton of some kinds of amides (J_{cis}=2.1 cps for formamide[9] and J_{cis}=1.8 cps for formtoluidide[7]). The signals, (c) and (d), were assigned to belong, respectively, to the imino and the formyl protons of the *trans*-form, because they were the doublet due to the spin-spin coupling between the *trans*-protons, and the value of the coupling constant was 11.3 cps (J_{trans}=11.4 cps, both for formamide[9] and for formtoluidide[7]).

Figure 2 shows the spectrum of the form-*p*-toluidide in dimethyl sulfoxide. All the resonance signals, except for that of the imino proton of the *trans*-form, correspond with those in carbon tetrachloride solution. When a small amount of dimethyl sulfoxide was added in the carbon tetrachloride solution of the formtoluidide, the signal (a) of the imino proton of the *cis*-form shifted to the lower field, whereas that of the *trans*-form, (c), remained almost constant. As the concentration of the dimethyl sulfoxide increased, the signal (a) approached to the signal (c). Accordingly, in dimethyl sulfoxide, the signal (c) may be concealed behind the signal (a). The low-field shift

8) J. A. Pople, W. G. Schneider and H. Bernstein, "High Resolution Nuclear Magnetic Resonance," McGraw-Hill, New York (1959), p. 102.

9) L. H. Piette, J. D. Ray and R. A. Ogg, *J. Mol. Spectroscopy*, **2**, 66 (1958).

of the signal (a) by the addition of dimethyl sulfoxide may be due to the hydrogen bonding between the imino hydrogen of the *cis*-form and the molecule of dimethyl sulfoxide. The independence of the concentration of the dimethyl sulfoxide in the case of the chemical shift of the imino proton of the *trans*-form may be ascribed to that the associated molecules of the *trans*-form make the ring dimer (See Fig. 11).

Although Figs. 1 and 2 do not so distinctly the doublet of the resonance signals of the ring protons, the spectrum of form-*p*-anisidide shows the typical AB-type doublet of the protons on the *para*-disubstituted benzene ring (Fig. 3). The signal (e) was ascribed to belong to the *cis*-form, while the signal (f), to the *trans*-form, from their relative intensities. In Fig. 1 the two resonance signals, (g) and (h), of the methyl protons, which appeared at slightly different positions, corresponded with the *cis*- and *trans*-forms respectively.

When the spectra in carbon tetrachloride (Fig. 1) and benzene are compared with those in dimethyl sulfoxide (Fig. 2) and acetone, the intensities of all resonance signals of the protons of the *trans*-form in the latter solvents are much smaller than those of the *cis*-form. This shows that the *cis*- and *trans*-forms exist in an equilibrium, and that the equilibrium inclines toward the *cis*-form in the polar solvent. The effect of varying the concentrations in carbon tetrachloride showed that the equilibrium favored the *cis*-form as the concentration increased.*5 The substituent effect on the

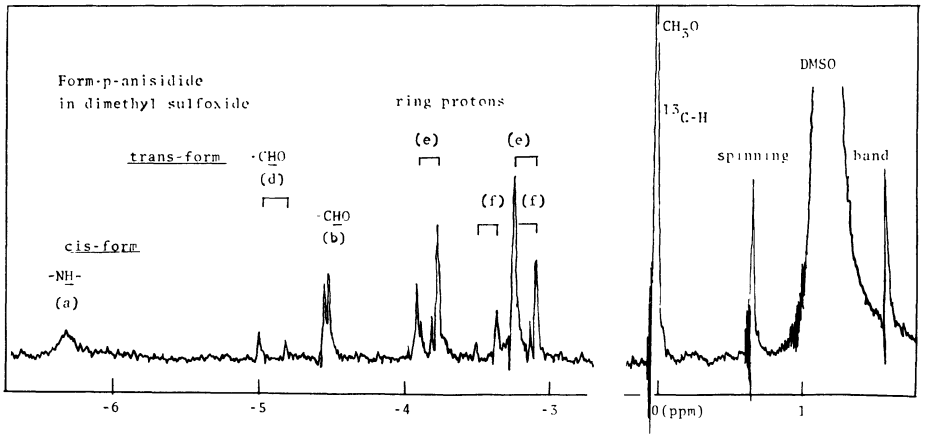

Fig. 3. Proton resonance spectrum (60 Mc/sec) of form-*p*-anisidide at 5 mol% in dimethyl sulfoxide at 20.0±0.5°C. The chemical shifts shown are relative to the low-field ^{13}C–H satellite of dimethyl sulfoxide.

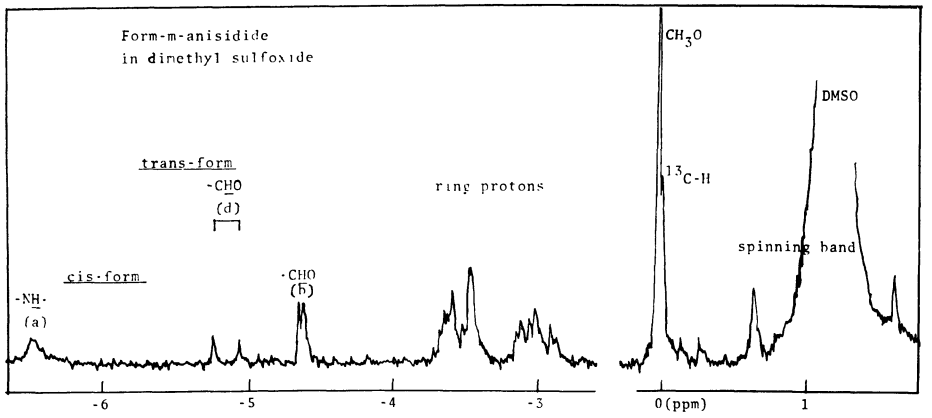

Fig. 4. Proton resonance spectrum (60 Mc/sec) of form-*m*-sanisidide at 5 mol% in dimethyl sulfoxide at 20.0±0.5°C. The chemical shifts are relative to the low-field ^{13}C–H satellite of dimethyl sulfoxide.

*5 With higher concentrations, the asymmetric polarized structure is favored by a dipoler-type interaction, as has been indicated for *N*,*N*-disubstituted formamide.

(Ref. 10).

10) T. Yonezawa and I. Morishima, This Bulletin, **39**, 2346 (1966).

equilibrium in dimethyl sulfoxide showed a trend that the *trans*-form was favored by the electron-releasing substituent. These results may be all explained by assuming an asymmetric polarized structure for the *cis*-form (Fig. 7), while, a non-polarized structure for the *trans*-form (Fig. 11), as will be discussed in detail later. The representative spectra of *meta*- and *para*-substituted formanilides in dimethyl sulfoxide are shown in Figs. 3 and 4.

Substituent Effect on the *cis*-Form. *(i) Correlation of the Chemical Shift of the Imino Proton with the σ^0-Constant.* Although the ^{14}N quadrupole makes the measurement of accurate chemical shifts difficult by broadening the imino proton signal, this disadvantage is offset by the wide range of the chemical shifts observed (about 70 cps). This enhanced sensitivity of the substituent effect on the imino proton signal can be understood in terms of hydrogen bonding to the solvent molecule.

In Fig. 5, the relative chemical shifts of the imino protons are plotted against the σ^0-values. The correlation is expressed by Eq. (4), which was derived from a least-squares fit of the data:

$$\Delta\delta = -40.3\sigma^0 + 2.1 \qquad (4)$$

for all the 18 substituents except five: *p*-NH_2, *m*-OH, *p*-OH, *m*-COOH and *p*-COOH. The correlation coefficient and the standard deviation have the respective values of 0.988 and 2.1. The plots for *p*-COOH and *m*-COOH are excluded from the figure, for their σ^0-values have not been established. The plots for such substituents as *p*-NH_2, *p*-OH, and *m*-OH deviate greatly above the correlation line. These substituents, whether in the *meta*-position or the *para*-position, are apparently much more electron-releasing than the ordinary σ^0-values predict. The effect may be a reflection of the alteration of the substituent by the specific solvation. The σ^0-values of these substituents in dimethyl sulfoxide, calculated from the regression line, are: -0.67 for *p*-NH_2, -0.41 for *p*-OH, -0.16 for *m*-OH, 0.50 for *p*-COOH, and 0.11 for *m*-COOH. The reliability of these σ^0-values will be examined in the succeeding sections.

This aspect of the substituent effect on the imino proton reveals that there is no extra conjugative interaction between the substituent and the side-chain in the *cis*-form. This result suggests that, the amide group not in the plane of the aromatic ring, can not interact with the aromatic *pi*-electron system. When we assume an asymmetric polarized structure for the *cis*-form, the departure from planarity can be explained as due to the steric repulsion between the hydrogen of the aryl group, in the ortho position shown, and the C–O$^-$ group,*6 The molecule of the *cis*-form is shown schematically in Fig. 7.

(ii) Correlation of the Chemical Shift of the Formyl Proton with the σ^0-Value. It is expected that the

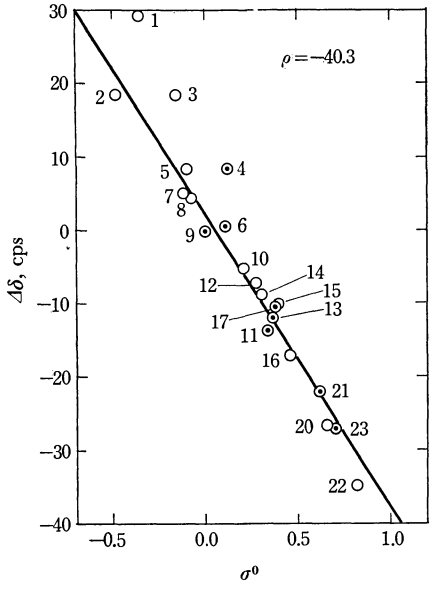

Fig. 5. Relative chemical shifts of the imino-protons of the *cis*-forms *vs.* Hammett σ^0. Numbered points correspond to entries in Table 1.
⊙: *meta*-substituent ○: *para*-substituent

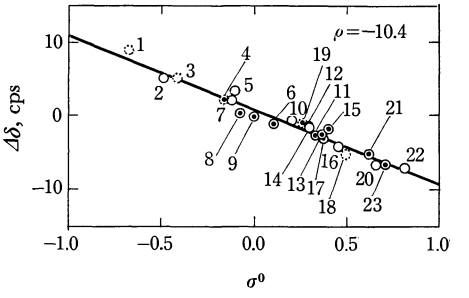

Fig. 6. Relative chemical shifts of the formyl-protons of the *cis*-forms *vs.* Hammett σ^0. Numbered points correspond to entries in Table 1. Substituents, NH_2, OH and COOH are shown by dotted circles.
⊙: *meta*-substituent ○: *para*-substituent

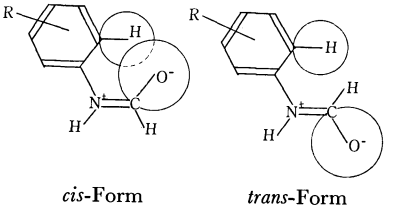

cis-Form *trans*-Form

Fig. 7. The *cis*- and *trans*-forms of *m*- and *p*-substituted formanilides. The radii of the circles correspond to the van der Waals' radii of the atoms.

*6 This type of steric repulsion has been suggested for formanilide by Mizushima *et al.* (Ref. 6).

chemical shifts of the formyl protons correlate with the σ^0-values, because even those of the imino protons exhibit no significant conjugative interaction between the substituent and the imino group. Thus, as is shown in Fig. 6, the relative chemical shifts can be expressed as:

$$\Delta\delta = -10.4\sigma^0 + 1.0 \qquad (5)$$

for all the 18 substituents except for five substituents mentioned above. The values of r*[7] and s*[7] were 0.974 and 0.8 respectively. This lack of good correlation is to be expected since the formyl protons of all the formanilides have a small spread of total chemical shift (about 16 cps). When the σ^0-values in dimethyl sulfoxide are used for the substituents mentioned above, all their plots fall close to the correlation line, as is shown by the dotted circles in the figure.

Substituent Effect on the *trans*-Form. Application of the Yukawa-Tsuno Equation to the Chemical Shift of the Formyl Proton. In the *trans*-form, a plot of the chemical shifts of the formyl protons against the Hammett σ^0-constants reveals a good correlation in the case of the *meta*-derivatives, as is shown in Fig. 8. This relation can be expressed as:

$$\Delta\delta_m = -12.0\sigma^0 + 0.5 \qquad (6)$$

In this case, too, the plots for *m*-OH and *m*-COOH fall close to the *meta*-correlation line when their σ^0-values in dimethyl sulfoxide are used. The ρ-value is compatible with the ρ-value (-10.4) in the case of the formyl proton in the *cis*-form, as is to be expected from the fact that the distance between the substituent and the proton observed is not very different in the two cases. As is shown in Table 1, however, the formyl protons of all the *trans*-forms have quite a large spread of total chemical shift (about 37 cps) compared with the case of the formyl proton of the *cis*-form. This must be a reflection of a strong extra conjugative interaction between the substituent and the side-chain in the *trans*-form.

It is characteristic that all the plots for the electron-releasing conjugative substituents at the para-position, such as *p*-NH_2, *p*-$N(CH_3)_2$, and *p*-CH_3, deviate seriously from the *meta*-correlation line in the direction to be predicted by the σ^+-value,[2] whereas those for the electron-withdrawing con-

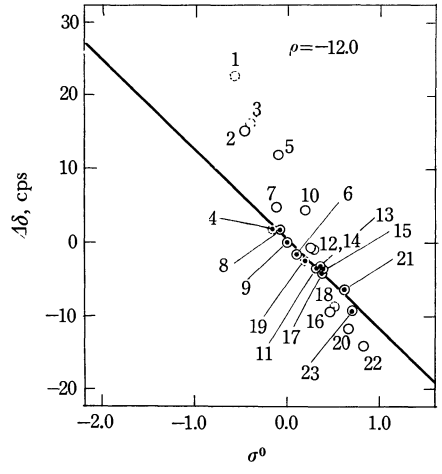

Fig. 8. Relative chemical shifts of the formyl protons in the *trans*-form *vs.* Hammett σ^0. Numbered points correspond to entries in Table 1. Substituents, NH_2, OH, and COOH are shown by dotted circles.
⊙: *meta*-substituent ○: *para*-substituent

*[7] r: the correlation coefficient; s: the standard deviation of experimental results from the regression line.

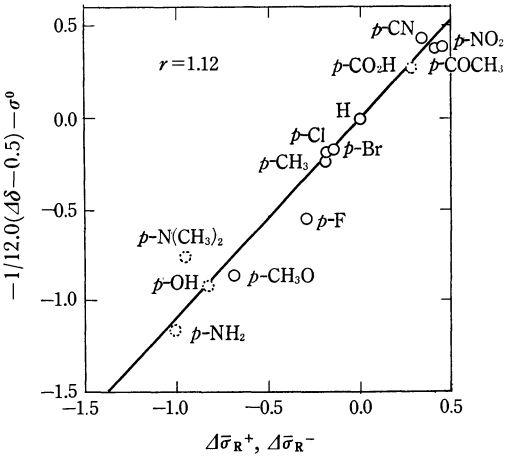

Fig. 9. Determination of the r-value for the chemical shifts of the formyl protons of the *trans*-forms.

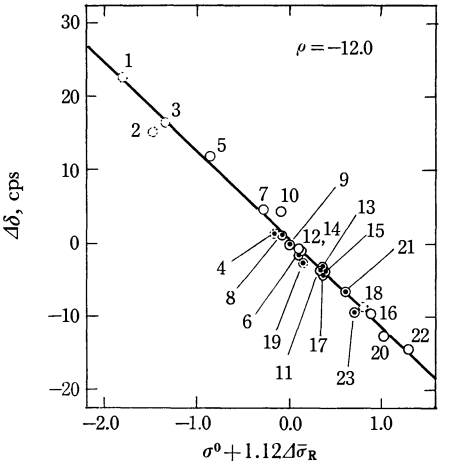

Fig. 10. Correlation of the chemical shifts of the formyl protons of the *trans*-forms with the Yukawa-Tsuno equation. Numbered points correspond to entries in Table 1. Substituents, $N(CH_3)_2$, NH_2, OH, and COOH are shown by dotted circles.
⊙: *mreta*-substituent ○: *para*-sbustituent

jugative substituents, such as *p*-$COCH_3$, *p*-CN, and *p*-NO_2, deviate considerably in the direction of the σ^--value.[3] When the σ^+-values are used for the former substituents and the σ^--values for the latter, all the plots except that for *p*-$N(CH_3)_2$ fall near the correlation line, but the correction seems yet to be insufficient. This result suggests that the Yukawa-Tsuno equation (3) may be applicable to the chemical shifts of the formyl protons if we adopt the σ^+-values for the former substituents and the σ^--values for the latter as a common reference of substituent constants, and if we assume that this system has the same *r*-value for both types of substituents. Thus, a good correlation is obtained as:

$$\Delta\delta = -12.0(\sigma^0 + 1.12\Delta\bar{\sigma}_R) + 0.5 \qquad (7)$$

for the 16 substituents, as is shown in Fig. 10. The values of r*[7] and s*[7] were 0.993 and 0.8 respectively. A plot for the *p*-fluoro derivative deviates somewhat above the correlation line, as has been observed by Yukawa and Yamada.[4] in the chemical shifts of the ethynyl protons in *meta*- and *para*-substituted phenylacetylenes.

When the σ^0-values in dimethyl sulfoxide and the ordinary $\Delta\bar{\sigma}_R$-values*[8] are used, the plots for *p*-NH_2, *p*-OH, and *p*-COOH*[9] fall close to the correlation line. Only the plot for *p*-$N(CH_3)_2$ deviates greatly down from the correlation line. Yukawa and Tsuno[10] have indicated a good correlation between the chemical shifts of *para*-protons on monosubstituted benzenes and the $\Delta\bar{\sigma}_R$-values, but in this case, too, the plot for *p*-$N(CH_3)_2$ deviates considerably from the correlation line. From the correlation line, the $\Delta\bar{\sigma}_R{}^+$-value for *p*-$N(CH_3)_2$ is calculated as -0.93. When this value is used in the present case, the plot for *p*-$N(CH_3)_2$ falls near the correlation line, as is shown by dotted circle, (2), in Fig. 10. The origin of the difference between the two $\Delta\bar{\sigma}_R{}^+$-values, one of which has been derived from the reactivity data and the other from the NMR data, is not yet evident.

The characteristic aspect of the substituent effect in the case of the *trans*-form is in contrast to the situation in the *cis*-form, and it implies that the aryl and the amide groups constitute a expanded conjugated system over the whole molecule. When we assume an asymmetric polarized structure for the *trans*-form (Fig. 7), this is explained as follows. First, in the *trans*-form, the aromatic ring and the amide groups lies in the same plane, because of the lack

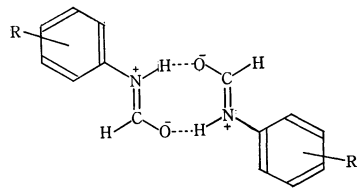

Fig. 11. The ring dimer of the molecules of the *trans*-form of *m*- and *p*-substituted formanilides.

of the steric interaction between the aryl and the amide groups. Second, as is shown schematically in Fig. 11, the molecules of the *trans*-form associate to make the ring dimer.*[10] All of these effects may cause that the formal charges on the nitrogen atom of the imino group and the oxygen atom of the C–O group are distributed along the bonds in the molecule, and that the composite *pi*-electron systems are delocalized along the entire body of the planar molecule.

Solvent Effect on Three Substituents, NH_2, OH, and COOH. Equation (7) shows that the normal $\Delta\bar{\sigma}_R$-values can also be applied in dimethyl sulfoxide to the substituents, such as NH_2, OH, and COOH, which form a strong hydrogen bonding with the solvent molecule. This result suggests that this specific solvation does not affect the term of the conjugative interaction. On the other hand, their σ^0-values in dimethyl sulfoxide differ remarkably from their normal σ^0-values. Which, then, the inductive or the mesomeric contribution of the σ^0-constant, does this solvation influence? We will now attempt to answer this question.

The σ^0-constant separated by Yukawa and Tsuno[1] is shown in Eq. (8):

$$\sigma^0 = \sigma_i + \sigma_\pi \qquad (8)$$

where the σ_i and σ_π terms are called the *sigma*-inductive and *pi*-electronic effects respectively. When the σ_i-and σ_π-values*[11] are used, Eq. (3) generally turns to:

$$\log k/k_0 = \rho(\sigma_i + r\sigma_\pi) \qquad (9)$$

where $\sigma_\pi = \sigma_\pi{}^+$*[12] and $\boldsymbol{r} = 1 + 2.4r$ for the electron-releasing conjugative substituent, and $\sigma_\pi = \sigma_\pi{}^-$*[12] and $\boldsymbol{r} = 1 + 1.2r$ for the electron-withdrawing conjugative substituent. Here, we will assume that this solvation affects only the term of the inductive effect by forming hydrogen bonding with the substituent group. Then. Eq. (8) can be expressed as:

$$\sigma^0_{(DMSO)} = \sigma_{i(DMSO)} + \sigma_\pi \qquad (10)$$

From Eq. (10), the σ_i-values in dimethyl sulfoxide are calculated to be: -0.25 for *p*-NH_2, -0.07 for

*[8] See Table 2.

*[9] Although the $\Delta\bar{\sigma}_R{}^-$ value for *p*-COOH has not been established, there may be little difference between the $\Delta\bar{\sigma}_R{}^-$ values for *p*-COOH and *p*-COOR. Therefore, the $\Delta\bar{\sigma}_R{}^-$ value for *p*-COOR (0.28) is used in this case.

11) Y. Yukawa and Y. Tsuno, "Jikken Kagaku Koza" (Handbook of Chemical Experiments), Supplemental Vol. 12, ed. by the Chem. Soc. Japan, Maruzen Co., Tokyo (1967), p. 462.

*[10] The presence of the ring dimer for formanilide has been suggested by Mizushima *et al.* (Ref. 6).

*[11] See Table 2.

*[12] $\sigma_\pi{}^+ = 0.415\Delta\bar{\sigma}_R{}^+$ and $\sigma_\pi{}^- = 0.81\Delta\bar{\sigma}_R{}^-$ (Ref. 1). If $0.415\Delta\bar{\sigma}_R{}^-$ is adopted, the plots for *p*-CN, *p*-$COCH_3$, *p*-COOH, and *p*-NO_2 fall on the correlation line.

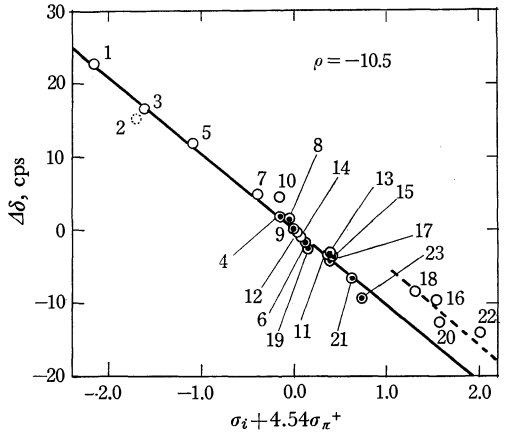

Fig. 12. Correlation of the chemical shifts of the formyl protons of the *trans*-forms with the equation, $\Delta\delta=\rho(\sigma_i+r\sigma_\pi)$. Numbered points correspond to entries in Table 1.
⊙: *meta*-substituent ○: *para*-substituent

p-OH, and 0.27 for *p*-COOH. If Eq. (9) holds for all the *para*-substituents which are electron-releasing conjugative, the use of these σ_i-values will prove the above assumption to be appropriate.

Figure 12 shows that Eq. (9) fits well for all the substituents mentioned above; the relation can be expressed as:

$$\Delta\delta = -10.5(\sigma_i + 4.54\sigma_\pi^+) \qquad (11)$$

In view of the error in the measurement of each chemical shift, we are probably justified in concluding that this ρ-value is almost equal to the ρ-value (−12.0) for the *meta*-derivatives. When the σ_π^--values are used for the electron-withdrawing conjugative substituents, *p*-$COCH_3$, *p*-CN, *p*-COOH, and *p*-NO_2, their plots fall on the other line. However, this result may be reasonable in view of the definition of the σ_π^--value.*[12] This fact does not essentially affect the above discussion. Accordingly, it may be concluded that this type of solvation influences not the mesomeric contribution but the inductive contribution of the substituent effect.

We wish to express our indebtedness to Mr. Mitsuru Yamazaki of Nagoya University for the measurement of the NMR spectra. Thanks are also due to Mr. Shozo Masuda of Tokyo University for his elemental analyses of the samples.

BULLETIN OF THE CHEMICAL SOCIETY OF JAPAN VOL. 42 1934—1937 (1969)

Macro Chelate Rings. I. Synthesis of 2,7-Dimethyl-4,5-bis-(salicylideneaminomethyl)acridone as a Quadridentate Chelating Agent and Its Metal Complexes

Hisashi OKAWA and Tamotsu YOSHINO

Department of Chemistry, Faculty of Science, Kyusyu University, Hakozaki, Fukuoka

(Received August 5, 1968)

2,7-Dimethyl-4,5-bis(salicylideneaminomethyl)acridone, which may form a quadridentate metal complex involving a ten-membered chelate ring, was synthesized by a sequence of steps and characterized. A monomeric cobalt(II) complex of the ligand was isolated and examined.

A number of six- or less-membered metal chelates have been synthesized, but there have been few, if any, characterized complexes with eight- or more-membered chelate rings in spite of the interest in the configuration of the complex.

In order to find a suitable metal complex which is sterically controlled for our ultimate object of making an asymmetric synthesis of an organic compound, we attempted to synthesize a novel quadridentate chelating agent, 2,7-dimethyl-4,5-bis-(salicylideneaminomethyl)acridone (I), which may form a ten-membered chelate ring in addition to two six-membered chelate rings by complex formation.

As is generally known, a purely organic macro ring compound is considered to be difficult to obtain without the selection of a suitable cyclization reaction and strict reaction conditions. In chelate compounds as well, an eight- or more-membered solitary chelate ring would not seem to form a stable metal complex because of the extreme weakness of the chelate effect. A considerably stable inner complex, however, may be formed if a macro chelate ring is fortified with an adjoining six-mem-

bered chelate ring on each side. Actually, some stable chelates of the ligand derived from salicylaldehyde and hexamethylenediamine have been obtained.

From this fact it seems possible to isolate a metal chelate of the liganed (I) in a stable form. However, no chelating agent similar to our ligand has ever been synthesized. The hydrogen atom attached to the nitrogen atom in the acridone nucleus may hinder the complex formation. Moreover, the ligand is unique in that the two phenolic oxygen atoms and two azomethin nitrogen atoms in the ligand molecule can not coordinate to the four sites of a square, planar central atom, as shown by a model consideration. Therefore, it seems necessary for the chelate to take a tetrahedral or octahedral configuration.

Therefore, in this work the synthesis of 2,7-dimethyl-4,5-bis(salicylideneaminomethyl) acridone (I) was explored as well as the complex formation.

Results and Discussion

The synthetic scheme of the organic moiety is shown in Chart 1. As the starting material, 2,7-dimethylacridone (V), in which the most reactive sites of acridone are blocked by methyl groups, was prepared by the Jourdan-Ullmann-Goldberg method from *p*-bromotoluene and 2-amino-5-methylbenzoic acid, which had been synthesized by a new method. Since the aminomethyl derivatives of acridone were not known, several routes were attempted. Among these, only direct aminomethylation was successful. 2,7-Dimethylacridone (V) was treated with *N*-hydroxymethylphthalimide or *N*-hydroxymethylbenzamide in concentrated sulfuric acid, and the condensation product (VI or VII) was hydrolyzed with hydrobromic acid to give 2,7-dimethyl-di(aminomethyl)acridone dihydrobromide (VIII). The di(aminomethyl)derivative was stable only in its salt form; the isolation of the free diamine was unsuccessful. Because of the instability of free diamine, the positions of the substitution were tentatively assigned to the 4 and 5 positions by analogy with the electrophilic substitutions of 2,7-dichloro and 2,7-dibromoacridone.[1] This 2,7-dimethyl-4,5-di(aminomethyl) acridone dihydrobromide was treated with salicylaldehyde to give 2,7-dimethyl-4,5-bis(salicylideneaminomethyl)acridone (I), the structure of which was confirmed by elementary analysis; its infrared spectrum supported the existence of a chelated azomethin group at 1625 cm^{-1}.

The compound (I) formed metal complexes with several metal salts, such as cobalt(II) and nickel(II) acetates. Of these the cobalt(II) complex (IX) was so stable as to be isolable in a pure state;

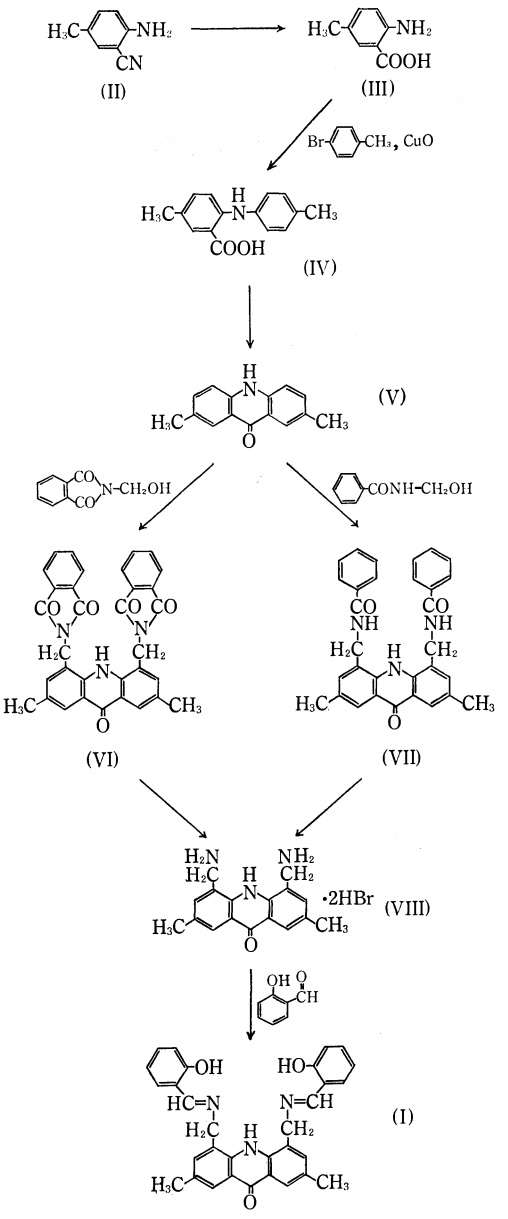

Chart 1.

its structure was determined by elementary analysis, by molecular-weight determination by vapor pressure in methanol, and by the shift of the C=N strectching vibration from 1625 to 1620 cm^{-1}. On the other hand, no recognizable shifts of the C=O and N–H stretching vibrations in the acridone nucleus were observed upon complex formation, the respective peaks being at 3270 and 1625 cm^{-1}. This fact means that the acridone nucleus does not change to the 9-hydroxyacridine nucleus upon prototropy; accordingly, the nitrogen atom in the acridone nucleus does not participate in the complex formation. The quinquedentate structure shown

1) M. Ionescu and D. Postescu, *Studia Univ. Babes-Bolyai, Ser. Chem.*, **11**(1), 73 (1966).

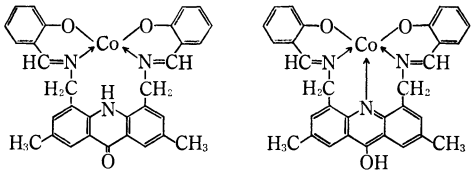

(IXa) (IXb)

Chart 2.

in formula (IXb) could thus be excluded, and the quadridentate structure (IXa) was chosen as that of the cobalt(II) complex (Chart 2*1). The hydrogen atom attached to the nitrogen atom in the acridone nucleus was, unexpectedly, shown not to hinder the complex formation. Although the cobalt(II) complex did not have sufficient stability because of the steric strain probably due to the macro ring, our experiments have shown that the matal complex involving a ten-membered chelate ring is possibly so stable as to be isolable in a pure state.

Experimental

2-Amino-5-methylbenzonitrile (II). A mixture of 3-bromo-4-aminotoluene (186 g, 1 mol) and cuprous cyanide (100 g, 1.1 mol) in *N,N*-dimethylformamide (250 m*l*) was refluxed. Cuprous cyanide was dissolved within about 10 min. After a period of 3 hr, the reaction mixture was poured into a solution of sodium cyanide (200 g) in water (700 m*l*). The entire mixture was heated on a water bath for 1 hr and then cooled. The upper organic layer was separated, and the aqueous layer was extracted with benzene (300 m*l*). After the combined mixture of the organic layers had been dried over anhydrous sodium sulfate and the solvent had been removed by distillation, the residue was subjected to vacuum distillation; a fraction (97 g) boiling at 94—102°C/2 mmHg and solidifying immediately on cooling was collected to give 2-amino-5-methylbenzonitrile. A sample crystallized from ethanol consisted of colorless needles with a mp of 60—61°C.

The compound obtained by this new method was identified by the coincidence of our description with that of Findeklee's report.[2]

2-Amino-5-methylbenzoic Acid (III). 2-Amino-5-methylbenzonitrile (61 g, 0.5 mol) was hydrolyzed in a solution prepared by adding ethanol (500 m*l*) to a solution of sodium hydroxide (80 g) in water (100 m*l*). The sodium salt which separated after 7 hr was collected and dissolved in water (500 m*l*). The aqueous solution was neutralized with hydrochloric acid to give 2-amino-5-methylbenzoic acid, the subsequent crystallization of which from benzene gave colorless needles with a mp of 173°C.

The product was identified by the coincidence of our descritpion with that of Findeklee's report.[3]

2-(*p*-Tolylamino)-5-methylbenzoic Acid (IV). A mixture of 2-amino-5-methylbenzoic acid (40 g, 0.25 mol), *p*-bromotoluene (43 g, 0.25 mol), copper(II) oxide (0.5 g), and anhydrous potassium carbonate (18 g) in quinoline (100 m*l*) was refluxed at 240°C for 3 hr. After the excess *p*-bromotoluene and quinoline had been removed by steam distillation, the remaining dark-brown reaction mixture was boiled with active charcoal (5 g) for 5 min and then filtered. The filtrate, on acidification with hydrochloric acid, separated a dark yellowish green precipitate which was then crystallized from ethanol to give pale yellow prisms (50 g) with a mp of 184—186°C.

Found: C, 74.89; H, 6.36; N, 5.87%. Calcd for $C_{15}H_{15}NO_2$: C, 74.67; H, 6.27; N, 5.80%.

2-Amino-5-methylbenzoic acid and excess *p*-bromotoluene formed yellow crystals of 2-bis(*p*-tolyl)amino-5-methylbenzoic acid, which in turn yielded *N*-*p*-tolyl-2,7-dimethylacridone with a mp of 217—219°C.

2,7-Dimethylacridone (V). A solution of 2-(*p*-tolylamino)-5-methylbenzoic acid (50 g) in concentrated sulfuric acid (200 m*l*) was heated on a water bath for 4 hr. After having been cooled, the reaction mixture was poured onto ice. The yellow precipitate was collected by filtration. After any impurities had been removed by boiling with a 10% aqueous sodium carbonate solution, the insoluble residue was crystallized from dioxane or acetic acid to give yellow needles (28 g) with a mp of above 300°C. The overall yield from 2-amino-5-methylbenzoic acid was 55%.

Found: C, 80.99; H, 5.99; N, 6.58%. Calcd for $C_{15}H_{13}NO$: C, 80.69; H, 5.87; N, 6.27%.

The use of an excess of sulfuric acid led to the formation of a compound of an unknown structure, the composition of which was close to $C_{15}H_{14}NO_5SNa$.

2,7-Dimethyl-4,5-bis(phthalimidomethyl)acridone (VI). 2,7-Dimethylacridone (2.23 g, 0.01 mol) and *N*-hydroxymethylphthalimide (3.54 g, 0.023 mol) were dissolved in concentrated sulfuric acid (50 m*l*), and then the solution was left standing at room temperature for a week. The reaction mixture was then poured onto ice to give a yellow precipitate; this precipitate was collected by suction, treated in a 10% sodium bicarbonate solution (300 m*l*), collected by filtration, and washed with water and then with ethanol. The yield was almost quantitative. An analytical sample was crystallized from acetic acid to give pale yellow needles with a mp of above 300°C.

Found: C, 72.93; H, 4.46; N, 7.46%. Calcd for $C_{33}H_{23}N_3O_5$: C, 73.19; H, 4.28; N, 7.76%.

The use of a large excess of *N*-hydroxymethylphthalimide resulted in the formation of an insoluble substance, of an unknown structure, apparently containing more than two, probably six, phthalimidomethyl groups.

Found: C, 69.11; H, 3.88; N, 7.89%. Calcd for $C_{69}H_{43}N_7O_{13}\cdot H_2O$: C, 69.29; H, 3.79; N, 8.20%.

2,7-Dimethyl-4,5-bis(benzamidomethyl)acridone (VII). A mixture of 2,7-dimethylacridone (1.1 g, 0.005 mol) and *N*-hydroxymethylbenzamide (1.8 g, 0.012 mol) in concentrated sulfuric acid (50 m*l*) was left standing at room temperature for ten days, and then the reaction mixture was poured onto ice. The yellow precipitate was collected by filtration. After having been boiled in a 10% aqueous sodium bicarbonate solution, it was collected, washed with water, and crystallized from a methanol-dioxane mixture to give pale yellow needles (2.2 g) with a mp of above 300°C.

Found: C, 75.81; H, 5.82; N, 8.42%. Calcd for $C_{31}H_{27}N_3O_3$: C, 76.03; H, 5.56; N, 8.58%.

*1 Two water molecules which may be coordinated to the cobalt atom are eliminated in this chart.

2) W. Findeklee, *Ber.*, **38**, 3544 (1905).

3) W. Findeklee, *ibid.*, **38**, 3555 (1905).

2,7-Dimethyl-4,5-di(aminomethyl)acridone Dihydrobromide (VIII). A mixture of 2,7-dimethyl-4,5-bis(phthalimidomethyl)acridone (5 g) in acetic acid (50 m*l*) and 40% hydrobromic acid (50 m*l*) was refluxed in an oil bath for 2 days. The yellow needles (400 mg) which separated were collected by filtration and washed with a small amount of ethanol.

Found: C, 43.87; H, 4.86; N, 8.98%. Calcd for $C_{17}H_{21}N_3OBr_2$: C, 44.27; H, 5.03; N, 9.11%.

This dihydrobromide (200 mg) was also obtained in a comparable yield by refluxing 2,7-dimethyl-4,5-bis-(benzamidomethyl)acridone (2 g) in a mixture of acetic acid (30 m*l*) and 40% hydrobromic acid (30 m*l*) for 7 hr. In this case, the reaction time could be shortened for a comparably easy hydrolysis. These dihydrobromides were confirmed to be the same by the coincidence of the two infrared spectra.

The diamine seemed to be stable only in its salt form; attempts to isolate the free diamine failed, giving only a black paste.

2,7-Dimethyl-4,5-bis (salicylideneaminomethyl)-acridone (I). An acidic solution of 2,7-dimethyl-4,5-di(aminomethyl)acridone dihydrobromide (50 mg) and salicylaldehyde (50 mg) in 50% ethanol (30 m*l*) was neutralized with a 10% sodium bicarbonate solution to separate dark pink needles; these needles were collected by filtration and recrystallized three times from dioxane to give pink needles (30 mg) with a mp of 227—229°C. UV (ethanol): 31600 (6770), 25600 (5460) and 24700 cm^{-1} (ε 6190). IR (KBr disk): 3270 (N–H) and 1625 cm^{-1} (C=O and C=N).

Found: C, 76.24; H, 5.63; N, 8.51%. Calcd for $C_{31}H_{27}N_3O_3$: C, 76.05; H, 5.56; N, 8.58%.

Cobalt(II) Complex of 2,7-Dimethyl-4,5-bis(salicylideneaminomethyl)acridone (IX). A mixture of 2,7-dimethyl-4,5-bis (salicylideneaminomethyl) acridone (30 mg) and cobalt(II) acetate tetrahydrate (25 mg) in ethanol (25 m*l*) was heated on a water bath for 3 hr to give a reddish-brown precipitate; this precpitate was collected by filtration and washed with a small amount of ethanol. It was soluble in pyridine, dioxane, and *N,N*-dimethylformamide. UV (ethanol): 20000 (2100), 17500 (1100) and 7300 cm^{-1} (ε 480). IR (KBr disk): 3270 (N–H), 1625 (C=O) and 1620 cm^{-1} (C=N).

Found: C, 64.29; H, 4.77; N, 7.21; Co, 10.15%, mol wt, 590 (methanol). Calcd for $C_{31}H_{25}N_3O_3Co\cdot 2H_2O$: C, 63.92; H, 5.02; N, 7.21; Co, 10.12%, mol wt, 582.5.

Nickel(II) Complex of 2,7-Dimethyl-4,5-bis(salicylideneaminomethyl)acridone (X). A mixture of 2,7-dimethyl-4,5-bis (salicylideneaminomethyl) acridone (30 mg) and nickel(II) acetate tetrahydrate (25 mg) in ethanol (25 m*l*) was heated on a water bath for 1 hr. The precipitate was collected by filtration and washed with a small amount of ethanol to give a yellowish-brown powder.

Found: C, 63.37; H, 4.57; N, 7.53%. Calcd for $C_{31}H_{25}N_3O_3Ni\cdot 2H_2O$: C, 63.94; H, 5.02; N, 7.22%.

BULLETIN OF THE CHEMICAL SOCIETY OF JAPAN VOL. 42 1937—1941 (1969)

Secondary Structure of Poly-L-arginine and Its Derivatives*1

Tadao HAYAKAWA, Yoshiyuki KONDO and Hiroyuki YAMAMOTO

Institute of High Polymer Research, Faculty of Textile Science and Technology, Shinshu University, Ueda

(Received August 12, 1968)

The conformations of poly-$N^{\omega,\omega'}$-dicarbobenzyloxy-L-arginine, poly-N^{ω}-carbobenzyloxy-L-arginine, and poly-L-arginine hydrobromide were studied by means of their infrared spectra (IR), X-ray photographs, optical rotatory dispersions (ORD), and circular dichroisms (CD). The presence of the α-helical conformation in poly-$N^{\omega,\omega'}$-dicarbobenzyloxy-L-arginine and poly-N^{ω}-carbobenzyloxy-L-arginine was confirmed by X-ray photographs and by their IR spectra. The ORD and the CD curves of these polymers were found to be characteristic of the α-helical conformation. It was also found that these polypeptides have a random coil conformation in trifluoroacetic acid. In the (2-chloroethanol : trifluoroacetic acid) solvent system, the typical helix-coil transition of poly-N^{ω}-carbobenzyloxy-L-arginine was observed at 20—30% trifluoroacetic acid. The ORD and the CD curves of poly-L-arginine showed that the polymer took a random coil structure in the pH range from 2.7 to 11.0. However, when the pH is increased from 11.0 to 11.5, the spectra gradually change into the α-helix structure. Moreover, the polypeptide predominantly took the α-helix structure at pH 12.5. From the ORD and CD data, the polypeptide can be considered to have a right-handed α-helix conformation.

Considerable interest has recently been shown in the secondary structure of many synthetic polypeptides and proteins in the solid state and in solution. The protamins are strongly basic proteins which have high arginine contents, and their con-

*1 Presented at the Annual Meeting of the Society of Polymer Science of Japan, Tokyo, May, 1968.

formations have been found by the NMR[1] and the ORD[2,3] measurements to be almost random coil structures in aqueous solutions. However, the physicochemical properties of poly-L-arginine and its derivatives have not been reported. Recently we have prepared poly-L-arginine as an useful model of the protamins and have also prepared, by the NCA method,[4] two kinds of protected polyarginine as intermediates. In this paper, the physical properties and the secondary structure of poly-$N^{\omega,\omega'}$-dicarbobenzyloxy-L-arginine, poly-N^{ω}-carbobenzyloxy-L-arginine, and poly-L-arginine hydrobromide in the solid state and in solution will be discussed using the date obtained from the IR spectra, the X-ray analyses, and the ORD and CD.

Experimenta

Materials. Poly-$N^{\omega,\omega'}$-dicarbobenzyloxy-L-arginine (I), poly-N^{ω}-carbobenzyloxy-L-arginine (II), and poly-L-arginine hydrobromide (III) were prepared by the NCA method described in a previous paper.[4] The degree of polymerization of these polypeptides is found to be *ca.* 70 by carboxyl end-group analysis.

Measurements. The IR spectra were recorded by the use of the potassium bromide-pellet technique on a Jasco IR spectrophotometer, Model DS-301. The X-ray diffraction photographs were taken with a Rigaku-denki Geigerflex, using a Cu-target. The ORD and CD were measured on a Jasco Model ORD/UV-5 ORD recorder with a CD attachment at room temperature, using the cells with light paths of between 0.1 and 100 mm. The aqueous solutions of poly-L-arginine for the ORD and CD measurements were prepared by dissolving poly-L-arginine hydrobromide in water and by adjusting the pH with 0.1N NaOH.

Results and Discussions

IR Studies and X-Ray Analyses. The IR absorption spectra of I, II, and III showed absorptions at 1655 cm^{-1} (Amide I) and 1545 cm^{-1} (Amide II), suggesting that the polymer could have the α-structure (Fig. 1). The absorption shoulder at 1545 cm^{-1} and the other absorptions at 1515cm^{-1}, 1615 cm^{-1} and 1725 cm^{-1} of the polymers I and II may be due to the influence of the protected guanido group in polyarginine. The spectrum of III is simplified in all regions because of the removal

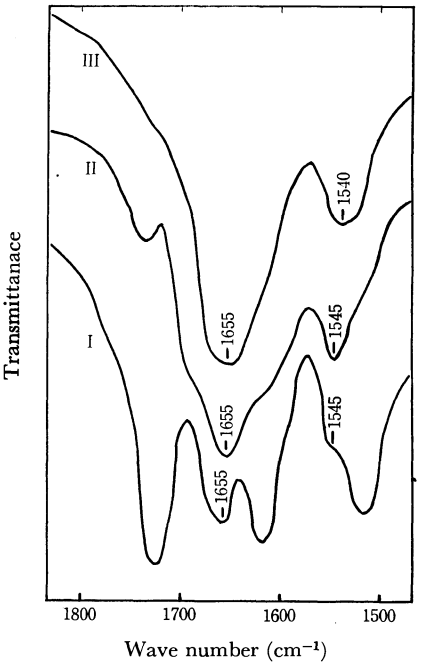

Fig. 1. IR spectra of poly-L-arginine hydrobromide and derivatives.
I: poly-$N^{\omega,\omega'}$-dicarbobenzyloxy-L-arginine;
II: poly-N^{ω}-carbobenzyloxy-L-arginine;
III: poly-L-arginine hydrobromide

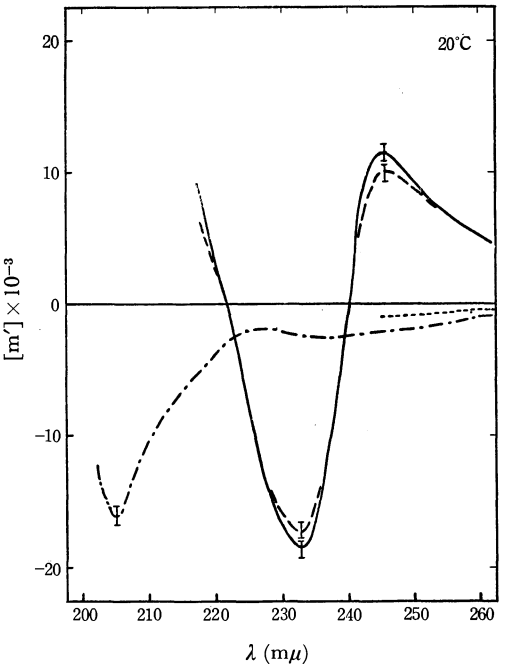

Fig. 2. ORD of poly-$N^{\omega,\omega'}$-dicarbobenzyloxy-L-arginine in THF (——), in dioxane (- - -), in TFA (- - - -) and in 2-chloroethanol (- · -).

1) E. M. Bradbury, C. Crane-Robinson, H. W. E. Rattle and R. M. Stephans, "Conformation of Biopolymers," ed. G. N. Ramachandam, Academic Press, London and New York (1967), p. 583.

2) B. Jirgensons and L. S. Hnilica, *Biochim. Biophys. Acta*, **109**, 241 (1965).

3) E. M. Bradbury, C. Crane-Robinson, H. Goldman, H. W. E. Rattle and R. M. Stephans, *J. Mol. Biol.*, **29**, 507 (1967).

4) T. Hayakawa, Y. Kondo, H. Yamamoto and Y. Murakami, This Bulletin, **42**, 479 (1969).

of the protecting group of the guanido group and showed absorptions at 1655 cm^{-1} and 1540 cm^{-1}. X-ray analyses of the polymers I, II, and III were also carried out. The X-ray diffraction patterns of I and II indicated the presence of a 18 Å reflection. Similarly, the X-ray photograph of poly-γ-benzyl-L-glutamate[5] in the α-helix structure shows the presence of a 13 Å reflection. This could be interpreted as indicating that a helix-helix interval of an α-helical polypeptide is broadened from 13 Å to 18 Å for poly-L-arginine derivatives (I and II) because of the bulky side chain. Poly-L-arginine hydrobromide (III) gives an almost amorphous photograph.

Optical Rotatory Dispersion and Circular Dichroism. *Poly-$N^{\omega,\omega'}$-dicarbobenzyloxy-L-arginine.* The ORD curves of poly-$N^{\omega,\omega'}$-dicarbobenzyloxy-L-arginine in tetrahydrofuran (THF), in dioxane, in 2-chloroethanol, and in trifluoroacetic acid (TFA) are shown in Fig. 2. In THF and in dioxane, the polypeptide exhibits a positive Cotton effect, with a strong peak at 245—247 mμ, followed by a deep trough at 233 mμ; the crossover point lies at 240 mμ. A second positive Cotton effect can be expected below 220 mμ with the crossover point at 222 mμ, but this is not clearly evident from the ORD curves. The CD curves of the polypeptide in THF and in dioxane are recorded in order to resolve

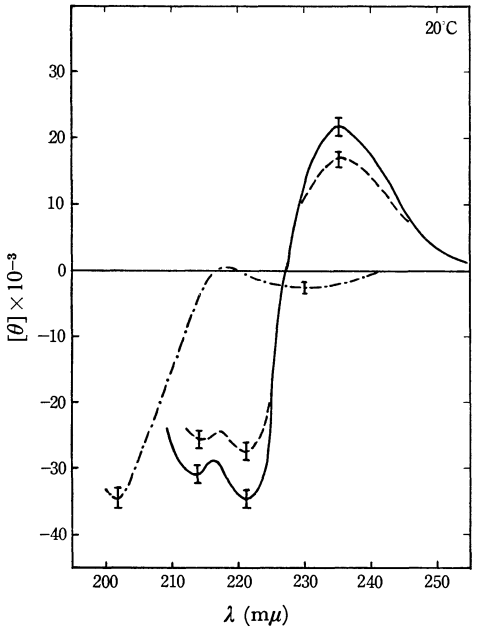

Fig. 3. CD of poly-$N^{\omega,\omega'}$-dicarbobenzyloxy-L-arginine in THF (——), in dioxane (– – –) and in 2-chloroethanol (– · –).

5) C. H. Bamford, A. Elliot and W. E. Hanby, "Synthetic Polypeptides," Academic Press, New York (1956), p. 263; Y. Mitsui, Y. Iitaka and M. Tsuboi, *J. Mol. Biol.*, **24**, 15 (1967).

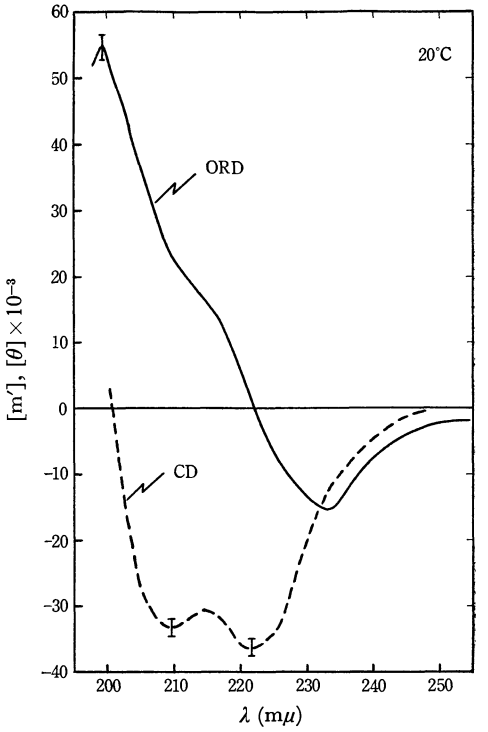

Fig. 4. ORD and CD of poly-N^{ω}-carbobenzyloxy-L-arginine in 2-chloroethanol.

any possible overlapping of Cotton effects in this region. The CD curves are shown in Fig. 3. The CD curves of the polypeptide reveal a strongly positive dichroism centered at 235 mμ in the wavelength range 250—200 mμ. Two negative dichroism bands, at 221 mμ and 214 mμ, are observed for these solutions; a positive dichroism band can also be expected below 200 mμ. The positive dichrosim band at 235 mμ can be assigned to the π–π^* exciton transition of the benzyl group. The negative ellipticity band at 221 mμ appears to be the n–π^* peptide electronic transition associated with the α-helical conformation of polypeptide, while the negative band at 214 mμ and the positive band below 200 mμ are to be assigned to the parallel-polarized and perpendicular-polarized π–π^* exciton transitions of the peptide groups respectively.[6] These dichroism bands are found in approximately the same positions and have the same signs and magnitudes as those observed in right-handed α-helix polypeptides. From these CD and ORD measurements, this polypeptide can be considered to have a right-handed α-helix conformation in THF and in dioxane.[6] When TFA and 2-chloroethanol are used as the solvents (Fig. 2), the peak at 245 mμ disappears. The ORD and the CD curves of the polypeptide in 2-chloroethanol (Figs. 2 and 3) are characteristic of the random coil conformation; there is a 238 mμ trough, a 226 mμ peak, and a 205 mμ trough in the ORD curve, and

a small negative dichroism band at 230 mμ, a small positive dichroism band at 217 mμ, and a large negative dichroism band at 202 mμ in the CD curve. These results suggest that the phenyl groups near the backbone of the main chain exist in a dissymmetric environment in helix-supporting solvents (THF, dioxane). In TFA and in 2-chloroethanol, the polypeptide exists as a random coil and the dissymmetry is lost.[7]

Poly-N^{ω}-carbobenzyloxy-L-arginine. The ORD and the CD curves of poly-N^{ω}-carbobenzyloxy-L-arginine in 2-chloroethanol are shown in Fig. 4. The polymer has a 233 mμ trough and a 199 mμ peak, with a shoulder near 213 mμ, on the ORD curve; it also has two negative dichroism bands, at 222 and 210 mμ.[6] These spectra suggest that the polypeptide has a right-handed α-helix structure. The Moffitt-Yang plot for poly-N^{ω}-carbobenzyloxy-L-arginine in mixed solvents (TFA-2-chloroethanol) is shown in Fig. 5. The ORD of this polypeptide in (TFA : 2-chloroethanol) solutions fits the Moffitt-Yang equation. The coefficient of the second term, b_0, is found to be dependent on the mol% of TFA. In 100% TFA, b_0 is zero and a_0 is −310, while in 100% 2-chloroethanol b_0 is −600 and a_0 is +360.

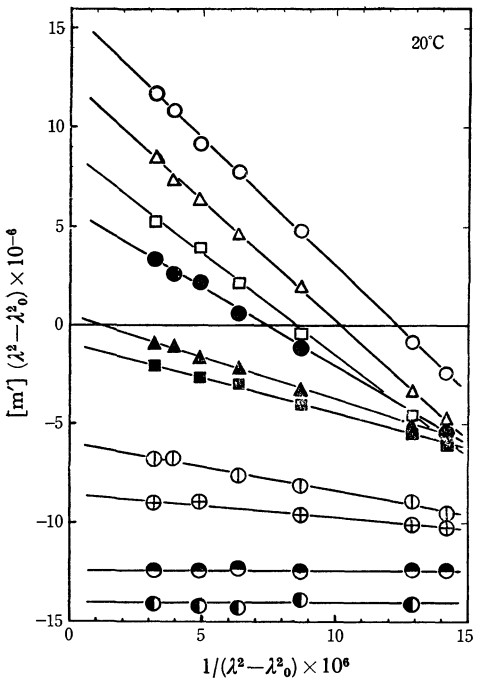

Fig. 5. Moffitt-Yang plot for poly-N^{ω}-carbobenzyloxy-L-arginine in mixed solvents (TFA-2-chloroethanol).
Volume per cent of TFA: ○, 0; △, 5; □, 10; ●, 20; ▲, 25; ■, 35; ⊕, 45; ⊕, 65; ◓, 80; ◐, 100

These results suggest that the polypeptide has a random coil structure in TFA and that it is a right-handed α-helix structure in 2-chloroethanol. More-

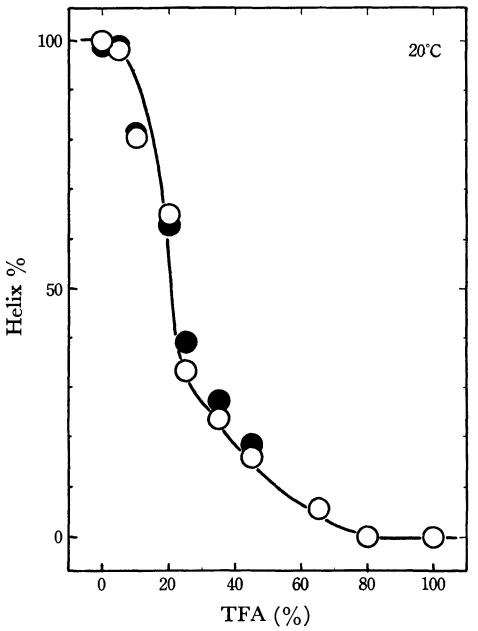

Fig. 6. Helix-coiled transition of poly-N^{ω}-carbobenzyloxy-L-arginine in TFA-2-chloroethanol mixtures.
○: from the b_0; ●: from the $[m']_{233}$

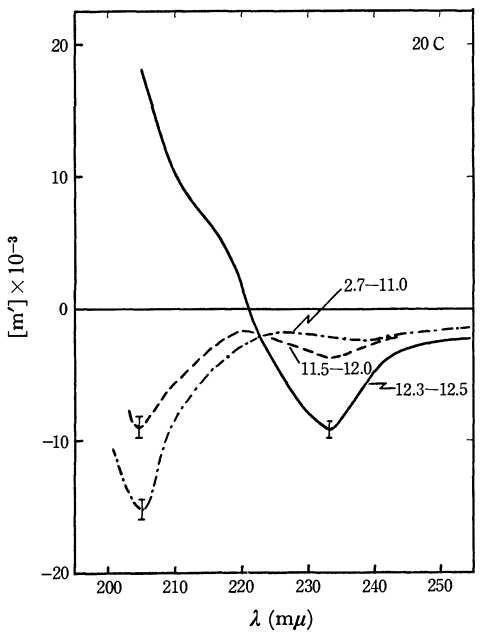

Fig. 7. ORD of poly-L-arginine as a function of pH in aqueous media.
pH 2.7—11.0 (-·-·-), pH 11.5—12.0 (------) and pH 12.3—12.5* (——).
*: water-methanol (2:1, v/v)

6) G. Holzwarth and P. Doty, *J. Am. Chem. Soc.*, **87**, 218 (1965).

7) M. Goodman and E. Peggion, *Biochemistry*, **6**, 1533 (1967).

over, the helix-coil transition of the polypeptide in mixed solvents typically takes place at 20—30% TFA (Fig. 6). The helical contents are calculated by two methods[8,9]: a) from the b_0 value for the Moffitt-Yang plot, and b) by using the magnitude, $[m']_{233}$, in the ultraviolet-region ORD measurements.

Poly-L-arginine. The ORD curves of poly-L-arginine as a function of the pH in aqueous media are shown in Fig. 7. In the pH range 2.7—11.0, the polypeptide is in a random coil structure which has a 238 mμ trough, a 227 mμ peak, and a 205 mμ trough. However, when the pH is increased from 11.0 to 11.5, a remarkable change in the ORD spectrum is observed: the peak at 227 mμ disappears and the trough at 238 mμ shifts to 233 mμ. The solubility of the polypeptide decreases at pH values higher than 12.0. Therefore, ORD and CD measurements were carried out in methanol-water media. In the pH range 12.3—12.5, the polypeptide has predominantly the α-helix conformation: a trough with $[m']_{233}\cong -9000$, a crossover point at 221 mμ, and a shoulder near 214 mμ. However, the magnitude of the $[m']_{233}$ value for the polypeptide is smaller than the magnitude of the $[m']_{233}\cong -15000$ values of poly-L-glutamic acid (pH 4)[9] and poly-L-lysine (pH 11)[10] in aqueous solutions. When the pH is increased to 12.6, the polypeptide precipitates. It could be assumed that the coil-helix transition of the polypeptide takes place in this solution (pH 12.5), but this was not evident from the ORD spectra. The CD curves of the polypeptide as a function of the pH are shown in Fig. 8. In the pH range 2.7—11.0 the CD spectrum shows the same curve as that observed in the ORD; *i. e.*, the polypeptide shows the characteristics of a random coil, a small negative dichroism band at 230 mμ, and a small positive dichroism band at 218 mμ, while a large negative dichroism band may be anticipated below 200 mμ. In the pH range 11.5—12.0 the CD spectrum shows that the polypeptide partially takes the α-helix structure.

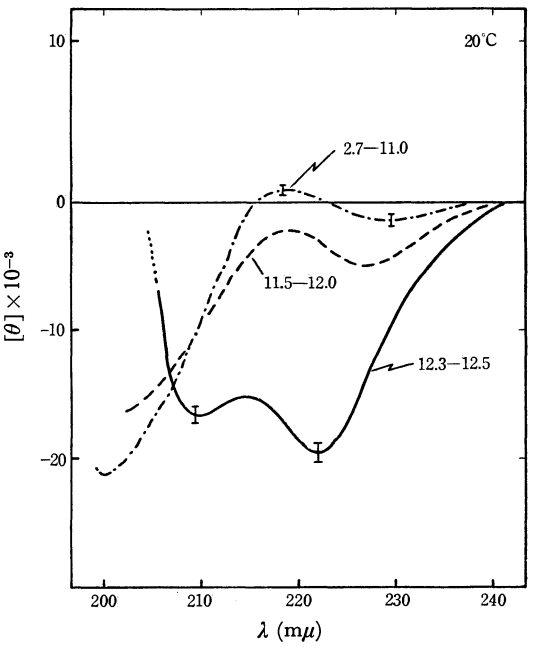

Fig. 8. CD of poly-L-arginine as a function of pH in aqueous media.
pH 2.7—11.0 (-·-·-), pH 11.5—12.0 (----) and pH 12.3—12.5* (——).
*: water-methanol (2 : 1, v/v).

The polypeptide has predominantly the right-handed α-helix conformation between the pH values of 12.3 and 12.5: two negative dichroism bands, at 222 and 209 mμ, with $[\theta]_{222}\cong -19000$ and $[\theta]_{209}\cong -17000$ values respectively. However, the $[\theta]_{222}$ and the $[\theta]_{209}$ values are smaller than those of usual polypeptides.[6,10] These results may be assumed to indicate either that the polypeptide mingle with some random coil conformation or that the molecular weight of the polypeptide is much smaller than that of usual polypeptides.

The authors wish to express their thanks to the Kaishin Kisei Domei of this Faculty for its financial support.

8) E. Iizuka and J. T. Yang, *Biochemistry*, **4**, 1249 (1965).

9) J. Y. Cassim and J. T. Yang, *Biochem. Biophys. Res. Commun.*, **26**, 58 (1967).

10) B. Davidson and G. D. Fasman, *Biochemistry*, **6**, 1616 (1967).

BULLETIN OF THE CHEMICAL SOCIETY OF JAPAN VOL. 42 1942—1947 (1969)

Studies on Stable Free Radicals. III.*1 Reactions of Stable Nitroxide Radicals with *S*-Radicals Derived from Benzenethiols and Thiamine

Keisuke MURAYAMA and Takao YOSHIOKA

Central Research Laboratories, Sankyo Co., Ltd., Shinagawa-ku, Tokyo

(Received September 5, 1968)

The reaction of the extremely stable free radical, 2,2,6,6-tetramethyl-4-oxopiperidine-1-oxyl (I), was carried out with benzenethiols (IV). The formation of diphenyl disulfides (VI), benzenesulfinic acids (VII), and 1-(*p*-substituted benzenesulfinyl)-2,2,6,6-tetramethyl-4-oxopiperidines (X) from the above reaction shows that the radical (I) can act as a hydrogen-abstracting agent, an oxidizing agent, and a radical scavenger. Possible mechanisms for the coupling reaction of the radical (I) with the *S*-radicals (V) to give the sulfinamides (X) were discussed. A substituent effect was observed in the formation of the disulfides (VI). The *N*-oxyl radical (I) and another stable free radical, such as 2,6-di-*t*-butyl-4-methylphenoxyl radical (XXV), were shown to react with the *S*-radical (XVII) derived from thiamine (XIV) to give new types of thiamine derivatives, *S*-(2,2,6,6-tetramethyl-4-oxopiperidino)thiamine (XX) and *S*-(2,6-di-*t*-butyl-4-methylphenoxy)thiamine (XXVI) respectively.

Many studies of the synthetic methods and physical properties of extremely stable *N*-oxyl radicals have recently been reported.[2,3] However, few papers have reported the roles of such radicals as oxidizing agents, hydrogen-abstracting agents, or radical scavengers. Especially, there have been few studies of the reactivities of radicals by means of isolating the coupled products of the radicals with the other free radicals.[1,4] In the preceding paper[1] we studied the reactive sites in such radicals as 2,2,6,6-tetramethyl-4-oxopiperidine-1-oxyl (I) and cyclohexane-1-spiro-2′-(4′-oxoimidazolidine-1′-oxyl)-5′-spiro-1″-cyclohexane (III) from the structure of the coupled products of I and III with a *C*-radical derived from α,α′-azo-bis(isobutyronitrile) (ABIN).

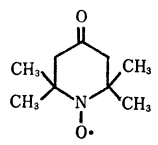

(I)

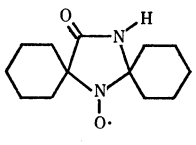

(III)

Chart 1

In this paper the authors wish to report that the radical (I) can act as a hydrogen-abstracting agent, an oxidizing agent, and a radical scavenger, by using the fact that the radical (I) reacts with benzenethiols (IV) to give diphenyl disulfides (VI), benzenesulfinic acids (VII), and 1-benzenesulfinyl-2,2,6,6-tetramethyl-4-oxopiperidine (X). Most importantly, the fact that the radical (I) acts as a radical scavenger is very interesting because this result can be applied to other experiments to determine whether a reaction proceeds *via* a free radical intermediate or not.

Todd and Sykes,[5] and Yurugi[6] have studied the pyrolysis of thiamine disulfide (XVIII) and the reaction of the *S*-anion (XV) of thiamine (XIV) with potassium ferricyanide to give thiochrome (XIX). Although they have postulated a reaction mechanism involving an *S*-radical intermediate in the above reaction, no coupled products of the *S*-radical (XVII) of thiamine with other free radicals have been obtained. We applied the reaction of the free radical (I) with the *S*-radical derived from benzenethiol to the case of another *S*-radical (XVII) derived from thiamine (XIV).

Results and Discussion

The reaction of the *N*-oxyl radical (I) with various benzenethiols (IV) was found to proceed

*1 Part II: Ref. 1.

1) K. Murayama, S. Morimura and T. Yoshioka, This Bulletin, **42**, 1640 (1969).

2) M. B. Neiman, Yu. G. Madedova and E. G. Rozantzev, *Azerb. Khim. Zh.*, **1962**, 37.

3) E. G. Rozantzev and M. B. Neiman, *Tetrahedron*, **20**, 131 (1964).

4) E. G. Rozantzev and V. A. Golubev, *Izv. Akad. Nauk SSSR, Ser. Khim.*, **1966**, 891.

5) a) P. Sykes and A. R. Todd, *J. Chem. Soc.*, **1951**, 534. b) P. Nesbitt and P. Sykes, *ibid.*, **1954**, 4584.

6) S. Yurugi, *Yakugaku Zasshi (J. Pharm. Soc. Japan)*, **77**, 259, 264 (1957).

vigorously in the absence of a solvent at room temperature. This reaction took place even at −55°C in an ethereal or a chloroform solution to give the disulfides (VI), the substituted benzenesulfinic acids (VII), and 1-(*p*-substituted benzenesulfinyl)-2,2,6,6-tetramethyl-4-oxopiperidines (X), as Chart 2 shows. Two reduction products, 2,2,6,6-tetramethyl-4-oxopiperidine (XII) (*ca.* 35% yield) and 1-hydroxy-2,2,6,6-tetramethyl-4-oxopiperidine (XI) (*ca.* 6% yield), were also isolated.

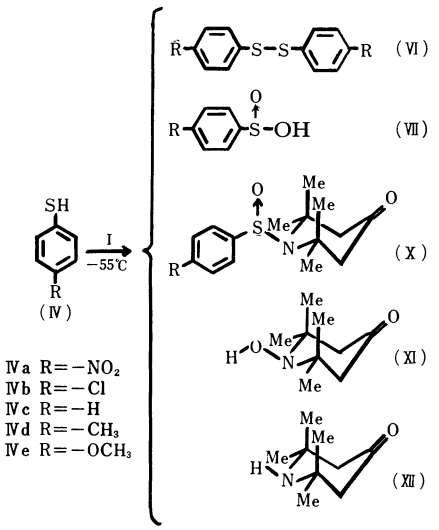

Chart 2[7-9]

The structural assignments of these products were based on the results of the elemental analyses and spectral data. The melting points of the products were identical with those of normal products produced by the independent syntheses of X from the corresponding sulfinyl chlorides and XII, or that of authentic samples.

Our preliminary communication showed that, in our NMR studies of the amides X, four methyl protons of the amides X gave rise to two broad absorptions indicative of magnetic non-equivalence.[10]

The reaction mechanism can be formulated as is shown in Chart 3. The sulfhydryl hydrogen of thiols (IV) was abstracted by the radical (I). The *S*-radicals (V) thus obtained then dimerized to give the dimer (VI). The *N*-oxyl radical (I) or (II) can further react with *S*-radicals (V) to give intermediate, (VIII) or (IX), which, on isomerization, furnish amides (X).

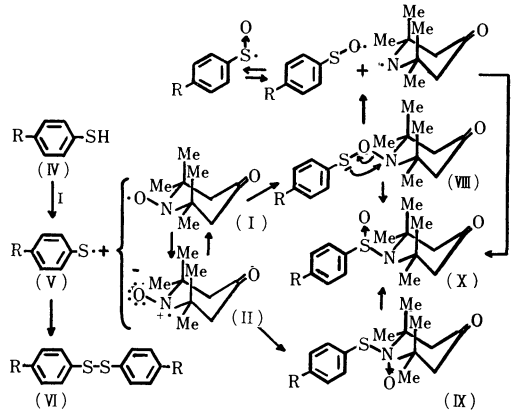

Chart 3[7-9]

The formally analogous thermal rearrangement of sulfenates to sulfoxides has been reported in racemization studies of optically-active sulfoxides by Mislow *et al.*,[11] who have proposed the following homolytic dissociation mechanism:

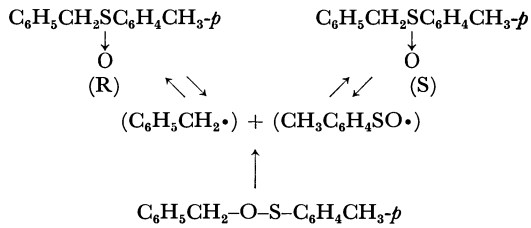

Similar mechanisms involving an –O–N< bond cleavage in VIII may also be possible.

Sulfinic acid formation, *i. e.*, VII, can hardly be explained by the hydrolysis of the sulfinamides (X), since the reaction of the *N*-oxyl radical (I) with the thiols proceeds in anhydrous media. The details of this reaction mechanism will be presented elsewhere.

Thus, the *N*-oxyl radical (I) appears to have the properties of a hydrogen-abstracting agent, an oxidizing agent, and a radical scavenger. The change of the *p*-substituent on the phenyl group from hydrogen to $-NO_2$, $-Cl$, $-CH_3$, or $-OCH_3$ had only a small effect. Table 1 shows that such an electron-donating group as *p*-OCH_3 tended to decrease the yield of the disulfides (VI). The yield was determined by UV-intensity measurements (λ_{max}) after separation using silica gel-column chromatography. This fact can be explained in terms of the small effect of the substituents on the stability

7) In this chart a piperidine ring was conveniently shown in a chair form as represented for the amine XII by Aroney *et al.*[8] However, Rozantzev and Cur'yanova[9] proposed a twist and a boat form for the *N*-oxyl radical (I) and 1,4-dihydroxy-2,2,6,6-tetramethylpiperidine respectively.

8) M. J. Aroney, C.-Y. Chen, R. J. W. Le Fèvre and A. N. Singh, *J. Chem. Soc. B*, **1966**,98.

9) E. G. Rozantzev and E. N. Cur'yanova, *Izv. Akad. Nauk SSSR, Ser. Khim.*, **1966**, 979.

10) K. Murayama and T. Yoshioka, *Tetrahedron Letters*, **1968**, 1363.

11) E. G. Miller, D. R. Rayner and K. Mislow, *J. Am. Chem. Soc.*, **88**, 3138, 3139 (1966).

TABLE 1. *p*-SUBSTITUENT EFFECT ON THE YIELD OF DIPHENYL DISULFIDE

Substituent (*p*)	$-NO_2$	-Cl	-H	$-CH_3$	$-OCH_3$
Yield (%)	55.0	51.5	51.5	52.0	30.5

of the *S*-radical, or on the rate of the hydrogen-abstraction from benzenethiols.

These results appeared to be inconsistent with those proposed by Kooyman *et al.*,[12] who have studied the hydrogen-abstraction reaction by the 1-methyl-1-cyanoethyl radical from substituted benzenethiols (ρ-value: -0.4). However, a direct comparison is impossible because of the uncertainty of the reaction mechanism; in the system studied, there was no evidence that the disulfides were kinetically-controlled products.

Since the free radical (I) was found to exhibit the property of a radical scavenger, we considered using it in the reaction of the radical (I) with the *S*-radical of thiamine (XIV) in a thiol form in order to investigate whether the reaction proceeds *via* a free radical intermediate (XVII) or not. As is

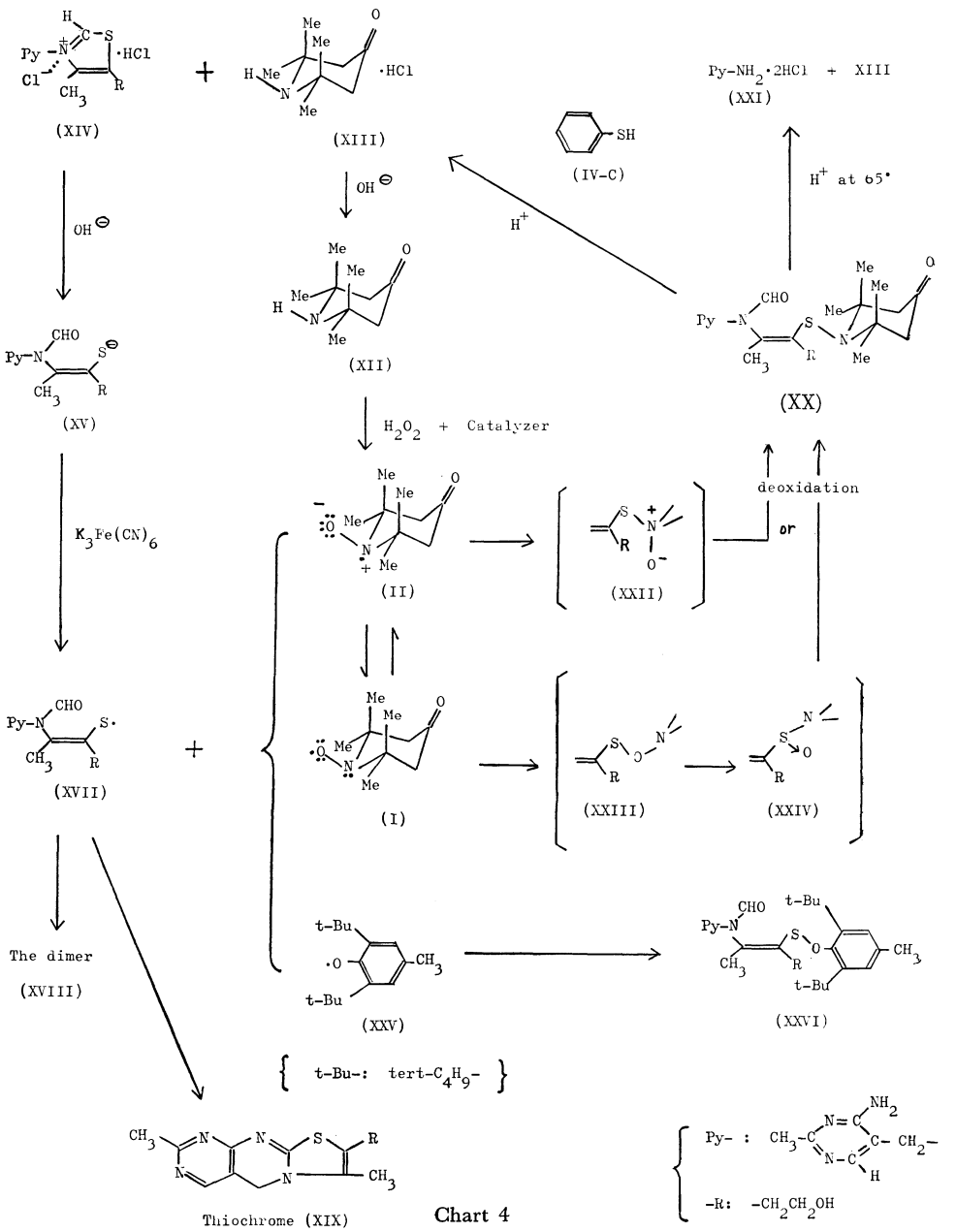

Chart 4

12) Y. Schaafsma, A. F. Bickel and E. C. Kooyman, *Rec. Trav. Chim.*, **76**, 180 (1957).

summarized in Chart 4, thiamine (XIV) was transformed into the *S*-anion (XV) by normal procedures.[13] This *S*-anion (XV) was oxidized with a 1-equivalent electron-abstracting agent, potassium ferricyanide, at 5°C to give the corresponding *S*-radical (XVII).[14] The reaction of the *N*-oxyl radical (I) with the *S*-radical (XVII) was expected to give a coupled product, a new thiamine derivative.[15] From the results of elemental analyses, the UV, IR, NMR, and mass spectra, and the R_f-value in paper chromatography and a thiochrome test,[16] (to be shown in the Experimental section), the structure of the isolated product, $C_{21}H_{33}N_5O_3S$, was deduced to be *N*-[(4-amino-2-methyl-5-pyrimidyl)methyl]-*N*-{4-hydroxy-1-methyl-2-[(2,2,6,6-tetramethyl-4-oxopiperidino)thio]-1-butenyl}-formamide (XX). Further, the hydrolysis of the new derivative, XX, with hydrochloric acid gave 2-methyl-4-amino-5-aminomethylpyrimidine dihydrochloride (XXI) and 2,2,6,6-tetramethyl-4-oxopiperidine hydrochloride (XIII). The reduction of XX with benzenethiol and hydrochloric acid gave thiamine hydrochloride (XIV) and 2,2,6,6-tetramethyl-4-oxopiperidine hydrochloride (XIII) quantitatively. These results are consistent with the structure XX. However, the above observations could not ascertain whether or not a sulfenamide group, –S–N<, was present in this molecule XX. Strong support for the existence of the sulfenamide group was given by the mass spectrometric fragmentation of XX using a high-resolution double-focussing mass spectra; the large fragment peaks at *m/e* 122.073, 186.098, and 249.136 corresponded with $C_6H_8N_3^+$, $C_9H_{16}NOS^+$, and $C_{12}H_{17}N_4O_2^+$ respectively, as is shown in Chart 5. Therefore, the isolated product, XX, was deduced to be a deoxy-form of the expected normal coupled product. Further, the structure of XX was established by X-ray analysis.[17]

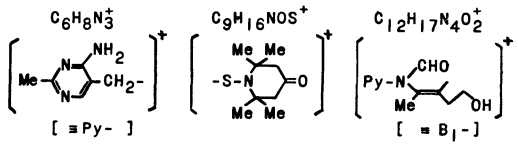

Chart 5

In the reaction of benzenethiols with the *N*-oxyl radical, the coupled products were isolated as sulfinamides, –S(=O)–N<, as has been described above.

On the other hand, the coupled product of the *N*-oxyl radical (I) with the *S*-radical (XVII) of thiamine was found to be a sulfenamide, –S–N<, (XX), which was considered to have been produced *via* a normal coupling intermediate, XXII, XXIII, or XXIV. The difference between the two cases will be reported on elsewhere.

Sulfenamides have been produced by Dunbar and Rogers by the following procedure.[18] Although the thiamine derivative in the RSO_2–S–R′ form could not be detected in our laboratory, the thiol-sulfonate, RSO_2–S–R, can be produced by the reaction of the *N*-oxyl radical (I) with the disulfide (XVIII). Therefore, it is possible to consider that

$$RSO_2\text{–}S\text{–}R' + 2\ HN\langle^{R''}_{R'''} \rightleftharpoons R'\text{–}S\text{–}N\langle^{R''}_{R'''} + RSO_2^{\ominus}\cdot{}^{\oplus}H_2N\langle^{R''}_{R'''}$$

the sulfenamide (XX) of thiamine was produced by such a process.

In order to exclude the possibility of the formation of the sulfenamide (XX) by such a course, and in order to prove the existence of the *S*-radical (XVII) of thiamine, it was felt necessary to carry out the reaction of XVII with a free radical other than the *N*-oxyl radical (I). The phenoxyl radical, the 2,6-di-*t*-butyl-4-methylphenoxyl radical (XXV), was chosen as the other free radical. As expected, the *S*-radical (XVII) of thiamine reacted with the phenoxyl radical (XXV) to give a coupled product XXVI, mp 197°C (from MeOH) and the disulfide XVIII under almost the same conditions as those used for the reaction of the *N*-oxyl radical (I) with the *S*-radical (XVII) of thiamine. The molecular formula of $C_{27}H_{40}N_4O_3S$, (XXVI) was assigned to the coupled product of the *S*-radical (XVII) with the phenoxyl radical (XXV) on the basis of the elemental analysis. The structures XXVI-a, XXVI-b, and XXVI-c were reasonable for the coupled products (XXVI), as Chart 6 shows.

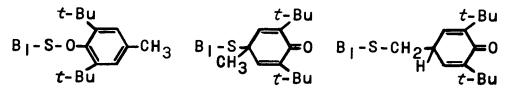

Chart 6

The UV spectrum of the product (XXVI) showed λ_{max}^{EtOH} 235 mμ (log ε 4.22) and 276 mμ (log ε 4.03) (shoulder) in an ethanol solution. The thiochrome test for the product (XXVI) was negaitve. After the reduction of the product (XXVI) with cysteine, the test was positive. Since a thiamine alkylsulfide with the partial structure of =C–S–C could not be

13) R. R. Williams, *Ergev. Vitamin u. Hormon Forsch.*, **1**, 256 (1938).

14) R. Stewart, "Oxidation Mechanisms," W. A. Benjamin, New York, N. Y. (1964), p. 85.

15) K. Murayama and T. Yoshioka, *Chem. Pharm. Bull. (Tokyo)*, **15**, 723 (1967).

16) W. Karrer, *Helv. Chim. Acta*, **20**, 369 (1937).

17) T. Tamura, S. Sato and T. Yoshioka, *Tetrahedron Letters*, **1969**, 547.

18) J. E. Dunbar and J. H. Rogers, *J. Org. Chem.*, **31**, 2842 (1966).

generally reduced with cysteine, the structures XXVI-b and XXVI-c may be excluded.[19]

Thus, the reaction of thiamine in the thiol form with potassium ferricyanide was understood to proceed *via* a free radical intermediate. In these results the existence of new types of thiamine derivatives was established.

Experimental

All the melting points were uncorrected.

The NMR spectra were obtained by means of a Varian A-60 NMR spectrometer, using tetramethylsilane as the internal standard at 32°C.

The mass spectra were obtained using a JEOL-JMS-OlS mass spectrometer with an ionizing voltage of 70 eV.

The paper chromatograms of thiamine derivatives were run with an *n*-butanol - acetic acid - water mixture (4 : 1 : 5) on Toyofilter paper No. 51, using the ascending technique, while spots were detected by spraying with a dilute Dragendorff reagent.

Materials. The benzenethiol (IV-c), *p*-nitro- (IV-a), *p*-chloro- (IV-b), and *p*-methylbenzenethiol (IV-d) used in this work were obtained from the Tokyo Kasei Kogyo Co., Ltd. Compound IV-a was twice recrystallized from dichloroethane after the solution of the corresponding potassium salt of IV-a had been treated with active charcoal at 5°C under a nitrogen atmosphere and then neutralized with a 10% hydrochloric acid solution to furnish an almost pure compound (IV-a). The other thiols, (IV-b), (IV-c), and (IV-d), were purified by distillation under diminished pressure. The *p*-methoxy derivative (IV-e) was prepared by the general method described in the literature.[20]

2,2,6,6-Tetramethyl-4-oxopiperidine-1-oxyl (I) was prepared by the oxidation of the corresponding amine (XII) by hydrogen peroxide in the presence of sodium tungstate and ethylenediaminetetraacetic acid (EDTA).[3]

General Procedure for the Reaction of *p*-Substituted Benzenethiols (IV) with 2,2,6,6-Tetramethyl-4-oxopiperidine-1-oxyl (I). Into a solution of 0.01 mol of IV in 15 m*l* of anhydrous chloroform, maintained at an internal temperature of −55——60°C with stirring under a dry nitrogen atmosphere, there was slowly added, drop by drop, a solution of 0.01 mol of I in 5 m*l* of anhydrous chloroform. After the addition was completed, the stirring was continued for 1 hr at −55°C; then the internal temperature was gradually raised to room temperature. The reaction mixture was allowed to stand at room temperature for 10 hr, and then the solvent was evaporated under diminished pressure at 30°C. The oily residues or crude crystals were chromatographed on 100 g of silica gel activated at 150°C for 2 hr. By using anhydrous *n*-hexane as the eluting solvent, *p*-substituted diphenyl disulfides (VI) were isolated. Then 1-(*p*-substituted benzenesulfinyl)-2,2,6,6-tetramethyl-4-oxopiperidines (X) (*ca.* 10%), 2,2,6,6-tetramethyl-4-oxopiperidine (XII) (*ca.* 35%), and 1-hydroxy-2,2,6,6-tetramethyl-4-oxopiperidine (XI) (*ca.* 6%) were eluted with benzene. Lastly, the salts of 2,2,6,6-tetramethyl-4-oxopiperidine with *p*-substituted benzenesulfinic acids (VII) was eluted with methanol. The disulfides (VI) were recrystallized from ethanol to give analytically-pure samples which were identical with authentic samples. The sulfinamides (X) were recrystallized from ethanol or ether to give analytically-pure samples which were identical with the normal samples produced by the reaction of *p*-substituted benzenesulfinyl chloride with 2,2,6,6-tetramethyl-4-oxopiperidine (XII) in dry triethylamine at 50°C. The sulfinamides (X) are listed in Table 2.

The benzenesulfinates of VII (*ca.* 20%) obtained from the last fraction were recrystallized from ethanol to give analytically-pure samples which were identical with authentic samples.

***N*-[(4-Amino-2-methyl-5-pyrimidyl)methyl]-*N*-{4-hydroxy-1-methyl-2-[(2,2,6,6-tetramethyl-4-oxopiperidino)thio]-1-butenyl}formamide (XX). [Abbr., *S*-(2,2,6,6-Tetramethyl-4-oxopiperidino)thiamine].** Into a mixture of 33.4 g (0.1 mol) of thiamine hydrochloride (XIV) and 17.0 g (0.1 mol) of the *N*-oxyl radical (I) in 100 m*l* of water, there was slowly added a solution of 12 g of sodium hydroxide in 50 m*l* of water at 5°C with vigorous stirring. After the reaction mixture was allowed to stand at 20°C for 30 min, a solution of 32.9 g (0.1 mol) of potassium ferricyanide in 100 m*l* of water was added at 5°C with vigorous stirring. The crude crystals which were separated after several hours were then filtered and washed with cold water three times. The crude product was recrystallized from wet

TABLE 2. *p*-SUBSTITUTED DERIVATIVES OF 1-BENZENESULFINYL-2,2,6,6-TETRAMETHYL-4-OXOPIPERIDINE

Compound	R	Mp (°C) (decomp.)		Analysis (%) Calcd C	H	N	S	Mw	Found C	H	N	S	Mw
X-a	$-NO_2$	179—180	$C_{15}H_{20}N_2O_4S$	55.55	6.17	8.64	9.88	324	55.35	6.20	8.60	9.92	328[c]
X-b	$-Cl$	163—164	$C_{15}H_{20}ClNO_2S$	57.42	6.34	4.47	10.21	313	57.38	6.51	4.44	10.09	345[a]
X-c	$-H$	116—117	$C_{15}H_{21}NO_2S$	64.51	7.53	5.02	11.47	279	64.30	7.58	5.01	11.41	286[a]
X-d	$-CH_3$	160—161	$C_{16}H_{23}NO_2S$	65.53	7.92	4.78	10.92	293	65.57	7.99	4.70	10.91	300[c]
X-e	$-OCH_3$	131—132	$C_{16}H_{23}NO_3S$	62.13	7.44	4.53	10.36	309	61.87	7.40	4.66	10.25	325[a]

Mw: VPO-method a: in an acetone solution, c: in a chloroform solution.

19) For the sake of less solubility, NMR spectrum of XXVI was not measured.

20) D. S. Tarbell and D. K. Fukushima, "Organic Syntheses," Coll. Vol. 3, p. 809 (1955).

methanol to afford colorless prisms with a mp of 179°C (monohydrate). The monohydrate was dried at 105—110°C for 10 hr under diminished pressure to give an analytically-pure sample (mp 179°C). Found: C, 57.78; H, 7.76; N, 16.29; S, 7.39%. Calcd for $C_{21}H_{33}N_5O_3S$: C, 57.91; H, 7.64; N, 16.08; S, 7.36%. UV λ_{max}^{EtOH} mμ (logε): 235 (4.17); 276 (3.77) (shoulder). IR cm^{-1} ($CHCl_3$ solution, 1.0 m/m NaCl, Grating):[21] ν_{O-H} 3620; $\nu_{as\ N-H}$ 3480; $\nu_{s\ N-H}$ 3335; $\nu_{C=O}$ 1715. NMR (τ) (in d-6 DMSO):[22] 2.08 (1H, singlet); 2.13 (1H, singlet). R_f (paper chromatography):[23] 0.70. The thiochrome test was negative, but became positive after reduction with cysteine.[24] High-resolution double-focussing mass spectra: molecular ion peak, *m/e* 435.230=$C_{21}H_{33}N_5O_3S$; large fragment peaks, *m/e* 122.073=$C_6H_8N_3^+$; *m/e* 186.098=$C_9H_{16}NOS^+$; *m/e* 249.136=$C_{12}H_{17}N_4O_2^+$.

The Hydrolysis of *S*-(2,2,6,6-Tetramethyl-4-oxopiperidino)thiamine (XX). A solution of 0.87 g (0.002 mol) of XX in 2 m*l* of methanol containing 0.5 g (0.005 mol) of concentrated hydrochloric acid (35% aq) was refluxed for 2 hr, and then the solvent was evaporated under diminished pressure. Scratching induced the oily residue to solidify upon the addition of absolute ethanol. The mixture thus obtained was filtered, and the solid was recrystallized from wet ethanol; mp 265—270°C (bubbling). Found: C, 34.25; H, 5.73; N, 26.48; Cl, 33.40%. Calcd for $C_6H_{12}N_4Cl_2$: C, 34.12; H, 5.69; N, 26.54; Cl, 33.65%. This compound was identical with authentic 4-amino-2-methyl-5-aminomethylpyrimidine·2HCl (XXI).[25] The filtrate was evaporated under diminished pressure. The oily residue, when scratched in ethyl acetate, gave a yellow semi-solid. After this semi-solid was filtered off, the filtrate was treated with fresh ethyl acetate to furnish a white precipitate which was then separated by filtration. To a suspension of this solid in ethyl acetate on a water bath, a small amount of ethanol was added until the solid dissolved. This solution was cooled at −30°C to give white crystals. This crystalline product was neutralized with potassium hydroxide in a methanol solution to give 2,2,6,6-tetramethyl-4-oxopiperidine (XII), which was identical with an authentic sample.

The Reduction of *S*-(2,2,6,6-Tetramethyl-4-oxopiperidino)thiamine (XX) with Benzenethiol. Into a mixture of 4.4 g (0.0101 mol) of XX and 4.4 g (0.0400 mol) of benzenethiol in 30 m*l* of methanol, 2.1 g of a 35% aqueous solution of hydrochloric acid (0.0101 mol) were slowly added, drop by drop, with stirring at 10°C. After the mixture had stood for 10 hr at 20°C, the solvent was evaporated under diminished pressure. The residue solidified upon being scratched in a small amount of ethanol (about 10 m*l*). As the solid was a mixture of thiamine hydrochloride (XIV) and diphenyl disulfide (VI), the solid was purified by fractional crystallization from ethanol. Thiamine hydrochloride monohydrate, mp 235°C was crystallized out first, and then the diphenyl disulfide, mp 61°C was obtained. These substances were identical with authentic samples. After the above filtrate was evaporated under diminished pressure, the residue, upon the addition of a small amount of ethyl acetate with scratching, furnished a small amount of a solid. The solids (crude VI and XIV) were removed, and then to the filtrate there was added a further amount of ethyl acetate. This solution deposited white crystals after standing for several hours. These crystals were treated with potassium hydroxide in methanol to afford 2,2,6,6-tetramethyl-4-oxopiperidine (XII), which was identical with an authentic sample.

***N*-[(4-Amino-2-methyl-5-pyrimidyl)methyl]-*N*-{4-hydroxy-2-[(2,6-di-*t*-butyl-4-methylphenoxy)thio]}-formamide (XXVI).** [*S*-(2,6-Di-*t*-butyl-4-methylphenoxy)thiamine]. To a solution of 6.7 g (0.0199 mol) of thiamine hydrochloride (XIV) in 50 m*l* of water, with the internal temperature maintained at 5°C by effective stirring under a nitrogen atmosphere, there was slowly added, drop by drop, a solution of 2.4 g (0.06 mol) of sodium hydroxide in 10 m*l* of water. After the addition was completed, stirring was continued for 1 hr at 20°C to afford the *S*-anion (XV) of thiamine (XIV), which was, for convenience, named the "-$S^{\ominus}$-solution." Separately, to a mixture of 4.4 g (0.020 mol) of 2,6-di-*t*-butyl-4-methylphenol in 20 m*l* of benzene and 4.4 g (0.110 mol) of sodium hydroxide in 20 m*l* of water, while controlling the internal temperature at 5°C by effective stirring (nearly an emulsion) under a nitrogen atmosphere, there was slowly added, drop by drop, a solution of 6.5 g (0.0198 mol) of potassium ferricyanide in 20 m*l* of water. After the addition was completed, stirring was stopped. The benzene-layer was carefully separated under a nitrogen atmosphere with a large pipette. Immediately, a portion of the benzene solution in the large pipette was slowly added, drop by drop, to the "-$S^{\ominus}$-solution" with effective stirring at 5°C (nearly an emulsion) under a nitrogen atmosphere; meanwhile, a solution of 6.6 g (0.0205 mol) of potassium ferricyanide in 20 m*l* of water was alternately added in an approximately equivalent amount to the above benzene solution. After this alternating addition was completed, the benzene layer was separated by means of a large pipette as soon as possible. Subsequently the benzene solution which separated was allowed to stand for several hours; the crude crystalline product was isolated and then recrystallized from methanol, mp 197°C. Found: C, 64.52; H, 8.04; N, 10.98; S, 6.26%. Calcd for $C_{27}H_{40}N_4O_3S$: C, 64.80; H, 8.00; N, 11.20; S, 6.40%. UV λ_{max}^{EtOH} mμ (logε): 234.5 (4.22); 276.5 (4.03). Thiochrome test: negative, but positive after reduction with cysteine.

21) These values were disagreement with the standard value in nonpolar dilute solution becuase of the measurement in concentrated chloroform solution.

22) K. Kotera, *Chem. Pharm. Bull. (Tokyo)*, **13**, 440 (1965).

23) S. Yoshida, *Yakugaku Zasshi (J. Pharm. Soc. Japan)*, **74**, 993 (1954).

24) O. Zima and K. Ritsert, *Z. Physiol. Chem.*, **267**, 210 (1941).

25) H. Hirano and H. Yonemoto, *Yakugaku Zasshi (J. Pharm. Soc. Japan)*, **76**, 230 (1956).

The authors wish to thank Professor Makoto Okawara of the Tokyo Institute of Technology for his valuable comments, Dr. Issei Iwai of these laboratories for his helpful guidance during the course of this work, and Mr. Susumu Higashida for his technical assistance.

BULLETIN OF THE CHEMICAL SOCIETY OF JAPAN VOL. 42 1948—1954 (1969)

Reaction of Xanthates with *t*-Amines. VI. The Reaction Mechanism

Hiroshi Yoshida

Department of Synthetic Chemistry, Faculty of Engineering, Shizuoka University, Hamamatsu

(Received September 11, 1968)

It was previously reported that xanthate reacted with *t*-amine to give quaternary ammonium salt at room temperature, and dithiolcarbonates at elevated temperatures. Precise study showed that these reaction products are formed by the following three reactions: the alkylation of *t*-amine with xanthate affords quaternary ammonium salt and the reaction of xanthate with quaternary ammonium salt yields dithiolcarbonate, while there is transesterification between thiolesters and quaternary ammonium salt. The rate constants and equilibrium constants of these reactions were calculated.

Xanthates are known to react with ammonia, prim-, and *s*-amines to give thioncarbamates and mercaptans:[1)]

$$ROCS_2R' + HNR''_2 \rightarrow ROCSNR''_2 + R'SH$$

However, no work has yet been reported on the reaction of xanthates with *t*-amines. In previous papers[2)] the present author has reported that xanthates react with *t*-amines at room temperature to give quaternary ammonium salts, and at elevated temperatures (70—80°C) to yield dithiolcarbonates and a small amount of ammonium salts. For example, *n*-propyl methylxanthate reacts with triethylamine thus:

$$MeOCS_2\,n\text{-Pr} + Et_3N \rightarrow Et_3\overset{\oplus}{N}(Me)\overset{\ominus}{S}COSMe + Et_3\overset{\oplus}{N}(Me)\overset{\ominus}{S}COS\,n\text{-Pr} + MeSCOSMe + MeSCOS\,n\text{-Pr} + n\text{-PrSCOS}\,n\text{-Pr}$$

The present paper will deal with the formation of the products obtained by the reaction of xanthates with *t*-amines by the following three successive reactions:

i) Alkylation of *t*-amines with xanthates (to give quaternary ammonium salts).

ii) The reaction of xanthates with the quaternary ammonium salts (to yield dithiolcarbonates).

iii) Transesterification between thiolesters (xanthates and/or dithiolcarbonates) and the quaternary ammonium salts.

Results and Discussion

t-Amine, a nucleophile, reacts with ordinary carboxylic esters to yield quaternary ammonium salts.[3),4)] Alkyl acylates are cleaved at their alkyl-

Table 1. Products of the reactions between thionesters and nucleophiles

Ester	Nucleophile	Reaction condition		Product
$MeOCS_2Me$[a)]	Et_3N	80°C	*	MeSCOSMe, $Et_3\overset{+}{N}(Me)\overset{-}{S}COSMe$ (7%)
	$Et_3\overset{+}{N}(Me)\overset{-}{S}COSMe$	80°C	*	MeSCOSMe, $Et_3\overset{+}{N}(Me)\overset{-}{S}COSMe$ (Recov.)
$EtOCS_2Et$	Et_3N	90°C	20 hr	EtSCOSEt, $Et_4\overset{+}{N}\overset{-}{S}COSEt$ (5%)
$MeOCS_2C_6H_5$[b)]	Et_3N	40°C	*	$MeSC_6H_5$
	$Et_3\overset{+}{N}(Me)\overset{-}{S}C_6H_5$	40°C	*	$MeSC_6H_5$, $Et_3\overset{+}{N}(Me)\overset{-}{S}C_6H_5$ (Recov.)
$MeOCSC_6H_5$	Et_3N	80°C	10 hr	$MeSCOC_6H_5$, $Et_3\overset{+}{N}(Me)\overset{-}{S}COC_6H_5$ (6%)
	$Et_3\overset{+}{N}(Me)\overset{-}{S}COC_6H_5$	80°C	5 hr	$MeSCOC_6H_5$, $Et_3\overset{+}{N}(Me)\overset{-}{S}COC_6H_5$ (Recov.)

Mole ratio 1:1, in each reaction no solvent was used.
* The reaction was quite facile at this temperature.
a) Ref. 2b.
b) Ref. 2c.

1) W. Walter and K. D. Bode, *Angew. Chem.*, **79**, 285 (1967).

2) a) H. Yoshida, S. Inokawa and T. Ogata, *Nippon Kagaku Zasshi (J. Chem. Soc. Japan, Pure Chem. Sect.)*, **86**, 950 (1965); b) *ibid.*, **86**, 1179 (1965); c) *ibid.*, **87**, 1209 (1966); d) *ibid.*, **87**, 1212 (1966).

3) a) B. Willstätter and W. Kahn, *Ber.*, **35**, 2757 (1902); b) L. P. Hammett and H. L. Pfluger, *J. Am. Chem. Soc.*, **55**, 4079 (1933); c) A. C. Pierce and M. M. Joullie, *J. Org. Chem.*, **27**, 3968 (1962).

4) J. H. Wernz, U.S. Pat. 3635100.

oxygen bond to afford the corresponding sulfides[5-7] by means of the action of mercaptides, while thiolacylates undergo ester interchange reactions[5,6] with mercaptides as a result of the nucleophilic attack of mercaptide ions on the carbonyl group. As has previously been reported,[2d] the alkylation of *t*-amines with xanthates resembled the Menschutkin reaction. At elevated temperatures xanthates react with *t*-amines to yield the rearranged dithiolcarbonates and a small amount of ammonium salts. As is shown in Table 1, not only xanthates but also thionesters give the rearranged thiolesters when they are treated with triethylamine or with the corresponding ammonium slats. The reactivity of alkyl thionesters decreased in the order: methyl$\gg$ ethyl$>$*n*-propyl with respect to the alkyl group. When thionesters were heated under similar conditions without any amines or ammonium salts, no detectable change was observed. These preliminary experiments indicated that ammonium salts formed in the initial step attack thionesters to give thiolesters.

Alkylation of *t*-Amines with Xanthates (to give Quaternary Ammonium Salts). It has been reported that the reaction of *t*-amines with ordinary esters yields quaternary ammonium salts at elevated temperatures.[3,4] Hammett and Pfluger[3b] have reported that the rates of the methylation of trimethylamine by various esters increase with an increase in the strength of the acid. However, no work has been reported on the reaction of *t*-amines and thion- or thiol-esters. In a previous paper,[2d] the kientics of the reaction of *S*-alkyl, -aryl, and -aralkyl xanthates with various amines in benzene has been reported (Table 3). The rates of the reaction of various esters with trimethylamine are compared with those of xanthates in Table 2. The rate constants (observed or extrapolated from higher temperatures) for the quaternization of trimethylamine with methylesters in benzene at 30°C are shown in Table 3. As the table shows, thionesters are more active than the corresponding oxygen-esters. The difference in activation energy between dimethylcarbonate and dimethylthioncarbonate, and that between methyl *p*-nitrobenzoate and methyl *p*-nitrothionbenzoate, are 5.2 and 3.6 kcal/mol respectively (Table 3); therefore, the activation energy of the alkylation of trimethylamine with an ordinary ester is 4—5 kcal/mol greater than the corresponding thionester which rearranges to form the thiolester. The summation of the bond energies shows that thion-thiol rearrangement should be exothermic, amounting to

Table 2. Rate constants of the alkylation of trimethylamine with esters in benzene

Ester	Temp. (°C)	k_2 (l/mol·hr)
$MeOCOC_6H_4NO_2$-(*p*)	100.0	0.0109
	110.0	0.0201
	120.0	0.0338
$MeOCSC_6H_4NO_2$-(*p*)	45.0	0.0421
	50.0	0.0575
	55.0	0.0850
$MeOCSC_6H_4Cl$-(*p*)	50.0	0.00985
$MeOCSC_6H_5$	45.0	0.00325
	50.0	0.00456
	55.0	0.00657
$MeOCSC_6H_4Me$-(*p*)	50.0	0.00251
$MeOCSC_6H_4OMe$-(*p*)	50.0	0.00171
MeOCSOMe	25.0	0.0149
	30.0	0.0224
	34.9	0.0332
MeOCOOMe	100.0	0.00749
	110.0	0.0144
	120.0	0.0296
MeSCOSMe	120.0	*
$MeSCOC_6H_5$	120.0	*

* No detectable reaction was observed.

Table 3. Rate constants of the alkylation of trimethylamine with esters in benzene at 30°C

Ester	k_2 (l/mol·hr)	Relative rate	E_a (kcal/mol)	ρ (°C)
MeOCS·SMe[a]	0.0731	1	12.1	
MeOCS·OMe	0.0112[c]	1/6.5	14.6	
MeOCO·OMe[b]	0.0000078[c]	1/9400	19.8	
MeOCS·SC_6H_5[a]	0.353	4.8		+1.65 (30)
MeOCS·$SCH_2C_6H_5$[a]	0.129	1.8		+0.82 (30)
$MeOCSC_6H_5$[b]	0.00119	1/61	13.1	+1.44 (50)
$MeOCSC_6H_4NO_2$-(*p*)[b]	0.0153	1/4.8	12.9	
$MeOCOC_6H_4NO_2$-(*p*)[b]	0.0000652	1/1120	16.5	

a) Ref. 2d.
b) Rate constant extrapolated from higher temperatures in Table 2.
c) The half value of the observed rate constant.

5) W. R. Vaughan and J. B. Baumann, *J. Org. Chem.*, **27**, 739 (1962).
6) G. S. Sasin, P. R. Schaeffer and R. Sasin, *ibid.*, **22**, 1183 (1957).
7) J. C. Sheehan and G. D. Daves, Jr., *ibid.*, **29**, 2006 (1964).

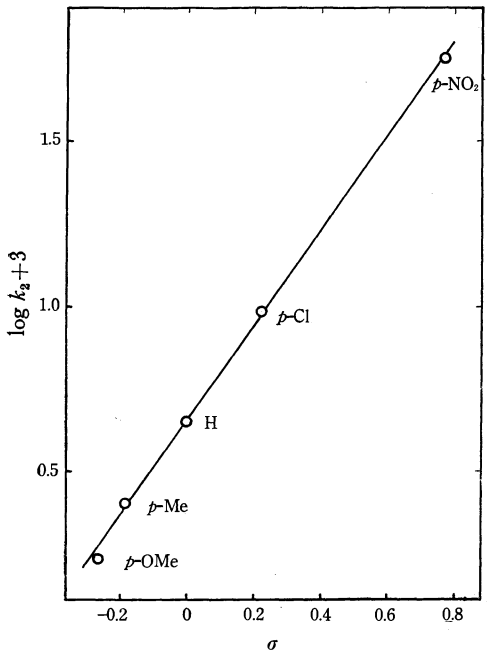

Fig. 1. Hammett plot of methyl thionbenzoates with trimethylamine in benzene at 50°C.

nearly 20 kcal/mol.[8] O'Connor and Nace[9a] have reported that the activation energies for the pyrolysis of the ethylcarbonate and methylxanthate of cholesterol are 41.0 and 32.9 kcal/mol respectively. This difference in activation energy (8.1 kcal/mol) is in good agreement with that between dimethyl carbonate and methyl methylxanthate for alkylation (7.7 kcal/mol. Table 3). The substitution of an electron-accepting group for the carbonyl carbon of the esters leads to an increase in the rate of alkylation (positive ρ values in Table 3). The ρ factor is +0.467 for the pyrolysis of *S*-benzyl cholesterylxanthates,[9a] and +0.82 for the alkylation of trimethylamine with *S*-benzyl methylxanthates. The difference may be due to the fact that the former is a cyclic *cis* intramolecular elimination reaction,[9c] and the latter, an S_N2. The smaller reactivity of dimethyl thioncarbonate than that of methyl methylxanthate may be due to the electron-releasing resonance effect of the methoxy group.[10]

Thus, the greater reactivity of xanthates may be based on the decreased activation energy due to the electron-accepting mercapto group and to thion-thiol rearrangement.

The Reaction of Methyl Methylxanthate (I) with Tetramethyl Ammonium Dithiocarbonate $Me_4\overset{\oplus\ominus}{N}SCOSR$ (II). The reaction product between I and trimethylamine gave no rearranged product in benzene. On the other hand, it gave dimethyldithiolcarbonate under homogeneous conditions in dimethylformamide (DMF) or dimethylsulfoxide (DMSO), even at room temperature. The rate constants of the following reactions in DMF at 30°C were determined by measuring the rates of the disappearance of I (the transesterification, described in the following section, was disregarded):

$$Me_3N + MeOCS_2Me \xrightarrow{k_2} Me_4\overset{\oplus\ominus}{N}SCOSMe \quad (1)$$

$$Me_4\overset{\oplus\ominus}{N}SCOSMe + MeOCS_2Me \xrightarrow{k_2'} Me_4\overset{\oplus\ominus}{N}SCOSMe + MeSCOSMe \quad (2)$$

The rate equations are:

$$d[X]/dt = -k_2[X][A] - k_2'[S][X]$$

$$d[S]/dt = k_2[X][A]$$

The concentrations are related thus:

$$[S] + [A] = [A_0]$$

$$[S] + [X] + [T] = [X_0]$$

where [X], [A], [S], and [T] indicate the concentrations of I, trimethylamine, II (R=Me), and dimethyl dithiolcarbonate respectively, and where $[A_0]$ or $[X_0]$ indicate the initial concentration. Put $[X_0]=[A_0]$; then, upon integration:

$$\left.\begin{aligned} x &= [(\kappa-1)/\kappa]\alpha + (1/\kappa)\ln\alpha + 1/\kappa \\ \tau &= \int_\alpha^1 \frac{d\alpha}{\alpha[(\kappa-1)\alpha + \ln\alpha + 1]} \\ \tau &= -\ln x \qquad (\kappa = 1), \end{aligned}\right\} \quad (3)$$

where $\tau=[A_0]k_2't$, $\kappa=k_2/k_2'$, $x=[X]/[X_0]$, and $\alpha=[A]/[A_0]$. x and τ, as functions of α for various κ's, can be calculated by Eq. (3); and x plotted against τ in Fig. 3.

The reaction (2) is pseudo-first-order, and the apparent first-order rate constant is proportional to the concentration of II (R=Me) (Fig. 2). The slope of the line gives k_2'. Equimolar reactions of I with trimethylamine proceed; data typical of those shown in Table 8 are plotted in Fig. 3, where they give $\kappa=0.19$. The results, summarized in Table 4, indicate that, toward I, $MeSCOS^-$ is a stronger nucleophile than trimethylamine by a factor of 5. As has been shown previously (Table 1), xanthates react with triethylamine to yield dithiolcarbonates at elevated temperatures. At lower temperatures crystalline quaternary ammonium salts have little reactivity, while at elevated temperatures they melt and dissolve in the reagent and react with xanthates. Trimethylamine reacts

8) C. H. DePuy and R. W. King, *Chem. Revs.*, **60**, 431 (1960).

9) a) G. L. O'Connor and H. R. Nace, *J. Am. Chem. Soc.*, **74**, 5454 (1952); b) *ibid.*, **75**, 2118 (1953); c) R. F. W. Bader and A. N. Bourns, *Can. J. Chem.*, **39**, 348 (1961).

10) A. W. Baker and G. H. Harris, *J. Am. Chem. Soc.*, **82**, 1923 (1960); C. C. Price and S. Oae, "Sulfur Bonding," Ronald Press, New York (1962), p. 10.

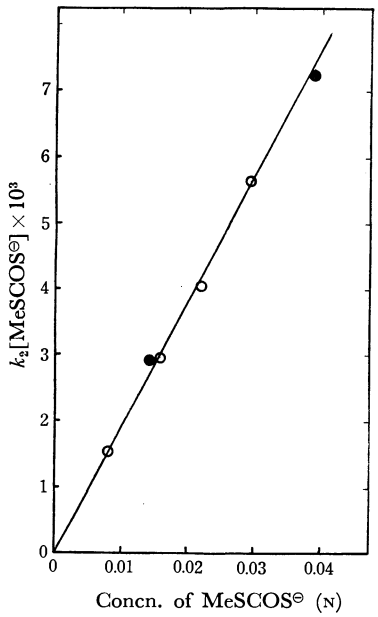

iFg. 2. The relation between the appararent first-order rate constant and concentration of I for reaction (2).

○: $Me_4\overset{+}{N}\overset{-}{S}COSMe$ ●: $Et_3\overset{+}{N}(Me)\overset{-}{S}COSMe$

30 times faster with I in DMF than in benzene (Table 4). This increase in rate agrees with the reported value[11] for the Menschutkin reaction (25.6). The rearrangement of thionesters to thiol-

Table 4. Second-order rate constants of the reaction of methylxanthate with nucleophiles

Nucleophile	Solvent	Temp. (°C)	Rate const. (l/mol·min)	Ratio
Me_3N	Benzene	30	k_2 0.0012	1
Me_3N	DMF	30	k_2 0.036	30
II (R=Me)	DMF	30	k_2' 0.186	155

esters has been reported by many workers, almost all of them concerned with intramolecular reactions (for example, the Schönberg rearrangement[12] or the thermal rearrangement of xanthates[13]). It was confirmed that the reactions of thionesters (such as xanthates and thionbenzoates) with *t*-amines to form thiolesters are second-order and that the initially-formed thiolate ions (monoalkyl dithiolcarbonate and thiolbenzoate ions) react as strong nucleophiles with thionesters to give rearranged thiolesters.

Transesterification between Thiolesters and II. It is well known that transesterification occurs when an ester is heated with alcohol in the presence of acid or base. Although some works[5-7,14] have reported the transesterification of thiolesters, the kinetics or equilibrium has not been investigated. The reaction between II and thiolesters in benzene (heterogeneous conditions) produced no detectable change, but the mixture of II and thiolesters in DMF or DMSO came to equilibrium in a few

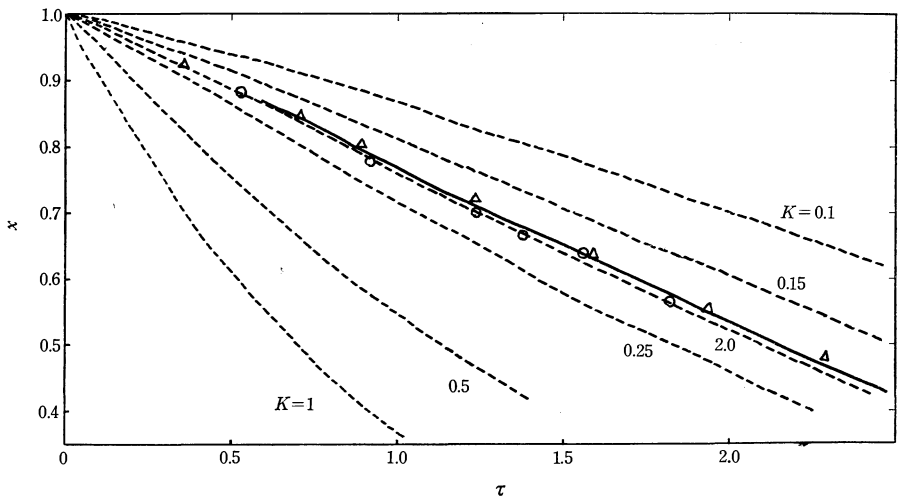

Fig. 3. The relation between τ and x.
△: $[A_0]=[X_0]=0.0466$N ○: $[A_0]=[X_0]=0.0344$N

11) E. L. Eliel, "Steric Effects in Organic Chemistry," ed. by M. S. Newman, John Wiley & Sons Inc., New York (1956), p. 70.

12) H. R. Al-Kajimi, D. S. Tarbell and D. Plat, *J. Am. Chem. Soc.*, **77**, 2479 (1955); D. H. Powers and D. S. Tarbell, *ibid.*, **78**, 70 (1956).

13) T. Taguchi, Y. Kawazoe, K. Yoshihara, H. Kanayama, M. Mori, K. Tabata and K. Harano, *Tetrahedron Letters*, **1965**, 2717.

14) H. Yoshida, S. Inokawa and T. Ogata, This Bulletin, **39**, 2055 (1966).

Table 5. Reaction products of the alkylthiolcarbonates with II

Ammonium salt	Thiol ester R′	Thiol ester X	Mole ratio	Reaction condition	Products (mol%) II R	II R′	X RSCSR	X RSCSR′	X R′SCSR′	K
II (R=Me)	Et	O	2 : 1	a	56	44	19	50	31	0.621
II (R=Et)	Me	O	2 : 1	a	43	57	30	51	19	0.578
II (R=Me)	Et	S	2 : 1	a	55	45	20	49	31	0.641
II (R=Et)	Me	S	2 : 1	a	45	55	29	50	21	0.658
II (R=Me)	*n*-Pr	O	2 : 1	a	58	42	18	49	34	0.515
II (R=Me)	*i*-Pr	O	2 : 1	a	62	38	14	50	36	0.380
II (R=Me)	*s*-Bu	O	2 : 1	a	67	33	10	51	39	0.316
$Me_4NSCSSMe$	Et	O	2 : 1	b						
II (R=Me)	*n*-$PrOCS_2Et$		1 : 1	a	56	44	*n*-$PrOCS_2Me$(45)		*n*-$PrOCS_2Et$(55)	0.610
EtSK	*n*-$PrOCS_2Me$		1 : 1	a			*n*-$PrOCS_2Me$(44)		*n*-$PrOCS_2Et$(56)	

a) 50°C for 15 min.
b) No detectable change was observed after 12 hr at 50°C.

minutes at room temperature. Table 5 shows that the amount of ammonium salts produced depends on thiol groups and not on the structure of the thiolesters (*i.e.*, xanthate, trithiocarbonate, and dithiolcarbonate).

The following equilibrium can be derived from Table 5:

$$Me_4\overset{\oplus\ominus}{N}SCOSMe + (Ester)\text{-}SR \rightleftarrows Me_4\overset{\oplus\ominus}{N}SCOSR + (Ester)\text{-}SMe$$

$$K = [Me_4\overset{\oplus\ominus}{N}SCOSR][(Ester)\text{-}SMe]/[Me_4\overset{\oplus\ominus}{N}SCOSMe][(Ester)\text{-}SR]$$

The slope of the straight line obtained by plotting $\log K$ *vs.* σ^* for R ($\rho^*=+2.2$) is shown in Fig. 4. The positive ρ^* value indicates that the equilibrium of the reaction depends on the relative basicities of $RSCOS^-$.[15]

The explanation that these reaction products are formed by an S_N2 attack of $RSCOS^-$ on the carbonyl carbon of the thiolester seems improbable, since the reaction of dialkyl trithiocarbonate (X=S) and II gave no trithiocarbonate ion ($RSCS_2^-$), while this ion should be formed in any reaction by mechanism (A) or (B):

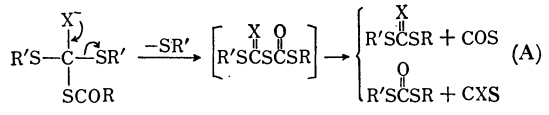

(A)

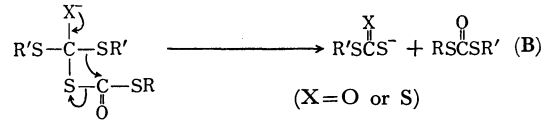

(B)

The reaction of methyl *n*-propylxanthate with potassium ethylmercaptide was found to yield ethyl *n*-propylxanthate by ester interchange under similar conditions (Table 5). Thus, it seems plausible that the mercaptide ion initially formed by the reaction (C):[16]

$$RSCOS^{\ominus} \rightleftarrows RS^{\ominus} + COS \qquad (C)$$

attacks the carbonyl carbon of the thiolesters to yield transesterification products. Thiolesters do not react with monoalkyl trithiocarbonate. The

15) Although free acids RSCOSH are not known, their pK_a values should give postive ρ^* for R groups considering the data of xanthic acids [V. Hejl and J. Pecher, *Chem. Zvensti*, **21**, 261 (1967); *Chem. Abstr.*, **67**, 85514 (1967); H. Majima, *Chem. Abstr.*, **56**, 2201f (1962)] and mercaptans [D. L. Yabroff, *Ind. Eng. Chem.*, **32**, 257 (1940); M. M. Kreevoy, E. T Happer, R. E. Duvall, H. S. Wilgus, III, and L. T. Ditsch, *J. Am. Chem. Soc.*, **82**, 4899 (1960)].

16) Although in a literature [Houben-Weyl "Methoden der Organischen Chemie" 9, Georg Thieme Verlag, Stuttgart (1955), p. 807] the salt is described to be unknown, the treatment of potassium ethylmercaptide with carbonyl sulfide in DMF or in benzene was found to yield $EtSCOS^-K^+$. The structure of the salt was determined by VPC analysis of the reaction product [EtSCOSMe] with methyl iodide. This finding also seems to suggest reaction (C).

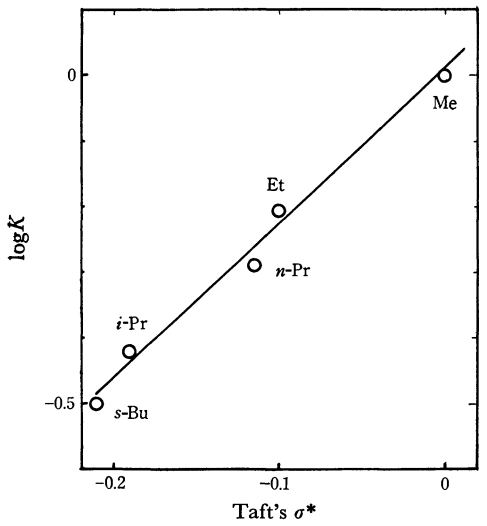

Fig. 4. The relation between Taft's σ^* and log K.

resonance energy[17] calculated by the author leads to the conclusion that the stability of the trithiocarbonate ion is greater than that of the dithiolcarbonate ion (II).

17) LCAO MO calculation of carbonate ions were carried out according to the procedure of M. J. Janssen [*Rec. Trav. Chim.*, **79**, 1066 (1960)] using following parameters.

	Coulomb integral (α_x)	Resonance integral (β_{C-x})
-S-	$\alpha+\beta$	0.6β
=S	$\alpha+0.5\beta$	
-O-	$\alpha+2.5\beta$	1.2β
=O	$\alpha+1.0\beta$	

The procedure was repeated until consistent result was obtained. The results was as follows:

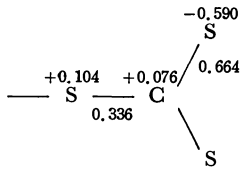

RE = 0.950β

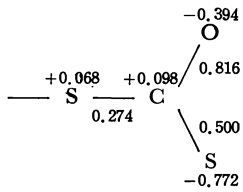

RE = 0.220β

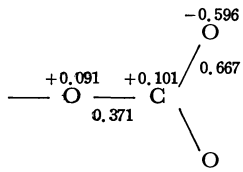

RE = 1.860β

Experimental

Materials. The newly-prepared compounds are shown in Table 6, together with the previously-reported ones.[2]

Kinetic Determination in Benzene. The accurately-weighed ester was dissolved in dry benzene. The concentration of trimethylamine in benzene was determined by titration.[18] The solution (the initial concentrations of the reagents were 0.2—0.5N) was sealed in stoppered test tubes (reactions at 25—35°C) or in ampoules (above 45°C). After appropriate times, ampoules were removed from the bath and cooled; the ammonium salts produced were collected on a glass filter, washed with ether, and then weighed. First-order rate constants with respect to esters and trimethylamine are shown in Tables 1 and 2.

The structure and purity of ammonium salts were tested as previously.[2] The newly-prepared ammonium salts are shown in Table 6. The physical constants of the *S*-methylesters obtained by the reaction of ammonium salts with methyl iodide agreed with those of authentic samples (Table 6).

Kinetic Determination in DMF. The concentrations of trimethylamine in DMF were determined by potentiometric titration,[18] while the solutions of methyl methylxanthate (I) and ammonium salts were prepared by dissolving accurately-weighed amounts of the solute in dry DMF. The solutions of ammonium salt are not stable at elevated temperatures, exhibiting a slight yellow color in a few hours at 50°C. Thus, the solutions should be prepared just before use.

The reaction rate was determined spectrometrically by measuring the rate of the disappearance of I (λ_{max} =275.5 mμ, ε=9020, ethanol). In the reaction, dimethyl dithiolcarbonate (λ_{max}=248 mμ, ε=4420, ethanol) was obtained in 60—80% yields. The reaction of I with tetramethyl ammonium dithiocarbonate $Me_4NSCOSR$ (II) was of a pseudo-first-order, and the rate constants were proportional to the concentration of II (R=Me) (Fig. 2). A typical example is shown in Table 7.

The rate constant, k_2, for the reaction of trimethylamine and I in DMF is obtained by the use of the curves shown in Fig. 3, which are drawn from data typical of those in Table 8. The data are listed in Table 4.

Determination of Equilibrium Constants. An equimolar mixture of II and thiolester (accurately weighed) in DMF (a 10% solution) was sealed in a stoppered test tube filled with nitrogen, and then left for 15 min at 50°C to let it come to equilibrium. Then the mixture was divided into two equal parts. To one part was added a large amount of a mixture of dry benzene and ether 1:1 (v/v), and the resulting precipitates (ammonium salts) were washed thoroughly with the solvent. The composition of the precipitates was determined by VPC after treating them with methyl iodide. The second part was poured into cold water and extracted with ether. The ethereal extract (thiolesters), after having been dried over sodium sulfate, was analyzed by VPC. The ratio of the products is listed in Table 5.

18) C. W. Pifer and E. G. Wallish, *Anal. Chem.*, **24**, 300 (1952).

Table 6. Physical constants of esters and tetramethyl ammonium salts

Ester	Bp °C/mmHg [mp °C]	n_D (°C)	Ref.
$MeOCSC_6H_5$	120/22	1.6118 (20)	a
$MeSCOC_6H_5$	127/18	1.5855 (20)	b
$MeOCSC_6H_4Cl$-(*p*)	[48—49]		b
$MeSCOC_6H_4Cl$-(*p*)	137—138/14 [21]		b
$MeOCSC_6H_4NO_2$-(*p*)	[71—73]		c
$MeSCOC_6H_4NO_2$-(*p*)	[97—98]		d
$MeOCSC_6H_4Me$-(*p*)	136—137/22	1.6068 (20)	e
$MeSCOC_6H_4Me$-(*p*)	133—135/13	1.5837 (20)	b
$MeOCSC_6H_4OMe$-(*p*)	[46—46.5]		b
$MeSCOC_6H_4OMe$-(*p*)	[43]		f
MeOCSOMe	119—120	1.4624 (25)	g
i-PrSCOS*i*-Pr	96.5—98/18	1.5100 (25)	h
s-BuSCOS*s*-Bu	124—125/17	1.5028 (23)	i
$Me_4\overset{+}{N}\overset{-}{S}COC_6H_5$	[113—114]		
$Me_4\overset{+}{N}\overset{-}{S}COC_6H_4Cl$-(*p*)	[153—155]		
$Me_4\overset{+}{N}\overset{-}{S}COC_6H_4NO_2$-(*p*)	[201—202]		
$Me_4\overset{+}{N}\overset{-}{S}COC_6H_4Me$-(*p*)	[144—145]		
$Me_4\overset{+}{N}\overset{-}{S}COC_6H_4OMe$-(*p*)	[126—129]		
$Me_4\overset{+}{N}\overset{-}{O}COC_6H_4NO_2$-(*p*)	[250—252]		

a) M. Matsui, *Mem. Coll. Sci. Kyoto*, **1**, 285 (1908).
b) R. Mayer, S. Scheithauser and D. Kunz, *Chem. Ber.*, **99**, 1393 (1966).
c) Found: C, 48.26; H, 3.39; N, 6.97%. Calcd for $C_8H_7NO_3S$: C, 48.72; H, 3.58; N, 7.10%.
d) A. M. Khaletskii and A. M. Yanovitskaya, *Zhur. Obschei Khim.*, **19**, 1193 (1949); *Chem. Abstr.*, **44**, 1952 (1950).
e) Y. Sakurada, *Mem. Coll. Sci. Kyoto*, [A] **10**, 73 (1927).
f) H. Gross and G. Mattey, *Chem. Ber.*, **97**, 2606 (1964).
g) M. Delepine, *Compt. rend.*, **150**, 878 (1910).
h) Found: C, 46.61; H, 8.27%. Calcd for $C_7H_{14}OS_2$: C, 47.15; H, 7.91%.
i) Found: C, 52.25; H, 9.16%. Calcd for $C_9H_{18}OS_2$: C, 52.38; H, 8.79%.

Table 7. The reaction of I with II (R=Me) in DMF at 30°C

Time (min)	Abs ($\lambda_{max}^{275.5}$)	Abs (λ^{248})	k (min^{-1})
0	1.046	0.044	
100	0.708	0.152	0.00405
120	0.658	0.167	0.00403
175	0.538	0.203	0.00401
230	0.441	0.235	0.00396
305	0.330	0.271	0.00404
365	0.251	0.281	0.00409
1440	0.034	(0.232)	

13.7 mg (I), 20.0 mg (II) (R=Me) in 5 m*l* DMF. Absorbance of 20 μl aliquot diluted with 5 m*l* ethanol in a 1 cm cell.

Table 8. The reaction of I with trimethylamine in DMF at 30°C

Time (min)	Abs ($\lambda^{275.5}$)
0	0.783
40	0.724
80	0.670
100	0.633
140	0.569
180	0.502
220	0.437
260	0.382
300	0.329
330	0.280
1740	0.006

$[A_0]=[X_0]=0.0466$N in DMF. Absorbance of 15 μl aliquot diluted with 10 m*l* of ethanol in a 1 cm cell.

The author wishes to express his gratitude to Professor Ryōzō Gotō of Kyoto University and Professor Saburo Inokawa and Dr. Tsuyoshi Ogata of Shizuoka University for their valuable discussions and encouragement throughout the work.

BULLETIN OF THE CHEMICAL SOCIETY OF JAPAN VOL. 42 1955—1958 (1969)

Reactions of Cycloalkanone Oxime *p*-Toluenesulfonates

Tadashi SATO and Hirohisa WAKATSUKA

Department of Applied Chemistry, Waseda University, Shinjuku-ku, Tokyo

(Received September 24, 1968)

The reactions of cyclohexanone and cyclopentanone oxime *p*-toluenesulfonates were studied. It was found that cyclohexanone oxime *p*-toluenesulfonate (IIIa) afforded a tetrahydroazepine derivative (Va), while cyclopentanone oxime *p*-toluenesulfonate (X) afforded *δ*-valerolactam *p*-toluenesulfonate (XIII), when both compounds were heated in benzene.

The rearrangement of ketoxime *p*-toluenesulfonates (I) into *N*-*p*-toluenesulfonamides (II) has been known as one type of Beckmann rearrangement and has been extensively studied. The rearrangements of cyclohexanone and cyclopentanone oxime *p*-toluenesulfonates have been reported by Heldt[1] and by Grob *et al.*[2] Cyclohexanone oxime *p*-toluenesulfonate (IIIa) is thermally unstable and defragnates at room temperature, particularly when its purity is not high. In connection with our studies of pyrolysis, we carried out reactions with these compounds and obtained results different from those reported.

Heldt reported that when IIIa was left standing in dry chloroform at 25°C for one year, it yielded a compound (named Compound A)to which the structure IV could be assigned. He showed that Compound A melted at 124.6—125°C, and had strong bands at 1710 and 1640 cm^{-1} in its infrared spectrum.

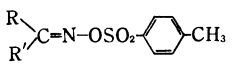

I

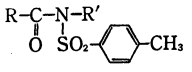

II

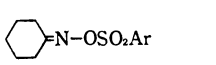

IIIa: Ar=H_3C-

b: Ar=

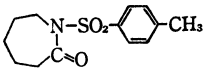

IV

We refluxed IIIa in dry benzene for 3 hr, and obtained in a 54% yield a compound (named Compound B) which showed characteristics similar to those of Compound A.*1 Compound B melted at 124°C and had strong bands at 1720 and 1640 cm^{-1} in its infrared spectrum. However, Compound B was confirmed to be 6-(3,4,5,6-tetrahydro-2*H*-azepin-7-ylamino)-hexanoic acid *p*-toluenesulfonate (Va) by the following evidence. The *p*-toluenesulfonyl moiety was assumed to be combined with the tetrahydroazepine moiety through salt-type linkage, not through sulfonamide-type linkage as is the case for the structure IV, because *p*-toluenesulfonic acid was immediately isolated as an addition compound with 2,4-dinitrophenylhydrazine (DNPH), upon the addition of a DNPH reagent[3] to Compound B. When Compound B was dissolved in 18% hydrochloric acid and the solution was concentrated *in vacuo* at room temperature, hydrochloride Vb crystallized out. Vb showed infrared bands at 1720 and 1640 cm^{-1} and had a pK_a value of 4.45. Furthermore, Vb was identical with the authentic sample prepared from *ε*-caprolactam and phosgene.[4] From the reaction

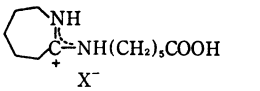

X^-

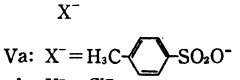

Va: X^-=H_3C-

b: X^-=Cl^-

c: X^-=

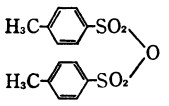

VI

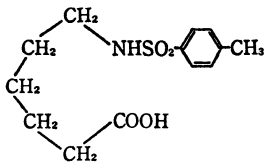

VII

1) W. Z. Heldt, *J. Am. Chem. Soc.*, **80**, 5880 (1958).

2) C. A. Grob, H. P. Fischer, W. Raudenbusch and J. Zergenyi, *Helv. Chim. Acta*, **47**, 1003 (1964).

*1 The identity of Compounds A and B was not established because neither Compound A nor its complete spectrum was available. The differences in elemental analyses between the two compounds were: C, 0.01—0.73; H, −0.02—0.07; N, 0.50—0.52%.

3) R. L. Shriner, R. C. Fuson and D. Y. Curtin, "The Systematic Identification of Organic Compounds," 4th ed., John Wiley & Sons, New York, N. Y. (1956), p. 219.

4) H. R. Meyer, *Kunststoffe-Plastics*, **3**, 160 (1956); *Chem. Abstr.*, **52**, 11781f (1958).

mixture of IIIa in benzene we isolated as by-products ε-caprolactam, *p*-toluenesulfonic anhydride (VI), and a compound with a mp of 123°C (named Compound C). Compound C showed only one absorption band at 1685 cm^{-1}, in the carbonyl region in the infrared spectrum; it was thus obviously different from Compounds A and B. The structure IV was assigned to Compound C because it was identical with the product obtained by the thermal dehydration of 6-(*p*-toluenesulfonamido)-hexanoic acid (VII).

The same results were obtained when chloroform or carbon tetrachloride was used in place of benzene as the solvent for the reaction of IIIa.

When cyclohexanone oxime benzenesulfonate (IIIb) was refluxed in benzene for 3 hr, a benzenesulfonate derivative, Vc, corresponding to Va was obtained. Vc was converted into the hydrochloride Vb by treating it with 18% hydrochloric acid. Diphenyl sulfone (VIII) was isolated in this case as the sole by-product. It was found that benzenesulfonyl peroxide (IX), when refluxed in benzene, afforded VIII. These facts induced us to suggest that the reaction IIIb→Vc proceeded through a

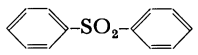

VIII

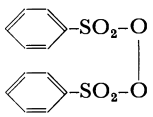

IX

radical fission in IIIb, although no further experimental evidence was obtained. The same type of reaction as those of IIIa→Va and IIIb→Vc has been reported by Oxley and Short[5] with benzophenone oxime *p*-toluenesulfonate.

The reaction of cyclopentanone oxime *p*-toluenesulfonate (X) was studied next. Grob and his coworkers[2] reported that when X was allowed to stand for 3.5 hr at 23°C in 80% ethanol containing an equivalent amount of triethylamine, it yielded δ-valerolactam and *N*-*p*-toluenesulfonyl-δ-valerolactam (XI, mp 144—145°C). Heldt[1] reported that the heating of X in glacial acetic acid at 35°C for 2 hr yielded a compound with a mp of 151—152°C (named Compound D); he assigned the structure XII to this compound.

When X was refluxed in benzene for 3 hr, an oil was obtained which, on standing in the air, crystallized to give a compound with a mp of 147°C (named Compound E). Compounds D and E were found to be identical by synthesizing Compound D according to the method reported by Heldt. It was found, however, that the assignment of the structure XII to Compound D, made by Heldt, was unacceptable, because the authentic compound with the structure XII (mp 92°C, named Compound F) which was prepared from 5-aminopentanoic acid

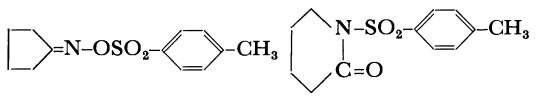

X XI

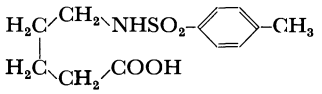

XII

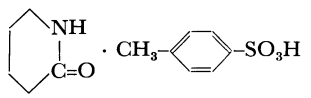

XIII

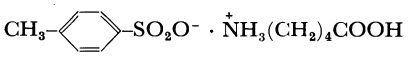

XIV

and *p*-toluenesulfonyl chloride was different from Compounds D and E*[2]. The structure XII for Compound F was confirmed by the fact that Compound F afforded XI (mp 144—145°C), upon thermal dehydration under the same conditions as those used for the dehydration of VII into IV. The infrared spectrum of XI was identical with that of IV.

It was concluded that the structure XIII should be assigned to Compounds D and E, because Compound E was prepared by just mixing δ-valerolactam and *p*-toluenesulfonic acid in acetone and afforded XIV on hydrolysis.

Reactions with other types of ketoxime *p*-toluenesulfonates are now being studied.

Experimental

Reaction of Cyclohexanone Oxime *p*-Toluenesulfonate (IIIa) in Benzene. A solution of cyclohexanone oxime *p*-toluenesulfonate (IIIa)[1] (5 g) in 50 m*l* of dry benzene was refluxed for 4 hr. The solution gradually turned yellow and then brown. The benzene was then evaporated *in vacuo*, and water was added. 0.3 g of a solid material was filtered out (solid: named M), and the filtrate was concentrated *in vacuo*. Acetone was added, and the solution was left to stand overnight. A solid material appeared which was recrystallized from a mixture of dioxane and 2-methoxyethanol to afford 2 g of pure Va, mp 124°C.

Found: C, 57.16; H, 7.57; N, 7.12%. Calcd for $C_{19}H_{30}O_5N_2S$: C, 57.29; H, 7.54; N, 7.04%.

IR spectrum (cm^{-1}): 1720 (s), 1640 (vs), 1217 (vs), 1160 (vs).

When a small amount of Va was added to the 2,4-dinitrophenylhydrazine reagent (DNPH),[3] an addition compound of DNPH and *p*-toluenesulfonic acid, mp

5) P. Oxley and W. F. Short, *J. Chem. Soc.*, **1948**, 1514.

*2 Heldt[1] reported that when δ-valerolactam was treated successively with 95% sulfuric acid, with aqueous sodium hydroxide, and with *p*-toluenesulfonyl chloride, crystals with a melting point of 143.5—144.5°C resulted. To these crystals he assigned a structure of XII in the monohydrated form. We followed his method, but we obtained Compound F, mp 92°C.

213°C, was obtained. This material did not show a melting point depression on admixture with an authentic sample of the addition compound.

The solid M obtained above was immediately recrystallized from ligroin to afford 0.2 g of crystals; mp 127°C (mother liquor: named N). The compound was found to be identical with the authentic sample of *p*-toluenesulfonic anhydride (VI)[6] from a study of its infrared spectrum and by a mixed-melting-point determination. The mother liquor N was then evaporated *in vacuo*, and water was added. The solution was kept overnight at room temperature, and the water was evaporated *in vacuo*. Ligroin was added to the residue and a small amount of an insoluble material (*p*-toluenesulfonic acid) was removed with charcoal. The ligroin was evaporated *in vacuo*, and a solid material was obtained. The material was recrystallized from ligroin to afford a compound with a mp of 121°C. The compound was found to be *N*-*p*-toluenesulfonyl-ε-caprolactam (IV) by a study of its infrared spectrum and by a mixed-melting-point determination with the authentic sample.

The Conversion of Va into the Hydrochloride Vb. A solution of Va (1 g) in 10 m*l* of 18% hydrochloric acid was concentrated *in vacuo* at temperature below 40°C, and then acetone was added to the residue. The solid material which appeared was recrystallized from a mixture of dioxane and 2-methoxyethanol to afford Vb, mp 150°C. This compound was found to be identical with the authentic sample of Vb by a study of its infrared spectrum and by a mixed-melting-point determination.

6-(3,4,5,6-Tetrahydro-2*H*-azepin-7-ylamino)-hexanoic Acid Hydrochloride (Vb). This compound was prepared in the following modification of a method described in the literature.[4] To a stirred solution of phosgene (4 g) in 10 m*l* of chloroform, there was added, drop by drop, ε-caprolactam (4.5 g) in 10 m*l* of chloroform at a temperature between 30°C and 40°C. After the addition was complete, the reaction mixture was stirred for an additional 3 hr at a temperature between 30°C and 40°C, and then the chloroform was evaporated *in vacuo*. When a small amount of ether was added, a solid appeared. This solid was filtered and dissolved in 50 m*l* of 18% hydrochloric acid. The solution was then refluxed for 30 min and concentrated *in vacuo*. Upon the addition of acetone to the residue, a solid was obtained which was recrystallized from a mixture of dioxane and 2-methoxyethanol to afford Vb, mp 148°C (lit[4] mp 152—153°C).

Found: C, 54.88; H, 8.85; N, 10.53%. Calcd for $C_{12}H_{22}N_2O_2 \cdot HCl$: C, 54.86; H, 8.76; N, 10.68%.

IR spectrum (cm^{-1}): 1730 (s), 1645 (vs), 1155 (vs).

NMR spectrum (in CF_3COOH): δ 7.6 (broad, 2H), δ 3.5 (multiplet, 4H), δ 2.7 (multiplet, 4H), δ 1.8 (multiplet, 12H).

pK_a: 4.45.

***N*-*p*-Toluenesulfonyl-ε-caprolactam (IV).** 6-(*p*-Toluenesulfonamido)hexanoic acid (VII)[1] (2 g) was heated in a small still under a vacuum (1 mmHg) at 125°C for 15 hr. The residue was then stirred in a 5% sodium bicarbonate solution for 2 days. The insoluble material was recrystallized from a mixture of water and acetone to afford a small amount of IV, mp 123°C.

Found: C, 58.43; H, 6.31; N, 5.32%. Calcd for $C_{13}H_{17}NO_3S$: C, 58.43; H, 6.34; N, 5.24%.

IR spectrum (cm^{-1}): 1685 (vs), 1354 (vs), 1170 (vs).

Cyclohexanone Oxime Benzenesulfonate (IIIb). To a stirred solution of cyclohexanone oxime (5.6 g) in 10 m*l* of pyridine, benzenesulfonyl chloride (8.8 g) in 15 m*l* of pyridine was added, drop by drop, at such a rate that the reaction temperature did not exceed 0°C. After the addition was complete, the reaction mixture was stirred for an additional 3 hr at 0°C. The reaction mixture was poured into a mixture of ice and sulfuric acid (containing 8 g of sulfuric acid). The yellow oil was immediately extracted with 80 m*l* of benzene. The benzene solution was washed with water two times and dried over anhydrous sodium sulfate in a refrigerator overnight. The solution was then used directly for the next process.

Reaction of Cyclohexanone Oxime Benzenesulfonate (IIIb) in Benzene. The benzene solution of cyclohexanone oxime benzenesulfonate (IIIb) obtained above was refluxed for 4 hr. The benzene was then evaporated *in vacuo*, and water was added. The solid material was filtered out (solid: named P), and the filtrate was evaporated *in vacuo*. Acetone was added to the residue, and the solution was left to stand overnight. The solid material thus obtained was recrystallized from a mixture of dioxane and 2-methoxyethanol to afford 2.4 g of Vc, mp 99°C.

Found: C, 56.27; H, 7.26; N, 7.06%. Calcd for $C_{18}H_{28}N_2O_5S$: C, 56.25; H, 7.30; N, 7.30%.

IR spectrum (cm^{-1}): 1720 (s), 1640 (vs), 1215 (vs), 1165 (vs), 1125 (vs).

Compound Vc was converted to the hydrochloride Vb in the same way as was Va converted into Vb.

The solid P was recrystallized from ligroin to afford a small amount of diphenyl sulfone (VIII), mp 121°C (lit[7] mp 125°C).

Found: C, 66.14; H, 4.60%. Calcd for $C_{12}H_{10}O_2S$: C, 66.06; H, 4.59%.

The infrared spectrum of this material was identical with the published spectrum of VIII.[8]

Reaction of Benzenesulfonyl Peroxide (IX) in Benzene. A solution of benzenesulfonyl peroxide (IX)[9] (3 g) in 30 m*l* of benzene was refluxed for 2 hr and then evaporated *in vacuo*. The residue was recrystallized from ligroin to afford 1 g of diphenyl sulfone (VIII), mp 121°C.

Reaction of Cyclopentanone Oxime *p*-Toluenesulfonate (X) in Benzene. A solution of cyclopentanone oxime *p*-toluenesulfonate (X)[1] (2 g) in 20 m*l* of dry benene was refluxed for 3 hr. The benzene was then evaporated *in vacuo*. The solid material which appeared when the solution was left in the air was recrystallized from dioxane to afford 1.9 g of δ-valerolactam *p*-toluenesulfonate (XIII), mp 147°C. The compound was found to be identical with the authentic sample by a study of its infrared spectrum and by mixed-melting-point determination.

δ-Valerolactam *p*-Toluenesulfonate (XIII). To a solution of δ-valerolactam (2.3 g) in 10 m*l* of acetone

6) H. Meyer, *Monatsh. Chem.*, **34**, 573 (1913).

7) F. Mauthner, *Ber.*, **39**, 3594 (1906).

8) DMS Card, "Documentation of Molecular Spectroscopy," Butterworths Scientific Publications, London.

9) R. F. Weinland and H. Lewkowitz, *Ber.*, **36**, 2702 (1903).

there was added a solution of *p*-toluenesulfonic acid (4 g) in 20 m*l* of acetone. The solid material which appeared was recrystallized from dioxane to afford 6 g of XIII, mp 147°C.

Found: C, 53.34; H, 6.56; N, 4.79%. Calcd for $C_{12}H_{17}NO_4S$: C, 53.14; H, 6.30; N, 5.17%.

IR spectrum (cm^{-1}): 2300 (w), 1685 (s), 1220 (vs), 1120 (vs), 1025 (vs), 1000 (s).

Reaction of Cyclopentanone Oxime *p*-Toluenesulfonate (X) in Acetic Acid. This reaction was carried out under conditions identical with those described by Heldt.[1] Crystals with a mp of 147°C were obtained; they were identical with the authentic sample of XIII. Repeated recrystallizations from glacial acetic acid did not raise the melting point.[1]

Hydrolysis of δ-valerolactam *p*-Toluenesulfonate (XIII). A solution of δ-valerolactam *p*-toluenesulfonate (XIII) (2 g) in 20 m*l* of water was refluxed for 2 hr. The water was then evaporated *in vacuo*; an oily residue, which soon solidified, was recrystallized from dioxane to afford 2 g of 5-aminopentanoic acid *p*-toluenesulfonate (XIV), mp 142°C. The compound was found to be identical with the authentic sample of XIV by a study of its infrared spectrum and by a mixed-melting-point determination.

5-Aminopentanoic Acid *p*-Toluenesulfonate(XIV). δ-Valerolactam (1 g) and *p*-toluenesulfonic acid (2 g) were dissolved in 50 m*l* of water. The solution was refluxed for 5 hr, and the water was evaporated *in vacuo*. An oily material soon solidified. Recrystallization from dioxane afforded 3 g of XIV, mp 142—142.5°C.

Found: C, 49.87; H, 6.73; N, 4.55%. Calcd for $C_{12}H_{19}NO_5S$: C, 49.83; H, 6.57; N, 4.84%.

IR spectrum (cm^{-1}): 1700 (s), 1215 (vs), 1164 (vs), 1115 (s), 1025 (s), 1000 (s), 810 (m).

5-(*p*-Toluenesulfonamido)pentanoic Acid (XII). To a solution of 5-aminopentanoic acid hydrochloride[10] (2.5 g) in a sodium hydroxide solution (1.4 g of sodium hydroxide in 7.5 m*l* of water), there was added a solution of *p*-toluenesulfonyl chloride (3.5 g) in 15 m*l* of acetone below 30°C. The solution was then stirred for 3 hr and neutralized with hydrochloric acid. The solution was freezing-dried, and the residue was extracted with ethyl acetate. After the ethyl acetate had been evaporated, the residual solid was recrystallized from water. Crystals with a mp of 92°C (1.25 g) were obtained.

Found: C, 53.44; H, 6.38; N, 5.21%. Calcd for $C_{12}H_{17}NO_4S$: C, 53.14; H, 6.30; N, 5.17%.

IR spectrum (cm^{-1}): 1686 (s), 1330 (s), 1155 (vs).

***N*-*p*-Toluenesulfonyl-δ-valerolactam (XI).** This compound was prepared by the dehydration of XII in the same way as was VII dehydrated into IV. Recrystallization from a mixture of benzene and ligroin afforded crystals of XI, mp 140°C (lit[2] mp 145°C).

IR spectrum: 1675 (vs), 1350 (vs), 1170 (vs), 825 (s), 675 (s).

10) L. E. Schniepp and C. S. Marvel, *J. Am. Chem. Soc.*, **57**, 1557 (1935).

BULLETIN OF THE CHEMICAL SOCIETY OF JAPAN VOL. 42 1959—1963 (1969)

Kinetic Study of the Polymerization of Diallyl Carbonate*1

Akira MATSUMOTO, Katsutoshi TAKASHIMA and Masayoshi OIWA

Department of Applied Chemistry, Faculty of Engineering, Kansai University, Senriyama, Suita-shi, Osaka

(Received October 2, 1968)

The polymerization of diallyl carbonate was carried out at 60°C, benzoyl peroxide being used as the initiator; here it has been discussed kinetically from the point of view of cyclopolymerization. The rate of polymerization, R_p, was not proportional to the square root or the first power of the initiator concentration, (I), but $R_p/(I)^{1/2}$ and $(I)^{1/2}$ bore a linear relationship. The rate of polymerization, the residual unsaturation, and the degree of polymerization decreased with a decrease in the monomer concentration. The relation between the rate of polymerization over the degree of polymerization, $R_p/\bar{P}_{n,0}$ and the monomer concentration, (M), was also linear, as in $R_p/(I)^{1/2}$ and $(I)^{1/2}$. The ratio of the rate constant of the unimolecular cyclization reaction to that of the bimolecular propagation reaction of the uncyclized radical, K_c, was estimated to be 4.0 mol/*l* from the dependence of the residual unsaturation on the monomer concentration.

It is well known that diallyl-compounds undergo cyclopolymerization.[1-9] It seems, however, that there have been few detailed studies of kinetic treatment on the basis of cyclopolymerization.

Holt and Simpson[1] have studied, with a number of diallyl esters, the statistical theory of gelation; they have found that the conversion at the gelation point was greater than would be calculated for the formation of networks from tetrafunctional monomers, and that the divergence from theory could be partly explained as resulting from a loss of unsaturation by cyclization. In their report they also proposed a reaction scheme for the polymerization of the diallyl ester; however, the kinetics based on the scheme were not clarified in detail, for their consideration contained the assumption that the reactivities of the uncyclized radical with an adjacent pendant double bond and of the cyclized radical were equivalent.

On the other hand, we have presented in detail the kinetics of the polymerization of diallyl phthalate;[10] in this paper the two radicals mentioned above were individually treated.

In the present experiment, the polymerization of diallyl carbonate was carried out; by employing the kinetic equations derived in a previous paper, we will kinetically discuss our results from the standpoint of cyclopolymerization.

Experimental

Materials. The diallyl carbonate was prepared by the ester exchange reaction of diethyl carbonate with allyl alcohol according to the procedure of Adelson and Dannenberg.[11] A portion of clean sodium (about 4 g) was cut into small pieces and then added to 230 g of absolute allyl alcohol. After all the sodium had been dissolved, 120 g of diethyl carbonate was added; the mixture was refluxed under a Vigreux column, and then ethyl alcohol was taken off overhead. The residue was taken up in 100 m*l* of benzene, and water-washed several times, after which the benzene was distilled off. The residue was distilled under reduced pressure and then redistilled just before use; bp 90—91°C/50 mmHg, d_4^{20} 0.969 (lit,[11] bp 95—97°C/57—61 mmHg). The purity of the diallyl carbonate was confirmed by the complete disappearance of the absorption due to the ethyl group in its NMR spectrum.

The benzoyl peroxide (BPO) was purified by repeated precipitations from a chloroform solution by the addition of methanol.

*1 Studies of the Polymerization of Diallyl-compounds. V.

1) T. Holt and W. Simpson, *Proc. Roy. Soc.*, **A238**, 154 (1956).

2) G. B. Butler and R. J. Angelo, *J. Am. Chem. Soc.*, **79**, 3128 (1957).

3) S. G. Matsoyan, G. M. Pogosyan, R. N. Skripnikova and A. V. Mushegyan, *Vysokomol. Soedin.*, **5**, 183 (1963).

4) S. G. Matsoyan, G. M. Pogosyan, A. O. Dzhagalyan and A. V. Mushegyan, *ibid.*, **5**, 854 (1963).

5) V. G. Ostroverkhov, L. A. Brumorsckaya and A. A. Korniyenko, *ibid.*, **6**, 1020 (1964).

6) S. G. Matsoyan, G. M. Pogosyan, R. K. Skripnikova and L. L. Nikogosyan, *Izv. Akad. Nauk Arm. SSSR Khim. Nauki*, **15**, 541 (1962).

7) G. B. Butler, A. Crawshaw and W. L. Miller, *J. Am. Chem. Soc.*, **80**, 3615 (1958).

8) G. B. Butler, *J. Polymer Sci.*, **48**, 279 (1960).

9) C. S. Marvel, *ibid.*, **48**, 101 (1960).

10) A. Matsumoto, K. Asano and M. Oiwa, *Nippon Kagaku Zasshi* (*J. Chem. Soc. Japan, Pure Chem. Sect.*), **90**, 290 (1969).

11) D. E. Adelson and H. Dannenberg, U. S. Pat. 2514354 (1950).

The benzene was washed thoroughly with concentrated sulfuric acid and then with distilled water until it became neutral; it was then dried on calcium chloride and distilled over metallic sodium.

Polymerization Procedure. Polymerizations were carried out in glass ampoules (10—50 ml capacity), using dry benzene as the solvent and BPO as the initiator. Measured amounts of diallyl carbonate, BPO, and benzene were placed in a glass ampoule, which was then degassed twice in the usual manner and flushed with nitrogen. The ampoule was then sealed under a vacuum and transferred into a thermostat regulated at the desired temperature.

After a definite reaction time, the ampoule was removed from the thermostat and the polymer was separated by pouring the contents into a tenfold volume of methanol containing hydroquinone, and also by centrifuging.

The polymer thus obtained was then washed repeatedly with methanol and dried *in vacuo* until a constant weight was attained. The conversion was calculated on the weight of the dry polymer obtained.

The polymer was then purified by dissolving it in benzene and by subsequent reprecipitation in methanol.

Analyses of the Polymer. The residual unsaturation of the purified polymer was determined by the method of Simpson *et al.*[12]; the polymer was dissolved in benzene, saponified in excess alcoholic potassium hydroxide, and neutralized with hydrochloric acid, and then the free allyl alcohol was determined by the bromide-bromate technique. Tests on pure diallyl esters showed that this could be done within an estimated error of ±1.5%. The results were expressed as percentages of pure diallyl carbonate.

The molecular weight of the polymer was measured with a vapor-pressure osmometer, Hewlett Packard 302.

Results and Discussion

Kinetics of the Diallyl Ester. In a previous paper,[10] the kinetics of the polymerization of diallyl phthalate was discussed in detail on the basis of cyclopolymerization; the kinetic equations were derived by assuming steady-state conditions, conditions which were based on the following reaction scheme:

Decomposition: $\mathrm{I} \longrightarrow 2\mathrm{R}\cdot$ $2k_d(\mathrm{I})$

Initiation: $\mathrm{R}\cdot + \mathrm{M} \longrightarrow \mathrm{M}\cdot$ $2k_i(\mathrm{R}\cdot)(\mathrm{M})$

Cyclization: $\mathrm{M}\cdot \longrightarrow \mathrm{M_c}\cdot$ $k_c(\mathrm{M}\cdot)$

Propagation:
$\mathrm{M}\cdot + \mathrm{M} \longrightarrow \mathrm{M}\cdot$ $2k_p(\mathrm{M}\cdot)(\mathrm{M})$
$\mathrm{M_c}\cdot + \mathrm{M} \longrightarrow \mathrm{M}\cdot$ $2k_{cp}(\mathrm{M_c}\cdot)(\mathrm{M})$

Chain transfer:
$\mathrm{M}\cdot + \mathrm{M} \longrightarrow \mathrm{P} + \mathrm{M}\cdot$ $2k_{t_1}(\mathrm{M}\cdot)(\mathrm{M})$
$\mathrm{M_c}\cdot + \mathrm{M} \longrightarrow \mathrm{P} + \mathrm{M}\cdot$ $2k_{t_2}(\mathrm{M_c}\cdot)(\mathrm{M})$

Re-initiation: $\mathrm{M}\cdot^* + \mathrm{M} \longrightarrow \mathrm{M}\cdot$ $2k_i'(\mathrm{M}\cdot^*)(\mathrm{M})$

Stabilization: $\mathrm{M}\cdot^* + \mathrm{M}\cdot^* \longrightarrow \mathrm{M}^* - \mathrm{M}^*$ $k_{t_3}(\mathrm{M}\cdot^*)^2$

where I denotes an initiator; M, a diallyl ester monomer; P, the polymer; R·, the initiator radical; M·, the uncyclized radical; $\mathrm{M_c}\cdot$, the cyclized radical, and M·*, the degraded radical.

If a steady state is assumed for the different types of radicals, Eqs. (1)—(4) can be obtained:

$$(\mathrm{R}\cdot) = fk_d(\mathrm{I})/k_i(\mathrm{M}) \tag{1}$$

$$(\mathrm{M}\cdot) = \frac{2fk_d(\mathrm{I}) + 2k_i'(2fk_d(\mathrm{I})/k_{t_3})^{1/2}(\mathrm{M})}{2k_{t_1}(\mathrm{M}) + k_ck_{t_2}/(k_{cp} + k_{t_2})} \tag{2}$$

$$(\mathrm{M_c}\cdot) = \frac{\{k_c/2(k_{cp} + k_{t_2})(\mathrm{M})\}\{2fk_d(\mathrm{I}) + 2k_i'(2fk_d(\mathrm{I})/k_{t_3})^{1/2}(\mathrm{M})}{2k_{t_1}(\mathrm{M}) + k_ck_{t_2}/(k_{cp} + k_{t_2})} \tag{3}$$

$$(\mathrm{M}\cdot^*) = (2fk_d(\mathrm{I})/k_{t_3})^{1/2} \tag{4}$$

The rate and the degree of polymerization were then obtained as Eqs. (5) and (6), in which it was assumed that the dimer, M*–M*, produced by stabilization was present in the polymer recovered.

$$\begin{aligned} R_p &= 2k_i(\mathrm{R}\cdot)(\mathrm{M}) + 2(k_p + k_{t_1})(\mathrm{M}\cdot)(\mathrm{M}) \\ &\quad + 2(k_{cp} + k_{t_2})(\mathrm{M_c}\cdot)(\mathrm{M}) + 2k_i'(\mathrm{M}\cdot^*)(\mathrm{M}) \\ &= \{2fk_d(\mathrm{I}) + 2k_i'(2fk_d(\mathrm{I})/k_{t_3})^{1/2}(\mathrm{M})\} \\ &\quad \times \left\{1 + \frac{2(k_p + k_{t_1})(\mathrm{M}) + k_c}{2k_{t_1}(\mathrm{M}) + k_ck_{t_2}/(k_{cp} + k_{t_2})}\right\} \end{aligned} \tag{5}$$

$$\begin{aligned} \bar{P}_{n,o} &= R_p/\{2k_{t_1}(\mathrm{M}\cdot)(\mathrm{M}) + 2k_{t_2}(\mathrm{M_c}\cdot)(\mathrm{M}) + k_{t_3}(\mathrm{M}\cdot^*)^2\} \\ &= \left\{1 + \frac{2(k_p + k_{t_1})(\mathrm{M}) + k_c}{2k_{t_1}(\mathrm{M}) + k_ck_{t_2}/(k_{cp} + k_{t_2})}\right\} \\ &\quad \times \left\{\frac{fk_d(\mathrm{I}) + k_i'(2fk_d(\mathrm{I})/k_{t_3})^{1/2}(\mathrm{M})}{2fk_d(\mathrm{I}) + k_i'(2fk_d(\mathrm{I})/k_{t_3})^{1/2}(\mathrm{M})}\right\} \end{aligned} \tag{6}$$

Here f denotes the efficiency of the initiation of the chain radicals by R·.

On the other hand, the rate of the formation of the pendant double bonds in the polymer is given by:

$$\begin{aligned} \mathrm{d}m/\mathrm{d}t &= 2k_i(\mathrm{R}\cdot)(\mathrm{M}) + 2k_p(\mathrm{M}\cdot)(\mathrm{M}) - k_c(\mathrm{M}\cdot) \\ &\quad + 2k_{cp}(\mathrm{M_c}\cdot)(\mathrm{M}) + 4k_{t_1}(\mathrm{M}\cdot)(\mathrm{M}) \\ &\quad + 4k_{t_2}(\mathrm{M_c}\cdot)(\mathrm{M}) + 2k_i'(\mathrm{M}\cdot^*)(\mathrm{M}) \\ &= \{2fk_d(\mathrm{I}) + 2k_i'(2fk_d(\mathrm{I})/k_{t_3})^{1/2}(\mathrm{M})\} \\ &\quad \times \left\{2 + \frac{2(k_p + k_{t_1})(\mathrm{M})}{2k_{t_1}(\mathrm{M}) + k_ck_{t_2}/(k_{cp} + k_{t_2})}\right\} \end{aligned} \tag{7}$$

By combining Eqs. (5) and (7), the following equation was obtained for evaluating K_c, the probability of cyclization which is characteristic of each monomer.

$$\left(F - \frac{2\beta}{1 + 2\beta}\right)^{-1} = \frac{(1 + 2\alpha)(1 + 2\beta)}{1 + 3\alpha + 2\alpha\beta} + \frac{(1 + 2\beta)^2}{2(1 + 3\alpha + 2\alpha\beta)(1 + \beta)} \cdot K_c \cdot \frac{1}{(\mathrm{M})} \tag{8}$$

12) W. Simpson, T. Holt and R. J. Zetie, *J. Polymer Sci.*, **10**, 489 (1953).

where F is the ratio of the amount of the residual pendant double bonds in the polymer to that of the polymerized diallyl ester monomer, $dm/d(M)$, while α, β, and K_c are k_{t1}/k_p, k_{t2}/k_{cp}, and k_c/k_p respectively.

If the kinetic chain length is sufficiently large and if the dimer, M*–M*, produced by stabilization is not present in the polymer recovered, the loss of the monomer by the initiation, chain transfer, and re-initiation reactions is negligible compared with that by the propagation reaction. The above equations may, therefore, be simplified as follows:

$$R_p = 2k_p(M\cdot)(M) + 2k_{cp}(M_c\cdot)(M)$$
$$= \{2fk_d(I) + 2k_i'(2fk_d(I)/k_{t3})^{1/2}(M)\} \times \left\{\frac{2k_p(M) + k_ck_{cp}/(k_{cp}+k_{t2})}{2k_{t1}(M) + k_ck_{t2}/(k_{cp}+k_{t2})}\right\} \quad (9)$$

$$\bar{P}_{n,o} = R_p/\{2k_{t1}(M\cdot)(M) + 2k_{t2}(M_c\cdot)(M)\}$$
$$= \frac{2k_p(M) + k_ck_{cp}/(k_{cp}+k_{t2})}{2k_{t1}(M) + k_ck_{t2}(k_{cp}+k_{t2})} \quad (10)$$

$$dm/dt = 2k_p(M\cdot)(M) - k_c(M\cdot) + 2k_{cp}(M_c\cdot)(M)$$
$$= \{2fk_d(I) + 2k_i'(2fk_d(I)/k_{t3})^{1/2}(M)\} \times \left\{\frac{2k_p(M) - k_ck_{t2}/(k_{cp}+k_{t2})}{2k_{t1}(M) + k_ck_{t2}/(k_{cp}+k_{t2})}\right\} \quad (11)$$

From Eqs. (9) and (11) we obtain:

$$(1-F)^{-1} = \frac{1}{1+\beta} + \frac{2}{K_c}\cdot(M) \quad (12)$$

The combination of Eqs. (9) and (10) gives:

$$R_p/\bar{P}_{n,o} = 2fk_d(I) + 2k_i'(2fk_d(I)/k_{t3})^{1/2}(M) \quad (13)$$

Polymerization Results. The bulk polymerization of diallyl carbonate was investigated under different initiator concentrations at 60°C; the time-conversion curves are shown in Fig. 1. The initial rates of polymerization as calculated from the slope of the straight lines shown in Fig. 1 are summarized in Table 1; they are not proportional to the square root or to the first power of the initiator concentration, as had been expected from Eq. (9).

Table 1. Influence of the initiator on the rate of polymerization of diallyl carbonate (in bulk, at 60°C)

(I) mol/l	$R_p\times10^5$ mol/l·sec	$(R_p/(I)^{1/2})\times10^5$ (mol/l)$^{1/2}$·sec^{-1}	$(R_p/(I))\times10^5$ sec^{-1}
0.4	6.84	10.24	16.2
0.2	3.64	8.13	18.2
0.1	2.05	6.47	20.5
0.06	1.44	5.91	24.1

The influence of the monomer concentration was studied by measuring the rate of polymerization, the residual unsaturation, and the degree of poly-

Table 2. Results of polymerization of diallyl carbonate at 60°C ((BPO)=0.2 mol/l, in benzene)

(M) mol/l	$R_p\times10^5$ mol/l·sec	R_{us}[a]	$\bar{P}_{n,o}$[b]	$(R_p/\bar{P}_{n,o})\times10^7$ mol/l·sec
6.82	3.64	0.379	77	4.72
4.54	3.12	0.341	75	4.16
3.41	2.47	0.306	67	3.69
2.27	2.05	0.253	63	3.25
1.70	1.82	0.237	56	3.25
1.14	—	0.224	51	—

a) The residual unsaturation is the degree of unsaturation of the molecule expressed as a percentage of pure diallyl carbonate and was obtained by the analysis of the polymer less than 10% conversion.

b) The initial degree of polymerization was obtained by the extrapolation from the experimental results shown in Fig. 2.

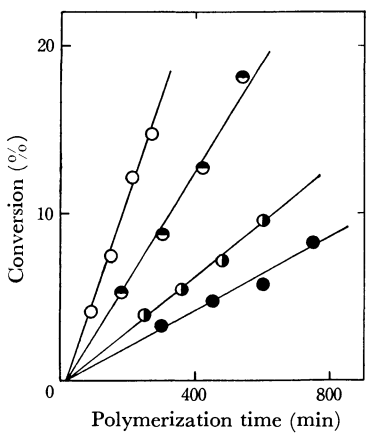

Fig. 1. Time-conversion curves in the bulk polymerization of diallyl carbonate at 60°C.
(I)=0.4(○), 0.2(◓), 0.1(◑), 0.06(●) mol/l

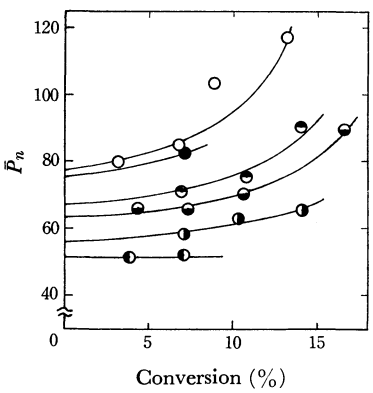

Fig. 2. Dependence of the degree of polymerization on conversion.
Polymerization temperature, 60°C
(I)=0.2 mol/l; (M)=6.82(○), 4.54(●), 3.41(◓), 2.27(◒), 1.70(◑), 1.14(◐) mol/l

merization at a constant initiator concentration ((I)=0.2 mol/l) at 60°C. The results obtained are given in Table 2.

The conversion dependence of the degree of polymerization is shown in Fig. 2. It had a tendency to increase with an increase in the conversion, and to become smaller with a decrease in the monomer concentration. Similar tendencies were observed in the previous work[10] for the polymerization of diallyl phthalate. These results may be attributed to an increase in the probability of the crosslinking reaction as the polymerization proceeds.

The values of the initial degree of polymerization, $\bar{P}_{n,o}$, as extrapolated from the experimental results shown in Fig. 2, are plotted against the monomer concentration in Fig. 3.

In Fig. 4, the relation between the residual unsaturation of the polymer, R_{us}, and the monomer concentration is plotted. Both $\bar{P}_{n,o}$ and R_{us} tend to decrease with a decrease in the monomer concentration.

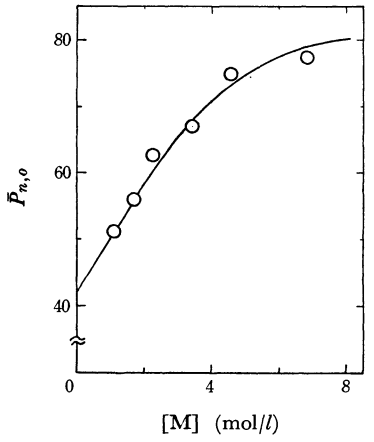

Fig. 3. Dependence of the initial degree of polymerization on monomer concentration.
Polymerization temperature, 60°C, (I)=0.2 mol/l

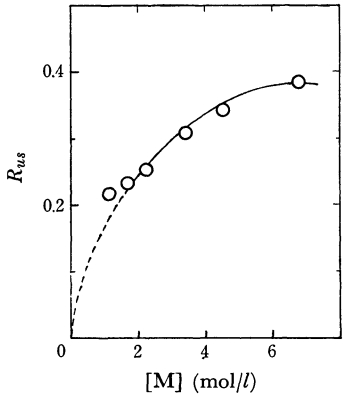

Fig. 4. Relation between the residual unsaturation and the monomer concentration.
Polymerization temperature, 60°C, (I)=0.2 mol/l

Also, as is shown in Figs. 2 and 3 and in Table 2, the initial degree of polymerization was sufficiently large; therefore, as has been mentioned above, the simplified kinetic equations, *e. g.*, Eqs. (9)—(12), can be used instead of the more elaborate ones, *e. g.*, Eqs. (5), (6) and (8), for the polymerization of diallyl carbonate.

Dependence of the Degree of Polymerization on the Initiator and Monomer Concentrations. From Eq. (10) it may be kinetically expected that the degree of polymerization will be independent of the initiator concentration. The degree of polymerization of the polymers obtained under different initiator concentrations, *e. g.*, (I)=0.4, 0.2, 0.1, and 0.06 mol/l, were determined to be 86, 82, 86, and 83 respectively; they were nearly identical, regardless of the initiator concentration. The polymers analyzed were all of about 5% conversion. This agreement between the kinetics and the experimental results may support the idea that the use of the simplified kinetic equations is justifiable.

On the other hand, the dependence of the initial degree of polymerization on the monomer concentration is shown in Fig. 3. By comparing the results with Eq. (10), we obtained the following results : $(\bar{P}_{n,o})_{M\to 0}=k_{cp}/k_{t2}\simeq 42$, $(\bar{P}_{n,o})_{M\to\infty}=k_p/k_{t1}\simeq 80$. These results suggest that the reactivities of the uncyclized radical and the cyclized radical are not equivalent. If the reactivities of the two radicals are equivalent, as has been shown by Holt and Simpson,[1] the degree of polymerization should be independent of the monomer concentration.

Influence of the Initiator and Monomer Concentrations on the Rate of Polymerization. When the monomer concentration is kept constant and the initiator concentration is varied, it may be kinetically expected from Eq. (9) that $R_p/(\mathrm{I})^{1/2}$ *vs.*

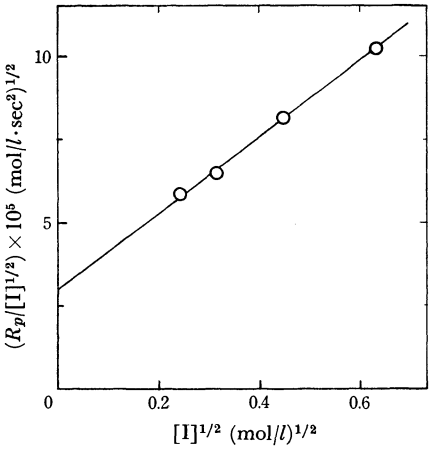

Fig. 5. Plot of $R_p/(\mathrm{I})^{1/2}$ *vs.* $(\mathrm{I})^{1/2}$.
Polymerization temperature, 60°C
(M)=6.82 mol/l

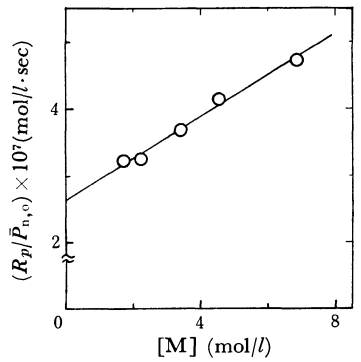

Fig. 6. Plot of $R_p/\bar{P}_{n,o}$ *vs.* (M).
Polymerization temperature, 60°C
(I)=0.2 mol/l

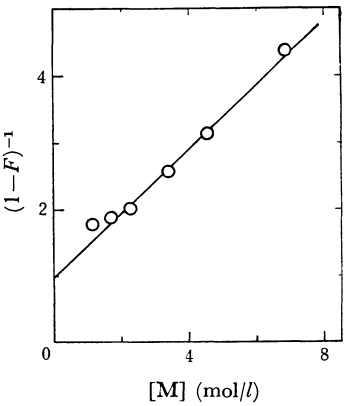

Fig. 7. Plot of $(1-F)^{-1}$ *vs.* (M).
Polymerization temperature, 60°C
(I)=0.2 mol/l

$(I)^{1/2}$ will be a straight line.*2

Similarly, if the initiator concentration is kept constant and the monomer concentration is varied, a linear relationship between $R_p/\bar{P}_{n,o}$ and (M) may be expected from Eq. (13).

These results are plotted in Figs. 5 and 6, in which the fit of the experimental data to the linear relationship is fairly good. From the slope and the intercept of the straight line shown in Fig. 5, fk_d and $k_i'/k_{t3}^{1/2}$ were estimated to be 0.74×10^{-6} sec^{-1} and 0.23×10^{-4} $(l/mol\cdot sec)^{1/2}$ respectively, while in Fig. 6, fk_d and $k_i'/k_{t3}^{1/2}$ were 0.67×10^{-6} sec^{-1} and 0.30×10^{-4} $(l/mol\cdot sec)^{1/2}$, values in good agreement with the values in Fig. 5.

Estimation of K_c. The ratio of the rate constant of the unimolecular cyclization reaction to that of the bimolecular propagation of the uncyclized radical, K_c, was evaluated by applying Eq. (12) to the experimental measurements of the dependence of the residual unsaturation on the monomer concentration.

The plot $(1-F)^{-1}$ *vs.* (M) is shown in Fig. 7; it has a good linear relationship, as was predicted by Eq. (12). K_c was estimated to be 4.0 mol/l from the slope of the straight line.

On the other hand, if the uncyclized and cyclized radicals were not individually treated as by Holt and Simpson,[1] the following equation would be obtained:

$$(1-F)^{-1} = (2k_p/k_c)(M)$$

It is obvious, however, that this equation is not sufficient to account for the experimental data shown in Fig. 7.

In cyclopolymerization, K_c is the critical factor determining the microstructure of the polymer; it may be interpreted as twice the monomer concentration necessary for the rate of the bimolecular propagation reaction to equal that of the unimolecular cyclization.[13] Thus, the monomer concentration of diallyl carbonate required for the two processes to proceed at an equal rate is 2.0 mol/l, which corresponds to about a 70% dilution of the pure monomer.

*2 Eq. (9) can be written as follows:

$$\frac{R_p}{(I)^{1/2}} = \{2fk_d(I)^{1/2} + 2k_i'(2fk_d/k_{t3})^{1/2}(M)\} \times \left\{\frac{2k_p(M) + k_ck_{cp}/(k_{cp}+k_{t2})}{2k_{t1}(M) + k_ck_{t2}/(k_{cp}+k_{t2})}\right\}$$

13) W. E. Gibbs, *J. Polymer Sci.*, **A2**, 4815 (1964).

BULLETIN OF THE CHEMICAL SOCIETY OF JAPAN VOL. 42 1964—1967 (1969)

The Basicities of Substituted Diphenyl Sulfoxides[1)]

Shigeru Oae, Kazuo Sakai and Norio Kunieda

Department of Applied Chemistry, Faculty of Engineering, Osaka City University, Sumiyoshi-ku Osaka

(Received October 11, 1968)

The basicities of nine *meta*- and *para*-substituted diphenyl sulfoxides have been determined spectrophotometrically in sulfuric acid media. The pK_{BH^+} values thus obtained indicate that these sulfoxides possess rather weak basicities (pK_{BH^+}; -3.67——-5.74). and these pK_{BH^+} values gave a good correlation with Brown-Okamoto's σ^+ values, ($\rho=-2.00$), instead of σ-values. These observations seem to suggest a considerable conjugative interaction between phenyl groups and sulfoxide group of these diphenyl sulfoxides.

Sulfoxides have been considered to be weakly basic because of their physical and chemical behavior, the remarkable solvating power of cationic species, semipolar nature of the S–O linkage, *etc.* But the basicities of only a few alkyl sulfoxides have hitherto been determined.[2)]

Recently, Andersen and his co-workers[3)] determined the basicities of *meta*- and *para*-substituted phenyl methyl sulfoxides by the potentiometric titration in acetic anhydride, and gave the pK_{BH^+} values which can be nicely correlated by Hammett's σ values with a large ρ value of -3.79. More recently, Haake and Cook[4)] determined the pK_{BH^+} values of phenyl methyl sulfoxide and dimethyl sulfoxide, -3.45 and -2.7 respectively, by the measurements of NMR chemical shift of methyl group and they showed the values to be considerably larger than those of Andersen's[3)] and earlier workers'.

During the course of our studies on the acid-catalyzed oxygen exchange reactions,[5)] we were interested in the basicities of diaryl sulfoxides and synthesized nine substituted diphenyl sulfoxides and determined their basicities. The measurements of the basicities of these substituted diphenyl sulfoxides were carried out spectrophotometrically in sulfuric acid media in a fashion similar to that described by Hammett[6)] and other workers,[7)] taking advantage of our earlier finding that sulfoxides ionize in a concentrated sulfuric acid in a following manner,[8)] since the UV spectra of diaryl sulfoxides are quite different from those of the corresponding protonated species.

$$R_2SO + H_2SO_4 \rightleftarrows R_2\overset{+}{S}OH + HSO_4^- \quad (i\text{-facter}=2) \qquad (1)$$

The pK_{BH^+} values for the substituted diphenyl sulfoxides thus obtained are listed in Table 2, and are found to be nicely correlated by Brown-Okamoto's[9)] σ^+ values, with ρ value of -2.00.

Experimental and Results

The Substituted Diphenyl Sulfoxides were prepared by the oxidation of the corresponding sulfides with the bromine complex of pyridine and water in acetic acid according to the same procedure as described in our previous paper.[10)] Their melting and boiling points (°C) were *p*-CH_3O, 60—60.5°C, lit,[11)] 55—57°C; *p*-C_2H_5O, 71— 72°C; *p*-CH_3, 69—70°C, lit,[11)] 71—72°C; *m*-CH_3, 44.5—45.5°C, lit,[11)] 46—47°C; H, 70—71°C, lit,[11)] 71°C; *p*-Cl, 44—45°C, lit,[11)] 45—46°C; *p*-I, 106—107°C, lit,[12)] 106°C; *p*-Br, 62—62.5°C; *m*-Cl, 165—

1) Paper XXXII on Sulfoxides.

2) P. Nylén, *Z. Anorg. Allgem. Chem.*, **246**, 227 (1941).

3) K. K. Andersen, W. H. Edward, J. B. Biasotti and R. A. Strecker, *J. Org. Chem.*, **31**, 2859 (1966).

4) a) P. Haake and D. Cook, *Tetrahedron Letters*, **1968** 427; b) S. Oae, K. Sakai and N. Kunieda, unpublished work.

5) a) S. Oae, T. Kitao and Y. Kitaoka, *Chem. & Ind.*, **1961**, 291; b) S. Oae, T. Kitao, T. Kitaoka and S. Kawamura, This Bulletin, **38**, 546 (1965); c) S. Oae and N. Kunieda, *ibid.*, **41**, 696 (1968).

6) a) L. P. Hammett and A. J. Deyrup, *J. Am. Chem. Soc.*, **54**, 2721 (1932); b) L. A. Flexser, L. P. Hammett and A. Dingwall, *ibid.*, **57**, 2103 (1925).

7) a) A. R. Katritzky, A. J. Waring and K. Yates, *Tetrahedron*, **19**, 465 (1963); b) K. Yates and H. Wai, *Can. J. Chem.*, **43**, 2131 (1965).

8) S. Oae, T. Kitao and Y. Kitaoka, This Bulletin, **38**, 543 (1965).

9) H. C. Brown and Y. Okamoto, *J. Am. Chem. Soc.*, **80**, 4979 (1959).

10) S. Oae, Y. Ohnishi, S. Kozuka and W. Tagaki, This Bulletin, **39**, 364 (1966).

11) G. Modena, *Gazz. Chem. Ital.*, **89**, 834 (1959).

12) D. L. Hammick and B. Wiliams, *J. Chem. Soc.*, **1938**, 211.

167°C/1.5 mmHg, lit,[11] 190—192°C/5 mmHg; *p*-NO_2, 106—107°C, lit.[11] 106—107°C.

Sulfuric Acid. Concentrations of sulfuric acid - water media were determined by titrating with a standard alkali solution. The H_0 values used here are Long and Paul's[13] with the corrections above 60% of concentrations given by Jorgensen and Harter.[14]

Measurement of pK_{BH^+}. The UV spectra of the sulfoxides in sulfuric acid media ranging from 0% to 91.3% acid were measured with a Hitachi EPS-2U model Spectrophotometer. The wave lengths and intensities of the absorption maxima of the unprotonated (A_B) and protonated (A_{BH^+}) forms of the sulfoxides are listed in Table 1. We can see from these UV charts, for example, shown in Fig. 1 that the intensities of the absorption maxima of the unprotonated sulfoxides increase while those of the protonated sulfoxides decrease with the decrease of the concentration of sulfuric acid.

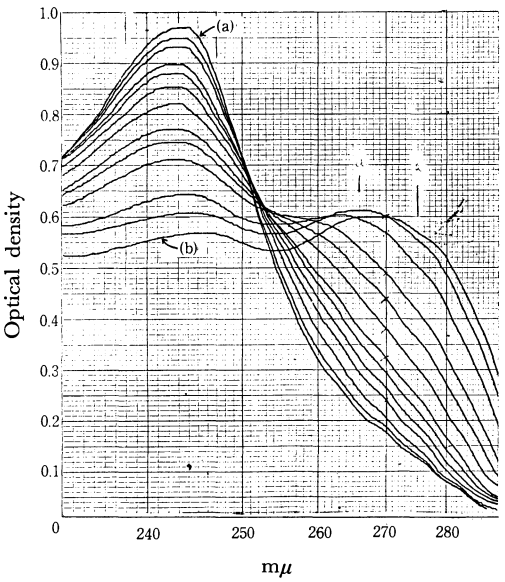

Fig. 1. UV chart of *p*-bromophenyl phenyl sulfoxide in sulfuric acid.
(a), in water and (b), in 90.2% sulfuric acid

Hammett used the following equation (Eq. (2)) to estimate the pK_{BH^+} values of such weak bases as acetophenone, benzoic acid and others in sulfuric acid media,[6a] but the equation could not be used for the measurement of pK_{BH^+} values of several other compounds[15] which do not behave as ideal Hammett bases,[7a,16] since a gradient of log [BH^+]/[B] *vs.* $-H_0$ for a non-Hammett base is not unity. Although numerous compounds have been shown to behave as Hammett bases, many compounds are not so, and our compounds were also found to be non-Hammett bases. In such cases it is more prudent to use the following equation (Eq. (3)) for the pK_{BH^+} calculation of the non-Hammett bases,[7a,16] namely substituted sulfoxides in this case.

$$pR_{BH^+} = H_0 - \log \frac{[BH^+]}{[B]} \qquad (2)$$

$$pK_{BH^+} = H_0 - n \log \frac{[BH^+]}{[B]} \qquad (3)$$

Incidentally this equation has been used for the estimation of pK_{BH^+} values of amides,[7a,b] acetophenone,[7b] benzoic acid,[7b] benzaldehyde,[7b] phosphine oxides,[16] phosphine sulfides,[16] and phenyl methyl sulfoxide,[4] *etc.*

In the spectrophotometric determination, [BH^+] and [B] can be rewritten as [$A-A_{BH^+}$] and [A_B-A] respectively, where A is an absorbance of a sulfoxide in sulfuric acid media of an adequate concentration. When the values of log[BH^+]/[B] obtained are plotted against H_0 values according to Eq. 3, one gets a straight line from which *n* and the pK_{BH^+} value can be obtained. This method was quite useful for the determination of pK_{BH^+} of most of the sulfoxides. However, we could not measure the pK_{BH^+} values of *para*- and *meta*-nitrophenyl phenyl sulfoxides by this method, since the absorption maxima of the UV spectra for the unprotonated and protonated forms of these sulfoxides are too near to be measured with reliable accuracy.

The *n*-values for the substituted diphenyl sulfoxides were found to be larger (1.8—2.4) than unity, like those for benzamide (1.51),[7b] acetophenone (1.37),[7b] benzaldehyde (1.22),[7b] benzoic acid (1.20),[7b] phosphine oxides

Table 1. Wave length maxima for substituted diphenyl sulfoxides (X-C_6H_4-SO-C_6H_5)

Substituent (X)	λ_{max} in water[a]		λ_{max} in 91.3 % sulfuric acid	
	mμ	log ε	mμ	log ε
p-CH_3O	245	4.21	281	4.05
p-C_2H_5O	246	4.22	283	4.11[b]
p-CH_3	237	4.20	264	4.02
m-CH_3	234	4.13	253	3.88
H	233	4.15	255	3.91
p-Cl	240	4.23	262	4.07
p-I	240	4.40	263	4.19[b]
p-Br	243	4.28	268	4.07[b]
m-Cl	232	4.10	245	3.94[b]

a) The values of UV spetcra in water in this column had close resemblance to those in ethanol solution.
b) In 90.2% sulfuric acid.

13) M. A. Paul and F. A. Long, *Chem. Revs.*, **57**, 1 (1957).

14) M. J. Jorgenson and D. R. Harter, *J. Am. Chem. Soc.*, **85**, 878 (1963).

15) a) For the uracil; A. R. Katritzky and A. H. Wuring, *J. Chem. Soc.*, **1962**, 1540; b) For the substituted benzamide; J. T. Edward, H. S. Chang, K. Yates and R. Stewart, *Can. J. Chem.*, **38**, 1518 (1960); c) R. Stewart and M. R. Granger, *ibid.*, **39**, 2508 (1961).

16) Recently, Haake and his co-workers have used this equation for the pK_{BH^+} measurement of phosphine oxides and others by NMR with less confusion; P. Haake, R. D. Cook and G. H. Hurst, *J. Am. Chem. Soc.*, **89**, 2650 (1967).

Table 2. The pK_{BH^+} values and H_0 dependence of substituted diphenyl sulfoxides

Substituent	$-pK_{BH^+}$	n[a]	Wavelength for detn. mμ[b]
p-CH_3O	3.67±0.18	1.81±0.20	240—290
p-C_2H_5O	3.67±0.16	1.81±0.20	240—290
p-CH_3	4.40±0.22	2.19±0.11	235—274
m-CH_3	4.73±0.13	1.68±0.20	231—270
H	4.92±0.18	2.39±0.12	230—265
p-Cl	5.15±0.18	2.26±0.11	238—270
p-I	5.13±0.26	2.19±0.20	235—270
p-Br	5.24±0.10	2.24±0.20	238—275
m-Cl	5.74±0.04	2.27±0.23	231—270
Benzophenone[c]	6.23±0.10	1.75±0.10	259—345
Acetophenone[c]	6.30±0.18	1.50±0.11	250—310

a) The correlation coefficient of all these values gave more than 0.990.
b) This is the wave length of UV spectra used to determine A.
c) These compounds were used as the standard of the pK_{BH^+} values of the sulfoxides.

(1.43—2.21),[16] *etc.*, indicating that the diphenyl sulfoxides also do not behave as Hammett bases. Recently Haake and Cook[4] also reported large n-values for phenyl methyl sulfoxide (1.62) and dimethyl sulfoxide (1.61).

All our pK_{BH^+} data of the substituted diphenyl sulfoxides obtained are listed in Table 2. Although we have also calculated the pK_{BH^+} values of our compounds by the method described by Davis and Geissmann,[17] these values are identical to those in Table 2.

Stretching Frequency of S–O Bond for Substituted Diphenyl Sulfoxides. The infrared spectra were determined in a set of 0.20 mm fixed path cells by means of JASCO-IR-C Infrared Spectrophotometer while the concentration of a sulfoxide was maintained as 0.05 mol/l in carbon tetrachloride. The stretching vibrations of S–O bonds of these substituted diphenyl sulfoxides obtained are listed in Fig. 2, and are found to be in a good correlation with Hammett σ values, with a correlation coefficient, r=0.990.

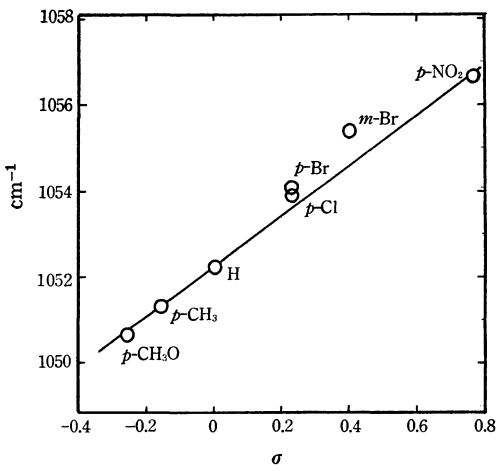

Fig. 2. Stretching frequencies of the S–O bond substituted diphenyl sulfoxides plotted against σ values.

Discussion

The pK_{BH^+} values of the diphenyl sulfoxides listed in Table 2 reveal that these sulfoxides possess rather weak basicities, and even the strongest base of this series, *i. e.*, p-anisyl phenyl sulfoxide, has its pK_{BH^+} of only −3.67. Recently, the pK_{BH^+} values of diphenyl sulfoxide has been measured in acetic anhydride by titration with perchloric acid by Andersen and his co-workers,[3] but their pK_{BH^+} value (−3.58) is considerably larger than that of ours (−4.97).[20] The pK_{BH^+} values of several other organic oxides are also listed in Table 3 for comparison.

Table 3. pK_{BH^+} Values of organic oxides

Compound	pK_{BH^+}		
$(C_6H_5)_2SO$	−4.97[a]	−3.58[b]	
$(C_6H_5)S(O)CH_3$	−0.488[b]	−3.45[c]	−3.60[d]
$(CH_3)_2SO$	0.911[b]	0[f]	−2.7[c]
$(C_6H_5)_2P(O)CH_3$	−3.2[c]		
$(C_6H_5)C(O)CH_3$	−6.15[e]	−6.30[a]	−6.51[c]
$(C_6H_5)_2CO$	−6.18[e]	−6.23[a]	
$(CH_3)_3NO$	4.65[f]		
$(CH_3)_3AsO$	3.75[f]		

a) This work.
b) By potentiometric titration method (Ref. 3).
c) By NMR method (Ref. 4a, 16).
d) Our unpublished work, by NMR (Ref. 4b).
e) By a similar method to ours (Ref. 18, 19).
f) Ref. 2.

The basicities of the sulfoxides resemble more closely those of the carbonyl compounds and phosphine oxides than those of the amine and arsine oxides. Probably a substantial 2p–3dπ interaction may be in operation between the two ends of the S–O bond to diminish the basicities of the sulfoxide as in the cases of carbonyl compounds and phosphine oxides. It is known incidentally that the basicity of an oxide would be diminished

17) C. T. Davis and T. A. Geissmann, *J. Am. Chem. Soc.*, **76**, 3507 (1954).

18) A. Fischer, B. A. Grigor, J. Packer and J. Vanghan, *ibid.*, **83**, 4208 (1962).

19) R. Stewart and K. Yates, *ibid.*, **80**, 6355 (1959).

20) The pK_{BH^+} value for phenyl methyl sulfoxide of Haake and Cook[4a] and ours[4b] which was measured by NMR in sulfuric acid media, are also smaller than that of Andersen and his co-workers'[3] which was measured by potentiometric titrations in acetic anhydride.

not only the semipolar character but also by the π-bonding character of the oxide bond.[21]

For example, the C–O bond of the carbonyl compounds which display the weakest basicities among several organic oxides possess almost complete π-bonding character, while the N–O and As–O bonds of amines and arsine oxides are known to be of a semipolar nature and quite basic.

It is interesting to note that the basicities of diphenyl sulfoxide is markedly smaller than that of dimethyl sulfoxide. In the case of dimethyl sulfoxide,[22] perhaps both electron-donating inductive and hyperconjugative effects of two methyl groups increase the electron density of the sulfoxide S–O linkage to enhance the basicity, while the low basicity of diphenyl sulfoxide may be due to the electron-withdrawing inductive effect of two phenyl groups which reduce the electron density of the S–O bond.

When the pK_{BH^+} values for the *meta*- and *para*-substituted diphenyl sulfoxides thus obtained were plotted against Brown–Okamoto's[9] σ^+ values, a good straight line was obtained with the correlation coefficient $r=0.990$, and the ρ value of -2.00.[24] Incidentally it is known that the plotting of the same pK_{BH^+} values against Hammett's σ values gives a very poor correlation, $r=0.920$.

These σ^+-correlations and the magnitude of ρ value of the diphenyl sulfoxides closely resembled those of substituted acetophenones (For $\sigma^+-pK_{BH^+}$; $\rho=-2.17$ ($r=0.983$). For $\sigma-pK_{BH^+}$; $\rho=-2.22$ ($r=0.903$))[19] and benzaldehydes (for $\sigma^+-pK_{BH^+}$; $\rho=-1.85$ ($r=0.994$)).[25] This suggests that similar resonance effects by the same substituents are possible for all these compounds. The two extremely delocalized formula for the protonated form of *p*-substituted diphenyl sulfoxides would be depicted as shown below.

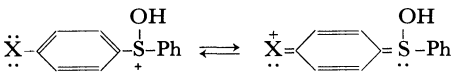

Since the sulfur atom can expand its valence shell beyond octet using its 3d orbitals, the C–S bond between the aromatic carbon atom and the sulfur atom could have another π bonding (2p–3d type) upon the protonation to create a discrete positive charge on the sulfur atom and the formation of this 2p–3dπ bonding may call for a large resonance effect of the substituent.

In the case of the unprotonated sulfoxides, however, such a large demand for resonance effect of substituent would be negligible, since the sulfur atom bears only a fraction of a positive charge and hydrogen bonding to the terminal oxygen atom would give only a perturbation on the electron localization along the C–S linkage. Therefore, the S–O stretching frequency would be very slightly affected by the resonance effect of the substituents.

21) The bond moment; average value $\mu_{SO}=3.0$ D and the shorter bond length; 1.45 Å (average) also indicate a considerable double bonding of sulfoxides. [See C. C. Price and S. Oae, "Sulfur Bonding," Chapter 4, Ronald Press Co., New York, N. Y. (1962).]

22) The dipole moments of diphenyl sulfoxide and dimethyl sulfoxide were 4.08 (D)[12] and 4.3 (D)[23] respectively, which also show a larger inductive effect of methyl substituents.

23) A. J. Parker, "The Use of Dipolar Aprotic Solvents in Organic Chemistry," in "Advances in Organic Chemistry," Vol. 5, ed. by R. A. Raphael, E. C. Taylor and H. Wynberg, Interscience Publishers, N. Y. (1965), p. 3.

24) The value for *p*-anisyl phenyl sulfoxide was found to be slightly lower than that predicted by the σ^+ values. This deviation would be caused by the solute-solvent hydrogen bonding in sulfuric acid acting to reduce the resonance effect of *p*-CH_3O group.[5a]

25) K. Yates and R. Stewart, *Can. J. Chem.*, **37**, 664 (1959).

BULLETIN OF THE CHEMICAL SOCIETY OF JAPAN VOL. 42 1968—1971 (1969)

The Mechanism of the Alkaline Decomposition of Triarylsulfonium Bromide with Phenyllithium[1]

Yong He Khim and Shigeru Oae

Department of Apllied Chemistry, Faculty of Engineering, Osaka City University, Sumiyoshi-ku, Osaka

(Received October 11, 1968)

Tritolylsulfonium bromide was subjected to alkaline decomposition in order to clarify the mechanism of the reaction of triarylsulfonium bromide with phenyllithium in ether. Diaryl sulfides, diaryls, and other aryl derivatives were obtained and the combined yield was nearly quantitative. On the basis of the ratio of the products formed in the reaction, the alkaline decomposition is considered to proceed through two mechanistic routes, *i. e.*, one involving the nucleophilic attack of phenyl anion on the sulfur atom (about 70%) and the other the "benzyne" route (about 20%).

The reaction of triarylsulfonium halide with phenyllithium has been studied by Franzen[2] and later by Andersen.[3] However, their experimental procedures are not identical and the results they obtained are also somewhat different. The mechanisms suggested are also entirely different.

Franzen reported that triphenylsulfonium bromide exchanges phenyl groups with phenyllithium very rapidly and involves the initial formation of an unstable tetravalent sulfur intermediate and the succeeding extrusion of the phenyl group. On the other hand, Andersen proposed a mechanism involving "benzyne" intermediate on the basis of their observation that the addition of phenyllithium to diphenyl sulfoxide in ethyl ether gives diphenyl sulfide and diphenyl.

Franzen and Joschek[4] later also presented evidence that tri-(2-methoxyphenyl)sulfonium chloride reacted with phenyllithium to give the corresponding aryne though in poor yield. Meanwhile, Sheppard[5] suggested that the reaction between phenylsulfur trifluoride with phenyllithium to give both phenyl sulfide and diphenyl proceeds *via* the initial formation of tetraphenylsulfur intermediate by the replacement of the fluorines by phenyl groups, similar to the reaction between triarylsulfonium halide and aryllithium. However, the mechanisms of all these reactions have remained totally unclarified. In addition to the two mechanistic pathways hitherto mentioned, *i. e.*, the one involving the tetravalent sulfur intermediate and the other which includes "benzyne" intermediate, there are two other possibilities; namely, the reaction may proceed *via* the initial nucleophilic attack of phenyllithium on the carbon atom (mechanism 3) or may proceed *via* an intramolecular decomposition (mechanism 4). All these possible mechanisms are schematically illustrated with tolyldiphenylsulfonium compound as shown below.

1) Nucleophilic attack on sulfur atom.

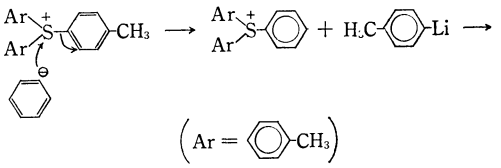

2) Benzyne mechanism.

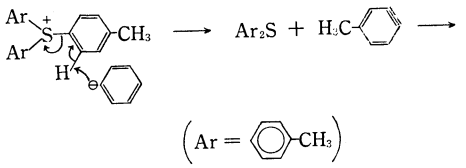

3) Aromatic S_N reaction.

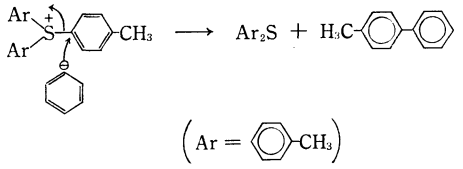

4) Intramolecular decomposition.

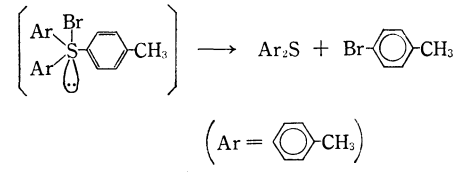

1) Paper II on Sulfonium Salt. Paper I, this Bulletin, **42**, 1622 (1969).

2) V. Franzen and C. Mertz, *Ann.*, **643**, 24 (1961).

3) K. K. Andersen and S. A. Yeager, *J. Org. Chem.*, **28**, 865 (1963).

4) V. Franzen, H. I. Joschek and C. Mertz, *Ann.*, **654**, 82 (1962).

5) W. A. Sheppard, *J. Am. Chem. Soc.*, **84**, 3058 (1962).

In order to make a choice among these possible mechanistic pathways for the reaction between triarylsulfonium compound and aryllithium, we have undertaken detailed analyses of the products formed in the reaction between tritolylsulfonium compound and phenyllithium. This paper will describe a detailed account of the investigation. In the previous studies by both Franzen and Andersen there was a technical difficulty in choosing a plausible mechanism, since the yields of reaction products in both cases were entirely different. However, by the use of tritolylsulfonium compound with phenyllithium, one can readily test the "benzyne" mechanism (Mechanism 2) and the intramoleclular decomposition (Mechanism 4), since the "benzyne" mechanism will require the formation of both *m*- and *p*-substituted ditolyls, while the intramolecular decomposition mechanism (4) will give tolyl bromide and diaryl sulfide.

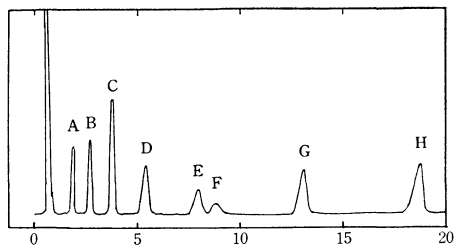

Fig. 1. Vapor phase chromatography (packing: 30%-PEGA, 70%-fiber brick) at 178°C.

A: 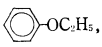 , B: , C: 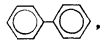 ,

D: 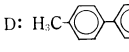 , E: 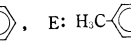 , F: 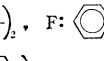 ,

G: 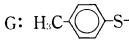 , H: 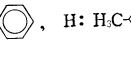

Results and Discussion

The products obtained are shown in Table 1. The reaction of tritolylsulfonium bromide with phenyllithium was carried out in boiling ether and after the reaction was completed the reaction mixture was carbonated. The products contained in ether layer were carefully fractionated by gas chromatography and identified by comparing their mp, infrared and NMR spectra with those of the authentic samples. A typical gas chromatogram of the products formed is shown in Fig. 1. One finds peaks of *p*-ditolyl sulfide, phenyl *p*-tolyl sulfide, ditolyl, *p*-methyldiphenyl, diphenyl, phenetole, phenol, and *p*-tolyl bromide in the vapor phase chromatogram. However, ditolyl and diphenyl sulfide were obtained as a mixture without being well-separated and their products ratio was determined by NMR spectra. Further, through the careful inspection of the infrared absorption spectra it was found that ditolyl consists of a mixture of two isomers, *i. e.*, *p,p'*-dimethyldiphenyl and *m,p'*-isomer in the ratio of about 1:3. Since *m,p'*-dimethyldiphenyl is formed only through the "benzyne" route (mechanism 2) through which nearly the same amount of *p,p'*-isomer would be also formed. Therefore, the "benzyne" route shown below would account for approximately 20% of the products formed in the reaction. Tolyllithium being a stronger nucleophile than phenyllithium, apparently reacts preferentially with "benzyne" formed. When the reaction was performed in the presence of a 2.0 molar equivalent of lithium thiophenoxide, a nucleophile which reacts more rapidly than phenyl-

Table 1. The reaction of tritolylsulfonium bromide with phenyllithium in ether

Sulfide group (yield %)	Diaryl group (yield %)	Aryl group (yield %)	Carboxylic acid (yield %)	Other product** (yield %)
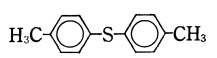 (57)	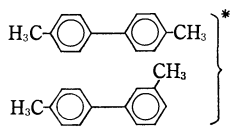 * (20)	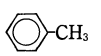 (small)	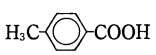 (26)	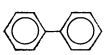 (5–8)
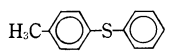 (33)	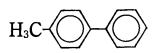 (29)	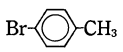 (1–2)		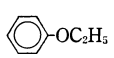 (~3)
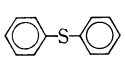 (7)				(3–5)

* The molar ratio of *m*- and *p*-isomers is about 1:1.

** All the products result in the formation of phenyllithium.

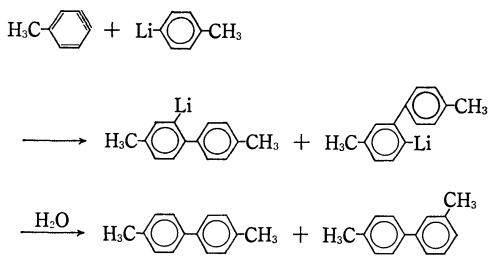

lithium with benzyne,[6] diphenyl sulfide (8%) and ditolyl (21%) were obtained. These yields of the two products do not differ much, regardless of the absence or presence of thiophenoxide in the reaction system. If the lithium thiophenoxide can compete with tolyllithium in the addition reaction to "benzyne," the yield of diphenyl sulfide would increase and the yield of ditolyl would decrease. If phenyllithium could compete with tolyllithium in addition to "benzyne," both *p*-methyldiphenyl and its *m*-isomer would be obtained; however, no such *m*-isomer could be detected. *p*-Tolyl phenyl sulfide and diphenyl sulfide are undoubtedly the products formed by the collapse of the tetravalent sulfur intermediate as shown below, while di-*p*-tolyl sulfide is formed not only *via* this route but also by other routes. The mechanistic route involving the aromatic nucleophilic substitution on the carbon atom with the phenyllithium with ditolyl sulfide as the leaving group (mechanism 3) could explain the formation of ditolyl sulfide and *p*-methyldiphenyl, but not that of *p*-tolyl phenyl sulfide. Therefore, this route, (mechanism 3) is rather unlikely.

Judging from the distribution of the whole product and the yields of tolyl compounds formed from the sulfonium bromide, the mechanism involving the nucleophilic attack on the sulfur atom (mechanism 1) seems to account for about 75% of the products formation. Previously Franzen calculated the portion of the reaction through the mechanistic route 1 only from the amount of benzoic acid formed by the carbonation in the reaction of triphenylsulfonium bromide with phenyllithium. By the use of tritolylsulfonium bromide with phenyllithium for the reaction, one can now include other tolyl compounds such as methyldiphenyl, ditolyl and toluene as the products formed by the mechanistic route 1.

In view of the substantial formation of ditolyl the exchange of aryl group *via* route 1 undoubtedly takes place very fast. Meanwhile, the formation of tolyl bromide could be explained in terms of the intramolecular decomposition[7] though the yield (2%) is very poor (mechanism 4). Another possible route for the formation of tolyl bromide would be the addition of bromide to aryne formed by the route 2.

Besides, diphenyl,[8,9] phenetole[10] and phenol[9] were obtained. These undoubtedly result from the reaction of phenyllithium formed in the reaction of bromobenzene with lithium in diethyl ether, since all these compounds can be found among the reaction mixture before the addition of the sulfonium salt and the amounts remain the same even after the addition of the salt.

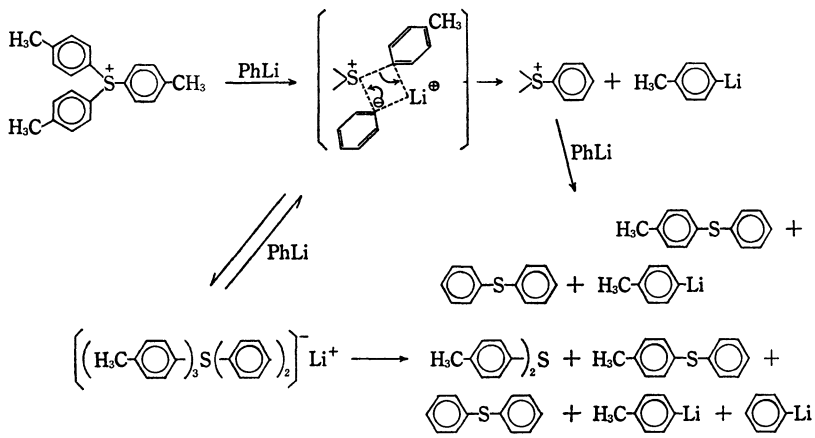

6) a) R. Huisgen in "Organometallic Chemistry," H. Zeiss, ed., Reinhold Publishing Corp., New York, N. Y. (1960), pp. 11, 36—87.

7) G. H. Wiegand and W. E. McEwen, *Tetrahedron Letters*, **1965**, 2639.

8) E. Muller and T. Topel, *Ber.*, **72B**, 273 (1939).

9) H. A. Pacevitz and H. Gilmann, *J. Am. Chem. Soc.*, **61**, 1603 (1939).

10) G. Wittig and U. Pockels, *ibid.*, **72B**, 884 (1939).

Experimental

Starting and Authentic Materials. Tritolylsulfonium bromide was prepared[11] from ditolylethoxysulfonium tetrafluoroborate[12] and tolyl Grignard reagent. mp 244—245°C (decomp.). *m*- And *p*-methyldiphenyls were prepared from the reaction of the corresponding diazonium salt with benzene and (*m*,*p*'- and *p*,*p*'-) dimethyldiphenyls were also obtained similarly. Diphenyl sulfide, phenyl tolyl sulfide and di-*p*-tolyl sulfide were prepared by the reaction of the corresponding aryldiazonium salts with thiophenolate.

The Reaction of Tritolylsulfonium Bromide with Phenyllithium. Tritolylsulfonium bromide (2.14 g, 0.0056 mol), in 10 m*l* of anhydrous ethyl ether was added to the ethereal solution of phenyllithium (0.024 mol) prepared from bromobenzene and lithium under a nitrogen stream. After the reaction mixture was refluxed for 45 min, it was poured onto dry ice, and hydrolyzed with 5% of hydrobromic acid. The ethereal layer was extracted with 10% sodium carbonate solution, and aqueous extract was acidified to isolate the mixture of benzoic and toluic acids. *p*-Toluic acid (0.2 g) was seperated by careful recrystallization from an alcohol-water mixture. The ethereal layer was washed, dried and fractionated by vapor phase chromatography. The identification and the determination of the yields of the products were performed using quantitative vapor phase chromatography and by comparison of their infrared spectra with those of authentic samples. The isolated compounds from the organic layer and their yields are shown in Table 1.

Meanwhile, the direct hydrolysis of the reaction mixture, after it was refluxed for 50 min, gave the products in almost same yields. However, in this case toluene (22%) was obtained instead of toluic acid.

The Reaction of Tritolylsulfonium Bromide with Phenyllithium-Thiophenoxide Mixture. Thiophenol (1.76 g, 0.008 mol) in 5 m*l* of anhydrous ethyl ether was added to the ethereal solution of phenyllithium (0.024 mol) and the mixture was kept stirring for 10 min at 40°C. Tritolylsulfonium bromide (1.4 g, 0.004 mol) in 10 m*l* of anhydrous ethyl ether was added to this mixture. After the reaction mixture was refluxed for 80 min, poured into ice water, acidified with 5% hydrobromic acid, and the ethereal layer was separated. The ether extract of the water layer was combined with it. Distillation of the organic layer gave almost the same products, and their yields in the case where only phenyllithium was used are shown in Table 1. The purities and yields of the products were checked by the usual quantitative vapor phase chromatography. (Diphenyl sulfide 8%, ditolyl 21%, toluene 20%.)

11) a) K. K. Andersen and N. E. Papanikolaov, *ibid.*, **1966**, 5445.

12) C. R. Johnson and D. Macants, Jr., *ilid.*, **87**, 5408 (1965).

BULLETIN OF THE CHEMICAL SOCIETY OF JAPAN VOL. 42 1971—1975 (1969)

Synthetic Studies of Sesamol Derivatives. XI.*1 Synthesis of 5,6-Methylenedioxy-2-isopropenylbenzo[*b*]furan*2

Kenji FUKUI, Mitsuru NAKAYAMA and Sachihiko TANAKA

Department of Chemistry, Faculty of Science, Hiroshima University, Higashi Sendamachi, Hiroshima

(Received October 25, 1968)

5,6-Methylenedioxy-2-isopropenylbenzo[*b*]furan, an analogue of the naturally-occurring 5,6-dimethoxy compound, has been synthesized by the dehydration of the corresponding 2-(1′-hydroxy)isopropyl derivative, which was obtained from 2-hydroxy-4,5-methylenedioxybenzaldehyde. By the catalytic hydrogenation of the benzofuran, its 2-isopropyl derivative and its 2-isopropyl-2,3-dihydrofurano-compound were prepared. The NMR spectra of these compounds have been compared.

Recently, a new naturally-occurring benzofuran derivative, 5,6-dimethoxy-2-isopropenylbenzo[*b*]-furan (I), has been isolated from *Ligularia stenocephala* Matsum. *et* Koidz. by Takahashi *et al.*[1] 5,6-Methylenedioxy-2-isopropenylbenzo[*b*]furan (II), an analogue of I containing a methylenedioxy group instead of two methoxyl groups, has a substitution pattern found in several naturally-occurring flavonoids, isoflavonoids and coumestans; it could, therefore, be expected to occur in nature. It was considered useful to synthesize II and record its properties in order to help in the identification of the compound when it is discovered. In continuation of a series of synthetic studies of sesamol deriv-

*1 Part X: K. Fukui and M. Nakayama, This Bulletin, **41**, 2733 (1968).

*2 Presented at the 21st Annual Meeting of the Chemical Society of Japan, Osaka, April, 1968.

1) T. Murae, Y. Tanahashi and T. Takahashi, *Tetrahedron*, **24**, 2177 (1968).

atives, the present paper will describe the syntheses of II and related compounds, and will present the spectral data of these compounds.

The reaction of methylmagnesium iodide with 5,6-methylenedioxy-2-acetylbenzo[*b*]furan (III), which was obtained by treating 2-hydroxy-4,5-methylenedioxybenzaldehyde (IV)[2] with monobromoacetone, afforded a benzofuran derivative V, $C_{12}H_{12}O_4$, mp 65—66°C. The same compound, V, was furnished by the reaction of this Grignard reagent with 5,6-methylenedioxy-2-carbethoxybenzo[*b*]furan (VI).[3] The infrared spectrum of V exhibited an absorption due to the hydroxyl group at 3320 cm^{-1}. In its NMR spectrum (Table 1),*3 a singlet signal at δ 2.10 (1H), which easily disappeared upon deuterium exchange, and a sharp singlet at δ 1.63 (6H) provided evidence for the presence of $-C(OH)(CH_3)_2$ grouping. Moreover, V has the NMR signals at δ 5.97 (singlet, 2H, $O-CH_2-O$), 6.46 (doublet, 1H, $J=0.75$ Hz, β-hydrogen atom of benzofuran ring),[4] 6.90 (singlet, 1H, aromatic proton), and 6.97 (doublet, 1H, $J=0.75$ Hz, aromatic proton). These NMR spectral data suggest the presence of one β-proton on the benzofuran ring and that the two isolated aromatic protons are in a 1,4-relationship. Therefore, the structure of V was established as 5,6-methylenedioxy-2-(1′-hydroxy) isopropylbenzo[*b*]-furan.

The dehydration of V by heating alone afforded an isopropenyl derivative II, $C_{12}H_{10}O_3$, mp 98—99°C, in a 41% yield. The NMR spectrum of II (Table 1 and Fig. 1) showed a methyl signal, δ 2.09 (3H, doublet, $J=$Hz), and signals due to two vinyl protons at δ 5.12 and 5.70 (each 1H, finely-split signal).

The catalytic hydrogenation of II over 5% Pd-C in ethyl acetate at room temperature gave the corresponding isopropylbenzofuran VII, $C_{12}H_{12}O_3$, mp 56—57°C; its NMR spectrum exhibited signals at δ 1.29 (6H, doublet, $J=7$ Hz), 3.02 (1H, multiplet, $(CH_3)_2$=CH–), 6.89 (1H, singlet), and 6.97 (1H, broad singlet). Elvidge and Foster[4] have reported that, in the NMR spectra of benzofurans, the 3-proton couples with the 7-proton with $J=0.9$ Hz. The singlet at δ 6.89 and the broad singlet at δ 6.97 mentioned above can, therefore, be attributed to the 4- and 7-protons respectively. This assumption is in accord with the spectral data (Table 1) of 4,5-methylenedioxybenzo[*b*]furan (VIII)[3] and its 3-methyl- (IX) and 2,3-dimethyl-derivative (X) prepared from sesamol.[5]

Next, VII was further reduced over 5% Pd-C in ethanol at an elevated temperature to give 2,3-dihydrobenzofuran, XI. The NMR spectrum of XI (Table 1 and Fig. 3) showed a two-proton

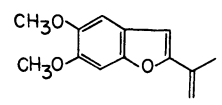

I

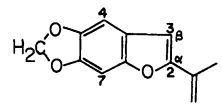

II

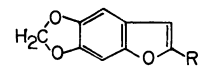

III R=$COCH_3$
V R=$C(OH)(CH_3)_2$
VI R=$CO_2C_2H_5$
VII R=$CH(CH_3)_2$

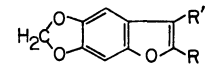

VIII R=R′=H
IX R=H, R′=CH_3
X R=R′=CH_3

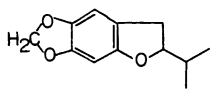

XI

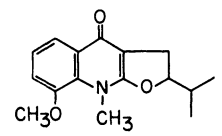

XII

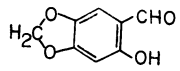

IV

TABLE 1. THE NMR SPECTRAL DATA OF BENZO[*b*]-FURANS*3,4

Benzo[*b*]-furan	Proton			
	C-2	C-4	C-3	C-7
II	—	6.93_s	6.57_{bs}	6.99_d ($J=1$)
III	—	7.02_m	7.42_d $J=0.75$)	7.02_m
V	—	6.90_s	6.46_d ($J=0.75$)	6.97_d ($J=0.75$)
VI	—	6.99_s	7.45_d ($J=1$)	7.07_m
VII	—	6.89_s	6.25_m	6.97_{bs}
XI	4.46_m	6.62_s	$2.56—3.28_m$	6.35_s
VIII	7.58_d ($J=2$)	6.99_s	6.68_{dd} ($J=2$, $J=1$)	7.05_d ($J=1$)
IX	7.35_q ($J=1.5$)	6.90_s or 6.97	—	6.97_s or 6.90_s
X	—	6.82_s or 6.92_s	—	6.92_s or 6.82_s

*4 s=singlet, bs=broad singlet, d=doublet, q=quartet, m=multiplet, and dd=double doublet and $J=$Hz value.

2) K. Fukui and M. Nakayama, This Bulletin, **35**, 1321 (1962).

3) K. Fukui, M. Nakayama and K. Okazaki, *Nippon Kagaku Zasshi* (*J. Chem. Soc. Japan, Pure Chem. Sect.*), **87**, 1096 (1966).

*3 The NMR spectra were measured with a Hitachi R-20 spectrometer, using tetramethylsilane as the internal standard (δ-value in $CDCl_3$).

4) J. A. Elvidge and R. G. Foster, *J. Chem. Soc.*, **1964**, 981.

5) K. Fukui and M. Nakayama, *J. Sci. Hiroshima Univ., Ser. A-II*, **26**, 131 (1963).

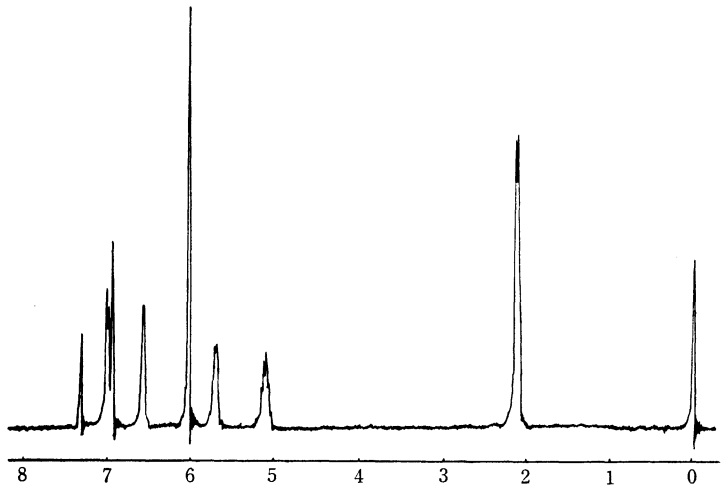

Fig. 1. NMR spectrum of II.

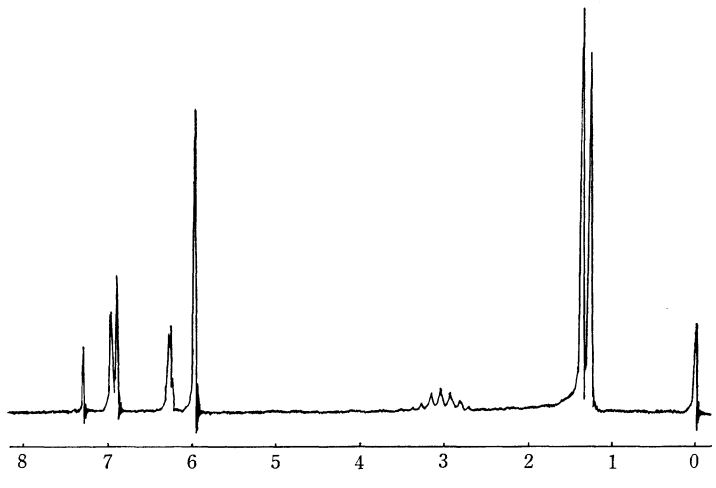

Fig. 2. NMR spectrum of VII.

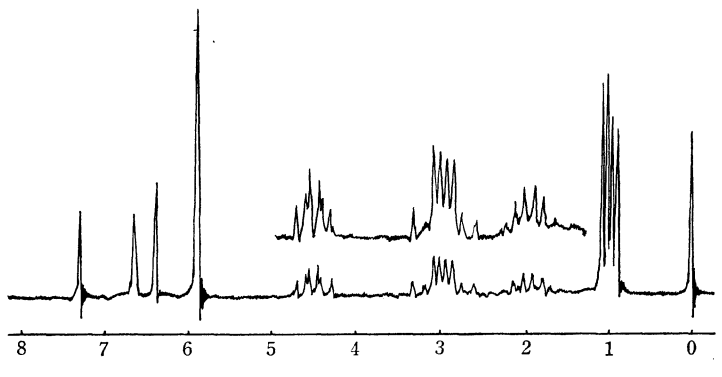

Fig. 3. NMR spectrum of XI.

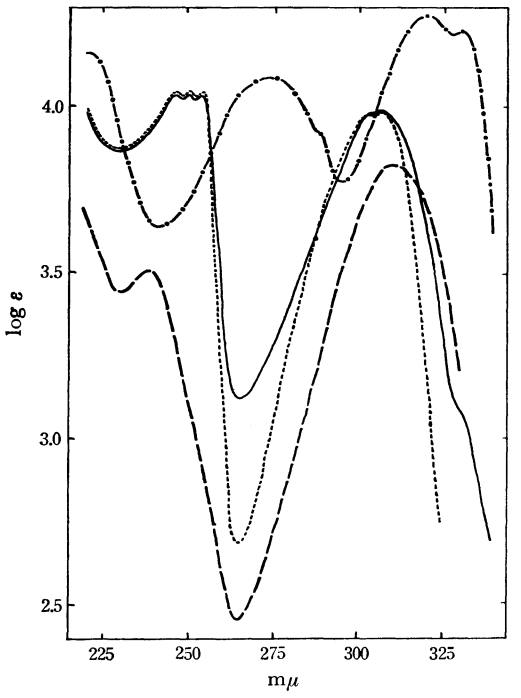

Fig. 4. Ultraviolet spectra of II (-·-·-), V (——), VII (------) and XI (— — —) in ethanol.

multiplet centered at δ *ca.* 2.9 and a one-proton multiplet centered at δ 4.46 attributable to the β- and α-protons of dihydrofuran-ring respectively. An interesting feature of the spectrum was provided by the signals (δ 0.93 and 0.99, each 3H, doublet, J=6.5 Hz) due to the two methyl groups of the isopropyl side chain; *e. g.*, these signals are quite similar to those of the isopropyldihydrofuran system in lunacrine (XII),[6] and these two methyl groups are magnetically nonequivalent.

The ultraviolet spectra of these compounds (II, V, VII, and XI) are shown in Fig. 4. The shape of the UV spectrum of V is very similar to that of VII. The bathochromic effect (about 11 mμ) observed in the spectrum of II could be explained as resulting from the isopropenyl double bond conjugated to the furan ring at the α-position. On the other hand, the spectrum of XI is very similar to that of 6-substituted-3,4-methylenedioxyanisole derivatives.[7]

Experimental*5

5,6-Methylenedioxy-2-acetylbenzo[*b*]furan (III). A hot solution of IV (mp 125—126°C)[2] (3.3 g) in absolute ethanol (40 m*l*) was treated with a solution of potassium hydroxide (1.2 g) in absolute ethanol (20 m*l*). Then, monobromoacetone (3.0 g) was stirred, drop by drop, into the hot solution over a 20-min period and the reaction mixture was refluxed for 1 hr on a steam bath. Again, potassium hydroxide (0.6 g) and monobromoacetone (1.5 g) were added to the mixture and the reaction was continued for 1 hr. The product was treated again with potassium hydroxide (0.3 g) and monobromoacetone (0.75 g). After the addition of water (20 m*l*), the organic solvent was evaporated. The resulting residue was repeatedly extracted with benzene. The combined benzene solutions were washed with a diluted sodium hydroxide solution, dried over anhydrous sodium sulfate, and evaporated. The residue was crystallized from ethanol to give colorless needles of III, mp 156.5—157°C; yield, 3.2 g. IR: 1672 (C=O); 1626, 1545, 1495 (aromatic); 1036, 945 cm^{-1} (O-CH_2-O). UV: λ_{max} mμ (log ε); 267 (3.76), 291.5 (4.00), 340 (4.27). NMR:*3,4 δ 6.05$_s$ (O-C$\underline{H}_2$-O), 2.55$_s$ (C$\underline{H}_3$CO) and Table 1.

Found: C, 64.95; H, 4.14%. Calcd for $C_{11}H_8O_4$: C, 64.70; H, 3.95%.

5,6-Methylenedioxy-2-(1′-hydroxy)isopropylbenzo[*b*]furan (V). *a) From III.* A solution of III (510 mg) in a mixture of anhydrous ether (10 m*l*) and anhydrous benzene (35 m*l*) was slowly stirred into a methylmagnesium iodide solution (from methyl iodide (1.56 g) and magnesium (270 mg) in anhydrous ether (15 m*l*)) for 0.5 hr in an ice-bath. After stirring for 1.5 hr, the reaction mixture was decomposed by the cautious addition of 1N sulfuric acid (20 m*l*). The aqueous layer was reextracted with benzene, and the combined benzene solution were washed with a 5% sodium hydrogen carbonate solution and a saturated sodium thiosulfate solution, and dried over anhydrous sodium sulfate. After the solvent had been evaporated *in vacuo*, the residue was purified by column chromatography over alumina with benzene. The elute was evaporated to yield yellow crystals. This was sublimated at 50°C *in vacuo* to give colorless crystals of V, mp 65—66°C; yield, 160 mg. IR: 3320 (OH); 1630, 1591, 1555, 1505 (aromatic); 1040, 938 cm^{-1} (O-CH_2-O). UV: λ_{max} mμ (log ε); 246.5 (4.03), 250.5 (4.03), 254.5 (4.03), 306$_{sh}$*6 (3.98), 309 (3.98), 331$_{sh}$ (3.10). NMR:*3,4 δ 5.97$_s$ (O-C$\underline{H}_2$-O); 2.10$_s$ (O$\underline{H}$); 1.63$_s$ (6H, C$\underline{H}_3$) and Table 1.

Found: C, 65.57; H, 5.29%. Calcd for $C_{12}H_{12}O_4$: C, 65.44; H, 5.49%.

b) From VI. A mixture of VI (mp 84—85°C)[3] (1.1 g) in anhydrous ether (10 m*l*) and anhydrous benzene (20 m*l*), and a methylmagenesium iodide solution (from methyl iodide (2.20 g) and magnesium (0.35 g) in anhydrous ether (10 m*l*)) was refluxed on a steam bath with stirring for 1.5 hr. The reaction mixture was then treated as above to give V, mp 65—66°C; yield, 0.55 g.

5,6-Methylenedioxy-2-isopropenylbenzo[*b*]furan (II). The hydroxy-compound V (160 mg) was heated at 150°C for 5 min in a stream of nitrogen. The viscous, orange yellow product was sublimated in a stream of nitrogen *in vacuo* at 90°C/1 mmHg to give colorless needles of II, mp 98—99°C; yield, 60 mg.

6) S. Goodwin, J. N. Shoolery and L. F. Johnson, *J. Am. Chem. Soc.*, **81**, 3065 (1959).

7) K. Fukui and M. Nakayama, *Nippon Kagaku Zasshi* (*J. Chem. Soc. Japan, Pure Chem. Sect.*), **84**, 606 (1963).

*5 All the melting points are uncorrected; the infrared spectra were measured in Nujol, while the ultraviolet spectra were measured in ethanol.

*6 sh=shoulder.

IR: 1620, 1555, 1502 (aromatic); 1038, 940 (O-C$\underline{H}_2$-O); 877 cm^{-1} ($H_2C{=}C\langle$). UV: λ_{max} mμ (log ε); 221 (4.16), 276 (4.07), 320 (4.26), 332 (4.22). NMR: *3,4 δ 6.00$_s$ (O-C$\underline{H}_2$-O); 5.70$_m$, 5.12$_m$ (each IH, $\rangle C{=}C\underline{H}_2$); 2.09$_d$ (J=1)(C$\underline{H}_3$) and Table 1.

Found: C, 71.14; H, 5.12%. Calcd for $C_{12}H_{10}O_3$: C, 71.28; H, 4.99%.

5,6-Methylenedioxy-2-isopropylbenzo[*b*]furan (VII). A solution of II (65 mg) in ethyl acetate (50 m*l*) was hydrogenated over 5% Pd-C (50 mg) at room temperature for 10 min; 1 molar equivalent of hydrogen was absorbed. After the catalyst had been filtered, the filtrate was evaporated under a weak vacuum. The residual oil was soon crystallized on cooling. This was sublimated *in vacuo* at 55°C/0.5 mmHg to give colorless prisms of VII, mp 56—57°C; yield, 57 mg. IR: 1625, 1588, 1555, 1500 (aromatic); 1036, 943 cm^{-1} (O-C$\underline{H}_2$-O). UV: λ_{max} mμ (log ε); 247 (4.04), 251 (4.03), 255 (4.04), 305 (3.97), 309 (3.97). NMR: *3,4 δ 5.96$_s$ (O-C$\underline{H}_2$-O); 3.02$_m$ (J=7)($\rangle C\underline{H}$); 1.29$_d$ (J=7)(6H, C$\underline{H}_3$) and Table 1.

Found: C, 70.39; H, 5.88%. Calcd for $C_{12}H_{12}O_3$: C, 70.57; H, 5.92%.

5,6-Methylenedioxy-2-isopropyl-2,3-dihydrobenzo[*b*]furan (XI). A solution of VII (40 mg) in ethanol was hydrogenated over 5% Pd-C at 70°C at atmospheric pressure for a few hours. After the same procedure as has been described above, the residue was crystallized from dilute ethanol to give colorless plates of XI; mp 92—93°C; yield, 37 mg. IR: 1616, 1498 (aromatic); 1047, 934 cm^{-1} (O-C$\underline{H}_2$-O). UV: λ_{max} mμ (log ε); 240 (3.51), 313 (3.82). NMR: *3,4 δ 5.85$_s$ (O-C$\underline{H}_2$-O); 1.93$_m$ (J=6.5) ($\rangle C\underline{H}$); 0.99$_d$, 0.93$_d$ (J=6.5) (each 3H, C$\underline{H}_3$) and Table 1.

Found: C, 70.09; H, 6.67%. Calcd for $C_{12}H_{14}O_3$: C, 69.88; H, 6.84%.

5,6-Methylenedioxy-3-methylbenzo[*b*]furan (IX). *a) 2-Acetyl-4,5-methylenedioxyphenoxyacetic Acid.* A mixture of 2-hydroxy-4,5-methylenedioxyacetophenone (mp 112—113°C)[8] (0.9 g), ethyl bromoacetate (0.9 g), and anhydrous potassium carbonate (4.0 g) in anhydrous acetone (100 m*l*) was refluxed for 7 hr in a steam bath, and then the inorganic precipitates were filtered off. After the filtrate had been evaporated, the residue was added to a 2N sodium hydroxide solution (60 m*l*). The mixture was heated in a steam bath for 0.5 hr and then acidified with 2N hydrochloric acid. The resulting precipitate was collected and recrystallized from ethyl acetate to give 2-acetyl-4,5-methylenedioxyphenoxyacetic acid as colorless needles, mp 205°C; yield, 0.6 g. IR: 1734, 1711, 1654 (C=O); 1620, 1500 (aromatic); 1043, 932 cm^{-1} (O-C$\underline{H}_2$-O).

Found: C, 55.69; H, 4.23%. Calcd for $C_{11}H_{10}O_6$: C, 55.46; H, 4.23%.

b) 5,6-Methylenedioxy-3-methylbenzo[b]furan (IX). A mixture of the above phenoxyacetic acid (0.6 g), anhydrous sodium acetate (10 g), and acetic anhydride (100 m*l*) was vigorously refluxed for 3 hr. The cooled mixture was then poured into water. The resulting precipitate was collected and recrystallized from ethanol to give IX as colorless needles, mp 56—56.5°C; yield, 0.4 g. IR: 1621, 1585, 1504 (aromatic); 1038, 939 cm^{-1} (O-C$\underline{H}_2$-O). UV: λ_{max} mμ (log ε); 248.5 (3.92), 256 (3.83), 303 (3.90), 308 (3.90). NMR: *3,4 δ 5.98$_s$ (O-C$\underline{H}_2$-O); 2.17$_d$ (J=1.5)(C$\underline{H}_3$).

Found: C, 67.92; H, 4.51%. Calcd for $C_{10}H_8O_3$: C, 68.18; H, 4.58%.

5,6-Methylenedioxy-2,3-dimethylbenzo[*b*]furan (X). To a solution of sesamol[5] (5.0 g) and 3-chlorobutanone-2 (3.9 g) in anhydrous methyl ethyl ketone (150 m*l*), anhydrous potassium carbonate (20 g) and potassium iodide (12 g) were added. The resulting mixture was refluxed for 17 hr in a steam bath, and then the inorganic precipitates were filtered off. After the filtrate had been evaporated, the residue was distilled *in vacuo* to give methyl α-(3,4-methylenedioxyphenoxy) ethyl ketone as a colorless oil, bp 163—165°C/23 mmHg; yiled, 3.0 g.

A mixture of the above ketone (3.0 g) and polyphosphoric acid (n=2.5; 18 g) was kept at room temperature for 2 days. The reaction mixture was then poured into a 2N sodium hydroxide solution. The resulting precipitate was collected and recrystallized from ethanol to give X as colorless needles, mp 82—83°C; yield, 1.5 g. IR: 1643, 1619, 1496 (aromatic); 1034, 938 cm^{-1} (O-CH_2-O). UV: λ_{max} mμ (log ε); 251 (3.96), 307 (3.95), 311 (3.95). NMR: *3,4 δ 5.96$_s$ ((O-C$\underline{H}_2$-O); 2.32$_s$, 2.07$_s$ (each 3H, C$\underline{H}_3$).

Found: C, 69.47; H, 5.14%. Calcd for $C_{11}H_{10}O_3$: C, 69.46; H, 5.30%.

The authors are indebted to Mr. Masaaki Fukumitsu for assistance with part of the experimental work. This work was supported in part by a grant-in-aid from the Ministry of Education.

8) K. Fukui and M. Nakayama, This Bulletin, **37**, 300 (1964).

BULLETIN OF THE CHEMICAL SOCIETY OF JAPAN VOL. 42 1976—1981 (1969)

The Reaction of Haloferrocenes with Copper(I) Salts in Pyridine

Masaru SATO, Takehiko ITO, Izumi MOTOYAMA, Ken-ichi WATANABE and Kazuo HATA

Department of Chemistry, Faculty of Science, Tokyo Metropolitan University, Setagaya, Tokyo

(Received November 5, 1968)

The halogen exchange reaction of haloferrocene series with copper(I) salts (halide, cyanide) in an organic base was studied in comparison with that of the halobenzene series, which is regarded as a kind of nucleophilic substitution. Chloro-, bromo-, and cyanoferrocene were all obtained from iodoferrocene by this reaction in good yields. The reactivity of the ferrocene series was much higher than that of the benzene series. The order of the reactivity of halogen, I>Br>Cl, was similar to that of the benzene series. On the other hand, the substituent effects in the comparative reactivity of 1′-substituted-1-chloroferrocene with copper(I) cyanide was observed to be as follows: Et>H>Cl>Ac. This order in the ferrocene series was opposite to that in the *p*-substituted bromobenzene series: CN>Ac>Br>H>Me. In view of the electrophilic tendency in the ferrocene series and its high reactivity, the reaction mechanism is discussed.

Since the discovery of the aromaticity of ferrocene many interesting findings on the reactions of ferrocene derivatives have been reported. Ferrocene itself has a greater reactivity in the electrophilic substitution than does benzene. For example, it is acetylated with acetyl chloride and anhydrous aluminum chloride 10^6 times faster than benzene.[1] However, the nucleophilic substitution of ferrocene derivatives seems to take place with much difficulty, and few have been reported. Chloroferrocene, for example, reacts neither with potassium amide in liquid ammonia[2] nor with potassium hydroxide or potassium acetate.[3] It is interesting to note, however, that copper or copper salts have been found to participate in the reactions of haloferrocenes. The Ullmann aryl-coupling reaction of iodoferrocene took place at 60°C to afford biferrocenyl in a high yield,[4] but that of iodobenzene took place only at 200°C. The reaction of bromo- and chloroferrocene with copper(II) acetate gave ferrocenyl acetate with ease.[3] Nesmeyanov *et al.* have obtained cyanoferrocene in a good yield by the reaction of bromo- or chloroferrocene with copper(I) cyanide.[3] Thus, the substitution reactions of haloferrocenes including chloroferrocene with copper(I) salts seem to occur more easily than those of the benzene series, while the reaction of chlorobenzene with copper(I) cyanide hardly ever takes place under ordinary reaction conditions, such as with iodo- or bromobenzene.

In our previous reports,[5,6] some information on the Rosenmund-von Braun reaction of halobenzene with a complex of copper(I) cyanide and an organic base in nitrobenzene was presented, along with a discussion of the reaction mechanism. It has been reported that this reaction proceeds easily in dimethylformamide or *N*-methylpyrrolidone.[7] The reactions of halobenzene with copper(I) halides as well as with cyanide in an organic base have also been reported by Bacon and Hill.[8]

In this study, haloferrocenes were submitted to similar reactions, and the results were examined in comparison with those in the benzene series.

Syntheses of Haloferrocenes

Haloferrocenes can not be synthesized by the direct halogenation of ferrocene. Therefore, they have hitherto been obtained through the reaction of chloromercuriferrocene with halogen[9,10] or

1) M. Rosenblum, J. O. Santer and W. G. Howells, *J. Am. Chem. Soc.*, **85**, 1450 (1963).

2) J. W. Huffman, L. H. Keith and R. L. Asbury, *J. Org. Chem.*, **30**, 1600 (1965).

3) A. N. Nesmeyanov, V. A. Sazonova and V. N. Drozd, *Chem. Ber.*, **93**, 2717 (1960).

4) M. D. Rausch, *J. Org. Chem.*, **26**, 1802 (1961).

5) T. Ito and K. Watanabe, This Bulletin, **41**, 419 (1968).

6) N. Akanuma, H. Amemiya, T. Hayashi, K. Watanabe and K. Hata, *Nippon Kagaku Zasshi* (*J. Chem. Soc. Japan, Pure Chem. Sect.*), **81**, 333 (1960).

7) L. Friedmann and H. Shechter, *J. Org. Chem.*, **26**, 2522 (1961); M. S. Newman and H. Boden, *ibid.*, **26**, 2525 (1961).

8) R. G. R. Bacon and H. A. O. Hill, *J. Chem. Soc.*, **1964**, 1097.

9) A. N. Nesmeyanov, E. G. Perevalova and O. A. Nesmeyanova, *Dokl. Akad. Nauk S. S. S. R.*, **100**, 1099 (1955).

10) H. Shechter and J. F. Helling, *J. Org. Chem.*, **26**, 1034 (1961).

Table 1. The halogen exchange reactions of haloferrocenes
Reaction temperature: 117°C

Exp. No.	Iodoferrocene	(g)	Copper(I) salt	(g)	Pyridine (ml)	Reaction time (hr)	Product	Yield (%)
1	Iodoferrocence	3.12	CuCl	1.98	30	3	Chloroferrocene	88.3
2	Iodoferrocence	3.12	CuBr	2.87	30	3	Bromoferrocene	94.2
3	Iodoferrocence	3.12	CuCN	3.6	20	3	Cyanoferrocene[a]	83
4	1,1′-Diiodoferrocene	18.0	CuCl	30	200	3	1,1′-Dichloroferrocene	77.4
5	1,1′-Diiodoferrocene	2.19	CuCN	2.24	20	2	1-Iodo-1′-cyanoferrocene[b]	40.2

a) Along with an unidentified product 0.15 g, mp 157—158°C.
b) Along with 37.5% recovery.

N-halosuccinimide,[11] or through the reaction of ferroceneboronic acid with copper(II) halide.[3,12] Among the haloferrocenes, however, iodoferrocene is easily obtained in a high yield by the treatment of chloromercuriferrocene with iodine.[10]

On the other hand, it is well known that iodobenzene easily undergoes a halogen exchange reaction with copper(I) halides to give bromo- or chlorobenzene in a good yield. Thus, chloro- and bromoferrocene may be expected to be successfully obtained by the reaction of iodoferrocene with copper(I) chloride and bromide respectively. The halogen exchange reactions were achieved only by refluxing the mixtures of iodoferrocene and copper(I) halides in pyridine for a few hours under an oxygen-free nitrogen atmosphere. Cyanoferrocene was also obtained using copper(I) cyanide instead of copper(I) halides.*1 The experimental results are summarized in Table 1.

Thus, these reactions are sufficiently useful as a method of synthesizing bromo-, chloro- or cyanoferrocene, since iodoferrocene is obtainable with considerable ease. On the other hand, the fact that the reaction of 1,1′-diiodoferrocene with copper(I) cyanide afforded 1′-cyano-1-iodoferrocene as the sole isolable product suggests a new method to synthesizing various 1′-substituted haloferrocenes.

The Rosenmund-von Braun Reaction of Haloferrocenes in Comparison with the Benzene Series. With a view to elucidating the character of the substitution reaction of haloferrocenes with copper(I) salts, the results of the reaction of haloferrocenes with copper(I) cyanide in pyridine under somewhat different conditions were compared with those of the same reaction with halobenzenes. The results of the experiments are shown in Tables 2 and 3. The relatively fast decomposition of iodoferrocene at 118°C may reduce the yield of cyanoferrocene to below that of benzonitrile from iodobenzene. Chloroferrocene gave a 34% yield of cyanoferrocene at 140°C (Exp. 5 in Table 2), while chlorobenzene did not react at all (Exp. 7 in Table 3).*2 A similar contrast was also evident in the reactions of bromo-compounds. In general, the higher the reaction temper-

Table 2. The reaction of haloferrocenes with copper(I) cyanide
Haloferrocenes: 0.4 g in each run, Reaction time: 2 hr

Exp. No.	Haloferrocene	CuCN (g)	Pyridine (ml)	Reaction temp. (°C)	Yield of cyanoferrocene	Recovered (%)
1	FcI	2	10	118	63	+
2	FcBr	2	10	118	32	35
3	FcBr	3	3	140	64	+
4	FcCl	2	10	118	Trace	*ca.* 100
5	FcCl	3	3	140	34	66

A small amount of unidentified product (mp 157°C) was obtained in every case.
The formation of ferrocene by the decomposition of haloferrocenes was observed in Exps. 1, 2 and 3.

Table 3. The reaction of halobenzenes with copper(I) cyanide
Halobenzenes: 0.5 ml in each run, Reaction time: 2 hr

Exp. No.	Halobenzene	CuCN (g)	Pyridine (ml)	Reaction temp. (°C)	Yield of benzonitrile[a] (%)
1	PhI	2	10	118	98
2	PhBr	2	10	118	Trace
3	PhBr	2	10	118	2.5[b]
4	PhCl	2	10	118	—
5	PhI	3	3	140	*ca.* 100
6	PhBr	3	3	140	43[c]
7	PhCl	3	3	140	—

a) Calculated by the gas chromatographic analysis.
b) The reaction time, 10 hr.
c) When heated for 9 hr at 140—150°C, the yield was 85%.

11) R. W. Fish and M. Rosenblum, *J. Org. Chem.*, **30**, 1253 (1965).
12) A. N. Nesmeyanov, V. A. Sazonova and V. N. Drozd, *Dokl. Akad. Nauk S. S. S. R.*, **126**, 1004 (1959).

*1 Nesmeyanov *et al.*[3] performed this reaction at 135—140°C without any solvent.

*2 Chlorobenzene was hardly ever changed by heating at 140—150°C for 14 hr. Upon reaction in an autoclave at 250°C for 9 hr, the yield of the nitrile was 34%.[5]

ature, the greater the increase in the yield of nitriles, and the reactivity of the halogens in both the ferrocene and the benzene series was in the same order: I>Br>Cl.*3

The ease of the displacement of halogens from the benzene nucleus was also shown to be the same order by Bacon and Hill.[8] This order is the inverse of that of the reactivities of activated aryl halides in the nucleophilic substitution. This implies that the reactions of haloferrocenes with copper(I) salts proceed in a manner similar to those of halobenzenes, at least at certain steps. On the other hand, the higher reactivity of the ferrocene series, together with that of the Ullmann coupling and Ullmann condensation of haloferrocenes,[4] suggests the contribution of a characteristic factor of ferrocene molecules to this reaction.

Effects of Substituents. In order to examine the electronic factor in this reaction, the reactions of *p*-substituted halobenzenes and of 1′-substituted haloferrocenes with copper(I) cyanide were carried out, and the effect of the substituents was discussed.

1′-Ethyl-, 1′-chloro-, and 1′-acetyl-1-chloroferrocene were synthesized, and competitive reactions of each of them with chloroferrocene were carried out in γ-picoline.*4 Similarly, the competitive reactions of *p*-methyl-, *p*-bromo-, and *p*-acetylbromobenzene with bromobenzene were all examined in the same solvent. The nitriles produced were analyzed by gas chromatography; the results are shown in Tables 4 and 5 in terms of the relative reactivity.

TABLE 4. THE RELATIVE REACTIVITY OF 1′-SUBSTITUTED CHLOROFERROCENE

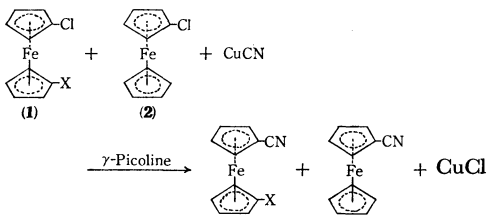

1: 0.0015 mol, **2**: 0.0015 mol, CuCN: 3.0 g, γ-Picoline: 3.0 m*l*, Biphenyl[a]: 0.0015 mol, Reaction temp.: 145°C, Reaction time: 2 hr, in N_2 atmosphere.

Exp. No.	Substituent X	Relative reactivity
1	C_2H_5	1.65
2	H	1.00
3	Cl	0.04[b]
4	$COCH_3$	—

a) Added as an internal standard in the gas chromatographic analysis.
b) Only 1′-chloro-1-cyanoferrocene was obtained.

TABLE 5. THE RELATIVE REACTIVITY OF *p*-SUBSTITUTED BROMOBENZENE

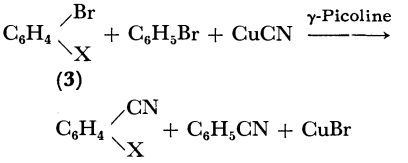

3: 0.02 mol, C_6H_5Br: 0.02 mol, CuCN: 3.0 g, γ-Picoline: 4.0 m*l*, Reaction temp.: 147°C, Reaction time: 3 hr

Exp. No.	Substituent X	Relative reactivity
1	CH_3	0.92
2	H	1.00
3	Br	1.21[a]
4	$COCH_3$	1.90
5	CN	2.03[b]

a) *p*-Bromobenzonitrile and terephthalonitrile were obtained.
b) The relative rate of *p*-bromobenzonitrile was calculated not from the direct competitive reaction, but from the result of No. 3 in this table, on the assumption that *p*-bromobenzonitrile is initially formed from *p*-dibromobenzene, followed by further substitution to terephthalonitrile.

It is very interesting that a remarkable electrophilic character was observed in the reaction of the ferrocene series, while the nucleophilic character was observed in that of the benzene series. Bacon and Hill also reported that the effect of substituents in the latter was slightly nucleophilic.[8] In view of the model proposed in our earlier paper,[5] the interaction of the cyano group with the carbon atom in benzene nuclei may be nucleophilic. Therefore, the trend and the order of substituent effcet shown in Table 5 seems reasonable. However, the nucleophilic character of this reaction, caused by the activation by the base-CuCN complex, is not as conspicuous as in an ordinary nucleophilic substitution of activated halobenzenes.

In the reactions of the ferrocene series (Table 4), the electron-withdrawing acetyl and also chloro groups exert a strong suppressive effect. The fact that dichloroferrocene only afforded a monocyano compound can be interpreted in terms of the interfering effect of a strong electron-withdrawing cyano group which has previously been substituted in another cyclopentadienyl ring. A similar result is found in the case of diiodo derivatives (Exp. 5 in Table 1). Thus, the fact that the electron-withdrawing group displays a suppressive effect on the substitution reaction of the ferrocene series, contrary to that of the benzene series,

*3 I>Br>Cl>F: Fluorobenzene is never replaced by this reaction.[5] The reactivity order was estimated on the basis of the yields of nitriles from the corresponding halides.

*4 It was used because its boiling point is higher than that of pyridine (bp 145°C).

offers an important suggestion for discussing the mechanism of this reaction in close relationship with the superior reactivity of the ferrocene series.

Discussion

The halogen exchange reaction of haloferrocene participated with copper(I) salt is considered to be a kind of nucleophilic substitution, analogous to that of halobenzene under the same conditions. Nevertheless, the displacement of halogen from the ferrocene nucleus was found to be facile in the order: I>Br>Cl, an order similar to that observed in halobenzenes. This kind of metal-assisted aromatic replacement reaction has been extensively studied by Bacon and Hill,[8] who established that the reaction was initiated by bonding between the halogen in aryl halide and copper, thus giving an "onium" structure (**4**), followed by the formation of a four-centered cyclic intermediate or an ion pair, or by a homolytic fission, and that an electron-withdrawing group on the aryl halide had only a small accelerating effect on the reaction rate.

$$ArBr + CuClL_2 \longrightarrow Ar\text{-}\overset{\oplus}{Br}\text{-}\overset{\ominus}{Cu}L_2 \quad (\mathbf{4})$$
$$\qquad\qquad\qquad\qquad\quad Cl$$

L: Ligand

It may be concluded that, within the range of conditions employed in this investigation, copper(I) salt is present in the reaction mixture in the form of a complex with a pyridine base.[5] It has also been shown that the nature of the pyridine base in the copper complex affects the rate of the substitution reaction remarkably. Under the circumstances, an electronic state of the halogen atom in aryl halide, like one of the copper atom in the complex, will seriously affect the first stage of the reaction. The cyclopentadienyl ring in ferrocene has a higher electron density than the benzene ring, so the halogen in haloferrocene may be expected to be more strongly coordinated to the copper atom than that in the corresponding halobenzene under the same conditions. The expected higher reactivities of haloferrocenes were actually observed in this investigation.

As is shown in Table 4, the effect of 1′-substituents observed in haloferrocenes was contrary to what was expected from the nucleophilic feature of this reaction. That is, the reaction was accelerated with an electron-releasing group, while it was retarded with an electron-withdrawing one.

In view of these results, the halogen exchange reaction in the ferrocene series seems to be more complicated than that in the benzene series. However, on the assumption that the principal mechanism of this reaction is not different between the two series, the anomalism observed in the substituent effect of haloferrocenes can reasonably be explained as follows: In haloferrocenes, a particular interaction between the copper(I) salt-base complex and haloferrocene precedes the formation of an "onium"-type intermediate (**4**) by an attack of the halogen in the haloferrocene on the copper atom in the complex, and exerts a controlling effect on the rate of the reaction. Since haloferrocene acts as an electron donor in this reaction, an electron-withdrawing substituent on haloferrocene retards the above-mentioned interaction, thus reducing the rate of the reaction. This explanation is consistent with the experimental results obtained in this study, and similar interaction has been observed in several members of the ferrocene series.[13] Therefore, it seems reasonable to assume a precedence of such an interaction in the halogen exchange reactions, although there is no direct evidence to support this assumption.

Further work on this subject is in progress and a more detailed discussion will be reported later.

Experimental

Materials. Commercial copper(I) chloride and bromide were used without any further purification. The copper(I) cyanide was prepared from copper(II) sulfate and potassium cyanide. Commercial pyridine, γ-picoline, and halobenzenes were purified by distillation under reduced pressure. The purity of all the organic reagents was checked by gas chromatography.

Iodoferrocene. Iodoferrocene was prepared, by a modification of the procedure reported by Shechter and Helling,[10] in a much improved yield, 71—91%; mp 48—49°C (lit. 44—45°C,[9] 49—49.5°C[4]).

Chloroferrocene. To a solution of 3.12 g (0.01 mol) of iodoferrocene in 30 m*l* of pyridine, 1.98 g (0.02 mol) of copper(I) chloride were added and then the mixture was refluxed with stirring for 3 hr under a nitrogen atmosphere. At the end of the reaction, 100 m*l* of *n*-hexane were added. Then, the reaction mixture was filtered, and the precipitate collected on a filter was washed several times with *n*-hexane. The filtrate and the washings were combined and washed with dilute hydrochloric acid and water successively. The organic layer was dried over anhydrous magnesium sulfate. After the removal of the solvent, the residual crude product was chromatographed on alumina to afford 1.95 g chloroferrocene. Yield, 88.3%; mp 56—56.5°C (lit. 58—59°C[3]).

Bromoferrocene. Following the procedure described above, bromoferrocene was prepared from iodoferrocene and copper(I) bromide in pyridine. Yield, 94%; mp 29—30°C (lit. 32—33°C[3]).

Cyanoferrocene. Iodoferrocene (3.1 g, 0.01 mol) and copper(I) cyanide (3.6 g, 0.04 mol) were treated in 20 m*l* of pyridine by the procedure used for the preparation of chloroferrocene. The crude product thus obtained was chromatographed on Florisil to give 1.75 g of cyanoferrocene. Yield, 83%; mp 106—107°C (lit.

13) V. L. Wolf and H. Hennig, *Z. Anorg. Allgem. Chem.*, **341**, 1 (1965).

107—108°C[3]). Unidentified yellow crystals were obtained as a by-product (0.15 g), mp 157—158°C.

1,1'-Diiodoferrocene. Following the procedure reported by Nesmeyanov *et al.*,[9] 1,1'-diiodoferrocene was prepared in a much improved yield. Purification by means of chromatography gave 5.77 g of 1,1'-diiodoferrocene as an orange liquid. Yield, 65.5%; bp 85°C/0.003 mmHg, n^{23} 1.6850.

1,1'-Dichloroferrocene. 1,1'-Dichloroferrocene was prepared by the reaction of 1,1'-diiodoferrocene with copper(I) chloride in pyridine following the procedure previously described for the preparation of chloroferrocene. Yield, 77.4%; mp 76—77°C (lit. 75—77°C[3]).

1'-Cyano-1-iodoferrocene. To a solution of 2.19 g (0.005 mol) of 1,1'-diiodoferrocene in 20 m*l* of pyridine, there were added 2.24 g (0.0025 mol) of copper(I) cyanide, and then the mixture was refluxed for 2 hr under a nitrogen atmosphere. After a treatment similar to that for chloroferrocene, the crude product was chromatographed on Florisil to give 0.8 g of the starting material and 0.68 g of 1'-cyano-1-iodoferrocene. The yield of the latter, 40.2%; mp 43.5—45°C.

Found: C, 39.72; H, 2.56; N, 4.25%. Calcd for $C_{11}H_8NIFe$: C, 39.20; H, 2.39; N, 4.16%.

1'-Acetyl-1-chloroferrocene. A solution of 7.6 m*l* (0.06 mol) of boron trifluoride etherate in 10 m*l* of dry dichloromethane was added to a solution of 5.5 g (0.025 mol) of chloroferrocene and 5.65 m*l* (0.06 mol) of acetic anhydride in 100 m*l* of dry dichloromethane over a 7-min period under a nitrogen atmosphere and in an ice bath. After the reaction mixture had been stirred for 30 min in the ice bath and then for 5.5 hr at room temperature, it was poured into ice water. The dichloromethane layer was washed repeatedly with water and dried over anhydrous magnesium sulfate. After the solvent had been removed, the residue was chromatographed on alumina to give 2.80 g of cholroferrocene and 3.20 g of 1'-acetyl-1-chloroferrocene. The yield of the acetyl compound, 48.6%; mp 55.5°—56.7°C (lit. 53—55°C[14]).

1'-Ethyl-1-chloroferrocene. Zinc (1.0 g) was amalgamated by stirring it with 0.1 g of mercury(II) chloride in 4 m*l* of dilute hydrochloric acid (1:20) for 10 min. After the aqueous phase had then been decanted off, a solution of 0.25 g of 1'-acetyl-1-chloroferrocene in 2.5 m*l* of conc. hydrochloric acid and 2.5 m*l* of acetic acid was added to the amalgamated zinc. The mixture was refluxed for 5 min and then cooled to room temperature. Then the zinc was filtered off and washed with ether. The filtrate was extracted with ether. The combined ethereal solution was washed with water, dilute aqueous potassium hydroxide, and water successively, and dried over anhydrous magnesium sulfate. After the ether had then been evaporated away, the residue was chromatographed on alumina with *n*-hexane, there was thus obtained 0.19 g of 1'-ethyl-1-chloroferrocene. Yield, 81.0%; bp 65—66°C/0.006 mmHg, n^{23} 1.6048.

Found: C, 58.10; H, 5.23%. Calcd for $C_{12}H_{13}ClFe$: C, 57.95; H, 5.23%.

1'-Ethyl-1-cyanoferrocene. To a solution of 0.67 g (0.0027 mol) of 1'-ethyl-1-chloroferrocene in 1.5 m*l* of γ-picoline, 1.21 g (0.0135 mol) of copper(I) cyanide were added. The reaction mixture was heated for 3 hr at 140—145°C under a nitrogen atmosphere, and cooled after the addition of 10 m*l* of pyridine at the end of the reaction. After a treatment similar to that described for the preparation of chloroferrocene, the crude product was chromatographed on silica gel to give 0.375 g of the starting material and 0.159 g of 1'-ethyl-1-cyanoferrocene. The yield of the cyano compound, 24.8%; 99—100°C/0.045 mmHg (lit. 152—156°C/5 mmHg[3]).

The Reaction of Haloferrocene with Copper(I) Cyanide (Table 2, Exp. 2). A mixture of 0.40 g of bromoferrocene, 2.0 g of copper(I) cyanide, and 10 m*l* of pyridine was stirred for 2 hr at 118°C. After the reaction was over, 30 m*l* of ether was added to the hot reaction mixture and the whole was refluxed for 10 min while being stirred well. The copper(I) salt-pyridine complex thus precipitated was filtered off and washed well with ether. The extraction with fresh ether was repeated three times in order to ensure the extraction of the product from the reaction mixture. All the ethereal solutions were then combined, washed three times with dilute hydrochloric acid and then with water, and dried over anhydrous magnesium sulfate. After the ether had been distilled off, the residue was chromatographed on silica gel with a mixture of *n*-hexane and benzene (1: 1) to give 0.10 g (32%) of cyanoferrocene, mp 106—107°C, and 0.14 g (35%) of the recovered bromoferrocene.

In the case of the reaction of chloroferrocene, the products were analyzed by gas chromatography; by this means the quantities of cyanoferrocene and the recovered chloroferrocene were determined precisely.

The Reaction of Halobenzene with Copper(I) Cyanide (Table 3, Exp. 6). A mixture of 0.5 m*l* of bromobenzene, 3.0 g of copper(I) cyanide and 3.0 m*l* of pyridine was stirred at 140°C for 2 hr. Then the reaction mixture was treated similarly as in the case of haloferrocenes. The ethereal solution thus obtained was analyzed by gas chromatography. The yield of benzonitrile was 43%.

The Competitive Reaction of Haloferrocenes (Table 4, No. 1). A mixture of 3.0 g of copper(I) cyanide, 3.0 m*l* of γ-picoline, 0.377 g (0.0015 mol) of 1'-ethyl-1-chloroferrocene, 0.336 g of chloroferrocene, and 0.203 g of biphenyl (internal standard for gas chromatography) was stirred for 2 hr at 145°C. After the reaction was over, 6 m*l* of pyridine and 20 m*l* of ether were added to the hot reaction mixture, and the whole was refluxed for 10 min while being stirred well. A copper(I) salt-pyridine complex precipitated from the reaction mixture. The precipitate was filtered off and washed with ether. To complete the collection of the product, the precipitate was extracted twice more. The ethereal solutions thus obtained were combined, washed with dilute hydrochloric acid, and then with water, and dried over anhydrous magnesium sulfate. The solution was concentrated and analyzed by gas chromatography.

The Relative Reactivities of Haloferrocenes. After the competitive reaction between chloroferrocene and 1'-substituted chloroferrocene, the yields of both nitriles were calculated from the ratio of each peak area of the nitriles to the internal standard (biphenyl). When a large excess of copper(I) cyanide over haloferrocene was used, the reaction was apparently first-order in haloferrocenes. Therefore, on the assumption

14) D. W. Hall and J. H. Richards, *J. Org. Chem.*, **28**, 1549 (1963).

that the reaction would be approximately first-order in haloferrocenes under the conditions employed in the present experiments, the rate constants were calculated from the yields of the nitriles. The relative reactivities of 1′-substituted chloroferrocene and chloroferrocene are shown in Table 4. Similarly, the relative reactivities of *p*-substituted bromobenzene and bromobenzene were found to be as shown in Table 5.

Analytical Conditions for Gas Chromatography. Apparatus: Ohkura Model 1100. Column: 2 m×6 mm stainless-steel column packed with 10% Silicon Grease on Daichrom W with 60—80 meshes. Temperature: 180—200°C (130°C for halobenzene). Carrier gas: H_2. Flow rate: 40—60 ml/min. Relative retention time: FcH (1); Biphenyl (1.16); FcCl (1.57); 1′-Et-1-Cl-ferrocene (2.43); 1,1′-Cl_2-ferrocene (2.48); FcCN (2.77); $FcCOCH_3$ (3.45); 1′-Et-1-CN-ferrocene (4.32); 1′-Cl-1-CN-ferrocene (4.43); 1′-Ac-1-CN-ferrocene (5.23).

For the substituted halobenzenes, the following conditions were employed. Column: 2 m×6 mm stainless-steel column packed with 10% Carbowax 1500 on Chromosorb W with 60—80 meshes. Temperature: 180—190°C. Carrier gas: H_2. Flow rate: 40 ml/min.

BULLETIN OF THE CHEMICAL SOCIETY OF JAPAN VOL. 42 1981—1986 (1969)

The Reaction of Carboxylic Acids and Hydrocarbons in a Silent Electric Discharge. I. The Reaction of Acetic Acid with Ethylene*1

Teruo HIRAKI

Institute of Commodities, Faculty of Economics, Kagawa University, Takamatsu

(Received November 11, 1968)

In order to ascertain the possibility of telomerization by a silent discharge, a mixture of acetic acid and ethylene was discharged in an ozonizer under various conditions. The α-*C*-alkylation of acetic acid which was expected to result from its discharge-induced reaction with ethylene was not observed; neither propionic acid nor higher carboxylic acids were identified by gas chromatography. However, *n*-butyl acetate was obtained in a good yield. The formation of the acetate can be explained as resulting from the combination of an acetoxy radical with two molecules of ethylene. The yield of the acetate, as well as those of the liquid and gaseous products, increased with a rise in the temperature and in the voltage, with the time, and with a rise in the ratio of ethylene to the acid concentration. Besides this acetate, the liquid products were confirmed to consist of ethyl methyl ketone, acetone, acetaldehyde, hydrocarbons, and ethyl and *n*-propyl acetates. The gaseous products were carbon dioxide, carbon monoxide, C_1—C_4-hydrocarbons, and hydrogen. Judging from the relative concentration of each compound in the reaction products, it may be said that the acetoxy radical ($CH_3COO\cdot$) and the acetyl radical ($CH_3CO\cdot$) are the main intermediates in this reaction system.

No detailed study has been reported on the reaction of an acetic acid-ethylene mixture by light or radiation, not to mention by silent discharge, although a study of the radiolysis[1] of acetic acid has been made.

Acetic acid has an active hydrogen atom, as well as alcohols (primary and secondary), carbonyl compounds, hydrocyanic acid, and mercaptans. Kawamoto[2] has shown that the acrylonitrile and higher cyanides are produced by the reaction of hydrocyanic acid having an α-H with ethylene in a silent discharge, although the author could not find telomers higher than the one-to-one adduct in the discharge-induced reaction of 2-propanol and ethylene.

It would be interesting to ascertain if a silent electric discharge initiates the telomerization of acetic acid and ethylene, and if it can be employed as a means to the direct synthesis of carbonyl compounds or acetates. In the present paper, the author wishes to report the direct formation of acetates in the silent discharge, and to establish, if possible, the optimum conditions for the preparation of these compounds.

*1 The major part of these research results were presented at the 21st Annual Meeting of the Chemical Society of Japan, Osaka, April, 1968.

1) A. S. Newton, *J. Chem. Phys.*, **26**, 1764 (1957); R. H. Johnsen, *J. Phys. Chem.*, **63**, 2041 (1957).

2) K. Kawamoto, This Bulletin, **41**, 2164 (1968).

Experimental

Materials. The acetic acid, which did not contain any impurities reducing a 0.1% potassium permanganate solution, was purified by column distillation after it had been refluxed over phosphorus pentoxide, while commercial ethylene (research grade) was used without further purification. No impurity was found by gas chromatographical analysis; the analyses of acetic acid and ethylene were performed by means of columns of DEGS (diethylene glycol succinate) and activated charcoal respectively.

Discharge Tube. The discharge tube used is shown in Fig. 1. This tube was a Pyrex tube of the Siemens type[3] with a gap length of 2.5 mm and an effective length of 45 cm. The outside (B) of the discharge tube was filled with water, while the inner tube (A) was filled with a 3% $CuSO_4$ solution. Electrodes (C) were inserted into both (A) and (B).

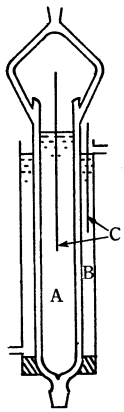

Fig. 1. The used discharge tube.

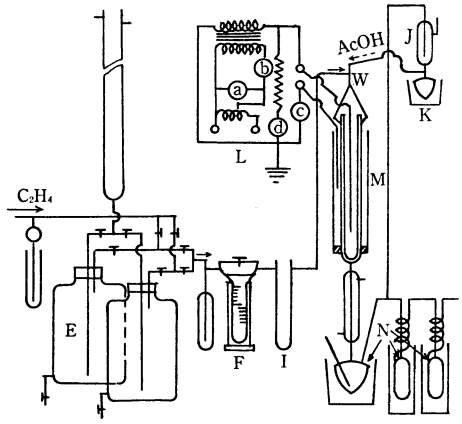

Fig. 2. The apparatus for a flow system.

a) Voltmeter, V b) Ammeter, A
c) Ammeter, mA d) Ammeter, μA

3) T. Matsuda, K. Oto and K. Sugino, *Nippon Kagaku Zasshi (J. Chem. Soc. Japan, Pure Chem. Sect.)*, **79**, 324 (1958).

Apparatus and Procedure. The experiment was performed in a flow system. The apparatus is shown in Fig. 2. As soon as acetic acid had been dropped, at regular time intervals, from a dropping funnel (J) into a pot, a heater (K) turned it into vapor, which was then introduced into a discharge tube (M). Ethylene coming from the reservoir (E) was passed through a solid sodium hydroxide tube (I) in order to remove the moisture in the ethylene, which was then introduced into the discharge tube along with the acetic acid vapor. The ethylene flow rate was measured by passing it through a calibrated flowmeter (F). The reaction products that passed through the discharge tube were separated into a condensable part and non-condensable gases by three traps (N) cooled to 0°C. The high tension was applied to the discharge tube from a transformer (L; capacity, 15 kV) which used a 60-cycle alternating current.

Analysis of the Products. The reaction products were identified by comparing their retention times on gas chromatography with those of authentic samples. The non-condensable products were analyzed by gas chromatography (column, 3 m activated charcoal at 100°C; carrier gas, hydrogen). For the analyses of C_3 and C_4-hydrocarbons and of hydrogen, a 3-m column of hexamethylphosphoramide and a 3-m column of molecular sieve-13X were used at 35°C (carrier gas, helium).

The condensable products were confirmed not only by gas chromatography (column, tricresyl phosphate, PEG-6000 and diethylene glycol succinate at 100°C; carrier gas, He), but also by the formation of the derivatives. Thus, ethyl methyl ketone, obtained as a fraction boiling at 80°C, was converted into its semicarbazone and 2,4-dinitrophenylhydrazone,*2 the melting points of the derivatives being 145.5—146°C and 116.8—117.3°C respectively. They showed no depression of their melting points when mixed with authentic specimens. The quantitative analysis of the liquid products was performed by gas chromatography (column, 3 m, diethylene glycol succinate at 100°C; carrier gas, helium).

Results and Discussion

The experimental conditions and the reaction products are listed in Tables 1 and 2. The main liquid products identified were acetaldehyde, acetone, ethyl methyl ketone, and ethyl, and *n*-propyl and *n*-butyl acetates. The percentage compositions of compounds shown in these tables are the average of three experiments; the fluctuations in the yields of these compounds were less than 1%. The gaseous products which were formed in this reaction were methane, ethane, acetylene, C_3 and C_4-hydrocarbons, carbon monoxide, carbon dioxide, and hydrogen.

*2 The semicarbazone and 2,4-dinitrophenylhydrazone of ethyl methyl ketone were prepared according to the procedure of R. L. Shriner, R. C. Fuson and D. Y. Curtin, "The Systematic Identification of Organic Compounds," 4th ed., John Wiley & Sons, New York (1956), pp. 218, 219.

TABLE 1. INFLUENCES OF A MOLAR RATIO OF ETHYLENE TO ACETIC ACID ON THEIR DISCHARGE REACTION

Experiment No.	1	2	3	4	5	6
Secondary voltage, kV	11.6	11.6	11.6	11.6	11.6	11.6
current, mA	3.0	2.0	2.2	2.2	2.2	2.2
Temp. of discharge tube						
Inside, °C	88	85	88	88	87	86
Outside, °C	84	84	85	84	78	81
Residence time, hr	6.5	6.5	6	6	6	6
Material						
Acetic acid {Amount, g	51.75	52.11	52.33	51.90	52.91	52.26
Acetic acid {Velocity, g/hr	8.6	8.7	8.7	8.7	8.8	8.7
Ethylene {Volume, *l*	0	7.40	7.80	9.70	11.45	13.50
Ethylene {Velocity, *l*/hr	0	1.23	1.30	1.62	1.91	2.25
Molar ratio (ethylene/AcOH)	0	0.38	0.40	0.49	0.58	0.69
Amount of liquid product, g	1.15	1.89	1.88	1.76	1.89	2.23
Conversion, %*	2.46	2.76	2.80	2.65	2.69	3.15
Composition of liquid product, %**						
Acetaldehyde	6.7	8.2	10.3	8.8	7.1	7.7
Acetone	63.5	11.4	9.2	8.4	9.6	10.2
Ethyl methyl ketone	7.1	11.4	11.9	12.3	12.9	12.2
Ethyl acetate	8.3	7.5	8.0	7.1	7.9	7.4
n-Propyl acetate	1.8	10.8	11.8	12.3	10.7	11.1
n-Butyl acetate	3.5	20.5	17.7	21.8	21.5	23.4
Hydrocarbons	9.1	30.2	31.1	29.3	30.3	28.0

Gaseous products: methane, ethane, acetylene, propane, *n*-butane, 1-butene, carbon monoxide, carbon dioxide and hydrogen.

TABLE 2. INFLUENCES OF DISCHARGE TEMPERATURE, VOLTAGE AND TIME ON THE REACTION BETWEEN ACETIC ACID AND ETHYLENE

Experiment No.	8	9	3	10	11
Secondary voltage, kV	10.3	10.3	11.6	11.6	11.6
current, mA	2.4	1.8	2.2	2.1	2.2
Temp. of discharge tube					
Inside, °C	41	83	88	82	88
Outside, °C	34	86	85	82	83
Residence time, hr	6	6	6	3	9
Material					
Acetic acid {Amount, g	51.60	51.38	52.33	52.10	51.11
Acetic acid {Velocity, g/hr	8.6	8.6	8.7	8.7	8.5
Ethylene {Volume, *l*	8.60	8.95	7.80	10.75	11.40
Ethylene {Velocity, *l*/hr	1.4	1.5	1.3	1.8	1.9
Molar ratio (ethylene/AcOH)	0.44	0.45	0.40	0.55	0.60
Amount of liquid product, g	0.60	0.95	1.88	0.95	2.83
Conversion, %*	1.11	1.61	2.80	1.40	4.21
Composition of liquid product, %**					
Acetaldehyde	3.1	6.5	10.3	8.3	9.1
Acetone	30.9	31.4	9.2	6.9	10.3
Ethyl methyl ketone	4.9	10.0	11.9	12.2	11.6
Ethyl acetate	6.4	8.3	8.0	9.2	8.3
n-Propyl acetate	8.0	6.8	11.8	9.4	12.0
n-Butyl acetate	7.8	20.3	17.7	19.4	16.0
Hydrocarbons	38.9	16.7	31.1	34.6	32.7

Gaseous products: see Table 1.

* The conversion efficiency was given by (grams of reaction product per grams acetic acid used) $\times 100$.

** The yields of each compound were given by (grams of each compound per grams of total reaction product) $\times 100$.

These compounds were obtained in every run (though in the case of the decomposition of acetic acid alone, the acetylene and C_3—C_4-hydrocarbons were not formed). However, the distribution of the products depended upon the voltage of discharge, the residence time, the temperature in the tube, and the molar ratio of the reactants.

Influences of teh Molar Ratio of Ethylene to Acetic Acid on the Yield. In order to check the molar ratio effects on the discharge reaction of acetic acid and ethylene, the reaction was carried out with various ratios of the ethylene to the acetic acid concentration. As may be seen from Experiment Nos. 1—6 in Table 1, the yields of liquid products increased with an increase in the molar ratio of ethylene to acetic acid. However, the distribution of the products depended on the molar ratio of reactants as follows. (1) Acetone was obtained in the highest yield in the absence of ethylene; the acetone yield decreased when acetic acid was mixed with ethylene. Up to the molar ratio of 0.58: 1, the yield decreased almost linearly with an increase in the ratio of ethylene to acetic acid. (2) The yield of ethyl methyl ketone increased at high ratios of ethylene to the acid concentration. These facts seem to indicate that acetone is formed by the combination of an acetyl radical with a methyl radical, and ethyl methyl ketone, by the addition of an acetyl radical to an ethylene, and that the C–OH-bond breaking in the acetic acid excited by the silent discharge is rather preferred in the absence of ethylene.

On the other hand, the yield of acetates identified was lowest in the decomposition of acetic acid; it was favored by high ratios of ethylene to the acid concentration. Thus, it is thought that the acetates are formed *via* an acetoxy radical ($CH_3COO\cdot$), a radical which is produced in large quantities by the free radicals derived from the excited ethylene; the free radicals attack this acetic acid to remove a hydrogen atom in the carboxyl. However, since carbon dioxide was obtained more in the absence of ethylene than in its presence, the high yields of acetates might result from the stabilization of the acetoxy radical in the presence of ethylene. This result also suggests that the decarboxylation is rather more preferred in the discharge decomposition of acetic acid than in the reaction of a mixture of acetic acid and ethylene.

The yield of ethyl acetate was almost the same regardless of the molar ratio of the reactants. The yield of the telomer with $n=2$ (*n*-butyl acetate) increased with an increase in the molar ratio of the ethylene to the acid. Thus, it may be said that the yield of the telomer with $n=2$ is favored by a low ratio of the acetic acid to the ethylene concentration.

Influences of the Discharge Temperature, Voltage, and Time on the Reaction between Acetic Acid and Ethylene. As is shown in Table 2, when the discharge reactions were carried out at 35 and 85°C, under the reaction conditions of a 0.4: 1 molar ratio of ethylene to acetic acid, 10.5 kV, and 6 hr, the yields of the liquid products increased with a rise in the temperature. *n*-Butyl acetate (1: 2 telomer) was obtained in an especially high yield when the ozonizer was kept "warm." This fact indicates that the telomerization of this sort is much affected by the discharge temperature.

On the other hand, the yields of the liquid products increased at a high voltage of discharge; the yields of all the carbonyl compounds except acetone, and of the acetates increased (the acetone yield, on the other hand, decreased very much). This suggests that the addition reaction occurs predominantly at a high tension.

Further, it has been found that increasing the residence time increases not only the reaction rate but also the yields of all the carbonyl compounds, including acetone, and of the acetates.

Thus, it has become apparent that the yields of the liquid and gaseous products increase with a rise in the temperature, the voltage, and the time, and at high ratios of the ethylene to the acetic acid concentration (a high yield of the telomer with $n=2$, *n*-butyl acetate, is especially favored by such a ratio).

Besides *n*-butyl acetate, liquid products were confirmed to consist of ethyl methyl ketone, acetone, acetaldehyde, and ethyl and *n*-propyl acetates, plus hydrocarbons. The gaseous products were C_1—C_4-hydrocarbons, carbon monoxide and dioxide, and hydrogen.

Judging from the relative concentration of each compound in the reaction products, it may be said that the acetoxy radical ($CH_3COO\cdot$) and the acetyl radical ($CH_3CO\cdot$) are the main intermediates in this reaction system.

The Assumed Radicals and Reaction Scheme. The characteristic of the action of silent discharge on a compound seems to be the electronic excitation of the molecule. Some of the molecules may be transformed by inelastic collisions into vibrationally-excited molecules. The activated molecules thus formed are considered to change into radicals or atoms, and into a very small amount of ionized molecules, as has been reported by many workers.[4] The radicals which are assumed to be formed from acetic acid under a silent discharge and a part of the postulated reaction scheme are shown in Table 3.

These precursor radicals, II—IV, might be

4) S. C. Lind and G. R. Schultze, *J. Phys. Chem.*, **42**, 547 (1938); H. Winer and M. Burton, *J. Am. Chem. Soc.*, **75**, 5815 (1953); J. C. Devins and M. Burton, *ibid.*, **76**, 2618 (1954); E. Inoue, *Denki Kagaku (J. Electrochem. Soc. Japan)* **23**, 574 (1955); S. Takahashi, *Nippon Kagaku Zasshi (J. Chem. Soc. Japan, Pure Chem. Sect.)*, **79**, 132 (1958).

TABLE 3. THE ASSUMED RADICALS AND REACTION SCHEME

$CH_3COOH + e^*$ (accelerated electron) $\longrightarrow$
CH_3COOH^* (excited AcOH) + e (electron deactivated by collision)

$CH_3COOH^* \longrightarrow$

- $\xrightarrow{\times}$ $\cdot CH_2COOH + H\cdot$ (I) (1)
- $\longrightarrow$ $CH_3COO\cdot + H\cdot$ (II) (2)
  - $\xrightarrow{\cdot CH_3}$ CH_3COOCH_3 (3)
  - $\xrightarrow{C_2H_4}$ $CH_3COO\dot{C}_2H_4 \xrightarrow{AcOH} CH_3COOC_2H_5$ (4)
  - $\xrightarrow{C_2H_4}$ $CH_3COO\dot{C}_4H_8 \xrightarrow{AcOH} CH_3COOC_4H_9$ (5)
  - $\longrightarrow$ $\cdot CH_3 + CO_2$ (6)
- $\longrightarrow$ $CH_3\dot{C}O + \cdot OH$ (III) (7)
  - $\xrightarrow{H\cdot}$ CH_3CHO (8)
  - $\xrightarrow{\cdot CH_3}$ CH_3COCH_3 (9)
  - $\xrightarrow{C_2H_4}$ $CH_3COC_2H_4 \xrightarrow{AcOH} CH_3COC_2H_5$ (10)
  - $\longrightarrow$ $\cdot CH_3 + CO$ (11)
- $\longrightarrow$ $\cdot COOH + \cdot CH_3$ (IV) (12)
  - $\longrightarrow$ $CO_2 + \cdot H$ (13)
- $\longrightarrow$ $\cdot CH_3 + CO_2 + \cdot H$ (14)

formed not only by the reactions shown in this table, but also by various reactions between acetic acid and the various radicals formed. The Radical (I) seems not to be derived from acetic acid excited by the silent discharge (even if the radical were formed, the radical would be too labile to exist), since propionic acid, butyric acid, and higher carboxylic acids were not identified by gas chromatography.

When acetic acid alone was discharged in an ozonizer, acetone and carbon monoxide were obtained in good yields. Accordingly, the C–OH-bond breaking in acetic acid (Eq. (7)) seems to occur rather preferably in the case of the decomposition of the excited acetic acid.

In the present reaction system, the (6), (13) and (14) processes seem to be those for forming carbon dioxide, but the processes to give CO_2 may not necessarily be these three, because Adams *et al.*[5] have shown, by the use of a radical scavenger, that 20% of the methane obtained in the radiolysis of acetic acid passes through the "molecule" process, $CH_3COOH^* \rightarrow CH_4 + CO_2$. Moreover, Ausloos and Steacie[6] have shown that 10% of the methane produced was derived from the dissociation of the acetic acid vapor excited by light.

Comparison with Peroxide-, Light-, and Gamma-Ray-Induced Reactions. The liquid products obtained in the decomposition of the acetic acid excited by the silent discharge are similar to those obtained in the radiolysis of acetic acid as shown by Bach,[7] Johnsen,[1] and Newton.[1] However, Burr[8] has shown that, in each radiolysis of the deuteriated and tritiated acetic acids, CD_3COOH and CT_3COOH, the methane and hydrogen produced were formed through the following processes:

5) G. E. Adams, J. H. Baxendale and R. P. Sedgwick, *J. Phys. Chem.*, **63**, 854 (1959).

6) P. Ausloos and E. W. R. Steacie, *Can. J. Chem.*, **33**, 1530 (1955).

7) Bach showed that the *G*-value of the acetone formed in the radiolysis of acetic acid vapor was 0.45; N. Bach, *Proc. Intern. Conf. Peaceful Uses Atomic Energy*, United Nations, New York, **7**, 538 (1956). In addition, Johnsen showed that the *G*-values of the gaseous products were 0.35 (H_2), 3.34 (CH_4), 0.62 (C_2H_6), 0.37 (CO), and 6.0 (CO_2). Further, Newton has reported that, besides these compounds, acetaldehyde and methyl acetate are obtained in such a reaction system.

$$\cdot CH_3 + CH_3COOH \rightarrow CH_4 + \cdot CH_2COOH$$

$$\cdot H + CH_3COOH \rightarrow H_2 + \cdot CH_2COOH$$

Namely, Burr[8] proposed the formation of the $\dot{C}H_2$-COOH radical. In addition, Roland and Harmon,[9] and Coffman[10] showed that the product was $H(C_2H_4)_nR'COOH$, in which R′ is R less H; this product was not formed by the discharge when a saturated organic acid (RCOOH) with an α-H is heated to 70—80°C with ethylene and a catalyst such as benzoyl peroxide under pressure at 895—950 atm.

It has been reported by Thomas *et al.*[11] that the radical from ethylene in the electrical discharge is a vinyl radical, and that it is produced by breaking a carbon-hydrogen bond. However, since the formations of vinyl acetate and methyl vinyl ketone were not observed, the vinyl radical is considered not to be formed here; the carbon-hydrogen bond in ethylene is not broken to give the vinyl radical, but is activated to give acetylene and 1-butene. These compounds were obtained in the gaseous products.

The main conclusion to be drawn from these results is that, by using a high-frequency current to energize the ozonizer, the nature of the reaction products can be controlled by controlling the experimental conditions. In one case the major product was acetone, and in another, *n*-butyl acetate.

8) J. G. Burr, *J. Phys. Chem.*, **61**, 1481 (1957).

9) J. R. Roland and J. Harmon, U. S. Pat. 2433015 (1947); *Chem. Abstr.*, **42**, 2268 (1948).

10) D. D. Coffman, U. S. Pat. 2433016 (1947); *Chem. Abstr.*, **42**, 2456 (1948).

11) Thomas *et al.* showed that the processes in the decomposition of ethylene excited by the silent discharge were as follows:

$$H_2C{=}CH_2 \rightarrow H_2C{=}\overset{H}{\overset{|}{C}}\text{–} + H \text{ (in extreme cases)}$$

$$H_2C{=}CH_2 \rightarrow H_2C{=}\overset{H}{\overset{|}{C}}\cdots H \xrightarrow{-H_2} HC{\equiv}CH$$

(in other cases) $\downarrow +CH_2{=}CH_2$

$$H_2C{=}\overset{H}{\overset{|}{C}}\text{–}CH_2CH_3$$

where C···H indicates an activated C–H-bond; C. L. Thomas, G. Egloff and J. C. Morrell, *Chem. Revs.*, **28**, 1 (1941).

BULLETIN OF THE CHEMICAL SOCIETY OF JAPAN VOL. 42 1986—1991 (1969)

Intramolecular Interaction between the Hydroxyl Group and the Cyclopropane Ring

Michinori Ōki, Hiizu Iwamura, Tetsuo Murayama and Isao Oka

Department of Chemistry, Faculty of Science, The University of Tokyo, Hongo, Tokyo

(Received November 20, 1968)

Cyclopropylcarbinol shows two absorption maxima due to the O–H stretching, the lower-frequency band being stronger than the higher. The results are interpreted on the basis of intramolecular interaction between the hydroxyl group and the cyclopropane ring. This kind of interaction is not clearly detected with 2-cyclopropylethanol, but 2,2-dicyclopropylethanol and 2-(1-methylcyclopropyl)ethanol give results which are best interpreted by assuming the presence of the interaction. It is concluded, from the findings on rigid molecules, that O–H···cyclopropane interaction is possible when the hydroxyl group approaches the edge within the plane of the ring. The steric effect of the methyl group is also discussed.

In view of the fact that the pi-electron system behaves as a proton acceptor in interaction with the hydroxyl group,[1] it seemed that it would be interesting to investigate the possible interaction between the three-membered ring and the hydroxyl group. The sigma-electrons forming the so-called "banana bond" are known to be rather mobile, and cyclopropane, oxirane, and aziridine are known to show properties like those of the pi-electron system.

A preliminary report[2] on the interaction of the oxirane ring was published by two of the present

1) See M. Ōki, H. Iwamura, T. Onoda and M. Iwamura, *Tetrahedron*, **24**, 1905 (1968) and earlier papers.

2) M. Ōki and T. Murayama, This Bulletin, **40**, 1997 (1967).

authors (M. O. and T. M.); this paper will deal with the intramolecular interaction between the hydroxyl group and the cyclopropane ring. The first observation on this phenomenon was reported some 10 years ago,[3] and a full paper appeared recently.[4] Although the other approaches were made using different model compounds, the conclusion derived by the present authors is in good agreement with that drawn in the aforementioned literature.

The investigation of the intramolecular rather than the intermolecular interaction is convenient for deducing the geometry of the interacting molecule, since the approach of the hydroxyl group can be regulated both in direction and in site. It will be shown that the most preferred conformation of the interacting molecule is such that the hydroxyl group approaches the edge of the cyclopropane ring within the plane of the ring (II). The structure of the protonated cyclopropane rings has previously been discussed with respect to the reaction mechanisms, and it has been suggested to be edge-protonated[5] (I). Olah *et al.* also postulated, from the Raman spectrum of protonated tricyclo-[2.2.1.$0^{2,6}$]heptanes,[6] the same structure. The present authors believe that their results support the structure, since the geometry of the interacting molecule corresponds to the first step of the protonation and may be supposed to be close to the protonated structure.

(I)

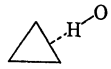

(II)

TABLE 1. ν_{O-H} DATA OF PRIMARY CYCLOPROPYLALKANOLS

Compound	ν_{max} (cm^{-1})	ε ($mol^{-1} \cdot l \cdot cm^{-1}$)	$A \times 10^{-3}$ ($mol^{-1} \cdot l \cdot cm^{-2}$)	A_l/A_h*
Cyclopropylcarbinol	3633.7 3619	27 26	2.3 2.6	1.1
2-Cyclopropylethanol	3637.5 3623	36 19	2.7 1.3	0.48
3-Cyclopropyl-1-propanol	3640.3 3627	58 23	3.6 1.2	0.33
2-(1-Methyl-cyclopropyl)ethanol	3637.7 3625	34 25	2.2 1.6	0.74
2,2-Dicyclopropyl-ethanol	3642 3623.4	21 45	1.5 3.9	2.6

* A_l and A_h denote integrated intensities of the bands at lower and higher frequencies, respectively.

3) P. von R. Schleyer, D. S. Trifan and R. Backskai, *J. Am. Chem. Soc.*, **80**, 6691 (1958).

4) L. Joris, P. von R. Schleyer and R. Gleiter, *ibid.*, **90**, 327 (1968).

5) G. J. Karabatsos, C. E. Orzech, Jr., and S. Meyerson, *ibid.*, **87**, 4394 (1965).

6) G. A. Olah, A. Commeyras and C. Y. Lui, *ibid.*, **90**, 3882 (1968).

Results and Discussion

The infrared spectral data of ω-cyclopropylalkanols are collected in Table 1.

The O–H stretching absorption of cyclopropylcarbinol was reported by Schleyer *et al.*[3,4]; their results are in good agreement with those obtained in the present study. The O–H stretching spectrum of cyclopropylcarbinol shows two maxima, the band at the lower frequency being stronger than that of the higher, in contrast to the case with saturated aliphatic alcohols[7] (see Table 2).

TABLE 2. ν_{O-H} DATA OF ALIPHATIC ALCOHOLS

Compound	ν_{max} (cm^{-1})	$A \times 10^{-3}$ ($mol^{-1} \cdot l \cdot cm^{-2}$)	A_l/A_h	Ref.
CH_3CH_2OH	3637.3 3627	2.8 1.6	0.56	7
$CH_3CH_2CH_2OH$	3639.7 3626	3.4 1.3	0.38	7
$(CH_3)_2CHCH_2OH$	3641.5 3628	3.6 1.8	0.50	7
$(CH_3)_2CHCH_2CH_2OH$	3639.9 3627	3.8 1.6	0.42	

The situation is similar to those of allyl alcohol[7] and benzyl alcohol[7,8]; it is best interpreted by assuming that the hydroxyl group and the cyclopropane ring interact with each other intramolecularly. The intensity of the lower-frequency band is stronger than that of the higher because of the interaction stabilizing the conformation (IV) relative to the free form (III).

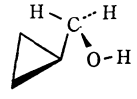

(III)

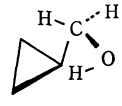

(IV)

2-Cyclopropylethanol (see also Fig. 1) shows two O–H stretching absorptions also, the $\Delta\nu$ (the difference in the wave numbers of the two absorption maxima) being 14.5 cm^{-1} and the (A_l/A_h) ratio of integrated intensities being 0.48. 3-Cyclopropyl-1-propanol likewise shows two maxima, the $\Delta\nu$ and A_l/A_h values being 13.3 cm^{-1} and 0.33 respectively. The saturated alcohols in Table 2 give $\Delta\nu$ values between 10.3 and 13.7 cm^{-1} and A_l/A_h values between 0.38 and 0.56. Thus, 3-cyclopropyl-1-propanol can be considered to have no detectable intramolecular interaction, and the origin of the doublet O–H bands can be attributed to the presence of rotational isomers about the C–O bond. Although the A_l/A_h ratio of 2-cyclopropylethanol is in the range of free primary alcohols, the

7) M. Ōki and H. Iwamura, This Bulletin, **32**, 950 (1959).

8) M. Ōki and H. Iwamura, *ibid.*, **32**, 955 (1959).

$\Delta\nu$ is a little larger than the normal value. Thus, 2-cyclopropylethanol is somewhat an intermediate case.

In order to test whether there is the intramolecular interaction in 2-cyclopropylethanol, it may be necessary to change the situation to a more favorable one. This can be done in many ways. One which the authors chose at the outset was adding one more cyclopropyl group at the β-position of ethanol to form 2,2-dicyclopropylethanol. This selection was made because of a previous success in pi-electron systems: triallylcarbinol showed a very strong interaction band due to the favorable entropy factor.[9] The data shown in Table 1 and in Fig. 1 indicate an increase in A_l/A_h (2.6 instead of 0.48), although $\Delta\nu$ remains almost intact.

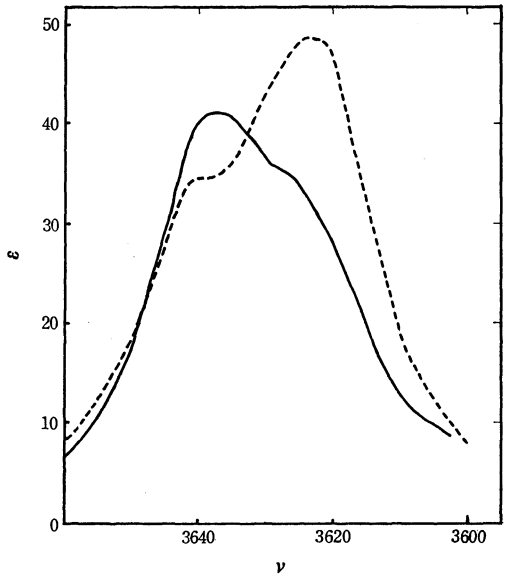

Fig. 1. ν_{O-H} Absorption bands of 2-cyclopropylethanol (——) and 2,2-dicyclopropylethanol (—·—).

Another proof of the presence of the interaction may be obtained by increasing the electron density of the ring, for the higher electron density should facilitate the interaction. Thus, a methyl group is introduced to the cyclopropane ring. 2-(1-Methylcyclopropyl)ethanol gives a slightly increased A_l/A_h ratio, as is shown in Table 1. Although this fact alone may not be taken as positive evidence, in combination with the above results with 2,2-dicyclopropylethanol it strongly indicates the presence of the intramolecular interaction. It may be concluded that the intramolecular interaction between the hydroxyl group and the cyclopropane ring exists in 2-cyclopropylethanol derivatives, although, because of a small stabilizing energy, it can not be clearly demonstrated unless the situation is favorable for the interaction: it can also be concluded that 3-cyclopropyl-1-propanol has no detectable interaction of this kind.

Fixing the conformation of a molecule favorable for the interaction should also facilitate the interaction. In addition, a molecule with a rigid geometry should give information on the conformation of the interacting molecule. Accordingly, the infrared spectra of tricyclo[3.2.1.$0^{2,4}$]octan-6-ols[10] and related compounds were measured; the results are listed in Tables 3 and 4.

The rotational isomers are possible for secondary alcohols about the C–O axis, as is shown by V and VI. It is known[7] that the ν_{O-H} of V appears at about 3626 cm^{-1}, and that of VI, at *ca.* 3617 cm^{-1}.

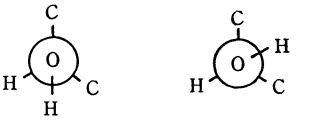

All the ν_{O-H} absorption bands of tricyclo[3.2.1.$0^{2,4}$]-octan-6-ols possess similar shapes, the lower-frequency side being a little greater than the symmetrical curve. It will be convenient to use the β/α ratio introduced by Aaron and Rader[11] in discussing the band shape. Here α and β denote the segments of the half band-width of the high- and low-frequency sides of ν_{max} respectively (Fig. 2).

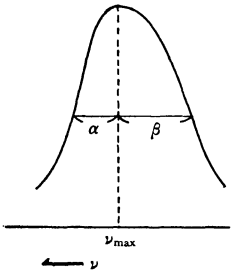

Fig. 2. Explanation of symbols α and β.

If the β/α ratio is greater than unity, the absorption band may be considered to be asymmetric, possibly indicating the presence of a small band at the lower-frequency.

An inspection of Table 3 will show that β/α value is very close to unity when no interaction of the hydroxyl group with the cyclopropane ring is possible because of the geometry of the molecule. The difference in the ratios of exo and endo isomers (VII and VIII) deserves special mention.

9) M. Ōki and H. Iwamura, This Bulletin, **33**, 1600 (1960).

10) These compounds were generously donated by Professor K. B. Wiberg, Yale University, to whom we wish to express our hearty thanks.

11) H. S. Aaron and C. P. Rader, *J. Am. Chem. Soc.*, **85**, 3046 (1963).

Table 3. ν_{O-H} Data of tricyclo-[3.2.1.$0^{2,4}$]octan-6-ols

Compound	ν_{max} (cm^{-1})	$\Delta\nu_{1/2}$ (cm^{-1})	β/α
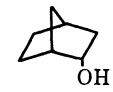	3625.2	26	0.94
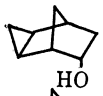	3627.1	29	1.34
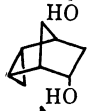	3627.2	25	1.10
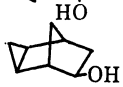	3624.0	20	1.13
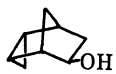	3624.0	19	1.15

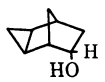
(VII)

(VIII)

While the β/α value of VIII is very close to unity, that of VII is distinctly higher than anything else in Table 3. This is indicative of the presence of another band on the lower-frequency side.

It will not be unnatural to consider, from the analogous situation of 2-cyclopropylethanol, that there are some portions of molecular species which have an internal O–H···cyclopropane interaction in compound VII, but not in compound VIII. It is now apparent, therefore, that if the O–H group approaches the edge of the cyclopropane ring from the side, the O–H···cyclopropane interaction is possible, while it is impossible if O–H approaches from the upper side to the face of the ring.

The same conclusion was drawn by Schleyer and his co-workers from the fact that tricyclo[3.2.1.$0^{2,4}$]-octan-8-ol derivatives (IX and X) possess bands corresponding to the interacting molecule.[4]

(IX)

(X)

Another evidence, though negative, for the geometry of the interacting molecule can be found in bicyclo[3.1.0]hexan-3-ol derivatives. The conformation of bicyclo[3. 1. 0]hexan-3-ol had been postulated by Winstein and Sonnenberg[12] to be a chair on the basis of the unusually fast solvolysis rate of the tosylate, but their suggestion was later amended to be, rather, a boat form.[13] The NMR data in hand agree with the latter, also. A rationale for this conformation may be the repulsion between axial hydrogens at the 2 and 6 positions, as revealed by the molecular model. Therefore, in thujyl alcohol[14] (XII), the hydroxyl group can not come close to the cyclopropane ring, thus eliminating the possibility of interaction. In neothujyl alcohol (XI) and *cis*-bicyclo[3.1.0]-hexan-3-ol, the interaction would be possible if the geometry were such that the hydroxyl group approached the ring from the upper side. Table 4 indicates this is not the case.

Table 4. ν_{O-H} Data of bicyclo[3.1.0]-hexan-3-ol derivatives

Compound	ν_{max} (cm^{-1})	β/α	$A\times10^{-3}$ ($mol^{-1}\cdot l\cdot cm^{-2}$)
cis-Bicyclo[3.1.0]-hexan-3-ol	3625.2	0.99	
Neothujyl alcohol	3624.6	1.0	
Thujyl alcohol	3632.1 3618		2.9 0.74
Cyclopentanol	3626.1	1.1	

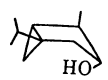
(XI)

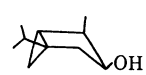
(XII)

However, these facts cannot be taken as evidence for rejecting the Walsh model of cyclopropane.[15] Although, in this model, the electron density must be high at the center of the ring, this does not necessarily mean that the O–H group can approach the site. The steric repulsion must be severe in order to effect the overlapping of the orbitals concerned, thus outweighing any stabilization by the O–H··· cyclopropane interaction. The present authors

Table 5. ν_{O-H} Data of secondary cyclopropylcarbinols

Compound	ν_{max} (cm^{-1})	ε ($mol^{-1}\cdot l\cdot cm^{-1}$)	$A\times10^{-3}$ ($mol^{-1}\cdot l\cdot cm^{-2}$)	A_l/A_h
1-Cyclopropylethanol	3631 3616.9	14 57	1.1 3.1	2.8
1-(2,2-Dimethyl-cyclopropyl)ethanol	3616.6	69	3.9	—
1-(*trans*-2-Methyl-cyclopropyl)ethanol	3628 3617.9	13 53	1.3 2.8	2.1
1-(*trans*-2-Methyl-cyclopropyl)-1-propanol	3633 3619.1	9 57	0.6 3.4	5.7

12) S. Winstein and J. Sonnenberg, *ibid.*, **83**, 3235, 3244 (1961).

13) S. Winstein, E. C. Friedrich, R. Baker and Y. I. Lin, *Tetrahedron, Suppl.*, **8**, 621 (1966).

14) Thujone was kindly donated by Dr. K. Tori of Shionogi & Co. to whom our sincere thanks are due.

15) A. D. Walsh, *Trans. Faraday Soc.*, **45**, 179 (1949).

would like to reserve their conclusion on the electronic structure of the cyclopropane ring until further experimental evidence is obtained.

Table 5 presents the ν_{O-H} data of 1-cyclopropylethanol derivatives. It is worthy pointing out that the A_l/A_h ratio is larger with 1-cyclopropylethanol than with cyclopropylcarbinol. These results can be understood when the favorable conformation is considered.

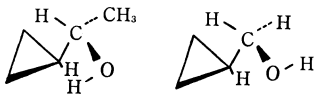

(XIII) (XIV)

As to the conformation determined by the rotation about the C–O bond, the one (XIV) in which the hydrogen of the O–H group is in between two hydrogens, when illustrated by Newman projection, is favored in primary alcohols, probably because of the steric effect. This conformation is undoubtedly not likely in the O–H···cylopropane interaction. In secondary alcohols, the situation changes and the conformation (XIII), in which O–H can come close to the ring is not unfavorable. This very conformation is necessary for establishing the intramolecular interaction.

The introduction of two methyl groups to the position 2 of the cyclopropane ring causes the free band of 1-cyclopropylethanol to disappear. These results may be explained when steric factor of the methyl group is considered. Due to the steric effect inserted by the methyl group *cis* to the 1-hydroxyethyl, the H-inside conformation (XV) is more stable than the CH_3-inside (XVI) or the O–H-inside (XVII) conformations. Whatever conformation is taken with respect to the C–O axis in XVII, the conformation is not good at establishing the O–H···cyclopropane interaction.

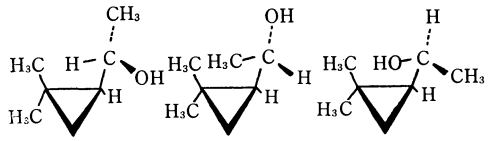

(XV) (XVI) (XVII)

These circumstances must reduce the possibility of the existence of the free form. These considerations are supported by the reappearance of the free O–H absorption on the removal of the *cis*-methyl group [1-(*trans*-2-methylcyclopropyl)ethanol], as is shown in Table 5. It is, then, not surprising to find that 1-(*trans*-2-methylcyclopropyl)-1-propanol having methyl and 1-hydroxypropyl groups *trans* to each other, like the corresponding ethanol derivative, shows very small absorption for the free O–H and gives a large A_l/A_h value.

One might argue that the configuration of the alcohol may be different from that shown. However, there are many examples showing the stereochemical outcome of the Simmons-Smith reaction. For example, the reaction of methylene iodide and copper-zinc couple with 2-cyclohexen-1-ol gives bicyclo[4.1.0.]heptan-*cis*-2-ol,[16] whereas 2-cyclohexen-1-ol affords *cis*-2,3-epoxycyclohexan-1-ol on epoxidation.[17] Thus, it may be postulated that epoxidation and Simmons-Smith reaction give the same steric outcome. Then, since it has been established in this laboratory that the oxidation of 4-methyl-3-penten-2-ol with perbenzoic acid affords the threo isomer of the corresponding epoxide,[18] it is natural to consider that the Simmons-Smith reaction of 4-methyl-3-penten-2-ol will give the product of the configuration as shown (the threo isomer).

There is another possibility, that the steric effect of the methyl groups prohibits the approach of the O–H group to the cyclopropane ring in the conformation XVI. However, further study will be necessary before we can discuss this sort of steric effect of the substituents.

Experimental

Spectral Measurements. A Perkin-Elmer 112G single-beam grating infrared spectrometer was used for measuring the infrared absorption spectra in the 3 μ region, the spectral slit width being 0.8 cm^{-1}.

Wako special-grade carbon tetrachloride was used as the solvent. The concentrations of the alcohols were *ca.* 0.003 mol/*l*, and the length of the quartz optical cell was 2 cm. The obtained absorption band was graphically separated into two symmetrical curves.

Materials. The compounds used in this study were known compounds unless otherwise stated, and their physical constants were checked prior to measurements.

3-Cyclopropyl-1-propanol was synthesized in the following way. Cyclopropylcarbinyl bromide was condensed[19] with diethyl malonate in the presence of sodium ethoxide, and the product was hydrolyzed. The dicarboxylic acid thus obtained lost carbon dioxide on distillation, and the resulting 3-cyclopropylpropionic acid was reduced with lithium aluminum hydride.

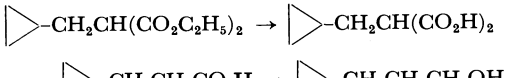

3-Cyclopropylpropionic Acid. Diethyl cyclopropylcarbinylmalonate (27 g) was heated with 120 m*l* of 10% aqueous sodium hydroxide until a homogeneous solution was obtained. The solution was acidified with hydrochloric acid, and the dicarboxylic acid was heated

16) W. G. Dauben and G. H. Berezin, *J. Am. Chem. Soc.*, **85**, 468 (1963).

17) H. B. Henbest and R. A. L. Wilson, *J. Chem. Soc.*, **1957**, 1958.

18) M. Ōki and T. Murayama, unpublished work. The epoxide thus prepared was identical with that obtained by G. B. Payne [*J. Org. Chem.*, **27**, 3819 (1962)].

19) J. A. Arvin and R. Adams, *J. Am. Chem. Soc.*, **50**, 1983 (1928).

in vacuo, thus affording 3-cyclopropylpropionic acid, bp 104—105°C/17 mmHg, $n_D^{17.5}$ 1.4375, in a 69% yield. This compound had been prepared[20] by the Arndt-Eistert reaction of cyclopropylacetic acid, and the boiling point reported to be 101°C/15 mmHg.

3-Cyclopropyl-1-propanol. 3-Cyclopropylpropionic acid (13 g) in 100 m*l* of ether was added to 6 g of lithium aluminum hydride in 250 m*l* of ether. The distillation of the product gave 7 g (61%) of 3-cyclopropyl-1-propanol, bp 66°C/18 mmHg.

Found: C, 72.18; H, 12.32%. Calcd for $C_6H_{12}O$: C, 71.95; H, 12.08%.

NMR (τ): 6.40 (singlet OH), 6.47 (triplet CH_2O), 8.2—9.1 (multiplet CH_2CH_2), 9.2—10.3 (multiplet ring H).

2,2-Dicyclopropylethanol. This was prepared by the hydroboration of 1,1-dicyclopropylethylene, followed by alkaline oxidation. Considering that the hydroboration of vinylcyclopropane, followed by oxidation, has been reported to yield 97 : 3 mixture of 2-cyclopropylethanol and 1-cyclopropylethanol,[21] and considering that 1,1-dicyclopropylethylene has an enhanced steric effect, the purity of the 2,2-dicyclopropylethanol thus prepared was expected to be good. The spectral evidence supported this expectation.

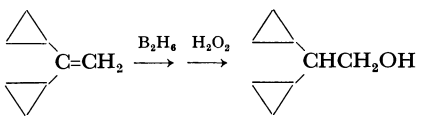

To a solution of 6 g of 1,1-dicyclopropylethylene[22] and 1 g of lithium aluminum hydride in 80 m*l* of dry tetrahydrofuran, was added 4 g of boron trifluoride etherate in 30 m*l* of tetrahydrofuran with cooling in an ice-salt bath. After the solution had been stirred for 3 hr, the excess hydride was decomposed with water. The mixture was treated with 10 m*l* of 3N sodium hydroxide and then with 10 m*l* 33% hydrogen peroxide. The distillation of the product gave 4.2 g (60%) of the crude alcohol. Redistillation afforded pure 2,2-dicyclopropylethanol; bp 106—106.5°C/41 mmHg, $n_D^{26.5}$ 1.4620.

Found: C, 76.04; H, 11.36%. Calcd for $C_8H_{14}O$: C, 76.14; H, 11.18%.

NMR (τ): 6.55 (doublet CH_2O), 7.22 (singlet OH), 9.30—10.20 (multiplet methine and ring H).

2-(1-Methylcyclopropyl)ethanol and 1-(*trans*-2-methylcyclopropyl)-1-propanol were prepared by the Simmons-Smith reaction of the corresponding olefinic alcohols.

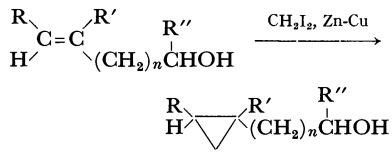

2-(1-Methylcyclopropyl)ethanol. To a suspension of a zinc-copper couple, prepared according to LeGoff[23] from 35 g of glannular zinc in 200 ml of ether, were added 24 m*l* of methylene iodide and 16 g of 3-methyl-3-buten-1-ol in 50 m*l* of ether. After having been refluxed for 2 days, the mixture was treated in the usual manner to afford 3.5 g of the crude product (bp 52—53°C/10 mmHg). A pure sample boiled at 51—52°C/11 mmHg and possessed an n_D^{16} value of 1.4370.

Found: C, 72.18; H, 12.15%. Calcd for $C_6H_{12}O$: C, 71.95; H, 12.06%.

NMR (τ): 6.20—6.60 (multiplet CH_2O and OH), 8.59 (triplet β-CH_2), 9.00 (singlet CH_3), 9.70—9.90 (multiplet ring H).

1-(*trans*-2-Methylcyclopropyl)-1-propanol. This was similarly prepared from 4-hexen-3-ol in 49% yield. Bp 45—47°C/8 mmHg, $n_D^{18.5}$ 1.4362.

Found: C, 73.38; H, 12.40%. Calcd for $C_7H_{14}O$: C, 73.63; H, 12.36%.

20) J. H. Turnbull and E. S. Wallis, *J. Org. Chem.*, **21**, 663 (1956).

21) S. Nishida, I. Moritani, K. Ito and K. Sakai, *ibid.*, **32**, 939 (1967).

22) I. A. D'yakonov and I. M. Stroiman, *Zh. Obshch. Khim.*, **33**, 4019 (1963); *Chem. Abstr.*, **60**, 9159 g (1964).

23) E. LeGoff, *J. Org. Chem.*, **29**, 2048 (1964).

BULLETIN OF THE CHEMICAL SOCIETY OF JAPAN VOL. 42 1992—1995 (1969)

Studies of the Organic Reactions of Metal Carbonyls. XVII.*1 The Reaction of Potassium Iron Carbonylates with Allyl Halide and Its Derivatives

Yoshinobu TAKEGAMI, Yoshihisa WATANABE, Takeaki MITSUDO and Toshiharu OKAJIMA

Department of Hydrocarbon Chemistry, Faculty of Engineering, Kyoto University, Sakyo-ku, Kyoto

(Received December 4, 1968)

The reactions of potassium iron carbonylates ($K_2Fe(CO)_4$, $KHFe(CO)_4$ and $K_2Fe_2(CO)_8$) with allyl halide and its derivatives have been studied. Allyl halide and its derivatives react readily with these carbonylates in ethyl alcohol at 30°C to give the corresponding and isomerized olefins. The reaction of allyl chloride in hydrous ethyl alcohol gives propylene in a good yield and 1,5-hexadiene as a by-product. In dry ethyl alcohol, the yield of propylene decreases. The reaction of *trans*-1-chloro-2-butene gives *trans*-2-butene (the major product), *cis*-2-butene, and 1-butene. The reaction of 1-chloro-3-methyl-2-butene and 3-chloro-3-methyl-1-butene gives 2-methyl-2-butene (the major product), 3-methyl-1-butene, and 2-methyl-1-butene. These reactions are considered to proceed *via* σ- and π-allyl iron carbonyl complexes.

Previous work in this laboratory has shown that potassium iron carbonylates, mainly $KHFe(CO)_4$, react with isoprene in alcohol to give three different monoolefins, and that the yields and the distribution of these monoolefins are remarkably affected by the reaction conditions (the solvents and the atmosphere).[1]

The present study deals with the reactions of iron carbonylates, mainly $K_2Fe(CO)_4$, with allyl halide compounds. The results obtained here indicate that allyl halide compounds react with the iron carbonyl complexes, which then decompose in such polar solvents as alcohol and water to the corresponding olefin and isomerized olefins.

Experimental

Three potassium iron carbonylates, $KHFe(CO)_4$, $K_2Fe(CO)_4$ and $K_2Fe_2(CO)_8$, were prepared according to the method described in a previous paper.[2] A 50 m*l* portion of a 0.011M $KHFe(CO)_4$, $K_2Fe(CO)_4$, or 0.0055M $K_2Fe_2(CO)_8$ solution was used in each run.

Materials. 1-Chloro-3-methyl-2-butene (A) and 3-chloro-3-methyl-1-butene (B) were prepared by bubbling hydrogen chloride into isoprene at −10°C. These products were fractionated by vacuum distillation into two fractions.*2 The allyl halides, *trans*-1-chloro-2-butene, 3-chloro-2-methyl-1-propene, iron pentacarbonyl, and the other compounds employed in this study were all commercial products.

Reaction Procedure. To the solution of the potassium iron carbonylate, a certain amount of allyl halide or its derivatives was added, and then the mixture was agitated vigorously at 30°C under an atmospheric pressure of nitrogen or carbon monoxide. After a certain reaction time, the reaction flask was connected with a cold trap immersed in liquid nitrogen and fitted with a vacuum pump. The gases in the reaction flask were collected in the trap at 30 mmHg. The trap was allowed to warm to room temperature and then heated to 80°C, and the gas evolved was submitted to analysis. The liquid reaction mixture was analyzed at the same time.

Analytical Procedures. The reaction products were gas-chromatographed. For the gaseous products, a column packed with active carbon (0.3 cmϕ, 3 m) or a column packed with dimethylsulfolan (0.3 cmϕ, 5 m) was used. For the liquid products, a Golay R 45 column (0.25 mmϕ, 45m) and a column packed with SE 30 on a chromasorb were used.

Results and Discussion

The Reactions of $K_2Fe(CO)_4$ and $K_2Fe_2(CO)_8$ with Allyl Halides. Table 1 summarizes the results of these reactions, which were carried out under an atmosphere of carbon monoxide or nitrogen at 30°C. $K_2Fe(CO)_4$ reacts readily with allyl chloride, while the light-brown reaction mixture immediately turns dark red, and then yellow brown. As the reaction products, propylene (the major product) and 1,5-hexadiene are obtained.

*1 Part XVI: This Bulletin, **42**, 206 (1969). Presented at the Symposium on Organometallic Compounds, Tokyo, October, 1968.

1) Y. Takegami, Y. Watanabe, H. Masada and T. Mitsudo, This Bulletin, **42**, 206 (1969).

2) Y. Takegami, Y. Watanabe, H. Masada and I. Kanaya, *ibid.*, **40**, 1456 (1967).

*2 One, A 79%, B 21%; the other, A 17%, B 83%.

TABLE 1. THE REACTION OF $KHFe(CO)_4$, $K_2Fe(CO)_4$ AND $K_2Fe_2(CO)_8$ WITH ALLYL HALIDES AT 30°C

Exp. No.	Allyl halide	Reaction conditions*				Products**	
		Iron carbonylate	Solvent	H_2O Content	Atmosphere	Propylene	1,5-Hexadiene
1	Allyl chloride***	$K_2Fe(CO)_4$	EtOH	1	N_2	1.90	0.18
2	Allyl chloride****	$K_2Fe(CO)_4$	EtOH	0	N_2	1.00	0.15
3	Allyl chloride	$K_2Fe(CO)_4$	EtOH	1	CO	1.75	0.13
4	Allyl chloride	$KHFe(CO)_4$	EtOH	1	CO	1.31	0.18
5	Allyl chloride	$K_2Fe_2(CO)_8$	EtOH	1	CO	1.22*****	0.15*****
6	Allyl bromide	$K_2Fe(CO)_4$	EtOH	1	CO	0.75	0.16
7	Allyl iodide	$K_2Fe(CO)_4$	EtOH	1	CO	0.84	0.19
8	Allyl chloride	$K_2Fe(CO)_4$	THF	0	N_2	0.42	0
9	Allyl chloride	$K_2Fe(CO)_4$	Benzene	0	N_2	0.27	0.02

* 1 atm, 3—4 hr, allyl halide 3.0 mol/mol-$Fe(CO)_4^{2-}$
** mol/mol-$Fe(CO)_4^{2-}$
*** CO_2 (0.43 mol/mol-$Fe(CO)_4^{2-}$) and CO (0.81 mol/mol-$Fe(CO)_4^{2-}$) were evolved.
**** CO_2 (0.07 mol/mol-$Fe(CO)_4^{2-}$) and CO (0.67 mol/mol-$Fe(CO)_4^{2-}$) were evolved.
***** mol/g-atm Fe

The yield of propylene amounts to about 2 mol*3 in hydrous ethyl alcohol (Exp. 1). However, in dry ethyl alcohol the yield of propylene decreases to 1 mol (Exp. 2). In both cases the yield of 1,5-hexadiene is almost 0.2 mol. Comparing Exp.1 with Exp. 3, the nitrogen atmosphere seems to be little more favorable to the production of propylene than the carbon monoxide atmosphere. Under carbon monoxide some side reactions, such as a carbonylation reaction, occur. The infrared spectrum of the reaction mixture treated with an alcoholic solution of iodide and hydrogen chloride has a band at 1738 cm^{-1} characteristic of an ester, indicating that some acyl-iron carbonyl complex is formed.

$KHFe(CO)_4$ and $K_2Fe_2(CO)_8$ also react with allyl chloride to give propylene and 1,5-hexadiene (Exps. 4 and 5), but the yields of propylene are less than that of the reaction of $K_2Fe(CO)_4$. The order of the reactivity of the iron carbonylates to the substitution reaction seems to be: $K_2Fe(CO)_4 > KHFe(CO)_4 > K_2Fe_2(CO)_8$.

As Exps. 6 and 7 show, allyl bromide and iodide also react with $K_2Fe(CO)_4$. However the yields of propylene are less than half of that of the reaction of allyl chloride.

The reaction of $K_2Fe(CO)_4$ with allyl halide is considered to proceed *via* σ- and π-allyl iron carbonyl complexes and to follow the following reaction scheme:

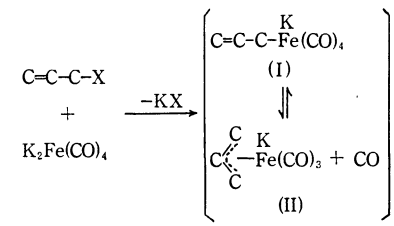

$$\xrightarrow{\text{solvent}} C{=}C{-}C \quad (1)$$

In the first step, $K_2Fe(CO)_4$ reacts with allyl halide to give the σ-allyl complex (I). This complex seems then to be converted to the π-allyl complex (II) with an evolution of carbon monoxide. These complexes may be unstable in an alcoholic solution, thus abstracting hydrogen from the solvent and giving propylene in a good yield. This reaction scheme is supported by the fact that, under nitrogen, a considerable amount of carbon monoxide evolves (Exps. 1 and 2).

When 1 mol of water is present in the reaction system, a considerable amount of carbon dioxide also evolves (Exp. 1). Thus, the water present in the system is more favorable to the formation of propylene and carbon dioxide. This fact seems to indicate that the water acts as one of the hydrogen sources and that a reaction between the water and carbon monoxide occurs to give hydrogen and carbon dioxide:

$$H_2O + CO \rightarrow 2(H) + CO_2 \quad (2)$$

This reaction mechanism is, however, not yet completely clear.

In dry tetrahydrofuran and in dry benzene the iron carbonylate is less reactive and the yield of propylene decreases to lees than half of that in dry ethyl alcohol (Exps. 8 and 9). These solvents are unsuitable for this reaction because the iron carbonylate is insoluble in benzene and only slightly soluble in THF. In these solvents, the formation of 1,5-hexadiene is also retarded.

The Reaction of *trans*-1-Chloro-2-butene and 3-Chloro-2-methyl-1-propene. The results of the reactions are summarized in Table 2. All of the reactions were carried out at 30°C in ethyl alcohol. *trans*-1-Chloro-2-butene reacts with $K_2Fe(CO)_4$ to give *trans*-2-butene (the major product), *cis*-2-butene, and 1-butene. The yield of the

*3 Hereafter mol means mole per mole of $Fe(CO)_4^{2-}$.

TABLE 2. THE REACTION OF $K_2Fe(CO)_4$ WITH THE DERIVATIVES OF ALLYL HALIDE IN ETHYL ALCOHOL AT 30°C

Exp. No.	Reagent	Reaction conditions****			Products**				
		H_2O Content*	Atmosphere	Reaction time (min)	1-Butene	*cis*-2-Butene	*trans*-2-Butene	2-Methylpropene	Total yield of monoolefins
10	*trans*-1-Chloro-2-butene	1	CO	10	0.16 (21)	0.14 (19)	0.44 (60)		0.74
11	*trans*-1-Chloro-2-butene	1	CO	60	0.15 (18)	0.15 (19)	0.51 (63)		0.81
12	*trans*-1-Chloro-2-butene	1	CO	240	0.20 (18)	0.20 (18)	0.72 (64)		1.12
13	*trans*-1-Chloro-2-butene	0	N_2	60	0.19 (19)	0.18 (19)	0.60 (62)		0.97
14	*trans*-1-Chloro-2-butene	0	N_2	4(d)***	0.17 (15)	0.16 (15)	0.78 (70)		1.11
15	3-Chloro-2-methyl-1-propene	1	N_2	180				1.75	

* mol/mol-$Fe(CO)_4^{2-}$
** mol/mol-$Fe(CO)_4^{2-}$ ( ): mol%, total monoolefins at each run=100%
*** (d): day
**** 3.0 mol/mol-$K_2Fe(CO)_4$

olefins amounts to 1.1 mol. The distribution of these monoolefins is approximately independent of the atmosphere, the presence of water, and the reaction time (10—240 min). After 4 days (Exp. 14), however, the percentage of *trans*-2-butene increases to 70%, while those of 1-butene and *cis*-2-butene decrease to 15% and 15% respectively, showing that under these conditions the isomerization among the butenes slowly occurs. This reaction is considered to proceed *via* σ- and π-allyl iron carbonyl complexes and to follow the following reaction scheme:

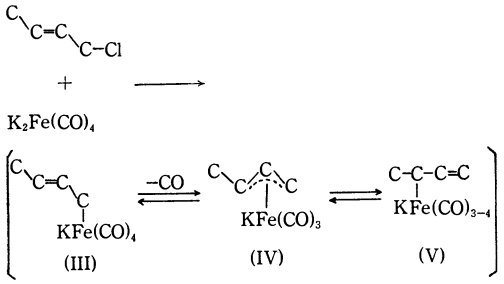

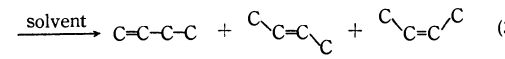

(3)

Thus, two σ-allylic compleexs (III and V) and one π-allylic complex (IV) are possible. For the formation of 1-butene, two routes from the complexes III and V are probable.
From the complex III:

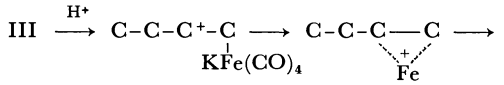

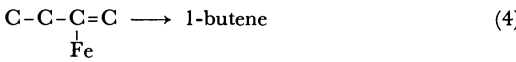

(4)

From the complex V:

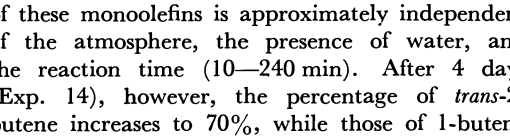

(5)

The π-allylic structure can reasonably be considered to be more stable than the σ-allyl structures. σ-Allyl manganese carbonyl has been suggested to decompose in the presence of an acid to give propylene in a way similar to that of Eq.(4).[3] In this case the reaction was carried out in a neutral or a rather basic solution. Moreover, it is safe to conclude that the complex III is more stable and more dominant than the complex V, which has a structure with larger steric hindrance. Accordingly, the route (5) is more probable for the formation of 1-butene. The complexes III and V seem to give 2-butene and 1-butene respectively. This consideration is supported by the facts that the percentages of 2-butenes are larger than that of 1-butene and that the isomerization among the the butenes occurs slowly under the conditions employed.

3-Chloro-2-methyl-1-butene also reacts with $K_2Fe(CO)_4$ to give 2-methylpropene in a good yield (Exp. 15).

The Reaction of 1-Chloro-3-methyl-2-butene and 3-Chloro-3-methyl-1-butene. The results of the reactions are summarized in Table 3. All of the reactions were carried out in ethyl alcohol at 30°C.

As Table 3 shows, 1-chloro-3-methyl-2-butene and 3-chloro-3-methyl-1-butene react with $K_2Fe(CO)_4$ and $KHFe(CO)_4$ to give three different

3) M. L. H. Green and P. L. I. Nagy, *J. Chem. Soc.*, **1963**, 189.

TABLE 3. THE REACTION OF $K_2Fe(CO)_4$ AND $KHFe(CO)_4$ WITH 1-CHLORO-3-METHYL-2-BUTENE AND 3-CHLORO-3-METHYL-1-BUTENE IN ETHYL ALCOHOL

Exp. No.	Reagent	Reaction conditions			Yield of mono-olefins*	Products: Distribution of monoolefins (%)		
		mol ratio Reagent/ $Fe(CO)_4^{2-}$	H_2O Content*	Reaction time**		3-Methyl-1-butene (A)	2-Methyl-1-butene (B)	2-Methyl-2-butene (C)
21	1-Chloro-3-methyl-2-butene	1	0	1.5	0.64	20	1	79
22	1-Chloro-3-methyl-2-butene	1	0	2(d)	0.59	5	5	90
23	1-Chloro-3-methyl-2-butene	3	1	1.5	0.98	7	7	86
24	1-Chloro-3-methyl-2-butene	3	0	1.5	0.82	5	5	90
25*	1-Chloro-3-methyl-2-butene	3	0	1.5	0.98	5	7	88
26	3-Chloro-3-methyl-1-butene	1	0	1.5	0.55	18	3	79
27	3-Chloro-3-methyl-1-butene	3	1	1.5	1.29	9	7	84
28	3-Chloro-3-methyl-1-butene	3	1	2(d)	1.23	9	6	85
29	3-Chloro-3-methyl-1-butnee	3	0	1.5	1.07	9	6	86

* mol/mol-$Fe(CO)_4^{2-}$
** hr, (d): day
*** $KHFe(CO)_4$ used

monoolefins, 2-methyl-2-butene (C), 3-methyl-1-butene (A), and 2-methyl-1-butene (B). At a high mole ratio ($RX/Fe(CO)_4^{2-}=3.0$), the distribution of the olefins is almost independent of the reaction conditions (the atmosphere, the presence of water, and the reaction time 1.5 hr —2 day). Under these conditions the olefin C is predominant, its percentage amounting to 85—90%; the olefins seem to be almost in an equilibrium because the distribution of the olefins remains unchanged with an increase in the reaction time.

When the mole ratio is 1.0 (Exps. 21 and 26), the olefins A and C predominate in the initial stage of the reactions. In this case the percentage of the olefin A amounts to 20%.

Judging from the similarity between the reactions of 1-chloro-3-methyl-2-butene and 3-chloro-3-methyl-1-butene, these reactions seems to have the same intermediates. Thus, the following reaction scheme seems reasonable:

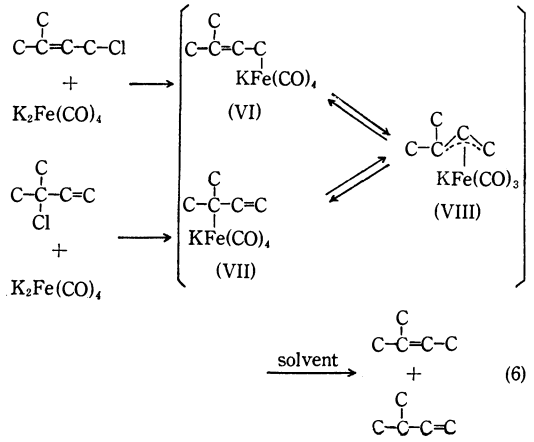

(6)

In these cases, two σ-allyl complexes and one π-allyl complex are possible. The complex VI may be more stable than the complex VII because the tertiary structure of the latter has a larger steric hindrance. Accordingly, the equilibrium between them may be much more favorable to the complex VI. Thus, starting with even 3-chloro-3-methyl-1-butene under the conditions employed, the complex VI seems to be readily formed, giving the olefin C as the major product. The formation of the π-complex VIII is supported by the evolution of carbon monoxide.

This work was supported in part by The Kawakami Foundation, to which our thanks are due.

BULLETIN OF THE CHEMICAL SOCIETY OF JAPAN VOL. 42 1996—2005 (1969)

Anionic Telomerizations of Styrene with Butylamines*1

Teruzo ASAHARA, Manabu SENŌ, Sadayoshi TANAKA and Norio DEN

Institute of Industrial Science, The University of Tokyo, Roppongi, Minato-ku, Tokyo

(Received December 5, 1968)

The anionic telomerizations of styrene with *n*-butylamine, *s*-butylamine, *t*-butylamine and isobutylamine catalyzed by sodium metal were investigated. The structures of the products were discussed by the NMR spectra obtained in carbon tetrachloride and identified to be *N*-butyl-2-phenylethylamines and *N*-butyldi(2-phenylethyl)amines. The general reaction scheme was proposed and interpreted with the concept of the anionic telomerization, where amine acts as a telogen and styrene as a taxogen.

The concept of telomerization was introduced for reactions of the type

$$XY + nM \rightarrow XM_nY$$

by Harmon in 1945.[1] Radical telomerizations have been actively investigated by many reseachers in the USA, Japan, USSR, Israel, *etc.*, and those of ethylene with carbon tetrachloride in particular. On the contrary, only a few papers on anionic and cationic telomerizations have appeared.

The hydrogen atoms attached to the nitrogen atom in ammonia NH_3, primary amines RNH_2 or secondary amines RR'NH are weakly acidic[2] and subject to the attack of strong alkalis such as sodium metal, phenyl potassium and *n*-butyllithium to form alkali amides. Some of these can add to styrene[3] or initiate the anionic polymerization of styrene.[4] Hence it was supposed that on taking one of the amines as a telogen and styrene as a taxogen, an anionic telomerization would take place with sodium metal as a catalyst.

In this paper investigation in telomerization of styrene with butylamines and the NMR spectra of the resulting *N*-butyl-2-phenylethylamines and *N*-butyldi(2-phenylethyl)amines are presented. Moreover, the reaction mechanism is discussed with the proposed scheme from the standpoint of anionic telomerization.

Results and Discussion

Reaction Products. Each of the butylamines $BuNH_2$ was reacted with syrene in the presence of sodium metal as a catalyst to produce N-butyl-2-phenylethylamine (**1**) and *N*-butyldi(2-phenylethyl)amine (**2**), but *N*-butyl-2,4-diphenylbutylamine (**3**) was not obtained.

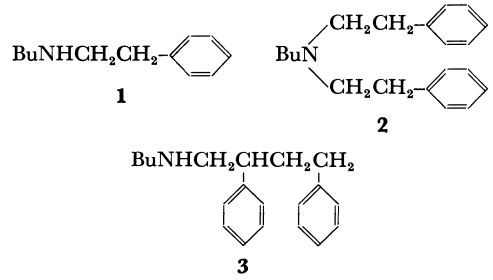

The reaction products are listed in Table 1, where column 1 shows the amines used and column 4 the reaction products isolated.

Structures of the Reaction Products. Figures 1, 2, 3 and 4 show the proton NMR spectra of the reaction products. The assignments of the signals to the protons are listed in Table 2. In the compound **2c** there is one conformation about a single bond between the nitrogen and the carbon (e), in which three methyl groups are not equivalent in the conformation.

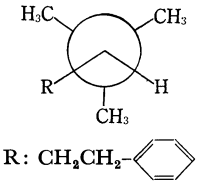

The splitting of the methyl singlet of the protons (f) into two signals would be caused by the restricted rotation about the single bond between the nitrogen and the carbon (e). If the rotation is as free as in the compound **1c**, three methyl groups would become equivalent in the NMR and show a single methyl singlet. The splitting of the phenyl

*1 Anionic Telomerizations. I.

1) J. Harmon, U. S. Pat. 2390099 (1945)

2) W. K. McEwen, *J. Am. Chem. Soc.*, **58**, 1124 (1936).

3) R. Wegler and G. Pieper, *Chem. Ber.*, **83**, 1 (1950).

4) W. C. E. Higginson and N. S. Wooding, *J. Chem. Soc.*, **1952**, 760.

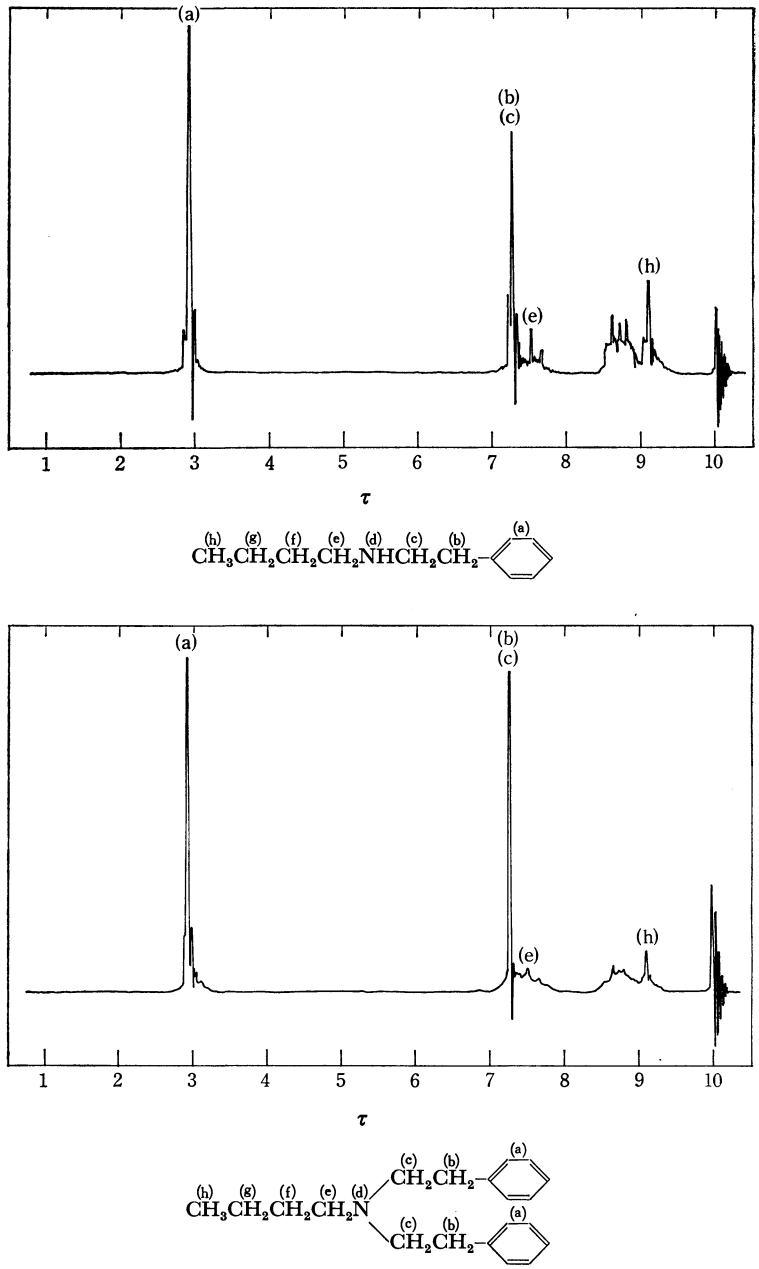

Fig. 1. NMR spectra of *n*-butyl-2-phenylethylamine and *n*-butyldi(2-phenylethyl)amine.

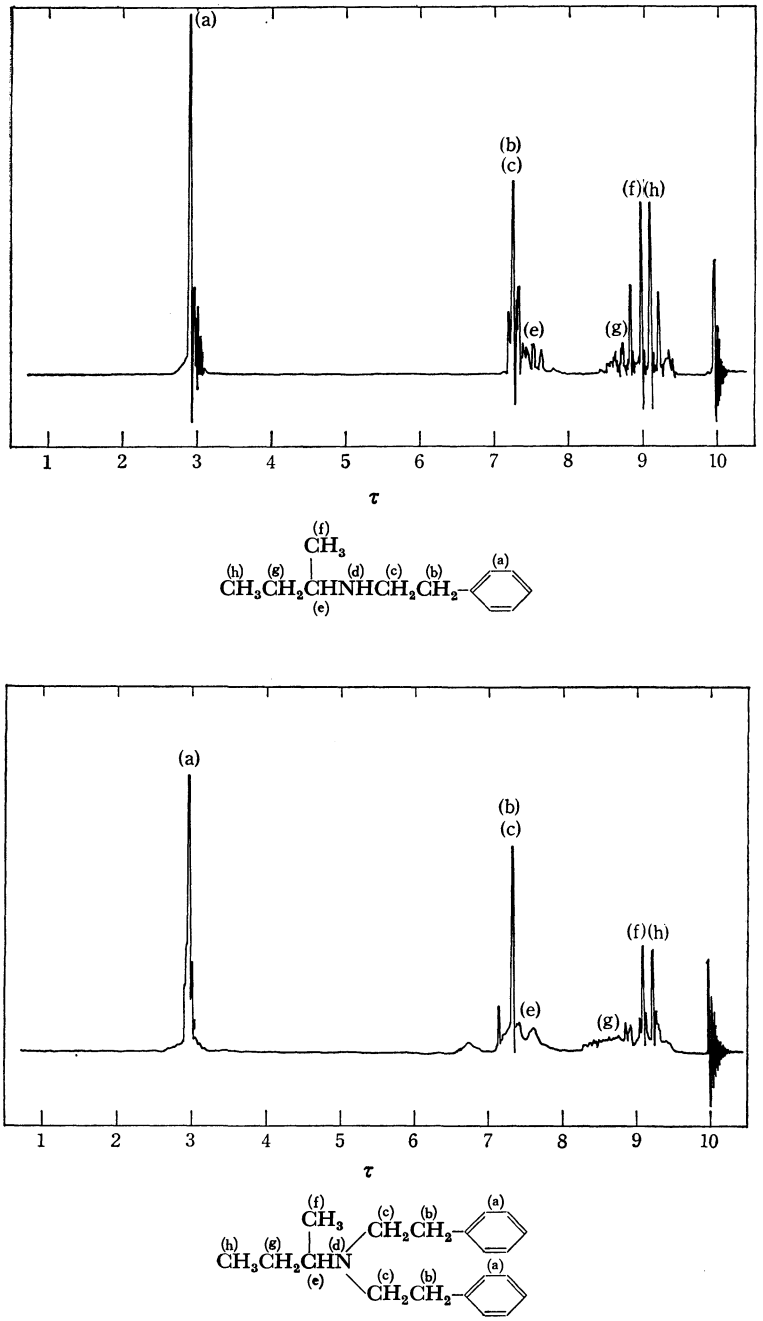

Fig. 2. NMR spectra of *s*-butyl-2-phenylethylamine and *s*-butyldi(2-phenylethyl)amine.

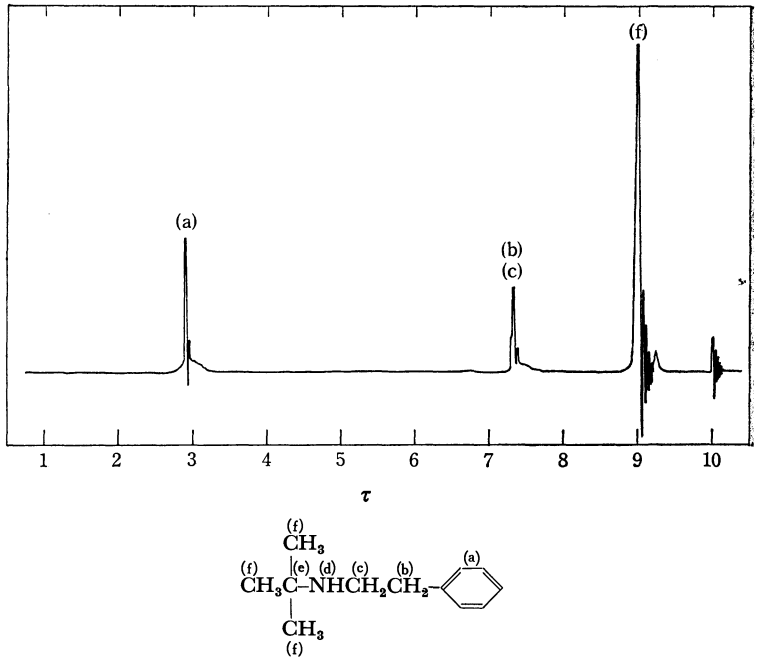

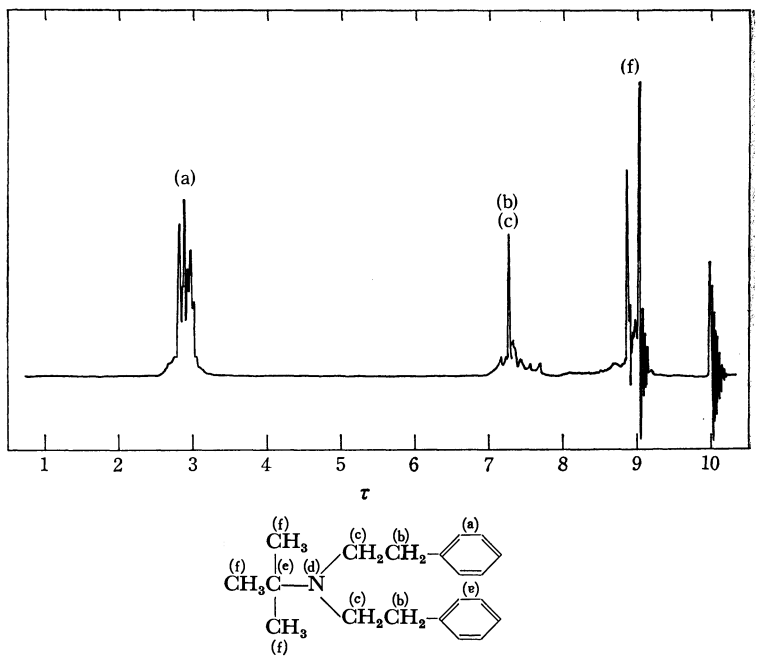

Fig. 3. NMR spectra of *t*-butyl-2-phenylethylamine and *t*-butyldi(2-phenylethyl)amine.

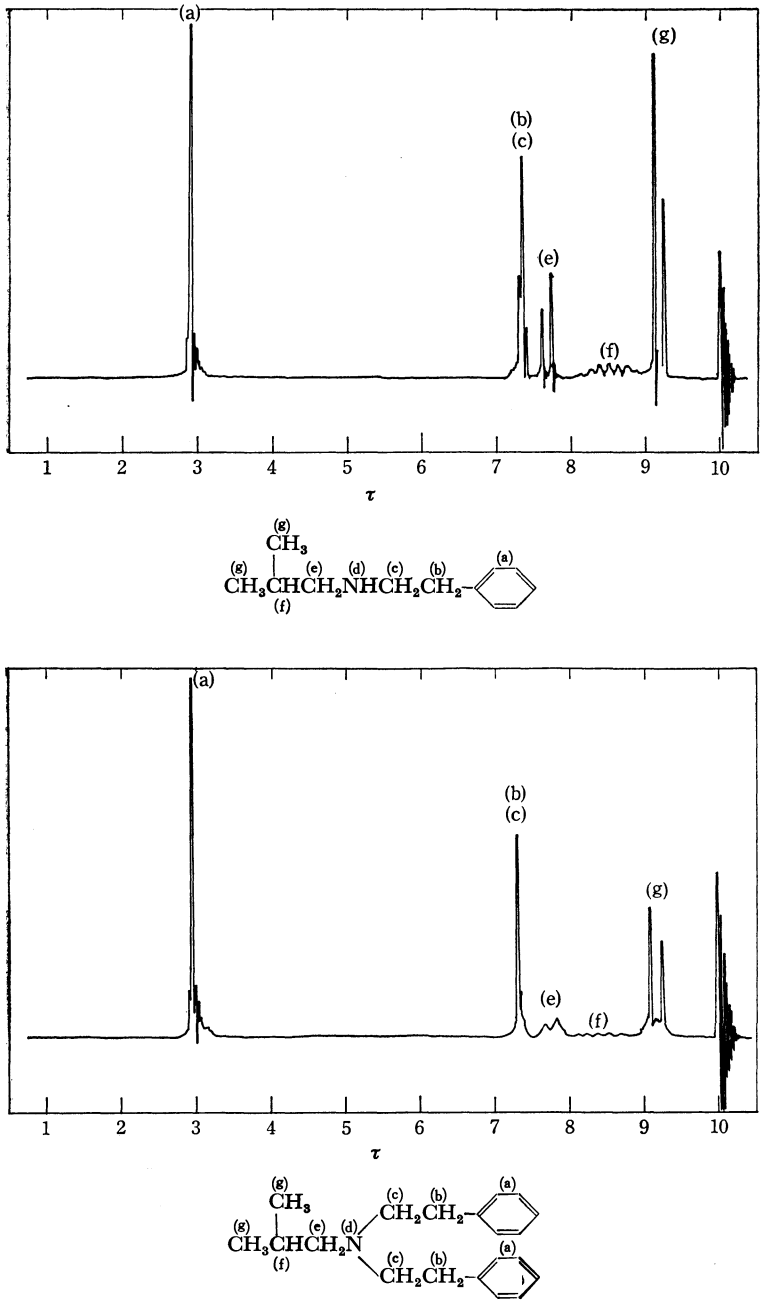

Fig. 4. NMR spectra of isobutyl-2-phenylethylamine and isobutyldi(2-phenylethyl)amine.

TABLE 1. REACTION PRODUCTS OBTAINED IN THE REACTIONS OF STYRENE WITH BUTYLAMINES[a)]

Amine	Reaction temp. °C	Reaction time hr	Reaction products		Bp[b)] °C/mmHg	Yield[c)] %
n-Butylamine	46.0±0.5	3.0	*n*-BuNHCH$_2$CH$_2$-C$_6$H$_5$	(**1a**)	104—105/4	26.3
			n-BuN(CH$_2$CH$_2$-C$_6$H$_5$)$_2$	(**2a**)	183—184/4	23.5
s-Butylamine	60.0±0.5	4.3	*s*-BuNHCH$_2$CH$_2$-C$_6$H$_5$	(**1b**)	90—91/4	11.1
			s-BuN(CH$_2$CH$_2$-C$_6$H$_5$)$_2$	(**2b**)	179—180/4	10.8
t-Butylamine	45.0±1.0	3.9	*t*-BuNHCH$_2$CH$_2$-C$_6$H$_5$	(**1c**)	86—87/4	11.6
			t-BuN(CH$_2$CH$_2$-C$_6$H$_5$)$_2$	(**2c**)	170—171/4	11.9
Isobutylamine	65.0±0.5	4.1	isoBuNHCH$_2$CH$_2$-C$_6$H$_5$	(**1d**)	91—92/4	21.5
			isoBuN(CH$_2$CH$_2$-C$_6$H$_5$)$_2$	(**2d**)	177—178/4	49.4

a) The molar ratio of styrene to amine was unity.
b) Boiling points were uncorrected.
c) Yields were calculated on the basis of styrene added.

protons (a) in the compound **2c**, which does not appear in the compound **1c**, is perhaps due to the different conformations that are brought about by the restricted rotations about single bonds between carbons (b) and (c) and between carbon (c) and nitrogen. The IR spectra and the NMR spectra are consistent with the structural formulas illustrated in Table 1.

General Reaction Scheme. The reaction scheme is considered as follows. The initiation reaction may be the addition of sodium to styrene **4**, and product **5** transmetalates with the primary amine to give sodium amide **7**.

$$2Na + CH_2{=}CH\text{-}C_6H_5 \longrightarrow CH_2NaCHNa\text{-}C_6H_5 \quad (1)$$

4 **5**

$$5 + 2RNH_2 \rightleftarrows CH_3CH_2\text{-}C_6H_5 + 2RNHNa \quad (2)$$

6 **7**

Sodium amide **7** is able to react with styrene, and the resulting sodium salt **8** changes into the amide **7** by reaction (4), thus a cycle of reactions is formed.

$$7 + 4 \longrightarrow RNHCH_2CHNa\text{-}C_6H_5 \quad (3)$$

8

$$8 + 6 \underset{}{\overset{k_1}{\rightleftarrows}} RNHCH_2CH_2\text{-}C_6H_5 + 7 \quad (4)$$

1

Compound **8** reacts with the secondary amine **1** as well as the primary amine **6**, and amide **9** adds to styrene.

$$8 + 1 \underset{}{\overset{k_2}{\rightleftarrows}} 1 + RNNaCH_2CH_2\text{-}C_6H_5 \quad (5)$$

9

Table 2. Assignments of the signals to the protons*

Reaction products		Protons (a)	(b)	(c)	(d)	(e)	(f)	(g)	(h)
n-BuNHCH$_2$CH$_2$-C$_6$H$_5$	(**1a**)	2.89	7.27	7.27	···	7.48	···	···	9.09
n-Bu(CH$_2$CH$_2$-C$_6$H$_5$)$_2$N	(**2a**)	2.94	7.33	7.33	—	7.53	···	···	9.12
s-BuNHCH$_2$CH$_2$-C$_6$H$_5$	(**1b**)	2.91	7.29	7.29	···	7.53	9.00	8.75	9.09
s-Bu(CH$_2$CH$_2$-C$_6$H$_5$)$_2$N	(**2b**)	2.96	7.38	7.38	—	7.50	9.07	8.76	9.17
t-BuNHCH$_2$CH$_2$-C$_6$H$_5$	(**1c**)	2.90	7.29	7.29	···	—	8.99	—	—
t-Bu(CH$_2$CH$_2$-C$_6$H$_5$)$_2$N	(**2c**)	2.84 2.90 2.93 2.94	7.28	7.28	—	—	8.93 9.04	—	—
isoBuNHCH$_2$CH$_2$-C$_6$H$_5$	(**1d**)	2.89	7.30	7.30	···	7.63 7.74	8.51	9.13 9.24	—
isoBu(CH$_2$CH$_2$-C$_6$H$_5$)$_2$N	(**2d**)	2.91	7.33	7.33	—	7.71 7.83	8.33	9.12 9.23	—

* Figures in Table are τ values

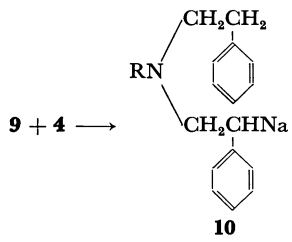

(6)

10

Compound **10** transmetalates with amines **6** and **1**.

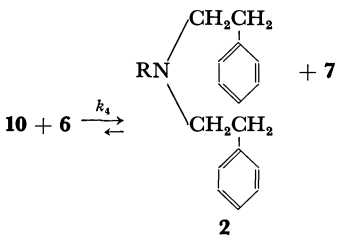

(7)

2

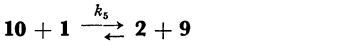

(8)

The organometallic compound **8** has a possibility to react with **4**, besides **6** and **1**, *i.e.* the propagation reaction may also take place.

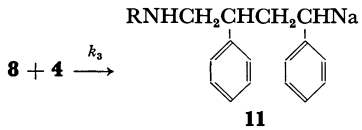

(9)

11

Compound **11** reacts with amines **6** and **1**.

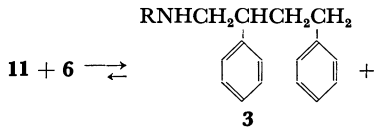

(10)

3

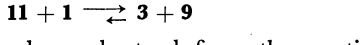

(11)

It may be understood from the reaction scheme that compounds **1**, **2** and **3** should be prepared in the reaction of amines and styrene catalyzed by sodium metal.

Anionic Telomerization. The reactions described in the preceding section can be interpreted as follows. We obtain Eq. (12) on combining Eqs. (3) and (4),

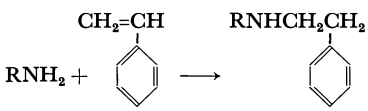

(12)

and Eq. (13) on combining Eqs. (3). (9) and (10).

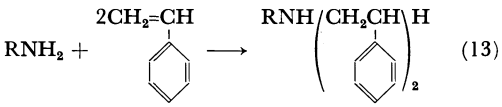

(13)

If RNH_2 acts as a telogen and styrene as a taxogen, the telomerization reaction may be expressed as follows,

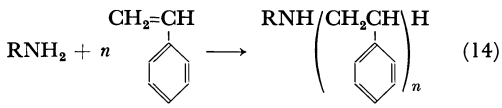

(14)

12

and the homolog **12** is obtained as a telomer. Hence, it is considered that Eqs. (12) and (13) are special cases of Eq. (14) and the products **1** and **3** are the telomers with $n=1$ and $n=2$, respectively. The secondary amine **12** has still an acidic hydrogen attached to the nitrogen atom and so **12** can react as a telogen. Therefore, another telomerization reaction may occur in RNH–CH_2=CH system,

i.e.,

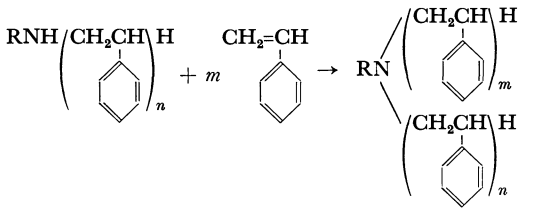

13 (15)

From Eqs. (6) and (8), Eq. (16) is obtained.

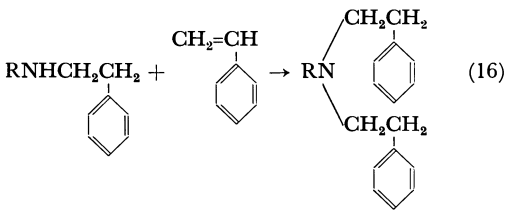

(16)

Reaction (16) is a special case of the telomerization reaction (15) and product **2** is one of the telomers **13**. Thus, the reaction products **1**, **2** and **3** may be interpreted as telomers in the telomerization reactions (14) and (15), and some part of the residue which remained undistilled in vacuum distillation is supposed to be a mixture of telomers **13** with $m+n \geqq 3$.

Reaction Scheme and Reactivity of Amines. Suppose k_1, k_2, k_3, k_4, k_5 and k_6 are the rate constants of reactions (4), (5), (9), (7), (8) and (17), respectivery. Compound **8** reacts with **6**, **1** and **4**, and so reactions (4), (5) and (9) are competitive each other. Other competitive reactions consist of reactions (7), (8) and (17).

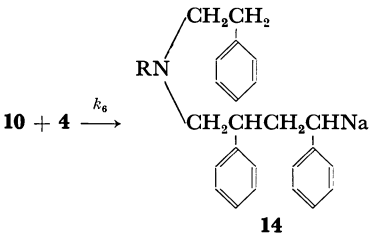

(17)

14

If k_3 [CH_2=CH] is smaller than k_1 [RNH_2] or

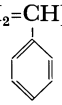

k_2 [$RNHCH_2CH_2$], the main product is not **3** but

1, while if k_3 [CH_2=CH] is greater than k_1[RNH_2]

and k_2 [$RNHCH_2CH_2$], product **3** and its higer

homologs 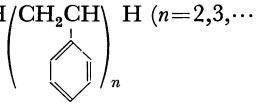 H ($n=2,3,\cdots$) areformed.

From similar consideration, if k_6[CH_2=CH] is smaller

than k_4[RNH_2] or k_5 [$RNHCH_2$=CH_2], product **12**

is hardly prepared, but compound **2** is prepared. On the contrary, if k_6 [CH_2=CH] is greater than

k_4[RNH_2] and k_5[$RNHCH_2CH_2$], compound **12**

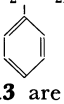

and its higher homologs **13** are formed.

Under the reaction conditions adopted, the rate of the chain transfer reaction may be considered to be faster than that of the propagation one, since compound **2** was obtained but not compound **3**, *i.e.* the amines with acidic hydrogens reacted more easily with the organosodium compound **8** than styrene.

Experimental

Physical Data. For mass spectral analysis, a Hitachi RMU-6D mass spectrometer was employed with the electron beam energy at 80 eV. The molecular weight determination by vapor pressure osmometry was car-

TABLE 3. CHARACTERIZATION OF FRACTION PRODUCTS

Molecular formula / Structural formula		Elementary analysis	Calcd	Found	Molecular weight Calcd	MS	VPO	Ref. I. (°C)	IR cm^{-1}
$C_{12}H_{19}N$ 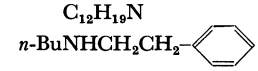	(**1a**)	C H N	81.30 10.80 7.90	80.78 10.81 7.91	177.28	177	184	1.4951 (25.0)	3290
$C_{12}H_{19}N$ 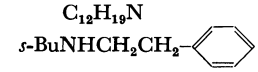	(**1b**)	C H N	81.30 10.80 7.90	80.75 10.99 8.11	177.28	177	171	1.4958 (24.5)	3310
$C_{12}H_{19}N$ 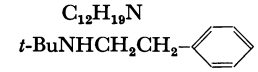	(**1c**)	C H N	81.30 10.80 7.90	80.71 11.06 7.69	177.28	177	182	1.4938 (24.5)	3290
$C_{12}H_{19}N$ 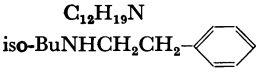	(**1d**)	C H N	81.30 10.80 7.90	81.28 10.85 7.89	177.28	177	173	1.4938 (24.5)	3315
$C_{20}H_{27}N$ 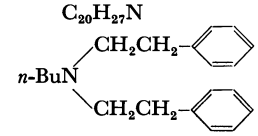	(**2a**)	C H N	85.35 9.67 4.98	85.10 9.89 4.78	281.42	281	272	1.5319 (25.0)	—
$C_{20}H_{27}N$ 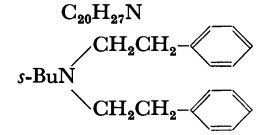	(**2b**)	C H N	85.35 9.67 4.98	84.86 10.01 5.17	281.42	281	286	1.5281 (24.5)	—
$C_{20}H_{27}N$ 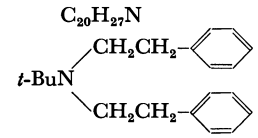	(**2c**)	C H N	85.35 9.67 4.98	84.88 10.18 5.09	281.42	281	277	1.5298 (24.5)	—
$C_{20}H_{27}N$ 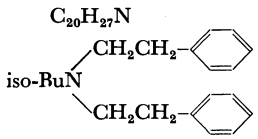	(**2d**)	C H N	85.35 9.67 4.98	85.14 9.78 5.00	281.42	281	279	1.5299 (24.5)	—

ried out in benzene at 37°C on a Hewlett Packard Model 302 vapor pressure osmometer. IR spectra were recorded on a Hitachi Perkin-Elmer 125 grating infrared spectrophotometer. Proton NMR spectra were obtained on a Japan Electron Optics Lab. JNM C-60 HL spectrophotometer using tetramethylsilane as internal standard in carbon tetrachloride.

Materials. Styrene was dried over anhydrous magnesium sulfate for a day or two and was distilled under reduced pressure. Amines were dried over sodium hydroxide and were collected by distillation under atmospheric or reduced pressure according to their boiling points.

General Procedure for Preparation. A primary amine and finely sliced sodium were placed in a four-necked round-bottomed flask, provided with a mechanical stirrer, a reflux condenser, a dropping funnel and an inlet of nitrogen. The flask was heated to a prescribed temperature in an oil bath. The oil was agitated mechanically and its temperature was controlled by a thermostat. Styrene was added dropwise to the amine for from one hour to three, and thereafter the mixture was kept standing for reaction for a further three to five hours. Then the solution was cooled to room temperature and the alkali was decomposed by adding an equivalent amount of methanol and was neutralized by a 0.1N hydrochloric acid. A small amount of benzene was added to this reaction mixture and the resulting solution was washed with water, dried over sodium carbonate and distilled *in vacuo*.

***N*-Butyl-2-phenylethylamine (1a) and *N*-Butyldi-(2-phenylethyl)amine (2a).** To 21.1 g of *n*-butylamine and 0.7 g of sodium which were heated to 46.0 ±0.5°C, 31.2 g of styrene was added dropwise during 3 hr and the reaction was carried out for a further 3 hr. To the reaction mixture that was cooled to room temperature were added 3.1 m*l* of methanol and 5.0 m*l* of water. Then the solution was neutralized with hydrochloric acid, diluted with 50 m*l* of benzene and washed with 50 m*l* of water, and the organic layer was separated, dried and distilled *in vacuo* to give **1a** (14.0 g, 26.3%) and **2a** (19.8 g, 23.5%). The other reactions were carried out in similar procedures.

Characterization of Reaction Products. Table 3 summarizes the results on the characterization of the reaction products. Column 1 lists the molecular formula and structural formula of these compounds. Columns 2 and 3 show the result of the elementary analysis. The

weight percents were calculated for the molecular formula described in column 1. Satisfactory agreement with measured values confirms the expected structures. Columns 4, 5 and 6 report the molecular weights which were calculated, determined by the mass spectrometry and measured by the vapor pressure osmometry, respectively. The theoretical molecular weight was calculated for the molecular formula listed in column 1. These molecular weights agree with one another, and support the molecular formula proposed. The refractive indices of these compounds are listed in column 7. Whether the product has the group -NH- or not was confirmed by IR spectra. Wave numbers of the absorption peak due to the -NH- stretching vibration are described in column 8.

BULLETIN OF THE CHEMICAL SOCIETY OF JAPAN VOL. 42 2005—2013 (1969)

Organic Reactions under High Pressure. IV. Effect of Pressure on the Competitive Nitration of Benzene and Monosubstituted Benzenes. Dependence of the Substitutent Effect on the Pressure

Tsutomu ASANO

Department of Chemistry, Faculty of Science, Kyoto University, Sakyo-ku, Kyoto

(Received December 12, 1968)

Partial rate factors for the nitration of six monosubstituted benzenes with nitric-sulfuric acid in acetic acid at 45°C have been determined over the 1—2000 kg/cm² pressure range. The ρ value for this reaction changed from −7.22 (1 kg/cm²) to −6.92 (2000 kg/cm²). This pressure dependency of the ρ value was not expected for this type of reaction. This phenomenon is interpreted in terms of the dependence of the degree of solvation of the transition states on the substituents. An abnormal deactivation due to pressure has been observed in the case of biphenyl. This deactivation has been attributed to an increase in the deviation from the coplanarity of the two phenyl groups. The dependence of the *ortho* : *para* ratios on the pressure is also discussed.

Since the last decade, pressure effects on the rates and product distributions of organic reactions have been extensively studied, and the results have offered much useful information about the reaction mechanisms.[1] The high-pressure technique is an especially powerful tool by which to investigate the solvation and steric hindrance in transition states.

For a liquid-phase reaction, the effect of pressure on the rate constant, k, can be expressed by Eq. (1);

$$(\partial \ln k/\partial P)_T = -\Delta V^{\neq}/RT \qquad (1)$$

where $\Delta V^{\neq}$ is the volume of the activation of the reaction, that is, the difference in the partial molar volumes between the transition state and the initial state. In considering the molecular theory of activation volumes, it is convenient to follow Evans and Polanyi[2] and to split $\Delta V^{\neq}$ into two terms:

$$\Delta V^{\neq} = \Delta_1 V^{\neq} + \Delta_2 V^{\neq} \qquad (2)$$

The change in the volume of the reacting molecules when they form the transition state is represented by $\Delta_1 V^{\neq}$, while $\Delta_2 V^{\neq}$ represents the accompanying change in the volume of the surrounding solvent. The magnitude of $\Delta_2 V^{\neq}$ is mainly determined by the difference in the total charge and in its distribution in the initial and transition states.[3] As a result, reactions in which the slow step leads to the formation of ions from neutral molecules and those in which ions combine to form neutral molecules have larger $\Delta_2 V^{\neq}$ values. On the other hand, reactions in which ions participate without either increasing or decreasing the net charge of the system have smaller $\Delta_2 V^{\neq}$ values. On the basis of this electrostriction theory, Ellis *et al.*[4] considered the effect of the pressure on the ρ value of the Hammett equation and predicted as follows:

1) For example, see E. Whalley, "Advances in Physical Organic Chemistry," Vol. 2, ed. by V. Gold, Academic Press, London and New York (1964), p. 93.

2) M. G. Evans and M. Polanyi, *Trans. Faraday Soc.*, **31**, 875 (1935).

3) S. D. Hamann "Physico-Chemical Effects of Pressure," Butterworths Scientific Publications, London (1957), Chapters 8 and 9.

4) A. J. Ellis, W. S. Fyfe, R. I. Rutherford, A. Fischer and J. Vaughan, *J. Chem. Phys.*, **31**, 176 (1959).

(A) For a reaction between an ion and a neutral molecule, pressure changes should have little effect on the value of ρ.

(B) For a reaction between ions or between neutral molecules leading to a dipolar transition state, the magnitude of ρ should be influenced by a change in the pressure.

In the case of B, the validity of the prediction was shown by examinations of the pressure effect on the dissociation constants. Fischer *et al.*[5] measured the pK values in water at 25°C of a number of substituted benzoic and phenylacetic acids over the pressure range from 1 to 3000 bars. In both series, the ρ values decreased with an increase in the pressure, as had been predicted. Imoto *et al.*[6] investigated the effect of the pressure on the rate of the saponification of ethyl benzoates in aqueous dioxane over the 1—1000 kg/cm^2 pressure range; they found that $\Delta V^{\neq}$ values were essentially unchanged by substituents (*p*-Cl, MeO, H). This result shoud support the above prediction of the case A.

As has been mentioned above, Ellis' prediction is based on the electrostriction theory; *i.e.*, for example, the $\Delta_2 V^{\neq}$ value for reactions (3) and (4) will be small because the net charge of the system does not change during the activation processes.*1

$$\underset{}{A_1 + B^+ \rightarrow \underset{I}{A_1^{+\delta} \cdots B^{+\delta}} \rightarrow P_1} \quad (3)$$

$$\underset{}{A_2 + B^+ \rightarrow \underset{II}{A_2^{+\delta} \cdots B^{+\delta}} \rightarrow P_2} \quad (4)$$

Hence, the difference in $\Delta V^{\neq}$ between reactions (3) and (4), $\delta\Delta V^{\neq}$,*2 will be negligible. Therefore, it may be concluded that pressure changes have little effect on the value of ρ.*3

However, it should be possible to consider as follows. The solvation in the initial states will be nearly the same in both reactions because of the intervention of the common ion, B^+, as an attacking entity. Consequently, the difference in $\Delta_2 V^{\neq}$ must come from the difference in solvation between the two transition states, I and II. The situation is the same for the dissociation of benzoic acids, (5) and (6):

$$C_6H_5COOH \rightarrow C_6H_5COO^- + H^+ \quad (5)$$

$$XC_6H_4COOH \rightarrow XC_6H_4COO^- + H^+ \quad (6)$$

In this case, the differences in $\Delta\bar{V}^{\circ}$ values are large enough for the ρ value to change with the pressure. Since the two carboxylic acids will be solvated to quite the same extent, the difference in the $\Delta\bar{V}^{\circ}$ values is mainly due to the difference in solvation between the two carboxylate ions. Therefore, if the degrees of charge distribution in the two transition states, I and II, are considerably different, $\delta\Delta V^{\neq}$ will be large enough to be detected experimentally.

The nitration of monosubstituted benzenes by nitric-sulfuric acid in acetic acid seems to be a suitable model reaction for studying the influence of the pressure upon the ρ value for a reaction between an ion and a neutral molecule for the following reasons:

(1) The value of $|\rho|$ for the nitration reaction is large (*ca.* 6.0).[7]

(2) The attacking entity is undoubtedly an ionic species, an incipient nitronium ion.[8]

(3) As the competitive method is applicable, uncertainties arising from imperfect and, consequently, unequal pressure and temperature control are avoided.

In addition, the effect of the pressure on the *ortho* : *para* ratios would give new information about the steric hindrance in ionic reactions. In many instances, it is observed that $\Delta V^{\neq}$ becomes more negative as the reacting center becomes more sterically hindered.[9] The most plausible explanation of such a phenomenon is Gonikberg's[10] suggestion that $\Delta V^{\neq}$ contains a negative term, $\Delta V^{\neq}_{\text{sterle}}$, arising from the overlap of interfering atoms in the transition state.*4 Coillet and Hamann[11] have reported, however, that the *ortho* : *para* ratios in the nitration of toluene and chlorobenzene decrease with an increase in the pressure, but the exact reason for this anomaly could not be ascertained.

This report will describe the studies in the competitive nitration of benzene and six monosubstituted benzenes by nitric-sulfuric acid in acetic

5) A. Fischer, B. R. Mann and J. Vaughan, *J. Chem. Soc.*, **1961**, 1093.

6) T. Imoto, Y. Ogo and H. Oka, presented at 8th High Pressure Symposium, Kobe, Oct., 1966; Abstracts, p. 104.

*1 A and P are the substrate and a product respectively, B^+ is a common attacking entity, and the subscripts 1 and 2 denote different substituents.

*2 $\delta\Delta V^{\neq} = \Delta V^{\neq}$ (recation (4)) $- \Delta V^{\neq}$ (reaction (3))

*3 For a discussion of the substituent effect on $\Delta_1 V^{\neq}$ values, see Ref. 4.

7) L. M. Stock and H. C. Brown, "Advances in Physical Organic Chemistry," Vol. 1, ed. by V. Gold, Academic Press, London and New York (1963), p. 99.

8) G. A. Olah, S. J. Kuhn, S. H. Flood and J. C. Evans, *J. Am. Chem. Soc.*, **84**, 3687 (1962).

9) For example, see S. D. Hamann, *Ann. Rev. Phys. Chem.*, **15**, 349 (1964).

10) M. G. Gonikberg, "Chemical Equilibria and Reaction Rates at High Pressures," Izdatel, Akad. Nauk, SSSR, Moscow (1960), English transl. Israel Program for Scientific Translations, Jerusalem, p. 106.

*4 There are some exceptions. See Refs. 11, 12 and 13.

11) D. W. Coillet and S. D. Hamann, *Nature*, **200**, 166 (1963).

12) W. J. leNoble, *J. Am. Chem. Soc.*, **85**, 1470 (1963).

13) R. Goto, T. Asano, K. Matsumoto and A. Sera, *Rev. Phys. Chem. Japan*, **37**, 16 (1967).

TABLE 1. EFFECT OF PRESSURE ON THE COMPETITIVE NITRATION OF BENZENE AND ACTIVATED MONOSUBSTITUTED BENZENES IN ACETIC ACID AT 45°C

Toluene							
P (kg/cm²)	k_{Me}/k_H [a]	*o*- %	*m*- %	*p*- %	f_o^{Me} [b]	f_m^{Me}	f_p^{Me}
1	27.2	55.9	2.7	41.4	45.6	2.2	67.7
1000	25.0	56.4	2.8	40.9	42.2	2.1	61.2
2000	23.2	56.4	2.9	40.7	39.3	2.0	56.6
t-Butylbenzene							
P (kg/cm²)	k_{Bu}/k_H	*o*- %	*m*- %	*p*- %	f_o^{Bu}	f_m^{Bu}	f_p^{Bu}
1	15.2	9.7	7.4	82.9	4.4	3.4	75.6
1000	13.6	10.4	7.7	81.8	4.3	3.2	66.7
2000	12.3	11.0	8.1	80.9	4.1	3.0	59.7
Biphenyl[c]							
P (kg/cm²)	k_{Ph}/k_H	*o*- %		*p*- %	f_o^{Ph}		f_p^{Ph}
1	30.3	62.2		37.8	28.2		34.3
600	26.5	62.6		37.4	24.9		29.7
1000	25.0	62.4		37.6	23.4		28.2
2000	22.7	62.1		37.9	21.1		25.8

a) Relative reactivity of toluene to benzene
b) Partial rate factor of *ortho* position to methyl group
c) It was assumed that the formed nitrobiphenyls consist of *o*- and *p*-nitrobiphenyl.

acid at 45°C over the 1—2000 kg/cm² pressure range; we undertook the studies in order to obtain new, detailed information about the solvation and steric hindrance in the transition states for aromatic electrophilic substitution reactions.

Experimental Results

The effects of the pressure on the competitive nitration of benzene and activated monosubstituted benzenes are summarized in Table 1.

While there are only small, but significant, changes in the isomer distribution (position selectivity), one can see rather a large change in the relative reactivity, k_X/k_H (substrate selectivity). As the pressure applied increases, the relative reactivity decreases appreciably. Although the *ortho* : *para* and *meta* : *para* ratios increase with an increase in the pressure in toluene and *t*-butylbenzene, this is not due to the increasing reactivity of the *ortho* and *meta* positions, but to the decreasing reactivity of the *para* position. In the case of biphenyl, the pressure independency of the *ortho* : *para* ratio is observed, while the relative reactivity diminishes more extensively than in alkylbenzenes.

TABLE 2. EFFECT OF PRESSURE ON THE COMPETITIVE NITRATION OF BENZENE AND DEACTIVATED MONOSUBSTITUTED BENZENES IN ACETIC ACID AT 45°C

Fluorobenzene							
P (kg/cm²)	k_F/k_H	*o*- %	*m*- %	*p*- %	f_o^F	$f_m^F \times 10^3$	f_p^F
1	0.142	9.23	0.210	90.6	0.0392	0.89	0.769
1000	0.140	9.32	0.239	90.5	0.0391	1.00	0.758
2000	0.140	9.26	0.268	90.5	0.0390	1.13	0.761
Chlorobenzene							
P (kg/cm²)	k_{Cl}/k_H	*o*- %	*m*- %	*p*- %	f_o^{Cl}	$f_m^{Cl} \times 10^3$	f_p^{Cl}
1	0.0400	23.1	0.669	76.2	0.0277	0.80	0.183
1000	0.0409	23.6	0.768	75.7	0.0290	0.94	0.186
2000	0.0409	23.6	0.844	75.6	0.0289	1.03	0.185
Bromobenzene							
P (kg/cm²)	k_{Br}/k_H	*o*- %	*m*- %	*p*- %	f_o^{Br}	$f_m^{Br} \times 10^3$	f_p^{Br}
1	0.0337	27.3	0.91	71.8	0.0277	0.92	0.145
1000	0.0354	27.8	1.03	71.2	0.0295	1.09	0.151
2000	0.0365	28.0	1.12	70.8	0.0306	1.23	0.155

Table 3. Reaction constant ρ and correlation coefficient r for the nitration by mixed acid in acetic acid at 45°C

P (kg/cm²)	1	1000	2000
ρ	−7.22	−7.05	−6.92
r	0.988	0.989	0.986

On the contrary, chlorobenzene and bromobenzene show an increasing relative reactivity with an increase in the pressure. The results are shown in Table 2. In all three cases in Table 2, the increase in f_m is striking; bromobenzene and chlorobenzene reveal an apparent increase in the *ortho* : *para* ratio with the pressure, as is also observed in alkylbenzenes.

The partial rate factors in Tables 1 and 2 are plotted against Brown-Okamoto's σ^+ value to give a straight line. The ρ values calculated by the method of least squares and the correlation coefficients, r, are listed in Table 3. (The values of biphenyl were not included in the calculations. This will be discussed below.) The correlation of these plots is not excellent, but it may be concluded that the ρ value increases appreciably with an increase in the pressure.

Fischer *et al.*[5] have pointed out that the magnitude of $\Delta V^{\neq}$ values could be an indication of anticipating whether or not ρ depends on the pressure. This can be interpreted as follows. Assuming that σ^+ is not a function of the pressure, one can obtain Eq. (9) from Eqs. (7) and (8):

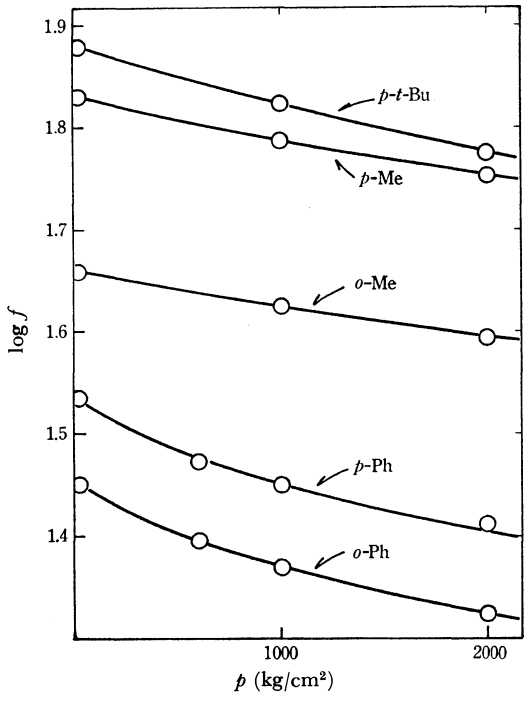

Fig. 1. $\log f$-p curves for the nitration of activated monosubstituted benzenes.

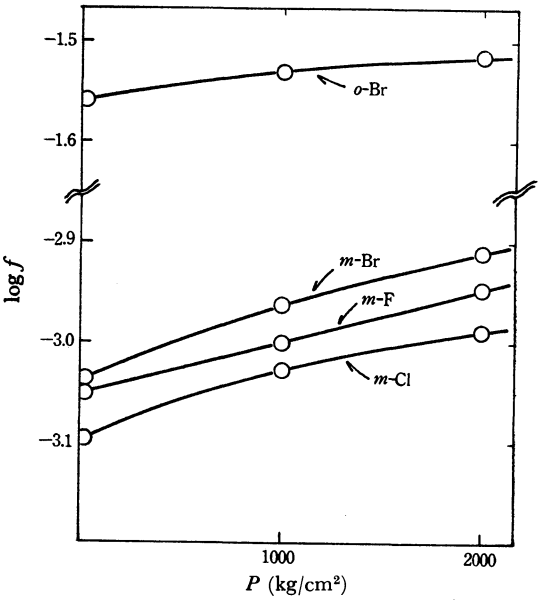

Fig. 2. $\log f$-p curves for the nitration of halobenzenes.

Table 4. $\delta\Delta V_1^{\neq}$ or $\delta\Delta\bar{V}_{1000}^{\neq}$ values for the nitration by mixed acid in acetic acid at 45°C (ml/mol)[a]

Substituent	*o*-	*m*-	*p*-
Methyl	2.1	1.2*	3.2
t-Butyl	0.6*	1.6*	3.5
Fluoro	0.1*	−3.1	0.4*
Chloro	−1.2*	−5.0	−0.5*
Bromo	−2.0	−5.2	−1.1*
Phenyl	6.2		6.6

*: $\delta\Delta\bar{V}_{1000}^{\neq}$ values

a) The error is estimated at most 0.5 ml/mol.

$$\Delta V^{\neq} = -RT(\partial \ln k/\partial P)_T \quad (7)$$

$$\log f = \rho\sigma^+ \quad (8)$$

$$\delta\Delta V^{\neq} = -RT(\partial \ln f/\partial P)_T = -2.3RT\sigma^+(\partial\rho/\partial P)_T \quad (9)$$

Thus, if σ^+ is independent of the pressure and if ρ varies with the pressure, then the plot of $\delta\Delta V^{\neq}$ at a constant pressure and temperature against σ^+ should give a linear line, including the point of origin. Figures 1 and 2 show the dependence of $\log f$ on the pressure. From the slopes of the curves at zero pressure, the $\delta\Delta V^{\neq}{}_1$*5 values were calculated; they are listed in Table 4, together with the values of $\delta\Delta\bar{V}_{1000}^{\neq}$*6 for the other positions.*7

*5 $\delta\Delta V^{\neq}$ values at 1 atm.

*6 $\delta\Delta\bar{V}_{1000}^{\neq} = -RT(\ln f_{1000} - \ln f_1)1/1000$. The numerals indicate the pressure.

*7 The values of $\delta\Delta\bar{V}_{1000}^{\neq}$ are adopted instead of $\delta\Delta V^{\neq}{}_1$ for the *meta* positions of alkylbenzenes and the *para* positions of halobenzenes because the changes in the reactivity of these positions with the pressure are relatively small; hence, $\delta\Delta V^{\neq}$ should change little with the pressure.

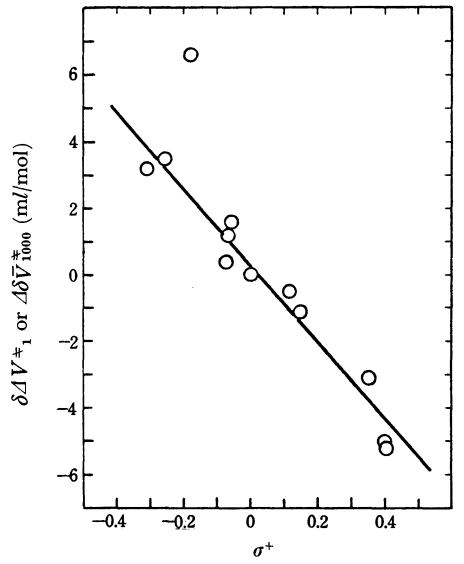

Fig. 3. Plot of $\delta\Delta V^{\neq}_1$ or $\delta\bar{V}^{\neq}_{1000}$ against σ^+.

Those values are plotted in Fig. 3 against σ^+; the line passes through the point of origin. The correlation shown in Fig. 3 reveals this relation:

$$\delta\Delta V^{\neq}_1 = -11.6\sigma^+ + 0.24.$$*8

The dependence of the ρ value for nitration by nitric-sulfuric acid in acetic acid on the pressure is evident.

Discussion

Effect of Pressure on f_m and f_p. Since no kinetic isotope effect was observed in the nitration of benzene and a number of its derivatives of widely differing reactivities,[14] the observed $\delta\Delta V^{\neq}$ values represent the difference in $\Delta V^{\neq}$ between the following two processes (in Eqs. (10) and (11), NO_2^+ represents a weaker electrophilic precursor of the nitronium ion):[8]

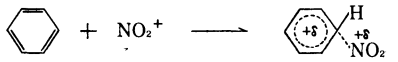

(10)

III

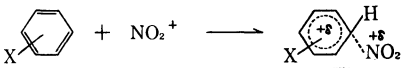

(11)

IV

According to Evans and Polanyi,[2] $\delta\Delta V^{\neq}$ is separated into two terms, $\delta\Delta_1 V^{\neq}$ and $\delta\Delta_2 V^{\neq}$ (Eq. (12)):

$$\delta\Delta V^{\neq} = \Delta V^{\neq}_X - \Delta V^{\neq}_H = (\Delta_1 V^{\neq}_X - \Delta_1 V^{\neq}_H) + (\Delta_2 V^{\neq}_X - \Delta_2 V^{\neq}_H) = \delta\Delta_1 V^{\neq} + \delta\Delta_2 V^{\neq} \quad (12)$$

When the replacement of a hydrogen atom of benzene molecule with a different substituent, X, occurs at a point sufficiently remote from the reaction site, a condition for the applicability of the $\rho\sigma^+$ equation is fulfilled; the first term, $\delta\Delta_1 V^{\neq}$, is decided by the difference in the C···N bond length in the two transition states, III and IV. The position of the trasition state on the reaction coordinate might change with the reactivity of the substrate; however, it is unlikely that the C···N bond length changes so greatly that $\delta\Delta_1 V^{\neq}$ amounts to several milliliters.*9 The detritiation of methylbenzenes seems a good example indicating that the position of the transition state does not change with the substituents. Ansell and Taylor[15] found that $\log f_o^{Me}$: $\log f_p^{Me}$ ratio for *m*-xylene is 0.885 ± 0.035, exactly the same as in toluene, in spite of the fact that the former is 200 times as reactive as the latter. From this result they concluded that the transition states are not sufficiently different for any effect of the differing stabilizations of the *ortho* and *para* positions to show up. Consequently, if the attack by a nitrating agent occurs at a position *meta* or *para* to the substituent X, the $\delta\Delta_1 V^{\neq}$ should be nearly equal to zero; *i.e.*, $\delta\Delta_2 V^{\neq}$ should be responsible to the observed $\delta\Delta V^{\neq}$. When the substituent X is more electron-donating than the hydrogen atom, the charge on the nitrogen atom disperses more extensively into the benzene ring in IV than in III. Thus, the desolvation attributable to charge dispersion during the activation step should be more extensive in IV. On the other hand, when X is more electron-attracting than the hydrogen atom, the desolvation during the activation step should be less extensive in IV. The $\delta\Delta V^{\neq}$ values listed in Table 4 clearly reveal that this is the case. The anomalous pressure dependence of the reactivity of biphenyl will be discussed later.

Thus, the extent of solvation in the transition state of the nitration of benzene derivatives changes with the substituents. Accordingly, the ρ value increases with an increase in the pressure. The reported independency of the ρ value of the saponification of ethyl benzoates[6] must have its origin in its relatively small ρ value ($\rho \fallingdotseq 2$), which makes the difference in $\Delta V^{\neq}$ small.

Abnormal Deactivation of Biphenyl by Pressure. The *para* and *ortho* positions to phenyl group are anomalously deactivated with an increase in the pressure. From the plot of $\delta\Delta V^{\neq}_1$ against σ^+, $\delta\Delta V_1^{\neq}$ may be expected to be approximately 2.5 ml/mol for the *para* position of biphenyl.

*8 The results for biphenyl were not included in the calculation.

14) Numerous investigations of kinetic isotope effects in nitration have been conducted. See H. Zollinger, Ref. 1, p. 163.

*9 If one arbitrarily assumes that the van der Waals cross-sectional area of the C···N bond is equal to $1.5^2\times3.14=7.07$ Å^2, there must be *ca.* 1 Å difference in the C···N bond length in order for $\delta\Delta_1 V^{\neq}$ to amount to 4.3 ml/mol.

15) H. V. Ansell and R. Taylor, *J. Chem. Soc.*, *B*, **1968**, 526.

The observed value, 6.6 ml/mol, is more than twice that expected. The deviation from the $\delta\Delta V^{\ddagger}_1$-$\sigma^+$ plot implies a pressure dependence of the substituent constant, $\sigma^+_{p\text{-Ph}}$.

Stock and Brown[16] pointed out that the reactivity of the *para* position in biphenyl increases significantly with an increase in the electron demand of the substitution reaction; that is, $\sigma^+_{p\text{-Ph}}$ decreases as the electrophile becomes less reactive. They attributed this anomaly to the variation in the angle between two rings and explained as follows: "..... the full contribution of the substitutent is not achieved because of steric repulsions among the four hydrogens.....As the selectivity of the electrophilic reaction increases, the steric forces are, in part, overcome by the increased energy requirements of the transition state."

As the other substituents do not show any anomaly, the anomalous deactivation of biphenyl by pressure must be due to the change of the angle between two rings. However, the cause of the increased angle should not be the increase in the reactivity of the attacking incipient nitronium ion as a result of the pressure, because an ion should be solvated more strongly at high pressures than at atmospheric pressure. It seems to be rather reasonable to consider that, as the angle between two phenyl groups at the transition (and ground) state becomes greater, the volume of the system decreases.

McCune *et al.*[17] have reported that the racemization of sodium salt of L-6-nitro-2,2'-carboxybiphenyl is retarded by an increase in the pressure to an extent corresponding to $\Delta V^{\ddagger}=2$ ml/mol at 1 atm in a 0.1 N aqueous sodium hydroxide solution. McKelvey and Brower[18] independently studied the effect of the pressure on the rate of the racemization of three compounds with the general strcture V, where Ar denotes an aryl group with hindering *ortho* substituents. In ethanol the rate constant decreased with an increase in the pressure ($\Delta V_1^{\ddagger}\fallingdotseq 2$ ml/mol). Although the exact

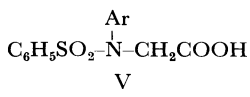

V

reason for these activation volumes could not be obtained, it may be quite all right to assume that as the angle between two phenyl groups in the transition (and ground) state decreases, the volume of the system increases. Consequently, under high pressure the angle will increase and the resonance contribution will decrease to some extent. We suggest that the observed $\delta\Delta V^{\ddagger}$ value reflects not only the volume change during the activation step, but also the decreased resonance contribution caused by an external pressure. In other words, the structure of the transition state changes with the pressure.

16) Ref. 7, p. 108.

17) C. C. McCune, F. Wm. Cagle, Jr., and S. S. Kistler, *J. Phys. Chem.*, **64** 1773 (1960).

18) D. R. McKelvey and K. R. Brower, *ibid.*, **64**, 1958 (1960).

Table 5. Effect of pressure on the *ortho* : *para* ratios in the nitration of monosubstituted benzenes by mixed acid in acetic acid at 45°C

Substituent	P (kg/cm²)		
	1	1000	2000
Methyl	1.35	1.38	1.39
t-Butyl	0.117	0.127	0.136
Phenyl	1.65	1.66	1.64
Fluoro	0.102	0.103	0.102
Chloro	0.303	0.312	0.312
Bromo	0.380	0.390	0.395

Effect of the Pressure on the *ortho* : *para* Ratio. The *ortho*: *para* ratios at various pressures are shown in Table 5. Except for the cases of biphenyl and fluorobenzene, the *ortho* nitration increases with the pressure, and as substituent becomes larger the tendency becomes even more remarkable. These results show a tendency the reverse of that reported by Coillet and Hamann.[11] They reported the nitration of toluene and chlorobenzene by anhydrous nitric acid in acetic acid at 0°C. Their results are quoted in Table 6.

Table 6. Effect of pressure on the isomer distributions in the nitration of toluene and chlorobenzene by nitric acid in acetic acid at 0°C

P (atm)	Toluene				Chlorobenzene		
	o- %	*m*- %	*p*- %	*o*-/*p*-	*o*- %	*p*- %	*o*-/*p*-
1	56.0	2.0	42.0	1.33	24.7	75.3	0.328
1200	55.0	2.2	42.8	1.29			
2000	54.3	2.4	43.3	1.25	20.4	79.6	0.256

Obviously, the *ortho* : *para* ratios decrease with the pressure and the tendency is more remarkable in chlorobenzene. These two inconsistent results can most plausibly be explained in terms of the difference in solvation in the two systems. The activation volume of the *ortho* nitration can be separated into four terms, as in Eq. (13).

$$\Delta V^{\ddagger}(ortho) = \Delta_1V^{\ddagger}+\Delta_2V^{\ddagger} = (\Delta_1V^{\ddagger}_{bond}+\Delta_1V^{\ddagger}_{steric}) + (\Delta_2V^{\ddagger}_{el}+\Delta_2V^{\ddagger}_{steric}) \quad (13)$$

$\Delta_1V^{\ddagger}_{bond}$: volume change of the reacting molecules due to changes in the bond length during the activation process. In the present case, $\Delta_1V^{\ddagger}_{bond}<0$.

$\Delta_1V^{\ddagger}_{steric}$: volume change of the reacting molecules due to the overlap of interfering atoms in the transition state. $\Delta_1V^{\ddagger}_{steric}<0$.

$\Delta_2V^{\neq}_{el}$: volume change of the solvent due to the changing electrostatic interaction of the reacting molecules with the solvent during the activation process. In the present case, $\Delta_2V^{\neq}_{el}>0$.

$\Delta_2V^{\neq}_{steric}$: volume change of the solvent due to the steric inhibition of solvation in the transition state. $\Delta_2V^{\neq}_{steric}>0$.

In the *para* nitration the $\Delta_1V^{\neq}_{steric}$ and $\Delta_2V^{\neq}_{steric}$ terms are not present; accordingly, $\Delta_1V^{\neq}=\Delta_1V^{\neq}_{bond}$ and $\Delta_2V^{\neq}=\Delta_2V^{\neq}_{el}$. It seems to be plausible to assume $\Delta_1V^{\neq}_{bond}$ (*para*) is equal to $\Delta_1V^{\neq}_{bond}$ (*ortho*). Although it is not obvious whether or not $\Delta_2V^{\neq}_{el}$ (*para*) is larger than $\Delta_2V^{\neq}_{el}$ (*ortho*), the difference, $\Delta_2V^{\neq}_{el}$ (*ortho*) $-\Delta_2V^{\neq}_{el}$ (*para*), will be small compared to the $\Delta_2V^{\neq}_{steric}$ term. In view of the above approximations, the difference in the activation volumes in the *ortho* nitration and *para* nitration may be represented as in Eq. (14). In Eq. (14) $\Delta_1V^{\neq}_{steric}$ is negative and $\Delta_2V^{\neq}_{steric}$ is positive.

$$\Delta V^{\neq}(ortho)-\Delta V^{\neq}(para)\fallingdotseq\Delta_1V^{\neq}_{steric}+\Delta_2V^{\neq}_{steric} \quad (14)$$

Accordingly, it depends on the relative magnitude of the above two terms whether the applied pressure increases the *ortho* : *para* ratio or decreases it. The solvation of an ionic species and a dipolar molecule should be more striking under Coillet and Hamann's conditions (acetic acid solution at 0°C) than in the present case (acetic acid solution at 45°C). Therefore, the volume increase due to the steric inhibition of solvation, $\Delta_2V^{\neq}_{steric}$, should be larger at 0°C than at 45°C and $\Delta_2V^{\neq}_{steric}$ should exceed the volume contraction arising from the overlap of interfering atoms, $\Delta_1V^{\neq}_{steric}$, at 0°C. As a result, the *ortho* : *para* ratios decrease with an increase in the pressure. On the other hand, under the present conditions $\Delta_1V^{\neq}_{steric}$ exceeds $\Delta_2V^{\neq}_{steric}$ and the applied pressure causes the increase in the *ortho* : *para* ratio.

If the above explanation is correct, the *ortho*: *para* ratio in chlorobenzene should decrease more extensively with the pressure than in toluene at 0°C for reasons to be outlined below.

The initial state solvation should be more striking for chlorobenzene because of the larger polarization of the C–Cl bond than of the C–CH_3 bond.*10 In the reaction of allyl chloride with phenoxide ion in water, the product ratio, (*o*-allylphenol)/(*p*-allylphenol), decreases with an increase in the pressure ($\delta\Delta V_1^{\neq}=5.4$ ml/mol at 30°C).[12] The data in Table 6 are in accordance with the above prediction; the fact that the changes in the *ortho*: *para* ratios with the pressure in chlorobezene and in toluene are nearly equal at 45°C indicates that the difference in the initial state solvation is small and does not play a principal role in the effect of the pressure on the *ortho* : *para* ratios. Since the values of $\Delta_1V^{\neq}_{steric}$ are not known, the extent of the volume increase due to the steric inhibition of solvation can not be discussed further on the basis of the data at hand.

*10 The dipole moments of chlorobenzene and toluene are 1.56 and 0.39 respectively.

Experimental

Materials. Unless otherwise stated, the materials used in the present experiment were prepared by standard methods; the purities were inspected by g.l.c. and had the following physical constants (all the melting and boiling points are uncorrected).

t-Butylbenzene, prepared by the method of Norris and Strugis[19]; bp 168.5°C, n_D^{27} 1.4889. Fluorobenzene, prepared by the method of Flood[20]; bp 85.5°C, n_D^{20} 1.4677. Nitrotoluenes, *o*- bp 110—111°C/28 mmHg, n_D^{27} 1.5424; *m*- bp 121°C/32 mmHg, n_D^{27} 1.5431; *p*- mp 51.9—52.1°C. *o*-Nitro-*t*-butylbenzene, prepared by the nitration of *t*-butylbenzene and collected by preparative g.l.c.; n_D^{27} 1.5141. *m*-Nitro-*t*-butylbenzene, prepared from *p*-*t*-butylaniline*11; n_D^{27} 1.5238. *p*-Nitro-*t*-butylbenzene, prepared by the nitration of *t*-butylbenzene and collected by preparative g.l.c.; mp 27°C, n_D^{27} 1.5305. Biphenyl; mp 70.0—70.5°C. *o*- and *p*-Nitrobiphenyls, purified by recrystallization, *o*-; mp 35.4—36.0°C from ethanol. *p*-; mp 114.3—115.0°C from methanol-chloroform. *m*-Nitrobiphenyl, prepared by the method of Elks *et al.*;[22] mp 59.9—60.0°C from ethanol. *o*-Nitrofluorobenzene, bp 95—96°C/15.5mmHg, $n_D^{22.6}$ 1.5292. *m*-Nitrofluorobenzene, kindly supplied by the Hashimoto Kasei Co., Ltd.; bp 82—83°C/19 mmHg, $n_D^{22.6}$ 1.5231. *p*-Nitrofluorobenzene, prepared by the method of Cheek *et al.*[23] from *p*-nitrobenzenediazonium tetrafluoroborate,[24] $n_D^{22.7}$ 1.5293. Nitrochlorobenzenes, *o*- mp 32.5—32.7°C; *m*- mp 44.7—44.9°C; *p*- mp 83.9—84.0°C. Nitrobromobenzenes, prepared by the method of Newman and Fones,[25] *o*- mp 41.6—

*11 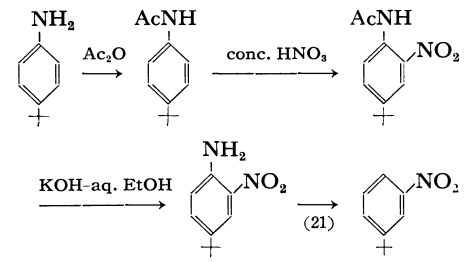

19) J. F. Norris and B. M. Strugis, *J. Am. Chem. Soc.*, **61**, 1415 (1939).

20) D. T. Flood, "Organic Synthesis," Coll. Vol. II, p. 295 (1963).

21) N. Kornblum, "Organic Reactions," Vol. 2, p. 294 (1960).

22) J. Elks, J. W. Haworth and D. H. Hey, *J. Chem. Soc.*, **1940**, 1285.

23) P. H. Cheek, R. H. Wiley and A. Roe, *J. Am. Chem. Soc.*, **71**, 1863 (1949).

24) K. Fukui, H. Kitano, R. Ijiri, Y. Inamoto and T. Matsufuji, *Nippon Kagaku Zasshi (J. Chem. Soc. Japan, Pure Chem. Sect.)*, **79**, 889 (1958).

25) M. S. Newman and W. S. Fones, *J. Am. Chem. Soc.*, **69**, 1221 (1947).

42.0°C; *m*- mp 54.6—54.9°C; *p*- mp 127.0°C.

All the other materials and solvents were purified by ordinary methods. Guaranteed-reagent-grade nitric acid (d=1.42) and sulfuric acid (d=1.84) were used.

High-pressure Apparatus. The high-pressure apparatus has been described previously.[13]

Nitration and Analytical Procedure. Nitrations were carried out by adding an acetic acid solution of nitric-sulfuric acid to a solution of benzene, substituted benzene, and a suitable internal standard at room temperature. The initial concentrations of acids and water were as follows; for alkyl- and aryl-benzenes, H_2O=1.3M, HNO_3=0.6N, H_2SO_4=2.6N; for halobenzenes, H_2O=2.3M, HNO_3=1.0N, H_2SO_4=4.7N. The substrate concentrations were in the range of 0.15—1.15M.

About 2.5 m*l* of the reaction mixture was transferred to a reaction vessel (sealed tube or glass syringe) and maintained at 45°C at the desired pressure. The reaction was stopped by adding water after a few hours depending on the pressure. The mixture was neutralized with aqueous sodium hydroxide and extracted repeatedly with methylene chloride. The extracts were washed, concentrated carefully, and analyzed by g.l.c. The validity of this procedure was previously proved using synthetic mixtures of nitrobenzenes. Analyses were made for nitro aromatics, and this value was subtracted from the initial concentration of the aromatic to obtain the value of the final concentration.

The relative reactivities were calculated by Eq. (15)[26]:

$$k_X/k_H = [\log [XC_6H_5]_0 - \log [XC_6H_5]_t]/[\log [C_6H_6]_0 - \log [C_6H_6]_t] \quad (15)$$

The *meta*: *ortho* ratios in the nitration of halobenzenes were determined independently in order to obtain the exact concentration of *m*-nitrohalobenzenes.

The kinetic runs were performed at least three times under each set of conditions; the averaged values are shown in Tables 1 and 2. A typical example is shown in Table 7.

Table 7. Competitive nitration of benzene and *t*-butylbenzene at 2000 kg/cm²

k_{Bu}/k_H	*o*- %	*m*- %	*p*- %	f_o^{Bu}	f_m^{Bu}	f_p^{Bu}
12.4	10.9	7.8	81.2	4.1	2.9	60.4
12.6	10.9	7.9	81.2	4.1	3.0	61.4
12.0	11.3	8.4	80.3	4.1	3.0	57.8
12.0	11.1	8.3	80.6	4.0	3.0	58.0
12.5	11.0	7.9	81.1	4.1	3.0	60.8

In the reaction of biphenyl, the remaining biphenyl was determined directly. It was assumed that nitrobiphenyls consist of *o*- and *p*-nitrobiphenyl, for the separation of *m*-nitrobiphenyl from the *para* isomer on g.l.c. was not enough to determine its quantity; however, the quantity is very small and the obtained partial rate factors for the *ortho* and *para* positions should be real ones.

Table 8. Gas chromatography analytical data

Nitrobenzene	Retention time (min)	Nitrobenzene	Retention time (min)
Toluene		**Chlorobenzene**	
Tricresyl phosphate 10%, 3 m, 158°C,		PEG 20M 10%, 3 m, 195°C, He 22.5 m*l*/min	
He 33 m*l*/min		Nitrobenzene	6.9
Nitrobenzene	5.4	*m*-Nitrotoluene[a]	9.2
o-Nitrotoluene	7.2	*m*-Nitrochlorobenzene	11.3
m-Nitrotoluene	8.7	*p*-Nitrochlorobenzene	12.7
p-Nitrotoluene	10.5	*o*-Nitrochlorobenzene	15.6
o-Nitrochlorobenzene[a]	14.7	**Bromobenzene**	
***t*-Butylbenzene**		PEG 20M 10%, 3 m, 210°C, He 21 m*l*/min	
Apiezon grease L 20%, 4.5 m, 198°C,		Nitrobenzene	4.3
He 15 m*l*/min		*p*-Nitrochlorobenzene[a]	7.6
Nitrobenzene	3.0	*m*-Nitrobromobenzene	10.9
p-Nitrotoluene[a]	4.6	*p*-Nitrobromobenzene	12.1
o-Nitro-*t*-butylbenzene	6.0	*o*-Nitrobromobenzene	14.6
m-Nitro-*t*-butylbenzene	7.9	**Biphenyl**	
p-Nitro-*t*-butylbenzene	10.1	Silicon oil KF 96 (Shinetsu Chemicals Co., Ltd.),	
Fluorobenzene		10%, 3 m, 163°C, He 25 m*l*/min.	
PEG 20M 10%, 3 m, 186°C, He 24 m*l*/min		Nitrobenzene	1.5
m-Nitrofluorobenzene	4.6	*p*-Nitrochlorobenzene[a]	2.5
p-Nitrofluorobenzene	5.5	Biphenyl	4.7
Nitrobenzene	6.4	219°C, He 22.5 m*l*/min.	
o-Nitrofluorobenzene	7.5	*o*-Nitrobiphenyl	3.2
m-Nitrotoluene[a]	8.5	*m*-Nitrobiphenyl	4.9
		p-Nitrobiphenyl	5.1

a) Internal standard substances

26) M. J. S. Dewar, T. Mole and E. W. T. Warford, *J. Chem. Soc.*, **1956**, 3576.

Gas-chromatographic Analysis. All analyses of the nitration mixtures were carried out on a Yanagimoto gas chromatograph Model GCG 5DH. A thermal-conductivity detector was used except for the determination of the *meta*: *ortho* ratio in the case of halobenzenes. For this purpose a flame-ionization detector was used. The analytical conditions and retention times are presented in Table 8.

The author wishes to express his appreciation to Professor Jiro Osugi for his courtesy of providing the high-pressure apparatus used in the present experiment. He is also indebted to Professors Ryozo Goto and Akira Sera for their helpful discussions and encouragement throughout this work.

BULLETIN OF THE CHEMICAL SOCIETY OF JAPAN VOL. 42 2013—2021 (1969)

Ring Expansion of Bicyclic *gem*-Dihalo- and Monohalocyclopropanes

Teiichi ANDO, Hirokazu HOSAKA, Hiroki YAMANAKA and Wataru FUNASAKA

Department of Industrial Chemistry, Faculty of Engineering, Kyoto University, Sakyo-ku, Kyoto

(Received December 13, 1968)

Some bicyclic *gem*-dichlorocyclopropanes (Ia through Id) and *gem*-chlorofluorocyclopropanes (IIa through IId) were prepared by the addition of dichloro- and chlorofluorocarbene, respectively, to the appropriate cyclic olefins. The reduction of these dihalocyclopropanes with tri-*n*-butyltin hydride gave the corresponding monochloro- (IIIa through IIId) or monofluorocyclopropanes (IVa through IVd) in fairly good yields. When treated with an excess of hot quinoline, the *endo*-chloro isomers of IIa, IIb, IId, IIIa, IIIb, and IIId were converted to their ring expansion products, whereas their *exo*-chloro isomers were recovered unchanged. In contrast, the *exo*-chloro isomers of IIc and IIIc decomposed more readily than their *endo*-chloro isomers under similar conditions. These results were discussed on the concept of a concerted disrotatory process.

The ring opening or ring expansion reactions of *gem*-dihalo- and monohalocyclopropanes have received much attention in recent years, and it has been found that the reaction rate is dependent not only on the kind of halogen[1] but also on the molecular geometry of the substrate.[2-9] Baird and Reese[2] have proved that *endo*-6-chlorobicyclo[3.1.0]hexane is converted to 3-chlorocyclohexene when heated at 120°C. Ghosez *et al.*,[3] have shown that the *endo*-chloro isomer of 3-chloro-8-oxatricyclo[3.2.1.$0^{2,4}$] octane undergoes ring expansion at 80°C, while the *exo*-chloro isomer remains unchanged after being heated at 150°C for 15 hr. Analogous results have been reported with the chlorofluorocarbene adduct to indene,[4] and the chloro-, bromo-, or chlorofluorocarbene adduct to norbornene.[5-7] Schweizer and Parham[8] showed that the *exo*-chloro isomer of 7-chloro-2-oxabicyclo[4.1.0]heptane decomposed at 120°C in quinoline to give 2,3-dihydro-öxepin, while the *endo*-chloro isomer remained unchanged at 176.5°C in quinoline.

This paper describes the synthesis of a series of *n*,*n*-dichloro-, *n*-chloro-*n*-fluoro-, *n*-chloro-, and *n*-fluorobicyclo[$n-3.1.0$]alkanes ($n=6$, 7, and 9) and their 2-oxa analogues ($n=7$) and the stereospecificity observed in some of their ring expansion reactions in quinoline. A part of the present work has already been reported in preliminary communications.[9,10]

1) P. S. Skell and S. R. Sandler, *J. Am. Chem. Soc.*, **80**, 2024 (1958).
2) M. S. Baird and C. B. Reese, *Tetrahedron Letters*, **1967**, 1379.
3) L. Ghosez, P. Laroche and G. Slinckx, *ibid.*, **1967**, 2767.
4) W. E. Parham and R. R. Twelves, *J. Org. Chem.*, **22**, 730 (1957).
5) C. W. Jefford, E. Huang-Yen and R. T. Medary, *Tetrahedron Letters*, **1966**, 6317.
6) C. W. Jefford and R. T. Medary, *Tetrahedron*, **23**, 4123 (1967).
7) L. Ghosez, G. Slinckx, M. Glineur, R. Hoet and P. Laroche, *Tetrahedron Letters*, **1967**, 2773.
8) E. E. Schweizer and W. E. Parham, *J. Am. Chem. Soc.*, **82**, 4085 (1960).
9) T. Ando, H. Yamanaka and W. Funasaka, *Tetrahedron Letters*, **1967**, 2587.
10) T. Ando, H. Yamanaka, S. Terabe, A. Horike and W. Funasaka, *ibid.*, **1967**, 1123.

Results and Discussion

Synthesis of *n,n*-Dichloro- and *n*-Chloro-*n*-fluorobicyclo[*n*−3.1.0]alkanes (*n*=6, 7, and 9) and Their 2-Oxa Analogues (*n*=7). 6,6-Dichlorobicyclo[3.1.0]hexane (Ia), 7,7-dichlorobicyclo[4.1.0]heptane (Ib), 9,9-dichlorobicyclo[6.1.0]nonane (Ic), and 7,7-dichloro-2-oxabicyclo[4.1.0]heptane (Id) were prepared by the reaction of dichlorocarbene with cyclopentene, -hexene, -octene, and 2,3-dihydro-4*H*-pyran, respectively. The corresponding chlorofluoro derivatives (IIa, IIb, IIc, and IId) were prepared similarly from chlorofluorocarbene. The dihalocarbenes were generated very conveniently by gradual addition of methanol to a mixture of sodium hydride and methyl trichloro- or dichlorofluoroacetate, which generally gave better yields of the dihalocarbene adducts than the conventional sodium methoxide - trihaloacetate method.[11,12] The yields and the properties of the *gem*-dihalocyclopropanes thus prepared are summarized in Table 1.

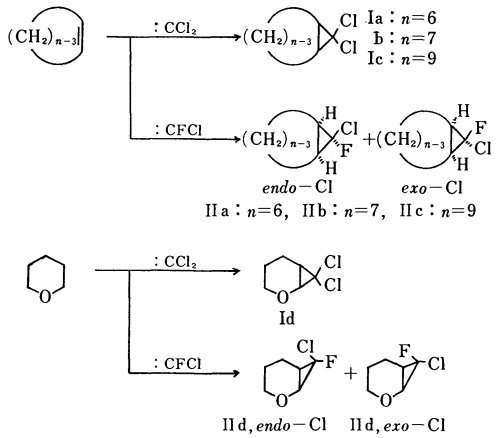

As is shown in Table 1, each of the chlorofluoro derivatives obtained was a mixture of the *endo*-chloro and the *exo*-chloro isomers, with the former predominating. Similar results have been reported in the addition of chlorofluorocarbene to other olefins.[13a] Probably, as Moss and Gerstl pointed out,[13] the electronic factor (difference in polarizability of the halogen substituent) plays a more important role than the steric factor in determining the stereoselectivity of the dihalocarbene addition.

The assignments of the configuration were made by NMR spectroscopy, based on the generalization that in fluorocyclopropanes $J_{HF,cis}$ is larger than $J_{HF,trans}$[14] and that cyclopropyl fluorines are shielded by *cis*-, and deshielded by *trans*-, alkyl groups.[9,13] Their NMR data are given in Tables 2 and 3.

Synthesis of *n*-Chloro- and *n*-Fluorobicyclo[*n*−3.1.0]alkanes (*n*=6, 7, and 9) and Their 2-Oxa Analogues (*n*=7). 6-Chlorobicyclo[3.1.0]hexane (IIIa), 7-chlorobicyclo[4.1.0]heptane (IIIb), 9-chlorobicyclo[6.1.0]nonane (IIIc), and 7-chloro-2-oxabicyclo[4.1.0]heptane (IIId) were prepared, as a mixture of the *endo*-chloro and the *exo*-chloro isomers, by partially reducing the corresponding dichloro derivatives (Ia, Ib, Ic, and Id) with an equimolar amount of tri-*n*-butyltin hydride in the

Table 1. Synthesis and properties of *n,n*-dichloro- and *n*-chloro-*n*-fluorobicyclo[*n*−3.1.0]-alkanes (*n*=6, 7, and 9), and their 2-oxa analogues (*n*=7)

Structure	*n*	Yield (%)	Isomer ratio (*endo*-Cl/*exo*-Cl)	Bp (°C/mmHg)	n_D (°C)
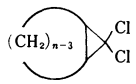	6 (Ia)	55		60—62/15	1.5910 (22)
	7 (Ib)	65		72—74/12	1.5003 (23)
	9 (Ic)	55		80—83/3.5	1.5006 (31)
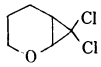	(Id)	70		72—73/8	1.4967 (24)
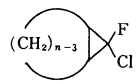	6 (IIa)	44	2.3—2.4	50—53/43	1.4495 (16)
	7 (IIb)	60	1.2—1.5	50—52/15	1.4560 (20)
	9 (IIc)	51	1.9—2.0	70—73/8	1.4660 (31)
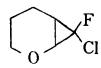	(IId)	78	1.5—1.6	68—69/20	1.4556 (20)

11) W. E. Parham and F. C. Loew, *J. Org. Chem.*, **23**, 1705 (1958).
12) R. A. Moore and R. Levine, *ibid.*, **29**, 1883 (1964).
13) a) R. A. Moss and R. Gerstl, *ibid.*, **32**, 2268 (1967). b) R. A. Moss and R. Gerstl, *Tetrahedron*, **23**, 2549 (1967).
14) a) H. M. Hutton and T. Schaefer, *Can. J. Chem.*, **40**, 875 (1962). b) J. D. Graham and M. T. Rogers, *J. Am. Chem. Soc.*, **84**, 2249 (1962). c) D. J. Patel, M. E. H. Howden and J. D. Roberts, *ibid.*, **85**, 3218 (1963). d) K. L. Williamson, Y. Li, F. H. Hall and S. Swager, *ibid.*, **88**, 5678 (1966).

TABLE 2. PARAMETERS OF NMR SPECTRA OF *n,n*-DIHALO- AND *n*-HALOBICYCLO[*n*−3.1.0]-ALKANES (*n*=6, 7, AND 9)

Structure	*n*	Chemical shift, ppm		Coupling constant, Hz		
		H_A*	F**	J_{HAF}	J_{HBF}	J_{HAHB}
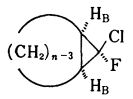	6		47.5		19.2	
	7		47.8		19.0	
	9		46.4		15.8	
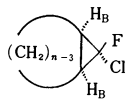	6		82.8		8.1	
	7		82.3		5.0	
	9		83.9		7.1	
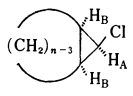	6	3.34				7.5
	7	3.22				7.5
	9	3.10				7.5
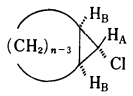	6	2.67				1.4
	7	2.70				3.3
	9	2.30				2.5
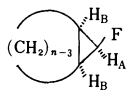	6	4.62	158.0	66.3	10.0	6.5
	7	4.47	156.0	68.0	9.0	6.3
	9	4.32	164.0	64.8	6.0	6.0
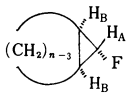	6	4.23	137.0	64.3	21.0	1.0
	7	4.25	126.2	65.0	18.0	2.0
	9	3.72	129.3	62.4	19.7	1.0

* Downfield from TMS.
** Upfield from trifluoroacetic acid.

presence of azobisisobutyronitrile.[15] The yields and the properties of the chlorocyclopropanes thus prepared are shown in Table 4, together with the isomer ratios determined by gas chromatography (glpc) before distillation.

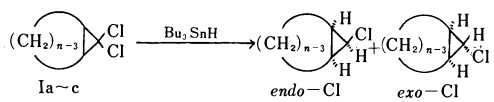

IIIa : *n*=6, IIIb : *n*=7, IIIc : *n*=9

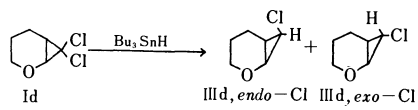

It is to be noted that the *endo*-chloro isomer predominates in IIIb and IIIc, whereas the *exo*-chloro isomer predominates in IIIa.[16]

Under similar conditions, an isomeric mixture of IIa was converted to a mixture of the *endo*-fluoro and the *exo*-fluoro isomers of 6-fluorobicyclo[3.1.0]-hexane (IVa). 7-Fluorobicyclo[4.1.0]heptane (IVb), 9-fluorobicyclo[6.1.0]nonane (IVc), and 7-fluoro-2-oxabicyclo[4.1.0]heptane (IVd) were obtained, as a mixture of isomers, from IIb, IIc, and IId, respectively. The reduction of these chlorofluorocyclopropanes required a longer reaction time than that of the corresponding dichlorocyclopropanes, and there was no sign of the monochloro derivative being formed. The yields and the properties of the products are shown in Table 5, together with the isomer distributions.

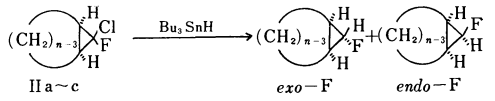

IVa : *n*=6, IVb : *n*=7, IVc : *n*=9

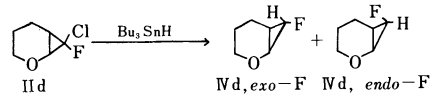

A comparison of Tables 1 and 5 reveals that the isomer ratio of the reduction product (IVa, IVb, and IVc) is quite close to that of the starting material (IIa, IIb, and IIc, respectively). This result is best explained by the stereospecific nature of the reduction of *gem*-halofluorocyclopropanes by organotin hydrides, which has already been demonstrated with IIa and IIb by isolating the pure isomers and reducing them separately.[17] In contrast, the reduction of IId did not occur stereospecifically, as is suggested by the disagreement of the isomer ratio of IVd with that of IId. The nonstereospecific nature of the reduction has been demonstrated by reducing the pure *endo*-chloro isomer of IId,[18] and will be discussed in a separate paper.

The configurations of the isomers of the chloro- and fluorocyclopropanes thus prepared were determined by their NMR spectra; in addition to the generalizations quoted above, use was made of the rule that $J_{HH,cis}$ is generally larger than $J_{HH,trans}$ in cyclopropanes.[19] The NMR data are presented in Tables 2 and 3. The NMR spectra of IId, IIId, and IVd were analyzed by the double resonance method.[20]

Ring Expansion of *n,n*-Dichloro- and *n*-Chloro-*n*-fluorobicyclo[*n*−3.1.0]alkanes (*n*=6,

15) D. Seyferth, H. Yamazaki and D. L. Alleston, *J. Org. Chem.*, **28**, 703 (1963).

16) The predominant formation of the *exo*-halo isomer has been observed also in the reduction of 6,6-dichloro-3-oxabicyclo[3.1.0]hexane (prepared from 2,5-dihydrofuran and dichlorocarbene) with tri-*n*-butyltin hydride; H. Yamanaka, T. Ando and W. Funasaka, unpublished.

17) T. Ando, F. Namigata, H. Yamanaka and W. Funasaka, *J. Am. Chem. Soc.*, **89**, 5719 (1967).

18) T. Ando, H. Yamanaka and W. Funasaka, unpublished.

19) W. G. Dauben and W. T. Wipke, *J. Org. Chem.*, **32**, 2976 (1967), and the references cited therein.

20) We thank Dr. M. C. Woods, Dept. of Chemistry, Tohoku Univ., for his measurements of proton NMR spectra at 100 MHz and his valuable discussion.

Table 3. Parameters of NMR spectra of 7-chloro-7-fluoro-, 7-chloro-, and 7-fluoro-2-oxabicyclo[4.1.0]heptane

Structure	Chemical shift, ppm			Coupling constant, Hz					
	H_M^*	H_X^*	F**	J_{HMF}	J_{HAF}	J_{HXF}	J_{HAHM}	J_{HAHX}	J_{HMHX}
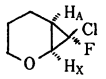			58.2		22	12			
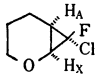			90.0		6	2			
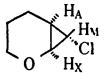	2.90	3.68					4.5	8.0	1.0
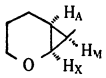	3.01	3.68					8.4	7.8	5.0
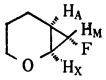	4.34	3.76	135.1	60.0	26.6	11.4	3.3	8.8	0
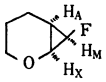	4.29	3.28	165.0	6.33	1.23	0	6.7	8.2	4.3

* Downfield from TMS.
** Upfiled from trifluoroacetic acid.

Table 4. Synthesis and properties of *n*-chlorobicyclo[*n*−3.1.0]alkanes (*n*=6, 7, and 9) and 7-chloro-2-oxabicyclo[4.1.0]heptane

Structure	*n*	Reaction temp. (°C)	Yield (%)	Isomer ratio (*exo*-Cl/*endo*-Cl)	Bp (°C/mmHg)	n_D (°C)
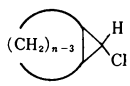	6 (IIIa)	80	82	1.6—1.7	65—70/63	1.4750 (21)
	7 (IIIb)	140	67	0.40—0.33	52—54/13	1.4860 (26)
	9 (IIIc)	90	72	0.45—0.46	77—79/8	1.4888 (31)
	(IIId)	85	67	1.0—1.3	40—45/4	1.4800 (24)

Table 5. Synthesis and properties of *n*-fluorobicyclo[*n*−3.1.0]alkanes (*n*=6, 7, and 9) and 7-fluoro-2-oxabicyclo[4.1.0]heptane

Structure	*n*	Reaction temp. (°C)	Yield (%)	Isomer ratio (*exo*-F/*endo*-F)	Bp (°C/mmHg)	n_D (°C)
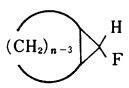	6 (IVa)	80	72	2.3—2.4	56—57/166	1.4234 (12)
	7 (IVb)	140	56	1.3—1.5	132—134/760	1.4400 (20)
	9 (IVc)	90	86	1.9—2.0	66—67/20	1.4519 (31)
	(IVd)	85	33	1.8—1.9	45—52/30	1.4383 (20)

7, and 9) and Their 2-Oxa Analogues ($n=7$). Recently, Lindsay and Reese[21] have found that the treatment of 7,7-dibromobicyclo[4.1.0]heptane with quinoline at 220—238°C gives 1,3,5-cycloheptatriene in 66—68% yield, while at 200°C under reduced pressure it gives a mixture of 1- and 2-bromo-1,3-cycloheptadiene in 38% yield. It has also been reported that 6,6-dibromobicyclo[3.1.0]-hexane or 6,6-dichlorobicyclo[3.1.0]hexane rearranges to the corresponding 2,3-dihalocyclohexene when heated at 150—180°C,[22] and that 7,7-dichlorobicyclo[4.1.0]heptane is converted to 1,3,5-cycloheptatriene when heated at 444—520°C.[23] These experimental results suggest that the thermal rearrangement of *n,n*-dihalobicyclo[$n-3.1.0$]alkanes is often accompanied by dehydrohalogenation, and is assisted by the presence of a base such as quinoline.

In accord with these findings, 6,6-dichlorobicyclo-[3.1.0]hexane (Ia) was converted to 2,3-dichlorocyclohexene (V) when heated at 120°C with an excess of quinoline. Further heating at 140°C resulted in the formation of 2-chloro-1,3-cyclohexadiene (VI). 7,7-Dichlorobicyclo[4.1.0]heptane (Ib) and 9,9-dichlorobicyclo[6.1.0]nonane (Ic) did not react at 120°C, and had to be heated at *ca.* 200°C in order to effect ring expansion. The products formed from Ib and from Ic were 1,3,5-cycloheptatriene (VII) and monochlorocyclononadiene (VIII),[24] respectively. Triene (VII) was probably formed *via* the intermediate chlorocycloheptadiene, which, however, could not be isolated under the reaction conditions. 7,7-Dichloro-2-oxabicyclo[4.1.0]heptane (Id) at 120°C in quinoline was converted to 2,3-dihydro-6-chloroöxepin (IX).

The lower temperature required for effecting the ring expansion of Ia, relative to that of Ib or Ic, may be due to the difference in ring strain between Ia (five-membered) and Ib or Ic (six- or eight-membered).

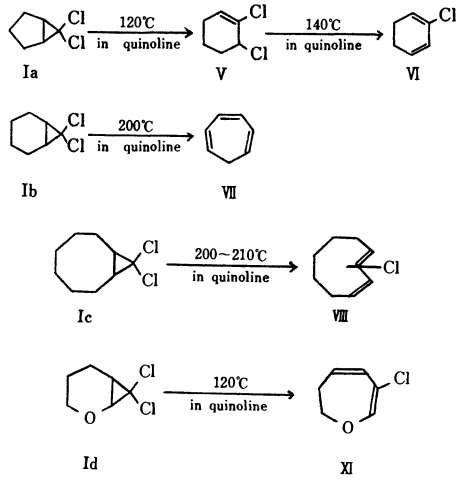

A similar ring expansion reaction occurred also when an isomeric mixture of 6-chloro-6-fluorobicyclo[3.1.0]hexane (IIa) was treated with quinoline at 110°C or at 140°C; 3-chloro-2-fluorocyclohexene (X) or 2-fluoro-1,3-cyclohexadiene (XI) were obtained, respectively. In these cases, the *exo*-chloro isomer was completely recovered. Similarly, the treatment of an isomeric mixture of 7-chloro-7-fluorobicyclo[4.1.0]heptane (IIb) and 7-chloro-7-fluoro-2-oxabicyclo[4.1.0]heptane (IId) with quinoline at 200°C or 120°C resulted in the formation of 1,3,5-cycloheptatriene (VII) and 2,3-dihydro-6-fluoroöxepin (XII), respectively, with complete recovery of the *exo*-chloro isomer. Fluorocycloheptadiene, the most probable precursor of VII in the ring expansion of IIb, was again not isolated.

These experimental facts indicate a much higher reactivity of the *endo*-chloro than that of the *exo*-chloro isomers. This stereospecificity, *i.e.*, the

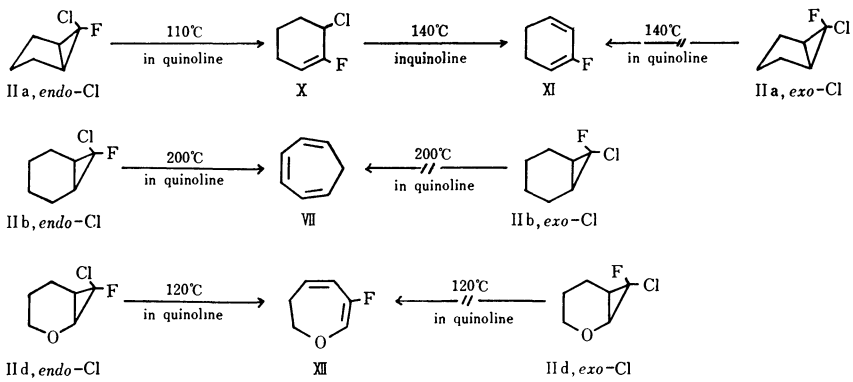

21) D. G. Lindsay and C. B. Reese, *Tetrahedron*, **21**, 1673 (1965).

22) a) J. Sonnenberg and S. Winstein, *J. Org. Chem.*, **27**, 748 (1962). b) E. Bergman, *ibid.*, **28**, 2210 (1963).

23) a) H. E. Winberg, *ibid.*, **24**, 264 (1959). b) G. C. Robinson, *ibid.*, **29**, 3433 (1964).

24) The structures of VIII, XV, and XVIII have not yet been fully established, but are only estimated; the results of their elemental analyses and their IR and NMR spectral data are in good agreement with the proposed structure (see Experimental), but the possibility that they might be a *cis*-diene or its derivative is not completely excluded.

strong dependence of the reaction rate upon the molecular geometry of the substrate, can be reasonably explained by assuming the rate-determining step of the ring opening of *gem*-chlorofluorocyclopropanes to be a "concerted disrotatory process,"[25] in which the chlorine is removed in preference to the fluorine, to form the corresponding 2-fluoroallyl cation. The selection rule advanced by DePuy *et al.*,[25] for such a process states that when the ring opening and the removal of the substituent occur simultaneously, the groups *trans* to the leaving group must rotate outward, and those *cis*, inward. If the same mechanism applies to the present reactions, the transition state (XIII) formed from the *exo*-chloro isomer of IIa, IIb, or IId would be sterically too much strained, as is shown below, for the ring expansion to occur. In contrast, the transition state (XIV) formed from the corresponding *endo*-chloro isomer would be much less strained.

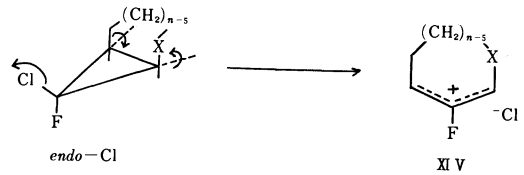

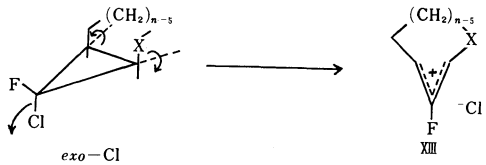

The above arguments predict that if the transition state of type XIII is more stable than that of type XIV, the ring expansion of the *exo*-chloro isomer of *gem*-chlorofluorocyclopropanes must occur faster than that of the *endo*-chloro isomer. This was proved to be the case in the ring expansion of 9-chloro-9-fluorobicyclo[6.1.0]nonane (IIc); the treatment of an isomeric mixture of IIc with quinoline at 215—225°C resulted in the formation of monofluorocyclononadiene (XV)[24] with the *endo*-chloro

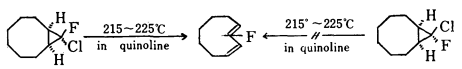

IIc, *exo*-Cl XV IIc, *endo*-Cl

isomer recovered. In view of the well-known higher stability of *trans*- than *cis*-cyclononene, and probably of *trans*- than *cis*-2-cyclononenyl cation, this result is by no means "anomalous." Similar apparent anomalies have been reported in the acetolysis of bicyclo[5.1.0]octyl and -[6.1.0]nonyl tosylates[26] as well as in the ring expansion of 9-bromobicyclo-[6.1.0]nonane by aqueous chromous sulfate.[27]

Ring Expansion of *n*-Halobicyclo[*n*−3.1.0]-alkanes (*n*=6, 7, and 9) and Their 2-Oxa Analogues (*n*=7) in Quinoline. As might be expected from the above discussion, the ring expansion of 6-chlorobicyclo[3.1.0]hexane (IIIa), 7-chlorobicyclo-[4.1.0]heptane (IIIb), 9-chlorobicyclo[6.1.0]nonane (IIIc) and 7-chloro-2-oxabicyclo[4.1.0]heptane (IIId) also occurred with distinct stereospecificity; it was only the *endo*-chloro isomers of IIIa, IIIb, and IIId, or the *exo*-chloro isomer of IIIc that underwent the ring expansion when treated with quinoline at 120—220°C.

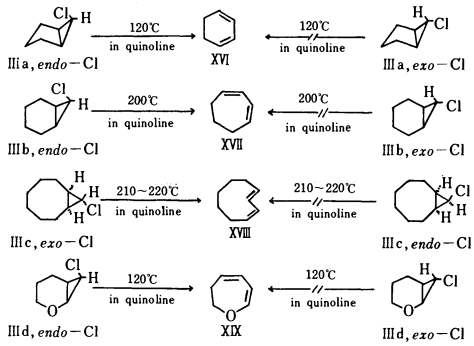

The more facile conversion of the *endo*-chloro, compared with the *exo*-chloro, isomer of IIId to 2,3-dihydroöxepin, does not agree with the experimental results reported by Schweizer and Parham,[8] who prepared an isomeric mixture of IIId by the addition of chlorocarbene, generated by the method of Closs and Closs,[28] to 2,3-dihydro-4*H*-pyran. They stated that the *exo*-chloro isomer of IIId decomposed more easily than the *endo*-chloro isomer, and attributed the difference in reactivity to an anchimeric assistance exerted by the *trans*-oxygen atom during the loss of the chlorine. Their structural assignment for the isomers of IIId, however, is tentative and lacks decisive evidence: it was based only on the idea that the sterically less hindered *exo*-chloro isomer must be formed in greater predominance than the more hindered *endo*-chloro isomer. In view of the findings by Closs[29] that chlorocarbene reacts with cyclohexene to yield more *endo*- than *exo*-chloronorcarane and with unsymmetrical olefins

25) C. H. DePuy, L. G. Schnack and J. W. Hausser, *J. Am. Chem. Soc.*, **88**, 3343 (1966).

26) a) P. von R. Schleyer, G. W. Van Dine, U, Schöllkopf and J. Paust, *ibid.*, **88**, 2868 (1966). b) U. Schöllkopf, K. Fellenberger, M. Patsch, P. von R. Schleyer, T. Su and G. W. Van Dine, *Tetrahedron Letters*, **1967**, 3639.

27) H. Nozaki, T. Aratani and R. Noyori, *Tetrahedron*, **23**, 3645 (1967).

28) G. L. Closs and L. E. Closs, *J. Am. Chem. Soc.*, **81**, 4996 (1959).

29) G. L. Closs, R. A. Moss and J. J. Coyle, *ibid.*, **84**, 4985 (1962).

to yield more *syn*-than *anti*-isomers, it is not surprising that the more hindered *endo*-chloro isomer is formed in greater predominance when it reacts with 2,3-dihydro-4H-pyran.

Both the *endo*-fluoro and the *exo*-fluoro isomers of 6-fluorobicyclo[3.1.0]hexane (IVa), 7-fluorobicyclo-[4.1.0]heptane (IVb), and 9-fluorobicyclo[6.1.0]-nonane (IVc) were quite stable under conditions similar to, or severer than, those used for the ring expansion of their chlorofluoro analogues. This is in good agreement with the observed lack of reactivity of the *exo*-chloro isomers of IIa, IIb, and IId or of the *endo*-chloro isomer of IIc, which evidently indicates the stability of the C–F bond, as compared with the C–Cl bond, in the ring expansion of halo- or dihalocyclopropanes.

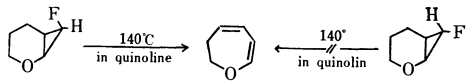

IVd, *endo*-F XIX IVd, *exo*-F

The *endo*-fluoro isomer of 7-fluoro-2-oxabicyclo-[4.1.0]heptane (IVd), however, was converted to 2,3-dihydroöxepin (XIX) when heated at 140°C for 5 hr with an excess of quinoline. The enhanced reactivity of the *endo*-fluoro isomer of IVd, relative to that of IVa, IVb, and IVc, may be accounted for by the resonance effect of oxygen to stabilize the transition state of type XIV. The *exo*-fluoro isomer of IVd was recovered unchanged under similar conditions.

Experimental

General. The infrared spectra were obtained with a Shimadzu IR 27B Spectrophotometer. The UV spectra were measured with a Beckmann DB Spectrophotometer. The proton NMR spectra were obtained with a Varian Associates A-60, H-100, or a JEOL JNM C-60H Spectrometer in duteriochloroform or carbon tetrachloride with TMS as internal reference. Chemical shift data are given in δ values. The fluorine NMR spectra were obtained with a Hitachi High-Resolution NMR Spectrometer H-60 or a JEOL JNM C-60 (at 56.4 MHz) in carbon tetrachloride with trifluoroacetic acid as external reference. Gas chromotography (glpc) was performed on a Shimadzu GC-2C or a Yanagimoto 5DH Chromatograph. The analytical columns were 3 m×3 mm of 7.5% apiezon grease L, 10% tricresyl phosphate, 5% silicone grease, or 10% polyethylene glycol 6000 on 60/80 mesh or 80/100 mesh celite 550 or chromosorb W; the preparative columns were 2 m×10 mm of either 30% apiezon grease L or 30% tricresyl phosphate on 60/80 mesh celite 550. The percentage composition of isomers was estimated from peak areas of glpc or NMR signals.

General Procedure for Preparation of *n*,*n*-Dichlorobicyclo[*n*−3.1.0]alkanes (*n*=6, 7, and 9) and Their 2-Oxa Analogues (*n*=7). In a 200-m*l* five-necked flask fitted with a reflux condenser, a stirrer, a thermometer, a dropping funnel and an inlet tube for nitrogen, was placed a mixture of 4.9 g (0.2 mol) of sodium hydride (as a 50% dispersion in mineral oil), 0.2 mol of the corresponding olefin, and 20 m*l* of anhydrous ether. To the mixture was added under nitrogen, 35.5 g (0.2 mol) of methyl trichloroacetate and then 7 g (0.22 mol) of methanol, both dropwise at *ca.* 0°C. The addition of methanol required about 2 hr. After the reaction mixture was let to stand overnight, a small amount of methanol, and subsequently 70 m*l* of water, were gradually added. The organic layer was separated, the aqueous layer was extracted with ether, and the combined organic layer was washed with aqueous sodium hydroxide and with water. After being dried over anhydrous calcium chloride, it was distilled in vacuum to give *gem*-dichlorocyclopropanes. In the distillation of Ia, care had to be taken in order to avoid its isomerization to V. The yields and the properties of the products are given in Table 1.

General Procedure for Preparation of *n*-Chloro-*n*-fluorobicyclo[*n*−3.1.0]alkanes (*n*=6,7, and 9) and Their 2-Oxa Analogues (*n*=7). The procedure was essentially the same as above, except that 32.2 g (0.2 mol) of methyl dichlorofluoroacetate was used instead of methyl trichloroacetate, and that methanol was added at *ca.* 25—35°C instead of *ca.* 0°C. The yields and the properties of the products are given in Table 1. The gas chromatograms of IIa and IIb thus prepared had two peaks, the ratio of the areas of which was taken to be equal to the ratio of the weights of the isomers. The isomer distribution of IIc and IId, which showed only a single peak in glpc under various conditions, was determined from the integrated areas of the fluorine NMR peaks.

General Procedure for Reduction of *n*,*n*-Dichloro- and *n*-Chloro-*n*-fluorobicyclo[*n*−3.1.0]alkanes (*n*=6,7, and 9) and Their 2-Oxa Analogues (*n*=7). A mixture of 0.1 mol of *n*,*n*-dichloro- or *n*-chloro-*n*-fluorobicyclo[*n*−3.1.0]alkane, 29.1 g (0.1 mol) of tri-*n*-butyltin hydride, and a small amount of azobisisobutyronitrile or di-*t*-butyl peroxide was heated, with stirring, at the temperature shown in Table 3 until an aliquot from the reaction mixture showed no IR absorption due to Sn–H stretching (near 1820 cm^{-1}). The product was isolated by distillation, and the isomer ratio was determined by glpc.

Ring Expansion of 6,6-Dichlorobicyclo[3.1.0]hexane (Ia). In a flask fitted with a reflux condenser and a thermometer, a mixture of 7.6 g (0.05 mol) of Ia and 18 g (0.15 mol) of quinoline was heated at 120°C for 5 hr. After distillation (85—95°C/20 mmHg), the product was purified by preparative gas chromatography, and identified to be 2,3-dichlorocyclohexene by comparison of its refractive index and IR spectrum with those of an authentic sample;[22b] n_D^{20} 1.5155, $\nu_{C=C}$ 1640 cm^{-1}.

Found: C, 47.80; H, 5.52%. Calcd for $C_6H_8Cl_2$: C, 47.71; H, 5.34%.

Further heating of the above reaction mixture at 140°C for 5 hr gave 82% yield of 2-chloro-1,3-cyclohexadiene, bp 70°C/78 mmHg, n_D^{20} 1.5055, IR (cm^{-1}): 3045 (m), 2940 (s), 2820 (s), 1632 (s), 1590 (w), 1440 (m), 1430 (s), 1390 (s), 1028 (s), 945 (s), 805 (s), and 720 (s).

Found: C, 62.85; H, 6.33%. Calcd for C_6H_7Cl: C, 62.90; H, 6.16%.

Ring Expansion of 7,7-Dichlorobicyclo[4.1.0]heptane (Ib). A mixture of 30 g (0.18 mol) of Ib and 77.4 g (0.6 mol) of quinoline was heated at 200°C in a

200-ml flask fitted with a reflux condenser and a thermometer. After 4 hr, the reflux of the reaction mixture became vigorous and the temperature in the flask lowered to below 180°C. At this temperature the mixture was heated for an additional 6 hr. Distillation of the reaction mixture gave 16 g (61% yield) of 1,3,5-cycloheptatriene which was identified by comparing its IR, UV, and NMR spectra with those of an authentic sample;[21] bp 108—110°C, n_D^{20} 1.5235, λ_{max}^{EtOH} 261 mμ (ε 3700).

Found: C, 91.46; H, 8.54%. Calcd for C_7H_8: C, 91.25; H, 8.75%.

Ib was heated at 200°C for 26 hr without quinoline. Although the generation of hydrogen chloride was noted, the glpc analysis of the reaction mixture showed no definite products. The starting material was almost completely recovered by distillation.

Ring Expansion of 7,7-Dichloro-2-oxabicyclo-[4.1.0]heptane (Id). A mixture of 8.3 g (0.05 mol) of Id and 50 g (0.39 mol) of quinoline was heated at 120°C for 6 hr. Distillation of the reaction mixture gave 5.2 g (80% yield) of 2,3-dihydro-6-chloroöxepin, bp 85—90°C/14 mmHg, n_D^{21} 1.5183.

Found: C, 55.31; H, 5.32%. Calcd for C_6H_7ClO: C, 55.19; H, 5.40%.

Ring Expansion of 6-Chloro-6-fluorobicyclo-[3.1.0]hexane (IIa). A mixture of 6.7 g (0.05 mol) of IIa (isomeric mixture) and 18 g (0.15 mol) of quinoline was heated at 110°C for 5 hr. Distillation of the reaction mixture afforded 70% yield of 2-fluoro-3-chlorocyclohexene (X) and the unchanged *exo*-chloro isomer, which were separated by preparative gas chromatography. IR (cm^{-1}) of X: 2940 (s), 1702 (s), 1380(s), 1150 (s), 975 (s), 885 (s), and 705 (s).

The above reaction mixture was heated at 140°C for an additional 5 hr. 2-Fluoro-1,3-cyclohexadiene was obtained in 49% yield; n_D^{20} 1.4520, IR (cm^{-1}): 3020 (w), 2970 (s), 2850 (m), 1670 (s), 1595 (w), 1410 (s), 1165 (s), 815 (m), 795 (m), and 730 (m).

Found: C, 73.61; H, 7.22%. Calcd for C_6H_7F: C, 73.45, H, 7.19%. The *exo*-chloro isomer was completely recovered.

Ring Expansion of 7-Chloro-7-fluorobicyclo-[4.1.0]heptane (IIb). A mixture of 30 g (0.2 mol) of IIb (isomeric mixture) and 90 g (0.7 mol) of quinoline was heated at 200°C for 10 hr. Distillation of the reaction mixture afforded 5.2 g (50% yield based on the *endo*-chloro isomer) of 1,3,5-cycloheptatriene and 12.5 g of the unchanged *exo*-chloro isomer.

A mixture of IIb (isomeric mixture), ethylbenzene (as internal reference), and quinoline was heated at 200°C. Glpc analysis indicated that the *endo*-chloro isomer was lost completely after 10 hr, while the *exo*-chloro isomer remained unchanged.

Ring Expansion of 7-Chloro-7-fluoro-2-oxabicyclo[4.1.0]heptane (IId). A mixture of 10 g (0.065 mol) of IId (isomeric mixture) and 42 g (0.33 mol) of quinoline was heated at 120°C for 3 hr. Distillation of the reaction mixture gave two fractions, (a) bp 51—57°C/45 mmHg, 3.5 g, and (b) bp 70—80°C/25—30 mmHg, 3.5g. Redistillation of fraction (a) gave 77% yield (based on the *endo*-chloro isomer) of pure 2,3-dihydro-6-fluoroöxepin; bp 58—60°C/65 mmHg, n_D^{21} 1.4706, IR (cm^{-1}): 3024 (m), 2995 (m), 2945 (m), 2913 (m), 1670 (m), 1628 (m), 1420 (s), 1290 (s), 1238 (s), 1126 (vs), 928 (s), and 740 (s).

Found: C, 63.30; H, 6.25%. Calcd for C_6H_7FO: C, 63.15; H, 6.18%. Fraction (b) was the unchanged *exo*-chloro isomer.

Ring Expansion of 6-Chlorobicyclo[3.1.0]hexane (IIIa). A mixture of 5.8 g (0.05 mol) of IIIa (isomeric mixture) and 18 g (0.15 mol) of quinoline was heated at 120°C for 4 hr. Distillation of the reaction mixture gave 80% (based on the *endo*-chloro isomer) of 1,3-cyclohexadiene; bp 78—80°C, n_D^{20} 1.4756, and the unchanged *exo*-chloro isomer which was recovered unchanged even after being heated at 140°C for an additional 10 hr.

Found: C, 89.80; H, 10.20%. Calcd for C_6H_8: C, 89.94; H, 10.06%.

Ring Expansion of 7-Chlorobicyclo[4.1.0]heptane (IIIb). A mixture of 14 g (0.11 mol) of IIIb (isomeric mixture) and 45 g (0.35 mol) of quinoline was heated at 140°C for 5 hr. Glpc analysis of the reaction mixture showed that no reaction had occurred. The mixture was then heated at 200°C for 10 hr. Distillation of the reaction mixture gave 6.2 g (80% yield based on the *endo*-chloro isomer) of 1,3-cycloheptadiene; bp 118—120°C, n_D^{20} 1.4970, λ_{max}^{EtOH} 246 mμ (ε 7500), and 3.0 g of the unchanged *exo*-chloro isomer.

Found: C, 89.15; H, 10.84%. Calcd for C_7H_{10}: C, 89.29; H, 10.71%.

Heating of IIIb (isomeric mixture) without quinoline at 165°C for 19 hr gave a small amount of black, tarry material, but no diene product.

Ring Expansion of 7-Chloro-2-oxabicyclo[4.1.0] heptane (IIId). A mixture of 8.5 g (0.064 mol) of IIId (isomeric mixture) and 20 g (0.16 mol) of quinoline was heated at 120°C for 3 hr. Distillation of the reaction mixture gave 2.0 g (70% yield based on the *endo*-chloro isomer) of 2,3-dihyroöxepin; bp 56°C/10 mmHg, n_D^{22} 1.4958, and 4.2 g of the unchanged *exo*-chloro isomer which was recovered unchanged even after heated in quinoline at 120°C for 10 hr.

Found: C 74.78; H 8.30%. Calcd for C_6H_8O: C, 74.97; H, 8.39%.

Ring Expansion of 6-Fluorobicyclo[3.1.0]hexane (IVa) and 7-fluorobicyclo[4.1.0]heptane (IVb). A mixture of IVa or IVb (isomeric mixture), ethylbenzene (internal reference), and quinoline was heated at 200°C for 10 hr in a sealed tube. Glpc analysis of the reaction mixture proved that neither of the isomers had decomposed under these conditions.

Ring Expansion of 7-Fluoro-2-oxabicyclo[4.1.0] heptane (IVd). An isomeric mixture of IVd did not show any appreciable change when heated in quinoline at 120°C for 10 hr, but prolonged heating at 140°C for an additional 5 hr resulted in the decomposition of the *endo*-fluoro isomer to yield 2,3-dihyroöxepin (in a low yield), with recovery of the *exo*-fluoro isomer.

Ring Expansion of 9,9-Dichloro- (Ic), 9-Chloro-9-fluoro- (IIc), 9-Chloro- (IIIc), and 9-Fluorobicyclo [6.1.0]nonane (IVc). A mixture of Ic, IIc, IIIc, or IVc and quinoline was heated at 200—220°C for 10 hr. After distillation of the reaction mixture, the products were purified by preparative gas chromatography. Chlorocyclononadiene (VIII); bp 94°C/17 mmHg, n_D^{22} 1.5130, IR (cm^{-1}): 3015 (m), 2940 (s), 2860 (s), 1625 (s), 1590 (w), 1460 (s), 1040 (s), 950 (s), and 785 (s), NMR: δ 1.3—2.5 (m) (10H) and δ 5.5—6.0 (m) (3H).

Found: C, 69.12; H, 8.28%. Calcd for $C_9H_{13}Cl$: C, 69.00; H, 8.37%. Fluorocyclononadiene (XV); bp

98°C/70 mmHg, n_D^{21} 1.4783, IR (cm^{-1}): 3015 (m), 2940 (s), 2860 (s), 1690 (s), 1640 (w), 1460 (m), 1450 (m), 1120 (s), 1115 (m), 840 (m), and 750 (m). NMR: δ 1.2—2.6 (m) (10H) and δ 4.8—6.0 (m) (3H).

Found: C, 77.16; H, 9.52%. Calcd for $C_9H_{13}F$: C, 77.10; 9.35%. Cyclononadiene (XVIII); bp 105°C/83 mmHg, n_D^{21} 1.4940, IR (cm^{-1}): 3020 (s), 2940 (s), 2860 (s), 1630 (w), 1458 (s), 770 (s), and 734 (s), NMR: δ 1.2—2.4 (m) (10H) and δ 5.1—5.9 (m) (4H).

Found: C, 88.23; H, 11.77%. Calcd for C_9H_{14}: C, 88.45; H, 11.55%.

The *endo*-chloro isomer of IIc or IIIc and both isomers of IVc remained unchanged after being heated at 220°C for an additional 10 hr.

BULLETIN OF THE CHEMICAL SOCIETY OF JAPAN VOL. 42 2021—2028 (1969)

1,3-*O*-Benzylidene-L-sorbose[1)]

Takashi MAEDA, Mitsuru KIMOTO, Shigeru WAKAHARA and Kanji TOKUYAMA

Shionogi Research Laboratory, Shionogi & Co., Ltd., Fukushima-ku, Osaka

(Received December 17, 1968)

It has been proposed that 1,3-*O*-benzylidene-L-sorbose (III) exists as an equilibrium mixture of a pyranose form (IIIp), a keto-form (IIIk) and a furanose form (IIIf) in solutions. The acetylation of III in pyridine afforded the acetates of IIIf; one of them (IV) is in a keto-form (IVk) in a crystalline state, and at a low temperature, while the acetates of IIIf and IIIp at higher temperatures. When a pyridine solution of III was allowed to stand for some time before acetylation, the yield of the acetate of IIIp increased. The recrystallization of III usually gave crystals of IIIf, however, while the addition of petroleum ether to the concentrated pyridine solution of III afforded a powder which was consisted mainly of IIIp. These results suggest that III exists as IIIf in a crystalline state and as an equilibrium mixture of IIIf, IIIk, and IIIp in solution; the existence of this equilibrium was also confirmed by proton magnetic resonance spectroscopy.

The 1,3-*O*-acetal of L-sorbose (I) is a key intermediate in the acetalation of I, which is an important reaction for L-ascorbic acid production.[2–4)] We have successfully isolated two examples of this kind of acetals, 1,3-*O*-ethylidene-α-L-sorbopyranose (II) from the ethylidenation[3)] and 1,3-*O*-benzylidene-L-sorbose (III) from the benzylidenation.[2)] It is quite natural that the ring structure of II has a pyranose form, for I is stable in an α-L-pyranose form.[5)] On the other hand, much attention should be paid to the surprising fact with III that a β-furanose form (IIIf) of the *cis*-decalin type is more likely than an α-pyranose form (IIIp) of the *trans*-decalin type (see Chart 2). III exists as IIIf in a crystalline state, while IIIp is considered to exist only as an equilibrium mixture with IIIf in solution. This paper will be concerned with the equilibrium of III. For this purpose, further studies of the

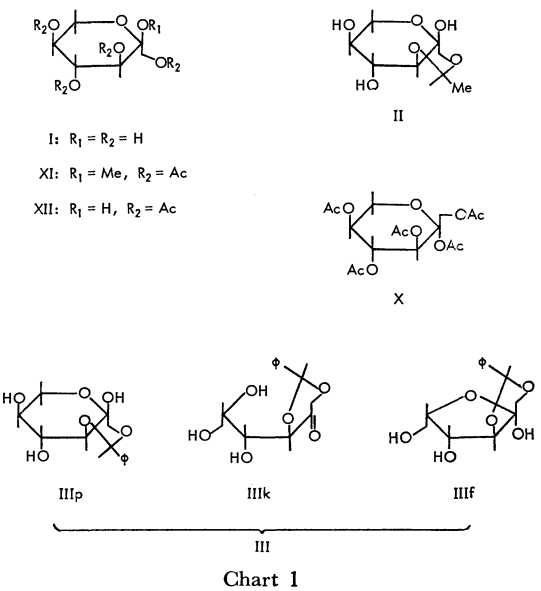

Chart 1

1) Sorboses XV. For Part XIV, See Ref. 2.

2) T. Maeda, M. Kimoto, S. Wakahara and K. Tokuyama, This Bulletin, **42**, 1668 (1969).

3) T. Maeda, M. Kiyokawa and K. Tokuyama, *ibid.*, **42**, 492 (1969).

4) T. Maeda and K. Tokuyama, *Tetrahedron Letters*, **1968**, 3079.

5) a) S. J. Angyal, "Conformational Analysis," ed. by E. L. Eliel, N. A. Allinger, S. J. Angyal and G. A. Morrison, John & Wiley, New York (1965), p. 351. b) J. C. Jochins, G. Taigel, A. Seelinger, P. Lutz and H. E. Driesen, *Tetrahedron Letters*, **1967**, 4363. c) I. Listowsky, S. Englard and G. Avigad, *Carbohyd. Res.*, **2**, 261 (1966).

acetylation of III and proton magnetic resonance spectroscopic studies were carried out.

The acetylation of III in pyridine with acetic anhydride at −5—6°C has been shown to give 4,6-di-*O*-acetyl- (V) and 2,4,6-tri-*O*-acetyl-1,3-*O*-benzylidene-β-L-sorbofuranose (VI), along with a limited amount of 4,5-di-*O*-acetyl-1,3-*O*-benzylidene-α-L-sorbopyranose (VII).[2] This fact suggests that III usually exists as IIIf in a pyridine solution at a low temperature. The acetylation at about −30°C gave strong support to this suggestion. The examination of the reaction by thin-layer chromatography (TLC) showed that a mono-acetate (IV) initially appeared and that V and VI then appeared at the expense of IV. No formation of detectable amount of VII was observed. The interuption of the reaction after 2 hr gave mainly IV, which was then converted into VI *via* V, by further acetylation, but not into VII.

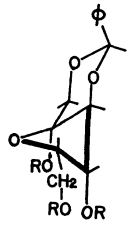

IIIf, IV, V, VI

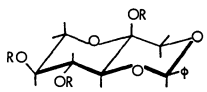

IIIp, VII, VIII

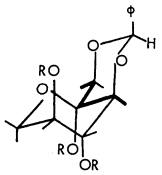

IX

Chart 2

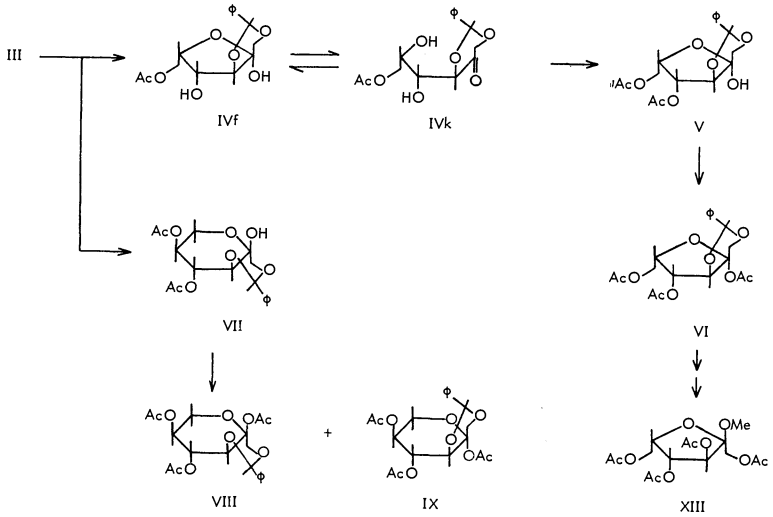

Chart 3

In view of the above facts, possibility of a pyranose structure for IV may be excluded. As the primary hydroxyl group at the C_6 position of IIIf must be more reactive for the acetylation than the secondary one at C_4,[6] the structure of IV is determined to be 6-*O*-acetyl-1,3-*O*-benzylidene-β-L-sorbofuranose. The PMR spectrum of IV in chloroform-d showing the absence of a proton on a tertiary carbon bearing an acetoxyl group (AcO$\underset{|}{\underset{|}{\text{C}}}$H), confirmed this structure (Fig. 1).

The behavior of IV is very interesting. The infrared (IR) spectrum of IV in a KBr disk, showing two strong absorption bands at 1720 and 1740 cm^{-1} due to carbonyl groups (Fig. 2), and the optical rotatory dispersion (ORD), showing no Cotton effect[7] (Fig. 3), made it clear that IV exists as a keto-form (IVk) in a crystalline state to a considerable extent and as a furanose form (IVf) in solution.

The acetylation of III, IV, and V with acetic anhydride in pyridine gave VI as the final product, even though weak conditions were used.[8] This unexpected acetylation of a tertiary hydroxyl group was not observed in the case of VII. For the formation of the 2-*O*-acetyl derivative of VII

6) R. H. Adkins, *J. Am. Chem. Soc.*, **49**, 2517 (1927); **55**, 299 (1933); **56**, 442 (1934).

7) Acyclic ketoses are known to show a Cotton effect. See T. Sticzay, C. Reciar, K. Babor, M. Fedoroňks and K. Linek, *Carbohyd. Res.*, **6**, 418 (1968).

8) This type of abnormal acetylation has been reported on a Noranisation-derivative by Hirata *et al.*, however, a longer reaction period was required. K. Yamada, S. Takada, S. Nakamura and Y. Hirata, *Tetrahedron*, **24**, 1267 (1968).

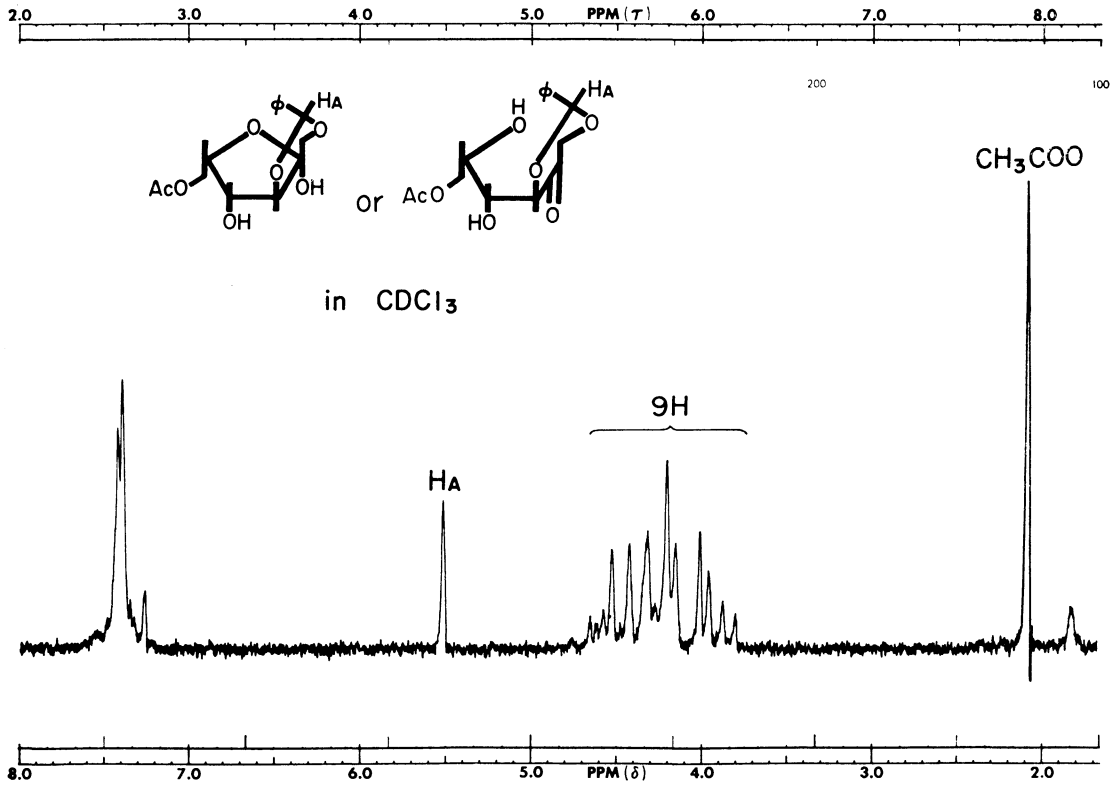

Fig. 1. PMR spectrum of IV in chloroform-d at 60 MHz.
H_A shows the signal due to a benzylic proton.

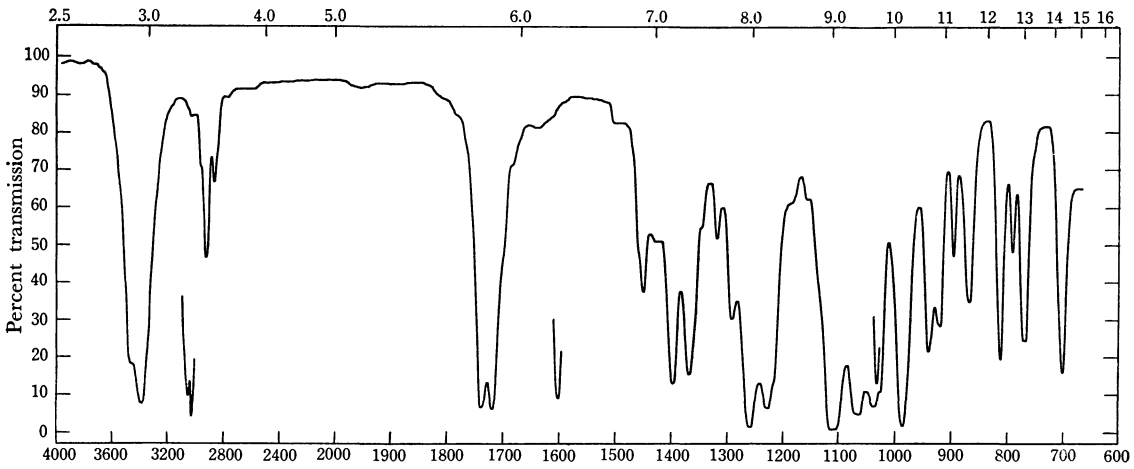

Fig. 2. IR spectrum of IV (KBr disk).

(VIII), ordinary reaction conditions were required, such as heating on a boiling-water bath or using sodium acetate and acetic anhydride under heating. In the case of the acetylation on a boiling-water bath, the β-anomer of VIII (IX) was also isolated.

The structures of VIII and IX were confirmed by the methods described below. The PMR spectrum of VIII in chloroform-d revealed the presence of one axial (τ 7.79) and two equatorial (τ 7.95) acetoxyl groups.[9] Two one-proton signals due to H_4 and H_5 appeared as a quartet (τ 4.41) and a multiplet (τ 4.90) respectively in the AcO-C-H range. The coupling constants ($J_{3,4}\simeq$10 and $J_{4,5}\simeq$9Hz) suggested that the pyranose structures was in the 1C chair form. Thus, the structure

9) L. D. Hall, *Advan. Carbohyd. Chem.*, **19**, 51 (1964).

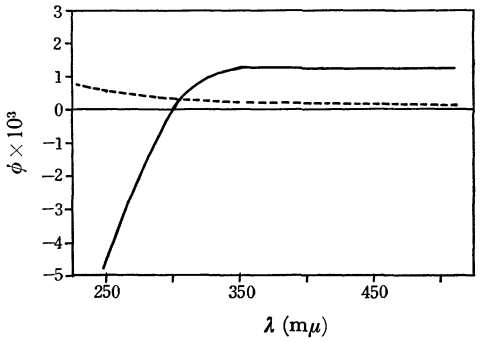

Fig. 3. ORD curves of IV and IX.
—— IV
--- IX

of VIII was determined to be 2,4,5-tri-*O*-acetyl-1,3-*O*-benzylidene-α-L-sorbopyranose.

The structure of IX should be compatible with either 2,4,5-tri-*O*-acetyl-1,3-*O*-benzylidene-β-L-sorbopyranose or 4,5,6-tri-*O*-acetyl-1,3-*O*-benzylidene-L-sorbose. However, the latter structure could de excluded because the ORD curve showed the absence of a carbonyl group[7] (Fig. 3). The positive value of the optical rotation and the fact that the PMR spectrum in chloroform-d was close to that of 1,2,3,4,5-penta-*O*-acetyl-β-L-sorbopyranose (X)[10] supported the former structure. The formation of IX was somewhat curious, for IX has an unstable *cis*-decalin type conformation in which its sugar moiety must also adopt the unlikely Cl chair form;[11] however, IX will be shown below to indeed possess this structure.

The easy acetylation of the tertiary hydroxyl group of V could not be attributed to the presence of the 1,3-*O*-benzylidene group, because the acetylation of the tertiary hydroxyl group of VII did not occur under similar reaction conditions. More especially, no acetylation of 1,3,4,6-di-*O*-benzylidene-β-L-sorbofuranose was obtained even on heating on a boiling-water bath. Therefore, the acetylation of the tertiary hydroxyl group of V must be caused by the closeness of the acetyl group at C_4 to the anomeric hydroxyl group. The closeness made possible the migration of the acetyl group from C_4 to C_2.

The existence of the long range coupling across 4 σ bonds between H_1 and H_3 also supported the structure of IX.[13] The coupling is usually observed in the 1,3-*O*-benzylidene-β-derivatives and suggests that the protons are in a zig-zag or W-letter arrangement (see Chart 2). The possibility of an epimerization on the C_3-configuration during the heating in pyridine was ruled out by the fact that the catalytic hydrogenation of IX in MeOH, followed by acetylation gave 1,3,4,5-tetra-*O*-acetyl-α-L-sorbopyranose (XII).[14]

In the hydrogenation of IX, methyl 1,3,4,5-tetra-*O*-acetyl-α-L-sorbopyranoside (XI)[15] was also isolated. This König-Knorr type glycosidation from IX to XI was also observed in the case of VI, which gave a fairly good yield of methyl 1,3,4,6-tetra-*O*-acetyl-α-L-sorbofuranoside (XIII).[16] However, the treatment of X under the same reaction conditions gave XI to a very limited extent. Accordingly, the existence of 1,3-*O*-benzylidene groups in VI and IX seems to enhance the rate of exchange of the acetoxyl group with the methoxyl group.

The above-described product analyses of the acetylations of III pointed out that IIIf is a predominant form in pyridine at low temperatures and that it transforms to IIIp with a rise in the temperature. The transformation from IIIf to IIIp was confirmed by the following PMR spectroscopic studies.

The PMR spectra of III in pyridine-d_5 are reported in Fig. 4. Two singlet signals (H_A) at τ 4.20 and 4.24, assignable to benzylic protons, appeared when measured at room temperature immediately after the dissolution of III in pyridine-d_5 (Fig. 4a). The third signal (H_B) at τ 4.09 assignable also to a benzylic proton which newly appeared when measured at 70°C (Fig. 4b), and its relative intensity increased synchronically with the decrease in the former two signals when the pyridine solution was heated at 100°C for 1 hr (Fig. 4c). An increase in the third signal was also obtained when the pyridine-d_5 solution was allowed to stand at room temperature for a long time (Fig. 4d).

The relative ratio of the signals (H_A) at τ 4.20 and 4.24 was constantly about 2 : 1 during the measurements. The one can reasonably be assigned to the benzylic proton of IIIf, and the other, to that of the keto-form of III (IIIk). The α-furanose form of III may be excluded, since a 1,3-*O*-acetal ring fused to an α-furanose can be expected to deform the furanose-ring conformation seriously.[16] On the other hand, the existence of IIIk is supported by the fact that IV adopts the keto-form IVk to

10) H. Paulsen, H. Köster and K. Heyns, *Chem. Ber.*, **100**, 2669 (1967).

11) Methyl 1,3,4,5-tetra-*O*-acetyl-β-L-sorbopyranoside was confirmed to exist as a conformer mixture of 1C and Cl chair forms.[12] The comparison of the PMR data of IX with those of the above pyranoside suggested that X may adopt mainly the Cl chair form.

12) K. Tokuyama, T. Maeda, K. Tori, S. Satoh and K. Kuriyama, paper presented at the 1st Symposium on Organic Structural Chemistry, Tokyo, Nov., 1968.

13) For example, see L. D. Hall, *Carbohyd. Res.*, **4**, 514 (1967).

14) Y. Khounine and A. Arragon, *Bull. Soc. Chim. France*, **1938**, 1404.

15) H. H. Schlubach and G. Graefe, *Ann.*, **532**, 211 (1937).

16) T. Maeda, K. Tori, S. Satoh and K. Tokuyama, This Bulletin, **41**, 2495 (1968).

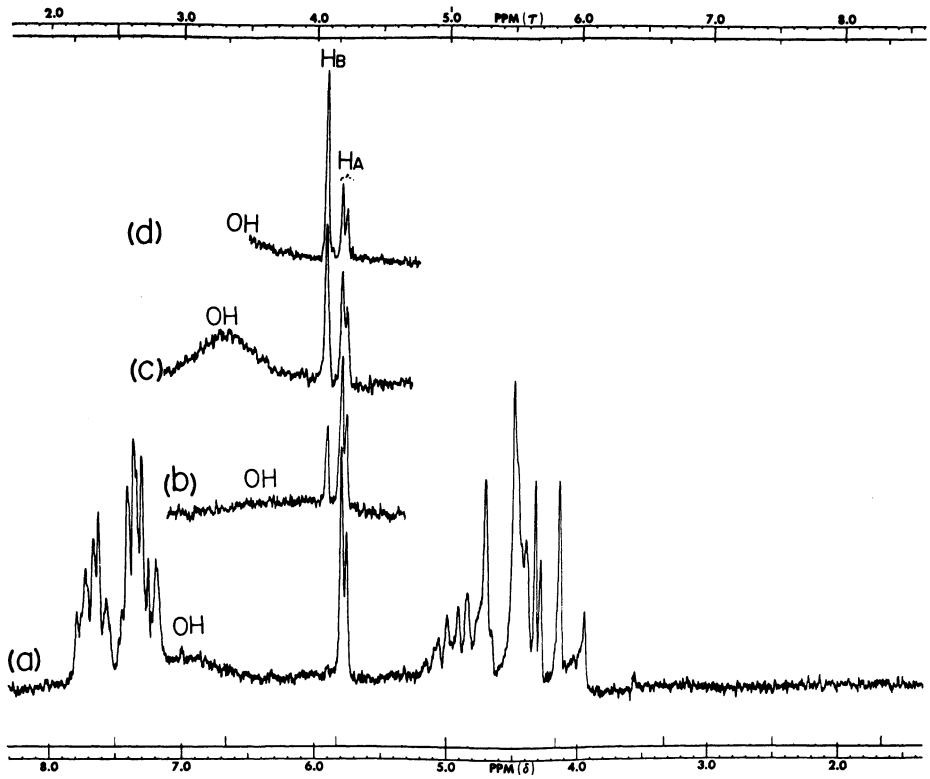

Fig. 4. PMR spectra of III in pyridine-d_5 at 60 MHz.
(a) Measured at room temperature immediately after dissolution of III
(b) Measured at 70°C
(c) Measured at room temperature after heating the solution at 100°C for 1 hr
(d) When the solution was allowed to stay at room temperature for 12 hr

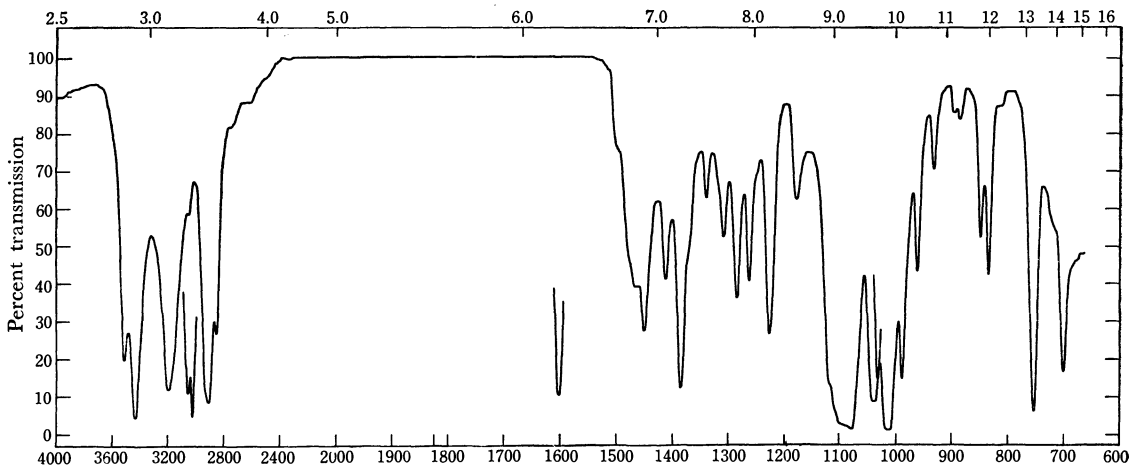

Fig. 5. IR spectrum of III (IIIf) (KBr disk).

some extent. However, as the absorption band due to the carbonyl group was hardly detected in the attenuated total reflection IR (ATR) spectrum of the pyridine solution of III, it was concluded that IIIk was a minor component compared to IIIf. Therefore, we could assign the signal at τ 4.20 to that of IIIf, and the one at τ 4.24, to IIIk. The third signal (H_B) at τ 4.09 was assigned to the benzylic proton of IIIp, since the acetylation of the pyridine solution, which showed a strong intensity of this signal, gave VII as the major product.

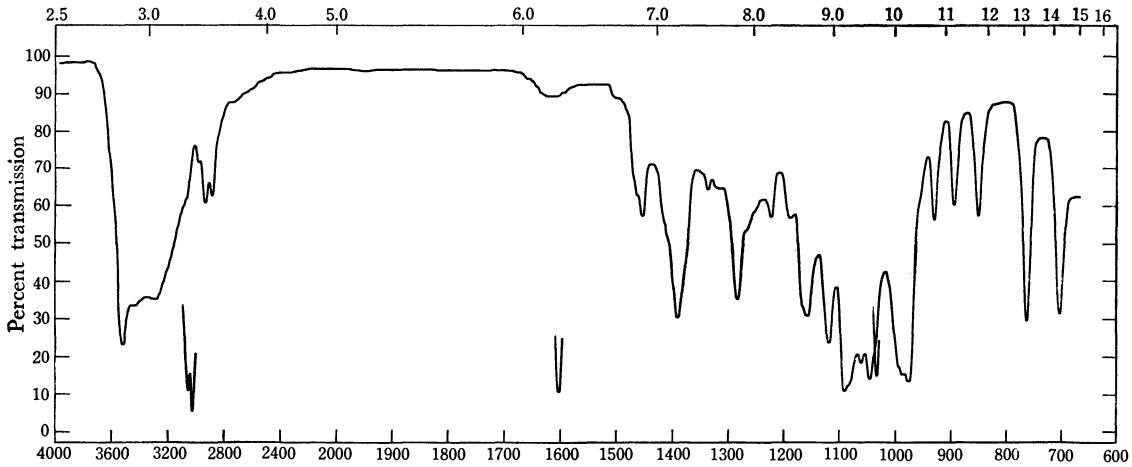

Fig. 6. IR spectrum of III (mainly IIIp) (KBr disk).

As has previously been reported, III adopts IIIf in a crystalline state. Further, the above-mentioned facts establish that III exists in solution as a mixture of IIIf, IIIk, and IIIp. As IIIp is the dominant form in pyridine we attempted to isolate it. Crystals of IIIf usually appeared upon the concentration of the pyridine solution, which showed a high concentration of IIIp. On the other hand, an amorphous powder was obtained on the addition of petroleum ether to the concentrated pyridine solution before any crystals started to appear. This powder had a low melting point, a negative optical rotation (which suggested the presence of IIIp), and it obviously differed from IIIf in its IR spectrum (see Figs. 5 and 6). The recrystallization of this powder from methanol gave IIIf, and the acetylation gave VII as the major product. Therefore, this powder is considered to contain considerable amount of IIIp. These data also supported the idea that IIIf is dominant in a crystalline state.

In conclusion, III usually crystallizes as IIIf and equilibrates among IIIf, IIIk, and IIIp in solution. It is obscure why IIIf of the unstable *cis*-decalin type can exist exceptionally in the case of benzylidene derivatives of L-sorbose (I). The presence of IV of the keto-form in a crystalline state is also surprising. We hope that these interesting fused-ring systems will be elucidated by thermodynamic treatments.

Experimental

All the melting points were recorded on a Kofler microstage apparatus and have been corrected.

The optical rotations were determined in chloroform containing 1% ethanol unless otherwise stated, and the concentrations were recorded in percentages. The ORD curves were obtained on a Nippon-Bunko ORD/UV 5 spectrometer.

The PMR spectra were measured on a Varian A-60A spectrometer equipped with a variable temperature probe using 5% solutions of samples and with TMS as the internal standard. The results obtained from first-order approximation are listed in Table 1.

Thin-layer chromatography (TLC) and preparative TLC (PTC) were carried out on a silica-gel plate in the

Table 1. Chemical shifts (τ) and coupling constants (J, Hz) in $CDCl_3$[a]

Compd.	H_1, $H_{1'}$	H_3	H_4	H_5	H_6	$H_{6'}$	Benzylic H	CH_3COO	Other H
IV	5.3 — 6.2[b]						4.48	7.90	OH 5.3—6.2[b]
VIII	4.88, 6.23	6.30	4.41	4.90	5.98	6.44	4.42	7.79, 7.95 (6H)	
	$J_{1,1'}=12.0$	$J_{3,4}=10.0$	$J_{4,5}=9.0$	$J_{5,6}=6.3$	$J_{5,6'}=10.7$				
					$J_{6,6'}=11.3$				
XI	5.43, 5.77	5.54	4.90	5.24	5.76	5.97	4.44	7.91 (6H), 7.97	
	$J_{1,1'}=12.0$	$J_{3,4}\simeq 2$	$J_{4,5}\simeq 3$	$J_{5,6}\simeq 2$	$J_{5,6'}\simeq 2$				
	$J_{1,3}\leqq 1.0$		$J_{4,6'}\leqq 1.0$		$J_{6,6'}\simeq 13.0$				
X	5.33, 5.52	4.53	4.82	5.12	5.68	6.09	—	7.90 (15H)	
	$J_{1,1'}=12.0$	$J_{3,4}\simeq 5$	$J_{4,5}\simeq 4$	$J_{5,6}\simeq 3$	$J_{5,6'}\simeq 2.5$				
			$J_{4,6'}\leqq 1.0$		$J_{6,6'}=13.0$				

a) Aromatic protons appeared at τ 2.5—2.8 as multiplets
b) Unresolved

same manner as has been previously described.[2] The solvent systems used were chloroform-acetone (9 : 1, v/v, solvent A), ether-petroleum ether (5 : 1, v/v, solvent B; 3 : 1, v/v, solvent C, 2 : 1, v/v; solvent D), and benzene-ether (2 : 1, v/v, solvent E).

General Procedure of Acetylation. A compound (1 part in weight) was treated with a mixture of pyridine and acetic anhydride (1 : 1 v/v; 10 parts in volume) at the cited temperature. The reaction mixture was then poured onto crushed ice, neutralized with sodium hydrogencarbonate, and extracted with chloroform. The chloroform was washed with water, 1N HCl and water, and then dried and evaporated. The acetate thus obtained was purified by recrystallization and/or by PTC.

Acetylation of III. a) III (1.00 g) was acetylated at −30°C for 2 hr. The recrystallization of the product from ethanol gave IV as needles (301 mg). V (60 mg)[2] was separated from the mother liquor (351 mg) by repeated PTC with solvents A and B.

IV: mp 153—155°C, $[\alpha]_D^{25}$ +16.5° (*c* 0.956). Found: C, 58.14; H, 5.86%; mol wt, 314. Calcd for $C_{15}H_{18}O_7$: C, 58.06; H, 5.85%; mol wt, 310. ORD: $[\phi]_{400}$ +172°; $[\phi]_{300}$ +298°; $[\phi]_{232}$ +616.

b) III (500 mg) was acetylated for 5 hr at room temperature and then for 1 hr at around 70°C. VI[2] was mainly obtained, it was purified by recrystallization from ethanol-water. The yield was 536 mg.

c) A solution of III (583 mg) in pyridine (6 m*l*) was heated on a boiling-water bath for 13.5 hr and then kept overnight at room temperature. Acetic anhydride (6 m*l*) was added to the solution. After having been kept at room temperature for 15.5 hr, the solution was worked up by the general procedure. A crystalline syrup (871 mg) was obtained. The recrystallization of the syrup from ether gave VII (126 mg). From the mother liquor, VI (212 mg) and VII (175 mg) were separated by PTC with solvent A. The total yield of VII was 311 mg.

d) III (1.00 g) was preliminarily heated in a way similar to the above and then acetylated at around 0°C for 4 hr. A syrup (1.20 g) was obtained. The recrystallization of the syrup from ether gave VII (697 mg). From the mother liquor, V (140 mg) was separated by PTC with solvent D.

Acetylation of VII. a) VII (600 mg) was acetylated on a boiling-water bath for 3 hr. The products were separated into VIII (131 mg) and IX (200 mg) by PTC with solvent D.

VIII (84 mg) was obtained as needles by further recrystallization from ether. It had mp 203.5—205°C, $[\alpha]_D^{23}$ −38.7° (*c* 0.988). Found: C, 57.58; H, 5.76%; mol wt, 394. Calcd for $C_{19}H_{22}O_9$: C, 57.86; H, 5.62%; mol wt, 394.

IX was a very hygroscopic syrup, $[\alpha]_D^{23}$ +14.7° (*c* 0.911). Found: C, 56.51; H, 5.65%; mol wt, 412. Calcd for $C_{19}H_{22}O_9$: C, 57.86; H, 5.62%; mol wt, 394. ORD: $[\phi]_{400}$ +1273°, $[\phi]_{350}$ +1307°, $[\phi]_{300}$ +89°, $[\phi]_{250}$ −4670°.

b) A solution of VII (30 mg) in acetic anhydride (3.0 m*l*) was heated at 70°C in the presence of sodium acetate (0.30 g). After 4.5 hr, the mixture was cooled to room temperature and kept overnight. Then the solution was worked up by the usual procedure. The recrystallization of crude crystals from ether (34 mg) gave VIII (21 mg). The lack of any formation of IX was confirmed by TLC.

Acetylations of IV, V and VII. These acetylations were carried out a) below 0°C and b) at 100°C for 3 hr. The reactions were checked by TLC with solvents A and D. The results are listed in Table 2.

Table 2. Acetylation products

Starting material	Reaction conditions	
	a)	b)
IV	V, VI	VI
V	VI	VI
VII	recovered	VIII, IX

Formation of XI from IX. A solution of IX (168 mg) in methanol (20 m*l*) was hydrogenated in the presence of 5% Pd-C (840 mg) at atmospheric pressure. After 1 hr, the catalyst was removed by filtration and washed with methanol. The combined solution of the filtrate and the washings were evaporated to give a syrup (77 mg). The syrup was acetylated without further purification. The product was separated into XII (31 mg) and XI (30 mg) by PTC with solvent C. A mixture of XII, methyl iodide (5 m*l*), and silver oxide (0.5 g) was refluxed for 4 hr and then kept overnight at room temperature. The precipitates were removed by filtration. The filtrate was concentrated to give XI (23 mg).

Preparation of X. 1,3,4,5-Tetra-*O*-acetyl-α-L-sorbopyranosyl chloride (3.59 g)[17] was treated with anhydrous acetic acid (100 m*l*) in the presence of mercuric acetate (5 g) at room temperature. After 70 min, the reaction mixture was poured into ice water and extracted with chloroform. The extract was subsequently washed with water, a 5% sodium hydrogencarbonate solution, and water. The solution was dried over $MgSO_4$ and then evaporated to give a syrup (4.6 g). X (0.26 g, R_f 0.38—0.45) was isolated by PTC with solvent E. The recrystallization of crude X from ether gave needles (97 mg); mp 108—109.5°C, $[\alpha]_D^{23}$ +71.6° (*c* 0.705) (lit.[15] mp 113.8°C, $[\alpha]_D$ +74.4°).

Preparation of XIII from VI. VI (767 mg) was hydrogenated by the same procedure as was used for IX. The acetylation of a crude product gave a syrup (432 mg) from which XIII (88 mg) was isolated by repeated PTC with solvents A and D.

Treatment of X under Hydrogenation Conditions. A solution of X (10.5 mg) in methanol was treated in a manner similar to that used for IX. Hardly any hydrogen up-take could be observed. The thin-layer chromatogram showed the existence of a trace of XI along with the unreacted X.

The Equilibrium of III in Pyridine. *a) Isolation of IIIp.* (i) A solution of crystals of IIIf (100 mg) in pyridine (0.2 m*l*) was allowed to stand at room temperature. After 6 days, the solution was poured into petroleum ether (10 m*l*). A precipitated syrup was separated by decantation and washed with petroleum ether. The addition of ether to the syrup gave an amorphous powder (67 mg) which consisted mainly of **IIIp.** It had mp 151—182°C, $[\alpha]_D^{23}$ −26.7°→−24.1°

17) K. Tokuyama and M. Katsuhara, This Bulletin, **39**, 2728 (1966).

(24 hr) (*c* 0.640, methanol). Found: C, 58.41; H, 5.99%. Calcd for $C_{13}H_{16}O_6$: C, 58.20; H, 6.01%. The acetylation of the powder (10 mg) at 0°C for 6 hr gave VII (9.6 mg).

(ii) A solution of crystals of IIIf (1 part) in pyridine (10 parts) was heated at 100°C for 15 hr and then kept at room temperature for 35 hr. The solution was concentrated to a brown syrup containing a small amount of pyridine. The syrup was washed with petroleum ether and then dissolved in methanol. Insoluble crystals of IIIf were removed by filtration. The filtrate was evaporated to give a syrup. Ether was added to the syrup and the powder thus precipitated, which contained IIIf and IIIp, was removed by filtration. The filtrate was evaporated to give a powder. The recrystallization of the powder from ether gave the powder of IIIp of a considerable purity. It had mp 150—158°C.

b) *Transformation of IIIp to IIIf.* (i) A solution of IIIf (21.5 mg) in pyridine (0.4 m*l*) was heated at 100°C for 13.5 hr and then kept at room temperature for 30.5 hr. The solution was evaporated under reduced pressure. Crystals of IIIf (21.4 mg) were thus obtained.

(ii) A solution of IIIp (7 mg), prepared by the above procedure (a-ii), in methanol was allowed to stand overnight at room temperature; then it was concentrated. Crystals of IIIf (6 mg) were obtained.

The authors wish to express their gratitude to Professor Toshihiko Okamoto, The University of Tokyo, and to Dr. Ken'ichi Takeda, Director of this Laboratory, for their encouragement. They are also indebted to Drs. Kaoru Kuriyama, Kazuo Tori and Shiroh Satoh for the ORD and PMR.

BULLETIN OF THE CHEMICAL SOCIETY OF JAPAN VOL. 42 2028—2032 (1969)

The Nucleophilic Substitution Reactions of 2-Aminotropone Derivatives

Takashi TODA, Shôji RYU[1] and Tetsuo NOZOE

Department of Chemistry, Faculty of Science, Tohoku University, Katahira-cho, Sendai

(Received December 31, 1968)

The nucleophilic substitution reactions of 2-aminotropone (I), 2-methylaminotropone (II), 2-dimethylaminotropone (III), and 2-troponyl trimethylammonium iodide (IV), and their alkyl derivatives were investigated. It was found that the properties of I and II are similar to those of tropolones. On the other hand, those of III are analogous to those of tropolone methyl ethers, while those of IV are, rather, comparable to those of 2-halotropones or tropolone tosylates.

2-Aminotropone (I) and its derivatives have been obtained early in the history of troponoid chemistry.[2-4] However, only a few examples of the electrophilic and nucleophilic substitution reactions of these compounds have been investigated[3,4] other than the syntheses of many 1-azaazulan-2-one derivatives from 2-aminotropones by the action of active methylene compounds.[3b,4,5] Recently, the present authors investigated the electrophilic substitution reactions[6] of I and its *N*-alkyl derivatives —2-methylaminotropone (II)[3a] and 2-dimethylaminotropone (III)[3a]— and found that the reaction of III caused the hydrolysis of the dimethylamino group, thus giving tropolone derivatives.[6] The reaction mechanism of the hydrolysis was later clarified.[7] In this paper, the authors wish to report their

1) Present address: Zenyaku Kogyo K. K., Oizumi-machi, Nerima-ku, Tokyo.

2) T. Nozoe, S. Seto, H. Takeda and K. Matsumoto, *Proc. Japan Acad.*, **27**, 566 (1951); W. von E. Doering and L. H. Knox, *J. Am. Chem. Soc.*, **73**, 828 (1951); J. Akroyd, R. D. Haworth and J. D. Hobson, *J. Chem. Soc.*, **1951**, 3427.

3) a) T. Nozoe, S. Seto, H. Takeda, S. Morosawa and K. Matsumoto, *Sci. Repts. Tohoku Univ, I*, **36**, 126 (1952). b) S. Ryu and T. Toda, *ibid.*, **51**, 105 (1968).

4) T. Nozoe, K. Takase and H. Matsumura, "Dai Yuki Kagaku" (Comprehensive Organic Chemistry), Vol 13, Asakura Shoten, Tokyo (1960).

5) T. Nozoe, S. Seto, S. Matsumura and T. Terasawa, *Chem. & Ind.*, **1954**, 1356; T. Nozoe, S. Seto and S. Nozoe, *Proc. Japan Acad.*, **32**, 472 (1956); S. Seto and S. Nozoe, *ibid.*, **32**, 756 (1956); S. Matsumura, This Bulletin, **34**, 1362 (1961); K. Ogura, H. Sasaki and S. Seto, *ibid.*, **38**, 306 (1965); T. Toda, S. Seto and T. Nozoe, *ibid.*, **41**, 2102 (1968); N. Soma and G. Sunagawa, *Yakugaku Zasshi (J. Pharm. Soc. Japan)*, **82**, 418 (1962); N. Soma *ibid.*, **82**, 892, 898 (1962).

6) T. Nozoe, S. Ryu and T. Toda, This Bulletin, **41**, 2978 (1968).

7) T. Toda, Y. Miura and T. Mukai, *Nippon Kagaku Zasshi (J. Chem. Soc. Japan, Pure Chem. Sect.)*, **89**, 804 (1968).

findings on the nucleophilic substitution reactions of I, II, III, and 2-troponyl trimethylammonium iodide (IV)[3a] and their alkyl derivatives; especially, the properties of these compounds in relation to nucleophiles will be compared with those of tropolones, tropolone methyl ethers, tropolone tosylates, and 2-halotropones.

I: R=NH_2 IV: R=$N(Me)_3^{\oplus}\cdot I^{\ominus}$
II: R=NHMe V: R=OH
III: R=$N(Me)_2$

It has been shown that I gives tropolone (V) by the action of aqueous alkali.[3c] II and III afforded V under the same reaction conditions; however, IV gave a rearrangement product, benzoic acid. Although the treatment of III and IV with hydrochloric acid in alcohol gave V in a good yield, the same treatment of I and II resulted in the recovery of the starting substances. The action of hydrogen chloride on I, II, and III in absolute dioxane gave the corresponding hydrochlorides; on the other hand, IV afforded 2-chlorotropone.[3a,8] When III was treated with sodium methoxide in methanol, V and its methyl ether were obtained in 74% and 25% yields respectively. The treatment of IV resulted in 59% methyl benzoate and 26% benzoic acid, but I and II were recovered unchanged under the same reaction conditions. I, II, and III are stable entities on heating. IV is recovered when heated in acetone, methanol, and ethanol for a short period; however, when it is heated in water or directly under reduced pressure, IV gives III, and methyl iodide is liberated. III was a detectable product only by the treatment of IV with silver oxide with heating; however, when IV was treated with silver oxide in ethanol, benzoic acid was obtained in a good yield.

I and II were recovered unchanged when treated with amines at room temperature or even when heated with aniline under reflux. On the other hand, III gave I, II, and 2-hydrazinotropone[3a] in good yields by treatment with ammonia, methylamine, and hydrazine respectively. IV also afforded I and II under the same conditions. The treatment of III with *p*-thiocresol, potassium cyanide, cupric cyanide, or potassium thiocyanate resulted in the recovery of the starting substance, while IV gave 2-(*p*-tolylthio)-tropone[8,9] with *p*-thiocresol and III with inorganic cyano compounds.

Generally, the reaction of tropolone methyl ethers with nucleophilic reagents gives normal substitution products.[4,10] On the other hand, the reaction of 2-halotropones and tropolone tosylates with nucleophiles affords abnormal substitution products.[4,10]

The reaction of 2-dimethylamino-4-isopropyltropone (VI)[11] and its methyl iodide (VII) with methylamine gave a normal substitution product, 2-methylamino-4-isopropyltropone, from the former, and an abnormal substitution product, 2-methylamino-5-isopropyltropone,[11] from the latter. Therefore, the reaction mode of 2-dimethylaminotropones is analogous to that of tropolone methyl ethers, and the reactions of their quaternary bases to nucleophilic reagents take place in abnormal ways, much as with 2-halotropones and tropolone tosylates.[12]

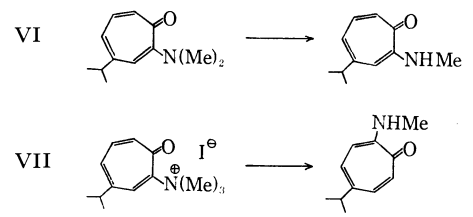

The Grignard reaction of tropolone methyl ethers gave 2-substituted tropone derivatives[13–15]; the reaction mechanism has been proved to proceed by way of 1,8-addition.[16]

The reactions of III with methylmagnesium bromide, phenylmagnesium bromide, and butyllithium afforded 2-methyltropone,[17] 2-phenyltropone,[13a,14] and 2-butyltropone[14] respectively in good yields. In order to clarify the mechanism of the above reaction, the reaction of VI with phenylmagnesium bromide was investigated and found to give 5-isopropyl-2-phenyltropone.[13,17] Therefore, the Grignard reaction of 2-dimethylaminotropone proceeds in the fashion of 1,8-addition, similar to that of tropolone methyl ethers.

8) a) B. A. Abadir, J. W. Cook, L D. Loudon and D. K. V. Steel, *J. Chem. Soc.*, **1952**, 2350. b) W. von E. Doering and L. H. Knox, *J. Am. Chem. Soc.*, **74**, 5683 (1952).

9) T. Nozoe, M. Sato and K. Matsuda, *Proc. Japan Acad.*, **28**, 407 (1952); *Nippon Kagaku Zasshi (J. Chem. Soc. Japan, Pure Chem. Sect.)*, **73**, 781 (1952).

10) Y. Kitahara, *Sci. Repts. Tohoku Univ., I*, **39**, 250 (1956).

11) T. Sato, *Nippon Kagaku Zasshi (J. Chem. Soc. Japan, Pure Chem. Sect.)*, **80**, 1056 (1959).

12) The reactions of deuterio derivatives of III and IV with several different kinds of nucleophiles were investigated by T. Kanno and S. Ito. The results obtained agreed with ours. The Master's thesis of T. Kanno, submitted to Tohoku University.

13) a) T. Nozoe, T. Mukai and J. Minegishi, *Proc. Japan Acad.*, **27**, 419 (1951). b) T. Nozoe, S. Seto, T. Ikemi, T. Sato and K. Watanabe, *ibid.*, **28**, 413 (1952).

14) W. von E. Doering and C.F. Hisky, *J. Am. Chem. Soc.*, **74**, 5688 (1952).

15) P. Akroyd, R. D. Haworth and P. R. Jefferies, *J. Chem. Soc.*, **1954**, 286.

16) R. D. Haworth and P. B. Tinker, *ibid.*, **1955**, 911.

17) T. Mukai, *Nippon Kagaku Zasshi (J. Chem. Soc. Japan, Pure Chem. Sect.)*, **79**, 1547 (1958).

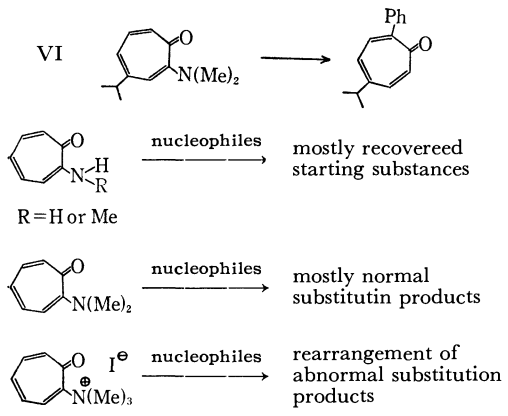

As has been shown above, 2-aminotropones and 2-methylaminotropones behave similar to tropolones[4] in both electrophilic[6] and nucleophilic substitution reactions. On the other hand, 2-dimethylaminotropones show different properties toward electrophiles compared with those of tropolone methyl ethers,[6] but they possess properties analogous with those of tropolone methyl ethers toward nucleophilic reagents. The properties of the quaternary bases of 2-dimethylaminotropones are similar to those of 2-halotropones and troplone tosylates.[4] The reason why alkaline hydrolyses are the only exchange reactions of the amino and methylamino groups of I and II with nucleophiles to take place is as follows: a hydrogen atom on the nitrogen in these compounds can be ionized, especially under the basic conditions, and the attack of nucleophiles on the formed aminotroponates is not easy, while the attacks of electrophiles on such entities occur readily.[6] A weak nucleophile such as the chloride anion can not be exchanged with amino groups of I, II, and III, even under acidic conditions. Only IV gives 2-chlorotropone, as has been mentioned above.

Experimental[18]

Base Hydrolyses. a) III (450 mg) was heated under reflux for 4 hr with 5 m*l* of 1.6N ethanolic potassium hydroxide. On the removal of the ethanol, a yellow crystalline mass was obtained; water was then added, and the solution was made slightly acidic (pH 6—6.5) with dilute hydrochloric acid and extracted with chloroform. On the evaporation of the solvent under reduced pressure, the residual oil crystallized in needles; it was recrystallized from petroleum ether - cyclohexane to give light yellow needles, mp 46—47°C (400 mg); undepressed when mixed with an authentic sample of tropolone.

b) From 450 mg of II, 400 mg of V were obtained by the same procedure.

c) VI was hydrolyzed as above to give light yellow plates, mp 49—50°C, which was identical with that of an authentic sample of hinokitiol. Yield, 150 mg from 200 mg of VI.

d) IV (600 mg) was refluxed for 3 hr on a water bath with 5 m*l* of 1.6N ethanolic potassium hydroxide. After the solution had been cooled, water was added; then the solution made weakly acidic with dilute hydrochloric acid and extracted several times with ether. An oily product solidified on the removal of the solvent, and recrystallization from benzene yielded white needles, mp 117—118°C (230 mg), which was undepressed on admixture with benzoic acid.

Acid Hydrolyses. a) I (243 mg) was heated under reflux with a mixture of 10% hydrochloric acid (5 m*l*), water (3 m*l*), and ethanol (5 m*l*) on a water bath for 6 hr. After the reaction mixture had cooled, it was made neutral and extracted with chloroform. The removal of the solvent and the recrystallization of the residue from cyclohexane yielded 220 mg of pale yellow needles, mp 105—106°C, identified as the recovered starting material from its IR and UV and by a mixed-melting-point determination with an authentic sample of I.

b) When the procedure described above was run using 270 mg of II, 250 mg of II, mp 76—77°C, were recovered.

c) When 300 mg of III were treated as above, 200 mg of V were obtained, mp 47—47.5°C. Its mixed melting point with an authentic sample of tropolone was undepressed.

The mother layer, after the separation of the tropolone, was made neutral with sodium bicarbonate, and extracted with chloroform, and the extract was dried over sodium sulfate. On the removal of the solvent, a brownish-yellow oily residue was obtained. Its IR and UV spectra were identical with those of III, and the oil gave a picrate, mp 144—146°C; yield, 75 mg.

d) When IV was treated as above, it gave tropolone; yield, 200 mg from 500 mg of IV.

Reactions with Anhydrous Hydrogen Chloride in Dioxane. a) I (365 mg) was dissolved in 5 m*l* of anhydrous dioxane in an ampoule through which dry hydrogen chloride was passed. The hydrogen chloride-saturated reaction mixture was then heated on a boiling-water bath for 3 hr. After the ampoule had been cooled, it was opened and the contents transferred to a small, round-bottomed flask. The removal of the solvent left white needles, mp 198—200°C; yield, 450 mg. IR: ν_{KBr} 3000—2400 cm^{-1} (broad, $\nu_{NH_3^+}$). This was dissolved in water, neutralized with aqueous sodium bicarbonate, extracted with benzene, and dried over sodium sulfate; the subsequent removal of the solvent gave a pale yellow solid. The recrystallization of the solid from cyclohexane-benzene afforded 320 mg of needles, mp 105—107°C, which had IR and UV spectra identical with those of an authentic specimen of 2-aminotropone.

b) When II (405 mg) was treated at above, a nearly quantitative yield of the hydrochloride (mp 250°C) was obtained as white needles. On the neutralization of the hydrochlorides, 350 mg of the starting substance (mp 74—76°C) were recovered.

c) From 450 mg of III, 530 mg of the hydrochloride (mp *ca.* 250°C) were obtained by the above procedure. On neuntralization with dilute sodium carbonate, followed by the usual working-up and alumina chromatography, 320 mg of III were regenerated.

18) All melting points are uncorrected.

d) IV (500 mg) was heated with 5 m*l* of hydrogen chloride-saturated dioxane in a sealed tube at 40—50°C for 4 hr. By the usual working-up and by purifying the reaction product through alumina chromatography, 200 mg of white needles were obtained, mp 59—60°C. This was found by a mixed-melting-point determination to be identical with and authentic sample of 2-chlorotropone.

Reactions with Sodium Methoxide. a) III (450 mg) was refluxed for 3 hr with a solution of sodium methoxide prepared by dissolving 90 mg of sodium in 5 m*l* of freshly-distilled absolute methanol, while moisture was carefully excluded. When the methanol was evaporated under reduced pressure, the reaction mixture partly solidified; it was washed three times with 2N potassium hydroxide and then extracted with benzene. The benzene layer was dried over sodium sulfate, and evaporated; the residue, on vacuum distillation, afforded a light yellow oil, 300 mg, whose IR spectrum was identical with that of 2-methoxytropone. From the product, a picrate, mp 115—117°C, was prepared in the usual way; its melting point was undepressed on admixture with an authentic sample of 2-methoxytropone picrate.

The water layer obtained in the alkaline washings described above was acidified, extracted with chloroform, dried, and evaporated to dryness. The residue crystallized from cyclohexane-light petroleum gave light yellow needles, mp 48—49°C, identified as tropolone by a mixed-melting-point determination.

b) I and II were treated by the procedure described above. The starting substances were recovered unchanged in nearly quantitative yields in both cases.

c) Metallic sodium (110 mg) was dissolved in 5 m*l* of absolute methanol, and to the resulting solution IV (600 mg) was added. The reaction mixture was allowed to stand at room temperature for 2 hr, and then refluxed on a water bath for one hour. The methanol was removed under reduced pressure, and to the residue water was added; the solution was washed three times with 2N potassium hydroxide to remove free benzoic acid, and it was extracted with benzene. The benzene layer was dried, and evaporated, and the residual oil was purified by vacuum distillation to afford a colorless oil (160 mg) which was found by a comparison of their IR spectra to be identical with an authentic sample of methyl benzoate.

From the water layer, benzoic acid was obtained (65 mg) following the same procedure after acidification with dilute hydrochloric acid and subsequent extraction with ether. The identification was made by a mixed-melting-point determination with an authentic sample.

Reactions with Amines and Hydrazine Hydrate. *2-Aminotropone.* a) III (450 mg) was allowed to react with an excess of liquid ammonia in a sealed tube at room temperature for 6 days. The removal of the excess ammonia and the liberated dimethylamine left a solid residue which was then recrystallized from cyclohexane-benzene to give 350 mg of pale yellow needles, mp 105—106°C; this substance was identified as I by a study of its IR spectrum and by a mixed-melting-point test with an authentic sample.

b) IV was treated as above to give 300 mg of I from 600 mg of IV.

c) II was treated in the same manner, but the starting substance was recovered quantitatively.

2-Methylaminotropone. a) III was allowed to react with a large excess of liquid methylamine in a sealed tube at room temperature for 6 days. The recryltallization of the solid residue obtained after the removal of the amine afforded yellow needles, mp 78—79°C, identified as 2-methylaminotropone; yield, 290 mg from 450 mg of III.

b) The treatment of IV (600 mg) with an excess of liquid methylamine yielded 350 mg of II.

c) I was recovered quantitatively when treated as above,

4-Isopropyl-2-methylaminotropone VI (200 mg) was allowed to react with liquid methylamine in a sealed tube for 4 days at room temperature. On the removal of the excess amine, the reaction mixture solidified; it was recrystallized from petroleum ether to give yellow crystals, mp 83—84°C (180 mg), undepressed on admixture with an authentic sample of 4-isopropyl-2-methylaminotropone.[19]

5-Isopropyl-2-methylaminotropone. VII (350 mg) was treated as above with liquid methylamine. After the excess amine had been removed, the product was dissolved in benzene and chromatographed on alumina. The benzene effluent gave a picrate in the usual way; the mp 208—210°C from ethanol did not show any depression on admixture with the authentic picrate of 5-isopropyl-2-methylaminotropone.

2-Hydrazinotropone. a) III (450 mg) was dissolved in 10 m*l* of ethanol, and to the resulting solution there were added 250 mg of 80% hydrazine hydrate. The reaction mixture was then refluxed on a water bath for 40 min, The evaporation of the solvent left a crystalline residue which was recrystallized from cyclohexane to give 400 mg of 2-hydrazinotropone, mp 94—95°C. The identification was made by study of its IR spectrum and by a mixed-melting-point determination with an authentic sample of 2-hydrazinotropone.

b) IV (600 mg) was treated with 170 mg of 80% of hydrazine hydrate in 10 m*l* of ethanol as above to gave 135 mg of 2-hydrazinotropone.

c) When I and II were treated under the same reaction conditions as above, the starting sudstances were recovered quantitatively.

Attempted Reaction of I and II with Aniline. a) A mixture of 365 mg of I and 5 m*l* of aniline was heated to reflux on an oil bath at 200°C for 3 days. The aniline was then expelled under reduced pressure, and the the black resinous residue was subjected to vacuum (0,1 mmHg) sublimation to give brownish-yellow prisms, mp 103—105°C. The crude crystals were further recrystallized from cyclohexane-benzene to afford 330 mg of recovered I, which was confirmed by a mixed-melting-point determination with an authentic sample of I.

d) The attempted reaction of II with aniline under the conditions described above gave rise to only the recovery of the starting materials unchanged.

Reaction with *p*-Thiocresol. a) IV (600 mg) and *p*-thiocresol (300 mg) were added to an ethanolic solution of sodium ethoxide prepared by dissolving metallic sodium (46 mg) in 10 m*l* of absolute ethanol. The reaction mixture was then refluxed, while all

19) Unpublished, prepared in the authors' laboratory.

moisture was excluded, on a water bath for 2 hr. After the solvent had been removed, the residual solid mass was recrystallized from cyclohexane to afford yellow crystals, mp 144—145°C (450 mg), identified as 2-(*p*-tolylthio)-tropone by a study of the IR spectrum and by a mixed-melting-point determination with an authentic sample.

b) When II was treated with a 1-equivalent mole of *p*-thiocresol and with 2-equivalent moles of sodium ethoxide under the same conditions, the starting substances were recovered in *ca.* a 90% yield.

Reaction with Silver Oxide. Silver nitrate (500 mg) was dissolved in 5 m*l* of water. To the resulting solution there was added a 1N sodium hydroxide solution until no more precipitation occurred. The grayish-brown precipitate was washed thoroughly until neutral to pH test paper and then used directly in the subsequent step.

To a stirred solution of IV (290 mg) in 50% aqueous ethanol, the moist silver oxide prepared above was added, portion by portion, at room temperature. Immediately after the addition of the reagent, a conspicuous evolution of trimethylamine was observed; it was detected from its odor, the alkaline reaction to pH test paper, and a picrate formation; mp 214—216°C.

The reaction mixture exhibited an alkalinity at pH *ca.* 8.5 (pH test paper) because of the dissolved trimethylamine. The reaction mixture, after having been stirred for 15 min at room temperature, was made acidic (pH *ca.* 4) and extracted with ether (20 m*l* ×4). The removal of the solvent and recrystallization from benzene afforded 110 mg of needles, mp 120—121.5°C, undepressed in a mixed-melting-point test with authentic benzoic acid.

b) When IV was reacted with dry silver oxide in xylene at 150°C for 5 hr and then worked-up as usual, *ca.* 90% of III was obtained.

Reaction with Organometallic Compounds. a) To a stirred solution of phenylmagnesium bromide prepared from bromobenzene (3.4 g) and magnesium ribbons (525 mg) in 50 m*l* of anhydrous ether under a nitrogen stream, there was added, drop by drop, a solution of III (1.0 g) in 30 m*l* of anhydrous ether; the reaction mixture was then heated under reflux for one hour. Upon the addition of the reactant, a solid yellowish mass attached to the wall of the vessel gradually turned grey white. After refluxing, 50 m*l* of a 40% ammonium chloride solution was added. The ether layer was separated, and the water layer was extracted several times with ether; then the combined organic layer was washed with water, dried over sodium sulfate, and evaporated under reduced pressure. The residue which solidified on cooling was purified through vacuum sublimation and then recrystallized from cyclohexane to give 1.05 g of needles (mp 84°C, which did not show any depression on admixture with authentic 2-phenyltropone).

b) An ethereal solution of III (1.0 g) was added to a stirred solution of methylmagnesium iodide, and then reacted as above. The residual oil, on vacuum distillation, gave 860 mg of a light yellow oil which was identified as 2-methyl tropone by a comparison of its IR spectrum with that of an authentic specimen.

c) III (500 mg) was dissoved in 100 m*l* of dry ether, and into the resulting solution there was vigorously stirred, drop by drop and in a nitrogen atmoshpere, an ethereal solution containing 7 m*l* of 1.8 mol *n*-butyllithium (supplied by Japan Chem. Industry K. K.). The reaction mixture was subjected to gentle reflux for 1.5 hr and then decomposed with dilute hydrochloric acid; the product was taken up in ether and dried. After the removal of the solvent, the residual oil was purified through vacuum distillation to give 500 mg of oil identified as 2-*n*-butyltropone by a comparison of its IR spectrum with that of an authentic specimen prepared by the reaction of 2-methoxytropone with *n*-butyllithium.[14]

d) VI (500 mg) was allowed to react with phenylmagnesium bromide prepared from magnesium ribbons (250 mg) and bromobenzene (1.57 g) in an ethereal solution with stirring for 2 hr under a nitrogen stream. After the usual working-up, the oily product thus obtained was chromatographed on alumina, and from the cyclohexane effluent, on the removal of the solvent, there were obtained pale yellow plates (mp 86—88°C, undepressed on admixture with an authentic sample of 5-isopropyl-2-phenyltropone).

Reaction with Potassium Thiocyanate. IV was dissolved in dimethylformamide, and to the resulting solution 2 equimoles of potassium thiocyanate were added. The reaction mixture was then refluxed for 3 hr and the excess solvent was removed under reduced pressure. After the usual working up, the residual oil was distilled under reduced pressure to give 89% of III, identified by a comparison of its IR spectrum with that of an authentic sample.

When potassium cyanide or cupric cyanide were used instead of potassium thiocyanate, almost the same results were obtained.

The treatment of III with these cyanides under the same conditions resulted in the recovery of the starting substances.

BULLETIN OF THE CHEMICAL SOCIETY OF JAPAN VOL. 42 2033—2037 (1969)

A Study of Valence Tautomerism of Cycloheptatriene-Norcaradiene

Teruji TSUJI, Shuji TERATAKE and Hiroshi TANIDA

Shionogi Research Laboratory, Shionogi & Co., Ltd., Fukushima-ku, Osaka

(Received January 22, 1969)

Rates of the Diels-Alder reaction of cycloheptatriene, tricyclo[4.3.1.0]deca-2,4-diene, 1,3-cyclohexadiene, and *cis*-bicyclo[4.3.0]nona-2,4-diene with excess of fumaryl chloride were measured using a dilatometer. Comparison of the rate of cycloheptatriene with that of other olefins raises the question of the free energy difference so far estimated between cycloheptatriene and norcaradiene, which has been proposed to exist in equilibrium. It is suggested that the most preferable mechanism of the Diels-Alder reaction of cycloheptatriene is not through the norcaradiene isomer, but through the transition state of the norcaradiene structure.

The valence tautomerism of unsaturated medium ring systems is of current interest,[1] and recent studies have indicated that cyclooctatetraene,[2] cyclooctatriene[2,3] and oxepine[4] are in equilibrium with their tautomeric isomers, bicyclo[4.2.0]octa-2,4,7-triene, bicyclo[4.2.0]octa-2,4-diene, and benzene oxide, respectively. In this kind of study for cyclooctatriene, the major technique was a kinetic study of the Diels-Alder reaction.[2] Regarding tropilidene, the spectroscopic studies have indicated that the principal species is 1,3,5-cycloheptatriene, whereas the product studies of the chemical reactions have suggested that norcaradiene is the reacting species.[5] The reaction of tropilidene with dienophile yields tricyclic products containing a cyclopropane ring formally derived from norcaradiene,[6] and the thermal isomerization of tropilidene gave toluene formed, presumably, by cleavage of the three-membered ring of norcaradiene.[7] For about twenty years, the chemistry of tropilidene and related compounds has been actively carried out in Japan.

These circumstances prompted us to carry out a kinetic study of the Diels-Alder reaction of tropilidene with fumaryl chloride[6a] in the hope that the norcaradiene isomer hypothetically existing in equilibrium with cycloheptatriene could be demonstrated.[8]

Kinetic Problem.

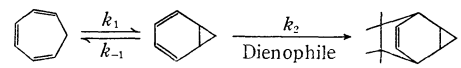

A B D C

If we assume an equilibrium ($K=k_1/k_{-1}$) between cycloheptatriene (A) and norcaradiene (B), followed by the Diels-Alder addition of B to a dienophile (D), that is a two-step mechanism, the rate of the adduct (C) formation, d[C]/dt, is denoted by k_2-[B][D]. Setting d[B]/dt=0 from steady state approximation, we have

$$d[B]/dt = k_1[A] - k_{-1}[B] - k_2[B][D] = 0$$

$$[B] = k_1[A]/(k_{-1}+k_2[D])$$

$$d[C]/dt = k_2[B][D] = k_1k_2[A][D]/(k_{-1}+k_2[D]) \quad (1)$$

Under the condition that the concentration of D is much larger than that of A, the concentration of D is constant throughout the reaction period.

$$k_1k_2[D]/(k_{-1}+k_2[D]) = k_c \quad (2)$$

k_c is the pseudo-first order rate constant varying with [D], and one can get the following equation.

$$d[C]/dt = k_c[A]$$

1) As recent reviews, a) E. Vogel, *Angew. Chem.*, **74**, 829 (1962); b) S. J. Rhoad, "Molecular Rearrangements," Vol, 1, ed. by P. de Mayo, John Wiley & Sons, New York, N. Y. (1963), p. 655.

2) R. Huisgen, F. Mietzsch, G. Boche and H. Seidl, "Organic Reaction Mechanisms," The Chemical Society, London (1965), p. 3.

3) a) A. C. Cope, A. C. Haven, F. L. Ramp and E. R. Trumbull, *J. Am. Chem. Soc.*, **74**, 4867 (1952); b) D. S. Glass, J. Zirner and S. Winstein, *Proc. Chem. Soc.*, **1963**, 276.

4) E. Vogel and H. Günther, *Angew. Chem. Internat. Edit.*, **6**, 385 (1967).

5) G. Maier, *ibid.*, **6**, 402 (1967); references cited therein.

6) a) K. Alder and G. Jacobs, *Chem. Ber.*, **86**, 1528 (1953); b) K. Alder, K. Kaiser and M. Schumacher, *Ann.*, **602**, 80 (1957); c) K. Alder, H. Jungen and K. Rust, *ibid.*, **602**, 94 (1957).

7) a) K. N. Klump and J. P. Chesick, *J. Am. Chem. Soc.*, **85**, 130 (1963); b) W. G. Woods, *J. Org. Chem.*, **23**, 110 (1958).

8) Interest in the kinetic studies of the Diels-Alder reactions was stimulated by the lecture given by Professor R. Huisgen at the Shionogi Research Laboratory in March 1962, and personal discussions one of the authors had with him later in October 1967. Our thanks are due to Professor Huisgen.

According to the magnitude of k_1,k_{-1} and k_2, the situation is further divided into three cases.

(a) $k_2[D] \ll k_1$ and k_{-1}. The slow combination of B with D compared to the rapid equilibrium is rate-determining. From Eqs. (1) and (2) we have $d[C]/dt = (k_1/k_{-1})k_2[A][D]$ and $k_c = (k_1/k_{-1})k_2[D]$.

(b) $k_2[D] \gg k_1$ and k_{-1}. The first equilibrium step becomes the rate-determining step. $d[C]/dt = k_1[A]$ and $k_c = k_1$.

(c) $k_2[D] \approx k_1$ and k_{-1}. This case corresponds to that between the two limiting cases (a) and(b), and both steps are effective on rate-determination. The relation is represented by Eqs. (1) and (2).

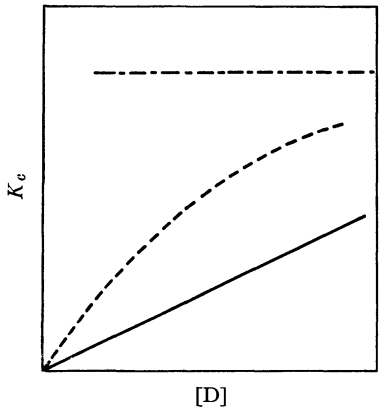

Fig. 1. Correlation of K_c and $[D]$.
—— Case (a) and (d)
---- Case (c)
———— Case (b)

Plotting k_c against the varying amounts of D, as shown in Fig. 1, provides, for the case (a), a straight line through the origin having a slope of $(k_1/k_{-1})k_2$, for (b), a straight line parallel to the abscissa corresponding to $k_c = k_1$, and for (c), a curve through the origin.

The case (d): if the Diels-Alder reaction proceeds without intervention of B and produces C with the second order rate constant of k_2', we have

$$d[C]/dt = k_2'[A][D]$$

When the concentration of D is much larger than that of C, we have $d[C]/dt = k_c'[A]$ where $k_c' = k_2'[D]$. This relation should be the same as the case (a).

Results

The kinetic studies were performed under such conditions that the concentration of fumaryl chloride[9] varied from ten to thirty times the concentration of cycloheptatriene. The rate was followed dilatometrically in dioxane by measuring the reduction in the total reaction volume due to the union of the two molecules to one.[10] A decrease of the meniscus height in the graduated capillary against the reaction time satisfied the correlation of the pseudo-first-order up to about three half-lives. As an example, rate constants, k_{obs} at 55.01°C, varying the concentration of fumaryl chloride are shown in Table 1.

Table 1. The Diels-Alder reaction of cycloheptatriene with fumaryl chloride

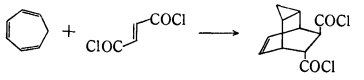

A D

$[A]\times10^2$ mol/l	[D] mol/l	[D]/[A]	K_{obs}· sec^{-1}
6.01	0.63	10.4	5.54×10^{-5}
6.01	1.20	20.0	1.16×10^{-4}
6.01	1.51	25.0	1.44×10^{-4}
6.01	1.79	29.8	1.84×10^{-4}

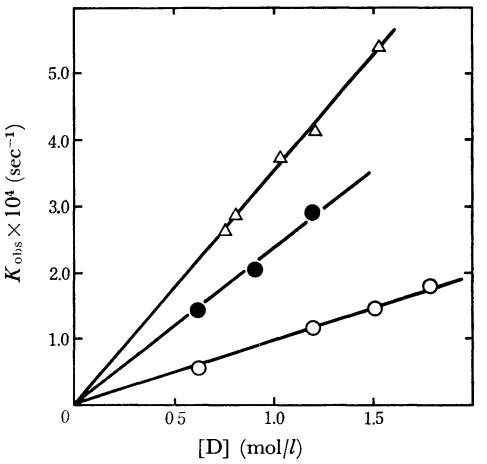

Fig. 2. Correlation of kobs and [D] at three temperatures.
○ 55.01°C ● 72.47°C △ 79.98°C

Plotting k_{obs} against increasing concentrations of fumaryl chloride at 55.01°C, 72.47°C and 79.98°C, yielded straight lines, as shown in Fig. 2. These linearities correspond either to the case (a) $k[D] \ll k_1$ and k_{-1} involving the intermediate (B), or the case (d) which is not through B. Similar lines were also obtained from the reaction with a more reactive dienophile, tetracyanoethylene.

Slopes of the straight lines represent the values of $(k_1/k_{-1})k_2$ or k_2' at the respective temperatures.

9) Fumaryl chloride is a very reactive dienophile. Its addition to cyclopentadiene proceeds (at 20°C in dioxane) 100 times more rapidly than the addition of maleic anhydride to the same diene. J. Sauer, H. Wiest and A. Mielert, *Chem. Ber.*, **97**, 3183 (1964).

10) R. Huisgen in "Methoden der Organischen Chemie," Vol. III, Part I, ed. by E. Muller, Georg Thieme Verlag, Stuttgart (1955), p. 120.

Table 2. Rates of the Diels-Alder reaction of cycloheptatriene with fumaryl chloride

Temp. °C	$(k_1/k_{-1})k_2$ or k_2' (l/mol·sec)	Calculated at 15°C: $\Delta H^{\neq}$ (kcal/mol)	$\Delta S^{\neq}$ (cal/deg)	$(k_1/k_{-1})k_2$ or k_2' (l/mol·sec)
55.01	1.08×10^{-4}			
72.47	2.50×10^{-4}	10.8	−44	9.7×10^{-6} a)
79.98	3.69×10^{-4}			

a) Calculated from the observed rates using the least square method.

Table 2 shows their values and the value extrapolated to 15°C by use of the Arrhenius equation.

If the Diels-Alder reaction of cycloheptatriene proceeds through an equilibrium with B, since $(k_1/k_{-1})k_2$ is now known, evaluation of k_2 leads to a determination of the equilibrium constant (k_1/k_{-1}). We wanted to evaluate k_2 from the Diels-Alder reactions of some compounds, which are structually related to norcaradiene, with fumaryl chloride. The compounds chosen were tricyclo[4.3.1.0]deca-2,4-diene (E),[11] 1,3-cyclohexadiene (F), *cis*-bicyclo-[4.3.0]nona-2,4-diene (G), and bicyclo[4.2.0]octa-2,4-diene (H), in which E has the norcaradiene structure fixed by an additional five-membered ring.

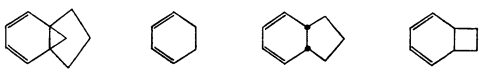

E F G H

G was prepared by us according to the schema shown below, although it had been synthesized by Alder through a different route.[12]

Under the conditions of the pseudo-first-order with excess of fumaryl chloride, the addition rates of the dienes were determined in the same way as above and summarized in Table 3.

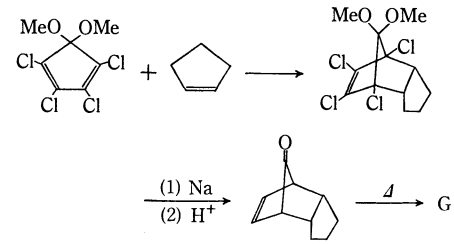

Discussion

If the cycloheptatriene-norcaradiene pre-equilibrium exists, the overall rate of the adduct formation from cycloheptatriene is shown as $(k_1/k_{-1})k_2=9.7\times10^{-6}$ l/mol·sec at 15°C. The second-order rate constants, k_E, k_F, k_G and k_H, obtained from E, F, G and H, respectively, are given in Table 4. Here, k_H was estimated on the fact that the addition of H to maleic anhydride is thirty times faster than that of cycloheptadiene (F) in dioxane at 30°C (by Huisgen[2] and Sauer[13]).

Table 4. Assumed equilibrium between cycloheptatriene and norcaradiene[a]

Compd.	k_2 (l/mol·sec)[b]	k_1/k_{-1}[c]	Norcaradiene at equilibrium (%)
E	1.2×10^{-5}	0.8	45
F	4.7×10^{-4}	2×10^{-2}	2
G	9.5×10^{-3}	10^{-3}	0.1
H	1.4×10^{-2}	7×10^{-4}	0.07

a) At 15°C.
b) Rate of the Diels-Alder reaction of the dienes with fumaryl chloride at 15°C (Table 3).
c) Calculated from the equation $(k_1/k_1)k_2=9.7\times10^{-6}$ l/mol·sec.

Table 3. Rates of the Diels-Alder reaction of various dienes with fumaryl chloride

Compd.	Temp. °C	K (l/mol·sec)	Calculated at 15°C: $\Delta H^{\neq}$ (kcal/mol)	$\Delta S^{\neq}$ (cal/deg)	K (l/mol·sec)
E	45.00	8.24×10^{-4} a)	11.0	−43	1.2×10^{-5} a,d)
	32.60	3.98×10^{-4} a)			
	19.97	1.77×10^{-4} a)			
F	25.42	9.62×10^{-4} b)	11.2	−35	4.7×10^{-4} b,d)
	15.00	4.48×10^{-4} b)			
	15.02	4.97×10^{-4} b)			
G	15.00	9.50×10^{-3} c)			9.5×10^{-4} c)

a) K_E. b) K_F. c) K_G.
d) Calculated from the observed rates using the least square method.

11) E. Vogel, W. Wiedemann, H. Kiefer and V. F. Harrison, *Tetrahedron Letters*, **1963**, 673.
12) K. Alder and H. A. Dortmann, *Chem. Ber.*, **87**, 1905 (1954).
13) J. Sauer, D. Lang and A. Mielert, *Angew. Chem. Internat. Ed.*, **5**, 211 (1966).

Replacement of k_2 by these second-order constants yields various estimations of k_1/k_{-1}, from which the equilibrium concentrations of norcaradiene are derived as 45, 2, 0.1 and 0.07% (Table 4). However, the former two values could be eliminated, because they are very unreasonable on the basis of the spectral properties of tropilidene reported.[5] Appropriate adoptions of the latter two values lead to the free energy differences of 4.0 and 4.5 kcal/mol respectively, existing between cycloheptatriene and norcaradiene.

On the other hand, the free energy difference of 11 ± 4 kcal has been proposed[14] basically from the table of bond-energy[15] and some discussions using this value have appeared frequently in literatures.[16] The value of 11 ± 4 kcal/mol corresponds to k_1/k_{-1} of 5×10^{-6}—4×10^{-12}. Thus, introduction of this k_1/k_{-1} value into the equation, $(k_1/k_{-1})k_2 = 9.7\times10^{-6}$ l/mol·sec, yields k_2 of 2—2×10^6 l/mol·sec as the addition rate of norcaradiene to fumaryl chloride at 15°C, which turns out to be an astonishingly large value referring to the second-order rate constants of E, F, G and H. Even the lowest value, 2 l/mol·sec, which corresponds to the free energy difference of 7 kcal/mol, is close to the rate of highly reactive cyclopentadiene with fumaryl chloride at 20°C in dioxane.[9] These lead to two alternative views; (i) the rate of the Diels-Alder reaction of norcaradiene is abnormally larger than we would expect on the basis of present organic theories, or (ii) the estimated value of 11 ± 4 kcal/mol is unreasonably large.

By comparison of the rate of G with that of F (Table 3), it might be considered that a fused five-membered ring accelerates the Diels-Alder reaction by a factor of twenty. If view (i) is taken, it is reasonable to regard that Vogel's compound (E) fusing a five-membered ring to the norcaradiene structure has also a great reactivity in the Diels-Alder reaction. However, it is found that E is less reactive by a factor of forty than F. Although there was no evidence that the reactivity of E should be compatible with that of norcaradiene, these discrepancies throw a serious doubt upon the free energy difference of 11 ± 4 kcal/mol.

Consequently, three basic limiting cases are derived for the relationship between cycloheptatriene and norcaradiene. (1) The free energy difference between both structures is much smaller than the previously proposed value of 11 ± 4 kcal/mol. (2) The difference of 11 ± 4 kcal/mol exists and then the addition rate of norcaradiene is abnormally great by presently unknown factors. (3) The Diels-Alder reaction of cycloheptatriene does not proceed through norcaradiene which has been proposed to exist in the ground state, but takes the norcaradiene structure in the transition state, pictured as

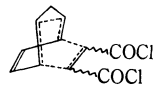

Although available data are insufficient to obtain a conclusion on the above alternatives, we prefer the possibility of (3) that transition into norcaradiene takes place only under the influence of the attacking agent.

Experimental

All melting points were corrected. Infrared spectra were recorded on a Nippon Bunko IR-S spectrometer. NMR spectra were determined at 60 Mc with a Varian A-60 Spectrometer using tetramethylsilane as an internal standard.

Materials and Apparatus. The cycloheptatriene used in this work was Shell chemical material which was obtained in a purity better than 95% by distillation (bp 114—115°C). Tricyclo[4.3.1.0]deca-2,4-diene (E), bp 71—73°C/15 mmHg, n_D^{24} 1.5248 (lit.[11] bp 61—62°C/11 mmHg, n_D^{20} 1.5267) was prepared by the procedure of Vogel. 1,3-Cyclohexadiene (F) (bp 79—80°C) was supplied by Dr. T. Nakata.[17] Dioxane was purified by the procedure of Hess and Frahm.[18]

The dilatometer used, whose desigh is explained in Ref. 10, is equipped with a reaction vessel of about 20 cc and a graduated capillary of inner-diameter of 0.5 mm. Thermostat was maintained in a range of ±0.01°C at the indicated temperatures.

Typical Rate Determination. The sample of 1.385 g of cycloheptatriene was weighed in a 20 ml volumetric flask and filled to 20 ml with dioxane. Fumaryl chloride (4.590 g) was accurately weighed in a 25 ml volumetric flask, to which *ca.* 20 ml of dioxane and an aliquot of 2 ml from the dioxane solution of cycloheptatriene previously prepared was added. The mixed solution was kept in thermostat at 55.01°C for a short time and filled to 25 ml with dioxane, so that the concentrations of cycloheptatriene and fumaryl chloride were 0.0601 and 1.200 mol/l. After cooling, the resulting solution was transferred into the dilatometer, whose meniscus in the capillary was adjusted to the desired height when the thermostat attained the reaction temperature. Then reading of the meniscus height was started and continued until ten-half lives. The difference in the meniscus height from start to ten-half lives was 6.67 cm.

Addition of Tetrachlorocyclopentadienone Dimethyl Ketal to Cyclopentene. A mixed solution of 10 g of cyclopentene and 41.7 g of tetrachlorocyclopen-

14) W. von E. Doering and M. R. Willcott, III, unpublished; M. R. Willcott, III, Ph. D. Dissertation, Yale University, 1963.

15) J. L. Franklin, *Ind. Eng. Chem.*, **41**, 1070 (1949).

16) a) J. A. Berson and M. R. Willcott, III, *J. Am. Chem. Soc.*, **88**, 2494 (1966); b) G. D. Sargent, N. Lowrry and S. D. Reich, *ibid.*, **89**, 5985 (1967).

17) T. Nakata and N. Choumei, *J. Macromol. Sci-Chem.*, **A1(8)**, 1433 (1967).

18) K. Hess and H. Frahm, *Ber.*, **71B**, 2627 (1938).

tadienone dimethyl ketal was sealed in a glass tube and heated to 170°C for 18 hr. After cooling, the solid residue was chromatographed on 100 g of standard Merck alumina with petroleum ether (bp 40—50°C) to exclude dark brown impurity. The eluent was concentrated. The residue solidified was recrystallized from petroleum ether to give 40.1 g (82.3% based on cyclopentene) of *endo*-1,7,8,9-tetrachlorotricyclo[5.2.1.$0^{2,6}$]deca-8-en-10-one dimethyl ketal, mp 83.5—84.5°C. NMR (CCl_4) at τ 6.44 and 6.52 (two methoxyls, 6H, singlet), 7.0 (two methines, 2H, multiplet) and 7.57 (three methylenes, 6H, multiplet). Found: C, 43.69; H, 4.27%. Calcd for $C_{12}H_{14}Cl_4O$: C, 43.41; H, 4.25%.

***endo*-Tricyclo[5.2.1.$0^{2,6}$]deca-8-en-10-one.** A solution of 33.2 g of the above adduct in 600 m*l* of tetrahydrofuran and 96.5 g of *t*-butyl alcohol was efficiently stirred at reflux temperature under nitrogen atmosphere. Sodium chip (57.5 g) was cautiously added for over one hour to the reaction mixture followed by stirring for an additional 5 hr. After cooling, the remaining sodium was decomposed with cold methanol and then with a large amount of cold water. The solution was extracted with ether, dried over sodium sulfate, and evaporated to yield 19.0 g of an oily residue, which was distilled at 98—103°C /8 mmHg to give 14.0 g of the dechlorinated ketal.

The ketal was dissolved in 30 m*l* of methanol and 50 m*l* of 70% aqueous acetic acid, and warmed to 80°C under stirring for 3.5 hr. The reaction mixture was poured into cold water and made alkaline with sodium hydroxide. After extraction with ether, evaporation gave 9.8 g of a solid residue, which was recrystallized from petroleum ether to give 8.5 g (57.5%) of white needles, mp 61.5—63.0°C (in sealed tube). NMR (CCl_4) at τ 3.62 (vinyl, 2H, triplet), 7.1 (two methines, 2H, at carbon 1.7, quintet), 6.58 (two methines at carbon 2.6, multiplet), and 8.0—9.2 (three methylenes, 6H, multiplet). IR $\nu_{max}^{CCl_4}$ 2985, 2940, 2858, 2866, and 1782 cm^{-1}. Found: C, 81.29; H, 8.20%. Calcd for $C_{10}H_{12}O$: C, 81.04; H, 8.16%.

***cis*-Bicyclo[4.3.0]nona-2,4-diene (G).** The ketone was vaporized at 120—130°C and reduced pressure (35 mmHg) in a stream of nitrogen introduced by means of a fine capillary tube. The vapor passed through a 30 cm section of 4 mm (diameter) tubing packed with glass grain of 30—40 mesh and maintained at 250—300°C by means of an externally heated coil of nichrome wire. The products were trapped at dry ice-acetone temperature. The crude pyrolysate was distilled at 101—102°C/123 mmHg to yield 4.5 g (79.2%) of the decarboxylated diene, n_D^{25} 1.5052. NMR (CCl_4) at τ 4.42 (vinyl, 4H, multiplet), 7.4 (two methines, 2H, multiplet) and 8.0—8.8 (three methylenes, 6H, multiplet). UV: $\lambda_{max}^{n\text{-heptane}}$ 260 mμ (ε 4200), IR $\nu_{max}^{CCl_4}$ 3030, 2942, 2868, 1640, 1585, 1449 and 690 cm^{-1}. Found: C, 89.95; H, 10.07%. Calcd for C_9H_{12}: C, 89.94; H, 10.06%.

NOTES

BULLETIN OF THE CHEMICAL SOCIETY OF JAPAN VOL. 42 2038—2040 (1969)

Kinetics of the Oxidation of Benzyl Alcohol by Acid Permanganate

K. K. BANERJI and P. NATH

Department of Chemistry, University of Jodhpur, Jodhpur, India

(Received January 29, 1968)

The observed kinetic isotope effect[1] in the oxidation of cyclohexanol by acid permanganate has indicated that probably oxidation involves a hydride ion transfer from alcohol to the oxidant. Recently Barter and Littler[2] suggested that oxidation of alcohols and ethers involves transfer of a hydride ion from the carbon atom carrying the functional group to the oxidant. Littler[1] indicated permanganic acid as the important oxidising species, however, Banerjee and SenGupta[3] have postulated manganese(III) as the active species in the acid permanganate oxidation of methanol and ethanol. No information is available on the acid permanganate oxidation of benzyl alcohol except a preliminary work reported by Cullis and Ladbury.[4] It was, therefore, considered fruitful to investigate the kinetics of the oxidation of benzyl alcohol by acid permanganate.

Experimental

Materials. Perchloric acid (60% E. Merck) was used as a source of hydrogen ions; sodium perchlorate (Reidel) was used to adjust ionic strength; permanganate solutions were prepared by dissolving 'AnalaR' potassium permanganate and acetic acid (99.5% B.D.H.) was used for preparing the solvent mixture. Benzyl alcohol (B.D.H.) was purified by fractionation. All other chemicals used were chemically pure.

Kinetic Measurement. The reactions were studied at constant temperature (±0.02°C). Unless otherwise stated, the solvent was 20% acetic acid. The concentration of benzyl alcohol was kept in excess to that of $KMnO_4$. Reaction mixtures containing requisite amounts of perchloric acid, acetic acid and benzyl alcohol were placed in thermostat for sufficient time. Reactions were started by adding permanganate solution rapidly through a pipette. Aliquots were withdrawn at known intervals of time and concentration of permanganate was estimated iodometrically.

Results

Product Study. Oxidation of benzyl alcohol by acid permanganate gives benzaldehyde as the main product. The amount of benzaldehyde formed was estimated by gravimetric method as 2,4-dinitrophenylhydrazone.[5] The recovery of benzaldehyde is about 85% based on the following reaction:

$$2MnO_4^- + 5C_6H_5CH_2OH + 6H^+ \rightarrow 2Mn^{2+} + 5C_6H_5CHO + 8H_2O$$

This shows that the further oxidation of benzaldehyde is not significant under the conditions

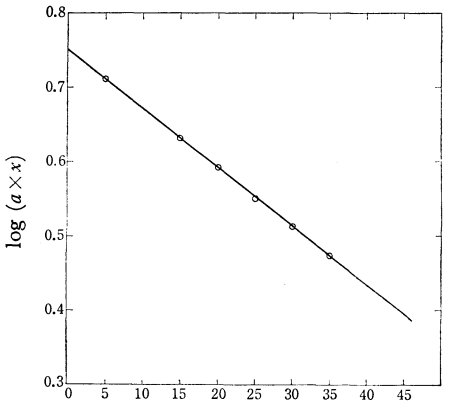

Fig. 1. Typical run.
[$PhCH_2OH$]: 2.0×10^{-3}M, [MnO_4^-]: 4.0×10^{-4}M, [H^+]: 0.61M, Temp. : 35°C, K_1 : $18.4\times10^{-3}min^{-1}$

1) J. S. Littler, *J. Chem. Soc.*, **1962**, 2190.
2) R. N. Barter and J. S. Littler, *J. Chem. Soc.*, (*B*), **1967**, 205.
3) J. Banerjee and K. K. SenGupta, *Curr. Sci.* (*India*), **34**, 14 (1965).
4) C. F. Cullis and J. W. Ladbury, *J. Chem. Soc.*, **1955**, 555.
5) J. Mitchell, Jr., "Organic Analysis," Vol. I Interscience Publishers, Inc., New York (1953), p. 279.

of the reaction.

Rate Laws. When benzyl alcohol and hydrogen ions are in excess the rate at which permanganate disappears follows the first order rate law. A typical kinetic run is illustrated in Fig. 1. In all cases the values of first order constants were determined graphically, for first 30—40 percent of the reaction.

Further the value of first order rate constant does not vary with the initial concentration of permanganate (Table 1).

Table 1. Variation of rate with concentration of manganese(VII)

$[PhCH_2OH]$: 2.0×10^{-3}M; $[H^+]$: 0.61M; Temp. 35°C					
$[MnO_4^-]\times10^4$ mol l^{-1}	4.0	6.0	8.0	10.0	12.0
$k_1\times10^3$ min^{-1}	18.4	18.4	18.6	17.3	18.0

Thus the order with respect to manganese (VII) is one.

The reaction is also of first order with respect to benzyl alcohol (Table 2).

Table 2. Variation of rate with concentration of benzyl alcohol

$[MnO_4^-]$: 4.0×10^{-4}M; $[H^+]$: 0.61M; Temp. 35°C.					
$[PhCH_2OH]\times10^3$ mol l^{-1}	1.0	2.0	3.0	4.0	5.0
$k_1\times10^3$ min^{-1}	9.1	18.4	27.7	36.8	46.1
$k_1/[PhCH_2OH]$	9.1	9.2	9.2	9.2	9.2

Under the conditions of constant ionic strength the rate varies linearly with concentration of hydrogen ions (Table 3).

Table 3. Variation of rate with concentration of hydrogen ions

$[MnO_4^-]$: 4×10^{-4}M; $[PhCH_2OH]$: 1×10^{-3}M; Temp. 35°C. Ionic strength (μ): 1.92M						
$[H^+]$ mol l^{-1}	0.48	0.72	0.96	1.44	1.68	1.92
$k_1\times10^3$ min^{-1}	10.0	13.8	17.5	26.5	30.9	26.8
$10^2\,k_1/[H^+]$	2.08	1.92	1.82	1.84	1.84	1.92

This indicates that increase in acidity brings about an increase in the rate of the oxidation. This may well be due to protonation of permanganate anion to give permanganic acid, a more powerful oxidant.

$$H^+ + MnO_4^- \rightleftarrows HMnO_4$$

This accords well with the suggestion of Littler[1] that acid catalysed path in the oxidation of cyclohexanol by permanganate involves a protonation in the pre-equilibrium. Stewart and Mocek also observed such an effect in the acid permanganate oxidation of formic acid.[6]

Effect of Manganese(II). Addition of manganous sulphate does not appreciably affect the rate of the oxidation (Table 4).

Table 4. Effect of manganese(II) on the rate of oxidation

$[MnO_4^-]$: 4×10^{-4}M; $[PhCH_2OH]$: 1×10^{-3}; $[H^+]$: 1.23M; Temp. 35°C					
$[Mn(II)]\times10^4$ mol l^{-1}	0.0	4.0	8.0	10.0	12.0
$k_1\times10^3$ min^{-1}	21.0	23.0	22.2	22.7	23.0

These results are contrary to that observed by Banerjee and SenGupta[3] in the acid permanganate oxidation of methanol and ethanol. They observed that the rate of oxidation is decreased by addition of manganese(II). The fact that the rate of the oxidation is unaffected by manganese(II) indicates that intermediate valency states of manganese are not important in this reaction.

Effect of Fluoride Ions. Addition of sodium fluoride also does not cause any change in the first order rate constant.

This also supports the view that intermediate valency states of manganese are not important in this oxidation, as fluoride ions are known to suppress the oxidation by manganese(III) and manganese(IV) by complexation.

Effect of Temperature. Data on the effect of temperature on the rate of oxidation are summarized in Table 5.

Table 5. Variation of rate with temperature

$[PhCH_2OH]$: 2.0×10^{-3}M; $[MnO_4^-]$: 4.0×10^{-4}M; $[H^+]$: 0.61M

Temp. °K	$k_1\times10^2$ min^{-1}	$k\times10^2$ l^2 m^{-2} sec^{-1}	
303	1.38	18.9	$\Delta S^{\neq}$
308	1.84	25.1	-27.2 e.u.
313	2.46	33.6	$\Delta H^{\neq}$
318	3.24	44.3	10.8 kcal mol^{-1}

It is found that a plot of $\log k$ against inverse of temperature is straight line. Arrhenius equation is therefore, valid for this reaction. The specific rate constant, k defined as

$$k = \frac{k_1\ (\text{min}^{-1})}{60\cdot[PhCH_2OH][H^+]}$$

Discussion

Absence of any effect of manganese(II) and

6) R. Stewart and M. M. Mocek, "Oxidation in Organic Chemistry," ed. by K. B. Wiberg, Academic Press, New York (1965), p. 56.

of fluoride ions on the rate of oxidation suggests that benzyl alcohol is mainly oxidzed by manganese-(VII). The linear increase in the rate of oxidation with increase in acidity accords well with the suggestion that probably permanganic acid is the active species.

$$H^+ + MnO_4^- \rightleftarrows HMnO_4$$

The entropy of activation and heat of activation data suggest that a C–H bond is ruptured in the rate-determining step (*cf.* Bakore and Narain[7,8]). The hydrogen may be removed by the oxidant either as a hydrogen atom or a hydride ion. It has been pointed out that known cases of hydride-ion transfer reactions seems to have a low isotope effect.[9] The value of 2.42 for the kinetic isotope effect in the oxidation of cyclohexanol by acid permanganate, observed by Littler,[1] suggests hydride transfer in the oxidation. This is, however, not conclusive and permanganate is known to function as a one-electron oxidant also, abstracting a hydrogen atom. Recently Barter and Littler[2] have shown that acid permanganate oxidation of alcohols involve a two-electron mechanism, with transfer of a hydride-ion from the carbon atom bearing the functional group to the oxidant. The values of heat of activation and entropy of activation for the oxidation of benzyl alcohol are of the same order as those of methanol and ethanol. This indicates that probably same mechanism operates in these oxidations.

If one accepts the hydride-transfer mechanism, the oxidation of benzyl alcohol by acid permanganate may be visualized as

$$HMnO_4 + H\text{–}\overset{\overset{C_6H_5}{|}}{\underset{\underset{H}{|}}{C}}\text{–}OH \xrightarrow{\text{slow}} H_2MnO_4^- + C_6H_5\overset{+}{C}HOH$$

(Mn(V))

$$C_6H_5\overset{+}{C}HOH \xrightarrow{\text{fast}} C_6H_5CHO + H^+$$

$$5Mn(V) \xrightarrow{\text{fast}} 2Mn(II) + 3Mn(VII)$$

The existance of manganese(V) as a reaction intermediate is well established.

7) G. V. Bakore and S. Narain, *J. Chem. Soc.*, **1963**, 3419.

8) G. V. Bakore and S. Narain, *Z. Physik. Chem.*, **227**, 8 (1964).

9) C. G. Swain, R. F. W. Bader, R. M. Esteve, Jr., and R. N. Griffin, *J. Am. Chem. Soc.*, **83**, 1951 (1961).

BULLETIN OF THE CHEMICAL SOCIETY OF JAPAN VOL. 42 2040—2041 (1969)

Hot-Atom Chemistry of Bromine. III.[1] The Use of Bromides and Bromate in an Attempt at the Recoil-Synthesis of Two Organic Radiobromides in Solid Mixture Systems

Chiro SHINOMIYA, Akira OYOSHI and Toshiaki KISHIKAWA

Department of Industrial Chemistry, Faculty of Engineering, Kumamoto University, Kumamoto

(Received July 10, 1968)

Since the early study of recoil syntheses with organic bromides in organic solutions,[2] many experiments on the recoil syntheses of ^{82}Br-labeled organic bromides have been undertaken in the liquid phase. A few, however, have been done in solid phase It has previously been reported that the radiative neutron capture and the isomeric transition produce bond disruption in irradiated aqueous bromate[3] and that the radiobromine-82 so produced in a pyrenebromanil-molecular compound could combine with the pyrene ring to produce ^{82}Br-labeled pyrene.[1] The present note describes an attempt at the recoil labeling of the ^{82}Br atoms in pyrene or *p*-benzoquinone, with potassium bromate, bromide or ammonium bromide used as the bromine source.

Experimental

The samples were composed of the organic target and the bromine source (in a molar ratio of 1 : 4[4]); the ingredients were mixed by pestling them together

1) Part II: C. Shinomiya *et al.*, This Bulletin, **42** (8), (1969), in press.

2) E. Glückauf and J. W. J. Fay, *J. Chem. Soc.*, **1936**, 390.

3) C. Shinomiya, A. Oyoshi and T. Kishikawa, This Bulletin, **42**, 1437 (1969).

4) The equal ratio of the quinone ring: bromine in bromanil reported in the previous paper.[1]

on an agate motar. They were then irradiated at the reactor temperature (*ca.* 40°C) in a pneumatic tube of KUR[5] for 1—80 min. The thermal neutron flux and the accompanying gamma-dose rate at 1 MW operation were 5×10^{12} n/cm²/sec and 2.7×10^{7} R/hr respectively. After standing for more than 2 hr[6] at room temperature, the samples were extracted into a two-phase mixture of a carbon disulfide solution of bromine and an aqueous mixture of potassium bromide and bromate; radioactivity measurements were then made with respect to the ^{82}Br activities. The organic yield was calculated in the manner described in a previous paper.[1]

Results

Table 1 shows the organic yields in the irradiated pyrene or *p*-benzoquinone and bromine compound mixtures at various irradiation times. No definite dependency of the irradiation time on the organic yield was established. In these heterogeneous mixtures a chance for a recoiled atom to escape from the bromide or bromate crystal may be small, and only the atoms recoiled at or near the surface of the crystal may be stabilized in both the organic crystal and the parent one. No dependency of the irradiation time can be supported by this explanation.

Table 1. Organic yields in irradiated mixtures

Bromine source	Irrad time min	Organic yield, % in organic targets	
		Pyrene	*p*-Benzoquinone
NH_4Br	20	4.4	2.1
KBr	1	0.7	1.3
	5	0.4	0.4
	10	2.7	3.3
	20	3.2	1.9
	30	3.6	4.3
$KBrO_3$	1	1.0	3.3
	5	2.4	4.4
	10	1.8	2.0
	30	3.7	2.2
	80	1.6	3.9

Ammonium bromide was considered to be more effective than potassium bromide on the organic yields in both pyrene and *p*-benzoquinone. Bromate was effective for a short period of irradiation, and bromide, for a long period.

The authors wish to express their appreciation to Dr. Shiro Iwata, Dr. Yoshiyuki Kiso, and the personnel of the Research Reactor Institute, Kyoto University, for their assistance in the irradiation.

5) Kyoto University Reactor.

6) The isomeric transition reaction of ^{82m}Br (half-life *ca.* 6 min) was completed during the time; O. U. Anders, *Phys. Rev.*, **138**, B1 (1965); J. F. Emery, *J. Inorg. Nucl. Chem.*, **27**, 903 (1965).

BULLETIN OF THE CHEMICAL SOCIETY OF JAPAN VOL. 42 2041—2042 (1969)

The Isotope Effect of Hydrogen on the Autoxidation of Benzene and Toluene in Aqueous Solutions*1

Hiroshi HOTTA, Nobutake SUZUKI and Takuji KOMORI

Japan Atomic Energy Research Institute, Takasaki, Gunma

(Received August 2, 1968)

As the result of studies of the autoxidation of benzene[1] and toluene[2] in aqueous solutions catalyzed by metal ions at elevated temperatures, it has been assumed that the main reaction of the propagation process is the abstraction reaction of hydrogen by peroxides:

$$ROO\cdot + RH \rightarrow ROOH + R\cdot \qquad (1)$$

where R represents the phenyl or benzyl radical. As an extension of this work, the autoxidation, initiated by Fenton's reagent, was carried out for an equimolar mixture of C_6H_6 and C_6D_6 and one of $C_6H_5CH_3$ and $C_6D_5CD_3$ in a previous work.[2] The isotope effect of hydrogen or the rate constant ratio of this reaction, k_H/k_D, was then estimated from the isotopic composition of the products at a low reaction conversion by using the equation:

$$\frac{k_H}{k_D} = \frac{(RD)}{(RH)} \times \frac{(Product)}{(d\text{-}Product)} \qquad (2)$$

where (RD)/(RH) is the initial mole ratio of the

*1 The Autoxidation of Aromatic Hydrocarbons in Aqueous Solutions. XII.

1) H. Hotta, N. Suzuki and T. Abe, This Bulletin, **39**, 417 (1966).

2) N. Suzuki and H. Hotta, *ibid.*, **40**, 1361 (1967).

deuterated reactant to the normal reactant, which was unity, while (Product)/(d-Product) is the mole ratio of the normal product to the deuterated product. This method should give the value of k_H/k_D, when the concentration of the reactant (RH or RD) in the aqueous phase is always high in comparison with that of ROO· in reaction (1).[3] For this purpose, acetone was added in the aqueous phase in order to increase the solubility of aromatic hydrocarbons.

The values in the previous work[2] (*i. e.*, *ca.* 1.4), however, seemed to be rather low for the confirmation of reaction (1). Recently, it has been found that direct mass spectrometry is not a good method for measuring the isotopic composition of the products, since the isotope effect of vaporization during sampling sometimes becomes effective for products with such low vapor pressures.[4] Therefore, the isotopic measurements were carried out by an entirely different procedure in the present work. Namely, the products, separated by gas chromatography, were converted to hydrogen and deuterium prior to the mass spectrometry. The present method is definitely a better way for the isotopic measurement, since it avoids the inherent error due to the above isotope effect of vaporization. The values of the present work, estimated by Eq. (2), are listed in Table 1.

Table 1. Isotope effect of hydrogen

Reactant	Product	Temp., °C	k_H/k_D
Benzene	Biphenyl	20	1.9
	Phenol	70	2.4±0.2
Toluene	Benzyl alcohol	70	4.6±0.3
	Dibenzyl	70	4.8

The values (4.5—4.8) obtained for toluene are similar to the values for the propagation process (reaction (1)) of the autoxidation of aromatic hydrocarbons, that is, 5.5 for cumene at 60°C[5] and 5.1 for diphenylmethane at 30°C.[6] Meanwhile, similar values (4.5—5.1) have also been reported for the oxidation of *p*-methoxytoluene by manganic acetate in acetic acid,[7] which involves the detachment of the hydrogen atom by an electron-transfer process.

As for the oxidation of benzene, Smith and Norman suggested, after a qualitative experiment, that there is no kinetic isotope effect on the hydroxylation of benzene to phenol by Fenton's reagent at room temperature.[8] Meanwhile, the addition of the hydroxyl radical to benzene has been confirmed as the primary process in the formation of phenol in the pulse radiolysis of an aqueous solution of benzene at room temperature.[9]

Contrary to the above observations of Smith and Norman, however, the present value for benzene at 70°C (2.4) appears somewhat unexpectedly high. In our previous preliminary study,[3] too, it was a general tendency for the value of k_H/k_D, obtained at 70°C to be relatively larger than that at 20°C. Since the kinetic isotope effect usually decreases with an increase in the temperature, the higher value at 70°C seems to suggest that the process at 70°C includes a different reaction route, which has a higher isotope effect. A few possible pathways have already been proposed as examples in reference (8). However, none of these mechanisms can explain the fact that more than one half of the oxygen in the produced phenol is originated from water.[4] Further investigation is necessary, for the mechanism is rather complicated for the case of benzene.

Experimental

The oxidation procedure was almost the same as an earlier one.[3] That is, 0.4 cc of benzene was dissolved in 75 cc of a 0.4N sulfuric acid solution containing 0.01M ferrous sulfate and 25 cc of acetone at 20°C, while 0.5 cc-portions of benzene and toluene were dissolved in 80 cc of the above ferrous solution and 20 cc of acetone at 70°C. Benzene or toluene was almost an equimolar mixture with the respective deuterated reagent, Benzene-d_6 and toluene-d_8, obtained from Merck, Sharp & Dohme of Canada, Ltd , were proved extremely pure chemically and isotopically by gas chromatography and mass spectrometry, 10 cc of 1.5% hydrogen peroxide were added, drop by drop, over a period of about 90 sec, to the above solutions in a 300 cc flask opened to the air.

After the mixture had been stirred for 10 min and then cooled, the products were separated by gas chromatography (PEG 6000). Then they were converted to water by being passed through cupric oxide pellets at 500°C with dry oxygen. This water was again reduced to hydrogen gas by passing it through zinc pellets at 370°C. The ratio of hydrogen to deuterium in this gas was determined by mass spectrometry.

3) H. Hotta, This Bullein, **40**, 687 (1967).
4) H. Hotta and N. Suzuki, *ibid.*, **41**, 1537 (1968).
5) G. A. Russell, *J. Am. Chem. Soc.*, **79**, 3871 (1957).
6) J. A. Howard and K. U. Ingold, *Can. J. Chem.*, **44**, 1119 (1966).
7) P. J. Andrulis, Jr., M. J. S. Dewar, R. Dietz and R. L. Hunt, *J. Am. Chem. Soc.*, **88**, 5473 (1966).
8) J. R. L. Smith and R. O. C. Norman, *J. Chem. Soc.*, **1963**, 2897.
9) L. M. Dorfman, I. A. Taub and R. E. Bühler, *J. Chem. Phys.*, **36**, 3051 (1962).

BULLETIN OF THE CHEMICAL SOCIETY OF JAPAN VOL. 42 2043—2044 (1969)

The Formation of 3-*n*-Butylamino-7-hydroxy-9-*n*-butyl-carbazolquinone(1, 4) in the Reaction of *p*-Benzoquinone with *n*-Butylamine

Kazuyuki SUGITA*1 and Ju KUMANOTANI

The Engineering Research Institute, Faculty of Engineering, The University of Tokyo, Yayoi, Bunkyo-ku, Tokyo

(Received September 5, 1968)

The reaction of *p*-benzoquinone with amines has been employed conveniently as a method of preparing 2,5-diamino-*p*-benzoquinoid compounds;[1] however, the details of the reaction remain to be elucidated. For instance, it is found in our laboratory that the reactions generally yield considerable amounts of resinous matter, especially with aliphatic amines.

We will report that, in the reaction of *p*-benzoquinone with alcoholic *n*-butylamine, a new compound, 3-*n*-butylamino-7-hydroxy-9-*n*-butyl-carbazolquinone(1,4) (IV), is formed in appropriate quantity, together with 2,5-bis(*n*-butylamino)-*p*-benzoquinone. The following scheme may be proposed for the formation of the carbazolquinone. I is formed through two steps:[1] (a) the nucleophilic 1,4-addition of the amine to the quinone to give an amino-quinol, and (b) the oxidation of the quinol with *p*-benzoquinone. III is obtained from I *via* a route similar to that described for I: the formation of III through II is due to the reductive potential of the diaminoquinone nucleus being more negative than that of the monoaminoquinone nucleus.

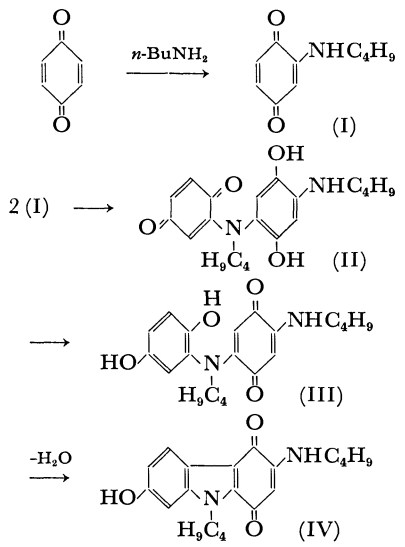

The compound (IV) was separated fractionally by recrystallization, and its molecular weight and formula were determined by the VPO method and by elementary analysis respectively. The structure of IV was confirmed as follows. The polarographic potential, −0.48 V (*vs.* SCE), measured at 25°C in a mixed solvent (1 : 1 v/v) of isopropanol and a phosphate buffer (pH, 6.0), indicates that IV has a diamino-*p*-benzoquinone nucleus.[2] This is supported by the following UV and IR spectral data: $\lambda_{max}^{CHCl_3}$ 354 mμ (ε, 17000), attributable to the π–π* transition band of the quinone nucleus; 3370 (m. ν_{N-H}), 1650 (m. $\nu_{C=C}$), 1590 (s. $\nu_{C=O}$), and 1510 cm^{-1} (s. amido II type band).[2] The intensity of the ν_{N-H} band of IV was found IR spectroscopically to be equivalent to one N–H group per mole unlike that of 2,5-bis(*n*-butylamino)-*p*-benzoquinone. The NMR spectrum in pyridine showed signals at 8.9—9.4 (triplet, 6H, $-CH_2-C\underline{H}_3$), 8.0—9.0 (multiplet, 8H, $>N-CH_2-C\underline{H}_2-C\underline{H}_2-CH_3$), 6.6—7.1 (quartet, 2H, $-NH-C\underline{H}_2-$), and 5.1—5.5 τ (triplet, 2H, $>N-C\underline{H}_2-$); in dimethyl sulfoxide it showed signals at 4.82 (singlet, 1H, quinoid ring proton), 2.4—3.3 (multiplet, 4H, three aromatic and one N–H protons), and 0.55 τ (singlet, 1H, O–H proton). The hydroxy proton was assigned by the deuterium substitution method. Further clear evidence obtained from the NMR spectrum of the *O*-acetate of IV proved the presence of three aromatic protons in the ABC system.

Experimental

Materials. *p*-Benzoquinone (mp 115—116°C) was utilized by submitting a commercially-available chemical to sublimation. *n*-Butylamine, obtained commercially, was of a chemically pure grade and was used without further purification.

Separation by TLC and Instrumental Analyses.

*1 Present address: Department of Graphic Engineering, Faculty of Engineering, Chiba University, Yayoi-cho, Chiba City.

1) See *e.g.*, L. F. Fieser and M. Fieser, "Advanced Organic Chemistry," Reinhold, New York (1961), p. 853.

2) J. Kumanotani, F. Kagawa, A. Hikosaka and K. Sugita, This Bulletin, **41**, 2118 (1968).

These proceedings were carried out in the same way as has already been described in a previous paper.[2)]

Purification and Identification of the Products. A solution of *p*-benzoquinone (25 g, 0.232M) in 250 m*l* of 98% ethanol was stirred into a solution of *n*-butylamine (9.73 g, 0.133M) in 50 m*l* of ethanol at room temperature for 25 min. Then the solution was refluxed for 1 hr and subsequently cooled to room temperature for 1 hr under stirring. The red crystals thus precipitated were filtered off, washed with a small amount of ethanol, and dried *in vacuo*; they amounted to 5.1 g (27% of the theoretical yield). Recrystallization from dioxane gave red rod crystals, mp 163.5—164.5°C (Found: N, 11.19%). This compound was identified with an authentic sample of 2,5-bis(*n*-butylamino)-*p*-benzoquinone prepared in our laboratory.[2)] When the mother liquor was evaporated to dryness at 30°C under reduced pressure, a black material was given as a residue. The light brown substance (10.7 g) obtained as an insoluble part after the black material had been washed several times with 100 m*l* of chloroform was recrystallized from water and submitted to sublimation to give white needles, mp 169.5—170.8°C. The needles were identified by comparing their IR spectrum and they showed no depression in a mixed-melting-point determination with an authentic sample of hydroquinone The solid material obtained by the removal of the chloroform from the solution under reduced pressure with an aspirator was dissolved in 60 m*l* of methanol and refrigerated for 12 hr. The crystals that precipitated were filtered off and dried *in vacuo* to yield 3.4 g (8.6%). Recrystallization from methanol and then from chloroform gave yellowish brown powders; mp 184.9—185.7°C (corr).

Found: C, 70.31; H, 7.20; N, 7.97%; mol wt, 345. Calcd for $C_{20}H_{24}O_3N_2$: C, 70.56; H, 7.11; N, 8.23%; mol wt, 340.

Derivation of the O-Acetyl Carbazolquinone. The carbazolquinone (300 mg) was dissolved in 30 m*l* of acetic anhydride, and then the solution was refluxed for 4 hr. The resulting solution was cooled and treated twice with 10 times as much as warm water (at *ca.* 50°C) to give precipitates. The crude acetate obtained by extraction with ether was dissolved in a small amount of chloroform, applied in lines on the silica-gel layers (thickness, 0 5 mm), anddeveloped with chloroform. A broad and dark brown zone at R_f 0.15—0.25 was scraped off and eluted with 30 m*l* of chloroform The elute was evaporated to dryness at room temperature under reduced pressure with an aspirator to give dark brown powders (145 mg). The powders were recrystallized from methanol; mp 147.5—149.0°C. Found: N, 7.11%; mol wt, 389. Calcd for $C_{22}H_{26}O_4N_2$: N, 7.34%; mol wt, 382. The saponification value was found to be 148.9 (*theor.* 147.4) by titrating the residual alkaline after refluxing a solution of the acetate (40 mg) dissolved in 20 m*l* of 0.05N aqueous sodium carbonate methanol (2 : 3 v/v) for 1 hr. The spectral data, *i.e.*, $\nu_{C=O}$ at 1760 cm^{-1} and the signal at 7.70 τ (3H, $-CO-C\underline{H}_3$), are in agreement with thoes of the acetate. In comparison with the NMR spectra between the acetate and its parent quinone, the three aromatic proton signals of the ABC-system are clearly seen in the range between 2 τ and 4 τ, and the proton signal of N-H is at 3.9 τ.

BULLETIN OF THE CHEMICAL SOCIETY OF JAPAN VOL. 42 2044—2046 (1969)

Synthesis and Spectrophotometric Observations of Ethyl *p*-(Acetylsalicylylamino)-benzoate*1

Yukinao NODA

Division of Chemistry, Osaka City University Medical Shool, Osaka

(Received September 10, 1968)

Ethyl *p*-(acetylsalicylylamino)-benzoate (AB) has been synthesized in a water medium.[1] This paper will describe a new simple method of synthesizing AB and will present its ultraviolet, infrared, fluorometric, and phosphorometric spectra.

Acetylsalicylic acid (1 g) and ethyl *p*-aminobenzoate (1 g) were dissolved in 40 m*l* of ethyl acetate, and then dicyclohexylcarbodiimide (1 g) in 5 m*l* of ethyl acetate was gradually stirred into the mixed solution at room temperature. As the reaction proceed, dicyclohexylurea was obtained as the precipitate. The reaction mixture was then allowed to stand at room temperature for 16 hr. The precipitated dicyclohexylurea was filtered off, and the filtrate was evaporated to dryness *in vacuo* below 40°C. The oily residue was dissolved in 5 m*l* of methanol, and 5 m*l* of ether and 100 m*l* of petroleum ether were added to the solution. Crystals were obtained after the solution had been kept in a refrigerator. This crystalline material was recrystallized from methanol, ether, and then petroleum ether; fine needles were thus obtained. The yield was 900 mg. Melting point: 140°C (uncorrected, this is identical with that in Reference 1).

Found: C, 66.03; H, 5.40; N, 4.45%. Calcd

*1 This is an anaesthetica.

1) D. Curtis, U. S. Pat. 2352691 (1944).

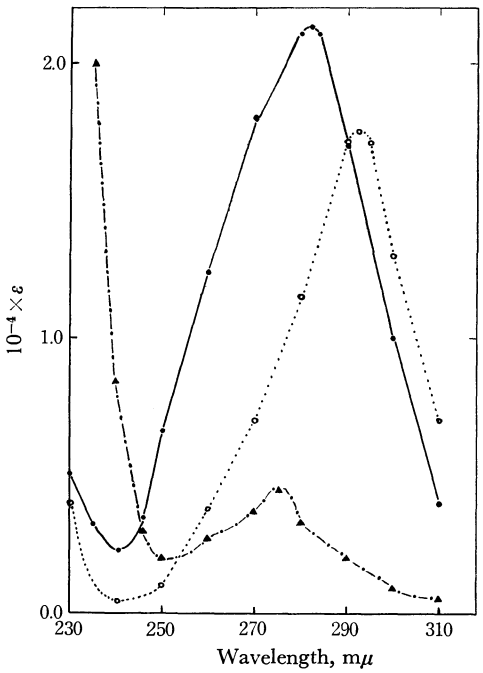

Fig. 1a. Ultraviolet spectra of AB, ethyl *p*-aminobenzoate and acetylsalicylic acid.
●——● AB
○·····○ Ethyl *p*-aminobenzoate
▲—·—·▲ Acetylsalicylic acid
Each concentration in methanol was 5×10^{-5}M.

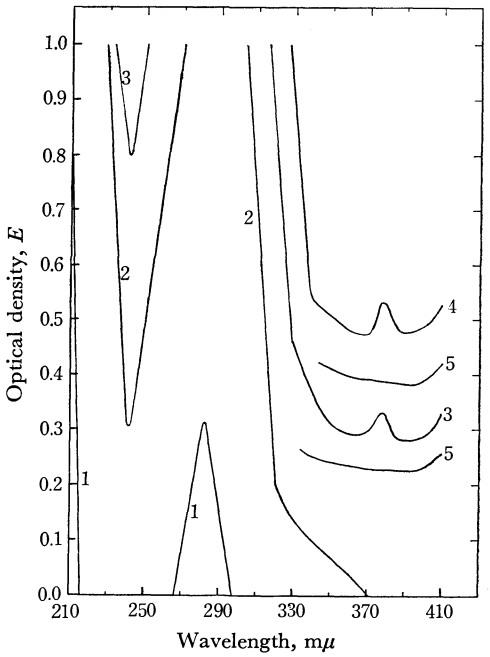

Fig. 1b. Ultraviolet spectrum of AB.
The concentration of AB in methanol was 5×10^{-5}M.
Curves 1, 2, 3 and 4 were determined at different sensitivities of spectrophotometer.
Curve 5 is methanol.

for $C_{18}H_{17}O_5N$: C, 66.06; H, 5.20; N, 4.28%.

One mg of AB is soluble in 5 m*l* of water at 100°C and in methanol, ethanol, and ether, and insoluble in petroleum ether. The ferric chloride reaction[2] was negative with this compound.

The ultraviolet spectrum of AB was determined in methanol using Beckman DU and Shimadzu MPS-50L spectrophotometers; the results are shown in Figs. 1a and 1b.

From the results, the λ_{max} of AB was located at 282.5 mμ (ε, 21400) and the λ_{min} at 241 mμ in methanol. AB may exist in the two forms of keto and enol isomers, shown below;

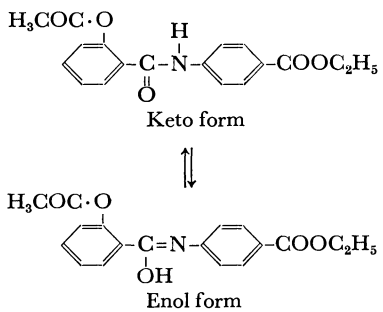

Figure 1b shows the presence of a band at 377.5 mμ, and the infrared spectrum of AB, as measured with a Hitachi infrared spectrophotometer, EPI-G type, showed characteristic absorption bands at 3320 cm^{-1} and 3070 cm^{-1} attributable to the *trans* form of the amide group,[3] as is shown in Fig. 2.

Consequently, it is probable that the steric structure of AB is mainly the keto form. If the band at 377.5 mμ is the enol form as shown in Fig. 1b, it is in a negligibly low concentration.

When AB was excited at 280 mμ or at 300 mμ

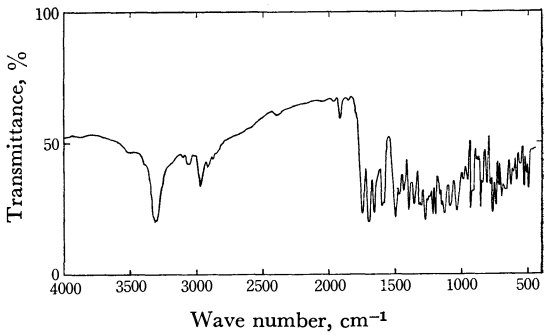

Fig. 2. Infrared spectrum of AB measured by the KBr tablet method.

2) Commentary of the Japanese Pharmacopoeia, 7th Ed. Nankodo Co., Tokyo (1962), p. 4.

3) K. Nakanishi, "Infrared Absorption Spectra," Nankodo Co., Tokyo (1967), p. 49.

in cyclohexane with a Hitachi fluorescence spectrophotometer, model MPF-2A, the maximum appeared in the fluorescence spectrum at 323 mμ as is shown in Fig. 3a, while the phosphorescence spectrum was observed at 77°K in ether : isopentane : alcohol (5 : 5 : 3, v/v); on the other hand, several peaks were observed between 400 mμ to 500 mμ. as Fig. 3b shows. This phenomenon may be inferred to be due to the effect of the temperature on the molecular distribution in the vibrational levels.

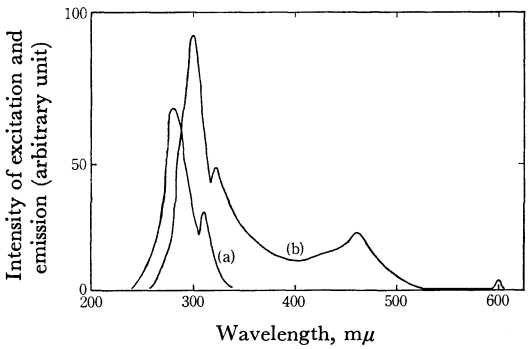

Fig. 3a. Fluorescence and excitation spectra of AB.
The concentration of AB in cyclohexane was 5 μg.
(a) Excitation spectrum
Emission at 310 mμ, slit width 1.29 mm, band path of wavelength 10 mμ.
(b) Fluorescence spectrum
Emission at 300 mμ, slit width 1.29 mm, band path of wavelength 10 mμ.
The peak at 300 mμ is due to the scattered light and the small peak at 600 mμ is also due to the scattered light.

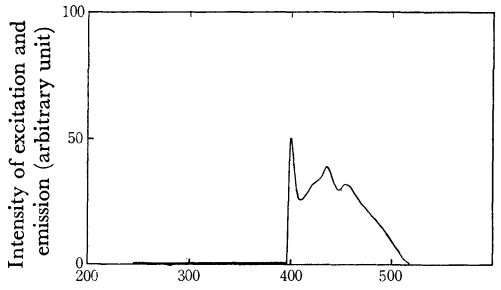

Fig. 3b. Phosphorescence spectrum of AB.
The concentration of AB in ether: isopentane : alcohol (5 : 5 : 3, v/v) was 5 μg.
The temperature of the solution of AB was 77°K.
Excitation at 280 mμ, slit width 2.58 mm, band path of wavelength 2 mμ.

BULLETIN OF THE CHEMICAL SOCIETY OF JAPAN VOL. 42 2046—2048 (1969)

The Effect of Impurities on the Whiteness of Lanthanum Oxide

Kazuhide MIYAZAKI

Central Research Laboratories, Mitsui Mining and Smelting Co., Mitaka-shi, Tokyo

(Received September 18, 1968)

The present paper will investigate how the whiteness of lanthanum oxide is affected by the presence of minor amounts of three common impurities, praseodymium, neodymium and calcium; the influence is expressed in terms of the Munsell Value scale.

Lanthanum oxide, La_2O_3, is a white, amorphous powder which has increasingly been used in many fields of industries; for instance, using it the glass industry has produced a silica-free optical glass with a high refractive index. The purity of the commercially available material is usually 99.5% or more.

However, it has been accepted that, from an industrial point of view, one of the most important factors in evaluating a white powdery product on the market is its appearance of whiteness. The case of lanthanum oxide is no exception; a visual comparison is one of the usual practices in judging the quality or marketability of the white product.

The element has been separated from a rare earth mixture, itself derived from monazite sand and consisting of the rare earth elements from La through Lu, by basicity separations[1,2] or by fractional crystallization.[3] Praseodymium and neodymium are frequent contaminants in the lanthanum due to the fact that these two elements are the closest neighbors of the lanthanum in the La-Lu series and so are the most difficult to separate.

1) E. V. Klever and B. Love, "The Technology of Scandium, Yttrium and the Rare Earth Metals," Pergamon Press, London and New York (1963), p. 19.
2) C. A. Hampel, *Glass Ind.*, **41**, No. 1, 15 (1960).
3) F. H. Spedding and A. H. Daane, "The Rare Earths," John Wiley and Sons, New York and London (1961), p. 137.

While the oxides of La, Ce^{3+}, Tb, and Lu are colorless, the coloring is most distinct in the case of Pr_6O_{11} and Nd_2O_3; Pr_6O_{11} is black, and Nd_2O_3 is lavender blue.[4] Therefore, the presence of these two elements in the La_2O_3, even in small quantities, will appreciably degrade the whiteness of the product; such presence usually gives a grayish shade to the product, which would otherwise be pure white.

Still another impurity which commonly accompanies this element is calcium coming from the monazite sand and the processing water used in the manufacturing plant. Calcium is also close to lanthanum in many characteristics, such as its basicity, its separability with ion exchange resins, and the solubility product of oxalate. Although the removal of calcium from the lanthanum is of prime importance for the manufacturer, the influence of this element on the coloring of La_2O_3 has previously been frequently overlooked, for the calcium oxide is also white in itself.

This paper will present the results of a study whereby a color difference meter was used to characterize the interdependence of the influence of three common impurities, Pr, Nd, and Ca, on the coloring of highly pure lanthanum oxide in an attempt to provide a convenient criterion in terms of the value scale in the Munsell color system. The purpose here is to establish a practical measure for judging which one of these three elements is the major source of the coloring and to help to improve the quality of the La_2O_3 product in terms of its whiteness as well as of its chemical purity.

Experimental

Materials. Spectrographic-grade highly pure oxides of lanthanum, neodymium, and praseodymium were commercially available from the Lindsay Chemical Division, American Potash and Chemical Corp., and from Johnson, Matthey & Co. Lanthanum oxide was graded as 99.997% La_2O_3, while praseodymium oxide and neodymium oxide were 99.9% Pr_6O_{11} and 99.9% Nd_2O_3 respectively. As for the calcium component, reagent-grade calcium oxide was used. Spectrographic examinations showed no evidence of unnecessary elements in this material.

Procedures. The component oxides are weighed into a beaker, dissolved with dilute hydrochloric acid, and stirred. An oxalic acid solution was then added, and a mixed oxalate precipitate was obtained and ignited at about 1000°C to give several samples of lanthanum oxides contaminated, to several degrees, with small amounts of neodymium, praseodymium, and calcium oxides. Contaminations with Pr_6O_{11} to the extent of 0.15%, Nd_2O_3 0.35%, and CaO 1.0% of the lanthanum oxide produced a dark-colored sample which no longer bore a commercial value in its appearance. The degradation of the lanthanum oxide due to the artificially incorporated impurities was measured with a Color Difference Meter using the Munsell value scale, and the values *versus* the impurity contents were plotted. However, no appreciable differences in the Chroma and Hue scales were observed because the produced colors were solely gray or dark, well fitting into the value scale from about 6.5 to 9.5, the latter of which was the reading for the lanthanum oxide as received.

4) *E.g.*, Catalogue for Products of The Rare Earth Group, Johnson, Matthey & Co., London.

Results and Discussion

Figure 1 shows the value of the lanthanum oxide against the CaO content in the presence of Nd_2O_3 and/or Pr_6O_{11}. It may be observed from curve (1) that the presence of 0.5% Nd_2O_3 exhibits no appreciable effect on the appearance of La_2O_3, even with an increase in the CaO content up to 1.0%. Therefore, a rather low-purity lanthanum oixde (about 98.5% La_2O_3) can retain its white appearance, with a value of about 9.0, if the La_2O_3 contains no impurities other than Nd_2O_3 and CaO.

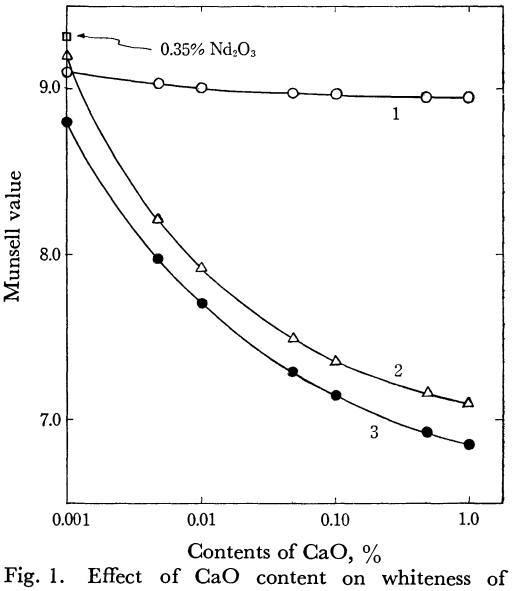

Fig. 1. Effect of CaO content on whiteness of La_2O_3 contaminated with Pr_6O_{11} and/or Nd_2O_3 expressed in terms of the Munsell Value scale.
(1): La_2O_3-0.5% Nd_2O_3 system, (2): La_2O_3-0.15% Pr_6O_{11} system, and (3): La_2O_3-0.15% Pr_6O_{11}-0.35% Nd_2O_3 system.

On the other hand, the situation is quite different in the case of Pr_6O_{11} as may be observed from curve (2). A contamination of La_2O_3 with only 0.15% Pr_6O_{11} and 0.01% CaO has much degraded the white appearance down to the value of 7.9, although the net La_2O_3 content is still higher (being 99.8% La_2O_3). It may also be seen from curve (2) that the presence of CaO to the extent of 1.0% together with the Pr_6O_{11}, gives the low value of 7.1, with which the product may no longer be marketable. It is to be noted from curves (1) and

(2), however, that the presence of 0.15% Pr_6O_{11} is less detrimental than that of 0.5% Nd_2O_3 if the CaO is not present at all or if only a trace is present.

From the initial position of curve (3) on the ordinate of Fig. 1 it may be seen that the combination of 0.15% Pr_6O_{11} and 0.35% Nd_2O_3 is more detrimental than 0.5% Nd_2O_3 alone. It can be naturally expected that the individual effect of 0.35% Nd_2O_3 will be less harmful than that of 0.5% Nd_2O_3, which gives a value reading of 9.3. 0.15% Pr_6O_{11} without calcium also does practically no harm, giving 9.2 However, the starting point of curve (3), positioned on the ordinate at a value less by about 0.3 than curves (1) and (2), indicates that the interaction of 0.35% Nd_2O_3 and 0.15% Pr_6O_{11} exists in spite of the fact that these elements individually behave much less harmfully. The additions of CaO to the La_2O_3-Pr_6O_{11}-Nd_2O_3 system remarkably decrease the value of the whiteness, and the curve (3) parallels the curve (2) down to about 6.9 with 1% CaO.

Most commercial rare-earth salts contain individual elements in about the same ratio as the ore treated.[5] After cerium has been removed by oxidation and hydrolysis, therefore, praseodymium and neodymium are the major impurities of lanthanum remaining until the last stages of the purification process, because these two elements are close to lanthanum in chemical and physical characteristics except in color. Moreover, they are present in the raw materials in amounts next to that of lanthanum. On the other hand, the rest of the impurities, from Sm through Sc, are relatively easier to separate because of their considerable difference in characteristics and their small amounts. Although it has been conventionally thought that the best way to obtain a pure white lanthanum oxide is simply to make the net La_2O_3 content as free as possible from these rare earth impurities, the results of Fig. 1 show that there is a possibility of a sample with 99.8% La_2O_3 (0.15% Pr_6O_{11}+ 0.01% CaO) being worse in color than one with 98.5% La_2O_3 (0.5% Nd_2O_3 + 1.0% CaO). It follows, accordingly, that emphasis should be placed on the removal of calcium in many cases in order to obtain a La_2O_3 product of high quality in both whiteness and chemical purity.

5) J. G Parker, "Mineral Facts and Problems, Rare Earths," Bull. 630, Bureau of Mines, 1965 ed., p. 753.

Summary

The detrimental effects of three common impurities, praseodymium, neodymium, and calcium, on the coloring of lanthanum oxide were investigated in terms of the Munsell value scale, using a color difference meter. The co-existence of praseodymium and calcium was most distinct in degrading the white color of lanthanum oxide, while neodymium was a minor coloring source even when combined with calcium. The effect of praseodymium present in a minor amount was not very pronounced without the simultaneous presence of calcium. The combination of praseodymium and neodymium did the most harm in the presence of calcium.

BULLETIN OF THE CHEMICAL SOCIETY OF JAPAN VOL. 42 2048—2050 (1969)

Triplet-Singlet Emission Spectrum of Acenaphthenequinone Vapour

S. Nath SINGH, M. G. JAYSWAL and R. S. SINGH

Department of Spectroscopy, Banaras Hindu University, Varanasi-5, India

(Received September 11, 1968)

The phosphorescence spectrum of acenaphthenequinone has been reported by Kuboyama and Yabe[1] at 77°K in various solvents and in the crystalline state. These authors have identified it as due to n–π^* (Triplet-Singlet) transition from the position of bands, solvent effect and life-time considerations. Recently, we have reported infrared and Raman spectra[2] of the molecule and the observed bands were assigned to different modes of vibrations. In the present work, the emission spectrum of the molecule in the vapour phase has been reported and discussed.

Experimental

The Eastman L. R. grade sample of acenaphthene-

1) A. Kuboyama and S. Yabe, This Bulletin, **40**, 2475 (1967).

2) S. Nath Singh and R. S. Singh, *Current Sci.*, **36**, 624 (1967).

quinone was sublimed before use and yellow needles were obtained. The emission was excited by using an uncondensed transformer discharge in the presence of flowing vapour of benzene, employing the conventional π-type of discharge tube. The yellowish emission glow was photographed by Fuess glass spectrograph with 60 μ slit width in 10 hr using Kodak I-F plates. Two different plates were measured on Hilger L-76 comparator and the average values of the measurements have been reported.

Results and Discussion

The emission spectrum of acenaphthenequinone lies in the region 5700—6900 Å and consists of thirteen diffuse but intense bands (Fig. 1). The intensity distribution of bands is unusual similar to those observed in various *p*-quinones[3] where the bands in the middle of the spectrum are more intense compared to those on the either sides. The wave numbers, visually estimated intensities and analysis of bands are given in Table 1.

The moderately strong band at 17552 cm^{-1} has been taken as the (0,0) band of the system. From the gross structure of bands, it is evident that the

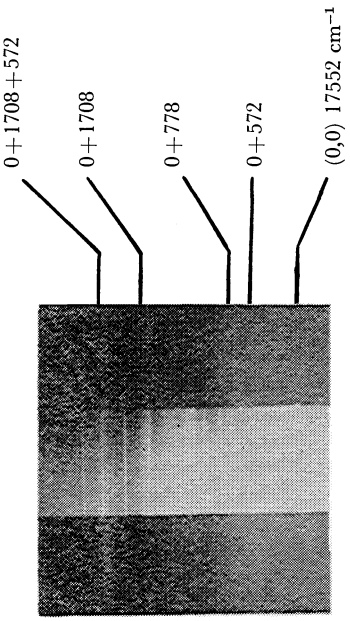

Fig. 1. Emission Spectrum of Acenaphthenequinone.

system is due to an allowed transition, as most of the totally symmetric fundamental frequencies are found to be superposed on this (0,0) band. Assuming C_{2v} symmetry for the molecule both in the ground as well as in the excited state, the spectrum has been analysed in terms of three totally symmetric vibrations: 572 (ring deformation), 778 (ring breathing) and 1708 cm^{-1} (C=O stretching) for which the corresponding Raman frequencies[2] have been reported at 575, 790 and 1723 cm^{-1}. The weak band at 17271 cm^{-1}, which is 281 cm^{-1} apart from the (0,0) band, may in all probability be due to excitation of a nontotally symmetric skeletal deformation type of vibration, the corresponding Raman value of which is 276 cm^{-1}. It is found that the ring breathing and C=O stretching mode of vibrations are predominent in the spectrum and most of the bands may be explained in terms of these two frequencies. The magnitude 1708 cm^{-1} for C=O stretching mode of vibration which has a higher value as compared to *p*-quinones[4] shows aliphatic character of the substituent group and molecule has been characterised not as a "true quinone.[5]"

Table 1. Emission bands of acenaphthenequinone

Wave number (cm^{-1})	Intensity	Difference from (0,0) band	Assignment
17552	(5)	0	(0,0)
17271	(1)	281	0+281
16980	(6)	572	0+572
16774	(6)	778	0+778
16493	(2)	1059	0+778+281
16194	(4)	1358	0+778+572
16009	(4)	1543	0+2×778
15844	(10)	1708	0+1708
15574	(5)	1978	0+1708+281
15264	(10)	2288	0+1708+572
15082	(2)	2470	0+1708+778
14793	(1)	2759	0+1708+778+281
14481	(1)	3071	0+1708+778+572

In the phosphorescence study[1] an intense band has been reported at 5990 Å (16690 cm^{-1}) in the crystalline state at 77°K and may be the electronic origin of the system. The (0,0) band identified at 5696 Å (17552 cm^{-1}) in the present vapour emission spectrum is at a higher energy value by 862 cm^{-1} as compared to the electronic origin in the phosphorescence spectrum in the crystalline state. This value is in conformity with the common observation that the electronic origin of the same system lies at a higher energy in the vapour phase as compared to the crystalline state. The two spectra seem to correspond to each other and the present vapour emission may be assigned as due

3) M. G. Jayswal and R. S. Singh, *Spectrochim. Acta*, **21**, 1597 (1965); *J. Mol. Spectry.*, **17**, 6 (1965); S. N. Singh, Ph. D. Thesis, B.H.U. (1968).

4) S. N. Singh and R. S. Singh, *Spectrochim. Acta*, **24A**, 1591 (1968); H. Stamureich and T. T. Sans, *J. Chem. Phys.*, **42**, 920 (1965).

5) C. N. R. Rao, "Chemical Application of Infrared Spectroscopy," Academic Press, New York (1963), p. 229.

to n–π^* (Triplet-Singlet) electronic transition. The life-time of the phosphorescence emission at low temperature[1] has been reported of the order of 10^{-2} sec which is a favourable value for observing a triplet-singlet emission even in the vapour state and such type of observation has been made in several *p*-quinones.[3] Moreover, the presence of benzene vapours seems to be quite important which possibly transfer its energy to excite the quinone molecule.[6]

The authors are thankful to Professor N. L. Singh for his keen interest in the work. One of them S. N. S. is grateful to N. B. S. (PL-480), U. S. A. for financial assistance.

6) R. S. Singh, *Indian J. Pure & Appl. Phys.*, **6**, 91 (1968).

BULLETIN OF THE CHEMICAL SOCIETY OF JAPAN VOL. 42 2050—2051 (1969)

Nuclear Quadrupole Resonance of α-Dimethyltellurium Dichloride

Seiichi KONDO, Emiko KAKIUCHI and Tsuyoshi SHIMIZU

Laboratory of Physical Chemistry, Osaka University of Education, Tennoji-ku, Osaka

(Received October 7, 1968)

Chlorine nuclear quadrupole resonance has been reported on several tellurium compounds such as tellurium tetrachloride[1] and complex salts[2]. The ionicity of Te–Cl bonds in these compounds differs from each other considerably. It is of interest to compare the ionicity of these compounds with that of an organotellurium compound, α-dimethyltellurium dichloride. It is also interesting to study the Zeeman effect of the single crystal whose structure has been determined by X-ray analysis by Christofferson, Sparks and McCullough.[3]

Experimental

The material was synthesized by the method of Vernon[4] from metallic tellurium and methyl iodide as raw material and was recrystallized twice from ethanol solution. Mp 96.6°C (lit.[4] 92°C). Found: Cl 31.85%. Calcd for $C_2H_6TeCl_2$: Cl 31.57%. X-Ray powder diffraction lines of this sample by X-ray diffractometer were in good agreement with those of literature.[3]

A single crystal was grown from the melt by slow cooling in the vacuum-sealed cylindrical ampoule and used for the Zeeman measurement. Since this material decomposes gradually by heating, the crystal thus obtained was slightly colored and opaque. The *b*-axis of this monoclinic crystal was found by Laue photographs to lie about 30° from the axis of the ampoule.

Resonance signals were recorded with the usual self-quenching superregenerative oscillator detector.[5] The Zeeman field was generated by a Helmholtz coil with an intensity of about 20 gauss.

Results and Discussion

Two resonance absorptions were recorded with approximately the same signal to noise ratio, *S/N*, within the searching range of 40 to 12 MHz, as shown in Table 1.

TABLE 1. THE NQR FREQUENCIES OF α-DIMETHYLTELLURIUM DICHLORIDE AT VARIOUS TEMPERATURES

Temp. °K	Freq., MHz Cl_1	*S/N*	Freq., MHz Cl_2	*S/N*
77	18.124	4	15.685	2
205	18.028	4	15.463	2
298.3	17.855	4	15.323	3
340.0	17.752	4	15.268	3

Single crystal Zeeman effect study showed two different orientations for each of the two resonance lines. These two sets of orientations seem to arise from two molecules in the unit cell being related to each other by the operation of two-fold axial symmetry as seen from the crystal stucture. The valence angles of Cl–Te–Cl bonds of these molecules observed were 176±3° and are almost equal to 172±0.3° determined by crystal structure analysis.[3] The loci of angles of Zero-splitting, θ_0, were searched to find the assymmetry parame-

1) A. Schmitt and W. Zeil, *Naturforsch.*, **18a**, 428 (1963).

2) D. Nakamura, K. Ito and M. Kubo, *J. Am. Chem. Soc.*, **84**, 163 (1962).

3) G. D. Christofferson, R. A. Sparks and J. D. McCullough, *Acta Cryst.*, **11**, 782 (1958).

4) R. H. Vernon, *J. Chem. Soc.*, **119**, 687 (1921).

5) C. Dean, *Phys. Rev.*, **96**, 1053 (1954).

ter, but it was difficult to obtain a more accurate value of θ_0 than $55\pm1°$ owing to an experimental error. The Zeeman effect study has guided us to the assignment of two resonances to each of the two chlorine nuclei in the molecule as shown in Table 2.

Table 2. The NQR frequencies of Cl atoms, the covalency $(1-i)$ of Te–Cl bonds, the effective charge ρ of Te atoms and the bond lengths of several Te compounds

	Freq. MHz	$(1-i)$	ρ	Te–Cl Å
α-$(CH_3)_2TeCl_2$	18.124	0.44	1.18	2.48[c]
	15.685	0.38		2.54[c]
$TeCl_4$[a]	28.166	0.68	1.30	2.27
	27.382	0.40		2.40
$(NH_4)_2TeCl_6$[b]	15.137	0.32	2.08	2.54

a) Ref. 1. b) Ref. 2. c) Ref. 3.

This conclusion is also supported by the fact that each chlorine atom in the molecule has only one equivalent position in the unit cell and that the frequency difference of the two resonance lines is much larger than that usually expected from the effect of crystalline field.

Table 2 shows (1) the NQR frequencies of Cl atoms of several Te compounds, (2) the respective covalency $(1-i)$ of Te–Cl bonds in which i is the ionicity, using Townes and Dailey relation[6] with s-hybridization character assumed as 0.15, and (3) the effective charge ρ of Te atom and their bond lengths. The ionicity of Te–Cl bond of α-dimethyltellurium dichloride is larger than that of tellurium tetrachloride by the influence of methyl groups.

This research was partly supported by a grant from the Ministry of Education.

6) C. H. Townes and B. P. Dailey, *J. Chem. Phys.*, **23**, 118 (1955).

BULLETIN OF THE CHEMICAL SOCIETY OF JAPAN VOL. 42 2051—2054 (1969)

The Spectrophotometric Determination of Scandium with Chromal Blue G

Katsuya UESUGI

Laboratory of Chemistry, Himeji Institute of Technology, Himeji

(Received October 8, 1968)

For the spectrophotometric determination of scandium, various workers have proposed many organic reagents including alizarin red S,[1,2] oxine,[3] tiron,[4] morin,[5] naphthyl azoxine S,[6] arsenazo,[7] sulfonazo,[8] pontachrome azure blue B, [9] eriochrome cyanine R,[10] xylenol orange,[11] pontacyl violet 4BSN,[12] and chromazurol S.[13]

In this paper, a new method for the spectrophotometric determination of scandium using chromal blue G (sodium-2″-chloro-4″-nitro-4′-hydroxy-3,3′-dimethylfuchsone-5,5′-dicarboxylate, color index 43835), similar in structure to pontachrome azure blue B, eriochrome cyanine R, and chromazurol S, will be described. The method is based on the highly-sensitive colored reaction of chromal blue G with scandium in an acetate

1) A. R. Eberle and M. W. Lerner, *Anal. Chem.*, **27**, 1551 (1951).
2) I. M. Korenman, V. P. Gunina and L. K. Trifonova, *Zhur. Analit. Khim.*, **14**, 547 (1959).
3) F. Umland and H. Puckelt, *Anal. Chim. Acta*, **16**, 334 (1957).
4) H. Hamaguchi, N. Onuma, R. Kuroda and R. Sugisita, *Talanta*, **9**, 563 (1962).
5) E. B. Sandell, "Colorimetric Determination of Traces of Metals," 3rd Ed., Interscience Publishers, New York (1959), p. 800.
6) T. Shimizu, *Bunseki Kagaku (Japan Analyst)*, **16**, 233 (1967).
7) H. Onishi and C. V. Banks, *Anal. Chim. Acta*, **29**, 240 (1963).
8) V. G. Brudz, V. I. Titov, E. P. Osiko, D. A. Drapkina and K. S. Smirnova, *Zhur. Analit. Khim.*, **17**, 568 (1962).
9) T. Shigematsu, K. Uesugi and M. Tabushi, *Bunseki Kagaku (Japan Analyst)*, **12**, 267 (1963).
10) T. Fujinaga, T. Kuwamoto, S. Tsurubo and K. Kuwabara, *ibid.*, **13**, 127 (1964).
11) S. S. Berman, G. R. Duval and D. S. Russell, *Anal. Chem.*, **35**, 1392 (1963).
12) T. Shigematsu and K. Uesugi, *Bunseki Kagaku (Japan Analyst)*, **16**, 467 (1967).
13) R. Ishida and N. Hasegawa, This Bulletin, **40**, 1153 (1967).

buffer solution. It will be found that chromal blue G is a more sensitive reagent for scandium than eriochrome cyanine R[10] or chromazurol S,[13] and that the proposed method is comparable in sensitivity to the method using pontachrome azure blue B.[9]

Experimental

Reagents. *Standard Scandium Solution.* The standard solution of scandium was prepared by dissolving 153 mg of scandium oxide (Mitsuwa Chemicals) in 50 m*l* of concentrated hydrochloric acid and then by diluting the solution to 1 *l*. This solution contained 100 μg of scandium per m*l*. This stock solution was then diluted to the concentration required for each experiment.

Chromal Blue G Solution. The chromal blue G (Geigy Company, Inc., New York, U.S.A.) was purified by recrystallization from ethanol before use, and 0.1 g of it was dissolved in 100 m*l* of 95% ethanol. This solution was stable for at least a month.

Buffer Solution (*pH* 6.0). A buffer solution of pH 6.0 was prepared by mixing a 0.2 M acetic acid solution and a 0.2 M sodium acetate solution.

All other reagents were analytical grade in quality and were used without further purification.

Apparatus. Absorbance measurements were made with a Hitachi spectrophotometer, model 139, using 1.00-cm matched quartz cells. The pH measurements were carried out with a Hitachi-Horiba glass electrode pH meter, model M-4.

The Standard Procedure for the Determination of Scandium. Transfer the sample solution containing 3—30 μg of scandium to a 25 m*l* volumetric flask and add 2 m*l* of the 0.1% chromal blue G solution. Then add 10 m*l* of the buffer solution (pH 6.0), shake well, and make up to the mark with distilled water. After 20 min, measure the absorbance at 590 mμ, using a reagent blank solution treated in a similar manner as a reference.

Results and Discussion

Absorption Curves. The absorption curves of the reagent solution at various pH values are shown in Fig. 1. The maximum absorption of the reagent solution are found at 480 mμ below pH 4.0, at 430 mμ over the pH range from 5.5 to 10.0, and at 590 mμ above pH 10.5. The absorption curves of the scandium complex at different pH are shown in Fig. 2. The curves in Fig. 2 were obtained by measuring the absorbance of colored solutions containing 0.6 ppm of scandium against a reagent blank containing the same amount of the reagent. The maximum absorption of the complex is found at 590 mμ in acidic media, above pH 7.0, the position of the maximum absorption shifts toward a longer wavelength.

Effect of the pH on Color Development. The effect of the pH on the color development of the scandium complex was examined by measuring the absorbance of a colored solution at 590 mμ. The results are shown in Fig. 3, from which it can be seen that the maximum intensity can be obtained in the pH range from 5.8 to 6.5. An acetic acid-acetate buffer solution, pH 6.0, was found to be satisfactory for this purpose.

Rate of the Color Development. The color of the scandium complex gradually develops at room temperature; the full color is obtained 15 minutes after preparation and then remains almost constant for at least an hour.

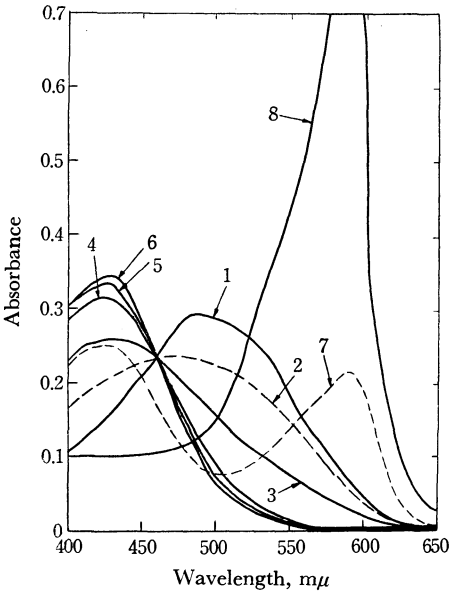

Fig. 1. Absorption spectra of reagent at various pH.
Reagent 20 ppm
pH 1: 4.0, 2: 4.5, 3: 5.0, 4: 5.5, 5: 6.0—6.5, 6: 7.5, 7: 11.5, 8: 12.5

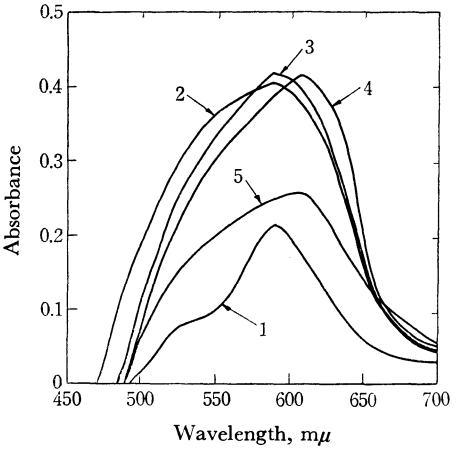

Fig. 2. Absorption spectra of scandium complex at various pH.
Sc 0.6 ppm, Reagent 80 ppm
Reference: Reagent blank
pH 1: 4.0, 2: 5.5, 3: 6.0—6.5, 4 :7.0, 5: 8.0

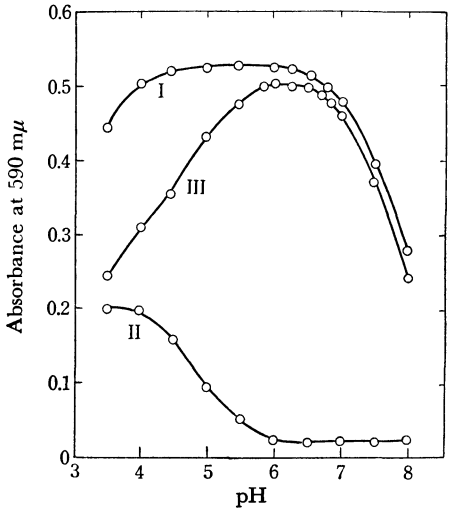

Fig. 3. Effect of pH on color intensity.
I: Reagent 80 ppm+Sc 0.72 ppm (Reference: water)
II: Reagent 80 ppm (Reference : water)
III: Reagent 80 ppm+Sc 0.72 ppm (Reference: Reagent blank)

Effect of Amount of the Reagent on Color Intensity. The effect of variable amounts of the reagent on the color development was examined for a definite concentration of scandium. The absorbance of the scandium complex at 590 mμ gradually increases at higher reagent concentrations. Therefore, it is necessary to keep constant the amount of the reagent added. Two milliliters of a 0.1% solution of the reagent were found to be sufficient for less than 1.2 ppm of scandium.

Effect of Temperature on the Color Development. There was no variation in the absorbance of the color system over the temperature range from 10 to 30°C.

Beer's Law. The scandium complex is found, using the standard procedure, to follow Beer's law up to 1.2 ppm of scandium. The molar extinction coefficient is 3.14×10^4 at 590 mμ. The spectrophotometric sensitivity of the reaction is 1.4×10^{-3} μg Sc/cm², corresponding to $\log I_0/I = 0.001$.

Effect of Diverse Ions. The effect of 28 cations and some anions on the determination of scandium were examined. Copper(II), cobalt(II), beryllium, iron(III), chromium(III), yttrium, and rare earth elements interfere. These cations give a positive error in the determination of scandium, as these also form colored complexes with the reagent in a slightly acidic medium. Chloride, nitrate, sulfate, and acetate do not interfere, even at a high concentration.

Complex Formation. The method of continuous variations was applied for the determination of the component of the proposed scandium complex with chromal blue G. The results are

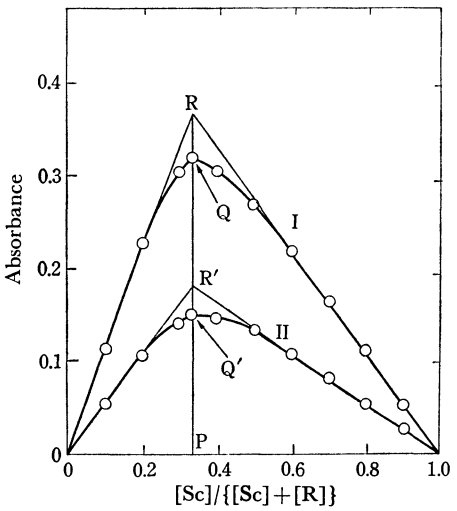

Fig. 4. Continuous variation method.
pH 6.0, 25°C
I: $[Sc]+[R]=7.0\times10^{-5}$M
II: $[Sc]+[R]=3.5\times10^{-5}$M

shown in Fig. 4, which indicates that a 1-to-2 complex is formed between scandium and chromal blue G. These results were confirmed by the mole-ratio method.

The formation constant was calculated from the curves obtained by the continuous-variation method. As the mole ratio of the scandium-chromal blue G complex is 1 : 2, the reaction can be expressed as:

$Sc + 2R \rightleftarrows ScR_2$			
0	0	C	initial concentration
αC	$2\alpha C$	$C(1-\alpha)$	equilibrium concentration

where C is the total concentration of the complex in moles per liter assuming no dissociation and where α is the degree of dissociation. The formation constant, K, was estimated from the curves shown in Fig. 4 on the basis of the following relationships:[14]

$$K = C(1-\alpha)/(\alpha C)(2\alpha C)^2$$

$$\alpha = (E_m - E_s)/E_m$$

where E_m is the maximum extinction of the complex when all the scandium is present in the form of the complex, and where E_s is the actual absorbance of the complex. The value of E_m and E_s correspond to PR or PR′ and PQ or PQ′ respectively. The formation constant at pH 6.0 and 25°C was estimated to be 2.8×10^{10}.

The proposed method using chromal blue G has several advantages as a reagent for scandium: the maximum absorbance can be obtained rapidly; no extraction of the complex is required, since the scandium complex is water-soluble; it is also comparable with the method using pontachrome

14) A. E. Harvey, Jr., and D. L. Manning, *J. Am. Chem. Soc.*, **72**, 4488 (1950).

azure blue B,[9] and this method is much more sensitive than any other of the methods mentioned above.

The author wishes to express his hearty thanks to Professor Tsunenobu Shigematsu and Dr. Masakazu Matsui of the Institute for Chemical Research, Kyoto University, for their kind guidance.

BULLETIN OF THE CHEMICAL SOCIETY OF JAPAN VOL. 42 2054—2056 (1969)

The Reaction of *N*-Acylmethylisoquinolinium Betain with Heterocumulens*1

Shigeru SATO and Masaki OHTA

Laboratory of Organic Chemistry, Tokyo Institute of Technology, Ookayama, Meguro-ku, Tokyo

(Received October 9, 1968)

Among the various methods of formation of mesoionic compounds, the 1,3-dipolar cycloaddition method has been widely investigated by Huisgen *et al.*[1,2] In an earlier paper,[3] we reported the preparation of mesoionic triazolone by means of the 1,3-dipolar addition between 3-phenylsydnone and phenyl isocyanate. Kroehnke and his coworkers prepared the mesoionic thiazolo[2,3-*a*]isoquinolinium ring system by treatment of *N*-arylmethyl- and *N*-acylmethylisoquinolinium salts with carbon disulfide and alkali, in which 1,3-dipolar cycloaddition followed by dehydrogenation occurred as shown below.[4,5]

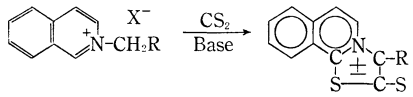

In this paper we wish to report the results of reactions of pyridinium and isoquinolinium betain with heterocumulens.

When triethylamine was added into the solution of *N*-phenacylisoquinolinium bromide (I) and an equimolar amount of phenyl isothiocyanate in dimethylformamide, the yellow precipitates were separated out immediately. The structure of this compound was assinged to be 2-(α-phenylthiocarbamoylphenacyl)isoquinolinium enol betain (II) based on the elementary and spectral analyses. II was obtained directly by the treatment of *N*-phenacyl-isoquinolinium enol betain (III) with phenyl isothiocyanate in quantitative yield. Similarly 2-(α-phenylcarbamoylphenacyl)isoquinolinium enol betain (IV) was obtained by the treatment of III with phenyl isocyanate. However, dicyclohexylcarbodiimide did not react with III.

The hydrolysis of II with hydrochloric acid gave 2-(phenylthiocarbamoyl) isoquinolinium chloride, while II was stable towards the hydrolysis with sodium hydroxide.

The oxidative ring closure of II by air did not occur by passing of air into the solution of II in ethanol for a day. However, II underwent cyclization and dehydrogenation on being heated in toluene for two hours to give anhydro-2-mercapto-3-benzoyl-imidazolo[2,3-*a*]isoquinolinium hydroxide (V) in 40% yield. Furthermore V was obtained by the oxidation of II with potassium ferricyanide

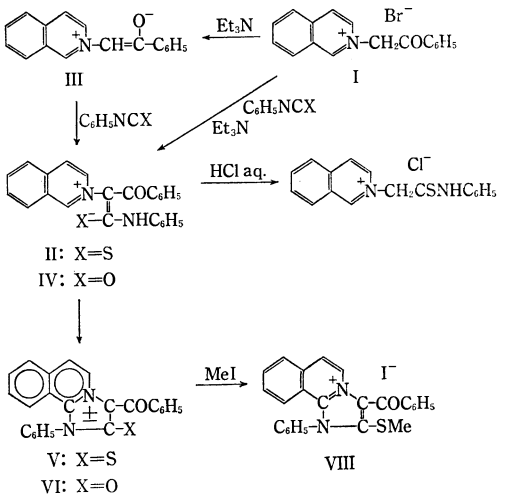

*1 This paper was presented at the 20th Annual Meeting of the Chemical Society of Japan, Tokyo, April, 1967.

1) R. Huisgen, E. Funke, F. C. Schaefer, H. Gotthardt and E. Brunn, *Tetrahedron Letters*, **1967**, 1809.

2) R. Huisgen, R. Grashey and R. Krishke, *ibid.*, **1962**, 387.

3) S. Sato and M. Ohta, *ibid.*, **1967**, 4261.

4) F. Kroehnke and H. Steuernagel, *Angew. Chem.*, **73**, 36 (1961); *Chem. Ber.*, **97**, 1118 (1964).

5) J. E. Baldwin, M. C. McDaniel, M. Newton and I. C. Paul, *Tetrahedron Letters*, **1966**, 4239.

in 50% yield. A similar treatment of IV with potassium ferricyanide gave anhydro-2-hydroxy-3-benzoyl-imidazolo[2,3-*a*]isoquinolinium hydroxide (VI).

The significant differences of the IR spectra between V and VI were as follows: V has strong absorptions at 1550 cm^{-1} and 1350 cm^{-1}. VI has strong absorptions at 1650 cm^{-1} and 1550 cm^{-1}, but no absorption at 1350 cm^{-1}. These absorptions are attributed as follows: the absorption at 1650 cm^{-1} is due to the ring-carbonyl group, 1350 cm^{-1} to the ring-thiocarbonyl group and 1550 cm^{-1} to the carbonyl group of the benzoyl group. These facts suggest that the carbonyl group of the benzoyl group is fairly polarized, and among the many canonical forms such as VIIa—c which are considered to contribute to the resonance of V and VI, VIIa may be the most important contributor.

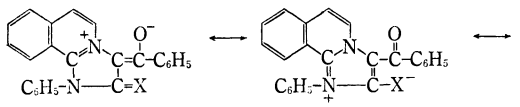

VIIa VIIb

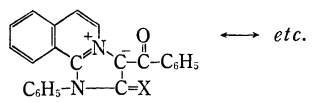

VIIc

V and VI did not melt at 300°C and did not undergo hydrolysis with hydrochloric acid or sodium hydroxide. V was converted to *S*-methyl derivative (VIII) by treatment with methyl iodide in an almost quantitative yield.

An unidentified resinous oil was obtained by oxidation of 2-(α-phenylcarbamoylphenacyl)- and 2-(α-phenylthiocarbamoylphenacyl)pyridinium enol betain[6] (IX) with potassium ferricyanide in boiling DMF. It may be produced by the decomposition of the corresponding mesoionic compounds or the starting material under oxidative reaction conditions.

In order to obtain 2-(α-phenylcarbamoylmethyl)-isoquinolinium enol betain (X), 2-benzylisoquinolinium chloride was reacted with phenyl isocyanate in the presence of triethylamine. However, the trimer of phenyl isocyanate was obtained instead of X. The hydrochloride (XI) of X was obtained by the treatment of isoquinoline and phenylchloroacetanilide. However, the treatment of XI with triethylamine gave the tarry substances from which nothing was obtained in pure state.

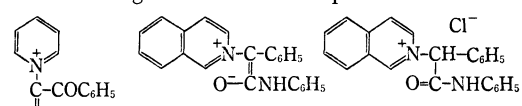

XI X XI

6) These compounds were prepared by Kroehnke's method: F. Kroehnke and H. Koebler, *Ber.*, **70**, 538 (1937).

When the benzylpyridinium chloride was reacted with phenyl isothiocyanate or phenyl isocyanate, *N*,*N'*-diphenylthiourea and carbanilide were obtained respectively.

Experimental[7]

Preparation of 2-(α-Phenylthiocarbamoylphenacyl)isoquinolinium Enol Betain (II). (A) Into a solution of 3.1 g of I and 1.3 g of phenyl isothiocyanate in 10 m*l* of water and 50 m*l* of dimethylformamide (DMF), 1.5 g of triethylamine was added dropwise with stirring. Immediately orange precipitates were separated out. After stirring for half an hour, 50 m*l* of water was added and the precipitates were collected by filtration and recrystallized from ethanol to give 3.5 g of II, yellow needles; mp 175—177°C. Found: C, 75.57; H, 4.34; N, 7.37%. Cacld for $C_{24}H_{18}N_2SO$: C, 75.39; H, 4.71; N, 7.33%.

(B) 0.3 g of phenyl isothiocyanate was added into a suspension of 0.5 g of III in 50 m*l* of DMF, which was stirred for half an hour. After removal of the solvent under reduced pressure, oily residue was crystallized by adding ether. After collecting by filtration, the precipitates were recrystallized from ethanol to give 0.65 g of II; mp 175—176°C.

The Hydrolysis of II with Hydrochloric Acid. A solution of 1 g of II in 80 m*l* of ethanol and 4 m*l* of concentrated hydrochloric acid was refluxed for 2 hr. After removal of the solvent under reduced pressure, the residual precipitates were recrystallized from ethanol to give 0.5 g of 2-(α-phenylthiocarbamoylmethyl)isoquinolinium chloride, pale yellow prisms; mp 230—232°C. Found: C, 64.73; H, 4.52; N, 8.82%. Calcd for $C_{17}H_{15}N_2SCl$: C, 64.86; H, 4.78; N, 8.96%.

Preparation of 2-(α-Phenylcarbamoylphenacyl)-isoquinolinium Enol Betain (IV). Into a suspension of 3.3 g of I and phenyl isocyanate in 50 m*l* of dry DMF, 2.5 g of triethylamine was added dropwise with stirring. After stirring for 5 hr, the solvent was removed under reduced pressure. The residual precipitate were collected and recrystallized from ethanol to give 4 g of IV; yellow needles, mp 190—192°C. Found: C, 78.28; H, 5.33; N, 7.66%. Calcd for $C_{24}H_{18}N_2O_2$: C, 78.67; H, 4.95; N, 7.65%.

The Oxidative Ring-closure of II and IV. (A) A suspension of 1 g of II and 1 g of potassium ferricyanide in 50 m*l* of DMF and 50 m*l* of water was refluxed for half an hour. After cooling, a large amount of water was added and separated precipitates were collected by filtration. Recrystallization from dimethyl sulfoxide (DMSO) gave 0.5 g of V, pale yellow needles; mp over 300°C. V was insoluble in ethanol, benzene and ether, and soluble in hot DMSO. Found: C, 75.27; H, 4.45; N, 7.51%. Calcd for $C_{24}H_{16}N_2OS$: C, 75.79; H, 4.21; N, 7.38%.

The same treatment of IV with potassium ferricyanide as mentioned above gave VI, pale yellow needles. VI did not melt at 300°C. Found: C, 78.24; H, 4.41; N, 7.89%. Calcd for $C_{24}H_{16}N_2O_2$: C, 79.12; H, 4.39; N, 7.69%.

(B) A suspension of 1.2 g of II in 100 m*l* of toluene

7) All melting points were determined on a hot plate and were not corrected.

was refluxed for 2 hr. After removal of the solvent, the residual crystals were recrystallized from DMSO to give 0.3 g of V; mp over 300°C.

The Methyl Derivative of V (VIII). A suspension of 0.5 g of V in 30 m*l* of acetic acid and 0.5 m*l* of methyl iodide was refluxed for a few minutes. After cooling, ether was added into the solution, and the separated precipitates were collected by filtration. The recrystallization from ethanol gave VIII. Yield was almost quantitative. VIII did not melt at 300°C. Found: N, 5.58%. Calcd for $C_{25}H_{19}IN_2OS$: N, 5.47%.

Preparation of 2-(α-Phenylcarbamoylbenzyl)-isoquinolinium Chloride (XI). A mixture of 0.6 g of isoquinoline and 1.2 g of phenylchloroacetanilide was heated at 120—125°C in an oil bath for 5 min. After cooling, the oily reaction mixture was crystallized by the addition of acetone, and was collected by filtration. The recrystallization from ethanol gave 1.4 g of XI, colorless silky needles; mp 245°C. Found: C, 73.33; H, 5.34; N, 7.53%. Calcd for $C_{23}H_{19}ClN_2O$: C, 73.80; H, 5.08; N, 7.49%.

Reaction of *N*-Benzylisoquinolinium Chloride with Phenyl Isocyanate in the Presence of Triethylamine. Into a solution of 5.2 g of *N*-benzylisoquinolinium chloride and 1.5 g of phenyl isocyanate in 100 m*l* of dry DMF, 2.5 m*l* of triethylamine was added dropwise with stirring. The solution was stirred for 5 hr. After removal of the solvent under reduced pressure, 50 m*l* of water and 20 m*l* of alcohol were added into the oily residue, and the separated precipitates were collected by filtration. The recrystallization from ethanol gave 1.2 g of the trimer of phenyl isocyanate; mp 288—289°C.

Reaction of *N*-Benzylpyridinium Chloride with Phenyl Isothiocyanate. Into a solution of 3 g of *N*-benzylpyridinium chloride and 3.7 g of phenyl isothiocyanate in 50 m*l* of acetonitrile, 3.7 g of triethylamine was added dropwise with stirring. After stirring for one hour, the reaction mixture was evaporated to dryness under reduced pressure. Into the residual mixture of triethylamine hydrochloride and oily product, 50 m*l* of water added. The separated precipitates were collected by filtration and recrystallized from ethanol to give 2 g of pale yellow needles; mp 157—158°C. No depression of the melting point on admixture with *N,N'*-diphenylthiourea was observed.

Similarly, by the treatment of *N*-benzylpyridinium chloride with phenyl isocyanate, carbanilide was obtained.

BULLETIN OF THE CHEMICAL SOCIETY OF JAPAN VOL. 42 2056—2058 (1969)

Selenium Dioxide Oxidation of Styrene and Norbornene

Khan A. JAVAID, Noboru SONODA and Shigeru TSUTSUMI

Department of Chemical Technology, Faculty of Engineering, Osaka University, Yamadakami, Suita, Osaka

(Received October 12, 1968)

Oxidation of olefins by selenium dioxide generally produces allylic derivatives resulting from the oxidation at α-methyl or α-methylenic carbon atom.[1-6] So it was interesting to study the behavior of the olefins like styrene and norbornene where such carbon atom is not present. Norbornene was selected also for studying the ionic nature of the reaction. Styrene reportedly did not react with selenium dioxide in a sealed tube.[7] Here we report the oxidation of these olefins using glacial acetic acid and some other solvents.

Results and Discussion

Oxidation of styrene with selenium dioxide in glacial acetic acid at 150—160°C in an autoclave produced styrene glycol diacetate in a good yield. The other products were phenylglyoxal and styrene glycol monoacetate.

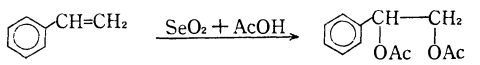

The identification of the products was carried out by IR and glc analyses by comparison with authentic samples. No organoselenium compound could be characterized. An almost stoichiometric amount of metallic selenium was deposited under suitably controlled experimental conditions. Base-catalyzed hydrolysis of the products gave styrene glycol.

When dioxane was used as the solvent phenyl-

1) N. Rabjohn, "Organic Reactions," Vol. 5, John Wiley & Sons, Inc., New York and London (1949), p. 331.
2) A. Guillemonat, *Ann. Chim.*, **11**, 143 (1939).
3) J. P. Schaefer and B. Horvath, and H. R. Klein, *J. Org. Chem.*, **33**, 2647 (1968).
4) J. P. Schaefer and B. Horvath, *Tetrahedron Letters*, **1964**, 2023.
5) K. Wiberg and S. D. Neilsen, *J. Org. Chem.*, **29**, 3353 (1964).
6) J. L. Huguet, Presented at International Oxidation Symposium, San Francisco, California, August 28, 1967.
7) H. L. Riley and N. A. Friend, *J. Chem. Soc.*, **1932**, 2342.

glyoxal was obtained in an 11% yield with a trace of benzaldehyde. To examine the possibility of styrene glycol formation, water was added to the dioxane, but styrene glycol could be obtained in trace only. Some other solvents like methyl alcohol, *t*-butyl alcohol and DMSO were also tried. The results are summarized in Table 2. Polymerization of styrene was observed in all cases except when the acetic acid was used as the solvent.

Oxidation of norbornene with selenium dioxide in glacial acetic acid under the similar conditions as employed for the oxidation of styrene produced 2,3-*exo-cis*-norbornane diacetate and 2,7-*exo-syn*-norbornane diacetate in the ratio of 2 to 1. Appreciable amounts of monoacetates could not be detected as the qualitative glc analysis remained almost the same after treatment of the reaction products with acetic anhydride. The base-catalyzed hydrolysis of the reaction products gave a mixture of 2,7-*exo-syn*-norbornane diol and 2,3-*exo-cis*-norbornanediol which showed a positive test for vicinal alcohols by periodic acid.

Our results are in good agreement with the mechanism postulated by Schaefer[3,4] which suggests the electrophilic attack of selenium dioxide itself or conjugate acid of selenium dioxide on the double bond of the olefin. Again, in the oxidation of norbornene the formation of rearranged product 2,7-*exo-syn*-norbornane diacetate apart from the 2,3-*exo-cis*-norbornane diacetate, indicates that oxidation is passing through a carbonium ion.

Strained olefins such as bicycloheptene or bicyclooctene usually add electrophiles with rearrangement,[8b] or with trans stereochemistry,[8a] but many reagents as mercuric acetate,[9] nitrosyl chloride[10] and hydrogen halides,[8b] *etc.* have been observed to add in cis fashion. In our experiments, both cis addition and rearrangement occurred with preference to cis addition.

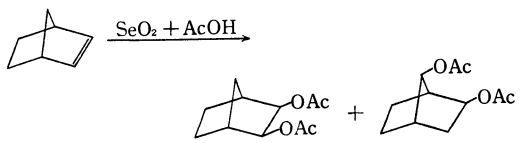

The formation of cis product can be attributed to the torsional and windshield wiper effects.[9] From the experimental data it can be further noted that the yields are very low in the solvents other than

Table 1. Oxidation of styrene and norbornene with selenium dioxide in glacial acetic acid

Olefin	Reaction Temp. °C	Reaction Time hr	Product	Yield %
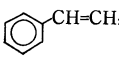	150	10	$C_6H_5CHOAcCH_2OAc$	52.0
			$C_6H_5CHOAcCH_2OH$	7.0
			C_6H_5COCHO	3.0
	150	10	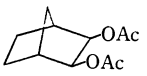	25.0
			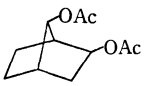	15.0

Table 2. Effect of solvents on the styrene oxidation

No.	Solvent	Reaction temp °C	Reaction time, hr	Product	Yield %
1	Dioxane	140—150	10	C_6H_5CHO	Trace
				C_6H_5COCHO	11.0
2	Dioxane water 15%	145—150	10	C_6H_5CHO	0.4
				C_6H_5COCHO	6.0
				$C_6H_5COCH_2OH$	2.0
				$C_6H_5CHOHCH_2OH$	1.0
3	Dioxane water 15% H_2SO_4 0.3%	145—150	10	C_6H_5CHO	0.8
				C_6H_5COCHO	6.0
				$C_6H_5COCH_2OH$	4.0
4	Dioxane CH_3OH 20%	120—130	11	No reaction	
5	Dioxane CH_3OH 20%	170—180	11	C_6H_5CHO	4.0
				C_6H_5COCHO	2.0
				Unknown	2.0
6	*t*-BuOH	120	10	C_6H_5CHO	Trace
				C_6H_5COCHO	8.0
				Unknown	6.0
7	*t*-BuOH	160—170	10	C_6H_5CHO	Trace
				C_6H_5COCHO	5.0
				Decomposition products	

8) a) H. Kwart and J. L. Nyce, *J. Am. Chem. Soc.*, **86**, 2601 (1964). b) H. Kwart and R. K. Miller, *ibid.*, **78**, 5678 (1956).

9) A. Factor and T. G. Traylor, *J. Org. Chem.*, **33**, 2607 (1968); T. Tidwell and T. G. Traylor, *ibid.*, **33**, 2614 (1968).

10) J. Meinwald, Y. C. Meinwald and T. N. Baker, *J. Am. Chem. Soc.*, **86**, 4074 (1964).

acetic acid. This catalytic effect of acetic acid has been well explained by Olson.[11]

Experimental

Oxidation of Styrene in Acetic Acid. In a 30 m*l* of glacial acetic acid 5 g of anhydrous selenium dioxide was dissolved and 5 g of freshly distilled styrene was added. The solution was put in a 50-m*l* autoclave and volume made up to 40 m*l* with acetic acid. Heating was continued at 150—160°C for 10 hr. The temperature was raised to 180°C for the last two hours. The metallic selenium was filtered off. Acetic acid was removed by distillation under reduced pressure. The fraction boiling at 118—125°C/2mmHg was identified to be a mixture of phenylglyoxal[12] (3%) bp 95—97°C/25mmHg, styrene glycol monoacetate[13] (7%) and styrene glycol diacetate[14] (52%) bp 159.5°C/18mmHg by comparison of their glc and IR with authentic samples. Base-catalyzed hydrolysis gave white needles after recrystallization from *n*-hexane. Its IR and mixture melting point were in complete agreement with that of authentic styrene glycol.[15]

Oxidation of Styrene in Different Solvents. The same procedure as mentioned above was repeated using dioxane, dioxane - water, dioxane - water - sulfuric acid, dioxane - methyl alcohol and *t*-butyl alcohol respectively. The experimental conditions are given in Table 2. Qualitative and quantitative analyses of the products were carried out by IR and glc.

Oxidation of Notbornene in Acetic Acid. Five grams of selenium dioxide was dissolved in 30 m*l* of acetic acid and 5 g of norbornene was added. The reactants were heated for 10 hr at 140—150°C in the 50-m*l* autoclave. After filtering off the metallic selenium and removing the acetic acid by distillation under vacuum, the distillate boiling at 70—99°C/2mmHg was collected. Product identification was carried mainly by glc techniques. S. E. 30 column was found suitable for separating the isomers of norbornane diacetate. 2,3-*exo-cis*-Norbornane diacetate (25%) and 2,7-*exo-syn*-norbornane diacetate (15%)[16] were found as main products by comparison with authentic samples. Authentic 2,3-*exo-cis*-norbornane diacetate was prepared by esterification of 2,3-*exo-cis*-norbornanediol.[17] Four grams of 2,3-diol was treated with 40 m*l* of acetic anhydride in 100 m*l* of pyridine for 4 hr under reflux.

Base-Catalyzed Hydrolysis of the Products. To 1 g of reaction products were added 50 m*l* of methyl alcohol, 5 g of sodium hydroxide and 5 m*l* of water. The mixture was refluxed for 4 hr. After filtration and adjusting the pH to 6, methyl alcohol was distilled off and the remaining liquid was extracted with hot *t*-butyl alcohol, dark sticky crystals were obtained which were dissolved in a small amount of ethyl alcohol and the solution was put in the sublimation tube. Ethyl alcohol was evaporated at 100°C and then sublimation was carried out at 120—130°C/20mmHg. White crystals melting near 165°C were obtained. The IR was analogous to a mixture of 2,3-*exo-cis*-norbornane diol and 2,7-*exo-syn*-norbornanediol and their presence was confirmed by glc analysis. The crystals also gave a positive periodic acid test for vicinal alcohols due to the presence of 2,3-exo-*cis*-norbornanediol.

Khan A. Javaid thanks the Ministry of Education, Japan for granting a scholarship.

11) D. H. Olson, *Tetrahedron Letters*, **1966**, 2053.
12) H. A. Riley and A. R. Grey, "Organic Syntheses," Vol. 15, p. 67 (1935).
13) T. Cohen, M. Dughi, V. A. Notaro and G. Pinkus. *J. Org. Chem.*, **27**, 814 (1962).
14) W. L. Evans and E. H. Morgan, *J. Am. Chem. Soc.*, **35**, 54 (1913).
15) M. A. Nicholas and S. Sussman, *ibid.*, **59**, 2345 (1937).
16) N. Sonoda and S. Tsutsumi, This Bulletin, **38**, 958, (1965).
17) H. Kwart and W. G. Vosbugh, *J. Am. Chem Soc.*, **76**, 5400 (1954).

BULLETIN OF THE CHEMICAL SOCIETY OF JAPAN VOL. 42 2059—2061 (1969)

On the Erlenmeyer Reaction. II. Mechanism of DL-*threo*-*N*-Benzal-diphenylhydroxyethylamine Formation[1]

Kaoru HARADA

Institute of Molecular Evolution and Department of Chemistry, University of Miami Coral Gables, Florida 33134 U.S.A.

(Received October 11, 1968)

Erlenmeyer reported that glycine condensed easily with benzaldehyde in strongly alkaline aqueous ethanol.[2,3] The rapid condensation reaction at room temperature resulted in the formation of sodium salt of *threo*-*N*-benzalphenylserine.[4] The mechanism of the *threo*-phenylserine formation was explained in the earlier report[5] by a second order asymmetric transformation.

From the reaction mixture of the Erlenmeyer phenylserine formation, *N*-benzalisodiphenylhydroxyethylamine (*threo*-isomer) was isolated. The *threo*-diphenylhydroxyethylamine (*threo*-DHEA) was found to be the main product when three moles (instead of two moles) of benzaldehyde were used.[6] The presence of the more soluble *erythro*-*N*-benzal-DHEA isomer in the reaction mixture was identified.[6] It was found in the previous study[5] that the amount of DHEA in the Erlenmeyer reaction increased steadily with time. It was also found that with long reaction time, the final product was crystalline *threo*-*N*-benzal-DHEA. From these results, it may be inferred that *erythro*-DHEA is converted into the *threo*-DHEA during the reaction.

In order to elucidate the stereochemical course of Erlenmeyer's DHEA formation, several sets of synthetic and conversion reactions were carried out. These reactions are: 1) glycine, benzaldehyde and alkali; 2) DL-*threo*-phenylserine, benzaldehyde and alkali; 3) DL-*erythro*-phenylserine, benzaldehyde and alkali; 4) DL-*erythro*-DHEA, benzaldehyde and alkali; 5) L-(+)-*erythro*-DHEA, benzaldehyde and alkali; 6) D-(+)-*erythro*-*N*-benzal-DHEA and alkali. These reactions were carried out in alcoholic aqueous solution at room temperature in a manner similar to that of the Erlenmeyer reaction. It was found that final products of reactions 1)—6) were all DL-*threo*-*N*-benzal-DHEA. Melting points, elemental analyses, and infrared absorption spectra all agreed with the authentic DL-*threo*-*N*-benzal-DHEA. Results are

TABLE 1. FORMATION OF DL-*threo*-DIPHENYLHYDROXYETHYLAMINE

	Starting material g(mol)	PhCHO ml (mol)	KOH g	Solvent EtOH ml	Solvent H_2O ml	*N*-Benzal-DHEA,*2 g	Mp*3 °C	Nitrogen analysis*4 Found, %
1	Gly 1.50 (0.02)	6.4 (0.04)	3.5	10	20	2.70	132—133	4.57
2	*threo*-Ph-Ser H_2O 3.08 (0.02)	3.2 (0.02)	3.5	10	20	2.65	132—133	4.64
3	*erythro*-Ph-Ser, 1/2 dioxane 4.50 (0.02)	3.2 (0.02)	3.5	10	20	2.58	132—133	4.80
4	DL-*erythro*-DHEA*1 4.26 (0.02)	3.2 (0.02)	3.5	35	5	2.58	132—133	4.84
5	L-*erythro*-DHEA*1 2.13(0.01)	1.6 (0.01)	1.6	17	2.5	1.78	131—132	4.67
6	*N*-Benzal-D-*erythro*-DHEA*1	—	0.9	9	1.3	0.28	131—132	4.80

*1 Reaction mixtures of 4) and 5) were heated at 60—65°C for 10 min to dissolve DHEA.
*2 The yields show the weights of crystal after washing.
*3 The melting points show after one recrystallization.
*4 The nitrogen analyses were carried out by Micro-Tech. Laboratories, Skokie, Illinois, U. S. A. Calculated value of the nitrogen analysis is 4.65%.

1) Contribution No. 113 of the Institute of Molecular Evolution, University of Miami.
2) E. Erlenmeyer, Jr., *Ber.*, **25**, 3455 (1892).
3) E. Erlenmeyer, Jr., and E. Frühstück, *Ann.*, **284**, 36 (1894).
4) K. Vogler, *Helv. Chim. Acta*, **33**, 2111 (1950).
5) T. Kaneko and K. Harada, This Bulletin, **34**, 1314 (1961).
6) E. Erlenmeyer, Jr., *Ann.*, **307**, 70 (1899).

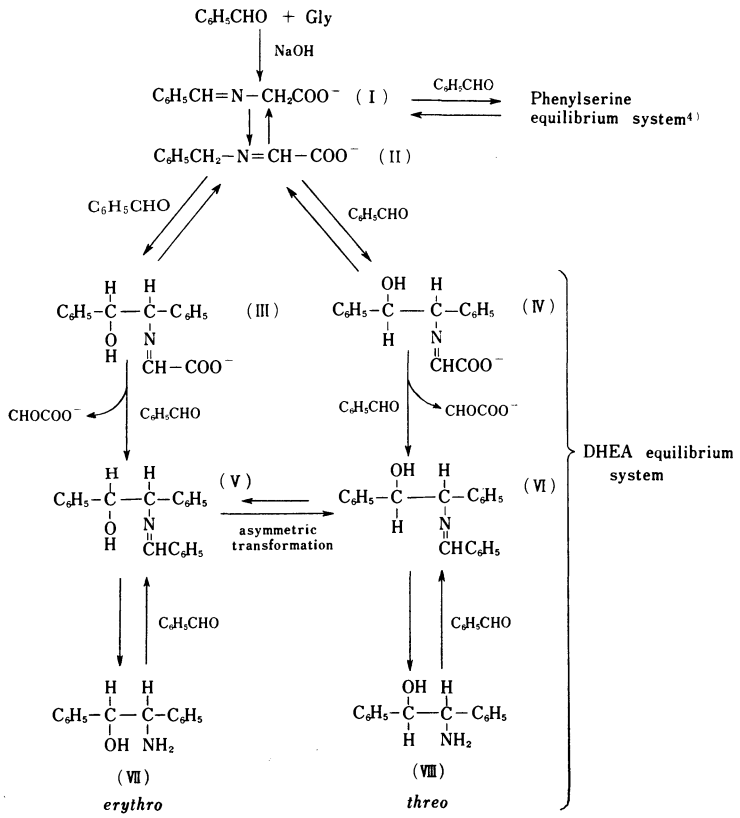

Fig. 1. Postulated mechanism of DL-*threo*-diphenylhydroxyethylamine formation in the Erlenmeyer reaction.

summarized in Table 1. These results suggest a possible mechanism for the formation of DL-*threo*-DHEA in the Erlenmeyer reaction. The postulated pathway of the reactions is shown in Fig. 1.

As described in the earlier study,[5] *N*-benzalglycine (I) was the starting material to form *threo*-phenylserine. The I could be tautomerized under strongly alkaline conditions into structure II, which was proven by isolation of benzylamine from a reaction mixture of the Erlenmeyer reaction.[6,7] The II reacts with benzaldehyde forming two racemic isomers, *erythro* (III) and *threo* (IV) isomers. These III and IV could be converted to *N*-benzal isomers V and VI in the presence of benzaldehyde. The solubility of V in the reaction mixture (alkaline aqueous ethanol) was found to be very large and it does not crystallize. However, the solubility of the corresponding diastereomeric isomer (VI) is small and it crystallized easily from the reaction solvent. Therefore, if there is an equilibrium between V and VI under the reaction conditions, the *erythro* isomer V could be converted into *threo* isomer VI by crystallization (second order asymmetric transformation). It has been reported that the reaction of benzaldehyde with phenylalanine, tyrosine, leucine, and aspartic acid resulted in the formation of corresponding α-keto acids and DL-*threo*-DHEA with no isolable phenylserine analogs.[6,8]

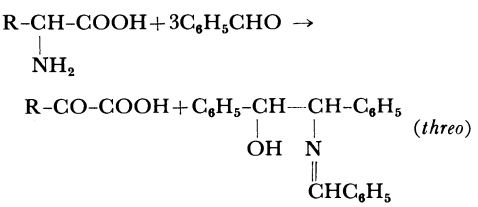

This finding also supports the inference that the DHEA formation is not dependent on the amino acid used but on the intermediate (II) which is tautomerized from the *N*-benzal-amino acid. Under conditions which were employed in this study, optically active *erythro*-DHEA was converted to racemic *threo*-DHEA. Solubility of the optically active *erythro*-*N*-benzal-DHEA was found to be much smaller than that of the racemic *N*-benzal-

7) Benzylamine was also isolated from the reaction mixture of glycine and benzaldehyde by heating at 130°C; T. Curtius and G. Lederer, *Ber.*, **19**, 2462 (1886).

8) E. Erlenmeyer, Jr., *Ann.*, **337**, 205 (1904); *Ber.*, **30**, 2896 (1897).

DHEA in the reaction solvent. Therefore, the reaction mixture was kept at 60—65°C for 10 min at the beginning of the reaction. This might be a reason for the racemization of both asymmetric carbons of optically active *erythro*-DHEA. However, another explanation of the racemization is possible, *i. e.*, a cleavage of α-β carbon linkage. Such a mechanism is conceivable since the α,β-linkage is rather weak.[9] However, at the present time it is difficult to decide whether the conversion pathway is a) direct (V→VI) or b) indirect (V→IX→VI).

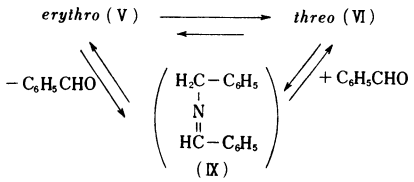

The results obtained in this study and also in the previous study[5] show that there are two large equilibrium systems in the Erlenmeyer reaction (Fig. 1). The one is the phenylserine equilibrium system[5] and the other is the DHEA equilibrium system. These two systems are connected to each other at structure I in Fig. 1. In a short reaction time, the Erlenmeyer reaction resulted in the formation of crystalline sodium salt of DL-*threo*-phenylserine from glycine and benzaldehyde by the second order asymmetric transformation. However, in a prolonged reaction, *threo*-*N*-benzal-DHEA was crystallized out from the reaction mixture by the second order asymmetric transformation.

Experimental

Reaction (1): Formation of DL-*threo*-*N*-benzal-DHEA from Glycine. Glycine, 1.50 g (0.02 mol), was dissolved in a solution of 3.50 g of potassium hydroxide in 20 m*l* of water. The solution was mixed with a solution of 4.75 m*l* of benzaldehyde and 10 m*l* of ethanol under cooling. Nitrogen gas was introduced in the reaction flask and the mixture was shaken until it became clear. Crystallization of *N*-benzal-*threo*-phenylserine sodium salt began after 30 min. The mixture was kept at room temperature. After two days, the crystals of *threo*-phenylserine sodium salt decreased in amount. It seems that the conversion reaction of phenylserine to DHEA took place during this time. In order to complete the conversion reaction, the reaction mixture was kept at room temperature for two more weeks. After the reaction was over, the crystals were filtered and washed with a small amount of cold ethanol, yield 2.70 g, mp 132—133°C. This was recrystallized from 24 m*l* of ethanol, yield 2.33 g, mp 132—133°C. Nitrogen analysis, found: 4.57%. Infrared absorption spectrum: 3480, OH; 2700—3000 monosubstituted benzene; 1650, C=N; 1605, 1590, benzene CH; 754, 700, monosubstituted benzene. The infrared absorption spectrum was found to be identical with that of authentic DL-*threo*-*N*-benzal-DHEA.

Reactions (2) and (3) were carried out in the same way as Reaction (1). In both reactions, DL-*threo*-*N*-benzal-DHEA was isolated after 16 days of reaction.

Reaction (4): Conversion of DL-*erythro*-DHEA to DL-*threo*-DHEA. A mixture of DL-*erythro*-DHEA, 4.26 g (0.02 mol), and 3.20 m*l* of benzaldehyde in 35 m*l* of ethanol was mixed with a solution of 3.5 g of potassium hydroxide and 5.0 m*l* of water. Nitrogen gas was introduced in the reaction flask and the mixture was heated in a water bath at 65°C to dissolve the DHEA under shaking. After the reaction mixture became clear, the solution was cooled by water and was kept at room temperature for 16 days. Crystallization began after 3 hr. Crystals were separated by filtration and were washed with a small amount of cold ethanol. Yield, 2.58 g, mp 130—131°C. This was recrystallized once from ethanol, mp 132—133°C. Infrared absorption spectrum was found to be identical to the authentic DL-*threo*-*N*-benzal-DHEA. Nitrogen analysis, found: 4.84%.

Reaction (5): Conversion of L-(+)-*erythro*-DHEA to DL-*threo*-DHEA. D-(−)- and L-(+)-*erythro*-DHEA was resolved by the use of L- and D-glutamic acid.[10] D-(−)-*erythro*-DHEA, mp 142.5—143°C, $[\alpha]_D^{25}$ −6.0° in absolute ethanol; D-*erythro*-DHEA hydrochloride, mp 213—214°C, $[\alpha]_D^{25}$ −62.8° in H_2O; D-*erythro*-*N*-benzal-DHEA, mp 109°C, $[\alpha]_D^{25}$ +76.9° in absolute EtOH. L-(+)-*erythro*-DHEA, mp 142.5—143°C, $[\alpha]_D^{25}$ +6.3° in absolute ethanol; L-*erythro*-DHEA hydrochloride, mp 213—214°C, $[\alpha]_D^{25}$ +64.2° in H_2O; L-*erythro*-*N*-benzal-DHEA, mp 109°C, $[\alpha]_D^{25}$ −77.3° in absolute EtOH. Reaction (5) was carried out in the same way as reaction (4). Starting from 2.13 g of L-*erythro*-DHEA, 1.78 g of DL-*threo*-*N*-benzal-DHEA was obtained after 6 days of reaction, mp 130—132°C. After one recrystallization, the melting point rose to 131—132°C. No optical rotation was observed. Infrared absorption spectrum was identical to that of the authentic DL-*threo*-*N*-benzal-DHEA. Nitrogen analysis, found: 4.67%.

This work was supported by Grant NGR 10-007-052 of the National Aeronautics and Space Administration, U. S. A., to which the author expresses gratitude. The author wishes to express his thanks to Dr. Takeo Kaneko for his discussion and encouragement.

9) DL-*threo*-DHEA resulted in benzylamine by heating at 130°C.

10) J. Weiland, K. Pfister, III, E. F. Swanezy, C. A. Robinson and M. Tishler, *J. Am. Chem. Soc.*, **73**, 1217 (1951). The literature reported that the specific rotation of D- and L-*erythro*-DHEA were −10.1° and +10.2° respectively. Attempts to obtain D- and L-*erythro*-DHEA which have the specific rotations of −10.1° and +10.2° were unsuccessful. Recent literature [M. Nakazaki, This Bulletin, **36**, 1204 (1963)] reported that the specific rotation of D-(−)-*erythro*-DHEA was −6.4°. However, other physical properties were found to be the same as in the literature by Weiland *et al.*

BULLETIN OF THE CHEMICAL SOCIETY OF JAPAN VOL. 42 2062—2064 (1969)

Fluorination of Inorganic Sulfur Compounds*1

Shunji NAGASE, Takashi ABE and Hajime BABA

Government Industrial Research Institute, Nagoya, Kita-ku, Nagoya

(Received October 22, 1968)

Sulfuryl fluoride has been prepared by a number of methods, including the fluorination of sulfur dioxide,[1-7] sulfur trioxide,[8,9] sulfuryl chloride,[2-4,10,11] and sodium sulfate or sodium sulfite[12] by the use of various inorganic fluorinating agents. The thermal decompostion of barium fluorosulfonate has been known to yield sulfuryl fluoride.[13] The formation of sulfuryl fluoride has also been observed in the electrochemical fluorination of fluorosulfonic acid[14] and in that of several inorganic sulfur compounds.[15] In the electrolysis of a liquid mixture of sulfur dioxide and hydrogen fluoride at a low temperature,[16] and in that of inorganic sulfur compounds in fused potassium-dihydrofluoride,[15] sulfuryl fluoride was found among the products.

Sulfuryl fluoride is a useful commercial fluorochemical; it is, for example, a good insecticidal fumigant.[17] In the course of our studies of the electrochemical fluorination of gaseous compounds,[18] we have now found that sulfuryl fluoride can be readily produced in a good yield directly from gaseous sulfur dioxide. This electrochemical process involves the bubbling of the starting material into anhydrous liquid hydrogen fluoride. In the present paper, emphasis will be placed on the application of this recently-developed electrochemical method of the fluorination of gaseous compounds for the production of sulfuryl fluoride.

The electrochemical fluorination of related sulfur compounds, such as thionyl fluoride, thionyl chloride, sulfuryl chloride, sulfur mono-, and dichlorides, was also carried out in order to clarify their behavior in the fluorination.

Experimental

Materials. Sulfur dioxide (99.9%) was obtained from the Takachiho Chemical Industrial Co. Thionyl fluoride was prepared by the procedure given in the literature.[19] Thionyl chloride, sulfuryl chloride, sulfur mono-, and dichlorides were redistilled under atmospheric pressure or at reduced pressure before use. Anhydrous hydrogen fluoride (99%) was used after preliminary electrolysis.

Fluorination of Sulfur Dioxide. The apparatus and procedures for the fluorination have previously been described.[20] The electrolysis was carried out without using a conductivity additive. The exit gases from the sodium fluoride tube were regularly monitored by gas chromatography by taking the sample through a sampling valve placed immediately after the tube. Chromatographic analyses were carried out with a Shimadzu GC-2C model chromatograph, using a 0.3 cm i.d. × 6 m column packed with 60% (by wt) perfluoro-tri-*n*-butylamine*2 on 60/80 mesh Celite 545 SK.*3 (Column temperature: 0°C; carrier gas: helium).

The products formed (in the order of their peak appearance in the chromatogram) were as follows:

*1 "Electrochemical Fluorination of Gases." Part VI.

1) H. Moissan and P. Lebeau, *Compt. rend.*, **132**, 374 (1901).
2) H. J. Emeléus and J. F. Wood, *J. Chem. Soc.*, **1948**, 2183.
3) M. M. Woyski, *J. Am. Chem. Soc.*, **72**, 919 (1950).
4) L. J. Belf, Brit. Pat. 727062 (1955).
5) R. Ruh, R. A. Davis and K. A. Allswede, U. S. Pat. 3092458 (1963).
6) L. G. Anello and C. Woolf, U. S. Pat. 3107979 (1963); Japanese Pat. Publ. 4051 (1963).
7) A. G. Bisignani and R. H. Edgecomb, U. S. Pat. 3320030 (1967).
8) H. A. Pacini and A. E. Pavlath, U. S. Pat. 3132925 (1964).
9) J. R. Soulen, U. S. Pat. 3146068 (1964).
10) K. Wiechert, *Z. anorg. allgem. Chem.*, **261**, 310 (1950).
11) W. Sundermeyer, *ibid.*, **314**, 100 (1962).
12) M. Picon and L. Domange, *Compt. rend.*, **236**, 704 (1953).
13) W. Traube, J. Hoerenz and F. Wunderlich, *Ber.*, **52**, 1272 (1919).
14) H. Schmidt and H. D. Schmidt, *Z. anorg. allgem. Chem.*, **279**, 289 (1955).
15) A. Engelbrecht, E. Mayer and Chr. Pupp, *Monatsh. Chem.*, **95**, 633 (1964).
16) E. Nachbaur and A. Engelbrecht, *ibid.*, **95**, 214 (1964).
17) E. E. Kenage, *J. Econ. Entomol.*, **50**, 1 (1957); D. Stewart, *ibid.*, **50**, 7 (1957).
18) Preceding paper: S. Nagase, H. Baba and T. Abe, This Bulletin, **40**, 2358 (1967).
19) U. Wannagat and G. Mennicken, *Z. anorg. allgem. Chem.*, **278**, 310 (1955).
20) S. Nagase, H. Baba and T. Abe, This Bulletin, **38**, 834 (1965).

*2 Synthesized by the electrochemical fluorination of tri-*n*-butylamine according to the method in the literature; E. A. Kauck and J. H. Simons, U. S. Pat. 2616927 (1952); Brit. Pat. 666733 (1952).

*3 Gaschro-Kogyo Co., Ltd.,

oxygen difluoride, a mixture of sulfuryl fluoride and sulfur hexafluoride,*4 and thionyl tetrafluoride. When the feed rate was high, unchanged sulfur dioxide appeared after oxygen difluoride. The gases from the sodium fluoride tube were led to and bubbled through an aqueous solution of sodium sulfite containing a small amount of potassium iodide, by which means the products other than sulfuryl fluoride and sulfur hexafluoride were removed.*5 These two products were guided to cold traps and then subjected to low-temperature distillation.

Fluorination of Thionyl Fluoride. An electrolytic cell with a capacity of 300 ml[18] was used. Among the several runs made, the best reaction conditions were as follows: thionyl fluoride (36 ml/min) and helium (15 ml/min) were led through the bubbler into anhydrous hydrogen fluoride containing sodium fluoride (5 g). The electrolysis was then conducted at −30°C with an anodic current density of 1.6 A/dm² and at a cell voltage of 6—7 V. However, even under these conditions, explosions in the reaction system frequently occurred and quantitative analyses of the products were not possible. The products consisted of a considerable amount of thionyl tetrafluoride and traces of sulfur hexafluoride and oxygen difluoride.

Fluorination of Thionyl Chloride, Sulfuryl Chloride, Sulfur Mono-, and Dichlorides. For these liquid samples, the fluorination was conducted in batches by the use of the electrolytic cell with a capacity of 1 *l*.[20] A conductivity additive, sodium fluoride (10 g), was necessary for the fluorination of sulfur mono-, and dichlorides. The products obtained from these materials were treated similarly to those obtained from the fluorination of sulfur dioxide. Thionyl tetrafluoride produced from thionyl chloride was yielded as sulfuryl fluoride by hydrolysis.

Results and Discussion

The reaction conditions for the electrochemical fluorination of sulfur dioxide and the results obtained are shown in Table 1. The reaction can be carried out easily; sulfuryl fluoride is produced as the principal product, along with cleaved by-products.

$$SO_2 \xrightarrow{[F]} SO_2F_2,\ SOF_4,\ SF_6,\ OF_2$$

The sulfur in the products is in the hexavalent state, as is usual in the electrochemical fluorination of sulfur-containing compounds. The composition of the products was not changed practically by the reaction time. A representative example of the composition*6 (Run 1) was sulfuryl fluoride, 62%; thionyl tetrafluoride, 23%; sulfur hexafluoride, 1%; and oxygen difluoride, 14%.

Table 1. Fluorination of sulfur dioxide

Run No.	SO_2 feed[a] rate ml/min	Total amount of SO_2 fed, mol	Electricity[b] passed A. hr	Cell temp. °C	SO_2F_2[c] Yield %
1	32	0.201	60	6—7	70.0
2	47	0.312	65	6—7	49.5
3	36	0.239	65	16	90.4
4	30	0.204	50	16—17	64.8

a) He flow rate: 15 ml/min.
b) Anodic current density: 2.8 A/dm², Cell voltage: 6—8 V
c) Calculated on the basis of the amount of SO_2 fed.

Generally, a lower feed rate with a higher cell temperature gave sulfuryl fluoride in a better yield. Under the conditions used, the highest yield of sulfuryl fluoride was given at a feed rate of 36 ml/min and at a cell temperature of 16°C. At this temperature, however, the reaction with the smaller feed rate did not proceed smoothly due to explosions in the apparatus, thus giving a lower yield of sulfuryl fluoride. The cause of the explosions may be the generation of free fluorine because of the insufficient concentration of sulfur dioxide in anhydrous hydrogen fluoride.

The sulfur-oxygen bond in the oxygen-containing sulfur compounds is relatively stable to fluorination, as may be seen in the poor yields (<1%) of sulfur hexafluoride. The sulfur-oxygen bond in sulfuryl fluoride is particularly inert; the thionyl tetrafluoride and sulfur hexafluoride formed from sulfur dioxide are not produced through the exhaustive fluorination of sulfuryl fluoride, which is found not to be fluorinated by the electrochemical fluorination,*7 just as it has been shown not to be fluorinated by the catalytic fluorination.[21]

The electrochemical fluorination of thionyl fluoride resulted in the formation of thionyl tetrafluoride, together with traces of sulfur hexafluoride and oxygen difluoride. However, more highly-fluorinated products such as pentafluorosulfur hypofluorite,[21,22] were not detected.

$$SOF_2 \xrightarrow{[F]} SOF_4,\ (SF_6,\ OF_2)^{*8}$$

The reaction conditions and the yields of the principal products obtained in the electrochemical fluorination of sulfur oxychlorides and sulfur chlorides are shown in Table 2. The several compounds were produced as follows:

*4 Can be separated by gas chromatography over silica gel.

*5 Thionyl tetrafluoride was converted into sulfuryl fluoride by hydrolysis [H. Jonas, *Z. anorg. allgem. Chem.*, **265**, 273 (1951)].

*6 The ratio of the peak areas in the chromatogram.

*7 The electrochemical fluorination of sulfuryl fluoride was examined by procedures similar to those used for thionyl fluoride. Sulfuryl fluoride was recovered, unchanged.

21) F. B. Dudley, G. H. Cady and D. F. Eggers, Jr., *J. Am. Chem. Soc.*, **78**, 1553 (1956).

22) J. K. Ruff and M. Lustig, *Inorg. Chem.*, **3**, 1422 (1964).

*8 The amounts of the compounds listed in parentheses in this and in the following equations were small.

Table 2. Fluorination of sulfur compounds

Run No.	Sample[a] mol	Electricity[b] passed A. hr	Main product Yield[c] %
5	$SOCl_2$ (0.25)	69	SOF_4 (31.7), SOF_2
6	SO_2Cl_2 (0.25)	97	SO_2F_2 (65.7)
7	S_2Cl_2 (0.125)	155	SF_6 (78.2)[d]
8	SCl_2 (0.25)	113	SF_6 (63.7)

a) He flow rate: 60 ml/min.
b) Anodic current density: 2.8 A/dm^2, Cell voltage: 5.5—7 V, Cell temperature: 5—6°C.
c) Calculated on the basis of the amount of the starting material charged.
d) A 100% yiled represents the formation of 2 mol of SF_6 from 1 mol of the starting material.

$$SOCl_2 \xrightarrow{[F]} SOF_2, SOF_4, (SF_6, OF_2, HCl)$$

$$SO_2Cl_2 \xrightarrow{[F]} SO_2F_2, Cl_2, (SO_2ClF, SF_6, OF_2)$$

$$S_2Cl_2 \xrightarrow{[F]} SF_6, Cl_2, (SOF_2, SOF_4)$$

$$SCl_2 \xrightarrow{[F]} SF_6, Cl_2, (SF_5Cl, SOF_2, SOF_4)$$

The compositions of the products varied with the reaction time. The amount of sulfur hexafluoride produced from thionyl chloride and sulfuryl chloride was small (1—2% yield). Chlorine in thionyl chloride appeared to be removed mostly as hydrogen chloride,*9 while in sulfuryl chloride most of the chlorine was removed as chlorine gas.

The electrochemical fluorination of sulfur monochloride which has been briefly described in a patent,[23] and that of sulfur dichloride afforded sulfur hexafluoride in substantial yields. Traces of thionyl fluoride and thionyl tetrafluoride might be produced from impurities in the sulfur chlorides.

*9 These oxychlorides are known to react with anhydrous hydrogen fluoride to yield the corresponding oxyfluorides and hydrogen chloride (Ref. 10). This fact was examined under the modified reaction conditions used for the present work; without passing the current through the anhydrous hydrogen fluoride solution in the cell, but with bubbling helium into it, the oxychlorides were subjected to fluorination at 6°C. Thionyl chloride gave thionyl fluoride, while sulfuryl chloride yielded sulfuryl chlorofluoride.

23) M. Prober, U. S. Pat. 2717235 (1955).

BULLETIN OF THE CHEMICAL SOCIETY OF JAPAN VOL. 42 2064—2066 (1969)

The Influence of Lanthanide Ions on the Polarographic Minima of Peroxodisulfate Ions

Akio IWASE and Tsuguo ITO

Department of Chemistry, Faculty of Science, Yamagata University, Koshirakawa-cho, Yamagata

(Received November 1, 1968)

It is generally known, from a report by Frumkin[1] on the effect of cations on the minimum wave of peroxodisulfate ions, that when the cationic charge is constant, the effect is more pronounced for larger ionic radii (r_c). This seems to demonstrate that the mutual electrostatic interaction between depolarizer and electrode depends on the size of the hydrated cations adsorbed on the electrode. The aim of the present study is to examine the behavior of this minimum wave of the $S_2O_8^{2-}$ anion in the presence of the lanthanide cations, which have similar ionic radii, in order to obtain some information about the hydration structure of these cations as they are adsorbed on the electrode surface. For comparison, the aluminum ion was also investigated.

1) A. Frumkin, *Z. Elektrochem.*, **59**, 807 (1955).

Experimental

D. c. polarograms were recorded using a Yanagimoto Polarograph PB, Type 4. The capillary constants used were: $m=1.432$ mg/sec, $t=5.1$ sec/drop, $m^{2/3}t^{1/6}=1.667$ $mg^{2/3}\,sec^{-1/2}$ in a 0.1N KCl solution with a mercury column height of 58.4 cm at -1.15 V *vs.* SCE. The temperature was 25 ± 0.1°C in all cases. The dissolved oxygen was removed by passing through nitrogen gas.

To prepare the 0.01M $K_2S_2O_8$ solution, $K_2S_2O_8$ of an analytical grade was dissolved in distilled water without further purification; the concentration was determined by indirect titration using a $KMnO_4$ standard solution. 0.01M lanthanide ion solutions and an aluminum ion solution were prepared by dissolving in 0.001N HCl the corresponding amounts of their chloride compounds, which had been prepared from the oxides (99.9% pure) by treatment with HCl. The concentrations were determined by chelatometric titration using an EDTA

standard solution. Each solution described above was diluted to the required concentration before use. All the other reagents used were reagent-grade.

Results and Discussion

D. C. Polarogram of Peroxodisulfate in the Presence of the Lanthanide Ion or the Aluminum Ion. In order to obtain a proper minimum wave of $S_2O_8^{2-}$, 0.01 M LiCl was chosen as the supporting electrolyte. D. c. polarograms of solutions containing 4.2×10^{-4}M $S_2O_8^{2-}$, 1×10^{-4}M HCl, and 1×10^{-5}M of Al, La, and Yb ions respectively are shown in Fig. 1. The current-voltage

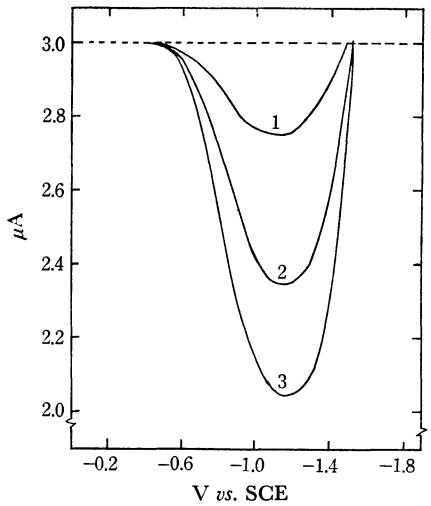

Fig. 1. D.c. polarograms of 0.42 mM $K_2S_2O_8$ in 0.01 M lithium chloride and 0.1 M hydrochloric acid, in the presence of 0.01 mM of (1) Al, (2) La, and (3) Yb.

curves were recorded by sweeping the voltage in the negative direction from −0.45 V, since the maxima appeared at *ca.* −0.3 V. In this case the plateau of the limiting current lay within a very small region, −0.45——0.50 V. The minimum current, i_{dep}, was obtained by measuring the current corresponding to the depth from the limiting current at −0.45 V to the minimum point. The voltage corresponding to the minimum was approximately −1.15 V. As is obvious from Fig. 1, i_{dep} increases in the order: $Al^{3+}<La^{3+}<Yb^{3+}$. The effect of cations on the minimum phenomena (for $S_2O_8^{2-}$) is due to their adsorption, as was noted by Frumkin. Also, the effect of the concentrations of La or Tb ions (Fig. 2) obviously shows that the relation between the persulfate current at the minimum and their concentration gives a saturated curve and that the adsorption equilibrium is of a Langmuir type. The temperature coefficient of i_{dep} was also examined between 30°C and 50°C in the presence of lanthanide ions, but no well-

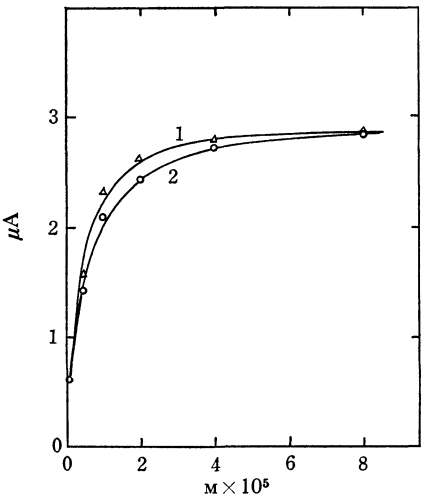

Fig. 2. Effects of (1) lanthanum and (2) terbium concentrations on persulfate current at the minimum in solutions containing 0.42 mM $K_2S_2O_8$ plus 10 mM LiCl and 0.1 mM HCl.

defined wave was observed.

The Relation between the Size of the Cation (III) and the Minimum Current. i_{dep}, measured in solutions containing 1×10^{-5}M cation (III), 4.2×10^{-4}M $K_2S_2O_8$, 1×10^{-2}M LiCl and 1×10^{-4}N HCl, and the Stokes radii,[2] r_s, of the cations(III) at 25°C are shown in Table 1. The r_s values were

Table 1. Relationship of i_{dep} to the ionic radius

0.42 mM $K_2S_2O_8$; 10 mM LiCl; 0.1 mM HCl; 0.01 mM lanthanide.

Cation(III)	i_{dep} (μA)	r_c Å	r_s Å	r_s-r_c Å
La	0.67	1.22	3.92	2.70
Pr	0.75	1.16	3.93	2.77
Nd	0.78	1.15	3.94	2.79
Sm	0.76	1.13	3.99	2.86
Eu	1.84	1.13	4.03	2.90
Gd	0.85	1.11	4.06	2.95
Tb	0.88	1.09		
Dy	0.85	1.07	4.16	3.09
Ho	0.89	1.05	4.12	3.07
Er	0.88	1.04	4.15	3.11
Tm	0.93	1.04	4.18	3.14
Yb	0.96	1.00	4.16	3.16
Lu	0.96	0.99		
Al	0.25	0.57	3.60	3.03

calculated from the equation: $r_s=(Z\varepsilon\times1/300)/6\pi\eta\mu$. The lanthanide ion mobilities used in

2) I. Oshita, "Electrophysical Property of Liquid," Maki Co., Tokyo (1964), p. 13.

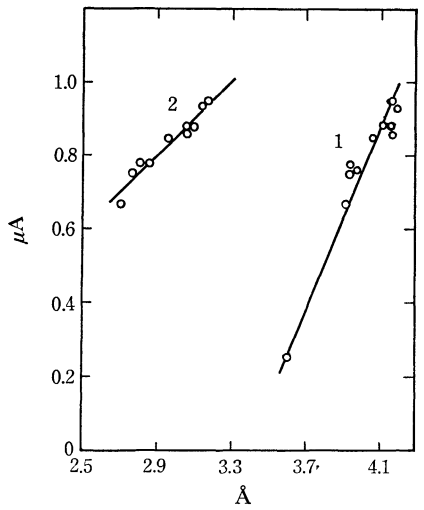

Fig. 3. Relation between i_{dep} and ionic radius : (1), r_s; (2), $r_s - r_c$.

calculating μ were obtained from the literature.[3] In Table 1, r_c are the ionic radii reported by Goldschmidt.[4] The value of r_s for the aluminum ion was calculated as follows. First, the value of the equivalent conductivity[5] of $AlCl_3$ at an infinite dilution was obtained by extrapolation. Second, the value of the Cl^- mobility, 76.3, was subtracted from the value obtained above. The value of the Al^{3+} mobility was then found to be 75.5 (at 25°C). Figure 3 shows the relation between i_{dep} and r_s. All the points on curve 1 in Fig. 3 apparently lie on an approximately straight line drawn from Al to La. However, the values of r_s in Table 1 are almost unchanged for La, Pr, and Nd, although there is a clear difference between the i_{dep} values of La and Pr. The same phenomenon is recognized in Dy, Ho, Er, Tm, and Yb. Curve 2 in Fig. 3 is a plot of the radius difference ($r_s - r_c$) *vs.* i_{dep}; this shows a better linear relation than does 1 (except for Al). Consequently, among the lanthanide ions with the same r_s values, it seems probable that the charge-transfer process of $S_2O_8^{2-}$ is more suppressed by thicker hydration layers. The increase in i_{dep}value in the presence of the Eu(III) ion can be interpreted as follows: the Eu(III) ion is reduced immediately to the Eu(II) ion at -1.15 V and is adsorbed as a bivalent hydrated cation, so it gives a relatively large value of i_{dep}.

3) R. A. Robinson and R. H. Stokes, "Electrolyte Solution," Butterworths Scientific Publications, London (1959).

4) R. G. Vickery, "Chemistry of the Lanthanons," Butterworths Scientific Publications, London (1953), p. 204.

5) Chem. Soc. of Japan, "Handbook of Chemistry," Maruzen Co., Tokyo (1952), p. 609.

BULLETIN OF THE CHEMICAL SOCIETY OF JAPAN VOL. 42 2066—2068 (1969)

The Rearrangement of 2-Aminobenzophenones

Kakuzo ISAGAWA, Takumi ISHIWAKA, (the late) Masamichi KAWAI and Yasaburo FUSHIZAKI

Department of Applied Chemistry, Faculty of Engineering, University of Osaka Prefecture, Sakai, Osaka

(Received November 6, 1968)

A previous paper[1] described how 2-amino-5-chlorobenzophenone (Ib) afforded the intermolecular condensation product, 2,8-dichloro-6,12-diphenyldibenzo[*b*,*f*]-1,5-diazocine (IIb), under the several sets of conditions.[2]

This report will deal with the rearrangement of aminobenzophenones (I) to benzanilides (III) by treating them with zinc chloride.

It has been reported that the migration of acetyl, propionyl, and benzoyl groups occurred when the *N*-monoacyl- or *N*,*N*-diacylaniline was heated for a long time with anhydrous aluminum chloride or zinc chloride, and that the migration groups entered into the *o*-position or, preferably, the *p*-position.[3-5] On the other hand, 9-acridone was prepared from 2-aminobenzophenone in the presence of lead

1) M. Kawai, *Nippon Kagaku Zasshi (J. Chem. Soc. Japan, Pure Chem. Sect.)*, **88**, 102 (1967).

2) W. Metlesics, T. Reanick, G. Silverman, R. Tavares and L. H. Sternbach, *J. Med. Chem.*, **9**, 633 (1966).

3) J. F. J. Dippy and J. H. Wood, *J. Chem. Soc.*, **1949**, 2719.

4) J. F. J. Dippy and V. Moss, *ibid.*, **1952**, 2205.

5) F. D. Chattaway, *ibid.*, **1904**, 386.

monoxide,[6] and a series of 2-amino-2′-fluorobenzophenones, upon treatment with potassium carbonate in *N,N*-dimethylformamide, underwent internal nucleophilic exchange to give the corresponding 9-acridones.[7]

We have now found that the treatment of I with zinc chloride gave benzanilides (III) and 9-acridones (IV), together with dibenzodiazocines (II). In this reaction, the rearrangement of I to III was brought about, and the benzoyl group migrated from the carbon of the aromatic nucleus to the nitrogen of the amino group. At the same time, I underwent dehydrocyclization to IV.

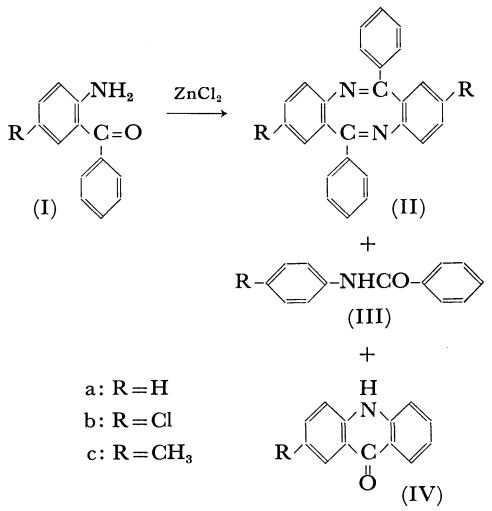

Table 1. Treatment of 2-aminobenzophenones with $ZnCl_2$ or $AlCl_3$

Attempted compound	Catalyst	Temp. °C	Products, %[a]		
			Diazocine	Anilide	Acridone
Ia	$ZnCl_2$	200	22.0	4.1	trace
Ia	$ZnCl_2$	220	21.5	3.8	trace
Ib	$ZnCl_2$	180	67.9	trace	—
Ib	$ZnCl_2$	200	43.3	7.9	trace
Ib	$ZnCl_2$	220	10.1	14.3	trace
Ib	$ZnCl_2$	240	8.2	4.8	trace
Ib	—	200	41.7	—	—
Ib	$AlCl_3$	200	77.5	trace	—
Ic	$ZnCl_2$	200	17.9	1.7	trace
Ic	$ZnCl_2$	220	11.4	trace	trace

a) Theoretical yield, based on aminobenzophenones.

Table 1 presents the results obtained under suitable conditions.

As may be seen in Table 1, Ib scarcely rearranged to IIIb at all in the presence of aluminum chloride. However, the rearrangement proceeded well when zinc chloride was used as the catalyst. When the mixture was heated at 200°C or 220°C, the yields of anilides increased in the following order: R= CH_3<H<Cl, where R is as shown in the synthetic scheme. As for the reverse reaction, Dippy and Moss reported that the percentage conversion into 2-aminobenzophenones was 15% for IIIb and 5% for IIIc.[4] Furthermore, these authors described how a monoacyl and a *N,N*-diacylaniline rearranged by an intermolecular mechanism, since the acyl group could be removed in the form of acyl chloride. In our experiment, a small amount of benzoic acid was produced upon the treatment of Ia with zinc chloride.

Experimental

Treatment of 2-Aminobenzophenones with $ZnCl_2$ or $AlCl_3$. Only a typical reaction will be described here. All of these reactions were carried out by a method similar to that described below.

To 4.63 g (0.02 mol) of Ib heated to 120°C there were added 2.6 g of zinc chloride. The mixture was then heated to the temperature shown in Table 1 for ten hours. After cooling to room temperature, 100 m*l* of warm water and 200 m*l* of chloroform were added to the reaction mixture; brownish, insoluble solids were filtered off. The aqueous layer was separated and discarded. The organic layer was dried over anhydrous potassium carbonate, filtered, and concentrated to dryness *in vacuo*. The residue was dissolved in a mixture of chloroform and carbon tetrachloride (1 : 1) and chromatographed on a column of silica gel. The residue remaining after the evaporation of the first eluate was added to 20 m*l* of methanol. The insoluble material, diazocine IIb, was recrystallized from a mixture of methanol and methylene chloride to give yellow prisms; mp 219—220°C (lit[1,2] mp 219—220°C). IR:*1 1615, 890, 854 cm^{-1}. (Found: C, 72.92; H, 3.60; N, 6.34; Cl, 16.59%).

The mother liquors were concentrated to dryness *in vacuo*, and the residue was added to carbon tetrachloride and filtered. The insoluble material, 4′-chloroben zanilide IIIb, was recrystallized from methylene chloride to give colorless needles; mp 190—192°C (lit[8] mp 192—193°C). IR: 3300, 1650 cm^{-1}. NMR:*2 δ 10.06 (broad singlet, 1H, NH), δ 8.06—7.27 (multiplet, 9H, aromatic protons). (Found: C, 67.59; H, 4.40; N, 6.33%).

2-Chloro-9-acridone (IVb) was afforded from an eluate of the second band (blue-violet fluorescence). The second eluate was concentrated to dryness *in vacuo*, and the residue was recrystallized from *N,N*-dimethylformamide to give bright yellow prisms; mp>320°C (lit[9] mp>360°C). IR: 1635, 1600, 1560 cm^{-1}. (Found: C, 67.78; H, 3.49; N, 6.23%).

Identification of the Other Products. The diazocines, anilides, and acridones were identified by

*1 Taken on KBr tablets.

*2 Measured in $CDCl_3$-DMSO (4:1); tetramethylsilane as the internal standard.

6) C. Graebe and F. Ullmann, *Ber.*, **27**, 3483 (1894).

7) R. I. Fryer, J. Early and L. H. Sternbach, *J. Chem. Soc.*, **1963**, 4979.

8) R. von Walther, *J. prakt. Chem.*, [2], **58**, 160 (1903).

9) F. Ullmann, *Ann.*, **355**, 339 (1907).

means of mixed-melting-point measurements, and by a comparison of these IR and/or NMR spectra with those of authentic samples synthesized by the methods cited below or by similar methods.

6,12-Diphenyldibenzo[b,f]-1,5-diazocine (*IIa*).[1,2] Mp: 190—192°C. IR: 1620, 770 cm^{-1}.

2,8-Dimethyl-6,12-diphenyldibenzo [b,f]-1,5-diazocine (*IIc*).[1] Mp: 195—196°C. IR: 1620, 870, 820 cm^{-1}.

Benzanilide (*IIIa*).[10] Mp: 162—163°C. IR: 3300, 1650 cm^{-1}. NMR: δ 9.82 (broad singlet, 1H, NH), δ 8.09—7.10 (multiplet, 10H, aromatic protons).

4'-Methylbenzanilide (*IIIc*).[10] Mp: 156—158°C. IR: 3320, 1650 cm^{-1}. NMR: δ 9.62 (broad singlet, 1H, NH), δ 8.05—7.08 (multiplet, 9H, aromatic protons), δ 2.32 (singlet, 3H, CH_3).

9-Acridone (*IVa*).[11] Mp: >320°C. IR: 1635, 1600, 1560 cm^{-1}.

2-Methyl-9-acridone (*IVc*).[11] Mp: >320°C. IR: 1635, 1600, 1560 cm^{-1}.

10) C. N. Webb, "Organic Syntheses," Coll. Vol. I, p. 82 (1941).

11) C. F. H. Allen and G. H. W. McKee, *ibid.*, Coll. Vol. II, p. 15 (1943).

BULLETIN OF THE CHEMICAL SOCIETY OF JAPAN VOL. 42 2068—2069 (1969)

Preparation of Epicamphor

Hitoshi TAKESHITA, Takeo MUROI and Shô ITÔ*1

Department of Chemistry, Tohoku University, Sendai

(Received November 18, 1968)

Although the stepwise reduction of camphorquinone (I) by aluminum and sodium amalgam is reported[1,2] to be the most convenient method for the preparation of epicamphor (II), we have found it to prove inadequate for large scale preparations, affording a mixture of *exo*-3-hydroxycamphor (III) and *exo*-2-hydroxyepicamphor (IV) in varying amounts.[3] In view of the extreme sensitivity of IV toward alkali, as was demonstrated by its conversion to III,[4] IV could not be expected to survive under the conditions used for the reduction even if the reaction first produced IV preferentially. In order to utilize II for other purposes, we have been trying to develop its convenient large-scale synthesis. The preparation and structure elucidation of exo-2-hydroxyepicamphor have recently been described by Fleming and Woodward.[5] Though the first step of our method is essentially the same as theirs, we wish to record in detail our synthesis of epicamphor II.

When I was heated with ethylene glycol and benzene in the presence of *p*-toluenesulfonic acid, monoketal (V) was obtained as the major product

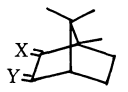

I: X = Y = O
II: X = H_2, Y = O
III: X = O, Y =
IV: X = , Y = O
V: X = O, Y = 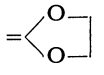
VI: X = Y =
VII: X = 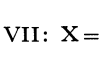 , Y =
VIII: X = , Y = O

together with a small amount of diketal (VI). These products were separated efficiently by crystallization and alumina column chromatography. V was subsequently reduced stereospecifically with lithium aluminum hydride[5] to yield *exo*-2-hydroxyepicamphor ketal (VII) which was then hydrolysed to IV by 12N sulfuric acid in five minutes with no indication of the presence of the product formed by acyloin rearrangement. Although direct reduction of IV by sodium amalgam afforded a mixture of II and camphor, the same reduction (pH adjusted to 6—8) of the corresponding acetate (VIII), which was obtained quantitatively by mild acetylation of IV, afforded II with a purity of more than 95%. The reaction sequence appears to be the most convenient way of preparing *l*-epicamphor from *d*-camphor.

*1 To whom all correspondence should be addressed.

1) J. Simonsen and L. N. Owen, "The Terpenes," Vol. II, Oxford Univ. Press, London (1957), p. 516.

2) J. Bredt and M. Bredt-Saveisberg, *Ber.*, **62**, 2216 (1929).

3) W. Hückel and O. Fechting, *Ann. Chem.*, **652**, 81 (1962).

4) J. Bredt and J. M. Fischer, *J. Prak. Chem.*, **131**, ii 56 (1931).

5) I. Fleming and R. B. Woodward, *J. Chem. Soc., C*, **1968**, 1289.

Experimental*2

Reaction of Camphorquinone (I) and Ethylene Glycol. I (prepared from *d*-camphor) (17 g), *p*-toluenesulfonic acid (0.5 g) and ethylene glycol (22 g) were dissolved in benzene (200 m*l*) and heated under reflux with azeotropic removal of water. The mixture was poured into water and extracted with benzene. Evaporation of the solvent gave a crystalline solid which was recrystallized from cyclohexane to give pure V (14 g) as colorless needles, mp 88—89.5°C, Found: C, 68.36; H, 8.69%. Calcd for $C_{12}H_{18}O_3$: C, 68.54; H, 8.68%. IR (KBr): 1752, 1399, 1375, 1041, 1024, 984, 974, 955, 938, 908, 780 cm^{-1}. NMR: 0.85 (3H, singlet), 0.99 (6H, singlet), 3.75—4.35 (4H, multiplet).

Alumina chromatography of the recrystallization mother liquor eluting with benzene - ethyl acetate mixture (3.0 g) gave additional V (4.4 g) and diketal VII (3.0 g) which after recrystallization from cyclohexane formed colorless needles, mp 63—63.5°C. Found: C, 65.97; H, 8.71%. Calcd for $C_{14}H_{22}O_4$: C, 66.11; H, 8.72%. IR (KBr): 1386, 1364, 1206, 1020, 996, 973, 953, 900, 820 cm^{-1}. NMR: 0.72 (3H, singlet), 0.83 (3H, singlet), 1.27 (3H, singlet), 3.47—4.10 (8H, multiplets).

Lithium Aluminum Hydride Reduction of Camphorquinone Monoketal (V). V (13.7 g) was dissolved in anhydrous ether (50 m*l*) and lithium aluminum hydride (1.5 g) in ether (15 m*l*) were added dropwise at 0°C. After excess of the reagent was decomposed in the usual manner, the reaction mixture was extracted with ether. Removal of the solvent and distillation of the residual oil yielded the hydroxyketal (VII) as a colorless oil, (13.1 g). Found: C, 67.91; H, 9.56%. Calcd for $C_{12}H_{20}O_3$: C, 67.89; H, 9.50%. IR (CCl_4): 3520, 1392, 1372, 1094, 1029, 1009, 990, 982, 950, 918, 811 cm^{-1}. NMR: 0.80 (3H, singlet), 0.84 (3H, singlet), 1.05 (3H, singlet), 2.07 (OH), 3.13 (1H, *sharp* singlet), 3.70—4.10 (4H, multiplet).

***exo*-2-Hydroxyepicamphor (IV).** VII (13.2 g) was shaken with aqueous 12N sulfuric acid for five minutes at room temperature and then extracted with ether. After removal of the solvent, the residue was recrystallized from ligroin to yield IV (8.3 g) as colorless prisms, mp 229—230°C. IR (KBr): 3395, 1745, 1395, 1375, 1096, 980, 809 cm^{-1}. NMR: 0.92 (3H, singlet), 1.00 (6H, singlet), 3.42 (1H, *sharp* singlet).

***exo*-2-Acetoxyepicamphor (VIII).** IV (4.0 g) was heated in acetic anhydride (15 m*l*) at 140°C for 4 hr. After removal of the excess reagent *in vacuo* the residual oil was distilled to give VIII (4.7 g), as a colorless liquid. (Found: C, 67.96; H, 8.53%. Calcd for $C_{12}H_{18}O_3$: C, 68.54; H, 8.68%. IR (CCl_4): 1758, 1748, 1397, 1376, 1230, 1070 cm^{-1}. NMR: 0.89 (3H, singlet), 0.93 (3H, singlet), 0.99 (3H, singlet), 2.06 (3H, singlet), 4.74 (1H, *sharp* singlet).

Sodium Amalgam Reduction of *exo*-2-Hydroxyepicamphor (IV). *a*) IV (500 mg) in methanol (100 m*l*) was reduced with 1.2% sodium amalgam (5 g) at room temperature. After dilution with water, the reaction mixture was extracted with ether to yield colorless crystals (300 mg), GLC of which showed the presence of more than 95% of epicamphor (II).

b) IV (30 g) in 25% methanol (2 *l*) was reduced with 1.5% sodium amalgam (220 g) at room temperature. The reaction was followed by GLC which indicated the formation of camphor even at an early stage. After completion of the reduction the colorless product isolated was composed of 59% of II and 41% of camphor.

Epicamphor (II). VIII (10 g) in 30% aqueous methanol (300 m*l*) was reduced with sodium amalgam (prepared from 19.2 g of sodium and 1500 g of mercury) the pH of the solution being maintained between 6 and 8 by addition of glacial acetic acid. The reaction was followed by GLC during the reaction period. After the reaction was completed, the reaction mixture was diluted with water and the aqueous layer was extracted with ether. Removal of the solvent yielded colorless crystals, which after sublimation *in vacuo* afforded colorless scales (II), mp 186°C. $[\alpha]_D$ −58.0° (5.1 g) (Found: C, 78.19; H, 10.47%). IR (KBr): 1744, 1415, 1388, 1373, 1200, 1005 cm^{-1}. NMR: 0.94 (6H, singlet), 1.01 (3H, singlet). 2,4-DNP, mp 190.5—191.5°C. (lit[2] mp 189—190°C).

*2 All NMR spectra were measured using a Varian A-60 spectrometer for carbon tetrachloride solutions. Chemical shifts are expressed in ppm from internal tetramethylsilane. Optical rotation was measured for 2.8% methanol solution.

H. T. and S. I. are indebted to the Matsunaga Science Foundation and Takeda Science Foundation, respectively, for their generous grants.

BULLETIN OF THE CHEMICAL SOCIETY OF JAPAN VOL. 42 2070—2071 (1969)

A Study of the Mechanism of the Carboxylation of Potassium Phenoxide by Means of the Carbon-14 Tracer Technique[1)]

Yutaka YASUHARA,* Tatsuo NOGI* and Hideo SAISHŌ**

* *Mishima Laboratory, Toyo Rayon Company, Ltd., Mishima, Shizuoka*

** *Central Research Laboratories, Toyo Rayon Company, Ltd., Otsu, Shiga*

(Received November 19, 1968)

A novel synthesis of *p*-hydroxybenzoic acid from potassium phenoxide, potassium carbonate, and carbon monoxide has previously been reported.[2)] The reaction mechanism has, however, not yet been established, it has not been made clear whether the carboxyl group of *p*-hydroxybenzoic acid is derived from either potassium carbonate or carbon monoxide. In the present study, potassium carbonate ^{14}C is used to throw light on the mechanism.

Results and Discussion

The radioactivities of the two products, *p*-hydroxybenzoic acid and formic acid, are listed in Table 1. The results lead to the conclusion that the carbon atom of potassium carbonate attacks the phenoxide nucleus and that carbon monoxide is converted into potassium formate:

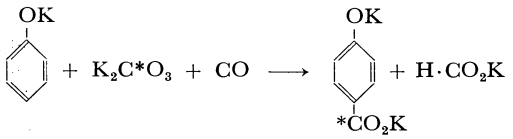

Since this reaction proceeds almost quantitatively, and since most of the carboxyl group seems to be introduced directly into the position *para* to the hydroxyl group,[2,3)] a possible mechanism of the reaction is:

TABLE 1. RADIOACTIVITIES OF *p*-HYDROXYBENZOIC ACID AND FORMIC ACID PRODUCED FROM POTASSIUM CARBONATE-^{14}C

Sample* mg	Radioactivity dpm	Specific activity μCi/mg
p-HBA: 2.92	50.17×10^{4}	7.8×10^{-2}
0.50	8.71×10^{4}	7.9×10^{-2}
FA: 56	9.13×10^{4}	7.4×10^{-4}

* *p*-HBA: *p*-hydroxybenzoic acid
FA: formic acid

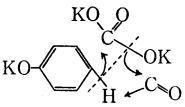

It is rather difficult to postulate that the termolecular complex is directly formed in such a smooth reaction. To study the mechanism of this reaction in detail, the reaction of potassium carbonate with carbon monoxide,[4)] that of potassium phenoxide with carbon monoxide, and that of potassium phenoxide with potassium carbonate were each examined at 250 and 350°C. Among these six cases, only in the case of potassium carbonate with carbon monoxide at 350°C was a chemical change observed. Oxalic acid (1.2 g, 11%) was obtained from 13.8 g of potassium carbonate under an initial carbon monoxide pressure of 90 kg/cm^2 (at room temperature) after 6 hr. By analogy with the Kolbe-Schmitt reaction,[5)] the formation of a complex of potassium phenoxide and carbon monoxide might be suggested. However, in view of the facts described above, together with the fact that phenol itself can also be carboxylated with potassium carbonate under a carbon monoxide atmosphere,[6)] such a possibility may be ruled out in this case.

Thus, the following assumption is the most probable. First, potassium carbonate and carbon monoxide form a complex, which may be a precursor of dipotassium oxalate. Secondly, the complex reacts with potassium phenoxide, and dipotassium *p*-hydroxybenzoate and potassium formate are formed:

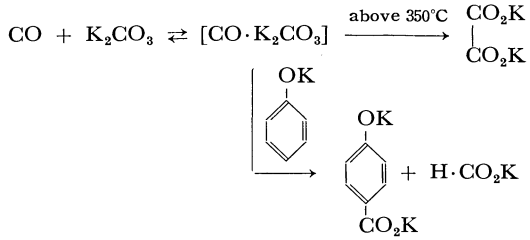

1) Carboxylation by Alkali Salts and Carbon Monoxide. IV. Paper III: Y. Yasuhara and T. Nogi, *Chem. & Ind. (London)*, **1969**, 77.

2) Y. Yasuhara and T. Nogi, *Chem. & Ind. (London)*, **1967**, 229.

3) Y. Yasuhara and T. Nogi, *J. Org. Chem.*, **33**, 4512 (1968).

4) C. Matignon and C. Faurholt, *Compt. Rend.*, **179**, 273 (1923).

5) J. L. Hales, J. I. Jones and A. S. Lindsey, *J. Chem. Soc.*, **1954**, 3145.

6) T. Nogi and Y. Yasuhara, in preparation.

The results shown in Table 1 indicate also that the exchange of the carboxyl group between dipotassium *p*-hydroxybenzoate and potassium formate is very slow. This is in contrast to the Kolbe-Schmitt reaction,[7] in which an appreciable exchange of the carboxyl group between dipotassium salicylate and potassium carbonate accompanies the rearrangement, and to the Henkel process,[8] in which the exchange between dipotassium phthalate and potassium carbonate takes place through carbon dioxide in the gas phase. However, it is not obvious whether such different results come from differences, alone or in combination, in the temperatures, in the atmospheres (CO and CO_2), or in the reagents (the formate and the carbonate).

Experimental

Materials. The potassium phenoxide was prepared by neutralizing phenol with potassium hydroxide in *n*-propanol. After filtration the crystals were dried at 130°C *in vacuo* (N_2, 20 mmHg). Potassium carbonate-^{14}C was prepared by heating a mixture of 6.9 g of potassium carbonate and 9.0 m*l* of an aqueous solution containing *ca.* 1 mCi of sodium carbonate-^{14}C (the Radiochemical Centre, England) to dryness.

Procedure. A glass vessel containing potassium phenoxide (6.6 g) and potassium carbonate-^{14}C (6.9 g) was placed in a stainless-steel autoclave (*ca.* 100 m*l*) and then dried *in vacuo* (N_2, 10 mmHg) at 220°C for 5.5 hr. The autoclave was then filled with carbon monoxide at a pressure of 85 kg/cm^2 (initial, at room temp.) and heated at 240—250°C for 6.0 hr (20 min preheating). The product was dissolved into 50 m*l* of water, and then the solution was acidified to pH 9.0 with 6N sulfuric acid. The regenerated phenol was extracted with ether. After further acidification with 12N sulfuric acid to pH 1.0, the aqueous solution was extracted again with ether. From the ether extract *p*-hydroxybenzoic acid was obtained, and, after treatment with activated charcoal, recrystallization from water, and drying, 3.0 g of purified *p*-hydroxybenzoic acid (mp 211—213°C) was recovered. Formic acid (bp 100—101°C) was obtained from the aqueous solution by exhaustive extraction with ether and fractional distillation. The reactions of three pairs, potassium carbonate and carbon monoxide, potassium phenoxide and potassium carbonate, and potassium phenoxide and carbon monoxide, were carried out analogously to that described above.

The radioactivities of *p*-hydroxybenzoic acid (in dioxane) and formic acid (in toluene) were measured on a Tracerlab LSC-20A liquid scintillation counter.

The authors wish to express their deep thanks to Mr. Hiroyuki Nagao of the Nippon Atomic Industry Group Co., Ltd., for his measurement of the radioactivities. Thanks are also due to Mr. Tadao Katō of the Toyo Rayon Co., Ltd., for his helpful suggestions and to Mr. Ikuzō Takahashi of the Toyo Rayon Co., Ltd., for his assistance in the experimental work.

7) S. E. Hunt, J. I. Jones, A. S. Lindsey, D. C. Killoh and H. S. Turner, *J. Chem. Soc.*, **1958**, 3152.

8) S. Furuyama, This Bulletin **40** 1212 (1967).

BULLETIN OF THE CHEMICAL SOCIETY OF JAPAN VOL. 42 2071—2074 (1969)

A Complex Formed by the Reaction of Ruthenium Tetroxide with 1,10-Phenanthroline in Carbon Tetrachloride

Toshio ISHIYAMA

Radiation Center of Osaka Prefecture, Shinke-cho, Sakai, Osaka

(Received November 29, 1968)

The synthesis and identification of the organic chelate compound of ruthenium in its higher oxidation states, for instance, Ru(IV), Ru(VI), Ru(VII), and Ru(VIII), are quite difficult since most organic compounds are oxidized by ruthenium tetroxide in the reaction mixture. Martin[1] obtained an interesting complex as an orange-brown precipitate by the reaction of ruthenium tetroxide with nitric oxide in carbon tetrachloride according to the following equation:

$$2RuO_4 + 8NO = Ru_2N_6O_{15} + N_2O$$

He suggested that it might be a nitrato complex containing two bis(nitrosyl)ruthenium groups linked by an oxo-bridge $[RuO_2(NO)_2NO_3]_2O$. Koda[2] reported obtaining an addition compound of ruthenium tetroxide with pyridine, $RuO_4 \cdot 2C_5H_5N$, as greenish-black crystals in carbon tetrachloride.

1) F. S. Martin, J. M. Fletcher, P. G. M. Brown and B. M. Gattehouse, *J. Chem. Soc.*, **1959**, 76.

2) Y. Koda, *Inorg. Chem.*, **2**, 1306 (1963).

A previous paper[3] reported obtaining a ruthenium tetroxide complex with 2,2′-bipyridine by the reaction of ruthenium tetroxide with 2,2′-bipyridine in carbon tetrachloride. In the present paper a binuclear complex of ruthenium(VII) will be reported, together with the electronic spectra of the previous complex, [RuO_4 bipy].

Experimental

Materials. Ruthenium(III) chloride monohydrate (extra pure grade) supplied by Mitsuwa Chemicals & Co. was used without further treatment, while commercial 1,10-phenanthroline was dried by heating it at 115°C for 3 hr and was then recrystallized from ethanol. The carbon tetrachloride was washed with a 1.5 per cent alcoholic solution of potassium hydroxide more than three times and repeatedly with pure water, and then distilled.

Preparation. *Ruthenium(VII) Oxide Complex with 1,10-Phenanthroline*, [Ru_2O_7 $phen_2$]. Ruthenium tetroxide in a nitric acid solution was prepared according to the method reported in a previous paper.[3] Ruthenium tetroxide in a nitric acid solution was extracted with carbon tetrachloride. To the organic solution, cooled in an ice bath, there was added a carbon tetrachloride solution of 1,10-phenanthroline. A dark green precipitate of the ruthenium(VII) oxide complex with 1,10-phenanthroline was separated immediately. After 20 hr, the precipitate was filtered, washed with carbon tetrachloride, and dried *in vacuo*. The mole ratio of 1,10-phenanthroline to ruthenium tetroxide employed in the reaction varied from 1:1 to 1:4, but the product obtained was the same in any case. The dried precipitate was dissolved in pure water, and an insoluble product was filtered off. After concentration on a hot water bath, the crystals formed were separated, recrystallized once again from water, and dried *in vacuo*. Yield: 10.2% on the basis of the ruthenium tetroxide. The complex is insoluble in carbon tetrachloride, chloroform, benzene, acetone, ether, ethanol, and acetic acid, but soluble in water and methanol.

The ruthenium content and the molecular weight of the complex were measured by a method reported previously.[3]

Found: Ru, 29.36; C, 42.60; H, 2.69; N, 8.41%; mol wt, 680. Calcd for [$Ru_2O_7(C_{12}H_8N_2)_2$]: Ru, 30.12; C, 42.62; H, 2.41; N, 8.21%; mol wt, 675.

Ruthenium(VIII) Oxide Complex with 2,2′-Bipyridine, [RuO_4 bipy]·$3H_2O$. This was synthesized according to the method reported in a previous paper.[3]

Found: Ru, 26.33; C, 31.07; H, 3.79; N, 7.80; H_2O, 15.00%; mol wt, 330. Calcd, for [$RuO_4(C_{10}H_8N_2)$]·$3H_2O$; Ru, 27.06; C, 31.81; H, 3.70; N, 7.46; H_2O, 14.70%; mol wt, 321 (anhydride).

Absorption Spectra. The infrared absorption spectra were obtained by the KBr disk method on a infrared spectrophotometer, Model IR-S, of the Japan Spectroscopic Co. The visible and ultraviolet absorption spectra were measured with a Beckmann Model DU spectrophotometer.

Magnetic Measurement. The mangetic susceptibility was measured at 27°C with a Gouy balance. The complex was found to be diamagnetic.

Results and Discussion

Composition of the Complex. From the results of the elemental analysis, the mole ratio of ruthenium to 1,10-phenanthroline was found to be 1:1. The observed molecular weight indicates that the complex is binuclear, [Ru_2O_7 $phen_2$].

Infrared Absorption Spectra. The main infrared absorption bands of the ruthenium(VII) oxide complex with 1,10-phenanthroline are shown in Table 1, together with those of the pure ligand. The C=N stretching peak is shifted to the higher frequency side by the ligation. This behavior is interpreted as an indication that the bond order of the carbon-nitrogen link is increased. The bands attributable to the C=C and C–H bonds are also shifted to the higher frequencies. Similar observations have also been reported for [Fe $phen_3$]Cl_2 and other phenanthroline complexes by Schilt and Taylor,[4] Inskeep,[5] and Busch and Bailor.[6]

Table 1. The characteristic infrared absorption bands of ruthenium(VII) oxide complex with 1,10-phenanthroline (cm^{-1})

Assignment	phen	[Ru_2O_7 $phen_2$]
ν (C=N)	1621	1630
ν (C=C)	1585	1606
	1560	1575
ν (C–H)	762	775
	730	738

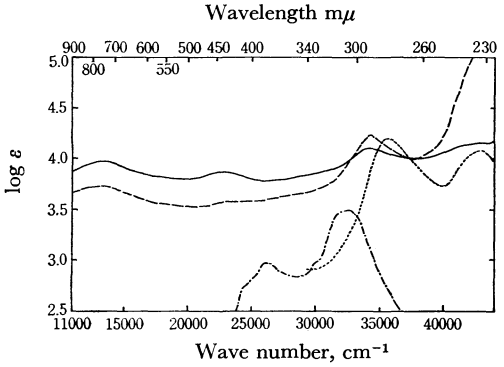

Fig. 1. Electronic absorption spectra of [RuO_4 bipy] and its components.
—— [RuO_4 bipy] in H_2O
– – – [RuO_4 bipy] in CH_3OH
------ bipy in H_2O
-·-·- RuO_4 in H_2O

3) T. Ishiyama, Annual Report of the Radiation Center of Osaka Prefecture, **8**, 40 (1967).

4) A. A. Schilt and R. C. Taylor, *J. Inorg. Nucl. Chem.*, **9**, 211 (1959).

5) R. G. Inskeep, *ibid.*, **24**, 763 (1962).

6) D. H. Busch and J. C. Bailor, Jr., *J. Am. Chem. Soc.*, **78**, 1137 (1956).

Electronic Absorption Spectra. The visible and ultraviolet absorption spectra of ruthenium-(VIII) and (VII) oxide complexes with 2,2′-bipyridine and 1,10-phenanthroline respectively were measured in water and methanol. They are shown in Figs. 1 and 2, together with those of pure ligands and ruthenium tetroxide in water.

The ruthenium(VIII) oxide complex with 2,2′-bipyridine has four absorption bands, at 740, 440, 292, and 245 mμ. A similar spectrum has also been reported by Koda[2] for bis(pyridine)ruthenium-(VIII) oxide. The two peaks of a higher intensity observed in the visible region may both be assigned to the charge transfer from ligand to metal. The two absorption bands observed for ruthenium tetroxide have also been attributed to the charge transfer from oxygen to ruthenium.[7] The two peaks at 292 and 245 mμ can be assigned to the π_1 and π_2-bands respectively, corresponding to the 279 and 233 mμ bands in the 2,2′-bipyridine. The red-shifts of the π_1 and π_2-bands by ligation to ruthenium(VIII) can be explained as follows. The molecule of 2,2′-bipyridine has been proved by Fielding and LeFèvre,[8] and by Krumholz[9] to assume the *trans*-form in a neutral or basic aqueous solution and also in organic solutions. The facts that *trans*-bipyridine was changed to the *cis*-form, and that the π_1 and π_2-bands were shifted to a longer wavelength by coordination to a metal atom, were confirmed by Nakamoto[10] in the case of the tris-(2,2′-bipyridine)nickel(II) complex. The same effect must be felt in the present case of the ruthenium(VIII)-2,2′-bipyridine chelate.

In an aqueous solution of the ruthenium(VII) oxide complex with 1,10-phenanthroline, three absorption bands and a shoulder are observed at 685, 450, 264, and 315 mμ respectively. The two peaks of a higher intensity observed in the visible region may both be assigned to the charge transfer from ligand to metal. The first charge-transfer bands of [RuO_4 bipy] and [Ru_2O_7 $phen_2$] are observed in a region of wavelength longer than those of [Ru $bipy_3$]Cl_2 and [Ru $phen_3$]Cl_2 which were reported by Crosby *et al.*[11] These facts show that the charge-transfer transitions in Ru-(VIII)-2,2′-bipyridine and Ru(VII)-1,10-phenanthroline chelates occur with a lower energy because the t_{2g} orbitals are not filled. A shoulder and a peak, observed at 315 and 264 mμ respectively, nearly coincide with the two absorption bands, at 320 and 265 mμ, of 1,10-phenanthroline. It should be noticed that the influence of ruthenium bonding on the spectrum of 1,10-phenanthroline is much less than in the case of 2,2′-bipyridine. The same situation was also observed in the case of mono-2,2′-bipyridine and mono-1,10-phenanthroline complexes of cobalt(II) and nickel(II) by Sone *et al.*[12]

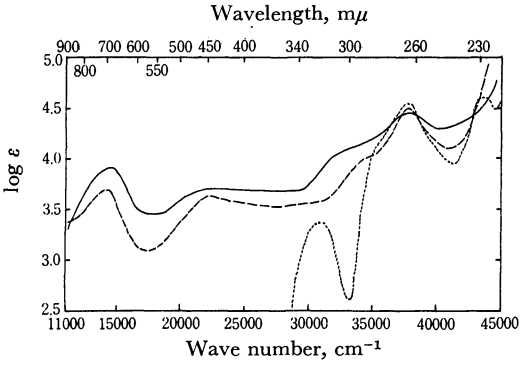

Fig. 2. Electronic absorption spectra of [Ru_2O_7-$phen_2$] and 1,10-phenanthroline.
—— [Ru_2O_7 $phen_2$] in H_2O
—— [Ru_2O_7 $phen_2$] in CH_3OH
------ phen in H_2O

Magnetic Property. The measured molecular weight suggests that the ruthenium(VII) oxide complex with 1,10-phenanthroline is binuclear. The observed diamagnetism of the binuclear complex, [Ru_2O_7 $phen_2$], may be explained as follows. When the Ru(VII) ions, each containing one unpaired d electron, form the binuclear complex with an oxygen-bridge between ruthenium atoms (presumably linear), one electron from each Ru-(VII) and two from the oxygen atom will be form two electron pairs occupying the lower two of the three center MO's. The molecular orbital treatments of $K_4Ru_2OCl_{10}$ and $[RuO_2(NO)_2NO_3]_2O$ which have been reported by Dunitz and Orgel[13] and by Martin *et al.*[1] can be applied to [Ru_2O_7-

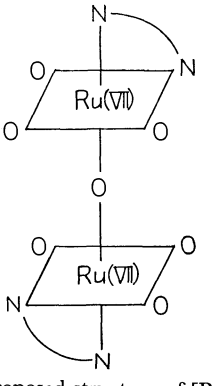

Fig. 3. The proposed structure of [Ru_2O_7 $phen_2$].

7) D. S. McClure, *Solid State Phys.*, **9**, 507 (1959).
8) P. E. Fielding and R. J. W. LeFèvre, *J. Chem. Soc.*, **1951**, 1811.
9) P. Krumholz, *J. Am. Chem. Soc.*, **73**, 3487 (1951).
10) K. Nakamoto, *J. Phys. Chem.*, **64**, 1420 (1960).
11) G. A. Crosby, W. G. Parkins and P. M. Klasser, *J. Chem. Phys.*, **43**, 1498 (1965).
12) K. Sone, P. Krumholz and H. Stammreich, *J. Am. Chem. Soc.*, **77**, 777 (1955).
13) J. D. Dunitz and L. E. Orgel, *J. Chem. Soc.*, **1953**, 2594.

$phen_2$]. The structure thus proposed for the present complex is shown in Fig. 3; its oxidation number is assumed to be 7.

The auther wishes to express his sincere thanks to Professor Shinichi Kawaguchi of Osaka City University for his kind guidance and encouragement throughout this work. His thanks are also due to Dr. Tetsuo Mamuro, the chief of the Department of Health Physics and Instrumentation of the Radiation Center of Osaka Prefecture, for his encouragement and support, and to Dr. Shichio Kawai, the University of Osaka, for his guidance in the measurement of the magnetic susceptibility.

BULLETIN OF THE CHEMICAL SOCIETY OF JAPAN VOL. 42 2074—2076 (1969)

The Separation Factor for Alkali Metals in Solvent Extraction with Hexyl

Shoji MOTOMIZU,* Tadashi IWACHIDO** and Kyoji TÔEI*

* *Department of Chemistry, Faculty of Science, Okayama University, Tsushima, Okayama*
** *College of Liberal Arts and Sciences, Okayama University, Tsushima, Okayama*

(Received December 16, 1968)

The extractions of alkali metals reported to date have almost all been based upon the ion-association principle. For example, polyiodide,[1] tetraphenylborate,[2,3] hexafluorophosphate,[4] and phenols[5,6] have been investigated. The extraction of alkali metals into nitrobenzene using Hexyl[7,8] is also related to the ion association. However, the mechanism for the extraction with Hexyl has not yet been extensively studied. In our previous paper,[9] the mechanism for the extraction of alkali metals using Hexyl was discussed, and the association constants of Hexyl salts in an aqueous solution and in a nitrobenzene solution, the partition coefficients of ion-pairs, and the extraction constants were reported.

In this paper, the separation factor of two alkali metals will be discussed and an equation for the extraction separation of alkali metals with Hexyl will be given theoretically and examined in the cases of sodium and potassium.

Calculations

The Separation Factor of Two Alkali Metals. The general equation for the separation factor, α, is given hereafter by using the extraction and the association constants.

The separation factors for alkali metals, M_1 and M_2, are written as:

$$\alpha_{M_2}^{M_1} = \frac{q_{M_1}}{q_{M_2}} = \left(\frac{[M_1R]_o+[M_1^+]_o}{[M_1R]_a+[M_1^+]_a}\right)\left(\frac{[M_2R]_o+[M_2^+]_o}{[M_2R]_a+[M_2^+]_a}\right)^{-1} \quad (1)$$

where q_{M1} and q_{M2} are the distribution ratios of M_1 and M_2 respectively, and where the subscripts o and a refer to the organic and aqueous phases respectively. [MR], [M^+], and [R^-] are the concentrations of the ion-pair, the metal ion, and the Hexyl anion respectively. $[M_1R]_o$ and $[M_2R]_o$ can be neglected compared with $[M_1^+]_o$ and $[M_2^+]_o$ respectively, because the association constants for M_1R and M_2R are very small. When $[R^-]_a$ is relatively small compared with the concentration of the alkali metal in the aqueous phase, $[M_1R]_a$ and $[M_2R]_a$ can also be neglected compared with $[M_1^+]_a$ and $[M_2^+]_a$ respectively. Therefore, Eq. (1) can be rearranged to Eq. (2):

$$\alpha_{M_2}^{M_1} = \frac{[M_1^+]_o}{[M_2^+]_o} \times \frac{[M_2^+]_a}{[M_1^+]_a} \quad (2)$$

The combination of the two association constants, $K_o^{M_1R}$ and $K_o^{M_2R}$, leads to Eq. (3):

$$\frac{[M_1^+]_o}{[M_2^+]_o} = \frac{K_o^{M_1R}}{K_o^{M_1R}} \times \frac{[M_1R]_o}{[M_2R]_o} \quad (3)$$

The combination of Eqs. (2) and (3) leads to Eq. (4):

1) M. Kyrš and S. Podesva, *Anal. Chim. Acta*, **27**, 183 (1962).
2) K. Haruyama and T. Ashizawa, *Japan Analyst*, **14**, 120 (1965).
3) R. C. Fix and J. W. Irvine, Jr., MIT Lab. Nuclear Science, Annual Progress Report (Nov. 30, 1955).
4) *Idem, ibid.*, Progress Report (May 31, 1955).
5) K. B. Brown, Oak Ridge National Laboratory Rept. ORNL-TM-449 (1963).
6) W. J. Ross and J. C. White, *Anal. Chem.*, **36**, 1998 (1964).
7) M. Kyrš, *Collection Czechoslov. Chem. Commun.*, **27**, 2380 (1962).
8) T. Iwachido and K. Tôei, This Bulletin, **37**, 1276 (1964).
9) K. Tôei, T. Iwachido and S. Motomizu, *ibid.*, **42**, 1006 (1969).

$$\alpha_{M_2}^{M_1} = \frac{K_o^{M_1R}}{K_o^{M_2R}} \times \frac{[M_1R]_o[M_2^+]_a}{[M_2R]_o[M_1^+]_a} = \frac{K_o^{M_1R} \cdot E_{M_1R}}{K_o^{M_2R} \cdot E_{M_2R}} \quad (4)$$

where E_{M_1R} and E_{M_2R} are the extraction constants of M_1R and M_2R respectively and are defined as:

$$E_{M_1R} = \frac{[M_1R]_o}{[M_1^+]_a[R^-]_a f_a^2} \quad (5)$$

$$E_{M_2R} = \frac{[M_2R]_o}{[M_2^+]_a[R^-]_a f_a^2} \quad (6)$$

where f_a indicates the activity coefficient.

Equation (4) is rearranged to Eq. (7):

$$[M_1^+]_a = \frac{1}{1+(q_{M_2} \cdot \alpha_{M_2}^{M_1})} \times T_{M_1} \quad (7)$$

where T_{M1} is the total concentration of metal, M_1.

Experimental

Reagents. The Hexyl sodium salt was prepared and purified by the method reported in the previous paper.[9] The Hexyl-Na nitrobenzene solution was prepared by dissolving the Hexyl-Na in nitrobenzene to give 1.0×10^{-3}M. All the other chemicals used were of a guaranteed reagent grade. Aqueous solutions were prepared by dissolving the sodium hydroxyde, the sodium, and the potassium chloride to give 0.001M, 0.1M, and 2×10^{-5}—1×10^{-3}M respectively.

Apparatus. The concentration of potassium in the aqueous phase after the extraction was determined flame-photometrically by using a Hitachi Flamephotometer, FPF-2.

Extraction Procedures. The extractions were all carried out at 25°C. Twenty milliliters of an aqueous solution containing sodium and potassium were placed into a 50-m*l* separatory funnel and shaken moderately for about thirty minutes with an equal volume of a nitrobenzene solution of Hexyl-Na (1.0×10^{-3}M) so as not to form an emulsion. The final equilibrated pH of the aqueous phase was 10—11. The potassium and Hexyl in the aqueous phase separated from the organic phase were determined flamephotometrically and spectrophotometrically respectively.

Table 1. The constants for hexyl salts

MR	K_o^{MR} *1	K_a^{MR} *2	D_{MR} *3	E_{MR}
Hexyl-Li	3.3	8.9	0.5	4.5
Hexyl-Na	4.0	9.4	3.4	3.2×10
Hexyl-K	4.6	174	20.4	3.5×10^3
Hexyl-Rb	4.7	365	22.2	8.1×10^3
Hexyl-Cs	2.3			

*1 The association constant in nitrobenzene saturated with water:

$$K_o^{MR} = [MR]_o/[M^+]_o[R^-]_o f_a^2$$

*2 The association constant in the aqueous solution:

$$K_a^{MR} = [MR]_a/[M^+]_a[R^-]_a f_a^2$$

*3 The partition coefficient:

$$D_{MR} = [MR]_o/[MR]_a$$

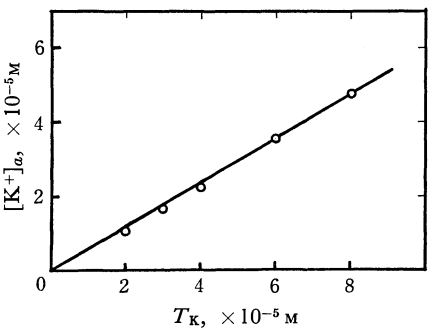

Fig. 1. The plot of $[K^+]_a$ *vs.* T_K.
Original concentration of sodium chloride in the aqueous phase: 1.0×10^{-1}M.
Original concentration of Hexyl-Na in the organic phase: 1.0×10^{-3}M.
In all extractions, the concentration of Hexyl salt in the aqueous phase was less than about 10^{-5}M.

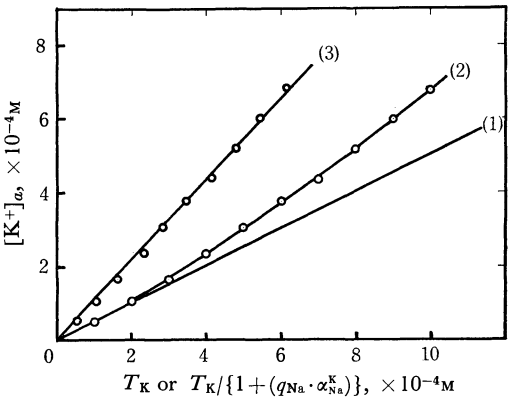

Fig. 2. The plot of $[K^+]_a$ *vs.* T_K or $T_K/\{1+(q_{Na}\cdot\alpha_{Na}^K)\}$.
(1): the line with a slope of 0.5.
(2): the plot of $[K^+]_a$ *vs.* T_K.
(3): the plot of $[K^+]_a$ *vs.* $T_K/\{1+(q_{Na}\cdot\alpha_{Na}^K)\}$.

Results and Discussion

As is shown in Table 1, which is reprinted from our previous report,[9] the association constants of Hexyl alkali metal salts in an organic phase are very small, so the theoretical equation (4) is useful. For example, if M_1 and M_2 are potassium and sodium respectively, the value of α_{Na}^K is calculated from the extraction constants and the association constants to be 9.5×10.

Figures 1 and 2 show the plot of $[K^+]_a$ against T_K. In the region where the concentration of potassium can be neglected in the organic phase, compared with the concentration of sodium, q_{Na} is thought to be kept at 0.01 and α_{Na}^K is 9.5×10, as has been mentioned above, so the slope may be expected to be about 0.5 $(1/(1+0.95))$. In Fig. 1 the slope is about 0.5, as expected. When q_{Na} seems to vary, the plot of $[K^+]_a$ against T_K gradually

deviates from the line of the 0.5 slope (Fig. 2). Figure 2 also shows the plot of $[K^+]_a$ against $T_K/\{1+(q_{Na}\cdot\alpha^K_{Na})\}$. This plot shows a good linearity, and the slope is 1.1.

Equation (7) has thus been found to be in good agreement with the experimental data. Therefore, Eq. (4) will be very useful in estimating the separation of alkali metals.

BULLETIN OF THE CHEMICAL SOCIETY OF JAPAN VOL. 42 2076—2077 (1969)

Proof of the Configuration at C_4 of Guaioxide

Yoshiaki TANAHASHI, Shûji TOMODA and Takeyoshi TAKAHASHI

Department of Chemistry, Faculty of Science, The University of Tokyo, Bunkyo-ku, Tokyo

(Received December 18, 1968)

Recent communications[1,2] on the structure of guaioxide have prompted us to report our results on this problem. Our attention to the structure of this compound has been drawn by isolation of two new sesquiterpene oxides ($C_{15}H_{26}O$) from "San-shion" of *Ligularia* genus (probably *L. sibirica*).[3] These oxides which we conventionally called LB and LC are both isomeric to guaioxide. One (LC) of these recently turned out to be identical with liguloxide.[4]

Guaioxide has been isolated from guaiac wood oil by Bates and Slagel.[5] They reported that acid treatment of guaiol (I) gave guaioxide for which the structure II or III was suggested. Later Ledoux *et al.*[6] assigned the structure IIa to guaioxide, provided that the hydroxyl group adds to the double bond at C_1—C_5 in *trans* manner, and that no isomerization occurs at the other centers (I→A→IIa). Ishii *et al.*[1] recently deduced the structure IIb for guaioxide in which the hydrogen at C_1 and the ether bridge are both β-oriented. One of the most probable courses of formation of guaioxide might be a migration of the double bond at C_1—C_5 to the position C_4—C_5 with addition of proton at C_1 from β-side followed by *srans* addition of the hydroxyl group (I→B→C→IIb′). Hence use of deuteriated acid in cyclization of guaiol (I) is expected to give information on the mechanism of formation of guaioxide and on the stereochemistry at C_4.

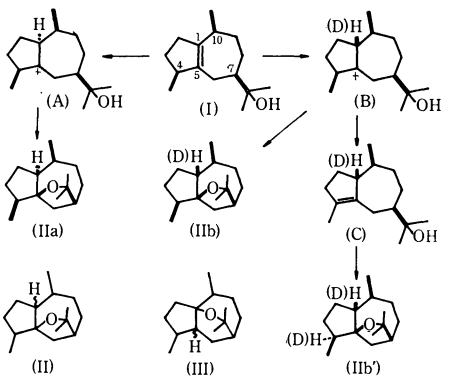

Guaiol (I) gave guaioxide-d_1 when treated with sulfuric acid-d_2 in acetic acid-d_1. The mass spectrum of deuteriated guaioxide shows a molecular ion peak at *m/e* 223, and the NMR spectrum is essentially the same with that of non-deuteriated guaioxide, showing no change in the region of methyl signals. One deuterium atom introduced is, therefore, located at C_1.

This result eliminates the possibility of any acid-catalyzed isomerizations of the double bond (*e.g.* I→B→C→IIb′) during the formation of guaioxide, and establishes that guaioxide has the same configurations at C_4, C_7 and C_{10} as those of guaiol, although no evidence is given as to the ring junction. The above result firmly confirms the 4β-methyl configuration which was previously given for guaioxide by Ishii *et al.*[1] on the basis of generally accepted considerations for microbial hydroxylation.

With Ishii's conclusion[1] admitted, guaioxide should be formed by the route I→B→IIb. *Cis* addition of hydroxyl group would be due to the

1) H. Ishii, T. Tozyo and H. Minato, *Chem. Commun.*, **1968**, 649.

2) C. Ehret and G. Ourisson, *Bull. Soc. Chim. France*, **1968**, 2629.

3) F. Patil, G. Ourisson, Y. Tanahashi, M. Wada and T. Takahashi, *ibid.*, **1968**, 1947.

4) H. Ishii, T. Tozyo and H. Minato, *Chem. Commun.*, **1968**, 106. The structure of liguloxide was recently shown to be 4-epiguaioxide: H. Ishii, T. Tozyo and H. Minato, *Chem. Commun.*, **1968**, 1534.

5) R. B. Bates and R. C. Slagel, *Chem. & Ind.*, **1962**, 1715.

6) P. Ledoux, B. P. Vaterlaus and G. Chiurdoglu, *Bull. Soc. Chim. Belges*, **75**, 551 (1966); P. Ledoux, *Ing. chim.*, **48**, 24 (1966).

conformational stability of an intermediate cation B in comparison with cation A. This evidence is important in view of the structural studies of the remaining oxide (LB) which are in progress in our laboratory and in the Shionogi Research Laboratory.[7]

Experimental

Treatment of Guaiol with Sulfuric Acid-d_2 in Acetic Acid-d_1. Guaiol (957 mg) was dissolved in 99% acetic acid-d_1 (CIBA Ltd. ; 19 g) containing sulfuric acid-d_2 (13 μl). The solution was left at room temperature (13—15°C) for 72 hr. Repeated chromatographies (eluted with petroleum ether) of the crude reaction product (763 mg) over silica gel, then over alumina, gave a hydrocarbon mixture (437 mg) and a colorless oil (41 mg). The latter, having the same retention time in VPC with that of guaioxide, showed essentially the same IR and NMR spectra with those of guaioxide respectively, and gave rise to a molecular ion peak at m/e 223 on its mass spectrum (measured using the Hitachi Mass Spectrometer, RMU-6D Type).

We thank Dr. H. Ishii of Shionogi Research Laboratory, Shionogi and Co., for his valuable discussion and for the identification of LC with liguloxide.

7) Private communication from Dr. H. Ishii.

BULLETIN OF THE CHEMICAL SOCIETY OF JAPAN VOL. 42 2077—2079 (1969)

Reactions of Isocyanides with Carbon Tetrahalogenides in the Presence of Dicobalt Octacarbonyl

Yasuhiro YAMAMOTO*1 and Nobue HAGIHARA

The Institute of Scientific and Industrial Research, Osaka University, Suita-shi, Osaka

(Received December 19, 1968)

It is well established that isocyanides, analogous to carbon monoxide, coordinate to transition metals to give the complexes of isocyanides. In previous papers we have reported on the catalytic polymerization of isocyanides by $BF_3O(C_2H_5)_2$ or transition metal complexes,[1] and on the reactions of isocyanides with various transition metal complexes.[2]

Bamford and Maltman reported some of the characteristic properties of metal carbonyl-organic halide systems as free radical initiators.[3] In the course of our studies on the polymerization of isocyanides with metal carbonyl-carbon tetrahalogenide systems, we found that isocyanides readily reacted with carbon tetrahalogenides in the presence of $Co_2(CO)_8$ to yield *N*-substituted dihaloacetamides and cobalt(II) complexes of isocyanides, suggesting the formation of carbene as intermediates.

Carbon tetrachloride containing a small amount of water was added to a mixture of cyclohexyl isocyanide and $Co_2(CO)_8$ in benzene at room temperature. The subsequent reaction was initiated with evolution of carbon monoxide and gave *N*-cyclohexyldichloroacetamide and dichlorotetrakis(cyclohexyl isocyanide)cobalt(II).

A similar reaction in methanol gave *N*-cyclohexyldichloroacetimidate and dichlorotetrakis(cyclohexyl isocyanide)cobalt(II). The use of other metal carbonyls or metal carbonyl derivatives, such as $Fe(CO)_5$, $Cr(CO)_6$, $Mo(CO)_6$, $[Co(PPh_3)_2(CO)_3]BPh_4$ and [Fe(morphorine)][$Fe(CO)_4$] did not promote the reactions. The use of $[Co(PPh_3)_2(CO)_3][Co(CO)_4]$ promoted the reaction to give *N*-cyclohexyldichloroacetamide, $Co(C_6H_{11}NC)_4Cl_2$ and $Co(PPh_3)_2(CO)_2Cl_2$. The results of the reaction are listed in Table 1.

It has been reported by Halleux that *N*-cyclohexyldichloroacetimidate was obtained from the reaction of cyclohexyl isocyanide with dichlorocarbene, prepared from potassium methoxide and chloroform, and it decomposed spontaneously to produce *N*-cyclohexyldichloroacetamide.[4]

*1 Present address: The Institute of Physical and Chemical Research, Yamatomachi, Saitama.

1) Y. Yamamoto, T. Takizawa and N. Hagihara, *Nippon Kagaku Zasshi (J. Chem. Soc. Japan, Pure Chem. Sect.)*, **87**, 1355 (1966); Y. Yamamoto and N. Hagihara, *ibid.*, **89**, 898 (1968).

2) Y. Yamamoto and N. Hagihara, This Bulletin, **38**, 1084 (1966); Y. Yamamoto, H. Yamazaki and N. Hagihara, *ibid.*, **41**, 532 (1968).

3) C. H. Bamford, *J. Polymer Sci., C*, 1571 (1964); C. H. Bamford and W. R. Maltman, *Trans. Faraday Soc.*, **62**, 2823 (1966).

4) A. Halleux, *Angew. Chem.*, **76**, 889 (1964).

TABLE 1. THE REACTIONS OF ISOCYANIDES WITH CARBON TETRAHALOGENIDES IN THE PRESENCE OF $Co_2(CO)_8$

Isocyanide	CX_4	Product	Yield[a] (%)	mp[b] (°C)	Analyses (%) C	H	N	IR[c] (cm^{-1})
$C_6H_{11}NC$	CCl_4	$C_6H_{11}NHCOCHCl_2$	37	140—141	45.61 (45.73)	6.56 (6.24)	6.24 (6.67)	
		$Co(CNC_6H_{11})_4Cl_2$	93	84—86	59.87 (59.36)	7.86 (7.83)	9.39 (9.35)	2220
	CBr_4	$C_6H_{11}NHCOCHBr_2$	28	172—173	32.65 (32.14)	4.26 (4.38)	4.88 (4.68)	
		$Co(CNC_6H_{11})_4Br_2$	96	116—118	51.27 (50.77)	6.79 (6.78)		2215
$(CH_3)_3CNC$	CCl_4	$(CH_3)_3CNHCOCHCl_2$	48	152—153	39.34 (39.15)	6.03 (6.03)	7.47 (7.61)	
		$Co(CNC(CH_3)_3)_4Cl_2$	94	*ca.* 298	51.59 (51.95)	7.73 (7.85)	11.83 (12.12)	2230
	CBr_4	$(CH_3)_3CNHCOCHBr_2$	25	182—184	27.01 (26.40)	4.38 (4.06)	5.26 (5.13)	
		$Co(CNC(CH_3)_3)_4Br_2$	92		43.91 (43.57)	6.71 (6.58)	10.55 (10.16)	2175
$C_6H_5CH_2NC$	CCl_4	$C_6H_{11}CH_2NHCOCHCl_2$	22	94.5—95.5	49.52 (49.57)	4.20 (4.16)	6.41 (6.42)	
		$Co(CNCH_2C_6H_5)_4Cl_2$	95	106—108	64.17 (64.24)	4.79 (4.79)	9.33 (9.36)	2215
	CBr_4	$C_6H_{11}CH_2NHCOCHBr_2$	23	123—125	35.25 (35.21)	2.89 (2.96)	4.54 (4.56)	
		$Co(CNCH_2C_6H_5)_4Br_2$	95	151—153	55.61 (55.91)	4.17 (4.11)		2215

a) Based on $Co_2(CO)_8$ employed. b) All complexes, $Co(CNR)_4X_2$, decomposed.
c) KBr method, N≡C band.

The fact that *N*-substituted dihaloacetamides or *N*-cyclohexyldichloroacetimidate was obtained in our reaction suggested the existence of dihaloketenimine as the intermediates of the reactions. In order to confirm the formation of carbenes, the reaction of $[Co(CO)_3(PPh_3)_2][Co(CO)_4]$ with carbon tetrachloride or carbon tetrabromide was carried out in cyclohexene. The reaction gave 7,7-dichloronorcarane and $Co(CO)_2(PPh_3)_2Cl_2$, or 7,7-dibromonorcarane and $Co(CO)_2(PPh_3)_2Br_2$. These results suggest the formation of the carbene intermediates.

The possible pathway for the reaction may be sketched in the following manner:

$$5R\text{-}N{\equiv}C + Co_2(CO)_8 \rightarrow Co(CNR)_5Co(CO)_4 + 4CO \quad (1)$$
$$(I)$$

$$I + 2CX_4 + 5RNC \rightarrow 2Co(CNR)_4X_2 + 4CO + 2RN{=}C{=}CX_2 \quad (2)$$

$$RN{=}C{=}CX_2 + H_2O \rightarrow RNHCOCHX_2$$
$$RN{=}C{=}CX_2 + CH_3OH \rightarrow RNC{=}C(OCH_3)CHX_2 \quad (3)$$

When $Co_2(CO)_8$ was added to excess isocyanide, it reacted with isocyanide, as was reported by Sacco,[5] to yield $Co(CNR)_5Co(CO)_4$ by the evolution of 4 mol of carbon monoxide, according to Eq. (1). In addition, the evolution of 4 mol more of carbon monoxide was observed, when carbon tetrahalogenide was added to the reaction mixture. This fact showed that *N*-substituted dihalokenimine and $Co(CNR)_4X_2$ were formed, according to Eq. (2). *N*-Substituted dihaloketenimine rapidly reacted with water or methanol to produce the corresponding amide or imidate.

Experimental

Materials. Various isocyanides[6] and transition metal complexes[7] were prepared according to the prescription given in literature.

The Reaction of Cyclohexyl Isocyanide with Carbon Tetrachloride in the Presence of $Co_2(CO)_8$. To a solution of 1.0 g of $Co_2(CO)_8$ in 25 ml of *n*-hexane was added 2.3 g of cyclohexyl isocyanide. After 20 min, into this was added 5.0 g of aqueous carbon tetrachloride (*ca.* 5% H_2O) with constant stirring at room temperature. The reaction was completed within 2 hr to give dark green solution, with the precipitaiton of a green solid. Precipitate was filtered and washed by *n*-hexane. It was found to be $Co(CNC_6H_{11})_4Cl_2$ and was soluble in acetone and chloroform, but was insoluble in petroleum ether. The evaporation of the filtrate gave raw products of *N*-cyclohexyl dichloroacetamide, which was recrystallizad by benzene-acetone mixture. The infrared spectrum and the melting point of this

5) A. Sacco, *Gazz. Chim. Ital.*, **83**, 632 (1953).

6) I. Ugi and R. Mayr, *Chem. Ber.*, **93**, 239 (1960).

7) R. B. King, "Organometallic Syntheses," Vol. 1, Academic Press Inc., New York (1965), p. 98.

product were identical with those of authentic *N*-cyclohexyldichloroacetamide.

By analogous procedure, other *N*-substituted dihaloacetamides and dihalotetrakis(isocyanide)cobalt(II) were obtained. Their melting points, analyses and infrared spectra are summarized in Table 1.

The Reaction of Carbon Tetrachloride with $[Co(CO)_3(PPh_3)_2][Co(CO)_4]$ in the Presence of Cyclohexene. Carbon tetrachloride (5.4 g) was added to a mixture of $[Co(CO)_3(PPh_3)_2][Co(CO)_4]$ (4.5 g) and cyclohexene (20 m*l*) at room temperature. After the reaction mixture had been kept for 2.5 hr with constant stirring, a pale green precipitate was filtered, and found to be $Co(CO)_2(PPh_3)_2Cl_2$(3.65 g, mp 82—83°C). Glpc analysis of the distillate of the filtrate showed the presence of 7,7-dichloronorcarane, which was identified by comparison of its glpc retention time with that of an authentic sample.

Found: C, 64.52; H, 4.39; Cl, 10.15%. Calcd for $Co(CO)_2(PPh_3)_2Cl_2$: C, 64.24; H, 4.26; Cl, 9.98%.

BULLETIN OF THE CHEMICAL SOCIETY OF JAPAN VOL. 42 2079—2081 (1969)

The Structure Theory of Water. II. The Thermodynamic Properties of Liquid Deuterium Oxide

Kiyoshi ARAKAWA, Katsutaka SASAKI and Yuko ENDO

Research Institute of Applied Electricity, Hokkaido University, Sapporo

(Received December 20, 1968)

In the preceding paper[1] (Part I), a statistical thermodynamic theory was successfuly applied to liquid water, based on a two state model which consists of an ice-like structure (class I) and unbonded monomers (class II). The same treatment has been applied to liquid deuterium oxide, with the intention to explain the thermodynamic properties of the liquid and to test the applicability of the two state model.

In the calculation of the partition function (Part I), the two quantities, *viz.*, the energy difference between class I and class II, ε, and the free volume for the molecule in class II, v_f, were used as adjustable parameters. The values of the parameters were estimated to be 3 kcal/mol and 4.0×10^{-25} cm^3 respectively. They are in line with the thermodynamic properties of the liquid water. In the present calculation the same value for v_f has been used, since the dimension of the molecule and the dipolar interactions *etc.* of D_2O are practically the same as those of H_2O.[2]

For the magnitude of ε for D_2O a higher value is required than for H_2O, since the energy of sublimation for the former ($\Delta E_{\text{subl}}^{D_2O}$: 12.08 kcal/mol) is larger than that of the latter ($\Delta E_{\text{subl}}^{H_2O}$: 11.65 kcal/mol).[2] Considering that the van der Waals interactions between D_2O molecules may be nearly the same as those between H_2O molecules, the magnitude of ε for D_2O is estimated to be 3.4 kcal/mol.

$$\varepsilon_{D_2O} - \varepsilon_{H_2O} \fallingdotseq \Delta E_{\text{subl}}^{D_2O} - \Delta E_{\text{subl}}^{H_2O} \tag{1}$$

Concerning the frequencies which have been attributed to intermolecular vibrations of the molecules in class I, a tentative assignment has been made with reference to the data from the infrared and Raman spectroscopy[3,4] and also by taking into account the difference in the mass and the principal moments of inertia between D_2O and H_2O molecules.[5] The ratio of librational frequencies, and that of the principal moments of inertia between D_2O and H_2O are estimated to be 1.38, and 1.91 respectively, according to Swain and Bader.[5] The values for ν_i and A, B, C are given in Table 1.

TABLE 1. INTERMOLECULAR VIBRATIONAL FREQUENCIES AND PRINCIPAL MOMENTS OF INERTIA FOR D_2O

Frequency (cm^{-1})			
Translational vibration	Rotational vibration		
$\nu_1=\nu_2=\nu_3$	ν_4	ν_5	ν_6
170	340	470	540
Moment of inertia			
A	B	C	
1.96×10^{-40}	3.67×10^{-40}	5.63×10^{-40}	

1) K. Arakawa and K. Sasaki, This Bulletin, **42**, 303 (1969).

2) G. Nemethy and H. A. Scheraga, *J. Chem. Phys.*, **41**, 680 (1964).

3) P. A. Giguére and K. B. Harvey, *Can. J. Chem.*, **34**, 798 (1956).

4) D. A. Draegert, N. W. B. Stone, B. Curnutte and D. Williams, *J. Opt. Soc. Am.*, **56**, 64 (1966).

5) G. Swain and R. F. Bader, *Tetrahedron*, **10**, 182 (1960).

TABLE 2. THERMODYNAMIC VARIABLES

Temp. (°C)	A_{calc} (kcal/mol)	A_{obs}	E_{calc} (kcal/mol)	E_{obs}	S_{calc} (cal/deg·mol)	S_{obs}	$(C_v)_{calc}$ (cal/deg·mol)	$(C_v)_{obs}$
4	−1.435	−1.58	3.205	3.04	16.74	16.6	28.88	20.5
10	−1.538	−1.68	3.374	3.15	17.34	17.1	27.64	20.3
20	−1.713	−1.85	3.633	3.36	18.23	17.8	26.64	20.1
30	−1.903	−2.03	3.883	3.57	19.08	18.4	23.17	19.9
40	−2.098	−2.22	4.103	3.77	19.80	19.1	21.05	19.7
50	−2.299	−2.42	4.307	3.97	20.44	19.7	18.94	19.4
60	−2.502	−2.62	4.478	4.17	20.95	20.4	17.26	19.1

Calculation of Thermodynamic Variables.

According to the statistical mechanical theory reported in Part I, calculations of thermodynamic variables for liquid D_2O have been made over the temperature range from 4—60°C, using the values of parameters described above. The calculated values of the Helmholtz energy, A, the internal energy, E, the entropy, S, and the specific heat at constant volume, C_v, are given in Table 2. The results calculated are compared with the experimental data for liquid D_2O and also with the results calculated by Némethy and Scheraga.[2] They are plotted against temperature in Figs. 1—4. The mole fraction x of hydrogen bonded portion is calculated and given in Table 3, together with the ratio, x_{D_2O}/x_{H_2O}.

TABLE 3. FRACTION OF HYDROGEN BONDED PORTION, x

Temp. (°C)	x_{D_2O}	x_{D_2O}/x_{H_2O}*
4	0.514	1.03
10	0.479	1.03
20	0.427	1.03
30	0.378	1.03
40	0.336	1.03
50	0.298	1.02
60	0.268	1.02

* The values of x_{H_2O} are those calculated in Part I.

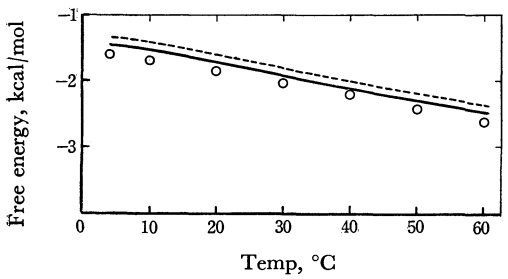

Fig. 1. Helmholtz energy, A, for liquid D_2O. Circle, observed: Solid ine, calculated; Dotted line, Némethy and Scherage[2]

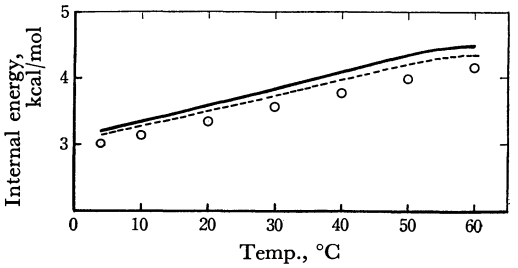

Fig. 2. Internal energy, E, for liquid D_2O. Circle, observed; Solid line, calculated; Dotted line, Némethy and Scheraga[2]

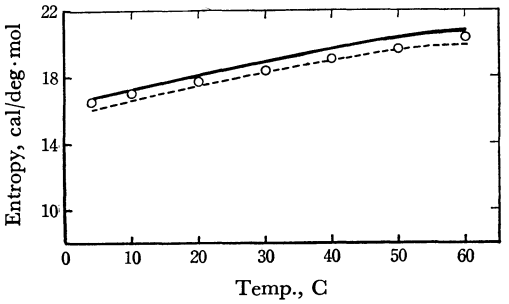

Fig. 3. Entropy, S, for liquid D_2O. Circle, observed; Solid line, calculated; Dotted line, Némethy and Scheraga[2]

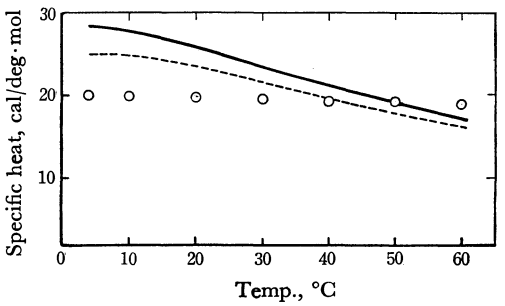

Fig. 4. Specific heat, C, for liquid D_2O. Circle, observed; Solid line, calculated; Dotted line, Némethy and Scheraga[2]

As seen in Figs. 1—4, the agreement between calculated and observed values for D_2O is fairly good, except that deviations are seen in the values of C_v. In the present calculation for D_2O, the parameters, ε, v_f, and v_t have been fixed theoretically as compared with those for H_2O. Thus we might say that agreement is satisfactory.[2,6]

It seems reasonable from observed data[2] that in liquid D_2O the degree of hydrogen bonding is higher than for liquid H_2O. The ratio, x_{D_2O}/x_{H_2O} given in Table 3 is in line with this view.

We see that the thermodynamical behavior of liquid D_2O is described adequately by using the value of ε_{D_2O} which is larger than ε_{H_2O}. The results support the idea that the bond strength of O—D···O is stronger than that of O—H···O.

It is concluded that the two state theory for liquid water (Part I) gives an adequate representation of thermodynamical behaviors of liquid D_2O.

6) M. R. Thomas and H. A. Scheraga, *J. Phys. Chem.*, **69**, 3722 (1965).

BULLETIN OF THE CHEMICAL SOCIETY OF JAPAN VOL. 42 2081—2083 (1969)

Metal Complexes of Amino Acids. IV.[1] The Circular Dichroism of Tetrammine Cobalt(III) Complexes Containing Two Unidentate L-Amino Acid Ligands

Takaji YASUI,* Junnosuke FUJITA** and Yoichi SHIMURA*

* *Department of Chemistry, Faculty of Science, Osaka University, Toyonaka, Osaka*

** *Department of Chemistry, Faculty of Science, Tohoku University, Katahira-cho, Sendai*

(Received December 24, 1968)

The preparation of a large number of pentammine and tetrammine cobalt(III) complexes containing L-amino acids as unidentate ligands were given in previous papers,[1,2] and the studies on the so-called vicinal effect due to the coordinated L-amino acids by means of rotatory dispersion (RD) and circular dichroism (CD) were reported.

From these studies, it was shown that the magnitude of inversive dispersion of RD and the intensity of CD in the d→d transition band region are enhanced by the sterical restriction of the conformational mobility of the coordinated L-amino acid. As a supplement to these studies, some new tetramminebis(amino-acid)cobalt(III) complexes are described in the present paper. The following abbreviations are used for the amino acid ligands: glyH = $CH_2(COO^-)NH_3^+$, alaH = $CH_3CH(COO^-)NH_3^+$, β-alaH = $CH_2(COO^-)CH_2NH_3^+$, sarH = $CH_2(COO^-)(NH_2CH_3)^+$, and proH = $CH(COO^-)CH_2CH_2CH_2NH_2^+$.

Experimental

cis-Tetrammine(β-alanine)(L-alanine)cobalt(III) Perchlorate and cis-Tetrammine(sarcosine)(L-alanine)cobalt(III) Perchlorate: cis-$[Co(NH_3)_4(\beta\text{-alaH})(L\text{-alaH})](ClO_4)_3$ and cis-$[Co(NH_3)_4(sarH)(L\text{-alaH})](ClO_4)_3$. The crude complexes were obtained by a method similar to that employed in the preparation of cis-$[Co(NH_3)_4(glyH)(L\text{-alaH})](ClO_4)_3\cdot 2H_2O$.[2] Purification was carried out by reprecipitation from their methanol solutions with dropwise addition of ether. These purple complexes are readily soluble in water and acetone, but insoluble in ether. The elemental analyses were made after dehydrating them on phosphorus pentoxide in a vacuum desiccator.

Found: C, 11.78; H, 4.37; N, 13.64%. Calcd for $C_6H_{26}N_6O_{16}Cl_3Co$: C, 11.94; H, 4.35; N, 13.93%.

Found: C, 12.02; H, 4.30; N, 13.67%. Calcd for $C_6H_{26}N_6O_{16}Cl_3Co$: C, 11.94; H, 4.35; N, 13.93%.

cis-Tetramminebis(L-proline)cobalt(III) Perchlorate: cis-$[Co(NH_3)_4(L\text{-proH})_2](ClO_4)_3$. A solution of cis-$[Co(NH_3)_4(OH_2)_2](ClO_4)_3$[3] and the calculated amount of L-proline in a small amount of water was warmed on a water-bath at 65°C for about seven hours. After the resulting solution had been kept for two days at room temperature, a large amount of methanol-ether mixture (2 : 1) was added to it. Purification of the crude product obtained was made from the methanol solution by the addition of ethanol-ether mixture (2 : 1). This was dehydrated on phosphorus pentoxide in a vacuum desiccator.

Found: C, 18.05; H, 4.54; N, 12.81%. Calcd for $C_{10}H_{30}N_6O_{16}Cl_3Co$: C, 18.32; H, 4.62; N, 12.82%.

The preparation of the other complexes studied has

1) Part III of this series: T. Yasui, J. Hidaka and Y. Shimura, This Bulletin, **39**, 2417 (1966).

2) J. Fujita, T. Yasui and Y. Shimura, *ibid.*, **38**, 654 (1965).

3) M. Linhard and M. Weigel, *Z. Anorg. Chem.*, **260**, 65 (1949).

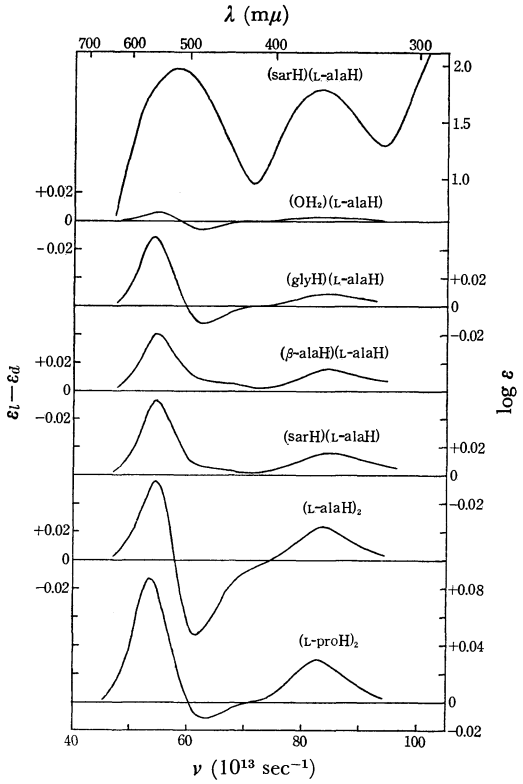

Fig. 1. Absorption and CD curves of the *cis*-[$Co^{III}(N)_4(O)_2$] type complexes containing one or two unidentate amino acid ligands.

already been reported.[2] The CD curves were obtained by a Model ORD/UV-5 spectrophotometer of Japan Spectroscopic Co. and the absorption spectra by a Shimadzu QR-50 spectrophotometer; the measurements were made in aqueous solutions at room temperature. The CD curves are shown in Fig. 1 and their extremum data are listed in Table 1.

Discussion

The analytical results and the absorption spectra of the complexes obtained obviously indicate that the amino acid ligands are coordinated to the cobalt(III) ion with the oxygen atom of the carboxyl group, and that the two oxygen donor atoms are situated at the *cis* positions of an octahedron. Therefore all of the complexes studied here have a general type of coordination, namely *cis*-[$Co(N)_4(O)_2$] structure.

In the first absorption band region, the CD bands of the *cis*-[$Co(OH_2)(NH_3)_4$(L-alaH)]$^{3+}$ complex are very weak in contrast to those of the other complexes (Fig. 1). The CD bands of the [$Co(NH_3)_5$(L-alaH)]$^{3+}$ complex, which contains only one L-alanine ligand, is also very weak.[1] If the aquo ligand in the (aquo)(L-alanine) complex is replaced by another amino acid ligand, the CD bands are considerably intensified (Fig. 1). In these complexes, the two amino acids in *cis* positions should take conformations somewhat restricted by the mutual interaction between them. The interaction between the L-alanine and the aquo ligands in the (aquo)(L-alanine) complex will be less than that between the two amino acid ligands in a bis(amino-acid)tetrammine complex. Thus the enhancement of the CD intensity may be attributed to the sterical restriction of the conformational mobility of the L-alanine ligand.

The *cis*-[$Co(N)_4(O)_2$] structure has a symmetry of C_{2v}, and two CD components are expected in the region of the first absorption band of these complexes. Indeed they show the two CD bands; the longer wavelength bands of all the complexes are positive in their signs. A positive CD band is also commonly observed in the second absorption band region for each L-amino acid complex. These CD bands of the bis(amino-acid) complexes will

Table 1. Absorption and CD data of the tetrammine complexes of [$Co^{III}(N)_4(O)_2$] type (the extremum positions are given in 10^{13} sec^{-1})

Ligand in *cis* positions	I Band		II Band	
	ν^{AB}_{max} (log ε_{max})	ν^{CD}_{ext} $(\varepsilon_l-\varepsilon_d)_{ext}$	ν^{AB}_{max} (log ε_{max})	ν^{CD}_{ext} $(\varepsilon_l-\varepsilon_d)_{ext}$
(OH₂)(L-alaH)	59.2 (1.86)	53.6 (+0.006)	84.0 (1.72)	83.3 (+0.002)
		61.2 (−0.006)		
(glyH)(L-alaH)	58.0 (1.97)	53.7 (+0.048)	82.4 (1.78)	83.3 (+0.007_4)
		61.8 (−0.013_5)		
(β-alaH)(L-alaH)	57.8 (1.98)	54.0 (+0.040_5)	82.6 (1.79)	84.5 (+0.014_5)
		ca. 62 (+0.007)		
(sarH)(L-alaH)	58.1 (1.97)	54.0 (+0.054)	82.5 (1.78)	85.7 (+0.016_5)
		ca. 62 (+0.006)		
(L-alaH)₂	58.2 (1.96)	53.6 (+0.057)	82.8 (1.77)	82.2 (+0.025_6)
		60.6 (−0.054)		
(L-proH)₂	58.0 (1.97)	54.0 (+0.089)	82.8 (1.79)	82.5 (+0.032)
		63.1 (−0.010_2)		

be useful in determining the absolute configurations of amino acids. It has already been reported that the complexes of *trans*-$[Co(en)_2(L\text{-amino-acid})_2]^{3+}$ type have positive CD signs in the longer wavelength component of the first absorption band, and also in the second absorption band. Dunlop and Gillard[4] proposed the use of the complexes of $[Co(NH_3)_5(OCOR)]^{n+}$ type for the determination of absolute configuration of the $RCOO^-$, and this was criticized by Hawkins and Lawson.[5] The latter authors stated that the pentammine type complexes with the L-ligands impose a positive sign to the $^1A_1 \rightarrow {}^1E$ and a negative sign to the $^1A_1 \rightarrow {}^1A_2$ transition in the first absorption band region. Almost all of the pentammine type complexes, however, show only one component in the first absorption band region.[1,5] It seems that the bis(amino-acid) type complexes are more suitable for the determination of the absolute configurations of amino acids.

4) J. H. Dunlop and R. D. Gillard, *Tetrahedron*, **23**, 349 (1967).

5) C. J. Hawkins and P. J. Lawson, *Chem. Commun.*, **1968**, 177.

SHORT COMMUNICATIONS

The Structure of a New Flavone, "Arthraxin"

Makoto KANETA and Noboru SUGIYAMA

Fukushima Technical College, Fukushima, and Department of Chemistry, Tokyo Kyoiku University, Otsuka, Tokyo

(Received April 7, 1969)

We have isolated from *Arthraxon hispidus* Makino, commonly called "Kobunagusa," a new flavonoid (I, mp 336°C, empirical formula $C_{21}H_{16}O_9$), which we wish to call "arthraxin." Kobunagusa has been used as a source of natural dyestuff for "Kihachijo," which is a traditionally well-known brilliant yellow silk cloth produced on Hachijo island. The only report on a chemical study of the dyestuff has been made by Hayashi *et al.*,[1] and they did not succeed in obtaining a pure substance because of the difficulty of purification.

Compound I has neither methoxyl nor methylenedioxy groups, and it forms a penta methyl ether (II), $C_{21}H_{11}O_4(OCH_3)_5$ and a penta acetate (III), $C_{21}H_{11}O_4(OCOCH_3)_5$. The ultraviolet absorption spectrum of I in ethanol showed characteristic absorption bands at 256, and 340 mμ and a pronounced inflection at 273 mμ. The λ_{max} of the band at 256 mμ did not shift with the addition of anhydrous sodium acetate. This fact indicated the absence of the hydroxyl group or the presence of the protected hydroxyl group at C^7.[2] The infrared absorption spectrum of I demonstrated the presence of the >CO of γ-pyrone by the band at 1645 cm^{-1} and the absence of a furan ring or a lactone grouping in the molecule. On fusion with caustic potash, I yielded protocatechuic acid and pholoroglucinol.

The NMR spectrum of I in deuterated DMSO indicated the presence of 1H at C^6 (τ 3.70, s), C^3 (τ 3.35, s),[3] C$^{5'}$ (τ 3.10—3.20,m), C$^{2'}$, and C^6 (τ 2.60—2.75, m).[4] The spectrum also suggested the presence of the CH_3–$\underset{\underset{OH}{|}}{CH}$–$CH_2$– grouping by the signals at τ 8.50 (d, 3H of –CH_3), τ 7.20—7.40 (m, 2H of –CH_2–), and τ 5.30 (m, 1H of –CH–). The NMR spectrum of II in $CDCl_3$ showed the presence of five OCH_3 groups by the signals at τ 6.50 (s, 3H), τ 6.15 (s, 3H), τ 6.10 (s, 3H), τ 6.05 (s, 3H), and τ 5.95 (s, 3H).[5] The mass spectra further showed the presence of five OH groups in I by the difference in the molecular weights of II (482) and I (412).[6]

On the basis of these results, it can be considered that I is a luteolin derivative with a $C_6H_8O_4$ residue attached at C^7 and C^8. As three OH groups are present in the benzene rings, the remaining two OH groups must be present in this $C_6H_8O_4$ residue. The mass spectrum of I gave the fragments of *m/e* 397 and 379, which were interpreted by the general pattern of fragmentation:

$$\underset{(412)}{R\text{-}\underset{\underset{OH}{|}}{CH}\text{-}CH_3} \xrightarrow[-CH_3]{} \underset{(397)}{[R\text{-}\underset{\underset{OH}{|}}{CH}]^+} \xrightarrow[-H_2O]{} \underset{(379)}{[R\text{-}CH{=}CH]^+}$$

From these data and the fragmentations of the mass spectra of I and II, the following structure was deduced to be the most probable one for arthraxin.

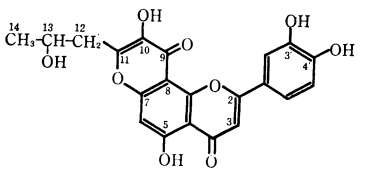

The structure of flavone, in which a side-chain, CH_3–$\underset{\underset{OH}{|}}{CH}$–$CH_2$– or a γ-pyrone ring is attached to the benzene ring, has not yet been established.

1) K. Hayashi and T. Inoue, *Acta Phytochimica*, **15**, 53 (1949).

2) L. Jurd and R. M. Horowitz, *J. Org. Chem.*, **22**, 1618 (1957).

3) J. Massicot and Jean-Pierre Marthe, *Bull. Soc. Chim. France*, **1962**, 1962; J. Massicot, Jean-Pierre Marthe and S. Heitz, *ibid.*, **1963**, 2712.

4) T. J. Batterham and R. J. Highet, *Australian J. Chem.*, **17**, 428 (1964); A. C. Waiss, Jr., R. E. Lundin and D. J. Stern, *Tetrahedron Letters*, **1964**, 513.

5) R. H. Bible, Jr., "Guide to the NMR Empirical Method," Plenum Press, New York (1967), pp. 106,158; R. I. Reed, *J. Chem. Soc*, **1963**, 5949.

An ESR Study of the Copper(II) Complexes of DL-α-Alanine and L-α-Alanine

Hiroshi Yokoi and Taro Isobe

Chemical Research Institute of Non-aqueous Solutions, Tohoku University, Katahira-cho, Sendai

(Received May 6, 1969)

The copper(II) complexes of α-amino acids contain almost planar chelate rings; therefore, no stereospecificity is expected.[1,2] An investigation of the properties of the copper(II) complexes of α-alanines, both in solution and in the solid state, has shown that there are almost no differences in properties between the copper(II) complexes of racemic- and *laevo*-α-alanines, except in some specific points.[1]

The purpose of this communication is to report the ESR results for the copper(II) complexes of racemic- and *laevo*-α-alanines, both in solution and in the solid state. Figure 1 shows the K-band ESR

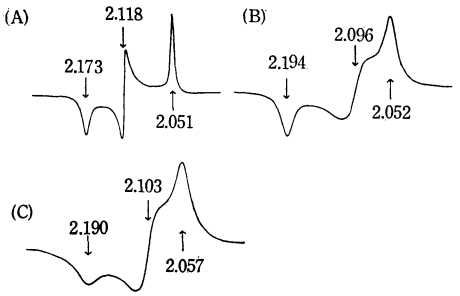

Fig. 1. The powder ESR spectra (K-band, 22°C). The numbers in this figure indicate *g* values.
(A) [Cu(DL-α-alanine)$_2$]·H_2O
(B) [Cu(DL-α-alanine)$_2$]
(C) [Cu(L-α-alanine)$_2$]

spectra of the powdered samples at room temperature. This figure indicates that the water of crystallization of [Cu(DL-α-alanine)$_2$]·H_2O, I, plays the very important role in determining the properties of the complex in a crystal, and that there is a clear difference in the absorption line shape between

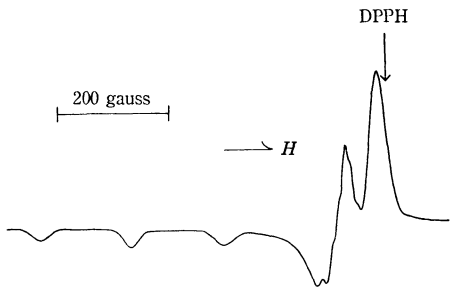

Fig. 2. The X-band ESR spectrum of [Cu(DL-α-alanine)$_2$] in aqueous-methanolic solution at 77°K.

[Cu(DL-α-alanine)$_2$], II, and [Cu(L-α-alanine)$_2$], III, the former bing prepared by the elimination of the water of crystallization of I at 165°C *in vacuo*.

Figure 2 shows the X-band ESR spectrum of I in an equivolume mixture of water and methanol at the temperture of liquid nitrogen. The results determined for the complexes in the solution are as follows:

I: $g_{//}=2.264$, $A_{//}=178\times10^{-4}\text{cm}^{-1}$,
$A_N^{\perp}=11.7\times10^{-4}\text{ cm}^{-1}$

III: $g_{//}=2.264$, $A_{//}=175\times10^{-4}\text{cm}^{-1}$
$A_N^{\perp}=11.1\times10^{-4}\text{ cm}^{-1}$

$A_N^{\perp}$ was determined from the super-hyperfine structure observed on the $g_{\perp}$ component by the second-derivative X-band ESR measurements. These results show that there is a significant difference in the values of $A_{//}$ and $A_N^{\perp}$ between I and III in solution.

In conclusion, all the ESR results obtained here indicate that there is some stereospecific difference in electronic structure between the copper(II) complexes of racemic- and *laevo*-α-alanines, both in solution and in the solid state. The details will be published elsewhere.

1) R. D. Gillard, H. M. Irving, R. Parkins, N. C. Payne and L. D. Pettit, *Chem. Commun. (London)*, **1965**, 81.

2) E. J. Corey and J. C. Bailar, *J. Am. Chem. Soc.*, **81**, 2620 (1959); W. E. Bennet, *ibid.*, **81**, 246 (1959).

Effect of Phase on the Trapped Radical in the Radiolysis of Solid Isobutane as Studied by ESR Spectroscopy

Tetsuo MIYAZAKI, Terunobu WAKAYAMA, Kenji FUEKI and Zen-ichiro KURI

Department of Synthetic Chemistry, Faculty of Engineering, Nagoya University, Chikusa-ku, Nagoya

(Received May 8, 1969)

The solvent radicals observed in the radiolysis of solid hydrocarbons are mostly formed by the C–H bond rupture. Since the yields of the radicals are generally not affected by the addition of electron scavengers[1] or by the photobleaching of trapped electrons,[1] the mechanism of their formation cannot be explained simply in terms of charge neutralization reactions. Recently the present authors reported that the addition of carbon tetrachloride to solid isobutane suppresses the production of the solvent radicals.[2,3]

In this work we have observed that quite different radicals are trapped in the radiolysis of isobutane depending on whether it is in the glassy or the crystalline state. The ESR spectrum of γ-irradiated pure isobutane, which is polycrystalline at 77°K, is shown in Fig. 1a. The spectrum can be assigned to the isobutyl radical.[4] An isobutane (92 mol%)—3-methylpentane (8 mol%) mixture can be frozen to a clear glass by rapid cooling or to a polycrystal by slow cooling at 77°K. Upon the γ-irradiation of the mixture in the polycrystalline state, the ESR spectrum shown in Fig. 1b was obtained; it is the same as the spectrum obtained in the radiolysis of pure isobutane at 77°K. A quite different ESR spectrum, however, was obtained by the γ-irradiation of the mixture in the glassy state (Fig. 1c). The spectrum consists of ten equally-spaced lines with a coupling constant of 22.3G; the value is consistent with the value of 22.5G for the t-C_4H_9 radical.[5] The spectrum coincides with the spectrum of t-C_4H_9 radicals produced by dissociative-electron attachment to t-C_4H_9Br in the radiolysis of 3-methylpentane containing 5 mol% t-C_4H_9Br at 77°K.

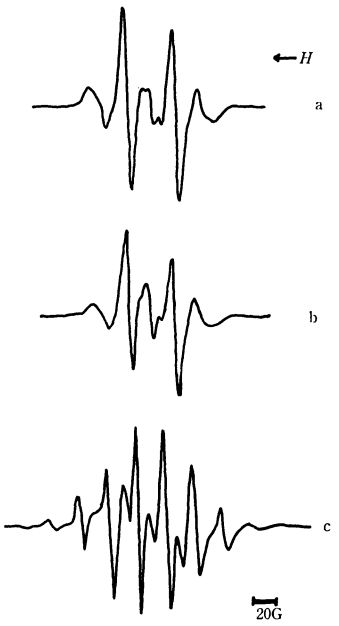

Fig. 1. (a) ESR spectrum of γ-irradiated isobutane at 77°K.
(b) ESR spectrum of γ-irradiated isobutane (92 mol%)–3-methylpentane (8 mol%) mixture in the polycrystalline state at 77°K.
(c) ESR Spectrum of γ-irradiated isobutane (92 mol%)–3-methylpentane (8 mol%) mixture in the glassy state at 77°K.
Irradiation dose: 3.7×10^5 rad, Spectrometer gain setting of figures a, b and c were 67 db.

Such a phase effect in the radiolysis of solid hydrocarbons has not been reported previously. Further studies of this phenomenon are now in progress.

1) M. Shirom and J. E. Willard, *J. Phys. Chem.*, **72**, 1702 (1968).
2) T. Wakayama, T. Miyazaki, K. Fueki and Z. Kuri, This Bulletin, **42**, 1164 (1969).
3) T. Wakayama, T. Kimura, T. Miyazaki, K. Fueki and Z. Kuri, presented at the 22nd Annual Meeting of Chemical Society of Japan, April, 1969.
4) J. Lin and F. Williams, *J. Phys. Chem.*, **72**, 3707 (1968).
5) P. B. Ayscough and C. Thomson, *Trans. Faraday Soc.*, **58**, 1477 (1962).

The Spectral Blue Shift of Li(TCNQ) at High Pressures

Ichimin SHIROTANI, Nobuko SAKAI, Hiroo INOKUCHI and Shigeru MINOMURA

The Institute for Solid State Physics, The University of Tokyo, Roppongi, Tokyo

(Received May 19, 1969)

The energies of the electronic transitions of most organic crystals are shifted toward the lower side with an increase in the pressure.[1-3] However, the absorption band at 540 mμ of quaterrylene ($C_{40}H_{20}$) evaporated film is less affected by the pressure,[4] and in the cases of azulene and ferrocene a small blue shift is observed at high pressures.[5]

The activation energy of Li(TCNQ) decreases from 0.32 eV at 1 bar to 0.07 eV at 169 kbar.[6] However, a large blue shift was observed with a change in the pressure on the absorption spectra of Li(TCNQ).

A hydrostatic pressure was applied to the optical cell by means of a pressure-transmitting medium, kerosene, up to 7 kbar at room temperature.

Figure 1 shows the absorption spectra of crystalline Li(TCNQ) at 1 bar and 5.4 kbar. Two bands situated in the visible region showed a large blue shift with an increase in the pressure. The rates of pressure shift are listed in Table 1. Since the crystalline absorption spectrum is similar to that of the dimer $(TCNQ^-)_2$ in an aqueous Li(TCNQ) solution,[7] the large blue shift may be explained by assuming a bimolecular association of $(TCNQ^-)$ ion radicals in the solid.

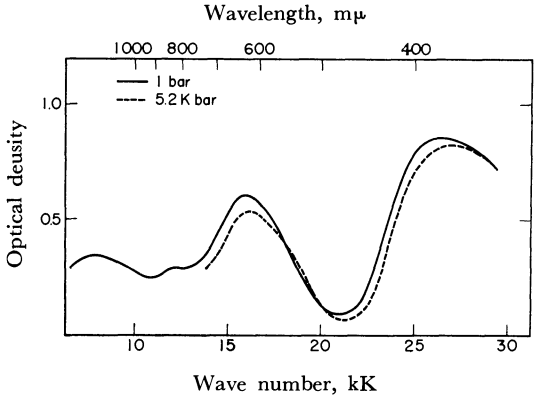

Fig. 1. The pressure dependece of the absorption spectra of Li(TCNQ).

Table 1. Pressure shift of the optical absorption peak for several anion radical salts

Compound	Absorption peak (kK)	Pressure shift (cm^{-1}/kbar)
Li(TCNQ)	26.5	+86
	16.0	+51
	7.7	—
K(TCNQ)	27.5	+58
	16.1	+45
	8.3	—
DAD(TCNQ)	25.8	+52
	11.6	—
Na(chloranil)	26.2	+62
	11.8	−58
Azulene	14.4	+ 6[a]
Ferrocene	23.3	+20[a]

a) Ref. 5

However, the absorption band of the salt in a PVA solid solution was insensitive to the applied pressure. Therefore, it is assumed that the major contribution to the blue shift does not arise from the bimolecular association in the crystalline state, but from the crystal field of metal-positive ions.

The near-infrared band at 7.7 kK observed in the solid Li(TCNQ) can be assigned to an inter-radical charge-transfer band.[8] The pressure effect on this peak could not be observed because of interference by the transmitting fluid. Generally, the charge-transfer bands of molecular complexes show a red shift at high pressures.[2] The low-energy band at 7.7 kK may be expected to be shifted to the red with a change in the pressure.

Similar results for K(TCNQ), diaminodurene (DAD) (TCNQ), and Na(chloranil) are listed in Table 1. The 11.8 kK band of Na(chloranil), which did not appear in solution spectra, showed a red shift at high pressures. This may be ascribed to the inter-radical charge-transfer band in the solid.

1) S. Wiederhorn and H. G. Drickamer, *J. Phys. Chem. Solids*, **9**, 330 (1959).
2) H. W. Offen, *J. Chem. Phys.*, **42**, 430 (1965).
3) H. Ohigashi, I. Shirotani, H. Inokuchi and S. Minomura, *J. Phys. Soc. Japan*, **19**, 1996 (1964); *J. Chem. Phys.*, **43**, 314 (1965); *Mol. Cryst.*, **1**, 463 (1966).
4) I. Shirotani, H. Inokuchi and S. Akimoto, This Bulletin, **40**, 2277 (1967).
5) R. B. Aust, W. H. Bentley and H. G. Drickamer, *J. Chem. Phys.*, **41**, 1856 (1964); J. C. Zahner and H. G. Drickamer, *ibid.*, **35**, 375 (1961).
6) I. Shirotani, T. Kajiwara, H. Inokuchi and S. Akimoto, This Bulletin, **42**, 366 (1969).
7) R. H. Boyd and W. D. Phillips, *J. Chem. Phys.*, **43**, 2927 (1969).
8) Y. Iida This Bulletin **42**, 71 (1969).

Natural Occurrence of Humuladienone, Humulenone-II, and α-Corocalene; New Constituents of Hop Oil

Yoko NAYA and Munio KOTAKE

The Institute of Food Chemistry, Dojimanaka, Kita-ku, Osaka

(Received May 23, 1969)

By a combination of fractionation, column chromatography over silica gel and neutral alumina-silver nitrate, and preparative GLC, it has now been possible to isolate the titled sesquiterpenes, (I), (IV), and (V), from the Japanese hop (*Humulus lupulus* L.).

Compound (I), $C_{15}H_{24}O$, $[\alpha]_D^{24}$ +5.0° (c=0.68, $CHCl_3$) is a colorless oil which exhibited carbonyl absorption (1705 cm^{-1}) in the infrared spectrum. Other peaks of diagnostic value were at 1380, 1363 (gem-dimethyl), and 975 and 840 cm^{-1} (C=C *trans*). Its NMR spectrum*1 showed a singlet at 1.01 (6H, tertiary methyl) and a doublet at 1.04 (3H, J=6.8 cps, secondary methyl); the doublet (3H, J=1 cps) at 1.59 is assignable to a methyl on a trisubstituted olefinic linkage; complex multiplets located between 4.80 and 5.25 accounted for three vinyl protons (HC=CH and CH_3C=CH–). Its MS spectrum exhibits the molecular ion peak at *m/e* 220 and the base peak at *m/e* 96, together with quite an abundant peak at *m/e* 138.

On catalytic hydrogenation over PtO_2 in ethanol, I took up one mole of hydrogen to yield (II), $C_{15}H_{26}O$ (M^+, *m/e* 222). Examination of its IR and NMR spectra revealed that the *trans* C=C bond has been reduced and that CH_3C=CH is still present. On the other hand, the hydrogenation of I by the same catalyst in acetic acid gave the saturated compound (III), $C_{15}H_{28}O$, (M^+, *m/e* 224).

All the above data are compatible with the structure (I) for humuladienone. Such a formulation was also supported by the co-occurrence of humulenone-II (IV), which is identical (IR, NMR) with the ketone derived from humulenol-II by Damodaran and Dev.[1] The final conclusion was obtained by the partial hydrogenation of IV over PtO_2 in ethanol-ether, where two products were provided. The main product of the hydrogenation had an IR spectrum completely superimposable on that of I, while the other was found to be identical with that of II.

In addition, it may be noted from the solvent effect on the NMR spectra that the methyl group adjacent (α) to a carbonyl function of humuladienone (I) seems to exist in a pseudo-axial nature: ($\Delta=\delta^{obs.}_{CCl_4}-\delta_{C_6H_6}$=0.1 ppm). A similar range of up-field shift is also observed for the hydrogenated derivatives, II and III.

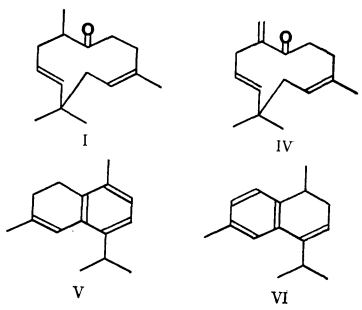

For compound (V), $C_{15}H_{20}$ (M^+, *m/e* 200), we propose the name α-corocalene. The other ingredient of the same fraction was γ-calacorene (VI), which afforded calamenene on catalytic hydrogenation and which was identical with the compound isolated from *Juniperus rigida* (IR, NMR, MS, UV).[2] The infrared spectrum of V showed a characteristic absorption for an aromatic compound (3050, 1875, 1650, 1595, 1480, 860, 815 cm^{-1}). Moreover, the NMR spectrum exhibited a doublet at 1.22 (6H, J=7.5 cps) and a singlet at 2.19 (3H) which are assignable to an isopropyl and a methyl on an aromatic ring respectively; a doublet (3H, J=1 cps) at 1.94 and a broad singlet at 6.48 (1H) accounting for the group, CH_3C=CH, conjugated to an aromatic ring, and a singlet at 6.86 (2H) and a complex signal located between 2.57 and 3.50 (4H) which are attributable to two aromatic protons and two allylic methylenes respectively. The catalytic hydrogenation of V resulted in the uptake of one mole of hydrogen to give a dihydro-α-corocalene (VII), $C_{15}H_{22}$ (M^+, *m/e* 202). The characteristics mentioned above support the structure of 1,6-dimethyl-4-isopropyl-7,8-dihydronaphthalene for α-corocalene. The IR spectra of V and VII were identical with those of authentic compounds, which were synthesized by Šorm *et al.*[3]

*1 All the NMR spectra were taken in CCl_4 on a JEOL C-60 spectrometer, with TMS as the internal reference. The values are reported in ppm.

1) N. P. Damodaran and Sukh Dev, *Tetrahedron Letters*, **1963**, 1941; *Tetrahedron*, **24**, 4133 (1968).

2) B. Tomita, Y. Hirose and Y. Nakatsuka, "Symposium papers, the 12th Symposium on the Chemistry of Terpenes, Essential Oils, and Aromatics," (Hamamatsu, 1968), p. 144.

3) F. Šorm, K. Vereš and V. Herout, *Coll. Czech. Chem. Commun.*, **18**, 106 (1953).

Preparation and Optical Resolution of μ-Amido-μ-superoxo and μ-Amido-μ-peroxo Tetrakis(α-di-imine) Dicobalt(III) Ions

Yoichi SASAKI and Junnosuke FUJITA

Department of Chemistry, Faculty of Science, Tohoku University, Katahita-cho, Sendai

(Received May 26, 1969)

New binuclear cobalt(III) complexes of the type, $[L_2Co(\mu\text{-}NH_2,O_2)CoL_2](ClO_4)_n$, where L is 1,10-phenanthroline (phen) or 2,2′-bipyridyl (bip), and $n=3$ and $n=4$ correspond to the so-called μ-peroxo and μ-superoxo form, respectively, were prepared and resolved into their optical isomers. These are first examples of binuclear cobalt(III) complexes involving conjugated aromatic ligands, and their circular dichroism (CD) spectra will provide useful information in elucidating the electronic state of binuclear complexes. The μ-peroxo complexes were precipitated by warming a mixture of $[(NH_3)_4Co(\mu\text{-}NH_2,O_2)Co(NH_3)_4](ClO_4)_4$ and phen or bip (molar ratio 1 : 4) in methanol at 60°C for 10 hr, and recrystallized from hot water. The μ-superoxo complexes were obtained by adding solid sodium perchlorate to 7N nitric acid solutions of the corresponding μ-peroxo complexes. Found: C, 47.75; H, 2.72; N, 10.29%. Calcd for $C_{48}H_{36}N_9O_{15}Co_2Cl_3=[(phen)_2Co(\mu\text{-}NH_2,O_2)Co(phen)_2](ClO_4)_3\cdot H_2O$: C, 47.76; H, 3.01; N, 10.44%. Found: C, 43.60; H, 2.94; N, 9.34%. Calcd for $C_{48}H_{38}N_9O_{20}Co_2Cl_4=[(phen)_2Co(\mu\text{-}NH_2,O_2)Co(phen)_2](ClO_4)_4\cdot 2H_2O$: C, 43.66; H, 2.90; N, 9.55%. Found: C, 42.99; H, 3.31; N, 11.45%. Calcd for $C_{40}H_{38}N_9O_{16}Co_2Cl_3=[(bip)_2Co(\mu\text{-}NH_2,O_2)Co(bip)_2](ClO_4)_3\cdot 2H_2O$: C, 42.71; H, 3.41; N, 11.21%. Found: C, 39.69; H, 3.11; N, 10.50%. Calcd for $C_{40}H_{36}N_9O_{19}Co_2Cl_4=[(bip)_2Co(\mu\text{-}NH_2,O_2)Co(bip)_2](ClO_4)_4\cdot H_2O$: C, 39.82; H, 3.01; N, 10.45%. The racemic μ-peroxo complexes were converted into chloride and treated with silver *d*-antimonyltartrate to be resolved into optical isomers. The optically active μ-superoxo complexes were prepared from the corresponding active μ-peroxo complexes.

As the figure shows, the CD spectrum of $(+)_D$-μ-superoxo-phen complex is similar to that of $(-)_D$-$\Lambda\Lambda$-$[(en)_2Co(\mu\text{-}NH_2,O_2)Co(en)_2]^{4+}$ (en= ethylenediamine)[1] in the visible region. Furthermore, the phen complex gives a strong negative and a positive CD component from longer to shorter wavelength corresponding to the π–π^* transition of chelated phen (34000—37000 cm^{-1}). These results lead to the conclusion that the $(+)_D$-μ-superoxo-phen complex has $\Lambda\Lambda$ absolute configuration.[2,3] The enantiomers, $(+)_D$-μ-peroxo-phen, $(+)_D$-μ-superoxo-bip and $(+)_D$-μ-peroxo-bip have also $\Lambda\Lambda$ configuration.

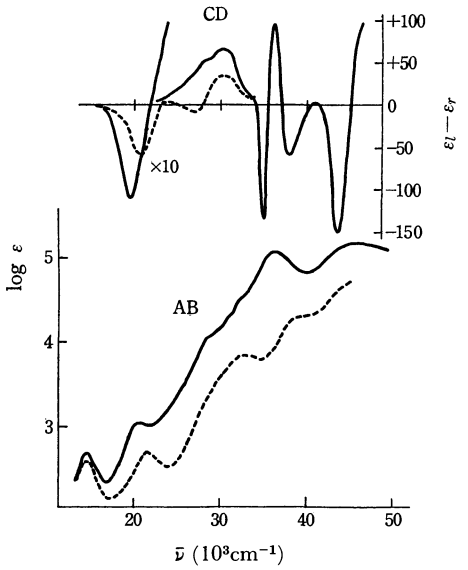

Fig, 1. The absorption (AB) and CD spectra of $(+)_D$-$[(phen)_2Co(\mu\text{-}NH_2,O_2)Co(phen)_2](ClO_4)_4$ in 60% perchloric acid (——) and $\Lambda\Lambda$-$[(en)_2Co(\mu\text{-}NH_2,O_2)Co(en)_2](NO_3)_4$ in water (------).

1) Y. Sasaki, J. Fujita and K. Saito, This Bulletin, **42**, 146 (1969).

2) S. F. Mason and J. W. Wood, *Chem. Commun.*, **1968**, 1512.

3) B. Bosnich, *Inorg. Chem.*, **7**, 178 (1968).

Luminol Amidine

Yoshimori OMOTE, Hiroshi YAMAMOTO, Shoji TOMIOKA and Noboru SUGIYAMA

Department of Chemistry, Tokyo Kyoiku University, Otsuka, Tokyo

(Received May 30, 1969)

Luminol, one of the most popular chemiluminescent compounds, has been used as an indicator in titration analysis.[1] Recently luminol was shown to be a mixture and not a pure compound, as had usually been believed.[2] It is very difficult to purify commercial luminol by recrystallization because it is sparingly soluble in most solvents.

During the course of synthetic studies of luminol derivatives we found that luminol reacts with the Vilsmeier reagent from dimethylformamide (DMF) and thionyl chloride to afford luminol amidine (I), which is moderately soluble in water and which is easily purified by recrystallization from water.

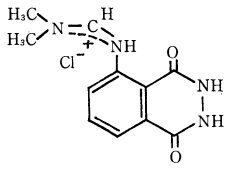

The luminol amidine (*N,N*-dimethyl-*N'*-diketophthalazine-5-yl-formamidine) was prepared as follows: 1.77 g of luminol was dissolved in 20 m*l* of DMF, into which the Vilsmeier reagent from 2.19 g of DMF and 3.57 g of thionyl chloride was stirred. The precipitates which appeared were recrystallized from water to give colorless needles, mp 271—272°C (dec).

Found: C, 49.15; H, 4.94; N, 20.93%. Calcd for $C_{11}H_{13}O_2N_4Cl$: C, 49.16; H, 4.87; N, 20.85%. UV: $\lambda_{max}^{H_2O}$ nm (log ε), 228 (4.53), 283 (4.17) and 318 (4.17). IR: ν_{max}^{KBr} cm^{-1} 1705, 1645. NMR δ^{D_2O} 3.35 (3H, s), 3.55 (3H, s), 7.7—7.9 (3H, m) and 8.87 (1H, s).

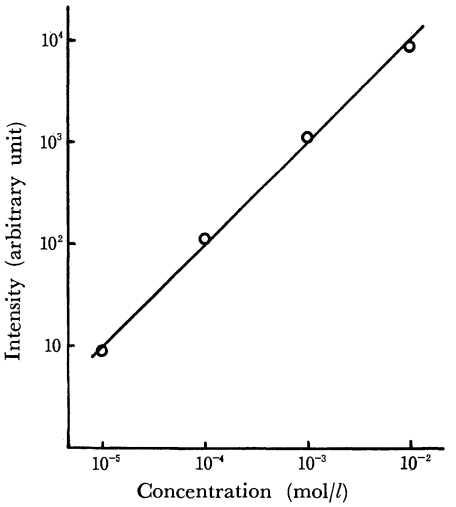

Fig. 1. The chemiluminescence intensity of luminol amidine (I) against molar concentration when the mixture of 0.3% aqueous hydrogen peroxide (0.5 m*l*) and 0.3% potassium ferricyanide aqueous solution (0.5 m*l*) was added to the solution of I in 0.1 N sodium hydroxide aqueous solution.

The chemiluminescence of luminol amidine was measured by Hitachi Photomultiplier. The relative intensity of light emission of luminol amidine is about one twenty-fifth that of luminol itself, the maximum of the chemiluminescence spectrum is 452 nm. The plot of the chemiluminescence intensity with the variation in concentration between 10^{-2} and 10^{-5} mol/*l* shows a straight line (Fig. 1). This suggests that luminol amidine will be useful as a standard compound for the chemiluminescence measurement.

1) F. Kenny and R. B. Kurtz, *Anal. Chem.*, **24**, 1218 (1952); L. Erdey and I. Buzas, *Anal. Chim. Acta*, **22**, 524 (1960).

2) D. S. Bersis and J. Nikokavouras, *Nature*, **217**, 451 (1968).

BULLETIN OF THE CHEMICAL SOCIETY OF JAPAN VOL. 42 2091—2098 (1969)

Infrared Study of the Conformational Equilibria of *meso*- and *racemic*-2,3-Dichlorobutanes

Kazuyoshi IIMURA, Naoto KAWAKAMI and Masatami TAKEDA

Department of Chemistry, Faculty of Science, Science University of Tokyo, Kagurazaka, Shinjuku-ku, Tokyo

(Received July 17, 1968)

The conformational equilibria of rotational isomers of *meso*- and *racemic*-2,3-dichlorobutanes were investigated in various solvents by an infrared method. The coexistence of three rotational isomers was found for each of the *meso* and *racemic*-2,3-dichlorobutanes. However, the equilibrium concentrations changed depending on the solvent dielectric constant. The equilibrium concentration of the less polar form of a rotational isomer, in which the conformation is extended *trans* with respect to the Cl–C–C–Cl linkage, decreased as the solvent dielectric constant increased. The energy differences between the rotational isomers in the gaseous state and in acetonitrile solvent were also discussed.

One of the present authors has examined the solvent effect on the unperturbed molecular dimensions of chlorinated *trans*- and *cis*-1,4-polybutadienes, and has found that those of chlorinated *trans*-1,4-polybutadiene changed depending on the solvent dielectric constant.[1] For chlorinated *cis*-1,4-polybutadiene the situation was obscure. These experimental findings, however, can be correlated with the solvent effect on the conformational changes of the polymer chain.

The chemical structure of chlorinated 1,4-polybutadiene manifests a head-to-head linkage of polyvinyl chloride and has adjacent CHCl groups in the polymer chain. If the *trans* chlorination takes place to the unsaturated double bond of 1,4-polybutadiene, the chemical structures of the chlorinated parts of *trans*- and *cis*-1,4-polybutadienes become the *meso* and *racemic* structures respectively. In solution, the conformation of the chlorinated part having adjacent polar C–Cl bonds would vary under the influence of an electrostatic interaction by the surrounding solvent molecules. However, the conformation of the ethylenic linkage of chlorinated 1,4-polybutadiene may not strongly depend on the solvents. The conformational structure of chlorinated 1,4-polybutadiene in solution may, therefore, be mainly subjected to the local conformations of the chlorinated parts.

An infrared study of the conformations of *meso*- and *racemic*-2,3-dichlorobutanes (hereafter abbreviated as *meso*-DCB and *racemic*-DCB respectively) should give basic information on the stable local conformations of chlorinated *trans*- and *cis*-1,4-polybutadienes respectively. Although quantitative investigations of the equilibrium concentrations of rotational isomers of *meso*- and *racemic*-DCB have been reported by Bothner-By and Naar-Colin[2] and by Anet[3] using NMR method, no detailed studies of the equilibrium concentrations in solvents with different dielectric constants have been reported. Taufen *et al.*[4] have reported on the Raman spectra of *meso*- and *racemic*-DCB and discussed the qualitative equilibrium concentrations of the rotational isomers in pure liquids only.

In the present study the infrared spectra of *meso*- and *racemic*-DCB are examined in different solvents and are discussed in terms of the solvent effect on the equilibrium concentrations of rotational isomers. In addition, the energy difference between the rotational isomers is also discussed.

Experimental

Preparations of *meso*- and *racemic*-DCB. Dried chlorine gas was reacted with *trans*- and *cis*-2-butenes (Matheson Co.; purity, 99.8%) at −20°C for 3 hr in order to prepare *meso*- and *racemic*-DCB respectively. The products were washed with water and then with a 10% sodium carbonate solution, and were dried over anhydrous calcium chloride. The *meso*- and *racemic*-DCB were distilled under atmospheric pressure, whereupon fractions with boiling points of 113—114°C and 116—118°C respectively were collected.[5] A gas-chromatographic analysis (stationary phase, Carbowax 20 M; column temperature, 117.5°C; column length, 1 m; carrier gas, helium with a speed of 40 ml/min) indicated that the amount of impurity due to

1) M. Takeda, R. Endo and K. Ishizaki, Preprints for the 20th Annual Meeting of The Chemical Society of Japan, (April, 1967), 4N-205.

2) A. A. Bothner-By and C. Naar-Colin, *J. Am. Chem. Soc.*, **84**, 743 (1962).

3) A. L. Anet, *ibid.*, **84**, 747 (1962).

4) H. J. Taufen, M. J. Murray and F. F. Cleaveland, *ibid.*, **65**, 1130 (1943).

5) H. J. Lucas and C. W. Gould, Jr., *ibid.*, **63**, 2541 (1941).

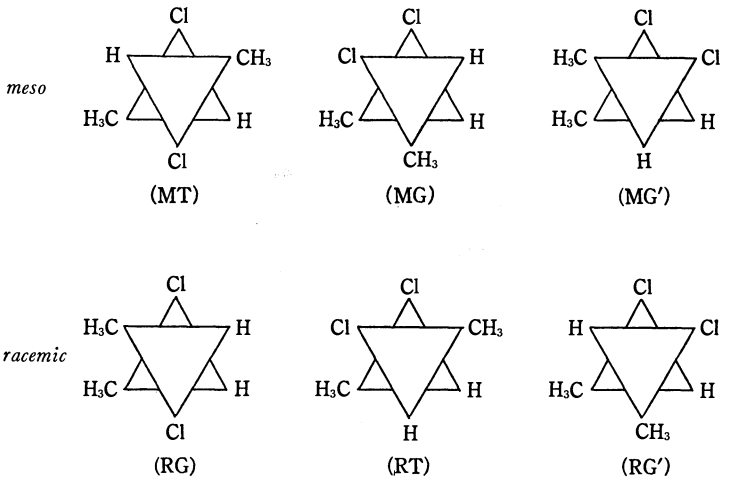

Fig. 1. The possible conformations for *meso*- and *racemic*-2,3-dichlorobutanes.

trichlorobutane is less than 1% for both isomers. The NMR spectra of the samples were completely identical with those observed by Bothner-By and Naar-Colin.[2]

Measurements of Infrared Spectra. The infrared spectra were recorded mainly for the region of 400—800 cm^{-1} using a Hitachi EPI-2 double-beam spectrophotometer with a KBr prism. Spectral observation was also made in the region of the NaCl prism for reference. In measuring the solution spectra, the absorption due to the solvent was compensated for by a variable-thickness cell filled with the solvent.

Results and Discussion

Spectra of Liquid State and the Existence of Rotational Isomers. The possible rotational isomers of *meso*- and *racemic*-DCB are shown in Fig. 1, and are designated by T, G or G'; in them the two terminal C–CH_3 bonds are located *trans* and *gauche* to each other. The *meso* and *racemic* isomers are identified by prefixing M and R respectively. In the case of the *meso* isomers, MG is a mirror image of MG'. Hence, both MG and MG' should give the same spectrum.

In general, the frequencies of C–Cl stretching vibrations, which will hereafter be abbreviated as ν(C–Cl), appearing in the region of 760—550 cm^{-1} are characteristic of the geometrical arrangments near the C–Cl bond of chlorohydrocarbons.[6-8] The number of absorption bands and their relative intensities in this region should, therefore, give information on the existence of rotational isomers of DCB. Actually, as Fig. 2 shows, two bands, at 695 and 650 cm^{-1} for *meso*-DCB, and four bands, at 703, 692, 652, and 596 cm^{-1}, for *recemic*-DCB are observed in the ν(C–Cl) region. No absorption band attributable to the ν(C–Cl) is observed in the range from *ca.* 700 cm^{-1} up to 850 cm^{-1} for either *meso*- or *racemic*-DCB. All the absorption bands appearing at frequencies higher than 850 cm^{-1} can be assigned to the C–H stretching and deformation, and C–C stretching, vibrations. The bands at 535 and 420 cm^{-1} of *meso*-DCB, like those at 559 and 522 cm^{-1} of *racemic*-DCB, can be assigned to the skeletal bending vibrations, because the frequencies of these bands are too low to be assigned to the ν(C–Cl) vibrations.

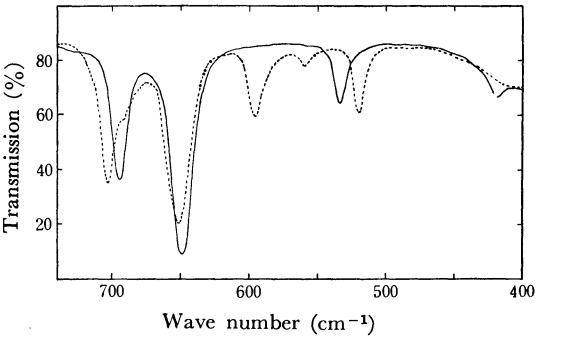

Fig. 2. The infrared spectra of liquid state.
Full line: *meso*, broken line: *racemic*

In the case of *meso*-DCB, MT should give only one infrared active ν(C–Cl) because of its C_t symmetry. The relative intensities of the two absorption bands observed in the ν(C–Cl) region would not depend on the solvents if these bands arose merely from MG and MG'. The relative intensities of these two bands, however, strongly depend on the solvents, as will be described below. This experimental finding suggests that these two bands are caused by two different components, namely, MT and MG or MG'.

6) T. Shimanouchi, S. Tsuchiya and S. Mizushima, *Kobunshi (High Polymers, Japan)*, **8**, 202 (1959).
7) K. Nakamura, *Nippon Kagaku Zasshi (J. Chem. Soc. Japan, Pure Chem. Sect.)*, **78**, 1164 (1957).
8) J. J. Shimpman, J. L. Folt and S. Krimm, *Spectrochim. Acta*, **18**, 1603 (1962).

As for the liquid *racemic*-DCB, two absorption bands due to the ν(C–Cl) may be expected for each of the rotational isomers. The four absorption bands observed in the ν(C–Cl) region indicate the existence of more than one rotational isomer.

Solvent Effect on the Spectra and Assignment of the ν(C–Cl) Bands. Using the method proposed by Miyagawa,[9] we have calculated the dipole moments of the rotational isomers of *meso*- and *racemic*-DCB. The calculated values are listed in Table 1. In accounting for the difference in dipole moments, it can be said that the equilibrium concentrations of rotational isomers in solution vary because they are affected by a reaction field induced from the solvent molecules;[10] the polar forms of rotational isomers are stabilized in the solvent with a larger dielectric constant.

It follows that the ν(C–Cl) bands can be assigned to a definite rotational isomer by observing the intensity change in the ν(C–Cl) bands in solvents with different dielectric constants. Indeed, the changes in the spectra of *meso*- and *racemic*-DCB with the solvents are remarkable as is shown in Fig. 3.

Table 1. Calculated dipole moments (in D.U.) for *meso*- and *racemic*-2,3-dichlorobutanes

Isomer	Chain conformation	Dipole moment
meso-DCB	MT	0
	MG	3.08
	MG′	3.08
racemic-DCB	RG	0.66
	RT	2.64
	RG′	3.33

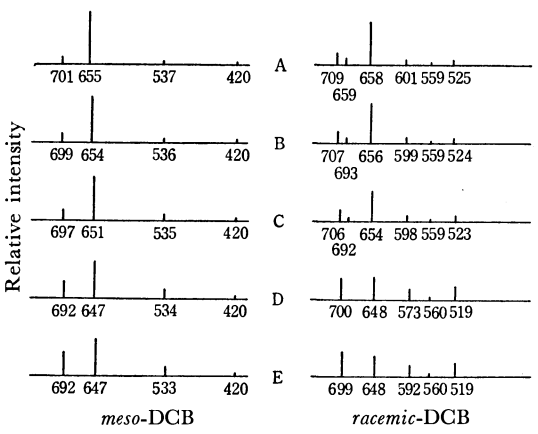

Fig. 3. The relative intensities of absorption bands in the various solvents (concentration: 0.8—0.5 mol/*l*, cell thickness: 0.047—0.055 mm).
A: *n*-Hexane, B: Cyclohexane,
C: Carbon disulfide, D: Cyclohexanone,
E: Acetonitrile

In the spectra of *meso*-DCB, the intensities of the bands at 695, 535, and 420 cm^{-1} increase, and that of the bands at 650 cm^{-1} decreases, as the dielectric constant of the solvent increases from 1.89 (*n*-hexane) to 37.5 (acetonitrile). At the same time, a downward shift of the absorption frequency is noted in the polar solvents.*1 In the light of the notations proposed by Shimanouchi *et al.*,[6] the types of ν(C–Cl) bands for DCB may be classified as S_C, S_{Cl} and S_H, where the subscripts represent the *trans* substituents on the C–C bond adjacent to a C–Cl bond. According to this classification, the types of ν(C–Cl) bands arising from the individual rotational isomers are denoted as S_{Cl} for MT and RG, as S_C for RG′, as S_H for RT, and as S_C and S_H for both MG and MG′.

In the spectrum of *meso*-DCB, the intense bands at 650 cm^{-1}, the intensity of which decreases in the solvent with the larger dielectric constant, is ascribed mainly to the antisymmetric S_{Cl}-type vibration of the nonpolar MT. The 695 cm^{-1} band is assigned to the S_C-type vibration of the polar MG and MG′ by taking account of the increase in its intensity in the solvent with the larger dielectric constant. A remaining band, due to the S_H-type vibration of MG and MG′, may be expected in the range around 640—600 cm^{-1}. In the Raman spectrum[4] of liquid *meso*-DCB, an intense band at 703 cm^{-1} and a somewhat weak band at 652 cm^{-1} are found in the ν(C–Cl) region. The antisymmetric S_{Cl}-type vibration of MT is a Raman inactive vibration and, hence, should not be observable in the Raman spectrum. The weak Raman band at 652 cm^{-1} must, therfore, be assigned to the infrared and Raman-active S_H-type vibrations of MG and MG′. The intense Raman band at 703 cm^{-1} probably involves the symmetric S_{Cl}-type vibration of MT and the infrared and Raman-active S_C-type vibrations of MG and MG′. The Raman-active symmetric S_{Cl}-type vibration should not give any infrared absorption because of the C_i symmetry of MT. Consequently, the infrared band at 695 cm^{-1} may be attributed to the S_C-type vibration of MG and MG′, while that at 650 cm^{-1} may be said to consist of two components of ν(C–Cl) bands; one arises from the S_{Cl}-type vibration of MT, and the other, from the S_H-type vibrations of MG and MG′.

The above assignments agree almost entirely with an empirical rule established by Shimanouchi

9) I. Miyagawa, *Nippon Kagaku Zasshi (J. Chem. Soc. Japan, Pure Chem. Sect.)*, **75**, 1061 (1954).
10) I. Watanabe, S. Mizushima and Y. Mashiko, *Nippon Kwagaku Kwaishi (J. Chem. Soc. Japan)*, **64**, 962 (1943).

*1 Hereafter, for convenience, the frequencies of absorption bands given are those observed in the liquid spectra.

et al.[6] and by Shipman *et al.*[8] According to this rule, the ν(C–Cl) *trans* to a C–Cl or C–C bond and that *trans* to a C–H bond usually appear in the frequency regions of 700—655 cm^{-1} and 640—600 cm^{-1} respectively. With respect to *racemic*-DCB, therefore, two ν(C–Cl) bands arising from each of RG and RG′ may be observed nearly in the former frequency region, and those arising from RT, in the latter one. The 692 and 652 cm^{-1} bands, the intensities of which decrease with an increase in the solvent dielectric constant, can be assigned to the S_{Cl}-type vibrations of the less polar RG. The 703 and 596 cm^{-1} bands can be assigned to the S_C and S_H-type vibrations of polar RG′ and RT respectively, since their intensities increase with an increase in the solvent dielectric constant. Although two S_C bands and two S_H bands must be expected for RG′ and RT respectively, in this case no bands except the 703 and 596 cm^{-1} bands are found in the ν(C–Cl) region. This absence of bands cannot be explained at present.

For liquid *racemic*-DCB, Taufen *et al.*[4] have observed the three Raman bands at 695, 653, and 599 cm^{-1} and have assigned them to RG, RG′, and RT respectively. The assignment for the former two bands is the reverse of our interpretation. However, the Raman band at 695 cm^{-1} is believed to be related not only to RG but also to RG′, for the more intense band at 703 cm^{-1} of RG′ and the weaker band at 692 cm^{-1} of RG in the infrared spectrum of the liquid state are so close in their frequencies (see Fig. 2) that the Raman bands corresponding to them could not be separately observed in the Raman spectrum. As is evident from the behavior of the infrared band at 652 cm^{-1} for the solvents, the Raman band at 653 cm^{-1} can be assigned to the S_{Cl}-type vibration of RG.

The empirically-established correlations between the infrared absorption bands and the structures of rotational isomers are summarized in Table 2.

TABLE 2. ASSIGNMENTS OF ABSORPTION FREQUENCY

Isomer	Frequency	Assignment[a]	Rotational isomer
meso-DCB	695	S_C	MG, MG′
	650	S_{Cl}	MT
		S_H	MG, MG′
	535	δ	
	420	δ	
racemic-DCB	703	S_C	RG′
	692	S_{Cl}	RG
	652	S_{Cl}	RG
	596	S_H	RT
	559	δ	
	522	δ	

a) S and δ denote C–Cl stretching and skeletal bending vibrations respectively.

Equilibrium Concentrations of Rotational Isomers in Various Solvents. We can determine the change in the equilibrium concentrations of rotational isomers in solution from the change in the intensity ratio of the ν(C–Cl) bands belonging to each of the rotational isomers.

In the case of *meso*-DCB, the optical densities of the 695 cm^{-1} and 650 cm^{-1} bands, D_{695} and D_{650}, can be represented with reference to the concentrations of rotational isomers as follows:

$$D_{695} = K_G C_G l \quad (1)$$

$$D_{650} = K_G' C_G l + K_{MT} C_{MT} l \quad (2)$$

where C_{MT} is the concentration of MT; C_G, the sum of the concentrations of MG and MG′, which are equal in population, and l, the optical pathlength of the cell. K_G is the absorption coefficient of the 695 cm^{-1} band, which arises from MG and MG′. Equation (2) is introduced by considering the 650 cm^{-1} band to be composed of two types of ν(C–Cl) bands belonging to MT and to MG and MG′; hence, K_{MT} and K_G' are the absorption coefficients arising from the component of MT and from that of MG and MG′ respectively. Dividing Eq. (2) by Eq. (1), we obtain:

$$C_{MT}/C_G = (K_G/K_{MT})(D_{650}/D_{695}) - (K_G'/K_{MT}) \quad (3)$$

We have at present no available information for determining the ratios of the absorption coefficients in Eq. (3). However, in the case of liquid *meso*-2,3-dibromobutane the values of K_G/K_{MT} and K_G'/K_{MT} are determined to be 0.534 and 0.223 respectively.*2 Taking into account the similarity in the molecular structures, the ratios of absorption coefficient which are experimentally determined for *meso*-2,3-dibromobutane can be transferred to those for *meso*-DCB; we thus obtain:

$$C_{MT}/C_G = 0.534(D_{650}/D_{695}) - 0.223 \quad (4)$$

Putting 2.27, the observed value of D_{650}/D_{695} for the liquid state, into Eq. (4), we obtain the equilibrium concentrations of the rotational isomers of liquid *meso*-DCB at 28°C as $C_{MT}=0.50$ and $C_G=0.50$. Further, it is also possible to determine the value of the equilibrium concentration by an independent method; *e. g.*, the mean dipole moment of the liquid state, which can be calculated from the dielectric constant of the liquid through

*2 Unlike the results obtained for *meso*-DCB, in the spectrum of liquid *meso*-2,3-dibromobutane the three ν(C–Br) bands are separately observed at 552 cm^{-1} for MT, and at 636 and 600 cm^{-1} for MG and MG′. Therefore, the determination of the values of K_G/K_{MT} and K_G'/K_{MT} becomes possible on the basis of the ratios of the observed optical densities, D_{636}/D_{552} and D_{600}/D_{552}, and the equilibrium concentrations of each rotational isomer, which are calculated from the dielectric constant (6.245) of the liquid.[11]

11) K. Iimura, to be published.

TABLE 3. EQUILIBRIUM CONCENTRATIONS OF THE ROTATIONAL ISOMERS IN THE VARIOUS SOLVENTS

Solvent	MT	MG	MG'	RT	RG	RG'	Method
n-Hexane (1.89)	0.74	0.13	0.13	0.24	0.58	0.18	IR study (at 28°C)
Cyclohexane (2.02)	0.71	0.14_5	0.14_5	0.24	0.58	0.18	present investigation
Carbon disulfide (2.64)	0.70	0.15	0.15	0.26	0.52	0.22	
Liquid sample*	0.50	0.25	0.25	0.34	0.39	0.27	
Cyclohexanone (18.3)	0.49	0.25_5	0.25_5	0.42	0.27	0.31	
Acetonitrile (37.5)	0.30	0.35	0.35	0.43	0.25	0.32	
Carbon disulfide	0.58	0.21	0.21			0.14	NMR study (at 29°C) by
Acetonitrile	0.33	0.33	0.33				Kondo *et al.*[17]
Carbon disulfide	0.64	0.18	0.18				NMR study by Bothner-By
Liquid sample	0.52	0.24	0.24	0.33	0.33	0.33	and Naar-Colin[2]

The numerals in parentheses indicate the dielectric constant of solvent.
* Dielectric constants of pure liquids are 8.823 and 9.761 for *meso*- and *racemic*-DCB, respectively.[5]

Onsager equation.*3 The equilibrium concentration at 25°C thus determined is $C_{MT}=0.49$ and $C_G=0.51$. It will be seen that the agreement with the equilibrium concentration observed by the infrared method is very satisfactory.

In estimating the equilibrium concentration in solution, it is necessary to examine the applicability of Eq. (4) since, in general, the value of the absorption coefficient of an infrared band changes depending upon the nature of the solvent.[13] According to the study by Hirota, however, the ratio of the absorption coefficients of an infrared band in two solutions is kept constant, is determined by the solvents, and is common to the absorption bands of any molecules.[14] The ratio of the absorption coefficient of the ν(C–Cl) bands of DCB in a solvent may, therefore, change little; hence, no serious error will be introduced into the values of the equilibrium concentrations in the various solvents obtained through Eq. (4). The equilibrium concentrations thus obtained for *meso*-DCB are listed in Table 3.

With respect to *racemic*-DCB, the values of the absorption coefficients can not be determined by the above-described method, for all three rotational isomers have different dipole moments. The ratios of absorption coefficients were, therefore, obtained from the equilibrium concentrations, which were themselves estimated by means of the energy difference between the rotational isomers in the gaseous state. Let D be the optical density; k, the absrption coefficient; C, the concentration or the number of molecules of the rotational isomer, and f, the partition function. We then have:

$$D_I/D_{II} = (k_I/k_{II})(C_I/C_{II}) = (k_I/k_{II})(f_I/f_{II})\exp(-\Delta E/\boldsymbol{R}T) \quad (5)$$

where ΔE is the energy difference between the two rotational isomers, which are discriminated by the subscripts I and II. The ratio of the partition function can be assumed to be approximately unity.[15] For the case of 1,2-dichloroethane, Watanabe *et al.*[16] have calculated the ratio of the partition function of the *gauche*-form to that of the *trans*-form, and they have determined the value to be 0.95 at 25°C. From the assumption above mentioned, the value of C_I/C_{II} can be estimated from ΔE, and then the ratio of the absorption coefficient, k_I/k_{II}, can be determined by means of the observed ratio of optical densities in Eq. (5).

The energy differences between RG' and RG and between RT and RG are found to be 1.1 kcal/mol and 1.0 kcal/mol respectively by measuring the temperature change in the absorption intensities, as will be described below. From these data, the values of $C_{RG'}/C_{RG}$ and C_{RT}/C_{RG} at 28°C are calculated as 0.159 and 0.188 respectively. The ratios of the absorption coefficients, $k_{RG'}/k_{RG}$ and k_{RT}/k_{RG}, are then determined to be

*3 The equilibrium concentration in the liquid stated is calculated from the following relation:

$$m^2 = (\mu^2_{MT}N_{MT} + \mu^2_G N_G)/(N_{MT} + N_G)$$

where, m is the mean dipole moment of the liquid; μ, the dipole moment, and N, the number of molecules which are discriminated by the subscripts (G shows two *gauche*-forms). The calculated dipole moments listed in Table 1 are used for μ_{MT} and μ_G. The value of m^2 was calculated by the Onsager equation:[12]

$$m^2 = (9\boldsymbol{k}T/4\pi\boldsymbol{N})(M/d)[(\varepsilon-n^2)(2\varepsilon+n^2)/\varepsilon(n^2+2)^2]$$

where $\boldsymbol{k}$ is the Boltzman constant; $\boldsymbol{N}$, the Avogadro number, and M, the molecular weight. The values of the dielectric constant (ε=8.823), the density (d=1.1023), and the refractive index (n=1.4386) at 25°C were taken from the paper of Lucas and Gould.[5]

12) L. Onsager, *J. Am. Chem. Soc.*, **58**, 1486 (1936).
13) T. Yoshino, This Bulletin, **27**, 592 (1954).
14) E. Hirota, *ibid.*, **27**, 295 (1954).
15) Y. Morino, I. Miyagawa, T. Haga and S. Mizushima, *ibid.*, **28**, 165 (1955).
16) I. Watanabe, S. Mizushima and Y. Morino, *Nippon Kagaku Zasshi (J. Chem. Soc. Japan, Pure Chem. Sect.)*, **63**, 1131 (1942).
17) S. Kondo, T. Tagami, K. Iimura and M. Takeda, This Bulletin, **41**, 790 (1968).

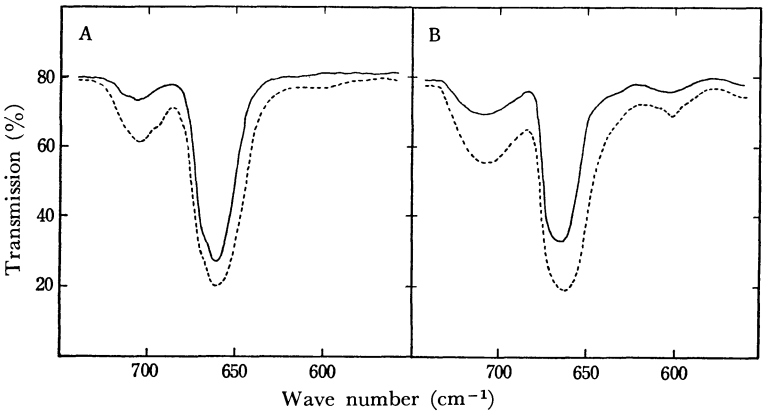

Fig. 4. The infrared spectra of gaseous state at the different temperatures.
A: *meso* (full line: 29°C, broken line: 146°C),
B: *racemic* (full line: 28°C, broken line: 151°C)

0.987 and 0.292 respectively from the observed ratios of the optical densities, $D_{RG'}/D_{RG}=0.157$ and $D_{RT}/D_{RG}=0.055$, at 28°C. The equilibrium concentrations of *racemic*-DCB in various solvents are obtained using these ratios of absorption coefficients; they are listed in Table 3, together with those obtained for *meso*- and *racemic*-DCB by the NMR investigations.[2,17]

Although there are only few solvents available to be compared commonly for both infrared and NMR method, a fair agreement between the data obtained by the two independent methods is noted for the liquid state and the acetonitile solution of *meso*-DCB. For the carbon disulfide solution, however, the data for MT obtained by the infrared method are slightly larger than those obtained by the NMR methods. With respect to liquid *racemic*-DCB, the data obtained by the infrared method agree almost entirely with those obtained by the NMR method. In our previous NMR investigation it was noted that the vicinal coupling constants of *racemic*-DCB depends little upon the solvents.[17] In contrast to the infrared results shown in Table 3, this experimental finding leads to the conclusion that the equilibrium concentrations of *racemic*-DCB does not remarkably change under the influence of solvents. However, as is shown in Fig. 3, the considerable changes in the intensity of the ν(C–Cl) bands in the different solvents suggest that the equilibrium concentrations change depending upon the solvents.

Spectra of the Gaseous State and the Energy Difference of Rotational Isomer. The spectra of gaseous *meso*- and *racemic*-DCB at different temperatures are shown in Fig. 4. The bands appearing at 706 and 661 cm^{-1} of *meso*-DCB correspond to those at 695 and 650 cm^{-1} respectively in the liquid state. For the gaseous *racemic*-DCB the bands corresponding to those at 703, 652, and 596 cm^{-1} of the liquid state are observed at 710, 665, and 603 cm^{-1} respectively. In general, from the temperature-dependence of the band intensities, the energy difference, ΔE, between the rotational isomers can be calculated by Eq. (5). Since, for *racemic*-DCB in the liquid state, the very weak 692 cm^{-1} band appears as a shoulder band on the more intense 703 cm^{-1} band, we have assumed that the broad band at 710 cm^{-1} in the geseous state arises mainly from the RG'.

In the case of *meso*-DCB the ratio of the intensity of the 661 cm^{-1} band to that of the 706 cm^{-1} band does not directly represent the abundance ratio of

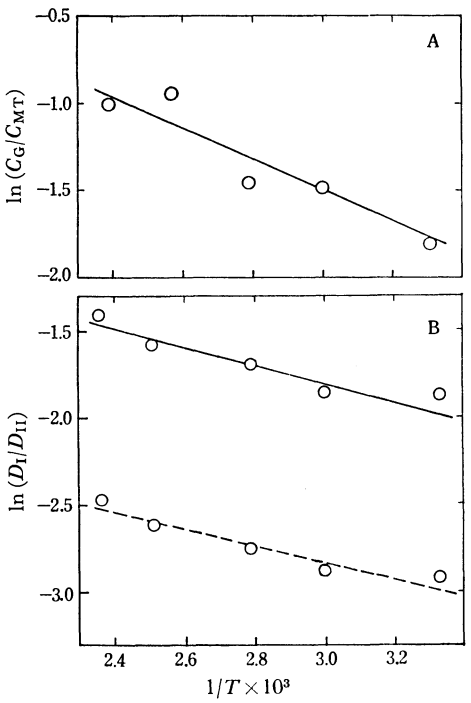

Fig. 5. The temperature dependences of abundance ratio and of intensity ratio in gaseous state.
A: *meso*, B: *racemic* (full line: $D_I/D_{II}=D_{710}/D_{665}$, broken line: $D_I/D_{II}=D_{603}/D_{665}$)

the two isomers. The abundance ratio, C_{MT}/C_G, was, therefore, estimated through Eq. (3), and then ΔE was obtained by means of Eq. (5).

As Fig. 5 shows, relations of the logarithmic values of the intensity ratios or the abundance ratio against $1/T$ were found to be linear. From the slope of the straight lines, the energy differences in the gaseous state are estimated; they are listed in Table 4.

Table 4. Energy differences between the rotational isomers in gaseous state
(kcal/mol)

Energy difference*	Observed value	Calculated value[17]
ΔE^{gas}_{MG-MT}	1.7	1.45
$\Delta E^{gas}_{RG'-RG}$	1.1	0.85
ΔE^{gas}_{RT-RG}	1.0	0.75

* The energy difference between two rotational isomers of which are shown by the subscripts.

The observed values of ΔE are of the same order as the calculated results of our previous report.[17] The value of ΔE^{gas}_{MG-MT} for *meso*-DCB is larger than the ΔE between *gauche* and *trans* forms of 1,2-dichloroethane (1.2 kcal/mol).[18] This is understandable, for the steric repuslion between the two methyl groups is somewhat larger than that between the chlorine atom and the methyl group,*4 and therefore the difference in steric potential between the MG of *meso*-DCB and the corresponding *gauche* form of 1,2-dichloroethane is to be larger than that between the *trans* forms of these two substances. In the case of *racemic*-DCB, the potential energies of RG' and RT are almost the same in magnitude, both higher than that of RG by approximately 1.0 kcal/mol. These results suggest that the energy difference between the rotational isomers of 2,3-dichlorobutane is mainly affected, just as in the case of 1,2-dichloroethane, by the skeletal conformations of the Cl–C–C–Cl linkage and an electrostatic interaction induced by the two C–Cl bonds.

Temperature Change in Spectra in the Acetonitrile Solution. Figure 6 shows the temperature dependence of the abundance ratio, C_G/C_{MT}, for *meso*-DCB, and the intensity ratio of the infrared band for *racemic*-DCB in the acetonitrile solvent. In contrast with the same relation for the gaseous state (see Fig. 5), in this case positive slopes are obtained against $1/T$. The results can be explained in terms of change in energy difference between the rotational isomers, a change which is caused by an interaction between the molecular dipole and its induced moment in the surrounding solvent medium. By taking Onsager's field[12] as the reaction field,[10] when a molecule of dipole moment, μ, in the gaseous state is transferred from the vacuum into the solvent medium of the dielectric constant, ε, the potential energy is lowered by:

$$E_r = (\varepsilon-1)\mu^2/(2\varepsilon+1)a^3 \qquad (6)$$

where a is the radius of the solute molecule.

Putting the dipole moments listed in Table 1 and the dielectric constant of acetonitrile (37.5) into Eq. (6), the energy differences between the rotational isomers in the solution can be calculated as $\Delta E^{sol}_{MG-MT} = 0.02$ kcal/mol, $\Delta E^{sol}_{RG'-RG} = -0.73$ kcal/mol, and $\Delta E^{sol}_{RT-RG} = -0.24$ kcal/mol.*5 The observed energy differences in the solution, which are determined from the linear relations shown

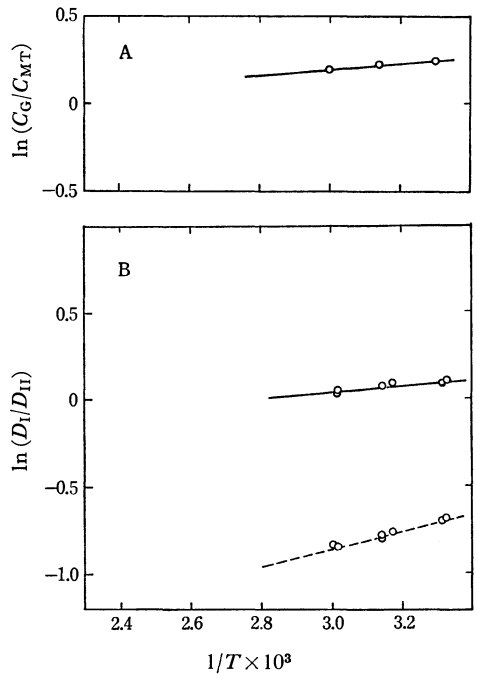

Fig. 6. The temperature dependences of abundance ratio and of intensity ratio in acetonitrile solution.
A: *meso*, B: *racemic* (full line: $D_I/D_{II}=D_{699}/D_{648}$, broken line: $D_I/D_{II}=D_{592}/D_{648}$)

18) T. Shimanouchi, H. Tsuruta and S. Mizushima, *Sc. Pap. Inst. Phys. Chem. Res. Tokyo*, **42**, 165 (1945).

*4 The van der Waals radii of the chlorine atom and the methyl group are 1.8 and 2.0 Å respectively (L. Pauling, "The Nature of the Chemical Bond," Cornell Univ. Press, Ithaca, New York (1940)).

*5 In calculating E_r, a is roughly estimated by the equation; $M/d=(4\pi a^3/3)N$, where M and d are the molecular weight and the density of the solute molecule, and N, the Avogadro number. As the values of the densities, 1.1023 and 1.1063 were used for *meso*- and *racemic*-DCB respectively.[5] To estimate the energy difference in the solution, ΔE^{sol}, the calculated ΔE^{gas} values listed in Table 4 were used.

in Fig. 6, are $\Delta E^{sol}_{MG\text{-}MT} = -0.3$ kcal/mol, $\Delta E^{sol}_{RG'\text{-}RG} = -0.3$ kcal/mol, and $\Delta E^{sol}_{RT\text{-}RG} = -1.0$ kcal/mol.

Although some discrepancies between the calculated and observed energy differences in the solution are noted, the decreases in the potential energy of the polar MG, RG' and RT conformations in the acetonitrile solvent can be explained qualitatively by appling Onsager's reaction field.

The authors are grateful to Professor T. Shimanouchi for his guidance and to Dr. S. Kondo and Mr. S. Shimogawara for their kind discussions and assistance.

BULLETIN OF THE CHEMICAL SOCIETY OF JAPAN VOL. 42 2098—2101 (1969)

Raman and Infrared Spectra of β-Alanine

R. S. KRISHNAN and R. S. KATIYAR

Department of Physics, Indian Institute of Science, Bangalore 12, India

(Received March 8, 1968)

The Raman spectrum of β-alanine has been recorded in the single crystal form employing λ 2537 technique. The infrared spectra in Nujol mull and KBr pellet have been taken for the range 400—4000 cm^{-1}. The spectra exhibit the characteristic lines of the zwitter ion and also hydrogen bond vibrations in the region 2400—3000 cm^{-1}. The tentative assignments of the observed lines are given and compared with those of other amino acids.

The study of the vibration spectra of amino acids by Raman and infrared spectroscopy is useful for getting information about their molecular configurations and the nature of hydrogen bonding in these substances. A systematic study of the Raman spectra of glycine and its addition compounds from this laboratory has been reported by Krishnan and Narayanan.[1] The infrared spectra of crystalline amino acids have been studied by Klotz and Green[2] and Thompson *et al.*[3] Edsall and his coworkers[4] have made extensive spectral measurements on a large number of amino acids in aqueous solution. Attempts have also been made to assign the vibrational frequencies of glycine molecule on the basis of the normal coordinate analysis.[5-7] The Raman and infrared spectra of β-alanine (β-amino propionic acid, $H_2N{\cdot}CH_2{\cdot}CH_2{\cdot}COOH$) in the crystalline state have, however, not been studied. The authors have recorded the Raman spectrum of β-alanine in the single crystal form and the infrared absorption spectrum in the powder form at the room temperature and the results are presented in this paper. A comparative study of the vibration spectra of α-glycine, γ-glycine, α-alanine and β-alanine has also been made.

Experimental

Single crystals of β-alanine were grown from aqueous solution of the pure substance. The biggest crystal grown had roughly the size, 6 mm^3. Using mercury λ 2537 excitation and a Hilger medium quartz spectrograph the Raman spectrum of the crystal was recorded on Ilford Zenith Astronomical plates with exposures of one day. The infrared absorption spectrum of the substance was recorded in the spectral region 4000—400 cm^{-1} in the form of the potassium bromide disc, using a Carl Zeiss UR-10 Infrared spectrometer.

Results

An enlarged photograph of the Raman spectrum of β-alanine is reproduced in Fig. 1, along with its microphotometer record. The positions and frequency shifts of the Raman lines are marked on the microphotometer tracing. The frequency shifts are also listed in Table 1. The figures in brackets represent the relative intensities of the Raman lines estimated visually. Thirty nine Raman lines have been recorded. Some of these lines fall very near some mercury lines and are therefore not clearly separated. However, their

1) R. S. Krishnan and P. S. Narayanan, "Crystallography and Crystal Perfection," Academic Press Ltd., London (1963), and references therein.

2) I. M. Klotz and D. M. Green, *J. Phys. Chem.*, **52**, 961 (1948).

3) H. W. Thompson, D. L. Nicholson and L. N. Short, *Discussions Faraday Soc.*, **9**, 22 (1950).

4) J. T. Edsall, *J. Am. Chem. Soc.*, **80**, 3807 (1958); **72**, 474 (1950); **62**, 1312, 1767 (1943).

5) S. Suzuki, T. Shimanouchi and M. Tsuboi, *Spectrochimica Acta*, **19**, 1195 (1963).

6) M. Tsuboi, T. Onishi, I. Nakagawa, T. Shimanouchi and S. Mizushima, *Spectrochimica Acta*, **12**, 253 (1958).

7) H. Baba, A. Mukai, T. Shimanouchi and S. Mizushima, *Nippon Kagaku Zassi (J. Chem. Soc. Japan, Pure Chem. Sect.)*, **70**, 333 (1949).

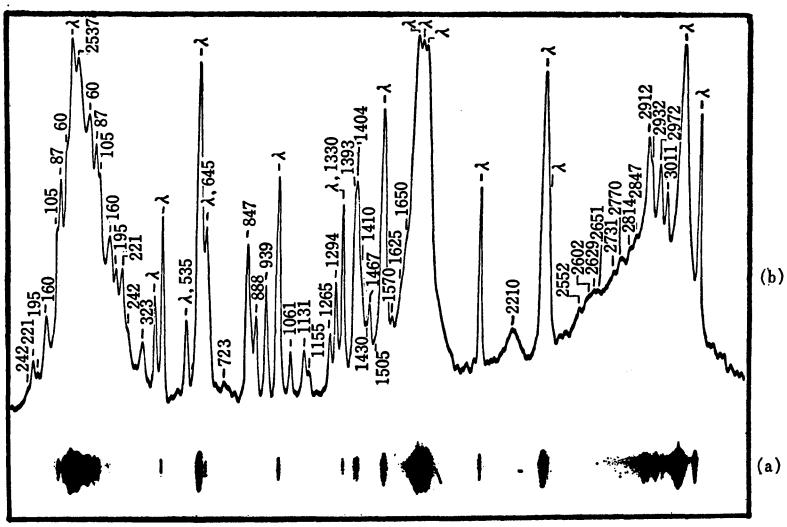

Fig. 1. (a) Raman spectrum of β-alanine, (b) Microphotometer record.

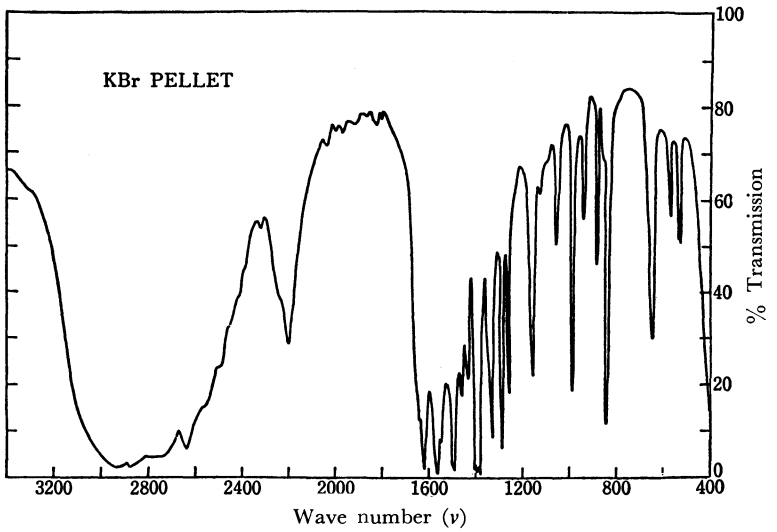

Fig. 2. Infrared absorption spectrum of β-alanine.

presence can be predicted from the infrared spectrum of the substance. The infrared absorption curve obtained for β-alanine is reproduced in Fig. 2. The observed infrared absorption frequencies are listed in Table 1. Forty nine absorption maxima have been identified.

Discussion

β-Alanine crystallises in the orthorhombic system (Jose and Pant[8]) with the space group D_{2h}^{15}-*Pbca*. The unit cell (a=9.865, b=13.8 and c=6.07 Å), has eight molecules occupying general positions. The molecule as such does not have any symmetry and therefore all the internal vibrations of the molecule should be both Raman and infrared active. Exclusive of the long wavelength acoustic modes, there are a total of 309 factor group fundamentals. Each molecule of β-alanine has 33 internal vibrations. Since there are eight molecules in the unit cell, each internal vibration will be further split. Since the intermolecular forces in the crystal are relatively weak, the splitting of the degeneracies would be small and difficult to be experimentally observed. One can expect to observe at least 33 vibrations in Raman effect and in infrared absorption. This is actually the case. The remaining 45 fundamentals are known as the external vibrations and can further be divided into 24 rotatory type and 21 translatory type of oscilations. Since the crystal has got the centre of symmetry, only 12 translatory type and 12 rotatory type of oscillations will be Raman active.

8) P. Jose and L. M. Pant, *Acta Cryst.*, **18**, 806 (1965).

TABLE 1. VIBRATION FREQUENCIES OF β-ALANINE

Raman shifts (in cm^{-1})	IR absorption maxima (in cm^{-1})	Assignments
60(2), 87(3), 105(2), 160(3), 195(3)		Lattice lines
221(4), 242(2)		N^+–H···O bonded
323(4)		C–CN^+ bending
535(—)	530(m), 537(m)	COO^- rocking and NH_3^+ torsion
	572(m)	COO^- wagging
645(—)	650(st)	COO^- bending
723(2)		
847(8)	850(st)	C–CN^+ stretch
888(6)	887(st)	
939(7)	947(m), 991(st)	CH_2 rocking
1061(5)	1060(m), 1100(w)	C–N^+ stretch
1131(4)	1130(w)	NH_3^+ rocking
1155(2)	1158(st)	
1265(5)	1261(st)	CH_2 wagging
1294(6)	1292(st)	CH_2 twisting
1330(—)	1332(st)	CH_2 wagging
1393(9)	1386(vs)	COO^- sym. stretching
1404(10)	1397(vs)	
1410(5)	1410(vs)	
1430(2)	1445(m)	CH_2 deformation
1467(5)	1462(st)	
1505(—)	1498(vs)	NH_3^+ sym. deformation
	1504(vs)	
1570(3)	1548(st)	NH_3^+ deg. deformation
	1565(vs)	
1625(—)	1623(vs)	COO^- asym. stretching
1650(—)	1645(w), 1810(w), 1835(w), 1880(w), 1930(w), 1983(w), 2005(w), 2050(w)	Combination frequencies
2210	2207(m), 2240(w), 2323(w), 2400(w), 2420(w), 2450(w), 2500(w)	
2552	2560(w)	
2602(3)		
2629(4)		
2651(4)	2640(vs)	N^+–H···O stretching
2731(4)		
2770(4)	2740—2800(vs)	N^+–H···O stretching
2814(2)		
2847(2)	2885(vs)	
2912(10)		
2932(9)	2932(vs)	CH_2 sym. stretching
2972(9)		
3019(8)	3025(vs)	CH_2 antisym. stretching
	3300(w), 3400(w)	Combination frequencies

The thirty three internal vibrations of the molecule can be classified as due to the vibrations of the various groups in the molecule. The assignments of the observed Raman and infrared frequencies are given in column 3 of Table 1. Theoretically the group $-CH_2-CH_2-$ should have two symmetric and two asymmetric CH_2 stretching vibrations. However, as one CH_2 group stretches in and out of phase, it disturbs the carbon atom of the next CH_2 group very little because of the insulating effect of the low frequency C–C vibration. Therefore the coupling between the two CH_2 groups is very weak. As a result, the two symmetric CH_2 stretching vibrations will have almost the same frequency and the two asymmetric stretching modes will also have nearly the same frequency which is somewhat higher than the symmetric stretching frequency. In the case of CH_2 bending vibrations such as wag and rock, the angle H–C–H does not change appreciably and the motions of the hydrogen atoms must be directly opposed by the motion of the carbon of the next CH_2 group which indicates a strong coupling between the two CH_2 groups and therefore they may be expected to have different rocking and wagging frequencies.

The absence of the C–O and NH_2 group frequencies and the presence of COO^- and NH_3^+ frequencies clearly indicate that the molecules exist in the zwitter ion form ($NH_3^+ \cdot CH_2 \cdot CH_2 \cdot COO^-$) in the crystal. Further, since the N–H stretching frequencies of NH_3^+ group are considerably lowered and are broad, the molecules are held together by strong hydrogen bonds of N^+–H···O type. According to Parimala Jose and Pant[8] the N···O distances are 2.76, 2.78 and 2.78 Å and three strong hydrogen bonds should therefore be present around the nitrogen atom. This view is confirmed in the present analysis. From the correlation curve of N^+–H···O stretching frequencies *versus* the H-bond lengths given by Krishnan and Krishnan,[9] the N^+–H···O stretching frequencies can be identified at 2651 and 2731 cm^{-1} in Raman spectrum corresponding to the N···O distances of 2.76 and 2.78 Å. The large number of subbands in this region quite possibly arises from an anharmonic interaction o the allowed overtone and summation frequencies. The presence of the hydrogen bonds must be accompanied by some low frequency N+H···O stretching oscillations. These low frequency stretching oscillations are calculated using the formula given by Pimentel and Sederholm.[10] The results of the calculation show that the frequency shifts 221 and 242 cm^{-1} may be attributed to the motions of the hydrogen bonds N+H···O. Similar low

9) R. S. Krishnan and K. Krishnan, *Proc. Ind. Acad. Sci.*, **A60**, 11 (1964).

10) G. C. Pimentel and C. M. Sederholm, *J. Chem. Phys.*, **24**, 639 (1956).

TABLE 2. COMPARISON OF VIBRATION SPECTRA OF AMINO ACIDS

α-glycine Raman shifts (in cm^{-1})	γ-glycine Raman shifts (in cm^{-1})	α-alanine IR maxima (in cm^{-1})	β-alanine Raman shifts (in cm^{-1})	Assignments
3008	2995	—	3011	CH stretching
2974	2964		2972	
			2932	
			2912	CH stretching
1640	1629	1597	1625	COO^- stretching
1563	1586	1623	1570	NH_3^+ deg. deformation
			1548 IR	
1506	1500	1534	1505	NH_3^+ sym. deformation
			1498 IR	
—	—	1455	—	CH_3 deformation
1441	1441	—	1467	CH_2 deformation
1459			1430	—
1414	1405	1412	1410	COO^- sym. stretching
1395	1391		1404	
			1393	
—	—	1355	—	CH_3 sym. deformation
1330	1341	—	1330	CH_2 wagging
1320	1326	—	1294	CH_2 twisting
—	—	—	1265	CH_2 wagging
1140	1165	1237	1155	NH_3^+ rocking
1112	1141	1131		
1038	1045	1148	1061	$C-N^+$ stretching
—	—	1026	—	CH_3 rocking
		1015		
925	924	—	991 IR	CH_2 rocking
			939	
896	895	918	888	$C-CN^+$ stretching
		852	847	
677	686	771	645	COO^- bending
588	—	648	572 IR	COO^- wagging
499	503	540	537 IR	COO^- rocking and
—	516	492	530 IR	NH_3^+ torsion
358	362	—	323	CCN^+ bending

frequency shifts due to hydrogen bond oscillations have been observed by Gross,[11] Balasubramanian, Krishanan and Iitaka[12] and Krishnan and Krishnan[13] in hydrogen bonded crystals.

The tentative assignments of the other Raman frequencies have been made by comparing the vibration spectra of β-alanine with that of glycine. A comparative study of the vibration spectra of α-glycine,[1] γ-glycine,[12] α-alanine[14] and β-alanine has been made in the Table 2. It is to be noted that the group frequencies do not vary much in these crystals except some frequencies in the case of β-alanine. All these crystals exist as dipolar (zwitter) ions in the crystalline state. There are some weak bands observed in the infrared spectrum in the region from 1800 to 2500 cm^{-1}. These can be explained as the overtones and combinations of some of the fundamental vibration frequencies.

The low frequency Raman lines are due to the external oscillations of the molecules in the crystal.

11) E. Gross, "Hydrogen Bonding by Madzi," Pergamon Press, London, p. 202, (1959).

12) K. Balasubramanian, R. S. Krishnan and Y. Iitaka, This Bulletin **35**, 1303 (1962).

13) K. Krishnan and R. S. Krishnan, *Proc. Ind. Acad. Sci.*, **55**, 153 (1962).

14) K. Fukushima, T. Onishi, T. Shimanouchi and S. Mizushima, *Spectrochimica Acta*, **14**, 236 (1959).

BULLETIN OF THE CHEMICAL SOCIETY OF JAPAN VOL. 42 2102—2106 (1969)

Optical Spectra of Transition Metals in Na_2O-P_2O_5 Glasses

Takashi MAEKAWA, Toshio YOKOKAWA and Kichizo NIWA

Department of Chemistry, Faculty of Science, Hokkaido University, Sapporo

(Received November 18, 1968)

The optical spectra and the magnetic susceptibilities were obtained in sodium phosphate glasses containing transition metal ions. It was shown that the content of the transition metal ions of higher valency states increases with an increase in that of Na_2O whenever an oxidation equilibrium occurs between two or more valency states. By combining the visible spectra analyzed from the viewpoint of the ligand field theory with the results of the magnetic susceptibility measurement, it was shown that most transition metals coordinate six oxygen atoms in the phosphates.

The studies of the coloration of the transition metal ions in fused salts have, so far, greatly progressed with regard to the halide and nitrate systems especially. Bates applied the ligand-field theory to the analysis of the spectra of the colored glass.[1] In a sodium silicate and a sodium borate, the variation of the visible spectra with the sodium concentration was observed by Bamford.[2] Recently, the concept of the formation of non-bridging oxygen ions in a borate was used in explaining the fact that the intensity of absorption rapidly changed at a definite alkali concentration.[3] In contrast with the borates and the silicates, however, those have been few experimental measurements of the phosphates. The ligand-field absorption of the manganous ion in $3K_2O{\cdot}7P_2O_5$ and $3Na_2O{\cdot}7P_2O_5$ glass was obtained by Bingham and Parke.[4] Recently, the optical spectra and the magnetic susceptibility of cobalt(II) ion in Na_2O-P_2O_5 glass at various sodium oxide concentrations were measured.[5]

In this experiment the variation in the intensity and position of the visible absorption spectra were examined in sodium phosphate glasses with various compositions of Na_2O in order to investigate the structure of the phosphate network as well as their relation to the transition metal ions. The magnetic susceptibilities of this glass were also measured, since those quantities provide important information on the valency states of transition metal ions as well as their coordination numbers.

1) T. Bates, "Modern Aspect of the Vitreous State," Vol. 2, Butterworths, London (1962), Chap. 5.
2) C. R. Bamford, *Phys. and Chem. of Glasses*, **3(6)**, 189 (1962).
3) A. Paul and R. Douglas, *ibid.*, **9(1)**, 21 (1968).
4) K. Bigham and S. Parke, *ibid.*, **6(6)**, 224 (1965).
5) M. Kuto *et al.*, Preprints for the 21st Annual Meeting of the Chemical Society of Japan (Osaka, 1968).

Experimental

Materials. The sample glass was prepared by melting $NaPO_3$, P_2O_5, and H_3PO_4 of a guaranteed reagent grade. The transition metals which were added as oxides were V_2O_5, Cr_2O_3, MnO_2, Co_2O_3, Fe_2O_3, NiO, and CuO. These were added, in amounts up to about 0.5 wt per cent, to the sodium phosphate, melted in a platinum crucible, and kept in the liquid state for 10 hr in order to get uniform mixtures.

Measurement of Optical Absorption Spectra. The melt in a crucible was cast into a mould of brass. The thickness of the sample plate was 0.5 cm. To avoid the moisture and the scattering caused by the rough surface, the sample was immersed in a benzene-chlorobenzene solution in an absorption cell.

Measurement of Magnetic Susceptibility. Use was made of a Gouy balance. The strength of the magnetic field was 15000 gauss. The net susceptibility due to the transition metal ions was obtained after the correction for the blank from the solvent glass was applied.

Determination of the Composition of the Glass Solvent. The sample was dissolved in an aqueous solution of nitric acid, and all the phosphates were converted to orthophosphate. From the quantity of NaOH required to neutralize the solution from the first to the second neutralization point, the quantity of P_2O_5 was determined. The Na_2O content was determined by the difference from the total weight.

Water Content in Glass. In the phosphate glass it is important to consider the presence of water. It is quite difficult to remove the water completely by the ordinary procedure. A considerable amount of water will still be present, especially when the sodium oxide concentration is low. This water was, however, ignored because water dissolves in glass not as H_2O molecules by as a network modifier, like sodium oxide. Although the presence of water alters the so-called basicity of the glasses, this doesn't have as much effect on transition metal ions as free H_2O molecules.

Results

Visible Absorption Spectra. *1) Vanadium.* The glasses containing vanadium were yellow when

the Na_2O content was high, but they turned green as the Na_2O content decreased. The extinction curves of the glasses are given in Fig. 1. The small absorption around 700 mμ increased in intensity as the Na_2O content decreased. Vanadium is able to have three valency states, V(III), V(IV), and V(V), in the glasses. V(V) has a $3d^0$ electronic configuration, so it has no absorption bands caused by the crystal field of oxygen ligands. V(IV) ($3d^1$) has a single spin-allowed band which occurs in the infrared region,[6] so it could not be detected in this experiment either. Therefore, it is considered that the small absorption is due to the V(III) ion in the glass and that the proportion of the V(III) decreases as the Na_2O

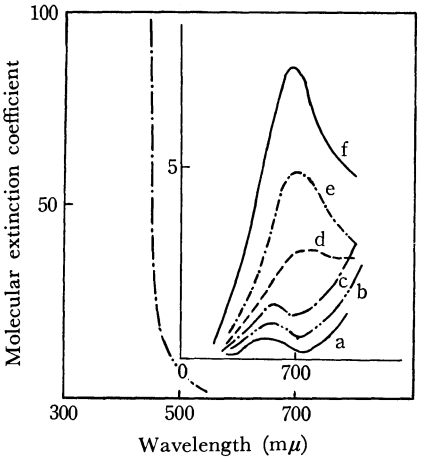

Fig. 1. The optical absorption of vanadium in sodium phosphate glasses with various sodium oxide concentration.

a 53.6 mol% Na_2O, b 52.5, c 50.3, d 27.7, e 17.4, f 0

content increases. The proportion of the higher valency state usually increases with the Na_2O content in glasses containing transition metals,[7] as may also be seen below.

2) Chromium. The glass containing chromium was green, and the color did not change with the composition. The extinction curves of the glasses are shown in Fig. 2. This glass has three prominent peaks, around 450, 635 and 600 mμ; they are considered to be three spin-allowed transitions in an octahedral crystal field of Cr(III). The assignment of these bands will be discussed later.

3) Manganese. The glasses changed from pale brown to pale purple with an increase in the Na_2O content. The extinction curves are shown in Fig. 3; they consist of a single band at 500 mμ. This band increases in intensity with an increase in the Na_2O

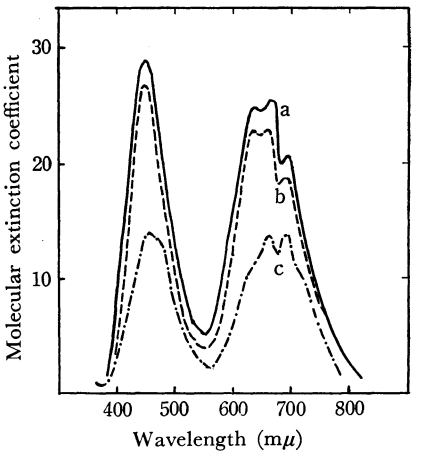

Fig. 2. The optical absorption of chromium in sodium phosphate glasses with various sodium oxide concentrations.

a 55.4 mol% Na_2O, b 50.8, c 0

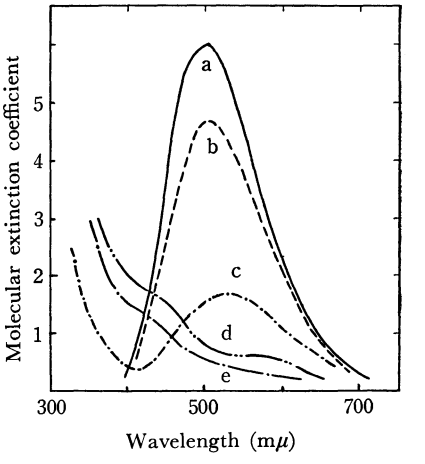

Fig. 3. The optical absorpion of manganese in sodium phosphate glasses with various sodium oxide concentrations.

a 56.1 mol% Na_2O, b 51.4, c 44.6, d 22.1, e 0

content. Manganese is present in glasses as divalent or trivalent ions. The absorption at 500 mμ is considered to be the spin-allowed transition of Mn(III), whose content increases with an increase in the Na_2O content. Mn(II) has a $3d^5$ electronic configuration and has no spin-allowed crystal-field bands.

4) Iron. The glasses were yellowish brown. The extinction curves are shown in Fig. 4. Iron is present in glasses as divalent or trivalent ions. Fe(II) ($3d^6$) has a single spin-allowed absorption band in the infrared region, but the band could not be detected in this experiment. Fe(III)($3d^5$) has an *iso*-electronic configuration with Mn(II) and has no spin-allowed crystal-field band. The weak absorption is due to the spin-forbidden crystal-field

6) W. Johnstone, *J. Am. Ceramic Soc.*, **48(12)**, 608 (1965).
7) R. W. Douglas, P. Nath and A. Paul, *Phys. and Chem. of Glasses*, **6(6)**, 216 (1965).

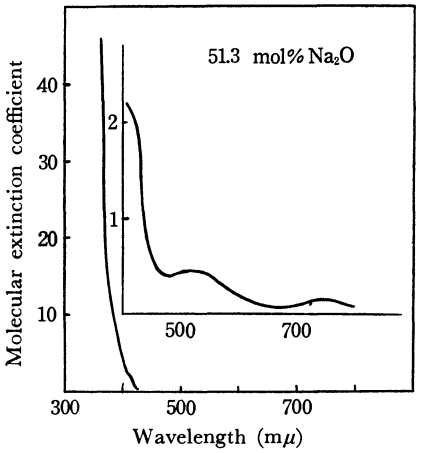

Fig. 4. The optical absorption of iron in sodium phosphate glass.

band. Chemical analysis showed that most of the iron ions are present as trivalent (about 95%) in the sodium metaphosphate glass.

5) Cobalt. The glasses change from pink to blue with an increase in the Na_2O content. The extinction curves are shown in Fig. 5. Cobalt is divalent in the glass. When the Na_2O content is low, Co(II) is surrounded by six oxygen atoms, but as the Na_2O content increases the proportion of the tetrahedrally-coordinated cobalt ion increases. The variation in color is consistent with this change. The change from octahedral to tetrahedral coordination occurs in other glasses.[3]

6) Nickel. The glasses were yellow but became greenish with an increase in the Na_2O content. The extinction curves are shown in Fig. 6. The nickel in the glasses is in the form of the divalent ion, which has a $3d^8$ electronic configuration. In the octahedral field, the nickel(II) ion has three spin-allowed bands.

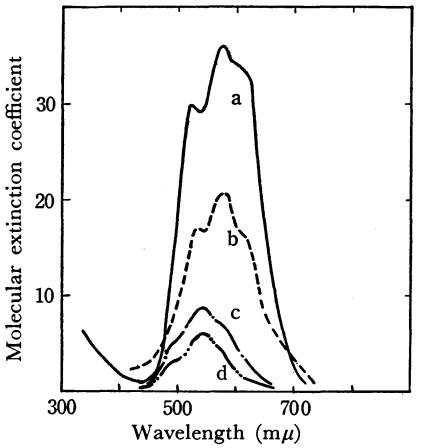

Fig. 5. The optical absorption of cobalt in sodium phosphate glasses with various sodium oxide concentrations.

a 57.4 mol% Na_2O, b 50.6, c 44.0, d 0

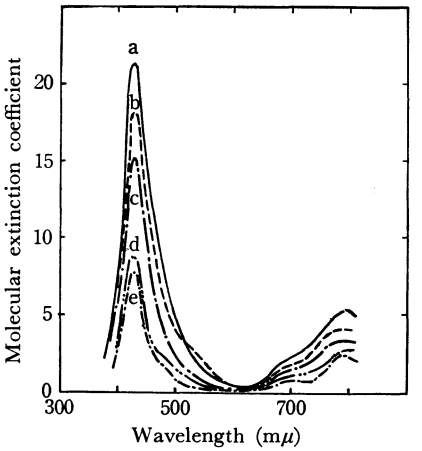

Fig. 6. The optical absorption of nickel in sodium phosphate glasses with various sodium oxide concentrations.

a 59.0 mol% Na_2O, b 55.5, c 51.4, d 36.6, e 0

The absorptions around 425 and 780 mμ correspond to these bands, and the other band appears in the infrared region. It was shown in the sodium borate glasses that the tetrahedrally-coordinated nickel ion is present in the higher-alkali-content glasses.[8] In the phosphate glasses this is shown by the variation in the intensity of the absorption, which will be discussed later.

7) Copper. All the sodium glasses containing copper were pale blue. The extinction curves of the glasses are shown in Fig. 7. The main absorp-

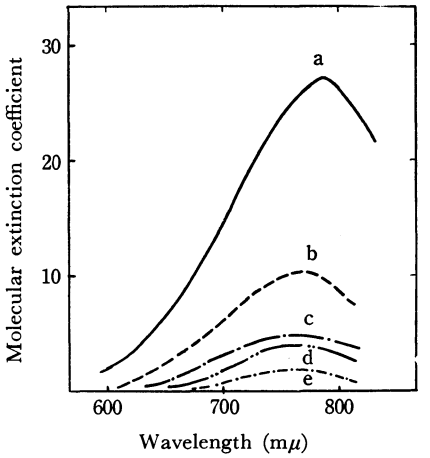

Fig. 7. The optical absorption of copper in sodium phosphate glasses with various sodium oxide concentrations.

a 50.9 mol% Na_2O, b 45.6, c 41.8, d 34.1, e 0

8) J. Berkes and W. White, *Phys. and Chem. of Glasses*, **7(6)**, 191 (1966).

Table 1. Assignment of the absorption band of transition metals in sodium phosphate glasses

Ion	Band assignment	$-6H_2O$ (mμ)	Na-Glass (mμ)
V +3	$^3T_1 \rightarrow {}^3T_2$	562	665
Cr +3	$^4A_2 \rightarrow {}^4T_1$	410	450
	$^2T_1$		634
	$^4T_2$		658
	^2E	671	690
Mn +3	$^5E \rightarrow {}^5T_2$	476	500
Fe +3	$^6A_1 \rightarrow {}^4E, {}^4A_1$	406	410
	$^4T_2$	540	520
	$^4T_1$	793	740
Co +2	$^4T_1 \rightarrow {}^4T_1$	465	490
		515	530
	$^4A_2 \rightarrow {}^4T_1$ (Tetrahedral)	600	620
Ni +2	$^3A_2 \rightarrow {}^3T_1$	395	425
	^1E	649	700
	$^3T_1$	741	782
Cu +2	$^2E \rightarrow {}^2T_2$	796	760

tion band appeared at 760 mμ, its intensity increasing with the Na_2O content. The copper in the glasses is in the divalent state with a $3d^9$ electronic configuration. This absorption band is due to the transition in an octahedral field. The apparent ligand field strength is 13000 cm^{-1}.

Discussion

The observed bands are summarized in Table 1. The corresponding values in octahedrally-coordinated aquo-complex are also included. A comparison of the two sets of data shows that the bands may be identified as transitions in the octahedral-ligand field. In Co and Ni, however, the tetrahedral-ligand field must be taken into consideration.

In general the field strength of the phosphate glass is smaller than tnat of the corresponding aquo-complex by about 10%. This fact is also seen in other glasses.[1] In copper, on the other hand, the splitting of *d* levels due to the ligand field is greater than that of the copper(II) aquo-complex. This result may be explained by considering that there occurs a large tetragonal distortion.[1]

Figure 8 shows the relation between the intensity of the absorption and the Na_2O content in nickel(II), copper(II), and chromium(III) glasses. The increase in intensity is probably caused by the following two effects:

(1) the increase in the portion of ions which occupy the sites under the octahedral and/or tetrahedral crystal field and cause the optical absorption. This increase is closely related to the structure of the glasses, and

(2) the increase in the number of the ions in the relevant valency state, which is related to redox equilibrium of the transition metal ions.

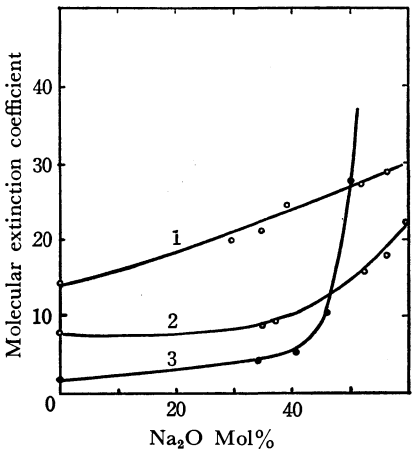

Fig. 8. The variation of the intensity with sodium oxide concentration.
1 Cr ~450 mμ, 2 Ni ~420 mμ, 3 Cu ~760 mμ

In chromium, the intensity increases moderately with the Na_2O content. This suggests that the proportion of Cr(III) increases with an increase in the Na_2O content, although no divalent chromium ions were detected. In copper, on the other hand, the intensity changes abruptly at an Na_2O content of 40 mol%. This shows that, in addition to a possible increase in the proportion of Cu(II), the structure of the glasses changes at this composition; that is, the glass network disintegrates into discrete ions so that the probability of occupying the octahedral site increases at this composition.

In nickel, an abrupt change in intensity occurs at the composition of 40 mol% Na_2O. As in the borate glasses, it is considered that the proportion of tetrahedral Ni(II) coordination increases from this point.

Magnetic Susceptibilities. From the magnetic susceptibilities, the effective magnetic moments of

Table 2. Effective magnetic moment of transition metal ions in sodium metaphosphate glasses

		$-6H_2O$ μ_{eff} (B.M.)	Sodium metaphosphate μ_{eff} (B.M.)	Ion
V	+4	1.70	1.10	V^{3+}, V^{4+}, V^{5+}
	+3	2.61		
	+2	3.80		
Cr	+3	3.80	3.77	Cr^{2+}, Cr^{3+}
	+2	4.80		
Mn	+3	4.80	5.62	Mn^{2+}, Mn^{3+}
	+2	5.83		
Co	+2	4.90	4.70	Co^{2+}
Ni	+2	3.12	3.21	Ni^{2+}
Cu	+2	1.83	2.02	Cu^{2+}

transition metal ions in sodium metaphosphate glasses were derived from the relation:

$$\mu_{eff} = 2.84\sqrt{\chi_M \cdot T}$$

where χ_M is the molar susceptibility, and T, the absolute temperature. These results are summarized in Table 2. The corresponding values in octahedral aquo-complex are included. In general, the effective magnetic moment of the transition metal ions in a crystal field can be represented by the following relation:

$$\mu_{eff} = \mu_0\left(1 - \alpha\frac{\lambda}{\Delta}\right)$$

where Δ is the strength of the crystal field, λ is a parameter of spin-orbit interaction, μ_0 is a spin-only magnetic moment, and α is a positive constant. λ is positive when there are fewer than five 3d electrons and is negative when there are more.

Therefore, if it is assumed that the transition metal ions in the glasses coordinate six oxygen atoms and that λ does not differ much between the glasses and aquo-complexes, the μ_{eff}'s of V, Cr, and Mn become smaller, and those of Co, Ni, and Cu become larger than those of the corresponding aquo-complex. Table 2 shows that this relation holds except in the case of Co. It is known that the magnetic moment in the tetrahedral field is smaller than that in the octahedral field.[9] Therefore, in cobalt this result can be explained by the existence of the tetrahedrally-coordinated cobalt ions, which is consistent with spectra results.

As to vanadium, the values suggest that the V(IV) and V(V) are predominant, as has also been implied from the spectral measurements. The μ_{eff} of Mn shows that there are a considerable number of Mn(II) ions which can not be detected spectroscopically. It may be concluded from the table that nickel and copper are predominant in the divalent state in the phosphate glasses.

In conclusion, the coordination of oxygen atoms on the transition metal ion is closely related to the structure of the glass. Thus, when the Na_2O content is low, most of the transition metal oxides act as network modifiers and the coordination number is 6, while some of them (Ni, Co) act as network formers at a high Na_2O content when the coordination number becomes 4. This is also reflected in the fact that, at a high basicity, transition metal ions of high valency state form stable coordination complexes.

9) R. L. Carlin, "Transition Metal Chemistry," Vol. 1, Marcel Dekker, New York (1965), Chap. 1.

BULLETIN OF THE CHEMICAL SOCIETY OF JAPAN VOL. 42 2106—2111 (1969)

Ignition Delay Time Studies of Hydrogen and Oxygen Reactions through Silent Electric Discharge

Kihei MORINAGA

Department of Chemistry, Defense Academy, Hashirimizu, Yokosuka

(Received November 25, 1968)

The ignition of hydrogen and oxygen could be induced by the so-called silent electric discharge, and the ignition delay time after the termination of the discharge was found to be proportional to a logarithm of the discharge intensity (pulse current). The proportionality constants in different diluents, argon and helium, were analyzed to yield the net effect of chain breaking in the reaction:

$$H + O_2 + M \xrightarrow{k_4} HO_2 + M$$

and the rate coefficient, k_1, for the reaction:

$$H + O_2 \xrightarrow{k_1} OH + O$$

assuming a third-body efficiency of the diluent gases. It was inferred from the results that the radical reproducing from HO_2 significantly lessened the effect of the above chain breaking reaction, the accumulation of radicals seemed to be persistent even in the low-temperature region, where the k_1 value was observed not to be above the assumed value of $k_1[M]/2$.

The ignition of hydrogen and oxygen by silent electric discharge was reported previously[1] regarding the effects of the gas composition and the pressure on the threshold of the ignition.

The present paper will attempt to estimate the net effect of the chain breaking reaction by com-

1) K. Morinaga, This Bulletin, **35**, 627 (1962).

paring the experimental results on the ignition delay time in an argon diluent and in a helium diluent, assuming a third-body efficiency of the diluent gases.

Unlike spark discharge, silent discharge can be characterized by numerous small discharges which continue for a certain period of time. These small discharge can be represented on the Lichtenberg figure[2] as numerous spots[3] sporadically distributed all over the electrode (which is a dielectric substance) surface and on the current diagram as numerous fringe-like pulses the summation of which can lead to pulse current.[3,4] These are essential features of the silent electric discharge.

The linear relationship between the pulse current and the extent of chemical reaction in silent discharge was confirmed in previous papers.[5,6]

In the present paper, the pulse current was adopted in order to show the extent of the discharge which brings about the silent-discharge ignition of hydrogen and oxygen.

Experimental

Hydrogen, oxygen, and inert gases over three-nine pure were dried over silica gel and were then manometrically mixed to the desired composition in a conventional vacuum system without further treatment. The mixture was left to stand for more than 48 hr ($p=1$ atm) in a glass vessel before use. The composition of the inert gas *i. e.*, argon or helium, ranged from 5 to 55%, while the hydrogen and oxygen remained stoichiometric. The initial pressure of the gas mixture for runs was kept at 250 mmHg in all cases.

The electric circuit system which actuated the one-shot silent electric discharge and the device for the observation of the current diagram of the discharge were similar to those in previous experiments.[1,7] Under the present experimental conditions, the pulses on the current diagram appeared satisfactorily separated for convenient pulse-height measurements.

The cylindrical test bomb of the preceding work[1] was replaced by a cubic bomb with a 3 cm×8 cm×8 cm interior. It was provided with a quartz window for observing the emission from the ignited gas. The former conventional spark plugs[1] through which a high voltage was applied to the inside electrodes were replaced by Teflon plugs for better insulation from surface leakage. A safety diaphragm and needle valves were attached to the bomb just as in the previous work. The leak rate of the bomb system was less than 2 mmHg per hour in any case, and the bomb was filled with the test gas after repeated washing operations which took less than 3 min.

The silent discharge electrodes were composed of two polished Toshiba Terex glass plates (hard glass of the boric oxide type) 5 cm×6 cm×1 mm. The discharge gap distance of the electrodes was maintained by means of cementing an appropriate glass piece in each corner of the plate, and the discharge gap width was within the limit of 2.05—2.12 mm. Tin foil (7.5 cm^2) was stuck on the outside of the glass electrodes. The entire set-up of the electrodes was sustained by two springs which acted as electric leads insulated from the test bomb by the Teflon plugs.

The pick-up system for the emission from the ignited gas between two electrodes consisted of two slits, an interference filter,*1 and a photomultiplier tube (RCA 1P-28). The slits were designed so as not to transmit any light from the electrode surface. The interference filter separated the band system of $OH(^2\Sigma-^2\Pi)_{v=0,0}$ from the other emission of the ignited gas. The signal from the photomultiplier tube and the current diagram of the discharge were recorded simultaneously on a dual-beam oscilloscope.

To avoid unnecessary disturbance of the light-emission trace due to the discharge noise, much care was taken and all the ground points were coordinated at a unified earth point while the test bomb was floating, entirely from the ground.

A primary DC current was applied to the primary coil of a transformer through a switch, the ON and OFF operation of which produced secondary high tension in the secondary circuit. The discharge intensity or the pulse current in the secondary circuit could be regulated by changing the primary DC current, while the discharge period was less affected. In the present experiment, the high tension in the secondary coil which accompanied the ON stage of the switch was used exclusively.

Results

Typical oscillographic patterns of the pulse current and of the signal from the photomultiplier tube are shown in Fig. 1, where t and τ_i denote the discharge period and the ignition delay time

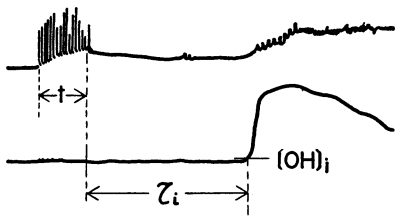

Fig. 1. Oscillographic pattern of current diagram (upper trace) and OH emission profile (lower trace).
t, discharge period; τ_i, ignition delay time; $[OH]_i$, a certain definite concentration of $OH(\Pi)$.

2) G. L. Lichtenberg, *Novi. Comment Gött.*, **8**, 168 (1777); Y. Toriyama, "Dust Figure of Surface Discharge and its Applications" (in English), Kinokuniya, Tokyo, Japan (1961).

3) M. Suzuki and Y. Naito, *Proc. Japan Academy*, **28**, 469 (1952).

4) K. Honda and Y. Naito, *J. Phys. Soc. Japan*, **10**, 1007 (1955).

5) K. Morinaga and M. Suzuki, This Bulletin, **34**, 157 (1961); **35**, 204, 429 (1962).

6) K. Morinaga, *ibid.*, **35**, 345, 625 (1962).

7) K. Morinaga and M. Suzuki, *Memoirs of the Defense Academy*, VII, 1031 (1967).

*1 Baird Atomic, Inc., U. S. A., A-31; Peak, 3070 Å; Half Peak Band Width, 100 Å.

respectively. The ignition delay time is determined by two cut-off points, one of which is the termination of the silent electric discharge and the other, the rise of the light emission to a definite value. In the figure, the ordinate of the upper trace can be represented by Coulomb units; the sum of the pulse heights divided by t gives the pulse current, I_p.

With an increasing in the pulse current, the ignition delay time decreased. Figures 2 and 3 show the relation between the ignition delay time and the logarithm of the pulse current in the argon diluent and the helium diluent respectively. The solid lines in the figures represent the least-square

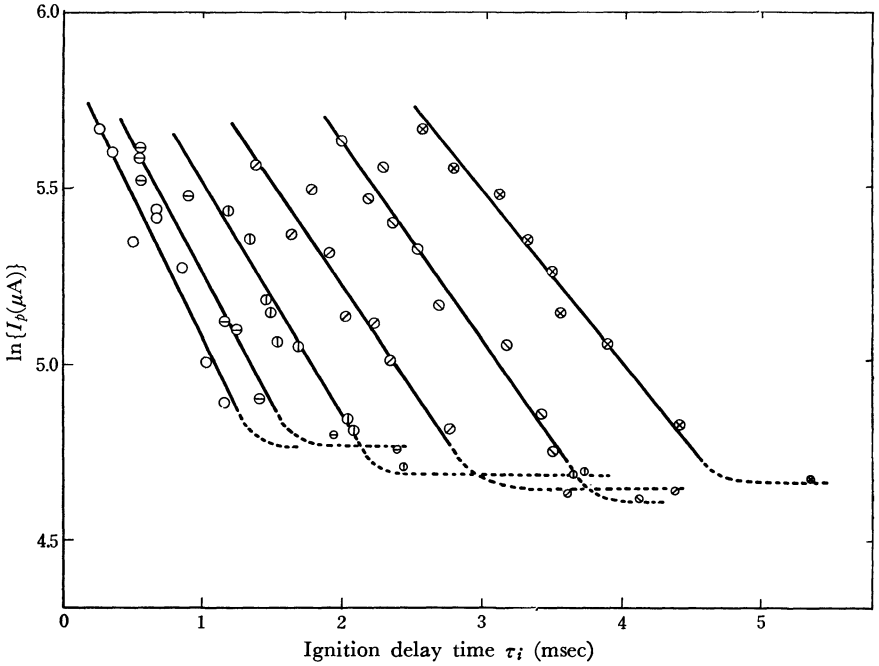

Fig. 2. Relation between ignition delay time and pulse current in argon diluent mixtures. Diluent composition is; ○, 5%; ⊖, 15%; ⓘ, 25%; ⊘, 35%; ⊘ 45%; ⊗, 55%.

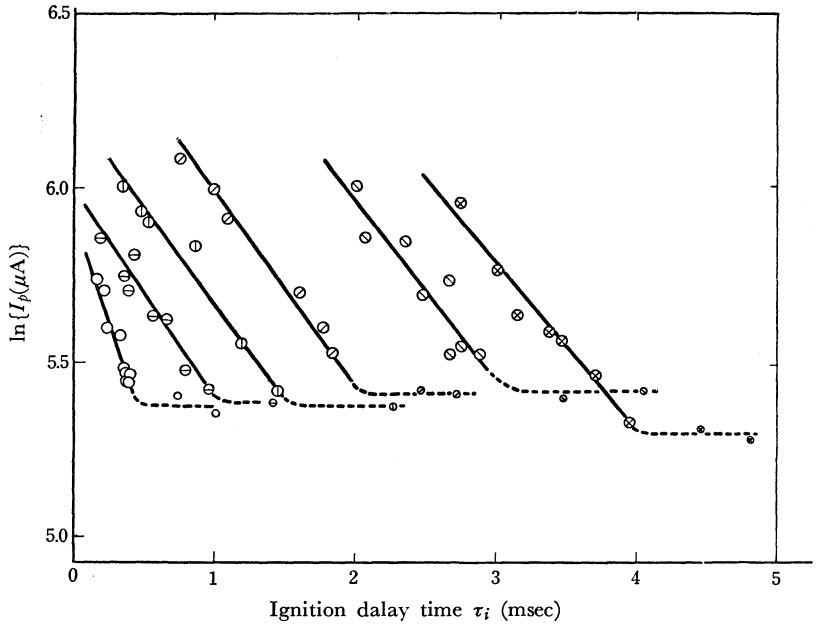

Fig. 3. Relation between ignition delay time and pulse current in helium diluent mixtures. Data points as in Fig. 2.

lines of the experimental results which are shown by the larger circles. The ignition delay time shows a linear relationship against the logarithm of the pulse current well above the threshold of the ignition, though the results most contiguous to the threshold manifest themselves in the longer delay time region, as are shown by the smaller circles.

The threshold pulse current value of the ignition in the helium diluent is of an order of magnitude higher than that in the argon diluent, while the threshold value in argon tends to decrease with an increase in the argon fraction; however, only the difference in the slopes of the solid lines in the argon diluent and the helium diluent will be discussed in the present paper.

To check indirectly whether or not any unexpected corona discharge occurred, electrodes, the outer surfaces and corners of which had been covered by paraffin wax, were tested. However, there was no significant difference in the experimental results between paraffin-coated and non-coated electrodes.

Two photomultiplier experiments, in which one of the photomultipliers was used for the observation of the outer side of the electrodes, and the other, for the inside, were conducted. It was confirmed that the ignition always started from the midst of the electrodes.

Discussion

In the course of the pre-induction period, where the silent electric discharge takes place, the chain-carrier radicals H, O, and OH, will be produced:

$$0)\quad H_2,\ O_2 \text{ and } M \xrightarrow{R_0} H,\ OH \text{ and } O$$

where R_0 denotes the rate of the formation of any specific chain-carrier radicals.

As far as the radical concentration at the termination of the discharge is concerned, the following two cases can be presumed as an approximation. If the discharge period, t, is long enough for the radicals to attain a saturated concentration through the discharge on condition that the forward rate is proportional to the pulse current[6,7] and that the decay of radicals is proportional to the concentration, then the radical concentration at the end of the discharge will be proportional to the pulse current. On the other hand, if the back reaction of decay of radicals can be ignored, then the radicals will accumulate through the discharge period, t, and the radical concentration at the end of the discharge will be proportional to $(R_0 \times t)$ or to the pulse current multiplied by t. However, under the present experimental conditions, the discharge period, t, was independent of the pulse current, as was stated formerly; therefore, the radical concentration at the end of the discharge will again be proportional to the pulse current.

Accordingly, we can estimate that the radical concentration at the end of the discharge is proportional to the pulse current, or:

$$[H]_0 \propto [O]_0 \propto [OH]_0 \propto I_p \qquad (1)$$

After the termination of the discharge, the reaction profile will be analogous to the shock-initiated induction-period reaction starting from the above radical concentration.

The elementary reaction in the hydrogen and oxygen system which should govern the induction period would appear to be the bimolecular reaction among H, O, OH, H_2 and O_2 and the three-body radical recombination reaction. However, in the present case we disregard the mutual reaction among H, O and OH because the concentrations of such species will be very low compared to those of hydrogen and oxygen during the induction period. Accordingly, we assume the following reaction scheme[8,9]:

$$1)\quad H + O_2 \xrightarrow{k_1} OH + O$$

$$2)\quad O + H_2 \xrightarrow{k_2} OH + H$$

$$3)\quad OH + H_2 \xrightarrow{k_3} H_2O + H$$

$$4)\quad H + O_2 + M \xrightarrow{k_4} HO_2 + M$$

Miyama and Takeyama[9] found that the gas-phase reaction of HO_2 came to play an important role in a low-temperature and high-pressure regime shock wave experiment. The fate of HO_2, which should be taken into consideration in the present experimental environment, will be:

$$5)\quad HO_2 + H_2 \xrightarrow{k_5} H_2O_2 + H$$

$$6)\quad HO_2 \xrightarrow[\text{wall}]{K_6} \text{destruction}$$

where K_6 is a function of the electrode dimensions, the diffusion coefficient, and the chain-breaking efficiency.

The steady-state assumptions for the O, OH, and HO_2 radicals will lead to the equation:

$$[H] = [H]_0 \exp[\{2k_1 - k_4[M]K_6/(K_6 + k_5[H_2])\}[O_2]\tau] \qquad (2)$$

and finally to:

$$[OH] = [OH]_0 \exp[\{2k_1 - k_4[M]K_6/(K_6 + k_5[H_2])\}[O_2]\tau] \qquad (3)$$

where the origin of time, τ, should coincide with the termination of the discharge and where $[H]_0$ and $[OH]_0$ are the concentrations of H and OH at $\tau = 0$. We had adopted the rise of OH emission to a definite value as to be used for a cut off point of the ignition delay time, τ_i.

8) G. L. Schott and J. L. Kinsey, *J. Chem. Phys.*, **29**, 1177 (1958).

9) H. Miyama and T. Takeyama, *ibid.*, **41**, 2287 (1964).

Belles and Lauver[10] referred to the possibility of using the emitted light as an indication of the progress of the main reaction to allow quantitative comparisons to be made between the induction times measured by following the concentration of the ground state OH(Π) with absorption spectroscopy and those measured by the easier method of observing the emitted light, regarding OH(Σ) as having been formed in the monoradical reaction: $H+O_2+H_2 \rightarrow H_2O+OH(\Sigma)$. Accordingly, we assumed that the ignition delay time, τ_i, was approximately the time interval between two cuts, namely, the termination of the discharge and the rise of OH(Π) radicals to a certain definite value of $[OH]_i$, though our recent shock-wave studies of the emission of OH($\Sigma-\Pi$)[11] ascribed the chemical excitation of OH(Σ) to the biradical reaction of $H+O+M \rightarrow OH(\Sigma)+M$.

Then:

$$[OH]_i = [OH]_0 \exp[\{2k_1-k_4[M]K_6/(K_6+k_5[H_2])\}[O_2]\tau_i] \quad (4)$$

Equations (1) and (4) lead to:

$$-\log(I_p) = \{2k_1-k_4[M]K_6/(K_6+k_5[H_2])\}[O_2]\tau_i+C \quad (5)$$

provided $[OH]_i$ is a certain definite value. The above relation can represent the experimental results of linear relationship between $\log(I_p)$ *vs.* τ_i.

The values of $2k_1-k_4[M]\times F$ which were obtained from the slopes of the least-square lines in Figs. 2 and 3 are listed on Table 1, where F is the abbreviation of the factor $K_6/(K_6+k_5[H_2])$. The difference between columns 2 and 3 on the same line of Table 1 can be expressed by: $([M]^{Ar}_{He}-[M]^{Ar}_{Ar})k^{Ar}_4\times F$, where $[M]^{Ar}_{Ar}$ and $[M]^{Ar}_{He}$ denote the third-body concentration of the two mixtures. The coefficients of the third-body ability of gas molecules on the reaction 4) had been established through experiments on the second explosion limit of hydrogen and oxygen. The coefficients of argon, helium, and oxygen, in comparison with that of hydrogen, are 0.20, 0.36 and 0.35 respectively.[12] If the coefficient of argon is taken to be unity, the coefficients of helium, hydrogen, and oxygen are 1.80, 5.00, and 1.75. The superscript Ar in the above expression denotes that the coefficient for the third-body ability of argon is taken to be unity.

Table 1. The values for $2k_1-k_4[M]\times F$ obtained from the slopes of the least square lines in Figs. 2 and 3

Diluent composition %	$2k_1-k_4^{Ar}[M]^{Ar}_{Ar}\times F$ (Ar diluent) ($sec^{-1}\,mol^{-1}\,l$)	$2k_1-k_4^{Ar}[M]^{Ar}_{He}\times F$ (He diluent) ($sec^{-1}\,mol^{-1}\,l$)
5	1.84×10^5	2.60×10^5
15	1.86×10^5	1.47×10^5
25	1.90×10^5	1.58×10^5
35	1.91×10^5	1.63×10^5
45	2.15×10^5	1.96×10^5
55	2.51×10^5	2.30×10^5

$F = K_6/(K_6+k_5[H_2])$

Reactant in the mixture is stoichiometric mixture of hydrogen and oxygen.

$[M]^{Ar}_{Ar}$, $[M]^{Ar}_{He}$: Third body concentration for reaction 4), of the mixtures with argon diluent and helium diluent. Superscript Ar denotes the third body ability of argon being stood for standard to express the third body concentration and the rate for reaction 4).

The test gas of a definite diluent composition contained a definite amount of a stoichiometric mixture of hydrogen and oxygen, and the features of the reaction may be expected to be essentially the same in both the argon-diluent and helium-diluent mixtures, and so $[M]^{Ar}_{He}-[M]^{Ar}_{Ar}$ can be attributed solely to the difference in the third-body efficiency of the diluent gases, argon and helium, or:

$$[M]^{Ar}_{He} - [M]^{Ar}_{Ar} = (1.8-1.0)[M]_0 f_{diluent}$$

where $f_{diluent}$ denotes the mole fraction of the diluent gas. The ignition took place in a constant volume system, and $[M]_0$ is obtainable assuming a negligible depletion of the reactant during the induction period. Thus, the values for $k^{Ar}_4\times F$ were derived from a comparison of the experimental results in columns 2 and 3 in Table 1 without any further assumptions.

The values for k_1 could also be derived from the values of column 2 and/or column 3 in Table 1 and the known $k^{Ar}_4\times F$ values, assuming the value for the third-body concentration $[M]^{Ar}_{Ar}$ and/or the concentration $[M]^{Ar}_{He}$, of the mixtures. In the course of the induction period the contribution of water to the reaction 4) is of no consequence, though its third-body ability is quite large.[12] The contribution of other intermediate species can reasonably be ignored. The third-body concentration for the mixture with the argon diluent will then be:

$$[M]^{Ar}_{Ar} = [M]_0(f_{Ar} + 5.00f_{H_2} + 1.75f_{O_2})$$

while for the mixture with the helium diluent it will be:

$$[M]^{Ar}_{He} = [M]_0(1.80f_{He} + 5.00f_{H_2} + 1.75f_{O_2})$$

where f_{Ar}, f_{He}, f_{H_2}, and f_{O_2} are the mole fractions of the subscribed gases. The values for k_1 thus derived from the experimental results are listed on

10) F. E. Belles and M. R. Lauver, *J. Chem. Phys.*, **40**, 415 (1964).

11) W. C. Gardiner, Jr., K. Morinaga, D. L. Ripley and T. Takeyama, Paper presented at the 6th International Shock Tube Symposium Freiburg Germany, April, 1967; Paper presented at the 21st Annual Meeting of the Chemical Society of Japan, Osaka, April, 1968.

12) B. Lewis and G. von Elbe, "Combustion, Flames and Explosions of Gases," 2nd Edition, Academic Press, New York and London (1961), p. 29.

Table 2. Derived values of k_1, F and k_5/K_6 at induction period

Diluent composition, %	k_1 ($sec^{-1} mol^{-1} l$)	F	k_5/K_6 ($mol^{-1} l$)
5	—	—	—
15	6.60×10^5	1.39×10^{-2}	0.89×10^4
25	3.50×10^5	0.68×10^{-2}	2.08×10^4
35	2.41×10^5	0.42×10^{-2}	3.85×10^4
45	1.76×10^5	0.22×10^{-2}	8.70×10^4
55	1.81×10^5	0.20×10^{-2}	10.65×10^4

Table 2.

The factor F represents the fraction of atoms H which are destroyed by reacting through the reaction 4); concurrently it will show the net effect of the chain breaking in the reaction 4). The estimation of F was made by assuming the value of k_4^{Ar} in the induction period. The activation energy for the reaction 4) is a small, negative value, and the k_4^{Ar} value in the induction period can be reasonably assumed from a literature expression available elsewhere[13] if we know the approximate temperature during the induction period. An attempt was made to assume the value for k_4^{Ar} with regard to the threshold temperature. The expressions[14] for k_1 and k_4^{Ar} which were used for the estimation of the threshold temperature were $k_1=10^{11.313}\exp(-16490/\boldsymbol{R}T)$ and $k_4^{Ar}=8.6\times10^8\exp(+1280/\boldsymbol{R}T)$, while the threshold expression used was $2k_1=k_4^{Ar}[M]^{Ar}$.

The values for F thus estimated and the values for k_5/K_6 reduced from F are listed on Table 2. The values for F which appear in the table are considerably smaller than unity, signifying that the reaction 5) is predominant over the reaction 6). Miyama and Takeyama[9] have shown that the reaction 5) became significant in reproducing chain carrier radicals in low-temperature, high-pressure regime shock wave experiments. These results as well as ours possibly suggest that chain-carrier reproduction from HO_2 is predominant over the surface destruction of HO_2 under our experimental conditions.

The values for k_1 in Table 2 obtained from the experimental results resembled the literature value[14] in the temperature range between the initial temperature and the second explosion-limit temperature. Due to the small value of F, the net effect of the chain-breaking reaction 4) becomes insignificant; the accumulation of radicals might be persistent resulting in the actuation of ignition even in the temperature range where the k_1 value was observed not to be above the value of $k_4^{Ar}[M]^{Ar}/2$. Fujimoto[15] had provided experimental evidence that in his reflected shock wave ignition, the ignition took place under the threshold temperature.

The variation in values for k_1 and k_5/K_6 in Table 2 is difficult to elucidate quantitatively because of a lack of experimental evidence about the induction-period temperature, which requires a more detailed investigation.

Summary

The induction-period reaction of silent discharge ignition in a hydrogen and oxygen system appears to be analogous to the shock-initiated reaction in a low-temperature high-pressure regime. The reaction in the discharge period may be likened to the 0th. reaction of shock-wave ignition. By comparing the argon diluent and the helium diluent systems, the net effect of chain breaking through the reaction 4) was estimated.

13) G. L. Schott and P. F. Bird, *J. Chem. Phys.*, **41**, 2869 (1964); R. W. Getzinger and G. L. Schott, *ibid.*, **43**, 3237 (1965); D. Gutman, E. A. Hardwidge, F. A. Dougherty and R. W. Lutz, *ibid.*, **47**, 4400 (1967).

14) W. C. Gardiner, Jr., K. Morinaga, D. L. Ripley and T. Takeyama, *ibid.* **48**, 1665 (1968).

15) S. Fujimoto, This Bulletin, **36**, 1233 (1963).

BULLETIN OF THE CHEMICAL SOCIETY OF JAPAN VOL. 42 2112—2119 (1969)

Theory of the Gel-forming Polymerization of Polyepoxy and Related Compounds

Tokio YAMABE and Kenichi FUKUI

Faculty of Engineering, Kyoto University, Sakyo-ku, Kyoto

(Received November 29, 1968)

A theory of the molecular-size distribution of cross-linked polymers to be formed from a mixture of polyfunctional monomers and mono-functional monomers through step-by-step polymerizations by certain initiators is presented on the assumption that all unconverted functional groups are equireactive for both initiations and propagations, which proceed without termination, transfer, or cyclization. The distribution is obtained by applying the statistical theory of gel formation with multifunctional interunit junctions, which are, in this case, equivalent to cross-linking chains. Some noticeable theoretical results are obtained: (1) the distribution obtained is quite different from that obtained for branched-chain polymers by condensation polymerization; (2) the fraction of converted functional groups at the gel point is independent of the initial concentration of the monofunctional monomer, while it is in proportion to the ratio of the initial concentration of the initiator to that of polyfunctional monomers; (3) there is a certain condition under which the gelation will never take place, even at complete conversion, and (4) the state to be reached after the gel point is quite different from the results obtained previously. The case of a mixture of monomers with any distribution of functionalities is also briefly presented. An explanation of the validity of the distribution beyond the gel point is discussed in the Appendix.

It happens that, in certain step-by-step polymerizations, the chain-initiation and the subsequent addition proceed with comparable velocities, without either termination or transfer. Such is the case in some ring-opening polymerizations of cyclic compounds, such as epoxy, cyclic imino, amide, or anhydride compounds, or in some anionic polymerizations of vinyl compounds.*1

The molecular-size distribution of linear polymers obtained from a monofunctional monomer such as ethylene oxide through the step-by-step polymerization was first given by Flory,[1] while the distribution of cross-linked polymers formed from f-functional monomers ($f \geqq 1$) was reported in our own previous paper.[2] Both were obtained by solving kinetic equations describing the polymerization processes.

In the present paper, a theory of the molecular-size distribution of cross-linked polymers to be formed from a mixture of polyfunctional and monofunctional monomers is presented. By this theory, one can sufficiently explain the characteristic features of such a polymerization process without any loss of generality. The condition for the gelation and the property of the sol fraction after the gel point are also investigated. In the last portion of this text, the case of a mixture of polyfunctional monomers with any distribution of their functionality is treated.

The distribution was obtained, not by solving the kinetic equations as in the previous paper, but by applying the statistical theory of polymerization with multifunctional interunit junctions.[3] A chain to be cross-linked may reasonably be regarded as a kind of interunit junction, as was treated previously.[3] With this idea, which is the essential point of the present paper, we are able to obtain the exact product distribution for the step-by-step polymerization process.

Let us treat first a mixture of f-functional monomers and monofunctional monomers, and then a mixture of monomers of various functionalities. The former and the latter are referred to as Case I and Case II respectively.

Case I. A System Composed of f-Functional and Monofunctional Monomers

Molecular-size Distribution. It should be remarked at the outset that the treatment presented below is applicable to all polymerization processes of this kind which fulfill the following assumptions, already set up in the previous paper:[2] (1) Each polyfunctional monomer possesses f identical

*1 For instance, see F. W. Billmeyer, Jr., "Textbook of Polymer Science," Interscience, New York (1962).

1) P. J. Flory, "Principles of Polymer Chemistry," Cornell Univ. Press, Ithaca, New York (1953).

2) K. Fukui and T. Yamabe, *J. Polymer Sci.*, **A2**, 3743 (1964).

3) K. Fukui and T. Yamabe, This Bulletin, **40**, 2052 (1967).

functional groups, and all unconverted functional groups on the monomers or polymers are equivalent and of the same reactivity. (2) Any unconverted functional group can react with the initiator to be changed into a growing chain, and the rate of the initiating step is equal to that of the subsequent addition step. (3) Moreover, reactions proceed without either termination or transfer. Therefore, the number of growing chains is equal to the number of initiators consumed. (4) No formation of rings, not even of the small ones formed by intra-inter polymerization, occurs through the process of polymerization.

Suitable examples may be supplied from the polymerizations of polyepoxides initiated by some hydroxy compounds or secondary amines, or catalyzed by some tertiary amines or boron trifluoride complexes.[4,5] Another ideal case may be realized in the anionic polymerization of some polyvinyl compounds by sodium.[6]

Under these assumptions, a polymeric molecule is composed of various lengths of growing chains. This may be visualized by the following scheme, in which the example taken is the ring-opening copolymerization of monoepoxide, Y–CH(–O–)–CH_2, and diepoxide, CH_2(–O–)–CH–Z–CH(–O–)–CH_2, where RI is the initiator and where Y and Z designate the residues of monoepoxide and diepoxide respectively:

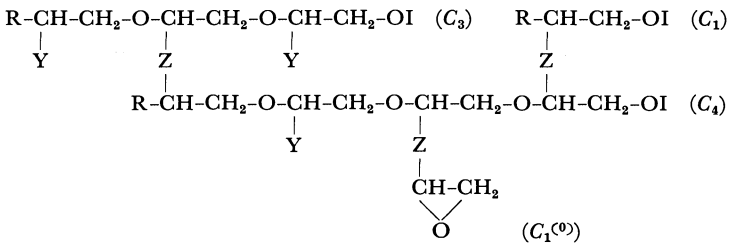

In this schematic presentation, C_k and $C_1^{(0)}$ stand for a growing chain containing k functional groups and an unconverted functional group respectively. The polymeric molecule can be described, therefore, by specifying the length of each growing chain, that is, the number of functional groups involved in it, if any further difference in the structure of the polymeric molecule is disregarded.

On the other hand, a previous paper[3] has treated, in general, the case where the polymerization proceeds with various kinds of interunit junctions being concurrently formed in a system. Here the term "interunit junction" indicates a junction connecting several functional groups, each in different monomeric units, irrespective of the order of combination. According to the number of functional groups involved in one interunit junction formed, they are named as mono-, bi-, ter-, ..., and, more generally, multifunctional interunit junctions. Following this definition, a growing chain composed of k functional units is a k-functional interunit junction.

Moreover, it should be noted here that there are two kinds of monofunctional interunit junctions. The one is apparently a growing chain produced from a functional group indicated by C_1, and the other is that of an unconverted functional group indicated by $C_1^{(0)}$ in the sense of the scheme mentioned above. In this fashion the molecular-size distribution of the polymerization of polyfunctional epoxy or vinyl compounds can be obtained exactly, as long as the polymerization satisfies the conditions already assumed.

Now, let I_0, N_1, and N_f be the numbers of initially-existing initiators, monofunctional monomers, and f-functional monomers respectively, in a system and let $M(n_1, n_f; \nu)$ be the number of polymeric molecules containing ν growing chains, n_1 monofunctional monomers, and n_f f-functional monomers.

Then, as the polymeric molecule has ν growing chains, it contains $(n_1+n_f+\nu-1)$ units of converted functional groups and, hence, $\{(f-1)n_f-\nu+1\}$ unconverted functional groups, since intramolecular reactions are excluded. According to this definition, $M(0, 0; 1)$, $M(1, 0; 0)$, and $M(0, 1; 0)$ represent the instantaneous values of the numbers of initiators, monofunctional monomers, and f-functional monomers respectively.

From the above definitions, we obtain:

$$I_0 = \sum M(n_1, n_f; \nu) \quad (1)$$

$$N_1 = \sum n_1 M(n_1, n_f; \nu) \quad (2)$$

$$N_f = \sum n_f M(n_1, n_f; \nu) \quad (3)$$

where the summation should cover all the integers of n_1, n_f, and ν satisfying $(f-1)n_f+1 \geqq \nu \geqq 0$.

Moreover, if we denote the total number of molecules at the initial state and at a given instant by M_0 and M, respectively, these can be obtained

4) H. Lee and K. Neville, "Epoxy Resin," McGraw Hill Book Co., New York (1957).

5) I. Skeist, "Epoxy Resins," Reinhold Publishing Co., New York (1958).

6) M. Szwarc, M. Levy and R. Milkovitch, *J. Am. Chem. Soc.*, **78**, 2656 (1956); R. Waack, A. Rembaum, J. D. Coombes and M. Szwarc, *ibid.*, **79**, 2026 (1957).

as follows:

$$M = \sum M(n_1, n_f; \nu) \tag{4}$$

$$M_0 = I_0 + N_1 + N_f = \sum (\nu + n_1 + n_f) M(n_1, n_f; \nu) \tag{5}$$

In order to formulate the molecular-size distribution, it is convenient to introduce two variables, α and ρ, in such a way as:

$$\alpha = F/I_0 \tag{6}$$

$$\rho = (1/F)\sum (n_1 + n_f + \nu - 1) M(n_1, n_f; \nu) = (M_0 - M)/F \tag{7}$$

where α stands for the initial number of functional groups per initiator, where ρ is the fraction of converted functional groups, and where $F = N_1 + fN_f$ is the total number of functional groups in the system.

Now let us attempt to obtain the distribution by the use of the statistical theory of polymerization with multifunctional interunit junctions previously proposed by the present authors.[3]

Let $m(n_1, n_f; \{j_k\})$ be the number of polymeric molecules which are composed of n_1 monofunctional monomeric units and n_f f-functional monomereric units and are also constructed by j_1 monofunctional, j_2 bifunctional, $\cdots$, j_k k-functional chains. The set of these numbers is designated as $\{j_k\}$. In particular, the number of unconverted functional groups is written as $j_1^{(0)}$. Also, we designate the probabilities that a functional group is involved in the growing chain composed of k functional chains ($k \geqq 1$) and in that of unconverted ones as P_k and $P_1^{(0)}$ respectively. It obviously follows that:

$$P_1^{(0)} + \sum_{k=1} P_k = 1 \tag{8}$$

According to Eq. (48) in Ref. 3, the most probable distribution of $m(n_1, n_f; \{j_k\})$ in equilibrium is given by:

$$m(n_1, n_f; \{j_k\}) = (N_1 + fN_f)((f-1)n_f)!(n_1 + n_f - 1)! \frac{w_1^{n_1}}{n_1!} \cdot \frac{w_f^{n_f}}{n_f!} \cdot \frac{P^{j_1^{(0)}}}{j_1^{(0)}} \cdot \prod_{k \geqq 1} \frac{P_k^{j_k}}{j_k!} \tag{9}$$

with these conditions:

$$j_1^{(0)} + \sum_k j_k - 1 = (f-1)n_f \tag{10}$$

and:

$$n_1 + n_f - 1 = \sum_k (k-1) j_k \tag{11}$$

where w_1 and $w_f (= 1 - w_1)$ are the weight fractions of monofunctional monomers and f-functional monomers respectively; namely,

$$w_1 = N_1/(N_1 + fN_f), \qquad w_f = fN_f/(N_1 + fN_f) \tag{12}$$

In the step-by-step polymerization, the number of growing chains composed of k functional groups, which is denoted hereafter by J_k, was given by Flory[7] as follows:

$$J_k = \frac{\lambda^k e^{-\lambda}}{k!} I_0 \qquad (k \geqq 1) \tag{13}$$

$$J_1^{(0)} = I_0 e^{-\lambda}$$

The probability of the formation of a k-functional interunit junction, P_k, is then given, according to the definition, by:

$$P_k = \frac{kJ_k}{F} = \frac{I_0}{F} \cdot \frac{\lambda^{k-1} e^{-\lambda}}{(k-1)!} \tag{14}$$

Therefore, the fraction of converted functional groups, ρ, is represented by the following relation:

$$\rho = \sum_{k \geqq 1} P_k = \frac{\lambda I_0}{F} \sum_{k \geqq 1} \frac{\lambda^{k-1} e^{-\lambda}}{(k-1)!} = \frac{\lambda I_0}{F} = \frac{\lambda}{\alpha}$$

which endows the $\lambda (= \alpha\rho)$ of Eq. (13) with the physical meaning as the mean length of a growing chain (see Eq. (25)). Then, the fraction of unconverted functional groups, $P_1^{(0)}$, is given by:

$$P_1^{(0)} = 1 - \sum_{k \geqq 1} P_k = 1 - \rho \tag{16}$$

By the use of these equations, the distribution, $m(n_1, n_f; \{j_k\})$, may be rewritten as follows:

$$m(n_1, n_f; \{j_k\}) = F \cdot \frac{(fn_f - n_f)!(n_1 + n_f - 1)!}{(fn_f - n_f + 1 - \sum_{k \geqq 1} j_k)!} \cdot \frac{w_1^{n_1}}{n_1!} \cdot \frac{w_f^{n_f}}{n_f!} \cdot \prod_k \frac{1}{j_k!((k-1)!)^{j_k}}$$

$$\times (1-\rho)^{fn_f - n_f + 1 - \sum_k j_k} \cdot \rho^{\sum_k j_k + n_1 + n_f - 1} \cdot e^{-(\sum_k j_k)\alpha\rho} \tag{9'}$$

According to the definition of $M(n_1, n_f; \nu)$ it is obvious that;

$$M(n_1, n_f; \nu) = \sum_{\sum_k j_k = \nu} m(n_1, n_f; \{j_k\}) \tag{17}$$

7) P. J. Flory, *J. Am. Chem. Soc.*, **62**, 1561 (1940).

where summation should cover all sets of positive integers (zero included), j_k, which satisfy the condition: $\sum_k j_k = \nu$.

On the other hand, the following mathematical relation is necessary in calculating the summation in Eq. (17):

$$\sum_{\sum_k j_k=\nu} \frac{(\sum j_k)!}{\prod_k j_k![(k-1)!]^{j_k}} = \left[\text{the coefficient of } Z^{\sum_k (k-1)j_k} \text{ in the expantion of } \left(\sum_{k\geqq 1}^{\infty} \frac{Z^{k-1}}{(k-1)!}\right)^{\sum_k j_k}\right]$$

$$= \frac{\nu^{\sum_k (k-1)j_k}}{(\sum_k (k-1)j_k)!} = \frac{\nu^{n_1+n_f-1}}{(n_1+n_f-1)!} \tag{18}$$

Using this relation, we finally obtain the size distribution as follows:

$$M(n_1,\ n_f;\ \nu) = (N_1+fN_f)\frac{(fn_f-n_f)!\,\nu^{n_1+n_f-1}}{(fn_f-n_f+1-\nu)!\,\nu!} \cdot \frac{{w_1}^{n_1}}{n_1!} \cdot \frac{{w_f}^{n_f}}{n_f!} \rho^{\nu}(1-\rho)^{(f-1)n_f+1-\nu}(\alpha\rho)^{n_1+n_f-1} \cdot e^{-\nu\alpha\rho} \tag{17'}$$

The resulting distribution is, however, by no means restricted to the case of equilibrium system; it should be equally applicable to unidirectionally changing systems, as long as the assumptions mentioned above are fulfilled. This point is supported by the fact that the distribution given by Eq. (17') can equally be derived from differential equations describing the polymerization kinetics, although they are too complex. Also, the following fact helps the present discussion. The distribution for the special case in which only f-functional monomers are contained is reduced to the equation:

$$M(0,\ n_f;\ \nu) = \frac{(fN_f)(fn_f-n_f)!\,\nu^{n_f-1}}{\nu!\,(fn_f-n_f+1-\nu)!\,n_f!} \rho^{\nu}(1-\rho)^{(f-1)n_f+1-\nu}(\alpha\rho)^{n_f-1}e^{-\nu\alpha\rho}$$

which agrees with the distribution function of our previous paper[2] derived from the kinetic method.

The instantaneous values of the initiators, the monofunctional monomers, and the f-functional monomers may be presented, respectively, as:

$$M(0,\ 0;\ 1) = I = I_0e^{-\alpha} \tag{19}$$

$$M(1,\ 0;\ 0) = N_1(1-\rho) \tag{20}$$

$$M(0,\ 1;\ 0) = N_f(1-\rho)^f \tag{21}$$

The number and weight-average molecular sizes can readily be obtained as:

$$\langle P_n\rangle = 1 + \frac{f\rho}{1-f\rho-(1-\rho)^f+f/\alpha} \tag{22}$$

$$\langle P_w\rangle = 1 + \frac{(f/\alpha)[(\alpha\rho)^2+2\alpha\rho+(f-1)\alpha\rho^2]}{[1-(1-\rho)^f+f/\alpha][1-(f-1)\alpha\rho^2]} \tag{23}$$

Both the unconverted monomers and the initiators are excluded in these averages.

The number- and the weight-average chain lengths, $\langle k_n\rangle$, $\langle k_w\rangle$, of cross-linked polymers are easily obtained from Eq. (14) as:

$$\langle k_n\rangle = \sum_{k=1}^{\infty} P_k / \sum_{k=1}^{\infty} (P_k/k) = \lambda/(1-e^{-\lambda}) \tag{24}$$

$$\langle k_w\rangle = \sum_{k=1}^{\infty} kP_k / \sum_{k=1}^{\infty} P_k = 1+\lambda \tag{25}$$

where the unconverted functional groups and the initiators are not taken into account.

The Condition for Gelation. The critical condition determining the gel point can be characterized by the following equation, derived from Eqs. (6) and (23):

$$\rho_c = \left[\frac{I_0}{f(f-1)N_f}\right]^{1/2} \tag{26}$$

where ρ_c is the extent of reaction at the gel point. It is remarkable that ρ_c is dependent on the amount of initiators as well as on that of f-functional monomers, while it is independent of the amount of monofunctional monomers.

It should be noted here, however, that there exists a restriction for the attainment of the gel point. This comes from the condition $\rho \leqq 1$, which implies that the fraction of converted functional groups should be less than unity. Therefore, it is necessary, on the basis of Eq. (26), that:

$$f(f-1)N_f \geqq I_0 \tag{27}$$

for the attainment of the gel point. If the system is initially prepared, irrespective of the amount of the monofunctional monomer, in such a way that

$$I_0 > f(f-1)N_f \geqq 0 \tag{28}$$

the critical conversion, ρ_c, can never be reached at any extent of reaction. Such an amount of f-functional monomers compared with that of initiators is too small for the gelation to occur, so such a system will remain as a sol phase. The circumstance mentioned above may be clarified by information as to the number and the weight averages of chains in a mixture of polymeric molecules. Using Eq. (17'), we obtain the number-average number of chains, $\langle \nu_n\rangle$, which is usually called by the crosslinking index, γ:

$$\langle \nu_n\rangle = \frac{\sum \nu M(n_1, n_f; \nu)}{\sum M(n_1, n_f; \nu)} = \left[1 - \frac{N_f}{I_0}\left(\frac{(1-\rho)^f-(1-f\rho)}{1-e^{-\alpha\rho}}\right)\right]^{-1} \tag{29}$$

while the weight-average number of chains, $\langle \nu_w\rangle$, is written:

$$\langle \nu_w \rangle = \frac{\sum \nu(n_1+fn_f)M(n_1, n_f; \nu)}{\sum (n_1+fn_f)M(n_1, n_f; \nu)} = \frac{1+(f-1)w_f}{(1-w_f(f-1)\alpha\rho^2)(1-w_f(1-\rho)-w_f(1-\rho)^f)} \tag{30}$$

Therefore, the number-average number of chains at the gel point, $\langle \nu_n \rangle_c$, can be represented by:

$$\langle \nu_n \rangle_c \cong \left[\frac{1}{2}+\frac{(f-2)}{3!}\rho_c-\frac{(f-2)(f-3)}{4!}\rho_c^2+\cdots\right]^{-1} \tag{31}$$

where the term of $e^{-\alpha\rho}$ is neglected.

If the initial condition, namely, the N_f/I_0, ratio is varied within the range indicated by Eq. (27) within which the gelation occurs, ρ_c will change from zero to unity. Then we have:

$$2 \geqq \langle \nu_n \rangle \geqq \frac{f}{f-1} \tag{32}$$

which shows that in the N_1 - N_f system the cross-linking index at the gel point keeps the value between two and $f/(f-1)$ as long as the gelation takes place. On the other hand, $\langle \nu_w \rangle$ tends to become infinite as ρ nears ρ_c, irrespective of the functionality, f, of the polyfunctional monomer.

At complete conversion ($\rho=1$) without gelation, which is attained by means of Eq. (28), the number-average number of branches is:

$$\langle \nu_n \rangle_{\rho=1} = \frac{I_0}{I_0-N_f(f-1)} \tag{33}$$

while the weight-average number is:

$$\langle \nu_w \rangle_{\rho=1} = \frac{N_1+f^2N_f}{N_1+fN_f} \cdot \frac{I_0}{I_0-f(f-1)N_f} \tag{34}$$

The weight-average molecular size is a finite value, as is given by:

$$\langle P_w \rangle_{\rho=1} = \frac{N_1+f^2N_f}{N_1+fN_f} \cdot \frac{I_0+N_1+fN_f}{I_0-f(f-1)N_f} \tag{35}$$

Likewise, according to the variation in the initial ratio, N_f/I_0, in the range of Eq. (28), $\langle \nu_n \rangle_{\rho=1}$ and $\langle \nu_w \rangle_{\rho=1}$ vary in the ranges:

$$\frac{f}{f-1} > \langle \nu_n \rangle_{\rho=1} \geqq 1 \tag{36}$$

and

$$\infty > \langle \nu_w \rangle_{\rho=1} \geqq 1 \tag{37}$$

respectively.

The small average number of branches indicated by Eq. (36) implies that a small amount of the functional groups of the f-functional monomers specified by the condition of Eq. (28) is consumed by the reaction with the initiator, thus preventing the branching. The chains in polymeric monomers can grow longer and longer by means of the reaction with monofunctional monomers, without any branching in the polymeric molecules. In this way, the average length of a chain, given by Eq. (24), in polymeric molecules finally reaches $\alpha=F/I_0$ at complete conversion.

Furthermore, at a given value of F for a fixed value of I_0, the range of N_1, where the gelation does not occur at any extent of reaction, can be rewritten from Eq. (28) as:

$$F \geqq N_1 \geqq F - \frac{I_0}{f-1} \tag{28'}$$

This equation presents the amount of monofunctional monomers which may be present without causing gelation; it may have practical significance since this equation gives the experimental condition under which the polymerization of polyfunctional monomers might be carried out without gelation. The equation determining the gel point reported in a previous paper[2] is completely consistent with Eq. (26).

The situation is different in the corresponding case of the selfcondensation between f-functional and bi-functional monomers. The fraction of converted functional groups at the gel point, ρ_c in our notation, expressed by Flory[7] and Stockmayer[8] as:

$$\rho_c = \frac{1}{1+(f-2)w_f}$$

can never exceed unity, so the gelation always takes place at a certain conversion. Compared with this result, one can recognize that the present treatment indicates the importance of the amount of initiator for the condition of gelation.

Relationships after the Gel Point. This section will be devoted to a discussion of the sol fraction after the gel point has been reached. Our general theory, presented previously,[3] will be used here.

In the present case, the generating function, $f(x)$, defined by Eq. (15) in Ref. 3 is expressed as follows:

$$f(x) = w_1 + w_f u^{f-1} \tag{38}$$

where:

$$u(x) = P_1^{(0)} + \sum_{k=1} P_k x^{k-1} \tag{39}$$

or, by the use of Eq. (14):

$$u(x) = 1 - \rho + \rho e^{-(1-x)\lambda} \tag{39'}$$

The characteristic equation defined by Eq. (26) in Ref. 3 can be readily obtained from Eqs. (38) and (39') as:

$$x = f(x) = w_1 + w_f\{1-\rho+\rho e^{-(1-x)\lambda}\}^{f-1} \tag{40}$$

It was proved also in Ref. 3 that, besides the trivial solution $x=1$, there exists another real positive root, $x_1<1$, of Eq. (38) beyond the gel point ($(f-1)\alpha^2>1$). In general, the root is obtained only by numerical methods except in a few special cases.

With this root, x_1, the sol fractions of the mono- and the f-functional monomers, $w_1^{(s)}$ and $w_f^{(s)}$,

8) W. H. Stockmayer, *J. Chem. Phys.*, **11**, 45 (1943).

are obtained as, respectively (see Eq. (25) in Ref. 3):

$$w_1^{(s)} = w_1 u_1 \tag{41}$$

$$w_f^{(s)} = w_f u_1^f \tag{42}$$

where $u_1 = u(x_1)$.

The total sol fraction, W_{sol}, is then given by:

$$W_{sol} = w_1^{(s)} + w_f^{(s)} = x_1\{1 - \rho + \rho e^{-(1-x_1)\lambda}\} \tag{43}$$

The soluble part, $P_k^{(s)}$, of the weight fraction of C_k-chains is given by:

$$P_k^{(s)} = P_k x_1^k \tag{44}$$

$${}^{(s)}P_1^{(0)} = P_1^{(0)} x_1 \tag{45}$$ *2

By the use of Eqs. (42) and (43), the probability, $P_k'^{(s)}$, of forming a C_k-chain in the sol phase is obtained as:

$$P_k'^{(s)} = P_k^{(s)}/W_{sol} = P_k x_1^k / W_{sol} \tag{46}$$

The number- and the weight-average lengths of the chains in the sol phase are expressed as follows:

$$\langle k_n \rangle^{(sol)} = \sum_{k=1}^{\infty} P_k'^{(s)} / \sum_{k=1}^{\infty} (P_k'^{(s)}/k) = \frac{x_1\lambda}{e^{-\lambda}(e^{x_1\lambda} - 1)} \tag{47}$$

$$\langle k_w \rangle^{(sol)} = \sum_{k=1}^{\infty} k P_k'^{(s)} / \sum_{k=1}^{\infty} P_k'^{(s)} = (1+\lambda x_1) e^{-(1-x_1)\lambda} \tag{48}$$

Equations (47) and (48) show that the average chain length varies with the progress of the reaction after the gel point.

Likewise, the fraction, ρ', of converted functional groups in the sol phase is:

$$\rho' = \sum_{k=1}^{\infty} P_k'^{(s)} = \frac{\rho e^{-(1-x_1)\lambda}}{1 - \rho + \rho e^{-(1-x_1)\lambda}} \tag{49}$$

The quantities of the gel phase are then obtained by their differences from the totals, namely:

$$\left.\begin{aligned} w_f^{(g)} &= w_f - w_f^{(s)} = w_f(1 - u_1^f) \\ w_1^{(g)} &= w_1 - w_1^{(s)} = w_1(1 - u_1) \\ W_{gel} &= 1 - W_{sol} = w_1^{(g)} + w_f^{(g)} \end{aligned}\right\} \tag{50}$$

Similarly, we get:

$$\left.\begin{aligned} P_k^{(g)} &= P_k - P_k^{(s)} = P_k(1 - x_1^k) \\ {}^{(g)}P_1^{(0)} &= P_1^{(0)} - {}^{(s)}P_1^{(0)} = P_1^{(0)}(1 - x_1) \end{aligned}\right\} \tag{51}$$

and, hence:

$$\left.\begin{aligned} P_k'^{(g)} &= P_k^{(g)}/W_{gel} \\ {}^{(g)}P_1'^{(0)} &= {}^{(g)}P_1^{(0)}/W_{gel} \end{aligned}\right\} \tag{52}$$

The fraction, ρ'', of converted functional groups in the gel phase is obtained from Eq. (52) as follows:

$$\rho'' = \sum_{k=1}^{\infty} P_k'^{(g)} = \frac{\rho(1 - x_1 e^{-(1-x_1)\lambda})}{(1-x_1) + \rho x_1(1 - e^{-(1-x_1)\lambda})} \tag{53}$$

The weight-average chain length $\langle k_w \rangle^{(gel)}$ forming the gel phase is presented from Eq. (52):

$$\langle k_w \rangle^{(gel)} = \frac{\sum_{k=1}^{\infty} k P_k^{(g)}}{\sum_{k=1}^{\infty} P_k^{(g)}} = \frac{(1+\lambda) - x_1(1+x_1\lambda)e^{-(1-x_1)\lambda}}{1 - x_1 e} \tag{54}$$

Especially, at the instant immediately after the gel point, *i. e.*, at the point where:

$$\rho = \rho_c + \Delta\rho \tag{55}$$

x_1 and u_1 are approximated to the first order of $\Delta\rho$ as follows:

$$x_1 \cong 1 - \frac{4(f-1)w_f}{1 + (f-2)\rho_c}\Delta\rho \tag{56}$$

$$u_1 \cong 1 - \frac{4}{1 + (f-2)\rho_c}\Delta\rho \tag{57}$$

With these values of x_1 and u_1, all the quantities expressed in Eqs. (41) to (54) may be approximated in explicit forms as functions of $\Delta\rho$. For example,

$$W_{gel} \cong \frac{4(w_1 + f w_f)}{1 + (f-2)\rho_c}\Delta\rho \tag{50'}$$

$$\rho'' \cong \frac{1 + (f-1)w_f\rho_c}{1 + (f-1)w_f} + \frac{(f-1)w_f\{2 - (2f-5)\rho_c + (f-6)\rho_c^2\}}{(1 - (f-1)w_f)(1 + (f-2)\rho_c)}\Delta\rho \tag{53'}$$

$$\langle k_w \rangle^{(gel)} \cong 1 + \alpha\rho_c + \frac{\alpha\rho_c}{1 + \alpha\rho_c} - \frac{\alpha}{2}(\alpha\rho_c + 2)(\alpha\rho_c - 1)\Delta\rho \tag{54'}$$

At the gel point, $\Delta\rho \to 0$, both ρ'' and $\langle k_w \rangle^{(gel)}$ have finite values, indicated by the first terms of Eqs (53') and (54').

Case II. A Mixture of Monomers of Various Functionalities

Molecular-size Distribution. Here let us consider briefly the system of a mixture of polyfunctional monomers with different numbers of equivalent functional groups; say, N_1 monofunctional, N_2 bifunctional, $\cdots$, and N_s s-functional monomers.

With the same treatment as in Case I, we can obtain the molecular size distribution of the copolymers formed under the same assumptions:

$$M(n_1, n_2, \cdots, n_s; \nu) = \frac{(\sum_s (s-1)n_s)!\, \nu^{\sum_s n_s - 1}}{(\sum_s s N_s)\, \nu!\, (\sum_s (s-1)n_s + 1 - \nu)!} \cdot \Pi \frac{w_s^{n_s}}{n_s!} \times \rho^{\nu}(1-\rho)^{\sum_s (s-1)n_s + 1 - \nu} \cdot (\alpha\rho)^{\sum_s n_s - 1} \cdot e^{-\nu\alpha\rho} \tag{58}$$

where:

*2 Only for $P_1^{(0)}$, the suffixes (s) and (g), indicating the soluble part and the gel respectively, are hereafter replaced by ${}^{(s)}P_1^{(0)}$ to avoid confusion.

$$w_s = \frac{sN_s}{\sum_s sN_s}, \quad \text{and} \quad \alpha = \frac{\sum_s sN_s}{I_0}$$

The fraction of converted functional groups at the gel point, ρ_c, is given by:

$$\rho_c = \sqrt{\frac{I_0}{\sum_s s(s-1)N_s}} \tag{59}$$

The sol fraction, W_{sol}, is represented by:

$$W_{sol} = \sum_{f=1}^{s} w_f u_1^f \tag{60}$$

where x_1 in Eq (39') defining u_1 is, instead, the lowest positive root of the following equation:

$$x = \sum_{f=1}^{s} w_f x^{f-1} \tag{61}$$

The other relationships after the gel point may be obtained in a similar fashion.

Discussion

First let us discuss the noticeable theoretical finding of Eq. (26), the finding that the fraction of converted functional groups at the gel point depends on the concentration of the initiator or the catalyst.

In the case of the polycondensation of polyfunctional monomers (and, hence, in the case of the radical polymerization of divinyl compounds, which has been considered by Flory and Stockmayer to be equivalent to the case of the self-condensation of tetrafunctional monomers), such a dependency on the initiator has been out of question from the theoretical point of view. Some experimental results show, however, in a few polymerizations of divinyl compounds[9] or diepoxy compounds,[10] a dependency of ρ_c on the initiator concentration which has been confirmed by a careful reinvestigation. For example, Kakurai and Noguchi[10] reported on the curing process of diepoxide (Epon 828) with tertiary amine, where the assumptions set up in the present theoretical treatment seemed to be roughly fulfilled. In their case, they found that $\rho_c=0.5$, independent of the amount of the catalyst employed, using a complicated treatment based on Flory's expectation method; they concluded, from Fig. 1, that this value agreed with the actual observations. Figure 1 seems to show, however, that in fact ρ_c depends upon the amount of the catalyst. If so, it may be of interest to reanalyze these results by means of the present theory, which requires that $\rho_c=1/\sqrt{\alpha}$. The theoretical gel points indicated in Fig. 1 appear to explain

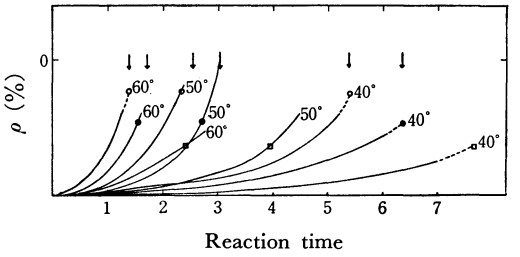

Fig. 1. The comparison between the total gel point (ρ_c) and the experimental ones obtained by Kakurai and Noguchi (from Fig. 4 in Ref. 10).
Theoretical gel points: ○ ($\alpha=7$, $\rho_c=0.37$), ● ($\alpha=14$, $\rho_c=0.28$), □ ($\alpha=28$, $\rho_c=0.18$)
Observed gelation time: ↓ (dotted lines are extrapolated by present authors)

the observed gel point satisfactorily.

The same paper also reports some experimental information on the sol fraction after the gel point, as is shown in Fig. 2. The theoretical value for the sol fraction of this case ($f=2$, $w_1=0$, $w_f=1$) given by Eq. (42) is presented in the same figure. The relationship between ρ and the reaction time, t, was obtained from Eq. (7a) of Ref. 2, *i. e.*, $\rho=1-\exp(-2kN_2t/\alpha)$ with $2kN_2=2.3$ 1/hr.*3 The agreement of the theory with the experimental results is satisfactory.

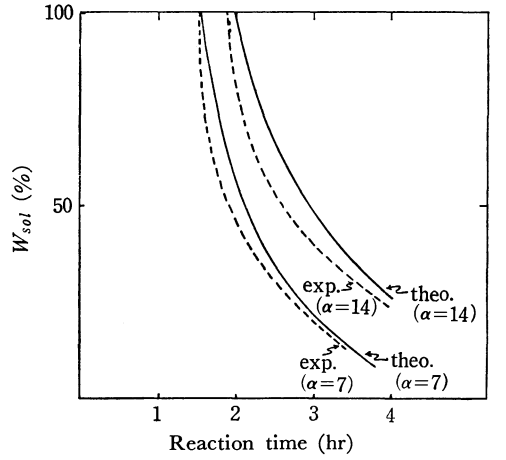

Fig. 2. The comparison between the theoretical sol fraction and the experimental ones obtained by Kakurai and Noguchi (Fig. 5 in Ref. 10).

Usually, the amount of catalysts directly affects the physical properties of the cured epoxy resins. For various kinds of catalysts, the favorable ratio of $\alpha=F/I_0$, *i. e.*, the number of epoxy groups per initiator, is determined through experiments; for instance, Bruin[11] observed that one amine

9) M. Gordon and R-J. Roe, *J. Polymer Sci.*, **21**, 27, 39, 57, 75 (1956); C. Walling, *J. Am. Chem. Soc.*, **67**, 441 (1945); L. Minnema and A. J. Staverman, *J. Polymer Sci.*, **29**, 281 (1958); B. T. Storey, *ibid.*, **A3**, 215 (1965).

10) T. Kakurai and T. Noguchi, *Kogyo Kagaku Zasshi (J. Chem. Soc. Japan, Ind. Chem. Sect.)*, **65**, 827 (1962).

*3 This value was determined from the observed value of the gelation time.

11) P. Bruin, *Chem. & Ind.*, **1957**, 616.

nitrogen atom in the catalyst is sufficient for from six to eight epoxide groups (namely, $\alpha=6$—8). It may be reasonable to attribute some physical properties of the gel to the average chain length (Eq. (54)) and the average number of active network chains, which can be calculated by the present theory.

In commercial practice, the epoxy resins are usually modified by reactive diluents, which are usually monoepoxides,[4] such as allylglycidyl ether and phenylglycidyl ether. To the extent that these diluents are incorporated, they lower the epoxide functionality of the resin, *i. e.*, the average number of epoxides per monomeric molecule. Since it is only the excess over one epoxide per molecule that can result in cross-linking, too large an amount of a reactive diluent ruins some physical properties of the cured resin.[12] In fact, it has been demonstrated that, in concentrations above 15 per cent, they much reduce the strength and solvent resistance of the cured resin.[5] The present theory can provide a basis for a quantitative discussion of this important diluent effect; such a detailed discussion will be undertaken elsewhere.

Appendix

It is well known that, in commenting on the earlier theory of Flory regarding gel formation, Stockmayer, in 1943,[8] threw doubt upon the validity of the application of the distribution equation beyond the gel point. Stockmayer pointed out the contradiction that the fraction of converted functional groups in the gel phase exceeds a limit which could not be surpassed if intramolecular reaction were forbidden (for instance, in the case of the self-condensation of f-functional monomers, the value of this limit is $2/f$). Notwithstanding Flory's protest,[1,13] it seems that no unequivocal explanation of this problem has yet been given. Therefore, we will present here a simple explanation of Stockmayer's paradox. For the convenience of explanation, let us consider the following "hypothetical" gel to be formed by the self-condensation of f-functional monomers ($f\geqq3$). All the functional groups are converted to form a single gel molecule in which *any* functional group is converted and is connected to paths to infinity without cyclization. Such a gel would have a structure of an infinite number of monomeric units with an infinite number of branches without end. In this gel, ρ'' is considered to be unity.

Therefore, according to our opinion, it may be considered that, from a purely theoretical point of view, there is no such limit of ρ''. However, physically, it is quite imperfect, since the number of units and the number of branches of the "physical" gel are finite after all. In conclusion, the validity of the distribution beyond the gel point in the present theory may have been verified only from a theoretical point of view. In this way, the Stockmayer paradox may be attributed to the fact that the "facsimile" of nature treated in physical theory is not nature itself.

12) P. Bruin, *Kunststoffe*, **45**, 383 (1955).

13) P. J. Flory, *Chem. Revs.*, **39**, 137 (1946).

BULLETIN OF THE CHEMICAL SOCIETY OF JAPAN VOL. 42 2120—2122 (1969)

The Mechanism of ESR Relaxation in Peroxylamine Disulfonate Ion $\cdot ON(SO_3)_2^{2-}$

Shizuo FUJIWARA and Kayoko SAKIOKA*1

Department of Chemistry, Faculty of Science, The University of Tokyo, Hongo, Tokyo

(Received December 4, 1968)

The mechanism of ESR relaxation in $\cdot ON(SO_3)_2^{2-}$ is discussed. As the line width in an aqueous solution is plotted against the concentration, it is almost concentration independent in the range lower than 7×10^{-3} mol/*l*, but the dependence increases in the higher range. Powles and Moseley showed that the anisotropy of the *g*-value contributes to the line width in the lower concentration range, but the line width in the higher-concentration range, which is investigated in the present investigation, can not be accounted for by the *g*-tensor anisotropy. Hence, it is supposed that electron spin exchange or nuclear quadrupole interaction contributes in the higher-concentration range. The latter can, however, be eliminated by the line width measurement in a deuterium measurement in a deuterium oxide solution, and so it may be concluded that electron spin exchange is the main contribution to the line width in the higher-concentration range. This is in accordance with the proposal of Jones. Furthermore, we could show that, by calculation of the line shape for Bloch's equation, including exchange interactions, the exchange frequency of 5.4×10^{7} sec^{-1} can give a line fitting the observed line shape for the 7.8×10^{-2} mol/*l* solution. This result can be taken as another evidence showing that the electron spin exchange is the main source of the line width in the higher-concentration range.

The widths of ESR hyperfine lines, ΔH, have attracted the interest of many investigators. For example, a very careful examination of ΔH in organic radicals has proven useful for the elucidation of molecular motion of free radicals.[1] Rogers and Pake[2] observed the dependence of ΔH on the nuclear quantum number, m_I; McConell interpreted this phenomena in terms of a model where the electron spin which carries anisotropy relaxes with the hyperfine field.[3] This model worked nicely and excited more detailed investigations.[4] For example, Powles and Moseley,[4a] working on the peroxylamine disulfonate ion ($\cdot ON(SO_3)_2^{2-}$) in mixed solvents of glycerine and water, noted viscosity dependence of the each hyperfine line width. Although this study presented several interesting features, they are not suitable for the general discussion of relaxation mechanisms, for the chemical surroundings of the paramagnetic ion change with the change in the concentration of glycerine. Kivelson classified the mechanisms of the spin relaxation in detail, and one of the present authors applied his results to the case of an aqueous solution of cupric ions. In the latter investigation, the relaxation of cupric ions in a dilute aqueous solution was found to be determined mainly by the perturbation of the spin-orbit interaction of isotropically-hydrated $[Cu(H_2O)_6]^{2+}$ ions and, in higher-concentration regions, by anisotropies of the *g*-values and by electron spin exchange.[5] A similar conclusion has also been obtained experimentally with respect to the Ti(III) ion.[6] Jones has studied an aqueous solution of $\cdot ON(SO_3)_2^{2-}$ and analyzed the line width, assuming that electron spin exchange is the main effect of the relaxation.[7]

Besides the electron spin exchange and the spin-orbit interaction, the nuclear quadrupole effect is a possible source of relaxation. Kubo presented a theoretical treatment of the contribution of the quadrupole effect to the nuclear spin relaxation, and much experimental evidence has been put forward with regard to this mechanism.[8,9] As this evidence

*1 Present address: The Institute of Industrial Science, The University of Tokyo, Roppongi, Tokyo.

1) G. H. Franfel, *J. Phys. Chem.*, **71**, 139 (1967).

2) R. N. Rogers and G. E. Pake, *J. Chem. Phys.*, **33**, 1107 (1960).

3) H. M. McConell, *ibid.*, **25**, 709 (1956).

4) a) J. G. Powles and M. H. Moseley, *Proc. Phys. Soc. (London)*, **77**, 729 (1961). b) P. W. Atkins and D. Kivelson, *J. Chem. Phys.*, **44**, 154 (1966). c) R. Wilson and D. Kivelson, *ibid.*, **44**, 169 (1966). d) R. Wilson and D. Kivelson, *ibid.*, **44**, 4440 (1966). e) R. Wilson and D. Kivelson, *ibid.*, **44**, 4445 (1966). f) D. C. McGain and R. J. Myers, *J. Phys. Chem.*, **71**, 192 (1967).

5) R. Fujiwara and H. Hayashi, *J. Chem. Phys.*, **43**, 23 (1965).

6) S. Fujiwara and T. Watanabe, *J. Magnetic Resonance*, **1**, in press.

7) M. T. Jones, *J. Chem. Phys.*, **38**, 2892 (1963).

8) M. Suzuki and R. Kubo, *Mol. Phys.*, **7**, 201 (1963).

is related to NMR, we have become interested in investigating to what extent, if any, this effect is related to the relaxation of the electron system which couples with a nucleus carrying quadrupole moment. We chose peroxylamine disulfonate ion $\cdot ON(SO_3)_2^{2-}$ as the sample, because it reveals a well-resolved hyperfine interaction with nitrogen,[10] and we can find pertinent results on such related compounds as di-tertiary butyl nitroxide (DTBN).[11] This paper will show that the contribution of the quadrupole interaction is small and that the line width is, as has been noted by Jones, dominated by the electron spin exchange.

Experimental

Spectra were measured on a Japan Electron Optics X-band ESR spectrometer, Model JES-3BS-X, with 100 kHz/sec field modulation. The modulation amplitude is 30 mgauss, and the microwave power is kept low so as not to saturate the signal. All measurements were carried out at room temperature (20°C).

Solutions of the peroxylamine disulfonate ion $\cdot ON(SO_3)_2^{2-}$ were made by dissolving Fremy's salt in a 0.1 N aqueous solution of sodium carbonate. The concentration of the sample was determined by optical method, taking the molar extinction coefficient of this compound as $\varepsilon=20.8$ (at 545 mμ).[12] Water and deuterium oxide were used as solvents. The ESR intensities of the sample solutions were found constant over several hours, hence, we assume that they are stable over the period of measurement. The concentration of the sample solutions varied from 5×10^{-4} to 8×10^{-2} mol/l. No degassing procedure was carried out.

For the calculation of the line shapes, the RA-5 electronic digital computer made by Japan Electron Optics Company was used.

Results and Discussion

The width was measured as the separation of the maximum slope points of the derivatives of the absorption spectrum, which can be shown as a function of the concentration shown in Fig. 1. The results in Fig. 1 suggest that, the lower concentration range, the width is almost independent of the concentration, having a value of 0.24 gauss. It is also found that the width is the same in both H_2O and D_2O, which have different viscosities 1.0 and 1.2 cps respectively. These findings eliminate the spin-spin dipole interaction, the quadrupole interaction, and the anisotrpy due to the nuclear quantum number as the dominant sources of the electron spin relaxation, because if the spin-spin interaction is working as the dominant factor, the line width should be concentration dependent, while if the quadrupolar interaction or the anisotropy due to the nuclear quantum number works, then the width should be viscosity dependent. Using the B. P. P.[13] model, the dipolar line width is evaluated as 0.18 gauss for the solution of 0.01 mol/l. This is about two-thirds of the observed line width of 0.3 gauss. Hence, we assume that complexity exists in the system; *i. e.*, the spin-orbit interaction or the electron spin exchange interaction contributes to the relaxation as well as the dipolar interactions, and also that the apparent features of the concentration dependence can not be simply interpreted. This can be presented in a different way by manipulating the line shape. We construct an absorption line of three hyperfine components, each of a Lorentzian shape and of a definite width, the hyperfine components being separated from each other by 13 gauss. The calculated line is as shown in Fig. 2, where the line width of the hyperfine component is given two values, 2.9 gauss and 4 gauss. It may be seen in the figure that the outer peak is higher than the central peak; moreover, the line width is broader than the latter, contrary to the experimental observations. In the latter, the

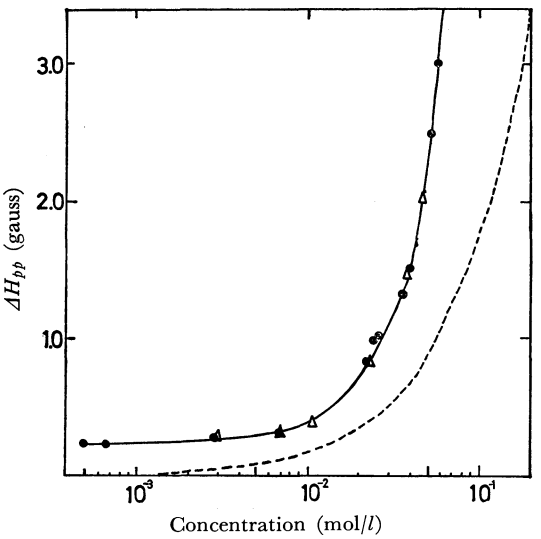

Fig. 1. Concentration dependence of line width in water (•) and in deuterium oxide (△). Dotted line is line width calculated on the bases of intermolcular dipole interaction.

9) a) R. A. Ogg and J. D. Ray, *J. Chem. Phys.*, **26**, 1515 (1957). b) E. L. Muetteries and W. D. Phillipios, *J. Am. Chem. Soc.*, **81**, 1074 (1959). c) R. A. Ogg, *J. Chem. Phys.*, **22**, 1933 (1954). d) J. N. Shoolrey, *Discussions Faraday Soc.*, **19**, 215 (1955). e) H. Watanabe, T. Toya, M. Ohzuru and M. Kubo, The 6th Symposium on Nuclear Magnetic Resonance, Kyoto, Japan, Octobor, 1967.

10) G. E. Pake, J. Townsend and S. I. Weissman, *Phys. Rev.*, **85**, 682 (1952).

11) W. Plachy and D. Kivelson, *J. Chem. Phys.*, **47**, 3312 (1967).

12) H. Murbi and D. M. Ritter, *J. Am. Chem. Soc.*, **74**, 3394, (1952).

13) N. Bloembergen, E. M. Purcell and R. V. Pound, *Phys. Rev.*, **73**, 679 (1948).

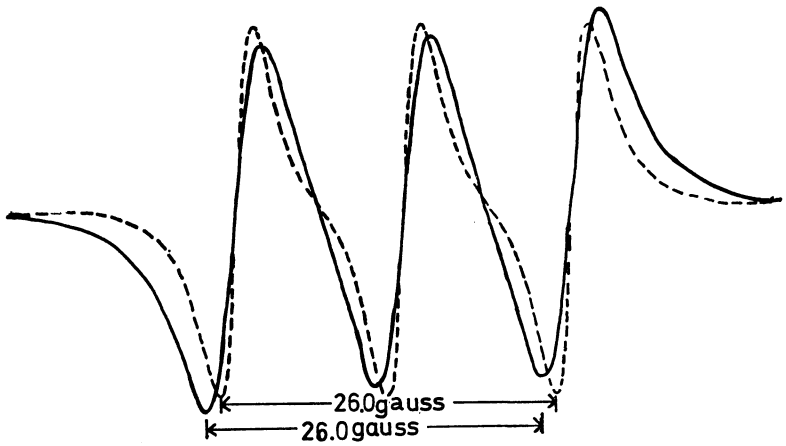

Fig. 2. Calculated line shape with the assumption of equal line width of each hyperfine component separated by 13 gauss from each other. Dotted curve refers to the line of 2.9 gauss of ΔH_{pp}, the peak to peak line width of the hyperfine component, and the full line to that of 4.0 gauss of ΔH_{pp}.

central line width is slightly narrower in the range of about 6×10^{-2} mol/l, and then it becomes broader in the higher concentration range ($\sim1\times10^{-1}$ mol/l). This suggests that the line shape could not be analyzed simply by the overlap of Lorentzian hyperfine lines of the same line width. This investigation supports that of Kivelson.[11] As to the nonequivalence of the hyperfine component, the line width in this system can be produced by the spin exchange mechanism. We manipulate the line shape on the basis of a modification of Bloch's equation which carries an exchange interaction term by which we can evaluate the magnitude of this interaction roughly. We write first modifications of the Bloch equation for three sites,[14] assuming that the fraction of each spin state is equal and that the spin state are mixed through electron exchange. The imaginary part, v, of the total magnetization, M, is given below;

$$v = \frac{M(PZ+RM)}{P^2+R^2}$$

where;

$$P = 3(\Delta\nu + 4\tau\Delta\nu/T_2 + 3\tau^2\Delta\nu/T_2^2 - \tau^2\Delta\nu^3 + \Delta\nu\tau^2\delta\nu^2)$$

$$R = 3/T_2 + 6\tau/T_2^2 - 6\Delta\nu^2\tau + 2\tau\delta\nu^2 + 3\tau^2/T_2^3 - 9\Delta\nu^2\tau^2/T_2 + 3\tau^2\delta\nu^2/T_2$$

$$W = 3 + 6\tau/T_2 + 3\tau^2/T_2^2 - 3\Delta\nu^2\tau^2 + \delta\nu^2\tau^2$$

$$Z = 6(\tau\Delta\nu + \Delta\nu\tau^2/T_2)$$

where T_2 refers to the spin-spin relaxation time in the absence of electron spin exchange, and where $1/\tau$ is the exchange frequency, $\delta\nu$, the coupling constant, and $\Delta\nu$, the frequency from the center.

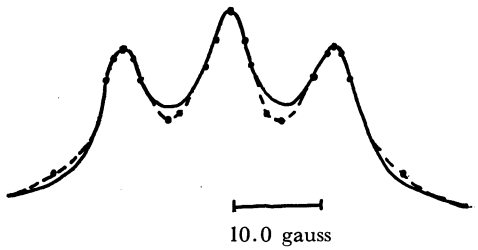

Fig. 3. —— The integrated line shape for a solution of 7.8×10^{-2} mol/l of $\cdot ON(SO_3)_2^{2-}$. -●- The calculated line shape for the modified Bloch's equation.

As the exchange frequency is taken as 5.4×10^7 sec^{-1}, $1/T_2$, as 0.36×10^7 sec^{-1}, and $\delta\nu$, as 3.6×10^7 sec^{-1}, the line shape is calculated to be as shown by the dotted curve in Fig. 3. It agrees fairly well with the curve observed with the solution of 7.8×10^{-2} mol/l, which is shown in Fig. 3 by the straight curve. Jones investigated the electron spin exchange in his study of the line width. However, the present analysis of the total line shape should be more efficient.

14) L. E. Piette and W. A. Anderson, *J. Chem. Phys.*, **30**, 899 (1959).

BULLETIN OF THE CHEMICAL SOCIETY OF JAPAN VOL. 42 2123—2128 (1969)

The Effects of Organic Additives on the Solubilities and CMC's of Potassium Alkyl Sulfates in Water. II. Effects of Some Nonhydroxy Compounds

Keishiro SHIRAHAMA*, Makoto HAYASHI** and Ryohei MATUURA***

* *Department of Chemistry, Faculty of Science and Engineering, Saga University, Honjo-machi, Saga*
** *College of Foreign Students, Chiba University, Yayoi-cho, Chiba*
*** *Department of Chemistry, Faculty of Science, Kyushu University, Hakozaki, Fukuoka*

(Received December 5, 1968)

Solubilities and critical micelle concentrations (CMC) of potassium dodecyl sulfate (KDS) and hexadecyl sulfate (KHS) were measured in aqueous solutions to which dioxane, acetone, urea, or dimethyl sulfoxide had been added over the temperature range of 5—40°C. It was found that all additives mentioned above raised solubility and CMC with an exception for dioxane which showed a slight minimum on a CMC-additive concentration curve. Solvent effects on the alkyl and ionic groups of a surfactant molecule were separated by considering the difference of the standard free energy change for the solution process of KHS and that of KDS. It was deduced that a primary effect on the alkyl group is the one that a strongly cohesive solvent, water, is replaced by a less cohesive organic solvent and other mechamisms, such as an effect on the water structure, follow as the secondary. In terms of the above considerations, effects on the Krafft point were also referred to.

In Part I of this series, the solvent effects on potassium alkyl sulfates of such compounds as lower alcohols and glycols were reported.[1] The present paper will describe solvent effects, on the same surfactants, of dioxane, acetone, urea and dimethyl sulfoxide which are characterized by the name, nonhydroxy compounds. The effects on CMC caused by these additives have been reported by many authors,[2-6] but the nature of the effects has not been elucidated. We believe that the phenomena should be understood in terms of solvent effects on single-ion dispersion as well as on micelle dipersion, as these two are equilibriated with each other. Then it was attempted to measure solubilities and CMC's of KDS and KHS (solubility only) in various mixed solvents of aqueous organic compounds mentioned above. Dioxane was employed because of the diverse dielectric constants of its aqueous solution, and other three are interesting for their related chemical structures.

Experimental

Materials. Potassium alkyl sulfates are the same samples as used in the previous work.[1] Dioxane was refluxed on metallic sodium for hours and distilled. Acetone was purified by distillation, after treated with a small amount of potassium permanganate. Urea was recrystallized twice from ethanol-water (2 : 1 in volume) mixture and dried in vacuum. Dimethyl sulfoxide was shaken and distilled in the presence of alumina under reduced pressure.

Procedures. Solubility and CMC measurements were performed by the same methods as in Part I. Urea solutions were kept in refrigerator and used within 10 days so as to avoid any error that may come from the hydrolysis of urea.

Results and Discussion

Solubilities and CMC's of KDS are plotted against temperature in Figs. 1—4.*1 It is evident from the figures that the increase in concentration of the additive results in increases both in solubility and in CMC except for the dioxane-water mixed solvent in which a slight CMC-decreasing effect was observed. These results are in contrast with the effects caused by hydroxy compounds,[1] where the solubility curve crosses that for pure water. Thus, the hydroxy additives caused increase in

1) K. Shirahama, M. Hayashi and R. Matuura, This Bulletin, **42**, 1206 (1969).
2) K. Shirahama and R. Matuura, *ibid.*, **38**, 373 (1964).
3) M. F. Emerson and A. Holtzer, *J. Phys. Chem.*, **71**, 3320 (1967).
4) J. M. Corkill, J. F. Goodman, S. P. Harrold and J. R. Tate, *Trans. Faraday Soc.*, **63**, 240 (1967).
5) M. J. Schick, *J. Phys. Chem.*, **68**, 3585 (1964).
6) P. Mukerjee and A. Ray, *ibid.*, **67**, 190 (1963).

*1 In Figs. 2 and 4, the CMC curves were completed by extrapolating the CMC's in the lower additive concentrations to the ones in the higher additive concentrations, *i. e.*, 7.34% acetone and 27.9% dioxane.

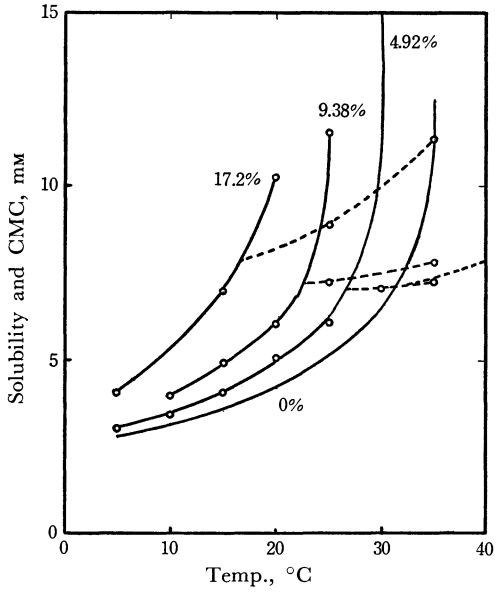

Fig. 1. Solubilities and CMC's of KDS in dioxane-water mixed solvents.
solid line: solubility curve
dotted line: CMC curve

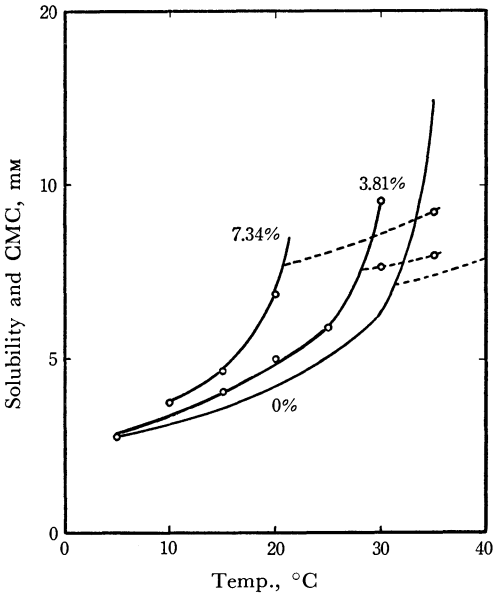

Fig. 2. Solubilities and CMC's of KDS in acetone-water mixed solvents.

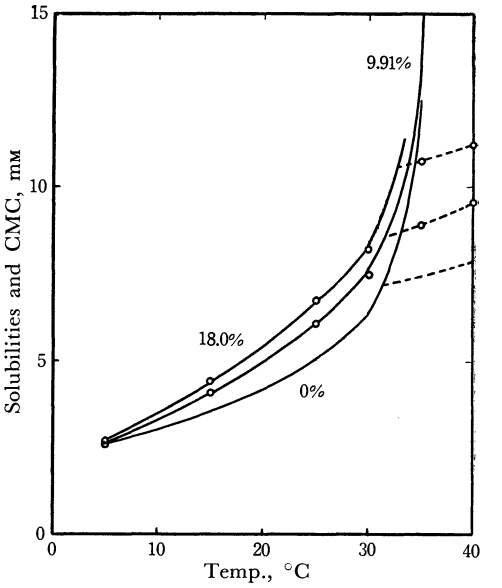

Fig. 3. Solubilities and CMC's of KDS in dimethyl sulfoxide - water mixed solvents.

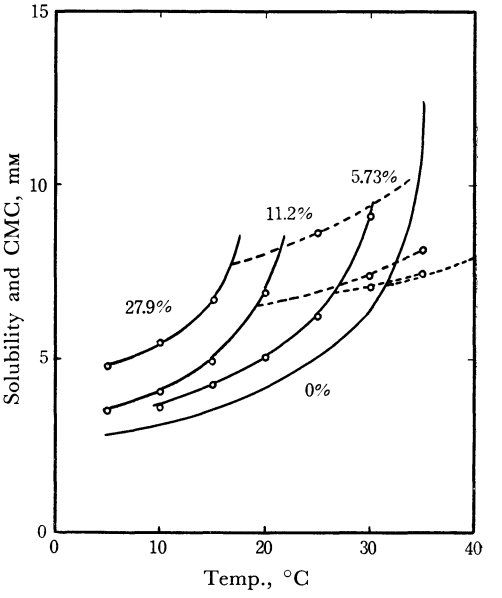

Fig. 4. Solubilities and CMC's of KDS in urea-water mixed solvents.

solubility at higher temperature ranges, but at lower temperature ranges they caused decrease in solubility, as compared with solubilities in pure water. On the other hand, the additives used in the present work enhance solubilities at all experimental temperatures, although for acetone-, and dimethyl sulfoxide - water systems, the solubility curves crossed at the lowest experimental temperature (near 5°C), and for dioxane- and urea - water mixed solvents, it may be expected that solubility curves will intersect each other at temperatures lower than 0°C. This enhanced solubility is a marked difference from the solubility of a simple electrolyte, for which electrostatic theory predicts reduced solubility in most organic solvent-water mixtures.[7] The organic additives in the

7) H. S. Harned and B. B. Owen, "The Physical Chemistry of Electrolyte Solutions," Reinhold Publ. Corp., New York (1958), p. 81.

present work, *i. e.*, nonhydroxy compounds would form hydrogen bond with water just as hydroxy compounds do and strengthen the net-work structure which limits the dissolution of hydrophobic solutes. But this effect is well compensated by the fact that the structuredness of liquid water, or clusters, are "molten" by the presence of the additives, just as by the thermal agitation, and bulky closed space is liberated for the dissolved solute.[8]

To be more quantitative, the standard free energy change for the solution process, and the corresponding enthalpy and entropy changes defined as

$$\Delta F^\circ = -2RT \ln X_s, \quad (1)$$

$$\Delta H^\circ = \frac{\partial \Delta F^\circ}{\partial (1/T)} \quad (2)$$

and

$$\Delta S^\circ = \frac{\Delta H^\circ - \Delta F^\circ}{T} \quad (3)$$

may be considered. Here X_s is a solubility in mole fraction, and other notations are usual ones. The values of ΔH° and $T\Delta S^\circ$ are shown as a function of weight percentage of the additives in Fig. 5, where the values in ethanol-water mixed solvents are also added for comparison. Both enthalpy and entropy changes are rather small as compared with those in alcohols-water mixed solvents. It is especially noted that the effect by urea is very small. This fact might suggest some different mechanism with this compound which is well-known for its protein denaturating ability, often discussed in connection with the structure of liquid water.[9] Another example of this difference

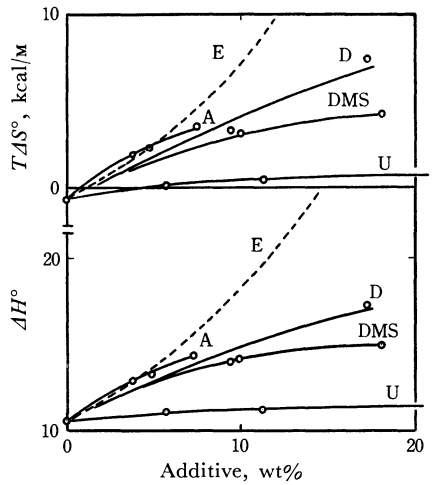

Fig. 5. The values of ΔH°'s and $T\Delta S^\circ$'s in mixed solvents.
E: ethanol, A: acetoxane, D: dioxane, DMS: dimethyl sulfoxide, U: urea

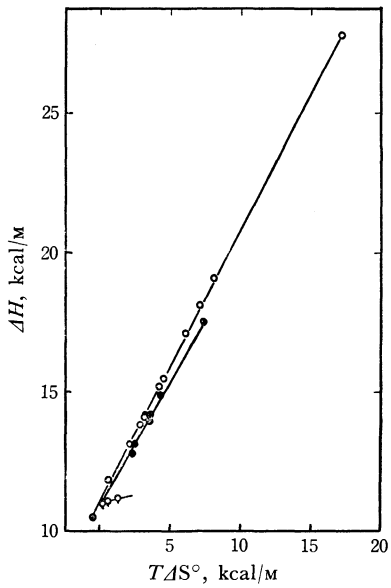

Fig. 6. ΔH°'s *vs.* $T\Delta S^\circ$'s plot.
○: hydroxy compound, ●: nonhydroxy compound, ○: urea, ⊙: water

would be seen in Fig. 6, where ΔH°'s are plotted against $T\Delta S^\circ$'s for the mixed solvents studied in both Parts I and II. Figure 6 represents that effects of hydroxy, nonhydroxy and urea fall on different lines, respectively. This fact may suggest that these additives would have some diverse roles in the solution process.

At the same enthalpy change, the entropy change is in order of urea, nonhydroxy and hydroxy compounds. These differences may arise from the difference in the net-work structure formation effect and the space-releasing effect of these compounds. It was reported by Nakanishi[10] that an effect on the partial molar volume of water by the addition of the compounds can be classified by the two categories of hydroxy and nonhydroxy compounds.

Solvent Effect on CMC. In view of the above explanations, the changes in CMC's given in Fig. 7 are understood: in a monomer-micelle equilibrium, if monomer becomes more stable but micelle does not by an additive, the equilibrium should displace to the monomer side, thus CMC is raised. This is clearly seen in Fig. 8, where a relative solubility (r_s) is plotted against a relative CMC (r_m). The relative solubility here means a ratio of a solubility of single-ion dispersion extrapolated to 35°C in a mixed solvent to that in pure water. The extrapolated values obtained by the logarithm of solubility *vs.* the reciprocal of temperature plot, and the ones by the graphical extrapolation tracing the smooth curve agreed each other. The relative CMC also has a similar meaning. An approximate

8) F. Franks and D. G. Ives, *Quart. Rev. (London)*, **20**, 1 (1966).
9) For example: G. C. Kresheck and L. Benjamin, *J. Phys. Chem.*, **68**, 2476 (1964).
10) K. Nakanishi, This Bulletin, **33**, 793 (1960).

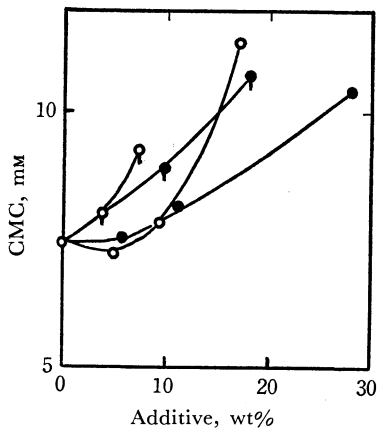

Fig. 7. CMC's of KDS in mixed solvents at 35°C.
○: dioxane, ○: acetone, ●: urea, ●: dimetyl sulfoxide

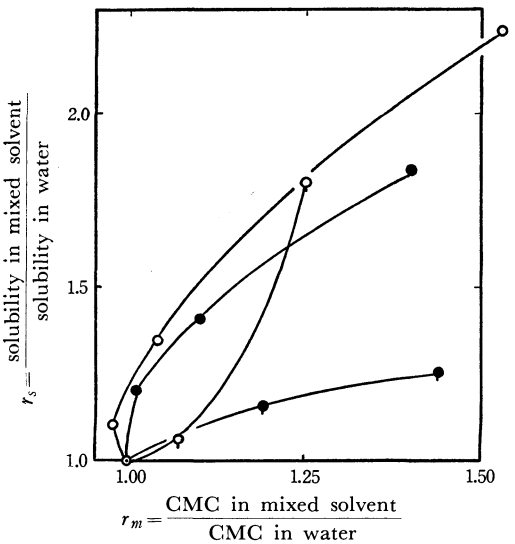

Fig. 8. Relative CMC (r_m) *vs.* relative solubility (r_s) plot.
⊙: water, ○: dioxane, ●: urea, ○: acetone, ●: dimethyl sulfoxide.

pararellism between the two ratios supports this idea. A less or non CMC-decreasing ability of dimethyl sulfoxide might be attributed to its highly hydrophilic nature as compared with others. The CMC-decreasing power of dioxane is, although slight, explicit in Fig. 7. Urea is also believed to be effective in breaking micelles because of high dielectric constant of its aqueous solutions.[3] The CMC-decreasing power of acetone might not be negligible, judging from its both hydrophilic and hydrophobic nature, but it would be overcome by a marked CMC-increasing effect. A shallow minimum of the CMC *vs.* additive concentration curve in dioxane-water mixed solvent was found for sodium dodecyl sulfates too,[2] and explained in term of solubilization of dioxane molecules into micelles just as seen in the cases of alcohols-water mixtures.[11,12]

Separation of Solvent Effects. As was done in Part I, solvent effects can be divided into two portions: a solvent effect on the nonpolar group and one on the ionic group of a surfactant molecule. In order to do so, solubilities of KHS in respective mixed solvents were measured (shown

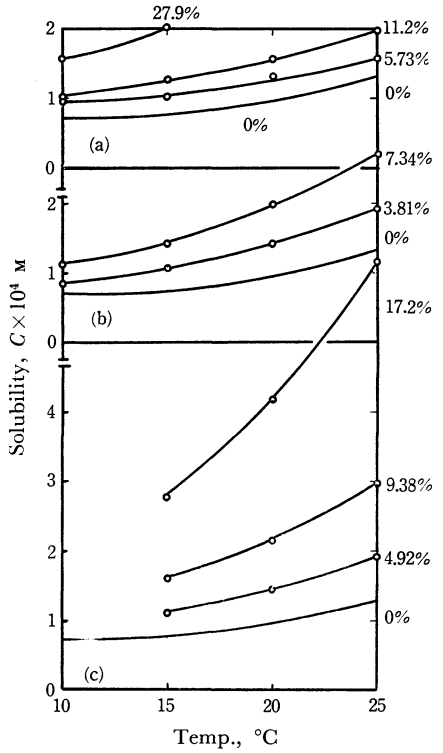

Fig. 9. Solubilities of KHS in mixed solvents.
(a) urea, (b) acetone, (c) dioxane

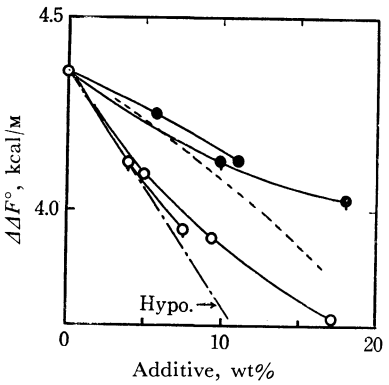

Fig. 10. Solvent effect on nonpolar group of a surfactant molecule.
○: dioxane, ○: acetone, ●: urea, ●: dimethyl sulfoxide
dotted line: ethanol
chain line: the hypothetical effect as reported in Part I.

11) K. Shinoda, This Bulletin, **26**, 101 (1953).
12) Y. Ooshika, *J. Colloid Sci.*, **9**, 254 (1954).

in Fig. 9, and for aqueous dimethyl sulfoxide, 0.110, 0.129 mM in 9.91 and 18.0 DMS wt% respectively, at 15°C only) and then the solvent effect on the nonpolar group $\Delta\Delta F^\circ$ was calculated by applying the following equation,

$$\Delta\Delta F^\circ = \Delta F^\circ_{KHS} - \Delta F^\circ_{KDS} = -2RT\ln\frac{C_{KHS}}{C_{KDS}}, \quad (4)$$

where subscripts refer to the respective surfactants, C's are solubilities of surfactant in a solvent, and other notations are usual ones. The values of $\Delta\Delta F^\circ$ are presented as a function of weight percentage of additives in Fig. 10, where a hypothetical solvent effect is drawn as before.[1] The hypothetical solvent effect is simply expressed as

$$\Delta\Delta F^\circ_{hypo} = \Delta F^\circ_w(1-\phi_H), \quad (5)$$

where ΔF°_w is the standard free energy change of the nonpolar group for the solution process in pure water, *i. e.*, a solvent effect of water, ϕ_H is a volume fraction of hexane which was taken as a hypothetical additive. Here is again a positive deviation from the hypothetical behavior. This deviation is relatively small for acetone and dioxane which enhance the solubilities of the surfactants, probably due to their space-releasing effect. Another useful indication is a $\Delta\Delta F^\circ$ *vs.* CED plot in Fig. 11, where CED's (cohesive energy density) are calculated from the pressure-temperature, and density data from various sources of the corresponding binary systems.[13]

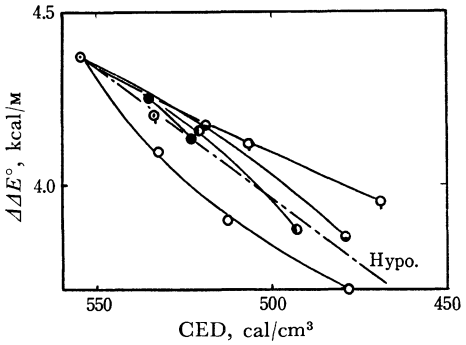

Fig. 11. $\Delta\Delta F^\circ$ *vs.* CED plot.
⊙: water, ○: dioxane, ○: acetone, ●: urea, ●: DMS, ◐: methanol, ◒: ethanol, ⊙: 1-propanol.

The CED of the hypothetical mixture was calculated by the equation,[14]

$$(CED)_{hypo} = (\phi_w\delta_w + \phi_H\delta_H)^2, \quad (6)$$

where subscripts w and H refer to water and a hypothetical solvent, respectively, and ϕ's and δ's are volume fractions and solubility parameters, respectively. Here hexane was taken as a hypothetical additive, for which the density and the solubility parameter are available. In Fig. 11, points are scattered around the hypothetical effect. This may indicate a primary solvent effect that the strongly cohesive liquid, water, becomes energetically loosened by adding any less cohesive compound. Both the net-work formation and the space-releasing effect would follow this primary effect and work against, or sometimes, for it. Urea which is solid and therefore the most cohesive shows a remarkable solvent effect and thus should hold a special position in affecting the structure of liquid water.

The solvent effect in the ionic group ΔF°_{ion} was calculated from the equation,

$$\Delta F^\circ_{ion} = \Delta F^\circ_{KDS} - \Delta\Delta F^\circ \times 3. \quad (7)$$

In Fig. 12, ΔF°_{ion}'s are plotted against the reciprocals of dielectric constants of the mixed solvents. A line was determined by the least square method. The slope gives the Born radius 0.5 Å.

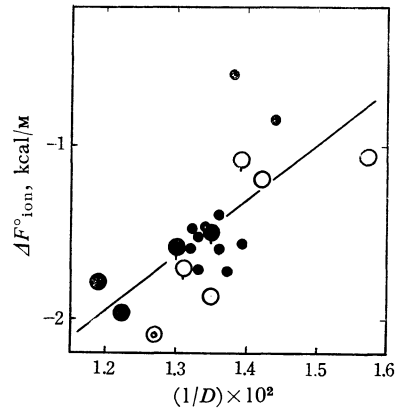

Fig. 12. Solvent effect on ionic group of a surfactant molecule.
⊙: water, ○: dioxane, ○: acetone, ●: DMS, ●: urea, small full circles are for hydroxy compounds as repoted in Part I.

Solvent Effects on the Krafft Point. The Krafft point is defined as the intersection of solubility curve and CMC curve. Thus detailed knowledge on the two curves might be required to predict the solvent effect on the Krafft point, but here, as in Part I, two simplified extremes are considered: (a) CMC curve changes (increase or decrease) with solubility curve fixed, (b) solubility curve changes with CMC curve fixed. These two extreme cases are schematically shown in Fig. 13. In Fig. 14, the observed Krafft points are plotted against the weight percentage of additives. It is noted that dimethyl sulfoxide affects only a little on the Krafft point probably due to a cancellation of the (a) and (b) effects.

13) a) For acetone and alcohols, "International Critical Tables," Vol. III, pp. 111, 292 (1928). b) For dioxane, F. Hovorka, R. A. Schaeffer and D. Dreisbach, *J. Am. Chem. Soc.*, **58**, 2264 (1936). c) For urea, G. Scatchard, W. J. Hamer and S. E. Wood, *ibid.*, **60**, 3016 (1938); H. M. Chadwell and F. W. Politi, *ibid.*, **60**, 1291 (1938).

14) J. H. Hildebrand and R. L. Scott, "The Solubility of Nonelectrolytes," Reinhold, New York (1950), p. 198.

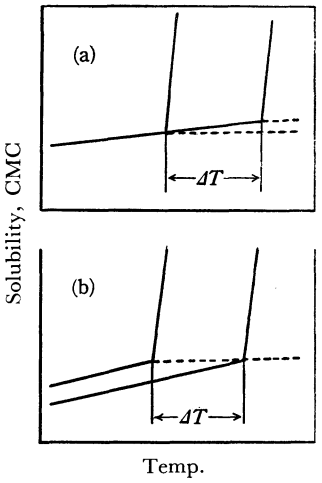

Fig. 13. The two extreme cases of the effects on the Krafft point.
solid line: solubility curve
dotted line: CMC curve
ΔT: change in the Krafft point.

On the other hand, dioxane, acetone and urea show the effects of the same magnitude. The lowering of the Krafft point might be brought about by the (b) mechanism exceeding the (a). This is also clear from Fig. 8 which shows a marked increase in solubility as compared with the CMC increase.

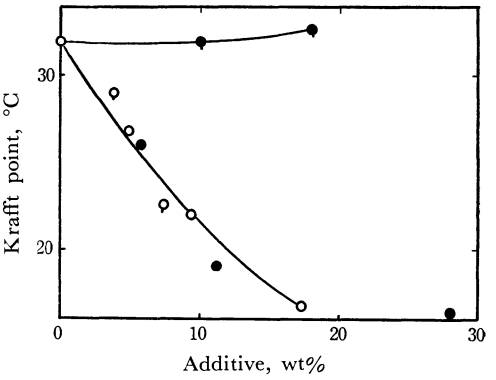

Fig. 14. Solvent effect on the Krafft point.
○: dioxane, ○: acetone, ●: urea, ●: dimethyl sulfoxide.

BULLETIN OF THE CHEMICAL SOCIETY OF JAPAN VOL. 42 2128—2131 (1969)

Reactions of Ions in the Radiolysis of Liquid Propane

Kuniyasu TANNO and Shoji SHIDA

Laboratory of Physical Chemistry, Tokyo Institute of Technology, Meguro-ku, Tokyo

(Received December 6, 1968)

The reactions of ions, especially fragmentation of excited ions and the subsequent reactions of fragment ions in the radiolysis of liquid propane have been investigated by the use of charge scavengers such as sulfur hexafluoride (SF_6) and ammonia (NH_3). It has been confirmed that the fragment ions are produced by the dissociation of the excited parent ion prior to the parent ion-electron recombination. The yields of $C_2H_5^+$ and $C_3H_7^+$ have been measured by the use of the reaction, $RH^+ + NH_3 \rightarrow R + NH_4^+$, with the results $G \geq 0.28$ and ~ 1.1 respectively. These ions neutralize with electrons to form ethylene or propylene. The hydride ion transfer reaction between $C_2H_5^+$ and propane may be competing with the neutralization of $C_2H_5^+$ by electron in the absence of an additive. The yields of fragment ions are compared in the radiolysis of several saturated hydrocarbons.

Studies of ionic reactions in the liquid-phase radiolysis of some branched saturated hydrocarbons using charge scavengers such as SF_6 and NH_3 were reported previously.[1,2] Some of the significant results found were (1) the fragmentation of excited molecular ions still occurs in the liquid phase, (2) the fragment ion (such as t-$C_4H_9^+$ and s-$C_3H_7^+$) neutralizes with an electron to form an olefin molecule, and (3) the hydride ion transfer reaction may not be so fast as in the gas phase. The present report of the radiolysis of liquid propane shows a similar pattern of ionic reactions. Koob and Kevan[3,4] studied extensively the liquid-phase

1) K. Tanno, T. Miyazaki, K. Shinsaka and S. Shida, *J. Phys. Chem.*, **71**, 4290 (1967).

2) K. Tanno, S. Shida and T. Miyazaki, *ibid.*, **72**, 3496 (1968).

3) R. D. Koob and L. Kevan, *Trans. Faraday Soc.*, **64**, 706 (1968).

4) R. D. Koob and L. Kevan, *ibid.*, **64**, 422 (1968).

radiolysis of propane by the use of deutrated propane and a radical scavenger (oxygen). However, we have employed a different technique to detect the ionic species, that is, proper use of charge scavengers.

Experimental

The propane supplied by Takachiho Shoji Co. was purified by gas chromatography and trap-to-trap distillations to reduce hydrocarbon impurities less than 10 ppm. SF_6 (>98%) (Matheson Co.) and NH_3 Takachiho Shoji Co.) of high purity were used without further purification. Propane was irradiated in Pyrex glass ampoules 5 mm in diameter fitted with break seals. Mole fraction of the gas-phase propane was less than 5% of the total in the ampoule. Samples were kept at 4°±1°C during irradiation in an ice-water mixture. Irradiations were carried out by ^{60}Co γ-rays, at a dose rate of 7.1×10^{19} eV/g hr. The total doses were 3.55×10^{20} eV/g. Other experimental details were described previously.[2] G Values reported here are based on the energy absorbed by propane only.

Results and Discussion

In Fig. 1 is shown the effect of SF_6 on the yield of ethane, ethylene and propylene. Other radiolytic yields are $G(H_2)=4.8$ and $G(CH_4)=0.68$ without SF_6, and $G(H_2)=2.5$ and $G(CH_4)=0.56$ with 4 mol% SF_6. The G values of fragment products obtained in the present work without an additive are somewhat smaller than those obtained by Koob and Kevan.[4]

An appreciable increase in the ethane yield is observed upon the addition of SF_6, while the yields of ethylene and propylene decrease rapidly. This

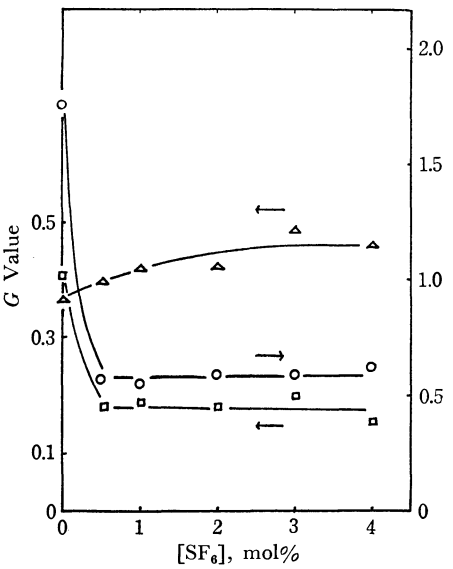

Fig. 1. Effect of SF_6 in the radiolysis of liquid propane.
△ C_2H_6, □ C_2H_4, ○ C_3H_6

phenomenon suggests the definite contribution of ionic reactions to the formation of these products. A similar increase in an alkane and the decrease in an olefin product yield upon the addition of an electron scavenger has also been observed in the radiolysis of liquid isobutane and isopentane where $G(C_3H_8)$ or $G(C_4H_{10})$ increases upon the addition of SF_6[2] or CCl_4.[5]

A possible mechanism of the ionic reactions for the formation of ethylene is

$$C_3H_8 \sim\!\!\!\rightarrow C_2H_5^+ + CH_3 \quad (1)$$

$$C_2H_5^+ + e^- \rightarrow C_2H_4 + H \quad (2)$$

$$C_3H_8^+ + e^- \rightarrow C_2H_4 + CH_4 \quad (3)$$

Ethylene is formed by neutralization with an electron of $C_2H_5^+$ as well as the parent ion such as reaction (3). We reported the formation of an olefin molecule by neutralization of a fragment carbonium ion in the radiolysis of several liquid hydrocarbons.[1,2] A part of $C_2H_5^+$ may form ethane by the hydride ion transfer reaction with propane, competing with the neutralization reaction (2).

$$C_2H_5^+ + C_3H_8 \rightarrow C_2H_6 + C_3H_7^+ \quad (4)$$

The decrease in ethylene yield caused by SF_6 is due to the capture of electrons by SF_6.

$$e^- + SF_6 \rightarrow SF_6^- \quad (5)$$

The increased yield of ethane upon the addition of SF_6 may be explained by the fact that the neutralization of $C_2H_5^+$ is delayed and that the hydride ion transfer reaction (reaction (4)) becomes predominant in place of the neutralization of $C_2H_5^+$. The decrement of ethylene exceeds the increment of ethane, because the ethylene formation by both reactions (2) and (3) is prevented by SF_6, while ethane formation is promoted only by reaction (4).

Although the possibility that SF_6 promotes the H_2^- transfer reaction could not be denied,

$$C_2H_4^+ + C_3H_8 \rightarrow C_2H_6 + C_3H_6^+ \quad (6)$$

the extent of reaction (6), if any, is estimated to be smaller than that of reaction (4), if one considers the result of gas-phase radiolysis of propane[6] or the mass spectral data,[7] where the relative abundance of $C_2H_5^+$ greatly exceeds that of $C_2H_4^+$. Actually Koob and Kevan[3] infrerred that the degree of reaction (6) is about half as much smaller than that of reaction (4) in the liquid-phase radiolysis of propane at 35°C. However, the following explanation for the increased yield of ethane could not be entirely excluded.

5) A. A. Scala and P. Ausloos, *J. Chem. Phys.*, **47**, 5129 (1967).
6) L. I. Bone, L. W. Sieck and J. H. Futrell, "The Chemistry of Ionization and Excitation," ed. by G. R. A. Johnson and G. Scholes, Taylor and Francis, Ltd., London (1967), pp. 223—235.
7) American Petroleum Institute Research Project 44

$$C_2H_5^+ + SF_6^- \rightarrow C_2H_5 + SF_6 \quad (7)$$

$$C_2H_5 + C_3H_8 \rightarrow C_2H_6 + C_3H_7 \quad (8)$$

Thus, following reaction (5), SF_6^- neutralizes with $C_2H_5^+$ to lead to the formation of ethyl radicals which then abstract hydrogen atom of propane to form ethane. Detailed discussion on this point was given in a previous paper.[2] We tentatively prefer reaction (4) for the increase in the ethane yield upon the addition of SF_6.

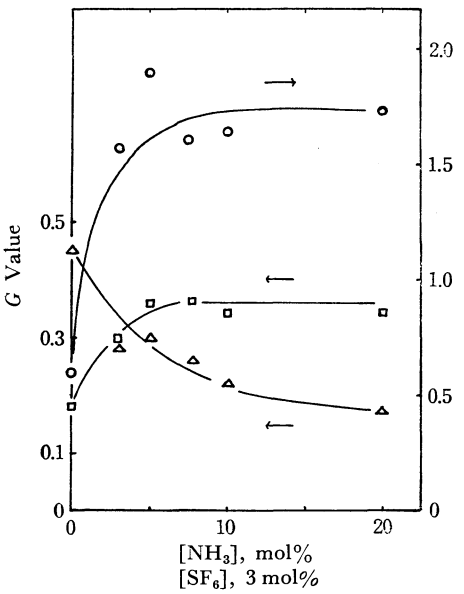

Fig. 2. Effect of NH_3 in the presence of SF_6 in the radiolysis of liquid propane.
△ C_2H_6, □ C_2H_4, ○ C_3H_6

The increased yield of ethylene and the decreased yield of ethane caused by NH_3 added together with SF_6 (Fig. 2) is undoubtedly attributed to the proton transfer from $C_2H_5^+$ to NH_3.

$$C_2H_5^+ + NH_3 \rightarrow C_2H_4 + NH_4^+ \quad (9)$$

Proton transfer reactions between several carbonium ions and NH_3 have been reported.[8,9] The G increment of ethylene at higher concentrations of NH_3 is 0.17, while the G decrement of ethane is 0.28. A plausible explanation for the difference is that the condensation reaction occurs between $C_2H_5^+$ and NH_3 which does not lead to the formation of ethylene.

$$C_2H_5^+ + NH_3 \rightarrow C_2H_5NH_3^+ \quad (10)$$

Ward and Hamill[10] reported the similar condensation reactions between several carbonium ions and methyl alcohol. If reaction (10) is assumed, $G(C_2H_5^+) \geqq 0.28$ may be estimated from the decrement of ethane at 20 mol%NH_3 allowing for the possibility that $C_2H_5^+$ cannot be captured completely even at 20 mol% NH_3.

Propylene is formed in the absence of an additive as

$$C_3H_7^+ + e^- \rightarrow C_3H_6 + H \quad (11)$$

The occurrence of the reaction may be supported by the fact that the yield of propylene increases with the addition of NH_3 in the presence of SF_6 (Fig. 2). The increase is due to the proton transfer from $C_3H_7^+$ to NH_3.

$$C_3H_7^+ + NH_3 \rightarrow C_3H_6 + NH_4^+ \quad (12)$$

Reaction (12) seems to be very efficient, because 5 mol% NH_3 is sufficient enough to capture almost all of $C_3H_7^+$ as seen in Fig. 2. The G increment of propylene is 1.12, and $G(C_3H_7^+) \approx 1.1$ is estimated.

$C_3H_7^+$ can be formed from the decomposition of the excited parent ion as well as the secondary reaction such as reaction (4). In the xenon-sensitized radiolysis of propane in the gas phase,[6] $C_3H_7^+$ produced by the secondary reaction (hydride ion transfer reactions of fragment ions with propane) was estimated as much as 0.91 in M/N yield. However, in the liquid phase, the yield of the fragment ions which undergo the secondary reaction to produce $C_3H_7^+$ is estimated not to greatly exceed $G(C_2H_5^+) \approx 0.28$, so $C_3H_7^+$ may be formed directly from the decomposition of the parent ion in the liquid phase.

We have so far investigated the ionic reactions in the radiolysis of several staurated hydrocarbons and were able to measure the approximate yields of the fragement carbonium ions. The results is summarized in Table 1. The yield of fragment ions differs from one hydrocarbon to another. A simplified theoretical treatment has been proposed by Miyazaki *et al.*[11] to explain the difference and they obtained the qualitative agreement with the experiment. In any case, there seem to be two factors governing the fragment ion formation prior to the parent ion-electron recombination in the radiolysis of liquid saturated hydrocarbons. The two factors are (1) the heat of formation of a carbonium ion from the parent ion and (2) the number of atoms in the hydrocarbon, that is, the number of degrees of vibrational freedom.

The internal energy distribution functions of excited parent ions were determined experimentally for only propane and *n*-butane.[12] However, if one assumes that the amount of the internal energy and its distribution of the excited parent ions do not differ greatly from one hydrocarbon to another,

8) T. Miyazaki and S. Shida, This Bulletin, **38**, 2114 (1965).
9) T. Miyazaki and S. Shida, *ibid.*, **39**, 2344 (1966).
10) J. A. Ward and W. H. Hamill, *J. Am. Chem. Soc.*, **89**, 5116 (1967).
11) T. Miyazaki, K. Tanno and S. Shida, This Bulletin, **42**, 362 (1969).
12) W. A. Chupka and M. Kaminsky, *J. Chem. Phys.*, **35**, 1991 (1961).

TABLE 1. THE G VALUES OF FRAGMENT IONS IN THE LIQUID-PHASE RADIOLYSIS OF SATURATED HYDROCARBONS*

Fragment ion	Saturated hydrocarbon					
	CCC	C CCC	C CCCC	C CCC C	CC CCCC	C C CCCCC C
$C_2H_5^+$	0.28 (30)	—	0.1 (19)	—	—	—
$C_3H_7^+$	1.1 (8)	1.15 (14)	0.23 (19)	—	0.5 (17)	—
$C_4H_9^+$	—	—	0.12 (20)	1.0 (8)	— —	0.36 (13)

* The values presented here, except for propane, are taken from Refs. 1 and 2. In the parentheses are shown the heat of formation of the fragment ion formed from the parent molecular ion in kcal/mol, taken from Ref. 13 or F. H. Field and J. L. Franklin, "Electron Impact Phenomena," Academic Press, Inc., New York (1957)

the smaller the number of bonds in a hydrocarbon, the greater the energy partitioned per one bond. If these two conditions are favorably satisfied, relatively high values of fragment ions may be obtained, for example, such as $G(C_3H_7^+)=1.1$ and 1.15 for propane and isobutane, and $G(C_4H_9^+)=1.0$ for neopentane.

The $C_4H_9^+$ is formed in the radiolysis of neopentane as well as isopentane, but in different yields. Both hydrocarbons have the same number of degrees of vibrational freedom. However, the heat of formation by reaction (13) is 20 kcal/mol,[13] while only 8 kcal/mol[13] is required for reaction (14).

$$iso\text{-}C_5H_{12}^+ \rightarrow C_4H_9^+ + CH_3 \qquad (13)$$
$$\Delta H = 20 \text{ kcal/mol}$$

$$neo\text{-}C_5H_{12}^+ \rightarrow t\text{-}C_4H_9^+ + CH_3 \qquad (14)$$
$$\Delta H = 8 \text{ kcal/mol}$$

Naturally the latter case gives the larger yield of $C_4H_9^+$. The C–C bond energy of a parent ion of a branched hydrocarbon is generally greatly weaker than that of a straight-chain alkane. Although we have not measured, except propane, the yield of fragment ions produced by the C–C bond rupture in the radiolysis of straight-chain alkanes, the yield of fragment ions may be expected smaller, if present, in the radiolysis of straight-chain alkanes such as *n*-pentane and *n*-hexane.

Reactions (15) and (16) require almost the same heat of formation.[13]

$$iso\text{-}C_4H_{10}^+ \rightarrow sec\text{-}C_3H_7^+ + CH_3 \qquad (15)$$
$$\Delta H = 14 \text{ kcal/mol}$$

$$iso\text{-}C_8H_{18}^+ \rightarrow t\text{-}C_4H_9^+ + C_4H_9 \qquad (16)$$
$$\Delta H = 13 \text{ kcal/mol}$$

However, if one compares the values in Table 1, $G(sec\text{-}C_3H_7^+)$ exceeds $G(t\text{-}C_4H_9^+)$. This may be because that the number of degrees of the vibrational freedom of C_4H_{10} is much smaller than that of C_8H_{18}, and that the energy partitioned per C–C bond is larger in the case of isobutane.

The authors wish to thank Dr. T. Miyazaki of Nagoya University for valuable suggestions.

13) J. L. Franklin and F. W. Lampe, *Trans. Faraday Soc.*, **57**, 1449 (1961).

BULLETIN OF THE CHEMICAL SOCIETY OF JAPAN VOL. 42 2132—2136 (1969)

ESR Studies of Carboxylic Acid- and Ester-Radical Anions Produced by γ-Irradiation at 77°K

Yukihiko NAKAJIMA, Shin SATO and Shoji SHIDA

Department of Applied Physics, Tokyo Institute of Technology, Ookayama, Meguro-ku, Tokyo

(Received December 10, 1968)

A series of monocarboxylic acids and esters have been γ-irradiated at 77°K, either pure or in the rigid matrix of 2-methyltetrahydrofuran, and the products have been examined by ESR spectroscopy. The spectra obtained in the pure state showed that the primary paramagnetic species in each case is the corresponding radical anion, $R-\dot{C}\begin{smallmatrix}O^-\\O-R'\end{smallmatrix}$. In the rigid matrix, these characteristic spectra have been obtained after illuminating the γ-irradiated sample with visible light at the expense of the spectra of trapped electrons. When ultraviolet light was used for the illumination, the spectra of the radical anions disappeared, but instead appeared the spectra of the radicals produced by the decomposition of the radical anions. The latter spectra were almost the same as those obtained by the direct photolyses of acids and esters.

Many radicals and ions in rigid matrices at low temperatures have been characterized by their optical and ESR spectra.[1-4] These unstable intermediates are usually produced by the irradiation of ultraviolet light or γ-rays. As the rigid matrix, 2-methyltetrahydrofuran (MTHF) has often been used; in it trapped electrons are easily formed by γ-irradiation. When electrophilic molecules are present in the matrix, electrons released from the traps by the illumination of visible light are captured by the solute molecules. In the present paper, a series of monocarboxylic acids and esters are used as the solutes.

In 1959, Alger, Anderson and Webb[5] examined X-irradiated formic and acetic acids and several esters of these acids by ESR spectroscopy; they observed doublet spectra in every case, but they did not assign the spectra. Miyagawa and Gordy[6] also studied X-irradiated acetic acid and discussed the paramagnetic species responsible for the doublet spectrum.

In connection with a study of the behavior of electrons in rigid matrices, we reinvestigated the radiolyses and the photolyses of carboxylic acids and esters, both pure and in the matrix of MTHF, by means of ESR spectroscopy. While the present research was being undertaken, a study[7] appeared on a series of carboxylic acid radical anions, where the anions were prepared by the reaction with alkali metals. Our results on the acids are almost entirely consistent with theirs, but quantitatively a few variances are observed.

Experimental

Commercially-available carboxylic esters, methyl formate, methyl acetate, ethyl acetate, propyl acetate, methyl propionate, ethyl propionate, methyl *n*-butyrate, and methyl pivalate were purified by trap-to-trap distillations. Formic acid, acetic acid, propionic acid, and fully-deuterated acetic acid commercially obtained were used without purification. MTHF was stored in a sodium mirror for more than a day before use. For irradiating samples, carboxylic acids, esters, and MTHF containing small amounts of esters were frozen in Spectrosil tubes at the temperature of liquid nitrogen. These tubes were irradiated at 77°K with ^{60}Co γ-rays for half an hour at the dose rate of 2.2×10^5 R/hr. After the irradiation, samples were examined in the dark by means of a JEP-1 X-band ESR spectrometer with a field modulation of 100 kc/sec. After the initial measurement, bleaching experiments were performed with visible light from a tungsten lamp, and then with ultraviolet light from a Toshiba SHL-100 UV-2 mercury lamp. On the other hand, direct photolyses of several esters with ultraviolet light were also performed. As the standard for determining the hyperfine splitting constants and the line widths observed, Mn^{2+} in MgO was applied to the cavity.

1) G. N. Lewis and D. Lipkin, *J. Am. Chem. Soc.*, **83**, 1036 (1961).
2) M. K. Carter and G. Vincow, *J. Chem. Phys.*, **47**, 292 (1967).
3) T. Shida and W. H. Hamill, *J. Am. Chem. Soc.*, **88**, 3683 (1966).
4) T. Shida and W. H. Hamill, *J. Chem. Phys.*, **44**, 2369 (1966).
5) R. S. Alger, T. H. Anderson and L. A. Webb, *ibid.*, **30**, 695 (1959).
6) I. Miyagawa and W. Gordy, *J. Am. Chem. Soc.*, **83**, 1036 (1961).
7) J. E. Bennett and L. H. Gale, *Trans. Faraday Soc.*, **64**, 1174 (1968).

Results

γ-Radiolyses of Pure Carboxylic Esters. An ESR spectrum of γ-irradiated ethyl acetate is shown in Fig. 1. The spectrum A was obtained immediately after γ-irradiation. This spectrum was little affected by the illumination of visible light, while 2 min illumination with ultraviolet light was enough to eliminate this characteristic spectrum of the doublet and produce instead a quartet due to methyl radicals, as is shown in the spectrum B of Fig. 1. The underlying weak spectra in the A and B consist of five lines which are probably due to the radical, $CH_3\dot{C}OOCHCH_3$.[8,9] Characteristic doublet spectra obtained with γ-irradiated ethyl acetate were also observed with other esters, such as methyl acetate, propyl acetate, methyl propionate, ethyl propionate, and methyl *n*-butyrate. As an example, the ESR spectrum of γ-irradiated propyl acetate is

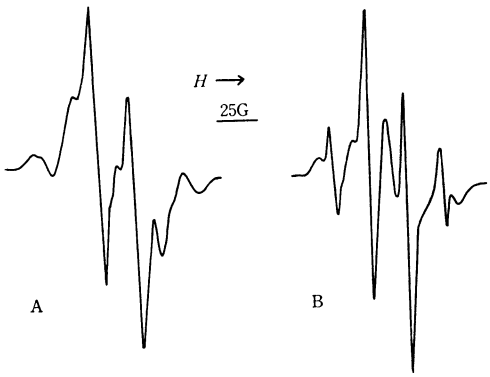

Fig. 1. ESR spectra of γ-irradiated ethyl acetate.
A: immediately after γ-irradiation
B: after bleaching by UV light

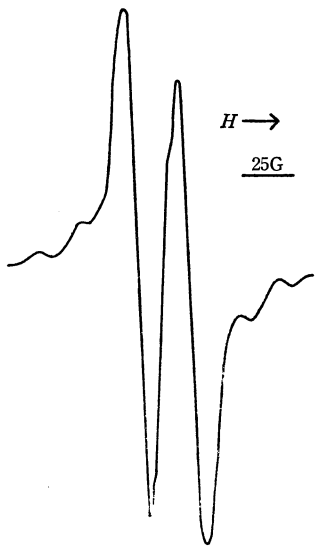

Fig. 2. ESR spectrum of γ-irradiated propyl acetate.

Table 1. Main ESR spectrum of γ-irradiated monocarboxylic esters and acids

Compound	No. of line	Hfs const. (oe)	Line widths (oe)
$HCOOCH_3$	1	—	6.3
CH_3COOCH_3	2	23.3	4.3
$CH_3COOC_2H_5$	2	23.3	6.1
$CH_3COOC_3H_7$	2	21.5	7.3
$C_2H_5COOCH_3$	2	20.7	6.4
$C_2H_5COOC_2H_5$	2	21.5	7.3
$C_3H_7COOCH_3$	2	21.5	6.4
$(CH_3)_3CCOOCH_3$	1	—	10.3
HCOOH	2	12.7	9.0
CH_3COOH	2	34.1	12.5
CD_3COOD	3	5	2.5
C_2H_5COOH	2	26.7	12.7

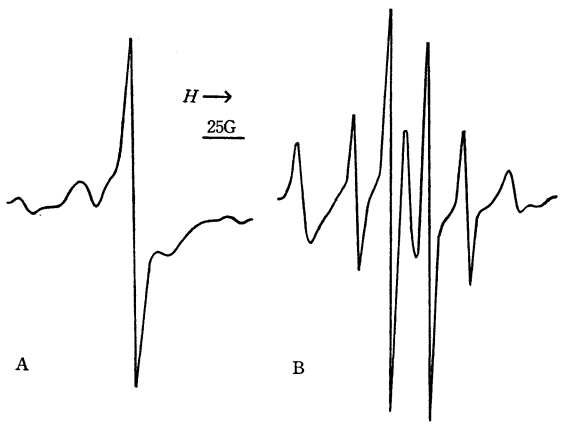

Fig. 3. ESR spectra of γ-irradiated methyl formate.
A: immediately after γ-irradiation
B: after bleaching by UV light

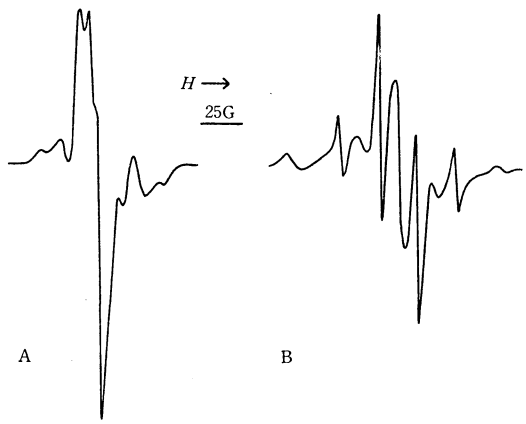

Fig. 4. ESR spectra of γ-irradiated methyl pivalate.
A: immediately after γ-irradiation
B: after bleaching by UV light

8) H. Zelde and R. Livingston, *J. Chem. Phys.*, **30**, 40 (1959).
9) W. A. Seddon and D. R. Smith, *Advan. Chem. Ser.*, **82**, 163 (1968).

shown in Fig. 2. All these doublet spectra were little affected by the visible light-illumination, but were converted to the spectra due to such radicals as methyl and formyl by the ultraviolet light-illumination. The underlying spectra for each ester were well explained as being due to the following radicals: $CH_3COO\dot{C}H_2$ or $\dot{C}H_2COOCH_3$ for methyl acetate, $CH_3COOCH_2\dot{C}HCH_3$ for propyl acetate, CH_3-$\dot{C}HCOOCH_3$ for methyl propionate, and CH_3-$\dot{C}HCH_2COOCH_3$ for methyl butyrate. Table 1 summarizes the hyperfine splitting constants and the line-widths of the doublets, including the results obtained with methyl formate, methyl pivalate, and several carboxylic acids. The ESR spectrum of γ-irradiated methyl formate is shown in Fig. 3. A strong singlet spectrum is seen at the center. This singlet was not affected by the visible light-illumination, but upon ultraviolet illumination for 2 min it changed to the spectra mainly due to methyl radicals. The underlying spectra in the A of Fig. 3 are probably due to $HCOO\dot{C}H_2$ and $\dot{C}HO$. These spectra became stronger after the ultraviolet illumination. Figure 4 shows the ESR spectrum of γ-irradiated methyl pivalate. The underlying spectra are probably due to the radicals, $\dot{C}H_3$ and $(CH_3)_2\dot{C}H_2CCOOCH_3$ or $(CH_3)_3CCOO\dot{C}H_2$. The singlet spectrum at the center decayed a little upon the visible light-illumination. Upon the ultraviolet illumination, however, it immediately changed to the spectra due to methyl and formyl radicals, as is shown in Fig. 4.

We also made observations with monocarboxylic acids under the same condition as for their esters. The results are included in Table 1. These characteristic spectra were almost the same as those already reported by Bennett and Gale using alkali metal-deposition on the acids in preparing the paramagnetic species.[7] The coincidence in the splitting constants and in the line-widths of the spectra is satisfactory.

Ultraviolet Photolyses of Esters. Most of the esters, when frozen at 77°K, become polycrystalline; this is not desirable for the photolyses. Therefore, the experiments were performed with only the five esters which become glassy or nearly glassy at 77°K. These samples were irradiated for about half an hour with a high-pressure mercury lamp. In the case of methyl formate, the spectra due to three radicals, $\dot{C}H_3$, $\dot{C}HO$, and $HCOO\dot{C}H_2$, were observed. Similar spectra were obtained with methyl acetate, and it was noticed that the spectrum due to methyl radicals decayed more rapidly in methyl formate than in methyl acetate at the temperature of liquid nitrogen. Figure 5 shows the ESR spectrum of UV-irradiated ethyl acetate. The spectrum may be identified as being due to the two radicals, $\dot{C}H_3$ and $\dot{C}H_3COO$-

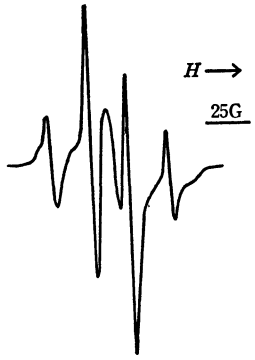

Fig. 5. ESR spectrum of UV-irradiated ethyl acetate.

$\dot{C}HCH_3$. The spectra obtained with other esters, methyl acetate, ethyl propionate, and methyl pivalate, were also well explained by the combination of those due to $\dot{C}H_3$ and $\dot{C}HO$ radicals and the radicals produced by the cleavage at the weakest C–H bond of esters. With ethyl propionate, the contribution of the formyl radical was extremely small and the spectrum due to ethyl radicals was observed instead of that due to methyl radicals.

As has been stated above, ultraviolet irradiation does not give the characteristic spectra obtained by γ-irradiation, such as the doublet with methyl acetate and the singlet with methyl pivalate.

γ-Radiolyses of Esters in the Rigid Matrix of MTHF. The ESR spectrum observed immediately after the γ-irradiation of pure MTHF consisted of a large singlet and a small seven-line spectrum. The singlet may be due to trapped electrons, while the underlying spectrum is probably due to MTHF radicals.[10] When a small quantity of a solute such as a carboxylic ester or sulfur hexafluoride was added to the matrix, the singlet spectrum was reduced. In Fig. 6, the peak height of the singlet

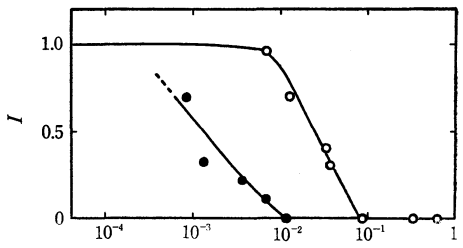

Fig. 6. Relative peak heights (I) of the spectra due to trapped electrons in γ-irradiated MTHF as a function of the mole fractions of additives.
○: ethyl acetate
●: sulfur hexafluoride

10) D. R. Smith and J. J. Pieroni, *Can. J. Chem.*, **43**, 876 (1965).

is plotted as a function of the concentrations of sulfur hexafluoride and ethyl acetate. In the present experiment, the concentration of esters in the matrix was always kept within the range of 1 to 2 mol%, so that the peak height of the singlet obtained immediately after γ-irradiation was almost the same as that obtained with pure MTHF. After the illumination with visible light, however, spectra characteristic of γ-irradiated pure esters appeared at the expense of this singlet spectrum. Figure 7 shows the spectra obtained with γ-irradiated

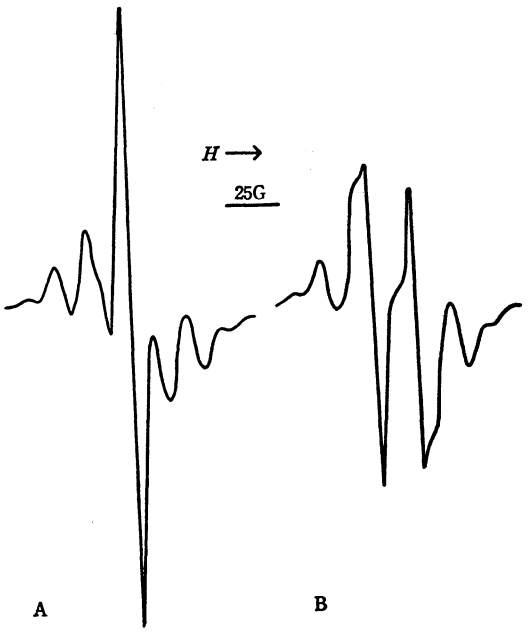

Fig. 7. ESR spectra of γ-irradiated MTHF containing 1 mol% ethyl acetate.
A: immediately after γ-irradiation
B: after bleaching by visible light

MTHF containing 1 mol% ethyl acetate before and after the illumination with visible light. Solute molecules with which the characteristic doublet was observed were methyl, ethyl and propyl acetate, ethyl and methyl propionate, and methyl butyrate. When ultraviolet light was used for the illumination, all the doublets disappeared and the spectra of such radicals as methyl and formyl appeared. These changes correspond exactly to those observed in the pure states previously described. The hyperfine splitting constants and the line-widths of the doublets are summarized in Table 2.

Acetic acid and propionic acid were also used for the solute molecules in the γ-irradiated MTHF glasses. The observed spectra correspond well to those obtained in the pure states. Fully-deuterated acetic acid was also examined. Judging from the spectrum obtained with the pure acid, the expected spectrum was a triplet with a hyperfine splitting constant of 5 G. However, the spectrum actually obtained was a broad singlet. This may be due to the overlap of the spectra due to various radicals produced by γ-irradiation. A similar result was obtained with formic acid; in the pure state a doublet

Table 2. Main ESR spectrum of γ-irradiated MTHF containing monocaboxylic esters or acids after bleaching by visible lights

Compound	No. of line	Hfs const. (oe)	Line widths (oe)
$HCOOCH_3$	1	—	6.7
CH_3COOCH_3	2	$23._6$	5.7
$CH_3COOC_2H_5$	2	$23._1$	7.6
$CH_3COOC_3H_7$	2	$23._0$	6.1
$C_2H_5COOCH_3$	2	$19._8$	5.3
$C_2H_5COOC_2H_5$	2	$21._2$	5.2
$C_3H_7COOCH_3$	2	$20._0$	5.5
$(CH_3)_3CCOOCH_3$	1	—	8.3
$HCOOH$	1	—	7.6
CH_3COOH	2	$32._0$	$10._3$
C_2H_5COOH	2	$25._4$	9.9
CD_3COOD	1	—	$12._5$

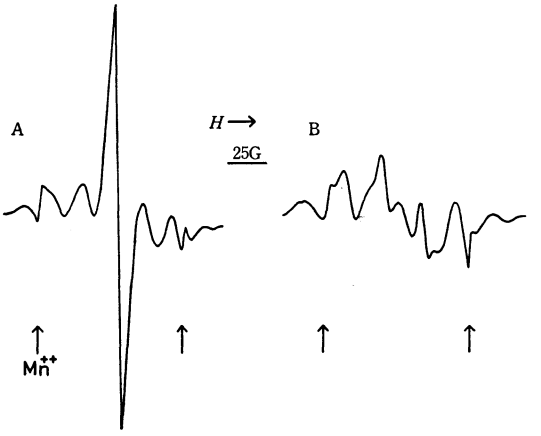

Fig. 8. ESR spectra of γ-irradiated MTHF containing 1 mol% methyl pivalate.
A: after bleaching by visible light
B: after bleaching by UV light

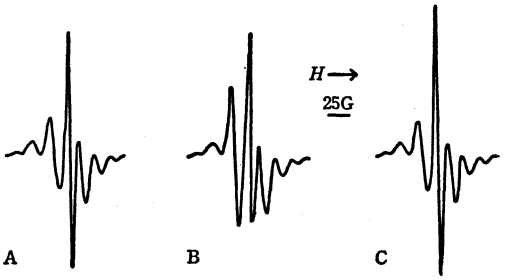

Fig. 9. ESR spectra of γ-irradiated MTHF containing 1 mol% methyl formate.
A: immediately after γ-irradiation
B: after 1-min illumination of visible light
C: after 3-min illumination of visible light

was obtained, but in the matrix a broad singlet was obtained. The spectra A and B in Fig. 8 show the ESR spectra obtained with γ-irradiated methyl pivalate-MTHF glass after the illumination with visible and ultraviolet light. The change from the spectrum A to B exactly corresponds to that observed in the pure state. Figure 9 shows the change in the spectrum obtained with a MTHF glass containing methyl formate during the illumination with visible light. At the beginning of the illumination, the singlet at the center decayed and a doublet appeared, but upon the continuous illumination the doublet diminished and the singlet increased again. The decreased singlet may be attributed to trapped electrons, but the cause of the increased one cannot be specified. This singlet may be the spectrum observed in the pure state. After the ultraviolet illumination, the singlet disappeared, leaving the spectra mainly due to methyl and formyl radicals.

Discussion

As may be seen in Tables 1 and 2, the spectra obtained with γ-irradiated pure carboxylic esters and acids are in good agreement with those obtained with γ-irradiated MTHF containing the corresponding esters and acids after the illumination with visible light. It is now well known that the singlet spectrum observed immediately after the γ-irradiation of a MTHF rigid glass is due to electrons trapped in the solvent and that this singlet is easily quenched by the illumination with visible light. Therefore, the spectra obtained with MTHF glass solutions after illumination with visible light are probably due to the paramagnetic species formed in the reaction of electrons with solute molecules.[3,4] Since carboxylic compounds have large electron affinities, the paramagnetic species above stated might be the corresponding radical anions. Bennett and Gale, using the technique of alkali metal deposition on the carboxylic acids at the temperature of liquid nitrogen, observed the spectra due to the products. The spectra they observed with acids are very similar to those we obtained with acids and esters. They assigned these spectra to the corresponding radical anions, $R-\dot{C}\begin{smallmatrix}O^-\\ O-R'\end{smallmatrix}$. This assignment exactly fits the present results, except for the case of methyl formate.

If radical anions, $R-\dot{C}\begin{smallmatrix}O^-\\ O-R'\end{smallmatrix}$, are responsible for the characteristic spectra obtained with γ-irradiated esters, the doublets observed with esters having β-protons in the substitute, R, suggest that the bond R–Ċ does not rotate freely at the temperature of liquid nitrogen. This has already been substantiated in the case of acetic acid by Bennett and Gale; when the sample was warmed up from the temperature of liquid nitrogen, the doublet observed at 77°K was converted to a quartet typical of that observed in a freely-rotating methyl group, while the reverse process occurred when it was cooled again at 77°K. In the case of methyl pivalate, the corresponding characteristic spectrum observed was a singlet. This is consistent with the above assignment, because this ester has no β-protons.

If the foregoing discussion is applicable to every acid and ester, formic acid and its esters should give a doublet spectrum because of the interaction of an α-proton. Bennett and Gale reported that they observed a doublet with methyl formate, although the details were not presented. As has been stated in the Results section, we observed a singlet with γ-irradiated methyl formate and a peculiar change in the spectrum with the MTHF rigid solution during the illumination with visible light, as is shown in Fig. 9. This change can tentatively be explained as follows; the decrease in the singlet by the illumination is due to the quenching of trapped electrons, while the increase in the doublet may be due to the formation of the radical anions, $H-\dot{C}\begin{smallmatrix}O^-\\ O-CH_3\end{smallmatrix}$. However, if this radical anion is unstable when illuminated with visible light, the following reaction may occur:

$$H-\dot{C}\begin{smallmatrix}O^-\\ O-CH_3\end{smallmatrix} \rightarrow CO_2^- + \text{residue} \qquad (1)$$

In the present interpretation, this reaction corresponds to the change from the spectra B to the C in Fig. 9. Carbon dioxide anions are known to show a singlet and to be stable in visible light.[11] Accordingly, the singlet observed with γ-irradiated methyl formate may be explained in terms of the reaction (1) under γ-irradiation.

In the experiments of Bennett and Gale, carboxylic acids were examined mainly. Therefore, the paramagnetic species they obtained were perhaps dimer anions but were not the monomer radical anions:

$$R-\dot{C}\begin{smallmatrix}O-H-O\\ O-H-O\end{smallmatrix}C-R^-$$

This consideration can also be applied to the present results obtained with acids. In the case of esters, however, the hydrogen bonding is not expected to be so strong that the characteristic spectra observed may be attributed to the monomer radical anions. This may explain the differences in the hyperfine splitting constants of acids and the corresponding esters.

The authors are indebted to Dr. K. Shimokoshi of this Institute for his valuable suggestion.

11) M. Shirom, R. F. C. Claridge and J. E. Willard, *J. Chem. Phys.*, **47**, 286 (1967).

BULLETIN OF THE CHEMICAL SOCIETY OF JAPAN VOL. 42 2137—2140 (1969)

Activity Coefficients of Aqueous Xylose and Maltose Solutions

Hatsuho UEDAIRA and Hisashi UEDAIRA

The Textile Research Institute of Japanese Government, Sawatari, Kanagawa-ku, Yokohama

(Received December 16, 1968)

Osmotic and activity coefficients of aqueous xylose and maltose solutions at 25°C are measured by the isopiestic vapor pressure method. Densities of these solutions are also determined at 25°C. The activity coefficients of water in these solutions show that both xylose and maltose solutions do not behave as regular solutions. Second virial coefficients for xylose and maltose are calculated from partial molar volumes of the solute and the solvent at infinite dilution and empirical equations of water activity coefficient. The coefficients calculated for xylose and maltose are 111 and 248 cc/mol, respectively. Second virial coefficients for these sugars and a few other sugars are approximately proportional to the molecular weight. This relation is explained by the van der Waals model.

The tendency of nonpolar solute to adhere to one another in aqueous environment is affected by the addition of sugars to the system. The protective action of sugars, including xylose, glucose and sucrose, in the coagulation of plasma proteins has been found by Hardt *et al.*[1] They showed that the degree of the action varied with sugars. In a previous paper,[2] we have reported that sucrose affected the hydrophobic bonding between dye ions and decreased the self-association of dyes.

The influence of the addition of sugars on the aqueous solutions of protein and nonpolar solute can be explained by the thermodynamic properties of aqueous sugar solutions. Activity coefficient has been obtained, however, so far only for glucose,[3] sucrose[4] and raffinose.[5] Stigter[6] and Kozak *et al.*[7] calculated the second virial coefficients for these three sugars from the activity and density data.

In the present work, osmotic and activity coefficients of maltose and xylose solutions were determined by the isopiestic vapor pressure method. Density was measured for these two systems. The second virial coefficients of these sugars were calculated by the method of Kozak *et al.*[8]

1) C. R. Hardt, I. F. Muddleson and C. D. Ball, *J. Biol. Chem.*, **163**, 211 (1946).

2) H. Uedaira and H. Uedaira, *Kolloid Z. Z. für Polym.*, **194**, 148 (1964).

3) J. B. Taylor and J. S. Rowlinson, *Trans. Faraday Soc.*, **51**, 73 (1955).

4) R. A. Robinson and R. H. Stokes, *J. Am. Chem. Soc.*, **65**, 1954 (1961).

5) H. D. Ellerton, G. Reinfelds, D. E. Mulcahy and P. J. Dunlop, *J. Phys. Chem.*, **68**, 398 (1964).

6) D. Stigter, *ibid.*, **64**, 118 (1960).

7) J. J. Kozak, W. S. Knight and W. Kauzmann, *J. Chem. Phys.*, **48**, 675 (1968).

8) R. A. Robinson and R. H. Stokes, "Electrolyte Solutions," Butterworth Scientific Publications, London (1959).

Experimental

Materials. Maltose (G. R.) and xylose (G. R.) were purified by crystallization repeated two or three times from water-ethanol solutions. Potassium chloride of analytical grade (Merck Co.) was used without further purification. These samples were dried *in vacuo* over phosphorus pentoxide at 100°C. Solutions were made up in conductance water which was air-freed by boiling before use.

Isopiestic Vapor Pressure Method. Osmotic and activity coefficients were determined with an apparatus similar to that employed by Robinson and Stokes.[4] About 2 m*l* of the sample solution was placed in each of two or three cylindrical silver dishes with lids. The reference potassium chloride solution was also placed in another set of silver dishes. These dishes were placed on a flat copper block contained in a vacuum desiccator, which was set in a thermostat bath at 25°C, controlled to ±0.01°C. At the start of the run, the hinged lids of the dishes were held open by a similar device as described by Robinson and Stokes.[4] The desiccator was evacuated to about 20 mmHg. In order to stir the solution the desiccator was rocked once every four or five seconds. Stirring was made by 3 mm pyrex glass spheres rolling across the bottom of the dishes. At the end of the run, after each dish was closed the vacuum was broken. Equilibrium concentration was measured by weighing the dishes. All the weights were corrected to vacuum. The time required for the equilibrium to be attained was 48 to 90 hr.

Calculation of the Osmotic and the Activity Coefficients. The osmotic coefficient of sugar, ϕ, is given by

$$\phi = 2m_R\phi_R/m, \quad (1)$$

where m_R and m are the molal concentrations of reference solute potassium chloride and sugar in isopiestic equilibrium, respectively. ϕ_R is the osmotic coefficient of potassium chloride at the concentration m_R. The values of the osmotic coefficient for potassium chloride solutions were tabulated by Robinson and Stokes.[8] The osmotic coefficients for each system were represented by the equations of the form

$$\phi = 1 + am + bm^2 + cm^3 . \quad (2)$$

The coefficients a, b and c were obtained by the method of least squares.

From the Gibbs-Duhem relation and the definition of ϕ, the activity coefficient of solute, γ, is shown by

$$\ln \gamma = (\phi - 1) + \int_0^m (\phi - 1) \mathrm{d} \ln m$$

$$= 2am + \frac{3}{2} bm^2 + \frac{4}{3} \mathrm{cm}^3 . \quad (3)$$

The activity coefficient of solvent water, γ_w, was expressed as a power series in the mole fraction of the solute, x. For solutions of nonelectrolytes we have

$$\ln \gamma_w = Bx^2 + Cx^3 + Dx^4 . \quad (4)$$

The coefficients B, C and D have the form[7],*1

$$B = -\left[\frac{1}{2} + a\frac{10^3}{W}\right], \quad (5)$$

$$C = -\left[\frac{2}{3} + 2a\frac{10^3}{W} + b\left(\frac{10^3}{W}\right)^2\right], \quad (6)$$

$$D = -\left[\frac{3}{4} + 3a\frac{10^3}{W} + 2b\left(\frac{10^3}{W}\right)^2 + c\left(\frac{10^3}{W}\right)^3\right], \quad (7)$$

where W is the molecular weight of water.

Density Measurements and the Calculation of Partial Molar Volumes. Density measurements were performed at 25±0.01°C with springel pycnometers of 30 m*l* capacity. At higher concentration of maltose solutions, that of 10 m*l* capacity was used. The density values for each system were fitted to the equations of the form

$$d = d_0 + A_1 m + A_2 m^2 + A_3 m^3 . \quad (8)$$

From Eq. (8), specific volume V is obtained.

$$V = \frac{1}{d_0} - \frac{A_1}{d_0} m + \left(\frac{A_1^2}{d_0^3} - \frac{A_2}{d_0^2}\right) m^2 + \left(-\frac{A_1^3}{d_0^4} + \frac{2A_1A_2}{d_0^3} - \frac{A_3}{d_0^2}\right) m^3 + \left(\frac{A_1^4}{d_0^5} - \frac{3A_1^2A_2}{d_0^4} + \frac{A_2^2 + 2A_1A_3}{d_0^3}\right) m^4 + \cdots . \quad (9)$$

Partial molar volumes of water, $\bar{v}_1$, and of solute, $\bar{v}_2$, can be calculated by the equations

$$\bar{v}_1 = W \cdot V - [(1000 + mM)mW/1000](\partial V/\partial m) , \quad (10)$$

$$\bar{v}_2 = M \cdot V + (1000 + mM)(\partial V/\partial m) , \quad (11)$$

where M is the molecular weight of the solute.

Results

The experimental values of the equilibrium molalities of xylose and maltose, and the molalities of the corresponding potassium chloride solutions are given in Table 1. The osmotic coefficients calculated by Eq. (1) are also given. These coefficients of xylose and maltose solutions are represented by the following equations.*2

$$\phi_{xy} = 1 + 0.01407m + 0.002288m^2 - 0.000482m^3 \quad (12)$$

$$\phi_{mal} = 1 + 0.03635m + 0.001818m^2 - 0.002405m^3 \quad (13)$$

The slope of the osmotic coefficient-concentration curves increases in the order

xylose < glucose < maltose < sucrose < raffinose.

From Eqs. (3), (4), (12) and (13), the expressions of activity coefficients of the solute and the solvent were obtained. They are for xylose solution,

$$\ln \gamma_{xy} = 0.02814m + 0.003432m^2 - 0.0006427m^3 , \quad (14)$$

$$\ln \gamma_{w,xy} = -1.281x^2 - 9.093x^3 + 65.61x^4 , \quad (15)$$

and for maltose solution

$$\ln \gamma_{mal} = 0.007270m + 0.02727m^2 - 0.003207m^3 , \quad (16)$$

$$\ln \gamma_{w,mal} = -2.518x^2 - 60.71x^3 + 302.5x^4 . \quad (17)$$

In contrast to glucose solutions,[3] none of xylose, maltose and sucrose[4] solutions behave as regular solutions.

Table 1. Isopiestic solutions of potassium chloride and xylose or maltose at 25°C

m_R	m_{xy}	ϕ_{xy}	m_R	m_{mal}	ϕ_{mal}
0.30924	0.55618	1.007_2	0.33268	0.58406	1.030_4
0.47150	0.83631	1.014_3	0.41508	0.72443	1.032_6
0.55423	0.97815	1.017_7	0.42119	0.73320	1.035_1
0.72969	1.2850	1.018_7	0.51480	0.88687	1.043_2
0.90713	1.5831	1.028_1	0.56039	0.96097	1.047_3
1.1436	1.9874	1.033_7	0.72969	1.2273	1.066_6
1.3158	2.2876	1.035_2	0.98979	1.6203	1.096_4
1.6413	2.8414	1.045_5	1.0114	1.6459	1.103_0
2.0112	3.4673	1.058_7	1.1436	1.8446	1.113_4
			1.3155	2.0844	1.135_9
			1.6379	2.5369	1.168_5
			2.0112	3.0356	1.209_2

*1 Two misprints are found in Kozak's equations (11) and (12). In the coefficient of the term of x^3, $b(10^3/W)$ should be $b(10^3/W)^2$, and in the coefficient of term of x^4, $3b(10^3/W)^2$ should be $2b(10^3/W)^2$.

*2 An IBM 7090 computer was used for all the calculations by the method of least squares.

TABLE 2. DENSITY OF AQUEOUS XYLOSE AND MALTOSE SOLUTIONS AT 25°C

m	d (g/ml)
Xylose	
0.026610	0.99854
0.039512	0.99922
0.053683	0.99997
0.067322	1.0007
0.13553	1.0044
0.27789	1.0120
0.50056	1.0232
0.99509	1.0465
1.5812	1.0715
2.2569	1.0971
2.9975	1.1221
Maltose	
0.30617	1.0352
0.59583	1.0670
0.99162	1.1049
1.4480	1.1421
2.3365	1.1996
2.8692	1.2275

Densities of xylose and maltose solutions are shown in Table 2, and are represented by the equations

$$d_{xy} = 0.99707 + 0.05505m - 0.00572m^2 + 0.000426m^3, \quad (18)$$

$$d_{mal} = 0.99707 + 0.13122m - 0.02505m^2 + 0.002551m^3. \quad (19)$$

From Eqs. (8), (9), (10), (11), (18) and (19), partial molar volumes of water and xylose in aqueous xylose solution are

$$\bar{v}_1 = 18.069 + 0.009003m^2 - 0.003251m^3 + 0.002313m^4, \quad (20)$$

$$\bar{v}_2 = 95.20 + 0.9994m + 0.2707m^2 - 0.1712m^3 + 0.01356m^4. \quad (21)$$

and those of water and maltose in maltose solution are

$$\bar{v}_1 = 18.069 + 0.9551m^2 + 0.03240m^3 - 0.01557m^4, \quad (22)$$

$$\bar{v}_2 = 211.3 - 106.0m + 8.025m^2 + 1.167m^3 - 0.8652m^4. \quad (23)$$

Discussion

Activity coefficients of xylose and maltose in aqueous solutions show deviations from ideality. The behavior of these aqueous solutions can be discussed more definitely by the second virial coefficient in the osmotic virial equations.

Recently Kozak *et al.*[7] proposed the method of calculation of the second virial coefficient from water activity coefficient and partial molar volume. If compressibility effects can be neglected, and concentrarions in the osmotic virial equation expressed in molecules per unit volume, then the second virial coefficient B_2^* can be calculated by

$$B_2^* = (v_2^* - v_1^0) + v_1^0\left(\frac{1}{2} - B\right)/N_A, \quad (24)$$

where N_A is the Avogadoro number, v_1^0 and v_2^* the partial molar volumes of solvent and solute at infinite dilution, and B the coefficient in Eq. (4). The values of v_1^0 and v_2^* are unchanged whether $\bar{v}_1$ and $\bar{v}_2$ are expressed as a power series in the molal concentration or molar concentration, so B_2^* be calculated from Eqs. (15), (17), (20), (21), (22), and (23). The values are

$$B_2^* \cdot N_A = 111 \text{ cc/mol for xylose in water},$$

$$B_2^* \cdot N_A = 248 \text{ cc/mol for maltose in water}.$$

The values of B_2^* for glucose and sucrose were calculated by Stigter,[6] and that for raffinose by Kozak *et al.*[7]

If we take the sugars as rigid spheres with attractive tails, the second virial coefficient $B_2^*(T)$ for such a van der Waals model is[9]

$$B_2^* = \left(4 - \frac{3}{64}\frac{h\nu_0}{kT}\frac{\alpha^2}{a^6}\right)\frac{4}{3}\pi a^3, \quad (25)$$

where a is the radius of a molecule, α the polarizability, other symbols have their usual meanings. As α and a^3 are proportional to the molecular weight, the quantity in the parenthesis of Eq. (25) is approximately independent of the molecular weight. Therefore, B_2^* will be proportional to

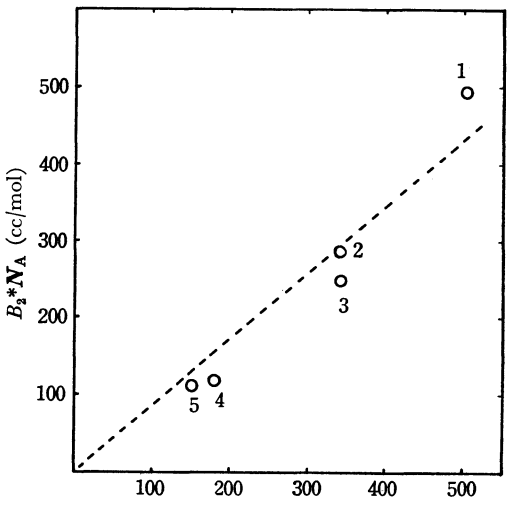

Fig. 1. The relation between second virial coefficient and molecular weight.
1: raffinose 2: sucrose 3: maltose 4: glucose 5: xylose

9) B. Chu, "Molecular Forces," Chap. 3, John Wiley & Sons, New York, London (1967).

the molecular weight. In Fig. 1, the plots of the second virial coefficients *versus* molecular weights are shown. The figure shows that the relation (25) holds approximately. While maltose and sucrose have the same molecular weight, B_2^* of maltose is smaller than that of sucrose. This may be caused by the larger attractive force between maltose molecules.

BULLETIN OF THE CHEMICAL SOCIETY OF JAPAN VOL. 42 2140—2142 (1969)

Diffusion Coefficients of Xylose and Maltose in Aqueous Solution

Hisashi UEADAIRA and Hatsuho UEDAIRA

The Textile Research Institute of Japanease Government, Sawatari, Kanagawa-ku, Yokohama

(Received December 16, 1968)

Diffusion coefficients for the systems aqueous xylose solution and aqueous malotse solution at 25°C were measured by the Rayleigh interference method. Viscosities of these systems were also determined. The concentration dependence of diffusion coefficient for maltose solution is well described by the Gordon relation. For xylose solution, however, a small deviation from this relation is observed. The translational frictional coefficient of maltose was calculated by the shell model of Bloomfield *et al.* If the effect of the local viscosity around a molecule of the solute is corrected, the agreement between the calculated and the observed values is satifsactory.

Only a small amount of data on diffusion of sugars in aqueous solution can be found in literature. Studies on such sugars are limited to the application of the Stockes-Einstein relation and the Gordon empirical relation. For example, the limiting diffusion coefficient of sucrose in aqueous solution is compared with the value calculated by the Stokes-Einstein relation,[1] though the molecule of sucrose has a non-spherical shape.

We present here the viscosity data and the diffusion coefficients for xylose and maltose in the aqueous solution at 25°C. Activity coefficients and densities for these systems have been presented previously.[2] The Gordon relation is tested by these data, and the translational frictional coefficient of maltose in the solution is calculated by the shell model of Bloomfield *et al.*,[3] a comparison being made between the observed and the calculated frictional coefficient.

Experimental

Materials. Xylose and maltose were purified as before.[2]

Viscosity Measurements. An Ubbelohde viscometer was used, the flow time for water at 25°C being 373.6 sec. The correction of the kinetic energy was not made. Viscosity measurement was made at 25.00±0.01°C.

Diffusion Measurements. The diffusion experiment was performed at 25.00±0.01°C using a Spinco Model H diffusion apparatus with a Rayleigh interferometer. For typical run, eight or nine photographic exposures were made at intervals ranging from 15 min to 4 hr; 4 inch by 5 inch Kodack type M glass photographic plates were used. The concentration difference of the solution on both sides of the diffusion boundary was adjusted so that the total number of Rayleigh fringes became 50 or 60. The plates were measured with a Shimadzu type SR-2 comparator. The zero time correction was the order of several seconds. The computation of diffusion coefficients was made by the method suggested by Creeth.[4]

Deionized water was employed as the solvent for these systems. All solutions were prepared by weight, and the weighing was corrected to vaccum. The molar concentrations of solutions were calculated from the density.

Results and Discussion

Reciprocals of relative viscosities of xylose and maltose solutions are represented by the following experimental equations.

$$\eta_0/\eta = 1 - 0.337c \quad (c<0.5) \tag{1}$$

for xylose solution, and

$$\eta_0/\eta = 1 - 0.851c \quad (c<0.3) \tag{2}$$

for maltose solution, where c is the molarity of solute.

In Table 1, the mean concentration of each diffusion experiment and the corresponding observed

1) J. K. Gladden and M. Dole, *J. Am. Chem. Soc.*, **75**, 3700 (1953).

2) H. Uedaira and H. Uedaira, This Bulletin, **42**, 2137 (1969).

3) V. Bloomfield, W. O. Dalton and K. E. Van Holde, *Biopolymers*, **5**, 135 (1967).

4) J. M. Creeth, *J. Am. Chem. Soc.*, **77**, 6428 (1955).

TABLE 1. AN EXPERIMENTAL TEST OF GORDON'S RELATION FOR XYLOSE SOLUTION AT 25°C

$D_0 = 7.495 \times 10^{-6}$ cm²/sec

c (mol/l)	$D_{exp} \times 10^6$ (cm²/sec)	$1+c\frac{d \ln y}{dc}$	η_0/η	$D_{calc} \times 10^6$ (cm²/sec)	D_{exp}/D_{calc}
0.095730	7.385	1.0121	0.968	7.341	1.006
0.18612	7.309	1.0238	0.937	7.191	1.016
0.19637	7.299	1.0252	0.934	7.177	1.017
0.27356	7.221	1.0356	0.908	7.048	1.025
0.44546	7.046	1.0598	0.850	6.752	1.044

TABLE 2. AN EXPERIMENTAL TEST OF GORDON'S RELATION FOR MALTOSE SOLUTION AT 25°C

$D_0 = 5.201 \times 10^{-6}$ cm²/sec

c (mol/l)	$D_{exp} \times 10^6$ (cm²/sec)	$1+c\frac{d \ln y}{dc}$	η_0/η	$D_{calc} \times 10^6$ (cm²/sec)	D_{exp}/D_{calc}
0.006305	5.179	1.0018	0.994	5.180	1.000
0.044895	5.072	1.0130	0.962	5.064	1.001
0.097604	4.910	1.0290	0.917	4.907	1.001
0.12398	4.825	1.0373	0.894	4.822	1.001
0.15109	4.755	1.0459	0.871	4.738	1.004
0.17387	4.662	1.0534	0.852	4.667	0.999
0.22598	4.496	1.0710	0.807	4.495	1.000
0.25272	4.408	1.0804	0.784	4.405	1.001

value of diffusion coefficient for the xylose solutions are given in the first two columns. The corresponding data for maltose solution are given in Table 2. Diffusion coefficients for the two systems decrease linearly with the increase of concentrations. Extrapolated diffusion coefficients are also given in these Tables. The concentration dependence of the diffusion coefficients is larger for maltose than for xylose solution.

Gosting and Morris[5] demonstrated that the observed diffusion coefficients of sucrose in dilute aqueous solutions agreed with diffusion coefficients calculated from the Gordon relation[6]

$$D = D_0\left(1 + c\frac{d \ln y}{dc}\right)\frac{\eta_0}{\eta}, \qquad (3)$$

where y was the molar activity coefficient of solute, η_0 and η the viscosities of water and the solution, and D_0 the limiting value of D as $c \to 0$.

In a previous paper,[2] we obtained the activity coefficients of xylose and maltose in aqueous solution at 25°C. Using the available density data,[2] we obtain the following experimental equations of the molar activity coefficients y

$$\ln y = 0.1237c + 0.01195c^2 \quad (c<3.0) \qquad (4)$$

for xylose solution, and

$$\ln y = 0.2856c + 0.05475c^2 + 0.02720c^3 \quad (c<2.0) \qquad (5)$$

for maltose solution.

It is of interest whether Eq. (3) may describe the dependence which we have observed in the diffusion coefficients upon the concentration for xylose and maltose solutions. In Table 1 for the xylose solution, the third column contains the values of $[1+c(d \ln y/dc)]$ computed by Eq. (4). The values of η_0/η, column 4, were calculated from Eq. (1). Substitution of these values of D_0, $[1+c(d \ln y/dc)]$ and η_0/η into Eq. (3) then gives the values of D_{calc}, column 5. The ratio D_{exp}/D_{calc} is given in the last column in Table 1. The arrangement of Table 2 for the maltose solution is similar to that of Table 1.

As seen from Table 2, Eq. (3) holds for the maltose solution. For the xylose solution, however, the value of D_{exp} is larger than that of D_{calc} (Table 1), and its deviation, though small, increases with the increase of concentration. It is thought that the effect of the kinetic correction term of Eq. (3) is overestimated.

Longsworth[7] suggested that the value of D_0 of different solution could be expressed by the Stokes-Einstein relation in the form

$$D_0 = \frac{kT}{6\pi\eta_0}\left(\frac{4\pi N_A}{3V}\right)^{1/3} \qquad (6)$$

where V is the apparent molar volume of solute, N_A the Avogadro number, and the other symbols have their usual meanings. The apparent molar volumes at the infinite dilution for the xylose and the maltose in the solutions are 95.2 and 211.3

5) L. J. Gosting and M. Morris, *ibid.*, **71**, 1998 (1949).

6) A. R. Gordon, *J. Chem. Phys.*, **5**, 522 (1937).

7) L. G. Longsworth, *J. Am. Chem. Soc.*, **74**, 4155 (1952).

cc/mol, respectively.[2] Using Eq. (6) to calculate the diffusion coefficients of xylose and maltose at infinite dilution we obtained 7.311 and 5.607×10^{-6} cm²/sec, respectively, whereas the values extrapolated from the observed data are 7.495 and 5.201 $10^{-6}\times$ cm²/sec (Tables 1 and 2). The differences between the calculated and the observed values amount to 2.5 and 7.8%. Gladden and Dole[1] found that the differences between the calculated and the observed diffusion coefficients of glucose and sucrose amounted to 2.3 and 7.8%. The differences between the calculated and the observed values for xylose and glucose are small in comparison with the differences between the corresponding values for maltose and sucrose, because the molecules of xylose and glucose are nearly spherical. From this result, even for a small molecule such as maltose and sucrose, the deviation from the spherical shape has a large effect on the application of Eq. (6).

The assumption of the solvent as a continuum in the derivation of the Stokes relation implies that the dimensions of the diffusing particles are large in comparison with those of the solvent molecules. This assumption does not hold in the case of the small molecule, and its frictional coefficient is affected by the structure of solvent. In the aqueous solution, the water structure in the immediate vicinity of the solute is different from that of bulk water. Therefore, the value of η_0 of Eq. (6) must be different from that of bulk water. The translational frictional coefficient for a small molecule with any structure is not given yet. Therefore, when the equation of the frictional coefficient for a large particle is applied to the small molecule, the effect of the local viscosity must be suitably corrected.

Recently, Bloomfield, Dalton and Van Holde,[3] using the shell model, proposed the following expression for the translational frictional coefficient of the macromolecule with a structure which can be visualized as composed of n spherical subunits.

$$f=\frac{6\pi\eta_0\left(\sum_{l=1}^{n}r_l^2\right)^2}{\sum_{l=1}^{n}r_l^3+\sum_{l=1}^{n}\sum_{s=1}^{n}{}'\,r_l^2r_s^2\langle R_{ls}^{-1}\rangle} \qquad (7)$$

where R_{ls} is the distance between centers of two spherical shells of radius r_l and r_s

As the molecule of maltose consists of two identical spherical shells (glucose), the translational frictional coefficient f_M of maltose can be calculated by Eq. (7). Thus we have the expression

$$f_M=1.3(6\pi\eta_0r_G), \qquad (8)$$

where r_G is the radius of glucose. Water structure around the glucose and the maltose in the aqueous solution is regarded as identical. Therefore, the ratio of the frictional coefficient of maltose and glucose is independent of the water structure around the solute. The frictional coefficient f_G of glucose is equal to $6\pi\eta_0r_G$, and so $f_M/f_G=1.3$. On the other hand, the diffusion coefficient is in inverse proportion to the frictional coefficient. The limiting diffusion coefficient of glucose in the aqueous solution at 25°C obtained by Gladden and Dole[1] is 6.75×10^{-6} cm²/sec. Thus the ratio of experimental frictional coefficient of maltose to that of glucose is

$$\frac{f_M}{f_G}=\frac{D_{0G}}{D_{0M}}=\frac{6.75\times10^{-6}}{5.201\times10^{-6}}=1.29_7.$$

Agreement between the calculated and the observed ratio is very good, and is not accidental. Recently, we obtained a good agreement between the calculated and the observed ratio for the β-cyclodextrin in aqueous solution.[8] Generally, the frictional coefficient of the small molecule with complex shape is calculated by expression (7), if the effect of the local viscosity around the solute is corrected.

The authors thank Dr. K. Tsuda in our Institute for helpful discussions, and Mr. S. Tomita (Government Chemical Industrial Research Institute) for the use of a Spinco Model H.

8) H. Uedaira, H. Uedaira and K. Tsuda, presented at the Autumn Meeting of the Chemical Society of Japan, October, 1968.

BULLETIN OF THE CHEMICAL SOCEITY OF JAPAN VOL. 42 2143—2148 (1969)

Studies of the Estimation of the Interfacial Energy of Embryo in Solid-Liquid Systems

Tasuku NAKAI

Department of Chemical Engineering, Faculty of Engineering, Hiroshima University, Senda-machi, Hiroshima

(Received December 18, 1968)

A novel method for the estimation of the interfacial energy of an embryo from the solubility data in solid-liquid systems has been proposed. The distribution function of embryos in solutions derived thermodynamically has been used as the base for the present treatment. The interfacial energies were calculated numerically for three different combinations of solute and solvent, namely, water-inorganic salt, water-organic compound, and organic solvent-organic compound. A fairly good linear relationship was observed between the interfacial energies calculated and the temperatures over the whole temperature range of solubility data. The semiempirical equation describing the relationship between the interfacial energy of the embryo and the temperature in the solid-liquid system was found to be exactly the same as that between the surface energy of the liquid in contact with gas through a free surface and the temperature. The size dependence of the interfacial energy has also been briefly described.

With regard to the nucleation phenomena in both gas and liquid phases, it has been concluded theoretically that the interfacial energy is an important physical property directly affecting the nucleation rate. In spite of the importance of the interfacial energy of embryo in solid liquid systems, however, few reports have been published so far. Accordingly, the determination of the interfacial energy of the embryo seems to be indispensable to developing the nucleation study in solid-liquid systems.

The interfacial energies of the embryo in solid-liquid systems have been sporadically determined from the measurements of the excess solubility of finely-divided crystals,[1-4] the waiting time in the critical nucleus formation,[5-7] and the nucleation rate.[8-10] Because of many theoretical and experimantal difficulties, the numerical values of the interfacial energy reported so far differ from one another depending on the method of measurement and the investigator, and the values are considered to be unreliable. Moreover, the temperature dependence of the interfacial energy in solid-liquid systems has not been studied at all. In this paper, a method of estimating the interfacial energy of the embryo from the solubility data is proposed, and its numerical values over the entire temperature ranges of the solubility data are calculated for a large number of solid-liquid systems. In addition, both the temperature- and the size-dependences of the interfacial energy are described.

Theoretical

It is generally recognized that a great number of embryos of various sizes are present in a supersaturated solution.*1 According to this concept, it is possible to derive a distribution function of the embryos in a supersaturated solution.

Let X_{nj} be the number fraction of embryos composed of j molecules of solute, and assume that the interfacial energy is independent of both the embryo size and the solution composition. For an ideal solution, the change in the Gibbs free energy due to the coagulation of j molecules is given by:[11,12]

1) G. A. Hulett, *Z. Phys. Chem.*, **37**, 385 (1901); **47**, 357 (1904).
2) A. R. Tourky and S. E. S. El Wakkad, *J. Phys. and Coll. Chem.*, **53**, 1126 (1949).
3) Van Zeggeren and G. C. Benson, *Can. J. Chem.*, **35**, 1150 (1957).
4) B. V. Enüstün and J. Turkevich, *J. Am. Chem. Soc.*, **82**, 4502 (1960).
5) G. Preckshot and G. G. Brown, *Ind. Eng. Chem.*, **44**, 1314 (1952).
6) A. C. Chatterji and R. N. Singh, *J. Phys. Chem.*, **62**, 1408 (1958).
7) R. Gindt and R. Kern, *Compt. Rend.*, **562**, 4186, 4400 (1963).
8) J. C. Fisher, J. H. Holloman and D. Turnbull, *Science*, **109**, 168 (1949).
9) H. Naono and M. Miura, This Bulletin, **38**, 80 (1965).
10) H. Naono, *ibid.*, **40**, 1104 (1967).

*1 An embryo is defined as a molecular aggregate the aggregation number of which ranges from two to a number less than that in a critical nucleus.

11) H. Reiss, *Ind. Eng. Chem.*, **44**, 1284 (1952).
12) A. E. Nielsen, "Kinetics of Precipitation," Pergamon Press, Oxford, London (1964), p. 7.

$$\Delta g = -j\phi + \beta\sigma j^{2/3} + \boldsymbol{k}T \ln Xn_j \quad (1)^{*2}$$

where Δg is the Gibbs free energy change per j molecules; ϕ, the Gibbs free-energy change per molecule; β, the geometric factor of the embryo; σ, the interfacial energy; $\boldsymbol{k}$, the Boltzmann constant, and T, the absolute temperature. The number fraction of embryos composed of j molecules of the solute, X_{nj}, is defined by:

$$Xn_j = \frac{n_j}{\sum_{j=2}^{j} n_j + n_1 + n_s} \quad (2)$$

where n_j is the number of embryos composed of j molecules of the solute; $\sum_{j=2}^{j} n_j$, the number of embryos of various sizes; n_1 the number of monomolecules of the solute, and n_s, the number of solvent molecules.

When the equilibrium of the embryo distribution in a supersaturated solution is accomplished, Δg becomes zero and Eq. (1) reduces to:

$$Xn_j = \frac{n_j}{\sum_{j=2}^{j} n_j + n_1 + n_s} = \exp\left(-\frac{\beta\sigma j^{2/3} - j\phi}{\boldsymbol{k}T}\right) \quad (3)$$

and

$$n_j = \left(\sum_{j=2}^{j} n_j + n_1 + n_s\right) \exp\left(-\frac{\beta\sigma j^{2/3} - j\phi}{\boldsymbol{k}T}\right) \quad (4)$$

If it is possible to extend this distrubition function to the saturated state, ϕ should become zero; Eq. (4) can then be rewritten as:

$$n_j = \left(\sum_{j=2}^{\infty} n_j + n_1 + n_s\right) \exp\left(-\frac{\beta\sigma j^{2/3}}{\boldsymbol{k}T}\right) \quad (5)$$

where the upper limit of the summation is taken to infinity, since the number of solute molecules in the critical nucleus is considered to be infinite in a saturated solution.

If the number of the monomolecules of the solute is also assumed to be expressed by Eq. (5), the total number of embryos of various sizes and monomolecules is given by:

$$\sum_{j=2}^{\infty} n_j + n_1 = \sum_{j=1}^{\infty} n_j = \left(\sum_{j=1}^{\infty} n_j + n_s\right)\left\{\sum_{j=1}^{\infty} \exp\left(-\frac{\beta\sigma j^{2/3}}{\boldsymbol{k}T}\right)\right\} \quad (6)$$

Accordingly, the number of solvent molecules is given by:

$$n_s = \left(\sum_{j=1}^{\infty} n_j + n_s\right) - \sum_{j=1}^{\infty} n_j = \left(\sum_{j=1}^{\infty} n_j + n_s\right)\left\{1 - \sum_{j=1}^{\infty} \exp\left(-\frac{\beta\sigma j^{2/3}}{\boldsymbol{k}T}\right)\right\} \quad (7)$$

When all the embryos of various sizes dissociate to monomolecular solutes, the total number of monomolecular solutes is given by:

$$\sum_{j=1}^{\infty} jn_j = \left(\sum_{j=1}^{\infty} n_j + n_s\right)\left\{\sum_{j=1}^{\infty} j \exp\left(-\frac{\beta\sigma j^{2/3}}{\boldsymbol{k}T}\right)\right\} \quad (8)$$

Finally, the so-called "*solubility*" in the mole fraction can be expressed as follows:*3

$$solubility = \frac{\sum_{j=1}^{\infty} jn_j}{\sum_{j=1}^{\infty} j \cdot n_j + n_s} = \frac{\sum_{j=1}^{\infty} j \exp\left(-\frac{\beta\sigma j^{2/3}}{\boldsymbol{k}T}\right)}{\sum_{j=1}^{\infty} j \exp\left(-\frac{\beta\sigma j^{2/3}}{\boldsymbol{k}T}\right) + 1 - \sum_{j=1}^{\infty} \exp\left(-\frac{\beta\sigma j^{2/3}}{\boldsymbol{k}T}\right)} \quad (9)$$

The average number of solute molecules per embryo in a saturated solution, j_{av}, may be estimated in the following manner:

$$j_{av} = \frac{\sum_{j=2}^{\infty} jn_j}{\sum_{j=2}^{\infty} n_j} = \frac{\sum_{j=2}^{\infty} j \exp\left(-\frac{\beta\sigma j^{2/3}}{\boldsymbol{k}T}\right)}{\sum_{j=2}^{\infty} \exp\left(-\frac{\beta\sigma j^{2/3}}{\boldsymbol{k}T}\right)} \quad (10)$$

where the lower limit of the summation is taken as two, since the aggregate composed of two or more molecules is defined as an embryo.

The dimensionless quantity included in the above equations is then replaced by:

$$\frac{\beta\sigma}{\boldsymbol{k}T} \equiv K \quad (11)$$

By substituting Eq. (11) into Eqs. (9) and (10), one obtains:

$$solubility = \frac{\sum_{j=1}^{\infty} j \exp(-Kj^{2/3})}{\sum_{j=1}^{\infty} j \exp(-Kj^{2/3}) + 1 - \sum_{j=1}^{\infty} \exp(-Kj^{2/3})} \quad (12)$$

$$j_{av} = \frac{\sum_{j=1}^{\infty} j \exp(-Kj^{2/3})}{\sum_{j=2}^{\infty} \exp(-Kj^{2/3})} \quad (13)$$

The relationship between the *solubility* or j_{av} and the K value can be determined by the numerical calculation using Eqs. (12) and (13), since the *solubility* and j_{av} are the functions of only K. If the embryo is assumed to be a sphere, β should be expressed as:

$$\beta = (4\pi)^{1/3}(3v)^{2/3} \quad (14)$$

*2 The present author is aware that the use of the term "interfacial energy" is not always appropriate, since the idea of an "interface" between a solution and an embryo composed of only a few solute molecules is purely formal. In such a case the term should simply be understood as a word meaning the excess energy which is inherent in the embryo formation.

*3 The solubility in the mole fraction is usually defined as the ratio of the number of monomolecular solutes to the number of both monomolecular solutes and solvents. In the present paper, however, the number fraction defined by Eq. (2) is used as the concentration. In order to avoid confusion, italic type is used for the former quantity.

where v is the molecular volume of the solute.

The results of the numerical calculation for the *solubility* and j_{av} as a function of K are shown in Figs. 1 and 2 respectively.

The interfacial energy and the average number of solute molecules per embryo in a saturated solution can be obtained through the following procedures: 1) the calculation of the *solubility* at an arbitrary temperature from the solubility data; 2) the determination of K corresponding to the *solubility* from Fig. 1; 3) the calculation of β by Eq. (14); 4) the calculation of σ corresponding to the K obtained by means of Eq. (11), and 5) the determination of j_{av} corresponding to K from Fig. 2.

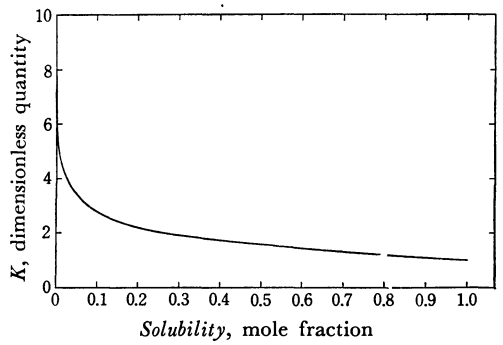

Fig. 1. Relationship between K and *solubilty*.

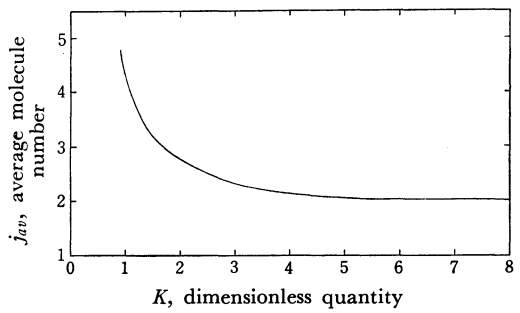

Fig. 2. Relationship between j_{av} and K.

Results

The present calculation was applied to the solid-liquid systems for which the solubility data were known over a wide temperature range. The systems were selected from "Kagaku Binran."[13] Since Eqs. (12) and (13) should hold for any combination of solute and solvent, the calculation was carried out for three different systems: 1) fifty inorganic salts in water, 2) fifteen organic compounds in water, and 3) fifteen organic compounds in organic solvents.

The interfacial energies for three sorts of inorganic salts, *i. e.*, easily-soluble anhydrides, easily-soluble hydrates, and sparingly-soluble anhydrates, were calculated. Some of the results are shown in Figs. 3, 4 and 5, where the interfacial energy is plotted against the centigrade temperature. As these figures show, a fairly good linearity in the plot of σ values against the centigrade temperatures was obtained for all fifty systems calculated.

Similar calculations were also carried out for both water-organic compound and organic solvent-organic compound systems. Some of the results are shown in Figs. 6 and 7. In these instances linearity was also obtained for all thirty systems.

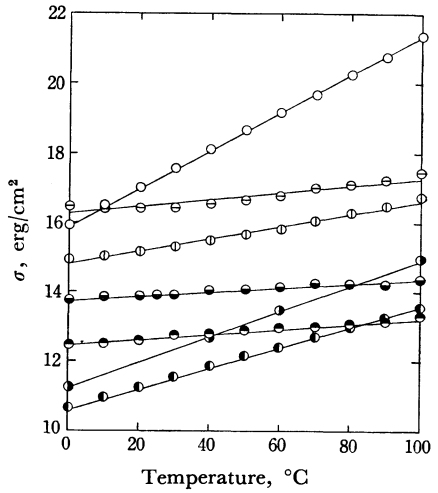

Fig. 3. Relationship between σ and the temperature for easily-soluble anhydrous salts in water.
○: NaCl ⊖: K_2SO_4 ◐: KCl ◑: ZnI_2
◒: NH_4Cl ◐: K_2CrO_4 ◓: NH_4Br

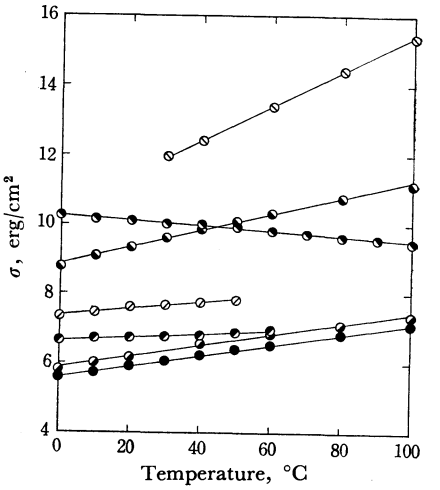

Fig. 4. Relationship between σ and the temperature for easily-soluble hydrous salts in water.
⊘: $Na_2CO_3 \cdot H_2O$ ◔: $CuSO_4 \cdot 5H_2O$
◔: $LiOH \cdot H_2O$ ⊘: $NaI \cdot 2H_2O$
◐: $SrCl_2 \cdot 6H_2O$ ◑: $MgCl_2 \cdot 6H_2O$
●: $MgBr_2 \cdot 6H_2O$

13) "Kagaku Binran," Maruzen, Tokyo (1958), p. 581.

Discussion

Temperature Dependence. The temperature dependence of the surface energy in the gas-liquid system has been studied theoretically by several authors[14,15] and a linear relationship has been concluded to hold. The temperature dependence of the surface energy of liquids which come in contact with gases through a free surface has been experimentally ascertained, and the following empirical equation has been proposed;[16,17]

$$\sigma\left(\frac{M}{\rho_l}\right)^{2/3} = \alpha(T_c - T - 6) \tag{15}$$

where M is the molecular weight; ρ_l, the density of the liquid; α, a constant; T_c, the critical absolute temperature of the liquid, and T, the absolute temperature corresponding to σ,

On the other hand, a linear relationship between the interfacial energy of embryo and the temperature was also obtained from the present study for solid-liquid systems. Since v in Eq. (14) is expressed by:

$$v = \frac{M}{N\rho_s} \tag{16}$$

one obtains, by substituting Eq. (16) into Eq. (14):

$$\beta = (4\pi)^{1/3}\left(\frac{3}{N}\right)^{2/3}\left(\frac{M}{\rho_s}\right)^{2/3} \tag{17}$$

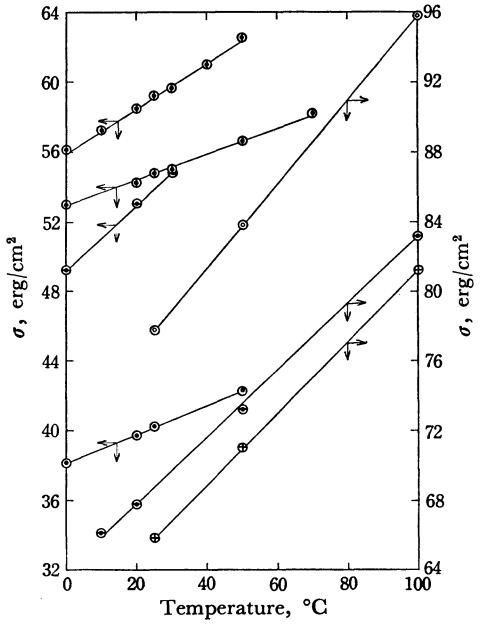

Fig. 5. Relationship between σ and the temperature for sparlingly-soluble anhydrous salt in water.
⊕: $PbSO_4$ ⊕: Ag_2CrO_4 ⊕: $SrSO_4$
◎: $CaCO_3$ (Aragonite) ⊙: $BaSiF_6$ ⊖: $BaSO_4$
⊕: $CaCO_3$ (Calcite)

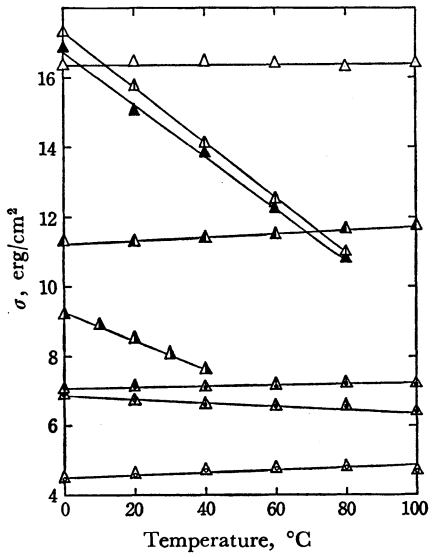

Fig. 6. Relationship between σ and the temperature for organic compounds in water.
△: Picric acid ▲: Oxalic acid ◭: Cyanamide ◮: Glycine
◬: Succinic acid ◭: Potassium oxalate ◮: Racemic acid ◬: Sucrose

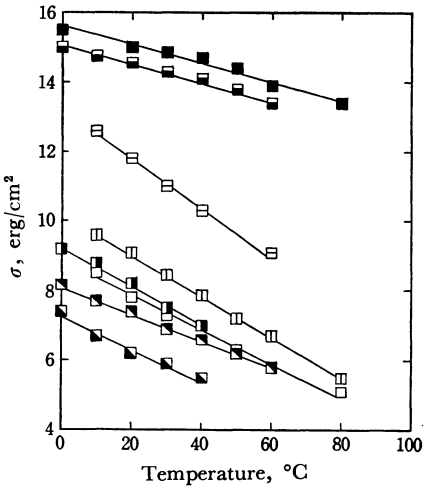

Fig. 7. Relationship between σ and the temperature for organic compound - organic solvent systems.
■: Anthraquinone-benzene
■: Anthracene-benzene
▤: Picric acid - benzene
▥: Benzoic acid - benzene
■: Acetamide-ethanol
□: Naphthalene-benzene
◥◣: Acetanilide-ethanol
◥◣: Urethan-ethanol

14) J. O. Hirschfelder, C. F. Curtiss and B. R. Bird, "Molecular Theory of Gases and Liquids," John Wiley, New York (1954), p. 342.
15) J. Frenkel, "Kinetic Theory of Liquids," Dover Publications, New York (1955), p. 310.
16) R. Eötvös, *Wied. Ann.*, **27**, 456 (1886).
17) W. Ramsay and J. Shields, *J. Chem. Soc.*, **1893**, 1089.

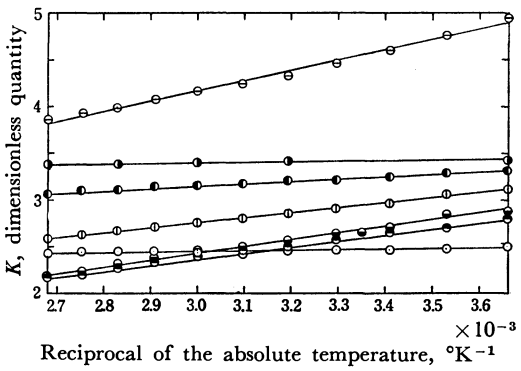

Fig. 8. Relationship between K and the reciprocal of the absolute temperature for easily-soluble anhydrous salts in water.
⊖: K_2SO_4 ◑: ZnI_2 ◐: K_2CrO_4 ⓘ: KCl
◒: NH_4Cl ◓: NH_4Br ○: NaCl

where ρ_s is the density of the solute at the solid state and N, the Avogadro number.

The K values lie on a straight line in the plot against the reciprocal of the absolute temperature, as is shown in Fig. 8, in which the same systems as those in Fig. 3 are selected. Therefore, the relationship between K and the absolute temperature is given as:

$$K = A + \frac{B}{T} \tag{18}$$

where both A and B are constants characteristic of their solid-liquid systems.

By substituting Eqs. (17) and (18) into Eq. (11), one can derive the following semi-empirical equation for solid-liquid systems;

$$\sigma\left(\frac{M}{\rho_s}\right)^{2/3} = \frac{Ak}{(4\pi)^{1/3}\left(\frac{3}{N}\right)^{2/3}}\left(T + \frac{B}{A}\right) \tag{19}$$

By comparing Eq. (15) with Eq. (19), one can conclude that the temperature dependence of the interfacial energy can be expressed by similar equations for both cases, *i. e.*, liquids coming into contact with gases through a free surface and solid embryos in saturated solutions.

Size Dependence. The size dependence of the surface energy of a small droplet in a gas-liquid system has been thermodynamically studied by Tolman,[18] and the following theoretical equation has been derived:

$$\frac{\sigma_r}{\sigma_\infty} = \frac{1}{1 + \frac{2\delta}{r}} \tag{20}$$

where σ_r is the surface energy of the droplet with the radius r; σ_∞, that of the liquid with a free surface, and δ, a constant. Although he suggested that δ should be of the same order as the molecular diameter of liquid species, he did not make any numerical examination, presumably because of the lack of the surface energy data on small droplets in gas-liquid systems.

Since the *solubilities* don't change greatly with the temperature in the systems calculated in the present study, the variation in j_{av} was not appreciable over the whole temperature range. For instance, when the *solubility* of potassium chloride varies from 0.0694 to 0.120, corresponding to the temperature elevation from 0°C to 100°C, the K value changes from 3.06 to 2.50. Accordingly, the J_{av} value obtained from Fig. 2 varies from 2.32 to 2.44 corresponding to the variation of K. Since the variations in j_{av} were unappreciable for all solid-liquid systems studied, it may be reasonable to say that the size effect of the interfacial energy of embryo does not appear in the σ values calculated by the present method.

Comparison with the Published Data. Although the interfacial energies of the finely-divided crystals in solid-liquid systems have been investigated by several authors[1-4,19] on the basis of measuring the excess solubility, the results seem questionable. This is an indication of the number of theoretical and experimental difficulties unavoidable in treating fine particles, as was pointed out by Harbury.[19] The interfacial energies calculated by the present method will be compared below with recently-published data.

Recently, the interfacial energy of strontium sulfate has been estimated by Enüstün and Turkevich[4] utilizing the dependence of the solubility on the particle size. They have given 84 ± 8 erg/cm² as the interfacial energy of the finely-divided crystals (radius, 9 Å) at 25°C. On the other hand, by means of the present method σ and j_{av} are determined to be 53.9 erg/cm² and 2.0 respectively in the saturated solution at 25°C. Assuming that the difference in σ values depends only on the difference in the number of molecules in the two embryos, one can determine δ in Eq. (20). If the embryo is spherical, the radius of the embryo composed of two molecules becomes 3.33 Å. By substituting the σ and r of both embryos into Eq. (20) and by then dividing the former by the latter, one can obtain;

$$\frac{84}{53.9} = \frac{1 + \frac{2\delta}{3.33}}{1 + \frac{2\delta}{9}} \tag{21}$$

From Eq. (21) δ is calculated to be 2.20 Å. As a result of the above examination, δ seems to be roughly equated to the molecular radius (2.64 Å) of strontium sulfate, where the molecular radius is calculated on the assumption of a spherical molecule.

18) R. C. Tolman, *J. Chem. Phys.*, **16**, 758 (1948). **17**, 333 (1949).

19) L. Harbury, *J. Phys. Chem.*, **50**, 190 (1946).

Van Zeggeren and Benson[3] have investigated, by means of the electric-conductivity method, the solubilities of sodium chloride specimens varying in specific surface in ethanol at 25°C. They have given 171 erg/cm^2 as the interfacial energy of the fine crystal with a radius of 325 Å. In the present study the value is 50.9 erg/cm^2 for the embryo with a radius of 2.78 Å. In this system the δ in Eq. (20) becomes 3.37 Å (molecular radius: 2.20 Å)

Fisher *et al.*[8] have shown that the interfacial energy for the critical nucleus in a water-sucrose system is about 6 erg/cm^2. In the present study the value is 4.6 erg/cm^2 for the sucrose embryo composed of solute molecules of 2.4 at 25°C.

As a whole, the present calculation of the interfacial energies gives somewhat smaller values than those previously reported. This is probably due to the fact that smaller values of the embryo size were here calculated. Since our knowledge of the size dependence of the interfacial energy is insufficient at the present stage, it is difficult to predict in detail the interfacial energies of the fine crystals of various sizes in solid-liquid systems.

The conclusions are that it is possible to estimate the interfacial energy of embryos from the solubility data for all solid-liquid systems and that the interfacial energies calculated are linear in the plot against the temperature, as has been ascertained in gas-liquid systems with a free surface.

The author wishes to thank Professor Shigefumi Fujita, Faculty of Engineering, Tokyo Institute of Technology, for his many helpful discussions and suggestions during this study. Thanks are also due to Professor Masaji Miura, Faculty of Science, Hiroshima University, for his continuing interest and encouragement.

BULLETIN OF THE CHEMICAL SOCIETY OF JAPAN VOL. 42 2148—2158 (1969)

Electron Diffraction Studies of Formaldehyde, Acetaldehyde and Acetone

Chuichi KATO,*1 Shigehiro KONAKA, Takao IIJIMA and Masao KIMURA

Department of Chemistry, Faculty of Science, Hokkaido University, Sapporo

(Received December 18, 1968)

The molecular structures of formaldehyde, acetaldehyde, and acetone have been investigated by the sector-microphotometer method of electron diffraction. Certain of the bonded interatomic distances, r_g, were determined to be as follows: for formaldehyde, $r(C-O)=1.209_3\pm0.003_3$ Å and $r(C-H)=1.096_7\pm0.053_5$ Å; for acetaldehyde, $r(C=O)=1.208_5\pm0.003_3$ Å and $r(C-C)=1.514_2\pm0.005_1$ Å; for acetone, $r(C=O)=1.211_0\pm0.004_1$ Å and $r(C-C)=1.516_7\pm0.004_8$ Å. The value of $r_g(C=O)$ for formaldehyde was perfectly consistent wth the zero-point average distance, $r_z(C=O)$, determined by microwave spectroscopy.

The structures of formaldehyde, acetaldehyde, and acetone have been the subject of a large number of structural investigations, for these compounds are the simple and elementary units of organic molecules containing carbonyl groups. Several structure determinations by microwave spectra have been published in the past decade.[1-3] In contrast to these studies by microwave spectra, however, studies by electron diffraction have so far been carried out[4-6] by the visual method and, necessarily, their results have included large uncertainties.

It is well known that bond lengths originally determined by microwave spectroscopy and by electron diffraction are not of the same physical siginificance, but can be related to each other by

*1 Present address: Fuji Iron and Steel Central Research Laboratory Co., Sagamihara, Japan.

1) HCHO: a) T. Oka, *J. Phys. Soc. Japan*, **15**, 2274 (1960); b) K. Takagi and T. Oka, *ibid.*, **18**, 1174 (1963).

2) CH_3CHO: a) R. W. Kilb, C. C. Lin and E. B. Wilson, Jr., *J. Chem. Phys.*, **26**, 1695 (1957); b) D. R. Herschbach, *ibid.*, **27**, 975 (1957).

3) $(CH_3)_2CO$: a) J. D. Swalen and C. C. Costain, *ibid.*, **31**, 1562 (1959); b) R. Nelson and L. Pierce, *J. Mol. Spectry.*, **18**, 344 (1965).

4) HCHO: D. P. Stevenson, J. E. LuValle and V. Schomaker, *J. Am. Chem. Soc.*, **61**, 2508 (1939).

5) CH_3CHO: D. P. Stevenson, H. D. Burnham and V. Schomaker, *ibid.*, **61**, 2922 (1939); R. H. Schwendeman, *Diss. Abs.*, **18**, 1645 (1958).

6) $(CH_3)_2CO$: O. Bastiansen and H. Viervoll, *Acta Chem. Scand.*, **2**, 702 (1948); M. Kimura and Y. Kurita, *Nippon Kagaku Zassi (J. Chem. Soc. Japan, Pure Chem. Sect.)*, **72**, 396 (1951); P. W. Allen, H. J. M. Bowen, L. E. Sutton and O. Bastiansen, *Trans. Faraday Soc.*, **48**, 991 (1952); C. Romers and J. E. G. Grentzberg, *Rec. Trav. Chim.*, **75**, 331 (1956).

taking into account the effect of thermal motions.[7] Since structure determinations for relatively complicated molecules must be performed on several assumptions when either method is used, microwave spectroscopy and electron diffraction may be considered to complement each other in determinations of molecular configurations.[8] Thus, the most reliable structures of formaldehyde, acetaldehyde, and acetone will be determined by combining information from electron diffraction with that from spectroscopy. The purpose of the present paper is to present the accurate molecular structures of these compounds as determined by the sector-microphotometer method of electron diffraction.

Experimental

The electron diffraction unit used in the present

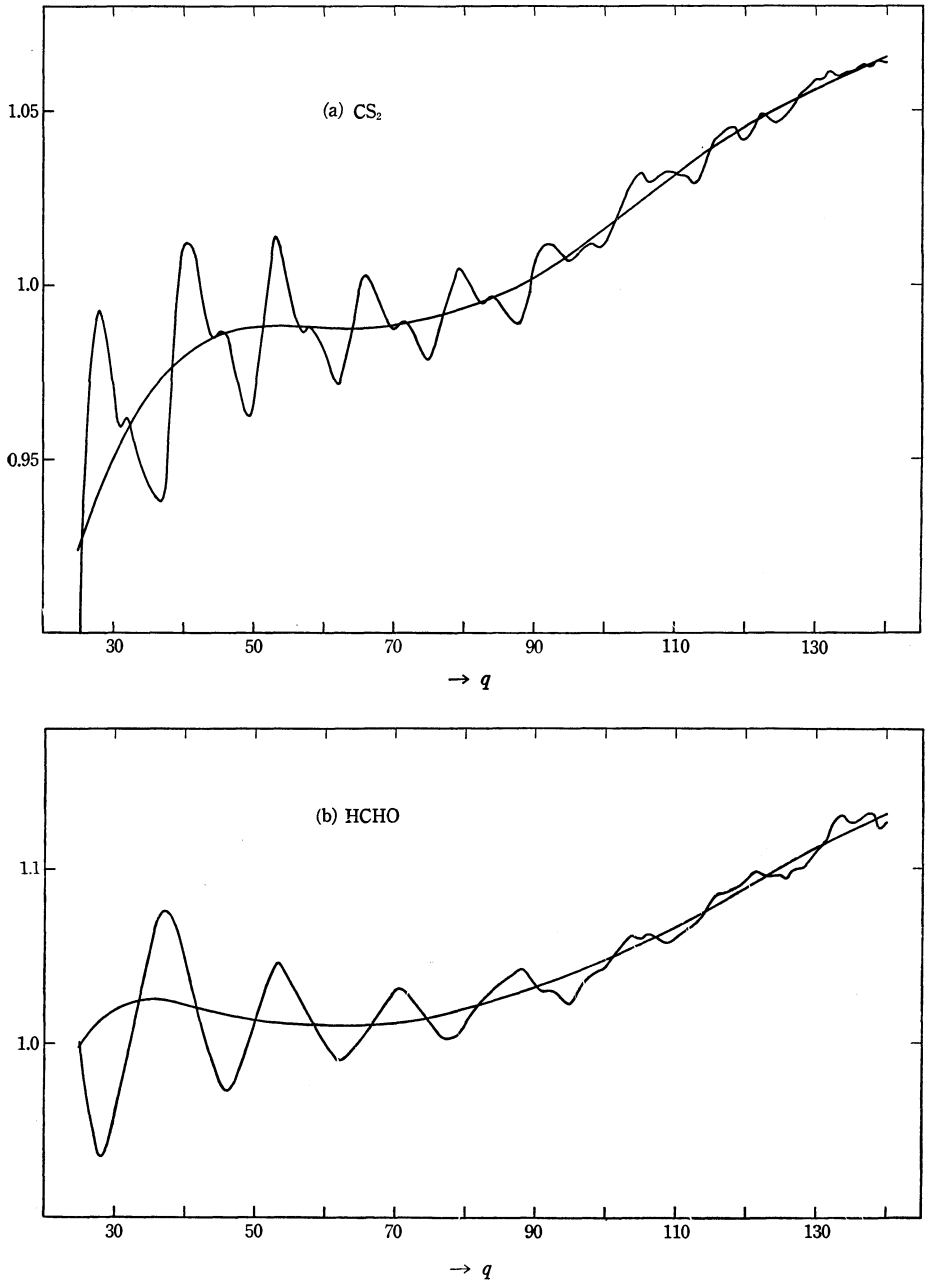

7) Y. Morino, K. Kuchitsu and T. Oka, *J. Chem. Phys.*, **36**, 1108 (1962).

8) K. Kuchitsu, T. Fukuyama and Y. Morino, *J. Mol. Structure*, **1**, 463 (1967—68).

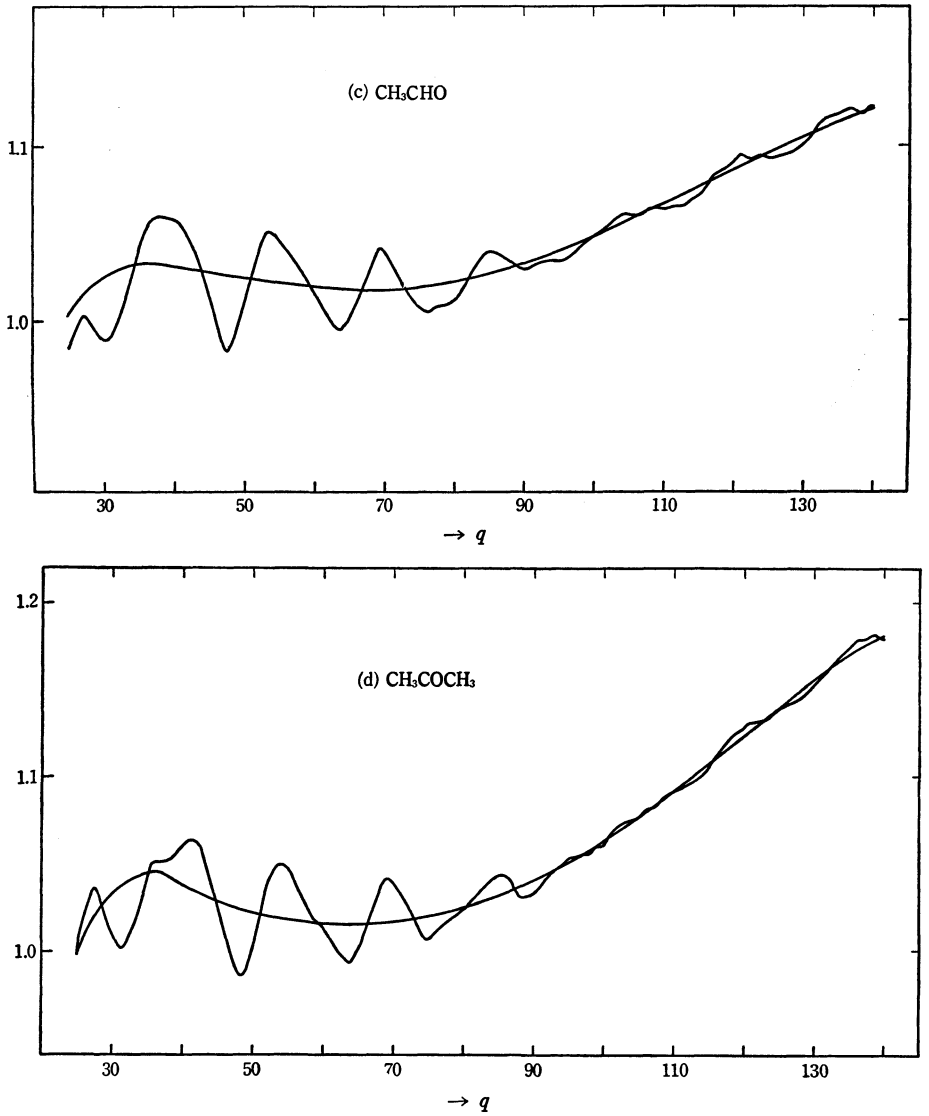

Fig. 1. Leveled intensities and backgrounds.
(a) CS_2, (b) HCHO, (c) CH_3CHO and (d) CH_3COCH_3.

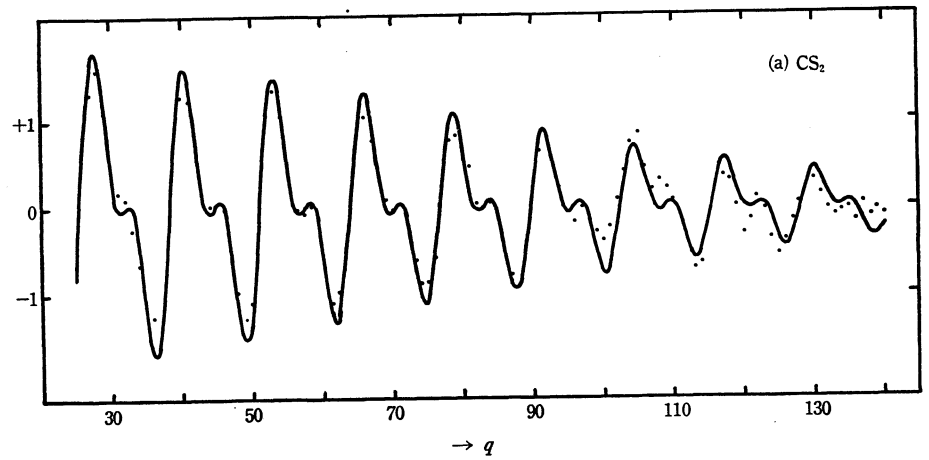

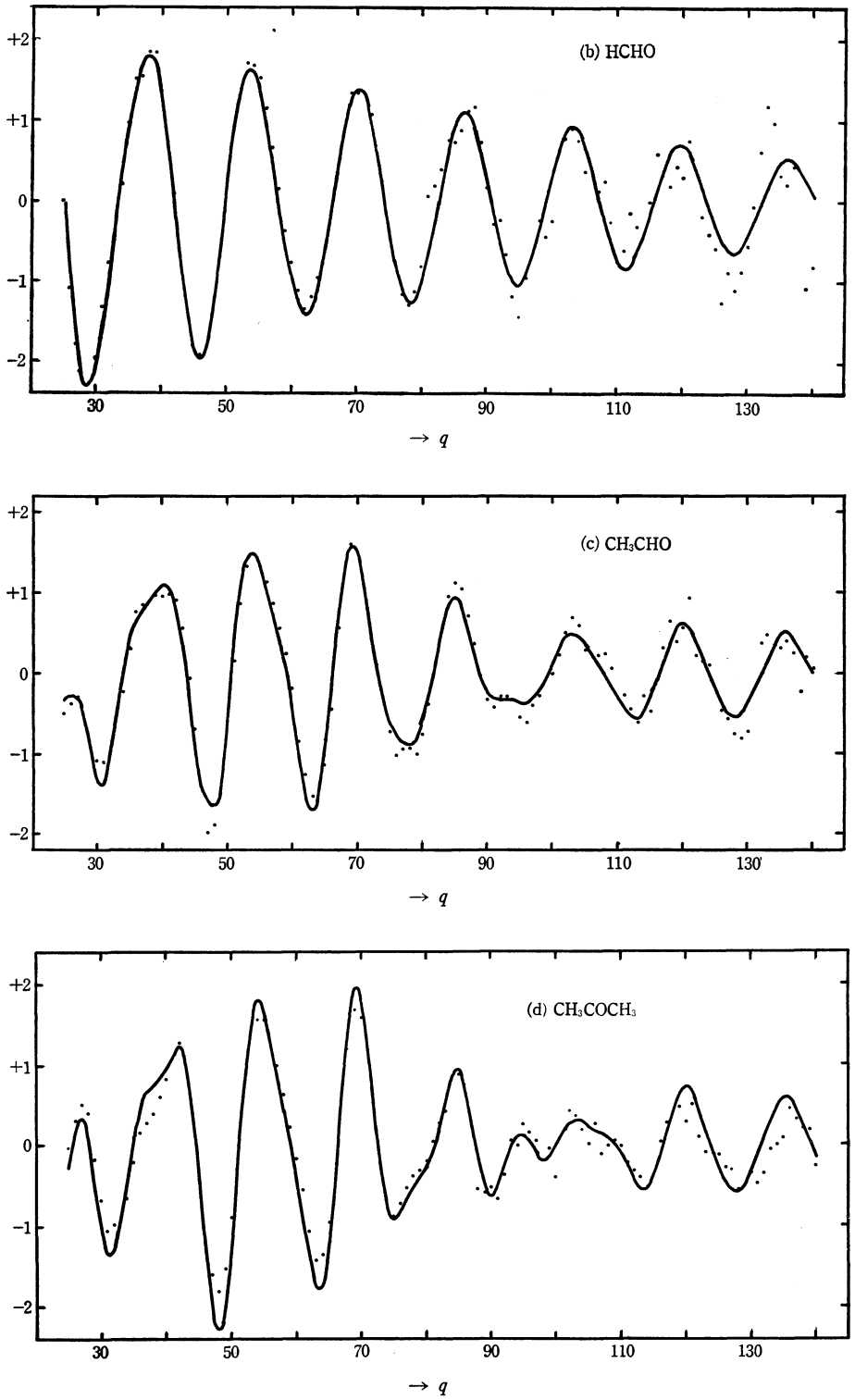

Fig. 2. Molecular intensity curves.
(a) CS_2, (b) HCHO, (c) CH_3CHO and (d) CH_3COCH_3.

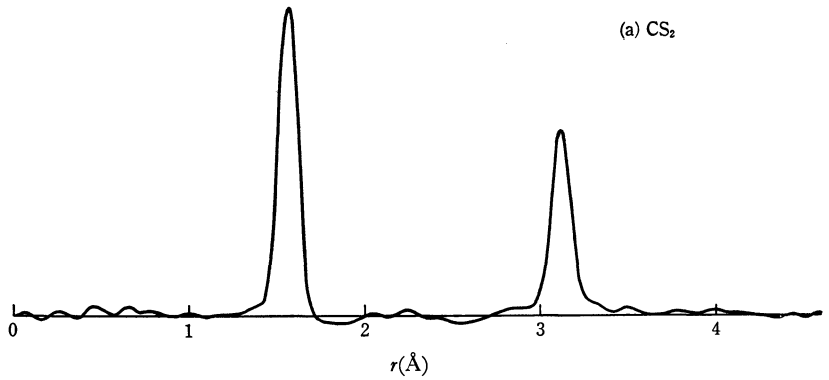
(a) CS_2
0
1
2
3
4
r(Å)

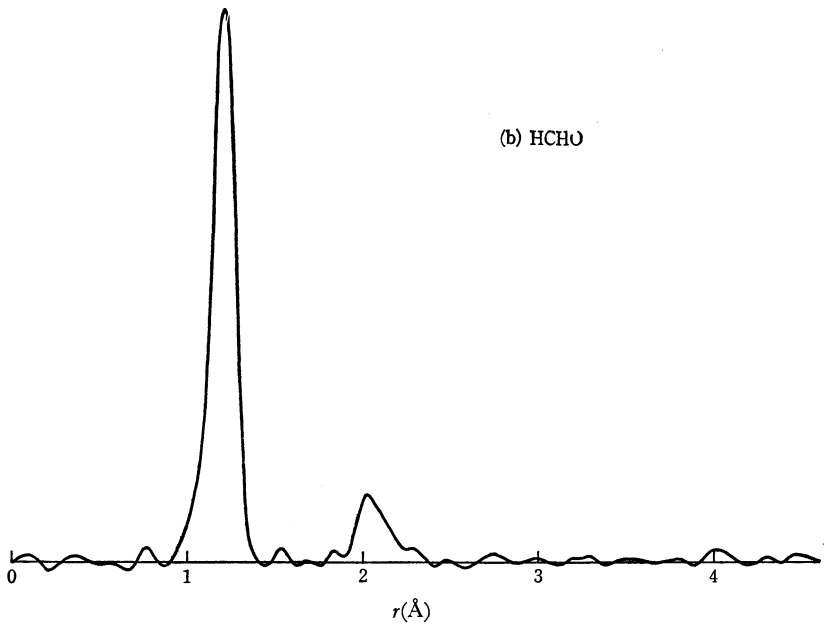
(b) HCHO
0
1
2
3
4
r(Å)

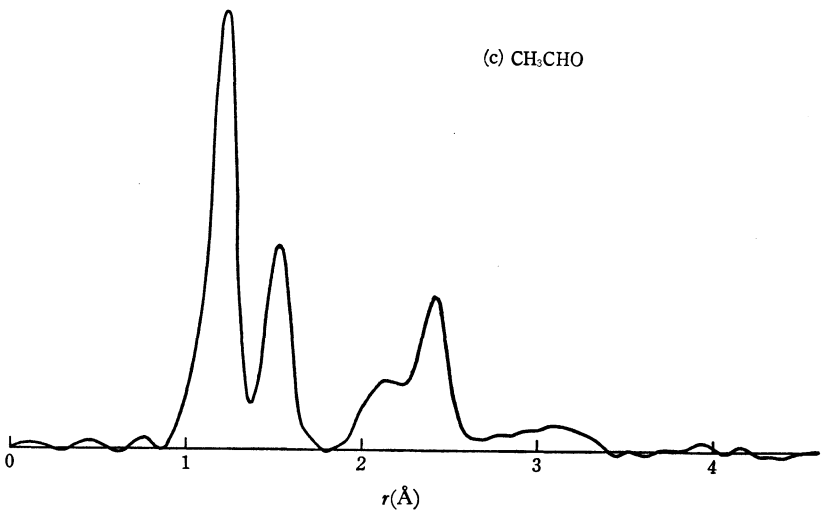
(c) CH_3CHO
0
1
2
3
4
r(Å)

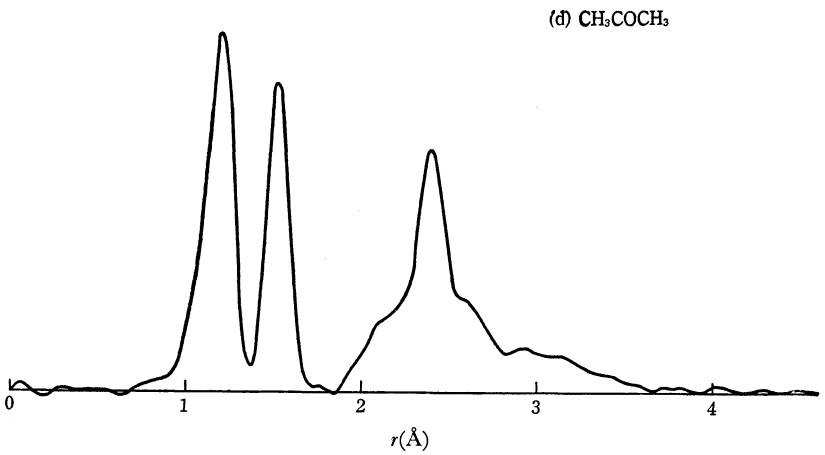

Fig. 3. Radical distribution curves.
(a) CS_2 (b) HCHO, (c) CH_3CHO and (d) CH_3COCH_3.

studies was newly designed and constructed. The camera lengths, the distance from the nozzle center to a plate, was perfectly fixed at 10.930 cm. Details about the unit will be reported elsewhere.[9] Diffraction photographs were taken with an r^3-sector at room temperature, 21.5°C. An accelerating voltage (~46 kV) was stabilized to within 0.1 percent throughout the sequence of exposures, which included a few pictures of the reference molecule and several pictures of sample molecules.

For the determinations of accelerating voltages, carbon disulfide was used as the reference material, for it has a suitable vapor pressure at room temperature and its distance parameters have been determined very accurately from spectroscopic data and confirmed by electron diffraction.[10] The use of a gaseous reference eliminates any systematic error due to the probable discrepancy between the nozzle and the actual diffraction centers and also some other systematic errors in the course of the experiment and analysis, for such errors are probably compensated for by employing the same procedure for both sample and reference gases.

The samples of carbon disulfide and acetone were special-grade reagents obtained from commercial sources. The sample of formaldehyde was prepared by the thermal depolymerization of commercial paraformaldehyde at 110°C according to the method of Spence and Wild.[11] Similarly, a sample of acetaldehyde was prepared by fractional distillation after depolymerizing commercial paraldehyde. The gases of carbon disulfide, formaldehyde, acetaldehyde, and acetone were stored in 1.5 *l* flasks at pressures of about 80 mmHg 120 mmHg, 135 mmHg, and 125 mmHg respectively, and then led into the diffraction chamber through a nozzle with an orifice 0.2 mm in diameter.

The photographic densities were measured by two different method: (1) with a double-beam microphotometer, model NLM-III, of the Narumi Co., Ltd, in our laboratory; this microphotometer was equipped with a cam converting transmission into optical density and a pen-recorder (pen-recording method), and (2) with a single-beam microphotometer, model MP-3, of the Rigaku Denki Co., Ltd., to which an integrating digital voltmeter was connected (digital method).[12],*2 Measurements were made by scanning across the full diameters of the diffraction patterns while the photographic plates were being rotated about the diffraction centers. The diffraction intensities were determined by averaging the corresponding points on both sides of the center; they covered the range $q=25$—150 at intervals of $\Delta q=1.0$.

Analysis and Results

After correction for the deviation of the sector shape from an ideal r^3-curve, the measured total intensities were leveled by dividing by the smooth theoretical backgrounds. Examples of the leveled experimental intensities are shown in Fig. 1a—d. The backgrounds on these intensity curves (solid lines in Fig. 1) were not in perfect agreement with the theoretical values. Since photographs taken without the injection of gases were perfectly transparent, the turned-up backgrounds at larger scattering angles may be due mainly to the reflection of scattered electrons from the inside wall of the sector mount.[9] The final leveled intensities, I_T, were obtained by subtracting these extraneous backgrounds, which were assumed to be given by the deviations of the experimental backgrounds from the theoretical values normalized to the experimental values at $q=65$.

By drawing smooth backgrounds, I_B, through

9) Y. Murata, K. Kuchitsu and M. Kimura, *Japan. J. Appl. Phys.*, to be published.

10) Y. Morino and T. Iijima, This Bulletin, **35**, 1661 (1962).

11) R. Spence and W. Wild, *J. Chem. Soc.*, **1935**, 338.

12) Y. Morino, K. Kuchitsu and T. Fukuyama, This Bulletin, **40**, 423 (1967).

*2 The present authors wish to thank Professor Morino and his collaborators of the University of Tokyo for allowing us to use the microphotometer.

the leveled intensity curves, I_T, the molecular intensities, $qM(q)^{obs}$, were obtained according to the equation:

$$qM(q)^{obs} = q(I_T/I_B - 1) \quad (1)$$

The final smooth backgrounds and the corresponding molecular intensity curves were determined after Karle's criterion[13] by the Fourier inverse transformation of the radial distribution curves.[14] The molecular intensity curves and the radial distribution curves thus obtained are shown in Fig. 2a—d and Fig. 3a—d respectively.

The structure determinations were carried out by the method of least-squares applied to the molecular intensities, $qM(q)^{obs}$, with a conventional weight function, as is shown in Fig. 4. The theoretical expression corresponding to the observed $qM(q)^{obs}$ value is:

$$qM(q)^{calc} = \kappa \sum_i \sum_j{}' A_{ij}\mu_{ij} \cos \Delta\eta_{ij} \times \exp\left[-\frac{1}{2}\left(\frac{\pi}{10}q\right)^2 l^2_{ij}\right] \sin\left[\frac{\pi}{10}q\left\{r_{aij} - \left(\frac{\pi}{10}q\right)^2 \kappa_{ij}\right\}\right], \quad (2)$$

$$A_{ij} = \left(\frac{10}{\pi}\right)\frac{1}{r_{aij}} \cdot \frac{Z_iZ_j}{\sum_k Z_k(Z_k+1)},$$

$$\mu_{ij} = \frac{|F_i||F_j|}{\sum_k |F_k|^2 + \sum_k S_k} \cdot \frac{\sum_k Z_k(Z_k+1)}{Z_iZ_j}, \quad (3)$$

$$|F| = (h^2s^2/8\pi^2 me^2)|f|, \; s = \frac{\pi}{10} \cdot q,$$

where all the notations have their usual significances. The atomic scattering factors for electrons, $|f|$, and the phase shifts, $\Delta\eta_{ij}$, were those calculated by Kimura *et al.*,[15] while the inelastic scattering factors, S_k, were taken from the table given by Tavard *et al.*[16],*3 The starting models for the least-squares fittings are given in Table 1. Simultaneous least-squares refinements were not successful for all parameters because the low-weight

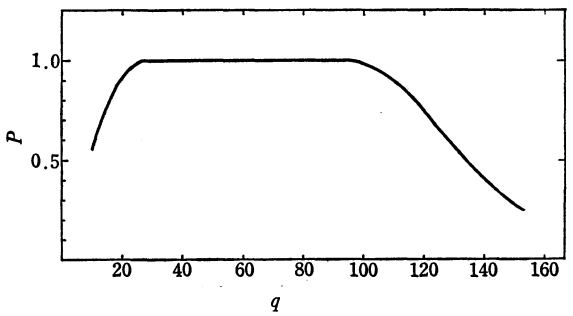

Fig. 4. Weight function.

TABLE 1.[a] MOLECULAR PARAMETERS CHOSEN AS THE STARTING MODELS FOR LEAST-SQUARES REFINEMENTS[b]

(a) CS_2: linear

	r_{ij}	l_{ij}	$\kappa_{ij}(\times 10^6)$
C-S	1.558	0.0391	(0.6)
S···S	3.109	0.0412	(0.5)

(b) HCHO: planar, C_{2v} symmetry

	r_{ij}	l_{ij}	$\kappa_{ij}(\times 10^6)$
C-O	1.208	0.0385	(0.7)
C-H	1.116	0.0802	(13.8)
O···H	2.032	0.0945	(8.8)

(c) CH_3CHO: C_s symmetry with the oxygen atom eclipsing a hydrogen atom of the CH_3 group.

	r_{ij}	l_{ij}	$\kappa_{ij}(\times 10^6)$
C-O	1.216	0.033	(0.4)
C···C	2.402	0.078	(4.1)
C-C	1.501	0.050	(2.1)
C-H(CH_3)	1.086	0.080	(13.7)
C-H	(1.114)	(0.080)	(13.7)
C···H(CH_3)	(2.142)	(0.098)	(10.2)
C···H(CHO)	(2.244)	(0.098)	(10.2)
O···H(CHO)	(2.004)	(0.091)	(7.6)
O:::H(CH_3)	(3.106)	(0.100)	(11.1)
O:::H(CH_3)	(2.707)	(0.100)	(11.1)

(d) CH_3COCH_3: C_{2v} symmetry with CH_3 groups eclipsed to a C=O bond.

	r_{ij}	l_{ij}	$\kappa_{ij}(\times 10^6)$
C-O	1.222	0.03	(0.3)
C···O	2.384	0.06	(1.4)
C-C	1.507	0.045	(1.4)
C···C	2.573	0.066	(2.1)
C-H	(1.085)	(0.077)	(11.7)
C···H	(2.145)	(0.100)	(11.1)
	(2.121)	(0.100)	(11.1)
C:::H	(2.863)	(0.11)	(16.3)
	(3.373)	(0.12)	(23.0)
O:::H	(3.067)	(0.100)	(11.1)
	(2.494)	(0.100)	(11.1)

a) Values associated with hydrogen-hydrogen pairs were dropped out from this table because of their very small contributions to molecular intensities.

b) In the least-squares treatment the values in parentheses were fixed, but the planarities of molecules were not assumed.

13) J. Karle and I. L. Karle, *J. Chem. Phys.*, **18**, 957 (1950); I. L. Karle and J. Karle, *ibid.*, **18**, 1963 (1950).

14) R. A. Bonham and L. S. Bartell, *ibid.*, **31**, 702 (1959).

15) M. Kimura, S. Konaka and M. Ogasawara, *ibid.*, **46**, 2599 (1967).

16) C. Tavard, D. Nicolas and M. Rouault, *J. chim. phys.*, to be published.

*3 The authors wish to thank Dr. Tavard who kindly sent the complete table before publication.

structure parameters are very insensitive to refinement and, also, certain parameters are strongly correlated with one another. Assuming equal interatomic distances and mean amplitudes for the equivalent pairs of atoms, the parameters refined by the present least-squares treatments were as follows: for CS_2, k, r_a(C–S), r_a(S–S) and their associated mean amplitudes; for formaldehyde, k, r_a(C=O), r_a(O···H), r_a(C–H) and their associated mean amplitudes; for acetaldehyde, k, r_a(C=O), r_a(C–C), r_a(C···O), r_a(C–H methyl) and their associated mean amplitudes; and for acetone, k, r_a(C=O), r_a(C–C), r_a(C···O), r_a(C···C) and their associated mean amplitudes. The other parameters were all fixed at the assumed values indicated in parentheses in Table 1. The interatomic distances and mean amplitudes in Table 1 were selected from those given in previous structural studies of these molecules[1-6,10] and other related compounds. The anharmonicity constants, κ_{ij}, for carbon disulfide were given by Kuchitsu.[17] The values for bonded atom pairs of the other molecules were estimated from the following approximate equation:[18]

$$\kappa_{ij} \approx (1/9)l^2_{ij}\langle \Delta z_{ij} \rangle \approx (1/6)al^4_{ij} \quad (4)$$

assuming the Morse potentials with the asymmetry constant, a, of $2\,\text{Å}^{-1}$.[19] Although no proper method of estimating κ's is available for non-bonded atom pairs, it was suggested by Kuchitsu[17] that they appear several-fold smaller than the diatomic estimates given by Eq. (4). Therefore, the κ_{ij}'s for non-bonded atom pairs were assumed to be one-third of the values estimated from Eq.

TABLE 2. DETERMINATION OF A SCALE FACTOR BY THE USE OF THE STRUCTURE OF CARBON DISULFIDE

		Plate 1 (I)	Plate 1 (II)	Average	σ_1[b]	σ_2[b]	2.5σ[b]
k		0.938 ±0.026	0.860 ±0.030	0.899	0.020	0.039	0.095
r_a' (Å)[a]	C-S	1.5647±0.0011	1.5631±0.0013				
	S···S	3.1244±0.0020	3.1241±0.0022				
l_a (Å)	C-S	0.0371±0.0015	0.0374±0.0017	0.0373	0.0011	0.0002	0.0028
	S···S	0.0468±0.0020	0.0444±0.0022	0.0456	0.0015	0.0012	0.0038
$r_g'=r_a'+l_a^2/r_a'$ (Å)[a]	C-S	1.5657	1.5641	1.5649	0.0009	0.0008	
	S···S	3.1249	3.1247	3.1248	0.0014	0.0001	
s. f.[c]	C-S	0.99508±0.00069	0.99610±0.00083				
	S···S	0.99491±0.00063	0.99498±0.00070				
		0.99500	0.99554	0.99527			0.00207[d]
δ_g (Å)[e]		0.0065	0.0035	0.0050			

a) r_a' and r_g' denote the values obtained by presuming the camera length of 10.930 cm, and an accelerating voltage of 46 kV. b) See text.
c) Scale factor$=r_g/r_g'$, r_g(C-S)=1.558, r_g(S···S)=3.109, Ref. 10. d) See text. e) Shrinkage.

TABLE 3. RESULTS FOR FORMALDEHYDE

		Plate 1	Plate 2	Average	σ_1	σ_2	2.5σ
k		0.989 ±0.027	0.990 ±0.017	0.990	0.016	0.001	0.040
r_a (Å)	C-O	1.2137±0.0015	1.2113±0.0010				
	O···H	2.0534±0.0216	2.0596±0.0150				
	C-H	1.1186±0.0156	1.0679±0.0171				
$r_a+l_a^2/r_a$ (Å)	C-O	1.2149	1.2125				
	O···H	2.0577	2.0639				
	C-H	1.1232	1.0782				
s. f.		0.99527	0.99753				
r_g (Å)	C-O	1.2092	1.2095	1.2093	0.0009	0.0001	0.0022
	O···H	2.0480	2.0588	2.0534	0.0131	0.0054	0.0337
	C-H	1.1179	1.0755	1.0967	0.0117	0.0212	0.0530
l_a (Å)	C-O	0.0417±0.0019	0.0408±0.0012	0.0413	0.0011	0.0005	0.0037
	O···H	0.0898±0.0173	0.0932±0.0119	0.0915	0.0104	0.0017	0.0260
	C-H	0.0721±0.0130	0.1050±0.0094	0.0886	0.0080	0.0165	0.0413

17) K. Kuchitsu, This Bulletin, **40**, 505 (1967).
18) Y. Morino and Y. Murata, *ibid.*, **38**, 104 (1965).
19) E. R. Lippincott and R. Schroeder, *J. Chem. Phys.*, **23**, 1131 (1955).

(4). At any rate, ambiguities in κ's have no substantial influence on the final results in the present studies.

The optical densities for each plate were measured by the two different methods described in the Experimental section. The least-squares refinements were applied to the individual molecular intensity curves. The results agreed with each other within their associated standard deviations, the interatomic distances especially being in perfect agreement. However, the standard deviations were smaller for the results obtained from optical densities by the digital method than for those obtained by the pen-recording method, for the former method gave the smoother intensity curves than the latter. Therefore, for the determinations of r_a and l_a we adopted only the results of the least-squares refinements applied to the whole range of observations by the digital method. The center of gravity of the probability function, r_g, can be obtained by the relation:

$$r_g = r_a + l_a^2/r_a. \quad (5)$$

The scale factors for each sequence of exposures were determined by the use of the diffraction patterns of carbon disufide. Examples are shown in Table 2. Since the scale factors were very close to unity, no correction was made of parameters

Table 4. Results for acetaldehyde

		Plate 1	Plate 2	Average	σ_1	σ_2	2.5σ
k		1.008 ±0.034	0.992 ±0.035	1.000	0.035	0.008	0.088
r_a (Å)	C-O	1.2122±0.0012	1.2147±0.0012				
	C-C	1.5190±0.0026	1.5217±0.0028				
	C···O	2.4088±0.0043	2.4136±0.0043				
	C-H	1.1045±0.0093	1.0828±0.0089				
$r_a+l_a^2/r_a$ (Å)	C-O	1.2134	1.2159				
	C-C	1.5206	1.5233				
	C···O	2.4104	2.4150				
	C-H	1.1100	1.0884				
s. f.		0.99527	0.99452				
r_g (Å)	C-O	1.2077	1.2092	1.2085	0.0009	0.0008	0.0022
	C-C	1.5134	1.5150	1.5142	0.0016	0.0008	0.0040
	C···O	2.3990	2.4004	2.3997	0.0031	0.0007	0.0078
	C-H	1.0948	1.0769	1.0859	0.0091	0.0090	0.0228
l_a (Å)	C-O	0.0391±0.0015	0.0371±0.0016	0.0381	0.0011	0.0010	0.0028
	C-C	0.0492±0.0024	0.0502±0.0027	0.0497	0.0018	0.0005	0.0045
	C···O	0.0619±0.0036	0.0590±0.0036	0.0605	0.0025	0.0015	0.0064
	C-H	0.0862±0.0062	0.0839±0.0063	0.0851	0.0045	0.0012	0.0111

Table 5. Results for acetone

		Plate 1	Plate 2	Average	σ_1	σ_2	2.5σ
k		0.930 ±0.028	0.930 ±0.030	0.930	0.021	0.000	0.051
r_a (Å)	C-O	1.2152±0.0017	1.2184±0.0021				
	C-C	1.5227±0.0018	1.5250±0.0023				
	C···O	2.3917±0.0031	2.3911±0.0039				
	C···C	2.6209±0.0128	2.6223±0.0141				
$r_a+l_a^2/r_a$ (Å)	C-O	1.2165	1.2197				
	C-C	1.5244	1.5267				
	C···O	2.3934	2.3927				
	C···C	2.6230	2.6244				
s. f.		0.99527	0.99309				
r_g (Å)	C-O	1.2107	1.2113	1.2110	0.0013	0.0003	0.0034
	C-C	1.5172	1.5162	1.5167	0.0015	0.0005	0.0038
	C···O	2.3821	2.3762	2.3792	0.0025	0.0030	0.0075
	C···C	2.6106	2.6063	2.6085	0.0095	0.0022	0.0237
l_a (Å)	C-O	0.0387±0.0017	0.0398±0.0021	0.0393	0.0013	0.0005	0.0034
	C-C	0.0495±0.0018	0.0487±0.0023	0.0491	0.0015	0.0004	0.0037
	C···O	0.0632±0.0026	0.0609±0.0033	0.0621	0.0021	0.0012	0.0053
	C···C	0.0750±0.0095	0.0739±0.0107	0.0745	0.0071	0.0005	0.0178

other than interatomic distances. The final values of r_g are given as averages of the r_g values determined separately for two selected plates. Tables 3, 4, and 5 show the results for formaldehyde, acetaldehyde, and acetone respectively.

The σ_1 and σ_2 values were estimated according to these two formulae: $\sigma_1^2=\langle\sigma^2\rangle/2$ and $\sigma_2^2=\sum v_i^2/n(n-1)$ respectively. Here, $\langle\sigma^2\rangle$ is the average of the square standard deviations for two plates, and v_i the residuals of the results of the ith plate subtracted from the average value. For most structure parameters, σ_2's were smaller than σ_1's. Taking the greater of σ_1 and σ_2 as a standard deviation, σ, for each parameter, random errors were given by 2.5 σ, representing 99% confidence intervals.

Five plates, one for each compound and two for carbon disulfide, were taken in a sequence of exposures; they are designated as plate 1 in the tables. Plate 2 for each compound was obtained in a separate sequence of exposures, one which included a plate for carbon disufide. The overall consistency in the results between plates 1 and 2 shows that the same experimental conditions were reproduced in the repeated exposures and that various systematic errors, such as errors originating from the drift of voltage, the uncertainty of the effective camera distance, *etc.*, may be regarded as being reflected in the error of the scale factor to be estimated below. Although a rigorous statistical meaning cannot be imposed on σ_2, which was estimated from only two plates in the present studies, σ_2 would coincide with σ_1 if a sufficiently large number of observations were made.

Since ach scale factor for plate 2 was determined by the analysis of only one plate of carbon disulfide, the largest standard deviation for individual scale factors may safely be taken as a standard deviation for all the scale factors used in the present studies. Thus, the error in the scale factor was given by 2.5 $\sigma=0.00207$, and $\sigma=0.00083$ for the C–S distance of plate 1 (II), corresponding to an error of 0.208 percent in interatomic distances. The total error for each parameter was considered to consist of two independent errors, the random error obtained in the least-squares fitting and the error in the scale factor. The final values of interatomic distances and their estimated total errors are given in Fig. 5. The interatomic distances obtained for acetone explain the planar frame of CCCO, as may clearly be seen by comparing them with the calculated values for a planar model shown in parentheses in Fig. 5.

The mean amplitudes, l_a, experimentally determined were not corrected for the effects of the sample size,[20] for the magnitudes of the corrections are much less than the total experimental errors. In Table 6 the final values of the mean amplitudes, l^{ED}, and their associated errors are summarized.

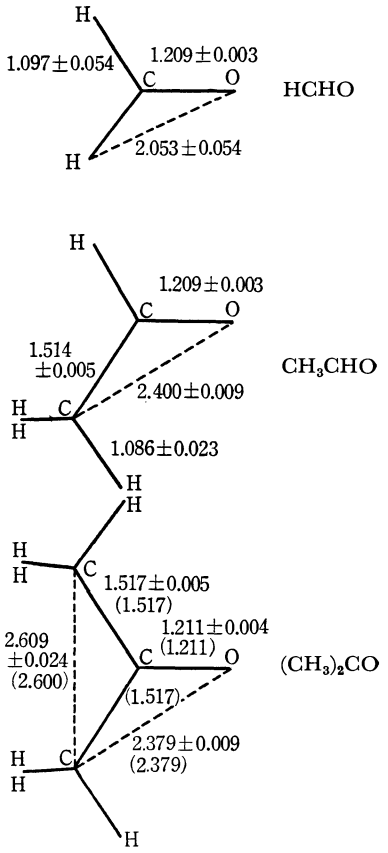

Fig. 5. The interatomic distances r_g in Å unit. The values in parentheses for acetone are interatomic distances calculated for a rigid model with the C_{2v} symmetry.

TABLE 6. MEAN AMPLITUDES OF FORMALDEHYDE, ACETALDEHYDE AND ACETONE AT 21.5°C

		l^{ED} a)	l^{spectr} b)
Formaldehyde	C-O	$0.041_3\pm0.004_0$	0.0385
	C-H	$0.088_6\pm0.041_3$	0.0802
	O···H	$0.091_5\pm0.036_5$	0.0945
Acetaldehyde	C-O	$0.038_1\pm0.004_0$	0.0389
	C-C	$0.049_7\pm0.006_5$	0.0493
	C-H	$0.085_1\pm0.015_8$	0.0778
	C···O	$0.060_5\pm0.009_0$	
Acetone	C-O	$0.039_3\pm0.004_8$	0.0399
	C-C	$0.049_1\pm0.005_3$	0.0513
	C···O	$0.062_1\pm0.007_5$	
	C···C	$0.074_5\pm0.025_3$	

a) The present study.
b) The fundamental frequencies and the set of force constants (VF. 3) of the valence force field in Ref. 22 were employed.

20) Y. Morino and Y. Murata, This Bulletin, **38**, 114 (1965).

TABLE 7. COMPARISON OF C=O AND C-C INTERATOMIC DISTANCES AS DETERMINED BY ELECTRON DIFFRACTION AND MICROWAVE SPECTROSCOPY

		C=O		C-C	
		ED	MW	ED	MW
HCHO	r_g	$1.209_3 \pm 0.003_3$	(1.2085)		
	r_z		$1.207_8 \pm 0.003$[a]		
CH_3CHO	r_g	$1.208_5 \pm 0.003_3$		$1.514_2 \pm 0.005_1$	
	r_0		1.2155 ± 0.0020[b]		1.501 ± 0.005[b]
CH_3COCH_3	r_g	$1.211_0 \pm 0.004_1$		$1.516_7 \pm 0.004_8$	
	r_s		1.222 ± 0.003[c]		1.507 ± 0.003[c]

a) Ref. 1b. b) Ref. 2a. c) Ref. 3a.

Discussion

The results of the present studies show there is no significant difference in the carbon-oxygen bond lengths of formaldehyde, acetaldehyde, and acetone in spite of their different environments. In other words, the difference between H and CH_3 as substituents does not affect the carbon-oxygen bond lengths. The carbon-carbon bond lengths in acetaldehyde and acetone were almost the same, their values being intermediate between about 1.54 Å for single bonds and about 1.47 Å for central C–C single bonds in conjugated systems.

The mean amplitude, l_a, is approximately equal to the value of l_g, which refers to r_g, and also to l_α, which refers to the harmonic oscillators.[17] Therefore, the observed values, l^{ED}, are in Table 6 compared with the values, l^{spectr}, calculated from the spectroscopic data, values which are equivalent to l_α. The l^{spectr} values were calculated by a usual method[21] by the use of the fundamental frequencies and the force constants of the valence force field (the VF3 set) reported by Cossee and Schachtschneider.[22] The agreements between l^{ED} and l^{spectr} are quite satisfactory.

Table 7 compares the bond lengths determined in the present study with those obtained from the rotational constants by microwave spectroscopy. For acetaldehyde and acetone, it is at this moment a question whether the bond lengths as determined by two different methods can be regarded as consistent with each other, for r_g, r_0, and r_s represent bond lengths with different physical significances.

Fortunately, the zero-point structure, r_z, for formaldehyde was given by Takagi and Oka.[1b] Since the conversion of r_z into r_g can be made rather straightforwardly, r_g was estimated from the r_z for the C=O bond of formaldehyde. To a good approximation, r_z can be related to r_g by the equation:[17,23]

$$r_g = r_z + \delta r + \frac{3}{2}a(l_T^2 - l_0^2) + [\langle \Delta x^2 \rangle_0 + \langle \Delta y^2 \rangle_0]/2r_a \quad (6)$$

Here, δr is the correction for the centrifugal distortion, $\langle \Delta x^2 \rangle_0$ and $\langle \Delta y^2 \rangle_0$ are the perpendicular mean amplitudes at 0°K, and l_T and l_0 are the parallel mean amplitudes at T °K and 0°K respectively. The values of $\langle \Delta x^2 \rangle$, $\langle \Delta y^2 \rangle$, and l_0 were calculated simultaneously in the calculations of l^{spectr}.[21,24] The estimation of δr was based upon a model in which the CH_2 group and the oxygen atom were bound with a force constant of 11 md/Å (K(C=O) in Ref. 22) at a distance of 1.2078 Å (r_z in Ref. 1b). The numerical values thus calculated were 0.00062 Å for δr, 0.00000 Å for $(3/2)a(l_T^2 - l_0^2)$ and 0.00004 Å for $[\langle \Delta x^2 \rangle_0 + \langle \Delta y^2 \rangle_0]/2r_a$. The value of r_g estimated from r_z then becomes 1.2085 Å, which agrees almost perfectly with the r_g value obtained by electron diffraction.

It has recently been shown that a cooperative use of diffraction and spectroscopic data is most useful in obtaining accurate structures of medium-sized molecules.[8] The present results for acetaldehyde and acetone must, therefore, be effectively combined with available spectroscopic informations. The application of this procedure to the structural studies of these molecules will be reported in separate papers.

The calculations of the least-squares analysis were carried out on the electronic computer, HITAC 5020 E, in the computing center of the University of Tokyo, to which the present authors' thanks are due.

21) Y. Morino, K. Kuchitsu and T. Shimanouchi, *J. Chem. Phys.*, **20**, 726 (1952).

22) P. Cossee and J. H. Schachtschneider, *ibid.*, **44**, 97 (1966).

23) Y. Morino, K. Kuchitsu and T. Oka, *ibid.*, **36**, 1108 (1962).

24) Y. Morino and E. Hirota, *ibid.*, **23**, 737 (1955).

BULLETIN OF THE CHEMICAL SOCIETY OF JAPAN VOL. 42 2159—2164 (1969)

Zero-point Average Structure of Acetaldehyde

Takao IIJIMA and Masao KIMURA

Department of Chemistry, Faculty of Science, Hokkaido University, Sapporo

(Received December 18, 1968)

The zero-point average structure of acetaldehyde has been determined by the use of the moments of inertia and the average distances, obtained by microwave spectroscopy and electron diffraction respectively. The following r_z parameters have been determined: 1.515±0.005 Å for C–C, 1.207±0.004 Å for C=O, 1.073±0.002 Å for C–H(methyl), 123°48′±9′ for ∠CCO, and 108°52′±17′ for ∠HCH of the methyl top.

The molecular structure of acetaldehyde was studied by Kilb, Lin, and Wilson[1] by means of microwave spectroscopy. They determined the structure parameters (the so-called r_0 structure) from the moments of inertia for normal acetaldehyde and its six isotopically-substituted molecules, assuming that the bond distances and angles, except for those of the methyl group, were the same for all isotopic species.

Recently the present authors and their collaborators made an electron diffraction study of the structure of this molecule.[2] The results were not in close agreement with those from the microwave study, as may be seen by comparing the C–C and C=O distances in Table 1. However, this does not necessarily mean that the results are inconsistent with each other, for the distance parameters reported do not have exactly the same physical significance.

TABLE 1. PREVIOUS RESULTS FOR r(C–C) AND r(C=O) OF ACETALDEHYDE (IN Å)

	r(C–C)	r(C=O)
r_0(MW)[a]	1.501±0.005	1.216±0.002
r_g(ED)[b]	1.514±0.005	1.209±0.003

a) Microwave spectroscopy. Ref. 1.
b) Electron diffraction. Ref. 2.

Recent theoretical studies[3-5] have provided methods of converting the original spectroscopic and diffraction results into common physical quantities in order to facilitate their comparison. One practical way is to reduce the structure parameters determined experimentally to those of the zero-point average structure. Furthermore, several investigations[6-10] have shown that the cooperative use of spectroscopic and diffraction results is successful in the determination of the accurate structures of gas molecules. In the present study, the zero-point average structure of acetaldehyde has been determined by a cooperative use of microwave and electron diffraction data.

Zero-point Moments of Inertia

The moments of inertia obtained by microwave spectroscopy are effective moments of inertia for the ground vibrational state. They are converted to zero-point moments of inertia by correcting for apparent variations due to intramolecular harmonic vibrations. The relations between the effective moments $(I_{\alpha\alpha})_{eff}$ and the moments of inertia of a non-vibrating rigid molecule, $I^0{}_{\alpha\alpha}$, are given by the following equations:[3,4],*1

$$\frac{1}{(I_{\alpha\alpha})_{eff}} = \frac{1}{I^0{}_{\alpha\alpha}} + \frac{1}{(I^0{}_{\alpha\alpha})^2}\sum_s \frac{h}{8\pi^2 c\omega_s} \times \left[\sum_{s'}{}' \frac{4\omega_{s'}{}^2}{\omega_s{}^2-\omega_{s'}{}^2}(\zeta_{ss'}{}^{(\alpha)})^2 + 3A_{ss}{}^{(\alpha\alpha)}\right] + \frac{h^3}{8\pi^2}(3\tau_{\beta\gamma\beta\gamma} - 2\tau_{\alpha\beta\alpha\beta} - 2\tau_{\alpha\gamma\alpha\gamma}) \quad (1a)$$

and:

$$\frac{1}{(I_{\alpha\beta})_{eff}} = \frac{1}{I^0{}_{\alpha\alpha} I^0{}_{\beta\beta}}\sum_s \frac{h}{8\pi^2 c\omega_s}$$

1) R. W. Kilb, C. C. Lin and E. B. Wilson, Jr., *J. Chem. Phys.*, **26**, 1695 (1957).
2) C. Kato, S. Konaka, T. Iijima and M. Kimura, This Bulletin, **42**, 2148 (1969).
3) T. Oka, *J. Phys. Soc. Japan*, **15**, 2274 (1960).
4) T. Oka and Y. Morino, *J. Mol. Spectry.*, **6**, 472 (1961).
5) K. Kuchitsu and L. S. Bartell, *J. Chem. Phys.*, **36**, 2460, 2470 (1962).
6) K. Kuchitsu, *ibid.*, **44**, 906 (1966).
7) Y. Morino, K. Kuchitsu, Y. Hori and M. Tanimoto, This Bulletin, **41**, 2349 (1968).
8) K. Kuchitsu, T. Fukuyama and Y. Morino, *J. Mol. Structure*, **1**, 463 (1967—68).
9) K. Kuchitsu, *J. Chem. Phys.*, **49**, 4456 (1968).
10) K. Kuchitsu and S. Konaka, *ibid.*, **45**, 4342 (1966).

*1 No degenerate mode of vibration exists in this molecule.

Table 2. Moments of inertia of acetaldehyde (in amu. Å²)

	CH_3CHO			CD_3CDO		
	a	b	c	a	b	c
I_{eff}(obs)[a]	8.933	49.741	55.553	14.456	58.936	67.123
$I_\alpha^{(z)}$(obs)[b]	8.887	49.773	55.589	14.387	58.957	67.178

	CD_3CHO			$^{13}CH_3{}^{13}CHO$		
	a	b	c	a	b	c
I_{eff}(obs)[a]	12.114	58.853	64.672	—	51.313	57.325
$I_\alpha^{(z)}$(obs)[b]	12.053	58.868	64.729	—	51.352	57.370

	$^{13}CH_3CHO$			$CH_3CH^{18}O$		
	a	b	c	a	b	c
I_{eff}(obs)[a]	—	51.292	57.130	—	52.245	58.157
$I_\alpha^{(z)}$(obs)[b]	—	51.328	57.168	—	52.282	58.196

a) Effective moments of inertia for the ground vibrational state observed by microwave spectroscopy (Ref. 1).
b) Zero-point moments of inertia reduced from I_{eff} by Eq. (3).

$$\times\left[\sum_{s'}{}'\frac{4\omega_{s'}{}^2}{\omega_s{}^2-\omega_{s'}{}^2}\zeta_{ss'}{}^{(\alpha)}\zeta_{ss'}{}^{(\beta)}+3A_{ss'}{}^{(\alpha\beta)}\right]. \quad (1b)$$

The last term of Eq. (1a) comes from the quadratic term of centrifugal distortion, where $\tau_{\alpha\beta\gamma\delta}$ is given by:[11]

$$\tau_{\alpha\beta\gamma\delta}=-\sum_s\frac{1}{I^0{}_{\alpha\alpha}I^0{}_{\beta\beta}I^0{}_{\gamma\gamma}I^0{}_{\delta\delta}}\cdot\frac{a_s{}^{(\alpha\beta)}a_s{}^{(\gamma\delta)}}{8\pi^2\boldsymbol{hc}^2\omega_s{}^2}. \quad (2)$$

All the notations are the same as in Ref. 4. The non-vanishing off-diagonal elements, $1/(I_{\alpha\beta})_{eff}$, indicate that the principal axes in a vibrating molecule deviate slightly from those in equilibrium. However, numerical calculations have shown that these terms are negligibly small for acetaldehyde and its isotopic species.

When the $(I_{\alpha\alpha})_{eff}$ represents the observed principal moments of inertia for the ground vibrational state, the $I^0{}_{\alpha\alpha}$ is the zero-point moment of inertia according to Oka[3] and Laurie and Herschbach.[12,13] In other words, $I^0{}_{\alpha\alpha}$ is the moment of inertia of such a rigid molecule that each atom is fixed at an average position which may be slightly different from an equilibrium position because of the first-order effect of anharmonicity. By using the observed moments of inertia, I_α(obs), of Table 2, the zero-point moments of inertia, $I_\alpha^{(z)}$(obs), were obtained by:

$$I_\alpha^{(z)}(\text{obs})=I_\alpha(\text{obs})-[(I_{\alpha\alpha})_{eff}-I^0{}_{\alpha\alpha}]_{calc}, \quad (3)$$

where $(I_{\alpha\alpha})_{eff}$ was calculated from Eq. (1a). The structure parameters determined by microwave spectroscopy[1] and the force constants determined by Cossee and Schachtschneider, the VF3 set,[14] were used in this calculation. The same force constants were assumed for all the isotopic species. Although there are, for some reason, slight discrepancies between the vibrational frequencies calculated in the present study and those reported

Table 3. Observed and calculated normal frequencies of acetaldehyde (in cm^{-1})

	CH_3CHO			CD_3CDO		
	obsd[a]	calcd	calcd[a]	obsd[a]	calcd	calcd[a]
In-plane modes						
1	3010	3008	3007	2265	2247	2247
2	2967	2961	2961	2130	2139	2139
3	2822	2802	2801	2060	2098	2098
4	1743	1769	1762	1737	1701	1700
5	1441	1440	1455	1151	1165	1164
6	1400	1409	1402	1045	1033	1044
7	1352	1307	1329	1028	955	1016
8	1113	1127	1089	938	941	930
9	919	931	917	747	752	720
10	509	511	510	436	454	456
Out-of-plane modes						
11	3010	3004	3003	2225	2236	2236
12	1420	1426	1426	1028	1029	1029
13	867	863	863	—	672	672
14	763	762	761	573	620	620
15	150	145	148	116	109	113

a) Reported by Cossee and Schachtschneider.[14]

11) D. Kivelson and E. B. Wilson, Jr., *ibid.*, **20**, 1575 (1952).
12) D. R. Herschbach and V. W. Laurie, *ibid.*, **37**, 1661 (1962).
13) V. W. Laurie and D. R. Herschbach, *ibid.*, **37**, 1687 (1962).
14) P. Cossee and J. H. Schachtschneider, *ibid.*, **44**, 97 (1966).

orignally by Cossee and Schachtschneider, as is shown in Table 3, no further refinement of the force constants was made. The mean-square amplitudes of vibration calculated by use of the force constants were in good agreement with those observed by electron diffraction (*cf.* Table 4 in Ref. 2).

The effects of the slipping rotation of the π-electrons of a C=O bond and the lone-pair electrons of the oxygen atom were corrected for in the case of formaldehyde by Oka.[3] His corrections were -0.003 amu.Å^2 at most. Although the effects are expected to be of a similar magnitude for acetaldehyde, the corrections are only a few in ten thousand or less since the moments of inertia of acetaldehyde are much greater than those of formaldehyde. Therefore, the corrections for these effects were ignored in the present study.

Isotope Effect on Zero-point Structure

In order to determine the r_z-structures from the moments of inertia, $I_\alpha^{(z)}$, of several isotopic species, the primary and secondary isotope effects*2 on r_z distances should be estimated. By defining the local Cartesian coordinates, x, y, and z, for a particular pair of atoms with a z axis taken in the direction of their equilibrium positions, r_z is expressed as:

$$r_z = r_e + \langle \Delta z \rangle_0 \tag{4}$$

in terms of the equilibrium distance, r_e, and the average increment of the distance along the z-axis, $\langle \Delta z \rangle_0$. The average is taken at 0°K, or for the ground vibrational state. By the diatomic approximation[8,15] $\langle \Delta z \rangle_0$ is given by:

$$\langle \Delta z \rangle_0 = (3/2)a_3 l_0^2 - K_0 \tag{5}$$

and:

$$K_0 = [\langle \Delta x^2 \rangle_0 + \langle \Delta y^2 \rangle_0]/2r_e\,, \tag{6}$$

where a_3 is the Morse anharmonicity parameter of the bond-stretching; l_0^2, the mean-square amplitude of vibration at 0°K, and $\langle \Delta x^2 \rangle_0$ and $\langle \Delta y^2 \rangle_0$, the perpendicular mean-square amplitudes of vibration at 0°K.

The anharmonicity parameters for C-H, C-C, and C=O bonds were assumed to be 1.98 Å^{-1}, 2.1 Å^{-1}, and 2.4 Å^{-1}, respectively.[15] The mean-square amplitudes and the perpendicular amplitudes needed for the estimation of K_0 were calculated by the use of l-matrix elements, which were obtained simultaneously with a computing program for the calculation of the I_{eff} values. The numerical values of $\langle \Delta z \rangle_0$ calculated for the bonded distances of several isotopic species are tabulated in Table 4.

Table 4. Isotope effects on r_z parameters. Calculated values of $\langle \Delta z \rangle_0$ (in Å units)

	C-H_{Me}	C-H_{Ald}	C-C	C=O
CH_3CHO	−0.005	0.001	0.0059	0.0026
CD_3CDO	−0.002	0.001	0.0056	0.0028
CD_3CHO	0.000	−0.001	a	0.0024
$^{13}CH_3{}^{13}CHO$	−0.005	a	0.0056	a
$CH_3CH^{18}O$	a	a	a	0.0025

a) Not calculated. This does not necessarily mean that the values are negligibly small.

The relatively large negative values of $\langle \Delta z \rangle_0$ for the methyl C–H distances are caused by the large perpendicular amplitudes due to the torsional motion of the methyl top. For the C–C and C=O distances, the differences in $\langle \Delta z \rangle_0$ for different isotopic species are negligibly small, as had been expected.

The values of $\langle \Delta z \rangle_0$ in the table might include large systematic errors, caused mainly by assuming the values of a_3.[9,16,17] Kuchitsu estimated an uncertainty of +0.002 Å for the difference between the $\langle \Delta z \rangle_0$ values of the C–C bonds in C_2H_6 and C_2D_6.[9] This amount of uncertainty in the isotope effect sometimes leads to large errors in the structure parameters determined by the least-squares adjustment, especially when the adjustment is made under the circumstances that a strong correlation exists among some of the parameters.[7] In the present study, the correlation between r_{C-C} and $r_{C=O}$ was very strong when only spectroscopic data were used, as will be shown in the following section. Therefore, the uncertainties in the parameters are expected to be yet larger than those listed in Table 6, column I, which appears later. When diffraction data are used cooperatively, however, the influence of the possible systematic errors in $\langle \Delta z \rangle_0$ would be unimportant. The isotope effect for bond angles was ignored in the present study.

Zero-point Structure from $I_\alpha^{(z)}$

The seven parameters shown in Fig. 1 determine the structure of acetaldehyde when C_{3v} symmetry is assumed for the methyl top. In the final results, the parameters h and x shown in the figure are converted into r_{C-H} and ∠HCH respectively. It was confirmed by Kilb, Lin, and Wilson[1] that one of the three hydrogen atoms of the methyl top is opposed by the oxygen atom.

By a simple geometrical consideration, the following equation is obtained:

$$I_a^{(z)} + I_b^{(z)} - I_c^{(z)} = 3m_H h_z^2\,, \tag{7}$$

where:

$$h_z = (2/\sqrt{3})r_z \sin(\alpha_z/2)\,, \tag{8}$$

*2 Primary and secondary isotope effects have the meaning defined in Ref. 17.

15) K. Kuchitsu and Y. Morino, This Bulletin, **38**, 805, 814 (1965).

16) L. S. Bartell and H. K. Higginbothom, *J. Chem. Phys.*, **42**, 851 (1965).

17) L. S. Bartell, *ibid.*, **42**, 1681 (1965).

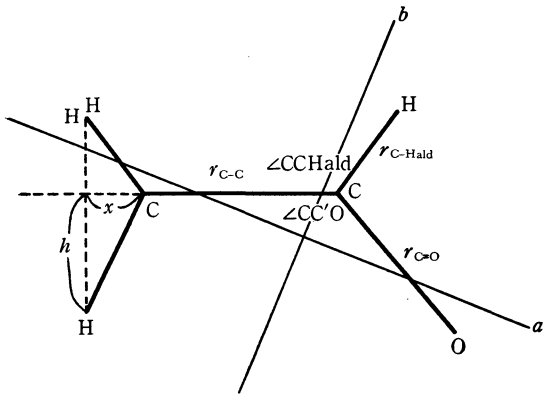

Fig. 1. Configuration and structure parameters of acetaldehyde.

and where r_z and α_z designate r_z(C–H) and ∠HCH respectively. From the observed $I_\alpha^{(z)}$ values of CH_3CHO, CD_3CDO, and CD_3CHO, the best-fit value of h_z, or the product of the parameters r_z and $\sin(\alpha_z/2)$, was determined, where slight differences in the h_z values of the three isotopic species were taken into consideration. The right-hand side of Eq. (7), calculated from the determined value of h_z, is compared with the observed value

Table 5. Comparisons of $I_a^{(z)}+I_b^{(z)}-I_c^{(z)}$ (in amu.Å²)

	obsd[a]	calcd[b]
CH_3CHO	3.071	3.072
CD_3CDO	6.176	6.170
CD_3CHO	6.192	6.196

a) Observed by microwave spectroscopy. Ref. 1.
b) Calculated by use of the adjusted parameters. (Eq. (7)).

of the left-hand side for each isotopic species in Table 5. As may be seen in the table, the agreement is quite satisfactory. This is one of the cases in which an isotope effect of r_z estimated on the basis of the mass difference accounts for the observed results. In this stage, r_z(C–H) and α_z were not determined separately.

The Jacobian matrix elements of twelve moments of inertia (two from each of the six isotopic species)*3 with regard to six in-plane parameters were calculated. The Jacobian matrix showed that $I_\alpha^{(z)}$'s were quite insensitive to ∠CCH(ald); hence, this angle was fixed at the value reported by Kilb, Lin, and Wilson,[1] and five parameters, r_{C-C}, $r_{C=O}$, ∠CCO, x, and $r_{C-H(ald)}$, were adjusted by the standard least-squares procedure. The parameters derived are listed in the column I of Table 6, along with their limits of error. The twelve

*3 The moments of inertia of $CH_3{}^{13}CHO$ were not included, because they probably depend more strongly on those of the other isotope species.

Table 6. Adjusted r_z parameters of CH_3CHO with limits of error (in Å units)[a]

	I	II
C–C	1.504±0.012	1.515±0.005
C=O	1.217±0.011	1.207±0.004
∠CCO	124°3′±25′	123°48′±9′
C–H(Me)	1.074±0.004	1.073±0.002
∠HCH	108°43′±34′	108°52′±17′
C–H(ald)	1.114±0.012	1.114±0.011
∠CCH(ald)	117°29′ (ass'd)	117°29′ (ass'd)

I. Obtained by using spectroscopic moments of inertia $I_{obs}^{(z)}$ only. The uncertainties should be larger if systematic errors in $\langle \Delta z \rangle_0$ are also taken into consideration.
II. Obtained by using r_z-values from electron diffraction in addition to the spectroscopic data.
a) 2.5 times standard deviation obtained by the least-squares procedure.

Table 7. Comparison of moments of inertia[a] (in amu. Å²)

		I		II	
		$I_{calc}^{(z)}$	dev.[b]	$I_{calc}^{(z)}$	dev.[b]
CH_3CHO	a	8.903	−0.016	8.900	−0.013
	b	49.760	0.013	49.758	0.015
	c	(55.590	−0.001)	(55.586	0.003)
CD_3CDO	a	14.383	0.004	14.376	0.011
	b	58.945	0.012	58.956	0.001
	c	(67.152	0.016)	(67.155	0.013)
CD_3CHO	a	12.040	0.013	12.029	0.024
	b	58.852	0.016	58.850	0.018
	c	(64.691	0.038)	(64.684	0.035)
$^{13}CH_3{}^{13}CHO$	a	—	—	—	—
	b	51.332	0.020	51.343	0.009
	c	57.368	0.002	57.375	−0.005
$^{13}CH_3CHO$	a	—	—	—	—
	b	51.313	0.015	51.321	0.007
	c	57.168	0.000	57.172	−0.004
$CH_3CH^{18}O$	a	—	—	—	—
	b	52.267	0.015	52.249	0.033
	c	58.199	−0.003	58.183	0.013

a) Calculated values of $I_\alpha^{(z)}$ by using the structure parameters adjusted by the least-squares procedure. See Table 6 for specifications I and II.
b) dev.$=I_{obs}^{(z)}-I_{calc}^{(z)}$.

observed $I_\alpha^{(z)}$'s are not independent enough to alleviate the strong correlation between the increase in r_{C-C} and the decrease in $r_{C=O}$; the correlation factor estimated from the elements of the error matrix*4 amounted to 100 percent. This is more

*4 A matrix $\boldsymbol{B}$ is defined in terms of the Jacobian matrix $\boldsymbol{J}$ and a diagonal weight matrix $\boldsymbol{W}$ as $\boldsymbol{B}=\boldsymbol{J}\boldsymbol{W}\tilde{\boldsymbol{J}}$. The inverse of B is called an error matrix. According to the theory of errors, a correlation factor between the ith and jth parameters which have been adjusted by the least-squares method is given by
correlation factor$=(B^{-1})_{ij}/[(B^{-1})_{ii}(B^{-1})_{jj}]^{1/2}$.

easily seen in Fig. 2, where the process of solving the normal equation in the least-squares adjustment is reduced to the determination of the cross point of two straight lines drawn on the r_{C-C} *versus* $r_{C=O}$ plane. However, because of the strong correlation between r_{C-C} and $r_{C=O}$ the two lines are almost identical. Large standard errors result from this correlation making the error matrix nearly singular.

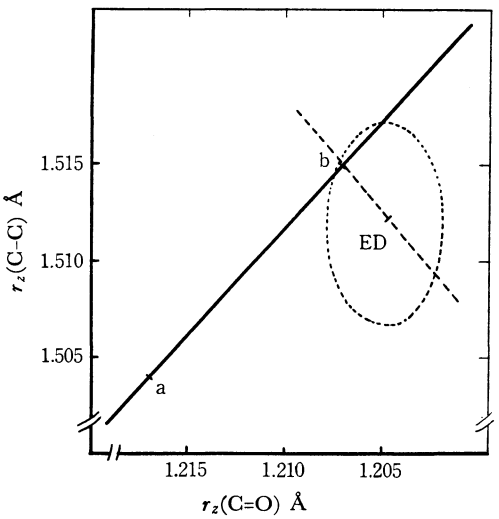

Fig. 2. Relation between r_z(C-C) and r_z(C=O). The cross point a of the two straight lines, indistinguishable in this figure, indicates the most probable values of r_z(C-C) and r_z(C=O) determined for spectroscopic moments of inertia. The point b indicates the most probable values determined by using electron diffraction data in addition to the spectroscopic data. The point ED indicates the results of electron diffraction for r_z(C-C) and r_z(C=O). The contour shows the limits of error of the diffraction data. The dashed line shows possible variation of r_z(C-C) and r_z(C=O) when a systematic error is allowed for in the scale factor of the diffraction data.

The moments of inertia, $I_\alpha^{(z)}$, calculated from the most probable values of the parameters are listed in Table 7, together with deviations from the observed moments of inertia. A deviation as large as 0.03 amu.Å^2 can originate from possible systematic errors in the isotope effects estimated for $\langle \Delta z \rangle_0$ and from the ignorance of anharmonicity in the deformation of bond angles, as has been mentioned in the preceding sections. Fractional deviations, however, are as small as a few parts per thousand or less. Therefore, uncertainties in the structure parameters due to these origins may also be expected to be a few parts per thousand unless correlations between parameters are as strong as in this case.

Zero-point Average Distance from Electron Diffraction

The distances, r_g(C–C) and r_g(C=O), determined by electron diffraction at room temperature were converted to r_z distances by the following equation;[9,10]

$$r_z = \lim_{T\to 0°K} r_g^T - K_0$$
$$\cong r_g^T - (3/2)a_3(l_T^2 - l_0^2) - \delta r_{cent} - K_0 \qquad (9)$$

where l_T^2 is the mean-square amplitudes and δr_{cent} the centrifugal stretching, both at room temperature, and where the other notations are as specified in Eqs. (5) and (6). This process is based on the assumption that a potential function associated with a bonded distance is well approximated by the Morse-type potential if the net distance between the two atoms, not the distance projected onto the equilibrium direction, is taken as a parameter of the potential function.[15] The non-bonded distances were not converted, for the uncertainties in their values are larger and, also, the anharmonicities for non-bonded atom pairs are not well known. The C–H distances were not determined with sufficient accuracy by electron diffraction.

The centrifugal stretching corrections were roughly estimated to be 0.000_4 Å for C–C and 0.000_2 Å for C=O by referring to the C=O bond of CO_2 calculated rigorously at room temperature, 0.0003 Å.[18] The numerical values for this conversion are summarized in Table 8. A comparison of the r_z-values in Table 8 with those in Table 6 reveals no inconsistency between the spectroscopic and diffraction r_z values; any inconsistency would be obscured by the large limits of error in the spectroscopic values.

Table 8. Conversion from r_g to r_z

	r_g^T (Å)	l_T^2 (Å^2)	l_0^2 (Å^2)	a_3 (Å^{-1})
C-C	1.514	0.00244	0.00237	2.1
C=O	1.209	0.00151	0.00150	2.4

	K_0 (Å)	δr_{cent} (Å)	r_z (Å)
C-C	0.0016	0.0004	1.512
C=O	0.0018	0.0002	1.205

T=300°K

Zero-point Structure with Additional r_2's Observed by Electron Diffraction

The strong correlation between the r_{C-C} and $r_{C=O}$ values was dissolved by a cooperative use of the r_z distances observed by electron diffraction

18) Y. Murata, K. Kuchitsu and M. Tanimoto, This Bulletin, to be published.

and the moments of inertia observed by microwave spectroscopy. The least-squares procedure was straightforward, and the two observed quantities, r_z^{ED}(C–C) and r_z^{ED}(C=O), were added to the twelve $I_\alpha^{(z)}$'s. Thus, five parameters were adjusted to fourteen observations. Obviously, the additional part of the Jacobian matrix had only two non-vanishing elements, one between the parameter r_{C-C} and the observed r_z^{ED}(C–C), and the other between r_{C-O} and r_z^{ED}(C=O). The relative weighting factors for observed quantities were identified as being inversely proportional to the square of the error of each observed value. The limits of error (99% confidence interval) in electron diffraction were reported to be ± 0.005 Å for r_z^{ED}(C–C) and ± 0.003 Å for r_z^{ED}(C=O). The errors arising from the conversion from r_g to r_z were ignored because they were considered to be less important. For the $I_\alpha^{(z)}$'s determined by microwave spectroscopy, the errors from which the weighting factors should be estimated are not only the original experimental errors in the moments of inertia, but also those including uncertainties in the conversion from I_{eff} to $I_\alpha^{(z)}$. However, most of the errors may be considered to arise from the conversion process. Therefore, these uncertainties are represented by the deviations of $I_\alpha^{(z)}$(obs) from $I_\alpha^{(z)}$(calc) calculated by use of the most probable values of the parameters. Corresponding to the 99% confidence interval in electron diffraction, the maximum deviation of $I_\alpha^{(z)}$(calc), ± 0.03 amu.Å^2, was taken as an error for $I_\alpha^{(z)}$.

The results of the least-squares adjustment are summarized in the second column of Tables 6 and 7. The adjusted values of r_{C-C} and $r_{C=O}$ are also indicated in Fig. 2 by the b point. Although there might be additional systematic errors which do not appear as a mutual inconsistency between the $I_\alpha^{(z)}$'s of several isotopically-substituted species, they were not taken into consideration, for their amounts are not well known. In the present case, however, even if the weighting factor for $I_\alpha^{(z)}$ were reduced to a quarter of the values used in view of the possible systematic error, the final set of parameters would remain almost unchanged, for the b point in Fig. 2 is the nearest point to the ED point on the solid line. The authors' view is that better estimates of errors for $I_\alpha^{(z)}$ will be established gradually through the further application to other molecules of the method of the cooperative use of diffraction and spectroscopic data.

Another method of this cooperative use is to eliminate a systematic error in the scale factor for diffraction results by the use of the spectroscopic moments of inertia, as was applied to the cyanogen molecule by Morino *et al.*[7] and to ethane by Kuchitsu.[9] In the present study this corresponds to finding a cross point of the two lines in Fig. 2: a dashed line passing the ED point so as to represent a proportional variation in r_{C-C} and $r_{C=O}$ according to a small deviation in the scale factor, and a solid line which represents the values of r_{C-C} and $r_{C=O}$ satsifying the least-squares condition for $I_\alpha^{(z)}$. Fortuitously, the cross point was very close to the b point, so the parameter values were identical with those obtained by the least-squares adjustment. Thus, the structure parameters listed in column II of Table 6 are considered to give the most reliable average structure of acetaldehyde.

From the values of $\langle \Delta z \rangle_0$ shown in Table 4 and the r_2 values determined in the present study, an approximate value of r_e was estimated by the use of Eq. (4), although it might include a large systematic error. The value of r_e obtained for the C–H bond of the methyl group was 1.078 Å, showing fair agreement with the 1.085 Å of CH_4[19] and the 1.080 Å of CH_3X.[20] When the r_z-value of the C–H(Me) of acetaldehyde, 1.073 Å, is compared with the r_2-value of the C–H in CH_4, 1.100 Å, one might erroneously conclude that there is a remarkable difference in the nature of the C–H bonds in acetaldehyde and methane. However, it must be noted that the r_z value depends not only on the nature of the bond but also on the environment of the bond in a molecule and the isotope effect. Judging from the agreement of the approximate r_e-values, it is probable that the C–H bonds in these molecules are similar in nature and that the difference between r_z-values arises mainly from the environment effect, *e. g.*, the torsional motion of the methyl top in acetaldehyde.

The authors wish to thank Mr. Chuichi Kato for his help in the early stage of this study. The numerical calculations were performed on a HITAC 5020E of the Computing Center of the University of Tokyo and on a FACOM 270-20 in the laboratory of Professor Kimio Ohno, Hokkaido University, to whom the authors' thanks are also due.

19) L. S. Bartell, K. Kuchitsu and R. J. deNeui, *J. Chem. Phys.*, **35**, 1211 (1961).

20) Y. Morino and J. Nakamura, This Bulletin, **38**, 443 (1965).

BULLETIN OF THE CHEMICAL SOCIETY OF JAPAN VOL. 42 2165—2169 (1969)

Temperature-jump Studies of the Kinetics of the Formation of the Monochloro and Monobromo Complexes of Iron(III)

Tatsuya YASUNAGA and Shoji HARADA

Department of Chemistry, Faculty of Science, Hiroshima University, Higashi-sendamachi, Hiroshima

(Received December 21, 1968)

The temperature-jump method was used to study the kinetics of $FeCl^{2+}$ and $FeBr^{2+}$ complex formations in aqueous solutions. Complex formation is composed of two paths. In the acid-independent path, the rate-determining step of complex formation may be the reaction between $Fe(H_2O)_5^{3+}$ and X^- ($X^- = Cl^-$, Br^-). The other path is that *via* the hydrolysis of ferric ions, and the rate-determining step is the loss of a water molecule from the inner coordination sphere of the metal ion. The kinetic values obtained are in good agreement with the results obtained by the flow method.

Many of the fast metal complex formation reactions in solution have been studied with the help of the relaxation methods developed mainly by Eigen and Mayer,[1] and a step-by-step association picture has been presented to explain their relaxation phenomena.

Some of the complex formation reactions of Fe(III) have also been studied by the flow method,[2-6] the pressure-jump method,[7] and, most recently, the temperature-jump method.[8,9] By the temperature-jump method Cavasino[8,9] has reexamined a few of the Fe(III) complex formation reactions previously studied by the flow method and has given the kinetic values and interpreted the reactions.

The present study was undertaken in order to obtain kinetic information on the $FeCl^{2+}$ complex formation reaction over a wide range of acidity and temperature by the temperature-jump method. Moreover, since there has been very little information on the kinetics of the $FeBr^{2+}$ complex formation reaction,[3] we aimed to establish the mechanisms in more detail and to obtain the kinetic values of the reaction. Another purpose was to test the operation of a newly-built device at the beginning of the temperature-jump study.

Experimental

All the inorganic chemicals were of a reagent grade. Stock solutions of $Fe(NO_3)_3$ and NaCl were prepared. The concentration of ferric ion was determined photometrically. The chloride concentration was checked by titration with a standard silver nitrate solution. The hydrogen ion concentration was changed by the addition of $HClO_4$. The ionic strength was adjusted to $\mu = 1.0$ by the addition of $NaClO_4$. The temperature-jump apparatus used was a modification of that described by Hammes and Fasella.[10] A schematic diagram of our apparatus is shown in Fig. 1. The 0.1 μF condenser was charged to 18000 V and discharged

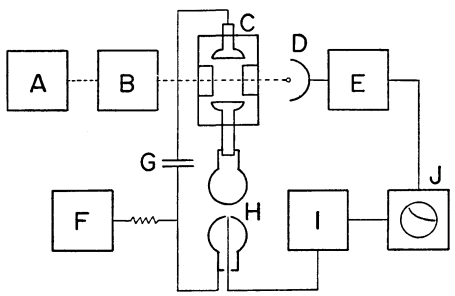

Fig. 1. Schematic diagram of temperature-jump apparatus.
(A) light source; (B) monochromator; (C) observation cell; (D) photomultiplier; (E) amplifier; (F) high voltage; (G) condenser; (H) spark gap; (I) trigger; (J) oscilloscope

1) M. Eigen and L. De Mayer, "Technique of Organic Chemistry," Vol. VIII, 2nd Ed., S. L. Friess, E. S. Lewis and A. Weissberger, Ed., Interscience Publishers, Inc., New York, N. Y. (1963), Part 2, p. 895.
2) R. E. Connick and C. P. Coppel, *J. Am. Chem. Soc.*, **81**, 6389 (1959).
3) P. Matthies and H. Wendt, *Z. Physik. Chem. (Frankfurt)*, **30**, 137 (1961).
4) J. F. Below, Jr., R. E. Connick and C. P. Coppel, *J. Am. Chem. Soc.*, **80**, 2961 (1958).
5) G. G. Davis and W. MacF. Smith, *Can. J. Chem.*, **40**, 1836 (1962).
6) D. Seewald and N. Sutin, *Inorg. Chem.*, **2**, 643 (1963).
7) H. Wendt and H. Strehlow, *Z. Elektrochem.*, **66**, 228 (1962).
8) F. Accascina, F. P. Cavasino and S. D'Alessandro, *J. Phys. Chem.*, **71**, 2474 (1967).
9) F. P. Cavasino, *ibid.*, **72**, 1378 (1968).
10) G. G. Hammes and P. Fasella, *J. Am. Chem. Soc.*, **84**, 4644 (1962).

through the air gap. The observation cell was connected in parallel with the condenser *via* two gold-plated electrodes. The concentration changes were observed by single-beam-designed optical techniques. The temperature jump of the solution between the two electrodes was 5±1°C. The magnitude of the temperature jump was calibrated by comparing the change in the absorbance value of a test sample induced by discharge with the values previously measured at various temperatures. The test sample was a 0.02 M glycine solution (μ=1.0) at pH 9 containing phenolphthalein; it was followed at 550 mμ.

In all the ferric chloride solutions, the relaxation spectrum was characterised by a single relaxation time. A representative relaxation effect is shown in Fig. 2. Blank solutions containing only $Fe(NO_3)_3$ or NaCl with $NaClO_4$ gave no relaxation phenomena in the same range of time. The reciprocal relaxation time was calculated from a plot of $-\log \Delta C$ *vs.* the time, where ΔC is the deviation of the concentration from its equilibrium value. The wavelength of observation was 390 mμ. The quoted relaxation times and rate constants are the mean values of several runs.

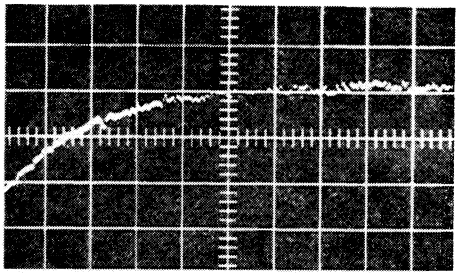

Fig. 2. Experimental relaxation curve at 27°C and μ=1.0.
$\sum$[Fe]=5×10^{-2} M; $\sum$[Cl]=5×10^{-} M; [H$^+$]= 0.10 M. The sweep rate is 5 msec per devision.

In the case of $FeBr^{2+}$ complex formation studies, $Fe(NO_3)_3$ and NaBr were used. Experiments were performed over the range of acidity of 0.1 M≤[H$^+$]≤ 0.8 M and at temperatures between 20°C and 40°C at μ=1.2.

Results

In the present studies, the following equilibria are assumed to be present and are attributed to the relaxation:

$$Fe^{3+} + X^- \rightleftarrows FeX^{2+} \qquad K_X = \frac{(FeX^{2+})}{(Fe^{3+})(X^-)} \qquad (1)$$

$$Fe^{3+} + H_2O \rightleftarrows FeOH^{2+} + H^+ \qquad K_{OH} = \frac{(FeOH^{2+})(H^+)}{(Fe^{3+})} \qquad (2)$$

Taking into account the low concentrations of Fe^{3+} and X^- and the high acidities, the following equilibria may be neglected:

$$FeX^{2+} + X^- \rightleftarrows FeX_2^+ \qquad (3)$$

$$FeOH^{2+} + H_2O \rightleftarrows Fe(OH)_2^+ + H^+ \qquad (4)$$

$$2FeOH^{2+} \rightleftarrows Fe_2(OH)_2^{4+} \qquad (5)$$

With these hypotheses, the overall mechanism for the complex formation of FeX^{2+} may be expressed as follows:

$$\begin{array}{ccc} H_2O + Fe^{3+} + X^- & \underset{k_{21}}{\overset{k_{12}}{\rightleftarrows}} & FeX^{2+} + H_2O \\ k_{13}\downarrow\uparrow k_{31} & & k_{42}\uparrow\downarrow k_{24} \\ Fe(OH)^{2+} + X^- + H^+ & \underset{k_{43}}{\overset{k_{34}}{\rightleftarrows}} & Fe(OH)X^+ + H^+ \end{array} \qquad (6)\ (7)$$

The protolytic reactions (vertical steps) will be very fast, and the other two processes may correspond to the rate-determining steps of complex formation.

Assuming that $Fe(OH)X^+$ is in a steady state, the rate of FeX^{2+} formation is given by:

$$\frac{d(FeX^{2+})}{dt} = k_{12}(Fe^{3+})(X^-) + k_{34}(FeOH^{2+})(X^-) - k_{21}(FeX^{2+}) - k_{43}(Fe(OH)X^+) \qquad (8)$$

and

$$\frac{d\Delta[FeX^{2+}]}{dt} = -\Delta[FeX^{2+}]([Fe^{3+}] + [X^-] + 1/K_X)(k_{12} + k_{34}\cdot K_{OH}/[H^+]) \qquad (9)$$

The reciprocal relaxation time is, then, related to the rate constants and the concentrations as follows:

$$\begin{aligned} 1/\tau &= (k_{12} + k_{34}\cdot K_{OH}/[H^+])([Fe^{3+}] + [X^-] + 1/K_X) \\ &= (k_f^\circ + k_f'/[H^+])([Fe^{3+}] + [X^-] + 1/K_X) \\ &= k_f([Fe^{3+}] + [X^-] + 1/K_X) \end{aligned} \qquad (10)$$

with $k_f^\circ = k_{12}$; $k_f' = k_{34}\cdot K_{OH}$; $k_f = k_f^\circ + k_f'/[H^+]$. The concentrations of Fe^{3+} and X^- are obtained from the total iron and halide concentrations and the corrected equilibrium constants, K_X and K_{OH}.

Table 1. Averaged $1/\tau$[a] values in ferric chloride solutions at μ=1.0 and 27°C

[H$^+$], M	$\sum$Fe, 10^{-2} M	5	5	5	3
	$\sum$Cl, 10^{-2} M	5	3	1	2
0.050		202	153	148	140
0.075		100	106	109	120
0.100		94	84	76	84
0.150		67	53	59	58
0.200		50	45	52	47
0.400		26	28	22	27

a) Unit, sec^{-1}

Table 2. Averaged $1/\tau$[a] values in ferric bromide solutions at μ=1.2 and 27°C

[H$^+$], M	$\sum$Fe, 10^{-2} M	5	5	5	2
	$\sum$Br, 10^{-2} M	5	5	1	2
0.10		1600	1670	1590	1380
0.20		940	1000	960	1040
0.40		525	550	540	530
0.60		370	375	430	415
0.80		295	290	310	280

a) Unit, sec^{-1}

The relaxation times were affected only very slightly by the ferric and halide concentrations, as is shown in Tables 1 and 2. This can easily be foreseen from the fact that the quantity of the concentration part, $([Fe^{3+}]+[X^-])$, is smaller than $1/K_X$ (maxima: 30% in the case of $FeCl^{2+}$ but only 3% in the case of $FeBr^{2+}$); therefore, it is not necessary to know the concentrations with any great accuracy.

A) $FeCl^{2+}$ Complex Formation Reaction. The formation rate constants were calculated by Eq. (10) with $1/\tau$ values in Table 1, the equilibrium concentrations of the ions, and the dissociation constant. As may be seen in Fig. 3, the observed rate constant depends greatly on the hydrogen ion concentration. The points are linear, with a finite intercept at $1/[H^+]=0$. The intercept and slope of Fig. 3 give values of $k_f^\circ=20\pm10$ $M^{-1}sec^{-1}$ and $k_f'=26\pm3$ sec^{-1} at 27°C.

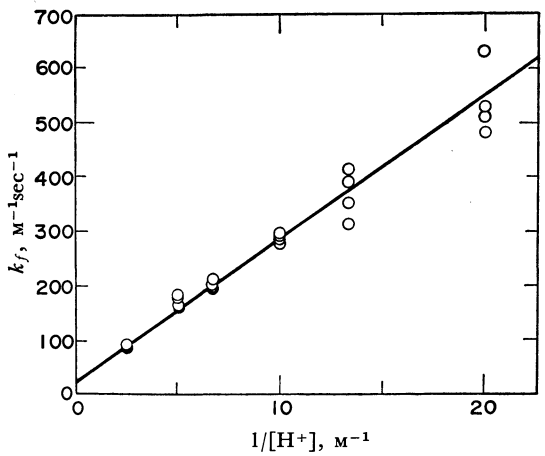

Fig. 3. The acid dependence of the formation rate constant of $FeCl^{2+}$ at 27°C and $\mu=1.0$.

In order to determine the enthalpies and entropies of activation, a series of experiments was run covering the temperature range from 20°C to 40°C. The equilibrium constants for ferric chloride at various temperatures have been estimated by the van't Hoff equation using the value at 25°C of 4.03 M^{-1} and $\Delta H=6.0$ kcal mol^{-1}.[2] K_{OH} has been estimated in the same way with the values of $\Delta H=10.2$ kcal mol^{-1} and $K_{OH}=1.60\times10^{-3}$ M^{-1} at 25°C.[11] The rate constants were calculated by means of Eq. (10), with the concentrations corrected for the temperatures; the results are shown in Fig. 4.

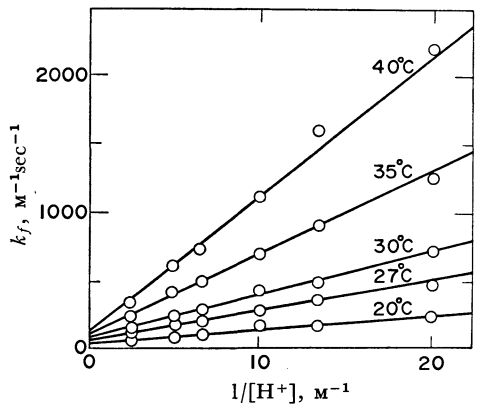

Fig. 4. k_f of $FeCl^{2+}$ *vs.* $1/[H^+]$ plot at various temperatures and $\mu=1.0$.

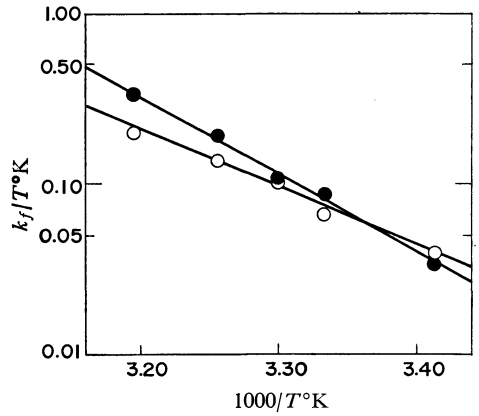

Fig. 5. Temperature dependence of k_f° (○) and k'_f (●) of $FeCl^{2+}$ at $\mu=1.0$.

Table 3. Kinetic data for $FeCl^{2+}$ formation and dissociation at $\mu=1.0$ and 25°C

Formation reaction		Dissociation reaction	
k_{12}, $M^{-1}sec^{-1}$	19 ± 10	k_{21}, $M^{-1}sec^{-1}$	4.7 ± 2
k_f', sec^{-1}	18.5 ± 3	k_b', sec^{-1}	4.6 ± 0.7
k_{34}, $M^{-1}sec^{-1}$	$1.15(\pm0.2)\times10^4$	k_{43}, $M^{-1}sec^{-1}$	$2.85(\pm0.5)\times10^3$
k^*_{FeOH}, sec^{-1}	1×10^4		
$\Delta H^\ddagger_{12}$, kcal. mol^{-1}	16 ± 5	$\Delta H^\ddagger_{21}$, kcal. mol^{-1}	10 ± 5
$\Delta H^\ddagger_{34}$, kcal. mol^{-1} a)	11 ± 2	$\Delta H^\ddagger_{43}$, kcal. mol^{-1}	15 ± 2
$\Delta S^\ddagger_{12}$, e. u.	1 ± 17	$\Delta S^\ddagger_{21}$, e. u.	-21 ± 17
$\Delta S^\ddagger_{34}$, e. u.	-3 ± 7	$\Delta S^\ddagger_{43}$, e. u.	8 ± 7

a) Calculated from $\Delta H^\ddagger_{f'}$ and the enthalpy change of reaction (12).

11) R. M. Milburn, *J. Am. Chem. Soc.*, **79**, 537 (1957).

Figure 5 shows a plot of log $k_f°/T$ °K *vs.* $1000/T$ °K, and similarly for k_f'. From the slopes of these lines, $\Delta H^{\ddagger}_{f°}=16\pm5$ kcal mol and $\Delta H^{\ddagger}_{f'}=21\pm2$ kcal mol^{-1} were calculated using the Eyring equation. $k_f°$ and k_f' at 25°C were taken to be $k_f°=19\pm10$ M^{-1} sec^{-1} and $k_f'=18.5\pm3$ sec^{-1} (*cf.* Fig. 5). These values are in good agreement with Connick's values,[2] $\Delta H^{\ddagger}_{f°}=16.6$ kcal mol^{-1}, $\Delta H^{\ddagger}_{f'}=23.3$ kcal mol^{-1}, $k_f°=9.5$ M^{-1} sec^{-1}, and $k_f'=18.0$ sec^{-1} at 25°C. The other kinetic values for $FeCl^{2+}$ formation and dissociation reactions are also listed in Table 3.

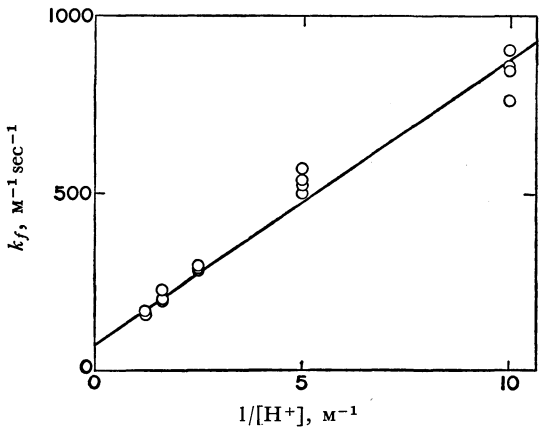

Fig. 6. The acid dependence of the formation rate constant of $FeBr^{2+}$ at 27°C and $\mu=1.2$.

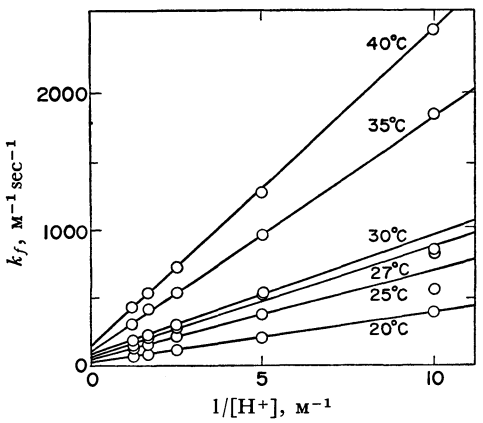

Fig. 7. k_f of $FeBr^{2+}$ *vs.* 1/[H$^+$] plot at various temperatures and $\mu=1.2$.

B) $FeBr^{2+}$ Complex Formation Reaction. The formation rate constants were calculated from the data in Table 2 and the equilibrium constants, $K_{Br}=0.56$ M^{-1} and $K_{OH}=1.78$ M^{-1} at $\mu=1.2$ and 27°C. Plots of the rate constants against 1/[H$^+$] in Fig. 6 gave values of $k_f°=73\pm20$ M^{-1} sec^{-1} and $k_f'=80\pm5$ sec^{-1} at 27°C. The enthalpies and entropies of activation were calculated from the data in Fig. 7. The kinetic values for the $FeBr^{2+}$ formation and for the dissociation reactions are listed in Table 4.

Discussion

Taking into account the fact that the rate constant of the complex formation is composed of two terms, one independent of hydrogen ion concentration and the other dependent on it, the complex formation reaction *via* rapid ion-pair formation, followed by the rate-determining loss of a water molecule in the inner coordination sphere of the metal ion, may be proposed as this reaction mechanism:

$$Fe(H_2O)_6^{3+} + X^- \overset{K°_{Fe}}{\rightleftharpoons} (H_2O)_5Fe^{3+}(H_2O)X^- \overset{k^*_{Fe}}{\rightleftharpoons} (H_2O)_5FeX^{2+} + H_2O \quad (11)$$

$$Fe(H_2O)_6^{3+} \overset{K_{OH}}{\rightleftharpoons} (H_2O)_5Fe(OH)^{2+} + H^+ \quad (12)$$

$$(H_2O)_5Fe(OH)^{2+} + X^- \overset{K°_{FeOH}}{\rightleftharpoons} (H_2O)_4Fe(OH)^{2+}(H_2O)X^- \overset{k^*_{FeOH}}{\rightleftharpoons} (H_2O)_4Fe(OH)X^+ + H_2O \quad (13)$$

$$(H_2O)_4Fe(OH)X^+ + H^+ \overset{\text{fast}}{\rightleftharpoons} (H_2O)_5FeX^{2+} + H_2O \quad (14)$$

where $K°$ is the ion-pair equilibrium constant and k^* is the rate constant for the rate-determining step of the inner coordinated water substitution. The two rate constants obtained above, k_{12} and k_{34}, have the following relationships:

$$k_{12} = K°_{Fe} \cdot k^*_{Fe} \quad (15)$$

Table 4. Kinetic data for $FeBr^{2+}$ formation and dissociation at $\mu=1.2$ and 25°C

Formation reaction		Dissociation reaction	
k_{12}, M^{-1} sec^{-1}	50 ± 20	k_{21}, sec^{-1}	94 ± 20
k_f, sec^{-1}	65 ± 5	k_b, sec^{-1}	125 ± 5
k_{34}, M^{-1} sec^{-1}	$(4.1\pm0.3)\times10^4$	k_{43}, M^{-1} sec^{-1}	$(7.9\pm0.3)\times10^4$
k^*_{FeOH}, sec^{-1}	4×10^4		
$\Delta H^{\ddagger}_{12}$, kcal. mol^{-1}	12 ± 2	$\Delta H^{\ddagger}_{21}$, kcal mol^{-1}	6 ± 2
$\Delta H^{\ddagger}_{34}$, kcal. mol^{-1} a)	6 ± 2	$\Delta H^{\ddagger}_{43}$, kcal mol^{-1}	10 ± 2
$\Delta S^{\ddagger}_{12}$, e. u.	-10 ± 7	$\Delta S^{\ddagger}_{21}$, e. u.	-29 ± 7
$\Delta S^{\ddagger}_{34}$, e. u.	-18 ± 7	$\Delta S^{\ddagger}_{43}$, e. u.	-2 ± 7

a) Calculated from $\Delta H^{\ddagger}_{f'}$ and the enthalpy change of reaction (12).

TABLE 5. RATE CONSTANTS[a] FOR Fe(III) COMPLEX FORMATION REACTIONS AT 25°C

Complex	μ	k_{12}	k'_{12}[b]	$k_{34}\times10^{-4}$	k'_{34}[c] $\times10^{-4}$	Ref.
$FeCl^{2+}$	1.0	19	—	1.2	—	This work
$FeCl^{2+}$	1.0	9.4	—	1.1	—	2
$FeBr^{2+}$	1.2	50	—	4.1	—	This work
$FeBr^{2+}$[d]	1.7	20	—	2.6	—	3
$FeCNS^{2+}$	0.4	127	—	1.0	—	4
$FeSO_4^{+}$	0.6	—	—	24	2.4	7
$FeSO_4^{+}$	0.5	—	—	—	14.5	5
FeF^{2+}	0.5	—	11	—	0.32	14
FeN_3^{2+}	1.0	—	4	—	0.68	6
FeN_3^{2+}	0.1	—	—	—	0.74	8

a) Unit, $M^{-1}\,sec^{-1}$

b) k'_{12} corresponds to $Fe^{3+}+HX \xrightarrow{k'_{12}} FeX^{2+}+H^+$

c) k'_{34} corresponds to $FeOH^{2+}+HX \xrightarrow{k'_{34}} Fe(OH)X^{+}+H^+$

d) $t=22$°C

$$k_{34} = K^{\circ}_{FeOH}\cdot k^{*}_{FeOH} \qquad (16)$$

Unfortunately, K° cannot be determined experimentally; therefore, it has become customary to estimate K° from the Fuoss equation.[12,13] Assuming that the distance of the closest approach of the ion-pair partners is about 5 Å, K°_{Fe} and K°_{FeOH} can be calculated to be about 5 and 1 respectively at $\mu=0.5$—1.0, for the corresponding type of ion pairs. The value of K° in this calculation is uncertain because of the large ionic strength correction made in the calculation. The value of k^* for some of the Fe(III) complex formation reactions can be estimated from K° and the rate constants in Table 5.

The rate constants for the rate-determining process of reaction (13), k^{*}_{FeOH}, lie approximately in the same order, $(1-4)\times10^4$, irrespective of the nature of the entering ligand. According to Connick and Genser,[15] the rate constant for the water exchange on $(H_2O)_5FeOH^{2+}$ is estimated to be of the same order as these values ($\sim10^4\,sec^{-1}$). These facts indicate that the substitution of a water molecule in the inner coordination sphere of the metal ion is the rate-determining process of the complex formation reaction.

On the other hand, we must admit that the k_{12} and k_{12}' values also fall in nearly the same order. With $K^{\circ}_{Fe}=5$, k^{*}_{Fe} can be calculated to be 1—25 sec^{-1} by Eq. (15). Comparing k^{*}_{Fe} with the rate constant for water exchange on $Fe(H_2O)_6^{3+}$, $2.8\times10^2\,M^{-1}\,sec^{-1}$,[15] these values are a little too small. This shows that Eq. (11) is not the best possibility for the mechanism of reaction (6). An alternate mechanism consistent with the data may be proposed:

$$Fe(H_2O)_6^{3+} \overset{fast}{\rightleftarrows} Fe(H_2O)_5^{3+} + H_2O \qquad (17)$$

$$Fe(H_2O)_5^{3+} + X^- \rightleftarrows Fe(H_2O)_5X^{2+} \qquad (18)$$

where the reaction (17) is fast and where the rate-determining step is the reaction (18). This mechanism seems reasonable in view of two facts: the water exchange reaction rate is faster than the complex formation rate, and the complex formation rate of Fe(III) depends on the nature of the entering ligand.

Among the activation parameters for the complex formations of Fe(III), Cavasino[9] indicated some discrepancy in the reaction with Cl^- and attributed it to the high ionic strength at which the kinetic studies were carried out. In this work, however, we could not observe any such discrepancy in either $FeCl^{2+}$ or $FeBr^{2+}$ formation reactions; this fact also suggests that the rates of Fe(III) complex formation reactions are controlled by the rate of loss of a coordinated water molecule from the cation.

Further studies with other complexes of Fe(III) are in progress and will be reported on in due course.

12) R. M. Fuoss, *J. Am. Chem. Soc.*, **80**, 5059 (1958),
13) G. G. Hammes and J. I. Steinfeld, *ibid.*, **84**. 4639 (1962).
14) D. Pouli and W. MacF. Smith, *Can. J. Chem.*, **38**, 567 (1960).
15) R. E. Connick and E. E. Genser, quoted in Ref. 6.

BULLETIN OF THE CHEMICAL SOCIETY OF JAPAN VOL. 42 2170—2173 (1969)

Orbital Electronegativities in Molecules and Ionic Character in Molecular Complexes

Yoshio MATSUNAGA

Department of Chemistry, Faculty of Science, Hokkaido University, Sapporo

(Received December 21, 1968)

The orbital electronegativities in the nine aromatic hydrocarbons were estimated on the basis of the ionization potentials and the appearance potentials of the doubly-charged ions. Then, by applying the principle of electronegativity equalization to molecular complexes, the orbital electronegativities in typical electron acceptors were evaluated. The ionic character in single and crystal complexes were discussed in terms of the electronegativities of the component molecules. Consideration of neither the ionization potential of the donor molecule, the electron affinity of the acceptor molecule, nor the orbital electronegativities appeared to be enough to define the ionic character in a complex.

The formation of molecular complexes by aromatic compounds has been interpreted in terms of weak covalent interaction between the π-electrons of the donor and acceptor.[1] The donor is a molecule with a relatively low ionization potential and the acceptor is a molecule with a relatively high electron affinity. The transfer of a negative charge from the donor to the acceptor takes place by the interaction. As the orbital electronegativity, defined as the derivative of the energy with respect to the charge, has been known to be a measure of the power of atoms and groups to attract an electron,[2,3] the extension of this concept to molecules might be useful in systematizing the experimental data and in gaining an understanding of the ionic character in molecular complexes.

The molecular electronegativity introduced by Becker and Wentworth is constant for aromatic hydrocarbons, 4.07 ± 0.05 eV,[4] and so is apparently different from the quantities considered in this paper.

Orbital Electronegativities in Molecules

We assume that the form:

$$\varepsilon(\rho) = a\rho + b\rho^2 \qquad (1)$$

is a good approximation of the true equation for representing the energies of molecules in various states of ionization. ε represents the total energy of all the electrons in a molecule, taking the energy of the neutral molecule to be zero. ρ is the charge on the molecule at a particular state of ionization. The differentiation of Eq. (1) with respect to ρ gives the electronegativity:

$$\chi(\rho) = a + 2b\rho \qquad (2)$$

Specifically for the neutral molecule:

$$\chi(0) = a \qquad (3)$$

As the compounds under consideration are neutral, closed-shell entities, the ε *vs.* ρ curve has a discontinuity in the slope at $\rho=0$. The electronegativity evaluated with $\varepsilon(1)$ and $\varepsilon(2)$ is for the highest occupied orbital and is different from that evaluated with $\varepsilon^*(-1)$ and $\varepsilon^*(-2)$. The latter is the electronegativity of the lowest vacant orbital. (Hereafter the quantities involving the lowest vacant orbital are indicated by asterisks.) Becker and Wentworth have defined their molecular electronegativity by an average of the ionization potential, $\varepsilon(1)$, and the electron affinity, $-\varepsilon^*(-1)$. Thus, theirs is not the property of a single orbital but concerns both the highest occupied and the lowest vacant orbitals.

The ionic character in donor-acceptor complexes may be defined by the following equation, which is based on the principle of electronegativity equalization or on the concept of bond electronegativity:[3]

$$\rho = \frac{a_A^* - a_D}{2(b_D + b_A^*)} \qquad (4)$$

where the subscripts D and A refer to the donor and the acceptor respectively. This approximation may not be poor provided that the ionic character is low. Equation (4) corresponds to the condition for minimizing the energy of the complex by charge transfer:

1) G. Briegleb and J. Czekalla, *Angew. Chem.*, **72** 401 (1960).

2) R. P. Iczkowski and J. L. Margrave, *J. Am. Chem. Soc.*, **83**, 3547 (1961).

3) J. Hinze, M. A. Whitehead and H. H. Jaffé, *ibid.*, **85**, 148 (1963).

4) R. S. Becker and W. E. Wentworth, *ibid.*, **85**, 2210 (1963).

$$\varepsilon_C(\rho) = a_D\rho + b_D\rho^2 - a_A^*\rho + b_A^*\rho^2 \quad (5)$$

By eliminating ρ from Eq. (5) using Eq. (4), we obtain the contribution of the charge transfer to the binding energy:

$$\varepsilon_C = -\frac{(a_A^*-a_D)^2}{4(b_D+b_A^*)} \quad (6)$$

Thus, the stabilization energy may be anticipated to be nearly proportional to the square of the difference in orbital electronegativity.

Once the parameters, a and b, for a typical donor (or acceptor) molecule are known, those in the acceptor (or donor) molecule may be estimated on the basis of the magnitude of the ionic character or the charge transfer, ρ, in the complex. Of course, the value of $\varepsilon^*(-1)$ for the acceptor (or $\varepsilon(1)$ for the donor) must be available, but generally it can be easily measured or estimated.

Aromatic Hydrocarbons. There are, at present, very few compounds for which both $\varepsilon(1)$ and $\varepsilon(2)$ or $\varepsilon^*(-1)$ and $\varepsilon^*(-2)$ are known. For several aromatic hydrocarbons the ionization potentials, $\varepsilon(1)$, and the appearance potentials of doubly-charged ions, $\varepsilon(2)$, have been measured by Wacks and Dibeler.[5,6] The electronegativities of the highest occupied orbitals can be evaluated by means of Eq. (1). The results are presented in Table 1 with the values of $\varepsilon(1)$ and $\varepsilon(2)$. The appearance potentials of doubly-charged ions have been reported to have an estimated probable error of ± 0.5 eV; therefore, the estimation of a_D and b_D cannot be very accurate. It must be noted that the electronegativity, a_D, is more variable than the ionization potential. Moreover, the changes in these two quantities are not quite parallel. The values of the b_D parameters are scattered in the range from 3 to 4 eV, and no correlation with the ionization potential is noted.

Table 1. Ionization potentials $\varepsilon(1)$, appearance potentials of doubly charged ions $\varepsilon(2)$ and electronegativities of the highest occupied orbitals in some aromatic hydrocarbons

Hydrocarbon	$\varepsilon(1)$ (eV)	$\varepsilon(2)$ (eV)	a_D (eV)	b_D (eV)
Benzene	9.38	26.4	5.56	3.82
Naphthalene	8.26	22.7	5.17	3.09
Anthracene	7.55	21.1	4.55	3.00
Phenanthrene	8.03	23.1	4.51	3.52
Pyrene	7.72	24.00	3.44	4.28
Tetracene	6.95	22.14	2.83	4.12
Tetraphene	7.53	22.03	4.04	3.49
Chrysene	8.01	23.35	4.35	3.67
Triphenylene	8.19	24.10	4.33	3.86

5) M. E. Wacks and V. H. Dibeler, *J. Chem. Phys.*, **31**, 1557 (1959).
6) M. E. Wacks, *ibid.*, **41**, 1661 (1964).

Acceptors. Electron affinities have been estimated for a number of acceptors by Briegleb.[7] Recent measurements of the affinity of *p*-benzoquinone by the magnetron technique have suggested that Briegleb's value is too low, probably by 0.8 eV.[8] We assume that this difference can be used in estimating the acceptors now under consideration.

If the wave function of the ground state of a single 1 : 1 complex is approximated by:

$$a\psi_0(D, A) + b\psi_1(D^+\text{-}A^-) \quad (7)$$

where $\psi_0(D, A)$ is the wave function for a no-bond structure and $\psi_1(D^+\text{-}A^-)$ is that for a dative structure formed by the transfer of one electron from the donor (D) to the acceptor (A) molecule, while the ionic character is given by b^2. Briegleb *et al.* have measured the dipole moments of the three naphthalene complexes in solution and estimated the coefficients, a and b, in Eq. (7).[9] The parameters, a_A^* and b_A^*, may then be calculated using Eq. (4), with the values of $b^2(=\rho)$ and the electron affinities, $-\varepsilon_A^*(-1)$, estimated separately. The results are summarized in Table 2. Contrary to the case of the electron donors, the electronegativity, a_A^*, is relatively constant in these three acceptors. The change in the electron affinity arises mostly from the change in the b_A^* parameter.

Table 2. Electron affinities of acceptors $-\varepsilon_A^*(-1)$, ionic character ρ estimated for the naphthalene complexes and electronegativities of the lowest vacant orbitals of acceptors

Acceptor	$-\varepsilon_A^*(-1)$ (eV)	ρ	a_A^* (eV)	b_A^* (eV)
s-Trinitrobenzene	1.5	0.028	5.57	4.07
p-Chloranil	2.2	0.041	5.71	3.51
TCNE	2.6	0.063	5.99	3.39

Ionic Character in Donor-Acceptor Complexes

Single Complexes. With the parameters listed in Tables 1 and 2, the ionic character in the tetracyanoethylene (TCNE) complexes can be estimated by means of Eq. (4), they are presented in Table 3. The values for the complexes of large hydrocarbons seem to be too high. For example, Kuroda *et al.* have reported that the dipole moment of the pyrene

7) G. Briegleb, *Angew. Chem.*, **76**, 326 (1964).
8) A. L. Farragher and F. M. Page, *Trans. Faraday Soc.*, **62**, 3072 (1966).
9) G. Briegleb, "Elektron-Donator-Acceptor-Komplexe," Springer-Verlag, Berlin, Göttingen, Heidelberg (1961), p. 22.

complex is 2.0 debye.[10] By adopting Eq. (7), an ionic character about a half of the present estimation is obtained. This disagreement is rather serious. It has also been pointed out that Eq. (7) is too simple to represent the true wave function of the donor-acceptor complex.[10,11] The

TABLE 3. IONIC CHARACTERS AND STABILIZATION ENERGIES ESTIMATED FOR THE TETRACYANOETHYLENE COMPLEXES

Hydrocarbon	ρ by Eq. (4)	$-\varepsilon_C$ (eV) by Eq. (6)
Benzene	0.030	0.006
Naphthalene	(0.063)	0.026
Anthracene	0.113	0.081
Phenanthrene	0.107	0.079
Pyrene	0.166	0.212
Tetracene	0.210	0.332
Tetraphene	0.142	0.149
Chrysene	0.116	0.095
Triphenylene	0.114	0.095

significance of higher-energy charge-transfer configurations, including back charge-transfer configurations, has been emphasized. Therefore, the a_A^* and b_A^* parameters should be accepted only with some reservations. The disagreement in the pyrene complex may be regarded as an indication that the contributions from back charge-transfer configurations, D^--A^+, involving higher-energy orbitals, to the ground state of the pyrene complex are more appreciable than those to the ground state of the naphtalene complex. Table 3 includes the stabilization energies calculated by Eq. (6). These energies differ from the resonance energies given by the quantum mechanical treatment. Nevertheless, the calculated energies are mostly in the right order of magnitude, suggesting that the classical charge-transfer stabilization may be of some importance in the formation of molecular complexes.

Crystal Complexes. McConnell *et al.* have elaborated a Hartree-Fock molecular-field approximation to the energy of a 1 : 1 crystal complex and have proposed the following equation:[12]

$$E(\rho) = N(\varepsilon_0\rho - \varepsilon_1\rho^2) \tag{8}$$

Here $N\varepsilon_0$ is the energy required to charge the lattice so that there is a unit positive charge on each donor molecule and a unit negative charge on each acceptor molecule, while $-N\varepsilon_1\rho^2$ indicates the total attractive energy in the lattice. ε_0 is related to the ionization potential of the donor, $\varepsilon_D(1)$, and the electron affinity of the acceptor, $-\varepsilon_A^*(-1)$, by:

$$\varepsilon_0 = \frac{1}{2}[\varepsilon_D(1) + \varepsilon_A^*(-1)] \tag{9}$$

Assuming that ρ has to be in the range of 0 to 1, the energy is found by Eq. (8) to be at its minimum at $\rho=0$ when $\varepsilon_1<\varepsilon_0$ and at $\rho=1$ when $\varepsilon_1>\varepsilon_0$. Accordingly, they have concluded that 1 : 1 crystal complexes must divide quite sharply into two classes, namely, $\rho=0$ and 1.

Using the present approach, however, we reach conclusions very different from these. Within the framework of the electronegativity equalization, the energy of a crystal complex consisting of $N/2$ molecules of the donor and $N/2$ molecules of the acceptor is simply Eq. (5) multiplied by $N/2$, namely:

$$E(\rho) = \frac{N}{2}[(a_D - a_A^*)\rho + (b_D + b_A^*)\rho^2] \tag{10}$$

As $(a_D - a_A^*)$ is small in the complexes to which this approximation is good, the second term dominates in this equation. Therefore, the general features of the E *vs.* ρ curve given by Eq. (10) bear no resemblance to those suggested by McConnell *et al.* In Fig. 1 the energy of the naphthalene-TCNE complex is plotted against the charge using the parameters listed in Tables 1 and 2. The curve given by Eq. (8) is also illustrated for the sake of comparison.

If the ionic character in a crystal complex is high, the electrostatic ion-ion interaction becomes of major importance, just like the energy required to charge the lattice. Then:

$$E(\rho) = \frac{N}{2}[(a_D - a_A^*)\rho + (b_D + b_A^*)\rho^2 - 2\varepsilon_i\rho^2] \tag{11}$$

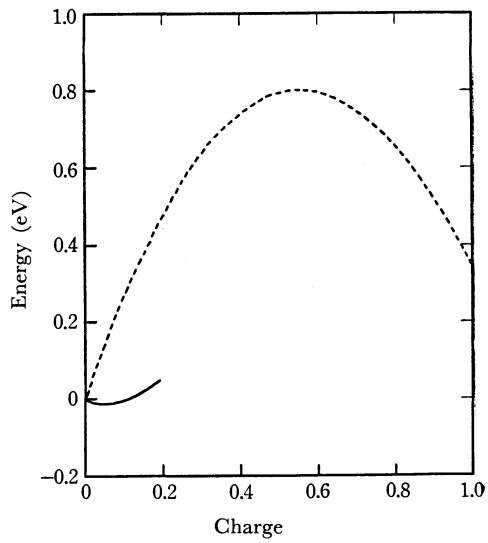

Fig. 1. Energy *vs.* charge as given by Eq. (10) (——) and by Eq. (8) (- - -) for naphthalene-TCNE complex.

10) H. Kuroda, T. Amano, I. Ikemoto and H. Akamatu, *J. Am. Chem. Soc.*, **89**, 6056 (1967).
11) R. S. Mulliken, *J. Chim. Phys.*, **61**, 20 (1963).
12) H. M. McConnell, B. M. Hoffman and R. M. Metzger, *Proc. Natl. Acad. Sci.*, **53**, 46 (1965).

where the ε_i has the same meaning as the ε_1 in Eq. (8). The amount of charge transfer in equilibrium is given by:

$$\rho = \frac{a_A^* - a_D}{2(b_D + b_A^* - 2\varepsilon_i)} \tag{12}$$

The condition $\varepsilon_i > [\varepsilon_D(1) + \varepsilon_A^*(-1)]/2$ leads to $\rho > 1/2$. As ε_i seems to be of the order of the magnitude of 2 eV,[13] among the donors and acceptors in Tables 1 and 2 the $\rho > 1/2$ condition is likely to be fulfilled when tetracene is combined with TCNE. Figure 2 presents the E *vs.* ρ curves given by Eqs. (8) and (11) with the parameters for this combination and with $\varepsilon_i = 2.5$ eV. If we employ Eq. (8), the assumption that $0 \leqq \rho \leqq 1$ is important. However, this does not seem very reasonable because each orbital may accommodate two electrons. It must be added that the presence of this particular complex is unlikely because of the chemical reaction between component compounds. Furthermore, as has been discussed in the preceding section, the ionic character defined by the parameters in Tables 1 and 2 may be too large and the $\rho > 1/2$ condition is not necessarily attained by the whole complex even if this complex could be prepared. Nevertheless, it should be emphasized that the presence of a number of crystal complexes in which $\varepsilon_i > [\varepsilon_D(1) + \varepsilon_A^*(-1)]/2$ is fulfilled has been indicated by the electronic and vibrational spectra.[14,15] The curves in Fig. 2 may be considered to present the general features of the ionic character in such complexes.

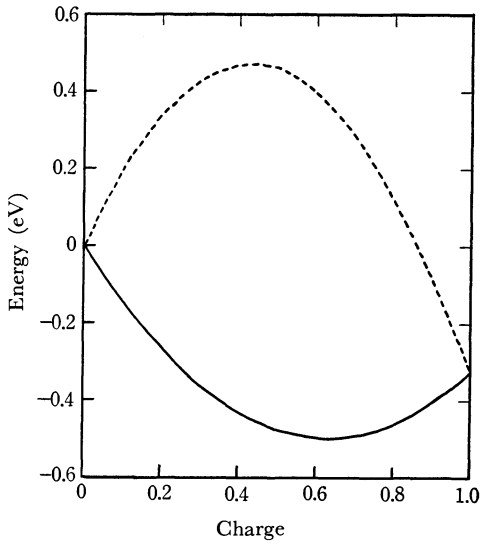

Fig. 2. Energy *vs.* charge as given by Eq. (11) (——) and by Eq. (8) (- - -) for tetracene-TCNE complex.

In conclusion, we wish to remark that consideration of neither the ionization potential of a donor, the electron affinity of an acceptor, nor the electronegativities represented by the a_D and a_A^* parameters is enough to define the ionic character in a complex. Let us therefore suppose the presence of some donors which have the same ionization potential as tetracene but which have a_D and b_D parameters different from those of the hydrocarbon, say, $a_D = 3.50$ and $b_D = 3.45$, and $a_D = 4.00$ and $b_D = 2.95$, respectively. Such donors may be considered to be more electronegative than tetracene; however, the ionic character in the TCNE complexes indicated by Eq. (12) may be anticipated to be higher than that in the tetracene complex, namely, 0.677 and 0.743 compared to 0.630.

13) Y. Matsunaga, This Bulletin, in press.

14) R. Foster and T. J. Thomson, *Trans. Faraday Soc.*, **59**, 296 (1963).

15) Y. Matsunaga, *J. Chem. Phys.*, **41**, 1609 (1964).

BULLETIN OF THE CHEMICAL SOCIETY OF JAPAN VOL. 42 2174—2179 (1969)

The Crystal and Molecular Structure of Carbazole

Masayasu KURAHASHI,*1 Makoto FUKUYO and Akira SHIMADA

Department of Chemistry, Faculty of Science, Osaka City University, Sumiyoshi-ku, Osaka

and Akio FURUSAKI and Isamu NITTA

Faculty of Science, Kwansei Gakuin University, Nishinomiya

(Received December 27, 1968)

The crystal structure of carbazole has been refined with three-dimensional X-ray data. Single crystals obtained from the melt are orthorhombic with four molecules in a unit cell of the dimensions $a=7.77_2$, $b=19.18_2$ and $c=5.72_5$ Å; space group is *Pnma*. Positional and thermal parameters were obtained by the least-squares method. The final discrepancy index R is 10.9% excluding zero intensity data. The e.s.d.'s in bond lengths not involving hydrogen atoms are 0.006—0.010 Å, and the corresponding errors in bond angles are about 0.5°. The molecule is planar within the deviation of 0.03 Å. A crystallographic mirror plane normal to the b-axis passes through the nitrogen atom and is perpendicular to the molecular plane. Comparison of the observed and theoretical bond lengths is made with discussion thereof. Some physical properties related to the crystal structure are also discussed by comparing its structure with that of fluorene. With the help of thermodynamical data, it has been argued that the hydrogen bond of N-H···N between molecules is not formed not only in the crystalline state but also in the liquid state.

A preliminary note on the crystal structure analysis of carbazole[1] was reported in 1966 by the authors. However, as the analysis was not sufficiently precise, a three-dimensional refinement has been undertaken. The main purpose of this investigation is to elucidate the molecular structure in detail, so as to obtain some information about the behavior of the hydrogen atom attached to the nitrogen. It will also be of significance to compare the experimental result with the theoretical one calculated by the MO method. It is further hoped that discussions may be given on some physical properties such as sublimation, cleavage, density and melting point in relation to the crystal structure.

Experimental

The crystals in colorless plates obtained from the melt belong to the orthorhombic system. The cell dimensions were determined from $hk0$ and $0kl$ Weissenberg photographs calibrated with silicon powder lines. The crystal data are summarized in Table 1. From systematic absences ($0kl$ with $k+l$ odd and $hk0$ with h odd) and intensity statistics, the space group of this crystal is determined to be *Pnma*. There are four molecules in the unit cell, and the molecule should have a mirror in it. The integrated intensities of 698 reflections were estimated visually from multiple-film equi-inclination Weissenberg photographs of the layers $hk0$ to $hk5$ and $0kl$ to $4kl$. Lorentz and polarization corrections were applied together with a spot-shape correction for upper layers, and all the intensities were placed on a common scale. Since the cross section of the crystals used was small enough(0.2×0.5 mm² for the a- and 0.3×0.5 mm² for the c-axis), no correction was made for the absorption effect.

Table 1. Crystal data

Compound:	Carbazole
	$C_{12}H_9N$
	MW = 167.2
	mp = 245°C
Unit cell:	(Cu$K\alpha$ radiation)
	Orthorhombic
	$a = 7.772\pm0.005$ Å
	$b = 19.182\pm0.010$ Å
	$c = 5.725\pm0.005$ Å
	$V = 853.5$ Å³
	$D_m = 1.29$ g/cm³
	$D_x = 1.301$ g/cm³
	$Z = 4$
	$\mu = 6.06$ cm⁻¹
Space group;	*Pnma*

Determination and Refinement of the Structure

The approximate coordinates of nitrogen and carbon atoms had already been found in the preliminary investigation. A least-squares refinement was started with the final parameters in that study. At first, hydrogen atoms were omitted from the calculations. After

*1 Present address: National Reserch Institute for Metals, Nakameguro, Meguro-ku, Tokyo.

1) M. Kurahashi, M. Fukuyo, A. Shimada, A. Furusaki and I. Nitta, This Bulletin, **39**, 2564 (1966).

four cycles of the refinement, R dropped from the initial value 22.0 to 17.6%. The positional parameters were further refined by the block-diagonal matrix least-squares method with the anisotropic temperature factors of the form $\exp\{-(B_{11}h^2+B_{22}k^2+B_{33}l^2+B_{12}hk+B_{23}kl+B_{31}lh)\}$, and R fell to 13.6% after four cycles. At this stage of refinement a three dimensional difference synthesis shown in Fig. 1 was calculated. In the map, the five of the eight highest peaks between 0.3 and 0.5 e.Å^{-3} corresponded to the hydrogen atoms. Including these, further four cycles of the refinement reduced R to 10.9%. Individual isotoropic temperature factors of 5.0 Å^2 had been assigned to these hydrogen atoms, and after the refinement those of the four hydrogen atoms attached to the benzene ring turned into 4.0—6.0 Å^2 and that of the hydrogen atom attached to the nitrogen increased to 7.3 Å^2.

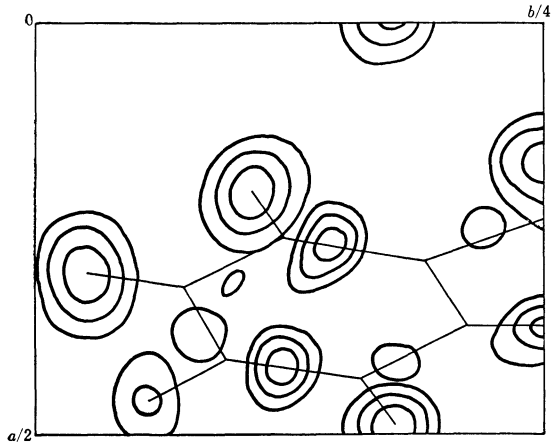

Fig. 1. Composite difference synthesis showing the hydrogen atoms. Contours at 0.1 e.Å^{-3} beginning at 0.2 e.A^{-3}.

Results and Discussion

Table 2 gives the final positional parameters of all the atoms with their e.s.d.'s evaluated in the least-squares calculations. The final temperature factors are listed in Table 3. The direction cosines and distances from the origin of the best planes through various sets of atoms in the molecule are presented in Table 4, together with the angles between these planes. The displacements of atoms from the various planes of Table 4 are given in Table 5. The electron density and difference syntheses in the molecular plane are shown in Fig. 2. The final calculated structure factors are compared in Table 6* with the observed values.

A crystallographic mirror plane normal to the b-axis passes through the nitrogen atom and is perpendicular to the molecular plane. Putting aside the positions of the hydrogen atoms, benzene rings and pyrrole ring in the carbazole molecule are respectively planar within the experimental error, less than 0.01 Å. Carbazole molecule itself is approximately planar within the deviations of 0.03 Å, though, strictly speaking, the two benzene rings in the molecule make an angle of 1.63°. The slightly bent structure might be due to the intermolecular interactions in the crystal field.

Table 2. Positional parameters and their e.s.d.'s

	x	σx	y	σy	z	σz
N	0.2373	(8)	0.2500	(*)	0.2346	(11)
C_1	0.2866	(6)	0.1911	(3)	0.3604	(8)
C_2	0.2596	(7)	0.1207	(3)	0.3047	(9)
C_3	0.3223	(8)	0.0734	(3)	0.4632	(11)
C_4	0.4075	(7)	0.0918	(3)	0.6682	(10)
C_5	0.4327	(6)	0.1618	(3)	0.7230	(9)
C_6	0.3698	(6)	0.2115	(3)	0.5679	(8)
H_N	0.1978	(128)	0.2500	(*)	0.0651	(175)
H_1	0.2160	(72)	0.1084	(27)	0.1505	(97)
H_2	0.3067	(75)	0.0293	(28)	0.4089	(104)
H_3	0.4297	(69)	0.0632	(29)	0.8130	(109)
H_4	0.4799	(72)	0.1743	(27)	0.9002	(94)

* Parameter constrained by symmetry requirements.

Table 3. Thermal vibration parameters for the expression $T = \exp\{-(B_{11}h^2+B_{22}k^2+B_{33}l^2+B_{12}hk+B_{23}kl+B_{31}lh)\}$ and their e.s.d.'s

	B_{11}	σ	B_{22}	σ	B_{33}	σ	B_{12}	σ	B_{23}	σ	B_{31}	σ
N	0.0179	(12)	0.0047	(2)	0.0231	(18)	0.0000	(*)	0.0000	(*)	−0.0116	(27)
C_1	0.0134	(7)	0.0039	(2)	0.0232	(15)	0.0004	(7)	0.0010	(9)	0.0029	(19)
C_2	0.0191	(10)	0.0045	(2)	0.0290	(18)	−0.0029	(8)	−0.0058	(10)	0.0012	(24)
C_3	0.0217	(12)	0.0034	(2)	0.0455	(23)	−0.0026	(8)	−0.0022	(12)	0.0113	(29)
C_4	0.0208	(11)	0.0038	(2)	0.0373	(20)	0.0013	(8)	0.0047	(11)	0.0037	(27)
C_5	0.0149	(9)	0.0045	(2)	0.0242	(15)	−0.0009	(7)	0.0010	(10)	0.0004	(20)
C_6	0.0105	(7)	0.0038	(2)	0.0229	(14)	−0.0009	(6)	−0.0012	(8)	−0.0008	(17)

* Parameter constrained by symmetry requirements.

* The complete data of the F_o-F_c table are kept as Document No. 6903 at the office of the Bulletin of the Chemical Society of Japan. A copy may be secured by citing the document number and by remitting, in advance, ¥250 for photoprints. Payment may be made by check or money order payable to: Chemical Society of Japan.

TABLE 4. EQUATIONS OF THE PLANES AND ANGLES BETWEEN DIFFERENT PLANES

1 Carbazole ring plane
2 Benzene ring plane (1)
3 Benzene ring plane (2)
4 Pyrrole ring plane

Equations of planes

1	$-0.8765X \quad -0.4815Z-1.0841=0$
2	$-0.8746X+0.0142Y-0.4847Z-1.1229=0$
3	$-0.8746X-0.0142Y-0.4847Z-0.9867=0$
4	$-0.8795X \quad -0.4760Z-1.0757=0$

Angles between different planes

	2	3	4
1	0.84°	0.84°	0.37°
2		1.63°	1.00°
3			1.00°

TABLE 5. DEVIATIONS OF ATOMS FROM VARIOUS PLANES

	1	2	3	4
N	−0.026*	−0.005	−0.005	−0.003*
C_1	−0.015*	−0.008*	0.024	0.003*
C_2	0.015*	0.002*	0.073	0.035
C_3	0.025*	0.003*	0.099	0.039
C_4	0.010*	−0.002*	0.084	0.015
C_5	−0.011*	−0.003*	0.045	−0.008
C_6	−0.010*	0.008*	0.029	−0.001*
C_6'	−0.010*	0.029	0.008*	−0.001*
C_5'	−0.011*	0.045	−0.003*	−0 008
C_4'	0.010*	0.084	−0.002*	0.015
C_3'	0.025*	0.099	0.003*	0.039
C_2'	0.015*	0.073	0.002*	0.035
C_1'	−0.015*	0.024	−0.008*	0.003*
H_N	−0.22*	−0.21	−0.21	−0.20
H_1	−0.11	−0.13	−0.06	−0.09
H_2	−0.02	−0.05	0.07	−0.00
H_3	0.26	0.24	0.34	0.26
H_4	0.16	0.17	0.21	0.15
H_4'	0.16	0.21	0.17	0.15
H_3'	0.26	0.34	0.24	0.26
H_2'	−0.02	0.07	−0.05	−0.00
H_1'	−0.11	−0.06	−0.13	−0.09

Least-squares plane is determined by the atoms with *.

Figure 3 shows the projection of the molecule upon its mirror plane. There the nitrogen atom and the hydrogen attached to it are given by the electron density contours, of which those for the hydrogen are drawn on the basis of a difference synthesis. As seen in the figure, electron density contours of the hydrogen atom are elongated in the direction normal to the molecular plane, where the peak is located. In view of the contour lines and anisotropic thermal parameters for the nitrogen clearly showing its oscillation in the direction normal to the molecular plane, the elongation mentioned above will imply that the hydrogen oscillates apparently more intensely than the nitrogen in the same direction.

It may be noted that such elongation can be interpreted as one of the two following possibilities. The first is to assume that the valence state of the nitrogen atom is mainly the sp^2 state and the equilibrium position of the hydrogen atom lies in the molecular plane, its out-of-plane oscillation being quite violent. The second is that the state is more or less sp^3 and the equilibrium position of

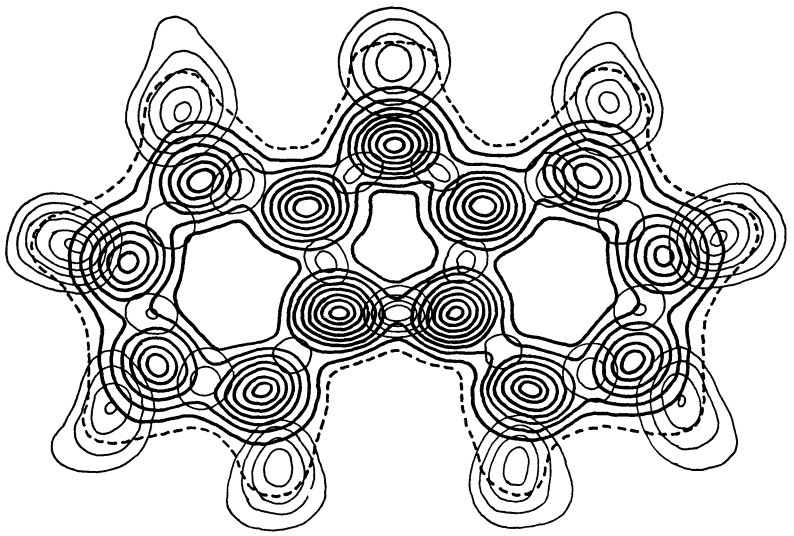

Fig. 2. Electron density and difference syntheses on the molecular plane. The contour lines, starting from 1.0 e.Å^{-3} are at intervals of 1.0 e.Å^{-3}. The broken line is 0.5 e.Å^{-3}. The fine lines, starting from 0.1 e.Å^{-3} are at intervals of 0.1 e.Å^{-3}.

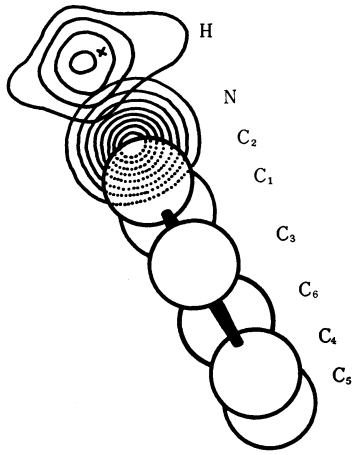

Fig. 3. Electron density for the nitrogen and difference synthesis for the attached hydrogen atom. The contour lines for the nitrogen, starting from 1.0 e.Å^{-3} are at intervals of 1.0 e.Å^{-3}, and for the hydrogen starting from 0.15 e.Å^{-3} at intervals of 0.1 e.Å^{-3}. The cross shows the position of the hydrogen atom determined by the least-squares method. The circles show the carbon atoms.

the hydrogen atom is on either side of the molecular plane and moves back and forth between these two positions somewhat like the umbrella inversion of ammonia molecule.

The cross in Fig. 3 indicates the position of the hydrogen determined by the least-squares method. It is deviated by 0.22 Å from the mean molecular plane (Table 5, 1), the e.s.d.'s of its positional parameters being of the order of 0.10 Å (Table 2). The temperature factor obtained by the least-squares method for this hydrogen atom is 7.33 Å^2, which is the largest of the hydrogen atoms in the molecule. Although it is not certain that the N–H bond is bent as the cross shows, there remains a possibility that this bending might be really due to the crystal field or some other reason. Anyhow, evidence that the hybridization state of the nitrogen is purely sp^3, can be excluded, for in such a case the deviation of the hydrogen from the molecular plane should be as large as 0.6 Å.

Bond lengths and angles are shown in Fig. 4. The e.s.d.'s of the bond distances are about 0.007 Å, except for 0.010 Å for the central C–C bond related to the mirror symmetry. The average C–C bond distance in the six-membered ring is 1.39_4 Å which is very close to the value found in crystalline benzene. Several theoretical treatments[2-4] have been made on carbazole. The observed bond lengths are compared with theoretical values

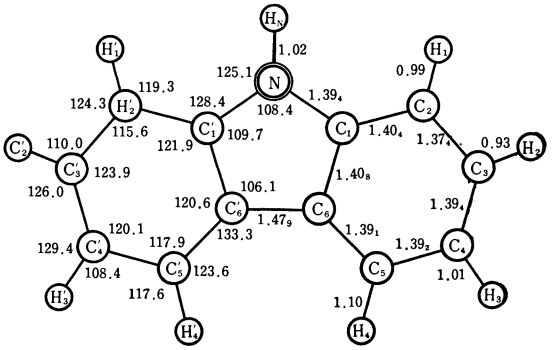

Fig. 4. Bond lengths and angles of carbazole.

Table 7. Comparison with theoretical investigation

	Bond order	Bond length		
		Theoretical*1	Observed*2	(e.s.d.)
N–C_1	0.420	1.375	1.394 (1.399)	0.006
C_1–C_2	0.572	1.414	1.404 (1.405)	0.008
C_2–C_3	0.722	1.387	1.374 (1.377)	0.008
C_3–C_4	0.607	1.408	1.394 (1.398)	0.008
C_4–C_5	0.719	1.388	1.392 (1.395)	0.008
C_5–C_6	0.584	1.412	1.391 (1.394)	0.007
C_6–C_1	0.593	1.410	1.408 (1.414)	0.006
C_6–C_6'	0.404	1.444	1.479 (1.484)	0.010

*1 Theoretical bond lengths were calculated by
r(C-C) = 1.517 − 0.18p
r(C-N) = 1.451 − 0.18p
r: bond length p: bond order

*2 Bond lengths corrected for thermal motion are in parentheses. The thermal parameters of the molecule were reasonably well explained on the basis of rigid-body motion.

calculated by SCFMO,[4] which is shown in Table 7. Observed C_5–C_6 is shorter by 0.02_1 Å, and C_6–C_6' and N–C_1 are longer by 0.03_5 and 0.01_9 Å respectively than theoretical values. It is suggestive that these are related to either C_6 or N, of which the hybridization state may be somewhat deviated from the standard sp^2 as seen in the bond angle distribution.

The bond angles in the five-membered ring ranges from 106.1° to 109.7° and that in the phenyl ring ranges from 115.6° to 123.8°. The e.s.d.'s are about 0.5°. Using the observed bond lengths and sp^2 orbital skeletons for nitrogen and carbon atoms, the observed distribution of the bond angles may be qualitatively explained by the molecular model based on the assumption that all the bonds

2) H. C. Longuet-Higgins and C. A. Coulson, *Trans. Faraday Soc.*, **43**, 87 (1947).
3) R. W. Schmid, *Helv. Chim. Acta*, **45**, 1982 (1962).
4) K. Nishimoto, private communication.

in the molecule share the strain force uniformly.

The crystal structure is shown in Fig. 5. The nearest approach between two nitrogen atoms of the neighboring molecules is 3.89 Å, and this shows that the hydrogen bond such as N-H···N is not formed in the crystal. This supports Aihara's conclusion from the measurement of the vapor pressure.[5] The position of the hydrogen atom attached to the nitrogen also shows this fact. In addition, it is sterically impossible to form hydrogen bond if the nitrogen is trigonally hybridized. Molecular packing seems to be uniform in *a*- and *c*-directions, and close contacts of 3.42—3.68 Å between molecules are found for any pair of neighboring molecules. On the other side there is considerably large space around $y=0$ and $y=1/2$, and the nearest approach between carbon atoms C_3 and C_4' of the neighboring molecules in the *b*-direction is as large as 3.87 Å. This is the reason why the crystal cannot elongate along the *b*-axis and shows excellent cleavage parallel to the (010) plane.

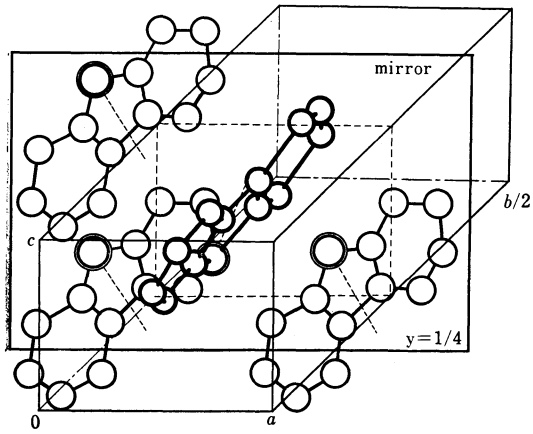

Fig. 5. Crystal structure of carbazole.

Carbazole crystal belongs to the same space group as fluorene[6] where N-H in carbazole is

TABLE 8. COMPARISON BETWEEN CARBAZOLE AND FLUORENE

	Carbazole $C_{12}H_9N$			Fluorene $C_{13}H_{10}$		
	MW 167.2			MW 166.2		
Crystal data						
	$a = 7.77_2$ Å			$a = 8.49$ Å		
	$b = 19.18_2$ Å			$b = 18.97$ Å		
	$c = 5.72_5$ Å			$c = 5.72$ Å		
	$V = 853.5$ Å^3			$V = 921.4$ Å^3		
	$D_m = 1.29_0$ g/cm^3			$D_m = 1.20_6$ g/cm^3		
	$D_x = 1.30_1$ g/cm^3 $z = 4$			$D_x = 1.19_7$ g/cm^3 $z = 4$		
Atomic parameters						
	x	y	z	x	y	z
N	0.237	1/4	0.235			
C_1	0.287	0.191	0.360	C_2	0.267	0.189	0.373
C_2	0.260	0.121	0.305	C_3	0.250	0.114	0.335
C_3	0.322	0.073	0.463	C_4	0.322	0.068	0.487
C_4	0.407	0.092	0.668	C_5	0.408	0.091	0.676
C_5	0.433	0.162	0.723	C_6	0.427	0.163	0.724
C_6	0.370	0.211	0.568	C_7	0.358	0.211	0.566
Thermodynamical data						
	mp = 245°C			mp = 115°C		
	bp = 355°C			bp = 293°C		
	ΔH_m*1 = 7.04 kcal/mol			ΔH_m*2 = 4.80 kcal/mol		
	ΔH_v*3 = 15.5 kcal/mol			ΔH_v*4 = 13.5 kcal/mol		
	$\Delta H_m + \Delta H_v = 22.5$ kcal/mol			$\Delta H_m + \Delta H_v = 18.3$ kcal/mol		
	ΔH_s*5 = 21.9 kcal/mol					
	ΔH_s*6 = 20.2 kcal/mol					

*1 *International Critical Table*, **5**, 134, (1929).
*2 "Coal Tar Data Book," Vols. 1 and 2, D2, The Coal Tar Research Association, England.
*3 *International Critical Table*, **3**, 226 (1928).
*4 *Ibid.*, **3**, 227 (1928).
*5 F. S. Mortimer and D. V. Murphy, *Ind. Eng. Chem.*, **15**, 1140 (1923).
*6 A. Aihara, *Nippon Kagaku Zassi (J. Chem. Soc. Japan, Pure Chem. Sect.)*, **76**, 492 (1955).

5) A. Aihara, *Nippon Kagaku Zassi (J. Chem. Soc. Japan, Pure Chem. Sect.)*, **76**, 492 (1955).

6) D. M. Burns and J. Iball, *Proc. Roy. Soc.*, **227A**, 200 (1955).

replaced by $C\langle^{H}_{H}$, and it resembles considerably that of fluorene in both cell dimensions and atomic parameters. Comparison of the crystal data, atomic parameters and thermodynamical data is shown in Table 8. Figure 6 shows the (010) projections of the crystal structure of both compounds. The plane of the fluorene molecules makes an angle of 55.2° to the *a*-axis, while the corresponding angle is 61.0° in carbazole. Intermolecular distances shown in Fig. 6 are generally shorter in carbazole than in fluorene.

As is easily expected from the crystal structure, subliming tendency of these compounds is related to the fact that strong intermolecular forces such as hydrogen bonds do not exist. However, effective partial volume around N-H will be smaller than that around $C\langle^{H}_{H}$, and carbazole, containing a nitrogen in a molecule, shows a dipole moment of 2.09 D.[7] Therefore the molecular arrangement would be influenced to some extent by such effects. Figure 6 shows such influence. In the crystal of carbazole, the dimension of *a*-axis is thus smaller, and this, in addition to the greater molecular weight by 1 than that of fluorene, leads to greater density.

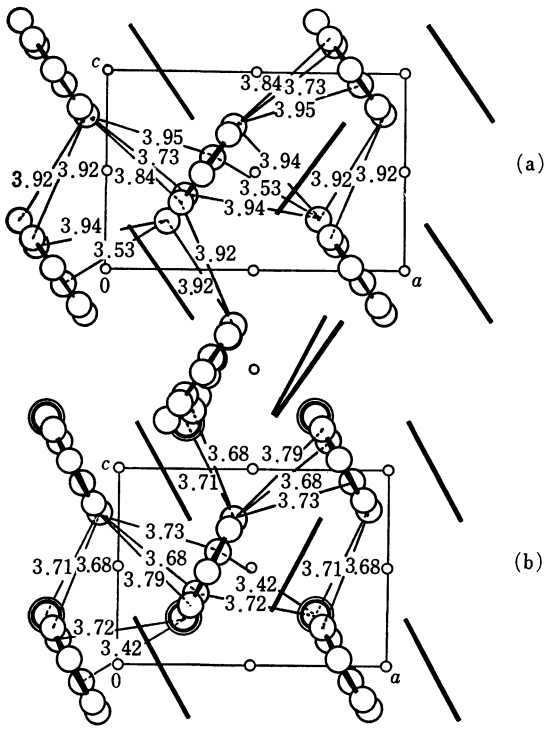

Fig. 6. Comparison of the crystal structure between fluorene (a) and carbazole (b).

The fact that the intermolecular distances are generally shorter in carbazole than in fluorene will imply stronger cohesive forces. In connection with this discussion, it is of interest to make comparison of thermodynamical data for these compounds. The lattice energy is directly related to ΔH_s (heat of sublimation). However, for lack of the datum on fluorene the sum of ΔH_m (heat of fusion) and ΔH_v (heat of vaporization) may be taken instead of ΔH_s and it comes out to be smaller by a few kcal/mol than the ΔH_s of carbazole.

Melting points of cabazole and fluorene are 245 and 115°C respectively. The large difference in melting points must depend on the difference either in ΔH_m or in ΔS_m (entropy change by fusion) because T_m (melting point) is given by $T_m = \Delta H_m / \Delta S_m$. ΔH_m's of carbazole and fluorene are reported to be 7.04 and 4.80 kcal/mol, so that ΔS_m's are calculated to be 13.6 and 12.4 e.u. respectively. It may be concluded that considerable difference in melting points is fairly due to the difference in ΔH_m connected to intermolecular interaction energy. On the other hand, comparison of the ΔS_m's will suggest that in the liquid state of carbazole there exists no perceptible hydrogen bond formation because in the latter case there would be some kind of ordering.

7) E. G. Cowlew and A. R. Parpington, *J. Chem. Soc.*, **1936**, 47.

BULLETIN OF THE CHEMICAL SOCIETY OF JAPAN VOL. 42 2180—2183 (1969)

Mössbauer Spectral Observation of α-Fe_2O_3 Supported on Silica Gel during Activation

Taro TACHIBANA and Toshie OHYA

Department of Chemistry, Ochanomizu University, Otsuka, Bunkyo-ku, Tokyo

and Tohru YOSHIOKA, Junji KOEZUKA and Hiroko IKOMA

Central Research Laboratory, Tokyo Shibaura Electric Co., Ltd., Komukai Toshiba-cho, Kawasaki

(Received December 28, 1968)

Mössbauer spectral studies were made of samples of α-Fe_2O_3 highly dispersed on silica gel before and after activation, which consisted of evacuated heating at 475°C. The spectra gave evidence that Fe^{2+} ions were produced from α-Fe_2O_3 during the activation process. Reduction was impossible after the activation and oxidation had been repeated three times. However, the inactivated sample came to be again reduced by activation after having been exposed to water vapor at room temperature. In order to explain these facts, a working hypothesis was advanced that the hydroxyl groups near the surface of the particles play a principal role in reacting with organic contamination from the vacuum system, as a result bringing about the partial reduction of α-Fe_2O_3.

Some metal oxide powders acquire adsorptive or catalytic activity by the activation process consisting of heating *in vacuo* at a high temperature. It is also known that some metal oxides produce non-stoichiometric oxide by the activation, thus changing their color. Very little work has, however, been done on these states of metal oxide. Blyholder and Richardson[1] reported, in their infrared spectral studies of the surface of α-Fe_2O_3, that the presence of Fe^{2+} ions near the surface might be expected as a results of a prolonged heating process at an evacuated atmosphere.

This report will describe some results of the Mössbauer spectral observation of supported α-Fe_2O_3 particles during activation.

Experimental

Two samples, A and B, of α-Fe_2O_3 supported on silica gel were prepared by impregnating silica gel with ferric nitrate solutions (enriched in Fe-57 for sample A), drying it at 120°C, and calcining it at 250°C for 16 hr in air. The Fe_2O_3 content was 2 wt% for sample A and 20 wt% for sample B. Both samples showed the spectrum[2] characteristic of α-Fe_2O_3. The average particle size was roughly estimated to be less than 130Å for sample A, and above 300Å for sample B, by comparing our spectra with the results of Shinjo *et al.*[3] and Kündig and Bömmel.[4] The broadening analysis of the X-ray diffraction patterns gave similar results.

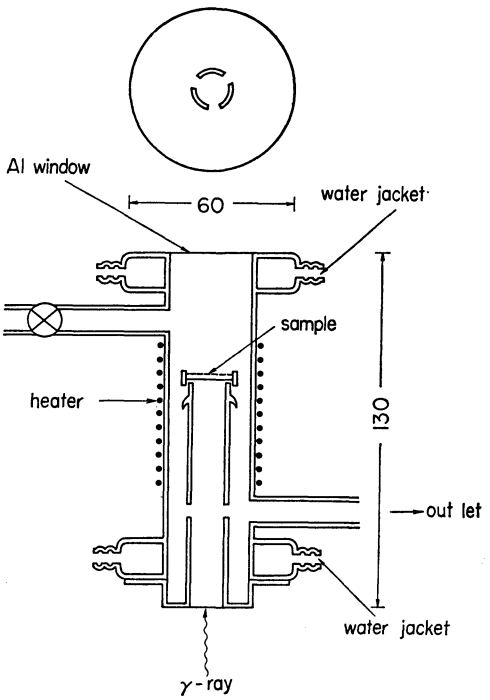

Fig. 1. A cross section of quartz-made cell.

In order to observe the effect of the activation, the sample was put into a small quartz-made supporter, which was mounted in a quartz cell equipped with windows of aluminum foil 100 μ thick as shown in Fig. 1. The activation was carried out by degassing the sample at room temperature for 3 hr, then heating it at 375°C in

1) G. Blyholder and E. A. Richardson, *J. Phys. Chem.*, **68**, 3882 (1964).

2) G. Constabaris, R. H. Rindquist and W. Kündig, *Appl. Phys. Letters*, **7**, 59 (1965).

3) T. Nakamura, T. Shinjo, Y. Endo, N. Yamamoto, M. Shiga and Y. Nakamura, *Phys. Letters*, **12**, 178 (1964).

4) W. Kündig and H. Bömmel, *Phys. Rev.*, **142**, 327 (1966).

an atmosphere of oxygen for one hour, and finally maintaining it at 475°C and under a pressure of 10^{-5} Torr for 8 hr. The spectra were measured after the sample had then been allowed to cool to room temperature. A time-mode Mössbaure spectrometer was used in this experiment.

Results

Figure 2 shows the Mössbauer spectra of sample A before and after the activation. The base lines of the spectral curves are all normalized to one. Curve (a) of the figure is the spectrum of normal sample A. It consists of only a quadrupole-split center line, indicating that the α-Fe_2O_3 is superparamagnetic. Curve (b), the spectrum of activated sample A, is a complex spectrum quite different from that of the original sample. This indicates that Fe atoms of α-Fe_2O_3 particles in the bulk as well as on the surface were changed into a state different from the original one by the activation.

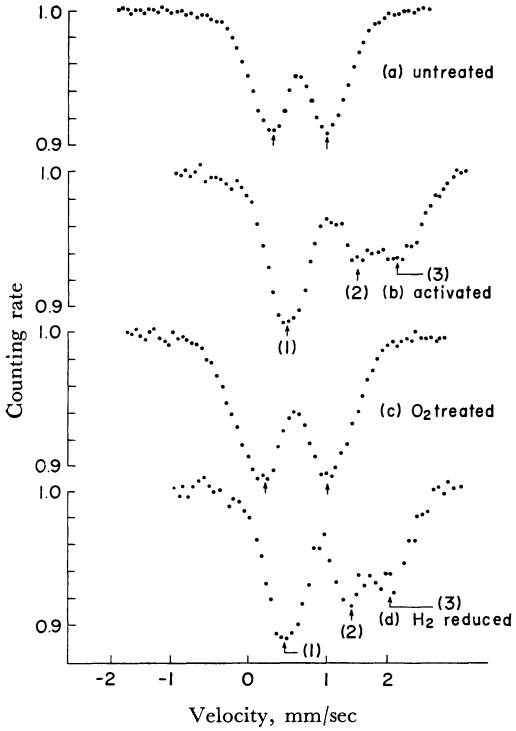

Fig. 2. Mössbauer spectra of a 2wt% α-Fe_2O_3-on-silica gel sample undergoing several treatments.

Figure 3 shows the spectra of sample B. Before the activation, sample B gave a spectrum of six hyperfine-split line, indicating antiferromagnetic characteristics, as is seen with α-Fe_2O_3 in bulk. Only the innermost doublet of the six lines appears in curve (a) of Fig. 3. This spectrum was replaced by curve (b) of the figure after the activation. However, the change was much smaller than that in the sample A. From this result, it follows

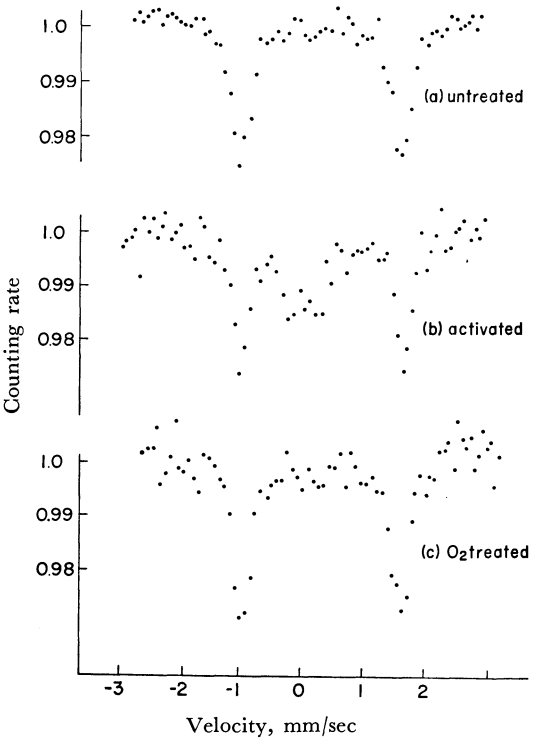

Fig. 3. Mössbauer spectra of a 20 wt%-α-Fe_2O_3-on-silica gel sample undergoing the activation and oxidation.

that, in observing the spectral change upon activation, it is more profitable to experiment with sample A. The following investigation was, therefore, completely conducted with sample A.

The spectrum was observed again after the activated α-Fe_2O_3 had been exposed to thoroughly-dried oxygen gas at 1 atm and at 200°C for about one hour. The resulting spectrum is curve (c) of Fig. 2, which is almost identical with curve (a) of the figure, though the parameters are somewhat larger than those of curve (a). This is shown in Table 1. Similar result was, though ample time is required, obtained also by the experiment at room temperature.

As the cycle of the oxygen treatment and the degassing was repeated, it was found to become

Table 1. Differential chemical shift* (δ), quadrupole splitting (Δ), and full width at half maximum (Γ) for curve (a) and (c) in Fig. 1

Curve	(a)	(c)
δ	0.60	0.63
Δ	0.75	0.88
Γ	0.63	0.80

Unite: (mm/sec) Error: $<\pm 0.02$ (mm/sec)

* Values relative to sodium nitropruside

gradually more difficult to obtain a sample which showed the activated-state spectrum. After the third cycle, the sample obtained no longer exhibited the activated-state spectrum. However, when this sample was placed in oxygen gas at 200°C and then exposed to water vapor at its saturation pressure at room temperature, it came to reproduce the activated-state spectrum (curve (b) of Fig. 2) upon evacuated heating.

Next, sample A was reduced by heating it in a hydrogen gas stream at 450°C for 8 hr. The resulting spectrum is curve (d) of Fig. 2, which is approximately the same as curve (b) of the figure, *i. e.*, the activated-state spectrum. This result gives evidence that some Fe ions of the activated sample were in a reduced state.

Discussion

The activated state spectrum (curve (b) of Fig. 2) was almost the same as the hydrogen-reduced spectrum which had previously been obtained by Hobson and Cambell.[5] The spectrum is apparently different from that of metallic iron. The spectra, (b) and (d), of Fig. 2 have three peaks, 1, 2, and 3, numbering from left to right. As with Hobson and Cambell, these spectra are resolved into two doublets, consisting of 1-3 and 1-2 peaks. The differential chemical shift, δ, and the quadrupole splitting, Δ, for the superposed doublets are given in Table 2. When we compare these data with the spectral data*1,[6] of many iron compounds, it is not unreasonable to conclude that the doublet 1-3 ($\delta = +1.37$ mm/sec, $\Delta = 1.77$ mm/sec) may be ascribed to a Fe^{2+} ion. The chemical shift of the 1-2 doublet ($\delta = +1.05$ mm/sec, $\Delta = 1.14$ mm/sec) has a value between the typical Fe^{2+} and Fe^{3+} states, with a rather large quadrupole splitting.

TABLE 2. DIFFERENTIAL CHEMICAL SHIFT* (δ) AND QUADRUPOLE SPLITTING (Δ) FOR CURVE (b) AND CURVE (d) IN FIG. 1

Curve	(b)		(d)	
peak	1-2	1-3	1-2	1-3
δ	+1.05	+1.37	+1.02	+1.36
Δ	1.14	1.77	1.01	1.65

Unite: (mm/sec) Error: $< \pm 0.02$ (mm/sec)

* Values relative to sodium nitropruside

The nature of this state was not yet been elucidated, but it is evident that two electronic states of the Fe ion, one of which is a typical Fe^{2+} state, exist in the activated α-Fe_2O_3. This activated state is recovered into the original α-Fe_2O_3 when it comes in contact with oxygen gas, so it is probably an unstable and non-stoichiometric iron oxide.

It should be interesting to consider the mechanism by which the Fe^{2+} state is produced from α-Fe_2O_3 by the evacuated heating. Some articles[7,8] show that powders of such metal oxides as TiO_2, MoO_3, are partially reduced by the evacuated heating into a lower oxidized state and that the reduction results from some organic contamination from the vacuum system or from an impurity carbon in the original sample. In our experiment, it is unreasonable to take the latter into consideration, since a considerable amount of carbon must be assumed to explain the complet change in the spectrum of the sample upon activation. Since our experiment was done in a conventional vacuum system equipped with a greased stopcock and an oil-diffusion pump, doubtless our sample was also exposed to an organic contamination. Nevertheless, in this atmosphere it was impossible to activate a sample which had been subjected to repeated degassing and oxidation. This fact suggests that some change was brought about on the surface of α-Fe_2O_3 particles by the repeated activation procedures. Here it is noticeable that such an inactivated sample has its reactivity restored upon exposure to water vapor at room temperature.

Evidence[9] has been given that the chemisorbed water is present in the form of the OH group on the surface of ferric oxide and that it provides the active site for a surface chemical reaction on ferric oxide. This leads us to assume that the OH group on the Fe atom of α-Fe_2O_3 particle surface might act as active sites in reacting with an organic contamination during the activation.

The surfaces of most oxide adsorbents have been found to be composed of hydroxyl groups which are removed during the activation and again formed immediately on exposure to water vapor at room temperature.[10] It is probable that an α-Fe_2O_3 sample which has lost its surface hydroxyl groups by means of the repeated activation procedure can no longer be activated by being in contact with organic contamination. Consequenly, it seems reasonable to assume that the hydroxyl groups on the surface of α-Fe_2O_3 particles play a principal role for reacting with organic contamination and that, as a result, the partial reduction of α-Fe_2O_3 occurs.

In order to draw a decisive conclusion, however,

5) M. C. Hobson, Jr., and A. D. J. Cambell, *J. Catalysis*, **8**, 294 (1967).

*1 $1.33 < \delta(Fe^{2+}) < 1.75$
$0.55 < \delta(Fe^{3+}) < 0.82$

6) A. R. Champion, R. W. Vanghan and H. G. Drickamer, *J. Chem. Phys.*, **47**, 2583 (1967).

7) J. Gebhardt and K. Herrington, *J. Phys. Chem.*, **62**, 120 (1958).

8) M. Onchi and I. Kusunoki, *Nippon Kagaku Zasshi (J. Chem. Soc. Japan, Pure Chem. Sect.,)* **85**, 612 (1964).

9) G. Okamoto, R. Furuichi and N. Sato, *Electrochim. Acta*, **12**, 1287 (1967).

10) T. Morimoto, M. Nagao and F. Tokuda, This Bulletin, **41**, 1533 (1968).

much remains to be done with the Mössbauer spectral measurements. However, since the application of the Mössbauer spectroscopy to surface work is at present yet in its infancy, it seems valuable to make this report as a preliminary step.

We wish to thank Dr. Kin-ichi Nohga of the Toshiba Central Research Laboratory for his continuous encouragement during this work. We are very grateful to Professor Tetsuo Takaishi of Saint Paul's University for his helpful discussions. The expenses of this work have been supported in part by a Scientific Research Grant from the Ministry of Education.

BULLETIN OF THE CHEMICAL SOCIETY OF JAPAN VOL. 42 2183—2186 (1969)

Microwave Spectrum, Barrier to Internal Rotation, and Dipole Moment of *trans*-Crotonaldehyde

Masao SUZUKI and Kunio KOZIMA

Laboratory of Molecular Spectroscopy, Tokyo Institute of Technology, Ookayama, Meguro-ku, Tokyo

(Received December 28, 1968)

The microwave spectrum of *trans*-crotonaldehyde has been measured in the frequency region from 8.2 to 36 kMc/sec. The R-branches for the a-type and the R- and Q-branches for the b-type have been assigned. The low J transitions of the a-type and all of the b-type transitions are split into the A-level and the E-level by the internal rotation of the methyl group. The apparent rotational constants for the A- and E-levels have been obtained from the pseudo-rigid rotor approximation as $A_A=32636.58$ Mc/sec, $A_E=32627.57$ Mc/sec, $B=2183.30$ Mc/sec, and $C=2073.32$ Mc/sec. From these values it can be concluded that this molecule is of the *s-trans* form. The barrier height of the hindering rotation of the methyl group is 1730 ± 10 cal/mol. The value of the total dipole moment is 3.72 ± 0.28 D.

As a result of studies of the microwave or the infrared spectra it has been reported that the conjugated molecules with the structure of $\rangle C{=}\overset{|}{C}{-}\overset{|}{C}{=}$, such as acrolein,[1] butadiene[2] and fluoroprene[3] are planar in form. Of the two planar forms, *i. e.*, the *s-cis* and the *s-trans* form, only the *s-trans* form exists in the vapor with these molecules. However, it has been found that both forms exist in the vapor with acrylic acid,[4] acryloyl fluoride[5] and acryloyl chloride.[6]

It seems that it would be interesting to ascertain the stable conformation of such conjugated molecules with the methyl group and to determine the height of the potential barrier to internal rotation. For these purposes this research was carried out.

Experimental

The spectrum was measured over the frequency range from 8.2 to 36.0 kMc/sec with a conventional Stark-modulation microwave spectrometer. The frequencies were measured by the method reported in previous papers.[7,8] For the frequency range from 32.0 to 36.0 kMc/sec, the klystron 35V11 (Oki) was employed. The measurements were made at the temperature of dry ice by using a 3-m absorption cell.

Commercial crotonaldehyde was dried over magnesium sulfate and distilled *in vacuo*. The purity of the sample was ascertained with a vapor-phase chromatograph.

Results and Discussion

Microwave Spectrum. It was found that the rotational spectrum of *trans*-crotonaldehyde is composed of both the a-type and the b-type, as in the cases of such similar molecules as acrolein[1] and methyl vinyl ketone.[9] The a-type spectrum is much more intense than the b-type spectrum.

1) E. A. Cherniak and C. C. Costain, *J. Chem. Phys.*, **45**, 104 (1966).
2) A. R. H. Cole, G. M. Mohay and C. A. Osborne, *Spectochim. Acta*, **23A**, 909 (1967).
3) D. R. Lide, Jr., *J. Chem. Phys.*, **37**, 2074 (1962).
4) K. Bolton, N. L. Owen and J. Sheridan, *Nature*, **218**, 266 (1968).
5) J. J. Keirns and R. F. Crul, Jr., *J. Chem. Phys.*, **48**, 3773 (1968).
6) J. E. Katon and W. R. Feairheller, Jr., *ibid.*, **47**, 1248 (1967).
7) A. Hatta, C. Hirose and K. Kozima, This Bulletin, **41**, 1088 (1968).
8) Y. Ohnishi and K. Kozima, *ibid.*, **41**, 1323 (1968).
9) P. D. Forster, V. M. Rao and R. F. Curl, Jr., *J. Chem. Phys.*, **43**, 1064 (1965).

Table 1. Observed and calculated frequencies in *trans*-$CH_3CH{=}CHCHO$

A-levels Transition	Mc/sec ν(observed)	Mc/sec ν(calculated)	Deviation
a-type			
1_{01}–2_{02}	8512.99*	8512.94	0.05
1_{11}–2_{12}	8403.32*	8403.26	0.06
1_{10}–2_{11}	8623.14*	8623.22	−0.08
2_{02}–3_{03}	12769.03	12768.67	0.36
2_{12}–3_{13}	12604.75*	12604.70	0.05
2_{11}–3_{12}	12934.76*	12934.64	0.11
3_{03}–4_{04}	17023.60	17023.50	0.10
3_{13}–4_{14}	16806.04	16805.92	0.12
3_{12}–4_{13}	17246.15	17245.84	0.31
5_{05}–6_{06}	25529.38	25529.31	0.07
5_{15}–6_{16}	25206.80	25207.41	−0.61
5_{14}–6_{15}	25867.80	25867.26	0.54
6_{06}–7_{07}	29779.50	29779.73	−0.23
6_{16}–7_{17}	29407.30	29407.53	−0.23
6_{15}–7_{16}	30177.70	30177.33	0.37
7_{07}–8_{08}	34028.80	34028.04	0.76
7_{17}–8_{18}	33606.52	33607.16	−0.54
7_{16}–8_{17}	34487.05	34486.88	0.17
b-type			
3_{03}–2_{12}	17574.90*	17574.92	−0.02
4_{04}–3_{13}	13156.05*	13156.12	−0.07
5_{05}–4_{14}	8684.56	8684.89	−0.33
8_{18}–9_{09}	9697.96	9696.97	0.99
9_{19}–10_{010}	14409.14	14408.49	0.65
7_{07}–7_{16}	32078.80	32076.99	1.81
8_{08}–8_{17}	32537.94	32535.83	2.11
9_{09}–9_{18}	33059.99	33057.83	2.16
10_{010}–10_{19}	33646.50	33644.13	2.37
11_{011}–11_{110}	34302.00	34299.01	2.99
12_{012}–12_{111}	35025.74	35022.51	3.23

* A, B and C were obtained from these transitions.

The assignments of the a-type transitions of the low rotational quantum numbers were determined by their Stark effect. The assignment and the splittings caused by the internal rotation of the methyl group are shown in Tables 1 and 2 respectively. The rotational constants of B and C for the A-levels were obtained from the $1_{10}\rightarrow 2_{11}$ and $1_{11}\rightarrow 2_{12}$ transitions, which occur at frequencies of $(3B+C)$ and $(B+3C)$ respectively. Because the a-type spectrum is characteristic of a near-prolate symmetric rotor, the rotational constant of A cannot be determined accurately by means of this spectrum.

For the a-type transitions, $J_{K,K'}\rightarrow J+1_{K,K'+1}$, the lines in which the value of K is equal to 2 or higher than 2 overlap closely. Therefore, this spectrum was not used to determine the rotational constants and has been omitted from the table.

Table 2. A-E splittings in *trans*-$CH_3CH{=}CHCHO$

Transition	$(\nu_A-\nu_E)_{obs.}$
a-type	
1_{10}–2_{11}	4.02 Mc/sec
1_{11}–2_{12}	−3.80
2_{11}–3_{12}	0.77
2_{12}–3_{13}	−0.85
3_{12}–4_{13}	0.35
3_{13}–4_{14}	−0.28
b-type	
3_{03}–2_{12}	11.05
4_{04}–3_{13}	10.30
5_{05}–4_{14}	9.67
8_{18}–9_{09}	−9.07*
9_{19}–10_{010}	−8.93
7_{07}–7_{16}	8.95*
8_{08}–8_{17}	8.99*
9_{09}–9_{18}	8.84*
10_{010}–10_{19}	8.20
11_{011}–11_{110}	9.28
12_{012}–12_{111}	9.35

* The difference of the rotational constants of A was determined from these transitions.

The splittings caused by the internal rotation of the methyl group could also be observed in the b-type spectrum. These splittings are much larger in the b-type spectrum. As was expected in view of similar molecules, it seems very probable that the framework of the molecule has the planar configuration. Therefore, in order to facilitate the assignments of the b-type spectrum, the rotational constant, A, was estimated from the relation:

$$I_c - I_a - I_b = \delta' - I_\alpha$$

where I_a, I_b, and I_c are the principal moments of inertia, I_α is the moment of inertia of the methyl group about its symmetry axis, and δ' is a pseudo-inertial defect. The $(I_\alpha-\delta')$ value was assumed tentatively to be 3.16 amu·Å^2 which is the same as that reported for propylene.[10] By using the A value thus estimated, the frequencies of the b-type lines of the $J_{0J}\rightarrow J_{1J-1}$ series were calculated and measured. The frequencies of the seven lines which show the Stark patterns of Q-branches and which split into the A- and the E-levels were found to be higher than 32 kMc/sec. By the aid of the Q-branch plot, these lines were identified as those of $J\geq 7$. By the plot, the values of $(A-C)/2$ and of Ray's κ were obtained as 15281 Mc/sec and -0.99279_5 for the A-levels and 15276 Mc/sec and -0.99279 for the E-levels. From this it is clear that the pseudo-rigid rotor approximation holds for the high J and low K transitions of both the E- and A-levels.

10) E. Hirota, *J. Chem. Phys.*, **45**, 1984 (1966).

By using the rotational constants of A estimated from these values, the low J R-branch transitions of the b-type were calculated and measured. The assignments of these transitions are shown in Table 1. From the low J transitions which are marked by a star in Table 1, the accurate pseudo-rigid rotational constants of A_A, B, and C were determined by the least-squares method. The results are listed in Table 3. The values of B and C agreed with those obtained above within the limits of experimental error. The frequencies calculated by the rotational constants thus determined are shown in Table 1 for the A-levels. From this table it can be seen that the effect due to the centrifugal distortion cannot be disregarded, especially for the b-type spectrum. However, the terms for these distortions were not determined, for only the $K=0\rightarrow1$ and $K=1\rightarrow1$ transitions were measured.

TABLE 3. ROTATIONAL CONSTANTS AND MOMENTS OF INERTIA OF *trans*-$CH_3CH{=}CHCHO$

Rotational constants	Moments of inertia*
$A_A=32636.58\pm0.2$ Mc/sec	$I_a^A=15.485$ amu·Å^2
$A_E=32627.57\pm0.2$	
$B=2183.30\pm0.06$	$I_b=231.474$
$C=2073.32\pm0.04$	$I_c=243.753$
$\kappa_A=-0.992803\pm0.000001$	
$(I_a^A+I_b)-I_c=3.206$ amu·Å^2	

* Conversion factor: 5.05377×10^5, corresponding to $^{12}C=12$ atomic scale.

By the use of the least-squares methods, the difference between the pseudo-rigid rotational constants of A could be determined from the splittings of the transitions marked by a star in Table 2, because it was shown by the Q-branch plot that the pseudo-rigid rotor approximation nearly holds for these transitions. The value of the rotational constant of A_E for the E-level was, then, estimated to be 32627.57 Mc/sec. The difference between the rotational constants of B for both levels is negligible, because the frequencies of the high J and low K lines of the R-branches do not split for the a-type transitions. The calculation mentioned below supports this. In view of the molecular structure, it can be easily seen that the rotational constants of C do not differ in the two levels.

Molecular Structure and Internal Rotation. Because the observed pseudoinertial defect, δ', is nearly zero, it is safe to consider that the molecular framework is planar. However, there are two possible planar forms, *i. e.*, the *s-cis* and the *s-trans* form, as is shown in Fig. 1. When the values of the r_s-structure of acrolein[10] were assumed for this molecule, with the additional assumptions that the CH_3–C bond length and $\angle CH_3$-C=C were 1.501 Å and 123.3° respectively by the use of the values of propylene[11] and that all the valency angles of the methyl group and all the C–H bond lengths were 109.47° and 1.090 Å, the calculated rotational constants of the *s-cis* form were as follows; $A=18580$ Mc/sec, $B=2677$ Mc/sec, and $C=2375$ Mc/sec. As these values are quite different from the observed values, the possibility of the *s-cis* form can be disregarded. However, for the *s-trans* form calculated under the same assumptions the rotational constants were very close to the observed values.

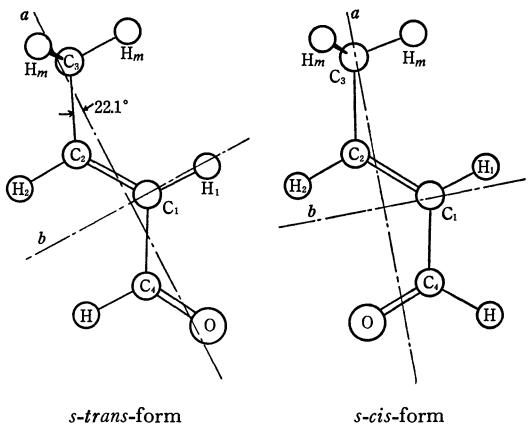

s-trans-form *s-cis*-form

Fig. 1. Two forms of *trans*-$CH_3CH{=}CHCHO$.

In order to ascertain whether or not the *s-cis* form exists in the vapor, the measurements were carefully made near the frequencies of the $J_{0J}\rightarrow J_{1J-1}$ transitions, which were calculated for the *s-cis* form by the use of the rotational constants described above. However, we could not observe any lines which might be assigned to the *s-cis* form. It was concluded that the stable form of *trans*-crotonaldehyde is the *s-trans* form.

To get the best fit between the observed and the calculated values for the rotational constants of B and C, the valency angles, $\angle CH_3$–C=C and $\angle CH_3$–C–H, of the carbon atom to which the methyl group attaches were determined by making the assumptions mentioned above except for these two angles. The probable structural parameters obtained are shown in Table 4. The table also shows that the calculated value for the rotational constant of A agrees with the unperturbed value to be estimated below.

Since the internal top has a threefold axis, the hindering potential, V, may be expanded in the Fourier series:

$$V=\frac{V_3}{2}(1-\cos3\alpha)+\frac{V_6}{2}(1-\cos6\alpha)+\cdots$$

In this paper only the V_3 term is considered, for

11) D. R. Lide, Jr., and D. Christensen, *J. Chem. Phys.*, **35**, 1374 (1961).

Table 4. Molecular structure of *trans*-$CH_3CH{=}CHCHO$

Assumed structural parameters			
$r(C_1-C_4)$	1.470 Å	$\angle C_2{=}C_1-C_4$	119.83°
$r(C_1{=}C_2)$	1.345	$\angle C_1-C_4{=}O$	123.28
$r(C_2-C_3)$	1.501	$\angle C_1-C_4-H$	115.10
$r(C_4{=}O)$	1.219	$\angle H_m-C_3-H_m$	109.47
$r(C_4-H)$	1.108	$\angle C_2-C_3-H_m$	109.47
$r(C_2-H_2)$	1.086	$\angle C_2{=}C_1-H_1$	122.83
$r(C_1-H_1)$	1.084		
$r(C_3-H_m)$	1.090		
Fitted structural parameters			
$\angle C_3-C_2{=}C_1$	125.64°	$\angle H_2-C_2-C_3$	116.09°
Calculated rotational constants			
$A=32630.46$ Mc/sec			
$B=2183.84$			
$C=2073.67$			

the V_6 term would introduce only a minor correction in the value of V_3.

The Hamiltonian can be written in the following manner:

$$H_A{}^0 = A_A P_z{}^2 + B_A P_y{}^2 + C P_x{}^2$$

and

$$H_E{}^0 = A_E P_z{}^2 + B_E P_y{}^2 + C P_x{}^2 + F W_{0E}{}^{(1)} \mathfrak{P}$$

where

$$F = \hbar^2/2rI_\alpha,\ r = 1 - \sum_{g=a,b} \lambda_g{}^2 I_\alpha / I_g$$

$$\alpha = \lambda_a I_\alpha / I_a,\ \beta = \lambda_b I_\alpha / I_b$$

$$\mathfrak{P} = \alpha P_z + \beta P_y$$

$$A_\sigma = A_0 + F\alpha^2 W_{0\sigma}{}^{(2)},\ B_\sigma = B_0 + F\beta^2 W_{0\sigma}{}^{(2)}$$

(σ=A or E)

The notations have the meanings given by Herschbach.[12] The values of the parameters described above are given in Table 5. By use of these values and Herschbach's Table (Appendix C),[12] the values of s, a parameter of the Mathieu equation, and the barrier height can be calculated from the frequency splittings of the $1_{10}\rightarrow 2_{11}$ and the $1_{11}\rightarrow 2_{12}$ transitions, by assuming that $I_\alpha = 3.160$ amu·Å^2. The value of V_3 is 1730±10 cal/mol, lower than that obtained for propylene.[13] The barrier height calculated from the difference, $A_A - A_E$, under the same assumptions is 1720±10 cal/mol. This value agrees with that determined above. The frequency splittings of the other transitions are not used for this calculation, for the contributions of the $FW_{0E}{}^{(1)}\mathfrak{P}$ term to the splittings are equal to or less than about 1 Mc/sec. By using the value of s, the unperturbed value, A_0, was calculated to be 32630.54 Mc/sec and the difference between B_A and B_E was found to be 0.002 Mc/sec in support of the experimental result.

For near-prolate symmetric top molecules like this, the contribution of the $F\alpha W_{0E}{}^{(1)} P_z$ term to the rotational energy ($K_{-1}=1$) of the E-level can be represented approximately as $2(F\alpha W_{0E}{}^{(1)})^2/\{J(J+1)(B-C)\}$. Small deviations from the rigid-rotor approximation for the low J transitions of the E-levels are due to this term. However, because for the high J transitions ($J \geq 7$), the correction due to this term is smaller than 0.2 Mc/sec, therefore, the pseudo-rigid rotor approximation holds.

Table 5. Barrier height and A-E splitting

	$(\nu_A-\nu_E)_{obs.}$	$(\nu_A-\nu_E)_{calc.}$	s
$1_{10}-2_{11}$	4.02	3.92	41.4
$1_{11}-2_{12}$	−3.80	−3.92	41.6
The results			
$s=41.5\pm0.2$			
$V_3=1730\pm10$ cal/mol			
$A_0=32630.54$ Mc/sec			
Parameters used in the calculation			
$I_\alpha=3.160$ amu·Å^2			
$\lambda_a=0.9239$		$\lambda_b=0.3773$	
$\alpha=0.1885$		$\beta=0.0052$	
$F=1.941\times10^5$ Mc/sec			

Dipole Moment. The Stark displacements of the $M=0$ component of seven transitions, shown in Table 6, were measured in order to determine the a and b components, μ_a and μ_b, of the electric dipole moment. These lines fit the quadratic Stark displacements nicely. The absoption cell was calibrated using the $J=0\rightarrow1$ transition of OCS, taking the dipole moment of OCS as 0.7152 D.[14] The observed and calculated Stark coefficients are given in Table 6. The value of the dipole moment obtained is 3.72±0.28 D. This value is in agreement with that of 3.67 D obtained by Debye's method.[15]

Table 6. Stark effect and dipole moment

Transition		$\delta\nu/\varepsilon^2$(obsd)[a]	$\delta\nu/\varepsilon^2$(calcd)[a]
$1_{01}-2_{02}$	$M=0$	−110.52	−110.28
$1_{10}-2_{11}$	$M=0$	87.50	87.96
$2_{02}-3_{03}$	$M=0$	−4.60	−5.31
$2_{20}-3_{21}$ $2_{21}-3_{22}$	$M=0$	34.60	34.02
$2_{12}-3_{13}$	$M=0$	−4.25	−4.36
$2_{11}-3_{12}$	$M=0$	−4.75	−4.98
$\mu_a{}^2=12.03\pm0.09$			
$\mu_b{}^2=2.47\pm1.78$			
$\mu=3.72\pm0.28$ D			

a) Unit is Mc(kV/cm)$^{-2}$.

12) D. R. Herschbach, *J. Chem. Phys.*, **31**, 91 (1959).
13) D. R. Lide, Jr., and D. E. Mann, *ibid.*, **27**, 868 (1957).
14) J. S. Muenter, *ibid.*, **48**, 4544 (1968).
15) E. C. Hurdis and C. P. Smyth, *J. Am. Chem. Soc.*, **65**, 89 (1943).

BULLETIN OF THE CHEMICAL SOCIETY OF JAPAN VOL. 42 2187—2193 (1969)

ESR and Optical Absorption Studies of the Copper(II) Complexes of Ethylenediamine and Its Alkyl Derivatives

Hiroshi Yokoi and Taro Isobe

Chemical Research Institute of Non-Aqueous Solutions, Tohoku University, Katahira-cho, Sendai

(Received January 7, 1969)

The ESR and the optical absorption of the copper(II) complexes of ethylenediamine and a series of alkylated ethylenediamines have been investigated in order to estimate the character of the chemical bonding in the copper(II) complex. The covalency of the bonding of the copper atom to the ligand nitrogen atoms in the complexes has been discussed in connection with the chemical and physical properties of the complexes or of their ligand molecules themselves. The ESR results indicate that the σ bonding of the complexes becomes more covalent as the number of alkyl groups in their ligand molecules increases; furthermore, the tendency toward the σ bonding becomes more pronounced when the alkyl groups are ethyl rather than methyl and when they are *N*-substituted alkyl groups rather than *C*-substituted ones. It is also indicated that there is a linear relationship between the energies of the ultraviolet absorption band for the complexes and the relative ionization potentials estimated for their ligand molecules, and that absorption band can be assigned to an electron transfer from a ligand σ orbital to an antibonding orbital associated with the copper atom. From these results, it may be concluded that, as the σ bonding becomes more covalent, this charge transfer band shifts to a longer wavelength.

The ESR spectra of a variety of copper(II) complexes have been measured in order to investigate the bonding character of copper-ligand bonds in the complexes. The bonding parameters showing the degree of covalency for the bonds have been estimated from the magnetic parameters, namely, the g and A values, determined from their ESR spectra.[1-4] Little attention has been paid to the interesting and important problem of finding some correlation between the degree of covalency thus obtained and the chemical and physical properties of the complexes or their ligand molecules themselves. However, it is not easy to do this because of the fact that the ESR of the complexes is substantially concerned with only the antibonding orbitals associated with the copper atom.

In the present work the copper(II) complexes of ethylenediamine and a series of alkylated ethylenediamines were examined systematically by the usual methods of ESR and optical absorption, and an attempt was made to find the above-mentioned correlation. Since only a few papers have been published on the behavior of the optical absorption bands of the complexes, the assignment of the bands in the ultraviolet region was also discussed.

Experimental

The copper(II) complexes employed in this study were: [I] $[Cu(en)_2](ClO_4)_2$, [II] $[Cu(pn)_2](ClO_4)_2$, [III] $[Cu(m\text{-bn})_2](ClO_4)_2$, [IV] $[Cu(d'men)_2](ClO_4)_2$, [V] $[Cu(eten)_2](ClO_4)_2$, [VI] $[Cu(d'een)_2](ClO_4)_2$, [VII] $[Cu(dmen)_2](ClO_4)_2$, and [VIII] $[Cu(deen)_2](ClO_4)_2$, where en, pn, *m*-bn, d'men, eten, d'een, dmen, and deen are ethylenediamine, 1,2-diaminopropane, *meso*-2, 3-diaminobutane, *N,N'*-dimethylethylenediamine, *N*-ethylethylenediamine, *N,N'*-diethylethylenediamine, *N,N*-dimethylethylenediamine, and *N,N*-diethylethylenediamine respectively. The first three copper(II) complexes had already been dealt with in our previous paper.[4] The ligand molecules were commercially available except for *m*-bn, eten, and d'een, which were prepared and purified according to the methods of the literature.[5]

The ESR spectra of the complexes were measured in solutions at room temperature and on frozen solutions at the temperature of liquid nitrogen with a Hitachi X-band and K-band ESR spectrometer, model MES-4001,

1) A. H. Maki and B. R. McGarvey, *J. Chem. Phys.*, **29**, 31, 35 (1958).

2) D. Kivelson and R. Neiman, *ibid.*, **35**, 149 (1961).

3) E. M. Robert and W. S. Koski, *J. Am. Chem. Soc.*, **82**, 3006 (1960); F. R. Gersman and J. D. Swalen, *J. Chem. Phys.*, **36**, 3221 (1962); S. J. T. Owen, K. J. Standley and A. Walker, *ibid.*, **40**, 183 (1964); B. G. Malmstom and T. Vanngard, *J. Mol. Biol.*, **2**, 118 (1960); A. K. Wiersma and J. J. Windle, *J. Phys. Chem.*, **68**, 2316 (1964); W. Schneider and A. V. Zelewsky, *Helv. Chim. Acta*, **48**, 1529 (1965); S. E. Harrison and J. M. Assour, *J. Chem. Phys.*, **40**, 365 (1964); D. Kivelson and S. Lee, *ibid.*, **41**, 1896 (1964).

4) H. Yokoi and T. Isobe, This Bulletin, **41**, 2835 (1968).

5) F. Basolo, Y. T. Chen and R. K. Murmann, *J. Am. Chem. Soc.*, **75**, 1478 (1953); R. C. O'Gee and H. M. Woodburn, *ibid.*, **73**, 1370 (1951).

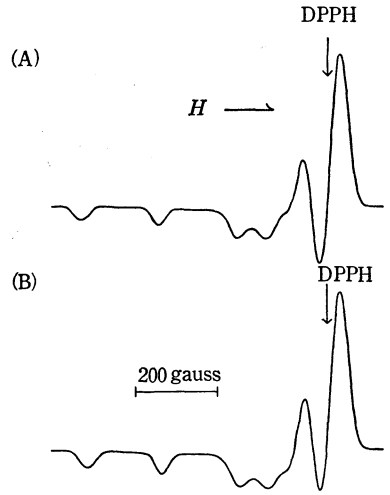

Fig. 1. ESR spectra (X-band) measured in 50% water - 50% methanol at 77°K.
(A) $[Cu(d'men)_2](ClO_4)_2$
(B) $[Cu(dmen)_2](ClO_4)_2$

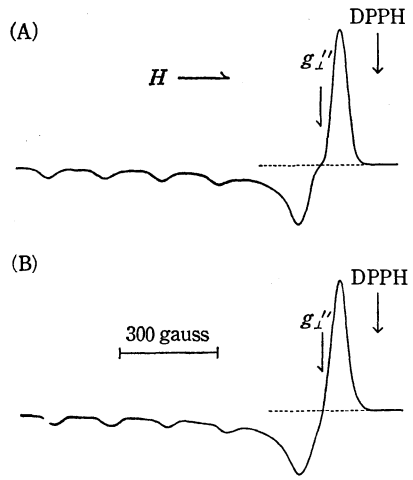

Fig. 2. ESR spectra (K-band) measured in 50% water-50% methanol at rigid state.
(A) $[Cu(d'men)_2](ClO_4)_2$
(B) $[Cu(dmen)_2](ClO_4)_2$

equipped with a 100 kc field modulation unit. The solvents were methanol and a 50% water - 50% methanol mixture (volume %). The field was calibrated with an NMR probe and then with a benzene solution of vanadyl acetylacetonate or with Mn(II) ions in MgO powder. Some of the ESR spectra observed are shown in Figs. 1—3. The optical absorption spectra of the complexes in an aqueous solution were measured with a Cary model 14 spectrometer; some of them are shown in Figs. 4 and 5.

Results and Discussion

Magnetic Parameters. The spin Hamiltonian and the methods of determining the magnetic parameters, the g and A values, had already been described in one of our previous papers.[4] It

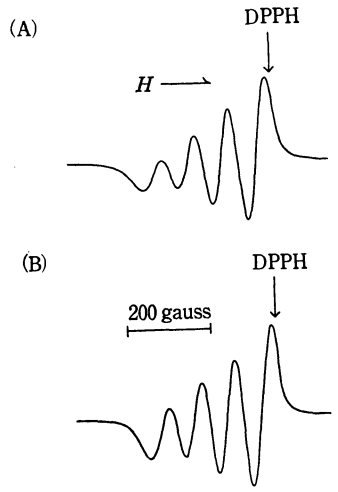

Fig. 3. ESR spectra (X-band) measured in 50% water - 50% methanol at room temperature.
(A) $[Cu(d'men)_2](ClO_4)_2$
(B) $[Cu(dmen)_2](ClO_4)_2$

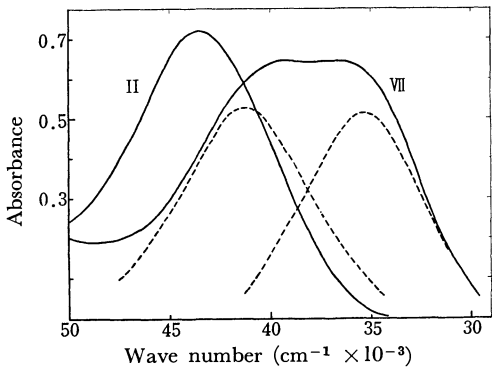

Fig. 4. The ultraviolet absorption spectra measured in aqueous solution at room temperature. Dotted lines represent the possible component bands obtained by approximate Gaussian analysis.

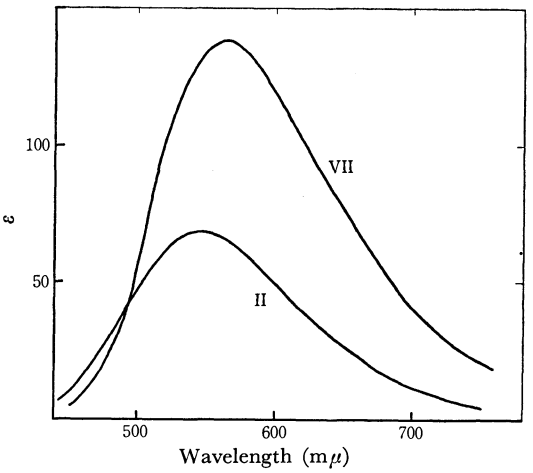

Fig. 5. The visible absorption spectra measured in aqueous solution at room temperature.

Table 1. Magnetic parameters

	Copper(II) complex[a]	Solvent[b]	$g_{//}$	$g'_{\perp}$[c]	$g''_{\perp}$[d]	$A_{//}$ $\times10^4$ cm^{-1}	$A_{\perp}$[c] $\times10^4$ cm^{-1}	g_0[e]	A_0[e] $\times10^4$ cm^{-1}
[I]	$[Cu(en)_2](ClO_4)_2$	MH	2.206	2.050	2.052	209	25	2.102	86
		M	2.209			207			
[II]	$[Cu(pn)_2](ClO_4)_2$	MH	2.208	2.050	2.051	210	26	2.103	87
		M	2.209			206			
[III]	$[Cu(m\text{-bn})_2](ClO_4)_2$	MH	2.203	2.050	2.050	205	27	2.101	86
		M	2.203			204			
[IV]	$[Cu(d'men)_2](ClO_4)_2$	MH	2.216	2.053	2.050	201	26	2.107	84
		M	2.210			205			
[V]	$[Cu(eten)_2](ClO_4)_2$	MH	2.213	2.052	2.044	202	27	2.106	85
		M	2.210			204			
[VI]	$[Cu(d'een)_2](ClO_4)_2$	MH	2.217	2.052	2.050	196	23	2.107	81
		M	2.214			198			
[VII]	$[Cu(dmen)_2](ClO_4)_2$	MH	2.209	2.053	2.048	198	24	2.105	82
		M	2.218			185			
[VIII]	$[Cu(deen)_2](ClO_4)_2$	MH	2.212	2.055	2.049	184	21	2.107	75
		M	2.208			186			

a) The data for the complexes [I], [II] and [III] were quoted from our previous paper.[4]
b) M: methanol, MH: 50% water, 50% methanol (volume %).
c) $g'_{\perp}$ was calculated using the following equation, $g_0=(1/3)(g_{//}+2g'_{\perp})$. $A_{\perp}$ was also calculated in the same way.
d) $g''_{\perp}$ was directly obtained from the ESR spectrum measured in rigid solution at K-band.
e) Measured at room temperature.

seems that the ligand field can not always be of an axial symmetry for the complexes [V], [VII], and [VIII], because, in their ligand molecules, alkyl groups are not substituted symmetrically on the two nitrogen atoms; this fact is certainly reflected in their ultraviolet absorption spectra, which will be discussed below. However, judging from the line shapes of such K-band ESR spectra as are shown in Fig. 2, it may well be said that the ligand field for the complexes does not deviate greatly from axial symmetry. Therefore, the average value, expressed as $g_{\perp}$, for two slightly different perpendicular g values was adopted for use in the following discussions. The $g_{\perp}$ value was determined according to the following two methods. One is the method of using the parameters, g_0 and A_0, obtained from the ESR spectra of a solution at room temperature, and the equation $g_0=(1/3)(g_{//}+2g_{\perp})$, where the $g_{\perp}$ value thus obtained is expressed as $g'_{\perp}$ in Table 1. The other is the method of determining the $g_{\perp}$ value directly from the K-band ESR spectra in the way shown by the arrow in Fig. 2. The $g_{\perp}$ value thus obtained is expressed as $g''_{\perp}$ in Table 1. All the magnetic parameters obtained in this work are listed in Table 1.

Bonding Parameters. The experimentally-determined magnetic parameters listed in Table 1 can be used for estimating the nature of the chemical bonding between the copper atom and the ligand nitrogen atoms in the complexes by means of the molecular orbital theory. This method had already been outlined in our previous paper on the copper(II) complexes of amines whose ligand field is of axial symmetry.[4] On the other hand, it is convenient to know that almost the same method for obtaining the bonding parameters is substantially applicable to the copper(II) complexes in which ligand field deviates to some extent from axial symmetry. The following wave functions can generally be written for the antibonding molecular orbitals associated with the copper atom;

$$\psi(x^2-y^2) = \alpha d_{x^2-y^2} - \alpha'\phi_L(x^2-y^2)$$
$$\psi(xy) = \beta_1 d_{xy} - \beta_1'\phi_L(xy)$$
$$\psi(z^2) = \alpha_1 d_{z^2} - \alpha_1'\phi_L(z^2)$$
$$\psi(xz) = \beta_x d_{xz} - \beta'_x\phi_L(xz)$$
$$\psi(yz) = \beta_y d_{yz} - \beta_y'\phi_L(yz)$$

The expressions which relate the experimental ESR data to the covalency parameters, α, β_1, β_x, and β_y, are:

$$g_z = 2 - \frac{8\lambda}{\Delta E_{xy}}(\alpha^2\beta_1^2 - f_1) \quad (1)$$

$$g_x = 2 - \frac{2\lambda}{\Delta E_{xz}}(\alpha^2\beta_x^2 - f_2) \quad (2)$$

$$g_y = 2 - \frac{2\lambda}{\Delta E_{yz}}(\alpha^2\beta_y^2 - f_3) \quad (3)$$

$$A_z = P\left\{-\frac{4}{7}\alpha^2 - \kappa + (g_z - 2) + \frac{3}{14}[(g_x - 2) + (g_y - 2)] + f_4\right\} \quad (4)$$

$$A_x = P\left\{\frac{2}{7}\alpha^2 - \kappa + (g_x - 2) - \frac{3}{14}(g_y - 2) + f_5\right\} \quad (5)$$

$$A_y = P\left\{\frac{2}{7}\alpha^2 - \kappa + (g_y - 2) - \frac{3}{14}(g_x - 2) + f_6\right\} \quad (6)$$

where κ is the Fermi contact term, $P=0.036\ cm^{-1}$, $\lambda=-828\ cm^{-1}$, f's are small constants (f_1, f_2, $f_3 \leqq 0.04$, $f_4 \leqq 0.03$, f_5, $f_6 \leqq 0.005$), and $\Delta E_s = E_{x^2-y^2} - E_s$ ($s=xy$, xz, yz). From the above equations, it can be understood that the values of α^2 and κ ($\kappa=\alpha^2\kappa_0{}^2$) can be calculated by the same method as we used previously if we can experimentally obtain the average values of g_x and g_y, and of A_x and A_y, expressed here as $g_\perp$ and $A_\perp$ respectively.[4] Furthermore, the average value of $\beta_x{}^2$ and $\beta_y{}^2$, expressed as β^2, can also be estimated by the above procedure. The approximate ligand field energies of the complexes under discussion were determined by the procedure in our previous paper,[4] assuming that the ligand field for the complexes is of axial symmetry; they are listed in Table 4. The bonding parameters thus calculated are listed in Table 2.

Table 2. Bonding parameters[a]

Copper(II) complex[b]	α^2	$\beta_1{}^2$	β^2	κ_0
[I]	0.83	0.58	0.72	0.42
[II]	0.84	0.58	0.70	0.42
[III]	0.82	0.58	0.72	0.43
[IV]	0.82	0.61	0.71	0.42
[V]	0.82	0.60	0.66	0.42
[VI]	0.81	0.58	0.70	0.42
[VII]	0.81	0.59	0.70	0.41
[VIII]	0.77	0.60	0.68	0.41

a) The parameters were calculated using the experimental data measured in the solvent MH. The mean of $g'_\perp$ and $g''_\perp$ listed in Table 1 were used for convenience as the essential $g_\perp$ value for calculation of the parameters.

b) The listed values for the complexes [I], [II] and [III] were quoted from our previous paper.

The results in Table 2 indicate that there is a clear correlation between the value of α^2 (the covalency parameter of σ bonding) and the structure of the ligand molecule. The more alkyl groups (methyl or ethyl groups) a ligand contains, the smaller the value of α^2 for its complex becomes. Especially, the *N*-substituted alkyl group shows a stronger tendency to make the value of α^2 decrease than the *C*-substituted alkyl group; furthermore, the tendency is more pronounced in the ethyl group than in the methyl group. This tendency

Table 3. Acid dissociation constants pK_{BH^+} of ethylenediamine and its alkyl derivatives and stability constants β_2 of the copper(II) complexes of these ligand molecules[a]

Ligand molecule	pK_{BH^+}	β_2
en	10.18	20.13
pn	10.00	20.06
m-bn	9.97	20.06
d'men	10.29 (10.16)	18.10 (16.34)
eten	10.56	18.57
d'een	10.46	15.62
dmen	10.00 (9.53)	19.58 (15.96)
deen	(10.02)	(13.72)

a) These data were cited from the literatures.[6] The measurements were carried out at 25°C in aqueous 0.5 N KNO_3 medium by the method of glass electrode. The values in parentheses are the data measured in aqueous 0.1 N KCl medium.

can be simply explained in terms of the inductive effect of alkyl groups, which increases the electron-donating power of the ligand nitrogen σ orbitals and, consequently, makes the σ orbitals interact more strongly with the $d_{x^2-y^2}$ orbital of the copper atom. The acid dissociation constants of the ligand molecules and the stability constants of their copper(II) complexes are cited in Table 3 from the literature.[6] From a comparison between the results of Tables 2 and 3, it follows that there seems to be little correlation between the acid dissociation constants of the ligand molecules and the values of α^2 for their complexes, but the stability constant decreases as the value of α^2 decreases, that is, as the σ bonding becomes more covalent. However, since the stability constant must be substantially related to the total energy of stabilization for complex formation, it is suggested that more important factors than the σ bonding contribute to the stability of the complex.

The values of $\beta_1{}^2$ and β^2 for all the complexes listed in Table 2 are much smaller than unity. This implies, as has been indicated previously,[2] that in-plane and out-of-plane π bondings must play an important role in determining the properties of the copper(II) complexes of amines.

Optical Absorption Spectra. The spectral data obtained for the complexes employed in this work are listed in Table 4. There have been fewer reports about the spectroscopy of copper(II) complexes than on other metal complexes, and

6) L. G. Sillen and A. E. Martell, "Stability Constants of Metal-ion Complexes" (Special Publication No. 7), The Chemical Society, Burlington, London (1964); F. Basolo, R. K. Murmann and Y. T. Chen, *J. Am. Chem. Soc.*, **75**, 1478 (1953); F. Basolo and R. K. Murmann, *ibid.*, **76**, 211 (1954); F. Basolo, Y. T. Chen and R. K. Murmann, *ibid.*, **76**, 956 (1954); H. Irving and J. M. M. Griffiths, *J. Chem. Soc.*, **1954**, 213, 4370.

TABLE 4. OPTICAL ABSORPTION SPECTRA[a] AND ESTIMATED LIGAND FIELD ENERGIES[b]

Copper(II) complex	λ_{max} (mμ): log ε			ΔE_{xy} (cm^{-1})	ΔE_{xz}
[I]	228 : 3.78		547 : 1.80	15200	19600
[II]	230 : 3.81		547 : 1.84	15200	19600
[III]	234 : 3.90		546 : 1.85	15200	19600
[IV]	262 : 3.77		566 : 1.98	15000	19300
[V][c]	242 : 3.49	265 : 3.40	558 : 1.96	14900	19200
[VI][c]	244 : 3.43	272 : 3.43	581 : 1.98	14200	18300
[VII]	243 : 3.56	283 : 3.55	563 : 2.14	14800	19000
[VIII][c]	244 : 3.32	283 : 3.41	588 : 2.12	14100	18200

a) The measurement was carried out in aqueous solution at room temperature.
b) The method for estimating these energy values had been described in our previous paper.[4]
c) Ultraviolet absorption bands were determined by approximate Gaussian analysis.

only a few papers on the ultraviolet spectroscopy for the copper(II) complexes of ethylenediamine and its analogues have been published so far. Basu and Basu reported that the intense absorption bands of the copper(II) complexes of amines in the 200—250 mμ region are the charge-transfer bands between the copper ion and the amines.[7] On the other hand, the single broad band generally observed in the visible region for copper(II) complexes in solution has been ascertained to be due to *d–d* absorption bands and to consist of three or four components.[8] The visible spectral bands of the copper(II) complexes of ethylenediamine and its analogues have already been discussed in our previous paper.[4]

The ultraviolet absorption spectrum of the complex [VII] in an aqueous solution, as is shown in Fig. 5, clearly consists of two absorption bands. For the complexes [V], [VIII], and also [VI] the observed ultraviolet absorption spectra may reasonably be considered to consist of two bands. The data listed in Table 3 for these complexes were obtained from their spectra by approximate Gaussian analysis. Since the structures of these complexes are considered to be lower in symmetry than those of the complexes [I], [II], and [III], the above-mentioned spectral fact seems to result from this decrease in symmetry; the ligand field for the complexes [V], [VI], [VII], and [VIII] deviates to some extent from axial symmetry.

The energy of the ultraviolet absorption band decreases in going from [I] to [VIII] in Table 3 when the lower energy band of the two ultraviolet bands is chosen in [V], [VI], [VII], and [VIII]. This tendency suggests that there is a correlation between the energies of the ultraviolet absorption band for the complexes and the structure of their ligand molecules; furthermore, the value of α^2 also decreases in the same order, as has been indicated above.

Molecular Orbitals and Chemical Bondings. The ESR results obtained for the copper(II) complexes of ethylenediamine and a series of alkylated ethylenediamines revealed that there is a clear correlation between the covalency of σ bonding for the complexes and the structure of their ligand molecules. However, the ESR method can not explain why there is such a correlation, because only antibonding molecular orbitals associated with the copper atom are treated in obtaining bonding parameters from the ESR data, whereas bonding and other antibonding orbitals are not entirely necessary in doing so. Ligand field energies themselves also reflect various aspects of the electronic structure of complexes. However, some of the ligand field energies determined experimentally from optical absorption are used for calculating bonding parameters using Eqs. (1)—(6) without deeply considering the original meanings of the ligand field energies themselves.

The molecular orbitals of the copper(II) complexes are built up by linear combinations of the 3*d*, 4*s*, and 4*p* atomic orbitals or the copper atom and the hybrid orbitals of the ligand atoms directly coordinated to the copper atom. It has generally been accepted that the ligand nitrogen atoms of amines have sp^3 hybrid orbitals or orbitals near to sp^3 hybrid orbitals.

The amount of mixing of atomic orbitals in the molecular orbitals, which shows the degree of covalency directly, is proportional to the atomic orbital overlap and inversely proportional to their Coulomb-energy difference.[9,10] Now, it was assumed that for all the complexes under considera-

7) G. Basu and S. Basu, *Anal. Chim. Acta*, **21**, 187 (1959).
8) J. Bjerrum, C. J. Ballhausen and C. K. Jorgensen, *Acta Chem. Scad.*, **8**, 1275 (1954); R. L. Belford, M. Calvin and G. Belford, *J. Chem. Phys.*, **26**, 1165 (1957); S. Yamada and R. Tsuchida, This Bulletin, **29**, 289 (1956).
9) R. S. Mulliken, *J. Chem. Phys.*, **23**, 1841 (1955); M. Wolfsberg and L. Helmholz, *ibid.*, **20**, 837 (1952).
10) C. J. Ballhausen and H. B. Gray, *Inorg. Chem.*, **1**, 111 (1962); C. J. Ballhausen and H. B. Gray, "Molecular Orbital Theory," W. A. Benjamin, New York (1964), p. 102.

Table 5. Ionization potentials (in units of eV) of various alkyl amines[a)]

Alkyl amine	R					
	H	CH_3	CH_2CH_3	$(CH_2)_2CH_3$	$CH(CH_3)_2$	$(CH_2)_3CH_3$
RNH_2	10.15	8.97	8.86	8.78	8.72	8.71
R_2NH		8.24	8.01	7.84	7.73	7.69
R_3N		7.82	7.50	7.23		

a) These were cited from Watanabe's data.[11)]

tion the values of the overlap integral, S, for the σ bonding are almost equal and that the Coulomb energies of copper atomic orbitals with which ligand orbitals mix to from molecular orbitals are not very different form each other; thus, we do not introduce such a complicated and refined concept as valence-state ionization energy.[10)] On the above assumption, the degree of covalency of the σ bonding for the complexes depends only upon the Coulomb energies of their ligand σ orbitals. As has already been mentioned in the foregoing paragraph, there is a clear correlation between the energies of the ultraviolet absorption band for the complexes and the structure of their ligand molecules. It can, therefore, be expected from this fact that all the ultraviolet absorption bands are of the same type, and that the Coulomb energies of the ligand orbital concerned with the ultraviolet absorption band undergo regular change in the order given in Table 3. Watanabe measured the ionization potentials of various small and simple molecules.[11)] We selected the ionization potentials of various amines from his data; they are listed in Table 5. It is clearly indicated in this table that the ionization potential of alkyl amine becomes smaller as the alkyl group changes from methyl to butyl and as the number of alkyl groups in the amine increases. The ionization potentials of the amines may be considered, on a first approximation, to correspond to the Coulomb energies of the nitrogen lone-pair electron orbital which is used as the ligand σ orbital in their complexes. It is reasonable to expect that the ionization potentials of ethylenediamine and its alkyl derivatives, which have not yet been measured, vary in just the same way as those of alkyl amines. As a trial, the relative values of the ionization potentials for ethylenediamine and its alkyl derivatives were estimated by the following procedure. The ionization potentials of ethylenediamine, 1,2-diaminopropane, *N*-ethylethylenediamine, and *N*,*N*-diethylethylenediamine were assumed to be equal to those of ethylamine, isopropylamine, diethylamine, and triethylamine respectively. The ionization potentials of other alkylated ethylenediamines were also estimated from the corresponding two alkyl amines, with a proportional allotment. The relative values of the ionization potentials thus estimated are listed in Table 6.

Table 6. The relative ionization potentials (in units of eV) estimated for ethylenediamine and its alkyl derivatives

en	$NH_2CH_2CH_2NH_2$	8.86
pn	$NH_2CH_2CH(CH_3)NH_2$	8.72
m-bn	$NH_2CH(CH_3)CH(CH_3)NH_2$	8.62
d'men	$CH_3NHCH_2CH_2NHCH_3$	8.13
eten	$NH_2CH_2CH_2NHCH_2CH_3$	8.01
d'een	$CH_3CH_2NHCH_2CH_2NHCH_2CH_3$	8.01
dmen	$NH_2CH_2CH_2N(CH_3)_2$	7.71
deen	$NH_2CH_2CH_2N(CH_2CH_3)_2$	7.50

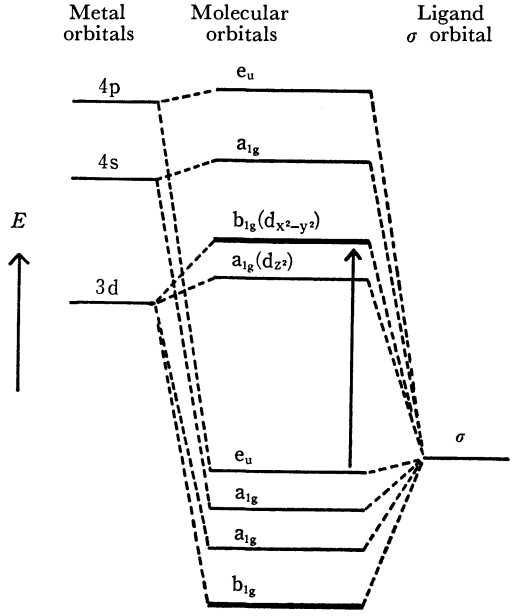

Fig. 6. Molecular orbital energy level scheme for square planar copper(II) complex (D_{4h} symmetry) in which ligand has a σ orbital system.

The energy-level scheme of the molecular orbitals concerned with ligand σ orbitals for the copper(II) complex whose ligand field has a D_{4h} symmetry is shown in Fig. 6. The ground state of the complex is, then, B_{1g}. From symmetry arguments, two allowed charge-transfer transitions may be anticipated for the complex, corresponding to the one-electron transitions:

$e_u \leftarrow b_{1g}$ ($B_{1g} \rightarrow E_u$) and $b_{2u} \leftarrow b_{1g}$ ($B_{1g} \rightarrow B_{2u}$)

11) K. Watanabe, *J. Chem. Phys.*, **26**, 1773 (1957).

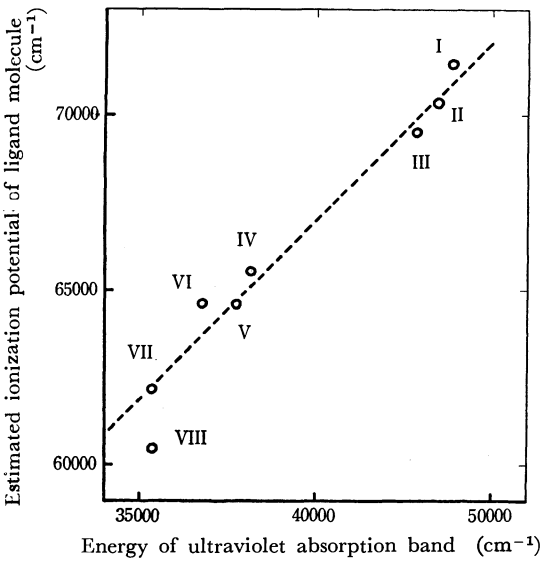

Fig. 7. Shifts in energies of ultraviolet absorption bands with changes in the estimated ionization potentials of ligand molecules.

These are transitions from molecular orbitals essentially localized on the ligands to molecular orbitals essentially localized on the metal atom. In order to ascertain whether or not the ultraviolet absorption band corresponds to the former charge-transfer band, the energies of the band were plotted against the ionization potentials estimated above, where the lower energy band of the two ultraviolet absorption bands was chosen for the complexes [V]—[VIII]; this is shown in Fig. 7. It is obvious in this figure that there is a linear relationship between the energies of the band and the ionization potentials with a slope of about 45°. This relationship is a characteristic feature of the charge-transfer band; it suggests that a dominant factor in determining the energy of the charge-transfer band is the energy difference between the Coulomb energies of copper 3*d* orbitals and ligand σ orbitals. Therefore, the band is assigned to the $B_{1g} \rightarrow E_u$ charge-transfer transition.

As has already been mentioned, the charge transfer bands of the complexes in Table 3 appear at lower energies as the number of alkyl groups in their ligand molecules increases; furthremore, the tendency of the band becomes more pronounced when the alkyl groups are ethyl rather than methyl and when they are *N*-substituted alkyl groups rather than *C*-substituted ones. The fact that the charge-transfer band shifts to a longer wavelength indicates that the energy difference between the levels of the copper 3*d* orbital and the ligand σ orbital becomes smaller and that, accordingly, the σ bonding becomes more covalent. This tendency toward covalency is perfectly consistent with the one derived from the ESR results. Therefore, it may be concluded that, for the metal complexes of ethylenediamine and its analogues, the σ bonding becomes more covalent as the charge-transfer bands appear at longer wavelengths.

BULLETIN OF THE CHEMICAL SOCIETY OF JAPAN VOL. 42 2193—2198 (1969)

Thermodynamic and X-Ray Studies of Solid Solutions of Silver Bromide and Sodium Bromide

Toshihide TSUJI, Kazuo FUEKI and Takashi MUKAIBO

Department of Industrial Chemistry, Faculty of Engineering, The University of Tokyo, Hongo, Tokyo

(Received January 14, 1969)

Activity, and partial molal free energy, enthalpy and entropy of AgBr in AgBr-NaBr solid solutions have been obtained at 350 and 400°C from the e.m.f. data of galvanic cells of the type Ag/AgBr-NaBr/Br_2. It has been found that the solid solution forms a regular solution defined by Hildebrand. A miscibility gap has been found by the study of galvanic cells and confirmed by high temperature X-ray diffraction. A new phase diagram of the AgBr-NaBr system is presented.

Kiukkola and Wagner[1] showed new potentialities and inherent limitations of e.m.f. measurements on galvanic cells with solid electrolytes for the determination of standard molal free energies of formation of halides, oxides, sulfides and other compounds at elevated temperatures. Although many e.m.f. studies were made for simple oxides, halides and sulfides, only a few studies have been carried out for the solid solutions consisting of

1) K. Kiukkola and C. Wagner, *J. Electrochem. Soc.*, **104**, 308, 379 (1957).

these simple salts.

Wachter,[2] and Panish and his co-workers[3] have reported the e.m.f. of the cell with solid electrolyte AgCl-NaCl and Pal'guev *et al.*[4] have measured the e.m.f. of electrochemical cells of a different type

$$Ag/AgBr//AgBr\text{-}NaBr/Br_2,$$
$$Ag/AgBr//AgBr\text{-}NaBr/Ag,$$
$$Br_2/AgBr//AgBr\text{-}NaBr/Br_2.$$

In the present paper, the result of studies on the activity, and partial molal quantities of AgBr in AgBr-NaBr solid solutions and miscibility gap by means of the galvanic cell $Ag/AgBr\text{-}NaBr/Br_2$ are given. For the determination of miscibility gap, high temperature X-ray diffraction study was also carried out.

Experimental

Samples. Sodium bromide and silver bromide of high purity were supplied from Junsei Pure Chemicals & Co., Ltd. and Kojima Chemical Co., Ltd., respectively. Silver bromide was prepared from pure silver nitrate and sodium bromide. No difference in e.m.f. due to the source of silver bromide was found in the experiment.

Silver bromide and sodium bromide were mixed in a desired proportion and ground together in an agate mortar. The mixture was melted in a quartz tube in bromine atmosphere, heated until the solution became clear, kept at about 400°C for several hours and then quenched. After cooling the sample was taken out from the quartz tube and ground again.

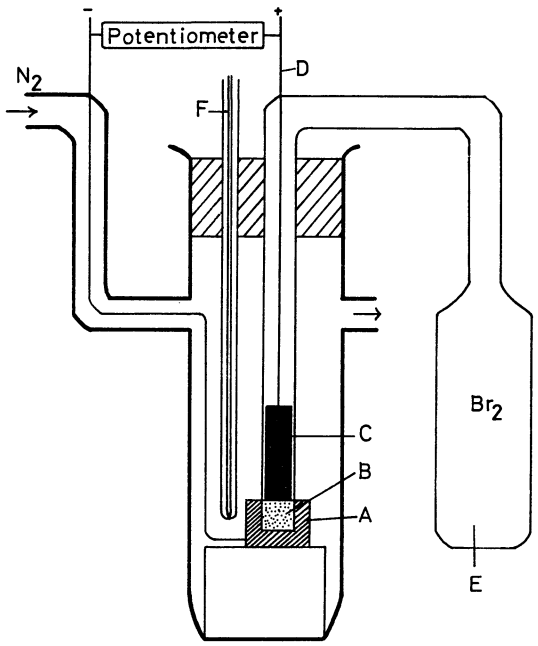

Fig. 1. Cell for the e.m.f. measurement.
A: silver crucible, B: AgBr-NaBr solid solution.
C: graphite, D: platinum wire,
E: bromine reservoir, F: thermocouple

E. M. F. Measurement. The apparatus used for the e.m.f. measurement of galvanic cells is shown in Fig. 1. Powder of solid solution was put into a silver crucible, A, which serves as the anode of the cell. This crucible also serves to keep the temperature of the electrolyte uniform. A quartz tube of 10 mm in diameter was inserted into the crucible. After the powder was melted, a graphite electrode of high purity, C, connected with platinum wire, D, was put into the fused solution. The salt was slowly solidified and kept at 400°C, and then the quartz tube was evacuated. After checking airtightness, bromine which had been purified by vacuum-distillation and dried with a magnesium perchlorate column, was introduced into the quartz tube and purified nitrogen stream was kept flowing along outside the tube.

The thermoelectric potential was measured on a cell which was constructed by replacing of the solid electrolyte with a silver block. It was found that the thermoelectric potential ranged from 1.4 to 4.1 mV depending on the temperature and was quite reproducible. Correction of the thermoelectric potential was made for all e.m.f. data.

The temperature of the furnace was maintained constant within ±0.5°C by means of an electronic controller. The e.m.f. of the thermocouple was measured with a P-42 type pyrometer of Murayama Denki Ltd. The temperature of the reservoir of bromine was controlled within ±0.05°C so that the fluctuation of the vapor pressure of bromine was less than 0.2% of the total pressure. The vapor pressure of bromine at each temperature was calculated from the temperature of the reservoir and the vapor pressure data in the Nesmeyanov table.[5] At a temperature range of 200 to 400°C the e.m.f. was measured by means of a potentiometer of Yokogawa Electric Works Ltd. in conjunction with a G-52 type galvanometer of Murayama Denki Ltd. When a new graphite electrode was employed, it took about 20 hr to attain a constant potential. When the vapor pressure of bromine was changed, the equilibrium was attained in two hours. The e.m.f. was reversible with regard to temperatures and the vapor pressure of bromine, but at low concentrations of silver bromide the conductivity of solid solutions was too small to measure the e.m.f.

High Temperature X-Ray Diffraction. In order to determine the exact solubility limit the powdered sample prepared in the same method as described above was mounted on a platinum sample holder and the lattice constant was measured by means of a high temperature X-ray diffractometer, type D-8C of Rigaku Denki Co., Ltd.

2) A. Wachter, *J. Am. Chem. Soc.*, **54**, 919 (1932).
3) M. B. Panish, F. F. Blankenship, W. R. Grimes and R. F. Newton, *J. Phys. Chem.*, **62**, 1325 (1958).
4) S. F. Pal'guev, S. V. Karpachev and L. D. Yushina, *Trudy Inst. Elektrokhim., Akad. Nauk S. S. S. R., Ural. Filial.*, **1**, 105 (1960).
5) A. N. Nesmeyanov, "Vapour Pressure of the Elements," translated and edited by J. I. Carasso, Academic Press, New York (1963), p. 366.

Results and Discussion

Figure 2 shows the plot of E *vs.* $\log P_{Br_2}$ for AgBr-NaBr solid solutions with various compositions at 400°C. A good linear relationship is seen between the vapor pressure of bromine and the e.m.f. within a pressure range 0.0864 and 0.650 Torr. A similar linear relationship was obtained at temperatures from 200 to 400°C.

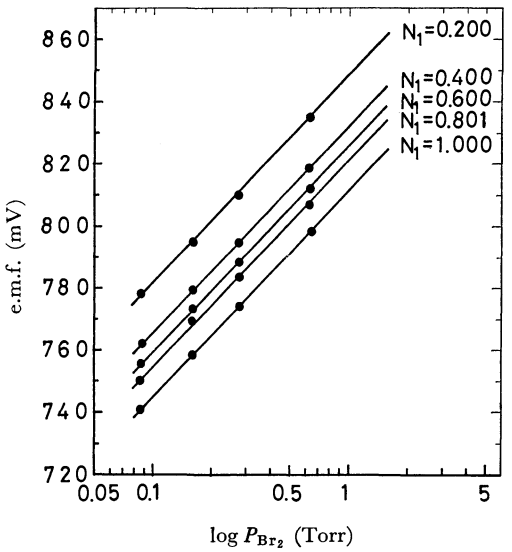

Fig. 2. Plot of E *vs.* $\log P_{Br_2}$ at 400°C.

TABLE 1. VALUES OF E_0 (mV)

N_1	°C				
	400	350	300	250	200
0.100	870.1	(885.2)	(898.2)		
0.200	849.1	865.8	(885.1)	(903.6)	
0.300	836.0	854.1	873.4	892.5	
0.400	832.4	851.4	870.9	886.5	906.9
0.500	826.5	846.9	867.6	889.1	910.8
0.600	826.6	847.4	869.4	885.9	904.0
0.700	823.5	845.3	869.5	890.2	914.0
0.801	821.7	844.8	870.5	888.5	906.5
0.901	818.5	841.4	864.6	885.1	907.6
1.000	811.9	835.3	858.9	878.2	895.3

Table 1 shows E_0, the e.m.f. at a bromine pressure of 1 Torr, which was obtained by extrapolating the plot of E *vs.* $\log P_{Br_2}$. The data with parentheses are those less reproducible.

According to Wagner[6] the open circuit potential, E, for an electrochemical cell, Ag/AgBr-NaBr/Br_2, is given by the equation

$$E = \frac{1}{F}\int_{\mu'_{Br_2}}^{\mu''_{Br_2}} (1-t_e)\mathrm{d}\mu_{Br_2}, \qquad (1)$$

where t_e is the transference number of electrons, μ'_{Br_2} and μ''_{Br_2} the chemical potentials of bromine at the metal-solid solution interface and at the gas-solid solution interface, respectively, and F the Faraday constant.

Using the free energy change ΔG_1 of the reaction $Ag+1/2Br_2=(AgBr)$ in solid solution, Eq. (1) is rewritten as

$$E = \frac{-\Delta G_1}{F} - \frac{1}{F}\int_{\mu'_{Br_2}}^{\mu''_{Br_2}} t_e\mathrm{d}\mu_{Br_2}. \qquad (2)$$

Wagner[7] has reported that the second term in Eq. (2) resulting from electronic conduction in pure silver bromide is 3.8 mV for $P_{Br_2}=0.23$ Torr at 277°C.

Tubandt and Reinhold[8] have shown that pure solid silver bromide is an entirely ionic conductor at temperatures from 200 to 300°C and Pal'guev *et al.*[9] have mentioned that according to the e.m.f. measurements of the electrochemical cell, Ag/AgBr/Br_2, the conductivity of the solid electrolyte were entirely ionic over a temperature range of 100 to 434°C.

In our experiment above 300°C the slope of the plots between E and $\log P_{Br_2}$ of pure silver bromide is close to the theoretical value, $2.303\,RT/2F$, where R is the gas constant and T the absolute temperature. Our experimental values of e.m.f. for pure silver bromide at 300°C is 1.1 mV lower than those calculated by Hamer *et al.*[10] From these results, it is concluded that pure silver bromide is a purely ionic conductor above 300°C. At lower temperatures our experimental data tend to deviate and are about 10 mV lower than those of Hamer *et al.*[10] because of the contribution of electronic conduction.

As shown in Fig. 2 the slope of the plot between E and $\log P_{Br_2}$ of AgBr-NaBr solid solutions with various compositions is the same as that of pure silver bromide. A similar relationship is found at 300 and 350°C. Since pure silver bromide is entirely ionic at the temperatures mentioned above, the solid AgBr-NaBr system is supposed to be also an ionic conductor above 300°C. Therefore, the second term in Eq. (2) can be eliminated for AgBr-NaBr solid solutions as well as pure silver bromide, and ΔG_1 is obtained from the e.m.f. data. If $\Delta G°$ denotes the free energy of formation of pure silver bromide, the partial molal free energy of silver bromide in solid solutions,

6) C. Wagner, *Proc. Intern. Comm. Electrochem. Thermodyn. Kinet.*, **7**, 361 (1957).

7) C. Wagner, "Advances in Electrochemistry and Electrochemical Engineering," Vol. 4, ed. by P. Delahay, Interscience, New York (1966), p. 1.

8) C. Tubandt and H. Reinhold, *Z. Elektrochem.*, **29**, 313 (1923); **31**, 84 (1925).

9) L. D. Yushina, S. F. Pal'guev and S. V. Karpachev, *Zh. Fiz. Khim.*, **35**, 342 (1961).

10) W. J. Hamer, M. S. Malmberg and B. Rubin, *J. Electrochem. Soc.*, **112**, 750 (1965).

Table 2. Thermodynamic data of the AgBr-NaBr system at 350 and 400°C

	N_1	ΔG_1, kcal	$\bar{G}_1$, kcal	$\bar{S}_1$, cal/°C	$\bar{H}_1$, kcal	a_1	a_2
400°C	0.100	−20.06	−1.34	3.83	1.24	0.367	0.912
	0.200	−19.58	−0.86	3.09	1.22	0.527	0.861
	0.300	−19.28	−0.56	2.45	1.09	0.660	0.801
	0.400	−19.19	−0.47	2.03	0.89	0.702	0.774
	0.500	−19.06	−0.34	1.38	0.59	0.778	0.707
	0.600	−19.06	−0.34	1.20	0.47	0.776	0.700
	0.700	−18.99	−0.27	0.74	0.23	0.819	0.628
	0.801	−18.95	−0.23	0.14	−0.13	0.845	0.569
	0.901	−18.87	−0.15	0.23	0.00	0.893	0.447
	1.000	−18.72	0	0	0	1.000	0
350°C	0.100	−20.41	−1.15	3.83	1.24	0.395	0.916
	0.200	−19.96	−0.70	3.09	1.22	0.567	0.867
	0.300	−19.69	−0.43	2.45	1.09	0.705	0.809
	0.400	−19.63	−0.37	2.03	0.89	0.741	0.786
	0.500	−19.53	−0.27	1.38	0.60	0.806	0.727
	0.600	−19.54	−0.28	1.20	0.47	0.798	0.724
	0.700	−19.49	−0.23	0.74	0.23	0.830	0.664
	0.801	−19.48	−0.22	0.14	−0.13	0.838	0.650
	0.901	−19.40	−0.14	0.23	0.00	0.893	0.501
	1.000	−19.26	0	0	0	1.000	0

$\bar{G}_1$, is obtained by the equation

$$\bar{G}_1 = \Delta G_1 - \Delta G^\circ. \quad (3)$$

From the temperature dependence of $\bar{G}_1$, the partial molal entropy and enthalpy of silver bromide in solid solutions are calculated. If pure silver bromide is chosen as the standard state, the activity of silver bromide in its solution is calculated by the relation

$$\bar{G}_1 = 2.303\,\boldsymbol{R}T \log a_1. \quad (4)$$

The activity of sodium bromide, a_2, is obtained by means of the Gibbs-Duhem equation in the integrated form

$$\log \frac{a_2}{N_2} = -\int_0^{N_1} \frac{N_1}{N_2} \mathrm{d} \log \frac{a_1}{N_1}. \quad (5)$$

Thermodynamic data of the AgBr-NaBr system at 350 and 400°C are shown in Table 2.

Kleppa and Meschel[11] have determined the heat of solution of AgBr-NaBr by high temperature solution calorimetry at 350°C using pure liquid silver nitrate as the solvent. Table 3 gives the data by Kleppa and Meschel together with those obtained by the present study. Agreement is fairly good except for the data at N_1=0.801.

The deviation from Raoult's law is illustrated in Figs. 3 and 4. As can be seen from the figures, the system shows positive deviations from Raoult's law. Figures 3 and 4 also show that the solid solution is completely miscible at 400°C, but partially miscible at 300°C.

Table 3. Partial molal enthalpies of AgBr in AgBr-NaBr solid solutions at 350°C

N_1	This work $\bar{H}_1$ kcal	Kleppa and Meschel[11] $\bar{H}_1$ kcal
0.100	(1.24)	2.01
0.200	1.22	1.50
0.300	1.09	1.08
0.400	0.89	0.74
0.500	0.60	0.48
0.600	0.47	0.28
0.700	0.23	0.15
0.801	−0.13	0.06
0.901	0.00	0.01

Zemczuzny[12] has reported that the AgBr-NaBr system forms a complete solid solution. A recent work by Stokes and Li[13] have indicated the existence of a miscibility gap with a critical temperature near 175°C for the AgCl-NaCl system. In view of the similarity of the AgCl-NaCl and AgBr-NaBr system, a miscibility gap can be expected.

11) O. J. Kleppa and S. V. Meschel, *J. Phys. Chem.*, **69**, 3531 (1965).

12) S. F. Zemczuzny, *Z. Anorg. Allgem. Chem.*, **153**, 47 (1926).

13) R. J. Stokes and C. H. Li, *Acta Met.*, **10**, 535 (1962).

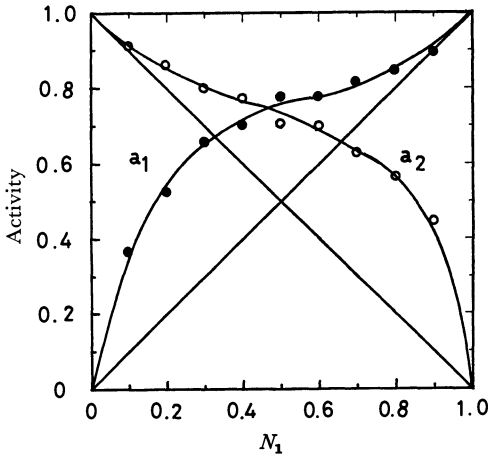

Fig. 3. Activity curves for AgBr-NaBr solid solutions at 400°C.

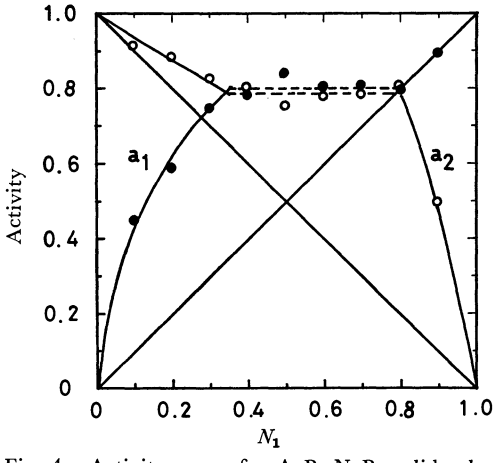

Fig. 4. Activity curves for AgBr-NaBr solid solutions at 300°C.

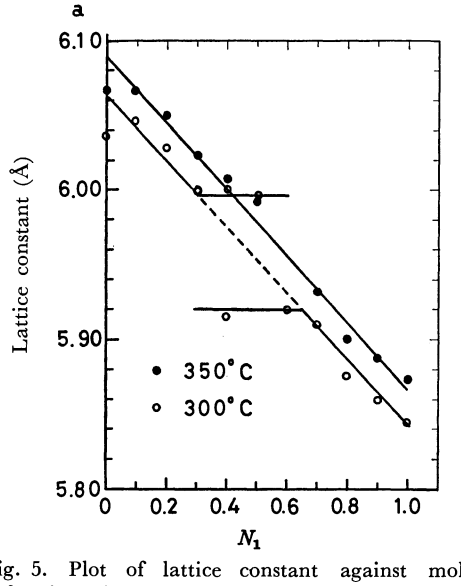

Fig. 5. Plot of lattice constant against mole fraction of AgBr.

In order to determine the exact solubility limit, a high temperature X-ray diffraction was carried out. Figure 5 shows lattice constants, a, plotted against mole fraction of silver bromide, N_1. As can be seen in Fig. 5, the lattice constant at 350°C decreases linearly with the increase in mole fraction of silver bromide (Vegard's law), but at lower temperatures such as 300°C the discontinuity in lattice parameter was found. The solubility limit

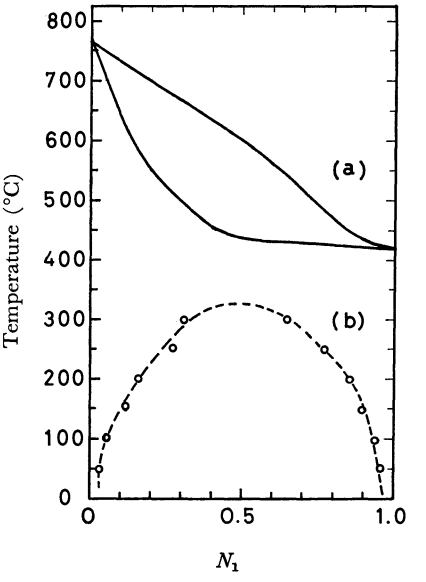

Fig. 6. Phase diagram of the AgBr-NaBr system. (a): Zemczuzny, (b): this work

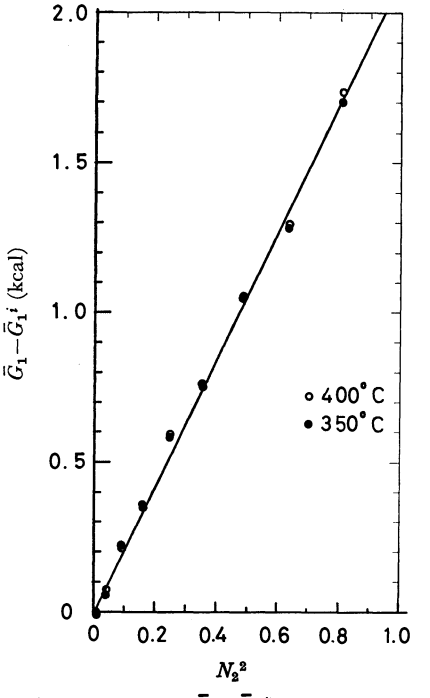

Fig. 7. Plot of $(\bar{G}_1-\bar{G}_1^i)$ against N_2^2.

was measured at an interval of 50°C from 50 to 350°C.

Figure 6 shows the phase diagram of the AgBr-NaBr system. The dotted line is the result of the present work and the liquidus and solidus lines are obtained from the data of Zemczuzny.[12]

Figure 7 gives the plot of $(\overline{G}_1-\overline{G}_1^i)$ *vs.* N_2^2, where $\overline{G}_1^i$ is the partial molal free energy of component 1 in the ideal solution. A good linear relationship exists between $(\overline{G}_1-\overline{G}_1^i)$ and N_2^2 and two sets of points for 350 and 400°C fall on a single straight line. This result clearly shows that the AgBr-NaBr system forms a regular solution which was defined by Hildebrand[14] above the critical temperature. It is concluded from this result that the partial molal entropy is the same as it would be in the ideal solution, *i. e.*, $\overline{S}_1=\overline{S}_1^i=R \ln N_1$, and that two kinds of positive ions are distributed at random in the solid solution.

14) J. H. Hildebrand, *J. Am. Chem. Soc.*, **51**, 66 (1929).

Summary

(1) The partial molal free energy of AgBr in the solid AgBr-NaBr system was determined by the e.m.f. measurement for the cell, Ag/AgBr-NaBr/Br_2, at 350 and 400°C.

(2) The partial molal entropy and the partial molal enthalpy of AgBr in the solid AgBr-NaBr system were calculated.

(3) From the e.m.f. measurement, a miscibility gap was found in the AgBr-NaBr system. The exact solubility limit was determined by high temperature X-ray diffraction.

(4) A new phase diagram of the AgBr-NaBr system was presented.

(5) The system was found to form a regular solution defined by Hildebrand.

BULLETIN OF THE CHEMICAL SOCIETY OF JAPAN VOL. 42 2198—2202 (1969)

Heat of Immersion of Titanium Dioxide in Water. II. The Effect of the Crystallinity of Anatase

Teiji OMORI, Junichiro IMAI, Mahiko NAGAO and Tetsuo MORIMOTO

Department of Chemistry, Faculty of Science, Okayama University, Tsushima, Okayama

(Received January 16, 1969)

Two kinds of anatase samples which have very large specific surface areas and low crystallinities were prepared, and the interaction between the solid surface and the water molecule was investigated by measuring the water content, the heat of immersion in water, and the infrared spectrum of each sample. Two characteristic features were found in these samples: first, the plot of the heat of immersion *vs.* the pretreatment temperature did not reveal such a maximum as had been found previously with the crystalline anatase, and second, the heat of surface hydration as calculated from the plot of the heat of immersion *vs.* the water content was found to be remarkably smaller than with the crystalline anatase. These facts have led us to conclude that, with the anatase samples of a low crystallinity, not only does the rehydration reaction of a surface oxide structure produced at an elevated temperature proceed more easily on immersion in water, but also the heat of rehydration is smaller, than in a sample of a high crystallinity. Moreover, it was found from an infrared spectroscopic investigation that the water molecules physisorbed on the surfaces of large-area samples could be desorbed more gradually than those on small-area samples and remained small in quantity up to near 300°C *in vacuo*.

Titanium dioxide is one of the most important white pigments produced on an industrial scale; it has been studied by many investigators from the surface-chemical point of view. Nevertheless, it seems that many problems remain to be worked out with this material. Recently, the investigations have been carried out on the vapor adsorption,[1-3] the heat of immersion,[4] the surface

1) C. M. Hollabaugh and J. J. Chessick, *J. Phys. Chem.*, **65**, 109 (1961).

2) P. T. Dawson, G. T. Rich and D. A. Haydon, *ibid.*, **68**, 3550 (1964).

3) T. Morimoto, M. Nagao and F. Tokuda, *ibid.*, **73**, 243 (1969).

4) W. H. Wade and N. Hackerman, *ibid.*, **65**, 1681 (1961).

charge,[5,6] and the catalytic activity[7,8] of titanium dioxide; consequently, it has become clear that the surface hydroxyl groups play an important role in these phenomena. The plot of the heat of immersion of most metal oxides in water against the pretreatment temperature reveals a maximum, this phenomenon being also closely related to the presence of surface hydroxyl groups. Since, by analysing the plot, we can estimate the heat of formation of a surface hydroxyl group (the heat of surface hydration), the measurement of the heat of immersion of metal oxides in water makes it possible to make an energetic interpretation of the chemisorption of water on the solid surfaces. Recently, we have discovered two types of heat-of-immersion curves on α-Fe_2O_3; one shows a maximum, while the other does not.[9]

In the present work, anatase samples with large surface areas have been prepared in order to clarify the conditions of the appearance of a non-maximum curve in the plot of the heat of immersion *vs.* the pretreatment temperature. Then the interaction between the solid surface and the water molecule has been investigated by measuring the surface water content, the heat of immersion in water, and the infrared spectroscopy and by comparing the results with those obtained previously for the crystalline anatase.[10] As a result, two typical non-maximum curves have been observed in the plot of the heat of immersion *vs.* the pretreatment temperature; one shows an almost straight line, while the other shows an intermediate type between a maximum curve and a straight line.

Experimental

Materials. Two kinds of anatase were prepared in this study. The first sample was made by repeatedly treating the precipitate of anatase made through the hydrolysis of titanium sulfate with 1 N ammonia water in order to remove a large quantity of contaminated sulfate ions. It was then washed thoroughly with distilled water, and finally treated by means of electrodialysis (sample FA). The second sample was produced by calcining titanium peroxide for 4 hr at 400°C in air; the titanium peroxide had been prepared by the oxidation of metallic titanium with hydrogen peroxide. This sample was washed with distilled water, and finally the contaminating trace of electrolytes was removed by means of electrodialysis (sample SA). These two samples were dried at 110°C for 10 hr. For the sake of comparison, the data on the sample AI obtained in the previous work[10] are also cited, and also some new data were taken on this sample.

Surface-area Measurements. The specific surface areas of the anatase samples were determined by applying the BET theory to the nitrogen adsorption data obtained at the temperature of liquid nitrogen, assuming the molecular area of nitrogen to be 16.2 Å^2.

Heat-of-immersion Measurements. A sample of *ca.* 10 m^2 was used for every immersion measurement. Prior to the calorimetric measurement, the sample was treated in an ampoule at a desired temperature for 4 hr in a vacuum of 10^{-5} Torr, and then the ampoule was sealed off. The calorimeter and the technique of the heat-of-immersion measurements have been reported previously.[11] The measurements were carried out at 25°C. The heat of the breaking of the vacant ampoule was found to be 0.28 J; this was calibrated for the heat-of-immersion data.

Water-content Measurements. The water content of the anatase samples was measured by the successive ignition-loss method reported previously.[11] When the samples of anatase were treated at elevated temperatures *in vacuo*, small amounts of gases other than water vapor were found to be evolved. The amounts of these gases were measured volumetrically by a method described previously;[10] these data were then calibrated for the water content data. For instance, the gases other than water vapor which were evolved at 300, 400, and 600°C for the samples FA and SA were 0.02, 0.10, and 0.16, and 0.39, 0.94, and 1.67 molecules/100 Å^2 respectively.

Infrared Spectroscopy. The apparatus used for the infrared spectroscopic study was one made by the Japan Spectroscopic Co. (IR-G), to which a cell for the powdered sample was attached. The cell was essentially the same as that utilized by Yates.[12] The disk was prepared by pressing the powdered sample under a pressure of *ca.* 300 kg/cm^2. The sample disk set in the cell was first treated at an elevated temperature in a vacuum of 10^{-5} Torr for 4 hr and cooled to room temperature; then an infrared absorption spectrograph was taken. The measurements were repeated successively on one and the same sample after heat treatment at increasing temperatures.

Results and Discussion

The specific surface area of anatase is plotted against the pretreatment temperature in Fig. 1. For the sake of comparison, the surface area of the sample AI in a preceding paper[10] is cited in Fig. 1. The surface area of the sample FA is extremely large at room temperature, but it decreases remarkably with a rise in the temperature of heat treatment, indicating a great sintering. In the case of the sample SA also, a considerable sintering occurs. As a whole, we may conclude about the relation illustrated in Fig. 1 as follows:

5) T. Morimoto and M. Sakamoto, This Bulletin, **36**, 1369 (1963).

6) T. Morimoto and M. Sakamoto, *ibid.*, **37**, 719 (1964).

7) A. A. Tolstopyatova, I. R. Konenko and A. A. Balandin, *Izv. Akad. Nauk SSSR, Otd. Khim. Nauk*, **1961**, 38.

8) A. A. Balandin, I. R. Konenko and A. A. Tolstopyatova, *ibid.*, **1961**, 45.

9) T. Morimoto, H. Naono, N. Katayama and M. Nagao, This Bulletin, **42**, 1490 (1969).

10) T. Morimoto, M. Nagao and T. Omori, *ibid.*, **42**, 943 (1969).

11) T. Morimoto, K. Shiomi and H. Tanaka, *ibid.*, **37**, 392 (1964).

12) D. J. C. Yates, *J. Phys. Chem.*, **65**, 746 (1961).

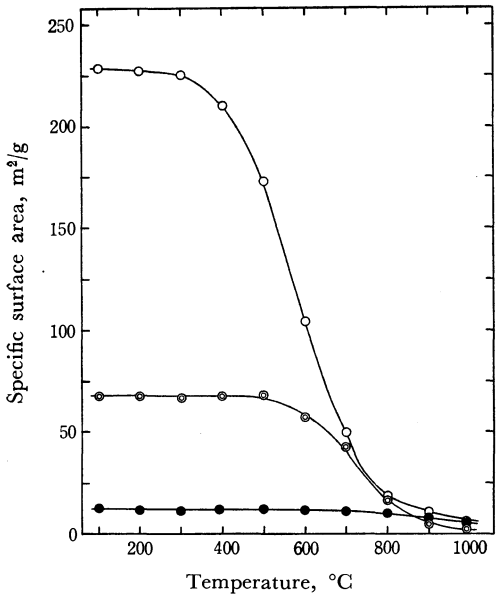

Fig. 1. Dependence of specific surface area of anatase on pretreatment temperature.
○, sample FA; ◎, sample SA; ●, sample AI

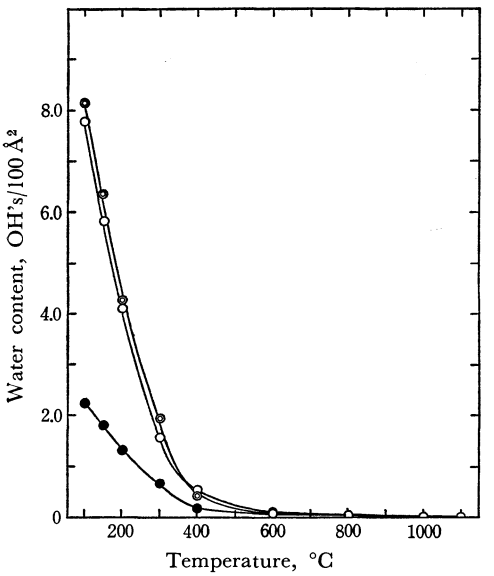

Fig. 2. Water content of anatase at various temperatures.
○, sample FA; ◎, sample SA; ●, sample AI

the larger the specific surface area, the lower the temperature at which the sintering starts.

Figure 2 gives the relation between the water content and the temperature of pretreatment. The water-content value of the samples decreases in the order: SA>FA>AI.

The heat of immersion of anatase in water is plotted as a function of the temperature of pretreatment in Fig. 3. In spite of the large differences

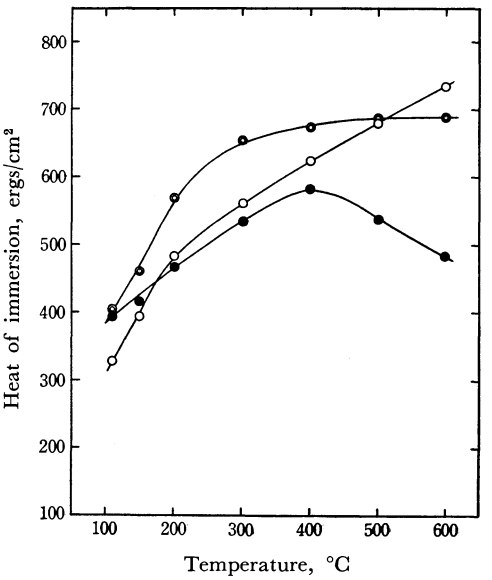

Fig. 3. Dependence of heat of immersion of anatase in water on pretreatment temperature.
○, sample FA; ◎, sample SA; ●, sample AI

between the particle sizes of the three kinds of anatase samples, the particle-size rule investigated in detail by Wade and Hackerman,[4] which states the increase in the heat of immersion with the increase in the particle size, does not hold in the present case. However, it should be noted that the samples FA and SA do not reveal any maximum in the heat-of-immersion curve, in contrast with the case of the sample AI. Most plots of the heat of immersion of metal oxides in water *vs.* the pretreatment temperature have revealed a maximum. For instance, in the cases of SiO_2,[13,14] TiO_2,[4,10] ZnO,[15] Al_2O_3,[11] and Fe_2O_3[9] all the heat-of-immersion curves showed a maximum, although the maximum value and the temperature at which the maximum appears vary with the nature of the metal oxides. Only in the case of Fe_2O_3, have samples showing no maximum in the heat-of-immersion curve been discovered besides samples showing a maximum. In the present case of anatase, two samples having large surface areas show no maximum in the heat-of-immersion curve, while the sample AI, which has a small surface area, shows a maximum. Moreover, a new type of characteristic feature can be seen from Fig. 3 — the heat of immersion of one sample (FA) increases sharply and almost linearly even after 400°C, whereas that of the other sample (SA) increases sharply at first, but slowly later. The

13) G. J. Young and T. P. Bursh, *J. Colloid Sci.*, **15**, 361 (1960).
14) J. W. Whalen, *Advan. Chem. Ser.*, **33**, 281 (1961).
15) T. Morimoto, M. Nagao and M. Hirata, *Kolloid-Z. Z. Polymere*, **225**, 29 (1968).

shape of the non-maximum curve observed on α-Fe_2O_3 rather resembles the case of anatase (the sample SA).

The appearance of the maximum in the heat-of-immersion curve has been elucidated as follows: the surface hydroxyl groups can be removed by pretreatment at elevated temperatures, and the resulting activated sites can easily be rehydrated to form hydroxyl groups on immersion in water. This additional heat evolution due to the rehydration reaction of the activated sites reaches a maximum value with the rise in the pretreatment temperature, since the number of the activated sites increases upon this pretreatment. Over a certain degree of pretreatment temperature, however, the activated surface oxide structure formed is stabilized, making it possible to retard the rehydration reaction on immersion in water. Thus the heat-of-immersion value decreases in the range of higher pretreatment temperatures. This heat of chemisorption of water which varies largely with the pretreatment temperature can be superimposed upon the wetting heat due to the physisorption of water.

When we reported, in a previous paper,[9] the first instance where two groups of samples showing both maximum curves and non-maximum curves in the plot of the heat of immersion were discovered in the same substance (α-Fe_2O_3), this phenomenon was not resolved satisfactorily. However, we suggested that the stabilization of the surface oxide structure formed by treatment at elevated temperatures is insufficient on the samples which give a non-maximum curve in the plot of the heat of immersion. With the sample FA in the present work the heat of immersion increases linearly over the range of pretreatment temperatures from 200 to 600°C; this suggests that little stabilization occurs on the surface oxide structure up to this, the highest temperature of treatment studied. With the sample SA, on the other hand, the heat of immersion increases sharply up to 300°C and then slowly, indicating that only weak stabilization takes place upon pretreatment at elevated temperatures.

The anatase samples were submitted to X-ray diffraction measurements. From these data the crystallite size of the samples can be estimated according to Scherrer's equation;[16] it amounts to 114, 258, and 2260< Å for the samples FA, SA, and AI respectively, with reference to the peak of the (101) plane of anatase. These values are those calibrated by using the data on a well-defined quartz crystal taken under the same conditions. It can be seen from these data that the sample with a larger surface area is of a lower crystallinity, as is to be expected. Thus, we may conclude that the stabilization of the surface oxide structure made by heat treatment occurs with more difficulty on the surface of the sample with a lower crystallinity. In other words, the stabilization of the $-Ti\langle^{O}_{O}\rangle Ti-$ structure on the surface of anatase which is produced by the reaction:

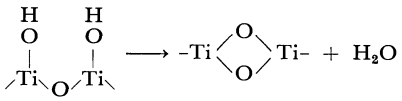

occurs with more difficulty; accordingly, the reverse reaction of this equation proceeds more easily on a surface with an ill-defined crystal structure than on a surface with a well-defined one. This phenomenon can probably be considered to be caused by the irregular bond length and the strained bond angle of the $-Ti\langle^{O}_{O}\rangle Ti-$ structure on the surface, both of which features arise from the lower crystallinity of the sample. The sample SA has the intermediate crystallinity among the three, produces a moderate stabilization of the surface oxide structure, and has a break in the heat-of-immersion curve at a temperature of about 300°C.

In Fig. 4 the heat of immersion of anatase is plotted against the water content in the treatment range up to 400°C. All the plots represent a linear relationship, the slope giving the heat of formation of a surface hydroxyl group, that is, the heat of surface hydration. The value of the heat of surface hydration can be read from Fig. 4 as 11.8 and 14.9 kcal/mol water for the samples FA and SA respectively, whereas the value is 26.4 kcal/mol water for the sample AI. The former two values are quite a bit smaller than the latter, which is the value of a representative crystalline anatase sample. This indicates that the heat of surface hydration is smaller on the surface with a lower crystallinity. Thus, we can conclude that the surface of the sample FA, whose crystallinity is the lowest, can be rehydrated most easily even

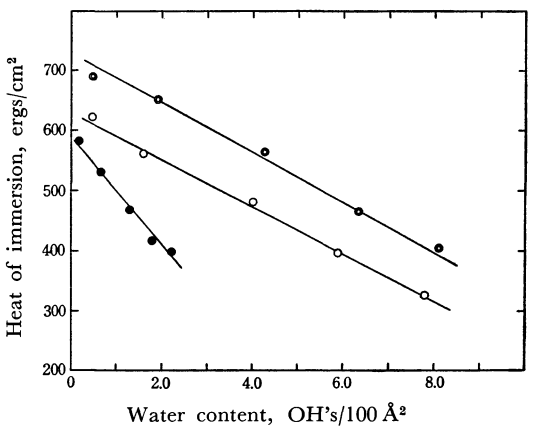

Fig. 4. Relation between heat of immersion and water content on anatase.
○, sample FA; ◎, sample SA; ●, sample AI

16) P. Scherrer, *Göttinger Nachrichten.*, **2**, 98 (1918).

after treatment at higher temperatures; moreover, its heat of surface hydration is the smallest. Since, when the activation energy of a reaction is small, the reaction proceeds rapidly, Fig. 3 suggests that the activation energy of the surface hydration reaction on the sample FA is the smallest, while that on the sample AI is the largest. It is known that, as for reactions with the same reaction mechanism, the activation energy of a reaction is larger on the reaction giving the larger reaction heat.[17] In the present examples it seems that this relation holds also in the case of the surface hydration reaction.

Figure 5a illustrates the infrared absorption spectra of the sample FA. After the sample has been degassed at 10^{-5} Torr for 4 hr at room temperature, the spectrum shows a broad absorption band in the range of 3700—2000 cm^{-1} and a shoulder near 3630 cm^{-1}. The former can be assigned to the stretching vibration of hydrogen-bonded hydroxyl groups, and the latter, to the stretching vibration of the isolated surface hydroxyl groups.[18] Another absorption band, near 1620 cm^{-1}, is considered to be due to the bending of hydroxyl groups, indicating the existence of physisorbed water.[12,18] After treatment at 110°C *in vacuo* the intensity of the spectrum generally decreases and the stretching vibration band of hydroxyl groups comes to separate into two parts, indicating a relative increase in the number of free hydroxyl groups. Even after treatment at 200°C there remains a slight bending vibration of hydroxyl groups, but it is extinguished completely after treatment at 300°C. This may be caused by the difficulty of the desorption of the capillary condensed water molecules. The reason why the heat of surface hydration of the sample FA is the least among these three samples may be partially that the desorption of the physisorbed water is most difficult from the sample FA because of the intensive capillary condensation; this results in an apparent increase in the water content at relatively low temperatures and in an apparent decrease in the heat of surface hydration calculated therefrom.

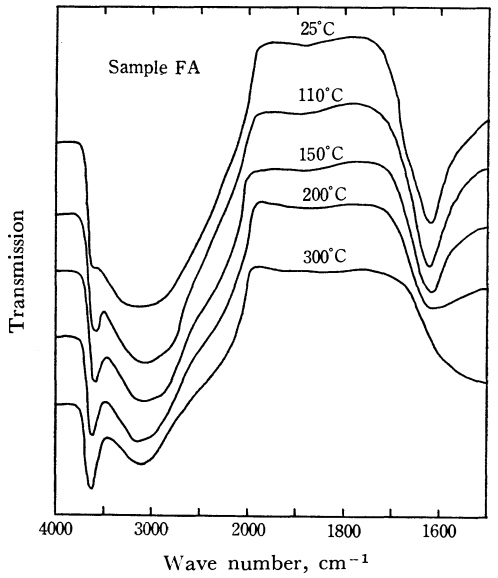

Fig. 5a. Infrared absorption spectra of sample FA under various conditions of treatment.

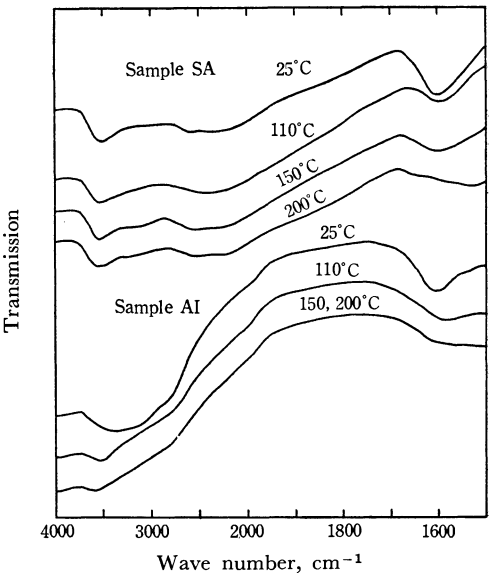

Fig. 5b. Infrared absorption spectra of samples SA and AI under various conditions of treatment.

Figure 5b shows that the water molecules physisorbed on the sample AI can be desorbed by heat treatment up to 150°C in a vacuum of 10^{-5} Torr, while those on the sample SA can be desorbed by heat treatment at a temperature higher than 200°C. Also, the large water content of the sample SA probably comes from the difficult desorbability of the physisorbed water, which may result in the small heat of surface hydration, as in the case of the sample FA.

17) S. Glasstone, K. J. Laidler and H. Eyring, "The Theory of Rate Processes," McGraw-Hill Book Co., New York, N. Y. (1941).

18) K. E. Lewis and G. D. Parfitt, *Trans. Faraday Soc.*, **62**, 204 (1966).

BULLETIN OF THE CHEMICAL SOCIETY OF JAPAN VOL. 42 2203—2208 (1969)

Theory of Photoselection for Zeeman Split Phosphorescence

Tohru AZUMI and Saburo NAGAKURA

The Institute for Solid State Physics, The University of Tokyo, Roppongi, Minato-ku, Tokyo

(Received January 23, 1969)

General equations applicable to photoselection experiments for Zeeman split phosphorescence are derived. The general equations are also extended to the cases where excitation and observation are effected with unpolarized light, and expressions for the ratio of phosphorescence intensities of the three split subcomponents are obtained. Some comments on experimentation are made.

As reported previously,[1,2] we have succeeded in observing the Zeeman splitting of the phosphorescence of pyrazine. By measuring the phosphorescence intensities of the three Zeeman split components, one is able to obtain matrix elements connecting the ground state and all of the three triplet subcomponents. An example of such treatment has been given in a previous paper for the pyrazine phosphorescence.[2] For more detailed analyses, an experiment under polarized light is necessary. Such polarization measurements, conjoined with the Zeeman effect, will provide us with invaluable information on the nature of spin subcomponents, the manner in which the triplet state acquires the singlet character, effect of coupled vibrations, and so on.

The methods for polarization measurements are divided into two major classes. In one method one uses an oriented sample such as single crystal. In the other, called the method of photoselection, samples of random orientation are used. The former method is usually considered superior in a sense that it provides the polarization nature uniquely. However, the use of single crystals, the very necessary condition for this method, limits the actual application for the following reasons: First, the crystal structure, especially the arrangement of molecules in a unit cell, is not known for a majority of organic molecular crystals. Second, it is extremely difficult to retain a relatively large single crystal uncracked at liquid helium temperature. Finally, most important and crucial of all, many organic molecules do not exhibit phosphorescence in pure crystalline states. This is especially relevant for molecules whose lowest triplet state is of π, π^* nature.[3] Any molecular phosphorescence for molecules of this class should therefore be investigated in solutions or in mixed crystals. Because of the three difficulties associated with the single crystal experiments the method of photoselection acquires greater importance. The general equations which have been used for photoselection work are, however, not valid when external magnetic field is applied. It is consequently required that the theory of photoselection be extended to include the effect of magnetic field. In this paper, general equations applicable to photoselection experiments for the Zeemen split phosphorescence are derived. The general equations and the manner of their derivation are of importance not only for the polarization work but also for ordinary Zeeman effect experiments with unpolarized light because the latter should be treated as a special case of the former.

Theoretical

1) Effect of Magnetic Field on the Phosphorescence Intensities. The effect of magnetic field on the triplet state of organic molecules was treated in a previous paper;[2] consequently, only the essence is outlined here.

Let the lowest triplet state be produced by an excitation of an electron from a molecular orbital ϕ_a to a molecular orbital ϕ_b. We choose the following zeroth order triplet eigenfunctions.

$$\left.\begin{aligned} |T_x> &= 2^{-1/2}(|\bar{\phi}_a\bar{\phi}_b| - |\phi_a\phi_b|) \\ |T_y> &= 2^{-1/2}(|\bar{\phi}_a\bar{\phi}_b| + |\phi_a\phi_b|) \\ |T_z> &= 2^{-1/2}(|\phi_a\bar{\phi}_b| + |\bar{\phi}_a\phi_b|) \end{aligned}\right\} \quad (1)$$

The Hamiltonian for Zeeman effect is represented by

$$\mathscr{H} = g\beta H(lS_x + mS_y + nS_z) \quad (2)$$

where l, m, and n are direction cosines of molecular axes, x, y and z, respectively, with the field direction. Further, the zero field splitting parameters D and E are neglected. This assumption

1) T. Azumi, Y. Udagawa, M. Ito and S. Nagakura, *J. Chem. Phys.*, **47**, 4850 (1967).

2) T. Azumi, M. Ito and S. Nagakura, This Bulletin, **42**, 685 (1969).

3) H. Sternlicht, G. C. Nieman and G. W. Robinson, *J. Chem. Phys.*, **38**, 1326 (1963).

may roughly be justified for many organic molecules when magnetic field is larger than, say, 15 kG. (See a previous paper[2]) When magnetic field is applied, triplet wave functions $|T_1>$, $|T_0>$ and $|T_{-1}>$ are now represented in terms of (1) as

$$\begin{pmatrix} |T_1> \\ |T_0> \\ |T_{-1}> \end{pmatrix} = \begin{pmatrix} \sqrt{\frac{1-l^2}{2}} & \frac{n+ilm}{\sqrt{2(1-l^2)}} & \frac{-(nl+im)}{\sqrt{2(1-l^2)}} \\ l & im & n \\ \sqrt{\frac{1-l^2}{2}} & \frac{n-ilm}{\sqrt{2(1-l^2)}} & \frac{-(nl-im)}{\sqrt{2(1-l^2)}} \end{pmatrix} \begin{pmatrix} |T_x> \\ |T_y> \\ |T_z> \end{pmatrix} \tag{3}$$

The spin-orbit interaction which allows spin-forbidden triplet-singlet transitions is approximated as

$$\mathscr{H}_{so} = \sum_i \xi_i l_i S_i \tag{4}$$

where two electron operators are neglected. Then, the singlet state which may mix with the triplet state is only of the type

$$|S> = 2^{-1/2}(|\phi_a\bar{\phi}_c| + |\phi_c\bar{\phi}_a|) \tag{5}$$

The matrix elements for the spin-orbit interaction betwen the singlet and the triplet states are now obtained as follows:

$$\begin{pmatrix} <S|\mathscr{H}_{so}|T_1> \\ <S|\mathscr{H}_{so}|T_0> \\ <S|\mathscr{H}_{so}|T_{-1}> \end{pmatrix} = \frac{\hbar}{2}\xi \begin{pmatrix} -\sqrt{\frac{1-l^2}{2}} & i\frac{n+ilm}{\sqrt{2(1-l^2)}} & \frac{nl+im}{\sqrt{2(1-l^2)}} \\ -l & -m & -n \\ -\sqrt{\frac{1-l^2}{2}} & i\frac{n-ilm}{\sqrt{2(1-l^2)}} & \frac{nl-im}{\sqrt{2(1-l^2)}} \end{pmatrix} \begin{pmatrix} <\phi_c|l_x|\phi_b> \\ <\phi_c|l_y|\phi_b> \\ <\phi_c|l_z|\phi_b> \end{pmatrix} \tag{6}$$

Let the phosphorescence intensities from the three subcomponents, $|T_1>$, $|T_0>$ and $|T_{-1}>$ be denoted by I_1 I_0, and I_{-1}. Then from (6)

$$\begin{pmatrix} I_1/g_1 \\ I_0/g_0 \\ I_{-1}/g_{-1} \end{pmatrix} = c \begin{pmatrix} \frac{1-l^2}{2} & \frac{1-m^2}{2} & \frac{1-n^2}{2} \\ l^2 & m^2 & n^2 \\ \frac{1-l^2}{2} & \frac{1-m^2}{2} & \frac{1-n^2}{2} \end{pmatrix} \begin{pmatrix} u_x \\ u_y \\ u_z \end{pmatrix} \tag{7}$$

where c is a proportionality constant, g's represent the Boltzmann populations of the respective components, and further, u_x, u_y and u_z represent the contribution to intensity from l_x, l_y and l_z in spin-orbit coupling (4).

2) Theory of Photoselection: Incorporation of the Effect of Magnetic Field. Theory of photoselection was presented in an elegant manner by Albrecht.[4] We shall closely follow his presentation, and here merely incorporate the effect of magnetic field.

We choose the two coordinate sets, the molecule-fixed set (x, y, z) and the laboratory-fixed set (a, b, c). Assigning these a common origin we then specify the orientation of a molecule in laboratory using Eulerian angles, θ, ϕ and ψ. The cosines of the angles between the axes of the two coordinates are

	x	y	z
a	$\cos\theta$	$\sin\theta\sin\psi$	$\sin\theta\cos\psi$
b	$\sin\theta\sin\phi$	$\cos\phi\cos\psi-\cos\theta\sin\phi\sin\psi$	$-\cos\phi\sin\psi-\cos\theta\sin\phi\cos\psi$
c	$-\sin\theta\cos\phi$	$\sin\phi\cos\psi+\cos\theta\cos\phi\sin\psi$	$-\sin\phi\sin\psi+\cos\theta\cos\phi\cos\psi$

These nine direction cosines are abbreviated as, for example, t_{ax}.

The experimental arrangement is shown schematically in Fig. 1. Namely, excitation is effected with the light incident along b axis onto ac face, polarized along a axis by an amount p and along c axis 1-p. The magnetic field is applied along c axis. The emitted phosphorescence may be viewed along a axis or along c axis. In the latter case, the Faraday rotarion may affect the polarization values. Hence, we had better avoid observation from c axis when magnetic field is large enough to cause the Faraday rotation.

We assume that at a given wavelength absorption takes place in x, y and z axes of the molecule

4) A. C. Albrecht, *J. Mol. Spectroscopy*, **6**, 84 (1961).

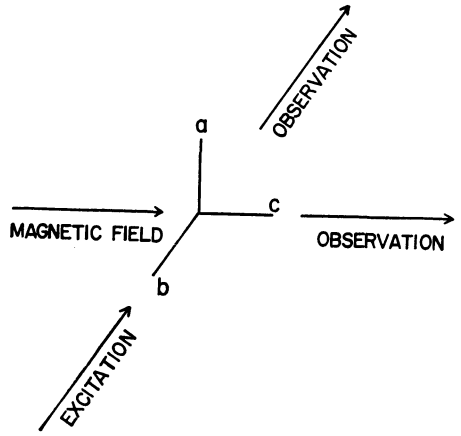

Fig. 1. Experimental arrangement.

with the fraction of r_x, r_y and r_z, respectively. Similarly, we assume that at a given wavelength the phosphorescence is polarized along x, y, and z axes with the fraction of q_x, q_y and q_z, respectively.

Now, the probability that a molecule at θ, ϕ and ψ is photoexcited is given by

$$p[r_x t_{ax}^2 + r_y t_{ay}^2 + r_z t_{az}^2] + (1-p)[r_x t_{cx}^2 + r_y t_{cy}^2 + r_z t_{cz}^2]$$

and the probability for viewing with light polarized, say, along a is

$$q_x t_{ax}^2 + q_y t_{ay}^2 + q_z t_{az}^2$$

with analogous expressions for viewing along b and c axes. Unsplit phosphorescence intensities are proportional to the product of these two expressions. In the presence of magnetic field, these quantities are split up according to (7). Namely, for I_1 and I_{-1} the above product is further multiplied by

$$g_{\pm 1}\left[\frac{1-l^2}{2}u_x + \frac{1-m^2}{2}u_y + \frac{1-n^2}{2}u_z\right]$$

and for I_0

$$g_0[l^2 u_x + m^2 u_y + n^2 u_z]$$

where $l=t_{cx}$, $m=t_{cy}$ and $n=t_{cz}$. In the sample of random orientation we integrate the product of the three expressions over Eulerian angles:

$$\int_0^{2\pi} \mathrm{d}\psi \int_0^{2\pi} \mathrm{d}\phi \int_0^{\pi} \sin\theta \, \mathrm{d}\theta$$

3) Results. Integration of the expressions described above yields the following results. Here, A, B, and C denote the phosphorescence intensities polarized along a, b and c axes, respectively. The subscript $+1$, 0 and -1 indicate the phosphorescence subcomponents.

$$
\begin{aligned}
A_0 &= g_0 r\left[u_x\left\{p\begin{bmatrix}6&4&4\\4&18&6\\4&6&18\end{bmatrix}+(1-p)\begin{bmatrix}4&20&18\\6&2&6\\4&6&4\end{bmatrix}\right\}+u_y\left\{p\begin{bmatrix}18&4&6\\4&6&4\\6&4&18\end{bmatrix}\right.\right.\\
&\quad\left.+(1-p)\begin{bmatrix}6&2&6\\16&8&18\\6&4&4\end{bmatrix}\right\}+u_z\left\{p\begin{bmatrix}18&6&4\\6&18&4\\4&4&6\end{bmatrix}+(1-p)\begin{bmatrix}4&6&4\\6&4&4\\18&18&6\end{bmatrix}\right\}\left.\right]q\\
B_0 &= g_0 r\left[u_x\left\{p\begin{bmatrix}4&4&6\\4&8&16\\6&16&6\end{bmatrix}+(1-p)\begin{bmatrix}4&20&18\\6&2&6\\4&6&4\end{bmatrix}\right\}+u_y\left\{p\begin{bmatrix}4&8&16\\8&0&6\\16&6&6\end{bmatrix}\right.\right.\\
&\quad\left.+(1-p)\begin{bmatrix}6&2&6\\16&8&18\\6&4&4\end{bmatrix}\right\}+u_z\left\{p\begin{bmatrix}6&16&6\\16&6&6\\6&6&2\end{bmatrix}+(1-p)\begin{bmatrix}4&6&4\\6&4&4\\18&18&6\end{bmatrix}\right\}\left.\right]q\\
C_0 &= g_0 r\left[u_x\left\{p\begin{bmatrix}4&6&4\\20&2&6\\18&6&4\end{bmatrix}+(1-p)\begin{bmatrix}34&2&6\\2&10&2\\6&2&6\end{bmatrix}\right\}+u_y\left\{p\begin{bmatrix}6&16&6\\2&8&4\\6&18&4\end{bmatrix}\right.\right.\\
&\quad\left.+(1-p)\begin{bmatrix}2&10&2\\10&26&6\\2&6&6\end{bmatrix}\right\}+u_z\left\{p\begin{bmatrix}4&6&18\\6&4&18\\4&4&6\end{bmatrix}+(1-p)\begin{bmatrix}6&2&6\\2&6&6\\6&6&30\end{bmatrix}\right\}\left.\right]q\\
A_{\pm 1} &= g_{\pm 1} r\left[u_x\left\{p\begin{bmatrix}18&5&5\\5&12&4\\5&4&12\end{bmatrix}+(1-p)\begin{bmatrix}5&4&5\\11&6&11\\12&11&5\end{bmatrix}\right\}+u_y\left\{p\begin{bmatrix}12&5&4\\5&18&5\\4&5&12\end{bmatrix}\right.\right.\\
&\quad\left.+(1-p)\begin{bmatrix}4&13&11\\6&3&5\\11&12&5\end{bmatrix}\right\}+u_z\left\{p\begin{bmatrix}12&4&5\\4&12&5\\5&5&18\end{bmatrix}+(1-p)\begin{bmatrix}5&11&12\\11&5&12\\5&5&4\end{bmatrix}\right\}\left.\right]q\\
B_{\pm 1} &= g_{\pm 1} r\left[u_x\left\{p\begin{bmatrix}5&12&11\\12&3&6\\11&6&4\end{bmatrix}+(1-p)\begin{bmatrix}5&4&5\\11&6&11\\12&11&5\end{bmatrix}\right\}+u_y\left\{p\begin{bmatrix}5&10&6\\10&7&11\\6&11&4\end{bmatrix}\right.\right.\\
&\quad\left.+(1-p)\begin{bmatrix}4&13&11\\6&3&5\\11&12&5\end{bmatrix}\right\}+u_z\left\{p\begin{bmatrix}4&6&11\\6&4&11\\11&11&6\end{bmatrix}+(1-p)\begin{bmatrix}5&11&12\\11&5&12\\5&5&4\end{bmatrix}\right\}\left.\right]q\\
C_{\pm 1} &= g_{\pm 1} r\left[u_x\left\{p\begin{bmatrix}5&11&12\\4&6&11\\5&11&5\end{bmatrix}+(1-p)\begin{bmatrix}4&6&4\\6&16&6\\4&6&18\end{bmatrix}\right\}+u_y\left\{p\begin{bmatrix}4&6&11\\13&3&12\\11&5&5\end{bmatrix}\right.\right.\\
&\quad\left.+(1-p)\begin{bmatrix}20&2&6\\2&8&4\\6&4&18\end{bmatrix}\right\}+u_z\left\{p\begin{bmatrix}5&11&5\\11&5&5\\12&12&4\end{bmatrix}+(1-p)\begin{bmatrix}18&6&4\\6&18&4\\4&4&6\end{bmatrix}\right\}\left.\right]q
\end{aligned}
\qquad (8)
$$

where

$$\boldsymbol{r} = [r_x \; r_y \; r_z]$$

and

$$\boldsymbol{q} = \begin{bmatrix} q_x \\ q_y \\ q_z \end{bmatrix}$$

Hence of cource

$$\boldsymbol{r}\begin{bmatrix} c_{11} & c_{12} & c_{13} \\ c_{21} & c_{22} & c_{23} \\ c_{31} & c_{32} & c_{33} \end{bmatrix}\boldsymbol{q} = \begin{matrix} c_{11}r_xq_x + c_{12}r_xq_y + c_{13}r_xq_z \\ +c_{21}r_yq_x + c_{22}r_yq_y + c_{23}r_yq_z \\ +c_{31}r_zq_x + c_{32}r_zq_y + c_{33}r_zq_z \end{matrix}$$

Extension to Unpolarized Work

The general equations derived above may readily be extended to the cases where both excitation and observation are made with unpolarized light. The results for two different observations are as follows.

(1) Straight view (observation along b axis)

$$\left.\begin{aligned} I_0 &= g_0\boldsymbol{r}\left\{u_x\begin{bmatrix}24 & 16 & 16\\ 16 & 16 & 10\\ 16 & 10 & 16\end{bmatrix} + u_y\begin{bmatrix}16 & 16 & 10\\ 16 & 24 & 16\\ 10 & 16 & 16\end{bmatrix} + u_z\begin{bmatrix}16 & 10 & 16\\ 10 & 16 & 16\\ 16 & 16 & 24\end{bmatrix}\right\}\boldsymbol{q} \\ I_{\pm1} &= g_{\pm1}\boldsymbol{r}\left\{u_x\begin{bmatrix}16 & 13 & 13\\ 13 & 20 & 16\\ 13 & 16 & 20\end{bmatrix} + u_y\begin{bmatrix}20 & 13 & 16\\ 13 & 16 & 13\\ 16 & 13 & 20\end{bmatrix} + u_z\begin{bmatrix}20 & 16 & 13\\ 16 & 20 & 13\\ 13 & 13 & 16\end{bmatrix}\right\}\boldsymbol{q} \end{aligned}\right\} \quad (9)$$

(2) Side view (observation along c axis)

$$\left.\begin{aligned} I_0 &= g_0\boldsymbol{r}\left\{u_x\begin{bmatrix}9 & 24 & 23\\ 10 & 15 & 17\\ 9 & 17 & 16\end{bmatrix} + u_y\begin{bmatrix}17 & 8 & 17\\ 22 & 11 & 23\\ 17 & 9 & 16\end{bmatrix} + u_z\begin{bmatrix}16 & 17 & 9\\ 17 & 16 & 9\\ 23 & 23 & 10\end{bmatrix}\right\}\boldsymbol{q} \\ I_{\pm1} &= g_{\pm1}\boldsymbol{r}\left\{u_x\begin{bmatrix}16.5 & 12.5 & 13\\ 19.5 & 13.5 & 16\\ 20 & 16 & 13\end{bmatrix} + u_y\begin{bmatrix}12.5 & 20.5 & 16\\ 13.5 & 15.5 & 13\\ 16 & 20 & 13\end{bmatrix} + u_z\begin{bmatrix}13 & 16 & 20\\ 16 & 13 & 20\\ 13 & 13 & 16\end{bmatrix}\right\}\boldsymbol{q} \end{aligned}\right\} \quad (10)$$

The above equations determine the ratio of the three split phosphorescence subcomponents when neither polarizer nor analyser is used. It is to be noted that the ratio is not simply a ratio of the Boltzmann populations.

An Example: Predictions for Pyrazine Phosphorescence

Because of the complexity of the general equations it may not be very clear as to how the polarization is affected by magnetic field. From this viewpoint, we shall take pyrazine phosphorescence as an example and illustrate how the phosphorescence intensities are divided among the three subcomponents and how the polarization values are affected by magnetic field.

Group theoretical consideration[2] predicts $u_y=1$ and $q_z=1$ for 0, 0 band of the pyrazine phosphorescence. (For details see a previous paper.[2]) Polarization observed by Krishna and Goodman[5] is in agreement with this prediction. The molecular axes are defined as recommended by Mulliken.[6] Namely, z axis lies in the molecular plane on the N-N axis and x axis is normal to the molecular plane. We consider two different wavelength regions of excitation, one for $^1B_{2u}$ (π, π^*) state (at 37839 cm^{-1}) and the other for $^1B_{3u}$ (n, π^*) state (at 30776 cm^{-1}). Further, we consider the case in which the exciting light is polarized either along a axis (vartical excitation) or along c axis (horizontal excitation).

In Fig. 2 are shown predicted phosphorescence intensities polarized either along a, b, or c axis under the four different modes of excitation. The length of the vertical lines and the numbers specified indicate the phosphorescence intensities divided by the population of the upper level. It is immediately seen how zero field intensities are split up into three subcomponents under the presence of magnetic field. Shown also in Fig. 2 are the values of polarization for straight view and for

Table 1. Predicted intensity ratio of the thrle phosphorescence subcomponents for pyrazine

	$I_1 : I_0 : I_{-1}$	
Excitation	Straight view	Side view
$^1B_{3u}(n, \pi^*)$	$16g_1 : 10g_0 : 16g_{-1}$	$16g_1 : 17g_0 : 16g_{-1}$
$^1B_{2u}(\pi, \pi^*)$	$13g_1 : 16g_0 : 13g_{-1}$	$13g_1 : 23g_0 : 13g_{-1}$
$^1B_{1u}(\pi, \pi^*)$	$20g_1 : 16g_0 : 20g_{-1}$	$13g_1 : 16g_0 : 13g_{-1}$

5) V. G. Krishna and L. Goodman, *J. Chem. Phys.*, **36**, 2217 (1961).

6) R. S. Mulliken, *ibid.*, **23**, 1997 (1955).

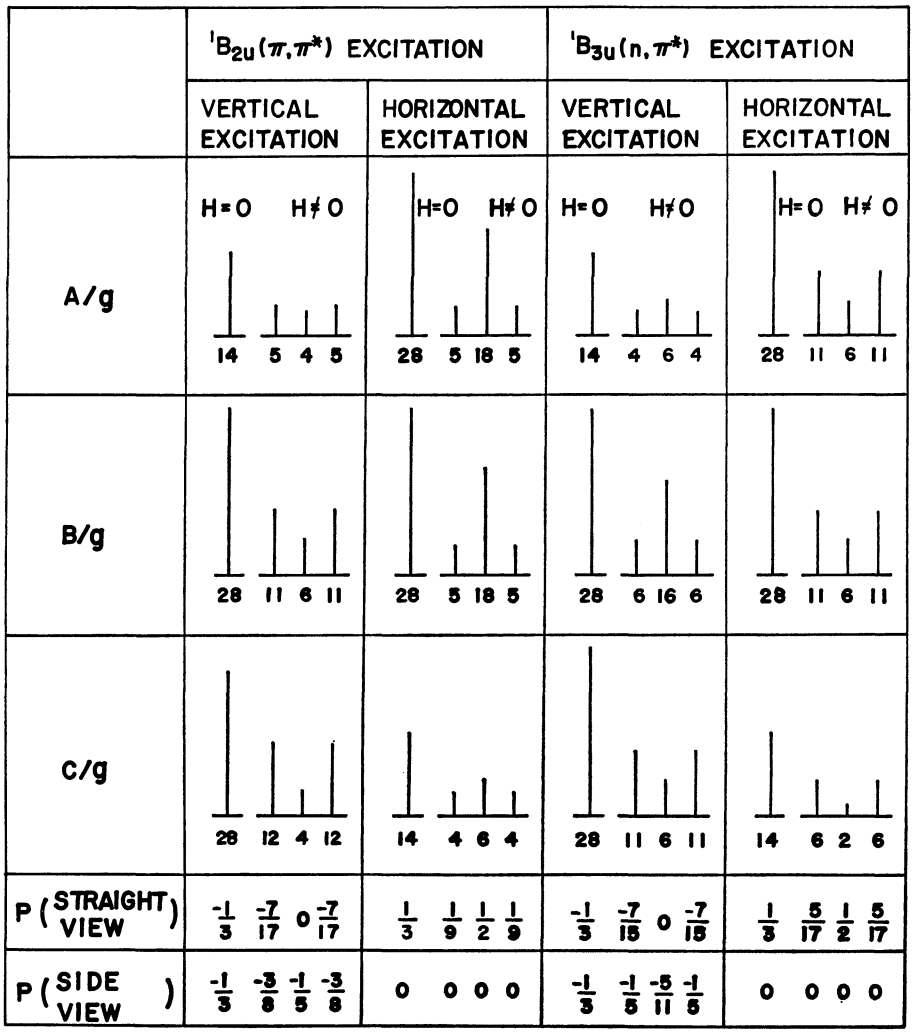

Fig. 2. Predicted phosphorescence intensities and polarizations for pyrazine phosphorescence under different modes of excitation (see the text).

side view. It is amazing to see how fertile informations are obtained by applying magnetic field. It is exactly for this reason that the polarization measurements under magnetic field are recommended. The predicted ratio of the phosphorescence intensities for unpolarized work is summarized in Table 1. A part of this result has been already presented in a previous paper.

Some Comments on Experimentation

The present paper aims only at presenting general equations which may be of use in ideal photoselection experiments. Whether or not ideal conditions for photoselection experiments are satisfied in reality and how to solve any difficulties that might occur is another question. We have not made any considerable effort in this regard so far; however, in the following, we point out our views on experimentation.

One of the difficulties inherent to polarization experiments is due to improper polarization caused by the apparatus. This difficulty is readily overcome in a similar manner to Azumi and McGlynn,[7] and Russel and Albrecht[8] calibrated their apparatus for improper polarization effect in ordinary (*i. e.*, without magnetic field) photoselection experiments. The correction involves a repetition of the experiment keeping everything unchanged except for the excitation which is effected horizontally and emission is observed from the side. Theoretically, the emission should in this case be unpolarized. This is easily seen

7) T. Azumi and S. P. McGlynn, *J. Chem. Phys.*, **37**, 2413 (1962).

8) P. G. Russell and A. C. Albrecht, *ibid.*, **41**, 2536 (1964).

from the fact that in the general equations (8) equating p to zero necessarily yields $A=B$ for all three phosphorescence subcomponents. Any observed polarization should, consequently, be regarded as due to instrumentation, and is served for the correction factor. Further, by observing this correction factor by varying the strength of magnetic field, one may be able to see, though indirectly, the effect of Faraday rotation.

Another difficulty in photoselection experiment is that one has to work with samples of random orientation. Further, the sample should be strain-free. In this connection, it is noted that in the Zeeman effect experiment, one has to lower the temperature to liquid helium temperature to narrow the bandwidth, since the Zeeman splitting at 50 kG may only amount to 5—6 cm^{-1}. Rigid glass solvents which may be used at liquid helium temperature are shown in Table 2. These media have been reported to form transparent glass at 4.2°K, but it is uncertain whether or not they are strain-free. Furthermore, it is doubtful if bandwidth becomes sufficiently narrow in these media. In fact, according to Armstrong,[9] in the isopentane-3-methylpentane mixed solvent no significant band narrowing has been attained by lowering temperature down to 4.2°K. In this regard, one may also try some rare gas matrices such as neon and xenon[10] and also so called "Shpolskii's solvents" such as cyclohexane and carbon tetrachloride[11] even though they are best considered polycrystalline.

Table 2. Rigid glass solvents at 4.2°K

Solvent	Reference
Isopentane + 3-Methylpentane (6 : 1 in volume)	9
Silicone (Dow-Corning 200 with 10^6 cs viscosity)	9
Trifluorobromomethane	12

Test of various solvents for use of photoselection experiments at liquid helium temperature is being attempted and will be reported in future publications.

We wish to express our appreciation to Professor Mitsuo Ito for constant encouragement and invaluable discussions.

9) A. T. Armstrong, private communications to T. A. (1968).
10) G. W. Robinson, *J. Mol. Spectroscopy*, **6**, 58 (1961).
11) E. V. Shpol'skii, *Soviet Phys. Usp.*, **5**, 522 (1963).
12) F. E. Dörr, *Angew. Chem.*, **78**, 457 (1966).

BULLETIN OF THE CHEMICAL SOCIETY OF JAPAN VOL. 42 2208—2211 (1969)

ESR Studies on the Reaction of an OH Radical in α,β-Unsaturated Aldehyde*[1]

Takahisa ICHIKAWA*[2] and Keiji KUWATA

Department of Chemistry, Faculty of Science, Osaka University, Toyonaka, Osaka

(Received January 27, 1968)

ESR studies on the UV irradiated α,β-unsaturated aldehyde - hydrogen peroxide mixtures have been done at low temperature in order to examine the reactions of an OH radical with aldehyde: formyl hydrogen-abstraction, methyl hydrogen-abstraction, and addition to an olefinic bond. It has been shown that abstraction of a methyl hydrogen by an OH radical occurs in crotonaldehyde, whereas β-addition of an OH radical to an olefinic bond takes place in methacrolein and acrolein. A formyl hydrogen is unreactive with an OH radical in any case. The distribution of unpaired electron in the radicals was also discussed.

Several ESR studies were carried out in this laboratory concerning the reaction of an OH radical at low temperature with an organic compound having hydroxyl groups.[1] It was found that the OH radical abstracts mainly an α-hydrogen. In some cases the possibility of hydrogen-abstraction from

*1 This work was presented at the 19th Annual Meeting of the Chemical Society of Japan in 1966, Tokyo.

*2 Present address: The Government Industrial Research Institute of Nagoya, Hirate-machi, Kita-ku, Nagoya.

1) K. Kuwata, T. Ichikawa and K. Hirota, *Nippon Kagaku Zasshi (J. Chem. Soc. Japan, Pure Chem. Sect.)*, **83**, 652 (1962); K. Kuwata, K. Nishikida, H. Kawazura and K. Hirota, This Bulletin, **36**, 925 (1963); T. Ichikawa, *Nippon Kagaku Zasshi (J. Chem. Soc. Japan, Pure Chem. Sect.)*, **85**, 736 (1964); T. Ichikawa and K. Kuwata, *Kogyo Kagaku Zasshi (J. Chem. Soc. Japan, Ind. Chem. Sect.)*, **68**, 1516 (1965); K. Nishikida and K. Kuwata, *J. Phys. Chem.*, in press.

a hydroxyl group was discussed. In derivatives of glycol, successive reactions, RCHOH–RCHOH $\xrightarrow{\dot{O}H}$ RCHOH–$\dot{R}$COH $\xrightarrow{h\nu}$ $\dot{R}$COH–RCO, were considered on the basis of ESR spectral changes and analysis of evolved gas. In connection with these results, it is interesting to examine the reaction of an OH radical in α,β-unsaturated aldehyde systems, because the aldehyde has a formyl hydrogen, methyl hydrogens, and an olefinic bond, which is expected to bring about a competition among formyl hydrogen-abstraction, methyl hydrogen-abstraction, and addition to an olefinic bond.

Experimental

Materials. Hydrogen peroxide (30 wt%) was concentrated under reduced pressure to 95 wt%, and the antioxidant was removed by distillation before use. Reagent-grade crotonaldehyde, methacrolein, and acrolein were purified by fractional distillation under reduced pressure.

Procedure. The aldehyde containing 10 mol% hydrogen peroxide was introduced into a quartz sample tube and deaerated by freezing and thawing under vacuum. The sample in a clear glassy state was illuminated in a quartz Dewar vessel at 77°K with the light from a low pressure mercury lamp. After illumination for 3hr the sample was transferred quickly into a cavity which was immersed in liquid nitrogen. Warming of the sample was carried out inside the cavity in the range 77—300°K. Details of the cavity have already been shown.[2] Measurements were done at X-band with a homemade spectrometer using 450kc/sec field modulation.

Results and Discussion

Crotonaldehyde. Figure 1a shows the ESR spectrum of an illuminated glass of a crotonaldehyde-hydrogen peroxide mixture at 80°K. On warming the sample to 160°K the spectrum changed as shown in Fig. 1b. The intensity of the signal was not reduced lower than 50% of the initial state. The spectrum consists of equally spaced four lines with the separation of 12.9 G, the intensity ratios of the lines being 1.2 : 2.8 : 2.8 : 1.0. Since the ratios are closer to 1 : 3 : 3 : 1, the radical should have equally interacting three protons.

The four line spectrum can be interpreted by the radical formed by abstraction of a methyl hydrogen; $\dot{C}H_2$–CH=CH–CHO↔CH_2=CH–$\dot{C}$H–CHO↔CH_2=CH–CH=CH–$\dot{O}$. The identification is based upon the following arguments. The molecular orbital calculation of pi-electron spin densities using McLachlan procedure[3] gave the values as follows;

	C_1	C_2	C_3	C_4	O_5
ρ=	0.6456	−0.1704	0.5051	−0.0324	0.0521
a(G)=	14.6	3.9	11.4	0.7	

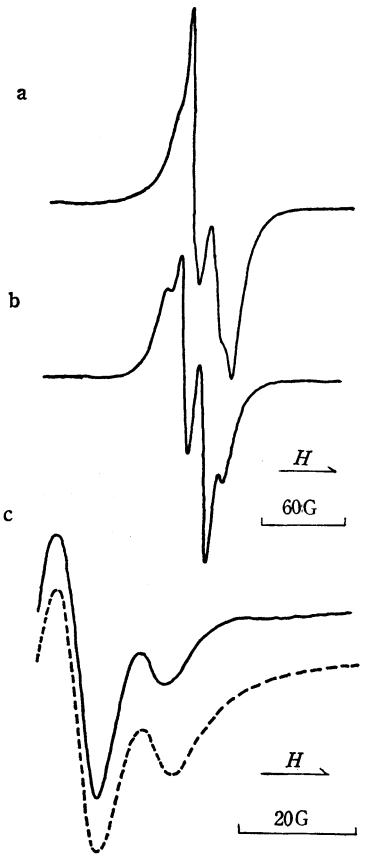

Fig. 1. ESR spectra of an illuminated glass of crotonaldehyde containing 10 mol% hydrogen peroxide.
a) Spectrum measured at 80°K
b) Spectrum measured at 160°K
c) Computed curve (dotted lines)

Hfs constants were estimated by taking into account McConnell's relation[4]

$$a = Q \cdot \rho \qquad (1)$$

where Q is a constant (23 G) and ρ is the spin density on the carbon. The results indicate that the C_2 and C_4 protons do not contribute strongly to the hfs and the difference between C_1 and C_3 proton hfs constants is not larger than the observed line width (5 G). Thus it seems probable that the postulated radical gives the four line spectrum due to the predominant interaction with two C_1

2) K. Kuwata and K. Hirota, This Bulletin, **34**, 458 (1961).

3) A. D. McLachlan, *Mol. phys.*, **3**, 233 (1960). The parameter λ in the procedure was given $\lambda=1.2\beta$. The coulomb integrals and the resonance integrals were assumed to be $\alpha_O=\alpha_C+1.5\beta$, $\alpha_C=\alpha_{C'}-0.15\beta$, $\beta_{CO}=1.6\beta$, and $\beta_{CC'}=\beta$, which were used in the calculation on the anion radicals of aromatic carbonyl compounds (P. H. Rieger and G. K. Fraenkel, *J. Chem. Phys.*, **37**, 2811 (1962)).

4) H. M. McConnell and D. B. Chesnut, *J. Chem. Phys.*, **28**, 107 (1958).

and one C_3 protons. The computed curve with Lorentzian line shapes in consideration of these results is shown in Fig. 1c.

It is apparent that another possible radical such as CH_3-CH=CH-$\dot{C}$=O (hydrogen-abstraction from a formyl group) and CH_3-CHOH-$\dot{C}$H-CHO (OH-addition to an olefinic bond) can not give the four line spectrum. The reason for this is that the former is a sigma radical in which an unpaired electron is localized on a sigma orbital of a carbon atom[5] and has only one interacting proton, and the latter has unequally interacting three protons, *i. e.*, α-, β-, and formyl protons.

Although the spectrum before warming of the sample exhibits asymmetric line shapes, it apparently already contains the characteristic features of the four lines in the spectrum, which suggests that the initial spectrum consists of the four lines and some additional lines. The spectral change, therefore, is likely due to the disappearance of more unstable radicals.

An ESR spectrum of illuminated crotonaldehyde without hydrogen peroxide was also examined, the results showing a relatively small radical yield, *i. e.*, one twentieth in the case containing hydrogen peroxide.

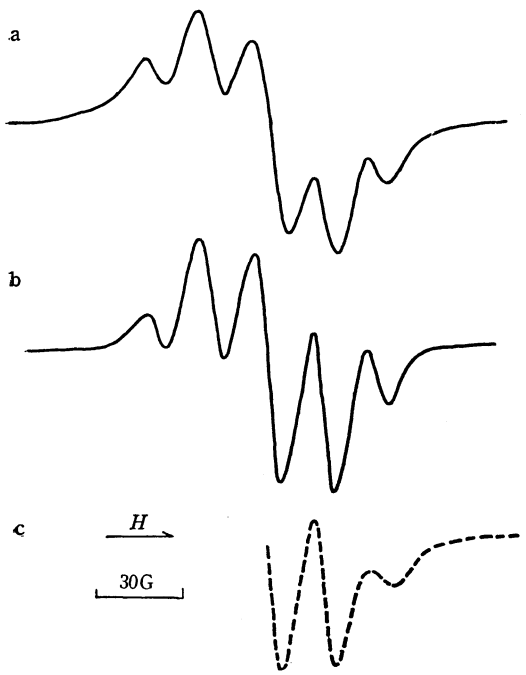

Fig. 2. ESR spectra of an illuminated glass of methacrolein containing 10 mol% hydrogen peroxide.
a) Spectrum measured at 80°K
b) Spectrum measured at 180°K
c) Computed curve

Methacrolein. An illuminated glass of methacrolein-hydrogen peroxide mixture gave the spectrum as shown in Fig. 2a. On warming the sample to 180°K, the spectrum became well resolved five lines with separations of 19.5 G whose intensity ratios were 1.1 : 3.7 : 5.5 : 3.4 : 1.0. The radical should have equally interacting four protons because the theoretical intensity ratios are 1 : 4 : 6 : 4 : 1.

If a methyl hydrogen is abstracted by an OH radical, the radical CH_2=C(CHO)-$\dot{C}H_2$↔$\dot{C}H_2$-C(CHO)=CH_2 would be formed. This radical would be essentially the allyl type with equally interacting four protons. The hfs constants of 19.5 G, however, are considerably larger than the expected value, *i. e.*, 14.4 G observed in the allyl radical.[6] It seems difficult to attribute the five line spectrum to the supposed radical.

In β-addition to an olefinic bond, the radical CH_2OH-$\dot{C}$(CH_3)-CHO↔CH_2OH-C(CH_3)=CH-$\dot{O}$ is formed. The five line spectrum may be accounted for by this radical on the assumption of a conformation as follows: 1) The methyl group rotates so rapidly that as all the hfs constants of the methyl protons are substantially equivalent. 2) The methylene group is fixed on such positions that one of the methylene protons has a hfs constant around 19.5 G, while the other less than the observed line width (8 G). According to Heller and McConnell,[7] the hfs constant of each β-proton is given by

$$a_{\beta_i} = 2Q_\beta \cdot \rho_\alpha \cdot \cos^2\theta_i \qquad (2)$$

where Q_β is a constant, ρ_α a spin density on an α-carbon, and θ_i an angle between a H_i-C_β-C_α plane and an axis of a p_z orbital occupied by an unpaired electron. For a rapidly rotating methyl proton, a value of $\cos^2\theta_{av}$ is equal to 1/2. Hence the hfs constants of the methyl protons are given by $a_\beta(CH_3)=Q_\beta\cdot\rho_\alpha=19.5$ G. Substitution of the values given above for a_{β_1} and $Q_\beta\cdot\rho_\alpha$ into Eq. (2) leads to a value of 45° for θ_1. Provided that the difference between θ_1 and θ_2 is 120°, θ_2 is either 75° or 15°. Taking the former, we found a value $a_{\beta_2}=2.6$ G from Eq. (2).

It is added here that as the π-electronic system of this radical resembles that of the allyl radical,[6] the spin density on the formyl carbon is expected to be small and also the hfs constant of a hydrogen attached to the formyl carbon is expected to be less than the observed line width. The computed curve is also shown in Fig. 2c for comparison with the observed spectrum.

5) F. J. Adrian, E. L. Cochran and V. A. Bowers, *ibid.*, **36**, 1661 (1962); *ibid.*, **43**, 462 (1965).

6) J. E. Bennett and A. Thomas, *Proc. Roy. Soc.*, **208A**, 123 (1964).

7) C. Heller and H. M. McConnell, *J. Chem. Phys.*, **32**, 1535 (1960).

Fessenden and Schuler[8] evaluate a value $Q_\beta = 29.3$ G from their results of a number of aliphatic hydrocarbon radicals. Using the value, we found 0.667 for ρ_α. Fischer[9] showed experimentally that ρ_α in a substituted alkyl radical $X_1-\dot{C}(-X_2)-X_3$ can be calculated by use of a product rule

$$\rho_\alpha = \prod_{i=1}^{3}(1-\Delta(X_i)), \qquad (3)$$

where $\Delta(X_i)$ is a fraction which expresses the spin-density withdrawing-power of an X_i group. Substituting the values given by Fischer[9] ($\Delta(CH_3)=0.081$ and $\Delta(CH_2OH)=0.079$) and authors[10] ($\Delta(CHO)=0.198$) into Eq. (3), we obtain a value $\rho_\alpha=0.678$, which is very close to the experimentally derived value.

Acrolein. An illuminated glass of an acrolein-hydrogen peroxide mixture gave the spectrum as shown in Fig. 3a together with the spectrum observed after warming of the sample to 160°K (Fig. 3b). The spectrum at 160°K consists of unequally spaced four lines with the separations of 17.0, 13.0, and 17.0 G in turns and the intensity ratios of 1.0 : 1.4 : 1.5 : 1.2. The results suggest that the radical formed has two unequally interacting protons with the hfs constants of 17.0 and 30.0 G, respectively.

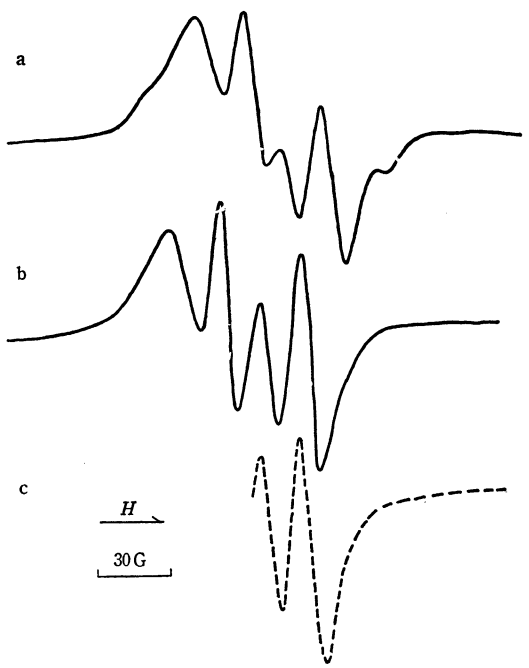

Fig. 3. ESR spectra of an illuminated glass of acrolein containing 10 mol% hydrogen peroxide.
a) Spectrum measured at 80°K
b) Spectrum measured at 160°K
c) Computed curve

The spectrum can be attributed to the radical produced by β-addition to an olefinic bond; $CH_2OH-\dot{C}H-CHO \leftrightarrow CH_2OH-CH=CH-\dot{O}$. The molecular orbital calculation[3] leads to predicted values for pi-electron spin densities on the radical as follows:

	C_1	C_2	O_3
ρ	0.758	0.048	0.194
a(G)	17.4	1.1	

On substituting a value $a_1=17.0$ G into Eq. (1), the spin density on C_1 is found to be 0.739, which shows good accordance with the calculated value.

The angle, θ_1 and θ_2 for the methylene proton can be calculated from Eq. (2) by using the values $a_{\beta_1}=30.0$ G, $Q_\beta=29.3$ G, and $\rho_\alpha=0.739$, which gives the values 34° and 86°, respectively. As a result, the angle $\theta_2=86°$ leads to a value $a_{\beta_2}=0.22$ G. The computed curve is shown in Fig. 3c.

Application of the values $\rho_\alpha=0.739$ and $\Delta(CH_2OH)=0.079$ to the Eq. (3) leads to a value $\Delta(CHO)=0.198$, which may be compared with the value $\Delta(CRO)=0.162$ given by Fischer.[8]

Summary and Conclusion

We have attempted to study by the ESR method the reaction of an OH radical in α,β-unsaturated aldehyde at low temperature. It has been found that abstraction of a methyl hydrogen by an OH radical occurs in crotonaldehyde, whereas β-addition of an OH radical to an olefinic bond takes place in methacrolein and acrolein. A formyl hydrogen seems to be unreactive with an OH radical in any case. Further work will be necessary to determine what factors are in favor of abstraction or addition especially in crotonaldehyde and methacrolein.

The values of pi-electron spin-densities obtained by the molecular orbital calculation using McLachlan procedure have shown good accordance with those estimated from experimental data on the radicals in crotonaldehyde and acrolein. Application of Fischer's treatment has been helpful for discussions on spin densities and hfs constants.

The authors wish to express their thanks to Professor Kozo Hirota for his encouragement throughout this study.

8) R. W. Fessenden and R. H. Schuler, *ibid.*, **39**, 2141 (1963).
9) H. Fischer, *Z. Naturforsch.*, **19a**, 866 (1964); *ibid.*, **20a**, 428 (1965).
10) See the next section of the text.

BULLETIN OF THE CHEMICAL SOCIETY OF JAPAN VOL. 42 2212—2219 (1969)

Anharmonic Potential Constants and Vibrational and Rotational Parameters for Hydrogen Cyanide

Toru NAKAGAWA and Yonezo MORINO

Department of Chemistry, Faculty of Science, The University of Tokyo, Hongo, Tokyo

(Received January 31, 1969)

The general fourth-order potential constants, f, for hydrogen cyanide were determined by a least-squares analysis applied to the observed values of the vibrational energies and the rotational constants for six isotopic species, $H^{12}C^{14}N$, $H^{13}C^{14}N$, $H^{12}C^{15}N$, $D^{12}C^{14}N$, $D^{13}C^{14}N$, and $D^{12}C^{15}N$. The normal frequencies, ω_i, the cubic and quartic potential constants, k_{ijk} and k_{ijkl}, the anharmonicity constants, x_{ij}, the vibration-rotation interaction constants, α_i, and the Coriolis coupling constants, ζ_{ij}^{x} were calculated for the six isotopic species.

The determination of the intramolecular potential function is one of the most important problems in molecular spectrosocpy. Once this has been done, various properties of molecules can be coordinated in a unified way upon this fundamental function. Suzuki, Pariseau, and Overend[1] determined the cubic and quartic potential constants for hydrogen cyanide by means of a least-squares fit to the observed values of the vibrational energies, ν, and the rotational constants, B_v, in various vibrational states. Though they used 87 observed values for two isotopic species, $H^{12}C^{14}N$ and $D^{12}C^{14}N$, the final values of the *nineteen* parameters still have intensive mutual correlations. Accordingly, a further refinement of the potential function is very desirable if one wants to predict various properties based on the potential function. Since the observed values of ν and B_v are available for four other isotopic species, *i. e.*, $H^{13}C^{14}N$, $H^{12}C^{15}N$, $D^{13}C^{14}N$, and $D^{12}C^{15}N$, they are also used in the least-squares analysis in the present study; the number of the observed values has increased to 124.

Another aim of the present study is to obtain the vibrational and rotational parameters, such as ω_i, k_{ijk}, k_{ijkl}, x_{ij}, and α_i and to predict the vibrational energies, ν, and the rotational constants, B_v, in various vibrational states of the six isotopic species. The uncertainties of these predicted values are also estimated on the basis of the probable errors of the potential constants, f, and their mutual correlation. It should be noticed that the estimated uncertainties of the calculated values will often become unreasonably large unless the correlations among the f constants are taken into account.

Determination of Anharmonic Potential Constants

The method described in our previous paper[2] on the anharmonic potential constants of OCS was applied to the present least-squares calculation as follows.

Observables. The observed values of the vibrational energies, ν, and the rotational constants, B_v-B_0, for the six isotopic species used in the least-squares fit are listed in Columns 2 and 6 of Table 1, together with their references.[3-10] The values for higher vibrational levels with $v_1+\frac{1}{2}v_2+v_3>4$ were not used in the analysis in order to avoid the influence of higher-order terms and accidental perturbations.

Parameters. The variable parameters to be determined were the nineteen potential constants, f, up to the fourth order in the expansion formula of:

$$V = \frac{1}{2}f_R\Delta R^2 + f_{Rr}\Delta R\Delta r + \frac{1}{2}f_r\Delta r^2 + \frac{1}{2}f_\alpha\Delta\alpha^2 + f_{RRR}\Delta R^3 + f_{RRr}\Delta R^2\Delta r + f_{Rrr}\Delta R\Delta r^2 + f_{rrr}\Delta r^3 + f_{R\alpha\alpha}\Delta R\Delta\alpha^2$$

1) I. Suzuki, M. A. Pariseau and J. Overend, *J. Chem. Phys.*, **44**, 3561 (1966).

2) T. Nakagawa and Y. Morino, *J. Mol. Spectry.*, **26**, 496 (1968).

3) A. G. Maki and L. R. Blaine, *ibid.*, **12**, 45 (1964).

4) A. G. Maki, E. K. Plyler and R. Thibault, *J. Opt. Soc. Am.*, **54**, 869 (1964).

5) D. H. Rank, G. Skorinko, D. P. Eastman and T. A. Wiggins, *ibid.*, **50**, 421 (1960).

6) H. C. Allen, Jr., E. D. Tidwell and E. K. Plyler, *J. Chem. Phys.*, **25**, 302 (1956).

7) A. E. Douglas and D. Sharma, *ibid.*, **21**, 448 (1953).

8) W. W. Brim, J. M. Hoffman, H. H. Nielsen and K. N. Rao, *J. Opt. Soc. Am.*, **50**, 1208 (1960).

9) C. A. Burrus and W. Gordy, *Phys. Rev.*, **101**, 599 (1956).

10) D. H. Rank, H. D. Rix and R. E. Kagarise, *J. Chem. Phys.*, **20**, 1437 (1952).

TABLE 1. OBSERVED AND CALCULATED VALUES OF ν AND B_v

Species State	Vibrational energy ν (cm^{-1})				Rotational constant $B_v - B_0 (10^{-3}\ cm^{-1})$			
	Obsd	Calcd	O-C	Weight[a]	Obsd	Calcd	O-C	Weight[b]
$H^{12}C^{14}N$								
00^00					1478.219 i	1478.205	0.014	12.5
10^00	2096.85 c	2096.85	0.00	5.0	-10.0_7 c	−10.068	-0.0_{02}	12.3
02^00	1411.43 d	1412.08	−0.65	0.078	7.59_8 c	7.385	0.21_3	0.78
00^01	3311.48 e	3311.45	0.03	5.0	-10.42_1 e	−10.418	-0.00_3	12.5
20^00	4173.07 e	4172.79	0.28	0.078		−20.135		
12^00	3502.13 c	3501.70	0.43	0.059	−2.748 c	−2.683	−0.065	0.595
04^00	2802.85 c, k	2804.63	−1.78	0.0012		14.770		
10^01	5393.70 e	5393.69	0.01	1.25	−20.286 e	−20.486	0.200	4.2
02^01	4684.32 e	4685.57	−1.25	0.059	-2.37_7 c	−3.033	0.65_6	0.595
00^02	6519.61 e	6519.48	0.13	0.078	−21.151 e	−20.836	−0.315	0.78
22^00	5571.89 f, k	5570.41	1.48	0.0195		−12.750		
12^01	6761.33 e	6760.59	0.74	0.0446		−13.101		
10^02	8585.57 e	8587.11	−1.54	0.059	−30.82 e	−30.904	0.08_4	0.595
00^03	9627.02 g	9624.08	2.94	0.0068	−32.21 e	−31.255	-0.95_5	0.154
12^02	9914.41 g	9916.05	−1.64	0.016	−24.02 g	−23.519	-0.50_1	0.219
10^03	11674.46 e	11677.11	−2.64	0.0061	−41.61 e	−41.322	-0.28_8	0.137
00^04	12635.90 e	12625.25	10.65	0.0012	−43.794 e	−41.673	−2.121	0.064
01^10	711.98 h	712.35	−0.37	2.5	3.549 c	3.693	−0.144	6.25
11^10	2805.58 c	2805.59	−0.01	0.83	−6.657 c	−6.375	−0.282	3.12
03^10	2113.46 c	2114.66	−1.20	0.0068	11.35_9 c	11.078	0.28_1	0.152
01^11	4004.17 e	4004.83	−0.66	0.83	-6.65_9 e	−6.726	0.06_7	3.12
21^10	4878.27 e	4877.93	0.34	0.056	-16.9_0 f	−16.443	-0.4_{57}	0.568
13^10	4201.29 e	4200.67	0.62	0.0060		1.010		
11^11	6083.35 e	6083.47	−0.12	0.38	−16.639 e	−16.793	0.154	1.79
03^11	5366.86 e	5369.19	−2.33	0.0060		0.659		
01^12	7192.75 e	7193.89	−1.14	0.056	−17.097 e	−17.144	0.047	0.568
11^12	9256.11 g	9257.92	−1.81	0.042	−26.82 g	−27.212	0.39_2	0.446
01^13	10280.30 g	10279.53	0.78	0.0060	−27.72 g	−27.562	-0.15_8	0.136
02^20	1426.53 c	1427.55	−1.02	0.039		7.385		
12^20	3516.88 c	3517.21	−0.33	0.0303	-3.52_6 c	−2.683	-0.84_4	0.338
04^20	2818.16 c	2820.07	−1.91	0.0012		14.770		
02^21	4699.21 e	4701.08	−1.87	0.0303		−3.033		
$H^{13}C^{14}N$								
00^00					1439.988 e	1439.978	0.010	12.5
10^00		2063.05				−9.741		
00^01	3293.51 e	3293.46	0.05	5.0	−9.63 d	−9.648	0.01_8	12.3
10^01	5343.66 e	5343.62	0.04	1.25	−19.19 e	−19.389	0.19_9	4.15
02^01	4655.86 e	4657.19	−1.33	0.059	−3.09 e	−3.058	-0.03_2	0.595
00^02	6483.28 e	6483.17	0.11	0.078	−19.55 e	−19.296	-0.25_4	0.78
10^02	8519.24 e	8520.43	−1.19	0.059		−29.037		
00^03	9571.73 j	9569.13	2.60	0.0068	−29.2 j	−28.944	-0.2_{56}	0.154
10^03	11591.42 j	11593.50	−2.08	0.0061	−38.8 j	−38.685	-0.1_{15}	0.137
00^04	12561.84 j	12551.35	10.49	0.0012	-40.6_6 j	−38.593	-2.0_{68}	0.064
01^10	707.39 e	706.34	1.05	2.5	3.20 e	3.295	-0.09_5	6.25
11^10	2765.32 c	2765.27	0.05	0.83		−6.446		
01^11	3982.22 e	3981.44	0.78	0.83		−6.353		
11^11	6028.79 e	6027.47	1.32	0.38		−16.094		
01^12	7153.07 e	7152.78	0.29	0.056	−15.949 e	−16.001	0.052	0.568
02^21	4675.03 e	4672.41	2.62	0.0303	−2.79 e	−3.058	0.26_8	0.338
$H^{12}C^{15}N$								
00^00					1435.27 d	1435.226	0.04_4	11.1
10^00		2064.35				−9.655		
00^01	3310.09 d	3310.13	−0.04	5.0	-10.02_8 d	−10.020	-0.00_8	12.3
01^10		711.41				3.541		

Table 1. (continued)

Species state	Vibrational energy ν (cm^{-1}) Obsd	Calcd	O-C	Weight[a]	Rotational constant $B_v - B_0$(10^{-3} cm^{-1}) Obsd	Calcd	O-C	Weight[b]
$D^{12}C^{14}N$								
00^00					1207.747 e	1207.692	0.055	25.0
10^00	1925.26 d	1925.24	0.02	6.67	−6.55 d	−6.542	-0.00_8	24.4
02^00	1129.98 d	1130.29	−0.31	0.104	8.87 d	8.783	0.08_7	1.56
00^01	2630.30 d	2630.34	−0.04	6.67	-10.32_9 d	−10.264	-0.06_5	24.4
20^00	3836.35 f	3836.79	−0.44	0.104	−13.63 f	−13.084	-0.54_6	1.56
12^00	3060.67 d	3061.56	−0.89	0.078	1.92_6 d	2.240	-0.31_4	1.19
10^01	4523.27 e	4523.18	0.09	1.67	-16.61_0 e	−16.807	0.19_7	8.26
02^01	3729.12 d	3729.03	0.09	0.078	−0.83 d	−1.482	0.65_2	1.19
00^02	5220.24 d	5219.69	0.55	0.104	−20.69 d	−20.529	-0.16_1	1.56
01^10	569.04 d	569.30	−0.26	3.33	4.34 d	4.391	-0.05_1	12.3
11^10	2497.14 d	2497.56	−0.42	1.11	−2.37 d	−2.151	-0.21_9	6.21
01^11	3183.67 d	3183.85	−0.18	1.11	−5.69 d	−5.873	0.18_3	6.21
21^10	4410.96 f, k	4412.13	−1.17	0.074		−8.693		
13^10	3623.94 d, k	3625.56	−1.62	0.0080		6.632		
11^11	5079.46 e	5079.71	−0.25	0.513	−12.056 d	~12.415	0.359	3.56
01^12	5757.88 d	5757.40	0.48	0.074	−15.79 d	−16.138	0.34_8	1.13
02^20	1137.94 d	1138.59	−0.65	0.052	8.66 d	8.783	-0.12_3	0.782
12^20	3068.63 d	3069.88	−1.25	0.040	1.56 d	2.240	-0.68_0	0.676
02^21	3736.94 d	3737.37	−0.43	0.040	−1.04 d	−1.482	0.44_2	0.676
$D^{13}C^{14}N$								
00^00					1187.073 d	1187.017	0.057	12.5
10^00	1911.84 d	1911.81	0.03	6.67		−6.420		
00^01	2590.07 d	2590.05	0.02	6.67	−9.74 d	−9.648	-0.09_2	24.4
01^10		561.60				4.054		
$D^{12}C^{15}N$								
00^00					1173.0 d	1173.080	-0.0_{79}	7.0
10^00		1900.12				−6.290		
00^01	2621.19 d	2621.22	−0.03	6.67	-10.00_8 d	−9.883	-0.12_5	24.4
01^10		568.06				4.236		

a) Statistical weights in the least-squares analysis, in cm^2 units.
b) Statistical weights in 10^6 cm^2 units.
c) Maki *et al.*, Ref. 3.
d) Maki *et al.*, Ref. 4.
e) Rank *et al.*, Ref. 5.
f) Allen *et al.*, Ref. 6.
g) Douglas *et al.*, Ref. 7.
h) Brim *et al.*, Ref. 8.
i) Burrus *et al.*, Ref. 9.
j) Rank *et al.*, Ref. 10.
k) Only the Q branch has been observed.

TABLE 2. FOURTH-ORDER POTENTIAL CONSTANTS f OF HCN DETERMINED BY LEAST-SQUARES METHODS

Potential constant	Suzuki *et al.*[a]	This work	Unit
f_R(CN)	18.776 ±0.17	18.707 ±0.016	md/Å
f_{Rr}	−0.216 ±0.08	−0.211 ±0.006	md/Å
f_r(CH)	6.230 ±0.03	6.244 ±0.003	md/Å
f_α	0.2592±0.003	0.2598±0.0004	md·Å
f_{RRR}	−19.227±0.36	−20.846 ±0.16	md/Å^2
f_{RRr}	−1.335±0.40	0.046 ±0.22	md/Å^2
f_{Rrr}	−0.322±0.27	−0.496 ±0.11	md/Å^2
f_{rrr}	−6.085±0.15	−5.626 ±0.07	md/Å^2
$f_{R\alpha\alpha}$	−0.272±0.05	−0.328 ±0.02	md
$f_{r\alpha\alpha}$	−0.134±0.07	−0.054 ±0.03	md

Potential constant	Suzuki *et al.*[a]	This work	Unit
f_{RRRR}	17.52 ±6.9	27.09 ±1.2	md/Å^3
f_{RRRr}	4.71 ±7.7	0.73 ±1.2	md/Å^3
f_{RRrr}	1.17 ±3.0	1.07 ±0.4	md/Å^3
f_{Rrrr}	1.05 ±2.0	1.35 ±0.4	md/Å^3
f_{rrrr}	8.79 ±0.7	6.38 ±0.3	md/Å^3
$f_{RR\alpha\alpha}$	−0.189 ±0.46	−0.010 ±0.10	md/Å
$f_{Rr\alpha\alpha}$	0.196 ±0.43	0.138 ±0.06	md/Å
$f_{rr\alpha\alpha}$	0.201 ±0.23	−0.110 ±0.07	md/Å
$f_{\alpha\alpha\alpha\alpha}$	0.0029±0.004	0.0014±0.0007	md·Å
$\hat{\sigma}^2$		0.130	

a) Ref. 1. Table 3, Column (iii).

TABLE 3. CORRELATION FACTORS AMONG THE f CONSTANTS ($\times 10^{-2}$)

	f_R	f_{Rr}	f_r	f_α	f_{RRR}	f_{RRr}	f_{Rrr}	f_{rrr}	$f_{R\alpha\alpha}$	$f_{r\alpha\alpha}$	f_{RRRR}	f_{RRRr}	f_{RRrr}	f_{Rrrr}	f_{rrrr}	$f_{RR\alpha\alpha}$	$f_{Rr\alpha\alpha}$	$f_{rr\alpha\alpha}$	$f_{\alpha\alpha\alpha\alpha}$
f_R																			
f_{Rr}	−44																		
f_r	−51	71																	
f_α	2	−1	1																
f_{RRR}	−8	−11	−10	−16															
f_{RRr}	−7	19	−19	20	−86														
f_{Rrr}	12	−29	−26	−20	59	−75													
f_{rrr}	−3	11	12	21	−85	92	−87												
$f_{R\alpha\alpha}$	−10	27	29	40	−34	37	−44	38											
$f_{r\alpha\alpha}$	11	−31	−32	−39	29	−38	43	−38	−95										
f_{RRRR}	−73	30	32	16	−55	55	−46	55	36	−32									
f_{RRRr}	0	−70	−44	−12	48	−56	56	−50	−38	42	−22								
f_{RRrr}	−51	3	5	−8	59	−60	32	−52	−24	27	6	52							
f_{Rrrr}	38	−43	−22	10	−32	36	−62	56	13	−9	−8	1	−35						
f_{rrrr}	13	−22	−24	−21	84	−93	87	−99	−42	42	−61	55	47	−47					
$f_{RR\alpha\alpha}$	−2	−8	−5	−50	32	−35	38	−37	−87	81	−35	30	18	−14	38				
$f_{Rr\alpha\alpha}$	2	−8	−10	27	−5	9	−17	15	31	−35	14	−29	−6	−3	−17	−51			
$f_{rr\alpha\alpha}$	−8	26	25	39	−18	26	−32	26	93	−98	26	−37	−20	1	−30	−83	44		
$f_{\alpha\alpha\alpha\alpha}$	−7	20	25	−56	−7	11	−14	10	34	−41	11	−16	−9	0	−12	−25	1	37	

$$+ f_{raa}\Delta r\Delta\alpha^2 + f_{RRRR}\Delta R^4 + f_{RRRr}\Delta R^3\Delta r + f_{RRrr}\Delta R^2\Delta r^2 + f_{Rrrr}\Delta R\Delta r^3 + f_{rrrr}\Delta r^4 + f_{RRaa}\Delta R^2\Delta\alpha^2 + f_{Rraa}\Delta R\Delta r\Delta\alpha^2 + f_{rraa}\Delta r^2\Delta\alpha^2 + f_{aaaa}\Delta\alpha^4, \quad (1)$$

where ΔR and Δr denote the stretching displacements of the CN and CH bonds respectively, and $\Delta\alpha$, the bending displacement. The force constants obtained by Suzuki, Pariseau, and Overend[1] were used as the initial values for the least-squares refinement. No account was taken of the resonance interactions, such as the Fermi resonance ($\omega_1 \sim 2\omega_2$ and $\omega_3 \sim 2\omega_2$) and a third-order anharmonic resonance ($3\omega_1 \sim 2\omega_3$). The equilibrium bond lengths were assumed to be $R_e(\mathrm{CN}) = 1.15313$ Å and $r_e(\mathrm{CH}) = 1.06593$ Å, according to Rank, Skorinko, Eastman, and Wiggins.[4]

Statistical Weights. The weights of ν and B_v in the least-squares analysis were evaluated by taking into account the uncertainties due to higher-order terms as well as the experimental uncertainties, according to the procedure suggested in our preceding paper.[2] The uncertainties of the former type were estimated on the basis that $\sigma_y^2 = 0.20\ (\mathrm{cm}^{-1})^2$ and $\sigma_r^2 = 0.08 \times (10^{-3}\ \mathrm{cm}^{-1})^2$ for HCN, and $\sigma_y^2 = 0.15 \times (\mathrm{cm}^{-1})^2$ and $\sigma_r^2 = 0.04 \times (10^{-3}\ \mathrm{cm}^{-1})^2$ for DCN. In Columns 5 and 9 of Table 1 the weights thus evaluated are shown in units of $(\mathrm{cm}^{-1})^{-2}$ and $(10^{-3}\ \mathrm{cm}^{-1})^{-2}$ respectively.

The calculation was carried out by using the computer program described in our preceding paper[2] on the HITAC 5020E computer at the Computer Centre, The University of Tokyo.

The general fourth-order portential constants determined are shown in Column 2 of Table 2, while their correlation factors are given in Table 3. The potential constants obtained in the present study are essentially the same as those obtained by Suzuki, Pariseau, and Overend,[1] but they are more precise than the latter, as may clearly be seen from the probable errors listed in Table 2. The calculated values of ν and $B_v - B_0$ are tabulated in Columns 3 and 7 of Table 1, and the deviations, in Columns 4 and 8.

Potential Constants in the Normal-Coordinate System and the Vibrational and Rotational Parameters

On the basis of the force constants, f, determined above, the potential constants, ω_i, k_{ijk}, and k_{ijkl}, in the normal-coordinate representation were calculated for the six isotopic species; the results are shown in Table 4. These calculated values have the advantage that the isotopic relations among them are fully taken into account. The standard errors for ω and k were evaluated according to Eq. (20) of Ref. 2, with account taken of the correlations among the f constants. The ω and k constants vary to a large extent for different isotopic species as a result of the change in normal coordinates. Table 5 shows the contributions of the f constants to the k constants; the main term is underlined for each k constant. One can see that the contributions of *bond-stretching* f constants are predominant in the cubic and quartic k constants, including even those related to the *bending* vibration. The contributions of the *cross* terms are much smaller

TABLE 4. POTENTIAL CONSTANTS IN THE NORMAL-COORDINATE SYSTEM (cm^{-1})

	$H^{12}C^{14}N$	$H^{13}C^{14}N$	$H^{12}C^{15}N$	$D^{12}C^{14}N$	$D^{13}C^{14}N$	$D^{12}C^{15}N$
ω_1	2128.67±0.80[a]	2094.16	2095.12	1952.12±0.63[a]	1938.52	1925.83
ω_2	727.10±0.51	720.71	726.01	579.85±0.41	571.82	578.49
ω_3	3441.16±0.44	3422.04	3439.85	2703.34±0.72	2661.58	2794.30
k_{111}	−106.9 ±0.5	−105.7	−104.6	−84.7 ±0.4	−83.8	−82.9
k_{113}	53.3 ±2.5	50.7	52.1	−3.7 ±2.0	4.4	1.5
k_{122}	96.2 ±1.4	85.0	92.7	184.7 ±1.1	174.4	178.6
k_{133}	−216.3 ±4.6	−198.0	−210.6	−329.6 ±3.3	−315.7	−321.6
k_{223}	608.9 ±1.3	613.7	612.7	269.7 ±1.1	278.3	277.1
k_{333}	−289.0 ±7.9	−291.6	−290.1	−90.1 ±5.5	−100.0	−97.3
k_{1111}	6.47±0.3	6.34	6.29	4.62±0.2	4.53	4.47
k_{1113}	−5.23±0.8	−4.86	−5.06	1.61±0.7	0.49	0.88
k_{1122}	−14.38±0.4	−12.45	−13.66	−37.45±0.6	−34.35	−35.39
k_{1133}	14.00±1.5	12.11	13.36	33.97±1.8	31.74	32.50
k_{1223}	−89.35±1.9	−82.56	−87.51	−90.64±0.6	−88.44	−89.52
k_{1333}	28.74±0.6	26.93	28.16	19.21±0.5	19.93	19.79
k_{2222}	58.97±2.0	59.69	59.56	23.40±2.1	23.62	23.75
k_{2233}	−244.79±4.8	−246.60	−246.30	−93.96±1.9	−95.79	−96.21
k_{3333}	33.14±1.5	33.44	33.29	11.00±0.7	11.39	11.39

a) Standard error calculated by taking into account the correlations among the f constants according to Eq. (20) of Ref. 2.

TABLE 5. CONTRIBUTIONS OF THE f CONSTANTS TO THE k CONSTANTS (cm^{-1})

(a) Cubic constants of $H^{12}C^{14}N$

	k_{111}	k_{113}	k_{133}	k_{333}	k_{122}	k_{223}
f_R(CN)					33.0	−9.8
f_{Rr}					−10.6	2.3
f_r(CH)					135.7	676.3
f_α					−16.2	−57.2
f_{RRR}	−104.1	93.1	−27.8	2.8		
f_{RRr}	0.1	0.4	−0.3	0.0		
f_{Rrr}	−0.5	−4.6	−10.5	3.5		
f_{rrr}	−2.4	−35.7	−177.8	−295.3		
$f_{R\alpha\alpha}$					−42.5	12.7
$f_{r\alpha\alpha}$					−3.1	−15.3
Total	−106.9	53.3	−216.3	−289.0	96.2	608.9

(b) Cubic constants of $D^{12}C^{14}N$

	k_{111}	k_{113}	k_{133}	k_{333}	k_{122}	k_{223}
f_R(CN)					53.0	−42.3
f_{Rr}					−6.2	3.1
f_r(CH)					194.3	323.5
f_α					−23.4	−27.6
f_{RRR}	−56.2	134.5	−107.3	28.5		
f_{RRr}	0.2	0.0	−0.3	0.2		
f_{Rrr}	−2.0	−4.9	−0.2	4.3		
f_{rrr}	−26.7	−133.2	−221.8	−123.1		
$f_{R\alpha\alpha}$					−27.6	22.0
$f_{r\alpha\alpha}$					−5.5	−9.1
Total	−84.7	−3.7	−329.6	−90.1	184.7	269.7

(c) Quartic constants of $H^{12}C^{14}N$

	k_{1111}	k_{1113}	k_{1133}	k_{1333}	k_{3333}	k_{1122}	k_{1223}	k_{2233}	k_{2222}
f_R						−1.32	0.79	−0.12	0.27
f_{Rr}						0.21	0.96	−0.31	−0.17
f_r						−2.59	−25.82	−64.34	70.76
f_α						0.59	3.40	7.84	−8.22
f_{RRR}						−5.11	3.04	−0.45	
f_{RRr}						0.11	−0.34	0.00	
f_{Rrr}						−1.01	−4.76	1.29	
f_{rrr}						−7.46	−74.40	−185.40	
$f_{R\alpha\alpha}$						1.90	6.13	−2.00	−0.70
$f_{r\alpha\alpha}$						0.14	1.17	2.41	−3.20
f_{RRRR}	6.27	−7.47	3.34	−0.66	0.05				
f_{RRRr}	0.07	0.31	−0.31	0.10	−0.01				
f_{RRrr}	0.05	0.45	0.90	−0.66	0.10				
f_{Rrrr}	0.03	0.39	1.86	2.70	−0.98				
f_{rrrr}	0.06	1.10	8.21	27.27	33.97				
$f_{RR\alpha\alpha}$						−0.06	0.04	−0.01	
$f_{Rr\alpha\alpha}$						0.36	1.71	−0.54	
$f_{rr\alpha\alpha}$						−0.13	−1.27	−3.17	
$f_{\alpha\alpha\alpha\alpha}$									0.22
Total	6.47	−5.23	14.00	28.74	33.14	−14.38	−89.35	−244.79	58.97

TABLE 5. (Continued)

(d) Quartic constants of $D^{12}C^{14}N$

	k_{1111}	k_{1113}	k_{1133}	k_{1333}	k_{3333}	k_{1122}	k_{1223}	k_{2233}	k_{2222}
f_R						−1.73	2.76	−1.10	1.05
f_{Rr}						0.26	0.22	−0.34	−0.22
f_r						−8.29	−27.61	−22.99	29.02
f_α						1.42	3.54	2.97	−3.86
f_{RRR}						−6.67	10.65	−4.25	
f_{RRr}						0.06	−0.28	0.01	
f_{Rrr}						−1.24	−1.27	1.33	
f_{rrr}						−23.90	−79.57	−66.24	
$f_{R\alpha\alpha}$						2.22	0.85	−2.10	−1.09
$f_{r\alpha\alpha}$						0.44	1.26	0.87	−1.64
f_{RRRR}	2.75	−8.78	10.51	−5.59	1.12				
f_{RRRr}	0.09	−0.07	−0.19	0.24	−0.08				
f_{RRrr}	0.16	0.27	−0.30	−0.36	0.28				
f_{Rrrr}	0.24	1.02	1.05	−0.49	−0.89				
f_{rrrr}	1.38	9.17	22.89	25.41	10.58				
$f_{RR\alpha\alpha}$						−0.03	0.05	−0.02	
$f_{Rr\alpha\alpha}$						0.53	0.46	−0.70	
$f_{rr\alpha\alpha}$						−0.51	−1.70	−1.41	
$f_{\alpha\alpha\alpha\alpha}$									0.14
Total	4.62	1.61	33.97	19.21	11.00	−37.45	−90.64	−93.96	23.40

TABLE 6. VIBRATIONAL AND ROTATIONAL ANHARMONIC TERMS (cm^{-1})

	$H^{12}C^{14}N$	$H^{13}C^{14}N$	$H^{12}C^{15}N$	$D^{12}C^{14}N$	$D^{13}C^{14}N$	$D^{12}C^{15}N$
x_{11}	−10.45 ±0.38[a]	−10.27	−10.13	−6.84 ±0.29[a]	−6.80	−6.69
x_{12}	−3.61 ±0.22	−4.13	−3.46	3.01 ±0.20	2.03	3.11
x_{13}	−14.61 ±0.22	−12.90	−14.08	−32.40 ±0.26	−30.29	−30.90
x_{22}	−2.44 ±0.17	−2.31	−2.46	−2.08 ±0.11	−1.91	−2.10
x_{23}	−18.98 ±0.21	−18.38	−18.91	−15.80 ±0.24	−14.91	−15.67
x_{33}	−51.71 ±0.21	−51.87	−51.88	−20.50 ±0.36	−20.74	−20.98
x_{ll}	5.35 ±0.09	5.24	5.40	3.29 ±0.64	3.13	3.33
$\alpha_1\times10^3$	10.068±0.068	9.741	9.655	6.542±0.051	6.420	6.290
$\alpha_2\times10^3$	−3.693±0.047	−3.295	−3.541	−4.391±0.038	−4.054	−4.236
$\alpha_3\times10^3$	10.418±0.043	9.648	10.020	10.264±0.037	9.648	9.883

a) Calculated standard error. See Footnote a of Table 4.

TABLE 7. CORIOLIS COUPLING CONSTANTS

	$H^{12}C^{14}N$	$H^{13}C^{14}N$	$H^{12}C^{15}N$	$D^{12}C^{14}N$	$D^{13}C^{14}N$	$D^{12}C^{15}N$
ζ_{12}^x	0.1529±0.0007[a]	0.1631	0.1536	−0.0871±0.0010[a]	−0.0645	−0.0719
ζ_{23}^x	0.9882±0.0001	0.9866	0.9881	0.9962±0.0001	0.9979	0.9974

a) Calculated standard error.

TABLE 8. BOND-STRETCHING ANHARMONICITIES FOR HCN IN COMPARISON WITH THOSE FOR CN AND CH (in $Å^{-1}$)

	Diatomic molec. CN or CH	HCN
CN bond a_3	2.268	2.229
a_4	2.294	2.228
CH bond a_3	1.981	1.802
a_4	2.087	1.872

than those of the *principal* terms.

The vibrational anharmonicity constants, x_{ij}, and the vibration-rotation interaction constants, α_i, were also calculated. They are tabulated in Table 6. The calculated values of the Coriolis coupling constants, ζ_{12}^x and ζ_{23}^x, are listed in Table 7.

The *l*-type doubling constants and the centrifugal distortion constants were also calculated, together with their *v*- and *J*-dependent terms. The cal-

TABLE 9. RATIO OF THE FERMI RESONANCE TERM $|k_{stt}/(\omega_s-2\omega_t)|$

	$H^{12}C^{14}N$	$H^{1}C^{14}N$	$H^{12}C^{15}N$	$D^{12}C^{14}N$	$D^{13}C^{14}N$	$D^{12}C^{15}N$
k_{122} (cm^{-1})	96.2	85.0	92.7	184.7	174.4	178.6
$\omega_1-2\omega_2$ (cm^{-1})	674.	653.	643.	792.	795.	769.
Ratio	0.143	0.130	0.144	0.233	0.219	0.232
k_{223} (cm^{-1})	608.9	613.7	612.7	269.7	278.3	277.1
$\omega_3-2\omega_2$ (cm^{-1})	1987.	1981.	1988.	1544.	1518.	1537.
Ratio	0.306	0.310	0.308	0.175	0.183	0.180

culated values of q_v and D_v are in good agreement with the observed values, as will be reported elsewhere.[11] This agreement offers positive support for the anharmonic potential constants obtained from ν and B_v in the present study.

Discussion

The two parameters a_3 and a_4 which are defined[12] by:

$$a_3 = -2f_{rrr}/f_r \tag{2}$$

and:

$$a_4 = [24f_{rrrr}/7f_r]^{1/2} \tag{3}$$

are convenient for expressing the bond-stretching anharmonicity. Their values for HCN are compared with those for CH and CN in Table 8. The table suggests that the potential function for a bond stretching in the HCN molecule is quite similar to that in the corresponding diatomic molecule, CH or CN.

As for the anharmonic resonance in HCN, an accidental perturbation of the $3\omega_1$—$2\omega_2$ type has been pointed out by Douglas and Sharma.[7] The perturbation of this type was disregarded in the present study without any serious effect on the potential constants determined above. This is because the perturbation mentioned above is significant only for highly-excited vibrational states, such as (00^04), (30^02), (10^04), and (40^02), and the weights of the observed values for these states were zero or small in the least-squares analysis.

Nevertheless, a problem was found in the present study concerning the Fermi resonance. In the present calculation the k_{122} and k_{223} terms were treated with a second-order perturbation theory without any special consideration of the Fermi resonances, $\omega_1-2\omega_2$ and $\omega_3-2\omega_3$. It was found, however, that the k_{122} and k_{223} constants thus obtained were not small enough compared with the energy differences, $\omega_1-2\omega_2$ and $\omega_3-2\omega_2$ respectively. Table 9 shows that the $|k_{stt}/(\omega_s-2\omega_t)|$ ratios for the $\omega_3-2\omega_2$ resonance of HCN and the $\omega_1-2\omega_2$ resonance of DCN are even larger than the ratio, 0.231, for the well-known case of the $\omega_1-2\omega_2$ resonance for OCS.[2] Rigorously speaking, these Fermi resonances must be treated separately from the usual perturbation calculation, as was done for OCS. According to such a treatment, some relations must be expected among the ν and B_v values; for instance:

$$B(02^00) - B_0 < 2[B(01^10) - B_0] \tag{4}$$

and:

$$B(02^20) > B(02^00). \tag{5}$$

The observed values, however, do not satisfy these relations. It seems likely that the discrepancies suggest the importance of such higher-order effects as the γ terms. In the present study no corrections for the third- and higher-order perturbation were taken into account; therefore, the exact diagonalization of the Fermi resonance terms remains to be done in the future.

11) T. Nakagawa and Y. Morino, *J. Mol. Spectry.*, to be published.

12) K. Kuchitsu and Y. Morino, This Bulletin, **38**, 805 (1965).

BULLETIN OF THE CHEMICAL SOCIETY OF JAPAN VOL. 42 2220—2227 (1969)

A Study of the Low-temperature Oxidation of Cumene in the Presence of Triphenylsulfonium Chloride. Propagation and Termination Steps

Katsutoshi OHKUBO, Tokio YAMABE and Kenichi FUKUI

Faculty of Engineering, Kyoto University, Sakyo-ku, Kyoto

(Received February 3, 1969)

The low-temperature liquid-phase oxidation of cumene using triphenylsulfonium chloride was studied in order to establish the nature of the activity of sulfonium catalysts and the oxidation mechanism. The oxidation occurs in an autocatalytic fashion below 70°C, while it proceeds in an auto-retarding fashion above 85°C. This is a characteristic feature of this oxidation. The cause of the deactivation at higher temperatures is mainly the deoxygenation of the assumed complex (Cat.$\cdots O_2$). The decomposition of cumene hydroperoxide and the subsequent formation of α-cumyl alcohol, acetophenone, and dicumyl peroxide were seriously affected by the presence of sulfonium salts. The formation of acetophenone was accelerated thermally, while that of α-cumyl alcohol was not accelerated much, though it was accelerated by the catalyst-oxygen complex. Dicumyl peroxide, once formed in an appreciable amount, was gradually decomposed, both thermally and catalytically. The catalyst was deactivated by the product formed. This phenomenon was attributed to the masking action of oxygen-containing products. The mechanism oxidation was discussed on the basis of these observations.

Our previous reports[1,2] revealed the outstanding nature of sulfonium salts as a catalytic substance for the liquid-phase oxidation of cumene with molecular oxygen in the low-temperature range (55—85°C). This type of oxidation is initiated through hydrogen abstraction from cumene by a complex which is postulated to form as a consequence of the reversible association of molecular oxygen with the sulfonium catalyst.

$$\text{Cat.} + O_2 \rightleftarrows \text{Cat.}\cdots O_2$$

$$\text{Cat.}\cdots O_2 + RH \longrightarrow R\cdot + \cdot O_2H + \text{Cat.}$$

At the beginning of the reaction, the oxidation of this type proceeds in a simpler fashion; in this period the oxygen absorbed is almost quantitatively used in the formation of hydroperoxide. However, the propagation reaction is composed of several steps, in which not only hydroperoxide, but also acetophenone, dicumyl peroxide, and α-cumyl alcohol are produced in appreciable amounts.

In recent years, the mechanism of cumene oxidation at propagating and terminating steps has received considerable attention.[3-5] Certain aspects of the mechanism, however, still remain obscure. Namely, it has been left unclarified how the behavior of free radicals ($RO\cdot$, $RO_2\cdot$, $CH_3\cdot$, *etc.*) changes at different temperatures with or without catalysts in their competing reactions, including intramolecular ones. Moreover, much work has been done by means of kinetic methods, which usually do not afford much reliable information, in particular about the termination reaction. In addition, a majority of the experiments in these works were carried out at relatively high temperatures (100—200°C) with heterogeneous metal compound catalysts, which inevitably complicated the results. In this regard, the present experimental conditions are quite favorable to make the mechanism clear because of the homogeneity of the reacting system and because of the low temperature employed.

This paper will attempt to clarify the low-temperature oxidation mechanism of cumene with triphenylsulfonium chloride and the nature of its catalytic action by investigating the effects of the temperature and of catalysts upon oxygen absorption and oxidation products.

The present study gives some noticeable results: (1) The propagation reaction proceeds through the decomposition of cumene hydroperoxide, which is caused not so much thermally as by triphenylsulfonium chloride; (2) The formations of acetophenone and dicumyl peroxide are strongly influenced by the temperature, while that of α-cumyl alcohol is not so much affected by the temperature but is, rather, promoted by sulfonium salts; on the contrary, dicumyl peroxide is rather

1) K. Fukui, K. Ohkubo and T. Yamabe, This Bulletin, **42**, 312 (1969).

2) K. Ohkubo, T. Yamabe and K. Fukui, *ibid.*, **42**, 1800 (1969).

3) P. D. Bartlett and T. G. Traylor, *J. Am. Chem. Soc.*, **85**, 2407 (1963).

4) T. G. Traylor, *ibid.*, **85**, 2411 (1963).

5) T. G. Traylor and C. A. Russell, *ibid.*, **87**, 3698 (1965).

decomposed by the catalyst; (3) The deactivation of the catalyst by certain oxidation products, especially by α-cumyl alcohol, is ascribed to thier masking actions, which retard the reaction.

Experimental

Material and Catalyst. Cumene was washed with concentrated sulfuric acid, dried on magnesium sulfate, and then rectified to collect the center fraction; bp 152.5°C, $n_D^{20}=1.4910$. The fraction was then filtered chromatographically through activated alumina (200—300 mesh) and stored under nitrogen at 0°C. As the oxidation catalyst, triphenylsulfonium chloride was synthesized by the method presented in our earlier report.[6]

Oxidation Procedure. Under a nitrogen atmosphere, triphenylsulfonium chloride and cumene (10 m*l*) were added to an oxidation flask (50 m*l* capacity) attached to a gas burette from which air was then evacuated and which was filled with oxygen several times. The oxidation flask was contained in a thermostated oil-bath, and oxygen absorption was followed in the way previously described.[2] The oxidation products were determined by the following analytical procedure.

Analytical Procedure. The main products, cumene hydroperoxide (CHP), dicumyl peroxide (DCP), acetophenone (AP), and α-cumyl alcohol (CA), were determined by the following methods.

Cumene Hydroperoxide (CHP). CHP was determined by an iodometric method which is essentially taken from Fordham and Williams,[7] but modified in the following points. A 0.5—2.0 m*l* portion of the oxidate was added to 5.0 m*l* of a saturated aqueous potassium iodide solution containing 10 m*l* of glacial acetic acid and 100 m*l* of isopropyl alcohol. The resultant mixture was flushed with nitrogen and then refluxed gently with occasional shaking for 3.0—4.0 min. The liberated iodine was titrated with a 0.1 N sodium thiosulfate solution until the yellow color disappeared. The amount of CHP was then determined from the difference between the titer of the blank and the oxidate-containing mixture.

Dicumyl Peroxide (DCP). A 0.5—1 m*l* portion of the oxidate was added to 50 m*l* of glacial acetic acid containing 3 g of sodium iodide, and then the entire mixture was heated in a nitrogen atmosphere at 110—115°C for 1 hr. After dilution by oxygen-free water (3.0 m*l*), the resulting iodine was titrated in nitrogen with a standard thiosulfate solution. The difference between this determination and that of CHP gave the amount of dicumyl peroxide.

Acetophenone (AP). AP was determined like the 2,4-dinitrophenylhydrazone; mp 248—249°C, mixed mp 249°C.

α-Cumyl Alcohol (CA). CA was determined as the reaction product with thioglycolic acid.[8]

The Solubility of Chlorides to Cumene. Commercially-pure alkali chlorides (LiCl, NaCl, KCl, RbCl, CsCl, and NH_4Cl) were calcined, fused, and then pulverized to about 200 mesh powder. The solubility of these chlorides and triphenylsulfonium chloride to cumene was determined by the following treatment. The chloride (500 mg) was added to cumene (50 m*l*); after the mixture had been vigorously stirred for one hour at two definite temperatures (20 ±0.5°C and 70±0.5°C), the upper layer (10 m*l*) of the mixture was titrated by an alcoholic solution of a N/100 silver nitrate solution, using potassium chromate as the indicator. Table 1 records the solubility of the chlorides to cumene.

Table 1. The solubility of various chlorides to cumene

Chloride (MCl) (M)	Solubility (mg-atom/100 mg of cumene)	
	Cl at 20±0.5°C	Cl at 70±0.5°C
Li	0.041	0.221
Na	0.017	0.116
K	0.017	0.116
Rb	0.029	0.150
Cs	0.029	0.231
NH_4	0.041	0.234
$(C_6H_5)_3S$	0.206	0.244

Results and Discussion

In the initial range of the reaction, the amount of oxygen absorbed is consumed only to form CHP, and the rate of its formation depends almost linearly upon the amount of the sulfonium catalyst.[2] In the propagation and termination steps, however,

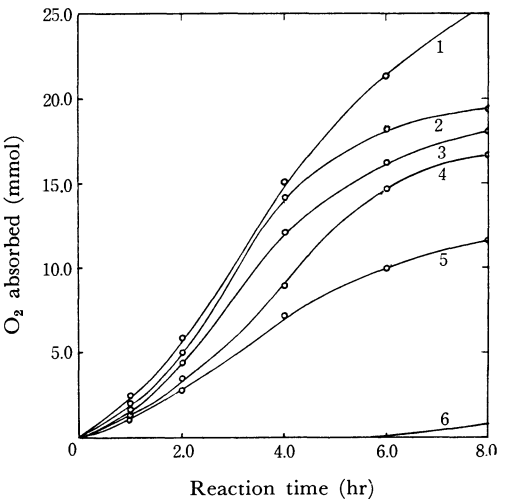

Fig. 1. The influence of the amount of triphenylsulfonium chloride on the oxygen absorption at 70°C.
The amount of $(C_6H_5)_3SCl$ (mmol/m*l*$\times 10^3$): 1, 36.85; 2, 26.80; 3, 16.65; 4, 10.05; 5, 3.35; 6, none

6) K. Fukui, K. Kanai, Takezono and H. Kitano, *Kogyo Kagaku Zasshi (J. Chem. Soc. Japan, Ind. Chem. Sect.)*, **67**, 1131 (1964).
7) T. W. L. Fordham and H. L. Williams, *Can. J. Research*, **B27**, 943 (1949).
8) B. Holmberg, *J. prakt. Chem.*, **141**, 93 (1934).

the hydroperoxide decomposes, both thermally and catalytically. The decomposition products (AP, DCP, and CA) complicate the oxidation mechanism. First, the catalytic effect of the sulfonium salt upon oxygen absorption and the composition of the oxidation products in these steps were investigated at 70 and 85°C. The oxygen absorption curves at 70°C in Fig. 1 indicate that the oxygen absorption of an autocatalytic nature increases monotonously with the amount of the catalyst. The dwindling of absorption began after *ca.* 4 hr, and the retardation appeared about 8 hr after the start. Therefore, the oxidation products after 4.0 and 8.0 hr may afford information about the propagation and the termination processes respectively. This point will be discussed below.

The decrease in oxygen absorption may be attributed to the deactivation of the catalyst, itself probably caused by the masking action of the accumulated CHP, as was discussed in our previous report.[2] Actually, the rates of absorption declined upon the addition of CHP, as is shown in Table 6. This may be connected with the fact that sulfonium catalysts are easily dissolved in polar solvents, especially those containing oxygen lone-pairs, which might cause a strong interaction with sulfonium ions. Namely, such molecules as CHP blocking the active sites of sulfonium ions may prevent oxygen molecules from approaching there; hence, they may depress the catalytic activity. This masking action of CHP might be assisted by the association of the hydroperoxides through hydrogen-bonds between them.*1 The circumstances of the masking action are illustrated schematically in Fig. 2.

Table 2 indicates that the accumulation of CHP diminishes in proportion to the amount of the catalyst. In fact, in the absence of any catalyst, CHP is preserved from secondary changes almost completely, even a 17.5 hr reaction. This fact suggests that CHP is decomposed essentially catalytically, whereas it is little converted thermally. Actually, the sulfonium catalyst decomposes CHP exclusively in this temperature range; this will be discussed in detail in a subsequent paper.

Mention should be made here of the decomposition of CHP. There are three possible paths to be considered for the generation of α-cumyloxy radicals, the main source of the formation of products. The first one is the unimolecular thermal decomposition:

$$\mathrm{ROOH} \xrightarrow{\text{unimol. decomp.}} \mathrm{RO}\cdot + \cdot\mathrm{OH} \qquad (1)$$

This is, however, hardly conceivable, because CHP is sufficiently stable in hydrocarbons up to 130—140°C.[10]

The second is the following bimolecular decomposition through dimer formation by the hydrogen bond when the concentrations of CHP are high:

$$2\mathrm{ROOH} \rightarrow \left[\mathrm{RO\cdots O\cdots H\cdots O_2R}\right] \xrightarrow{\text{bimol. decomp.}} \mathrm{RO}\cdot + \mathrm{RO_2}\cdot + \mathrm{H_2O} \qquad (2)$$

This implies that the hydrogen-bond formation

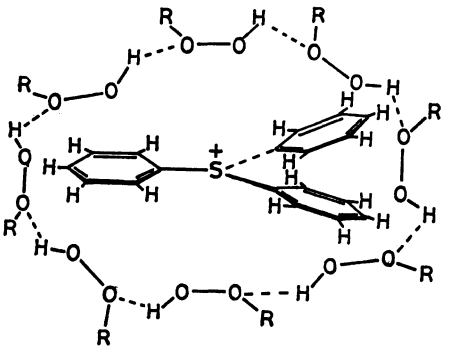

$R = C_6H_5C(CH_3)_2-$

Fig. 2. A proposed model for the makings effect of CHP on triphenylsulfonium ion catalyst.

TABLE 2. EFFECT OF CATALYST AMOUNT UPON CHP FORMATION AT 70°C

Catalyst amount (mmol/ml $\times 10^3$)	Reaction time (hr)	O_2 absorbed (mmol)	CHP (mmol)	CHP (%)*
3.35	1.0	0.98	0.95	97.2
	4.0	7.10	5.71	80.5
	8.0	11.80	8.9	75.4
10.05	1.0	1.25	1.17	93.5
	4.0	8.90	6.20	68.6
	8.0	16.7	9.2	55.1
16.65	1.0	1.60	1.47	92.1
	4.0	12.1	7.25	59.9
	8.0	18.1	9.4	51.9
26.80	1.0	2.07	—	—
	4.0	14.2	7.10	50.0
	8.0	19.5	9.5	48.7
36.85	1.0	2.38	2.16	91.0
	4.0	15.0	—	—
	8.0	25.5	9.0	35.5
None	17.5	5.73	5.63	98.20

* Calculated as mol CHP per 100 mol oxygen absorbed.

*1 In fact, Bateman and Hughes,[9] in their study of the infrared spectrum of cyclohexenyl hydroperoxide, showed that, in a diluted hydroperoxide solution in benzene, OH groups appear at 3500 cm^{-1}, while in an undiluted solution they appear at 3350 cm^{-1}; this apparently indicates the formation of intermolecular hydrogen bonds between them.

9) L. Bateman and H. Hughes, *J. Chem. Soc.*, **1952**, 4594.

10) M. S. Kharasch, A. Fono and W. Nundenberg, *J. Org. Chem.*, **16**, 113 (1951).

promotes the fission of the oxygen-oxygen bond of CHP.*2 At any rate, the thermal decomposition of CHP in cumene is actually very small in the temperature range of 60—80°C.*3

Hence, the only reasonable path is the third one (reaction (3)). This may, then, be proposed as the main reaction giving α-cumyloxy radicals. A more detailed discussion of this will be presented in a subsequent paper.

$$\mathrm{ROOH} + (\mathrm{C_6H_5})_3\mathrm{SCl} \rightarrow \left[\mathrm{R}\diagup\mathrm{O}\cdots\overset{\overset{\mathrm{H}^+}{\diagup}}{\mathrm{O}}\cdots\mathrm{S}(\mathrm{C_6H_5})_3\cdots\mathrm{Cl}^- \right]$$

$$\rightarrow \mathrm{RO}\cdot + \cdot\mathrm{OH} + (\mathrm{C_6H_5})_3\mathrm{SCl} \qquad (3)$$

Products of Oxidation. The α-cumyloxy radicals thus formed are readily converted to the major products through chain-transfer reactions (4a and 4b) or a chain-terminating reaction (4c).

$$\mathrm{RO}\cdot \xrightarrow[\mathrm{RH}]{\text{hydrogen abstraction}} \mathrm{ROH(CA)} + \mathrm{R}\cdot \qquad (4a)$$

$$\mathrm{RO}\cdot \xrightarrow{\beta\text{-scission}} \mathrm{AP} + \mathrm{CH_3}\cdot \qquad (4b)$$

$$\mathrm{RO}\cdot \xrightarrow[\mathrm{RO}\cdot]{\text{coupling}} \mathrm{ROOR(DCP)} \qquad (4c)$$

$$(\mathrm{R} = \mathrm{C_6H_5C(CH_3)_2}-)$$

CA Formation. Among these products, CA was apparently formed in an amount comparable with those of AP and DCP, as is shown in Table 3. This fact is worthy of emphasis since CA formation through hydrogen abstraction by RO· from cumene is difficult in low-temperature thermal oxidation without a catalyst, even if cumene is a good hydrogen donor. This is supported by the study of Blanchard[11] on cumene oxidation at 60°C by the use of α,α'-azodiisobutyronitrile, in which CA is formed only in an extremely small amount compared with AP and DCP. Table 3 also shows, however, that the accumulation of CA gradually lessened, whereas that of AP increased remarkably, as the reaction proceeded.

Such a remarkable CA formation as is described above may be attributed to the co-existence of oxygen and the catalyst. This is because the amount of CA is very small in the thermal and catalytic decomposition of CHP in cumene at 65°C without oxygen.*4 Therefore, it may be taken into account that molecular oxygen would participate in the CA formation as a natural consequence of its free radical character in the following "concerted" single-step process:

$$\mathrm{RO}\cdot + \mathrm{RH} + \mathrm{O_2} \xrightarrow[\text{liquid phase}]{} \mathrm{ROH} + \mathrm{RO_2}\cdot \qquad (5)$$

A possible alternate pathway may be a consequent process which comprises:

$$\mathrm{RH} + \mathrm{O_2} \rightarrow \mathrm{R}\cdot + \mathrm{HO_2} \qquad (5a)$$

$$\mathrm{RO}\cdot + \mathrm{HO_2}\cdot \rightarrow \mathrm{ROH} + \mathrm{O} \qquad (5b)$$

If we simply assume that the activation energy of the reverse process of (5a) is small, then, accordingly, the activation energy for (5a) is equal to the heat of this step—it is estimated to be about 38 kcal/mol.*5 This value is nearly equal to the energy of the oxygen-oxygen bond cleavage of CHP. Considering the fact that the thermal decomposition of CHP does not take place below 100°C, the reaction (5a) is also unlikely to occur appreciably at similarly low temperatures. The circumstances are almost same for the former mechanism (5), since, from the energetic point of view, (5) might be not so very different from the combination of the reactions (5a) and (5b).

As a matter of fact, the hydrogen abstraction from RH by O_2 is difficult without activation, as in the form of (Cat.$\cdots O_2$), as was reported in the previous paper.[2] However, this "activated form" of oxygen may also promote the formation of CA as might be readily expected from the ability of hydrogen abstraction of activated O_2. This point has already been discussed.[1,2]

$$\mathrm{RO}\cdot + \mathrm{RH} + \mathrm{Cat.}\cdots\mathrm{O_2} \rightarrow \mathrm{ROH} + \mathrm{RO_2}\cdot + \mathrm{Cat.} \qquad (6)$$

On the other hand, we may consider the process to be divided into three elementary steps:

$$\mathrm{RH} + \mathrm{Cat.}\cdots\mathrm{O_2} \rightarrow \mathrm{R}\cdot + \mathrm{Cat.} + \mathrm{HO_2}\cdot \qquad (6a)$$

$$\mathrm{RO}\cdot + \mathrm{HO_2}\cdot \rightarrow \mathrm{ROH} + \mathrm{O_2} \qquad (6b)$$

$$\mathrm{R}\cdot + \mathrm{O_2} \rightarrow \mathrm{RO_2}\cdot \qquad (6c)$$

Reaction (6) would be very easy because of its small activation energy (below 5.25—6.15 kcal/mol).[2] Therefore, reaction (6) is considered to be more plausible than (5) for the mechanism of CA formation. The saturation phenomena in the CA

*2 Reaction (2) is supported by the study of Bateman and Hughes[9] on olefin oxidation, in which the bimolecular mechanism appears at a temperature lower than about 80°C.

*3 Following our preliminary experiments, the thermal decomposition of CHP (22.5 mmol) in cumene (20 ml) occurred in the amounts of 0.50 mmol for 10.3 hr and 1.20 mmol for 9.0 hr at 65 and 80°C respectively.

*4 0.50 mmol of CHP was subjected to thermal decomposition to produce 5.2 mol% of CA and 63.8 mol% of AP after 10.3 hr, while 12.5 mmol of CHP was decomposed by the use of the sulfonium catalyst to produce 9.6 mol% of CA and 41.2% of AP.

*5 The bond dissociation energies of H-O_2. and R-H are 47.1 ± 2 kcal[12] and 85 kcal respectively. Therefore, the activation energy of the reaction (5a) is estimated to be *ca.* 38 kcal. On the other hand, by the use of the D(H-O_2·)=36 kcal/mol estimated by Uri,[13] it is estimated to be *ca.* 49 kcal/mol.

11) H. S. Blanchard, *J. Am. Chem. Soc.*, **81**, 4548 (1959).

12) S. N. Fonor and R. L. Hudson, *J. Chem. Phys.*, **36**, 2681 (1962).

13) N. Uri, *Chem. Revs.*, **50**, 375 (1952).

TABLE 3. EFFECT OF CATALYST AMOUNT UPON PRODUCT COMPOSITION AT PROPAGATION AND TERMINATION STEPS* (reaction temperature: 70°C)

Catalyst amount (mmol/ml × 10^3)	Reaction time (hr)	O_2 absorbed (mmol)	CHP (%)**	DCP (%)**	AP (%)**	CA (%)**
3.35	4.0	7.10	80.5	5.4	3.7	9.7
	8.0	11.80	75.4	5.2	5.4	12.4
10.05	4.0	8.90	68.5	5.1	15.5	10.0
	8.0	16.7	55.1	4.4	22.8	14.6
16.65	4.0	12.1	59.9	—	15.57	—
	8.0	18.1	51.9	7.0	25.6	14.1
26.80	4.0	14.2	50.0	6.1	21.60	13.2
	8.0	19.5	48.7	4.2	32.4	14.9
36.85	4.0	15.0	—	—	—	—
	8.0	25.5	35.5	—	48.8	—

* For choice of reaction time of 4 and 8 hr as representing the propagation and termination steps respectively, see the text.

** Percents of CHP, AP and CA are defined by (mol of compound found)/(mol of O_2 absorbed), while DCP% is defined by 2×(mol of DCP found)/(mol of O_2 absorbed).

TABLE 4. OXIDATION PRODUCTS AT TERMINATION STEPS (reaction temperature: 85°C, reaction time: 4.0 hr)

Catalyst amount (mmol/ml × 10^3)	O_2 absorbed (mmol)	Weight increase (mg)	CHP (%)*	DCP (%)*	AP (%)*	CA (%)*
3.35	4.88	114.0	41.0	11.4	32.7	11.5
16.65	7.43	143.8	31.6	9.55	37.4	11.1
20.10	7.81	209.8	29.1	10.0	39.6	17.8
33.5	6.85	168.3	20.5	—	40.2	—
67.0	8.99	233.9	23.4	3.68	41.2	20.5

* Percents of CHP, AP and CA are defined by (mol of compound found)/(mol of O_2 absorbed), while DCP (%) is defined by 2×(mol of DCP found)/(mol of O_2 absorbed).

formation as the reaction proceeds, as may be observed in Table 3, may thus be explained by the deactivation of the catalyst as a result of the masking action of the products.

Traylor and Russell[5] emphasized that CHP was a better hydrogen atom source than cumene, proposing the reaction:

$$RO\cdot + ROOH \rightarrow ROH + RO_2\cdot \qquad (7)$$

on the basis of the fact that CH_3OD was isolated from the decomposition of deuterated hydroperoxide (CH_3OOD).[14] However, the bond-dissociation energy of ROO–H (~89.5 kcal[15]) is rather larger than that of hydrocarbon (RH) (~85 kcal). This implies that reaction (7) is not easier than (4a), particularly at low temperatures. Moreover, reaction (7) is not probable at low concentrations of the hydroperoxide.

Further possible paths to CA, for example, $CH_3O_2\cdot + RO_2\cdot \rightarrow CH_2O + ROH + O_2$, seem not to be dominant for a reason to be discussed later.

AP Formation. Acetophenone (AP) is formed through a β-scission of the methy radical, (4b). Reaction (4b) is predominant rather than reaction (4a), as is indicated in Table 4. The difference in activation energies (about 7.3 kcal) between (4a) and (4b) was also reported by Bailey and Godin.[16]

Formation of DCP. Under the conditions of low-temerature oxidation, a chain-terminating step by coupling, (4c), is also to be taken into account. DCP is thermally stable at 70—85°C, but it should be noticed that the scission of the O–O linkage of common peroxides is easier than that of hydroperoxides. The activation energy of the O–O bond fission of dialkyl peroxides (~36.2 kcal[17]) is smaller than that of alkyl hydroperoxide (~38.5 kcal[18]). Actually, the rate of the thermal decomposition of DCP is found to be appreciably faster than that of CHP.[18] As is shown in Table 3, the amount of DCP decreases as the reaction proceeds, corresponding to the decomposition of DCP accumulated.

14) C. Walling, "Free Radicals in Solution," John Wiley and Sons, New York, N. Y. (1957), p. 444.

15) S. W. Benson, *J. Am. Chem. Soc.*, **86**, 3922 (1964).

16) H. C. Bailey and G. W. Godin, *Trans. Faraday Soc.*, **52**, 68 (1956).

17) A. D. Kirk and J. H. Knox, *ibid.*, **56**, 1296 (1960).

18) A. V. Tobolsky and R. B. Mesrobian, "Organic Peroxides," Interscience Publishers, New York (1954), pp. 88—89.

Table 4 indicates that the catalyst lessens the formation of DCP. Here it must be remarked that the catalyst accelerates the decomposition of CHP to produce RO·. Accordingly, it may rather be expected that the DCP formation would increase on that account, especially at a low temperature, provided that the catalyst does not force the decomposition of DCP. In reality, DCP is considerably decomposed by the catalyst in cumene without O_2 at 85°C, forming AP predominantly and also CA in an appreciable amount,*6 whereas thermally the decomposition is far smaller.

$$ROOR \xrightarrow{\text{sulfonium catalyst}} 2RO\cdot \rightarrow \text{(4a) or (4b)} \quad (8)$$

The decomposition of DCP is, therefore, one of the pathways to AP and CA.*7 The thermal decomposition of DCP in cumene has been studied by Bailey and Godin,[14] who reported that the ratio of AP to CA varied from 0.68 to 1.95 in the range from 111.2°C to 160°C. This phenomenon may suggest that AP formation is more strongly accelerated by the temperature than is CA formation. This point will be discussed again later.

Formation of RO_4R. Mention should be made here of the possible coupling of cumylperoxy radicals ($RO_2\cdot$) to form unstable intermediates (RO_4R).*8

$$RO_2\cdot + RO_2\cdot \longrightarrow \left[R-O-\overset{\overset{O}{\uparrow}}{O}-\overset{\overset{O}{\uparrow}}{O}-R \right] \longrightarrow 2RO\cdot + O_2 \quad (9)$$

The RO· radical produced will undergo reactions according to the three schemes (4a), (4b), and (4c).

Besides the process (4c), there seems to be another direct route to ROOR possible, as has been pointed out by Russel[19] in the case of secondary alkyl tetroxide:

$$RO_4R \rightarrow ROOR + O_2 \quad (10)$$

Boozer and his co-workers[21] suggested the following reaction in their study using deutrocumene at 65°C:

$$RO_4R \rightarrow ROOH + C_6H_5C(CH_3)=CH_2 + O_2 \quad (11)$$

This reaction is, however, doubtful in the present case because no α-methylstyrene is detected in our experiments. The unreliability of reaction (11) can also be concluded in view of the result of an ^{18}O-tracer study by Bartlett[3] of the recombination of the cumyloxy radical.

Behavior of the Methyl Radical. Methyl radicals are produced through the β-scission of RO·. They are converted to the peroxy radical in the following way:

$$CH_3\cdot + O_2 \rightarrow CH_3OO\cdot \quad (12)$$

Other possibilities for the disappearance of $CH_3\cdot$ involve various chain-transferring and chain-terminating reactions:

$$CH_3\cdot + RH \rightarrow CH_4 + R\cdot \quad (13a)$$

$$CH_3\cdot + ROOH \rightarrow CH_4 + RO_2\cdot \quad (13b)$$

$$CH_3\cdot + CH_3\cdot \rightarrow C_2H_6 \quad (14)$$

$$CH_3\cdot + RO\cdot \rightarrow CH_3OR \quad (15)$$

$$CH_3\cdot + RO_2\cdot \rightarrow CH_3OOR \quad (16)$$

Of these, (15) and (16) are not likely in the present low-temperature oxidation since neither cumylmethyl ether nor cumylmethyl peroxide was detected. Also, reaction (14) may be discarded in this case because of the low concentration of $CH_3\cdot$ radicals. Consequently, the hydrogen abstraction reactions, (13a) and (13b), seem to be almost the only pathway of $CH_3\cdot$ consumption.

The activation energy of (13a) is relatively small.*9 Actually, methane is detected in the decomposition of CHP by triphenylsulfonium chloride at 65°C.*10 Also, reaction (13b) can not be disregarded. Kharasch and his co-workers have confirmed the methane formation from thermal decomposition of CHP in decane at 140°C. In that case, however, decane can not be a good hydrogen source. In the present case, (13a) seems to be preferable.

In the presence of an appreciable amount of molecular oxygen, however, reaction (12) might be preferable to (13). The behavior of methyl-

*6 92% of the DCP (initial amount=22.5 mmol) in cumene is decomposed by triphenylsulfonium chloride (22.5 mmol) in about 11.0 hr at 85°C, thus forming AP (52.3%) and CA (36%), but thermally it decomposes only about 34% of the initial amount during the same reaction time.

*7 DCP melts at 39°C and is less stable than CHP. The scission of the O-O bond of DCP has a smaller energy of activation (34.5 kcal/mol)[16] than that of CHP (~38 kcal).

*8 The formation of RO_4R was first proposed by Russell[19] for *s*-alkylperoxy radicals. The transitory existence of this intermediate has also been supported by Milas and Djokic[20] in their study of the ozonization of potassium *t*-perbutoxide. A crystalline solid isolated at −78°C, which might be expected to be di-*t*-butyl tetroxide, decomposed spontaneously at −30 to 0°C to give equivalent amounts of di-*t*-butyl peroxide and oxygen molecules. The possibility of the presence of RO_4R is suggested by a recent thermochemical calculation by Benson.[11]

19) G. A. Russell, *J. Am. Chem. Soc.*, **79**, 3781 (1957).

20) N. A. Milas and S. M. Djokic, *Chem. Ind. (London)*, **1962**, 405.

21) C. E. Boozer, B. W. Pounder, J. C. Trisler and C. E. Wightman, *J. Am. Chem. Soc.*, **78**, 1506 (1956).

*9 We assume that $R=\alpha$-cumyl is almost equal to or less than $R=t$-butyl in reaction (13) and cite the value of 7.7 kcal after Tikhomirova.[22]

22) N. N. Tikhomirova and V. V. Voevodskii, *Chem. Abstr.*, **45**, 9940 (1951) (*Doklady Akad. Nauk S.S.S.R.*, **79**, 993 (1951)).

*10 Some CHP (4.50 mmol) in cumene (20 ml) is decomposed by $(C_6H_5)_3SCl$ (0.27 mmol) for 9.0 hr to produce about 30 mol% of methane.

peroxy radicals thus formed is still obscure. Traylor and Russell[5] have proposed the following path:

$$CH_3OO\cdot + RO_2\cdot \rightarrow CH_2O + ROH(CA) + O_2 \quad (17)$$

In the low-temperature oxidation, however, CA formation is depressed remarkably, as has been reported by Blanchard,[11] while AP is produced dominantly. If all of the methyl radicals formed are converted to methylperoxy radicals according to reaction (12), the amount of CA should, stoichiometrically, be not less than that of AP. In reality, however, the quantity of CA is much less than that of AP. By means of scheme (17) only, this fact can not be explained. Another route to AP may, for instance, be of the following type:

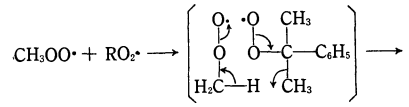

$$CH_2O + AP + CH_4 + O_2 \quad (18)$$

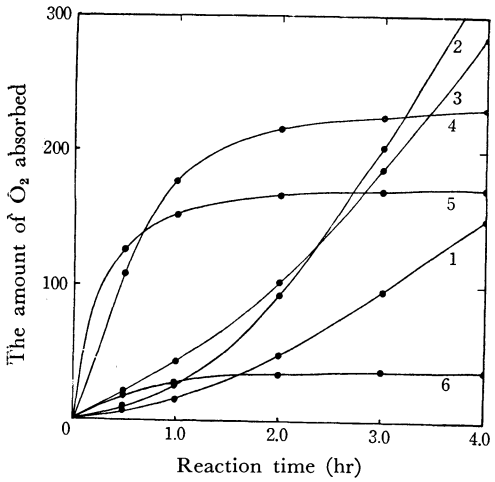

Fig. 3. temperatuee effect on oxygen absorption by the use of $(C_6H_5)_3SCl$ (16.65×10^{-3} mmol/m*l*). 1: 55°C; 2: 65°C; 3: 70°C; 4: 80°C; 5: 100°C; 6: 120°C

Such a concerted, complicated process may be possible in the solvent cage, just as in the case of Eq. (9).

Temperature Effect. The present experiment was carried out in the temperature range from 55 to 85°C; in this range sulfonium catalysts are relatively stable. In order to specify the influences of temperature on the oxidation process, a higher-temperature range up to 120°C was also employed. Figure 3 indicates that the reactions below 70°C are clearly autocatalytic, while those above 80°C are auto-retarding. The latter ones may be ascribed to the deoxygenation of the catalyst-oxygen complex according to the increase in the temperature*11 and by means of the masking action of products. The variation in the products with the reaction temperature is indicated in Table 5. The decrease in CHP with the temperature is remakable, while AP and CA apparently increase as the temperature rises, the former more than the latter. Such a difference in the temperature effect of AP and CA is reasonable. The former arises from an intramolecular reaction of RO· in which the vibrational cleavage of the carbon-methyl bond takes place as a result of the participation of adjacent π orbitals. The latter is produced by an intermolecular hydrogen abstraction from RH; the rate of such a process may be controlled by the steric hindrance of two bulky reactants. The temperature dependence of the (AP/CA) ratio has been found to be 7.3 kcal.[16] In the present catalytic process, it is noted that the CA formation through reaction (6) is also depressed with the increase in the temperature as a result of the deoxygenation of the catalyst complex.

Additive Effect. The deactivation of the sulfonium catalyst, possibly caused by a masking action of oxidation products, is deduced from the effect of various additives on the rate of oxygen absorption. Table 6 displays the decrease in the initial maximum rate[2] of oxygen absorption and the lengthening of the induction period. The decrease in the rate is particularly remarkable in

TABLE 5. EFFECT OF TEMPERATURE UPON PRODUCT COMPOSITION
(catalyst amount: 16.65×10^{-3} mmol/m*l*; reaction time: 4.0 hr)

Reaction temperature (°C)	O_2 absorbed (mmol)	Weight increase (mg)	CHP (%)*	DCP (%)*	AP (%)*	CA (%)*
55	6.26	166.9	78.3	6.37	8.10	7.8
65	13.1	247.8	60.7	5.42	21.1	12.6
80	9.46	315.4	38.47	11.7	34.4	20.8
100	6.58	—	4.57	—	56.0	28.5
120	1.25	13.1	1.44	17.0	63.2	26.2

* Per cents of CHP, AP and CA are defined by (mol of compound found)/(mol O_2 absorbed), DCP (%) is defined by $2\times$(mol of DCP found)/(mol of O_2 absorbed).

*11 The large optical density of the absorption band of a possible methyl-cyclohexane-oxygen complex is observed at lower temperatures (H. Tsubomura and R. P. Lange, *J. Chem. Phys.*, **36**, 2155 (1962)).

the case of CA. The reason may be the masking action of the additives through their shielding of *d* orbitals of the catalyst, as has been described previously.[1,2] It has been ascertained that the sulfonium catalysts are not decomposed by these reaction products.[1]

Table 6. The effect of addition of product molecules upon initial maximum rate[a] and the length of induction period at 70°C (catalyst amount 3.35×10^{-4} mmol/ml)

Product	Amount (mmol)	Rate (max.) (mol l^{-1} $sec^{-1}\times10^4$)	Induction period[b] (sec)
None	—	1.76 (0.29)*	0 (450)*
CHP	6.75	1.12 (0.31)*	70 (300)*
	9.00	1.04	75
	18.0	0.64	180
DCP	6.75	1.54 (0.33)*	40 (270)*
	18.0	1.50	60
AP	1.70	0.894 (0.26)*	30 (480)*
	4.28	0.745	70
	8.55	0.706	120
	17.0	0.297	190
CA	1.70	0.12 (0.19)*	360 (600)*
	4.28	0.00	—

a) The maximum rate appeared at the initial step in the oxidation[2] using $(C_6H_5)_3SCl$.
b) The period was determined as the time passed from the start of oxygen absorption.
* The values in the parentheses were those obtained without use of catalyst. In this case, the maximum rate was calculated from the oxygen absorption curve at the reaction time of 1.0 hr.

Table 7. The amount of oxygen absorbed and cumene hydroperoxide content in the oxidation of cumene saturated with various chlorides (reaction temperature: 70°C; reaction time: 8.0 hr)

Catalyst (MCl) (M)	O_2 absorbed (mmol)	CHP (%)[a]
Li	18.2	35.6
Na	0.64	98.7
K	1.27	100
Rb	1.36	98.5
Cs	1.48	96.6
NH_4	0.43	100
$(C_6H_5)_3S$	18.6	50.6
None	5.73[b]	98.2

a) Calculated as mol CHP per 100 mol oxygen absorbed.
b) Reaction time was 17.5 hr.

It should be taken into account that the effect of product addition appears even in autoxidation without a catalyst. The promoting effect observed in the cases of CHP and DCP might be attributed to their action as initiators. Inhibitory action of CA (and, less remarkably, of AP) in thermal processes is observed, but the extent never exceeds the usual alcohol effect.[23] It is of interest that the catalyst activity of triphenylsulfonium chloride is almost independent of the chloride anion concentration. Table 7 compares the catalytic activities of various alkali chlorides and triphenylsulfonium chloride in the oxidation of cumene saturated with them. The oxygen absorption is never in proportion to the content of the chloride anion, a proportion to be expected from Table 1.*12

Summarized Scheme of the Reaction. In conclusion, the reaction mechanism is summarized schematically in Fig. 4 for help in understanding it.

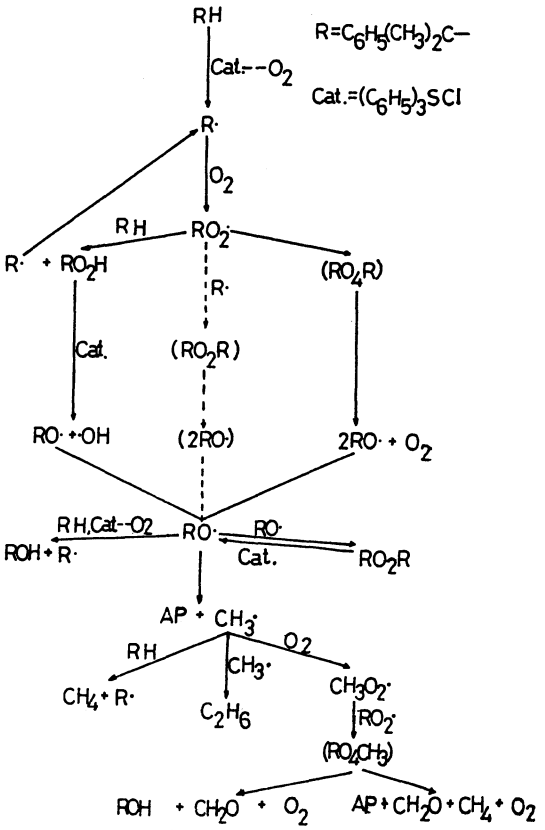

Fig. 6. A scheme for the mechanism of cumene oxidation by the use of $(C_6H_5)_3SCl$.

23) For instance, see a) K. U. Ingold, *Chem. Revs.*, **61**, 563 (1961). b) K. Negoro and T. Sawada, *Kyogyo Kagaku Zasshi (J. Chem. Soc. Japan, Ind. Chem. Sect.)*, **67**, 1105, 1172 (1964). c) J. Yamashita, K. Kurashima, M. Tobita and H. Hashimoto, *ibid.*, **67**, 1153 (1964).

*12 The activity of lithium chloride will be discussed later.

BULLETIN OF THE CHEMICAL SOCIETY OF JAPAN VOL. 42 2228—2232 (1969)

The Mechanism of the Scintillation from a Benzene Solution of *p*-Terphenyl

Tsunenari SAITO and Shin SATO

Department of Applied Physics, Tokyo Institute of Technology, Ookayama, Meguro-ku, Tokyo

(Received February 4, 1969)

The luminescence from a benzene solution containing *p*-terphenyl induced by γ-ray irradiation has been compared with that induced by UV irradiation at 2500 Å in the presence of various quenchers. The quenching efficiencies of electron and positive ion scavengers (SF_6, N_2O, CO_2 and NH_3) were found to be greater for the γ-ray excitation than for the UV excitation, while 1,3-butadiene, which is known as a quencher for excited benzene, ($^1B_{2u}$), showed almost the same efficiency for both modes of excitation. These results suggest that, even in a benzene solution, a series of ionic reactions is partly responsible for the formation of the scintillating state of *p*-terphenyl, and that the apparent quenching effect of ion scavengers is mainly due to their interference in the formation of the excited state of the benzene which is produced by the recombination reaction between the benzene cation and an electron. It was estimated that more than 30% of the excited state of benzene is formed by the recombination reaction.

In previous papers[1] we have shown that the luminescence from a cyclohexane solution containing *p*-terphenyl (*p*TP) irradiated with γ-rays is quenched by electron and positive ion scavengers and have suggested that the following ionic processes occur in this scintillator solution:

$$C \begin{cases} \xrightarrow{\sim\sim} C^+ + e & (1) \\ \xrightarrow{\sim\sim} C^* & (2) \end{cases}$$

$$T + e \rightarrow T^- \quad (3)$$

$$T + C^+ \rightarrow T^+ + C \quad (4)$$

$$T^- + C^+ \rightarrow T^* + C \quad (5)$$

$$T^+ + e \rightarrow T^* \quad (6)$$

$$T^+ + T^- \rightarrow T^* + T \quad (7)$$

Here, C, T, and T* denote cyclohexane, *p*TP, and a scintillating state of *p*TP respectively. The conclusions obtained in the previous papers are that the reaction (2) does not much contribute to the luminescence, and that the scintillating state of *p*TP is mainly formed by the neutralization reactions of the anions or cations of *p*TP. A similar conclusion has recently been reached by several groups of investigators. Thomas *et al.* used a pulse technique to elucidate the origin of the triplet state of scintillator molecules,[2] Ludwig analyzed the decay curve of the γ-ray induced luminescence in terms of ionic reactions,[3] and Hentz and Knight[4] used an electron-scavenging method similar to ours.

The present paper will show the results obtained by using a benzene solution containing *p*-terphenyl as a scintillator solution and will discuss the role of charged species in the γ-ray induced luminescence. Hitherto, many investigations have been carried out on this scintillator solution, but most of the investigations have not paid any attention to the participation of charged species in the mechanism of the scintillation.

Experimental

Dotite Spectrosol benzene and scintillation-grade *p*TP supplied by the Nakai Chemical Co. were used without purification. Nitrous oxide, ammonia, sulfur hexafluoride, 1,3-butadiene, and carbon dioxide purchased from the Takachiho Trading Co. were used after bulb-to-bulb distillation. The cyclohexane was purified in a manner described previously.[1]

Figure 1 shows the arrangement of the apparatus for measuring the intensity of the luminescence from a solution. A Toshiba UV-31 filter was inserted between the solution vessel and a photomultiplier (Toshiba SY-99) in order to cut off the luminescence from benzene itself. The source of γ-rays was 1.3 mCi-^{60}Co sealed in a glass tube. As the UV light sources at 3100 Å and 2400—2600 Å, a Hitachi hydrogen discharge lamp and a Beckman monochromator were used. When we

1) Yoshida and S. Sato, This Bulletin, **40**, 2216 (1967). T. Saito, K. Takahashi and S. Sato, *ibid.*, **41**, 2603 (1968).

2) J. W. Hunt and J. K. Thomas, *J. Chem. Phys.*, **46**, 2954 (1967); J. K. Thomas, K. Johnson, T. Klippert and R. Lowers, *ibid.*, **48**, 1608 (1968); R. Cooper and J. K. Thomas, *ibid.*, **48**, 5097 (1968).

3) P. K. Ludwig, *Mol. Cryst.*, **4**, 147 (1968); P. K. Ludwig and M. M. Huque, *J. Chem. Phys.*, **49**, 805 (1968).

4) R. R. Hentz and R. J. Knight, *J. Phys. Chem.*, **72**, 1783 (1968).

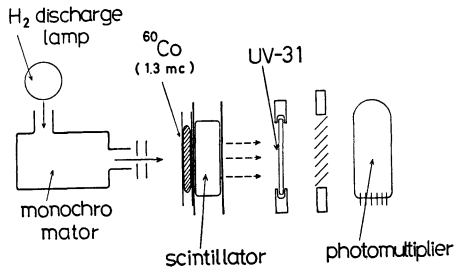

Fig. 1. Arrangenment of the apparatus.

used the lights at 3100 Å, which excite only *p*TP molecules in a solution, the arrangement of the apparatus was changed so that the excitation beam could not directly enter the photomultiplier. When the UV lights used were in the 2400—2600 Å range and the apparatus was arranged as is shown in Fig. 1, essentially all the light impinging into the vessel was absorbed by benzene, since the concentration of *p*TP used in this experiment did not exceed 4.0×10^{-4} moll^{-1}, while the ratio of the optical density of benzene to that of *p*TP at 2400 Å was 250 : 1. In preparing the solutions, benzene containing a certain amount of *p*TP was degassed by freeze-and-thaw cycles in a mercury-free high-vacuum manifold. The concentration of an added gas in a solution was calculated by using the Ostwald absorption coefficient separately measured. The method of the measurement has already been described.[1] The Ostwald absorption coefficients in benzene obtained at 30°C were as follows: 2.7 for nitrous oxide, 0.67 for sulfur hexafluoride, 2.4 for carbon dioxide, and 7.5 for ammonia. 1,3-Butadiene was assumed to be completely soluble.

In order to ascertain the reactivity of electrons to nitrous oxide and sulfur hexafluoride in benzene, the *G*-value of the nitrogen from a benzene solution of nitrous oxide in the presence of sulfur hexafluoride was measured by using a method previously described.[5,6]

Results

Direct Excitation of *p*-Terphenyl. Figure 2 summarizes the effects of electron and positive ion scavengers and 1,3-butadiene on the luminescence from a cyclohexane solution of *p*-terphenyl when excited by light at 3100 Å. These experiments were carried out in order to establish whether or not any direct interaction between excited *p*TP and quenchers exists. Obviously, all the ion scavengers do not interact with the scintillating state of *p*TP, but 1,3-butadiene does a little, as was expected. The data obtained with 1,3-butadiene were well in accord with the Stern-Volmer relation (I):

$$I_0/I = 1 + \gamma[Q] \qquad (I)$$

The constant, γ, was obtained to be 0.68 $l$mol^{-1}. Here, [Q] denotes the concentration of the quencher.

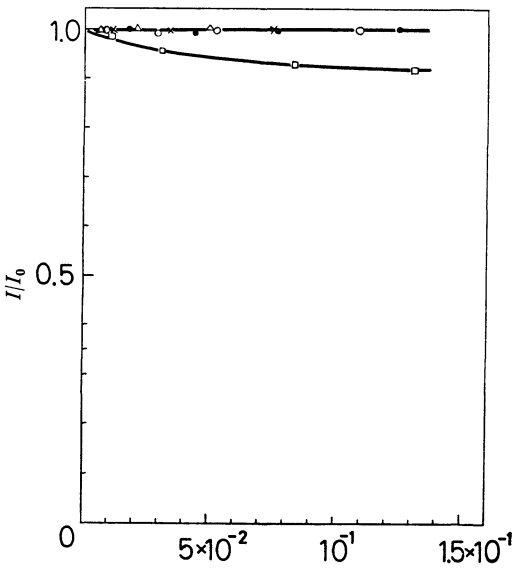

Concentration of quenchers, (mol/l)

Fig. 2. Quenching curves obtained with a cyclohexane solution.
[*p*TP]$=10^{-5}$ mol l^{-1}, excited by 3100Å;
□, 1,3-butadiene; ●, NH_3; ×, CO_2; Δ, SF_6; ○, N_2O

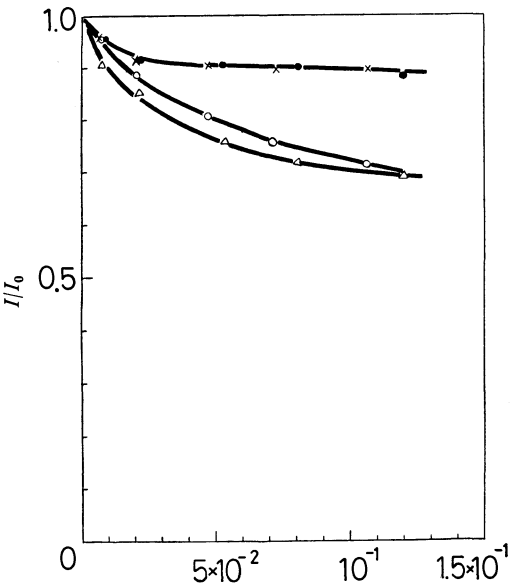

[N_2O], (mol/l)

Fig. 3. Quenching by nitrous oxide.
[*p*TP]$=4.4\times10^{-3}$ mol l^{-1}, ○, excited by γ-rays; ×, excited by UV; [*p*TP]$=4.0\times10^{-4}$ mol l^{-1}; Δ, γ-rays; ●, UV

I and I_0 are the intensities of the luminescence in the presence and in the absence of the quencher respectively.

Quenching Efficiencies of Electron and Positive Ion Scavengers. In Fig. 3, the relative emission intensities from *p*TP-benzene solutions

5) S. Sato, R. Yugeta, K. Shinsaka and T. Terao, This Bulletin, **39**, 156 (1966).

6) S. Sato, T. Terao, M. Kono and S. Shida, *ibid.*, **40**, 1818 (1967).

excited by light at 2500 Å and by γ-rays are plotted as a function of the nitrous oxide concentration. The concentrations of pTP used were 4.4×10^{-3} and 4.0×10^{-4} moll^{-1}. Here, two points should be noticed. First, the quenching ability of nitrous oxide under γ-rays is much greater than that under the UV lights. Second, the quenching ability does not depend much on the concentration of pTP.

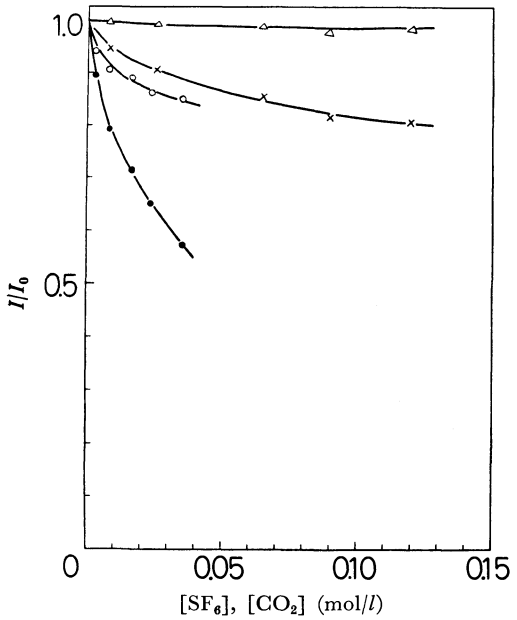

Fig. 4. Quenching by electron scavengers.
[pTP]$=4.0\times10^{-4}$ mol l^{-1}; △, CO_2(UV); ×, CO_2(γ-rays); ○, SF_6(UV); ●, SF_6(γ-rays)

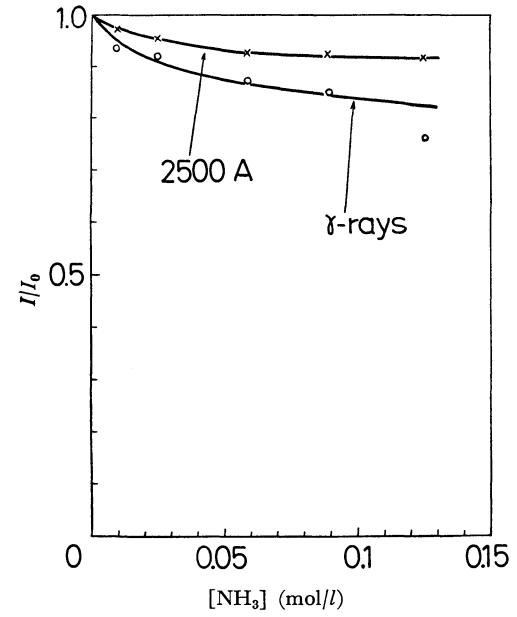

Fig. 5. Quenching by ammonia.
[pTP]$=4.0\times10^{-4}$ mol l^{-1}, ×, UV, ○, γ-rays

Similar experiments were also carried out using sulfur hexafluoride, carbon dioxide, and ammonia in place of nitrous oxide. The results are shown in Figs. 4 and 5. Obviously, the quenching abilities are in the following order: sulfur hexafluoride, nitrous oxide, carbon dioxide, and ammonia. All these quenchers are more effective under γ-rays than under UV light. Although the only UV lights used here were at 2500 Å, exactly the same quenching curves for each quencher were obtained by using the wavelengths of 2400 and 2600 Å.

Quenching by 1,3-Butadiene. Figure 6 shows the relative emission intensity as a function of the concentration of 1,3-butadiene. The quenching curves obtained under UV light and under γ-rays practically coincide with each other. This coincidence contrasts with the results obtained by using ion scavengers as the quencher.

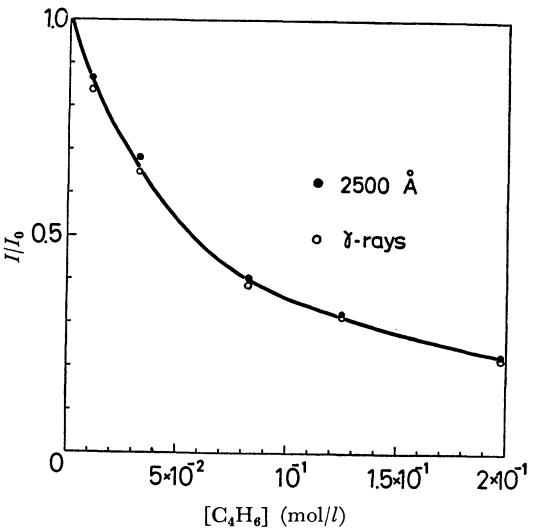

Fig. 6. Quenching by 1,3-butadiene.
[pTP]$=4.0\times10^{-4}$ mol l^{-1}

***G*-Values of Nitrogen from a Benzene Solution of Nitrous Oxide in the Presence of Sulfur Hexafluoride.** Table 1 summarizes the G-values of nitrogen from a benzene solution of nitrous oxide and sulfur hexafluoride. The significance of these data will be discussed later.

TABLE 1. EFFECT OF SULFUR HEXAFLUORIDE ON $G(N_2)$ FROM A BENZENE SOLUTION OF NITROUS OXIDE

N_2O mol l^{-1}	SF_6	$G(N_2)$
0.34	0	2.5
0.33	0.011	2.3
0.35	0.027	2.0
0.37	0.15	1.1
0.36	0.35	0.84
0.37	0.59	0.57

Discussion

As is shown in Fig. 2, ion scavengers did not interact with the scintillating state of *p*TP in the range of the concentrations of *p*TP and scavengers studied. On the other hand, these scavengers did quench the luminescence induced by UV at 2500 Å, although they were not strong. The quenching by carbon dioxide was practically negligible. Since the excitation energies of these scavenger molecules are not smaller than that of the $^1B_{2u}$ state of benzene, the simple energy-transfer mechanism cannot be used in the interpretation. One possible mechanism is that involving the formation of a charge-transfer complex between an excited benzene molecule and an ion scavenger molecule in the process. Since the quenching effects were not strong, the participation of impurities cannot be excluded.

When the excitation was made by γ-rays, the quenching effects of ion scavengers became prominent, as is shown in Figs. 3, 4, and 5. Even carbon dioxide showed the effect. This compound is now known as an electron scavenger in radiation chemistry.[6] These quenching effects may, therefore, be attributed to the interference of ion scavengers in the ionic process by which the scintillating state of *p*TP is formed. There are two possible mechanisms for such interference. One (Mechanism 1) is the competition between *p*TP and ion scavengers for the charged species produced in the system. This mechanism satisfactorily explains the quenching effect of ion scavengers in a *p*TP-cyclohexane scintillator.[1] If this mechanism plays a major role in the quenching, a strong dependence on the concentration of *p*TP should be observed, as has actually been observed in a *p*TP-cyclohexane scintillator. The other mechanism (Mechanism 2) is the interference of ion scavengers in the ionic process by which excited benzene is formed. This reaction scheme may be described as follows:

$$B \begin{cases} \xrightarrow{\sim\sim} B^+ + e_B & (8) \\ \xrightarrow{\sim\sim} B^* & (9) \end{cases}$$

$$B^+ + e_B \rightarrow B^* \quad (10)$$

$$e_B + S \rightarrow S^- \quad (11)$$

$$B^+ + S \rightarrow B + S^+ \quad (12)$$

$$B^+ + S^- \rightarrow B + S \quad (13)$$

$$B^* + T \rightarrow B + T^* \quad (14)$$

Here, B, S, and T denote, respectively, benzene, scavenger, and *p*-terphenyl molecules. The suffix B is attached to the electron e, in order to indicate that the electron is in benzene. If this mechanism is operative, the quenching curves should not depend strongly on the concentration of *p*TP, but this was actually observed. This discrimination, however, is not conclusive. Another support for Mechanism 2 will be given later.

Regardless of the mechanism of the interference of ion scavengers in the ionic processes occurring in the system, the quenching curves obtained under γ-ray irradiation suggest that a large part of the luminescence results from the ionic reactions. Since the luminescence from UV-irradiated benzene solutions was quenched by ion scavengers, as is shown in Figs. 3 and 4, the following tentative correction was made in an attempt to visualize the purely ionic effects of ion scavengers:

$$(I/I_0)_{corr} = (I/I_0)_\gamma / (I/I_0)_{UV} \quad (II)$$

Here, the subscripts γ and UV denote γ-ray and UV irradiations respectively. The results are plotted in Fig. 7. If sulfur hexafluoride behaves only as an electron scavenger, the corrected curve indicates that more than 30% of the excited benzene, which is the precursor of the scintillation, is formed by an ionic reaction, probably the recombination reaction between benzene cations and electrons.

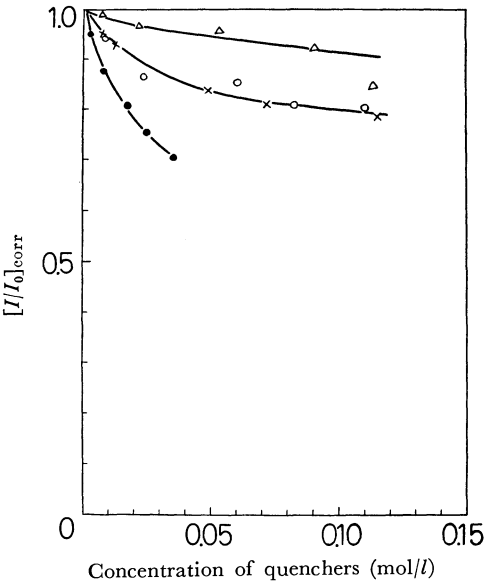

Fig. 7. $[I/I_0]_{corr}$ as a function of the concentrations of ion scavengers.
△, NH_3; ×, N_2O; ○, CO_2; ●, SF_6

According to Fig. 7, the electron-scavenging ability of sulfur hexafluoride is stronger than those of nitrous oxide and carbon dioxide. In cyclohexane solutions, however, the abilities were estimated to be almost the same for these three scavengers.[6] In order to interpret this discrepancy, we have measured the *G*-values of nitrogen from a benzene solution of nitrous oxide in the presence of various amounts of sulfur hexafluoride. The results are shown in Table 1. If a simple relation (III) is applicable to these data:[6]

$$\frac{1}{G(N_2)} = \frac{1}{G_0(N_2)}\left(1 + k\frac{[SF_6]}{[N_2O]}\right) \quad (III)$$

the slope k should show the ratio of the rate constant of the reaction of electrons with sulfur hexafluoride to that with nitrous oxide. As is shown in Fig. 8,

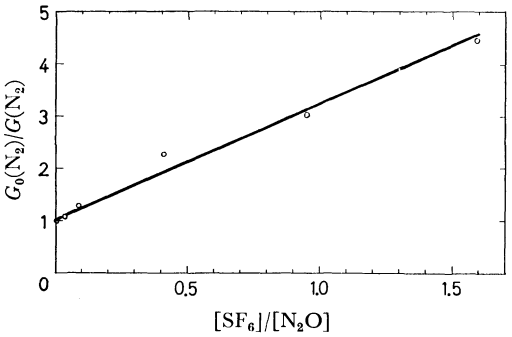

Fig. 8. Dependence of $G(N_2)$ on the concentration of sulfur hexafluoride.

a linear relationship has been obtained and the slope k has been calculated to be 2.2; this value should be compared with that of 1.0 obtained in a cyclohexane solution.[6] This difference qualitatively explains the difference between the two quenching curves obtained with sulfur hexafluoride and nitrous oxide. Electrons in benzene may be solvated more strongly than those in cyclohexane. This is not unreasonable, since aromatic hydrocarbons larger than benzene, such as naphthalene and biphenyl, are known to capture electrons to form anions.[7] Therefore, the reaction between electrons and electron scavengers in benzene may not be diffusion-controlled.

The quenching curves obtained with 1,3-butadiene are shown in Fig. 6. In the case of UV excitation, the species being quenched must be the $^1B_{2u}$ state of benzene.[8] If the ion-molecule reaction between the benzene cation and 1,3-butadiene is important in the present system, the quenching curve obtained by γ-ray irradiation should deviate from the curve obtained by UV irradiation, because the benzene cation must be the precursor of the $^1B_{2u}$ state of benzene and both the cation and the excited state of benzene are subject to the interference of 1,3-butadiene. The coincidence of the two quenching curves strongly suggests, therefore, that most of the benzene cations produced in the system are neutralized before the ion-molecule reaction with 1,3-butadiene occurs. In other words, Mechanism 2 is at least predominant in this system over Mechanism 1. However, a detailed inspection reveals that the quenching ability of 1,3-butadiene under γ-rays is a little stronger than that under UV light. This suggests that the participation of Mechanism 1 cannot be excluded conclusively. Recently, the G-value of "free electrons" in benzene has been measured as 0.053 by the conductivity method.[9] These electrons must contribute to the scintillation by the formation of p-terphenyl anions (Mechanism 1).

7) S. Arai and L. M. Dorfman, *J. Chem. Phys.*, **41**, 2190 (1964).

8) A. Morikawa and R. J. Cvetanović, *ibid.*, **49**, 1214 (1968).

9) W. F. Schmidt and A. O. Allen, *J. Phys. Chem.*, **72**, 3730 (1968).

BULLETIN OF THE CHEMICAL SOCIETY OF JAPAN VOL. 42 2232—2238 (1969)

ESR Studies of Bis-(*N*,*N*-diethylethylenediamine)copper(II) Perchlorate

Hiroshi Yokoi, Mitsuru Sai and Taro Isobe

The Chemical Research Institute of Non-Aqueous Solutions, Tohoku University, Katahira-cho, Sendai

(Received February 10, 1969)

The ESR of bis-(*N*,*N*-diethylethylenediamine)copper(II) perchlorate has been examined in the polycrystalline state at three temperatures corresponding to the color change in the copper(II) complex due to thermochromism, in the glassy state of an aqueous solution at the temperature of liquid nitrogen, and in the magnetically-diluted state in diamagnetic bis-(*N*,*N*-diethylethylenediamine)nickel(II) perchlorate powder at three temperatures corresponding to the color change of the diluent due to thermochromism. The g and A values for square planar copper(II) complexes have been discussed in connection with the strength of the axial ligand field. The ESR results indicate that the structure of bis-(*N*,*N*-diethylethylenediamine)copper(II) perchlorate changes remarkably according to its circumstances, and possible mechanisms for the thermochromism have been suggested.

The bis-(*N*,*N*-diethylethylenediamine)copper(II) perchlorate was found to exhibit many interesting properties: (1) It is one of the few red copper(II) complexes, while it turns purplish-blue in an aqueous

solution.[1,2] (2) The copper(II) complex exhibits thermochromism, a phenomenon which accompanies changes in crystal form and color.[1,3] (3) This copper(II) complex is known to be isomorphous to the diamagnetic nickel complex bis-(*N,N*-diethylethylenediamine)nickel(II) perchlorate, which also exhibits two steps of thermochromism.[3,4]

The copper(II) complex is *trans*-square coplanar, and two perchlorate anions are located at the axial position.[2,3] As to the structure of the complex, this is the only information so far reported. No satisfactory explanation for the structural mechanism of the thermochromism has yet been given. Therefore, more detailed and reliable information on the structure of the complex in various states is needed before we can understand the many interesting properties of the complex. The ESR technique is very useful for the study of the ligand field in metal complexes, and it has been widely applied to various copper(II) complexes.[5-9] The purpose of this paper is to discuss the ESR results on the copper(II) complex with the aim of estimating its structure and properties in various states, and their dependence on its molecular circumstances.

Experimental

The *N,N*-diethylethylenediamine, represented below, was a commercially-available substance. The bis-deen copper(II) perchlorate was prepared by the method in the literature[1] and was then recrystallized from methanol. In order to obtain magnetically-diluted samples, diamagnetic nickel complexes, bis-deen nickel(II) perchlorate, bis-deen nickel(II) tetrafluoroborate, diiodo-bis-deen nickel(II), and dinitrato-bis-deen nickel(II), were prepared using nickel(II) salt containing 1% of the cupric salt of the same anion, according to the method of the literature.[4] These samples are represented as Ni-ClO_4, Ni-BF_4, Ni-I, and Ni-NO_3 respectively. Although the amount of copper in each of these samples was not determined accurately in this investigation, proper magnetical dilution seemed to have been done for all the samples judging from the resolution of hyperfine structures and the S/N ratio of their ESR spectra, as shown, for example, in Figs. 2 and 3.

The ESR spectra were measured with a Hitachi X-band and a K-band ESR spectrometer, Model MES-4001, equipped with a 100 kc/s field modulation unit; furthermore, the second derivative ESR spectra were obtained using 100 kc/s-40 c/s field modulations in order to resolve the nitrogen super-hyperfine structure clearly. The field was calibrated with an NMR probe, and then with a benzene solution of vanadyl acetylacetonate. The ESR measurements were carried out at the temperatures of −196, 22, and 80—125°C for powdered samples and at −196°C in the glassy state for a *ca.* 0.01 M solution, using an equivolume mixture of water and methanol as the solvent. The ESR spectra thus obtained are shown in Figs. 1—5.

Results and Discussion

Polycrystalline State. The ESR line shapes for the polycrystalline samples of $S=1/2$ have been studied extensively by several authors.[10-12] From the ESR spectrum of the polycrystalline copper(II) complex, three approximate principal g values can be obtained, and a rough estimate for the line width along each of the principal axes may be made. The latter is, of course, connected with the spin interaction among neighboring cupric ions in a crystal.[13]

Figure 1 shows the ESR spectra of the polycrystal of bis-deen copper(II) perchlorate measured at three temperatures. This complex is brick red at room temperature and blue above 44°C. Furthermore, the complex has been found in this study to become pale red on cooling to the temperature of liquid nitrogen. This suggests that one more step of phase transition exists between room temperature and −196°C, although the phase-transition point was not determined precisely. This fact is also strongly supported by the clear differences in line shape among the three ESR spectra shown in Fig. 1, each being measured in the temperature range corresponding to each of the transition phases. These phases are called, in the order of temperature, the lower-temperature phase, the

1) P. Pfeiffer and H. Glasser, *J. prakt. Chem.*, **151**, 134 (1938).
2) S. Yamada and S. Miki, This Bulletin, **36**, 680 (1963).
3) W. E. Hatfield, T. S. Piper and U. Klabunde, *Inorg. Chem.*, **2**, 629 (1963).
4) D. M. L. Goodgame and L. M. Venanzi, *J. Chem. Soc.*, **1963**, 616.
5) A. Abragam and M. H. L. Pryce, *Proc. Roy. Soc. (London)*, **A205**, 135 (1951); K. W. H. Stevens, *ibid.*, **A219**, 542 (1953).
6) A. H. Maki and B. R. McGarvey, *J. Chem. Phys.*, **29**, 31, 35 (1958).
7) D. Kivelson and R. Neiman, *ibid.*, **35**, 149 (1961).
8) H. Yokoi and T. Isobe, This Bulletin, **41**, 2835 (1968).
9) B. G. Malmstom and T. Vanngard, *J. Mol. Biol.*, **2**, 118 (1961); A. H. Maki, N. Edelstein, A. Davison and R. H. Holm, *J. Am. Chem. Soc.*, **86**, 4580 (1964); M. Sharnoff, *J. Chem. Phys.*, **42**, 3383 (1965); R. C. Slade, A. A. G. Tomlinson, B. J. Hathaway and D. E. Billing, *J. Chem. Soc.*, **1968**, 61.
10) E. L. Cochran, F. J. Adrian, and V. A. Bowers, *J. Chem. Phys.*, **34**, 1161 (1961); R. Lefebre, *ibid.*, **33**, 1826 (1960).
11) F. K. Kneubuhl, *ibid.*, **33**, 1074 (1960).
12) J. W. Searl, R. C. Smith and S. J. Wyard, *Proc. Phys. Soc.*, **78**, 1174 (1961).
13) P. W. Anderson and P. R. Weiss, *Rev. Mod. Phys.*, **25**, 269 (1953); H. Abe, K. Ono, I. Hayashi, J. Shimada and K. Iwanaga, *J. Phys. Soc. Japan*, **9**, 814 (1954).

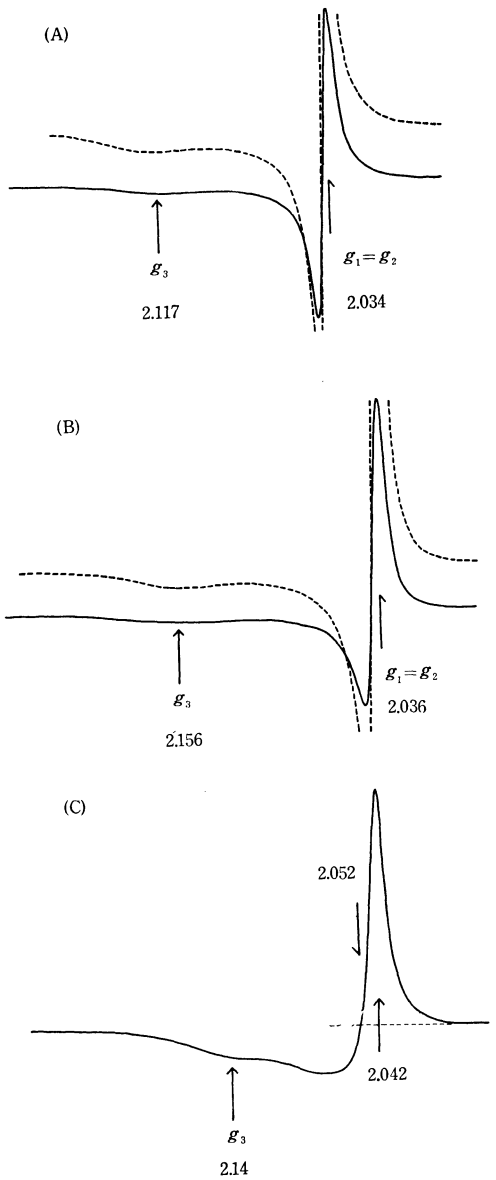

Fig. 1. The K-band ESR spectra of bis-(*N*,*N*-diethylethylenediamine)copper(II) perchlorate in poly-crystalline state. The spectra of dotted line are in case where amplification increased. The numbers represent *g* values.
(A) at −196°C, (B) at 22°C, (C) at 80°C

room-temperature phase, and the higher-temperature phase respectively.

The line shapes for all of the ESR spectra shown in Fig. 1 consist of one very intense absorption in the high-field part and one very weak and broad absorption in the low-field part, the latter being hardly observable by X-band measurement. This spectral feature apparently agrees with that of square planar copper(II) complexes, where the relation among three principal *g* values (assumed as $g_1 \leq g_2 \leq g_3$) is $g_1 \fallingdotseq g_2 < g_3$, which results from an axial or near axial symmetry in the ligand field. The numbers in the ESR spectra of Fig. 1 represent the results analyzed. Spectrum (A) in this figure is quite similar in line shape to (B) except that the *g* values are somewhat greater in (B) than in (A). However, Spectrum (C) is quite different in line shape from the (A) and (B) spectra, especially in the line shape of the intense absorption in the high-field part. A possible explanation for this is that the difference between the values of g_1 and g_2 is somewhat larger in (C) than in (A) and (B). In (C) the mean value of g_1 and g_2 could be estimated to be about 2.05. Furthermore, g_3 was smaller in (C) than in (B). Accordingly, although the phase-transition of the crystal is necessarily accompanied

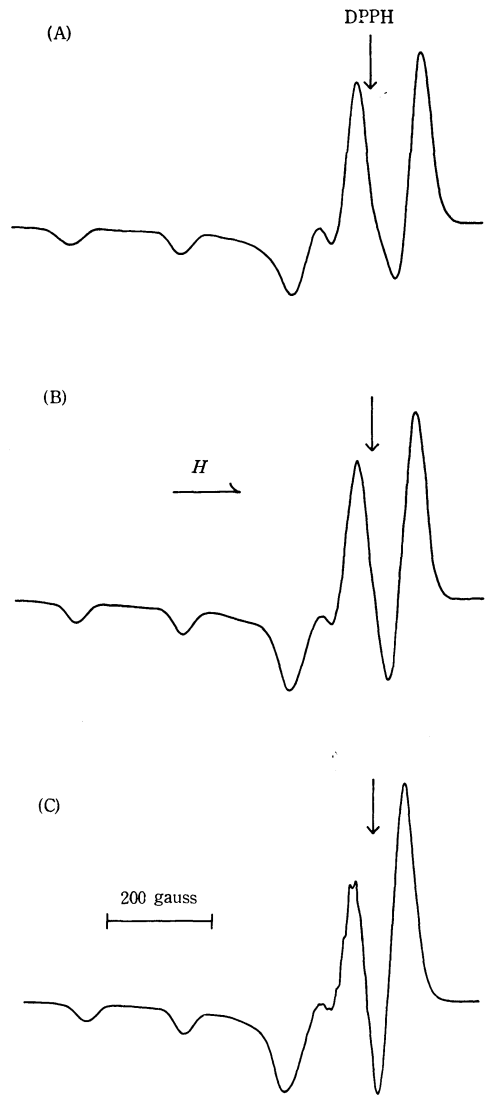

Fig. 2. The X-band ESR spectra of bis-(*N*,*N*-diethylethylenediamine)copper(II) perchlorate magnetically diluted in bis-(*N*,*N*-diethylethylenediamine) nickel(II) perchlorate powder.
(A) at −196°C, (B) at 22°C, (C) at 120°C

by some structural change in the constituent molecules, the structural change in this copper(II) complex from the room-temperature phase to the higher-temperature phase is not of the same type as that from the lower-temperature phase to the room-temperature phase.

Magnetically-diluted Powdered Samples. Bis-deen nickel(II) perchlorate is known to be isomorphous to bis-deen copper(II) perchlorate.[3] Interestingly, the nickel complex also exhibits two steps of thermochromism: it is reddish-orange above about 90°C, orange near room temperature, and pale yellow upon being cooled to the temperature of liquid nitrogen. Figure 2 shows the ESR spectra of the copper(II) complex magnetically diluted in diamagnetic bis-deen nickel(II) perchlorate, measured using the X-band in the three temperature ranges corresponding to the transition phases of the diluent. These ESR spectra are very similar to each other in line shape except that the super-hyperfine structure observed in the high-field part is clearly resolved as the transition phase becomes a higher-temperature phase. This property of the super-hyperfine structure is also clearly indicated in the second derivative spectra shown in Fig. 3. This tendency of the super-hyperfine structure is contrary to the general rule that the line width narrows, because of the lengthening of the spin-lattice relaxation time, with a lowering in the temperature. Accordingly, it seems most reasonable that the tendency is closely related to the fact that the resolution of this kind of super-hyperfine structure depends upon the relative values among the magnetic parameters of g, A, and A_N. The super-hyperfine structure under discussion is considered to be due to the interaction of a copper unpaired electron with ligand nitrogen nuclei.[6-8]

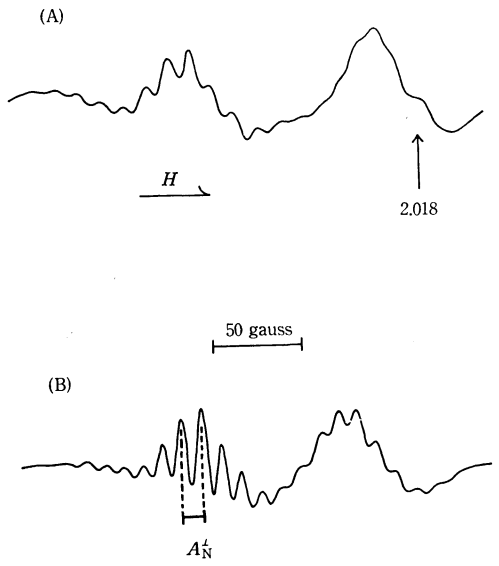

Fig. 3. The second derivative X-band ESR spectra enlarged at the high field part of the ESR spectra shown in Fig. 2.
(A) at 22°C, (B) at 120°C

The K-band ESR spectra for two temperature phases are shown in Fig. 4. These two spectra are similar to each other in line shape. The purpose of this K-band measurement is to eliminate as far as possible the complexity of absorption observed in the high-field part of the X-band spectra of Fig. 2. Judging from the line shape of these K-band ESR spectra of Fig. 4,[11] it seems reasonable to determine the values of g_1 and g_2 in such a way as is indicated by the arrows in the figure. Then, g_1 differs from g_2 by about 0.03; therefore, axial symmetry in the ligand field decreases to a certain extent in Ni-ClO_4.

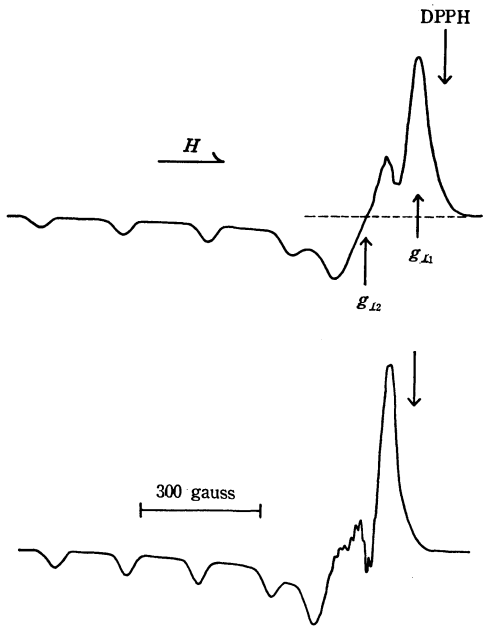

Fig. 4. The K-band ESR spectra of bis-(*N*,*N*-diethylethylenediamine)copper(II) perchlorate magnetically diluted in bis-(*N*,*N*-diethylethylenediamine)nickel(II) perchlorate powder.
(A) at 22°C, (B) at 120°C

Bis-deen nickel(II) tetrafluoroborate, diiodo-bis-deen nickel(II), and dinitrato-bis-deen nickel(II) are diamagnetic; all of these also exhibit two steps of thermochromism, much like bis-deen copper(II) perchlorate.[4] They were used as diluents in order to dilute magnetically the copper(II) complex of the same anion. The behavior of the ESR spectra for these samples, namely, Ni-BF_4, Ni-I and-NO_3, was almost the same as that of Ni-ClO_4. It is worth noting that the change in magnetic parameters for the copper(II) complexes takes place at the transition temperatures of diluents, for the change in bis-deen copper(II) perchlorate did not occur at its transition temperature of 44°C. This result indicates that the structural change in the copper(II) complexes takes place simultaneously

Table 1. The magnetic parameters of $[Cu(deen)_2]X_2$[a] magnetically diluted in the powder of $[Ni(deen)_2]X_2$

Temperature (°C)	Magnetic parameter	X			
		ClO_4^-	BF_4^-	I^-	NO_3^-
−196	$g_{//}$	2.171	2.172	2.178	2.170
	$A_{//}\times10^4\,cm^{-1}$	213	213	202	212
22	$g_{//}$	2.172	2.175	2.179	2.171
	$g_{\perp 1}$	2.018	2.018	2.021	2.015
	$g_{\perp 2}$	2.045	2.046	2.049	2.049
	$A_{//}\times10^4\,cm^{-1}$	206	205	198	206
	$A_N{}^{\perp}\times10^4\,cm^{-1}$	11.3	11.3	10.8	11.6
120	$g_{//}$	2.180	2.182	2.180	2.173
	$A_{//}\times10^4\,cm^{-1}$	193	192	190	201
	$A_N{}^{\perp}\times10^4\,cm^{-1}$	10.6	10.7	11.0	11.0

a) For example, bis-(*N*,*N*-diethylethylenediamine)copper(II) perchlorate is expressed as $[Cu(deen)_2]X_2$ where $X=ClO_4^-$.

with those of the diluents. All of the magnetic parameters experimentally determined for the magnetically-diluted samples are listed in Table 1.

The results listed in Table 1 indicate that the g and A values gradually change in one direction as the phase changes from the lower-temperature phase to the higher-temperature phase. This fact implies that the structural changes accompanied by each of the phase transitions are of the same kind and increase in one direction with the transition from the lower-temperature phase to the higher. The super-hyperfine splitting constants decrease slightly for almost all of the samples as the phase transfers from the room-temperature phase to the higher-temperature phase. This suggests that the σ covalency of copper-ligand nitrogen bonds decreases somewhat with the same phase transition.[6-8] The table also reveals that all the anions of Ni-ClO_4, Ni-BF, Ni$_4$-I, and Ni-NO_3 have almost the same effect on the cupric ion.

Solution. Figure 5 shows the X-band and K-band ESR spectra of bis-deen copper(II) perchlorate in the glassy state of an aqueous-methanolic solution measured at the temperature of liquid nitrogen. When spectrum (B) in this figure is compared with the spectra of Fig. 4, the difference between g_1 and g_2 seems to be smaller in the former than in the latter; the ligand field for the copper(II) complex is nearer to being of an axial symmetry in solution than in the diamagnetic nickel(II) complex. The spectra of Fig. 5 were analyzed as follows:

$$g_{//} = 2.212$$
$$g_{\perp} = 2.048$$
$$A_{//} = 184\times10^{-4}\,cm^{-1}$$

Attention should be given to the point that the structure of the copper(II) complex changes considerably according to its circumstances.

Ligand Field and Magnetic Dilution. In this paragraph the structure of bis-deen copper(II)

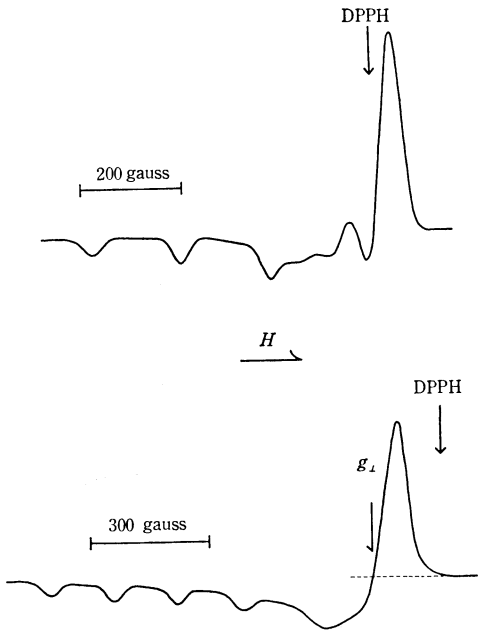

Fig. 5. The ESR spectra of bis-(*N*,*N*-diethylethylenediamine)copper(II) perchlorate in aqueous-methanolic solution at −196°C.
(A) X-band, (B) K-band

perchlorate will be discussed from the point of view of ESR. The copper(II) complex is known to be purplish-blue in an aqueous solution and red in crystal.[1,2] This color change has been speculated, on a simplified basis, to be due to the difference in strength of ligand field along the axis normal to the molecular plane.[2] Although the copper(II) complex is of a planar structure in both states, in an aqueous solution water molecules, being small in volume, can come close to the cupric ion, but in crystal perchlorate anions can not come so closely to the cupric ion as can water

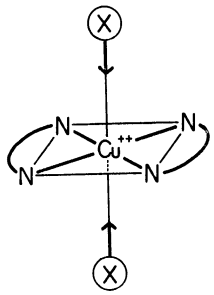

Fig. 6. The schematically represented structure of the copper(II) complex under discussion. X (ClO_4^- or H_2O) presents axial ligand field to cupric ion.

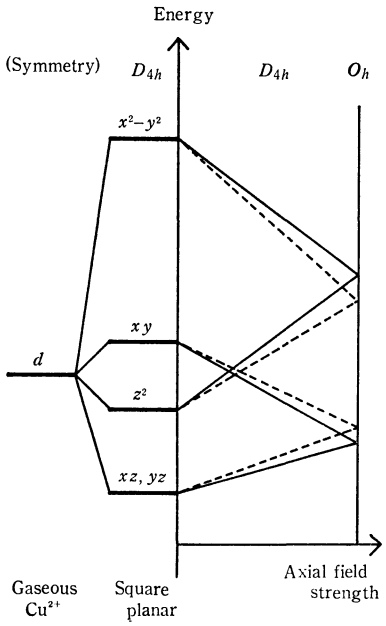

Fig. 7. Schematic representation of the energy levels cupric ion in axial ligand field of various streng of ths.

molecules because of the remarkable steric hindrance by ligand ethyl groups on the bulky anions.

In Fig. 6 the above situation is schematically pictured. Figure 7 also schematically represents, using, for convenience, the crystal field theory, the energy levels of the cupric ion of the square planar complex (D_{4h} symmetry) when two axial ligands coordinate to the cupric ion in various strengths. The dotted line in this figure represents the energy levels in a more practical case; when the axial coordination strengthens, the equatorial coordination weakens. In the planar copper(II) complex, the uppermost level of the $d_{x^2-y^2}$ orbital is half filled, and the other levels, completely occupied, with electrons, and the *d*-*d* absorption bands correspond to a one-electron transfer from the lower levels to the uppermost level. The fact that the bands shift to longer wavelengths as the axial coordination strengthens has been confirmed both theoretically and experimentally.[14]

It will be assumed that the following wave functions describe the system:

$$\left.\begin{aligned}
\psi_{x^2-y^2} &= \alpha d_{x^2-y^2} - \alpha' \sigma_L(x^2-y^2) \\
\psi_{xy} &= \beta d_{xy} - \beta' \phi_L(xy) \\
\psi_{xz,yz} &= \beta_1 d_{xz,yz} - \beta_1' \phi_L(xz, yz) \\
\psi_{z^2} &= \alpha_1 d_{z^2} - \alpha_1' \sigma_L(z^2)
\end{aligned}\right\} \quad (1)$$

In each of the wave functions, the second term on the right-hand side represents the proper ligand orbital which can be mixed with the copper *d* orbital expressed in the first term. The relations between the ESR data and the covalency parameters, α, β, and β_1, can then be expressed approximately as follows:[5-9]

$$g_{//} = 2 - \frac{8\lambda}{\Delta E_{xy}}\alpha^2\beta^2 \quad (2)$$

$$g_{\perp} = 2 - \frac{2\lambda}{\Delta E_{xz,yz}}\alpha^2\beta_1^2 \quad (3)$$

$$A_{//} = P\left[-\frac{4}{7}\alpha^2 - \kappa + (g_{//}-2) + \frac{3}{7}(g_{\perp}-2)\right] \quad (4)$$

where κ is the Fermi contact term, $\Delta E_{xy} = E_{x^2-y^2} - E_{xy}$, $\Delta E_{xz,yz} = E_{x^2-y^2} - E_{xz,yz}$, and $P = 0.036$ cm^{-1}.

It is interesting and important to learn how the *g* and *A* values change as the axial coordination varies in strength. The following theory may be derived from Fig. 7 and the three equations (2)—(4); All of the following discussion is concerned with the case in which the axial ligand field strengthens. α^2 increases remarkably, β_1^2 increases to a smaller extent, and the change in β^2 is quite small. $\Delta E_{xz,yz}$ decreases remarkably, and ΔE_{xy} decreases slightly. Therefore, $g_{//}$ remarkably increases. $g_{\perp}$ also increases, but the amount of increase is not large because of the small factor, 2, in the second terms on the right-hand side of Eq. (3). On the other hand, the situation for $A_{//}$ is rather complicated. When the axial coordination varies in strength, the change in the value of $|A_{//}|$ is dependent on the relative changes in the value of α^2, κ, and *g* in Eq. (4). However, it was experimentally indicated that, for some planar copper(II) complexes, the value of $|A_{//}|$ decreases as the axial coordination is strengthened.[15] Furthermore, cupric ions in MgO or CaO, which may be regarded as extreme cases in which the axial coordination becomes almost equal in strength to the equatorial coordination, have a very small value of $|A_{//}|$.[16] From the above-mentioned facts, it may be considered, as a general rule, that the value of $|A_{//}|$ decreases

14) R. L. Belford, M. Calvin, and G. Belford, *J. Chem. Phys.*, **26**, 1165 (1957); D. P. Graddon, *J. Inorg. Nucl. Chem.*, **14**, 161 (1960).

15) H. Yokoi and T. Isobe, This Bulletin, **39**, 2054 (1966).

16) P. Azurin, J. W. Orton and J. E. Wertz, "Paramagnetic Resonance," Vol. 1, ed. by W. Low, Academic Press, New York (1963), p. 90; W. Hayes and J. W. Orton, *Rept. Progr. Phys.*, **22**, 204 (1959).

as the axial coordination strengthens.

The samples employed in this work are numbered as follows: the polycrystal at −196°C is I: the polycrystal are 22°C, II; the polycrystal at 80°C, III; Ni-ClO_4 at −196°C, IV: Ni-ClO_4 at 22°C, V; Ni-ClO_4 at 120°C, VI, and the aqueous-methanolic solution at −196°C, VII. For I, II, IV, V, VI, and VII, the $g_{//}$ or g_3 values are 2.117, 2.156, 2.171, 2.172, 2.180, and 2.212 respectively, and the $g_\perp$ values, or the mean values of g_1 and g_2, are 2.034, 2.036, 2.03−2.04, 2.03—2.04, 2.03—2.04, and 2.048 respectively. For IV, V, VI, and VII, the values of $|A_{//}|$ ($\times 10^4$ cm^{-1}) are 213, 206, 193, and 184 respectively. From these results it may reasonably be concluded that, among I, II, IV, V, VI, and VII, the difference in structure lies mainly in the axial coordination and that the axial ligand field is strengthened in this order of samples. The tendency of the super-hyperfine splitting constant for V and VI, which had already been discussed, also supports this conclusion indirectly. It is a very interesting suggestion that the phase transitions from I to II, from IV to V, and from V to VI accompany such a structural change as the access of the perchlorate anion to the cupric ion. However, the phase transition from II to III is of a different kind and possibily accompanies the structural change in the equatorial coordination. It may also be noted that IV, V, and VI in the above-mentioned series of samples decreases in axial symmetry to a slightly larger extent than the others.

It should be emphasized here that, as has been described, the properties of bis-deen copper(II) perchlorate vary to a larger extent according to its circumstances. Therefore, the meaning of magnetical dilution for the metal complex of a flexible structure is rather complicated.

BULLETIN OF THE CHEMICAL SOCIETY OF JAPAN VOL. 42 2238—2242 (1969)

The Kinetics of the Autoxidation of Ferrous Ions in Aqueous Tripolyphosphate Solutions

Yoshimi KURIMURA and Hideo KURIYAMA

Chemical Laboratory, College of General Education, Ibaraki University, Watari-machi, Mito, Ibaraki

(Received July 8, 1968)

The kinetics of the autoxidation of ferrous ions in tripolyphosphate solutions (pH 2—8) at an ionic strength of 0.20 M $NaClO_4$ was studied using a spectrophotometric technique. The rate expression for the oxidation reaction is given by:

$$d[Fe(III)]/dt = 4k_I[Fe^{II}(Htpp^{4-})][O_2] + 4k_{II}[Fe^{II}(Htpp^{4-})_2][O_2],$$

and $4k_{II}$ found is to be 1.0×10^2 M^{-1} sec^{-1} at 15°C. The simultaneous reaction paths of

$$Fe^{II}(Htpp^{4-}) + O_2 \xrightarrow{k_I} Fe^{III}(Htpp^{4-}) + O_2^- \text{ and } Fe^{II}(Htpp^{4-})_2 + O_2 \xrightarrow{k_{II}} Fe^{III}(Htpp^{4-})_2 + O_2^-$$

are consistent with the results obtained. When there is an excess of the triphosphate solution in the pH range from 6 to 8, the latter may be the rate-determining step. The acceleration of the oxidation of the ferrous ions in the triphosphate solution may be due to the fact that the stabilization of the oxidation products, $Fe^{III}(Htpp^{4-})$ and $Fe^{III}(Htpp^{4-})_2$, is greater than that of the corresponding ferrous triphosphate complexes. As the activation parameters for the latter reaction, the experiments gave the values of $\Delta H^{\neq} \sim 10$ kcal mol^{-1} and $\Delta S^{\neq} \sim -25$ cal mol^{-1}. deg^{-1}. The negative and relatively small value of the entropy of activation suggests that the activated complex is more extensively hydrated than is the ferrous complex of $Fe^{II}(Htpp^{4-})_2$.

Many workers have reported that the rate of the autoxidation of ferrous ions is dependent upon the species of anions present and on the pH's of the solutions.[1-9] The observed oxidation rates

1) J. H. C. Smith and H. A. Spoehr, *J. Am. Chem. Soc.*, **48**, 107 (1926).
2) H. A. Spoehr, *ibid.*, **46**, 1494 (1924).
3) J. King and N. Davidson, *ibid.*, **80**, 1542 (1958).
4) S. Utsumi and K. Muroshima, *Nippon Kagaku Zasshi (J. Chem. Soc. Japan, Pure Chem. Sect.)*, **86**, 593 (1965).
5) M. Cher and N. Davidson, *J. Am. Chem. Soc.*, **77**, 793 (1955).
6) A. M. Posner, *Trans. Faraday Soc.*, **49**, 382 (1953).
7) A. B. Lamb and L. W. Elder, *J. Am. Chem. Soc.*, **53**, 137 (1931).
8) R. O. Huffman and N. Davidson, *ibid.*, **78**, 4836 (1956).
9) P. George, *J. Chem. Soc.*, **1954**, 4349.

of Fe(II), at a given pH, decrease in the order: pyrophosphate,[1-4] phosphate,[5] chloride,[6] sulfate,[7,8] and perchlorate.[9] The rate, $-d[Fe(II)]/dt$, is first-order with respect to [Fe(II)] and p_{O_2} for the first three anions, while it is second-order with respect to [Fe(II)] and first-order with respect to p_{O_2} for the last two.

King and Davidson demonstrated that the rate for the oxidation of Fe(II) in an acid solution of pyrophosphate at pH's from 1 to 2 is first-order with respect to Fe(II), $H_2P_2O_7^{2-}$, and dissolved oxygen.[3] They also suggested that the effect of the pyrophsophate anions on the oxidation of Fe(II) may be due to the stabilization of such a transition state as $PP\cdots Fe\cdots O_2$, where PP is the pyrophosphate anion. It was also suggested that the rate, at a given pH, increases with an increase in the affinity of the anion towards ferric ions.[3]

In the previous work of this series, our finds on the oxidation of Fe(II) by dissolved oxygen in aqueous solutions in the presence of a chelating-agent were reported; these findings showed a linear relationship between the logarithmic rate constant and the $\log R_f$ value.[10],*1 Further extension of the work on the autoxidation of Fe(II) accelerated by the triphosphate anion was attempted spectrophotometrically; in this paper the mechanism of the reaction will be postulated.

Experimental

Materials. The ferrous ammonium sulfate, perchloric acid, sodium perchlorate, ferric ammonium sulfate, and sodium hydroxide were available G. R.-grade reagents. The sodium triphosphate was recrystallized five times from a 25% aqueous solution of ethanol. The purity of the sodium triphosphate ($Na_5P_3O_{10}\cdot 6H_2O$), as determined by means of anion exchange chromatography,[11] was above 98%. Redistilled water was used in preparing all the solutions.

Determination of Total Fe(III). The effect of the pH upon the absorption spectra of ferric ion species at wavelengths from 230 mμ to 350 mμ in an excess of triphosphate (TPP) is shown in Fig. 1. The isosbestic point at 260 mμ is invariable throughout the pH region between 2 and 7. Within this pH region, the total concentration of the ferric ions produced by the oxidation of ferrous ions can be determined by the absorption intensity at 260 mμ, whose molar extinction coefficient is 4620 $M^{-1}cm^{-1}$. In order to estimate the concentration of ferric ions at a pH value higher than 7, the value of a molar extinction coefficient at 260 mμ depending on the pH was found and used. For the purpose of determining the composition of the TPP

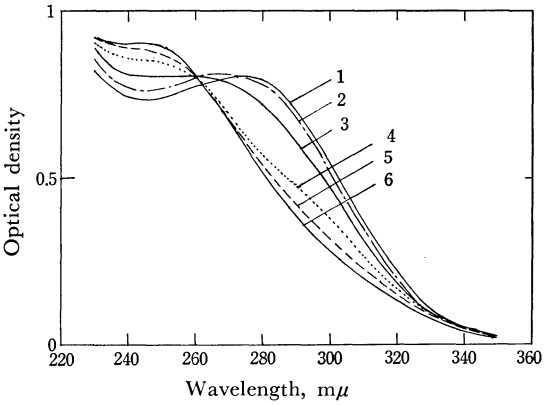

Fig. 1. Absorption spectra of the Fe(III)-TPP complex in exess of the TPP solutions.
1.33×10^{-4} M Fe(III), 1.66×10^{-2} M TPP,
0.20 M $NaClO_4$, 15°C
pH : 1 7.93 2 5.68 3 4.35
4 2.95 5 2.35 6 1.92

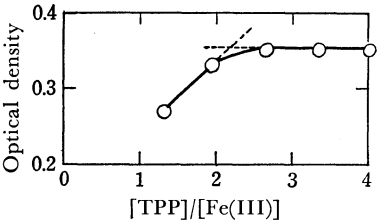

Fig. 2. Variation of the optical densities with [TPP]/[Fe(III)].
7.60×10^{-5} M Fe(III), 0.20 M $NaClO_4$,
pH=5.62±0.02, room temperature

complex of ferric ions, the molar-ratio method was applied; the results are shown in Fig. 2. The evidence shown in Fig. 2, in which the optical density becomes nearly constant at [TPP]/[Fe(III)] values higher than 2, suggests that the composition of the Fe(III) complex with the highest number of complexing agents is $Fe^{III}(TPP)_2$.

Rate Determination. Except for a few cases, the ionic strength of the TPP solutions was kept at 0.207 by sodium perchlorate. About 50 m*l* of the TPP solution was taken into a 100-m*l* beaker and the pH of this solution was adjusted by the addition of a few drops of dilute perchloric acid or dilute sodium hydroxide. Appropriate amounts of a freshly-prepared aqueous solution of ammonium ferrous sulfate and 25 m*l* of the TPP solution were kept in a thermostated bath at 15°C for about one hour in order to saturate these solutions with air. Then, reaction was initiated by the addition of 1 m*l* of the Fe(II) solution into the stirred TPP solution by means of an injection syringe. The ionic strength of the reaction mixture was 0.20. The progress of the oxidation reaction was followed spectrophotometrically at 260 mμ using a Hitachi recording spectrophotometer. The recording of the absorption intensity of the Fe(III) produced could be started within nine seconds after the initiation of the reaction. The pH value of the reaction mixture was measured using a Hitachi-Horiba F-5-type pH meter. The reaction rate

*1 R_f represents the ratio of the chelate formation constant for the Fe(III) to that for the Fe(II) ($K_{Fe^{III}L}/K_{Fe^{II}L}$).

10) Y. Kurimura, R. Ochiai and N. Matsuura, This Bulletin, **41**, 2234 (1968).

11) N. Matsuura, Y. Kurimura and K. Kiyokawa, *Bunseki Kagaku (Japan Analyst)*, **16**, 612 (1967).

in an oxygen-saturated solution was observed according to a procedure described previously.[10]

Results and Discussion

Variations in the optical densities of the Fe(III)-triphosphate complex at 260 mμ in aerated solutions initially containing TPP and various initial concentrations of Fe(II) are shown in Fig. 3. The initial oxidation rate, d[Fe(III)]/dt, was determined from the slope of the starting curve. A linear relationship between the oxidation rate and the Fe(II) concentration holds well except when the total concentration of the Fe(II) is relatively higher than that of the TPP. This linear relationship indicates a pseudo-first-order dependence of the rate on the Fe(II) concentration at any particular pH value.

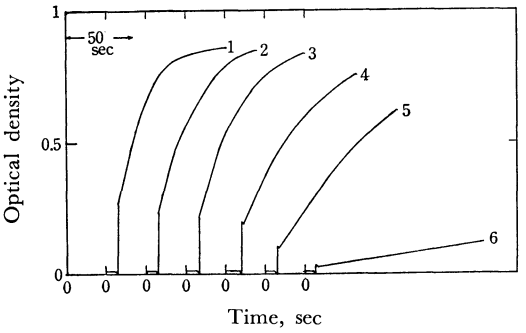

Fig. 3. Variation of the optical densities with the reaction times.
2.0×10^{-2} M TPP, 2.0×10^{-4} M Fe(II), 0.20 M $NaClO_4$, 15°C
pH : 1 8.77 2 8.29 3 6.36
4 5.31 5 4.61 6 3.41

A comparison of the oxidation rates in aerated and oxygenated solutions is tabulated in Table 1. A first-order dependence of the rate on the oxygen concentration is observed since the ratio of the obtained rates on these two solutions, R_O/R_A, is about 4.9; this value agrees with the theoretical value of the ratio of the oxygen concentration in the oxygenated and in the aerated solutions, which is evaluated as 4.76 : 1. The results obtained by varying the pH value are shown in Fig. 4. With an increase in the pH value, the rate increases

TABLE 1. COMPARISON OF THE OXIDATION RATES IN THE AERATED (R_A) AND THE OXYGENATED (R_O) SOLUTIONS (10^{-6} M sec^{-1})
2.0×10^{-4} M Fe(II), 2.0×10^{-2} M TPP, pH=4.01±0.02, room temperature

R_A	R_O	R_O/R_A
0.63	3.10	4.93
0.64	3.05	4.86
	mean	4.89

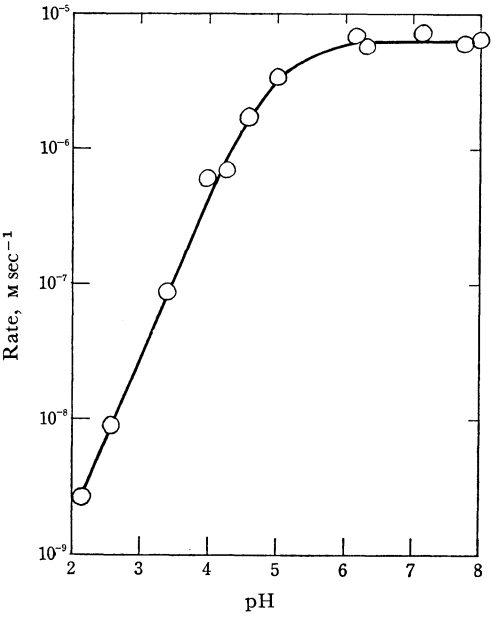

Fig. 4. Dependence of the oxidation rate on the pH.
2.0×10^{-2} M TPP, 2.0×10^{-4} M Fe(II), 0.20 M $NaClO_4$, 15°C

markedly in the pH region between 2 and 6, finally attaining a limiting value at a pH higher than 6. Simillar rate dependences on the pH were observed in the oxygen oxidation of such Fe(II)-chelates as Fe(II)NTA and Fe(II)-EDTAOH.[10]

In these Fe(II)-chelates systems, such an increase in the rate may be attributed to an increase in the concentration of the chelated Fe(II) with the pH value. Generally, Fe(II)-chelates are oxidized more rapidly by oxygen molecules in acid and neutral aqueous solutions than are aquo ferrous ions.[10]

In order to obtain information on the order of the oxidation reaction, Job's continuous variation method[12] was employed. The results with this method are shown in Fig. 5. In this figure, the oxidation rates are plotted against the ratio of the concentrations, [Fe(II)]/{[Fe(II)]+[TPP]}, which is represented by R, the dominator of which is kept at a constant value of 5.0×10^{-4} M. A maximum is observed at R ~0.3 on the curve; this indicates that the reaction is first-order with respect to the free Fe(II) concentration and second-order with respect to the free TPP concentration at a given pH and at a given concentration of the dissolved oxygen. The small shoulder observed around R ~0.5—0.7 suggests the other rate dependence, which is first-order with respect to the concentrations of the free Fe(II) and the free

12) P. Job, *Ann. Chim.*, **6**, 97 (1936).

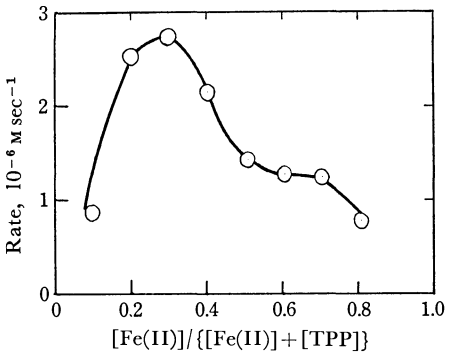

Fig. 5. Kinetic method of continuous variations. [Fe(II)]+[TPP] = 5.0×10^{-4} M, 0.20 M $NaClO_4$, pH=6.80±0.03, 15°C

TPP respectively.

From the results obtained, the rate equation at a given pH can be written as:

$$\frac{d[Fe(III)]}{dt} = k_a[Fe(II)]_f[TPP]_f[O_2] + k_b[Fe(II)]_f[TPP]_f^2[O_2] \quad (1)$$

where $[Fe(II)]_f$ and $[TPP]_f$ are the concentrations of the free ferrous ion and the free triphosphate ion respectively, and where k_a and k_b are apparent rate constants.

Under the present experimental conditions, five species of the triphosphate, H_5tpp, H_4tpp^-, H_3tpp^{2-}, H_2tpp^{3-}, and $Htpp^{4-}$, must be considered in the solution, while the completely dissociated species of tpp^{5-} can be disregarded. Fractions of the triphosphate species are calculated using the stability constants of triphosphoric acid;*2 these are plotted in Fig. 6 as a function of the pH value.

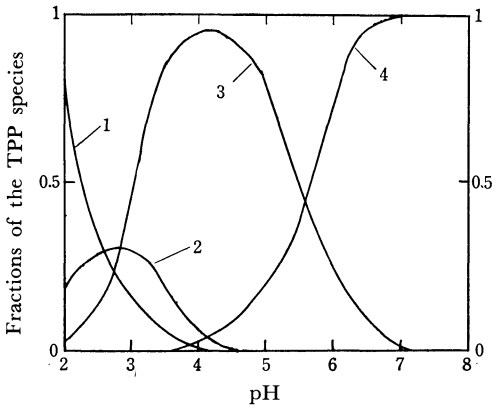

Fig. 6. Fractions of the TPP species *vs.* pH curve.
1: H_4tpp^- 2: H_3tpp^{2-} 3: H_2tpp^{3-} 4: $Htpp^{4-}$

*2 $\log K^H_{H_4L}=0$, $\log K^H_{H_3L}=2.6$, $\log K^H_{H_2L}=2.7$ and $\log K^H_{HL}=5.6$ and $\log K^H_L=7.9$ ($\mu=0.1$).[13]

13) A. E. Martell and G. Schwarzenbach, *Helv. Chim. Acta*, **39**, 653 (1956).

From a comparison of the rate-pH curve (Fig. 4) and the fraction-pH curve (Fig. 6), it is clear that the increase on the oxidation rate corresponds to the increase in the fraction of the H_4tpp^{4-}. This evidence suggests that the free TPP species in the rate equation (1) is $Htpp^{4-}$. It is reasonable to conclude from the results obtained that complex species of $Fe^{II}(Htpp^{4-})_2$ and $Fe^{II}(Htpp^{4-})$ are formed in the Fe(II)-TPP solution and that these are oxidized predominantly by dissolved oxygen. The quadratic dependence of the rate on the $Htpp^{4-}$ concentration, seen in the rate equation (1), is quite difficult to explain from kinetic point of view if complex formation between the Fe(II) and the TPP is not considered.

The reaction scheme most suited to the experimental results indicates two pre-equilibrium reactions, (2) and (3), and the simultaneous reaction paths of (4) and (5) (the (4) and (5) reactions are the rate-determining steps of the oxidation reaction):

$$Fe^{2+} + Htpp^{4-} \rightleftarrows Fe^{II}(Htpp^{4-}) \quad (2)$$

$$Fe^{II}(Htpp^{4-}) + Htpp^{4-} \rightleftarrows Fe^{II}(Htpp^{4-})_2 \quad (3)$$

$$Fe^{II}(Htpp^{4-}) + O_2 \xrightarrow{k_I} Fe^{III}(Htpp^{4-}) + O_2^- \quad (4)$$

$$Fe^{II}(Htpp^{4-})_2 + O_2 \xrightarrow{k_{II}} Fe^{III}(Htpp^{4-})_2 + O_2^- \quad (5)$$

$$O_2^- + H^+ \rightleftarrows HO_2 \quad (6)$$

$$Fe(II) + HO_2(\text{or } O_2^-) \rightarrow \text{further oxidation (fast)} \quad (7)$$

The oxidation of the Fe(II) by the HO_2 or O_2^- radical may proceed by means of Weiss's mechanism.[14,15] If so one molecule of O_2 oxidizes four atoms of the Fe(II). The above mechanism is also consistent with the results shown in Table 2, which shows little dependence of the rate on the ionic strength of the solution. Although the formation constant of the triphosphate complex of the ferrous ion has not yet been reported, complex formation between Fe(II) and TPP can be expected from the evidence that several divalent metal ion (Ba^{2+}, Cd^{2+}, Ca^{2+}, and Co^{2+}) complexes of the triphosphate with relatively greater stabilities

Table 2. Relationship between the oxidation rate and the ionic strength
2.0×10^{-2} M TPP, 2.0×10^{-4} M Fe(II), pH=5.90±0.02, 15°C

Ionic strength	Oxidation rate, 10^{-6} M sec^{-1}
0.20	7.8
0.25	8.0
0.50	8.4
1.00	10.0

14) J. Weiss, *J. Chim. Phys.*, **48**, C-6 (1951).
15) J. Weiss, *Experientia*, **IX**, 61 (1953).

have been reported.[16-18] The proposed rate expression for the oxidation reaction is:

$$\frac{d[Fe(III)]}{dt} = 4k_I[Fe^{II}(Htpp^{4-})][O_2] + 4k_{II}[Fe^{II}(Htpp^{4-})_2][O_2] \quad (8)$$

The first term in this quation may be neglected in an excess of the TPP solution in the pH region between 6 and 8 since the concentration of the $Fe^{II}(Htpp^{4-})_2$ is nearly equal to the total concentration of the Fe(II) (Fig. 5). The k_{II} value is then evaluated by dividing the oxidation rate, which is obtained in an excess of the TPP solution at pH 6—8, by the total concentration of the Fe(II) and by the oxygen concentration.*3 The k_{II} value thus obtained is 25 $M^{-1}sec^{-1}$ at 15°C.

As has previously been reported,[10] the accelaration of the oxidation of ferrous ions in the presence of such chelating agents as EDTA, EDTAOH, and DTPA may be attributed to the lowering of the free energy of the activation ($\Delta G^{\neq}$) of the rate-determining step of the reaction of the following type due to the fact that the ferric state is more stable than the corresponding ferrous state:

$$Fe^{II}Z + O_2 \rightarrow Fe^{III}Z + O_2^- \quad (9)$$

where $Fe^{II}Z$ and $Fe^{III}Z$ are ferrous and ferric chelates respectively. The effect of the triphosphate anion on the oxidation of ferrous ions also seems to be attributable to a lowering of the $\Delta G^{\neq}$ values of the reaction (4) and reaction (5) by complex formations. As the activation parameters for the reaction (5), $\Delta H^{\neq} \sim 10$ kcal mol^{-1} and $\Delta S^{\neq} \sim -24$ cal mol^{-1} deg^{-1} are obtained from the temperature dependence of the rate constant, as may be seen in Table 3. The relatively small negative value of the activation entropy suggests that the activated complex formed at the transition state in (5) is more extensively hydrated than the ferrous complex, probably as a result of the cleavage of the Fe–O bond in the ferrous complex. Analogous to the oxidation reaction discussed here, it is reasonable to suggest that the acceleration of the oxidation of the Fe(II) by the pyrophsophate anion in a relatively high pH region is due to complexation between the Fe(II) and the pyrophosphate anion.

Table 3. Temperature dependence of the oxidation rate

2.0×10^{-2} M TPP, 2.0×10^{-4} M Fe(II), pH=4.51±0.01, 0.20 M $NaClO_4$

$(1/T)\times10^3$	Rate constant (k_{II}, $M^{-1}sec^{-1}$)
3.47	25
3.37	41
3.31	53

16) J. A. Wolhoff and J. T. G. Overbeek, *Rec. Trav. Chim.*, **78**, 759 (1959).
17) J. I. Watters and S. M. Lambert, *J. Am. Chem. Soc.*, **81**, 3201 (1959).
18) A. Jansson and E. Wännien, *Tranta*, **10**, 769 (1963).
*3 The concentration of oxygen in the air-saturated solution is estimated to be 2.9×10^{-4} M at 15°C.

BULLETIN OF THE CHEMICAL SOCIETY OF JAPAN VOL. 42 2243—2246 (1969)

Oscillopolarographic Behaviour of Lanthanide Ions at the Dropping and Hanging-drop Mercury Electrodes

Akio IWASE and Chieko YOKOYAMA

Department of Chemistry, Faculty of Science, Yamagata University, Koshirakawa-cho, Yamagata

(Received August 21, 1968)

The oscillopolarographic behaviour of lanthanide ions at the dropping mercury electrode and hanging-drop mercury electrode was discussed. The variations of incision depth on the oscillopolarograms with a dropping mercury electrode in KSCN, KCl, KBr and $NaClO_4$ at pH 3.65 and 4.65 were found to depend on the first ionization potentials and the basicity of the lanthanide. On the basis of the results obtained it can therefore be presumed that the electrode reaction rate increases with the increase of the first ionization potentials.

It hat been reported[1,2] that the curves, $dE/dt = f(E)$, for the tervalent lanthanide ions, lanthanum, praseodymium and samarium in KI or KCl solutions, are affected by dissolved oxygen; the cathodic incision potential shifts in the negative direction and the anodic one in the positive direction and the incision depth decreases upon removal of the dissolved oxygen. This behaviour was attributed to the effect, as a catalyst, of hydroxide ions produced by the reduction of dissolved oxygen. However, little attention has been paid to the dependence of the incision depth on the characteristics of tervalent lanthanide ions.

The present investigation was undertaken to elucidate the relation between characteristics of the lanthanide ions, La^{3+}, Pr^{3+}, Nd^{3+}, Sm^{3+}, Gd^{3+}, Tb^{3+}, Dy^{3+}, Ho^{3+}, Er^{3+}, Tm^{3+} and Lu^{3+} and the incision depths in KSCN, KCl, KBr and $NaClO_4$ solutions. The data on the depolarization effect of the lanthanides reported herein indicate that the incision depths of the lanthanide ions are dependent on the first ionization potentials and the basicity.

Experimental

0.01 M solutions of lanthanide(III) chloride were prepared as follows: 99.9% lanthanide oxide was converted to the chloride and dissolved in diluted hydrochloric acid. Its concentration was standardized by a titration method[3] using an EDTA standard solution. Other reagents were all guaranteed grade and used without further purification. Adjustment of pH of the solution was done by adding 0.01 N hydrochloric acid or 0.01 N potassium hydroxide.

The curves, $dE/dt = f(E)$, were recorded with a manual Heyrovsky-Forejt type oscillopolarography constructed in this laboratory. A dropping mercury electrode (DME) and a hanging-drop mercury electrode (HME) were used as the polarizable electrode. The alternating current had a main frequency of 50 cps at 150 V. A direct current voltage in the range, -1.0 to -2.0 V, was superimposed on the alternating current. The alternating current intensities passing through the electrode were 0.12 mA for DME (surface area: 0.013 cm^2) and 0.23 mA for HME (surface area: 0.027 cm^2).

An Iwasaki SS-5051 synchroscope with WB-4 amplifier was employed and the photographs of the oscilloscope display were recorded with a Polaroid-Land camera and an Iwasaki UP-7 photo oscilloscope unit. The deflection sensitivities of the vertical axis were 3.5(DME) and 2.5 (HME) mV/cm except for Fig. 1. The positions of all incisions were measured directly on the oscilloscope and referred to a saturated calomel electrode by a comparative method[4] using the thallous or lead ions. The curves with the DME were photographed just before detachment of the mercury droplet when the surface area did not change appreciably with time. The capillary characteristics of DME used were an m value of 0.936 mg/sec and a drop time of 1.7 sec in an oxygen free 1 M potassium chloride solution for a mercury height of 57.6 cm. In order to ensure satisfactory reproducibility of the oscillopolarograms with HME, it was necessary to maintain a constant volume for the hanging-drop mercury. This was achieved by using a polarographic capillary with a mercury reservoir; after separation by means of gravitation, the mercury was caught on a glass spoon and attached to a silver wire by contact only. The weight of the mercury drop was 0.0058 g. For all experiments, the temperature was regulated at 25.0 ± 0.1°C.

1) J. Heyrovsky and R. Kalvoda, "Oscillographische Polarographie mit Wechselstrome," Akademie Verlag, Berlin (1960), p. 107.

2) S. Misumi and Y. Ide, *Mem. Faculty Sci., Kyushu Univ., Ser. C. Chem.*, **3**, 205 (1961).

3) K. Ueno, "Chelatometric Titration," Nankodo, Tokyo (1964), p. 327.

4) R. Kalvoda, "Techniques of Oscillographic Polarography," Elsevier, New York (1965), p. 168.

Results and Discussion

Oscillopolarographic Characteristics of Lanthanide Ions in Potassium Thiocyanate Solutions. The typical curves, $dE/dt=f(E)$, for 5×10^{-4} M lanthanide in a solution containing 1 M potassium thiocyanate at pH 3.65±0.05, are shown in Fig. 1. In this figure, curves (a) and (b) are the oscillopolarograms obtained with DME and with HME respectively. When DME was used the incision is observed for the Nd^{3+} ion only, whereas when HME was used the incision was observed for all ions in Fig. 1. It is obvious from comparison between the curves (a) and (b) that the incision depth is a function of the electrode reaction rate of the lanthanide ion. The oscillopolarographic characteristics of the lanthanide ions are shown in Tables 1*1,*2 and 2.*1,*2 In Table 1, the cathodic and anodic incision potentials obtained with DME were nearly constant and had a value of −1.41 and −1.40 V respectively. This is in agreement with the results reported by Dolezal[1] for several lanthanide ions. The incision was negligible with the removal of the dissolved oxygen in studies of the lanthanum and samarium ions, but no measurable incision was formed with Er, Tm and Lu irrespective of the presence of dissolved oxygen at pH 3.65±0.05 in an unbuffered solution. Generally, the incision depth of these ions in presence of the dissolved oxygen was greater than that with removal of the dissolved oxygen, and constant for La^{3+}, Pr^{3+} and Nd^{3+}, but for other ions studied, no regularity was found.

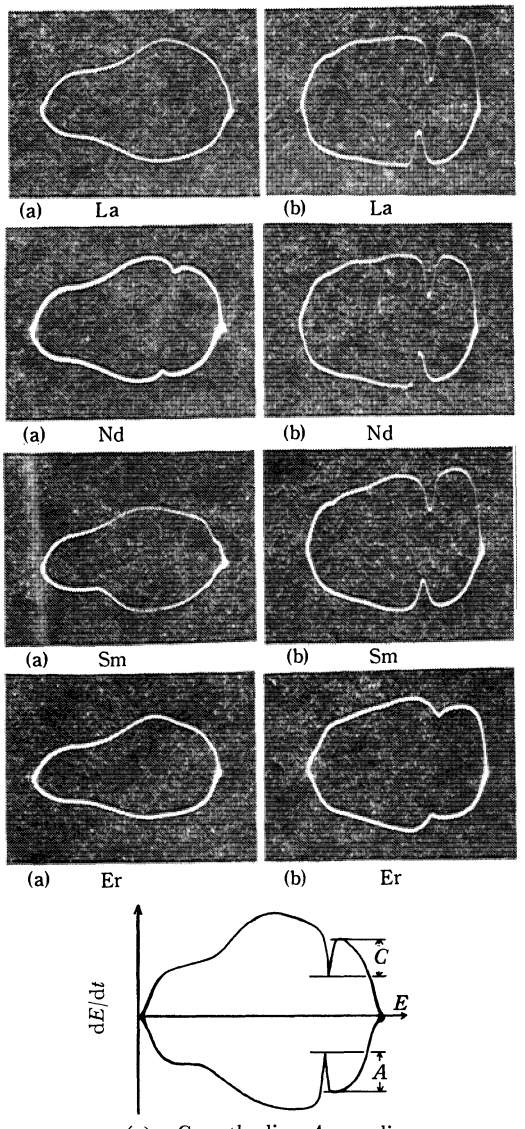

(c) C, cathodic; A, anodic

Fig. 1. Typical curves of the dE/dt *versus* the potential, E, of the lanthanide ions in a deoxygenated 1 M KSCN solulion. The curves were obtained with (a) a dropping and (b) a hanging-drop mercury electrode; (c), shows the method of measuring the incision depth. The deflection sensitivities of vertical axis were 10.0 (DME) 10.0 (DME) and 5.5 (HME) mV/cm.

As shown in Table 2, for the $dE/dt=f(E)$ curves obtained with HME, the quotients Q agreed with those obtained with the dropping mercury electrode and the incision depths were constant in the series, lanthanum to gadolinium, and independent of the presence of dissolved oxygen. On the basis of these observation, it seems that the electrode reaction rate of the lanthanum and samarium ions is slower than that of the other lanthanide ions (for example; Pr^{3+}, Nd^{3+}, Gd^{3+}, Tb^{3+}, Dy^{3+} and Ho^{3+}). As for erbium, thulium and lutetium, it was very difficult to identify a well-defined incision both with DME and HME because these ions may be hydrolyzed at the electrode surface under the above conditions.

In Fig. 2, curve D shows the plot of the cathodic incision depth with DME (with removal of dissolved oxygen) against the atomic numbers. This curve has two maxima, each of which is coincident with a similar maximum in the curve of the first ionization potentials[5] (curve E). As shown in Fig.3, the incision depth just before the detachment of the drop is dependent on the concentration of lanthanide ions. To determine the incision depths of neodymium, samarium and terbium, oscillopolarograms were measured on 0.5 to 5×10^{-4} M (HME), 0.5 to 5×10^{-3} M (DME, Nd^{3+}) and 0.5 to 3×10^{-3} M (DME, Tb^{3+}) lanthanide solutions containing 1 M KCl or 1 M KSCN at pH 3.65±

*1 The quotient Q is equal to the ratio of the distance between the left limiting point and the peak of the incision to the distance between the two limiting points (Fig. 1-c).

*2 Q values of the depolarization potential, incision depth and depolarization potential without removal of dissolved oxygen are shown in parentheses.

5) A. Cotton, "Progress in Inorganic Chemistry," Vol. 3, Interscience Publishers, New York (1962), p. 330.

Table 1. Depolarization potentials, incision depths and Q-quotients of lanthanides in 1 M potassium thiocyanate solutions with DME (pH: 3.65±0.05)

Lanthanide	Incision depth, mm				Q		Incition potential, V	
	C		A		C	A	C	A
La	disappear	(13.0)	disappear	(10.0)	(0.68)	(0.67)	(−1.41)	(−1.40)
Pr	1.0	(12.5)	1.0	(10.5)	0.69	0.67	−1.43	−1.40
Nd	2.0	(13.5)	2.0	(10.5)	0.69	0.67	−1.43	−1.40
Sm	disappear	(11.0)	disappear	(9.0)	(0.68)	(0.67)	(−1.41)	(−1.40)
Gd	4.5	(9.0)	4.0	(8.0)	0.68	0.67	−1.42	−1.40
Tb	6.0	(7.5)	4.0	(6.0)	0.68	0.67	−1.41	−1.40
Dy	4.0	(6.0)	3.5	(4.0)	0.68	0.67	−1.41	−1.40
Ho	2.0	(3.0)	1.0	(2.0)	0.68	0.67	−1.42	−1.40
Er, Tm, Lu	no measurable incision formed							

Table 2. Incision depths and Q-quotients of lanthanides in 1 M potassium thiocyanate solutions with HME (pH: 3.65±0.05)

Lanthanide	Incision depth, mm		Q	
	C	A	C	A
La	16.5 (17.0)	14.5 (15.0)	0.69	0.67
Pr	17.0 (16.5)	12.0 (12.0)	0.68	0.67
Nd	17.5 (17.0)	12.0 (12.0)	0.68	0.67
Sm	17.5 (17.0)	12.5 (12.0)	0.68	0.67
Gd	17.5 (17.0)	12.0 (12.0)	0.68	0.67
Tb	16.0 (14.5)	9.0 (10.0)	0.68	0.67
Dy	16.0 (13.5)	10.0 (9.0)	0.68	0.67
Ho	16.0 (10.0)	10.0 (6.5)	0.68	0.67
Er	3.5	2.0		
Tm	1.8			
Lu	no measurable incision formed			

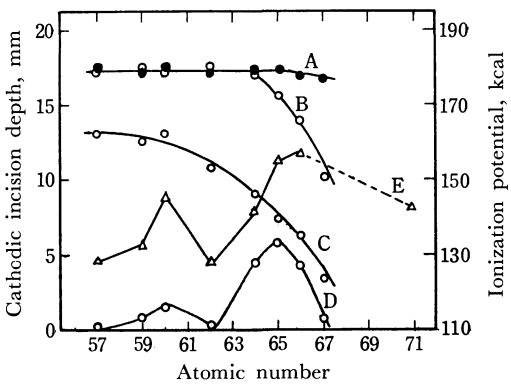

Fig. 2. Variation of cathodic incision depth with the lanthanides in 1 M KSCN solution at pH 3.65±0.05: curves A and B (without deaeration), with a HME; curve C (without deaeration) and D with a DME; curve E, the value of first ionization potential. The concentration of lanthanide added, A to D, was 0.0005 M.

0.05. As seen in Fig. 3, the incision depth increases proportionally to the lanthanide concentration

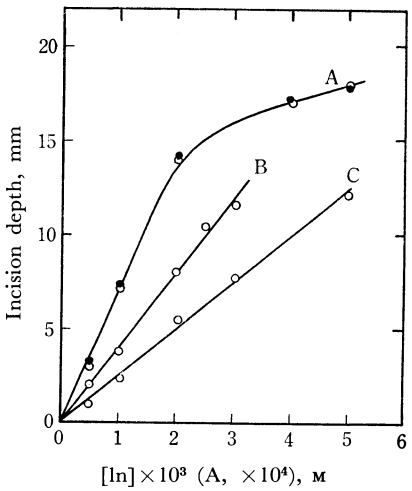

Fig. 3. Calibration curves of the lanthanides: curve A, with a HME (1 M KSCN and KCl; Tb, Sm and Nd); curves B and C, with a DME (1 M KCl; B, Tb; C, Nd).

for the range, 0.5 to 3×10^{-3} M (Tb^{3+}) and 0.5 to 5×10^{-3} M (Nd^{3+}) with the DME, and in the range, 0.5 to 2×10^{-4} M (Nd^{3+}, Sm^{3+} and Tb^{3+}) with HME.

Consequently, the variation of incision depth on curve D, Fig. 2, may be attributed to the difference in electrode reaction rate of each of the lanthanide ions.

Oscillopolarographic Characteristics of Lanthanide Ions in Potassium Chloride, Bromide and Perchlorate Solutions. The relation between the atomic number and the cathodic incision depth of the lanthanides at pH 3.65± 0.05 are shown in Fig. 4 to 6. In Fig. 4, oscillopolarograms were recorded in the range of potassium chloride concentration, 0.5 to 2.0 M. These oscillopolarograms have tendencies similar to those of the potassium thiocyanate solutions which have cathodic and anodic potentials of incision equal to

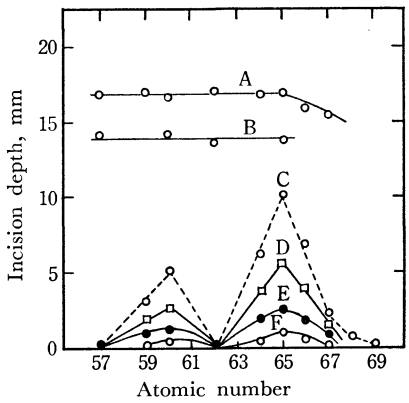

Fig. 4. Variation of the cathodic incision depth with the lanthanides in KCl solution at pH 3.65±0.05: the concentration of KCl added: A, B, C and E 1 M; D 0.5 M; F 2.0 M. The concentration of lanthanide added: A, D, E and F 0.0005; B 0.0002 M; C 0.0025 M. The kind of polarizable electrode used for A and B was a HME and C to F was a DME.

−1.42 and −1.40 V respectively. The curves C to F in Fig. 4 consist mainly of two peaks. This behaviour is also exhibited in the case of potassium thiocyanate solutions. Furthermore, the incision depths decrease to some extent as the concentration of potassium chloride increases. This effect may be attributed to the change of the potential ϕ_2[6] (which becomes less negative with increasing concentration). Curve A in Fig. 4, obtained with the HME, was similar to curve A in Fig. 2. The results measured at pH 4.65±0.05 in 1 M potassium chloride solutions are shown in Fig. 5.

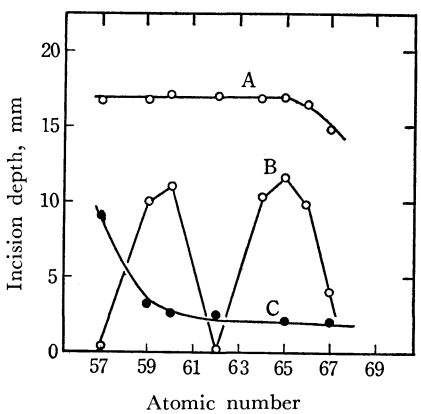

Fig. 5. Variation of the cathodic incision depth with lanthanide in 1 M KCl solution at pH 4.65±0.05. The concentration of lanthanide added was 0.0005 M and curve A was measured with a HME and curves B and C with a DME (C, without deaeration).

The value of the incision depth with HME in Fig. 5, 17.0±0.5 mm (La to Dy), was nearly equal to the value in the cases of 1 M potassium thiocyanate and of 1 M potassium chloride solutions at pH 3.65±0.05. The curve B in Fig. 5 shows the incision depths of lanthanide obtained with DME. These values were rather larger than those in the same supporting electrolyte at pH 3.65. It seems that the cathodic incision of lanthanides is attributable to the reduction of H^+ in hydrated water molecules[2] and that the anodic incision is attributable to the oxidation of lanthanide-halogeno hydride complexes,[1] which are formed by the hydride ions produced at the cathode. Consequently, the increase in the hydrogen ion concentration on the electrode surface might supress the formation of lanthanide-halogeno hydride complexes. Incision depths, without deaeration at pH 4.65, decreased with the decrease in the basicity and such behaviour may be caused by an increase of hydrolysis at the electrode surface. The incision potential was constant at −1.41±0.01 V *vs.* SCE.

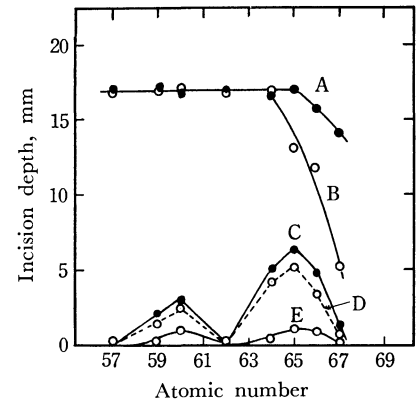

Fig. 6. Variation of the cathodic incision depth with lanthanide in 1 M KBr and $NaClO_4$ solution at pH 3.65±0.05. Supporting electrolyte: A and C, KBr; B, D (0.5 M) and E, $NaClO_4$. A and B, with HME; C to E, with DME.

In Fig. 6, curves A and B represent the results of analyses of the oscillopolarograms obtained on the solution containing 5×10^{-4} M lanthanide, 1 M potassium bromide, and 1 M sodium perchlorate, at pH 3.65±0.05 with HME. In curve B, the values of the incision depth from Tb to Ho are smaller than those of curve A. Curves C and E represent the results of analyses of the curves obtained on these solutions with DME. The values of the incision depth shown by curve C are larger than those by curve E (1 M sodium perchlorate). These results suggest the existence of halide and thiocyanato complexes of lanthanide at the electrode surface.

The authors are grateful to Professor M. Kobayashi for his interest in this work.

6) P. Delahay, "Double Layer and Electrode Kinetics," Interscience Publishers, New York (1966), p. 209.

BULLETIN OF THE CHEMICAL SOCIETY OF JAPAN VOL. 42 2247—2249 (1969)

Refinement of the Structure of Tohdite $5Al_2O_3 \cdot H_2O$

Goro YAMAGUCHI and Masataro OKUMIYA

Department of Industrial Chemistry, Faculty of Engineering, The University of Tokyo, Hongo, Tokyo

and Shuichiro ONO

Government Chemical Industrial Research Institute, Tokyo, Shinjuku-ku, Tokyo

(Received October 17, 1968)

The structure of tohdite, $5Al_2O_3 \cdot H_2O$, was determined by Yamaguchi Yanagida, and Ono (1964). Least-squares refinements based on their structure have been carried out using X-ray powder data. The final R factor of the reflection intensity reduced to 0.08 from the initial value of 0.26.

In previous papers the present authors reported on a new phase of alumina hydrate, tohdite $5Al_2O_3 \cdot H_2O$,[1] the conditions of its formation,[2] and its crystal structure as determined from the X-ray powder diffraction data.[3] After these articles, the authors learned of Torkar's study,[4] in which he described a mineral denoted "Al_2O_3-Form K1," but did not determine its chemical formula or atomic arrangement. The mineral described by Torkar seemed identical with tohdite.[5]

The structure of tohdite as determined by Yamaguchi, Yanagida, and Ono is as follows:

Cell dimensions: $a=5.576$ Å, $c=8.768$ Å

Space group : $P6_3mc$

O(1) 0 0 0	Al(1) 1/6 1/3 3/8
O(2) 1/2 0 0	Al(2) 2/3 1/3 1/8
O(3) 1/3 1/6 1/4	Al(3) 1/3 2/3 1/16
O(4) 1/3 2/3 1/4	

Overall temperature factor: 1.62 Å^2

These parameters were obtained on the following assumptions: the unit cell is composed of the ideal stacking of oxygen layers, every O–O distance being equal, and aluminium atoms are placed exactly at the centers of the oxygen polyhedra.

The intensities were calculated for fifty reflections (up to $\sin\theta/\lambda=0.456$ Å^{-1}), and the reliability factor, $R_I=\sum(I_o-I_c)/\sum I_o$, of 0.26 was obtained by omitting unobserved reflections. In the present paper the least-squares refinements of the structure of tohdite by means of the powder data will be reported.

Experimental

A polycrystalline sample of tohdite was prepared from Eta-Alumina by hydrothermal treatment.[3] In this powder sample the effect of the preferred orientation on the integrated intensities was confirmed to be negligible.[3] The X-ray diffraction diagrams were obtained by means of a Rigaku Denki diffractometer equipped with a Geiger counter using Cu$K\alpha$ radiation. The intensities relative to the intensity of the 202 reflection were obtained by measuring the areas of the peaks. The intensities of 51 peaks could be measured up to $\sin\theta/\lambda=0.621$ Å^{-1}. In addition, 35 reflections with negligible intensities were expected.

Structure Refinement

First, the lattice dimensions were refined from a least-squares fit of 32 reflections as follows:

$$a=5.575\pm0.001 \text{ Å}, \quad c=8.761\pm0.001 \text{ Å}.$$

Next, a least-squares analysis program was written for a HITAC 5020E computer in which the atomic parameters were varied so as to minimize $R_I'=\sum(I_o-I_c)^2$, where:

$\sum$=the summation of all peaks which can be separated in the diagram;

I_o=integrated intensity;

The calculated intensity, I_c, is presented as: $I_c=K\cdot Lp\cdot\sum_i m_i|F_i|^2$, where:

K=scale factor

Lp=Lorentz and polarization factor

m=multiplicity

F=structure factor.

In the calculation of the structure factors, only an overall isotropic temperature factor was used because the individual temperature factor for each atom did not give any physically significant results.

1) G. Yamaguchi, H. Yanagida and S. Ono, This Bulletin, **37**, 752 (1964).

2) G. Yamaguchi, H. Yanagida and S. Ono, *J. Ceram. Assoc. Japan*, **74**, 84 (1966).

3) G. Yamaguchi, H. Yanagida and S. Ono, This Bulletin, **37**, 1555 (1964).

4) K. Torkar and H. Krischner, *Ber. Deut. Keram. Ges.*, **39**, 131 (1962).

5) K. Torkar and H. Krischner, This Bulletin, **39**, 1356 (1966).

As was mentioned in a previous paper,[3] the possible space groups are $P6_3mc$ and $P31c$. Therefore, refinement was undertaken in both these cases.

In $P6_3mc$ 11 parameters could be varied: that is, the x and z coordinates of Al(1), O(2) and O(3), the z coordinate of Al(2), Al(3), and O(4), the overall isotropic temperature factor, and the scale factor. The calculation was performed starting from the previous parameters[3] and by omitting hydrogen atoms. After several least-squares cycles, the reliability factor, R_I, could be reduced to 0.08 for 115 reflections. The final atomic coordinates, their standard deviations, and the overall isotropic temperature factor are listed in Table 1. The values of I_o and I_c calculated from the final parameters are given in Table 2.

TABLE 1. ATOMIC COORDINATES WITH THEIR STANDARD DEVIATIONS ($\times 10^4$)

	x	y	z
Al(1)	0.1647(9)	$2x$	0.3708(19)
Al(2)	2/3	1/3	0.1533(27)
Al(3)	1/3	2/3	0.0611(29)
O(1)	0	0	0
O(2)	0.5098(10)	$2x$	0.0143(19)
O(3)	0.8291(23)	$2x$	0.2666(20)
O(4)	1/3	2/3	0.2638(28)

Overall temperature factor 0.46(0.03)Å^2

Refinement was also attempted according to $P31c$, in which the Al(1), O(2), and O(3) atoms can shift out of the mirror plane, while the Al(2), Al(3), O(1), and O(4) atoms have to remain in the same position as in $P6_3mc$. This refinement was unsatisfactory, probably because the calculation was performed using the intensity values obtained by summarizing the hkl and $hk\bar{l}$ reflections; this was done since it is impossible to distinguish the hkl and the $hk\bar{l}$ reflections of $P31c$ in the powder diagram, although these reflections have different structure factors.

It, therefore, still remains conceivable that the atoms are slightly displaced from these special positions of $P6_3mc$ and that $P31c$ should be taken for this crystal.

Discussion

This refinement shows that the packing deviates from the postulated ideal model of the previous work. The oxygen atoms are closely packed in layers perpendicular to the c axis and are situated at z=0, 1/4, 1/2, and 3/4 but the individual atoms have different z parameters. Consequently, the oxygen layers are deformed; the first layer (at $z\approx 0$, O(1): z=0, O(2): z=0.014) and the third layer, which is symmetrically equivalent to the first layer,

TABLE 2.

hkl	I_o	I_c	hkl	I_o	I_c
1 0 0	10	10	4 0 4	5	5
0 0 2	23	23	4 1 0		1 } 6
1 0 1	11	11	4 1 1	0	0
1 0 2	60	61	3 2 3	11	5
1 1 0	12	10	2 1 7		8 } 13
1 0 3	54	55	4 1 2	12	11
2 0 0	12	12	1 1 8		3 } 14
1 1 2	77	79	2 2 6	8	6
2 0 1	38	42	2 0 8	23	0
0 0 4	4	8	4 0 5		21 } 21
2 0 2	100	96	4 1 3	0	0
1 0 4	0	1	2 3 4	0	0
2 0 3	48	46	1 3 6	0	0
1 2 0	0	1	0 3 7	0	0
1 2 1	0	1	5 0 0	0	0
1 1 4	0	1	5 0 1	0	0
1 2 2	13	16	1 0 9	0	0
1 0 5	4	4	1 4 4	0	0
2 0 4	26	28	5 0 2	6	1
3 0 0	0	2	2 1 8		2 } 4
3 0 1	0	0	3 2 5		1
1 2 3	34	36	4 0 6	7	2
3 0 2	20	20	3 3 0		0 } 2
0 0 6	4	4	5 0 3	15	5
2 0 5	76	74	3 1 7		8 } 15
3 0 3	0	0	4 2 0		2
1 2 4	0	0	3 3 2	20	5
1 0 6	0	0	4 2 1		7
2 2 0	73	73	3 0 8		3 } 19
1 3 0	0	0	2 0 9		4
2 2 2	5	4	4 1 5	0	0
1 3 1		1 } 5	4 2 2	6	6
3 0 4	0	0	3 2 6	0	0
1 1 6	0	1	5 0 4	0	0
1 3 2	6	6	0 0 10	3	3
1 2 5	3	4	4 2 3	9	7
2 0 6	7	4	4 0 7		2 } 9
1 3 3	21	11	5 1 0		0
1 0 7		8 } 21	1 5 1	18	0
4 0 0		2	1 0 10		1
4 0 1	5	6	2 2 8		15 } 16
3 0 5	0	0	2 1 9		0
2 2 4	1	2	3 3 4	0	0
4 0 2	6	6	4 1 6	0	1
1 3 4	0	0	5 1 2	7	2
1 2 6	0	0	3 1 8		3 } 6
4 0 3	9	5	5 0 5		1
2 0 7		2 } 7	4 2 4	8	9
2 3 0	0	0	1 1 10	0	2
2 3 1	4	1	3 0 9	0	0
0 0 8		3 } 4	5 1 3	22	8
3 0 6	0	1	3 2 7		11 } 19
3 2 2	6	4	2 0 10	14	15
1 0 8		2 } 6	4 0 8	51	0
3 1 5	1	2	4 2 5		54
			5 1 4		0 } 54
			4 1 7		0
			5 0 6	0	0
			6 0 0	29	29
			6 0 1	0	0

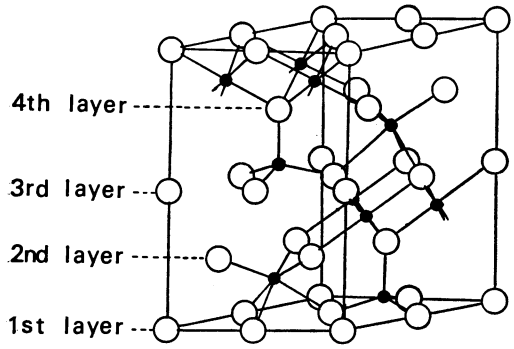

Fig. 1. The unit cell of the tohdite structure. Oxygen atoms are shown as large and aluminum atoms as small spheres.

are more deformed than the second layer (at $z \approx 1/4$, O(3): $z=0.267$, O(4): $z=0.264$) and the fourth. The distance between the first and second layers (0.26 Å) is larger than that between the second and the third layer (0.24 Å).

The interatomic distances were calculated from the coordinates of Table 1. The calculated standard deviations of the Al–O and O–O distances are from 0.01 to 0.03 Å.

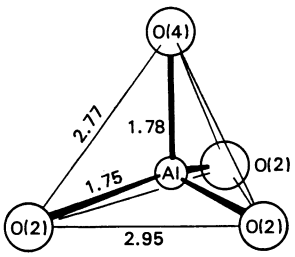

Fig. 2. Interatomic distances (Å) in $Al(3)O_4$.

The Al(3)–O distances are within the range of 1.78—1.75 Å, indicating that the $Al(3)O_4$ tetrahedra are slightly distorted (Fig. 2). In the $Al(2)O_6$ octahedra, aluminium atoms are placed at $z=0.153$, deviating from the $z=0.125$ of the ideal model, and are closer to the oxygen atoms of the upper face (in the second layer), 1.86 Å, than to the oxygen atoms of the lower face (in the first layer), 1.94 Å. The $Al(1)O_6$ octahedra are more distorted than the $Al(2)O_6$ octahedra.

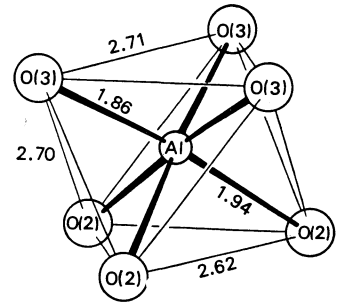

Fig. 3. Interatomic distances (Å) in $Al(2)O_6$.

The Al–O and the O–O distances in these AlO_6 octahedra are shown in Fig. 3 and Fig. 4. For comparison, the interatomic distances in AlO_6 octahedra for α-Al_2O_3[6] are also given; the Al–O distances are 1.86 and 1.97 Å, and to O–O 2.52, 2.87, 2.62, and 2.73 Å.

This refinement supports the expected nature of the distortion caused by local ionic attraction and repulsion.

All the calculations were performed with a HITAC 5020E computer of the Computation Center of Tokyo University, using programs written by the authors.

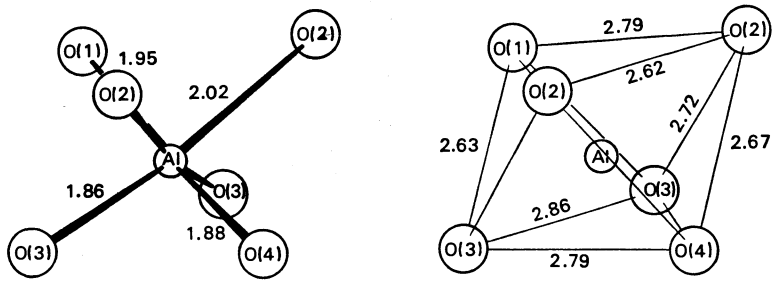

Fig. 4. Interatomic distances (Å) in $Al(1)O_6$.

6) R. E. Newnham and Y. M. de Haan, *Z. Krist.*, **117**, 235 (1962).

BULLETIN OF THE CHEMICAL SOCIETY OF JAPAN VOL. 42 2250—2254 (1969)

The Reaction between Mercury(II) and Organic Compounds. VII. The Formation Constant and Analytical Application of the *o*-(2-Thiazolylazo)-4-chlorophenol-Mercury(II) Complex

Fumiaki KAI

Department of Chemistry, Faculty of Science, Kumamoto University, Kurokami-machi, Kumamoto

(Received October 31, 1968)

The formation constants of the complex formed between *o*-(2-thiazolylazo)-4-chlorophenol, TACL, and mercury(II) in 2% v/v dioxane-water were log $K_{HgR^+}=6.2_1$ and log $K_{HgR_2}=6.1_0$ at $\mu=0.1$ and at room temperature. TACL was suggested as a suitable metallochromic indicator for the direct titrimetric determination of mercury(II) ions at pH 6.7—8.7 with an EDTA titrant. This optimum pH range was rather wide compared with that of the other metallochromic indicators, such as Cu-PAN, XO, and MTB. There were marked colour changes from deep blue to reddish-yellow or to violet at equivalence points. The mercury(II) ions up to 210 mg in 100 m*l* can be determined within an error of ±0.3% by this method.

o-(2-Thiazolylazo)-phenols have been found to be as excellent chromogenic reagents as pyridilazo phenols, and the properties of related chelates and analytical applications of them have hitherto been reported.

In preceding papers[1,2] the formation constants of the complexes formed between *o*-(2-thiazolylazo)-4-methoxy phenol (TAM) and *o*-(2-thiazolylazo)-cresol (TAC) and mercury(II) were shown. Moreover, these reagents were reported to be suitable metallochromic indicators for the direct titration of mercury(II) in a slightly alkaline medium. (In the case of the other indicators, such as Cu-PAN,[3] XO,[4] and MTB,[5] the optimum pHs of the direct titration for mercury(II) are pH 3—3.5(Cu-PAN) and pH 6 (XO and MTB).)

The present communication will describe the formation constant of the TACL-Hg(II) complex and its applicability to the metallochromic indicator for the determination of mercury(II) by titrimetry.

Experimental

Reagents. TACL was prepared according to the method reported in the literature[6] and was doubly recrystallized from hot ethanol. The purification of dioxane, the preparation of solutions of an EDTA titrant and of a stock solution of mercury(II), and the method of pH control were the same as those described previously.[1,2]

Instruments. The absorption spectra and the absorbances were measured with the Hitachi recording spectrophotometer (EPS-2) and a Hitachi photoelectric spectrophotometer (EPU-2) with 10-mm silica cells respectively. The pH was measured with a glass electrode pH meter (Hitachi-Horiba F-5).

Results and Discussion

Acid Dissociation Constant of TACL in a 2% v/v Dioxane-Water Solution. The dissociation scheme of TACL is as follows:

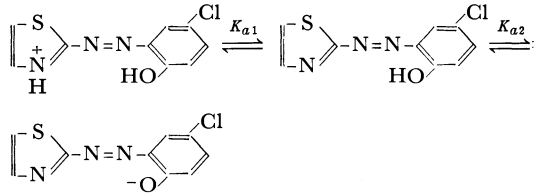

Each constant is given by Eq. (1):

$$K_{a1}=\frac{[HR][H^+]}{[H_2R^+]} \text{ and } K_{a2}=\frac{[R^-][H^+]}{[HR]} \quad (1)$$

The acid dissociation constants were obtained spectrophotometrically. For the second step only, Eq. (2) is given:

$$\log\frac{A-\varepsilon_{HR}C_{R^-}}{\varepsilon_{R^-}C_{R^-}-A}=\text{pH}+\log K_{a2} \quad (2)$$

where A is the total absorbance, C_{R^-}, the analytical concentration of TACL, and ε_{HR} and ε_{R^-}, the molar absorptivities of the HR and R^- species respectively.

The molar absorptivity was calculated from the horizontal lines of the pH-absorbance plot.

1) F. Kai, *Anal. Chim. Acta*, **44**, 129 (1969).
2) F. Kai, *ibid.*, **44**, 242 (1969).
3) H. Flaschka and H. Abdine, *Chemist-Analyst*, **45**, 58 (1956).
4) H. Körble, R. Pribil and A. Emf, *Chem. Listy*, **50**, 1440 (1956).
5) H. Körble, R. Pribil and A. Emf, *ibid.*, **51**, 1061 (1957).
6) A. Kawase, *Bunseki Kagaku* (*Japan Analyst*), **11**, 621 (1962).

TABLE 1. ACID DISSOCIATION CONSTANT OF TACL AND FORMATION CONSTANT OF Hg(II)-TACL CHELATE

Acid dissociation constant of TACL	Chelate			
	Composition	λ_{max}, mμ	ε_{max}	Formation constant
$pK_{a1}<0.5$	1 : 1	650	8.71×10^3	$\log K_{HgR^+}=6.2_1$
$pK_{a2}=7.7_0$	1 : 2	665	1.51×10^4	$\log K_{HgR_2}=6.1_0$

2% v/v dioxane-water solution; $\mu=0.1$ with potassium nitrate; room temp.

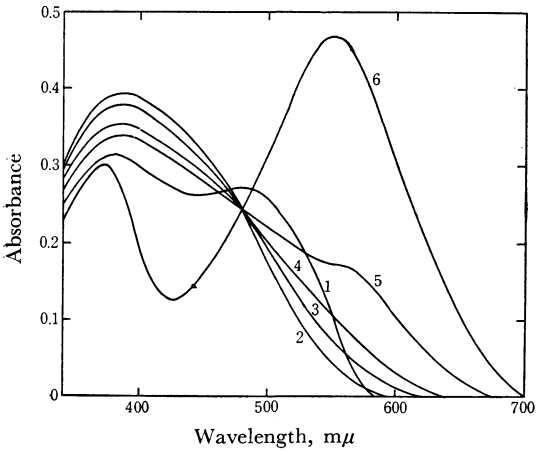

Fig. 1. Absorption spectra of TACL at different pH values. Concn.=4.00×10^{-5} M, $\mu=0.1$, Solvent=2% v/v dioxane-water.
Curve 1=pH 0.58 Curve 4=pH 7.00
2= 1.0—4.47 5= 7.60
3= 6.45 6= 10.15

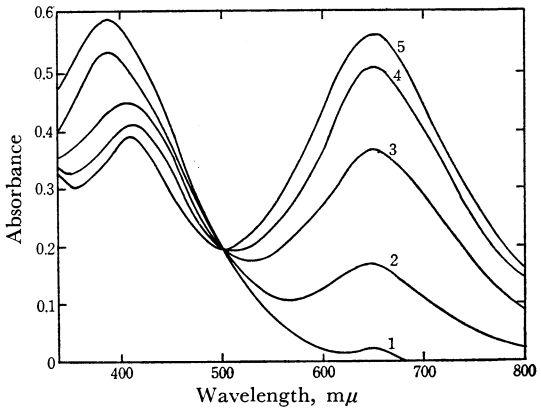

Fig. 2. Absorption spectra of Hg(II) and TACL mixture consisting of excess Hg(II) against TACL at different pH values. Concn.: TACL=6.66×10^{-5} M, Hg(II)=6.66×10^{-4} M, $\mu=0.1$, Solvent =2% v/v dioxane-water.
Curve 1=pH 3.60 Curve 4=pH 6.22
2= 4.72 5= 7.20—7.69
3= 5.53

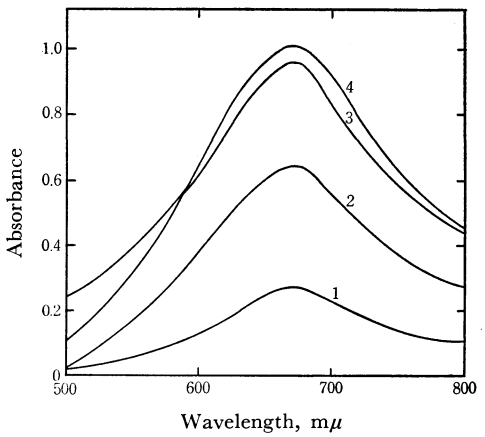

Fig. 3. Absorption spectra of Hg(II) and TACL mixture consisting of excess TACL against Hg(II) at different pH values. Concn.: TACL =6.66×10^{-4} M, Hg(II)=6.66×10^{-5} M, $\mu=0.1$, Solvent=2% v/v dioxane-water,
Curve 1=pH 5.40 Curve 3=pH 6.26
2= 6.01 4= 7.09

The absorption spectra of TACL in a 2% v/v dioxane-water solution at various pHs are shown in Fig. 1. They have the isosbestic point at 478 mμ and the absorption maxima at 550 mμ. At about pH> 7.6, TACL is red in colour due to the R^- species. By Eq. (2), the pK_{a2} value was obtained from the absorbances at 550 mμ. The precise pK_{a1} value was, however, not estimated because it may be considered to be in the pH<0 region. The values, which almost entirely conformed to those obtained in 20% v/v dioxane-water,[6] are listed in Table 1.

Absorption Spectra of Hg(II)-TACL Chelate in the Dioxane-Water Solution. The spectra of the mercury chelates were scanned for a 2% v/v dioxane-water solution containing various concentrations of the components at different pHs. Figure 2 shows the spectra of the mixture composed of excess mercury(II) and TACL (ten times as much mercury as TACL). From a pH of about 4.5 spectra were obtained with the isosbestic point at 502 mμ and the absorption maxima at 650 mμ, which was attributed to deep blue colour. Besides the mercury(II)-TACL chelate, an analogous blue colour was shown in the case of only the Ni(II)-TACL chelate,[6] TACL has, therefore, been suggested as a suitable metallochromic indicator for the titrimetric determination of mercury(II) ions with a proper titrant.

The spectra in the case of a reagent excess (ten times as much TACL as mercury) are illustrated in

Fig. 3. They were scanned using the TACL solution as the reference because the mixture showed a strong absorption caused by the predominant concentration of TACL itself.

Composition of the Chelate. By comparing the spectra shown in Figs. 2 and 3 it was found that almost all the figures of the curves, the wavelength, and the pH at the absorption maxima coincided; only their molar absorptivities differed. The molar absorptivities in Fig. 3 were nearly twice those in Fig. 2. Therefore the formation of the 1 : 1 chelate, HgR^+, was considered in the case of the mercury(II) excess (Fig. 2), and that of 1 : 2, HgR_2, in the case of the TACL excess (Fig. 3). The same situations have been described with respect to the analogous chelates formed between mercury(II) and thiazolylazo dyestuffs.[1,2]

Formation Constants of the Chelate. When the concentration of mercury(II) is in great excess in comparison with that of TACL, the successive formation constant can be calculated by Eq. (3):[1,2]

$$\log K_{HgR^+} = \log \frac{[HgR^+]}{[HR]} + pHg + pK_{a2} - pH \quad (3)$$

Equation (3) indicates that the plot of $\log[HgR^+]/[HR]$ against pH should give a straight line with a slope of unity, and that the formation constant can be calculated from the pH at which $\log[HgR^+]/[HR]$ equals zero, the acid dissociation constant of TACL, and the initial concentration of mercury(II) ions. Figure 4a shows the plot of $\log[HgR^+]/[HR]$ *versus* pH. The pHg value was estimated here on the assumption that it should be decreased by 10% from the initial concentration belonging to the 1 : 1 chelate formation because of the initial ratio of the components, $[Hg^{2+}]/[TACL]=10$. As a result, the successive formation constant, $\log K_{HgR^+}$, calculated was 6.2_1.

The second successive formation constant can be obtained indirectly from the over-all formation constant using Eq. (4):[1,2]

$$\log \frac{[HgR_2]}{[Hg^{2+}]} = \log K_{HgR^+} \cdot K_{HgR_2} + 2\log[HR]_t - 2pK_{a2} + 2pH \quad (4)$$

where $[HR]_t$ is the total concentration of TACL. Equation (4) shows that the over-all formation constant can be calculated by the pH at which $\log[HgR_2]/[Hg^{2+}]$ equals zero, the acid dissociation constant of TACL, and an experimental concentration of $[HR]_t$. Figure 4b shows the plot of $\log[HgR_2]/[Hg^{2+}]$ *versus* pH. In this case of a reagent excess, the $[HR]_t$ value was calculated by assuming that the initial concentration of the ligand may be decreased by 20% due to the 1 : 2 chelate formation because the initial mixture was composed of $[TACL]/[Hg^{2+}]=10$. The over-all formation constant obtained was $\log K_{HgR^+} \cdot K_{HgR_2} = 12.3_1$; therefore the second successive formation constant, $\log K_{HgR_2}$, was 6.1_0. These values are listed in Table 1.

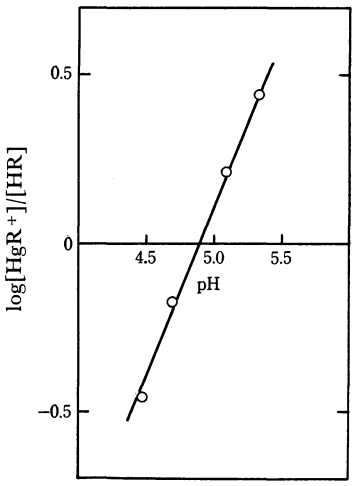

Fig. 4a. Plot of $\log [HgR^+]/[HR]$ *vs.* pH.

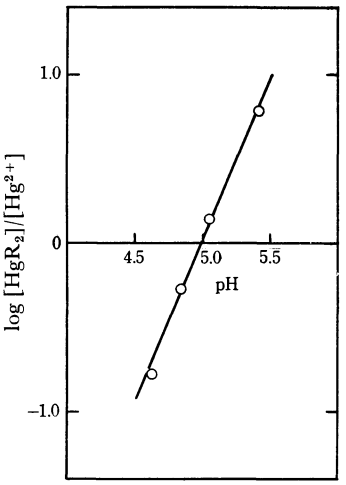

Fig. 4b. Plot of $\log [HgR_2]/[Hg^{2+}]$ *vs.* pH.

Applicability of TACL as a Metallochromic Indicator for Hg(II). In the case of the titrimetric determination of mercury(II) ions with a proper titrant (EDTA), and with TACL as the indicator, a sharp colour change may be expected because of the large difference in formation constant between the TACL-Hg(II) obtained as above and the HgY ($\log K_{HgY}=21.8$).

pH. Photometric titrations were carried out at various pHs. The concentration of mercury(II) was 5×10^{-4} M and several drops of an alcoholic TACL solution (*ca.* 10^{-2} M) were added to the sample solution. A deep blue solution was thus obtained. The concentration of the aqueous EDTA titrant was 10^{-2} M. The pH was adjusted with a 0.1 M phosphate buffer. As can be seen in Fig. 5, in the pH range of 6.7—8.7 the sharp colour changes were observed at the equivalence point. This optimum pH range seems to be rather wider than that indicated by the other indicators (BT:

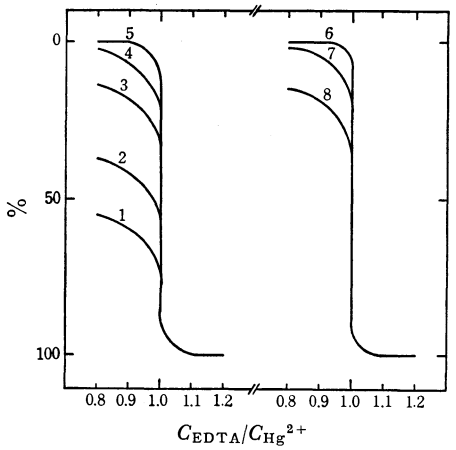

Fig. 5. Photometric titration curves.
$C_{Hg^{2+}}=5\times10^{-4}$ M, TACL$=4\times10^{-5}$ M, EDTA$=0.1$ M, Buffer$=$phosphate system.
Curve 1$=$pH 4.1 Curve 5$=$pH 6.9
2$=$ 5.0 6$=$ 8.2
3$=$ 5.9 7$=$ 8.7
4$=$ 6.5 8$=$ 9.1

pH 3—3.5; XO and MTB: pH 6). At the other pHs tested, colour changes were observed before the equivalence point, whereas no colour change such as a tailing of the colour after the equivalence point was shown at any of the tested pHs.

Error. Recovery tests were carried out at various concentrations of mercury(II) ions at pH 8.0. Table 2 shows that only a small error, within ±0.3, was given at the concentrations of mercury(II) up to 211.04 mg/100 m*l* (corresponding to 1.05×10^{-2} M as Hg^{2+}). The negative error was increased at concentrations of mercury(II) higher than about 10^{-2} M. Accordingly, it is desirable to keep the concentration of mercury(II) below *ca.* 10^{-2} M.*1

Effect of Diverse Ions. An interference study was also carried out. The depression of the absorbances at 650 mμ was checked after the titration of aqueous sample solutions containing various amounts of diverse ions with the EDTA titrant (10^{-2} M). A 100 m*l* of the sample solution (5×10^{-4} M as Hg(II) ions) was kept at pH 8.0. The results are listed in Table 3. Negative errors were given by anions which can form complex ions with mercury(II), whereas positive errors were given by metal ions which can form complexes with the EDTA titrant. Cyanide, thiocyanate, ammonium, and halide except considerable amounts of chloride gave the negative errors. On metal ions, a large positive error was given by nickel(II); the Ni(II)-TACL chelate showed a blue colour analogous to that of the Hg(II)-TACL chelate. Cobalt(II), zinc(II), cadmium(II), and copper(II)

Table 2. Recovery of mercury(II) at various concentration at pH 8.0

Taken mg as Hg^{2+}/100 m*l*	Found mg as Hg^{2+}/100 m*l*	Recovery %	Error %
10.28	10.25	99.7	−0.3
20.50	20.50	100.0	0.0
25.76	25.73	99.9	−0.1
34.62	34.55	99.8	−0.2
40.18	40.22	100.1	+0.1
48.05	48.00	99.8	−0.2
103.55	103.99	100.3	+0.3
211.04	210.97	99.9	−0.1
274.52	258.31	94.1	−5.9
334.31	312.23	93.4	−6.6

Table 3. Effects of diverse ions (100 m*l* of 5×10^{-4} M mercury(II), pH$=$8.0)

Ion	Added amounts as ion, mg	Recovery of mercury(II), %	Error %
Cl^-	5.0	100.0	0.0
	10.0	100.2	+0.2
	20.0	99.7	−0.3
Br^-	0.5	98.2	−1.8
	1.0	90.4	−9.6
I^-	0.5	92.7	−7.3
	1·0	90.4	−9.6
CN^-	0.1	98.5	−1.5
	0.5	95.6	−4.4
SCN^-	0.1	99.6	−0.4
	0.5	93.2	−6.8
NH_4^+	5.0	99.7	−0.3
	7.0	98.4	−1.6
Ag^+	10.0	100.0	0.0
Ca^{2+}	10.0	100.1	+0.1
Sr^{2+}	10.0	100.0	0.0
Ba^{2+}	10.0	99.8	−0.2
Co^{2+}	1.0	99.5	−0.5
	2.0	102.9	+2.9
Ni^{2+}	0.5	101.3	+1.3
	1.0	109.5	+9.5
Cu^{2+}	1.0	100.1	+0.1
	2.0	101.7	+1.7
	3.0	109.8	+9.8
Zn^{2+}	0.5	100.0	0.0
	1.0	101.1	+1.1
Cd^{2+}	0.5	99.9	−0.1
	1.0	100.9	+0.9
Al^{3+}	10.0	100.0	0.0
Cr^{3+}	10.0	99.9	−0.1
Fe^{3+}	10.0	99.9	−0.1

Metal ions were added as nitrate.

*1 At concentrations higher than 10^{-2} M, mercury(II) oxide was apt to form. The excess ammoniacal buffer system may be suitable in this case: *cf.* N. Iritani, T. Tanaka and H. Sakai, *Nippon Yakugaku Zassi (J. Pharm. Soc. Japan)*, **76**, 1068 (1956); *ibid.*, **77**, 106 (1957).

ions gave errors. However, no interference was caused by the presence of silver(I), calcium(II), strontium(II), barium(II), chromium(III), iron-(III), and aluminium(III) ions up to 10 mg.

The titration could be carried out accurately without heating the sample solution.

In view of the above data, it may be suggested that TACL can also be utilized as a metallochromic indicator of mercury(II), for its sensitivity and accuracy are as good as those of TAC[1] and TAM.[2]

On the basis of the above results, the recommended procedure for the direct titrimetric determination of mercury(II) ions using TACL as the indicator is as follows: Take about 100 m*l* of a sample solution containing not more than 10^{-2} M as mercury(II) ions at pH 6.7—8.7, adjusted with a 0.1 M phosphate buffer system. Add several drops of an alcoholic solution of TACL (*ca.* 10^{-2} M) to the sample solution, and then titrate with the EDTA titrant (10^{-2} M aq. soln.). Near the end-point, carry out the titration slowly and with constant shaking. The colour change is sharp and reversible.

The author wishes to express his deep gratitude to Professor D. Yamamoto of Kumamoto University for his useful discussions and encouragement throughout this work.

BULLETIN OF THE CHEMICAL SOCIETY OF JAPAN VOL. 42 2254—2258 (1969)

Photochemical Analysis. I. Photonometric Titration of Thallic Ion by Uranyl Photoreduction Reaction

Yu YOKOYAMA and Shigero IKEDA

Department of Chemistry, Faculty of Science, Osaka University, Toyonaka

(Received November 7, 1968)

Photonometric titration of thallic ion is described, in which uranous ion, the titrant, is generated by photoreduction of uranyl ion in a sulfuric acid solution containing sodium lactate. Uranyl ion could be reduced with the light at wavelengths longer than 300 mμ, whereas thallic ion could not be reduced with the light in this wavelength range. Selective photoreduction of uranyl ion was accomplished by eliminating wavelengths below 300 mμ with a filter. In this photonometric titration, reaction solutions were irradiated without stirring at 29.5±0.5°C. The absorbance of uranous ion produced was measured at 655 mμ every fixed irradiation time, and the absorbance was plotted against the irradiation time. Induction period, which means the period during which the absorbance remains actually zero, was in a linear relation with thallic concentration. Thus the titration of thallic ion was satisfactorily carried out in the concentration range from 0.01 to 0.1 mM. The results proved the feasibility of titration in a completely sealed container and suggest a possibility of titration on a microvolume of reaction solution.

Photonometric titration was first proposed by Bricker and Schonberg.[1] In photonometric titration, titrant is photochemically generated in a solution containing a substance to be determined. However, no titration systems have been investigated except ferric-ferrous,[1] cobaltic-cobaltous,[2] and anthraquinone-reduced anthraquinone[3] systems. In the present paper, a photonometric titration by uranyl-uranous redox system is described. The photoreduction of uranyl to uranous ion has been utilized as preliminary treatment in volumetric titration of uranium by Rao *et al.*,[4,5] but in the present case this reaction is performed for generation of titrant.

The previous experiments on potentiometric titration[6,7] showed that, in spite of effective stirring of reaction solution, there existed a time lag (approximately less than one second) between addition of a titrant and indication of potential, as is the case with all conventional titrations. In the photochemical reaction, it is possible to generate a titrant homogeneously. In the present work,

1) C. E. Bricker and S. S. Schonberg, *Anal. Chem.*, **30**, 922 (1958).

2) H. D. Drew and J. M. Fitzgerald, *ibid.*, **38**, 778 (1966).

3) T. Kuwana, *ibid.*, **35**, 1398 (1963).

4) G. G. Rao, V. P. Rao and M. V. R. Rao, *Anal. Chim. Acta*, **15**, 97 (1956).

5) G. G. Rao, V. P. Rao and N. C. Venkatamma, *Z. anal. Chem.*, **150**, 178 (1956).

6) Y. Yokoyama, N. Tsuji and S. Suzuki, *Bunseki Kagaku (Japan Analyst)*, **15**, 20 (1966).

7) N. Tsuji and Y. Yokoyama, *ibid.*, **17**, 939 (1968).

therefore, an attempt was made to perform the titration in a stoppered reaction vessel without stirring. A reaction vessel of 10 mm in light path length and 5 m*l* in volume, provided with a ground stopcock, was designed, and used throughout the present work.

In photochemical reactions, some substances react with a product of the photochemical reaction and some take part in the reaction as a quencher. In a series of our photochemical experiments, these actions of coexisting substances were found to be applicable to the determination of microamounts of substances. These results will be published in succession, and hereafter *the chemical analysis based on the photochemical reaction will be called "the photochemical analysis."*

The photochemical analysis has the following advantages over other analytical methods. (1) The titrant is generated in a reaction vessel, as the titration proceeds. Consequently, unstable substances can be utilized as titrant. (2) The determinable concentration range is of the same order as, or less than, that in the coulometric titration. (3) The titration can be performed in a completely sealed container and, therefore, there is a possibility of titration on a microvolume of reaction solution. On the other hand, the shortcomings are as follows. (1) The temperature of reaction solution must be kept constant, as is usual in experiments of reaction rate measurement. (2) Interference of coexisting substances could occur in two different ways, that is, the reaction with a photochemical reaction product and the quenching reaction.

Experimental

Reagents. Uranyl standard solution (0.05 M) was prepared by dissolving G. R. uranyl acetate in water containing a small amount of sulfuric acid. The factor of this solution was determined to be 0.965 by gravimetry as uranyl oxinate. Thallic standard solution (0.025 M, f=0.937) and thallous standard solution (0.05 M, f=0.993) were prepared by dissolving thallic oxide of 99.9% purity and E. P. thallous sulfate in 1.2 N sulfuric acid solution, respectively. The factors of these solutions were determined iodometrically. Sodium lactate solution (0.2 M), and sulfuric acid solution (5 N) were also used in phtochemical reaction. In addition, sulfuric acid (1 N) solutions of the following salts were prepared: bismuth nitrate, mercuric sulfate, silver sulfate, zinc sulfate, and cadmium sulfate. The following reagents were prepared for iodometric titration of thallium: 0.01 M thallous chloride standard solution, 0.01 N sodium thiosulfate solution, 1% potassium iodide solution, 1% starch indicator solution, 20% phenol-glacial acetic acid solution, bromine mixture which was prepared by dissolving 50 g of sodium dihydrogenphosphate monohydrate and 50 g of ammonium chloride in 450 m*l* of saturated bromine water, and phosphate-chloride mixture containing 50 g of sodium dihydrogenphosphate monohydrate and 50 g of ammonium chloride in 450 m*l* water.

Apparatus. In order to follow the photoreduction of uranyl ion, a Shimadzu Ltd. Model QV-50 spectrophotometer was utilized with some modification. A side wall of the absorption cell compartment was replaced with a new side wall equipped with a window and a shutter. In front of the shutter a 120 W medium pressure mercury lamp, which was employed as the light source for photochemical reaction, was attached together with a lens system, and the optical axis was addjusted so as to intersect that of the monochromator at right angles. The cell holder was positioned at the intersection. A 10 mm × 10 mm quartz absorption cell with four transparent sides was used in place of a usual absorption cell, and also served as a photochemical reaction vessel. The cell was fitted with a ground stopcock. The mercury lamp and its power unit were components of a Hitachi Ltd. Model 203 fluorescence spectrophotometer. The light intensity from the lamp stabilized within 15 min from initial ignition. Absorption spectra were recorded with a Hitachi Ltd. Model EPS-2 automatic recording spectrophotometer.

Procedure. The reagent solutions were mixed in a 25 m*l* measuring flask, and diluted to 25 m*l*. Approximately 5 m*l* of the mixed solution was transferred into a reaction vessel, which was then set in the cell holder. For photochemical reaction, the reaction vessel was irradiated with the mercury lamp with the shutter open. After irradiation for a definite time, the absorption of uranous ion produced was measured at a wavelength of 655 mμ with the shutter closed. Irradiation was continued with the shutter open for further reaction.

Total thallium was determined according to the following procedure, which was a modification of the method proposed by Sill *et al.*[8] To a solution containing thallium was added 15 m*l* of 5 N sulfuric acid, 30 m*l* of water and 50 m*l* of the bromine mixture. The solution was boiled to oxidize completely thallous to thallic ion until the coloration of the solution became light yellow. After being cooled, 0.4 m*l* of the phenol solution was added to remove free bromine and then total thallium was titrated with 0.01 N sodium thiosulfate solution. Before titration of thallium, 0.01 N sodium thiosulfate solution was standardized against 0.01 M thallous chloride standard solution. Titration of thallic ion in the presence of thallous ion was carried out in the same way as for the determination of total thallium, except that bromine mixture was replaced with phosphate - chloride mixture and heating was omitted. The titration of thallic ion could be performed in the presence of uranyl ion without any interference of uranyl ion.

Results

Measurement of Absorption Spectra. Transmittance curves of uranyl, uranous and thallic ions were recorded in the wavelength range from 250 to 700 mμ. They are shown in Fig. 1. The curve of uranyl ion was that of a solution containing 10 mM uranyl ion, and 40 mM sodium lactate in 1 N sulfuric acid (hereafter called the uranyl mixed solution), and the curve of uranous ion was

8) C. W. Sill and H. E. Peterson, *Anal. Chem.*, **21**, 1268 (1949).

obtained with the uranyl mixed solution after exposure to the mercury lamp until the absorption characteristic of uranous ion was no further increased. Uranous ion has an absorption maximum at 655 mμ (molar absorptivity $\varepsilon=48.9$), and hence the ion was determined spectrophotometrically at this wavelength. For comparison a transmittance curve of a solution containing merely 10 mM uranyl ion in 1 N sulfuric acid was also recorded, and found to be identical with the curve for the uranyl mixed solution. The curve of thallic ion was recorded with a solution containing 10 mM thallic ion, and 40 mM sodium lactate in 1 N sulfuric acid (hereafter called the thallic mixed solution). A transmittance curve of thallous ion was also measured, which is not shown in Fig. 1, and was found merely to shift to a shorter wavelength by approximately 40 mμ compared with the curve of thallic ion.

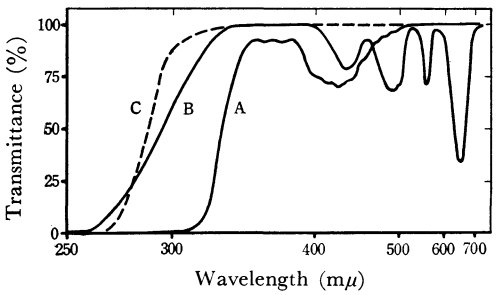

Fig. 1. Absorption spectra of uranyl, uranous, and thallic ions.

A: 10 mM uranyl ion (with 40 mM Na lactate and 1 M H_2SO_4)
B: 10 mM uranous ion (obtained by exposing the solution A to mercury lamp)
C: 10 mM thallic ion (with 40 mM Na lactate and 1 N H_2SO_4)

Irradiation without Filter. The uranyl mixed solution was transferred into the reaction vessel, and irradiated with the mercury lamp without any filter. The absorbance of uranous ion was measured every fixed irradiation time, and the amount of uranous ion produced was calculated by using the molar absorptivity of uranous ion. The thallic mixed solution was also irradiated under the same conditions. Thallous ion thus produced was determined by iodometric titration every fixed irradiation time. Results are presented in Fig. 2. Uranyl ion was reduced to a considerable extent within the irradiation time, as would be expected, and also the reduction of thallic ion took place, even if only slightly.

Irradiation with Filter. The uranyl and the thallic mixed solutions were irradiated through a soft glass filter for eliminating the light of wavelength shorter than 300 mμ. Other conditions were the same as mentioned above. The relation

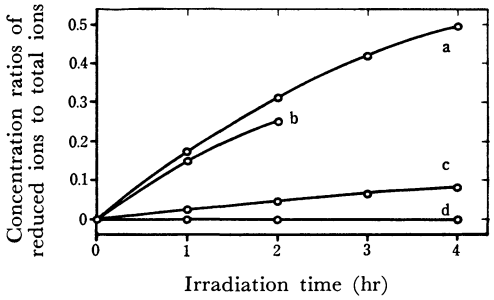

Fig. 2. Photochemical reaction of uranyl and thallic ions.

a and b: 10 mM uranyl ion (same solution as A in Fig. 2)
c and d: 10 mM thallic ion (same solution as C in Fig. 3)
a and c: without filter, b and d: with filter

between the amount of ion reduced and the irradiation time is shown in Fig. 2. The reaction of thallic ion could not be observed, and at the same time the efficiency of uranyl photoreduction was slightly lowered.

Stoichiometry of Reaction between Thallic and Uranous Ions. The uranyl mixed solution was exposed to the light of the mercury lamp to produce uranous ion. Exposure was continued until uranyl ion was completely reduced. To each 10 m*l* of the solution (containing 10 mM uranous ion) was added an aliquot of the 25 mM thallic standard solution and then water to make up to 13 m*l*. After mixing, the absorbance of of the mixture was measured. The results showed that one mole of thallic ion reacted with one mole of uranyl ion. Therefore, it is considered that the overall reaction proceeds according to the following equation.

$$U^{4+} + Tl^{3+} + 2H_2O = UO_2^{2+} + Tl^{+} + 4H^{+}$$

Photonometric Titration Curve and Calibration Curve. Uranyl ion was photochemically reduced in the presence of thallic ion. Test solutions contained various amounts of thallic ion together with 10 mM uranyl ion, 40 mM lactate and 1 N sulfuric acid. The solutions were irradiated through the filter in the cell compartment kept at 29.5±0.5°C under the same conditions as before, and the absorbance of uranous ion produced was measured at 655 mμ every fixed irradiation time. An example of a photonometric titration curve is shown in Fig. 3. It is seen that the curve consists of two parts, that is, the first part where the absorbance remains actually zero, and the second part where the absorbance steadily increases. In order to follow the change in concentration of thallic ion during irradiation, thallic ion in the test solution was iodometrically determined. While thallic ion existed before the point where the titration curve begins to rise, the ion was not detected after the

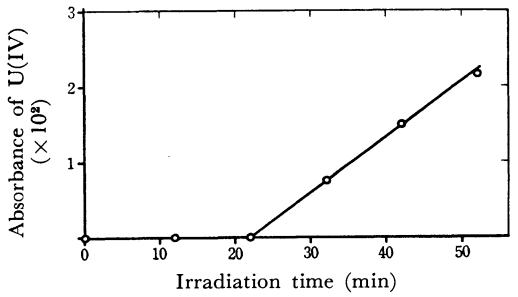

Fig. 3. Photonometric titration curve of thallic ion.
0.1 mM thallic ion (in the solution containing 10 mM uranyl ion, 40 mM Na lactate, and 1 N H_2SO_4). Measurement was made at 29.5± 0.5°C.

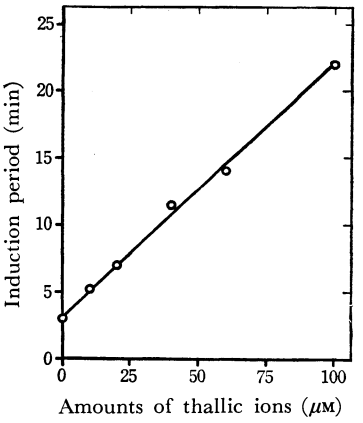

Fig. 4. Calibration curve of thallic ion.
Induction periods were obtained from a set of photonometric titration curves as shown in Fig. 3.

point. The induction period was dependent on the amount of coexisting thallic ion. Photonometric titration curves were constructed for thallic ion in a concentration range of 0 to 0.1 mM, and the induction periods were obtained from each of the curves. The measurement of the induction period was repeated three times for each thallic concentration, and the values observed were averaged. Figure 4 shows a plot of the induction periods against the concentration of thallic ion. Nearly linear relationship was obtained in the concentration range, but the plot did not pass through the origin. The effect of other metal ions on the photonometric titration of thallic ion was tested. Bi(III), Zn(II), and Cd(II) ions in concentration of 0.4 mM had no influence on the determination of thallic ion. But Hg(II) and Ag(I) were reduced under the same conditions as for the photonometric titration of thallic ion.

Discussion

Absorption Spectra. The uranyl spectrum obtained was similar in profile to those reported by Bell *et al.*,[9] Betts *et al.*[10] and others. Betts *et al.* showed that an absorption maximum of noncomplexed uranyl ion at approximately 415 mμ shifted to the vicinity of 420 mμ on complex formation with sulfate ion. Since the uranyl spectrum in Fig. 1 has the absorption maximum at 420 mμ regardless of the presence of lactate, it is reasonable to think that uranyl ions formed a sulfate complex. Bell *et al.* have recently reported that uranyl ion in two excited state energy levels (at 21270 and 20502 cm^{-1}) can be responsible for the photochemistry of uranyl ion. In the present investigation, therefore, the photochemical reaction of uranyl ion was carried out by use of the light in the wavelength range longer than 300 mμ (approximately 33000 cm^{-1}).

Thallic and thallous ions show no light absorption above approximately 320 mμ, and, therefore, in the longer wavelength range do not interfere with light absorption of uranyl ion. An intense absorption band exists below approximately 300 mμ. In consideration of the fact that thallic ions underwent the photochemical reduction by irradiation with unfiltered mercury lamp, the intense absorption band below approximately 300 mμ is supposed to be involved in the photochemical reaction of thallic ion.

Photoreduction of Uranyl and Thallic Ions. The initial concentration of uranyl ion affects not only the reaction rate of the uranyl photoreduction, but also the homogeneity of the photoreduction in the reaction solution. The number of photons absorbed by uranyl ion in the reaction vessel is diminished as the incident light from the mercury lamp proceeds from the front of the vessel to the back. Consequently there should be some difference in the amount of uranous ion produced along the path length of the incident light. An excessive increase in the uranyl concentration would enlarge the difference to such an extent that the homogeneity of the reaction solution can not be maintained by the diffusion process of the solutes. In consideration of the two factors, the reaction rate and the homogeneity of the photoreduction, the uranyl concentration of 10 mM was chosen in the present work, since in this concentration the reaction rate is moderate and a difference was not seen in the absorbance before and after vigorous mixing of irradiated reaction solutions.

The work by Rao *et al.*[4] of the photoreduction of uranyl ion in the sodium lactate-sulfuric acid system showed that the reduction rate of uranyl ion was constant over sulfuric acid concentration from 0.10 to 2.0 N and that the reduction rate

9) J. T. Bell and R. E. Biggers, *J. Mol. Spectry.*, **25**, 312 (1968).
10) R. H. Betts and R. K. Michels, *J. Chem. Soc.*, **1949**, 286.

reached a maximum value at a lactate-to-uranyl ratio as high as 4 to 1. Therefore, subsequent experiments were performed with 40 mM of sodium lactate and 1 N of sulfuric acid.

The fact that thallic ion undergoes photoreduction under certain conditions has already been reported by Benrath,[11] who observed that thallic ion was photochemically reduced in the presence of oxalic acid, tartaric acid, or alcohol. Figure 2 shows that the photoreduction took place in the presence of sodium lactate, also. However, the reaction could not be observed on irradiation through the soft glass filter.

Photonometric Titration Curve. In the photonometric titration, the absorption at 655 mμ could not be observed until the absorbance began to increase steadily, and thallic ion did not exist after the rising point of the titration curve. Thus this point could be considered to be the end point. The mechanism of the photoreduction of uranyl ion has not been made clear, and there is some possibility that thallic ion reacts with an intermediate of the photochemical reaction. Accordingly it seems that uranous ion is formed as a final product of the photochemical reaction in the absence of other reducible substances, and that, when thallic ion coexists, it is reduced preferentially before reduction of uranyl ion owing to the more positive oxidation potential of thallic ion.

The fact that the reaction solution containing no thallic ion showed a blank induction period suggests that a part of uranous ion is oxidized by something other than thallic ion. Hitherto it has been reported that uranous ion is oxidized by the air or oxygen dissolved in the solution, and the mechanism of this reaction has been studied by Halpern and Smith.[12] As a check, the uranyl mixed solution was irradiated with the mercury lamp after removal of the air with a rotary vacuum pump. The photonometric titration curve of this solution revealed that the absorbance at 655 mμ began to increase from the start of irradiation. In addition experiments done at temperatures down to 15°C indicated that there was a parallel relationship between the blank induction period and the solubility of oxygen. Thus it is certain that oxygen dissolved in solutions consumes uranous ion. However, because the temperature of reaction solutions is kept at 29.5±0.5°C, the effect of dissolved air would be unchanged for each reaction solution, and thus the plot for each thallic concentration should be shifted equally by a constant value, that is, a blank induction period.

Application. Table 1 shows the results of determination of thallic ion by use of the calibration curve presented in Fig. 4. Although the measurement for 0.15 mM thallic ion was also tried and the result showed that the plot for this concentration still lay in the extension of the calibration curve, it seems that the measurement of a too long induction period is incovenient for practical use. On the other hand, for thallic ion less than 0.01 mM the reproducibility would become relatively worse.

TABLE 1. RESULTS OF DETERMINATION OF THALLIC ION

Concentration of thallic ion, μM		
Present	Found	Average
10	13, 8, 6	9
20	19, 22, 17	20
40	41, 43, 46	43
100	107, 96, 102	102

Hence it is found that photonometric titration can satisfactorily be applied to microdetermination of thallic ion in the concentration range from 0.01 to 0.1 mM. Further improvement of accuracy would be effected by increase in the optical path length of reaction vessel for absorption measurement.

The rise of temperature increases the reaction rate of the uranyl photoreduction, and, hence, affects the induction period. Therefore, the calibration curve shown in Fig. 4 can not be applied to the data obtained at other temperatures. Hg(II) and Ag(I) interfered with the determination of thallic ion owing to their reactivity against the photoreduction product, but there was no interference from such ions as Zn(II), Cd(II), and Bi(III).

For the first time in photonometric titration, and probably in all kinds of titration, the titration procedure could be carried out without stirring the reaction solution. This fact indicates that titration can be performed in a far smaller volume of reaction solution, when allowed to make use of microspectrophotometric technique, and that it is possible to carry out titration in a cell isolated completely from outside, because both the generation of titrant and the measurement of concentration of a reaction product can be made without breaking the isolation of the reaction system.

11) A. Benrath, *Z. Wiss. Phot., Photophysik Photochem.*, **14**, 217 (1915).

12) J. Halpern and J. G. Smith, *Can. J. Chem.*, **34**, 1419 (1956).

BULLETIN OF THE CHEMICAL SOCIETY OF JAPAN VOL. 42 2259—2263 (1969)

Syntheses and Properties of Some Metal Bromo-Dithiolium Complexes*1

Akira OUCHI, Hiroshi EGUCHI, Toshio TAKEUCHI and Akiko FURUHASHI*2

Department of Chemistry, College of General Education, The University of Tokyo, Komaba, Meguro-ku, Tokyo

(Received November 9, 1968)

The bromo-3-methyl-5-phenyl-1,2-dithiol-1-ium complexes were obtained from metal benzoylacetonate, using hydrogen sulfide and bromine with a catalyst of hydrogen bromide. These complexes resemble bromo-bis(3,5-dimethyl-1,2-dithiol-1-ium) complexes and many of them are of the high-spin type. The Zn(II) and Cd(II) complexes are of the ML_2Br_4 type (where M=metal and L=3-methyl-5-phenyl-1,2-dithiol-1-ium), like 3,5-dimethyl-1,2-dithiol-1-ium complexes, while Cu(I) is of the $MLBr_2$ type. However the analytical results shows that the Mn(II), Fe(II) and Co(II) complexes are of the ML_2Br_3 type. Infrared spectra as well as electronic spectra are shown and discussed.

The tetrachloro-[1,2] and tetrabromo-[3] bis(3,5-dimethyl-1,2-dithiol-1-ium) complexes have already been synthesized and discussed, and the cobalt(II) and iron(II) tetrachlorobis(3,5-dimethyl-1,2-dithiol-1-ium) complexes were also reported on recently.[4] As the tetrabromobis(3,5-dimethyl-1,2-dithiol-1-ium) complexes are synthesized from many kinds of metal acetylacetonates without difficulty, it seemed that it would be very interesting to apply this synthesis technique in an attempt to obtain other bromo-dithiolium complexes. Consequently, the present authors have examined syntheses using many kinds of β-diketonates, including cobalt(II), nickel(II), zinc(II) complexes of benzoylacetone, trifluoroacetylacetone, dibenzylmethane, trifluorobenzoylacetone, methyl acetoacetate, and ethyl acetoacetate. However, the expected products were obtained only from the benzoylacetonates; the syntheses using other β-diketonates have not yet been successful.

Attempts to synthesize chloro(3-methyl-5-phenyl-1,2-dithiol-1-ium) complexes using hydrogen chloride and chlorine in place of hydrogen bromide and bromine were all unsuccessful. This seems due to the facts that: 1) the dithiolium ring is not easily formed from these β-diketones under the experimental condition presented above; 2) some β-diketones are more easily destroyed by free chlorine or bromine than is acetylacetone, and some side-reaction occurs predominantly; 3) steric hindrance owing to the introduced radicals on 2- or 4- carbons seriously affects the formation of complexes.

From the syntheses, two types of complexes of bivalent metals were obtained; ML_2Br_4 (where M=Zn(II) or Cd(II)) and ML_2Br_3 (where M=Mn(II), Fe(II) and Co(II)). The former seems to be isostructural to tetrabromo-bis(3,5-dimethyl-1,2-dithiol-1-ium) complexes. However, the latter compounds are of the new type. The cuprous salt has the $CuLBr_2$ formula and not the CuL_2Br_3 formula; the compound of the latter type was obtained from acetylacetonate.

Recently in our laboratory we have been successful in synthesizing some halogeno(3-methyl-5-phenyl-1,2-dithiol-1-ium) complexes by means of the reaction of metal halide and dithiolium perchlorate.[5] The products are ML_2X_4 or MLX_3-type complexes for bivalent metals and MLX_4-type complexes for tervalent metals. From manganese(II) and cobalt(II) bromides, regular ML_2X_4-type complexes and not ML_2X_3-type complexes were obtained. The colors of these two types of complexes are a little different; the ML_2X_4-type manganese(II) complex is light yellow, while the ML_2X_3-type one is deeper yellow; the former type of cobalt(II) complex is yellowish green, and the latter type is grass green. From ferric bromide a MLX_4-type complex was obtained, while a ML_2X_4-type complex was obtained from cupric bromide, as the redox reaction does not occur in the synthetic process using dithiolium salt. On the other hand, the direct synthesis of the halogeno-(dithiolium)-complex may include some different reactions because of the use of an excess of strong

*1 This paper was presented at the 18th Symposium on Coordination Chemistry, Kyoto, October, 1968.

*2 Department of Chemistry, College of Engineering and Science, Aoyama Gakuin University, Meguri-sawa, Setagaya-ku, Tokyo.

1) K. Knauer, P. Hemmerich and J. D. W. Van Voorst, *Angew. Chem. Intern. Ed. Engl.*, **6**, 262 (1967).

2) A. Furuhashi, K. Watanuki and A. Ouchi, This Bulletin, **41**, 110 (1968).

3) A. Furuhashi, T. Takeuchi and A. Ouchi, *ibid.*, **41**, 2049 (1968).

4) A. Ouchi, M. Nakatani and Y. Takahashi, *ibid.*, **41**, 2044 (1968).

5) Y. Takahashi, M. Nakatani and A. Ouchi, *ibid.*, **42**, 274 (1969).

reagents, such as hydrogen sulfide or bromine.

The infrared spectra and electronic spectra of the complexes of all these types, *i.e.*, ML_2X_4, ML_2X_3, MLX_2, and MLX_4, are almost identical, and so their structures are probably not very different from one another.

Experimental

Materials and Instruments. The starting materials were of a G. R. grade and were used without purification. The infrared spectra were obtained by a nujol and hexachloro-1,3-butadiene mull procedure using a DS-301-type infrared spectrophotometer of the Japan Spectroscopic Co., Ltd. Electronic spectra were obtained with a Hitachi EPS-2-type automatic recording spectrophotometer. The reflectance spectra were obtained with an Ito Model QU-3 spectrophotometer using a reflectance attachment and a magnesium oxide standard. The magnetic moments were measured with a Gouy balance at room temperature (21°C).

Synthesis of Tetrabromo-bis(3-methyl-5-phenyl-1,2-dithiol-1-ium)cadmium(II). Two and seven-tenths grams (0.010 mol) of anhydrous cadmium(II) bromide and three grams (0.018 mol)*3 (or less) of benzoylacetone were mixed with 30 m*l* of absolute ethanol. After the dissolution, a precipitate appeared. To the mixture cooled on ice dry hydrogen bromide was added over a 1 hr period; the precipitate was completely dissolved during this procedure. Then about 1.0 m*l* (0.04 mol) of bromine*4 was stirred in, drop by drop. Finally hydrogen sulfide was passed through for about 5 min until a little precipitate appeared.*5 The precipitate was filtered off and the filtrate was mixed with a half volume of petroleum ether and kept in a cold room (—about 5°C) overnight. The needle-like yellow precipitate thus obtained was filtered off, and the product was washed with ethanol, carbon disufide, chloroform, and diethyl ether (in that order) to remove the mother liquor, sulfur, the dimer of the dithiobenzoylacetone, and the washing solvents respectively. The product was then dried in a vacuum desiccator at room temperature. The yield was about 2.1 g (36.0% calculated from the quantity of benzoylacetone used).

Though the product is soluble in such polar solvents as water or alcohol, it reacts with them; on the other hand it is hardly soluble in non-polar solvents. For this reason recrystallization has not yet been successful.

The syntheses of the zinc(II) complex and of ML_2Br_3-type complexes of manganese(II) and cobalt(II) were carried out by almost the same method. The yields are shown in Table 1.

The iron(II) complex, FeL_2Br_3, was obtained from iron(III) bromide without using bromine as the ferric ion itself worked as the oxidizing agent. The copper(I) complex, $CuLBr_2$, was obtained from copper(II) bromide by the same process without bromine. In both cases no product was isolated if bromine was added during the process.

The Analyses of Bromine in Complexes. The analysis of the bromine in these complexes was difficult; the Volhard method and the iodometry, both to be described below, were examined.

i) Volhard Method. The solid sample was stirred with a silver nitrate-nitric acid aqueous solution for about 10 min and the excess silver ion was titrated with a thiocyanate solution.

Table 1. Analysis and yield of complexes (Figures are given in %.)

		Metal	C	H	S	Br	Yield
MnL_2Br_3	Calcd	8.06	35.26	2.66	18.83	35.19	19
	Found	8.16	35.30	2.70	19.08	33.00	
FeL_2Br_3	Calcd	8.19	35.21	2.66	18.80	35.14	19
	Found	7.75	35.39	2.62	18.08	33.41	
CoL_2Br_3	Calcd	8.60	35.05	2.65	18.72	34.98	19
	Found	8.86	35.02	2.72	19.15	34.90	
ZnL_2Br_4	Calcd	8.47	31.13	2.33	16.63	41.43	16
	Found	8.27	31.99	2.72	16.48	42.60	
CdL_2Br_4	Calcd	13.73	29.34	2.22	15.67	39.04	36
	Found	14.14	29.22	2.29	15.84	39.20	
$CuLBr_2$	Calcd	15.25	28.83	2.18	15.39	38.35	20
	Found	15.30	29.11	2.53	16.36	38.30	

HL = dithiobenzoylacetone ($C_{10}H_{10}S_2$)

*3 In these syntheses metal salt should be present in excess, as: i) the trapping effect of the dithio-chelate is better; ii) the dimerization reaction is minimized, and iii) the excess of metal halide is easily washed out by ethanol after the reaction.

*4 A little excess is necessary as the reaction solution contains a great excess of hydrogen sulfide. The bromine added reacts first with hydrogen sulfide to produce sulfur; then the sulfur bromine and hydrogen sulfide seem to undergo a complicated reaction (polysulfide may be produced on the way), and finally the complexes are obtained. To add too much bromine destroys the product, and the yield is not good either.

*5 If hydrogen sulfide was passed through too long, the complex precipitate on the step, the impurities, and the yield were seriously lowered.

ii) Iodometry. The solid sample was dissolved into water and oxidized with potassium permanganate in the presence of phosphoric acid at room temperature. The isolated bromine was extracted with carbon tetrachloride, the organic solvent layer was shaken and introduced into the aqueous solution of potassium iodide, and the freed iodine was titrated with a standard sodium thiosulfate solution.

Both analytical techniques were applicable to ML_2Br_4-type complexes. However, for ML_2Br_3-type complexes the Volhard method gave too high values, about 30% higher than the expected values; on the other hand, the iodometry gave us too low values, about 30—50% lower than the calculated values.

The results of the bromine analyses of ML_2Br_3 complexes given in Table 1 were obtained by the usual elemental analysis technique for organic compounds-measuring as silver bromide after other interfering substances had been removed. This method is not very suitable, either, and considerable error is inevitable. However, the results of the analyses of the other elements, metal, sulfur, carbon, and hydrogen of these complexes coincide with the expected values within the range of experimental error, thus confirming the formulae shown here.

Results and Discussion

The analytical data as well as the yields of the synthesis process are shown in Table 1. Their magnetic moments are given in Table 2.

Table 2. Magnetic moments of complexes
(Figures are given in B. M. per 1 mol of metal.)

	B. M.	Valence of the central metal
MnL_2Br_3	5.95	II
FeL_2Br_3	5.35	II
CoL_2Br_3	4.68	II
ZnL_2Br_4	diamagnetic	II
CdL_2Br_4	diamagnetic	II
$CuLBr_2$	diamagnetic	I

From the magnetic data, the manganese(II), iron(II), and cobalt(II) complexes all seem to be high-spin complexes. ML_2Br_4-type complexes of zinc(II) and cadmium(II) are diamagnetic and bivalent. The copper complex is also diamagnetic and univalent.

The colors of the solids and the reflectance spectra between 12500 and 28500 cm^{-1} are shown in Table 3. The manganese(II), zinc(II), and cadmium(II) complexes are yellow, and very little absorption is recognized in the 12500—22000 cm^{-1} region. On the other hand, iron(II) and copper(I) complexes have a deep color and have considerable absorption in this region, although the band is too broad and the wave numbers of the maximum points are not clear. The cobalt(II) complex has an absorption maximum at 14300 cm^{-1} which is probably a d–d band.

All of these complexes have the intense band at about 24000—25000 cm^{-1} which is characteristic of all of this type of compound, but it is not seen in their absorption spectra in ethanol, probably because of the dissociation of the complexes in the solution.

The absorption spectra of the ethanol solution of these complexes are shown in Table 4. The absorptions in the visible region are very weak; the absorption peaks are seen almost only in the ultraviolet region.

The wavelengths and the molar absorption coefficients of the absorption maxima of the solutions coincide with those of 3-methyl-5-phenyl-1,2-dithiol-1-ium perchlorate, which is synthesized by the method of Schmidt and Schulz.[6] Judging from these facts, the complex seems to dissociate completely into ions in the solution.

If the pure ethanol which does not contain perchloric acid was used as the solvent, the color of the solution gradually turned red at room temperature; this is due to the decomposition of the dithiolium ion, because the same color change is also seen in the solution of pure dithiolium salt.

The infrared spectra data of the complexes and the 3-methyl-5-phenyl-1,2-dithiol-1-ium perchlorate are summarized in Table 5, together with those of some related compounds.[4] The general features of the infrared spectra of these complexes, both ML_2Br_4 and ML_2Br_3-type complexes, resemble those of tetrachloro-bis(3-methyl-5-phenyl-1,2-dithiol-1-ium)iron(II) and not those

Table 3. Reflectance spectra of complexes
(Figures are given in cm^{-1}. s: strong, m: medium, w: weak, sh: shoulder, br: broad)

	Color				
MnL_2Br_3	light yellow	25000 s, sh	22400 w, sh		
FeL_2Br_3	greenish brown	24400 s, sh			18200 br 15350 m
CoL_2Br_3	light green	24400 s, sh	22210 w, sh	21200 m, sh	14300 s
ZnL_2Br_4	light yellow	24400 s, sh	21730 w, sh		15750 w, sh
CdL_2Br_4	light green	24100 s, sh			
$CuLBr_2$	dark reddish brown	24400 s, sh	22200 br 18850 m		16100 br, m, sh

6) M. Schmidt and H. Schulz, *Chem. Ber.*, **101**, 277 (1968).

Table 4. Electronic spectra of complexes
(Figures are given in cm^{-1} for wave numbers and $\log \varepsilon$ for intensities (in parenthese).)

	Broad	Shoulder	Peak	Sharp peak
$LClO_4$	45200 (3.92)	41200 (3.66)	34100 (3.80)	28300 (4.29)
MnL_2Br_3	45200 (4.15)	41200 (3.96)	34100 (4.05)	28250 (4.56)
FeL_2Br_3	44900 (4.38)	41300 (4.20)	34100 (4.20)	28250 (4.66)
CoL_2Br_3	45100 (4.26)	41200 (4.04)	34100 (4.14)	28250 (4.61)
ZnL_2Br_4	45100 (4.26)	41200 (4.05)	34100 (4.16)	28250 (4.61)
CdL_2Br_4	45100 (4.24)	41200 (4.07)	34100 (4.13)	28300 (4.58)
$CuLBr_2$	45100 (3.88)	41200 (3.68)	34100 (3.69)	28300 (4.14)

$L=C_{10}H_9S_2$
Solvent: 35%(volume) ethanol solution of 60% perchloric acid

of bis-(dithiobenzoylacetonato)nickel(II). Moreover, the 3-phenyl-5-methyl-1,2-dithiol-1-ium perchlorate shows a very similar pattern as well, though the absorption in the 1050—1130 cm^{-1} region is not clear because of the overlapped absorption of the perchlorate ion.

From these facts, it can be said that in ML_2X_4-type complexes halogen atoms do not seriously effect the infrared spectra of the dithiolium ion. Therefore, their structure should be isostructural to tetrabromo-bis(3,5-dimethyl-1,2-dithiol-1-ium) complexes,[3] though an X-ray crystallographic study of them is necessary to clarify the structure in detail. By analogy, $Cu(I)LBr_2$ may have a $(-M-Br-)_n$ chain structure, where one more bromine and probably dithiolium ion bond to each tetracoordinated metal atom.

In the case of ML_2X_3-type complexes, as the central metal atom is bivalent and not abnormally charged, how the charge is distributed in the whole molecule is a problem. One dithiolium ion is

Table 5. Infrared frequencies of the complexes (cm^{-1})
br=broad, s=strong, m=medium, w=weak, sh=shoulder, $L=C_{10}H_9S_2$. *=absorption by ClO_4^-

$LClO_4$	NiL_2	FeL_2Cl_4	MnL_2Br_3	FeL_2Br_3	CoL_2Br_3	ZnL_2Br_4	CdL_2Br_4	$CuLBr_2$	Tentative assignment
		1593w	1590w	1588w	1588w	1587w	1590w	1585w	aryl
1500w	1470 s	1500w	1495w	1498w	1495w	1490w	1500w		ν(C=C),
1478 s	1465 s	1475 s	1478 s	1475 s	1475 s	1475w	1480 s	1478 s	δ(C-H)
1452m	1445 s	1455w	1455w	1455w	1455w	1455w	1455w	1455 s	
1380w	1360m	1372w	1378w	1370w	1378w	1373w	1383w	1342	$\delta(CH_3)$ and
1340w	1350 s	1340w	1340w	1340w	1340w	1338 br	1338w	1333 br	others
1317w	1298 s	1312w			1305w	1300w	1315w	1311w	ν(C=C)
1255 s	1273m	1258 s	1256 s	1256 s	1257 s	1255 s	1255 s	1250 s	ν(C-R)
1190w	1219m								ν(C=S), or
1170w	1209w								the mix.
	1180m								of them
1150w	1155w	1145m	1148m	1147m	1145m	1146m	1163	1145m	
							1153 m		aryl
							1145		
1080 vs*	1108w	1098w	1098w	1098w	1095w	1095w	1097w	1095w	δ(C-H),
br	1073w								ν(C-C)
									or others
1005w	1025m		1025 br	1020 br	1020 br	1015 br	1020 br	1020w	$\rho(CH_3)$
	1018m	1018m							ν(C-CH_3)
995w	998m	998m	999m	998m	998m	996m	999m	996m	
			975w	972w	970w	968w	973w		aryl
933m	908m	923 s	927m	925m	925m	923m	927	921w	
							920 w		
860 s		877 s					880m		
	840m	865 s	865 s	862 s	865 s	860 s	850	860 s	$\nu(C=S)^+$
							835 m		δ(C-H)
770 s	763 s	760 s	763 s	761 s	760 s	757 s	772	761 s	aryl or π
	736 s						762 s		
685m	690 s	708w	710w	708w	707w	703w	708w		π(C-H)
	677m	675 s	680 s	681 s	680 s	673 s	676 s	675 s	aryl

unipositive, so the other one should be zero valent. The monomer of the free dithio-β-diketone is unstable, and the dimer and the complex containing the dimers, $(Cu^{I}(C_5H_7S_2)Cl)_n$, for example,[3] show very different infrared spectra. Judging from this fact, this complex does not contain the dimer.

When the dithiolium complexes are synthesized directly from the dithiolium salt, the formulae of the products of the complexes of these metals are ML_2Br_4 and there is no difficulty in making a bromine analyses of them. Consequently, one dithiobenzoylacetone of the ML_2X_3-type complexes is not a usual dithiolium ion but is more easily hydrolyzed, and the sulfur atoms in it are apt to be isolated as sulfide ions.

As for benzoylacetone adducts, Rosenheim synthesized $SbCl_5(C_{10}H_{10}O_2)$;[7] the benzoylacetone is zero valent in it. Really the $MLCl_3$-type dithiolium compounds have already been synthesized;[5] these ML_2Br_3-type compounds may be the adducts of the zero valent dithiole to the $MLBr_3$-type complexes; then the dithiole-type ligand, which is less stable than the dithiolium type in the case of dithiobenzoylacetone, can easily be destroyed.

From these results, the other dithio-β-diketone is probably a 1,2-dithiole derivative, 3*H*-3-methyl-5-phenyl-1,2-dithiole, for example, although the evidence is not decisive. During the process of synthesis the coexistence of the Mn(II), Fe(II), or Co(II) ions in the solution may prevent the perfect oxidation of the ligand to the dithiolium cation.

However, the presence of a uni-negative-valent brominated dithiole ion, for example, cannot be denied completely. Really, such compounds may be easily produced as intermediates of the synthetic process.[8] The 3-methyl-4-bromo-5-phenyl-1,2-dithiole, for example, should be uni-negative, and its infrared spectra may be expected not to be very different from those of the usual dithiolium ion, as in the case of halogenated acetylacetonates.[9] On the other hand, if the bromine atom is attached to the 3- or 5-carbon of the ditholium ion, more serious deviations of the infrared spectra may be expected. These brominated dithiolium ions seem to be easily hydrolyzed by water or alcohol.[10] However, as our attempt to synthesize ML_2Br_2-type compounds failed, the presence of the LBr^- ion was not proved.

The authors wish to thank the Biochemistry Section of our college for doing the infrared spectra measurements. The authors wish also to express their appreciation to Professor Yasumasa Hayakawa and the staff of the Department of Chemistry of Aoyama Gakuin University and to acknowledge gratefully their helfpful discussions with Professors Yukichi Yoshino, Kunihiko Watanuki, and their laboratory colleagues.

A part of this research was carried out with a Scientific Research Grant from the Ministry of Education to which the authors' thanks are due.

7) A. Rosenheim, W. Loewenstamm and L. Singer, *Ber.*, **36**, 1833 (1903).

8) D. Leaver, D. M. McKinnon and W. A. H. Robertson, *J. Chem. Soc.*, **1962**, 5104; **1965**, 32.

9) D. Givson, C. Oldham, J. Lewis, D. Lawton, R. Mason and G. B. Robertson, *Nature*, **208**, 580 (1965).

10) J. Faust and R. Mayer, *Angew. Chem.*, **75**, 573 (1963).

BULLETIN OF THE CHEMICAL SOCIETY OF JAPAN VOL. 42 2264—2267 (1969)

Electronic Absorption Spectra of the Alkali Metal Complexes with Bipyridine

Yasuo TORII, Takanori YAZAKI, Youkoh KAIZU, Shigetaka MURASATO and Hiroshi KOBAYASHI

Department of Chemistry, Tokyo Institute of Technology, Ookayama, Meguro-ku, Tokyo

(Received November 18, 1968)

Electronic absorption spectra of the alkali metal complexes with 2,2'-bipyridine, 4,4'-dimethyl-2,2'-bipyridine or 5,5'-dimethyl-2,2'-bipyridine have been observed in tetrahydrofuran solutions. Each spectrum has four major bands in the near infrared, visible and near ultraviolet regions, and is essentially due to the π–π^* transitions in the negative ion (extra π electron trapping state) of bipyridine or its dimethyl derivatives coordinating to a metal ion. The band about 18000 cm^{-1} is the most sensitive to the metal ion species involved and assigned to a transition with the polarization parallel to the short axis of the bipyridine molecule. Each absorption band of the bipyrdine negative ion shows characteristic spectral shift upon CH_3-substitutions in its peripheral positions. This CH_3-substitution effect on the absorption spectra of bipyridine negative ion is quite different from that of complexes including neutral bipyridines and gives a basis of the criterion to determine whether the coordinating bipyridine in a certain bipyridine complex do exist in negative ion (π electron trapping state) or not.

Alkali metals (M) react with 2,2'-bipyridine (bipy) in tetrahydrofuran (THF), dioxane, liquid ammonia and others, forming two kinds of complexes, M_2(bipy) and M(bipy). They have been isolated as various types of crystals with some solvent molecules.[1] Some studies have been done by measuring magnetic susceptibility[2] and electron spin resonance[3-6] in the solid state and the solution, but nothing has been reported on their electronic absorption spectra in detail.*1 In this paper electronic absorption spectra of the 1:1 complexes of alkali metals such as lithium, sodium and potassium with 2,2'-bipyridine, 4,4'-dimethyl-2,2'-bipyridine (4dmbip) or 5,5'-dimethyl-2,2'-bipyridine (5dmbip) in tetrahydrofuran solutions are reported.

These complexes are of reddish violet and Na-complexes, for example, show spectra given in Fig. 1. Since Li- and K-complexes also give absorption curves similar to those of Na-complexes, whole curves need not be presented, and only four major absorption maxima are tabulated in Table 1. These bands, except those near 18000 cm^{-1}, are virtually invariant in their positions with the change of metal ion species. ESR studies[5,6] have shown that the alkali metal complex is rather an ion-pair formed by a metal ion, M^+, and a negative ion, $bipy^-$, an unpaired electron being predominantly delocalized in the antibonding π^* molecular orbitals of bipyridine but partly transferred to the atomic orbitals of metal ion. These lead to an assignment of the absorption bands to the π–π^* transitions in the coordinating bipyridine negative ion.

The spectral shift of the 18000 cm^{-1} band upon metal subsitution is small but is not out of resolution. Figure 2 shows the relation between the band positions and ionic radii (r) of the metal ions,*2 where $R+r$ is the distance from the center of the metal ion to the center of bipyridine molecule. If $bipy^-$ acts as a bidentate ligand which coordinates to a metal ion through two nitrogen atoms, the π–π^* transitions may be polarized parallel to either the long axis or the short axis of bipyridine molecule. Since the latter axis passes through the metal ion, the electronic transitions polarized parallel to this are expected to be more sensitive to a positive charge on the metal ion than those

1) S. Herzog and R. Taube, *Z. Chem.*, **2**, 208 (1962).
2) R. Perthel, *Z. Physik. Chem.*, **211**, 74 (1959).
3) B. Elschner and S. Herzog, *Arch. Sci.*, **11**, 160 (1958).
4) A. Zahlan, F. W. Heineken, M. Bruin and F. Bruin, *J. Chem. Phys.*, **37**, 683 (1962).
5) V. E. König and H. Fischer, *Z. Naturforsch.*, **17a**, 1063 (1962).
6) J. Dos Santos Veiga, W. L. Reynolds and J. R. Bolton, *J. Chem. Phys.*, **44**, 2214 (1966).

*1 Absorption curve of Na(bipy) has been reported by C. Mahon and W. L. Reynolds: *Inorg. Chem.*, **6**, 1927 (1967).

*2 Goldschmidt's ionic radii; L. Bragg, "The Crystalline State," Vol. 1, G. Bell and Sons Ltd., London (1949).

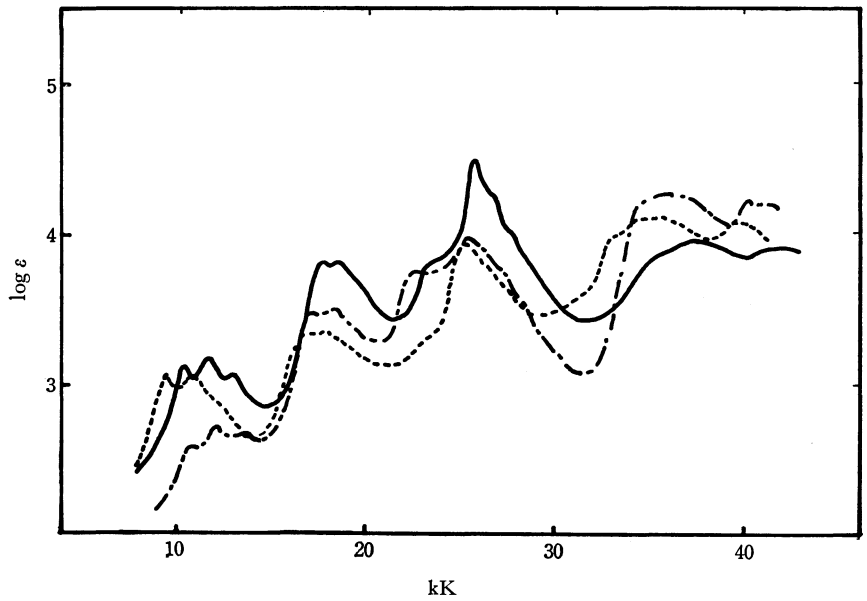

Fig. 1. Electronic absorption spectra in THF solutions.
——: Na(bipy), —·—: Na(4dmbip), - - -: Na(5dmbip)

TABLE 1. ABSORPTION MAXIMA OF THE COMPLEXES
(Absorption maxima are given in $10^3\,cm^{-1}$ or kK and intensities, $\log \varepsilon$ in parentheses.)

Li(bipy)	Na(bipy)	K(bipy)	Na(4dmbip)	Na(5dmbip)
10.6	10.5 (3.13)	10.4 (3.42)	11.1 (2.6)	9.5 (3.06)
12.0	12.0 (3.19)	11.9 (3.48)	12.4 (2.7)	10.9 (3.07)
13.0	13.3 (3.06)	13.2 (3.36)	13.7 (2.7)	12.3 (2.90)*
18.2	17.8 (3.81)	17.6 (3.97)	17.1 (3.5)	17.0 (3.35)
19.2	18.8 (3.79)	18.7 (3.97)	18.3 (3.5)	17.9 (3.36)
	23.7 (3.80)*		22.5 (3.8)*	23.0 (3.25)*
26.0	25.9 (4.47)	25.8 (4.58)	25.4 (4.0)	25.3 (3.94)
	37.4 (3.94)	37.7 (3.91)	35.5 (4.3)	35.5 (4.08)

* shoulder

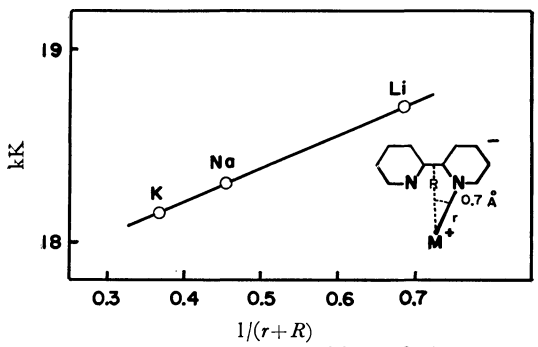

Fig. 2. Relation between positions of the bands near 18000 cm^{-1} and ionic radii of alkali metal ions.*1
Li, Na and K denote Li(bipy), Na(bipy), and K(bipy), respectively.

polarized perpendicular to this axis. The facts that the 18000 cm^{-1} band is the most sensitive to the metal ion species and its position is proportional to $1/(r+R)$, seem to be interpreted as followes. Spectral shift due to an electrostatic interaction between a positive charge on the metal ion, Ze and the transition dipole moment μ is approximately given by

$$\delta\varepsilon = \frac{Ze\mu}{(r+R)}\cos\theta\left[1 + \frac{l^2}{8(r+R)^2}(5\cos^2\theta - 3) + \cdots\right],$$

for $r+R > (1/2)l$, where θ is an angle between the transition dipole moment and the straight line connecting both centeres of the ligand and the metal ion, and l is the real dimension of the transition dipole. If the transtion moment orients perpendicular to the ligand-metal line, the electro-

static spectral shift seems to be very small, since $\cos\theta=0$, and $\delta\varepsilon=0$. The transition moment in the direction of the line gives relatively large electrostatic shift, since $\cos\theta=1$, and $\delta\varepsilon$ is maximum. The 18000 cm^{-1} band is caused by a π-π^* transition polarized toward the metal ion, while the others insensitive to the metal substitution are polarized perpendicular to the 18000 cm^{-1} transition.

The whole absorption curve of Na(bipy) does not change its shape so much upon CH_3-substitutions at 4 and 4' or 5 and 5' positions of the conjugated system. However, each band does change its position and intensity in a characteristic way of each wave number region. This is known by Fig. 1. The lowest wave number bands, for example, are shifted to the higher wave number in the order 5dmbip<bipy<4dmbip, while the second lowest ones near 18000 cm^{-1} are in the order 5dmbip< 4dmbip<bipy. Therefore the effects of the CH_3-substitutions on the conjugated system can not be explained in terms of simple rules, whithout knowing the actual electronic structure of each energy state. The CH_3-substitution, a very weak perturbation to the π electron system, however, is reasonably expected not to give a drastic change in the whole π electronic structure but only to change slightly the energy scheme of the molecular orbitals. Experimental rules of the spectral behaviors observed upon the CH_3-substitutions in the bipyridine negative ion, rather weakly binding to the metal ion, are expected to be held even in fairly strong coordination to the metal ion with higher oxidation number than one, unless the coordination enhances drastically π electron delocalization between the coordinating negative ion and the metal ion or gives rise to a crucial electron transfer from negative ion to the metal ion.

On the other hand, in some cases where the ligand is molecular bipyridine but not negative ion, electronic absorption bands with $\log\varepsilon\geq3$ have been frequently observed in the near infrared and visible regions. $[Cr^{II}(bipy)_3]^{2+}$ ion is an example of this case. These bands are to be approximately assigned to charge transfer transitions from the d orbitals of the central metal ion to the lowest vacant π^* orbitals of bipyridine molecules.[7] The CH_3-substitutions give quite different spectral effects on the metal-ligand charge transfer bands from effects on the π-π^* bands in the coordinating bipyridine negative ion. The lowest wave number bands near 9000 cm^{-1}, for example, are shifted to the higher wave number in the order 4dmbip< bipy<5dmbip, which is reverse to the effect observed in the lowest wave number bands of the coordinating negative ion near 11000 cm^{-1}.

Tris bipyridine metal complexes with lower abnormal valency[1] such as $[M(bipy)_3]$, where M=Ti, V, Cr, Mn, Fe, Co or Al, may be divided into two extreme types; the one includes bipyridine molecules coordinating to a metal ion with abnormal oxidation number, and the other includes bipyridine negative ions coordinating to a metal ion with rather normal oxidation number, although electron delocalization possibly makes this distinction a little bit indistinguishable. They both show generally deep color and have absorption bands with $\log\varepsilon\geq3$ in the near infrared and visible regions. Their absorption curves are very complicated and apparently similar to each other, but by the use of the method of CH_3-substitutions described above, we can determine whether they include negative ion or not.[8]

Experimental

Materials. Na(bipy), Na(4dmbip), Na(5dmbip) and K(bipy) were prepared in the apparatus shown in Fig. 3. Equimolar metallic sodium and bipyridine or its dimethyl derivatives were placed at the part marked a in a branch of the H-tube, apparatus I. THF, which was used as a solvent, had been previously purified by the usual method and stored on $LiAlH_4$ in an atmosphere of nitrogen free from oxygen. A flask containing THF was connected to a vacuum system at the joint C. THF was distilled into the tube A or B from the storing flask, degassed under freezing to remove a trace of oxygen in the solvent, and distilled into the tube a. The H-tube was sealed off at the point d. All the procedures were carried out under vacuum. The tube was shaken. Bipyridine or its dimethyl derivatives were reduced by metal sodium in THF

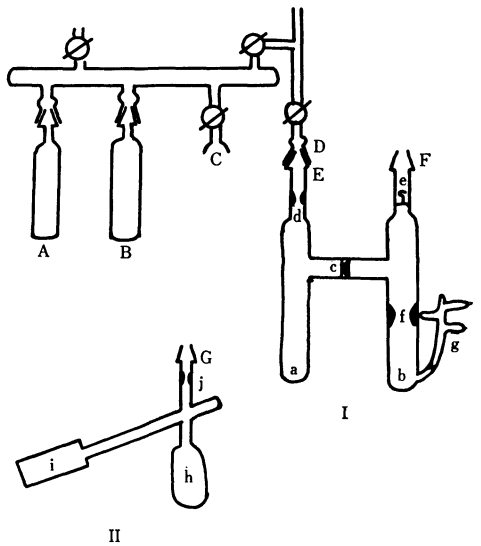

Fig. 3. Apparatus for the preparation of the materials (I) and of the sample solutions of absorption spectrum measurements (II).

7) I. Fujita, T. Yazaki, Y. Torii and H. Kobayashi, This Bulletin, to be published.

8) Y. Kaizu, T. Yazaki and Y. Torii, This Bulletin, to be published.

and reddish violet solutions were obtained. The reduction was completed in about one day at room temperature. The solution was then filtrated through the glass filter c and the filtrate was collected in the tube b. Again the H-tube was connected with the vacuum system at the joint F. After the breakable seal e was broken, THF was completely distilled off and the tube was sealed off at the point f. Compounds thus obtained were stored in the tube g under vacuum. The tube g has several branches which are used to take a portion of material.

Li-complex was prepared by a method virtually identical with that described above, except for the use of apparatus II instead of the H-tube. The preparation was carried out in the flask h, and solution thus obtained were not evaporated to isolate crystalline substance but directly transferred to the quartz cell i for the measurement of its electronic absorption spectra.

Electronic Absorption Spectra. Sample solutions for spectral measurement were prepared with apparatus II connected to the vacuum system through the joints D and G. A capsule containing a small amount of the sample was placed in the quartz cell i and solvent THF was distilled directly into the flask h, in which the volume of the solvent was measured. The apparatus was then sealed off at the point j. The capsule was broken by a breaker, previously enclosed in the apparatus, in the flask h, and the compound was dissolved into the solvent. The amount of compound was estimated from the difference between weight of the unbroken capsule containing the compound and that of the capsule, taking into account the buoyancy correction for the unbroken capsule. The sample solution thus obtained in the flask h was transferred into the quartz cell i, the light path of which is 0.1 cm or 1 cm long, and electronic absorption spectra were measured using a Shimadzu multipurpose recording spectrophotometer model MPS-50.

BULLETIN OF THE CHEMICAL SOCIETY OF JAPAN VOL. 42 2267—2272 (1969)

Polarographic Study of the Cadmium(II)-Ethylenediaminetetrapropionate Chelate

Mutsuo KODAMA and Yayoe TOMINAGA

Department of Chemistry, Ibaraki University, Mito, Ibaraki

(Received November 20, 1968)

The d.c. polarographic behavior of the cadmium(II) ion in ethylenediaminetetrapropionate (EDTP) was studied in the pH range from 8.30 to 10.30. Over the entire range of experimental conditions employed, the cadmium(II)ion invariably gave a single well-defined wave corresponding to the following reversible two-electron reduction:

$$\begin{array}{l} CdZ^{2-} + nH^+ + Hg + 2e^- \rightleftarrows Cd(Hg) + H_nZ^{n-4} \\ \quad \downarrow\uparrow \\ CdZ_2^{6-} \end{array}$$

Even in the presence of ammonia or the alaninate ion, the cadmium(II) ion in the EDTP solution also behaves reversibly in a polarographic electrolysis. However, the half-wave potential was found to be shifted to the more negative potentials by the addition of ammonia or alaninate. This was ascribed to the formation of a mixed ligand chelate involving ammonia or the alaninate ion. From the relation between the shift of the half-wave potential and the concentration of ammonia or alaninate, the composition and the stability constant of the mixed ligand chelate were determined and the electrode reaction was established as:

$$\begin{array}{l} Cd(A)Z^{2-m} \rightleftarrows CdZ^{2-} + nH^+ + Hg + 2e^- \rightleftarrows Cd(Hg) + H_nZ^{n-4} \\ \qquad\qquad\quad \downarrow\uparrow \\ \qquad\qquad\quad CdZ_2^{6-} \end{array}$$

where A means the ammonia or the alaninate ion. The K_2, K^{NH_3}, and K^{ala} values determined were 5.5×10^2, 1.38×10^2, and 2.61×10^4 respectively.

The cadmium(II) chelates of ethylenediaminetetraacetic acid (EDTA) and its related compounds have been studied by numerous investigators.[1-4] The cadmium(II) chelates of several aminopolycarboxylic acids have been found to give two waves frequently. The reversible first wave is kinetic in

1) N. Tanaka, R. Tamamushi and M. Kodama, *Z. Phys. Chem., N. F.*, **14**, 141 (1958).

2) J. Koryta, *Collection Czech. Chem. Commun.*, **24**, 3057 (1959).

3) N. Tanaka, K. Ebata, T. Takahari and T. Kumagai, This Bulletin, **35**, 1836 (1962).

4) Y. Koike and H. Hamaguchi, *J. Inorg. Nucl. Chem.*, **29**, 437 (1967).

nature and may be attributed to the reduction of the cadmium(II) ion dissociated from the cadmium-(II)-aminopolycarboxylate chelate. The second wave, which corresponds to the direct reduction of the cadmium(II)-aminopolycarboxylate chelate is, however, irreversible. Generally, the direct reduction of the cadmium(II)-aminopolycarboxylate chelate is irreversible. Therefore, the polarographic wave due to the direct reduction of the cadmium(II)-aminopolycarboxylate chelate can hardly be used for the establishment of the electrode reaction mechanism or for the determination of an equilibrium between the cadmium(II) ion and aminopolycarboxylate. Exceptionally, the cadmium(II) chelate of ethylenediaminetetrapropionic acid (EDTP) was found to behave reversibly in a polarographic electrolysis. In this paper, the polarographic behavior of the cadmium(II) ion in the EDTP solution will be investigated systematically and the solution equilibria between the cadmium(II) ion and EDTP will be determined.

The effects of ammonia and the alaninate ion on the polarographic behavior of the cadmium(II)-EDTP chelate were also studied. The half-wave potential of the cadmium(II)-EDTP chelate shifted to more negative potentials with an increase in the concentration of ammonia or the alaninate ion. This was ascribed to the formation of a mixed ligand chelate involving ammonia or the alaninate ion.

Experimental

Reagents. The purification of EDTP and the preparation of its solution have been described previously.[5] The methods of preparing and standardizing a cadmium(II) perchlorate solution were also given in a previous paper.[6] All the other chemicals were of an analytical reagent grade and were used without further purification. The ionic strength of the sample solution was adjusted to 0.30 by adding an appropriate volume of a 1.0 M sodium perchlorate solution. The alanine used in this study was a racemic mixture.

Apparatus and Experimental Procedure. All the apparatus (mannual and pen-recording polarographs and the dropping mercury electrode (DME)) and the experimental procedures were the same as those employed previously.[5] All the polarographic measurements were conducted at 25°C.

Results and Discussion

Polarographic Behavior of the Cadmium(II) Ion in an Ethylenediaminetetrapropionate Solution in the Absence of Ammonia or Alaninate. The d. c. polarographic behavior of the cadmium(II) ion in an EDTP solution not containing ammonia or alaninate was studied in the pH range from 8.30 to 10.30. In the present study, no buffer reagent was used, because the present system always contains a large excess of un-complexed EDTP over cadmium(II) ions and, hence, is considered to have enough of a buffer capacity to maintain the pH value of the solution constant in this pH range. Over the entire pH range employed, the cadmium(II) ion invariably gave a well-defined single wave. A typical polarogram is reproduced in Fig. 1. As is shown in Fig. 2, a conventional plot of $\log(i/(i_l-i))$ against the applied d.c.

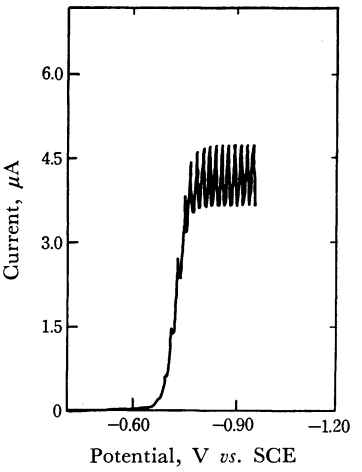

Fig. 1. D. c. polarogram of cadmium(II) ion in EDTP solution.
μ=0.30, pH=9.31
Concentration of cadmium(II)=0.920 mM
Concentration of EDTP=20.0 mM

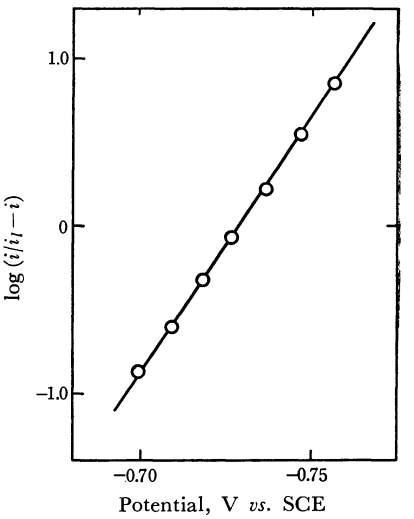

Fig. 2. A conventional plot of $\log(i/(i_l-i))$ against the applied d. c. potential.
μ = 0.30, pH=9.31
Concentration of cadmium(II)=0.920 mM
Concentration of EDTP=20.0 mM

5) M. Kodama and A. Kimura, This Bulletin, **40**, 1639 (1967).

6) M. Kodama and C. Sasaki, This Bulletin, **41**, 127 (1968).

potential, E, gave straight lines with reciprocal slopes falling in the range from 32 to 35 mV. This clearly indicates that the electrode reaction is a reversible two-electron reduction process.

The wave-height was found to be exactly proportional to the bulk concentration of the cadmium(II) ion and the square-root of the effective pressure on the DME (The results are not shown here). These facts also support the above conclusion that the electrode reaction of the cadmium(II) ion in EDTP solution proceeds reversibly.

In the present pH range, the wave-height was almost independent of the pH value of the sample solution and the concentration of un-complexed EDTP, but slightly lower than that observed in an acid medium. The decrease in the wave-height may correspond to the chelate formation of the cadmium(II) ion with EDTP, because the diffusion-current constant of a complexed metal ion is usually smaller than that of un-complexed metal ion.

An EDTP is a weak acid with $pK_1=2.96$, $pK_2=3.32$, $pK_3=6.58$, and $pK_4=9.33$,[7,8] where the pK's are the acid dissociation constants of EDTP. Therefore, the conditional formation constant of the cadmium(II)-EDTP chelate must be a function of the hydrogen ion concentration; hence, the half-wave potential of the cadmium(II) ion in an EDTP solution would greatly depend on the pH value of the solution. This prediction was examined experimentally. Some typical results are shown in Table 1. The half-wave potential shifted to more negative potentials with an increase in the pH value of the solution. As was discussed in connection with the polarography of the copper(II)-*N*-(2-hydroxyethyl)-ethylenediamine-*N*,*N*',*N*'-triacetate chelate,[9] when only a normal chelate with a 1-to-1 composition is formed, the half-wave potential, $(E_{1/2})_{CdZ}$ may be expected to shift to negative potentials with a decrease in the log (α_H) value of EDTP, log $(\alpha_H)_Z$, corresponding to the following relation:

$$\frac{\Delta(E_{1/2})_{CdZ}}{\Delta \log(\alpha_H)_Z} = 29.6\,\text{mV} \qquad (1)$$

Here, $(\alpha_H)_Z$ is given by $1+[H^+]/k_4+[H^+]^2/k_4\cdot k_3+\cdots+[H^+]^4/k_4k_3k_2k_1$ and k's are the dissociation constants of EDTP. As is shown by the data in Table 1, however, the negative shift of the half-wave potential with a decrease in the log $(\alpha_H)_Z$ value was much greater than that expected from the (1) relation.

The dependence of $(E_{1/2})_{CdZ}$ on the concentration of EDTP was also investigated. The results are given in Table 2. $(E_{1/2})_{CdZ}$ shifted to more negative potentials with an increase in the concentration of un-complexed EDTP, $[Z]_f$. The shift of the half-wave potential, however, was much greater than that to be expected for the reversible two-electron reduction of the normal

Table 1. $(E_{1/2})_{CdZ}$ and pH

$\mu=0.30$, Concentration of EDTP=20.0 mM
Concentration of cadmium(II)=0.920 mM

pH	log $(\alpha_H)_Z$	$(E_{1/2})_{CdZ}$ V *vs.* SCZ	$\Delta(E_{1/2})_{CdZ}$, mV	
			Calcd ($29.6\,\Delta \log(\alpha_H)_Z$)	Obsd
8.33	1.024	−0.695	0	0
8.84	0.612	−0.714	12.2	19
9.31	0.311	−0.729	21.1	34
9.69	0.158	−0.738	25.6	43
10.01	0.082	−0.743	27.9	48

Table 2. $(E_{1/2})_{CdZ}$ and $[Z]_f$

$\mu=0.30$, pH=9.33
Concentration of cadmium(II)=0.920 mM

$[Z]_f$	$(E_{1/2})_{CdZ}$ V *vs.* SCE	$\Delta(E_{1/2})_{CdZ}$, mV		
		Calcd ($29.6\,\Delta \log[Z]_f$)	Calcd (with the aid of Eq. (3'''))	Obsd
10.0	−0.710	0	0	0
20.0	−0.729	−8.9	−16.0	−19
30.0	−0.741	−14.1	−29.0	−31

7) R. C. Courtney, S. Chaberek, Jr., and A. E. Martell, *J. Am. Chem. Soc.*, **75**, 4814 (1953).
8) M. Kodama and Y. Tominaga, This Bulletin, **42**, 721, 724 (1969).
9) M. Kodama and Y. Tominaga, *ibid.* **42**, 394 (1969).

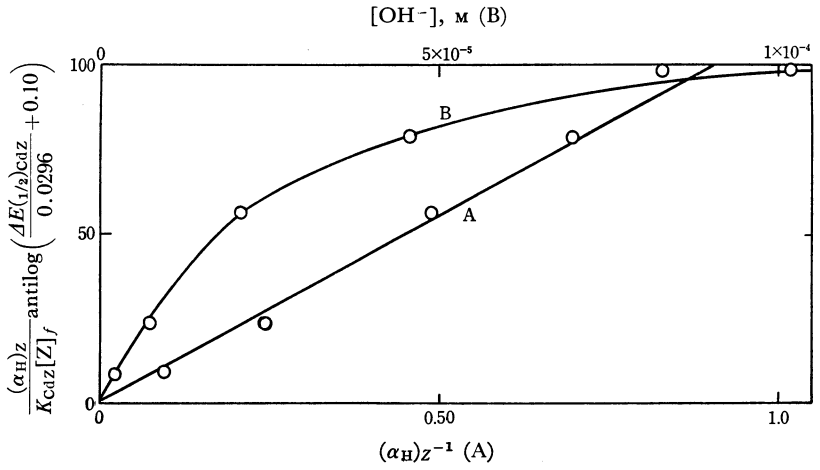

Fig. 3. The plot of $\frac{(\alpha_H)_Z}{K_{CdZ}[Z]_f}$ antilog$\left[\log\frac{k_{Cd^{2+}}}{k_{CdZ}}+\frac{\Delta(E_{1/2})_{CdZ}}{0.0296}\right]$ against $[Z]_f/(\alpha_H)_Z$ or $[OH^-]$.

chelate with a composition of 1-to-1, $\Delta(E_{1/2})/\Delta\log[Z]_f=-29.6$ mV.

Since the present study was conducted at higher pH's, the above two facts clearly indicate that, under the present experimental conditions, the cadmium(II) ion forms normal chelate with a 1-to-2 composition as well as that with a 1-to-1 composition with EDTP. Therefore, the electrode reaction can be assumed to be:

$$\begin{array}{l} CdZ^{2-} + nH^+ + Hg + 2e^- = Cd(Hg) + H_nZ^{n-4} \\ \quad\downarrow\uparrow \\ CdZ_2^{6-} \end{array} \qquad (2)$$

with the half-wave potential corresponding to:

$$(E_{1/2})_{CdZ} = E^\circ_{Cd} + 0.0296\left[\log f_{Cd^{2+}} + \log\frac{k_{Cd(Hg)}}{k_{CdZ}} - \log\frac{K_{CdZ}}{(\alpha_H)_Z}\left(1+\frac{K_2}{(\alpha_H)_Z}[Z]_f\right)[Z]_f\right] \qquad (3)$$

where E°_{Cd}, $f_{Cd^{2+}}$, $k_{Cd(Hg)}$, k_{CdZ}, and K_{CdZ} have their usual meanings and where $K_2=[CdZ_2^{6-}]/[CdZ^{2-}]\cdot[Z^{4-}]$.

From Eq. (3), the shift of the half-wave potential of the cadmium(II) ion due to the chelate formation with EDTP, $\Delta(E_{1/2})_{CdZ}$, can be derived as:

$$\Delta(E_{1/2})_{CdZ} = 0.0296\left[\log\frac{k_{CdZ}}{k_{Cd^{2+}}} + \log\frac{K_{CdZ}}{(\alpha_H)_Z}\left(1+\frac{K_2[Z]_f}{(\alpha_H)_Z}\right)\right] \qquad (3')$$

By rearranging Eq. (3') and by casting the resulting relation into antilog form, (3'') can be easily derived:

$$1+\frac{K_2}{(\alpha_H)_Z}[Z]_f = \frac{(\alpha_H)_Z}{K_{CdZ}[Z]_f} \times \text{antilog}\left[\log\frac{k_{Cd^{2+}}}{k_{CdZ}}+\frac{\Delta(E_{1/2})_{CdZ}}{0.0296}\right] \qquad (3'')$$

On the other hand, if the fact that the shift of the half-wave potential is much greater than that to be expected for the reversible two-electron reduction of the chelate with a 1-to-1 composition can be ascribed to the formation of a mixed ligand chelate involving the hydroxyl ion, OH^-, the left-hand side of Eq. (3'') should be replaced by $1+K^{OH}\cdot[OH^-]$, where K^{OH} is $[CdZ(OH)^{3-}]/[CdZ^{2-}]\cdot[OH^-]$. Using some typical data, the right-hand side of Eq. (3'') was plotted against $[Z]_f/[\alpha_H]_Z$ or $[OH]^-$. As is shown in Fig. 3, only the plot of the right-hand side of Eq. (3'') against $[Z]_f/(\alpha_H)_Z$ gave a linear relation with an intercept of 1. Furthermore, as is shown by the data in Table 2, with the increase in the concentration of un-complexed EDTP, the half-wave potential was found to shift to more negative potentials corresponding exactly to Eq. (3''). These facts strongly confirm the formation of a normal chelate with a composition of 1-to-2 and, hence, the electrode reaction (2). In the calculation of the right-hand side of Eq. (3'') the K_{CdZ} value of 2.51×10^5 ($\mu=0.30$) estimated from the K_{CdZ} value obtained in a solution with an ionic strength of 0.10 by Courtney *et al.*[7] and the activity coefficients of the ion calculated by means of the Davies equation[10] were used. From the slope of the linear relation in Fig. 3, K_2 was estimated to be 5.5×10^2.

D.C. Polarographic Behavior of the Cadmium(II) Ion in EDTA Solutions Containing Ammonia or Alanine. The d.c. polarographic behavior of the cadmium(II) ion in EDTP solutions containing ammonia or the alaninate ion was also investigated systematically. The limiting current of the cadmium (II)-EDTP chelate was little affected by the presence of ammonia or the alaninate ion, but the half-wave potential was found to shift to more negative potentials with an

10) J. N. Butler, "Ionic Equilibrium," Addison-Wesley Publishing Co., Reading, Massachusetts (1964), p. 437.

increase in the concentration of ammonia or alaninate. Considering the magnitude of formation constants of cadmium(II)-ammine, -alaninate, and -EDTP complexes,[11] it may safely be concluded that even 0.1 M ammonia or alaninate ions can not displace the EDTP anion from the cadmium(II)-EDTP chelate under the present experimental conditions. The conditional formation constant of the mixed ligand chelate involving both EDTP and ammonia or the alaninate ion is larger than that of the normal EDTP chelate, and in the polarography of the metal complexes, the increase in the value of the conditional formation constant always results in a negative shift of the half-wave potential. Therefore, the above negative shift caused by the addition of ammonia or the alaninate ion can be attributed to the formation of a mixed ligand chelate involving ammonia or the alaninate ion.

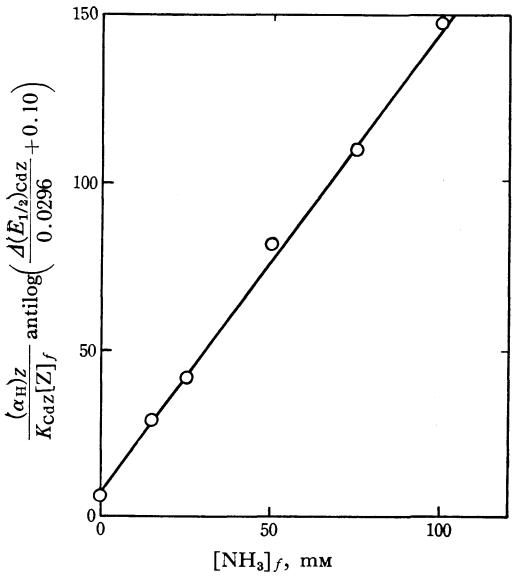

Fig. 4. The plot of $\frac{(\alpha_H)_Z}{K_{CdZ}[Z]_f}\text{antilog}\left[\log\frac{k_{Cd^{2+}}}{k_{CdZ}}+\frac{\Delta(E_{1/2})_{CdZ}}{0.0296}\right]$ against $[NH_3]_f$.
pH=9.33, Concentration of EDTP=20.0 mM

If a mixed ligand chelate with the composition of $Cd(A)Z^{2-m}$ is also formed (where A indicates ammonia or the alaninate ion), the left-hand side of Eq. (3'') should be replaced by $1+K_2[Z]_f/(\alpha_H)_Z+K^A[A]_f$. Here, K^A denotes $K^{NH_3}=[Cd(NH_3)Z^{2-}]/[CdZ^{2-}][NH_3]_f$ of $K^{ala}=[CdZ(ala)^{3-}]/[CdZ^{2-}][ala]_f$, and $(A)_f$ denotes the concentration of un-complexed ammonia, $[NH_3]_f$ or that of the un-complexed alaninate ion, $[ala]_f$. Therefore, provided that the concentration of un-complexed EDTP and the solution pH are kept constant, the plot of the right-hand side of Eq. (3'') against $[A]_f$ will give a linear relation with a intercept of $1+K_2[Z]_f/(\alpha_H)_Z$. This relation was examined successfully by means of the experimental data. The results are shown in Figs. 4 and 5. From the slopes of the linear relations in Figs. 4 and 5, K^{NH_3} and K^{ala} were estimated to be 1.38×10^2 and 2.61×10^4 respectively. On the basis of the above results and discussion, the electrode reaction of the cadmium(II)-EDTP chelate at the mercury electrode in the presence of ammonia

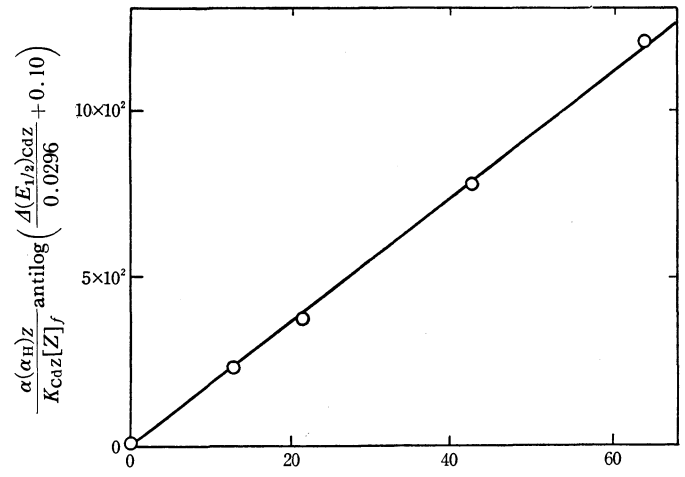

Fig. 5. The plot of $\frac{(\alpha_H)_Z}{K_{CdZ}[Z]_f}\text{antilog}\left[\log\frac{k_{Cd^{2+}}}{k_{CdZ}}+\frac{\Delta(E_{1/2})_{CdZ}}{0.0296}\right]$ against $[ala]_f$.
pH=9.45, Concentration of EDTP=10.0 mM

11) L. G. Sillen and A. E. Martell, "Stability Constants of Metal Ion Complexes," The Chemical Society, London (1964).

or the alaninate ion can be established to proceed thus:

$$\begin{aligned} Cd(A)Z^{2-m} &\rightleftharpoons CdZ^{2-} + nH^+ + Hg + 2e^- \\ &\quad \downarrow\uparrow \\ &\quad CdZ_2^{6-} \\ &\rightleftharpoons Cd(Hg) + HnZ^{n-4} \end{aligned} \qquad (4)$$

where $Cd(A)Z^{2-m}$ means $Cd(NH_3)Z^{2-}$ or $CdZ(ala)^{3-}$.

Here, it can be mentioned that the K^{ala} value found was almost identical with the K_1 value of the cadmium(II) - alaninate chelate.[12] If an alaninate anion functions as a monodentate ligand in the present mixed ligand-chelate formation, the equilibrium constant, K^{ala}, can be expected to be considerably smaller than the K_1 value of cadmium(II)-alaninate chelate. As has been reported by several authors,[11] K_1 values of cadmium(II) complexes of monodentate ammonia and the acetate ion can be expected to be thermodynamically considerably smaller than that of the cadmium(II) chelate of the bidentate alaninate anion. The steric and other effects may also reduce the stability of the mixed ligand chelate appreciably. Therefore, the above fact may indicate that an alaninate anion acts as a bidentate ligand in the present mixed-ligand-chelate formation.

12) D. J. Perkins, *Biochem. J.*, **57**, 702 (1954).

BULLETIN OF THE CHEMICAL SOCIETY OF JAPAN VOL. 42 2272—2275 (1969)

The Spectrophotometric Determination of Zirconium(IV) with Bromopyrogallol Red*[1]

Takayoshi SAKAI*[2] and Yûko FUNAKI*

Chemical Department, Faculty of Science, Hirosaki University, Bunkyô-chô, Hirosaki

(Received November 25, 1968)

Zirconium(IV) reacts with an excess of bromopyrogallol red to form a violet complex. The constant absorbance of a solution containing the complex is obtained in the pH range from 5.0 to 5.4 at 670 mμ. About 25 min is required to complete the chelate formation in a boiling water bath. The complex thus formed is stable for at least 3 hr. The color system obeys Beer's law in the range from 4 to 35 μg zirconium in 25 ml. The sensitivity of the reaction is 0.002 μg per cm^2 for an absorbance of 0.001. In composition the complex has a metal-to-ligand ratio of 1:2. The molar absorptivity and the apparent formation constant of the complex are calculated to be 7.01×10^4 at 670 mμ and 1.11×10^9 at pH 5.2 respectively. The effect of diverse ions on the determination is examined.

Bromopyrogallol red (BPR or H_4L) has been used as a reagent for the spectrophotometric determination of many metallic cations, including silver(I),[1] uranium(IV),[2] yttrium(III) and cerium(III),[3] titanium(IV)[4] bismuth(III),[5] indium(III),[6] niobium(V),[7] scandium(III),[8] and thorium(IV).[9] It is found that BPR reacts with zirconium(IV) under heating to form a violet complex. The present paper describes the fundamental conditions for applying the reaction to the spectrophotometric determination of zirconium.

Experimental

Reagents and Apparatus. *Standard Zirconium Solution.* About a 1×10^{-2} M zirconium(IV) solution

*1 This work was partly presented at the Tohoku Branch Meeting of the Chemical Society of Japan, Yamagata, October, 1966.

*2 Present address: Hachinohe Technical College, Tamonoki, Hachinohe, Aomori.

*3 Present address: Department of Chemical Engineering, Faculty of Engineering, Tohoku University, Aramaki, Sendai.

1) R. H. Dagnall and T. S. West, *Talanta*, **8**, 711 (1961).

2) V. F. Lukjaov and E. P. Duderova, *Zh. Analit. Khim.*, **16**, 60 (1960).

3) J. Herrington and K. C. Steed, *Anal. Chim. Acta*, **22**, 180 (1960).

4) V. Suk, I. Nemcova and M. Malat, *Collect. Czech. Chem. Commun.*, **30**, 2538 (1965).

5) V. Suk and M. Smetanava, *ibid.*, **30**, 2535 (1965).

6) Sn. T. Talipan, Kr. S. Abdultaeva and G. P. Gorkovaya, *Uzbeksk. Khim.*, **6**, 16 (1962): *Chem. Abstr.*, **58**, 12122 (1963).

7) R. Belcher, T. V. Ramakrishna and T. S. West, *Talanta*, **12**, 681 (1965).

8) T. Shimizu, *ibid.*, **14**, 473 (1967).

9) K. Tonosaki and T. Sakai, This Bulletin, **42**, 456 (1969).

was prepared by dissolving a guaranteed zirconyl nitrate dihydrate in 0.2 N perchloric acid. The solution was standardized by EDTA titration, using xylenol orange[10] as the indicator.

The solutions of BPR, diverse ions, and the buffer, and the apparatus were the same as those used in a previous work.[9]

All the measurements were made at 25±0.5°C.

Standard Procedure. To a sample solution containing up to 32 μg of zirconium in a 50 ml Erlenmeyer flask, 1.2 ml of a 1×10^{-3} M BPR solution and 10 ml of a 0.25 M acetate buffer solution with a pH value of 5.2 were added. The mixture was then heated in a boiling water bath for 25 min. The solution was cooled with running water to room temperature, transferred into a 25 ml volumetric flask, and then diluted to the mark with water. After 10 min, the absorbance of the solution was measured at 670 mμ using a reagent blank as the reference.

Results and Discussion

Absorption Curves. Figure 1 shows that the maximum absorption of the zirconium - BPR complex is found at 670 mμ.

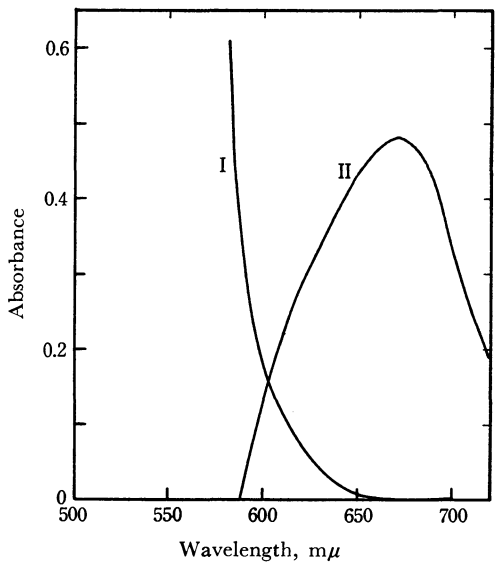

Fig. 1. Absorption curves of BPR and its zirconium complex.

BPR: 4.80×10^{-5} M, Zr(IV): 18.2 μg in 25 ml (7.97×10^{-6} M), μ: 0.1, I: BPR *vs.* water, II: zirconium-BPR complex *vs.* BPR, pH: 5.23.

The Effect of pH. As is shown in Fig. 2, the maximum absorbance is obtained in the pH range from 4.7 to 4.8. The complex formed below pH 4.9 showed a tendency to precipitate on standing, probably because of its uncharged form.*4

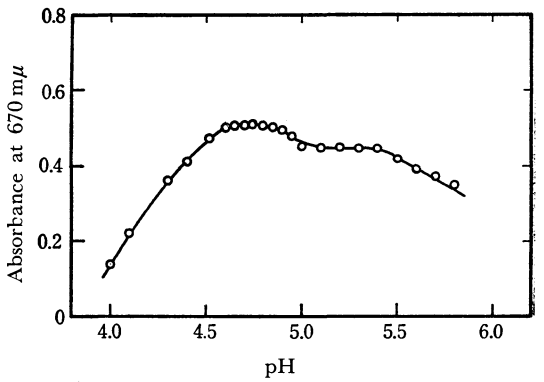

Fig. 2. Effect of pH.
Zr(IV): 18.2 μg, BPR: 4.00×10^{-5} M, μ: 0.1, Reference: Reagent blank

A constant absorbance is obtained over the pH range from 5.0 to 5.4. All the absorbance readings were taken within this range, since the absorbance of the solution containing the complex remains almost constant for at least 3 hr after heating.

The Effect of Heating Time. It requires several hours at room temperature to complete the reaction between zirconium and BPR. The reaction was, however, accelerated by heating. The maximum absorbance was obtained when a solution containing zirconium and BPR was heated in a boiling water bath for from 20 to 35 min.

The Effect of the Amount of Reagent. The maximum, and almost constant, absorbance was obtained when from 1 to 3 ml of a 1×10^{-3} M BPR solution was added to a solution containing 18.2 μg of zirconium. The order of the addition of the reagents was not critical.

Calibration Curve. Beer's law is found to hold in the range from 4 to 35 μg of zirconium in 25 ml. The sensitivity of the reaction was calculated according to Sandell's notation[11] and found to be 0.002 μg of zirconium per cm^2. The reproducibility of the method was examined using a solution containing 18.2 μg of zirconium. From the data obtained by eleven determinations, the standard deviation was calculated to be 0.003 (2.8%) in absorbance.

The Effect of Diverse Ions. The results are listed in Table 1.

A Comparison with Other Methods. Table 2 indicates that the proposed method is comparable with the morin method[16] in sensitivity.

10) K. Ueno "Kireto Tekitei (Chelatometric Titration)" (in Japanese), Nankodo, Tokyo (1960), p. 325.

*4 It was found experimentally that zirconium forms a 1 : 1 complex with BRR at lower pH values. Since, as will be mentined below, BPR may exist mainly as the anionic species, H_3L^-, in the pH range from 1 to 4, the formula of the 1 : 1 complex may be represented as an uncharged form, $ZrO(H_2L)$.

11) E. B. Sandell, "Colorimetric Determination of Traces of Metals," Interscience Publishers, New York (1950), p. 49.

TABLE 1. EFFECT OF DIVERSE IONS AT pH 5.2

Zirconium taken: 18.2 μg (0.20 μmol) Tolerance limit* μmol	Ions
large excess	chloride
0.2	sulfate, Co, Pb
0.1—0.05	Ag, Cd, In, fluoride, oxalate
0.04—0.01	Be, Bi, Ce(III), Cu, Ga, Hg, La, Mn, Ni, Pd, Sm, Th(IV), Ti(IV), Tl(I), Tl(III), U(VI), V(IV), W(VI), Y, Yb, Zn, phosphate, tartrate, citrate
0	Cr, Fe(III), Nd, EDTA

* Value which gives less than 3% relative error

Composition of the Complex. The method described by Benesi and Hildebrand[20] is used to determine the composition of the complex. Since BPR may exist mainly as the anionic form, H_2L^{2-}, in the pH range from 5 to 8,*5 and zirconium(IV), as ZrO^{2+}, the formation of the complex with a metal-to-ligand ratio of $1:n$ can be represented as;

$$ZrO^{2+} + nH_2L^{2-} \rightleftarrows ZrO(HL)_n^{(3n-2)-} + nH^+ \quad (1)$$

$$K' = [\{ZrO(HL)_n\}^{(3n-2)-}]/[ZrO^{2+}][H_2L^{2-}]^n \quad (2)$$

where K' is the apparent formation constant at a given pH value. The following relation may finally be derived as a result of the transformation of

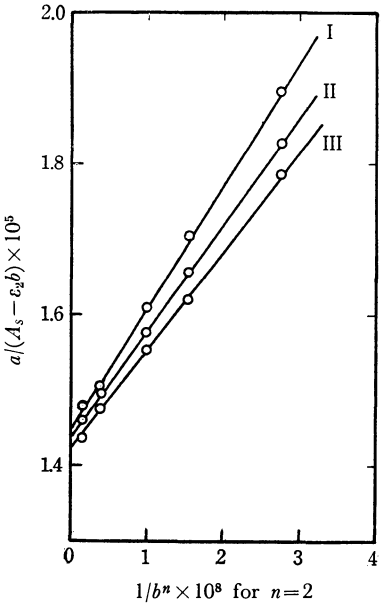

Fig. 3. Plots of $a/(A_s-\varepsilon_2 b)$ *vs.* $1/b^n$ at pH 5.5. Zr: 3.87×10^{-6} M, BPR: 7.74×10^{-5}—2.32×10^{-4} M, μ: 0.5, I: 680 mμ, II: 665 mμ, III: 670 mμ

Eq. (2):

$$a/(A_s-\varepsilon_2 b) = 1/\varepsilon_3 + 1/K'\varepsilon_3 b^n \quad (3)$$

where A_s is the absorbance of the solution containing the complex and ligand added in excess to a definite

TABLE 2. COMPARISON WITH OTHER METHODS

Reagent	Molar absorptivity $\times 10^4$	Sensitivity μg/cm²
Bromopyrogallol Red	7.01 (670 mμ)	0.002
Pyrocatechol Violet[12]	4 (655 mμ)	
Gallein[13]	0.77 (530 mμ)	0.02
N-Methyl anabasine-α-azoresorsinol[14]	1.05 (530 mμ)	
Arsenazo III[15]	12.5±0.3 (670 mμ)	
Morin[16]	7.30 (420 mμ)	
8-Hydroxyquinoline[17]	1.47 (386 mμ)	
Chromazurol S[18]	4.1±0.04 (560 mμ)	
Molybdate[19]	0.475 (725 mμ)	

12) J. P. Young and J. C. White *Talanta*, **1**, 263 (1958).
13) L. Kekedy and G. Balogh, *Studia Univ. Babes-Bolyai, Ser. Chem.*, **8**, 204 (1963); *Chem. Abstr.*, **61**, 12631 (1964).
14) Sh. T. Talipov, R. Kh. Dzhiynbaeva and M. Abdurakhmanov, *Nauchn Tr. Tashkentsk. Gos. Univ. No.* **264**, 146 (1964); *Chem. Abstr.*, **65**, 14427 (1966).
15) N. V. Mel'chakova, M. N. Stanislavskaya and V. M. Peshkova, *Zh. Analit. Khim.*, **19**, 701 (1964); *Chem. Abstr.*, **61**, 7699 (1964).
16) T. Ito and Y. Hoshino, *Bunseki Kagaku (Japan Analyst)*, **13**, 257 (1964).
17) R. T. Van Santen, J. H. Schlewitz and C. H. Toy, *Anal. Chim. Acta*, **33**, 593 (1965).
18) I. S. Mustafin and V. S. Shchukina, *Zh. Analit. Khim.*, **21**, 309 (1966); *Chem. Abstr.*, **65**, 3000 (1966).
19) J. C. Guyon and C. C. Clowers, *Anal. Chim. Acta*, **37**, 401 (1967).
20) M. A. Benesi and J. H. Hildebrand, *J. Am. Chem. Soc.*, **71**, 2703 (1949).
*5 The stepwise acid dissociation constants of BPR have been determined by Suk[21] as $K_1=(6.92\pm0.27)\times10^{-1}$, $K_2=(4.07\pm0.09)\times10^{-5}$, $K_3=(7.41\pm0.10)\times10^{-10}$, and $K_4=(5.37\pm0.32)\times10^{-12}$.
21) V. Suk, *Collect. Czech. Chem. Commun.*, **31**, 3127 (1966).

amount of zirconium, where a and b are the total concentrations of zirconium and the ligand respectively, and where ε_2 and ε_3 are the molar absorptivities of the ligand and the complex respectively. Only a choice of n equal to two made the data interpretable, showing that a 1 : 2 complex is formed between zirconium and BPR. Some of the results are shown in Fig. 3. From the intercept of the straight line, ε_3 was calculated to be 7.01×10^4 at 670 mμ, and K', as a mean value of the values obtained at five wavelengths between 660 and 680 mμ, was found to be 1.11×10^9 at pH 5.2.

The authors wish to express their hearty thanks to Professor Kôichi Tonosaki for his kind advice and instruction throughout this study. They also wish to extend their thanks to Dr. Makoto Otomo for his valuable suggestions.

BULLETIN OF THE CHEMICAL SOCIETY OF JAPAN VOL. 42 2275—2281 (1969)

Methods of Preparing the 2,2'-Dipyridyl and 1,10-Phenanthroline Cobalt(III) Complexes of the $[CoX_2dip_2]$- and $[CoX_2phen_2]$-Type[1)]

Nobufumi MAKI

Department of Chemistry, Faculty of Engineering, Shizuoka University, Johoku, Hamamatsu

(Received November 25, 1968)

The bis(2,2'-dipyridyl) and bis(1,10-phenanthroline)cobalt(III) complexes of the $[CoX_2N_4]$-type, including the following new compounds, have been prepared: $[Co(CN)_2dip_2]NO_3\cdot 7H_2O$, $[Co(CN)_2dip_2]_2SO_4\cdot 12H_2O$, $Na[Co(SO_3)_2dip_2]\cdot 5H_2O$, $Na[Co(S_2O_3)_2dip_2]\cdot 7H_2O$ $[Co(N_3)_2dip_2]N_3\cdot 2H_2O$, $[Co(N_3)_2dip_2]ClO_4$, $[Co(N_3)_2dip_2]_2SO_4\cdot 5H_2O$, $[Co(N_3)_2dip_2]NO_3\cdot 2H_2O$, $[Co(N_3)_2dip_2]Cl\cdot 3H_2O$, $[Co(SCN)_2dip_2]NCS\cdot 5/2\ H_2O$, $[Co(SCN)_2dip_2]ClO_4\cdot 2H_2O$, $[Co(SCN)_2dip_2]Cl\cdot 3H_2O$, $K[Co(SO_3)_2phen_2]\cdot 5H_2O$, $[Co(NO_2)_2phen_2]Cl\cdot 4H_2O$, $Na[Co(S_2O_3)_2phen_2]$, $[Co(N_3)_2phen_2]N_3$, $[Co(CN)_2phen_2]NO_3\cdot 6H_2O$, $[Co(CN)_2phen_2]Cl\cdot 4H_2O$. The known compounds, including the cobalt(II) and cobalt(III) complexes of the luteo type, have also been prepared by methods other than those described hitherto in the literature. The absorption spectra in the visible and ultraviolet regions have been measured and compared with those of the bis(ethylenediamine)cobalt-(III) complexes. The rhodanato-cobalt(III) complexes, $[Co(SCN)_2dip_2]ClO_4\cdot 2H_2O$ and $[Co(SCN)_2phen_2]NCS$, have been ascertained to be the sulfur-bonded thiocyanato complexes on the evidence of the absorption spectra in the visible and infrared regions.

A number of papers have been published concerning the preparation and the absorption spectra of the bis(ethylenediamine)cobalt(III) complexes, but very few concerning the corresponding cobalt-(III) complexes with 2,2'-dipyridyl and 1,10-phenanthroline have appeared.[2)]

The purpose of this work was to prepare the cobalt(III) complexes of the $[CoX_2dip_2]$- and $[Co\ X_2phen_2]$-type and to elucidate the difference between their absorption spectra and those of the ammine and amine cobalt(III) complexes. Above all, an effort was made to solve the problem of whether or not the rhodanate ligand, SCN^-, is bound to the cobalt(III) ion by the sulfur atom within the coordination sphere of the 2,2'-dipyridyl and 1,10-phenanthroline cobalt(III) complexes, in which the contribution of the π-bonding character to their coordinate bonds is considered to be fairly large.

In addition, the cobalt(III) and cobalt(II) complexes of the $[CoN_6]$-type were prepared by a more convenient and simple method than those described hitherto in the literature.

Experimental

The dichloro complexes, *trans*-$[CoCl_2dip_2]Cl$[3)] and *trans*-$[CoCl_2phen_2]Cl\cdot 4H_2O$,[4)] were used as the starting complexes for the preparation.

Preparation of $[Co(SCN)_2dip_2]NCS\cdot 5/2H_2O$. A water solution (100 m*l*) containing 0.46 g of KNCS was stirred, a drop by drop, into 300 m*l* of a water solution of $[CoCl_2dip_2]Cl$ (1.0 g). First, a green precipitate

1) Presented in part at the 9th Symposium on the Coordination Chemistry, held at Kyushu University, October 21, 1959.

2) A. A. Vlček, *Inorg. Chem.*, **6**, 1425 (1967).

3) F. M. Jaeger and J. A. van Dijk, *Z. anorg. u. allgem. Chem.*, **227**, 273 (1936).

4) P. Pfeiffer and Br. Werdelmann, *ibid.*, **236**, 31 (1950).

immediately separated from the solution; then, its gradually turned a reddish brown. The product was filtered and washed with water several times. The crude complex was recrystallized from hot 60% ethanol twice. Ruby-like red crystals were thus obtained. Found: Co, 9.71; C, 46.93; N, 16.60; H, 3.81%. Calcd for $[Co(SCN)_2dip_2]NCS\cdot\frac{5}{2}H_2O$: Co, 9.98; C, 46.78; N, 16.60; H, 3.58%.

The perchlorate and chloride salts were obtained by treating the complex with 10% $HClO_4$ and 6 N HCl respectively. Found: Co, 9.31; C, 42.37; N, 13.53; H, 3.48%. Calcd for $[Co(SCN)_2dip_2]ClO_4\cdot 2H_2O$: Co, 9.46; C, 42.42; N, 13.49; H, 3.24%.

Found: Co, 10.19; C, 45.88; N, 14.71; H, 4.02%. Calcd for $[Co(SCN)_2dip_2]Cl\cdot 3H_2O$: Co, 10.21; C, 45.79; N, 14.57; H, 3.84%. The complex is insoluble in water, but soluble in alcohol.

Preparation of $[Co(NO_2)_2dip_2]Cl\cdot 5H_2O$. One gram of *trans*-$[CoCl_2dip_2]Cl$, dissolved in 40 m*l* of water, was mixed with 0.4 g of KNO_2 dissolved in 10 m*l* of water, and the mixture was heated on a water bath for half an hour. The yellow product was recrystallized from hot water containing acetic acid.[5] Found: Co, 9.87; C, 40.77; N, 14.32; H, 4.23%. Calcd for $[Co(NO_2)_2dip_2]Cl\cdot 5H_2O$: Co, 10.01; C, 40.80; N, 14.27; H, 4.45%.

Preparation of $Na[Co(SO_3)_2dip_2]\cdot 5H_2O$. A water solution (100 m*l*) of $[CoCl_2dip_2]Cl$ (1.0 g) was mixed with 0.53 g of Na_2SO_3 dissolved in 20 m*l* of water, and the mixture was warmed on a water bath below 60°C. The yellow precipitate which deposited from the solution was filtered and washed with water, ethanol, and ether. The complex is scarcely soluble in water or ethanol. Found: Co, 9.02; C, 37.05; N, 8.80; H, 3.89%. Calcd for $Na[Co(SO_3)_2dip_2]\cdot 5H_2O$: Co, 9.14; C, 37.27; N, 8.69; H, 4.07%.

Preparation of $[Co(N_3)_2dip_2]N_3\cdot 2H_2O$. A water solution (100 m*l*) of *trans*-$[CoCl_2dip_2]Cl$ (1.0 g) was heated on a water bath (60—70°C) with 0.26 g of NaN_3. On cooling, lustrous brown crystals deposited on the wall of the beaker. The crude complex was recrystallized twice from hot water below 70°C. The azido complex is very soluble in both water and ethanol. Found: Co, 11.00; C, 44.94; N, 34.21; H, 3.89%. Calcd for $[Co(N_3)_2dip_2]N_3\cdot 2H_2O$: Co, 11.05; C, 45.04; N, 34.14; H, 3.75%.

By treating the complex with 5% $HClO_4$, 3 N H_2SO_4, 3 N HNO_3, and 3 N HCl, the salts of each the respective acid were obtained. Found: Co, 10.71; C, 43.28; N, 25.18; H, 3.05%. Calcd for $[Co(N_3)_2dip_2]ClO_4$ (anhydrous): Co, 10.62; C, 43.30; N, 25.25; H, 2.91%.

Found: Co, 11.02; C, 43.76; N, 25.40; H, 3.97%. Calcd for $[Co(N_3)_2dip_2]_2SO_4\cdot 5H_2O$: Co, 10.93; C, 43.80; N, 25.54; H, 3.86%.

Found: Co, 10.71; C, 43.34; N, 27.95; H, 3.80%. Calcd for $[Co(N_3)_2dip_2]NO_3\cdot 2H_2O$: Co, 10.65; C, 43.41; N, 27.84; H, 3.62%.

Found: Co, 11.20; C, 45.49; N, 26.63; H, 3.99%. Calcd for $[Co(N_3)_2dip_2]Cl\cdot 2H_2O$: Co, 11.19; C, 45.60; N, 26.59; H, 3.80%.

Preparation of $Na[Co(S_2O_3)_2dip_2]\cdot 7H_2O$. Two grams of *trans*-$[CoCl_2dip_2]Cl$, suspended in 30 m*l* of water, were mixed with 20 m*l* of a water solution containing 2.1 g of $Na_2S_2O_3\cdot 5H_2O$. The mixture was then heated on a water bath at 55°C for ten minutes. The solution assumed a brown color. When the solution was then allowed to stand under ice cooling, bright brown crystals separated from the solution, they were filtered and washed with cold 80% ethanol and ether. More crystals were obtained by the drop-by-drop addition of cold absolute ethanol to the mother liquor. The complex solution tends to decompose slowly, even at room temperature, evolving hydrogen sulfide. The complex is very soluble in water, but less soluble in ethanol. Found: Co, 7.99; C, 32.13; N, 7.60; H, 4.21%. Calcd for $Na[Co(S_2O_3)_2dip_2]\cdot 7H_2O$: Co, 7.91; C, 32.23; N, 7.52; H, 4.03%.

Preparation of $[Co(CN)_2dip_2]NO_3\cdot 7H_2O$. Fifteen grams of *trans*-$[CoCl_2dip_2]NO_3$(anhydrous), suspended in 500 m*l* of distilled water, were mixed with 10 g of AgCN, and the mixture was heated on a water bath (80°C) for three hours. The color of the solution changed from green to yellow. The solution was filtered, and the residue containing AgCl was repeatedly extracted with hot water. Then, the filtrate and the extracted solution were joined and concentrated into one-third in the former volume by evaporation. When the solution was then allowed to stand, lustrous, needle-shaped yellow crystals deposited from the solution; they were filtered and washed with cold water, ethanol, and ether. The crude product was recrystallized from hot water. Found: Co, 9.58; C, 43.15; N, 15.97; H, 5.03%. Calcd for $[Co(CN)_2dip_2]NO_3\cdot 7H_2O$: Co, 9.64; C, 43.22; N, 16.04; H, 4.95%. Before elementary analysis, the complex was dried overnight at room temperature in a vacuum desiccator on silica gel. In a preliminary report,[6] however, the elementary analysis was carried out on a sample of the complex which had been dried out *in vacuo* for three hours at 110°C, because the complex lost part of its crystallization water in the vacuum desiccator on concentrated sulfuric acid. The anhydrous complex is hygroscopic.

The corresponding sulfate of the complex was obtained by treating *trans*-$[CoCl_2dip_2]_2SO_4$ (anhydrous) with an excess of AgCN at 80°C. Found: Co, 10.12; C, 45.54; N, 14.45; H, 5.01%. Calcd for $[Co(CN)_2dip_2]_2SO_4\cdot 12H_2O$: Co, 10.17; C, 45.60; N, 14.50; H, 4.88%.

The attempt to react the dithiosulfato complex, $Na[Co(S_2O_3)_2dip_2]\cdot 7H_2O$, with KCN has failed due to the disruption of the complex. Hence, the analogous method of synthesis for *cis*-$[Co(CN)_2en_2]Cl$[7] is not suitable for obtaining the dicyanobis(2,2'-dipyridyl)-cobalt(III) complex.

Preparation of $[Co(gly)dip_2]Cl_2$.*1 To a water solution (100 m*l*) containing 9.56 g of *trans*-$[CoCl_2dip_2]$-Cl (anhydrous) **1.6** g of glycine were added, and the mixture was heated on a water bath (80°C) for three hours. When the reaction was over, the solution was further concentrated *in vacuo* with a rotatory evaporator

5) Independent of this work, another method of preparation has already appeared in R. G. Pearson, R. E. Meeker and F. Basolo, *J. Inorg. Nucl. Chem.*, **1**, 341 (1955).

6) N. Maki, T. Hamazaki and S. Sakuraba, This Bulletin, **41**, 1735 (1968).

7) P. R. Rây and B. Sarma, *J. Indian Chem. Soc.*, **28**, 59 (1951).

*1 gly=a glycinato ligand, $NH_2CH_2COO^-$

below 50°C. Into the deep-violet viscous liquid thus obtained there were then stirred, in small portions, 50 ml of ethanol containing 30% ether. Violet or almost black powders were thus obtained; they were stocked in the vacuum desiccator over concentrated sulfuric acid. The purifications were carried out in the usual manner, *i. e.*, by the addition of ethanol and ether to a water solution of the complex, since the solubility of the complex in water is quite large. The complex is hygroscopic. The absorption spectrum in the visible and ultraviolet regions agrees with that obtained by Murakami *et al.*[8] Found: Co, 11.31; C, 51.09; N, 13.37; H, 3.80%. Calcd for $[Co(gly)dip_2]Cl_2$: Co, 11.42; C, 51.18; N, 13.57; H, 3.90%.

The carbonato complexes, $[Co(CO_3)dip_2]Cl\cdot 3H_2O$ and $[Co(CO_3)dip_2]NO_3\cdot 5H_2O$, were prepared according to the directions of Jaeger and van Dijk.[9] Found: Co, 11.03; C, 48.51; N, 10.70; H, 4.09%. Calcd for $[Co(CO_3)dip_2]Cl\cdot 3H_2O$: Co, 11.32; C, 48.43; N, 10.76; H, 4.26%.

Found: Co, 10.04; C, 43.11; N, 11.93; H, 4.58%. Calcd for $[Co(CO_3)dip_2]NO_3\cdot 5H_2O$: Co, 10.10; C, 43.24; N, 12.01; H, 4.49%.

The 2,2'-dipyridyl reagent used was synthesized according to the method of Badger and Sasse.[10] Namely, the pyridines undergo condensation in the presence of Raney nickel to yield 2,2'-dipyridyl. As a by-product, 2,2',2''-terpyridyl (black powder) was obtained. The crude dipyridyl was purified by sublimations.

Preparation of $[Co(NO_2)_2phen_2]Cl\cdot 4H_2O$. Analogously to the case of the dipyridyl complex, a solution (100 ml) of *trans*-$[CoCl_2phen_2]Cl\cdot 4H_2O$ (5.98 g) was treated with 1.8 g of KNO_2 at 80°C for half an hour. The product was recrystallized from hot water containing acetic acid. Found: Co, 9.42; C, 46.83; N, 13.55; H, 4.02%. Calcd for $[Co(NO_2)_2phen_2]Cl\cdot 4H_2O$: Co, 9.52; C, 46.58; N, 13.58; H, 3.91%.

Preparation of $[Co(CO_3)phen_2]Cl\cdot 5H_2O$. A solution (150 ml) of *trans*-$[CoCl_2phen_2]Cl\cdot 4H_2O$ (5.98 g) was treated with 1.4 g of K_2CO_3 at 80°C for fifteen minutes. Orange-red crystals were thus obtained.[11] Found: Co, 9.80; C, 50.00; N, 9.29; H, 4.42%. Calcd for $[Co(CO_3)phen_2]Cl\cdot 5H_2O$: Co, 9.74; C, 49.64; N, 9.26; H, 4.33%.

Preparation of $K[Co(SO_3)_2phen_2]\cdot 5H_2O$. By treating *trans*-$[CoCl_2phen_2]Cl\cdot 4H_2O$ (5.98 g) with 3.2 g of K_2SO_3 in 100 ml of water at 60°C, lustrous brown crystals were obtained. The product was purified by recrystallization from hot water below 60°C. Found: Co, 8.40; C, 40.81; N, 8.01; H, 3.87%. Calcd for $K[Co(SO_3)_2phen_2]\cdot 5H_2O$: Co, 8.32; C, 40.68; N, 7.91; H, 3.70%.

Preparation of $[Co(CN)_2phen_2]NO_3\cdot 6H_2O$. Analogously to the case of the dicyano-bis(2,2'-dipyridyl) cobalt(III) complex, 20 g of *trans*-$[CoCl_2phen_2]NO_3$ were treated with 15 g of AgCN in 500 ml of distilled water at 70—80°C for three hours. The suspension was filtered, and the filtrate was concentrated by evaporation. When the solution was then allowed to stand, silky yellow crystals deposited on the wall of the beaker. The complex was stored in the vacuum desiccator over silica gel.[12] Found: Co, 9.11; C, 48.39; N, 15.17; H, 4.67%. Calcd for $[Co(CN)_2phen_2]NO_3\cdot 6H_2O$: Co, 9.19; C, 48.68; N, 15.29; H, 4.40%.

The chloride of the complex was obtained by treating the nitrate with a solution of KCl, because the chloride of the complex is less soluble in water than the nitrate. Found: Co, 10.08; C, 54.07; N, 14.66; H, 4.52%. Calcd for $[Co(CN)_2phen_2]Cl\cdot 4H_2O$: Co, 10.18; C, 53.95; N, 14.52; H, 4.18%.

Preparation of $[Co(bathophen)_3]Cl_3$ (anhydrous). To a suspension (50 ml) of $[CoCl(NH_3)_5]Cl_2$[13] (0.25 g) there were added 1.1 g of bathophenanthroline,*2 and the mixture was heated on a water bath (80—85°C) for an hour. The starting complex dissolved slowly in solution and reacted, evolving ammonia, to yield the tris(bathophenanthroline)cobalt(III) complex. The product was purified by recrystallizations in ethanol, since the complex is more soluble in ethanol than in water. The complex was dried out *in vacuo* on concentrated sulfuric acid before the elementary analyses. Found: Co, 4.95; C, 74.48; N, 7.03; H, 4.33%. Calcd for $[Co(bathophen)_3]Cl_3$: Co, 5.07; C, 74.39; N, 7.23; H, 4.16%.

Preparation of $[Co\ trip_2]Cl_3\cdot 7H_2O$. Quite analogously to the previous case, the bis(2,2',2''-terpyridyl)cobalt(III) chloride was prepared directly from the pentamminecobalt(III) complex. Namely, the suspension (80 ml) of $[CoCl(NH_3)_5]Cl_2$ (0.54 g) in a 50% ethanol-water solution was refluxed for ten hours with 1.05 g of terpyridyl in a flask equipped with a reflux condenser. Lustrous brown crystals separated from the solution when the reaction was over. Found: Co, 7.83; C, 47.44; N, 10.96; H, 4.91%. Calcd for $[Co\ trip_2]Cl_3\cdot 7H_2O$: Co, 7.78; C, 47.54; N, 11.09; H, 4.79%. The absorption spectrum agreed with that of the complex obtained by the method of Morgan and Burstall.[14]

Preparation of $[Co(N_3)_2phen_2]N_3$. A water solution (100 ml) containing 5.98 g of *trans*-$[CoCl_2phen_2]Cl\cdot 4H_2O$ was treated with 1.9 g of NaN_3 dissolved in 50 ml of water at 70°C for half an hour. The product was recrystallized from ethanol and dried out *in vacuo* on $CaCl_2$. Found: Co, 10.92; C, 52.84; N, 33.42; H, 3.05%. Calcd for $[Co(N_3)_2phen_2]N_3$: Co, 10.81; C, 52.85; N, 33.39; H, 2.96%. The complex is more soluble in ethanol than in water.

Preparation of $Na[Co(S_2O_3)_2phen_2]$ (anhydrous). A water solution (100 ml) of 5.98 g of *trans*-$[CoCl_2$-

8) M. Murakami, S. Senoh, N. Matsusato, H. Itatani and J.-W. Kang, *Nippon Kagaku Zasshi (J. Chem. Soc. Japan, Pure Chem. Sect.)*, **83**, 823 (1962).

9) F. M. Jaeger and J. A. van Dijik, *Proc. Acad. Amsterdam*, **39**, 164 (1936).

10) G. M. Badger and W. H. Sasse, *J. Chem. Soc.*, **1956**, 616 (1956).

11) The description of this compound is found in the following report: A. V. Ablov and S. M. Palade, *Z. neorg. Chem.*, **6**, 601 (1961).

12) The elementary analyses reported promptly in the preliminary communication (see Ref. 6) were carried out on a sample of the anhydrous compound which had been dried out in a vacuum drying chamber at 110°C for three hours, because the crystallization water was partly lost *in vacuo* on concentrated sulfuric acid.

13) W. A. Hynes and L. K. Yanaoski, *J. Am. Chem. Soc.*, **30**, 3053 (1938).

*2 bathophen=4,7-diphenyl-1,10-phenanthroline

14) G. Morgan and F. H. Burstall, *J. Chem. Soc.*, **1937**, 1649.

$phen_2]Cl\cdot 4H_2O$ was treated with 5.0 g of $Na_2S_2O_3\cdot 5H_2O$ at room temperature. The mixture turned dark brown. To this solution there were added drop by drop under ice cooling 100 m*l* of a mixture of ethanol and ether. The brown powder which separated from the solution was filtered and washed with ethanol and ether. The product was purified in the same manner. Found: Co, 8.92; C, 43.38; N, 8.57; H, 2.61%. Calcd for $Na[Co(S_2O_3)_2phen_2]$: Co, 8.84; C, 43.24; N, 8.41; H, 2.42%. The complex is unstable in solution and tends to decompose in itself, evolving hydrogen sulfide, thus producing the metallic cobalt.

Preparation of $[Co(bathophen)_3]Cl_2\cdot 8H_2O$. The water solution (30 m*l*) of 0.13 g of hexaquocobalt(II) chloride was treated with 1.0 g of bathophenanthroline at 80°C for five minutes. On cooling, brown crystals were obtained. Found: Co, 4.58; C, 67.95; N, 6.58; H, 5.24%. Calcd for $[Co(bathophen)_3]Cl_2\cdot 8H_2O$: Co, 4.64; C, 68.03; N, 6.61; H, 5.08%. The complex is more soluble in ethanol than in water.

Preparation of $[Co\,dip_3]Cl_2\cdot 3H_2O$. To a 30% methanol-water solution (100 m*l*) in which 5 g of $[CoCl(NH_3)_5]Cl_2$ had been suspended, 9.4 g of 2,2'-dipyridyl were added; the mixture was then refluxed on a water bath for eight hours. The crude product was recrystallized from hot water containing acetic acid. Found: Co, 8.52; C, 52.43; N, 12.41; H, 4.51%. Calcd for $[Co\,dip_3]Cl_3\cdot 3H_2O$: Co, 8.59; C, 52.38; N, 12.22; H, 4.40%.

Preparation of $[Co\,phen_3]Cl_3\cdot 7H_2O$. A suspension (130 m*l*) of a 30% methanol-water solution containing 5 g of $[CoCl(NH_3)_5]Cl_2$ and 12.1 g of 1,10-phenanthroline was refluxed on a water bath for ten hours. Dark brown crystals were thus obtained. Found: Co, 6.97; C, 51.98; N, 9.98; H, 4.80%. Calcd for $[Co\,phen_3]Cl_3\cdot 7H_2O$: Co, 7.08; C, 51.97; N, 10.10; H, 4.60%.

Preparation of $[Co(SCN)_2phen_2]NCS$ (anhydrous). To a hot water solution (50 m*l*) containing 1.2 g of *trans*-$[CoCl_2phen_2]Cl\cdot 4H_2O$ there were added 1.1 g of KNCS dissolved in 50 m*l* of water, and the mixture was heated on a water bath for an hour. Dark brown precipitates separated from the solution, they were filtered and washed with water several times, and then with ethanol and ether. Found: Co, 9.79; C, 54.80; N, 16.72; H, 2.86%. Calcd for $[Co(SCN)_2phen_2]$-NCS: Co, 9.93; C, 54.63; N, 16.52; H, 2.72%. The complex is insoluble in both water and alcohol, but soluble in dimethyl sulfoxide.

Measurement. The absorption spectra in the visible and ultraviolet regions were determined manually with a Beckmann DU spectrophotometer. The IR spectra were recorded on a Perkin-Elmer grating infrared spectrophotometer, Model 337, equipped with a KBr-pellet.

Results and Discussion

Figure 1 shows the absorption spectra of the cobalt(III) complexes of the $[Co^{III}X_2dip_2]$-type measured in the aqueous phase except that of the thiocyanato complex. The first spin-allowed band, which is assigned to a d–d transition, shifts towards a shorter wavelength according to this order of the ligands: $S_2O_3^{2-}$, SCN^-, N_3^-, CO_3^{2-}, gly$^-$, dip, NO_2^-, CN^-. This order of the ligands agrees with that of the spectrochemical series[15] except for the SCN^- ligand. The absorption intensity of the first band for the $[Co(SCN)_2dip_2]^+$ ion is seen to be abnormally larger than those of the corresponding 2,2'-dipyridyl cobalt(III) complexes of the nitrogen-hexacoordinated $[Co\,N_6]$-type. This fact may be explained as being due to the hyperchromic effect of the sulfur-bonded ligand, SCN^-. As far as the cobalt(III) complexes are concerned, the rhodanato-ligand has been well known to be

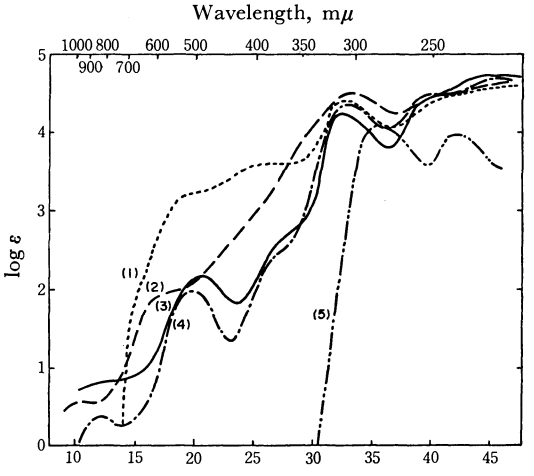

Fig. 1. The absorption spectra of the bis(2,2'-dipyridyl)cobalt(III) complexes of the $[CoX_2\,dip_2]$-type: (1) ---- $[Co(SCN)_2dip_2]ClO_4\cdot 2H_2O$ in methanol; (2) —— $Na[Co(S_2O_3)_2dip_2]\cdot 7H_2O$ in methanol; (3) —— $[Co(gly)dip_2]Cl_2$; (4) ——— $[Co(CO_3)dip_2]Cl\cdot 3H_2O$; (5) —·— 2,2'-dipyridyl in ethanol.

bound to the central cobalt(III) ion by the nitrogen atom; indeed, the isothiocyanatocobalt(III) complexes are more familiar than the thiocyanato complexes, in which the SCN^- ligand is bound by the sulfur atom.

Several years ago, however, the pentacyanocobaltate(III) complex, $K_3[Co(CN)_5SCN]$, was described as belonging to the group of thiocyanato complexes.[16] Recently, Stotz *et al.*[17] have reported the synthesis of an isothiocyanato complex, $K_3[Co(CN)_5NCS]$ (a linkage-isomer).

The dithiocyanato-bis(2,2'-dipyridyl) and bis(1,10-phenanthroline)cobalt(III) complexes, $[Co(SCN)_2dip_2]ClO_4\cdot 2H_2O$ and $[Co(SCN)_2phen_2]$-NCS, prepared here have also been ascertained to

15) Y. Shimura and R. Tsuchida, This Bulletin, **29**, 311 (1956).
16) N. Maki, J. Fujita and R. Tsuchida, *Nature*, **183**, 458 (1959).
17) I. Stotz, W. K. Wilmarth and A. Haim, *Inorg. Chem.*, **7**, 1250 (1968).

TABLE 1. THE ABSORPTION MAXIMA OF THE COBALT(III) COMPLEXES WITH 2,2'-DIPYRIDYL AND 1,10-PHENANTHROLINE

Compound	I-band	II-band	III-band	IV-band	V-band
$Na[Co(S_2O_3)_2dip_2]\cdot 7H_2O$	*ca.* 18(1.98)*	*ca.* 23(2.50)*	33.0(4.49)	40.0(4.48)	
$[Co(SCN)_2dip_2]ClO_4\cdot 2H_2O$	*ca.* 19(3.18)*	26.3(3.60)	32.8(4.40)	——*	
$[Co(N_3)_2dip_2]N_3\cdot 2H_2O$	19.4(2.60)	*ca.* 30(3.99)*	33.1(4.43)	*ca.* 41(4.37)	47.2(4.74)
$[Co(CO_3)dip_2]Cl\cdot 3H_2O$	20.0(2.01)	*ca.* 27(2.5)*	32.8(4.35)	40.5(4.80)	
$[Co(gly)dip_2]Cl_2$	20.8(2.18)	*ca.* 28(2.6)*	32.2(4.24)	45.0(4.75)	
$[Co\ dip_3]Cl_3\cdot 3H_2O$	22.1(1.82)	*ca.* 29(3.14)*	32.6(4.48)	*ca.* 41(4.80)	
$[Co(NO_2)_2dip_2]Cl\cdot 5H_2O$	22.3(2.30)	*ca.* 29(3.9)*	33.0(4.68)	40.7(4.84)	
$[Co(CN)_2dip_2]NO_3\cdot 7H_2O$	*ca.* 24(2.02)*	*ca.* 27(2.34)*	31.8(4.32)	32.9(4.34)	41.0(4.34)
$Na[Co(S_2O_3)_2phen_2]$	*ca.* 18(2.16)*	*ca.* 28(4.0)*	——*	36.3(4.77)	43.3(4.82)
$[Co(SCN)_2phen_2]NCS$	*ca.* 19(2.98)*	*ca.* 26(3.42)*	*ca.* 29(3.55)*	*ca.* 32(4.08)	*ca.* 34(4.24)
$[Co(N_3)_2phen_2]N_3$	18.9(2.43)	*ca.* 28(3.80)*	——*	36.3(4.48)	——**
$K[Co(SO_3)_2phen_2]\cdot 5H_2O$	*ca.* 19(2.26)*	*ca.* 28(3.67)*	——*	36.3(4.49)	45.7(4.71)
$[Co(CO_3)phen_2]Cl\cdot 5H_2O$	19.6(2.04)	*ca.* 26.7(2.40)*	*ca.* 29(3.2)*	36.3(4.67)	——**
$[Co\ phen_3]Cl_3\cdot 7H_2O$	*ca.* 21.5(2.0)*	27.9(3.54)		36.3(4.90)	44.7(5.16)
$[Co(NO_2)_2phen_2]Cl\cdot 4H_2O$	*ca.* 23(2.60)*	*ca.* 29(3.35)*	*ca.* 32(3.90)*	36.3(4.58)	*ca.* 40(4.8)
$[Co(CN)_2phen_2]NO_3\cdot 6H_2O$	*ca.* 24(2.14)*	*ca.* 27(2.56)*	28.7(3.30)	*ca.* 31(3.49)*	*ca.* 34(4.22)* 36.8(4.77)
$[Co\ trip_2]Cl_3\cdot 7H_2O$	22.5(2.53)	28.1(4.04)	29.3(4.18)	35.7(4.48)	47.0(4.76)
$[Co(bathophen)_3]Cl_3$	*ca.* 23(2.3)*	*ca.* 25.8(3.3)*	*ca.* 29(4.25)*	35.2(5.21)	46.7(5.06)
2,2'-dipyridyl				35.5(4.08)	42.3(3.96)
1,10-phenanthroline		31.0(2.81)	38.0(4.51)	43.3(4.82)	44.3(4.68)
2,2',2''-terpyridyl			35.5(4.30)	43.0(4.32)	
bathophenanthroline			*ca.* 32(4.14)	36.1(4.61)	45.4(4.60)

* Shoulder band; ** Broad band; Unit=Wave number 10^3/cm ($\log \varepsilon$)

be bound by the sulfur atom on the evidence of the absorption spectra in the far-infrared regions.

Table 1 shows the numerical data of the absorption maxima and intensities ($\log \varepsilon$) of the cobalt(III) complexes with 2,2'-dipyridyl and 1,10-phenanthroline.

Table 2 summarizes the frequencies of the C–N and C–S stretching-vibrations for the rhodanato-cobalt(III) complexes. The values of the stretching-vibration, C–S, for the 2,2'-dipyridyl and 1,10-phenanthroline complexes fall within the range, 690—720 cm^{-1}, characteristic of sulfur-bonded thiocyanato-complexes, while the values for the usual isothiocyanato-ammine and amine complexes come within the range, 780—860 cm^{-1}, characteristic of nitrogen-bonded isothiocyanato-complexes.[18]

TABLE 2. THE FREQUENCIES OF THE C–N AND C–S STRETCHING VIBRATIONS FOR THE THIOCYANATO- AND ISOTHIOCYANATO-COBALT(III) COMPLEXES IN A SOLID STATE

Compound	C–N	C–S
$[Co(SCN)_2dip_2]ClO_4\cdot 2H_2O$	2080_s	705_w
$[Co(SCN)_2dip_2]Cl\cdot 3H_2O$	2075_s	704_w
$[Co(SCN)_2dip_2]NCS\cdot 5/2H_2O$	2070_s	705_w
$K_3[Co(SCN)(CN)_5]$	2110_s	719_w
$[Co(SCN)_2phen_2]NCS$	2060_s	695_w
cis-$[Co(NCS)_2en_2]Cl\cdot H_2O$	2110_m 2060_s	803_w 788_m
trans-$[Co(NCS)_2en_2]Cl\cdot H_2O$	2120_s 2080_w	788_m
$[Co(NCS)(NH_3)_5]Cl_2$	2140_s	850_m 808_m
$[Co(NCS)(NH_3)_5]SO_4\cdot 2H_2O$	2140_s	848_m 803_m

s=strong; m=medium; w=weak

The linkage-isomers of the rhodanato-complexes can be distinctly distinguished from each other on the evidence of their polarographic behavior in solution. The isothiocyanato-complexes, such as *trans*-$[Co(NCS)_2en_2]Cl\cdot H_2O$ and $[Co(NCS)(NH_3)_5]Cl_2$, exhibit the strong adsorption on the surface of the dropping mercury electrode (DME) which was pointed out by Tanaka *et al.*[19] as being due to interaction between the naked sulfur and the mercury of the electrode, while the thiocyanato complexes, which have no naked sulfur on the outside of the coordination sphere, show no adsorption at the DME. The adsorptions of *trans*-$[Co(NCS)_2en_2]^+$ and $[Co(NCS)(NH_3)_5]^{2+}$ ions were observed to exist at the range +0.2——0.5 V *vs.* SCE on the electrocapillary curves and on the current-time curves. No adsorptions were observed for the $[Co(SCN)_2dip_2]^+$ ion on the

18) A. Turco and C. Pecile, *Nature*, **191**, 66 (1961).
19) N. Tanaka, E. Kyuno, G. Sato and R. Tamamushi, *J. Phys. Chem.*, **66**, 2706 (1962); N. Tanaka, T. Ito and R. Tamamushi, This Bulletin, **37**, 1430 (1964).

DME in the 80% methanol-water solution containing 1 M lithium chloride.

The 2,2'-dipyridyl and 1,10-phenanthroline are considered to have a strong π-bonding character as ligands in the sphere of coordination; *i. e.*, these are considered to have the nature of the "back coordination." In such mixed ligand cobalt(III) complexes, the rhodanate ion is interpreted as having a tendency to coordinate to the cobalt(III) ion by means of the sulfur atom rather than by means of the nitrogen atom, since the six coordinate bonds also tend, in general, to resemble each other in the nature of bonding as far as possible within the same coordination sphere.

Figure 2 shows the absorption spectrum of the bis(2,2',2''-terpyridyl)cobalt(III) complex, [Co-trip$_2$]Cl$_3$·7H$_2$O, in comparison with that of [Co-dip$_3$]Cl$_3$·3H$_2$O.[20] The first absorption band is located at a shorter wavelength than that of the corresponding tris(2,2'-dipyridyl)cobalt(III) ion.

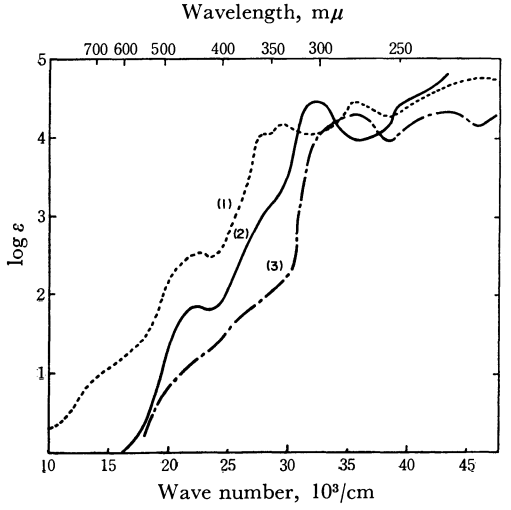

Fig. 2. The absorption spectra of the bis(2,2',2''-terpyridyl)cobalt(III) complex and of its ligand only: (1) ---- [Co trip$_2$]Cl$_3$·7H$_2$O; (2) —— [Co dip$_3$]Cl$_3$·3H$_2$O; (3) —·— 2,2',2''-terpyridyl in ethanol.

Figure 3 shows the absorption spectra of the tris(bathophenanthroline)cobalt(III) complex and of its ligand only.

The first d-d band for the d^6-complexes of the [Co N$_6$]-type shifts to a shorter wavelength according to this order of the ligands: phen, dip, trip, bathophen.

Figure 4 shows the absorption spectra of the bis-(1,10-phenanthroline)cobalt(III) complexes of the [CoX$_2$ phen$_2$]-type. The first band shifts towards a shorter wavelength in this order of the ligands: $S_2O_3^{2-}$, N_3^-, SO_3^{2-}, CO_3^{2-}, phen, NO_2^-, CN^-.

Figure 5 shows the absorption spectra of the dinitro-bis(2,2'-dipyridyl) and bis(1,10-phenanthroline)cobalt(III) complexes in relation to the *cis*- and *trans*-bis(ethylenediamine)cobalt(III) complexes. The d-d bands shift to a shorter wavelength according to this order of the ligands: phen, dip, en.

Figure 6 shows the absorption spectra of the dicyano-bis(2,2'-dipyridyl) and bis(1,10-phenanthroline)cobalt(III) complexes and their respective

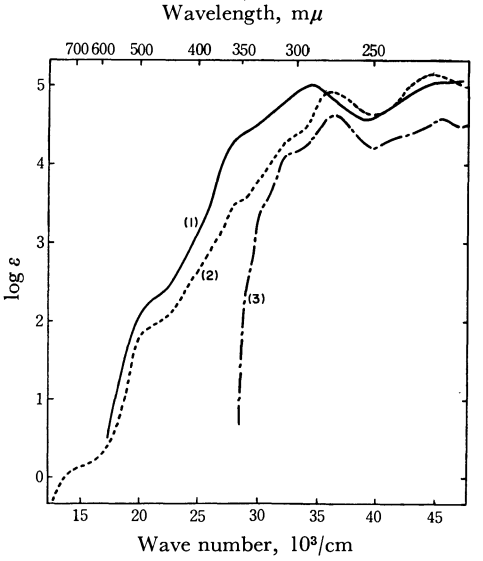

Fig. 3. The absorption spectra of tris(bathophenanthroline) and tris(1,10-phenanthroline)cobalt(III) complexes: (1) —— [Co(bathophen)$_3$]Cl$_3$ in ethanol; (2) ---- [Co dip$_3$]Cl$_3$·3H$_2$O; (3) —·— bathophenanthroline in ethanol.

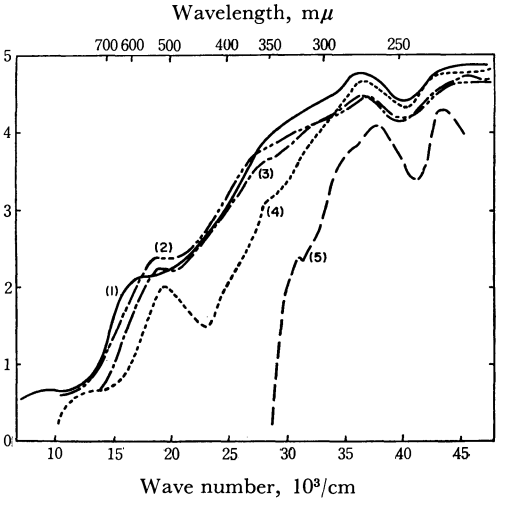

Fig. 4. The absorption spectra of the bis(1,10-phenanthroline)cobalt(III) complexes of the [CoX$_2$ phen$_2$]-type: (1) —— K[Co(S$_2$O$_3$)$_2$phen$_2$] in methanol; (2) —·— [Co(N$_3$)$_2$phen$_2$]N$_3$ in methanol; (3) —·— K[Co(SO$_3$)$_2$phen$_2$]·5H$_2$O in water; (4) ---- [Co(CO$_3$)phen$_2$]Cl·5H$_2$O in water; (5) - - - 1,10-phenanthroline in ethanol.

20) K. Yamasaki, This Bulletin, **12**, 390 (1937).

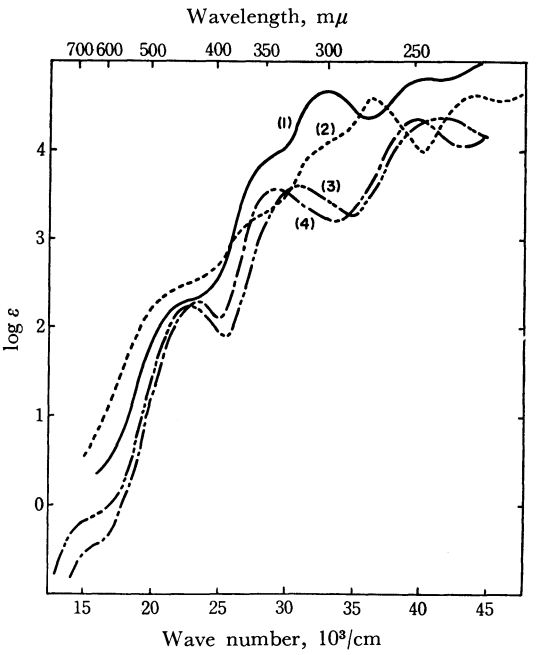

Fig. 5. The absorption spectra of the dinitrocobalt(III) complexes obtained in water: (1) —— $[Co(NO_2)_2dip_2]Cl \cdot 5H_2O$; (2) - - - $[Co(NO_2)_2phen_2]Cl \cdot 4H_2O$; (3) —·— *trans*-$[Co(NO_2)_2en_2]ClO_4$; (4) —— *cis*-$[Co(NO_2)_2en_2]ClO_4$.

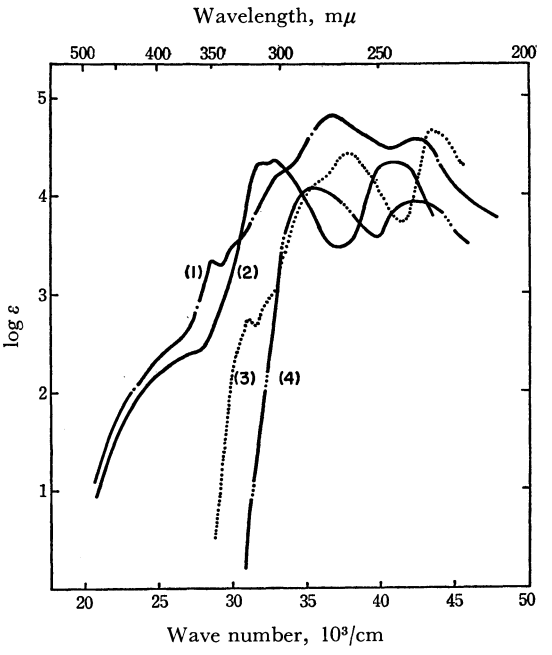

Fig. 6. The absorption spectra of the dicyanocobalt(III) complexes with 2,2'-dipyridyl and 1,10-phenanthroline: (1) —·— *cis*-$[Co(CN)_2phen_2]NO_3 \cdot 6H_2O$; (2) —— *cis*-$[Co(CN)_2dip_2]NO_3 \cdot 7H_2O$; (3) ····· 1,10-phenanthroline in ethanol; (4) —···— 2,2'-dipyridyl in ethanol.

ligands only. The spectrum of the latter agrees with that reported by Favini *et al.*[21] as a whole, but it does not necessarily coincide in detail, especially in the matter of a small peak present at around 27—29 kK.*3

21) G. Favini and E. Paglia, *J. Inorg. Nucl. Chem.*, **8**, 155 (1958); G. Favini and E. Paglia, Proceedings of the 4th I. C. C. C., Rome (1957), ed. by L. Cambi, Pergamon Press, New York, N. Y. p. 155.

*3 No description of the preparation of $[Co(CN)_2phen_2]OH \cdot 7H_2O$ has been found, but the complex might have been prepared by treating the praseo-salt with KCN in solution.

The author is indebted to Mr. Taihei Hamazaki for his experimental assistance of preparing the dicyano cobalt(III) complexes. The author also wishes to express his appreciation to the late Professor Ryutaro Tsuchida and Professor Shukichi Sakuraba for their encouragements and discussions throughout this work.

BULLETIN OF THE CHEMICAL SOCIETY OF JAPAN VOL. 42 2282—2286 (1969)

Spectrophotometric Determination of L-Ascorbic Acid*[1]

Yoshiro OGATA and Yoshio KOSUGI

Department of Applied Chemistry, Faculty of Engineering, Nagoya University, Chikusa-ku, Nagoya

(Received January 16, 1969)

A novel quantitative determination of L-ascorbic acid by UV spectrophotometry in a HCl-KCl buffer has been developed. Ascorbic acid (λ_{max} 244 mμ) of over 2×10^{-5} M can quantitatively be determined by this method. Several oxidizing, reducing, acidic or basic reagents and other organic compounds which may be present together with ascorbic acid in ordinary drugs and drinks do not interfere the determination.

A considerable amount of L-ascorbic acid (Vitamin C) is now consumed as medicine and also as an antioxidant and additive in drinks and foods. A number of estimations of ascorbic acid assay have been developed, *i. e.*, visual titration,[1] spectrophotometry (or colorimetry),[1] polarography,[2] gas chromatography,[3] gravimetry,[4] bioassay method,[5] *etc.* have been postulated. Among them, titration and spectrophotometry are prevailing. The color change of indicators such as Tillman's reagent (2,6-dichlorophenolindophenol), Folin's reagent (phosphomolybdate), methylene blue and iodine are often employed for titration and colorimetry. Although some modifications of these methods have been reported,[6] they have shortcomings; *i.e.*, they are difficult to carry out, when a sample is either colored or contaminated with acidic or reducing substances which may react with the indicators. Fujita *et al.*[7] used a metaphosphoric acid solution and Robertson[8] added KCN to the sample solution, and they determined ascorbic acid content by the estimation of difference of absorbances before and after disappearance of ascorbic acid by oxidase or cupric ion. Reducible substances, however, often react with other reducing agents as well as ascorbic acid. In view of a large absorbance of ascorbic acid in UV region, the spectrophotometry was examined in detial. The present paper is a summary of our data concerning the suitable conditions of this very simple procedure for the spectrophotometric analysis in the presence of a number of additives.

Ascorbic acid (H_2A) is unstable in aqueous solutions, especially in the presence of heavy meta ions such as cupric and ferric ions. Though the rate of autoxidation to dehydroascorbic acid (DA) decreases in less polar organic solvents,[9] the solubility of the acid is generally small in these solvents, but the common organic compounds are very often soluble and their UV absorption bands overlap that of ascorbic acid.

The authors have previously studied kinetics of the copper-salt catalyzed autoxidation of ascorbic acid (H_2A) to dehydroascorbic acid (DA).[10]

$$H_2A + \tfrac{1}{2}O_2 \rightarrow DA + H_2O \qquad (1)$$

According to our mechanism,[10] ascorbic acid should be more stable in more acidic media. However, the cuprous ion formed by the reaction of cupric ion with ascorbic acid may easily be oxidized in acidic media to cupric ion (Eq. (2)), a catalyst for the autoxidation.

$$Cu(I) + \tfrac{1}{4}O_2 + H^+ \rightarrow Cu(II) + \tfrac{1}{2}H_2O \qquad (2)$$

It is known[11] that halide ion, *e. g.*, chloride ion, retards reaction (2) and also inhibits the formation of complex of ascorbic acid and cupric ion. These mechanisms suggest that hydrochloric acid free of metal ion is effective to prevent autoxidation. Even a trace of cupric ion, *e. g.*, 1.5×10^{-9} M,

*1 Contribution No. 120.

1) The Association of Vitamin Chemists, Inc. Ed., "Method of Vitamin Assay," 2nd ed., Interscience Publishers, Inc., New York (1951), Chap. 4, p. 71.

2) H. Woggon, *Ernährungsforschung*, **4**, 35 (1959).

3) T. Uno and H. Okuda, *Yakugaku Zasshi (J. Pharm. Soc. Japan)*, **86**, 1148 (1966).

4) J. H. Roe and M. J. Oesterling, *J. Biol. Chem.*, **152**, 511 (1944).

5) M. E. Reid, "Estimation of the Vitamins, Biological Symposia XII," The Jacques Cattell Press, Lancaster, Pa. (1947), p. 373.

6) I. Onishi and T. Hara, This Bulletin, **37**, 1314 (1964); R. Charonnat and L. B. Beauquesne, *Ann. Pharm. France*, **16**, 96 (1958); M. Schmall, C. W. Pifer, E. G. Wollish, R. Duschinsky and H. Gainer, *Anal. Chem.*, **26**, 1521 (1954).

7) A. Fujita and T. Sakamoto, *Biochem. Z.*, **297**, 10 (1938).

8) E. B. Robertson, *J. Soc. Chem. Ind.*, **53**, 277 (1934).

9) Y. Ogata and Y. Kosugi, Solvent Effect on the Autoxidation of L-Ascorbic Acid, *Tetrahedron*, **25**, 1055 (1969).

10) Y. Ogata, Y. Kosugi and T. Morimoto, *ibid.*, **24**, 4057 (1968).

11) L. W. Mapson, *Biochem. J.*, **39**, 228 (1945).

however, acts as an effective catalyst[12] and the complete removal of these metallic ions are often difficult. Furthermore, the very low concentration of chloride ion accelerates the autoxidation,[11] but its high concentration retards the overall reaction. Thus, as a source of chloride ion a large amount of alkali chlorides besides HCl should be advantageous for the stabilization of ascorbic acid.

Experimental

Ultraviolet Spectroscopy. An automatic recording spectrophotometer (Type Simadzu SV-50A) equipped with quartz cells (light path of 10 mm) was used.

Materials. Ascorbic acid was of 99.5% pure with decomposition point of 190.9°C [lit. 190—192°C (dec.)[13]] and optical rotation of $[\alpha]_D^{25}$ +20.94° [lit. 20.5—21.5°[13]]. Dehydroascorbic acid was prepared from ascorbic acid by the method of Fujimura *et al.*,[14] and crystallized from acetic acid[15]: decomposition point 218—222°C (dec.) [lit. 196°C (dec.),[14] 225°C (dec.),[16] 237—240°C (dec.)[15]]. Potassium chloride and the following organic compounds were of commercial guaranteed reagent grade; saccharose, oxalic acid, nicotinamide, sodium cyclohexylsulfamate, D-fructose, DL-methionine. Hydrochloric, phosphoric, metaphosphoric acids and other organic compounds were of commercial extra pure grade and were used without further purification. Oxygen and nitrogen gases were of over 99.7% and 99.95% pure, respectively. Distilled water was used. Cupric and ferric chlorides were estimated by iodometry and chelation with EDTA, respectively.

Procedure. Sample solutions of given concentrations in stoppered volumetric flasks were kept standing at constant temperature (20°C) for a known period. There was no appreciable difference in the decreasing rate of ascorbic acid concentration between 2—3 day's storage of samples in a glass flask and that in a polyethylene bottle. After being kept for a certain period, ascorbic acid was diluted to *ca.* 5×10^{-5} M and the absorption curve ranging 238—255 mμ was drawn. The ascorbic acid concentrations in the dilute solutions were obtained by means of a calibration curve.

Titration with the Indophenol Method.[1] Samples were diluted to the concentration of *ca.* 10^{-1} M ascorbic acid and titrated with a 0.012% 2,6-dichlorophenolindophenol solution.

Results and Discussion

Absorption Spectrum and Molar Extinction Coefficient. Ultraviolet absorption peak (λ_{max}) of ascorbic acid varies with solvent, pH and temperature. The variation of λ_{max} may be caused by the change of the degree of solvation, ionization and/or association of ascorbic acid. The peak (λ_{max}) was 244 mμ in these acidic solutions in the present experiment. In a solution of 0.4 N HCl and 0.4 M KCl, the absorbance (E_{244}) at 244 mμ of various concentrations of ascorbic acid had the relation $E_{244}=10^4[H_2A]-0.035$ with the concentration ($[H_2A]$), at least, at 2×10^{-5}—9×10^{-5} M. Molar extinction coefficient (ε_{244} or ε_{max}) was found to be 10000.

Acidic Solutions. Acids can suppress the dissociation of ascorbic acid. The stability of ascorbic acid was examined under various conditions in a mixture of 0.4 N HCl and 0.4 M KCl, 0.1 N HCl, 0.4 N HCl, 0.1 N H_3PO_4 or *ca.* 2% metaphosphoric acid.

In all of these solutions, λ_{max} and ε_{max} were the same, *i. e.*, 244 mμ and 10000, respectively. Metaphosphoric acid may be advantageous in the presence of cupric chloride of *ca.* 15 ppm in a dilute solution. However, polymerization degree (n) of commercial metaphosphoric acid, $(HPO_3)_n$, and hence the degree of dissociation in solution is not measurable by means of the usual titration method. Further, the solution of metaphosphoric acid for UV measurements should be filtered to remove the turbidity and stored in a refrigerator to prevent depolymerization. Because of this troublesome treatment as well as instability of the solution (safe storage is within a week), metaphosphoric acid was less suitable as a stabilizer of ascorbic acid. A mixture of aqueous HCl and KCl (a modified Clark-Lubs buffer solution) was found to be the most advantageous solution. All experiments described below were carried out in this buffer solution of 0.4 N HCl and 0.4 M KCl.

Effects of Other Factors. Our kinetic study[10] shows that the rate of autoxidation of ascorbic acid decreased at high concentration of ascorbic acid and at lower partial pressure of oxygen. These facts imply that ascorbic acid is more stabilized at its high concentration and in the absence of oxygen. These effects are shown in Table 2 combined with the result in Table 1. Ascorbic acid is more stable in nitrogen than in air or oxygen, but the effect was too low to necessitate determination under nitrogen atmosphere, except for the presence of a large amount of metallic ion.

Ferric ion also catalyzes the autoxidation of ascorbic acid, but the examination of the effect of ferric chloride (Table 3) shows that ferric ion of the concentration below *ca.* 13 ppm in a dilute solution does not affect stabilization.

Absorption of Organic Compounds. For the application of this analytical method to drugs, drinks and foods, it is necessary to know the possibility of the overlap of the absorption band with those of organic compounds which may be present

12) L. W. Mapson, *ibid.*, **35**, 1332 (1941).
13) P. G. Stecher, "The Merck Index," 7th ed., Merck & Co., Inc., Rahway, N. J., U. S. A. (1960), p. 106.
14) K. Fujimura and A. Matsuda, *Memoirs Research Inst. Food Science, Kyoto Univ.*, No. 8 (1954), p. 17.
15) H. Staudinger and W. Weis, *Z. Physiol. Chem.*, **337**, 284 (1964).
16) P. G. Stecher, "The Merck Index," 7th ed., Merck & Co., Inc., Rahway, N. J., U. S. A. (1960), p. 323.

TABLE 1. STABILITY OF ASCORBIC ACID IN VARIOUS ACIDIC SOLUTIONS IN THE ABSENCE OR PRESENCE OF CUPRIC CHLORIDE AT 20°C

Solution	Added $CuCl_2$ (10^{-4} M)	Concentration of ascorbic acid (10^{-5} M)				
		Initial	1 hr	5 hr	1 day	2 day
0.4 N HCl	0	3000	2980	2940	2900	2620
0.4 M KCl		6.01	5.89	5.68	4.49	3.71
	2.3	3000	2940	2930	2500	2330
		6.01	5.84	4.22	2.16	—
0.1 N HCl	0	3040	2930	2890	2740	2550
		6.00	5.97	5.62	5.32	3.55
	2.3	3040	3000	2890	2590	2100
		6.00	4.83	1.22	0.22	—
0.4 N HCl	0	2990	2910	2910	2780	2550
		6.03	5.82	5.61	5.51	4.27
	2.3	2990	2920	2880	2610	2340
		6.03	5.90	3.06	0.48	—
0.1 N H_3PO_4	0	3000	3000	2870	2750	2510
		6.00	5.87	5.78	5.40	4.15
	2.3	3000	3000	2760	2550	1790
		6.00	5.93	5.67	5.21	4.92
ca. 2% $(HPO_3)_n$	0	2950	2920	2860	2770	2770
		5.83	5.80	5.75	5.46	5.19
	2.3	2950	2950	2910	2870	2770
		5.83	5.83	5.58	5.54	4.90
Water	0	3000	2920	2980	2850	2540
	2.3	3.00	2.82	2.80	2.60	2.33

TABLE 2. EFFECTS OF CONCENTRATION OF ASCORBIC ACID AND NITROGEN OR OXYGEN ON THE STABILITY IN A BUFFER SOLUTION OF 0.4 N HCl - 0.4 M KCl

Atmosphere	Added $CuCl_2$ (10^{-4} M)	Concentration of ascorbic acid (10^{-2} M)				
		Initial	1 hr	5 hr	1 day	2 day
Air	0	12.0	12.0	11.9	11.6	10.8
	2.3	12.0	12.0	11.7	10.7	—
N_2	0	3.00	2.96	2.95	2.94	2.74
	2.3	3.00	2.95	2.84	2.83	2.67
O_2	0	3.00	2.95	2.95	2.70	2.64
	2.3	3.00	2.87	2.74	2.60	2.21

TABLE 3. EFFECT OF FERRIC CHLORIDE ON THE STABILITY OF ASCORBIC ACID

Added $FeCl_3$ (10^{-4} M)	Concentration of ascorbic acid (10^{-2} M)				
	Initial	1 hr	5 hr	1 day	2 day
2.3	3.00	2.99	2.98	2.78	2.47
2300	3.00	1.76	1.69	1.49	1.13

together with ascorbic acid.

Results are shown in Table 4 as ε_{244}, ε_{max} and ε_{275}, where ε_{275} of ascorbic acid is only 400. Common vitamins are usually slightly soluble in the buffer solution and hence they are not examined. Extraction of ascorbic acid from solid samples with a small amount of the buffer solution can avoid contamination of such less soluble substances. If a sample is liquid, extraction with diethyl ether is recommended to remove vitamins A, D, E, *etc.*, and other many organic compounds.

A given amount of ascorbic acid was mixed with organic compounds whose ε's at suitable wavelengths were known (*e. g.*, see Table 4) and analyzed

TABLE 4. MOLAR EXTINCTION COEFFICIENTS AT λ_{244}, λ_{275} AND λ_{max} OF SOME ORGANIC COMPOUNDS IN A BUFFER OF 0.4 N HCl - 0.4 M KCl

Compound	ε_{244}	ε_{275}	λ_{max}	ε_{max}
Dehydroascorbic acid	9.4×10	1.1×10^2	302	1.3×10^2
Nicotinamide	2.05×10^3	8.3×10^2	261.5	5.6×10^3
Aspartic acid	0.1>	0.1>	—	—
Pantothenic acid	1.4×10	4.6	—	—
DL-Methionine	1.7×10	0.1>	—	—
Taurine	0.1>	0.1>	—	—
Glycine	0.1>	0.1>	—	—
Dextrose	0.1	0.1	—	—
D-Fructose	0.8	2.7	280.5	2.8
Saccharose	1.2	1.1	258	1.3
D-Sorbitol	0.6	0.7	264	0.1
Saccharin	1.8×10^3	7.5×10^2	278.5	7.7×10^2
Sodium cyclohexylsulfamate	3.1	0.1>	—	—
Citric acid	4.7	0.1>	—	—
DL-Malic acid	1.6×10	1.6	—	—
Tartaric acid	6.5	0.1>	—	—
Oxalic acid	3.7×10	1.1×10	244	3.7×10
Succinic acid	6.5	1.2	—	—
Tannic acid	2.5×10^3	6.9×10^3	275	6.9×10^3
Caffeine	2.8×10^3	7.5×10^3	269.5	8.0×10^3
Tartrazine	1.3×10^4	1.3×10^4	(Visible region)	

TABLE 5. MODELS OF APPLICATION

Sample	Composition	Concentration prepared (10^{-5} M)	$E_{244}^{calc.}$	$E_{244}^{obs.}$	$E_{275}^{calc.}$	$E_{275}^{obs.}$
A	ascorbic acid	6.435	0.608	—	0.026	—
	nicotinamide	5.70	0.117	—	0.045	—
	total absorption		0.725	0.730	0.071	0.073
B	ascorbic acid	4.52	0.417	—	0.018	—
	tannic acid	5.64	0.141	—	0.378	—
	caffeine	3.61	0.101	—	0.274	—
	total absorption		0.659	0.671	0.670	0.669

spectrophotometrically.

The results in Table 5 indicate that this method is satisfactory, when two absorbances at 244 mμ and at an appropriate wavelength of additives are known.

Applications. A commercial vitamin pill (Sample I) contains many organic compounds. For example, the indicated composition was as follows: vitamin A palmitate 2500 I. U., calciferol 250 I. U., thiamine tetrahydrofurfuryl disulfite 2 mg, vitamin B_2 2.5 mg, nicotinamide 10 mg, vitamin B_6 2.5 mg, folic acid 0.25 mg, calcium pantothenate 5 mg, vitamin B_{12} 0.001 mg, vitamin C 37.5 mg, DL-α-tocopherol acetate 1 mg in one tablet. The pill (0.5506 g) was powdered and extracted with the KCl-HCl buffer solution of less than 20 m*l*. The filtrate was further extracted twice with diethyl ether (each *ca.* 50 m*l*). The residual aqueous solution was diluted to 1 tablet/6250 m*l* buffer solution and its absorbance at 244 mμ was measured to be 0.357. Accordingly, the content of ascorbic acid in the pill was calculated to be 37.7 mg/tablet using a calibration curve. The observed content agreed with the indicated content (37.5 mg/tablet) of ascorbic acid and also with the content estimated by indophenol method (37.0 mg/tablet).

Besides ascorbic acid, tannic acid and caffeine are main components of green tea (Sample II). The sum of these two components was estimated to be 2.68×10^{-4} mol/g using $E_{275}=0.495$, assuming that they have the same ε_{275} and ε_{244} values of 7.2×10^3 and 2.65×10^3, respectively (*cf.* Table 4). Thus the ascorbic acid content was calculated from $E_{244}-0.316$ and dilution degree of 1 g/4 *l*.

E_{244}(obs.)$-E_{244}$(tannic acid + caffeine)$=0.316-0.177=0.139$

This value of 0.139 corresponds to 1.67×10^{-5} M ascorbic acid solution and the concentration gives an approximate content of the acid in Sample II

to be *ca.* 11.8 mg/g. The sample was diluted to 1 g/100 m*l* and titrated with indophenol method. The content of ascorbic acid was determined to be 9.6—13.1 mg/g. This uncertainty may be due to the coloration of the sample.

Ascorbic acid content in an orange juice (Sample III) or a purified drink (Sample IV) was also difficult to be estimated exactly by the indophenol method even by employing the xylene extraction technique.[1] But the UV method is not interfered by coloring materials; moreover the sample is so diluted (*ca.* 5×10^{-5} M of ascorbic acid) that it is almost colorless. In addition, the additive property of the UV absorbance enables the accurate determination of the acid content. In the present experiments, a known amount of ascorbic acid (0, 1.25×10^{-5}, 2.5×10^{-5} or 3.5×10^{-5} M) was added to a sample and a straight line, obtained from plots of *E vs.* concentration, afforded an exact value of the acid content.

In these two cases of drinks (Samples III and IV), the values found were higher than the labeled values. This may be caused by the fact that the makers added the acid in a greater amount than that indicated on the label taking the consumption of ascorbic acid during storage into consideration.

Conclusion

The strong UV absorption band of ascorbic acid (λ_{max} 244, ε_{max} 10000 in an acidic solution) enables its facile quantitative determination with a very simple procedure, even if a sample contains a small amount of the acid (10^{-4} M). Oxidizing agents (*e. g.*, some metallic ions) and reducing agents (*e. g.*, oxalic acid and dextrose) which may react with ordinary titration indicators do not interfere with this direct spectophotometry. Also, colored materials which may sometimes be contained, do not interfere with it. Even when their compositions are unknown, the following circumstances may take place: (i) some components of drugs, drinks or foods have only small absorbance at 244 mμ on high dilution of the sample, (ii) some components of the sample are slightly soluble in a buffer solution consisting of 0.4 N HCl and 0.4 M KCl, and (iii) the total absorbance of a sample is known, as is often the case, before adding ascorbic acid.

The authors would like to thank Takeda Pharmaceutical Ind. Co., Sankyo Pharmaceutical Co. and The Aichi Food Research Institute for their gifts of some of the materials, and also Mr. M. Gotoh for his helpful assistance.

BULLETIN OF THE CHEMICAL SOCIETY OF JAPAN VOL. 42 2286—2291 (1969)

Separation Factors of Adjacent Rare Earths between the Aqueous and Resin Phases in the Presence of EDTA

Masaru NOGUCHI,*1 Akashi YOSHIFUJI*1 and Zenzi HAGIWARA

Department of Chemical Engineering, Tohoku University, Sendai

(Received January 21, 1969)

In order to find the accurate separation factors of two adjacent rare earths between the aqueous and resin phases, measurements were performed at 30°C in the presence of EDTA and using Dowex 50W, X-8, 50—100 mesh. The following results were obtained under the same experimental conditions as were employed in ion-exchange system for the isolation of the rare earth series. The separation factors were 2.05 for Er-Tm, 1.88 for Dy-Ho, 1.61 for Y-Dy, 1.76 for Tb-Y, 1.30 for Eu-Gd, and 3.77 for Sm-Nd. In the Er-Tm separation factor, a fairly large discrepancy was observed between the calculated and experimental values. It is concluded from the experimental results that the separation factors of pairs of lanthanons should be directly measured.

A successful ion-exchange process[1] was first developed by the Reasearch Group of the Ames Laboratory, USAEC, in combination with a cation exchanger and using EDTA (ethylenediamine-*N,N,N',N'*-tetraacetic acid: H_4Y) as the eluant. In order to treat theoretically the elution system[2,3] of the rare earths with the EDTA eluant, it is

*1 Present address: Takefu Factory, Shinetsu Chemical Industry Corp.

1) J. E. Powell and F. H. Spedding, *Trans. Met. Soc. AIME*, **215**, 457 (1959).

2) F. H. Spedding and A. H. Danne, "The Rare Earths," John Wiley, New York (1961).

3) Z. Hagiwara, *Bull. Japan Inst. Metals*, **4**, 311 (1965); Z. Hagiwara, *Asahi Glass Industry-Kogyo-Gijitsu-Shorei-Kai*, **9**, 183 (1963).

necessary to get precise information on the separation factors of the lanthanide elements in the presence of a chelating agent.

The separation factor (α) of adjacent rare earths, Ln_1 and Ln_2, is approximately expressed as the ratio of the two stability constants: $\alpha^{Ln_2}_{Ln_1} \cong K_{Ln_1Y}/K_{Ln_2Y}$ It is possible to calculate the α-value using the stability constants[4,5] measured at an ionic strength of 1/10 M. In the isolation of rare earths from each other, a dilute eluant such as approximately 0.015 M EDTA buffered with ammonium hydroxide (pH$\cong$8.5) is widely used. Therefore, it may be valuable to find more accurate separation factors of the lanthanide series suitable for a real system and to compare them with the calculated values. For the complete solution of the Eu-Gd pair, the minimum elution distance calculated by using $v=(1+\varepsilon N_0)/\varepsilon$ and $\varepsilon=\alpha^{Eu}_{Gd}-1=(K_{GdY}/K_{EuY})-1$ is quite different from the experimental results. The symbol v indicates the minimum number of displacements of the mixed adsorption band necessary to carry out separation, while N_0 represents the mole fraction of the Eu component in the binary mixture of Eu and Gd being separated. Powell[6] indicated that the reason for this is the utilization of the separation factor unsuitable for the real exchange system, and that the Eu-Gd separation factor appears to be approximately 1.1.

The principal purpose of this research is to find the separation factor for pairs of adjacent lanthanons and to use them for analyzing the elution system of rare earth with EDTA.

Experimental

Materials Used. The rare earth oxides, such as Nd_2O_3, Sm_2O_3, Eu_2O_3, Gd_2O_3, Tb_4O_7, Y_2O_3, Dy_2O_3 Ho_2O_3, Er_2O_3, and Tm_2O_3, had high purities, greater than 99.9%. They were produced by the Shinetsu Chemical Industry Corp. Each oxide was dissolved with hydrochloric acid, and the rare earth ion was adsorbed in a resin bed of the hydrogen form in order to prepare the rare earth form. All the other chemicals used were of an analytical grade, and Dowex 50W, X-8, 50—100 mesh, was employed as the cation exchanger.

Experimental Procedures. An I.D.-22 mm Pyrex glass column containing Dowex 50W,X-8, 50—100 mesh was used for the elution experiment (Fig. 1). The resin was supported by a sintered glass disk.

Prior to the equilibrium experiment, a saturated form of the rare earth band was first prepared by passing the rare earth chloride solution through a Pyrex glass column involving a hydrogen form of Dowex 50W, X-8, 50—100 mesh; the column was then connected to the copper retaining bed (B-column). The latter was further connected to the C-column in the copper form. Using the 0.015 M EDTA buffered with ammonium hydroxide (pH$\cong$8.5) and the flow rate of 2 ml/min,

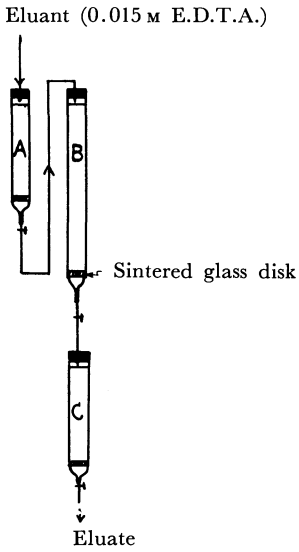

Fig. 1. Ion-exchange columns used for the preparation of rare earth type of resin containing ammonium and hydrogen.
Dimension of columns as hydrogen form of resin:
A: Rare earth adsorption bed (2.2×25 cm)
B: Copper retaining bed (2.2×50 cm)
C: Copper retaining bed (2.2×20 cm)
Resin used: Dowex 50W, X-8, 50—100 mesh
Flow rate: 2 ml/min

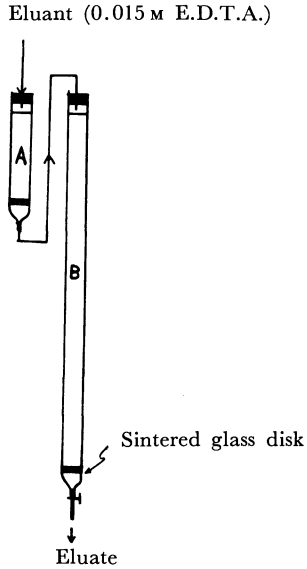

Fig. 2. Ion-exchange columns for the preparation of rare earth eluate.
Dimension of columns as hydrogen form of resin:
A: Rare earth adsorption bed (2.2×25 cm)
B: Copper retaining bed (2.2×100 cm)
Resin used: Dowex 50W, X-8, 50—100 mesh
Flow rate: 2 ml/min

4) E. J. Wheelwright, F. H. Spedding and G. Schwarzenbach, *J. Am. Chem. Soc.*, **75**, 4196 (1953).
5) G. Schwarzenbach, R. Gut and G. Anderegg, *Helv. Chim. Acta*, **37**, 937 (1954).
6) E. Eyling, "Progress in the Science and Technology of the Rare Earths," Vol. 1, Pergamon Press, New York (1964).

Table 1. Composition of the aqueous and resin phases before equilibrium

Rare earth pair	Composition of resin phase (Equivalent fraction)				Composition of aqueous phase (mol/l)				
	Ln	Ln	NH_4	H	Ln	Y_f	Ln	NH_4	pH
Tm-Er	Tm	0.9101	0.0121	0.0783	Er	0.00082	0.01488	0.00353	2.00
Ho-Dy	Ho	0.8666	0.0344	0.0991	Dy	0.00143	0.01487	0.00575	2.05
Dy-Y	Dy	0.8779	0.0412	0.0809	Y	0.00138	0.01415	0.00610	2.23
Y-Tb	Y	0.9210	0.0312	0.0475	Tb	0.00169	0.01440	0.00650	2.21
Gd-Eu	Gd	0.8784	0.0559	0.0657	Eu	0.00193	0.01461	0.00745	2.41
Sm-Nd	Sm	0.8472	0.0547	0.0981	Nd	0.00250	0.01374	0.00997	2.59

Total concn. of anionic EDTA species: $Y_T = L_n + Y_f$ (mol/l)

the rare earth band was displaced to a distance corresponding to several band lengths. After the C-column had been completely displaced by the rare earth, the elution was stopped. The steady-state band of the rare earth in the C-column was then washed with a 60% ethyl alcohol solution and then dried. The dried resin was finally used for the experiments. By employing the above method, various rare earth forms of resins involving ammonium and hydrogen were prepared; they are listed in Table 1.

On the other hand, a rare earth solution containing ammonium and hydrogen was prepared by the column method, shown in Fig. 2. After making the rare-earth-saturated bed, it was eluted with the 0.015 M EDTA (pH≅8.5). After a movement proportional to approximately 3-4 band lengths, the rare earth fraction from the main column was collected for the equilibrium experiments. Several types of rare earth fractions prepared are listed in Table 1, in which the two symbols Ln and NH_4 express the total concentrations of rare earth and ammonium in the aqueous phase.

Equilibrium Experiment. After mixing definite portions of the prepared rare earth form of resin containing small amounts of ammonium and hydrogen with 300, 450, and 600 ml of the rare earth fraction, the mixtures were maintained at 30°C for 96 hr in a thermostat under occasional stirring. After equilibration, the resin was separated from the aqueous phase, and both phases were analyzed in order to find the separation factor in the presence of EDTA.

Analysis. The constituents in the resin were eluted with 2 M NaCl. The rare earth in the resin and aqueous phases was determined as a mixed oxide after precipitating the oxalate. Further, each rare earth in the mixed oxide was determined by spectrophotometry as well as by X-ray fluorescent spectrometry. The determination of ammonium was performed by the Kjeldahl method, and the excess of EDTA (Y_f), which was present in the uncombined form with rare earth, was determined volumetrically with a standard solution of $NdCl_3$, using an arzenoazo indicator [3-(2-arzono-phenylazo)-4,5-dihydroxy-2,7-naphthalene-disulfonic acid] and pyridine as the buffer solution.

Results and Discussion

The compositions of adjacent rare earths at equilibrium are given in Tables 2 to 7, in which the rare earths in both phases are expressed in the mole fraction:

$$m_{Ln_1} + m_{Ln_2} = 1, \quad m_{\overline{Ln}_1} + m_{\overline{Ln}_2} = 1$$

where the barred quantities refer to the resin phase, and the unbarred, the aqueous phase. The observed separation factors are also represented; these are found by the following relation:

$$\alpha_{Ln_1}^{Ln_2} = \left(\frac{m_{\overline{Ln}_2}}{m_{\overline{Ln}_1}}\right)\left(\frac{m_{Ln_1}}{m_{Ln_2}}\right)$$

whether or not a chelating agent is present in the system, the separation factor of the two adjacent rare earths is defined as the concentration ratio of these species in the resin and aqueous phases. The dimensionless separation factor is not affected by the selection of the concentration units. The average values of the separation factors for the two adjacent rare earths are tabulated in Table 8. The values calculated from the stability constants of the rare earth-EDTA chelates also appear in the same table.

In this study, the Er-Tm separation factor showed 2.05. This is too far from the value calculated using the stability constants ($\alpha_{Tm}^{Er} \cong K_{TmY}/K_{ErY}$). The α_{Tm}^{Er}-value[7] at 60°C is 2.02 under almost the same experimental conditions at 30°C. Powell[8] pointed out that a linear relation is seen in the plot of the logarithm of the stability constants as a function of the ionic radius of rare earth from Gd through Lu (See Table 8). Considering a regular decrease in stability with an increase in the radius and the difference in cationic radius between the tripositive rare earth ions, one would speculate that the differences between K_{Ln_1Y}/K_{Ln_2Y} and K_{Ln_2Y}/K_{Ln_3Y} will be small. The differences in radius are 0.02 Å for Ho^{3+}–Er^{3+}, 0.01 Å for Er^{3+}–Tm^{3+}, and 0.01 Å for Tm^{3+}–Yb^{3+}. The following sequence can be estimated for pairs of elements from Ho through Yb:

$$\alpha_{Yb}^{Tm} < \alpha_{Tm}^{Er} < \alpha_{Er}^{Ho}$$

7) Z. Hagiwara, A. Banno and A. Kamei, *J. Inorg. & Nucl. Chem.*, submitted for publication (Feb., 1969).

8) J. E. Powell, *J. Chromatog.*, **29**, 210 (1967).

The α-value of 2.05 at 30°C is concluded to be reasonable on the basis of the following facts. The Er-Tm separation factor at 30°C can be calculated employing the thermodynamic quantities ($\Delta H°$, $\Delta S°$ and $\Delta F°$) obtained by a calorimetric study[9] of the formation of the rare earth-EDTA chelate

Table 2. Ion exchange equilibrium and separation factor (Tm-Er system)

Exp. No.	Sample* taken		Mole fraction of adjacent rare earths** at equilibrium (30°C)				α_{Tm}^{Er}
			Resin phase		Aqueous phase		
	Tm-resin (meq.)	Er-soln. (m*l*)	Tm	Er	Tm	Er	
3-1	17.48	300	0.462	0.538	0.648	0.352	2.15
3-2	17.42	450	0.343	0.657	0.531	0.469	2.17
3-3	17.43	600	0.294	0.706	0.433	0.567	1.83

* Detail compositions are given in Table 1.
** Ratios of the two adjacent rare earths in both phases were determined by absorption method.

Table 3. Ion exchange equilibrium and separation factor (Dy-Ho system)

Exp. No.	Sample* taken		Mole fraction of adjacent rare earths** at equilibrium (30°C)				α_{Ho}^{Dy}
			Resin phase		Aqueous phase		
	Ho-resin (meq.)	Dy-soln. (m*l*)	Ho	Dy	Ho	Dy	
5-1	16.20	300	0.449	0.551	0.611	0.389	1.93
5-2	16.13	450	0.337	0.663	0.487	0.513	1.87
5-3	16.23	600	0.269	0.731	0.405	0.595	1.85

* Detail compositions are given in Table 1.
** Determined by absorption method.

Table 4. Ion exchange equilibrium and separation factor (Y-Dy system)

Exp. No.	Sample* taken		Mole fraction of adjacent rare earths** at equilibrium (30°C)				α_{Dy}^{Y}
			Resin phase		Aqueous phase		
	Dy-resin (meq.)	Y-soln. (m*l*)	Dy	Y	Dy	Y	
1-1	19.11	300	0.547	0.453	0.662	0.338	1.62
1-2	19.08	450	0.428	0.572	0.549	0.451	1.63
1-3	18.70	600	0.356	0.644	0.465	0.535	1.57

* Detail compositions are given in Table 1.
** Determined by X-ray fluorescent spectrometry.

Table 5. Ion exchange equilibrium and separation factor (Tb-Y system)

Exp. No.	Sample* taken		Mole fraction of adjacent rare earths** at equilibrium (30°C)				α_{Y}^{Tb}
			Resin phase		Aqueous phase		
	Y-resin. (meq.)	Tb-soln. (m*l*)	Y	Tb	Y	Tb	
4-1	19.40	300	0.520	0.480	0.659	0.341	1.78
4-2	19.40	450	0.400	0.600	0.525	0.475	1.66
4-3	19.39	600	0.303	0.693	0.448	0.552	1.85

* Detail compositions are given in Table 1.
** Determined by X-ray fluorescent spectrometry.

9) J. L. Mackey, J. E. Powell and F. H. Spedding, *J. Am. Chem. Soc.*, **84**, 2047 (1962).

Table 6. Ion exchange equilibrium and separation factor (Eu-Gd system)

Exp. No.	Sample* taken		Mole fraction of adjacent rare earths** at equilibrium (30°C)				α_{Gd}^{Eu}
	Gd-resin (meq.)	Eu-soln. (m*l*)	Resin phase		Aqueous phase		
			Gd	Eu	Gd	Eu	
6-1	16.72	300	0.524	0.476	0.591	0.409	1.31
6-2	16.76	450	0.417	0.583	0.484	0.516	1.31
6-3	16.65	600	0.347	0.653	0.407	0.593	1.29

* Detail compositions are given in Table 1.
** Determined by absorption method.

Table 7. Ion exchange equilibrium and separation factor (Nd-Sm system)

Exp. No.	Sample* taken		Mole fraction of adjacent rare earths** at equilibrium (30°C)				α_{Sm}^{Nd}
	Sm-resin (meq.)	Nd-soln. (m*l*)	Resin phase		Aqueous phase		
			Sm	Nd	Sm	Nd	
2-1	17.91	300	0.440	0.560	0.748	0.252	3.78
2-2	17.88	450	0.306	0.694	0.619	0.381	3.68
2-3	17.89	600	0.226	0.774	0.528	0.472	3.84

* Detail compositions are given in Table 1.
** Determined by absorption method.

Table 8. Comparison of separation factors in presence of EDTA

Rare earth pair (Ln_1-Ln_2)	$\alpha_{Ln_1}^{Ln_2} \cong \frac{K_{Ln_1Y}}{K_{Ln_2Y}}$		$\alpha_{Ln_1}^{Ln_2} = \frac{m_{Ln_1}\, m_{\overline{Ln_2}}}{m_{Ln_2}\, m_{\overline{Ln_1}}}$	Ion	Radius (Å)
	Calcd Value*	Calcd value**	Observed mean value (30°C)		
Lu-Yb	2.00	1.82	—	Lu^{3+}	0.84
Yb-Tm	1.55	2.09	—	Yb^{3+}	0.85
Tm-Er	2.95	3.31	2.05	Tm^{3+}	0.86
Er-Ho	1.86	1.74	—	Er^{3+}	0.87
Ho-Dy	1.90	3.63	1.88	Ho^{3+}	0.89
Dy-Y	1.62	1.55	1.61	Dy^{3+}	0.91
Y-Tb	1.45	1.51	1.76	Tb^{3+}	0.92
Tb-Cd	3.63	4.79	—	Gd^{3+}	0.94
Gd-Eu	1.05	1.02	1.30	Eu^{3+}	0.96
Eu-Sm	1.62	1.38	—	Sm^{3+}	0.97
Sm-Nd	3.39	3.09	3.77	Pm^{3+}	0.98
Nd-Pr	1.62	2.04	—	Nd^{3+}	0.99
Pr-Ce	2.63	2.29	—	Pr^{3+}	1.00
Ce-La	3.02	4.68	—	Ce^{3+}	1.02
				La^{3+}	1.04
				Y^{3+}	0.88
				Sc^{3+}	0.68

* Stability constants measured by G. Schwarzenbach *et al.*,[5] are used.
** Stability constants measured by E. J. Wheelwright *et al.*,[4] are used.

(LnY) in solutions at 25°C and $\mu=0.1$.

$$\Delta F^\circ_{Er} = -\boldsymbol{R}T \ln K_{ErY} = \Delta H^\circ_{Er} - T\Delta S^\circ_{Er}$$
$$\Delta F^\circ_{Tm} = -\boldsymbol{R}T \ln K_{TmY} = \Delta H^\circ_{Tm} - T\Delta S^\circ_{Tm}$$

The above relation lead to the following form:

$$\log \alpha_{Tm}^{Er} = \log \frac{K_{TmY}}{K_{ErY}} = -\frac{(\Delta H^\circ_{Tm} - \Delta H^\circ_{Er}) - T(\Delta S^\circ_{Tm} - \Delta S^\circ_{Er})}{2.303\boldsymbol{R}T}$$

Introducing $\Delta H^\circ_{Tm} = -1870$ cal/mol, $\Delta H^\circ_{Er} = -1708$ cal/mol, $\Delta S^\circ_{Tm} = 79.1$ cal/mol per deg. and $\Delta S^\circ_{Er} = 78.3$ cal/mol per deg., a value of 1.96 is obtained as the separation factor of the Er-Tm pair at 303°K. Further, the same treatment as above gives 1.91 as the α_{Tm}^{Er}-value at 333°K. The α_{Tm}^{Er}-values found experimentally at temperatures of 30°C and 60°C are in fair agreement with the calculated values.

The observed separation factor of 1.30 for Eu and Gd is greater than the calculated value; the former approaches 1.1,[6] as predicted from the results of the ion exchange elution of a mixture of Eu and Gd. On the other hand, slight differences in the separation factors for pairs of rare earths, such as Y–Dy, Tb–Y, and Nd–Sm, are observed between the calculated and experimental values. This may be attributed to the following facts: the α-measurement was performed at an ionic strength of *ca.* 0.015 M in order to get suitable values for the real exchange system, while the stability constants of the rare earth-EDTA chelates were determined at $\mu=0.1$. However, the difference in the separation factor due to the ionic strength may be insignificant between the adjacent rare earth pair. As may be clear from the stability constants of Ln-EDTA chelates,[4,5,9] fairly large differences have been reported in the literature. The accuracy in determining the stability constant is naturally limited to some degree by the very stable chealte formation. The above factors are considered to exert a serious effect on the calculation of the separation factor using the values of the stability constants.

It is convenient to calculate the separation factor by means of the difference in the stabilities of two adjacent rare earths. However, the experimental results show that the separation factor should be directly measured under conditions similar to those in the ion-exchange system employed for the elution.

The authors wish to thank Mr. Matsuji Sato for his X-ray fluorescent analysis.

BULLETIN OF THE CHEMICAL SOCIETY OF JAPAN VOL. 42 2291—2295 (1969)

Preparation and Properties of Di-μ-alkoxo-bis(3-alkyl-5-methylsalicylaldehydato)dicopper(II)

Takako INAZU, Hisashi OKAWA, Takahiko INAZU and Tamotsu YOSHINO

Department of Chemistry, Faculty of Science, Kyushu University, Hakozaki, Fukuoka

(Received January 24, 1969)

In this paper, the syntheses of copper(II) complexes of 3-alkylsalicylaldehydes, B, as well as the syntheses and properties of dimeric copper(II) complexes, C, with bridged alkoxy groups are reported.

In the course of our studies of the effects of large-membered chelate rings on the stabilities of such complexes as A, copper(II) complexes of 3-alkylsalicylaldehydes were synthesized as reference compounds. The copper(II) complexes thus obtained were normal, monomeric copper(II) chelates, B (ligand: Cu=2 : 1); when these copper(II) complexes, B, were refluxed with alcohol without any bases, the monomeric complexes could be converted to dimeric copper(II) complexes, C. The structures of the dimeric copper(II) complexes, C, with bridged alkoxy groups were verified by the study of the infrared spectrum, the ultraviolet spectrum, the nuclear magnetic resonance spectrum, by elementary analysis, a molecular-weight determination, electrophoresis, and by considering the magnetic moment of di-μ-ethoxo-bis(3-ethyl-5-methylsalicylaldehydato)dicopper(II), XVII, as a representative of the dimeric copper(II) complexes, C.

Several complexes containing alkoxide, especially methoxide, have been reported,[1,2] but very few

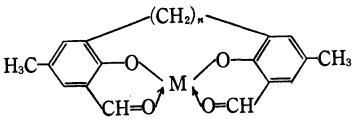

Fig. 1. [A]

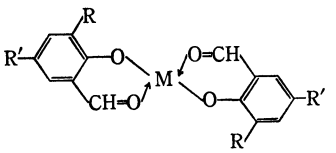

R′=H; R=*t*-C_4H_9 (XII).
R′=CH_3; R=CH_3 (VIII), R=C_2H_5 (IX),
R=*n*-C_3H_7 (X), R=*n*-C_4H_9 (XI),
R=*n*-C_5H_{11} (XIII), R=*cyclo*-C_6H_{11} (IV).

Fig. 2. [B]

1) J. A. Bertrand and R. I. Kaplan, *Inorg. Chem.*, **4**, 1657 (1965).

2) R. M. Klein and J. C. Bailar, Jr., *ibid.*, **2**, 1187 (1963).

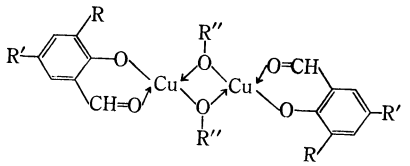

$R''=C_2H_5$, $R'=H$; $R=t\text{-}C_4H_9$ (XXI)
$R''=C_2H_5$, $R'=CH_3$; $R=CH_3$ (XV),
$R=C_2H_5$ (XVII), $R=n\text{-}C_3H_7$ (XIX),
$R=n\text{-}C_4H_9$ (XX), $R=n\text{-}C_5H_{11}$ (XXII),
$R=cyclo\text{-}C_6H_{11}$ (XXIII)
$R''=CH_3$, $R'=CH_3$; $R=C_2H_5$ (XVI)
$R''=n\text{-}C_8H_{17}$, $R'=CH_3$; $R=C_2H_5$ (XVIII)

Fig. 3. [C]

stable dimeric copper(II) complexes with bridged alkoxy groups have been reported. In some cases,[1] dimeric copper(II) complexes have been obtained by refluxing with a base such as potassium hydroxide. In these experiments, the dimeric copper(II) complexes could be obtained by merely refluxing with alcohol without any bases. In the case of monomeric copper(II) complexes of salicylaldehydes without an alkyl group at the 3 position, such as salicylaldehyde or 5-methylsalicylaldehyde, dimeric copper(II) complexes could not be isolated by refluxing in alcohol without any bases.[3] Therefore, the alkyl group in the 3 position must have exerted some steric effects.

Four 3-alkyl-5-methylsalicylaldehydes, II, III, IV, and VI, were synthesized as is shown in Fig. 4 by the Duff reaction of 2-alkyl-4-methylphenols, XXVI,[4] with boric acid and hexamethylenetetramine in glycerol. The 2-alkyl-4-methylphenols were synthesized by the Clemmensen reduction of 2-acyl-4-methylphenols, XXV, which had themselves been obtained from the aryl ester, XXIV, by the Fries rearrangement.

In each case, a monomeric copper(II) complex, B, was obtained by the addition of an ethanolic

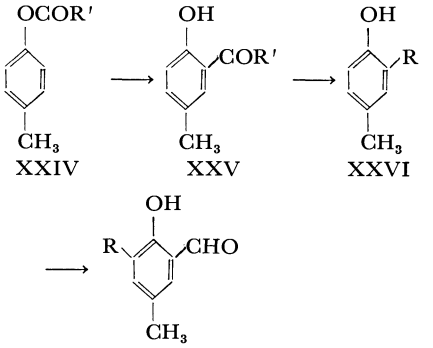

XXIV $R'=CH_3$, C_2H_5, $n\text{-}C_3H_7$, $n\text{-}C_4H_9$
XXV $R'=CH_3$, C_2H_5, $n\text{-}C_3H_7$, $n\text{-}C_4H_9$
XXVI $R=C_2H_5$, $n\text{-}C_3H_7$, $n\text{-}C_4H_9$, $n\text{-}C_5H_{11}$

Fig. 4. Synthetic route of aldehydes I—VII.

Table 1. C-O Stretching vibration of the bridged alkoxy groups over the 1040—1070 cm^{-1} range

	R	R''	C-O, cm^{-1}
XV	CH_3	C_2H_5	1060, 1048
XVII	C_2H_5	C_2H_5	1068, 1054
XIX	$n\text{-}C_3H_7$	C_2H_5	1059, 1050
XX	$n\text{-}C_4H_9$	C_2H_5	1060, 1054
XXI*	$t\text{-}C_4H_9$	C_2H_5	1055
XXII	$n\text{-}C_5H_{11}$	C_2H_5	1063, 1055
XXIII	$cyclo\text{-}C_6H_{11}$	C_2H_5	1060, 1050
XVI	C_2H_5	CH_3	1070, 1040
XVIII	C_2H_5	$n\text{-}C_8H_{17}$	1069, 1055

* No methyl group in the 5 position.

solution of a ligand. By refluxing the brown-colored monomeric complexs, B, with alcohol, green complexes were obtained. The green crystals thus obtained were suggested to be dimeric

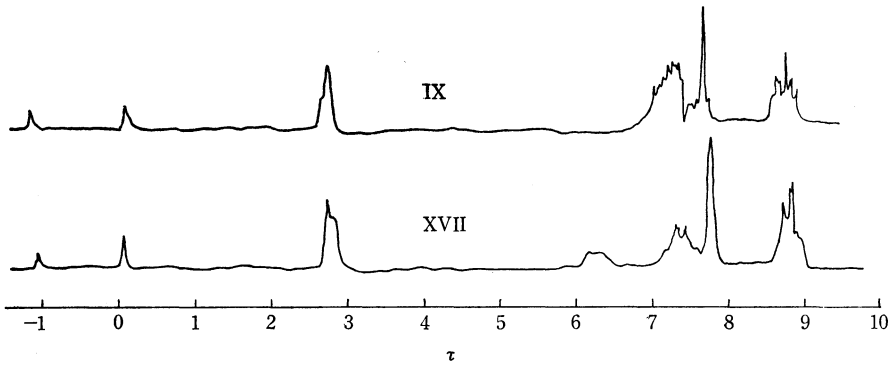

Fig. 5. The NMR spectra of the monomeric complex, IX and the dimeric complex, XVII.

3) The dimeric complexes can be obtained by refluxing in alcohol with potassium hydroxide; T. Shono, M. Mori and K. Shinra, Paper presented at the 18th Symposium on Coordination Chemistry, Kyoto, October, 1968.

4) The $R=CH_3$ in XXVI was commercially obtained. The $R=$cyclo-C_6H_{11} in XXVI was obtained by the Friedel-Crafts reaction of *p*-cresol with cyclohexene. See Y. Koike, H. Okawa, T. Inazu and T. Yoshino, *Mem. Fac. Sci., Kyushu Univ., Ser. C, Chem.*, **6**, 5 (1967).

by elementary analyses and by molecular-weight determinations. In the infrared spectra of the dimeric complexes, C, the bands over the 1040—1070 cm^{-1} range are assigned to the C–O stretching vibration of the bridged alkoxy groups, which are not observed in the case of the monomeric complexes, B. The data of the infrared spectra are given in Table 1.

The magnetic moments of the compounds were calculated using the expression; $\mu_{eff}=(8\chi_A T)^{1/2}$. The value obtained, 1.36 B. M., for the dimeric copper(II) complex, XVII, was considerably below the value for one unpaired electron. The value obtained for the monomeric copper(II) complex, IX, was 2.03 B. M. The dimeric nature, the low magnetic moment, and the tendency of copper(II) to achieve four-coordination suggest that there are bridging groups present in the complex.

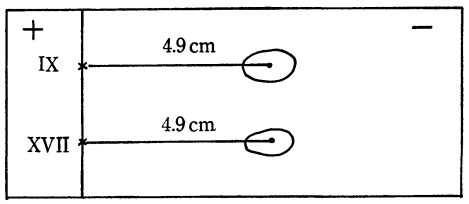

Fig. 6. Paper electrophoresis of the monomeric complex, IX and the dimeric complex, XVII.

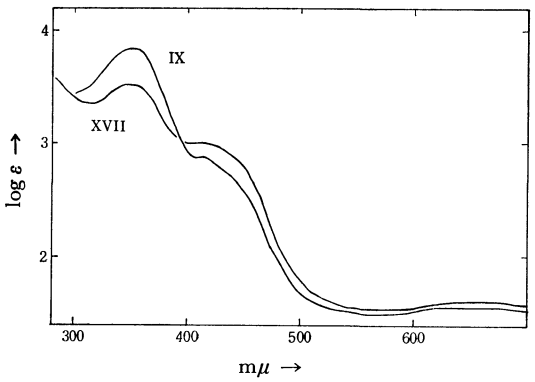

Fig. 7. Visible and ultraviolet spectra of the monomeric complex, IX, and the dimeric complex, XVII, in benzene.

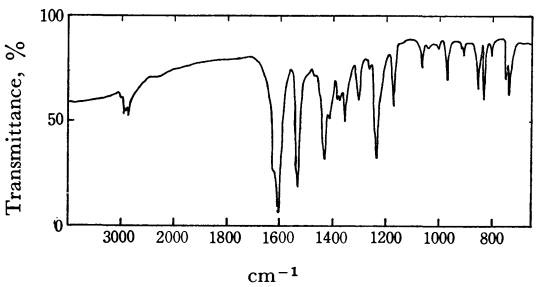

Fig. 8. Infrared spectrum of the monomeric complex, IX, in KBr disk.

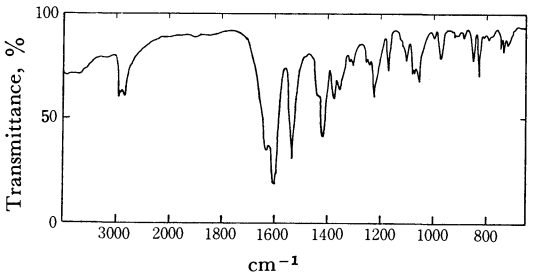

Fig. 9. Infrared spectrum of the dimeric complex, XVII, in KBr disk.

The NMR spectrum of the dimeric copper(II) complex, XVII, was in accord with that assumed for the dimeric structure; $\tau=8.75$ multiplet for terminal methyl protons at the 3 position and the bridged ethoxy groups, $\tau=7.67$ singlet for methyl at the 5 position, $\tau=7.40$ quartet for methylene protons at the 3 position, $\tau=6.27$ broad for methylene groups of the bridged ethoxy groups, and $\tau=0.12$ singlet for aldehyde protons. In the NMR spectrum of the monomeric copper(II) complex, IX, the absorption bands in the region $\tau=6.3$ were not observed, while other bands were observed at comparative positions. In both cases, protons for the dissociated salicylaldehyde, $\tau=-1.13$ for the dimeric complex, XVII, and -1.17

Table 2. Properties of aldehydes

	Aldehyde R	Aldehyde R′	Cryst. form*	Mp, Bp	Yield %
I	CH_3	CH_3	py. liq	99—111°C/22 mmHg	19.6
II	C_2H_5	CH_3	py. liq	133—137°C/33 mmHg	23
III	n-C_3H_7	CH_3	py. liq	140—148°C/34 mmHg	21
IV	n-C_4H_9	CH_3	py. liq	141—153°C/38 mmHg	10.4
V	t-C_4H_9	H	py. liq	126—131°C/22 mmHg	4
VI	n-C_5H_{11}	CH_3	py. liq	163—184°C/40 mmHg	13.6
VII	$cyclo$-C_6H_{11}	CH_3	py. n.	127°C	41

* b=brown, g=green, liq=liquid, n=needles, p=powder, pl=plates, py=pale yellow y=yellowish.

Table 3. Properties and analytical data of the monomeric complexes, B

	Cryst. form*	Mp	Formula	Analyses, % Found C	Found H	Found Cu	Calcd C	Calcd H	Calcd Cu	Yield %
VIII	b.n.	231—232°C	$C_{18}H_{18}O_4Cu$	59.89	5.18	17.43	59.74	5.01	17.56	54.2
IX	b.n.	152—154°C	$C_{20}H_{22}O_4Cu$	61.50	5.89	16.33	61.60	5.69	16.30	27
X	b.n.	173—174°C (decomp)	$C_{22}H_{26}O_4Cu$	62.97	6.27	15.10	63.22	6.27	15.20	29.8
XI	b.n.	149—151°C (decomp)	$C_{24}H_{30}O_4Cu$	64.53	6.74	14.26	64.63	6.78	14.25	29
XII	b.pl.	226.5—228°C	$C_{22}H_{26}O_4Cu$	63.00	6.27	14.96	63.22	6.27	15.20	29.2
XIII	b.n.	142—145.5°C (decomp)	$C_{26}H_{34}O_4Cu$	65.75	7.46	13.33	65.87	7.23	13.40	19.7
XIV	b.n.	232—233°C	$C_{28}H_{34}O_4Cu$	67.51	6.92	12.52	67.52	6.88	12.76	62.6

* b=brown, g=green, liq=liquid, n=needles, p=powder, pl=plates, py=pale yellow, y=yellowish.

Table 4. Properties and analytical data of the dimeric complexes, C

	Cryst. form*	Mp	Formula	Analyses, % Found C	Found H	Found Cu	Calcd C	Calcd H	Calcd Cu	Mol wt Found	Mol wt Calcd	Yield %
XV	g.p.	182—196°C (decomp)	$C_{22}H_{28}O_6Cu_2$	50.95	5.75	24.89	51.20	5.47	24.65		515.56	48.1
XVI	y.g.p.	202°C (decomp)	$C_{22}H_{28}O_6Cu_2$	51.04	5.45		51.26	5.47	24.65		515.56	
XVII	g.n.	180—183°C	$C_{24}H_{32}O_6Cu_2$	52.78	5.99	23.64	53.03	5.93	23.38	520.1	543.61	73.9
XVIII	g.p.	108°C (decomp)	$C_{36}H_{56}O_6Cu_2$	59.40	7.93	18.80	60.74	7.93	17.85		711.89	
XIX	g.p.	171—172°C	$C_{26}H_{36}O_6Cu_2$	54.72	6.57	22.38	54.63	6.34	22.23	589	571.67	75.5
XX	y.g.n.	165°C	$C_{28}H_{40}O_6Cu_2$	55.82	6.81	21.00	56.08	6.72	21.19		599.72	
XXI	y.g.n.	171—181.5°C	$C_{26}H_{36}O_6Cu_2$	54.51	6.64	20.64	54.63	6.35	22.23		571.67	56.4
XXII	g.p.	132—133°C	$C_{30}H_{44}O_6Cu_2$	57.22	7.36	20.18	57.40	7.06	20.24		627.77	54.9
XXIII	y.g.p.	216°C (decomp)	$C_{32}H_{44}O_6Cu_2$	58.61	7.19	19.67	58.97	6.80	19.50	696	651.80	59.9

* b=brown, g=green, liq=liquid, n=needles, p=powder, pl=plates, py=pale yellow, y=yellowish.

for the monomeric complex, IX, were observed.

A large number of copper(II) compounds, including bissalicylaldehydato copper(II), are square-planar. The visible spectra of the IX and XVII complexes consist of a broad band centered around 650 mμ. The absorption is similar in wavelength and in intensity to that of square-planar complexes of copper(II).[1] The close resemblance of the ultraviolet and visible spectrum of the dimeric copper(II) complex, XVII, to that of the monomeric copper(II) complex, IX, revealed that the dimeric complex, XVII, is square-planar. With the aid of paper electrophoresis, it was proved that copper atoms in the dimeric complex, XVII, are not in a reduced univalent state. All the experimental evidence is consistent with a planar, dimeric structure.

Experimental

All the melting points are uncorrected. The physical properties and analytical data of the products are summarized in Tables 2, 3, and 4. The ultraviolet and visible spectra were measured on a Hitachi EPS-3T spectrophotometer. The infrared spectra were measured on a Hitachi EPI-S2 spectrophotometer. The NMR spectra were recorded on a Varian Associates A-60 model, using tetramethylsilane as the internal standard and $CDCl_3$ as the solvent. The molecular weights were obtained with a Hitachi 115 vapor-pressure osmometer, using benzene as the solvent.

Magnetic Moment Determination. The magnetic susceptibilities of the compounds were measured with a Gouy balance at 27°C. The corrected molar susceptibilities were 771.5×10^{-6} c.g.s. unit for the dimeric complex, XVII, and 1725.4×10^{-6} c.g.s. unit for the monomeric complex, IX.

Paper Electrophoresis. Toyo Roshi No. 51 filter paper was used, with a solvent system of 8% formic acid - acetic acid - methanol - water (1 : 3 : 6 : 10 by vol) (600 V, 3 mA, 30 min). Without further treatment, pale blue spots of cupric ions were obtained.

3-Ethyl-5-methylsalicylaldehyde, II. The mixture of 150 g of glycerol and 35 g of boric acid was heated on a water bath under diminshed pressure for 2 hr and then on an oil bath at 200°C for 30 min. To the mixture there were added 25 g of hexamethylenetetramine and 36.2 g of 2-ethyl-*p*-cresol. The mixture thus obtained was heated at 150—165°C for 50 min. After cooling, 25 m*l* of concentrated sulfuric acid in 75 m*l* of water was added to the reaction mixture. The mixture was steam-distilled, and the 3-ethyl-5-methylsalicylaldehyde thus obtained was extracted with ether. The organic layer was washed with water and dried over anhydrous sodium sulfate, and the ether was removed. The residual oil was distilled, bp 122—124°C/20 mmHg, in a 12.5% yield (5.45 g).

Bis(3-ethyl-5-methylsalicylaldehydato)copper(II), IX. A solution of 2.00 g of 3-ethyl-5-methylsalicylaldehyde in 10 m*l* of ethanol was mixed with a solution of 1.60 g of copper(II) acetate monohydrate in 30 m*l* of ethanol. The mixed solution was left standing under diminished pressure at room temperature. The brown needles thus formed were collected and washed with a little ethanol. Yield, 516 mg, 21.7%. Mp 152—154°C.

Conversion of the Monomeric Complex, IX, to the Dimeric Complex, XVII. A mixture of 305 mg of the monomeric complex, IX, and 30 m*l* of ethanol was refluxed for 30 min. After cooling, 157 mg of green needles of the dimeric complex, XVII, were collected and washed with a little ethanol. They were soluble in chloroform and insoluble in water.

BULLETIN OF THE CHEMICAL SOCIETY OF JAPAN VOL. 42 2296—2300 (1969)

Deprotonation of Oxime Complexes: Dimethylglyoxime-Cobalt(III) Complexes*[1]

Isao MASUDA, Mitsuhiro SAKANO and Koichiro SHINRA

Department of Applied Chemistry, Faculty of Engineering, Osaka University, Yamada, Suita, Osaka

(Received February 4, 1969)

Dimethylglyoxime-Co(III) complexes with the formula $[Co(dmgH)_2A_2]^n$ (I), where dmgH is dimethylglyoximato mono-anion, A is an axial ligand such as aniline, *p*-anisidine, pyridine, γ-picoline, imidazole, NH_3, CN^-, and NO_2^-, and n is -1, 0, or $+1$, were found to change their electronic absorption spectra reversibly depending on the pH of the solution. These changes have been attributed to the dissociation of the proton from the intramolecular hydrogen bridges of the complex; the changes are accompanied by the formation of the complex $[Co(dmgH)(dmg)A_2]^{n-1}$, where dmg represents the dimethylglyoximato di-anion. The proton dissociation constants (pK_a) obtained by the spectrophotometric method indicated that the complex I is generally a weak acid of $pK_a=7.7$—12.6. With the exception of the pyridine and the γ-picoline ligand, axial ligands do not appreciably affect the pK_a values. However, axial pyridine and the γ-picoline ligand increase the tendency of the hydrogen bridges to dissociate the proton.

Some metal chelate-complexes coordinated with oxime derivatives are thought to dissociate the proton reversively depending upon the pH of the solutions. The reaction can be generally represented as follows:

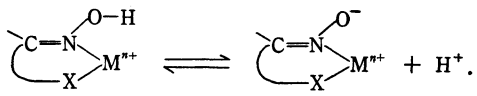

This phenomenon has been observed in Fe(III) complexes of Schiff bases derived from 1,2-diketonemonoximes and amines[1] and in complexes of methyl-2-pyridyl ketoxime.[2] As for pyridine-2-aldoxime complexes of Fe(II), Fe(III), Ni(II), Pd(II), and Pt(II), proton dissociation constants (pK_a) corresponding to the above reaction have been determined.[3,4]

In the present paper an extensive investigation with respect to such proton dissociation as is described above has been made on Co(III)-dimethylglyoxime complexes of the $[Co(dmgH)_2A_2]^n$*[2] type, this investigation has revealed that the hydrogen in the intramolecular, hydrogen bridges of the complexes can be ionized as an proton depending on the pH of the aqueous solution. Moreover, the ionization constants have been expeditiously obtained by the spectrophotometric method.[5]

Experimental

Measurements. The electronic absorption spectra were measured with a Hitachi EPS-3 spectrophotometer. An aqueous complex solution was buffered to a desirable pH by adding a Mcllavine or Kolthoff's buffer solution. The pH measurements of the solution was made on a glass-electrode pH meter calibrated against the standard buffer. All measurements of both the spectra and pH were carried out at room temperature from 20 to 25°C.

Complexes. *Bis(dimethylglyoximato)-di(imidazole)cobalt(III) Chloride*, $[Co(dmgH)_2(imidazole)_2]Cl\cdot 2H_2O$. This complex was newly prepared for the present study. Into an aqueous solution containing 5 g of cobalt(II) chloride hexahydrate, 5 g of dimethylglyoxime and 7 g of imidazole dissolved in ethanol were added. The subsequent passing of air through the solution for 30—40 min at room temperature resulted in the precipitation of a reddish-brown complex. This complex was recrystallized from hot water.

Found: Co, 11.66; C, 33.89; H, 5.19; N, 22.51; Cl, 6.81%. Calcd for $Co(C_{14}H_{18}N_8O_4)Cl\cdot 2H_2O$: Co, 11.86; C, 33.85; H, 5.27; N, 22.56; Cl, 6.70%.

The other complexes studied were prepared and purified according to the methods in the articles noted in Table 1.

*[1] Part of this work has been communicated: Y. Yamano, I. Masuda, K. Shinra, *Inorg. Nucl. Chem. Letters*, **4**, 581 (1968).

1) I. Masuda, *Nippon Kagaku Zasshi (J. Chem. Soc. Japan, Pure Chem. Sect.)*, **82**, 563, 1350 (1961).

2) D. K. Banerjea and K. K. Tripathi, *Anal. Chem.*, **32**, 1196 (1960).

3) G. I. H. Hanania and D. H. Irvine, *J. Chem. Soc.*, **1962**, 2745.

4) I. Masuda and K. Shinra, *Science Reports, Osaka University*, **11**, 3 (1962).

*[2] Mono-, and di-valent dimethylglyoximato anion are abbreviated as dmgH, and dmg, respectively. "A" represents axial ligand such as amine, CN^- or NO_2^-. And "n" denotes $+1$, 0, or -1.

5) W. Stenström and N. Goldsmith, *J. Phys. Chem.*, **30**, 1683 (1926).

Table 1. pK_a values of the complexes associated with the equillibrium (1)

Complex	pK_a	Isosbestic point (mμ)
$[Co(dmgH)_2(Aniline)_2]Cl\cdot 4H_2O$[6]	10.5	250, 347
$[Co(dmgH)_2(p\text{-}Anisidine)_2]Cl\cdot H_2O$[7]	10.9	249
$[Co(dmgH)_2(Pyridine)_2]Cl\cdot H_2O$[6,8]	7.7	250
$[Co(dmgH)_2(\gamma\text{-}Picoline)_2]Cl\cdot H_2O$	8.0	248
$[Co(dmgH)_2(Imidazole)_2]Cl\cdot 2H_2O$	9.9	246
$[Co(dmgH)_2(NH_3)_2]Cl\cdot 5H_2O$[6]	10.5	245
$[Co(dmgH)_2NH_3\cdot Cl]$[8,9]	12.0	248
$K[Co(dmgH)_2(CN)_2]\cdot 1.5H_2O$[10]	12.6	242
$NH_4[Co(dmgH)_2(NO_2)_2]\cdot H_2O$[9,11]	12.6	240

Results

The complexes of the type $[Co(dmgH)_2A_2]^{n*2}$ listed in Table 1 change their electronic absorption spectra with a change in the pH in an aqueous solution. For instance, the spectrum of the aniline complex with A=aniline in an alkaline medium differs from that in an acid medium, as is shown in Fig. 1. With a change in the pH the complex undergoes a series of reversible spectrum changes, with the isosbestic points at 250 and 347 mμ, as may be seen in Fig. 2. Moreover, a plot of the absorbances at 280 mμ against the pH values gave the curve shown in Fig. 4-a. These spectral evidences seem to indicate that the complex exists

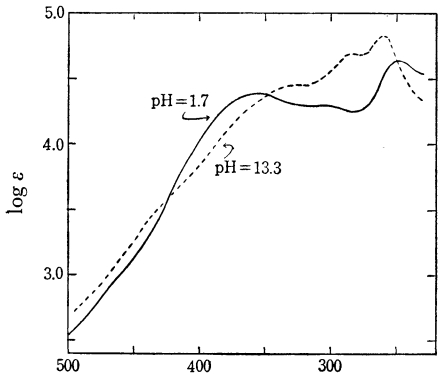

Fig. 1. Electronic spectra of $[Co(dmgH)_2(Aniline)_2]Cl\cdot 4H_2O$ in acid (pH=1.7) and alkaline (pH=13.3) solutions.

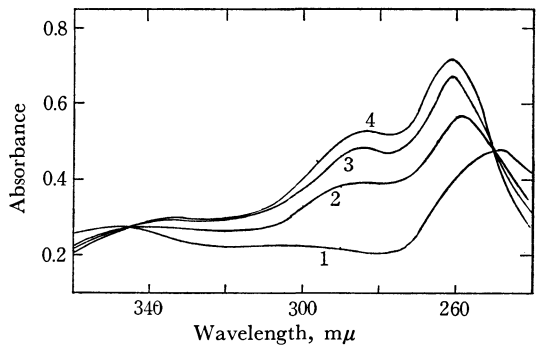

Fig. 2. Electronic spectra of $[Co(dmgH)_2(Aniline)_2]Cl\cdot 4H_2O$ in solutions of various pH.
Initial concentration: 2.18×10^{-5} M
Cell length: 1 cm.
pH: curve 1=5.4, curve 2=10.6, curve 3=11.1, curve 4=12.9

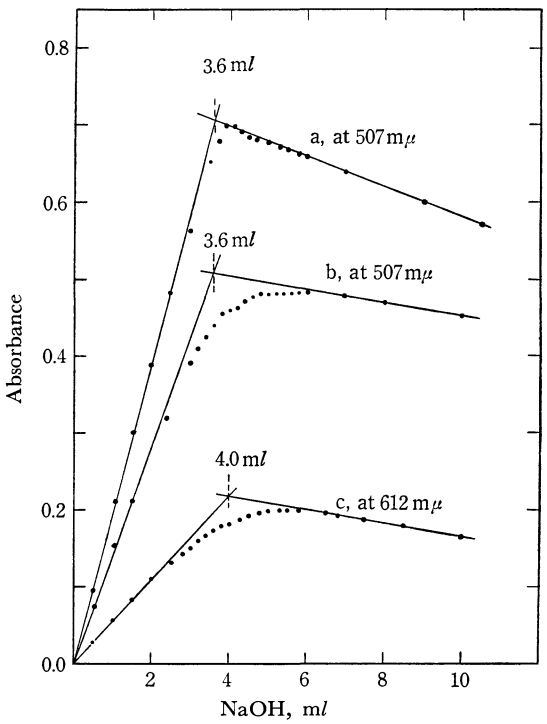

Fig. 3. Photometric titration curves of aqueous complex solutions by standard (0.0416 N) NaOH solution.

	NaOH, ml*
a: $[Co(dmgH)_2(Pyridine)_2]Cl\cdot H_2O$, 0.160 mmol	3.8
b: $[Co(dmgH)_2(NH_3)_2]Cl\cdot 5H_2O$, 0.160 mmol	3.8
c: $[Co(dmgH)_2(Aniline)_2]Cl\cdot 4H_2O$, 0.168 mmol	4.1

* Calculated amount of NaOH, ml

in two types of structures in solutions: the type A in solutions with pH<9, and the type B in solutions with pH >11.5.

6) Y. Nakatsuka and H. Iinuma, This Bulletin, **11**, 48 (1936).
7) C. Matsumoto, T. Kato and K. Shinra, *Nippon Kagaku Zasshi (J. Chem. Soc. Japan, Pure Chem. Sect.)*, **86**, 1266 (1965).
8) L. Tschgaeff, *Ber.*, **39**, 2701 (1906).
9) H. Kuroya, *J. Institute Polytechnics, Osaka City University*, **1**, C1 (1950).
10) N. Maki, This Bulletin, **38**, 2013 (1965).
11) L. Tschgaeff, *Ber.*, **41**, 2230 (1908).

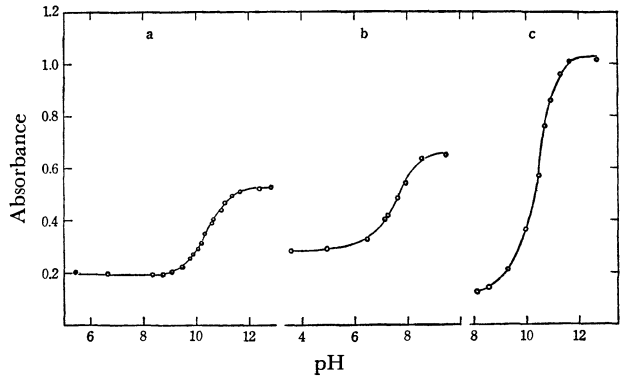

Fig. 4. Absorbance : pH curves.
a: $[Co(dmgH)_2(Aniline)_2]Cl \cdot 4H_2O$, initial concentration $=2.18\times10^{-5}$ M, $\lambda=280$ mμ
b: $[Co(dmgH)_2(Pyridine)_2]Cl \cdot H_2O$, initial concentration $=1.01\times10^{-4}$ M, $\lambda=300$ mμ
c: $[Co(dmgH)_2(NH_3)_2]Cl \cdot 5H_2O$, initial concentration $=1.00\times10^{-3}$ M, $\lambda=420$ mμ
Cell length $=1.0$ cm

The complex thus isolated, given in Table 1, has the formula $[Co(dmgH_2)(aniline)_2]Cl$; in an aqueous solution it shows a spectrum which quite agrees with that of the type A described above. Moreover, the photometric titration of this complex on an aqueous solution with a standard aqueous sodium hydroxide indicated that one mole of the complex is equivalent to one mole of sodium hydroxide, as is shown in Fig. 3.

Thus the above experimental results show that the conversion of the type A to the type B is accompanied by an proton dissociation of the complex. The ionization constants (pK_a) associated with this proton dissociation for the aniline complex was, then, spectrophotometrically obtained as 10.5 on the basis of the following relation: in the absorbance : pH curve shown in Fig. 4-a the pH value corresponding to the absorbance which is equal to $(D_A+D_B)/2$ should represent the pK_a. In this equation, D_A and D_B are the absorbances due to the complexes of the type A and of the type B respectively; they can be evaluated from the curve extrapolated according to the method of Stenström and Goldsmith.[5]

All the other complexes listed in Table 1 display spectral changes analogous to those of the aniline complex. The isosbestic points of the spectral changes are shown in Table 1. Also listed in Table 1 are the pK_a values with respect to each complex determined from the absorbance : pH curves shown in Figs. 4 and 5.

Discussion

It has been considered on the basis of NMR[12,13] and IR[13,14] spectroscopic studies and the chemical

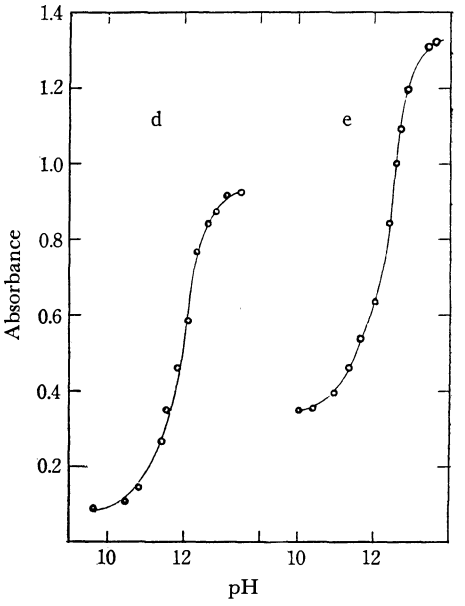

Fig. 5. Absorbance : pH curves.
d: $[Co(dmgH)_2NH_3 \cdot Cl]$, initial concentration $=1.02\times10^{-3}$ M, $\lambda=440$ mμ
e: $NH_4[Co(dmgH)_2(NO_2)_2] \cdot H_2O$, initial concentration $=1.00\times10^{-3}$ M, $\lambda=420$ mμ
Cell length $=1.0$ cm

characteristics,[6] that, in a series of cobalt(III)-dimethylglyoxime complexes with the formula $[Co(dmgH)_2A_2]^n$,*2 the central cobalt ion coordinates two dimethylglyoximato radicals to form a planar configuration including stable, intramolecular hydrogen bridges and two moles of A as

12) H. A. O. Hill, K. G. Morallee and R. E. Collis, *Chem. Commun.*, **1967**, 888; Y. Yamano, I. Masuda and K. Shinra, *Inorg. Nucl. Chem. Letters*, **4**, 581 (1968).

13) R. D. Gillard and G. Wilkinson, *J. Chem. Soc.*, **1963**, 6041.

14) A. Nakahara, J. Fujita and R. Tsuchida, This Bulletin, **29**, 296 (1956).

axial ligands. As for the ammine complex with A=NH_3, X-ray crystallography has confirmed it to have a planar chelate structure.[15]

The electronic spectra of the complexes with A=NH_3, NO_2^-, or a halide anion have also been reported by several workers.[16] Matsumoto[7] has stated that the complexes with A=aniline derivatives are characterized by two intense ($\log \varepsilon \doteqdot 4$) absorption bands; one is due to the Co(III)→dmgH charge transfer observed around 300 mμ, and the other, to the axial ligand A→Co(III) charge transfer in the range of 350—410 mμ. However, there seems to have been no study which has dealt, in detail, with the spectral changes in the complexes.

As has been shown in the present study, the $[Co(dmgH)_2A_2]^n$ complexes, listed in Table 1 change their electronic spectra reversibly depending on the pH of the solution. From such spectral changes as those shown in Figs. 4 and 5, the complexes may be considered to exist in the solution in two forms, the type A in acid and neutral media and the type B in an alkaline medium. The isolated complexes with the $[Co(dmgH)_2A_2]^n$ composition show, in aqueous solutions, electronic spectra which agree with those of the corresponding A-type complex, and they consume one equivalent of an aqueous sodium hydroxide to change into a B-type complex.

From a consideration of these experimental results and in view of the structure of the complexes, it seems most reasonable to conclude that the electronic spectral changes of the $[Co(dmgH)_2A_2]^n$ are due to the proton dissociation of hydrogen in the hydrogen bridges of the complexes, as is shown in Eq. (1).

Further support for the above conclusion comes from the fact that, in the case of 1,2-cyclohexanedionedioxime (niH_2), which is analogous to the dimethylglyoxime, two types of complexes, $[Co(niH)_2(p\text{-anisidine})_2]Cl$ and $[Co(niH)(ni)(p\text{-anisidine})_2]$, have been isolated.[17] As to α-benzildioxime(bzH_2), the complex with the $[Co(bzH)(bz)(p\text{-anisidine})_2]$ formula is also known.

The dissociation constants, pK_a(Table 1), associated with Eq. (1) indicate that the $[Co(dmgH)_2A_2]^n$ complex is generally a very weak acid. With the exception in the pyridine complex, monovalent complex-cation always shows pK_a=9.9—10.9, and the monovalent complex-anion, pK_a=12.6, while a neutral complex shows pK_a values between them (Table 1).

In the cobalt complexes with dimethylglyoxime, the tendency to form O–H–O hydrogen bonding shown in Fig. A has been considered to be very strong. In fact, the complex with the $Co(dmgH)_3$ composition, where a similar hydrogen bonding is lacking, can be synthesized only in a strong alkaline solution.[14] However, as has been seen in the present work, the $[Co(dmgH)_2A_2]^n$ complexes (Fig. A) may be characterized as acids, though they are very weak (Table 1). As for their conjugate bases $[Co(dmgH)(dmg)A_2]^{n-1}$ (Fig. B), the remaining hydrogen bridge was not observed to dissociate the proton under the experimental conditions (pH≦13) employed. This seems to be mainly due to the stronger hydrogen bonding in the $[Co(dmgH)(dmg)A_2]^{n-1}$ than in the corresponding $[Co(dmgH)_2A_2]^n$, since the increase in the negative charges of a complex ion of this type may only slightly increase the pK_a value in 1—2, as is indicated in Table 1.

In general, an oxime group may be expected to increase its tendency to dissociate the proton when coordinated to a transition metal ion. The iron(II) complex with pyridine-2-aldoxime, $[Fe(PAO)_3H_2]^+$,*3 dissociates proton showing pK_a=3.36, and as to $[Fe(PAO)_3H]$, its pK_a=7.13; in the case of the palladium complex, $[Pd(PAO)_2H]^+$, the pK_a is 4.0, though a free pyridinealdoxime gives pK_a=10.22 referred to its oxime group.[3,4]

In comparison with the above facts, in the case of dimethylglyoxime-Co(III) complexes, the oxime group shows a much larger pK_a value than that expected from the pK_a value of free dimethylglyoxime, which is known to be about 11.[18] The

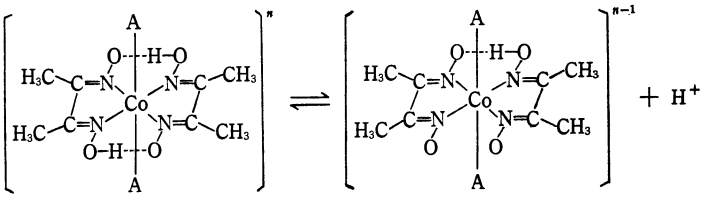

Fig. A Fig. B (1)

15) K. S. Viswanathan and N. R. Kunchur, *Acta Cryst.*, **14**, 675 (1961).

16) A. Nakahara, This Bulletin, **28**, 207 (1955).

*3 Pyridine-2-aldoximato anion is abbreviated as PAO.

17) C. Matsumoto, I. Masuda and K. Shinra, *Nippon Kagaku Zasshi (J. Chem. Soc. Japan, Pure Chem. Sect.)*, **88**, 46 (1967).

18) T. V. Parke and W. W. Davis, *Anal. Chem.*, **26**, 642 (1954).

larger pK_a values for the complexes may be attributable to the hydrogen bonding in the dimethylglyoxime-Co(III) complexes (Fig. A).

Finally, it is of interest to note that pyridine and γ-picoline complexes show somewhat lower pK_a values than those of the other complexes, as may be seen in Table 1; this indicates that axial pyridine derivatives tend to facilitate the proton dissociation of hydrogen bridges in the complexes. It appears that this can be understood by assuming a double bonding character between the nitrogen atom in the pyridine ring and the central cobalt, which would make easy the transmittance of an electronic effect of the axial ligand to the oximato radical. A study of this point in some detail will be presented in a subsequent paper.

BULLETIN OF THE CHEMICAL SOCIETY OF JAPAN VOL. 42 2300—2302 (1969)

Electrochemical Behavior of Platinum in Solutions Containing Ethylenediaminetetraacetate

Nobuyuki TANAKA

Department of Chemistry, Faculty of Science, Tohoku University, Katahira-cho, Sendai

and Tadashi FUJISAWA

Department of Applied Chemistry, Yamagata Technical Junior College, Jonan, Yonezawa

(Received February 21, 1969)

The electrochemical behavior of platinum in solutions of ethylenediaminetetraacetate(EDTA) has been investigated by the measurements of current-potential and current-time curves and by the controlled-potential electrolysis. EDTA gives the anodic limiting current, which is much smaller than that of one-electron transfer obtained for the ordinary diffusion-controlled electrode reaction. Platinum was detected by the spectrophotometric method in the solution which was subjected to the electrolysis at controlled potential. The results suggest that the anodic current is due to the electrolytic dissolution of the platinum electrode by the reactions,

$$Pt + 2H_2O \rightarrow Pt(OH)_2 + 2H^+ + 2e \quad (1)$$

$$Pt(OH)_2 + H_2Y^{2-} \rightarrow PtY^{2-} + 2H_2O \quad (2)$$

where Y^{4-} represents a quadrivalent anion of EDTA.

The anodic limiting current of ethylenediaminetetraacetate (EDTA) which was obtained at the platinum electrode was found to be much smaller than the diffusion-controlled limiting current obtained for the electrode reaction of one-electron transfer and to be independent of the rate of rotation of the platinum electrode. Recently, Stulik and Vydra[1] have investigated the electrode reaction of EDTA at the platinum electrode and stated that the anodic limiting current is due to the oxidation of EDTA itself.

However, our preliminary experiments suggested that the anodic limiting current was due to the electrolytic dissolution of the platinum electrode in the solution of EDTA.

This paper describes the electrochemical behavior of platinum in the solution of EDTA which was revealed from the voltammetric measurements and the controlled-potential electrolysis.

Experimental

Apparatus. A recording polarograph, Yanagimoto Model P 102 was used for the measurements of current-potential and current-time curves. A Hokuto Denko linear scanning unit Model LS-1D, potentiostat PS-500 B and XY recorder F-3B were used for the measurements of cyclic voltammetric curves and for the electrolysis at controlled potential. A Hitachi-Horiba pH meter Model F was used for the measurement of pH. All measurements were made in a thermostat at 25.0°± 0.1°C except those which were made at various temperatures. The measurement of absorbancy was made with a Hitachi Model 139 spectrophotometer.

Electrode. A platinum wire electrode was sealed into a glass tube which was filled with mercury for electrical contact. The electrode was 0.7 mm in diameter and 5 mm in length, its geometric surface area being approximately 0.11 cm^2. The electrode was rotated with a synchronous motor at a rate of 600 rpm. The counter electrode which was used for the

1) K. Stulik and F. Vydra, *J. Electroanal. Chem.*, **16**, 385 (1968).

electrolysis at controlled potential was a platinum spiral of 0.7 mm in diameter and 40 mm in length.

Pretreatment of Electrode. The platinum wire electrode was treated with 10 N nitric acid and washed with distilled water. Before use, it was subjected to several cycles from −0.5 to +1.5 V *vs.* the saturated caromel electrode (SCE) in a deaerated 0.1 M perchloric acid. Then the electrode which was finally polarized anodically was short-circuited against SCE. If the electrode showed such a characteristic that the current decreased practically to zero within 2 or 3 min, it was called a "clean electrode."[2] When the electrode did not show such a characteristic, the cycled polarization was repeated. The clean electrode was stored usually in a deaerated distilled water.

Reagents. All reagents used were of reagent grade.

Spectrophotometric Measurements. The solution (50 m*l*) which was subjected to the controlled potential electrolysis was concentrated to about 1 m*l* in volume. The residual solution was treated with bromine water and concentrated hydrochloric acid and evaporated to almost dryness in order to convert Pt(II) to Pt(IV).[3] Ten milliliters of 1 : 1 hydrochloric acid was added and the solution was concentrated again to about 1 m*l* to remove bromine completely. The residual solution was treated according to Ayres and Meyer:[4] 10 m*l* of 6 N hydrochloric acid, 10 m*l* of 20% ammonium chloride solution and 10 m*l* of 1.0 M tin(II) chloride solution containing 3.5 N hydrochloric acid were added and the developed color was extracted with isoamyl acetate containing 1% resorcinol, of which absorption spectra were obtained.

Results and Discussion

Current-potential Curves. Current-potential curves of 5 mM EDTA in 0.1 M acetate buffer solutions were obtained with the rotated or stationary platinum electrode in the absence of oxygen, which are shown in Fig. 1. An arrow sign represents the direction of scanning potential. In both cases, the anodic limiting currents gave almost the same value which was independent of the rate of rotation of the electrode and was much smaller than that of one-electron transfer of ordinary compounds at this electrode. This indicates that the anodic current is not controlled by diffusion. In addition, the cathodic peak current was smaller in the presence of EDTA than in the absence of EDTA in the solution. This may indicate that the oxide film produced on the electrode surface was dissolved partly by the chemical reaction with EDTA.

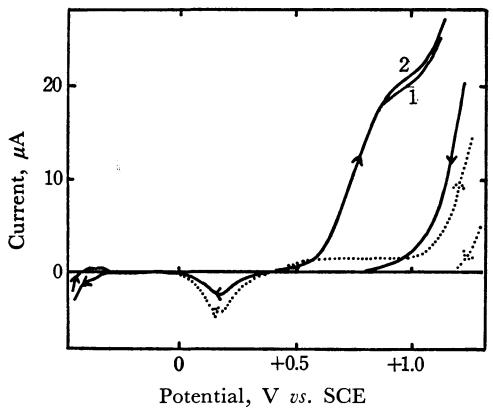

Fig. 1. Voltammetric curves of 5 mM EDTA in 0.1 M acetate buffer solutions at (1) rotated and (2) stationary Pt electrode. ····· indicates voltammetric curve of 0.1 M acetate buffer.

The anodic current increased with the increase of the concentration of EDTA, but it was not exactly proportional to the latter, as is given in Table 1. In the acetate buffer solution, the anodic current decreased with increasing pH's, and at higher pH's adjusted with other buffers no anodic current could be obtained. (Fig. 2).

The above results suggest that the anodic current is due to the electrode reaction given by

$$Pt + 2H_2O \rightarrow Pt(OH)_2 + 2H^+ + 2e \quad (1)$$

$$Pt(OH)_2 + H_2Y^{2-} \rightarrow PtY^{2-} + 2H_2O \quad (2)$$

Table 1. Anodic currents at 0.9 V at various EDTA concentrations in 0.1 M acetate buffer solutions

Concentration of EDTA, mM	Anodic current at +0.9 V, μA	
	Observed	Corrected for residual current*
1	6.0	3.5
5	14.5	12.0
10	23.0	20.5
20	36.5	34.0

* Residual current due to platinum oxide formation.

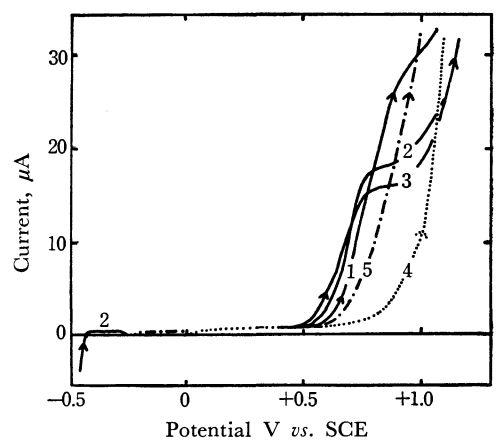

Fig. 2. Voltammetric curves of 5 mM EDTA at pH (1) 3.6 (2) 4.7 (3) 5.1 (4) 9.3 (0.1 M borate buffer) and (5) 13 (0.1 M NaOH).

2) I. M. Kolthoff and N. Tanaka, *Anal. Chem.*, **26**, 632 (1954).

3) D. T. Napp and S. Bruckenstein, *ibid.*, **40**, 1036 (1968).

4) G. H. Ayres and A. S. Meyer, Jr., *ibid.*, **23**, 299 (1951).

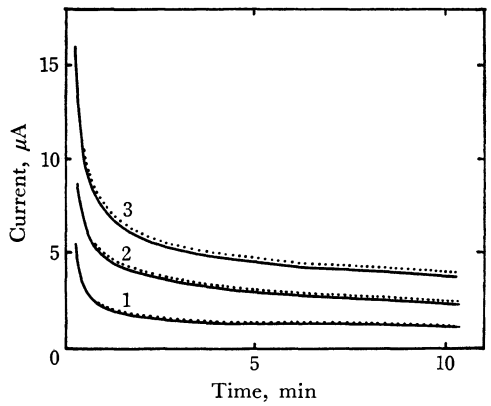

Fig. 3. Current-time curves of (1) 1×10^{-3} M, (2) 3×10^{-3} M and (3) 5×10^{-3} M EDTA obtained at 0.9 V *vs.* SCE in 0.1 M acetate buffer solution. ····· indicates $i-t$ curves at stationary and ——, at rotated Pt electrode.

The species H_2Y^{2-} is predominant in a pH range where the anodic current is obtained.

Current-time Curves. Current-time curves of EDTA were measured with the rotated and the stationary electrodes at +0.9 V. They are shown in Fig. 3 after correction for the residual current. Although the current decreased rapidly at first, it was nearly constant after the elapse of 5 min. There was practically no difference in current at the rotated and at the stationary electrode. The product $it^{1/2}$ which was found not to be constant also supports that the anodic current is not diffusion-controlled.[5]

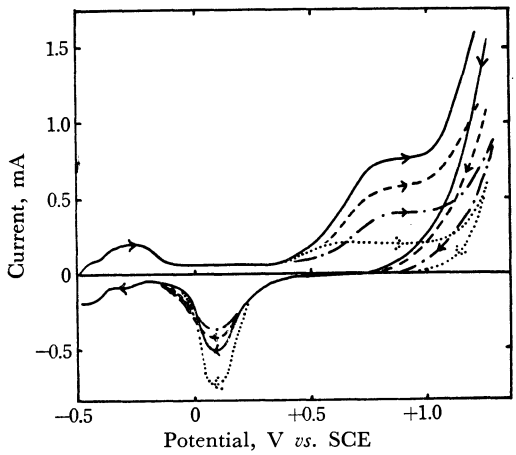

Fig. 4. Cyclic voltammetric curves of 5 mM EDTA in 0.1 M acetate buffer solutions at 25°C (—·—), 40°C (——) and 55°C (——). ····· indicates that of base electrolyte at 55°C. Scan rate is 0.2 V/sec.

5) P. Delahay, "New Instrumental Methods in Electrochemistry," Interscience, New York (1954), p. 51.

Cyclic Voltammetric Curves. Cyclic voltammetric curves of 5 mM EDTA in 0.1 M acetate buffer solutions were measured at various temperatures. Some of the curves are given in Fig. 4. The cathodic peak current obtained in the presence of EDTA was found to be always smaller than that obtained in the absence of EDTA. The anodic limiting current was enhanced with increasing temperature.

Electrolysis at Controlled Potentials. The solutions containing 5 or 10 mM EDTA and 0.1 M acetate buffer were electrolyzed for 10 hr at controlled potential of +0.9 V or at potentials cycled in the range of −0.1 V to +1.3 V, and the ultraviolet absorption spectra were obtained with the procedure mentioned above, which are shown in Fig. 5. The absorption band is considered to be due to the formation of Pt(IV)-Sn(II) complexes. In Fig. 5, the absorption spectra of the solution which was prepared with a standard platinum(IV) solution and a tin(II) chloride solution are shown. These spectra clearly indicate that platinum is dissolved electrochemically into the solution to a greater amount in the presence of EDTA than in the absence of EDTA.

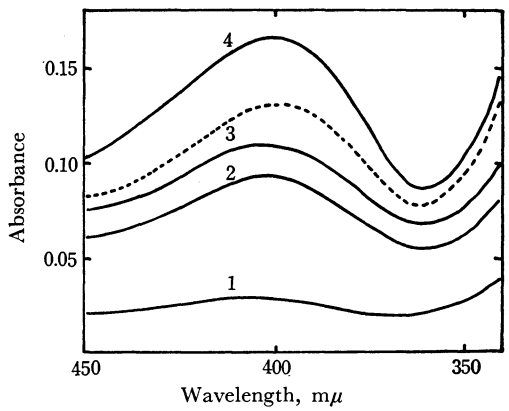

Fig. 5. Absorption spectra of Pt(IV)-Sn(II) chloride complex in isoamyl acetate solution. —— indicates absorption spectra of the solutions which were prepared with the solution subjected to the electrolysis at potentials cycled in the range of −0.1 to +1.3 V (1, 2 and 3) and at controlled potential at +0.9 V (4) for 10 hr. The concentrations of EDTA in electrolysis solutions were 0(1), 5(2) and 10 (3 and 4) mM. ---- indicates absorption spectra of the solution which was prepared with 2.45 mM Pt(IV) standard solution and tin(II) chloride solution.

Conclusion. From all of the results obtained in this study, it may be concluded that the anodic current obtained in the solution of EDTA is not due to the oxidation of EDTA itself but due to the electrolytic dissolution of platinum electrode with EDTA.

BULLETIN OF THE CHEMICAL SOCIETY OF JAPAN VOL. 42 2303—2307 (1969)

Oligomerization of Isoprene by Zirconium Catalysts

Akira MISONO, Yasuzo UCHIDA, Ken-ichi FURUHATA and Shohei YOSHIDA

Department of Industrial Chemistry, Faculty of Engineering, The University of Tokyo, Hongo, Tokyo

(Received August 6, 1968)

The oligomerization of isoprene by catalyst systems consisting of a zirconium compound and an organoaluminum compound was studied. Isoprene was dimerized to 2,6-dimethyl-1,*trans*-3,6-octatriene by a catalyst system consisting of zirconium(IV) *n*-butoxide and diethylaluminum chloride. The selectivity for this dimer was increased to more than 90% by adding triphenylphosphine or tetrahydrofuran to this catalyst system. The effects of the molar ratio of the catalyst components and those of catalyst species were studied.

It is well known that the oligomerizations of olefins are catalyzed by transition metal complexes. The structures of the oligomers are affected by the transition metal and other catalyst components. We reported previously the cyclic dimerization of isoprene to a mixture of 1,5- and 2,5-dimethyl-1,5-cyclooctadiene with a catalyst system consisting of iron(III) acetylacetonate, 2,2'-dipyridyl, and triethylaluminum.[1]

Some catalyst systems containing titanium or chromium have been reported to give a linear dimer of isoprene, 2,6-dimethyl-1,3,6-octatriene along with other oligomers.[2,3]

We now wish to report on the selective linear dimerization of isoprene by catalyst systems consisting of zirconium(IV) *n*-butoxide, diethylaluminum chloride, and an additive, such as triphenylphosphine or tetrahydrofuran. The dimer was 2,6-dimethyl-1, *trans*-3,6-octatriene. The effects of the molar ratios of the catalyst components on the selectivity for the dimer were studied.

Experimental

Reagents. Isoprene was dried over anhydrous sodium sulfate, distilled, and deoxygenated by the freeze-thaw method with pumping.

Allyl chloride was dried over calcium sulfate and distilled under an atmosphere of nitrogen.

Organoaluminum compounds were distilled at reduced pressures and dissolved in benzene.

Benzene, toluene, tetrahydrofuran, and ethyl ether were purified by conventional procedures.

Zirconium(IV) *n*-butoxide was prepared according to the reported method.[4]

Zirconium(IV) acetylacetonate was prepared by the reaction of pyridinium hexachlorozirconate and excess acetylacetone in benzene, to which mixture triethylamine was added, drop by drop, over a 30-min period, and was then purified by recrystallization from acetylacetone.

Tetra-π-allylzirconium was synthesized according to the method reported by Wilke.[5]

Triphenylphosphine and 2,2'-dipyridyl were commercial reagents.

Reactors. The reaction was carried out in a 30 m*l* glass tube, a 200 m*l* glass autoclave, or a 100 m*l* stainless steel autoclave.

Reaction Procedure. In a typical reaction, 5.4 mmol of triphenylphosphine were put into a stainless steel autoclave; the autoclave was swept several times with dry nitrogen, and then 6.28 g of benzene, 50 mmol of isoprene, 0.5 mmol of zirconium(IV) *n*-butoxide (16.7 wt% benzene solution), and 5.0 mmol of diethylaluminum chloride (19.9 wt% benzene solution) were added, in this order, under a dry nitrogen stream. The total amount of benzene was controlled so as to be 8.3—8.5 g. Then the autoclave was closed and kept at 100°C for 2 hr.

Analysis. For the separation of the products, the reaction solution was washed with diluted hydrochloric acid and with water, and then dried over anhydrous sodium sulfate and fractionally distilled. For the determination of the products, gas chromatography, infrared spectrography and nuclear magnetic resonance spectrography were applied, together with elementary analysis and molecular weight measurement. The gas chromatography was also used in calculating the conversion percent of isoprene and the yields of the products. A 2 m stainless steel column, 4-mm in diameter and packed with polydiethylene glycol succinate on Shimalite, was used. Operation conditions: column temperature, 112°C and 180°C for dimers and trimers respectively; Flash evaporator temperature, 300°C;

1) A. Misono, Y. Uchida, M. Hidai and Y. Ohsawa, This Bulletin, **39**, 2425 (1966).

2) a) L. I. Zakharkin, *Dokl. Akad. Nauk, S.S.S.R.*, **131**, 1069 (1960). b) H. Takahashi and M. Yamaguchi, *Osaka Kogyo Gijutsu Shikensho Kiho*, **15**, 271 (1964).

3) G. Wilke, *J. Polymer Sci.*, **38**, 45 (1959).

4) D. C. Bradley, F. M. Abd-El Halim, E. A. Sadek and W. Wardlaw, *J. Chem. Soc.*, **1952**, 2032.

5) G. Wilke, B. Bogdanovic, P. Heimbach, W. Keim, M. Kroner, W. Oberkirch, K. Tanaka, E. Steinrucke, D. Walter and H. Zimmermann, *Angew. Chem.*, **78**, 157 (1965).

carrier gas (helium) speed, 30 ml/min. Benzene was used as the internal standard.

Infrared spectra of the products were taken with a Nihon Bunko Model DS-301.

Nuclear magnetic resonance spectra were recorded on a Nihon Denshi Model C-60.

Molecular weights were measured by the cryoscopic method in benzene.

Results and Discussion

Structures of the Products. The reaction mixtures were analyzed by gas chromatography (Table 1).

Table 1. Gas chromatographic results of dimers and trimers of isoprene

Column temp., °C	Relative retention time of product based on benzene					
	Dimer		Trimer			
112	2.8	3.4				
180			2.9	4.9	6.8	9.9

Table 2. NMR spectra assignment of 2,6-dimethyl-1,*trans*-3,6-octatriene

NMR (τ-value)		Assignment*
8.45	doublet	h
8.40	singlet	f
8.25	singlet	b
7.25	doublet	e
5.12	singlet	a
4.67	quartet	g
4.42	sextet	d
3.75	doublet	c

* The protons of 2,6-dimethyl-1,*trans*-3,6-octatriene are represented as follows.

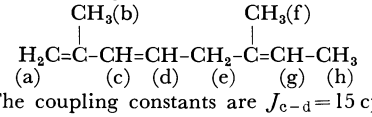

The coupling constants are $J_{c-d}=15$ cps, $J_{d-e}=6$ cps, and $J_{g-h}=6$ cps.

A product with the relative retention time of 2.8 (112°C) was the main product. For analysis, it was isolated by distillation. The structure of the product was identified as 2,6-dimethyl-1,*trans*-3,6-octatriene by means of its nuclear magnetic resonance spectra, shown in Table 2; this structure was supported by the infrared spectra, which showed absorptions due to methyl and methylene groups (2960, 2905, 2840, 1455, 1440, and 1375 cm^{-1}), conjugated and isolated double bonds (1655, 1645, and 1610 cm^{-1}), a *trans* double bond (965 cm^{-1}), a terminal methylene group (885 cm^{-1}), and a tri-substituted double bond (815 cm^{-1}). A mixture of the products whose relative retention times were 4.9, 6.8, and 9.9 (180°C) was also separated by distillation. These compounds were confirmed to be trimers by molecular weight measurements (Found: 200, Calcd for $C_{15}H_{24}$: 204). The products whose relative retention times were 4.9 and 9.9 (180°C) were obtained in a relatively highly pure state by the fractional distillation. The infrared spectra of the product whose relative retention time was 9.9 showed absorptions due to methyl and methylene groups (2960, 2910, 2840, 1440, and 1375 cm^{-1}), a *trans* di-substituted double bond (965 cm^{-1}), and a tri-substituted double bond (810 cm^{-1}). No absorption was observed due to a terminal methylene or a vinyl group. The structure of this trimer has not yet been confirmed, but we assume it to be as shown below:

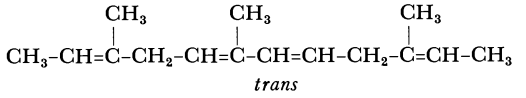

trans

The absorption characteristic of a conjugated double bond was not observed, but this can be explained by the fact that this compound has a nearly symmetric structure. The nuclear magnetic resonance spectra of this compound showed absorptions at about $\tau=8.4$ due to a methyl group which was attached to an unsaturated carbon atom, at $\tau=7.3$ (doublet) due to methylene protons between double bonds, and at $\tau=4$—5 (multiplet) due to olefinic protons; these absorptions do not contradict the structure shown above. This compound might be formed by the addition of isoprene to the 1-position of the dimer, 2,6-dimethyl-1,*trans*-3,6-octatriene. The infrared spectra of the trimer whose relative retention time was 4.9 showed absorptions due to methyl and methylene groups (2960,

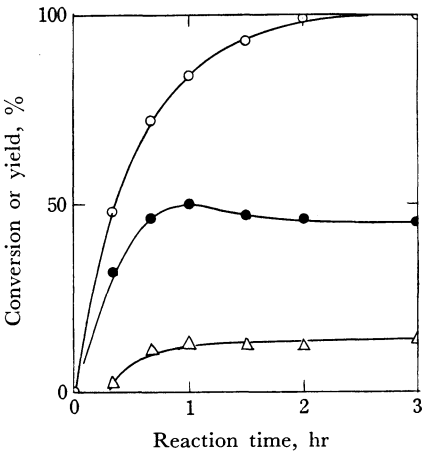

Fig. 1. Time dependence of the reaction.

○: Conversion of isoprene, %
●: Yield of 2,6-dimethyl-1,*trans*-3,6-octatriene, %
△: Yield of trimers, %
Reaction temp.: 100°C
Isoprene/$Zr(O^nC_4H_9)_4$ mol ratio: 100
$AlEt_2Cl/Zr(O^nC_4H_9)_4$ mol ratio: 10

2910, 2840, 1455, 1440, and 1380 cm^{-1}), *trans* di-substituted, tri-substituted, and conjugated double bonds (1660, 1645, 1610, 965, and 815 cm^{-1}), and a terminal methylene group (885 cm^{-1}). This trimer can be considered to be linear, but its structure has not yet been confirmed. The trimer with a relative retention time of 6.8 could not be isolated in sufficient purity for its structure to be studied in detail.

The Time Dependence of the Reaction. The time dependence of the reaction of isoprene by the catalyst system consisting of zirconium(IV) *n*-butoxide, and diethylaluminum chloride was studied (Fig. 1). The conversion of isoprene became almost 100% in 2 hr. The yield of 2,6-dimethyl-1,*trans*-3,6-octatriene reached a maximum at about 1 hr, and then it decreased slightly. It is probable that the dimer was consumed in the successive reaction to higher oligomers.

The Effects of the Molar Ratio of the Catalyst Components. The effects of the molar ratio of the components of the catalyst consisting of zirconium(IV) *n*-butoxide and diethylaluminum chloride or triethylaluminum are shown in Figs. 2 and 3 respectively.

In the case of diethylaluminum chloride, the conversion of isoprene increased with the increase in the molar ratio. The yield of 2,6-dimethyl-1,*trans*-3,6-octatriene reached a maximum at the molar ratio of 10. The yield of trimers was almost constant when the molar ratio exceeded 10, and the polymer yield was increased as the molar ratio was increased. On the other hand, in the case of

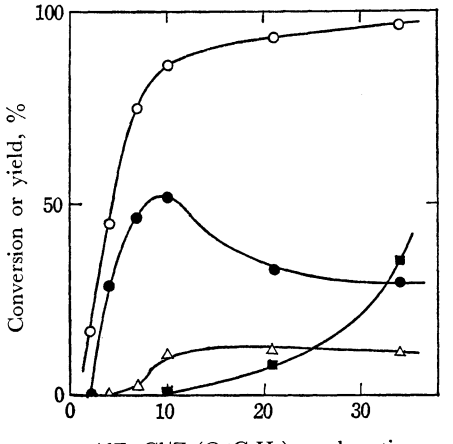

Fig. 2. Effect of the molar ratio of diethylaluminum chloride to zirconium(IV) *n*-butoxide.
○: Conversion of isoprene, %
●: Yield of 2,6-dimethyl-1,*trans*-3,6-octatriene, %
△: Yields of trimers, %
■: Yield of polymer, %
Reaction temp.: 100°C, Reaction time: 2 hr
Isoprene/$Zr(O^nC_4H_9)_4$ mol ratio: 100

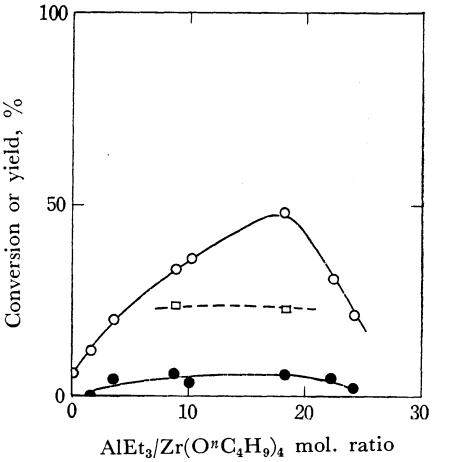

Fig. 3. Effect of the molar ratio of triethylaluminum to zirconium(IV) *n*-butoxide.
○: Conversion of isoprene, %
●: Yield of 2,6-dimethyl-1, *trans*-3,6-octatriene, %
□: Yield of polymer, %
Reaction temp.: 100°C, Reaction time: 2 hr
Isoprene/$Zr(O^nC_4H_9)_4$ mol ratio: 100

triethylaluminum the maximum conversion of isoprene appeared at the molar ratio of 18. By this catalyst system, isoprene was consumed mainly by high polymerization, and the yield of 2,6-dimethyl-1,*trans*-3,6-octatriene was small (0—7%) at the molar ratios between 7 and 22.

As other organoaluminum compounds, diethylaluminum ethoxide and ethylaluminum dichloride were used. In the case of diethylaluminum ethoxide, however, the reaction of isoprene did not take place. The binary system of zirconium(IV) *n*-butoxide and ethylaluminum dichloride polymerized isoprene immediately. The infrared spectrum of the polymer obtained by this binary catalyst system showed only methyl and methylene absorptions and did not show any absorption due to carbon-carbon double bonds. This spectrum was identical with that of the polymer obtained by ethylaluminum dichloride only. Ethylaluminum dichloride was reported to cause the cationic polymerization of isoprene to a ladder polymer.[6]

The best organoaluminum compound as a catalyst component was thus found to be diethylaluminum chloride, and the best yield of the dimer of isoprene was accomplished when the molar ratio of diethylaluminum chloride to zirconium(IV) *n*-butoxide was about 10.

The Effects of Additives. In the oligomerization of olefins, the addition of an electron donor to the reaction system strongly affects the reaction

6) B. A. Dolgoplosh, G. P. Belonovskaja, I. I. Boldgreva, E. N. Kropacheva, K. V. Nelson, Ja. M. Rosinoer and J. D. Chernova, *J. Polymer Sci.*, **53**, 209 (1961).

products, *e.g.*, in the oligomerization of butadiene with iron complex catalysts.[7] In the present study some electron donors were added to the catalyst system consisting of zirconium(IV) *n*-butoxide and diethylaluminum chloride (Al/Zr; 10). The results are shown in Fig. 4.

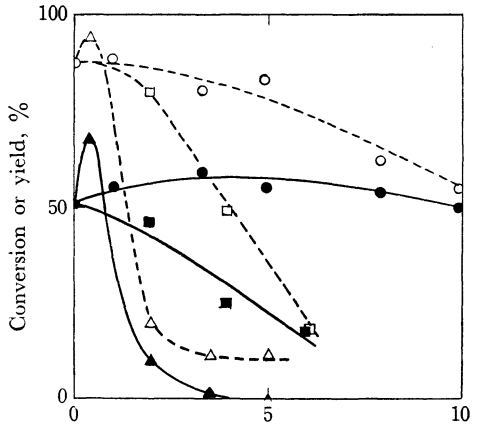

Fig. 4. Effects of additives.
----: Conversion of isoprene, %
——: Yield of 2,6-dimethyl-1,*trans*-3,6-octatriene, %
Additives are represented by
○●: PPh_3, □■: THF, △▲: 2,2'-dipyridyl.
Reaction temp.: 100°C, Reaction time: 2 hr
Isoprene/Zr(O^{n}C$_4$H$_9$)$_4$ mol ratio: 100
$AlEt_2Cl$/Zr(O^{n}C$_4$H$_9$)$_4$ mol ratio: 10

The addition of triphenylphosphine lowered only the conversion of isoprene, while the yield of 2,6-dimethyl-1,*trans*-3,6-octatriene was slightly increased. In the case of tetrahydrofuran, both the conversion and the yield were decreased. The formation of higher oligomers was strongly suppressed in both cases, and the selectivity for the dimer increased to more than 90%. The addition of 2,2'-dipyridyl suppressed the reaction of isoprene.

The Reaction with Catalyst Systems Consisting of Other Zirconium Compounds. Zirconium(IV) acetylacetonate, zirconium(IV) chloride, and tetra-π-allylzirconium were used in place of zirconium(IV) *n*-butoxide in the reaction of isoprene.

When zirconium(IV) acetylacetonate and diethylaluminum chloride were used as catalysts, no oligomerization of isoprene took place, but polymerization did occur. The polymer obtained was a white powder melting at 123°C; the infrared spectrum of the polymer showed methyl and methylene absorptions and two absorptions at 890 cm^{-1} and 980 cm^{-1}.

In the case of the catalyst system consisting of zirconium(IV) chloride and triethylaluminum or diethylaluminum chloride, the reaction solution was not homogeneous and only a small amount of polymer was formed at the surface of zirconium(IV) chloride.

In tetra-π-allylzirconium, the π-allyl ligand is supposed to be replaced with isoprene. In the reaction of isoprene by tetra-π-allylzirconium alone, the dimerization of isoprene to 2,6-dimethyl-1,*trans*-3,6-octatriene was observed along with the polymerization reaction. When diethylaluminum chloride was employed as a catalyst component, the conversion of isoprene and the yield of the dimer increased as the molar ratio of diethylaluminum chloride to tetra-π-allylzirconium increased. However, the formation of the dimer became constant at the higher molar ratio. The effect of the molar ratio of diethylaluminum chloride to tetra-π-allylzirconium is shown in Fig. 5. From this result, the addition of diethylaluminum chloride seemed to be necessary to produce an effective catalyst for the dimerization.

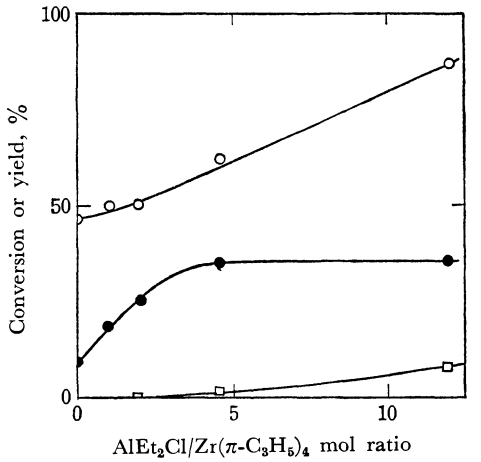

Fig. 5. Effect of the molar ratio of diethylaluminum to tetra-π-allylzirconium.
○: Conversion of isoprene, %
●: Yield of 2,6-dimethyl-1,*trans*-3,6-octatriene, %
□: Yields of trimers, %
Reaction temp.: 100°C, Reaction time: 2 hr
Isoprene/Zr(π-C$_3$H$_5$)$_4$ mol ratio: 100

In the oligomerization of dienes with the catalyst system consisting of a transition metal and an alkylaluminum, the alkylaluminum is considered to act as an alkylating reagent of the transition metal. A low-valent transition metal species is then formed by the homolytic splitting of the carbon-metal bond. The catalyst systems consisting of zirconium(IV) *n*-butoxide and diethylaluminum chloride, with or without a stoichiometric amount of isoprene, were diamagnetic at room temperature and after having been heated at 100°C for 30 min.

7) M. Hidai, K. Tamai, Y. Uchida and A. Misono, This Bulletin, **39**, 1357 (1966).

From these results, we assume that zirconium is in its four-valent state during the dimerization reaction.

The small difference between triphenylphosphine and tetrahydrofuran in the effects on the dimerization of isoprene by the catalyst system consisting of zirconium(IV) *n*-butoxide and diethylaluminum chloride can be explained on the assumption presented above. If zirconium is in its four-valent state (d^0), the back donation to ligands does not play an important part in the catalytic reaction.

BULLETIN OF THE CHEMICAL SOCIETY OF JAPAN VOL. 42 2307—2309 (1969)

Studies on Stable Free Radicals. IV.*[1] Decomposition of Stable Nitroxide Radicals

Keisuke MURAYAMA and Takao YOSHIOKA

Central Research Laboratories, Sankyo Co., Ltd., Shinagawa-ku, Tokyo

(Received December 4, 1968)

Decomposition studies of extremely stable free radicals such as 2,2,6,6-tetramethyl-4-oxopiperidine-1-oxyl (I), 2,2,6,6-tetramethylpiperidine-1-oxyl (VIII) and 2,2,6,6-tetramethyl-4-hydroxypiperidine-1-oxyl (IX) were carried out: although radical I decomposed to give 1-hydroxy-2,2,6,6-tetramethyl-4-oxopiperidine (IV) both in the light and dark, radicals VIII and IX were more stable under these reaction conditions. Therefore it was confirmed that i) a source of hydrogen was the ketonic α-methyene hydrogens, ii) a radical which could give a thermodynamically stable conjugated product by a cycloelimination was easily decomposed and iii) the decomposition of radical I was only accelerated by heating and was independent of the action of light.

In a previous study on reactivity of extremely stable free radicals,[1] it was reported that the reaction of stable free radicals such as 2,2,6,6-tetramethyl-4-oxopiperidine-1-oxyl (I) and cyclohexane-1-spiro-2'-(4'-oxoimidazolidine-1'-oxyl)-5'-spiro-1''-cyclohexane (II) with a *C*-radical derived from α,α'-azo-bis(isobutyronitrile) (ABIN) (III) gave the corresponding coupled products. Although the reaction of II with III proceeded in a high yield, the reaction of I with III only gave a coupled product in a poor yield and a by-product, 1-hydroxy-2,2,6,6-tetramethyl-4-oxopiperidine (IV), in 38.4% yield.[1] We wish to explain the differences in the mechanism in the case of I and II in this paper.

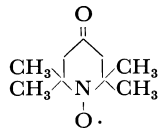

(I)

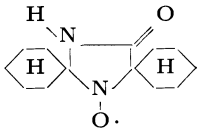

(II)

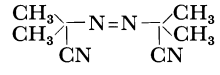

ABIN (III)

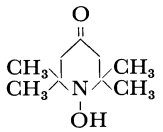

(IV)

Results and Discussion

It appears that the by-product (IV) arose from a hydrogen abstraction reaction of I. *A priori* following sources of hydrogen would be possible: i) hydrogen from the solvent (MeOH), ii) a trace of water, iii) a methyl-hydrogen in ABIN (III), iv) that in radical I, v) a methylene-hydrogen in I. In order to exclude the possibilities i) ii) and iii), a solution of radical I in anhydrous benzene was refluxed for 30 hr under a dry nitrogen atmosphere. Under these conditions radical I afforded the >N–O–H (IV) and a polymeric substance[2] in 60% and 30% yields, respectively. A trace of 2,6-dimethyl-2,5-heptadien-4-one (phorone) (V) was also isolated and identified by comparison of melting point, IR and NMR spectra and vpc retention time with those of an authentic sample. Furthermore heating of radical I at 105—110°C in the absence of solvent for 3 hr under a

*1 Part III: K. Murayama and T. Yoshioka, This Bulletin, **42**, 1942 (1969).

1) K. Murayama, S. Morimura and T. Yoshioka, This Bulletin, **42**, 1640 (1969).

2) The structure of a polymeric substance was uncertain.

dry nitrogen atmosphere, gave the same results. These observations would suggest the following mechanism. The stable radical I abstracts a hydrogen atom from an α-methylene of the ketone in another radical I (=I') to give a reactive intermediate (VI). A second stable radical I abstracts a hydrogen atom from the intermediate VI to give a second >N–O–H (IV), a thermodynamically stable conjugated ketone (phorone) (V) and nitric oxide (VII).[3] Thus three moles of I give two moles of IV and therefore the theoretical yield of IV is 66.6% based on the weight of the starting material. This supposition is therefore compatible with our observation. Phorone (V) prepared from I may be further polymerized by nitric oxide (VII).[4]

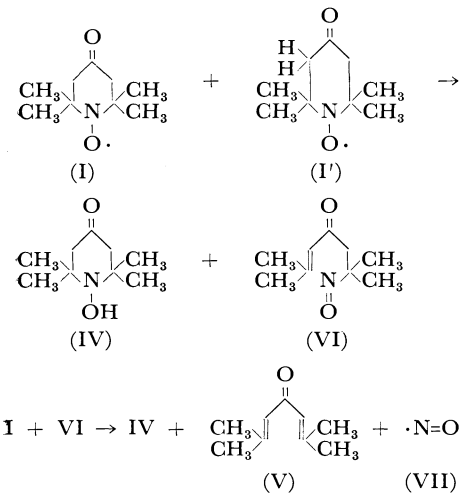

I + VI → IV + (V) + ·N=O

Thus : 3·(I) → 2·(IV)

The following additional argument was made for the sake of confirming the action of a hydrogen atom on a α-carbon of the ketone group in the piperidine ring. If such α-methylene hydrogens were effective, 2,2,6,6-tetramethylpiperidine-1-oxyl (VIII) and 2,2,6,6-tetramethyl-4-hydroxypiperidine-1-oxyl (IX), which had no ketone group, should be more stable than radical I.

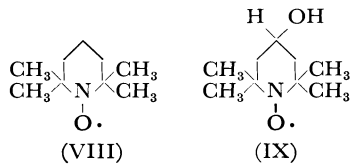

Under the same reaction conditions, as expected, radicals VIII and IX were almost recovered, and additionally no ketonic compound I was detected by the vpc technique, although the ketone I was anticipated to be prepared from the corresponding secondary alcohol IX by the attack of the *N*-oxyl radical IX just as acetone was prepared from isopropyl alcohol by the attack of the free radicals derived from diacetyl peroxide.[5] Similarly, no formation of acetone was observed during the hydrogen abstraction reaction by the radical IX from isopropyl alcohol.

A similar cycloelimination has been reported by Keana *et al.*[6] They have attempted a photolysis of the stable free radical, *e.g.* 3-carbamoyl-2,2,5,5-tetramethylpyrroline-1-oxyl, to obtain the thermodynamically stable conjugated corresponding ketone and nitric oxide (VII). This fact suggests that the stable free radical I may decompose photochemically. In order to investigate the possibility of photocycloelimination of radical I, a solution of I in anhydrous benzene was refluxed in the dark for 30 hr under a dry nitrogen atmosphere. Thus radical I converted into the >N–O–H (IV) in a high yield just as in the light. Accordingly, the photocycloelimination observed in the study of 3-carbamoyl-2,2,5,5-tetramethylpyrroline-1-oxyl[6] was excluded in a case of the

TABLE 1. REACTION CONDITIONS AND PROPERTIES OF PRODUCTS

Entry	Solvent	Reaction time (hr)	Reaction temperature	Light	Product
i	b	15	reflux	light	IR-OH
ii	b	30	reflux	light	crystal
iii	b	15	reflux	dark	IR-OH
iv	b	30	reflux	dark	crystal
v	non	4	95—100°C	light	crystal
vi	non	4	95—100°C	dark	crystal
vii	non	3	105—110°C	light	crystal
viii	non	3	105—100°C	dark	crystal

b: in a benzene solution; non; without solvent; light: under a room light; IR-OH: detected ν_{O-H} (IR) in a crude oil: crystal: isolated as crystals (mp 90—91°C).

3) No attempt was made to isolate and identify this gas VII as well as in a case of Ref. 6.

4) Polymerization of phorone (V) with nitric oxide (VII) was not attempted in this work.

5) M. S. Kharasch, J. L. Rowe and W. H. Urry, *J. Org. Chem.*, **16**, 905 (1951).

6) J. F. W. Keana and F. Baitis, *Tetrahedron Letters*, **1968**, 365.

stable free radical I. Table 1 shows reaction conditions and properties of products.

It was therefore confirmed that i) a source of hydrogen was the α-methylene hydrogen of the ketone group in the piperidine ring (I), ii) a stable radical which could give a thermodynamically stable conjugated product by a cycloelimination was easily decomposed and iii) the decomposition of radical I was only accelerated by heating and was independent of the action of light.

Experimental

Melting points were uncorrected.

The NMR spectra were obtained with a Varian A-60 NMR spectrometer, using tetramethylsilane as an internal standard at 32°C.

The IR spectra were determined by means of Nujol mull and liquid film.

Materials. 2,2,6,6,-Tetramethyl-4-oxopiperidine-1-oxyl (I) was prepared by the oxidation of the corresponding amine by hydrogen peroxide in the presence of sodium tungstate and ethylenediaminetetraacetic acid (EDTA).[7] 2,2,6,6-Tetramethylpiperidine-1-oxyl (VIII) and 2,2,6,6-tetramethyl-4-hydroxypiperidine (IX) were derived from I.[8,9]

General Procedure for the Decomposition of the Extremely Stable Free Radicals. a) A solution of 17.0 g (0.10 mol) of radical I in anhydrous benzene was refluxed for several hours under a dry nitrogen atmosphere. After the solvent was evaporated under reduced pressure and the IR spectrum of the residue was taken, the residue was distilled under reduced pressure at low temperature (below 80°C). The distillate ($bp_{0.05}$ 75—80°C) was scratched to induce crystallization and the solid obtained was filtered and recrystallized from petroleum benzine to give an analytically pure sample which was identified by comparison of a melting point, IR and NMR spectrum and vpc retention time with that of an authentic 1-hydroxy-2,2,6,6-tetramethyl-4-oxopiperidine (IV),[10] mp 90—91°C. A mixed melting point with the authentic IV was undepressed. Found: C, 63.47; H, 10.19; N, 7.98%. Calcd for $C_9H_{17}NO_2$: C, 63.16; H, 10.04; N, 8.19%.

b). After heating radical I at 110°C for 3 hr under a dry nitrogen atmosphere, the oil was distilled under reduced pressure below the reaction temperature, 105—110°C. In the same manner as a), 1-hydroxy-2,2,6,6-tetramethyl-4-oxopiperidine (IV) was obtained, mp 90—91°C. A mixed melting point with the authentic sample was undepressed.

The Detection and the Identification of a Trace of 2,6-Dimethyl-2,5-heptadien-4-one (Phorone) (V). Phorone (V) was detected from the first distillate (bp_5 60—70°C) both in the general procedure a) and b), and was identical with the authentic V (mp 28°C, IR, NMR, vpc retention time). A mixed melting point with the authentic V was undepressed.

The authors wish to thank Dr. I. Iwai of these laboratories for his helpful guidance during the course of this work and Mr. S. Higashida for his technical assistance.

7) M. B. Neiman, Yu. G. Madedova and E. G. Rozantzev, *Azerb. Khim. Zh.*, **1962**, 37.

8) E. G. Rozantzev and M. B. Neiman, *Tetrahedron*, **20**, 131 (1964).

9) E. G. Rozantzev, *Izv. Akad. Nauk SSSR, Ser. Khim.*, **1966**, 770.

10) E. G. Rozantzev and V. A. Golubev, *ibid.*, **1966**, 891.

BULLETIN OF THE CHEMICAL SOCIETY OF JAPAN VOL. 42 2310—2312 (1969)

Synthetic Studies of 4-Oxo- and 4-Imino-3,4-dihydro-1,3-oxazoles*[1]

Akiko CHINONE, Shigeru SATO, Toshiyasu MASE and Masaki OHTA

Laboratory of Organic Chemistry, Tokyo Institute of Technology, Ookayama, Meguro-ku, Tokyo

(Received December 14, 1968)

For the purpose of synthesizing new mesoionic compounds of oxazole ring system having oxo group at 4 position, reaction of *N*-phenylbenzimidoyl chloride with glycolic acid was examined. Only an unexpected rearranged product was obtained. The reaction of *N*-phenylbenzimidoyl chloride with glycolonitrile successfully afforded the intermediate, which was treated with hydrogen chloride or with picric acid or with acetyl perchlorate to give 4-imino-3,4-dihydro-1,3-oxazole derivatives. Condensation of *N*-phenylbenzimidoyl chloride with mandelonitrile followed by treatment with acetyl perchlorate gave 4-imino-3,4-dihydro-1,3-oxazole derivative.

Of the possible mesoionic oxazoles, only 5-oxo-[1,2] and 5-imino-3,5-dihydro-1,3-oxazoles[3] have been reported. Though they are unstable in comparison with mesoionic thiazoles, some reactions were reported.[4] In the present study, we undertook the synthesis of 4-oxo- and 4-imino-3,4-dihydro-1,3-oxazoles because their structural relationship to 4-oxo- and 4-imino-3,4,-dihydro-thiazoles[5] is of considerable interest.

As a possible route towards a synthesis of 4-oxo-3,4-dihydro-1,3-oxazole (IV), we tried the reaction of *N*-phenylbenzimidoyl chloride (I) with glycolic acid (IIa) anticipating the formation of an intermediate **III**. When this reaction was carried out in an ether solution in presence of triethylamine, the reaction product was benzoyloxyacetanilide (Va), its structure being deduced from its elementary analysis and infrared spectrum. Treatment of I with lactic acid (IIb) or mandelic acid (IIc) under the same conditions gave also rearranged products, Vb and Vc respectively.

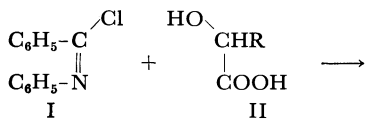

I II

IIa: R=H
IIb: R=CH_3
IIc: R=C_6H_5

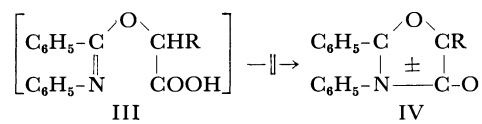

III IV

V

Va: R=H
Vb: R=CH_3
Vc: R=C_6H_5

The reaction of *N*-phenyl-*p*-methoxybenzimidoyl chloride with IIa also afforded the rearranged product. Attempts to obtain III and IV under various conditions were unsuccessful. For the formation of V the C=N bond in I must be cleaved. The same type of rearrangement has been reported for the reaction of thiobenzanilide with bromoacetic acid in boiling benzene.[5] The formation of V may proceed through the intermediate III which is not stable enough to be isolated, presumably due to the enhanced electrophilic character of imidate carbon atom as compared with thio-analog. The rearrangement occurred even in the presence of less equimolar triethylamine. As a possible mechanism, it seems that the reaction is initiated by a nucleophilic attack of carboxyl oxygen toward imidate carbon atom as shown below.

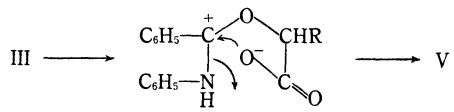

As a first step in the formation of 4-imino-3,4-dihydro-1,3-oxazole (VIII), I was condensed with glycolonitrile (VIa) in the presence of sodium hydride in THF to yield VIIa. Relatively unstable intermediate without purification gave undetectable brownish oil.

*1 Studies of mesoionic compounds. XXXII.

1) R. Huisgen, H. Gotthardt, H. O. Bayer and F. C. Schaefer, *Angew. Chem.*, **76**, 185 (1964).

2) M. Ohta and T. Mase, *Nippon Kagaku Zasshi (J. Chem. Soc. Japan, Pure Chem. Sect.)*, **89**, 714 (1968).

3) S. Sato and M. Ohta, This Bulletin, **41**, 2218 (1968).

4) R. Huisgen, E. Funke, F. C. Schaefer, H. Gotthardt and E. Brunn, *Tetrahedron Letters*, **1967**, 1809.

5) M. Ohta, H. Chosho, C. Shin and K. Ichimura, *Nippon Kagaku Zasshi, (J. Chem. Soc. Japan, Pure Chem. Sect.)*, **85**, 440 (1964).

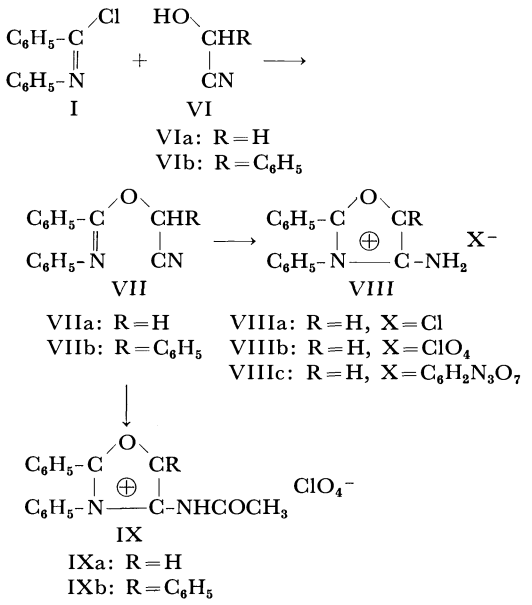

Treatment of this intermediate with hydrogen chloride in benzene gave the expected product, 4-imino-2,3-diphenyl-3,4-dihydro-1,3-oxazole hydrochloride (VIIIa). The infrared spectrum was consistent with that expected for VIIIa, but the elementary analysis indicated that the solid contained a small amount of dihydrochloride. The hydrochloride VIIIa, which was unstable and decomposed gradually into an unknown brownish compound, was converted to stable perchlorate (VIIIb) by treatment with silver perchlorate. The perchlorate showed a characteristic band at 308 mμ (ε, 9200) in its ultraviolet spectrum suggestive of its heteroaromatic system. On treating VIIa with picric acid, ring formation took place to produce the picrate (VIIIc) as yellow needles. *N*-Acetyl derivative IXa was obtained by treatment of VIIa with perchloric acid in acetic anhydride. Condensation of I with mandelonitrile followed by addition of acetyl perchlorate, without isolation of the intermediate (VIIb) because of its unstability, gave 5-phenyl derivative of *N*-acetyl perchlorate (IXb). These ring formations seem to proceed as a result of interaction of two polar groups, by a mechanism similar to that of sydnone imine salts.[6] The treatment of IXa and IXb with sodium bicarbonate afforded benzanilide, sodium perchlorate and an unidentified compound, and did not give free bases, probably because it has a high unstability unlike *N*-acylthiazone-imines.[7] The ring formation of VIIa with acetyl chloride, benzenesulfonyl chloride, oxalyl chloride and malonyl chloride was unsuccessful.

The structure of these products were established by infrared spectra, which showed strong bands at 3150—3350 cm^{-1} resulting from N–H stretching vibration, and at 1630—1680 cm^{-1} resulting from oxazole ring. They are very similar to those of 4-thiazone-imines. *N*-Substituted carbonyl group showed absorption band at relatively high frequency, 1690—1705 cm^{-1}, probably due to the effect of positive charge of the ring.

Some 4-imino-3,4-dihydro-1,3-oxazole salts showed absorption maxima in their ultraviolet spectra at about 300 mμ just as 4-thiazone-imine salts.

Experimental

All melting points were determined on a micro hot stage, and are not corrected. Infrared spectra were taken on KBr tablets.

Benzoyloxyacetanilide (Va). To a solution of 0.8 g of glycolic acid (IIa) and 2.0 g of triethylamine in 30 m*l* of dry ether, 2.2 g of *N*-phenylbenzimidoyl chloride (I) was added. The precipitates which separated out gradually were allowed to stand overnight, filtered and washed repeatedly with water. Recrystallization of the solid from benzene gave 2.2 g of white needles; mp 152—153°C. IR: 3295, 1725, 1670 cm^{-1}.

Found: C, 70.33; H, 4.78; N, 5.49%. Calcd for $C_{15}H_{13}NO_3$: C, 70.59; H, 5.13; N, 5.49%.

Benzoyloxymethylacetanilide (Vb). To a solution of 4.3 g of I and 1.8 g of lactic acid in 30 m*l* of dry ether, 6.0 g of triethylamine was added dropwise and the solution was stirred for an hour at room temperature. The precipitates which separated out were collected by filtration, washed with water, recrystallized from benzene to give 4.3 g of white needles; mp 154—155°C. IR: 3260, 1725, 1670 cm^{-1}.

Found: C, 71.15; H, 5.90; N, 5.46%. Calcd for $C_{16}H_{15}NO_3$: C, 71.38; H, 5.61; N, 5.20%.

Benzoyloxyphenylacetanilide (Vc). A solution of 2.3 g of I in 10 m*l* of dry ether was added to a solution of 1.5 g of mandelic acid and 1.2 g of triethylamine in 30 m*l* of dry acetonitrile under cooling with water. The precipitates separated out gradually. After stirring for an hour, the precipitates were filtered off and the filtrate was concentrated under vacuum. Then the crystalline product was collected and washed repeatedly with ether. The product was recrystallized from benzene to give 2.8 g of white needles; mp 170.5—171.5°C. IR: 3220, 1723, 1663 cm^{-1}.

Found: C, 76.24; H, 5.41; N, 4.07%. Calcd for $C_{21}H_{17}NO_3$: C, 76.12; H, 5.17; N, 4.23%.

***p*-Methoxybenzoyloxyacetanilide.** A solution of 0.8 g of IIa and 2.0 g of triethylamine and 2.5 g of *N*-phenyl-*p*-methoxybenzimidoyl chloride was allowed to stand overnight at room temperature. Precipitates which separated out gradually were collected and washed with water repeatedly. The solid was reprecipitated from benzene solution with ligroin to give 1.5 g of white needles; mp 104—105°C. IR: 3280, 1728, 1673 cm^{-1}.

Found: C, 67.05; H, 5.26; N, 5.56%. Calcd for $C_{16}H_{15}NO_4$: C, 67.36; H, 5.30; N, 4.91%.

***o*-Cyanomethyl-*N*-phenylbenzimidate (VIIa).** To a solution of 2.8 g of I and 2.8 g of glycolonitrile (VIa) in 30 m*l* of THF, a suspension of 4.8 g of sodium

6) P. Brookes and J. Walker, *J. Chem. Soc.*, **1957**, 4409.

7) H. Chosho, K. Ichimura and M. Ohta, This Bulletin, **37**, 1670 (1964).

hydride in THF was added dropwise under cooling with an ice-salt bath, resulting in a violent evolution of hydrogen gas. After stirring for an hour, the solid was filtered off and the filtrate was concentrated under vacuum without heating. The resulting oily product was washed a few times with *n*-hexane, which was cooled with dry ice in acetone, in order to crystallize the product. Recrystallization of the product from the minimum amount of *n*-hexane gave 2.2 g of white needles; mp 61—62°C. IR: 1680 cm^{-1}.

Found: C, 76.06; H, 4.95; N, 11.76%. Calcd for $C_{15}H_{12}N_2O$: C, 76.25; H, 5.12; N, 11.86%.

4-Imino-2,3-diphenyl-3,4-dihydro-1,3-oxazole hydrochloride (VIIIa). To a solution of 0.7 g of VIIa in 15 m*l* of benzene, 10 m*l* of benzene containing 0.2 g of gaseous hydrogen chloride was added and an exothermic reaction took place. The precipitates which separated out were collected and recrystallized from chloroform to give 0.27 g of VIIIa; mp 116—122°C. IR: 1680, 1650 cm^{-1}. The elementary analysis of the product was slightly inconsistent with that expected for VIIIa, probably because of a small amount of dihydrochloride.

4-Imino-2,3-diphenyl-3,4-dihydro-1,3-oxazole perchlorate (VIIIb). To a solution of 0.27 g of VIIIa in 15 m*l* of dry acetonitrile, was added dropwise a solution of 0.20 g of silver perchlorate in chloroform-ethanol. The precipitated silver chloride was filtered off and the filtrate was concentrated under vacuum to give a white solid. Reprecipitation from chloroform solution with ether gave 0.16 g of white needles; mp 160—166°C. $\lambda_{max}^{CH_3CN}$ 298 mμ (ε, 13600).

Found: C, 53.50; H, 3.89; N, 8.32%. Calcd for $C_{15}H_{13}N_2O_5Cl$: C, 53.49; H, 3.86; N, 8.32%.

4-Imino-2,3-diphenyl-3,4-dihydro-1,3-oxazole picrate (VIIIc). A benzene solution of VIIa was treated with a solution of picric acid in benzene to yield picrate which was recrystallized from isopropyl alcohol to give yellow needles; mp 108—109°C. IR: 3320, 3150, 1660, 1628 cm^{-1}.

Found: C, 53.86; H, 2.94; N, 15.15%. Calcd for $C_{21}H_{15}N_5O_8$: C, 54.20; H, 3.25; N, 15.05%.

***N*-Acetyl-4-imino-2,3-diphenyl-3,4-dihydro-1,3-oxazole perchlorate (IXa).** To a solution of 1.6 g of VIIa in 40 m*l* of acetic anhydride, 2 g of 70% aqueous perchloric acid was added dropwise with stirring and cooling with ice-salt bath. After 10 min ether was poured into the solution to give white precipitates, which were reprecipitated from chloroform solution with ether to give 1.1 g of white needles; mp 178—178.5°C. IR: 3260, 3215, 1690, 1640 cm^{-1}. $\lambda_{max}^{CH_3CN}$ 308 mμ (ε, 9200), 244 mμ (ε, 9200).

Found: C, 53.23; H, 3.97; N, 7.02%. Calcd for $C_{17}H_{15}N_2O_6Cl$: C, 53.62; H, 3.99; N, 7.40%.

***N*-Acetyl-4-imino-2,3,5-triphenyl-3,4-dihydro-1,3-oxazole Perchlorate (IXb).** To a solution of 5.4 g of I and 3.3 g of mandelonitrile (VIIb) in 20 m*l* of benzene, 5 g of triethylamine was added dropwise. After stirring for 2 hr at room temperature, precipitates which separated out were filtered off and the filtrate was concentrated under vacuum, until no triethylamine was detected. The concentrated solution was diluted with 30 m*l* of acetic anhydride, to which 7 g of 70% aqueous perchloric acid was added under cooling with ice-salt bath. Precipitates, which gradually separated out, were collected and recrystallized from ethanol to give 2.6 g of white needles; mp 228.5—230°C. IR: 3215, 3170, 1705, 1670 cm^{-1}.

Found: C, 60.48; H, 4.54: N, 5.97%. Calcd for $C_{23}H_{19}N_2O_6Cl$: C, 60.73; H, 4.18; N, 6.16%. $\lambda_{max}^{CH_3CN}$ 312 mμ (ε, 17600), 251 mμ (ε, 21900).

BULLETIN OF THE CHEMICAL SOCIETY OF JAPAN VOL. 42 2312—2318 (1969)

Cooxidation of Hydrocarbons in Liquid Phase. VI. Reactivities of Hydrocarbons and Peroxy Radicals

Etsuo NIKI, Yoshio KAMIYA and Nobuto OHTA

Department of Fuel Engineering, The University of Tokyo, Hongo, Tokyo

(Received December 14, 1968)

Cooxidation of all the combinations of two hydrocarbons among styrene, α-methylstyrene, tetralin and cumene was studied at 70°C in the presence of azobisisobutyronitrile as a thermal initiator. The reactivity ratios for each binary mixture were determined by several appropriate methods. The relative reactivities of styrene, α-methylstyrene, tetralin and cumene toward the peroxy radicals were approximately in the ratio 15 : 10 : 5 : 1. It was also concluded that the secondary peroxy radicals were more reactive than the tertiary peroxy radicals and that the polymeric peroxy radicals were more reactive than the normal alkylperoxy radicals.

The cooxidation of the binary mixtures of styrene, α-methylstyrene, tetralin and cumene was studied and the reactivity ratios were determined by several methods in order to obtain an information on the reactivities of the hydrocarbons and of the peroxy radicals toward each other.

Results

The rates of cooxidations of 6 systems are shown in Fig. 1. In all cases, the observed rates of oxygen absorption were corrected for nitrogen evolved by the decomposition of AIBN, oxygen absorbed by the dimethylcyanomethyl radical, and oxygen evolved in the termination step.[1] The reactivity ratios, r, were determined by several methods discussed in a previous paper.[1]

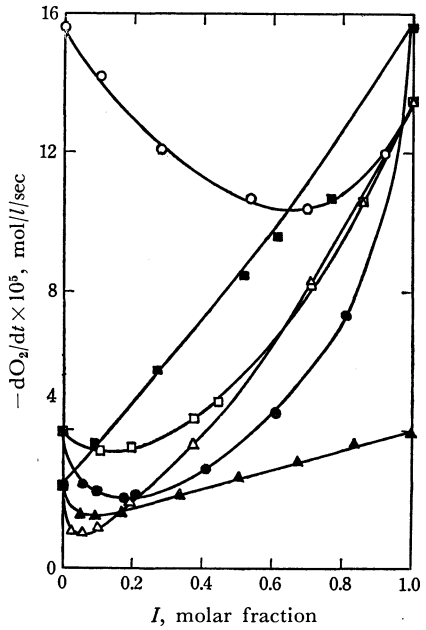

Fig. 1. Cooxidation of hydrocarbons.
70°C, oxygen pressure=760 mmHg,
AIBN=1.00×10^{-2} M
○: Styrene (I) - α-methylstyrene (II)
□: Styrene (I) - tetralin (II)
△: Styrene (I) - cumene (II)
●: α-Methylstyrene (I) - tetralin (II)
■: α-Methylstyrene (I) - cumene (II)
▲: Tetralin (I) - cumene (II)

Styrene (S) and α-Methylstyrene (M). The reactivity ratios were determined from the rates of cooxidations by our rate method[1,2] and the values of 1.6 and 0.71 were obtained for r_S and r_M respectively. The product of the two reactivity ratios is 1.1.

Styrene (S) and Tetralin (T). This system was studied previously.[1] Our rate method gave the values of $r_S=2.7$ and $r_T=0.49$, while the Fineman-Ross method gave the values of $r_S=3.0$ and $r_T=0.45$.[1]

Styrene (S) and Cumene (C). The reactivity ratios were determined by measuring the oxygen uptake and hydroperoxide formed, which was first employed by Mayo and his co-workers.[3] The results are summarized in Table 1. Hydroperoxide was determined by the Wibaut method.[4] The oxidation of styrene gives mostly styrene polyperoxide with small amounts of benzaldehyde and formaldehyde.[5] The Wibaut method[4] gives little titer for the oxidation of styrene,[1] while cumyl hydroperoxide can be determined quantitatively by this method (Table 1). The slightly greater yield of cumyl hydroperoxide than expected in the oxidation of cumene may be ascribed to the oxidation which proceeds after the absorption measurement is completed, while the product is being removed from the reaction vessel for analysis. It was demonstrated that the titrable hydroperoxide was unstable in the oxidizing styrene.[6] In order to minimize this complication, the conversions were kept very low. Thus, the hydroperoxide determined by the Wibaut method was taken as the amount of cumene reacted, and styrene reacted was calculated from the difference between oxygen uptake and hydroperoxide formed. The reactivity ratios were determined by the Fineman-

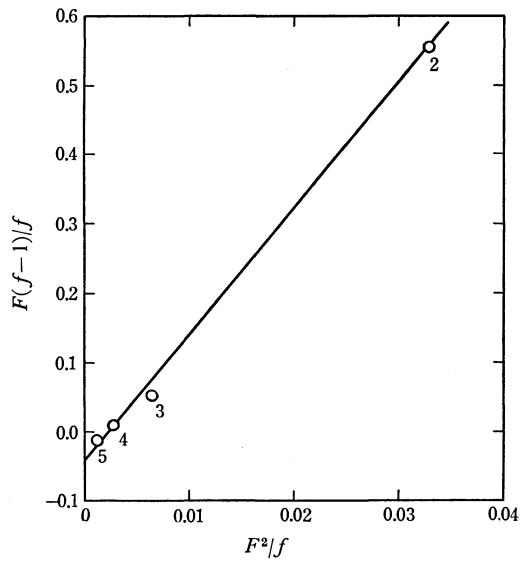

Fig. 2. Fineman-Ross plot for the cooxidation of styrene and cumene.
70°C, oxygen pressure=760 mmHg

1) E. Niki, Y. Kamiya and N. Ohta, This Bulletin, **42**, 512 (1969).
2) E. Niki, M. Kuwata, Y. Kamiya and N. Ohta, *Kogyo Kagaku Zasshi (J. Chem. Soc. Japan, Ind. Chem. Sect.)*, **70**, 1679 (1967).
3) F. R. Mayo, M. G. Syz, T. Mill and J. K. Castleman, "Advances in Chemistry Series," Vol. 75, Am. Chem. Soc., Washington D. C. (1968), p. 38.
4) J. P. Wibaut, H. B. van Leeuwen and B. van der Wal, *Rec. Trav. Chim.*, **73**, 1033 (1954).
5) A. A. Miller and F. R. Mayo, *J. Am. Chem. Soc.*, **78**, 1017 (1956); F. R. Mayo, *ibid.*, **80**, 2465 (1958).
6) R. Hiatt, C. W. Gould and F. R. Mayo, *J. Org. Chem.*, **29**, 3461 (1964).

TABLE 1. COOXIDATIONS OF STYRENE (S) AND CUMENE (C) AT 70°C

Run No.	1	2	3	4	5
$[S]_0$, M	0.00	2.92	0.730	0.398	0.208
$[C]_0$, M	7.20	4.80	6.60	6.87	7.02
S, molar fraction	0.000	0.378	0.0995	0.0548	0.0288
Time, min	30	24	45	36	33
$(-O_2)_{observed}$, mM	42.5	46.1	30.5	22.4	19.7
$(-O_2)_{corrected}$, mM[a]	42.8	46.3	30.9	22.7	20.0
Conversion, %[b]	0.59	0.60	0.43	0.30	0.28
$(hpo)_{observed}$, mM	46.4	3.78	10.8	10.1	11.7
$(hpo)_{corrected}=\Delta C$, mM[c]	46.4	3.76	10.7	10.1	11.7
ΔS, mM[d]		42.54	20.2	12.6	8.3
$(hpo)/(-O_2)$	1.08	0.0811	0.346	0.445	0.585
$F=[S]_0/[C]_0$		0.609	0.111	0.0580	0.0296
$f=\Delta S/\Delta C$		11.3	1.89	1.25	0.710

a) $(-O_2)_{corrected}=(-O_2)_{observed}+R_i(1/e-1)/2$. R_i and e represent the rate of initiation and the efficiency of the radical production from initiator respectively. The correction was made for nitrogen evolved in the initiation step, and for oxygen absorbed and evolved in the initiation and termination steps.
b) (Initial hydrocarbon concentration)/$(-O_2)$.
c) $(hpo)_{corrected}=(hpo)_{observed}-$(hpo from AIBN), where hpo represents hydroperoxide. ΔC means cumene reacted.
d) ΔS=Styrene reacted.

TABLE 2. COOXIDATIONS OF α-METHYLSTYRENE (M) AND TETRALIN (T) AT 70°C

Run No.	6	7	8	9
$[M]_0$, M	2.56	1.78	0.905	0.700
$[T]_0$, M	4.90	5.65	6.50	6.68
M, molar fraction	0.344	0.240	0.122	0.0948
Time, min	70	80	60	50
$(-O_2)_{observed}$, mM	104	103	76.1	68.0
$(-O_2)_{corrected}$, mM	105	104	76.6	68.4
Conversion, %	1.41	1.40	1.03	0.93
$(hpo)_{observed}$, mM	32.6	46.9	57.1	55.5
$(hpo)_{corrected}=\Delta T$, mM[a]	31.4	44.8	53.5	51.0
ΔM, mM[b]	73.6	59.2	23.1	17.4
$F=[M]_0/[T]_0$	0.522	0.315	0.139	0.105
$f=\Delta M/\Delta T$	2.34	1.32	0.432	0.341

a) ΔT=tetralin reacted. b) ΔM=α-methylstyrene reacted.

Ross method:[7]

$$\frac{F}{f}(f-1) = r_S\frac{F^2}{f} - r_C, \qquad (1)$$

where $F=[S]_0/[C]_0$ and $f=\Delta S/\Delta C$. Figure 2 gives the values of 18 and 0.045 for r_S and r_C respectively. These values are reasonably in agreement with the values of $r_S=20$ and $r_C=0.05$ at 60°C obtained by Mayo and his co-workers.[3]

α-Methylstyrene (M) and Tetralin (T). Previously, we obtained the values $r_M=5.5$ and $r_T=0.70$ by our rate method.[2] Since the product of these two reactivity ratios exceeds unity considerably, the reactivity ratios for this binary mixture were determined by two other methods.

The amounts of oxygen uptake and hydroperoxide formation determined by the Wibaut method in the cooxidations of α-methylstyrene and tetralin are shown in Table 2. This method is the same as that employed in the cooxidations of styrene and cumene. The Fineman-Ross plot obtained by the results in Table 2 is shown in Fig. 3, which gives the values of 6.1 and 0.41 for r_M and r_T respectively. The product of the two reactivity ratios is 2.5.

The r_T value was determined separately by the hydroperoxide method which was first employed

7) M. Fineman and S. D. Ross, *J. Polymer Sci.*, **5**, 259 (1950).

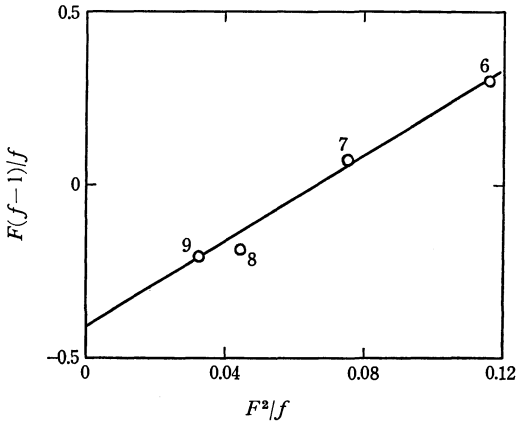

Fig. 3. Fineman-Ross plot for the cooxidation of α-methylstyrene and tetralin.
70°C, oxygen pressure=760 mmHg

by Howard, Schwalm and Ingold.[8] This method was devised on the basis that the peroxy radicals abstract the hydrogen atom from hydroperoxides much faster than they abstract the hydrogen atom from the hydrocarbons or add to the double bond.

When enough tetralyl hydroperoxide is added in the oxidation of α-methylstyrene, the tetralylperoxy radical contributes as a chain carrier, and the rate of oxidation is given by

$$-dO_2/dt = k_{TM}[M]R_i^{1/2}/(2k_{tTT})^{1/2} = k_{TM}[M](ek_i[AIBN]/k_{tTT})^{1/2}, \quad (2)$$

where R_i is the rate of initiation, e the efficiency of the radical production, and k_{TM} and k_{tTT} the rate constants of the following reactions:

$$TO_2\cdot + M \xrightarrow{k_{TM}} TOOM\cdot ,$$

$$TO_2\cdot + TO_2\cdot \xrightarrow{k_{tTT}} \text{tetralone} + \text{tetralol} + O_2 .$$

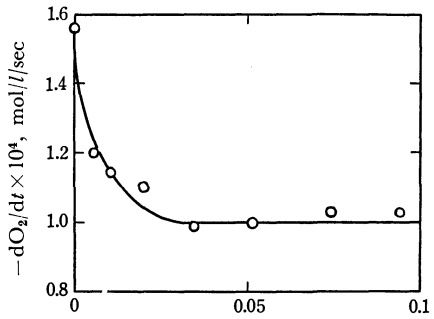

Fig. 4. Oxidation of α-methylstyrene in the presence of tetralin hydroperoxide.
70°C, oxygen pressure=760 mmHg,
AIBN=1.00×10⁻² M

The rates of the oxidation of α-methylstyrene in the presence of tetralyl hydroperoxide are shown in Fig. 4 as a function of the concentration of tetralyl hydroperoxide. The rates of the oxidation of α-methylstyrene decrease with an increase in the concentration of tetralyl hydroperoxide; this is because the rapid termination by the two secondary tetralylperoxy radicals replaces the slower termination by the tertiary α-methylstyrylperoxy radicals. But when the concentration of tetralyl hydroperoxide exceeds 3.5×10^{-2} mol/l, the rates of the oxidation of α-methylstyrene are virtually constant, 1.00×10^{-4} mol/l/sec. The rate constants for the individual step in the oxidation of tetraline were determined by several investigators,[9-11] and the compilation and extrapolation to 70°C of the reported data give the values 30 and 8.0×10^6 l/mol/sec for k_p and k_t respectively. Substitution of the values 1.00×10^{-4} mol/l/sec, 7.70 mol/l, 0.65, 3.96×10^{-5} sec^{-1}, 1.00×10^{-2} mol/l, and 8.0×10^6 l/mol/sec for the rate of oxidation, [M], e, k_t, [AIBN], and k_{tTT}, respectively, into the Eq. (2) gives k_{TM} to be 72. Therefore, the r_T is calculated to be 30/72=0.42.

α-Methylstyrene (M) and Cumene (C). In a previous paper[12] of this series, we have obtained the reactivity ratios for this system as $r_M=9.3$ and $r_C=0.10$ by using Mayo-Lewis method.[13]

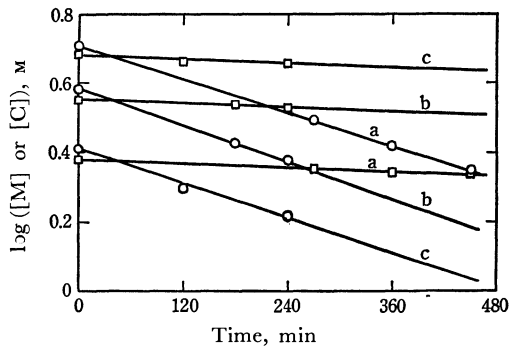

Fig. 5. Cooxidation of α-methylstyrene and cumene.
70°C, oxygen pressure=760 mmHg,
AIBN=1.00×10⁻² M
○: α-Methylstyrene, □: cumene
a: $[M]_0=5.13$, $[C]_0=2.40$
b: $[M]_0=3.85$, $[C]_0=3.60$
c: $[M]_0=2.57$, $[C]_0=4.80$

8) J. A. Howard, W. J. Schwalm and K. U. Ingold, "Advances in Chemistry Series," Vol. 75, Am. Chem. Soc., Washington D. C. (1968), p. 6.

9) C. H. Bamford and M. J. S. Dewar, *Proc. Royal Soc.*, **A198**, 252 (1949).

10) J. A. Howard and K. U. Ingold, *Can. J. Chem.*, **44**, 1119 (1966).

11) H. Berger, A. M. W. Blaauw, M. M. Al and P. Smael, "Advances in Chemistry Series," Vol. 75, Am. Chem. Soc., Washington D. C. (1968), p. 346.

12) E. Niki and Y. Kamiya, *Kogyo Kagaku Zasshi (J. Chem. Soc. Japan, Ind. Chem. Sect.)*, **70**, 42 (1967).

13) F. R. Mayo and F. M. Lewis, *J. Am. Chem. Soc.*, **66**, 1594 (1944).

Table 3. The rates of oxidations of α-methylstyrene and cumene in their cooxidations
70°C, oxygen pressure=760 mmHg, [AIBN]=1.00×10^{-2} M

$[M]_0$ M	$[C]_0$ M	$-dM/dt\times10^4$ mol/l/sec	$-dC/dt\times10^5$ mol/l/sec	$F=[M]_0/[C]_0$	$f=\frac{(-dM/dt)}{(-dC/dt)}$
5.13	2.40	1.58	0.815	2.14	19.4
3.85	3.60	1.26	1.26	1.07	10.0
2.57	4.80	0.872	1.77	0.535	4.92

The rates of disappearance of α-methylstyrene and cumene were followed by gas-liquid chromatography, and as a result the conversion of the hydrocarbons, especially that of α-methylstyrene, was rather high. In order to avoid the complicated effects of the oxidation products and of the variation of the medium, the r values were determined using the rates of oxidation of both hydrocarbons at the initial stage. The concentrations of the two hydrocarbons were measured periodically and the in logarithm was plotted against time as shown in Fig. 5. The calculated rates of oxidations of α-methylstyrene and cumene are given in Table 3, and the Fineman-Ross plot obtained from these data are shown in Fig. 6. The solid line in Fig. 6 corresponds to $r_M=9.3$ and $r_C=0.10$.

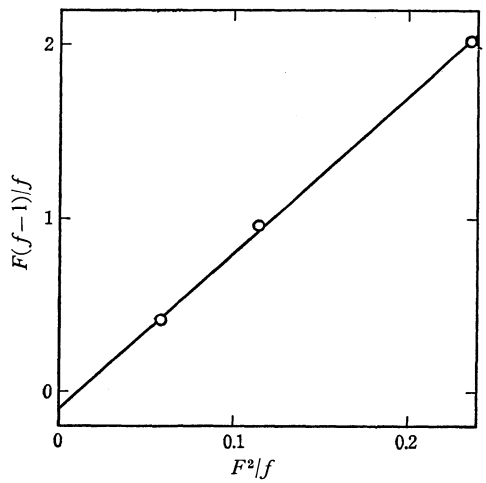

Fig. 6. Fineman-Ross plot for the cooxidation of α-methylstyrene and cumene.
The solid line corresponds to $r_M=9.3$ and $r_C=0.10$.
70°C, oxygen pressure=760 mmHg

Tetralin (T) and Cumene (C). The values 4.2 and 0.19 were obtained for r_T and r_C respectively at 70°C from the rates of cooxidations using our rate method.[14]

Discussion

In the past, it was generally accepted that the peroxy radicals derived from the hydrocarbons had approximately the same reactivities independent of their structures, and the rates of the reactions of peroxy radicals with hydrocarbons were determined solely by the hydrocarbons. If the reactivities of the peroxy radicals are really independent of their nature, the product of the two reactivity ratios is necessarily unity, since, in the cooxidations of the binary mixture of the hydrocarbons A and B,

$$k_{AA} = k_{BA},\ k_{BB} = k_{AB}$$

hence,

$$r_A r_B = (k_{AA}/k_{AB})(k_{BB}/k_{BA}) = (k_{AA}/k_{BA})(k_{BB}/k_{AB}) = 1$$

Alagy *et al.* determined the reactivity ratios for several systems and concluded that the reactivities of the peroxy radicals were dependent on the structure on the basis that the products of the two reactivity ratios deviated from unity.[15] On the contrary, Russell and Willamson[16] concluded that the reactivities of the peroxy radicals are fairly independent of their nature. Recently, this problem has received much attention. Howard and Ingold demonstrated by determining the absolute rate constants for hydrocarbon oxidations that the reactivities of the peroxy radicals are dependent on their structure, and that the primary peroxy radicals are more reactive than the secondary peroxy radicals and in turn the secondary peroxy radicals are more reactive than the tertiary ones.[10,17-19] They attributed the differences in the reactivities of the peroxy radicals to the steric effect. On the other hand, Mayo and his coworkers reported that the relative reactivities of the hydrocarbons toward various peroxy radicals were nearly independent of the alkylperoxy radicals involved.[3]

It is worth pointing out that the fact that the product of two reactivity ratios is unity does not always imply the same reactivities of the various peroxy radicals. Even if the absolute reactivities

14) E. Niki, Y. Kamiya and N. Ohta, *Kogyo Kagaku Zasshi (J. Chem. Soc. Japan, Ind. Chem. Sect.)*, **71**, 859 (1968).

15) J. Alagy, G. Clement and J. C. Balaceanu, *Bull. Soc. Chim. France*, **1960**, 1495; **1961**, 1303, 1792.

16) G. A. Russell and R. C. Williamson, Jr., *J. Am. Chem. Soc.*, **86**, 2364 (1964).

17) K. U. Ingold, Intern. Symp. Free Radicals in Solution, Univ. of Michigan, Ann Arbor, Mich., 1966.

18) B. S. Middleton and K. U. Ingold, *Can. J. Chem.*, **45**, 191 (1967).

19) J. A. Howard and K. U. Ingold, *ibid.*, **46**, 2655, 2661 (1968).

of the peroxy radicals are different, the product of two reactivity ratios can be unity. For example, when the peroxy radical $AO_2\cdot$ is more reactive than the peroxy radical $BO_2\cdot$ by a factor of p toward both hydrocarbons A and B, the product of r_A and r_B is:

$$r_A \times r_B = (k_{AA}/k_{AB})(k_{BB}/k_{BA}) = (k_{AA}/k_{BA})(k_{BB}/k_{AB}) = p/p = 1$$

Another problem is the error involved in the reactivity ratios. It is extremely difficult to obtain accurate r values in the cooxidation of the hydrocarbons. If it is assumed that the reactivity ratios contain 10, 20, 30, and 50% of error, then the product of two r values lies in the range of 0.81—1.2, 0.64—1.4, 0.49—1.7, and 0.25—2.3, respectively. Thus, it would be risky to estimate whether the reactivities of the different peroxy radicals are the same or not from the product of two reactivity ratios.

After all, the reactivities of the peroxy radicals may be evaluated from the absolute propagation rate constants and the reactivity ratios. In Table 4 are summarized the reactivity ratios obtained for the cooxidation of styrene, α-methylstyrene, tetralin and cumene at 70°C.

Table 4. The reactivity ratios at 70°C

Hydrocarbon A	Hydrocarbon B	r_A	r_B	$r_A r_B$
Styrene	α-Methylstyrene	1.6	0.71	1.1
Styrene	Tetralin	2.9	0.47	1.4
Styrene	Cumene	18	0.045	0.81
α-Methylstyrene	Tetralin	5.7	0.51	2.9
α-Methylstyrene	Cumene	9.3	0.10	0.93
Tetralin	Cumene	4.2	0.19	0.80

The calculated rate constants for the reactions of styryl, α-methylstyryl, tetralyl and cumyl peroxy radicals with these four hydrocarbons are shown in Table 5. The absolute rate constants at 70°C for styrene,[20] α-methylstyrene[10,21] tetralin,[9-11] and cumene[11,22-26] were calculated from the compilation of the values in literature. Table 5 indicates that the rate constants for the reactions of hydrocarbons with peroxy radicals are dependent on both of them. The relative reactivities of the hydrocarbons toward the peroxy radicals and *vice versa* calculated from Table 5 are shown in Tables 6 and 7 respectively. Table 6 indicates that the relative reactivities of styrene, α-methylstyrene, tetralin, and cumene are approximately in the ratio 15 : 10 : 5 : 1. On the other hand, Table 7 shows that the secondary peroxy radicals are more reactive than the tertiary peroxy radicals, and that the polymeric peroxy radicals are more reactive than the usual monomeric aralkylperoxy radicals.

The results and discussion given above suggest that the rates of the reactions between hydrocarbons and peroxy radicals depend not only on the hydrocarbons being attacked but also on the attacking peroxy radicals. The reactivities of the hydrocarbons may be determined mostly by the bond dissociation energy of the bond being broken and the degree of the resonance stabilization of the radical newly formed. Probably, both steric and polar effects may be responsible for the differences in the reactivities of the peroxy radicals. Howard and Ingold[10,18] emphasized the steric effects to explain the differences in the reactivities of the peroxy radicals. Indeed the relative reactivities of cumene and tetralin toward various free radicals and atoms suggest the considerable steric effects of the attacking species,[27] but it is not clear whether

Table 5. Rate constants for the reactions of peroxy radicals with hydrocarbons at 70°C

Hydrocarbon	$(k_p/(2k_t)^{1/2})\times 10^3$ $(l/\text{mol/sec})^{1/2}$	Rate constants in l/mol/sec[b]			
		$SO_2\cdot$	$MO_2\cdot$	$TO_2\cdot$	$CO_2\cdot$
Styrene	22.2	210[a]	69	64	27
α-Methylstyrene	28.1	130	48[a]	59	12
Tetralin	7.70	72	8.4	30[a]	6.3
Cumene	4.63	12	5.2	7.1	1.2[a]

a) Calculated by extrapolation from literature values; see text.
b) $SO_2\cdot$, $MO_2\cdot$, $TO_2\cdot$, and $CO_2\cdot$ represent styryl-, α-methylstyryl-, tetralyl-, and cumylperoxy radicals respectively.

20) J. A. Howard and H. U. Ingold, *ibid.*, **43**, 2729, 2737 (1965).
21) J. A. Howard and K. U. Ingold, *ibid.*, **44**, 1113 (1966).
22) H. W. Melville and S. Richards, *J. Chem. Soc.*, **1954**, 944.
23) J. R. Thomas and C. A. Tolman, *J. Am. Chem. Soc.*, **84**, 2079 (1962)
24) J A. Howard and J. C. Robb, *Trans. Faraday Soc.*, **59**, 1590 (1963).
25) J. A. Howard and K. U. Ingold, *Can. J. Chem.*, **45**, 793 (1967).
26) D. G. Hendry, *J. Am. Chem. Soc.*, **89**, 5433 (1967).
27) E. Niki, Y. Kamiya and N. Ohta, *Kogyo Kagaku Zasshi (J. Chem. Soc. Japan, Ind. Chem. Sect.)*, **71**, 1187 (1968).

Table 6. Relative reactivities of hydrocarbons toward peroxy radicals at 70°C

Hydrocarbon	Peroxy radical			
	$SO_2\cdot$	$MO_2\cdot$	$TO_2\cdot$	$CO_2\cdot$
Styrene	18	13	8.9	22
α-Methylstyrene	11	9.3	8.2	10
Tetralin	6.2	1.6	4.2	5.3
Cumene	1	1	1	1

Table 7. Relative reactivities of peroxy radicals toward hydrocarbons at 70°C

Hydrocarbon	Peroxy radical			
	$SO_2\cdot$	$MO_2\cdot$	$TO_2\cdot$	$CO_2\cdot$
Styrene	7.8	2.6	2.4	1
α-Methylstyrene	11	4.0	4.9	1
Tetralin	11	1.3	4.8	1
Cumene	10	4.3	5.9	1

the volume of the hydrocarbon portion of the peroxy radicals is so important in determining the reactivities of the peroxy radicals. The thermodynamic data also throw doubt upon the importance of the steric effects of the peroxy radicals. Most alkyl-alkyloxy bond strengths are about 78 kcal.[28] But the bond strength of the *t*-butyl - *t*-butoxy bond is 69 kcal.[28] The 9 kcal lowering of the C–O bond dissociation energy observed in the *t*-butyl ether is attributed to the repulsion of closely bound bulky *t*-butyl groups.[28] On the other hand, the O–O bond dissociation energies of dimethyl, diethyl, dipropyl, and di-*t*-butyl peroxides are approximately the same.[28] These facts suggest that the volume of R in ROOR does not give a significant steric effect in contrast with ROR. Howard and Ingold related the differences in the reactivities of the primary, secondary and tetrtiary peroxy radicals to the chain termination reactions of these peroxy radicals.[10] However, the rates of chain terminating bimolecular interactions of the peroxy radicals may be dependent more on the mechanism of the reaction and statistical factors, *i. e.*, absence or presence of α-hydrogen atoms and their number than on the steric effects.

If the steric effects of the attacking peroxy radicals are really important, the steric structure of the hydrocarbons being attacked may also have at least large effects. In this case, the product of two reactivity ratios is expected to deviate from unity. For example, if cumylperoxy radical is less reactive than tetralylperoxy radical due to the steric factors, then the steric effects may be more significant when the peroxy radicals abstract a hydrogen atom from cumene than from tetralin. That is

$$k_{TT}/k_{CT} < k_{TC}/k_{CC}\,.$$

Hence

$$r_T r_C = (k_{TT}/k_{TC})(k_{CC}/k_{CT}) < 1\,.$$

Thus, if the steric factors affect the reactivities of the hydrocarbons and the peroxy radicals, the product of the two reactivity ratios deviates from unity.

Experimental

Styrene and α-methylstyrene were washed with dilute alkali and water, dried, and distilled under reduced pressure of nitrogen. Tetralin and cumene were washed successively with sulfuric acid, water, alkali and water, dried, and then distilled under reduced pressure of nitrogen. All these four hydrocarbons were passed down the activated alumina column before use. Tetralyl hydroperoxide was prepared by the air oxidation of tetralin at 65°C for 50 hr in the presence of AIBN followed by the repeated recrystallization from *n*-hexane. Commercial AIBN was recrystallized from methanol.

The rate of cooxidation was measured by following the oxygen uptake periodically in a constant pressure closed system. The formation of hydroperoxide was measured by the iodometric titration employed by Wibaut *et al.*[4] In the cooxidation of α-methylstyrene and cumene, the disappearance of the two hydrocarbons was determined by the gas - liquid chromatography using Apiezon-L column at 170°C. The calculation of the data was performed at the Data Processing Center of the University of Tokyo.

A part of this work was supported by The Kawakami Foundation.

28) S. W. Benson, *J. Chem. Educ.*, **42**, 502 (1965).

BULLETIN OF THE CHEMICAL SOCEITY OF JAPAN VOL. 42 2319—2323 (1969)

Coumarins. VI. The Acid-catalyzed Reaction of Phenols with β-Aminocrotononitrile[1]

Kikumasa SATO and Masao ŌHASHI

Department of Applied Chemistry, Faculty of Engineering, Yokohama National University, Minami-ku, Yokohama

and Takeshi AMAKASU and Katsuhiko TAKEDA

Chemical Laboratory, Seimi Chemical Co., Ltd., Chigasaki, Chigasaki-shi, Kanagawa

(Received December 19, 1968)

A new synthesis of 4-methylcoumarins has been developed by means of the acid-catalyzed condensation of phenols with β-aminocrotononitrile. Such monohydric phenols as phenol or cresols reacted with β-aminocrotononitrile in polyphosphoric acid (PPA) to give 4-methylcoumarins in poor yields, along with a good yield of 6-amino-3-cyano-2,4-lutidine (III). In contrast, 7-substituted-4-methylcoumarins were obtained in 23—44% yields from resorcinol and its monomethyl ether. On the other hand, when β-aminocrotononitrile was heated in PPA, the lutidine (III) was obtained in a high yield. Its precursor, 4-amino-1,3-dicyano-2-methylpenta-1,3-diene (XI), was isolated under mild conditions. These results suggest that β-aminocrotononitrile may undergo the preferential self-dimerization to the lutidine (III) rather than the intermolecular condensation with phenols.

The preceding paper in this series[2] described the direct synthesis of several coumarins by the acid-catalyzed reaction of phenols with β-oxonitriles. These studies have now been extended to β-aminocrotononitrile, *i. e.*, diacetonitrile. Although the hydrogen chloride-catalyzed reaction of polyhydric phenols such as resorcinol with β-aminocinnamonitriles has previously been shown[3] to give the corresponding 4-phenylcoumarins, we could find no report concerning the acid-catalyzed reaction of phenols with such aliphatic β-amino-α,β-unsaturated nitriles as β-aminocrotononitrile.

The sodium-induced dimerization of acetonitrile has been shown[4-6] to give β-amino-*cis*-crotononitrile (Ia) and mixture (Ic) of Ia and Ib. The *cis*-isomer (Ia) may be readily isomerized, in part, to the *trans*-configuration (Ib) by placing it in contact with a protic solvent such as ethanol.[5,6] The conversion is subject to an acid-base catalyst.[6]

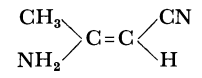

Ia

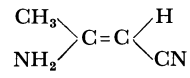

Ib

In the present study we have examined the acid-catalyzed reaction of phenols with β-aminocrotononitrile (Ic), using polyphosphoric acid (PPA).

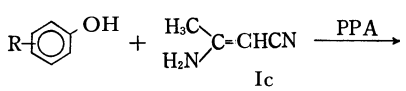

Ic

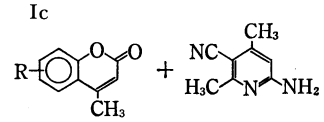

IIa, R=H
b, R=6-CH_3
c, R=7-CH_3
d, R=7-OCH_3
e, R=7-OH

III

When equimolar amounts of resorcinol and Ic were treated in a PPA solution, 4-methylumbelliferone (IIe) (44%) was obtained along with 6-amino-3-cyano-2,4-lutidine (III). Resorcinol monomethyl ether behaved analogously when treated with Ic under the same conditions and gave the corresponding coumarin, IId, as well as III.

In contrast, a poor yield of 4-methylcoumarins (IIa—c) was isolated from the reaction of such less reactive phenols as cresols with Ic under similar conditions. The structure of the coumarins II follows from the infrared spectra, which showed

1) This investigation was presented at the 21st Annual Meeting of the Chemical Society of Japan, Osaka, April, 1968.

2) K. Sato and T. Amakasu, *J. Org. Chem.*, **33**, 2446 (1968).

3) E. Von Meyer, *J. Prakt. Chem.*, [2] **67**, 342 (1903); A. Sonn, *Ber.*, **51**, 821 (1918).

4) a) R. Holtwart, *J. Prakt. Chem.*, [2] **39**, 230 (1889). b) J. Moir, *J. Chem. Soc.*, **81**, 111 (1902).

5) J. J. Conn and A. Taurins, *Can. J. Chem.*, **31**, 1211 (1953).

6) E. Bullock and B. Greogry, *Can. J. Chem.*, **43**, 332 (1965).

Table 1. The acid-catalyzed reaction of phenols with diacetonitrile (Ic)[a]

No.	Phenol	Reaction[b] Temp., °C	Time, hr	Product	Yield, %
1	Phenol	125—130	3	IIa	4
2	*p*-Cresol	125—130	4	IIb	7
3	*m*-Cresol	125—130	4	IIc	7
4	Resorcinol monomethyl ether	115—120	4	IId	23
5	Resorcinol	100—105	3	IIe	44

No.	Mp, °C Obsd[c]	Lit	IR (KBr) cm^{-1} C=O	UV (EtOH) λ_{max} mμ (ε)
1	82—82.5	83—84[d]	1705	213 (19000) 274 (9000) 315 (5000)
2	148.5—149	151[e]	1710	218 (24000) 276 (12000) 324 (6000)
3	132—132.5	132[e]	1700	222 (19000) 282 (11000) 319 (10000)
4	158.5—159	158.5—159[e]	1730	222 (16000) 252 ± 2(2000)[f] 324 (14000)
5	184—184.5	185	1680	222 (14000) 254 ± 2(2300)[f] 326 (13000)

a) 6-Amino-3-cyano-2,4-lutidine (III) was isolated along with II.
b) See Experimental Section for molar ratio of reagents.
c) Recrystallized from aqueous ethanol.
d) E. W. Woodruff, "Organic Syntheses," Coll. Vol. III, p. 581 (1955).
e) See Ref. 2.
f) Flat.

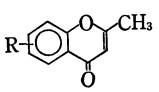

IV

lactone C=O bands at 1680—1730 cm^{-1}, and the ultraviolet data, which make it possible to distinguish[7] clearly between coumarins II and isomeric chromones IV. These results, summarized in Table 1, indicate that the reactions proceed through the addition of phenols to Ic, as is shown below:

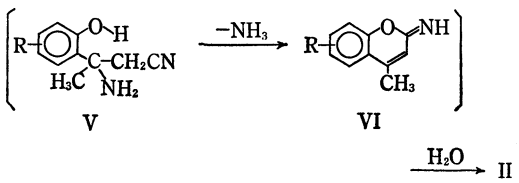

V VI II

The resulting addition product (*i.e.*, V) is then converted, by the intramolecular cyclization, to an iminocoumarin, VI. The intermediate VI then readily undergoes acid hydrolysis to II. Neither V nor VI could be isolated in any case, whereas the acid-promoted condensation of phenols with benzoylacetonitrile has been demonstrated[2] to furnish 4-phenyl-2-iminocoumarins, VII, corresponding to VI, while 3-cyano-4-methyliminocoumarin (VIII)[8] and 3-substituted-2-iminocoumarins, IXa—d,[9] may be obtained by the base-catalyzed condensation of 2-hydroxyacetophenone as malononitrile. This is probably to be attributed and salicylaldehyde respectively, with such cyano compounds to the difference in resonance stability between the intermediate VI and VII, VIII, or IX. It is interesting to note that no para condensation product, X, could be isolated from the reaction of phenol, while the acid-catalyzed reaction of phenol

7) a) B. K. Ganguly and P. Bagchi, *J. Org. Chem.*, **21**, 1415 (1956). b) K. Sen and P. Bagchi, *ibid.*, **24**, 316 (1956); c) L. L. Wood and J. Sapp, *ibid.*, **27**, 3703 (1962).

8) H. Junek, *Monatsh.*, **95**, 234 (1964).

9) R. Kuhn and D. Weiser, *Ann.*, **600**, 144 (1956); G. P. Schiemenz, *Ber.*, **95**, 483 (1962); H. Junek, *Monatsh.*, **94**, 192 (1963).

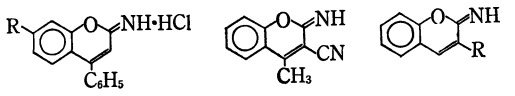

VII
R=-OH, -OCH$_3$, -CH$_3$

VIII IXa, R=-C$_6$H$_5$
b, R=-CONH$_2$
c, R=-CN
d, R=
-CCH(CN)$_2$
||
NH

with benzoylacetonitrile may furnish β-(*p*-hydroxyphenyl)cinnamonitrile as the sole product.[2]

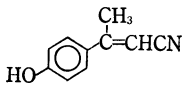

X

Although the dimerization of β-aminocrotononitrile (Ic) under various conditions has previously been reported to give the lutidine III[4,10] *via* 4-amino-1,3-dicyano-2-methylpenta-1,3-diene (XI),[6,11] no report could be found concerning the use of PPA for the condensation.

The nitrogenous product, III, described above, was obtained together with 4-methylcoumarins, II, when phenols were treated with Ic in the presence of PPA. The analytical data agreed with the formula $C_8H_9N_3$, which is itself in accord with the structure of the lutidine derivative, III, and the precursor, XI. The physical properties, along

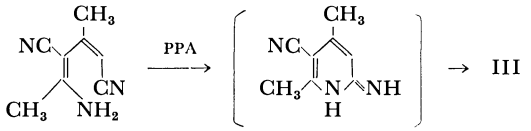

XI

with the infrared and ultraviolet spectra, suggest that the product is assignable to the cyclic compound III. When treated with 12 N hydrochloric acid, the product, III, was converted to the salt, XII, while treatment with acetic anhydride gave the N-acetyl-derivative, XIII. Moreover, this lutidine, III, when refluxed with 75% sulfuric acid, yielded 6-amino-2,4-lutidine (XIV), while when it was refluxed with 48% hydrobromic acid, it afforded

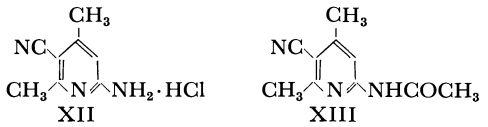

XII XIII

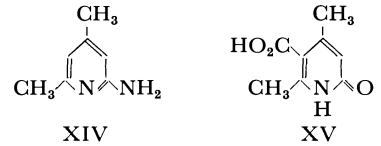

XIV XV

2,4-lutid-6-on-3-carboxylic acid (XV). These results confirm the structure III for 6-amino-3-cyano-2,4-lutidine. On the other hand, we have found a convenient method for preparing III by means of the PPA-catalyzed self-condensation of Ic. When the nitrile Ic was heated in PPA at 160—165°C for 1 hr, the lutidine, III, was obtained in an 81% yield. In contrast, under mild conditions Ic gave a dienaminonitrile, XI (13%), as well as III. The dienaminonitrile, XI, readily underwent intramolecular cyclization, through isomerization, to III when heated in PPA or an alkaline solution. The results, along with the infrared spectra and the ultraviolet spectra, confirm the structures of III and XI for the lutidine and pentadiene derivatives respectively.

The following discussion is presented to account

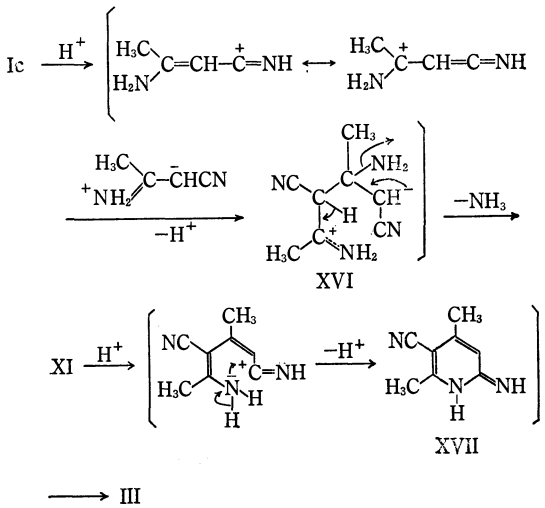

XVI XVII

for the formation of XI and III from β-aminocrotononitrile (Ic). The protonation of Ic, followed by interaction between the electrophilic β- and nucleophilic α-centers of Ic, provides, *via* deprotonation, the unstable betaine XVI, which then undergoes deamination to XI. Furthermore, compound XI is converted to III through intramolecular cyclic addition to XVII and subsequent isomerization. The data are consistent with this view.

Accordingly, the usual poor yield of 4-methylcoumarins II, is due to such a predominant dimerization of Ic as is shown above.

Experimental[12]

Materials. β-Aminocrotononitrile (Ic), mp 52—53°C, was prepared by the dimerization of acetonitrile

10) E. Von Meyer, *J. prakt. Chem.*, [2] **52**, 89 (1895).
11) a) E. von Meyer, *ibid.*, [2] **78**, 517 (1908). b) E. von Meyer, *ibid.*, [2] **90**, 41 (1914). c) P. J. Brignell, E. Bullock, U. Einsner, B. Gregory, A. W. Johnson and H. Williams, *J. Chem. Soc.*, **1963**, 4819.

12) All melting points, determined on a Shimadzu Type MM-2 micro hot stage, are uncorrected. Infrared and ultraviolet spectra were recorded, respectively, on a Hitachi Model EPI-S2 and Hitachi Model EPS-3T spectrophotometers. NMR spectra were taken in d_6-dimethylsulfoxide on a JEOL Model C-60H instrument with tetramethylsilane as an internal standard.

with sodium metal.[4b] The monoetherification of resorcinol with dimethylsulfate was carried out by means of the procedure of Kinugawa and his co-workers.[13] 3-Cyano-2,4-lutid-6-one was obtained by the treatment of Ic with boiling water.[4a]

PPA-Catalyzed Reaction of Phenols with Ic; 4-Methylcoumarins. *General Procedure.* Finely-powdered Ic (4.1 g, 0.05 mol) was added slowly to a mixture of the phenol (0.05 mol) and 41 g of PPA at 90°C, after which stirring was vigorously continued at 90—100°C. Then the mixture was gradually heated on an oil bath and kept under the conditions shown in Table 1. Thereafter the resulting mixture was chilled, poured into water containing crushed ice (200—300 m*l*), and extracted with ether. After the extract had been washed with water and dried over anhydrous magnesium sulfate, the removal of the solvent, followed by recrystallization from aqueous ethanol, gave the pure 4-methylcoumarin (II). The results with individual compounds are presented in Table 1.

The aqueous layer was basified with 10% sodium hydroxide and then filtered to afford orange crystals. Recrystallization from 95% ethanol furnished 6-amino-3-cyano-2,4-lutidine (III) as colorless needles; mp 226—227°C (lit[6] 227—228°C); sublimed at *ca.* 160°C; ν_{max}^{KBr} 3400, 3330 (N–H), 3130, 2200 (C≡N), 1665 (C=N), 1605, 1492 (C=C), 1413, 1380 (CH_3), 1175, and 840 cm^{-1}; NMR: τ 7.76 (2-CH_3), 7.60 (4-CH_3), 6.50 (NH_2), and 3.75 (nuclear proton).

Found: C, 65.39; H, 6.43%. Calcd for $C_8H_9N_3$: C, 65.31; H, 6.12%.

4-Amino-1,3-dicyano-2-methylpenta-1,3-diene (XI). *a)* Compound Ic (1.0 g) was added to 10 g of PPA at room temperature. A vigorously exothermic reaction occurred. The mixture was allowed to stand at 30—50°C for 1.5 hr, during which time the solution was sometimes stirred by means of a glass rod. The neutralization of the resulting mixture with an alkaline solution, followed by filtration, gave quantitatively a mixture of crude-orange products, III and XI. Fractional crystallization from water afforded III, mp 226—227°C. XI (0.12 g, 13%) was obtained from the mother liquor; mp 167—168°C (lit[6] mp 166—166.5°C) (from water). ν_{max}^{KBr}: 3380, 3320, 3200 (NH_2), 2200 (C≡N), 1655 (C=N), 1600, 1545 (C=C), 1250 cm^{-1}; λ_{max}^{EtOH} mμ (ε): 220 (6920), 256 (4530), 327 (9920); NMR: τ 7.83 (CH_3, 6H), 6.57 (NH_2, 2H), and 4.57 (olefinic proton, 1H).

Found: C, 65.51; H, 6.44%. Calcd for $C_8H_9N_3$: C, 65.31; H, 6.12%.

b) Acetyl chloride (5.0 g) was stirred, drop by drop, into a solution of Ic (2.5 g) in absolute ether (30 m*l*) over a period of 10 min and then kept for 30 min at room temperature. Thereafter the yellow mass which was deposited was filtered to afford the adduct, which was then washed with ether. The treatment of the adduct with water (7 m*l*), followed by filtration, gave the crude XI; this product was recrystallized from water to provide the pure XI (0.7 g, 31%) as colorless needles, mp 167—168°C. The infrared spectrum was identified with that of XI presented above.

6-Amino-3-cyano-2,4-lutidine (III). *a) From Ic.* The nitrile Ic (2.1 g) was added slowly to 21 g of PPA at 90—100°C over a period of 10 min; the mixture was then gradually heated and stirred on an oil bath at 160—165°C for 1 hr. After the resulting mixture had cooled to about 90°C, it was poured into an ice-water slurry (80 g), and neutralized with 10% sodium hydroxide; then the mixture was allowed to stand for a long time. Filtration gave a yellow crystal mass, which was recrystallized from aqueous ethanol to provide the pure III (1.5 g, 81%) as colorless needles, mp 226—227°C; λ_{max}^{EtOH} 272 mμ (ε=7200). A mixed-melting-point determination with an authentic sample such as that already prepared (mp 226—227°C) showed no depression.

b) From XI. A mixture of XI (140 mg) and PPA (1.4 g) was heated on an oil bath at 160°C for half an hour. A treatment of the resulting mixture similar to that shown above gave III (80 mg, mp 226—227°C).

c) The Base-catalyzed Cyclization of XI.[6] A mixture of XI (100 mg) and 5% potassium hydroxide (10 m*l*) was stirred at 100°C for 3 hr chilled to room temperature, and allowed to stand for some time. Filtration, followed by recrystallization from ethanol, afforded the pure III (28 mg); mp 226—227°C.

6-Amino-3-cyano-2,4-lutidine Hydrochloride (XII). A mixture of III (130 mg) and 12 N hydrochloric acid (5 m*l*) was heated at 100—105°C for 2.5 hr. The removal of the hydrochloric acid furnished the crude salt XII (160 mg), which was then recrystallized from ethanol to give the pure product as colorless needles; mp 248—249°C; ν_{max}^{KBr}: 3300 (N-H), 2650—2750 ($-\overset{+}{N}H_3\overset{-}{Cl}$) cm^{-1}.

Found: C, 52.04; H, 5.74%. Calcd for $C_8H_{10}ClN$: C, 52.32; H, 5.45%.

6-Acetylamino-3-cyano-2,4-lutidine (XIII). A solution of III (140 mg) in acetic anhydride was warmed at 80°C for 1 hr and then chilled. After the solution had stood in an ice-box for 1 day, filtration and subsequent recrystallization from ethanol provided the product, XIII, as colorless needles; mp 255—256°C (lit[10] mp 250°C); ν_{max}^{KBr}: 3230 (N–H), 2230 (C≡N), 1680 (C=O), 1580, 1530 (C=C) cm^{-1}.

Found: C, 63.22; H, 6.11; N, 21.97%. Calcd for $C_{10}H_{11}N_3O$: C, 63.47; H, 5.86; N, 22.21%.

6-Amino-2,4-lutidine (XIV). A mixture of III (1.0 g) and 75% sulfuric acid (10 g) was heated at 150—160°C for 3 hr. The cooled mixture was neutralized with dilute sodium hydroxide and extracted with ether (30 m*l*). After the extract had been washed with water and dried over anhydrous magnesium sulfate, the solvent was removed; recrystallization from ethanol then gave colorless plates (0.6 g, 72%); mp 66—67°C (lit[14] 65—67°C); ν_{max}^{KBr}: 3450, 3350 (NH_2), 3130, 1615 (C=C), 1570, 1450, 1390, 1380 (CH_3), 1235, 820, and 810 cm^{-1}.

2,4-Lutid-6-on-3-carboxylic Acid (XV). A solution of III (1.0 g) in 48% hydrobromic acid (10 m*l*) was heated at 120—130°C for 3 hr. The removal of the hydrobromic acid gave the crude product; this was recrystallized from ethanol to give pure XV (0.62 g, 55%) as colorless needles; mp 271—272°C (dec); ν_{max}^{KBr}: 3400 (w. OH), 3000, 2800, 1670, 1640—1620, 1460, 1420, 1385 (CH_3), 1350, 1240, 955, 905, 825, and 710 cm^{-1}.

Found: C, 57.25; H, 5.71; N, 8.12%. Calcd for

13) J. Kinugawa, M. Ochiai and H. Yamamoto, *Yakugaku Zasshi (J. Pharm. Soc. Japan)*, **79**, 931 (1959).

14) B. Rudner, U. S. Pat. 2892841 (1959).

$C_8H_9NO_3$: C, 57.48; H, 5.43; N, 8.38%.

3-Cyano-2,4-lutid-6-one. This compound was prepared from III according to the procedure of Bullock and Gregory.[6] The treatment of III with sodium nitrite in dilute hydrochloric acid gave the product; mp>300°C (lit mp 293°C[4]; mp 305—307°C[6]). A mixed-melting-point determination with an authentic sample from III[4] (mp>300°C) indicated no depression. ν_{max}^{KBr}: 3400 (w. OH), 1660 (C=O), 1615 (C=C), 1410, 1370 (CH_3), 870, and 720 cm^{-1}.

BULLETIN OF THE CHEMICAL SOCIETY OF JAPAN VOL. 42 2323—2326 (1969)

Photochemical Reactions of Some Thioparabanates

Teijiro YONEZAWA, Masakatsu MATSUMOTO, Yoichi MATSUMURA and Hiroshi KATO

Department of Hydrocarbon Chemistry, Faculty of Engineering, Kyoto University, Kyoto

(Received December 23, 1968)

1,3-Disubstituted thioparabanates (I) were reduced with ethanol under the action of light tc yield 2-mercaptoimidazolidine-4,5-diones (II) with or without 2-(1-hydroxyethyl)-2-mercaptoimidazolidine-4,5-dione (III). It seems that these reactions may be initiated by the n–π^* transition of the lone pair in the 2-thiocarbonyl group. When dimethylthioparabanate (Ic) was irradiated with a high-pressure mercury arc in a chloroform solution of amylene, a photocycloaddition product, a trimethylene sulfide (IVa), was obtained.

Recently several investigations[1-3] into the photochemical reduction of thiobenzophenone in alcoholic solvents and the photocycloaddition of the same compound with such olefins as 1-butene and 1,3-cyclooctadiene have been made. Its photochemical behavior has been found to be considerably different from that of benzophenone; in the photochemical reduction reaction, the former gave benzhydryl mercaptan, dibenzhydryl disulfide, and a tetrasulfide as reduction products,[1] whereas dibenzopinacol was produced from the latter.[2] In the photocycloaddition reaction thiobenzophenone with olefins gave 1:1 adducts and 2:1 adducts, or olefins formed by the decomposition of these adducts,[3] while it is well known that oxetanes are produced from many carbonyl compounds.

However, the photochemical reactivities of the ureid carbonyl group and the thioureid group have scarcely been studied at all. A purpose of the present work is to compare the photochemical reactions of thioparabanates containing a thioureid group with those of thiobenzophenone and benzophenone.

Results

Electronic Spectra. All the thioparabanates (I) are yellow. The ultraviolet and visible spectra of these compounds are shown in Table 1, together with those of thioparabanic acid, parabanic acid, and tetramethylthiourea. For all the derivatives of thioparabanic acid (I), the electronic spectra in ethanol showed an n–π^* absorption band at 400—440 mμ and a π–π^* absorption band at about 300 mμ. The former is probably due to an n–π^* transition which is mainly localized on the thiocarbonyl group in thioparabanates (I); parabanic acid has an n–π^* absorption band due to the carbonyl group of the oxalyl group at 314 mμ, and thioparabanates (I) are expected to have an n–π^* absorption band of the oxalyl group in the same region. The n–π^* absorption band of the thiocarbonyl group in tetramethylthiourea is at 324 mμ[4] and the imidazolidinetrione molecule is nearly planar,[5] so if the thioparabanic acid molecule has a similar structure, the π orbitals of 2-thiocarbonyl group may overlap with the lone-pair orbitals of N atoms and also with the π orbitals of the oxalyl group. Consequently, the n–π^* absorption band of the thiocarbonyl group is thought to shift longer wavelength region than that of tetramethylthiourea. The results of the ASMO SCF calculation[6] (zero differential approximation) indicate that the singlet-singlet transitions for thioparabanic acid are as follows; the $n_{C=S}$–π^* transition at 341 mμ,

1) G. Oster, L. Citarel and M. Goodman, *J. Am. Chem. Soc.*, **84**, 703 (1962).

2) *E. g.*, N. J. Turro, "Molecular Photochemistry," W. A. Benjamin, New York (1965), p. 140.

3) a) E. T. Kaiser and T. F. Wuifers, *J. Am. Chem. Soc.*, **86**, 1897 (1964); b) K. Yamada, M. Yoshika and N. Sugiyama, *J. Org. Chem.*, **33**, 1240 (1968).

4) M. J. Janssen, *Rec. Trav. Chim.*, **79**, 454 (1960); *Chem. Abstr.*, **55**, 104i (1961).

5) L. E. Sutton, "Tables of Interatomic Distances and Configuration in Molecules and Ions," Chemical Society, London (1958), p. 144.

6) T. Yonezawa, H. Konishi and H. Kato, to be published.

TABLE 1. ELECTRONIC SPECTRA OF THIOPARABANATES (I)

R	R'	π-π*[a] λ_{max} (mμ)	π-π*[a] ε	n-π*[a] λ_{max} (mμ)	n-π*[a] ε
H	H	304	10400	416	40
C_6H_5	H	302	13200	422	49
$C_6H_5CH_2$	H	302	12800	415	30
C_6H_5	C_6H_5	305	15300	432	44
CH_3	CH_3	298	13900	402	25
C_2H_5	C_2H_5	301	14600	405	35
C_6H_5	$C_6H_5CH_2$	302	14000	421	38
parabanic acid		—	—	314	40
$((CH_3)_2N)_2C=S$[b]		—	—	324	2.41[c]

a) Measured in ethanol at 25°C.
b) In diethyl ether.
c) log ε

TABLE 2. PHOTOREDUCTION PRODUCTS OF THIOPARABANATES (II)

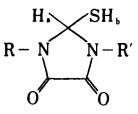

	R	R'	Mp (°C)	NMR spectra* (τ) H_a	NMR spectra* (τ) H_b	J_{ab} (Hz)
(II-a)	Ph	Ph	200	2.50	4.28	9.0
(II-b)	Ph	$PhCH_2$	173	2.53	4.28	9.0
(II-c)	CH_3	CH_3	—	2.82	4.89	9.0
(II-d)	C_2H_5	C_2H_5	—	2.83	4.89	9.0

* in d_6-DMSO solutions

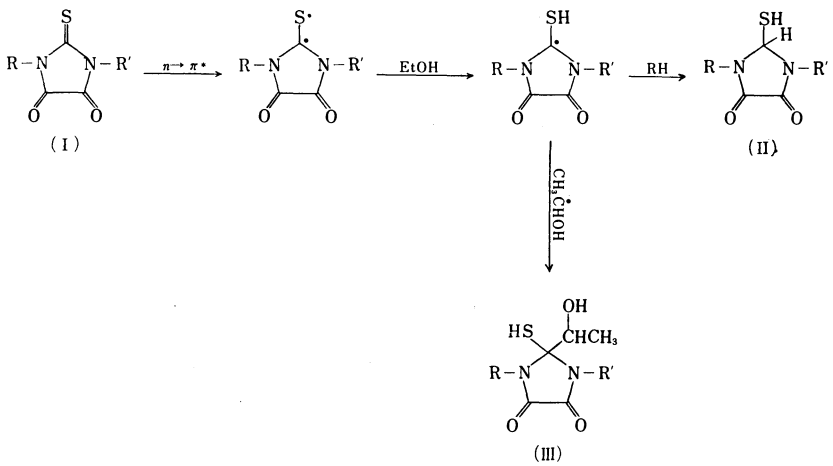

Scheme 1.

the lowest π-π* transition at 286 mμ, and a very weak σ-π* absorption at 436 mμ (though this third transition has never been detected).

Photoreduction. 1,3-Diphenylthioparabanate (Ia) in an ethanol solution was irradiated under a nitrogen atmosphere with a 200-W high-pressure mercury arc. The yellow color of the solution gradually faded, and the reduction product, 1,3-diphenyl-2-mercapto-imidazolidine-1,5-dione (IIa) was formed in a quantitative yield. As in the case of diphenylthioprarabanate, the irradiation of most 1,3-disubstituted thioparabanates led to the corresponding mercaptans (II). The melting points and NMR parameters of these reduction products

are shown in Table 2. In Table 2, when the substituent group is a methyl or an ethyl group, the reduction product (IIc or IId) could not be obtained in a pure form. The mercaptan (IIc) and (IId) were very unstable and were oxidized by air to form the corresponding thioparabanate.

When the substrate had one or two active hydrogen atoms bonded to the nitrogen, the photochemical reactions of these compounds gave complex products. In the case of thioparabanic acid, thiourea, carbon monoxide, and trace of formaldehyde were obtained, while in the case of monoesters, tarry products were obtained. In these photoreductions, active protons bonded to the nitrogen atom may labilize the reduction form (II) of thioparabanate containing an active mercapto proton.*1

In the reduction of diethylthioparabanate, the mercaptan (IId) was obtained, plus 2-(1-hydroxyethyl)-1,3-diethyl-2-mercapto-imidazolidine-4,5-dione (III) as a by-product. The mercaptan (III) can reasonably be assumed to be produced by a combination of the thioketyl radical (A) and the α-hydroxyethyl radical (B). Moreover, the thioketyl radical (A) may be produced from the excited molecule of I resulting from the n–π^* transition of the thiocarbonyl group, but not from a π–π^* transition. Thus, the mechanism of the photochemical reduction of thioparabanates (I) may be considered to be as is shown in Scheme 1.

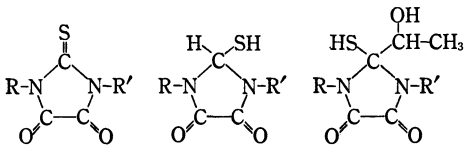

(I) (II) (III)

In the photochemical reduction in ethanol, thioparabanates seem to behave in a considerably different fashion from thiobenzophenone; in the case of thiobenzophenone, it is significant that the benzhydryl-thiyl radical $(C_6H_5)_2CHS\cdot$ is formed through the abstraction of the hydrogen atom from the solvent,[2] while in the case of thioparabanates the ketyl radical seems to be formed through the reaction.

Photocycloaddition. The photochemical addition reaction of dimethylthioparabanate (Ic) with amylene was attemtped in chloroform with a 200-W high-pressure mercury arc under a nitrogen atmosphere. A 1 : 1 addition product (IV) of dimethylthioparabanate and amylene was obtained as colorless crystals melting at 136.0—137.0°C. The mass spectrum of the adduct (IV) gave fragment ions at m/e 169.098 ($^{12}C_8{}^1H_{13}{}^{14}N_2{}^{16}O_2$ requires 169.0982) and m/e 103.058 ($^{12}C_5{}^1H_{11}{}^{32}S$ requires 103.0576). The NMR spectrum showed a quartet (a-methyne proton, 1H, J=6 Hz) at τ=6.54, a doublet (b-methyl protons, 3H, J=6 Hz) at τ=8.71, and four singlets, due to c-, d-, e-, and f-methyl protons, at τ=6.63, 6.78, 8.70, and 8.95. From these results, the adduct (IV) was identified as a trimethylenesulfide (IVa). The fragmentation patterns in the mass spectrum exclude the isomer (IVb) as a product since the fragment, C_3H_6S, coming from the C–S and C–C bond fission could not be detected.

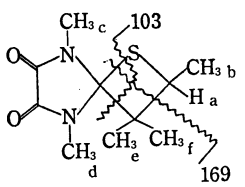

(IVa)

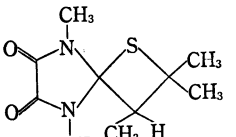

(IVb)

In the cases of the other thioparabanates, no photocycloaddition reaction occurred.

Experimental

Materials. The thioparabanates (I) were prepared by the treatment of a ethylene dichloride solution of the corresponding thiourea with oxalyl chloride.[7] The thiourea were obtained from the reaction of the corresponding isothiocyanate and amine. The thioparabanates were purified by recrystallization from ethanol.

Amylene was prepared by treating t-amyl alcohol with concentrated H_2SO_4. This was purified by fractional distillation; bp 37.0—38.5°C.

Spectra. The visible and ultraviolet spectra were measured in an ethanol solution at 25°C using a Shimadzu UV50M spectrophotometer.

Irradiation of Diphenylthioparabanate (Ia). A solution of 7.0 g (0.025 mol) of the ester (Ia) in 500 m*l* of absolute ethanol was purged with nitrogen for 1 hr and then irradiated under nitrogen with a 200-W high-pressure mercury arc. The yellow solution of Ia completely faded within 15 hr. From the reaction mixture, ethanol was evaporated *in vacuo;* then the white residue was recrystallized from benzene, giving 1,3-diphenyl-2-mercapto-imidazolidine-4,5-dione (IIa) as silky crystals melting at 200.0°C; yield, 98%. The infrared spectrum in KBr showed the absorption of the oxalyl group at 1745 cm^{-1}. The NMR spectrum in hexadeuterio-dimethyl sulfoxide (d_6-DMSO) showed one proton at τ=2.51 as a sharp doublet (J=9.0 Hz), one proton at τ=4.28 (a sharp doublet, J=9.0 Hz), and a complex absorption (10H) centered at τ=2.75. Upon the addition of D_2O, the doublet at τ=2.51 disappeared and the doublet at τ=4.28 turned into a singlet at τ=4.28.

Found: C, 63.38; H, 4.26; N, 9.86; S, 11.26%. Calcd for $C_{15}H_{12}O_2N_2S$: C, 63.60; H, 4.04; N, 9.79;

*1 Most α-aminomercaptans, –NHC(SH)–, like these analogs, *gem*-diols and α-hydroxymercaptans, are unstable and have never been isolated.

7) T. Yonezawa, M. Matsumoto, S. Tanimoto and H. Kitano, *Nippon Kagaku Zasshi (J. Chem. Soc. Japan, Pure Chem. Sect.)*, **89**, 784 (1968).

S, 11.01%.

Irradiation of Benzylphenylthioparabanate (Ib). A solution of 7.4 g (0.025 mol) of the ester (Ib) in absolute ethanol (500 m*l*) was irradiated under a nitrogen atmosphere for 15 hr. In this case the solution was not faded. After irradiation the solvent was evaporated from the reaction mixture *in vacuo*. The oily residue was chromatographed on alumina in benzene, thus giving 1-benzyl-3-phenyl-2-mercapto-imidazolidine-4,5-dione (IIb) (5.9 g), mp 173.0°C after crystallization. The NMR spectrum showed complex absorption due to two phenyl groups centered at τ=2.61 (11H), containing a signal of the mercapto proton, a sharp doublet at τ=4.28 (1 H, J=9.0 Hz), and a singlet at τ=6.82 (2H).

Found: C, 65.68; H, 4.59: N, 9.11%. Calcd for $C_{17}H_{14}O_2N_2S$: C, 65.80; H, 4.55; N, 9.03%.

Irradiation of Dimethylthioparabanate (Ic). A 0.05 mol/*l* solution of the ester (Ic) in ethanol (500 m*l*) was irradiated under a nitrogen atmosphere for 2 hr. Then the solution was concentrated under nitrogen at reduced pressure. The almost colorless oily residue was used for the measurement of its NMR spectrum. In this case the expected mercaptan (IIc) was very unstable and was easily oxidized by air to form the starting materials. The mercaptan (IIc) was characterized only by its spectroscopic properties, the NMR spectrum of the oil described previously showed a mercapto proton (a sharp doublet, J=9.0 Hz) at τ=2.82 and a 2-methyne proton (a sharp doublet, J=9.0 Hz) at τ=4.89.

Irradiation of Diethylthioparabanate (Id). The ester (Id) was treated by the similar manner to that employed in the case of dimethylthioparabanate (Ic). The NMR spectrum of the crude mercaptan (IId) showed a mercapto proton as a sharp doublet (J=9.0 Hz) at τ=2.93 and a 2-methyne proton as a sharp doublet (J=9.0 Hz) at τ=4.89. The crude reaction products was chromatographed on alumina in chloroform, and when the resultant pale yellow oil was allowed to stand for two weeks, colorless needles separated out, giving 2-(1-hydroxyethyl)-1,3-diethyl-2-mercapto-imidazolidine-4,5-dione (III), mp 134.0—135.0°C, by crystallization from cyclohexane. The NMR spectrum in d_6-DMSO showed a singlet (mercapto proton, 1H) at τ=3.02, a doublet (hydroxy proton, 1H, J=4.5 Hz) at τ=4.87, a complex absorption composed of a multiplet (methyne proton, 1H) centered at τ=6.35 and a quartet (two methylene protons, 4H, J=6.3 Hz) at τ=6.38, and a complex absorption composed of two triplets (methyl protons of two ethyl groups, 6H, J=6.3 Hz) at τ=8.75 and 8.91 and a doublet (methyl protons of hydroxyethyl group, 3H, J=6.3 Hz) at τ=8.85. These assignment were confirmed by spin-decoupling experiments.

Found: C, 46.39; H, 6.99; N, 12.25%. Cacld for $C_9H_{16}O_3N_2S$: C, 46.54; H, 6.94; N, 12.06%.

Irradiation of Thioparabanic Acid. A 0.05 mol/*l* solution of thioparabanic acid in ethanol was irradiated with a 200-W high-pressure mercury arc under a nitrogen atmosphere for 10 hr. During irradiation the evolution of carbon monooxide and hydrogen sulfide was observed. A trace of formaldehyde was also detected in the reaction mixture by Denigès' method. The evaporation of ethanol from the solution gave crude thiourea in the yield of 73%.

Irradiation of Some Monoesters of Thioparabanic Acid. The photochemical reduction reactions were attempted for phenylthioparabanate and benzylthioparabanate. In these cases the formation of acetaldehyde was recognized and no corresponding mercaptan (II) was obtained, only a tarry product.

Irradiation of Dimethylthioparabanate (Ic) with Amylene in Chloroform. A solution of dimethylthioparabanate (Ic) (5.0 g, 0.032 mol), and amylene (40.0 g, 0.57 mol) in chloroform (25 m*l*) was irradiated with a 200-W high-pressure mercury arc under a nitrogen atmosphere for 20 hr. After irradiation, the unreacted amylene and solvent were distilled off from the reaction mixture. Then an oily residue was dissolved in 20 m*l* of chloroform and chromatographed on alumina (150 g) in 1:1 chloroform and petroleum ether. This gave, successively, colorless needles (IV) (210 mg), colorless leaflects (V) (30 mg), and dimethylparabanate (200 mg) as a colorless leaflets which showed a mp of 152.0°C, after crystallization from cyclohexane (Biltz and Topp[8] give mp 154.0°C). The recrystallization of IV from cyclohexane yielded the trimethylenesulfide (IVa), mp 136.0—137.0°C. The NMR spectrum in deuteriochloroform showed a complex absorption comprised of a quartet (a-methyne proton, 1H, J=6.0 Hz) at τ=6.54, two singlets (c- and d-methyl protons, 6H) at τ=6.63 and τ=6.78, a doublet (b-methyl protons, 3H, J=6.0 Hz) at τ=8.71, and two singlets (e- and f-methyl protons, 6H) at τ=8.70 and τ=8.95. These assignments were confirmed by spin-decoupling experiments. The infrared spectrum in chloroform showed $\nu_{C=O}$ at 1740 cm^{-1}. The mass spectrum exhibited fragment ions at *m/e* 103.058 ($^{12}C_5{}^1H_{11}{}^{32}S$ requires 103.0576) and *m/e* 169.098 ($^{12}C_8{}^1H_{13}{}^{14}N_2{}^{16}O_2$ requires 169.0982).

Found: C, 52.45; H, 6.92; N, 12.20%. Calcd for $C_{10}H_{16}O_2N_2S$: C, 52.55; H, 7.00; N, 12.25%.

The identification of V is not yet complete, but we presume, from its NMR and mass spectra, and from the results of elemental analysis, that V is a 2 : 2 adduct of dimethylthioparabanate (Ic) and amylene.

8) H. Biltz and E. Topp, *Ber.*, **47**, 1387 (1913).

BULLETIN OF THE CHEMICAL SOCIETY OF JAPAN VOL. 42 2327—2330 (1969)

Synthetic Studies of the Flavone Derivatives. XII.*1 The Synthesis of 8,3'-Dimethoxy-5,7,4'-trihydroxyflavone

Kenji FUKUI and Mitsuru NAKAYAMA

Department of Chemistry, Faculty of Science, Hiroshima University, Higashi Sendamachi, Hiroshima

and Tokunaru HORIE

Department of Applied Chemistry, Faculty of Engineering, University of Tokushima, Tokushima

(Received December 28, 1968)

The partial benzylation of 3-methoxy-2,4,6-trihydroxyacetophenone gave a mixture of 2,4-dibenzyloxy-6-hydroxy- and 4,6-dibenzyloxy-2-hydroxy-3-methoxyacetophenone. The latter was esterified with 4-benzyloxy-3-methoxybenzoyl chloride, and the resulting ester was converted into 8,3'-dimethoxy-5,7,4'-tribenzyloxyflavone *via* the corresponding diketone. The catalytic debenzylation of the flavone gave 8,3'-dimethoxy-5,7,4'-trihydroxyflavone. Its diethyl ether was also prepared from 3,6-dimethoxy-4-ethoxy-2-hydroxyacetophenone by an unambiguous method.

Recently, several new 5,7-dihydroxy-8-methoxyflavone derivatives have been isolated in nature[1] and their structures have been identified on the basis of spectral comparison with the known flavones. The synthesis of 3,8,3'-trimethoxy-5,7,4'-trihydroxyflavone (I) and related compounds have previously been reported.[2] It was considered useful to synthesize 8,3'-dimethoxy-5,7,4'-trihydroxyflavone (II), which may be expected to occur in nature, and to compare its properties with that of I and related compounds. The present paper will report on the synthesis of II from 3-methoxy-2,4,6-trihydroxyacetophenone (III).[3]

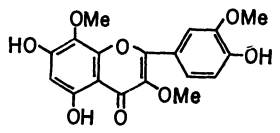

I

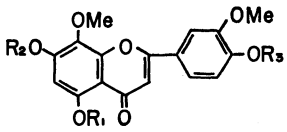

II $R_1=R_2=R_3=H$
VII $R_1=R_2=R_3=C_6H_5CH_2$
VIII $R_1=R_2=R_3=CH_3CO$
IX $R_1=H$, $R_2=R_3=Et$
XII $R_1=Me$, $R_2=R_3=Et$

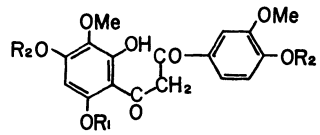

VI $R_1=R_2=C_6H_5CH_2$
XIII $R_1=Me$, $R_2=Et$

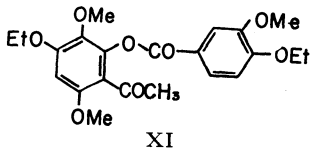

XI

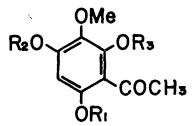

III $R_1=R_2=R_3=H$
IV $R_1=H$, $R_2=R_3=C_6H_5CH_2$
V $R_1=R_2=C_6H_5CH_2$, $R_3=H$
X $R_1=Me$, $R_2=Et$, $R_3=H$

When the III ketone was treated with benzyl chloride in the presence of anhydrous potassium carbonate in anhydrous acetone, two kinds of benzylated ketones, A (a crystalline fraction, mp 140—141°C) as the minor portion and B (an oily fraction) as the major portion, were separated from the reaction mixture. The former, A, shows

*1 Part XI of this series: K. Fukui, T. Matsumoto and S. Tanaka, This Bulletin, **42**, 2380 (1969).

1) C. A. Henrick and P. R. Jefferies, *Tetrahedron*, **21**, 3219 (1965); E. L. Ghisalberti, P. R. Jefferies and C. A. Stacey, *Australian J. Chem.*, **20**, 1049 (1967).

2) K. Fukui, M. Nakayama and T. Horie, *Experientia*, **24**, 417, 769 (1968); K. Fukui, T. Matsumoto, M. Nakayama and T. Horie, This Bulletin, **41**, 2805 (1968); T. Horie, *Experientia*, **24**, 880 (1968).

3) P. S. Phadke, A. V. Rama Rao and K. Venkataraman, *Indian J. Chem.*, **5**, 131 (1967).

the analytical data for $C_{23}H_{22}O_5$ corresponding to the dibenzyl ether of III and a positive ferric chloride reaction. The latter, B, could not be crystallized, but it was identified as crude 2,4-dibenzyloxy-6-hydroxy-3-methoxyacetophenone (IV) on the basis of further experiments.[4] Consequently, the structure of A was postulated to be 4,6-dibenzyloxy-2-hydroxy-3-methoxyacetophenone (V).

The V dibenzyloxyketone was esterified with 4-benzyloxy-3-methoxybenzoyl chloride in the presence of anhydrous pyridine, and then the resulting ester was converted into 4,6-dibenzyloxy-2-hydroxy-3-methoxy-ω-(4-benzyloxy-3-methoxybenzoyl)-acetophenone (VI) by Baker-Venkataraman transformation.[5] The cyclodehydration of the VI diketone with anhydrous sodium acetate in acetic acid afforded a flavone, mp 149.5—150.5°C, which gave a red color when treated with magnesium and hydrochloric acid. The NMR spectrum*2 of the flavone indicated the presence of two methoxyl groups, three benzyloxy groups, and five aromatic protons (Table 1). Further, a set of proton signals at 6.51 and 6.64 (each 1 H, singlet) in the aromatic region could, by the application of the study of Farid,[6] be assigned to the C-6 and C-3 protons*3 respectively. Therefore, this flavone may be formulated as 8,3'-dimethoxy-5,7,4'-tribenzyloxyflavone (VII). The debenzylation of VII with hydrogen gave the desired flavone II, which was then easily derived to triacetate (VIII) by the usual method.

In order to establish the structure of the trihydroxyflavone (II), the diethyl derivative (IX) of II was also synthesized by the following unambiguous method. 2-Hydroxy-3,6-dimethoxy-4-ethoxyacetophenone (X),[7] when esterified with 4-ethoxy-3-methoxybenzoyl chloride, yielded 2-(4-ethoxy-3-methoxybenzoyloxy)-3,6-dimethoxy-4-ethoxyacetophenone (XI). The subsequent reaction of the XI ester gave 7,4'-diethoxy-5,8,3'-trimethoxyflavone (XII) *via* the corresponding diketone, XIII. The partial demethylation of XII with anhydrous aluminum chloride afforded 7,4'-diethoxy-8,3'-dimethoxy-5-hydroxyflavone, which was found to be identical with the IX mentioned above by a mixed-melting-point determination and by infrared spectra comparison. The NMR spectra of VIII and IX (Table 1) show one proton signal corresponding to the C-6 proton at 6.86 and 6.40 respectively; these spectra were in accordance with those of the flavone derivatives described in earlier reports.[1,6,8]

TABLE 1. NMR DATA OF FLAVONES*2,*4

Proton	Compounds		
	VII	VIII	IX
C-3	6.64_s	6.68_s	6.58_s
C-6	6.51_s	6.86_s	6.40_s
C-2'	$6.8—8.1_m$	7.50_{bs}	7.43_d
C-5'		$7.22_{d'}$	$6.98_{d'}$
C-6'		7.57_q	7.69_q

*4 s, singlet; bs, broad singlet; d, doublet (J_{meta}=2.5 Hz); d', doublet (J_{ortho}=9.0 Hz); q, quartet (J_{ortho}=9.0 Hz, J_{meta}=2.5 Hz); m, multiplet.

Experimental*5

4,6-Dibenzyloxy-2-hydroxy-3-methoxyacetophenone (V). A mixture of the acetophenone III[3] (2.5 g), anhydrous potassium carbonate (7.0 g), and benzyl chloride (3.5 g) in anhydrous acetone (50 ml) was refluxed for 16 hr and then diluted with water (150 ml). After the solution had been concentrated in a vacuum to *ca.* 50 ml, the residue was extracted with ether. The ether layer was washed with a 3% sodium hydroxide solution and with water, and the solvent was removed. After the oily residue had then been dissolved with methanol-ether (20 : 1), the mixture was kept overnight in a refrigerator. The resulting precipitate was collected, washed with methanol, and recrystallized from ethyl acetate to give V as pale yellow prisms, mp 140—141°C, which gave a dark brown color with ferric chloride; yield, 290 mg (6%). UV: λ_{max} mμ (log ε); 289.5 (4.24), 322 (3.53).

Found: C, 72.94; H, 5.70%. Calcd for $C_{23}H_{22}O_5$: C, 73.00 H, 5.86%.

The acetate: acetic anhydride-pyridine method; mp 87—88°C (colorless needles from aqueous methanol). UV: λ_{max} mμ (log ε); 263.5 (3.85), 302 (3.71).

Found: C, 71.64; H, 5.52%. Calcd for $C_{25}H_{24}O_6$: C, 71.41; H, 5.75%.

The solvent of the mother liquor was removed by evaporation to give crude 2,4-dibenzyloxy-6-hydroxy-3-methoxyacetophenone (IV) (*ca.* 1.5 g), which had been converted into some 5,7-dihydroxy-6-methoxyflavone derivatives in a previous paper.[4]

4,6-Dibenzyloxy-2-hydroxy-3-methoxy-ω-(4-benzyloxy-3-methoxybenzoyl)-acetophenone (VI). A mixture of V (0.5 g) and 4-benzyloxy-3-methoxybenzoyl

4) K. Fukui, M. Nakayama and T. Horie, *Experientia,* **25**, 355 (1969).

5) W. Baker, *J. Chem. Soc.,* **1933**, 1381; K. Venkataraman and H. S. Mahal, *ibid.,* **1934**, 1767.

*2 All the NMR spectra in this paper were measured with a Hitachi R-20 spectrometer (60 MHz), using tetramethylsilane as the internal standard (δ-value in $CDCl_3$).

6) S. Farid, *Tetrahedron,* **24**, 2121 (1968).

*3 The C-6 proton signal is broader than that of the C-3 proton.[6]

7) T. Horie, M. Masumura and S. Okumura, *Nippon Kagaku Zasshi (J. Chem. Soc. Japan, Pure Chem. Sect.),* **83**, 468 (1962).

8) C. A. Henrick and P. R. Jefferies, *Australian J. Chem.,* **17**, 934 (1964); J. Massicot and J-P. Marthe, *Bull. Soc. Chim. France,* **1962**, 1962; J. Massicot, J-P. Marthe and S. Heitz, *ibid.,* **1963**, 2712.

*5 All the melting points are uncorrected. The ultraviolet spectra were measured in ethanol.

chloride (0.8 g) in pyridine (6 ml) was heated for 2 hr in an oil bath at 120°C. The cooled reaction mixture was poured into diluted hydrochloric acid. The mixture was extracted with ether, and the ether layer was washed with a sodium carbonate solution and then with water. The solvent was removed, and the resulting semi-solid was dried in a desiccator.

A mixture of the above crude ester, powdered potassium hydroxide (1.0 g), and pyridine (10 g) was heated for 4 hr at 60°C with stirring. The reaction mixture was acidified with diluted hydrochloric acid and then solidified by the addition of ether. The resulting precipitate was collected and recrystallized from ethyl acetate to give VI as yellow needles; mp 146.5—148°C; yield, 330 mg (40%). From the ether layer, VI was also obtained according to the ordinary procedure; yield, 135 mg (17%). It gave a green color with ferric chloride. UV: λ_{max} mμ (log ε); 301 (4.17), 390 (4.44), 408_{sh} (4.39).*6

Found: C, 73.96; H, 5.68%. Calcd for $C_{38}H_{34}O_8$: C, 73.77, H, 5.54%.

8,3′-Dimethoxy-5,7,4′-tribenzyloxyflavone (VII). A mixture of VI (225 mg) and anhydrous sodium acetate (1.0 g) in acetic acid (10 ml) was heated for 2 hr at 140°C. The reaction mixture was then diluted with water and extracted with ether. The ether layer was washed with a sodium carbonate solution and with water, and allowed to stand overnight in a refrigerator. The separating crystals were collected, and recrystallized from ethyl acetate to give VII as colorless needles, mp149.5—150.5°C, which gave a negative ferric chloride reaction; yield, 155 mg (71%). IR: 1635 cm^{-1} (KBr). UV: λ_{max} mμ (log ε); 247_i (4.36),*7 272 (4.37), 338 (4.40). NMR:*2,*4 5.28_s (2H); 5.19_s (4H) (C_6H_5-$C\underline{H}_2$); 3.99_s (6H, $C\underline{H}_3O$); (Table 1).

Found: C, 76.20; H, 5.16%. Calcd for $C_{38}H_{32}O_7$: C, 75.98; H, 5.37%.

8,3′-Dimethoxy-5,7,4′-trihydroxyflavone (II). A solution of VII (130 mg) in ethyl acetate - methanol (1 : 1; 50 ml) was submitted to catalytic hydrogenolysis at room temperature in the presence of Pd-C (10%: 75 mg). After the catalyst had been filtered, the filtrate was evaporated under a vacuum. The residue was recrystallized from diluted ethanol to give II as yellow plates, mp 274—276°C, which gave a dark green color with ferric chloride; yield, 60 mg (91%). IR: 3540, 3470, 3400, 1649, 1613, 1578, 1556, 1508 cm^{-1} (KBr). UV: λ_{max} mμ (log ε); 244.5 (4.18), 253 (4.19), 276 (4.27), 343 (4.28).

Found: C, 61.61; H, 4.10%. Calcd for $C_{17}H_{14}O_7$: C, 61.82; H, 4.27.

The triacetate (VIII): hot acetic anhydride - pyridine method; mp 196—196.5°C (colorless needles from ethanol). IR: 1762, 1644 cm^{-1} ($CHCl_3$). UV: λ_{max} mμ (log ε); 241 (4.35), 263 (4.28), 316 (4.28). NMR:*2,*4 4.05_s, 3.94_s (each 3H, $OC\underline{H}_3$); 2.45_s, 2.40_s 2.36_s (each 3H, $OCOC\underline{H}_3$); (Table 1).

Found: C, 60.79; H, 4.40%. Calcd for $C_{23}H_{20}O_{10}$: C, 60.52; H, 4.42%.

2-(4-Ethoxy-3-methoxybenzoyloxy)-3,6-dimethoxy-4-ethoxyacetophenone (XI). A mixture of X[7] (2.5 g), 4-ethoxy-3-methoxybenzoyl chloride (2.8 g), and anhydrous pyridine (8.0 ml) was heated in an oil bath at 110°C for 2.5 hr. The cooled mixture was poured into ice-cold dilute hydrochloric acid and then solidified by the addition of ether. The resulting precipitate was collected and recrystallized from ethanol to give XI as colorless plates; mp 132.5—133.5°C; yield, 2.75 g (63%). From the ether layer, XI was also obtained according to the ordinary procedure; yield, 0.75 g (17%). UV: λ_{max} mμ (log ε); 265 (4.17), 300 (3.99).

Found: C, 63.30; H, 6.38%. Calcd for $C_{22}H_{26}O_8$: C, 63.15; H, 6.26%.

3,6-Dimethoxy-4-ethoxy-2-hydroxy-ω-(4-ethoxy-3-methoxybenzoyl)-acetophenone (XIII). A mixture of the XI ester (2.3 g), powdered potassium hydroxide (4.0 g), and pyridine (16 g) was treated by the procedure described for VI. The product was then recrystallized from ethanol to give XIII as pale yellow needles, mp 145—146°C, which gave a green color with ferric chloride; yield, 1.65 g (72%). UV: λ_{max} mμ (log ε); 298 (4.31), 387 (4.17), 405_{sh} (4.10).*6

Found: C, 63.32; H, 6.28%. Calcd for $C_{22}H_{26}O_8$: C, 63.15; H, 6.26%.

7,4′-Diethoxy-5,8,3′-trimethoxyflavone (XII). To a solution of XIII (1.17 g) in acetic acid (15 ml), a solution of acetic acid - concentrated sulfuric acid (5 : 1; 6 ml) was added, and then the mixture was heated at 70°C for 3 min. The cooled mixture was diluted with water (200 ml) and then heated on a steam-bath for 10 min. The resulting precipitate was collected and recrystallized from ethyl acetate to give XII as colorless prisms; mp 158—159°C; yield, 930 mg (83%). IR: 1652 cm^{-1} (Nujol). UV: λ_{max} mμ (log ε); 249 (4.21), 271.5 (4.23), 339 (4.25). NMR:*2,*4 7.59_q (C-6′); 7.46_d (C-2′); $6.99_{d'}$ (C-5′); 6.63_s (C-6); 6.46_s (C-3); 4.26_q, 4.19_q (each 2H, $CH_3C\underline{H}_2$, J=7.0 Hz); 3.97_s (9H, $C\underline{H}_3O$); 1.52_t (6H, $C\underline{H}_3CH_2$, J=7.0 Hz).

Found: C, 66.05; H, 6.06%. Calcd for $C_{22}H_{24}O_7$: C, 65.99; H, 6.04%.

7,4′-Diethoxy-8,3′-dimethoxy-5-hydroxyflavone (IX). *a) From II.* A mixture of II (33 mg), anhydrous potassium carbonate (500 mg), and diethyl sulfate (200 mg) in anhydrous acetone (15 ml) was refluxed for 6 hr and then diluted with water (50 ml). The resulting precipitate was collected and recrystallized from ethanol to give IX as colorless needles, mp 178—179.5°C, which gave a green color with ferric chloride; yield, 25 mg (65%). IR: 1663, 1613 cm^{-1} (Nujol). UV: λ_{max} mμ (log ε); 253.5 (4.26), 275 (4.32), 339 (4.31). NMR:*2,*4 12.6_{bs} (O$\underline{H}$); 4.19_q (4H, $CH_3C\underline{H}_2$, J=7.0 Hz); 3.96_s, 3.93_s (each 3H, $C\underline{H}_3O$); 1.51_t (6H, $C\underline{H}_3CH_2$, J=7.0 Hz); (Table 1).

Found: C, 65.19; H, 5.80%. Calcd for $C_{21}H_{22}O_7$: C, 65.27; H, 5.74%.

b) From XII. To a solution of XII (760 mg) in anhydrous nitrobenzene (8 g), a solution of anhydrous aluminum chloride (4 g) in ether (12 g) was added. The mixture was heated at 47°C for 3 hr. After the mixture had then been poured into 1% hydrochloric acid (250 ml), the solution was concentrated in a vacuum to 150 ml. The resulting precipitate was collected and recrystallized from ethanol to give IX, mp 178—179.5°C; yield, 360 mg (49%), which was identical with that of the sample a.

Found: C, 65.33; H, 5.82%. Calcd for $C_{21}H_{22}O_7$: C, 65.27; H, 5.74%.

The acetate: hot acetic anhydride - pyridine method; mp 175.5—176.5°C (colorless needles from ethyl acetate).

*6 sh=Shoulder.

*7 i=Inflection point.

IR: 1753, 1645 cm^{-1} (Nujol). UV: λ_{max} mμ (log ε); 246 (4.39), 263.5 (4.27), 340 (4.41). NMR:[*2,*4] 7.67_q (C-6′); 7.43_d (C-2′); $6.98_{d'}$ (C-5′): 6.67_s (C-3); 6.55_s (C-6); 4.20_q (4H, $CH_3C\underline{H}_2$, J=7.0 Hz); 4.02_s, 3.96_s (each 3H, $C\underline{H}_3O$); 2.44_s ($OCOC\underline{H}_3$); 1.52_t (6H, $C\underline{H}_3CH_2$, J=7.0 Hz).

Found: C, 64.63; H, 5.74%. Calcd for $C_{23}H_{24}O_8$: C, 64.48; H, 5.65%.

BULLETIN OF THE CHEMICAL SOCIETY OF JAPAN VOL. 42 2330—2332 (1969)

Studies of the *N*-Oxides of *N,N*-Dialkylamino Acids. II. The Syntheses of *N,N*-Dialkylglycine and Corresponding *N*-Oxides

Yoshikazu IKUTANI

Department of Chemistry, Osaka Kyoiku University, Tennoji-ku, Osaka

(Received December 31, 1968)

The reductive condensations of glycine with various aliphatic straight-chain aldehydes, such as acetaldehyde, propionaldehyde, and *n*-butyraldehyde, give the corresponding *N,N*-dialkyl derivatives. The *N*-monoalkyl derivative has not been obtained in any case. In another type of reactions, those with aliphatic branched-chain aldehydes, such as isobutyraldehyde and isovaleraldehyde, considerable *N*-monoalkylation takes place besides the dialkylation. The oxidations of *N,N*-dialkylglycine to the corresponding *N*-oxides have been successfully performed using an aqueous mixture of hydrogen peroxide and acetic acid except in the case of *N,N*-diisobutylglycine. Similar reductive condensations of sarcosine with various aliphatic aldehydes, such as acetaldehyde, propionaldehyde, *n*- and iso-butyraldehyde, and isovaleraldehyde, gave the corresponding *N*-alkylsarcosines. *N*-Isobutyl and *N*-isoamyl sarcosine were also obtained by the methylation of the corresponding *N*-monoalkylglycine. The *N*-oxides of *N*-alkylsarcosine were synthesized by a procedure similar to that described above.

In the preceding paper of this series,[1] the *N,N*-dimethylations of various neutral amino acids, such as glycine, L-alanine, DL-alanine, L-valine, DL-valine, L-leucine, L-phenylalanine, and L-tyrosine, and the oxidations to the corresponding *N*-oxides were investigated. In the present study, the preparations of *N,N*-dialkylglycine *N*-oxides have been studied. The alkylations of glycine by the catalytic reductive condensation with various aliphatic aldehydes were performed by a procedure similar to that reported in the preceding paper. The results obtained are summarized in Table 1.

These results clearly indicate that the corresponding *N,N*-dialkyl derivatives were obtained as the alkylation products when aliphatic straight-chain aldehydes were employed in these reactions. The *N*-monoalkyl derivatives initially formed seem to be more reactive to the carbonyl group of the aldehydes and readily react with an excess of aldehydes to give the corresponding *N,N*-dialkyl derivatives.

On the other hand, in the case of the reductive alkylation of glycine with aliphatic branched-chain aldehydes, such as isobutyraldehyde and isovaleraldehyde, considerable monoalkylation took place besides the dialkylation. However, when an excess of the aldehyde was used, the *N,N*-dialkyl derivative was obtained in a nearly quantitative yield. These results show the bulkiness of the substituent of aliphatic branched-chain aldehydes considerably inhibits the condensation reaction of the *N*-monoalkyl glycine initially formed and the aldehyde. This assumption is supported by the fact that the *N,N*-dialkylation of glycine with isovaleraldehyde proceeds more rapidly than that of the similar reaction with isobutyraldehyde. The analytical data and some properties of *N,N*-dialkylglycine are summarized in Table 2.

The oxidations of *N,N*-dialkyl derivatives of glycine to the corresponding *N*-oxides were performed successfully by the method described in the preceding paper. However, in the case of *N,N*-diisobutylglycine, all attempts to obtain the corresponding *N*-oxide were unsuccessful and the unchanged *N,N*-diisobutylglycine was recovered. This unfavorable result is probably brought about by the steric hindrance of the bulky isobutyl residue. The analytical data and some properties of the *N*-oxides of *N,N*-dialkylglycine are summarized in Table 3.

Similar reductive condensations of sarcosine with various aliphatic aldehydes, such as acetaldehyde, propionaldehyde, *n*- and iso-butyraldehyde, and isovaleraldehyde, gave the corresponding

1) Y. Ikutani, This Bulletin, **41**, 1679 (1968).

N-alkylsarcosines. These analytical data and some properties are summarized in Table 4.

N-Isobutyl and *N*-isoamyl sarcosine were also synthesized by the reductive methylation of the corresponding *N*-monoalkylglycine with formaldehyde.

The oxidations of *N*-alkylsarcosine to the *N*-oxides were performed by a procedure similar to

Table 1. The catalytic reductive condensation of glycine with various aliphatic aldehydes

Aldehyde	Molar ratio (aldehyde/glycine)	Reaction conditions		Recovery of glycine (%)	Yield of the product (%)	
		Temp. (°C)	Time (hr)		Monoalkyl	Dialkyl
Acetaldehyde	2	40—45	4	6	none	85
Propionaldehyde	2	40—45	4	13	none	80
n-Butylaldehyde	1	45—50	5	46	trace	41
	2	45—50	6	11	none	83
Isobutyraldehyde	1	50—55	4	65	23	7
	1.5	50—55	7	36	40	20
	2	50—55	9	22	40	36
Isovaleraldehyde	1	50—55	3	32	38	25
	2	50—55	6	16	19	59

Table 2. *N, N*-Dialkylglycine

Alkyl group	Mp (°C)	R_f Value*	Formula	C, %		H, %		N, %	
				Found	Calcd	Found	Calcd	Found	Calcd
Ethyl	123	0.65	$C_6H_{13}O_2N$	55.00	54.94	9.92	9.99	10.59	10.68
n-Propyl	129	0.68	$C_8H_{17}O_2N$	60.22	60.34	10.81	10.76	8.80	8.80
n-Butyl	135	0.83	$C_{10}H_{21}O_2N$	64.01	64.13	11.24	11.30	7.30	7.48
Isobutyl	98	0.76	$C_{10}H_{21}O_2N$	64.49	64.13	11.23	11.30	7.44	7.48
Isoamyl	172	0.88	$C_{12}H_{25}O_2N$	67.10	66.93	11.81	11.70	6.35	6.51

* A *n*-butanol - acetic acid - water (60 : 15 : 25) solvent system was used. The location of the paper chromatogram was performed by spraying of alkaline aqueous ethanol solution of thymol blue.

Table 3. *N, N*-Dialkylglycine *N*-oxide

Alkyl group	Yield (%)	Mp (dec. °C)	R_f Value	C, %		H, %		N, %		ν_{N-O} cm^{-1}
				Found	Calcd	Found	Calcd	Found	Calcd	
Ethyl	70	110	0.76	48.69	48.96	8.95	8.90	9.41	9.52	999
n-Propyl	87	93	0.81	54.81	54.83	9.80	9.78	7.94	7.99	987
n-Butyl	90	92	0.87	58.99	59.08	10.41	10.41	6.94	6.89	975
Isoamyl	92	148	0.93	62.15	62.30	10.83	10.89	5.97	6.05	1010

Table 4. *N*-Alkylsarcosine

Alkyl group	Yield (%)	Mp (°C)	R_f Value	C, %		H, %		N, %	
				Found	Calcd	Found	Calcd	Found	Calcd
n-Propyl	83	113	0.53	54.99	54.94	10.09	9.99	10.66	10.68
n-Butyl	87	95	0.66	58.09	57.90	10.44	10.41	9.42	9.65
Isobutyl (from sarcosine)	93	111	0.64	57.68	57.90	10.48	10.41	9.48	9.65
Isobutyl (from glycine *via* *N*-isobutyl glycine)	—	110	—	58.12	57.90	10.37	10.41	9.41	9.65
Isoamyl (from sarcosine)	87	132	0.71	60.13	60.34	11.02	10.76	8.65	8.80
Isoamyl (from glycine *via* *N*-isoamyl glycine)	—	136	—	60.50	60.34	10.84	10.76	8.65	8.80

TABLE 5. *N*-ALKYSARCOSINE *N*-OXIDE

Alkyl group	Yield (%)	Mp (°C)	R_f Value	C, % Found	C, % Calcd	H, % Found	H, % Calcd	N, % Found	N, % Calcd	ν_{N-O} cm^{-1}
n-Propyl	63	91	0.64	49.57	48.96	9.30	8.90	9.50	9.52	997
n-Butyl	67	98	0.78	52.01	52.15	9.41	9.38	8.89	8.69	985
Isobutyl (from sarcosine)	71	137 (dec.)	0.74	52.38	52.15	9.41	9.38	8.67	8.69	952
Isobutyl (from glycine *via* *N*-isobutyl glycine)	—	135 (dec.)	—	52.24	52.15	9.47	9.38	8.62	8.69	—
Isoamyl (from sarcosine)	65	130	0.79	54.80	54.83	9.58	9.78	7.78	7.99	994
Isoamyl (from glycine *via* *N*-isoamyl glycine)	—	127	—	54.54	54.83	9.75	9.78	7.73	7.99	—

that described in the preceding paper. The analytical data and some properties of *N*-alkylsarcosine *N*-oxides are summarized in Table 5. The optical resolutions of *N*-alkylsarcosine *N*-oxides are currently under investigation, the results will be reported in detail elsewhere.

Experimental

The Dialkylation of Glycine with Various Aliphatic Straight-chain Aldehydes. The *N,N*-dialkyl derivatives of glycine were obtained by the catalytic reductive condensation of glycine with various aliphatic straight-chain aldehydes, such as acetaldehyde, propionaldehyde, and *n*-butyraldehyde, according to a procedure smilar to that described in the preceding paper.

The Alkylation of Glycine with Aliphatic Branched-chain Aldehydes. A mixture of 15 g of glycine, 1.5 g of the silk-palladium catalyst, 29 g of isobutyraldehyde, 100 m*l* of ethanol, and 130 m*l* of water was shaken with hydrogen in an autoclave at 50—55°C for 9 hr. The catalyst was then removed by filtration, and the filtrate was evaporated to dryness under reduced pressure. The residue was suspended to a small volume of ethanol, and the suspension was dried up under reduced pressure to remove a trace of water. The residue was then extracted with two 50 m*l* portions of hot ethanol to dissolve the *N*-isobutyl and *N,N*-diisobutyl glycine. Unreacted glycine was removed as a precipitate. The combined extract was dried up under reduced pressure. The residue was then re-extracted with two 50 m*l* portions of hot acetone to dissolve *N,N*-diisobutyl glycine, while *N*-isobutylglycine remained as a precipitate. The yield of crude *N*-isobutylglycine was 10.5 g. The pure substance was obtained by the recrystallization of the crude product from hot ethanol, it melted at 207°C with decomposition.

Found: C, 54.52; H, 9.95; N, 10.71%. Calcd for $C_6H_{13}O_2N$: C, 54.94; H, 9.99; N, 10.68%.

When the extracted filtrate was dried up under reduced pressure, 13.5 g of crude *N,N*-diisobutylglycine was obtained. The product was dissolved in a minimum volume of a hot mixture of acetone and isopropyl ether (1 : 1), decolorized with a small amount of charcoal, and filtered. About the same volume of isopropyl ether was then added in small portions, and the mixture was stored in a refrigerator overnight. Fine crystals of *N,N*-diisobutylglycine were then collected by filtration, washed with a small amount of isopropyl ether, and dried under reduced pressure.

The reductive alkylation of glycine with isovaleraldehyde was performed in the same manner. The dialkyl derivative was extracted using three 100 m*l* portions of a hot mixture of acetone and ethanol (9 : 1). The *N*-isoamylglycine melted at 235°C with decomposition.

Found: C, 58.12; H, 10.37; N, 9.41%. Calcd for $C_7H_{15}O_2N$: C, 57.90; H, 10.41; N, 9.65%.

***N,N*-Dialkylglycine *N*-Oxides.** These substances were prepared by the oxidation of the corresponding *N,N*-dialkylglycine with an aqueous mixture of hydrogen peroxide and acetic acid according to a procedure similar to that described in the preceding paper except in the case of *N,N*-diisobutylglycine.

***N*-Alkylsarcosine.** The *N*-alkylsarcosines were obtained by the catalytic reductive condensation of sarcosine with the corresponding aliphatic aldehyde. For example, a mixture of 15 g of sarcosine, 1.5 g of the silk-palladium catalyst, 12 g of propionaldehyde, and 150 m*l* of water was shaken with hydrogen in an autoclave at 45—50°C for 6 hr. The catalyst was then removed by filtration, and the filtrate was evaporated to dryness under reduced pressure. The residue was dissolved in a small volume of ethanol, and the solution was dried up to remove a trace of water. After this procedure had been repeated three times, the residual syrup was stored in a desiccator for a week. The crude *N*-*n*-propylsarcosine thus crystallized was filtered with a small amount of isopropyl ether and recrystallized from a hot mixture of acetone and isopropyl ether. Other *N*-alkyl derivatives of sarcosine were obtained by a similar procedure.

The author is indebted to Professor Eizo Matsumura for his constant guidance in the course of the work, and to Professor Yoshiharu Izumi of Osaka University for his valuable advice and encouragement.

BULLETIN OF THE CHEMICAL SOCIETY OF JAPAN VOL. 42 2333—2336 (1969)

An Automatic Chromatographic Method for the Separation of Flavonoid Compounds

Masatake HORI

Research and Development Division, Takeda Chemical Ind., Ltd., Juso, Higashiyodogawa-ku, Osaka

(Received Junuary 6, 1969)

A new chromatographic method for the separation of flavonoids was developed using Amberlite XAD-2 adsorption resin as the stationary phase and a gradient system of ethanol-water as the eluent. The advantage of the method lies in the fact that a number of flavonoids can be separated by a single operation with good reproducibility. The accuracy of this method determined with pure flavonoids was within ±2%. In addition, the method is useful for preparative purposes, because the solvents used are readily removable by evaporation. The elution time of 56 flavonoids was determined by this method; moreover, the method was applied to the determination of flavonoids in crude methanol extracts from plants (*Scutellaria baicalenisis, Citrus aurantium* and *Crataegus cuneata*).

The chemistry of flavonoids has been a subject of interest for many organic chemists, and hence a number of the compounds have been recorded, which differ considerably in structure. In general, flavonoids can be separated by the chromatography on Magnesol, silica gel, cellulose powder, or alumina, *etc.*[1] These adsorbents, however, have to be selected for each experiment, because the polarity of flavonoids differs considerably among these compounds. Moreover, the adsorbents mentioned above have to be refilled in each experiment.

In this paper the author wishes to report a new method for the separation of flavones, flavonols, flavanones, and flavanonols, *etc.* by the use of an Amberlite XAD-2 column an dethanol-water as an eluant, with a gradient increase of the ethanol concentration from 20% to 90%.

Experimental

Instruments. All the experiments in this work were carried out using Beckman Model-130 Spectrochrom Analyzer.

Procedure. A glass column (9×1600 mm, with jacket) was packed with Amberlite XAD-2 adsorption resin (200—400 mesh) up to 1500 mm in height, and was kept at 45°C by circulating water in the jacket, except when investigation of the effect of column temperatures was made. Then the column was allowed to equilibrate with 20% ethanol at a flow rate of 60 ml/hr.

A solution of two to four flavonoids, each less than 500 μg in 1 m*l* of 20% ethanol solution, was placed on top of the column. If the sample was sparingly soluble in 20% ethanol, a suspension of the sample in the same solvent was applied. In the case of morin, the UV-absorbancy of which is very low, 2 mg of the sample was applied; by the same reason myricetin was applied as much as 20 mg. As for the solvent, 100 m*l* of 20% ethanol was run first; a successive linear gradient elution then followed with a total volume of 1 *l* raising the ethanol concentration from 20 to 90%. The eluate was determined automatically at three wavelengths, 270, 300 and 330 mμ, and collected by a fraction collector every ten minutes.

Materials. The flavonoids used in this study, except morin (E. Merck), myricetin (Fluka A. G.), naringenin (Tokyo Kasei), were all supplied by courtesy of Drs. S. Imai and N. Morita.*1

Methanol extracts of *Scutellaria baicalensis, Citrus aurantium* and *Crataegus cuneata* were prepared by repeated extraction of the dried plants with methanol at 70°C, followed by evaporation of the solvent. The residue was then dissolved in 20% ethanol and subjected to chromatography. The yields of extracts are shown in Table 1.

Results and Discussion

As is clear from theoretical plate concept in chromatography that the use of smaller granules as a stationary phase results in more efficient separation of the peaks, the resin used in this investigation was granulated and sieved in water and 200—400 mesh granules were collected. It is also known that the temperature of a column affects the separation and the elution time of the peaks. By a preliminary investigation, it was found that the peaks are tailing at low temperatures such as 25°C and the elution time becomes shortened with the rise in temperature (Fig. 1). However, the temperature of the column was maintained at 45°C to prevent bubble formation in the column at higher temperatures.

The chromatograms obtained with 56 authentic

1) M. K. Seikel, "The Chemistry of Flavonoid Compounds," ed. by T. A. Geissman, Pergamon Press, New York (1962), p. 34.

*1 Faculty of Pharmacology, Toyama University.

Table 2. Flavonoids used in this investigation

Sample	Name	Type of compound*	$\frac{E_{270\,m\mu}}{E_{300\,m\mu}}$	$\frac{E_{330\,m\mu}}{E_{300\,m\mu}}$	Sample	Name	Type of compound*	$\frac{E_{270\,m\mu}}{E_{300\,m\mu}}$	$\frac{E_{330\,m\mu}}{E_{300\,m\mu}}$
1	Apigenine-7-glucuronide	E	1.55	2.16	29	Phellamurin	G	0.79	0.34
2	Scutellarin	E	1.38	2.10	30	Morin	A	3.13	0.88
3	Nelumboside	E	1.48	1.43	31	Aromadendrin	A	0.56	0.38
4	Baicalin	E	1.77	1.10	32	Myricetin	A	1.79	1.41
5	Homoorientin	G	1.80	1.82	33	Linarin	G	1.07	1.61
6	Saponarin	G	1.66	1.86	34	Pectolinarin	G	1.44	2.04
7	Robinin	G	1.79	1.79	35	Cirsimarin	G	2.28	2.81
8	Rutin	G	1.13	1.43	36	Pedalitin	A	1.32	1.98
9	Scoparin	G	1.44	1.72	37	Chrysosplenin	G	1.72	1.82
10	Lonicerin	G	1.75	1.85	38	Fisetin	A	0.89	1.42
11	Rhoifolin	G	1.69	2.00	39	Fukugetin	G	1.12	0.85
12	Hyperin	G	1.49	1.49	40	Chrysosplenetin	A	1.32	1.90
13	Liquiritin	G	1.79	0.57	41	Quercetin	A	1.67	1.33
14	Tagetin	G	2.32	2.57	42	Amurensin	G	2.28	1.50
15	Pedaliin	G	1.68	2.07	43	Luteolin	A	1.43	1.71
16	Plantaginin	G	1.31	2.10	44	Neolinarin	G	1.38	2.10
17	Quercitrin	G	0.60	0.53	45	Genistein	A	2.11	0.36
18	Luteolin-7-glucoside	G	1.73	1.87	46	Naringenin	A	0.67	0.34
19	Trifolin	G	1.49	1.31	47	Kaempherol	A	1.91	1.67
20	Narcissin	G	1.57	1.52	48	Apigenin	A	1.20	1.54
21	Avicularin	G	1.53	1.53	49	Hesperetin	A	0.65	0.31
22	Kaempheritrin	G	1.45	1.36	50	Baicalein	A	1.96	1.30
23	Bakkoside	G	1.56	1.79	51	Cirsimaritin	A	1.41	2.19
24	Reynoutrin	G	1.39	1.33	52	2-Methylthio-chromone	A	2.04	5.11
25	Hesperidin	G	1.84	0.53	53	Wogonin	A	1.62	0.64
26	Apiin	G	1.37	1.79	54	Swertianol	A	1.79	1.59
27	Cosmosiin	G	1.27	1.68	55	Flavone	A	0.49	0.18
28	Juglanin	G	1.33	1.34	56	Euparin	A	2.92	0.37

* A: Aglycone, G: Glycoside, E: Sugar acid ester.

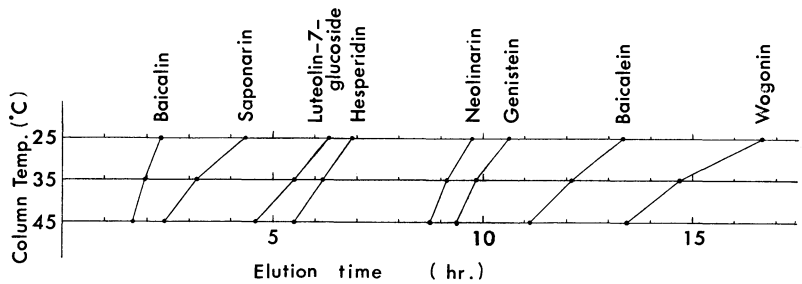

Fig. 1. Effect of the column temperature on the elution time of flavonoids.

flavonoids are summarized in Fig. 2. The number given to each peak corresponds to the sample number listed in Table 2.

In the actual chromatography each peak was drawn at three wavelengths. However, the peaks in Fig. 2 were drawn schematically to avoid complication of the chromatogram.

The elution curve of apiin (No. 26) consisted of two peaks, indicating that both peaks were due to an impurity. The broad peak of morin (No. 30) was far from being a Gaussian distribution. The fact suggests that the shape of the elution curve might be affected by an impurity.

Correlation of the elution time of these substances with their structure led to the conclusion that in this chromatography the polar flavonoids elute with shorter elution time. Thus, the following generalizations are possible.

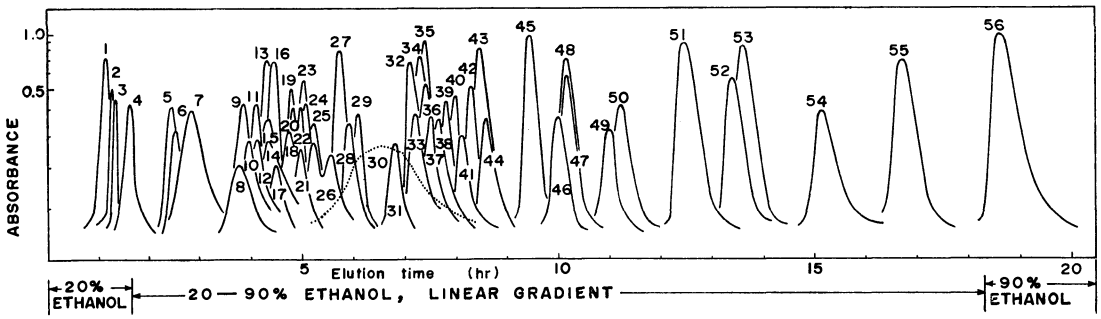

Fig. 2. The elution time of flavonoids.

Column: Amberlite XAD-2, 200—400 mesh, 9×1500 mm, 45°C
Solvent: Aqueous ethanol
Flow rate: 60 ml/hr

Table 1. Yields of methanol extracts from plant sources

Samples	Dry plant (g)	Methanol extract (g)	Amount applied to the column (mg)	Flavonoids determined	%/extract
Scutellaria baicarensis	3.0	0.8648	9.88	Baicalin	7.37
				Baicalein	3.38
				Wogonin	1.39
Citrus aurantium	1.2	0.1653	13.08	Hesperidin	39.6
Crataegus cuneata	3.0	0.2018	67.09	—	—

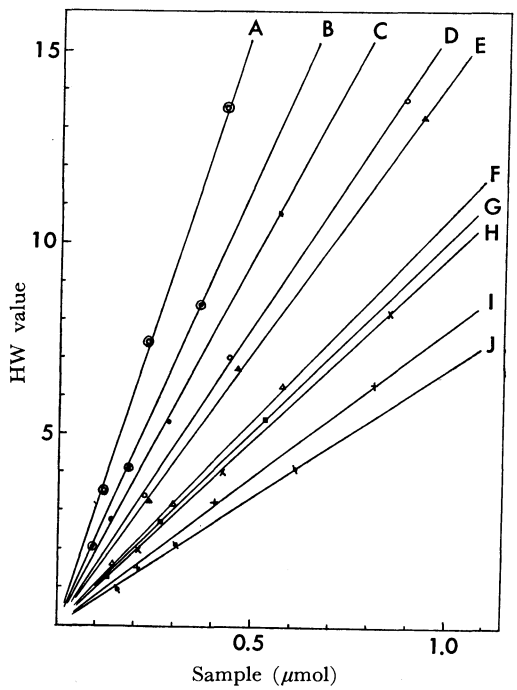

Fig. 3. Calibration curves determined by the HW method from the peak area.

A: Wogonin (53), B: Saponarin (6), C: Flavone (55), D: Kaempherol (47), E: Baicalein (50), F: Rutin (8), G: Baicalin (4), H: Hesperidin (25), I: Quercetin (41), J: Quercitrin (17).

i) The elution is in the order of sugar esters→glycosides→aglycones.

ii) Among the aglycones the compounds having more hydroxyl groups elute faster than the compounds having fewer hydroxyl groups. The stereochemical nature of the hydroxyl groups also affects the elution time of these aglycones.

iii) The elution time of glycosides varies considerably depending on the position where the sugar moiety is attached, even if the aglycone and the sugar are the same among the glycosides.

iv) The elution time for glycosides is greatly affected by the number of hydroxyl groups and sugars.

As is seen in Fig. 2, many of the glycosides and aglycones, which are eluted in the range of retention time, 4—8 hr, are difficult to be separated if they are present in one sample. In such a case, the measurement of the absorbances at three different wavelengths on the chromatogram becomes very significant, because the shape of the absorption spectra differs considerably from one flavonoid to another.[2] The ratios of the absorbance ($E_{270\,m\mu}/E_{300\,m\mu}$, $E_{330\,m\mu}/E_{300\,m\mu}$) calculated from chromatograms are listed in the right column of Table 2. The calibration curves of ten flavonoids calculated by the height-width

2) L. Jurd, "The Chemistry of Flavonoid Compounds," ed. by T. A. Geissman, Pergamon Press, New York (1962), p. 107.

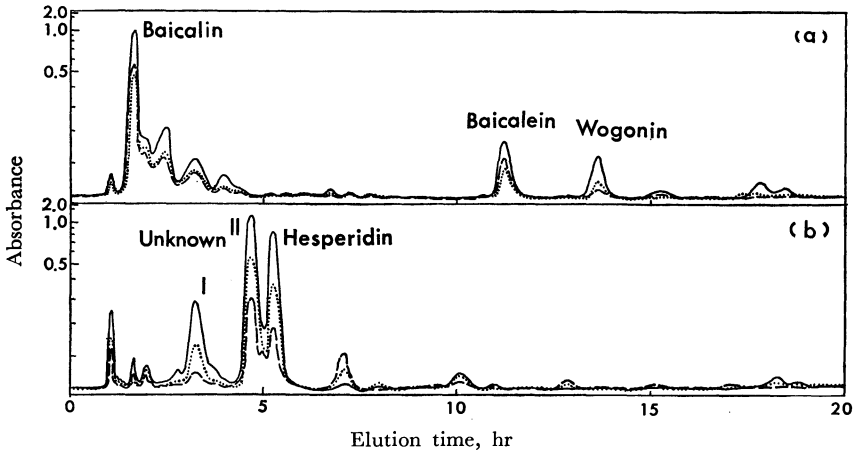

Fig. 4. Chromatograms of the methanol extracts of *Scutellaria baicarensis* (a) and *Citrus aurantium* (b).
——: 270 mμ ·····: 300 mμ — — —: 330 mμ

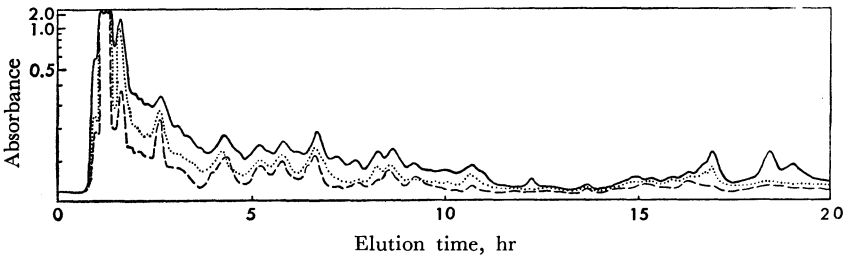

Fig. 5. Chromatogram of the methanol extract of *Crataegus cuneata*.

method*2 are shown in Fig. 3. The accuracy of these measurements lies within ±2%.

Application in the Chromatography of Plant Extracts. Methanol extracts of *Scutellaria baicalensis*, *Citrus aurantium* and *Crataegus cuenata* were prepared by the method as described above. The chromatogram of the extract from *Scutellaria baicalensis*, Fig. 4(a), indicates the presence of baicalin, baicalein and wogonin, all of which have been isolated from these plants. Similarly, the chromatogram of *Citurs aurantium* indicates the presence of hesperidin. Other peaks, which are seen in Fig. 4(b) and designated as peaks I and II, have not yet been characterized. These compounds, however, seem to be akin to hesperidin in their structures, because the absorption spectra resemble that of hesperidine. The chromatogram of the extract from *Crataegus cuneata* was complex as shown in Fig. 5, and the peaks of quercetin and vitexin, which have been isolated from this plant, were indistinguishable. The complexity is due to a large quantity of impurities extracted by methanol, and some pretreatment would be needed.

The author is grateful to Professor Hiroyuki Hatano (Kyoto University) and Dr. Katsura Morita (these laboratories) for valuable discussions. The author is also grateful to Drs. Shunji Imai and Naokata Morita for providing the samples. Thanks are due to Miss Michiyo Miyazaki for her assistance in the experimental work.

*2 The height-width method has been used in the amino acid analysis.

BULLETIN OF THE CHEMICAL SOCIETY OF JAPAN VOL. 42 2337—2342 (1969)

Anionic Telomerizations of Styrene with Some Secondary Amines*1

Teruzo ASAHARA, Manabu SENŌ, Sadayoshi TANAKA and Norio DEN

Institute of Industrial Science, The University of Tokyo, Roppongi, Minato-ku, Tokyo

(Received January 7, 1969)

The anionic telomerizations of styrene with some secondary amines catalyzed by sodium metal were investigated. In this reaction a secondary amine was used as a telogen and styrene as a taxogen. Three telomers, *i. e.* *N,N*-disubstituted 2-phenylethylamine, *N,N*-disubstituted 2,4-diphenylbutylamine and *N,N*-disubstituted 2,4,6-triphenylhexylamine were separated from the mixture of the produced telomers under vacuum distillation. Proton NMR spectra of these telomers in carbon tetrachloride were consistent with the expected structural formulas. The reaction scheme was proposed to explain the formation of telomers.

Anionic telomerization may be characterized to be an anionic polymerization of vinyl, vinylidene and diene compounds so that the initiation reaction, the propagation reaction and the chain transfer reaction can take place to a comparable extent in the polymerization reaction. If the propagation reaction exceeds the chain transfer one, polymerization reaction, in the ordinary sense, would occur to produce high polymers, and if the chain transfer reaction overcomes the propagation one, the anionic addition reaction would be realized. In fact many of the anionic addition reactions of vinyl and diene compounds with alkylaromatic compounds which contain the α-hydrogens in the side chain have been reported by Pine and his coworkers[1-11] and by other authors.[12-15]

The small unbalance between the rate constants of the initiation, the propagation and the chain transfer reactions can sometimes be compensated by controlling the concentrations of a telogen and a taxogen. In other words the molar ratio of a telogen to a taxogen during the telomerization reaction influences the composition and the average molecular weight of the produced telomers.

In this paper the results on the telomerization of styrene with some secondary amines, the separation of the telomers and NMR spectra of the separated telomers will be reported. The formation of the telomers will be discussed with the proposed reaction scheme.

Results and Discussion

Reactions of Styrene with Secondary Amines. Secondary amines were subjected to reaction with styrene to produce telomers, from which were separated the telomers with $n=1$, 2 and 3, respectively, *i.e.* *N,N*-disubstituted 2-phenylethylamines (**1**), *N,N*-disubstituted 2,4-diphenylbutylamines (**2**) and *N,N*-disubstituted 2,4,6-triphenylhexylamine (**3**).

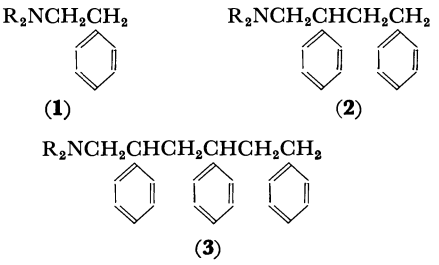

The higher homologs of these telomers were formed at the same time, but remained undistilled in residue under vacuum distillation. Diethylamine, di-*n*-propylamine, di-*n*-butylamine and diisobutylamine were reacted as a telogen. The reaction products obtained are listed in Table 1. The molar ratio of styrene to the amine influenced greatly the

*1 Anionic Telomerizations. II.

1) H. Pines, J. A. Vesely and V. N. Ipatieff, *J. Am. Chem. Soc.*, **77**, 554 (1955).
2) H. Pines and V. Mark, *ibid.*, **78**, 4316 (1956).
3) L. Schaap and H. Pines, *ibid.*, **79**, 4967 (1957).
4) H. Pines and L. Schaap, *ibid.*, **80**, 3076 (1958).
5) H. Pines and D. Wunderlich, *ibid.*, **80**, 6001 (1958).
6) H. Pines and D. Wunderlich, *ibid.*, **81**, 2568 (1959).
7) H. Pines and B. Notari, *ibid.*, **82**, 2209 (1960).
8) B. Notari and H. Pines, *ibid.*, **82**, 2945 (1960).
9) H. Pines and J. Shabtai, *J. Org. Chem.*, **26**, 4220 (1961).
10) H. Pines and N. C. Sih, *ibid.*, **30**, 280 (1965).
11) H. Pines and J. Oszczapowicz, *ibid.*, **32**, 3183 (1967).
12) R. Wegler and G. Pieper, *Chem. Ber.*, **83**, 6 (1950).
13) H. Hart, *J. Am. Chem. Soc.*, **78**, 2619 (1956).
14) R. D. Closson, J. P. Napolitano, G. G. Ecke and A. J. Kolka, *J. Org. Chem.*, **22**, 646 (1957).
15) G. G. Eberhardt and H. J. Peterson, *ibid.*, **30**, 82 (1965).

Table 1. Telomers obtained in the telomerization of styrene with secondary amines

Telogen	Telomer **1**	Telomer **2**	Telomer **3**
Diethylamine	$Et_2N\overset{(a)\ (b)}{C}H_2\overset{(c)}{C}H_2$ (**1a**)	$Et_2N\overset{(a)\ (b)\ (d)\ (e)}{C}H_2\overset{(c)\ (f)}{C}HCH_2CH_2$ (**2a**)	$Et_2N\overset{(a)\ (b)\ (d)\ (e)\ (g)\ (h)}{C}H_2\overset{(c)\ (f)\ (i)}{C}HCH_2CHCH_2CH_2$ (**3a**)
Di-*n*-propylamine	*n*-Pr$_2$NCH$_2$CH$_2$ (**1b**)	*n*-Pr$_2$NCH$_2$CHCH$_2$CH$_2$ (**2b**)	*n*-Pr$_2$NCH$_2$CHCH$_2$CHCH$_2$CH$_2$ (**3b**)
Di-*n*-butylamine	*n*-Bu$_2$NCH$_2$CH$_2$ (**1c**)	*n*-Bu$_2$NCH$_2$CHCH$_2$CH$_2$ (**2c**)	*n*-Bu$_2$NCH$_2$CHCH$_2$CHCH$_2$CH$_2$ (**3c**)
Diisobutylamine	isoBu$_2$NCH$_2$CH$_2$ (**1d**)	isoBu$_2$NCH$_2$CHCH$_2$CH$_2$ (**2d**)	isoBu$_2$NCH$_2$CHCH$_2$CHCH$_2$CH$_2$ (**3d**)

Et: $\overset{(k)\ (j)}{CH_3CH_2}$, *n*-Pr: $\overset{(l)\ (k)\ (j)}{CH_3CH_2CH_2}$, *n*-Bu: $\overset{(m)\ (l)\ (k)\ (j)}{CH_3CH_2CH_2CH_2}$, isoBu: $\overset{(l)\ \ (j)}{CH_3\overset{|}{\underset{(k)}{C}}HCH_2}$,

Table 2. Reaction conditions and reaction products

Secondary amine reacted	Moles of reactants [Styrene]/[Amine]	Dropping time min	Reaction time and temp. min	Reaction time and temp. °C	Telomer **1**[a] %	Tolomer **2**[a] %	Tolomer **3**[a] %
Diethylamine	0.3/0.3	100	180	50.0±0.5	76.9	2.0	0
	0.6/0.3	30	180	50.0±0.5	39.7	6.9	6.2
	3.0/1.5	80	180	50.0±0.5	39.2	11.3	2.5
Di-*n*-propylamine	0.6/0.3	35	180	100.0±0.5	29.4	25.2	10.3
Di-*n*-butylamine	0.6/0.3	20	180	150.0±0.5	13.7	26.4	23.5
Diisobutylamine	0.54/0.27	24	180	120.0±0.3	8.5	30.6	18.0

a) Yields were calculated on the basis of styrene added.

compositions of telomers. Table 2 gives the reaction conditions and the reaction products. Column 1 lists the amines used, and columns 6, 7 and 8 report the yields of the separated telomers.

Structures of the Separated Telomers. The telomer **1a** has a methyl triplet (1 : 2 : 1) at 9.03 τ and a methylene quartet (1 : 3 : 3 : 1) at 7.52 τ. These are the typical signals of ethyl group and are assigned to the two equivalent ethyl groups of the telomer **1a**. The signal at 7.38 τ is that of the methylene protons (a) and (b) between the nitrogen atom and the phenyl group. The protons constituting the phenyl group show a singlet at 2.94 τ. The telomer **2a** gives the signals at 9.12, 2.92 and 2.99 τ which are assigned to methyl protons (k), phenyl protons (c) and phenyl protons (f), respectively. The signals due to five methylene and a methine groups were not assigned completely, but the signals at 7.45, 7.56, 7.68 and 7.80 τ seem to form a methylene quartet due to protons (j). The telomer **3a** shows a methyl triplet and three phenyl singlets at 9.16, 2.93, 2.96 and 3.01 τ which are assigned to protons (k), (c), (f) and (i), respectively. The NMR signals of other telomers were assigned, and the results on the assignments of the signals to the protons of the separated telomers **1**, **2** and **3** are listed in Table 3. It was confirmed from IR spectra that none of the separated telomers has a –NH– group. The results on the

Table 3. Assignment of the signals to the protons

Telomers	The τ values of the signals of the protons in ppm												
	(a)	(b)	(c)	(d)	(e)	(f)	(g)	(h)	(i)	(j)	(k)	(l)	(m)
1a	7.38	7.38	2.94	—	—	—	—	—	—	7.33 7.45 7.56 7.68	8.91 9.03 9.15	—	
2a	···	···	2.92	···	···	2.99	—	—	—	7.45 7.56 7.68 7.80	9.00 9.12 9.24	—	
3a	···	···	2.93	···	···	2.96	···	···	3.01	7.54 7.56 7.68 7.80	9.03 9.16 9.27	—	
1b	7.34	7.34	2.84	—	—	—	—	—	—	7.48 7.59 7.71	8.40 8.52 8.65 8.76	9.03 9.15 9.27	
2b	···	···	2.81	···	···	2.88	—	—	—	···	8.49 8.61 8.74 8.86	9.12 9.23 9.35	
3b	···	···	2.79	···	···	2.85	···	···	2.91	···	8.52 8.64 8.77 8.89	9.14 9.26 9.37	
1c	7.39	7.39	2.86	—	—	—	—	—	—	···	···	···	9.03 9.13 9.23
2c	···	···	2.86	···	···	2.86	—	—	—	···	···	···	9.03 9.13 9.24
3c	···	···	2.87	···	···	2.87	···	···	2.87	···	···	···	9.03 9.14 9.23
1d	7.38	7.38	2.77	—	—	—	—	—	—	7.86 7.95	8.27	9.04 9.09 9.16 9.27	—
2d	···	···	2.78	···	···	2.86	—	—	—	7.94 8.03	8.40	9.05 9.13 9.25 9.36	—
3d	···	···	2.81	···	···	2.87	···	···	2.93	8.00 8.10	8.46	9.06 9.16 9.27 9.30 9.40	—

NMR and IR spectra of the produced telomers are consistent with the structural formulas of the telomers **1**, **2** and **3** listed in Table 1.

Reaction Scheme. The reaction scheme is considered as follows. The initiation reaction may be the addition of sodium to styrene (**4**), and the organometallic compounds **5** transmetalates with a secondary amine **6** to give the compound **7**.

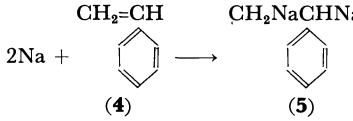

(1)

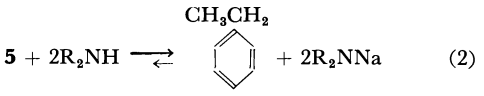

(2)

The compound **7** is able to react with styrene.

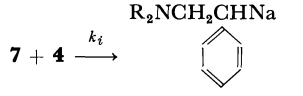

(3)

The resulting sodium salt **8** transmetalates with the amine **6** to produce the compound **1** and at the same time reacts with styrene (**4**).

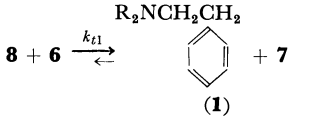

(4)

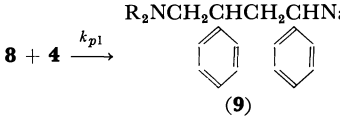

(5)

The reactions (4) and (5) compete for the compound **8**. Both the chain transfer reaction (6) and the propagation reaction (7) take place also competitively for the compound **9**.

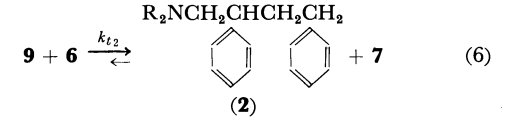

(6)

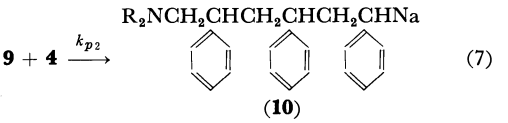

(7)

Generally, the competitive reactions (8) and (9) take place for the organosodium compound **11**.

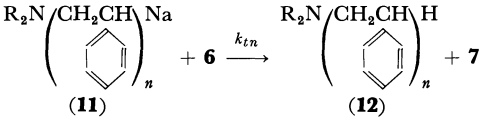

(8)

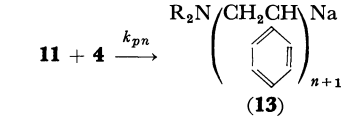

(9)

In the above equations, the notations k_t, k_{tn} and k_{pn} express the rate constants of the initiation reaction (3), the transfer reaction (8) and the propagation reaction (9), respectively. The reactions (3), (4), (5), (6), (7), (8) and (9) constitute a typical telomerization reaction. In fact, on combining Eqs. (3), (8) and (9) for $n=1, 2, \cdots, n-1$, the general equation of telomerization is obtained.

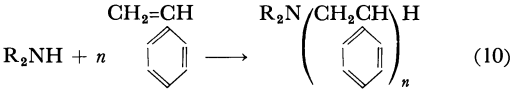

(10)

It may be understood from this reaction scheme that the telomers **1**, **2** and **3** are prepared by the anionic telomerization of styrene with the secondary amines.

Compositions of the Telomers. The reaction scheme proposed in the preceding section may be described as follows.

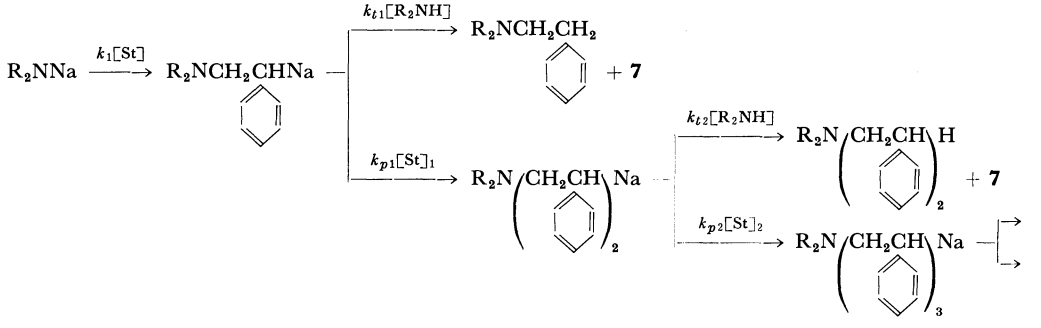

In the reaction styrene was added dropwise, and so the concentrations of styrene with which the organometallic compounds **7**, **8**, **9**, **10** and **11** reacted were different and were in the following order.

$$[St] > [St]_1 > [St]_2 > [St]_3 > \cdots \quad (11)$$

If we suppose that the rate constants of the propagation reactions and the chain transfer reactions are approximately independent of n and the concentration of amine remains almost unchanged in a few minutes, the ratios of the rates of the transfer reactions to those of the propagation reactions

TABLE 4. CHARACTERIZATION OF THE TELOMERS

Molecular formula Structural formula		Elementary analysis	Calcd %	Found %	Molecular weight Calcd	Mass	VPO	Refractive index	Bp °C/mmHg
$C_{12}H_{19}N$ $Et_2NCH_2CH_2$	(**1a**)	C H N	81.30 10.80 7.90	81.16 10.86 7.64	177.28	177	183	1.4972	77/0.1
$C_{20}H_{27}N$ $Et_2NCH_2CHCH_2CH_2$ 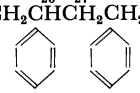	(**2a**)	C H N	85.35 9.67 4.98	85.63 9.92 4.81	281.42	281	277	1.5367	136/0.1
$C_{28}H_{35}N$ $Et_2NCH_2CHCH_2CHCH_2CH_2$ 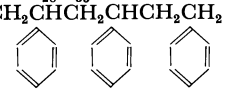	(**3a**)	C H N	87.22 9.15 3.63	86.94 9.31 3.36	385.57	385	377	1.5576	212/0.1
$C_{14}H_{23}N$ $n\text{-}Pr_2NCH_2CH_2$	(**1b**)	C H N	81.89 11.29 6.82	81.86 11.36 7.00	205.33	205	202	1.4889	94/0.03
$C_{22}H_{31}N$ $n\text{-}Pr_2NCH_2CHCH_2CH_2$ 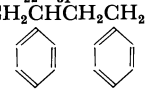	(**2b**)	C H N	85.38 10.10 4.53	85.27 10.07 4.58	309.48	309	313	1.5257	155/0.03
$C_{30}H_{39}N$ $n\text{-}Pr_2NCH_2CHCH_2CHCH_2CH_2$ 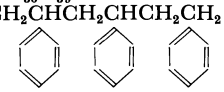	(**3a**)	C H N	87.11 9.50 3.39	87.04 9.07 3.05	413.62	···	408	1.5490	199/0.03
$C_{16}H_{27}N$ $n\text{-}Bu_2NCH_2CH_2$	(**1c**)	C H N	82.34 11.66 6.00	82.15 11.93 5.58	233.38	233	233	1.4990	148/4
$C_{24}H_{35}N$ $n\text{-}Bu_2NCH_2CHCH_2CH_2$ 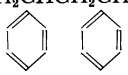	(**2c**)	C H N	85.40 10.45 4.15	85.89 10.04 4.20	337.53	338	334	1.5336	217/4
$C_{32}H_{43}N$ $n\text{-}Bu_2NCH_2CHCH_2CHCH_2CH_2$ 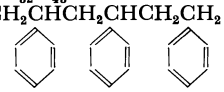	(**3c**)	C H N	87.02 9.81 3.17	87.63 9.24 3.19	441.67	···	444	1.5565	232/0.02
$C_{16}H_{27}N$ $isoBu_2NCH_2CH_2$	(**1d**)	C H N	82.34 11.66 6.00	82.06 11.87 5.81	233.38	233	235	1.4883	130/4
$C_{24}H_{35}N$ $isoBu_2NCH_2CHCH_2CH_2$ 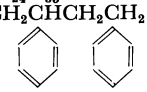	(**2d**)	C H N	85.40 10.45 4.15	85.58 10.17 4.10	337.53	338	318	1.5221	202/4
$C_{32}H_{43}N$ $isoBu_2NCH_2CHCH_2CHCH_2CH_2$ 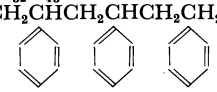	(**2d**)	C H N	87.02 9.81 3.17	87.10 9.84 3.01	441.67	···	432	1.5403	194/0.04

give the following inequality.

$$\frac{k_{t1}[R_2NH]}{k_{p1}[St]_1} < \frac{k_{t2}[R_2NH]}{k_{p2}[St]_2} < \frac{k_{t3}[R_2NH]}{k_{p3}[St]_3} < \cdots \quad (12)$$

Equation (12) shows that there may be a maximum in the yields of the telomers. The reactivities of the amines in the transfer reactions are supposed to be in the following order mainly because of the steric effects of the alkyl groups attached to nitrogen atoms.

$$k_{tn(Et_2NH)} > k_{tn(n\text{-}Pr_2NH)} > k_{tn(n\text{-}Bu_2NH)} > k_{tn(IsoBu_2NH)} \quad (13)$$

The smaller the rate constants of the transfer reactions, the larger the average degrees of polymerization or the average degree of telomerization become. In this experiment only the telomers with $n=1$, 2 and 3 were separated, but some of the higher homologs of telomers are considered to have been formed and to have remained undistilled in residue. On controlling the ratio of styrene to the amine during the reaction, one can prepare the mixture of telomers with arbitrary average molecular weight in the region of oligomers.

Experimental

Physical Data. For mass spectral analysis, a Hitachi RMU-6D mass spectrometer was employed with the electron beam energy at 80 eV. The molecular weight determination by vapor pressure osmometry was carried out in benzene at 37°C on a Hewlett Packard Model 302 vapor pressure osmometer. IR spectra were recorded on a Hitachi Perkin-Elmer 125 grating infrared spectrophotometer. Proton NMR spectra were obtained on a Hitachi Model R-20 spectrophotometer using tetramethylsilane as an internal standard in carbon tetrachloride.

Materials. Styrene was dried over anhydrous magnesium sulfate for a day or more and was distilled under reduced pressure. Amines were dried over sodium hydroxide and were distilled under atmospheric or reduced pressure according to their boiling points.

General Procedure for Telomerization. In a four-necked round-bottomed flask, provided with a mechanical stirrer, a reflux condenser, a dropping funnel and an inlet of nitrogen, are placed a secondary amine and finely sliced sodium. The flask was heated to a prescribed temperature in an oil bath. The oil was agitated mechanically and its temperature was controlled by a thermostat. Styrene was added dropwise to the amine in 0.3 to 1.3 hr, and thereafter the mixture was kept standing for reaction for further 3 hr. Then the solution was cooled to room temperature and the alkali was decomposed by adding an equivalent amount of methanol and was neutralized by a 0.1 N hydrochloric acid. A small amount of benzene was added to this reaction mixture, if necessary, in order to make the solution uniform and the resulting solution was washed with water, dried and distilled *in vacuo*.

Diethyl-2-phenylethylamine (1a), Diethyl-2,4-diphenylbutylamine (2a) and Diethyl-2,4,6-triphenylhexylamine (3a). To 21.1 g of diethylamine and 0.7 g of sodium which were heated to 50.0±0.5°C, 62.3 g of styrene was added dropwise during 0.5 hr and the reaction took place for a further 3 hr. To the reaction mixture that was cooled to room temperature were added 3.1 m*l* of methanol and 10.0 m*l* of water. Then the solution was neutralized with 0.1 N hydrochloric acid, washed with 50 m*l* of water, and the organic layer was separated, dried and distilled *in vacuo* to give 42.2 g (39.67%) of the telomer **1a** at 77°C/4 mmHg, 5.78 g (6.84%) of the telomer **2a** at 136°C/4 mmHg and 4.74 g (6.18%) of the telomer **3a** at 212°C/0.02 mmHg. The other telomers were obtained in similar procedures.

BULLETIN OF THE CHEMICAL SOCIETY OF JAPAN VOL. 42 2343—2347 (1969)

Copolymerization of Formaldehyde and Succinic Anhydride in the Presence of Carbon Dioxide

Hisao YOKOTA and Yahiko TORIUCHI

Takarazuka Laboratory, Sumitomo Chemical Co., Ltd., Takarazuka, Hyogo

and Tsutomu KAGIYA and Kenichi FUKUI

Faculty of Engineering, University of Kyoto, Sakyo-ku, Kyoto

(Received January 20, 1969)

A Study of the copolymerization of formaldehyde and succinic anhydride was carried out in a liquid carbon dioxide solution without adding any catalyst. A copolymer, in which a small number of succinic units was inserted into the sequence of oxymethylene units because of the low rate of copolymerization of succinic anhydride, was formed. With enhancing the concentration of succinic anhydride, the content of succinic units in the copolymer slightly increased. At reaction temperatures up to 120°C, the molecular weight of the copolymer decreased with a rise in the temperature, whereas the content of succinic units increased to about 3 mol%. The copolymerization proceeded rapidly, so the reaction immediately reached equilibrium. From the results of the study by X-ray diffractiometry, the crystal structure of the copolymer can be said to be similar to that of polyoxymethylene, but the crystallinity of the copolymer decreased as the content of succinic units increased. The rate of thermal degradation, which started from the end-groups of the copolymer was decreased by ester linkgae. The thermal-degradation temperature was enhanced as the content of succinic units increased. The copolymer also showed a high resistivity to the folding of the film, even though it had not been treated so as thoroughly to esterify the endgroups of the copolymer.

The present authors have studied the polymerization of formaldehyde in a liquid carbon dioxide solution in the presence of acetic anhydride. They have thus determined that the resulting polyoxymethylene can easily and thoroughly be acetylated by discharging the unreacted monomer and carbon dioxide from the reaction system and then heating, *in situ*, the remains.[1] A perfect acetylation of the polymer end-groups is achieved with acetic anhydride, which is added, in advance of polymerization, into the reaction system at a concentration of only 5 mol% to the monomer. This fact suggests that the acetic anhydride added is selectively located in the neighborhood of the growing polymer chain end in the stage of propagation. If a cyclic acid anhydride is used instead of acetic anhydride, the formation of a copolymer in which the sequence of oxymethylene units is connected with both ends of the ring-opening acid anhydride may be inferred. This work is devoted to a study of how to prepare the copolymer composed of oxymethylene and ester units by the copolymerization of formaldehyde and succinic anhydride in the presence of carbon dioxide; it will also attempt to establish the properties of the copolymer.

Experimental

Preparation of Materials. The formaldehyde monomer was prepared by the pyrolysis of dried α-polyoxymethylene from 150 to 180°C in a stream of carbon dioxide, after which the gas mixture thus produced was cooled at −78°C in order to condense the formaldehyde and carbon dioxide, as has been described before.[2] The concentration of formaldehyde in the thus-prepared solution of carbon dioxide was 60.1 wt%. The succinic anhydride was purified by recrystallization from a chloroform solution.

Procedure of Polymerization. A stainless-steel pressure vessel, with a capacity of 30 ml was used for the polymerization. The weighed succinic anhydride was placed in the vessel, after which the vessel was evacuated at room temperature and then cooled by liquid nitrogen. The monomer solution, which had previously been prepared in a monomer reservoir, was fed into the evacuated pressure vessel through a tube connecting the vessel to the monomer reservoir. The amount of the monomer solution thus fed in was determined by weighing the vessels before and after the feeding. The polymerization was carried out by keepting the pressure vessel in an oil-bath controlled within ±1°C. After the polymerization, the pressure vessel was cooled to 20°C; the unreacted monomer and carbon dioxide were then purged out.

After it had been cooled at −78°C, the product was

1) H. Yokota, M. Kondo, T. Kagiya and K. Fukui, This Bulletin, **41**, 1668 (1968).

2) H. Yokota, M. Kondo, T. Kagiya and K. Fukui, *J. Polymer Sci.*, **A-1**, **6**, 425 (1968).

washed with ethyl ether cooled at −78°C and then with acetone. The succinic anhydride remaining in the resulting polymer was extracted with chloroform for 24 hr by using a Soxhlet extractor. The obtained polymer was dried *in vacuo* at room temperature.

Procedure for Measuring Properties of the Copolymer. The inherent viscosity, η_i was determined by an Ostwald viscometer; the starting solution contained 0.5 g of the copolymer in 100 m*l* of *p*-chlorophenol in which 2% of α-pinene had been dissolved at 60°C.

The thermal stability of the copolymer was evaluated by the first-order reaction rate constant, k_{222} for thermal degradation at 222°C in an inert atmosphere. By heating the copolymer in a nitrogen atmosphere, which was kept at 222°C by means of a vapor bath of boiling methyl salicylate, the weight loss of the copolymer was followed continuously. The rate constant was estimated from the slope of the linear relation between the heating time and the logarithm of the weight loss of the polymer.

The folding endurance was represented by the number of creasing cycles which the copolymer film withstood before breaking when a film 120 μ thick was subjected to the creasing test of ASTM D-643-43. The film was prepared by pressing under heating.

The X-ray diffraction spectra were measured by the powdered-crystal method with a Rigaku-Denki DF-3 automatic X-ray diffractiometer. Filtered Cu$K\alpha$ radiation was used in this study.

Differential thermal analysis was carried out by a Shimadzu DT-10 differential thermoanalyzer. The powdered copolymer was dispersed in α alumina at a concentration of 20 wt%.

Determination of Copolymer Composition. The mole fraction of the copolymers was determined by measuring the infrared absorption intensity at 1737 cm^{-1} of the carbonyl group of the ester linkage. The absorption intensity at 1740 cm^{-1} of the carbonyl group, which was divided by the absorption intensity at 2930 cm^{-1} of the methylene group in order to eliminate the influence of sample thickness, was measured at a variety of compositions in a mixture of polyoxymethylene and methyl succinate, and the calibration curve thus obtained served to quantify the carbonyl group in the resulting copolymer. The infrared spectrum was measured by using a Hitachi EPI-2 infrared spectrometer. The polymer sample was molded as a KBr pellet or film. The film was prepared by pressing the copolymer powder at room temperature.

Results and Discussion

Influence of the Monomer Composition on the Copolymerization. The influence of the monomer composition on the copolymerization of formaldehyde and succinic anhydride in a liquid carbon dioxide solution at 100°C was investigated; the results are shown in Table 1.

Figure 1 shows a typical example of the infrared spectrum for the resulting polymer, in which the absorption band of the carbonyl group is exhibited only at 1740 cm^{-1}. This band was ascribable to the ester carbonyl group. This fact indicates that succinic anhydride gives ester linkage in the copolymer by means of ring-opening reaction. The present authors have already presented the following equation for the relation of the inherent viscosity, η_i and the number-average degree of polymerization, $\overline{P}_n$ to polyoxymethylene[2]:

$$\eta_i = 2.14\times10^{-2}\overline{P}_n^{0.61}$$

Assuming this equation to be applicable also in the case of a copolymer containing a low content of succinic anhydride as a comonomer, the number-average degree of polymerization of the copolymer shown in Figure 1 was found to be 1500. On the other hand, the determined content of succinic units in the copolymer was 0.71 mol%. Admittedly, the concentration of succinic units was about six times that of the polymer end-groups, the latter figure having been calculated from the number-average degree of polymerization.

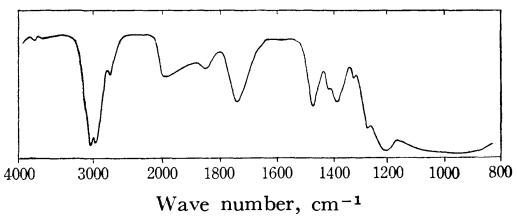

Fig. 1. Infrared spectrum of formaldehyde-succinic anhydride copolymer.
The sample; η_i 1.6 d*l*/g, succinic unit content 0.71 mol%.

TABLE 1. INFLUENCE OF MONOMER COMPOSITION ON COPOLYMERIZATION

CH_2O g	SAH*1 g	SAH/CH_2O mol ratio	CO_2 g	Polymer yield g	Conversion*2 wt%	η_i d*l*/g	k_{222}*3 %/min	Content of succinic unit, mol%
0.5	5.8	3.0	0.3	0.26	4.3 (52.0)	1.4	6.3	0.49
1.9	2.8	0.50	1.2	1.13	24.1 (59.5)	1.6	5.2	0.62
3.5	1.1	0.091	2.4	2.17	47.2 (62.0)	1.3	7.1	0.59
2.7	0.11	0.012	1.8	1.55	55.4 (57.4)	1.6	6.7	0.71

Reaction conditions; temperature 100°C, time 60 min.
*1 Succinic anhydride.
*2 Values calculated to formaldehyde are shown in parentheses.
*3 Values in an earlier stage of thermal decomposition.

Table 2. Influence of reaction time on copolymerization

Reaction time min	Polymer yield g	Conversion wt%	η_i dl/g	k_{222}* %/min	Content of succinic unit, mol%
5	2.92	54.2	1.7	3.3	0.73
10	3.19	59.1	1.7	4.0	0.51
20	2.93	54.4	1.8	3.5	0.40
40	2.78	51.3	1.6	6.7	0.43
60	3.09	57.4	1.9	4.6	0.59
180	2.83	52.4	1.3	4.4	0.63

Reaction conditions: formaldehyde 4.3 g, succinic anhydride 1.1 g, carbon dioxide 2.9 g, temperature 100°C.
* The definition is the same as in Table 1.

Table 3. Influence of reaction temperature on copolymerization

Reaction temp. °C	Polymer yield g	Conversion*1 wt%	η_i dl/g	k_{222}*2 %/min	Mp °C	Content of succinic unit, mol%
20	2.43	56.4 (76.0)	2.7	2.6	173—178	0.091
50	2.28	53.0 (71.3)	2.2	3.4	174—179	0.19
80	2.33	54.2 (72.8)	1.5	7.4	167—174	0.34
100	2.10	48.8 (65.6)	1.3	5.2	168—174	0.64
120	2.48	58.7 (77.4)	0.98	8.1	166—171	2.04

Reaction conditions: formaldehyde 3.2 g, succinic anhydride 1.1 g, carbon dioxide 2.1 g, time 60 min.
*1 Values in parentheses are defined the same as in Table 1.
*2 The definition is the same as in Table 1.

Thus, it was concluded that succinic units are inserted at several places in the sequence of oxymethylene units.

The results shown in Table 1 indicate that the content of succinic units in the resulting copolymer increased slightly with an increase in the concentration of succinic anhydride, but the content was, in general, lower than 1 mol%. Regarding formaldehyde as M_1 and succinic anhydride as M_2, it seems that the monomer reactivity ratio r_1 is extremely large and that r_2 is nearly zero.

The polymer yield increased as the concentration of succinic anhydride became less. However, the polymer yield based on the formaldehyde monomer was almost independent of the concentration of succinic anhydride. The degree of polymerization was also constant in a like manner. These facts were ascribed to the fact that the addition polymerization of formaldehyde proceeded predominantly, because the monomer reactivity ratio r_2 was extremely small.

Influence of the Reaction Time. The influence of the reaction time on the copolymerization was also studied as is shown in Table 2. The degree of polymerization, the inherent viscosity, and the content of succinic units were not at all affected by the reaction time. Accordingly, it seems that the rate of polymerization was very large at the temperature of 100°C, so that the reaction immediately reached equilibrium.

Influence of the Reaction Temperature. Table 3 shows the influence of the reaction temperature on the copolymerization of formaldehyde with succinic anhydride. The inherent viscosity and the succinic-unit content of the resulting copolymer are plotted against the reaction temperature in Fig. 2. The succinic-unit content rapidly increased with an enhancement in the reaction temperature, although it was less than 3 mol% even in the copolymer resulted at 120°C. This fact indicates an increase in the monomer reactivity ratio r_2 with the reaction temperature. The copolymer yield was independent of the temperature, whereas the inherent viscosity decreased reciprocally with the temperature. It seems, therefore, that the initial concentration of initiating species increases with an enhancement of the temperature.

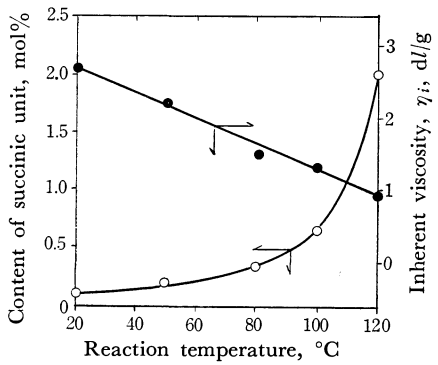

Fig. 2. Influence of reaction temperature on the degree of polymerization and succinic unit content of the copolymer.

Mechanism of Copolymerization. As has been mentioned above, formaldehyde and succinic anhydride copolymerized in a liquid carbon dioxide solution under pressure, while the addition polymerization of formaldehyde proceeded predominantly because of the low value of the monomer reactivity ratio r_2. Accordingly, it was concluded that an occasional insertion of succinic anhydride into the growing polyoxymethylene chain took place by means of the following schemes:

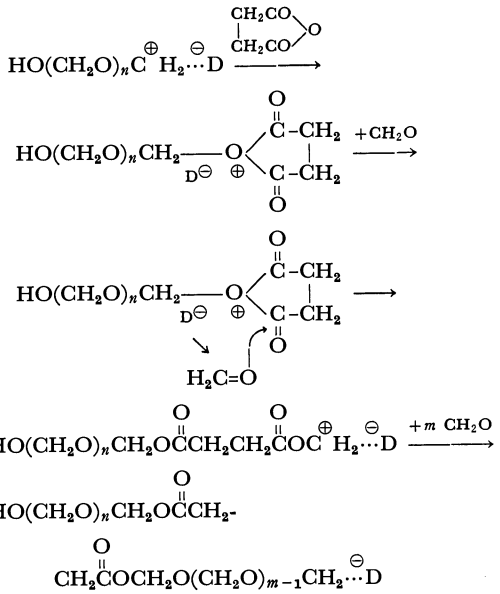

Structure and Properties of the Copolymer. It has been disclosed by infrared-spectrometric study that there is formed a copolymer into which succinic units are inserted in some places in the sequence of formaldehyde units. In this section, the structure and properties of the above copolymer will be discussed. The X-ray diffraction spectrum of the copolymer, which contained 0.68 mol% of succinic units, is shown in Fig. 3; the spectrum of α-polyoxymethylene, which was chosen as an example of the homopolymer of formaldehyde, is also shown in the same figure for the sake of comparison. The maximum peak for α-polyoxymethylene occurred at a scattering angle of 22.6°, whereas it occurred at 22.7° and there was an extra peak at 20.5° for the copolymer. The peak at 20.5° was ascribed to the amorphous part in the copolymer.[3] Furthermore, the crystallinity of the copolymers, which contained a variety of succinic units, was studied; the results are shown in Table 4. The crystallinity decreased as the succinic unit content rose. This fact indicates that a disturbance of the crystal lattice took place because of the insertion of succinic-units into the polymer chain.

3) C. F. Hammer, T. A. Koch and J. F. Whitney, *J. Appl. Polymer Sci.*, **1**, 170 (1959).

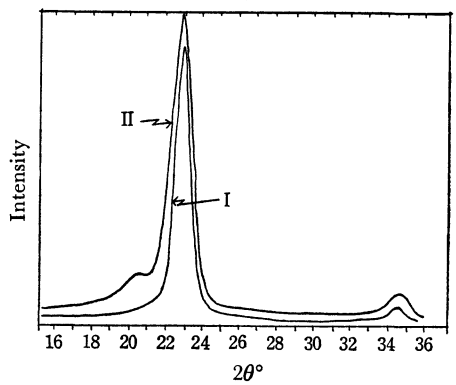

Fig. 3. X-ray diffraction spectra of the copolymer and α-polyoxymethylene.
(I) α-polyoxymethylene
(II) copolymer (succinic unit content, 0.68 mol%)

TABLE 4. INFLUENCE OF COPOLYMER COMPOSITION ON CRYSTALLINITY OF THE COPOLYMER

Content of succinic unit, mol%	η_i dl/g	Crystallinity %
0	0.95	98.0
0.40	1.79	94.6
0.67	1.75	88.7
1.1	0.30	82.1

The thermal properties of the copolymer were also investigated. A typical thermal degradation curve of a copolymer which had been constantly heated at 222°C in a nitrogen atmosphere is shown in Fig. 4. It was found that the rate constant of thermal degradation decreased with the heating time. The thermal degradation of polyoxymethylene, in general, follows a first-order rate equation; therefore, the rate constant does not vary

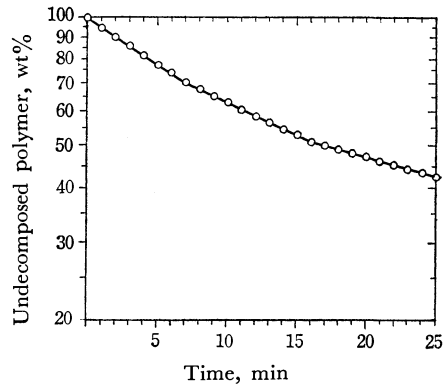

Fig. 4. Thermal decomposition of the copolymer in nitrogen atmosphere at 222°C.
Sample; η_i 1.34 dl/g, succinic unit content 0.64 mol%, initial rate constant of decomposition 5.2 wt%.

with the time.[4] On the contrary, the thermal stability of the copolymer investigated improved with heating. This may be ascribed to the fact that the successive degradation begun at the endgroups of the copolymer chain was lowered at the ester linkage, which is thermally more stable than the ether linkage.

Figure 5 shows the curves for the differential thermal analysis of the copolymer. With an increase in the content of succinic units, the melting point shown by the first peaks did not vary, but the degradation temperature by the second peaks increased. This may be caused by the thermal stability of the ester linkage in the copolymer chain.

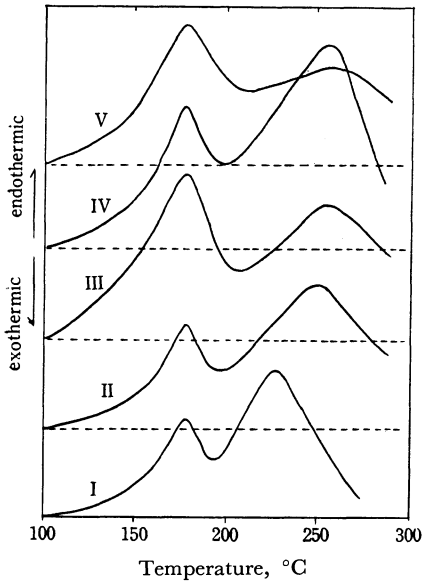

Fig. 5. DTA curves of the copolymer.
Succinic unit content and η_i of the sample: (I) 0.091 mol%, 2.7 dl/g; (II) 0.19 mol%, 2.2 dl/g; (III) 0.33 mol%, 1.5 dl/g; (IV) 0.64 mol%, 1.3 dl/g; (V) 2.04 mol%, 0.98 dl/g.

Table 5. Folding endurance of the copolymer

Sample*1		Folding endurance*2 $\times 10^{-3}$ times
Content of succinic unit, mol%	η_i dl/g	
3.5	1.8	87
2.0	1.8	78
1.1	1.7	92

*1 Sample thickness 120 μ
*2 Mean value for five runs

Lastly, the folding endurance of the copolymer film was studied; the results are shown in Table 5. Although there was no treatment for esterifying the endgroups in the copolymer, the film showed a high resistivity to folding. On the other hand, the folding endurance of polyoxymethylene diglycol has been reported to be less than 100 times.[5] The high resistivity of the film to folding may be a characteristic of the copolymer.

The authors wish to express their gratitude for the guidance and encouragement received from Dr. K. Fujimura. They also wish to express their thanks to Mr. T. Nishida, who carried out much of the experimental work.

4) T. A. Koch and P. E. Lindvig, *ibid.*, **1**, 164 (1959).

5) R. N. MacDonald, U. S. Pat. 2768994 (1956).

BULLETIN OF THE CHEMICAL SOCIETY OF JAPAN VOL. 42 2348—2351 (1969)

Kinetic Studies of the Triethylenediamine-catalyzed Transamidation of 1,3-Diphenylurea with *n*-Butylamine in Dioxane

Yoshiaki FURUYA,* Kazuo ITOHO** and Harue MIYAGI**

* *Department of Industrial Chemistry, Faculty of Engineering, Kumamoto University, Kumamoto*
** *Daiichi College of Pharmaceutical Sciences, Fukuoka*

(Received February 6, 1969)

The rates of the transamidation of 1,3-diphenylurea (abbreviated as DPU) with *n*-butylamine (BA) in dioxane in the presence of triethylenediamine (TED), forming *n*-butylphenylurea (BPU), aniline and carbon dioxide, were followed ultraviolet-spectrophotometrically. The rate of the reaction satisfied the following equation:

$$v = \{k_1' + k_2'[\mathrm{TED}]\}[\mathrm{DPU}] + \{k_2'' + k_3[\mathrm{TED}]\}[\mathrm{BA}][\mathrm{DPU}] .$$

The first and second terms correspond to the non- and the TED-catalyzed hydrolysis of diphenylurea, while the third and fourth terms represent, respectively, the non- and the TED-catalyzed transamidation. In both the non- and the TED-catalyzed transamidation, a probable mechanism which involves the nucleophilic attack of the lone pair of the N-atom on the carbonyl C-atom of diphenylurea, followed by the formation of ion pairs of quaternary ammonium salt and of quaternary ammonium type salt, was discussed.

The transamidation of 1,3-diphenylurea with primary amines in the presence of tertiary amine in dioxane has been previously reported.[1] In the present paper, the TED-catalyzed transamidation of 1,3-diphenylurea with *n*-butylamine will be measured by means of ultraviolet spectrophotometry, and its probable mechanism discussed.

Experimental

Materials. 1,3-Diphenylurea (DPU) was recrystallized three times from aqueous methanol; mp 244°C. *n*-Butylamine (BA) was rectified; bp 182°C. *n*-Butylphenylurea (BPU) was prepared by the reaction of phenyl *N*-phenylcarbamate with BA[2] and recrystallized from aqueous methanol; mp 130—131°C (Found: N, 14.3%; Calcd: 14.6%). Triethylenediamine (TED) obtained from Meisei & Co., Ltd., was purified by sublimation under reduced pressure; mp 110°C. Dioxane was refluxed for 7 hr with 10% of its volume of 1 N aqueous hydrochloric acid, while a slow stream of air was passed through the condenser in order to remove the acetaldehyde formed. The organic layer was then separated after treating it with potassium hydroxide. It was then distilled from metal sodium; bp 102°C.

Ultraviolet Spectrophotometry and Chemical Analysis. The absorption maxima of DPU and BPU were 255 and 238 mμ, while the minima of DPU and BPU were 227 and 217 mμ, respectively (see Fig. 1). The absorptions of BA, TED, and aniline are negligible at these wavelengths. Mixtures of DPU, BA, TED, and BPU of known concentrations (corresponding to 0, 20, 40, 60, 80, and 100% conversion) were prepared at 90°C; a plot of the difference in extinctions, $(E_{255}-E_{227})$ *vs.* $(E_{255}-E_{238})$, gave a straight line,[3] and the conversions calculated from the values of $(E_{255}-E_{238})$ at 0 and 100% conversion agreed well with the conversions calculated from the composition of the mixture within a 1% error.

The aniline liberated from DPU in a reaction mixture was detected by paper chromatography[1] and by Anger's reaction.

A Typical Run for the Rate Measurements. A solution of 1.6 m*l* of 0.5 M BA in dioxane was added to a solution of 34.4 m*l* of 0.0233 M DPU in dioxane; then

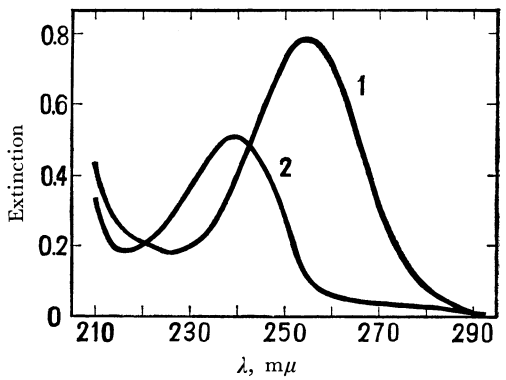

Fig. 1. Ultraviolet spectra of reactant and product in 2×10^{-5} M methanolic solution: 1, DPU; 2, BPU.

1) Y. Furuya and K. Itoho, *Chem. & Ind.*, **1967**, 359.

2) Y. Furuya, S. Goto, K. Itoho, I. Urasaki and A. Morita, *Tetrahedron*, **24**, 2375 (1968).

3) Y. Ogata, Y. Furuya and M. Ito, *J. Am. Chem. Soc.*, **85**, 3649 (1963).

a solution of 4.0 m*l* of 0.05 M TED in dioxane was poured into this mixture in order to start the reaction after the three solutions had attained temperature equilibrium at 90°C. Aliquots (0.2 m*l* each) were pipetted out at appropriate time intervals; for spectrophotometry each one was diluted with methanol to a 2×10^{-5} M initial concentration of the reactant. Then, the extinctions at 255, 238, and 227 mμ were measured. The conversion was calculated graphically from the observed value of $(E_{255}-E_{238})$, and the value of the first-order rate constant, $k_{1\,obs}$, was calculated.

Determination of the Water in the Reaction Medium. The remaining water in the dioxane was determined to be 0.047 M by the Karl Fischer method.

A Typical Procedure for the Conductivity Measurement. A 20 m*l* portion of the dioxane solution of DPU (0.02 M), BA (0.02 M), and TED (0.005 M) was heated at 90°C for 40 hr, after which the solution was diluted with 20 m*l* of conductivity water. The precipitate thus formed was filtered off by a glass filter. Then the conductivity of the solution was measured by means of a Yokogawa-Hewlett-Packard universal bridge 4255A(BV-Z-13C) at 25±0.2°C. The values of the conductivity of each member and couple for the reaction of DPU with BA in the presence of TED are indicated in Table 1.

Table 1. Specific conductivities of the reactants and products at 25±0.2°C

Reaction concn. of DPU, BA and aniline: 0.02 M
concn. of TED: 0.005 M
Measurement concn.: half of the values described above

Substance or couple of substances	Specific conductivity $\kappa\times10^6\ \Omega^{-1}\,cm^{-1}$ at 0 hr		at 40hr	at 90 hr
Cond. water	1.553			
Dioxane	2.848			
DPU	5.180			
BA	21.41			
TED	3.023			
Aniline	3.075			
DPU+TED	10.87	(1.33)*	(1.56)	(1.36)
DPU+BA	69.64	(2.62)	(0.88)	(0.46)
BA+TED	21.95	(0.90)	(0.56)	(0.89)
Aniline+TED	7.880	(1.29)	(2.95)	(2.75)
DPU+BA+TED	33.69	(1.14)	(0.40)	(0.40)

* The values in parentheses are the ratios of an actual value of each couple by the sum of the components.

Results and Discussion

The reaction follows the first-order kinetics with DPU, as is shown in Fig. 2. The plots of the first-order rate constant *vs.* the concentration of BA gives a straight line which does not pass through the point of origin, as is illustrated in Fig. 3. Therefore, the observed first-order rate constant is given by the following equation:

$$k_{1\,obs} = k_1 + k_2[BA] \qquad (1)$$

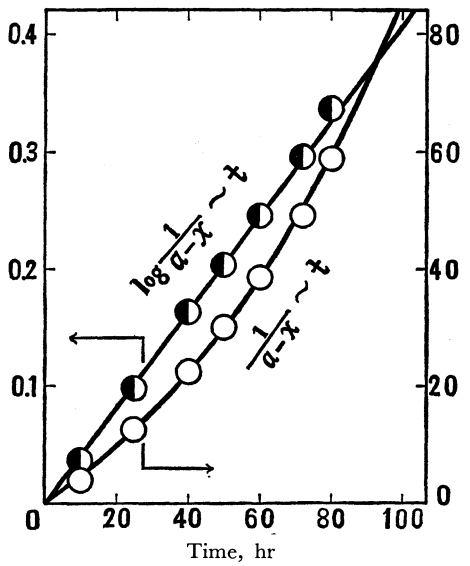

Fig. 2. Determination of reaction order in dioxane at 90°C.
Initial concn. of DPU and BA: 0.02 M,
concn. of TED: 0.005 M

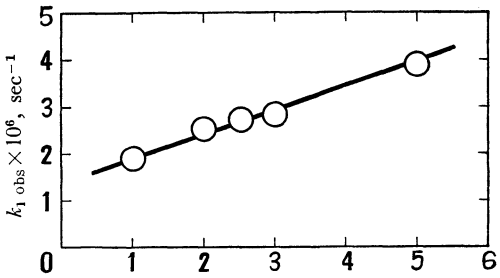

Fig. 3. The plots of $k_{1\,obs}$ *vs.* concentration of BA for the TED-catalyzed transamidation of DPU with BA in dioxane at 90°C.
Initial concn. of DPU: 0.02 M,
concn. of TED: 0.005 M

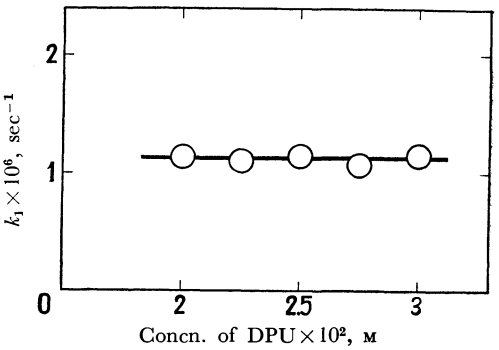

Fig. 4. The plots of k_1 *vs.* concentration of DPU for the TED-catalyzed transamidation of DPU with BA in dioxane at 90°C.
Initial concn. of BA: 0.02 M,
concn. of TED: 0.005 M

The values of k_1 and k_2 did not vary with the concentration of DPU (Figs. 4 and 5). However, these values contain the concentration of TED, as is obvious in Figs. 6 and 7.

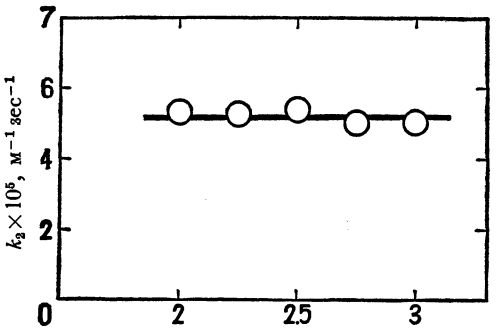

Fig. 5. The plots of k_2 *vs.* concentration of DPU for the TED-catalyzed transamidation of DPU with BA in dioxane at 90°C.
Initial concn. of BA: 0.02 M,
concn. of TED: 0.005 M

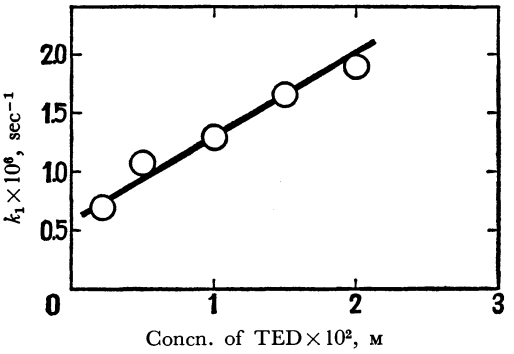

Fig. 6. The plots of k_1 *vs.* concentration of TED for the TED-catalyzed transamidation of DPU with BA in dioxane at 90°C.
Initial concn. of DPU and BA: 0.02 M

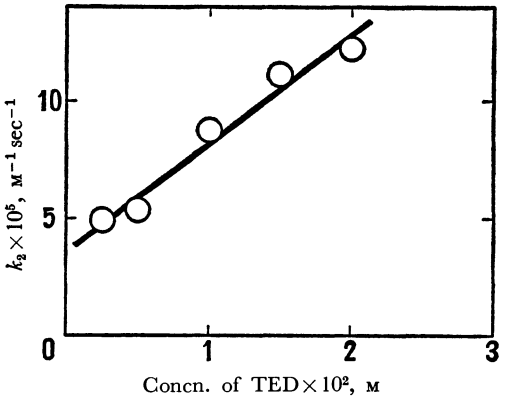

Fig. 7. The plots of k_2 *vs.* concentration of TED for the TED-catalyzed transamidation of DPU with BA in dioxane at 90°C.
Initial concn. of DPU and BA: 0.02 M

Hence, the k_1 and k_2 rate constants should be expressed as follows:

$$k_1 = k_1' + k_2'[\mathrm{TED}] \quad (2)$$

$$k_2 = k_2'' + k_3[\mathrm{TED}] \quad (3)$$

The total kinetics is, therefore, given by following equation:

$$v = \{k_1' + k_2'[\mathrm{TED}]\}[\mathrm{DPU}] + \{k_2'' + k_3[\mathrm{TED}]\}[\mathrm{BA}][\mathrm{DPU}] \quad (4)$$

The values of $k_1'\times10^6$ sec^{-1}, $k_2'\times10^5$ M^{-1} sec^{-1}, $k_2''\times10^5$ M^{-1} sec^{-1}, and $k_3\times10^3$ M^{-2} sec^{-1} were 0.57, 7.00, 3.50, and 4.69 respectively. The first and second rate constants are those of the hydrolysis of DPU in the absence and in the presence of TED as a catalyst. The values agree well with the experimental values of 0.56×10^{-6} sec^{-1} and 6.85×10^{-5} M^{-1} sec^{-1} obtained by the non- and the TED-catalyzed hydrolysis of DPU respectively (see Fig. 8). The conversions of the non- and the TED-catalyzed hydrolysis were *ca.* 6 and 30% respectively in the reaction heated at 90°C for 90 hr.

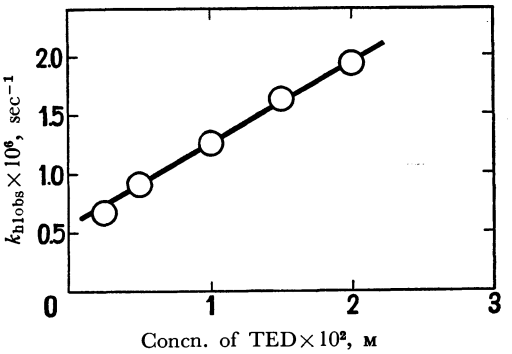

Fig. 8. The plots of k_{h1obs} *vs.* concentration of TED for the TED-catalyzed hydrolysis of DPU in dioxane at 90°C.
Initial concn. of DPU: 0.02 M.

The reaction is accelerated by a tertiary amine, especially TED. The conductivities of the couples of (DPU+TED) and (DPU+BA) are larger than the sum of the conductivities of the components, as is shown in Table 1. In the couples of (DPU+TED) heated at 90°C for 0 and 90 hr, the existence of quaternary ammonium salt was indicated by Wagner's and Dragendorff's reagents. The couple of (BPU+TED) heated for 0 hr indicates weakly the formation of quaternary ammonium salt by Dragendorff's reagent. No positive results were obtained in the couple of (DPU+BA) and/or (Aniline+TED) by Wagner's, Mayer's, and Dragendorff's reagents, for these couples do not form the quaternary ammonium salt. The conductivities of these couples probably depend on the formation of the ion pairs like a quaternary ammonium salt.

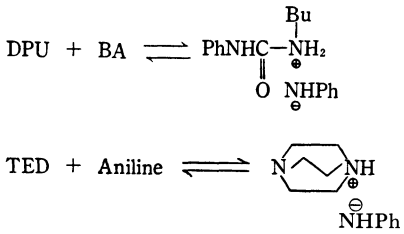

From these findings, a probable mechanism, which involves the nucleophilic attack by the lone pair of the N-atom of amine on the carbonyl C-atom of DPU, followed by the formation of a quaternary ammonium-type ion pair, may be suggested as follows:

Transamidation

Non-catalyzed

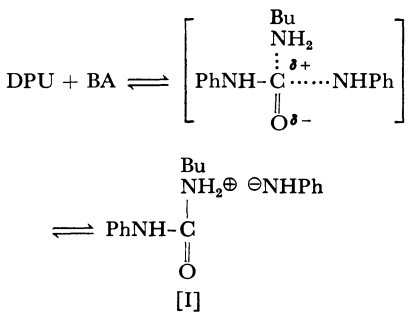

TED-catalyzed

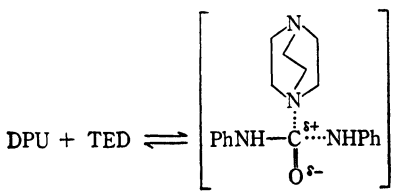

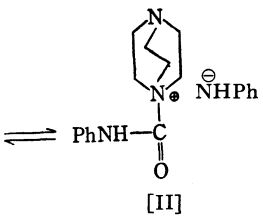

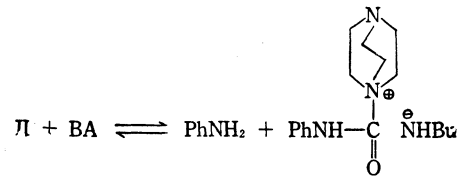

Hydrolysis

non-catalyzed

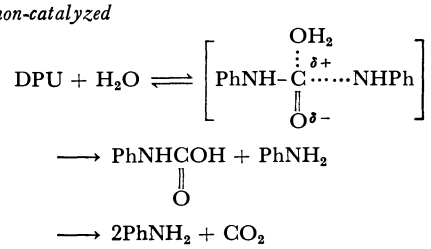

TED-catalyzed

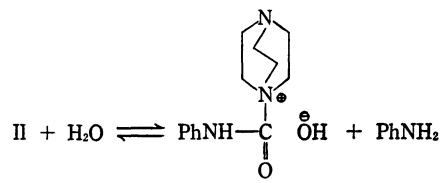

The authors are grateful to Mr. U. Ueda and Miss N. Araki for their aids in performing the work, and also to Mesei & Co. Ltd. for his gift of material.

BULLETIN OF THE CHEMICAL SOCIETY OF JAPAN VOL. 42 2352—2356 (1969)

Aminosugars. XVII. Synthesis of Benzyl 2-Acetamino-2-deoxy-α-D-glucopyranosiduronic Acidamides and *N*-(2-Acetamino-2-deoxy-D-glucuronyl)-aminoacids[1]*

Juji YOSHIMURA, Tadahide SATO and Hiroaki ANDO

Laboratory of Chemistry for Natural Products, Faculty of Science, Tokyo Institute of Technology, Meguro-ku, Tokyo

(Received February 13, 1969)

Benzyl 2-acetamino-2-deoxy-α-D-glucopyranosiduronic acid was obtained by direct oxidation of the corresponding glucoside, and converted to esters (methyl, ethyl and benzyl) and amides (methyl, ethyl, phenyl and benzyl). Condensation of the uronic acid with aminoacid benzylesters (gly, L-ala, L-asp, and L-glu) by dicyclohexylcarbodiimide gave the corresponding amides, some of which were hydrogenated to *N*-(2-acetamino-2-deoxy-D-glucuronyl)-aminoacids. Acid hydrolysis of the peptides were examined.

Hexosaminuronic acids which attract attentions as a polyfunctional sugar have been recently found in V_1-antigen of *Salmonella typhosa*[1] and other natural sources.[2] Heyns and Paulsen[3] first succeeded in the catalytic oxidation of methyl and benzyl 2-(benzyloxycarbonyl)amino-2-deoxy-α-D-glucopyranoside to the corresponding uronic acid in about 40% yield, using gaseous oxygen in the presence of platinum charcoal in a weakly alkaline solution, but had no success in the catalytic oxidation of the corresponding 2-acetamino-2-deoxy derivative. A few years later, Marsh and Levvy[4] obtained phenyl 2-acetamino-2-deoxy-α- and -β-D-glucopyranosiduronic acid in a yield of 29 and 49%, respectively, by a similar method using platinum oxide. Recently, Weidmann and Zimmerman[5] improved the method of Heyns and Paulsen,[3] and synthesized several derivatives of 2-acetamino-2-deoxy-D-glucuronic acid, starting from benzyl 2-(benzyloxycarbonyl)amino-2-deoxy-α-D-glucopyranosiduronic acid.

We synthesized several esters and amides of benzyl 2-acetamino-2-deoxy-α-D-glucopyranosiduronic acid (**1**) which was derived from the corresponding glucoside by direct oxidation, and in connection with our studies[6] on the carbohydrate-aminoacid linked compounds, carried out synthetic and hydrolytic works on *N*-(2-acetamino-2-deoxy-D-glucuronyl)aminoacids.

Results

Benzyl 2-acetamino-2-deoxy-α-D-glucopyranoside which was obtained in an excellent yield by an improved method of Kuhn *et al.*,[7] was oxidized by the method of Heyns and Paulsen[3] until the starting material was consumed, and the solution was filtered, deionized, and evaporated to give **1** in 70—90% yield. The use of secondary alcohols as an antiforming agent and antioveroxidant improved the yield.

Condensation of **1** with methanol, ethanol or benzyl alcohol in benzene by refluxing and azeotropic removal of water formed gave the corresponding esters (**2**, **3** and **4**) in about 50% yield. Treatment of **1** with saturated methanolic ammonia in a sealed tube at 90°C for 2 hr gave the corresponding amide (**5**) in a quantitative yield, which was identical with that synthesized by Weidmann and Zimmerman[8] from benzyl 2-(benzyloxycarbonyl)amino-2-deoxy-α-D-glucopyranosiduronic acid

*1 Part of this work was presented at the 21st Annual Meeting of The Chemical Society of Japan, April 1968. The main subject of this series of papers was revised from "Studies on D-Glucosamine Derivatives." Part XVI: *Carbohyd. Res.*, **4**, 435 (1967).

1) W. R. Clark, J. Mclaughlin and M. E. Webster, *J. Biol. Chem.*, **230**, 81 (1958).

2) T. H. Haskell and S. Hanessian, *Nature*, **199**, 1075 (1963); K. Heyns, G. Kiessling, W. Lindenberg, H. Paulsen and M. W. Webster, *Chem. Ber.*, **92**, 2435 (1959).

3) K. Heyns and H. Paulsen, *ibid.*, **88**, 188 (1955).

4) C. A. Marsh and G. A. Levvy, *Biochem. J.*, **68**, 617 (1958).

5) H. Weidmann and H. K. Zimmerman, *Ann.*, **639**, 198 (1961); *ibid.*, **684**, 226 (1965).

6) J. Yoshimura, M. Funabashi, S. Ishige and T. Sato, *Carbohyd. Res.*, **3**, 214 (1966); J. Yoshimura and M. Funabashi, This Bulletin, **39**, 2009 (1966); J. Yoshimura, H. Hashimoto and H. Ando, *Carbohyd. Res.*, **5**, 82 (1967).

7) R. Kuhn, H. H. Baer and A. Seelinger, *Ann.*, **611**, 236 (1958).

8) H. Weidmann and H. K. Zimmerman, *ibid.*, **641**, 138 (1961).

methylester by ammonolysis, *N*-debenzyloxycarbonylation and *N*-acetylation. **5** was also successfully converted to the corresponding nitrile by *O*-acetylation and dehydration with *p*-toluenesulfonyl chloride,[9] instead of triphenylphosphine dibromide.[8] Treatment of **1** with methylamine or ethylamine in methanol for 12 hr at room temperature, or with aniline or benzylamine and dicyclohexylcarbodiimide (DCC) gave the corresponding *N*-substituted amides (**6, 7, 8** and **9**) in about 50% yield, respectively.

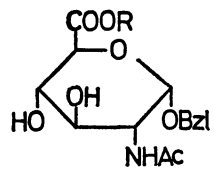

1 : R=H
2 : R=CH_3
3 : R=C_2H_5
4 : R=$CH_2C_6H_5$

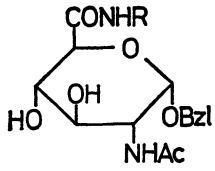

5 : R=H
6 : CH_3
7 : R=C_2H_5
8 : R=C_6H_5
9 : R=$CH_2C_6H_5$
10 : R=$CH_2COOC_7H_7$
11 : R=$CHCOOC_7H_7$ (CH_3)
12 : R=$CHCOOC_7H_7$ ($CH_2COOC_7H_7$)
13 : R=$CHCOOC_7H_7$ ($CH_2CH_2COOC_7H_7$)

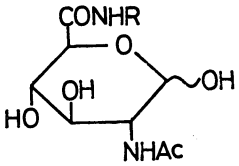

14 : 2R=CH_2COOH
15 : R=$CHCOOH$ (CH_2CH_2COOH)

Comparison of the NMR spectra (Figs. 1 and 2) of 3,4-di-*O*-acetyl derivative of **6** and **9** (**6'** and **9'**) made the first-order analysis possible. Common signals to both figures, *i. e.*, the doublet at 4.28τ (J_{2,C_2-NH}=9.8 Hz), the quintet at *ca.* 4.81 τ (H_3: 4.72 τ; H_4: 4.90τ; $J_{2,3}=J_{3,4}=J_{4,5}$=10.0 Hz), the doublet at 5.01 τ ($J_{1,2}$=3.2 Hz), the AB-quartet at 5.30 and 5.53 τ ($J_{A,B}$=12 Hz), the sextet at 5.75 τ, and the doublet at *ca.* 5.80 τ in the former, and those at 4.25 τ ($J_{2,-C_2NH}$= 9.5 Hz), at *ca.* 4.69 τ (H_3: 4.61 τ; H_4: 4.76 τ; $J_{2,3}=J_{3,4}=J_{4,5}$=9.5 Hz), at 4.95 τ ($J_{1,2}$=3.5 Hz), at 5.23 and 5.46 τ ($J_{A,B}$=12 Hz), at *ca.* 5.66 τ, and at *ca.* 5.53 τ in the latter were respectively assigned to C_2-NH, partly superimposed H_3 and H_4, H_1, C_1-OCH_2, H_2, and H_5 protons from the intensity ratio and the aids of the double resonance technique. The broad signal at *ca.* 3.7 τ and the doublet at 7.22 τ in the former and the broadend-triplet at 3.30 τ in the latter were assigned to C_6-NH, N-CH_3 ($J_{C_6-NH,\ N-CH_3}$=6Hz), and C_6-NH protons, respectively.

Condensation of **1** with *p*-toluenesulfonates of amino acid benzylester (amino acid: glycine, L-alanine, L-aspartic acid, and L-glutamic acid) in pyridine by DCC method gave the corresponding amides (**10, 11, 12** and **13**) in 20–30% yield, of which **10** and **13** were successfully hydrogenated in the presence of palladium-charcoal and a small amount of hydrochloric acid in methanol to give *N*-(2-acetamino-2-deoxy-D-glucuronyl)-glycine and L-glutamic acid (**14** and **15**), but the corresponding compounds for **11** and **12** could not be purely isolated.

The physical constants, analyses and yield of new compounds obtained here are summarized in

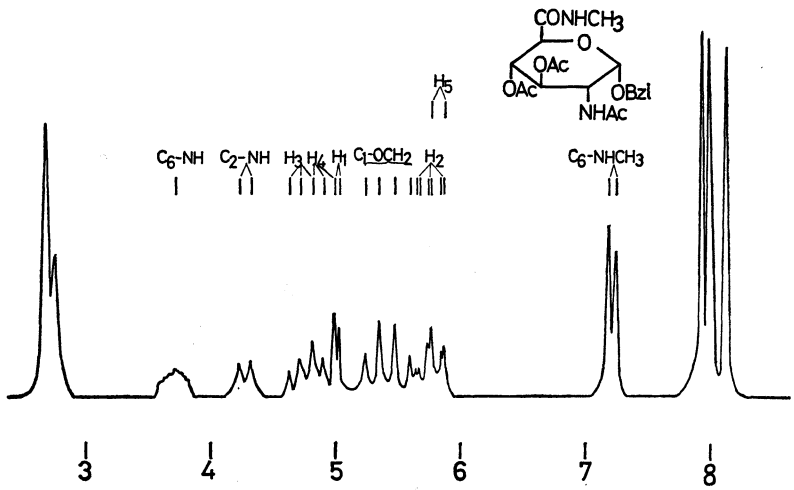

Fig. 1. MNR spectra of benzyl 2-acetamino-2-deoxy-3,4-di-*O*-acetyl-α-D-glucopyranosiduronic acid methylamide (100 Mc, $CDCl_3$).

9) H. Weidmann, *ibid.*, **679**, 178 (1964).

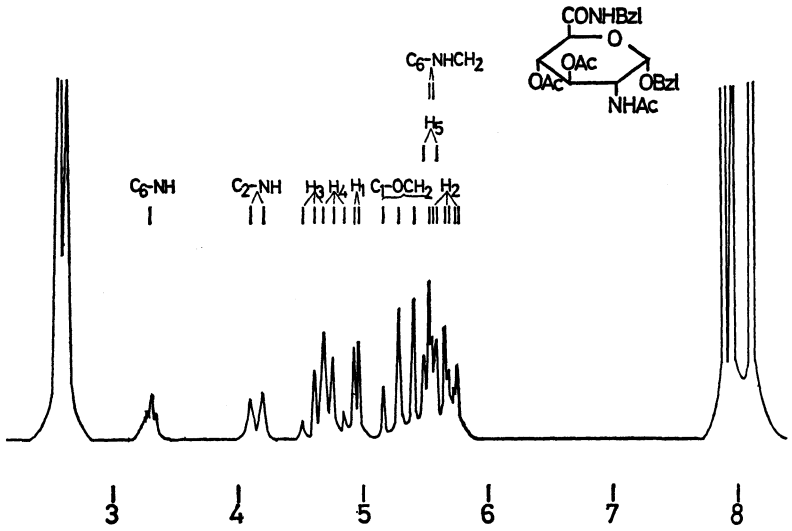

Fig. 2. NMR spectra of benzyl 2-acetamino-2-deoxy-3,4-di-*O*-acetyl-α-D-glucopyranosiduronic acid benzylamide (100 Mc, $CDCl_3$).

TABLE 1. THE PHYSICAL CONSTANTS AND ANALYSES OF NEW COMPOUNDS

Compd.	Formula	Mp, °C	Optical rotation			Found			Calcd			Yield %
			$[\alpha]_D^{23}$	Solvent	*c*	C%	H%	N%	C%	H%	N%	
1	$C_{15}H_{19}O_7N$	198	133	H_2O	1	55.30	7.18	4.49	55.38	5.89	4.31	90
2	$C_{16}H_{21}O_7N$	186—187	159	MeOH	1	56.69	6.22	4.12	56.63	6.24	4.13	52
3	$C_{17}H_{23}O_7N$	154—155	159	MeOH	1.13	57.57	6.44	3.99	57.78	6.56	3.96	49
4	$C_{22}H_{25}O_7N$	183—184	158	MeOH	0.98	63.42	6.02	3.57	63.60	6.07	3.37	51
6	$C_{16}H_{22}O_6N_2 \cdot 3/4H_2O$	203—204	140	EtOH	0.54	54.76	6.57	7.85	54.56	6.68	7.98	52
7	$C_{17}H_{24}O_6N_2 \cdot 3/4H_2O$	178—179	127	EtOH	0.45	55.50	7.13	7.72	55.75	6.97	7.65	54
8	$C_{21}H_{24}O_6N_2 \cdot 3/4H_2O$	204—205	70.1	$CHCl_3$	0.44	60.90	6.01	6.61	60.88	6.16	6.76	51
9	$C_{22}H_{26}O_6N_2 \cdot 3/4H_2O$	207—208	99.7	$CHCl_3$	0.47	61.32	6.23	6.77	61.23	6.45	6.54	50
6'	$C_{20}H_{26}O_8N_2$	198—199	120	MeOH	0.47	56.72	6.02	6.66	56.86	6.20	6.63	92
9'	$C_{26}H_{30}O_8N_2$	200—201	110	MeOH	1.08	62.73	5.95	5.87	62.64	6.07	5.67	90
10	$C_{24}H_{28}O_8N_2 \cdot H_2O$	170—171	140.7	MeOH	1	58.54	6.50	5.61	58.76	6.17	5.71	22
11	$C_{25}H_{30}O_8N_2 \cdot H_2O$	181—182	83.0	MeOH	1	59.67	6.82	5.52	59.51	6.39	5.55	21
12	$C_{33}H_{36}O_{10}N_2 \cdot H_2O$	125—126	35.8	MeCOMe	1	62.13	6.11	4.61	62.06	6.00	4.39	30
13	$C_{34}H_{38}O_{10}N_2$	186—187	60.5	$HCON(Me)_2$	1.17	64.66	6.14	4.69	64.34	6.04	4.41	20
14	$C_{10}H_{16}O_8N_2 \cdot H_2O$	sirup	57.3	MeOH	1.15	38.98	5.93	9.11	38.71	5.85	9.03	85
15	$C_{13}H_{20}O_{10}N_2 \cdot H_2O$	sirup	30.6	MeOH	1.21	40.83	6.12	7.19	40.85	5.80	7.33	88

Table 1.

In order to compare the stability of *N*-(2-acetamino-2-deoxy-D-glucuronyl)-amino acid with that of other carbohydrate-amino acid compounds having peptide bond, **14** and **15** was hydrolysed in 2 N hydrochloric acid at 100°C, and glycine and L-glutamic acid liberated was estimated at suitable intervals with an amino acid analyser. The first-order rate constant of **14** and **15** was 4.45 and 4.25×10^{-3} min^{-1}, respectively. These values indicate that the stability of the peptide bond between the uronic acid and amino acid is the same order as that of *N*-aminoacyl-D-glucosylamine and *N*-aminoacyl-D-glucosamine,[10] and consequently, the oxo-structure of sugar moiety has no effect on the stability of the peptide bond in the same molecule.

Experimental

All melting points were uncorrected. The solutions were evaporated under diminished pressure at a bath temperature usually not exceeding 45°C. Optical rotations were measured in a 0.5-dm tube at 578 mμ with a Carl-Zeiss Polarimeter. The content of water of crystallization was calculated from the analytical

10) G. S. Marks, R. D. Marshall and A. Neuberger, *Biochem. J.*, **87**, 274 (1963); J. Yoshimura and H. Hashimoto, *Carbohyd. Res.*, **4**, 435 (1967).

values.

Benzyl 2-Acetamino-2-deoxy-α-D-glucopyranoside. A suspended solution of 2-acetamino-2-deoxy-D-glucose (80 g, 0.36mol) in benzyl alcohol (900 m*l*) and boron trifluoride etherate (10 m*l*) was heated for 2 hr at 95—100°C, and after the addition of hydrogen chloride (2 g) in benzyl alcohol (100 m*l*) the solution was again heated for 1 hr at the same temperature. After cooling, the reaction mixture was poured into ether (500 m*l*) and filtered. The precipitate was dissolved in water (1 *l*) and the solution was extracted with ether to remove benzyl alcohol. The water layer was evaporated, and the residue was treated with charcoal in ethanol, crystallized by the addition of ether to give 80 g (67%) of fine crystals. Mp 182—183°C, $[\alpha]_D^{23}$ 178° (*c* 1, water) (Lit,[7] mp 183—184°C).

When the reaction mixture was directly evaporated without being poured into ether, and treated by the same procedure, the crystals weighed 97 g (85%). In the course of evaporation, the deposition of a small amount of benzyl 2-acetamino-2-deoxy-4,6-*O*-benzylidene-α-D-glucopyranoside[11] was always observed.

Benzyl 2-Acetamino-2-deoxy-α-D-glucopyranosiduronic Acid (1). In a four-necked flask equipped with stirrer, reflux condenser, dropping funnel, and in-let capillary was placed benzyl 2-acetamino-2-deoxy-α-D-glucopyranoside (25 g, 80 mmol) and platinum-charcoal (10%, 15 g) in water (500 m*l*), and air or oxygen was blown into the solution with violent stirring at 95°C, under the adjustment of pH at 6.8—7.7 with sodium bicarbonate solution. A secondary alcohol such as isopropyl alcohol or isobutyl alcohol was added at a suitable interval as an antifoaming agent and antioveroxidant, and the reaction was continued until the starting material had disappeared on TLC. After cooling, the catalyser was filtered off, and the solution was evaporated. The residue was extracted with ethanol to remove the starting material and dissolved in water. The solution was deionised with Amberlite IR-120 and evaporated to give a sirup which was decolorized and crystallized from ethanol. Yield, 19 g (77.3%). The second crop (3.7 g, 15.6%) was obtained from the mother liquid.

Benzyl 2-Acetamino-2-deoxy-α-D-glucopyranosiduronic Acid Esters (2, 3 and 4). The solution of benzyl 2-acetamino-2-deoxy-α-D-glucopyranosiduronic acid (2 g, 6.2 mmol) in an alcohol (20 m*l* of methanol, ethanol or benzyl alcohol) and benzene (200 m*l*) was refluxed on a boiling water bath for 3 hr, and the water formed was removed azeotropically. The solution was evaporated and the sirup obtained was crystallized from a small amount of hot ethanol and ether. The physical constants, analytical data and yields of these compounds are shown in Table 1.

Benzyl 2-Acetamino-2-deoxy-α-D-glucopyranosiduronic Acidamide (5). The uronic acid (28 g, 86 mmol) was heated with methanolic ammonia (200 m*l*) at 90°C for 2 hr in a sealed tube, and the solution was evaporated. Crystallization of the residual sirup from ethanol (20 m*l*) gave the amide in a quantitative yield. Mp 242°C, $[\alpha]_D^{17}$ 178° (*c* 1, water) (Lit,[9] mp 243°C)

Found: C, 55.86; H, 6.43; N, 8.57%. Calcd for $C_{15}H_{20}O_6N_2$: C, 55.55; H, 6.22; N, 8.64%.

Benzyl 2-Acetamino-2-deoxy-α-D-glucopyranosiduronic Acid Methyl- and Ethylamide (6 and 7). A solution of the uronic acid (2 g, 6.2 mmol) and methylamine or ethylamine (2 m*l* of 40% aqueous solution) in a large amount of methanol was stirred at room temperature for 12 hr, and evaporated to give a sirup which was crystallized from a small amount of hot acetone and ether. The physical constants, analytical data and yields are shown in Table 1.

Benzyl 2-Acetamino-2-deoxy-α-D-glucopyranosiduronic Acid Anilide and Benzylamide (8 and 9). A solution of the uronic acid (3.2 g, 9.9 mmol), dicyclo-hexylcarbodiimide (2.5 g, 12 mmol) and aniline (1.1 g, 12 mmol) or benzylamine (1.3 g, 12 mmol) in pyridine was agitated for 2 days, and dicyclohexylurea deposited was filtered off. The filtrate was evaporated, and the sirup obtained was crystallized from a small amount of methylene chloride and ether. Several data on these compounds are shown in Table 1.

Benzyl 2-Acetamino-2-deoxy-3,4-di-*O*-acetyl-α-D-glucopyranosiduronic Acidnitrile. Benzyl 2-acetamino-2-deoxy-3,4-di-*O*-acetyl-α-D-glucopyranosiduronic acidamide (0.5 g, 1.2 mmol) prepared from **5** by the procedure of Zimmerman *et al.*[9] was heated with *p*-toluenesulfonyl chloride (1.17 g, 6 mmol) in pyridine (7 m*l*) for 3 hr at 80—90°C. After cooling, the solution was poured into ice-water (100 m*l*) and extracted three times with chloroform (50 m*l*). The combined extracts was washed in turn with 1 N hydrochloric acid, sodium bicarbonate and water, dried and then evaporated. The sirup (0.5 g) obtained was crystallized from ethanol and ether. Yield, 0.3 g (63%), mp 165—165.5°C (Lit,[9] mp 159°C).

Found: C, 58.15; H, 5.33; N, 6.98%. Calcd for $C_{19}H_{22}O_7N_2$: C, 58.45; H, 5.68; N, 7.18%.

Benzyl 2-Acetamino-2-deoxy-3,4-di-*O*-acetyl-α-D-glucopyranosiduronic Acid Methylamide and Anilide (6′ and 9′). Acetylation of **6** and **9** with 4 mol equivalent of acetic anhydride in the same amount of pyridine was carried out in the usual manner. The physical constants, analyses and yield are shown in Table 1.

***N*-(Benzyl 2-Acetamino-2-deoxy-α-D-glucopyranosiduronyl)-aminoacid Benzyl Esters (10, 11, 12 and 13).** A solutions of the uronic acid (6.5 g, 20 mmol) and DCC (5 g, 24 mmol) in pyridine was added to a chilled solution of amino acid benzyl ester *p*-toluene sulfonate (each 20 mmol of gly, L-ala, L-asp and L-glu) and triethylamine (2 g, 20 mmol) in pyridine with stirring. After standing the solution at room temperature for 2 days, dicyclohexylurea separated was filtered off, and the filtrate was evaporated to give a sirup which was crystallized from a small amount of hot ethanol, and recrystallized from methylene chloride. The physical constants, analytical data and yield are listed in Table 1.

***N*-(2-Acetamino-2-deoxy-D-glucuronyl)-glycine and -L-glutamic Acid (14 and 15).** A solution of **10** or **13** (0.5 g) and palladium-charcoal (0.5 g) in aqueous ethanol was adjusted to pH 2 with diluted hydrochloric acid and hydrogenated until the theoretical amount of hydrogen was taken up. The catalyst was filtered off, and the filtrate was evaporated to give a sirup which was purified from ethanol and ether. Several data on these compounds are listed in Table 1.

Hydrolysis of *N*-(2-Acetamino-2-deoxy-D-glucu-

11) J. Yoshimura, M. Funabashi, S. Ishige and T. Sato, This Bulletin, **39**, 1760 (1966).

ronyl)-glycine and -L-Glutamic Acid. Each sample (22.5 μmol) was dissolved in 2 m*l* of 2 N hydrochloric acid, and the solution was heated at 100°C in a sealed tube. After 40, 60 and 80 min, the hydrolysate was analyzed with an amino acid analyzer Hitachi Model KLA-2, using a column packed with Amberlite CG-120 Type III, 1×50 cm; the eluent was 0.2 N citric buffer (pH 3.25) percolating at 30 m*l*/hr at 30°C. Glycine and glutamic acid were eluted with an elution time of 3.8 and 5.3 hr, and the amount was determined by comparison with standard. The first-order rate constant of **14** and **15** was 4.45 and 4.25×10^{-3} min^{-1}, respectively.

The authors are indebted to Mr. Kiyofumi Fukukawa of our Laboratory for the NMR measurements.

NOTES

BULLETIN OF THE CHEMICAL SOCIETY OF JAPAN VOL. 42 2356—2359 (1969)

Hot-Atom Chemistry of Bromine. II.[1] Application of the Szilard-Chalmers Process to Organic Molecular Compound-Pyrenebromanil and Related Compounds[2]

Chiro SHINOMIYA, Akira OYOSHI and Toshiaki KISHIKAWA

Department of Industrial Chemistry, Faculty of Engineering, Kumamoto University, Kurokami-cho, Kumamoto

(Received July 10, 1968)

In spite of a number of investigations of the application of the Szilard-Chalmers process[3] to organic halogen compounds, no organic molecular compounds have been tested. Two of the present authors (C. S. and T. K.) have previously reported[4] the formation of organic radiobromides activated by the ^{82m}Br-isomeric transition in a solid mixture of a bromine-benzene-molecular compound and benzene. The present note will deal with the chemcial effects of the recoil bromine atoms in pyrenebromanil (1 : 1).[5] It has a sandwich-type structure composed of pyrene and bromanil (tetrabromo-*p*-benzoquinone) molecules. The result will be compared with those on its related compounds—bromanil, bromopyrene, a pyrene-bromanil mixture, and others.

Experimental[6]

Materials. The 1 : 1 molecular compound-pyrene-bromanil (P−B) was prepared by mixing equimolar solutions of pyrene (P) and bromanil (B), both in toluene. The 1 : 1 mixture of P and B (P+B) was prepared by pestling the components on an agate mortar. Bromo derivatives[7] of P (PBr_n) were prepared and purified according to Lock[8] and Hock[9] respectively. 2-Bromohydroquinone (HQBr) was prepared according to Sarauw.[10]

Neutron Irradiation. Irradiation was carried out at the reactor temperature (*ca.* 40°C) in a pneumatic tube of KUR[11] with a thermal neutron flux of 5×10^{12} n/cm^2/sec and with an accompanying γ-dose rate of 2.7×10^7 R/hr.

Extraction and Measurement of Radioactivity. After having been cooled for more than two hours[12] at room temperature, the sample was transferred into a separatory funnel containing a carbon disulfide solution of bromine. Then the inorganic species were separated by means of extraction into an aqueous mixture of bromide and bromate (I). The bromine (II) was back-extracted from the carbon disulfide layer (III). A carbon disulfide-insoluble residue which was filtered out was extracted, first with ethyl ether[13] (IV),

1) Part I: C. Shinomiya, A. Oyoshi and T. Kishikawa, This Bulletin, **42**, 1437 (1969).

2) Presented at the 20th Annual Meeting of the Chemical Society of Japan, Tokyo, March, 1967.

3) L. Szilard and T. A. Chalmers, *Nature*, **134**, 462 (1934).

4) C. Shinomiya and T. Kishikawa, This Bulletin, **41**, 3026 (1968).

5) B. Turcsanyi and F. Tudos, *Magy. Chem. Folysirat*, **71**, 39 (1965).

6) All the melting points of the synthesized materials are uncorrected.

7) 3-Bromo, 3,8- and 3,10-dibromo derivatives were obtained.

8) G. Lock, *Ber.*, **70B**, 926 (1937).

9) H. Hock, *Chem. Ber.*, **92**, 2735 (1959).

10) M. Sarauw, *Ann.*, **209**, 105 (1881).

11) Kyoto University Reactor.

12) The ^{82m}Br(I. T.)^{82}Br reaction was completed during the time; O. U. Anders, *Phys. Rev.*, **138**, Bl (1965); J. F. Emery, *J. Inorg. Nucl. Chem.*, **27**, 903 (1965).

13) 2-Bromo-, 2,5- and 2,6-dibromo-*p*-benzoquinones are soluble in ethyl ether.

and then with benzene[14] (V).

The ^{82}Br activities in each layer were then measured. The total organic yield, defined as the percentage of activities remaining in the organic layers, is given by;

$$OY\ (\%) = \frac{\text{Activities in (III, IV and V)} \times 100}{\text{Activities in (I, II, III, IV and V)}}$$

Paper Chromatography and Paper Electrophoresis. In order to evaluate the distribution of the activities distributed in the layer (III), paper chromatography was carried out (on Toyoroshi No. 50 filter-paper by the ascending method, with *i*-AmOH-Py-H_2O 3 : 2 : 1.5 in V/V as developer). The distribution of the activities on the paper strips was examined by autoradiography. Readioactive bands on them corresponding to the autoradiograph patterns were cut in pieces, and the activities were counted.

The water-soluble species distributed in the layer (I) were analyzed by paper electrophoresis[1] (on Toyoroshi No. 50 filter-paper with a potential gradient of 54.5 V/cm and with 0.1 M aqueous ammonium acetate as the electrolyte solution), followed by autoradiography and measurement of the activity.

Results and Discussion

The relationship between the percentage of the ^{82}Br atoms remaining in the organic layers and the irradiation time is shown in Fig. 1. The extraction curve vary over a short period of irradiation (1—10 min), but the curves (except for P+B) seem to show no remarkable change with an increase in the irradiation time. This exception may be due to the difference in the composition of the target; *i. e.*, it is heterogeneous (mixture), where the others are all homogeneous (compounds).

The percentages of the activity distributed on the chromatographed strips are listed in Table 1.[15] In each sample, the relative activity in the components of R_f 0.12—0.17 decreased with an increase in the irradiation time, and *vice versa*. This may indicate that the distribution of the activities distributed in the layer (III) is affected by the irradiation period in the reactor.

Table 1. Distribution of ^{82}Br-labeled recoil products parted in carbon disulfide layer at two irradiation times

Target	Irra. time min	Yield, %, at R_f 0.12—0.17	Yield, %, at R_f 1
P−B	10	43.6	56.4
	30	41.5	58.5
P+B	10	70.7	29.3
	30	64.1	35.9
B	10	71.3	28.7
	30	69.4	30.6
PBr	10	0	100
	30	0	100
PBr_2[a]	10	35.8	64.2
	30	25.8	74.2
HQBr[a]	10	71.5	28.5
	30	62.0	38.0

a) Dissolved in carbon disulfide. No extraction.

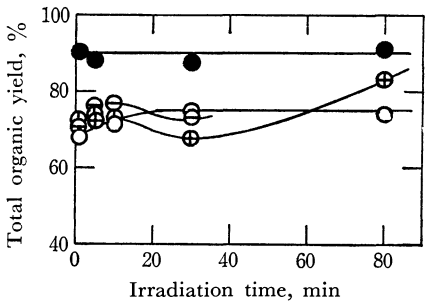

Fig. 1. Total organic yield as a function of the irradiation time.
⊖: pyrenebromanil, ⊕: pyrene-bromanil mixture, ○: bromanil, ●: bromopyrene

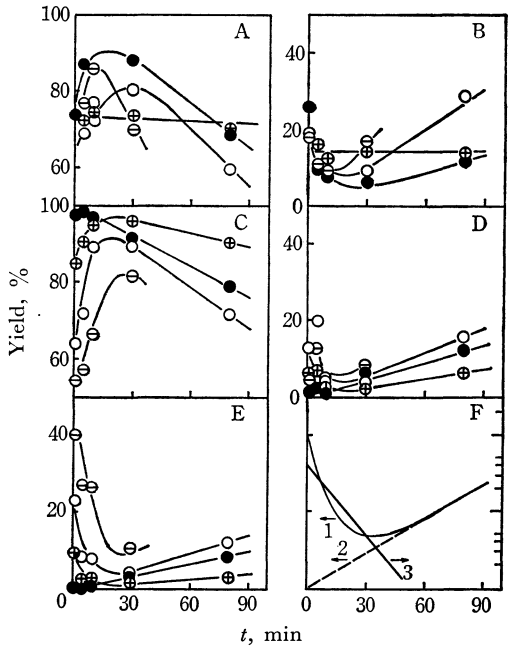

Fig. 2. Distribution of activities parted in aqueous or organic layers as a function of the irradiation time. A and B are distribution of bromide and bromine in the aqueous layers respectively. C, D and E are distribution of activities parted in the carbon disulfide, the ethyl ether and the benzene layers respectively. F is a schematic view of the analysis of a curve.
⊖: pyrenebromanil, ⊕: pyrene-bromanil mixture, ○: bromanil, ●: bromopyrene.

14) 1-Bromo-, 1,6- and 1,8-dibromo-, and 1,3,6-tribromopyrenes are soluble in benzene.

15) The standard R_f values were not determined. The present research was made on the distinction of distribution patterns of the recoil products for the two irradiation times.

TABLE 2. DISTRIBUTION OF ^{82}Br-LABELED RECOIL PRODUCTS PARTED IN AQUEOUS LAYERS AT VARIOUS IRRADIATION TIMES

Target	Irra. time, min	Yield,[a] %			
		Br_2	Br^-	Sum of unknowns	Origin[b]
P−B	5	10.5	76.8	6.4	6.3
	10	9.4	85.5	4.2	0.0
	30	16.6	70.1	12.4	0.8
P+B	5	15.3	72.2	9.6	3.1
	10	13.1	74.8	8.3	1.9
	30	14.2	73.6	14.5	1.4
	80	13.9	70.0	10.5	4.7
B	5	10.7	68.2	—	6.4
	10	12.9	72.6	10.2	1.0
	30	8.5	80.0	8.8	1.2
	80	28.6	59.2	10.2	1.8
PBr	5	9.9	87.0	0	0.6
	10	8.4	83.5	0	7.4
	30	6.2	87.9	0	2.1
	80	11.9	68.4	0	19.5
PBr_2[c]	10	—	41.8	0	53.7
	30	—	55.8	0	37.4
	80	—	56.3	0	33.5
HQBr[c]	5	—	39.8	27.4	20.1
	10	—	65.1	12.4	19.2
	30	—	58.3	19.7	26.5
	80	—	47.1	4.7	31.4

a) The relative yield was calculated from activities in the aqueous layers I and II. The values of Br^-, sum of unknowns and origin were calculated from activities distributed on the paper electrophoregrams. The sum of less than 100% was due to a "smear" of activity extending.[16]

b) Yield on an original spot may be of bromine and/or an organic bromide which has remained in the layer I.

c) Dissolved in carbon disulfide. The paper electrophoresis was carried out without extraction.

Among the samples, PBr, PBr_2, and P−B showed higher relative activities at the component of R_f 1, while the rest, B, HQBr, and P+B, showed more at the components of R_f 0.12—0.17. As compared with B, the distribution of P+B is not definitely affected when P is mixed in. When P−B is compared with P+B, on the other hand, the contribution of P is clear. The greater values at the component of R_f 1 in the irradiated P−B suggest the presence of a pyrene-radiobromine combination.

Table 2 lists the distribution of the ^{82}Br-labeled recoil products among the irradiated samples distributed in the aqueous layers (I and II) at various irradiation periods. In each case the major portion of the activities was found in the form of bromide. Three or four components, the mobilities of which were comparatively small, were obtained on paper strips of B, P−B, P+B, and HQBr. These components were not obtained on strips of PBr and PBr_2. These facts suggest that the components may be fragments of organic radiobromides originating in bromanil.

Figure 2 shows the relationship between the percentages of the ^{82}Br activities distributed in the aqueous or the organic layers and the irradiation time. The curves of the bromide and the bromine in P+B (see Figs. 2A and B) show a less remarkable change with the irradiation time. This may be because of the different behavior of the curve of its total organic yield.

The curves decreased (or increased) with an increase in the irradiation time. The longer the irradiation period, the better the (negative) proportionality to the irradiation time the curves seemed to show. To analyze the curve (see Fig. 2F) the final proportional portion was extrapolated back to time zero; on substracting the extrapolated line (2) from the original curve (1), another straight line (3) on a semilogarithmic scale was obtained. From the analyses of the curves, the following experimental equations were established;

$$Y = Y_0 \cdot e^{-rt} + mt \qquad (m>0)$$

16) J. Jack and G. Harbottle, *Trans. Faraday Soc.*, **54**, 520 (1958).

or; $Y = Y_0 \cdot e^{-rt} + mt + (1 - e^{-rt}) \quad (m<0)$

where Y, Y_0, m, and r are the yield at time t, the initial yield, the proportion constant, and the inclination of the semilogarithmic plot respectively. The quantitative treatment of such values as Y_0, m, and r should be discussed primarily on the basis of the theoretical derivation as functions of the reactor irradiation time and other considerable parameters. This question will be discuss in another paper.

The authors are indebted to Dr. Shiro Iwata, Dr. Yoshiyuki Kiso, and the personnel of the Research Reactor Institute, Kyoto University, for their assistance in the irradiation, and also to Mr. Masaya Tanizaki of their laboratory for his assistance in the experimental work.

BULLETIN OF THE CHEMICAL SOCIETY OF JAPAN VOL. 42 2359—2361 (1969)

Benzyne Addition Induced Rearrangement to *N*-Methyl-*N*-(1-phenethyl)aniline*[1]

Angelo G. GIUMANINI

Istituto di Chimica Organica ed Industriale, Università di Bologna, 40136 Bologna, Italy

and Arthur R. LEPLEY

Department of Chemistry, Marshall University, Huntington, West Virginia 25701, U.S.A.

(Received April 25, 1968)

In a continuing interest in the chemistry of α-dialkylamino carbanions and nitrogen ylids, we have studied the reaction between *N,N*-dimethylbenzylamine (DMBA) and benzyne, the latter being generated *in situ* by means of the reaction of a phenyl halide (Hal=F or Cl) and *n*-butyllithium. This technique, previously applied by the present authors to the system fluorobenzene/*n*-butyllithium/*N,N*-dimethylaniline,[1] allowed to predict that an *ortho*-ylid I formed which, in turn, could quickly isomerize to the *N*-ylids II and III by a prototropic shift. The ylids II and III are the postulated intermediates to the observed products IV and V of the reaction of the benzyldimethylanilinium ion VI with *n*-butyllithium[2] (Scheme 1). In the frame of this schematic and simplified picture, the environmental and physicochemical conditions for the generation of II and III should be closely similar for the two routes. It was therefore expected that the rates of the possible reactions involved[2] would closely parallel for the two cases, a fact that must be reflected into final product distribution. In a series of experiments with VI and *n*-butyllithium, we found[2] V to VI ratios between 0.81: 1 and 9.4 : 1 depending on experimental conditions.

In a related work by Jones *et al.* using VI and sodamide, only V was detected.[4]

We have now found in a preliminary study of the reaction in question that the benzyne generated betaine I affords practically a single (Stevens) rearrangement product, IV, as inequivocably shown by vapour phase chromatographic analysis[5] of the crude mixture combined with product separation and conventional analytical techniques. It also appears that no significant amounts of *o*-rearranged amine VII (Sommelet rearrangement) are present. Infrared and nuclear magnetic resonance spectral evidences ruled out that the isolated amine contained either product of 1,3 migration directly derived from the primary betaine I, apparently a very elusive compound, namely VIII and IX. Authentic IV was synthetized through an independent route[6] for definitive comparison.

There still remain the possibilities of direct displacement of the halogen atom by metallated

*1 This work was supported by U. S. Public Health Service grant GM-09136 from the National Institute of General Medical Science and the National Research Council of Italy. Parts of the work were presented before the 145th National Meeting of the American Chemical Society and the 10th National Meeting of the Italian Chemical Society.

1) A. R. Lepley, A. G. Giumanini, A. B. Giumanini and W. A. Khan, *J. Org. Chem.*, **31**, 2051 (1966).

2) A. G. Giumanini and A. R. Lepley, X Congresso Nazionale della Società Chimica Italiana, Padova 1968, comm. XIII/25 (1968).

3) G. C. Jones, W. Q. Beard and C. R. Hauser, *J. Org. Chem.*, **28**, 199 (1963).

4) Amine V is not stable in the presence of $NaNH_2$, which cleaves it to *N*-methylaniline and styrene. But this is the only source of these two compounds.[3]

5) A. H. Wagg, T. S. Stevens and D. M. Ostlo, *J. Chem. Soc.*, **1958**, 4057.

6) W. H. Puterbaugh and C. R. Hauser, *J. Am. Chem. Soc.*, **86**, 1396 (1964).

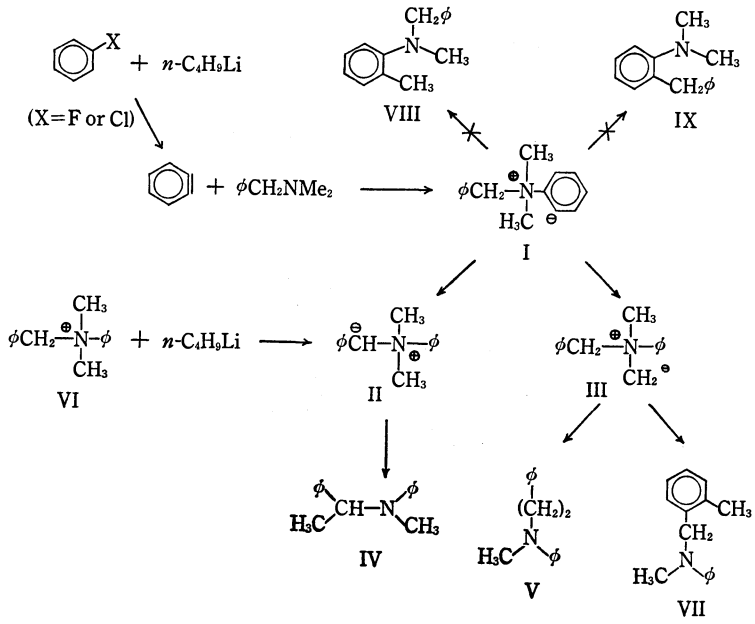

Scheme 1.

amine and of a benzyne reaction of the latter.[7] Indeed, BDMA reacts with *n*-butyllithium as evidenced by the bright colour appearing upon mixing with *n*-butyllithium. Once again the spectral characteristics of the separated amine ruled out such a hypothesis. The proton resonance spectrum indicated two methyls (a doublet centered at 1.46 ppm and split by methine with $J=6.7$ cps and a singlet at 2.56 ppm), a methine (quartet centered at 5.03 ppm and split by methyl with $J=7.0$ cps) and a phenyl (broad multiplet centered at 6.92 ppm) with relative intensities in the ratio 3/3/1/10.

Since the chromatic reaction between BDMA and *n*-butyllithium is instantaneous, it seems reasonable to conclude that either the metallated amine generates the benzyne to which it subsequently adds or the benzyne generated by excess butyllithium reacts with the metallated amine to yield the benzyl betaine anion X.

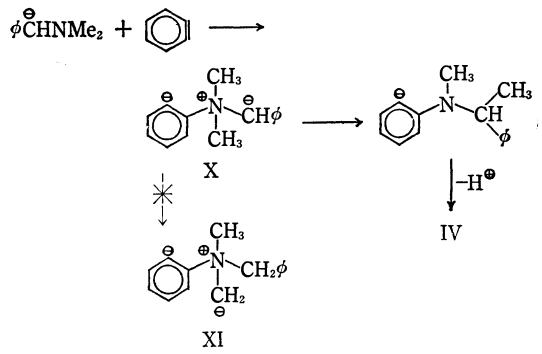

Scheme 2.

Since only a methyl shift occurs to produce IV, it is likely that the dianion X is involved in the rearrangement and at such a rate that prototropic shift to the methyl betaine anion XI cannot compete. Formation of ylid anions in the reactions of quaternary ammonium salts was previously advanced.[8]

To generate the benzyne, both chlorobenzene and fluorobenzene were used. The latter gave a better absolute yield in the rearranged amine (33% *vs.* 18%).

Experimental[9]

Chemicals. The best available grades of halobenzenes were used without purification. BDMA was a greatly appreciated gift of Miles Chemical Co. *n*-Butyllithium, 15% in hexane, was obtained from Foote Mineral Co. or prepared from 1-chlorobutane (Erba, Italy) and Li (Merk, W. Germany) in hexane under hydrogen.

Preparation of *N*-Methyl-*N*-(1-phenethyl)aniline (IV). *n*-Butyllithium (200 m*l*, 15%) was stirred and a solution of 200 m*l* BDMA in 400 m*l* anhydrous ether was rapidly added. The solution instantly turned bright yellow. Fluorobenzene (0.2 mol) in 150 m*l* ether

8) A. R. Lepley and A. G. Giumanini, *J. Org. Chem.*, **32**, 1706 (1967).

9) Essential experimental data are presented here. Further details and progresses of the research will be given at a later date. Physical properties (infrared and PMR spectra, refractive indexes and specific gravities) were measured in the standardized method previously described, *loc. cit.* and related analytical methods: A. R. Lepley, *Anal. Chem.*, **34**, 322 (1962); A. R. Lepley and W. A. Khan, *J. Org. Chem.*, **31**, 2064 (1966).

was added in one lot. After 15 min a heavy precipitation of salt was observed. The stirring was continued at 26°C for 24hr. Then 150 m*l* of water was added slowly with cooling, the ether layer was separated, dried over potassium hydroxide and distilled. A 33% yield was obtained of product boiling 181—2°C/20 Torr, $n_D^{25°}$ 1.5946. Gas chromatography showed less than 3% impurity in this product. The product was identical with material prepared by reaction of 1-bromoethylbenzene and *N*-methylaniline.

BULLETIN OF THE CHEMICAL SOCIETY OF JAPAN VOL. 42 2361—2362 (1969)

The Paramagnetism of Violanthrone-B

Tsuneo MAEKAWA

Department of Chemistry, College of General Education, The University of Tokyo, Komaba, Meguro-ku, Tokyo

(Received September 18, 1968)

It is well established that the compound named violanthrone-B is a mixture of $C_{34}H_{18}O$ (I) and $C_{34}H_{17}O$ (II). The formula (I) has been suggested by Aoki[1] and the shape of the carbon skeleton of (I) and (II) has been proved to be right by the author with X-ray analysis.[2] In a previous paper[3] the magnetic and some other physicochemical behaviors of violanthrone-B were reported. The present paper deals with the temperature dependence of the paramagnetism of the compound in a lower temperature region.

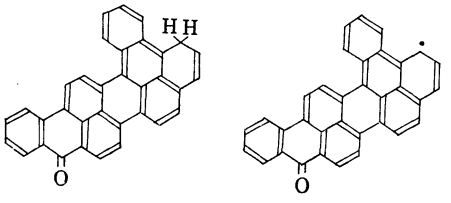

(I) (II)

Violanthrone-B was recrystallized from a solution in *o*-dichlorobenzene. Washed by ethanol, the precipitate was dried for several hours at 80°C under a pressure of 10^{-5} mmHg. Although this procedure of purification was much shorter than that reported in the previous paper, this method was sufficient to prepare the specimens for the measurement of the magnetic susceptibility.

The magnetic susceptibility was measured by the Faraday method. For the measurement of force on the specimen, the vacuum microbalance of Sartorius was used. The powdered sample was placed in a quartz container, which was suspended with a fine quartz rod from the balance arm and was placed at the point of the maximum field strength. A Faraday type magnet was used. For the temperature measurement the gold-cobalt alloy *vs.* copper thermocouple was used. The measuring-junction was placed under the quartz container as close as possible, since the maximum safe load of the balance was so small that we could not hang the thermocouple wire on the balance arm. In order to make uniform the temperature around the specimen and the thermocouple junction, a cylinder of copper foil was inserted around the specimen. The cryostat used was a simple double Dewar vessel type.

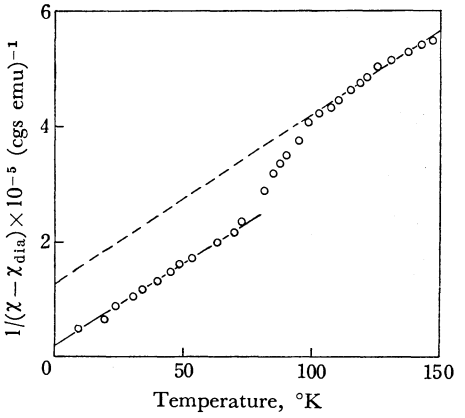

Fig. 1. The temperature dependence of the specific susceptibility of violanthrone-B.

We can summarize the result in Fig. 1, plotting the curve $1/(\chi-\chi_{dia})$ against T, where χ is the specific susceptibility, χ_{dia}, the diamagnetic part, for which the value estimated in the previous paper[3] is used, and T, the absolute temperature. The curve consists of two linear parts and both can be described by the Curie-Weiss law.

$$\chi = \frac{C}{T-\theta} + \chi_{dia} \qquad (1)$$

From the higher temperature region the Curie constant and the Curie temperature can be decided

1) J. Aoki, This Bulletin, **34**, 1817, 1820 (1961).
2) T. Maekawa, to be published.
3) H. Akamatu, T. Maekawa, Y. Iida and M. Kinoshita, This Bulletin, **37**, 849 (1964).

as

$$C=0.343\times10^{-3}\ \text{emu°K/g}$$
$$\theta=-41\text{°K}$$

which are nearly equal to the values reported before,[4] while from the lower temperature region we obtain

$$C=0.344\times10^{-3}\ \text{emu°K/g}$$
$$\theta=-5\text{°K}$$

It has been often observed that the magnetic susceptibility of the impure species becomes predominant at low temperature especially for the system of the singlet-triplet equilibrium.[5] In our case, however, the Curie constant observed at low temperature is equal to that of higher temperature, and consequently we obtain the constant density of the magnetic species in all the temperature region. It is accordingly conceivable that the magnetic behavior at low temperature of violanthrone-B is not because of any impurities but due to its own nature. It has been also observed for DPPH[6] that the Curie temperature changes very slightly at low temperature. These phenomena may be due to the phase transition of the crystal.

The author wishes to express his thanks to Professor Hiroo Inokuchi and Dr. Noriko Ohigashi for use of the equipment.

4) In the previous paper, Ref. 3, we decided the values $C=0.306\times10^{-3}$ emu°K/g and $\theta=-45$°K, where the magnetic susceptibility was measured also by the Faraday method over the temperature of liquid nitrogen up to the room temperature.

5) D. D. Thomas, H. Keller and H. M. McConnell, *J. Chem. Phys.*, **39**, 2321 (1963).

6) H. Inokuchi and N. Ohigashi, Private communication.

BULLETIN OF THE CHEMICAL SOCIETY OF JAPAN VOL. 42 2362—2363 (1969)

Contribution of Charge Transfer Structure to Exchange Interaction in the Crystal of Organic Free Radical

Tsuneo MAEKAWA

Department of Chemistry, College of General Education, The University of Tokyo, Komaba, Meguro-ku, Tokyo

(Received September 18, 1968)

It has been well known that the relatively high negative Curie temperature θ is often obtained from the susceptibility *vs.* temperature data for the crystalline-stable free radicals. For instance, $\theta=-17°K$[1] and $-45°K$[2] for DPPH and violanthrone-B, respectively. Furthermore, for a number of solid ionic aromatic free radicals such as TCNQ ionic radical[3] the large singlet-triplet splitting Δ has been observed in the ESR measurement. Both θ and Δ can be related to the exchange interaction J in the crystal. If we assume that every molecule in solid has interaction with one nearest neighbor, the relation can be derived by the Weiss field theory as

$$\Delta=2J=4k|\theta| \tag{1}$$

It seems improbable for the molecular crystals that such values of the Curie temperature or the S-T splitting are attributable to the simple exchange interaction. The large S-T splitting has been discussed by Hausser and Murrell[4] and McConnell[5] introducing the charge transfer structure of Mulliken type.

In the present paper we discuss the problem by the LCMO approach, which will give a simpler physical image.

The orbitals of the unpaired electrons of two interacting radicals A and B may be written in the form of LCMO as

$$\left.\begin{aligned}\varphi_A&=a\varphi_A{}^\circ+b\varphi_B{}^\circ\\ \varphi_B&=a\varphi_B{}^\circ+b\varphi_A{}^\circ\end{aligned}\right\} \tag{2}$$

in which $\varphi^\circ{}_{A,B}$ is the orbital for the isolated molecule. Then we have the wave function for a pair of radicals

$$\Psi_{AB}(1,2)=C[\varphi_A(1)\varphi_B(2)\pm\varphi_A(2)\varphi_B(1)] \tag{3}$$

1) J. Turkevich and P. Selwood, *J. Am. Chem. Soc.*, **63**, 1077 (1941).

2) H. Akamatu, T. Maekawa, Y. Iida and M. Kinoshita, This Bulletin, **37**, 849 (1964).

3) D. B. Chesnut and P. Arthur, Jr., *J. Chem. Phys.*, **36**, 2969 (1962).

4) K. H. Hausser and J. N. Murrell, *ibid.*, **27**, 500 (1957).

5) H. M. McConnell, "Molecular Biophysics," ed. by B. Pullman and M. Weissbluth, Academic Press, New York and London (1965), p. 317.

or

$$\Psi_{AB}(1,2) = c_1\Psi_1(1,2) + c_2\Psi_2(1,2) + c_3\Psi_3(1,2) \quad (4)$$

where

$$\left.\begin{aligned}\Psi_1(1,2) &= \varphi_A^\circ(1)\varphi_B^\circ(2)\\ \Psi_2(1,2) &= \varphi_A^\circ(2)\varphi_B^\circ(1)\\ \Psi_3(1,2) &= C'[\varphi_A^\circ(1)\varphi_A^\circ(2) + \varphi_B^\circ(1)\varphi_B^\circ(2)]\end{aligned}\right\} \quad (5)$$

C and C' are the normalization constants.

The secular equation derived from (4) is

$$\begin{vmatrix} H_{11}-W & H_{12}-S_{12}W & H_{13}-S_{13}W \\ H_{12}-S_{12}W & H_{11}-W & H_{13}-S_{13}W \\ H_{13}-S_{13}W & H_{13}-S_{13}W & H_{33}-W \end{vmatrix} = 0 \quad (6)$$

where the relations $H_{22}=H_{11}$, $H_{23}=H_{13}$ and $S_{23}=S_{13}$ are used. Readily factorized, Eq. (6) can be reduced to

$$\begin{vmatrix} \dfrac{H_{11}+H_{12}}{1+S_{12}} - W & \dfrac{H_{13}-S_{13}W}{1+S_{12}} \\ 2(H_{13}-S_{13}W) & H_{33}-W \end{vmatrix} = 0 \quad (7)$$

and

$$(H_{11}-H_{12}) - (1-S_{12})W = 0 \quad (8)$$

Equation (7) can be solved by the ordinary method of approximation and gives the energy of the lowest singlet state

$$W_s = W_s^\circ - \frac{2(H_{13}-S_{13}W_s^\circ)^2}{(1+S_{12})(H_{33}-W_s^\circ)} \quad (9)$$

corresponding to

$$c_1 = c_2, \quad c_3 \neq 0$$

where

$$W_s^\circ = \frac{H_{11}+H_{12}}{1+S_{12}} \quad (10)$$

On the other hand, from Eq. (8) we can obtain the solution for the triplet state

$$W_T = W_T^\circ = \frac{H_{11}-H_{12}}{1-S_{12}} \quad (11)$$

corresponding to

$$c_1 = -c_2, \quad c_3 = 0$$

W_S° and W_T° are the eigenvalues corresponding to the wave functions

$$\Psi_0^s(1,2) = \frac{1}{\sqrt{2+2S_{12}}}[\varphi_A^\circ(1)\varphi_B^\circ(2) + \varphi_A^\circ(2)\varphi_B^\circ(1)] \quad (12)$$

and

$$\Psi_0^T(1,2) = \frac{1}{\sqrt{2-2S_{12}}}[\varphi_A^\circ(1)\varphi_B^\circ(2) - \varphi_A^\circ(2)\varphi_B^\circ(1)] \quad (13)$$

respectively. Furthermore, it can be readily verified that Eq. (9) is equivalent to the equation obtained by Mulliken's method, that is, the eigenvalue for $\Psi = a\Psi_0^s + b\Psi_3$, while the triplet state is unaffected by the introduction of the charge transfer structure. This is the natural consequence resulting from Pauli's principle.

Finally, we can obtain the energy of the S-T splitting

$$\Delta = W_s - W_T = W_s^\circ - W_T^\circ - \frac{(H_{03}^s - S^s{}_{03}W_s^\circ)^2}{H_{33}-W_s^\circ} \quad (14)$$

where

$$H^s{}_{03} = \int \Psi_0{}^s H \Psi_3 d\tau, \quad S^s{}_{03} = \int \Psi_0{}^s \Psi_3 d\tau \quad (15)$$

If the higher orbitals $\varphi_A{}^1$ and $\varphi_B{}^1$ are taken into consideration, starting from

$$\left.\begin{aligned}\varphi_A &= a\varphi_A{}^\circ + b\varphi_B{}^\circ + c\varphi_B{}^1\\ \varphi_B &= a\varphi_B{}^\circ + b\varphi_A{}^\circ + c\varphi_A{}^1\end{aligned}\right\} \quad (16)$$

we can finally obtain

$$W_s - W_T = W_s^\circ - W_T^\circ - \frac{(H^s{}_{03} - S^s{}_{03}W_s^\circ)^2}{H_{33}-W_s^\circ} - \frac{(H^s{}_{01} - S^s{}_{01}W_s^\circ)^2}{H^s{}_{11}-W_s^\circ} + \frac{(H^T{}_{01} - S^T{}_{01}W_T^\circ)^2}{H^T{}_{11}-W_T^\circ} \quad (17)$$

where $H^s{}_{01}$, $S^s{}_{01}$, $H^T{}_{01}$, $S^T{}_{01}$, $H^s{}_{11}$ and $H^T{}_{11}$ are the quantities related to

$$\Psi_1{}^s = C''[\varphi_A^\circ(1)\varphi_A{}^1(2) + \varphi_A^\circ(2)\varphi_A{}^1(1) + \varphi_B^\circ(1)\varphi_B{}^1(2) + \varphi_B^\circ(2)\varphi_B{}^1(1)] \quad (18)$$

$$\Psi_1{}^T = C'''[\varphi_A^\circ(1)\varphi_A{}^1(2) - \varphi_A^\circ(2)\varphi_A{}^1(1) - \varphi_B^\circ(1)\varphi_B{}^1(2) + \varphi_B^\circ(2)\varphi_B{}^1(1)] \quad (19)$$

in which C'' and C''' are the normalization constants.

In Eq. (17) the fourth and the fifth terms on the right-hand side are the correcting terms of small value and tend to cancel each other. Thus, it seems to be probable that Eq. (14) is a good approximation for the S-T splitting. In Eq. (14) the last term on the right-hand side is the contribution of the intermolecular charge transfer structure. It should be noted that in this approximation the intermolecular charge transfer in the triplet state is absent owing to Pauli's principle.

BULLETIN OF THE CHEMICAL SOCIETY OF JAPAN VOL. 42 2364—2367 (1969)

Ultrasonic Effect on Phosphate Coating Formation*1

Takao UMEGAKI, Hiroshi ITO*2 and Taijiro OKABE

Department of Applied Chemistry, Faculty of Engineering, Tohoku University, Sendai

(Received October, 5, 1968)

The recent development of high power generators of ultrasonic wave has broadened its scope of application. If it is applied to the phosphatizing process, the cavitation caused by ultrasonic radiation in the phosphatizing solution is expected to prevent passivation of iron, and, removing hydrogen gas from the iron surface, to bring about a stirring effect. Ultrasonic cavitation is considered to eliminate the hindrance of Al^{3+} which has been recognized as one of the most undesirable contaminators when wet-process phosphoric acid is used as raw material for phosphatizing solution.[1] A few investigations of the ultrasonic effects[2-4] on the phosphate coating have been already reported, but the pH range of the phosphatizing solution and the condition of radiation for these investigations are limited. The present investigation has been undertaken to obtain the optimum condition for the formation of the phosphate coating under ultrasonic radiation.

Experimental

A) Phophatizing Solution. The phosphatizing solution was prepared by diluting phosphoric acid and dissolving a certain amount of $NaNO_3$, Na_2CO_3 and $Zn_3(PO_4)_2$. Differing from a commercial phosphatizing solution, the solution used in this experiment contained a large amount of zinc phosphate precipitates. The relationship between Na_2CO_3 and H_3PO_4 is shown in Fig. 1. The concentrations of $NaNO_3$ and $Zn_3(PO_4)_2{\cdot}4H_2O$ were fixed at 3.3 g/*l* and 19.3 g/*l*, respectively. The pH of the solution, as shown in Fig. 1 varied largely with the composition of the solution.

B) Apparatus and Procedure for Measurement. The apparatus consisted of a high frequency oscillator of alternate current and several magneto-restriction vibrators. The frequency of ultrasonic wave was altered by changing magneto-restriction vibrators within the range from 16 kc to 100 kc. The intensity of ultrasonic wave was continuously changeable from 0 W to 500 W. A polyethylene beaker containing the phosphatizing solution was placed on the radiation plane of the vibrator and a metal specimen was suspended with nylon fiber in the solution. The apparatus is schematically show in Fig. 2. Before the phosphatization the specimens were treated by the method describ-

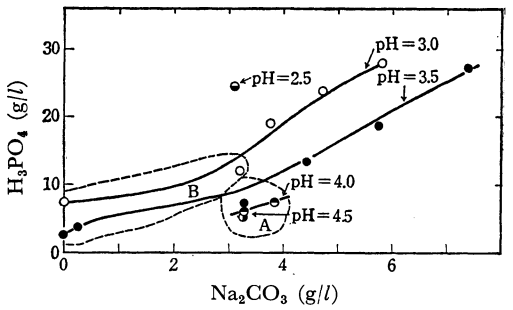

Fig. 1. Relationship among concentrations of H_3PO_4 and Na_2CO_3 and pH's of phosphatizing solutions.

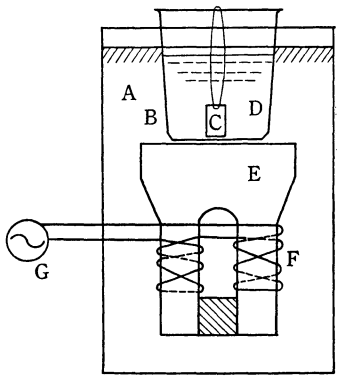

Fig. 2. Apparatus for ultrasonic radiation. A. thermostatic bath, B. polyethylene-made beaker, C. specimen, D. phosphatizing solution, E. magneto-restriction vibrator, F. exciting coil, G. ultrasonic oscillator

TABLE 1. COMPOSITION OF MILD STEEL USED

C	Si	Mn	P
0.20	trace	0.80	0.016

S	Cu	Cr	Ni
0.024	0.06	0.06	0.03

1) T. Umegaki, H. Ito and T. Okabe, This Bulletin, **42**, 1555 (1969).
2) L. E. C. Gandil, Brit. Pat. 885686 (1961).
3) T. Kataoka, Japanese Pat. 8509 (1958).
4) A. M. Ginberg and M. A. Naishuller, *J. Appl. Chem. USSR,* **37**, 551 (1964).

*1 Presented at the 21st Annual Meeting of the Chemical Society of Japan, Osaka, April, 1968.

*2 Present Address: Fukushima Technical Collge, Taira, Iwaki, Fukushima.

ed in a previous paper.[1] The composition of the specimens is shown in Table 1.

C) Amount of Phosphate Film. The weight of the coating was estimated by measuring the weight change of the specimens by dipping in a stripping solution containing 20% of CrO_3.

D) Corrosion Test. The corrosion resistivity of the phosphate coating was tested in the same manner as described in the preceding paper.[1] In this test the dipping time was cut to 5 hr, whereas the ten-hour test has been adopted previously.

Results and Discussion

The optimum composition of the phosphatizing solution under radiation of ultrasonic wave was sought at 50°C by microscopic observation on the phosphate coating. All experiments were done under radiation of ultrasonic wave with a frequency of 20 kc and an intensity of 25 W/cm². This ultrasonic radiation was adopted, taking the stability and feasibility in the generation of ultrasonic wave into consideration. As a preliminary experiment, commercial phosphatizing solutions were used for

Table 2. Relationship between coating weight and the composition of phosphating solution

Phosphating soln. No.	pH	H_3PO_4 (g/l)	Na_2CO_3 (g/l)	Coating weight (mg·cm²)
1	2.5	24.5	3.11	—
2	3.0	7.79	0.00	0.23
3	3.0	12.1	3.23	0.26
4	3.0	19.0	3.77	—
5	3.0	23.8	4.73	—
6	3.0	28.2	5.84	—
7	3.5	2.90	0.00	0.38
8	3.5	3.85	0.25	0.17
9	3.5	7.79	3.30	0.34
10	3.5	13.3	4.45	0.17
11	3.5	18.6	5.77	0.05
12	3.5	27.6	7.39	0.10
13	4.0	6.34	3.30	0.09
14	4.0	7.79	3.85	0.11
15	4.5	6.04	3.30	0.11

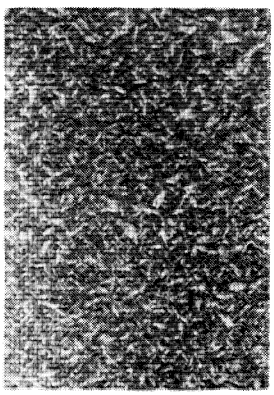

Fig. 3. Phosphate coating from the solution belonging to region B.
(5 min) (×180)

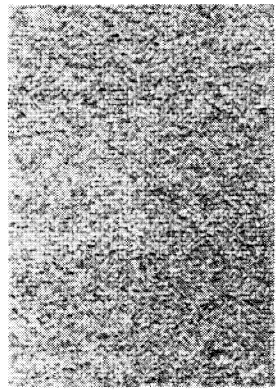

Fig. 4. Phosphate coating from the solution belonging to region A.
(5 min) (×180)

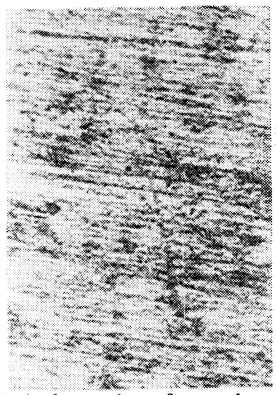

Fig. 5. Typical coating from the phosphating solutions of Nos. 10, 11, 12 and 14.
(5 min) (×180)

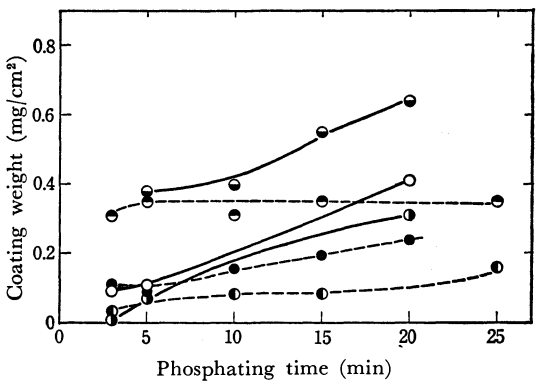

Fig. 6. Variation of coating weight with phosphating time at 50°C.
soln. No. 9, soln. No. 13, soln. No. 15
solid line: ultrasonic radiation
broken line: without radiation

phosphatization. So far as the microscopic observation on the phosphate coating showed, under ultrasonic radiation, no excellent coating was obtained in these solutions with considerably low pH. In the course of experiments under ultrasonic radiation, however, a slurry solution containing insoluble zinc phosphate was found to give a thin but sturdy coating. The relationship between the weight of the phosphate coating and the composition of the phosphatizing solution is shown in Table 2. At high concentration of H_3PO_4 and at low concentration of Na_2CO_3, a bulky and coarse coating was obtained. The solution which belonged to region B of Fig. 1 gave a coating such as shown in Fig. 3. Figure 4 shows the typical coating produced in the solution belonging to region A in Fig. 1. Compared with the solution in region B, the solution in region A gave thin coating, and the specimen used was uniformly covered with fine crystals. As shown in Fig. 5, a uniform coating was not obtained in the phosphatizing solutions of Nos. 10, 11, 12 and 14 listed in Table 1, the compositions of which belonged to neither of those in region A nor in region B. From microscopic observation of the coating surfaces, the solution region A was assumed to have the optimum composition under ultrasonic radiation. The optimum

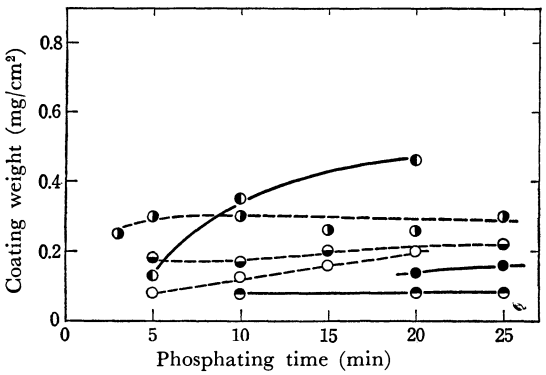

Fig. 7. Variation of coating weight with phosphating time at 75°C.
◐◑ soln. No. 9 ◒◓ soln. No. 13
○● soln. No. 15
solid line: ultrasonic radiation
broken line: without radiation

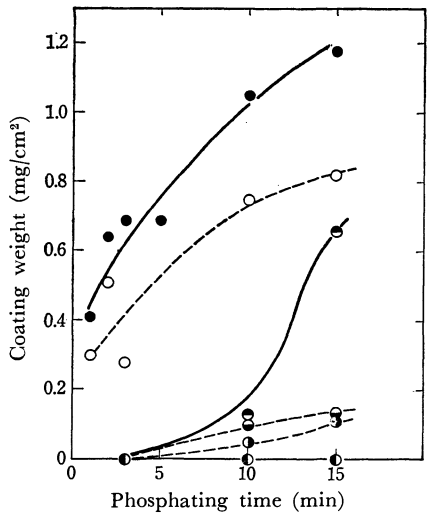

Fig. 8. Variation of coating weight with phosphating time at 95°C.
●○ soln. No. 9 ◒◓ soln. No. 13
◑◐ soln. No. 15
solid line: ultrasonic radiation
broken line: without radiation

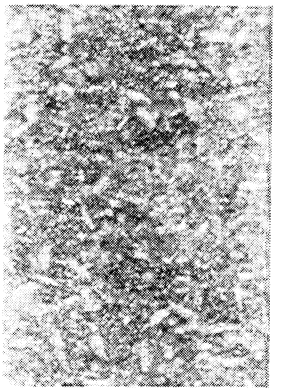

Fig. 9. Phosphate coating under ultrasonic radiation 95°C. (5 min) (×180)

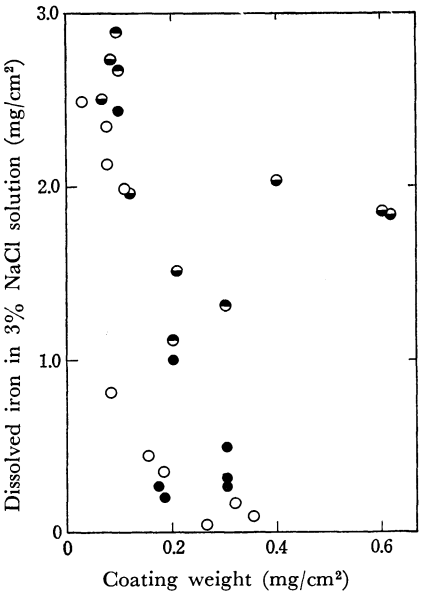

Fig. 10. Plot of relative resistivity against coating weight.
● 50°C ○ 75°C ultrasonic radiation
◑ 50°C ◐ 75°C without radiation

pH range of the solution of the phosphatizing process under ultrasonic radiation is 3—4, which is favorable for the precipitation of Al^{3+} and the elimination of its hindrance. The changes of the coating weight with the duration of phosphatization at 50, 75 and 95°C are shown in Figs. 6, 7 and 8. Figures 6 and 7 indicate that, under ultrasonic radiation, the saturation of the coating weight was present in the phosphatizing process, whereas the coating weight without radiation of ultrasonic wave increased gradually with time. The coating surface obtained at 95°C, in spite of its large thickness, was coarse and deficient in uniformity as shown in Fig. 9. On the other hand, the coatings obtained at 50 and 75°C were thin but sturdy. In Fig. 10, the amount of dissolved iron indicating the relative resistivity of coating, in the air-bubbled 3% NaCl solution, is plotted against the coating weight. The coating obtained under radiation of ultrasonic wave was found to be more sturdy than that treated by the ordinary dipping method, as is shown in Fig. 10. Figures 11 and 12 show the films obtained on the surfaces which had been oxidized by concentrated HNO_3 before phosphatization. In spite of the presence of oxide film on the specimen, a uniform film, shown in Fig. 11 was obtained by ultrasonic radiation. From comparison of Fig. 13 with Fig. 14, it has been revealed that ultrasonic wave also facilitated the film formation on the surface stained with mineral oil.

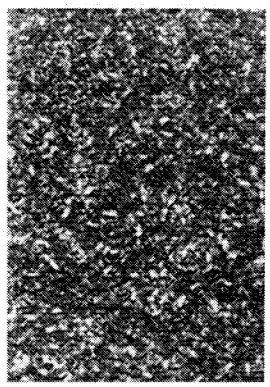

Fig. 11. Phosphate coating on oxide-covered surface under ultrasonic radiation. (5 min) (×180)

Fig. 12. Phosphate coating on oxide-covered surface without ultrasonic radiation. (5 min) (×180)

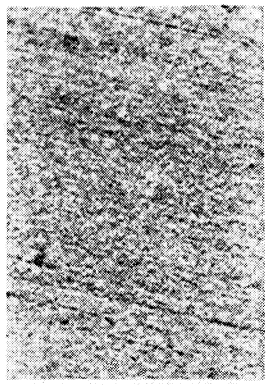

Fig. 13. Phosphate coating on oil-stained surface under ultrasonic radiation. (5 min) (×180)

Fig. 14. Phosphate coating on oil-stained surface. without ultrasonic radiation. (5 min) (×180)

This investigation was supported by a grant from Nippon Kokan (Japan Steel and Tube) Corp., for which the authors wish to express their sincere appreciation. The authors also wish to thank Mr. Chiharu Kasai in the Research Institute of Electrical Communication, Tohoku University, for suggestions on the design of ultrasonic wave generator.

BULLETIN OF THE CHEMICAL SOCIETY OF JAPAN VOL. 42 2368 (1969)

Studies on Cow's Urine. V. Determinaton by Gas-liquid Chromatography of an Acidic Part Obtained from Cow's Urine (Supplement)*1

Rikisaku SUEMITSU, Shin-ichi FUJITA, Mitsuo YOSHIMURA and Isao KONDO

Department of Applied Chemistry, Faculty of Engineering, Doshisha University, Kamikyo-ku, Kyoto

(Received November 14, 1968)

In the recent literature studies of aromatic acids in human urine[1-3] and amino acids in healthy rabbit urine[4,5] have been reported.

In a previous paper[6] we examined, by gas-liquid chromatography, phenolic and acidic parts obtained from the urine of Nihon-ushi (*Bos taurus* Linneaus) and presented a new metabolic pathway of phenylalanine and its derivatives.

In the present paper, seven components were newly identified in addition to nineteen compounds detected previously;[6] all are shown in Table 1.

The peak numbers are the same as those of Table 1 in a previous report.[6] Peak No. 25 was previously reported as unidentified, and No. 26, as 3-indoleacetic acid (?); however, the former is corrected to 3-indoleacetic acid, and the latter is here regarded as unidentified.

It is noteworthy that a small amount of 3-indoleacetic acid and β-3-indolepropionic acid are newly detected in the urine. They may be supposed to be degradation products of tryptophan *in vivo*.

Experimental

The gas-chromatographic analysis was performed as has been previously described.[6] In this experiment, 25% SE-60, coated on 80—100 mesh Diasolid L, was also used as the polar stationary phase in order to effect a good separation.

TABLE 1. AROMATIC ACIDS ADDITIONALLY DETECTED IN COW'S URINE

Peak No.	Rt.	Component	%
4	3.5	*o*-Hydroxyphenylacetic acid	trace
6_1	5.0	*m*-Methoxybenzoic acid	trace
7	5.2	*o*-Methoxyphenylacetic acid	0.65
16_1	13.1	3-Methoxy-4-hydroxyphenylacetic acid	trace
19	18.5	β-3-Methoxy-4-hydroxyphenylpropionic acid	0.35
25	32.4	3-Indoleacetic acid	0.15
26	38.9	Unidentified	0.1
27	48.5	β-3-Indolepropionic acid	0.15

*1 Presented at the 21st Annual Meeting of the Chemical Society of Japan, Osaka, April, 1968.

1) M. D. Armstrong, *J. Biol. Chem.*, **218**, 293 (1956).
2) C. M. Williams, *Anal. Biochem.*, **4**, 423 (1962).
3) C. E. Dalgliesh, E. C. Horning and M. G. Horning, *Biochem. J.*, **70**, 101, 792 (1966).
4) I. Tanaka, *Hoan Eisei*, **1**, 343 (1964).
5) H. Kato, *Shinshu Igaku Zasshi*, **1**, 53 (1952).
6) Part IV: R. Suemitsu, S. Fujita, Y. Mishima and M. Yoshimura, This Bulletin, **41**, 1381 (1968).

BULLETIN OF THE CHEMICAL SOCIETY OF JAPAN VOL. 42 2369—2371 (1968)

Stability Constants of Dimethyltin Dichloride and Tin Tetrachloride Complexes of *p*-Substituted Benzaldehydes, Acetophenones and *N,N*-Dimethylbenzamides

Gen-etsu MATSUBAYASHI, Noboru NISHII and Toshio TANAKA

Department of Applied Chemistry, Faculty of Engineering, Osaka University, Yamadakami, Suita, Osaka

(Received November 16, 1968)

Many stable dimethyltin dichloride - organic donor adducts have been isolated and their configurations in the solid state discussed by several workers.[1] Only a few quantitative data on them[1-3] in solution have been reported, however, although the stability constants of other organotin chlorides[4-7] and tin tetrachloride adducts[8] have been obtained. Recently we have reported that dimethyltin dichloride forms stable 1 : 1 adducts with some aromatic carbonyl donors and that their stability constants are quite small.[1] The present report will describe the stability constants for several dimethyltin dichloride and tin tetrachloride-aromatic carbonyl donor (XC_6H_4COR) complexes and the effect of the substituents, X and R groups.

Experimental

Materials. *N,N*-Dimethylbenzamide and its *p*-substituted derivatives were prepared according to the methods in the literature.[9] *p*-Nitro-*N,N*-dimethylbenzamide. Found: C, 55.90; H, 5.18; N, 14.87%. Calcd for $C_9H_{10}N_2O_3$: C, 55.66; H, 5.19; N, 14.42%. *p*-Chloro-*N,N*-dimethylbenzamide. Found: C, 58.53; H, 5.61; N, 7.84%. Calcd for $C_9H_{10}ClNO$: C, 58.86; H, 5.49; N, 7.62%. *N,N*-Dimethylbenzamide. Found: C, 72.12; H, 7.43; N, 9.41%. Calcd for $C_9H_{11}NO$: C, 72.45; H, 7.43; N, 9.39%. *p*-Methyl-*N,N*-dimethylbenzamide. Found: C, 73.18; H, 7.80; N, 8.64%. Calcd for $C_{10}H_{13}NO$: C, 73.59; H, 8.03; N, 8.58%. *p*-*N,N*-Dimethylamino-*N,N*-dimethylbenzamide. Found: C, 68.42; H, 8.59; N, 14.52%. Calcd for $C_{11}H_{16}N_2O$: C, 68.72; H, 8.39; N, 14.57%. The *p*-methoxy-*N,N*-dimethylbenzamide, kindly supplied by Professor Komori of this Department, was also analytically pure. The *p*-*N,N*-dimethylacetophenone was prepared according to the literature, and excellent analyses for carbon, hydrogen, and nitrogen were obtained on it.[1] The other acetophenone- and benzaldehyde derivatives were commercially-available materials and were distilled under nitrogen before use. Dimethyltin dichloride and dibromide, tin tetrachloride and 1,2-dichloroethane were purified according to the conventional methods.[3]

Spectrophotometers. The IR and UV spectrophotometers used here were previously described.[1]

Results and Discussion

The stability constants (K) of the complexes are defined by the following equation;

$$K = [A \cdot D]/[A] \cdot [D], \text{ in } A + D = A \cdot D$$

where A is dimethyltin dichloride or tin tetrachloride and where D is a carbonyl donor. The K values were determined from the infrared (Fig. 1) or ultraviolet spectra (Fig. 1 in Ref. 1) for the carbonyl donor molecules with varying amounts of the tin(IV) compounds in 1,2-dichloroethane, according to the method described previously.[1]

The results obtained for the dimethyltin dichloride and tin tetrachloride complexes are summarized in Tables 1 and 2, respectively. Dimethyltin dichloride - carbonyl donor complexes were isolated stably as 1 : 1 adducts rather than as 1 : 2 adducts,[1] and under the present experimental conditions a large excess of dimethyltin dichloride exists in

1) G. Matsubayashi, T. Tanaka and R. Okawara, *J. Inorg. Nucl. Chem.*, **30**, 1831 (1968), and the references therein.

2) M. Komura, Y. Kawasaki, T. Tanaka and R. Okawara, *J. Organometal. Chem.*, **4**, 308 (1965).

3) G. Matsubayashi, Y. Kawasaki, T. Tanaka and R. Okawara, *J. Inorg. Nucl. Chem.*, **28**, 2937 (1966).

4) N. A. Matwiyoff and R. S. Drago, *Inorg. Chem.*, **3**, 337 (1964).

5) T. F. Bolles and R. S. Drago, *J. Am. Chem. Soc.*, **87**, 5015 (1965); **88**, 3921, 5730 (1966).

6) J. L. Wardell, *J. Organometal. Chem.*, **9**, 89 (1967); **10**, 53 (1967).

7) Y. Kawasaki, M. Hori and K. Uenaka, This Bulletin, **40**, 2463 (1967).

8) M. H. Dilke and D. D. Eley, *J. Chem. Soc.*, **1949**, 2609; S. T. Zenchelsky and P. R. Segatto, *J. Am. Chem. Soc.*, **80**, 4796 (1958); F. T. Cioffi and S. T. Zenchelsky, *J. Phys. Chem.*, **67**, 357 (1963); T. L. Brown and M. Kubota, *J. Am. Chem. Soc.*, **83**, 331 (1961); J. Laane and T. L. Brown, *Inorg. Chem.*, **3**, 148 (1964); D. P. N. Sachell and J. L. Wardell, *Proc. Chem. Soc.*, 86 (1963), 405 (1964); *J. Chem. Soc.*, **1964**, 4134, 4300; *Trans. Faraday Soc.*, **61**, 1127, 1132 (1965); A. Mohammad and D. P. N. Sachell, *Chem. Ind.*, **1965**, 2069; *J. Chem. Soc., B*, **1964**, 527; J. J. Myher and K. E. Russell, *Can. J. Chem.*, **42**, 1555 (1964); G. Leclere and Duyckaerts, *Spectrochim. Acta*, **22**, 403 (1966); A. Kemula and R. T. Iwamoto, *J. Phys. Chem.*, **72**, 1334 (1968).

9) R. L. Carlson and R. S. Drago, *J. Am. Chem. Soc.*, **85**, 505 (1963).

Table 1. Stability constants (log K) of dimethyltin dichloride - aromatic carbonyl donor complexes in 1,2-dichloroethane at 25±2°C

D	X					
	$(CH_3)_2N$	CH_3O	CH_3	H	Cl	NO_2
$XC_6H_4COCH_3$	0.50±0.02[a,b] (0.11±0.03)[a,c]	0.03±0.02[a,b]		−0.22±0.08		
XC_6H_4COH	0.89±0.02[a,b]	0.52±0.10[a]	0.21±0.02[a]	−0.19±0.03		
$XC_6H_4CON(CH_3)_2$	1.64±0.03	1.37±0.02	1.45±0.02	1.34±0.02	1.16±0.02	0.86±0.02

a) Determined from UV spectra and the others from IR spectra.
b) Ref. 1.
c) The value of dimethyltin dibromide complex.

Table 2. Stability constants (log K) of tin tetrachloride - aromatic carbonyl donor complexes in 1,2-dichloroethane at 25±2°C

D	X			
	CH_3O	CH_3	H	Cl
$XC_6H_4COCH_3$	2.62±0.02		1.65±0.04	
XC_6H_4COH	3.27±0.02	2.60±0.02	2.16±0.06	1.93±0.03

Determined from UV spectra.

Table 3. C=O stretching frequencies of aromatic carbonyl donors and their frequency lowerings (in parentheses) accompanied by the complex formation with dimethyltin dichloride in 1,2-dichloroethane (in cm^{-1})

D	X				
	$(CH_3)_2N$	CH_3O	H	Cl	NO_2
$XC_6H_4COCH_3$	1665	1680	1686		
	(24)	(20)	(16)		
XC_6H_4COH	1665	1688	1706		
	(26)	(24)	(16)		
$XC_6H_4CON(CH_3)_2$	1626	1630	1633	1637	1643
	(41)	(36)	(36)	(37)	(29)

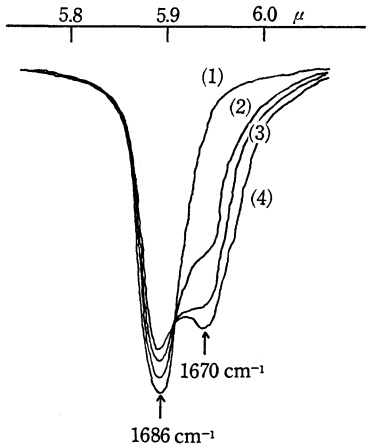

Fig. 1. The infrared spectrum of $C_6H_5COCH_3$ (0.0438 mol/l) with various concentrations of $(CH_3)_2SnCl_2$ in 1,2-dichloroethane.
$(CH_3)_2SnCl_2$: (1) 0, (2) 0.344, (3) 0.728, (4) 1.037 mol/l

solution in comparison with the donors. Therefore, the formation of the 1 : 1 adducts may be predominant in solution. In the cases of tin tetrachloride, the 1 : 2 adducts were isolated stably.[10,11] However, the K values obtained here may also be considered to be those for the 1 : 1 adducts, because of the large excess of tin tetrachloride compared with the donors. Tables 1 and 2 indicate that the acceptor strength of tin chlorides toward carbonyl donors is; $SnCl_4$: $(CH_3)_2SnCl_2$ ≒500—100 : 1. Furthermore, we can compare the acceptor strength of the latter toward *N,N*-dimethylbenzamide derivatives with that of iodine studied by Drago:[9] $(CH_3)_2SnCl_2$: I_2 ≒5 : 1.

Generally, the order of the electron-releasing tendency of R in XC_6H_4COR is known to be $H < CH_3 < N(CH_3)_2$. This is indicated in the C=O

10) G. A. Olah, "Friedel-Crafts and Related Reactions," Interscience, New York (1964).
11) I. R. Beattie, *Quart. Rev.*, **17**, 382 (1963).

stretching frequencies of the free ligands (Table 3); the frequency decreases with a stronger electron-releasing group, R or X. Table 3 also shows the C=O frequency shift to a lower region due to the complex-formation with dimethyltin dichloride. The magnitudes of the frequency lowering are compared with the K values. The association constants of the substituted acetophenones with protons were reported to be larger than those of substituted benzaldehydes.[12,13] In the cases of tin chloride complexes, however, the K value and the C=O frequency lowering become larger in the following order of R groups; $CH_3<H<N(CH_3)_2$, as may be seen in Tables 1, 2, and 3. This order for H and CH_3 groups may be due to the steric effect of the methyl group on the complex formation of tin chlorides.

There is an almost linear relationship between the $\log K$ and σ^+ values of p-substituents, X, in XC_6H_4COR (R=H, CH_3 and $N(CH_3)_2$). Similarly, linear relationships of $\log K$ against σ^+ values have been previously mentioned for boron trifluoride complexes of substituted benzamides[14] and for the protonation of substituted acetophenones and benzaldehydes.[12,13]

12) R. Stewart and K. Yates, *J. Am. Chem. Soc.*, **80**, 6355 (1958).

13) K. Yates and R. Stewart, *Can. J. Chem.*, **37**, 664 (1959).

14) B. M. J. Ellul and R. B. Moodie, *J. Chem. Soc., B*, **1967**, 253.

BULLETIN OF THE CHEMICAL SOCIETY OF JAPAN VOL. 42 2371—2372 (1969)

Intensity Ratio between (00*l*) Diffraction Lines of a Coke and a Simple Model of Carbon Layer Plane

Michio INAGAKI

Faculty of Engineering, Nagoya University, Chikusa-ku, Nagoya

(Received November 16, 1968)

It is known that the (004) diffraction line of non-graphitizing carbon is hardly detectable and that it develops gradually to become so with the increase in heat treatment temperature.

In the present work, the X-ray diffraction intensities of (00*l*) lines were measured on polyvinylchloride cokes heat-treated at different temperatures and the change of the intensity ratio between the (00*l*) lines was discussed from the standpoint that it was caused by the change of displacement of carbon atoms in the *c*-direction from the carbon layer plane.

Experimental and Results

The original sample was PV-7, a polyvinylchloride coke carbonized at 680°C. This sample was heat-treated at different temperatures between 1000 and 2600°C for 60 min in the flow of nitrogen by using a graphite resistance tube furnace. The heat treatment temperature (HTT) was measured by an optical pyrometer, which was calibrated by a standard lamp for optical pyrometry. For the heat-treated samples, intensities of (002) and (004) diffraction lines were measured by a fixed counting technique, using a goniometrer with Geiger counter. The measured intensity at each diffraction angle θ was corrected, being divided by Lorentz-polarization, the square of atomic scattering and absorption factors. The corrected intensities were plotted as a function of $\sin\theta$. The area under the profile of (00*l*) line, measured by a planimeter, is the integrated intensity of diffracted beames $I(00l)$ and is proportional to the square of the geometrical structure factor of the line. This proportionality for (002) and (004) lines must be equal to each other since both profiles of the lines were measured on the same specimen. Therefore, the ratio of intensities of (004) to (002) lines, $I(004)/I(002)$, is equal to the ratio of the square of geometrical structure factors of (004) to (002) lines, $|A(004)|^2/|A(002)|^2$.

The observed ratio $I(004)/I(002)$ is shown in

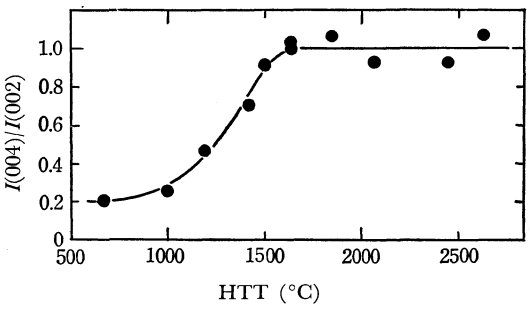

Fig. 1. Change of the observed intensity ratio $I(004)/I(002)$ with HTT.

Fig. 1, as a function of HTT. The ratios for the carbon subjected to heat treatment at low temperature are practically smaller than 1.00. They appear to equal 1.00 above 1600°C.

For the heat-treated samples, the c_0-spacing was measured by using the inner standard of silicon and a recording goniometrer. In Fig. 2, the intensity ratio $I(004)/I(002)$ is plotted against the c_0-spacing of the sample. The sample having c_0-spacing larger than 6.86 Å has an intensity ratio smaller than 1.00.

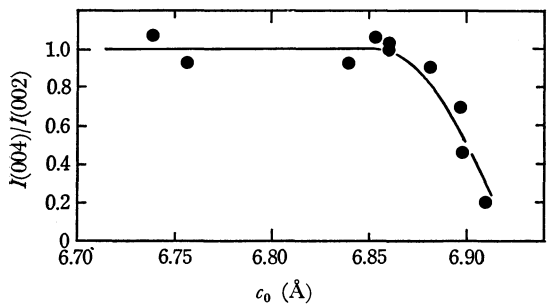

Fig. 2. Change of the observed intensity ratio $I(004)/I(002)$ with c_0-spacing.

Discussion

The measured intensity ratio can have a relatively large error, about ± 0.05 for the sample heat-treated at 2600°C and even greater for the samples subjected to heat treatment at low temperature such as 1400°C. Though no corrections for the instrumental factors were performed, the omission of such corrections was not the cause of the error in the ratio. A large part of the error resulted from the ambiguity of the determination of the background of X-ray diffraction. Even if the ratio $I(004)/I(002)$ has a relatively large ambiguity, the ratios of the carbons heat-treated at low temperatures were found to be actually smaller than the value of graphite 1.00.

The geometrical structure factor of $(00l)$ diffraction lines is given by

$$|A(00l)|^2 = \{\sum \cos 2\pi lz\}^2 + \{\sum \sin 2\pi lz\}^2$$

It depends only on relative position z along c-axis of carbon atoms in a unit cell. In graphite, all carbon atoms are coplanar, having the z-value of 0 and 1/2. The geometrical structure factors of $(00l)$ lines, of which l-index is even, equal one another and the ratio of the two of them equals unity. If some carbon atoms displace from the normal position of graphite by Δz along c-axis, the value of the geometrical structure factor becomes smaller than that of ideal graphite. The effect of reduction is greater for larger l-index lines. Therefore, the observed small ratio of $I(004)/I(002)$ can be interpreted as the result of out-of-plane displacements of carbon atoms. This means that the carbon layers are uneven or wrinkled.

According to the idea mentioned above, the present result shows that the displacement of carbon atoms disappears, in other words, all carbon atoms in carbon layer become coplanar, at about 1600°C or when the c_0-spacing becomes 6.85—6.86 Å. With the idea that the graphitization process is divided into two stages at the c_0-spacing of about 6.85 Å,[1-3] the present result suggests that the structural change in the first stage of the graphitization process ($c_0 > 6.85$ Å) is the decrease in the displacement of carbon atoms, in other words, "dewrinkling" of carbon layer planes, and that the three-dimensional ordering proceeds only after the carbon layer planes are straightened.

The idea of the displacement of carbon atoms is similar to that of Ruland.[4] However, he considered the displacement of carbon atom not only on the first stage but also on the second stage of graphitization process. This wrinkling model presented herewith is also consistent qualitatively with the electron microscopic observation by Kuroda.[5] He observed mosaic structure in a flake of carbon. In the present model, however, wrinkling of carbon is in the atomic scale.

The author wishes to thank Dr. T. Noda, president of Mie University, for his valuable discussions and thorough review of the paper, and Professor Y. Takagi and Professor S. Naka of Faculty of Engineering, Nagoya University, for their valuable discussions.

1) M. Mazza, H. Gasparoux and J. Amiell, *J. Chim. Phys.*, **61**, 729 (1964).
2) A. Forchioni, F. Boisard and P. Delhaes, *ibid.*, **61**, 1289 (1964).
3) M. Inagaki, *Tanso (Carbons)*, No. **53**, 61 (1968); M. Inagaki, Y. Murase and T. Noda, *ibid.*, No. **54**, 80 (1968).
4) W. Ruland, *Acta Cryst.*, **18**, 992 (1965).
5) H. Kuroda, This Bulletin, **32**, 728 (1959).

BULLETIN OF THE CHEMICAL SOCIETY OF JAPAN VOL. 42 2373—2375 (1969)

Asymmetric Hydrogenation of C=O Double Bond with Modified Raney Nickel. XII

Yoshiharu IZUMI, Susumu TATSUMI and Masami IMAIDA

Division of Organic Chemistry, Institute for Protein Research, Osaka University, Kita-ku, Osaka

(Received December 6, 1968)

The asymmetric hydrogenation of methyl acetoacetate to optically active methyl 3-hydroxybutyrate with a Raney nickel catalyst modified with optically active α-amino or α-hydroxy acid has been reported in previous papers of this series.[1,2] In these previous papers, the correlation between the asymmetric activity of the catalyst and the structure of modifying reagent, and the roles of the substituents at the α-asymmetric carbon of a modifying reagent have been discussed, and it has been found that the direction of the asymmetric activity of the catalyst with respect to the optical rotation of the product is decided by the absolute configuration of α-carbon and by the nature of the α-substituents of the modifying reagent. However, the asymmetric activities of the catalysts modified with α-substituted α-amino acids have not been discussed except with 2-methyl- and 2-benzylglutamic acids.

In the present paper, the asymmetric activities of the catalysts modified with (+)-isovaline and with (−)-2-methylaspartic acid are decribed; the results are compared with those obtained with 2-aminobutyric acid and aspartic acid in Table 1 and Fig. 1 respectively, in order to investigate the effect on the asymmetric activity of the replacement of an α-hydrogen of the modifying reagent with a methyl group. Moreover, as the absolute configuration of (+)-2-benzylglutamic acid was confirmed by means of the X-ray diffraction method by Kakudo *et al.*,[3] the relationship between the direction of the asymmetric activity of the catalyst with respect to the optical rotation of the product and the absolute configuration of the α-substituted amino acid used for modification is discussed in this report.

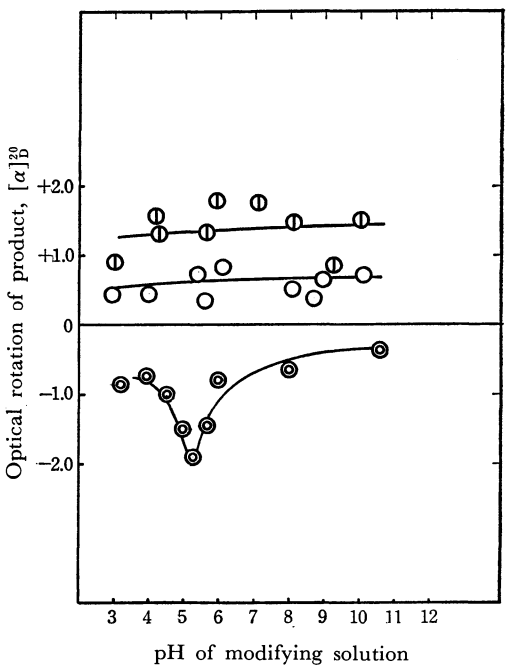

Fig. 1. Modifications with (−)-2-methylaspartic acid and L-aspartic acid.
—◑— (−)-2-Methylaspartic acid (modifying temp.: 100°C)
—○— (−)-2-Methylaspartic acid (modifying temp.: 0°C)
—◎— L-Aspartic acid (modifying temp.: 0°C)

TABLE 1. MODIFICATIONS WITH (+)-ISOVALINE AND L-2-AMINOBUTYRIC ACID

Modifying reagent	Modifying conditions		$[\alpha]_D$ of methyl 3-hydroxybutyrate
	pH	Temp. °C	
(+)-Isovaline	6.0	0	−0.66
	6.0	100	−0.65
L-2-Aminobutyric acid	6.05	0	−1.46
	5.85	100	−1.61

Experimental

Preparation of Catalyst. One and a half grams of Raney nickel alloy (Ni : Al=40 : 60) were added in small portions to 20 m*l* of a 20% sodium hydroxide solution over a 5-min period, and then the solution was allowed to stand for 45 min at 80°C. The nickel catalyst was washed several times with water.

Modification of Catalyst. An aqueous solution of the modifying reagent, the pH and the temperature of

1) Part X: Y. Izumi, K. Matsunaga, S. Tatsumi and M. Imaida, This Bulletin, **41**, 2515 (1968); Part XI: Y. Izumi, M. Imaida, T. Harada, T. Tanabe, S. Yajima and T. Ninomiya, *ibid.*, **42**, 241 (1969).

2) S. Tatsumi, *ibid.*, **41**, 408 (1968).

3) T. Ashida, Y. Sasada and M. Kakudo, This Bulletin, **40**, 476 (1967).

which had been adjusted to specified values, was added to a newly-prepared Raney nickel catalyst, and then the mixture was allowed to stand at the specified temperature, with occasional shaking, for 1.5 hr. After the modifying solution had been removed by decantation, the catalyst was washed once with water and twice with methanol.

Measurement of the Asymmetric Activity of the Catalyst. Redistilled methyl acetoacetate (18 ml) was hydrogenated in the presence of a modified Raney nickel catalyst which had been prepared from 1.5 g of an alloy. The reaction was run at 60°C under an initial hydrogen pressure of 80—100 kg/cm² in a shaking autoclave. The reduction product was filtered to remove the catalyst and then distilled under reduced pressure (bp 61—62°C/12 mmHg). The purity of the methyl 3-hydroxybutyrate was tested by gas chromatography. The optical rotatory power of the distilled product was measured by a conventional polarimeter in 1-dm tube at 20°C without dilution; the value was taken as the specific rotation because the density of methyl 3-hydroxybutyrate is nearly 1.0. According to Levene and Haller,[4] the optical rotatory power of methyl D-3-hydroxybutyrate is $[\alpha]_D^{20}$ −20.9.

Results and Discussion

Effect of the Modifying Temperature.[*1]

1) Isovaline. The effect of the modifying temperature on the catalyst modified with isovaline is shown in Table 1. No remarkable change in the asymmetric activity of the catalyst with the modifying temperature was found.

2) 2-Methylaspartic Acid. As is shown in Fig. 1, the asymmetric acitivity of the catalyst increases with the elevation of the modifying temperature, while on modification with aspartic acid it decreases with the elevation of the modifying temperature.[5] The tendency found in the modification with 2-methylaspartic acid was also observed in the cases of modification with 2-methyl- and 2-benzylglutamic acid, as has been reported in a previous paper.[6]

Effect of the Modifying pH.[*2]

The modifying pH does not so strongly affect the asymmetric activity of the catalyst in the case of modification with 2-methylaspartic acid as in the case of modification with 2-methyl- or 2-benzylglutamic acid,[6] as is shown in Fig. 1.

Correlation of the Direction of the Asymmetric Activity of the Catalyst and the Absolute Configuration of α-Substituted α-Amino Acid.

The configurations of (+)-isovaline,[7] (−)-2-methylaspartic acid,[8] and (+)-2-benzylglutamic acid[3] are written in the conventional Fischer diagram as follows:

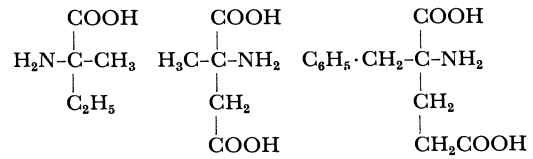

(+)-isovaline (−)-2-methylaspartic acid (+)-2-benzylglutamic acid

Thus, (+)-isovaline can be assigned either an L- or a D-configuration, depending on whether it is considered as a derivative of L-2-aminobutyric acid or of D-alanine. In a like manner, (+)-2-benzylglutamic acid and (−)-2-methylaspartic acid can be considered as a derivative of L-phenylalanine or of D-glutamic acid and as a derivative of L-alanine or of D-aspartic acid respectively. Moreover, Meister and his co-workers have suggested, after investigations using the biochemical method, that the (+)-isomer of 2-methylglutamic acid can be considered as a derivative of L-glutamic acid.[9] Meanwhile, catalysts modified with (+)-isovaline, with (−)-2-methylaspartic acid, and with (+)-2-benzylglutamic acid at 0°C gave predominantly methyl D-(−)-, L-(+)- and L-(+)-3-hydroxybutyrate respectively as the hydrogenation products.

These facts show that the direction of the asymmetric activity of the catalyst modified with α-substituted α-amino acid conforms to the general rule that the catalyst modified with L (or D)-α-amino acid at 0°C gives methyl D (or L)-3-hydroxybutyrate as the hydrogenation product when the α-substituted α-amino acid is considered as a derivative of the α-amino acid, which is more effective for the preparation of a catalyst with a high asymmetric activity. For example, the catalyst modified with optically active 2-aminobutyric acid at 0°C has a higher asymmetric activity than that modified with optically active alanine, and so in the case of the catalyst modified with (+)-isovaline at 0°C, the direction of the optical rotation of the product conforms to the general rule when the compound is considered as a derivative of L-2-aminobutyric acid.

Effect of the α-Alkyl Substituent of α-Amino Acid on the Formation of the Asymmetrically Active Center. The asymmetric activities of the catalysts modified with isovaline and with 2-methylaspartic acid are increased or

4) P. A. Levene and H. L. Haller, *J. Biol. Chem.*, **65**, 51 (1925).

*1 "Modifying temperature" means the temperature of the aqueous solution of the modifying reagent.

5) Y. Izumi, M. Imaida, H. Fukawa and S. Akabori, This Bulletin, **36**, 155 (1963).

6) Y. Izumi, S. Tatsumi, M. Imaida, Y. Fukuda and S. Akabori, *ibid.*, **38**, 1206 (1965).

*2 "Modifying pH" means the pH of the aqueous solution of the modifying reagent.

7) S. Yamada and K. Achiwa, *Chem. Pharm. Bull. Tokyo*, **12**, 1525 (1964).

8) S. Terashima, K. Achiwa and S. Yamada, *ibid.*, **14**, 572 (1966).

9) H. M. Kagan, L. R. Manning and A. Meister, *Biochemistry*, **4**, 1063 (1965).

at least not affected with the elevation of the modifying temperature. On the contrary, those with 2-aminobutyric acid and with aspartic acid decrease with the elevation of the modifying temperature. As the same results were obtained with α-substituted amino acids and with β-alkyl substituted amino acids, it can be assumed that the α-substituent has the same effect as the β-alkyl substituent on the formation of an asymmetrically active center on the surface of the catalyst. That is, in the case of modification with α- or β-alkyl substituted α-amino acid, the proportion of the (−)- to the (+)-asymmetrically active centers*3 on the surface of the catalyst does not greatly change with the modifying temperature.

The authors wish to express their thanks to Professor Masao Kakudo for the determination of the absolute configuration of (+)-2-benzylglutamic acid by means of the X-ray diffraction method.

This research was supported by the Kawaken Fine Chemicals Co., Ltd., Tokyo.

*3 "(+) (or (−))-asymmetrically active center" means the asymmetric center on the surface of the catalyst in which methyl L-(+) (or D-(−))-3-hydroxybutyrate is preferentially produced in hydrogenation of methyl acetoacetate. For example, on modification with L-glutamic acid, the catalyst modified at 0°C, which produces predominantly methyl D-(−)-3-hydroxybutyrate, contains predominantly (−)-asymmetrically active center, while the catalyst modified at 100°C, which produces predominantly methyl L-(+)-3-hydroxybutrate, contains predominantly (+)-asymmetrically active center.

BULLETIN OF THE CHEMICAL SOCIETY OF JAPAN VOL. 42 2375—2376 (1969)

Studies of Japanese Lacquer: Isolation of a Diphenyl Dimer of Urushiol

Takashi KATO and Ju KUMANOTANI

The Engineering Research Institute, Faculty of Engineering, The University of Tokyo, Bunkyo-ku, Tokyo

(Received December 9, 1968)

It is well known that Japanese lacquer oxidatively polymerizes under the action of laccase to form dried films with excellent properties. Previously, in order to elucidate the behavior of urushiol in the drying process, we have separated by thin-layer chromatography (TLC) three unknown components (with R_f 0.37, 0.27 and 0.20; 1 : 1 : 0.5 by wt, respectively) from a mildly-oxidized sap of the Japanese lacquer tree (*Rhus vernicifera* D. C. in Japan).[1]

It is the aim of the present paper to clarify the point that the component with R_f 0.20 (designated as D) is a diphenyl derivative (Ia) of urushiol. This has been proved by the separation of the hydrogenated D (Ib; 3,4,3',4'-tetrahydroxy-5,5'-dipentadecyldiphenyl) from the hydrogenated polymeric urushiol by TLC and by its derivation to the acetyl derivative (Ic). The identification of (Ic) was performed as follows: It is evident that the acetyl derivative of the hydrogenated D was a derivative of a dimeric urushiol on the basis of the results of elemental analysis and molecular weight measurement. The diphenyl structure was confirmed by the UV spectral absorption (λ_{max}^{EtOH} 256 mμ, ε 2.15×10^4).[2] Among the possible six isomers the identity of the compound with Ic was established by the NMR spectrum of the phenyl protons. A quartet (4H, $J=2$ cps) characteristic of the AB system[3] was observed in the region of τ 2.5—2.8. The small J-value indicates that two protons in the AB system were present in the meta position.[3]

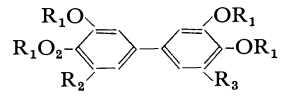

(I)

a: $R_1=H$; R_2, R_3=arbitrary side chain of urushiol
b: $R_1=H$; R_2, $R_3=C_{15}H_{31}$
c: $R_1=COCH_3$; R_2, $R_3=C_{15}H_{31}$

It is already known that tetrahydroxydiphenyl is formed in the reaction of *o*-quinone with cate-

1) T. Kato and J. Kumanotani, *J. Polymer Sci.* Part A-1, accepted, "Studies of Japanese Lacquer: Urushiol Dimerization by the Coupling Reaction between Urushiol Quinone and a Triolefinic Component of Urushiol."

2) K. Hirayama, "Handbook of Ultraviolet and Visible Absorption Spectra of Organic Compounds," Plenum Press Data Division, A Division of Plenum Publishing Corporation, New York (1967), p. 113.

3) R. M. Silverstein and G. C. Bassler, "Spectrometric Identification of Organic Compounds," John Wiley & Sons, Inc., New York, N.Y. (1967), pp. 118, 145.

chol in an aqueous medium,[4,5] and that urushiol quinone is formed[6] at an early stage of the oxidative polymerization of the sap of the Japanese lacquer tree. It seems, therefore, reasonable to assume that D (Ia) was formed by the reaction between urushiol and urushiol quinone.

Experimental[7]

Separation of a Diphenyl Dimer of Urushiol. The polymeric urushiol was obtained by the method reported previously[1] from a mildly-oxidized sap of the Japanese lacquer tree. The polymeric urushiol was hydrogenated at room temperature under an atmospheric pressure of hydrogen over 5% Pd-on-charcoal. The hydrogenated polymeric urushiol was dissolved in chloroform and applied as a spot on the silica-gel layer (thickness, 0.25 mm), which was made from Silica Rider (silica-gel with 12—14% calcium sulfate, purchased from the Daiichi Pure Chemicals Co.) and activated at 105°C for 1.5 hr. It was then chromatographed in a chloroform - ethyl acetate (87 : 13 v/v) solvent tank using the ascending technique. The developing distance was 12—14 cm. A filter paper (20×20 cm) impregnated with the developing solvent was inserted into the tank in order to saturate the atmosphere with the solvent-vapor. The chromatogram gave, when sprayed with a methanol-1% $FeCl_3$ solution, spots with R_f values of 0.50 (urushiol, dark violet), 0.37 (dark brownish green), 0.27 (dark violet) and 0.20 (dark violet), and others with smaller R_f values including a spot of the starting point. The compound with R_f 0.20 (the hydrogenated D) was then collected by TLC in the same manner as that described previously.[1] About 0.1 g of the purified, hydrogenated D which gave only one spot (with R_f 0.20) in its TLC, was obtained from 4 g of the hydrogenated polymeric urushiol. The hydrogenated D (91 mg) was acetylated at 50—60°C for 1 hr in a mixture of acetic anhydride (5 m*l*) and phosphoric acid (0.1 m*l*) under stirring, and the solution was further allowed to stand overnight at room temperature. The reaction mixture was shaken well with water (50 m*l*, *ca.* 60°C), and extracted with benzene (50 m*l*). The benzene extract was then washed with water (50 m*l*×3), and dried over calcium chloride. An oily material was obtained by the removal of the benzene in vacuum. It was examined by TLC (Silica Rider: thickness, 0.25 mm; developing solvent, chloroform - *n*-hexane, 3 : 2 v/v). The spots were detected by spraying with an aqueous sulfuric acid solution (1 : 1) and by heating at 150°C for 30 min, and the compound with R_f 0.26 was found to be a major product. It was collected by TLC using two silica-gel plates (1 mm thick). The separated material was crystallized from *n*-hexane - ether, and a white crystal (20 mg) was obtained, mp 99—100°C (corr.). UV λ_{max}^{EtOH} 256 mμ (ε 2.15×10^4); IR ν(KBr) 2920 (vs), 2860(s), 1770 (vs), 1599(w), 1478(s), 1378(s), 1259(m), 1208(vs), 1175(vs) 1113(w), 1030(m), 1014(m), 900(m), 873(w), 826(w), 775(w) and 720 cm^{-1} (w); NMR ($CDCl_3$) τ 2.5—2.8 (4H, quartet, J=2 cps, phenyl protons), 7.42 (4H, triplet, J=7 cps, protons of methylenes adjacent to benzene ring), 7.65 and 7.70 (each 6H, singlet, acetyl protons), 8.1—8.9 (52H, methylene protons), 9.11 (6H, triplet, J=5 cps, methyl protons).

Found: C, 74.48; H, 10.46%; mol wt, 760. Calcd for $C_{50}H_{78}O_8$: C, 74.40; H, 9.74%: mol wt, 807.2.

4) E. J. Grossman, Dissertation Columbia Univ., 1960, Mic 60-3076, Univ. Microfilms, Inc., Ann Arbor, Michigan.

5) W. G. C. Forsyth and V. C. Quesnel, *Biochim. Biophys. Acta*, **25**, 155 (1957).

6) J. Kumanotani, T. Kato and A. Hikosaka, paper presented at International Symposium on Macromolecular Chemistry, Tokyo and Kyoto, 1.5.01, 1966; *J. Polymer Sci.* Part C, in press.

7) The infrared spectra were obtained with a Nihon-Bunko IR-spectrophotometer, Model IR-S. The ultraviolet spectra were taken with a Hitachi spectrophotometer, EPS-2. The NMR spectra were determined with a Nihon-Denshi NMR spectromteter, JMN C-60. The chemical shifts are described in τ values relative to tetramethylsilane as an internal standard. The molecular weights were measured in methyl ethyl ketone with a vapor pressure osmometer, Model 301-A, Mechrolab., Inc.

BULLETIN OF THE CHEMICAL SOCIETY OF JAPAN VOL. 42 2377—2379 (1969)

Laser-induced Chemical Reaction. II. Reaction Induced by a Giant Pulse Laser

Ko TAKI, Pil Hyon KIM and Susumu NAMBA

The Institute of Physical and Chemical Research, Yamato-machi, Saitama

(Received December 9, 1968)

In a previous paper,[1] the reaction of hydrocarbons with carbon vapor produced by the irradiation of a normal laser on graphite carbon has been reported. From the distribution of the reaction products and from the results of a spectroscopic analysis, it was assumed that diatomic carbon (C_2) plays a dominant role. In this paper, the investigation of the reaction induced by a giant pulse ruby laser is described.

Experimental

The output power and the pulse width of the giant pulse laser used were 30 MW and 20 nsec respectively. The total output energy was 0.6 J, one-fifth of that of the normal laser in the previous report. The laser beam was focused by a lens 30 mm in focal length upon a carbon target placed in a 7 cc Pyrex cell filled with the vapor of hydrocarbons. After a 10—20 pulse irradiation, an analysis was peformed by gas chromatography using a silica gel and a squalane column. A quantitative analysis was also performed by mixing standards in the sample.

Results and Discussion

The reaction products in hydrogen are listed in Table 1, while the reaction products in ethylene and methane vapor at 10 Torr pressure are shown in Table 2. The gas pressure of 10 Torr was chosen so as to avoid any breakdown caused by the focused giant pulse laser. At a pressure higher than 100 Torr a breakdown was observed, as will be described later. Although the main products were C_2 compounds, as in the case of a normal laser reaction,

TABLE 1. REACTION PRODUCTS IN HYDROGEN

Product	Yield ($\times 10^{-6}$ mol)	
	Normal laser (10 pulse irradiation in 700 Torr H_2)	Giant pulse laser (20 pulse irradiation in 720 Torr H_2)
Methane	0.3—0.4	0.1
Ethane	0	0.01
Ethylene	0	0
Acetylene	15.0—20.0	0.4

the ratios of methane and ethane to acetylene were higher than those in normal laser reactions. This fact suggests that the distribution of carbon oligomers produced by the giant pulse laser is different from that produced by the normal laser; that is, the fraction of the monoatomic carbon (C_1) is larger in the former than in the latter. This may be due to the difference in the surface temperature of the carbon target. The estimated temperature[2,3] in the giant pulse laser is higher than in the normal laser.

The breakdown[4,5] of the gas is known to be caused by the focused giant pulse laser. When the laser beam was focused on a carbon target, a breakdown of gases was observed in the focused-on region. In this case, the product ratios were a little different from those in the breakdown without a target. This may be due to the fact that most of the energy of the laser beam is spent producing the breakdown. The yields of products in the breakdown of various substrates are shown in Table 3.*1 Spectroscopically, C_2 Swan bands were observed in the breakdown of these gases, as had previously been observed by Adelman.[6] These facts suggest that the products are mainly formed by the reaction of the substrate with the C_2 produced in the breakdown.

It is hard to produce the breakdown in gas at a low pressure.[5] No breakdown was, for instance, observed at 10 Torr ethylene or methane. However, in a mixture of 10 Torr ethylene and 750 Torr argon (ethylene mol fraction is 0.013), a breakdown was observed and argon lines were detected spectroscopically.

The product ratios, CH_4/C_2H_2 and C_2H_6/C_2H_2, and that of C_3 products to C_4 products are plotted as a function of the partial pressure of ethylene in the mixture with argon in Fig. 1. The figure shows

1) K. Taki, P. H. Kim and S. Namba, This Bulletin, **42**, 823 (1969).

*1 The breakdown was not observed in the case of a normal laser.

2) S. Namba, P. H. Kim and A. Mitsuyama, *J. Appl. Phys.*, **37**, 3330 (1966).

3) S. Namba, P. H. Kim, T. Itoh, T. Arai and H. Schwarz, *Sci. Papers I.P.C.R.*, **60**, 101 (1966).

4) R. G. Meyer and A. F. Haught, *Phys. Rev. Letters*, **11**, 401 (1963).

5) R. W. Minck, *J. Appl. Phys.*, **35**, 252 (1964).

6) A. H. Adelman, *J. Chem. Phys.*, **45**, 3152 (1966).

Table 2. Reaction products in ethylene and methane vapor at 10 Torr pressure

Substrate	Product	Yield ($\times 10^{-6}$ mol)	
		Normal laser (10 pulse irradiation)	Giant pulse laser (12 pulse irradiation)
Ethylene	Methane	0.007	0.014
	Ethane	trace	0.009
	Acetylene	1.6	0.47
	C_3-Compounds	trace	0.018
	C_4-Compounds	0.48	0.19
Methane	Ethane	0.022	0.084
	Acetylene	1.52	0.32
	C_3-Compounds	0.02	0.024
	C_4-Compounds	0.5	0.19

Table 3. Products yields in the breakdown of various substrates

Product	Yield ($\times 10^{-6}$ mol) in 10 pulse irradiation			
	Substrate			
	Methane	Ethane	Ethylene	Cyclopropane
Methane		0.5—0.7	0.05—0.08	0.4—0.5
Ethane	0.1—0.2		0.2—0.3	0.02
Ethylene	0	0.3—0.5		0
Acetylene	0.5—0.7	1.1—1.4	1.7—2.7	0.8—1.2
C_3-Products	0.1	0.3	0.03	
C_4-Products	0.1	0.2	0.4—0.5	0
Propane				0.1
Propylene				1.5—2.0

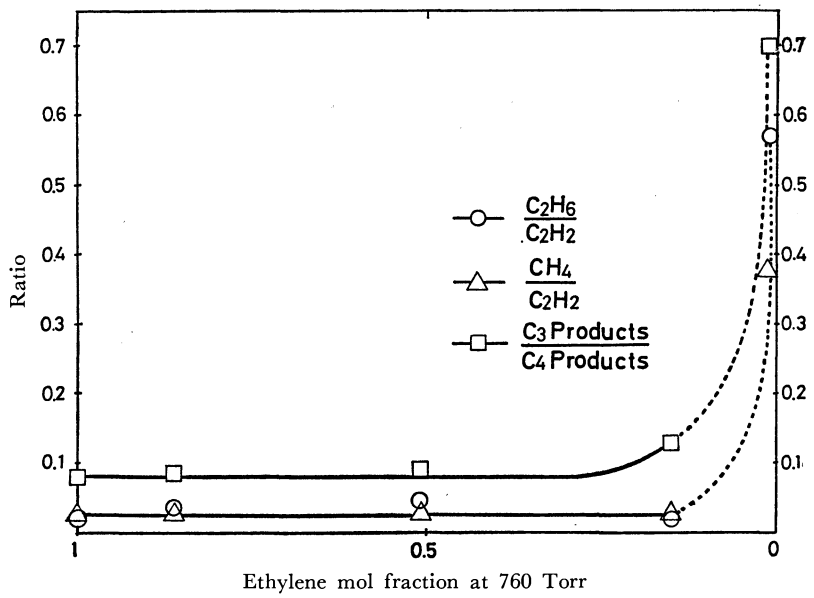

Fig. 1. Relation between product ratios and gas pressure in the mixture of ethylene and argon.

TABLE 4. RELATIVE YIELD IN THE γ-RADIOLYSIS AND IN THE LASER IRRADIATION IN THE MIXTURE OF ETHYLENE AND ARGON

Product	Relative G value in γ-radiolysis			Relative yield in laser irradiation
	Ethylene mol fraction in Ar			
	1.0*	0.7*	0.013	0.013
Methane			0.13	0.38
Ethane	0.26	0.18	0.16	0.57
Acetylene	1.00	1.00	1.00	1.00
n-Butane	0.33	0.26	0.18	0.35
C_3-Products			0.17	0.27

* From Ref. 7.

that the product ratios remain constant in the region of higher mol fractions (0.15) of ethylene, but at lower concentrations (0.013) these ratios rise sharply. At a higher partial pressure of ethylene, a breakdown reaction may occur on the ethylene molecule because its ionization potential (10.5 eV) is lower than that of argon (15.7 eV). On the other hand, at a lower concentration, breakdown may occur mainly on the argon rather than on the ethylene molecule, and the reaction products may be almost entirely formed by the decomposition of the excited ethylene produced by energy transfer to ethylene from the excited argon formed by the breakdown. The radiolysis of an inert gas and hydrocarbon mixture has been known to involve energy transfer reaction. However, the product ratios in the radiolysis of a 10-Torr-ethylene and 750-Torr-argon mixture are different from those in laser irradiation, as Table 4 shows. Radiolysis was performed at room temperature, and the total dose was about 10^{19} eV. This difference might be due to the difference between the reactions in the excited states of ethylene.

The methane and argon system showed almost identical results; ethane was the only condensable product at the pressure of 10 Torr methane and 750 Torr argon. In the presence of nitric oxide (4 Torr), the breakdown of the mixture of methane (12 Torr) and argon (744 Torr) did not give ethane. This suggests that the reaction involves free radical processes, as in the case of radiolysis. The radiolysis of methane[8-10] and a methane-argon mixture[11] has been known to involve free radical processes and to produce hydrogen and ethane, but not acetylene.

In the giant pulse laser-induced reaction, diatomic carbon (C_2) is considered to play a dominant role, but at a low concentration of the substrate in the argon mixture the reaction process may be due to the energy transfer from argon.

The authors wish to express their appreciation to Miss Kumiko Motegi for her valuable assistance.

7) F. W. Lampe, *Rad. Research,* **10**, 691 (1959).

8) F. W. Lampe, *J. Am. Chem. Soc.*, **79**, 1055 (1957).

9) S. C. Lind and D. C. Bardwell, *ibid.*, **48**, 2335 (1926).

10) K. Yang and P. J. Manno, *J. Phys. Chem.*, **63**, 752 (1959).

11) G. G. Meisels, W. H. Hamill and R. R. Williams, Jr., *ibid.*, **61**, 1456 (1957).

BULLETIN OF THE CHEMICAL SOCIETY OF JAPAN VOL. 42 2380—2382 (1969)

Synthetic Studies of the Flavone Derivatives. XI.*1 The Synthesis of 4′,5,7-Trihydroxy-3,8-dimethoxyflavone, A Pigment from *Cyanostegia angustifolia* Turcz.

Kenji FUKUI, Takashi MATSUMOTO and Sachihiko TANAKA

Department of Chemistry, Faculty of Science, Hiroshima University, Higashi-sendamachi, Hiroshima

(Received December 17, 1968)

Recently, Ghisalberti *et al.*[1] reported the isolation of two new pigments from the leaves and terminal branches of *Cyanostegia angustifolia* Turcz.; they proposed, on the basis of chemical and spectral studies, that the structures of these pigments were 4′,5,7-trihydroxy-3,3′,8-trimethoxyflavone (I) and 4′,5,7-trihydroxy-3,8-dimethoxyflavone (II).

In a previous paper,[2] we reported on the total synthesis of I and its identity with a natural pigment. The present paper will describe a total synthesis of II. The experimental details of the present work are essentially the same as those of the previous paper,[2] involving an oxidative demethylation[3] of the 5,8-dimethoxyflavone derivative with nitric acid.

According to Allan-Robinson's flavone synthesis,[4] the condensation of 2,4-dihydroxy-3,6,ω-trimethoxyacetophenone[5] (III) with 4-benzyloxybenzoic anhydride[6] (IV) gave 4′-benzyloxy-7-hydroxy-3,5,8-trimethoxyflavone (V), which was then benzylated to the 7-benzyl ether (VI). The compound VI was also obtained by a similar condensation of 4-benzyloxy-2-hydroxy-3,6,ω-trimethoxyacetophenone[5] (VII) with IV. The oxidative demethylation of VI with nitric acid gave the 5,8-quinone derivative (VIII) as an intermediate; this was then easily reduced to the corresponding 5,8-dihydroxy compound (IX). The partial methylation of IX with diazomethane gave 4′,7-dibenzyloxy-5-hydroxy-3,8-dimethoxyflavone (X), which was then debenzylated to give the desired flavone (II), mp 247—249°C and 257—258°C, by catalytic hydrogenolysis over Pd-C. The synthetic flavone (II) was shown to be identical with the natural pigment by a mixed-melting-point determination and by a comparison of their IR and UV spectra.

We next turned our attention to an investigation of another effective method. Since it is well known that 3,5-dimethoxyflavone derivatives are demethylated at the 5-position with anhydrous aluminum chloride in ether,[7] a partial demethylation of 4′,7-dihydroxy-3,5,8-trimethoxyflavone (XI), prepared from V, with anhydrous aluminum chloride in ether was carried out in the hope of obtaining the 5-hydroxy compound (II). The product obtained was yellow crystals, mp above 300°C, which were characterized as triacetate, mp 173—175°C,*2 and trimethylated ether (XIII). The flavone (XIII) was also obtained by the methylation of XI with diazomethane; this proved that there was no isomeric change during the demethylation of XI.

The physical properties of the demethylated flavone did not agree with those of the natural pigment. The NMR spectrum of the demethylated flavone in dimethyl sulfoxide-d_6 showed the presence of two methoxyl groups, at δ 3.84 and 3.87 (each a 3H singlet); of five aromatic protons, at δ 6.51 (singlet, C_6–H), 7.01 (doublet, $C_{3'}$–H and $C_{5'}$–H) and 8.12 (doublet, $C_{2'}$–H and $C_{6'}$–H), and three hydroxyl groups, at δ 8.74, 10.04, and 10.50 (each a 1H singlet). In the UV spectra summarized in Table 1, a long-wavelength band of the demethylated flavone in ethanol undergoes a large bathochromic shift (59 mμ) upon the addition of aluminum chloride;[8] this shows the presence of a free 3-hydroxyl group. The demethylated flavone is unstable in an alkaline solution, for when

*1 Part X: K. Fukui, T. Matsumoto and S. Tanaka, This Bulletin, **42**, 1398 (1969). Parts of this work have been briefly communicated: K. Fukui, T. Matsumoto, M. Nakayama and T. Horie, *Experientia*, **25**, 349 (1969).

1) E. L. Ghisalberti, P. R. Jefferies and C. I. Stacey, *Australian J. Chem.*, **20**, 1049 (1967).

2) K. Fukui, T. Matsumoto, M. Nakayama and T. Horie, This Bulletin, **41**, 2805 (1968).

3) M. Krishnamurti, T. R. Seshadri and P. R. Shankaran, *Tetrahedron*, **22**, 941 (1966), and the references cited therein.

4) J. Allan and R. Robinson, *J. Chem. Soc.*, **1924**, 2192.

5) V. D. N. Sastri and T. R. Seshadri, *Proc. Indian Acad. Sci.*, **24A**, 238 (1946).

6) S. E. Flores, J. Herran and H. Menchace, *Tetrahedron*, **4**, 132 (1958).

7) J. Gripenberg, "The Chemistry of Flavonoid Compound," ed. by T. A. Geissman, Pergamon Press, Oxford (1962), Chap. 13.

*2 The natural pigment gave triacetate; mp 167—168°C.[1]

8) L. Jurd, Ref. 7, Chap. 5.

Table 1. Ultraviolet spectea of XII, synthetic and natural II

	λ_{max} mμ (log ε)				
	EtOH	$AlCl_3$*3	NaOH*4	NaOH-HCl*5	NaOAc*6
XII	270 (4.25)	267 (4.35)	297 (4.22)	269 (4.25)	280 (4.33)
	294 (3.98)	341 (3.79)	316 (4.24)	295*7 (4.04)	381 (4.15)
	369 (4.24)	428 (4.28)	340 (4.23)		
Synthetic II	274 (4.36)	284 (4.30)	284 (4.42)	274 (4.18)	284 (4.42)
	310*7 (4.16)	313 (4.19)	334 (4.15)	310*7 (3.89)	304*7 (4.23)
	326 (4.19)	352 (4.25)	412 (4.42)	330 (4.21)	371 (4.06)
	360 (4.15)	417 (4.02)		361 (4.00)	
Natural II	274 (4.28)	284 (4.23)	284 (4.38)	274 (4.26)	281 (4.31)
	310*7 (4.08)	313 (4.13)	335 (4.08)	310*7 (4.04)	304*7 (4.14)
	326 (4.13)	352 (4.20)	412 (4.36)	328 (4.10)	369 (4.00)
	360 (4.09)	417 (3.95)		360 (4.08)	

*3 0.002 mol/*l*.
*4 Added one drop of aqueous sodium hydroxide (4%).
*5 The alkaline solution was acidified with dilute hydrochloric acid.
*6 Saturated with fused sodium acetate.
*7 Inflection.

the alkaline solution is acidified, the long-wavelength band of the parent spectrum in ethanol disappears. This suggests the presence of a free 3,4'-dihydroxyl group.[8] The presence of a free 7-hydroxyl group is also indicated by the bathochromic shift (10 mμ) of the short-wavelength band in the presence of fused sodium acetate.[8] From this spectral evidence, the structure of the demethylated flavone was established to be 3,4',7-trihydroxy-5,8-dimethoxyflavone (XII).

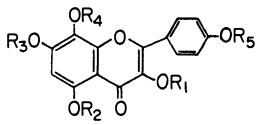

II $R_1=R_4=Me$, $R_2=R_3=R_5=H$
V $R_1=R_2=R_4=Me$, $R_3=H$, $R_5=C_6H_5CH_2$
VI $R_1=R_2=R_4=Me$, $R_3=R_5=C_6H_5CH_2$
IX $R_1=Me$, $R_2=R_4=H$, $R_3=R_5=C_6H_5CH_2$
X $R_1=R_4=Me$, $R_2=H$, $R_3=R_5=C_6H_5CH_2$
XI $R_1=R_2=R_4=Me$, $R_3=R_5=H$
XII $R_1=R_3=R_5=H$, $R_2=R_4=Me$
XIII $R_1=R_2=R_3=R_4=R_5=Me$

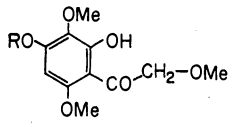

III R=H
VII R=$C_6H_5CH_2$

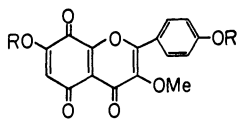

VIII R=$C_6H_5CH_2$

Experimental*8

4'-Benzyloxy-7-hydroxy-3,5,8-trimethoxyflavone (V). A mixture of III (7.2 g), IV (33.0 g), and potassium 4-benzyloxybenzoate (16.0 g) was ground together and heated at 180°C in an oil bath for 5 hr. The reaction mixture was cooled, powdered, and then refluxed for 30 min with a solution of ethanol (300 m*l*) and potassium hydroxide (30 g) in water (60 m*l*). The solvent was removed under a vacuum and washed with water; then the residue was again treated with an ethanolic alkaline solution as described above. The crude product was washed with hot water and hot acetone successively. The acetone-insoluble part was recrystallized from acetic acid to give yellow needles of V; mp 240—242°C; yield 2.0 g.

Found: C, 68.85; H, 4.97%. Calcd for $C_{25}H_{22}O_7$: C, 69.11; H, 5.10%.

4',7-Dibenzyloxy-3,5,8-trimethoxyflavone (VI). *a) From V.* The compound V (30 mg) was benzylated to give colorless needles of VI, mp 149—150°C (from aqueous methanol), which gave a negative ferric chloride reaction in ethanol; yield, 20 mg.

Found: C, 73.12; H, 5.39%. Calcd for $C_{32}H_{28}O_7$: C, 73.27; H, 5.38%.

b) From VII. A mixture of VII (1.9 g), IV (4.0 g), and potassium 4-benzyloxybenzoate (2.5 g) was treated by a method similar to that used for V. The crude product was recrystallized from methanol to give VI mp 149—150°C, which was undepressed on admixture with the sample of a); yield, 0.5 g.

4',7-Dibenzyloxy-5,8-dihydroxy-3-methoxyflavone (IX). A suspension of VI (320 mg) in nitric acid (45%: 7.0 m*l*) was stirred vigorously at 40°C for 10 min. After the mixture had been cooled, the dark brown precipitate (VIII) was collected, washed with water, and dissolved in acetic acid (10 m*l*). The solution was heated on a steam bath with sodium sulfite heptahydrate (1.5 g) for 1 min, and then diluted with water. The yellow precipitate was collected, washed

*8 All the melting points are uncorrected. The NMR spectra were taken on a Hitachi Model R-20 NMR spectrometer (60 Mc/sec), using tetramethylsilane as the internal standard; their chemical shifts are presented in terms of δ values; s: singlet, d: doublet.

with water, and recrystallized from acetone to give yellow needles of IX, mp 201—203°C, which gave a green ferric chloride reaction in ethanol; yield, 180 mg.

Found: C, 72.39; H, 4.68%. Calcd for $C_{30}H_{24}O_7$: C, 72.57; H, 4.87%.

4′,7-Dibenzyloxy-5-hydroxy-3,8-dimethoxyflavone (X). The flavone IX (120 mg) was methylated with diazomethane to give yellow needles of X, mp 161—162°C (from acetone-methanol), which gave a green ferric chloride reaction in ethanol; yield, 100 mg.

Found: C, 73.19; H, 5.11%. Calcd for $C_{31}H_{26}O_7$: C, 72.93; H, 5.13%.

4′,5,7-Trihydroxy-3,8-dimethoxyflavone (II). A solution of X (80 mg) in ethyl acetate (25 m*l*) was submitted to catalytic hydrogenolysis at room temperature in the presence of Pd-C (10%: 100 mg). The product was recrystallized from aqueous methanol to give yellow needles of II, mp 247—249°C and 257—258°C, which gave a green ferric chloride reaction in ethanol; yield, 35 mg. This flavone was shown to be identical with the natural pigment (mp 246—248°C and 256—258°C)*[9] by a mixed-melting-point determination and by a comparison of their IR and UV spectra.

Found: C, 61.82; H, 4.39%. Calcd for $C_{17}H_{14}O_7$: C, 61.82; H, 4.27%.

4′,7-Dihydroxy-3,5,8-trimethoxyflavone (XI). A mixture of V (1.8 g), Pd-C (5%: 1.5 g), and acetic acid (350 m*l*) was treated by a method similar to that used for II. The crude product was recrystallized from acetic acid to give XI, mp 290—292°C; yield, 1.0 g.

Found: C, 62.67; H, 4.55%. Calcd for $C_{18}H_{16}O_7$: C, 62.79; H, 4.68%.

3,4′,7-Trihydroxy-5,8-dimethoxyflavone (XII). A mixture of XI (600 mg), anhydrous aluminum chloride (5.0 g), and dry ether (60 m*l*) was refluxed for 8 hr. The mixture was poured into dilute hydrochloric acid (3 N: 200 m*l*). After the ether had been removed, the precipitate was collected, washed with water, and then recrystallized from aqueous pyridine to give pale yellow needles of XII, mp above 300°C, which gave a brown ferric chloride reaction in ethanol; yield, 250 mg.

Found: C, 62.12; H, 4.33%. Calcd for $C_{17}H_{14}O_7$: C, 61.82; H, 4.27%.

Triacetate of XII. Hot acetic anhydride - pyridine method; mp 173—175°C (from aqueous methanol); the substance gave a negative ferric chloride reaction.

Found: C, 60.30; H, 4.29%. Calcd for $C_{23}H_{20}O_{10}$: C, 60.52; H, 4.42%.

3,4′,5,7,8-Pentamethoxyflavone (XIII). The compound XI was methylated with diazomethane to give colorless needles of XIII, mp 157—159°C (from aqueous methanol) (lit,[9] 156—158°C), which gave a negative ferric chloride reaction. This compound was also obtained by the methylation of XII. NMR in $CDCl_3$: 3.92, 3.97 and 4.03 (each s, 5MeO), 6.49 (s, C_6-H), 7.10 (d, J=9.5 cps, $C_{3'}$-H and $C_{5'}$-H), 8.26 (d, J= 9.5 cps, $C_{2'}$-H and $C_{6'}$-H).

Found: C, 64.43; H, 5.35%. Calcd for $C_{20}H_{20}O_7$: C, 64.51; H, 5.41%.

The authors are grateful to Professor P. R. Jefferies, the University of Western Australia, for his gift of the natural pigment. This work was supported by a grant-in-aid from the Ministry of Education.

*[9] The melting point was observed in this laboratory.

9) S. Rangaswami, P. S. Rao and T. R. Seshadri, *Proc. Indian Acad. Sci.*, **9A**, 133 (1939).

BULLETIN OF THE CHEMICAL SOCIETY OF JAPAN VOL. 42 2382—2384 (1969)

A Method of Synthesizing Pyrimidine Derivatives

Isao SHIBUYA and Masahiro KURABAYASHI

Government Chemical Industrial Research Institute, Tokyo, Mita, Meguro-ku, Tokyo

(Received December 18, 1968)

The reaction of nitriles (2 mol), 1 mol of acid chlorides, and 1 mol of metal chlorides (Lewis acids) gives 1,3,5-oxadiazin-1-ium salts (I), while I gives various heterocyclic compounds, such as *s*-triazine, triazole, and oxadiazole derivatives, when treated with ammonia, hydrazine, hydroxylamine, and urea.[1)]

The present report is concerned with the reaction of Ia with substituted acetonitriles (XCH_2CN), *i. e.*, malonitrile (X: CN), methyl cyanoacetate (X: $COOCH_3$), and benzoylacetonitrile (X: COC_6H_5).

When Ia was refluxed with each of the above-mentioned reagents under basic conditions, II, III, and IV respectively were obtained in good yields. The molecular weights of II, III and IV were

$$2RCN + RCOCl + MeCl_n \rightarrow$$

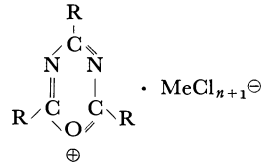

(I)

Ia: $R = C_6H_5$
$MeCl_n = SnCl_4$

1) R. R. Schmidt, *Chem. Ber.*, **98**, 334 (1965).

determined to be 376, 409, and 455 respectively by the mass spectrometric method. These results and the elementary analysis showed that these compounds are the adducts of the cation from Ia and of the anions from substituted acetonitriles. The fact that the IR spectra of these compounds were very similar to one another except for the characteristic absorptions of substituted groups of acetonitriles strongly suggests that these compounds all have a structure containing the same heterocyclic ring.

On the other hand, 1,3-oxazin-1-ium salt (V), which is regarded as a compound analogous to I, gives the acylaminopyridine derivative (VI) when treated with malononitrile;[2] the mechanism of this reaction has been proposed to be as follows;

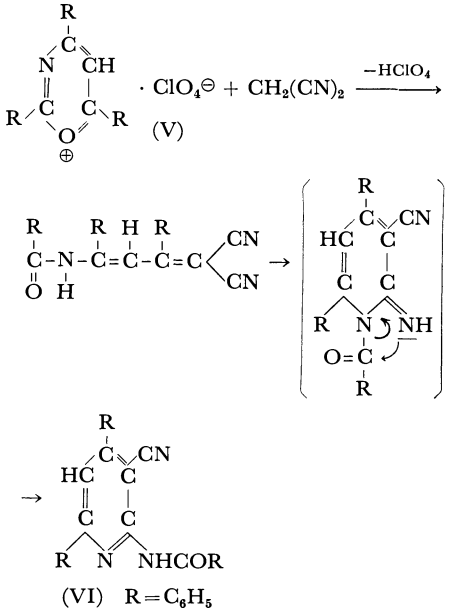

(V) (VI) $R=C_6H_5$

Therefore, it was supposed that the reaction of Ia with substituted acetonitriles would proceed in a manner similar to that of the above reaction, and that II, III, and IV would be the corresponding pyrimidine derivatives.

II was identified as follows:

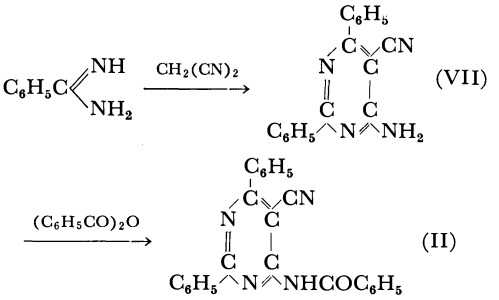

(VII)

(II)

4-amino-5-cyano-2,6-diphenylpyrimidine (VII) was derived from benzamidine and malononitrile,[3] and its benzoyl derivative was prepared by heating VII with benzoic anhydride. The IR and mass spectra of II were in good agreement with those of this benzoyl derivative. A mixed-melting-point determination with both samples showed no depression. It was, consequently, concluded that II was 4-benzoylamino-5-cyano-2,6-diphenylpyrimidine, and that III and IV were the corresponding pyrimidine derivatives. It was thus proved that pyrimidine derivatives are synthesized from 1,3,5-oxadiazin-1-ium salt in good yields by the treatment with substituted acetonitriles, and it was inferred that the mechanism of these reactions is similar to that of the reaction of 1,3-oxazin-1-ium salt with malononitrile.

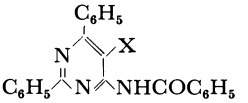

(II), (III), (IV)

II: X=-CN
III: =-$COOCH_3$
IV: =-C_6H_5

Experimental

4-Benzoylamino-5-substituted-2,6-diphenylpyrimidine (II), (III), and (IV). To a solution of 0.002 mol of each of the substituted acetonitriles and 0.30 g of triethylamine in 10 ml of dioxane, 1.30 g of Ia were added, and then the mixture was refluxed for 1 hr. The solvent was distilled off under reduced pressure, and the residue was washed with dilute hydrochloric acid, aqueous sodium hydroxide, and water, and recrystallized from acetic acid (II), ethanol (III), and acetone

TABLE 1. 4-BENZOYLAMINO-5-SUBSTITUTED-2,6-DIPHENYLPYRIMIDINES

	Substituent (X)	Yield (%)	Mp (°C)	Mol wt*	Elementary analysis						
					Found			Calcd for			
					C(%)	H(%)	N(%)	Fomula	C(%)	H(%)	N(%)
II	CN	95	240.5	376	76.64	4.35	14.65	$C_{24}H_{16}N_4O$	76.58	4.29	14.88
III	$COOCH_3$	86	186	409	73.18	4.84	10.21	$C_{25}H_{19}N_3O_3$	73.34	4.68	10.26
IV	COC_6H_5	66	200	455	79.11	4.50	9.35	$C_{30}H_{21}N_3O_2$	79.10	4.65	9.22

* Parent peaks of the mass spectra.

2) R. R. Schmidt, *ibid.*, **98**, 3892 (1965).
3) G. W. Kenner, B. Lythgoe, A. R. Todd and A. Topham, *J. Chem. Soc.*, **1943**, 388.

(IV) respectively. IR (II): 3240, 2210 (CN), 1671, 1559, 1475, 1380, 1269 cm^{-1}, (III): 3320, 1721 (ester), 1686, 1588, 1468, 1372, 1268, 1243 (ester) cm^{-1}, (IV): 3270, 1680, 1662 (C=O), 1559, 1478, 1382, 1277 cm^{-1}. The yield, mp, mol wt, and results of elementary analysis of these compounds are listed in Table 1.

4-Benzoylamino-5-cyano-2,6-diphenylpyrimidine (II) from VII. A mixture of 100 mg of VII and 0.5 g of benzoic anhydride was heated at 170—175°C for 30 min; the mixture was then washed with ethanol and recrystallized from acetic acid to give 105 mg of II; yield 78%; mp 240.5°C. Found: C, 76.80; H, 4.12; N, 14.82%. Calcd for $C_{24}H_{16}N_4O$: C, 76.58; H, 4.29; N, 14.88%.

BULLETIN OF THE CHEMICAL SOCIETY OF JAPAN VOL. 42 2384—2386 (1969)

On the Ionic Association of Alizarine Saphirol SE in Water-dioxane Mixtures

Masaru MITSUISHI, Yasuko FUNATSU and Nobuhiko KUROKI*[1]

Faculty of Fiber Science and Technology, Shinshu University, Ueda, Nagano

(Received December 19, 1968)

In the previous paper, we have concluded from spectroscopic and conductance measurements that Alizarine Saphirol SE (sodium salt of 1,5-dihydroxy-4,8-diaminoanthraquinone-2-sulfonic acid) exists in the form of ionic associates in water-ethanol mixtures with a low dielectric constant.[1] This association was ascribed to the increase of Coulombic attraction between the dye ion and the counter ion. It may be reasonable to expect that Alizarine Saphirol also exists in the ionic associate in water-dioxane mixtures having lower dielectric constants than those of water-ethanol mixtures. Such interactions between the dye ion and the counter ion in the mixtures is supposed to be expressed quantitatively in terms of ion association constant of the dye ion with the counter ion in the solution.

Since literatures on the association constant of a dye in water-organic solvent mixtures can hardly be found, it seems valuable to examine the dissociation constant of Alizarine Saphirol in water-dioxane mixtures in order to obtain some suggestive information not only on the dispersed state of the dye but also on the effect of dioxane on the ultraviolet and visible spectra of the dye in the mixtures.

In this paper, the conductance data were used to determine the equivalent conductance at infinite dilution and ion association constant by means of Shedlovsky's treatment[2] based on Onsager's limiting theory.

Experimental

Materials. The Alizarine Saphirol SE (sodium salt of 1,5-dihydroxy-4,8-diaminoanthraquinone-2-sulfonic acid) was taken from the laboratory stock used in the previous work[1]. The dioxane was purified as follows. Dioxane of a guaranteed reagent grade was boiled with potassium hydroxide under reflux for several hours. It was distilled after dehydration with metallic sodium through a 40 cm refluxing column.

Conductance Measurements. The conductance measurements were made with a Yokogawa-Hewlett Packard Universal Bridge BV-2-13 B. A simple dilution cell with cell constant 0.0688 was used. All the measurements were made at 25±0.01°C. The specific conductance of the solvents was always less than 1.0×10^{-6} mhos.

Dielectric Constant Measurements. Dielectric constant measurements were made by means of heterodynebeat method at 500 Kc/sec. The heterodyne circuit was prepared in our laboratory, and an oscilloscope was used as a detector. The electric capacity was determined with a precision condenser of Ando Electric Co., Ltd. The sample cell was Yamato Kagaku's Dielectric cell EL-25. Benzene ($\varepsilon=2.273$) was used as a standard material.

Viscosity Measurements. The viscosity of the solvent was determined with an Ostwald type viscometer.

Results and Discussion

Shedlovsky's equation to obtain the association constant K_A and the equivalent conductance at infinite dilution Λ_0 of 1-1 electrolyte is based on Onsager limiting theory expressed as

$$\frac{1}{\Lambda S_{(z)}}=\frac{1}{\Lambda_0}+\frac{c\Lambda S_{(z)}f_{\pm}^{2}}{K\Lambda_0^{2}}, \qquad (1)$$

where Λ is the equivalent conductance at concentration c, and $f_{\pm}^{2}$ is given by the Debye-Hückel limiting law. The values of $S_{(z)}$ have been tabulated by Daggett.[3] K is the dissociation constant and equal to $1/K_A$.

According to Eq. (1), the plot of $1/(\Lambda S_{(z)})$ against $c\Lambda S_{(z)}f_{\pm}^{2}$ should give a straight line,

*1 College of Engineering, University of Osaka Prefecture, Sakai, Osaka

1) M. Mitsuishi and G. Aida, This Bulletin, **39**, 246 (1966).

2) T. Shedlovsky, *J. Franklin Inst.*, **225**, 739 (1938).

3) H. M. Daggett, *J. Am. Chem. Soc.*, **71**, 1497 (1949).

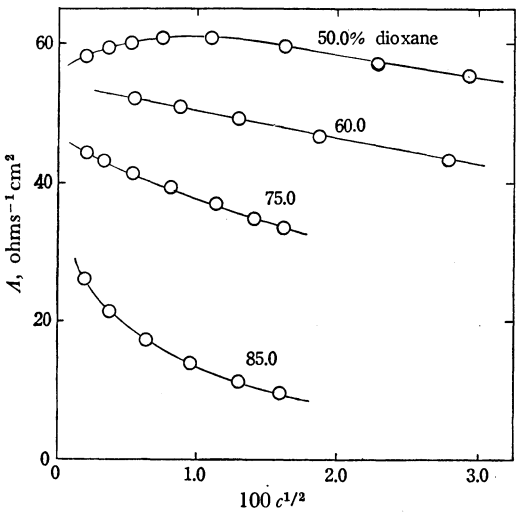

Fig. 1. Conductance of Alizarine Saphirol SE in water-dioxane mixtures.

passing through $1/\Lambda_0$ with a slope equal to $1/(K\Lambda_0)^2$; thus the association constant K_A and the equivalent conductance at infinite dilution Λ_0 can be determined.

The conductance of Alizarine Saphirol in water-dioxane mixtures is plotted against $\sqrt{c}$ in Fig. 1. In the solutions above 60% dioxane, the so-called McBain effects are not found on the Λ - $\sqrt{c}$ curves, so that Alizarine Saphirol is supposed to be monomeric in the solution.

In the previous paper, Alizarine Saphirol has been considered to be in the form of ionic associate in water-ethanol mixtures with a low dielectric constant from the conductance data.[1] It is reasonable to expect that Alizarine Saphirol exists in the form of ionic associate in the water-dioxane mixtures having dielectric constant lower than that of the water-ethanol mixtures. As shown in Fig. 1, the Λ - $\sqrt{c}$ curve of alizarine Saphirol in 85% dioxane is similar to that of weak electrolyte; thus the association constant is supposed to be appreciable.

Shedlovsky's treatment was used to determine Λ_0 and K_A, and the parameters resulting from the data analysis are given in Table 1.

The dielectric constants of the solvents in Table 1 are a little lower than those of Kunze and Fuoss,[4] and the viscosities of the solvents are comparable to those of Kunze and Fuoss

From Table 1, the ionic association constant K_A is seen to become larger with the increase of the proportion of dioxane in the mixtures; thus K_A becomes larger with the lowering of the dielectric constant of the solvent. This indicates obviously that the interaction between the dye ion and the counter ion increases with the lowering of the dielectric constant of the solvent.

In an attempt to analyze the data further, log K_A was plotted against $1/\varepsilon$ for the dye, and the result is shown in Fig. 2. Since the resulting plot is quite linear, the ionic associate in water-dioxane mixtures is considered to be formed entirely by the electrostatic interaction between the dye ion and the counter ion.

The Walden products ($\Lambda_0\eta$) are given in Table 1. It is found that $\Lambda_0\eta$ decreases steeply with the lowering of the dielectric constant of the solvent. The Walden products of some inorganic electrolytes in water-organic solvent mixtures have been found to become smaller than those in pure water by Atkinson *et al.*[5] who reported on the behavior of $MnSO_4$ in the mixtures of dioxane, methanol or acetone with water. A similar result has been obtained by Yokoi *et al.*[6] on Cu-*m*-benzenedisul-

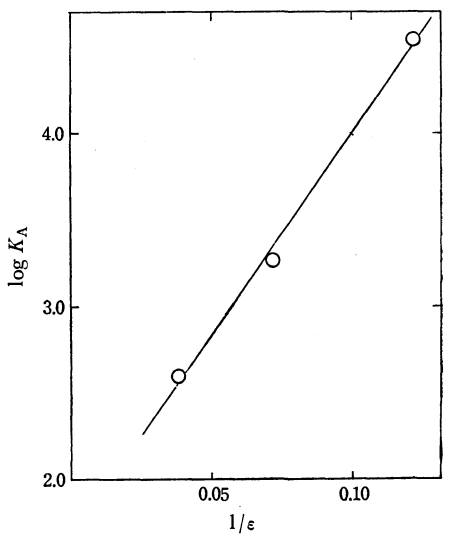

Fig. 2. Dependence of association constant on the reciprocal dielectric constant of the solvent.

Table 1. Calculated parameters

Dioxane in mixtures	ε	η	Λ_0	$\Lambda_0\eta$	K_A
60.0 wt %	25.9	1.949×10^{-2} poise	52.7 ohms^{-1} cm^2	1.02	3.98×10^2
75.0	14.0	1.819	44.3	0.802	1.88×10^3
85.0	8.2	1.557	29.2	0.455	3.46×10^4

4) R. W. Kunze and R. M. Fuoss, *J. Phys. Chem.*, **67**, 914 (1963).
5) G. Atkinson and S. Petrucci, *J. Am. Chem. Soc.*, **86**, 7 (1964).
6) M. Yokoi and E. Kubota, *Nippon Kagaku Zasshi (J. Chem. Soc. Japan, Pure Chem. Sect.)*, **86**, 894 (1965).

fonate in water-methanol mixtures. These results have been explained in terms of the competition between water and polar organic molecules for positions in the first coordination sphere of the ions. In addition to this effect, in the case of Alizarine Saphirol, the dye contains electron donating or electron accepting groups, such as $>C=O$, $-NH_2$ and $-OH$, so that there would be strong and specific interactions between dioxane and these groups, and these interactions presumably affect the conductance behavior of the dye.

The conductance data alone, however, will not be sufficient to clarify the specific interactions between the dye ion and solvent molecule, so that it is necessary to investigate further by ultraviolet-visible, ESR and NMR spectroscopic measurements.

The authors wish to thank Professor Haruo Gotoh and Professor Masatoki Yokoi for their helpful discussions.

BULLETIN OF THE CHEMICAL SOCIETY OF JAPAN VOL. 42 2386—2387 (1969)

The Synthesis and Physical Properties of 1,6-Dimethyl-8,8-dicyanoheptafulvene

Masaji ODA, Makoto FUNAMIZU and Yoshio KITAHARA

Department of Chemistry, Faculty of Science, Tohoku University, Katahira-cho, Sendai

(Received December 27, 1968)

In the course of our investigation of 8,8-dicyanoheptafulvenes, we needed to prepare 1,6-dimethyl-8,8-dicyanoheptafulvene (**1**). We wish here to report the synthesis of **1** and on its abnormalities in physical properties.

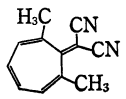

(**1**)

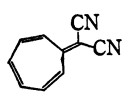

(**2**)

According to the method of the convenient synthesis[1] of 8,8-dicyanoheptafulvenes from tropones, refluxing 2,7-dimethyltropone[2] with malononitrile in acetic anhydride gave **1** in a 17% yield upon the separation of the reaction mixture by silica-gel-column chromatography. The IR, UV, and NMR spectra showed marked changes compared to those of 8,8-dicyanoheptafulvene (**2**)[3] (*cf.* Table 1). That is, the infrared absorption of the cyano group (2225 cm^{-1}) of **1** is at a higher frequency and its intensity is relatively weaker, while the ultraviolet absorption at the longest wavelength (390 mμ) is markedly weaker in intensity and the chemical shifts of ring protons are higher than those of **2**. These observations indicate that the conjugation of the cyano group with the seven-membered ring is appreciably hindered. This hindrance could be attributed to the deviation of **1**[4] from the planarity observed in **2**[5] by X-ray analysis, a deviation resulting from the intramolecular steric interaction between the methyl and the cyano groups. This is further supported by the fact that the dipole moment, 5.68 D (in benzene at 25°C), is far smaller than the value, 6.94 D,[6] calculated by regarding the seven-membered ring as a planar and regular heptagonal.

Experimental

8,8-Dicyanoheptafulvene (2). A solution of tropone (1.125 g, 10.6 mmol) and malononitrile (1.05 g, 15.9 mmol) in 10 m*l* of acetic anhydride was heated to reflux for 1.5 hr. The volatile substances were then removed *in vacuo*, leaving reddish crystals. The crystals were collected by filtration and washed with ethyl alcohol, giving 0.860 g of **2** as orange needles. The filtrate was concentrated and chromatographed on silica-gel eluted with benzene, this provided a further 0.315 g. Total yield, 1.175 g (72%). The melting point (201—202°C) and spectral data are all identical with those of an authentic sample.

1) K. Doi and Y. Kitahara, Tohoku Local Meetings of the Chemical Society of Japan, 1959. As for the procedure, see Experimental Section.

2) N. J. Leonard, L. A. Miller and J. W. Berry, *J. Am. Chem. Soc.*, **79**, 1482 (1957).

3) T. Nozoe, T. Mukai, K. Osaka and N. Shishido, This Bulletin, **34**, 1384 (1961).

4) This was finally confirmed by X-ray analysis to be a boat form-like structure in the seven-membered ring. H. Shimanouchi, Y. Sasada, C. Kabuto and Y. Kitahara, *Tetrahedron Letters*, **1968**, 5053.

5) H. Shimanouchi, T. Ashida, Y. Sasada, M. Kakudo, I. Murata and Y. Kitahara, This Bulletin, **39**, 2322 (1966).

6) Values of 7.49D[7] of **2** and 0.35 D of toluene were taken for the base moment and the C-CH_3 bond moment respectively.

7) M. Yamakawa, H. Watanabe, T. Mukai, T. Nozoe and M. Kubo, *J. Am. Chem. Soc.*, **82**, 5665 (1960).

Table 1. IR, UV and NMR spectral data

Compound	ν_{max}(KBr) cm^{-1}	λ_{max}(MeOH) mμ (log ε)	τ($CDCl_3$)
1	2225, 1612, 1580 1525, 766	245(4.04), 390(3.96)	3.43 s 4H 7.59 s 6H ($-CH_3$)
2[3]	2205, 1633, 1585 1520, 763	225(4.01), 255(4.08) 384(4.36)	2.5—3.2 m

1,6-Dimethyl-8,8-dicyanoheptafulvene (1). A solution of 2,7-dimethyltropone (1.34 g, 10 mmol) and malononitrile (0.90 g, 13.5 mmol) in 15 m*l* of acetic anhydride was heated to reflux for 45 min. The volatile substances were then removed *in vacuo*, and the red-brownish oily residue was chromatographed on silica-gel eluted with benzene. The yellow fraction collected provided 0.310 g (17%) of **1**. Recrystallization from methylene chloride - cyclohexane gave an analytical sample; yellow prisms, mp 102—103°C.

Found: C, 79.34; H, 5.69; N, 15.09%. Calcd for $C_{12}H_{10}N_2$: C, 79.09; H, 5.53; N, 15.38%.

BULLETIN OF THE CHEMICAL SOCIETY OF JAPAN VOL. 42 2387—2389 (1969)

Fluorescence Spectra of Aromatic Hydrocarbons in Polystyrene under High Pressure

Ichimin SHIROTANI, Takashi KAJIWARA and Hiroo INOKUCHI

The Institute for Solid State Physics, The University of Tokyo, Roppongi, Tokyo

(Received January 9, 1969)

The effect of pressure on the fluorescence spectra of aromatic compounds in the solid phase has been studied. Under pure hydrostatic pressures up to 8 kbar, ordinary fluorescence spectra of crystalline anthracene were observed.[1] However, when a quasi-hydrostatic pressure*1 of 7—10 kbar was applied to an anthracene crystal placed in the optical cell, a new broad emission band located in the 600 mμ wavelength region appeared.[2-4]

Between the new fluorescence band and the absorption spectra, no mirror image symmetry was found[5]; this new anomalous emission can be explained as an excimer fluorescence produced at high pressure. Similar phenomena were found on the fluorescence spectra of naphthalene, chrysene, 1,2-benzanthracene, 9,10-diphenylanthracene, and 2-methylanthracene. The increase in the fluorescence intensity of naphthacene doped in the anthracene host crystal with an increase in the pressure may be produced predominantly by the increment in the probability of energy transfer from the host to the guest.[6]

In this note, the fluorescence spectra of aromatic hydrocarbons dissolving in polystyrene under high pressure will be presented.

The high-pressure apparatus and the optical measurement attachment have already been reported.[6] A pressure up to 52 kbar was applied to the optical cell. A polystyrene sample containing aromatic hydrocarbons of about 0.05 wt% was prepared by the thermal polymerization of the monomer styrene containing dissolved hydrocarbons. The hydrocarbons used in this experiment were anthracene, perylene, benzo[*g,h,i*]perylene, and violanthrene B.

Figures 1 and 2 illustrate the fluorescence spectra of benzo[*g,h,i*]perylene and violanthrene B in polystyrene at several isobars. The fluorescence intensity of anthracene increased remarkably in the pressure range of 0—30 kbar,[6] but the intensity for perylene and violanthrene B decreased with an increase in the pressure. The peak shifts were smaller than that of the crystalline states, and a similar pressure effect has been found on their absorption spectra.[7] As is shown in Figs. 1 and 2, diffuse bands were observed at 52 kbar, but

*1 As a pressure transmitting medium, sodium chloride was used.

1) I. Shirotani, T. Kajiwara and H. Inokuchi, unpublished.

2) J. Tanaka, T. Koda, S. Shionoya and S. Minomura, This Bulletin, **38**, 1559 (1965).

3) P. F. Jones and M. Nicol, *J. Chem. Phys.*, **43**, 3759 (1965).

4) H. W. Offen, *ibid.*, **44**, 699 (1966).

5) H. Ohigashi, I. Shirotani, H. Inokuchi and S. Minomura, *Molecular Crystal*, **1**, 463 (1966).

6) H. Ohigashi, I. Shirotani, H. Inokuchi and S. Minomura, *J. Phys. Soc., Japan*, **19**, 1996 (1964).

7) I. Shirotani, H. Inokuchi and S. Akimoto, This Bulletin, **40**, 2277 (1967).

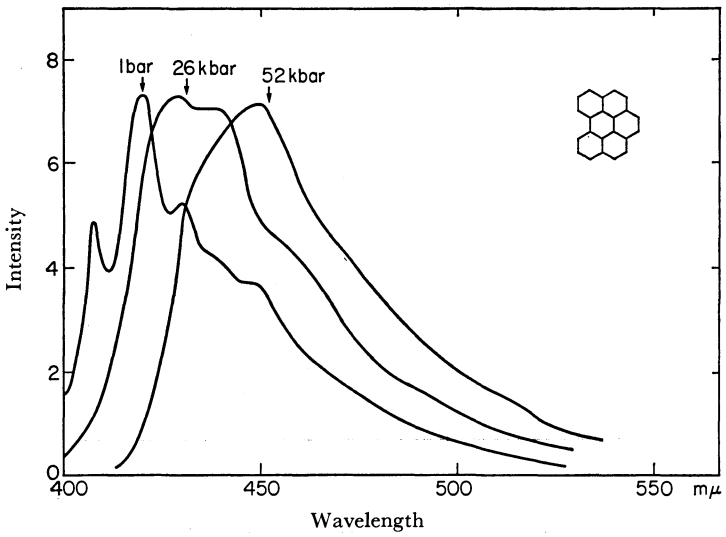

Fig. 1. The fluorescnce spectra of benzo[*g,h,i*] perylene in polystyrene matrix as a function of applied pressure.

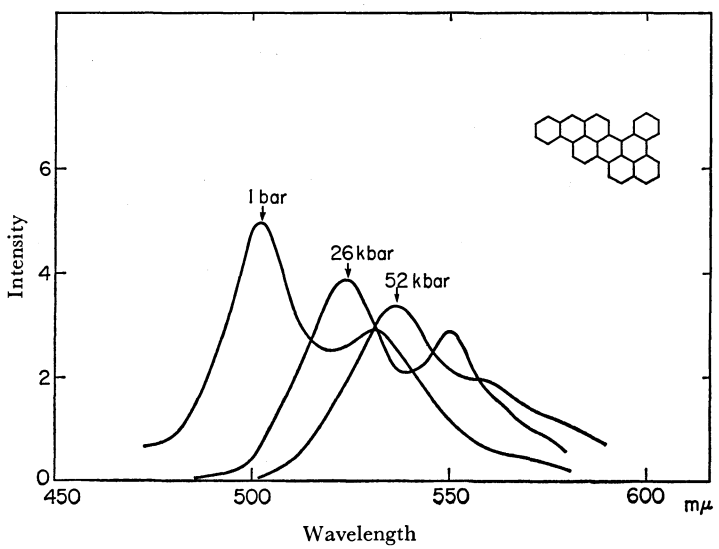

Fig. 2. The fluorescence spectra of violanthrene B in polystyrene under high pressure.

these broad emissions cannot be identified as the fluorescence of an excimer formed under high pressure. When benzo[*g,h,i*]perylene of 10^{-3}mol/*l* dissolved in polystyrene, the average intermolecular distance is not less than 30 Å, which is too large to form an "excimer." From the relation between the pressure and the volume given by Samara and Drickamer,[8] the average intermolecular distance at 52 kbar was estimated to be 94% of that at atmospheric pressure. Therefore, since the decrease in the molecular distance of the aromatic hydrocarbon-polystyrene system with the pressure is very small compared with the distance among the molecules in the polystyrene matrix, the formation of an excimer is difficult even at high pressure.

Figure 3 shows the fluorescence spectra at several isobars when two components—anthracene (5×10^{-2} mol/*l*) and perylene (10^{-4} mol/*l*)—were dissolved in polystyrene. The emission from anthracene was quenched with an increase in the pressure. On the contrary, the fluorescence intensity of perylene increased as the applied pressure increased. This behavior may arise from the energy transfer from anthracene to perylene. However, as has

8) G. A. Samara and H. G. Drickamer, *J. Chem. Phys.*, **37**, 474 (1962).

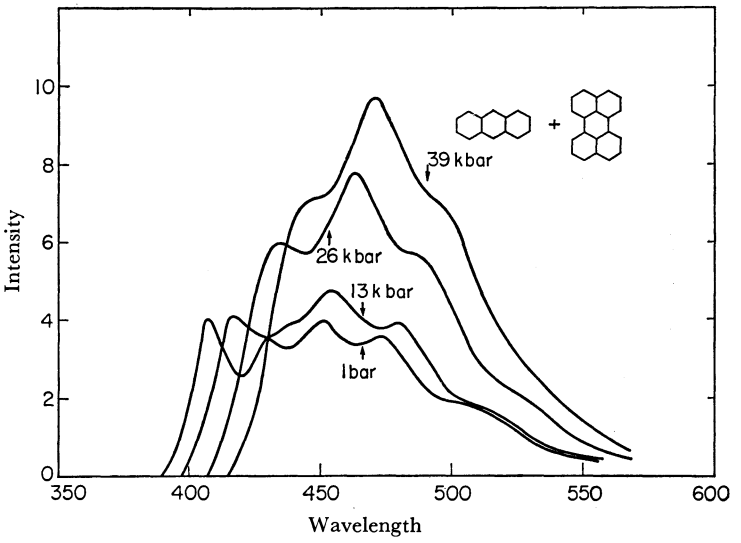

Fig. 3. The fluorescence spectra of anthracene-perylene mixture (guest)-polystyrene-(host)system under high pressure.

been mentioned previously, the discrepancy between the experimental and theoretical results for the anthracene-naphthacene mixed crystal system is very large.[6] For the anthracene-perylene mixture (guest) in polystyrene (host), a large discrepancy was also found. Therefore, the increase in energy transfer from anthracene to perylene may partly contribute to the effect of the pressure on these fluorescence phenomena.

The authors wish to thank Professor Junji Aoki and Mr. Satoshi Iwashima for their gift of the chemicals.

BULLETIN OF THE CHEMICAL SOCIETY OF JAPAN VOL. 42 2389—2391 (1969)

A New Synthetic Method of 4(1*H*)-Pyridones

Choji KASHIMA, Makoto YAMAMOTO, Susumu KOBAYASHI and Noboru SUGIYAMA

Department of Chemistry, Tokyo Kyoiku University, Otsuka, Tokyo

(Received January 16, 1969)

β-Diketones have been condensed with some nucleophilic reagents, such as ketones, aldehydes and esters, in the presence of alkali amide in liquid ammonia.[1,2] It has also been reported that Schiff bases have been condensed with β-diketones to give the corresponding dihydropyridiones.[3] Much like Schiff bases, nitrile is expected to condense with β-diketone to give 4(1*H*)-pyridone. Hauser and his co-workers reported[4] that acetanilide condensed with benzonitrile in the presence of two equivalents of butyllithium in *n*-hexane-tetrahydrofuran to give only ω-benzimidoylacetanilide. By the use of β-diketones instead of acetanilide in liquid ammonia, we obtained 4(1*H*)-pyridones directly. Many reports of 4(1*H*)-pyridone syntheses have appeared in the literature,[5-8] but this kind of 4(1*H*)-pyridone synthesis

1) C. R. Hauser and T. M. Harris, *J. Am. Chem. Soc.*, **80**, 6360 (1958).

2) N. Sugiyama, M. Yamamoto, T. Takano and C. Kashima, This Bulletin, **40**, 2909 (1967).

3) N. Sugiyama, M. Yamamoto and C. Kashima, *ibid.*, **42**, 1357 (1969).

4) R. L. Gay and C. R. Hauser, *J. Am. Chem. Soc.*, **89**, 1647 (1967).

5) J. Chauvelier, *Bull. soc. chim. France*, **1954**, 734.

6) J. Chauvelier and M. Gaudemar, *Compt. rend.*, **232**, 167 (1951).

7) S. Hunig and G. Kobrich, *Ann.*, **617**, 203 (1958).

8) A. F. Thomas and A. Marxer, *Helv. Chim. Acta*, **43**, 469 (1960).

has never before been described.

Results and Discussion

In liquid ammonia, acetylacetone (I) was condensed with benzonitrile (IV) in the presence of alkali amide. When three moles of lithium amide were used, neither imino compounds nor 4(1*H*)-pyridones were obtained, but when two moles of sodium amide were used 6-methyl-2-phenyl-4(1*H*)-pyridone hydrochloride (VIII) was obtained in a 35% yield. When three moles of potassium amide were used, the yield of VIII increased to 42%. The structure of VIII was proved by a study of the spectral data and by elemental analyses. The treatment of VIII with sodium carbonate in a 90% ethanol solution gave 6-methyl-2-phenyl-4(1*H*)-pyridone (V) quantitatively; it was identified with an authentic sample.[9]

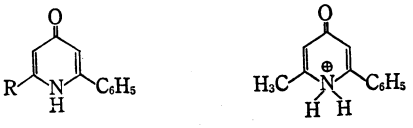

VIII

Scheme 1

In the same way, 6-phenyl-2,4-hexanedione (II) was condensed with IV. II has an activated terminal methyl group at C-1 and two activated methylene groups, at C-3 and C-5. Much as with the reaction of II with benzylidene aniline,[3] the reaction was effected to occur at the C-1 or C-5 position. However, the reaction of II occurred at C-1 and it afforded only one product, 6-phenethyl-2-phenyl-4(1*H*)-pyridone (VI).

The structure of VI was supported by the spectral data and by the elemental analyses. The infrared absorption spectrum of VI showed bands at 3260 (νNH), 1615 (conjugated ketone), 1580, 1520 (a pyridone-ring double bond), 1590, and 690 cm^{-1} (phenyl). The ultraviolet absorption spectrum showed absorption maxima at 242 and 261 mμ in an ethanol solution. The nuclear magnetic resonance spectrum in a deuterochloroform solution showed signals at τ 7.10 (singlet, 4H, phenethyl ethylene group), a doublet centered at τ 3.86 (2H, olefinic protons), a singlet at τ 2.85 (5H, aromatic protons of phenethyl group), and a multiplet centered at τ 7.32 (5H, C-2 substituted phenyl protons). These data supported the idea that the structure of VI is 6-phenethyl-2-phenyl-4(1*H*)-pyridone.

The condensation of benzoylacetone (III) with IV gave 2,6-diphenyl-4(1*H*)-pyridone (VII). The structure of VII was identified with that of an authentic sample.[10] It is considered that VII was

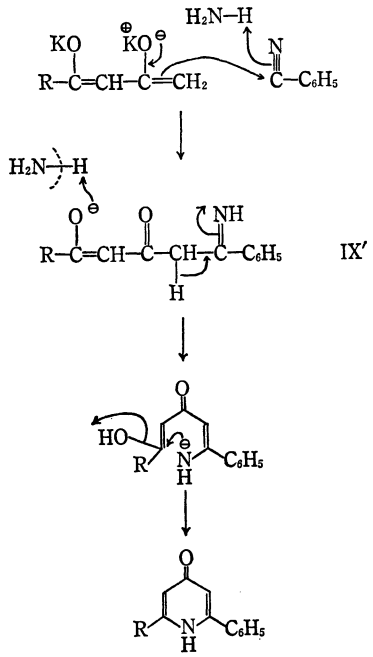

IX′

Scheme 2

produced *via* an intermediate imino compound (IX). However, an attempt to detect IX failed. This fact suggests that the cyclization of IX was accomplished before the neutralization.

We speculated that the reaction mechanism of this series is as follows: β-diketone and benzonitrile condense to give imino β-diketone (IX′) in the first step, and then IX′ is cyclized by dehydration to yield X, as is illustrated in Scheme 2.

Experimental

6-Methyl-2-phenyl-4(1*H*)-pyridone (V). *The Selection of the Reaction Conditions. A)* In a 500-m*l* three-necked flask, 300 m*l* of anhydrous liquid ammonia was placed. A small amount of potassium was then added and dissolved completely. Into the blue solution there was stirred a catalytic amount of ferric chloride, and then 5.85 g (0.15 g atom) of potassium were added in small portions. The resulting blue solution turned dark gray within 60—90 min. To this solution there was added 0.05 mol of I in 30 m*l* of anhydrous ether in small portions. After stirring for 60 min, 5.51 g (0.05 mol) of IV in 20 m*l* of anhydrous ether were added. After having been stirred for three hours at −33°C, the reaction mixture was neutralized with ammonium chloride. The liquid ammonia was evaporated rapidly on a water bath, and 100 m*l* of water was added from a dropping funnel. After 15 minutes' stirring, the ethereal layer was separated. To the alkaline aqueous layer 100 m*l* ether were added, and then the solution again extracted. To the remaining aqueous layer was added 100 m*l* of 2 N hydrochloric acid were added, after with the solution was allowed to stand at room temperature for 30 min. The resulting precipitate was recrystallized from hot water to give 4.94 g (42%)

9) S. Ruhemann, *J. Chem. Soc.*, **93**, 1281 (1908).
10) L. Neelakantan, *J. Org. Chem.*, **23**, 741 (1958).

of VIII as a white powder; mp 235—237°C, Beilstein test (+).

Found: C, 64.69; H, 5.64; N, 6.25%. Calcd for $C_{12}H_{12}NOCl$: C, 64.99; H, 5.43; N, 6.32%.

IR(KBr): 3250, 3400 (νNH), 1645, 1630 (νC=O, conjugated ketone and double bond) and 700 cm^{-1} (phenyl).

UV: λ_{max}^{EtOH} 235, 277 mμ.

B) According to the method *A*, 0.10 mol of sodium amide was used; 4.12 g (35%) of VIII was thus obtained.

C) According to the method *A*, 0.15 mol of lithium amide was used; VIII was not obtained.

To a solution of 1.0 g of VIII in 50 m*l* of 90% ethanol 5 g of anhydrous sodium carbonate was added; this mixture was then refluxed for two hours in a water bath. The resulting solution was filtered, and the solvent was removed under reduced pressure. The residue was recrystallized from hot water to give 0.75 g (93%) of V as a white powder; mp 174—176°C (lit 177—178°C[9]).

IR(KBr): 3300, 1625, 1580, 1525 and 700 cm^{-1}.

UV: λ_{max}^{EtOH} 240 mμ (ε 24800), 262 mμ (ε 15100).

NMR(in $CDCl_3$): τ 7.64 (3H, methyl, singlet), τ 4.00 (1H, olefinic proton, doublet), τ 3.73 (1H, olefinic proton, doublet), τ 2.35—2.72 (5H, aromatic protons, multiplet) and τ 1.50—1.90 (1H, NH, broad singlet).

6-Phenethyl-2-phenyl-4(1*H*)-pyridone (VI). According to the method *A*, VI was prepared from 8.0 g (0.05 mol) of II and 0.05 mol of IV. The product was dried in the air and then recrystallized from ethanol-acetone to give 7.1 g (51%) of VI as pale yellow plates; mp 172—173°C.

Found: C, 82.53; H, 6.36; N, 5.07%. Calcd for $C_{19}H_{17}NO$: C, 82.88; H, 6.22; N, 5.09%.

UV: λ_{max}^{EtOH} 241 mμ (ε 37500), 261 mμ (ε 25000).

2,6-Diphenyl-4(1*H*)-pyridone (VII). According to the method *A*, VII was prepared from 8.1 g (0.05 mol) of III and 5.15 g (0.05 mol) of IV. After the solution had been stirred for three hours at −33°C, the liquid ammonia was evaporated without neutralization. To the residue a 100 m*l* portion of water was added, and then 7.5 g (0.14 mol) of ammonium chloride in 100 m*l* of water. The ethereal layer was separated. The alkaline aqueous layer was extracted with three 100 m*l* portions of chloroform. After dried over calcium chloride, the chloroform solution was evaporated; the residue was chromatographed on a silica gel column (Merck 7734, 0.05—0.2 mm) with a benzene - ethyl acetate (4 : 1 v/v) mixture. The fraction (R_f-value: 0.18*[1]) was collected and concentrated to give only VII, which was then recrystallized from benzene to yield 3.83 g (31%) as white crystals: mp 178—179°C (lit 178°C[11]). No imino compound was detected.

IR(KBr): 3250, 1615, 1517, 1535 and 690 cm^{-1}.

UV: λ_{max}^{EtOH} 249 mμ (ε 32200), 280 mμ (ε 15000).

NMR (in $CDCl_3$): τ 3.25 (2H, olefinic protons, singlet), τ 3.00—3.80 (1H, NH, broad singlet) and τ 2.10—2.68 (10H, aromatic protons, multiplet).

---

*1 Thin layer chromatography: Wakogel B-500, Solvent: benzene.

11) R. J. Light and C. R. Hauser, *J. Org. Chem.*, **25**, 538 (1960).

BULLETIN OF THE CHEMICAL SOCIETY OF JAPAN VOL. 42 2391—2394 (1969)

The Epoxidation of α,β-Unsaturated Terpene Ketones

Jun KATSUHARA

Sun Star Dentifrice Company, Research Laboratory, Takatsuki, Osaka

(Received January 23, 1969)

It has recently been reviewed by Klein and Ohloff[1] that in a variety of α,β-unsaturated cyclic terpene ketones, the base-catalyzed epoxidation of exocyclic double bonds in conjunction with carbonyl groups proceeds in a non-stereoselective manner to produce a mixture of two diastereomeric epoxides, whereas in endocyclic double bonds, the steric course of epoxidation is highly stereoselective, resulting in the formation of a single product. However, they did not refer to the factors which govern the steric course of the epoxidation reaction.

The epoxidation of polarized double bonds with hydrogen peroxide in aqueous alkaline media was first reported by Weitz[2] and the reaction mechanism involving the intervention of a hydroperoxycarbanionic intermediate was proposed by Bunton.[3]

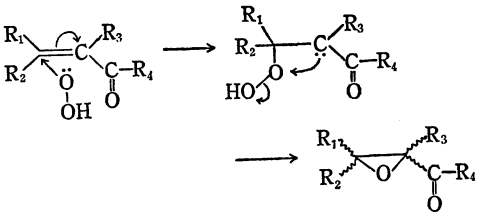

Dewar[4] advanced a theory for a facile bimolecular nucleophilic displacement of halogen α to

1) E. Klein and G. Ohloff, *Tetrahedron*, **19**, 1091 (1963).

2) F. Weitz and A. Scheffer, *Ber.*, **54**, 2327 (1921).

3) C. A. Bunton and G. J. Minkoff, *J. Chem. Soc.*, **1949**, 665.

4) M. J. S. Dewar, "The Electronic Theory of Organic Chemistry," Oxford University Press, Oxford (1949), p. 73.

a keto group and his theory states that the transition state is stabilized by overlap and conjugation of the C=O π-orbital with the orbitals of the bonds being formed and broken at the α-carbon atom. This concept was successfully applied by Zimmerman[5] for the stereochemical interpretation of the alkaline epoxidation reaction, in which the stereochemical preference in epoxide products was overlap controlled.

We wish herewith to mention that the Zimmerman overlap-control theory holds for the epoxidation of α,β-unsaturated cyclic terpene ketones as well, and that the conformational analysis of the transition state carbanion, which fulfilled the stereoelectronic requirements for the maximum stabilization by orbital overlap and charge delocalization, may provide a useful means of assigning an absolute configuration to the epoxide to be expected from the epoxidation of cyclic terpene ketones containing either endocyclic or exocyclic ethylene linkage.

In accordance with this view, the available data[1] actually indicate that upon epoxidation, cyclic terpene ketones containing α,β-endocyclic double bonds afford stereospecifically the enantiomer to be expected from the intermediate hydroperoxycarbanion which was stabilized by the orbital-overlap and charge delocalization in the conformation with the minimized non-bonded repulsive interactions of substituents in the preferred equatorial disposition. This may be exemplified in detail by (−)-(4R)-piperitone (**1**) which upon epoxidation, yielded exclusively (+)-(1R : 2R : 4R)-piperitone oxide (**2**): the nucleophilic attack of hydroperoxide anion to the β-carbon (here $C_{(1)}$) of the polarized double bond in **1** would produce two conceivable transition state carbanions *i. e.* **A** resulted from the attack of the anion to the 1 *re*-2 *re* face of the double bond and **C** resulted from that to the 1 *si*-2 *si* face. The transition state carbanion **A** in which both the anchoring isopropyl and methyl groups are disposed equatorially and the hydroperoxy group is in an axial position, should naturally be in a conformational equilibrium with **B** where both isopropyl and methyl groups are disposed axially and hydroperoxy group is in an equatorial position. A similar conformational equilibrium should obtain in the diastereomeric transition state conformer **C**. Of the four conceivable transition states **A**, **B**, **C** and **D**, only **A** and **D** can fulfill the stereoelectronic requirements for oxirane ring formation by intramolecular nucleophilic displacement since in these two conformations, the axial hydroperoxy group is so disposed as to permit the cyclization and also to possess the maximum stabilization by orbital overlap and charge delocalization. Further choice of these two conformers, then, would be made from a purely steric point of view, *i. e.* the comparison of relative conformational stability as demonstrated by inspection of scale models clearly indicates that the transition state carbanion **A** with both the anchoring isopropyl and methyl groups oriented equatorially should be more favored than the diastereometric counterpart **D** with the bulky isopropyl group disposed in an axial position and methyl group in an equatorial position. Since the first step of hydroperoxide anion attack is reversible, the steric course of the epoxidation should be directed to proceed through the most favored transition state **A** and the chemical consequence of this situation should naturally be the exclusive

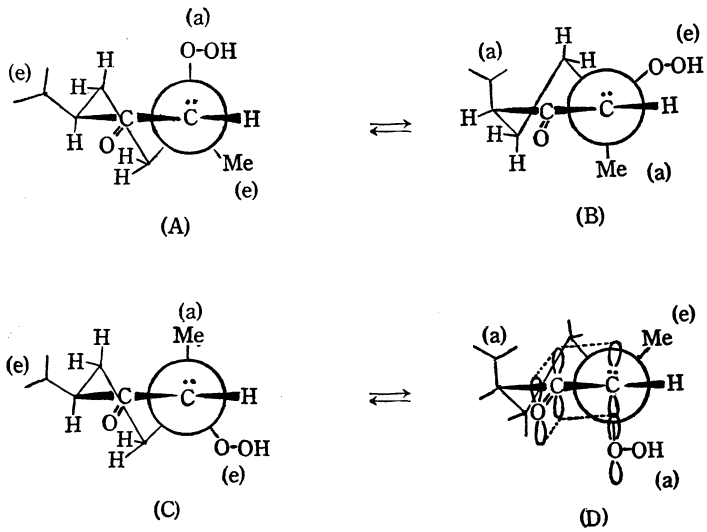

Scheme I

5) H. E. Zimmerman, L. Singer and B. S. Thyagarajan, *J. Am. Chem. Soc.*, **81**, 108 (1959).

formation of (+)-(1R:2R:4R)-piperitone oxide **2**. This is just what was found experimentally by the product analysis and the absolute assignment of configuration to **2**: the conformation of the most favored transition state **A** has been reflected as such in the epoxide product **2**.

Literature[1] affords cogent support for the stereochemical interpretation of epoxidation in terms of the overlap-control stabilization combined with conformational analysis, as demonstrated by the epoxidation of (−)-(4R)-piperitone (**1**) into (+)-(1R : 2R : 4R)-piperitone oxide (**2**); of (+)-(4S)-**1** into (−)-(1S:2S:4S)-**2**; of (−)-(4R)-carvone (**3**) into (+)-(1R : 2R : 4R)-carvone oxide (**4**); of (+)-(4S)-**3** into (−)-(1S : 2S : 4S)-**4**; of (−)-(4S)-perillaldehyde (**5**) into (−)-(1S : 2R : 4S)-perillaldehyde oxide (**6**); of (−)-(1R : 5S)-verbenone (**7**) into (−)-(1R : 2R : 3S : 5S)-verbenone oxide (**8**); of (+)-(1S:5R)**7** into (+)-(1S : 2S : 3R : 5R)-8; of (−)-(1R: 5S)-myrtenal (**9**) into (−)-(1R : 2R : 3S : 5S)-myrtenal oxide (**10**); of (−)-(1R : 5S)-umbellulone (**11**) into (−)-(1R : 3S : 4S : 5R)-umbellulone oxide (12),[6,7] respectively.

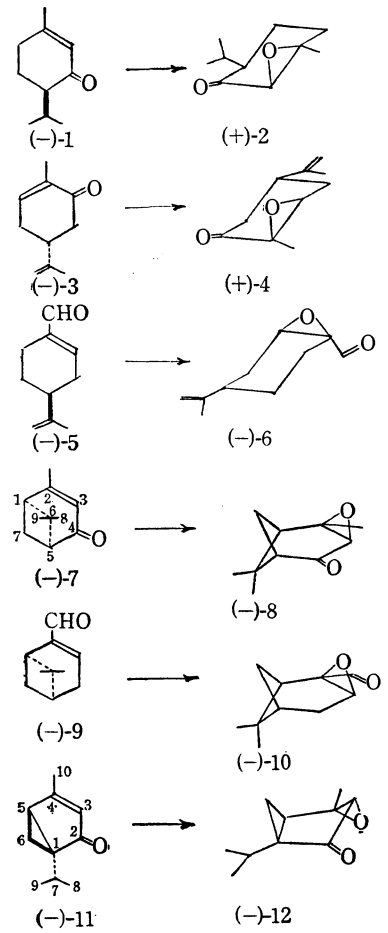

Scheme II

In a manner similar to the above-mentioned piperitone (**1**), the chair conformation of the intermediate hydroperoxy-carvone anion, with the isopropyl group disposed in an equatorial position and the hydroperoxy group in an axial position and thus with the advantage of overlap stabilization, would be more favored than the othewise-conformed counterpart, so that it would result in the end product **4** with the oxirane ring *trans* to the isopropyl group. What has been mentioned with carvone holds for (−)-perillaldehyde (**5**) as well. Verbenone (**7**) permits readier access to the 2 *si*-3 *re* face of the double bond because of the smaller bulkiness of $C_{(7)}$-hydrogen than the geminal dimethyl in the opposite side, thus naturally proceeding through the overlap-stabilized intermediate and resulting in the formation of the corresponding epoxide (**8**) (*trans* relative to geminal dimethyl). The situation is also the same with myrtenal which gave the *trans*-epoxide (**8**). (−)-Umbellulone (**11**), in which the bicyclo(3,1,0) system adopts the boat conformation as demonstrated by NMR-analysis,[8,9] also gave the corresponding *cis*-epoxide (**12**) (relative to isopropyl group) *via* the overlap-stabilized intermediate.

Based on these data, it may be generalized that in the epoxidation of endocyclic double bond involved in pinane skeleton, the isomer with the oxirane ring *trans* relative to geminal dimethyl groups is formed exclusively, and in other terpene ketones, the oxirane ring is stereospecifically introduced to the double bond so as to enable sterically the most favored intermediate conformation to be

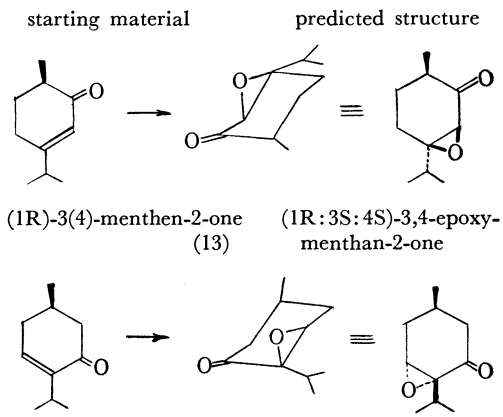

Scheme III

6) R. T. Gray and H. E. Smith, *Tetrahedron*, **23**, 4229 (1967).

7) H. E. Richard and C. S. James, *J. Am. Chem. Soc.*, **76**, 4118 (1954).

8) M. S. Bergqvist and T. Norin, *Arkiv for Kemi*, **22**, 137 (1964).

9) K. Tori, *Chem. Pharm. Bull. (Tokyo)*, **12** 1439, (1964).

stabilized by an effective and concomitant orbital-overlap stabilization.

When this generalization is applied to some endocyclic α,β-unsaturated terpene ketones, (1R)-3(4)-menthen-2-one (**13**) and (1R)-4(5)-menthen-3-one (**14**), the following configurations of the exclusive epoxide products may be predicted, experimental verification of which will be the subject of future publications.

Although available data for the epoxidation of exocyclic double bonds are scarce in literature, the epoxidation of (+)-(1R)-pulegone[10] (**15**), (+)-(1S : 5R)-pinocarvone[11] (**16**), (+)-(1R : 4S)-isopropylidenecamphor[12] (**17**) and (+)-(1S : 2S)-piperitenone oxide[10] (**18**) clearly shows that a mixture of diastereomeric epoxides is always obtained in a definite isomer ratio except in the last example, the sterically more favored and therefore the more stable isomer being dominant in every case. Since the exocyclic double bonds are not locked in a rigid cyclic skeleton and consequently the rotation around the single bond connecting the carbanionic sp^2-carbon (α) with the β-carbon carrying the hydroperoxy group is quite free, the hydroperoxy group is capable of fulfilling the stereoelectronic requirements for the maximum orbital overlap at both sides of the carbanionic sp^2-carbon and consequently to undergo nucleophilic displacement to form oxirane ring in two ways—one with axial oxirane-oxygen and equatorial carbon, and the other with the reversed conformational orientation of oxirane ring. The energy difference between these two diastereomeric transition states is thus purely steric in origin and is not so great as in the endocyclic counterparts, so that the stereoselectivity of epoxidation is dependent on the relative conformational stability of these two conformers, as was actually observed in product distribution.

Table 1

Starting material	Product isomers	Yield %
(+)-Pulegone	(−)-(1R:4R)-*trans*-**19**	64.5
	(+)-(1R:4S)-*cis*-**20**	35.5
(+)-Pinocarvone	(−)-(1R:2S:5R)-*trans*-**21**	35.5
	(+)-(1R:2R:5R)-*cis*-**22**	64.5
(+)-Isopropylidenecamphor	(−)-(1R:3S:4S)-*trans*-**23**	67
	(+)-(1R:SR:4S)-*cis*-**24**	33
(+)-Piperitenone oxide	(−)-(1S:2S:4S)-*cis*-**25**	

In pulegone oxide, the *trans* epoxide (**19**) (relative to $C_{(7)}$ and $C_{(10)}$) with the conformation involving both isopropyl and methyl groups in equatorial position is preferred to the *cis*-**20** with an axial methyl. The red shift in CD found for diastereomeric pinocarvone oxides showed the axial orientation of the oxirane-oxygen atom in both *trans*-**21** (relative to $C_{(6)}$ bridge carrying geminal dimethyl and $C_{(10)}$ methyl group) and *cis*-products (**22**) and on the basis of such conformations, the non-bonded interactions between the oxirane-oxygen and the $C_{(6)}$-dimethyl grouping favor the *cis*-**22** more than the *trans* epoxide (**21**), thus the former being the major product of epoxidation. The oxirane ring, $O-C_{(3)}-C_{(11)}$, in isomeric isopropylidenecamphor oxides is so situated as to be bisected by the carbonyl group and then the isomers differ in the non-bonded interactions between $C_{(7)}$-geminal dimethyl and isopropyl moiety of oxirane. Model inspection reveals that the the *trans* isomer (**23**) (relative to $C_{(7)}$ and $C_{(11)}$) is sterically more favored and stable than the *cis* **24**, in accordance with the result of product analysis. In the case of piperitenone oxide, the sole dioxide isolated (42%) was (−)-(1S : 2S : 4S)-diastereomer[10] (**25**) which has sterically the more favored conformation with both isopropyl moiety of oxirane and $C_{(1)}$-methyl group disposed equatorially. Although another diastereomeric *trans*-dioxide product was missing, the failure of its isolation may probably be due to experimental difficulties; this highly strained system containing two sensitive epoxide functions in an unfavorable conformation and a carbonyl group in a single C_{10}-molecule would supposedly be too labile to permit successful separation without any decay.

The author wishes to thank Professor T. Matsuura of Hiroshima University and Professor Y. Inouye of Kyoto University for many helpful discussions during this work.

10) J. Katsuhara, *J. Org. Chem.*, **32**, 797 (1967).
11) J. Katsuhara, This Bulletin, **41**, 2700 (1968).
12) J. Katsuhara, *ibid.*, **42**, No. 9 (1969), in press.

BULLETIN OF THE CHEMICAL SOCEITY OF JAPAN VOL. 42 2395—2396 (1969)

Syntheses of Pterocarpans. IV.*1 A New Synthesis of 3,8,9-Trimethoxypterocarpan*2

Kenji FUKUI, Mitsuru NAKAYAMA and Kenji TSUZUKI

Department of Chemistry, Faculty of Science, Hiroshima University, Higashi-sendamachi, Hiroshima

(Received January 24, 1969)

In previous papers, the present authors reported a new method for synthesizing pterocarpans (*e.g.*, (±)-pterocarpin (I),[1] (±)-maackiain (II)[2] and (±)-4-methoxypterocarpin (III)[3]) from the corresponding benzofuro[3',2':3,4]coumarins. This paper will describe the synthesis of 3,8,9-trimethoxypteocarpan (IV) from 7,5',6'-trimethoxybenzofuro[3',2' : 3,4]coumarin (V)[4] in a manner similar to that described earlier.[1-3]

The coumarin (V) was subjected to lithium aluminum hydride reduction in refluxing tetrahydrofuran. As expected, the reduction proceeded smoothly, giving the expected product, 5,6-dimethoxy-2-(2-hydroxy-4-methoxyphenyl)-3-hydroxymethylbenzo[*b*]furan (VI), in a 50% yield. The infrared spectrum of VI exhibits absorption bands at 3450 and 3200 cm^{-1} which are attributable to two hydroxyl groups. The diacetate of VI was easily prepared with acetic anhydride in pyridine. The subsequent dehydration of the diol (VI) in boiling diethyleneglycol afforded 3,8,9-trimethoxy-6a,11a-dehydropterocarpan (VII), mp 145—146°C. The NMR spectrum*3 of VII is closely similar to that of anhydropisatin (*O*-methyl anhydrosophorol) (VIII)[1,5] in having a methylenedioxyl group instead of dimethoxyl groups. Then, VII was hydrogenated in acetic acid with 10% Pd-C to the desired pterocarpan (IV), mp 135—136°C. This substance was found to be identical with an authentic sample which had been obtained by a different route[6] in a mixed melting-point determination and by infrared, ultraviolet, and NMR spectral comparisons.

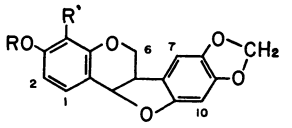

I R=Me, R'=H
II R=R'=H
III R=Me, R'=MeO

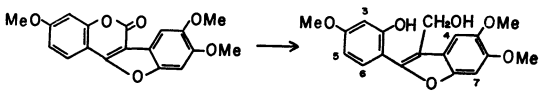

V VI

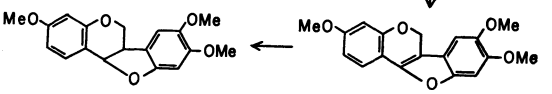

IV VII

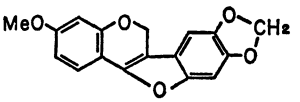

VIII

Experimental*4

5,6-Dimethoxy-2-(2-hydroxy-4-methoxyphenyl)-3-hydroxymethylbenzo[*b*]furan (V). A suspension of lithium aluminum hydride (300 mg) in anhydrous tetrahydrofuran (50 m*l*) was stirred into a solution of benzofurocoumarin (mp 248—249°C)[4] (IV) (500 mg) in anhydrous tetrahydrofuran (100 m*l*), and the mixture was then refluxed for 1 hr. The excess lithium alumi-

*1 Part III: K. Fukui, M. Nakayama and T. Harano, This Bulletin, **42**, 1693 (1969).

*2 Presented at the Okayama Meeting of the Chemical Society of Japan, Okayama, October, 1967.

1) K. Fukui and M. Nakayama, *Tetrahedron Letters*, **1966** 1805; This Bulletin, **42**, 1408 (1969).

2) K. Fukui, M. Nakayama, H. Tsuge and K. Tsuzuki, *Experientia*, **24**, 536 (1968).

3) K. Fukui, M. Nakayama and K. Tsuzuki, *ibid.*, **25**, 122 (1969).

*3 The NMR spectra were measured with a Hitachi R-20 spectrometer, using tetramethylsilane as the internal standard (δ-value in $CDCl_3$).

4) a) K. Fukui and M. Nakayama, *Nippon Kagaku Zasshi (J. Chem. Soc. Japan, Pure Chem. Sect.)*, **85**, 790 (1964); b) K. Fukui, M. Nakayama and H. Sesita, This Bulletin, **37**, 1887 (1964).

5) a) D. R. Perrin and W. Bottomley, *J. Am. Chem. Soc.*, **84**, 1919 (1962); b) D. D. Perrin and D. R. Perrin, *ibid.*, **84**, 1922 (1962); c) H. Suginome, This Bulletin, **39**, 1525 (1966).

*4 The melting points are uncorrected. The infrared spectra were measured in Nujol, while the ultraviolet spectra measured in an ethanol solution.

6) a) V. K. Kalra, A. S. Kukla and T. R. Seshadri, *Indian J. Chem.*, **5**, 607 (1967); b) K. Fukui, M. Nakayama and T. Harano, This Bulletin, **42**, 233 (1969).

num hydride was destroyed by the careful addition of ethyl acetate (2 ml) and water (50 ml). The cooled mixture was acidified with dilute hydrochloric acid and then extracted with ether. After the solvent had been removed under a vacuum, the resulting solid was recrystallized from hot water to give colorless needles of V, mp 130—131°C (250 mg, 50%). IR: 3450, 3200 cm^{-1} (OH). UV: λ_{max} mμ (log ε); 270.5 (4.25), 314 (4.40).

Found: C, 65.21; H, 5.57%. Calcd for $C_{18}H_{18}O_6$: C, 65.44; H, 5.49%.

The diacetate: acetic anhydride - pyridine method; mp 119.5—120.5°C (colorless prisms from methanol). IR: 1788, 1748 cm^{-1} (C=O). NMR:[*3] 7.57 (doublet, J=8.5 Hz, C-6′); 7.15 (singlet, C-4); 7.06 (singlet, C-7); 6.93 (quartet, J=2.5, 9.0 Hz, C-5′); 6.77 (doublet, J=2.5 Hz, C-3′) 5.25 (2H, singlet, CH_2O); 3.92, 3.90, 3.83 (each 3H, singlet, CH_3O); 2.07, 2.11 (each 3H, singlet, CH_3CO).

Found: C, 63.83; H, 5.43%. Calcd for $C_{22}H_{22}O_6$: C, 63.76; H, 5.35%.

3,8,9 - Trimethoxy - 6a, 11a - dehydropterocarpan (VII). A solution of VI (300 mg) in pure diethyleneglycol (10 ml) was refluxed for 10 min. During boiling, a slow separation of water was noted. The mixture was then cooled, diluted with water (30 ml), extracted with ether, and washed with a 1 N aqueous sodium hydroxide solution. After the ether had been removed under a vacuum, the resulting solid was recrystallized from ethanol to give colorless microcrystals of VII, mp 145—146°C (120 mg, 42%). IR: 1645, 1619, 1589, 1567, 1513, 1491 cm^{-1} (C=C, aromatic). UV: λ_{max} mμ (log ε); 250_i (4.11),[*5] 274 (3.95), 337 (4.39), 355 (4.32).

Found: C, 68.97; H, 5.28%. Calcd for $C_{18}H_{16}O_5$: C, 69.22: H, 5.16%.

3,8,9-Trimethoxypterocarpan (IV). A mixture of VII (100 mg) and 10% Pd-C (40 mg) in acetic acid (100 ml) was shaken in an atmosphere of hydrogen until 1.1 mol of hydrogen had been absorbed. After the catalyst had then been removed, the filtrate was evaporated under a vacuum. The resulting solid was recrystallized from ethanol to give colorless needles of IV (50 mg, 50%); mp 135—136°C (lit, mp 138—139°C;[6a] mp 136—137°C[6b]), identical with that of an authentic sample.[6b]

[*5] i=inflection point.

BULLETIN OF THE CHEMICAL SOCIETY OF JAPAN VOL. 42 2396—2398 (1969)

Infrared Spectra of Bis(2,4-dichloro-6-ethoxymercapto-isocyano-*s*-triazino-*N*,*S*) Copper(II)

Kiyoyasu KAWAI, Fujio MIZUKAMI and Yutaka KODAMA*1

Faculty of Literature and Science, Toyama University, Gofuku, Toyama

(Received February 3, 1969)

In a previous paper, the infrared and Raman spectra of 2,4-dichloro-6-isocyanodichloro-*s*-triazine(tetrameric cyanogen chloride: DCT-$NCCl_2$) have been reported[1]. The present paper will deal with the preparation of the bis(2,4-dichloro-6-ethoxymercaptoisocyano-*s*-triazino-*N*,*S*) copper(II) complex, [Cu(DCT-$NCSOC_2H_5)_2$], and with the infrared spectra of the complex and 2,4-dichloro-6-ethoxythiocarbamido-*s*-triazine, DCT-$NHCSOC_2H_5$, which is a derivative of DCT-$NCCl_2$ and the parent molecule of the ligand of the complex, in order to assign the observed spectra.

Experimental

2,4-Dichloro-6-ethoxythiocarbamido-*s*-triazine: DCT-$NHCSOC_2H_5$. This was prepared by the method described previously[2] and was identified analytically.

By the addition of sodium hydroxide to an aqueous solution of cupric nitrate (0.02 mol), its pH was adjusted to 7.4; it was kept at about 0°C. A solution of DCT-$NHCSOC_2H_5$ (0.02 mol) in chloroform was stirred drop by drop into the aqueous solution of cupric nitrate. The stirring continued for about five hours. The reaction mixture was then placed in a separatory funnel in order to separate the chloroform portion from the aqueous one. By evaporating the chloroform portion under reduced pressure, the red-brown colored crystal was precipitated and dried *in vacuo*. Recrystallization from carbon tetrachloride gave bis(2,4-dichloro-6-ethoxymercaptoisocyano-*s*-triazino-*N*,*S*) copper(II).

Found: Cu, 10.01; C, 25.34; N, 19.56; H, 1.90%. Calcd for $CuC_{12}N_8O_2S_2H_{10}Cl_4$: Cu, 11.19; C, 25.39; N, 19.74; H, 1.90%.

The infrared spectra were recorded by a Nujol or hexachloro-1,3-butadiene mull from 4000 to 250 cm^{-1} with Hitachi-Perkin-Elmer 125 and Hitachi EPI-L spectrometers. The frequencies of the observed bands may be expected to be accurate to ± 2 cm^{-1}; they may tentatively be assigned as is shown in Table 1.

*1 Present address: Toyama Chemical Co., Ltd., Shimookui, Toyama.

1) K. Kawai, Y. Kodama and F. Mizukami, *Spectrochim. Acta*, **24A**, 1013 (1968).

2) Y. Kodama and S. Shinohara, *Yuki Gosei Kagaku Kyokai-shi (J. Soc. Org. Synth. Chem. Japan)*, **22**, 669 (1964).

Table 1. The assignment of the infrared spectra of 2,4-dichloro-6-ethoxythiocarboamido-*s*-triazine and bis(2,4-dichloro-6-ethoxymercaptoisocyano-*s*-triazino-*N*,*S*) copper(II) (cm^{-1})

DCT-$NHCSOC_2H_5$	[Cu(DCT-$NCSOC_2H_5$)$_2$]	Assignment
3430 w		ν(N-H)
3138 m	3205 w	ν(C-H)
3065 m		
2990 w	2985 m	
2935 w	2825 m	
	1703 w	1241+465=1706
1646 vw		1001+646=1647
1575 s		δ(N-H)
1526 vs		ν(C=N) triazine ring
1503 vs	1488 vs, b	
1470 w		1036+435=1471
1440 w		797+646=1443
1403 s		ν(C=S)
1386 s	1389 s	$\delta(CH_3)$
	1355 m	ν(C=N)as. chelate ring
1311 w, sh		855+460=1315
1295 vs		ν(C-N)as.
	1291 s	ν(C=N)s. chelate ring
1280 w		646+635=1281
1249 vs	1241 vs	ν(C=N) triazine ring
1218 vs	1216 vs	
1159 vs	1159 m	ν(C-O)as.
	1112 m	ν(C=S)
1100 m		ν(C-N)s.
1036 m	1032 m	ν(C-O)s. or CH_3 rocking
1001 m	1000 m	triazine ring breathing
965 w	968 w	ν(C-C)
911 vw		
899 vw		
894 vw, sh		460+435=895
855 s	851 s	ν(C-Cl)
	805 w	
797 s	794 s	triazine ring out-of-plane
783 m	762 m	
688 m		
646 w	677 m	
635 m	624 m	
	596 w, sh	
	546 w	
	538 w	
472 w		
460 w	465 w	
435 w		
	419 w	ν(Cu-N)
273 vw	311 vw	

vs=very strong, s=strong, m=medium, w=weak, vw=very weak, sh=shoulder, b=broad, s.=symmetric and as.=asymmetric.

The NMR spectra were also recorded, using a Japan Electron Optics C-60H spectrometer at the frequency of 60 Mcps in deuterium-chloroform, with tetramethylsilane as an internal standard; this examination revealed the signals of two groups, a quartet at τ 5.38 and a triplet at τ 8.60, in the complex, and the signals of three groups, a singlet at τ 1.18, a quartet at τ 5.45, and a triplet at τ 8.55, in DCT-$NHCSOC_2H_5$.

Results and Discussion

The absence of the band assigned to the N-H stretching vibration in the infrared spectra of the complex is confirmed by its NMR spectra, in which only the signals due to the presence of a typical ethyl group have been observed.

A very strong and broad band at 1488 cm^{-1} assigned to the triazine ring-stretching vibration of the complex may be the overlap of two or more bands; the frequency has shifted toward frequencies lower than the 1526 and 1503 cm^{-1} of DCT-$NHCSOC_2H_5$ or those assigned to the ring-stretching vibration in several triazine derivatives.[1,3-5] This frequency shift suggests that there may be small differences in the nature of the bonds in the triazine ring and a decrease in the C=N stretching force constant of the ring as a result of the formation of the complex with the chelate ring.

The great difference between the infrared spectra of DCT-$NHCSOC_2H_5$ and those of the complex may arise from the C=S and C=N stretching frequencies in the chelate ring. By comparing the spectra of the two compounds, the strong band at 1403 cm^{-1} and the two bands at 1100 and 1295 cm^{-1} of DCT-$NHCSOC_2H_5$ may be assigned to the C=S stretching vibration and the symmetric and asymmetric C-N stretching vibrations of the $-\overset{\|}{C}(ring)-\overset{|}{N}-\overset{\|}{C}-$ group respectively; the C=S stretching frequency of the complex shifts lower by means of the coordination of the sulfur atom, that is, by the contribution of $C-S^- \rightarrow Cu$. On the other hand, the C=N stretching frequencies in the chelate ring shift higher because of the increase in the double-bond character. On the basis of the above facts and the assignment of other bands, the three bands at 1112, 1291, and 1355 cm^{-1} of

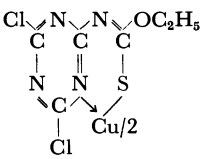

I

3) J. C. Lorquet, *Bull. Soc. Royale Science Liege*, **29**, 298 (1960).

4) J. E. Griffithe and D. E. Irish, *Can. J. Chem.*, **42**, 690 (1964).

5) T. S. Hermann, *Spectrochim. Acta*, **21**, 663 (1965).

the complex may be assigned to C=S stretching, symmetric C=N stretching, and asymmetric C=N stretching vibrations of the chelate ring respectively. Although some of the observed bands, including most of those in the lower frequency region, have not been assigned, the infrared spectra suggest that the complex is the chelate compound shown in Scheme I.

The authors are greateful to the members of the laboratory of Microanalysis, Faculty of Pharmacology of this University, for their microanalyses.

BULLETIN OF THE CHEMICAL SOCIETY OF JAPAN VOL. 42 2398—2401 (1969)

The Spectrophotometric Determination of Scandium with Eriochrome Azurol G

Katsuya UESUGI

Laboratory of Chemistry, Himeji Institute of Technology, Himeji

(Received February 3, 1969)

Some dyes of the triphenylmethane series react with many metallic ions in a weakly or a slightly acidic medium to form colored complexes. In preceding papers,[1,2] the present author and his co-workers described how pontachrome azure blue B and chromal blue G, dyes of this series, were excellent reagents for the spectrophotometric determination of scandium.

This paper will describe a spectrophotometric determination of scandium using eriochrome azurol G (sodium-2'',5'',6''-trichloro-4'-hydroxy-3,3'-dimethylfuchsone-5,5'-dicarboxylate, color index 43855), which is one of the compounds of this series. It is based on the reddish-violet complex formation between scandium ions and eriochrome azurol G in a slightly acidic medium. Several conditions under which small amounts of scandium can be determined, the influences of diverse ions, and the composition of the complex will be investigated. This reagent has been examined as an indicator of the titrimetric determination of potassium by tetraphenylborate and benzalkonium chloride.[3]

Experimental

Reagents and Apparatus. *Standard Scandium Solution.* 153 mg of scandium oxide (Mitsuwa Chemicals) were dissolved in small amounts of concentrated hydrochloric acid, and the solution was diluted to 1 *l* with water. This standard stock solution (100 ppm of scandium) was diluted further as required.

0.1% Eriochrome Azurol G Solution. Eriochrome azurol G (Tokyo Kasei Kogyo Co., Ltd., Tokyo) was further purified by recrystallization from ethanol before use, and then 0.1 g of it was dissolved in 100 m*l* of 95% ethanol. This reagent solution was stable for at least a month.

All the other reagents and apparatus used were the same as those reported previously.[2]

Procedure. Into a 25 m*l* volumetric flask place the standard solution or a sample solution containing 2.5—25 μg of scandium, and then add 2 m*l* of the 0.1% eriochrome azurol G solution. Add 10 m*l* of the buffer solution (pH 6.0, 0.2 M in acetate), mix thoroughly, and then dilute to the volume with distilled water. Measure the absorbance at 610 mμ using a reagent blank as a reference. Calculate the amount of scandium from the calibration curve.

Results and Discussion

Absorption Spectra. The absorption spectra of the reagent at various pH's are shown in Fig. 1. The maximum absorption of the reagent solution is found at 490 mμ below pH 4.5, at 430 mμ between pH 5.5 and 10, and at 590 mμ above pH 10.5. The absorbance curves of the scandium-eriochrome azurol G complex at various pH are shown in Fig. 2. The maximum absorption of the complex between 450 and 700 mμ is found at 610 mμ above pH 5.0. At pH 4.0, the complex in the visible region has two maxima, one at 600 mμ and another at 530 mμ. Below pH 3.5,however, the absorption maximum is found at 530 mμ.

Effect of the pH. The effect of the pH on the color reaction was investigated by taking absorbance measurements at 610 mμ of solutions containing scandium and eriochrome azurol G at various pH values. The results are shown in Fig. 3, from which it can be seen that the maximum absorbance of the scandium complex occurs in the pH range from 5.6 to 6.6. The reagent blank curve was

1) T. Shigematsu, K. Uesugi and M. Tabushi, *Bunseki Kagaku (Japan Analyst)*, **12**, 267 (1963).
2) K. Uesugi, This Bulletin, **42**, 2051 (1969).
3) T. Murakami, *Bunseki Kagaku (Japan Analyst)*, **14**, 880 (1965).

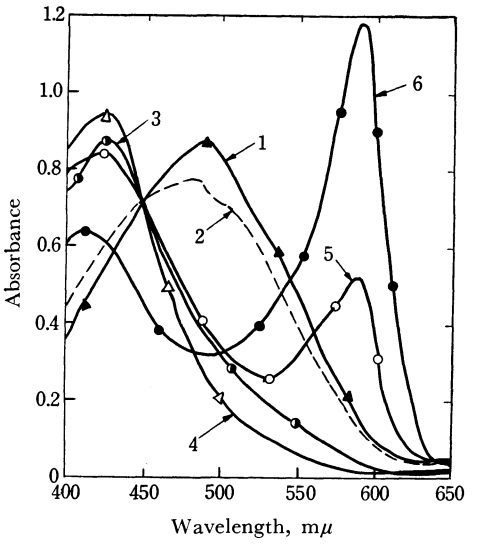

Fig. 1. Absorption spectra of reagent at various pH.
Reagent 80 ppm.
pH 1: 4.0, 2: 4.5, 3: 6.0, 4: 6.5—7.0, 5: 11.5, 6: 12.0

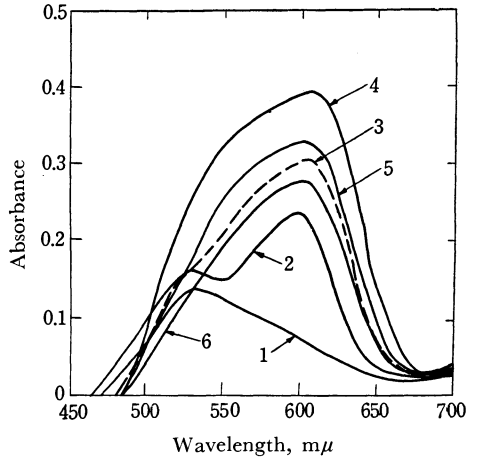

Fig. 2. Absorption spectra of scandium complex at various pH.
Reagent 80 ppm, Sc 0.6 ppm,
Reference: Reagent blank
pH 1: 3.4, 2: 4.0, 3: 5.0, 4: 6—6.4, 5: 7.0, 6: 8.0

obtained in the same manner, using the same amount of reagent. The acetate - acetic acid buffer, pH 6.0, was found to be satisfactory. The volume of the pH 6.0 buffer used was found to have no effect on the absorbance of a 0.5-ppm scandium solution over the range from 5 to 10 m*l* per 25 m*l* of solution.

Effect of Eriochrome Azurol G Concentration. The effect of the reagent concentration on the complex was investigated by measuring the absorbance at 610 mμ on solutions containing constant concentrations of scandium and the buffer and varying amounts of eriochrome azurol G. The absorbance increases as the reagent concentration increases. Therefore, it is desirable to keep the reagent concentration constant. Two milliliters of a 0.1% reagent solution was found to be sufficient for less than 1.0 ppm of scandium.

Color Stability. At room temperature, the formation of the scandium-eriochrome azurol G complex is substantially instantaneous, and its intensity is stable for at least one hour; only a 2% decrease in absorbance occurs after one hour when measured against a reagent blank.

Effect of the Temperature. The effect of the temperature on the color development was investigated by measuring the absorbance of solutions kept for 20 min at various temperatures. The absorbance does not change over the temperature range of 10 to 40°C. Over 40°C, the absorbance gradually decreases. Hence, normal temperature changes in the laboratory seem to have no effect.

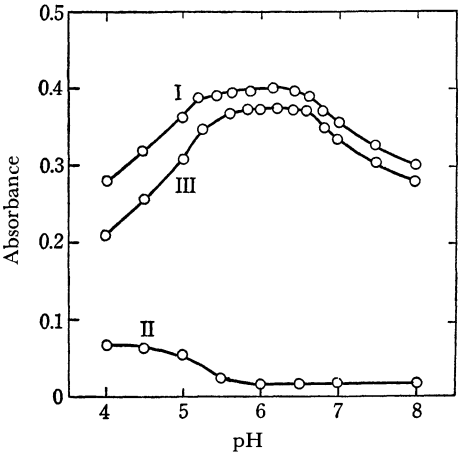

Fig. 3. Effect of pH on color intensity.
I: Reagent 80 ppm + Sc 0.6 ppm (Reference:water)
II: Reagent 80 ppm (Reference: water)
III: Reagent 80 ppm + Sc 0.6 ppm (Reference: Reagent blank)

Beer's Law and Sensitivity. Various amounts of a standard scandium solution containing up to 35 μg of scandium were used following the procedure mentioned above. Beer's law is obeyed over the range from 0.1 to 1.0 ppm of scandium. At 610 mμ the molar extinction coefficient is 29600. The spectrophotometric sensitivity is estimated to be 1.5×10^{-3} μg of scandium per cm², corresponding to log $I_0/I=0.001$.

The present method is very sensitive. Its sensitivity is much greater than that of the methods using eriochrome cyanine R (molar extinction

coefficient, $\varepsilon=19000$),[4] pyrocatechol violet ($\varepsilon=17300$),[5] arsenazo I ($\varepsilon=17000$),[6] pontacyl violet 4BSN ($\varepsilon=13700$),[7] tiron ($\varepsilon=8000$),[8] and naphthyl azoxine S ($\varepsilon=8000$);[9] its sensitivity is slightly higher than that of chromazurol S ($\varepsilon=27000$),[10] and it is comparable with that of the method using pontachrome azure blue B ($\varepsilon=31500$),[1] chromal blue G ($\varepsilon=31400$),[2] and xylenol orange ($\varepsilon=29410$).[11]

Table 1. Effect of diverse ions

Ion	added	as	Sc found (μg)
Ba(II)	100 μg	$BaCl_2$	9.9
Sr(II)	100 μg	$SrCl_2$	9.8
Mg(II)	100 μg	$MgCl_2$	10.1
Ca(II)	100 μg	$CaCl_2$	10.0
Mn(II)	100 μg	$MnSO_4$	10.0
Cu(II)	10 μg	$CuSO_4$	11.5
Zn(II)	100 μg	$ZnCl_2$	10.5
Cd(II)	100 μg	$CdCl_2$	9.9
Ni(II)	100 μg	$NiSO_4$	10.8
Co(II)	100 μg	$CoSO_4$	10.3
Pb(II)	100 μg	$Pb(NO_3)_2$	10.8
Hg(II)	100 μg	$HgCl_2$	9.8
Be(II)	5 μg	$BeCl_2$	28.9
Al(III)	5 μg	$Al(NO_3)_3$	22.3
Fe(III)	10 μg	$FeCl_3$	20.4
Cr(III)	100 μg	Cr-alum	8.0
Mo(VI)	100 μg	Na_2MoO_4	10.0
UO_2(II)	10 μg	$UO_2(NO_3)_2$	10.3
Y(III)	10 μg	YCl_3	12.1
La(III)	10 μg	$LaCl_3$	11.0
Ce(III)	10 μg	$CeCl_3$	11.2
Nd(III)	10 μg	$NdCl_3$	11.5
Gd(III)	10 μg	$GdCl_3$	11.1
Dy(III)	10 μg	$DyCl_3$	11.5
Er(III)	10 μg	$ErCl_3$	11.7
Th(IV)	10 μg	$Th(NO_3)_4$	11.0
Sulfate	100 mg	Na_2SO_4	10.5
Chloride	100 mg	NaCl	10.1
Nitrate	100 mg	KNO_3	10.2

Sc : 10.0 μg/25 ml

Precision and Accuracy. Nine determinations of 0.5 ppm of scandium gave a standard deviation of ±0.0074 ppm or a relative standard deviation of $\pm1.5\%$.

Effect of Diverse Ions. The effect of 26 cations and some anions on the determination of scandium was examined (Table 1). Many diverse cations, especially beryllium, copper(II), aluminum, iron(III), yttrium, thorium, and rare earth elements, interfere seriously with the determination of scandium, for they form complexes with eriochrome azurol G under the present experimental conditions (Fig. 4). The following anions do not interfere under the conditions described: sulfate, chloride, nitrate, and acetate, even when they are present in an anion-to-scandium ratio of 1 to 6000. The presence of oxalate, fluoride, citrate, and EDTA bleaches the color of the complex.

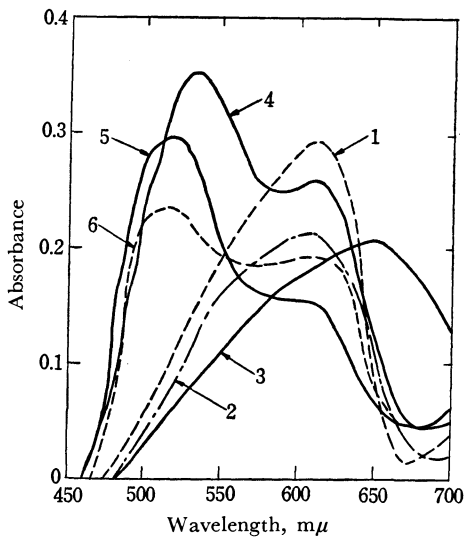

Fig. 4. Absorption spectra of beryllium, aluminum, iron(III), yttrium, lanthanum, and neodymium complexes at pH 6.0.
Reagent 80 ppm, Reference: Reagent blank
1: Be 0.15 ppm, 2: Al 0.13 ppm, 3: Fe(III) 0.3 ppm, 4: Y 2 ppm, 5: La 2 ppm, 6: Nd 2ppm

The absorption curves of the complexes of beryllium, aluminum, iron(III), yttrium, and some rare earth elements at pH 6.0 are shown in Fig. 4. The maximum absorbances of the beryllium and aluminum complexes are at 610 mμ, much like that of the scandium complex, and that of iron(III) complex is shifted toward a longer wavelength. The complexes of yttrium, lanthanum, gadolinium, and erbium have two absorption maxima, as is shown in Fig. 4.

Complex Formation. The composition of the scandium-eriochrome azurol G complex was

4) T. Fujinaga, T. Kuwamoto, S. Tsurubo and K. Kuwabara, *Bunseki Kagaku (Japan Analyst)*, **13**, 127 (1964).
5) S. P. Onosova and G. K. Kuntsevich, *Zh. Anal. Khim.*, **20**, 802 (1965).
6) H. Onishi and C. V. Banks, *Anal. Chim. Acta*, **29**, 240 (1963).
7) T. Shigematsu and K. Uesugi, *Bunseki Kagaku (Japan Analyst)*, **16**, 467 (1967).
8) H. Hamaguchi, N. Onuma, R. Kuroda and S. Sugisita, *Talanta*, **9**, 563 (1962).
9) T. Shimizu, *Bunseki Kagaku (Japan Analyst)*, **16**, 233 (1967).
10) R. Ishida and N. Hasegawa, This Bulletin, **40**, 1153 (1967).
11) O. V. Kon'kova, *Zh. Anal. Khim.*, **19**, 73 (1964).

determined by the continuous-variation method[12] and the mole-ratio method.[13] The results indicated that a 1 : 2 complex between scandium and eriochrome azurol G is formed at pH 6.0, and a 1 : 1 complex below pH 4.0. The formation constant of the scandium complex was determined spectrophotometrically by the same method as in a previous paper.[2] The formation constant for the complex at pH 6.0 and 25°C was calculated, from the curves of the continuous variation, as 2.6×10^{10}.

The author wishes to thank Professor Tsunenobu Shigematsu of the Institute for Chemical Research, Kyoto University, for his kind guidance, and Dr. Masayuki Tabushi and Dr. Masakazu Matsui for their valuable advice.

12) P. Job, *Ann. Chem.* **9**, 113 (1928).
13) J. H. Yoe and A. I. Jones, *Ind. Eng. Chem., Anal. Ed.*, **16**, 111 (1944).

SHORT COMMUNICATIONS

Mechanochemical Spin Generation in a Solid Charge Transfer Complex

Masatake OHMASA, Minoru KINOSHITA and Hideo AKAMATU

Department of Chemistry, Faculty of Science, The University of Tokyo, Hongo, Bunkyo-ku, Tokyo

(Received May 27, 1969)

In a previous paper, we have reported on electronic interactions in the solid charge-transfer complexes formed between tetracyanoquinodimethan (TCNQ) and a series of aromatic diamines, and have shown that most complexes can be divided into two main groups according to whether their ground electronic state is non-bonding or ionic.[1] In the course of the study, however, we found that the solid complex of benzidine and TCNQ could not be classified definitely to either of these two groups, as its infrared absorption spectrum was not explained either by a superposition of the spectra of neutral components or by a superposition of the spectra of ionic components.

We report here an interesting phenomenon found during the course of the work to elucidate the character of the ground electronic state of the benzidine-TCNQ system. Solid samples were precipitated from a solution in a similar manner to that described before[1] using several different solvents. Spectroscopic analysis of these solid complexes has indicated that there are two kinds of complexes with respect to occlusion of solvent molecules. The results obtained from the analysis of solution spectra in the UV and visible region are given in Table 1. As an example, the complex prepared in chloroform does not contain any solvent molecule, whereas that prepared in dichloromethane contains solvent molecules in mole ratios of approximately 1 : 1 : 1.5 (benzidine: TCNQ: solvent).*1

These two types of complexes are quite different in their infrared and ESR behaviors. As is shown in Fig. 1, the solid complex composed only of the donor and acceptor molecules exhibits the infrared absorption spectrum well explained by a superposition of the spectra of neutral component molecules, but, in the case of the complexes containing solvent molecules, the spectrum is distinctly different from that for the solvent-free complexes even apart from the bands assigned to the solvent molecules. (See also Fig. 2(c) of Ref. 1.)

TABLE 1. COMPOSITION OF THE BENZIDINE-TCNQ-SOLVENT SYSTEM AS DETERMINED SPECTROSCOPICALLY

Solvent used in preparation	Mol ratio*
$CHCl_3$	1.0 : 1.0 : 0
CH_3CHCl_2	1.0 : 1.1 : 0
CH_2Cl_2	1.0 : 1.1 : 1.6
$(CH_3)_2CO$	1.0 : 0.8 : 0.8
CH_3CH_2Br	1.0 : 1.1 : 1.6

* (Benzidine) : (TCNQ) : (Solvent)

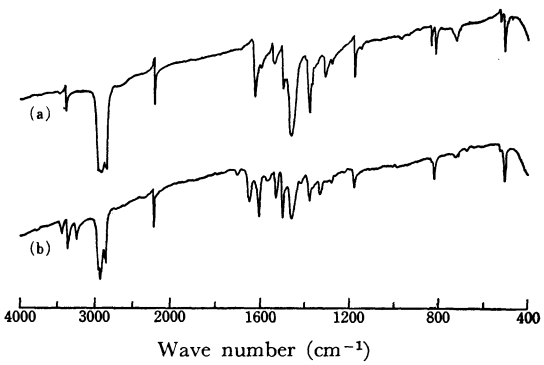

Fig. 1. Infrared absorption spectra of the benzidine - TCNQ complexes; (a) Solvent-free complex and (b) Solvent(acetone)-occluded complex.

In the ESR experiments, a well-grown crystalline sample of benzidine - TCNQ complex containing dichloromethane showed no ESR absorption, but it did give a strong ESR absorption signal (g= 2.0027) when it was ground to fine powder. On the other hand, the solvent-free complexes did not show ESR absorption at all, whether they were ground to fine powder or not.

Preliminary measurements showed that the electrical conductivities for the solvent-occluded samples were always higher by a factor of 10^4—10^5 compared to those for the solvent-free samples. These prominent effects of solvent occlusion on the electronic properties of the system are of great interest and further detailed studies including structural analysis are now in progress in our laboratory.

1) M. Ohmasa, M. Kinoshita, M. Sano and H. Akamatu, This Bulletin, **41**, 1998 (1968).

*1 An elementary analysis resulted in C, 58.45; H, 4.15; N, 15.58; Cl, 18.75, while calculated values for 1 : 1 : 1.5 were C, 59.37; H, 3.71; N, 16.30; Cl, 20.62%.

Preparation of a Dimeric Copper(II) Complex with Dithio α-Diketone

Seizo MISUMI and Kazuo KOYA

Inorganic Chemistry Laboratory, Faculty of Science, Kyushu Universiy, Fukuoka

(Received June 2, 1969)

Stilbenedithiol is a bidentate ligand containing two sulfur atoms. Several metal complexes with this ligand have been prepared by Schrauzer.[1] Regarding the copper(II) complex, however, only bis(maleonitrile dithiolato)Cu(II)[2] and bis(toluene-3,4-dithiolato)Cu(II)[3] have been reported. In this paper, we will describe the preparation of a novel copper(II) complex with stilbenedithiol as a dithio α-diketone complex.

By using the benzoin-P_4S_{10} method,[4] a copper(II)-stilbenedithiolate complex was prepared through the reaction of the thiophosphoric ester of stilbenedithiol and an excess of copper(II) in benzene; a dark violet complex was thus isolated. This complex, recrystallized from dioxane, is soluble in dichloroethane, chloroform, and ethanol, and it was found by elementary analysis to have the formula of $Cu_2S_2(S_2C_2(C_6H_5)_2)_2$. (Found: C, 49.98; H, 3.22; S, 26.95±3; Cu, 19.1%. Calcd for $Cu_2S_2(S_2C_2(C_6H_5)_2)_2$: C, 49.75; H, 2.99; S, 28.46; Cu, 18.08%). A molecular-weight determination by the use of the "Vapour Pressure Osmometer" showed that this compound was dimeric (Found: 661, Calcd: 676) and had a sulfur-bridged structure, one similar to the dimeric compounds of iron(II)[5] and molybdenum.[6] The structure may be supposed, as is shown in Fig. 1, to be a dimeric copper(II)-stilbeneditiolate complex.

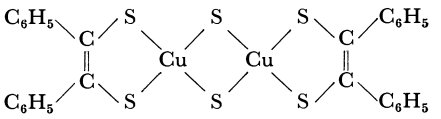

Fig. 1

It was found that this complex is diamagnetic. The absorption spectrum of the complex in dichloromethane shows that all the electronic transitions are at slightly longer wavelengths than those of the monomer; this fact is probably due to the dithion resonance *via* the sulfur bridges.

In the infrared spectrum, the C=C band was observed at 1445 cm^{-1}; this indicates about a 75% double-bond character, according to Schrauzer's relationship between the C=C stretching frequencies and the calculated % of the C=C character.[5] The peak at 328 cm^{-1} in the far-infrared region is probably to be assigned to the Cu-S stretching frequency. The detailed results will be reported shortly.

1) G. N. Schrauzer and V. P. Mayweg, *J. Am. Chem. Soc.*, **84**, 3221 (1962).

2) H. B. Gray and R. Williams, *ibid.*, **84**, 3596 (1962).

3) H. B. Gray and E. Billig, *ibid.*, **85**, 2019 (1963).

4) G. N. Schrauzer and V. P. Mayweg, *Inorg. Chem.*, **4**, 1615 (1965).

5) G. N. Schrauzer and V. P. Mayweg, *J. Am. Chem. Soc.*, **88**, 4604 (1966).

6) G. N. Schrauzer and V. P. Mayweg, *ibid.*, **88**, 5174 (1966).

Isotope Effects on the Reactions of ^{82}Br Activated by Isomeric Transition between CH_4 and CD_4

Enzo TACHIKAWA

Division of Chemistry, Japan Atomic Energy Research Institute, Tokai-mura, Ibaraki

(Received June 9, 1969)

^{82}Br activated by the isomeric transition originally has a high charge and a high energy resulting from the Auger process following the internal conversion.[1] Thus, it can react with a reactant *via* the energetic process and also *via* the thermal ionic process.

Spicer and Gordus[2] studied the reaction of ^{80}Br activated by the (I.T.) process with CH_4 and CD_4 and found that the total organic yield in the reaction with CH_4 is higher than in that with CD_4 by a factor of 1.5. On the other hand, Nicholas and Rack[3] attempted to prove that equal organic yields result from both the ^{82m}Br-CH_4 and ^{82m}Br-CD_4 systems. However, these measurements do not offer any information concerning the isotope effects in the individual reaction processes, energetic and thermal ionic.

This paper will described the study of the influence of the moderator gas on the individual products from both the ^{82m}Br-CH_4 and the ^{82m}Br-CD_4 systems; this study was undertaken in order to ascertain the isotope effects on each reaction process separately. The details of the experimental methods may be found elsewhere.[4] In all samples the ratio of Br_2 as a scavenger relative to CH_4 or CD_4 was kept constant, 0.11 ± 0.01, and the total pressure was 51 ± 1 cmHg.

Figure 1 shows the moderator effects on the products. $CH_3{}^{82}Br$ and $CD_3{}^{82}Br$ are $5.0\%\pm0.5\%$ and $2.1\%\pm0.2\%$ respectively at zero mole fraction of the moderator, and both can be extrapolated to $0.5\%\pm0.2\%$ at a 1.0 mol fraction of the moderator. On the other hand, $CH_2{}^{82}BrBr$ and $CD_2{}^{82}BrBr$ are constant at $1.1\%\pm0.2\%$ at any mole fraction of the moderator. This indicates that the $CH_3{}^{82}Br$ and $CD_3{}^{82}Br$ formed *via* the energetic process are $4.5\%\pm0.5\%$ and $1.6\%\pm0.2\%$ respectively. It may, then, be concluded that there is an isotope effect between CH_4 and CD_4 in the energetic reaction but not in the thermal ionic reactions.

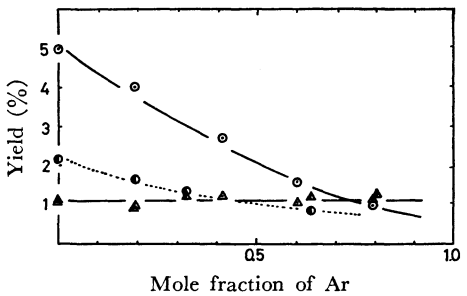

Fig. 1. Moderator effects on the yields of CH_3Br and CH_2Br_2.
system: ^{80m}Br-CH_4 ◐ $CH_3{}^{80}Br$ ◭ $CH_2{}^{80}BrBr$
system: ^{82m}Br-CH_4 ⊙ $CH_3{}^{82}Br$ △ $CH_2{}^{82}BrBr$

Several possible sources for the observed isotope effect in the energetic reaction can be considered, such as in the case of the reaction of the recoil tritium atom[5]: the moderator isotope effect, the probability-integral isotope effect, and the average-energy isotope effect. The present results demonstrate that the yeild of $CH_3{}^{82}Br$ is consistently higher than that of $CD_3{}^{82}Br$ at any mole fraction of the moderator and that the $CH_3{}^{82}Br/CD_3{}^{82}Br$ ratio for the energetic reaction is rather constant (3.0 ± 1.0). These findings are consistent with the moderator isotope effect and /or the probability-integral isotope effect. However, the moderator isotope effect is particularly important in the low mole fraction of the moderator; it becomes less important with an increase in the mole fraction of the moderator, since the energy loss through the nonbonding collisions with the moderator then become predominant. Thus, it would appear that the probability integral isotope effect is more important than the moderator isotope effect.

At this moment, it is not clear why the isotope effect was not found for the total organic yields in the work by Rack et al.[3] One possible reason is the inclusion of a polymer tagged with ^{82}Br in their analytical results.

1) S. Wexler and G. Anderson, *J. Chem. Phys.*, **33**, 850 (1960).
2) L. D. Spicer and A. A. Gordus, "Chemical Effects of Nuclear Transformations," Vol. I, IAEA, Vienna (1965), p. 185.
3) J. B. Nicholas and E. P. Rack, *J. Chem. Phys.*, **48**, 4085 (1968).
4) J. Okamoto and E. Tachikawa, This Bulletin, **42**, 1504 (1969).
5) E. K. C. Lee, G. Miller and F. S. Rowland, *J. Am. Chem. Soc.*, **87**, 190 (1965).

Natural Occurrence of Humulol and Tricyclohumuladiol

Yoko NAYA and Munio KOTAKE

The Institute of Food Chemistry, Dojimanaka, Kita-ku, Osaka

(Received June 11, 1969)

In our series papers[1] we have reported new constituents of hop oil. This communication will deal with two sesquiterpene alcohols, humulol (I) and tricyclohumuladiol (II), isolated from the same source.

The alcohol (I) is a viscous oil, $C_{15}H_{26}O$, $[\alpha]_D^{24}$ $-1.2°$ ($c=0.87$, MeOH), which exhibited hydroxyl group absorptions (3370 and 1110 cm^{-1}) in the IR spectrum. The other characteristic absorption bands were shown at 1380, 1365 (*gem*-dimethyl), and 980 cm^{-1} (C=C *trans*). The IR and NMR spectra of the compound I were identical with those of the alcohol, which had been isolated by Buttery *et al.*[2] They suggested[3,4] that the alcohol might be the same as Chapman's luparenol,[5] also isolated from hop oil; this suggestion was made on the basis of the molecular formula, $C_{15}H_{24}O$. If the two are the same, the molecular formula must be corrected. However, the identity of the compound (I) and "luparenol" can not be confirmed because of insufficient evidence. To avoid confusion, therefore, we propose the name "humulol" for the compound (I).

Its NMR spectrum*1 showed two singlets, at 1.05 and 1.10 (each 3H), and a doublet at 1.59 (3H, $J=1$ Hz), due to tertiary methyl groups and a vinyl methyl group respectively; and a singlet at 1.15 (3H) assignable to a methyl attached to a carbon atom bearing a hydroxyl group; complex multiplets located between 4.90—5.20 account for three vinyl protons (HC=CH and $CH=CCH_3$). The mass spectrum exhibited its molecular ion peak at *m/e* 222 and its base peak at *m/e* 82.

The hydrogenation of I with PtO_2 in acetic acid gave the saturated compound, $C_{15}H_{30}O$ (M^+, *m/e* 226).

When the alcohol (I) was injected in a preparative GLC (SF-96) at 220°C, the greater part of it was converted into β-humulene, which was identical with the authentic compound (IR, NMR, and MS). The above evidence indicates the structure I for humulol.

The diol II, named tricyclohumuladiol, $C_{15}H_{26}O_2$, $[\alpha]_D^{24}$ 0° ($c=2.7$, MeOH), was recrystallized from methanol - ether as colorless plates; mp 207°C. II exhibited hydroxyl absorptions (3300, 1135 cm^{-1}) and bands (1010, 895 cm^{-1}) assignable to cyclopropane ring in the IR spectrum; other peaks of diagnostic value were at 1360 and 1375 (*gem*-dimethyl). Its NMR spectrum ($(CD_3)_2SO$) showed singlets at 0.89, 0.95, 0.96, and 1.03 (each 3H, tertiary methyls); a multiplet centered at 2.98 (1H) is assignable to a proton on the carbon atom bonded to a hydroxyl group; a complex multiplet located between 0.10—0.70 accounts for three protons on a cyclopropane ring. The mass spectrum exhibited its molecular ion peak at *m/e* 238 and its base peak at *m/e* 43.

On acetylation with acetic anhydride and pyridine, II gave a monoacetate (III), $C_{17}H_{28}O_3$ (M^+, *m/e* 280), mp 69—70°C (rhombic). Upon treatment with $SOCl_2$ - pyridine or hydrochloric acid in a methanol solution, a tertiary hydroxyl group of III was replaced by chlorine; yielded was a viscous oil (IV), $C_{17}H_{27}O_2Cl$, which did not exhibit any hydroxyl absorption in its IR spectrum.

When II was oxidized with CrO_3 - pyridine, it afforded a hydroxy-ketone (V), $C_{15}H_{24}O_2$, which could be purified by GLC. The IR and UV spectra indicated that V is a macro-cyclic ketone conjugated with a cyclopropane ring (1670 cm^{-1} (C=O); λ_{max}^{hexane} 203 mμ (ε 2800)). V was characterized as a chloro-compound (VI), $C_{15}H_{23}OCl$, mp 115—116°C, by the method described above.

The chemical properties and physical constants of the diol (II) were quite simiar to those of the authentic compound[6] prepared from humulene; the absolute conformation is shown as the formula (II).

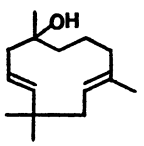

I

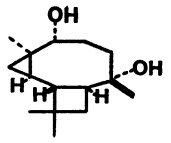

II

1) Previous paper: Y. Naya and M. Kotake, This Bulletin, **42**, 2088 (1969).

2) R. G. Buttery, W. H. McFadden, R. E. Lundin and M. P. Kealy, *J. Inst. Brew.*, **70**, 396 (1964).

3) R. G. Buttery and L. C. Ling, *Brewers Digest*, **1966**, 71.

4) R. G. Buttery, R. E. Lundin and L. Ling, *Agri. Food Chem.*, **15**, 58 (1967).

5) A. C. Chapman *J. Chem. Soc.*, **1928**, 1303.

*1 All NMR spectra were taken in CCl_4 on a JEOL Model C-60 spectrometer with TMS as an internal reference. The values are reported in ppm.

6) J. M. Greenwood, M. D. Solomon, J. K. Sutherland and A. Torre, *J. Chem. Soc., C*, **1968**, 3004.

Living Anionic Polymerization of 3-Vinylpyrene with Sodium-Naphthalene Complex

Kiyoshi TANIKAWA, Hirotaka HIRATA, Shigekazu KUSABAYASHI and Hiroshi MIKAWA

Department of Chemical Technology, Faculty of Engineering, Osaka University, Yamada-Kami, Suita, Osaka

(Received June 11, 1969)

With the cationic, radical and Ziegler-Natta catalysts we have already succeeded in polymerizing 3-vinylpyrene (3-VP), a vinyl monomer having the largest aromatic group hitherto known.[1] We have now found that the living anionic polymerization of this monomer is possible if the monomer is purified finally by sublimation in high vacuum and used without being exposed to air.

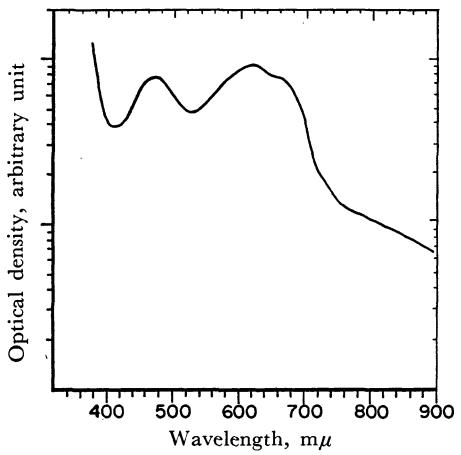

Fig. 1. Absorption spectrum of living PVP in THF at room temperature.

Polymerization was carried out by using high vacuum technique, and by adding the tetrahydrofuran (THF) solution of the sublimed monomer into the THF solution of the initiator, sodium-naphthalene, at room temperature. Typical results are shown in Table 1.

On addition of the monomer solution (pale yellow color), the green color of the solution of the initiator changed immediately to blue, showing absorption maximum at 620 mμ (Fig. 1). This band is attributed to the absorption of the living poly-3-vinylpyrene (PVP) for the following reasons. (1) The wavelengths of the absorption peaks of the living polystyrene,[2] polyvinylbiphenyl,[3] and poly-1-vinylnaphthalene[4] are 342, 405 and 558 mμ, respectively. It seems, therefore, reasonable that the spectrum of the living PVP shows a maximum at 620 mμ. (2) The color of the solution of the living PVP does not change appreciably by further addition of the monomer solution, while the total polymer yield increases considerably with the simultaneous increase of the intrinsic viscosity of the isolated polymer, as shown in Table 1.

TABLE 1. POLYMERIZATION OF 3-VINYLPYRENE

The 1st addition of the monomer g (mol $\times 10^4$)	The 2nd addition of the monomer g (mol $\times 10^4$)	Initiator (mol $\times 10^5$)	Yield g	Softening range °C	Intrinsic viscosity*
0.18 (7.9)	—	1.0	0.17	281<	0.23
0.16 (7.0)	0.15 (6.6)	0.9	0.28	300<	0.31

* in THF at 25°C.

1) a) K. Tanikawa, S. Kusabayashi, H. Hirata and H. Mikawa, *J. Polymer Sci., B*, **6**, 275 (1968); b) K. Tanikawa, T. Ishizuka, K. Suzuki, S. Kusabayashi and H. Mikawa, This Bulletin, **41**, 2719 (1968).

2) D. N. Bhattacharyya, C. L. Lee, J. Smid and M. Szwarc, *J. Phys. Chem.*, **69**, 612 (1965).

3) M. Szwarc, "Carbanions Living Polymers and Electron Transfer Processes," Interscience Publishers, New York (1968).

4) F. Bahsteter, J. Smid and M. Szwarc, *J. Am. Chem. Soc.*, **85**, 3909 (1963).

Electronic Spectra of Organic Charge Transfer Salts of 2-Dicyanomethylene-1,1,3,3-tetracyanopropane

Seiki SAKANOUE, Toshiaki TAMAMURA, Shigekazu KUSABAYASHI, Hiroshi MIKAWA, Nobutami KASAI, Masao KAKUDO and Haruo KURODA*

Department of Chemical Technology, Faculty of Engineering, Osaka University, Yamada-kami, Suita, Osaka
** Department of Chemistry, Faculty of Science, The University of Tokyo, Hongo, Bunkyo-ku, Tokyo*

(Received June 21, 1969)

In some compounds charge transfer bands between organic cation and organic anion have been observed in the electronic spectrum.[1] However, there has been no explanation of these charge transfer bands on the basis of the crystal structure.

The absorption spectra of quinolinium 2-dicyanomethylene-1,1,3,3-tetracyanopropanediide (Q_2DMTP) in various solvents are shown in Fig. 1. In chloroform-ethanol solution, two new shoulder bands appeared near 380 and 410 mμ in addition to the absorption of the component ions. The apparent extinction coefficient of these shoulder bands decreased with the increase of the polarity of the solvents. In the same solvent the apparent extinction coefficient of the absorption in 410 mμ increased with the increase of the concentration, while that of the absorption in 380 mμ decreased. This may be explained from the equilibrium between the dissociated ions and the ion-pairs, Q_2DMTP and/or QDMTP$^-$, and the new absorption bands due to the ion-pairs.

To elucidate the origin of the new absorption band, the polarized absorption spectrum of a single crystal was measured by means of a microspectrophotometer. The crystal of this salt is orthorhombic with the unit cell dimensions, $a=13.18$, $b=15.40$, $c=11.56$ Å; $Z=4$, and the space group, *Pbcn*. In the crystal, one unit consists of the propeller-shaped DMTP anion sandwiched with two planar quinolinium cations on both sides, and the unit is stacked in finitely along the *a*-axis. The tilt angle of the plane of the cation to the *a*-axis is about 60°. In the solid absorption spectrum, a new band was also observed. The spectrum of *a*-polarization and that of *c*-polarization are shown in Fig. 2. It can be seen that the optical density is higher in the *a*-polarization spectrum than in the *c*-polarization spectrum. In connection with the crystal structure, this result proves that the new band in solid is a charge transfer band between ions within an ion-pair.

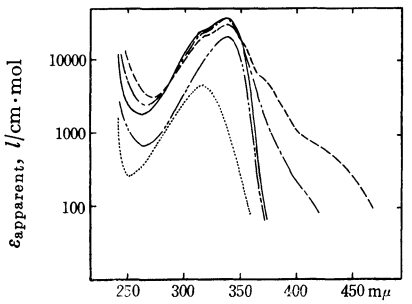

Fig. 1. The absorption spectra of Q_2DMTP in various solvents and its component ions (Q^+, $DMTP^{2-}$) in water.
····· Quinoline in HCl aqueous solution
–––– Na_2DMTP in H_2O
—— Q_2DMTP in H_2O 3.24×10^{-4} mol/l
—— Q_2DMTP in C_2H_5OH 3.16×10^{-4} mol/l
---- Q_2DMTP in $CHCl_3$-C_2H_5OH 5.00×10^{-4} mol/l

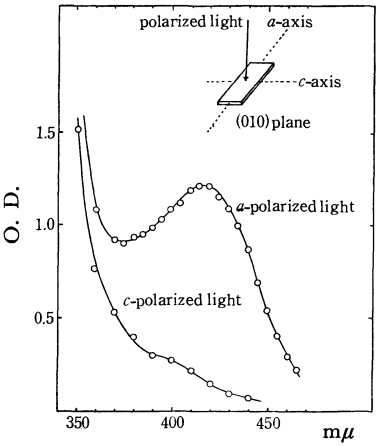

Fig. 2. Polarized absorption spectrum of Q_2DMTP.

Several other salts of DMTP were also prepared with *N*-heteroaromatic cations, such as pyridinium, quinolinium and *N*-methylacridinium. These salts showed characteristic colors, white, yellow and red, respectively. The wavelengths of the new absorption bands of these salts increased as the electron affinity of the *N*-heteroaromatic cations increased. Therefore the color of the salts may be also attributed to the electronic transition from the anion to the cation.

The results show that the new absorption band both in solid and in solution is a charge transfer band between ions within an ion-pair.

1) M. Feldman and S. Winstein, *Tetrahedron Letters*, **19**, 853 (1962); E. L. Goff and R. B. LaCount, *J. Am. Chem. Soc.*, **85**, 1354 (1963).

The Crystal Structure of an Organic Charge Transfer Salt, $[2(C_9H_8N)^+ \cdot (C_{10}N_6)^{2-}]$

Seiki SAKANOUE, Noritake YASUOKA, Nobutami KASAI, Masao KAKUDO, Shigekazu KUSABAYASHI and Hiroshi MIKAWA

Department of Applied Chemistry, Osaka University, Yamada-Kami, Suita, Osaka

(Received June 23, 1969)

The crystal of quinolinium 2-dicyanomethylene-1,1,3,3-tatracyanopropanediide, $[2(C_9H_8N)^+ \cdot (C_{10}N_6)^{2-}]$, is orthorhombic with the unit cell dimensions of $a=13.18$, $b=15.40$, $c=11.56$ Å; $Z=4$, $D_m=1.31_8$, and $D_c=1.31_4$ g/cm^3, and with the space group *Pbcn*. The intensities of 2003 reflections were measured visually from the multiple-film equi-inclination Weissenberg photographs taken with nickel-filtered Cu$K\alpha$ radiation around the *a* and *c* axes. The structure was solved by the symbolic addition, phase-determining procedure developed by Karle and Karle.[1] The $\sum_2$ formula was applied to 247 reflections with $|E| \geqq 1.60$. After six cycles, the signs of 161 reflections were determined; the *E*-map based on these signs allowed us to locate all the non-hydrogen atoms. The positional and thermal parameters of each atom were refined by the block-diagonal least-squares method ($R=15.2\%$).

Figure 1 shows the structures of the anion and the cation. The $(C_{10}N_6)^{2-}$ anion in this crystal has a C_2-2 symmetry instead of the C_3-3 symmetry (or approximately D_3-32) found in crystals of the hexahydrated calcium salt.[2] The four central carbon atoms are exactly co-planar. The three cyano-substituents, $-C(CN)_2$ are, however, tilted out of this plane, and the anion takes a propeller-shape. The one arm which lies on the 2-fold axis is rotated by 13° from the completely planar conformation, the other two being 24°. On the other hand, in the calcium salt[2] the three angles of tilt are all 24°. The decrease in the angle from 24° to 13° may be due to weak interaction between the anion and the cation. The bond distances and angles in the anion are similar to those found in the calcium salt. The quinolinium cation is co-planar within the limits of experimental error.

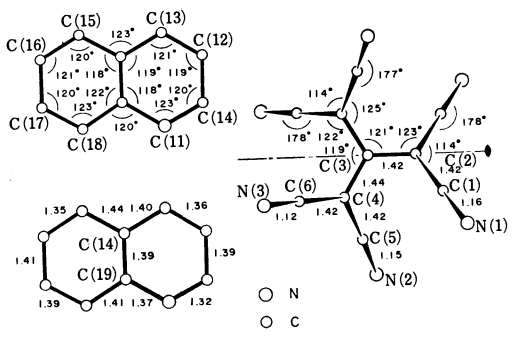

(a) (b)

Fig. 1. Structure of component ions.
(a) Quinolinium cation, $(C_9H_8N)^+$
(b) 2-Dicyanomethylene-1,1,3,3-tetracyanopropane anion, $(C_{10}N_6)^{2-}$
(Estimated standard deviations in distances are 0.013–0.02Å, and those in angles are 0.83–1.4°.)

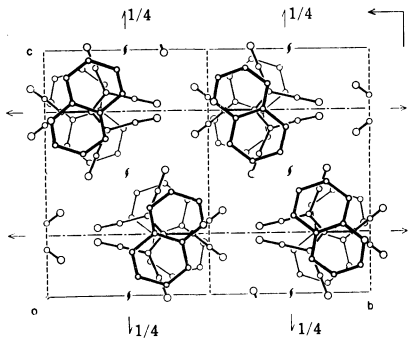

Fig. 2. Crystal structure of $[2(C_9H_8N)^+ \cdot (C_{10}N_6)^{2-}]$ projected onto the (010) plane.

Figure 2 shows the projectional view along the *a* axis. The packing unit consists of one di-anion and two mono-cations, and the anion lies on a 2-fold axis between two identical cations forming a sandwich. The N(1)–N(11) distance is 3.00 Å, which is the closest atomic contact between ions in this unit. These units stack infinitely along the *a* axis. In the contacts between these stacks along the *b* axis, a hydrogen bond exists between the N(3) of one unit and the N(11) of the other unit; the distance is 2.84 Å. The other intermolecular contacts are almost comparable with the sum of the van der Waals radii.

These results are interesting compared with the structures of other charge-transfer salts, 1-ethyl-2-methylquinolinium iodide[3] and tropylium iodide.[4]

1) For example, J. Karle and I. L. Karle, *Acta Cryst.*, **21**, 849, (1966).

2) D. A. Bekoe, P. K. Gantzel and K. N. Trueblood, *ibid.*, **22**, 657, (1967).

3) S. Sakanoue, Y. Kai, N. Yasuoka, N. Kasai, M. Kakudo and H. Mikawa, *Chem. Commun.*, **1969**, 176.

4) A. I. Kitaigorodskii, Yr. T. Struchlov, T. L. Khotsyanova, M. E. Vol'pin and D. N. Kursanov, *Izvest. Akad. Nauk S.S.S.R., Otdel. Khim. Nauk*, **1**, 32, (1960).

New Empirical Formulae for the Mass Effect in the Countercurrent Electromigration of Molten Metal Halides

Nobufusa SAITO and Hitoshi KANNO

Department of Chemistry, Faculty of Science, The University of Tokyo, Hongo, Bunkyo-ku, Tokyo

(Received June 23, 1969)

The mass effect of the cation in the countercurrent migration of molten metal halides has long been known to correlate with the cation-to-anion mass ratio according to Klemm's formulae:[1,2]

$$\mu = -0.15/(1+m_+/2.1m_-)$$
(for halides with layer lattices)

and $\mu = -0.078/(1+m_+/2.1m_-)$
(for halides with coordination lattices)

where μ, m_+, and m_- stand for the mass effect, the mass of the cation, and the mass of the anion, respectively.

However, recent investigations[3-6] have revealed that there are several cases in which the values of μ calculated by the Klemm formulae deviate considerably from the experimental values. Although a new empirical formula for the same sort of correlation was proposed by Jordan and Klemm[5] in 1966, it applies only to a group of alkali halides.

After a careful examination of the available data on μ, we have found that a clear correlation exists between the mass effect and the cation-to-anion radius ratio of the halide. In Fig. 1, the experimental values of μ for various metal halides are plotted as a function of the cation-to-anion radius ratio.

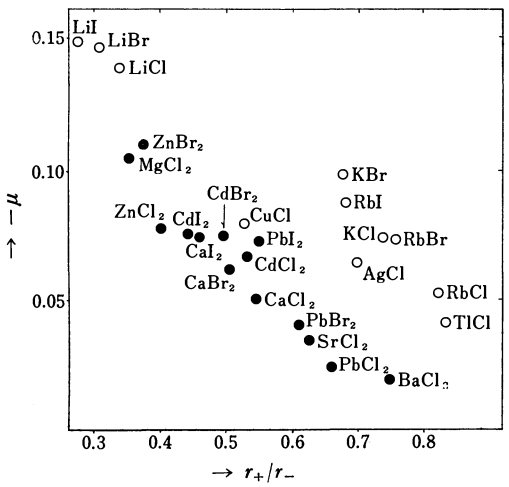

Fig. 1. Correlation of the mass effect of molten halides with the cation-to-anion radius ratio.
○ monovalent metal halide
● divalent metal halide
Sources of data: KBr and RbI—N. Saito, H. Kanno and I. Tomita, unpublished work; CaI_2, CdI_2 and PbI_2—J. Romanos and A. Klemm, *Z. Naturforsch.*, **19a**, 1000 (1964); $CdBr_2$—I. Holmlid, *ibid.*, **21a**, 270 (1966); other data—A. Klemm, "Molten Salt Chemistry," ed. by M. Blander, Interscience Publishers, New York, N. Y. (1964), p. 597.

We may see from Fig. 1 that a linear correlation exists between the mass effect and the cation-to-anion radius ratio of the halide. In addition, it is clear that the data for a group of monovalent metal halides show a linear correlation similar to, but clearly displaced from, the correlation line for a group of divalent metal halides.

Fitting the set of the data for each group of the halides in Fig. 1 to an equation of a linear form, $\mu = a(r_+/r_-)+b$, where a and b are constants, by a standard least-square procedure, we have obtained two empirical formulae:

$$\mu = 0.181(r_+/r_-) - 0.203$$
(for monovalent metal halides)

$$\mu = 0.233(r_+/r_-) - 0.185$$
(for divalent metal halides)

The experimental μ values of several halides are listed in Table 1, along with the values calculated by both Klemm's and our formulae.

TABLE 1. COMPARISON OF THE CALCULATED μ VALUES WITH EXPERIMENTAL DATA

Salt	$-\mu$ Found by experiments	$-\mu$ Calculated by Saito-Kanno's formulae	$-\mu$ Calculated by Klemm's formulae
RbCl	0.052	0.054	0.070
RbBr	0.073	0.065	0.099
RbI	0.087	0.079	0.113
LiCl	0.140	0.142	0.138
AgCl	0.064	0.077	0.061
$CaCl_2$	0.051	0.058	0.050
$CaBr_2$	0.062	0.067	0.060
CaI_2	0.075	0.079	0.130

Detailed discussions of our formulae will appear in a full paper to be published elsewhere.

1) A. Klemm, *Z. Naturforsch.*, **6a**, 487 (1951); *ibid.*, **8a**, 397 (1953).
2) A. Neubert and A. Klemm, *ibid.*, **16a**, 685 (1961).
3) J. Romanos and A. Klemm, *ibid.*, **19a**, 1000 (1964).
4) I. Holmlid, *ibid.*, **21a**, 270 (1966).
5) S. Jordan and A. Klemm, *ibid.*, **21a**, 1581 (1966).
6) N. Saito, H. Kanno and I. Tomita, unpublished work.

Pulse Radiolysis with Electric Conductivity. A Method of Obtaining the Rates of Propagation in the Radiation-induced Polymerization of α-Methylstyrene*[1]

Meiseki KATAYAMA, Hatsuo YAMAZAKI and Yasutomo OZAWA

Department of Chemistry, Faculty of Science, Hokkaido University, Sapporo

(Received June 24, 1969)

The present authors previously studied intermediates in irradiated dry α-methylstyrene by means of pulse radiolysis with optical absorption measurements.[1] Following that work, similar studies have been reported by Swallow and Schneider[2] and by Metz and his coworkers[3] for styrene as well as α-methylstyrene. All three groups agreed that one of the intermediates is the anion radical of these compounds. Now we wish to report on further investigations in which we applied a method of electric conductivity measurements after a pulse irradiation in order to obtain the rates of propagation in the reaction. The method is, in principle, similar to that used for determining the mobilities of a carrier in semiconductors[4] and later applied to the studies of radiation chemistry by Hummel and Allen[5] in order to obtain the yield of ions in some liquid hydrocarbons.

As is shown in Fig. 1, a very thin layer of ions, both anion and cation, is produced by a single pulse of X-rays in a sample very close to one electrode, E_1, which is negatively polarized in the present case. The cation then discharges on the electrode immediately after its formation, while the anion moves to the other electrode, E_2, for measurements over rather a long period of time. In this way, the mobility of anion can, in principle, be measured separately. The mobility of the cation can also be measured by simply reversing the polarity of E_1. When a polymerizing system is studied, an anion, or an anion radical, will polymerize as it moves to E_2. Since the diffusion constant, or the mobility, of ions generally decreases as their molecular weights increase, we can compare the rate of the propagation of anionic species directly with that of cationic species by comparing the respective measured mobilities by just changing the polarity of E_1. An example of such measurements is shown in Fig. 2.

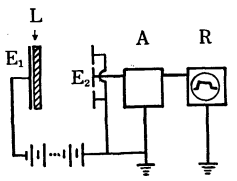

Fig. 1. The diagram of mobility measurements. E_1, E_2; electrode, L; layer of ions, A; ammeter and R; recorder.

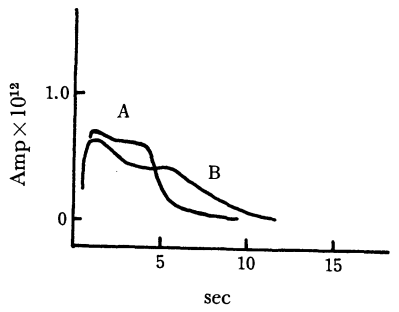

Fig. 2. The current-time curves with dry α-methylstyrene. A, positive ions and B, negative ions.

TABLE 1. THE MOBILITIES OF IONS IN α-METHYLSTYRENE
$[cm^2 V^{-1} sec^{-1}] \times 10^4$

Cation	Anion	Condition
5.0	1.9—1.4	dry[G(-monomer)≥7300]
5.0	4.0	saturated with water

Some data on mobility thus obtained in α-methylstyrene are given in Table 1. From these data and from the fact that the polymerization proceeds much faster in a dry sample than in wet ones,[6] it may be concluded that the anionic reaction is more important than the cationic one in the radiation-induced polymerization of α-methylstyrene.

*1 Presented at the 9th Japan Conference on Radioisotopes, Tokyo, May, 1969.

1) M. Katayama, M. Hatada, K. Hirota, H. Yamazaki and Y. Ozawa, This Bulletin, **38**, 851 (1965); M. Katayama, *ibid.*, **38**, 2208(1965); M. Katayama, H. Yamazaki, Y. Ozawa and K. Hirota, *Nippon Kagaku Zasshi (J. Chem. Soc. Japan, Pure Chem. Sect.)*, **87**, 37 (1966).

2) C. Schneider and A. J. Swallow, *J. Poly, Sci. B*, **4**, 277 (1966); C. Schneider and A. J. Swallow, *Macromol. Chem.*, **144** 155 (1968).

3) D. J. Metz, R. C. Potter and J. K. Thomas, *J. Poly. Sci. A-1*, **5**, 877 (1967).

4) For example, J. R. Haynes and W. Shockley, *Phys. Rev.*, **81**, 835 (1951).

5) A. Hummel and A. O. Allen, *Discussions Faraday Soc.*, **36**, 95 (1963); A. Hummel and A. O. Allen, *J. Chem. Phys.*, **44**, 3426 (1966).

6) P. Ausloos, "Fundamental Processes in Radiation Chemistry," Interscience Publishers, New York (1968), p. 576.

Anodic Oxidations. I. The Electrochemical Cyanation of 2,5-Dimethylfuran

Kunihisa YOSHIDA and Takayuki FUENO

Faculty of Engineering Science, Osaka University, Toyonaka, Osaka

(Received June 30, 1969)

Koyama and co-workers developed a method for the electrochemical cyanation of aromatic compounds.[1-4] With the exception of anisole, however, this method affords very poor yields of aromatic nitriles, and according to circumstances methoxylation is predominant. An improved approach to cyanation of aromatic compounds has recently been reported by Andreades and Zahnow.[5] Cyanation of olefins has also been studied without much success.[3,6,7]

We wish to report a new cyanation reaction of 2,5-dimethylfuran to olefinic cyano ethers.

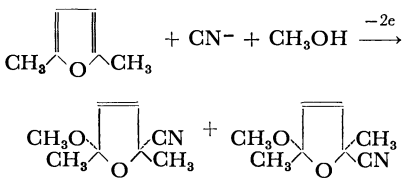

The over all reaction involves the attack of the cyanide ion on an anodically generated electrophilic intermediate.

Electrolysis was carried out by using a two-compartment cell which was equipped with a platinum wire electrode in the cathode compartment, and with the saturated calomel reference electrode and a platinum plate electrode having an area of 8 cm^2 in the anode compartment. A methanolic solution (40 m*l*) of 2,5-dimethylfuran (0.8 M) and sodium cyanide (0.8 M) was electrolyzed at 21°C for 7.5 hr, using an anode potential of 1.3 V *vs.* SCE. The catholyte was a methanolic solution of sodium cyanide (0.8 M). The current was about 60 mA. Vacuum distillation of the electrolyzed mixture afforded 0.92 g of colorless liquid boiling at 80°C/10 mmHg. The products were identified by infrared, mass and NMR spectroscopy to be a 2.4 : 1 mixture of the *cis* and *trans* isomeric 2,5-dihydro-2-cyano-2,5-dimethyl-5-methoxyfurans[8]; the molecular weight 153, the current yield 74%. Found: C, 62.78; H, 7.30; N, 9.06%. Calcd for $C_8H_{11}NO_2$: C, 62.73; H, 7.24; N, 9.14%.

Current-potential measurements were also carried out on a 0.8 M solution of sodium cyanide in methanol at 25°C, both in the presence and absence of 2,5-dimethylfuran, by using the same cell as that used for electrolysis. The measurements clearly showed that at 1.3 V the cyanide ion was not discharged to any discernible extent. Under the present conditions, therefore, it is 2,5-dimethylfuran that has predominantly been discharged at the anode. The electrophilic intermediate thus formed may have then reacted with both cyanide ion and methanol to form olefinic cyano ethers.

One major advantage of the present reaction lies in its relatively high yield in producing cyanated derivatives. Under the experimental conditions here adopted, the current yield was as high as 74% although the total yield of the cyano ethers based on 2,5-dimethylfuran used was *ca.* 20%. Another merit is that the reaction is accompanied by no undesirable side reactions.

Investigations of the mechanistic details of the reaction and its extension to other substrates are now under way and will be reported elsewhere.

1) K. Koyama, T. Susuki and S. Tsutsumi, *Terahedron Letters*, **1965**, 627.

2) V. D. Parker and B. E. Burgert, *ibid.*, **1965**, 4065.

3) K. Koyama, T. Susuki and S. Tsutsumi, *Tetrahedron*, **23**, 2675 (1967).

4) T. Susuki, K. Koyama, A. Omori and S. Tsutsumi, This Bulletin, **41**, 2663 (1968).

5) S. Andreades and E. W. Zahnow, Abstracts of Papers, Electrochemical Society Meeting, Electroorganic Division, Dallas, Texas, 1967, p. 15.

6) H. Schmidt and H. Meinert, *Z. Anorg. Allgem. Chem.*, **295**, 173 (1958).

7) K. Yoshida and S. Tsutsumi, *Tetrahedron Letters*, **1966**, 2501.

8) The NMR spectra of these products were compared with those of the known 2,5-dihydrofurans and the *cis* configuration was tentatively assigned to the major isomer: a) A. Aito, T. Matsuo and C. Aso, This Bulletin, **40**, 130 (1967); b) A. J. Baggaley and R. Brettle, *J. Chem. Soc., C*, **1968**, 969.

The Crystal Structure of Diamminecadmium(II) Tetracyanoniccolate(II) Benzene Clathrate, $Cd(NH_3)_2Ni(CN)_4 \cdot 2C_6H_6$*[1]

Yukiyoshi SASAKI

The Institute for Solid State Physics and Department of Chemistry, Faculty of Science, The University of Tokyo, Hongo, Tokyo

(Received July 16, 1969)

During the course of our studies on "Hofmann-type" benzene clathrates, $M(NH_3)_2M'(CN)_4 \cdot 2C_6H_6$ where M=Mn(II), Fe(II), Co(II), Ni(II), Cu(II), Zn(II), or Cd(II) and M'=Ni(II), Pd(II) or Pt(II),[1] it was assumed that these complexes would have structures similar to that of $Ni(NH_3)_2Ni(CN)_4 \cdot 2C_6H_6$ known as Hofmann's clathrate.[2] And it was considered highly desirable to carry out additional studies using single crystals.

The present communication reports results of the crystal structure determination which proved the above mentioned structure in the case of M=Cd and M'=Ni which has been already subjected to IR[3] and NMR[4] studies.

The crystals are tetragonal, with the space group of $P_{4/m}$-C'_{4h}. One formula unit is contained in a cell of the dimension: $a=b=7.575\pm0.006$ Å and $c=8.317\pm0.005$ Å. No piezo-electricity was observed.

The intensities of the three-dimensional reflections were measured visually from equi-inclination Weissenberg photographs around the a and c axes taken with Ni-filtered Cu$K\alpha$ radiation. In total, 356 reflections were collected. Table 1 shows the atomic parameters which give the R-factor of 11.8%.

On the whole, the crystal has a lameller structure, inorganic polymer sheets and layers of benzene being alternated. As shown in Fig. 1, the cadmium atom at 0, 0, 0 and the nickel atom at 1/2,1/2,0 are joined together by cyanide bridges to form planar sheets parallel to the plane (001). Four nitrogen atoms of cyanide anions and two ammonia molecules at *trans*-positions coordinate to a cadmium atom forming an octahedron. Four carbon atoms of cyanide ligands take square planar configuration in a $Ni(CN)_4$ unit. Benzene molecules are arranged between these sheets with their molecular planes parallel to the c axis making an angle of 58°30′ to a or b axis.

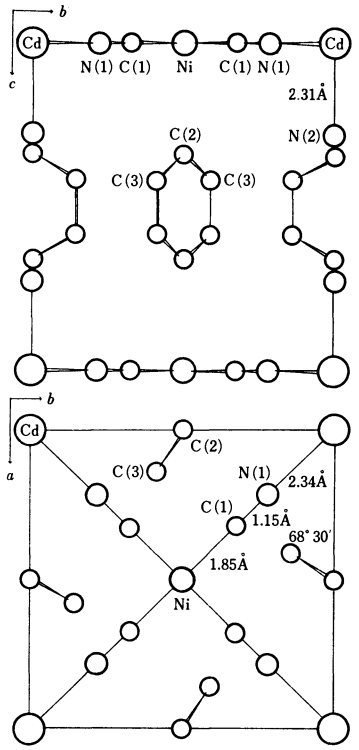

Fig. 1. Projections of the unit cell along a and c axes.
The standard deviations of the bond lengths are 0.03 Å for C-N and Cd-NH_3 and 0.02 Å for Ni-C and Cd-N(C).

TABLE 1. ATOMIC PARAMETERS WITH STANDARD DEVIATIONS

	$10^4X/a$	$10^4Y/b$	$10^4Z/c$	B(Å^2)
Cd	0000(0)	0000(0)	0000(0)	0.472(0.039)
Ni	5000(0)	5000(0)	0000(0)	1.909(0.108)
C(1)	3276(29)	3261(29)	0000(0)	1.422(0.368)
C(2)	0000(0)	5000(0)	3410(59)	4.451(0.267)
C(3)	1427(55)	4153(58)	4179(50)	7.447(0.891)
N(1)	2203(29)	2180(29)	0000(0)	2.389(0.409)
N(2)	0000(0)	0000(0)	2777(37)	1.804(0.466)

The electron clouds of the benzene molecules seem to be closely packed and are almost in contact with each other. These layers thus can be regarded as two-dimensional crystals of benzene between inorganic polymer sheets, $[Cd(NH_3)_2Ni(CN)_4]_\infty$.

*[1] The Metal Ammine Cyanide Aromatics Clathrates. VIII

1) T. Iwamoto, T. Nakano, M. Morita, T. Miyoshi, T. Miyamoto and Y. Sasaki, *Inorg. Chim. Acta*, **2**, 313 (1968).

2) J. H. Rayner and H. M. Powell, *J. Chem. Soc.*, **1952**, 319.

3) T. Miyoshi, T. Iwamoto and Y. Sasaki, *Inorg. Chim. Acta*, **2**, 329 (1968).

4) T. Miyamoto, to be published.

BULLETIN OF THE CHEMICAL SOCIETY OF JAPAN VOL. 42 2413—2416 (1969)

The Autoxidation of Ethylbenzene in the Presence of the Aqueous Phase

Hiroshi HOTTA, Masayuki ITO and Hiroaki MURASHIMA

Japan Atomic Energy Research Institute, Takasaki, Gunma

(Received May 6, 1968)

Ethylbenzene was oxidized to acetophenone and a small amount of benzaldehyde in the presence of the aqueous phase under oxygen pressure at 190°C. The yield of acetophenone decreased in the presence of sulfuric acid, sodium sulfate, and iron and copper sulfates. The formation of benzaldehyde was promoted in the presence of iron and copper sulfates and sulfuric acid. These effects can be explained mainly by the decomposition of α-phenylethyl hydroperoxide by the solutes in the aqueous phase.

The autoxidation of benzene and toluene in the aqueous phase catalyzed by metal ions have been studied between 100°C and 200°C, and their reaction mechanisms have been confirmed by using stable isotopes.[1-4] In contrast, the autoxidation of ethylbenzene occurs without any metal ions in the aqueous phase. The yields of the products are affected by various solutes in the aqueous phase. In the present paper, these effects will be discussed in comparison with the results of previous studies.

Experimental

The oxidation procedure, using a 50 cc stainless-steel reactor, has been described in detail in a previous paper.[1] That is, 3 cc of ethylbenzene was placed in a hard-glass tube with 15 cc of an aqueous solution, containing various solutes, under an oxygen pressure of 30 atm, then the mixture was kept at 190°C for 30 min by a controlled heater.

The products were analyzed by gas chromatography using a column of PEG 6000 at 170°C; they were identified mainly by the retention time, but partly also by means of the mass spectrum and the NMR spectrum. An amount less than 10^{-4} mol is meaningless quantitatively in the present paper; it means just "less than 10^{-4} mol." The amount of iron species was analyzed by spectrophotometry by previously-reported methods.[5]

Results

The products were acetophenone, benzaldehyde, and a small amount of a product which has a longer retention time than that of acetophenone and which is produced upon the autoxidation of acetophenone. Although benzoic acid could not be detected by gas chromatography under the present conditions, the amount produced for each run may be the highest in the order of 10^{-5} mol, as estimated from the pH change in the aqueous phase after experimentation.

The autoxidation of ethylbenzene was carried out with the aqueous phase at various pH's, which were controlled by the addition of sulfuric acid or sodium hydroxide. After experimentation, the pH was nearly 3 for the runs; the pH was more than 3 initially. The yield of acetophenone decreased for an acidic medium of less than pH 3. Since the pH was measured at room temperature, the pH at 190°C is not known.

The effect of sodium sulfate is shown in Fig. 1 as a function of its concentration in the aqueous

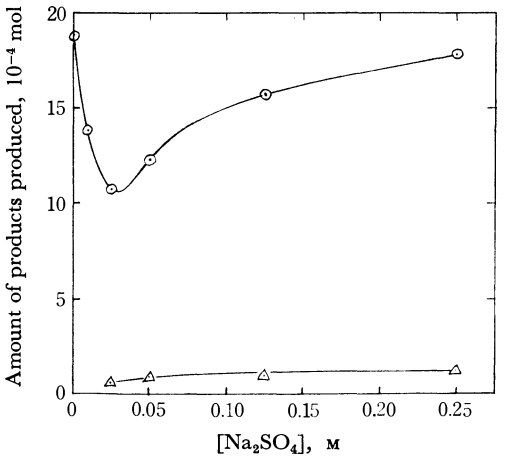

Fig. 1. The yields of acetophenone (⊙) and benzaldehyde (△) at 190°C in the sodium sulfate aqueous solution of various concentrations.

1) H. Hotta, A. Terakawa, K. Shimada and N. Suzuki, This Bulletin, **36**, 721 (1963).
2) H. Hotta, N. Suzuki and T. Abe, *ibid.*, **39**, 417 (1966).
3) N. Suzuki and H. Hotta, *ibid.*, **40**, 1361 (1967).
4) H. Hotta and N. Suzuki, *ibid.*, **41**, 1537 (1968).
5) H. Hotta and N. Suzuki, *ibid.*, **36**, 717 (1963).

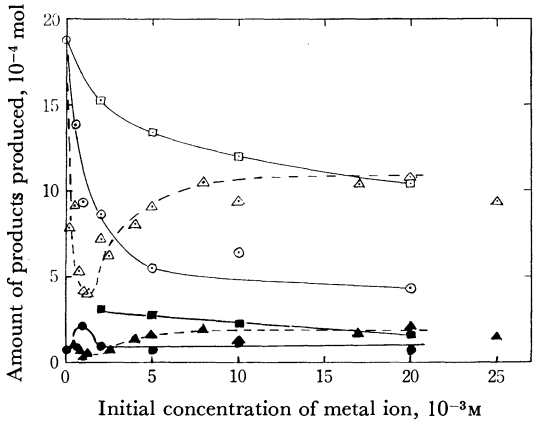

Fig. 2. The yields of acetophenone (open marks) and benzaldehyde (solid marks) at 190°C in the aqueous solution of ferrous (⊙ and ●), ferric (△ and ▲) and cupric (⊡ and ■) sulfates.

phase. The yield of acetophenone decreases at first and then increases upon further addition.

The effects of iron and copper sulfates were also examined. The amounts of acetophenone (open marks) and benzaldehyde (solid marks) produced are shown in Fig. 2 as a function of the initial concentrations of ferrous (⊙ and ●), ferric (■ and ▲), and cupric (⊡ and ■) sulfates. The yield of acetophenone decreases in the presence of these sulfates; especially, it gives a minimum at 0.001M in the case of ferric sulfates. On the other hand, the amounts of the total iron species and ferrous species, dissolved in the aqueous phase after experimentation, are shown in Fig. 3 as a function of the initial concentration of iron sulfates. The initial concentration in Figs. 2 and 3 is represented not by that of sulfate, but by that of iron.[1]

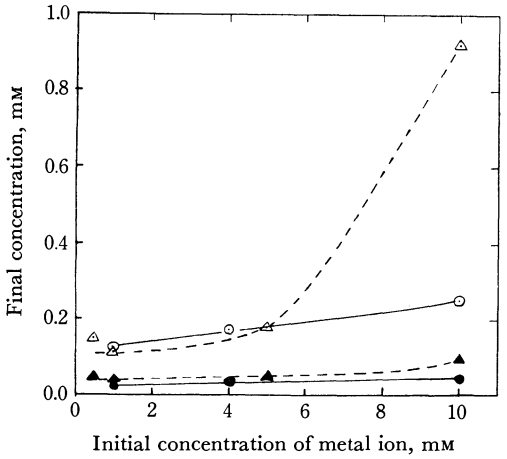

Fig. 3. The concentration of total iron species (open marks) and ferrous species in it (solid marks), dissolved in the aqueous phase after experimentation at 190°C in the aqueous solution of ferrous (⊙ and ●) and ferric (△ and ▲) sulfates.

When the autoxidation of ethylbenzene was initiated at 70°C by Fenton's reagent, as has been described in a previous paper,[4] the yield of methyl phenyl carbinol was more than twice that of acetophenone.

Discussion

So far, commercially-available ethylbenzene of a special grade was used without further purification. When this reagent was shaken several times with an aqueous solution of 0.1M ferrous sulfate, washed with water, and then distilled carefully, the amount of the products, oxidized with water at 190°C, decreased gradually with further purification, as is shown in Table 1. The amount of benzaldehyde produced was less than 10^{-5} mol in all the cases. The gas chromatogram of the reagent did not change with the purification.

Table 1. Purification of ethylbenzene

Shaking times	Acetophenone, 10^{-4} mol
0	17.7
4	12.1
10	9.7

When the autoxidation of ethylbenzene was carried out by adding it up to 7 cc to 15 cc of water, the yield of acetophenone increased linearly with the amount of ethylbenzene added. On the other hand, when 0.5 cc of ethylbenzene was oxidized without water, the yield of the products decreased with further purification. The pattern of the products was almost the same as in the presence of water.

These facts indicate that the autoxidation is not initiated by the thermal decomposition of ethylbenzene itself, but by that of a trace amount of some hydroperoxide in ethylbenzene; this substance is probably α-phenylethyl hydroperoxide to be stable at room temperature:

$$\mathrm{ROOH} \rightarrow \mathrm{RO\cdot} + \cdot\mathrm{OH} \qquad (1)$$

where R represents α-phenylethyl radical (ϕ–$\dot{\mathrm{C}}$H–$\mathrm{CH_3}$). The bond dissociation energy of this reaction is much less than that required for either hydrogen abstraction or C–C bond scission.[6-8]

The autoxidation is propagated in both the ethylbenzene and aqueous phases. On the other hand, the present findings indicate that the yield of the products is remarkably affected by solutes in the aqueous phase. This means that at least the main part of the propagation processes in a

6) L. A. Muzychenko, *Chem. Abstr.*, **59**, 5782d (1963).
7) J. A. Kerr, *Chem. Revs.*, **66**, 465 (1966).
8) S. W. Benson and J. Buss, *J. Chem. Phys.*, **29**, 546 (1958).

system containing the aqueous phase occur in the aqueous phase or in the participation of the hydrated solutes dispersed in the ethylbenzene phase. Since the oxygenated species are hydrophilic, they prefer either to be extracted in the aqueous phase or to be oriented to the hydrated solutes in the ethylbenzene phase. In the present paper, the effects of the solutes will be illustrated below by reactions in the above aqueous environment. Although some reactions independent of the solutes might occur in the non-aqueous phase, reactions with the solutes occur in the aqueous envivonment in the above meaning.

After reaction (1), the autoxidation is propagated as follows:

$$RH + \cdot OH \rightarrow R\cdot + H_2O \quad (2)$$

$$R\cdot + O_2 \rightarrow ROO\cdot \quad (3)$$

$$ROO\cdot + RH \rightarrow ROOH + R\cdot \quad (4)$$

with reaction (1). Furthermore, the following reactions may be expected in the aqueous phase, containing metal ions, M^+ (ferrous or cuprous ions) and M^{2+} (ferric or cupric ions):

$$H_2O \xrightarrow{M^+,O_2} \cdot OH \quad (5)$$

$$ROOH + M^+ \rightarrow RO\cdot + OH^- + M^{2+} \quad (6)$$

$$ROOH + M^{2+} \rightarrow ROO\cdot + H^+ + M^+ \quad (7)$$

The chain process is terminated by:

$$RO\cdot \rightarrow \text{Acetophenone} \quad (8)$$

$$2ROO\cdot \rightarrow RO\cdot \textit{ etc.} \quad (9)$$

The yield of acetophenone decreases upon the addition of a small amount of sodium sulfate, as may be seen in Fig. 1. Since the sulfate group becomes sulfur trioxide as a transient state at higher temperatures due to equilibrium thermal decomposition, according to studies as using oxygen-18:[9,10]

$$Na_2SO_4 \rightleftarrows \cdot SO_3 + NaO \quad (10)$$

This intermediate might scavenge the hydroxyl radical from reaction (1) as an initiator of the propagation process (reaction (2)) in this manner:

$$OH + \cdot SO_3 \rightarrow \cdot HSO_4 \quad (11)$$

The curve between 0 and 0.02M in Fig. 1 is almost identical with the curve of cupric sulfate in Fig. 2, as suggesting that these curves correspond to this effect of the sulfate group.

On the other hand, the sulfate group can initiate the autoxidation of hydrocarbons at higher temperatures, as has been discussed in a previous paper,[9] because the sulfur trioxide of reaction (10) becomes a sulfur peroxide in the oxygenated aqueous phase. This peroxide can abstract the hydrogen atom of ethylbenzene, as in reaction (4). It has been reported that various aromatics are oxidized by sulfuric acid and aqueous sulfates.[11,12] The increase in the yield at the higher concentrations of sodium sulfate in Fig. 1 may be attributed to this action. Since the sulfur peroxide is not very reactive, and since the propagation step of reaction (7) is lacking in this system, as may be seen in Fig. 1, the yield decreases abruptly, and then gradually rises.

The decrease in the yield in the acidic medium, as has been mentioned already, can be interpreted by the following acid-catalyzed decomposition of the hydroperoxide for reaction (1);

$$ROOH + H^+ \rightarrow RO^+ + H_2O \quad (12)$$

Then, spontaneously;

$$RO^+ \rightarrow \text{acetophenone} + H^+ \quad (13)$$

These reactions give only stable species. In a previous paper,[4] reaction (8) in the presence of metal ions was illustrated as;

$$RO + M^{2+} \rightarrow \text{acetophenone} + H^+ + M^+ \quad (14)$$

Reaction (14) is analogous with reactions (12) and (13).

In Fig. 2 the yield of acetophenone in the iron sulfate solution is seen to decrease to a greater extent than in the cupric sulfate solution. Since iron sulfates are precipitated as ferric oxides at temperatures higher than 150°C, as is shown in Fig. 3,[1,5] an aqueous solution of iron sulfates becomes an aqueous solution of sulfuric acid containing a small amount of iron species. Therefore, the effect of iron sulfates in Fig. 2 can be attributed to the superposition of the actions of sulfate and acid (reactions (11) and (12)). On the other hand, since cupric sulfate is not decomposed even at 190°C, the aqueous solution is still neutral. Therefore, the curve of cupric sulfate in Fig. 2 is almost identical with that of neutral salt, namely, sodium sulfate, as has been mentioned already.

In Fig. 2, the yield of acetophenone in the ferric solution is smaller at first, and then it becomes larger in a more concentrated solution than in the ferrous solution. In the ferrous solution, the autoxidation is initiated by the production of the hydroxyl radical (reaction (5)), while it is terminated through reaction (6). On the other hand, in the ferric solution it is propagated by reaction (7). The phenomena in Fig. 2 result from these effects in addition to the above effects of sulfate and acid.

In Fig. 3, the fraction of ferrous species in the

9) N. Suzuki, H. Hotta and H. Hashimoto, This Bulletin, **39**, 422 (1966).

10) A. E. Brodsky and N. A. Vysotskaya, *Zh. Fis. Khim.*, **32**, 1521 (1958).

11) M. Kilpatrick, M. W. Meyer and M. L. Kilpatrick, *J. Phys. Chem.*, **64**, 1433 (1960).

12) W. G. Toland, *J. Am. Chem. Soc.*, **82**, 1911 (1960).

total iron sepcies is low in comparison with benzene[1] and toluene.[3] This suggests that most of the acetophenone is formed by some termination process independent of metal ions, for example, reaction (12) rather than reaction (14) and/or some reaction in the non-aqueous phase.

Some benzaldehyde is produced with acetophenone under all conditions. The ratio of benzaldehyde to acetophenone is comparatively large in the presence of iron and copper sulfates and sulfuric acid, and it increases with an increase in the temperature. Since benzaldehyde was not formed from acetophenone under the present conditions, it might be formed competitively from the same intermediate with that for acetophenone.

The authors wish to express their appreciation to Dr. Toshio Sugiura for his cooperation in the mass spectrometry and to Mr. Hironao Hayakawa for his measurement of the NMR spectrum.

BULLETIN OF THE CHEMICAL SOCIETY OF JAPAN VOL. 42 2416—2421 (1969)

Electrolytic Polymerization of Acrylonitrile. Kinetic Approach and Effect of Supporting Electrolytes

Teruzo ASAHARA, Manabu SENŌ and Mitsuru TSUCHIYA

The Institute of Industrial Science, The University of Tokyo, Roppongi, Minato-ku, Tokyo

(Received June 6, 1968)

The electrolytic polymerization of acrylonitrile in constant current was examined by using several supporting electrolytes and the reaction mechanism was discussed. An explanation was given for the anomaly characteristic of the cathodic polymerization using sodium nitrate as a supporting electrolyte, which was reported by Funt. It was revealed that the polymerization is initiated by a radical mechanism at the anode and by an anionic mechanism at the cathode. The termination reaction of the anionic polymerization was analyzed by a kinetic approach and from the structural information of polymers obtained.

Recently, studies have been carried out on the electrode reaction and the following chemical reactions of acrylonitrile.[1] However, no definite conclusion has been obtained as to how many electrons are transferred in the electrolytic reduction, what chemical species are formed at the electrode, and what chemical reactions and termination follow.

In order to clarify these problems, the electrode reduction of acrylonitrile was studied by means of polarography, coulometry and electron spin resonance and the results were examined.

Experimental

Materials. Acrylonitrile was dried with barium oxide and calcium sulfate and distilled under reduced pressure. Sodium nitrate and sodium perchlorate of reagent grade were used without further purification. Tetrabutylammonium perchlorate was prepared from tetrabutylammonium hydroxide and perchloric acid and purified by recrystallization. Tetraethylammonium *p*-toluenesulfonate was synthesized by the reaction of ethyl *p*-toluenesulfonate and triethylamine and recrystallized.

Apparatus. The 500 m*l* cell used for electrolysis has no separatory membrane, because it has been confirmed that no polymer formation takes place in the anodic side. A source of direct current connected with a voltage stabilizer was used. The reaction temperature was maintained at 30°C and the solution was stirred with a magnetic stirrer. During electrolysis nitrogen gas was bubbled in. The electrolysis cell was equipped with a stirrer, a reflux condenser, an inlet tube of N_2 gas, a thermometer and a tube for sampling.

Reaction Kinetics. Every one hour, 10 m*l* of the reaction solution was taken out and poured into 100 m*l* of an aqueous sodium hydrosulfite solution. The resulting polymer precipitate was then separated and weighed after drying.

Measurement of ESR and Absorption Spectra. The ESR measurement was done on a Varian or a Japan Electron Optics Laboratory apparatus with an electrolysis cell. The anode was a platinum wire and the cathode a mercury pool. The measurement of absorption spectra was carried out with a Shimadzu Multipurpose Spectrophotometer using a 1 cm cell equipped with platinum electrodes. The viscosity of the

1) B. L. Funt and F. D. Williams, *J. Polymer Sci.*, **A2**, 865 (1964).

solution of resulting polymers in dimethylformamide was measured as usual at 30°C.

Results and Discussion

Electrode Reaction. Generally, an electrolytic reaction consists of two steps. One is the electrode reaction involving the electron-transfer reaction between ions or neutral molecules and the electrode. The other is the chemical reaction following or followed by the electrode reaction.

The reactivity on electrode changes with the electronic structure of reactants. It has been recognized in many cases that the electronic structures have certain relations to the half-wave potential.[2] The electronic energy state may be estimated by the molecular orbital theory.

The application of this procedure to vinyl compounds gives results as shown in Fig. 1. This shows a good correlation between the energy of the lowest unoccupied level and the half-wave potential of the polarographic reduction.

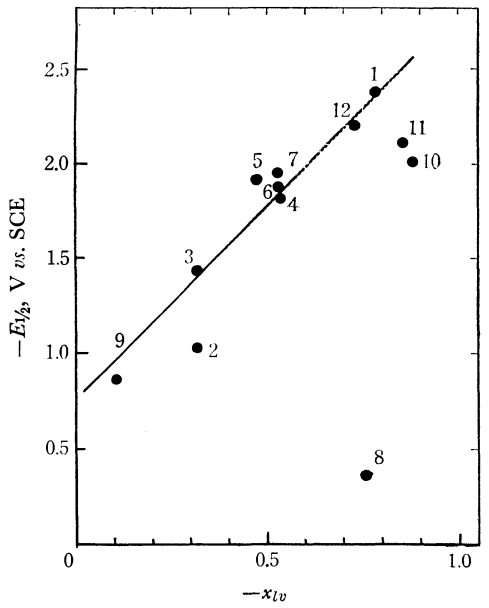

Fig. 1. The relation of coefficient of resonance integral in the lowest vacant orbital and the half-wave potential of various vinyl compounds.
1 styrene, 2 acrolein, 3 methyl vinyl ketone, 4 methyl acrylate, 5 acrylamide, 6 ethyl acrylate, 7 *n*-butyl acrylate, 8 vinyl acetate, 9 diethyl phthalate, 10 acrylonitrile, 11 methacrylonitrile, 12 1,2-dicyanoethylene

The ESR measurement during the electrolysis of acrylonitrile did not give any signal under the conditions shown in Table 1. The potentiostatic

Table 1. Conditions of ESR measurements

Acrylonitrile	Supporting elecrtolyte	Solvent	Cathode
10^{-3} mol/*l*	McKee's salt, 1 (g/50 m*l*)	H_2O	Hg
10^{-3} mol/*l*	McKee's salt, 1 (g/50 m*l*)	CH_3CN	Hg
10^{-3} mol/*l*	McKee's salt, 1 (g/50 m*l*)	DMF	Hg
10^{-3} mol/*l*	$N(CH_3)_4I$ 1 (g/50 m*l*)	$EtNH_2$	Hg
20 g	$NaNO_3$ 1 g	DMF 30 g	Hg
10 m*l*	$NaNO_3$ 1 g	DMF 40 ml	Pt

coulometry showed that two electrons were consumed for the reduction of one acrylonitrile molecule. The polarogram of acrylonitrile has a simple one-step reduction wave; the number of electrons for reduction was two from the limiting diffusion current density. On the other hand, the analysis of polarogram using the Nernst equation shows that the apparent number of electrons is 0.6. If the number of electrons is assumed to be 2, the transfer coefficient becomes 0.3, a reasonable value.[3] All these results lead to the conclusion that the two-electron reduction of acrylonitrile would be reasonable. Therefore, the following reaction mechanism could be proposed for the cathodic reduction:

$$CH_2=CHCN + 2e \rightarrow \overset{\ominus}{C}H_2\text{-}\overset{\ominus}{C}HCN$$

$$\overset{\ominus}{C}H_2\text{-}\overset{\ominus}{C}HCN + CH_2{=}CHCN \rightarrow$$

$$(2CH_2\text{-}\overset{\ominus}{C}HCN) \rightarrow NC\overset{\ominus}{C}H(CH_2)_2\overset{\ominus}{C}HCN$$

It is expected from the energy consideration that the reverse reaction, a disproportionation, hardly occurs. The formation of propionitrile and adiponitrile would take place according to the following reactions:

$$H_2O \rightleftarrows H^+ + OH^-$$

$$\overset{\ominus}{C}H_2\text{-}\overset{\ominus}{C}HCN + 2H^+ \rightarrow CH_3CH_2CN$$

$$NC\overset{\ominus}{C}H(CH_2)_2\overset{\ominus}{C}HCN + 2H^+ \rightarrow NC(CH_2)_4CN$$

It follows from this mechanism that the increase in water content gives rise to an increase in the yield of propionitrile. On the contrary, the decrease in water content gives an increase in the yield of adiponitrile and oligomers such as hydrotrimer. At a higher current density the formation rate of acrylonitrile dianion increases and the yield of propionitrile is depressed.

Beck[4] examined this reaction by the analysis of Tafel line in many systems containing acrylonitrile, and proposed the following reaction mechanism.

2) K. Higasi and H. Baba, "Quantum Organic Chemistry," Asakura Publishing Co., Tokyo (1965).

3) T. Asahara, M. Senō and H. Kaneko, *Denki Kagaku*, (*J. Electrochem. Soc. Japan*), **35**, 882 (1967).

4) F. Beck, *Chem. Ing. Tech.*, **37**, 607 (1967).

$$CH_2{=}CHCN + e + H_2O \xrightarrow{\text{slow}} \cdot CH_2CH_2CN + OH^-$$

$$\cdot CH_2CH_2CN + e \rightarrow : \overset{\ominus}{C}H_2CH_2CN$$

$$: \overset{\ominus}{C}H_2CH_2CN + CH_2{=}CHCN \rightarrow NCCH_2CH_2CH_2\overset{\ominus}{C}HCN$$

$$NCCH_2CH_2CH_2\overset{\ominus}{C}HCN + H_2O \rightarrow NC(CH_2)_4CN + OH^-$$

He considered that cyanoethyl iodide is reduced more easily than acrylonitrile, and that therefore cyanoethyl radical also would be reduced more easily than acrylonitrile, and reported that a weak signal was observed in the ESR measurement during electrolysis. However, there are ambiguities in his argument; for example, a cyanoethyl radical is an unstable primary radical and, if this was formed, it would enter into polymerization. Actually, polymer formation was scarcely observed. As to the ESR spectrum, the *g*-value and the hyperfine structure were not reported, and therefore the observed signal could not be assigned to a cyanoethyl radical. From these considerations, together with the polarographic result it could not be expected that the complex mechanism proposed by Beck is reasonable.

Electrolytic Polymerization of Acrylonitrile. Many researches have been carried out recently on the electrolytic polymerization of vinyl compounds. The principal feature of this method lies in the possibility of the control of the initiation reactions at electrodes by electrode potential and of the reaction rate by current density.

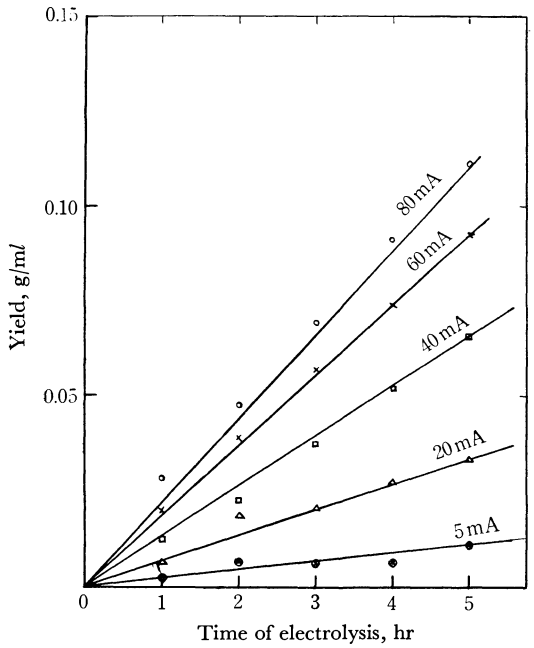

Fig. 2. The time dependence of the yield of polymers.

Funt and Williams[1] reported the anomaly in the electrolytic polymerization of acrylonitrile in dimethylformamide, using sodium nitrate as a supporting electrolyte. That is, there is a decrease in the rate of the formation of polymer with the increasing monomer concentration over a certain value. It should be noted that sodium nitrate is not soluble in acrylonitrile, but in dimethylform-

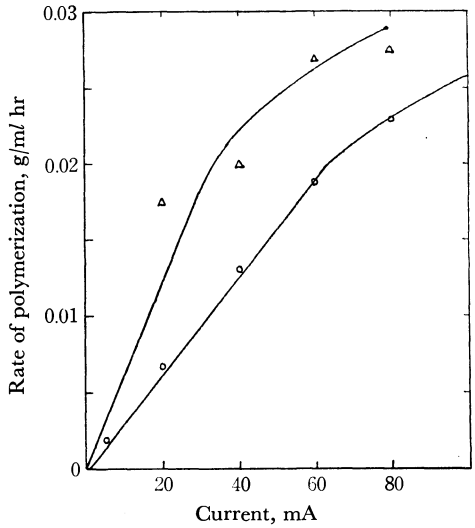

Fig. 3. The relation between the current and the rate of polymerization.
○ AN-$NaNO_3$, △ AN-McKee's salt

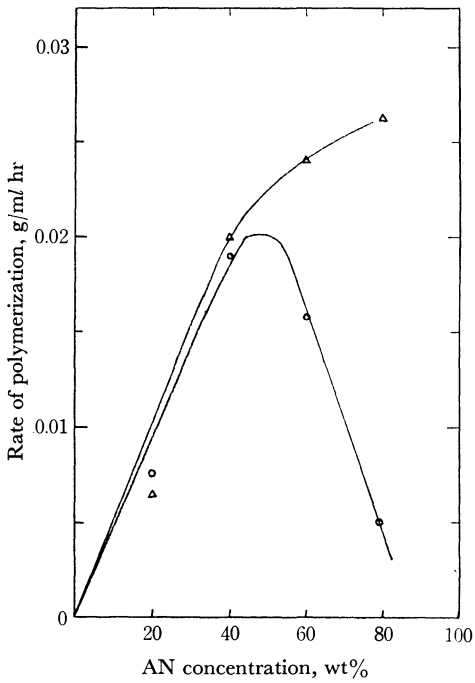

Fig. 4. The dependence of the rate of polymerization on AN concentrations.
○ AN-$NaNO_3$, △ AN-McKee's salt

amide, and sodium perchlorate is soluble both in acrylonitrile and dimethylformamide. It is of interest to use tetraethylammonium *p*-toluenesulfonate as a supporting electrolyte. However, Funt neither reported the structural analysis of the polymer obtained nor examined the reaction kinetics. As this reaction is interesting as a typical example of anionic addition reaction, the electrolytic polymerization of acrylonitrile was investigated.

AN-DMF-$NaNO_3$ System. A typical result in the system of acrylonitrile(AN)-dimethylformamide-(DMF)-$NaNO_3$ is shown in Fig. 2, where polymer yields are plotted against the reaction time corresponding to various current densities. When the molar ratio of AN to DMF is less than unity, the experimental results are expressed by the following equations (Figs. 3, 4, 5 and Table 2).

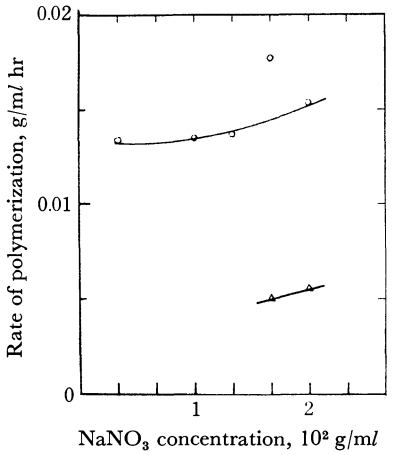

Fig. 5. The dependence of the rate of polymerization on $NaNO_3$ concentrations.
○ AN 60 wt%, △ AN 80 wt%

TABLE 2. INTRINSIC VISCOSITIES OF POLYMERS

AN-DMF-$NaNO_3$			AN-DMF-McKee's salt		
Current density mA/cm²	AN concn. wt%	$[\eta]$	Current density mA/cm²	AN concn. wt%	$[\eta]$
1.04*	40	1.2	4.16	40	0.18
2.08*	40	1.4	8.33	40	0.14
8.33	40	0.2	12.5	40	0.12
12.5	40	0.2	16.7	40	0.10
16.7	40	0.2			
8.33	20	0.2	8.33	20	0.11
8.33	60	0.2	8.33	60	0.24
8.33	80	0.3	8.33	80	
8.33	100	0.8	8.33	100	0.29

*In these cases, polymers are formed at anode and the analysis of IR spectrum of polymers suggests the following initiation mechanism:

$$NO_3^- \xrightarrow{-e} NO_3\cdot$$
$$NO_3\cdot + CH_2{=}CH{-}CN \rightarrow \text{polymers}$$

Rate of polymer formation: $\frac{d[P]}{dt} = k[M]\,[I]$

Degree of polymerization: DP = const.

The reaction might be assumed to consist of the following steps:

$$M + I \xrightarrow{k_i} C^* \quad (1)$$
$$C^* + M \xrightarrow{k_p} C^* \quad (2)$$
$$C^* + M \xrightarrow{k_{t1}} P \quad (3)$$
$$C^* \xrightarrow{k_{t2}} P \quad (4)$$

where M is monomer, C* active species with growing ends and P polymers. This reaction process was analyzed kinetically, using the stationary state method, and the following equations are obtained:

$$\frac{d[P]}{dt} = k_i\,[M][I]$$
$$DP = \frac{k_p\,[M]}{k_{t1}[M] + k_{t2}}$$

The experimental result requires that $k_{t1}[M]$ is much larger than k_{t2}. Therefore, the significance of the termination reaction (3) must be recognized. During electrolysis the bulk solution becomes yellow which remains after the electrolysis. This coloration would be caused not by reaction intermediates, but by resulting polymers, because polymers are yellow after purification. However, a question remains as to whether the color is due to the decomposition of supporting electrolytes. In order to confirm the possibility, the change in absorption

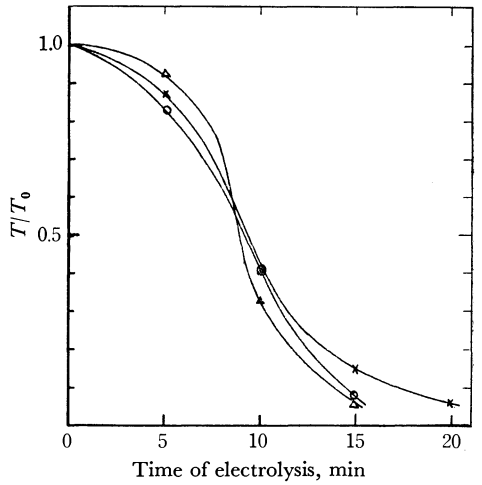

Fig. 6. Relation between the transmittance and the time of electrolysis.
○ 270 mμ, △ 310 mμ, ×340 mμ in DMF
T: Transmittance of sampe solution at given times
T_0: Transmittance of reference (t=0)

spectra of products was measured during electrolysis at various AN concentrations. The result is shown in terms of transmittance at the absorption peak (270 mμ) and other two wavelengths in Fig. 6. The change in transmittance T with time (t) obeys the exponential law $T=T_0e^{-\alpha/t}$, where T_0 is the transmittance at $t=0$. In Fig. 7, the values of α are plotted against the AN concentration. From this result it may be concluded that the decomposition of the supporting electrolyte has no correlation with the observed coloration.

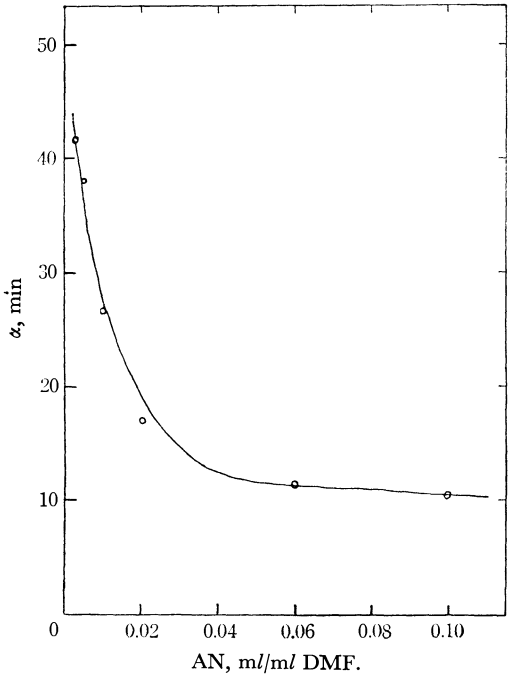

Fig. 7. The dependence of rate of coloration at 270 mμ on AN concentration in DMF.

Moreover, the identification of IR spectrum of polymers shows the existence of methyl and imino groups. Therefore, it seems that the coloration is due to the cyclization of nitrile groups. These observations suggest clearly the following termination reaction:

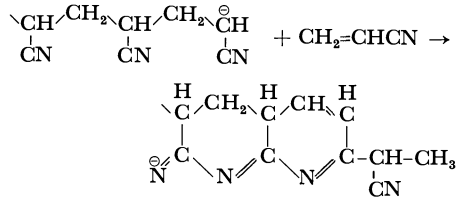

The anomaly in Fig. 4 might be attributed to the presence of the supporting electrolyte which is hardly soluble in acrylonitrile and causes an increase in the activation energy of the initiation step. This might be explained as follows. The dissociation of sodium nitrate is in equilibrium.

$$NaNO_3 \overset{K_1}{\rightleftarrows} Na^+ + NO_3^-$$

On the other hand, we have

$$[Na^+] = [NO_3^-] + [C^*]$$

An excess charge discharges at electrodes. If C* is small enough, we get

$$[Na^+] = \sqrt{K_1[NaNO_3]} \equiv K_1'$$

The following equilibrium would take place also for the active anions

$$C_f^* + Na^+ \overset{K_2}{\rightleftarrows} C_{nf}^*$$

where C^*_f and C^*_{nf} refer to the free active anions and the active ion-pairs respectively. C^*_f would be more active than C^*_{nf}.
Then

$$[C^*] = [C_f^*] + [C_{nf}^*]$$

$$= [C_f^*](1 + K_1'K_2)$$

Therefore

$$DP = \frac{k_p[C_f^*][M]}{k_{t1}[M][C^*] + k_{t2}[C^*]}$$

$$= \frac{k_p[M]}{(k_{t1}[M] + k_{t2})(1 + K_1'K_2)}$$

When the AN concentration increases, K_1' decreases and DP increases. In addition, it is suggested that the loss in the solvation energy of sodium cations results in the relative instability of the reactive point according to the linear free energy relationship, and the activation energy for the initiation reaction increases and the reaction rate decreases. This anomaly is not observed when McKee's salt is used as a supporting electrolyte.

AN-DMF-McKee's Salt System. In the system of AN, McKee's salt, and DMF, the polarogram of AN suggests the complex formation of AN with *p*-toluenesulfonate anion.[5] In this system, the current effect shows saturation for the rate of polymer formation at a certain current density as shown in Fig. 3. This would be interpreted on the assumption that the complex has a negative charge and the polymerization process in the neighborhood of the electrode is of the diffusion control even at a relatively low electrode potential. However, the decomposition of the supporting electrolyte would lead to the same result.

The increasing AN concentration causes an increase in the rate of polymer formation and the degree of polymerization as shown in Fig. 4 and

5) T. Arai, private communication.

Table 2. This behavior may be described as follows:

$$\frac{d[P]}{dt} = k_i[M][I] \qquad DP = k[M]$$

The kinetic analysis agrees with the result when $k_{t2} \gg k_{t1}[M]$, and suggests that the termination reaction (4), *i. e.*, the self-consumption of the reactive points, predominates. The IR spectrum of polymer obtained has no absorption assigned to methyl groups and the UV spectrum shows that the polymer has a cyclic unit. From these observations, the following termination seems reasonable.

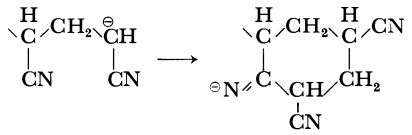

Electrolysis without Solvents. When sodium nitrate was used as a supporting electrolyte, the IR spectrum of the polymer obtained suggests the following reaction scheme:

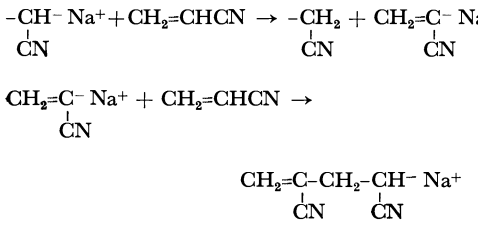

The electrolysis of acrylonitrile at the cathode without solvent using sodium perchlorate as a supporting electrolyte would proceed according to the following scheme:

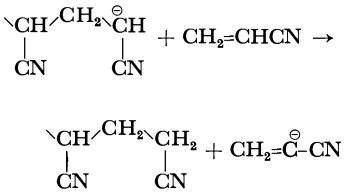

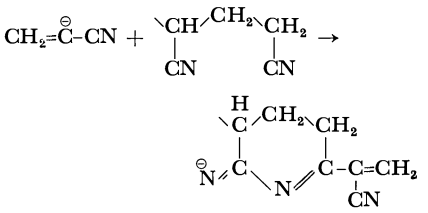

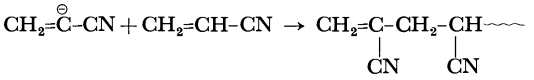

In this system, the polymerization proceeds at the anode through a radical mechanism, that is

$$ClO_4^- - e \rightarrow ClO_4\cdot$$

$$ClO_4\cdot + CH_2{=}CH{-}CN \rightarrow \text{polymers}$$

This is supported by the observation that the IR spectrum of the polymer formed at the anode has an absorption assigned to perchloro groups and the polymer has a very high molecular weight (the intrinsic viscosity in DMF is 4.0) and no coloration.

The information obtained in the present investigation is summarized as follows:

(1) The half-wave potentials and therefore the reactivity of vinyl compounds could be estimated from the molecular orbital calculation.

(2) Acrylonitrile undergoes a two-electron reduction in the cathode reaction.

(3) The lowering of the rate in the formation of polymer over a certain AN concentration in the system AN-DMF-$NaNO_3$ would be caused by the decrease in the rate constant of the initiation step.

(4) When the polymer is obtained at the cathode in the electrolysis of acrylonitrile, it is formed by the anionic polymerization mechanism. The termination reaction involves the cyclization of nitrile groups, and results in the formation of yellow-colored polymers.

(5) When the polymer is obtained at the anode it is initiated by the radical which is formed by the oxidation of supporting electrolytes. The degree of polymerization of polymers formed at the cathode is much lower than that of polymers formed at the anode.

BULLETIN OF THE CHEMICAL SOCIETY OF JAPAN VOL. 42 2422—2425 (1969)

Evaluation of the Activation Energies of Radical Substitution Reactions in the Gaseous Phase. II. An Approximate Formula with Two Constants

Tsutomu KAGIYA, Yūzō SUMIDA and Tokuji INOUE

Faculty of Engineering, Kyoto University, Sakyo-ku, Kyoto

(Received October 31, 1968)

The following approximate formula for evaluating the activation energies of radical substitution reactions has been derived from the formula proposed in a previous paper:

$$E_a = D_i - \varepsilon D_f(1 + \delta D_i)$$

where D_i and D_f are the bond dissociation energies of the initial and the final bonds. The calculated values are in good accordance with the observed values within ± 2.0 kcal/mol. The empirical formulae, proposed by Evans-Polanyi and Semenov *et al.*, between the activation energy and the reaction heat have been derived from this approximate formula. The Hammett-type rule has also been observed to hold in radical substitution reactions, and the substituent constants and the reaction constants have been determined by the use of the formula. A good correlation between the bond dissociation energy of the initial molecule and the radical reactivity index, delocalizability, based on the quantum chemical standpoint, has also been observed.

Evans and Polanyi have made a theoretical investigation of the activation energy of the radical substitution reaction and have obtained, in a homologous reaction, a quantitative relation between the activation energies and the reaction heats.[1] Bagdasaryan,[2] Tikhomirova-Voevodskii,[3] and Semenov[4] indicated that the correlation between the activation energies and the reaction heats is roughly independent of the kind of reaction components.

In a previous paper,[5] the present authors made an empirical study of the energy changes along the radical substitution reaction path, and proposed a theoretical equation for the evaluation of the activation energies employing the Morse potential energy functions. The equation is very useful, but it is rather complicated.

The purpose of this report is to present an approximate formula for the theoretical equation obtained in the previous paper, and to discuss the above empirical rules in connection with this formula.

1) M. G. Evans and M. Polanyi, *Trans. Faraday Soc.*, **34**, 11 (1938).

2) Kh. S. Bagdasaryan, *Zh. Fiz. Khim.*, **23**, 1375 (1949).

3) N. N. Tikhomirova and V. V. Voevodskii, *Dokl. Akad. Nauk, USSR*, **79**, 993 (1951).

4) N. N. Semenov, "Some Problems in Chemical Kinetics and Reactivity," English Ed., Princeton Univ. Press, Princeton, New Jersey (1958).

5) T. Kagiya, Y. Sumida, T. Inoue and F. S. Dyachkovskii, This Bulletin, **42**, 1812 (1969).

Derivation of Approximate Formula

The reactions with which we are concerned in this paper are radical substitution reactions of the three-center type, such as

$$A + BC \rightarrow AB + C \qquad (1)$$

where A, B, and C are reacting atoms or groups.

As has been described previously,[5] the energy of the transition state and the activation energy of any reaction (1) may, respectively, be given as follows:

$$E^* = \frac{4\alpha(1-\alpha)D_iD_f(D_f - \alpha D_i)}{(D_f - \alpha^2 D_i)^2} \qquad (2)$$

$$E_a = \frac{D_i\{(1-2\alpha)D_f + \alpha^2 D_i\}^2}{(D_f - \alpha^2 D_i)^2} \qquad (3)$$

where D_i and D_f are the bond dissociation energies of the initial and the final molecules, and where α is related to the reaction heat Q (in kcal/mol) by $\alpha = \exp(\beta Q)$, where β is a constant equal to 0.0190.

For the reaction heats, Q, ranging from -20 to 20 kcal/mol, α and α^2 are approximated as:

$$\left.\begin{aligned} \alpha &= 1 + \beta Q \\ \alpha^2 &= 1 + 2\beta Q \end{aligned}\right\} \qquad (4)$$

By substituting Eq. (4) into Eq. (2) and by using the two relations: $Q \simeq D_f - D_i$ and $\beta Q \ll 1$, we obtain:

$$E^* = \varepsilon D_f \times \frac{D_i(\beta D_i - 1)}{(1 - 2\beta D_i)^2} \qquad (5)$$

where $\varepsilon = 4\beta = 0.0760$. The second factor on the

right side of Eq. (5), $D_i(\beta D_i-1)/(1-2\beta D_i)^2$, is a function only of the bond dissociation energy, D_i, of the initial molecule. In order to approximate this factor by a simpler expression, let us use:

$$\frac{D_i(\beta D_i-1)}{(1-2\beta D_i)^2} \simeq 1+\delta D_i \qquad (6)$$

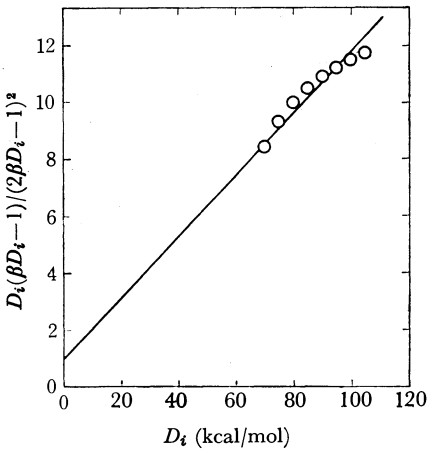

Fig. 1. Plot of $D_i(\beta D_i-1)/(2\beta D_i-1)^2$ *versus* D_i. The straight line represents the equation, $\frac{D_i(\beta D_i-1)}{(2\beta D_i-1)^2} = 1+0.108D_i$

Figure 1 shows that the linear approximation (6) with $\delta=0.108$ holds fairly well in the range of D_i with which we are concerned, *i. e.*, $D_i=70$ to 105 kcal/mol. By substituting Eq. (6) into Eq. (5), we obtain:

$$E^* = \varepsilon D_f(1+\delta D_i) \qquad (7)$$

Hence,

$$E_a = D_i - \varepsilon D_f(1+\delta D_i) \qquad (8)$$

and

$$\frac{D_i-E_a}{D_f} = \varepsilon + \varepsilon\delta D_i \qquad (9)$$

The linear relation (9) between $(D_i-E_a)/D_f$ and D_i has been checked by using the available experimental values of E_a for radical substitution reactions such as those given in the legend of Fig. 2. The results indicate that Eq. (9) works well when the constants ε and δ are chosen to be 0.0850 and 0.0944 respectively. These values are in good agreement with those of $\varepsilon=0.0760$ and $\delta=0.108$ which we have obtained earlier. By using $\varepsilon=0.0850$ and $\delta=0.0944$, we obtain:

$$E_a = D_i - 0.0850D_f(1+0.0944D_i) \qquad (10)$$

Results and Discussion

The activation energies of the various types of radical substitution reactions are calculated by means of Eq. (10); they are plotted against the observed values in Fig. 2. For both exothermic and endothermic reactions, the calculated values of

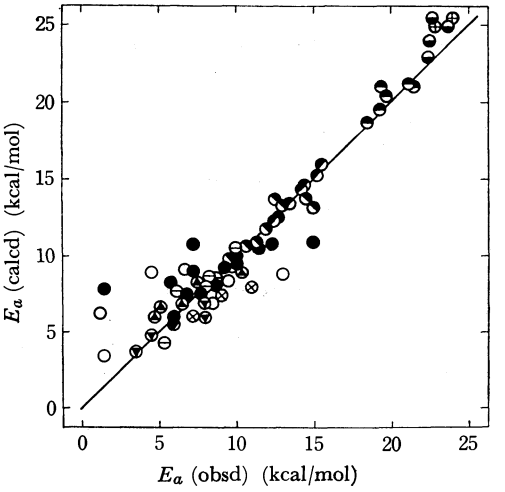

Fig. 2. Comparison of the calculated values of the activation energies of radical substitution reactions with the observed ones.
○ H+RH→H_2+R, ⊗ D+RH→HD+R,
● CH_3+RH→CH_4+R,
◔ C_2H_5+RH→C_2H_6+R,
◩ *n*-C_3H_7+RH→C_3H_8+R,
◓ *i*-C_3H_7+RH→C_3H_8+R,
◒ *t*-C_4H_9+RH→*t*-C_4H_{10}+R,
▲ CF_3+RH→CF_3H+R,
⊕ CH_3CO+RH→CH_3CHO+R,
▼ H+RCl→HCl+R, ⊖ Na+RCl→NaCl+R

the activation energies are in good agreement with the observed values within ±2.0 kcal/mol. It may be concluded from the results that Eq. (10) is a good approximate formula for evaluating the activation energies of radical substitution reactions.

The Evans-Polanyi Rule. Evans and Polanyi have studied the reactions of various alkyl chlorides with a sodium atom:[1]

$$\mathrm{Na} + \mathrm{RCl} \rightarrow \mathrm{NaCl} + \mathrm{R} \qquad (11)$$

and have found a simple parallelism between the activation energies and the reaction heats; *i. e.*,

$$\Delta E_a = -x\Delta Q \qquad (12)$$

where ΔE_a is the increase in the activation energy; ΔQ, the increase in the reaction heat, and x, a constant equal to about 0.25.

From Eq. (8) we may calculate the change in the activation energy of a radical substitution reaction (such as those taken up in Fig. 2) caused by changing the alkyl group, R:

$$\Delta E_a = E_a - E_{a_0} = (1-\varepsilon\delta D_f)(D_i - D_{i,0}) \qquad (13)$$

where the subscript "0" indicates the value in a certain standard reaction. The $(D_i-D_{i,0})$ factor may be equated to $-(Q-Q_0)$; hence,

$$\Delta E_a = -(1-\varepsilon\delta D_f)\Delta Q \qquad (14)$$

which may be brought into the form of Eq. (12) by setting:

$$x = 1 - \varepsilon\delta D_f \tag{15}$$

The x value calculated with $\varepsilon=0.0850$, $\delta=0.0944$, and $D_f=97.5$ kcal/mol,[6] that is the bond dissociation energy of the Na-Cl bond, is 0.22; this is nearly equal to the Evans-Polanyi value, 0.25. It is also found from Eq. (15) that the x value in Eq. (12) does not change with the bond dissociation energy of the initial molecule, while it does with that of the final molecule.

The Semenov Rule. Bagdasaryan,[2] Voevodskii,[3] and Semenov[4] have extended the Evans-Polanyi rule and have found that the activation energy can be calculated from Eq. (16) for exothermic reactions and from Eq. (17) for endothermic reactions:*1

$$E_a = A - yQ \tag{16}$$

$$E_a = A + (1-y)Q \tag{17}$$

where $A=10$ to 18 kcal/mol and $y=0.2$ to 0.4.

By substituting the relation, $D_i \simeq D_f - Q$, into Eq. (8),

$$E_a = (1 - \varepsilon - \varepsilon\delta D_f)D_f - (1 - \varepsilon\delta D_f)Q \tag{18}$$

for both exothermic and endothermic reactions. By comparing Eq. (18) with Eqs. (16) and (17), we obtain:

$$A = (1 - \varepsilon - \varepsilon\delta D_f)D_f \tag{19}$$

$$y = 1 - \varepsilon\delta D_f \text{ (for exothermic reactions)} \tag{20}$$

$$y = 2 - \varepsilon\delta D_f \text{ (for endothermic reactions)} \tag{20'}$$

From Eqs. (19) and (20) we find that the calculated values of A and y of exothermic reactions are in the ranges $11<A<19$ kcal/mol and $0.20<y<0.32$ respectively, provided that $85<D_f<100$ kcal/mol. This is in accordance with the Semenov empirical rule.

The Hammett-type Rule. The following is a list of various types of radical substitution reactions (1) changing a reacting radical in three reactions (A, B, and C):

$$A + BC_j \rightarrow AB + C_j \tag{21}$$

$$A_j + BC \rightarrow A_jB + C \tag{22}$$

$$A + B_jC \rightarrow AB_j + C \tag{23}$$

where the subscript j indicates the changing radical.

The increase in the activation energy, ΔE_a, of (21) caused by changing the standard radical, C_0, to C_j is given by:

$$\Delta E_a = (1 - \varepsilon\delta D_f)(D_{i,j} - D_{i,0}) = \dot{\rho}\dot{\sigma} \tag{24}$$

$$\dot{\rho} \equiv k(1 - \varepsilon\delta D_f) \tag{25}$$

$$\dot{\sigma} \equiv (1/k)(D_{i,j} - D_{i,0}) \tag{26}$$

In Eqs. (25) and (26) above, which define $\dot{\rho}$ and $\dot{\sigma}$, k is a constant whose value is chosen so that the value of $\dot{\rho}$ for the $CH_3+RH \rightarrow CH_4+R$ reaction is 10.0 (see below and Table 2). Notice that $\dot{\rho}$ and $\dot{\sigma}$ depend only on the final and the initial molecules respectively. We may regard them as analogues of Hammett's ρ and σ; we shall, then, call $\dot{\rho}$ the reaction constant, and $\dot{\sigma}$, the substituent constant.

Similarly, the increase in the activation energy, ΔE_a, of (22) caused by changing the attacking radical, A_0 to A_j is given by:

$$\Delta E_a = -\varepsilon(1 + \delta D_i)(D_{f,j} - D_{f,0}) \tag{27}$$

The $-\varepsilon(1+\delta D_i)$ and $(D_{f,j}-D_{f,0})$ are the factors depending only on the initial and the final molecules respectively. It may be considered that the former corresponds to the reaction constant, $\dot{\rho}'$, and the latter, to the substituent constant, $\dot{\sigma}'$.

When changing the parent radical B_0 to B_j, however, the increase in the activation energy, ΔE_a, is represented by a complicated expression and is not given by a simple Hammett-type formula:

$$\Delta E_a = (D_{i,j} - D_{i,0}) - \varepsilon(D_{f,j} - D_{f,0}) - \varepsilon\delta(D_{i,j}D_{f,j} - D_{i,0}D_{f,0}) \tag{28}$$

TABLE 1. THE SUBSTITUENT CONSTANTS IN RADICAL SUBSTITUTION REACTIONS

Substituent	$\dot{\sigma}$	Substituent	$\dot{\sigma}$
CH_3	0	i-C_4H_9	−0.21
C_2H_5	−0.03	t-C_4H_9	−0.26
$C(CH_3)_3CH_2$	−0.04	$CHCl_2$	−0.31
n-C_3H_7	−0.08	CH_3CO	−0.35
n-C_4H_9	−0.10	CH_2=$CHCH_2$	−0.38
i-C_3H_7	−0.16	CCl_3	−0.39
CH_2Cl	−0.16		

TABLE 2. THE REACTION CONSTANTS OF RADICAL SUBSTITUTION REACTIONS

Reaction	$\dot{\rho}$
$CH_3+RH \rightarrow CH_4+R$	10.0
$C_2H_5+RH \rightarrow C_2H_6+R$	11.0
n-$C_3H_7+RH \rightarrow C_3H_8+R$	11.8
i-$C_3H_7+RH \rightarrow C_3H_8+R$	14.0
t-$C_4H_9+RH \rightarrow t$-$C_4H_{10}+R$	17.0
$H+RCl \rightarrow HCl+R$	11.5
$Na+RCl \rightarrow NaCl+R$	12.8

6) A. G. Gaydon, "Dissociation Energies and Spectra of Diatomic Molecules," 1st Ed., Dover Publications, N. Y. (1947).

*1 Equation (16) for exothermic reactions holds fairly well, but Eq. (17) for endothermic reactions is not very good. Knox *et al.* have observed that y should be 0.91 for hydrogen abstraction reactions by a chlorine atom (endothermic reaction).[7] This value is in good agreement with the y value, 1.18, calculated by using (20') and $D_f=102$ kcal/mol,[8] which is the bond dissociation energy of the H-Cl bond.

7) G. C. Fettis and J. H. Knox, "Progress in Reaction Kinetics," Vol. 2, Pergamon Press, p. 1. (The Rate Constants of Halogen Atom Reactions)

8) G. Herzberg, "Spectra of Diatomic Molecules," 2nd Ed., D. Van Nostrand Company, N. Y. (1950).

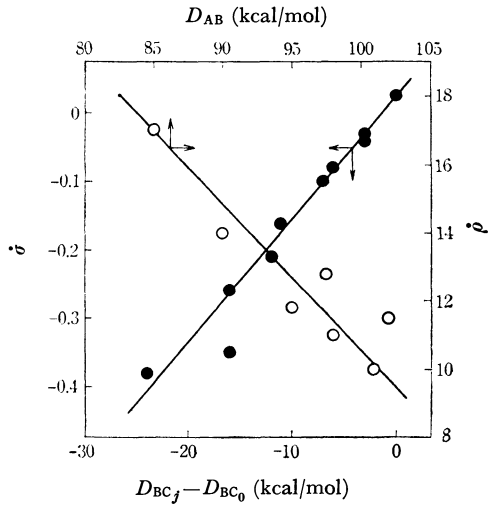

Fig. 3. Relation between the substituent constant $\dot{\sigma}$ or the reaction constant $\dot{\rho}$ and the bond dissociation energy.

$$\Delta E_a=(1-\varepsilon\delta D_{AB})(D_{BC_j}-D_{BC_0})=\dot{\rho}\dot{\sigma}$$

In fact, the increase in the activation energy caused by the change in the radical B_j is not expressed by a simple functional formula of the reaction heat.

In order to evaluate the substituent constants and the reaction constants of the type (21) of reactions, we choose the hydrogen abstraction reactions ($\dot{\rho}=10.0$) by a methyl radical as the standard reactions and a methyl group ($\dot{\sigma}=0$) as a standard substituent, C_0. By substituting the differences in the observed activation energies of the standard reactions into the relation, $\dot{\sigma}=\Delta E_a/\dot{\rho}$, where $\Delta E_a=E_{a(CH_3-H)}-E_{a(R-H)}$, we can evaluate the substituent constants, $\dot{\sigma}$ (Table 1). Moreover, the reaction constants, $\dot{\rho}$, of the other reactions are evaluated by the use of the substituent constants determined by such operations (Table 2).

As has been defined above, the substituent constants, $\dot{\sigma}$, and the reaction constants, $\dot{\rho}$, are, respectively, proportional to the $(D_{i,j}-D_{i,0})$ and $(1-\varepsilon\delta D_f)$ factors. As Fig. 3 shows, each constant can be expressed as a function of the bond dissociation energy.

The Radical Reactivity Index, D_r^R. Fukui *et al.*,[9] from the quantum chemical point of view, have proposed the delocalizability, D_r^R, as a radical reactivity index of radical substitution reactions (1):

$$D_r^R=\sum_j^{occ}\frac{(C_r^j)^2}{\lambda_j}+\sum_j^{unocc}\frac{(C_r^j)^2}{-\lambda_j} \qquad (29)$$

where C_r^j is the coefficient of the rth atomic orbital in the jth molecular orbital of the BC molecule, and λ_j, the coefficient of β in the energy of the jth molecular orbital of the BC molecule. Using this index, it has been assumed that the activation energy is written in the form:[10]

$$E_a=c_1-c_2D_r^R \qquad (30)$$

where it has been assumed that c_1 is a constant for a definite type of reactions and that c_2 is a constant depending only on the radical A.[10]

Equation (8) is rewritten as:

$$E_a=(1-\varepsilon\delta D_f)D_i-\varepsilon D_f \qquad (31)$$

For the hydrogen abstraction reactions by a methyl radical, $CH_3+RH\rightarrow CH_4+R$, the final bond dissociation energy, D_f, in Eq. (31) is constant, and the coefficient, c_2, in Eq. (30) should not change if the above assumption is satisfied. Therefore, the values of $D_r^R(H)$ should be expressed as a linear function of $D_{i(RH)}$, with a negative slope. This linear relation between $D_r^R(H)$ and $D_{i(RH)}$ has been checked in Fig. 4.

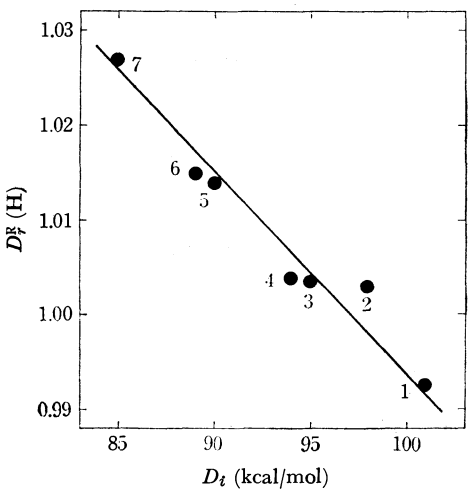

Fig. 4. Relation between the delocalizability of hydrogen abstraction reaction and the bond dissociaion energy. B=hydrogen atom
$E_a=(1-\varepsilon\delta D_f)D_i-\varepsilon D_f$
$E_a=c_1-c_2D_r^R$
1 Me–H, 2 Et–H, 3 *n*-Pr–H, 4 *n*-Bu–H, 5 *i*-Pr–H, 6 *s*-Bu–H, 7 *t*-Bu–H

On the basis of the above considerations, it may be concluded that Eq. (8) is not only a good approximate formula for the evaluation of the activation energies of radical substitution reactions, but also corresponds well with the empirical rules described previously.

9) K. Fukui, H. Kato and T. Yonezawa, This Bulletin, **34**, 1111 (1961).

10) K. Fukui, H. Kato and T. Yonezawa, *ibid.*, **35**, 1475 (1962).

BULLETIN OF THE CHEMICAL SOCIETY OF JAPAN VOL. 42 2426—2431 (1969)

Studies on Formaldehyde-Condensation Resin. VII.*1 Isolation of Mono-, Di-, Tri-, and Tetramethylolacetoguanamines

Tadashi URAGAMI and Masayoshi OIWA

Department of Applied Chemistry Faculty of Engineering, Kansai University, Senriyama, Suita-shi, Osaka

(Received November 11, 1968)

The reaction of acetoguanamine with formaldehyde was carried out in the presence of basic catalyst under various conditions, and mono-, di-, tri-, and tetramethylol derivatives of acetoguanamine were purely isolated. Their structures were identified by elemental analyses, infrared absorption spectra, NMR spectra, and chemical analyses of methylol groups.

The isolation of some intermediates of phenol, urea, melamine, and guanamine resins, well-known as the addition-condensation resin, has been studied by many workers.[1-9] Recently, there have been interesting presentations[10,11] on the syntheses of some kinds of benzoguanamine-formaldehyde resin intermediates, but no reports on any detailed studies of the methylol derivatives of acetoguanamine.

Acetoguanamine can be hydroxymethylated to form mono-, di-, tri-, tetramethylolacetoguanamines as follows:

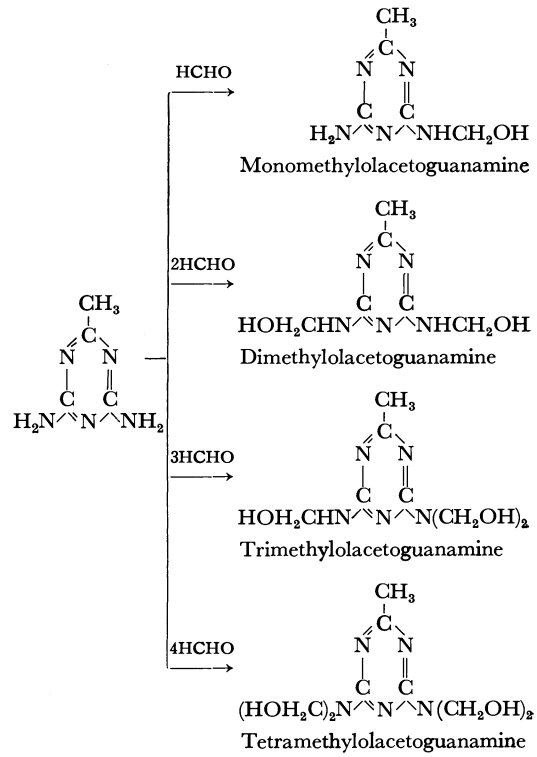

The present paper deals with the isolation of the methylol derivatives which were obtained from the base-catalyzed reaction of acetoguanamine with formaldehyde under various conditions.

Experimental

Materials. Nippon Gosei Chem. Ind. Co. best grade acetoguanamine was recrystallized from water, mp 269—271°C. Commercial formaline (*ca.* 37 wt%) was used. Pure commercial dimethylsulfoxide (DMSO) was purified by the usual method[12]: bp 88°C/25 mmHg.

*1 Part VI: T. Uragami and M. Oiwa, *Kogyo Kagaku Zasshi* (*J. Chem. Soc. Japan, Ind. Chem. Sect.*), **71**, 596 (1968).

1) M. Imoto, H. Kakiuchi and K. Kō, "Formaldehyde," Asakura-Shoten, Tokyo (1965), p. 209 and others.

2) H. Kakiuchi, "Urea Resin," Kobunshibunko 19, Kobunshi-Kankokai, Kyoto (1965), p. 35 and others.

3) S. Seto, *Osaka-Shiritsu Kogyo Kenkyusyo Hokoku* (*Bull. Osaka Mun. Tech. Research Institute*), Vol. **24** (1960); *Kobunshi Tenbo*, No. **11**, 13 (1954).

4) K. Koeda, *Kobunshi Tenbo*, No. **11**, 39 (1954).

5) H. Ohno, *Kobunshi Kagaku* (*Chem. High Polymers Japan*), **20**, 443 (1963).

6) T. Tashiro and R. Murase, *Sen'i Kogyo Shikensyo Hokoku* (*Bull. Textile Research Institute of Japanese Government*), **56**, 65 (1961).

7) M. Gordon *et al.*, *Soc. Chem. Ind.* (*London*), *Monograph*, No. **20**, 187 (1966).

8) M. Tajima and R. Shiba, Preprint for the 17th Annual Meeting of the Thermosetting Resin Lecture Discussion of Japan (September, 1967), p. 107.

9) S. Takeuchi and E. Ninagawa, Preprint for the 21th Annual Meeting of the Chemical Society of Japan (April, 1968), No. 4, p. 2772.

10) B. Ogaki, A. Yotsutsuji and Y. Sato, Preprint for the 15th Annual Meeting of the Thermosetting Resin Lecture Discussion of Japan (September, 1965), p. 5, *ibid.* (September, 1966), p. 99.

11) B. Ogaki, A. Yotsutsuji and T. Nakamura, *ibid.* (September, 1968), p. 239.

12) C. A. Kingsbury, *J. Org. Chem.*, **29**, 3262 (1964).

Hydroxymethylation of Acetoguanamine. In a four-necked flask equipped with a reflux condenser and a stirrer, formaline was added to 1 mol of acetoguanamine in the formaldehyde/acetoguanamine molar ratio of 1—8 (in some cases, water was added), and the pH was adjusted to the desired value with sodium hydroxide solution (the pH was measured with a glass electrode using Hitachi Horiba M-5 pH meter.). This mixture was heated for an hour with stirring in a thermostat regulated at 80°C, and then the flask containing the reaction products was cooled in ice-water or allowed to stand at room temperature until crystals precipitated. The obtained crystals [A] were collected on a Büchner funnel and the filtrate was allowed to stand for 1—2 days (in the cases of the formaldehyde/acetoguanamine molar ratio of 7 and 8, the filtrate was allowed to stand for a week) in a refrigerator. The crystals [B] deposited from the filtrate were filtered off, and the filtrate was treated again as mentioned above.

The conditions for preparation of methylol acetoguanamines are shown in Table 1.

Table 1. The conditions for preparation of methylolacetoguanamines

No.	AG g	F ml	Water ml	Molar ratio AG: F	pH
1	90	54.1	360	1 : 1	9.04
2	31	22	50	1 : 1.2	9.40
3	125	150.1	287	1 : 2	8.81
4	125	225.2	0	1 : 3	9.00
5	87.5	210	0	1 : 4	9.20
6	75	270	0	1 : 6	9.01
7	50	210	277	1 : 7	9.00
8	50	240	309	1 : 8	9.00

Acetoguanamine and formaldehyde are abbreviated as AG and F respectively.

Monomethylolacetoguanamine. To a suspension of 31 g (0.248 mol) of acetoguanamine in 50 m*l* of water was added 22 m*l* (0.2976 mol) of formaline. The mixture was adjusted to pH 9.40, heated at 80°C for about an hour after complete dissolution, and then cooled to 10°C. The deposited crystals were collected and dissolved in methyl cellosolve to remove unreacted acetoguanamine monomer. The crystals 2-A (see Table 2) recrystallized from acetone were separated, washed with cold water, air-dried and then dried at room temperature *in vacuo*.

Dimethylolacetoguanamine. A mixture of 125 g (1 mol) of acetoguanamine and 225.2 m*l* (3 mol) of formaline was adjusted to pH 9.00. This mixture became a transparent solution within a few minutes, and after 20 min, the reaction solution changed into a milky turbid solution, and then the reaction was continued for 40 min. The separated product 4-A was washed with petroleum ether and dried *in vacuo* (room temperature). The pure crystals 4-A′ were obtained by repeated crystallization from DMSO.

Trimethylolacetoguanamine. A mixture of 87.5 (0.7 mol) of acetoguanamine and 210 m*l* (2.8 mol) of formaline was heated for an hour at pH 9.20 and 80°C. This mixture became homogeneous after 10 min, and the reaction solution was clear until the reaction came to an end. The resulting solution was allowed to stand at room temperature until crystals formed, then the crystalline product 5-A was separated by filtration and the filtrate was kept to stand for 2 days in a refrigerator. The crystals 5-B obtained from this filtrate were collected, washed with cold water and methanol, and air-dried.

Tetramethylolacetoguanamine. Acetoguanamine (50 g, 0.4 mol) was suspended in 240 m*l* (3.2 mol) of formaline and about 310 m*l* of water. This mixture immediately became clear by heating at 80°C and pH 9.00. The product 8-A was obtained by setting the reaction solution for a week in a refrigerator. The

Table 2. The quantitative estimation of methylol groups in methylolacetoguanamines

No.	Cryst. No.	Methylol F% Found	Methylol F% Calcd	Methylol + Methylene F%	Observed F/AG ratio	Mp (°C)	N% Found	N% Calcd	Yield (%)
1	1-A	18.03	19.35	—	0.92	—	46.64	45.13	—
2	2-A	19.45		19.36	1.01	193—194	45.14		65.54
	2-B	20.61		—	1.07	—	44.56		—
	2-C	21.09		—	1.11	—	44.08		—
3	3-A	29.17	32.42	—	1.71	—	38.73	37.81	—
	3-B	29.68		—	1.82	—	38.35		—
	3-C	30.83		—	1.89	—	35.81		—
4	4-A	31.86		32.33	1.95	—	37.93		—
	4-A′	32.11		32.59	1.98	175—176	37.89		46.71
	4-B	35.37		—	2.28	—	32.76		—
5	5-A	39.39	41.85	—	2.74	—	34.53	32.54	—
	5-B	41.56		41.41	2.97	170—172	32.62		56.05
6	6-A	44.65	48.97	—	3.51	—	30.55	28.56	—
	6-B	46.95		—	3.69	—	29.76		—
7	7-A	46.96		—	3.69	—	29.78		—
	7-B	47.71		—	3.80	—	29.36		—
8	8-A	48.95		48.93	3.99	166—167	28.59		—
	8-B	48.87		48.88	3.98	166—167	28.59		20.96

Calcd % of methylol F and N are for pure mono-, di-, tri-, and tetramethylolacetoguanamines.

yield of crystals 8-A was lower than those of crystals 2-A, 4-A′, and 5-B. The filtrate, after the crystals 8-A were separated off, was kept for a week in a refrigerator and a small amount of the product 8-B was obtained.

Analyses of the Products. The products were analyzed by the iodometric[13] and the Levenson (phosphoric acid decomposition[14-16]) methods; the molar ratio of the hydroxymethylated formaldehyde and the combined total formaldehyde to acetoguanamine were calculated respectively. The amount of the methylene linkage was estimated from the difference between the two values obtained by the two methods. The infrared absorption spectra were observed by KBr disk method using the IR-27G infrared spectrophotometer of Shimadzu Co., Ltd. The NMR spectra of acetoguanamine derivatives in DMSO were recorded on a Japan Electron Optics Lab. NMR spectrometer, model JNM-3H (60 Mc), using tetramethylsilane as an internal reference.

The analyses of No. 2-A, 4-A′, 5-B, and 8-A crystals and their yields and melting points are shown in Table 2.

Results and Discussion

Chemical Analysis of Methylol Derivatives. It may be first considered from Table 2 that in products No. 2-A, 4-A′, 5-B, and 8-A the methylene linkage is not found at all, because the content of the methylol group agrees very closely with that of the combined total formaldehyde. Tollens reagent was reduced by these compounds, indicating the presence of the methylol groups. The molar ratio of the hydroxymethylated formaldehyde of these compounds were 1.01, 1.98, 2.97, and 3.99 respectively. It was also recognized that the agreement between the calculated and found values (elemental analyses) of No. 2-A, 4-A′, 5-B, and 8-A is within the error of the analysis and that the sharp melting point of each compound indicates a good quality. Accordingly, each of the crystals No. 2-A, 4-A′, 5-B, and 8-A was assumed to be a pure methylol derivative of mono-, di-, tri-, and tetramethylolacetoguanamines, respectively. Henceforth, they will be represented as AGF, AG2F, AG3F, and AG4F respectively.

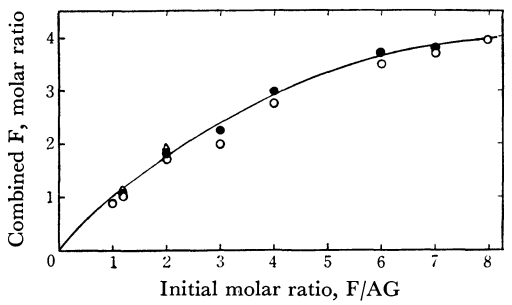

Fig. 1. The relationship between the initial molar ratio, F/AG and the observed molar ratio in methylol compounds.
○: crystal A, ●: crystal B, △: crystal C

The relationship between the initial molar ratios of formaldehyde and acetoguanamine and the observed molar ratios in methylol compounds is plotted in Fig. 1 based on data in Table 2. As can be seen from Fig. 1, the molar number of the combined formaldehyde to acetoguanamine increases with the increase of the reaction molar ratio. But in all the above results, each expected methylol compound is formed when an excess amount of formaldehyde is present in the reaction system, and especially in the preparation of AG4F, 8 mol of formaldehyde is needed which corresponds to two equivalents of acetoguanamine. This fact may easily be understood from the presence of four equilibriums in the formation of AG4F.

An increase of the content of the methylol group in the order of crystals [A], [B], and [C] in Table 2 indicates the formation of the higher order methylol compound.

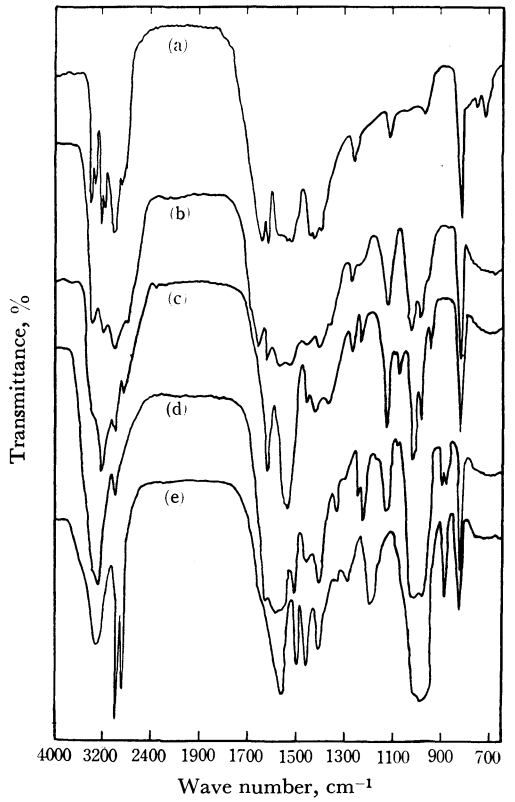

Fig. 2. Infrared absorption spectra of acetoguanamine (a), mono- (b), di- (c), tri- (d), and tetramethylolacetoguanamine (e).

13) A. Takahashi and I. Yamazaki, *Kobunshi Kagaku (Chem. High Polymers Japan)*, **15**, 232 (1958).
14) I. J. Levenson, *Ind. Eng. Chem. Anal. Ed.*, **12**, 332 (1940).
15) T. Kitagawa, *Kogyo Kagaku Zasshi (J. Chem. Soc. Japan, Ind. Chem. Sect.)*, **53**, 181 (1950).
16) K. Koeda, *Nippon Kagaku Zasshi (J. Chem. Soc. Japan, Pure Chem. Sect.)*, **75**, 571 (1954).

Infrared Absorption Spectra of Mono-, Di-, Tri-, and Tetramethylolacetoguanamines. In Fig. 2 are shown the infrared absorption spectra of acetoguanamine and its methylol derivatives, AGF, AG2F, AG3F, and AG4F. In these spectra, the absorption bands near 3000 cm^{-1} can not definitely be assigned, because in acetoguanamine (Fig. 2(a)) the $-NH_2$ and C–H stretching vibrations overlap with each other and in methylol derivatives (Fig. 2(b)—(e)) the N–H and O–H stretching bands[17,18] additionally overlap. The characteristic absorption bands at 1655 and 1626 cm^{-1} are assigned to the $-NH_2$ scissor vibration[19] and decreased with an increase of the number of methylol groups. The absorption at 1620 cm^{-1} shown in Fig. 2(c) (AG2F) is due to the N–H deformation vibration. The variation of the characteristic bands in the region of 1655 to 1620 cm^{-1} in Fig. 2(a)—(c) indicate that $-NH_2$ and –NH– groups on acetoguanamine take part in a series of reactions leading to the formation of methylol compounds, especially in Fig. 2 (e) (AG4F) where these peaks disappeared completely. The absorption in 1555—1400 cm^{-1} region seems to be due to the overlaps of the C–H stretching vibrations[19-21] of the triazine ring system and the side chain, and the C–H deformation band of the substituent group, $-CH_3$ on the triazine ring. It is known[22] that the bands of the C–H stretching vibration corresponding to primary, secondary, and tertiary amines appear at 1360—1250 cm^{-1}, but in these spectra, it is difficult to distinguish each peak clearly. The absorption near 1000 cm^{-1} due to the C–O stretching[23,24] indicates the presence of methylol group, which has been known[25] in the infrared absorption spectra of *o*- and *p*-methylolphenol. The intensity of this peak shows a prominent increase in proportion to the number of methylol groups. This fact suggests in connection with the absorption bands of

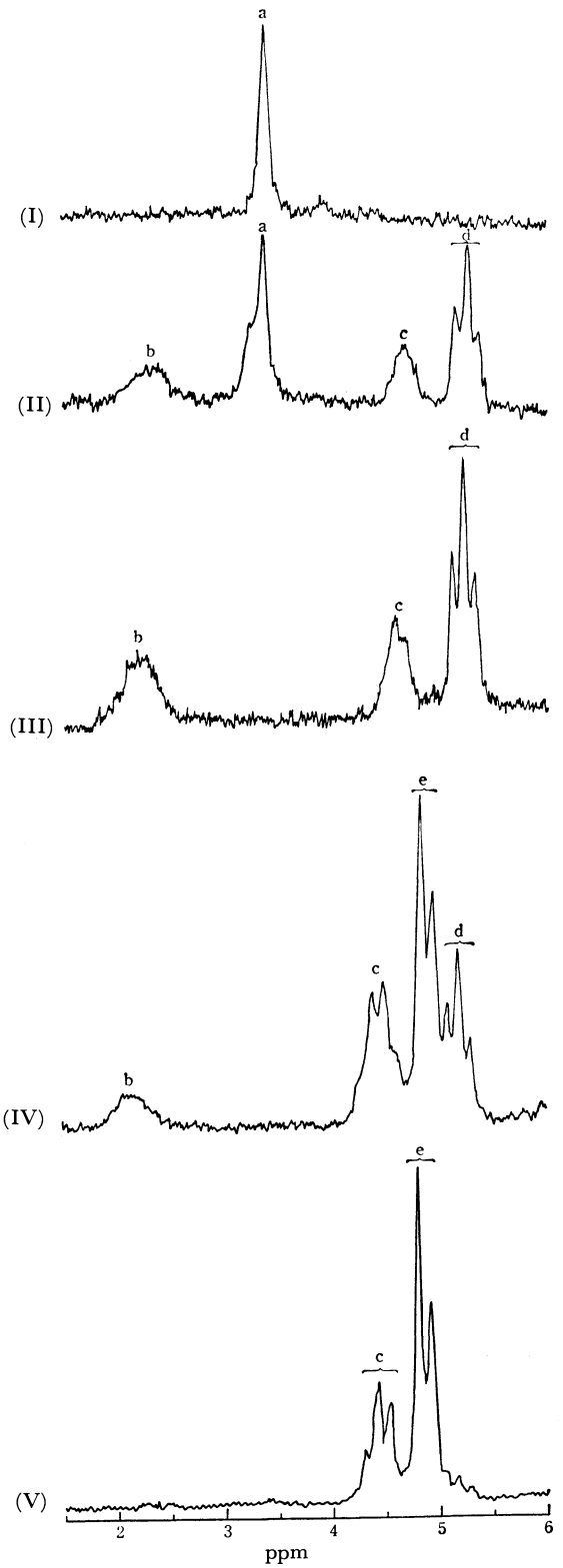

Fig. 3. NMR spectra of acetoguanamine (I), mono- (II), di- (III), tri- (IV), and tetramethylolacetoguanamine (V).

17) Y. Ogata, Y. Izawa, T. Itoh and S. Matsui, *Kogyo Kagaku Zasshi* (*J. Chem. Soc. Japan, Ind. Chem. Sect.*), **70**, 124 (1967).

18) R. M. Silverstein and G. C. Bassler, "Spectrometric Identification of Organic Compounds," John Wiley and Sons, Inc., New York (1963), p. 56.

19) G. Morimoto, *Nippon Kagaku Zasshi* (*J. Chem. Soc. Japan, Pure Chem. Sect.*), **87**, 797 (1966).

20) W. F. Jones and W. J. Orivelle-Tomas, *Trans. Faraday Soc.*, **55**, 208 (1957).

21) M. Takimoto, *Nippon Kagaku Zasshi* (*J. Chem. Soc. Japan, Pure Chem. Sect.*), **85**, 168 (1964).

22) A. D. Cross, "An Introduction to Practical Infrared Spectroscopy," published by Butterworth & Co., Ltd. Copyright, London (1964).

23) L. J. Bellamy, "The Infrared Spectra of Complex Molecules" (1958).

24) K. Nakanishi, "The Infrared Absorption Spectra," Nankodo, Tokyo (1960), p. 66 and others.

25) N. Yoshimi, M. Yamano and M. Tanaka, *Kogyo Kagaku Zasshi* (*J. Chem. Soc. Japan, Ind. Chem. Sect.*), **66**, 286, 1602 (1963).

TABLE 3. NMR DATA OF ACETOGUANAMINE AND ITS METHYLOL DERIVATIVES

Peak No. / ppm / Compound	a 3.4	b 2.3	c 4.3	d 5.1—5.4	e 4.7—5.0
AG	○	×	×	×	×
AGF	○	○	○	○	×
AG2F	×	○	○	○	×
AG3F	×	○	○	○	○
AG4F	×	×	○	×	○
Assignment proton	$-N\underline{H}_2$	$-N\underline{H}-$	$-NHCH_2O\underline{H}$	$-NHC\underline{H}_2OH$	$-N(C\underline{H}_2OH)_2$

Where the circle and saltire-cross marks indicate the presence and absence of the signals respectively.

the $-NH_2$ scissor and the N–H deformation that the number of methylol groups increases in the order of Fig. 2(a)—(e). It has been known[20,21,26] that the sharp band at 815 cm^{-1} is assigned to out-of-plane deformation vibration of the triazine ring.

The results of the infrared spectra may allow us to conclude, at least qualitatively, that the characteristic absorption bands, especially the peaks in 1655—1620 cm^{-1} region and at 1000 cm^{-1}, can be used as a measure of the degree of hydroxymethylation of acetoguanamine with formaldehyde.

NMR Spectra of Mono-, Di-, Tri-, and Tetramethylolacetoguanamine. The measurements of NMR spectra were also carried out to identify the above results. Since the signals of the methylene protons from acetoguanamine and DMSO (solvent) overlapped with each other, the signals of $-NH_2$ groups, –NH–, $-CH_2-$, and –OH on $-NHCH_2OH$ groups, and $-CH_2-$ on $-N(CH_2OH)_2$ were inquired. These spectra are shown in Fig. 3 and their chemical shifts are given in Table 3, in which the circle and saltire-cross marks indicate the presence and absence of the signals, respectively.

The signal at 3.4 ppm is observed both in the spectrum of acetoguanamine and AGF but not in that of the other compounds, and acetoguanamine has only this peak (Fig. 3(I)). Therefore, this singlet signal can be identified due to protons of primary amine. The protons which are possessed in AGF, AG2F, and AG3F, but not in acetoguanamine and AG4F, correspond to the imino proton and methylene protons of $-NHCH_2OH$ groups. It has been revealed[27] that the broad signal centered at 2.5 ppm can be assigned to a proton of secondary amine. From these results, the peak at about 2.3 ppm mentioned above may be assigned to the imino proton. On the other hand, the appearance of the triplet in the region of 5.1 to 5.4 ppm is due to the absorption for the methylene protons on $-NHCH_2OH$. The signal near 4.5 ppm can be identified with the hydroxyl group proton on methylol group, because this signal does not appear in acetoguanamine (Fig. 3(I)) but appears in AGF, AG2F, AG3F, and AG4F possessing the methylol group (Fig. 3(II)—(V)). The doublet signal in the region of 4.7 to 5.0 ppm appears in AG3F and AG4F as shown in Fig. 3(IV) and (V), in the spectrum of AG4F, the other absorption other than this doublet peak (e) and the hydroxyl group proton peak (c) can not be detected. Thus the peak (e) may be assigned as coming from the methylene protons on $-N(CH_2OH)_2$. It has become apparent that if the methylene protons on the methylol groups are the same, the methylene protons on $-NHCH_2OH$ and on $-N(CH_2OH)_2$ give the different signals respectively, and from the difference of these signals that the AG2F isomer of $-N(CH_2OH)_2$ type is not contained in the AG2F, *i.e.* the AG2F isomer is very difficult to be formed compared with AG2F bonding two methylol groups on both sides of amino groups. This fact may be explained by the difference of the reactivity of $-NH_2$ and –NH– groups as found by Jong and Jonge[28] on urea resin. If this isomer exists in the obtained AG2F compound, the absorption peaks of a primary amine should remain and that of the methylene on $-N(CH_2OH)_2$ should appear in Fig. 3(III).

The assignment of each proton in acetoguanamine and its methylol derivatives is shown in Table 3. The ratio of the absorption intensities of the signals is recognized to be in reasonable harmony with the calculated one for pure methylol compounds. It may be concluded that the results of the NMR spectra can be used as an indicator of the degree of hydroxymethylation by observing the characteristic absorption signals.

26) W. M. Padgett and N. F. Hammer, *J. Am. Chem. Soc.*, **80**, 803 (1958).

27) N. Yasaku and J. Kumanotani, Preprint for the 16th Annual Meeting of the Thermosetting Resin Lecture Discussion of Japan (September, 1966), p. 23.

28) J. I. de Jong and J. de Jonge, *Rec. Trav. Chim.*, **72**, 88 (1953).

From results of chemical analysis, infrared absorption spectra and NMR spectra analyses, it was found that four kinds of pure methylol derivatives of acetoguanamine, *i.e.*, mono-, di-, tri-, and tetramethylolacetoguanamines, can easily be synthesized by selecting the reaction conditions, especially the molar ratio of formaldehyde and acetoguanamine.

The authors wish to express their thanks to Professor Masaya Ogawa and Dr. Fukiko Yamada for their valuable discussions and encouragement, Mr. Isao Niwa for his experimental assistance, Mrs. Toshiko Kōno for her measurements of NMR spectra, and Miss Hisako Nishikawa for her elemental analysis. They are also grateful to Nippon Gosei Chem. Ind. Co., Ltd., for the generous gift of acetoguanamine.

BULLETIN OF THE CHEMICAL SOCIETY OF JAPAN VOL. 42 2431—2437 (1969)

ESR Spectra of the System of the Transition Metal Compound and Trialkyl Aluminum. II.*1 The System of the Vanadium Compound and Trialkyl Aluminum*2

Yasuo NOZAWA and Masatami TAKEDA

Department of Chemistry, Faculty of Science, Science University of Tokyo, Shinjuku-ku, Tokyo

(Received January 16, 1969)

The ESR spectra of the homogeneous organometallic catalyst system of VOA_2-$AlEt_3$ (I) and VCl_4-$AlEt_3$ (II) were measured in benzene, toluene, *n*-hexane and tetrahydrofuran solutions. A superhyperfine structure of nine lines with a *g*-value of 1.9917, and with a hyperfine splitting of 4.2 gauss on each eight line due to the ^{51}V nucleus, was observed in the systems of I and II in the aromatic solvents at any Al/V ratio from 1 to 15. The same type of spectrum was observed in the VA_3-$Al(isoBut)_3$ system in a benzene solution at Al/V ratios higher than 3. In the system of II, the single line was observed at Al/V ratios up to 5. At higher ratios the superhyperfine structure appeared to overlap on the single line. On the basis of these facts, it may be considered that the vanadium atom was reduced to the zerovalent state and was then complexed with aromatic solvents in these systems. This suggests the presence of a sandwich complex such as where X=H or CH_3.

Homogeneous catalytic systems of the vanadium (V) compound and aluminum alkyl for the polymerization of ethylene and its copolymerization with α-olefin have been investigated in detail.[1-4] Natta[5] has shown, by means of electron spin resonance (ESR) measurements, that the active species of vanadium complexes for the syndiotactic polymerization of polypropylene have a valence state of 3. The active oxidation state of the V compound has also been extensively discussed by Lehr.[6] The formation of a chlorine-bridged complex as the reaction product of vanadium tetrachlolide (VCl_4) and triethylaluminum ($AlEt_3$) in the VCl_4-$AlEt_3$ system has been proposed by Sciulydin.[7] The same type of ESR spectrum has, however, been obtained in the system of vanadyl acetylacetonate (VOA_2) and $AlEt_3$, in which chlorine atoms are not present. Therefore, it seems to be worthwhile to study further the chemical structure of the complex produced in the system of the V compound and $AlEt_3$.

The present paper describes ESR measurements

*1 Part I of this series: Y. Nozawa and M. Takeda, *Kogyo Kagaku Zasshi* (*J. Chem. Soc. Japan. Ind. Chem. Sect.*), **71**, 189 (1968).

*2 Presented at the 7th symposium on ESR held by the Chemical Society of Japan, Sapporo, September, 1968.

1) G. Natta, G. Mazanti, A. Valvassori, G. Sartori and D. Fiumani, *J. Polym. Sci.*, **51**, 411 (1961).

2) F. D. Otto and G. Parravano, *J. Polym. Sci.*, **A-2**, 5131 (1964).

3) L. C. Anand, S. S. Dixit and S. L. Kapur, *J. Polym. Sci.*, **A-1**, **6**, 909 (1968).

4) I. Pasquon, *Pure and Applied Chem.*, **6**, 465 (1968).

5) G. Natta, A. Zambelli, G. Lanzi, I. Pasquon, A. L. Segre and P. Centola, *Macromol. Chem.*, **81**, 161 (1965).

6) M. H. Lehr, *Macromolecular*, **1**, No. 2, 178 (1968).

7) S. V. Sciulydin, N. N. Tikhomirova, A. E. Shilov and A. K. Shilova, *Zh. Struk. Khim.*, **2**, 740 (1961).

of the VOA_2-$AlEt_3$ (I) and VCl_4-$AlEt_3$ (II) systems in various organic solvents; the formation of a sandwich complex of the V atom with aromatic solvents will be discussed on the basis of our observations.

Experimental

Reagent and Preparation of Samples. Vanadium trisacetylacetonate was prepared as described in the literature[8] and was purified by recrystallization from benzene. Commercially-obtained vanadium tetrachloride and triethylaluminum (Ethyl Co) were used without further purification. The solvents used were refluxed over a sodium ribbon and distilled immediately before use.

The samples for ESR measurements were prepared in a 30-milliliter glass vessel under a dried nitrogen atmosphere at room temperature. One milliliter of the 1/5 mol/*l* solution of the V compound was taken into the vessel and a predetermined aliquot of an $AlEt_3$ solution with the same concentration as the V compound was added; then the solvent was added to bring the total volume to 20 m*l*. Thus the concentration of the sample solution was 0.01 mol/*l* with respect to the V compound. The solution was introduced into a sample tube for ESR measurements by means of a hypodermic syringe. The concentration of the sample solution for the VOA_2-$AlEt_3$ system in *n*-hexane was small because of the low solubility of the species involved.

ESR Measurements. The ESR spectrometer used was a JES-3BSX-type apparatus (Japan Electron Optics Co. Ltd.) with 100 kHz field modulation and TE_{011} mode cavity. The *g*-value was determined by the aid of DPPH.

Results

1. The VOA_2-$AlEt_3$ System (I). The ESR spectra of VOA_2 and the VOA_2-$AlEt_3$ system in a benzene solution are shown in Fig. 1 and Fig. 2-a respectively. The eight-line signal with a *g*-value of 1.9843 and with a hyperfine (hf) splitting of 109 gauss was observed in a benzene solution of VOA_2. In the VOA_2-$AlEt_3$ system in benzene, similar line spectra with a *g*-value of 1.9917 and with a hf splitting of 62 gauss were obtained at an Al/V ratio from to 15. The eight-hf signal in each spectra is due to the interaction between an odd electron and the ^{51}V of the nuclear spin moment, 7/2. As is shown in Fig. 2-b, with a lower sweep rate a superhyperfine (shf) structure which apparently has nine-line signal with a splitting of 4.2 gauss was obtained on each line of the eight hf components in this system. The same spectral feature appeared also in the region where the Al/V ratio was higher than 15. The nine-shf structure, however, could not be detected in a benzene solution of VOA_2.

The spectra of this system in toluene are given in Fig. 3, the nine-line shf signal that overlapped on each component of the eight hf lines was also observed at Al/V ratios from 3 to 15. The spectrum was exactly the same as that obtained in the benzene solution.

The ESR spectra of this system in an *n*-hexane solution at an Al/V ratio of 7 are shown in Fig. 4. A signal with a *g*-value of 1.9928 containing an eight-line signal (a splitting of about 66 gauss) was observed on samples with Al/V ratios from 1 to 15. The shf structure could not, however, be detected at all on any eight-hf component. This spectrum is different from those of benzene and toluene solutions in that the eight-hf structure is missing in the former, apparently indicating that the radical species in an *n*-hexane solution is different from those in benzene and toluene.

The ESR signal of the system of VOA_2 and $AlEt_3$ could not be observed at any Al/V ratio when tetrahydrofuran was used as the solvent.

2. The VCl_4-$AlEt_3$ System (II). The ESR spectrum of the VCl_4-$AlEt_3$ system in a benzene

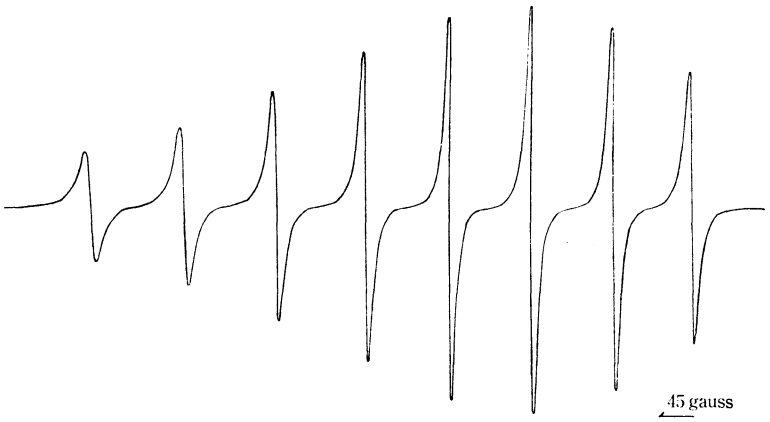

Fig. 1. The ESR spectrum of VOA_2 in benzene solution.

8) R. Rowe and M. Jones, *Inorg. Syn.*, **5**, 114 (1957).

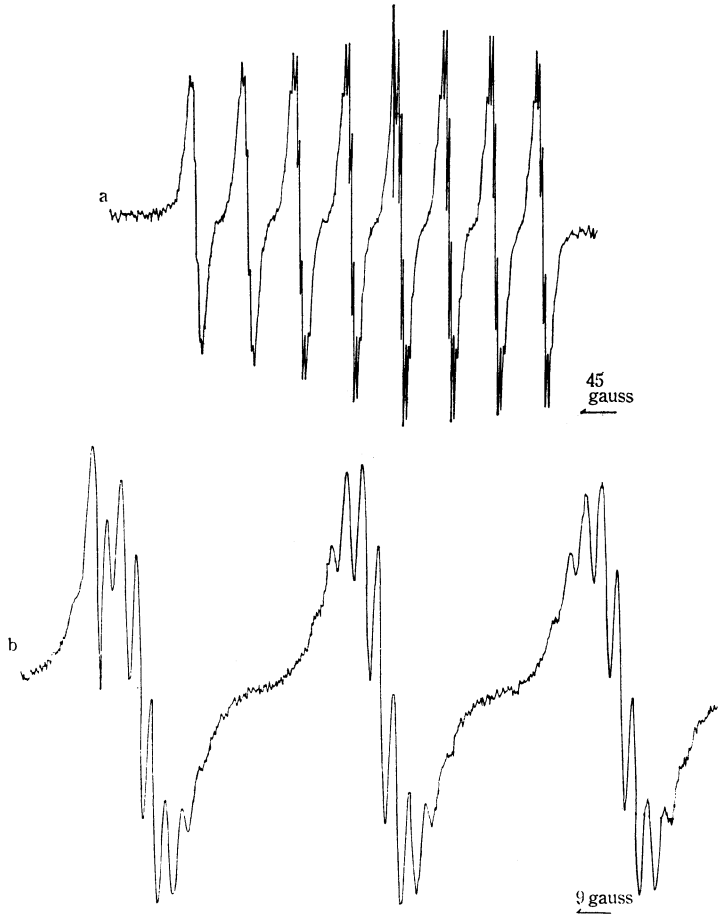

Fig. 2. The ESR spectra of the system of VOA_2-$AlEt_3$ in benzene solution. Al/V=15. When measured with higher sweep (a), lower sweep (b).

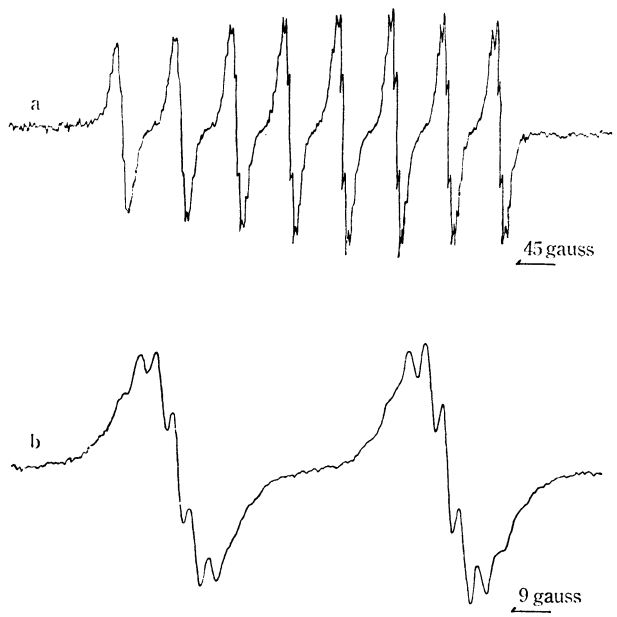

Fig. 3. The ESR spectra of the system of VOA_2-$AlEt_3$ in toluene solution. Al/V=3. When measured with higher sweep (a), and lower sweep (b)

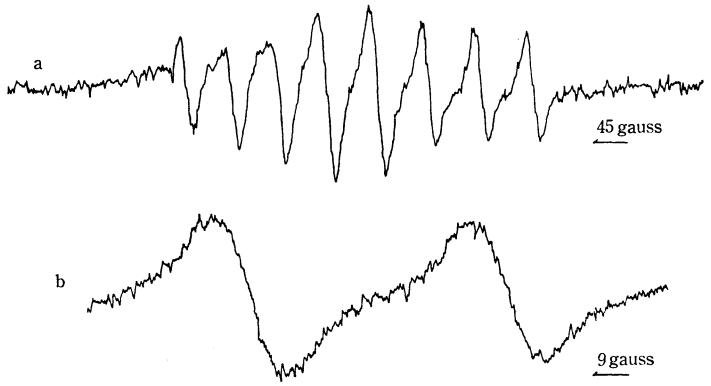

Fig. 4. The ESR spectra of the system of VOA_2-$AlEt_3$ in *n*-hexane solution. Al/V=7. When measured with higher sweep (a) and lower sweep (b).

solution at Al/V ratios up to 5, as shown in Fig. 5, consists of a single line signal with a *g*-value of 1.9775 and has a maximum slope width of approximately 170 gauss. At higher Al/V ratios, as is shown in Fig. 6, an eight line signal with a *g*-value of 1.9917 and containing a nine shf structure on each hf component similar to that found in the system I was superimposed on the single line signal described above.

In a toluene solution of this system, only a single line was observed at Al/V ratios up to 5. At higher ratios (7 and 15), the single line and the eight-line signal were observed again, the two signals overlapping.

The spectrum in an *n*-hexane solution has only a single line signal with a *g*-value of 1.9771, and its maximum slope width is approximately 200 gauss. No other signal (*e. g.*, the nine line shf signal) could be observed when the Al/V ratio was varied from 1 to 15. These single-line spectrum of this system can be exactly assigned to the signal of the VCl_2 compound by reference to those observed in a solid state and in a hydrocarbon solution.[5]

In view of the present observations, it is clear that the ESR-active species in a benzene and a toluene solution are different from that in *n*-hexane solution, as is the case for the system I. The results observed in both systems are summarized in Table 1.

The addition of various alcohols to the system I and II did not alter the line shapes of the spectra and the *g*-values of the signals, though the signal intensity decreased. This is in sharp contrast to the system of bis-cyclopentadienyltitanium dichloride ($(C_5H_5)_2TiCl_2$) and AlR_3, which will be described again later.

Discussion

As Fig. 1 and Fig. 2 show, the hf splitting of the eight-line signal for the benzene solution of VOA_2 is approximately 109 gauss, but the splitting width changes to 62 gauss in the systems of both I and II when $AlEt_3$ is added. It is, therefore, apparent that vanadium is reduced to a lower oxidation state from its initial state, +4, as a result of the reaction of the original compound with $AlEt_3$. A

Table 1. Summary of *g*-values and hyperfine coupling constants in various systems

System	Solvent	Al/V	*g*-Value	hf constant (8) (gauss)	shf constant (9) (gauss)
VOA_2	Benzene	—	1.9843	109	—
VOA_2-$AlEt_3$ (I)	Benzene	1—15	1.9917	62	4.2
	Toluene	3—15	1.9916	63	4.3
	n-Hexane	1—15	1.9928	66	—
	THF	1—15	—	—	—
VCl_4-$AlEt_3$ (II)	Benzene	1— 5	1.9705	(170)*	—
	Benzene	7—15	1.9917	62	4.3
	Toluene	1— 3	1.9705	(170)*	—
	Toluene	5—15	1.9915	63	4.3
	n-Hexane	1—15	1.9771	(200)*	—
VOA_2-$Al(i\text{-}But)_2$	Benzene	3— 8	1.9918	62	4.1
VA_3-$Al(i\text{-}But)_3$	Toluene	>3	1.9917	62	4.3

* The values in parentheses are maximum slope width of single resonance line.

correlation of the hf splitting with the oxidation state of ^{51}V has been reported,[9] it was found that the separations for V^{4+}, V^{3+} and V^{2+} in α-Al_2O_3 are 140, 110, and 88 gauss, respectively. The steady decrease in the splittings in this series also supports the idea of the formation of a reduced vanadium compound in the present system.

In the ESR spectrum for the system of VOA_2-Al(isoBut)$_3$ in toluene, eight-line signal with an hf splitting of 63 gauss, each of the signal with an shf structure of nine line similar to the spectra shown in Fig. 2, were also observed at Al/V ratios from 3 to 8. The oxidation state of vanadium is reduced to a lower state by Al(isoBut)$_3$ also.

For the system of vanadium trisacetylacetonate (VA_3) and Al(isoBut)$_3$ in benzene solution, no ESR signal was observed at Al/V ratios of 1 and 2.

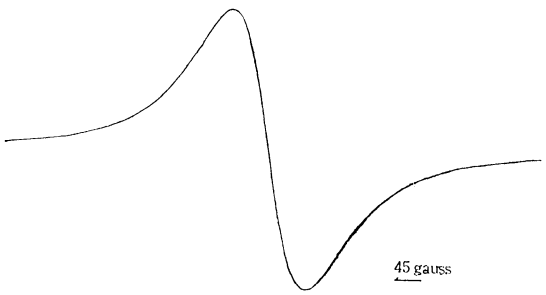

Fig. 5. The ESR spectrum of the system of VCl_4-$AlEt_3$ in benzene solution. Al/V=5.

The oxidation state of vanadium in VA_3 may be regarded as +3, and the species does not give rise to any ESR signal. Apparently, VA_3 is not reduced by Al(isoBut)$_3$ under such conditions. If the Al/V ratio was raised to above 3, however, the same spectra as those of I and II were obtained.

In the system of II in benzene and toluene, only a single broad line is observed at the Al/V ratio of 5, as is shown in Fig. 5. The spectra may be assigned to that of VCl_2. As Fig. 6 shows, at Al/V ratios higher than 5 the shf structure appears to overlap on the single line. The spectra with an shf structure may be attributed to the signal of vanadium, which has been reduced further from the divalent state to possibly that of zerovalent vanadium.[10]

Note that the nine-line shf structure described above could not be observed when *n*-hexane was used as a solvent instead of benzene and toluene.

Sciulydin[7] reported that the eight-line signal with a *g*-value of 1.992 aws observed in the VCl_4-$AlEt_3$ system in a benzene solution and that each hf component of the eight-line signal gave an shf structure of 11 or 13 lines; be proposed a chlorine-bridged structure such as $R_2Al\langle^{Cl}_{Cl}\rangle V\langle^{Cl}_{Cl}\rangle AlR_2$ its hf structure being attributable to interaction between an odd electron of the vanadium atom and four chlorine and two aluminum atoms. However, since we have observed the same spectral features in the VOA_2-$AlEt_3$ system in which no chlorine

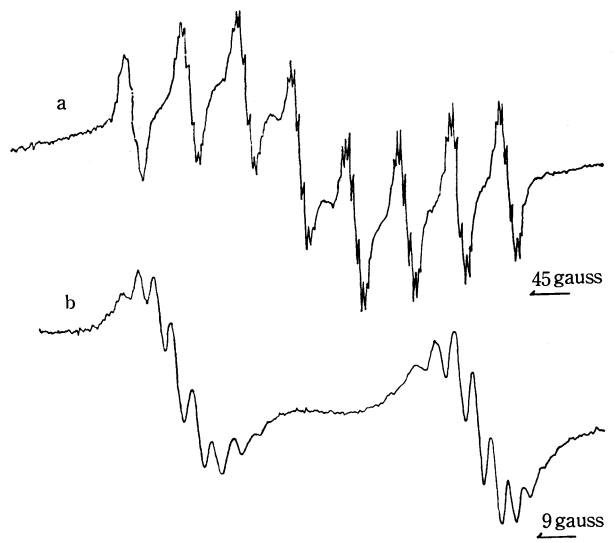

Fig. 6. The ESR spectra of the system of VCl_4-$AlEt_3$ in benzene solution. Al/V=15. When measured with higher sweep (a), and lower sweep (b).

9) J. Lambe and C. Kikuchi, *Phys. Rev.*, **118**, 71 (1960).

10) E. O. Fischer and H. P. Kögler, *Chem. Ber.*, **90**, 250 (1957).

atom is involved, the structure postulated above is not adequate to explain the spectra.

To aid the investigation of the complex formation of the V atom in the system, ESR measurements of the system of chromium trisacetylacetonate (CrA_3) and $AlEt_3$, analogous to the system of the vanadium compound and $AlEt_3$, were carried out. As is shown in Fig. 7, a nine-line spectrum[11] with a *g*-value of 1.986 was detected for the sample in a benzene solution at Al/Cr ratios higher than 4. The same type of spectrum consisting of a seven- or nine-line signal with a *g*-value of 1.987 in various aromatic solvents at the Al/Cr ratio of 10, was also reported by Angelescu *et al.*[12] They proposed the formation a sandwich-type complex of the chromium atom with aromatic species in these systems; they did so on the basis of the evidence that the shapes of the signals and the values of the *g*-factor were in agreement with those of $Cr(C_6H_6)_2^+$ [13] and its derivatives.[14]

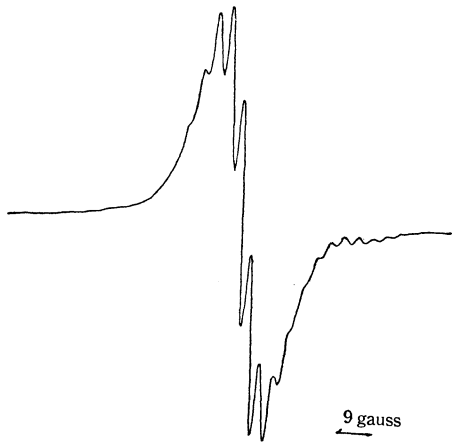

Fig. 7. The ESR spectrum of the system of CrA_3-$AlEt_3$ in benzene solution. Al/Cr=4.

By analogy with Angelescu's interpretation, the formation of a certain complex similar to $Cr(C_6H_6)_2^+$ may be expected for the system of the V Compound and $AlEt_3$ also. In fact, the shape of nine line signal observed in the system I and II (benzene and toluene being used as solvents) was apparently similar to that of the CrA_3-$AlEt_3$ system in various solvents.

Hence, we propose that the V compound in these systems is in the form of a sandwich-type complex with aromatic solvent molecules, as in the cases of CrA_3 and $AlEt_3$. The shf structure appearing in the spectra may, then, be attributed to the hf interaction between an odd electron and 12 (or 10) equivalent protons on the aromatic ring. Such an interaction would give rise to 13 equally-spaced lines with an intensity ratio of 1, 12, 66, 220, 495, 792, 924, 792, 495, 220, 66, 12 and 1 if $V(C_6H_6)_2$ is produced in the systems. Only nine-line signal was observed, however, this disagreement may be attributed to the poor signal-to-noise ratio of the spectra.

On the other hand, Hausser[15] has measured the ESR spectrum of $V(C_6H_6)_2$ in a mixed solvent (toluene and methylcyclohexane, (1 : 1)); he has observed eight-line signal due to the ^{51}V nucleus with a *g*-value of 1.9920, having an hf separation of 63.5 ± 1 gauss and an shf structure of nine line with a splitting of 4.0 ± 0.1 gauss superimposed on each hf component. The results obtained in our experiments are in good agreement with those obtained by Hausser with respect to the *g*-value, the shf splitting constant, and the pattern of the spectra.

In conclusion, the presence of an shf structure on eight-line spectrum observed in these systems (I and II) suggests the formation of a sandwich structure such as where X=H or CH_3, in which the chlorine-bridged structure proposed by Sciulydin is not involved.

Previously, in the system of $(C_5H_5)_2TiCl_2$-AlR_3 the six-line spectrum caused by hf interaction between an odd electron of the Ti^{3+} and the Al^{27} nucleus had been observed when methyl alcohol and the like were added to this system. This fact was interpreted by assuming the structure of the product to involve a di-μ-alkoxo bridge between the Ti and Al atoms.[16] On the other hand, as has been mentioned before, the *g*-value and the line shape of the spectra for the systems of I and II did not change when methyl alcohol was added, except for the decrease in the signal intensity. Therefore, as far as the results of the ESR measurement are concerned, it seems that the V atom does not form a di-μ-alkoxo bridge complex with the Al atom upon the addition of alcohol.

Conclusion

From the study of the ESR spectra in the systems of VOA_2-$AlEt_3$ (I) and VCl_4-$AlEt_3$ (II), the formation of a sandwich complex of zerovalent vanadium with aromatic solvents has been suggested; the

11) M. Takeda, K. Iimura, Y. Watanabe and Y. Nozawa, Preprints for the 14th Symposium on High Polymer (Oct.), 1965.

12) E. Angelescu, C. Nicolau and Z. Simon, *J. Am. Chem. Soc.*, **88**, 3910 (1966).

13) R. D. Feltham, P. Sogo and M. Calvin, *J. Chem. Phys.*, **26**, 1354 (1957).

14) B. Elschner and S. Herrog, *Z. Naturforsh.*, **12a**, 860 (1957).

15) K. Hausser, *ibid.*, **16a**, 1190 (1961).

16) Y. Nozawa and M. Takeda, *Kogyo Kagaku Zasshi* (*J. Chem. Soc. Japan, Ind. Chem. Sect.*), **71**, 189 (1968).

formation of an oxo-complex involving Al and V atoms could not be deduced in these systems, even in the presence of alcohol, as long as the ESR spectra of such systems were used as the criterion.

The authors wish to express their deep gratitude to Professor Goji Kodama, Science University of Tokyo, for his valuable advice and encouragement.

BULLETIN OF THE CHEMICAL SOCIETY OF JAPAN VOL. 42 2437—2449 (1969)

Semi-empirical Unrestricted SCF-MO Treatment for Valence Electron Systems. I. Application to Small Doublet Radicals

Teijiro YONEZAWA, Hiroshi NAKATSUJI, Takashi KAWAMURA and Hiroshi KATO*1

Department of Hydrocarbon Chemistry, Faculty of Engineering, Kyoto University, Kyoto

(Received January 20, 1969)

A semi-empirical SCF method for valence electron systems including a differential overlap previously proposed by the present authors is here extended to molecules with an open-shell structure. The unrestricted Hartree-Fock method is applied, and the one-centre and part of two-centre σ–π-type exchange repulsion integrals, playing an essential role in spin-density calculations, are included in the calculations. The calculated spin densities are divided into the mechanistic (spin-polarization and spin-delocalization) contributions. The spin-polarization mechanism is shown to be important even in cases where the spin delocalization mechanism has usually been considered to be dominant (*e. g.*, ethyl and vinyl radicals). The calculated spin densities of π-electron radicals (methyl, ethyl, allyl, and *trans*-butadienyl anion radicals) and of σ-electron radicals (vinyl, formyl, NO_2, CO_2^-, CN) are discussed. Their *hfs* constants and mechanistic contributions are calculated; for the methyl and vinyl radicals these are shown to be strongly angular-dependent. The calculated potential curve and the *hfs* constants of the vinyl radical lead to the CCH_α angle, $\theta \simeq 135°$; furthermore, the H_α and C_β *hfs* constants are shown to be negative. Generally, the calculated proton *hfs* constants agree satisfactorily with the experimental data and with other calculations except in the case of the formyl radical. The atomic dipoles of some σ-electron radicals are calculated, and some interesting features common to all the σ-electron radicals studied are found.

Recently semi-empirical SCF methods for valence electron systems have been generally applied[1-5] to calculations of certain physical and chemical properties of molecules. We have previously proposed a semi-empirical SCF method including differential overlaps for valence electron systems and applied it to various closed-shell molecules.[4] Here, we extend this method to molecules with an open-shell structure. As in the preliminary reports,[5] the unrestricted Hartree-Fock (UHF) method[6] is applied. Since the UHF wave function is not an eigenfunction of the spin-squared operator, S^2, the lowest contaminating spin functions are annihilated[7] after energy minimization.

The spin density calculated by the UHF method originates from two main mechanisms,[8] the spin-polarization (SP) and spin-delocalization (SD) mechanisms. In order to clarify the nature of the spin-density, these mechanistic contributions are

*1 Present adress: Department of General Education, Nagoya University, Chikusa-ku, Nagoya.

1) a) J. A. Pople, D. P. Santry and G. A. Segal, *J. Chem. Phys.*, **43**, S129 (1965). b) J. A. Pople and G. A. Segal, *ibid.*, **44**, 3289 (1966). c) J. A. Pople, D. L. Beveridge and P. A. Dobosh, *ibid.*, **47**, 2026 (1967). d) J. A. Pople, D. L. Beveridge and P. A. Dobosh, *J. Am. Chem. Soc.*, **90**, 4201 (1968).

2) N. M. Atherton and A. Hinchliffe, *Mol. Phys.*, **12**, 349 (1967).

3) T. Yonezawa, H. Konishi and H. Kato, This Bulletin, **41**, 1031 (1968).

4) a) T. Yonezawa, K. Yamaguchi and H. Kato, *ibid.*, **40**, 535 (1967). b) T. Yonezawa, H. Konishi and H. Kato, *ibid.*, **40**, 1071 (1967). c) H. Kato, H. Konishi, H. Yamabe and T. Yonezawa, *ibid.*, **40**, 2761 (1967). d) T. Yonezawa, H. Nakatsuji and H. Kato, *J. Am. Chem. Soc.*, **90**, 1239 (1968).

5) a) T. Yonezawa, H. Nakatsuji, T. Kawamura and H. Kato, This Bulletin, **40**, 2211 (1967). b) T. Yonezawa, H. Nakatsuji T. Kawamura and H. Kato, *Mol. Phys.*, **13**, 589 (1967).

6) J. A. Pople and R. K. Nesbet, *J. Chem. Phys.*, **22**, 571 (1954).

7) a) T. Amos and G. G. Hall, *Proc. Roy. Soc. (London)*, **A263**, 483 (1961). b) A. T. Amos, *Mol. Phys.*, **5**, 91 (1962). c) T. Amos and L. C. Snyder, *J. Chem. Phys.*, **41**, 1773 (1964). d) L. C. Snyder and T. Amos, *ibid.*, **42**, 3670 (1965).

separated by the method reported previously.[8] In π-electron radicals, the SP mechanism is dominant and is reduced to small σ–π-type electron repulsion integrals. In the present calculation, the one-center and part of two-center σ–π-type exchange repulsion integrals are included, although the latter was neglected previously.[5]

The method is applied mainly to the spin-density calculations of π-electron radicals, such as the methyl, ethyl, allyl, and *s-trans*-butadienyl anion radicals, and of some σ-electron radicals, such as vinyl, formyl, NO_2, CO_2^- and CN radicals. The mechanistic contributions to the spin density are separated, and some interesting features of spin density are revealed. Lastly, the dipole moments of the σ-electron radicals are analyzed.

Method

An unrestricted wavefunction for a system with p α-spin and q β-spin electrons has the form:

$$\psi_{\mathrm{uhf}} = |\varphi_1^\alpha(1)\alpha(1)\cdots\varphi_p^\alpha(p)\alpha(p)\varphi_1^\beta(p+1)\beta(p+1)\cdots \varphi_q^\beta(n)\beta(n)|, \quad (1)$$

where $n=p+q$. For the doublet radicals considered here $p=q+1$. The molecular orbital is expanded as a linear combination of all the valence atomic orbitals (VAO's), χ_r, of the constituent atoms:

$$\varphi_i^\alpha = \sum_r C_{ir}^\alpha \chi_r$$

and:

$$\varphi_i^\beta = \sum_r C_{ir}^\beta \chi_r. \quad (2)$$

The unrestricted SCF equations of the LCAO approximation are:

$$F^\alpha C_i^\alpha = \varepsilon_i^\alpha S C_i^\alpha$$

and:

$$F^\beta C_i^\beta = \varepsilon_i^\beta S C_i^\beta \quad (3)$$

in the usual notations.[6]

Estimation of Integral Valeus. One of the main features of the unrestricted SCF theory is its inclusion of spin correlation, thus enabling us to calculated negative spin densities. In the case of π-electron radicals, the spin densities appearing in the σ-type AO's are due to the σ–π-type spin-polarization mechanism.[9,10] In order to study these radicals, the following exchange integrals are considered in the calculations:

(a) The one-center exchange repulsion integrals*2 are evaluated by the approximate relations:[4c]

$$(sp|sp) = 0.045 Z_A (ss|pp)$$

and:

$$(pp'|pp') = 0.011 Z_A (pp|pp), \quad (4)$$

where s denotes the $2s$ AO.

(b) A part of the two-center σ–π-type exchange repulsion integrals is approximated by the following semi-empirical estimation:

$$(h\pi_X|h\pi_X)_{\text{semi-empirical}} = k(h\pi_X|h\pi_X)_{\text{Slater}}$$
$$(\mu_X\bar{\pi}_{X'}|\mu_X\bar{\pi}_{X'})_{\text{semi-empirical}} = k(\mu_X\bar{\pi}_{X'}|\mu_X\bar{\pi}_{X'})_{\text{Slater}} \quad (5)$$
$$(\mu_X\nu_{X'}|\mu_Y\nu_{Y'}) = \{(\mu_X\nu_{X'}|\mu_X\nu_{X'})\cdot(\mu_Y\nu_{Y'}|\mu_Y\nu_{Y'})\}^{1/2}$$

where h is a hydrogen $1s$ AO, where μ is a $2s$, $2p\sigma$ or $2p\pi$ AO, and where X and Y denote the first-row elements of the periodic table. The value of the parameter, k, is chosen so that the calculated proton spin densities of the methyl and ethyl radicals obtained before annihilation may reasonably be compared with the experimental results; the value is equal to 0.58 throughout these calculations.*3 For the $2s$ AO spin density of the carbon atom, the above two-center σ–π-type exchange repulsion integrals are not so important as are those for the proton spin density.*4

Note that many other two-center σ–π-type electron repulsion integrals are omitted. However, the parameter k, introduced in Eq. (5), may effectively include these neglected integrals for the proton-spin density in the C–H bond;*5 this assumption will, however, break down for heteropolar cases such as for the N–H and O–H bonds,

8) a) T. Yonezawa, H. Nakatsuji, T. Kawamura and H. Kato, *Chem. Phys. Letters*, **2**, 454 (1968). b) T. Yonezawa, H. Nakatsuji, T. Kawamura and H. Kato, *J. Chem. Phys.*, in press. c) H. Nakatsuji, H. Kato and T. Yonezawa, *ibid.*, in press.

9) a) H. M. McConnell, *J. Chem. Phys.*, **24**, 764 (1956). b) H. M. McConnell and D. B. Chesnut, *ibid.*, **27**, 984 (1957); **28**, 107 (1958). c) H. M. McConnell, *ibid.*, **28**, 1188 (1958). d) S. I. Weissman, *ibid.*, **25**, 890 (1956).

10) M. Karplus and G. K. Fraenkel, *J. Chem. Phys.*, **35**, 1312 (1961).

*2 The inclusion of one-center exchange repulsion integrals destroys the invariance[1a] of the Mulliken approximation, since $(pp|p'p') = (pp|pp) - 2(pp'|pp')$. Therefore, the one-center exchange repulsion integrals are included in the method after the Mulliken approximation for $(rs|tu)$ is completed, and the term $-2(pp'|pp')$ is introduced as a correction to $(pp|p'p')$. Thus, the present method is invariant to rotation around local atomic axis.

*3 The ratios of the adopted one-center exchange integrals to the theoretical values calculated from Slater AO's are 0.51 for $(pp'|pp')$ and 0.58 for $(sp|sp)$.

*4 For the methyl radical, the contributions of the one- and the two-center σ–π-type exchange repulsion integrals are -0.0787 and $+0.0512$ for the proton-spin density, and 0.1788 and -0.0301 for the carbon $2s$ AO spin-density (before annihilation).

*5 The contribution of the σ–π-type ionic integrals is zero if the C–H bond is assumed to be homopolar. For example, the configuration interaction treatment of the methyl radical, using the simple MO's based on the hybrid orbitals, showed that the contribution due to the two center σ–π-type ionic integrals amounts to only 6% of the total proton spin density.

where the omitted σ–π type ionic integrals may become important.

The method of estimating all the other integral values is the same as has been previously reported.[4-5]

Spin-polarization and Spin-delocalization Contributions. As has been shown in previous papers,[8] the spin-polarization (SP) contribution to the calculated spin density at the i position is given by the following equations for doublet radicals:

$$(\rho^i_{ba})_{SP} = \frac{3}{2}(\rho^i_{ba} - \rho^i_{aa}),$$

$$(\rho^i_{aa})_{SP} = \frac{1}{2}(\rho^i_{ba} - \rho^i_{aa}). \quad (6)$$

$(\rho^i_{ba})_{SP}$ is the SP contribution to the spin density, ρ^i_{ba}, calculated by the UHF method, and $(\rho^i_{aa})_{SP}$ is the SP contribution to the spin density, ρ^i_{aa}, obtained after annihilation.*6 The spin-delocalization (SD) contributions are the same for both stages (ba and aa) and are approximated[8] by:

$$(\rho^i)_{SD} = \rho^i - (\rho^i)_{SP}. \quad (7)$$

Estimation of the Isotropic *hfs* Constants. The isotropic proton *hfs* constant, a, is expressed approximately by: $a_H = A_H\rho_H$,[9c] while the values for the first-row nuclei of the periodic table are given as the sum of the $2s$ contribution ($A_{2s(N)} \cdot \rho_{2s(N)}$) and of the inner $1s$ contribution.

In the present calculations, A_H is regarded as a proportionality constant determined by "best fitting" the calculated spin densities (before annihilation) to the observed *hfs* constants.*7 A_H is set equal to 743 gauss throughout this paper. The $2s$ contribution to the *hfs* constant of the ^{13}C nucleus is calculated by setting $A_{2s(C)} = 1110$ gauss.[11] However, the present method does not give the quite important contributions to *hfs* constants by inner $1s$ AO's.[10,12] These contributions are opposite in sign to those of the $2s$ AO's.[10,12]

Application of the Method

In this section we will present the results obtained by applying the above method to three types of radicals: 1) organic π-electron radicals, such as methyl, ethyl, allyl, and *trans*-butadienyl anion radicals; 2) organic σ-electron radicals, such as vinyl and formyl radicals, and 3) inorganic σ-electron radicals, such as NO_2, CO_2^-, and CN radicals. The geometries and the numberings are illustrated in Fig. 1. In this section we will first show the general features common to the three types of radicals. Secondly, the characteristic features of each type of radical will be compared with the experimental results, and lastly, the dipole moments of the σ-electron radicals will be analyzed.

General Features. The calculated ionization potentials and electron affinities are given in Table 1, together with the experimental values. The calculated ionization potentials are generally larger than the observed values.

Table 2 gives the expectation values of the spin-squared operator, S^2, before and after the annihilation of the quartet spin function. The annihilation of the lowest contaiminating spin state yields a sufficiently pure eigenstate of S^2. If the sextet and higher spin states are neglected, the UHF wavefunction for doublet radicals may be written as:

$$\psi_{uhf} = C_{1/2}\psi_{1/2} + C_{3/2}\psi_{3/2},$$

and the relative weight, $(C_{3/2})^2/(C_{1/2})^2$, may be calculated by:[7]

$$(C_{3/2})^2/(C_{1/2})^2 = \frac{4\langle S^2\rangle_{uhf} - 3}{15 - 4\langle S^2\rangle_{uhf}}. \quad (8)$$

In the last column of Table 2, these values are given for various radicals; they are less than 0.04 for all the cases studied here.

That annihilation of the lowest contaminating spin state weakly influences the total charge densities[7b] is shown in Table 3 for the methyl and NO_2 radicals. This fact can be deduced generally.[8c] However, the annihilation causes large changes in the spin-density distributions, as will be shown below.

Organic π-Electron Radicals. *i) Methyl Radical.* The geometry, *hfs* constants, and some other properties of the methyl radical have been examined theoretically[1d,10,12,13] and experimental-

*6 Hereafter, the spin densities calculted befor and after annihilation will be wyitten as $\langle\rho\rangle_{ba}$ and $\langle\rho\rangle_{aa}$, and the charge densties, as $\langle q\rangle_{ba}$ anb $\langle q\rangle_{aa}$, $\langle\rho\rangle_{ba}$ has the same meaning as the ρ_{uhf} in the previous paper.[8]

*7 For the proton, the *hfs* constants calculated only from $(\rho_h)_{ba}$ are compared with the experimental results. The reasons for this are as follows: As may be seen from Eq. (6), the SP contributions satisfy the relation: $(\rho^i_{ba})_{SP} = 3(\rho^i_{aa})_{SO}$, while the SD contributions satisfy $(\rho^i_{ba})_{SD} = (\rho^i_{aa})_{SD}$. For example, in the ethyl radical, the spin density of the H_7 atom is due to both mechanisms, while that of the H_3 atom is due only to the SP mechanism. (See Fig. 1 and Table 4.) Thus, $\rho_{ba} \simeq 1.2\rho_{aa}$ for the H_7 atom and $\rho_{ba} \simeq 3\rho_{aa}$ for the H_3 atom. This example shows that, if the σ–π-type electron repulsion integrals are so adjusted that ρ_{ba} correlates well with the experimental values, then ρ_{aa} correlates poorly with the observed values in the least-mean-square's sense. For a comparison of the spin densities calculated by the various methods, see the article by Harriman and Sando (*J. Chem. Phys.*, **48**, 5138 (1968)).

11) J. R. Morton, *Chem. Revs.*, **64**, 453 (1964).

12) A. L. H. Chung, *J. Chem. Phys.*, **46**, 3144 (1967).

13) a) M. Karplus, *J. Chem. Phys.*, **30**, 15 (1959). b) D. M. Schrader and M. Karplus, *ibid.*, **40**, 1593 (1964). c) D. M. Schrader, *ibid.*, **46**, 3895 (1967). d) K. Morokuma, L. Pedersen and M. Karplus, *ibid.*, **48**, 4801 (1968). e) D. L. Beveridge and K. Miller, *Mol. Phys.*, **14**, 401 (1968).

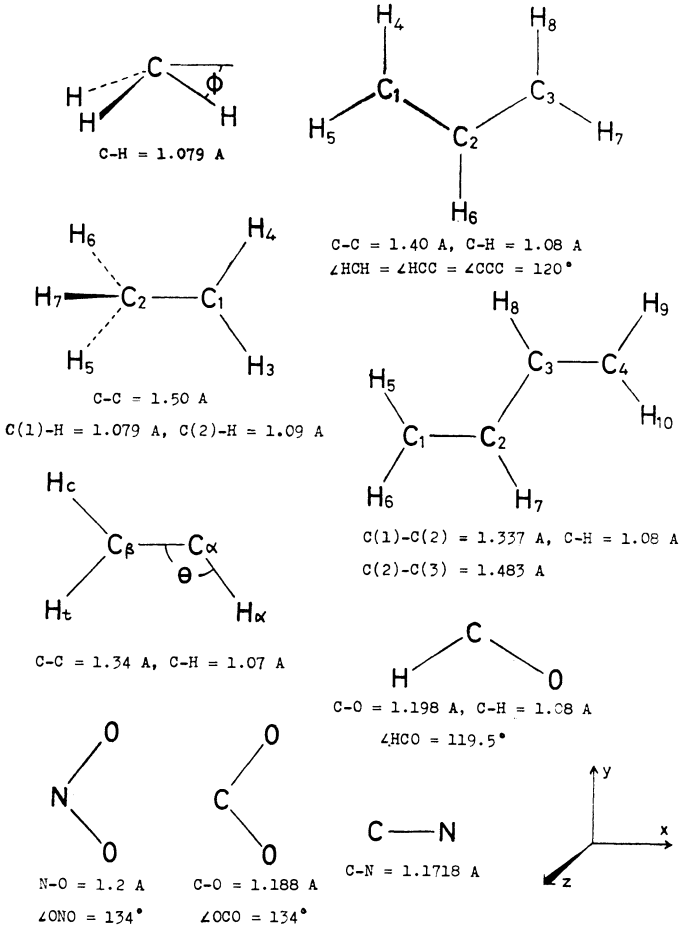

Fig. 1. Geometries (L. E. Sutton Ed., "Tables of Interatomic Distances and Configuration in Molecules and Ions," Chem. Soc. (London), (1956) and (1965)).

TABLE 1. IONIZATION POTENTIAL (*IP*) AND ELECTRON AFFINITY (*EA*) (eV)

Radical	*IP*		*EA*	
	Exptl.	Calcd	Exptl.	Calcd
CH_3	9.86,[a] 9.95[a]	10.310	1.1,[d] 1.4[e]	−0.813
C_2H_5	8.67,[a] 8.78[a]	10.062	0.9,[d] 0.94[e]	−0.690
C_3H_5	8.16,[a] 8.755[a]	9.202	2.1,[d] 2.21[e]	0.050
$C_4H_6^-$	−0.34[b]	−0.164	—	−7.728
C_2H_3	9.45[c]	10.223	—	−0.665
HCO	9.82,[a] 9.88[a]	9.854	—	0.200
NO_2	11.3,[a] 9.78[a]	11.967	2.34,[f] 1.62[d]	2.18
CO_2^-	—	1.820	—	−8.041
CN	14.55,[a] 15.13[a]	11.307	3.21[g]	0.445

a) R. W. Kiser, "Tables of Ionization Potentials", United States Atomic Energy Commission, TID-6142 (1960).
b) The value cited is the calculated *EA* of trans-butadiene: N. S. Hush and J. A. Pople, *Trans. Faraday Soc.*, **51**, 600 (1955).
c) F. W. McLafferty, "Mass Spectrometry of Organic Ions," Academic Press Inc., New York (1963), p. 240.
d) H. O. Pritchard, *Chem. Revs.*, **52**, 529 (1953); H. O. Pritchard and H. A. Skinner, *ibid.*, **55**, 745 (1955).
e) F. M. Page, Symp. Combust. 8-th, Pasadena, Calif., 1960, p. 160.
f) D. F. C. Morris, *J. Inorg. Nucl. Chem.*, **6**, 295 (1958).
g) J. T. Herron and V. H. Dibeler, *J. Am. Chem. Soc.*, **82**, 1555 (1960).

Table 2. The expectation values of S^2 before and after annihilation of the quartet spin function

Radical	$\langle S^2 \rangle$ Before annihilation	$\langle S^2 \rangle$ After annihilation	$\frac{(C_{3/2})^2}{(C_{1/2})^2}$ a)
Methyl			
$\phi=$ 0.0°	0.7544	0.7500	0.0014
6.0°	0.7542	0.7500	0.0014
12.0°	0.7537	0.7500	0.0012
19.47°	0.7529	0.7500	0.0010
Ethyl	0.7564	0.7500	0.0021
Allyl	0.8584	0.7510	0.0399
(*t*-Butadiene)$^-$	0.7828	0.7502	0.0113
Vinyl			
$\theta=$120°	0.7880	0.7502	0.0132
135°	0.7892	0.7503	0.0137
150°	0.7906	0.7504	0.0142
180°	0.7922	0.7506	0.0148
Formyl	0.7713	0.7502	0.0071
NO_2	0.7563	0.7500	0.0021
CO_2^-	0.7529	0.7500	0.0009
CN	0.7562	0.7500	0.0020

a) See Eq. (8).

Table 3. Total charge densities of the CH_3 and NO_2 radicals calculated before and after annihilation

CH_3 Atomic orbital	$\langle q \rangle_{ba}$	$\langle q \rangle_{aa}$	NO_2 Atomic orbital	$\langle q \rangle_{ba}$	$\langle q \rangle_{aa}$
2*s*	1.1152	1.1126	2*s*(N)	1.4906	1.4900
$2p_x$, $2p_z$	0.4200	0.4200	$2p_x$(N)	1.0690	1.0686
$2p_y$	1.0000	1.0000	$2p_y$(N)	0.2588	0.2578
h	0.7611	0.7602	$2p_z$(N)	0.7605	0.7603
			2*s*(O)	2.0238	2.0239
			$2p_x$(O)	1.5712	1.5712
			$2p_y$(O)	1.1459	1.1454
			$2p_z$(O)	1.4142	1.4141

ly[14] in great detail. In this paper we examine its structure, force constant, and *hfs* constants.

In Fig. 2, the calculated potential curve for the out-of-plane bending of the methyl radical is shown. The present calculation predicts a planar configuration[14] and gives a force constant of 0.183 mdyn/A, which is comparable with the experimental values, 0.2527 in a solid-argon matrix[14f] and 0.177 in a nitrogen matrix.[14g]

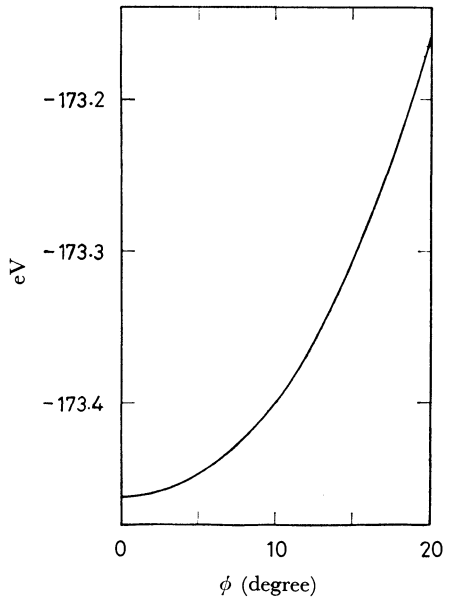

Fig. 2. Potential curve for out-of-plane bending of the methyl radical.

Recently, the isotope effects on the *hfs* constants of the methyl radicals have been reported by Fessenden;[14e] the spin densities on both the proton and the carbon nuclei have been seen to increase with an increase in the angle ϕ of Fig. 1. Here, we will examine the angular dependence of the spin densities in order to clarify the mechanism of these angular dependencies. The results are summarized in Table 4, while those for the carbon 2*s* AO are illustrated in Fig. 3. They predict reasonably well the angular dependences of the spin densities on both the hydrogen 1*s* and the carbon 2*s* AO's, which is in accordance with the experiments. Note that as the angle ϕ increases, the $(\rho_{2s(C)})_{SD}$ value increases, and that this increase exceeds the decreasing tendency of $(\rho_{2s(C)})_{SP}$, *vis.* Fig. 3. For the proton-spin density, the observed tendency may be explained by the increasing contribution of the SD mechanism with an increase in the angle. Note that the SP contribution is almost constant over the angular range considered and that the SD contribution is very small, even in the tetrahedral configuration.

In Table 5, these isotope effects of the methyl radicals are summarized and compared with the experimental values,[14e] the temperature effects[13] are neglected and the calculated *hfs* constants are averaged over the zero-point vibration, and the force constant of the CH_3 radical obtained by Milligan and Jacox[14g] is used for all the isotopical-

14) a) T. Cole, H. O. Pritchard, N. R. Davidson and H. M. McConnell, *Mol. Phys.*, **1**, 406 (1958). b) G. Herzberg and J. Shoosmith, *Can. J. Phys.*, **34**, 523 (1956). c) G. Herzberg, *Proc. Roy. Soc.* (*London*), **A262**, 291 (1961). d) R. W. Fessenden and R. H. Schuler, *J. Chem. Phys.*, **39**, 2147 (1963). e) R. W. Fessenden, *J. Phys. Chem.*, **71**, 74 (1967). f) W. L. S. Andrews and G. C. Pimentel, *J. Chem. Phys.*, **44**, 2527 (1966). g) D. E. Milligan and M. E. Jacox, *ibid.*, **47**, 5146 (1967).

TABLE 4. SPIN DENSITIES IN THE METHYL RADICAL

Geometry ϕ	Atomic orbital	Before annihilation			After annihilation		
		$\langle\rho\rangle_{ba}$	$(\rho)_{SP}$	$(\rho)_{SD}$	$\langle\rho\rangle_{aa}$	$(\rho)_{SP}$	$(\rho)_{SD}$
0°	$2s$(C)	0.1487	0.147	0.002[a]	0.0510	0.049	0.002[a]
	$2p_x$(C), $2p_z$(C)	0.0115	0.012	0.000	0.0038	0.004	0.000
	$2p_y$(C)	1.0000	0.000	1.000	0.9990	0.000	0.999
	h	−0.0275	−0.028	0.000	−0.0089	−0.009	0.000
6°	$2s$(C)	0.1523	0.143	0.009	0.0570	0.048	0.009
	$2p_x$(C), $2p_z$(C)	0.0117	0.012	0.000	0.0039	0.004	0.000
	$2p_y$(C)	0.9909	0.001	0.990	0.9897	0.000	0.990
	h	−0.0270	−0.028	0.001	−0.0084	−0.009	0.001
12°	$2s$(C)	0.1622	0.132	0.030	0.0739	0.044	0.030
	$2p_x$(C), $2p_z$(C)	0.0126	0.013	0.000	0.0042	0.004	0.000
	$2p_y$(C)	0.9653	0.003	0.962	0.9635	0.001	0.962
	h	−0.0258	−0.028	0.002	−0.0071	−0.009	0.002
19.47°[b]	$2s$(C)	0.1812	0.114	0.067	0.1052	0.038	0.067
	$2p_x$(C), $2p_z$(C)	0.0145	0.015	0.000	0.0049	0.005	0.000
	$2p_y$(C)	0.9164	0.004	0.912	0.9138	0.001	0.912
	h	−0.0241	−0.029	0.005	−0.0050	−0.010	0.005

a) This value must be zero by symmetry, and the error results from the approximation used to derive Eq. (7) (See Ref. 8).
b) Tetrahedral angle.

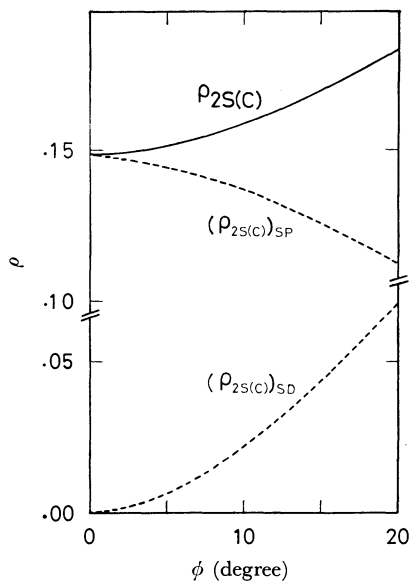

Fig. 3. $\langle\rho_{2s(C)}\rangle_{ba}$ and its mechanistic contributions *versus* the bending angle ϕ in the methyl radical. Only the curves obtained bofore annihilation are given, but the characteristic features are the same in both stages.

ly-substituted methyl radicals. As Table 5 shows, the rate of the change in the calculated *hfs* constants with an increase in the number of the deuterium atom is less than that required to explain the observed *hfs* constants; this has also been noted by Morokuma, Pedersen and Karplus.[13d] The vibrational corrections to the spin density are +0.0004 (0.29 gauss) and +0.0156～+0.0052 (17.31～5.77 gauss) for the hydrogen 1*s* AO and for the carbon 2*s* AO respectively. (See also Table 7.)

ii) Ethyl, Allyl and Butadienyl Anion Radicals. In this section, the spin densities of the ethyl, allyl, and *s-trans*-butadienyl anion radicals are discussed. The calculated spin densities and their mechanistic contributions are summarized in Table 6, while the proton *hfs* constants calculated from $\langle\rho_h\rangle_{ba}$ are shown in Table 7.

Previously,[8] the methyl proton *hfs* constants of the ethyl radical have been shown to be due to a major SD contribution and a minor SP contribution. When we assume the experimentally observed relation[15] for the methyl proton *hfs* constant, $a_H = B_0 + B_1\cos^2\theta$, where θ is the rotational angle about the C–C single bond, the values of B_0 and B_1 may be calculated as −1.49 and 55.28 gauss respectively.*8 The average a_H value over the rotational angle, θ, is 26.15 gauss, which may be compared with the observed value,[14d] 26.87 gauss.

15) a) C. Heller and H. M. McConnell, *J. Chem. Phys.*, **32**, 1535 (1960). b) A. Horsfield, J. R. Morton and D. H. Whiffen, *Mol. Phys.*, **4**, 425 (1961).

*8 B_0 is calculated from the results previously reported (Ref. 8)).

TABLE 5. ISOTOPE EFFECTS FOR THE *hfs* CONSTANT (gauss)

Radical	$\overline{\langle\rho_h\rangle_{ba}}$	$\overline{\lvert a_H\rvert}$ Calcd	$\overline{\lvert a_H\rvert}$ Exptl.[b]	Radical	$\overline{\langle\rho_{2s(C)}\rangle}$ ba	$\overline{\langle\rho_{2s(C)}\rangle}$ aa	$\Delta a(^{13}C)$[a] Calcd ba	$\Delta a(^{13}C)$[a] Calcd aa	$\Delta a(^{13}C)$[a] Exptl.[b]
$^{12}CH_3$	-0.0271_2	20.15	23.038	$^{13}CH_3$	0.1518_0	0.0562_3	0.00	0.00	0.00
$^{12}CH_2D$	-0.0271_5	20.17	23.10	$^{13}CH_2D$	0.1515_9	0.0558_7	−0.24	−0.41	−0.52
$^{12}CHD_2$	-0.0271_8	20.19	23.21	$^{13}CHD_2$	0.1513_5	0.0554_7	−0.50	−0.85	−1.28
$^{12}CD_3$	-0.0272_1	20.22	23.29[c]	$^{13}CD_3$	0.1511_0	0.0550_4	−0.78	−1.33	−2.36

a) $\Delta a(^{13}C)=a(^{13}C)-a(^{13}C \text{ in } ^{13}CH_3)$
b) Ref. 14e.
c) The relation, $a_H=6.514a_D$, is used.

TABLE 6. SPIN DENSITIES IN THE ETHYL, ALLYL, AND *trans*-BUTADIENYL ANION RADICALS

Radical	Atomic orbital	Before annihilation $\langle\rho\rangle_{ba}$	Before annihilation $(\rho)_{SP}$	Before annihilation $(\rho)_{SD}$	After annihilation $\langle\rho\rangle_{aa}$	After annihilation $(\rho)_{SP}$	After annihilation $(\rho)_{SD}$
Ethyl	$2s(C_1)$	0.1614	0.159	0.002[a]	0.0555	0.053	0.002[a]
	$2p_z(C_1)$	1.0001	0.002	0.998	0.9985	0.001	0.998
	$2s(C_2)$	−0.0123	−0.012	0.000	−0.0040	−0.004	0.000
	$2p_z(C_2)$	−0.0130	−0.013	0.000	−0.0042	−0.004	0.000
	h_3, h_4	−0.0345	−0.035	0.000	−0.0111	−0.011	0.000
	h_5, h_6	0.0165	0.003	0.013	0.0142	0.001	0.013
	h_7	0.0724	0.020	0.052	0.0593	0.007	0.052
Allyl	$2s(C_1)$	0.0988	0.099	0.000	0.0335	0.034	0.000
	$2p_z(C_1)$	0.6840	0.173	0.511	0.5686	0.058	0.511
	$2s(C_2)$	−0.0534	−0.054	0.000	−0.0175	−0.018	0.000
	$2p_z(C_2)$	−0.3414	−0.356	0.015[a]	−0.1043	−0.119	0.015[a]
	h_1, h_3	−0.0188	−0.019	0.000	−0.0061	−0.006	0.000
	h_5, h_7	−0.0191	−0.019	0.000	−0.0062	−0.006	0.000
	h_6	0.0049	0.005	0.000	0.0016	0.002	0.000
Butadienyl Anion	$2s(C_1)$	0.0674	0.067	0.000	0.0228	0.022	0.000
	$2p_z(C_1)$	0.5022	0.095	0.407	0.4387	0.032	0.407
	$2s(C_2)$	0.0157	0.016	0.000	0.0053	0.005	0.000
	$2p_z(C_2)$	0.1330	−0.094	0.227	0.1957	−0.031	0.227
	h_5, h_{10}	−0.0132	−0.013	0.000	−0.0043	−0.004	0.000
	h_6, h_9	−0.0125	−0.013	0.000	−0.0041	−0.004	0.000
	h_7, h_8	−0.0070	−0.007	0.000	−0.0023	−0.002	0.000

a) See Ref. a) of Table 4.

The allyl radical has been extensively studied[16] using the π-approximation method. The π-spin densities calculated by the UHF method by Berthier[16a] are 0.812 for $2p_z(C_1)$ and −0.619 for $2p_z(C_2)$ AO, and the projected values[16b] are 0.609 and −0.185 respectively. The corresponding values obtained by the present method are given in Talbe 6. The SP contribution to the spin density in the $2p_z(C_1)$ AO is as great as 10—25%.[16d] The spin densities on the $2p_z(C_2)$ and the h_6 AO's are calculated to be negative and positive in sign respectively, which is in agreement with earlier theoretical works.[16]

The electron-spin resonance study by Fessenden and Schuler[14d] of the allyl radical in a liquid medium showed a slight difference in the *hfs* constants for the two methylene protons (H_4 and H_5 in Fig. 1). Obviously, McConnell's relation,[9a] $a_H=Q_H\rho_c^\pi$, can not interpret this observed difference. However, the present valence electron treatment yields a small difference in the spin densities on the H_4 and H_5 nuclei. Therefore, the observed *hfs* constants of 13.93 and 14.83 gauss may be assigned

16) a) G. Berthier, *J. chim. Phys.*, **52**, 141 (1955). b) H. M. McConnell, *J. Chem. Phys.*, **29**, 244 (1958). c) C. Heller and T. Cole, *ibid.*, **37**, 243 (1962). d) D. Lazdins and M. Karplus, *ibid.*, **44**, 1600 (1966).

TABLE 7. ISOTROPIC PROTON *hfs* CONSTANTS

Radical	Position	*hfs* Constant (gauss) Calcd[a]	Exptl.[b]
Methyl ($\phi=0°$)	H	−20.43	(−) 23.04
Ethyl	$H(CH_2)$	−25.63	(−) 22.38
	$H(CH_3)$	26.15[c]	(+) 26.87
Allyl	H_4, H_8	−13.97	(−) 13.93
	H_5, H_7	−14.19	(−) 14.83
	H_6	3.64	(+) 4.06
t-Butadienyl Anion	H_5, H_{10}	−9.81	(−) 7.62
	H_6, H_9	−9.29	(−) 7.62
	H_7, H_8	−5.21	(−) 2.79
Vinyl ($\theta=135°$)	H_c	32.54	(+) 34
	H_t	72.37	(+) 68
	H_α	−15.83	(−) 16, (−) 13.4
Formyl	H	38.63	(+) 137.0

a) Calculated from $\langle\rho\rangle_{ba}$. See footnote *6.
b) Refs. 14e, 18, and 22.
c) The relation, $a_H=B_0+B_1\cos^2\theta$, is assumed.

to the H_4 (H_8) and H_5 (H_7) nuclei respectively. This assignment is the same as the one previously reported.[5a] However, the recent calculations by Hincliffe and Atherton[17] and by Pople, Beveridge, and Dobosh[1d] gave an assignment opposite to that reported here. Further experimental work is necessary to settle this point.*9

The proton *hfs* constants of the butadienyl anion radical have been observed by Levy and Myers.[18] The calculated values, assuming the *s-trans* configuration, are shown in Table 6. The CH_2 protons of butadiene are non-equivalent and different *hfs* constants are predictd; this is in contrast to the observed identical *hfs* constants for these protons.[18]

As is well known, the spin densities in the σ-type AO's of planar π-electron radicals and in the $2p_z(C_2)$ AO of the allyl radical are due only to the SP mechanism. Therefore, the $\langle\rho\rangle_{ba}=3\langle\rho\rangle_{aa}$ relation,[7c,8] is fairly satisfactory, except for the $2p_z(C_2)$ AO of the allyl radical.*10

Organic σ-Electron Radicals. *i) Vinyl Radical.* The *hfs* constants of the vinyl radical have recently been observed,[14d,14e,19] and its structure and the sign of the *hfs* constant of its α-proton have been intensely investigated.[2,5a,19,20] Previously,[5a] we suggested that the *hfs* constant of the α-proton is negative in sign. Here, we will examine theoretically the structure*11 and the *hfs* constants of this radical.

The calculated potential curve with respect to the bending of the θ angle of Fig. 1 is illustrated in Fig. 4. The minimum in the potential curve appears near 135°, the calculated barrier to inversion:

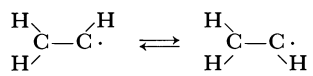

is 1.6 kcal/mol, which is comparable with the value, ~2 kcal/mol, estimated by the ESR technique.[14d]

One of the main features of the present method lies in its consistent applicability to the spin-density calculations of both σ- and π-electron radicals. Good examples in which the σ–π-type SP mechanism, the "bulk" SP mechanism, and the SD mechanism are all competing with one another are the spin densities on the α-hydrogen and the α- and β-carbon atoms of the vinyl radical. None of these mechanisms can be ignored. This may be understood from the fact that the unpaired orbital of this radical

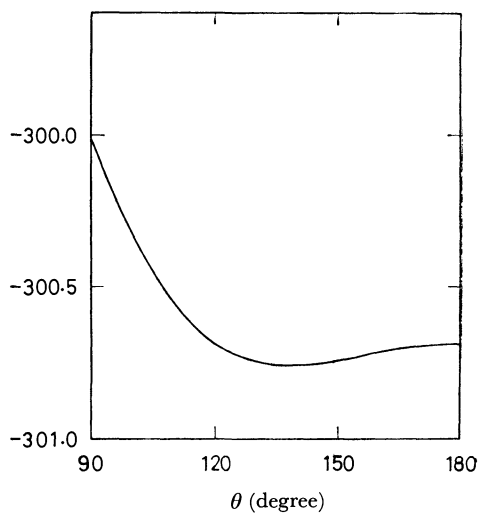

Fig. 4. Total energy (eV) on bending of CCH_α in the vinyl radical.

17) A. Hincliffe and H. M. Atherton, *Mol. Phys.*, **13**, 89 (1967).

*9 Recent experiments by Kochi and Krusic (*J. Am. Chem. Soc.*, **90**, 7157 (1968)) support the present assignment.

18) D. H. Levy and R. J. Myers, *J. Chem. Phys.*, **41**, 1062 (1964).

*10 This exception may be attributed to the rather large value of $(C_{3/2})^2/(C_{1/2})^2$ shown in Table 2, since the assumption used to derive Eq. (6) becomes crude in this case (see Ref. 8b).

19) E. L. Cochran, F. J. Adrian and V. A. Bowers, *J. Chem. Phys.*, **40**, 213 (1964).

20) a) W. T. Dixon, *Mol. Phys.*, **9**, 201 (1965). b) G. A. Peterson and A. D. McLachlan, *J. Chem. Phys.*, **45**, 628 (1966). c) R. S. Drago and H. Petersen, Jr., *J. Am. Chem. Soc.*, **89**, 5774 (1967). d) A. Hinchliffe, *Theoret. chim. Acta (Berl.)*, **8**, 300 (1967). e) Y. Ellinger, A. Rassat, R. Subra and G. Berthier, *ibid.*, **10**, 289 (1968).

*11 The present method predicts the angular geometry of ethylene in fair agreement with the experiment; this will be reported in detail at a later date.

at $\theta=135°$, calculated with the open-shell restricted Hartree-Fock (RHF) method,*[12] is

$$\varphi_{\mathrm{rhf}} = 0.2848(2s(\mathrm{C}_\alpha)) + 0.3542(2p_x(\mathrm{C}_\alpha)) + 0.8630(2p_y(\mathrm{C}_\alpha)) - 0.0609(2s(\mathrm{C}_\beta)) - 0.0664(2p_x(\mathrm{C}_\beta)) + 0.0368(2p_y(\mathrm{C}_\beta)) - 0.1910(h_c) + 0.2737(h_t) - 0.1319(h_\alpha),$$

and is mainly localized in the $2p_x(\mathrm{C}_\alpha)$ and $2p_y(\mathrm{C}_\alpha)$ AO's.

The spin densities and their mechanistic contributions are given in Table 8 for various configurations of the vinyl radical. The dependence of the carbon $2s$ AO spin density on the θ angle is illustrated in Fig. 5, while that of the proton spin density is illustrated in Fig. 6.

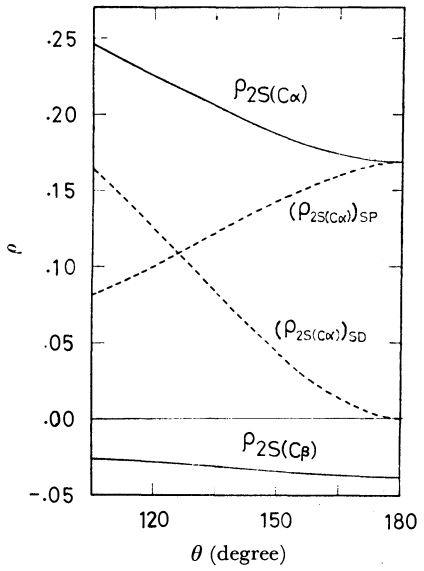

Fig. 5. $2s$ AO spin densities of carbon atoms *versus* the bending of CCH_α in the vinyl radical. Only the curves obtained before annihilation are shown, but the characteristic features are the same in both stages.

Figure 5 shows that the angular dependence of the SD contribution to the α-carbon $2s$ AO spin density is opposite to that of the SP contribution, and that it determines the dependence of the total spin density. At $\theta=135°$, $\rho_{2s}(\mathrm{C}_\alpha)$ is due to the 41—67% SD and 59—33% SP contributions. For the β-carbon atom, the angular dependence is exceptionally small and its $2s$ AO spin density is always negative.

Figure 6 shows that the spin density on the α-proton is the sum of the negative SP and the positive

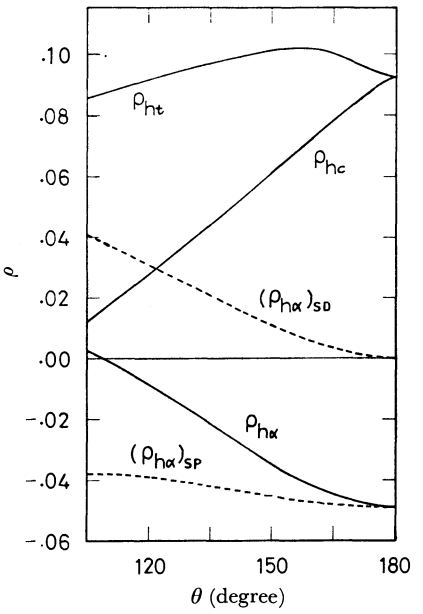

Fig. 6. Proton spin densities (ba) *versus* bending of CCH_α in vinyl radical.

SD contributions. They depend oppositely on the angle θ, and at $\theta=135°$, where the minimum potential lies, the α-proton spin density is due to the 97% SD and -197% SP contributions. For the *cis*- and *trans*-protons, their spin densities also show a large angular dependence, and they are also due to both the SD and SP mechanisms. At $\theta=135°$, the spin density of the *trans*-proton is due to the 73% SD and 27% SP contributions, while that of the *cis*-proton is due to the 80% SD and 20% SP contributions.

The calculated proton *hfs* constants at the minimum potential ($\theta=135°$) are $a_{\mathrm{H}c}=32.54$, $a_{\mathrm{H}t}=72.37$, and $a_{\mathrm{H}\alpha}=-15.83$ gauss (Table 7). These values agree satisfactorily with the experimental values. Moreover, as may be seen in Table 8 and Fig. 6, the calculated proton *hfs* constants obtained near $\theta=135°$ agree most reasonably with the experimental values, thus lending support to the vinyl radical configuration with $\theta=135°$.

Note that the calculated *hfs* constant of the α-proton is negative in sign.[5a] However, recent INDO calculations by Pople, Beveridge and Dobosh[1d] have predicted the opposite sign. Further experimental work, such as with isotope effects,[14e] will be necessary to settle this point. Figures 5 and 6 will be very useful when one experimentally determines the sign of the α-proton *hfs* constant. When the α-proton is replaced by deuterium, a smaller *hfs* constant (except for a constant factor $g_{\mathrm{H}}/g_{\mathrm{D}}=6.514$) should be observed if $a_{\mathrm{H}\alpha}$ is negative, and *vice versa*.

Let us now comment on the recent theoretical spin-density studies of the vinyl radical, in which

*[12] C. C. J. Roothaan, *Rev. Mod. Phys.*, **32**, 179 (1960). The estimations of the integral values are the same as for the present UHF calculations, except that the two center σ-π-type exchange repulsion integrals are not included in the RHF calculation.

TABLE 8. SPIN DENSITIES IN THE VINYL RADICAL

Geometry θ	Atomic orbital	Before annihilation			After annihilation		
		$\langle\rho\rangle_{ba}$	$(\rho)_{SP}$	$(\rho)_{SD}$	$\langle\rho\rangle_{aa}$	$(\rho)_{SP}$	$(\rho)_{SD}$
120°	$2s(C_\alpha)$	0.2251	0.100	0.125	0.1581	0.033	0.125
	$2s(C_\beta)$	−0.0286	−0.033	0.004	−0.0063	−0.011	0.004
	h_c	0.0286	0.005	0.024	0.0255	0.002	0.024
	h_t	0.0913	0.024	0.067	0.0752	0.008	0.067
	h_α	−0.0083	−0.039	0.031	0.0175	−0.013	0.031
135°	$2s(C_\alpha)$	0.2051	0.122	0.083	0.1240	0.041	0.083
	$2s(C_\beta)$	−0.0315	−0.035	0.004	−0.0082	−0.012	0.004
	h_c	0.0438	0.009	0.035	0.0381	0.003	0.035
	h_t	0.0974	0.026	0.071	0.0799	0.009	0.071
	h_α	−0.0213	−0.042	0.021	0.0064	−0.014	0.021
150°	$2s(C_\alpha)$	0.1870	0.143	0.044	0.0917	0.048	0.044
	$2s(C_\beta)$	−0.0348	−0.037	0.002	−0.0102	−0.012	0.002
	h_c	0.0614	0.013	0.048	0.0525	0.004	0.048
	h_t	0.1013	0.027	0.074	0.0832	0.009	0.074
	h_α	−0.0345	−0.045	0.011	−0.0042	−0.015	0.011
180°	$2s(C_\alpha)$	0.1690	0.166	0.003[a]	0.0583	0.055	0.003[a]
	$2s(C_\beta)$	−0.0384	−0.038	0.000	−0.0125	−0.013	0.000
	h_c, h_t	0.0926	0.023	0.070	0.0774	0.008	0.070
	h_α	−0.0487	−0.050	0.001[a]	−0.0153	−0.017	0.002[a]

a) See Ref. a) of Table 4.

only the SD contribution was taken into account.[20b,20c] For instance, if the SP mechanism is neglected, the α-proton spin density will be about +0.021 ($(\rho_{H\alpha})_{SD}$ shown in Table 8), which is of the same magnitude, but of the opposite sign, as the present result, −0.0213. Thus, even if the SP contribution is neglected, a value which is apparently reasonable in magnitude can be obtained for the α-proton spin density. Furthermore, neglect of the SP contribution leads to serious errors in the calculation of the spin densities even of other protons and of the carbon 2*s* AO's, as is shown in Table 8, Fig. 5, and Fig. 6. This is probably true for other σ-electron radicals as well; namely, one should not neglect the spin polarization mechanism even in σ-electron radicals, especially in AO's near the radical-center atom.[8b,20a]

ii) Formyl Radical. Recently, the results of a non-empirical UHF calculation of the formyl radical *hfs* constants have been reported by Hincliffe and Cook[21] to be in good agreement with the experimental values.[22] However, most of the semi-empirical MO calculations[1d,2,20b,20d] have failed to yield such a large proton *hfs* constant as was experimentally observed value, 137.0 gauss.[22] As may be seen in Table 9, the present result for the proton *hfs* constant is also disappointing. It is necessary to examine the present result to determine its failing by comparing it with the result of the non-empirical calculation.

From the $(\rho)_{SD}$ shown in Table 9 we can see that the unpaired orbital consists mainly of the $2p_y$(C) and $2p_y$(O) AO's. This implies that the SP mechanism is very important to the *hfs* constant of this radical. The nonempirical calculation of the proton *hfs* constant gave 154.58 gauss before annihilation and 133.95 gauss after single annihilation. The SP and SD contributions calculated from these values (see Eq. (20) of the previous report.[8b]) are 61.89 and 92.69 gauss before annihilation. In the present calculations, they are −5.94 and 44.58 gauss respectively. Very large differences exist in both contributions. The SP contributions of both methods differ especially even in sign. The reason for this is perhaps that σ–π-type exchange repulsion integrals other than those included in the present calculation (especially the two center σ–π-type ionic integrals which make a positive contribution to the proton *hfs* constant) can not be neglected in this case.

Inorganic σ-Electron Radicals. We chose here, as sample calculations for the inorganic σ-electron radicals, the isoelectronic NO_2 and CO_2^- radicals, where the spin densities on the VAO's

21) A. Hincliffe and D. B. Cook, *Chem. Phys. Letters*, **1**, 217 (1967).

22) a) F. J. Adrian, E. L. Cochran and V. A. Bowers, *J. Chem. Phys.*, **36**, 1661 (1962). b) J. A. Brivati, N. Keen and M. C. R. Symons, *J. Chem. Soc.*, **1962**, 237. c) F. J. Adrian, E. L. Cochlan and V. A. Bowers, *J. Chem. Phys.*, **44**, 4626 (1966).

TABLE 9. SPIN DENSITIES IN THE FORMYL RADICAL

Atomic orbital	Before annihilation			After annihilation		
	$\langle\rho\rangle_{ba}$	$(\rho)_{SP}$	$(\rho)_{SD}$	$\langle\rho\rangle_{aa}$	$(\rho)_{SP}$	$(\rho)_{SD}$
$2s$(C)	0.1603	0.029	0.131	0.1409	0.010	0.131
$2p_x$(C)	−0.0169	−0.021	0.004	−0.0029	−0.007	0.004
$2p_y$(C)	0.5028	−0.014	0.517	0.5124	−0.005	0.517
$2p_z$(C)	−0.1118	−0.114	0.002[a)]	−0.0356	−0.038	0.002[a)]
h	0.0522	−0.008	0.060	0.0574	−0.003	0.060
$2s$(O)	0.1106	0.109	0.002	0.0378	0.036	0.002
$2p_x$(O)	0.0593	0.020	0.039	0.0457	0.007	0.039
$2p_y$(O)	0.4802	0.012	0.468	0.4725	0.004	0.468
$2p_z$(O)	0.1310	0.128	0.003[a)]	0.0457	0.043	0.003[a)]

a) See Ref. a) of Table 4.

TABLE 10. SPIN DENSITIES IN NO_2, CO_2^-, AND CN RADICALS

Radical	Atomic orbital	$\langle\rho\rangle_{ba}$	$\langle\rho_{SP}\rangle_{ba}$	$\langle\rho_{SD}\rangle_{ba}$	$\langle\rho\rangle_{aa}$	Experimental[a)]
NO_2	$2s$(N)	0.1900	0.057	0.133	0.1522	0.106, 0.097
	$2p_x$(N)	0.4576	0.001	0.457	0.4570	0.452, 0.371
	$2p_z$(N)	0.0497	0.049	0.000	0.0169	0.019
	$2s$(O)	0.0505	0.048	0.003	0.0185	——
	$2p_x$(O)	0.3495	0.012	0.337	0.3412	——
	$2p_z$(O)	−0.0250	−0.025	0.000	−0.0082	——
CO_2^-	$2s$(C)	0.2652	0.012	0.253	0.2571	0.14
	$2p_x$(C)	0.5421	−0.006	0.548	0.5460	0.66
	$2p_z$(C)	0.0131	0.013	0.000	0.0044	0.08
	$2s$(O)	0.0641	0.056	0.008	0.0271	——
	$2p_x$(O)	0.2746	0.008	0.267	0.2690	——
	$2p_z$(O)	−0.0080	−0.008	0.000	−0.0026	——
CN	$2s$(C)	0.0884	−0.026	0.115	0.1060	——
	$2p_x$(C)	0.3377	−0.003	0.341	0.3398	——
	$2p_y$(C), $2p_z$(C)	−0.0494	−0.050	0.001	−0.0162	——
	$2s$(N)	0.0876	0.054	0.034	0.0515	——
	$2p_x$(N)	0.4994	0.006	0.493	0.4956	——
	$2p_y$(N), $2p_z$(N)	0.0563	0.056	0.000	0.0191	——

a) Ref. 23a.

are assumed from the anisotropy of the ESR parameters[23)] and the CN radical, which is especially interesting in its dipole moment. Table 10 summarizes the spin densities calculated on the various VAO's of these radicals, along with those estimated from the experiments.[23)] The NO_2 spin densities theoretically calculated by McEwen[24a)] and by Green and Linnett[24b)] gave small magnitudes (0.263 and 0.222 respectively) for the spin density on the $2p_x$(N) AO, but the present method gave $\rho_{2px(N)}=0.457$, which is in closer agreement with the experimental estimations.

Table 10 shows that the present calculation qualitatively predicts almost all features of the spin densities of the isoelectronic NO_2 and CO_2^- radicals. For example, the spin density on the $2p_x$(N) AO of NO_2 is smaller than that on the $2p_x$(C) AO of CO_2^-, the delocalization of the unpaired spin to oxygens is greater in NO_2 than in CO_2^-, *etc.*

23) a) P. W. Atkins, N. Keen and M. C. R. Symons, *J. Chem. Soc.*, **1962**, 2873. b) H. Zeldes and R. Livingston, *J. Chem. Phys.*, **35**, 563 (1961). c) H. Zeldes and R. Livingston, *ibid.*, **37**, 3017 (1962). d) D. W. Ovenall and D. H. Whiffen, *Proc. Chem. Soc.*, **1960**, 420. e) D. W. Ovenall and D. H. Whiffen, *Mol. Phys.*, **4**, 135 (1961). f) J. A. Brivati, N. Keen, M. C. R. Symons and P. A. Trevalion, *Proc. Chem. Soc.*, **1961**, 66.

24) a) K. L. McEwen, *J. Chem. Phys.*, **32**, 1801 (1960). b) M. Green and J. W. Linnett, *Trans. Faraday Soc.*, **57**, 1 (1961).

Note that the $2s$ spin densities shown in the last column of Table 10 are estimated from the observed values without paying any attention to the inner $1s$ contributions. Hence, these $2s$ contributions cannot be compared directly with the calculated contributions.

Analyses of Dipole Moments of σ-Electron Radicals. The dipole moment of a neutral molecule may be expressed approximately as the sum of the atomic dipole (μ_{AD}) and the charge dipole (μ_{CD}). The atomic dipole (x-direction) of the first-row atoms of the periodic table is given by:

$$\mu_{AD}(x) = -7.3370\sum_A(P^A_{sp(x)}/\zeta_A)$$

in debye units, and the charge dipole is:

$$\mu_{CD}(x) = 4.8029\sum_A(Z_A-N_A)x_A,$$

if we adopt the Mulliken approximation:

$$(\chi_r|x|\chi_s) = \frac{1}{2}S_{rs}\{(\chi_r|x|\chi_r)+(\chi_s|x|\chi_s)\}.$$

ζ_A is the Slater exponent, and N_A is the atomic population of the A atom. $P^A_{SP(x)}$ is the off-diagonal density matrix element between the $2s$ and $2p_x$ AO's of the A atom.

The analyses of the dipole moment of vinyl, formyl, NO_2, and CN radicals are given in Table 11; they were obtained by using the values obtained before annihilation. μ^α_{AD} and μ^β_{AD} are the contributions to the atomic dipole from all the occupied α- and β- spin orbitals respectively. These contributions may be further divided into those due to the first-row atoms in the molecule. As is shown in the forth and fifth columns of the table, μ^α_{AD} due to the radical center atom (*e.g.*, C_α in vinyl) surpasses the μ^α_{AD} due to the other atoms and the μ^α_{AD} values of all the constituent atoms. The values of μ^α_{AD}(HO) in the sixth column give contributions to the atomic dipole only from the highest occupied (HO) α-spin orbital. Note that the μ^α_{AD} (HO) at the radical-center atom makes the dominant contribution to μ^α_{AD} and even to μ_{AD}. Thus, the most unstable HO orbital of the σ-electron radical extends considerably out of the molecule from the radical center atom. The direction of the $-\mu^\alpha_{AD}$ (HO) of the vinyl radical is 113° from the C_α–C_β bond.

In NO_2 and CN radicals, the contributions due to the charge dipole cancel those due to the atomic dipole. In the CN radical especially, these two contributions are almost the same in magnitude, but reverse in direction, so the resultant dipole moment is very small. This should be compared with the well-known example of the CO molecule, where its atomic dipole surpasses its charge dipole and makes it a powerful ligand in the chemistry of metal complexes. The calculated dipole moment of NO_2 is -1.301 debye, which is too large if compared with the oserved value, -0.29 debye. However, the above qualitative discussion will not be altered by more rigorous calculations.

Summary and Conclusions

As has been seen in the previous sections, the semi-empirical method for valence electron systems including differential overlap can be satisfactorily extended to systems with open-shell structures.

TABLE 11. ANALYSES OF DIPOLE MOMENTS OF σ-ELECTRON RADICALS (in debye units)

Radical	Atom	Direction	Analyses of atomic dipole				Total
			μ^α_{AD} [a]	μ^β_{AD}	μ^α_{AD}(HO) [b]	μ_{AD} [c]	
Vinyl (θ=135°)	C_α	x	−0.36	0.06	−0.31	−0.31	μ_{AD}=0.68
		y	−0.85	0.16	−0.71	−0.69	μ_{CD}=0.52
	C_β	x	0.16	0.09	−0.02	0.24	μ=1.19
		y	0.01	0.01	−0.01	0.02	
Formyl	C	x	0.31	0.36	−0.13	0.67	
		y	−1.58	−0.36	−1.09	−1.93	μ_{AD}=1.42
	O	x	−0.36	−0.55	0.01	−0.91	μ_{CD}=3.07
		y	0.23	0.30	0.04	0.53	μ=3.16
NO_2 [d]	N	x	1.17	0.32	0.59	1.49	μ_{AD}=0.52
	O	x	−0.17	−0.31	0.02	−0.48	μ_{CD}=−1.83
							μ=−1.30
CN	C	x	1.87	0.90	1.03	2.77	μ_{AD}=1.13
	N	x	−1.01	−0.63	−0.31	−1.64	μ_{CD}=−1.18
							μ=−0.05

a) μ^α_{AD} denotes the contribution to atomic dipole (μ_{AD}) from all the occupied α-spin orbitals.
b) μ^α_{AD}(HO) denotes the contribution to atomic dipole from the highest occupied α-spin orbital.
c) $\mu_{AD} = \mu^\alpha_{AD} + \mu^\beta_{AD}$.
d) The experimental value is −0.29 debye; C. H. Townes and A. L. Schawlow, "Microwave Spectroscopy," McGraw-Hill Book Co., New York (1955).

The results of the present study are as follows:

(1) The separation of the mechanistic contributions to spin density makes it possible to enter into detailed discussions of the nature of the spin density; *e.g.*, the spin-polarization mechanism is shown to be very important even when the spin-delocalization mechanism has hitherto been considered dominant (*e.g.*, ethyl and vinyl radicals).

(2) A good correlation between the calculated *hfs* constants and the configurations of radicals is found for methyl and vinyl radicals. The geometry of the vinyl radical is predicted to be $\theta \simeq 135°$ from both the potential curve and the calculated *hfs* constants. Since there are many radicals with known *hfs* constants, but with unknown configurations, the agreement between the configuration expected from the calculated potential curve and that expected from the calculated *hfs* constants is ideal for a reliable prediction of the configuration of the radical from the theoretical point of view.

(3) The analyses of the atomic dipole moments of the σ-electron radicals revealed some interesting features. For example, the highest occupied orbitals of these σ-electron radicals make decisive contributions to the total atomic dipole.

The calculations were carried out on a HITAC 5020 E computer at the computation center of the University of Tokyo.

BULLETIN OF THE CHEMICAL SOCIETY OF JAPAN VOL. 42 2449—2453 (1969)

The Acidic Nature of Synthetic Zeolites: Acid Strength and Its Correlation with the Catalytic Activity

Hiroshi OTOUMA, Yoshimasa ARAI and Hiroshi UKIHASHI

Research Laboratory, Asahi Glass Co., Ltd., Hazawa-cho, Kanagawa-ku, Yokohama

(Received January 22, 1969)

The acidic characters of the X and Y zeolites exchanged by hydrogen, calcium, and lanthanum ions were investigated. Very characteristic features of the acid sites were found as compared with those of an amorphous silica-alumina cracking catalyst. The acidity is generally larger in the zeolites (2—3 meq/g) than in a silica-alumina (0.5 meq/g). The acid strength is more widely distributed in the zeolites ($H_0 = +3.3$ —< -8.2) than in a silica-alumina ($H_0 < -8.2$). Very important is the fact that the acid site increases not only in number but also in strength with an increase in the degree of ion exchange. The results on cumene cracking are in line with these results.

Zeolite catalysts exchanged by hydrogen ion or metal cations have been widely used in various reactions,[1] especially in the industrial cracking of gas oil.[2,3] The ion-exchanged zeolite catalyst has the ability to crack various hydrocarbons, the product distribution of which is similar to that obtained with a silica-alumina cracking catalyst.[4,5] These facts suggest that the zeolite catalyst is an acid solid. However, few data are available in the literature regarding the acidic character of zeolites, *i. e.*, the acid strength and its distribution, their correlation with the catalytic activity, and the difference in acidic character from amorphous silica-alumina.

The present work aims at clarifying the acidic characters of ion-exchanged zeolites by comparing them with that of silica-alumina.

Experimental

Materials. The X and Y zeolites were used, the former being Molecular Sieve 13X (a commercial product of Linde Co.) and the latter having been prepared in our laboratory by a method given in the literature.[6] Chemical analysis showed the compositions of $Na_2O \cdot$

1) P. B. Venuto and P. S. Landis, "*Advances in Catalysis*," Vol. 18 Academic Press, New York and London (1968), p. 259.

2) C. J. Plank, E. J. Rosinski and W. P. Hawthorne, *Ind. and Eng. Chem., Product Research and Development*, **3**, 165 (1964).

3) C. J. Plank and E. J. Rosinski, U. S. Pat. 3140253 (1964).

4) V. J. Frilette, P. B. Weisz and R. L. Golden, *J. Catalysis*, **1**, 301 (1962).

5) P. B. Weisz, V. J. Frilette, R. W. Maatman and E. B. Mower, *ibid.*, **1**, 307 (1962).

6) D. W. Breck, U. S. Pat. 3130007 (1964).

$Al_2O_3 \cdot 2.69SiO_2$ and of $Na_2O \cdot Al_2O_3 \cdot 4.73SiO_2$ for the X and Y zeolites respectively. X-ray diffraction examination revealed a good crystallinity in both types of zeolites. A commercial amorphous silica alumina catalyst which was 13% Al_2O_3 (a fluidized cracking catalyst) was used.

Ion Exchange. The cation-exchange on zeolites was carried out by bringing the sodium ion form of zeolites in contact with a 0.2N solution of nitrates or of chlorides. The desired degree of ion exchange was controlled by the number of repeating the ion exchange process. The ion exchanged zeolite was calcined after repeated washings with pure water and after drying at 110°C. Zeolites exchanged by the calcium and the lanthanum ions were also prepared as has been described above. The protonated zeolite was obtained in a different way, by the calcination of the ammonium ion form of zeolite, which was prepared by bringing zeolite in contact with an ammonium chloride solution.

Acidity and Acid Strength. The acidic character was determined by the Benesi method[7,8] by the use of *n*-butylamine as a titer and Hammett indicators. Samples were calcined at 10^{-3}—10^{-4} mmHg for 2 hr and then transferred into weighing bottles in a dry box and measured.

The total acidity was defined as the amount of the acid determined with Butter Yellow ($pK_a = +3.3$). The acid strength was determined by using indicators of various pK_a's.

Catalysts and Cumene Cracking. Ion-exchanged zeolite powders (1—5 μ in diameter) were pressed into pellets, and then they were crushed into pilled catalysts 60—100 in mesh size. The cumene-cracking reaction was carried out over a pilled catalyst calcined at 600°C for 2 hr prior to use. This activity test was carried out in a flow system. Figure 1 shows a schematic diagram of the apparatus used for cracking.

A simple cracking reaction was conducted over various cationic forms of zeolites under definite conditions: weight of catalyst 0.6 g; reaction temperature, 450°C; LHSV, 1.2. The products were condensed for 1 hr after the start of the reaction. The condensate was then analyzed by gas chromatography in order to determine the amount of the conversion of cumene to benzene.

In the case of the lanthanum ion exchanged form of the X zeolite, a more detailed experiment was undertaken in order to determine the correlation between the catalytic activity and the acidic character of zeolite. The reaction was carried out when the conversion of cumene was below ten percent, in which region the reaction rate was proportional to the amount of catalyst employed. Nitrogen gas was passed over the La–X catalyst for 1 hr at the reaction temperature, and then the cumene-nitrogen mixture was intoduced. The cracking activity was so high at the start that the sampling of products for 1 hr was begun 1 hr after the introduction of the reactant.

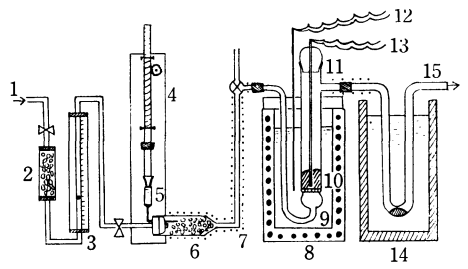

Fig. 1. Schematic diagram of apparatus for cumene cracking.

1	nitrogen gas	9	molten salt
2	drying tube	10	catalyst
3	rotameter	11	reactor tube of pyrex
4	cumene feeder	12, 13	thermocouple
5	syringe containing cumene		
6	cumene evaporator		
7	tape heater	14	dry ice bath
8	electric furnace	15	trap

7) H. A. Benesi, *J. Phys. Chem.*, **61**, 970 (1957).
8) H. A. Benesi, *J. Am. Chem. Soc.*, **78**, 5490 (1956).

Results and Discussion

Acidic Character. The color changes of Hammett indicators, showing the end point of titration, were similar in both silica-alumina and zeolites, except that some of the latter catalysts showed less obvious color changes in the indicators. This is probably due to the difference in acid strength, as will be discussed below.

The distribution curve of the acid strength is cumulatively shown in Figs. 2 to 4 as a function of H_0, together with that of a FCC silica-alumina. In the figures and hereafter the symbols M–X and M–Y refer to the X and Y zeolites exchanged by the cation of the element, M. Figure 2 indicates that, in general, the zeolites have, in striking contrast to the silica-alumina, which has a strong acid site only, acid sites over a wide range of strengths and a larger acidity. The dotted line for the Ca–X (95.7) in Fig. 2 denotes that the detection of the color change of the indicators (benzalacetophenone, $pK_a = -5.6$; anthraquinone, $pK_a = -8.2$) was disturbed because of the yellow surface of this sample.

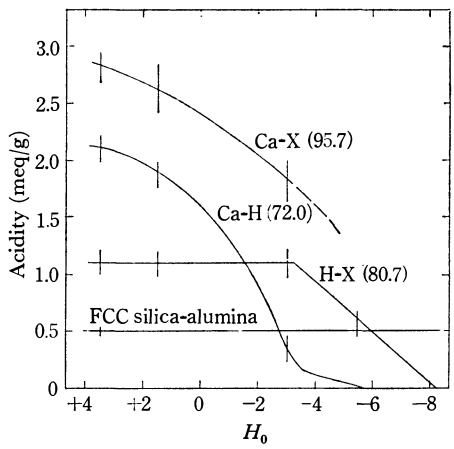

Fig. 2. Distribution of acid strength of the H–X, Ca–X and FCC silica-alumina.
The vertical lines and figures in bracket denote the uncertainty in titration and degree of the ion exchange, respectively. These remarks are also used in Figs. 3 and 4.

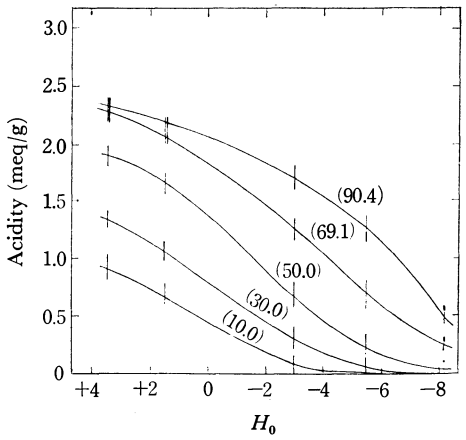

Fig. 3. Distribution of acid strength of the La–X with various degree of the ion exchange.

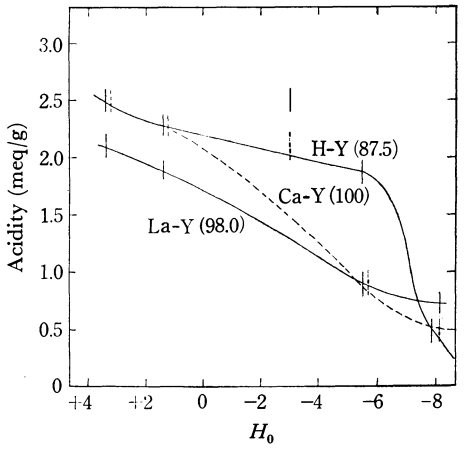

Fig. 4. Distribution of acid strength of the H–Y, Ca–Y and La–Y

Figure 3 shows the dependence of the distribution of the acid strength for the La–X on the degree of the ion exchange. The uniform crystalline structure of the zeolite leads us to expect that the distribution of the acid strength will be the same at any level of the ion exchange, whereas the total amount of acid will increase in proportion to the degree of the ion exchange. However, this is not the case. As may be seen in Fig. 3, stronger acid sites appear with an increase in the degree of ion exchange. Moreover, Figs. 2 and 3 show that the acid strength is dependent upon the kind of cation. These acidic characters are reasonable if the structure of the zeolite is considered. It has been established[9,10] that there are three kinds of sites occupied by sodium ions in the X and Y zeolites. It has also been found that, in the Ca–X, calcium ions occupied two kinds of sites, S_I and S_{II}, differing from each other in the number of oxygen atom coordinated to the calcium ion. The former site was located in the interior of the hexagonal prism, positioned between two puckered O_6 rings. It was effectively hidden from the surface of the large pore. The latter one was found in the O_6 ring, which formed a hexagonal face. It was positioned on the surface of the large pore. The results of the calculation of the electrostatic field strengths at these sites revealed that the charge distribution differed between the two sites, with the S_I site being energetically more stable than the S_{II} site. Thus, it follows that the calcium ion prefers the S_I site to the S_{II} site at a lower level of ion exchange.

Although the origin of the acid site in the zeolites has not been clarified well,[1] it is conceivable that the different states of the cation sites causes the occurrence of acid sites of different strengths.

Figure 4 indicates that the distribution of the acid strength also depends on the type of zeolite. A large proportion of the acid sites is distributed in the strong region in the Y zeolite, unlike as in the X zeolite. The total quantity of acid sites in the Y zeolite is less than that in the X zeolite, except for the protonated zeolite, corresponding to the difference in their ion exchange capacities. The X and Y zeolites are nearly the same in structure. The ratio of the silicon atom to the aluminum atom is higher in the Y zeolite. Rabo and his associates[9,10] have pointed out, however, that the electrostatic field strength at cation sites is much larger in the Y zeolite. It seems reasonable, therefore, that there is a difference in acid strength between the two types of zeolites.

In the case of the protonated zeolites, the H–X has less acidity than the H–Y. This can reasonably be explained by the results of the experiment given below. The crystalline structure of the NH_4–X collapsed, as was revealed by an X-ray diffraction

Table 1. Cumene cracking activity for various types of zeolites

Reaction temp. 450°C; LHSV=1.2; weight of catalyst; 0.6 g

Sample	Degree of ion exchange (%)	Amount of cations in zeolite (meq/g)	Conv. of cumene (%)
H-X	80.7	4.48	79.8
H-Y	87.5	3.73	95.3
Ca-X	72.0	4.02	8.7
Ca-X	95.7	5.37	68.3
Ca-Y	100	4.26	96.3
La-X	95.7	5.37	86.0
La-Y	86.0	3.67	97.1

9) P. E. Pickert, J. A. Rabo, E. Dempsey and V. Shomaker, Proc. 3rd Intern. Congr. Catalysis, Amsterdam, 1964, Vol. I, Wiley, New York (1965), p. 714.

10) J. A. Rabo, C. L. Angell, P. H. Kasai and V. Shomaker, *Discussions Faraday Soc.*, **41**, 328 (1966).

examination, during the formation of the H-X from the NH_4-X (NH_4-X $\xrightarrow{heat}$ H-X + $NH_3\uparrow$), while the surface area of the zeolite was being lowered. The surface area of the H-X was found to be 371 m^2/g, only one half those of the Na-X (723 m^2/g) and Na-Y (898 m^2/g). On the other hand, the H-Y remains crystalline in spite of undergoing the same calcination step as in the H-X.

Cumene Cracking. Table 1 lists the results of cumene cracking conducted over various forms of zeolites under the definite reaction conditions described above. Figures 6 and 7 show the cumene cracking activity for the La-X as functions of degree of ion exchange and of the reaction temperature.

The kinetics of the reaction was analyzed as follows. The mechanism of cumene cracking may be supposed to be:[11]

$$\text{Cumene} + \text{free site} \underset{k_2}{\overset{k_1}{\rightleftharpoons}} \text{cumene-site complex} \xrightarrow{k_3} \text{benzene} + \text{propylene} + \text{free site}$$

Assuming the adsorption step in equilibrium during the reaction, the following relationship is derived:

$$P_c/r = 1/k_3B_0 \cdot P_c + 1/k_3B_0K, \quad K = k_1/k_2 \qquad (1)$$

where:

P_c: partial pressure of cumene,
r: reaction rate,
B_0: number of active sites,
K: adsorption equilibrium constant.

The rate constant, k_3, is a measure of the ability to crack the complex. However, it is not determined directly because the value of B_0 is unknown. The value of k_3B_0, which is also a measure of the cracking activity, is determined from a reciprocal of the slope of a straight line plotted P_c/r *vs.* P_c, as is shown in Fig. 5.

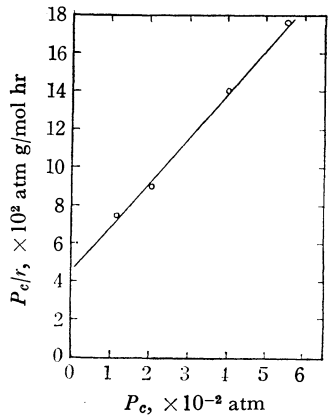

Fig. 5. Plots of P_c/r *vs.* P_c.
Catalyst: La-X (50.0);
Reaction temp.: 330°C

In the X zeolite the catalytic activity is in the following order:

La-X (percentage of the ion exchange: 95.7) > H-X (80.7) > Ca-X(95.7) > Ca-X(72.0); in the Y zeolite, although the amount of the cation exchange is less than that in the X zeolite, there is a very high activity in any cationic form. These results are in good agreement in order with the acid strength and not with the acidity, as is shown in Figs. 2 to 4. It is obvious from Figs. 6 and 7 that the catalytic activity increases more than linearly with an increase in the degree of ion exchange. Such a phenomenon,

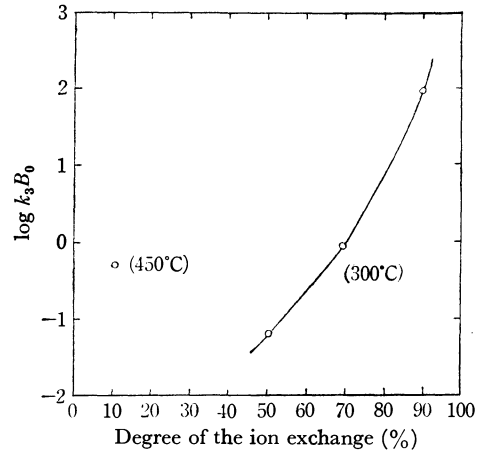

Fig. 6. Correlation between cumene cracking activity and degree of the ion-exchange for the La-X.
Figures in bracket denote the reaction temperature.

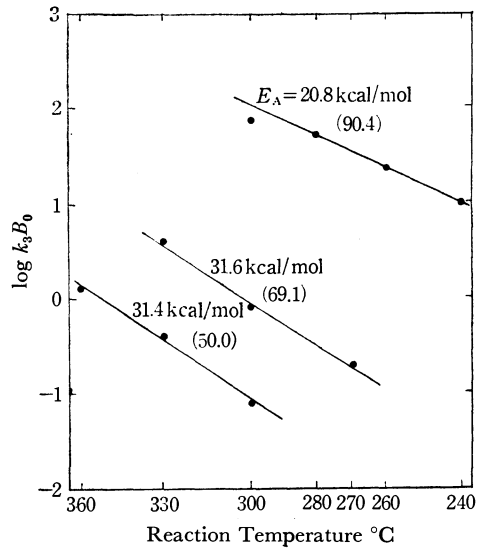

Fig. 7. Temperature dependence of cumene cracking activity and apparent activation energy for the La-X.
Figures in bracket denote degree of the ion-exchange.

11) W. F. Pansing and J. B. Malloy, *Ind. and Eng. Chem., Process Design and Development*, **4**, 181 (1965).

suggesting the heterogeneity of the zeolite surface, has been observed with, for example, the benzene propylation over the Rare-earth-Y,[12] the cumene cracking over the H-Y[13] and over the Ca-X,[14] and the hexane isomerization over the Pt/Ca-Y.[15] These results may be interpreted in terms of the variation in acid strength with an increase in the degree of ion exchange, as may be seen in Figs. 2 and 3 for the Ca-X and La-X respectively.

The apparent activation energy for the cumene cracking over the La-X, shown in Figs. 7, seems to decrease at a high level of ion exchange. The change in the activation energy with the degree of ion exchange may be a reflection of the difference in the nature of the two kinds of active sites, S_I and S_{II}. At a lower level of ion exchange calcium ions occupy mainly the S_I site, while at a higher level they occupy S_I and S_{II} sites. The catalytic activities originate from the S_I and S_{II} sites at lower and higher levels of ion exchange respectively. Accordingly, there has been found a change in the activation energy from 32 kcal/mol for the La-X (50.0) to 23 kcal/mol for the La-X (90.4), dependent upon the degree of ion exchange.

12) P. B. Venuto, L. A. Hamilton, P. S. Landis and J. J. Wise, *J. Catalysis*, **5**, 81 (1966).

13) J. Turkevich, F. Nozaki and D. Stamires, Proc. 3rd Intern. Congr. Catalysis, Amsterdam, 1964, Vol. I, Wiley, New York (1965), p. 586.

14) E. G. Boreskova, K. V. Topschiva and L. I. Piguzova, *Kinetika i Kataliz*, **5**, 903 (1964).

15) J. A. Rabo, P. E. Pickert, D. N. Stamires and J. E. Boyle, Actes 2nd Congr. Intern. Catalyse, Paris, 1960, Vol. 2, Editions Technip., Paris (1961), p. 2055.

BULLETIN OF THE CHEMICAL SOCIETY OF JAPAN VOL. 42 2453—2458 (1969)

Vacuum-ultraviolet Absorption Spectra of Aliphatic Ketones

Hiroyuki Ito,*1 Yoshihiko Nogata,*2 Sanae Matsuzaki and Akira Kuboyama

Government Chemical Industrial Research Institute, Tokyo, Shibuya-ku, Tokyo

(Received January 31, 1969)

The molar-absorptivity curves of various aliphatic ketones, mainly methyl alkyl ketones, in the gaseous state in the region from 1650 to 2000 Å have been obtained. In these ketones the absorption bands near 1950 Å and 1700 Å are denoted as A and B bands respectively. Di-*n*-propyl and diisopropyl ketones show, besides the A and B bands, an absorption band near 1650 Å (C band). The relations between the obtained spectra and the molecular structures of these ketones have been studied. On the basis of this study, the characteristics of the electronic transitions of A, B, and C bands have been discussed.

Up to now, there have been few data about absorption spectra in the vacuum-ultraviolet region. The number of molar absorptivity curves of organic compounds reported in this region have been especially few. Though the absorption spectra in this region are not so easily obtainable as those in the visible and near-ultraviolet regions, they may well provide much important information about structural and analytical chemistry.

Aliphatic ketones have, beside the $n\rightarrow\pi^*$ bands near 2800 Å and the $\pi\rightarrow\pi^*$ bands near 1550 Å, two or three moderately intense absorption bands in the range from 2000 to 1650 Å.[1-5] As for these absorption bands in the range from 2000 to 1650 Å, no accurate molar-absorptivity curves have been reported except for that of acetone.[2] In this work the molar-absorptivity curves of various aliphatic ketones, mainly methyl alkyl ketones, in the gaseous state, have been measured in the region from 2000 to 1650 Å; their relations to the molecular structures of the ketones will be discussed.

*1 Present address: The Research Development Corporation of Japan, Chiyoda-ku, Tokyo.

*2 Present address: Toyo Jozo Co., Ltd., Tagata-gun, Shizuoka Prefecture.

1) R. S. Holdsworth and A. B. F. Duncan, *Chem. Revs.*, **41**, 311 (1947).

2) J. S. Lake and A. J. Harrison, *J. Chem. Phys.*, **30**, 361 (1959).

3) E. E. Barnes and W. T. Simpson, *ibid.*, **39**, 670 (1963).

4) J. F. Horwood and J. R. Williams, *Spectrochim. Acta*, **19**, 1351 (1963).

5) A. Udvarhazi and M. A. El-Sayed, *J. Chem. Phys.*, **42**, 3335 (1965).

Experimental

Measurements. The absorption spectra were measured with a VUV-3 vacuum-ultraviolet self-recording spectrophotometer (the radius of the curvature of the concave grating was one meter) of the Japan Spectroscopic Co., Ltd., at room temperature. This apparatus has a ratio-recording double-beam system using the rotating-cell method.[6] In this method, 30-mm gas-cell blocks, made of stainless steel and containing a sample cell on one side and a reference cell on the other, rotate at 8 Hz and function as "rotating sectors." Fluorite plates 1 mm thick were used as the windows of the cells. As the light source and light detector, a MH-225 Mitsubishi Deuterium Lamp and a photomultiplier (EMI 6256B) were used. The absorption peak of mercury vapor at 1849.6 Å was used for the wavelength calibration. The pressures of sample gases were measured with a mercury manometer with an inner diameter of 16 mm.[7] The mercury levels were read with a measuring microscope. The sensitivity of the pressure reading was *ca.* 0.01 mm. Each absorption spectrum was measured several times.

Materials. The ketones used were obtained from the Tokyo Kasei Kogyo Co., Ltd. Spectro-grade acetone and methyl ethyl ketone were used. Their purity was checked by gas chromatography. Methyl isopropyl, methyl *s*-butyl, methyl *t*-butyl, and diisopropyl ketones were purified by gas chromatography. Deuteroacetone (acetone-d_6) of Ciba Products, Ltd., the isotopic purity of which was greater than 99.5 per cent, was used without further purification.

Results

The molar absorptivity curves obtained are shown in Figs. 1—6. The wavelengths and molar absorptivities of the absorption peaks in these absorptivity curves are given in Table 1. In Table 1 the accuracy of the wavelengths is ±1 Å, and the reproducibility of the molar absorptivities is within 10 per cent. The oscillator strengths (*f*-values) of the A and B bands are given in Table 2. Some photodecomposition of these ketones was found to occur during the measurements. This decomposition was the most remarkable in methyl *n*-amyl and methyl *n*-butyl ketones. In these cases several per cent of the original part was decomposed during the measurements. None of peaks obtained are believed to be characteristic of the photodecomposition products since they all decreased in intensity on continued irradiation. The obtained molar absorptivities of the longest-wavelength absorption peak of the band, near 1950 Å, of acetone and of the absorption maximum of the band, near 1950 Å, of diethyl ketone are in good agreement with those reported by Lake and Harrison[2] and by Barnes and Simpson[3] respectively. The shapes of the absorption bands near 1950 Å of these ketones are in good agreement with those of the transmittance curves of these ketones reported by Horwood and Williams.[4]

Discussion

As may be seen in Figs. 1—6, methyl alkyl ketones and diethyl ketone show two absorption bands, near 1950 Å and 1700 Å. Di-*n*-propyl and diisopropyl ketones show an absorption band near 1650 Å besides these two absorption bands. In this paper these three kinds of absorption bands, near 1950 Å, 1700 Å, and 1650 Å, will be denoted as A, B, and C bands respectively. In these ketones

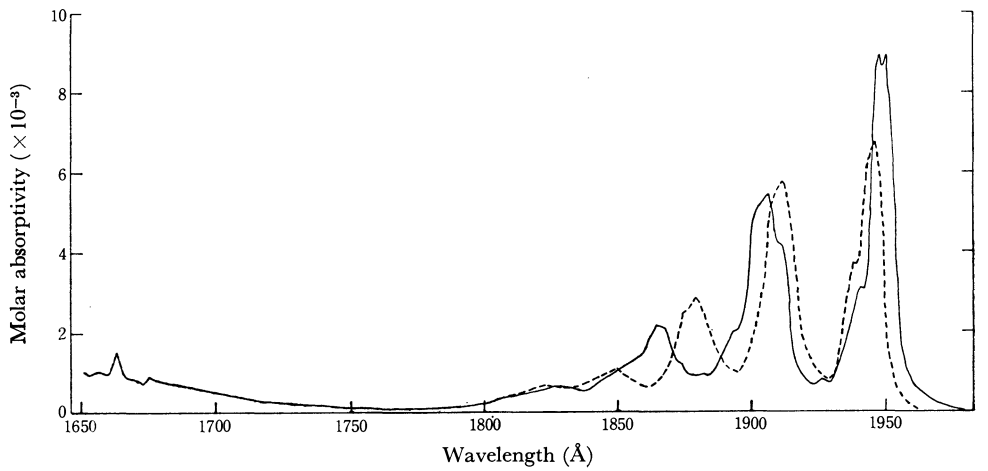

Fig. 1
—— Acetone ------ Acetone-d_6

6) Y. Nihei, S. Oda, E. Niki and H. Kamada, *Spectrochim. Acta*, **24A**, 457 (1968).

7) The gas-sampling apparatus has been constructed according to the method of Tsubomura *et al.* (H. Tsubomura, K. Kimura, K. Kaya, J. Tanaka and S. Nagakura, This Bulletin, **37**, 417 (1964)).

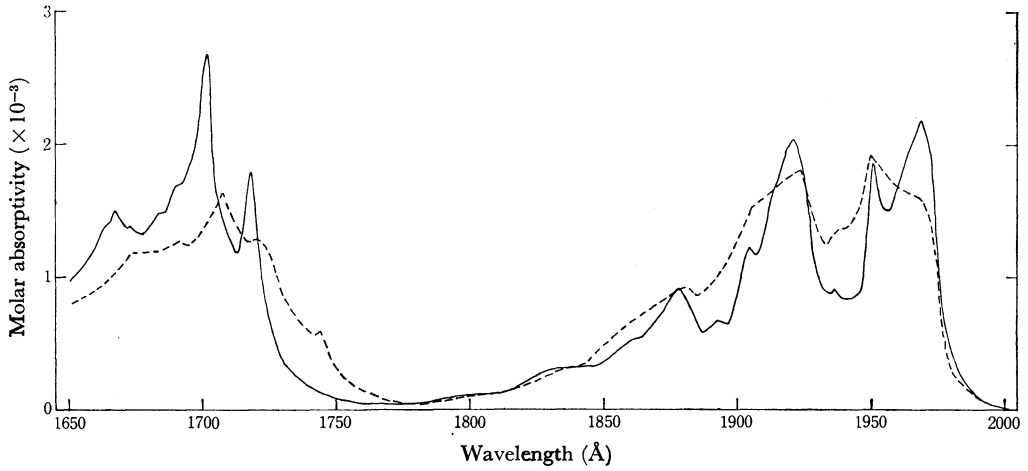

Fig. 2

—— Methyl ethyl ketone ------ Methyl *n*-propyl ketone

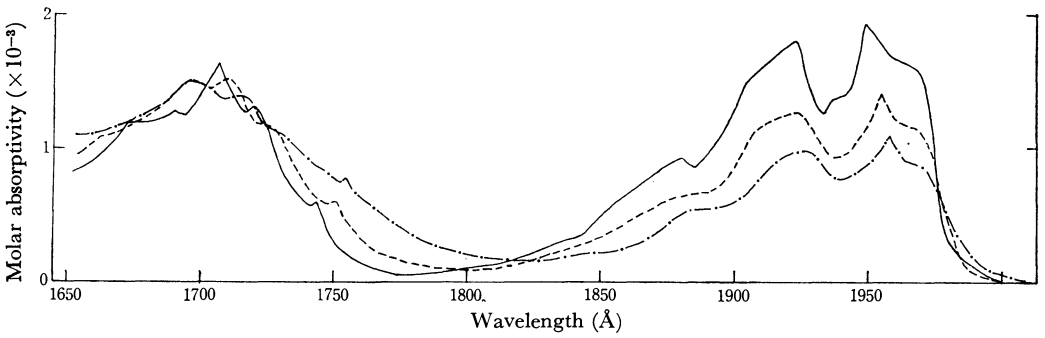

Fig. 3

—— Methyl *n*-propyl ketone ------ Methyl *n*-butyl ketone —·— Methyl *n*-amyl ketone

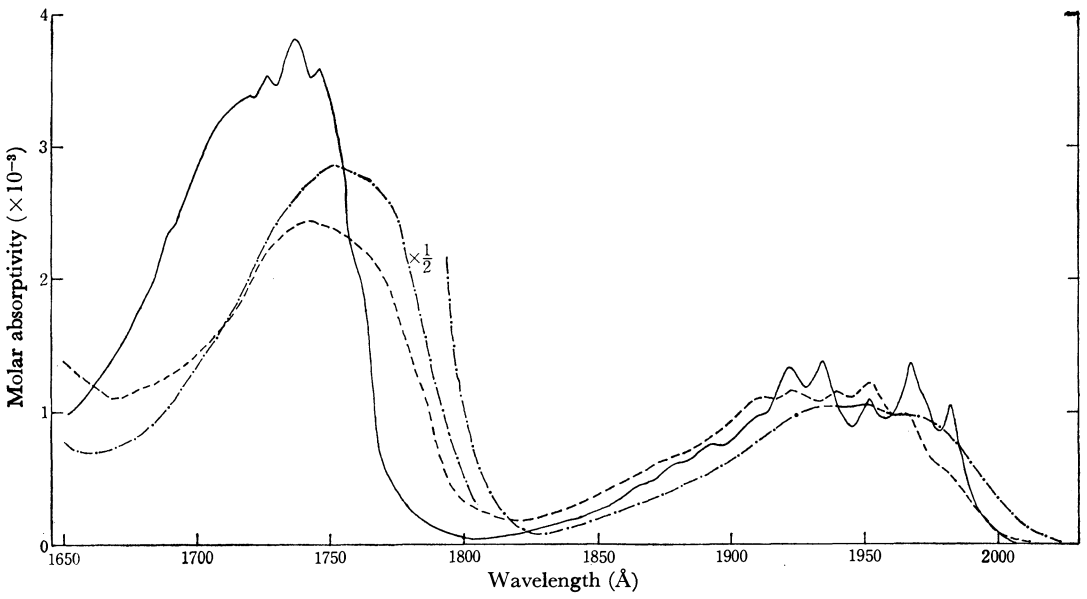

Fig. 4

—— Methyl isopropyl ketone ------ Methyl isobutyl ketone —·— Methyl *t*-butyl ketone

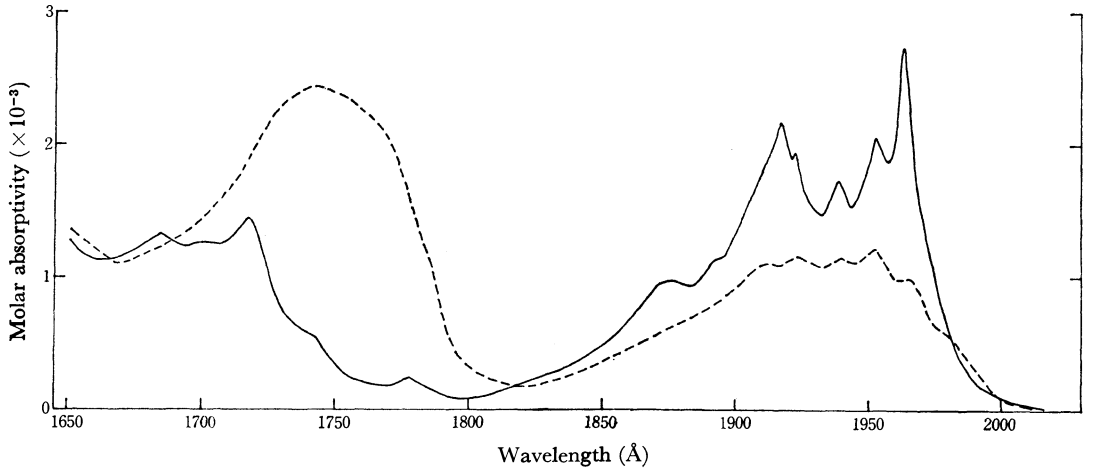

Fig. 5

—— Methyl *s*-butyl ketone ------ Methyl isobutyl ketone

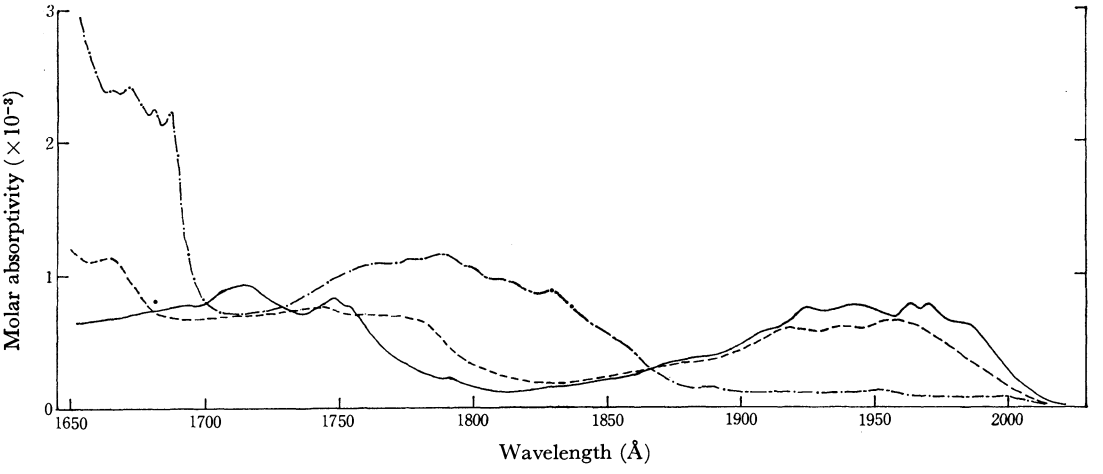

Fig. 6

—— Diethyl ketone ------ Di-*n*-propyl ketone —·— Di-isopropyl ketone

each of the three kinds of absorption bands is thought to have similar characteristics of the electronic transitions.

Methyl *n*-alkyl ketones, the methyl alkyl ketones in which the α-carbons of the alkyl groups are the secondary or tertiary carbons, and di-(non-methyl)alkyl ketones are classified into Group I, II, and III respectively for convenience. Methyl *s*-butyl ketone is classified in Group I. The following distinct points about the positions and intensities of A and B bands may be found by comparing Fig. 1—6 and Table 2.

(1) As for the position of the A band, the A band of acetone is at wavelengths a little shorter than those of the other ketones.

(2) As for the intensity of the A band, that of acetone is considerably greater than those of other ketones. In methyl *n*-alkyl ketones the intensity generally decreases with the number of carbon atoms in the *n*-alkyl groups. Those of Group II and III are weak, that of diisopropyl ketone bing especially weak.

(3) As for the position of the B band, the B bands of Group II and III are at wavelengths considerably longer than those of Group I, that of diisopropyl ketone being at a wavelength especially much longer than those of Group I.

(4) As for the intensity of the B band, that of acetone is very weak and all those of Group I except for acetone are similar to each other. Those of Group II, especially that of methyl *t*-butyl ketone, are remarkably greater than those of Group I, while those of Group III are close to those of Group I (except for acetone).

TABLE 1. THE WAVELENGTHS AND MOLAR ABSORPTIVITIES OF THE ABSORPTION PEAKS

	λ_{max} (Å)	ε_{max}		λ_{max} (Å)	ε_{max}
Acetone	1951	9000	Methyl isobutyl	1964	1000
	1948.5	9000	ketone	1952	1220
	1906	5600		1940	1150
	1865	2150		1924	1150
	1663	1500		1912	1100
				1742	2450
Acetone-d_6	1946	6900			
	1911	5700	Methyl *s*-butyl	1963	2730
	1879	2850	ketone	1952	2100
	1849	1100		1940	1770
	1663	1500		1923	2030
				1917	2170
Methyl ethyl ketone	1968.5	2200		1878	1050
	1951	1870		1777	300
	1936	930		1719	1450
	1921	2100		1685	1350
	1905	1270			
	1878	930	Methyl *t*-butyl	1950	1100
	1718	1800	ketone	1750	5800
	1701.5	2700			
	1666	1500	Diethyl ketone	1970	770
				1962	770
Methyl *n*-propyl	1950	1950		1942	770
ketone	1924	1800		1924	770
	1881	930		1748	830
	1744	600		1716	900
	1707	1650			
			Di-*n*-propyl ketone	1958	650
Methyl *n*-butyl	1955	1400		1920	600
ketone	1924	1270		1745	800
	1752	550		1667	1150
	1712	1450			
			Diisopropyl ketone	1949	100
Methyl *n*-amyl	1958	1100		1829	950
ketone	1927	1000		1790	1150
	1756	700		1687	2250
	1697	1500		1681	2300
				1672	2500
Methyl isopropyl	1982	1070		1665	2400
ketone	1967	1400			
	1951	1130			
	1935	1330			
	1922	1300			
	1746	3600			
	1737	3800			
	1727	3500			

As for the shapes of the A and B bands of each ketone, the A band shows a relatively sharp vibrational structure and its shape is very sensitive to the alkyl group. In the B band only that of methyl ethyl ketone shows a sharp vibrational structure. In acetone the frequency of the main vibrational progression is *ca.* 1140 cm^{-1}. On the other hand, that in deuteroacetone is *ca.* 940 cm^{-1}. On the basis of this fact, Lawson and Duncan[8] have safely assigned these frequencies to the C–H(D) bending vibration of the methyl groups. In the A bands of methyl ethyl and methyl *s*-butyl ketones the frequencies of the main vibrational progressions are *ca.* 1240 cm^{-1} and 1220 cm^{-1} respectively. These progressions may be similar to that in acetone. Besides these progressions, we found distinct progressions of two frequencies, 470 cm^{-1} in the A band and 580 cm^{-1} in the B band in methyl ethyl ketone, and two other frequencies, 290 cm^{-1} and 660 cm^{-1}, in the A band of methyl *s*-butyl ketone. The 470 cm^{-1} frequency in the A band of methyl

8) M. Lawson and A. B. F. Duncan, *J. Chem. Phys.*, **12**, 329 (1944).

Table 2. The oscillator strengths of A and B bands

	A Band f	B Band f
Acetone	0.035	
Acetone-d_6	0.033	
Methyl ethyl ketone	0.018	0.017
Methyl *n*-propyl ketone	0.020	0.016
Methyl *n*-butyl ketone	0.015	0.018
Methyl *n*-amyl ketone	0.011	0.022
Methyl isopropyl ketone	0.015	0.043
Methyl isobutyl ketone	0.015	0.031
Methyl *s*-butyl ketone	0.023	0.015
Methyl *t*-butyl ketone	0.013	0.072
Diethyl *t*-butyl ketone	0.010	0.014
Di-*n*-propyl ketone	0.008	0.012
Diisopropyl ketone	0.001	0.018

ethyl ketone is probably that of the C–O bending vibration.[9] The sharp vibrational structure of that of methyl *s*-butyl ketone is remarkable in view of the complex structure of this ketone. This is thought to be due to the particular, rigid three-dimensional molecular structure of this ketone. Recently a study of the infrared spectra of these ketones has shown that the various rotational isomers exist in the liquid and gaseous states.[9,10] The relation between the existence of the various rotational isomers and the band shapes is not clear at this stage. The co-existence of the various rotational isomers in the gas phase may contribute to the broadening of the absorption peaks.

The assignments of the A and B bands have been discussed by many authors. Heretofore, the A band has been identified as the $n\rightarrow\sigma^*$ band on the basis of its position and intensity by many people.[5,11,12] As has been described before, the fact that the frequency of the main vibrational progression in the A band of acetone is that of the C–H bending vibration of the methyl groups is to show that the hyperconjugation of the methyl groups to the carbonyl π-bond plays an important role in the electronic transition of the A band. The large intensity of the A band of acetone, and the very small intensity of the A band of diisopropyl ketone, where the hypercojugation of the isopropyl groups to the CO π-bond is thought to be weak, offer strong support for this theory. Since these hyperconjugations seem not to play an important role in the $n\rightarrow\sigma^*$ transition, this theory does not support the assignment of the A band to the $n\rightarrow\sigma^*$ band. Therefore, further theoretical and experimental examination for this assignment are desireable.

As for the electronic transition of the B band, there are two possible explanations of the remarkable difference in the intensity of the B band between acetone and methyl ethyl ketone. One is that a C–C bond combining with the CO bond plays an important role in the electronic transition of the B band. The other one is that the nonequivalency of the two alkyl groups favors this transition. The fact that the intensity of the B band of methyl isopropyl ketone is far greater than that of diisopropyl ketone seems to support the latter possibility. On the other hand, it is also remarkable that the B band of diisopropyl ketone is at a wavelength considerably longer than that of methyl isopropyl ketone. As for the electronic transition of the C band, its intensity seems to be too weak to assign the C band to the $\pi\rightarrow\pi^*$ band. Further theoretical and experimental examinations for the assignments of B and C bands are also desirable.

In these ketones the Rydberg transitions are expected to appear in the region shorter than 1800 Å. For example, the peak at 1663 Å in acetone and the four peaks in the C band of diisopropyl ketone may be those of Rydberg transitions. However, the Rydberg-transition peaks can not be discussed at this stage.

The authors are grateful to Mr. H. Tomita and Mr. I. Takeda of this Institute for their help with the gas chromatography, and to Dr. K. Kaya of the Institute of Physical and Chemical Research for his helpful advice.

9) T. Shimanouchi, Y. Abe and M. Mikami, *Spectrochim. Acta*, **24A**, 1037 (1968).

10) M. Hirota, T. Hagiwara and H. Satonaka, This Bulletin, **40**, 2439 (1967).

11) H. L. McMurry, *J. Chem. Phys.*, **9**, 231 (1941).

12) W. C. Johnson, Jr., and W. T. Simpson, *ibid.*, **48**, 2168 (1963).

BULLETIN OF THE CHEMICAL SOCIETY OF JAPAN VOL. 42 2459—2463 (1969)

Studies of Ion Exchange Membranes. XXX. The Tetrahydrofuran Extraction of the Ion-exchange Membrane and Its Base Membrane Prepared by the "Paste Method"

Yukio MIZUTANI

Tokuyama Soda Co., Ltd., Tokuyama-shi, Yamaguchi-ken

(Received February 3, 1969)

In order to throw light on the chemical structure of the ion-exchange membrane prepared by the "Paste Method," the ion-exchange membrane and its base membrane were extracted with tetrahydrofuran. The base membrane was composed of polyvinyl chloride and the resin component of the styrene-divinyl benzene system or of the 2-methyl-5-vinyl pyridine-divinyl benzene system, the ion-exchange group was introduced into this resin component. It was established that the resin component was partially extractable through a filter paper. Although the resin component and polyvinyl chloride should be entwined with each other, and although the resin component might be grafted on polyvinyl chloride, it could be concluded that the chemical structure of the ion-exchange membrane prepared by the "Paste Method" is different from that of Amberlite IR-120, *i. e.*, the homogeneously crosslinked gel-structure.

Many procedures have been proposed for the preparation of an ion-exchange membrane.[1-8] However, in most of these procedures the base membrane, with a functional group appropriate for the introduction of an ion-exchange group, is prepared beforehand, and then an ion-exchange group is introduced. Therefore, the preparation of the base membrane has thus far been an important theme.[2-8] The present author has already reported on the "Paste Method."[5-8] Namely, a fine powder of polyvinyl chloride (PVC) and a monomer mixture, consisting mainly of styrene (St)-divinyl benzene (DVB) or 2-methyl-5-vinyl pyridine (MVP)-DVB, was mixed to prepare the paste, and then a Teviron cloth (a reinforcing material) was coated with this paste. This resultant polymer composite was heated in order to polymerize the monomers. An ion-exchange group was introduced to the base membrane by sulfonation or quarternization with methyl iodide. The ion-exchange membrane thus prepared has been used in the electrophoretic concentration[9,10] or desalination[11] of sea water.

Furthermore, this ion-exchange membrane is flexible and thermoplastic. This characteristic of ion-exchange membranes prepared by the "Paste Method" suggests that the structure of the membrane may be different from the homogeneously crosslinked gel-structure.

The base membranes for the cation-exchange membrane (base membrane-C) and for the anion-exchange membrane (base membrane-A) show quite a good transparency. For example, the base membrane-C consists mainly of PVC and the resin component of the St-DVB system. Considering that PVC is immiscible with polystyrene and that the mixture of both polymers is an opaque white, the quite good transparency of the base membrane-C has been explained by the presence

1) H. Nakazawa, Y. Onoue and Y. Mizutani, *Kogyo Kagaku Zasshi* (*J. Chem. Soc. Japan, Ind. Chem. Sect.*), **61**, 789 (1958); Y. Onoue, Y. Mizutani and S. Akiyama, *Denki Kagaku* (*J. Electrochem. Soc. Japan*), **29**, 223 (1961); Y. Onoue, Y. Mizutani, W. Tesima, R. Yamane and S. Akiyama, *ibid.*, **29**, 468 (1961).

2) W. K. W. Chen, R. B. Mesrobian, D. S. Ballantine, D. J. Metz and A. Glines, *J. Polym. Sci.*, **23**, 903 (1957).

3) Y. Mizutani, *Kogyo Kagaku Zasshi* (*J. Chem. Soc. Japan, Ind. Chem. Sect.*), **65**, 1124 (1962).

4) Y. Mizutani, *ibid.*, **65**, 1128 (1962).

5) Y. Mizutani, R. Yamane, H. Ihara and H. Motomura, This Bulletin, **36**, 361 (1963).

6) Y. Mizutani, W. Tesima and S. Akiyama, Japanese Pat., 410368.

7) Y. Mizutani, W. Tesima, S. Akiyama, R. Yamane and H. Ihara, Japanese Pat., 481838.

8) Y. Mizutani, R. Yamane and H. Motomura, This Bulletin, **38**, 689 (1965).

9) R. Yamane, T. Sata and Y. Mizutani, *Nippon Kaisui Gakkai-Shi*, (*Bull. Soc. Sea Water Science Japan*), **20**, 313 (1967).

10) R. Yamane, H. Motomura, T. Sata and Y. Mizutani, *ibid.*, **20**, 327 (1967).

11) T. Matsuda, S. Ogawa and Y. Onoue, "Demineralization of Sea Water by Electrodialysis," Presented at the Second European Symposium on Fresh Water from the Sea, May, 9—12, 1967, Athens, Greece, European Federation of Chemical Engineering.

of the graft copolymer of PVC and the resin component.[5]

In order to elucidate the correlation between PVC and the resin component (M-resin) of the St-DVB system or the MVP-DVB system, in this study the ion-exchange membrane and its base membrane were extracted with tetrahydrofuran (THF).

Experimental

The Sample. The ion-exchange membrane and its base membrane were prepared by the "Paste Method."[5-8] Previous to the THF extraction, the sample was extracted with methanol in order to expel the unpolymerized monomer, *etc.*, by using a Soxhlet extractor.

The THF Extraction. The sample was extracted with THF for 30 hr by the use of a Soxhlet extractor.

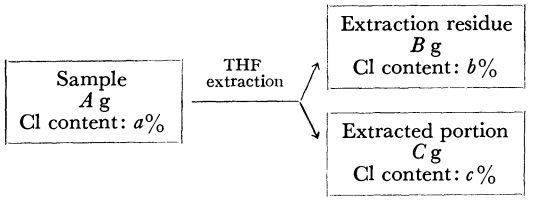

E_p and E_R were defined as follows:

$$E_p = \frac{\text{Quantity of chlorine in the extraction residue}}{\text{Quantity of chlorine in the base membrane}}$$

$$E_R = \frac{\text{Quantity of the M-resin in the extracted portion}}{\text{Quantity of the M-resin in the base membrane}}$$

The cylindric filter paper used was Toyo Filter Paper No. 84 (Size, 25×90 mm); the particle size retainable by this filter paper is 8 μ.

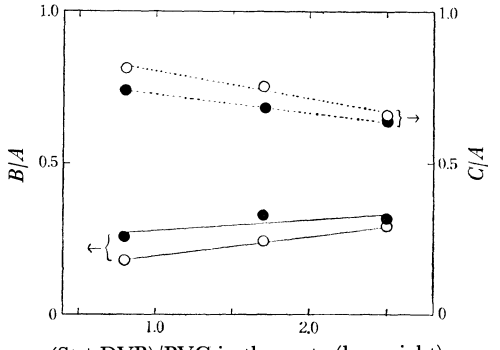

Fig. 1. The effect of the monomer content in the paste on B/A and C/A.
The composition of the paste:
DVB/(St+DVB)=0.025
Dioctylphthalate/PVC=0.31—0.4
Polymerization temperature: 110°C
-○-: Observed value
-●-: Calculated value of (St+DVB)/Base membrane-C (for B/A) or of PVC/Base membrane-C (for C/A)

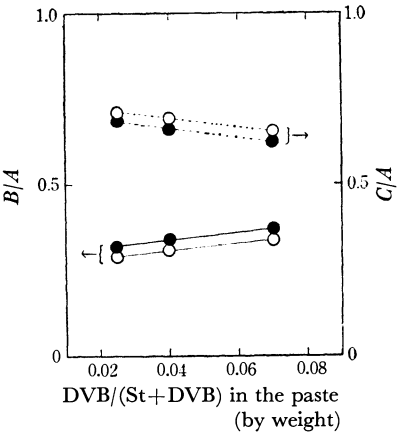

Fig. 2. The effect of the DVB content in the paste on B/A and C/A.
The composition of the paste:
(St+DVB)/PVC=2.5
Dioctylphthalate/PVC=0.31
Polymerization temperature: 110°C
-○-, -●- : Shown in Fig. 1

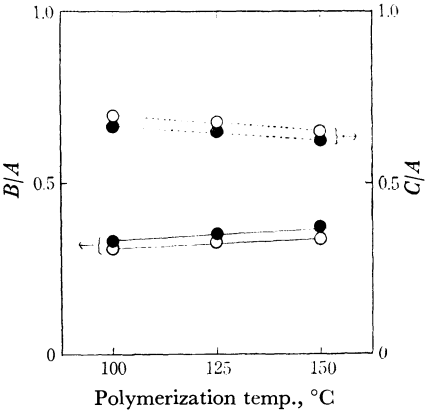

Fig. 3. The effect of the polymerization temperature on B/A and C/A.
The composition of the paste:
(St+DVB)/PVC=2.5
DVB/(St+DVB)=0.04
Dioctylphthalate/PVC=0.31
-○-, -●-: Shown in Fig. 1

Results and Discussion

The recovering ratio of the polymer after the THF extraction $[(B+C)/A]$ was larger than 0.98, and the chlorine balance $[(B\cdot b+C\cdot c)/A\cdot a]$ was 1.0 ± 0.2.

The Base Membrane-C. Figures 1—3 show the results of the THF extraction. With the increase in the monomer content [(St+DVB)/PVC] and in the DVB content [DVB/(St+DVB)] of the paste, and with the elevation of the polymerization temperature, the quantity of the extraction residue

increased linearly. The chlorine content of the extracted portion also increased linearly with the increase in the monomer content, but the DVB content in the paste and the polymerization temperature had no effect on the chlorine content in the extracted portion (Figs. 4—6). In all cases, the content of the extracted portion in the base membrane-C (C/A) was smaller than the PVC content of the base membrane-C and the chlorine content of the extracted portion was smaller than that of PVC itself (56.4%). These facts can be explained by the presence of the M-resin in the extracted portion. On the other hand, the chlorine content of the extraction residue was small (1.5—3%), but it showed the presence of PVC inextractable with THF.

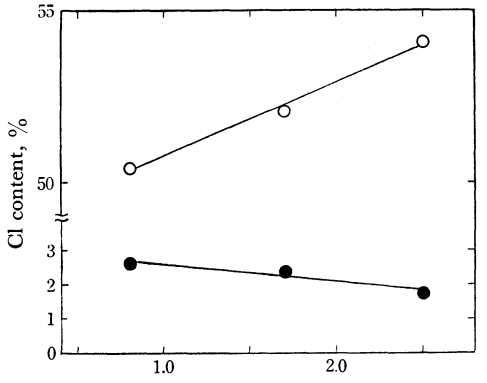

Fig. 4. The relation between the monomer content in the paste and the chlorine content of the extracted portion and the extraction residue.
The experimental condition is the same as shown in Fig. 1.
○ : Extracted portion ● : Extraction residue

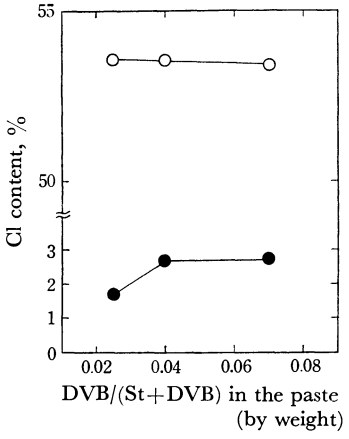

Fig. 5. The relation between the DVB content in the paste and the chlorine content of the extracted portion and the extraction residue.
The experimental condition is the same as shown in Fig. 2.
○: Extracted portion ●: Extraction residue

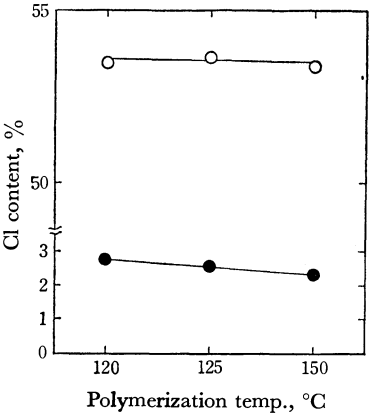

Fig. 6. The relation between the polymerization temperature and the chlorine content of the extracted portion and the extraction residue.
The experimental condition is the same as shown in Fig. 3.
○: Extracted portion ●: Extraction residue

It is very significant that a large quantity of the M-resin was found in the extracted portion. Since the M-resin should have a crosslinked structure, the presence of the M-resin in the extracted portion can be understood if the M-resin is very fine. This explanation is supported by Photo 1, which shows

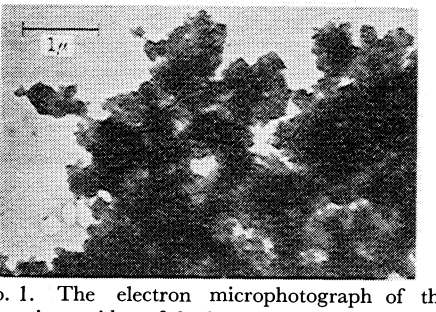

Photo. 1. The electron microphotograph of the extraction residue of the base membrane-C.

that the extraction residue was the aggregate of the fine particle and that its size was less than 50 mμ. When a monomer and DVB polymerize in a medium in which the monomer is soluble, while its polymer is insoluble, a fine powdery polymer with crosslinkage is obtained.[12,13] The formation of the spherical particle of the M-resin is explainable by considering PVC as a polymerization medium in which St and DVB are soluble, while polystyrene is insoluble. The network of the M-resin, formed by the polymerization of St and DVB, may be entwined with the PVC chain, and, furthermore, the M-resin may be grafted onto

12) Y. Mizutani, This Bulletin, **39**, 1088 (1966).
13) Y. Mizutani, *ibid.*, **40**, 1519 (1967).

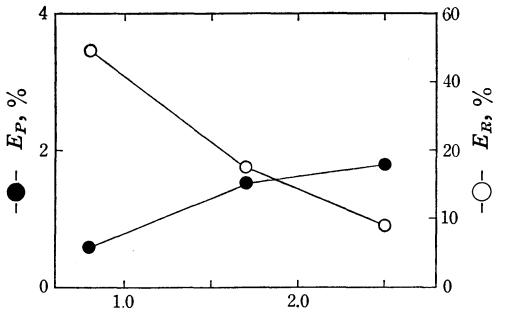

Fig. 7. The relation between the monomer content in the paste and the values of E_P and E_R.
The experimental condition is the same as shown in Fig. 1.

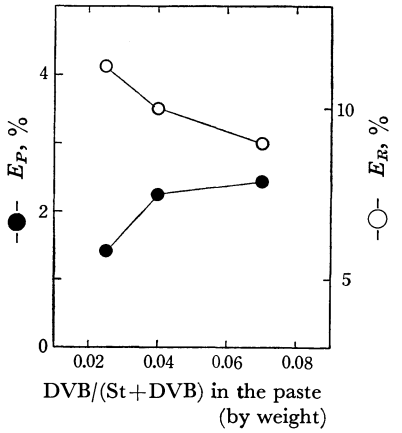

Fig. 8. The relatoin between the DVB content in the paste and the values of E_P and E_R.
The experimental condition is the same as shown in Fig. 2.

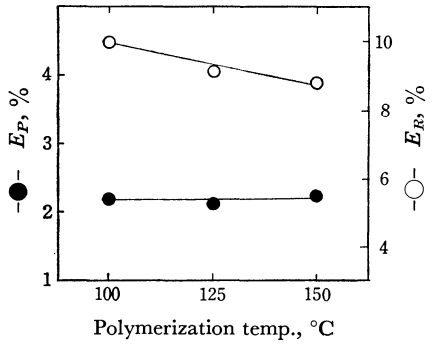

Fig. 9. The relation between the polymerization temperature and the values of E_P and E_R.
The experimental condition is the same as shown in Fig. 3.

PVC. The formation of the graft copolymer is confirmed by the graft copolymer prepared by the polymerization of St in the PVC film.[3] Thus, the presence of the M-resin in the extracted portion is explainable, but the degree of participation of the graft copolymer is still obscure, since the crosslinked M-resin was extracted through the filter paper.

Figures 7—9 show the E_R and E_P values. The E_P values show that the quantity of PVC in the extraction residue was 0.5—2% of the total PVC in the base membrane-C. With the increase in the monomer content of the paste, the E_P value increased and the E_R value decreased from 50% to 10%. These facts can be explained by the tendency for the increase in the monomer content to promote the swelling of the M-resin in the polymerization system, the entanglement of the network of the M-resin with the PVC chain, and the aggregation of the fine powdery resin. This explanation is supported by the observation that the extraction residue, although the E_R value was small, became fibrous or textural more distinct with the increase in the monomer content in the paste. With the increase in the DVB content in the paste, the E_P value increased and the E_R value decreased. These changes can be explained by the increase in the entanglement of the M-resin with the PVC chain. With the elevation of the polymerization temperature, the E_R value decreased, but this factor had no effect on the E_P value.

Table 1. The result of the THF extraction of the cation-exchange membrane

Sample	Base Membrane-C	Cation-exchange membrane	
		H^+ form	Na^+ form
B/A	0.152	0.423	0.525
E_t/E_0	—	0.731	0.878

E_t: Number of the ion-exchange site in the extraction residue.
E_0: Number of the ion-exchange site in the ion-exchange membrane.

The Cation-exchange Membrane. Table 1 shows the results of the THF extraction. By sulfonation with concentrated sulfuric acid, the ratio of the extraction residue (B/A) became larger than that of the base membrane-C. This may be explained by the reaction between PVC and the M-resin during the sulfonation and/or by the fact that the swelling of the cation-exchange membrane in THF is smaller than that of the base membrane-C. Furthermore, it was an important finding that the extracted portion had an ion-exchange capacity. This finding shows that the M-resin with the ion-exchange group was extracted; these observations are consistent with the finding concerning the base membrane-C. The presence of the fine powdery M-resin should be a reason why the cation-exchange membrane and its base

TABLE 2. THE RESULT OF THE THF EXTRACTION OF THE BASE MEMBRANE-A

	B/A	C/A	N content %	Cl content %	PVC content %	E_P %	E_R* %
Base membrane-A	—	—	2.74	39.34	69.75	—	—
Extraction residue	0.619	—	4.39	28.71	50.90	45.1	—
Extracted portion	—	0.380	0.2>	55.18	97.80	—	2.7

* Calculated from chlorine content.

TABLE 3. THE RESULT OF THE THF EXTRACTION OF THE ANION-EXCHANGE MEMBRANE (Cl^- form)

Sample	B/A	C/A	Cl content %	N content %	E_P %	E_R* %
Anion-exchange membrane	—	—	40.97	2.32	—	—
Extraction residue	0.731	—	36.68	3.04	65.6	—
Extracted portion	—	0.371	54.85	0.24	—	2.8

* Calculated from nitrogen content.

membrane have flexibility and thermoplasticity.

The Base Membrane-A. Table 2 shows the results of the THF extraction. The presence of the M-resin in the extracted portion was confirmed by the presence of nitrogen. Furthermore, the chlorine content of the extracted portion was clearly smaller (55.18%) than that of PVC itself (56.4%), and the E_R value showed that a little of the M-resin was extracted. On the other hand, much PVC was found in the extraction residue, as was shown by both the chlorine content and the E_P value, and the residue was fibrous or textural. The finding concerning the base membrane-A was considerably different from that of the base membrane-C; this difference is probably to be attributed to the difference between the affinity of St for PVC and that of MVP for PVC.

The Anion-exchange Membrane (Chloride-ion Form). Table 3 shows the results of the THF extraction. The membrane does not swell as much as the base membrane-A in Table 2. Also, the shape of the anion-exchange membrane was not destroyed by the THF extraction. The M-resin was partially extractable. This important finding can be explained by the fact, presented above, that there were fine particles of the M-resin extractable through a filter paper.

Conclusion

In order to elucidate the chemical structure of the ion-exchange membrane prepared by the "Paste Method," the ion-exchange membrane and its base membrane were extracted with tetrahydrofuran. Although the matrix of the ion-exchange resin component was complicatedly entwined with the polyvinyl chloride chain, and although the former should be grafted on the latter, the presence of fine particles of the ion-exchange resin component, extractable through a filter paper with tetrahydrofuran, was confirmed. This fact shows conclusively a characteristic of this ion-exchange membrane; it also suggests that the chemical structure of the ion-exchange membrane is different from that of Amberlite IR-120, *i.e.*, the homogeneously crosslinked gel-structure. Furthermore, this characteristic may be a reason why the ion-exchange membrane is flexible and thermoplastic.

BULLETIN OF THE CHEMICAL SOCIETY OF JAPAN VOL. 42 2464—2470 (1969)

Determination of S*–T Transition Probabilities of Some Xanthene and Thiazine Dyes on the Basis of T-Energy Transfer. II. Results in the Aqueous Solution

Masae NEMOTO, Hiroshi KOKUBUN and Masao KOIZUMI

Department of Chemistry, Faculty of Science, Tohoku University, Katahira-cho, Sendai

(Received February 3, 1969)

Intersystem crossing probability φ_{ST}^{A} for fluorescein, eosin, erythrosin, methylene blue and thionine in the aqueous solution of pH 7.2 (only for fluorescein 0.05N NaOH solution) has been determined by comparing the quantum yield of the nonsensitized (Φ) and the sensitized photoreduction (Φ^{S}) on the basis of the relations

$$\Phi = \varphi_{ST}^{A}\beta^{A} \qquad \Phi^{S} = \varphi_{ST}^{D}\beta\gamma^{A},$$

where β^{A} is the fraction of triplet dye molecules that undergo reduction, φ_{ST}^{A} and φ_{ST}^{D} are respectively for acceptor (dye) and donor (sensitizer), and γ is the energy transfer efficiency. This was assumed as unity. ATU and EDTA were used as a reducing agent. 1,5-Naphthalenedisulfonic acid and 1-anthracenesulfonic acid were used as sensitizers. The above relations and assumption have been found to hold satisfactorily. The φ_{ST}^{D} values for two sensitizers were determined using erythrosin as a reference substances for which φ_{ST}^{A} was assumed to be unity. φ_{ST}^{D} obtained was 0.88 for 1,5-naphthalenedisulfonic acid, and 0.82 for 1-anthracenesulfonic acid. φ_{ST}^{A} values for dyes obtained were: fluorescein (0.021) eosin (0.64) erythrosin (1.0) methylene blue (0.52) thionine (0.55). Using these φ_{ST}^{A} values, the rate constants for the following elementary reactions have been evaluated (A, dye: RH_2, reducing agent): $A^{T}+RH_2 \rightarrow$reaction, $A^{T}+RH_2 \rightarrow$deactivation, $A^{T}+A \rightarrow$reaction or deactivation.

In a previous paper[1] the application of the T-energy transfer was successfully applied to the determination of the S*-T transition probabilities of some xanthene and thiazine dyes in ethanol solutions. The method consists of comparison of the quantum yield for the direct photoreduction of dyes (Φ), with that of the sensitized reduction in otherwise similar conditions (Φ^{S}), using suitable aromatic hydrocarbons as sensitizers (donors). In an ideal case, Φ and Φ^{S} are written as

$$\Phi = -\mathrm{d[A]}/\mathrm{d}t/I_{ab} = \varphi_{ST}^{A}\beta^{A} \quad (1)$$

$$\Phi^{S} = -\mathrm{d[A]}/\mathrm{d}t/I_{ab} = \varphi_{ST}^{D}\gamma\beta^{A}, \quad (2)$$

where φ_{ST}^{A} and φ_{ST}^{D} are respectively the transition probabilities of S*–T transition for acceptor (dye) and donor, and β^{A} the fraction of the triplet dye which undergoes the reaction. γ is the efficiency of T-energy transfer between donor and acceptor and is regarded to be unity when the T-energy level of donor is much higher than that of acceptor. By combining (1) and (2) one can easily evaluate φ_{ST}^{A}, since the value of φ_{ST}^{D} is known for many aromatic hydrocarbons.

The purpose of the present paper is to extend the above method to the aqueous solutions. Hitherto there have been reported very few φ_{ST} values for dyes or for the substances dissolved in water. As far as we know, the only reliable data ever published for dyes are Bowers and Porter's.[2] However, their method which relies upon flash technique, appears to require some skill and caution in experiments.

Our method is very simple in principle and requires no particular technique but at present there is no report concerning the suitable sensitizers with the known φ_{ST}^{D} values. Once a set of such sensitizers are found, the method will have a wider scope of application.

As sensitizers, we have employed 1-anthracenesulfonic acid and 1,5-naphthalenedisulfonic acid. To determine the φ_{ST}^{D} value of the latter, erythrosin has been chosen as a reference substance, because its φ_{ST} value in the aqueous solution is, according to Bowers and Porter,[2] 1.0 and the same value has also been found by our experiment in ethanol.[1] In practice, the φ_{ST} value of 1,5-naphthalenedisulfonic acid has been determined by comparing Φ^{S} and Φ for the photoreduction of erythrosin using allylthiourea (ATU) or EDTA as a reducing agent. Then with the use of this φ_{ST}^{D} value, the φ_{ST}^{A} values

1) M. Nemoto, H. Kokubun and M. Koizumi, This Bulletin, **42**, 1223 (1969).

2) P. G. Bowers and G. Porter, *Proc. Roy. Soc.*, **A299**, 348 (1967).

Table 1. Quantum yield of photoreduction

Reducing agent, EDTA

EDTA	Fluorescein	Eosin	Erythrosin	Methylene blue	Thionine
2.0×10^{-2}M	——	——	4.52×10^{-2}	8.4×10^{-2}	3.7×10^{-1}
1.5×10^{-2}	——	——	4.26×10^{-2}	6.6×10^{-2}	3.5×10^{-1}
1.0×10^{-2}	1.1×10^{-3}	5.25×10^{-2}	3.76×10^{-3}	4.6×10^{-2}	2.95×10^{-1}
5.0×10^{-3}	0.64×10^{-3}	2.42×10^{-2}	1.9×10^{-2}	2.6×10^{-2}	1.9×10^{-1}
2.5×10^{-3}	0.30×10^{-3}	——	1.05×10^{-2}	——	——
1.0×10^{-3}	——	0.53×10^{-2}	——	0.54×10^{-2}	0.6×10^{-1}

Reducing agent, ATU

ATU	Fluorescein	Eosin	Erythrosin	Methylene blue	Thionine
2.0×10^{-2}M	——	——	2.1×10^{-2}	2.9×10^{-3}	1.14×10^{-2}
1.5×10^{-2}	——	——	1.7×10^{-2}	2.1×10^{-3}	1.1×10^{-2}
1.0×10^{-2}	4.7×10^{-4}	1.4×10^{-2}	1.4×10^{-2}	1.4×10^{-3}	0.93×10^{-2}
5.0×10^{-3}	2.9×10^{-4}	0.89×10^{-2}	1.02×10^{-2}	——	——
3.0×10^{-3}	1.8×10^{-4}	——	——	——	——
2.5×10^{-3}	——	0.45×10^{-2}	0.56×10^{-2}	——	——

of other dyes have been determined. Erythrosin can not be used as a reference substance for 1-anthracenesulfonic acid, because its T-state has almost the same energy as that of the dye. Hence its φ_{ST} value has been determined in reference to methylene blue. The results have been found to be quite consistent and satisfactory.

Experimental

Materials. All the dyes and ATU are the same as in the previous paper.[1] EDTA (Dotile 2NA) of G. R. grade was used without further purification. 1-Anthracenesulfonic acid sodium salt of G. R. grade of Wakojunyaku was passed through a column of activated alumina. 1,5-Naphthalenedisulfonic acid sodium salt of G. R. grade of Wakojunyaku was subjected to recrystallization from 3N HCl solution twice.

Apparatus and Procedures. The apparatus and the method of measurement are the same as in the previous paper.[1] The measurement was usually made at pH 7.2 by employing a phosphate buffer except fluorescein for which 0.05N NaOH solution was used. The concentrations of substances are as follows unless otherwise described: xanthene dyes, 1.0×10^{-5}M; thiazine dyes, 1.5×10^{-5}M; 1,5-naphthalenedisulfonic acid, 2.25×10^{-4}M; 1-anthracenesulfonic acid, 1.0×10^{-4}M; EDTA, 2.0×10^{-2}—1.0×10^{-3}M; ATU, 2.0×10^{-2}—2.5×10^{-3}M. Temperature was 30 ± 0.5°C. The fluorescence measurement was made by a Hitachi MPF-2A spectrofluorimeter whose spectral response was calibrated using standard substances.[3]

Results

Quantum Yields for the Direct Photoreduction of Dyes. Quantum yields for the photoreduction of fluorescein, eosin, erythrosin, methylene blue and thionine by EDTA and ATU in several concentrations are summarized in Table 1. The data for fluorescein,[4] eosin,[5] erythrosin[6] and methylene

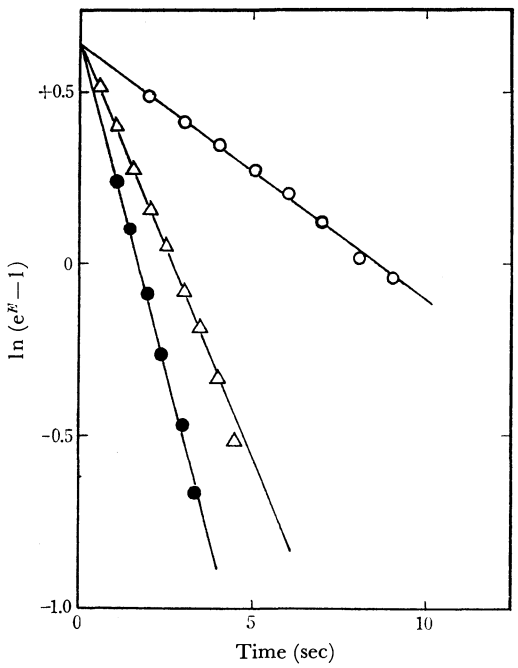

Fig. 1. Plots of ln (e^E-1) *vs.* t for thionine.
[thionine] $=1.5\times10^{-5}$ M
concentration of EDTA
○, 1.0×10^{-3}M △, 5.0×10^{-3}M
●, 1.0×10^{-2}M

3) E. Lippert, W. Nägele, I. Seibold-Blankenstein, U. Staiger and W. Voss, *Z. Anal. Chem.*, **170**, 1 (1959).

4) Y. Momose, K. Uchida and M. Koizumi, This Bulletin, **38**, 1601 (1965).

5) T. Ohno, Y. Usui and M. Koizumi, *ibid.*, **38**, 1022 (1965).

6) A. H. Adelman and G. Oster, *J. Am. Chem. Soc.*, **78**, 3977 (1956).

Table 2. Some reference data for the donors

	Solvent	Absorption cm^{-1}	Phosphorescence cm^{-1}	Decay[d] const. of T sec^{-1}	Quantum yield of fluorescence
Anthracene	EtOH	26700	14700[a]	7.0×10^{2}	0.3[e]
1-Anthracenesulfonic acid	H_2O (pH 7.2)	25900	—	1.0×10^{3}	0.18
Naphthalene	EtOH	31400	21250[b]	$\gtrsim10^{4}$	0.19[f]
1,5-Naphthalenedisulfonic acid	H_2O (pH 7.2)	29400	20800[c]	1.0×10^{3}	0.12

a) D. P. Craig and I. G. Ross, *J. Chem. Soc.*, **1954**, 1589.
b) in EPA at 77°K
c) in ethanol-water mixture
d) from the decay of T–T absorption at room temp.
e) T. Medinger and F. W. Wilkinson, *Trans. Faraday Soc.*, **61**, 620 (1965).
f) C. A. Parker *et al.*, *Proc. Chem. Soc.*, **1962**, 142.

blue[7] agree with the published ones within experimental error. There is no value in literature to compare with for thionine. Figure 1 gives the $\ln(e^{E}-1)$ *vs.* t plot (E, optical density), the linearity of which supports the occurrence of D-R mechanism.

Examination on the Applicability of the Method. For the present method to be applicable, there should be no interaction between donor and other components including transient intermediates, except for the energy transfer between donor and acceptor. Thus in the first place, reducing agents must in no sense react with donors. Secondly, donors must react neither with the triplet state of dye nor with any other transient intermediates such as semiquinones of dyes. In addition, high efficiency of the energy transfer is very much desired. In these respects, nothing is known on the system consisting of the present donors and dyes.

Table 2 gives some reference data on the present donors as compared with the mother hydrocarbons.

The fluorescence quantum yields of the two sulfonic acids have been determined by comparing the fluorescence intensities of the aqueous solutions of these two substances with those of the ethanol solutions of naphthalene and anthracene.

The conditions mentioned above have been examined for all the systems. Firstly, it was ascertained that the triplet decays of the donors are not affected by $\sim1.0\times10^{-2}$M of ATU or EDTA of the same concentration. However, it was found by flash experiment that the decays of the triplet state for some dyes are affected by the existence of donor to some extent. In line with this finding, the quantum yield for the direct photoreduction of erythrosin, methylene blue and thionine was found to decrease with the addition of a larger quantity of donor. Figure 2 gives the result for erythrosin. The type of this deactivation seemed to be a mere deactivation, because no decrease in donor concentration was observed after reaction. It was ascertained, however, that in the system of 1,5-naphthalenedisulfonic acid and erythrosin, for example, the concentration of donors two or three times larger than that of the standard concentration, does

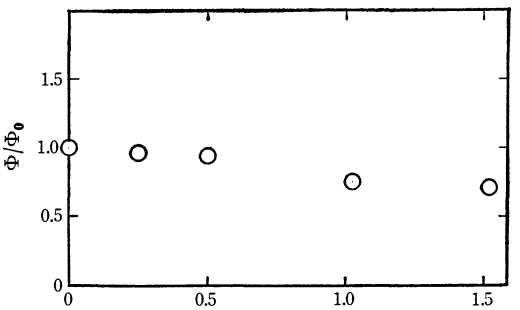

Fig. 2. Effect of the sensitizer's concentration on quantum yield of direct photoreduction.
[erythrosin] $=1.0\times10^{-5}$M
[EDTA] $=1.0\times10^{-2}$M

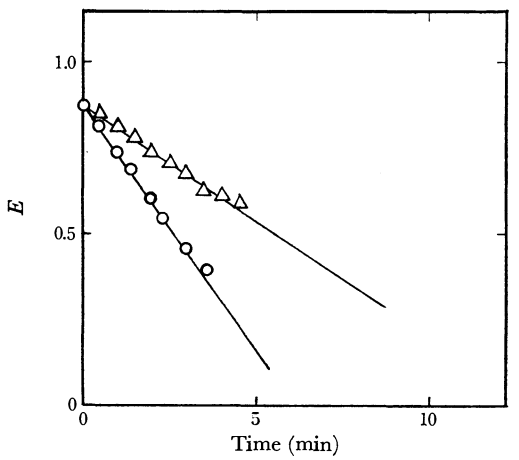

Fig. 3. An example of the plots of E *vs.* t for the sensitized reaction.
[eosin] $=11.0\times10^{-5}$M
[1,5-naphthalenedisulfonic acid] $=2.25\times10^{-4}$M
concentration of EDTA : △, 5.0×10^{-3}M
○, 1.0×10^{-2}M

7) N. Kosui, K. Uchida and M. Koizumi, This Bulletin, **38**, 1958 (1965).

not affect the Φ^S value, if the concentration of reductant is larger than 1.0×10^{-2}M.

Lastly, mention should be made on the behavior of energy transfer. Figure 3 gives the plots of optical density against time for eosin as an example, under different conditions.

The linearity of the plot for [dye] $>1.0\times10^{-5}$M ensures that I_{ab}, φ_{ST}^{D} γ and β^A remain constant during the run. In view of the triplet lifetime given in Table 2, the constancy of γ is expected to be secured, if the energy transfer occurs as a diffusion controlled process. Figure 4 gives the decay of the donor triplet in the absence and in the presence of erythrosin; from these data the rate constant for deactivation by erythrosin is estimated to be of the order of 10^9M^{-1} sec^{-1}. Although the exact value of the energy transfer efficiency is yet unknown, the assumption will be made in the following that γ is unity in view of a large difference in triplet energy level between donor and dye.

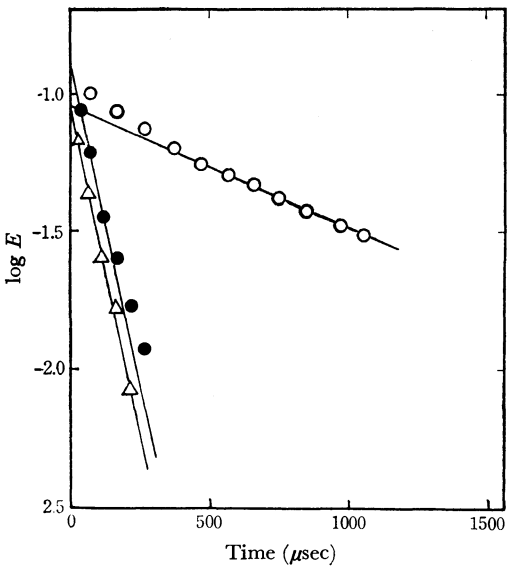

Fig. 4. Effect of the addition of the acceptor on the donor's triplet decay.
[1,5-naphthalenesulfonic acid]$=2.25\times10^{-4}$M
●, [erythrosin]$=1.0\times10^{-5}$M at 440 nm
△, at 580 nm
○, [erythrosin]$=0$ at 440 nm

Determination of φ_{ST}^{D} of the Two Donors. Firstly, φ_{ST}^{D} of 1,5-naphthalenedisulfonic acid has been determined by comparing the Φ^S values of the photoreduction of erythrosin sensitized by this donor, with those of the direct photoreduction of erythrosin listed in Table 1.

Table 3 gives the values of Φ^S of erythrosin and those of φ_{ST} of 1,5-naphthalenedisulfonic acid obtained on the assumption that φ_{ST} of erythrosin is unity.

Table 3. φ_{ST} of 1,5-naphthalenedisulfonic acid and Φ^S

Reductant	[Reductant]	Φ^S	φ_{ST}
EDTA	2.0×10^{-2}M	4.0×10^{-2}	0.89
	1.5×10^{-2}	3.8×10^{-2}	0.89
	1.0×10^{-2}	3.5×10^{-2}	0.93
	5.0×10^{-3}	1.55×10^{-2}	0.82
ATU	2.0×10^{-2}	1.9×10^{-2}	0.83
	1.5×10^{-2}	1.4×10^{-2}	0.90
	1.0×10^{-2}	1.25×10^{-2}	0.92
		Average	0.88 ± 0.05

Next, φ_{ST} of methylene blue was determined using 1,5-naphthalenedisulfonic acid as a donor. Then from the combination of methylene blue and 1-anthracene sulfonic acid, φ_{ST} of the latter was obtained by use of φ_{ST} of methylene blue, 0.52 ± 0.01. The result was that φ_{ST} of 1-anthracene-

Table 4. Quantum yield of sensitized photoreduction of xanthene dyes

donor; 1,5-naphthalenedisulfonic acid

Reductant	[EDTA]	Fluorescein	Eosin	Erythrosin
EDTA	2.0×10^{-2}M	—	—	4.0×10^{-2}
	1.5×10^{-2}	—	—	3.8×10^{-2}
	1.0×10^{-2}	4.04×10^{-2}	7.6×10^{-2}	3.5×10^{-2}
	5.0×10^{-3}	2.25×10^{-2}	3.4×10^{-2}	1.6×10^{-2}
	2.5×10^{-3}	1.3×10^{-2}	—	—
	1.0×10^{-3}	—	0.66×10^{-2}	—
	[ATU]			
ATU	2.0×10^{-2}	—	—	1.95×10^{-2}
	1.5×10^{-2}	—	—	1.43×10^{-2}
	1.0×10^{-2}	2.3×10^{-2}	2.1×10^{-2}	1.25×10^{-2}
	5.0×10^{-3}	1.17×10^{-2}	1.28×10^{-2}	—
	3.0×10^{-3}	0.75×10^{-2}	—	—
	2.5×10^{-3}	—	0.66×10^{-2}	—

Table 5. Quantum yield of sensitized photoreduction of thiazine dyes

Donor / Reductant	[Reductant]	I Methylene blue	I Thionine	II Methylene blue
EDTA	2.0×10^{-2}M	1.4×10^{-1}	5.7×10^{-1}	1.24×10^{-1}
	1.5×10^{-2}	1.14×10^{-1}	5.4×10^{-1}	1.1×10^{-1}
	1.0×10^{-2}	0.79×10^{-1}	5.0×10^{-1}	0.88×10^{-1}
ATU	2.0×10^{-2}	4.87×10^{-3}	1.79×10^{-2}	4.46×10^{-3}
	1.5×10^{-2}	3.45×10^{-3}	1.70×10^{-2}	3.38×10^{-3}
	1.0×10^{-2}	2.36×10^{-3}	1.49×10^{-2}	2.12×10^{-3}

I, 1,5-naphthalenedisulfonic acid
II, 1-anthracensulfonic acid

sulfonic acid is 0.82 ± 0.02 (As to the experimental data, see below).

The sums of Φ_F and φ_{ST} for 1,5-naphthalenedisulfonic acid and 1-anthracenesulfonic acid are respectively $0.88+0.12=1.0$ and $0.82+0.18=1.0$. Thus the internal conversion is negligible in these two donors.

Quantum Yields of the Sensitized Photoreduction Φ^S and the φ_{ST} Values of Dyes. Tables 4 and 5 give respectively the quantum yields of the sensitized photoreduction of xanthene and thiazine dyes. The experimental condition was always so selected that the reaction took place in an ideal way. The 1-anthracenesulfonic acid-thionine system was omitted, since the concentration of thionine in the aerated solution gradually decreased even in dark.

In Table 6 are summarized the φ_{ST} values of fluorescein, eosin, methylene blue and thionine obtained by applying Eqs. (1) and (2) to a set of two corresponding experimental data given in Tables 1, 4 and 5. The φ_{ST} values of methylene blue listed in the column of 1-anthracenesulfonic acid are the ones recalculated by putting φ_{ST} for 1-anthracenesulfonic acid as 0.82. Table 6 clearly shows that the φ_{ST} value of each dye is essentially the same independent of reducing agent and donor.

Discussion

Table 7 gives the comparison of the φ_{ST} values of the present work (pH 7.2) with the published data.

The values for xanthene dyes in the aqueous solution are somewhat larger than those in ethanol. The values for thiazine dyes on the other hand are about the same in both solvents. The present value for eosin is very close to Bowers and Porter's in spite of the entirely different method. Gollnick and Schenck's values are somewhat smaller than the present ones (except fluorescein). Their values were based on the assumption that the reaction $A^T+{}^3O_2\rightarrow A+{}^1O_2$ occurs in the presence of ample oxygen, with efficiency 1. It is unlikely that this assumption is correct.

According to our previous investigations, the

Table 6. φ_{ST} Values of dyes

Donor / Reductant	[Reductant]	I Fluorescein	I Eosin	I Methylene blue	I Thionine	II Methylene blue
EDTA	2.0×10^{-2}M	—	—	0.52	0.55	0.55
	1.5×10^{-2}	—	—	0.51	0.57	0.50
	1.0×10^{-2}	0.022	0.64	0.51	0.52	—
	5.0×10^{-3}	0.025	0.63	—	—	—
	2.5×10^{-3}	0.021	—	—	—	—
	1.0×10^{-3}	—	0.70	—	—	—
	Average	0.022 ± 0.003	0.66 ± 0.03	0.51 ± 0.01	0.54 ± 0.03	0.52 ± 0.03
ATU	2.0×10^{-2}	—	—	0.52	0.56	0.53
	1.5×10^{-2}	—	—	0.51	0.57	0.51
	1.0×10^{-2}	0.018	0.60	0.53	0.55	0.55
	5.0×10^{-3}	0.021	0.61	—	—	—
	3.0×10^{-3}	0.022	—	—	—	—
	2.5×10^{-3}	—	0.61	—	—	—
	Average	0.020 ± 0.002	0.61 ± 0.01	0.53 ± 0.01	0.56 ± 0.02	0.53 ± 0.02

I, 1,5-naphthalenedisulfonic acid
II, 1-anthracenesulfonic acid

Table 7. Comparison of φ_{ST} values

	Present work (pH 7.2)	Bowers and Porter[2] (pH 9.0)	in C_2H_5OH[1]	Gollnick and Schenck[8] in alcohols
Fluorescein	0.021±0.02[a]	0.05	0.0045±0.005[b]	0.03
Eosin	0.64 ±0.02	0.71	0.42 ±0.04	0.25~0.3
Erythrosin	(1.0)	1.07	1.05 ±0.03	0.62~0.6
Methylene blue	0.52 ±0.01		0.52 ±0.03	
Thionine	0.55 ±0.02		0.62 ±0.4	

a) 0.05N NaOH
b) 30 vol.% aq. alkaline ethanolic solution

Table 8. Comparison of the $(k_9+k_{10})/(k_7+k_8[A])$ values (R) and β_{max}

Acceptor / Donor	Fluorescein		Eosin		Erythrosin		Methylene blue		Thionine	
	R	β_{max}	R	β_{max}	R	β_{max}	R	β_{max}	R	β_{max}
EDTA										
None	50	0.1	54	0.13	73	0.08	84	0.4	100	0.89
1,5-Naphthalenedisulfonic acid	30	0.11	47	0.19	86	0.08	115	0.3	160	0.91
1-Anthracenesulfonic acid	—	—	—	—	—	—	100	0.3	—	—
ATU										
None	60	0.09	55	0.067	60	0.035	100	0.032	50	0.04
1,5-Naphthalenedisulfonic acid	57	0.077	40	0.07	60	0.029	110	0.024	50	0.03
1-Anthracenesulfonic acid	—	—	—	—	—	—	100	0.024	—	—

scheme for the present reaction can be described as follows,

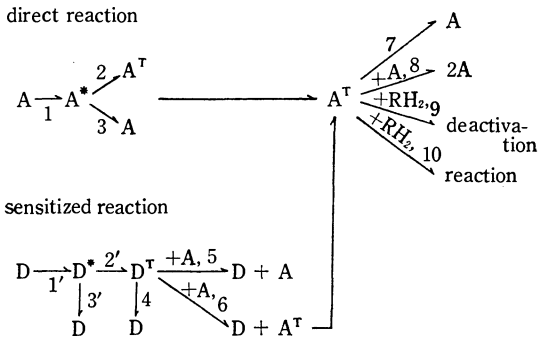

Then γ and β in Eqs. (1) and (2) are expressed as follows,

$$\gamma = \frac{k_6[A]}{k_4+(k_5+k_6)[A]} \tag{3}$$

$$\beta_A = \frac{k_{10}[RH_2]}{k_7+k_8[A]+k_9[RH_2]+k_{10}[RH_2]} \tag{4}$$

Insertion of (3) and (4) into Eqs. (1) and (2) allows us to expect that both the $1/\Phi$ *vs.* $1/[RH_2]$ plot and the $1/\Phi^S$ *vs.* $1/[RH_2]$ plot should give the same value for (intercept)/(slope), *i.e.* $(k_9+k_{10})/(k_7+k_8[A])$, if the donor does not interfere with the reaction scheme after the formation of A^T. Table 8 clearly shows that this really holds in all cases.

Furthermore the intercepts of the $1/\Phi$ *vs.* $1/[RH_2]$ plot and $1/\Phi^S$ *vs.* $1/[RH_2]$ plot give respectively $\varphi_{ST}^A\ \beta_{max}$ and $\varphi_{ST}^D\ \gamma\beta_{max}$, and if the relation $\gamma=1$ really holds, the same β_{max}, *i. e.* $k_{10}/(k_9+k_{10})$ should result irrespective of sensitized and nonsensitized reaction and also independent of the kind of sensitizer. In Table 8 are listed also the values of β_{max} evaluated from the intercepts by putting $\gamma=1$. It is evident that β_{max} for each dye-reductant system agree within experimental error. As in the ethanol solution mere deactivation is much larger for ATU than for EDTA. It is remarkable that mere deactivation scarcely occurs in the case of thionine-EDTA.

In the case of eosin and fluorescein, the (k_9+k_{10}) and k_7 values are known from the flash experiments and so the k_9, k_{10} and k_8 values are obtained. The results are given in Table 9.

Lastly, the tentative data reported in the previous papers will be corrected using the reliable φ_{ST} values obtained in the present paper. Since the equation

$$\frac{1}{\Phi} = \frac{1}{\varphi_{ST}^A}\left\{\frac{k_9+k_{10}}{k_9} + \frac{k_7}{k_{10}[RH_2]} + \frac{k_8[A]}{k_{10}[RH_2]}\right\}$$

holds, and $(k_9+k_{10})/k_9$ can be evaluated from the

8) K. Gollnick and G. O. Schenck, *Pure Appl. Chem.*, **9**, 507 (1964); K. Gollnick, *Advances in Photochem.*, Vol. 6, ed. by W. A. Noyes, Jr., G. S. Hammond and J. N. Pitts, John Wiley & Sons, New York (1968).

TABLE 9

	k_7 (sec^{-1})		k_8 ($sec^{-1}\cdot M^{-1}$)	k_9+k_{10} ($sec^{-1}\cdot M^{-1}$)	k_9 ($sec^{-1}\cdot M^{-1}$)	k_{10} ($sec^{-1}\cdot M^{-1}$)
Eosine	5.4×10^{2} a)	EDTA	$7.3—10\times10^{8}$	5.0×10^{5} b)	4.2×10^{5}	8.3×10^{4}
		ATU	$5.6—7.9\times10^{8}$	3.4×10^{5} b)	3.1×10^{5}	2.4×10^{4}
Fluorescein	5.10×10 c)	ATU	$2.8—4.5\times10^{8}$	2.0×10^{5} c)	1.8×10^{5}	1.8×10^{4}

a) V. Kasche and L. Lindqvist, *Photochem. Photobiol.*, **4**, 923 (1965).
b) T. Ohno, S. Kato and M. Koizumi, This Bulletin, **39**, 232 (1966).
c) L. Lindqvist, *Arkiv för Kemi*, **16**, 79 (1960).

TABLE 10. CORRECTED VALUES FROM THE PREVIOUS DATA

Reduction	[A]	$\frac{k_7+k_8[A]}{k_{10}}$	$\frac{k_{10}}{k_9+k_{10}}$	k_{10} $sec^{-1}\cdot M^{-1}$	k_8 $sec^{-1}\cdot M^{-1}$
Eosin*					
ATU	1.16×10^{-5}M	5.75×10^{-1}	0.23	7.8×10^{4}	4.4×10^{9}
	8.0×10^{-6}	4.47×10^{-1}	0.08	2.7×10^{4}	1.2×10^{9}
	4.0×10^{-6}	1.41×10^{-1}	0.05	1.7×10^{4}	2.4×10^{8}
	2.4×10^{-6}	0.9×10^{-1}	0.05	1.7×10^{4}	1.0×10^{8}
EDTA	8.0×10^{-6}	9.1×10^{-2}	0.125	6.0×10^{4}	6.2×10^{8}
	5.5×10^{-6}	4.6×10^{-2}	0.125		2.1×10^{8}
Fluorescein[4]					
ATU	0.09N NaOH	3.48×10^{-2}	0.23	4.52×10^{4}	1.5×10^{8}
	0.1N NaOH	2.6×10^{-2}	0.23		
EDTA	0.05N NaOH	1.79×10^{-2}	0.39		
	0.1N NaOH	2.04×10^{-2}	0.64		
Methylene blue[7]					
EDTA	9.0×10^{-6}	8.3×10^{-3}	0.45	6.1×10^{6}	3.0×10^{9}
ATU	8.2×10^{-6}		0.024	1.3×10^{4}	2.7×10^{9}

* The values of intercept for the $1/\Phi$ *vs.* $1/[RH_2]$ plot in the previous paper[5] appears to depend on the dye concentration. But in view of the present result, this is most likely due to experimental error. Hence $\varphi_{ST}=0.64$ was used in all the data.

intercept of the $1/\Phi$ *vs.* $1/[RH_2]$ plot, k_8, k_9 and k_{10} can be evaluated from the experimental data for the dependence of Φ on $[RH_2]$ and on [A], only if k_7 is known from the flash experiment. The knowledge of the (k_9+k_{10}) value from the flash experiment will make the evaluation of these constants more simple and more reliable. The corrected values from the previous data for fluorescein, eosin and methylene blue are given in Table 10.

It is seen that in general the previous k_{10} values are much too large while the k_8-value is correct in the order of magnitude. Moderate agreement is apparent between the data in Tables 9 and 10.

One of the authors (H.K.) wishes to thank the Matsunaga Science Foundation for financial support.

BULLETIN OF THE CHEMICAL SOCIETY OF JAPAN VOL. 42 2471—2475 (1969)

Adsorption of Surface Active Substance at Aqueous Surface Using Tritium Labeled Compounds: Adsorption from Mixed Aqueous Solution of Sodium Dodecylsulfate and Dodecanol

Kazuo TAJIMA, Mitsuo MURAMATSU and Tsunetaka SASAKI

Department of Chemistry, Faculty of Science, Tokyo Metropolitan University, Setagaya-Ku, Tokyo

(Received February 10, 1969)

Adsorbed amount of sodium dodecylsulfate (SDS) and *n*-dodecanol (DOH) at the gas-solution interface of their mixed aqueous solution was directly measured as a function of bulk concentration of DOH by the radiotracer method. For this purpose the surface radioactivity of the mixed solution in which either SDS or DOH was labeled with tritium, was counted by using a 2π windowless gas-flow counter. It was found that the adsorbed amount of DOH rapidly increases with increasing bulk concentration of DOH, while that of SDS gradually decreases. The adsorption of DOH and desorption of SDS are not a simple 1 : 1 replacement. A maximum total adsorption of about 13×10^{-10} mol/cm^2, which exceeds the amount of close-packed monolayer adsorption extends over a wide range of concentration studied. It was suggested that the adsorbed film consists of mixed monolayer or double layers. The latter film is composed of mixed monolyaer of SDS and DOH with adsorbed layer of SDS beneath. The molar ratio of adsorbed amount of DOH to SDS in the surface became unity, when the ratio of the bulk concentration of DOH to SDS was about one hundredth, which shows a stronger adsorption tendency of DOH than that of SDS.

It was reported in a previous paper[1] that the soft β-rays of tritium are very useful for the measurements of the amount of adsorption of a detergent at the surface of an aqueous detergent solution. By using a tritiated SDS it has been confirmed that the amount of saturate adsorption of SDS at the aqueous surface is 5.9×10^{-10} mol/cm^2 at 20°C. In the present paper, the measurements have been extended for studying the competitive adsorption between SDS and DOH at the surface of their mixed solution. It has been reported that the addition of a small amount of alcohol causes marked changes in the surface-chemical properties of a detergent solution, such as foam stability,[2] mechanical strength of adsorbed film,[3,4] and surface tension lowering.[5] These phenomena have been explained by the preferential or mixed adsorption of alcohol for the adsorbed film of the detergent at the aqueous surface.[6] Few papers, however, deal with the direct measurement of adsorption of these components in the mixed film at gas-solution interface under the static condition.

The experiments were carried out to determine the composition of this mixed adsorbed film by the adsorption measurement of the aqueous SDS-DOH system in which either SDS or DOH was labeled with tritium.

Experimental

The tritiated samples were synthesized according to the method reported in the previous papers[1,7] which gave the product of sufficiently high purity both surface-chemically and radiochemically. The solutions were prepared by dissolving in thrice distilled water the solid mixture of the samples, which had been obtained by evaporating to dryness the ethanol solutions of TSDS (tritium-labeled SDS) and DOH or SDS and TDOH (tritium-labeled DOH) of a desired composition. The surface radioactivity was measured by a 2π windowless gas-flow counter (Aloka DC-1001) using a humidified propane gas to prevent the evaporation of solution. The detailed procedures of the adsorption measurement were described.[1] In the present study special precaution was made further for the measurement of TDOH at the surface, since it is slightly volatile even in solution,[8,9]

1) M. Muramatsu, K. Tajima and T. Sasaki, This Bulletin, **41**, 1279 (1968).

2) G. Miles, J. Ross and L. Shedlovsky, *J. Am. Oil Chemists Soc.*, **27**, 286 (1950).

3) A. G. Brown, W. C. Thuman and J. W. McBain, *J. Colloid Sci.*, **8**, 491 (1953).

4) K. J. Mysels, M. C. Cox and J. D. Skewis, *J. Phys. Chem.*, **65**, 1107 (1961).

5) G. Miles and L. Shedlovsky, *ibid.*, **48**, 57 (1944).

6) K. Shinoda and J. Nakanishi, *ibid.*, **67**, 2547 (1963).

7) M. Muramatsu and K. Tajima, *J. Labelled Compounds*, **2**, 304 (1966).

8) J. H. Brooks and A. E. Alexander, Proceedings of the 3rd International Congress of Surface Activity, Vol. II, p. 196 (1960).

9) G. Nilsson, *J. Phys. Chem.*, **61**, 1635 (1957).

as mentioned in the later section. The pH of the solution was in the range of 5.8—6.2, and the temperature was kept at 20±0.5°C.

Throughout the measurements, the concentration of the detergent was kept at 5.63×10^{-3} mol/1000 g solution. The value corresponds to the minimum concentration for saturate adsorption attained below the CMC (critical micelle concentration). The amounts of adsorption of SDS and DOH were measured for DOH-TSDS and TDOH-SDS systems respectively.

Results and Discussions

Mixed Solution of TSDS and DOH. The time dependence of surface radioactivity due to TSDS in the mixed solution was measured and the result is shown in Fig. 1. It is noted in this figure that

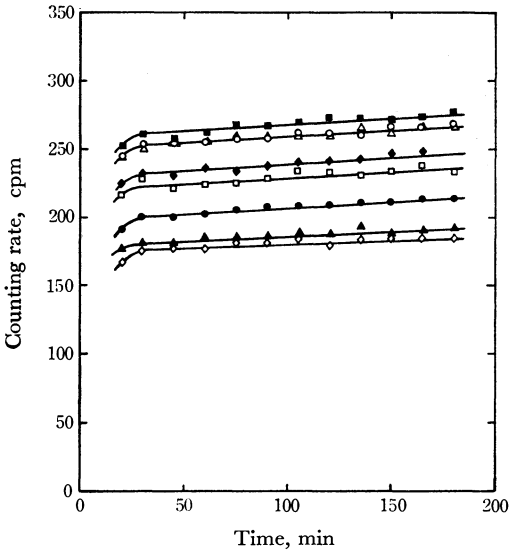

Fig. 1. Time dependence of surface radioactivity of TSDS due to adsorption of SDS from SDS-DOH mixed solution.
Concentration of SDS: 5.63×10^{-3} mol/1000 g solution.
Concentration of DOH (in mol/100 g solution):
■ 0 □ 3.61×10^{-4} △ 6.02×10^{-6}
● 6.02×10^{-4} ○ 6.02×10^{-5} ◇ 8.43×10^{-4}
◆ 2.41×10^{-4} ▲ 1.08×10^{-3}

the radioactivity first increases rapidly, then slowly and linearly with time after about 30—40 min. This seems to indicate both the rapid increase of adsorption towards the equilibrium and the rapid approach of counting efficiency to its steady state as mentioned previously.[1] Therefore, the radioactivity in adsorption equilibrium was evaluated by extrapolating the linear portion of the curve to time zero. The adsorbed amount of SDS in the mixed solution, Γ_{SDS}, was obtained by subtracting the radioactivity due to the bulk of the solution from the counting rate obtained above and multiplying the value obtained by the specific activity.[10] The value of Γ_{SDS} thus obtained is shown as a function of DOH concentration by the curve A of Fig. 2. The

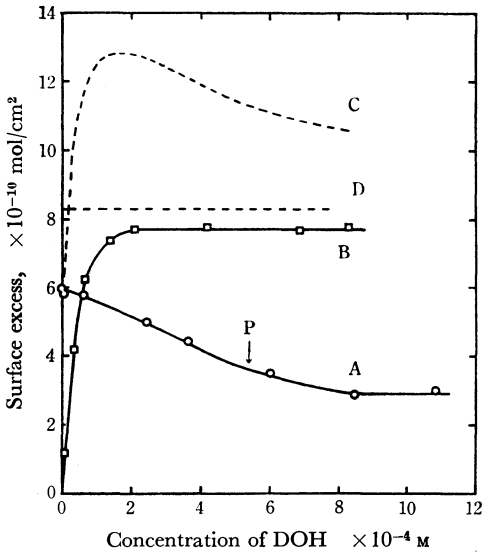

Fig. 2. Adsorbed amounts of SDS (curve A) and DOH (curve B) at aqueous surface for SDS-DOH mixed solution, as a function of DOH concentration at 20°C. Total adsorbed amount (curve C) and monolayer adsorption (curve D).

curve A shows the decrease in Γ_{SDS} with increasing concentration of DOH from the initial value of 5.9×10^{-10} mol/cm² (saturate adsorption from the solution containing SDS alone) to 2.9×10^{-10} mol/cm² and becomes constant beyond the DOH concentration of 8.4×10^{-4} mol/1000 g solution, where the opalesence evidently appeared in the solution. We can confirm from these facts that the amount of adsorption of SDS decreases with an increasing amount of the addition of DOH. The maximum effect appeared in the region beyond the saturation of DOH where its effective concentration became constant.

Mixed Solution of SDS and TDOH. Similar experiments as mentioned above were carried out, except for the use of tritiated DOH instead of SDS. Surface radioactivity due to TDOH in the mixed solution is shown in Fig. 3. It is seen that radioactivity decreases gradually with time over the range of DOH concentration of the mixed solution, approaching a constant value at higher DOH concentration and after sufficient lapse of time (about 90 min). This gradual decrease of radioactivity was considered to be due to the volatile

10) G. Aniansson and O. Lamm, *Nature*, **165**, 357 (1950); D. J. Salley, A. J Weith, Jr., A. A. Argyle and J. K. Dixon, *Proc. Roy. Soc.*, **A203**, 42 (1950).

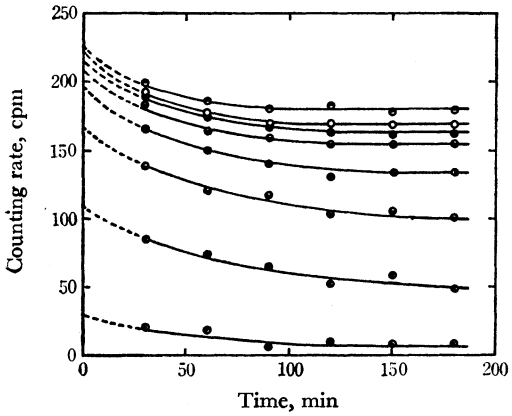

Fig. 3. Time dependence of surface radioactivity of TDOH due to adsorption of DOH from SDS-DOH mixed solution. Dotted lines show extrapolated value to zero time.
Concentration of DOH (in mol/100 g solution):
⊙ 6.86×10^{-6} ⊖ 2.06×10^{-4}
◐ 3.43×10^{-5} ● 4.12×10^{-4}
◒ 6.86×10^{-5} ○ 6.86×10^{-4}
◑ 1.36×10^{-4} ◓ 8.23×10^{-4}

nature of adsorbed DOH film at the surface.[8,11] In this connection the surface radioactivity of saturate TDOH solution without the addition of SDS is shown in Fig. 4. It is seen from Fig. 4

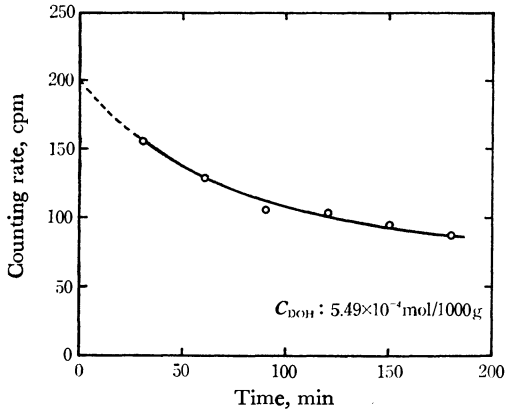

Fig. 4. Time dependence of surface radioactivity of TDOH due to the adsorption of DOH from its aqueous solution.

that surface radioactivity exhibited a similar tendency as in the case of Fig. 3. From these facts, it is presumed that the variation of surface radioactivity in Fig. 3 is partly due to the difference in adsorption rate between SDS and DOH, and partly to the evaporation of adsorbed DOH film as is shown in Fig. 4. The plateau appearing in the curve of Fig. 3 for DOH concentration of more than 2.06×10^{-4} mol/1000 g solution may be explained as a result of the dynamic equilibrium between the rate of adsorption of DOH into the surface layer from the bulk of solution and the rate of evaporation of it from the surface.

Thus, the value of counting rate of DOH corresponding to the equilibrium adsorption over the mixed solution was reasonably obtained by the extrapolation of the curve (as shown by the dotted line in Fig. 3). The extrapolation was made assuming an exponential decrease of the surface radioactivity (A) with time (t). The exponential relation was adopted since it was confirmed to hold fairly well for all experimental data of Figs. 3 and 4 as shown in Fig. 5. The adsorbed amount of DOH

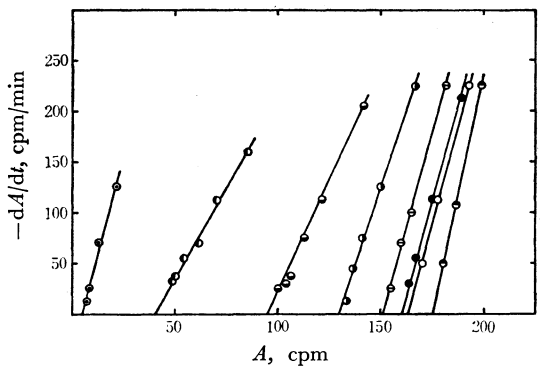

Fig. 5. A *versus* dA/dt plot.

in mixed solution, Γ_{DOH}, was calculated similarly as in the case of Γ_{SDS}. The results are shown by the curve B in Fig. 2. We can confirm in Fig. 2 that in the mixed adsorbed film Γ_{DOH} steeply increases with the DOH concentration contrary to the gradual decrease of Γ_{SDS} and reaches the saturate adsorption of 7.8×10^{-10} mol/cm² in the region of DOH concentration greater than 2.5×10^{-4} mol/1000 g solution. The curves show a strong tendency of DOH adsorption with no marked desorption of SDS.

Composition of Adsorbed Film. Few studies have been reported on the amount of adsorption at the surface of mixed aqueous solution of SDS and DOH by a direct and reliable method.[6,12] As an instance, we can cite the data of Wilson *et al.* obtained by foaming method. They reported $\Gamma_{SDS}=3.4\times10^{-10}$ mol/cm² and $\Gamma_{DOH}=3.9\times10^{-10}$ mol/cm² at 25°C for the mixed aqueous solution containing 8.7×10^{-3} mol/1000 g of SDS and 5.3×10^{-4} mol/1000 g of DOH. Corresponding data of the present study are $\Gamma_{SDS}=3.6\times10^{-10}$ mol/cm² and $\Gamma_{DOH}=7.7\times10^{-10}$ mol/cm² for the aqueous solution containing the same concentration of DOH

11) G. L. Gaines, Jr., Ed., "Insoluble Monolayers at Liquid-Gas Interface," Interscience Publishers, New York (1966), p. 208.

12) A. Wilson, M. B. Epstein and J. Ross, *J. Colloid Sci.*, **12**, 345 (1957).

as that of Wilson and 5.63×10^{-3} mol/1000 g of SDS as estimated from Fig. 2.

It is confirmed from these data that the two values of Γ_{SDS} are nearly equal, but those of Γ_{DOH} are largely different from each other. This discrepancy will be explained by the solubilization of DOH in aqueous SDS beyond CMC and resulting decrease in DOH activity in Wilson's measurement. A similar effect of the decrease in adsorption due to the solubilization has been reported by Aniansson[13] in the case of solubilization of sodium hexadecysulfate by SDS. Also, the effects of fatty alcohol on CMC and on surface tension *vers.* concentration curve of soap and other surface active substances may be closely related to the phenomena mentioned above.[5,14]

In Fig. 6, the fraction of DOH in the adsorbed

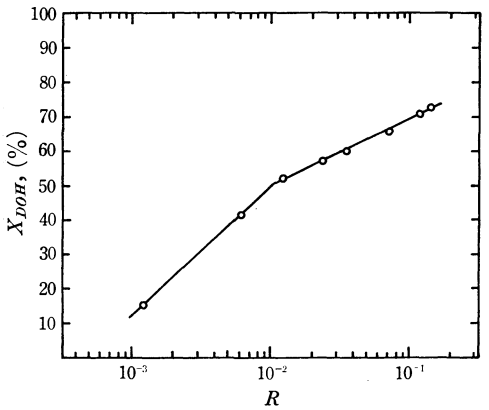

Fig. 6. Relation between X_{DOH} and R.
X_{DOH}: fraction of DOH in adsorbed film,
R: ratio of DOH concentration to SDS concentration in solution.

film, X_{DOH}, is plotted against the logartithm of the ratio, R, of DOH concentration to SDS concentration (constant) in the solution. It is seen in this figure that X_{DOH} shows a high value, although the value of R is still rather small: for instance, at $R=0.01$, $X_{DOH}=0.5$, *i. e.*, Γ_{SDS} is nearly equal to Γ_{DOH}. This means a strong tendency of DOH adsorption already at the small value of X_{DOH}, even in the presence of adsorbed film of SDS. Similar phenomena have been reported by Shinoda.[6] These facts may reasonably explain the remarkable effects of the addition of small amounts of DOH on the surface chemical properties of SDS solution.[2-4]

As for the mixed adsorption layer, the simple replacement of SDS by DOH in the layer cannot be conceivable, since the adsorption of DOH and the desorption of SDS did not occur in a simple ratio. The total amounts of adsorption of Γ_{DOH} and Γ_{SDS} together with the amount of adsorption corresponding to the close-packed monolayer are shown by dotted lines C and D respectively in Fig. 2. This figure shows that it is impossible for such a mixed adsorbed film to form a close-packed monolayer. This suggests that all molecules of SDS and DOH are not in the monomolecular layer at the surface of solution. In this connection it is noticed that the addition of SDS to the sufficiently concentrated solution of DOH (5.49×10^{-4} mol/1000 g solution) hardly affects the amount Γ_{DOH} (comparision of the extrapolated value of $\Gamma_{DOH}=7.4\times10^{-10}$ mol/cm^2 in Fig. 4 with the saturated value of $\Gamma_{DOH}=7.6\times10^{-10}$ mol/cm^2 for the mixed solution P in Fig. 2 containing the same amounts of DOH as in Fig. 4), while the addition of the same amounts of DOH to a solution of SDS markedly decrease the amount of Γ_{SDS} (from 5.9×10^{-10} mol/cm^2 at DOH concentration being zero to 3.6×10^{-10} mol/cm^2 for the mixed solution P in Fig. 2). These facts may suggest that adsorbed SDS molecules in excess of close-packed monolayer go beneath the monolayer at the surface of the solution while all adsorbed DOH appear in the monolayer. As to the structure of such a mixed adsorbed film, Fowkes reported[15] that the transition point is always observed in the pressure—area curve of the insoluble mixed monolayer composed of alkylsulfate and alcohol, when the alcohol content in the film exceeds 50%. He suggested the structure of film from the theory of ideal two-dimensional solution, in which the polar heads of sulfate are considered to be hydrated and placed beneath the surface of water, when the alcohol content of the film is less than 50%, but sulfate ions are dehydrated and occupy the same position as alcohol in the adsorbed film, when the alcohol content is over 50%.

In the present experiments, somewhat different behavior can be observed in the case of soluble adsorbed film composed of surfactant and alcohol. Namely, in the case of DOH composition being less than 50% in film, DOH molecules strongly penetrate into the adsorbed SDS film forming mixed monolayer, without marked desorption of SDS. In case of DOH composition being more than 50%, a mixed monolayer is likely to form, but here the mixed monolayer alone can not explain the total sum of Γ_{SDS} and Γ_{DOH} which exceeds the adsorbed amounts corresponding to the close-packed monolayer indicated by the dotted line D in Fig. 2. In this case a part of adsorbed SDS molecules are considered to form a mixed monolayer with DOH, while the rest of SDS molecules lie beneath the mixed monolayer as mentioned above. Thus, the structure of adsorbed layer is confirmed to be not a monolayer, contrary

13) G. Aniansson, *J. Phys. and Colloid Chem.*, **55**, 1286 (1951).
14) K. Shinoda, *J. Phys. Chem.*, **58**, 1136 (1954).
15) F. M. Fowkes, *ibid.*, **67**, 1982 (1963).

to the suggestion of Fowkes in the region of sufficiently large concentration of DOH, and the Fowkes' transition phenomena if it appears may be understood as the change from monolayer to double layers formation.

In order to study the composition of adsorbed mixed film further in detail, it is necessary to use a more improved method of measuring radioactivity. The work is being continued along this direction.

This work was supported by the Scientific Research Expenditure Grant of the Ministry of Education.

BULLETIN OF THE CHEMICAL SOCIETY OF JAPAN VOL. 42 2475—2479 (1969)

Kinetics of the Adsorption of Water and Electrical Conduction in Amorphous Ferric Oxide

Ryusaburo FURUICHI, Norio SATO and Go OKAMOTO

Department of Applied Chemistry, Faculty of Engineering, Hokkaido University, Sapporo

(Received February 19, 1969)

Amorphous ferric oxide was prepared by precipitation in a mixture of ammonium hydroxide and ferric nitrate at 90°C, after which it was calcinated in air at a constant rate of 10°C/min up to 200°C. The rate of the adsorption on the amorphous oxide was measured by a gravimetric method. An equation of the Elovich type was obtained: $dq/dt=k'p^{0.63}\exp(-\alpha' q/RTp^{0.5})$, where k' and α' are constants; q, the amount of adsorbed water, and p, the pressure. This kinetics can be interpreted by a model of a two-stage adsorption process, the van der Waals adsorption and the charge-transfer adsorption, the latter stage being assumed to be rate-determining. The effect of adsorbed water on the direct-current conductivity of the oxide, i, is formulated as $i=i_0\exp(aq)$. Assuming that the adsorbed water is acting as a donor-type impurity and that the ionization energy decreases with the concentration of impurity, the relation between i and q can be derived from the theory of the semiconduction of an n-type conductor.

Many investigators have reported the adsorption of water on ferric oxide.[1-6] Jurinak,[6] drawing a line between chemisorption and physical-adsorption, measured the amounts of water in the two adsorption states. Blyholder and Richardson[4] have shown, in a study of the infrared absorption, that the water molecule chemisorbs by dissociating to form an OH^- ion and an H^+ ion, the latter of which reacts with a surface O^{2-} ion to form another OH^- ion. Onoda and DeBruyn[7] have suggested the possibility of the transformation of anhydrous ferric oxide to goethite in a study of proton adsorption at the ferric oxide/aqueous solution interface. Kawasaki, Minowa, and Inamatsu[8] found, in studying the "Metallic Oxide Electric Hygrometer," that electrical resistance of oxide decreased with an increase in the relative humidity in the range from 50 to 100%. On the other hand, with various kinds of proteins the effect of adsorbed water on the electrical conductivity has been studied[9,10]; it has been found that the electrical conductivity, i, increased with an increase in the amount of adsorbed water, q, obeying an empirical equation, $i=A\exp(\alpha q)$, where A and α are constants.

It is to be noticed that the water adsorption affects the conductivity in a similar fashion in both inorganic and organic materials. The semiconductivity of inorganics is known to play an important role in the catalytic activity of the inorganic solids.

1) A. G. Foster, *J. Chem. Soc.*, **1945**, 360.
2) K. S. Rao, *J. Phys. Chem.*, **45**, 500 (1941).
3) F. H. Healey, J. J. Chessick and A. V. Fraioli, *ibid.*, **60**, 1001 (1956).
4) G. Blyholder and E.A. Richardson, *ibid.*, **66**, 2597 (1962).
5) S. J. Gregg, "Chemisorption," ed. by W. E. Garner, Butterworths Scientific Publications, London (1957), p. 68.
6) J. J. Jurinak, *J. Colloid Sci.*, **19**, 477 (1964).
7) G. Y. Onoda, Jr., and P. L. DeBruyn, *Surface Science*, **4**, 48 (1966).
8) T. Kawasaki, Z. Minowa and T. Inamatsu, *J. Appl. Phys. Japan*, **35**, 355 (1966).
9) D. D. Eley and R. B. Leslie, "Advances in Chemical Physics," Vol. VII, ed. by J. Duchesne, Interscience Publishers, New York (1964), p. 238.
10) B. Rosenberg, *J. Chem. Phys.*, **36**, 816 (1962).

In the present experiment, the kinetics of water adsorption on the amorphous ferric oxide prepared by heating the ferric oxide gel at 200°C, and the effect of water on the semiconductivity of the oxide, were investigated in an attempt to elucidate the interaction between the oxide and the adsorbed water.

Experimental

Materials. Ferric oxide gel was prepared by mixing 54 ml of a 6N NH_4OH solution and 750 ml of a 0.1 M $Fe(NO_3)_3$ solution at 90°C. The pH of the solution in which the hydroxide gel was suspended was 9.05. The precipitate obtained as above was carefully washed with distilled water and dried for two days at room temperature and for 6 hr at 100°C in 20 mmHg. After drying, it was calcinated in air at a fixed heating rate of 10°C/min up to 200°C and kept at this temperature for 10 min. The sample to be studied was ground to a powder with a mesh size of 200—300. This oxide was found to be amorphous by X-ray diffraction examination, and its surface area was 162 m^2/g (BET method).

Measurements. The rate of the adsorption of water vapor was measured gravimetrically using a quartz spring microbalance and a cathetometer. The water vapor was supplied by a sulfuric acid solution placed in a constant-temperature bath, while the pressure was controlled by changing the concentration of the acid solution. Before the adsorption experiment, the specimen was evacuated at 150°C for 3 hr at 10^{-5} mmHg. The cell used for the measurement of the electrical conductivity was of the sandwich type, with two platinum electrodes (contact area, 0.95 cm^2) and a stainless-steel spring to press the oxide between electrodes at a pressure of 1 kg/cm^2. The voltage supplied across the cell was 10 V d. c., and the conducting current was measured in a vacuum of 10^{-6} mmHg at various fixed temperatures ranging from 5°C to 50°C. The conducting current was measured by an electrometer (Ohkura Electric Co.). Before the measurement of the conductivity, the specimen was subjected to the adsorption of water vapor in a desiccator containing the sulfuric acid solution for various periods of time in order to change the amount of adsorbed water which could be determined by weighing the specimen before and after the adsorption.

Results

Kinetics of Adsorption. Typical adsorption-time curves are shown in Fig. 1, in which the amount of water adsorbed, q, is represented in units of mg H_2O per m^2 of the oxide surface and the time, t, in minutes. The q values in the initial stage of the adsorption, *i.e.*, for 1 or 1.5 min after the introduction of water vapor into the adsorption chamber, are not so accurate as in the later stage because of the oscillation of the quartz spring.

To analyze these adsorption-time curves in the figure, q is plotted against $\log(t+t')$ in Fig. 2, where t' is chosen to linearize the q-$\log t$ relation by a

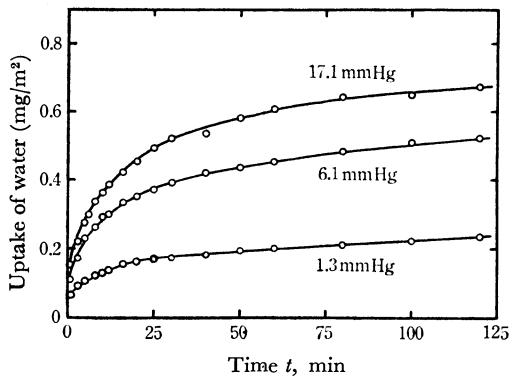

Fig. 1. Adsorption-time curves for amorphous ferric oxide at 30°C at various pressures.

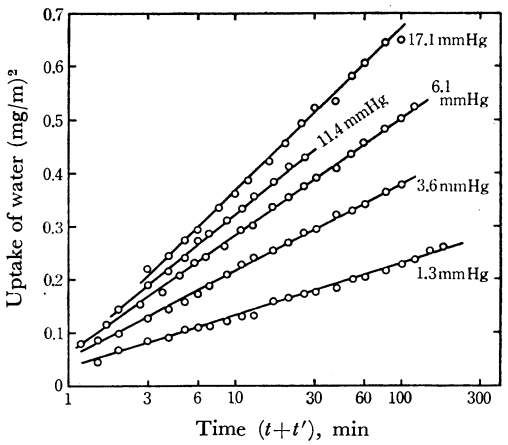

Fig. 2. Kinetics of the water vapor uptake at 30°C at various pressures.

trial-and-error method. It may be seen in Fig. 2 that the kinetics of water adsorption on the amorphous ferric oxide obeys the Rozinsky-Zeldovich or Elovich equation, which can be formulated as follows in the differential and integrated forms respectively:

$$dq/dt = k \exp(-\alpha q/\boldsymbol{RT}) \quad (1)$$

$$q = 2.303(\boldsymbol{RT}/\alpha)\log(t + \boldsymbol{RT}/\alpha k) - 2.303(\boldsymbol{RT}/\alpha)\cdot\log \boldsymbol{RT}/\alpha k \quad (2)$$

where k is the initial rate when q is zero and α is constant. The value of t' on the abscissa $\log(t+t')$ in Fig. 2, therefore, corresponds to the $\boldsymbol{RT}/\alpha k$ term, and the slope of the straight lines, to $2.303(\boldsymbol{RT}/\alpha)$ in Eq. (2). Accordingly, α and k can be calculated from the values of t' and the slope of the lines. However, it has been shown by Taylor and Thon[11] that the initial rate of adsorption, k, calculated t' is smaller than the experimentally-measured rate

11) H. A. Taylor and N. Thon, *J. Am. Chem. Soc.*, **74**, 4169 (1952).

in many cases. In the present paper, because of the difficulty in measuring the initial velocity, the calculated k has been assumed to be the initial rate of adsorption.

As may be seen in Fig. 2, the solpe of the line, that is $2.303(RT/\alpha)$ in Eq. (2), increases with the pressure of the water vapor, p. The slope of the line, when plotted as in Fig. 3, is seen to increase

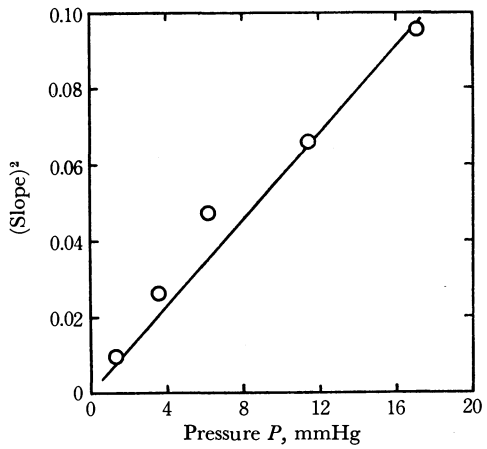

Fig. 3. Pressure dependence of the slope of lines in Fig. 2.

linearly with $p^{0.5}$, so α can be writted as $\alpha=\alpha'/p^{0.5}$. To examine the pressure-dependence of k, which can be calculated from Eq. (2), log k is plotted as a function of log p in Fig. 4. Thus, the relation

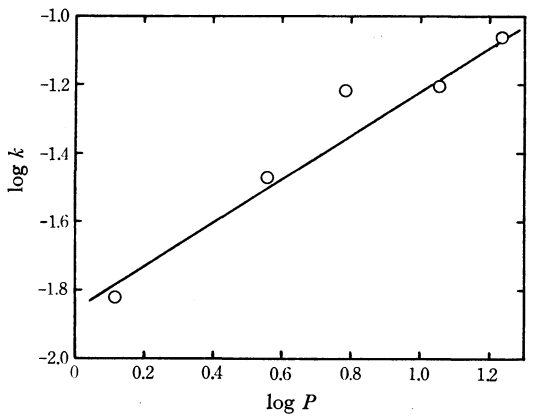

Fig. 4. Pressure dependence of the initial velocity calculated from the data in Fig. 2.

between k and p can be represented as $k=k'p^{0.63}$. The substitution of new pressure-dependent parameters, α and k, into Eq. (1) yields:

$$dq/dt = k'p^{0.63} \exp(-\alpha' q/RTp^{0.5}) \quad (3)$$

Electrical Conductivity. The results of the measurement of the electrical conductivity as a function of the temperature are shown in Fig. 5,

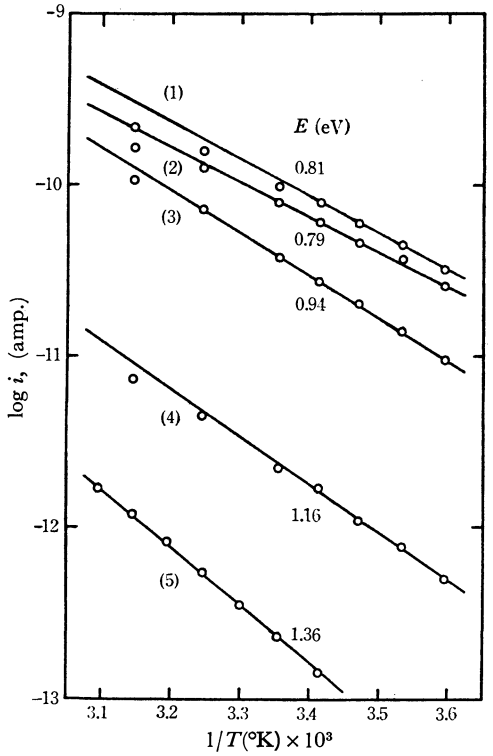

Fig. 5. Conductivity of amorphous ferric oxide as a function of temparature. Curves (1), (2), (3), (4) and (5) correspond, respectively, to the conductivity of samples containing 0, 4.9, 8.7, 12.0 and 14.5 wt% of adsorbed water.

in which the logarithm of the conducting current through the cell has been plotted against the reciprocal absolute temperature. Five curves, denoted in this figure by (1) to (5), represent the conductivity of specimens containing different amounts of adsorbed water, that is 0, 4.9, 8.7, 12.0 and 14.5 wt% of water respectively. The results in Fig. 5 show that the conducting current, i, at a given temperature, T, can be formulated by Eq. (4);

$$i = i_0 \exp(-E/kT) \quad (4)$$

where i_0 and E are constants and k, the Boltzman constant. Furthermore, it was found that, although no variation in the current with time occurred at 5°C in a vacuum, some decrease in the current did occur when air entered the conductivity cell. These results imply that the ferric oxides are n-type semiconductors. Accordingly, the slope of the lines Fig. 5 is considered to give the activation energy, E, for semiconduction. At higher temperatures the conducting currents of the wet oxides, as seen in Fig. 5, deviates downward from the stright line, probably because of the desorption of the adsorbed water.[10]

It may also be seen in Fig. 5 that as the amount of adsorbed water increases, E decreases and i

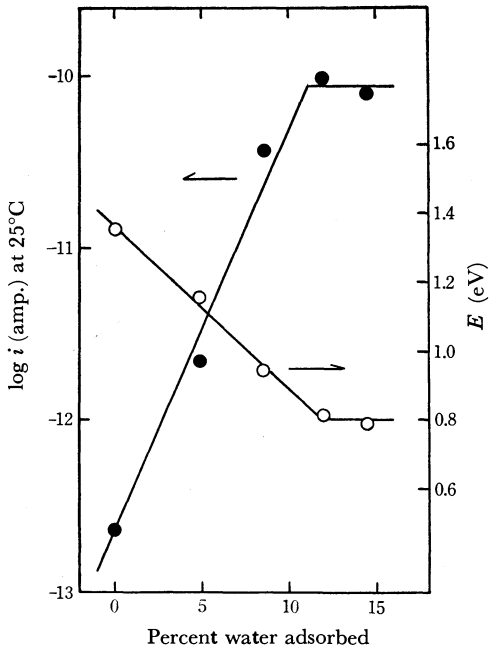

Fig. 6. Relation between conducting current at 25°C, activation energy and amount of adsorbed water.

increases in the temperature range examined. This is quantitatively shown in Fig. 6, in which the values of the conducting current at 25°C are given as examples. The change in the conducting current, i, with the amount of adsorbed water, q, at a fixed temperature is seen to obey the equation:

$$\log i = i' + aq \tag{5}$$

where i' and a are constants. Furthermore, the activation energy of semiconduction, E, can be expressed by:

$$E = E_0 - bq \tag{6}$$

where E_0 corresponds to the activation energy of the dried oxide and where b is constant.

From Eqs. (5) and (6) the relation:

$$\log i = \text{const.} - \text{const.} \times E \tag{7}$$

can be obtained. Equation (7) satisfies Mayer's rule,[12] which, in general, has been interpreted as follows: the activation energy of electronic conduction in semiconductors decreases with an increase in the concentration of carriers and donor centers. Accordingly, it may be concluded that the adsorbed water acts as a donor-type impurity in the oxide, the oxide being a semiconductor of the n type.

Discussion

As has been mentioned above, the amorphous ferric oxide is an n-type semiconductor and the adsorption of water on it causes the electrical conductivity to increase. Therefore, the adsorption which, in the present case, may be referred to as the cumulative or cationic chemisorption must be accompanied by the charge transfer. Hauffe, Morrison and Stone[13] have discussed the kinetics of the cationic adsorption on the basis of the boundary-layer theory of chemisorption. On the other hand, Eley and Leslie[14] postulated in their recent study that the adsorption kinetics of water vapor on proteins may be regarded as a two-stage process: the van der Waals adsorption and the charge-transfer adsorption, with the rate-determining step being the latter. On the basis of this adsorption model, they derived theoretically the equation indicated by Eq. (8) and gave a qualitative description of the rate of adsorption experimentally obtained (Eq. (9)):

$$dq/dt = K'N_{VW}p^{0.6}\exp[-(E_0 + \beta q - \gamma p)/RT] \tag{8}$$

$$dq/dt = Kp^{0.6}\exp(-\alpha' q/RTp) \tag{9}$$

where K, K', β, γ nad α' are constants; N_{VW}, the number of sites on the surface of the adsorbent, E_0, the energy barrier of the charge-transfer step at $q=0$. In Eq. (8), the activation energy, E, is assumed to increase linearly with the amonut of adsorbed water, the additional term, γp, is the contribution to E of the dipole moment of water molecules in the van der Waals adsorption state. By comparing Eq. (3) with Eq. (9), it can easily be seen that these two equations are almost the same except for a difference in the exponent of p in the exponential term. Accordingly, the adsorption of water on the amorphous ferric oxide may be explained by the two-stage model proposed for the adsorption on protein. On the basis of the above discussion, the adsorption process can be represented as follows:

$$H_2O + \text{oxide} \rightleftarrows [H_2O\cdots\text{oxide}]_{VW} \xrightarrow{-A\rightarrow} [H_2O \rightarrow {}^{-}\text{oxide}]_{CT}$$

Pearson and Bardeen[15] found, for boron in silicon, that the ionization energy, E_D, of the donors decreased with an increase in the concentration of the donors, n_D, in the semiconductor. Assuming the interaction energy between the impurity atoms to be inversely proportional to the average distance between these atoms, they derived this relation between E_D and n_D:

12) W. Meyer, *Z. Physik*, **38**, 1014 (1937); F. A. Kroger, "The Chemistry of Imperfect Crystals," North-Holland Publishing Co., Amsterdam (1964), p. 475.

13) K. Hauffe, "Advances in Catalysis," Vol. VII, Academic Press, New York (1955), p. 213; S. R. Morrison, *ibid.*, p. 259; F. S. Stone, "Chemistry of the Solid State," ed. by W. E. Garner, Butterworths Scientific Publications, London (1955), p. 367.

14) D. D. Eley and R. B. Leslie, *Trans. Faraday Soc.*, **62**, 1002 (1966).

15) G. L. Peason and J. Bardeen, *Phys. Rev.*, **75**, 865 (1949).

$$E_D = E_{DC} - n_D^{1/3} \quad (10)$$

If it can be assumed that, as has been described above, the adsorbed water is acting as an impurity producing donor centers, and that the amount of adsorbed water, q, is proportional to n_D to the one-third power, the change of E with q in Eq. (6) can be interpreted in terms of the interaction between the adsorbed waters. Moreover, the conductivity[16] is given by the theory of the impurity mechanism of semiconduction:

$$\sigma = e\mu(4n_D)^{1/2}(2\pi mkT/h^2)^{4/3} \exp(-E_D/2kT) \quad (11)$$

where e is the electronic charge, and μ, the mobility, while the others are well-known symbols. By substituting Eq. (10) into Eq. (11), and by assuming $n_D^{1/3}$ to be proportional to q, the logarithm of σ can be given by:

$$\log \sigma = \text{const.} + \log q^{3/2} + \text{const.} \times q \quad (12)$$

Neglecting log $q^{3/2}$ term, Eq. (12) fits the relation between i and q in Eq. (5) obtained experimentally in the present investigation.

One of the authors (R. F.) especially wishes to thank the Sakkokai Foundation for his scholarship.

16) N. F. Mott and R. W. Gurney, "Electronic Processes in Ionic Crystals," Clarendon Press, Oxford (1948), p. 165.

BULLETIN OF THE CHEMICAL SOCIETY OF JAPAN VOL. 42 2479—2485 (1969)

The Crystal and Molecular Structure of the High-melting-point Isomer of Bis-(1,2-diethoxycarbonyl-ethyl)tin Dibromide

Toshihide KIMURA, Tatzuo UEKI,[*1] Noritake YASUOKA, Nobutami KASAI[*2] and Masao KAKUDO

Department of Applied Chemistry, Faculty of Engineering, Osaka University, Yamada-Kami, Suita, Osaka

(Received February 20, 1969)

The high-mp isomer crystal of bis-(1,2-diethoxycarbonyl-ethyl)tin dibromide (mp 122—123°C) is monoclinic: $a=19.46$, $b=10.25$, $c=13.20$ Å, $\beta=121.1°$; space group $C2/c$; four molecules are contained in a unit cell. The molecule has the C_2 symmetry. The tin atom lies on the two-fold axis, and the coordination about the tin atom is nearly octahedral. Similar to the low-mp isomer, two bromine atoms attached to the tin atom are in *cis*-positions; also, two ligands, both 1,2-diethoxycarbonyl-ethyl groups, are bound to the tin atom by oxygen and carbon atoms, forming rather puckered five-membered rings. Both rings are in either the *d*- or *l*-form, instead of consisting of one *d*- and one *l*-form, as in the low-mp isomer.

Bis-(1,2-diethoxycarbonyl-ethyl)tin dibromide was prepared by a direct reaction between tin foil and diethyl bromosuccinate;[1] the two isomers thus

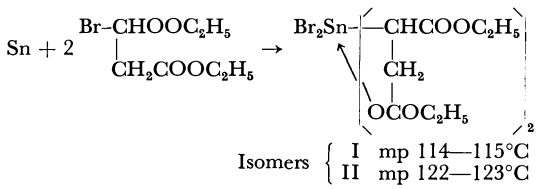

Isomers { I mp 114—115°C
II mp 122—123°C

isolated had mp's of 114—115°C and 122—123°C.

We undertook a three-dimensional structure analysis of these isomers by means of X-rays, and have already reported on the structure of I, the low-mp isomer.[2] In the present paper the molecular and crystal structure of II, the high-mp isomer, and the differences between the structure of these two isomers will be described.

Experimental

The crystals were obtained by recrystallization from an ethanol solution. They were colorless needles developed along the *c* axis. In order to determine the lattice parameters, oscillation and Weissenberg photographs were taken around the *b* and *c* axes. Debye lines of aluminum were superposed on the Weissenberg photographs for calibration.

For the intensity data collection, the layers from 0 through 7 around the *b* axis were recorded by the

*1 Present address: Institute for Protein Research, Osaka University, Joancho, Kita-ku, Osaka, 530.

*2 To whom any correspondence should be addressed.

1) S. Matsuda, S. Kikkawa and I. Omae, *Kogyo Kagaku Zasshi* (*J. Chem. Soc. Japan, Ind. Chem. Sect.*), **69**, 646 (1966).

2) M. Yoshida, T. Ueki, N. Yasuoka, N. Kasai, M. Kakudo, I. Omae, S. Kikkawa and S. Matsuda, This Bulletin, **41**, 1113 (1968).

multi-film equi-inclination Weissenberg technique, using nickel-filtered Cu$K\alpha$ radiation. The reflections of the layers from 0 through 2 around the c axis were also collected, mainly for the inter-layer scaling.

The intensities were estimated visually by using a calibrated standard scale. Lorentz and polarization corrections were carried out, but no absorption correction was made. In all, 1546 (1536 non-zero) reflections were obtained. The density was measured by the floatation method.

Crystal data are summarized in Table 1. For reference, those of the low-mp isomer are also shown in Table 1.

TABLE 1. CRYSTAL DATA OF THE TWO ISOMERS OF BIS-(1,2-DIETHOXYCARBONYL-ETHYL)TIN DIBROMIDE, $Br_2SnC_{16}H_{26}O_8$*

High-mp isomer (Present study)	Low-mp isomer[2]
mp=122—123°C	mp=114—115°C
MW=624.9	MW=624.9†
(Cu$K\alpha$ radiation, λ=1.5418 Å)	
a=19.46 Å	a=11.85 Å
b=10.25	b=20.24
c=13.20	c=9.79
β=121.1°	β=101.3°
U=2254 Å^3	U=2302 Å^3
D_m=1.82 g·cm^{-3}	D_m=1.80 g·cm^{-3}
Z=4	Z=4
D_x=1.83 g·cm^{-3}	D_x=1.80 g·cm^{-3} †
$C2/c$	$P2_1/a$

* This formula was printed, by the authors' mistake, as $Br_2SnC_{16}H_{22}O_8$ in the Ref. 2, for which the authors were very regret. Accordingly, the values of the MW and D_x in the Ref. 2 should be corrected as those in this table marked by dagger.

Determination and Refinement of the Structure

From the systematic absence of the reflections, the possible space group is either $C2/c$ or Cc. If the space group is $C2/c$, the general positions in the unit cell are eight-fold. In this case, however, four molecules are present, and the molecules must occupy special positions. Therefore, the molecule has either C_i or C_2 symmetry. In the case of Cc, the molecules lie on general positions. From these considerations, the following four possible cases may be considered:

1) the space group is $C2/c$, the molecule has the C_2 symmetry, and the two bromine atoms are in the *trans*-position;

2) the space group is $C2/c$, the molecule has the C_2 symmetry, and the two bromine atoms are in the *cis*-position;

3) the space group is $C2/c$, the molecule has the C_i symmetry, and the two bromine atoms are in the *trans*-position;

4) the space group is Cc, and the molecule has no symmetry.

The three-dimensional Patterson function was interpreted successfully in the case of 2), and so the space group was determined to be $C2/c$. The tin atom lies on the two-fold axis.

The crystal structure was established by the heavy-atom method. By starting with approximate parameters of tin and bromine atoms, the positions of all the light atoms except hydrogen were found in the three-dimensional Fourier maps. Successive block-diagonal least-squares refinement was carried out on a HITAC 5020E computer at the University of Tokyo, using a program written by Dr. T. Ashida. After two cycles of refinement for the heavy atoms, Sn and Br, the discrepancy factor, $R=\sum||F_o|-|F_c||/\sum|F_o|$, was reduced to 0.348. In this refinement, the unit weight was assigned for all reflections. Then, the refinement was made for all atoms except hydrogen. The following weighting scheme was applied: $w=(23.1/|F_o|)^2$ for $|F_o|>23.1$, $w=1.0$ for $23.1\geqq|F_o|\geqq1.0$, and $w=0.2$ for $|F_o|<1.0$. After three cycles, anisotropic temperature factors for the heavy atoms were introduced. Six cycles of refinement gave the R value of 0.167 for all reflections.

The atomic and thermal parameters are listed in Table 2, while the observed and calculated structure factors are listed in Table 3. The atomic scattering factors used in the structure-factor calculation were those of Hanson *et al.*[3]

TABLE 2. THE FINAL ATOMIC AND THERMAL PARAMETERS

Atom	x	y	z	β_{11}	β_{22}	β_{33}	β_{12}	β_{13}	β_{23}
Sn	0.0000	0.0521	0.2500	36	84	56	0	53	0
Br	0.0987	−0.1031	0.4029	64	141	103	41	96	43
O(1)	0.0894	0.2403	0.3580	4.8					
O(2)	0.1685	0.3821	0.3471	7.3					
O(3)	0.1036	−0.0946	0.1506	5.4					
O(4)	0.1969	0.0580	0.2583	7.0					
C(1)	0.0613	0.1115	0.1528	3.5					
C(2)	0.0831	0.2570	0.1813	6.5					
C(3)	0.1293	0.0212	0.1925	5.0					
C(4)	0.1091	0.2868	0.3005	4.1					
C(5)	0.1595	−0.1999	0.1843	7.9					
C(6)	0.1174	−0.3191	0.1628	9.8					
C(7)	0.1951	0.4299	0.4628	7.0					
C(8)	0.1509	0.5391	0.4641	11.2					

The anisotropic thermal parameters for heavy atoms are $\times10^4$ and are of the form:
$\exp\{-(\beta_{11}h^2+\beta_{22}k^2+\beta_{33}l^2+\beta_{12}hk+\beta_{13}hl+\beta_{23}kl)\}$.
Thermal parameters for light atoms are isotropic B in Å^2. The estimated standard deviations, $\sigma(r)$ for Sn is 0.0028 Å and for Br is 0.0043 Å.

3) H. P. Hanson, F. Herman, J. D. Lea and S. S. Skilman, *Acta Cryst.*, **17**, 1040 (1964).

TABLE 3. THE OBSERVED AND CALCULATED STRUCTURE FACTORS

K	FO	FC	K	FO	FC	K	FO	FC	K	FO	FC	K	FO	FC	K	FO	FC	K	FO	FC
H,L=-23	3		0	24	-11	4	29	25	0	41	11	4	15	14	H,L=-11	12		1	37	25	3	174	-149	4	34	39
1	7	2	2	27	-21	6	24	4	2	64	-60	6	64	61	1	73	71	3	44	39	5	117	-97	6	69	68
H,L=-23	4		4	15	-16	H,L=-16	9		4	57	-56	8	34	22	3	38	34	5	88	78	7	49	-28	H,L= -6	12	
1	8	17	H,L=-18	3		2	37	-27	6*	0	-22	H,L=-12	3		5	22	-2	7	49	43	9	68	70	0	74	65
H,L=-23	5		2	38	21	4	47	-54	H,L=-14	7		2	80	86	H,L=-11	13		H,L= -9	8		H,L= -7	3		2	41	38
1	15	-9	4	22	38	6	38	-39	2	57	53	4	93	90	1	15	6	1	45	34	1	21	-10	4	29	10
H,L=-23	6		H,L=-18	4		H,L=-16	10		4	74	73	6	26	20	3	22	-25	3	54	49	3	104	91	6	23	-19
1	14	-18	0	94	47	0	111	-113	6	46	40	H,L=-12	4		5	35	-40	5	56	52	5	125	97	H,L= -6	13	
H,L=-22	2		2	65	23	2	55	-57	H,L=-14	8		0	50	-15	H,L=-11	14		7	47	-41	7	78	73	2	56	-54
0	22	-21	4	16	3	4	23	24	0	87	95	2	50	46	1	59	-78	H,L= -9	9		H,L= -7	4		4	49	-50
H,L=-22	4		H,L=-18	5		6	34	36	2	70	67	4	94	85	3	28	-9	1	62	-57	1	299	292	6	14	-23
0	19	11	2	23	4	H,L=-16	11		4	24	-8	6	18	24	H,L=-11	15		3	145	-141	3	27	24	H,L= -6	14	
2	17	16	4	16	-22	2	22	9	6	26	-26	H,L=-12	5		1	20	7	5	61	-66	5	136	-112	0	21	-23
H,L=-22	5		H,L=-18	6		4	34	33	H,L=-14	9		2	169	-147	3	28	34	7	25	-2	7	20	-63	2	20	-20
2	21	-24	0	65	-58	6	33	41	2	23	18	4	151	-124	H,L=-11	16		H,L= -9	10		H,L= -7	5		H,L= -6	15	
H,L=-22	6		2	40	-31	H,L=-16	12		4	42	-38	6	32	-11	1	12	22	1	58	-46	1	15	12	2	25	28
0	21	-38	4	16	-8	0	64	63	6	56	-56	H,L=-12	6		H,L=-10	1		3	59	-51	3	90	68	H,L= -5	1	
2	19	-20	H,L=-18	7		2	37	34	H,L=-14	10		0	83	-72	2	23	-15	5	34	-32	5	124	-106	1	46	-47
H,L=-22	7		2	37	46	H,L=-16	13		0	110	-103	2	87	-83	4	50	-58	7	42	36	7	103	-92	3	316	-324
2	22	2	4	16	34	2	47	-55	2	38	-39	4	32	-20	6	74	-67	H,L= -9	11		H,L= -7	6		5	126	-111
H,L=-22	8		H,L=-18	8		4	39	-50	4	17	-3	6	18	2	8	57	-49	1	43	-28	1	147	-139	7	43	-39
0	51	56	2	28	32	H,L=-16	14		6	39	34	H,L=-12	7		H,L=-10	2		3	39	34	3	18	-24	H,L= -5	2	
2	21	21	4	35	34	0	18	-25	H,L=-14	11		2	37	-31	0	76	-61	5	45	43	5	14	19	1	277	-309
H,L=-22	9		H,L=-18	9		2	16	-23	2	61	60	4	43	34	2	73	-67	7	49	51	7	51	40	3	51	-46
2	20	-11	2	60	-64	H,L=-16	15		4	53	66	6	82	86	4	76	-75	H,L= -9	12		H,L= -7	7		5	32	26
H,L=-21	1		4	37	-51	2	13	22	6	16	18	H,L=-12	8		6	17	22	1	97	110	1	156	145	7	78	80
1	13	-2	H,L=-18	10		H,L=-15	1		H,L=-14	12		0	189	191	8	57	62	3	29	14	3	173	163	9	39	38
3	7	-6	2	46	-45	1	49	-29	0	24	24	2	110	98	H,L=-10	3		5	46	-39	5	116	95	H,L= -5	3	
H,L=-21	2		4	20	4	3	66	-73	2	28	10	4	37	-29	2	192	218	H,L= -9	13		7	29	-7	1	195	-181
1	18	-21	H,L=-18	11		5	42	-49	4	44	45	6	66	-52	4	207	186	1	22	12	H,L= -7	8		3	104	-67
3	10	-17	2	20	-2	7	16	-14	6	21	-4	H,L=-12	9		6	16	-8	3	23	-23	1	27	2	5	140	152
H,L=-21	3		H,L=-18	12		H,L=-15	2		H,L=-14	13		2	23	-10	H,L=-10	4		5	39	-43	3	85	74	7	123	151
1*	0	15	2	46	50	1	88	-95	2	52	-55	4	54	-48	0	18	15	H,L= -9	14		5	85	73	H,L= -5	4	
3	19	26	H,L=-18	15		3	24	-19	4	44	-53	6	74	-72	2	64	58	1	50	-47	7	35	-28	1	321	344
H,L=-21	4		2	12	36	5	17	19	H,L=-14	14		H,L=-12	10		4	84	69	3	32	-24	H,L= -7	9		3	10	12
1	21	12	H,L=-17	1		7	23	21	0	55	-53	0	61	-52	6	17	7	H,L= -9	15		1	54	-45	5	105	-99
H,L=-21	5		1	32	-22	H,L=-15	3		2	29	-30	2	50	-44	H,L=-10	5		1	38	34	3	107	-100	7	71	-74
1	40	-19	3	46	-58	1	28	-12	H,L=-14	15		4	60	-50	2	64	-52	3	33	53	5	58	-50	H,L= -5	5	
H,L=-21	6		5	15	-22	3	30	7	2	15	-3	6	18	7	4	139	-118	H,L= -9	16		7	17	-20	1	56	-49
1	34	-41	H,L=-17	2		5	59	59	H,L=-13	1		H,L=-12	11		6	60	-54	1	12	17	H,L= -7	10		3	128	-123
3	12	-15	1	28	-24	7	41	53	1	26	-17	2	95	97	H,L=-10	6		H,L= -8	1		1	94	-93	5	158	-153
H,L=-21	7		3	29	-20	H,L=-15	4		3	23	-23	4	65	78	0	260	-252	2	144	-132	3	45	-26	7	61	-53
3	12	7	5	15	-8	1	111	108	5	54	-60	6	24	19	2	110	-100	4	90	-106	5	44	30	H,L= -5	6	
H,L=-21	8		H,L=-17	3		3	17	31	7	17	-32	H,L=-12	12		4	70	55	6	58	-43	7	46	37	1	133	-105
1	41	52	1	28	-4	5	34	-24	H,L=-13	2		0	40	31	6	88	70	8	41	-22	H,L= -7	11		3	147	-136
3	25	16	3	17	20	7	38	-41	1	108	-114	2	47	39	H,L=-10	7		H,L= -8	2		1	54	-35	5	81	-65
H,L=-21	9		5	36	40	H,L=-15	5		3	23	-12	4	16	33	2	49	-30	0	39	13	3	17	3	7	54	41
3	12	-28	H,L=-17	4		1	42	-23	5	41	34	6	16	-4	4	59	59	2	102	-99	5	87	91	H,L= -5	7	
H,L=-21	10		1	70	78	3	59	-64	7	25	32	H,L=-12	13		6	110	112	4	79	-87	7	97	88	1	164	141
3	27	-22	3	17	2	5	39	-44	H,L=-13	3		2	15	-30	H,L=-10	8		6	42	-35	H,L= -7	12		3	228	209
H,L=-20	1		5	23	-24	7	17	-29	1	33	30	4	33	-43	0	151	153	8	40	70	1	70	79	5	94	82
2	11	-7	H,L=-17	5		H,L=-15	6		3	32	45	6	13	-35	2	82	77	10	52	54	3	42	21	7	23	-5
H,L=-20	2		1	28	9	1	32	-19	5	45	52	H,L=-12	14		4	32	19	H,L= -8	3		5	32	-26	H,L= -5	8	
0	28	-15	3	17	3	3	61	-60	7	39	35	0	67	-75	6	49	-36	2	87	82	H,L= -7	13		1	105	97
2	25	-20	5	23	-43	5	49	-41	H,L=-13	4		2	42	-48	H,L=-10	9		4	115	83	1	15	-19	3	105	86
H,L=-20	3		H,L=-17	6		7	38	33	1	44	43	H,L=-12	15		2	96	-100	6	64	55	3	39	-45	5	15	-2
2	41	28	1	47	-42	H,L=-15	7		3	61	68	2	11	5	4	82	-82	H,L= -8	4		5	39	-41	7	46	-33
4	12	35	3	24	-21	1	51	40	5	29	19	H,L=-12	16		6	50	-46	0	187	192	H,L= -7	14		H,L= -5	9	
H,L=-20	4		5	16	-6	3	96	106	7	30	-28	0	25	29	H,L=-10	10		2	113	104	1	14	-19	1	33	-22
0	34	21	H,L=-17	7		5	49	44	H,L=-13	5		H,L=-11	1		0	30	-11	4	70	-57	3	28	-32	3	52	-44
2	20	20	1	43	42	7	29	12	1	60	-50	1	18	-19	2	64	-60	6	84	-99	H,L= -7	15		5	73	-73
H,L=-20	5		3	63	77	H,L=-15	8		3	116	-119	3	15	12	4	68	-69	H,L= -8	5		1	26	31	7	64	-68
2	32	-15	5	23	34	1	62	58	5	34	-41	5	73	-87	6*	0	-10	2	58	46	3	29	43	H,L= -5	10	
4	19	-34	H,L=-17	8		3	35	30	7	30	-10	7	68	-63	H,L=-10	11		4	45	-35	H,L= -7	16		1	126	-131
H,L=-20	6		1	28	10	5	34	2	H,L=-13	6		H,L=-11	2		2	67	74	6	143	-126	1	19	33	3	31	-33
0	71	-71	3	40	37	7	28	-20	1	47	-40	1	126	-117	4	60	65	H,L= -8	6		H,L= -6	1		5	67	53
2	20	-29	5	36	31	H,L=-15	9		3	76	-73	3	32	-34	6	48	47	0	203	-198	2	183	-188	7	24	26
4*	0	0	H,L=-17	9		3	24	-26	5	34	-21	5	38	31	H,L=-10	12		2	84	-83	4	244	-177	H,L= -5	11	
H,L=-20	7		3	61	-69	5	56	-57	7	30	10	7	49	44	0	86	87	4	47	25	6	48	-49	1	33	22
2	20	12	H,L=-17	10		7	38	-46	H,L=-13	7		9	25	37	2	78	81	6	92	80	8	22	7	3	17	29
4	13	24	1	60	-72	H,L=-15	10		1	15	-15	H,L=-11	3		4	16	-10	H,L= -8	7		H,L= -6	2		5	67	65
H,L=-20	8		3	23	-17	1	89	-100	3	37	32	1	95	95	6	16	-23	2	105	104	0	104	-113	7	56	44
0	60	57	H,L=-17	11		3	24	-7	5	64	68	3	145	140	H,L=-10	13		4	94	79	2	182	-147	H,L= -5	12	
2	40	32	1	21	-7	5	40	44	7	53	67	5	73	56	2	16	-3	6	56	40	4	53	-28	1	16	30
4	13	12	H,L=-17	12		7	20	25	H,L=-13	8		7	24	-2	4	26	-29	H,L= -8	8		6	12	-8	3	45	41
H,L=-20	9		1	50	47	H,L=-15	11		1	123	132	H,L=-11	4		6	41	-52	0	82	-65	8	48	66	5	22	14
2	34	-46	3	14	20	1	32	24	3	29	23	1	22	21	H,L=-10	14		2	14	20	10	21	47	H,L= -5	13	
4	25	-38	H,L=-17	13		3	16	25	5	67	-59	3	80	73	0	67	-67	4	101	102	H,L= -6	3		1	41	-43
H,L=-19	1		1	32	-21	5	43	47	7	17	-23	5	60	50	2	44	-52	6	18	14	2	16	-10	3	47	-57
1	19	-8	H,L=-17	14		7	18	22	H,L=-13	9		7	17	-17	H,L=-10	15		H,L= -8	9		4	76	66	5	42	41
3	13	-20	1	15	-20	H,L=-15	12		1	23	9	H,L=-11	5		2	41	40	2	140	-135	6	159	169	H,L= -5	14	
H,L=-19	2		H,L=-17	15		1	27	36	3	17	19	1	73	-61	H,L=-10	16		4	97	-98	H,L= -6	4		1	19	-25
1	14	-11	1	8	23	3	31	34	5	60	-58	3	178	-163	0	27	16	6	18	-18	0	390	463	3	19	-27
3	14	-25	H,L=-16	1		5	20	5	7	55	-61	5	106	-86	H,L= -9	1		H,L= -8	10		2	200	195	H,L= -5	15	
H,L=-19	3		2	66	-67	H,L=-15	13		H,L=-13	10		7	35	-26	1	20	-24	0	59	-36	4	60	-54	1	22	6
1	26	22	4	57	-53	1	48	-49	1	62	-61	H,L=-11	6		3	18	-23	2	74	-64	6	122	-114	H,L= -4	1	
3	37	41	6	24	-18	H,L=-15	14		3	39	-36	1	140	-150	5	75	-70	4	24	-18	H,L= -6	5		2	161	-160
H,L=-19	4		H,L=-16	2		1	22	-27	5	29	4	3	52	-42	7	56	-56	6	18	8	2	70	-60	4	183	-150
1	37	21	0	42	-49	H,L=-15	15		7	16	25	5	59	42	H,L= -9	2		H,L= -8	11		4	68	-61	6	82	-89
3*	0	19	2	34	-45	1	10	5	H,L=-13	11		7	24	30	1	33	-26	2	37	-25	6	133	-121	8*	0	-6
H,L=-19	5		4	24	-8	H,L=-15	16		1	75	75	H,L=-11	7		3	119	-109	4	17	23	H,L= -6	6		H,L= -4	2	
1	31	-7	6	25	5	1	21	47	3	73	86	1	53	-42	5	48	-28	6	63	65	0	132	-120	0	167	-187
3	22	-6	H,L=-16	3		H,L=-14	1		5	43	48	3	22	-14	7	35	29	H,L= -8	12		2	104	-90	2	174	-161
H,L=-19	6		2	29	9	2	53	-56	7	14	-4	5	87	83	9	61	73	0	116	117	4	110	-95	4	8	25
1	58	-63	4	42	31	4	52	-61	H,L=-13	12		7	81	93	H,L= -9	3		2	65	70	6	32	28	6	78	83
3	22	-15	6	57	49	6	42	-50	1	16	5	H,L=-11	8		1	152	142	4	50	-35	H,L= -6	7		8	39	42
H,L=-19	7		H,L=-16	4		H,L=-14	2		3	47	40	1	153	153	3	202	212	6	41	-34	2	236	249	10	39	27
1	31	18	0	132	110	0	136	-133	5	34	31	3	51	50	5	106	75	H,L= -8	13		4	185	166	H,L= -4	3	
3	57	19	2	77	99	2	66	-65	H,L=-13	13		5	59	-44	7	22	-2	2	22	-9	6	17	17	2	99	-79
H,L=-19	8		4	17	-17	4	17	22	1	34	-32	7	56	-50	H,L= -9	4		4	34	-37	H,L= -6	8		4	49	45
1	30	33	6	44	-41	6	42	36	5	30	-35	H,L=-11	9		1	67	70	6	33	-41	0	20	8	6	135	160
3	34	28	H,L=-16	5		H,L=-14	3		H,L=-13	14		1	55	-46	3	73	59	H,L= -8	14		2	83	75	H,L= -4	4	
H,L=-19	9		2	29	-5	2*	0	-6	1	51	-59	3	72	-74	5	19	9	0	27	-33	4	101	82	0	265	277
3	51	-62	4	17	-24	4	17	15	H,L=-13	15		5	73	-73	7	22	-23	2	20	-26	6	18	6	2	125	105
H,L=-19	10		6	51	-50	6	73	72	1	16	-11	7	35	-34	H,L= -9	5		H,L= -8	15		H,L= -6	9		4	26	20
1	32	-36	H,L=-16	6		H,L=-14	4		H,L=-13	16		H,L=-11	10		1	47	-33	2	45	51	2	54	-47	6	62	-62
3	40	-25	0	25	-32	0	112	110	1	24	40	1	39	-26	3	45	-40	H,L= -8	16		4	98	-84	H,L= -4	5	
H,L=-19	12		2	44	-47	2	53	84	H,L=-12	1		3	72	-77	5	102	-82	0	24	29	6	65	-61	2	163	-153
1	47	57	4	30	-33	4	17	4	2	52	38	5	64	-53	7	61	-63	H,L= -7	1		H,L= -6	10		4	156	-147
H,L=-19	14		H,L=-16	7		6	19	-30	4	16	-32	7	33	27	H,L= -9	6		1	74	-58	0	170	-156	6	49	-44
1	17	-26	2	78	85	H,L=-14	5		6	73	-68	H,L=-11	11		1	181	-185	3	263	-263	2	98	-97	H,L= -4	6	
H,L=-18	1		4	79	80	2	86	-84	8	34	-34	1	65	60	3	24	6	5	66	-53	4	94	37	0	71	-63
2	30	-25	H,L=-16	8		4	68	-69	H,L=-12	2		3	99	107	5	95	74	7	10	-6	6	66	52	2	52	-44
4	29	-30	0	11	13	6	19	-38	0	158	-168	5	48	55	7	60	60	H,L= -7	2		H,L= -6	11		4	122	-102
H,L=-18	2		2	24	37	H,L=-14	6		2	55	-53	7	27	10	H,L= -9	7		1	23	-3	2	44	-25	6	47	-29

TABLE 3. THE OBSERVED AND CALCULATED STRUCTURE FACTORS (continued)

K	FO	FC	K	FO	FC	K	FO	FC	K	FO	FC	K	FO	FC	K	FO	FC	K	FO	FC	K	FO	FC
H,L= -4	7		H,L= -2	3		1	8	1	1	67	-68	5	27	-15	1	68	-60	3	48	-45	4	47	-42	1	37	-16
2	121	106	2	47	38	H,L=	0	0	3	102	-107	7	17	27	3	52	-48	5	17	-9	6	95	-95	3	24	-28
4	135	129	4	93	117	2	161	193	5	17	-45	H,L=	3	7	5	100	-103	7	17	23	8	37	-41	5	17	-23
6	48	40	6	69	83	4	97	-92	7	17	4	1	67	64	7	39	-32	H,L=	7	7	H,L=	10	2	H,L=	13	3
H,L= -4	8		H,L= -2	4		6	167	-193	H,L=	1	10	3	112	104	H,L=	5	6	1	33	17	0	170	-91	1	28	-4
0	235	233	0	221	-208	8	24	-19	1	23	-32	5	72	77	1	33	-37	3	24	27	2	93	-91	3	29	26
2	124	117	2	29	11	10	12	-3	3	46	-37	7	25	7	3	62	-58	5	17	27	4	40	-34	5	23	21
4	34	-26	4	102	123	H,L=	0	1	5	23	-13	H,L=	3	8	5	41	-19	7	27	23	6	18	7	7	14	23
6	63	-50	6	48	48	2	47	47	H,L=	1	11	1	27	8	7	17	19	H,L=	7	8	H,L=	10	3	H,L=	13	4
H,L= -4	9		H,L= -2	5		4	117	-127	1	28	8	3	59	57	H,L=	5	7	1	56	53	2	99	96	1	49	50
2	49	35	2	173	-186	6	74	-161	3	23	29	5	60	57	1	63	59	3	17	18	4	92	86	3	16	10
4	57	-46	4	169	-168	8	101	-93	5	15	24	7	17	-20	3	72	71	5	15	-25	6	26	37	5	15	-17
6	80	-76	6	14	-15	H,L=	0	2	H,L=	3	9	5	60	55	H,L=	7	9	H,L=	7	9	H,L=	10	4	H,L=	13	5
H,L= -4	10		H,L= -2	6		2	50	-51	1	56	60	1	28	-30	7	34	8	1	21	5	0	35	22	1	26	9
0	135	-130	0	83	-70	4	82	-102	3	21	9	3	60	-60	H,L=	5	8	3	15	-4	2	58	57	H,L=	13	6
2	62	-60	2	140	-171	6	9	19	5	13	-26	5	24	-35	1	52	51	H,L=	7	10	4	17	35	1	27	-26
4	34	4	4	18	-17	8	67	60	H,L=	2	0	7	22	-16	3	55	50	1	23	-25	6	26	4	H,L=	14	0
6	46	32	6	27	16	10	48	51	0	222	239	H,L=	3	10	5	24	1	H,L=	8	0	H,L=	10	5	0	39	13
H,L= -4	11		H,L= -2	7		H,L=	0	3	2	76	65	1	57	-63	7	22	-25	0	120	125	2	48	-41	2	33	36
2	67	61	2	49	-33	2	259	320	4	16	1	3	16	-23	H,L=	5	9	2	92	98	4	42	-40	4	38	35
4	76	75	4	32	34	4	228	265	6	53	-70	5=	0	15	1	33	-2	4	36	31	6	25	-26	6	32	6
6	40	38	6	73	75	6	11	20	8	21	-26	H,L=	3	11	3	17	-19	6	52	-25	H,L=	10	6	H,L=	14	1
H,L= -4	12		H,L= -2	8		H,L=	0	4	10	25	-30	1	15	-5	5	16	-37	8	46	-52	0	64	-64	2	60	-69
0	25	6	0	209	212	0	80	-61	H,L=	2	1	3	21	12	H,L=	5	10	H,L=	8	1	2	58	-58	4	45	-55
2	29	22	2	87	93	2	162	150	2	219	-263	5	19	28	1	53	-5=	2	49	43	4=	0	12	6	17	-12
4	57	59	4	73	-63	4	156	153	4	125	-152	H,L=	3	12	3	22	-18	4	30	-28	6	23	18	H,L=	14	2
6	23	5	6	72	-65	6	42	34	6	24	-20	1	42	43	H,L=	5	11	6	92	-89	H,L=	10	7	0	24	-18
H,L= -4	13		H,L= -2	9		H,L=	0	5	8	35	3	3=	0	8	3	18	24	8	65	-65	2	22	13	2	41	-38
2	55	-53	2	41	-26	2	105	-102	H,L=	2	2	H,L=	4	0	H,L=	6	0	H,L=	8	2	4	15	27	4	16	-20
4	29	-45	4	58	-59	4	120	-121	0	180	11	0	214	-256	0	37	-30	0	198	-183	6	14	32	H,L=	14	3
6	13	-18	6	73	-41	6	64	-70	2	82	-76	2	133	124	2	134	155	2	60	-63	H,L=	10	8	2	23	5
H,L= -4	14		H,L= -2	10		H,L=	0	6	4	122	-143	4	104	100	4	99	93	4	20	0	0	43	34	H,L=	14	4
0	29	-34	0	69	-63	0	128	-134	6	43	-41	6	47	41	6	53	47	6	61	44	2	19	26	0	57	49
2	26	-30	2	16	-33	2	165	-161	8	88	83	8	96	-84	8	108	-92	H,L=	8	3	H,L=	11	0	2	26	28
H,L= -3	1		4	49	-41	4	38	41	10	64	62	10	80	-73	10	69	-60	2	67	60	1	139	130	4	14	-5
1	15	5	6	26	5	6	65	61	H,L=	2	3	H,L=	4	1	H,L=	6	1	4	92	93	3	26	14	H,L=	14	6
3	77	74	H,L=	-2	11	H,L=	0	7	2	182	174	2	259	-284	2	100	-94	6	48	46	5	56	-51	0	29	-25
5	89	-106	2	97	88	2	13	-9	4	120	114	4	198	-172	4	157	-138	H,L=	8	4	7	47	-36	H,L=	15	0
7	87	-107	4	68	70	4	51	48	6	34	26	6	17	-15	6	67	-68	0	32	20	H,L=	11	1	1	33	26
H,L= -3	2		6	24	18	6	106	108	H,L=	2	4	8	21	31	8	29	-25	2	21	20	1	29	-28	3	42	36
1	173	-186	H,L=	-2	12	H,L=	0	8	0	185	207	H,L=	4	2	H,L=	6	2	4	74	63	3	39	-27	5	16	23
3	74	53	0	30	30	0	105	97	2	139	141	0	25	-85	0	91	-189	6	32	15	5	63	-73	7	15	-11
5	90	112	2	36	32	2	78	76	4	11	-6	2	172	-186	2	122	-114	H,L=	8	5	7	17	-34	H,L=	15	1
7	53	56	4	42	39	4	23	-9	6	51	-40	4	10	2	4	69	48	2	82	-90	H,L=	11	2	1	23	-27
9	37	11	6	15	-4	6	37	-30	H,L=	2	5	6	38	32	6	83	68	4	72	-83	1	31	-23	3	45	-64
H,L= -3	3		H,L= -2	13		H,L=	0	9	2	62	67	8	28	64	H,L=	6	3	6	26	-4	3	98	-52	5	38	-28
1	44	46	2	20	-18	2	93	-92	4	46	-32	10	54	43	2	44	-24	H,L=	8	6	5	30	-27	H,L=	15	2
3	18	-12	H,L=	-2	14	4	175	-172	6	126	-122	H,L=	4	3	4	52	51	0	35	-48	7	17	23	1	48	-44
5	92	114	0	48	-47	6	50	-40	H,L=	2	6	2	15	-2	6	97	87	2	47	-43	H,L=	11	3	3	33	-25
7	79	89	2	32	-36	H,L=	0	10	0	160	-162	4	38	40	H,L=	6	4	4	17	-11	1	45	37	5	15	4
H,L= -3	4		H,L= -1	1		0	36	-33	2	73	-77	6	118	115	0	144	155	6	26	16	3	94	85	H,L=	15	3
1	21	-6	1	86	-79	2	54	-41	4	32	21	H,L=	4	4	2	54	51	H,L=	8	7	5	39	37	1	26	0
3	109	110	3	82	68	4	34	-34	6	43	36	0	276	305	4	15	2	2	29	-2	7	17	9	3	15	7
5	69	70	5	152	-180	6	25	7	H,L=	2	7	2	118	115	6	62	-50	4=	0	20	H,L=	11	4	H,L=	15	4
7	71	-41	7	104	-116	H,L=	0	11	2	42	43	4	105	-91	H,L=	6	5	6	24	29	1	49	39	1	28	33
H,L= -3	5		H,L= -1	2		2	58	51	4	72	74	6	96	-98	2	108	-102	H,L=	8	8	3	42	40	3	19	11
1	129	-132	3	86	-117	4	43	41	6	78	68	H,L=	4	5	4	91	-92	0	60	63	5	17	9	H,L=	15	5
3	234	-225	5	20	27	6	28	25	H,L=	2	8	4	48	-44	6	18	-27	2	39	37	7	16	-25	1	24	-9
5	64	-56	7	34	55	H,L=	0	12	0	29	4	6	104	-102	H,L=	6	6	4	15	-16	H,L=	11	5	H,L=	16	0
7	28	14	9	56	54	0	66	62	2	39	36	H,L=	4	6	0	33	-18	6	14	-22	1	28	5	0	31	17
H,L= -3	6		H,L= -1	3		2	41	42	4	68	65	0	112	-107	2	22	-19	H,L=	8	9	3	24	-33	2	33	40
1	11	-3	1	225	246	H,L=	0	13	6	33	12	2	45	-44	4	73	-62	2	20	-4	5	16	-24	4	23	21
3	131	-110	3	219	247	2	18	-1	H,L=	2	9	4	68	-56	6	19	2	H,L=	8	10	7	20	-30	6	16	1
5	48	-48	5	87	115	H,L=	0	14	2	76	-84	6	18	13	H,L=	6	7	0	13	-14	H,L=	11	6	H,L=	16	1
7	47	35	7	11	10	0	39	-36	4	65	-65	H,L=	4	7	2	58	53	H,L=	9	0	1	57	-60	2	42	-34
H,L= -3	7		H,L= -1	4		H,L=	1	0	6	32	-18	2	104	111	4	55	50	1	208	200	H,L=	11	7	4	15	-33
1	27	-8	1	62	-57	1	284	402	H,L=	2	10	4	95	96	6	18	18	3	56	56	1	25	1	6	21	-16
3	87	72	3	168	170	3	53	47	0	31	-34	6	26	27	H,L=	6	8	5	85	-86	H,L=	11	8	H,L=	16	2
5	57	54	5	122	122	5	140	-155	2	48	-42	H,L=	4	8	0	59	67	7	44	-45	1	21	24	0	31	-47
7	53	54	7	31	-31	7	77	-69	4	16	-11	0	30	17	2	48	44	9	29	-23	H,L=	12	0	2	37	-32
H,L= -3	8		H,L= -1	5		9	12	-9	6	17	14	2	29	34	4	17	4	H,L=	9	1	0	115	114	H,L=	16	3
1	192	186	1	89	-94	H,L=	1	1	H,L=	2	11	4	67	65	6	24	-24	1	18	17	2	35	28	2	14	1
3=	0	19	3	220	-197	1	66	-65	2	16	7	6	18	4	H,L=	6	9	3	47	36	4	23	-4	H,L=	16	4
5	93	-88	5	67	-69	3	70	-87	4	21	20	H,L=	4	9	2	32	9	5	93	-112	6	18	-33	0	30	33
7	43	-34	7	32	-38	5	107	-164	6	20	28	2	29	-31	H,L=	6	10	7	94	-94	8	20	-9	H,L=	17	0
H,L= -3	9		H,L= -1	6		7	36	-57	H,L=	2	12	4	34	-46	0	55	-47	H,L=	9	2	H,L=	12	1	1	27	29
1	26	25	1	142	-142	H,L=	1	2	0	54	58	6	17	-27	2	20	-28	1	101	-105	2	50	-48	3	22	27
3	23	5	3	44	-39	1	176	-179	2	31	36	H,L=	4	10	H,L=	6	12	3	40	-43	4	99	-64	5	14	0
5	93	-74	5	76	98	3	149	-162	H,L=	3	0	0	74	-71	0	19	14	5	22	17	6	19	-41	H,L=	17	1
7	69	-69	7	53	47	5	58	-60	1	149	139	2	43	-47	H,L=	7	0	7	17	17	H,L=	12	2	1	21	-9
H,L= -3	10		H,L= -1	7		7	35	39	3	69	57	H,L=	4	11	1	55	45	H,L=	9	3	0	80	2	3	14	-21
1	95	-89	1	80	-64	9	79	79	5	13	4	2	20	3	3	103	106	1	53	62	2	33	-30	H,L=	17	2
3	17	-29	3	40	-14	H,L=	1	3	7	37	-36	H,L=	4	12	5	50	52	3	106	96	4	42	-39	1	30	-35
5	24	10	5	86	77	1	96	85	9	66	-57	0	37	37	7	55	-48	5	58	69	6	18	-3	3	13	-13
7	17	16	7	109	107	3	268	280	H,L=	3	1	2	23	23	9	71	-64	7	21	12	H,L=	12	3	H,L=	17	3
H,L= -3	11		H,L= -1	8		5	101	108	1	146	-142	H,L=	5	0	H,L=	7	1	H,L=	9	4	2	38	39	1	21	10
1	70	57	1	168	179	7	12	4	3	247	-272	1	56	-61	1	29	39	1	34	20	4	24	30	H,L=	17	4
3	74	74	3	27	11	H,L=	1	4	5	71	-74	3	152	123	3	34	-27	3	66	62	6	25	20	1	17	14
5	58	58	5	75	-72	1	104	98	7	10	10	5	167	161	5	72	-63	5	49	44	H,L=	12	4	H,L=	18	0
7	27	4	7	39	-42	3	78	78	H,L=	3	2	7	43	-45	7	78	-80	7	24	-18	0	40	33	0	42	36
H,L= -3	12		H,L= -1	9		5	39	33	1	26	3	9	111	-98	H,L=	7	2	H,L=	9	5	2	47	48	2	20	24
1	28	9	1	34	-30	7	50	-41	3	123	-89	H,L=	1	1	1	163	-192	1	36	-43	4	23	0	4	27	-1
3	44	42	3	68	-69	H,L=	1	5	5	41	-51	1	116	-121	3	26	-4	3	80	-93	6	17	-15	H,L=	18	1
5	44	36	5	75	-69	1	66	61	7	43	33	3	300	-304	5	68	63	5	24	-30	H,L=	12	5	2	13	-4
H,L= -3	13		7	39	-24	3	39	-40	9	56	65	5	48	-47	7	43	36	7	16	-8	2	28	-6	4	12	-17
1	26	-25	H,L=	-1	10	5	95	-83	H,L=	3	3	7	22	-7	9	38	9	H,L=	9	6	H,L=	12	6	H,L=	18	2
3	40	-38	1	28	-28	7	104	-101	1	19	-11	H,L=	5	2	H,L=	7	3	1	57	-61	0	43	-38	0	61	-38
5	23	-33	3	42	-40	H,L=	1	6	3	84	90	1	159	-168	1	25	19	3	24	-25	2	21	-30	H,L=	19	0
H,L= -3	14		5	38	-30	1	208	-203	5	65	52	3	67	-55	3	24	22	5	16	8	H,L=	12	7	1	18	32
1	38	-43	7	23	24	3	19	-21	7	54	49	5	53	40	5	100	95	7	21	24	2	13	21	3	12	9
H,L= -3	15		H,L= -1	11		5	66	51	H,L=	3	4	7	76	75	7	63	55	H,L=	9	7	H,L=	12	8	H,L=	19	1
1	13	-5	1	57	49	7	63	54	1	205	238	9	39	44	H,L=	7	4	1	23	-7	0	12	16	1	16	-2
H,L= -2	1		3	79	82	H,L=	1	7	3	41	39	H,L=	5	3	1	53	50	3	16	19	H,L=	13	0	H,L=	19	2
2	108	120	5	40	41	1	19	4	5	98	-84	1	15	3	3	21	18	H,L=	9	8	1	38	41	1	16	-22
4	23	-26	H,L=	-1	12	3	47	46	7	71	-67	3	12	2	5	16	6	1	49	49	3	17	15	H,L=	20	0
6	92	-159	1	55	48	5	88	80	H,L=	3	5	5	95	85	7	17	-10	H,L=	10	0	5	24	15	0	40	34
8	87	-83	3	39	30	7	63	60	1	42	42	7	93	89	H,L=	7	5	0	225	246	7	17	-19	2	20	18
H,L= -2	2		5	20	4	H,L=	1	8	3	30	15	H,L=	5	4	1	70	-76	2	98	85	H,L=	13	1	1	6	22
2	167	-141	H,L=	-1	13	1	30	27	5	95	-93	1	166	197	3	90	-86	4	39	-26	1	39	-33			
4	43	46	1	14	1	3	40	37	7	90	-85	3	13	15	5	45	-47	6	81	-86	3	67	-74			
6	83	121	H,L=	-1	14	5	45	37	H,L=	3	6	5	87	-87	7	25	7	8	35	-27	5	34	-38			
8	67	24	1	37	-43	7	17	-25	1	77	-86	7	47	-43	H,L=	7	6	H,L=	10	1	7	23	-2			
10	53	25	H,L=	-1	15	H,L=	1	9	3	42	-38	H,L=	5	5	1	22	-26	2	20	16	H,L=	13	2			

Description of the Molecular Structure and Discussion

The molecular structure is shown in Fig. 1. The geometry around the tin atom is shown in Fig. 2,*3 while the bond lengths and angles in the environment of the tin atom are listed in Table 4. Such as in the low-mp isomer, the two bromine atoms attached to the tin atom are in *cis*-positions. The two ligands, both 1,2-diethoxycarbonyl-ethyl groups, are bound to the tin atom by carbon and oxygen atoms, and form rather puckered five-membered rings. The coordination about the tin atom is a six-coordinated, distorted octahedron. In the $(CH_3)_2Sn(C_9H_6NO)_2$ compound, it was found that, though the tin atom seems to be six-coordinated, the C–Sn–C angle is nearly tetrahedral (110.7°); Schlemper postulated a theory that the bonding involves sp^3 hybrid orbitals on the tin atom participating in two normal covalent bonds to the methyl groups and in two three-center bonds to the oxinate groups.[4] In the high-mp isomer, however, the C–Sn–C angle (147.4°) and the other angles around the tin atom take values different from those in the oxinate chelate.

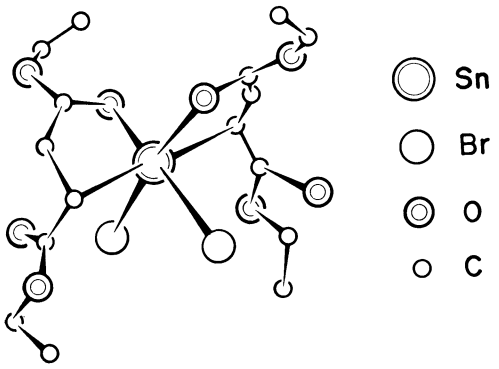

Fig. 1. The molecular structure of the high mp isomer of bis-(1,2-diethoxycarbonyl-ethyl)tin dibromide.

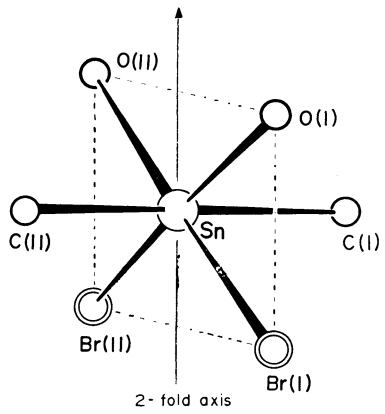

Fig. 2. The geometry around the tin atom.

*3 The Br(11), C(11), ···, C(18) and O(11), ···, and O(14) stand for the equivalent positions related by the two-fold axis at the $(0, y, 1/4)$ of Br(1), C(1),···, C(8) and O(1), ···, O(4) respectively.

Table 4. Bond lengths and angles in the environment of the tin atom

Bond length		Bond angle	
Sn–Br(1)	2.504 Å	Br(1)–Sn–Br(11)	101°
Sn–C(1)	2.24	Br(1)–Sn–C(1)	103
Sn–O(1)	2.49	Br(1)–Sn–O(1)	91
		Br(1)–Sn–C(11)	97
		Br(1)–Sn–O(11)	166
		C(1)–Sn–O(1)	72
		C(1)–Sn–C(11)	148
		O(1)–Sn–C(11)	83
		O(1)–Sn–O(11)	79

The estimated standard deviations of the bond lengths in Sn–Br is 0.005 Å, in Sn–C 0.03 Å, and in Sn–O 0.02 Å. Those for angles are all less than 2.5°.

The Sn–Br distance, 2.504 Å, is slightly shorter than the sum of the covalent radii of Sn and Br, 2.540 Å, and is also shorter than those in the low-mp isomer, 2.52 Å and 2.58 Å.[2] The Sn–Br distance of 2.507 Å observed in (4-bromo-1,2,3,4-tetraphenyl-*cis,cis*-1,3-butadienyl)dimethyltin bromide[5] is, however, close to this value. The Sn–C distance, 2.24 Å, is not much different from that in the low-mp isomer,[2] 2.26 Å, nor from that in (4-bromo-1,2,3,4-tetraphenyl-*cis*-1,3-butadienyl)dimethyltin bromide,[5] 2.24 Å. All these values are slightly longer than the sum of the covalent radii (2.17 Å) and also longer than those in $(CH_3)_3SnMn(CO)_5$[6] (2.16 Å) and those in $(CH_3)_2Sn(C_9H_6NO)_2$[4] (2.17 Å). The Sn–O bond distance, 2.49 Å, is considerably longer than the sum of the covalent radii (2.06 Å) and also longer than those in $(CH_3)_2Sn(C_9H_6NO)_2$[4] (2.10 Å) and those in $[\pi\text{-}C_5H_5Fe(CO)_2]_2Sn(ONO)_2$ (2.14 Å).[7] This suggests that the Sn–O bond is a weak coordination bond similar to that of the low-mp isomer (Sn–O, 2.45 Å). The bond angles shown in Table 4 are similar to those observed in the low-mp isomer.

The largest deviations from the least-squares planes, Br(1)–O(1)–O(11)–Br(11), Br(1)–C(1)–O(11)–C(11), and O(1)–C(1)–C(11)–Br(11), all centered by the tin, are 0.20 Å, 0.28 Å, and 0.24 Å respectively. These three planes make dihedral angles, 88°, 87°, and 87°, with each other.

The bond lengths and angles in the ligand, the

4) E. P. Schlemper, *J. Inorg. Chem.*, **6**, 2012 (1967).
5) F. P. Boer, J. J. Flynn, H. H. Freedman, S. V. Mckinley and V. R. Sandel, *J. Am. Chem. Soc.*, **89**, 5068 (1967).
6) R. E. Bryan, *Chem. Commun.*, **1967**, 355.
7) B. P. Bir'yukov, Yu. T. Struchkov, K. N. Anisimov, N. E. Koloeova, O. P. Osipova and M. Ya. Zakharov, *ibid.*, **1967**, 750.

1,2-diethoxycarbonyl-ethyl group, are listed in Table 5.

TABLE 5. THE BOND LENGTHS AND ANGLES OF THE LIGAND GROUP

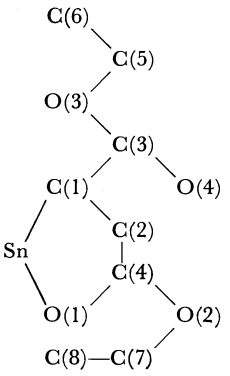

Bond length		Bond angle	
Sn-C(1)	2.24 Å	O(1)-Sn-C(1)	72°
Sn-O(1)	2.49	Sn-O(1)-C(4)	109
O(1)-C(4)	1.12	C(4)-O(2)-C(7)	118
O(2)-C(4)	1.39	C(3)-O(3)-C(5)	120
O(2)-C(7)	1.42	Sn-C(1)-C(2)	106
O(3)-C(3)	1.30	C(2)-C(1)-C(3)	116
O(3)-C(5)	1.43	C(1)-C(2)-C(4)	112
O(4)-C(3)	1.20	O(3)-C(3)-O(4)	129
C(1)-C(2)	1.54	O(3)-C(3)-C(1)	110
C(1)-C(3)	1.47	O(4)-C(3)-C(1)	120
C(2)-C(4)	1.41	O(1)-C(4)-C(2)	127
C(5)-C(6)	1.42	O(1)-C(4)-O(2)	120
C(7)-C(8)	1.42	O(2)-C(4)-C(2)	112
		O(3)-C(5)-C(6)	109
		O(2)-C(7)-C(8)	114

The estimated standard deviations for bond lengths are 0.02—0.08 Å, and for angles are 2.0—3.7°.

Each of the two ligands, both 1,2-diethoxycarbonyl-ethyl groups, has an asymmetric carbon atom, C(1) and C(11) respectively. In the low-mp isomer,[2] one of the two asymmetric carbons is in the *d*-form and the other, in the *l*-form. In the high-mp isomer, however, since the molecule has C_2 symmetry, both of them are in either the *d*-form or the *l*-form. The molecule must possess optical activity. Since there are glide planes in the unit cell (space group: $C2/c$), there are equal numbers of molecules of two optical antipodes (Fig. 3) in the crystal. The crystal exhibits no optical activity as a whole.

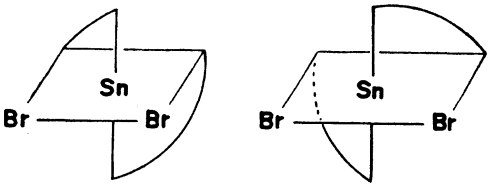

Fig. 3. Two optical antipodes.

Figure 4 shows the crystal structure of the high-mp isomer projected onto the (010) plane. Intermolecular atomic contacts of less than 4.0 Å are listed in Table 6. The shortest distances are O(4)-C(15)^{II}, 3.15 Å, O(4)-C(17)^{IV}, 3.16 Å, and C(7)-O(14),^{IV} 3.16 Å. These values are similar to those found in the low-mp isomer. However, the number of close intermolecular contacts in the high-mp isomer exceeds those in the low-mp isomer. Therefore, it seems that the molecules are packed more densely in the high-mp isomer than in the low-mp isomer. This is supported by the fact that the density of the high-mp isomer (D_m=1.82, D_x=1.83 g·cm^{-3}) is larger than that of low-mp isomer (D_m=1.80, D_x=1.80 g·cm^{-3}). The difference in the melting points of the two isomers, 8°C, may be

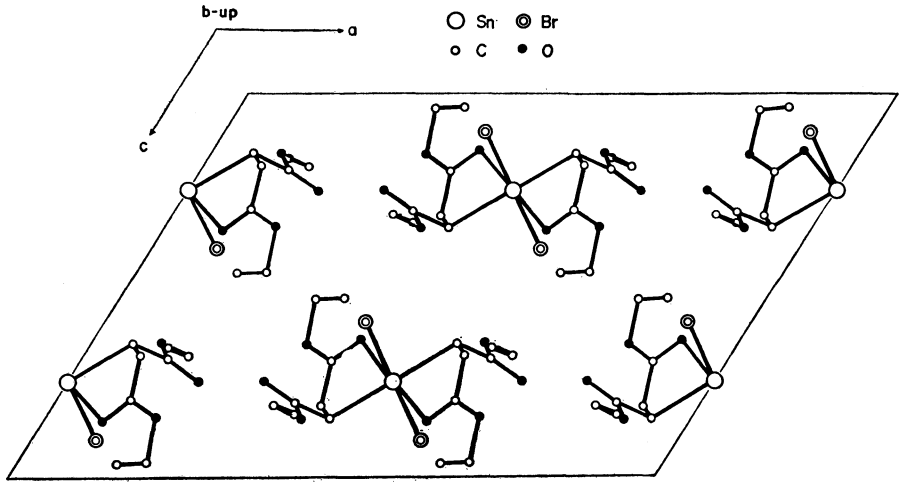

Fig. 4. The crystal structure of the high-mp isomer of bis-(1,2-diethoxycarbonyl-ethyl)tin dibromide.

TABLE 6. INTERMOLECULAR ATOMIC CONTACTS (LESS THAN 4.0 Å) OF THE HIGH-mp ISOMER

Br–C (van der Waals distance, 3.95 Å)				C(7)–O(14)^{iv}	3.16	O(4)–C(16)^{ii}	3.44
Br(1)–C(3)^{iii}	3.65 Å	C(13)–Br(11)^{iii}	3.65 Å	C(8)–O(14)^{iv}	3.45	O(4)–C(18)^{iv}	3.45
Br(1)–C(1)^{iii}	3.70	C(11)–Br(11)^{iii}	3.70	O(13)–C(1)^{iii}	3.61	C(11)–O(3)^{iii}	3.61
C(8)–Br(1)^{v}	3.78	C(18)–Br(11)^{v}	3.78	O(2)–C(15)^{ii}	3.68	O(2)–C(6)^{v}	3.71
Br(1)–C(17)^{iv}	3.88	C(7)–Br(11)^{iv}	3.88	O(12)–C(16)^{v}	3.71	C(15)–O(11)^{iii}	3.81
Br–O (van der Waals distance, 3.35 Å)				O(1)–C(5)^{iii}	3.81	O(1)–C(6)^{iii}	3.86
Br(1)–O(3)^{iii}	3.81 Å	O(13)–Br(11)^{iii}	3.81 Å	C(16)–O(11)^{iii}	3.86	O(1)–C(17)^{iv}	3.99
C–C (van der Waals distance, 4.00 Å)				C(7)–O(11)^{iv}	3.99		
C(8)–C(6)^{iii}	3.76 Å	C(16)–C(18)^{iii}	3.76 Å				
C(7)–C(6)^{iii}	3.83	C(16)–C(17)^{iii}	3.83	Code for superscript			
C(8)–C(6)^{v}	3.96	C(18)–C(16)^{v}	3.96	i	x,	y,	z
O–O (van der Waals distance, 2.80 Å)				ii	$1/2+x$,	$1/2+y$,	z
O(2)–O(14)^{ii}	3.98 Å			iii	x,	$-y$,	$1/2+z$
C–O (van der Waals distance, 3.40 Å)				iv	$1/2+x$,	$1/2-y$,	$1/2+z$
O(4)–C(15)^{ii}	3.15 Å	O(4)–C(17)^{iv}	3.16 Å	v	x,	$1.0+y$,	z

attributed to the above-mentioned difference between the intermolecular contacts of the two isomers.

The authors are very grateful to Professor S. Matsuda, Professor S. Kikkawa and Dr. I. Omae for providing them with the samples used in this study. The authors wish to express their thanks to Dr. T. Ashida for the use of computer programs (HBLS IV and DAPH).

BULLETIN OF THE CHEMICAL SOCIETY OF JAPAN VOL. 42 2485—2489 (1969)

The Ultrasonic Study of Aqueous Solutions of Alkyl-Substituted Urea

Katsutaka SASAKI and Kiyoshi ARAKAWA

Research Institute of Applied Electricity, Hokkaido University, Sapporo

(Received February 22, 1969)

An ultrasonic investigation of aqueous solutions of alkyl-substituted urea was made by means of an ultrasonic pulse technique in order to study the influence of the solutes upon the structure of solvent. The ultrasonic velocity and absorption were measured in solutions of 1,3-dimethylurea and 1,3-diethylurea in the frequency range from 5 to 45 Mc/sec. The temperature was varied from 10 to 40°C, and the concentration from 0.2 to 4 mol/*l*. Within the range of frequency no relaxation frequency was observed for both solutions. From the data on absorption coefficent and viscosity, the magnitude of absorption due to structural relaxation was calculated. It was found that structural absorption in dimethylurea solutions is slightly larger, and in diethylurea solutions much larger than that of the urea solutions. From these results, it is concluded that 1,3-dimethylurea is a structure breaker for the open-packed structure in water, the ability being smaller than that of urea, and that, for the behavior of 1,3-diethylurea molecule in water, the structure-forming ability of the ethyl group is found to surpass the structure-breaking effect of the residual part of the molecule.

In the preceding paper[1] one of the authors reported the results of an ultrasonic study on aqueous solutions of urea, and stated from experimental grounds that urea behaves as a structure breaker for the "open-packed structure" or the "ice-like structure" in liquid water. Recently, H. S. Frank and coworker[2] have discussed the behavior of urea molecules in water and have concluded that urea is a structure breaker for water, based on a two state model of water,[3] which has been made clear

1) K. Arakawa and N. Takenaka, This Bulletin, **40**, 2739 (1967).

2) H. S. Frank and F. Franks, *J. Chem. Phys.*, **48**, 4746 (1968).

3) L. Hall, *Phys. Rev.*, **73**, 775 (1948).

by the authors[4] to be a useful model for thermodynamical behaviors of liquid water. Urea is well known as a typical reagent for the denaturation of protein.[5] The effect of the addition of urea in aqueous solutions of polymers is said to consist of two factors;[6] the direct interactions between polymer molecules and urea[7,8] and the influence upon the configuration of polymer molecules through the change of the structure of water caused by the addition of urea.[1,9]

We have studied the structure of water[4] and the influence of the various addends upon it.[1,10] It is interesting to investigate the behavior of alkyl-substituted urea in water in comparison with those of urea, aiming at the effect of alkyl-substitution, especially the change in the ability as structure breaker which is attributed to the introduction of alkyl group. We measured the ultrasonic velocity and absorption of aqueous solutions of alkyl urea.

The denaturation effect of Lysozyme by 1,3-dimethylurea has recently been investigated by Hamaguchi and Sasaki.[11] Concerning the influence of alkane molecules upon the structure of water, Wetlaufer *et al.* have studied the solubility of hydrocarbons in 7M urea and 4.9M guanidine hydrochloride solutions,[12] and appreciable differences have been observed between the behavior of methane and that of higher homologues. Thus we carried out an ultrasonic study of aqueous solutions of 1,3-dimethylurea and 1,3-diethylurea.

Experimental

An ultrasonic pulse method was used for the measurements of the sound velocity and of the absorption. The apparatus used and the procedure for the measurements were described in the preceding paper.[13] The absorption coefficient was determined over the fequency range of 15—45 Mc/sec and at temperatures from 10 to 40°C with 10°C intervals. The sound velocity was measured at 5 Mc/sec. The temperature was held constant to within ±0.1°C. The absorption data were reproducible within 2% and the velocity data within 1 m/sec. Two commercial samples, 1,3-dimethylurea*1 and 1,3-diethylurea,*2 were used without further purification. The melting points of the samples were 106.6 ±0.5°C and 103.8±0.5°C, respectively. The viscosity coefficient, η, was measured on the aqueous solutions by means of an Ostwald capillary viscometer (flow time for pure water 77.7 sec at 20°C). From the values of η the classical absorption (Stokes loss) was calculated.

Results

Ultrasonic Velocity. The results obtained for the aqueous solutions of 1,3-dimethylurea and of 1,3-diethylurea are plotted against temperature in Figs. 1(a) and (b), respectively. The sound velocity data obtained for pure water by Greenspan and Tschiegg[14] are also given. We see that the concentration dependence of the velocity *vs.* temperature curves is similar to that for urea solutions.[1]

Ultrasonic Absorption. The absorption coefficient, α, was measured for solutions of 1,3-dimethylurea in the concentration range, 0.2—4 mol/*l*, and for solutions of 1,3-diethylurea in the range, 0.5—2 mol/*l*. The frequency dependency of α is given

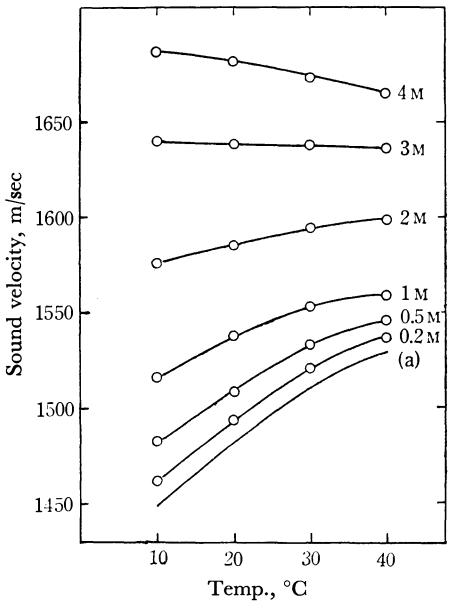

Fig. 1(a). Sound velocity of aqueous solutions of 1,3-dimethylurea.
(a) Pure water

4) K. Arakawa and K. Sasaki, This Bulletin, **42**, 303 (1969).
5) W. Kauzmann, *Advances Protein Chem.*, **14**, 1 (1959).
6) M. Watase and K. Arakawa, *Nippon Kagaku Zasshi* (*J. Chem. Soc. Japan, Pure Chem. Sect.*), **89**, 383 (1968).
7) D. R. Robinson and W. P. Jencks, *J. Am. Chem. Soc.*, **87**, 2462 (1965).
8) J. A. Gordon and W. P. Jencks, *Biochemistry*, **2**, 47 (1963).
9) G. G. Hammes and P. R. Schimmel, *J. Am. Chem. Soc.*, **89**, 442 (1967).
10) K. Arakawa and N. Takenaka, This Bulletin, **42**, 5 (1969).
11) K. Hamaguchi and H. Sakai, *J. Biochem.*, **57**, 721 (1965).
12) D. B. Wetlaufer, S. K. Malik, C. Stoller and R. L. Coffin, *J. Am. Chem. Soc.*, **86**, 508 (1964).
13) K. Arakawa and N. Takenaka, This Bulletin, **39**, 447 (1966); **40**, 2063 (1967).

*1 Aldrich Chemical Co., Inc., Milwaukee, Wisconsin, U.S.A.
*2 Tokyo Chemical Industry Co., Ltd., Tokyo.
14) M. Greenspan and C. E. Tschiegg, *J. Res. Natl. Bur. Std.*, **58**, 249 (1957); *J. Acoust. Soc. Am.*, **31**, 75 (1959).

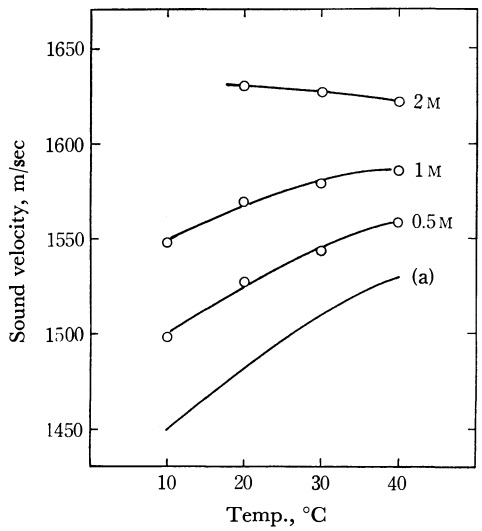

Fig. 1(b). Sound velocity of aqueous solutions of 1,3-diethylurea.
(a) Pure water

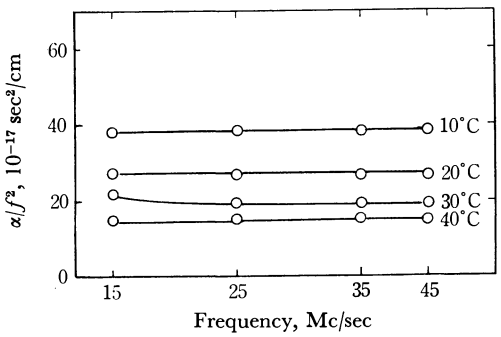

Fig. 2(a). Ultrasonic absorption of aqueous solutions of 1,3-dimethylurea.
Concn., 2 mol/*l*

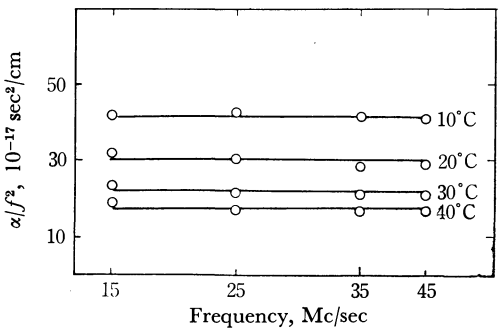

Fig. 2(b). Ultrasonic absorption of aqueous solutions of 1,3-diethylurea.
Concn., 1 mol/*l*

in Figs. 2(a) and (b) in the form of α/f^2 *vs.* $\log f$ relation, where f is frequency, for 2 mol/*l* solution of dimethyl urea and for 1 mol/*l* solution of diethyl urea, as examples. Both groups of curves are flat throughout the frequency range. This means that no relaxation frequency is observed.

In Figs. 3(a) and (b) the (α/f^2) *vs.* concentration curves are given for the solutions of dimethylurea and diethylurea, respectively. For solutions of diethylurea the magnitude of α/f^2 is seen to increase more rapidly than for solutions of dimethylurea with the increase in concentration. The (α/f^2) *vs.* concentration curves for aqueous solutions of urea, 1,3-dimethylurea, and 1,3-diethylurea at 20°C and 40°C are compared in Figs. 4(a) and (b). Concentrations are given in volume %. The dotted lines represent the magnitude of absorption,*3 which is attributed only to water as solvent when no structural change is assumed.

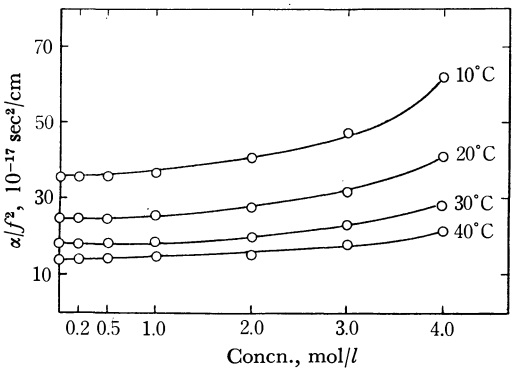

Fig. 3(a). α/f^2 *vs.* concn. relation 1,3-dimethylurea solution.

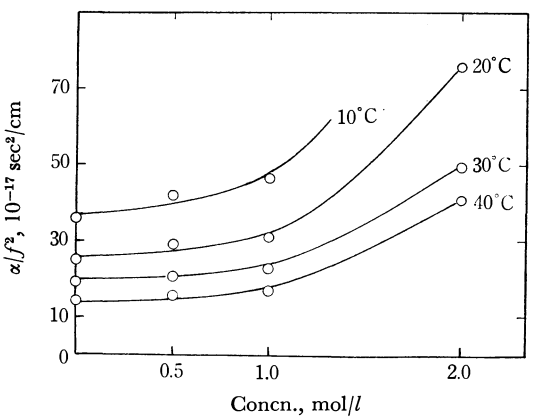

Fig. 3(b). α/f^2 *vs.* concn. relation 1,3-diethylurea solution.

In order to calculate the classical absorption $(\alpha/f^2)_\eta$, the viscosity coefficient η, was measured. The result is given in Fig. 5. The classical absorption is given by

$$(\alpha/f^2)_\eta = \frac{8\pi^2\eta}{3\rho V^3} \qquad (1)$$

*3 This is calculated according to the volume fraction of water as solvent from the absorption of pure water.

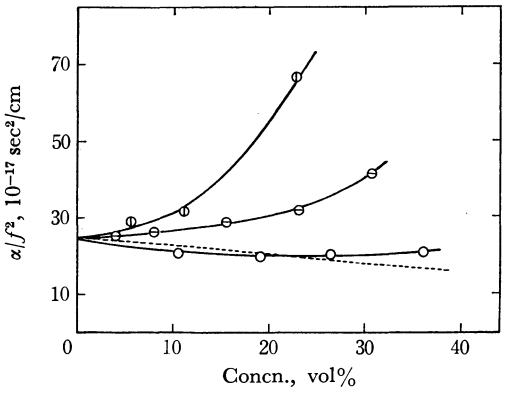

Fig. 4(a). α/f^2 *vs.* concn. relation at 20°C.
○ urea solution,
◒ 1,3-dimethylurea solution
◐ 1,3-diethylurea solution

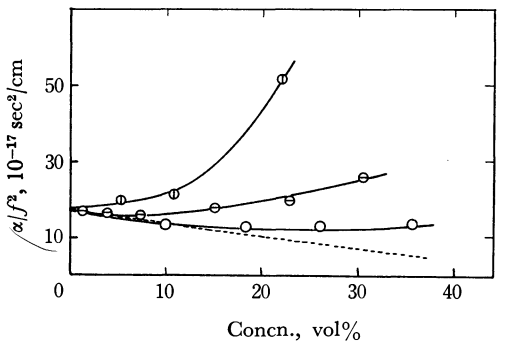

Fig. 4(b). α/f^2 *vs.* concn. relation at 40°C.
○ urea solution
◒ 1,3-dimethylurea solution
◐ 1,3-diethylurea solution

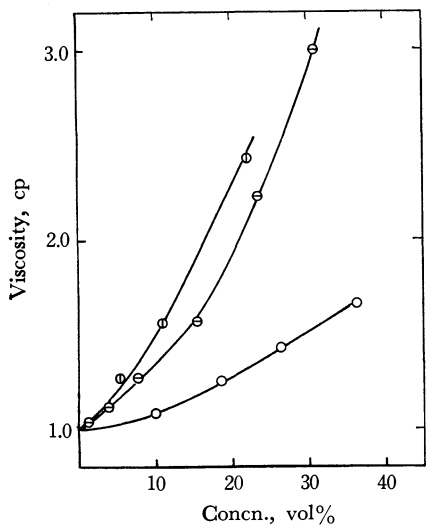

Fig. 5. Viscosity of solutions at 20°C.
○ urea solution
◒ 1,3-dimethylurea solution
◐ 1,3-diethylurea solution

where ρ is density and V is sound velocity. The absorption due to structural relaxation, $(\alpha/f^2)_{\text{struct.}}$ is given by subtracting $(\alpha/f^2)_\eta$ from $(\alpha/f^2)_{\text{obs.}}$

$$(\alpha/f^2)_{\text{struct.}} = (\alpha/f^2)_{\text{obs.}} - (\alpha/f^2)_\eta \qquad (2)$$

The result is shown in Figs. 6(a) and (b) for each temperature.

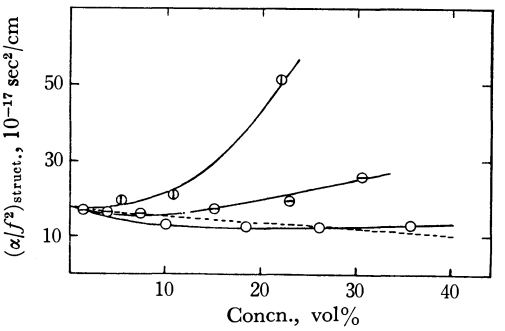

Fig. 6(a). $(\alpha/f^2)_{\text{struct.}}$ *vs.* concn. relation at 20°C.
○ urea solution
◒ 1,3-dimethylurea solution
◐ 1,3-diethylurea solution

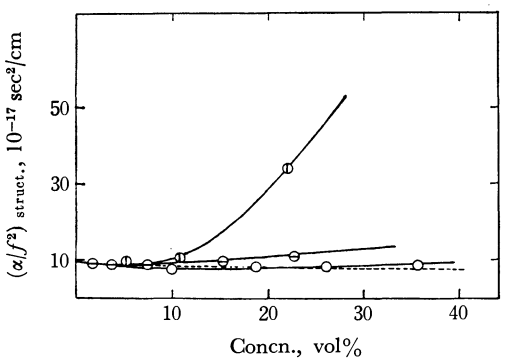

Fig. 6(b). $(\alpha/f^2)_{\text{struct.}}$ *vs.* concn. relation at 40°C.
○ urea solution
◒ 1 3-dimethylurea solution
◐ 1 3-diethylurea solution

Discussion

The Influence of Solute Molecules upon the Structure of Liquid Water. Urea is known as hydrogen bond breaker. However, there is some ambiguity[15] about the behavior of urea in water. From recent studies by us[1] and by Hammes *et al.*,[9] it has been concluded that urea behaves as a structure breaker for the ice-like structure in liquid water. In the case of alkyl-substituted urea the situation is different, because, in addition to the effect of substitution of hydrogen attached to amino radical, the alkyl group is believed to cause iceberg-

15) M. Abu-Hamdiyyah, *J. Phys. Chem.*, **69**, 2720 (1965).

formation around it in water.[16,17] That is, alkyl-substituted urea has two opposite functions, *viz.*, as a structure breaker and as a structure former.

It is clearly seen from Figs. 6(a) and (b) that the magnitude of ultrasonic absorption due to structural relaxation becomes larger in the order 1,3-diethylurea > 1,3-dimethylurea > urea. As pointed out previously,[1] the absorption in urea solutions decreases with the addition of the solute to water, and becomes smaller than the absorption caused by water component only (shown by dotted curves as seen in Figs. 4(a) and (b)). It is similar in the case of structural absorption as seen in Figs. 6(a) and (b). This fact supports definitely the idea that the urea molecules behave as the structure breaker for the ice-like structure in liquid water. This also seems to be the case in 1,3-dimethylurea solutions. The absorption of the solution of 1,3-dimethylurea due to structural relaxation is nearly equal to that in the solutions of urea for a concentration less than about 10 vol%. The magnitude of $(\alpha/f^2)_{\text{struct.}}$ for dimethylurea solutions decreases first with the increase in concentration, and is nearly equal to or a little smaller than that shown by the dotted line for a concentration range of less than about 10 vol%. This behavior is similar essentially to that of urea solutions, though the features observed are not so striking. 1,3-Dimethylurea molecules may be said to act as the structure breaker for the ice-like structure in water, though that ability is supposed to be smaller than that of urea.

In the case of the 1,3-diethylurea solutions, the situations are definitely different. The structural absorption in the solution is found to be much larger than that in the dimethylurea solution within the whole range of concentration. The difference between diethylurea solutions and the other two solutions becomes appreciable in the range of concentration greater than 0.1 volume fraction. This difference is, of course, ascribed to the presence of ethyl groups in place of methyl groups. In order to investigate the change of ultrasonic absorption accompanying the increase in the number of carbon atoms in homologous series, the absorption data for various compounds are given in Table 1. No appreciable change of absorption is observed. It seems that the variation of ultrasonic absorption induced by the introduction of C_2H_5 group in place of CH_3 is not great. Therefore, from the absorption data given in Figs. 6(a) and (b), the fact that the absorption in diethylurea solutions is greater than that in dimethylurea solutions is explained by the structure-forming effect of C_2H_5 group in liquid water. This is in line with the suggestion given by Wetlaufer *et al.*,[12] based on the solubility data of hydrocarbons in urea and guanidine hydrochloride solutions. According to their data, an essential difference between CH_4 and C_2H_6 has been observed with respect to the interaction of alkane molecules with water around themselves. It has been suggested that, at temperatures above about 20°C, C_2H_6 molecules and those of higher homologues have a structure-forming effect upon water molecules around them, with the exception of CH_4. Thus we conclude that in the diethylurea solution the comparatively large absorption is attributed at least partly to the local water structure around C_2H_5 groups, and that the structure-forming effect of C_2H_5 groups may surpass the structure-breaking effect of residual groups in the diethylurea molecule.

Table 1. Ultrasonic absorption of various liquids

Liquid	Temp. °C	f Mc/sec	α/f^2 10^{-17} sec^2/cm
C_6H_{14}	20	5—30	57.6[a]
C_7H_{16}	20	5—30	58[a]
C_8H_{18}	20	5—30	51[a]
$C_{10}H_{22}$	20	21	56.7[b]
$HCOOCH_3$	24.1	104	49.3[c]
$HCOOC_2H_5$	24.1	104	49.9[c]
$C_3H_7COOCH_3$	24.5	104	35.5[c]
$C_3H_7COOC_2H_5$	24.5	104	38.6[c]
CH_3COCH_3	24.4	104	25.7[c]
$CH_3COC_2H_5$	25	10—100	26.5[d]

a) N. I. Koshkin, *Primenenie ultraakustiki k issledovaniyo beshchestva*, **1**, 101 (1955).
b) S. Parthasarathy, M. Pancholy and A. F. Chapgar, *Nuovo Cimento* **10**, 111, 118, 1053 (1958).
c) E. L. Heasell and J. Lamb, *Pro. Phys. Soc.*, **B69**, 869 (1956).
d) M. S. de Groot and J. Lamb, *ibid.*, **A242**, 36 (1957).

Summary and Conclusion

From the ultrasonic data obtained by means of a pulse technique, it is concluded that in the aqueous solution of 1,3-dimethylurea the solute molecules behave as a structure breaker for the ice-like structure in liquid water, though the structure-breaking ability is smaller than that of urea. For the aqueous solution of 1,3-diethylurea it may be said that the structure-forming ability of ethyl group surpasses the structure-breaking effect of the residual part in the solute molecule.

The authors wish to thank Mr. Nobuo Takenaka and Miss Yuko Endo for their cooperation in performing this study.

16) G. Némethy and H. A. Scheraga, *J. Chem. Phys.*, **36**, 3401 (1962).
17) H. S. Frank and M. W. Evans, *J. Chem. Phys.*, **13**, 507 (1945).

BULLETIN OF THE CHEMICAL SOCIETY OF JAPAN VOL. 42 2490—2493 (1969)

The Size and Shape of the Component Molecules as the Factors Determining the Electronic Structure of Crystal Complexes

Yoshio MATSUNAGA

Department of Chemistry, Faculty of Science, Hokkaido University, Sapporo

(Received February 27, 1969)

The molecular complexes of six aromatic diamines with various acceptors were classified into those complexes having essentially non-bonding ground states and those having dative ground states on the basis of their vibrational spectra. A method to arrange the complexes by the difference between the ionization potential of the donor molecule and the electron affinity of the acceptor molecule was proposed to demonstrate how important the size and shape of the component molecules are as the factors determining the electronic structures of crystal complexes. The electrostatic energies per molecule in 1 : 1 crystal complexes were found to range from 2.3 to 2.6 eV.

On the basis of the electronic and vibrational spectra, it has been shown that most donor-acceptor crystal complexes can be rather sharply divided into two groups, namely, those having essentially non-bonding ground states and those having essentially dative ground states.[1,2] The complexes in the former group are often called as weak or non-ionic complexes and those in the latter group as strong or ionic complexes. In general, when the ionization potential of the donor molecule is low and the electron affinity of the acceptor molecule is high, the resulting complex tends to have a dative ground state. However, the formation of such a crystal complex must be governed not only by the energy needed to charge the molecules, but also by the electrostatic energy of the charged lattice. The latter quantity depends on the packing of the component ions, which in turn depends on the molecular size and on the shapes of the donor and the acceptor. The present work was started with the hope of demonstrating how important the molecular size and shape can be as factors determining the electronic structures of donor-acceptor crystal complexes.

The crystal complexes were characterized in the following way. If the vibrational spectrum of a complex is well approximated by a superposition of the spectra of the component compounds, the complex has a non-bonding ground state. There are slight shifts in frequency and some alternation of intensity, reflecting the molecular association; however, it is generally easy to point out the pattern due to each component.[3,4] When the vibrational spectrum consists of the spectra of the ionized components, namely, D^+ and A^- free-radical ions, the ground state of the complex is considered to be essentially dative. The difference in the vibrational spectrum between the D molecule and the D^+ ion or that between the A molecule and the A^- ion is generally so remarkable that the characterization of crystal complexes by their spectra is not difficult.[2]

The method of selecting the component compounds must be now mentioned. It is highly desirable to have component compounds of similar nature but with different molecular sizes and shapes. The following six aromatic diamines were thought to best fulfill these requirements: *N,N,N',N'*-tetramethyl-*p*-phenylenediamine (TMPD) (I), 1,6-diaminopyrene (II), *N,N,N',N'*-tetramethylbenzidine (III), diaminodurene (IV), 1,5-diaminonaphthalene (V), and *p*-phenylenediamine (VI). The donor I has the lowest ionization potential, and VI, the highest, among these compounds. Fortunately, even the latter is known to be able to form some authentic cation-radical salts with vibrational spectra comparable with those of the complexes. The donors II, III, and V represent diamines with pyrene, biphenyl, and naphthalene nuclei respectively. The donor IV, the ionization potential of which is presumably not far from that of I, was also included because of the higher stability of its crystal complexes. The acceptors must cover a range so wide that the diamine complexes with some acceptors have essentially non-bonding ground states, while those with some others have dative ground states. The following compounds were chosen: 2,3-dichloro-5,6-dicyano-*p*-benzoquinone (DDQ) (a), tetracyano-*p*-benzoquinodimethane (TCNQ) (b), tetracyanoethylene (TCNE) (c), 2,3-dicyano-α-naphthoquinone (d), 9-dicyanomethylene-2,4,7-trinitrofluorene (e), *p*-chloranil (f), *p*-fluoranil (g), 2,5-dichloro-*p*-benzoquinone (h), 2,4,7-

1) R. Foster and T. J. Thomson, *Trans. Faraday Soc.*, **59**, 296 (1963).
2) Y. Matsunaga, *J. Chem. Phys.*, **41**, 1609 (1964).
3) H. Kainer and W. Otting, *Chem. Ber.*, **88**, 1921 (1955).
4) J. W. Eastman, G. M. Androes and M. Calvin, *J. Chem. Phys.*, **36**, 1197 (1962).

trinitrofluorenone (i), and dichloro-*p*-xyloquinone (j).

Experimental

All the crystal complexes were prepared by crystallization or by precipitation from solutions. The solvents used were mostly benzene and chloroform. The vibrational spectra in the NaCl region were recorded as Nujol mulls using a Hitachi EPI-S2 infrared spectrophotometer. The visible absorption spectra of systems containing combinations of appropriate amounts of the donors and acceptors dissolved in chloroform were measured with a Beckman DK2A spectrophotometer.

Results and Discussion

Earlier the present author discussed the ionic character and charge transfer in molecular complexes in terms of the electronegativity of the highest occupied orbital of the donor molecule and that of the lowest vacant orbital of the acceptor molecule.[5] The condition;

$$\varepsilon_i < (I_D - A_A)/2 \qquad (1)$$

was obtained in the case where the charge on each molecule, ρ, in a 1:1 crystal complex is less than one half and:

$$\varepsilon_i > (I_D - A_A)/2 \qquad (2)$$

in the case where $\rho > 1/2$. Here, ε_i is the electrostatic energy per molecule when there is a unit positive or negative charge on each molecule, I_D is the ionization potential of the donor molecule, and A_A is the electron affinity of the acceptor molecule. It is apparent that the condition (1) is fulfilled in complexes having essentially non-bonding ground states and the condition (2), in those complexes with essentially dative ground states.

If one could arrange complexes placing the ionization potentials of donors on the abscissa and the electron affinities of acceptors on the ordinate, lines with a slope of -1 would become the scale for $I_D - A_A$. Such an arrangement of complexes seems to be convenient for demonstrating how the electrostatic energy, ε_i, can vary with the kind of component molecules. Unfortunately, the ionization potentials and the electron affinities are not available in the desired accuracy.

The energy of the charge-transfer absorption, $h\nu_{CT}$, in a 1:1 single complex with an essentially non-bonding ground state may be given by:

$$h\nu_{CT} = I_D - A_A - C + W + R + R', \qquad (3)$$

where C is the electrostatic energy in the dative bond structure, W is the energy due to van der Waals interaction in the no-bond structure, and R and R' are the energy changes due to the resonance interaction between these two structures in the ground and excited states respectively.[6] In a series of complexes of a given acceptor with various donors, when A_A is constant, it has been well established that a plot of $h\nu_{CT}$ against I_D yields a straight line. Therefore, $C - W - R - R'$ is a relatively insensitive function of the donor, and one may write as a good approximation;[7]

$$h\nu_{CT} \fallingdotseq I_D - A_A - C'. \qquad (4)$$

Here the electrostatic energy, C, in Eq. (3) is supposed to make the major contribution to the term C'. The energy of charge-transfer absorptions in complexes of a given donor with various acceptors may also be approximated by Eq. (4). Consequently, the energy of the charge-transfer absorption in the *s*-trinitrobenzene complex, X, measured in a chloroform solution was taken in this experiment as a measure of the ionization potential, and that in the pyrene complex, Y, as a measure of the electron affinity. The complexes on line of $Y = -X +$ constant in Fig. 1 must all exhibit charge-transfer absorptions at nearly the same energy. For example, the upper line corresponds to an energy of 15kK, and

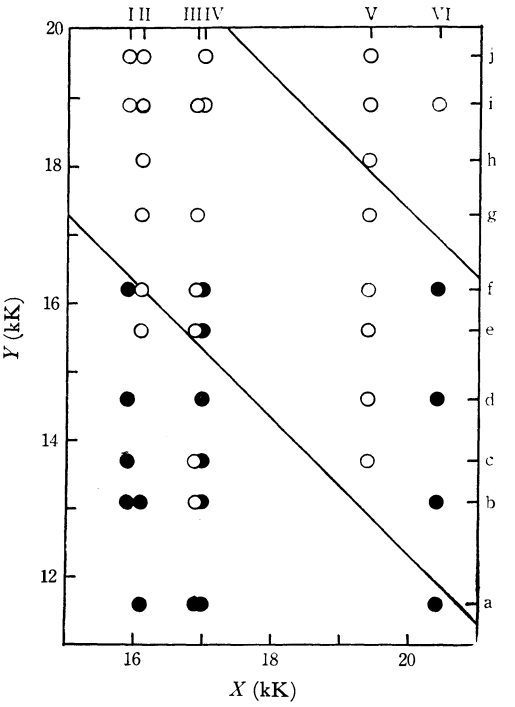

Fig. 1. Electronic structures of molecular complexes as revealed by the vibrational spectra. The complexes having non-bonding ground states are indicated by open circles and those having dative ground states by shaded circles. As to notations I—VI, a—f, and X and Y, see text.

5) Y. Matsunaga, This Bulletin, **42**, 2170 (1969).

6) G. Briegleb and J. Czekalla, *Z. Elektrochem.*, **59**, 184 (1955).

7) H. M. McConnell, J. S. Ham and J. R. Platt, *J. Chem. Phys.*, **21**, 66 (1953).

the lower one, to 10 kK. To check the validity of this diagram, the energies of charge-transfer absorptions observed in a solution for possible combinations of the donors I—VI and the acceptors a—j were plotted against the energies read on the diagram. As Fig. 2 shows, the agreement is generally excellent.

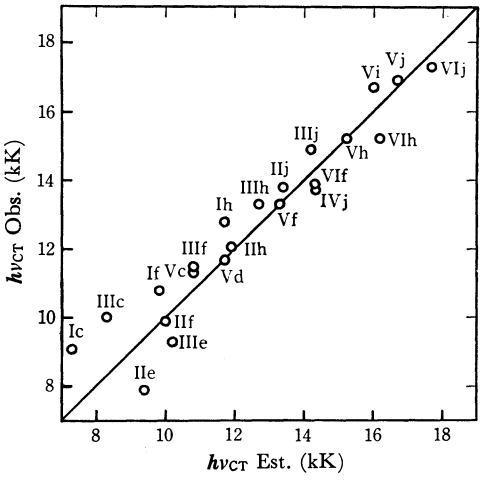

Fig. 2. Comparison between the observed energies of charge-transfer bands measured in solutions and the energies estimated by Fig. 1.

In Fig. 1 the complexes which were found to have essentially non-bonding ground states are indicated by open circles, and those found to have dative ground states, by shaded circles. The data for the DDQ (a) and *p*-chloranil (f) complexes were taken from the author's previous papers.[2,8] The independent characterization of some TCNQ (b) complexes is available in the literature.[9-11] Foster and Thomson have examined the visible absorption spectra of a number of TMPD (I) complexes and suggested that ionization by the complete transfer of an electron from the donor to the acceptor molecule occurs in the ground state of those complexes with several acceptors, including a, b, c, f, and h.[1] The present characterization by vibrational spectra is almost entirely consistent with theirs. Attempts to prepare well-defined complexes were not successful for the combinations missing from this figure. As expected, most of the complexes in the region where both X and Y are high are expressed by open circles, and those in the region where both X and Y are low, by shaded circles.

However, there are many exceptions which reflect the effects of the size and shape of component molecules on the electronic structure of the crystal complexes. Among these, *p*-phenylenediamine (VI), which is supposed to have the highest ionization potential, shows a strong tendency to form complexes with dative ground states, *e. g.*, the complex VIf. On the other hand, the tetramethylbenzidine (III) complexes tend to have non-bonding ground states in spite of the low ionization potential of the donor, *e. g.*, the complex IIIb. The difference in ε_i between these two extremes can be estimated using the following relations;

$$\varepsilon_i(\mathrm{VIf}) > [I_D(\mathrm{VI}) - A_A(\mathrm{f})]/2 \fallingdotseq [h\nu_{CT}(\mathrm{VIf}) + C']/2$$
$$\varepsilon_i(\mathrm{IIIb}) < [I_D(\mathrm{III}) - A_A(\mathrm{b})]/2 \fallingdotseq [h\nu_{CT}(\mathrm{IIIb}) + C']/2.$$

Although the crystal complex VIf has a dative ground state, the energy, $h\nu_{CT}$ (VIf), in the complex in solution can be measured using suitable solvents, or the value may be estimated by Fig. 1. Hence;

$$\varepsilon_i(\mathrm{VIf}) - \varepsilon_i(\mathrm{IIIb}) > [h\nu_{CT}(\mathrm{VIf}) - h\nu_{CT}(\mathrm{IIIb})]/2$$
$$= 3.3\,\mathrm{kK} \text{ or } 0.41\,\mathrm{eV}$$

Judging from the results presented in Fig. 1, this difference may be considered to be close to the maximum variation of ε_i.

One might feel that this difference is merely imaginary because, in the process of the estimation of ε_i, a possible change in the term C' in Eq. (4) was not taken into consideration at all. As will be discussed in the following paragraph, the electrostatic term in an ion pair in which the components are different in size and shape is generally smaller than that in which both the components are derivatives of benzene. If the doners to be compared are such as III and VI, the difference in X may be predicted to be smaller than that in I_D. Therefore, the above-mentioned value for ε_i (VIf) $-\varepsilon_i$ (IIIb) is rather underestimated.

It is very desirable to know even roughly how large ε_i itself can be. Taking the ionization potential of pyrene as 7.72 eV,[12] the following values were estimated by Eq. (4) using the energies of charge-transfer absorptions in the *s*-trinitrobenzene complexes; 7.0 eV for donor III and 7.5 eV for VI. The electron affinities were assumed to be 2.5 eV for the acceptor b and 2.2 eV for f following the discussion presented in a preceding paper.[5] Then, ε_i (VIf) $>$ 2.6 eV and ε_i (IIIb) $<$ 2.3 eV were obtained. Considering the uncertainties mentioned above, one may conclude that ε_i is of the order of magnitude of 2 eV. The electrostatic energy per molecule in a crystal, ε_i, is obtained by multiplying the Madelung constant by the electrostatic energy per molecule in an ion pair, C, in which the relative configuration is supposed to be kept the same.

8) Y. Matsunaga, *Nature*, **205**, 72 (1965).
9) H. Scott, P. L. Kronick, P. Chairge and M. M. Labes, *J. Phys. Chem.*, **69**, 1740 (1965).
10) M. Kinoshita and H. Akamatu, *Nature*, **207**, 291 (1965).
11) M. Ohmasa, M. Kinoshita, M. Sano and H. Akamatu, This Bulletin, **41**, 1998 (1968).
12) M. E. Wacks, *J. Chem. Phys.*, **41**, 1661 (1964).

This assumption does not seem to be strictly realized; however, the change in ε_t by the kind of component molecule may be nearly parallel to the corresponding change in C. The values of C were computed for combinations of benzene ion and three other hydrocarbon ions, locating a fractional point charge on each carbon atom. The charge distribution are those given by the Hückel MO theory. The molecular planes were assumed to be parallel to each other and to be separated by 3.40 Å. The results are presented in Fig. 3.

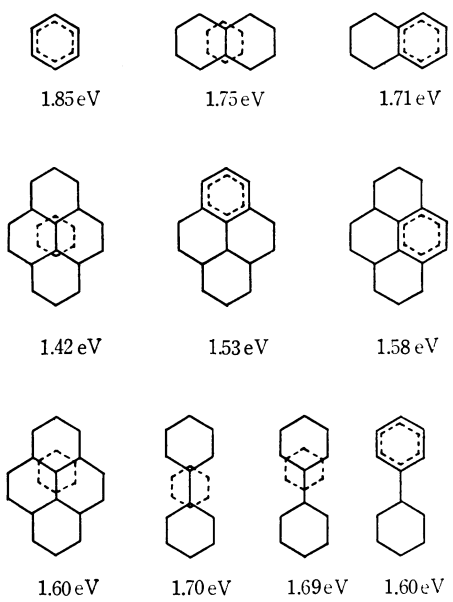

Fig. 3. The electrostatic energies per molecule in ion pairs consisting of aromatic hydrocarbon ions with a separation of 3.40 Å. All the C-C bonds were assumed to be 1.40 Å long.

The larger the difference in molecular size and shape, the smaller the electrostatic energy, C; therefore, one may expect a greater probability of finding complexes with non-bonding ground states. Although the component compounds used in the present work are not as simple as the hydrocarbons, the prediction is in fairly good agreement with the observed trends shown in Fig. 1. Assuming 1.85 eV for C in the complex VIf and 1.66 eV for C in the complex IIId, the Madelung constants were found in the range from 1.35 to 1.40. It may be worthwhile to note that these values are almost equal to the constant for a one-dimensional ionic lattice.

Most of the quinone complexes with electrical resistivities of 10^6 ohm cm or less were reported to have dative ground states. The only exceptions occurred in the case of 1,6-diaminopyrene-*p*-chloranil (IIf) and related molecular complexes.[8] On the basis of the results presented in Fig. 1, one may conclude that the complex IIf is located near the border line between 1,6-diaminopyrene complexes with non-bonding ground states and those with dative ground states. Furthermore, it has been established that the complex crystallized from benzene can be easily transformed into a new form exhibiting only a few ohm cm. The vibrational spectra indicated that, in this form, the electronic structure of the complex itself is intermediate between no-bond and dative.[13] The tetramethylbenzidine-*p*-chloranil (IIIf), which exhibits a resistivity of 10^6 ohm cm, is located near the 1,6-diaminopyrene complex. Thus, complexes with non-bonding ground states seem to exhibit relatively low resistivities only when the charge-transfer absorptions are in an exceptionally low-energy region. To prepare such complexes, the use of component compounds with a biphenyl or pyrene nucleus may be of great advantage. Attempts in this direction are now in progress.

The author wishes to express his thanks to Professor Hiroaki Baba of the Research Institute of Applied Electricity for the use of the Hitachi EPI-S2 infrared spectrophotometer, to Mr. Yoichi Iida for his help in the computation of the electrostatic energies presented in Fig. 3, and to Mr. Nobuhiko Miyajima for recording the infrared spectra.

13) Y. Matsunaga, *Nature*, **211**, 183 (1966).

BULLETIN OF THE CHEMICAL SOCIETY OF JAPAN VOL. 42 2494—2498 (1969)

Effects of Metallic Surfaces on the Thermal Decomposition of Ethane

Yoshiyuki NISHIYAMA

Chemical Research Institute of Non-Aqueous Solutions, Tohoku University, Sendai

(Received February 27, 1969)

The thermal decomposition of ethane was conducted in a static system at 700°C, using a silica vessel packed with a sheet of metal. Various sorts of metals were tested. The rate of ethylene formation decreased notably in the presence of metals as compared with the rate in an unpacked vessel, the decrease being larger at lower pressures. The activity of metals to reduce the rate was in order: Zr>Ti>Fe>Cu>W,Ag>Pt,Mo. The rate of methane formation did not change with the packing of metals. The main reactions were assumed to be radical reactions in the gas phase. From the observed order of reaction, it was concluded that the action of metal is to catalyze the recombination of hydrogen atoms and therefore to terminate the radical-chain reactions. A similar action was noted in hydrogen dissolved in a titanium sheet.

A metallic surface placed in hydrocarbon gases at a high temperature may catalyze the decomposition of the hydrocarbon on the surface. There is also another aspect of influence, which is the subject of the present report, *i. e.*, the metal surface may alter the rate of radical reactions in the gas phase by taking part in the formation and the quenching of radicals. This type of catalytic behavior of the reactor wall was first suggested by Rice and Herzfeld.[1] Laidler and Wojciechowski[2] attributed the change in the reaction order of ethane decomposition by the increase of the surface-to-volume ratio of quartz reactors to the termination process at the wall. Marshall and Quinn[3] made a kinetic analysis of ethane decomposition, assuming that homogeneous quadratic and heterogeneous linear termination occur simultaneously. The dependence of the rate of propane decomposition on the nature and the area of the surface was shown by Voevodsky.[4] However, no metallic surface seems to have been examined, so the present investigation was undertaken in order to clarify whether metals accelerate or retard the decomposition and to correlate the observed effects with the nature of the surface.

Experimental

Apparatus. The decomposition was carried out by a static method using a silica reaction vessel (shown in Fig. 1), which had a volume of 8.6 cc and an effective surface area of 31.6 cm². To see the effect of the metal, sheets of various metals, rectangular in shape and 0.1 mm thick, were bent and packed in turn into the vessel. Three different sizes of sheets were used: S-1, 1.0×7.0 cm²; S-2, 2.0×7.0 cm², and S-3, 4.0×7.0 cm². The packed states of the sheets are illustrated in Fig. 1. The packing of a silica plate was used for comparison. The reaction vessel was placed in an electric furnace and was maintained at 700±2°C for whole runs.

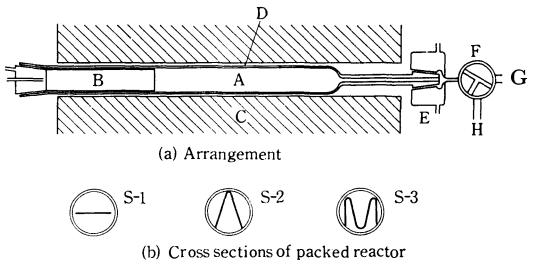

Fig. 1. Reaction vessel.

A: space for reaction, B: silica plug to exclude the space in temperature gradient, C: electric furnace, D: thermocouple, E: water-cooled joint, F: switching valve, G: piping connected to reservoir, H: piping connected to expansion bulb.

Materials. A research-grade ethane (>99.7%) was frozen in liquid air, and the non-condensable gases were removed by evacuation; then the ethane was evaporated slowly to leave the heavier impurities and was led into a reservoir. The metals used were obtained from commercial sources and were at least 99.9% pure, with the exception of titanium (99.3%). The pretreatment of metals will be individually described below.

Procedure. After the evacuation of the reaction vessel, ethane was introduced into the vessel and the pressure was equilibrated with that of the reservoir. This pressure will be referred to as the initial pressure of ethane, p_0. The reaction was stopped by expanding the gas in the reaction vessel into a pre-evacuated bulb

1) F. O. Rice and K. F. Herzfeld, *J. Phys. Colloid Chem.*, **55**, 975 (1951).

2) K. J. Laidler and B. W. Wojciechowski, *Proc. Roy. Soc. (London), Ser. A*, **260**, 91 (1961).

3) R. M. Marshall and C. P. Quinn, *Trans. Faraday Soc.*, **61**, 2671 (1965).

4) V. V. Voevodsky, *ibid.*, **61**, 2671 (1965).

(320 cc), and then the product was compressed by the use of a Teopler pump into the sampling tube of the gas chromatograph and analyzed.

Four to eight runs were made at the same pressure of ethane. The reaction time was usually 2 to 10 sec, and less than 20% of the ethane was decomposed. The gas chromatograph was equipped with 1.5 m of an active alumina column at 30°C; helium was used as the carrier, and the amounts of hydrogen, methane, ethane, and ethylene were determined quantitatively.

Results

Main Course of Reaction. The gaseous products were composed of nearly equal moles of ethylene and hydrogen, a small amount of methane (4 to 10% of ethylene), and unreacted ethane. In the cases of titanium or zirconium packing, the yield of hydrogen was somewhat less than that of ethylene, perhaps because of the dissolution of hydrogen into the metal. Also, the weight of these metals increased slightly, indicating that about 4% of the reacted ethane was fixed in a form of carbide. As the rate of the carbide formation of these metals with ethane is no less than that with ethylene,[5] the surface decomposition may be supposed not to disturb the gaseous-product distribution. In the other metals, no measurable change in the weight was observed and a lustrous appearance was retained. From these facts and from a tendency of the results described below which seems reasonable, it was assumed that the course of the decomposition in the gas phase in the presence of metal surface was similar to that reported for the reaction in silica vessels, at least so far as the initial rates were concerned.

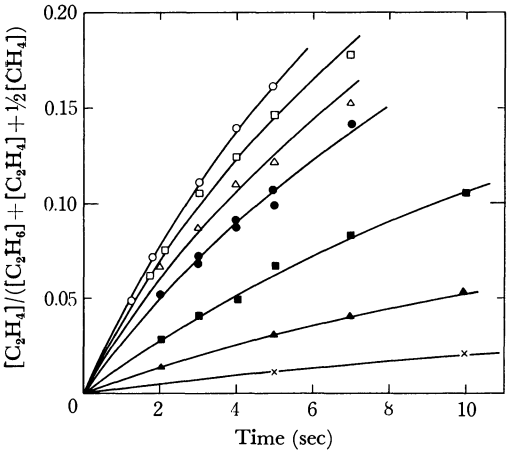

Fig. 2. Ethylene yield against time, in the presence of iron (S-2).
The p_0 values are: ○ 425, □ 288, △ 213, ● 153, ■ 73, ▲ 39, × 19 mmHg

The ethylene yield-time curve for each p_0 was similar to the reported pattern.[2] Typical plots are shown in Fig. 2. From the initial slope of the plots in Fig. 2, the initial rate of ethylene formation, r_0, was determined.[6] The initial rate of methane formation, r_0', was obtained in a similar manner. The rates so obtained have a probable error of about 10%, which is allowable for the present purposes.

Rate of Ethylene Formation. The rate of ethylene formation in the silica vessel is plotted against p_0 in the logarithmic scale in Fig. 3. This shows that the reaction is nearly first order with respect to ethane at higher pressures and 3/2 at

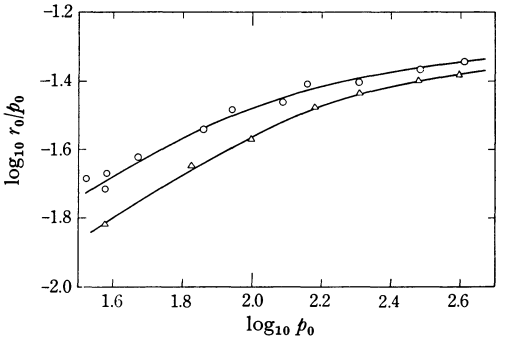

Fig. 3. Rate of ethylene formation in silica vessel.
○ unpacked (S/V=3.7 cm^{-1})
△ packed with a plate (S/V=7.1 cm^{-1})

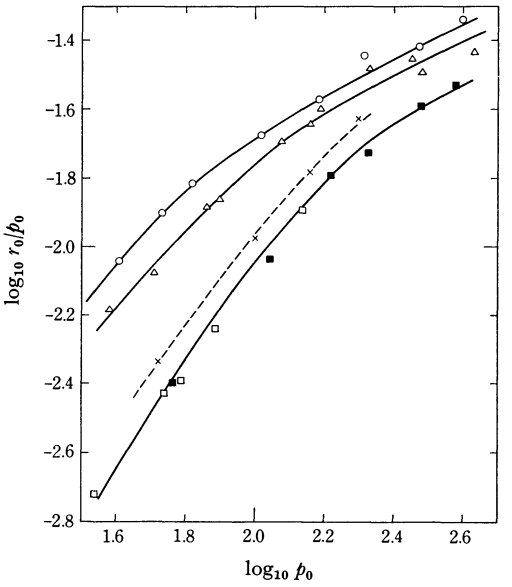

Fig. 4. Rate of ethylene formation in the presence of iron.
○ S-1, △ S-2 normal, × S-2 abraded, □ S-3 normal, ■ S-3 without hydrogen reduction

5) Y. Tamai, Y. Nishiyama, A. Abe and M. Takahashi, *Kogyo Kagaku Zasshi* (*J. Chem. Soc. Japan, Ind. Chem. Sect.*), **72**, 1933 (1969).

6) The initial slope itself means r_0/p_0 and this is used in preference to r_0 for convenience.

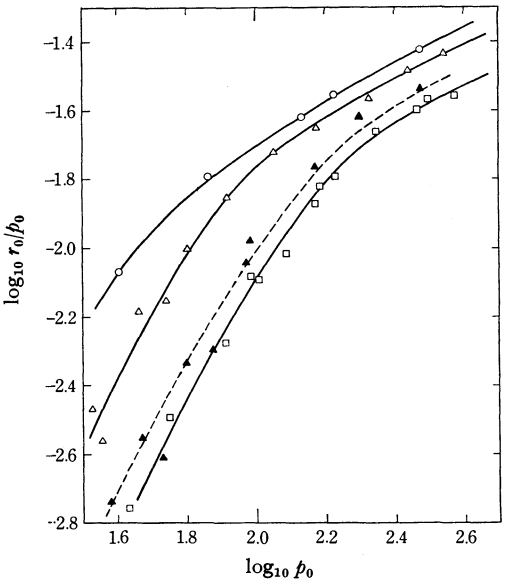

Fig. 5. Rate of ethylene formation in the presence of titanium.
○ S-1, △ S-2, ▲ S-2 with dissolved hydrogen, □ S-3

lower pressures, and that the order is altered slightly by the increase in the surface area, though the reaction rate is reduced somewhat.

The results for the cases of packing with iron sheets are shown in Fig. 4. Before use, the packed sheets were normally heated in 200 mmHg of hydrogen at 700°C for 30 min in order to reduce the oxidized surfaces. The same treatment was repeated frequently between the decomposition runs to keep the surface clean. A few runs were carried out using an iron sheet which had not been treated with hydrogen, but they showed essentially the same trend. The rate was decreased markedly by the packing of iron, and the order of reaction was 2 to 5/2 at 50 mmHg, the larger order for the larger sheet.

A check was made on the surface roughness by using an iron sheet abraded by Emery paper (#1). The results show a more pronounced decrease in the rate.

The titanium sheets were normally used without hydrogen treatment, for this is irrelevant to the reduction of oxide. The effect of hydrogen was tested by using titanium sheets packed in the reaction vessel and equilibrated with about 300 mmHg of hydrogen at 700°C (110 cc STP/g was absorbed). After this, the vessel was evacuated for 5 min and ethane decomposition conducted as usual.

The packing of titanium exerted an influence on the rate similar to that of iron, as is shown in Fig. 5, but the effect was more remarkable. The reaction order at 50 mmHg was from 2.1 to 3.0. It is interesting to note that titanium with dissolved hydrogen behaved as if the area of the sheet had been enlarged.

Various metals with the same dimensions are compared in Fig. 6. All the metals had smooth surfaces, and copper, silver, and platinum were treated with hydrogen, as iron had been. In every case, the rate was more or less reduced and the activity was in the order: Zr>Ti>Fe>Cu>W≅Ag>Pt≅Mo.

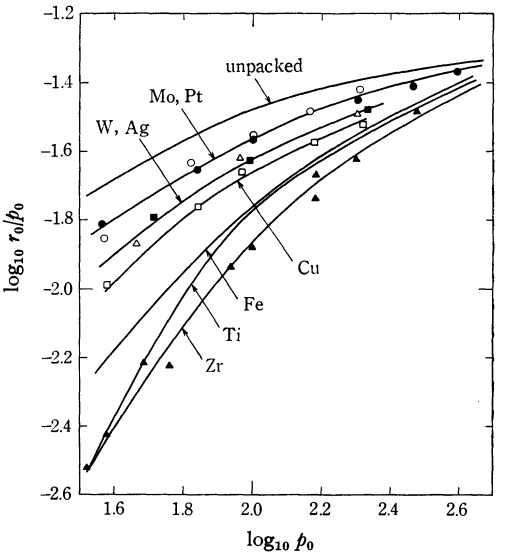

Fig. 6. Comparison of metals.
▲ Zr, □ Cu, △ W, ■ Ag, ○ Mo, ● Pt; S-2 for each

Rate of Methane Formation. The rates of methane formation in several cases are shown in Fig. 7. This figure indicates that the rates are only slightly affected by the presences of metallic surfaces, in contrast to the simultaneous large variation in the rate of ethylene formation. The reaction order was approximately 3/2 at higher pressures and increased to about 2 as the pressure was reduced.

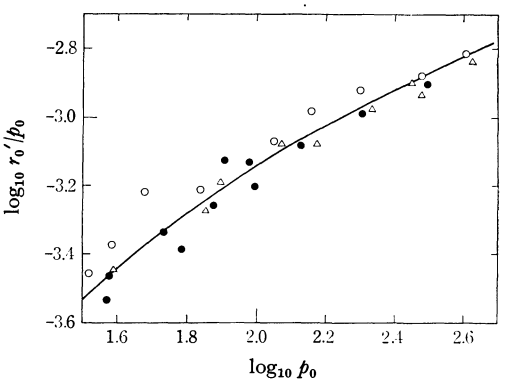

Fig. 7. Rate of methane formation.
○ unpacked, △ packed with iron S-2, ● Packed with titanium S-2 with dissolved hydrogen

Discussion

Kinetic Consideration of the Reaction Order. The thermal decomposition of ethane in the gas phase is usually explained on the basis of the radical mechanism as follows:

$$C_2H_6 \rightarrow 2CH_3\cdot \quad (1)$$

$$CH_3\cdot + C_2H_6 \rightarrow CH_4 + C_2H_5\cdot \quad (2)$$

$$C_2H_5\cdot \rightarrow C_2H_4 + H\cdot \quad (3)$$

$$H\cdot + C_2H_6 \rightarrow H_2 + C_2H_5\cdot \quad (4)$$

$$C_2H_5\cdot + C_2H_5\cdot \rightarrow C_4H_{10} \text{ or } C_2H_6 + C_2H_4. \quad (5)$$

The rate of methane formation is said to be a measure of the initiation step.[7] The order of this reaction was from 3/2 to 2 under the present condition; this order is in accord with the pressure-dependent nature of reaction (1).[7-9] The secondary production of methane from ethylene was noted in some cases,[10-12] but this is less important at present, for the rate of methane formation differed little among the cases in which the rate of ethylene formation differed remarkably.

The order of the decomposition of the ethyl radical is said to change from 1 to 3/2 as the pressure is reduced.[8,13] For the termination, the following processes involving hydrogen atoms were taken into account in addition to (5):

$$H\cdot + C_2H_5\cdot \rightarrow C_2H_6 \quad (6)$$

$$H\cdot + H\cdot \rightarrow H_2 \quad \text{(2nd order)} \quad (7)$$

$$H\cdot \rightarrow H_{ad} \text{ or } {}^1/_2\, H_2. \quad \text{(1st order)} \quad (8)$$

The reaction (6) is said to be quite slow in the gas phase.[8,14] The step (7) corresponds to a situation in which concentration of adsorbed hydrogen on the metal surface is relatively small and is in equilibrium with that in the gas phase. The step (8) reflects the situation either when the surface coverage of the adsorbed hydrogen is near unity and the recombination of hydrogen atoms occurs in the Rideal mechanism, or when every hydrogen atom is trapped by the surface when it collides.

For each case, the order of ethylene formation with respect to ethane was calculated, assuming the predominance of a particular termination step; the results are tabulated in Table 1.

Table 1. Calculated reaction order

Order of (1)	Order of (3)	Overall order for termination by (5)	(6)	(7)	(8)
3/2	1	3/4	5/4	7/4	5/2
3/2	3/2	5/4	3/2	7/4	5/2
2	1	1	3/2	2	3
2	3/2	3/2	7/4	2	3

The involvement of hydrogen in the termination increases the reaction order, as has been supposed by Marshall and Quinn[3] and others.[8,13] The present results seem to show clearly the contribution of hydrogen in termination. The highest order observed was 3 for titanium packing at lower pressures; it can be explained by the linear termination of hydrogen atoms. At higher pressures, termination by (6) seems to predominate. The order in the presence of iron indicates that the recombination of hydrogen is between linear and quadratic concentration dependence.

Other Possible Contributions of Metals. There is a possibility that the metallic wall initiates the radical chain. However, methyl radical formation seems not to occur on metal surfaces, as the rate of methane formation is scarcely affected by metals. Another mode of initiation might be the inverse step of (6), but this could play a role only at a very early stage of the decomposition, since the radical concentrations at the steady state favor recombination.

Also, the heterogeneous dehydrogenation of ethane might take place to some extent. However, at present this cannot be discriminated from homogeneous processes, as metallic surfaces exerted a stronger influence on termination, resulting in a reduction of the overall rate over the entire pressure range.

Effects of the Nature of the Surfaces. If the above explanation is correct, the negative catalytic activity of metals might have a close correlation with that of the recombination of hydrogen atoms in a hydrogen atmosphere. However, this activity would depend on the state of the surface. For a quantitative comparison, it is necessary to define the geometry of packing and to ascertain the rate of diffusion of each component. The metal surfaces in the present experiment were by no means clean and the crystallographic characteristics were not defined, so only a qualitative discussion is possible here. In spite of these imperfections, the present trend among metals seems reasonable and is, though only partly, in accord with that reported by Wood and Wise;[15] *i. e.*, the catalytic activity of metals for hydrogen-atom recombination is roughly in the order: Ti>(Ni)>

7) A. B. Trenwith, *Trans. Faraday Soc.*, **63**, 2452 (1967).
8) A. B. Trenwith, *ibid.*, **62**, 1538 (1966).
9) M. C. Lin and M. H. Back, *Can. J. Chem.*, **44**, 2537 (1966).
10) C. P. Quinn, *Proc. Roy. Soc.* (*London*), *Ser. A*, **275**, 190 (1963).
11) C. P. Quinn, *Trans. Faraday Soc.*, **59**, 2543 (1963).
12) M. C. Lin and M. H. Back, *Can. J. Chem.*, **44**, 2369 (1966).
13) M. C. Lin and M. H. Back, *ibid.*, **44**, 505 (1966).
14) D. W. Setser and B. W. Rabinovitch, *J. Chem. Phys.*, **40**, 2427 (1964).
15) B. J. Wood and H. Wise, *J. Phys. Chem.*, **65**, 1976 (1961).

Cu>W>Pt. The packing of a nickel sheet was attempted in this study, but the reaction rate varied considerably from run to run, so it was impossible to determine the rate with the desired precision. Roughly speaking, however, the effect of nickel was in the same range as that of iron. The accordance except in the case of nickel seems to indicate that the catalytic action of metals for hydrogen recombination is relatively insensitive to the adsorbed hydrocarbons. The weak activity of molybdenum may be associated with the weak interaction of this with hydrogen.[16]

The above trend holds only for metals of similar appearance; alteration of the surface state by abrasion changed the activity, as is usual in catalysis.

The action of hydrogen dissolved in titanium can be interpreted by assuming that hydrogen atoms emerging from bulk metal combine much more easily with hydrogen from the gas phase. The enhanced activities of dissolved hydrogen were noted in the the recombination of hydrogen atoms[15] and in other reactions, for example, in the dehydrogenation of cyclohexane.[17]

The author is grateful to Professor Yasukatsu Tamai for his helpful discussions and encouragement.

16) The solubility of hydrogen in molybdenum is less than that in silver, at 700°C; S. Dushman and J. M. Lafferty, "Scientic Foundation of Vacuum Technique," 2nd ed., John Wiley and Sons, New York (1962), p. 537.

17) B. J. Wood, *J. Catalysis*, **11**, 30 (1968).

BULLETIN OF THE CHEMICAL SOCIETY OF JAPAN VOL. 42 2498—2502 (1969)

The Effects of Tetraalkylammonium Salts on the Structure and the Temperature of the Maximum Density of Water

Goro WADA and Masako MIURA

Department of Chemistry, Nara Women's University, Nara

(Received March 1, 1969)

The effects of the tetraalkylammonium halides on the temperature of the maximum density of water were measured by means of dilatometry. Contrary to the expectation that the hydrophobic nature of the alkyl radicals would elevate the temperature of the maximum density of water, these salts lowered it, as other, more usual salts do, obeying the Despretz rule. Among the salts represented as R_4NBr, where R is either H or an *n*-alkyl radical, the Despretz constant, k_D, increases in the sequence: $H < CH_3 < C_2H_5 < n\text{-}C_3H_7 \ll n\text{-}C_4H_9$, while the deviation of k_D from k, which is a hypothetical constant of the ideal mixing where there is no interaction between the solute and the solvent, varies in the following sequence: $H \simeq CH_3 \simeq C_2H_5 \simeq n\text{-}C_3H_7 \ll n\text{-}C_4H_9$. The latter fact is attributable to the specific occurrence of a clathrate-like structure formed in the aqueous solution, only when R is $n\text{-}C_4H_9$. This is in accordance with another peculiarity of $(n\text{-}C_4H_9)_4NBr$ which shows a minimum in its partial molar volume at a certain concentration in water.

The phenomenon of the maximum density exhibited by water at 3.98°C under an atmospheric pressure is affected by the addition of a small amount of an electrolyte to it; this is in obedience to the Despretz rule,[1] which states that the lowering of the temperature of the maximum density (abbreviated as TMD) of water caused by a solute is linear with respect to its concentration. The rule has been almost uniformly confirmed by previous measurements of various electrolytes.[2] Recently, however, some alcohols, most markedly *t*-butyl alcohol, have been found to be in contradiction to the rule; their TMD is even elevated at dilute concentrations.[3] These observations have been interpreted as being attributable to the structure-promoting nature of the hydrophobic alkyl radicals bonded with the hydrophilic hydroxyl radical.

The present work has been undertaken in order to see how the tetraalkylammonium ions affect the TMD of water as the kind of the alkyl radicals is varied. As has been the recent trend, the characteristic properties of aqueous solutions of several

1) M. C. Despretz, *Ann. Chim. Phys.*, **70**, 49 (1839); **73**, 296 (1840).

2) "International Critical Tables," Vol. III, McGraw-Hill Book Co., New York, (1933), p. 107.

3) G. Wada and S. Umeda, This Bulletin, **35**, 646 (1962).

tetraalkylammonium salts have been investigated from various points of view——the partial molar volumes,[4-10] the adiabatic compressibilities,[4,6] the transport properties,[11-14] the heats of dilution,[15] the solubilities,[16,17] the near-infrared spectra,[18] and the association equilibria.[19,20] According to their experimental results, the alkyl radicals generally interact with water molecules, with a structure-promoting tendency through the hydrophobic bonds, which sometimes leads to the formation of a clathrate-like structure around the solute ions. Simply judging from the fact that the structure-breaking nature of ions lowered the TMD of water, as in the case of simple ions,[2] while, on the contrary, the structure-promoting nature of the hydrophobic radicals in non-electrolytes elevated it, as in the case of some alcohols,[3] one might expect a slight elevation of the TMD by tetraalkylammonium ions. However, this was not found to be the case, as will be described below.

Experimental

Materials. The crystals used were of a guaranteed reagent grade and were obtained from the Tokyo Kasei Kogyo Co., Ltd., Tokyo, or from the Nakarai Chemicals, Ltd., Kyoto. Commercial NaSCN, NH_4Br, $(CH_3)_4NBr$, $(C_2H_5)_4NBr$, and $(C_2H_5)_4NI$ were recrystalized from water, $(n\text{-}C_3H_7)_4NI$, from ethanol, and $(n\text{-}C_4H_9)_4NBr$, from ethyl acetate. Pure water was prepared by repeating twice the cycles of treatment with ion-exchange resin and distillation.

Procedure. The TMD values of solutions were determined by the use of a dilatometer especially made for the present purpose; it had a capacity of about 300 m*l*, thus enabling us to detect a volume change of 3×10^{-5}%, as has been described in detail elsewhere.[3]

The thermal expansion coefficients, α, and the molar volumes at 0°C, V_{S_0}, of the salts were determined by measuring the volumes of the crystals at various temperatures. In order to do that, a specific gravity bottle with a ground-in perforated glass stopper was used. In it a weighed amount of the crystal was put, after

Table 1. The increase in the TMD, ΔT, at the mole fraction x of various salts

Salt	$x\times10^3$	ΔT °C
NaSCN	0.10	−0.10
	0.73	−0.83
	1.46	−1.62
	2.33	−2.53
	2.94	−3.22
NH_4Br	0.11	−0.04
	1.16	−0.54
	2.34	−1.00
	2.87	−1.38
	4.14	−1.96
	5.22	−2.41
$(CH_3)_4NBr$	1.15	−0.67
	1.75	−0.97
	2.39	−1.33
	3.33	−1.85
	4.88	−2.64
$(C_2H_5)_4NBr$	0.67	−0.39
	1.11	−0.63
	1.76	−1.05
	2.48	−1.45
	2.90	−1.73
	4.55	−2.73
$(C_2H_5)_4NI$	0.43	−0.30
	1.17	−0.71
	1.38	−0.93
	2.18	−1.60
	2.93	−2.13
	3.68	−2.73
$(n\text{-}C_3H_7)_4NI$	0.34	−0.20
	0.68	−0.45
	0.91	−0.64
	1.11	−0.83
	1.54	−1.21
$(n\text{-}C_4H_9)_4NBr$	0.23	−0.18
	0.47	−0.42
	1.07	−1.12
	1.79	−1.89
	2.36	−2.52
	3.42	−3.80

4) B. E. Conway and R. E. Verral, *J. Phys. Chem.*, **70**, 3952, 3961 (1966).
5) J. Padova and I. Abrahamer, *ibid.*, **71**, 2112 (1967).
6) S. Schiavo, B. Scrosati and A. Tommasini, *Ric. Sci.*, **37**, 211, 219 (1967).
7) F. Franks and H. T. Smith, *Trans. Faraday Soc.*, **63**, 2586 (1967).
8) J. E. Desnoyers and M. Arel, *Can. J. Chem.*, **45**, 359 (1967).
9) F. J. Millero and W. Drost-Hansen, *J. Phys. Chem.*, **72**, 1758 (1968).
10) I. Lee and J. B. Hyne, *Can. J. Chem.*, **46**, 2333 (1968).
11) R. L. Kay, T. Vituccio, C. Zawoyski and D. F. Evans, *J. Phys. Chem.*, **70**, 2336 (1966).
12) D. F. Evans, G. P. Cunningham and R. L. Kay, *ibid.*, **70**, 2974 (1966).
13) R. A. Horne and R. P. Young, *ibid.*, **72**, 1763 (1968).
14) R. Fernandez-Prini, *Trans. Faraday Soc.*, **64**, 2146 (1968).
15) R. H. Wood, H. L. Anderson, J. D. Beck, J. R. France, W. E. de Vry and L. J. Soltzberg, *J. Phys. Chem.*, **71**, 2149 (1967).
16) F. Franks and D. L. Clarke, *ibid.*, **71**, 1155 (1967).
17) H. E. Wirth and A. Lo Surdo, *ibid.*, **72**, 751 (1968).
18) K. W. Bunzl, *ibid.*, **71**, 1358 (1967).
19) H. E. Wirth, *ibid.*, **71**, 2922 (1967).
20) P. R. Danesi, F. Orlandini and G. Scibona, *J. Inorg. Nucl. Chem.*, **30**, 2513 (1968).

which it was filled with an inert liquid, such as toluene or cyclohexane. The bottle was filled with the liquid under reduced pressure to prevent bubbles from being occluded in the small openings between the pieces of the crystal. The temperature variation of the molar volumes in the temperature range of about 2—25°C was linear and gave the α from the slope and the V_{S_0} from the intercept at 0°C, as calculated by the method of the least squares.

Results and Discussion

The observed shifts in the TMD from 3.98°C, ΔT, at various concentrations expressed in mole fractions, x, are listed in Table 1. Some of them agree well with the data appearing in the literature.[21,22] The good linear relationships between ΔT and x

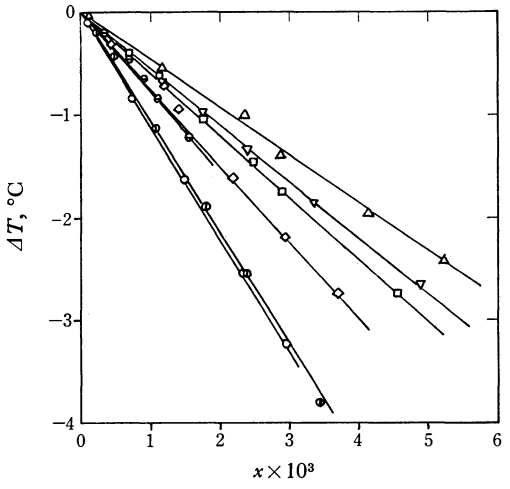

Fig. 1. The linear relationships between ΔT and x for various salts.
○ NaSCN, △ NH_4Br, ▽ $(CH_3)_4NBr$,
□ $(C_2H_5)_4NBr$, ◇ $(C_2H_5)_4NI$, ⊖ $(n\text{-}C_3H_7)_4NI$,
◐ $(n\text{-}C_4H_9)_4NBr$

TABLE 2. VARIOUS CONSTANTS FOR THE SALTS

Those in the parentheses are estimated values

Salt	k_D	$\alpha\times10^4$ deg^{-1}	V_{S_0} ml/mol	k	Δk
NaSCN	1095	1.83	46.0	30	1065
NH_4Br	465	1.99	40.1	28	437
$(CH_3)_4NBr$	549	1.97	98.7	69	480
$(C_2H_5)_4NBr$	596	3.15	150	169	427
$(n\text{-}C_3H_7)_4NBr$	(610)	—	—	(210)	(400)
$(n\text{-}C_4H_9)_4NBr$	1086	2.47	280	246	840
$(C_2H_5)_4NI$	726	2.25	164	131	595
$(n\text{-}C_3H_7)_4NI$	747	2.14	237	181	566

21) G. Wada and S. Umeda, This Bulletin, **35**, 1797 (1962).
22) A. J. Darnell and J. Greyson, *J. Phys. Chem.*, **72**, 3021 (1968).

for the individual salts may be seen in Fig. 1. Therefore, the Despretz constant, k_D, may be defined empirically as:

$$\Delta T = -k_D x \tag{1}$$

Its values for the salts are shown in Table 2.

When it is assumed that there is no interaction between the ions and the solvent molecules, and that, consequently, the resultant volume after the solute and the solvent have been mixed is the algebraic sum of the volumes of the components, the ideal depression of the TMD, ΔT_n, may be expressed as follows:[3]

$$\Delta T_n = -\frac{x}{1-x}\frac{\alpha}{2\beta}\frac{V_{S_0}}{V_{W_m}} \tag{2}$$

where V_{W_m} is the molar volume of water at 3.98°C, 18.016 ml/mol, and where β is also a constant, 7.80×10^{-6} deg^{-2}, related to the thermal expansion of water near the TMD, as defined by the equation:

$$V_W = V_{W_m}\{1+\beta(\theta-3.98)^2\} \tag{3}$$

in which θ is the temperature in Celsius. This equation is only applicable at temperatures close to the TMD of water. According to Eq. (2), ΔT_n is approximately linear with respect to x, with a proportional constant of $k=(\alpha/2\beta)(V_{S_0}/V_{W_m})$ at concentrations so dilute that $1-x$ can be regarded as being equal to unity. Then, the following relationship can be established:

$$\Delta T_n = -kx \tag{4}$$

For the calculation of k's, the values of α and V_{S_0}, tabulated in Table 2, are necessary.

Generally, the observed k_D and the calculated k do not coincide with each other; rather, the former predominates over the latter. Therefore, the difference between them, $\Delta k=k_D-k$ (shown in the last column of Table 2), is a useful clue for any discussion of the discrepancy from the ideal mixing.

In the present work, since experimental data on $(n\text{-}C_3H_7)_4NBr$ are lacking because of the difficulty of purifying it, $(n\text{-}C_3H_7)_4NI$ was used instead, with $(C_2H_5)_4NI$ as a reference.

TABLE 3. COMAPRISON OF THE VALUES OF k_D BETWEEN BROMIDES AND IODIDES

Cation	Br^-	I^-	Diff (I^-–Br^-)
Li^+ [2]	390	460	70
Na^+ [2]	820	950	130
K^+ [2]	740	860	120
$(C_2H_5)_4N^+$	596	726	130

Table 3 lists the values of k_D for the bromides and iodides of several common cations; it indicates that the differences between the bromides and iodides are almost constant unless the size of the cation is extremely small.

Because of this additive nature of ions, the k_D of $(n\text{-}C_3H_7)_4NBr$ can be roughly estimated as is shown in the parentheses in Table 2. The k value for the same salt can also be estimated by simply assuming that it may come in the middle between those for $(C_2H_5)_4NBr$ and $(n\text{-}C_4H_9)_4NBr$. Consequently, its Δk may be supposed to be approximately 400.

A survey of the Δk values of tetraalkylammonium bromides (R_4NBr) in Table 2 will show that Δk does not vary greatly so long as R corresponds to either H, CH_3, C_2H_5, or $n\text{-}C_3H_7$, but that it suddenly doubles when R is altered to $n\text{-}C_4H_9$.

According to the general tendency already found in the cases of simple salts, Δk is always positive and is larger for the stronger structure-breakers or for the weaker structure-formers. Water is considered to be an equilibrium mixture between the molecules of an ice-like structure (iceberg) and of a structure without hydrogen bondings.[23] When the ice-like structure is destroyed by ions, the TMD of water must be lowered to a larger extent than could be expected on the basis of k; this corresponds to the transition of the ice-like structure to a more packed one, because the water in the ice-like structure has a larger molar volume than otherwise. Since the alkyl radicals have a hydrophobic nature, and, since, therefore, they may be considered to promote the ice-like structure around them, the Δk's for tetraalkylammonium bromides have been expected to be negative, much as *t*-butyl alcohol really behaves.[3] However the facts found here are quite contrary to this expectation.

Among many tetraalkylammonium salts, only some tetra-*n*-butyl-ammonium salts are known to form clathrate hydrate crystals, such as $(n\text{-}C_4H_9)_4NBr\cdot 32.8H_2O$ and $(n\text{-}C_4H_9)_4N\text{-}C_6H_5COO\cdot 39.5H_2O$, in which the four $n\text{-}C_4H_9$ radicals are wrapped in individual polyhedral cages composed of water molecules and in which the nitrogen atom of the ammonium is located at the point of contact of these four cages.[24] Alkyl radicals smaller than the *n*-butyl do not form such clathrates because they are too small in comparison with the cage.

When the partial molar volumes of $(n\text{-}C_4H_9)_4NBr$ in its aqueous solutions are plotted against the square root of the concentrations, the curve exhibits a minimum value at the concentration of about 1 mol/*l*. The ratio of the number of moles of the solute to that of the solvent at this concentration corresponds to $(n\text{-}C_4H_9)_4NBr\cdot(60\pm 10)H_2O$.[25] In the cases of other simpler salts, no phenomenon like this is seen; in such cases there are only the monotonous curves of the partial molar volumes *vs.* the square root of the concentration approximately obeying the Debye-Hückel law.[26,27]

Therefore, the characteristic behavior of $(n\text{-}C_4H_9)_4NBr$ in exhibiting both an extraordinarily large value in Δk and a minimum value in the partial molar volume in aqueous solutions might be closely related to the fact that $(n\text{-}C_4H_9)_4NBr$ is the only one among the tetraalkylammonium bromides used that forms the clathrate hydrate. The number of water molecules involved in the clathrate-like structure in solution at the concentration of the minimum partial molar volume is approximately twice as many as in the crystal. Although the clathrate-like structure of $(n\text{-}C_4H_9)_4NBr$ in water is, therefore, in a less-established order than in the crystalline state, the water molecules around the $n\text{-}C_4H_9$ radicals are more ordered and more effectively packed than in the free water, similarly as the structure-breaking ions break the bulky, ice-like structure up into a more packed one. However, one important difference between the shrinks of the volumes due to the formation of the clathrate-like structure and to the destruction by the structure-breaking ions is that the former is accompanied by an increased order, but the latter, by an increased disorder.

The chemical shifts in the NMR signals due to the protons in the water molecules caused by the structure-promoting ions are usually negative, while they are positive upon the disappearance of the hydrogen bonds caused by the structure-breaking ions. The observed chemical shifts caused by the tetraalkylammonium ions are, on the contrary, positive, as if they were weak structure-breakers.[28] The tetraalkylammonium ions are large enough for them to be a likely kind of structure-breaker. However, the hydrophobic nature of the alkyl radicals must promote the structure around the ions by the so-called hydrophobic bonds.[29] This contradiction can be clearly interpreted by the fact that the covalent character of the hydrogen bonds in water causes a chemical shift towards a higher applied field of the water-proton resonance, as has been revealed by the measurements of the sodium alkyl sulfate solutions.[30]

Thus, in summary, the phenomena observed on the shifts in the TMD by the tetraalkylammonium ions may be said to be affected by three factors. First, the tetraalkylammonium ions are ions of such

23) G. Wada, This Bulletin, **34**, 955 (1961).

24) G. A. Jeffrey and R. K. McMullan, *J. Chem. Phys.*, **37**, 2231 (1962); R. K. McMullan, M. Bonamico and G. A. Jeffrey, *ibid.*, **39**, 3295 (1963).

25) W. Y. Wen and S. Saito, *J. Phys. Chem.*, **68**, 2639 (1964); S. Saito, *Hyomen (Surface)*, **4**, 584 (1966).

26) L. G. Hepler, J. M. Stokes and R. H. Stokes, *Trans. Faraday Soc.*, **61**, 20 (1965).

27) B. J. Levien, *Australian J. Chem.*, **18**, 1161 (1965).

28) H. G. Hertz and W. Spathoff, *Z. Elektrochem. Ber. Bunsenges. Phys. Chem.*, **63**, 1096 (1959).

29) W. Kauzmann, *Advances in Protein Chem.*, **14**, 1 (1959).

30) J. Clifford and B. A. Pethica, *Trans. Faraday Soc.*, **60**, 1483 (1964).

large radii that they behave like structure-breakers, making k_D larger than k. Second, the alkyl radicals are hydrophobic and so are likely to have the effect of depressing k_D. Third, only the tetra-*n*-butylammonium ion specifically serves to form a clathrate-like structure, a structure which makes the apparent partial molar volume of water smaller; consequently, the k_D of $(n\text{-}C_4H_9)_4NBr$ is one of the largest k_D's among the salts of the 1 : 1 type. Sodium thiocyanate was chosen as a typical structure-breaking salt; it has the very high k_D value of 1095, as is shown in Table 2.

BULLETIN OF THE CHEMICAL SOCIETY OF JAPAN VOL. 42 2502—2505 (1969)

Catalytic Vapor-Phase Ammoxidation of Substituted Toluenes over Chromium Oxide[1]

Katsumasa SAKANISHI and Yoshiro OGATA

Department of Applied Chemistry, Faculty of Engineering, Nagoya University, Chikusa-ku, Nagoya

(Received March 1, 1969)

Ammoxidation of substituted toluenes over a chromium oxide catalyst has been studied in a flow system at atmospheric pressure. The reactions give satisfactory yields (*ca.* 70%) of corresponding nitriles at high conversion of toluenes. The rate constant for the reaction of substrate adsorbed on the catalyst surface, k^0_T, is independent of the substituent of substrate, while the adsorption equilibrium constant of gaseous substrate, K_T, depends on the substituent, affording Hammett's ρ of -0.9 for σ^+. These results support our mechanism reported previously for the analogous oxidation of toluene and ethylbenzene over Cr_2O_3, which involves an electron transfer from adsorbed hydrocarbons to dissociated oxygen.

In previous papers, we have reported the kinetic study on the ammoxidation of toluene[2] and ethylbenzene[3] over chromium oxide and interpreted the results in terms of the Langmuir-Hinshelwood mechanism.[2,3] The rate constant for the reaction of substrate on the catalyst surface, k°, and the adsorption equilibrium constants, K, were estimated and it is proposed that the rate-determining step is the reaction between adsorbed hydrocarbon and adsorbed oxygen in a dissociated form.[3] The present paper is an extention of the study to the ammoxidation of substituted toluenes over chromium oxide; the reaction gave satisfactory yields of substituted benzonitriles, the data being interpreted in terms of k°_T and K_T.

Experimental

Materials. Toluene (bp 110.6°C), ethylbenzene (bp 135.8—136.0°C), *o*-xylene (bp 144.0—144.5°C), *m*-xylene (bp 137.2—137.5°C) and *p*-xylene (bp 136.5—137.0°C) were purified as previously described.[2,3] *p*-*t*-Butyltoluene (bp 108.5°C/60 mmHg) was purified by rectification. Commericial *o*-chlorotoluene was employed. *m*-Chlorotoluene (bp 59.5—61.0°C/23 mmHg),[4] *p*-chlorotoluene (bp 160.8—161.1°C),[5] *o*-bromotoluene (bp 76.5—77.7°C/23 mmHg),[6] *m*-bromotoluene (bp 104°C/65 mmHg),[7] *p*-bromotoluene (bp 79.5—79.9°C/24 mmHg),[8] *o*-tolunitrile (bp 93—94°C/20.5 mmHg),[9] *m*-tolunitrile (bp 104—104.5°C/24 mmHg),[9] and *p*-tolunitrile (bp 105.5°C/23 mmHg)[9] were synthesized by well-known methods. Commercial ammonia, N_2 and O_2 were employed. The same catalyst as that in the previous papers[2,3] was used for kinetic studies. The catalyst of 5 wt% Cr_2O_3 on Al_2O_3, used for synthetic studies, was prepared by a method similar to that in the previous paper[2] and was allowed to age under reaction conditions for 35 hr in order to stabilize its activity.

Apparatus and Procedures. The apparatus and procedure for kinetic studies were similar to those employed before,[2] but a column of 30 wt% Silicone D.C. 550 on Chamelite CK 40 cm was used for gas chromatographic analysis of the substituted toluenes.

For synthetic purposes, a reactor of stainless steel, 19 mm inner diameter, with a concentric thermowell

1) Contribution No. 134.

2) Y. Ogata and K. Sakanishi, *Tetrahedron*, **24**, 4881 (1968).

3) K. Sakanishi and Y. Ogata, *ibid.*, 6277.

4) F. Reverdin and P. Crepieux, *Chem. Ber.*, **33**, 2505 (1900).

5) C. S. Marvel and S. M. McElavain, "Organic Syntheses," Coll. Vol. I (1956), p. 170.

6) L. A. Bigelow, *ibid.*, p. 135.

7) L.A. Bigelow, J. R. Johnson and L. T. Sandborn, *ibid.*, p. 133.

8) L. A. Bigelow, *ibid.*, p. 136.

9) H. T. Clark and R. R. Read, *ibid.*, p. 514.

(4 mm outer diameter), was immersed in a thermostated alkali nitrates bath. The substrates of *ca.* 2 m*l* were charged by a microfeeder, and introduced with the mixed reaction gas into the reactor for about 2 hr. When the reaction was over, N_2 gas was fed into the ractor for 30 min. The products were collected by a trap cooled by air and traps cooled by a freezing mixture. Recrystallized products were identified by means of their melting points as well as GLC analysis.

Results

Preparative Ammoxidation of Substituted Toluenes. Ammoxidation of substituted toluenes[10] to prepare benzonitriles were carried out over the stabilized catalyst of 40 m*l* at the standard composition of reaction gas, *i. e.*, partial pressure of substrate (p_T) was 1.3×10^{-2} atm, that of oxygen (p_0) 13.3×10^{-2} atm, and that of ammonia (p_A) 6.7×10^{-2} atm. Nitrogen gas was used as a diluent.

Table 1. Ammoxidation of substituted toluenes at bath temperature of 370°C with gas space velocity of 450 hr^{-1}

Substrate	Product	Yield (mol %)[a]
p-Chlorotoluene	*p*-Chlorobenzonitrile	68
m-Chlorotoluene	*m*-Chlorobenzonitrile	69
o-Chlorotoluene	*o*-Chlorobenzonitrile	72
p-Bromotoluene	*p*-Bromobenzonitrile	75
m-Bromotoluene	*m*-Bromobenzonitrile	69
o-Bromotoluene	*o*-Bromobenzonitrile	74
p-Tolunitrile	Terephthalonitrile	66
m-Tolunitrile	Isophthalonitrile	63
o-Tolunitrile	Phthalonitrile	36
	+Phthalimide	15
p-Xylene	Terephthalonitrile	45
m-Xylene	Isophthalonitrile	29
	+*m*-Tolunitrile	5.6
o-Xylene	Phthalonitrile	26
	+Phthalimide	10
Toluene	Benzonitrile	45
Toluene[b]	Benzonitrile	72
Ethylbenzene	Benzonitrile	36
	+Styrene	8.2
Ethylbenzene[c]	Benzonitrile	50
	+Styrene	20

a) Based on the fed substrate. The conversions of all substrates were 100%, except for footnote b and c.
b) The conversion of toluene was 86% at bath temperature of 356°C, with gas space velocity of 930 hr^{-1} and catalyst volume of 19.3 m*l*.
c) The conversion of ethylbenzene was 77% at bath temperature of 360°C with gas space velocity of 930 hr^{-1} and catalyst volume of 19.3 m*l*.

As shown in Table 1, *o*-, *m*- and *p*-chlorotoluenes, bromotoluenes, and *m*- and *p*-tolunitriles gave fairly high yields of corresponding nitriles (*ca.* 70%). Relatively low yields of nitriles were obtained in ammoxidation of xylenes and unsubstituted toluene at 370°C under these conditions. However, at moderate reaction conditions (footnotes b and c in Table 1), toluene gave higher yield of benzonitrile (72%), its selectivity being 84%, while ethylbenzene gave 50% benzonitrile and 20% styrene, their selectivities being 65% and 26%, respectively.

Kinetics of Ammoxidation of Substituted Toluenes. The reaction conditions for kinetics were as follows: p_T, $0.67-2.67\times10^{-2}$ atm; p_A, 6.7×10^{-2} atm; p_0, 13.3×10^{-2} atm; reaction temperature, 400°C; catalyst volume, 2.5 m*l*; and gas space velocity, 7200 hr^{-1}.

Treatment of experimental data was similar to that of our previous reports,[2,3] *i. e.*, the rate of consumption of substrate, v_T, is expressed as:

$$v_T = -\frac{d[\text{substrate}]}{dt} = -\frac{d\left(\frac{p_{T_0}(1-x_T)}{RT_0}\right)}{d\left(\frac{V}{F}\right)} = k_T p_T^{t}\cdot p_0^{n}\cdot p_A^{a} \quad (1)$$

$p_0 \gg p_T$ and $p_A \gg p_T$, and hence p_0 and p_A are virtually constant under experimental conditions. Therefore, integration of Eq. (1) leads to

$$p_{T_0}\cdot x_T \simeq k_T R T_0 p_{T_0}^{t}\cdot p_0^{n}\cdot p_A^{a}(V/F) \quad (2)$$

or

$$v_T \simeq \frac{p_{T_0}\cdot x_T}{RT_0\left(\frac{V}{F}\right)} \quad (3)$$

Hence, the t value (kinetic order in substrate) can be estimated from the slope of line in the plot of $\log(p_{T_0}x_T)$ *vs.* $\log(p_{T_0})$. Also, applying Langmuir-Hinshelwood mechanism, v_T is expressed as follows.[2,3]

$$v_T = k_T^{\circ}\frac{K_T p_0\sqrt{K_0 p_0}}{(1+K_T p_{T_0}+\sqrt{K_0 p_0})^2} \quad (4)$$

Introduction of Eq. (3) into Eq. (4) gives

$$x_T^{-1/2} = \{1+\sqrt{(K_0 p_0)}+K_T p_{T_0}\} \times \{k^{\circ}_T RT_0 K_T\sqrt{(K_0 p_0)}V/F\}^{-1/2} \quad (5)$$

Relative values of K_T and k°_T can be obtained by means of the plot of $x_T^{-1/2}$ *vs.* p_{T_0} at various p_{T_0} with constant and known p_0, p_A and V/F as shown in Fig. 1. Values of K_0 and $k^{\circ}_T RT_0$ were estimated by using the value of 0.15 atm^{-1} for K_0, as obtained previously.[2]

These values are shown in Table 2. The values of K_T, $k^{\circ}_T RT_0$ and t were comparable with those obtained previously.[2] The values of $k^{\circ}_T RT_0$ are

10) For literature on ammoxidation of halotoluenes, see U. S. Pat. 2499055 (1950); German Pat. 1189976 (1965); and for *p-t*-butyltoluene, see S. D. Mekhtiev, R. G. Rizaev and A. S. Movruzova, *Dokl. Akad. Nauk Azerb. SSR*, **21**, (5), 17 (1965); E. Fischer, *Chem. Ingr.-Tech.*, **38**, 1203 (1966); and for a mixture of *m*-tolunitrile and *m*-xylene, see S. D. Mekhtiev, G. N. Suleimanov, Sh. F. Sharifova and Kh. S. Samedov, *Azerb. Khim. Zh.* (5), 73 (1966).

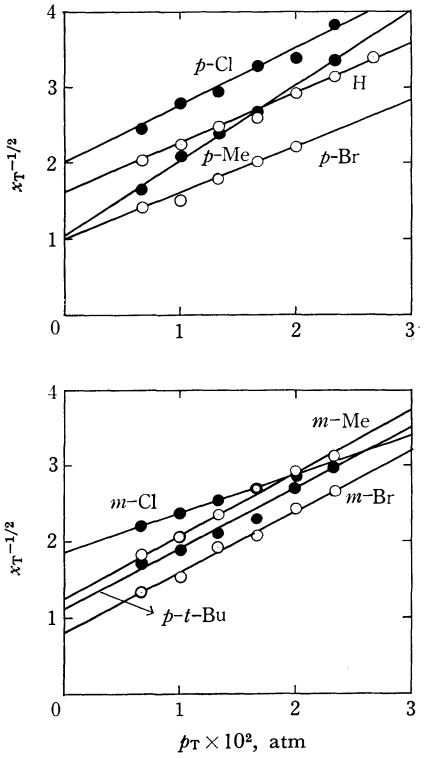

Fig. 1. Calculations of K_T and $k°_T$ at 400°C by means of Eq. (5).

TABLE 2. KINETIC PARAMETERS IN AMMOXIDATION OF SUBSTITUTED TOLUENES AT 400°C

Substituent	Conversion[a] (mol %)	K_T[b] (atm^{-1})	$k°RT_0$[b] (10^2 atm hr^{-1})	t[c]
p-CH_3	14.5	107	5.6	−0.1
p-t-Bu	16.7	72	6.2	~0
m-CH_3	13.9	77	5.4	0
H	14.8	48	5.6	+0.42
p-Cl	9.2	43	4.0	$+0.4_0$
m-Cl	13.9	31	6.3	$+0.5_2$
p-Br	24.3	63	11.0	-0.1_5
m-Br	22.8	114	9.3	−0.3

a) At p_{T_0} of 16.7×10^{-2} atm
b) Calculated by using K_O=0.15 atm^{-1}, see Ref. 2
c) Kinetic order in substrate

nearly constant except bromotoluenes. Values of K_T depend on the substituent of toluene. Hammett's plot of log K_T *vs.* Brown's σ^+ gave a straight line, from which the ρ value was estimated to be −0.9, except for bromotoluenes.

Discussion

Since the selectivities to nitriles are high at moderate reaction conditions (Table 1), kinetic data can clarify the mechanistic feature of the ammoxidation of substituted toluenes to the corresponding nitriles. As suggested previously,[3] the mechanism for the oxidation would be expressed as follows, where the rate is determined by step 8 or 9:

$$\mathrm{Hc\ (gas) + Catalyst^+ \overset{K_{Hc}}{\rightleftarrows} Hc^+(ads) + Catslyst} \quad (6)$$

$$\mathrm{O_2\ (gas) + 2\ Catalyst \overset{K_O}{\rightleftarrows} 2O^-(ads) + 2Catalyst^+} \quad (7)$$

$$\mathrm{Hc^+(ads) + O^-(ads) \underset{k_{-8}}{\overset{k_8}{\rightleftarrows}} [Hc^+(ads)O^-(ads)]\ I\ (transition\ state)} \quad (8)$$

$$\mathrm{[Hc^+(ads)O^-(ads)] \overset{k_9}{\longrightarrow} Intermediates\ or\ Products} \quad (9)$$

Here Hc means hydrocarbon and (ads) means adsorbed gas on the catalyst. Hence, $K_{Hc} \equiv K_T$ and $k°_T \equiv k_8 \cdot k_9/k_{-8}+k_9$.

The effect of substituent of toluenes on K_T gives ρ of −0.9 and the effect is expected from Eq. (6), where adsorbed hydrocarbons act as electron-donors to the catalyst. The relation between t and K_T in Table 2 implies that the stronger adsorption of substrate corresponds to the lower reaction order substrate.[3]

Equation (9) may be a hydrogen abstraction reaction. Factors influencing the selectivity in the hydrogen abstraction reaction are (i) the bond dissociation energy of the breaking C–H bond, (ii) the ionization potential of the formed radical, and (iii) the factor of entropy.[11] The transition state, I, seems to be resonating as follows.

$$\underset{II}{[(ads)^+ArCH_2{:}H\cdot O^-(ads)]} \leftrightarrow \underset{III}{[(ads)^+ArCH_2\cdot \dot{H}\cdot O^-(ads)]}$$

$$\leftrightarrow \underset{IV}{[(ads)^+ArCH_2{}^+\dot{H}{:}^-O^-(ads)]} \quad (10)$$

However, the contribution of the carbonium ion-type structure, IV, to stabilize the transition state may be negligible. Hence, the ionization potential of the substituted benzyl radical is not important for the reactivity of substrate. The bond dissociation energies of the substituted benzylic C–H bonds are almost constant.[12,13] Therefore, if the factor of entropy and others are nearly constant, $k°_T RT_0$ would not be affected by substituents. As shown in Table 2, the observed values of $k°_T RT_0$ are almost independent of substituent, except bromotoluene. This substituent effect on $k°_T RT_0$ and K_T supports the mechanism shown in Eqs. (6)—(9).

11) H. Sakurai and K. Tokumaru, "Chemistry of Free Radicals," Nankodo Ltd., Tokyo (1967), Chap. 17
12) M. Szwarc, *Chem. Rev.*, **47**, 75 (1950).
13) T. L. Cottrell, "The Strengths of Chemical Bonds," 2nd. Ed., Butterworths Scientific Publ., London (1958).

The unusual behavior of bromotoluenes may be explained as follows: The adsorption of substrates seems to need the charge transfer of π-donor type involving π- or pseudo π-electron and/or the charge transfer of n-donor type involving lone pair electron; in bromotoluenes, the latter may be more important and change the factor of entropy. Further, the decomposition of bromotoluenes may cause the intervention of Br· in the reaction system.[14]

Nomenclature

A Ammonia
O Oxygen
T Substrate, *i. e.*, substituted toluenes
a, n, and t Kinetic orders in A, O and T, respectively
p_T, p_0 and p_A Partial pressures of subscripted substance
0 Subscript 0 means initial stage of reaction
v_T Rate of consumption of substate, mol ml^{-1} hr^{-1}
k°_T Rate constant for the reaction of substrate on catalyst surface
x_T Conversion of substrate, mol mol^{-1}
K_i Adsorption equilibrium constant of i gas, atm^{-1}
V Volume of catalyst, ml
F Flow rate of gas (STP), ml hr^{-1}

14) K. Tarama, K. Hattori and Y. Kobayashi, Preprints for the 17th Annual Meeting of the Chemical Society of Japan (Tokyo, April 1964), p. 336.

The authors are indebted to Dr. T. Morimoto for the materials, and to Nissan Chem. Ind. Co. and Seitetsu Chem. Ind. Co. for their aid in the experiments.

BULLETIN OF THE CHEMICAL SOCIETY OF JAPAN VOL. 42 2505—2509 (1969)

Photoconductive Properties of Organic Polyiodides

Toshihiko SANO,*1 Kenichi OKAMOTO, Shigekazu KUSABAYASHI and Hiroshi MIKAWA

Department of Chemical Technology, Faculty of Engineering, Osaka University, Yamadakami, Suita-shi, Osaka

(Received March 5, 1969)

The photoconductive properties of $(CH_3)_4N^+I_5^-$, $(CH_3)_3(C_6H_5)N^+I_5^-$, *N*-methylacridinium pentaiodide and *N*-methylquinolinium pentaiodide were investigated by both a sandwich type cell and a single crystal cell. In the former arrangement, the photoresponse observed was the overlap of photoconductive response and photovoltaic response. The single crystal gave pure photoconductive response. Tetramethylammonium pentaiodide was the most photoconductive among the polyiodides. Spectral dependence of the photocondutcivity of this compound revealed that the threshold is at about 1000 mμ (1.24 eV). This value is in good agreement with the band gap energy 1.36 eV obtained from the temperature dependence of the dark current and 1.20—1.26 eV from calculation. Semiconductive properties of the organic polyiodides are explained by applying the band model.

Semiconductive properties of thirteen organic polyiodides including tetramethylammonium, trimethylphenylammonium, *N*-methylpicolinium, and *N*-methylacridinium polyiodides were investigated.[1,2] Two inorganic polyiodides, caesium triiodide[3] and tetraiodide,[4] were investigated. The effect of X- and γ-irradiations on the electrical conductivity of tetramethylammonium pentaiodide was also investigated.[5] Specific resistivity of the polyiodides was of the order 10^5—10^{12} Ωcm and had close connection with the number of the iodine atoms of the polyiodide anion. The framework of the polyiodide anion in the crystal is, therefore, considered to be of primary importance in determining the electrical

*1 Present address: Ueno Pharmaceutical Co., Ltd., Shimoichiba, Itami-shi, Hyogo.

1) S. Kusabayashi, H. Mikawa, S. Kawai, M. Uchida and R. Kiriyama, This Bulletin, **37**, 811 (1964).

2) S. Kusabayashi and H. Mikawa, *ibid.*, **38**, 1410 (1965).

3) M. Hayashi, H. Mikawa and S. Kusabayashi, Preprints for the 19th Annual Meeting of the Chemical Society of Japan (Yokohama, 1966), 1S010.

4) R. Matsuyama, S. Kusabayashi and H. Mikawa, Preprints for the 21st Annual Meeting of the Chemical Society of Japan (Suita, 1967), 2O227.

5) S. Kawai, R. Kiriyama, M. Uchida, S. Kusabayashi and H. Mikawa, This Bulletin, **38**, 799 (1965).

conductivity of the crystals. Energy band calculation of tetramethylammonium pentaiodide was carried out by the simple LCAO approximation method.[6] Calculation of the energy band was carried out with caesium triiodide[3] and caesium tetraiodide (Cs_2I_8).[4] Although in these calculations only the iodine framework was considered, without taking into consideration the effect of cations, values of the energy gap were found to be nearly the same as the observed value. This fact confirmed again the primary importance of the iodine framework in determining the electrical properties of the polyiodides.

The authors have already pointed out that some of the organic polyiodides have photoconductive response. In the present investigation, the photoconductive properties of tetramethylammonium pentaiodide (I), trimethylphenylammonium pentaiodide(II), *N*-methylquinolinium pentaiodide(III) and *N*-methylacridinium pentaiodide (IV) are reported. The threshold wavelength of the photoconductivity of I is in agreement with the band gap energy from the dark conductivity and the calculated band gap energy.

Experimental

Materials. The pentaiodides (I—IV) were prepared by the method reported[1,2] and used as the samples for photoconductivity measurement after recrystallizing repeatedly from water-alcohol (I, II, III) or alcohol-tetrahydrofuran (IV).

Sandwich-type Cell. The sandwich type cell (0.3—0.6 cm^2 in area and 10^{-2} cm in thickness) was made by melting and solidifying the polyiodide material between two nesa quartz plates (Fig. 1). The polyiodide materials sandwiched were in polycrystalline state.

Single Crystal Cell. The single crystal cell was made by putting between two quartz plates a single crystal (1.5 mm in width, 1 mm in thickness and 4 mm in length) with the electrodes attached by using silver paste (Fig. 1). The light illumination was effected perpendicular to the cleavage plane (*ab*-plane) of the crystal. To prevent the incident light from reaching the electrodes area an appropriate screen was attached to the single crystal cell. The sample was shut out from air with a paraffin seal between the two quartz plates, as shown in Fig. 1.

A monochromatic light from a 500 W xenon lamp with the intensity distribution shown in Fig. 2 was used, its intensity being controlled by neutral filters. Electrical measurements were carried out as usual at 20°C. In measuring the photocurrent, the dark current was potentiometrically compensated when necessary.

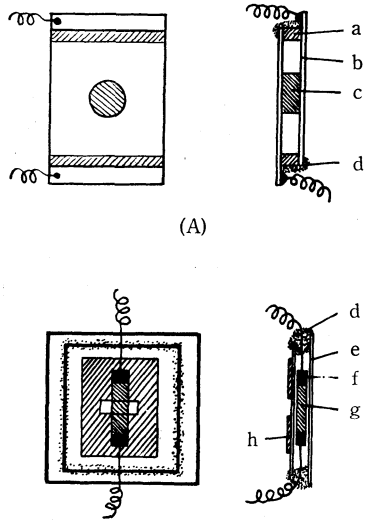

Fig. 1. Sandwich cell (A) and Single crystal cell (B).
a mica sheet, b nesa coated glass or quartz, c sample (melted and solidified), d paraffin, e glass or quartz, f silver paste, g crystal, h mask for the light

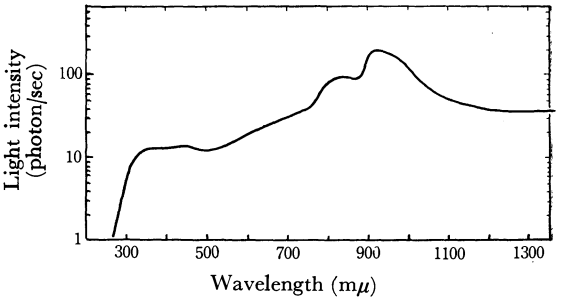

Fig. 2. Energy distribution of the light of the xenon lamp measured by a thermopile (Reedeer 8858 USA) using a monochrometer. For light of 300—320 mμ and 500—1200 mμ the slit width was kept 2 mm and 0.48 mm respectively. For 320—500 mμ the width of the wave length was kept 10 mμ. Absolute intensity of the light with this wave length width at 350—450 mμ region is 3.3×10^{14} photon/sec, when measured at the outlet of the monochrometer.

Results and Discussion

With the sandwich type cell the photoresponse consisted of both photoconductive response and photovoltaic response. It was revealed that the photoresponse of tetramethylammonium pentaiodide (I) is two to three orders of magnitude larger than the other three pentaiodides (II—IV). The photoresponse of I is very large when the positive side is illuminated, and small when illuminated at the negative side. Then sign of this rectifying effect in photoconductivity is in agreement with the positive sign of the thermoelectric power.[1] The predominant carrier in this material seems to be a hole rather

6) S. Kusabayashi and H. Mikawa, This Bulletin, **39**, 736 (1966); S. Kusabayashi, H. Mikawa, M. Konda and M. Hayashi, *ibid.*, **39**, 1383 (1966).

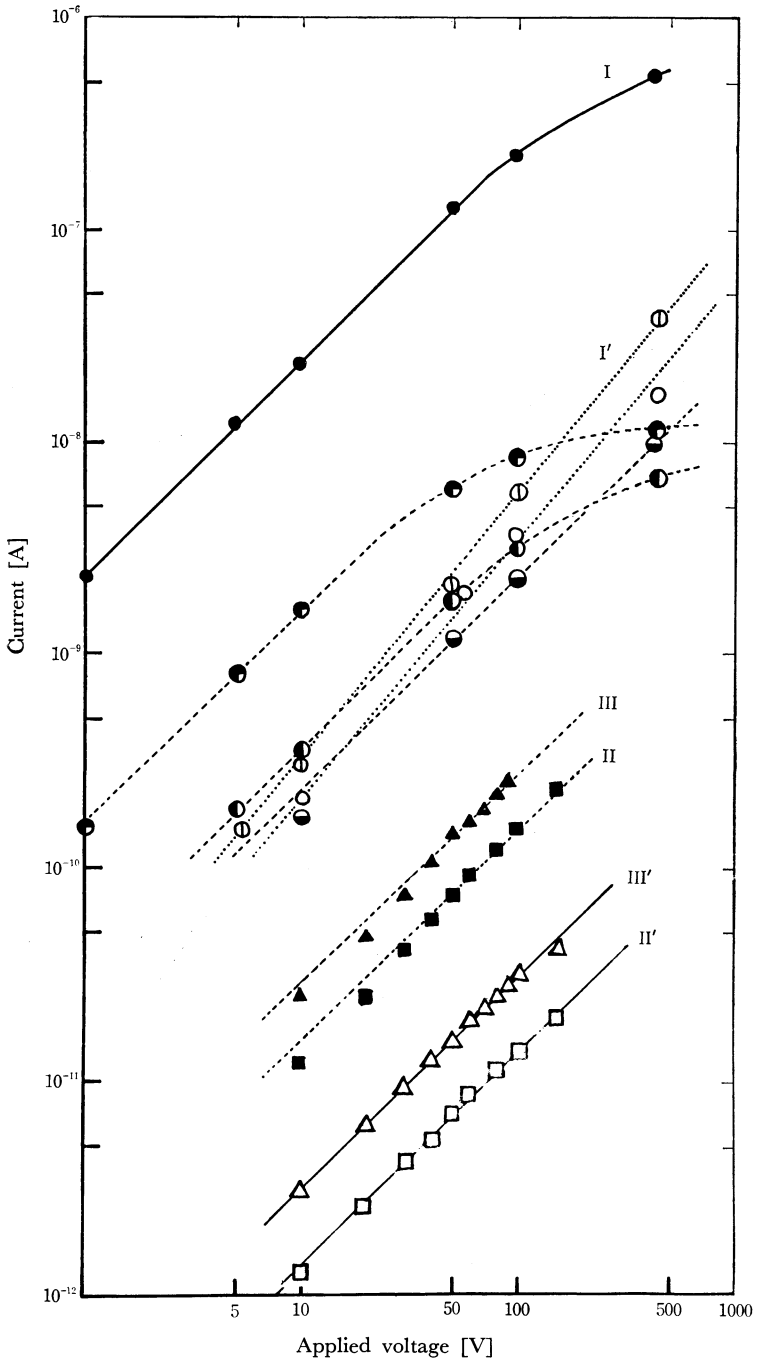

Fig. 3. Voltage dependence of the dark current I, II and III and the photocurrent I′, II′ and III′.
Tetramethylammonium pentaiodide (I and I′) with the monochromatic light of ◔ 850 mμ, ◐ 700 mμ, ◒ 600 mμ, ◑ 450 mμ, ○ 350 mμ. Trimethylphenylammonium pentaiodide (II and II′) and *N*-methylquinolinium pentaiodide (III and III′) with the light from a 500 W xenon lamp with the filter passing the light longer than 550 mμ. All values of the photocurrent are not normalized for the light intensity.

than an electron. At the higher applied voltage region, the photocurrents of II, III and IV are very small in comparison with the dark current, and the photocurrent due to the photovoltaic effect seems to be predominant.

With the single cyrstal cells no photoresponse was observed when illuminated with no applied potential. Under applied potential the steady state photocurrent with comparatively sharp rise and decay characteristics was observed with the light on or off. As the contact area between the electrode and the material is not illuminated in the single crystal cell, it might be concluded that the polyiodide materials are photoconductive. Photoresponse was in the order I $\gg$ II, III, IV, being in the same order as for the sandwich type cell.

The photocurrent with the monochromatic light was very small for the compounds II, III and IV, when compared with the dark current, being in the order of 10^{-11}—10^{-12} A. Total light with $\lambda > 550$ mμ was, therefore, used to measure the voltage dependence of the photocurrent of these compounds. Both the dark current and the photocurrent thus measured were proportional to the applied voltage, as shown by the curves II, II′, III and III′ in Fig. 3. The dark current and the photocurrent of compound I was nearly proportional to the applied voltage, as shown by the curves I and I′ in Fig. 3. As the photocurrent of this compound is rather large, monochromatic light was used. When illuminated with the light of the longer wavelength (700 mμ and 850 mμ), saturation of the photocurrent occurs in the higher voltage region. As the length of the single crystal was about 4 mm, the field strength remained within several hundred volt per cm even when 100 V was applied.

The light intensity dependence of the photocurrent changes as shown in Fig. 4 and Table 1 according to the applied voltage and the wave-

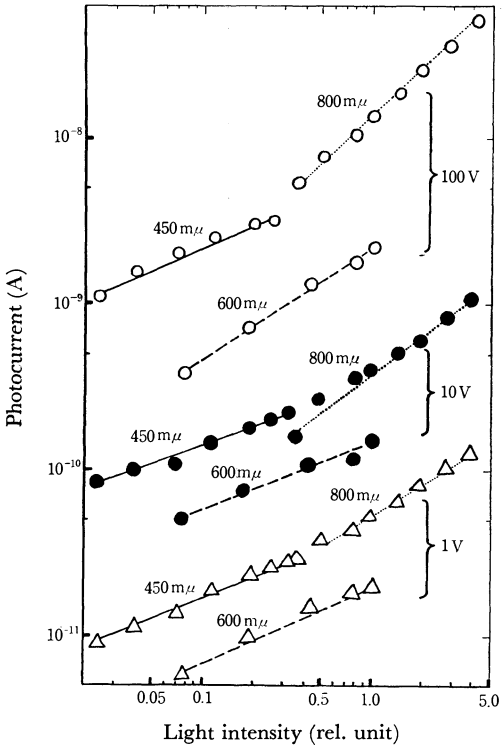

Fig. 4. Dependence of the photocurrent of tetramethylammonium pentaiodide on light intensity. Voltages shown in the figure are the potentials applied across the crystal of *ca.* 4 mm length.

TABLE 1. THE LIGHT INTENSITY (L) DEPENDENCE OF THE PHOTOCURRENT OF $(CH_3)_4{}^+I_5{}^-$

The numbers represent n in $I_{pn} \propto L^n$.

Voltage		Wavelength mμ		
		$\lambda<500$	$500<\lambda<700$	$700<\lambda$
High	(100—450 V)	0.5	0.5—1.0	1.0
Low	(1—100 V)	0.4—0.5	0.5—0.7	0.7—0.9

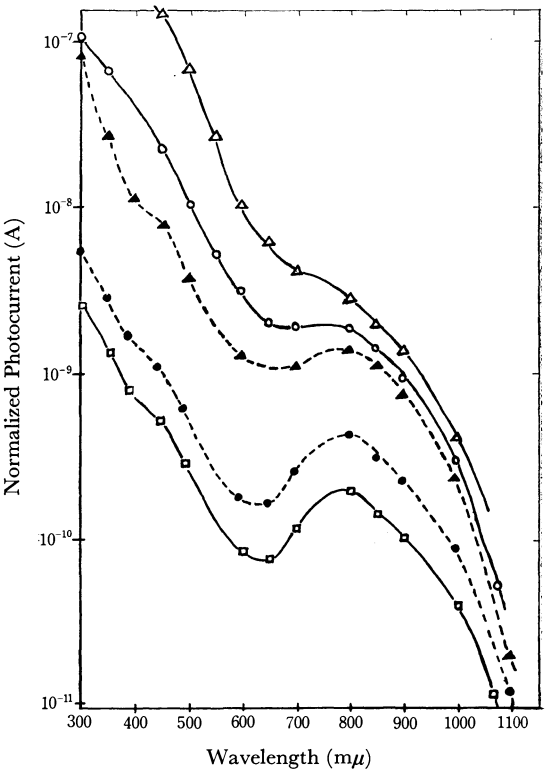

Fig. 5. Spectral dependence of the photocurrent of tetramethylammonium pentaiodide normalized for light intensity. Voltages shown in the figure are the potentials applied across the crystal of *ca.* 4 mm length.

—△— 450 V —○— 100 V
—▲— 50 V ------●------ 10 V
—□— 5 V

length. When illuminated with the light shorter than 500 mμ, the photocurrent was proportional to the 0.5 power of the light intensity, probably because the photocurrent was recombination limited in this region, the light being strongly absorbed, generating the carriers in very high concentration at the crystal surface. On the other hand the wavelength longer than 700 mμ is absorbed weakly, generating the carriers penetrating rather deep in the bulk of the crystal. This condition gives $n=1.0$. In the intermediate region from 500—700 mμ, n becomes 0.5—1.0.

The wavelength dependence of the photocurrent normalized for the light intensity L is shown in Fig. 5. The normalization was made by assuming the relation $I_{ph} \propto L^{1.0}$, the current at 600 mμ being taken as the standard. As the photocurrent is proportional to the light intensity in the region longer than 700 mμ at 100—450 V as shown in Fig. 4, this normalization may be reasonable at least in this region.

The apparent quantum yield of the photocurrent of tetramethylammonium pentaiodide was calculated to be 1.5×10^{-5} at 1000 mμ under 450 V. The threshold of the photocurrent seems to be about 1000 mμ. If the mechanism of the photoconduction is to be explained by the band model, the energy of the threshold (1.24 eV) must be equal to the band-gap energy. This value is in good agreement with the band-gap energy value 1.36 eV[1] estimated from the temperature dependence of the dark current and the band-gap energy value 1.20—1.26 eV estimated from the calculation.[6] These facts suggest that the band model is applicable to the photoconduction of the tetramethylammonium pentaiodide. Moreover, this result gives additional support to our previous suggestion that the iodine framework in the crystal structure is of primary importance in determining the conductivity of polyiodides.

BULLETIN OF THE CHEMICAL SOCIETY OF JAPAN VOL. 42 2509—2513 (1969)

The Bond Character of the Sn–Cl Bonds in the Hydrates of Tin(IV) Chloride

Hisao NEGITA, Tsutomu OKUDA and Mitsuo MISHIMA*1

Department of Chemistry, Faculty of Science, Hiroshima University, Higashi-Senda-machi, Hiroshima

(Received March 7, 1969)

Several hydrates of tin(IV) chloride, *e.g.*, $SnCl_4 \cdot xH_2O$ ($x=2$, 3, 4 and 5) and $SnCl_4 \cdot yD_2O$ ($y=3$, 4 and 5), were investigated by means of the nuclear quadrupole resonance (NQR) due to ^{35}Cl and the Mössbauer effect due to ^{119}Sn. The NQR-frequencies were observed at the temperature of liquid nitrogen and room temperature; they were found to range from 17.656 to 21.439 MHz. The Mössbauer effect was investigated only at the temperature of liquid nitrogen; it resulted in isomer shifts ranging from 0.275 to 0.350 mm/sec. The NQR-frequency and the isomer shift decreased with an increase in the number of water molecules in the hydrates, and the relationship between the NQR-frequency and the isomer shift was nearly linear. This relation was interpreted in terms of the transfer of the *s*-electrons of the tin atom to the chlorine atoms. Furthermore, it was revealed that there was a significant difference between the Sn-Cl bond of the hydrates and that of ammonium chlorostannate.

It is well-known that tin(IV) chloride forms various hydrates but their structures have not been determined by any means except the Raman spectra.[1] Tin(IV) chloride and its hydrates are suitable for investigating the Sn–Cl bond, since the electronic structures of the tin and chlorine atoms can be investigated by means of the Mössbauer effect due to ^{119}Sn and the nuclear quadrupole resonance due to ^{35}Cl.

The molecular complexes of tin(IV) chloride with organic or inorganic compounds containing oxygen or nitrogen atoms have thus far investigated by means of NQR[2,3] and the Mössbauer effect.[4–8]

*1 Present address: Department of Chemistry, Faculty of Literature and Science, Shimane University, Matsue.

1) H. S. Brune and W. Zeil, *Z. Physik. Chem. Neue Folge*, **32**, 384 (1962).

2) D. Biedenkapp and A. Weiss, *Z. Naturforsch.*, **19a**, 1518 (1964).

3) B. Haas, Thesis, Technischen Hochschule Karlsruhe (1965).

However, the hydrates of tin(IV) chloride was investigated at the temperature of liquid nitrogen.[2,3,9] Only the pentahydrate $SnCl_4 \cdot 5H_2O$ has been investigated by means of the Mössbauer effect[6,10–16] at both the temperature of liquid nitrogen and room temperature. A variety of values have been reported for the isomer shift of the hydrate, ranging from 0.2 to 0.3 mm/sec with respect to tin(IV) oxide except for the value of 0.09 mm/sec observed by Lees and Flinn.[17] These authors observed a small quadrupole splitting for that hydrate, although others did not. Our value for the isomer shift of the hydrate is 0.275 mm/sec, while the value for $SnCl_4 \cdot 5D_2O$ is 0.300 mm/sec.

Brune and Zeil[1] investigated several hydrates of tin(IV) chloride, $SnCl_4 \cdot xH_2O$ ($x=2$, 3, 4, 5 and 8) and $SnCl_4 \cdot yD_2O$ ($y=5$ and 8) by Raman spectroscopy. They concluded from the spectra that chlorine atoms are arranged octahydrally around the central tin atom and that two of the hydrated water molecules occupy the *trans*-position, that is, the hydrate molecules possess the D_{4h} symmetry in the liquid state and in solution. This is consistent with the conclusion drawn from the NQR-frequencies in the solid state.

The molecular configuration described above will be ascertained in this paper. The ionic character of the Sn–Cl bonds increases with the number of water molecules in the hydrates, and the bond character of the Sn–Cl bond in a similar compound, such as ammonium chlorostannate, is different from those of the hydrates.

Experimental

Materials. The hydrate of tin(IV) chloride was prepared by mixing tin(IV) chloride and light or heavy water in a proper molar ratio and in a sealed tube, but attempts to prepare the dihydrate, $SnCl_4 \cdot 2D_2O$, were unsuccessful. Ammonium chlorostannate was prepared by a method reported previously.[18]

Measurements. The NQR-spectrometer used for measuring the ^{35}Cl resonance consisted of a superregerative oscillator, an amplifier, and a detector. The resonance frequencies were determined at both room temperature and the temperature of liquid nitrogen.

The Mössbauer apparatus employed was essentially the same as that described previously.[4] Tin(IV) oxide containing 0.6 mCi of ^{119m}Sn was used as the γ-radiation source; it was kept at room temperature. The hydrate of tin(IV) chloride was mounted as an absorber; for tin it was about 15 mg/cm^2 thick and was cooled with liquid nitrogen.

Results and Discussion

Nuclear Quadrupole Resonance. The hydrates, $SnCl_4 \cdot 2H_2O$, $SnCl_4 \cdot 3H_2O$, and $SnCl_4 \cdot 3D_2O$, have a single resonance line due to ^{35}Cl at both room temperature and at the temperature of liquid nitrogen. The pentahydrates, $SnCl_4 \cdot 5H_2O$ and $SnCl_4 \cdot 5D_2O$, have two resonance lines at room temperature. The resonance of the latter hydrates could not be measured at the temperature of liquid nitrogen because of the piezo effect which appeared on cooling. The resonance lines in the tetrahydrates, $SnCl_4 \cdot 4H_2O$ and $SnCl_4 \cdot 4D_2O$, could not be found. The NQR-frequencies and the ionic characteristics found for the rest of the hydrates

TABLE 1. THE NQR-FREQUENCIES DUE TO ^{35}Cl FOR THE HYDRATES OF TIN(IV) CHLORIDE AND THE IONIC CHARACTER

Hydrate	Resonace frequency, MHz		Ionic character[a] %
	77°K	293°K	
$SnCl_4 \cdot 2H_2O$	21.439	21.039	55
$SnCl_4 \cdot 3H_2O$	20.384	20.173	57
$SnCl_4 \cdot 5H_2O$		18.054 17.656	62
$SnCl_4 \cdot 3D_2O$	20.438	20.208	57
$SnCl_4 \cdot 5D_2O$		18.102 17.735	62

a) The percent ionic character was obtained by neglecting the double bond character and the asymmetry parameter.

4) S. Ichiba, M. Mishima, H. Sakai and H. Negita, This Bulletin, **41**, 49 (1968).
5) S. Ichiba, M. Mishima and H. Negita, *ibid.*, **42**, 1486 (1969).
6) V. I. Gol'danskii, E. F. Makarov, R. A. Stukan, T. N. Sumarokova, V. A. Trukhanov and V. V. Khrapov, *Dokl. Acad. Nauk SSSR*, **156**, 400 (1964); *Dokl. Phys. Chem., Proc. Acad. Sci. USSR*, **156**, 474 (1964).
7) D. Khristrov, Tsv. Bonchev and Kl. Burin, *Compt. Rend. Acad. Bulgale Sci.*, **19**, 293 (1966).
8) N. N. Greenwood and J. N. R. Ruddick, *J. Chem. Soc. (A)*, **1967**, 1679.
9) R. Livingston, *J. Phys. Chem.*, **57**, 496 (1953).
10) Y. F. Lee, *Ho Tsu K'o Hsueh*, **4**, No. 3, 25 (1965).
11) O. C. Kistner, J. Jaccarino and L. R. Walker, "Isomer Shift in Sn-119," in "Proceedings of the Second International Conference on the Mössbauer Effect," ed. by D. M. J. Compton and A. H. Schoen, John Wiley and Sons, New York (1962), p. 264.
12) A. J. R. Boyle, D. St. P. Bunbury and C. Edwards, *Proc. Phys. Soc. (London)*, **79**, 416 (1962).
13) V. A. Bukarev, *Zh. Eksperim. i Teor. Fiz.*, **44**, 852 (1963); *Soviet Phys. JETP*, **17**, 579 (1963).
14) V. A. Bryukhanov, N. N. Delyagin, A. A. Opalenko and V. S. Shpinel, *Zh. Eksperim. i Teor. Fiz.*, **43**, 432 (1962); *Soviet Phys. JETP*, **14**, 1256 (1963).
15) M. Cordey-Hayes, *J. Inorg. Nucl. Chem.*, **26**, 915 (1964).
16) V. S. Shpinel, V. A. Gryukhanov and N. N. Delyabin, *Zh. Eksperim. i Teor. Fiz.*, **41**, 1767 (1962); *Soviet Phys. JETP*, **14**, 1256 (1962).
17) J. K. Lees and P. A. Flinn, *J. Chem. Phys.*, **48**, 882 (1968).
18) J. G. F. Druce, *Chem. News*, **117**, 193 (1918).

are summarized in Table 1. The ionic character is determined by neglecting the double-bond character and by estimating the *s*-electron character of the chlorine atom is 15%. As may be seen in Table 1, the NQR-frequency decreases with an increase in the number of water molecules; that is, the ionic character of the Sn–Cl bonds in the hydrates increases with the number of water molecules. In general, the hydrates of tin(IV) chloride with heavy water show slightly higher frequencies than those with light water. This result, however, shows no appreciable difference in the ionic character between the corresponding hydrates.

The atomic arrangement around the central tin atom in the dihydrates, $SnCl_4 \cdot 2H_2O$ and $SnCl_4 \cdot 2D_2O$, seems to be coordinated octahedrally by sp^3d^2-hybridization. If this is the case, the two water molecules must occupy either the *cis*- or the *trans*-position of an octahedron, as is shown in Fig. 1.

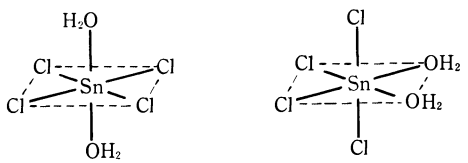

Fig. 1. The configuration of the dihydrate, $SnCl_4 \cdot 2H_2O$.
(a) *trans*-form (b) *cis*-form

From the fact that only a single NQR line was observed in the hydrates, the two water molecules may be considered to occupy the *trans*-position, since all the Sn–Cl bonds must be equivalent. Brune and Zeil suggested that the dihydrate takes the octahedral configuration in the liquid state.[1] Consequently, the D_{4h} symmetry of the dihydrate is preserved in the solid state.

The trihydrates, $SnCl_4 \cdot 3H_2O$ and $SnCl_4 \cdot 3D_2O$, also exhibit a single resonance line. Consequently, it may be assumed that two of the three water molecules are bonded to the central tin atom and occupy the *trans*-positions of the octahedron. The influence of non-coordinated molecules on the Sn–Cl bonds is quite significant, since the resonance frequency of the trihydrate, $SnCl_4 \cdot 3H_2O$, is considerably lower than that of the dihydrate, $SnCl_4 \cdot 2H_2O$, the difference being 1.055 MHz at the temperature of liquid nitrogen. The difference in ionic character between the two hydrates is 2%.

In the pentahydrates, the two resonance lines are situated close together; the difference between them is 0.398 MHz for $SnCl_4 \cdot 5H_2O$ and 0.367 MHz for $SnCl_4 \cdot 5D_2O$. This indicates the existence of two non-equivalent Sn–Cl bonds in the pentahydrates. The findings on the Raman spectra for the hydrates, $SnCl_4 \cdot xH_2O$ and $SnCl_4 \cdot yD_2O$, show that all the hydrates possess the D_{4h} symmetry with regard to the arrangement of the atoms bonded to the central tin atom in the liquid state. If the atomic configuration around the tin atom is the *cis*-form in the pentahydrates, the symmetry class must be C_{2v}. This contradicts the results of the Raman spectra. Consequently, it may be concluded that the small deviation in the resonance frequencies is not caused by the *cis*-form, but is brought about by the crystal field due to the three non-coordinated water molecules as well as the neighboring octahedrons.

In addition, the resonance frequencies of the pentahydrates, $SnCl_4 \cdot 5H_2O$ and $SnCl_4 \cdot 5D_2O$, are considerably lower than those of the dihydrate and trihydrates. Taking into account this lowing and the appearance of the two lines in the pentahydrate, the influence of the non-coordinated water molecules on the Sn–Cl bonds seems to be significant. On the other hand, the resonance frequencies of all the hydrates are much lower than those of pure tin(IV) chloride, 24.294, 24.226, 24.140, and 23.179 MHz at 77°K. The four chlorine atoms are spatially directed to the corners of a distorted tetrahedron in the crystal state, forming sp^3-hybrid orbitals, although Sn–Cl bonds have an ionic character of 48% if the double-bond character is disregarded. According to Haas[3] and Schawlow,[19] the ionic character is estimated to be 41 and 38% respectively. When tin(IV) chloride is hydrated, the atoms around the tin atom are arranged almost octahedrally, forming sp^3d^2-hybrid orbitals quite ionic in character. The *d*-electrons necessary for this hybridization are brought from the lone-pair electrons of the oxygen atoms of water molecules. The Sn–Cl bonds in the hydrates are more ionic than those of pure tin(IV) chloride, since the resonance frequencies of the former are lower than those of the latter.

Mössbauer Effect. The results of the Mössbauer effect are summarized in Table 2. The values of the isomer shift at the temperature of liquid nitrogen are shown with respect to tin(IV) oxide. These values fall in a range from 0.275 to 0.350 mm/sec and decrease with an increase in the number of water molecules in the same way as do the NQR-

Table 2. The Mössbauer effect due to ^{119}Sn of the hydrates of tin(IV) chloride

Hydrate	δ,[a] mm/sec	Hydrate	δ,[a] mm/sec
$SnCl_4 \cdot 2H_2O$	0.350		
$SnCl_4 \cdot 3H_2O$	0.325	$SnCl_4 \cdot 3D_2O$	0.350
$SnCl_4 \cdot 4H_2O$	0.300	$SnCl_4 \cdot 4D_2O$	0.330
$SnCl_4 \cdot 5H_2O$	0.275	$SnCl_4 \cdot 5D_2O$	0.300

a) δ is the isomer shift at liquid nitrogen temperature relative to the source of SnO_2 crystal. The accuracy is $\pm 5\%$ in the measurement.

19) A. L. Schawlow, *J. Chem. Phys.*, **22**, 1211 (1954).

frequencies. It may be noted again that the values for the hydrates of light water are slightly smaller than those of the hydrates of heavy water, but this fact will not be taken into account. From the tendency of the isomer shift, it is evident that the *s*-electron density at a tin nucleus decreases with an increase in the number of water molecules. The decrease in the *s*-electron density is caused by either losing *s*-electrons directly to other atoms or by receiving *p*- and/or *d*-electrons, the shielding effect of which decreases the *s*-electron density indirectly. The latter theory would mean an increase in the covalent character, and this is in conflict with the NQR results. Therefore, the tin atom is becoming a complete stannic ion with an increase in the number of water molecules. The increase in the ionic character results in a decrease in the covalent character and bring about a variation in the shielding effect.

According to the NQR results, the increase in the number of water molecules causes an increase in the electron density around the chlorine nucleus. Supposing that the *s*-electrons in the tin atom move to the chlorine atoms, the *s*-electron density at the tin nucleus should decrease, and hence the isomer shift should be diminished. This interpretation fits well with the findings on the Mössbauer effect.

The $(x-2)$ non-coordinated water molecules in the hydrates, $SnCl_4 \cdot xH_2O$, affect the nature of the Sn–Cl bonds significantly. However, these molecules do not take part directly in the decrease in the electron density at the tin nucleus, since they are located outside the octahedron centered about the tin nucleus. They seem to affect the tin atom through the coordinated chlorine atoms and/or water molecules, which may form hydrogen bonds with one another.

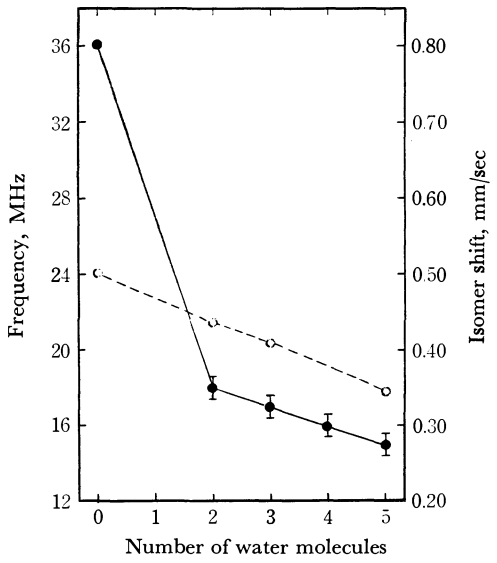

Fig. 2. The relation between the number of water molecules and the NQR-frequency or the isomer shift for the hydrate $SnCl_4 \cdot xH_2O$ at 77°K.

○: NQR-frequency ●: isomer shift

Figure 2 shows how the isomer shift and the NQR-frequency vary with the number of water molecules in the hydrate; the literature values of the pure tin(IV) chloride, 0.7,[6] 0.78,[20] 0.8,[7] 0.85,[13] and 0.9[15] mm/sec, have been averaged. It is apparent that there is a sudden decrease in the isomer shift from $x=0$ to $x=2$. This seems to be attributable to the shielding due to the *d*-electrons and to the increased ionic character of the tin atom. The gradient of the curve of the NQR-frequency *versus* the number of water molecules from $x=0$ to $x=2$ is almost the same as that from $x=2$ to $x=5$. The NQR-frequency of pentahydrates at the temperature of liquid nitrogen was roughly estimated from the value at room temperature. Taking the gradual decrease in the NQR-frequency into consideration, the sudden decrease of the isomer shift from $x=0$ to $x=2$ can be attributed to the shielding effect due to the *d*-electrons.

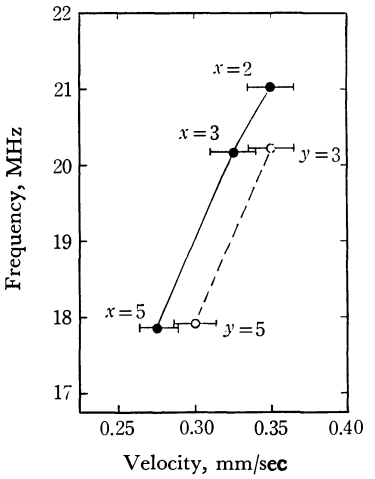

Fig. 3. The isomer shift at 77°K *versus* the NQR-frequency at 293°K for the hydrates, $SnCl_4 \cdot xH_2O$ and $SnCl_4 \cdot yD_2O$.

Figure 3 shows that the NQR-frequency increases almost linearly with the isomer shift in the two series of hydrates, $SnCl_4 \cdot xH_2O$ and $SnCl_4 \cdot yD_2O$. From this relation it may be concluded that the *s*-electrons of the tin atom move to the chlorine atoms. In other words, the less the isomer shift due to ^{119}Sn, the more ionic is the Sn–Cl bond. The resonance frequencies of the tetrahydrates, $SnCl_4 \cdot 4H_2O$ and $SnCl_4 \cdot 4D_2O$, which could not be observed in the present investigation are assumed

20) A. Yu. Aleksandrov, N. N. Delyagin, N. P. Mitrofanov, L. S. Polak and L. S. Shpinel, *Zh. Eksperim. i Teor. Fiz.*, **43**, 1242 (1962); *Soviet Phys. JETP*, **16**, 879 (1963).

to be as follows: The frequency for $SnCl_4 \cdot 4H_2O$ lies in the immediate neighborhood of 19 MHz, while that for $SnCl_4 \cdot 4D_2O$ is about 0.05 MHz higher than this value.

Ammonium hexachlorostannate, $(NH_4)_2SnCl_6$, shows two resonance lines at the temperature of liquid nitrogen, *i.e.*, 15.61 and 15.65 MHz. The value of the isomer shift for this compound is 0.475 mm/sec with respect to tin(IV) oxide in our experiment, although its literature values are 0.3,[15] 0.40,[14] 0.42,[16] 0.49,[21] and 0.50.[13] The crystal structure was analyzed by X-ray diffraction.[22] The tin atom is surrounded octahedrally by six equivalent chlorine atoms, but the NQR results show that two groups of slightly different bonds exist. The atomic arrangement around the tin atom in the hydrates can be obtained by substituting water molecules for chlorine in the hexachlorostannate ion. The NQR-frequencies reveal that the chlorine atoms in the ammonium hexachlorostannate are more ionic than that in the dihydrate. On the other hand, the Mössbauer effect reveals that the *s*-electron density at the tin nucleus in the chlorostannate is greater than in the dihydrate. Consequently, the tin atom is not as ionic as we had expected, although anions are coordinated to the tin atom. In other words, the Sn–Cl bonds in the chlorostannate are quite covalent. The conclusion that the more ionic the chlorine atoms, the more ionic is the tin atom does not apply to ammonium hexachlorostannate. $[SnCl_6]^{2-}$ ion has two minus charges distributed among the six chlorine atoms almost uniformly, while each chlorine atom has a charge of $-1/3$. Assuming that most of these charges participate in the ionic bond with an ammonium ion, the charges do not have a great influence upon the tin atom. This assumption is consistent with the NQR results and the Mössbauer effect.

The Sn–O bond is expected to be more ionic than the Sn–Cl bond in the dihydrate since the oxygen atom is more electronegative than the chlorine atom, and the isomer shift due to the ^{119}Sn of the dihydrate is smaller than those of $M^{I}_2SnCl_6$ or $M^{II}SnCl_6$ (M^{I}=H, K, NH_4; M^{II}=Mg, Ca, Ni), which are reported to be 0.42—0.49 mm/sec.[10,20]

The authors wish to express their thanks to Miss T. Shimazu for her help in checking some of the results.

21) G. Blinznakov and K. Petrov, *Z. anorg. allge. Chem.*, **354**, 307 (1967).

22) R. G. Dickinson, *J. Am. Chem. Soc.*, **44**, 276 (1922). Ammonium chlorostannate is the crystal of the cubic system with the space group O_h^5 and the lattice constant a_0=10.05 Å. The unit cell contains four molecules and the bond length of the Sn–Cl bond is 2.46 Å.

BULLEEIN OF THE CHEMICAL SOCITTY OF JAPAN VOL. 42 2514—2519 (1969)

Measurement of Negative Ions Formed by Electron Impact. IV. Negative Ion Mass Spectra and Ionization Efficiency Curves of Negative Ions of *m/e* 17 and 16 from *n*-Propyl and Isopropyl Alcohols

Satoru TSUDA, Akira YOKOHATA and Michihiro KAWAI

Department of Chemisrty, Faculty of Engineering, University of Hiroshima, Senda-machi, Hiroshima

(Received March 10, 1969)

The negative ion mass spectra of *n*- and iso-propyl alcohols, with emphasis on their relative yields to the positive ions under 80 eV, 40 eV and 15 eV electron energies, and the ionization efficiency (IE) curves of OH^- and O^- ions to the extent of 50 eV electron energies were measured. In both cases, the electron impacts of 80 eV and 40 eV gave almost the same negative ion mass spectra, in which the relatively strong peaks of *m/e* 16 (O^-), *m/e* 17 (OH^-) and *m/e* 25 (C_2H^-) ions except for the decrement of C_2H^- ions in 40 eV for isopropyl alcohol were characteristic. For *n*-propyl alcohol, the ratio of the yield of CH_2OH^+ ions to that of O^- ions (CH_2OH^+/O^-) gave the values of 6.9×10^4 and 1.9×10^5 in 80 eV and 40 eV. For isopropyl alcohol the values of $C_2H_4OH^+/OH^-$ were 3.3×10^4 and 6.4×10^4 in 80 eV and 40 eV, respectively. The comparison of the yield of negative ion in 10 eV with that of positive ion in 15 eV gave $CH_2OH^+/O^-=2.0\times10^4$ and $C_2H_4OH^+/OH^-=2.3\times10^3$. Each appearance potential observed in IE curves is well interpreted by the following reactions. [OH^- ions], for the first process C_3H_7OH(*n*- or iso-)$+e^-\rightarrow OH^-+C_2H_4+CH_2+H$, for the second process C_3H_7OH(*n*- or iso-)$+e^-\rightarrow OH^-+CH_3+CH_2+CH_2^++e^-$ or $OH^-+C_2H_4+CH_2+H^++e^-$. [O^- ions], for the first process C_3H_7OH(*n*- or iso-)$+e^-\rightarrow O^-+C_2H_5+CH_3$, for the second process C_3H_7OH(*n*- or iso-)$+e^-\rightarrow O^-+C_2H_4+CH_3+H$ or $O^-+C_2H_3+CH_3+H_2$ and for the third process C_3H_7OH(*n*- or iso-)$+e^-\rightarrow O^-+C_3H_7$(*n*- or iso-)$+H^++e^-$ or $O^-+C_3H_5+H_2+H^++e^-$.

Recently, several studies have been reported on the measurement of negative ion mass spectra by the electron impact method.[1-6] However, they were only made for limited kinds of compounds. Furthermore, data of the ionization efficiency (IE) curves of negative ions are very limited.[7-9] On the other hand, the role of negative ions is attracting increasing attention in the field of radiation chemistry. Compounds containing oxygen atom are of particular interest. Warman *et al.*[10,11] have pointed out the occurrence of the negative ion-molecule reactions containing O^- ions.

The authors reported previously the results of measurement of negative ion mass spectra obtained from nitroalkanes in relation to electron energies,[12] and of IE curves of NO_2^-, O^-, $CH_2NO_2^-$,[12] CN^- and CNO^-[13] ions.

This work was extended to *n*- and iso-propyl alcohols. Emphasis was placed on the relative yields of negative ions to the positive ions and on the measurement of the IE curves of OH^- and O^- ions.*1

1) C. E. Melton, "Mass Spectrometry of Organic Ions," ed. by F. W. McLafferty, Academic Press, New York, N. Y. (1963), p. 163.

2) E. W. McDaniel, "Collision Phenomena in Ionized Gases," John Wiley & Sons Inc., New York (1964), p. 368.

3) F. Fiquat-Fayard, *Actions Chim. Biol. Radiations*, **8**, 31 (1965).

4) R. T. Aplin, H. Budzikieweiz and C. Djerassi, *J. Am. Chem. Soc.*, **87**, 3180 (1965).

5) C. E. Melton and P. S. Rudolf, *J. Chem. Phys.*, **47**, 1771 (1967).

6) D. F. Munro, J. E. Ahnell and W. S. Koski, *J. Phys. Chem.*, **72**, 2682 (1968).

7) L. G. Christophorou, R. N. Compton, G. S. Hurst and P. W. Reinhardt, *J. Chem. Phys.*, **45**, 536 (1966).

8) L. G. Christophorou and R. N. Compton, *Health Physics*, **13**, 1277 (1967).

9) T. Sugiura, T. Seguchi and K. Arakawa, This Bulletin, **40**, 2992 (1967).

10) J. M. Warman, *Nature*, **213**, 382 (1967); *J. Phys. Chem.*, **72**, 52 (1968).

11) S. J. Rzad and J. M. Warman, *ibid.*, **72**, 3013 (1968).

12) S. Tsuda, A. Yokohata and M. Kawai, This Bulletin, **42**, 614 (1969).

13) S. Tsuda, A. Yokohata and M. Kawai, *ibid.*, **42**, 1515 (1969).

*1 Recently, the measurement of ethyl alcohol was reported. However, no detailed discussion was made. (H. Hotta, T. Sugiura and H. Kurihara, The 11th Meeting of Radiation Chemistry, Tokyo (1968)).

Experimental

Experiments were performed on a Hitachi RMU-6D mass spectrometer equipped with the T-2M ion source having a rhenium filament. The ion detection circuit consisted of a ten stage electron multiplier and of a Faraday collector. Conditions for the experiment and the method for correction of the electron energy scale were the same as those described previously[12] except for the use of accelerating voltage of 2.4 kV and electron multiplier voltage of 1.8 kV. The compounds used were of research grade and no further purifications were made.

Results and Discussion

Negative Ion Mass Spectra. Figures 1 and 2 show the negative ion mass spectra for *n*- and iso-propyl alcohols in 80 eV, 40 eV and 10 eV electron energies, in relation to the positive ion mass spectra in 80 eV, 40 eV and 15 eV.*2

For the electron impact of 80 eV and 40 eV, the peaks of negative ions obtained commonly in both samples are as follows; *m/e* 12 (C^-), *m/e* 13 (CH^-), *m/e* 14 (CH_2^-), *m/e* 16 (O^-), *m/e* 17 (OH^-), *m/e* 24 (C_2^-), *m/e* 25 (C_2H^-), *m/e* 41 (C_2HO^-), *m/e* 43 ($C_2H_3O^-$), *m/e* 57 ($C_3H_5O^-$) and *m/e* 59 ($C_3H_7O^-$).

The formation of *m/e* 41, 43, 57 and 59 ions shows that loss of hydrogen by negative ion formation is almost entirely restricted to that of an odd

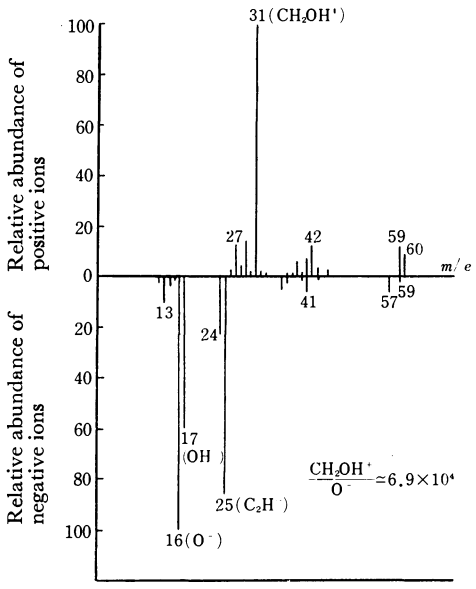

Fig. 1a.

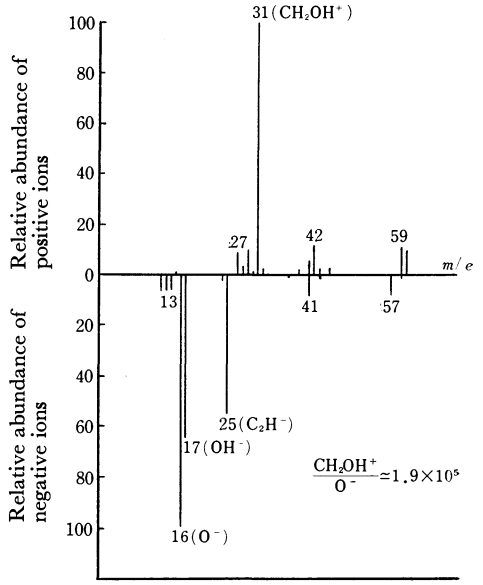

Fig. 1b.

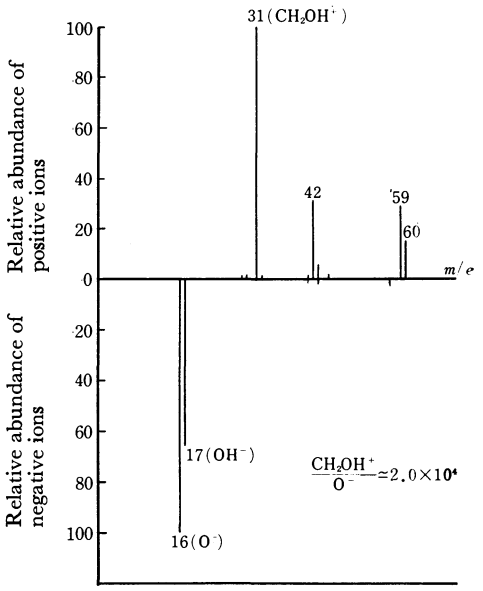

Fig. 1c.

Fig. 1. Positive and negative ion mass spectra of *n*-propyl alcohol.
(a) 80 eV
(b) 40 eV
(c) 15 eV for positive ions, 10 eV for negative ions

number of hydrogen atoms.

The most intense peaks were O^- ions for *n*-propyl alcohol and OH^- ions for isopropyl alcohol. A relatively large change in their relative yields with electron energies (80→40 eV) was found especially in C^-, C_2^- and C_3^- ions for *n*-propyl alcohol, and O^-, C_2^-, C_2H^-, C_3^- and C_2O^- ions for isopropyl alcohol. The general patterns of spectra in 80 eV

*2 Since the positive ions obtained in 10 eV electron energies are very limited, the data for 15 eV were conveniently used for comparison with the yield of negative ions in 10 eV.

showed a relatively good consistency with those obtained by Melton[1] in 90 eV except for a smaller peak of $C_3H_7O^-$ ions for the two samples.

The comparsion of the yield of O^- ions with of CH_2OH^+ ions (the most intense peak among the positive ions) for *n*-propyl alcohol and of OH^- ions with $C_2H_4OH^+$ ions (the most intense peak among the positive ions) for isopropyl alcohol gave $CH_2OH^+/O^-=6.9\times10^4$ and $C_2H_4OH^+/OH^-=3.3\times10^4$ for 80 eV electron energies, $CH_2OH^+/O^-=1.9\times10^5$ and $C_2H_4OH^+/OH^-=6.4\times10^4$ for 40 eV electron energies respectively.

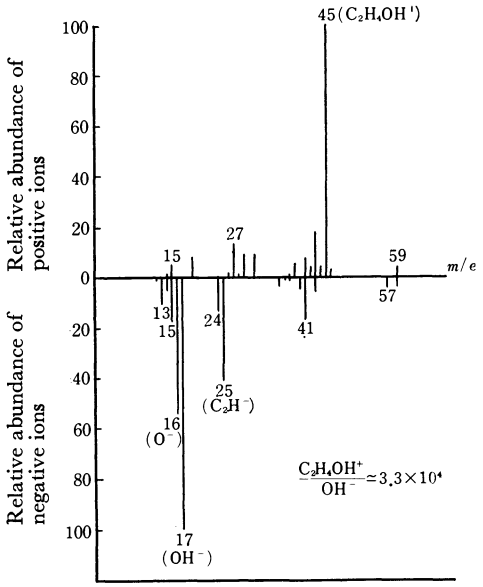

Fig. 2a.

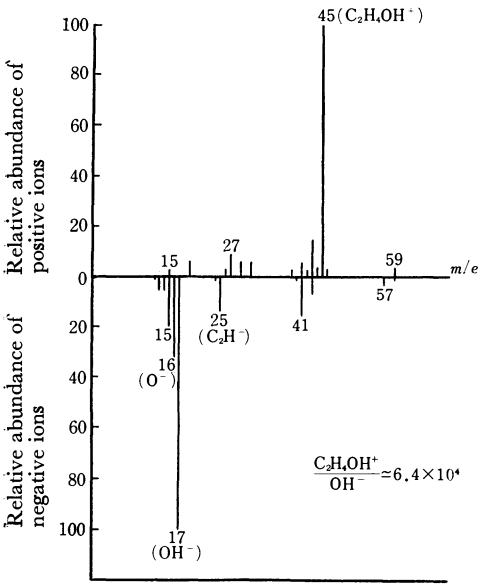

Fig. 2b.

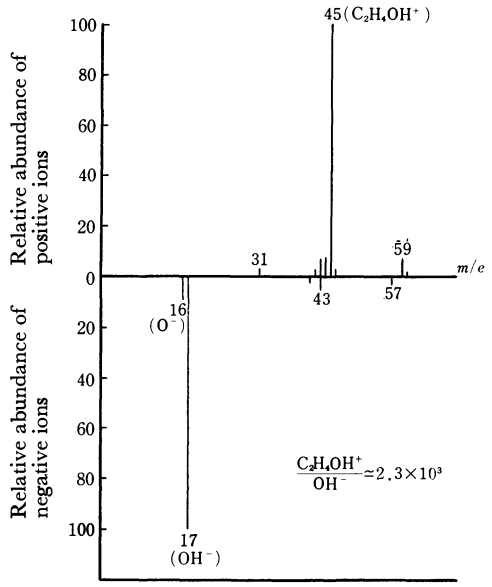

Fig. 2c.

Fig. 2. Positive and negative ion mass spectra of isopropyl alcohol.
(a) 80 eV
(b) 40 eV
(c) 15 eV for positive ions, 10 eV for negative ions

In 10 eV electron energies, O^- and OH^- ions for *n*-propyl alcohol and OH^- ions for isopropyl alcohol predominated other negative ions. When the yields of O^- and OH^- ions in 10 eV electron energies are compared with those of positive ions of the most intense peak obtained in 15 eV electron energies, $CH_2OH^+/O^-=2.0\times10^4$ for *n*-propyl alcohol and $C_2H_4OH^+/OH^-=2.3\times10^3$ for isopropyl alcohol were obtained respectively.

Since the data were taken at a pressure of $\sim10^{-6}$ mmHg, the possibility of ions induced by ion-molecule reactions would be ruled out.

The differences in negative ion mass spectra in both samples, especially of O^- and OH^- ions, will be also discussed later in relation to electron energies on the basis of measurement results of IE curves.

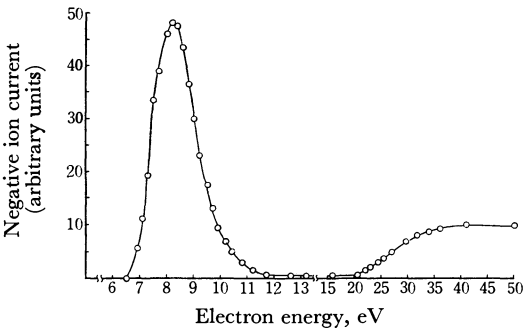

Fig. 3. Ionization efficiency curve of OH^- ions from *n*-propyl alcohol.

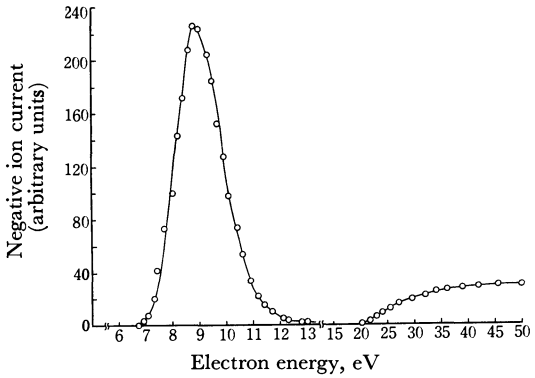

Fig. 4. Ionization efficiency curve of OH^- ions from isopropyl alcohol.

IE Curves. *OH^- Ions.* Figures 3 and 4 show the IE curves for *m/e* 17 (OH^-) ions obtained from *n*- and iso-propyl alcohols respectively. It can be understood that in both cases two processes contribute to their formation. The first process appears at ~6.5 eV for *n*-propyl alcohol and at ~6.7 eV for isopropyl alcohol. The second process appears at ~20.5 eV and ~20.1 eV. The shape of IE curves suggests clearly the dissociative electron capture for the first process and the ion pair formation for the second process.

Generally speaking, the appearance potential (AP) of reaction (1) can be experssed by Eq. (2), if the kinetic energies of fragment are ignored and the ions formed are in ground state.

$$XYZ + e^- \rightarrow X^- + Y + Z \quad (1)$$

$$AP_{calc} = \Delta H = \Delta H_f(X^-) + \Delta H_f(Y) + \Delta H_f(Z) - \Delta H_f(XYZ) \quad (2)^{*3}$$

In the case of ion pair formation ($Y \rightarrow Y^+$), the following equation holds.

$$AP_{calc} = \Delta H = \Delta H_f(X^-) + \Delta H_f(Y^+) + \Delta H_f(Z) - \Delta H_f(XYZ) \quad (3)$$

From Eqs. (2) and (3), the schemes of the most plausible reactions expected to occur at the onset values of each AP_{obs} were sought.

For the first process, the following reactions may be considered.

$$n\text{-}C_3H_7OH + e^- \rightarrow OH^- + C_3H_7 \quad (AP_{calc}=2.22\ eV) \quad (4)$$

$$\rightarrow OH^- + CH_3 + C_2H_4 \quad (AP_{calc}=3.19\ eV) \quad (5)$$

$$\rightarrow OH^- + C_2H_5 + CH_2 \quad (AP_{calc}=4.86\ eV) \quad (6)$$

$$\rightarrow OH^- + CH_2 + H + C_2H_4 \quad (AP_{calc}=6.56\ eV) \quad (7)$$

$$\rightarrow OH^- + CH_3 + 2CH_2 \quad (AP_{calc}=7.65\ eV) \quad (8)$$

*3 $\Delta H_f(X)$: heat of formation of X.

In the estimation of AP_{calc}, the values of ΔH_f (*n*-C_3H_7OH) = −2.70 eV, $\Delta H_f(OH^-)$ = −1.44 eV,*4 $\Delta H_f(C_3H_7)$ = 0.96 eV, $\Delta H_f(CH_3)$ = 1.39 eV, $\Delta H_f(C_2H_4)$ = 0.54 eV, $\Delta H_f(C_2H_5)$ = 1.10 eV, $\Delta H_f(CH_2)$ = 2.5 eV and $\Delta H_f(H)$ = 2.26 eV were used.[14] Among reactions (4)—(8), the reaction (7) is strongly expected because the consistency of AP_{calc} with AP_{obs} (~6.5 eV) is best for reaction (7).

For the second process,*5 the following reactions may be considered.

$$n\text{-}C_3H_7OH + e^- \rightarrow OH^- + C_3H_7^+ + e^- \quad (AP_{calc}=10.91\ eV) \quad (9)$$

$$\rightarrow OH^- + CH_3^+ + C_2H_4 + e^- \quad (AP_{calc}=13.03\ eV) \quad (10)$$

$$\rightarrow OH^- + C_2H_5^+ + CH_2 + e^- \quad (AP_{calc}=13.64\ eV) \quad (11)$$

$$\rightarrow OH^- + C_2H_4^+ + CH_3 + e^- \quad (AP_{calc}=13.70\ eV) \quad (12)$$

$$\rightarrow OH^- + CH_2^+ + C_2H_5 + e^- \quad (AP_{calc}=16.76\ eV) \quad (13)$$

$$\rightarrow OH^- + CH_3^+ + 2CH_2 + e^- \quad (AP_{calc}=17.49\ eV) \quad (14)$$

$$\rightarrow OH^- + CH_2^+ + CH_3 + CH_2 + e^- \quad (AP_{calc}=19.55\ eV) \quad (15)$$

$$\rightarrow OH^- + H^+ + CH_2 + C_2H_4 + e^- \quad (AP_{calc}=20.16\ eV) \quad (16)$$

A relatively good consistency of AP_{calc} of reaction (16) with AP_{obs} (~20.5 eV) suggests the possibility of the occurrence of reaction (16). A small allowance of the excess kinetic energies of the fragment ions, however, may also permit the possibility of reaction (15). In the present stage when their details are not well known, it is difficult to discuss this problem further.

The same reactions would also be assigned for the first and second processes in isopropyl alcohol, in which the use of ΔH_f(*i*-C_3H_7OH) = −2.84 eV is required.*6

O^- Ions. Figures 5 and 6 show the IE curves for *m/e* 16 (O^-) ions obtained from *n*- and iso-propyl alcohols respectively. The two samples gave similar curves except for a small peak at ~11.2 eV for *n*-propyl alcohol. If this peak is ignored, we see that the first process appears at ~6.2 eV and ~6.4 eV, the second process at the same value,

*4 To be estimated from $\Delta H_f(OH)$ = 0.39 eV and EA(OH) = 1.83 eV (L. M. Branscob, *Phys. Rev.*, **148**, 11 (1966)).

14) R. R. Bernecker and F. A. Long, *J. phys. Chem.*, **65**, 1565 (1961).

*5 For the value of $H_f(Y^+)$, see Ref. 14.

*6 In some cases, rearrangement should be taken into consideration.

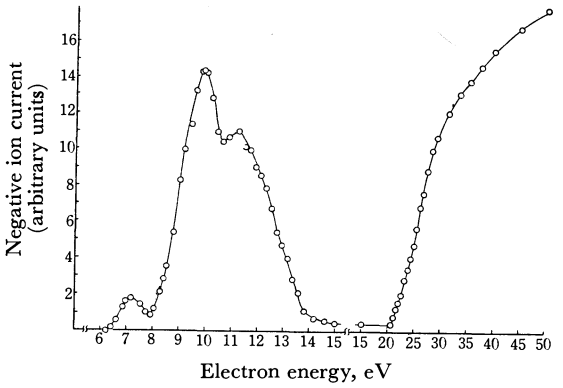

Fig. 5. Ionization efficiency curve of O^- ions from *n*-propyl alcohol.

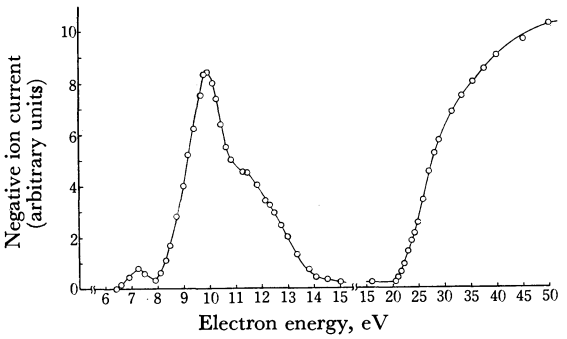

Fig. 6. Ionization efficiency curve of O^- ions from isopropyl alcohol.

~7.9 eV*[7] and the third process at ~20.8 eV and ~20.5 eV.

In the same manner as OH^- ions, the reaction schemes which correspond to each AP_{obs} value were sought by using $\Delta H_f(O^-)=1.09$ eV*[8] and the known values of ΔH_f(products).[14] For the first process, the following reactions may be considered.

$$n\text{-}C_3H_7OH + e^- \rightarrow O^- + C_3H_6 + H_2 \quad (AP_{calc}=4.00\ eV) \quad (17)$$

$$\rightarrow O^- + C_2H_5 + CH_3 \quad (AP_{calc}=6.28\ eV) \quad (18)$$

For the second process,

$$n\text{-}C_3H_7OH + e^- \rightarrow O^- + C_3H_7 + H \quad (AP_{calc}=7.01\ eV) \quad (19)$$

$$\rightarrow O^- + C_3H_5 + H_2 + H \quad (AP_{calc}=7.35\ eV) \quad (20)$$

$$\rightarrow O^- + C_2H_4 + CH_3 + H \quad (AP_{calc}=7.98\ eV) \quad (21)$$

$$\rightarrow O^- + C_2H_3 + H_2 + CH_3 \quad (AP_{calc}=8.01\ eV) \quad (22)$$

$$\rightarrow O^- + C_3H_6 + 2H \quad (AP_{calc}=8.52\ eV) \quad (23)$$

$$\rightarrow O^- + C_3H_4 + H_2 + 2H \quad (AP_{calc}=10.23\ eV) \quad (24)$$

For the third process,

$$n\text{-}C_3H_7OH + e^- \rightarrow O^- + CH_3^+ + H + C_2H_4 + e^- \quad (AP_{calc}=17.82\ eV) \quad (25)$$

$$\rightarrow O^- + C_2H_4^+ + H + CH_3 + e^- \quad (AP_{calc}=18.49\ eV) \quad (26)$$

$$\rightarrow O^- + H^+ + C_3H_7 + e^- \quad (AP_{calc}=20.61\ eV) \quad (27)$$

$$\rightarrow O^- + H^+ + C_3H_5 + H_2 + e^- \quad (AP_{calc}=20.95\ eV) \quad (28)$$

Among these reactions, the possibility of reaction (18) for the first proc of reaction (21) or (22) for the second process ar of reaction (27) or (28) for the third process can be strongly expected because their AP_{calc} values are almost consistent with each AP_{obs} value of ~6.2 eV, ~7.9 eV and ~20.8 eV respectively. For the same reason as described in the case of OH^- ions, however, we cannot exclude the possibility of reactions (19), (20) or (25) and (26). The same interpretation is also applied for isopropyl alcohol. Reaction (24) might correspond to the process appearing at ~11.2 eV of the third peak observed for *n*-propyl alcohol. This is, however, a tentative interpretation and still open to question.

The yield of negative ions (OH^-, O^- ions) depends on the cross section of formation process of negative ions. Figures 3 and 4 show that the maximum yield of OH^- ions is obtained at 8.2 eV for *n*-propyl alcohol and at 8.7 eV for isopropyl alcohol and is larger in isopropyl alcohol. The cross section of reaction (7) expected to occur at 8.2 eV and 8.7 eV electron energies is larger by a factor of 5 in isopropyl alcohol. On the other hand, Figs. 5 and 6 show that the maximum yield of O^- ions is obtained at almost the same electron energies, ~10 eV in the range of zero to 30 eV, and their yield is larger by a factor of ~1.6 in *n*-propyl alcohol.

It should be noted that (1) O^- ions for *n*-propyl alcohol and OH^- ions for isopropyl alcohol showed always the most intense peaks irrespective of electron energies used, (2) their yields under 80 eV and

*[7] Since the tailing due to the first process might overlap with the appearance of the second process, the exact determination of appearance potential of the second process is difficult. In this work, the minimum values in IE curves have been taken into consideration (G. J. Schulz, *Phys. Rev.*, **113**, 816 (1959)).

*[8] $\Delta H_f(O^-)=\Delta H_f(O)-EA(O^-)=2.56-1.47=1.09$ (eV) (L. M. Baranskob, D. S. Burch, S. J. Smith and S. Geltman, *Phys. Rev.*, **111**, 504 (1958)).

40 eV electron energies were lower by a factor of 10^5—10^4 than those of positive ions, (3) even if the energy is decreased to 10 eV, their yields were still lower by a factor of 10^4—10^3 compared with those of positive ions in 15 eV, and (4) contrary to our expectation, the simple dissociative electron capture and ion pair processes such as reactions (4) and (9)*[9] could not be found.

*[9] An apparatus with extremely high sensitivity seems to be required for the detection of reaction (9), $C_3H_7^+ + OH^- + e^-$. The cross section of this reaction appears to be extremely small. (S. Tsuda and W. H. Hamill, *Advan. Mass Spectry.*, **3**, 249 (1965))

BULLETIN OF THE CHEMICAL SOCIETY OF JAPAN VOL. 42 2519—2523 (1969)

Bond Lengths of Dimethylacetylene as Determined by Gas Electron Diffraction

Mitsutoshi TANIMOTO, Kozo KUCHITSU and Yonezo MORINO

Department of Chemistry, Faculty of Science, The University of Tokyo, Hongo, Tokyo

(Received March 14, 1969)

The bond distances of dimethylacetylene have been determined by electron diffraction to be r_g(C–C)$=1.467_5\pm0.001_3$ Å, r_g(C≡C)$=1.213_5\pm0.001_3$ Å, r_g(C–H)$=1.115_8\pm0.005_9$ Å, and ∠C–C–H$=110.7\pm0.4°$, the uncertainties representing the limits of experimental error. The carbon-carbon single bond length has been found to be in good agreement with that in butadiene, as was qualitatively to be expected from Stoicheff's empirical rule. The carbon-carbon triple bond length appears to be longer than that of acetylene and shorter than that of diacetylene by a few thousandths of an angstrom. The dependence of the triple-bond lengths on the environment is discussed in terms of the change in conjugation and hyperconjugation.

Abundant experimental data from spectroscopy and electron diffraction accumulated over three decades are of basic importance to a systematic understanding of molecular structure. A marked dependence of the carbon-carbon single bond lengths on environment was first recognized by Herzberg *et al.*[1] in 1937. A distinct but less conspicuous difference in C=C double bond lengths in allene and ethylene was later shown by Overend and Thompson.[2] A subsequent analysis of the available data led Stoicheff[3] to determine empirical regularities for the "normal" behavior of C–C and C=C bond lengths, which vary nearly linearly with the number of atoms attached to the carbon atoms in question. While a majority of the C–C and C=C lengths in hydrocarbons seem to follow his rule to 0.005 Å, this does not necessarily preclude an appreciable deviation due to adjacent heteroatoms, *i.e.*, a "secondary" effect, about which little is known at present. Recently a series of molecules with C–C bonds adjacent to two double bonds (butadiene, acrolein and glyoxal) were studied by Kuchitsu, Fukuyama, and Morino,[4] who demonstrated a systematic variation of the single-bond lengths. A similar difference was observed in the C–C bonds adjacent to two triple bonds (cyanogen[5] and diacetylene[6]). The purpose of the present study is to extend such investigations to C≡C triple-bond systems.

The lengths of ordinary C≡C bonds have been supposed to be insensitive to their environment. For example, the C≡C lengths (r_0) in acetylene, methylacetylene, and cyanoacetylene were found to be nearly equal (1.207 Å),[7] so that any increase in the length due to conjugation or hyperconjugation should be extremely small (probably not over 0.005 Å),[8] whereas Stoicheff remarked a slight decrease when halogen atoms were adjacent to a C≡C bond.[3] The constancy of the C≡C length

1) G. Herzberg, F. Patat and H. Verleger, *J. Phys. Chem.*, **41**, 123 (1937).

2) J. Overend and H. W. Thompson, *J. Opt. Soc. Am.*, **43**, 1065 (1953).

3) B. P. Stoicheff, *Tetrahedron*, **17**, 135 (1962).

4) K. Kuchitsu, T. Fukuyama and Y. Morino, *J. Mol. Structute*, **1**, 463 (1968).

5) Y. Morino, K. Kuchitsu, Y. Hori and M. Tanimoto, This Bulletin, **41**, 2349 (1968).

6) Y. Morino, K. Kuchitsu and M. Tanimoto, to be published.

7) G. Herzberg and B. P. Stoicheff, *Nature*, **175**, 79 (1955).

8) D. R. Lide, Jr., *Tetrahedron*, **17**, 125 (1962).

has had practical utility in the spectroscopic determination of molecular structure; when the number of independent structural parameters exceeded that of rotational constants available, the r_0(C≡C) length has often been set equal to that in simple acetylenic compounds, say, 1.206 Å, since this assumption was one of the most plausible. The r_s(C≡C) distances in a number of molecules measured by Costain and others seem to offer further support for this invariance, since they range from 1.205 Å (cyanoacetylene)[9] to 1.209 Å (tert-butylacetylene).[10]

However, if one intends to study the dependence of the bond lengths on the environment more carefully (say, with an accuracy better than 0.005 Å), one has to investigate the equilibrium or average distances instead of the r_0 or r_s distances. Since the latter parameters for polyatomic molecules are based on only operational definitions, they are not always suitable for such a critical comparison of bond lengths.

In this connection, the structure of diacetylene was examined in our laboratory. The *thermal average* C≡C length determined by electron diffraction was found to be r_g(C≡C)$=1.217_6\pm0.001_4$ Å,[6] about 0.006 Å longer than the corresponding value in in acetylene, r_g(C≡C)$=1.212\pm0.001$ Å.[6] This suggests that the *equilibrium* bond lengths (r_e) also differ by a similar amount, so that a further experimental study of molecules with C≡C bonds seems to be worthwhile.

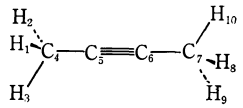

Fig. 1. The structure and numbering convention of dimethylacetylene.

The bond lengths in dimethylacetylene (2-butyne) have been investigated by gas electron diffraction in the present study. The structure of this molecule was first studied by means of electron-diffraction measurements by Pauling *et al.*,[11] who gave r(≡C–C≡)$=1.47\pm0.02$ Å on the assumptions that the other bond lengths were r(C≡C)$=1.20$ Å and r(C–H)$=1.09$ Å. The rotational constant, B_0, was determined by Callomon and Stoicheff[12] on the basis of an analysis of their pure rotational Raman spectrum. They could not, however, determine the dimensions of dimethylacetylene since they obtained the B_0 constant of the normal species alone. From a comparison of the observed moment of inertia with that calculated from the methylacetylene parameters, which was significantly smaller than the observed value, they concluded that at least one of the carbon-carbon bonds was longer than in the closely related molecule, methylacetylene.

Experimental

Two millilitres of a 99% pure liquid sample of dimethylacetylene were purchased from the Tokyo Kagaku Seiki Co., Ltd., and were used after vacuum distillation. Diffraction photographs were taken at room temperature using an apparatus with an r^3-sector.[13] The accelerating voltage (about 40 kV), stabilized to within 0.01%, was monitored during the exposure and was further calibrated with reference to the C=O length of carbon dioxide.[5] Four plates were chosen from each camera distance (107.78 ± 0.02 mm or 243.23 ± 0.02 mm), and their photographic densities, measured by a microphotometer, were analyzed in order to obtain the molecular intensities.

Analysis

The molecular intensities were analyzed by a conventional least-squares method[14] with some modifications.[4] The alterations involved a choice of independent parameters and corrections for vibrational effects. The calculations were made by using the HITAC 5020E at the Computer Centre of the University of Tokyo.

As a result of molecular vibration, the r_g distances determined by electron diffraction are not additive. The so-called shrinkage effect[15] should disappear in regard to the r_α distances, which are obtained from r_g by subtracting the perpendicular and centrifugal contributions:[16]

$$r_\alpha = r_g - \frac{\langle \Delta\rho^2 \rangle}{2r_e} - \delta r. \qquad (1)$$

Since the r_α structure represents the thermal-average positions of constituent atoms,[4] it corresponds to the equilibrium symmetry of the molecule. In other words, provided the molecular symmetry is known from spectroscopy, the number of distance parameters (r_α) can be decreased by assuming the symmetry as a constraint. In the present analysis, the bond lengths, r(C–H), r(C–C) and r(C≡C), and the angle θ(CCH) with regard to the r_α structure were taken as independent parameters.

9) C. C. Costain, *J. Chem. Phys.*, **29**, 864 (1958).
10) L. J. Nugent, D. E. Mann and D. R. Lide, Jr., *J. Chem. Phys.*, **36**, 965 (1962).
11) L. Pauling, H. D. Springall and K. J. Palmer, *J. Am. Chem. Soc.*, **61**, 927 (1939).
12) J. H. Callomon and B. P. Stoicheff, *Can. J. Phys.*, **35**, 373 (1957).
13) Y. Morino, M. Kimura, K. Kuchitsu and Y. Murata, *Japan. J. Appl. Phys.*, to be published.
14) Y. Morino, K. Kuchitsu and Y. Murata, *Acta Cryst.*, **18**, 549 (1965).
15) Y. Morino, J. Nakamura and P. W. Moore, *J. Chem. Phys.*, **36**, 1050 (1962).
16) Y. Morino, K. Kuchitsu and T. Oka, *ibid.*, **36**, 1108 (1962).

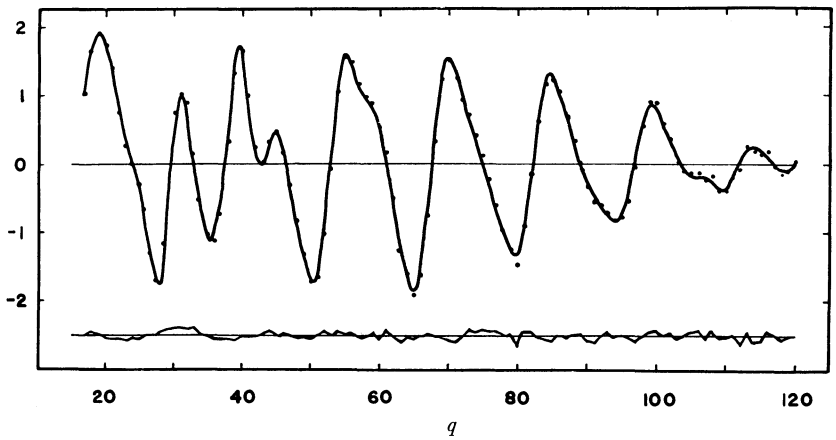

Fig. 2. Reduced molecular intensity curves (dots for observed values and the solid curve calculated from the best-fit model) and the residuals (below)

Since longer nonbonded H···H atom pairs contribute only a negligible amount to the reduced molecular intensity in the observed q range, the reduced molecular intensity is insensitive to the internal rotation of the methyl groups. Since the infrared spectra lead us to believe that the two methyl groups undergo a nearly free internal rotation,[17] the present analysis was based on the assumption of free rotation.

The asymmetry parameters, κ, were calculated by the diatomic approximation[18] to be 2.0×10^{-5} Å^3 for the CH bonded pairs and 8×10^{-7} Å^3 for the C≡C and C–C bonded pairs. The parameters for the other atom pairs were ignored since their effects were unimportant.

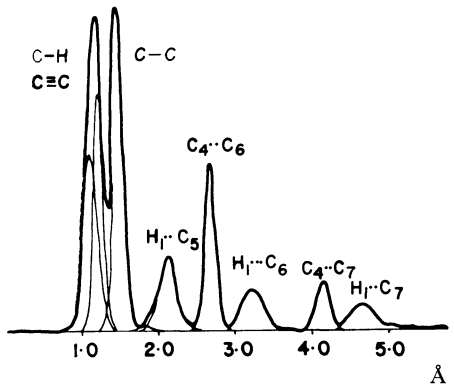

Fig. 3. Radial distribution curve. The atom pairs contributing to individual peaks are shown.

Table 1 lists the values of independent parameters obtained in the above analysis, together with their estimated limits of error (2.5 times the random standard errors plus systematic errors). The observed mean amplitudes given in Table 2 agree with the parallel amplitudes calculated by a conventional method[19] within the range of experimental error.

Table 1. Bond lengths and bond angle in dimethylacetylene[a]

	r_a	r_a^0	r_g	Limits of error
C–H	1.099_7	1.102_3	1.115_8	0.005_9 Å
C–C	1.458_9	1.462_7	1.467_5	0.001_3
C≡C	1.206_3	1.208_2	1.213_5	0.001_3
θ(CCH)	110.7°			0.4°

a) See Eqs. (1) and (2) for the definition of distances.

Table 2. Comparison of observed mean amplitudes with calculated values (in Å units)

Atom pair[a]	l_{obsd}	l_{calcd}
C_4–H_1	$0.073_0\pm0.002_3$	0.0784
C_5≡C_6	$0.035_2\pm0.002_8$	0.0365
C_4–C_5	$0.046_7\pm0.001_7$	0.0467
H_1•H_2	0.1260 (fixed)	0.1260
H_1•C_5	$0.100_7\pm0.005_1$	0.1062
C_4•C_6	$0.052_8\pm0.002_0$	0.0510
H_1••C_6	$0.122_6\pm0.009_7$	0.1301
C_4••C_7	$0.061_2\pm0.007_2$	0.0593
H_1•••C_7	$0.13_8\pm0.01_7$	0.1461

a) See Fig. 1 for the numbering of the atoms.

Discussion

Average Structure. The distances between the atoms in the vibrational ground state, r_a^0, were

17) D. Papoušek, J. Adams and K. N. Rao, Symposium on Molecular Structure and Spectroscopy O6, Columbus, Ohio, 1968.

18) K. Kuchitsu, This Bulletin, **40**, 498 (1967).

19) Y. Morino and E. Hirota, *J. Chem. Phys.*, **23**, 737 (1955).

obtained from the r_a distances by:[20]

$$r_a^0 = \lim(T \to 0°K) r_a$$
$$= r_a - (\langle \Delta z \rangle_T - \langle \Delta z \rangle_0), \quad (2)$$

where $\langle \Delta z \rangle = \langle \Delta r \rangle - (\langle \Delta x^2 \rangle + \langle \Delta y^2 \rangle)/2r_e$. The $\langle \Delta r \rangle$ term was calculated by assuming a Morse-type potential function for a bond, the anharmonicity parameter being taken from the corresponding diatomic molecule. The generalized mean amplitudes, $\langle \Delta x^2 \rangle$, $\langle \Delta y^2 \rangle$, and $\langle \Delta z^2 \rangle$, were calculated by the use of the quadratic force constants.[21] The values of the r_a^0 distances are given in Table 1.

The rotational constant, B_z, calculated from the r_a^0 structure was compared with the ground-state rotational constant, B_0, by correcting for vibration-rotation interactions.[20] The correction, -3×10^{-5} cm^{-1}, was an order of magnitude smaller than the experimental error. The rotational constant, B_0, calculated from the diffraction structure was 0.1116 $\pm$0.0002 cm^{-1}, which was 0.5$\pm$0.2% smaller than the spectroscopic B_0 constant,[12] 0.1122$\pm$0.0002 cm^{-1}.

This difference is probably due to the systematic error in the rotational-Raman measurement, since, for similar molecules[22-25] listed in Table 3, the

TABLE 3. ROTATIONAL CONSTANTS B_0 DERIVED FROM RAMAN AND INFRARED SPECTROSCOPY (in cm^{-1} units)

	Rotational Raman	Ref.	Infrared	Ref.	Δ[a]	ν[b]
C_2H_2	1.1769	12	1.17660	24	3	625.6
C_2N_2	0.15752	22	0.15712	26	4	233
$H_2C{=}C{=}CH_2$	0.2965_3	23	0.29632	25	2_1	354
C_4H_6	0.1122	12	(0.1117)[c]		5[c]	194

a) Difference in B_0 : B_0(RR) $-$ B_0 (IR) (in 10^{-4}cm^{-1} units).
b) Frequency of the lowest bending vibration.
c) Estimated.

rotational constants obtained from the Raman spectra are about 3×10^{-4} cm^{-1} larger than those derived from the infrared spectra, the difference exceeding their limits of error. The origin of the discrepancy for cyanogen was ascribed by Maki[26] to the Raman measurement biased by overlapping lines due to molecules in the low-lying vibrational excited states. If this is also the case for dimethylacetylene, a proper spectroscopic B_0 value should be smaller than the observed value[12] by about 5×10^{-4} cm^{-1}; it is thus estimated to be 0.1117$\pm$0.0002 cm^{-1}, in reasonable agreement with the present diffraction result.

Comparison of Bond Lengths. As was recently discussed by Kuchitsu,[27] distance parameters can be compared most conveniently in terms of the thermal-average (r_g) distances, since the differences in r_g for analogous molecules correspond to those in r_e within the range of experimental error; the effect of thermal vibration ($r_g - r_e$) on a certain bond distance should be essentially equal to its counterparts for analogous molecules. The r_g parameters determined above afford a clue to the problem set up in the introduction, *i. e.*, the effect of the environment on carbon-carbon triple and single bond lengths.

The change in multiple bond lengths by conjugation has been discussed from a theoretical point of view. Mulliken[28] argued that the multiple-bond length should increase only slightly since π-electrons delocalized into adjacent bonds as a result of conjugation should return to the original bonds because of mutual repulsion. In consideration of the effects of hybridization and electron delocalization on the CC bond lengths, Bak and Hansen-Nygaard[29] estimated a multiple-bond lengthening of a few thousandths of an angstrom from the corresponding shortening of the neighboring bonds. A number of experimental data indicating such lengthenings in multiple-bonds were given; those data were in rough agreement with what they expected. At the same time, however, they stressed the usefulness of further, more accurate experiments in order to make the structure comparison less ambiguous.

The present study has confirmed that the C≡C bond length in dimethylacetylene is significantly shorter than that in diacetylene[6] and longer than that in acetylene[6] (Table 4). Furthermore, the value for dimethylacetylene is in good agreement with the bond length in vinylacetylene.[30] The

TABLE 4. COMPARISON OF CARBON-CARBON TRIPLE BOND LENGTHS (in Å units)

Molecule		r_g (C≡C)
Acetylene	HC≡CH	1.212 $\pm$0.001
Dimethylacetylene	CH_3–C≡C–CH_3	$1.213_5\pm0.001_3$
Vinylacetylene	CH_2=CH–C≡CH	1.215 $\pm$0.003
Diacetylene	HC≡C–C≡CH	$1.217_6\pm0.001_4$

20) K. Kuchitsu and S. Konaka, *ibid.*, **45**, 4342 (1966).
21) K. Abe and T. Shimanouchi, to be published. The authors are indebted to their information prior to publication.
22) C. K. Møller and B. P. Stoicheff, *Can. J. Phys.*, **32**, 635 (1954).
23) B. P. Stoicheff, *Can. J. Phys.*, **33**, 811 (1955).
24) W. J. Lafferty and R. J. Thibault, *J. Mol. Spectry.*, **14**, 79 (1964).
25) A. G. Maki and R. A. Toth, *ibid.*, **17**, 136 (1965).
26) A. G. Maki, *J. Chem. Phys.*, **43**, 3193 (1965).
27) K. Kuchitsu, *ibid.*, **49**, 4456 (1968).
28) R. S. Mulliken, *Tetrahedron*, **6**, 68 (1959).
29) B. Bak and L. Hansen-Nygaard, *J. Chem. Phys.*, **33**, 418 (1960).
30) T. Fukuyama, K. Kuchitsu and Y. Morino, This Bulletin, **42**, 379 (1969).

above results are consistent with simple intuition in terms of the effect of conjugation and hyperconjugation on bond lengths. According to Mulliken,[31] the effect of conjugation should be larger than that of hyperconjugation. Thus, the C≡C distance in dimethylacetylene should fall in between those of diacetylene and acetylene. For a number of other molecules the lengths of CC triple bonds have been reported in terms of r_s distances. (For example, see Ref. 9). Presumably the r_s(C≡C) distances are shorter than the r_g(C≡C) distances by a few thousandths of an angstrom.

The C–C distance (r_g) determened in this study, $1.467_5 \pm 0.001_3$ Å, is equal to that in butadiene[32] (r_g(C–C) = 1.465±0.003 Å) within the range of experimental uncertainty. This observation agrees qualitatively with Stoicheff's rule, which says they should be identical. The C–C bond length in methylacetylene is also expected to be similar to those in dimethylacetylene and butadiene, whereas the r_s(C–C) distance was reported by Costain[9] to be 1.4589 Å. An electron-diffraction study of this molecule is now in progress.

The r_g(C–H) distance determined above (r_g(C–H) = $1.115_8 \pm 0.005_9$ Å) seems to be slightly longer than the CH bond length in ethane (r_g(C–H) = $1.110_8 \pm 0.002$ Å[27,33]), but the large limit of error attached to the former bond length forbids a quantitative comparison. The CCH angle in dimethylacetylene, 110.7±0.4°, appears to be only slightly smaller than that in ethane[27] (111.5±0.3°). A similar value has been reported for methylacetylene[9] (110.2° in r_s structure).

31) R. S. Mulliken, *Tetrahedron*, **17**, 247 (1962).

32) K. Kuchitsu, T. Fukuyama and Y. Morino, *J. Mol. Structure*, **4**, 41 (1969).

33) L. S. Bartell and H. K. Higginbotham, *J. Chem. Phys.*, **42**, 851 (1965).

BULLETIN OF THE CHEMICAL SOCIETY OF JAPAN VOL. 42 2523—2531 (1969)

The Chemistry of Protactinium. VIII. Synergistic Effect of Di-isobutyl Carbinol on the Pa(V)-TTA-Benzene Solvent Extraction System

Shin SUZUKI and Yasushi INOUE

The Research Institute for Iron, Steel and Other Metals, Tohoku University, Katahira-cho, Sendai

(Received January 8, 1969)

For the purpose of understanding the behavior of protactinium in a perchloric acid solution toward TTA-benzene extraction, the effect of di-isobutyl carbinol (DIBC) on the extraction was studied. A marked synergism was observed. As a result of a detailed investigation of such things as the effects of the TTA concentration, of the DIBC concentration, and of the acidity, the unified mechanism of TTA-benzene and TTA-DIBC-benzene extraction is considered to be a series of successive reactions, (1) through (4), with an increase in the DIBC concentration:

$PaO_m(OH)_n^{5-2m-n} + 4HT = Pa(OH)_2T_3(HT) + (m+n-2)H_2O + (5-2m-n)H^+$

$Pa(OH)_2T_3(HT) \rightarrow PaOT_3(HT)$ (slow, irreversible) (1)

$PaO_m(OH)_n^{5-2m-n} + 4HT + B = Pa(OH)_2T_3(HT)B + (m+n-2)H_2O + (5-2m-n)H^+$

$Pa(OH)_2T_3(HT)B \rightarrow PaOT_3(HT)B$ (slow, irreversible) (2)

$PaO_m(OH)_n^{5-2m-n} + 3HT + B = Pa(OH)_2T_3B + (m+n-2)H_2O + (5-2m-n)H^+$

$Pa(OH)_2T_3B \rightarrow PaOT_3B$ (slow, irreversible) (3)

$PaO_m(OH)_n^{5-2m-n} + 3HT + 2B = Pa(OH)_2T_3B_2 + (m+n-2)H_2O + (5-2m-n)H^+$

$Pa(OH)_2T_3B_2 \rightarrow PaOT_3B_2$ (slow, irreversible) (4)

The slow, irreversible reaction in each step indicates the irreversible formation of unstrippable species in the organic phase with aging. The absorption spectral measurements gave results consistent with this conclusion.

It was stated earlier[1] that when the protactinium concentration was lower than 10^{-6}M and the perchloric acid concentration was 0.3—2.0M, the reaction of TTA extraction of protactinium from a perchloric acid solution proceeded as:

$$PaO_m(OH)_n^{5-2m-n} + 4HT = Pa(OH)T_4 + (m+n-1)H_2O + (5-2m-n)H^+ \quad (1)$$

where $2m+n$ is 3 and 4, or as:

1) S. Suzuki and Y. Inoue, This Bulletin, **39**, 1705 (1966).

$$PaO_m(OH)_nT^{4-2m-n} + 4HT = PaT_5 + (m+n)H_2O + (4-2m-n)H^+ \quad (2)$$

where $2m+n$ is 2 and 3.

We have been unable to distinguish between the two reactions from the experimental evidence. Reaction (1) may, however, be considered to be more probable than reaction (2) because of the very low solubility of TTA in the aqueous phase. In any case, protactinium(V) in a perchloric acid solution is present as species which have +2 and +1 charges. $Pa(OH)T_4$, which is used in Eq. (1) to represent the extracted species, is not the only form which it is possible to deduce from the experimental results. In general, the addition compounds of HT should be taken into account. Thus the extracted form may generally be written as $PaO_p(OH)_qT_{5-2p-q}(HT)_d$, where $2p+q-d$ is unity. That is, $PaOT_3(HT)$ or $Pa(OH)_2T_3(HT)$, $PaO(OH)T_2(HT)_2$ or $Pa(OH)_3T_2(HT)_2$ and $Pa(OH)_4T(HT)_3$, $PaO_2T(HT)_3$ or $PaO(OH)_2T(HT)_3$, ··· are possible as well as $Pa(OH)T_4$, depending on the d value, which cannot be determined by a simple TTA extraction experiment. In the above investigation, discussion has been restricted to the qualitative aspect because the reproducibility of the experimental data is not good enough to provide quantitative information. One of the reasons for this irreproducibility has been considered to be the complex behavior of TTA extraction, which depends greatly on the method of preparing the perchloric acid solution of protactinium. In order to elucidate the complex behavior more clearly, an elaborate investigation was carried out. Definite differences in the extraction behavior were observed among four kinds of the solutions which were prepared by different methods. Moreover, it was shown that a stripping equilibrium was established only when a freshly-prepared protactinium solution in TTA-benzene was used. Unstrippable species are formed when the Pa-TTA-benzene stands for a long period.[2]

The investigation of a synergistic effect is one of the means to determine the d values mentioned above. Guillaumont[3] studied the synergistic effect of TBP on the extraction of protactinium by TTA-benzene. The mechanism of the effect was understood by the following reaction:

$$Pa(OH)_3T_2(HT)_2 + 2TBP = Pa(OH)_3T_2(TBP)_2 + 2HT \quad (3)$$

and the extraction mechanism of protactinium by TTA was:

$$Pa(OH)_3^{2+} + 4HT = Pa(OH)_3T_2(HT)_2 + 2H^+ \quad (4)$$

As a result of the investigation of the synergism by *n*-amyl alcohol in the TTA extraction system, Kolarich and his co-workers[4] concluded that the extracted species was $PaOT_3(HT)$.

In the present investigation, the effect of di-isobutyl carbinol (DIBC) on the TTA-benzene extraction of protactinium has been examined; a marked synergism was observed. The consideration of the mechanism of the synergistic effect enables us to determine the d value and to make a hypothesis concerning the reasons for the irreversible change of the protactinium species in the TTA-benzene solution.

Experimental

Reagents and Apparatus. ^{231}Pa *and* ^{233}Pa. Stock solutions of these isotopes in hydrochloric acid and hydrofluoric acid mixtures were prepared by a method reported previously.[5] The concentration of protactinium in the ^{231}Pa solution was determined by gravimetry as protactinium pentoxide. The benzene was purified by distillation, and doubly-distilled water was used throughout this experiment. The acidity of the solution was determined by titration with a standard sodium hydroxide solution. The highest-purity-grade lithium perchlorate was used for the adjustment of the ionic strength, and the concentration of its solution was determined gravimetrically as lithium sulfate. The other chemicals, such as thenoyl trifluoroacetone, perchloric acid and di-isobutyl carbinol, were also all of the highest purity.

For the solvent-extraction procedure, an Iwaki universal mechanical shaker, Model V-S, was used. A Kôbe Kôgyo Model PS-400 well-type scintillation probe coupled with a Kôbe Kôgyo Model SA-400 scaler was used for the γ-ray measurement. For the measurement of the absorption spectra, a Hitachi Model EPS-3 recording spectrophotometer with a 1 cm photometric cell was used.

Procedure. All the experiments were carried out at room temperature. Ordinary separatory funnels made of glass were used for the solvent extraction. To eliminate distortions of the experimental results arising from adsorption on glass, the walls of the funnels were preliminarily saturated with protactinium by shaking the test solution for a time sufficient for adsorption equilibrium to be reached. Care was taken to ascertain the material balance in each experiment, and each value given was the average of the results of at least two determinations. For all solvent extractions except with Fomin's method,[2,6] 5 m*l* portions of the aqueous and of the organic phase were used; after the separation of the two phases, a 2 m*l* aliquot of each phase was taken into a polyethylene test tube and counted for γ radioactivity. The distribution ratio was calculated by means of the usual relationship:

$$D = \frac{\gamma \text{ activity per 1 m}l \text{ of the organic phase}}{\gamma \text{ activity per 1 m}l \text{ of the aqueous phase}}$$

2) S. Suzuki and Y. Inoue, This Bulletin, **42**, 1916 (1969).

3) R. Guillaumont, *Bull. Soc. Chim. France*, **1965** (1) 132.

4) R. T. Kolarich, V. Y. Ryan and R. P. Schuman, *J. Inorg. Nucl. Chem.*, **29**, 783 (1967).

5) S. Suzuki and Y. Inoue, This Bulletin, **39**, 490 (1966).

6) V. V. Fomin, E. P. Maiorova, M. I. Krapivin and V. G. Yudina, *Zh. Neorg. Khimiya*, **3**, 2113 (1958).

Forward Extraction. The protactinium solution in 1M perchloric acid for the forward extraction experiments was prepared as follows.

Aliquots of ^{231}Pa and of ^{233}Pa stock solutions (a total of 5 m*l*) and a small amount of hydrofluoric acid were transferred into a platinum dish and evaporated almost to dryness, initially on a hot plate and finally on a water bath. The residue was dissolved in 5M perchloric acid with slight heating and diluted to make the protactinium concentration 10^{-7}M.

Backward Extraction. A protactinium solution in the organic solvent for the backward extraction was prepared by the following procedure.

Aliquots of ^{231}Pa and of ^{233}Pa stock solutions were transferred into a platinum dish and heated to dryness on a hot plate. The residue was dissolved in 0.64 m*l* of 1.17M hydrofluoric acid, and then 0.99 m*l* of 5.05M perchloric acid and 1.7 m*l* of a 1.33M aluminum perchlorate solution were added, in this order. The resulting solution was diluted to 50 m*l* with distilled water. This solution was then placed in contact with 200 m*l* of a DIBC-TTA-benzene solution of a suitable composition for 20 min. The concentration of protactinium in the TTA-DIBC-benzene solution thus prepared was 0.99×10^{-7}M.

Absorption Spectra. A ^{231}Pa solution containing 6.17×10^{-6} Mole was transferred into a platinum dish and heated to dryness on a water bath. The residue was dissolved in 0.96 m*l* of 1.17M hydrofluoric acid, and then 0.53 m*l* of 4.71N sulfuric acid and distilled water were added to make 25 m*l*. This solution was then transferred into a separatory funnel containing 25 m*l* of a 0.5M TTA-benzene solution and 25 m*l* of a 0.136M aluminum perchlorate solution. Then the separatory funnel was shaken with a mechanical shaker for 15 min. The organic phase was withdrawn from the funnel and an aliquot of the solution was diluted with DIBC-benzene of a suitable concentration. This solution was used for the absorption spectral measurement. The protactinium concentration was about 2.5×10^{-5}M.

Results

The Effect of Contact Time in the Forward Extraction. The effect of the contact time on the distribution ratio of protactinium in 1M perchloric acid was investigated as a function of the DIBC concentration, as is shown in Figs. 1a and 1b. When the DIBC concentration is lower than 0.1% (the concentration of DIBC is represented by volume%), the distribution ratio reaches constant after about 10 min of contact, whereas the extraction rate becomes slower with an increase in the concentration of DIBC. Longer than an hour's contact is necessary for the extractant 1% in DIBC to reach a constant distribution ratio.

The Effect of Aging on the Distribution Ratio in the Forward Extraction. The effect of aging time on the distribution ratio was investigated for the forward extraction of protactinium in a 1M perchloric acid solution by both 2×10^{-2}M TTA-0.07%DIBC and 5×10^{-2}MTTA-0.02%DIBC in benzene solutions. Curves similar to that of

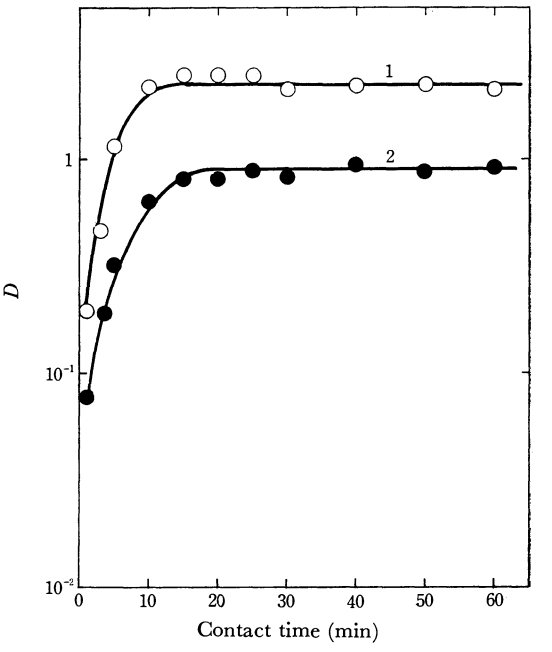

Fig. 1a. The effect of contact time on the extraction of Pa. I.
Aq. phase: 10^{-7}M Pa in 1M $HClO_4$
Org. phase: 1, 0.1% DIBC, 0.032M TTA
2, 0.4% DIBC, 0.0136M TTA

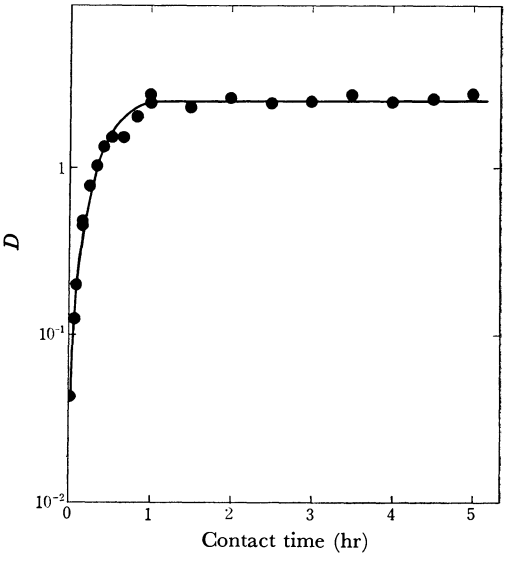

Fig. 1b. The effect of contact time on the extraction of Pa. II.
Aq. phase: 10^{-7}M Pa in 1M $HClO_4$
Org. phase: 1% DIBC, 0.0096M TTA

No. 1 in Fig. 3 of the 7th report of this series[2] were obtained; that is, the distribution ratio remains constant for about a week after the preparation of the sample, and then it begins to decrease. This constant value coincides with

one obtained from the backward distribution of the fresh protactinium solution in TTA-DIBC-benzene. The conditions used in the preparation of the protactinium solution are as suitable as those used for No. 1 in a previous report.[2] The reason why the No. 1 preparation method has not been used is that in it the control of the acidity is very difficult.

The Relation between the Distribution Ratio and the TTA Concentration. The influence of the TTA concentration on the distribution ratio was investigated for a 1M solution in perchloric acid at various DIBC concentrations. The logarithm of the distribution ratio was plotted as a function of the logarithm of the TTA activity in the benzene phase, as is shown in Fig. 2. Provided the nature of TTA is not affected by the presence of DIBC at such low concentrations as 1%, the activity of TTA in the benzene phase at equilibrium can be calculated from its initial concentration by the following equations:

$$\frac{(HT)_I}{(HT)_B} = 1.02 + 10^{-8}/(H^+)^{7)} \quad (5)$$

$$f_{HT} = 1 - 0.25(HT)_B^{0.48\ 8)} \quad (6)$$

where f_{HT} is the activity coefficient of TTA in benzene; $(HT)_B$, the final concentration in benzene when equilibrated with an equal volume of an aqueous phase, and $(HT)_I$, the initial concentration. It is clear from Fig. 2 that the log-log plot of the distribution ratio and the activity of TTA shows a good linearity, with varying slopes, depending on the DIBC concentration, over a wide range of TTA concentrations. As Table 1 shows, the slope is about 4 when the DIBC concentration is lower than 0.0003% and decreases with an increase in the DIBC concentration from 0.0003% upwards.

The Relation between the Distribution Ratio and the DIBC Concentration. The effect of the DIBC concentration on the distribution ratio was examined in 1M perchloric acid solution, with the TTA concentration kept constant. The logarithm of the distribution ratio was plotted as a function of the logarithm of the DIBC concentration in the benzene phase, as is shown in Fig. 3. Though the protactinium in the 1M perchloric acid solution was not extracted at all, even by pure DIBC, the distribution ratio increases remarkably upon the addition of a small amount of DIBC; that is, synergism is observed. The linear relationship does not hold between the log of the distribution ratio and that of the DIBC concentration, but the curves asymptotically approach straight lines with an increase in the DIBC concentration. When the concentrations of TTA were 0.02M, 0.05M, and 0.1M, the slopes of the curves approached 1.0, 1.4 and 1.8 respectively.

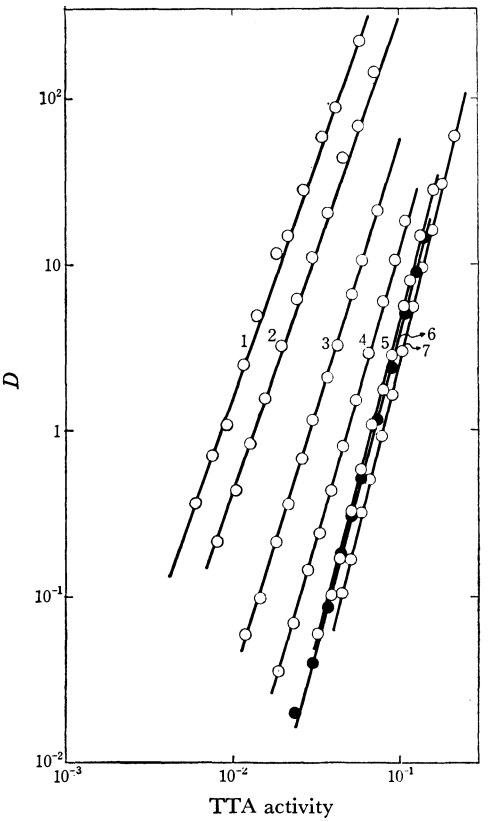

Fig. 2. Dependence of distribution ratio on TTA activity.
$HClO_4$ concn.: 1M, Pa concn.: 10^{-7}M
DIBC concn.: 1, 1%; 2, 0.4%; 3, 0.1%; 4, 0.02%
5, 0.005%; 6 0.001%; 7, 0.0003%

Table 1. The effect of DIBC concn. on slope

DIBC conc. (%)	Ratio of two species		Slope	
	T4	T3	Calcd	Exp.
0.0	100.0	0.0		4.00
0.0003				4.03
0.001	73.2	26.8	3.73	3.70
0.005				3.73
0.01	52.7	47.3	3.53	
0.02				3.61
0.1	29.9	70.1	3.30	3.27
0.4	13.8	86.2	3.14	3.02
1.0				2.85

The Relation between the Distribution Ratio and the Hydrogen-ion Concentration. The effect of acidity was studied by the backward extraction technique at a constant ionic strength of 1.967 by using various mixtures of perchloric acid and lithium perchlorate. Up to a hydrogen

7) A. M. Poskanzer and B. M. Foreman, *J. Inorg. Nucl. Chem.*, **16**, 323 (1961).
8) E. L. King and W. H. Reas, *J. Am. Chem. Soc.*, **73**, 1804 (1951).

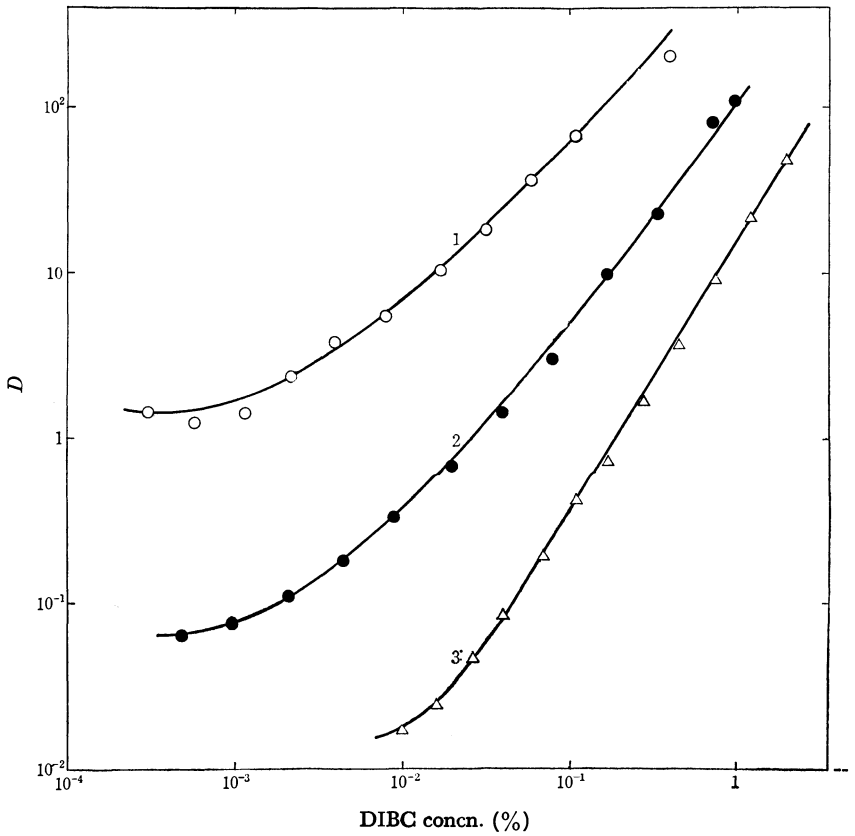

Fig. 3. Dependence of distribution ratio on DIBC concentration.
$HClO_4$ concn.: 1M, Pa concn.: 10^{-7}M
TTA concn.: 1, 0.1M; 2, 0.05M; 3, 0.02M

ion concentration of 1.5M, the log-log plots of the distribution ratio and the hydrogen ion concentration show a linear relationship with a slope of −1.7, except in the case of No. 5, as is clearly shown in Fig. 4. In the case of Curve 5, with TTA and DIBC concentrations of 0.1M and 0.0004% respectively, an exact linearity does not hold.

The Effect of Contact Time in the Backward Extraction. The effect of the contact time on the backward extraction carried out by using a freshly-prepared protactinium solution in 0.05M TTA and 0.02% DIBC-benzene was investigated; the results are shown in Fig. 5. The stripping solution was 1.0M perchloric acid. It is apparent from the figure that about an hour's contact is necessary to get a constant distribution ratio.

The Effect of Time of Standing of a Protactinium Solution in TTA-DIBC-Benzene on the Distribution Ratio. A protactinium solution in TTA-DIBC-benzene was stored in a brown bottle in the dark, and the change in the distribution ratio during the standing was followed. The protactinium in a 0.05M TTA-0.02% DIBC-benzene solution was stripped by 1M perchloric acid for 1.5 hr. It is apparent from Fig. 6 that, at first, the distribution ratio remained constant for about several hours and then gradually increased, finally reaching a constant 5 days after the preparation. The curve was analyzed by Fomin's method. As is shown in Fig. 7, the P value (the percentage of unstrippable species which are not in rapid equilibrium with the strippable species) observed for a fresh Pa-TTA-DIBC solution was only a few percent. It increases remarkably with the standing, however, and reaches a constant value of about 40% after 10 days of standing. The distribution ratio of strippable species does not change with standing, so that the increase in distribution ratio can be explained on the basis of the formation of unstrippable species alone.

Absorption Spectra of Protactinium in TTA-DIBC-Benzene Solution. The absorption spectra of protactinium in the TTA-DIBC-benzene mixture were measured from 340 to 650 mμ in relation to the DIBC concentration, as is shown in Fig. 8. The concentrations of protactinium and of TTA are *ca.* 2.5×10^{-5}M and 0.05M respectively. It is observed that, in the absence of DIBC, an absorption maximum appears at 408 mμ; it shifts to a shorter wavelength with an increase in the DIBC

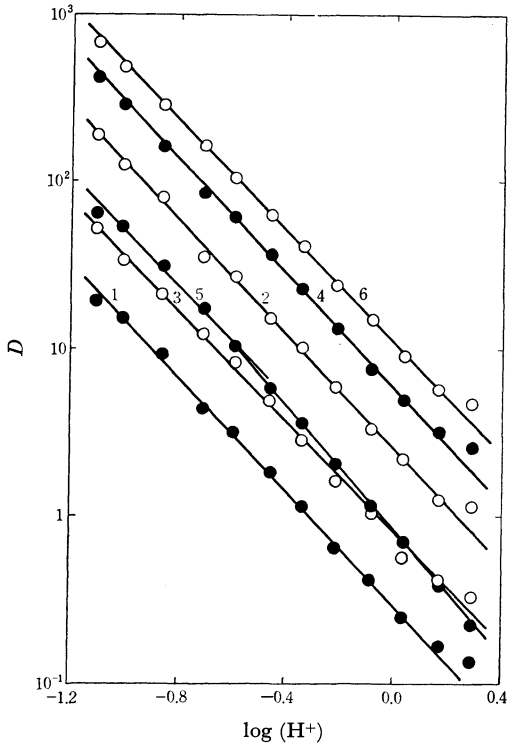

Fig. 4. Dependence of distribution ratio on hydrogen ion concentration.

Ionic strength: 1.967, Pa concn.: 10^{-7}M
Org. phase: 1, 0.02M TTA, 0.1% DIBC
2, 0.02M TTA, 0.4% DIBC
3, 0.05M TTA, 0.02% DIBC
4, 0.05M TTA, 0.1% DIBC
5, 0.1M TTA, 0.0004% DIBC
6, 0.1M TTA, 0.02% DIBC

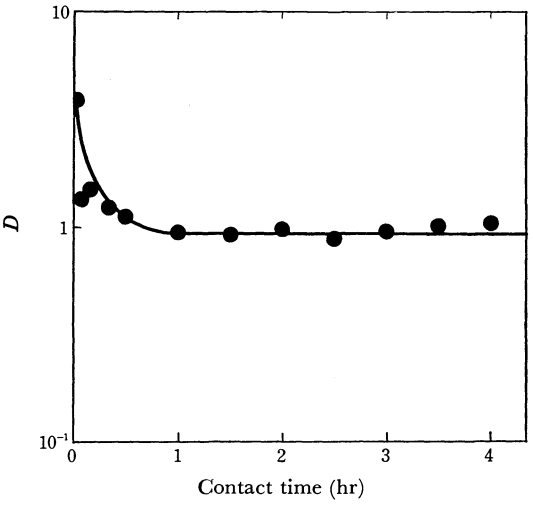

Fig. 5. The effect of contact time on the stripping of Pa.

Aq. phase: 1M $HClO_4$
Org. phase: 10^{-7}M Pa, 0.05M TTA, 0.02% DIBC

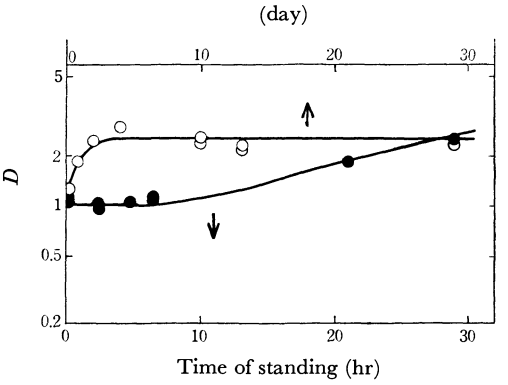

Fig. 6. The effect of time of standing on the stripping of Pa.

Aq. phase: 1M H IO_4
Org. phase: 10^{-7}M Pa, 0.05M TTA, 0.02% DIBC

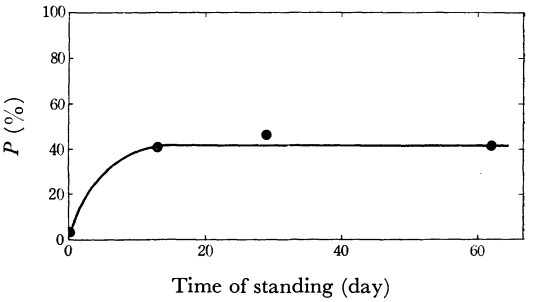

Fig. 7. P as a function of time of standing.

Aq. phase: 1M $HClO_4$
Org. phase: 10^{-7}M Pa, 0.05M TTA, 0.02% DIBC

concentration, reachir g 403 mμ when the DIBC concentration becomes higher than 1%. The absorbance also decreased with the DIBC concentration. The change in the absorption spectra with the DIBC concentration is negligible when the DIBC concentration is higher than 1%.

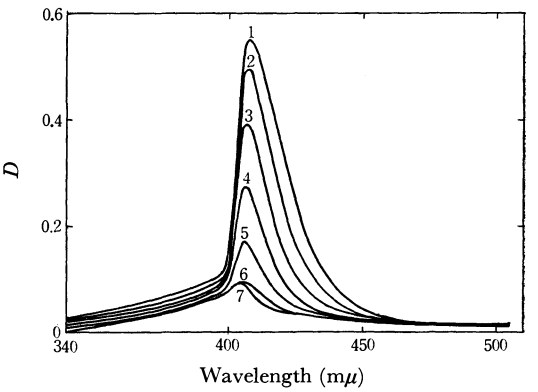

Fig. 8. Absorption spectra.

TTA concn.: 0.05M, Pa concn.: *ca.* 2.5×10^{-5}M
DIBC concn.: 1, 0%; 2, 0.001%; 3, 0.01%;
4, 0.1%; 5, 0.4%; 6, 1.0%; 7, 10.0%

Discussion

If the species extractable into the organic phase are considered to have no charge, the general equation for the TTA-DIBC extraction reaction can be written as:

$$\mathrm{PaO}_m(\mathrm{OH})_n^{5-2m-n}(\mathrm{aq.}) + (5-q-2p+d)\mathrm{HT}(\mathrm{org.}) + b\mathrm{B}(\mathrm{org.}) = \mathrm{PaO}_p(\mathrm{OH})_q(\mathrm{HT})_d\mathrm{T}_{5-2p-q}\mathrm{B}_b(\mathrm{org.}) + (m+n-p-q)\mathrm{H_2O} + (5-2m-n)\mathrm{H^+}(\mathrm{aq.}) \quad (5)$$

where HT, T^-, and B are used to denote the TTA molecule, the dissociated TTA anion, and the di-isobutyl carbinol molecule respectively. The equilibrium constant of this reaction can then be defined as:

$$K_{m,n,p,q,d} = \frac{[\mathrm{PaO}_p(\mathrm{OH})_q(\mathrm{HT})_d\mathrm{T}_{5-2p-q}\mathrm{B}_b][\mathrm{H_2O}]^{m+n-p-q}[\mathrm{H^+}]^{5-2m-n}}{[\mathrm{PaO}_m(\mathrm{OH})_n^{5-2m-n}][\mathrm{HT}]^{5-q-2p+d}[\mathrm{B}]^b} \quad (6)$$

where brackets have been used to represent the activities of the enclosed species. (The designation of the phase in which each species exists has been omitted in order to simplify the writing of the equation.) A distribution ratio expressed in terms of activities is defined as the sum of the activities of the protactinium species in the benzene phase divided by the sum of the activities of the protactinium species in the aqueous phase:

$$K_d = \frac{\sum_{p,q,d,b}[\mathrm{PaO}_p(\mathrm{OH})_q(\mathrm{HT})_d\mathrm{T}_{5-2p-q}\mathrm{B}_b]}{\sum_{m,n}[\mathrm{PaO}_m(\mathrm{OH})_n^{5-2m-n}]} \quad (7)$$

If the activity coefficients of TTA and DIBC are independent of the concentrations of DIBC and TTA respectively, one can derive the following relationships by the same procedure as was used before:[1]

$$-\frac{\partial \ln K_d}{\partial \ln [\mathrm{HT}]} = 5 - \sum(2p+q-d)f_{p,q,d,b} \quad (8)$$

$$\frac{\partial \ln K_d}{\partial \ln [\mathrm{H^+}]} = -\sum(5-2m-n)f'_{m,n} \quad (9)$$

$$\frac{\partial \ln K_d}{\partial \ln [\mathrm{B}]} = \sum bf_{q,p,d,b} \quad (10)$$

where $f_{p,q,d,b}$ is the fraction of the total activity of the protactinium species in the benzene phase contributed by the $\mathrm{PaO}_p(\mathrm{OH})_q(\mathrm{HT})_d\mathrm{T}_{5-2p-q}\mathrm{B}_b$ species, and $f'_{m,n}$ is that in the aqueous phase contributed by the $\mathrm{PaO}_m(\mathrm{OH})_n^{5-2m-n}$ species.

Hence,

$$\sum_{p,q,d,b} f_{q,p,d,b} = 1 \quad (11)$$

$$\sum_{m,n} f'_{m,n} = 1 \quad (12)$$

If the activity coefficients of the protactinium species and of the hydrogen ion are assumed to be constant over the entire range of acidity when the ionic strength of a solution is kept constant, the distribution ratio (D) obtained empirically can be replaced by the thermodynamic distribution ratio (K_d) expressed in terms of activity; no appreciable error should be introduced by this assumption. As is clearly shown in Fig. 4, a linear relationship with a slope of -1.7 holds between the logarithm of the distribution ratio and the logarithm of the hydrogen-ion concentration.

Therefore,

$$-5 + \sum(2m+n)f'_{m,n} = -1.7 \quad (13)$$

$$\sum(2m+n)f'_{m,n} = 3.3 \quad (14)$$

Therefore, in agreement with the results of the TTA extraction,[1] the protactinium in a perchloric acid solution may be found in the forms of $\mathrm{Pa(OH)_3^{+2}}$ or $\mathrm{PaO(OH)^{+}}$ and of $\mathrm{Pa(OH)_4^{+}}$, $\mathrm{PaO(OH)_2^{+}}$, or $\mathrm{PaO_2^{+}}$.

If the activity coefficients of the protactinium species are assumed to be constant, irrespective of the TTA concentration, the distribution ratio (D) obtained empirically can be replaced by the thermodynamic distribution ratio (K_d) in terms of activity; no appreciable error should be introduced by this assumption.

If DIBC is absent,

$$5 - \sum(q+2p-d)f_{p,q,d,b} = 4$$

$$\sum(q+2p-d)f_{p,q,d,b} = 1 \quad (15)$$

When DIBC is added, the slope of the log-log plot of the distribution ratio and the TTA activity in the organic phase changes from 4 to 3, depending on the DIBC concentration.

Thus,

$$3 \leqq 5 - \sum(q+2p-d)f_{p,q,d,b} \leqq 4$$

that is,

$$2 \geqq \sum(q+2p-d)f_{p,q,d,b} \geqq 1 \quad (16)$$

holds. In this experiment, we can not determine the d value. Depending on the postulated d value, one can obtain the following relationships:

When

$$d = 0 \quad 2 \geqq \sum(q+2p)f_{p,q,0,b} \geqq 1 \quad (17)$$

$$d = 1 \quad 3 \geqq \sum(q+2p)f_{p,q,1,b} \geqq 2 \quad (18)$$

$$d = 2 \quad 4 \geqq \sum(q+2p)f_{p,q,2,b} \geqq 3 \quad (19)$$

$$d = 3 \quad \sum(q+2p)f_{p,q,3,b} = 4 \quad (20)$$

In Eq. (20), the value of $\sum(q+2p)f_{p,q,3,b}$ over 4 is impossible because an improbable assumption must be made concerning the degree of hydrolysis, which is higher in the organic phase than in the aqueous phase. For the same reason, a d value of over 3 is impossible.

Next, in Eq. (10), if the activity coefficients of the protactinium species are assumed to be constant over the entire range of DIBC concentration, the

Table 2. Possible forms of extracted species

No.	DIBC concn.			
	Low	Intermediate		High
1	$Pa(OH)T_4$	$Pa(OH)T_4B$		
2	$Pa(OH)_2T_3(HT)$ $PaOT_3(HT)$	$Pa(OH)_2T_3(HT)B$ $PaOT_3(HT)B$	$Pa(OH)_2T_3B$ $PaOT_3B$	$Pa(OH)_2T_3B_2$ $PaOT_3B_2$
3	$Pa(OH)_3T_2(HT)_2$ $PaO(OH)T_2(HT)_2$	$Pa(OH)_3T_2(HT)_2B$ $PaO(OH)T_2(HT)_2B$	$Pa(OH)_3T_2(HT)B$ $PaO(OH)T_2(HT)B$	$Pa(OH)_3T_2(HT)B_2$ $PaO(OH)T_2(HT)B_2$
4	$Pa(OH)_4T(HT)_3$ $PaO(OH)_2T(HT)_3$ $PaO_2T(HT)_3$	$Pa(OH)_4T(HT)_3B$ $PaO(OH)_2T(HT)_3B$ $PaO_2T(HT)_3B$	$Pa(OH)_4T(HT)_2B$ $PaO(OH)_2T(HT)_2B$ $PaO_2T(HT)_2B$	$Pa(OH)_4T(HT)_2B_2$ $PaO(OH)_2T(HT)_2B_2$ $PaO_2T(HT)_2B_2$

distribution ratio (D) obtained empirically can be replaced by the thermodynamic distribution ratio (K_d) expressed in terms of activity. As is clear from Fig. 3, the relation:

$$0 \leqq \sum bf_{p,q,a,b} < 2 \qquad (21)$$

holds. When the DIBC concentration is very low, the distribution ratio is independent of the DIBC concentration, whereas the dependence of the distribution ratio on the TTA concentration is of the power of 4. When the concentration of DIBC is extremely high as compared with the concentration of TTA, the slope of the log-log plot of the distribution ratio and the DIBC concentration is 1.8. At such a high concentration of DIBC, it is clear from Fig. 3 that the TTA dependence on the distribution ratio is of the power of 3. From the above considerations, the possibilities for the species extracted into the organic phase in relation to the concentration of DIBC may be summarized as is shown in Table 2.

The degree of the hydrolysis of the extracted protactinium species may not increase with an increase in the DIBC concentration, for synergism is observed in spite of the decrease in the TTA dependence with an increase in the DIBC concentration. Nor does it decrease, for it is difficult for the less basic DIBC to replace the more basic hydroxy anion. This implies that the change in the extracted species with an increase in the DIBC concentration occurs from the left to the right of the same row in Table 2. These considerations naturally obviate the possibility of the first row. The series of reactions described in the third row was also not warranted, for the following reasons. In this case, two molecules of TTA are assumed to be combined loosely with the chelate. If this is the case, the TTA dependency of 2 should be easily attained with an increase in the DIBC concentration. This is, however, contrary to observation. The same argument is applicable in the case of the series of reactions in the last row. Accordingly, the most probable species extracted into the organic phase are those listed on the second row.

On the second row, two series of the extracted species are possible, depending on p or q, but their values cannot be determined from the experimental results. If one compares the species containing $Pa(OH)_2^{3+}$ and PaO^{3+}, the former is considered to be more hydrophilic than the latter. On the other hand, it is known that, in a benzene solution saturated with water, 11% of TTA is present as the hydrate and that, in a benzene solution which has been neither dried nor equilibrated with water, there is present 3% hydrate. The rate of conversion of the enole form to ketohydrate is very slow, taking 2 or 3 days to reach equilibrium.[9] As the two phases were in contact for only thirty minutes in the preparation of the protactinium solution in TTA-DIBC-benzene, the equilibrium between the enole and ketohydrate forms is not attained. Therefore, the benzene solution has the potentiality of absorbing water. For this reason or for another, if one considers that the forms composed of $Pa(OH)_2^{3+}$, which will participate in the extraction equilibrium, undergo dehydration to form that composed of PaO^{3+}, the irreversible formation of unstrippable species in the organic phase with the time of standing can be well understood. The same is applicable to the interpretation of the similar findings in the TTA extraction reported in the previous report.[2] The difference in the amount of irreversible species formed during a long period of standing between the TTA and the TTA-DIBC extractions (80% and 40% respectively) is attributable to the difference in the TTA concentration used. This irreversible change in the extraction behavior cannot be attributed to the polymerization of the extracted TTA chelate, nor to the decomposition of the chelate by some such means as thermal or radiation decomposition, as has been pointed out previously.[2] These arguments do not violate the validity of the hypothesis mentioned above.

The continuous change in the slope of the log-log plot of the distribution ratio and the TTA acitivity

9) E. L. King and W. H. Reas, *J. Am. Chem. Soc.*, **73**, 1806 (1951).

with the change in the DIBC concentration can be understood if we consider the extracted species to be a mixture of forms containing four TTA and three TTA, the mixing ratio continuously changing with the concentration of DIBC. In the study of the synergism of the UO_2^{2+} -TTA extraction system by TBP, Healy and his co-workers[10,11] showed that the absorption spectra of $UO_2(TTA)_2$ and $UO_2(TTA)_2TBP$ are essentially the same. In view of this fact, it can naturally be assumed that the solvation of DIBC to the protactinium TTA chelate does not affect the absorption spectrum of protactinium in the organic phase; that is, the spectra depend only on the number of TTA present in the extracted species. If we consider Curve No. 1 in Fig. 8 to be the spectrum of the protactinium species containing four molecules of TTA, and Curve No. 7 to be that of the species containing three molecules of TTA, as the spectrum does not change with an increase in the DIBC concentration above 1%, the intermediate curves can be constructed by an appropriate combination of the two curves, No. 1 and No. 7. Therefore, we can estimate the mixing ratio of the species containing three and four molecules of TTA from the absorption spectra. This calculation was done by the method of successive approximation, as is shown in the second and third columns of Table 1. From these values, the slope of the log-log plot of the distribution ratio and the TTA activity can be estimated. The results of the calculation, listed in the fourth column of Table 1, agree well with the empirical value presented in the same table.

In conclusion, one can say in summary that reactions (22) through (25) proceed in this order with the increase in the DIBC concentration:

$$PaO_m(OH)_n^{5-2m-n} + 4HT = Pa(OH)_2T_3(HT) + (m+n-2)H_2O + (5-2m-n)H^+$$
$$Pa(OH)_2T_3(HT) \rightarrow PaOT_3(HT) \quad \text{(slow, irresversible)} \tag{22}$$

$$PaO_m(OH)_n^{5-2m-n} + 4HT + B = Pa(OH)_2T_3(HT)B + (m+n-2)H_2O + (5-2m-n)H^+$$
$$Pa(OH)_2T_3(HT)B \rightarrow PaOT_3(HT)B \quad \text{(slow, irreversible)} \tag{23}$$

$$PaO_m(OH)_n^{5-2m-n} + 3HT + B = Pa(OH)_2T_3B + (m+n-2)H_2O + (5-2m-n)H^+$$
$$Pa(OH)_2T_3B \rightarrow PaOT_3B \quad \text{(slow, irreversible)} \tag{24}$$

$$PaO_m(OH)_n^{5-2m-n} + 3HT + 2B = Pa(OH)_2T_3B_2 + (m+n-2)H_2O + (5-2m-n)H^+$$
$$Pa(OH)_2T_3B_2 \rightarrow PaOT_3B_2 \quad \text{(slow, irreversible)} \tag{25}$$

where $2m+n=3$ and 4.

10) T. V. Healy and J. R. Ferraro, *J. Inorg. Nucl. Chem.*, **24**, 1449 (1962).

11) T. V. Healy, D. F. Peppard and G. W. Mason, *ibid.*, **24**, 1429 (1962).

BULLETIN OF THE CHEMICAL SOCIETY OF JAPAN VOL. 42 2532—2537 (1969)

Kinetics of Multidentate Ligand Substitution Reactions. VI. The Substitution Reaction of Diethylenetriaminepentaacetic Acid with the Nitrilotriacetato Nickelate(II) Chelate

Mutsuo KODAMA

Department of Chemistry, Ibaraki University, Mito, Ibaraki

(Received June 20, 1969)

The kinetics of the substitution reaction of diethylenetriaminepentaacetic acid (DTPA) with the nitrilotriacetato nickelate(II) chelate have been studied polarographically in both acid and alkaline media. The reaction was found to be first-order with respect to DTPA and also first-order with respect to the nitrilotriacetato nickelate(II) chelate with 1-to-1 composition. In an acid solution the reaction proceeds mainly through tervalent and quadrivalent DTPA anions. On the other hand, in an alkaline solution the reaction proceeds through quadrivalent and quinquevalent DTPA anions. The heat of activation and the entropy of activation for the three elementary reactions were estimated, and the effect of the protonation of the quinquevalent DTPA anion on the reaction rate was discussed.

In previous investigations,[1-4] kinetic studies of the nucleophilic substitution reactions between Eriochrom Black T (BT) and cobalt(II)- and nickel(II)-aminopolycarboxylate chelates were carried out spectrophotometrically. From a comparison of the rate constants of the reactions with chelates of *N*-(2-hydroxyethyl)-ethylenediamine, *N*,*N*′,*N*′-triacetic acid (EDTA-OH), cyclohexanediaminetetraacetic acid (CyDTA), and diethylenetriaminepentaacetic acid (DTPA) with those of the corresponding reactions involving EDTA chelates, a detailed reaction mechanism was formulated, and the steric effect was quantitatively discussed on the basis of the proposed reaction intermediates.

It now seems to be important and necessary to extend the study to the investigation of the effect of various ligands on the reaction mechanism and the rate of the nucleophilic substitution reaction involving the metal(II) aminopolycarboxylate chelate. This paper will describe a polarographic study of the kinetics on the reaction of diethylenetriaminepentaacetic acid with the nitrilotriacetato nickelate(II) chelate.

Experimental

Reagents. The nickel (II) nitrate solution was prepared by dissolving a known amount of metallic nickel (99.99% pure) in dilute nitric acid (1+1) and by removing the excess nitric acid by distillation under reduced pressure. The standardization of the concentration of nickel (II) solution was described in a previous paper.[2] The recrystallization of nitrilotriacetic acid (NTA) and DTPA and the preparation of their solutions were also described previously.[2,4] The other reagents were of analytical-reagent grades and were used without further purification.

Apparatus and Experimental Procedure. All the polarograms and the current-time curves were obtained with a Yanagimoto PA-102 pen-recording polarograph, using a dropping mercury electrode which had an *m* value of 0.837 mg/sec and a drop time of 4.02 sec in an air-free acetate buffer solution (total concentration of acetate ions=0.10M, μ=0.20) with a pH of 4.80 at 25°C at −0.50 V *vs.* SCE at the mercury height of 75 cm. The experimental procedures were the same as have previously been described by Tanaka, Kato and Tamamushi.[5] In this study, all the measurements were conducted in solutions with an ionic strength of 0.20 ($NaClO_4$). In the pH range from 4.50 to 5.80, an acetate buffer was employed. In the alkaline region (8.50<pH <10.00), however, no buffer reagent was used, for sample solutions contained a large excess of uncomplexed NTA and so had a sufficient buffer capacity already. Uncomplexed DTPA develops a well-defined anodic wave over the entire pH range covered,[6] so the rate of the reaction was followed by measuring the change in the diffusion current of DTPA with the time. In the potential range where the anodic wave due to the uncomplexed DTPA can be observed, nickel (II)-DTPA and NTA chelates are non-reactive in the polarographic electrolysis. Therefore, neither nickel (II) chelate has any effect on the determination of the concentration

1) M. Kodama, This Bulletin, **40**, 2575 (1967).
2) M. Kodama, C. Sasaki and M. Murata, *ibid.*, **41**, 1333 (1968).
3) M. Kodama, C. Sasaki and T. Noda, *ibid.*, **41**, 2033 (1968).
4) M. Kodama, C. Sasaki and K. Miyamoto, *ibid.*, **42**, 163 (1969).
5) N. Tanaka, K. Kato and R. Tamamushi, This Bulletin, **31**, 283 (1958).
6) M. Kodama and A. Kimura, *ibid.*, **40**, 1639 (1967).

of uncomplexed DTPA.[6] As the reaction rate was determined in this study by measuring the wave height of the uncomplexed DTPA, DTPA is also consumed by the polarographic electrolysis. However, the amount of DTPA consumed by the polarographic electrolysis is negligibly small as compared with that consumed by the substitution reaction with the nickel(II)-NTA chelate. The contribution of the polarographic electrolysis to the whole DTPA concentration change is only 0.05%, even under the experimental conditions where the present reaction proceeds at its slowest rate. In the polarographic electrolysis, a small amount of the mercury(II)-DTPA chelate is also formed at the electrode surface. However, the formation of the mercury(II)-DTPA chelate may be expected to give no effect on the rate of the substitution reaction, because the amount of mercury(II)-DTPA chelate formed is negligible as compared with those of the chemical species involved in the substitution reaction, and also because its stability constant is much greater than that of the nickel(II)–DTPA chelate.[7] This prediction was also confirmed experimentally by adding a small amount of the mercury-(II)-DTPA chelate (2×10^{-6}M). The presence of the mercury(II)-DTPA chelate had no effect on the rate of reaction.

Results and Discussion

All the exchange reactions were studied in solutions containing a large excess of complexed and uncomplexed NTA. Therefore, the exchange reaction (Reaction (1)) can be treated as a pseudo-first-order reaction.

$$H_nZ^{n-5} \underset{k^-}{\overset{k^+}{\rightleftharpoons}} \begin{cases} NiZ^{3-} + nH^+ \\ NiHZ^{2-} \end{cases}$$

where H_nZ^{n-5} denotes the incompletely-deprotonated DTPA anion and NiZ^{3-} and $NiHZ,^{2-}$ normal and protonated nickel(II)-DTPA chelates respectively.

The stability constants of nickel(II)-DTPA chelates are much greater than those of the corresponding nickel(II)-NTA chelates.[7] Therefore, the apparent rate constant of the forward reaction, k^+, must be much greater than that of the backward reaction, k^-, hence, it seemed that rate of the backward reaction may be neglected as compared with that of the forward reaction. This theory was examined experimentally. The presence of the 10.0 mM nickel(II)-DTPA chelate was found to have no effect on the rate of the substitution reaction of DTPA with the nickel(II)-NTA chelate. Consequently, if the present reaction proceeds through simultaneous reaction pathways which involve the dissociation of the nickel(II)-NTA chelate as well as the second-order nucleophilic substitution reactions involving completely- and incompletely-dissociated DTPA anions, the rate of the disappearance of uncomplexed DTPA should be a function of the uncomplexed DTPA concentration and the apparent rate constant, k^+, in a solution of a given pH and with given concentrations of the nickel(II)-NTA chelate and uncomplexed NTA will be given by:

$$k^+ = k_\alpha + \frac{k_\beta}{[\mathrm{DTPA}]_f} \quad (2)$$

where $[\mathrm{DTPA}]_f$ indicates the concentration of uncomplexed DTPA and where the k's are constants.

Consequently, the rate law for the disappearance of uncomplexed DTPA can be expressed as:

$$-\frac{d[\mathrm{DTPA}]_f}{dt} = k^+[\mathrm{DTPA}]_f = k_\alpha[\mathrm{DTPA}]_f + k_\beta \quad (3)$$

By integrating Eq. (3), we obtain:

$$-\ln\left([\mathrm{DTPA}]_f + \frac{k_\beta}{k_\alpha}\right) = -k_\alpha \cdot t - \ln\left([\mathrm{DTPA}]_f^0 + \frac{k_\beta}{k_\alpha}\right) \quad (4)$$

where $[\mathrm{DTPA}]_f^0$ and $[\mathrm{DTPA}]_f$ are the concentrations of uncomplexed DTPA at time=0 and t respectively.

As was reported previously,[6] the limiting current of the anodic wave due to uncomplexed DTPA is proportional to the concentration of uncomplexed DTPA over the entire pH range studied. Therefore, Eq. (4) can be rewritten as:

$$-\log\left(i_t + \frac{k_\beta \cdot k}{k_\alpha}\right) = \frac{k_\alpha}{2.303} - \log\left(i_0 + \frac{k_\beta \cdot k}{k_\alpha}\right) \quad (5)$$

where i_0 and i_t are the wave heights of DTPA at $t=0$ and $t=t$ respectively and where k is the constant,

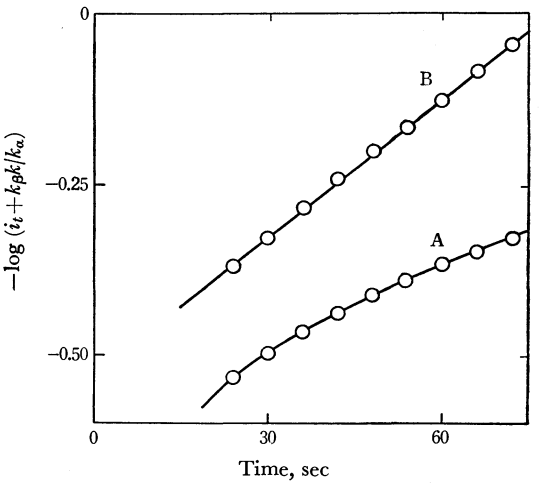

Fig. 1. The plot of $-\log(i_t+k_\beta k/k_\alpha)$ against t.
Concentration of Ni(II)-NTA chelate=6.90 mM
Concentration of uncomplexed NTA=9.53 mM
Concentration of acetate ion=9.15×10^{-2}M
Initial concentration of DTPA=0.453 mM
pH=5.00, μ=0.20, at 25°C
A. $k_\beta k/k_\alpha=1.00$, B. $k_\beta k/k_\alpha=0$

7) L. G. Sillen and A. E. Martell, "Stability Constants of Metal-Ion Complexes," The Chemical Society, London (1964), pp. 507, 693.

defined as $i=k\cdot[\mathrm{DTPA}]_f$.

If the present reaction mechanism does not involve the dissociation of the nickel(II)-NTA chelate, $k_\beta\cdot k/k_\alpha$ in Eq. (5) should be zero. Equation (5) was examined by using typical experimental data. As is illustrated in Fig. 1, the log-plot gave a linear relationship only when $k_\beta\cdot k/k_\alpha$ was zero over the entire pH range covered in this study. This fact clearly indicates that the reaction of DTPA with the nickel(II)-NTA chelate does not involve the dissociation of the nitrilotriacetato nickelate(II) chelate. This conclusion could also be confirmed by the fact that the k_α value determined from the slope of the linear relationship of $-\log i_t$ *versus* t was independent of the concentration of uncomplexed DTPA. The results obtained in the acid media (acetate buffer) are shown in Table 1.

TABLE 1. DEPENDENCE OF THE SLOPE ON THE DTPA CONCENTRATION

Concentration of uncomplexed NTA=9.53 mM
Concentration of nickel(II)-NTA chelate=6.90 mM
Concentration of acetate ion=9.15×10^{-2}M
μ=0.20, 25°C, pH=5.00

Initial concentration of DTPA, mM	Slope sec^{-1}
0.275	6.12×10^{-3}
0.453	6.12×10^{-3}
0.641	6.10×10^{-3}

With regard to the k_α value estimated from the above linear relationship, the following facts can also be established in acid media ($4.50<\mathrm{pH}<5.80$):
1) In solutions of a given pH and with given concentrations of acetate ion and uncomplexed NTA, k_α is proportional to the concentration of the nickel(II)-NTA chelate (Table 2).

TABLE 2. DEPENDENCE OF THE SLOPE ON THE CONCENTRATION OF NICKEL(II)-NTA CHELATE

Concentration of uncomplexed NTA=9.53 mM
Initial concentration of DTPA=0.453 mM
Concentration of acetate ion=9.15×10^{-2}M
μ=0.20, 25°C, pH=5.00

Concn. of Ni(II)-NTA, mM	Slope sec^{-1}	Concn. ratio	Slope ratio
6.90	6.12×10^{-3}	1.00	1.00
10.35	9.10×10^{-3}	1.50	1.49
13.80	$12.2_5\times10^{-3}$	2.00	2.00

2) In solutions of a given pH and with given concentrations of uncomplexed and complexed NTA, k_α is independent of the concentration of the acetate ion (Table 3).
3) In solutions of a given pH and with given concentrations of the acetate ion and the nickel(II)-NTA chelate, k_α is independent of the concentration of uncomplexed NTA (Table 4).

TABLE 3. DEPENDENCE OF THE SLOPE ON THE CONCENTRATION OF ACETATE ION

Concentration of uncomplexed NTA=9.53 mM
Concentration of nickel(II)-NTA chelate=6.90 mM
Initial concentration of DTPA=0.453 mM
μ=0.20, 25°C, pH=5.00

Concentration of acetate, ion, M	Slope, sec^{-1}
4.57×10^{-2}	6.12×10^{-3}
9.15×10^{-2}	6.12×10^{-3}
1.32×10^{-1}	6.15×10^{-3}

TABLE 4. DEPENDENCE OF THE SLOPE ON THE CONCENTRATION OF UNCOMPLEXED NTA

Concentration of nickel(II)-NTA chelate=6.90 mM
Concentration of acetate ion=9.15×10^{-2}M
Initial concentration of DTPA=0.453 mM
μ=0.20, 25°C, pH=5.00

Concentration of NTA, mM	Slope, sec^{-1}
9.53	6.12×10^{-3}
14.30	6.10×10^{-3}
19.10	6.10×10^{-3}

4) In solutions with given concentrations of the acetate ion and complexed and uncomplexed NTA, the plot of $k_\alpha\cdot(\alpha_H)_Z/[\mathrm{H}^+]$ against $[\mathrm{H}^+]$ gives a linear relationship (Fig. 2). Here, $(\alpha_H)_Z$ is the (α_H) value of DTPA.

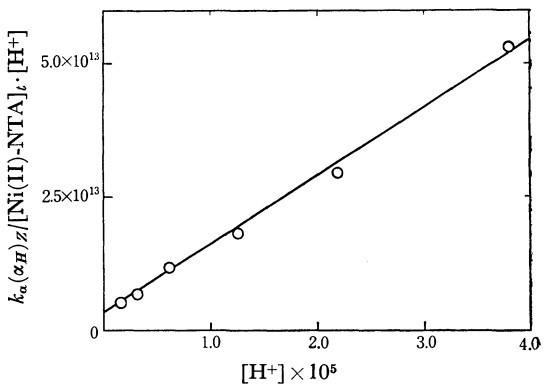

Fig. 2. The plot of $k_\alpha(\alpha_H)_Z/[\mathrm{Ni(II)\text{-}NTA}]_t\cdot[\mathrm{H}^+]$ against $[\mathrm{H}^+]$
Concentration of Ni(II)-NTA chelate=6.90 mM
Concentration of uncomplexed NTA=9.53 mM
Concentration of acetate ion=9.15×10^{-2}M
Initial concentration of DTPA=0.453 mM
μ=0.20, at 25°C

Thermodynamic calculation reveals that nickel (II) ions in solutions with pH's from 4.50 to 5.80 containing 10 mM uncomplexed NTA form only the chelate with a 1-to-1 composition, that the

predominant uncomplexed DTPA species are tervalent and quadrivalent anions, and that their concentrations are given by $[DTPA]_f[H^+]^2/k_5 \cdot k_4$ and $[DTPA]_f[H^+]/k_5$ respectively. Here, k_4 and k_5 denote the fourth and fifth dissociation constants of DTPA. Therefore, the above facts indicate that the present substitution reaction proceeds mainly through the following two simultaneous reaction pathways in the pH range from 4.50 to 5.80:

$$\text{i)}\quad NiX^- + H_2Z^{3-} \overset{k_1^+}{\rightleftharpoons} NiZ^{3-} + H^+ + HX^{2-}$$
$$\Big\Updownarrow \text{rapid}$$
$$NiHZ^{2-}$$

$$\text{ii)}\quad NiX^- + HZ^{4-} \overset{k_2^+}{\rightleftharpoons} NiZ^{3-} + HX^{2-}$$
$$\Big\Updownarrow \text{rapid}$$
$$NiHZ^{2-}$$

where NiX^- is the nickel(II)-NTA chelate with a 1-to-1 composition; HZ^{4-} and H_2Z^{3-}, quadrivalent and tervalent DTPA anions respectively, and HX^{2-}, the doubly-deprotonated NTA anion. On the basis of the above reaction mechanism, k_a in an acid medium can be written as:

$$k_a = \left(\frac{k_2^+[H^+]}{k_5} + \frac{k_1^+ \cdot [H^+]^2}{k_4 \cdot k_5}\right)\frac{[Ni(II)\text{-}NTA]_t}{(\alpha_H)_Z} \qquad (6)$$

In an alkaline medium ($8.50 < pH < 10.00$), as is illustrated by Tables 5 and 6, the k_a value determined from the linear relationship between $\log i_t$ and t was also found to be proportional to the total concentration of the nickel(II)-NTA chelate, but to be inversely proportional to the value of $1+k_{NiX_2} \cdot [X]_f/(\alpha_H)_X$, provided that the other experimental conditions are kept constant. Here, K_{NiX_2}, $(\alpha_H)_X$ and $[X]_f$ have the same meanings as have been used previously.[2] The above facts clearly indicate that the k_a value is linearly proportional to the concentration of the nickel(II)-NTA chelate with a 1-to-1 composition. $[X]_f$ was calculated from the total concentrations of NTA and nickel(II) ions with the aid of Eq. (2) of Ref. 2. As was found in the acid medium, k_a was also independent of the DTPA concentration (these results are not shown here). This fact clearly indicates that, in the pH range from 8.50 to 10.00, the substitution reaction of DTPA with the nitrilotriacetato nickelate(II) chelate does not proceed through the reaction pathway in which the dissociation of the nickel(II)-NTA chelate is involved.

The k_a value was also a function of the hydrogen ion concentration, and there was a linear relationship between $k_a \cdot (\alpha_H)_Z[1+k_{NiX_2} \cdot [X]_f/(\alpha_H)_X]/[Ni(II)NTA]_t$ and the hydrogen ion concentration, $[H^+]$ (Fig. 3). Here, $[Ni(II)NTA]_t$ indicates the total concentrations of nickel(II)-NTA chelates. All the facts stated above clearly indicate that, in an alkaline solution, the present reaction mainly proceeds through the following two reaction pathways.

Table 5. Dependence of the slope on the total concentration of nickel(II)-NTA chelate

Concentration of uncomplexed NTA=11.7 mM
Initial concentration of DTPA=0.453 mM
μ=0.20, 25°C, pH=9.50

Total concn. of Ni(II)-NTA, mM	Slope, sec^{-1}	Concn. ratio	Slope ratio
6.90	8.50×10^{-3}	1.00	1.00
10.35	12.8×10^{-3}	1.50	1.51
13.80	16.7×10^{-3}	2.00	1.97

Table 6. Dependence of the slope on the $[1+K_{NiX_2}[X]_f/(\alpha_H)_X]$ value

Initial concentration of DTPA=0.453 mM
Total concentration of nickel(II)-NTA chelate=6.90 mM
μ=0.20, 25°C, pH=9.50

Concn. of uncomplexed NTA, mM	Slope, sec^{-1}	Slope$\times[1+K_{NiX_2}[X]_f/(\alpha_H)_X]$
11.70	8.50×10^{-3}	1.19
27.3	3.58×10^{-3}	1.25
37.7	2.68×10^{-3}	1.21

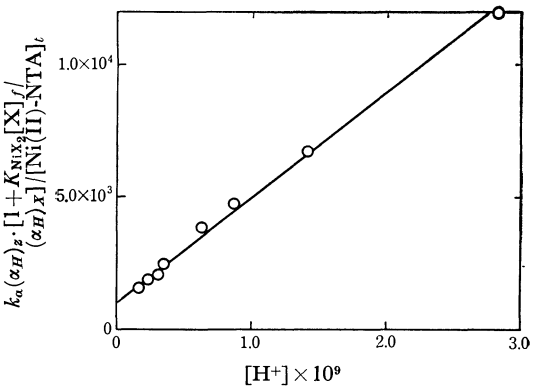

Fig. 3. The plot of $k_a(\alpha_H)_Z \cdot [1+K_{NiX_2}([X]_f/(\alpha_H)_X]/[Ni(II)\text{-}NTA]_t$ against $[H^+]$
Total concentration of nickel(II)-NTA chelate=6.90 mM
Total concentration of NTA=28.0 mM
Initial concentration of DTPA=0.453 mM
μ=0.20, at 25°C

$$\text{ii)}\quad NiX^- + HZ^{4-} \overset{k_2^+}{\rightleftharpoons} NiZ^{3-} + HX^{2-}$$
$$\Big\Updownarrow \text{rapid}$$
$$NiX_2^{4-}$$

$$\text{iii)}\quad NiX^- + Z^{5-} \overset{k_3^+}{\rightleftharpoons} NiZ^{3-} + X^{3-}$$
$$\Big\Updownarrow \text{rapid}$$
$$NiX_2^{4-}$$

where NiX_2^{4-} indicates the nickel(II)-NTA chelate with a 1-to-2 composition. Therefore, k_a in Eq. (5) can be written as:

$$k_a = \left(k_3^+ + k_2^+ \cdot \frac{[H^+]}{k_5}\right) \times \frac{[\text{Ni(II)-NTA}]_t}{(\alpha_H)_Z \cdot [1 + K_{NiX_2} \cdot [X]_f/(\alpha_H)_X]} \quad (7)$$

From the slopes and intercepts shown in Figs. 2 and 3, k_1^+, k_2^+ and k_3^+ were determined at 25°C. The k_2^+ value determined from the slope in Fig. 3 agreed well with that obtained from the intercept in Fig. 2. This agreement strongly supports the proposed reaction mechanism.

Similar results were also obtained in the experiments at 18°C and 9°C. The k^+ value determined at 18°C and 9°C are given in Table 7, along with

TABLE 7. RATE CONSTANTS, HEAT OF ACTIVATION AND ENTROPY OF ACTIVATION FOR REACTIONS i), ii) AND iii)

k^+ value	Temperature, °C 9.0	18.0	25.0	ΔH^{++} kcal/mol	ΔS^{++} e.u.
k_1^+	0.499	0.175	1.78	12.2	−16.5
k_2^+	2.77×10^1	7.24×10^1	3.06×10^2	19.3	20.5
k_3^+	3.1×10^2	7.0×10^2	9.1×10^2	10.0	−11.2

the results obtained at 25°C. Linear relationships were found between the log k^+ value and $1/T$ for three elementary reactions, i), ii) and iii); this made it possible to calculate the heat and entropy of activation. The results are given in Table 7. The k^+ values given in Table 7 are much greater than the corresponding rate constants for the reaction of the nickel(II)-NTA chelate with EDTA-OH,[8] lending strong support to the present author's conclusion that the exchange reaction of DTPA with the nickel(II)-NTA chelate proceeds predominantly through three simultaneous reaction pathways, all of which involve a second-order nucleophilic substitution reaction without any dissociation of the nickel(II)-NTA chelate. The greater rate constants probably mean that the present exchange reaction proceeds by a mechanism which involves a reaction intermediate more stable than that for the nickel-(II)-NTA-EDTA-OH reaction.

On the basis of the conclusion reached by Rorabacher and Margerum concerning the reaction of nickel(II)-polyamine complexes with EDTA,[9] the reaction intermediate expected for the present exchange reaction may involve the DTPA anion, all three nitrogen groups of which are coordinated to the nickel(II) ion, as well as the tervalent NTA anion. If the DTPA anion in the reaction intermediate forms only two nickel(II)-nitrogen bonds or less, the k^+ values of the present reaction should be smaller than the corresponding rate constants for the nickel(II)-NTA–EDTA-OH reaction, because the less stable reaction intermediate due to the larger steric effect of DTPA would make the reaction more sluggish.

It is also interesting to note that the heat of activation for the elementary reaction ii) is much larger than those for i) and iii) reactions, and that the entropy of activation for the ii) reaction is positive, whereas those for the i) and iii) reactions are negative. Generally, the entropy of activation for a second-order nucleophilic substitution reaction involving a multidentate ligand may be expected to be negative, because the conformational, translational, and rotational freedom of an entering multidentate ligand would be lost in the formation of a mixed ligand intermediate chelate. The negative entropy for the elementary reaction iii) may be responsible for this effect. An NMR study of the protonation of the quinquevalent DTPA anion (Fig. 4) in an aqueous solution[10] gave the conclu-

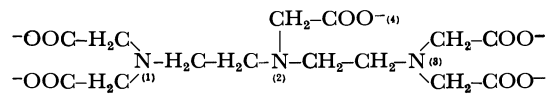

Fig. 4. Quinquevalent DTP Aanion.

sion that, after the addition of one proton equivalent, the terminal nitrogen groups, (1) and (3), are each protonated 26% of the time each; the central nitrogen group (2) is protonated 41% of the time, and the central acetate group (4) is protonated 7% of the time, while the terminal acetate groups are not protonated to any detectable extent. On the other hand, when a second proton equivalent is added, the two terminal nitrogen groups are each protonated 85% of the time, the central nitrogen group (2) is protonated only 15% of the time, and four terminal acetate groups are protonated 4% of the time. The fact that the first proton is almost equally bonded among the three nitrogen groups of the DTPA anion probably indicates that the intramolecular hydrogen bonding arranges the DTPA anion in a favorable position to form the reaction intermediate. Thus, less conformational and rotational freedom is lost in the formation of the mixed ligand intermediate chelate, corresponding to the positive entropy of activation for the e ementary reaction ii). The tervalent DTPA anion, H_2Z^{3-}, where the two terminal nitrogen groups are almost completely-protonated and where the central nitrogen group is protonated only 15% of the time, may have a conformation less favor-

8) M. Kimura, *Nippon Kagaku Zasshi* (*J. Chem. Soc. Japan, Pure Chem. Sect.*), **89**, 1209 (1968).

9) D. B. Rorabacher and D. W. Margerum, *Inorg. Chem.*, **3**, 382 (1964).

10) J. L. Sudmeier and C. N. Reilley, *Anal. Chem.*, **36**, 1698 (1964).

able to the formation of the reaction intermediate, because the electrostatic repulsion between the positively-protonated sites would prevent the DTPA anion from having a favorable conformation to react with the nickel(II)-NTA chelate. Thus, a remarkable decrease in entropy for the elementary reaction i) can be expected.

Finally, it can also be mentioned that, with an increase in the extent of the protonation of the central nitrogen and acetate groups, the heat of activation becomes greater. This probably suggests that the deprotonation of these groups is inherently required for the formation of a mixed ligand chelate intermediate, through which the exchange reaction of the nickel(II)-NTA chelate with DTPA proceeds. The importance of the conformation of the attacking group will be discussed in a subsequent paper.

The present author wishes to express his hearty thanks to Mr. Tomohiko Noda and Miss Yayoe Tominaga for their help during this experiment.

BULLETIN OF THE CHEMICAL SOCIETY OF JAPAN VOL. 42 2537—2543 (1969)

Role of the Solvent in the Distribution of the Zinc-TTA Chelate and the Adduct Formation with TBP

Kenichi AKIBA, Nobuo SUZUKI and Takuji KANNO

Research Institute of Mineral Dressing and Metallurgy, Tohoku University, Sendai

(Received January 28, 1969)

The distributions of the zinc chelate with thenoyltrifluoroacetone (TTA) between an aqueous solution and twelve inert organic solvents were investigated. After it had been confirmed that the distributed species were ZnA_2, the distribution coefficients of the chelate (P_M) and those of TTA (P_{HA}) were compared; it was found that there is a correlation which can be expressed as $\log P_M = n \log P_{HA} + \text{const.}$ When TTA and TBP are in the extraction system, the adduct formation constants of chelate were obtained. The activities of all the species which take part in the adduct formation were evaluated on the basis of the regular solution theory. It was found that the adduct formation constant in terms of activity (K_S°) is constant in all the organic solvents; namely, $\log K_S^\circ$ was found to be 4.05. Finally, the role of the solvent in the synergistic extraction system is explained systematically by a combination of the regularity in the distribution and that in the adduct formation.

The extraction processes of metal complexes have been studied qualitatively in several extraction systems, but there have been few works on the role of organic solvents in connection with the physical chemistry of a solution. The properties of solvents governing the distribution coefficient have never been clarified, and the solvents have been chosen empirically without even a qualitative measure.

In the previous papers the relation between the distribution coefficient and the solubility parameter of solvents was examined on the basis of the regular solution theory;[1] the regularities in the distributions of β-diketones and their scandium chelates have thus been explained in the various solvent systems.[2-6] A similar treatment is applicable not only to β-diketone but to a distributed species in general; the distribution coefficients of oxine and its derivatives have been explained in relation to the solubility parameter.[7]

However, the regularity in the distribution can be hardly explained in the same manner when such organic-phase reactions as adduct formation, dimerization, and solvation take place. A synergism on the distribution of the metal chelate has been observed in several extraction systems, but no general explanation of the role of the solvent has

1) T. Wakabayashi, S. Oki, T. Omori and N. Suzuki, *J. Inorg. Nucl. Chem.*, **26**, 2255 (1964).

2) T. Omori, T. Wakabayashi, S. Oki and N. Suzuki, *ibid.*, **26**, 2265 (1964).

3) N. Suzuki, K. Akiba, T. Kanno and T. Wakabayashi, *ibid.*, **30**, 2521 (1968).

4) N. Suzuki, K. Akiba, T. Kanno, T. Wakabayashi and K. Takaizumi, *ibid.*, **30**, 3047 (1968).

5) T. Wakabayashi, K. Takaizumi, K. Seto, N. Suzuki and K. Akiba, This Bulletin, **41**, 1854 (1968).

6) N. Suzuki, K. Akiba and T. Kanno, *Anal. Chim. Acta*, **43**, 311 (1968).

7) T. Wakabayashi, This Bulletin, **40**, 2836 (1967).

been given. The physicochemical properties of the solvent will, however, influence both the distribution coefficients and the equilibrium constants of the organic-phase reactions. The synergistic effect should be discussed in relation to not the over-all extraction constant but the equilibrium constants of the organic-phase reactions.

This work was undertaken in order to clarify the role of the organic solvent in the distribution of the chelate and in the adduct formation with a neutral ligand. The distribution coefficients of the zinc-TTA chelate between an aqueous perchlorate medium and several organic solvents are determined, and the relation between the distribution coefficients of TTA is examined. The adduct formation constants of the zinc-TTA chelate with tributyl phosphate (TBP) are obtained by the distribution method.

The activity coefficients of the species related to the organic-phase reaction are estimated with the aid of the regular solution theory,[8] and the adduct formation constants are correlated to changes in the activity coefficients. The role of solvents in synergistic extraction may be explained systematically by the regularity in the distribution and that in the adduct formation.

Experimental

Reagents. The zinc-65 was obtained from the New England Nuclear Corp. (USA) as a hydrochloric acid solution. After a portion of this solution had been dried on a water bath, the tracer was taken in 0.1M perchloric acid; the concentration of zinc ions was controlled by the addition of an inactive zinc solution.

TTA was purified as before.[6]

TBP was refluxed for 5 hr with an equal volume of a 0.5M sodium hydroxide solution on the water bath; the TBP phase was washed with water and dried over anhydrous sodium sulfate, and the washed product was distilled under reduced pressure.

All the solvents were purified by ordinary methods.

The apparatus used was the same as that described previously.[4]

Distribution Ratio of TTA (D_{HA}). The desired organic solution of TTA was shaken for 16 hr with an aqueous perchloric acid solution with an ionic strength of 0.1. After centrifuging, a portion of the aqueous phase was pipetted out, and the concentration of TTA was determined spectrophotometrically. An aqueous solution saturated with an organic solution free from TTA was used as a reference for the measurement of the absorbance.

Distribution Ratio of Zinc (D_M, $D_{M,S}$). An organic solution containing TTA was agitated for 20 hr with an acetate buffer solution (pH 3.5—5.5) containing ^{65}Zn. The ionic strength was adjusted to 0.1 with sodium perchlorate. After the two phases had been separated, the γ-activity of each phase and the pH of the aqueous phase were measured.

All the experiments were carried out at 25°C.

Concentration of Acetate Ions. The distribution ratios of zinc decreased slightly with an increase in the concentration of acetate ions up to about 0.05M, but they were constant below 0.01M. Accordingly, the concentration of acetate ions was kept at 0.002M.

Concentration of Zinc Ions. As the distribution ratios are independent of the zinc-ion concentration below about 5×10^{-6}M, the concentration of zinc was kept at 10^{-6}M. The recovery of the total γ-activity was always checked, and the losses of zinc were found for a few paraffinic solvents. To avoid the loss of zinc, the concentration of zinc was held constant at 10^{-7}M for these solvents.

Results and Discussion

The extraction processes of the zinc-TTA chelate may be expressed as follows:

$$Zn^{2+}_{aq} + nA^{-}_{aq} \overset{\beta_n}{\rightleftharpoons} ZnA^{(2-n)+}_{n,aq} \quad (1)$$

$$ZnA_{2,aq} \overset{P_M}{\rightleftharpoons} ZnA_{2,org} \quad (2)$$

$$ZnA_{2,org} + jHA_{org} \overset{K_j}{\rightleftharpoons} ZnA_2\cdot jHA_{org} \quad (3)$$

$$ZnA_{2,org} + mS_{org} \overset{K_{S,m}}{\rightleftharpoons} ZnA_2\cdot mS_{org} \quad (4)$$

where HA and S stand for the undissociated TTA and the neutral ligand respectively. The subscripts aq and org refer to the aqueous and organic phases.

The distribution of zinc in the absence of the neutral ligand, D_M, is given by:

$$D_M = \frac{P_M\beta_2[A^-]^2_{aq}\{1 + \sum K_j[HA]^j_{org}\}}{1 + \beta_n[A^-]^n_{aq}} \quad (5)$$

If no mixed adduct complexes, $ZnA_2\cdot jHA\cdot mS$, are formed, and distribution ratio in the presence of the neutral ligand, $D_{M,S}$, is written as:

$$D_{M,S} = \frac{P_M\beta_2[A^-]^2_{aq}\{1+\sum K_j[HA]^j_{org}+\sum K_{S,m}[S]^m_{org}\}}{1+\sum\beta_n[A^-]^n_{aq}} \quad (6)$$

The extraction of zinc complexes with the neutral ligand alone is negligibly small. If the undissociated TTA does not react with the chelate and if the only adduct with S is predominant, the following equation is obtained from Eqs. (5) and (6):

$$K_S = \frac{D_{M,S}}{D_M}\cdot\frac{1}{[S]^m_{org}} \quad (7)$$

where K_S is the overall adduct formation constant.

Distribution of the Zinc Chelate. The extraction mechanism of the zinc-TTA chelate has been studied for a few solvent systems, and it has been shown that bivalent zinc is extracted into the organic phase as the formally neutral species

8) J. H. Hildebrand and R. L. Scott, "Solubility of Nonelectrolytes," 3rd Ed., Dover, New York (1964).

ZnA_2.[9-11] In this study it was important to confirm that the distributed species is the same one for all solvents. Plots of log D_M measured at various pH values against pA ($=-\log[A^-]_{aq}$) gave a series of straight lines with a slope of -2. As an example that for benzene is given in Fig. 1; the same line

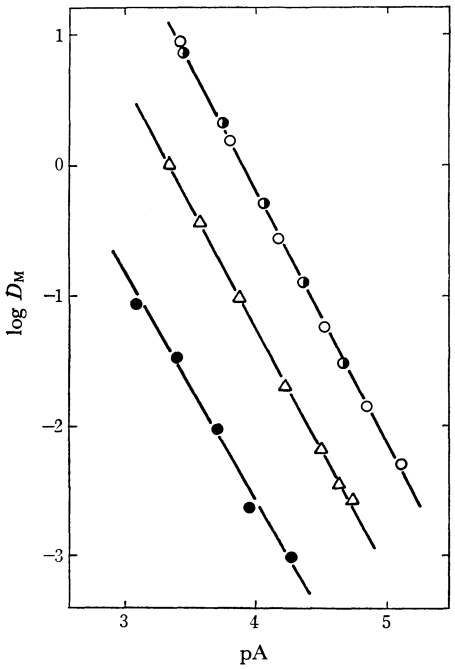

Fig. 1. Distribution ratio of zinc-TTA chelate as a function of pA.
Ionic strength, 0.10; $[HA]_{org,\,init.}=0.1M$
●, *n*-hexane; △, carbon tetrachloride;
○, benzene; ◑, benzene (pH=5.08)

was obtained at different concentrations of HA. In all cases, the distributed species is ZnA_2 and there is no additive compound with HA. The concentration of the dissociated TTA anion (A^-) in the aqueous phase can be calculated by the following equation:

$$[A^-]=\frac{[HA]_{org,init.}}{(P_{HA}+1)[H^+]/K_a+1} \qquad (8)$$

where K_a represents the apparent dissociation constant of TTA, $K_a=6\times10^{-7}$,[12] and where P_{HA} is the distribution coefficient of TTA. When the concentration of zinc is over 10^{-6}M, losses of radioactivities were observed in *n*-hexane, *n*-heptane, and cyclohexane. Even in this case, however, the distribution ratios are independent of the zinc concentration and the same straight lines, log D_M *vs.* pA, are obtained. After the two phases were discarded, the extracting tube was washed with an organic solvent other than the paraffinic solvent or with an acidic aqueous solution; a great portion of the lost activity could be thus recovered. It seems that both the phases were saturated with such complexes as $ZnA_2\cdot nH_2O$ and that a portion of the complexes was removed from the system as a precipitate. The possibility of the formation of the higher complexes, $ZnA_n^{(2-n)+}$ ($n>2$), seems to be eliminated. The measured distribution ratio may be regarded as a contribution of only one species, that shown as ZnA_2. The distribution coefficients of the chelate are too large to be measured experimentally. As the distribution ratio written in Eq. (5) is expressed as a simple function of pA, the distribution ratio is proportional to the distribution coefficient at a definite pA. The distribution ratios at pA 4.0 for each solvent are given in Table 1. The following relation

Table 1. Distribution ratio of zinc-TTA chelate and adduct formation constant with TBP at 25°C, ionic strength, 0.10

No.	Solvent	δ	log P_{HA}	log D_M (pA= 4.0)	log K_S
1	*n*-Hexane	7.3	0.68*	−2.54	5.17
2	*n*-Heptane	7.4	0.57	−2.74	5.26
3	Cyclohexane	8.2	0.56	−2.45	5.01
4	Chloroform	9.3	1.73*	−0.44	2.78
5	Methylene chloride	9.7	1.84*	0.21	3.03
6	Carbon tetrachloride	8.6	1.30*	−1.24	4.43
7	Benzene	9.2	1.62*	−0.23	4.01
8	Monochlorobenzene	9.5	1.65*	−0.30	3.73
9	*o*-Dichlorobenzene	10.0	1.59*	−0.30	3.90
10	Isopropylbenzene	8.5	1·37**	−0.99	4.09
11	Bromoform	10.5			2.84
12	Toluene	8.9	1.60*	−0.32	4.03

* Values from Ref. 1.
** Values from Ref. 2.

between the distribution coefficients of the chelating agent and those of the metal chelate has been derived from the regular solution theory[2] (the distributions of scandium β-diketonates were satisfactorily explained in the various solvent systems):[2,4-6]

$$\log P_M=\frac{V_M}{V_{HA}}\log P_{HA}+\text{const.} \qquad (9)$$

where V_{HA} and V_M denote the molar volume of the chelating agent and that of the metal chelate respectively. This relation is expected to hold for the zinc chelate also. Plots of log D_M at pA 4.0

9) T. Sekine and D. Dyrssen, *J. Inorg. Nucl. Chem.*, **26**, 1727 (1964).
10) H. M. N. H. Irving and D. N. Edgington, *ibid.*, **27**, 1359 (1965).
11) R. L. Scruggs, T. Kim and N. C. Li, *J. Phys. Chem.*, **67**, 2194 (1963).
12) J. C. Reid and M. Calvin, *J. Am. Chem. Soc.*, **72**, 2948 (1950).

against log P_{HA} give a straight line with a slope of 2.1, as is shown in Fig. 2. It is reasonable that the ratio of the molar volume of the chelate to that of TTA is about two, because two molecules of TTA combine with zinc ion.

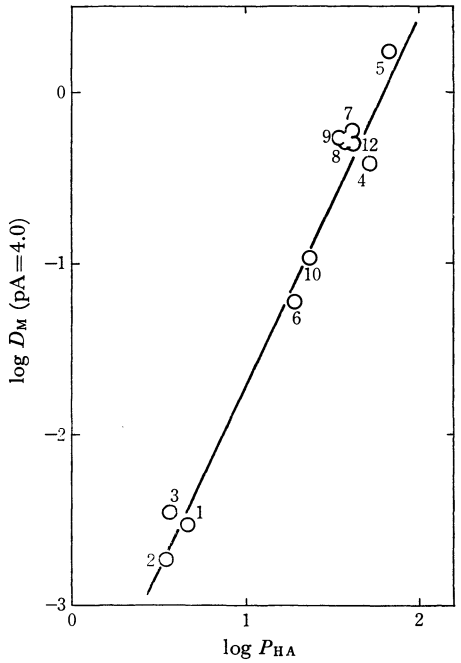

Fig. 2. Correlation between the distribution coefficient of TTA and that of zinc chelate.
The numbers in Figs. 2, 6 and 7 correspond to those in Table 1.

Distribution of Zinc Chelate in the Presence of the Neutral Ligand. When a formally neutral donor (S) is added to the chelate extraction system, the extraction is extremely enhanced.[9-11] The distribution behavior was examined in the presence of TBP in order to obtain a reliable adduct formation constant. At first, the distribution ratio of TTA was measured with the change in the concentration of TBP in order to examine whether or not TBP affects TTA; the results are shown in Fig. 3. The distribution ratios of TTA are independent of the TBP concentration up to 0.01M for *n*-hexane, 0.02M for carbon tetrachloride and benzene, and 0.1M for chloroform. In these concentration ranges of TBP, the UV spectra of TTA are essentially the same as those in the absence of TBP. At higher TBP concentrations, the distribution ratio increases with an increase in the concentration of TBP; the rate of increase is different for each solvent, being especially remarkable for *n*-hexane. It can be considered that the distributed species of TTA is affected by TBP. TTA exists almost entirely as the enol form in the inert solvent or at low TBP concentrations, while the ratio of the keto form increases with an increase in the cocentration of TBP. Therefore, the TBP concentration ranges where there is no effect of TBP were employed. As the distribution coefficients of TBP between the aqueous and the organic phases are very large,[13] the initial concentration of TBP may be regarded as the equilibrium concentration.

In order to examine the contribution of TBP to the adduct formation, the change in the distribution ratio of zinc ($D_{M,S}$) with the change in the concentration of TBP was examined as in Fig. 4.

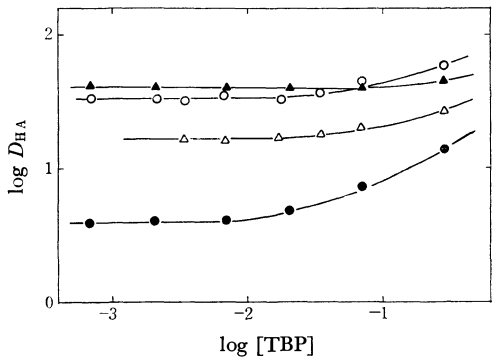

Fig. 3. Distribution ratio of TTA as a function of TBP concentration.
$[HA]_{org,\ init.}$=0.01M; ●, *n*-hexane; △, carbon tetrachloride; ○, benzene; ▲, chloroform

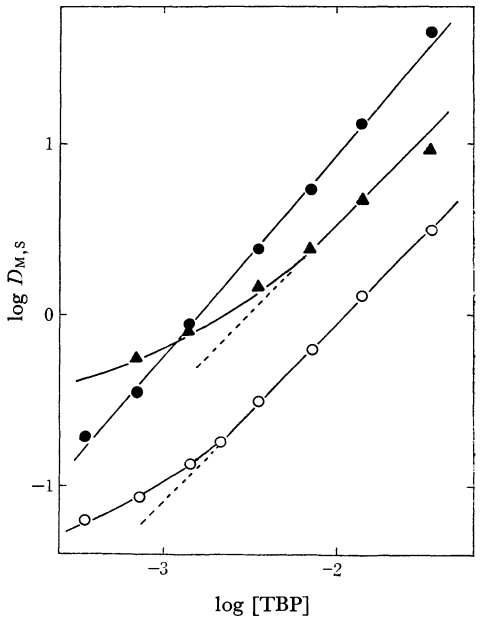

Fig. 4. Distribution ratio of zinc complex as a function of TBP concentration.
$[HA]_{org,\ init.}$=0.01M; ●, *n*-hexane (pA=3.98); ○, benzene (pA=4.82); ▲, chloroform (pA=4.05)

13) K. Alcock, S. S. Grimley, T. V. Healy, J. Kennedy and H.A.C. McKay, *Trans. Faraday Soc.*, **52**, 39 (1956).

The limiting slope was unity for each solvent. It seems that one molecule of TBP adds to one molecule of chelate; there is no evidence that two or more molecules of TBP add to the zinc chelate. The deviation from the straight line with a slope of 1 is evident at low concentrations of TBP, especially in the case of chloroform, because the assumption that the adduct is predominant is not applicable at low concentrations of TBP.

The plots of log $D_{M,S}$ against pA at a constant [TBP] gave a series of straight lines with a slope of -2, as is shown in Fig. 5. It is clear that the

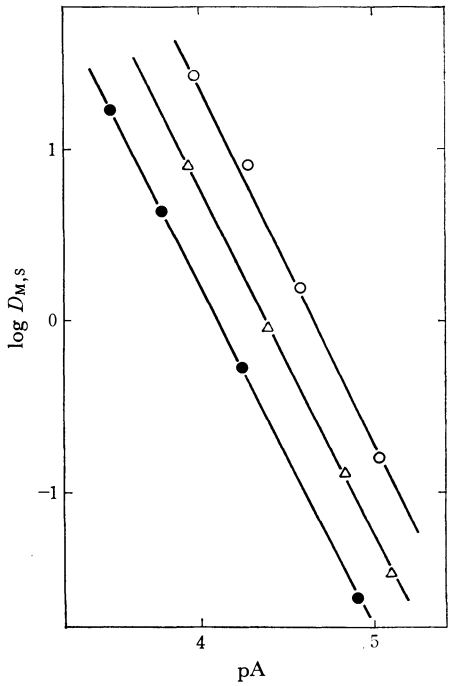

Fig. 5. Distribution ratio of zinc complex in the presence of TBP.
$[HA]_{org,\,init.}=0.01$M; [TBP]$=0.00366$M;
●, *n*-hexane; △, carbon tetrachloride;
○, benzene

adduct is predominant as compared with the case of no TBP, and that the adduct formation constant can be obtained from D_M and $D_{M,S}$.

The log K_S values are given in Table 1; they are close to the values obtained by Sekine and Dyrssen, 2.69 for chloroform and 4.34 for carbon tetrachloride.[9] Although there is a tendency toward large K_S values for simple paraffinic solvents and small ones for halogen-substituted solvents, the values of K_S are very different for each solvent. This means that the adduct formation constants are strongly influenced by the nature of the organic solvent, and that the role of the solvent in synergism is complicated. One can not simply relate the K_S values to the physicochemical properties of the solvent. The change in the activity with the solvent nature plays a very important role in the adduct formation. Therefore, the activity coefficients of all the species in the organic phase must be taken into account. Up to the present, it has been sometimes assumed that the activity coefficient of the species in the organic phase is close to unity, and there has been no consideration of the change in the activity with the nature of the solute and/or the solvent.

The interaction among the molecules in the organic solution should be estimated as the activity coefficient for each species. The overall adduct formation constant, expressed in terms of activities defined as K_S°, is:

$$K_S^\circ = \frac{a_{ZnA_2\cdot mS}}{a_{ZnA_2}a_S^m} = K_S\frac{\gamma_{ZnA_2\cdot mS}}{\gamma_{ZnA_2}\gamma_S^m} \tag{10}$$

where a represents the activity; γ, the activity coefficient, and the subscripts, chemical species. When the activity coefficient of a pure component is assumed to be unity, as is standard, the K_S° values do not depent on the medium. If the activities of all species can be evaluated in several organic solvents, the applicability of Eq. (10) may be considered. The activities of TBP have been measured in several organic solvents,[13,14] but those of the others have never been established. We have insufficient data on these organic solutions to evaluate the activity.

As the solvents used in this work may be regarded as so-called inert solvents, it seems that there are no specific interactions among the components of the solutions. These solutions are usually considered to be reasonably regular. It is practical to evaluate the activity according to the equation of Hildebrand-Scott:[8]

$$\begin{cases} \boldsymbol{R}T\ln a_A = \boldsymbol{R}T\ln x_A + V_A\varphi_B^2(\delta_A-\delta_B)^2 & \text{(11a)} \\ \boldsymbol{R}T\ln a_A = \boldsymbol{R}T\left[\ln\varphi_A + \varphi_B\left(1-\frac{V_A}{V_B}\right)\right] + V_A\varphi_B^2(\delta_A-\delta_B)^2 & \text{(11b)} \end{cases}$$

where the subscripts A and B denote the components A and B respectively, and where x represents the mole fraction; V, the molar volume, φ, the volume fraction, and δ, the solubility parameter. If the entropy of mixing is ideal, Eq. (11a) is appropriate. Where the molar volumes of components A and B are quite appreciably different, it seems that Eq. (11b) is more reasonable,[8] so Eq. (11b) is used in this study. The solubility parameters of the solvents have been listed in a monograph, or they can be calculated from the thermodynamic quantity.[8] However, as there are no fundamental data on, *e. g.*, the heat of vaporization and the solubility for the chelate and the adduct, it is difficult to evaluate the solubility parameter.

As for the chelate, the correlation between the

14) S. Siekierski, *J. Inorg. Nucl. Chem.*, **24**, 205 (1962).

distribution coefficients of TTA and of chelate shown in Fig. 2 would lead us to suppose that the molar volume of the chelate is twice that of TTA and that the solubility parameter of chelate is equal to that of TTA. Consequently, the activity of the chelate may be calculated from the two values V_M 320 m*l* and δ_{ZnA_2} 9.9. Next, the activity of adduct must be assessed one way or another. Here, taking into account that the concentration of the component A is sufficiently low, A and B represent the molecules of the solute and the solvent respectively in Eq. (11b). If the difference in the ratio of the molar volume of the solute to that of the solvent is small for each solvent, Eq. (11b) can be put into a simpler form:

$$\log \gamma_A = C + D(\delta_A - \delta_B)^2 \qquad (12)$$

where C and D are constants. When the activity coefficients of the component A, γ_A, or the values which are proportional to γ_A are plotted against the solubility parameters of the solvents, δ_B, the curve which indicates a minimum at $\delta_A=\delta_B$ will be drawn. Accordingly, the solubility parameter of the component A can be obtained at the minimum in the curve. Equation (10) can be rewritten as by adopting $m=1$:

$$\gamma_{ZnA_2\cdot S} = K_S^\circ \cdot \frac{\gamma_{ZnA_2}\gamma_S}{K_S} \qquad (13)$$

The combination of Eq. (12) ($ZnA_2\cdot S$ was taken as A) and Eq. (13) leads to Eq. (14):

$$\log \frac{\gamma_{ZnA_2}\gamma_S}{K_S} = C' + D(\delta_{ZnA_2\cdot S} - \delta_B)^2 \qquad (14)$$

where C' is a constant. The values of γ_{ZnA_2} may be calculated as above. Alcock and his co-workers[13] reported that TBP forms an ideal solution up to about a 1% TBP solution with paraffinic solvents and up to 10% with benzene and others. In calculating the activity coefficient of TBP, the experimental data on a 1% solution of TBP were used for *n*-hexane, *n*-heptane, and cyclohexane,[13] while those on a 5% solution obtained by Siekierski[14] were used for most of the solvents. The relation of Eq. (14) is shown in Fig. 6. The solubility parameter of the adduct was obtained as 9.4. The molar volume of the adduct may be got from the curvature of Fig. 6, but it is hard to get the accurate value because of an insufficient number of the experimental data on the solvents with large solubility parameters. In the present study the molar volume of the adducts was assumed to be equal to the algebraic sum of the molar volume of the chelate and that of TBP. This seems a reasonable assumption because Eq. (4) is the addition reaction, and, practically, the effect of the small difference in molar volume on the activity coefficient is small except when value of $|\delta_A-\delta_B|$ is large. Accordingly, the activity coefficient of the adduct can also be calculated from the two values $\delta_{ZnA_2\cdot S}$ 9.4 and $V_{ZnA_2\cdot S}$ 593 m*l*.

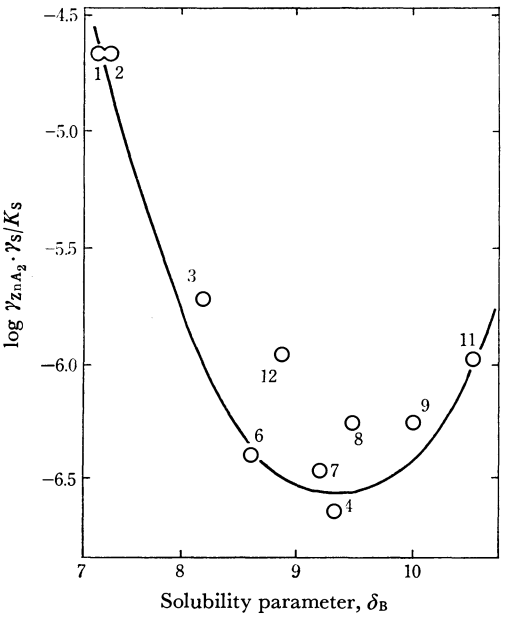

Fig. 6. Relation between the activity coefficient and the solubility parameter of solvent.

Since the activity coefficients of all the species were evaluated, the relation of Eq. (10) is illustrated in Fig. 7. The plots of log K_S against the logarithm of the activity coefficients are close to a straight line with a slope of −1 for most of the solvents, as was to be expected. The deviations from the

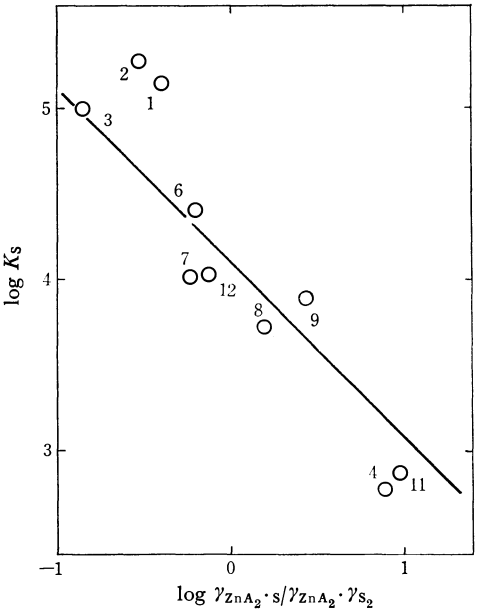

Fig. 7. Relation between the adduct formation constant and the activity coefficients in the organic phase.

line for *n*-hexane and *n*-heptane with large $|\delta_A-\delta_B|$ values appears to be due to the uncertainty concerning the molar volume of adduct. If the molecules of the chelate and TBP form a more compact adduct than the postulated one, the deviations are small. The value of $\log K_S^\circ$ was obtained as 4.05. Although the activity coefficients have been estimated on the base of a simplifing assumption, it is significant that the adduct formation constant in terms of activity is constant for each solvent. If the K_S value is measured for one solvent, that for the other can be estimated by considering the activity coefficient of the species.

Eq. (7) can be related to Eq. (10) as follows:

$$D_{M,S} = K_S^\circ D_M [S]_{org}^m \frac{\gamma_{ZnA_2}\gamma_S^m}{\gamma_{ZnA_2 \cdot mS}} \quad (16)$$

The distribution ratio in the presence of a neutral ligand can be pre-estimated from that in the absence of one according to Eq. (16). In this manner the role of the solvent in the synergistic extraction system can be explained systematically by a combination of the regularity as in the distribution of the metal chelate and that in the adduct formation.

The authors are grateful to Dr. T. Wakabayashi for his interest during this study. Thanks are also due to Miss H. Asano for her assistance in the experimental work.

BULLETIN OF THE CHEMICAL SOCIETY OF JAPAN VOL. 42 2543—2546 (1969)

Palladium(II) Complexes of *N*-Substituted Salicylideneimines

Shoichiro YAMADA and Kuniko YAMANOUCHI

Institute of Chemistry, College of General Education, Osaka University, Toyonaka, Osaka

(Received February 21, 1969)

Many new palladium(II) complexes (abbreviated as M(X-SAL·R)$_2$) of Schiff bases obtained from substituted salicylaldehydes and alkyl and aryl amines were prepared as yellow-orange or red crystals, where X denotes H, 3-CH_3O and 5,6-benzo. For R=*n*-alkyl and aryl groups, the complexes Pd(X-SAL·R)$_2$ in non-donor solvents consist of square-planar molecules. The complexes of the type Pd(X-SAL·*t*-C_4H_9)$_2$ show electronic spectra which are different from those of the complexes of the type Pd(X-SAL·*n*-alkyl)$_2$, but all these complexes are diamagnetic. This difference between the two kinds of complexes is discussed in connection with the bonding in, and the structure of, the complexes on the basis of the spectral and magnetic properties. The results for the palladium(II) complexes are compared with those for the corresponding nickel(II) complexes.

Many detailed studies have been reported on nickel(II) complexes (Fig. 1) with Schiff bases

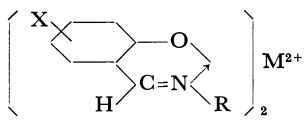

Fig. 1. M(X-SAL·R)$_2$

obtained from substituted salicylaldehydes.[1-3] Having a d^8 configuration, the palladium(II) ion forms complexes which are similar to the nickel(II) complexes, but there are also many examples of palladium(II) complexes which are remarkably different from the corresponding nickel(II) complexes. On the palladium(II) complexes with the Schiff bases, however, only a few papers have so far been published,[4,5] and systematic studies in particular seem to be lacking.

The present paper deals with preparation of the palladium(II) complexes with the Schiff bases and examination of their stereochemistry for comparison with the results about the corresponding nickel(II) complexes. It is also one of the purposes of the present work to examine the effect of steric hindrance of various degrees on the stereochemistry of these palladium(II) complexes.

1) R. H. Holm, G. W. Everett, Jr., and A. Chakravorty, "Progress in Inorganic Chemistry," Vol. VII, ed. by F. A. Cotton, Interscience Publishers, New York, N. Y. (1966), p. 83.

2) S. Yamada, *Coordin. Chem. Revs.*, **1**, 415 (1966).

3) L. Sacconi, "Essays in Coordination Chemistry," ed. by W. Schneider, G. Anderegg and R. Gut, Birkhäuser Verlag, Basel (1964), p. 148.

4) L. Sacconi, M. Ciampolini, F. Maggio and G. Del Re, *J. Am. Chem. Soc.*, **82**, 815 (1960).

5) S. Yamada, H. Nishikawa and K. Yamasaki, This Bulletin, **36**, 483 (1963).

Experimental

Materials. The palladium(II) complexes of the type $Pd(X\text{-}SAL\cdot R)_2$, which are shown in Tables 1

TABLE 1. ANALYTICAL DATA OF THE COMPLEXES OF THE TYPE $Pd(X\text{-}SAL\cdot alkyl)_2$

X	Alkyl	Calcd, %			Found, %		
		C	H	N	C	H	N
H	*i*-C_3H_7	55.72	5.57	6.50	55.84	5.65	6.52
	t-C_4H_9	57.55	6.10	6.10	57.36	6.10	6.28
	i-C_4H_9				57.26	6.09	6.44
5,6-Benzo	*n*-C_3H_7	63.31	5.31	5.27	63.46	5.17	5.15
	i-C_3H_7				63.50	5.19	5.43
	n-C_4H_9	64.42	5.77	5.01	63.98	5.77	5.13
	t-C_4H_9				63.59	5.81	4.80
3-CH_3O	*n*-C_3H_7	53.80	5.75	5.70	54.09	5.78	5.61
	i-C_3H_7				53.26	5.62	5.59
	n-C_4H_9	55.52	6.21	5.40	55.04	6.19	5.39
	t-C_4H_9				55.55	6.35	5.19

and 2, were prepared according to methods similar to those previously reported.[5] A typical example of preparation is as follows. To a solution of potassium tetrachloropalladate(II) (0.01 mol) and potassium hydroxide (0.02 mol) in a small amount of water were added a solution of salicylaldehyde or substituted salicylaldehyde (0.02 mol) in ethanol and an appropriate amine. The resulting solution was stirred at about 50°C for about one hour. The precipitate was collected by filtration and recrystallized from ethanol, chloroform or benzene.

The complexes $Pd(H\text{-}SAL\cdot R)_2$ with R=CH_3, C_2H_5, *n*-C_3H_7 and *n*-C_4H_9, which were first reported by Sacconi and others,[4] were prepared in the present work as previously reported.[5]

TABLE 2. ANALYTICAL DATA OF THE COMPLEXES OF THE TYPE $Pd(H\text{-}SAL\cdot aryl)_2$

Aryl	Calcd, %			Found, %		
	C	H	N	C	H	N
Ph*	62.81	3.62	5.64	62.08	3.96	5.48
o-CH_3Ph	63.79	4.56	5.32	63.37	4.61	5.04
m-CH_3Ph				63.57	4.52	5.32
p-CH_3Ph				63.73	4.65	5.32
o,o'-$(CH_3)_2Ph$	64.90	5.05	5.05	64.56	5.06	5.05
o-ClPh	55.00	3.20	4.93	54.89	3.42	4.63
m-ClPh				54.61	3.32	5.07
p-ClPh				55.08	3.26	4.79

* The notation Ph denotes a phenyl group.

All these palladium(II) complexes are yellow or yellowish orange, with the exception of the *N*-*t*-butyl-substituted complexes, which are brownish red. They are insoluble in water but soluble in methanol, ethanol, chloroform, benzene and acetone.

Analytical data of the new compounds are given in Tables 1 and 2.

Measurements. The electronic absorption spectra of the compounds in solution were determined with a Shimadzu MPL-50 and a Shimadzu QR-50 spectrophotometer.

Diamagnetism of the complexes was detected by the Gouy method.

Results and Discussion

Many new compounds, which are listed in Tables 1 and 2, have been prepared in the present work. Sacconi and others[4] formerly prepared the complexes of the type $Pd(H\text{-}SAL\cdot R)_2$ with R=CH_3, C_2H_5, *n*-C_3H_7 and *n*-C_4H_9, and concluded them to be *trans*-planar. Moreover, it is well known that the palladium(II), in general, takes a planar, four-coordinated configuration. It seems, therefore, to be most likely that the complexes of the type $Pd(X\text{-}SAL\cdot n\text{-}alkyl)_2$ prepared in the present work may also be planar. Electronic spectra of these complexes, as shown in Figs. 2 and 3, are quite

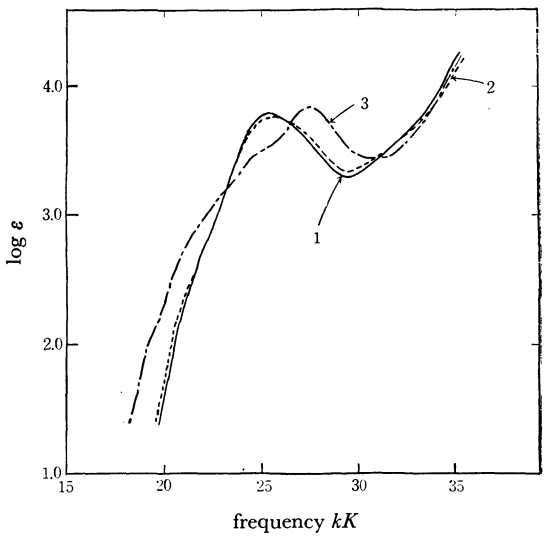

Fig. 2. Electronic absorption spectra of $Pd(H\text{-}SAL\cdot R)_2$ in chloroform; 1, R=*n*-C_4H_9 (——); 2, R=*i*-C_3H_7 (----); 3, R=*t*-C_4H_9 (— — —).

similar to each other, showing that their configuration is all alike. The absorption peak at about 25.5 kK may be due to an electronic transition within the ligand bound with the palladium(II) ion. The ligand field bands mainly due to the palladium(II) ion are considered to be hidden by the strong absorption bands of other origins. In a similar way, it is considered that the planar configuration is most likely for the complexes of the type $Pd(H\text{-}SAL\cdot R)_2$ with R=phenyl and substituted phenyl groups.

It is to be noted that Beer's law holds for all these palladium(II) complexes, so that no association of the square-planar complexes occurs in solution, in contrast to the behavior of the correspond-

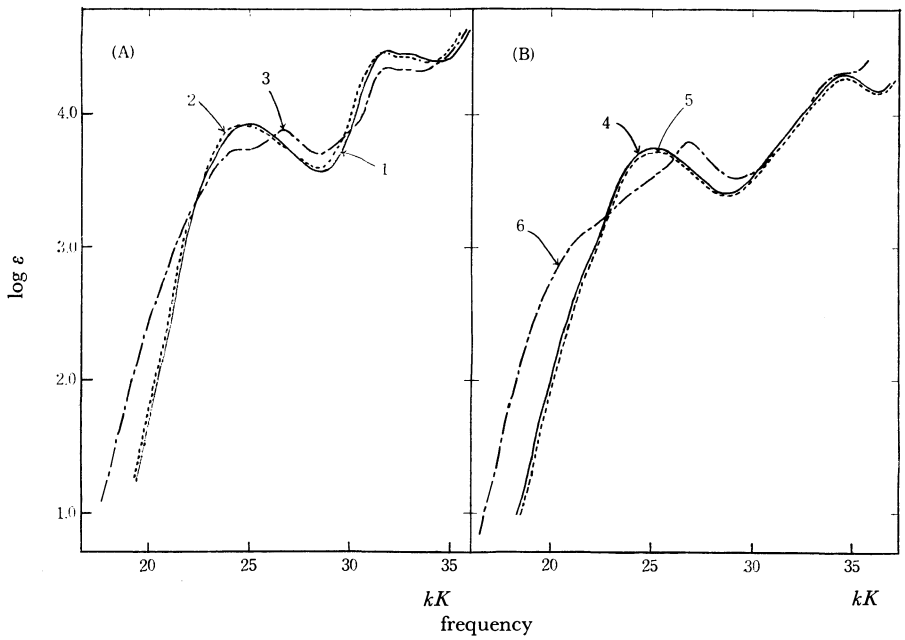

Fig. 3. Electronic absorption spectra in chloroform of (A) Pd(5,6-benzo-SAL·R)$_2$; 1, R=*n*-C_4H_9; 2, R=*i*-C_3H_7; 3, R=*t*-C_4H_9 and (B) Pd(3-CH_3O-SAL·R)$_2$; 4, R=*n*-C_4H_9; 5, R=*i*-C_3H_7; 6, R=*t*-C_4H_9.

ing nickel(II) complexes. This finding is in agreement with the current view that the tendency of palladium(II) to take coordination number larger than four is extremely low and, in fact, much lower than that of nickel(II).

With Pd(H-SAL·2,6-$(CH_3)_2$Ph)$_2$, the steric condition is not quite favorable for the square-planar configuration. However, since the corresponding nickel(II) and copper(II) complex have been found to be square-planar,[6] the square-planar configuration may also be most likely for Pd(H-SAL·2,6-$(CH_3)_2$Ph)$_2$ in spite of the possible steric hindrance. This is borne out by the electronic spectrum of this palladium(II) complex, which is quite similar to those of Pd(H-SAL·CH_3Ph)$_2$ and related complexes, as shown in Fig. 4.

For Pd(X-SAL·*i*-C_3H_7)$_2$, the steric condition is not quite favorable for the square-planar configuration. However, these complexes are diamagnetic, and their electronic spectra are similar to those of Pd(X-SAL·*n*-alkyl)$_2$, as may be seen in Figs. 2 and 3. It is, therefore, presumed that all these complexes are square-planar. It is to be noted that this is not the case with the corresponding nickel(II) complexes. The nickel(II) complexes of the type Ni(X-SAL·*i*-C_3H_7)$_2$ are square-planar or distorted-tetrahedral, depending upon the nature of X.[3,7]

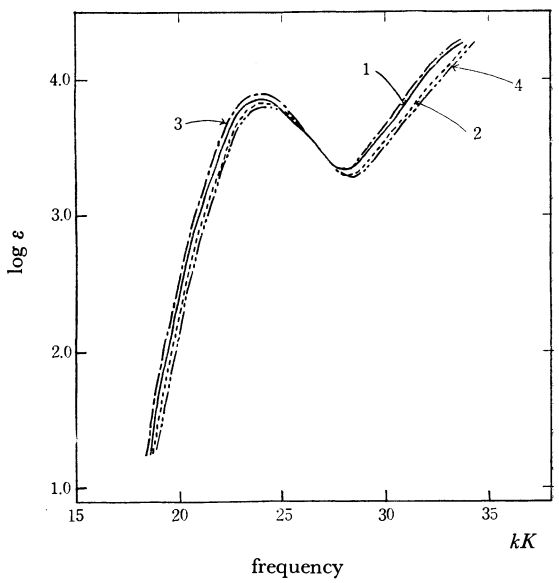

Fig. 4. Electronic absorption spectra of Pd(H-SAL·R)$_2$ in chloroform; 1, R=Ph (——); 2,R=*o*-CH_3Ph (– – –); 3, R=*p*-CH_3Ph (— — —); 4, R=*o*, *o*′-$(CH_3)_2$Ph (— · — · —).

For Pd(X-SAL·*t*-C_4H_9)$_2$, the steric condition is considered to be highly unfavorable for the planar configuration. Their electronic spectra are apparently different from those of the complexes of the type Pd(X-SAL·*n*-alkyl)$_2$, as clearly seen in Figs. 2 and 3. This difference in the spectrum between the complexes of the above two types may

6) S. Yamada, H. Nishikawa and E. Yoshida, This Bulletin, **39**, 994 (1966).

7) S. Yamada and H. Nishikawa, *ibid.*, **36**, 755 (1963).

be ascribed to either of the following two possibilities.

(1) The configuration of Pd(X-SAL·t-C_4H_9)$_2$ is distorted from the planar one.

(2) In Pd(X-SAL·t-C_4H_9)$_2$, the coordination configuration of the palladium(II) ion, namely [Pd(N)$_2$-(O)$_2$], is planar, but the remarkable steric hindrance in this case is exerted to the ligands, giving rise to considerable perturbation in the electronic state of the ligand.

Since the present work reveals that all these palladium(II) complexes are diamagnetic, the latter possibility seems to be higher than the former. The diamagnetism fo Pd(X-SAL·t-C_4H_9)$_2$, however, might also be explained, if we assume that the deviation from the planar coordination of [Pd(N)$_2$-(O)$_2$] is so small that the energy separation between the highest $d_{x^2-y^2}$ and the next highest d orbital of the palladium(II) ion is still large enough to allow the spin-paired state to remain the lowest. Definite conclusion on the precise configuration of the complexes Pd(X-SAL·t-C_4H_9)$_2$ must await X-ray examination.

The conclusion on the configurations of Pd(X-SAL·t-C_4H_9)$_2$ and Pd(X-SAL·i-C_3H_7)$_2$ is found to be different in many respects from that obtained previously about the corresponding nickel(II) complexes. This difference may be considered to arise from the following two points.

(1) The ionic radius of the palladium(II) ion is known to be considerably larger than that of the nickel(II) ion.

(2) The stability of the planar configuration *vis-a-vis* the tetrahedral one is higher for the palladium(II) than for the nickel(II) ion.

The spectra of all these Schiff base palladium(II) complexes in a donor-solvent like pyridine are nearly the same as those of the same complexes in non-donor solvents. It is, therefore, most likely that their configuration in non-donor solvents may be retained in pyridine, namely that the coordination of the pyridine molecule with the palladium(II) ion does not take place. It was previously shown that this was not the case with the nickel(II) complexes.[8] This difference between the nickel(II) and the palladium(II) complexes seems to show that the palladium(II) ion has less tendency to form sexa-coordination than the nickel(II) ion, as was also observed with related ligands as well as many others.[9]

In these respects, the platinum(II) ion is similar to the palladium(II) ion, and the difference between the platinum(II) and the nickel(II) ion is known to be even more marked than that between the palladium(II) and the nickel(II) ion. Therefore, with the platinum(II) complexes Pt(H-SAL·R)$_2$, a similar result to that with the corresponding palladium(II) complexes may be expected. This is borne out by the electronic spectra of these platinum(II) complexes. Thus the spectrum of Pt(H-SAL·n-alkyl)$_2$ is similar to that of Pt(H-SAL·i-C_3H_7)$_2$ but different from that of Pt(H-SAL·t-C_4H_9)$_2$.[5] The details of this phase of the study will be published later.

We wish to thank Mrs. Kayo Fujita for her experimental assistance at the earlier stage of the present work. Financial assistance of the Education Ministry of Japan is also gratefully acknowledged.

8) S. Yamada, E. Ohno, Y. Kuge, A. Takeuchi, K. Yamanouchi and K. Iwasaki, *Coordin. Chem. Revs.*, **3**, 247 (1968).

9) E. Yoshida and S. Yamada, This Bulletin, **38**, 2179 (1965).

BULLETIN OF THE CHEMICAL SOCIETY OF JAPAN VOL. 42 2547—2549 (1969)

The Viscosities of Aqueous Solutions Containing Metal Complexes. II. *trans*-1,2-Cyclohexanediaminetetraacetato Complexes*1

Motoo YASUDA

Department of General Education, Nagoya University, Chikusa-ku, Nagoya

(Received March 5, 1969)

The viscosities of aqueous solutions containing metal chelate formed with *trans*-1,2-cyclohexanediaminetetraacetic acid (H_4cydta) were measured with a Cannon-Fenske capillary viscometer. Measurements were made in a Shibata viscosity bath maintained at 25±0.01°C. The Jones-Dole viscosity *B*-coefficient of the cydta^{4-} chelates is larger than that of the corresponding ethylenediaminetetraacetato (edta^{4-}) chelates, as may be expected. The *B*-value of the Co(III) chelate [Co cydta]$^-$ is much smaller than that of any of the divalent metal cydta^{4-} chelates studied. This fact, the same as in the case of the edta^{4-} chelates, may indicate that the Co(III) chelate has a marked stable hexa-coordinated structure, while divalent metal chelates do not have such a stable hexa-coordinated structure as the Co(III) chelate.

In part I of this series,[1] the viscosities of aqueous solutions containing several cobalt complexes were measured with a capillary viscometer. The results showed that there was a distinct difference between the *B*-coefficients of Co(II) and Co(III) chelates formed with ethylenediaminetetraacetic acid (H_4edta); this suggested that there might be a marked difference between the structures of [Co edta]$^{2-}$ and [Co edta]$^-$ ions. In order to confirm this, a viscosity study was made of aqueous solutions of metal chelates formed with 1,2-cyclohexanediaminetetraacetic acid (H_4cydta), whose structure is very similar to that of H_4edta.

Experimental

Measurements. The viscosity *B*-coefficients of Co(III) and eleven divalent metal chelates were determined with a Cannon-Fenske capillary viscometer with an efflux time of *ca.* 240 sec for distilled water. The viscosities and densities of the solutions were measured in a Shibata viscosity bath maintained at 25±0.01°C.

Complexes. Potassium (cyclohexanediaminetetraacetato)cobaltate(III) trihydrate was obtained as red-violet crystals following the method in the literature.[2] However, divalent metal chelates were not isolated as crystals. Instead, solutions of these chelate were made up using metal nitrate (or chloride) and K_4cydta stock solutions. The concentrations of the metal nitrate (or chloride) solutions were determined by chelatometric titrations. The concentration of the K_4cydta stock solution, made from Dotite H_4cydta and potassium hydroxide, was also determined by chelatometric titration.

Calculations. For each of the chelates studied, the variations in the viscosity with the solute concentration was expressed by the Jones-Dole equation:[3]

$$\frac{\eta}{\eta_0} = 1 + A\sqrt{C} + BC \qquad (1)$$

where η and η_0 are the viscosities of the solution and of water respectively; and where *A* and *B* are constants characteristic of the solute. Only the *B*-coefficient will be discussed in this paper, for the *B*-coefficient seems to be a manifestation of the hydrated ionic volume; this is supported by the linearity of the *BC* term in the concentration. On the other hand, the *A*-coefficient, which is thought to represent the amount of the interionic electrostatic forces, will not be discussed here, for the *A*-values are very small compared with the *B*-values and are almost independent of the metal included in the chelate.

Results and Discussion

The viscosity and density data for K_2[Cu cydta] (+2KNO_3) and K[Co cydta] are listed in Tables 1 and 2. Table 3 contains the *B*-values of cydta^{4-} complex anions at 25°C, together with the stability constants for these complex ions reported by Anderegg.[4]

The solubility of the lead chelate, which was the least soluble in water of the metal chelates studied, was only 0.01 mol/*l*; thus, the *B*-value of

*1 Presented at the 10th International Conference on Coordination Chemistry, Tokyo and Nikko, Sept., 1967.

1) M. Yasuda, This Bulletin, **41**, 139 (1968).

2) F. P. Dwyer and F. L. Garvan *J. Am. Chem. Soc.*, **83**, 2610 (1961).

3) G. Jones and M. Dole, *ibid.*, **51**, 2950 (1929).

4) G. Anderegg, *Helv. Chim. Acta*, **46**, 1833 (1963).

Table 1. Viscosity and density data for K_2[Cu cydta] (+2KNO_3)*

C	d	η/η_0
0.0600	1.01855	1.05201
0.0300	1.00816	1.02639
0.0200	1.00474	1.01846
0.0150	1.00278	1.01392

* The B-value of the complex ion is obtained by subtracting a relatively small correction for the K^+ and NO_3^- ions. The B-values given by Gurney were used for these ions; $B_{K^+} = -0.007$, $B_{NO_3^-} = -0.046$. R.W. Gurney, "Ionic Processes in Solution," McGraw-Hill Book Co., New York (1953).

Table 2. Viscosity and density data for K[Co cydta]

C	d	η/η_0
0.04401	1.00802	1.02405
0.03081	1.00474	1.01639
0.02427	1.00323	1.01287
0.01592	1.00109	1.00814

Table 3. B-Coefficients and stability constants (k) of *trans*-1,2-cyclohexanediaminetetraacetato chelates

Metal	B	log k[4]
Cu^{2+}	0.92	21.95
Zn^{2+}	0.98	19.32
Ni^{2+}	1.01	19.4*
Co^{2+}	1.03	19.57
Cd^{2+}	1.13	19.88
Mn^{2+}	1.15	17.43
Mg^{2+}	1.20	10.97
Ca^{2+}	1.21	13.15
Sr^{2+}	1.24	10.54
Ba^{2+}	1.27	8.64
Pb^{2+}	~1.0	20.33
Co^{3+}	0.54	——

* J. H. Holloway and C. N. Reilly, *Anal. Chem.*, **32**, 249 (1960).

[Pb cydta]$^{2-}$ is the least accurate.

Now it may be very interesting to compare the B-values of the cydta^{4-} chelates with those of the edta^{4-} chelates, reported by Charles[5] and by the present author.[1] Their relation is shown in Fig. 1; the ordinates are the B-values of the cydta^{4-} chelates, and the abscissas, those of the edta^{4-} chelates. The rather good agreement of all the points except those for Mg^{2+} and Mn^{2+} chelates with the straight line may indicate that Mcydta^{n-} and Medta^{n-} chelates have similar structures.

5) R. G. Charles, *J. Am. Chem. Soc.*, **78**, 3946 (1956).

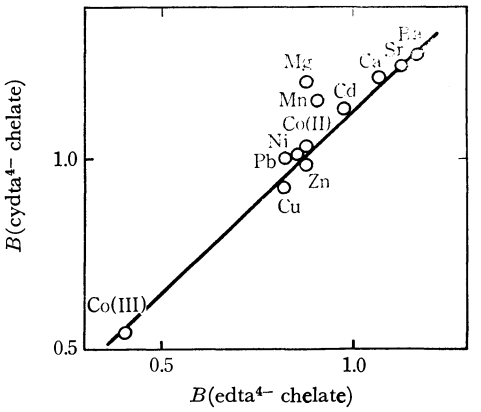

Fig. 1. Relation between the B-coefficients of cydta^{4-} and edta^{4-} Chelates

Next, Einstein's equation,[6] derived for the viscosity of the solution, must be taken into account. According to Einstein, the viscosity of a solution which contains, in suspension, rigid spherical particles which are large compared with the size of the solvent molecules is given by the following equation;

$$\eta = \eta_0(1 + 2.5\,\phi) \tag{2}$$

where ϕ is the volume-fraction occupied by the particles.

If it is assumed that his theory can be applied to large molecules in solution,*2 Eq. (3) is obtained from Eqs. (1) and (2);

$$A\sqrt{C} + BC = 2.5\,\phi \tag{3}$$

The volume fraction, ϕ, may then be expressed by:

$$\phi = CV \tag{4}$$

where V is the molar volume of the solute, including an attached solvent (in l/mol). Further the $A\sqrt{C}$ term is very small in comparison with BC, and so it can safely be neglected. Accordingly, we obtain:*3

$$B = 2.5\,V \tag{5}$$

Eq. (5) leads to:

$$v_h = \frac{4000\,B}{6.02}\ \text{Å}^3 \tag{6}$$

where v_h is the volume of the hydrated solute. Thus, the average radius can be calculated from the B-coefficient. The values obtained for the Co(II) and Co(III) chelates of edta^{4-} and cydta^{4-} are listed in Table 4.

6) A. Einstein, *Ann. Phys.*, **19**, 289 (1906); **34**, 591 (1911).

*2 This was confirmed by Fuoss and Tuan and by Stokes and Mills for $C(CH_2OH)_4$, Bu_4N^+, Ph_4B^-, *etc.*

*3 This relation was derived by Stokes and Mills; R. H. Stokes and R. Mills, "Viscosity of Electrolytes and Related Properties," Pergamon Press, Oxford (1965).

Table 4. *B*-Coefficients and average radii (r) of the Co chelates

	$[Co\ edta]^{2-}$	$[Co\ edta]^{-}$	$[Co\ cydta]^{2-}$	$[Co\ cydta]^{-}$
B	0.85	0.41	1.03	0.54
r(Å)	5.1	4.0	5.5	4.4

As may be seen from Table 4, the radius of the Co(III) chelate is about 1 Å smaller than that of the corresponding Co(II) chelate. Co-N interatomic distances have been measured for several Co(II) and Co(III) complexes derived from ligands with nitrogen donors. Since there are few data available on the Co(II)-N interatomic distance, it may be improper to draw a conclusion concerning the difference between the Co(II)- and Co(III)-N distances. However, it may be safely assumed that there is no marked difference between them. Further, since the $cydta^{4-}$ chelates have very large stability constants, it may be assumed that there is no apprreciable change in the viscosity of the solution due to the dissociation of the chelate. Accordingly, the large difference between *B*-coefficients of Co(III) and divalent metal chelates may imply that the structure of the Co(III) chelate is different from that of divalent metal chelates, as with the $edta^{4-}$ chelates. Thus, it may be assumed that the Co(III) chelate has a markedly stable hexa-coordinated structure, but that the divalent metal $cydta^{4-}$ chelates, not having so stable a hexa-coordinated structure as the Co(III) chelate, are present as a penta-coordinated chelate or as an equilibrium mixture of hexa- and penta-coordinated structures.

BULLETIN OF THE CHEMICAL SOCIETY OF JAPAN VOL. 42 2549—2551 (1969)

Dioxouraniun(VI) Complexes of Schiff Bases Obtained from Substituted Salicylaldehydes and Alkyl Amines[1)]

Shoichiro YAMADA and Akira TAKEUCHI

Institute of Chemistry, College of General Education, Osaka University, Toyonaka, Osaka

(Received March 5, 1969)

Dioxouranium(VI) complexes have been examined with Schiff bases obtained from substituted salicylaldehydes and alkyl amines. Many new complexes of the type abbreviated as $UO_2(NO_3)_2$(X-SAL·R·H)$_2$ have been prepared as orange-red crystals. The notation X denotes H, 5,6-benzo and 3-CH_3O, and R represents alkyl groups. Infrared spectra indicate that there is no uncoordinated nitrate ion, and that the nitrate ions are coordinated with the uranium(VI) ion as unidentate ligands in these complexes. It is to be noted that the molecules, and not anions, of the Schiff bases are coordinated with the metal ions, as in many other dioxouranium(VI) complexes.

A number of studies have been carried out on the Schiff base complexes of various metal ions.[2-4] These studies, however, were mainly concerned with the 3*d* transition elements, and comparatively little has been reported on the corresponding complexes of the heavier transition elements.

In the present work, dioxouranium(VI) ion has been taken up, and its complexes (Fig. 1) with

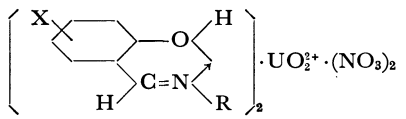

Fig. 1. $UO_2(NO_3)_2$(X-SAL·R·H)$_2$.

Schiff bases*1 obtained from substituted salicylaldehydes have been examined. The dioxouranium(VI) complexes are interesting, particularly in that the coordination number exceeding six may normally be expected for the uranium(VI) ion. Only a few papers[2,3,5)] have so far been published about dioxouranium(VI) complexes with the Schiff bases, and systematic studies were thought to be desirable.

1) Presented, in part, at the 18th Symposium on Coordination Chemistry, September, 1968, Kyoto.

2) P. Pfeiffer, E. Breith, E. Lübbe and T. Tsumaki, *Ann. Chem.*, **503**, 84 (1933).

3) R. H. Holm, G. W. Everett, Jr., and A. Chakravorty, "Progress in Inroganic Chemistry," Vol. VII, ed. by F. A. Cotton, Interscience Publishers, New York, N. Y. (1966), p. 83.

4) S. Yamada, *Coordin. Chem. Revs.*, **1**, 415 (1966).

*1 These Schiff bases are abbreviated as X-SAL·R·H in the present paper.

5) I. A. Savich, A. K. Pikaev, V. G. Lebedov and V. I. Spitsyn, *Zh. Neorg. Khim.*, **1**, 2736 (1956).

TABLE 1. ELEMENTAL ANALYSES OF THE DIOXOURANIUM (VI) COMPLEXES OF THE TYPE $UO_2(NO_3)_2(X\text{-}SAL\cdot R\cdot H)_2$

X	R	Calcd, %			Found, %			Method of prepara.
		C	H	N	C	H	N	
H	CH_3	28.92	2.73	8.43	28.67	2.54	8.11	(a)
	C_2H_5	31.22	3.20	8.09	31.93	3.18	7.64	(a)
	n-C_3H_7	33.34	3.63	7.76	33.10	3.39	7.84	(a)
	i-C_3H_7				32.80	3.65	7.51	(a), (b)
	n-C_4H_9	35.30	4.04	7.48	35.00	3.88	7·82	(b)
	t-C_4H_9				34.51	3.87	7.13	(a), (b)
5,6-Benzo	CH_3	37.70	2.90	7.33	38.01	2.62	6.68	(b)
	C_2H_5	39.40	3.31	7.07	39.49	2.98	7.43	(a), (b)
	n-C_3H_7	40.98	3.69	6.83	41.20	3.61	7.13	(b)
	i-C_3H_7				40.73	3.58	6.45	(b)
	n-C_4H_9	42.44	4.04	6.60	42.28	3.92	6.63	(b)
	t-C_4H_9				42.05	3.80	6.61	(a)
3-CH_3O	CH_3	29.84	3.06	7.73	29.91	2.97	7.47	(b)

Experimental

Materials. Dinitratobis(*N*-alkyl-salicylideneimine)-, dinitratobis(*N*-alkyl-5,6-benzosalicylideneimine)- and dinitratobis(*N*-alkyl-3-methoxysalicylideneimine)-dioxouranium(VI) complexes of the general formula $UO_2(NO_3)_2(X\text{-}SAL\cdot R\cdot H)_2$ were prepared according to the methods (a) and/or (b) given below. The notation X denotes H, 5,6-benzo and 3-CH_3O, and R represents alkyl groups. The elemental analyses of these complexes are given in Table 1.

(a) To a luke-warm solution of dioxouranium(VI) nitrate hexahydrate (0.01 mol) in ethanol (200 m*l*) was added a solution of a substituted salicylaldehyde (0.02 mol) in ethanol (100 m*l*). The solution immediately changed colour from orange-yellow to red. To this solution was added with stirring drop by drop a solution of an appropriate amine (0.02 mol) in ethanol (50 m*l*). The resulting red solution was allowed to stand for a few hours at about 30°C to 40°C. The orange-red crystals, which separated out, were collected by filtration and washed with ethanol.

(b) To a solution of dioxouranium(VI) nitrate hexahydrate (0.01 mol) in ether-ethanol (1 : 1, 300 m*l*) was added a solution of an appropriate Schiff base (0.02 mol) in ethanol (150 m*l*) with stirring at room temperature. The resulting solution was allowed to stand at about 5°C for a few hours. The orange-red crystals, which separated out, were collected by filtration, and washed with ethanol.

These dioxouranium(VI) complexes, the elemental analyses of which are given in Table 1, are slightly soluble in methanol, ethanol, chloroform and benzene, and a little more soluble in pyridine. Recrystallization from methanol, ethanol or chloroform was sometimes successful, but some of these complexes were so unstable against heat that they often underwent thermal decomposition during the process of recrystallization.

Measurements. The electronic absorption spectra of these complexes in solution were determined with a Shimadzu QR-50 spectrophotometer and a Shimadzu MPS-50 spectrophotometer. The infrared spectra in the region from 700 to 4000 cm^{-1} were measured with a Hitachi-EPI-2 infrared spectrophotometer using the Nujol mull technique.

The diamagnetism of the dioxouranium(VI) complexes in the solid state was detected by the Gouy method at room temperature.

Results and Discussion

Many new complexes of the type $UO_2(NO_3)_2(X\text{-}SAL\cdot R\cdot H)_2$, as shown in Table 1, have been prepared in the present work. They are stable against light and atmosphere in a solid state, and are all diamagnetic.

The infrared spectra of these complexes show no absorption band near about 1380 cm^{-1}, where the free nitrate ion is known to absorb. It is concluded, therefore, that there is no nitrate ion which is not bound with the uranium(VI) ion. Since these complexes show absorption peaks at about 1480 cm^{-1} and 1280 cm^{-1}, which are assigned to the ν_1 (NO stretching) and ν_4 (NO_2 asymmetric stretching) vibration, respectively,[6] it is presumed that in these complexes the nitrate ions are coordinated with the metal ion as unidentate ligands. It is thus found that the uranium(VI) ion takes an eight-coordination. A considerable number of dioxouranium(VI) complexes were previously reported which have nitrate ions coordinated with the uranium(VI) ion.[7] It is also to be noted that in the complexes of the type $UO_2(NO_3)_2(X\text{-}SAL\cdot$

6) E. P. Bertin, R. B. Penland, S. Mizushima, C. Curran and J. V. Quagliano, *J. Am. Chem. Soc.*, **81**, 3818 (1959); J. E. Fleming and H. Lynton, *Chem. Ind. (London)*, **1963**, 1416; C. C. Addison and W. B. Simpson, *J. Chem. Soc.*, **1965**, 598; A. B. Lever, *Inorg. Chem.*, **4**, 1042 (1965).

7) L. Sacconi and G. Giannoni, *J. Chem. Soc.*, **1954**, 2751; F. J. Frere, *J. Am. Chem. Soc.*, **55**, 4362 (1933).

$R\cdot H)_2$ the *neurtal molecules*, and not anions, of the Schiff bases are considered to be coordinated with the metal ion. Such was the case previously reported with dioxouranium(VI) complexes of 8-hydroxyquinoline, β-diketones and so on, in which the ligand *molecules* were considered to be bound with the metal ion.[7]

The electronic spectra of these dioxouranium(VI) complexes in the same solvent are all alike, independent of the nature of R, if comparison is made for the complexes with the same substituent X. The spectra of the complexes in chloroform are quite similar to those of the benzene solutions. In these solvents, Beer's law is found to hold, and it is most likely that these complexes may exist as eight-coordinated molecules, no decomposition or dissociation taking place. Since their solubility in organic solvents was considerably low, the absorption curves for the lower molar extinction coefficient was not very accurate. The absorption curves in Figs. 2 and 3 are regarded as superposition of the absorption due to the dioxouranium(VI) group[8] and that mainly due to the Schiff base molecules bound with the metal ion. The absorption of the former type is much stronger than that of the latter type, which is considered to be hidden by the former. Precise assignment of the absorption bands of these complexes is not possible at the present stage.

The electronic spectra of the methanol and the ethanol solution are different from those of the chloroform and the benzene solution. Some of the typical spectra in different solvents are also shown in Figs. 2 and 3. It is most likely that in methanol or in ethanol there occurs dissociation of the nitrate ions, and subsequent combination of the methanol or the ethanol molecule with the uranium(VI) ion. Incidentally, the combination of the methanol or the ethanol molecule with the uranium(VI) ion has often been observed, and indeed the alcohol adducts have been isolated as crystals, for example, with the dioxouranium(VI) complexes of the Schiff bases.[2,9]

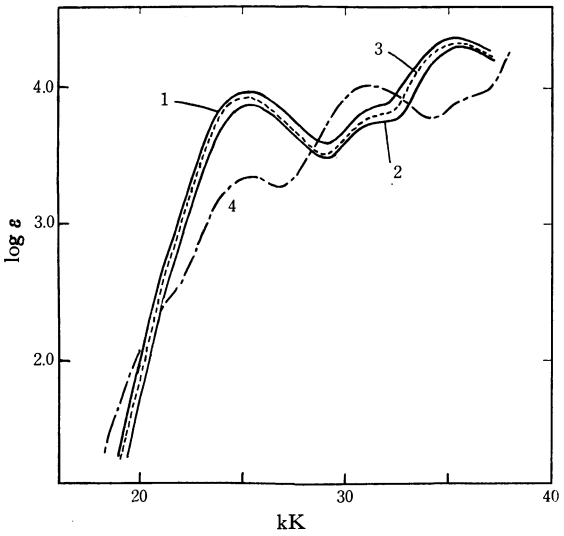

Fig. 2. Electronic absorption spectra of $UO_2(NO_3)_2$-(H-SAL·R·H)$_2$ in solution.
1, R=C_2H_5, in chloroform; 2, R=t-C_4H_9, in chloroform; 3, R=n-C_4H_9, in chloroform; 4, R=n-C_4H_9, in methanol

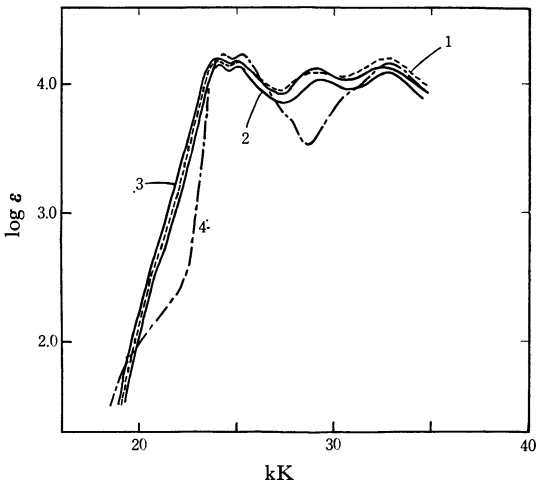

Fig. 3. Electronic absorption spectra of $UO_2(NO_3)$-(5,6-benzo-SAL·R·H)$_2$ in solution.
1, R=C_2H_5, in chloroform; 2, R=t-C_4H_9, in chloroform; 3, R=n-C_4H_9, in chloroform; 4, R=n-C_4H_9, in methanol

It is to be noted that the complexes of the type $UO_2(NO_3)_2$(X-SAL·t-C_4H_9·H)$_2$ were readily prepared and that their properties resemble those of the corresponding complexes with n-alkyl groups for R, all having an eight-coordinated configuration. This finding seems to be significant, particularly because it is known that the steric effect arising from the t-butyl group often favors the geometry which is different from that of the corresponding complex having an n-alkyl group instead of the t-butyl group.[10–12]

Financial support of the Ministry of Education is gratefully acknowledged.

8) S. P. McGlynn and J. K. Smith, *J. Mol. Spectry.*, **6**, 164 (1961); C. K. Jørgensen, *Acta Chem. Scand.*, **11**, 166 (1957).

9) S. Yamada and A. Takeuchi, unpublished.

10) L. Sacconi "Essays in Coordination Chemistry," ed. by W. Schneider, G. Anderegg and R. Gut, Birkhäuser Verlag, Basel (1964), p. 148.

11) S. Yamada and H. Nishikawa, This Bulletin, **36**, 755 (1963).

12) S. Yamada and K. Yamanouchi, *ibid.*, **42**, 2543 (1969).

BULLETIN OF THE CHEMICAL SOCIETY OF JAPAN VOL. 42 2552—2555 (1969)

The Syntheses and the Structure of Triethanolamine Complexes with Cobalt(II) and Nickel(II)[1)]

Yoshio KUGE*[1] and Shoichiro YAMADA

Institute of Chemistry, College of General Education, Osaka University, Toyonaka-shi, Osaka

(Received March 18, 1969)

Triethanolamine complexes with cobalt(II) and nickel(II) have been synthesized as crystals and examined on the basis of analytical data, electronic absorption spectra, and magnetic moments. A complex, $Ni\{N(CH_2CH_2OH)_3\}(ClO_4)_2$, which is formed with $Ni(ClO_4)_2$, is concluded to have a six-coordinated configuration, similar to that previously reported for the corresponding chloride, bromide, and nitrate complexes. In cobalt(II) complexes, $Co\{N(CH_2CH_2OH)_2(CH_2CH_2O)\}X$, which are formed with CoX_2 ($X=Cl^-$, Br^-, or NCS^-), the cobalt(II) ion is concluded to take a five-coordinated configuration.

A number of papers have been published concerning the behavior of metal complexes with triethanolamine (Formula I) in solution, but little

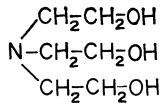

Formula I

is known about these complexes in the solid state.[2–4)]

Examining these complexes in the solid state by magnetic, spectroscopic, and X-ray powder techniques, Hughes and Rutt[5)] recently reached some significant conclusions about their stoichiometry and stereochemistry. Independently, the present authors have also carried out a similar study of this subject. Many of our conclusions agree with the conclusions of the earlier reports, but our study has also yielded some conclusions which are different from those in the previous works, or which seem to be of a more conclusive nature than those of the previous papers. Moreover, among the previous workers there has been some disagreement event about the stoichiometry of the solid compounds. The present paper is concerned with the syntheses and the structures of the triethanolamine complexes with cobalt(II) and nickel(II), but emphasis will be placed upon the new and more significant results and on those of our conclusions which are different from those of the previous papers.

Experimental

Materials. Since the composition of the solid complexes reported in the present paper markedly depends upon the precise conditions of preparation, it seems wise to give here a detailed account of the preparation.

Cobalt(II) complexes of triethanolamine were prepared as purple crystals in the following manner. Into a solution of $CoX_2 \cdot 6H_2O$ ($X=Cl^-$, Br^-, or NCS^-) (0.0125 mol) in 95% ethanol (100 m*l*), triethanolamine (0.025 mol) was stirred at room temperature. Purple crystals immediately began to separate out in the solution. After the solution had been stirred for about 30 min, the purple crystals of $Co\{N(CH_2CH_2OH)_2(CH_2CH_2O)\}X$ were collected by filtration, washed with cold ethanol, and dried overnight in a vacuum desiccator.

The solubility of these complexes in solvents like water, methanol and ethanol is quite low.

Employing a method essentially the same as that described above, Duff and Steer[4)] obtained crystals of the same compositions as ours, but Hughes and Rutt[5)] reported compounds with the $[Co\{N(CH_2CH_2OH)_3\}_2]X_2$ formula.

Nickel(II) complexes of triethanolamine of the $[Ni\{N(CH_2CH_2OH)_3\}_2]X_2$ formula ($X=Cl^-$, Br^-, NO_3^-, or ClO_4^-), were prepared as pale-blue crystals in the present work. The former three ($X=Cl^-$, Br^-, or NO_3^-) had been reported previously,[2,3,5)] but the complex with $X=ClO_4^-$ had not been.

The method in the present work was as follows. Into a solution of $NiX_2.6H_2O$ ($X=Cl^-$, Br^-, NO_3^-, or ClO_4^-) (0.025 mol) in 95% ethanol (100 m*l*), we stirred triethanolamine (0.055 mol) in small portions at about 60°C. After being kept at this temperature

*1 Present address: Osaka Public Health Institute, Mori-machi, Higashi-ku, Osaka.

1) Presented, in part, at the 17th Symposium on Coordination Chemistry, Hiroshima, December, 1967.

2) W. Hieber and E. Levy, *Z. anorg. Chem.*, **219**, 225 (1934).

3) H. Tettamanzi and B. Carli, *Gazzetta Chim. Ital.*, **63**, 566 (1933); *ibid.*, **64**, 315 (1934).

4) J. C. Duff and E. H. Steer, *J. Chem. Soc.*, **1932**, 2861.

5) M. N. Hughes and K. J. Rutt, *J. Chem. Soc., A*, **1968**, 2788.

TABLE 1. ANALYTICAL DATA OF COBALT (II) AND NICKEL (II) COMPLEXES OF TRIETHANOLAMINE

Compound		C(%)	H(%)	N(%)	Metal	halogen	μ*
$[Ni\{N(CH_2CH_2OH)_3\}_2](ClO_4)_2$	Found	25.47	5.23	5.14	10.20	—	3.05
	Calcd	25.92	5.44	5.04	10.55	—	
Co(TEA')Cl**	Found	30.13	6.05	6.09	23.80	14.18	4.35
	Calcd	29.73	5.82	5.77	24.29	14.61	
Co(TEA')Br	Found	25.25	4.77	4.89	20.14	27.74	4.30
	Calcd	25.11	4.57	4.88	20.53	27.84	
Co(TEA')NCS	Found	31.06	5.46	10.45	21.67	—	4.38
	Calcd	31.71	5.32	10.56	22.22	—	

* μ: magnetic moment at room temperature in B. M.
** The notaiton, TEA', represents an anionic ligand, $N(CH_2CH_2OH)_2(CH_2CH_2O)$.

for about 30 min, the solution was allowed to stand overnight at room temperature. A pale-blue precipitate which was formed in the solution was recrystallized from methanol. Pale-blue crystals of $[Ni\{N(CH_2CH_2OH)_3\}_2]X_2$ were thus obtained.

These complexes with $X=Cl^-$, Br^-, or NO_3^- are slightly soluble in methanol, but are almost insoluble in other solvents. The complex with $X=ClO_4^-$ is more soluble in methanol than are the othet three complexes.

With $X=ClO_4^-$, Hughes and Rutt[5] isolated a solid complex with a complicated formula.

Elemental analyses of those cobalt(II) and nickel(II) complexes whose composition remains still in dispute are given in Table 1.

Measurements. The electronic absorption spectra of the complexes in the solid state were determined with a Shimadzu QR-50 and a Shimadzu MPS-50L spectrophotometer. The measurement of the solution spectrum was possible only with $[Ni\{N(CH_2CH_2OH)_3\}_2](ClO_4)_2$. The solubilities of the other complexes in suitable solvents were too low for any accurate determination of the solution spectrum.

The X-ray diffraction diagrams were obtained with a Toshiba ADX-103 X-ray diffractometer.

The magnetic moments of the complexes were determined by the Gouy method at room temperature.

Results and Discussion

It was previously concluded, from the electronic spectra,[5] that the nickel(II) complexes $[Ni\{N(CH_2CH_2OH)_3\}]X_2$ with $X=Cl^-$, Br^-, or NO_3^- consisted of six-coordinated complex-ions.

The new complex, $[Ni\{N(CH_2CH_2OH)_3\}_2](ClO_4)_2$, in the solid state shows a spectrum which is quite similar to those of the corresponding complexes with $X=Cl^-$, Br^-, and NO_3^-, as is shown in Fig. 1. Since all these nickel(II) complexes in the solid state show absorption bands at nearly the same frequencies, they may be considered to take a quite similar configuration. The absorption bands at about 11.0, 16.7, and 26.5 kK may be assigned to $^3T_{2g}\leftarrow{}^3A_{2g}$, $^3T_{1g}(F)\leftarrow{}^3A_{2g}$, and $^3T_{1g}(P)\leftarrow{}^3A_{2g}$ in the scheme of the O_h-field symmetry. As has also been concluded previously,[5] it is most likely that triethanolamine normally acts as a

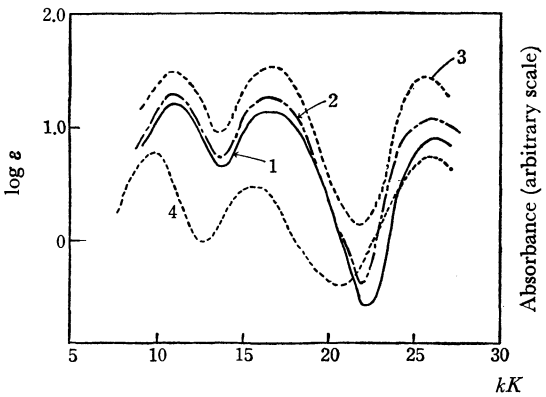

Fig. 1. Electronic absorption spectra of $[Ni\{N(CH_2CH_2OH)_3\}_2]X_2$.
1, $X=Br^-$, reflectance; 2, $X=NO_3^-$, reflectance; 3, $X=ClO_4^-$, reflectance; 4, $X=ClO_4^-$, in methanol. The scale on the right hand side refers to the curves 1, 2, and 3, and the scale on the left hand side the curve 4.

terdentate ligand with one hydroxyl-group remaining uncoordianted, although this ligand is structurally related to β,β',β''-triaminotriethylamine, which can function as a quadridentate ligand.

The absorption spectrum of $[Ni\{N(CH_2CH_2OH)_3\}_2](ClO_4)_2$ in methanol is found to be consistent with the octahedral configuration, but the band maxima in the solution spectrum are shifted toward much lower frequencies, indicating that the configuration of $[Ni\{N(CH_2CH_2OH)_3\}_2](ClO_4)_2$ in methanol may be considerably distorted compared with that in the solid state as well as with the regular octahedron.

The cobalt(II) complexes, $Co\{N(CH_2CH_2OH)_2(CH_2CH_2O)\}X$ ($X=Cl^-$, Br^-, and NCS^-), show quite similar spectra, as is shown in Fig. 2. It is found that these spectra cannot be consistently interpreted in terms of tetrahedral or an octahedral configuration.[6] Instead, they are similar to the

6) S. Buffagni and T. M. Dunn, *Nature*, **188**, 937 (1960); D. L. M. Goodgame, M. Goodgame and F. A. Cotton, *J. Am. Chem. Soc.*, **83**, 1161 (1961).

spectra of some cobalt(II) complexes of high-spin type, for which a five-coordinated structure has been established with certainty.[7]

The magnetic moments of these cobalt(II) complexes, as shown in Table 1, seem to be too low for the six-coordinated cobalt(II) complexes,

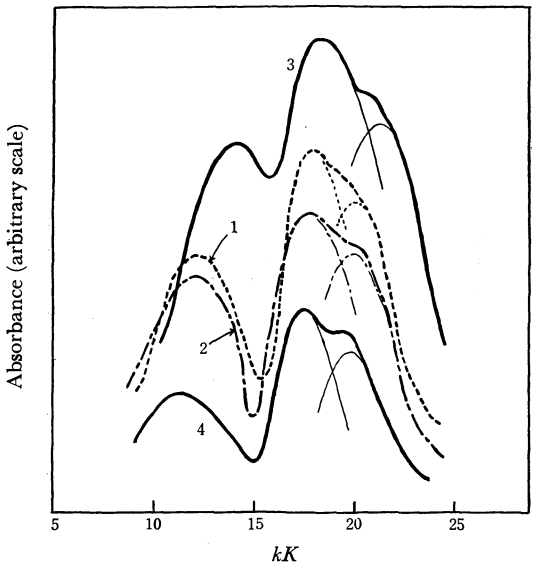

Fig. 2. Electronic absorption spectra of Co{N-$(CH_2CH_2OH)_2(CH_2CH_2O)$}X (compound I) and [Co(Me$_4$daeo)NCS]NCS (compound II) in the solid state. The notation Me$_4$daeo denotes a molecule of O{$CH_2CH_2N(CH_3)_2$}$_2$.
1, compound I, X=Cl$^-$; 2, compound I, X=Br$^-$; 3, compound I, X=NCS$^-$; 4, compound II. The curve 4 is taken from Ref. 7 in the text.

but they lie in a range which may reasonably be expected for the moments of the five-coordinated cobalt(II) complexes with ligands of this kind.[7] It may, therefore, be presumed that in the Co{N-$(CH_2CH_2OH)_2(CH_2CH_2O)$}X complexes (X=Cl$^-$, Br$^-$, or NCS$^-$), the cobalt(II) ion takes a five-coordinated configuration.

The close similarity of the spectra of these cobalt(II) complexes seems to indicate that they have a similar configuration, one in which the cobalt(II) ions take five-coordination. In agreement with this may be the fact that the X-ray powder diagram of Co{$N(CH_2CH_2OH)_2(CH_2CH_2O)$}Cl has been found in the present work to be quite similar to that of the bromide analogue.*2

For the configuration of the five-coordinated cobalt(II) complexes, the (A) configuration in Fig. 3 might at first sight be considered to be possible. This configuration, however, seems to be unlikely, since it is more likely that the ligand, $N(CH_2CH_2OH)_2(CH_2CH_2O)$, is a terdentate rather than a quadridentate ligand, judging from the findings on the corresponding nickel(II) complexes. The presence of one negatively-charged alcoholate group in the ligand suggests that these cobalt(II) complexes are binuclear or polynuclear, with bridging oxygen in the alcoholate group and with the chloride ion also coordinated to the cobalt(II) ion. The binuclear structure (B) in Fig. 3, like that found for

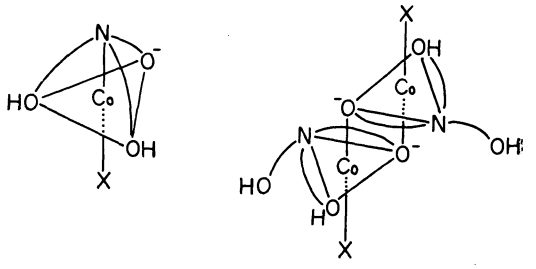

(A) (B)

Fig. 3. Some possible configurations of Co{$N(CH_2CH_2OH)_2(CH_2CH_2O)$}X, in which the cobalt(II) ion takes a five-coordination.

the cobalt(II) complex with *N*-methylsalicylideneiminate,[8] may be considered to be one of the most probable for the present cobalt(II) complexes. Any final conclusion about the precise configuration must, however, await further studies, based, for example, upon the X-ray crystal analysis.

It should be noted that a difference is observed between the cobalt(II) and the nickel(II) ion in the stereochemistry of their triethanolamine complexes. This difference seems to be in agreement with previous studies showing that the stability of the five-coordinated configuration *vis-à-vis* the six-coordinated configuration is higher for the cobalt(II) than for the nickel(II) ion.[9]

It is also interesting to compare the triethanolamine complexes with the corresponding complexes of N{$CH_2CH_2N(C_2H_5)_2$}$_3$. The present work reveals that NiX_2 (X=Cl$^-$, Br$^-$, or NO_3^-) forms six-coordinated complexes with the former ligand, while it has previously been shown[7] that five-coordinated complexes are formed with the latter ligand. The former and the latter ligands are found to function as terdentate and quadridentate

7) M. Ciampolini, N. Nardi and G. P. Speroni, *Coordin. Chem. Rev.*, **1**, 222 (1966); M. Ciampolini and N. Nardi, *Inorg. Chem.*, **6**, 445 (1967); *ibid.*, **5**, 1150 (1966).

*2 The low solubility of these complexes in suitable solvents did not allow any accurate determination of the conductivity or the molecular weight.

8) P. L. Orioli, M. Di Vaira and L. Sacconi, *Chem. Commun.*, **1965**, 103; *Inorg. Chem.*, **5**, 400 (1966).

9) S. Yamada, E. Ohno, Y. Kuge, A. Takeuchi, K. Yamanouchi and K. Iwasaki, *Coordin. Chem. Rev.*, **3**, 247 (1968); S. Yamada, A. Takeuchi, K. Yamanouchi and K. Iwasaki, This Bulletin, **42**, 131 (1969).

ligands, respectively. The difference between the two ligands lies only in the terminal groups, the ability of the OH-group to combine with the metal ion being considered to be lower than that of the NR_2-group.

The present authors wish to thank the Ministry of Education for its financial support.

BULLETIN OF THE CHEMICAL SOCIETY OF JAPAN VOL. 42 2555—2562 (1969)

Shielding Effect of *Ortho*-Substituents on Magnetic Moments and d–d Bands in Chloro-*N*-phenylsalicylideneiminatocopper(II)[*1]

Michinobu KATO,* Yoneichiro MUTO,** Hans B. JONASSEN,*** Kyoko IMAI,* Kazuko KATSUKI** and Seishi IKEGAMI**

* *Aichi Prefectural University, Mizuho-ku, Nagoya*
** *Department of Chemistry, Saga University, Saga*
*** *Department of Chemistry, Tulane University, New Orleans, La., U.S.A.*

(Received March 20, 1969)

Complexes with the formula, $Cu(\overset{1}{O}\cdot C_6H_4\cdot \overset{2}{C}H{=}N\text{-}Ph\text{-}X)Cl$, where Ph-X is a mono- or di-substituted phenyl group, were prepared. A dimeric structure was postulated for these complexes based on the observed subnormal magnetic moments and the chemical formula. For these complexes, a linear relation was observed to exist between the magnetic moments, $\mu_{eff}^{25°C}$, and the d–d band positions, $\tilde{\nu}_{max}$. The d–d bands of the dimeric complexes with *o*-substituents appeared at shorter wavelengths than those with *m*- or *p*-substituents irrespective of the polar nature of the substituents. A similar *ortho*-effect was also observed for the magnetic moments; complexes with *o*-substituents were observed to have smaller moment values than those with *m*- or *p*-substituents. The *ortho*-effect was also observed in the d–d bands of the monomeric bis-complexes $Cu(\overset{1}{O}\cdot C_6H_4\cdot \overset{2}{C}H{=}N\text{-}Ph\text{-}X)_2$ and their d–d bands when X=*o*-substituents appeared at shorter wavelengths than those with *m*- or *p*-substituents. These *ortho*-effects decreased for the solution spectra of the monomeric complexes.

In a previous paper,[1] it was reported that, despite the wide variation in the polar nature of the substituents in dimeric pyridine *N*-oxides copper(II) chloride complexes a linear relation exists between the magnetic moments, $\mu_{eff}^{25°C}$, and the d–d band positions, $\tilde{\nu}_{max}$. No such correlation, however, is found between the polar nature of the substituents in terms of Hammett's σ constants and the magnetic moments of the d–d band positions. The breakdown of Hammett's rule in these dimeric systems was correlated to a steric effect of the substituents on the central metal atom overlapped by their polar effect. The substituents in the aromatic ring which rotates around the N–C bond perpendicular to the coordination plane, will, depending on their size or positions, shield the fifth coordinating site of the central metal atom from the influences of other molecules or ions. This type of shielding effect makes the d–d bands shift towards shorter wavelengths and lowers the magnetic moments compared to those of the parent complexes.

In order to test the validity of these observations for other dimeric complexes, we have prepared copper(II) complexes with the formula, Cu(Sal·N–Ph–X)Cl[*2] and studied their magnetic and spectral properties. Spectral measurements were also made for the parent bis-complexes $Cu(Sal\cdot N\text{-}Ph\text{-}X)_2$.

[*1] A part of this study was presented by a) M. Kato, Y. Muto, H. N. Ramaswamy, H. B. Jonassen and K. Imai at the 16th Conference on Coordination Chemistry of the Chemical Society of Japan, Tokyo, November, 1966, Proceedings, p. 68. b) M. Kato, Y. Muto, K. Imai and H. B. Jonassen at the 20th Annual Meeting of the Chemical Society of Japan, Tokyo, April, 1967, Proceedings II, p. 75. c) Y. Muto, M. Kato H. B. Jonassen, H. N. Ramaswamy and K. Imai at the 10th International Conference on Coordination Chemistry, Nikko, September, 1967, and d) M. Kato, Y. Muto, H. B. Jonassen, K. Imai, K. Katsuki and S. Ikegami at the 18th Conference on Coordination Chemistry of the Chemical Society of Japan, Kyoto, October, 1968, Proceedings, p. 319.

1) Y. Muto, M. Kato, H. B. Jonassen and L. C. Cusachs, This Bulletin, **42**, 417 (1969).

[*2] $Sal\cdot N{=}\cdot\overset{1}{O}\cdot C_6H_4\cdot\overset{2}{C}H{=}N\cdot$ and Ph–X=mono- or di-substituted phenyl group with substituent X.

TABLE 1. ANALYTICAL DATA OF $Cu(\overset{1}{O}\cdot C_6H_4\cdot\overset{2}{C}H{=}N\text{-}Ph\text{-}X)Cl$*

Substituent X	C%		H%		N%		Cu%	
	Found	Calcd	Found	Calcd	Found	Calcd	Found	Calcd
H	53.15	52.89	3.64	3.41	4.76	4.74	21.38	21.52
2-CH_3	54.29	54.38	4.06	3.91	4.81	4.53	20.60	20.55
3-CH_3	54.42	54.38	4.04	3.91	4.51	4.53	20.64	20.55
4-CH_3	54.46	54.38	4.00	3.91	4.50	4.53	20.60	20.55
2-Cl	47.67	47.36	3.17	2.75	4.32	4.25	19.24	19.27
3-Cl	47.51	47.36	3.03	2.75	4.16	4.25	19.27	19.27
4-Cl	47.66	47.36	2.99	2.75	4.18	4.25	19.33	19.27
2-NO_2	45.47	45.89	2.81	2.67	8.54	8.23	18.79	18.68
3-NO_2	46.17	45.89	3.04	2.67	8.10	8.23	18.34	18.68
4-NO_2	45.77	45.89	2.98	2.67	8.02	8.23	18.73	18.68
2,6-$(CH_3)_2$	55.53	55.73	4.50	4.37	4.26	4.33	19.59	19.65
2,4-$(CH_3)_2$ ($\frac{1}{4}C_2H_5OH$)	56.08	55.61	4.65	4.67	4.43	4.18	18.88	18.98
2,6-Cl_2	43.88	42.88	2.30	2.21	4.05	3.85	17.45	17.45
2,3-Cl_2 ($\frac{1}{4}C_2H_5OH$)	42.81	43.17	2.60	2.55	3.87	3.73	17.12	16.92
2,5-Cl_2 ($\frac{1}{4}C_2H_5OH$)	43.01	43.17	2.52	2.55	3.86	3.73	16.99	16.92
3,4-Cl_2 ($\frac{1}{2}C_2H_5OH$)	43.58	43.43	2.49	2.86	3.92	3.62	16.63	16.41

* Ph-X=mono- or di-substituted phenyl group with substituent X.
Indications in the parentheses in the first column are the solvent molecules combined with the complexes for the chemical formula.

The present study also compares the difference in the pathways of polar effect transmittance in pyridine *N*-oxide and *N*-phenylsalicylaldimine complexes, and the magnetic interactions between copper(II) ions in a dimer.

Experimental

Materials. Salicylaldehyde, various aryl amines and anhydrous cupric chloride (Fisher certified reagent) were obtained commercially.

Preparation of the Copper(II) Complexes. *a) Parent Bis(N-phenylsalicylideneiminato)copper(II) Complexes.* These were prepared by the general method.[2,3] In most cases, methanol or ethanol was used as solvent but in the preparation of complexes with *o*-chloro or *o*-nitro group, dimethylformamide was employed instead of alcohols to elevate the reaction temperature. The purity of the recrystallized complexes was checked by copper analysis.

b) Chloro Copper(II) Complexes. In a typical preparation, a filtered solution of anhydrous cupric chloride in ethanol was added to one of the recrystallized parent complexes in a flask. The mole ratio of cupric chloride to each complex was 1.1 : 1, *i. e.*, ten percent excess of $CuCl_2$ over the stoichiometric quantity was used. The alcoholic mixture in the flask equipped with a condenser was stirred on a hot plate for two hours. The precipitated product was filtered off from solvent on a glass filter, washed several times with ethanol and once with ether, and dried at 70—80°C. The analytical data are listed in Table 1.

Magnetic Susceptibility Determinations. These data were obtained by the Gouy method at room temperature. The effective magnetic moment, μ_{eff}, per copper atom was calculated from the expression $\mu_{eff}=2.83\sqrt{\chi_M\cdot T}$ B.M., where χ_M is the molar susceptibility corrected using Pascal's constants,[4,5] for the diamagnetism of all the atoms in the compounds. The temperature-independent paramagnetism associated with the copper ions was not included in the calculation of μ_{eff} throughout this work. The magnetic moments observed at room temperature were corrected for minor room temperature variations to those at 25°C, $\mu_{eff}^{25°C}$, by using Bleaney and Bowers' equation assuming $g=2.2$.[6,7] These results are given in Table 2.

Spectral Measurements. These were made in 340—2000 mμ region on the automatic recording Hitachi EPS-3T spectrophotometer. The diffuse reflectance spectra of the parent bis-complexes and the copper(II) chloride complexes were measured with a reflectance attachment. Magnesium oxide or lithium fluoride of optical grade was used as the standard of light reflectance. Instead of diluting the compounds with the reference material, appropriate absorbancy ranges were selected by controlling the sensitivity knobs on the spectrophotometer. The band maxima of these complexes are recorded in Tables 3 and 5. Spectral measurements were also made for some of the paren bis-complexes in chloroform. The data of these solution

2) S. Yamada, *Coordin. Chem. Rev.*, **1**, 415 (1966).
3) P. Pfeiffer and H. Krebs, *J. prakt. Chem. N.F.*, **155**, 77 (1940).
4) G. Foëx, C. J. Gorter and L. J. Smits, "Constantes Sélectionnées, Diamagnétisme et Paramagnétisme, Relaxation Paramagnétique," Masson & Cie, Paris (1957), p. 222.
5) P. W. Selwood, "Magnetochemistry," Interscience Publishers, New York (1956), pp 78 and 91.
6) B. Bleaney and K. D. Bowers, *Proc. Roy. Soc. (London)*, **A214**, 451 (1952).
7) M. Kato, Y. Muto, H. B. Jonassen, K. Imai and A. Harano, This Bulletin, **41**, 1864 (1968).

Table 2. Magnetic data of $Cu(\overset{1}{O}\cdot C_6H_4\cdot \overset{2}{C}H{=}N\text{-}Ph\text{-}X)Cl$*

Substituent X	Susceptibility $\chi_g\cdot 10^6$ (cgs, emu)	Temperature (°K)	μ_{eff} (B.M.)	$\mu_{eff}^{25°C}$ (B.M.)
H	2.23	295	1.38	1.39
2-CH_3	1.57	303	1.26	1.24
3-CH_3	2.74	302	1.56	1.56
4-CH_3	1.96	287	1.33	1.35
2-Cl	1.17	295	1.14	1.15
3-Cl	1.55	299	1.28	1.27
4-Cl	1.67	302.5	1.32	1.31
2-NO_2	0.92	296	1.06	1.06
3-NO_2	2.47	296	1.54	1.54
4-NO_2	0.71_5	300	0.98	0.97
2,6-$(CH_3)_2$	1.70	290	1.30	1.32
2,4-$(CH_3)_2$ ($1/4\,C_2H_5OH$)	1.51	290	1.26	1.28
2,6-Cl_2	1.15	285	1.17	1.21
2,3-Cl_2 ($1/4\,C_2H_5OH$)	1.26	286	1.24	1.27
2,5-Cl_2 ($1/4\,C_2H_5OH$)	1.02	286	1.15	1.18
3,4-Cl_2 ($1/2\,C_2H_5OH$)	1.29	286	1.27	1.30

* See the footnote of Table 1.

Table 3. Data of reflectance spectra of $Cu(\overset{1}{O}\cdot C_6H_4\cdot \overset{2}{C}H{=}N\text{-}Ph\text{-}X)_2$**

Substituent X	Band maxima, λ_{max}, mμ
H	385 vs,sh 465 vs,sh 530 s,sh 694 s* 1690 vw
2-CH_3	375 vs,br 465 vs,sh 673 s* 1710 vw
3-CH_3	377 vs,br 485 vs,br,sh 733 s* 1715 vw
4-CH_3	362 vs 390 vs,br,sh 470 vs,sh 560 s,sh 710 s* 1710 vw
2-Cl	375 vs,br 460 vs,sh 545 s,sh 693 s* 1690 vw
3-Cl	370 vs,br,sh 500 vs,br,sh 736 s* 1685 vw
4-Cl	380 vs,br 495 vs,sh 730 s* 1690 vw
3-NO_2	(~ 405) vs,br,dp 495 vs,br,sh 737 s* 1680 vw
4-NO_2	(405 505) vs,br,dp 750 s* 1690 w
2,6-$(CH_3)_2$	390 vs,sh 465 s,sh 669 s* 1705 w
2,4-$(CH_3)_2$	390 vs,sh 460 vs,sh 668 s* 1710 w
2,6-Cl_2	385 vs,br,sh 470 vs,sh 690 s* 1690 w
2,3-Cl_2	(400 430) vs,dp 495 vs,sh 590 s,sh 748 s* 1685 w
2,5-Cl_2	400 vs,br,sh 480 vs,sh 600 vs,sh 794 s* 1690 vw
3,4-Cl_2	(385 445) vs,br,sh 530 vs,sh 776 s* 1690 vw

** See the footnote of Table 1. vs=very strong s=strong w=weak vw=very weak sh=shoulder br=broad dp=double peak, two bands in contiguity.
*=the d–d band which was employed in the discussion of substituent effect in text.

Table 4. Data of absorption spectra in $CHCl_3$ solution of $Cu(\overset{1}{O}\cdot C_6H_4\cdot \overset{2}{C}H{=}N\text{-}Ph\text{-}X)_2$*

Substituent X	Absorption maxima and extinction coefficients λ_{max}, mμ (log ε_{max})		
2-CH_3	394(4.08)	460 br,sh	647(2.16)*
3-CH_3	399(4.09)	470 br,sh	674(2.40)*
4-CH_3	396(4.23)	475 br,sh	677(2.42)*
2-Cl	397(3.89)	470 sh	659(2.09)*
3-Cl	402(3.94)	470 br,sh	668(2.32)*
4-Cl	401(4.21)	480 br,sh	669(2.32)*

* See the footnotes of Tables 1 and 3.

Table 5. Data of diffuse reflectance spectra of $Cu(\overset{1}{O}\cdot C_6H_4\cdot \overset{2}{C}H{=}N\text{-}Ph\text{-}X)Cl$*

Substituent X	Band maxima, λ_{max}, mμ
H	(380 425 515) vs,br,sh 890 s* 1690 vw
2-CH_3	(366 440 520) vs,br,sh 830 s* 1700 vw
3-CH_3	(365 445 525) vs,br,sh (680 s,sh 920 s*)dp 1695 vw
4-CH_3	370 vs 440 vs,br,sh 535 vs,br,sh 870 s* 1700 vw
2-Cl	360 vs 415 vs,sh 530 s,br,sh (664 825*) s,dp 1690 vw
3-Cl	370 vs,sh 420 vs,br,sh 525 s,sh 830 s* 1685 vw
4-Cl	(370 vs 445 vs 530 s) br,sh 880 s* 1690 vw
2-NO_2	410 vs,br (780 880 br*) s,dp 1690 vw
3-NO_2	(380 vs 465 vs 540 s) br,sh (686 915*) s,dp 1675 vw
4-NO_2	385 vs,br,sh 440 vs,br,sh 900 vs,br* 1670 vw
2,6-$(CH_3)_2$	440 vs,br,sh 871 s* 1690 vw
2,4-$(CH_3)_2$ ($1/4\,C_2H_5OH$)	440 vs 530 vs,sh 855 s* 1710 vw
2,6-Cl_2	(380 525) vs,br,sh (673 857*) s,dp 1680 vw
2,3-Cl_2 ($1/4\,C_2H_5OH$)	385 vs, sh 535 s, sh (675 875*) s, dp 1685 vw
2,5-Cl_2 ($1/4\,C_2H_5OH$)	390 vs,sh 540 s,sh (680 885*) s,dp 1680 vw
3,4-Cl_2 ($1/2\,C_2H_5OH$)	(380 435 530) vs,br,sh 868 s* 1690 vw

* See the footnotes of Tables 1 and 3.

spectra are given in Table 4. The bands listed in these tables may be resolved into more than one component.

Results and Discussion

Parent Monomeric Complexes. The parent monomeric complexes give rise to several bands in 340—2000 mμ region in the diffuse reflectance spectra (*cf.* Tables 3 and 4). Many of these bands are not well characterized. The bands at wave-

lengths shorter than about 500 mμ can probably be attributed to charge-transfer or intra-ligand transition.[8,9] The bands recorded at wavelengths longer than about 1200 mμ, are difficult to assign[10] and do not seem to be important in this discussion. The bands appearing around 700 mμ are the most distinct (marked with an asterisk in Tables 3 and 4), and most of these are considered to be the well-known d–d bands of the planar type of copper(II) complexes.[7–12]

Those of the complexes with a substituent in the *ortho*-position appeared at shorter wavelengths than those with a substituent at the *meta*- or *para*-position, *i. e.*,

$$\lambda_{max}\ (o\text{-}) < \lambda_{max}\ (m\text{-}) \sim \lambda_{max}\ (p\text{-})$$

The difference in λ_{max} between *meta*- and *para*-complexes is small compared to that between the *ortho*- and *meta*- or *para*-complexes. This is illustrated by the spectral curves of the complexes with methyl group in Fig. 1. On the other hand, essentially no difference in λ_{max} of d–d bands was observed among complexes with different substituents at the same ring positions. Figure 2 shows this for the absorption bands of complexes with *m*-Cl, *m*-CH_3 and *m*-NO_2, all at about 740—745 mμ.

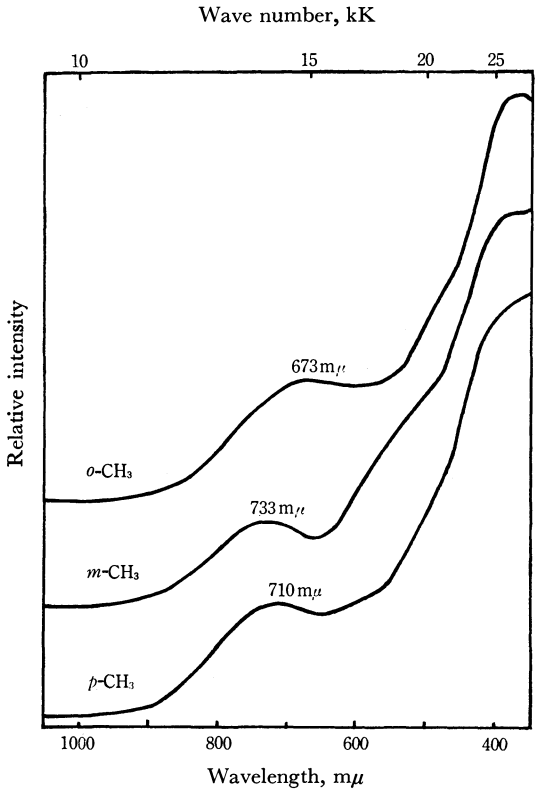

Fig. 1. Diffuse reflectance spectra of Cu(Sal·N-Ph-CH_3)$_2$.

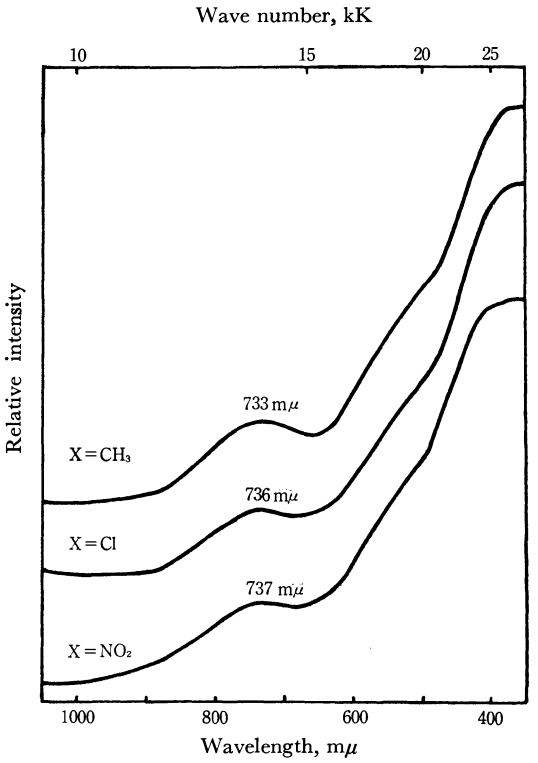

Fig. 2. Diffuse reflectance spectra of Cu(Sal·N-Ph-X)$_2$ with X=*m*-CH_3, *m*-Cl, and *m*-NO_2.

An X-ray analysis of the parent compound, bis(*N*-phenyl-salicylideneiminato)copper(II)[13] has shown that the plane of the *N*-phenyl group is nearly perpendicular to the $\begin{pmatrix}O\\N\end{pmatrix}Cu\begin{pmatrix}N\\O\end{pmatrix}$ plane. Under such conditions, substituents attached in the *ortho*-position of the phenyl group should have a great tendency to shield the fifth coordination site of the copper(II) ions. Such shielding effect is said to stabilize the complexes and to produce the observed "blue shift" of the d–d band.[1,14–17]

The "blue shift" effect of *ortho*-substituents on the d–d bands in chloroform solution was apparently retained even though it decreased compared to

8) L. Sacconi and M. Ciampolini, *J. Chem. Soc.*, **1964**, 276.
9) S. J. Gruber, C. M. Harris and E. Sinn, *J. Inorg. Nucl. Chem.*, **30**, 1805 (1968).
10) W. J. Eilbeck, F. Holmes, C. E. Taylor and A. E. Underhill, *J. Chem. Soc., A*, **1968**, 128.
11) J. Ferguson, *J. Chem. Phys.*, **35**, 1612 (1961).
12) The present authors, unpublished data.
13) L. Wei, R. M. Stogsdill and E. C. Lingafelter, *Acta Cryst.*, **17**, 1058 (1964).
14) J. Chatt and B. L. Shaw, *J. Chem. Soc.*, **1960**, 1718.
15) J. Chatt and B. L. Shaw, *ibid.*, **1961**, 285.
16) S. Yamada and S. Miki, This Bulletin, **36**, 680 (1963).
17) S. Miki and S. Yamada, *ibid.*, **37**, 1044 (1964).

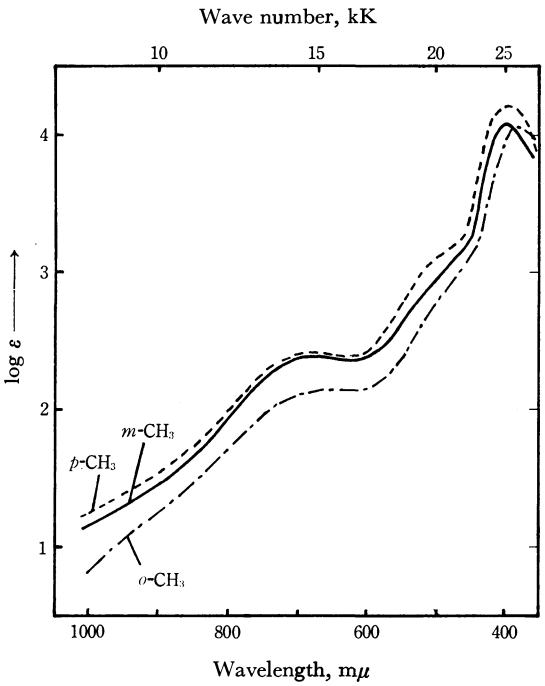

Fig. 3. Spectra of $Cu(Sal\cdot N\text{-}Ph\text{-}CH_3)_2$ in $CHCl_3$.

that in the solid state (*cf.* Fig. 3).

In solid complexes the vacant coordination sites of the copper(II) ion are subjected to the influences of adjacent atoms, ions, or molecules. However, in solutions of weak-coordinating solvents such as chloroform, these influences should decrease as the distances between the complexes increases. Since the solvent molecules display a kind of shielding effect, it is then quite probable that the shielding effect due to the steric condition of the *ortho*-substituents is much decreased. Since the copper(II) ion has one unpaired electron, a continuous variation in the influence of the ligand field or in the stereochemistry, seems to be possible.[18] The *ortho*-substituent effect for the di-substituted complexes, was retained in some cases (those with methyl group) but in other cases it became obscure (those with the chloro group) (*cf.* Table 3). This may be due to an additional steric effect which interferes with the existence of stable planar complex due to the preparatory method used for the solid complexes.[1,8,18,19]

Dimeric Chloro Copper(II) Complexes. No X-ray analysis for dimeric chloro copper(II) complexes similar to those we prepared has been reported. On the basis of the chemical formula of these complexes which contain only three coordinating atoms, and of the observed low magnetic moments,

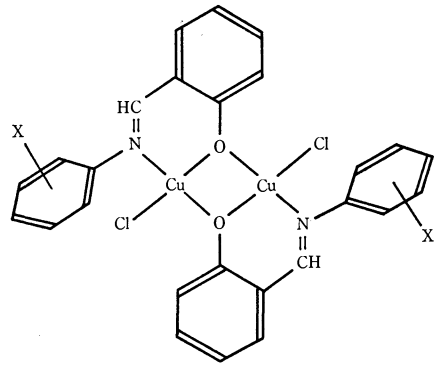

Fig. 4. The assumed dimeric structure of Cu(Sal·N-Ph-X)Cl.

we have assumed a dimeric structure of the type given in Fig. 4. Of the three types of coordinating atoms in the dimeric complexes, the phenolic oxygen atom is most probably the bridging atom because (1) the imino-nitrogen atom can not span the copper(II) ions because of steric hindrance of the *N*-phenyl group, and (2) a low magnetic moment of 1—1.5 B.M. recorded for these dimeric complexes has never been observed in copper(II) complexes with chlorine-bridges.[20]

a) Diffuse Reflectance Spectra. The diffuse reflectance spectra of the chloro copper(II) complexes revealed several bands in the 340—2000 mμ region similar to the parent monomeric complexes (*cf.* Table 5). The main d–d band which corresponds to that of the parent complexes can easily be distinguished from the other bands. The d–d band maximum occurs at a much longer wavelengths (800—900 mμ) than that of the monomeric complexes suggesting a distorted planar or pseudo-tetrahedral structure for these complexes.[8–10,19,21–23] Sacconi found that the salicylideneiminato-copper(II) of pseudo-tetrahedral type are maroon,[8] and these dimeric copper(II) chloride complexes are all maroon or brown. Chloro(*N*-alkylsalicylideneiminato)copper(II) complexes which we studied previously[*1-b,24] are closely related to chloro(*N*-phenylsalicylideneiminato)copper(II); they also are brown. They showed three bands in the 340—1500 mμ range with essentially the same spectral features as those of bis(*N*-alkylsalicylideneiminato)-

18) M. Kato, *Bull. Aichi Gakugei Univ.*, **9**, 95 (1960).

19) S. Yamada and H. Nishikawa, This Bulletin, **36**, 755 (1963).

20) M. Kato, H. B. Jonassen and J. C. Fanning, *Chem. Revs.*, **64**, 99 (1964).

21) L. Sacconi, "Essays in Co-ordination Chemistry," ed. by W. Schneider, G. Anderegg and R. Gut, Birkhaüser, Basel (1964), p. 148.

22) A. van der Avoird and P. Ros, *Theoret. chim. Acta (Berl.)*, **4**, 13 (1966).

23) C. M. Harris, H. R. H. Patil and E. Sinn, *Inorg. Chem.*, **6**, 1102 (1967).

24) Y. Muto, M. Kato, H. B. Jonassen, H. N. Ramaswamy and K. Imai, the paper presented at the 10th International Conference on Coordination Chemistry, Nikko, September, 1967, Proceedings, p. 337.

copper(II) with pseudo-tetrahedral structure.[8,21] The magnetic moments and the main d–d band positions of these chloro copper(II) complexes with *N*-alkyl groups fall in the range of 1—1.4 B.M. and of 800—900 mμ respectively, the same ranges as those observed for the dimeric complexes with *N*-phenyl groups of the present study.

Each copper(II) ion in these dimeric complexes is effectively surrounded by three coordinating atoms, one of which is the chloride ion which has a position in the early part of the spectrochemical series.[25] The ligand field strength is therefore much weaker than that of the monomeric complexes. The diffuse reflectance spectra of the dimeric complexes with mono-substituted *N*-phenyl group, showed a "blue shift" effect of *ortho*-substituents just as the parent monomeric complexes (*cf.* Fig. 5 and Table 5). This suggests that a structural

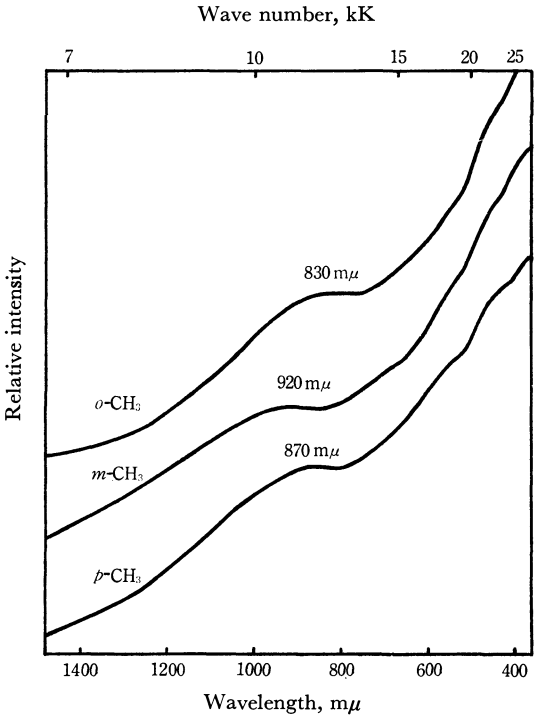

Fig. 5. Diffuse reflectance spectra of Cu(Sal·N-Ph-CH_3)Cl.

feature important in bis(*N*-phenylsalicylideneiminato)copper(II), namely the upward rotation of the *N*-phenyl group perpendicular to the coordination plane, is substantially retained in these dimeric complexes. The same type of *ortho*-substituent effects was observed in the d–d bands and in the magnetic interaction between copper(II) ions in a pair[1] for the dimeric copper(II) chloride complexes with pyridine *N*-oxides. The structure of the parent copper(II) chloride complex with pyridine *N*-oxide shows that the pyridine ring is rotated about the O–N bond such that its plane is essentially perpendicular to the coordination sphere of a distorted square-planar geometry.[26,27]

In the dimeric chloro copper(II) complexes with *N*-phenylsalicylaldimines, as for copper(II) chloride complexes with pyridine *N*-oxides, no correlation was observed to exist between Hammett's σ constants of substituents and the d–d band positions.

b) Magnetic Moments. For the complexes with a disubstituted *N*-phenyl group, the *ortho*-substituent effect of "lowering at magnetic moment" was observed in these dimeric complexes (*cf.* Table 2), with a few exceptions

$$\mu_{\mathrm{eff}}^{25^\circ\mathrm{C}}(o\text{-}) < \mu_{\mathrm{eff}}^{25^\circ\mathrm{C}}(m\text{-}) \sim \mu_{\mathrm{eff}}^{25^\circ\mathrm{C}}(p\text{-})$$

However, no correlation exists between the polar nature of the substituents in terms of Hammett's constants and the moments. These observations are the same as those in copper(II) chloride complexes with pyridine *N*-oxides.[1]

c) Linear Relation between d–d Band Positions and Magnetic Moments. Even though no correlation exists between Hammett's σ constants of substituents and the d–d band positions, $\tilde{\nu}_{\max}$, or the magnetic moments corrected to those at 25°C, $\mu_{\mathrm{eff}}^{25^\circ\mathrm{C}}$, a linear relation between $\tilde{\nu}_{\max}$ and $\mu_{\mathrm{eff}}^{25^\circ\mathrm{C}}$ (*cf.* Fig. 6) is found, the same relation observed for the copper(II) chloride complexes with pyridine *N*-oxides.[1,28] In the postulated structure of [Cu(Sal·N-Ph-X)Cl]$_2$ (Fig. 4) the magnetic interac-

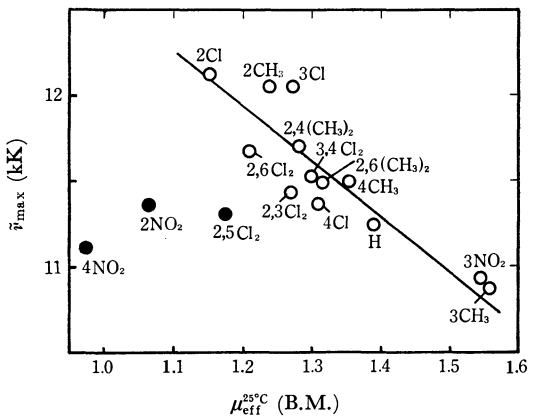

Fig. 6. The plot of the wave number ($\tilde{\nu}_{\max}$ in kK) of d–d bands of Cu(Sal·N-Ph-X)Cl against the corrected magnetic moments ($\mu_{\mathrm{eff}}^{25^\circ\mathrm{C}}$ in B.M.).

25) C. K. Jørgensen, "Absorption Spectra and Chemical Bonding in Complexes," Pergamon Press, Oxford (1962), p. 107.

26) H. L. Schäfer, J. C. Morrow and H. M. Smith, *J. Chem. Phys.*, **42**, 504 (1965).

27) R. S. Sager, R. J. Williams and W. H. Watson, *Inorg. Chem.*, **6**, 951 (1967).

28) M. Kato, Y. Muto and H. B. Jonassen, This Bulletin, **40**, 1738 (1967).

tion between copper(II) ions in a dimeric molecule will most probably occur by a superexchange mechanism through the bridging phenolic oxygen atoms.[29–32] Since the orbital overlap scheme of relevant orbitals for the superexchange interaction should essentially be the same for these two systems, a σ type and a π type pathway for the superexchange interaction are possible. The σ type seems to be more important for the same reason as that given for copper(II) chloride complexes with pyridine *N*-oxides.[1]

In the dimeric complexes with pyridine *N*-oxides, the polar effect of substituents transmits directly to the oxygen atoms which are in the superexchange pathway. On the other hand in $[Cu(Sla\cdot N\text{–}Ph\text{–}X)Cl]_2$, the substituent effect should transmit to the coordinating nitrogen atoms not in the superexchange pathway. Despite such difference in the transmittance of substituent-polar effect, the steric effect of the substituents appears to be more important in the determination of physicochemical properties of these complexes than the electronic effect of the substituents.

The anomalous properties of *o*-NO_2 and *p*-NO_2 complexes may be due to a different structure (*cf.* Table 2 and Fig. 6). These compounds have magnetic moments smaller than those expected from the linear relation between $\tilde{\nu}_{max}$ and $\mu_{eff}^{25°C}$; furthermore, whereas the other complexes are brown, these two complexes are greenish-orange in color and their d–d bands are broad. The *o*-NO_2 and *p*-NO_2 compounds are thus seemingly quite similar to the orange one of the two modifications of $Cu(Sal\cdot N\text{–}CH_3)Cl$*[1-b,24]; the orange compound has a moment of 0.9 B.M. and the brown one a moment of 1.47 B.M. at room temperature. The spectral curves of these two modifications are given with those of *p*-NO_2 and *m*-NO_2 compounds in Fig. 7. The compound with *m*-NO_2 group is brown and its spectral feature is essentially the same as that of all other complexes.

The reason for the deviation from linearity for the 2,5-Cl_2 compound is not clear at present. However, it is one of the disubstituted compounds and its d–d band is composed of two bands in contiguity (double peak).

The extent of magnetic interaction found in $[Cu(Sal\cdot N\text{–}Ph\text{–}X)Cl]_2$ ranges from 1 to 1.5 B.M. This is weaker than that observed for the copper(II) chloride complexes with pyridine *N*-oxides (0.2—1 B.M.). On the basis of the p*K* values of ligand

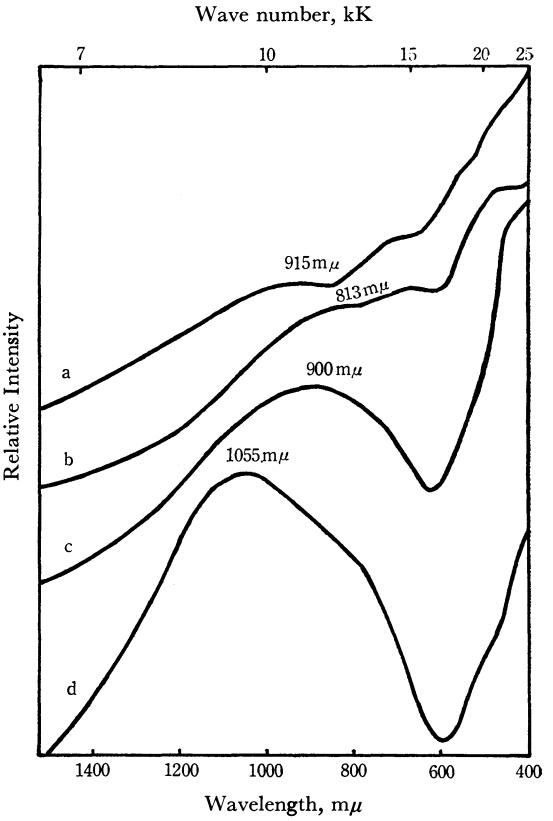

Fig. 7. Diffuse reflectance spectra of (A) $Cu(Sal\cdot N\text{–}Ph\text{–}X)Cl$ and (B) $Cu(Sal\cdot N\text{–}CH_3)Cl$.
(A): curve a, X=*m*-NO_2 and curve c, X=*p*-NO_2.
(B): curve b, brown modification and curve d, orange modification (*cf.* text).

molecules[33–36] the Cu–O coordinate bonds in the bridging framework is considered to be stronger in salicylideneiminato-complexes than in pyridine *N*-oxide complexes.

In the preceding paper, we suggested that the most important factor in the determination of the electron exchange is the bond angle rather than the bond strengths in a pathway, because an effective electron exchange requires a successive overlapping of the relevant orbitals of atoms in a superexchange pathway.[37]

A comparison of the total coordinate bonds in the two complexes shows in $[Cu(PyO)Cl_2]_2$*[3] one

29) G. A. Barclay, C. M. Harris, B. F. Hoskins and E. Kokot, *Proc. Chem. Soc.*, **1961**, 264.
30) G. A. Barclay and B. F. Hoskins, *J. Chem. Soc.*, **1965**, 1979.
31) W. E. Hatfield and F. L. Bunger, *Inorg. Chem.*, **5**, 1161 (1966).
32) A. P. Ginsberg, R. C. Sherwood and E. Koubek, *J. Inorg. Nucl. Chem.*, **29**, 353 (1967).
33) H. H. Jaffé and G. O. Doak, *J. Am. Chem. Soc.*, **77**, 4441 (1955).
34) T. J. Lane and A. J. Kandathil, *J. Am. Chem. Soc.*, **83**, 3782 (1961).
35) C. K. Jφrgensen, "Inorganic Complexes," Academic Press, Inc., New York, N. Y. (1963), p. 109.
36) Y. Muto and H. B. Jonassen, This Bulletin, **39**, 58 (1966).
37) J. B. Goodenough, "Magnetism and the Chemical Bond," Interscience Publishers, New York, N. Y. (1963), p. 165.
*3 PyO=pyridine *N*-oxide or its derivatives.

Cu–O (PyO–O) and two Cu–Cl bonds *versus* one Cu–O (phenolic-O), one Cu–N (imino-N) and one Cu–Cl bond for $[Cu(Sal\cdot N\text{–}Ph\text{–}X)Cl]_2$. This would indicate greater total covalent bond strength in the latter, however, their d–d bands are practically at the same energy (760—900 mμ) for $[Cu(PyO)Cl_2]_2$ and (830—900 mμ) for $[Cu(Sal\cdot N\text{–}Ph\text{–}X)Cl]_2$. This seeming contradiction can be resolved if it is postulated that the stereochemistry of the $[Cu(Sal\cdot N\text{–}Ph\text{–}X)Cl]_2$ complexes has a greater tetrahedral distortion than $[Cu(PyO)Cl_2]_2$.[8,21,22]

This assumption is consistent with the lower range of magnetic moments (0.2—1 B.M.) in the pyridine *N*-oxide and with the higher range (1—1.5 B.M.) in *N*-phenylsalicylideneiminato-complexes. On the basis of the assumed pathways the orbital overlap effective for the superexchange interaction should be weaker in the system with a greater pseudo-tetrahedral framework than in that with greater planar framework.

A linear relationship between d–d band position and magnetic moments in dimeric $[Cu(Sal\cdot N\text{–}Ph\text{–}X)Cl]_2$ has been established similar to that found previously for dimeric $[Cu(PyO)Cl_2]_2$. It holds even though in the two complexes there is a difference in the position of the coordinate bonds through which the substituent polar effect is transmitted in the superexchange pathway.

A shielding effect of the substituents on d–d band position and magnetic moments has also been observed which is greatest for *ortho* substitution (*ortho*-effect) even though a change in polarity of the substituents has no effect on either d–d band position or magnetic moments.

BULLETIN OF THE CHEMICAL SOCIETY OF JAPAN VOL. 42 2562—2566 (1969)

Metal Complexes of Schiff Bases Obtained from Substituted Salicylaldehydes and 2-Aminopyridine Derivatives[1)]

Shoichiro YAMADA and Kuniko YAMANOUCHI

Institute of Chemistry, College of General Education, Osaka University, Toyonaka, Osaka

(Received March 28, 1969)

Numerous metal complexes (abbreviated as $M(X\text{-}SAL\cdot R)_2\cdot nH_2O$) of Schiff bases obtained from substituted salicylaldehydes and 2-aminopyridine derivatives were prepared as crystals, where X=H, 5,6-benzo, 5-Cl, 5-Br, 5-NO_2 and 3-CH_3O, R=2-pyridyl, 2-(3-methylpyridyl), 2-(4-methylpyridyl) and 2-(6-methylpyridyl), and M=Co(II), Ni(II), Cu(II), Zn(II) and Pd(II). It is concluded, mainly from the electronic absorption spectra, that the cobalt(II) complexes are tetrahedral, with one exception, which has an octahedral configuration with two water molecules coordinated to the cobalt(II) ion. The nickel(II) complexes are octahedral, and the copper(II) and the palladium(II) complexes are planar. In these metal complexes, the Schiff bases are bidentate, except bis(*N*-2-(6-methylpyridyl)-salicylideneiminato)nickel(II), in which the ligand functions as a terdentate.

Ligands represented by Formula I*[1] contain three atoms capable of coordinating to one metal ion, but the steric condition does not seem to be favorable for them to act as terdentate ligands. However, there still remains a possibility that these ligands behave as terdentate ligands, and it seems interesting to examine in what compounds this may, in fact, occur. The present work concerns the preparation of Schiff base complexes with some transition metal ions and examination of their structure in relation to the coordination mode of these ligands.

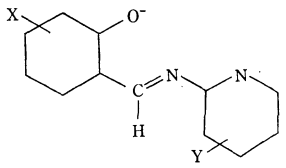

Formula I

1) Presented, in part, at the 18th Symposium on Coordination Chemistry, Kyoto, October, 1968.

*[1] Abbreviated as X-SAL·2-Py for Y=H and as X-SAL·CH_3-Py for Y=CH_3.

Experimental

Materials. Schiff base metal complexes newly prepared in the present work are shown in Tables 1, 2 and 3. The cobalt(II) complexes with the ligands

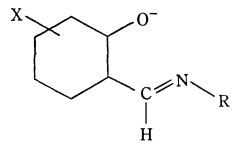

Formula II

represented by Formula II*[2] were prepared as previously reported,[2,3] either from cobalt(II) acetate tetrahydrate, substituted salicylaldehydes and amines, or from bis-(substituted salicylaldehydato)cobalt(II) and amines. One of the typical methods is given below for Co-(H-SAL·2-Py)$_2$ as an example. To a solution of cobalt-(II) acetate tetrahydrate (0.005 mol) in ethanol (10 m*l*) was added a solution of a Schiff base (0.01 mol) in ethanol (10 m*l*). The reaction was continued at about 65°C for about one hour. When the solution was cooled, crude product of the complex separated out. The pure compound was obtained as red crystals by recrystallization of the crude product from such solvents as chloroform, acetone, ethanol and benzene.

Table 1. Analytical data of Co(X-SAL·2-Py)$_2$

X	Calcd %			Found %			μ*
	C	H	N	C	H	N	
H	63.58	4.00	12.49	63.55	3.73	12.28	4.39
5,6-Benzo	69.44	4.01	10.12	69.28	3.77	9.86	4.17
5-Cl	55.19	3.09	10.73	54.61	2.77	10.58	4.31
5-Br	47.24	2.64	9.18	46.85	2.46	8.88	4.47
5-NO_2	53.05	2.97	15.47	52.54	2.59	15.46	4.51
3-CH_3O	60.82	4.32	10.91	60.48	4.11	11.30	4.35

* μ: magnetic moment in Bohr magneton at room temperature

The other cobalt(II) complexes were obtained in a similar way. Nickel(II), copper(II) and zinc(II) complexes given in Tables 2 and 3, were prepared by methods similar to those for the cobalt(II) complexes described above. Some of the cobalt(II) and nickel(II) complexes were obtained as dihydrate, which may be recrystallized from benzene or chloroform without decomposition.

Table 2. Analytical data of M(X-SAL·2-Py)$_2$

M	X	Calcd %			Found %		
		C	H	N	C	H	N
Cu*	H	62.94	3.96	12.23	63.31	3.77	12.11
	5,6-Benzo	68.87	3.97	10.04	68.49	3.73	9.70
	3-CH_3O	60.30	4.09	11.21	60.28	4.29	10.82
Zn**	H	62.69	3.95	12.19	63.42	3.42	11.91
	5,6-Benzo	68.64	3.96	10.01	69.28	3.59	9.56
Pd**	H	57.52	3.62	11.18	57.97	3.24	11.08
	5,6-Benzo	63.92	3.69	9.32	62.94	3.42	9.86

* The Cu(II) complexes are brown or dark-brown.
** The Zn(II) and the Pd(II) complexes are orange.

Palladium(II) complexes given in Table 2, were prepared by a method similar to that previously reported.[4]

All these complexes are insoluble in water, but soluble in methanol, ethanol, chloroform, dichloromethane and benzene, except Co(5-NO_2-SAL·2-Py)$_2$, which is almost insoluble in these organic solvents.

Measurements. The electronic absorption spectra of these complexes in solution and in the solid state were determined with a Shimadzu QR-50 and a Shimadzu MPS-50L spectrophotometer. In Tables 4 and 5 are listed only those data of the solution spectra, for which Beer's law was confirmed to hold.

The X-ray powder diagrams were obtained with a Toshiba ADX-103 diffractometer. The magnetic moments were determined at room temperature by the Gouy method using $CoHg(SCN)_4$ as a standard.

Table 3. Analytical data of M(H-SAL·Y-Py)$_2$(H_2O)$_n$

M	Y	n	Colour		C,%	H,%	N,%	μ
Co	3-CH_3	2	brown	calcd	60.35	5.06	10.83	
				found	60.19	4.97	10.68	4.79
	4-CH_3	0	red	calcd	64.87	4.61	11.64	
				found	64.51	4.55	11.45	4.38
	6-CH_3	0	red	calcd	64.87	4.61	11.64	
				found	64.61	4.55	11.76	4.42
Ni	3-CH_3	2	green	calcd	60.38	5.07	10.83	
				found	59.91	4.88	10.81	3.10
	4-CH_3	2	green	calcd	60.38	5.07	10.83	
				found	60.31	4.96	11.02	3.17
	6-CH_3	0	orange	calcd	64.90	4.61	11.64	
				found	64.73	4.63	11.83	3.25
Cu	3-CH_3	0	dark-green	calcd	64.25	4.56	11.53	
				found	64.53	4.26	11.45	—

Results and Discussion

Cobalt(II) and Zinc(II) Complexes. The complexes of the type Co(X-SAL·2-py)$_2$ are paramagnetic with magnetic moments ranging from 4.17 to 4.50 B.M., the values which lie in the range expected for tetrahedral cobalt(II) complexes of a high-spin type. The octahedral cobalt(II) complexes with the related Schiff bases are known to have magnetic moments near 5.0 B.M.,[2] which are evidently larger than the values for the tetrahedral complexes.

The electronic absorption spectra of these cobalt-(II) complexes in the solid state and in non-donor solvents, as shown in Fig. 1 and Table 4, are typical

*2 Abbreviated as X-SAL·R.

2) S. Yamada, *Coordin. Chem. Rev.*, **1**, 415 (1966).

3) R. H. Holm, G. W. Everett, Jr., and A. Chakravorty, "Progress in Inorganic Chemistry," Vol. VII, ed. by F. A. Cotton, Interscience Publishers, New York, N. Y. (1966), p. 83.

4) S. Yamada, H. Nishikawa and K. Yamasaki, This Bulletin, **36**, 483 (1963); S. Yamada and K. Yamanouchi, This Bulletin, **42**, 2543 (1969).

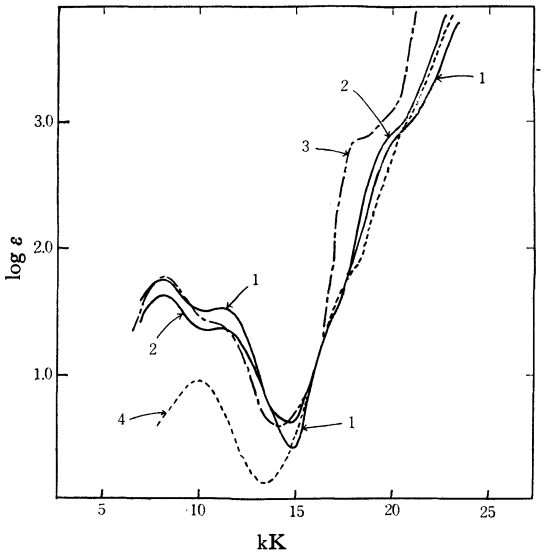

Fig. 1. Electronic absorption spectra of Co(X-SAL·R)$_2$ in solution.
1 X=H, R=Ph, in chloroform
2 X=H, R=2-Py, in chloroform
3 X=5,6-benzo, R=2-Py, in chloroform
4 X=H, R=2-Py, in pyridine

TABLE 4. SPECTRAL DATA OF Co(X-SAL·2-Py)$_2$

X	State	ν (log ε)	ν (log ε)
H	solid	8.1	10.7 sh
	chloroform	8.1(1.62)	11.0(1.37) sh
	pyridine	9.9(0.96)	
5,6-Benzo	solid	8.2	11.0 sh
	chloroform	8.2(1.76)	11.0(1.36) sh
	pyridine	10.1(1.21)	
5-Cl	solid	8.2	11.1 sh
	chloroform	8.2(1.77)	11.1(1.48) sh
5-Br	solid	8.2	11.0 sh
	chloroform	8.2(1.60)	11.0(1.34) sh
5-NO_2	solid	8.0	10.8 sh
	chloroform	insoluble	
3-CH_3O	solid	8.2	11.3
	chloroform	8.2(1.67)	11.4(1.48)

ν: 10^3 kK
sh: shoulder

of the tetrahedral cobalt(II) complex and different from that of the octahedral complex.[2,5] It is, therefore, concluded that the complexes of the type, Co(X-SAL·2-Py)$_2$, are tetrahedral with a high-spin. It is to be noted that the spectrum of Co-H-SAL·2-Py)$_2$ is quite similar to that of Co(H-SAL·Ph)$_2$,*3 which was previously concluded to be tetrahedral.[2] The absorption band at about 8.1 kK with a small shoulder at about 11 kK may be assigned to the transition $^4T_1 \leftarrow {}^4A_2$. It is also found that the configuration of these cobalt(II) complexes is tetrahedral, irrespective of the nature of the substituent X.

In all these cobalt(II) complexes, the ligands X-SAL·2-Py are found to act as bidentate ligands and not as terdentate ligands, the nitrogen atom in the heterocyclic ring not being bound with the metal ion. It is considered that the steric condition is not favorable for these ligands to act as terdentate ligands.

For R=4-CH_3-Py and 6-CH_3-Py, complexes of the type Co(H-SAL·R)$_2$ were obtained. It is concluded, from the electronic spectra, that they are tetrahedral with a high-spin. On the contrary, for R=3-CH_3-Py, a similar method yielded Co(H-SAL·R)$_2$(H_2O)$_2$ instead of Co(H-SAL·R)$_2$. The electronic spectra, as shown in Table 5, indicate that this complex in the solid state and in non-donor solvents consists of octahedral cobalt(II) with the two water molecules bound to the cobalt(II) ion. The magnetic moment of 4.79 B. M. for this complex may be understood on the basis of the octahedral configuration, although the value seems to be a little too low.

The electronic spectra, as shown in Tables 4 and 5, and Fig. 1, also indicate that, when dissolved in pyridine, these cobalt(II) complexes exist as bis-(pyridine)-complexes Co(X-SAL·R)$_2$(*py*)$_2$, where *py* denotes a pyridine molecule. This behavior is similar to that with the corresponding complexes for R=phenyl and substituted phenyl groups.[2]

It is known that the complexes of the type Zn(X-SAL-R)$_2$, in general, take a similar configuration to that of the corresponding cobalt(II) complexes. It may be, therefore, reasonable to assume that the zinc(II) complexes prepared in the present work also take a tetrahedral configuration. This seems to agree with the finding that the X-ray powder diagram of Zn(H-SAL·2-Py)$_2$ is quite similar to that of Co(H-SAL·2-Py)$_2$, showing that these two complexes are isomorphous with each other.

Complexes of Nickel(II) and Other Metal Ions. For R=2-Py, all the methods, which have been applicable to the synthesis of complexes of the other ions, proved to be unsuccessful for isolating the nickel(II) complexes of the type Ni(X-SAL·2-Py)$_2$. Thus those methods only yielded crystals of nickel(II) complexes with a complicated composition.

For R=3-CH_3-Py and 4-CH_3-Py, the nickel(II) complexes of the type Ni(H-SAL·R)$_2$(H_2O)$_2$ were obtained. They are all of a high-spin type with a magnetic moment ranging between 3.10 and 3.17 B.M. The electronic absorption spectra indicate, as shown in Fig. 2 and Table 5, that these nickel(II) complexes are octahedral in the solid state and in non-doner solvents. It is most likely that the two water molecules are bound with the nickel(II) ion.

*3 The notation Ph represents a phenyl group.

5) S. Yamada, *Coordin. Chem. Rev.*, **2**, 83 (1967).

Heating these complexes at about 100°C for many hours gave rise to neither decomposition nor loss of the water molecules. This indicates that the linkage of the water moleculrs with the nickel(II) ion may be considerably strong.

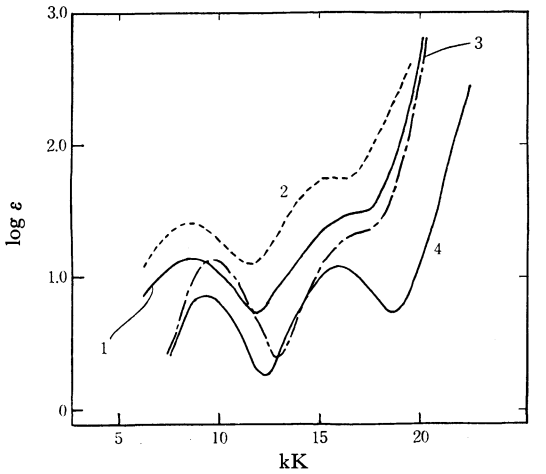

Fig. 2. Electronic absorption spectra of Ni(H-SAL·R)$_2$(H$_2$O)$_n$ in
1 R=6-CH$_3$-Py, n=0, in chloroform
2 R=6-CH$_3$-Py, n=0, solid
3 R=6-CH$_3$-Py, n=0, in pyridine
4 R=4-CH$_3$-Py, n=2,in chloroform

Table 5. Spectral data of M(H-SAL·Y-Py)$_2$(H$_2$O)$_n$

M	Y	n	State	ν (log ε)	ν (log ε)
Co	3-CH$_3$	2	solid	9.6	
			dichloro-methane	9.7(0.93)	
	4-CH$_3$	0	solid	8.0	9.9 sh
			chloroform	8.3 (1.75)	10.4(1.51) sh
	6-CH$_3$	0	solid	7.9	10.6 sh
			chloroform	8.2 (1.75)	10.6(1.46) sh
			pyridine	10.0(0.95)	
Ni	3-CH$_3$	2	solid	9.5	16.2
			dichloro-methane	9.4 (0.88)	16.0 (1.05)
	4-CH$_3$	2	solid	9.5	16.3
			chloroform	9.3 (0.86)	15.9 (1.08)
	6-CH$_3$	0	solid	8.1	15.2 sh
			chloroform	8.2 (1.13)	15.7 (1.45)sh
			pyridine	9.8 (1.13)	16.8 (1.28)sh

ν: 10^3kK
sh: shoulder

For R=6-CH$_3$-Py the nickel(II) complex Ni(H-SAL·R)$_2$ was obtained. This complex is paramagnetic with a magnetic moment of 3.25 B.M., which corresponds to a moment expected for the nickel(II) complex of a high-spin type. The electronic spectra indicate, as shown in Fig. 2 and Table 5, that this nickel(II) complex is octahedral in the solid state and in non-doner solvents. Since Beer's law holds for this as well as the other complexes, the association of the planar molecules in solution may be excluded for this complex. The band maxima lie in much lower frequency regions than the mixima of the related nickel(II) complexes, as may be seen in Table 5. The low frequency of the d-d band maxima, together with the comparatively high magnetic moment, seems to indicate that the configuration of Ni(H-SAL·6-CH$_3$-Py)$_2$ may be considerably distorted from the regular octahedron. It is to be noted that the ligand in this complex functions as a terdentate ligand with the nitrogen atom in the heterocyclic ring coordinated to the nickel(II) ion. It is also concluded, from the electronic spectrum, that this nickel(II) complex, when dissolved in pyridine, forms an octahedral pyridine adduct Ni(N-SAL·6-CH$_3$-Py)$_2$-(py)$_2$ in which the ligand H-SAL·6-CH$_3$-Py acts as a bidentate ligand.

The palladium(II) ion is similar to the nickel(II) ion in the sense that both ions have a d^8 configuration. Difference between these two ions, however, is remarkable in some respects; the palladium(II) ion forms stable quadri-coordinated planar complexes with various ligands, and the tendency of the palladium(II) ion to take coordination number exceeding four is much lower than that of the nickel-(II) ion. In the present work, the complexes of the type Pd(X-SAL·2-Py)$_2$ were obtained. Since the complexes of the type Pd(X-SAL·R)$_2$ so far obtained are known to have a square-planar con-

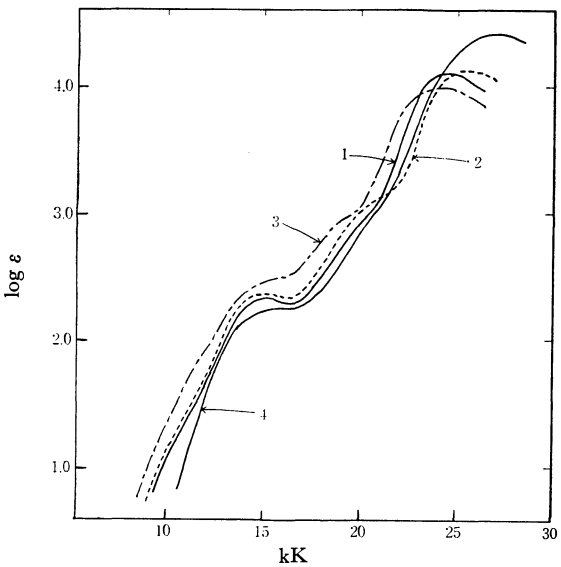

Fig. 3. Electronic absorption spectra of Cu(X-SAL·R)$_2$ in solution.
1 X=H, R=Ph, in chloroform
2 X=H, R=2-Py, in chloroform
3 X=3-CH$_3$O, R=2-Py, in chloroform
4 X=H, R=3-CH$_3$-Py, in dichloromethane

figuration for R=*n*-alkyl and aryl groups, it is most likely that the palladium(II) complexes may also be planar. In fact, the electronic spectrum of Pd(H-SAL·2-Py)$_2$ in solution is similar to that of Pd(H-SAL·Ph)$_2$ in solution, with a band at about 23.6 kK (log ε 3.8).

In contrast to the nickel(II) complexes, the copper(II) complexes of the type Cu(X-SAL·R)$_2$ were readily obtained as crystals. Since, for R=*n*-alkyl and aryl groups, the complexes of the type Cu(X-SAL·R)$_2$ so far obtained, in general, are known to take an essentially planar configuration,*4 it is expected that the copper(II) complexes obtained in the present work may also be planar. This seems to agree with the finding that the electronic absorption spectrum of Cu(H-SAL·2-Py)$_2$ is quite similar to that of Cu(H-SAL·Ph)$_2$, which was previously concluded to be planar, as shown in Fig. 3. The spectra of the other copper(II) complexes prepared in the present work are also found to be quite similar to the spectrum of Cu(H-SAL·2-Py)$_2$.

It is found that the ligands of the types X-SAL·2-Py and H-SAL·CH$_3$-Py function as bidentate ligands in the metal complexes prepared in the present work, with the exception of one nickel(II) complex, in which the ligand might act as a terdentate ligand. The steric condition does not seem to be favorable for these ligands to function as terdentate ligands, since in this case there should be formed the unstable four-membered ring containing the metal ion and the nitrogen atom in the pyridine ring. In this connection, it is interesting to note that for R=(2-pyridyl)-methyl Oehmke and Bailar[6] obtained a compound of a formula Ni(H-SAL·R)$_2$, in which the nickel(II) ion has coordination number six. The steric condition is obviously favorable for this ligand to act as a terdentate ligand.

Support of this work by the Ministry of Education is gratefully acknowledged.

*4 Some complexes are also known to form associated species in the solid state, yielding five-coordinated copper(II) complexes.

6) R. W. Oehmke and J. C. Bailar, Jr., *J. Inorg. Nucl. Chem.*, **27**, 2209 (1965).

BULLETIN OF THE CHEMICAL SOCIETY OF JAPAN VOL. 42 2566—2570 (1969)

Reactions of Thiamine Disulfide Monosulfoxides with Mercaptans[1)]

Goro Tsukamoto, Toshio Watanabe and Isamu Utsumi

Pharmaceutical Research Laboratory, Tanabe Seiyaku Co., Ltd., Kashima-cho, Higashiyodogawa-ku, Osaka

(Received September 16, 1968)

It was found that the reaction of thiamine disulfide monosulfoxide (I) with mercaptan is a competitive reaction between the so-called mercaptan-thiolsulfinate reaction and the apparent oxidation reduction reaction. This reaction offers an excellent method for the preparation of the mixed disulfides of thiamine and *t*-mercaptan or the unstable mixed disulfides, such as thiamine-glutathione disulfides.

In a previous paper,[2)] we showed that thiolsulfinate-type thiamine (I) gave 2-(2-methyl-4-amino-5-pyrimidyl)methylformamido-2-pentene-3-sulfinic acid (II, hereinafter called hypothiaminic acid) in alkaline or neutral hydrolysis as represented by

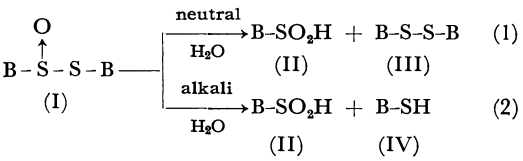

where

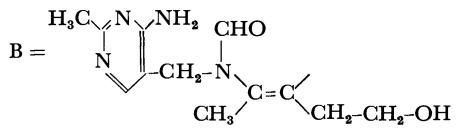

Yurugi *et al.* obtained thiamine butyl disulfide (VI, R=C_4H_7) in low yield on the oxidation of thiamine disulfide (III) in acetic acid with hydrogen peroxide, followed by reaction with butyl mercaptan in alkaline condition, and they suggested an intermediate in this reaction to be thiolsulfinate-type thiamine (I).[3)] In the meantime, we reported that

1) Part XXXII in a series on "Studies on Thiamine Disulfide."

2) I. Utsumi, T. Watanabe, K. Harada and G. Tsukamoto, *Chem. Pharm. Bull.* (*Tokyo*), **15**, 1485 (1967).

3) S. Yurugi, H. Kawasaki and S. Noguchi, *Yakugaku Zasshi* (*J. Pharm. Soc. Japan*), **75**, 498 (1955).

the oxidation of III with hydrogen peroxide did not give the corresponding thiolsulfinate (I).[4,5] This result and the observation described in this paper suggest that thiamine butyl disulfide produced in Yurugi's experiment is formed not through thiolsulfinate (I) but through an other mechanistic route,[6] which will be reported in near future. In this paper, we would like to report the reaction of I with mercaptans.

Result and Discussion

When thiolsulfinate (I) is allowed to react with mercaptans as reported for the reaction of alkyl alkanethiolsulfinate with thiamine in thiol form (IV),[7] compound I is expected to produce the unsymmetrical disulfide-type thiamines (VI). In fact, compound I reacts smoothly and very rapidly with mercaptans at room temperature to give the unsymmetrical disulfides (VI) within a few minutes.

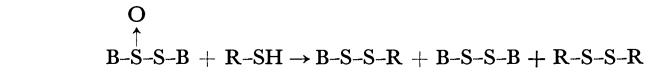

(I) (V) (VI) (III) (VII)

However, it was also found that symmetrical disulfides (III, VII) are concomitantly formed even under a stream of nitrogen.

It has been proposed that one mole of thiolsulfinate reacts with two moles of mercaptan to give two moles of unsymmetrical disulfide.[8] Whereas, Schöberl and Grafje, and Carson and Wong have suggested that a part of sulfenic acid, which is presumably formed in the reaction of thiolsulfinate with mercaptan, gives rise to disproportionation to give mercaptan and sulfinic acid.[9] If a similar reaction takes place in this case, the formation of hypothiaminic acid (II) and thiamine in thiol form (IV) would be observed.[2] However, these compounds (II, IV) can not be detected by paper electrophoresis[2] in the reaction solution.

The product analyses were carried out in detail by means of paper partition and gas chromatography, and the formation of the following compounds were observed: (1) in the case of molar ratio, V/I=2, three compounds, *i. e.*, unsymmetrical disulfide (VI) and symmetrical disulfides (III, VII), (2) in the case of V/I <2, starting compound (I) in addition to these three compounds, (3) in the case of V/I $\gg 2$, thiamine (IV) and thiothiamine (3-(2-methyl-4-amino-5-pyrimidyl)methyl-4-methyl-5-β-hydroxyethylthiazoline-2-thione) as the secondary decomposed products.

The yield of thiamine propyl disulfide obtained from the reaction of I with propyl mercaptan in 80% ethanol are listed in Table 1.

Table 1. Effect of amount of PrSH on yield of BSSPr

PrSH/I	1.0	1.2	1.4	1.6	1.8	2.0	2.1	3.0
Yield(%) of BSSPr	29	37	46	51	58	65	55	trace
PrSH(%) used in the formation of BSSPr	56	61	64	63	63	62	51	—

The reaction was carried out in 80% ethanol, and the main features of the reaction were the same even in absolute ethanol and acetic acid. Therefore, the predominant form of mercaptan should be undissociated acid which would either protonate or hydrogen-bond with sulfinate oxygen in the ground or transition state of the reaction, depending on the acidity of mercaptan.

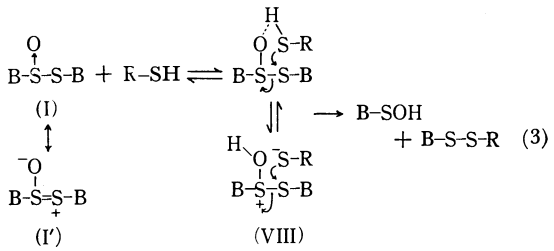

(I) (I') (VIII)

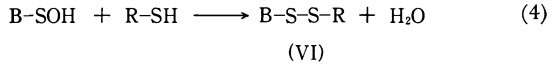

(VI)

Both protonation and hydrogen bonding would make the sulfinyl group a better leaving group which would favor the nucleophilic attack of mercaptan on sulfenyl sulfur resulting in the formation of sulfenic acid and unsymmetrical disulfide.

The symmetrical disulfides (III, VII) were produced in the same ratio as indicated in Table 2. The production of III suggests the possibility that III might be formed through oxidation-reduction reaction between I and mercaptan in accordance with the previous report in which the thiolsulfinate (I) and its *O*-benzoyl ester (IX, OH in structure I is $OCOC_6H_5$) were proved to behave as an

4) I. Utsumi, K. Harada, G. Tsukamoto and I. Daira, *J. Vitaminol. (Kyoto)*, **11**, 234 (1965).

5) I. Utsumi, K. Harada, K. Kohno and G. Tsukamoto, *ibid.*, **13**, 26 (1967).

6) The formation of VI would be due to mixed reactions between disproportionation reaction of disulfides with mercaptans and oxidation reactions of mercaptans in the presence of hydrogen peroxide.

7) T. Matsukawa and H. Kawasaki, *Yakugaku Zasshi (J. Pharm. Soc. Japan)*, **73**, 216 (1953).

8) L. D. Small, J. H. Bailey and C. J. Cavallito, *J. Am. Chem. Soc.*, **69**, 1710 (1947); *ibid.*, **71**, 3565 (1949); W. E. Savige, J. Eager, J. A. Maclen and C. M. Bocburgh, *Tetrahedron Letters*, **1964**, 3289.

9) A. Schöberl and H. Grafje, *Ann.*, **67**, 71 (1958); J. F. Carson and F. F. Wong, *J. Org. Chem.*, **26**, 3028 (1961).

Table 2. Effect of acidity of mercaptans on the reaction of I with RSH (RSH/I=2)

RSH	*p*-NO_2-phenyl	Phenyl	Benzyl	*n*-Pr
pK_a	5.11[10]	6.7[11]	9.43[11]	10.63[11]
Yield(%) of BSSR	trace[a]	15	58	65
Yield(%) of RSSR	97	80	41	38[b]
Yield(%) of BSSB	90	85	40	35

a) The unsymmetrical disulfide was detected only by paper partition chromatography (BuOH·AcOH·H_2O=4:1:5).
b) Produced PrSSPr was measured by gas chromatography (Column: Diethylene Glycol Succinate (1.5 m), Carrier gas: He(60 m*l*/min), Column temp.: 100°C, (Retention time: 6 min)

Table 3. Effect of each BuSH on yield of BSSBu (RSH/I=2)

RSH	*n*-Bu	*s*-Bu	*t*-Bu
Yield(%) of BSSR	75	86	90[a]

a) *t*-BuSSBu-*t* (yield: 5%) produced in this case was detected by gas chromatography (Retention time under the same condition as abvove: 3.8 min).

oxidizing reagent.[5,12]

In connection with the forgoing results, Tables 2 and 3 show that the mercaptans of higher acidity are oxidized more readily to the symmetrical disulfide (VII) than those of lower acidity, while the mercaptans of lower acidity yield a larger amount of unsymmetrical disulfide (VI) than the mercaptans of higher acidity. *O*-Benzoylthiamine disulfide monosulfoxide (IX) and thiamine benzyl disulfide monosulfoxide (ester of thiamine in thiol form (IV) and benzyl thiolsulfinic acid)[13] also showed similar reactivities to those of I.

The formation of the symmetrical disulfides (III, VII) would be dependent on the following reaction initiated by the attack of mercaptan to protonated oxygen. However, the attacking site of mercaptan is thought to be protonated oxygen and sulfinyl sulfur in the transition state (VIII). Namely, mercaptan attacks protonated oxygen to give symmetrical disulfides (III) and the corresponding sulfenic acid of the attacking mercaptan.

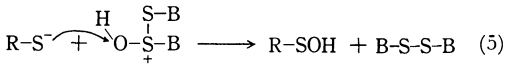

$$R\text{-}S^- + \overset{H}{\underset{+}{O}}\text{-}\overset{S\text{-}B}{\underset{+}{S}}\text{-}B \longrightarrow R\text{-}SOH + \underset{(III)}{B\text{-}S\text{-}S\text{-}B} \quad (5)$$

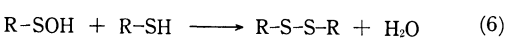

$$R\text{-}SOH + R\text{-}SH \longrightarrow \underset{(VII)}{R\text{-}S\text{-}S\text{-}R} + H_2O \quad (6)$$

This apparent oxidation-reduction presumably depends on the acidity of attacking mercaptan, *i. e.* the more acidic mercaptan can protonate oxygen more strongly and the resulting mercapto anion is more strongly nucleophile than the undissociated mercaptan. Similar trends have also been observed in the oxidation of mercaptan by sulfoxide to give disulfide, in which the order of reactivity of mercaptan is ArSH>$ArCH_2SH$>alkylSH.[14]

An important question remains as to the possible disproportionation reaction of the disulfides (VII, III) as follows:

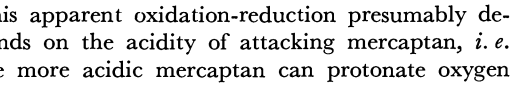

$$B\text{-}S\text{-}S\text{-}R + R\text{-}SH \longrightarrow B\text{-}SH + R\text{-}S\text{-}S\text{-}R \quad (7)$$

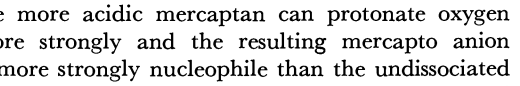

$$\overset{O}{\uparrow}\ B\text{-}S\text{-}S\text{-}B + B\text{-}SH \longrightarrow B\text{-}SOH + B\text{-}S\text{-}S\text{-}B \quad (8)$$

This must certainly be important when mercaptan is used more than two moles as indicated in Table 1.

Therefore, it can be concluded that the reaction of thiolsulfinate (I) with mercaptans is competitive reactions between the so-called mercaptan-thiolsulfinate reaction (Eq. (9)) and the apparent oxidation reduction (Eq. (10)).

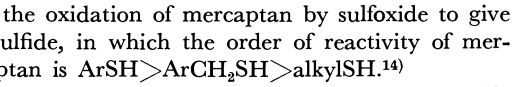

$$\underset{(I)}{\overset{O}{\uparrow}\ B\text{-}S\text{-}S\text{-}B} + 2\ \underset{(V)}{R\text{-}SH} \begin{cases} \longrightarrow 2\ \underset{(VI)}{B\text{-}S\text{-}S\text{-}R} + H_2O & (9) \\ \longrightarrow \underset{(III)}{B\text{-}S\text{-}S\text{-}B} + \underset{(VII)}{R\text{-}S\text{-}S\text{-}R} + H_2O & (10) \end{cases}$$

It is of interest to note that these thiolsulfinate remained unchanged after four years at room temperatures. This pronounced stability which seems unusual for this type of compound would be due to the conjugation of $-S(O^-)=S^+-$ double bond with both sides of olefinic double bonds.

Up to the present time, a number of thiamine alkyl disulfides have been prepared by a variety of methods,[15] but hardly any are suitable for the preparation of the mixed disulfides of thiamine and *t*-mercaptan. In contrast, the reaction of I with *t*-mercaptan offers an excellent method for the preparation of the mixed disulfides.

Reduction of the mixed disulfides of thiamine and *t*-mercaptan by sulfhydryl compounds to

10) L. Lumper and H. Zahn, "Advances in Enzymology," Vol. 27, ed. by F. F. Nord, John Wiley and Sons, New York (1965), p. 202.
11) M. M. Kreevoy, E. T. Harper, R. E. Duvall, H. S. Wilgus, III, and L. T. Ditsch, *J. Am. Chem. Soc.*, **82**, 4899 (1960).
12) We also knew that the thiolsulfinates (I, IX) were immediately reduced with triphenylphosphine in chloroform at room temperatures to give quantitatively the corresponding disulfides and triphenylphosphine oxide respectively. See J. F. Carson and F. F. Wong, *J. Org. Chem.*, **26**, 1467 (1961).
13) H. Kawasaki and H. Yonemoto, *Yakugaku Zasshi* (*J. Pharm. Soc. Japan*), **77**, 640 (1957).
14) T. J. Wallace, *J. Am. Chem. Soc.*, **86**, 2018 (1964).
15) T. Matsukawa and S. Yurugi, "Review of Japanese Literature on Beriberi and Thiamine," ed. by N. Shimazono and E. Katsura, Vitamin B Research Committee of Japan, Kyoto (1965), p. 107—114.

thiamine in thiol form proceeds with some difficulty in comparison with thiamine *n*-alkyl disulfides. This observation of biological interest will be reported elsewhere.

In addition to the preparation of the mixed disulfides, this reaction is also suitable for preparing unstable unsymmetrical thiamine disulfides such as thiamine-glutathione disulfide[16] and thiamine pyridylmethyl disulfide derivatives.[17]

Experimental

Melting points are not corrected. Infrared absorption spectra were measured with a Hitachi Infrared Spectrophotometer, EPI-S_2. Gas chromatographic analyses were carried out with a Shimadzu Model GC-1C.

Since thiamine disulfide (III), which was formed when thiolsulfinate (I) was allowed to react with mercaptans, could not be isolated quantitatively as crystals, it was measured as follows: Amounts of thiamine disulfide in the filtrates were determined by thiochrome method after the filtrates, from which unsymmetrical disulfides of thiamine (VII) were filtered off, were proved to contain only thiamine disulfide (III).

An Alternative Method for Preparation of Thiolsulfinates (I, VIII). The following procedure for the preparation of thiolsulfinates is favorable in comparison with that described previously.[5]

To a stirred solution of thiamine disulfide or its O-benzoyl ester (0.10 mol) dissolved in 2N H_2SO_4 (500 m*l*) was added peracetic acid (0.12 mol) under cooling with ice-water. The reaction mixture was allowed to stand overnight at room temperature. The adjustment of the reaction solution to pH 6—7 with Na_2CO_3 or $NaHCO_3$ gave the corresponding thiolsulfinates (I, IX), free from other oxidation product contaminants, as pale yellow crystals in satisfactory yield (80—85%).

Reaction of Thiolsulfinate (I) with Propyl and Butyl Mercaptans. *i) With Propyl Mercaptan.* To a suspension of I (580 mg) in 80% ethanol (10 m*l*) was added molar equivalent of propyl mercaptan (Table 1) with stirring under a stream of nitrogen at room temperature, and the mixture was allowed to stand for 10 min. The reaction solution, in which the mole ratio of the thiolsulfinate to the mercaptan was 1 : 1—1.8, was filtered and the filtrates were condensed under reduced pressure. The resulting residues to which water (5 m*l*) was added were allowed to stand for a day at room temperature to give colorless prisms in yields shown in Table 1. The crystals obtained were confirmed to be nearly pure by thin layer chromatography. Recrystallization of the crystals from benzene gave colorless prisms, mp 128—129°C, which were identical in infrared spectrum with the authentic thiamine propyl disulfide prepared by the known method.[6]

The reaction solutions, in which the mole ratio of the thiolsulfinate to the mercaptan was 1 : 2.0, 2.1, were similarly treated without having been filtered.

In a case where the mole ratio of the thiolsulfinate to the mercaptan was 1 : 3.0, a similar treatment of the reaction solution to the above-mentioned method afforded colorless needles (50 mg), mp 233—234°C (decomp.). Recrystallization from water gave colorless needles, mp 237—238°C (decomp.), which were identical in infrared spectrum with authentic 3-(2-methyl-4-amino-5-pyrimidyl)methyl-4-methyl-5-β-hydroxyethyl-thiazoline-2-thione. The mother liquor was condensed under reduced pressure to remove water and the resulting residue was dissolved in ethanolic HCl to afford colorless needles (560 mg), mp 246—247°C (decomp.), which were found to be identical with authentic thiamine hydrochloride by infrared spectrum.

ii) With n-Butyl Mercaptan. The procedure was the same as above. The reaction of I (580 mg) with *n*-butyl mercaptan (180 mg) gave 0.55 g (75%) of colorless prisms, mp 139—140°C. Recrystallization of the crystals from benzene gave colorless prisms, mp 135—136°C, which were found by infrared spectrum to be identical with authentic thiamine butyl disulfide prepared by the known method.[7]

iii) With s-Butyl Mercaptan. The procedure was the same as above except that the reaction time was 30 min. The reaction of I (580 mg) with *s*-butyl mercaptan (180 mg) yielded 640 mg (86%) of colorless prisms, mp 121—123°C. Recrystallization of the crystals from ethyl acetate gave thiamine *s*-butyl disulfide as colorless prisms, mp 121—123°C.

Found: C, 51.99; H, 7.11; N, 15.11; S, 17.41%. Calcd for $C_{16}H_{26}O_2N_4S_2$: C, 51.88; H, 7.08; N, 15.13; S, 17.28%.

IR ν_{max}^{Nujol} cm^{-1}: 3300, 3100, 1670, 1645, 1065.

Hydrochloride: Colorless needles (ethanol-ether), mp 160—161° C(decomp.).

Found: C, 47.44; H, 6.73; N, 13.75%. Calcd for $C_{16}H_{27}O_2N_4S_2Cl$: C, 47.22; H, 6.69; N, 13.77%.

iv) With t-Butyl Mercaptan. The procedure was the same as above except that the reaction time was 1 hr. The reaction of I (580 mg) with *t*-butyl mercaptan (180 mg) gave 660 mg (90%) of colorless prisms, mp 151—152°C. Recrystallization from ethyl acetate gave thiamine *t*-butyl disulfide as colorless prisms, mp 151—152°C.

Found: C, 51.84; H, 7.06; N, 15.09; S, 16.79%. Calcd for $C_{16}H_{26}O_2N_4S_2$: C, 51.88; H, 7.08; N, 15.13; S, 17.28%.

IR ν_{max}^{Nujol} cm^{-1}: 3310, 3150, 1670, 1060.

Hydrochloride: Colorless needles (ethanol-ether), mp 182—184°C.

Found: C, 47.48; H, 6.80; N, 13.87%. Calcd for $C_{16}H_{27}O_2N_4S_2Cl$: C, 47.22; H, 6.69; N, 13.77%.

Reaction of Thiamine Benzyl Disulfide Monosulfoxide with Trityl Mercaptan. To a solution of thiamine benzyl disulfide monosulfoxide (420 mg) in 80% ethanol (10 m*l*) was added trityl mercaptan (550 mg) and the mixture was stirred at 50°C for 30 min. After the reaction, the reaction solution, in which oily precipitate separated, was condensed to dryness under reduced pressure and the resulting residue which was washed with petroleum ether was crystallized from ethanol to give crystals, 400 mg, mp 171—173°C. Recrystallization from ethanol gave thiamine trityl disulfide as colorless prisms, mp 171—173°C.

Found: C, 67.15; H, 5.93; N, 10.13; S, 11.40%. Calcd for $C_{31}H_{32}O_2N_4S_2$: C, 66.88; H, 5.79; N, 10.06; S, 11.52%.

16) K. Kohno, G. Tsukamoto, Y. Kakie and I. Utsumi, *Vitamins (Kyoto)*, **36**, 336 (1967).

17) I. Utsumi, T. Watanabe and G. Tsukamoto, *ibid.*, **37**, 276 (1968).

IR ν_{max}^{Nujol} cm^{-1}: 3275, 3175, 1660, 1065, 730, 700.

This compound was found by infrared spectrum to be identical with authentic thiamine trityl disulfide prepared by the reaction of I with trityl mercaptan.

Reaction of I with Benzyl Mercaptan. To a stirred suspension of I (580 mg) in 80% ethanol (10 m*l*) was added benzyl mercaptan (248 mg) in nitrogen at room temperature, and a clear solution was immediately obtained. The reaction solution was condensed under reduced pressure. Water (5 m*l*) was added to the resulting residue and left to stand for a day to give crystals, 570 mg. After the crystals were dried under reduced pressure, they were washed with ether to give crystals, 470 mg (58%). Recrystallization from ethyl acetate gave 450 mg of thiamine benzyl disulfide as colorless prisms, mp 152°C, which were found to be identical with authentic samples by infrared spectrum.

Evaporation of the washed ether solution gave crystals, 100 mg (41%), mp 71—72°C, undepressed on admixture with authentic dibenzyl disulfide.

Reaction of I with Phenyl Mercaptan. The reaction between I (580 mg) and phenyl mercaptan (220 mg) was carried out with a similar procedure to that described in the reaction of I with benzyl mercaptan.

Ethanol as solvent of the reaction mixture was removed under reduced pressure and to the resulting residue was added water (5 m*l*) to separate crystals, which were extracted with chloroform. The chloroform solution was dried over sodium sulfate and chromatographed over alumina (10 g). The column was eluted with chloroform-ethanol (99 : 1) tracing with Dragendorff's reagent. The first fraction which is negative toward the reagent was condensed to dryness under reduced pressure to yield crystals (178 mg, 80%), mp 61—62°C, which were found to be identical with authentic diphenyl disulfide by infrared spectrum. The second fraction which is positive toward the reagent was treated similarly. The residue thus obtained was crystallized from benzene to yield colorless crystals (115 mg, 15%), mp 137°C (decomp.), which were found to be identical with authentic thiamine phenyl disulfide by infrared spectrum.

Reaction of I with *p*-Nitrophenyl Mercaptan. To a stirred suspension of I (580 mg) in 80% ethanol (10 m*l*) was added *p*-nitrophenyl mercaptan (310 mg). Separated colorless needles, 300 mg, mp 181—182°C, were filtered. Recrystallization from ethanol gave colorless needles, mp 182°C, which were found to be identical with authentic di-*p*-nitrophenyl disulfide by infrared spectrum.

The mother liquor from which di-*p*-nitrophenyl disulfide was filtered off was submitted to paper partition chromatography, which showed two spots, one R_f 0.37 assignable to thiamine disulfide and the other R_f 0.72 presumed to be thiamine *p*-nitrophenyl disulfide.

The authors are indebted to Professor S. Oae and Assistant Professor W. Tagaki of Osaka City University for their valuable discussions and their kindness to read the manuscript.

BULLETIN OF THE CHEMICAL SOCIETY OF JAPAN VOL. 42 2570—2573 (1969)

Alkoxysilanes. III. Preparation of Alkoxysiloxyaminosilane and Some of Its Reactions

Yoshimoto ABE and Ichiro KIJIMA

Department of Industrial Chemistry, Faculty of Engineering, Science University of Tokyo, Kagurazaka, Shinjuku-ku, Tokyo

(Received September 19, 1968)

Bis(tri-*t*-butoxysiloxy)diaminosilane was prepared by the reaction of the corresponding dichlorosilane with ammonia. It was also obtained by the reaction of silicon tetrachloride with tri-*t*-butoxysilanol in the presence of pyridine as a dehydrochloric acid agent, followed by the subsequent reaction of the mixture with ammonia. The alcoholysis, transamination reaction, hydrolysis, and acetolysis of this compound with *n*-butyl alcohol, phenol, aniline, *n*-butylamine, water, and acetic acid led to the formation of the corresponding bis(tri-*t*-butoxysiloxy)silane derivatives. In these reactions, the measurement of the ammonia evolved made it possible examine the relative reactivity of the reactants. An attempt to isolate the triaminosilane by the reaction of tri-*t*-butoxysiloxytrichlorosilane with ammonia resulted in the formation of tetraaminocyclotetrasilazane and a polymeric substance containing the silicon-nitrogen bond.

It has been previously established that the hydroxy or amino group attached to the silicon atom in alkoxy or alkylsilanes is apt to be susceptible to condensation to form a siloxane or silazane bond,[1] but these groups are stabilized in the silicon com-

1) P. Fessenden and J. S. Fessenden, *Chem. Revs.*, **61**, 316 (1961).

pounds containing two or three secondary or tertiary alkyl groups.[2,3]

We have reported that the hydroxy group can be stabilized remarkably by introducing the tributoxysiloxy group into silicon compounds; thus silanediol and even-triol can be obtained.[4] Therefore, it was also expected that the introduction of this substituent into silicon compounds would stabilize the amino groups and permit the isolation of di- or triaminosilane with tributoxysiloxy groups.

In the present work, the preparation of the aminosilanes and its reactions with alcohols, amines water, and acetic acid were investigated.

Results and Discussion

Bis(tri-*t*-butoxysiloxy)diaminosilane was prepared in about an 80% yield by the reaction of bis(tri-*t*-butoxysiloxy)dichlorosilane with ammonia. The same compound was also obtained in about a 65% yield by the reaction of silicon tetrachloride with tri-*t*-butoxysilanol in the presence of pyridine, followed by treatment of the reaction mixture with ammonia;

$$[(Bu^tO)_3SiO]_2SiCl_2 \xrightarrow{NH_3} [(Bu^tO)_3SiO]_2Si(NH_2)_2$$

$$SiCl_4 + 2(Bu^tO)_3SiOH + 2C_5H_5N \xrightarrow{NH_3} [(Bu^tO)_3SiO]_2Si(NH_2)_2 + 2C_5H_5NHCl$$

It could be distilled as a white crystalline solid without condensation, and it had a low melting point (55—57°C) and a high solubility in common organic solvents.

The diaminosilane reacted easily with water and acetic acid to give the corresponding silanediol and diacetoxysilane. However, alcoholysis and transamination reaction appear to occur step by step, for the reaction of the diaminosilane with phenol and *n*-butyl alcohol afforded only monobutoxy and monophenoxy derivatives when *n*-hexane was used as a solvent, whereas diphenoxy and dibutoxy derivatives were obtained by the reaction at the boiling point of each reactant. Similar results were obtained from transamination; the reaction of the diaminosilane with *n*-butylamine and aniline under the reflux of each reactant gave di-*n*-butylaminosilane and monoanilinosilane, but the further replacement of the amino group by aniline was difficult under the present conditions (Scheme 1).

Results similar to our findings that alcoholysis takes place step by step had been reported by Miner *et al.*,[2] who investigated the reaction of di-*t*-butoxydiaminosilane with alcohols and suggested that the reaction depends on the steric effect of the alkyl group of the alcohol. Therefore, the formation of mono-substituted derivatives when *n*-hexane is used as the solvent seems attributable to the steric effect of the *n*-butyl or phenyl group. Figure 1 shows the relative rates of transamination and alcoholysis determined by measuring the ammount of ammonia evolved. Apparently the reaction rate of *n*-butyl amine is faster than that of aniline, but the readiness of alcoholysis is not always in the phenol $>$ *n*-butyl alcohol order since the reaction temperatures are not taken into consideration.

In order to obtain tri-*t*-butoxysiloxytriaminosilane, the reaction of the corresponding trichlorosilane with ammonia was carried out. This reaction afforded, instead of the desired compound, a cyclosilazane containing a free amino group, which was identified as tetraaminotetra(tri-*t*-butoxysiloxy)cyclotetrasilazane $[(Bu^tO)_3SiOSi(NH_2)(NH)]_4$. Identification was made on the basis of the evidence from elemental analysis, the molecular-weight determination, and the infrared absorption peaks at 3450 and 3350 (ν_{NH}), 1530 (δ_{NH_2}), 1050 ($\nu_{Si-O-Si}$), and 950 ($\nu_{Si-N-Si}$) cm^{-1}.

In general, the reaction between trichlorosilane and ammonia leads to the formation of silsesquiazene;[5] nevertheless, in this case the cyclosilazane containing free amino groups was obtained.

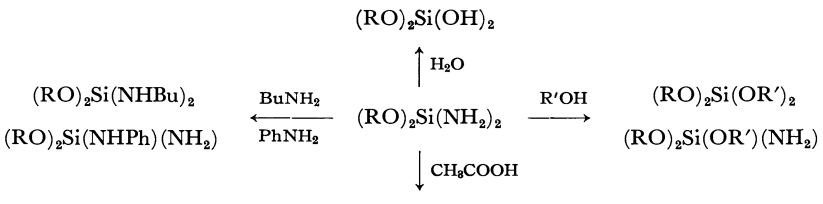

where R=$(BuO)_3Si$ and R'=Bu or Ph

Scheme 1

2) C. S. Miner, L. A. Bryan, R. P. Holysz and G. W. Pedlow, *Ind. Eng. Chem.*, **39**, 1368 (1947).

3) J.E. Wright, R.O. Bolt, A. Goldschmidt and A.D. Abbott, *J. Am. Chem. Soc.*, **80**, 1733(1951); C. R.(1951). Morgan, W. F. Olds and A. L. Rafferty, *ibid.*, **73**, 5193

4) Presneted at the 20th Annual Meeting of the Chemical Society of Japan, Tokyo, April, 1967.

5) U. Wannagat, E. Bogush and F. Hofler, *J. Organometal. Chem.*, **7**, 203 (1967); K. A. Andrianov and G. V. Kotrelev, *ibid.*, **7**, 217 (1967).

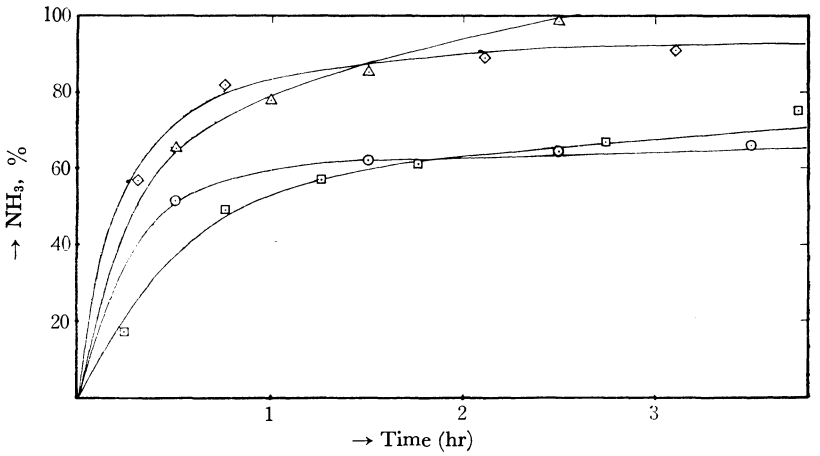

Fig. 1. The relative rate of the reaction of diaminosilane with *n*-butyl alcohol (⊡), aniline (⊙), phenol (◇), and *n*-butylamine (△). Reaction temperature, boilling points of reagents

This unexpected result is probably due to the large steric effect of tri-*t*-butoxysiloxy groups.[6,7]

In the couse of the distillation of the cyclosilazane, a solid was obtained as a residue; it was then purified to give a white powder (mp 240—243°C). Its IR spectrum was essentially identical with that of the cyclosilazane except for the absence of the absorption peaks at 1354 and 860 cm^{-1}. This product seems, therefore, to be a polymer formed by the condensation of the amino group in the cyclosilazane.

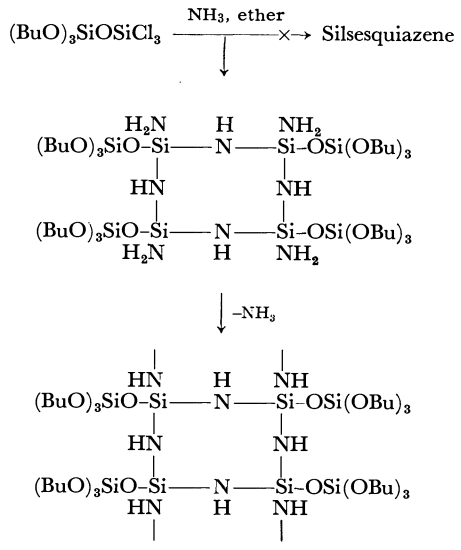

6) R. Schwarz and F. Weigel, *Z. Anorg. Allg. Chem.*, **268**, 251 (1952).

7) H. R. Allcock, "Heteroatom Ring Systems and Polymers," Academic Press, New York (1967), p. 146; D. N. Hunter, "Inorganic Polymers," John Willey & Sons Inc., New York (1963).

Experimental

All the experiments were carried out in a dry atmosphere or nitrogen. The melting points and boilling points were uncorrected.

Materials. The alcohols and amines were dried on calcium oxide or sodium hydroxide and were purified by distillation. The acetic acid was purified by fractional distillation. Bis(tri-*t*-butoxysiloxy)dichlorosilane and tri-*t*-butoxysiloxytrichlorosilane were prepared by a method previously described.[4]

Preparation of Bis(tri-*t*-butoxysiloxy)diaminosilane. To a solution of bis(tri-*t*-butoxysiloxy)dichlorosilane (28 g) in 200 m*l* of benzene, dry ammonia gas was introduced at 0—5°C with stirring. After the completion of the absorption of the ammonia, the mixture was refluxed for 1 hr. This treatment was repeated, and then the ammonium hydrochloride was filtered out and washed with benzene. The solvent was reomved, and the residue was distilled under reduced pressure to give 20 g of a crystalline solid (76.5%), bp 150°C/1 mmHg, mp 55—57°C. Found: C, 49.11; H, 9.96; N, 4.48; Si, 14.32%. Calcd for $C_{24}H_{58}O_8N_2Si_3$: C, 48.48; H, 10.40; N, 4.77; Si, 14.36%.

The preparation of the diaminosilane from silicon tetrachloride and tri-*t*-butoxysilanol proceeded in the following way: to a mixture of 74.6 g (0.283 mol) of silanol, 22.4 g (0.283 mol) of pyridine, and 400 m*l* of benzene, 23.8 g (0.141 mol) of silicon tetrachloride in 100 m*l* were stirred in, drop by drop, at about 0°C. The mixture was refluxed for 1 hr. Then the combined solution was cooled at about 0°C and ammonia gas was introduced. The distillation of the filtrate gave 53.8 g (64.0%) of the diaminosilane, 154°C/1 mmHg. IR: 3400 and 3350 (doublet, w, ν_{NH}), 1535 (m, δ_{NH_2}), 1385 and 1362 (doublet, *t*-butyl group), 1065 (s, $\nu_{Si-O-Si}$) cm^{-1}.

The Reaction of Diaminosilane with *n*-Butyl Alcohol. A solution of 3.4 g of *n*-butyl alcohol in 20 m*l* of *n*-hexane was added to a solution containing 15.2 g of diaminosilane. The mixture was refluxed for 1.5 hr with stirring, and the ammonia thus evolved

was trapped by introducing it into a sulfuric acid solution. The ratio of the recovery of ammonia was 47.4%. The removal of the solvent, followed by fractional distillation *in vacuo*, gave 14.6 g (88.1%) of a liquid; bp 156—157°C/0.6 mmHg, n_D^{20} 1.4125. Found: N, 2.07; Si, 12.93%. Calcd for $C_{28}H_{65}O_9NSi_3$: N, 2.17; Si, 13.00%. IR: 3400 and 3350 (doublet, w, ν_{NH}), 1530 (w, δ_{NH_2}) cm^{-1}.

Dibutoxy derivatives were obtained when the above reaction was carried out without any solvent; the diaminosilane (10.5 g) was heated with *n*-butyl alcohol (4.5 g) at 140—150°C for 10 hr under stirring (93%, ammonia evolved). The reaction mixture, on fractionation, gave 9.9 g (79.0%) of a pale yellow solid; bp 164—165°C/1 mmHg, mp 38—40°C (recrystallized with acetone). Found: C, 54.49; H, 11.22; Si, 12.03%. Calcd for $C_{32}H_{72}O_{10}Si_3$: C, 54.82; H, 10.30; Si, 11.87%. NMR: 8.71 (singlet, Bu^t), 6.32 (triplet, CH_2), 9.10 (doublet, CH_3) τ.

The Reaction of Diaminosilane with Phenol. To a solution of 13.4 g of diaminosilane in 50 m*l* of *n*-hexane, a solution of 4.4 g of phenol in 20 m*l* of *n*-hexane was added. The combined solution was then refluxed for 1.5 hr with stirring (45.6%, ammonia evolved). After the solvent had been removed, the residue was fractionated to give 9.9 g of a viscous liquid (75.7%); bp 182—183°C/1 mmHg, n_D^{20} 1.4361. Found: N, 1.74; Si, 12.78%. Calcd for $C_{30}H_{61}O_9NSi_3$: N, 2.16; Si, 12.80%.

The reaction was carried out without any solvent to obtain a diphenoxy derivative; a mixture of 16.0 g of diaminosilane and 7.7 g of phenol was heated at 170—180°C for 3.5 hr with stirring (94.0%, ammonia evolved). The residue was submitted to fractional distillation; this gave 15.6 g of a pale yellow solid (77.6%), bp 230—231°C/1 mmHg, mp 74—76°C (recrystallized with petroleum ether). Found: C, 57.10; H, 9.02; Si, 11.17%. IR: 1595, 1490, and 750 (m, phenyl group) cm^{-1}. NMR: 8.74 (singlet, Bu^t), 2.94 (single, phenyl protons) τ.

Hydrolysis of Diaminosilane. To 150 m*l* of a sulfuric acid solution (5%), 17.0 g of diaminosilane in 50 m*l* of *n*-hexane were added, drop by drop, at 7—8°C with agitation. The oily layer was separated, washed with a sodium bicarbonate solution and then water, and dried over anhydrous sodium sulfate. After the removal of the solvent, the residue was distilled *in vacuo*, giving 13.0 g (76.0%) of a white solid, bis(tri-*t*-butoxysiloxy)silanediol,[4] bp 154—155°C/1 mmHg.

The Reaction of Diaminosilane with Acetic Acid. Into a solution of 16.2 g of diaminosilane in 100 m*l* of *n*-hexane, a solution of 6.7 g of acetic acid in 50 m*l* of *n*-hexane was stirred, drop by drop, at 5—10°C for 45 min. The mixture was further stirred at room temperature for 1.5 hr, and then the ammonium acetate was filtered out. The removal of the solvent from the filtrate gave a solid, which was then dissolved into 20 m*l* of *n*-hexane. A white crystal was obtained from the solution when it was left standing under cooling; yield, 13.3 g (71.5%), mp 57—62°C. Found: C, 49.73; H, 9.29; Si, 12.30%. Calcd for $C_{28}H_{60}O_{12}Si_3$: C, 49.97; H, 8.98; Si, 12.52%. IR: 1734 (s, calbonyl group) cm^{-1}. NMR: 8.70 (Bu^t), 9.79 ($OCOCH_3$) τ.

Transamination Reaction of Diaminosilane with Aniline. A mixture of diaminosilane (13.7 g) and aniline (8.7 g) was heated at 140—150°C for 2.5 hr under stirring (54.5%, ammonia evolved). After the removal of the excess aniline, the mixture was distilled under reduced pressure, giving 13.0 g (80.7%) of a pale yellow liquid, bp 190.5°C/0.5 mmHg. The product partially solidified at room temperature. Found: C, 54.60; H, 10.10; N, 4.09; Si, 12.54%. Calcd for $C_{30}H_{62}O_8N_2Si_3$: C, 54.35; H, 9.42; N, 4.32; Si, 12.72%. IR: 3450 and 3350 (doublet, w, ν_{NH}), 1530 (w, δ_{NH_2}), 1487, 1590, and 750 (m, phenyl group) cm^{-1}. NMR: 8.66 (Bu^t), 5.75 (NHPh), 3.13 and 3.16 (doublet, phenyl protone) τ.

Transamination Reaction of Diaminosilane with *n*-Butylamine. A mixture of 6.5 g of *n*-butylamine and 13.1 g of diaminosilane was refluxed for 2.5 hr with stirring. The mixture was fractionally distilled under reduced pressure, giving 9.2 g (65.0%) of a pale yellow liquid, which solidified at room temperature; bp 192—193°C/0.5 mmHg, n_D^{20} 1.4217. Found: C, 54.45; H, 10.99; N, 3.73; Si, 11.86%. Calcd for $C_{32}H_{74}O_8N_2Si_3$: C, 54.97; H, 10.66; N, 4.01; Si, 11.86%. IR: 3350 (w, ν_{NH}) cm^{-1}. NMR: 9.12 (doublet, CH_3), 8.72 (Bu^t), 7.22 (quartet, CH_2) τ.

The Reaction of Tri-*t*-butoxysiloxytrichlorosilane with Ammonia. To a solution of 22.6 g of tri-*t*-butoxysiloxytrichlorosilane in 300 m*l* of dry ethyl ether, dry ammonia gas was introduced at −5 to −10°C for about 1 hr with agitation. After the absorption of ammonia had ceased, the mixture was stirred for 30 min at room temperature. After the above treatment had been repeated, ammonium hydrochloride was filtered out and the product washed with ehter. The evaporation of the solvent *in vacuo* gave a transparent, colorless, viscous liquid (14.3 g). This residue was submitted to analysis without further purification. Found: C, 44.47; H, 9.81; N, 8.36; Si, 17.30%, mol wt 1190, n_D^{20} 1.4270. Calcd for $(C_{12}H_{15}O_4N_2Si_2)_n$: C, 44.86; H, 9.39; N, 8.69; Si, 17.41%, mol wt 1289 (n=4).

This residue (7.9 g) was distilled *in vacuo* to give a transparent, highly viscous liquid (4.0 g); bp 220—222°C/0.5 mmHg, n_D^{20} 1.4250. Found: C, 44.58; H, 9.91; N, 7.68; Si, 17.30%, mol wt 1280. IR: 3450 and 3350 (doublet, m, ν_{NH}), 1530 (m, δ_{NH_2}), 1050 (vs, $\nu_{Si-O-Si}$), 950 (s, $\nu_{Si-N-Si}$) cm^{-1}.

After the distillation of the above product, 3.0 g of a white solid remained as a residue. The solid was further purified by the following procedure: to 50 m*l* of vigorously-stirred methanol, 3.0 g of the solid dissolved in 10 m*l* of benzene was added, drop by drop; then the precipitate was filtered and dried *in vacuo*, giving 2.6 g of a white powder, mp 240—243°C. Found: C, 43.02; H, 9.17; N, 6.07; Si, 19.90%. IR: 3450 and 3350 (w, ν_{NH}), 1050 (vs, $\nu_{Si-O-Si}$), 950 (s, $\nu_{Si-N-Si}$) cm^{-1}.

The authors wish to thank Professor Yojiro Tsuzuki for his helpful advice, and Mr. Takeo Takeuchi for his assistance in the experiments. Acknowledgement is also made to the Ministry of Education for its financial support.

BULLETIN OF THE CHEMICAL SOCIETY OF JAPAN VOL. 42 2574—2577 (1969)

Metal-Containing Initiator Systems. XVI. Radical Polymerization with Metal Carboxylates

Shuzo Aoki, Seitaro Matsumura and Takayuki Otsu

Department of Applied Chemistry, Faculty of Engineering, Osaka City University, Sugimoto-cho, Sumiyoshi-ku, Osaka

(Received October 3, 1968)

The polymerization of vinyl monomers with metal carboxylates has been investigated in benzene at 60°C. Cobalt(III) cyclohexanecarboxylate behaved as an effective initiator of the polymerization, and its activity was higher than that of corresponding salts of manganese (III) and copper(II), and than that of cobalt(III) acetylacetonate in the polymerizations of styrene (St) and methyl methacrylate (MMA). It was found that the overall rate of polymeriaztion (R_p) of MMA with cobalt(III) cyclohexanecarboxylate was expressed by the following equation, indicating that the polymerization proceeded through a free redical intermediate:

$$R_p = k[\mathrm{MMA}]^{1.4}[\mathrm{Co(III)}]^{0.5}$$

The free radical propagation of this polymerization was also supported by the results of the copolymerizations of St with MMA and with vinyl acetate; *i.e.*, the resulting copolymer composition curves agreed with the typical free radical ones. It was assumed that the initiation of polymerization occurred by means of a radical produced by the homolysis of the metal-oxygen bond in the carboxylate. The reaction order with respect to MMA in the above equation, which was higher than unity, suggested the participation of the MMA molecule in initiating the radical formation.

It is well known that some metal acetylacetonates can act as free radical initiators of vinyl polymerization. The initiation of polymerization has been considered to take place with a ligand radical resulting from the homolysis of the metal-oxygen bonds in metal acetylacetonates (Eq. (1)).[1-3]

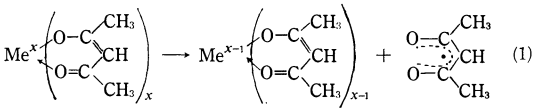

(1)

In previous papers,[3-5] the initiation of vinyl polymerizations by various metal acetylacetonates and copper(II) ethyl acetoacetate was investigated, and it was suggested that it occurs *via* the participation of the monomer used.

It can be predicted that certain metal carboxylates which consist of a similar structure of metal acetylacetonates may serve in a similar manner to initiate the vinyl polymerization. Indeed, lead tetraacetate[6] and ferric laurate[7] have been found to initiate the polymerization of methyl methacrylate (MMA).

The present paper will describe the polymerization of vinyl monomers with metal cyclohexanecarboxylates, especially that of MMA with cobalt(III) cyclohexanecarboxylate.

Experimental

Materials. The monomers and the solvents were purified by ordinary methods and were redistilled before use.

Copper(II) cyclohexanecarboxylate was prepared by the reaction of sodium cyclohexanecarboxylate with copper sulfate. Cobalt(III) cyclohexanecarboxylate was obtained through the reaction of sodium cyclohexanecarboxylate with cobalt sulfate in the presence of hydrogen peroxide, much as in the preparation of cobalt(III) acetylacetonate.[8] Manganese(III) cyclohexanecarboxylate was also prepared according to the method used for the preparation of manganese(III) acetylacetonate;[9] *i.e.*, sodium cyclohexanecarboxylate was reacted with manganese chloride in the presence of potassium permanganate. All of the metal cyclohexanecarboxylates

1) E. M. Arnett and M. A. Mendelsohn, *J. Am. Chem. Soc.*, **84**, 3821, 3824 (1962).

2) E.-G. Kastning, H. Naarmann, H. Reis and Ch. Berding, *Angew. Chem.*, **77**, 313 (1965).

3) C. H. Bamford and D. J. Lind, *Proc. Roy. Soc.*, **A 302**, 145 (1968).

4) T. Otsu, M. Minamii and Y. Nishikawa, *J. Macromol. Sci.*, **A2**, 902 (1968).

5) T. Otsu, Y. Nishikawa and S. Aoki, *Kogyo Kagaku Zasshi* (*J. Chem. Soc. Japan, Ind. Chem. Sect.*), **71**, 1067 (1968).

6) S. Aoki, R. Nakatani and T. Otsu, *ibid.*, **71**, 1756 (1968).

7) V. Lingamurty and S. R. Palit, *J. Sci. Ind. Res. (India)*, **18B**, 140 (1959).

8) B. E. Bryant and W. C. Fernelius, "Inorganic Syntheses," Vol. V, p. 188, (1957).

9) R. G. Cherles, *ibid.*, Vol. VII, p. 183, (1963).

obtained were thoroughly washed with water; they were then dried in a vacuum desiccator:

$Cu(OCOC_6H_{11})_2$; light blue powder, Cu (calcd) 20.0%, Cu (found) 20.7%.

$Co(OCOC_6H_{11})_3$; dark green powder, Co (calcd) 13.4%, Co (found) 13.8%.

$Mn(OCOC_6H_{11})_3$; dark brown powder, Mn (calcd) 12.6%, Mn (found) 13.3%.

Analytical-grade cobalt(III) acetylacetonate was used without further purification. Azobisisobutyronitrile was recrystallized from ethanol.

Polymerization. The polymerization was carried out in a sealed glass tube without diffused light in a thermostat maintained at given temperatures. The resulting polymer was isolated by pouring the polymerization mixture into a large amount of methanol.

The number-average molecular weight ($\bar{M}_n$) of the resulting polymers was determined from the intrinsic viscosity measurements in benzene at 30°C by using the following equations:[10]

$$[\eta] = 8.69 \times 10^{-5}\bar{M}_n^{0.76} \text{ for poly (MMA)}$$

$$[\eta] = 1.13 \times 10^{-4}\bar{M}_n^{0.73} \text{ for polystyrene}$$

Results and Discussion

Initiating Activity of Metal Cyclohexanecarboxylates. Styrene and MMA were polymerized by using copper(II), cobalt(III) and manganese(III) cyclohexanecarboxylates as initiators in bulk at 60°C. The results are shown in Table 1. Cobalt(III) cyclohexanecarboxylate was observed to show the highest initiating activity among these cyclohexanecarboxylates. For the MMA polymerization the activity decreased in the order: $Co^{III} > Mn^{III} > Cu^{II}$; this order agreed with that of the redox potential of the corresponding metal ions in aqueous solutions.[11]

Table 1. Bulk polymerizations of styrene and MMA with metal cyclohexanecarboxylates at 60°C

Carboxylate (1×10^{-2} mol/l)	Monomer	Time (hr)	Yield (%)	$\bar{M}_n\times10^{-5}$
Cu^{II}	Styrene	8	1.2	7.34
	MMA	5	trace	—
Co^{III}	Styrene	8	2.7	6.68
	MMA	2.5	6.6	8.55
Mn^{III}	Styrene	8	trace	—
	MMA	5	2.3	8.94

As can be seen from Table 2, the initiating activity of cobalt(III) cyclohexanecarboxylate was found to be higher than that of cobalt(III) acetylacetonate in the polymerizations of the vinyl monomers used. However, in the polymerization of butadiene, the initiating activity of cobalt(III) cyclohexanecarboxylate was very low.

Table 2. Bulk polymerizations of vinyl monomers with Co(III) cyclohexanecar boxylate and Co(III) acetylacetonate at 60°C

Monomer	Initiator	Time (hr)	Yield (%)
MMA	Carboxylate	5	11.0
	Acetylacetonate	5	2.2
Styrene	Carboxylate	5	1.9
	Acetylacetonate	5	1.0
Acrylonitrile[b]	Carboxylate	5	2.9
	Acetylacetonate	5	trace
Vinyl acetate	Carboxylate	2	2.0
	Acetylacetonate	2	trace
Butadiene[c]	Carboxylate	15	trace

a) Initiator 30 mg and monomer 10 ml were used.
b) Polymerized in 50 vol% benzene solution.
c) Polymerized in 70 vol% benzene solution using 100 mg of the carboxylate at 80°C.

Polymerization of MMA with Cobalt(III) Cyclohexanecarboxylate. The course of the MMA polymerization with cobalt(III) cyclohexanecarboxylate was investigated kinetically in bulk or in a benzene solution.

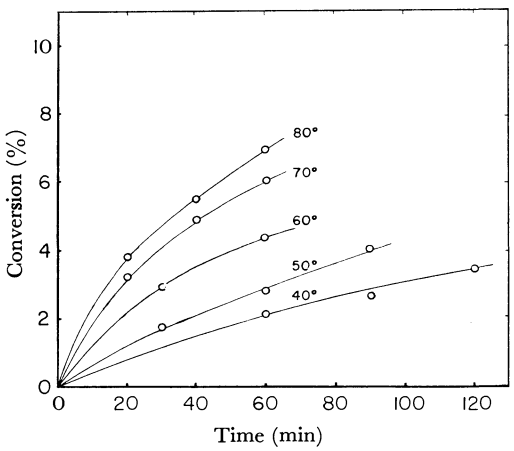

Fig. 1. Time-conversion curves in the bulk polymerization of MMA with cobalt(III) cyclohexanecarboxylate ([Co]=6.8×10^{-3} mol/l).

Figure 1 shows the time-conversion relations in the bulk polymerization of MMA at different temperatures. The linear relationship between the polymer yield and the time was not observed even at the initial stage of the polymerization, and the rate of polymerization decreased gradually with the time, much as in the MMA polymerization with lead tetraacetate.[6] Therefore, as a matter of convenience, the rate of polymerization was estimated approximately from the ratio of the polymer yield and the time at about a 5% polymer yield.

10) "Polymer Handbook," J. Brandrup and E. H. Immergut Ed., Interscience, New York (1966).
11) "Handbook of Chemistry," N. A. Lange Ed., McGraw-Hill, New York (1961).

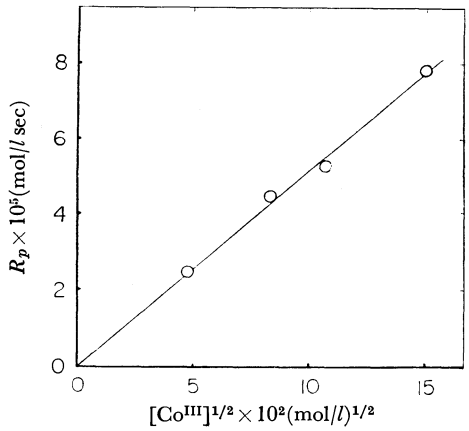

Fig. 2. Relationship between R_p and $[Co^{III}]^{1/2}$ at 60°C ([MMA]=4.7 mol/l in benzene).

Figure 2 shows the straight-line relationship between the rate of polymerization and the square-root concentration of the initiator at a constant MMA concentration in benzene at 60°C. Figure 3

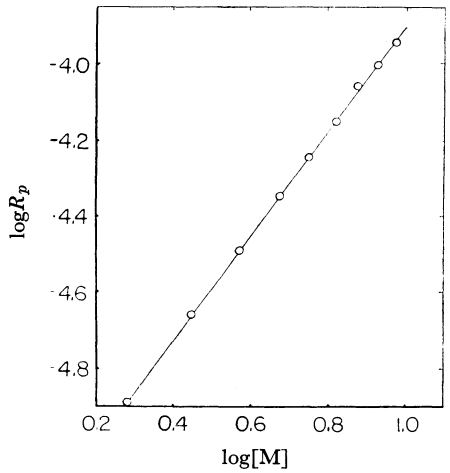

Fig. 3. Relationship between R_p and [MMA] in benzene at 60°C ($[Co^{III}]=6.8\times10^{-3}$ mol/l).

shows the log-log plot between the rate of polymerization and the monomer concentration at a constant initiator concentration in benzene at 60°C. From this figure, the kinetic order with respect to the MMA concentration was found to be 1.4.

Therefore, the overall rate of polymerization (R_p) of MMA with cobalt(III) cyclohexanecarboxylate was expressed by the following equation:

$$R_p = k[\text{MMA}]^{1.4}[\text{Co}]^{0.5} \quad (2)$$

The observed order with respect to the initiator concentration in Eq. (2) indicated that this polymerization proceeded through a free radical intermediate. The order of the MMA concentration, which was higher than unity, suggests that the MMA molecule participates in the radical formation from the cobalt(III) initiator.

The poly(MMA) obtained by using the metal cyclohexanecarboxylates showed the same infrared spectra as the typical radical polymer, indicating that there was no difference in stereoregularity between them.

Copolymerization of Styrene with MMA or Vinyl Acetate. Styrene (M_1) was copolymerized with MMA or vinyl acetate by using cobalt(III) cyclohexanecarboxylate as an initiator in bulk at 60°C. The monomer-copolymer composition curves obtained are shown in Fig. 4. From this figure

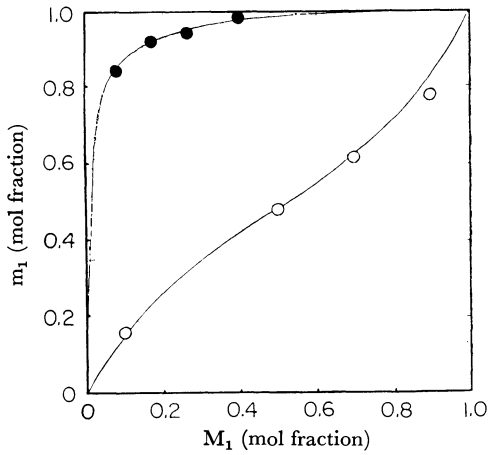

Fig. 4. Monomer-copolymer composition curves in the copolymerizations of styrene (M_1) with MMA (—○—) and with vinyl acetate (—●—) at 60°C.

the monomer reactivity ratios in these copolymerization systems were determined to be $r_1=0.40$ and $r_2=0.50$ for the styrene-MMA system, and $r_1=55$ and $r_2=0$ for the styrene-vinyl acetate system. These values were in accordance to those obtained by using peroxides and azo compounds as radical initiators,[10] indicating that this cobalt(III) initiator did not influence the propagation step of the radical polymerization.

Absorption Spectra of Cobalt(III) Cyclohexanecarboxylate. Cobalt(III) cyclohexanecarboxylate showed the characteristic absorption maximum at about 650 mμ based on the Co^{III} ion.

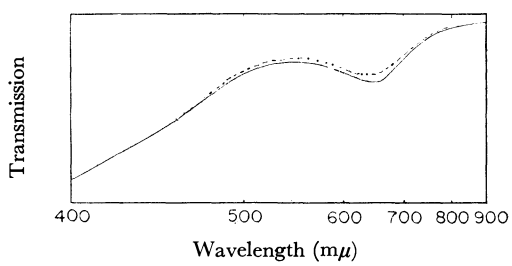

Fig. 5. Absorption spectra of cobalt (III) cyclohexanecarboxylate in benzene-MMA mixture (9 : 1). (——): Before heating, (-----): After heating

The intensity of this absorption peak did not change upon heating in benzene at 80°C for 18 hr. As can be seen from Fig. 5, however, it decreased slightly upon being heated in a benzene-MMA mixture. This result indicates that cobalt(III) cyclohexanecarboxylate does not decompose in benzene, much like cobalt(III) acetylacetonate,[12] but it decomposes in the presence of the MMA monomer.

Chain Transfer to Cobalt(III) Cyclohexanecarboxylate. Figure 6 shows the plot between the rate of the polymerization of MMA and the reciprocal degree of polymerization ($1/\bar{P}_n$) of the polymer obtained. Although this plot gave a straight line when azobisisobutyronitrile was used as an initiator, that obtained by using cobalt(III) cyclohexanecarboxylate showed a concave curve, indicating that considerable chain transfer to the cobalt(III) initiator occurred. According to the treatment by Tobolsky *et al.*,[13] the apparent chain transfer constant of this initiator toward the poly(MMA) was estimated to be 0.06.

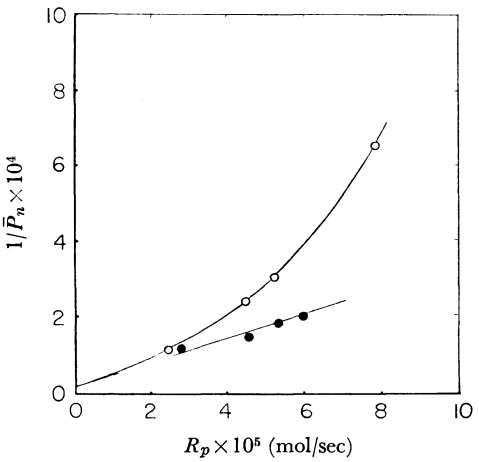

Fig. 6. $1/\bar{P}_n$ *vs.* R_p.
(—○—): Polymerized with cobalt(III) cyclohexanecarboxylate,
(—●—): Polymerized with azobisisobutyronitrile
(Polymerization conditions were the same with in Fig. 2.)

Conclusions

The following conclusions were derived from the results presented above: (i) cobalt(III) cyclohexanecarboxylate could serve as an effective free radical initiator of the MMA polymerization; (ii) this carboxylate did not influence the propagation step in the radical polymerization of MMA, and (iii) this carboxylate decomposed to produce the initiating radical species when the MMA monomer participated.

The initiation with cobalt(III) cyclohexanecarboxylate in the MMA polymerization might resemble that of metal acetylacetonates.[4,5] The polymerization was thought to be initiated with a radical produced by the homolysis of the metal-oxygen bond in metal carboxylate, with the participation of the MMA monomer, as follows:

$$Me^{x}\text{-}(\text{-O-}\overset{\overset{O}{\|}}{C}\text{-R})_x + M \rightarrow Me^{x-1}\text{-}(\text{-O-}\overset{\overset{O}{\|}}{C}\text{-R})_{x-1} + R\text{-}\overset{\overset{O}{\|}}{C}\text{-O-M}\cdot \text{ (or R-M}\cdot\text{)}$$

12) J. Itakura, H. Tanaka and H. Ito, *Kogyo Kagaku Zasshi* (*J. Chem. Soc. Japan, Ind. Chem. Sect.*), **70**, 1227 (1967).

13) B. Baysal and A. V. Tobolsky, *J. Polymer Sci.*, **8**, 529 (1952).

BULLETIN OF THE CHEMICAL SOCIETY OF JAPAN VOL. 42 2578—2583 (1969)

Kinetic Features of the Redox-polymerization of Acrolein with the Potassium Persulfate - Silver Nitrate System

Tsutomu KAGIYA, Shigeru MORITA and Kenichi FUKUI

Faculty of Engineering, Kyoto University, Sakyo-ku, Kyoto

(Received November 4, 1968)

The polymerization of acrolein initiated by the potassium persulfate-silver nitrate redox system in water was studied at 0°C from the point of view of kinetics. The potassium persulfate concentration was varied over the range from 15.75 to 157.5 mmol/*l*, and that of the initial monomer, from 0.462 to 2.675 mol/*l*, while the concentration of silver nitrate was 31.5 mmol/*l*. Both the polymerization rate and the molecular weight of the polymer were found to increase with the reaction time in the early stage, while in the stage of higher conversion the polymerization rate was gradually reduced and the molecular weight remained constant. In the early stage of the polymerization, the polymer yield showed a first-order dependence on the potassium persulfate and initial monomer concentrations. The molecular weight of the polymer was proportional to the monomer concentration, independent of the catalyst concentration. From these results, the kinetic features were discussed.

Some detailed studies of the redox-polymerization with potassium persulfate-silver nitrate catalyst system have been reported, especially focused on the polymerization of a monomer such as acrolein[1] and methyl vinyl ketone.[2] Little attention, however, has been paid to the kinetic mechanism of these polymerizations. In order to make clear the mechanism of the redox-type polymerization, the acrolein polymerization with the potassium persulfate - silver nitrate system was studied. The purpose of this report is to describe the characteristic features of this polymerization.

Experimental

Materials. Commercial acrolein was distilled under nitrogen, using a 50-cm column, immediately before use; boiling point, 52.5°C/760 mmHg. Commercial potassium persulfate and silver nitrate (G. R. Grade) were used without purification. The water was purified through ion-exchange resin.

Polymerization Procedure. Definite amounts of potassium persulfate and water were placed into a glass ampoule; then, after cooling to 0°C, acrolein and an aqueous solution of silver nitrate were added to this system under a nitrogen atmosphere. The ampoule was sealed and maintained at 0°C for a definite reaction time. The product was poured into a large quantity of water, separated by filtration or centrifuge, and washed with water. In order to remove the silver salts, the filter cake was dispersed in an aqueous sodium thiosulfate solution of 1 wt%. After several hours, it was filtered, washed several times with water, and finally dried *in vacuo* at room temperature.

Characterization of the Polymer. The infrared spectrum was measured with a Shimadzu Infrared Spectrophotometer (Model IR-27) on KBr pellets. For the viscosity measurements, 100 mg of polyacrolein were mixed with 5 m*l* of a 10% aqueous sulfur dioxide solution in a 10 m*l* volumetric flask. This was allowed to stand overnight at room temperature and then filled to the mark with a 10% aqueous sodium chloride solution. Using this solution, the specific viscosity was measured at 25°C with an Ostwald viscometer. The number-average molecular weight was calculated by using the equation determined with the date reported by Schulz,[3] the η_{sp}/C ranging from 0.02 to 0.10 *l*/g:

$$\bar{M}_n = 16.8 \times 10^5(\eta_{sp}/C) - 2.8 \times 10^4$$

For the quantitative determination of the aldehyde group, the polyacrolein was reacted quantitatively with phenylhydrazine by the usual method.[4,5] The nitrogen content of the product (polyacrolein-phenylhydrazone) was also measured. In order to determine the C–C double-bond content, the polyacrolein was reduced with sodium borohydride, $NaBH_4$, to give a soluble polymer of polyallylalcohol,[6,7] and then the product was hydrogenated with hydrogen in the presence of platinum

1) R. C. Schulz, H. Cherdron and W. Kern, *Makromol. Chem.*, **24**, 141 (1957).

2) G. S. Whitby, M. D. Gross, J. R. Miller and A. J. Costanza, *J. Polymer Sci.*, **16**, 549 (1955).

3) R. C. Schulz and H. Cherdron, private communication.

4) R. C. Schulz, R. Hollander and W. Kern, *Makromol. Chem.*, **40**, 16 (1960).

5) R. C. Schulz and W. Passmann, *ibid.*, **60**, 139 (1963).

6) R. C. Schulz, J. Kovacs and W. Kern, *ibid.*, **52**, 236 (1962).

7) R. C. Schulz and P. Elzer, *ibid.*, **42**, 205 (1961).

dioxide in acetic acid.[8] The amount of hydrogen consumed was also measured.

Results and Discussion

Characterization of the Polymer. The polymer is a white powdery amorphous solid insoluble in organic solvents at room temperature. The infrared spectrum of the polymer showed the peaks characteristic of the vinyl-type polymer $(-CH_2-\underset{\underset{CH=O}{|}}{CH}-)_n$[9] and was very similar to that of the polymer formed by radical initiators (Fig. 1.). The elementary analysis of the product by the reaction of polyacrolein with phenylhydrazine showed that the polymer contains 97.5 mol% vinyl-type units (N 18.93, H 6.80, C 73.65%). Since there was no hydrogen absorption in the reaction product with $NaBH_4$, it can be said that the C–C double bond was not present in this system. From these results, it can be concluded that not the aldehyde-type polymer but only the vinyl-type polymer is formed by the redox-pair potassium persulfate-silver nitrate system.

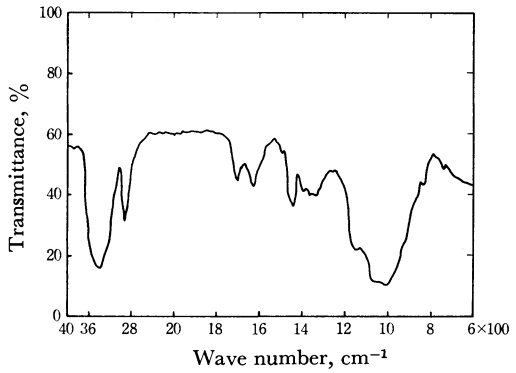

Fig. 1. Infrared spectrum of the polyacrolein formed with the redox system $AgNO_3/K_2S_2O_8$

Characteristic Effects of the Monomer and Potassium Persulfate Concentrations. The effect of the monomer concentration on the polymer yield and the molecular weight of the polymer was investigated; the results are shown in Table 1. Figure 2 indicates that the polymer yield at a constant time increases proportionally with the monomer concentration. The number-average degree of polymerization at a constant time is plotted against the monomer concentration in Fig. 3. It can be seen that the increase in the degree of polymerization with the monomer concentration becomes more pronounced with the reaction time; namely, the polymerizations in the earlier period (until 20 min) are characterized by a proportional increase in the degree of polymerization with the monomer concentration, while in the latter period (after 20 min) the exponent of the monomer concentration becomes more than unity.

Table 1. Effect of monomer concentration and time on polymer yield and molecular weight

Monomer concn. mol/l	Reaction time hr	Polymer yield mol/l	Molecular weight $\bar{M}_n \times 10^{-3}$
2.675	0.17	0.040	13.5
2.675	0.33	0.11	28.5
2.675	0.5	0.21	45.0
2.675	1.0	0.66	69.5
2.675	2.0	1.44	72.0
2.675	3.0	1.84	71.0
2.675	18.0	2.47	67.0
2.12	0.17	0.03	18.4
2.12	0.33	0.11	29.7
2.12	0.5	0.21	36.5
2.12	1.0	0.46	52.7
1.65	0.17	0.011	8.4
1.65	0.33	0.08	14.9
1.65	0.5	0.15	19.4
1.65	0.67	0.21	21.7
1.65	0.83	0.28	23.3
1.65	1.0	0.36	26.5
1.65	1.33	0.51	26.2
1.65	1.67	0.80	20.5
1.65	3.0	1.28	19.1
1.65	4.0	1.28	23.7
1.65	5.0	1.28	18.5
1.205	0.17	0.009	3.6
1.205	0.33	0.042	3.6
1.205	0.5	0.080	4.2
1.205	1.0	0.20	5.5
0.46	0.17	0.006	—
0.46	0.33	0.019	2.6
0.46	0.5	0.037	2.4
0.46	0.67	0.052	2.8
0.46	0.83	0.075	2.6
0.46	1.0	0.10	2.6
0.46	1.33	0.12	2.5
0.46	1.67	0.14	2.7
0.46	2.0	0.17	2.7
0.46	3.0	0.23	2.7
0.46	4.0	0.27	2.5
0.46	5.0	0.30	2.5

Reaction temperature=0°C; $[K_2S_2O_8]_0=[AgNO_3]_0=$ 31.5 mmol/l

The dependence of the polymer yield and the molecular weight of the polymer on the catalyst concentration is shown in Table 2. Figure 4 shows that the polymer yield increases proportionally with the catalyst concentration in the early stage (until 0.5 hr), while in the later stage

8) R. C. Schulz, J. Kovacs and W. Kern, *ibid.*, **54**, 146 (1962).

9) R. C. Schulz, *Kunststoffe*, **47**, 303 (1957).

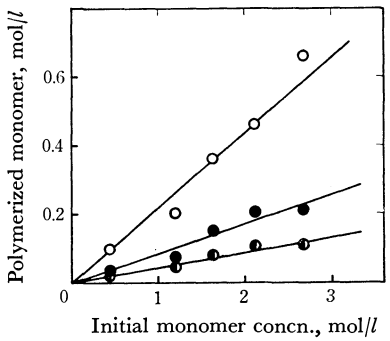

Fig. 2. The amount of polymerized monomer *vs.* initial monomer concentration.
T=0°C; $[K_2S_2O_8]_0=[AgNO_3]_0$=31.5 mmol/*l*; reaction time, 0.33 (◐), 0.5 (●), 1.0 hr (○)

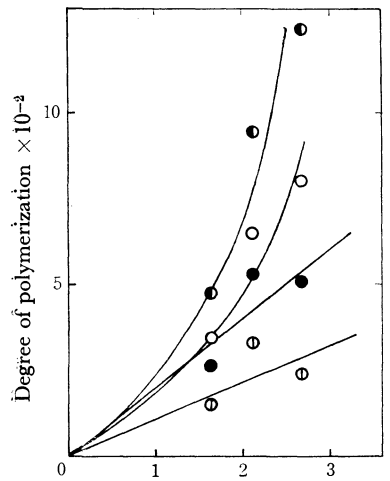

Fig. 3. Degree of polymerization *vs.* initial monomer concentration.
T=0°C; $[K_2S_2O_8]_0=[AgNO_3]_0$=31.5 mmol/*l*; reaction time, 0.17 (◑), 0.33 (●), 0.5 (○), 1.0 hr (◐)

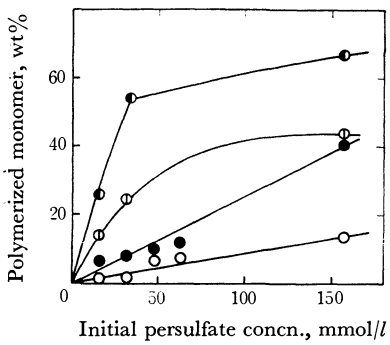

Fig. 4. The amount of polymerized monomer *vs.* initial potassium persulfate concentration.
T=0°C; $[AgNO_3]_0$=31.5 mmol/*l*; reaction time, 0.17 (○), 0.5 (●), 1.0 (◑), 2.0 hr (◐)

Table 2. Effect of persulfate concentration and time on polymer yield and molecular weight

$K_2S_2O_8$ concn. mmol/*l*	Reaction time hr	Polymer yield mol/*l*	Molecular weight $\bar{M}_n \times 10^{-3}$
15.75	0.17	0.026	3.7
15.75	0.25	0.033	4.2
15.75	0.5	0.09	8.6
15.75	0.75	0.13	7.0
15.75	1.0	0.19	11.3
15.75	2.0	0.35	12.3
15.75	3.0	0.51	9.0
23.6	0.77	0.13	11.1
23.6	0.92	0.22	10.0
31.5	0.52	0.11	5.6
31.5	0.73	0.18	5.6
47.25	0.30	0.08	2.9
47.25	0.44	0.12	4.0
63.0	0.23	0.06	2.8
63.0	0.43	0.12	4.3
94.5	0.10	0.02	1.3
94.5	0.33	0.13	2.6
157.5	0.11	0.26	0.6
157.5	0.17	0.18	0.9
157.5	0.33	0.44	0.9
157.5	0.5	0.54	1.8
157.5	0.67	0.51	3.0
157.5	0.83	0.68	2.7
157.5	1.0	0.58	3.6
157.5	1.5	0.88	4.5
157.5	2.0	0.90	5.1

Reaction temperature: 0°C; $[AgNO_3]_0$=31.5 mmol/*l*; Initial monomer concentration: 1.34 mol/*l*

the increase becomes less pronounced. It is noted that the degree of polymerization at a constant time is almost independent of the catalyst concentration.

Classification of the Polymerization.[10] The polymer yields at various monomer concentrations are plotted against the reaction time in Fig. 5. In each of several monomer concentrations, S-shape curves are obtained; in the early stage (until 0.5—1.0 hr), there is a marked acceleration in rate, while the polymerization rate is gradually reduced in the later stage.

Figure 6 shows the variation in the molecular weight of the polymer formed with the reaction time. It is a characteristic phenomenon that, in the early stage, the molecular weight of the polymer formed increases proportionally with the reaction time, as does the rate acceleration. In the later stage, however, the molecular weight is shown to remain constant, independently of the reaction time.

10) T. Kagiya, M. Izu and K. Fukui, This Bulletin, **40**, 1045 (1967).

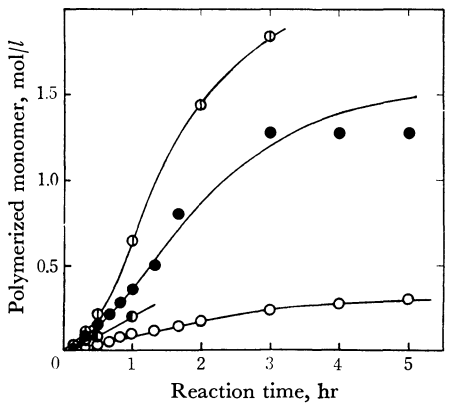

Fig. 5. The amount of polymerized monomer *vs.* reaction time.
T=0°C; $[K_2S_2O_8]_0=[AgNO_3]_0$=31.5 mmol/*l*; initial monomer concentration, 2.675 (◑) 1.65 (●), 1.205 (◐), 0.46 mol/*l* (○)

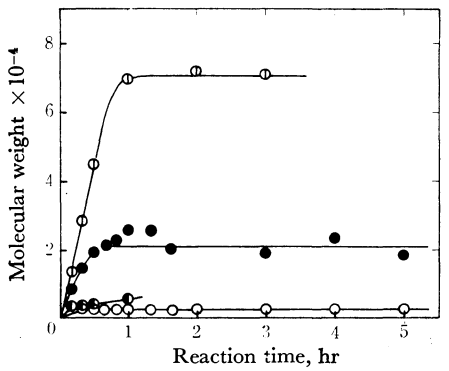

Fig. 6. Molecular weight *vs.* reaction time. Reaction conditions and notes are the same as shown in Fig. 5.

The rate acceleration in the early stage shows the accumulation of propagating species. The initiation reaction may, therefore, be considered to occur continuously in the course of the polymerization; that is, this system is a polymerization with a slow initiation. Since the mole of the propagating species increases with the reaction time, the non-stationary state is realized in this case. Moreover, from the fact that the number-average degree of polymerization increases with the reaction time in the early stage, this stage is a successive polymerization.

On the other hand, the polymerization in the later stage is a chain polymerization, for the degree of polymerization is independent of the reaction time. In order to determine whether the polymerization in the later stage has a rapid or a slow initiation, and whether it has a stationary or a non-stationary state, the following experiments were carried out. At first, it was shown that the addition of excess amounts of sodium chloride inhibits the polymerization reaction completely. Three-fold sodium chloride, NaCl, of silver nitrate, $AgNO_3$, was added at various times in the course of the reaction, while the total reaction time was five hours. We term the reaction before and after the adding of NaCl period I and period II respectively. Table 3 shows that the increase in

Table 3. Results of two-stage polymerization by the addition of NaCl[a)]

Reaction time hr		Polymerized monomer mol/*l*		
Period I	Period II	Overall[b)]	Period I[c)]	Period II[d)]
0.167	4.833	0.007	0.006	0.001
0.334	4.666	0.006	0.019	−0.013
0.5	4.5	0.014	0.037	−0.023
0.766	4.234	0.055	0.067	−0.012
1.0	4.0	0.104	0.099	0.005
2.0	3.0	0.152	0.172	−0.020
3.0	2.0	0.194	0.235	−0.041
5.0	0	0.279	0.297	−0.018

a) Reaction conditions: T = 0°C; $[K_2S_2O_8]_0$ = $[AgNO_3]_0$=31.5 mmol/*l*; initial monomer concentration: 0.462 mol/*l*; total reaction time: 5 hr; $NaCl/AgNO_3$=3.0 (molar ratio).
b) Overall polymerized monomer was obtained by subtracting the theoretical amount of AgCl (31.5 mmol/*l*) from the total yield.
c) The first-stage polymerization (Period I) was carried out as a blank polymerization in the same reaction conditions as that described above.
d) Polymerized monomer in Period II was obtained by subtracting the polymer yield in Period I from the overall polymer yield.

the polymer yield in period II was not observed in any case. This fact indicates that NaCl reacts with the Ag^+ ion to form a precipitate of AgCl, and that the formation of a new radical is stopped because of the disappearance of the reductant. The lack of any increase in the polymer yield in period II also leads to the consideration that there is a termination of the propagating species which had already been formed before the addition of sodium chloride.

In order to make clear the termination reaction, the polymerization was carried out by a two-stage monomer addition method as follows. The definite monomer was divided into two parts (14.7% and 85.3%). In the first stage the polymerization was carried out with the use of a 14.7% monomer for various reaction times, and then, after the addition of a residual monomer, polymerization (the second stage) was continued for one hour. The experimental results are given in Table 4. The polymer yield in the second stage is plotted in Fig. 7 against the reaction time in the first stage. The polymer yield increased with the time until about three hours, but it decreased thereafter.

TABLE 4. RESULTS OF TWO-STAGE POLYMERIZATION BY THE ADDITION OF MONOMER[a)]

Reaction time in lst-stage hr	Polymer yield mol/l				Degree of polymerization of final polymer $\times 10^{-3}$
	Overall (P_T)	lst-stage (P_1)	2nd-stage[b)] (P_2) ($=P_T-P_1$)	$[M_p]_2$[c)]	
0	0.54	0	0.54	0.54	2.1
0.33	0.67	0.02	0.65	0.55	2.9
0.5	0.81	0.04	0.78	0.67	3.2
1.0	1.05	0.10	0.95	0.84	3.4
2.0	1.30	0.17	1.13	1.01	3.0
5.0	1.12	0.30	0.82	0.77	2.7
8.0	0.79	0.34	0.45	0.43	2.5
23.0	0.67	0.48	0.19	0.19	1.1

a) Reaction conditions: $T = 0°C$; $[K_2S_2O_8]_0 = [AgNO_3]_0 = 31.5$ mmol/l; monomer concentration added in the first-stage, $[M_1]_0 = 0.462$: in the second-stage, $[M_2]_0 = 2.675$ mol/l; reaction time in the lst -stage: variable, the 2nd-stage: 1 hr.

b) P_2, the total polymer yield in the second-stage, was obtained by subtracting P_1 from P_T.

c) $[M_p]_2$, the polymer yield in the second-stage, was corrected as follows by eliminating the small amount of polymer formed during the second-stage with $[M_1]_0$.

$$[M_p]_2 = P_2 \times [M_2]_0 / ([M_1]_0 + [M_2]_0 - P_1)$$

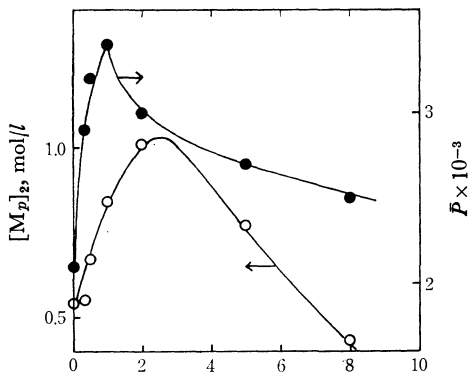

Fig. 7. Polymer yield in the second-stage and the degree of polymerization of the total polymer *vs.* reaction time in the first-stage. Reaction conditions are shown in Table 4.

This indicates that the propagating species accumulate until about three hours have passed, while, after three hours, the number of moles of the propagating species decreases with the reaction time because of the increase in the termination reaction and in the consumption of the catalyst.

It may be concluded from these facts that this redox polymerization is a non-stationary state accompanied by the accumulation of the propagating species in the early stage, and by the consumption of the propagating species in the later stage. The fact that the propagating species increase for three hours leads to the consideration that, in both the early and later stages, this system has a polymerization with a slow initiation.

The polymerization rate and the molecular weight of the polymer, as has been described before, increase continuously with the reaction time in

TABLE 5. EFFECT OF MONOMER CONCENTRATION ON THE NUMBER OF POLYMER CHAIN

Monomer concentration mol/l	Reaction time min	Polymerized monomer mol/l	Degree of polymerization	Number of[a)] moles of polymer chains $\times 10^4$ mol/l
1.65	10	0.011	150	0.73
1.65	20	0.08	270	3.07
1.65	30	0.15	350	4.45
1.65	40	0.21	390	5.39
1.65	50	0.28	420	6.66
1.65	60	0.36	470	7.57
2.12	10	0.03	330	1.00
2.12	20	0.11	530	2.03
2.12	30	0.21	650	3.16
2.12	60	0.46	940	4.90
2.62	10	0.05	480	1.08
2.62	20	0.11	690	1.65
2.62	30	0.23	950	2.48
2.675	10	0.04	240	1.67
2.675	20	0.11	510	2.19
2.675	30	0.21	800	2.64
2.675	60	0.66	1240	5.32

Reaction temperature=0°C, $[K_2S_2O_8]_0 = [AgNO_3]_0 = 31.5$ mmol/l

a) Number of moles of polymer chains was calculated from the ratio of the amount of polymerized monomer to the number-average degree of polymerization.

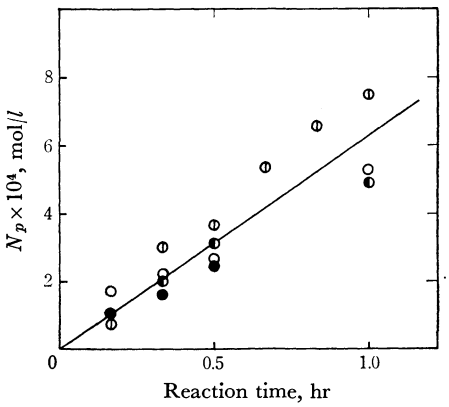

Fig. 8. Number of moles of polymer chains (N_p) *vs.* reaction time at various monomer concentration. $T = 0°C$; $[K_2S_2O_8]_0 = [AgNO_3]_0 = 31.5$ mmol/l; $[M]_0 = 1.65$ (◑), 2.12 (◐), 2.62 (●), 2.68 mol/l (○)

the early stage. This fact suggests that, in the early stage, neither the chain transfer nor the termination reaction is very remarkable, and that the initiation and the propagation reaction are the main elementary reactions. The effect of the monomer concentration on the number of moles of polymer chains is summarized in Table 5. From the experimental data, the number of moles of polymer chains is plotted against the reaction time in Fig. 8. The fact that an almost linear relation was found between them suggests that these redox systems have polymerizations with slow initiations. Since the number of moles of polymer chains was independent of the monomer concentration, the rate-determining step of the initiation reaction may be considered to be the decomposition reaction of the catalyst.

A more quantitative discussion of this polymerization will be given in a subsequent paper.

BULLETIN OF THE CHEMICAL SOCIETY OF JAPAN VOL. 42 2583—2588 (1969)

Graphical Evaluation of the Rate Constants of the Elementary Reactions in the Acrolein Polymerization with the Potassium Persulfate - Silver Nitrate Redox System

Tsutomu KAGIYA, Shigeru MORITA and Kenichi FUKUI

Faculty of Engineering, Kyoto University, Sakyo-ku, Kyoto

(Received November 4, 1968)

A quantitative study was made of the redox-polymerization of acrolein initiated by the potassium persulfate - silver nitrate system. The reaction mechanism of this polymerization was proposed on the basis of the results of the time-conversion, time-molecular weight curves, and also on the basis of the characteristic features of this polymerization, reported in a previous paper. The rate constants of the elementary reactions in this polymerization were estimated by a graphical method. In the early stage, neither the termination nor the transfer reaction is very remarkable as the initiation reaction, but in the later stage the termination reaction by a recombination of the polymer radical and the transfer reaction increase with the reaction time, as does the initiation reaction also.

In a previous paper[1] on the acrolein polymerization with the potassium persulfate - silver nitrate system, it was reported that the polymerization may be classified as a non-stationary state with a slow initiation in both the early and later stages. This paper will attempt to evaluate the rate constants of elementary reactions on the basis of quantitative kinetic measurements and to discuss the mechanism of this polymerization.

Results and Discussion

The Reaction Mechanism. In the previous paper[1], the redox-polymerization of acrolein with a potassium persulfate - silver nitrate catalyst was classified from a kinetic point of view. This polymerization has the non-stationary state showing an accumulation of the propagating species in the early stage (until 0.5～1.0 hr), and a consumption of the propagating species in the later stage. Moreover, this system is a polymerization with a slow initiation in both the early and later stages. Further, this system was found to show successive polymerization in the early stage, and chain polymerization in the later stage.

The following elementary reactions may, therefore, be assumed for the redox polymerization of acrolein on the basis of the experimental results reported in the previous paper[1] and the results of catalyst decomposition obtained by Bawn *et al.*[2] The respective rate expressions are also shown at the right.

1. Decomposition:

$$\underset{(C)}{Ag^+ + S_2O_8^{2-} + OH^-} \xrightarrow{k_d} SO_4^{2-} + \underset{(C^*)}{SO_4^-\cdot} + \underset{(C^*)}{HO\cdot} + Ag^+$$

$$R_d = k_d[C] \qquad (1)$$

1) T. Kagiya, S. Morita and K. Fukui, This Bulletin, **42**, 2578 (1969).

2) C. E. H. Bawn and D. Margerison, *Trans. Faraday Soc.*, **51**, 925 (1955).

2. Initiation:

$$C^* + M \xrightarrow{k_i} \underset{(P_1^*)}{CM\cdot} \qquad R_i = k_i[C^*][M] \tag{2}$$

3. Propagation:

$$P_n^* + M \xrightarrow{k_p} P_{n+1}^* \qquad R_p = k_p[P^*][M] \tag{3}$$

4. Termination:

$$P_m^* + P_n^* \xrightarrow{k_t} P_{m+n},\ P_m + P_n \qquad R_t = k_t[P^*]^2 \tag{4}$$

5. Transfer:

$$P_n^* + XY \xrightarrow{k_{tr}} P_nX + Y^* \qquad R_{tr} = k_{tr}[P^*][XY] \tag{5}$$

where C represents the potassium persulfate; C*, an anion radical, $SO_4^{-}\cdot$, and an HO· radical; M, the acrolein monomer; P_n^*, an active polymer chain composed of n monomers; [P*], the total concentration of all the active polymer chains, irrespective of size ($\sum_{n=1}^{\infty}[P_n^*]$); P_n, a dead polymer composed of n monomers; XY, the substance to which the activity of P_n^* is transferred; R_d, R_i, R_p, R_t, and R_{tr} the rates of decomposition, initiation, propagation, termination and transfer, and k_d, k_i, k_p, k_t and k_{tr}, the rate constants of these reactions.

It was reported by Bawn *et al.* that the catalyzed decomposition of potassium persulfate in an aqueous solution by the Ag^+ ion occurs according to:

$$Ag^+ + S_2O_8^{2-} \rightarrow Ag^{2+} + SO_4^{-}\cdot + SO_4^{2-}$$
$$Ag^{2+} + OH^- \rightarrow Ag^+ + HO\cdot$$

the second step is very fast compared with the first step, which is the rate-determining step, so that the silver ion (Ag^+) concentration remains constant during the reaction. The rate constant of the decomposition reaction at 0°C was obtained as k_d=0.15 *l*/hr.

The following equations are derived from the elementary reactions described above, when the $SO_4^{-}\cdot$ and HO· have the same reactivity for initiation:

$$-\mathrm{d[C]}/\mathrm{d}t = k_d[C] \tag{6}$$
$$\mathrm{d[C^*]}/\mathrm{d}t = 2R_d - R_i = 2k_d[C] - k_i[C^*][M] \tag{7}$$
$$\mathrm{d[P^*]}/\mathrm{d}t = R_i - 2R_t = k_i[C^*][M] - 2k_t[P^*]^2 \tag{8}$$

Since the polymer formed has a high molecular weight, the overall rate of polymerization is approximately equal to the rate of propagation:

$$R = \mathrm{d[M}_p\mathrm{]}/\mathrm{d}t \fallingdotseq R_p = k_p[P^*][M] \tag{9}$$

were R represents the overall polymerization rate, and [M_p], the amount of monomer polymerized. By integrating Eq. (6), the concentration of potassium persulfate is expressed as a function of the reaction time:

$$[C] = [C]_0 e^{-k_d t} \tag{10}$$

were $[C]_0$ represents the concentration of potassium persulfate at a definite reaction time, 0. The rate-determining step of the initiation reaction is the decomposition reaction of the catalyst, as was pointed out in the previous paper[1]; accordingly, Eq. (7) becomes:

$$\mathrm{d[C^*]}/\mathrm{d}t = 2R_d - R_i = 0 \tag{11}$$

By integrating Eq. (11), and by considering Eq. (10), the sum of polymer chains produced by initiation, $\int R_i \mathrm{d}t$, can be expressed by the following equation:

$$\int R_i \mathrm{d}t = 2\alpha[C]_0(1 - e^{-k_d t}) \tag{12}$$

where α is an efficiency factor of the catalyst.

The Evaluation of the Rate of Elementary Reactions in the Early Stage. The rate constant of the elementary reaction proposed above was determined by means of a graphical method in the non-stationary polymerization.[3] [P*] is given by Eq. (8):

$$[P^*] = \int R_i \mathrm{d}t - 2\int R_t \mathrm{d}t \tag{13}$$

From the facts that the polymerization rate and the molecular weight of the polymer increase with the reaction time, the termination rate may be considered to be smaller than the initiation rate.

When R_t is zero, Eq. (13) becomes:

$$[P^*] = \int R_i \mathrm{d}t = 2\alpha[C]_0(1 - e^{-k_d t}) \tag{14}$$

By a combination of Eqs. (9) and (14), the rate of polymerization is given as:

$$R_p = 2\alpha k_p[C]_0[M](1 - e^{-k_d t}) \tag{15}$$

In general, the number-average degree of polymerization at a given reaction time is defined by the following:

$$\bar{P} = \int R_p \mathrm{d}t \Big/ \left(\int R_i \mathrm{d}t + \int R_{tr} \mathrm{d}t - \int R_t \mathrm{d}t\right) \tag{16}$$

where $\bar{P}$ represents the number-average degree of polymerization. Since, in the early stage, the consumption of the monomer is very small and the value of $k_d t$ is smaller than unity, $\int R_p \mathrm{d}t$ without termination and $\int R_i \mathrm{d}t$ are given as follows by Eqs. (15) and (12) respectively:

$$\int R_p \mathrm{d}t = [M_p] = \alpha k_d k_p [C]_0 [M]_0 t^2 \tag{17}$$
$$\int R_i \mathrm{d}t = 2\alpha k_d [C]_0 t \tag{18}$$

If the transfer reaction to the monomer occurs, Eq. (19) is obtained:

$$\int R_{tr} \mathrm{d}t = \int k_{tr}[P^*][M]\mathrm{d}t = (k_{tr}/k_p)\int R_p \mathrm{d}t \tag{19}$$

From a combination of Eqs. (16), (17), (18) and

3) T. Kagiya, M. Izu, S. Machi and K. Fukui, This Bulletin, **40**, 1049 (1967).

(19), Eq. (16) becomes:

$$1/\bar{P} = 2/(k_p[M]_0 t) + k_{tr}/k_p \qquad (20)$$

The following evaluation of the rate constants of elementary reactions was made in the polymerization which was carried out under a monomer concentration of 2.68 mol/l and under a redox-pair concentration of 31.5 mmol/l (mol ratio 1 : 1). According to Eq. (20), $1/\bar{P}$ is plotted in Fig. 1 against

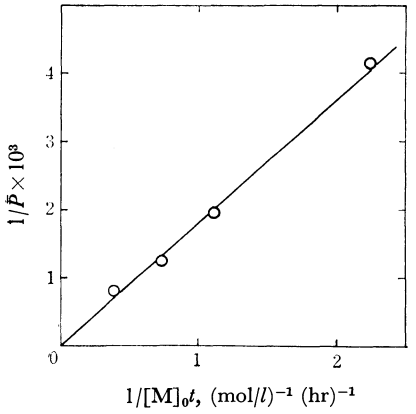

Fig. 1. Reciprocal of degree of polymerization *vs.* $1/[M]_0 t$
T=0°C; $[K_2S_2O_8]_0=[AgNO_3]_0=31.5$ mmol/l; initial monomer concentration, 2.675 mol/l

$1/[M]_0 t$ to give a straight line through the point of origin. This indicates either that the transfer and the termination reaction do not take place or that these reactions compensate each other in Eq. (16). In both cases, k_p was determined from the slope of the straight line in Fig. 1:

$$k_p = 1.1 \times 10^3 \ l/\text{mol}\cdot\text{hr}.$$

As was reported in the previous paper,[1] it was found, from the results obtained using a two-stage polymerization method, that termination reactions occur both in the early and later stages. It may be concluded, therefore, that the termination reaction compensates the transfer reaction in the early stage.

Equation (21) is derived from Eq. (15):

$$R_p/[M] = 2\alpha k_p[C]_0(1 - e^{-0.15t}) \qquad (21)$$

The plot of the $R_p/[M]$ term against the value of $2[C]_0(1-e^{-0.15t})$ gives a straight line through the point of origin, as is shown in Fig. 2. From the slope of the line, $\alpha k_p = 67.5$ l/mol·hr. Since the value of k_p was 1.1×10^3 l/mol·hr according to Eq. (20), as has been mentioned above, the efficiency factor of the catalyst is:

$$\alpha = 6.14 \times 10^{-2}$$

The value of $\int R_i dt$ is thus given by the following equation instead of by Eq. (12):

$$\int R_i dt = 12.28 \times 10^{-2}[C]_0(1 - e^{-0.15t}) \qquad (22)$$

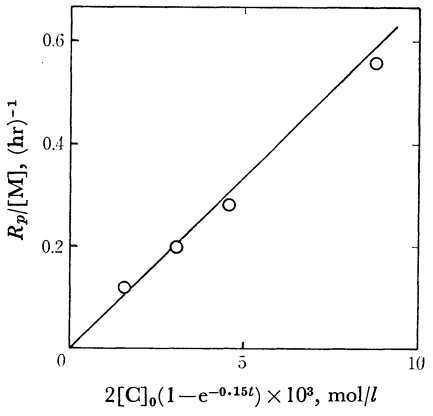

Fig. 2. $R_p/[M]$ *vs.* $2[C]_0(1-e^{-0.15t})$
Reaction conditions are the same as shown in Fig. 1.

The Evaluation of the Rate of Elementary Reactions in the Later Stage. The quantitative evaluation of the rate of elementary reactions in the later stage was continued as follows.

As has been described before, both the transfer and termination reactions take place in this polymerization and compensate each other. When the second-order termination by the polymer radical takes place, the following equation can be derived by integrating Eq. (4):

$$\int R_t dt = \int k_t[P^*]^2 dt = (k_t/k_p^2)\int (R_p^2/[M]^2)dt \qquad (23)$$

By combining Eqs. (9), (13), (22) and (23), Eq. (24) is derived:

$$\frac{R_p}{[M]\int \frac{R_p^2}{[M]^2}dt} = \frac{4.25(1-e^{-0.15t})}{\int \frac{R_p^2}{[M]^2}dt} - \frac{2k_t}{1.1\times 10^3} \qquad (24)$$

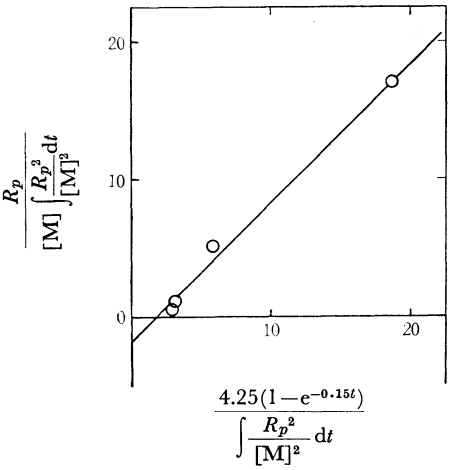

Fig. 3. $\frac{R_p}{[M]\int \frac{R_p^2}{[M]^2}dt}$ *vs.* $\frac{4.25\,(1-e^{-0.15t})}{\int \frac{R_p^2}{[M]^2}dt}$
Reaction conditions are the same as shown in Fig. 1.

By plotting the value of the left side against the first term on the right side in Eq. (24), a straight line with a slope of unity was obtained, as is shown in Fig. 3. From the value of the intercept of the ordinate axis, k_t was found to be 9.9×10^2 l/mol·hr.

Since the ratio of the consumption of the catalyst is 36% in a reaction period of three hours, it can be assumed that the concentration of the catalyst (potassium persulfate) remains almost constant for about three hours after the start of the polymerization. Eq. (25) can then be derived by combining Eqs. (7), (8) and (11);

$$d[P^*]/dt = 2\alpha k_d[C]_0 - 2k_t[P^*]^2 \quad (25)$$

The following equation is obtained by resolving the differential equation[4]:

$$[P^*] = (\alpha k_d[C]_0/k_t)^{1/2} \tanh\left[(4\alpha k_d k_t[C]_0)^{1/2}t\right] \quad (26)$$

By substituting the values of k_d, k_t, $[C]_0$ and α obtained above into Eq. (26), [P*] can be plotted against the reaction time as is shown in Fig. 4.

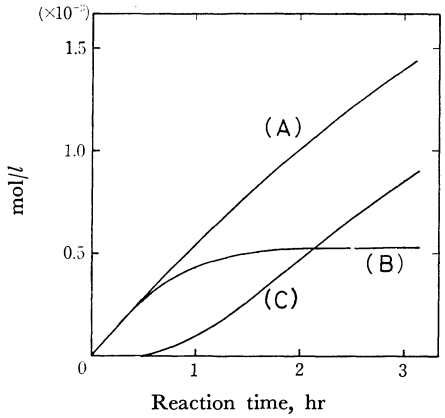

Fig. 4. $\int R_i dt$, [P*] and $2\int R_t dt$ *vs.* reaction time.
(A), $\int R_i dt$; (B), [P*]; (C), $2\int R_t dt$
Reaction conditions are the same as shown in Fig. 1.

$\int R_i dt$ [Eq. (22)] and $2\int R_t dt$ $(=\int R_i dt - [P^*])$ are also plotted in the same figure, Fig. 4. When the consumption of the catalyst is negligible, it is found that [P*] increases with the reaction time, therefore, the termination reaction becomes remarkable after thirty minutes. Since [P*] decreases, however, with the reaction time after about three hours from the start of the polymerization, as was shown in the previous paper,[1] it must be considered in practice that the consumption of the catalyst is not negligible in the later period.

When the recombination between propagating species prevails in the termination, Eq.(27) is derived from Eq.(16):

$$1/\bar{P} = \left(\int R_i dt - \int R_t dt\right)\Big/\int R_p dt + \int R_{tr} dt \Big/ \int R_p dt \quad (27)$$

In Eq.(27), when:

$$h(t) \equiv \int R_i dt - \int R_t dt \quad (28)$$

the value of $h(t)$ can be calculated from Fig. 4, assuming that the termination reaction occurs by means of a recombination between propagating species. When a chain transfer to XY (chain-transfer reagent) takes place with a constant concentration,

$$\int R_{tr} dt = k_{tr}[XY]\int [P^*]dt = (k_{tr}[XY]/k_p)\int \frac{R_p}{[M]}\,dt \quad (29)$$

By a combination of Eqs. (27), (28) and (29), the following equation is derived:

$$\frac{[M_p]}{\bar{P}\int \frac{R_p}{[M]}dt} = \frac{h(t)}{\int \frac{R_p}{[M]}dt} + \frac{k_{tr}[XY]}{k_p} \quad (30)$$

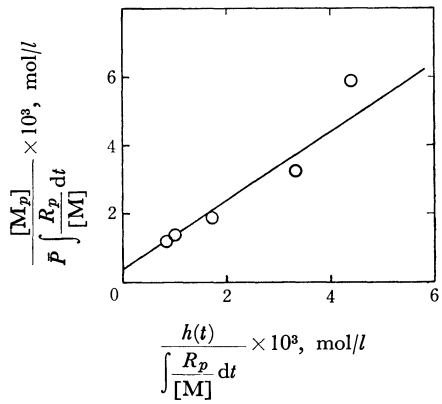

Fig. 5. $\dfrac{[M_p]}{\bar{P}\int \frac{R_p}{[M]}dt}$ *vs.* $\dfrac{h(t)}{\int \frac{R_p}{[M]}dt}$
Reaction conditions are the same as shown in Fig. 1.

The left side is plotted in Fig. 5 against the first term on the right side to give a straight line with the slope of unity. From the intercept on the ordinate axis, $k_{tr}[XY]/k_p$ can be obtained. By substituting the k_p value obtained before into $k_{tr}[XY]/k_p$, $k_{tr}[XY]$ is obtained as 0.44 $(hr)^{-1}$.

The rate equations and the rate constants of the elementary reactions obtained above are summarized in Table 1.

Comparison of Experimental Results with Theoretical Results. The experimental results on both the polymer yield and the degree of polymerization were compared with the equations which had been theoretically derived from the proposed elementary reactions.

The following relationship on the polymer yield is derived from combining Eqs.(9) and (26):

4) M. Magat, *J. Polymer Sci.*, **16**, 491 (1955).

TABLE I. THE RATE EQUATIONS AND THE RATE CONSTANTS OF THE ELEMENTARY REACTIONS

Elementary reaction		Rate equation	Rate constant
Decomposition	$Ag^+ + S_2O_3^{2-} + OH^- \rightarrow SO_4^{2-} + SO_4^{-}\cdot + HO\cdot + Ag^+$	$R_d = k_d[C]$	$k_d = 0.15$ (1/hr)
Initiation	$C^* + M \rightarrow P_1^*$	$R_i = k_i[C^*][M]$	$\int R_i dt = 2\alpha[C]_0(1-e^{-k_d t})$ (mol/l)
Propagation	$P_n^* + M \rightarrow P_{n+1}^*$	$R_p = k_p[P^*][M]$	$k_p = 1.1\times10^3$ (l/mol·hr)
Transfer	$P_n^* + XY \rightarrow P_nX + Y^*$	$R_{tr} = k_{tr}[P^*][XY]$	$k_{tr}[XY] = 0.44$ (l/mol·hr)
Termination	$P_m^* + P_n^* \rightarrow P_{m+n}$	$R_t = k_t[P^*]^2$	$k_t = 9.9\times10^2$ (l/mol·hr)

$$[M_p] = \int k_p(\alpha k_d[C]_0/k_t)^{1/2} \tanh [(4\alpha k_d k_t[C]_0)^{1/2}t][M]dt \quad (31)$$

By substituting various constants, and by graphically integrating with the reaction time, the theoretical value of $[M_p]$ is plotted against the time, and compared with the empirical data, in Fig. 6. A good agreement between observation and theory is observed.

On the other hand, when termination takes place by a recombination of polymer radicals, the following equation can be derived:

$$\bar{P} = \int R_p dt \Big/ \left(\int R_i dt + \int R_{tr} dt - \int R_t dt\right) \quad (16)$$

By substituting Eqs. (31), (12), (29) and (23) into Eq. (16) and by assuming that the [XY] is constant, the following equation is obtained.

The values of each term at various reaction times in Eqs. (32) and (33) are listed in Table 2. Table 2 shows that, in the early stage, both the termination

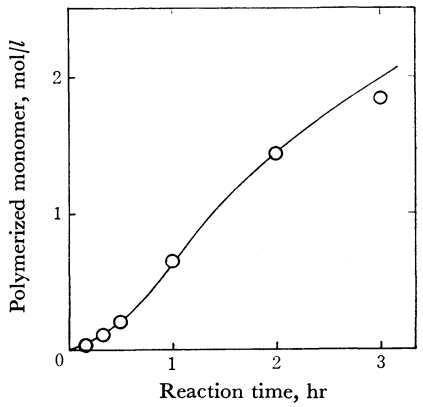

Fig. 6. The amount of polymerized monomer *vs.* reaction time.
(○), experimental data
(—), theoretical curve
Reaction conditions are the same as shown in Fig. 1.

$$\bar{P} = \frac{\int k_p[P^*][M]dt}{2\alpha[C]_0(1-e^{-k_d t}) + k_{tr}[XY]\int [P^*]dt - k_t\int [P^*]^2 dt}$$

$$= \frac{(\alpha k_d k_p^2[C]_0/k_t)^{1/2}\int \tanh [(4\alpha k_d k_t[C]_0)^{1/2}t][M]dt}{2\alpha[C]_0(1-e^{-k_d t}) + (k_{tr}[XY]/2k_t)\ln\cosh[(4\alpha k_d k_t[C]_0)^{1/2}t] - \alpha k_d[C]_0 t + (\alpha k_d[C]_0/4k_t)^{1/2}\tanh[(4\alpha k_d k_t[C]_0)^{1/2}t]}$$

$$= \frac{595\int \tanh(1.07t)[M]dt}{38.7(1-e^{-0.15t}) + 5.13\log\cosh(1.07t) - 2.9t + 2.71\tanh(1.07t)} \quad (32)$$

$$= \frac{[M_p]\times10^4}{38.7(1-e^{-0.15t}) + 5.13\log\cosh(1.07t) - 2.9t + 2.71\tanh(1.07t)} \quad (33)$$

TABLE 2. VARIATION OF $\int R_i dt$, $\int R_{tr} dt$, $\int R_t dt$ AND THE POLYMER YIELD WITH THE REACTION TIME

Reaction time hr	Initiation reaction $\int R_i dt\times10^4$ mol/l $38.7(1-e^{-0.15t})$	Transfer reaction $\int R_{tr} dt\times10^4$ mol/l $5.13\log\cosh(1.07t)$	Termination reaction $\int R_t dt\times10^4$ mol/l $2.9t-2.71\tanh(1.07t)$	Polymer yield mol/l $[M_p]$	$0.595\int\tanh(1.07t)[M]dt$
0.167	0.953	0.035	0.006	0.040	0.022
0.333	1.88	0.139	0.041	0.111	0.086
0.50	2.79	0.304	0.127	0.212	0.193
1.0	5.38	1.09	0.765	0.66	0.625
2.0	10.0	3.25	3.17	1.44	1.46
3.0	14.0	5.60	6.00	1.84	2.06

Reaction conditions are the same as Fig. 1.

and transfer reactions are very small compared with the initiation reaction and that they compensate each other in both the early and later stages. Therefore, in order to evaluate the propagation rate, it is adequate to adopt the method described above, using $R_t=R_{tr}=0$.

The empirical data is shown in Fig. 7 to agree

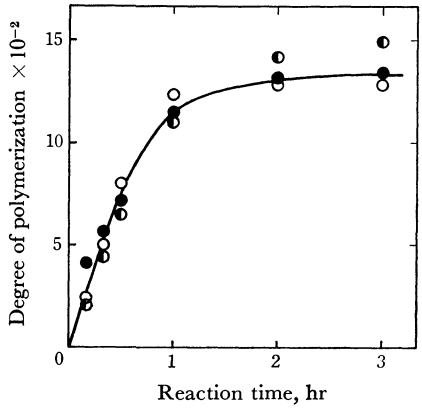

Fig. 7. Degree of polymerization *vs.* reaction time.
(○), experimental data
(◐), theoretical value obtained from Eq. (32)
(●), theoretical value obtained from Eq. (33)
Reaction conditions are the same as shown in Fig. 1.

with the theoretically-derived value. The deviation of the theoretical value in Eq.(32) from the experimental data in the later period is due to the consumption of the catalyst.

The values of k_{tr}[XY] in the polymerization at various monomer and catalyst concentrations are summarized in Table 3. The value of k_{tr}[XY] decreases with the initial monomer concentration, independently of the potassium persulfate concentration. The mechanism of the chain-transfer reaction is not clear, but it may be ascribed to impurities in water. The fact that the value of k_{tr}[XY] decreases remarkably with the initial monomer concentration suggests that the activity of XY is markedly decreased by the formation of the polymer.

TABLE 3. THE VALUE OF k_{tr}[XY]

Initial monomer concentration (mol/l)	k_{tr}[XY] $(hr)^{-1}$
0.449	7.7
1.230[a)]	3.0
1.486	2.0
2.272	0.5

Reaction condition: T=0°C,
$[AgNO_3]_0=[K_2S_2O_8]_0=31.5$ mmol/l
a) $[K_2S_2O_8]_0=15.75$ mmol/l

In the view of the fact that the experimental results on both the polymer yield and the degree of polymerization under several reaction conditions coincide with the equation theoretically derived, the proposed elementary reactions and the rate constants evaluated in the non-stationary-state polymerization may be accepted.

BULLETIN OF THE CHEMICAL SOCIETY OF JAPAN VOL. 42 2589—2592 (1969)

Synthetic Studies of the Derivatives of Acetylene. I. Reactions of 5-Bromopent-3-en-1-yne[1]

Kikumasa SATO and Masao HIRAYAMA

Department of Applied Chemistry, Faculty of Engineering, Yokohama National University, Minami-ku, Yokohama

(Received November 28, 1968)

The preparation of pent-2-en-4-ynylamine and pent-2-en-4-ynylthiol and their derivatives from 5-bromopent-3-en-1-yne was studied. Moreover, in connection with the preparation of the bromide, the rearrangement-bromination of vinylethynylcarbinol was found to give three isomeric bromides, 5-bromopent-*trans*-3-en-1-yne, 5-bromopent-*cis*-3-en-1-yne, and 3-bromopent-1-en-4-yne. Pent-2-en-4-ynylamine was obtained from 5-bromopent-3-en-1-yne by two methods, by the hydrolysis of the hexaminium salt and by the cleavage of *N*-(pent-2-en-4-ynyl)phthalimide. The reaction of 5-bromopent-3-en-1-yne with potassium hydrosulfide and the decomposition of ethyl pent-2-en-4-ynylxanthate by alcoholic ammonia gave pent-2-en-4-ynylthiol.

In previous papers, it was reported that propargyl bromide could be converted to propargylamine and propargyl mercaptan and their derivatives.[2a-c] These studies have now been extended to such a vinylogous bromide as 5-bromopent-3-en-1-yne (I). Compound I may be expected to be useful for some synthetic reactions because it has two different functional groups. It is well known that the bromine atom has so enhanced a reactivity that it undergoes Reformatskii reaction with carbonyl compounds,[3] but there have been only a few other studies, such as those of the reactions with potassium acetate,[4] ethyl acetoacetate,[5] potassium cyanide,[6] and diethylamine.[7] In the present study we examined various substitution reactions of I in order not only to synthesize the conjugated vinylacetylenic amine, thiol, and their derivatives, but also to investigate the difference in the reactivity of the bromine atom between I and propargyl bomide. Almost all of the reaction products prepared were new substances.

The common methods of preparing the bromide involve the rearrangement-bromination of vinylethynylcarbinol[6] and the direct bromination of the corresponding alcohol, pent-2-en-4-yn-1-ol.[3] According to the study of Bohlmann and Viehe,[6] the former method gave a mixture of two isomers, unrearranged bromide and rearranged bromide, judging from the ultraviolet spectrum of the mixture. When we re-examined the rearrangement-bromination reaction, we found that a mixture of three isomeric bromides, rearranged *trans*-5-bromopent-3-en-1-yne (I), *cis*-5-bromopent-3-en-1-yne (II), and unrearranged bromide (III), was obtained in a 49.2% yield. The ratio of I : II : III was

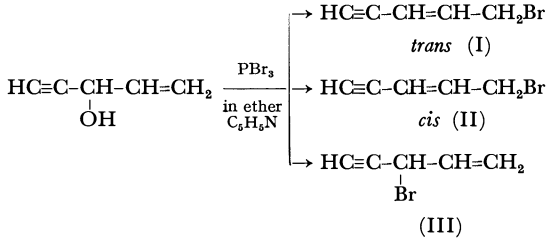

found to be about 2 : 1 : 1 by gas chromatography. The structures of these three isomers were confirmed by their infrared, ultraviolet, and NMR spectra, and by microanalyses of their hexaminium salts. Compound III was identified by its ultraviolet spectrum, which showed no absorption maximum. However, the final confirmation of *cis*- and *trans*-isomers depended on their NMR and ultraviolet spectra. The coupling constants of the olefinic protons of the two isomers are 10.5 and 17.0 Hz values which are characteristic of *cis*- and *trans*-olefinic protons respectively. Moreover, the absorption peaks of the ultraviolet spectra are

1) This investigation was presented at the 21st Annual Meeting of the Chemical Society of Japan, Osaka, April, 1968.

2) a) K. Sato, *Nippon Kagaku Zasshi* (*J. Chem. Soc. Japan, Pure Chem. Sect.*), **76**, 1404 (1955). b) K. Sato and O. Miyamoto, *ibid.*, **77**, 1409 (1956). c) K. Sato, *ibid.*, **77**, 1411 (1956).

3) H. B. Henbest, E. R. H. Jones and I. M. S. Walls, *J. Chem. Soc.*, **1950**, 3646.

4) I. M. Heilbron, E. R. H. Jones, R. N. Lacey, J. T. McCombie and R. Raphael, *ibid.*, **1945**, 77.

5) L. Crombie, S. H. Harper and D. Tompson, *ibid.*, **1951**, 2906.

6) F. Bohlmann and H. G. Viehe, *Chem. Ber.*, **87**, 712 (1954).

7) R. H. Jones, R. N. Lacey and P. Smith, *J. Chem. Soc.*, **1946**, 940.

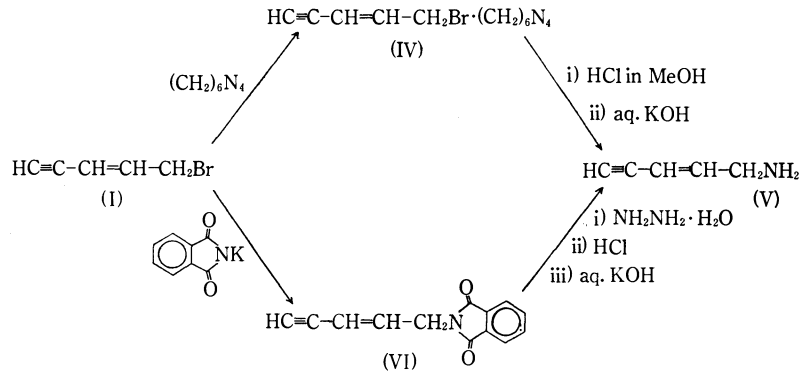

238.5 mμ ($\varepsilon=11400$) and 238 mμ ($\varepsilon=14400$); these values are also complete agreement with the *cis*- and *trans*-structures of the conjugated vinylacetylenic system.[8] Although vinylethynylcarbinol was obtained in a good yield, it is very troublesome to separate the three isomers formed in the following rearrangement-bromination reaction, as will be described in the Experimental section. Therefore, we were obliged to prepare the bromide I by the other direct bromination method[3] of pent-2-en-4-yn-1-ol, which had been obtained in the pure *trans*-form from sodium acetylide and epichlorohydrin.[4]

Allylamine and propargylamine derivatives were prepared from the corresponding halides by Delépine and Gabriel reactions but conjugated vinylacetylenic amines such as V have not been prepared. 5-Bromopent-3-en-1-yne reacted with hexamine in methanol to give the hexaminium salt (IV), which was warmed with concentrated hydrochloric acid to give brown crystals. When the crystals were treated with aqueous potassium hydroxide, pent-2-en-4-ynylamine (V) was obtained as a colorless liquid. On the other hand, the reaction of I with potassium phthalimide gave *N*-(pent-2-en-4-ynyl)phthalimide (VI) in a 92% yield. This result is interesting, for it contrasts with the fact that *N*-propargylphthalimide was obtained in only a 10% yield in a similar reaction.[2a] Compound VI was refluxed with hydrazine hydrate in ethanol and then treated with hydrochloric acid to yield pale brown crystals. The treatment of the crystals with aqueous potassium hydroxide gave the corresponding amine, V, in a 32% yield. Compound V was identified from its infrared and ultraviolet spectra and by the microanalyses of its derivatives. Especially, the location of the absorption maximum in the ultraviolet spectrum indicated that V had the expected conjugated vinylacetylenic structure. Compound V reacted normally with benzoyl chloride, sodium cyanate, phenyl isocyanate, and carbon disulfide to give the corresponding derivatives.

No report has also been found concerning the preparation of such vinylacetylenic thiols as VII. We found that VII could be obtained by two methods, the reaction of I with potassium hydrosulfide and the decomposition of the ethyl xanthate, though VII was not obtained by the hydrolysis of the isothiuronium bromide (IX). Compound I reacted with potassium hydrosulfide in acetone-water to give VII in a 47% yield, and ethyl pent-2-en-4-ynylxanthate (VIII), prepared in a 59.7% yield by the reaction of I with sodium xanthate, was decomposed by alcoholic ammonia also to yield VII in a 55% yield. However, VII could not be obtained by the hydrolysis of *S*-(pent-2-en-4-ynyl)isothiuronium bromide (IX) (itself obtained in a high yield by the reaction of I with thiourea) by aqueous sodium hydroxide because of the resinification of the reaction mixture upon distillation. *p*-Tolyl

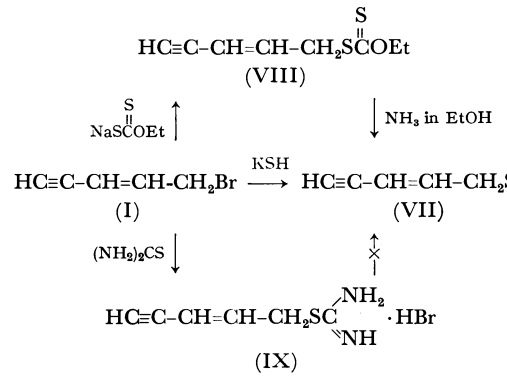

pent-2-en-4-ynyl sulfide (X) and pent-2-en-4-ynylthioacetic acid (XI) were prepared by the reaction of I with *p*-thiocresol and thioglycolic acid respectively.

From these results, the present authors conclude that compound I behaves almost like allyl bromide in the substitution reactions presented above, while I also shows a characteristic property with propargyl bromide in such reactions with carbonyl compounds as the Reformatskii reaction.

8) I. Bell, E.R.H. Jones and H.C. Whiting, *J. Chem. Soc.*, **1957**, 2597.

Experimental[9]

Materials. Vinylethynylcarbinol was obtained by the method of Bohlmann and Viehe.[6] 5-Bromopent-3-en-1-yne was prepared by the bromination of pent-2-en-4-yn-1-ol,[3] which had itself been obtained from sodium acetylide and epichlorohydrin.[4] The other materials were obtained from commercial sources.

Bromination of Vinylethynylcarbinol. The bromination was carried out by a slight modification of the method of Bohlmann and Viehe.[6] A solution of phosphorus tribromide (35.0 g) (0.13 mol) in 50 m*l* of dry ether was stirred, drop by drop and at 10±2°C, into a mixture of vinylethynylcarbinol (24.6 g) (0.3 mol) in 100 m*l* of dry ether containing 2.5 g of pyridine. After the mixture had been heated for 2.5 hr under reflux, the resulting mixture was chilled, poured over ice water, and extracted with ether. The ether was washed with water and saturated aqueous sodium bicarbonate, dried over sodium sulfate, and evaporated. The residue was distilled, giving mixed isomers (21.4 g) (49.2%) of a pale yellow liquid, bp 66—76°C/84 mmHg. The gas chromatography showed three peaks, and the ratio of I : II : III was 0.48 : 0.25 : 0.26. This mixture was distilled into three fractions through a 30 cm column.

Fraction 1 was 3-bromopent-1-en-4-yne (III) (6.3 g) (14.5%); bp 70—74°C/124 mmHg, n_D^{20} 1.5102; ν_{max}^{film} 3270, 2100, 1632, and 890 cm^{-1} (C=CH$_2$); and NMR peaks at δ 2.74 (the acetylenic proton), 4.98 (–CHBr–), 5.18 and 5.49 (terminal olefinic protons *cis* and *trans* to the vicinal olefinic proton respectively), and 6.09 ppm (the last olefinic proton). The ultraviolet spectrum had no absorption peak.

Fraction 2 was 5-bromopent-*cis*-3-en-1-yne (II) (3.5 g) (8.1%); bp 83—84°C/124 mmHg, n_D^{20} 1.5319; ν_{max}^{film} 3280, 2100, 1610, and 765 cm^{-1} (*cis* CH=CH); λ_{max}^{EtOH} 238.5 mμ (ε=11400); NMR peaks at δ 3.23 (the acetylenic proton), 4.11 (bromomethyl protons), 5.51 (the olefinic proton adjacent to the triple bond), and 6.19 ppm (the last olefinic proton); $J_{CH=CH}$=10.5 Hz. Moreover, it was identified as hexaminium bromide; mp 176—177.5°C (Found: N, 19.83%. Calcd for $C_{11}H_{17}N_4Br$: N, 19.64%).

Fraction 3 was 5-bromopent-*trans*-3-en-1-yne (I) (5.6 g) (12.9%); bp 85—87°C/124 mmHg, n_D^{20} 1.5422 (lit.[3] n_D^{17} 1.5430); ν_{max}^{film} 3300, 2080, 1620, and 955 cm^{-1} (*trans* CH=CH); λ_{max}^{EtOH} 238 mμ (ε=14400); NMR peaks at δ 2.90 (the acetylenic proton), 3.93 (bromomethyl protons), 5.65 (the olefinic proton adjacent to the triple bond), and 6.31 ppm (the last olefinic proton); $J_{CH=CH}$=17.0 Hz. These characteristic absorption peaks were in complete accord with those of *trans* authentic bromide prepared according to the method of Henbest and his co-workers.[3]

5-Bromopent-3-en-1-yne-hexamethylenetetramine (IV). A solution of 5-bromopent-3-en-1-yne (36.1 g) (0.25 mol) in 110 m*l* of ether was added, portion by portion, to a hot solution of hexamine (35.2 g) (0.25 mol) in 350 m*l* of methanol. After the solution had been refluxed for 10 min and then left to stand overnight, pale yellow crystals precipitated (54.7 g, mp 183—184°C (dec.)); from the filtrate, after the removal of the solvent, 6.4 more grams of crystal were obtained, mp 179—181°C (dec.). The yield was 86.0%. Recrystallization from methanol gave the pure IV; mp 184—185°C (dec.), ν_{max}^{KBr} 3180, 2080, 1630, and 945 cm^{-1}; λ_{max}^{EtOH} 219 (ε=12000), 228 (ε=15400), and 237 mμ (ε=12000). Found: C, 46.03; H, 6.28%. Calcd for $C_{11}H_{17}N_4Br$: C, 46.33; H, 6.01%.

***N*-(Pent-2-en-4-ynyl)phthalimide (VI).** A mixture of 5-bromopent-3-en-1-yne (4.4 g) (0.03 mol), potassium phthalimide (5.6 g) (0.03 mol), and 30 m*l* of ethanol was stirred for 12 hr under reflux. The removal of ethanol, followed by treatment with dilute aqueous potassium hydroxide, gave white crystals (5.8 g) (92.1%), mp 119—120.5°C. Recrystallization from ethanol provided the pure VI, mp 125—126°C; ν_{max}^{KBr} 3250, 2070, 1770, 955, 800, and 720 cm^{-1}. Found: C, 73.93; H, 4.62%. Calcd for $C_{13}H_9O_2N$: C, 73.92; H, 4.30%.

Pent-2-en-4-ynylamine (V). *A) From 5-Bromopent-3-en-1-yne-hexamethylenetetramine.* To a hot solution of 5-bromopent-3-en-1-yne-hexamethylenetetramine (28.5 g) (0.1 mol) in 330 m*l* of methanol, a 50 m*l* portion of concentrated hydrochloric acid was added, portion by portion, the mixture was then heated for 20 min under reflux. After the mixture had stood overnight, the precipitated ammonium chloride was filtered out; the removal of the solvent from the resulting filtrate gave brown crystals. Recrystallization from methanol gave 14.5 g of pale brown crystals, mp above 250°C; ν_{max}^{KBr} 3220, 3100—2900, 2070, 1600, 1565, 1490, and 955 cm^{-1}.

To a solution of the crystals (8.0 g) in 10 m*l* of water, a solution of potassium hydroxide (4.5 g) in 20 m*l* of water was added at 0—5°C; the resulting solution was extracted with ether. After drying over potassium hydroxide and evaporating, the distillation of the residue gave 1.8 g (40.3% based on hexaminium salt) of a liquid, bp 51°C/20 mmHg, n_D^{20} 1.5078; ν_{max}^{film} 3400—3150, 3300, 2080, 1590, 955, and 850 cm^{-1}; λ_{max}^{EtOH} 226 mμ (ε=14500).

B) From N-(Pent-2-en-4-ynyl)phthalimide. *N*-(Pent-2-en-4-ynyl)phthalimide (4.2 g) (0.02 mol) was treated for 1.5 hr with 80% aqueous hydrazine (1.4 g) (0.02 mol) in 60 m*l* of boiling 95% ethanol. Concentrated hydrochloric acid (3.5 m*l*) was added to the resulting mixture, which was then heated for 20 min under reflux. After the reaction mixture had then cooled and been filtered, the concentration of the filtrate gave 2.1 g (89.2%) of pale brown crystals, mp above 250°C. The infrared spectrum of this crystal was in complete accord with that of the hydrochloride salt obtained by passing hydrogen chloride into an ethereal solution of pent-2-en-4-ynylamine.

These crystals (5.9 g) (0.05 mol) were treated with aqueous potassium hydroxide such as in method A to yield 1.3 g (32.2%) of V, bp 55—56°C/28 mmHg.

This amine gave the following derivatives. Reaction with benzoyl chloride gave *N*-benzoylpent-2-en-4-ynylamine, mp 107—107.5°C (dil. MeOH); Found: C, 77.74; H, 6.05%. Calcd for $C_{12}H_{11}ON$: C, 77.81;

9) All melting points and boiling points are uncorrected and all distillations were carried out in a nitrogen atmosphere. Infrared and ultraviolet spectra were recorded on a Hitachi Model EPI-S2 spectrometer and Hitachi Model EPS-3T spectrometer, respectively. Gas chromatographic analyses were carried out on a Shimadzu Model GC-1C chromatograph and NMR spectra were taken on a JEOL C-60H instrument with tetramethylsilane as an internal reference.

H, 5.99%. Treatment with sodium cyanate and phenyl isocyanate afforded *N*-pent-2-en-4-ynylurea, mp 103—104°C (EtOH); Found: C, 57.49; H, 6.64%. Calcd for $C_6H_8ON_2$: C, 58.05; H, 6.50%, and *N*-phenyl-*N'*-pent-2-en-4-ynylurea, mp 137—137.5°C (EtOH); Found: C, 71.81; H, 6.33%. Calcd for $C_{12}H_{12}ON_2$: C, 71.98; H, 6.04%, respectively. Reaction with carbon disulfide gave pent-2-en-4-ynylammonium pent-2-en-4-ynyldithiocarbamate, mp 89—90°C; Found: C, 55.19; H, 6.21%. Calcd for $C_{11}H_{14}N_2S_2$: C, 55.43; H, 5.92%.

Ethyl Pent-2-en-4-ynylxanthate (VIII). 5-Bromopent-3-en-1-yne (14.5 g) (0.1 mol) was added at 5—8°C to a solution of sodium ethylxanthate in 60 m*l* of ethanol. After the mixture had been stirred for 1.5 hr at room temperature, sodium chloride was filtered out and the filtrate was concentrated *in vacuo*. The residue was distilled to give 11.1 g (59.7%) of a pale yellow liquid, bp 82—84°C/0.3 mmHg, n_D^{20} 1.5880; ν_{max}^{film} 3260, 2100, 1625, 1050 (–S–C(=S)–O–),[10] and 950 cm^{-1}; λ_{max}^{EtOH} 227.5 (ε=21500) and 282.5 mμ (ε=12800).[10] Found: C, 50.78; H, 5.71%. Calcd for $C_8H_{10}OS_2$: C, 51.58; H, 5.41%.

***S*-Pent-2-en-4-ynylisothiuronium Bromide (IX).** 5-Bromopent-3-en-1-yne (14.5 g) (0.1 mol) was added, portion by portion, to a hot solution of thiourea (7.6 g) (0.1 mol) in 180 m*l* of ethanol. After the mixture had been warmed for 3 hr at 50°C, the ethanol was evaporated to give white crystals (25.7 g) (97.0%), mp 142—144°C. Recrystallization from ethanol-isopropyl ether gave the pure IX, mp 146.5—147°C; ν_{max}^{KBr} 3300, 3100, 2100, and 958 cm^{-1}; λ_{max}^{EtOH} 229 mμ (ε=21600). Found: C, 32.63; H, 4.35%. Calcd for $C_6H_9N_2OBr$: C, 32.59; H, 4.10%.

Pent-2-en-4-ynylthiol (VII). *A) Reaction of 5-Bromopent-3-en-1-yne with Potassium Hydrosulfide.* A solution of 5-bromopent-3-en-1-yne (7.5 g) (0.05 mol) in 5 m*l* of acetone was added at room temperature for 30 min to aqueous potassium hydrosulfide prepared by the passage of hydrogen sulfide into a solution of potassium hydroxide (2.8 g) (0.05 mol) in 10 m*l* of water. After the mixture had been stirred for an additional hour, the resulting mixture was extracted with ether. The ether was dried over anhydrous sodium sulfate; the concentrate was distilled *in vacuo* to give 2.3 g (47.0%) of a colorless liquid, bp 46—47°C/15 mmHg, n_D^{20} 1.5580; ν_{max}^{film} 3300, 2550, 2050 ,1625, and 955 cm^{-1}; λ_{max}^{EtOH} 229 mμ (ε=9700).

Reaction with 2,4-dinitrochlorobenzene gave the 2,4-dinitrophenyl sulfide, mp 106.5—107.5°C (EtOH). Found: C, 49.68; H, 3.42%. Calcd for $C_{11}H_8O_4N_2S$: C, 50.00; H, 3.30%.

B) From Ethyl Pent-2-en-4-ynylxanthate. A saturated ammonia solution in 16 g of ethanol was stirred, drop by drop, into pent-2-en-4-ynylxanthate (4.2 g) (0.02 mol) at 55—60°C, then the mixture was stirred for 1.5 hr. The residue obtained after evaporating the solvent was distilled to give 1.1 g (55.0%) of a colorless liquid, bp 48—49°C/16 mmHg. The infrared spectrum of the product was in complete accord with that of the VII prepared by method A.

p-Tolyl Pent-2-en-4-ynyl Sulfide (X). 5-Bromopent-3-en-1-yne (7.1 g) (0.05 mol) was added at room temperature to a solution of *p*-thiocresol (6.2 g) (0.05 mol) and sodium ethoxide, prepared from sodium (1.2 g) (0.05 mol) and 35 m*l* of ethanol. After the mixture had been warmed for 1 hr, the precipitated sodium bromide was filtered; after the ethanol had been evaporated, the filtrate was extracted with ether. The ether extract was dried over anhydrous sodium sulfate and evaporated. The residue was distilled, giving 7.3 g (77.7%) of a liquid, bp 91—93°C/0.3 mmHg, n_D^{20} 1.5944; ν_{max}^{film} 3300, 2050, 1625, 1600, 1495, 955, and 800 cm^{-1}; λ_{max}^{EtOH} 227 mμ (ε=20700). Found: C, 75.92; H, 6.65%. Calcd for $C_{12}H_{12}S$: C, 76.55; H, 6.42%.

Pent-2-en-4-ynylthioacetic Acid (XI). 5-Bromopent-3-en-1-yne (15.2 g) (0.11 mol) was added at room temperature to a solution of sodium hydroxide (8.0 g) (0.2 mol) and thioglycolic acid (9.2 g) (0.1 mol) in 200 m*l* of water, after which the mixture was stirred for 20 hr at room temperature. The reaction mixture extracted with ether to remove the unreacted bromide. The water layer was acidified with 20% dilute sulfuric acid and extracted with ether. The ethereal extract, after being washed with water, dried over calcium chloride, and evaporated, was distilled to give 5.3 g (34.0%) of pale yellow liquid, bp 111—113°C/0.3 mmHg, n_D^{20} 1.5537; ν_{max}^{film} 3250, 3100—2900, 2070, 1710, and 955 cm^{-1}; λ_{max}^{EtOH} 229 mμ (ε=12200). Mol; Found by alkali titration: 157.1. Calcd for $C_7H_8O_2S$: 156.2.

10) E. Klein, J. K. Bosarbe and I. Norman, *J. Phys. Chem.*, **64**, 1666 (1960).

BULLETIN OF THE CHEMICAL SOCIETY OF JAPAN VOL. 42 2593—2595 (1969)

The Absolute Configuration of Isopropylidenecamphor Oxide

Jun KATSUHARA

Sun Star Dentifrice Company, Research Laboratory, Takatsuki, Osaka,

(Received December 5, 1968)

The conversion of (+)-isopropylidenecamphor derived from (+)-camphor into (1R:2S:4S)-isopropylideneborneol and (1R:2R:4S)-isopropylideneisoborneol was described. In light of this configurational correlation, it was concluded that (+)-isopropylidenecamphor oxide derived from isopropylideneborneol has (1R:3R:4S)-, and (−)-isopropylidenecamphor oxide derived from isopropylideneisoborneol, (1R:3S:4S)-configurations.

Djerassi and coworkers[1] have shown that the reversed octant rule is applicable to the Cotton effect at n-π^* transition of transoid cyclopropyl- and epoxy-ketones. To date, however, the optical rotatory dispersion curves of cisoid epoxy-ketones have been reported only with scanty examples and it has not yet been known whether or not the reversed octant rule is applicable to cisoid epoxy-ketones. With a view to formulating the relationship between the Cotton effect and the absolute configuration of cisoid epoxy-ketones, the author has recently reported the assignment of absolute configuration of *trans*- and *cis*-pulegone oxides,[2] *trans*- and *cis*-pinocarvone oxides[3] and discussed the ORD data obtained with these epoxides.

We wish, to describe the determination of absolute configurations of *trans*- and *cis*-isopropylidenecamphor oxides and to report the ORD and CD spectra thereof.

(+)-α-Bromocamphor (**2**), obtained by the bromination of (+)-camphor in the presence of anhydrous aluminum chloride, was grignardized and condensed with acetone in tetrahydrofuran to give a mixture of (+)-camphor (**1**), (+)-α-bromocamphor (**2**), 3-α-hydroxyisopropylcamphor (**3**) and (+)-isopropylidenecamphor (**4**) in the ratio of 44 : 16 : 16 : 24 as determined by VPC analysis. (+)-Isopropylidenecamphor (**4**) was obtained pure from the mixture and was then oxidized with 30% hydrogen peroxide in methanolic 30% sodium hydroxide solution to afford a mixture of *trans*- and *cis*-isopropylidenecamphor oxides. Separation of the mixed isomers was achieved by preparative VPC which afforded chemically pure (+)-**5** (oily) and (−)-**6** (mp 42°C) in an isomer ratio of 33:67.

(+)-Isopropylidenecamphor (**4**) was reduced with lithium aluminum hydride to yield the corresponding alcohol mixture consisting of the crystalline **7** (mp 88°C) in 9 parts and the liquid diastereomeric alcohol **8** in 91 parts.

Beckmann[4] reported that the lithium aluminum hydride reduction of camphor gave isoborneol (exo alcohol) which resulted from the attack of the hydride reagent to the less hindered side of camphor, *i. e.* opposite the geminal dimethyl group. Accordingly, judging from the product ratio found for the present reduction, it may be deduced that the major product **8** is (1R:2R:4S)-isopropylideneisoborneol and the minor diastereomer **7** is (1R:2S:4S)-isopropylideneborneol.

This assignment is supported also by the NMR analysis[5] of these diastereomeric alcohols **7** and **8**. The Δ value, 17.4 Hz, found for chemical shift of C-8 methyl group in **8** reasonably supported the *cis*-configuration of hydroxyl group relative to the methyl group. (See Table 1)

TABLE 1. CHEMICAL SHIFT (τ) OF METHYL GROUP

	7 (endo)			8 (exo)		
	H-8	H-9	H-10	H-8	H-9	H-10
$CDCl_3$ soln	9.12	9.23	9.00	9.02	9.17	9.05
Pyridine soln	9.10	9.15	8.97	8.73	9.12	8.90
Δ Value (c/sec)	1.2	4.8	1.8	17.4	3.0	9.0

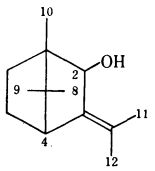

1) C. Djerassi, W. Klyne, T. Norin, G. Ohloff and E. Klein, *Tetrahedron*, **21**, 163 (1965).
2) J. Katsuhara, *J. Org. Chem.*, **32**, 797 (1967).
3) J. Katsuhara, This Bulletin, **41**, 2700 (1968).
4) C. Beckmann and R. Mezger, *Chem. Ber.*, **89**, 2738 (1956).
5) K. Tori and K. Aono, *Annual Report of Shionogi Research Laboratory*, **14**, 136 (1964).

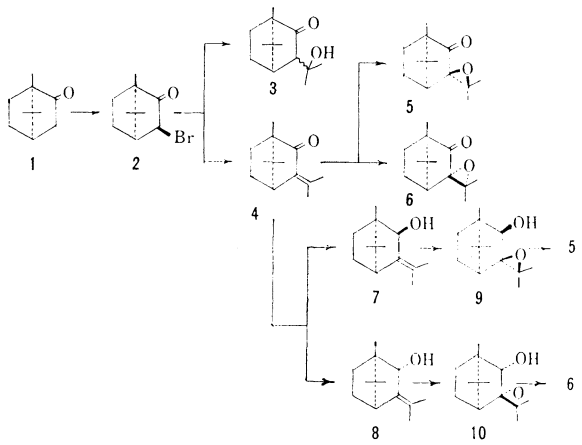

Scheme I.

Epoxidation with perbenzoic acid of **7** and **8** in chloroform afforded the *β*-epoxide (**9**)[6] of the (1R:2R:3R:4S)-configuration and the *α*-epoxide (**10**) having the (1R:2S:3S:4S)-configuration, respectively. These diastereomeric epoxides **9** and **10** were then oxidized with chromic acid in acetone, when (+)-*cis*-(1R:3R:4S)-isopropylidenecamphor oxide (**5**) was obtained from **9** and (−)-*trans*-(1R:3S:4S)-isopropylidenecamphor oxide (**6**) from **10**, the absolute configurations naturally having followed from the respective parent compounds. Compounds **5** and **6**, which were derived *via* an alternative route of transformation from the same parent ketone (**4**), were identified by means of IR- and VPC-comparison with (+)-*cis*-**5** and (−)-*trans*-**6** (See Scheme 1.).

Based on the ORD-studies of various bicyclo-[2.2.1]heptanone systems, Klyne[7] suggested that the octant rule is applicable to bicycloheptanone systems and accounted for the contribution of substituents to the overall ORD of the systems. For example, the ORD contributions of C-8 ,C-9 and C-10 in camphor was estimated as $a=+96$, by comparing the molar amplitude (+71) found for camphor[8] with that (−25) for camphenilone.

When this empirical generalization is applied to the systems **5** and **6**, whose octant projection diagrams are shown in Scheme II, the contribution of oxirane ring to the overall ORD of the respective diastereomeric isopropylidenecamphor oxides may be calculated in the same way: the *β*-oxirane group in **5** has a positive contribution (in ORD), $a=72-71=+1$ whereas the *α*-oxirane in **6** has a negative one, $a=41-71=-30$.

The magnitude of the amplitude contribution by the substituents in the ORD curve of the present

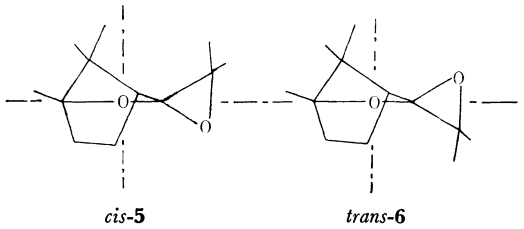

cis-**5** *trans*-**6**

Scheme II.

cisoid epoxy-ketone is too small to draw any definite conclusion on the validity of the reversed octant rule being applied to transoid epoxy-ketones in general.

Experimental[9]

Bromination of Camphor (1). Bromine (121 g) was added dropwise with stirring during 2 hr into a mixture of camphor (mp 178°C, $[\alpha]_D^{25}$ +44.18° (*c* 0.94, ethanol): 100 g, 0.66 mol) and anhydrous aluminum trichloride in 200 m*l* of dried carbon tetrachloride and the reaction mixture was stirred for further 6 hr at 60°C. After removal of solvent *in vacuo*, the crude product was washed with chilled *n*-hexane to give (+)-*α*-bromocamphor (**2**), mp 77°C, $[\alpha]_D^{20}$ +136.0±0.4° (*c* 0.89, ethanol), UV λ_{max}^{MeOH} m*μ* (*ε*), 306 (97): CD m*μ* ([*θ*]) in methanol, 350 (0), 315 (+5645), 265 (0), 220 (−1392), 212 (0), 205 (+5721), 34% yield.

Preparation of Isopropylidenecamphor (4). *α*-Bromocamphor (**2**) (35 g, 0.15 mol) in 280 m*l* of tetra-

6) H. B. Henbest and R. A. L. Wilson, *J. Chem. Soc.*, **1957**, 1958.

7) W. Klyne, *Tetrahedron*, **13**, 29 (1961).

8) G. Jacob, G. Ourisson and A. Rassat, *Bull. Soc. Chim. France*, **1959**, 1374.

9) Infrared spectra were recorded on a Shimadzu Model 27-G spectrophotometer. Optical rotatory dispersion and circular dichroism measurements were made on a Nippon Bunko Spectropolarimeter Model ORD/UV-5. Optical rotation measurements were recorded on a Perkin-Elmer Model 141 with a 10 cm-cell. Gas-liquid partition chromatography analyses were carried out using a Shimadzu 2-C gas chromatograph. A 3 mm×2.25 m column of 20% Hyporose-80 on Celite-545 served for VPC analyses. Nuclear magnetic resonance spectra were recorded with a Varian A-60 spectrometer.

hydrofuran was added to 3.5 g (0.14 g atom) of magnesium in 20 m*l* of THF under a nitrogen atmosphere during 1 hr. After 3 hr stirring, acetone (41 m*l*, 0.64 mol) was added to the reaction mixture and was reacted for 4 hr. The reaction mixture was poured onto ice-water and the organic layer was extracted with ether after ammonium chloride solution was added. Ethereal extracts were combined, washed and dried. Removal of solvent under reduced pressure yielded a crude product (27.9 g, 99%), which was analyzed by VPC. The product consisted of 44% **1**, 16% **2**, 16% 3-α-hydroxyisopropylcamphor (**3**),[10] mp 88°C, Found: C, 74.58; H, 10.61%. Calcd for $C_{13}H_{22}O_2$: C, 74.22; H, 10.56%, and 24% (+)-isopropylidenecamphor (**4**), liquid, $[\alpha]_D^{22}$ +201.1±6.6° (*c* 0.36, methanol), UV λ_{max}^{MeOH} mμ (ε), 248 (9110), 332 (70): CD mμ ([θ]) in methanol, 377 (0), 335 (+980), 305 (+1076), 250 (+21573), 210 (0).

Preparation of Mixture of Isopropylidenecamphor Oxides. A mixture of (+)-**4** (5 g, 0.038 mol) in methanol (50 m*l*) and 50 m*l* of 30% hydrogen peroxide in 50 m*l* of water was kept at 60°C, and to this was added dropwise a 30% aqueous solution (50 m*l*) of sodium hydroxide over a 30 min period. Stirring was continued for 7 hr, the temperature being maintained at 60°C. The reaction mixture was poured into 100 m*l* portion of ether, and the organic layer was separated and worked up as usual to give a crude product (4.5 g). The VPC analysis indicated that the crude product contained 33% of **5** and 67% of **6**.

Isolation and Properties of Pure Isopropylidenecamphor Oxides (5) and (6). Isolation of each diastereomer from the mixture was effected by preparative VPC. Further purification of the fraction on a silica gel column gave pure **5**: the IR-spectrum exhibited the following peaks ν_{max} 1760, 1380, 910 cm^{-1}: $[\alpha]_D^{28}$ +176.3±2.4° (*c* 0.9, methanol): ORD mμ ([φ]) in methanol, 400 (+1300), 333 (+5312), 295 (−1887), 228 (+7316), 210 (−7712): CD mμ ([θ]) in methanol, 350 (0), 316 (+5536), 255 (+184), 215 (+12263), 208 (+9073): UV λ_{max}^{MeOH} mμ (ε), 310 (50), Found: C, 74.37; H, 9.71%. Calcd for $C_{13}H_{20}O_2$: C, 74.94; H, 9.70%, and **6**: the IR-spectrum main bands ν_{max} 1750, 1380, 1015, 960, 930, 920, 830, 770 cm^{-1}; $[\alpha]_D^{28}$ −21.7±0.7° (*c* 0.9, methanol): ORD mμ ([φ]) in methanol, 400 (+343), 334 (+1532), 298 (−2475), 294 (−2541), 276 (−2312), 226 (−7728), 206 (+8608): CD mμ ([θ]) in methanol, 347 (0), 318.5 (+2477), 265 (0), 213 (−9554), 207 (−6176): UV λ_{max}^{MeOH} mμ (ε), 310 (49), mp 42°C, Found: C, 74.70; H, 9.70%. Calcd for $C_{13}H_{20}O_2$: C, 74.94; H, 9.70%.

Lithium Aluminum Hydride Reduction of Isopropylidenecamphor (4). Isopropylidenecamphor (5 g, 0.038 mol) dissolved in absolute ether (30 m*l*) was added dropwise with stirring to a chilled (−10°C) slurry of lithium aluminum hydride (3 g, 0.079 mol) in ether. Upon completion of addition, the reaction mixture was stirred at 0°C for an additional hr and then at 15—20°C for 10 hr, and finally, refluxed for 2 hr. Excess hydride was then decomposed by addition of moistened ether under effective cooling. The organic layer was separated, filtered and dried. Removal of ether gave a mixture of **7** and **8** (yield 4.5 g, 89%). The alcohols **7** and **8** were obtained pure by means of silica gel chromatography: **7**, 9 parts, mp 88°C, Found: C, 80.27; H, 11.39%. Calcd for $C_{13}H_{22}O$: C, 80.35; H, 11.41%, and its NMR spectrum indicated in $CDCl_3$ three three-hydrogen singlets (τ 9.23, 9.12, 9.00) for methyl at C-9, C-8, C-10, a three-hydrogen doublet (τ 8.36, *J*=1.5 Hz) for methyl at C-12, a three-hydrogen singlet (τ 8.25) for methyl at C-11, one-hydrogen doublet (τ 7.69, *J*=4.0 Hz) at C-4, and one-hydrogen singlet (τ 5.77) for the hydrogen on the carbon bearing the hydroxyl group; in pyridine three three-hydrogen singlets (τ 9.15, 9.10, 8.97) for methyl at C-9, C-8, C-10, a three-hydrogen doublet (τ 8.30, *J*=1.5 Hz) for methyl at C-12, a three-hydrogen singlet (τ 8.05) for methyl at C-11, one-hydrogen doublet (τ 7.60, *J*=4.0 Hz) at C-4, and one-hydrogen singlet (τ 5.55) for the hydrogen on the carbon bearing the hydroxyl group; **8**, 91 parts, liquid, $[\alpha]_D^{20}$ +127.7±0.8° (*c* 0.4 ethanol), and its NMR spectrum indicated in $CDCl_3$ three three-hydrogen singlets (τ 9.17 9.05, 9.02) for methyl at C-9, C-10, C-8, a three-hydrogen doublet (τ 8.32, *J*=1.0 Hz) for methyl at C-12, a three-hydrogen singlet (τ 8.18) for methyl at C-11, one-hydrogen doublet (τ 7.59, *J*=4.0 Hz) at C-4, and one-hydrogen singlet (τ 6.12) for the hydrogen on the carbon bearing the hydroxyl group; in pyridine three three-hydrogen singlets (τ 9.12, 8.90, 8.73) for methyl at C-9, C-10, C-8, a three-hydrogen doublet (τ 8.27, *J*=1.0 Hz) for methyl at C-12, a three-hydrogen singlet (τ 8.03) for methyl at C-11, one-hydrogen doublet (τ 7.53, *J*=4.0 Hz) at C-4, and one-hydrogen singlet (τ 5.87) for the hydrogen on the carbon bearing the hydroxyl group.

Preparation of *cis*- (5) and *trans*-Isopropylidenecamphor Oxide (6). To an ice-cold solution of perbenzoic acid in chloroform was added 0.26 g of **7** in 5 m*l* of chloroform. The reaction mixture was kept at 0°C for 16 hr. The reaction mixture was then washed with 5% sodium carbonate solution and dried over anhydrous sodium sulfate. Removal of solvent under reduced pressure gave an oily residue, which upon purification on an alumina column, afforded the epoxide **9** (0.13 g). A solution of **9** (100 mg) in acetone (1 m*l*) was added to a solution of chromic acid (55 mg) in water (1 m*l*) containing sulfuric acid (0.2 m*l*) with stirring at 0°C for 1 hr. Water (5 m*l*) was added and the reaction mixture was extracted with ether. The combined ether extract was washed with a 3% sodium hydrogencarbonate solution, water, and then dried over anhydrous sodium sulfate. Removal of solvent yielded a crude product (82 mg), which was then purified by silica gel column chromatography to give pure **5**. In exactly the same manner as described above, epoxidation of **8** (0.64 g) with perbenzoic acid furnished an oily epoxide (**10**) (0.42 g), which in turn, was further oxidized with chromic anhydride to give **6** (0.31 g).

The author wishes to thank Professor T. Matsuura of Hiroshima University, Professor Y. Inouye of Kyoto University, Dr. H. Minato, Dr. K. Kuriyama and Dr. K. Tori of Shionogi Research Laboratory, Dr. M. Kobayashi, Mr. M. Yasufuku, Mr. K. Hashimoto and Mr. H. Watanabe of Sun Star Research Laboratory, for many helpful discussions during this work, and to Shiono Koryo Co., Ltd. for their generous gift of authentic samples.

10) S. M. Malmgren, *Ber.*, **35**, 3910 (1902).

BULLETIN OF THE CHEMICAL SOCIETY OF JAPAN VOL. 42 2596—2599 (1969)

The Cobalt Carbonyl-catalyzed Hydroesterification of 3-(β-Cyanoethoxy)propene with Carbon Monoxide and Methanol

Akio MATSUDA

Government Chemical Industrial Research Institute, Tokyo, Mita, Meguro-ku, Tokyo

(Received December 20, 1968)

The cobalt carbonyl-catalyzed hydroesterification of 3-(β-cyanoethoxy)propene with carbon monoxide and methanol occurred in the presence of a small amount of hydrogen at a moderate temperature, methyl 4-(β-cyanoethoxy)butyrate being produced in a much larger amount than methyl 2-methyl-3-(β-cyanoethoxy)propionate. The double-bond isomerization leading to the formation of propionaldehyde dimethylacetal and ethylene cyanohydrin occurred simultaneously. The selectivity to the double-bond isomerization was very large at a low pressure; it decreased as the pressure was increased, with a corresponding increase in selectivity to the hydroesterification. The reaction rate was not increased by the addition of pyridine, but it was increased about tenfold by the addition of palladium chloride. Thus, the reaction could be carried out at a lower temperature in the presence of palladium chloride. The selectivity to the hydroesterification, however, did not increase upon the addition of palladium chloride, as the double-bond isomerization was also accelerated by its addition.

In a preceding paper on the intramolecular hydroesterification of allyl alcohol with carbon monoxide,[1] it was reported that the selectivity to the hydroesterification product, γ-butyrolactone, could not exceed 60% because of the simultaneous isomerization of allyl alcohol into propionaldehyde.

In the present study, in this connection, the hydroesterification of 3-(β-cyanoethoxy)propene, an etheric derivative of allyl alcohol, is studied with the intention of obtaining methyl 4-(β-cyanoethoxy)-butyrate in a good yield. The reaction proceeds in the presence of a small amount of hydrogen at a moderate temperature; methyl 4-(β-cyanoethoxy)-butyrate and methyl 2-methyl-3-(β-cyanoethoxy)-propionate are produced as the hydroesterification products, there being much more of the former than of the latter. However, an unexpected side-reaction leading to the formation of propional-dehyde dimethylacetal and ethylene cyanohydrin occurs to a considerable extent.

Experimental

The 3-(β-cyanoethoxy)propene was prepared by the cyanoethylation of allyl alcohol with acrylonitrile in the presence of sodium methoxide, and then distilled (73°C/3 mmHg). The propoxypropionitrile and methoxypropionitrile were also prepared by the cyanoethylation of propanol and methanol with acrylonitrile. The propionaldehyde dimethylacetal and isobutyraldehyde dimethylacetal were prepared by the reaction of methanol with propionaldehyde and isobutyraldehyde. The carbon monoxide and dicobalt octacarbonyl were prepared by a procedure described previously.[2] The palladium chloride and the other reagents were obtained commercially. The methanol and pyridine were rectified before use.

The reactions were carried out in the same 300-cc stainless-steel autoclave and with the same technique as was described previously;[2,3] the reaction was started at a desired temperature by dropping in dicobalt octacarbonyl, packed in a stainless-steel saucer, from a wing of the stirrer. The total pressure was kept constant during the reaction by supplying carbon monoxide from a pressure-storage vessel through a pressure regulator; the reaction temperature was controlled within ±1°C. The product composition was quantitatively determined by the gas-chromatographical method in a manner similar to that already described.[1]

Product Identification. The NMR spectra were measured at 100 Mc in carbon tetrachloride, with tetramethylsilane as the internal standard.

Methyl 4-(β-cyanoethoxy)butyrate: bp *ca.* 100°C/10^{-2} mmHg. IR spectrum: C=O (ester) 1735 cm^{-1}, C≡N 2240 cm^{-1}. NMR spectrum: $CH_2(-CN)$ τ 7.46 (triplet), $CH_2(-COOCH_3)$ τ 7.63 (triplet), $CH_2(-CH_2COOCH_3)$ τ 8.13 (quintet), OCH_3 τ 6.38 (singlet), CH_2OCH_2 τ 6.3—6.8 (overlapped multiplet).

Found: C, 55.96; H, 7.10; N, 8.24%. Calcd for $C_8H_{13}NO_3$: C, 56.12; H, 7.65; N, 8.18%.

Methyl 2-methyl-3-(β-cyanoethoxy)propionate: The sample was obtained by gas-chromatographic separation from the reaction product: the IR and the NMR spectra were compared with those of methyl 4-(β-cyanoethoxy)-butyrate. In the NMR spectrum there was no absorption due to $CH_2CH_2(-COOCH_3)$, but there was a strong

1) A. Matsuda, This Bulletin, **41**, 1876 (1968).

2) A. Matsuda and H. Uchida, *ibid.*, **38**, 710 (1965).

3) A. Matsuda, *ibid.*, **40**, 135 (1967).

Table 1. The effect of bases

1/4 mol 3-(β-cyanoethoxy)propene, 1/2 mol methanol, 2 mmol $Co_2(CO)_8$; total pressure 200 kg/cm²; hydrogen content of the gas used, 3% (Expt. No. 1—5), 0.8% (Expt. No. 6)

Expt. No.	1	2	3	4	5	6
Reaction temp. (°C)	120	120	120	120	110	120
Base	None	Py	Py	CH_3ONa	Py	Py
(mmol)	0	2	4	2	2	2
$k\times10^2$ (min^{-1})	2.3	2.0	1.2	2.7	0.84	0.81
Reaction time (min)	120	120	180	120	180	240
Conversion (%)	99	99	93	98	97	93
Selectivity (%)[a]						
$CH_2CH_2CH_2COOCH_3$ | OCH_2CH_2CN	52	60	63	62	67	70
$CH_2CH(CH_3)COOCH_3$ | OCH_2CH_2CN	1.4	1.5	2.2	1.6	2.0	2.3
$CH_3CH_2CH(OCH_3)_2$	28	26	28	28	24	27
γ-butyrolactone	0.9	3.3	1.7	1.0	1.1	—
$CH_2CH_2CH_3$ | OCH_2CH_2CN	0.3	0.8	0.6	0.4	0.5	—
$CH_3OCH_2CH_2CN$	—	—	—	0.4	—	—
The residue	17	8	4	6	5	1

a) Each product contained an amount of ethylene cyanohydrin equimolar to propionaldehyde dimethylacetal.

absorption(doublet) due to CH_3(–CH), indicating that this compound was the branched isomer of methyl 4-(β-cyanoethoxy)butyrate. IR spectrum: C=O (ester) 1738 cm^{-1}, C≡N 2240 cm^{-1}. NMR spectrum: CH_2(–CN) τ 7.47 (triplet), CH_3(–CH) τ 8.82 (doublet), CH(–$COOCH_3$) τ 7.25 (quartet), OCH_3 τ 6.35 (singlet), CH_2OCH_2 τ 6.3—6.8 (overlapped multiplet),

Results and Discussion

The Effect of Bases. In connection with the previous finding that the rate of the hydroesterification in the presence of a small amount of hydrogen is selectively increased by the addition of pyridine(Py),[1-4] the effects of such bases as Py and sodium methoxide on the present reaction were first examined.

The results are shown in Table 1. The first-order rate constant, k, was calculated according to the half-time method by means of this equation: $k=\ln 2\,/t_{1/2}$. The half-time, $t_{1/2}$, was estimated from the gas-supplying curve during the reaction and the final conversion, on the assumption that the amount of gas supplied was proportional to the amount of the reacted olefin. The ratio of methyl 4-(β-cyanoethoxy)butyrate to methyl 2-methyl-3-(β-cyanoethoxy)propionate was very large (30—40), indicating that the terminal methoxycarbonylation predominated in this case; this trend is the same as that observed in the hydroesterification of propylene and methyl acrylate.[2,4] The selectivity to β-propoxypropionitrile resulting from the hydrogenation of 3-(β-cyanoethoxy)propene was less than 1%. Propionaldehyde dimethylacetal and ethylene cyanohydrin were produced in equimolar amounts. Propionaldehyde dimethylacetal may result from the double-bond isomerization of 3-(β-cyanoethoxy)-propene, followed by the reaction with methanol. The other possible route involving the formation of allyl alcohol as an intermediate is not important, since, if such a route were important, γ-butyro-

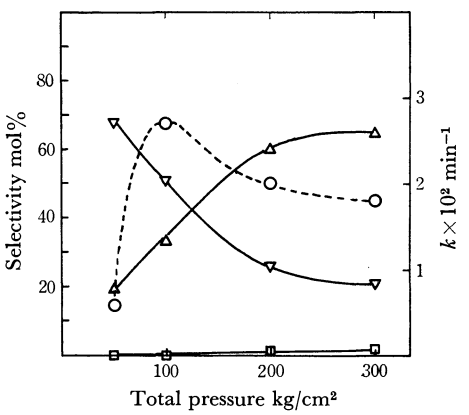

Fig. 1. The effect of total pressure
--○-- : $k\times10^2$ (min^{-1})
—△— : methyl 4-(β-cyanoethoxy)butyrate (mol%)
—□— : methyl 2-methyl-3-(β-cyanoethoxy)propionate (mol%)
—▽— : propionaldehyde dimethylacetal (mol%)

4) A. Matsuda, *ibid.*, **42**, 571 (1969).

lactone would result from the intramolecular hydroesterification of the intermediate allyl alcohol in a yield comparable with that of propionaldehyde dimethylacetal,[1] whereas the amount of γ-butyrolatone in the product was very small compared with the amount of propionaldehyde dimethylacetal.

The results of experiments carried out at various pressures, keeping the other conditions equal to those in Expt. No. 2, are shown in Fig. 1. The double-bond isomerization is presumed to be catalyzed by cobalt hydrotricarbonyl, since the selectivity to propionaldehyde dimethylacetal was very large at a low pressure, as had been observed in the previous study.[1]

$$\begin{array}{l} CH_2CH{=}CH_2 \\ \quad | \\ OCH_2CH_2CN \end{array} \xrightarrow{HCo(CO)_3} \begin{array}{l} CH{=}CHCH_3 \\ \quad | \\ OCH_2CH_2CN \end{array} \xrightarrow[-HOC_2H_4CN]{+2CH_3OH} CH_3CH_2CH(OCH_3)_2 \qquad (1)$$

As the pressure increased from 50 to 300 kg/cm^2, the selectivity to propionaldehyde dimethylacetal decreased and the selectivity to the hydroesterification products increased. The rate constant, k, showed a peak at 100 kg/cm^2; it began to decline as the pressure increased from 100 to 300 kg/cm^2. These effects of the total pressure are clearly due to the carbon monoxide partial pressure, since the rate constant, k, decreases by decreasing the hydrogen partial pressure, while the selectivity to propionaldehyde dimethylacetal remains unchanged (compare Expt. No. 6 with No. 2).

The addition of such bases as Py and sodium methoxide did not affect the reaction rate, but it increased the selectivity to the hydroesterification products. This increase in the selectivity seems to be the direct consequence of the fact that the residue is remarkably reduced by the addition of these bases. The residue is a mixture of unidentified polymers, probably resulting from the hydroformylation of 3-(β-cyanoethoxy)propene, followed by the polymerization of the resulting aldehydes; this is in accordance with the fact that the residue is considerably reduced by decreasing the hydrogen content of the gas used (Expt. No. 6), since the selectivity to the hydroformylation decreases upon a decrease in the hydrogen partial pressure.[2] The residue also decreases upon a decrease in the reaction temperature, resulting in an increased selectivity to the hydroesterification products.

In a preceding study of the hydoesterification of acrylonitrile, it was found that the addition of Py is effective in increasing the rate of the hydroesterification because it accelerates the formation of an acylcobalt carbonyl-intermediate, and that the methanolysis of this intermediate is very fast.[3] Consequently, the rate-determining step in the present reaction is not the formation of an acylcobalt carbonyl-intermediate, since the reaction rate in this case does not increase with the addition of pyridine. Therefore, the most probable rate-determining step in the present reaction is the formation of an alkylcobalt carbonyl-intermediate from olefin and cobalt hydrocarbonyl. If the formation of an alkylcobalt carbonyl-intermediate from olefin and cobalt hydrocarbonyl is really the rate-determining step, the reaction rate would probably be affected by weakening the olefinic double-bond by coordination.

The Effect of Palladium Chloride. Olefins can be activated by the π complex formation with palladium chloride to undergo reactions with various nucleophiles.[5] It has also been said that a palladium-compex can catalyze the carbonylation of olefins because it can activate the olefinic double-bond by the π complex formation.[6] Therefore, it seems probable that the reaction between an olefin and cobalt hydrocarbonyl can also be catalyzed by palladium chloride.

The results of experiments carried out in the presence of palladium chloride are shown in Table 2. Expectedly, the effect of palladium chloride on the rate was very remarkable. The rate constant, k, increased about tenfold upon the addition of a small amount of palladium chloride. The rate constant, k, in the presence of a small amount of palladium chloride was further increased by the addition of Py equimolar to dicobalt octacarbonyl. Thus, the reaction could be carried out at 90°C in the presence of small amounts of palladium chloride and Py (Expt. No. 9).[7] However, the selectivity to the hydroesterification products decreased upon the addition of palladium chloride, while the selectivity to propionaldehyde dimethylacetal increased; this is because palladium chloride accelerates the double-bond isomerization to a larger extent than it does the hydroesterification. The fairly large amount of γ-butyrolactone which is found in the products of the reactions carried out in the presence of palladium chloride probably results from the decomposition of methyl 4-(β-cyanoethoxy)butyrate, since the formation of allyl alcohol as an intermediate is unlikely, as has been mentioned before. In fact, such a decomposition took place when the products were distilled at a high temperature:

$$\begin{array}{l} CH_2CH_2CH_2COOCH_3 \\ \quad | \\ OCH_2CH_2CN \end{array} \longrightarrow \begin{array}{l} H_2C{-}CH_2 \\ \quad | \quad | \\ H_2C \quad C{=}O \\ \quad \backslash O / \end{array} + (CH_2{=}CHCN)_n + CH_3OH \qquad (2)$$

5) J. Tsuji, *Yukigosei Kagaku Kyokaishi* (*J. Synth. Organic Chem., Japan*), **25**, 984 (1967).

6) K. Bittler, N. Kutepow, D. Neubauer and H. Ries, *Angew. Chem.*, **80**, 352 (1968).

7) In the absence of palladium chloride, almost no reaction occurs at such a low temperature as 90°C.

TABLE 2. THE EFFECT OF PALLADIUM CHLORIDE

1/4 mol 3-(β-cyanoethoxy)propene, 1/2 mol methanol, 2 mmol $Co_2(CO)_8$; total pressure 200 kg/cm²; hydrogen content of the gas used, 3%

Expt. No.	1	7	2	8	9
Reaction temp. (°C)	120	120	120	120	90
$PdCl_2$ (mmol)	0	1	0	1	1
Py (mmol)	0	0	2	2	2
$k \times 10^2$ (min^{-1})	2.3	20	2.0	35	0.91
Reaction time (min)	120	15	120	5	120
Conversion (%)	99	100	99	100	71
Selectivity (%)[a,b]					
$CH_2CH_2CH_2COOCH_3$ | OCH_2CH_2CN	52	26	60	24	47
$CH_2CH(CH_3)COOCH_3$ | OCH_2CH_2CN	1.4	0.9	1.5	1.0	7.6
$CH_3CH_2CH(OCH_3)_2$	28	34	26	36	28
γ-Butyrolactone	0.9	23	3.3	26	3.6
$CH_2CH_2CH_3$ | OCH_2CH_2CN	0.3	0.4	0.8	0.3	0.5
$CH_3OCH_2CH_2CN$	—	—	—	0.3	0.4
The residue	17	15	8	12	12

a) *Cf.* Table 1.
b) The selectivity to isobutyraldehyde dimethylacetal in each run was less than 1%.

That the amount of γ-butyrolactone produced was small in the reaction carried out at 90°C (Expt. No. 9) is understandable, since the decomposition of methyl 4-(β-cyanoethoxy)butyrate would be slow at such a low temperature.

Although the reaction rate in the presence of palladium chloride increased upon the addition of Py, this is not because the carbon monoxide-insertion steps are accelerated by Py, for the selectivity to the hydroesterification product is not affected by the addition of Py. The effect of Py on the rate in this case should, therefore, be quite different from those observed in former studies;[1-4] this effect may be attributable to, for example, the activation of palladium chloride by Py.

In conclusion, it can be said to be certain that the formation of an alkylcobalt carbonyl-intermediate can be accelerated by palladium chloride, but not by Py alone; this is consistent with the former assumption that Py was effective in increasing the rate of the hydroesterification because it accelerated the carbon monoxide-insertion step by forming the acylcobalt carbonyl-Py complex:[3]

$$RCo(CO)_4 + Py \rightarrow RCOCo(CO)_3(Py) \xrightarrow[\text{fast}]{+CH_3OH} RCOOCH_3 + HCo(CO)_3 + Py$$

A more extensive study of the effect of palladium chloride is now in progress.

The author is indebted to Professor A. Ozaki, Tokyo Institute of Technology, for his helpful suggestions.

BULLETIN OF THE CHEMICAL SOCIETY OF JAPAN VOL. 42 2600—2604 (1969)

Coumarins. VII. The Acid-catalyzed Reaction of Aromatic Compounds with β-Chlorocarboxylic Acids[1]

Kikumasa SATO,* Yau-Shin LIN* and Takeshi AMAKASU**

* *Department of Applied Chemistry, Faculty of Engineering, Yokohama National University, Ohka-machi, Minami-ku, Yokohama*

** *Chemical Laboratory, Seimi Chemical Co., Ltd., 2645, Chigasaki, Chigasaki-shi, Kanagawa*

(Received December 31, 1968)

The aluminum chloride-catalyzed reaction of aromatic compounds, such as benzene and phenols, with β-chlorocarboxylic acids was investigated. Although the reactions of benzene, toluene, and chlorobenzene with β-chloropropionic acid were found to give the corresponding dihydrocinnamic acids in high yields, attempts to prepare dihydrocoumarin by a similar reaction of phenol were unsuccessful. Similarly, β-arylbutyric acids were obtained in good yields by means of the aluminum chloride-induced reaction of aromatic hydrocarbons with β-chlorobutyric acid (Ib). In contrast, phenols, such as phenol, *o*- and *m*-cresols, reacted with Ib under similar conditions to provide the corresponding β-(*p*-hydroxyphenyl)butyric acids in 22—60% yields, while a 51% yield of β-(5-hydroxy-2-methylphenyl)butyric acid was obtained upon a similar treatment of *p*-cresol with the acid Ib.

An earlier paper in this series[2] has demonstrated that the aluminum chloride-catalyzed reaction of phenols with crotonic acid gives 4-methydihydrocoumarins or their isomers and that dihydroumbelliferone is obtained by the reaction of resorcinol with acrylic acid in the presence of the ethyl ester of polyphosphoric acid. These studies have been extended to the corresponding β-chlorocarboxylic acids. Whereas the acid-catalyzed reactions of aromatic compounds with α,β-unsaturated acids have been extensively studied, little attention has been given to the similar reaction with β-chlorocarboxylic acids.

It has been shown[3] that the condensation of aromatic compounds, such as benzene, toluene, and chlorobenzene, with β-chlorocarboxylic acids, such as β-chloropropionic acid (Ia) and β-chlorobutyric acid (Ib), in the presence of aluminum chloride gives the corresponding indanones; no yields have been given, however. The aluminum chloride-catalyzed reactions of benzene with Ia[4] and with its ethyl ester[5] have previously been shown to provide dihydrocinnamic acid. Recently Dann and his coworkers[6] have reported that phenols condense with Ia in hydrofluoric acid to afford β-chloro-2-hydroxypropiophenones. No method of preparing dihydrocoumarins by the acid-catalyzed reaction of phenols with I has yet appeared in the literature.

In the present study we have examined the condensation of such aromatic compounds as phenols with Ia and Ib, using anhydrous aluminum chloride or boron trifluoride etherate.

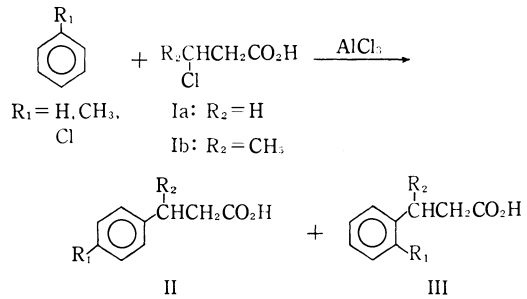

II III

A convenient method of preparing dihydrocinnamic acid (II, $R_1=R_2=H$) was developed by the use of at least two molecular proportions of aluminum chloride for the reaction of benzene with Ia. Similarly, toluene reacted with Ia at 50—55°C for 5 hr to give a high-total yield of the corresponding

1) This investigation was presented at the 21 st Annual Meeting of the Chemical Society of Japan, Ohsaka, April, 1968; and was supported mainly by Asahi Glass Co., for which we are grateful. Part VI of this series: K. Sato, M. Ōhashi, T. Amakasu, and K. Takeda, This Bulletin, **42**, 2319 (1969).

2) T. Amakasu and K. Sato *J. Org. Chem.*, **31**, 1433 (1966).

3) I. G. Farbenindustrie Akt.-Ges., German Pat. 485309 (1929).

4) K. Nagakubo, Y. Iwakura, K. Takei and T. Okada, *Nippon Kagaku Zassi* (*J. Chem. Soc. Japan, Pure Chem. Sect.*), **78**, 1209 (1957).

5) I. P. Tskervanic and I. V. Terent'eva, *Dokl. Akad. Nauk SSSR*, **50**, 257 (1945).

6) O. Dann, G. Volz and O. Huber, *Ann.*, **587**, 16 (1954).

TABLE 1. THE ALUMINUM CHLORIDE-CATALYZED REACTION OF AROMATIC COMPOUNDS WITH β-CHLOROCARBOXYLIC ACIDS (Ia, b)

No.	Compound R_1	Compound R_2	Aromatic compound	I (mol)	$AlCl_3$ (mol)	Reaction temp, °C	Reaction hr	Total yield (%)	Product composition, mol fraction II	Product composition, mol fraction III
1	H	H	120 ml	0.2	0.42	55—60	5	84		
2	CH_3	H	500 ml	1	2	55—60	5	90	0.6	0.4
3	Cl	H	1 mol	0.2	0.5	70—75	7	52	0.6	0.4
4	H	CH_3	50 ml	0.1	0.25	55—60	6	70		
5	CH_3	CH_3	40 ml	0.1	0.25	55—60	5	41	0.31	0.69
6	Cl	CH_3	0.1 mol[a]	0.1	0.3	50—55	5	33	b)	b)

a) The inert solvent used was *sym*-tetrachloroethane (50 m*l*).
b) Attempts to isolate the individual compounds were unsuccessful.

dihydrocinnamic acids, II and III ($R_1=CH_3$, $R_2=H$), in the same ratio as that of II to III ($R_1=$ Cl, $R_2=H$). On the other hand, Ib, when treated with benzene in the presence of 2 equivalents of aluminum chloride at 65—70°C, furnished β-phenylbutyric acid (II, $R_1=H$, $R_2=CH_3$) in a 70% yield. Toluene behaved analogously when treated with Ib, giving the corresponding butyric acids, II and III ($R_1=R_2=CH_3$). While the reaction of chlorobenzene with Ib at 100°C gave the corresponding indanones, IVa (56%) and IVb (16%), under mild conditions a mixture of their precursors, II and III ($R_1=Cl$, $R_2=CH_3$), was obtained in a 33% yield. These results, summarized in Table 1, indicate the predominant alkylation rather than acylation of aromatic compounds with I; they also confirm, along with the infrared spectra and their physical properties, the II and III structures for the β-arylacids.

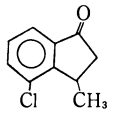

IVa

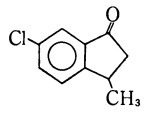

IVb

Although attempts to prepare dihydrocoumarin by extending the above results from Ia to phenol failed, phenyl β-chloropropionate (V) was obtained in a 26% yield when phenol was treated with Ia at 85—95°C for 4 hr in boron trifluoride etherate. The infrared spectrum was identical with that of an authentic sample of V.

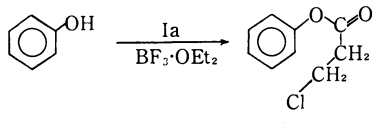

V

In contrast, when phenol was treated with Ib in the presence of 3 equivalents of anhydrous aluminum chloride in *sym*-tetrachloroethane, β-(4-hydroxyphenyl)butyric acid (VIa) was obtained in a 52% yield. The structure follows from the infrared spectrum, which clearly shows hydroxyl and acid C=O bands and an out-of-plane deformation of aromatic C–H at 3100, 1700, and 820 cm^{-1} respectively.

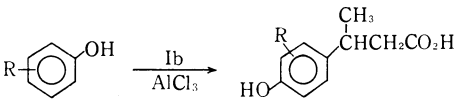

VIa, R=H
b, R=2-CH_3
c, R=3-CH_3

o-Cresol, when treated similarly with Ib, gave the corresponding butyric acid, VIc (22%). The new compound, VIc, was verified by a study of its infrared spectrum and by elemental analysis. With *m*-cresol white crystals, mp 123—124°C, were obtained. The analytical data agreed with the formula $C_{11}H_{14}O_3$, which is in accord with the structure of the *p*-alkylated product, VIb, and the *o*-isomer, VII.

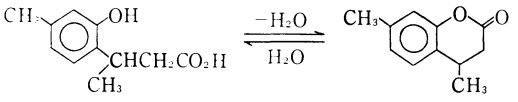

VII VIII

The infrared spectrum exhibited hydroxyl and carbonyl absorptions at 3150 and 1690 cm^{-1} respectively, along with aromatic deformations (860, 820 cm^{-1}). This spectrum does not make it possible to distinguish clearly between VIb and VII. The compound VII, obtained by the hydrolysis of the corresponding dihydrocoumarin, VIII, is known[7] to undergo an intramolecular dehydration cyclization to VIII. Accordingly, attempts to prepare VIII from the product resulted in the recovery of the starting material, VIb. Thus, it may be concluded that the product is β-(4-hydroxy-

7) T. Nakabayashi, *Yakugaku Zasshi* (*J. Pharm. Soc. Japan*), **74**, 23 (1954).

2-methylphenyl)butyric acid (VIb).

On the other hand, *p*-cresol behaved abnormally when similarly treated with Ib, giving crystals with a melting point of 111—112°C. The product was shown by elemental analysis to have the formula $C_{11}H_{14}O_3$, which is in accord with those of IX and X. The infrared spectrum showed hydroxy and acid C=O absorptions respectively at 3200 and 1710 cm^{-1}, in addition to an out-of-plane deformation of aromatic C–H at 860 and 800 cm^{-1}. The experimental fact that an attempt at cyclization to XI results in the recovery of the starting material may eliminate the possibility of such a structure as the *o*-alkylated product, X. Furthermore, in order to obtain evidence for the structure (IX), conversion to the indanone derivative XII was attempted. Compound IX, upon treatment in polyphosphoric acid (PPA) at 60—70°C for 1 hr, was converted into the corresponding indanone, XII, which gave its semicarbazone. The infrared spectrum of compound XII indicated the presence of a hydroxyl group (3300 cm^{-1}), a ketone carbonyl group (1675 cm^{-1}), and two adjacent hydrogen atoms of substituted benzene (820 cm^{-1}). Thus, the product,

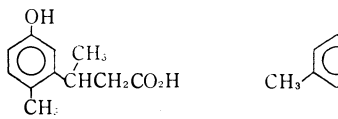

IX

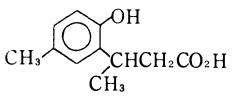

X

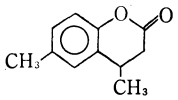

XI

IX, was proved to be *β*-(5-hydroxy-2-methylphenyl)butyric acid.

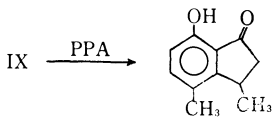

XII

When resorcinol was similarly treated with Ib in the presence of 3.3 equivalents of aluminum chloride at 85—90°C for 5 hr, 7-hydroxy-2-methylchromanone (XIII) was obtained in a 34% yield. The product, XIII, identical in properties with that previously reported, showed an infrared spectrum consistent with the structure of the chromanone derivative.

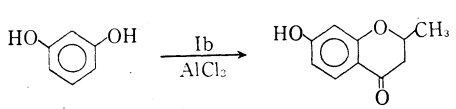

XIII

From the results obtained in this experiment, the following conclusions can be reached. While *β*-chlorocarboxylic acid, Ib, reacts not only with aromatic hydrocarbons and chlorobenzene, but also with phenols (but not resorcinol) to give *β*-arylbutyric acids, the aluminum chloride-catalyzed reaction of Ia takes place only with aromatic compounds, except for the cases of phenols and their ethers. In addition, it should be noted that the formation ratios of II to III are remarkably different between the reaction of Ia and that of Ib (Table 1). These facts suggest that the transition state (*i. e.*, XIV) in the attack of the electrophilic *β*-carbon of Ib on an aromatic nucleus might differ from that of Ia (*i. e.*, XV).

Anhydrous aluminum chloride is believed, of course, to coordinate with a chloro group and not only with a carboxylic group[2,8] but also with the hydroxyl group[9] of a phenol. The observation that the use of at least two and three molecular proportions of aluminum chloride in the reaction of

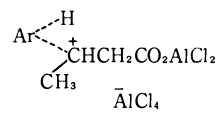

XIV

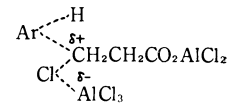

XV

aromatic hydrocarbons and of phenols respectively are necessary in order to obtain good yields of the products (II, III and VI, IX) supports this suggestion. In addition, the liberation of hydrogen chloride observed on the cold treatment of I acids with aluminum chloride results from the first step, in which the aluminum salt of I may be formed.

Experimental

All the melting points, determined on a Shimadzu Type MM-2 micro hot stage, and all the boiling points are uncorrected. The infrared spectra were recorded on a Hitachi Model EPI-S2 spectrophotometer, while gas chromatographic analysis were carried out on a Shimadzu Model GC-1C chromatograph.

Materials. *β*-Chloropropionic acid (Ia) (72.5%) was prepared by the addition of dry hydrogen chloride to acrylic acid at 10—20°C[10]; bp 101—103°C/12 mmHg; mp 38.5—40°C (from ligroin) (lit[10] mp 40.5°C). *β*-Chlorobutyric acid (Ib) was obtained in a quantitative yield by the similar treatment of the dry gas with crotonic acid in ether at 0°C for three days; bp 111—112°C/20 mmHg (lit[11] bp 98.5—99.5°C/12 mmHg). The other materials were obtained from commercial sources.

Dihydrocinnamic Acid (II, R_1=R_2=H). *Typical Procedure A.* Fine-powdered anhydrous aluminum chlo-

8) a) P. H. Groggins and P. H. Nagel, *Ind. Eng. Chem.*, **26**, 1313, 1317 (1934); b) P. H. Gore, *Chem. Revs.*, **55**, 229 (1955); c) W. R. Edwards and E. C. Sibille, *J. Org. Chem.*, **28**, 674 (1963).

9) H. W. Johnston and F. J. Gross, *J. Org. Chem.*, **22**, 1264 (1957).

10) E. Linnermann, *Ann.*, **163**, 96 (1872).

11) A. M. Cloves, *ibid.*, **319**, 357 (1901).

ride (56.1 g, 0.42 mol) was added slowly to a solution of Ia (21.7 g, 0.2 mol) in 120 ml of benzene, after which stirring was vigorously continued. The mixture was gradually heated on an oil bath and kept under the conditions shown in Table 1. The resulting mixture was chilled and poured over water containing crushed ice and concentrated hydrochloric acid. The organic layer was separated from the aqueous layer, which was then shaken with benzene. The extract was combined with the separated organic material, and then washed with water. After the extract had been dried over anhydrous magnesium sulfate and the solvent had been removed, the residue was distilled under reduced pressure to afford 50.8 g (84%) of a colorless oil; bp 153—155°C/12 mmHg (lit[4] bp 125—126°C/4 mmHg). It solidified after standing for some time. Recrystallization from ligroin gave the pure product; mp 48°C (lit[4] mp 48—49°C): ν_{max}^{KBr} 1700 (C=O), 750, 700 cm^{-1} (mono-substituted).

The product (23 g) was heated in PPA (280 g) at 70°C for 1 hr. The subsequent treatment of the mixture according to the usual manner provided indanone (14.6 g, 70%); mp 38.5°C (from ligroin) (lit[12] mp 40°C).

***p*- and *o*-Methyldihydrocinnamic Acids (II and III; $R_1=CH_3$, $R_2=H$).** The Procedure A shown above was followed, using the molar ratios of the reagents and the conditions listed in Table 1. The fractional recrystallization of the crude products (bp 140—143°C/3 mmHg, mp 50—80°C) from aqueous acetic acid (1 : 1.5, vol) and ligroin furnished II ($R_1=CH_3$, $R_2=H$); mp 115—116°C (lit[13] mp 117°C); ν_{max}^{KBr} 1700 (C=O), 810 cm^{-1} (aromatic C-H).

The recrystallization-mother liquor was extracted with ether and dried. The removal of the ether, followed by fractional distillation, gave 59.2 g of III ($R_1=CH_3$, $R_2=H$), which was then recrystallized from 95% ethanol to afford the pure product; mp 100—102°C (lit[14] mp 102°C); ν_{max}^{KBr} 1700 (C=O), 780 cm^{-1} (ortho-disubstituted).

***p*- and *o*-Chlorodihydrocinnamic Acids (II and III; $R_1=Cl$, $R_2=H$).** These compounds were prepared by means of Procedure A. The reaction was carried out under the conditions presented in Table 1. The resulting organic material, like that described above, was washed with diluted sodium hydroxide (50 ml × 3). Acidification, followed by filtration, gave 8 g of the crude product, II. Recrystallization from water provided colorless crystals; mp 94—96°C (lit[15] mp 91—93°C).

The filtrate was extracted with ether. Drying and the removal of the solvent afford 12 g of the crude compound, III, which was then recrystallized from aqueous ethanol to provide colorless crystals; mp 118—120°C (lit[16] mp 123°C).

Found: C, 58.80; H, 5.19%. Calcd for C_9H_9ClO: C, 58.55; H, 4.91%.

Phenyl β-Chloropropionate (V). To a mixture of 9.4 g (0.1 mol) of phenol and 10.8 g (0.1 mol) of Ia, boron trifluoride etherate (21.3 g, 0.15 mol) was added, drop by drop. The mixture was stirred and heated on an oil bath at 85—95°C for 4 hr. The resulting mixture was poured onto an ice-water slurry. The organic layer was separated from the aqueous layer, which was shaken with ether. The extract was washed with water and with saturated sodium bicarbonate, and then dried over magnesium sulfate. The removal of the ether, followed by distillation, gave V (3.9 g, 26%) as a colorless oil; bp 94—95°C/2 mmHg (lit[17] bp 132—135°C/12 mmHg); ν_{max}^{film} 1750 (ester, C=O), 750, 690 cm^{-1} (monosubstituted).

Found: C, 58.43; H, 5.10%. Calcd for $C_9H_9ClO_2$: C, 58.55; H, 4.91%.

β-Phenylbutyric Acid (II, $R_1=H$, $R_2=CH_3$). This compound was prepared according to Procedure A using the conditions shown in Table 1. The resulting extract was shaken with diluted sodium hydroxide, and the alkaline layer was acidified with hydrochloric acid. Extraction with ether, drying, and the subsequent removal of the solvent gave a crude oil, which was fractionated to yield the pure product (11.5 g, 70%); bp 145—148°C/5 mmHg (lit[18] bp 168°C/17 mmHg). It solidified and was recrystallized from ligroin, providing the pure compound as colorless crystals; mp 35—36°C (lit[18] mp 36—38.5°C); ν_{max}^{film} 1700 (C=O), 750, 690 cm^{-1} (aromatic C-H).

β-(*p*-Tolyl)butyric Acid (II, $R_1=R_2=CH_3$) and Its *o*-Isomer (III, $R_1=R_2=CH_3$). Procedure A was followed, using the molar ratios of the reagents and the conditions listed in Table 1. A mixture (7.3 g, 41%) of the compounds II and III was obtained, through such a workup as has been described above, from the resulting reaction mixture; bp 165—167°C/15 mmHg. It solidified after standing in an ice-box. Filtration gave the *p*-isomer (2.3 g), which was recrystallized from petroleum ether to afford the pure compound; mp 88—89°C (lit[19] mp 91°C); ν_{max}^{KBr} 1700 (C=O), 810 cm^{-1} (*p*-substituted).

The filtrate was fractionated to give the *o*-isomer (5 g); bp 168—169°C/13 mmHg (lit[20] bp 166—167.5°C/12 mmHg); ν_{max}^{film} 1700 (C=O), 780 cm^{-1} (*o*-substituted).

4-Chloro-3-methylindanone (IVa) and Its Isomer (IVb). These compounds were prepared according to Procedure A, using 40 ml of chlorobenzene, 12 g (0.1 mol) of Ib, and 33 g (0.25 mol) of aluminum chloride. The reaction was carried out at 100°C for 5 hr. The resulting mixture was treated such as has already been described, giving an organic material which was then shaken with an aqueous alkaline solution. After drying and the removal of the solvent, the residual oil was distilled to afford a mixture of IVa and IVb (13 g, 72%); bp 134—135°C/18 mmHg. A part of it solidified after standing at 0°C for a while. Filtration gave IVa (4.5 g), which was recrystallized from petroleum ether, providing the pure compound; mp 45—46°C (lit[3] mp 47°C); ν_{max}^{KBr} 1705 (ketone C=O), 840, 790, 780 cm^{-1} (1,2,3-trisubstituted).

The product gave the semicarbazone; mp 220—223°C.

12) K. von Auwers, *ibid.*, **415**, 160 (1918).
13) R. Huisgen and V. Vossius, *Monatsh. Chem.* **88**, 517 (1957).
14) C. Grundmann, *Chem. Ber*, **81**, 513 (1948).
15) T. F. Dankova, T. N. Bokova, N. A. Preobrazhenskii, A. E. Petrushchenks, I. A. Il'shtein and N. I. Shvetsov, *Zhur. Obshch. Khim.*, **21**, 787 (1951).
16) A. N. Nesmeyanov, R. Kh. Freidlina and N. A. Semenov, *Izvest. Akad. Nauk, SSSR, Otdel. Khim. Nauk*, **1955**, 993.
17) F. Mayer and L. v. Zütphen, *Ber.*, **57B**, 200 (1924).
18) D. H. Hey, J. Honeyman, D. H. Kohn and W. J. Peal, *J. Chem. Soc.*, **1953**, 2021.
19) T. Wagner-Jauregg and H. Hippchen, *Ber.*, **76B**, 694 (1943).
20) V. P. Gol'mov and C. Kun, *Zhur. Obshch. Khim.*, **29**, 3705 (1959).

Attempts to isolate the analytical sample, IVb, from the filtrate by repeated distillations failed; bp 136—140°C. Gas-chromatographic analysis showed the distillate (8.5 g) to consist of IVa (60%) and IVb (40%). The formation ratio of IVa to IVb is, accordingly, 0.78/0.22.

β-(*p*-Chlorophenyl)butyric Acid (II, R_1=Cl, R_2=CH_3) and Its *o*-Isomer III (R_1=Cl, R_2=CH_3). The procedure involves the use of an inert solvent such as *sym*-tetrachloroethane. Procedure A was followed, except for the use of such a solvent, using the molar ratio of the reagents and the conditions presented in Table 1. Fractional distillation gave a colorless oil (6.5 g, 33%), which was shown by means of gas-chromatographic analysis to be a mixture of the corresponding II and III. Attempts to isolate the individual compounds by a variety of means such as gas chromatography were unsuccessful; bp 170—173°C.

Found: C, 60.39; H, 5.81%. Calcd for $C_{10}H_{11}ClO_2$: C, 60.46; H, 5.53%.

β-(*p*-Hydroxyphenyl)butyric Acid (VIa). *Typical Procedure B.* A solution of phenol (9.4 g) and Ib (12 g, 0.1 mol) in *sym*-tetrachloroethane (25 m*l*) was added, drop by drop, to a stirred suspension of anhydrous aluminum chloride (40 g, 0.3 mol) in the solvent (25 m*l*) at 0—5°C for 1 hr, after this period stirring was vigorously continued until the evolution of hydrogen chloride subsided. The mixture was then gradually heated on an oil bath and kept at 70—75°C for 6 hr; the resulting mixture was chilled and poured over an ice-water slurry (300 m*l*) containing concentrated hydrochloric acid (100 m*l*). The organic layer was separated from the aqueous layer, which was then shaken with three 100 m*l* portions of ether. The extract was combined with the separated organic material and then washed with a saturated sodium bicarbonate solution and water. After it had been acidified with hydrochloric acid and extracted with ether, the extract was dried over anhydrous magnesium sulfate. The removal of the solvent gave a viscous oil contaminated with the starting Ib, which could be removed by means of high-vacuum distillation. It solidified after standing in an ice-box for some time. Filtration, followed by recrystallization from benzene, provided VIa (9.4 g, 52%): mp 136—138°C (lit[21] mp 136°C); ν_{max}^{KBr} 3100 (OH), 1700 (C=O) and 820 cm^{-1} (*p*-disubstituted).

Found: C, 66.59; H, 6.94%. Calcd for $C_{10}H_{12}O_3$: C, 66.65; H, 6.71%.

β-(4-Hydroxy-3-methylphenyl)butyric Acid (VIb). Procedure B for the preparation of VIa was followed, using 10.8 g (0.1 mol) of *o*-cresol, 12 g (0.1 mol) of Ib, 40 g (0.3 mol) of anhydrous aluminum chloride, and 50 m*l* of the solvent. The reaction was carried out at 70—75°C for 7 hr. VIb (4.2 g, 22%) was obtained as the product, through a work-up such as that shown above; mp 107—108°C (from benzene); ν_{max}^{KBr} 3400 (OH), 1680 (C=O) and 850, 800 cm^{-1} (1,3,4-trisubstituted).

Found: C, 67.71; H, 7.36%. Calcd for $C_{11}H_{14}O_3$: C, 68.02; H, 7.27%.

β-(4-Hydroxy-2-methylphenyl)butyric Acid (VIc). Compound VIc was prepared by means of Procedure B. The reaction was carried out under the same conditions as were shown in the preparation of VIb, using 5.4 g (0.05 mol) of *m*-cresol, 6 g (0.05 mol) of Ib, 20 g (0.15 mol) of aluminum chloride, and 25 m*l* of the solvent. When a viscous oil, obtained from the reaction mixture through the same work-up, was allowed to stand in an ice-box for two weeks, it solidified. Recrystallization from benzene afforded VIc (11 g, 60%): mp 123—124°C; ν_{max}^{KBr} 3150 (OH), 1690 (C=O), and 860, 820 cm^{-1} (1,2,4-trisubstituted).

Found: C, 67.80; H, 7.33%. Calcd for $C_{11}H_{14}O_3$: C, 68.02; H, 7.27%.

β-(5-Hydroxy-2-methylphenyl)butyric Acid (IX). This compound was prepared according to Procedure B, using 21.6 g (0.2 mol) of *p*-cresol, 24 g (0.2 mol) of Ib, 80 g (0.6 mol) of aluminum chloride, and 100 m*l* of the solvent. The reaction was carried out at 70—85°C for 7 hr. Recrystallization from benzene gave IX (19.8 g, 51%); mp 111—112°C; ν_{max}^{KBr} 3200 (OH), 1710 (C=O), 860, 800 cm^{-1} (1,2,5-trisubstituted).

Found: C, 67.77; H, 7.38%. Calcd for $C_{11}H_{14}O_3$: C, 68.02; H, 7.27%.

7-Hydroxy-3,4-dimethylindan-1-one (XII) A mixture of IX (3 g) and PPA (40 g) was stirred at 60—70°C for 1 hr, poured over cold water, and then extracted with ether. After it had been washed with a saturated sodium bicarbonate solution and with water, and dried over anhydrous magnesium sulfate, the solvent was removed to give a crude product; mp 35°C (lit[22] mp 53—54°C); ν_{max}^{KBr} 3300 (OH), 1675 (C=O) and 820 cm^{-1} (1,2,3,4-tetrasubstituted). The compound gave the semicarbazone; mp 203—205°C (from water) (lit[22] mp 217°C).

Found: C, 61.94; H, 6.67%. Calcd for $C_{12}H_{15}N_3O_2$: C, 61.78; H, 6.48%.

7-Hydroxy-2-methylchromanone (XIII). Procedure B was followed, using 11 g (0.1 mol) of resorcinol, 12 g (0.1 mol) of Ib, 45 g (0.33 mol) of aluminum chloride, and 50 m*l* of the solvent. The reaction was carried out at 85—90°C for 5 hr. The extract, obtained in the usual manner, was washed with a sodium hydroxide solution, and the alkaline layer was acidified with hydrochloric acid. Filtration, followed by recrystallization from water, afforded XIII (6 g, 34%); mp 174—176°C (lit[6] mp 175—176°C); ν_{max}^{KBr} 3100 (OH), 1600 (C=O), 850, 780 cm^{-1} (aromatic C–H). The compound gave the semicarbazone; mp 205—207°C (from aqueous ethanol).

Found: C, 66.90; H, 5.89%. Calcd for $C_{10}H_{10}O_3$: C, 67.40; H, 5.50%.

21) J. F. Bunnett and J. L. Marks, *J. Am. Chem. Soc.*, **74**, 5893 (1952).

22) K. von Auwers, *Ber.*, **44**, 3692 (1911); *Ann.*, **421**, 36 (1920).

BULLETIN OF THE CHEMICAL SOCIETY OF JAPAN VOL. 42 2605—2610 (1969)

Argentation Constants of Styrene Derivatives*1

Yoshiaki INAKI, Shun-ichi NOZAKURA and Shunsuke MURAHASHI

Department of Polymer Science, Faculty of Science, Osaka University, Toyonaka, Osaka

(Received January 22, 1969)

Equilibrium constants for the formation of silver ion complexes (argentation constants) of styrene derivatives in water were measured at 0 and 25°C by Andrews and Keefer's solubility method. The argentation constants for the 1 : 1 complex (K_1) decreased in this order: *cis*-β-alkylstyrene>α-alkylstyrene>*trans*-β-alkylstyrene, for a given alkyl group. This order was related to differences in the resonance stabilization of the double bond. The K_1 values of the α- and β-alkylstyrene series did not seem to correlate with Taft's steric substituent constant, E_s, within the respective series. However, when the hyperconjugation effect of alkyl substituents was considered, a good linearity between log K_1 and Hancock's parameter, E_s^c, was obtained. Thus, the steric effect was separated from the hyperconjugation effect, and it was found that the steric effects for the three series are nearly identical. Thermodynamic data indicated that an isokinetic relationship holds between ΔH and ΔS and that the argentation equilibrium is controlled mainly by the entropy factor. The degree of methyl substitution at the double bond of styrene slightly influenced the K_1 values, although 1,2-dihydronaphthalene had an abnormally large K_1 value.

The argentation (silver ion complexation) equilibria of unsaturated compounds have been investigated by several groups of workers.[1-6] The stabilities of the complexes of the silver ion with unsaturated compounds may be interpreted as the sum of the independent contributions of polar, resonance, and steric effects of substituents. The polar effects were discussed in terms of the Hammett ρ–σ relation for benzene derivatives by Andrews and Keefer[1] and for ring-substituted styrenes and other olefins by Fueno and his co-workers.[2-4] For the resonance effect, it has already been established that the argentation equilibria are affected by the conjugation of substituents with the reaction center.[5] Although the literature contains references to the steric effect of substituents on the argentation equilibria, the investigations have not been extended beyond qualitative discussions. Both Winstein and Lucas[5] and Fueno *et al.*[2] suggested that the reason for the reluctance of β-methylstyrene to argentate is the steric effect of the substituent. Muhs and Weiss[6] measured the argentation constants of many unsaturated compounds by the gas chromatographic method and discussed the steric effects of substituents qualitatively.

The present investigation was undertaken to obtain information concerning the steric effects in the argentation of styrene derivatives. In separate reports,[7,8] we have previously reported on our observations of the steric effects in the radical copolymerizations of α- and β-alkylstyrenes with acrylonitrile. From the difference in the steric effects of α- and β-alkylstyrenes in the radical copolymerizations, it was deduced that the transition state of the radical polymerization is not of the π-complex type but of the σ-complex type. Since it is known that the silver ion forms a π-complex with an unsaturated compound, the steric effect in the argentation of styrene derivatives may also give information concerning the transition state of the radical polymerizaion.

In the present investigation, the argentation constants of α- and β-alkylstyrenes in water were measured by Andrews and Keefer's solubility method.[1] Also, the argentation constants of *cis*- and *trans*-α,β-dimethylstyrenes, β,β-dimethylstyrene, 1,2-dihydronaphthalene, and indene were determined and compared with the values of the above styrenes.

*1 Presented at the 21st Annual Meeting of the Chemical Society of Japan, Osaka, March, 1968, and at the Meeting of Polymer Science, Kobe, June, 1968.

1) L. J. Andrews and R. M. Keefer, *J. Am. Chem. Soc.*, **72**, 3113 (1950).

2) T. Fueno, T. Okuyama, T. Deguchi and J. Furukawa, *ibid.*, **87**, 170 (1965).

3) T. Fueno, O. Kajimoto and J. Furukawa, This Bulletin, **41**, 782 (1968).

4) T. Fueno, O. Kajimoto, T. Okuyama and J. Furukawa, *ibid.*, **41**, 785 (1968).

5) S. Winstein and H. J. Lucas, *J. Am. Chem. Soc.*, **60**, 836 (1938).

6) M. A. Muhs and F. T. Weiss, *ibid.*, **84**, 4697 (1962).

7) S. Hirose, S. Nozakura and S. Murahashi, to be published.

8) K. Yasufuku, S. Nozakura and S. Murahashi, This Bulletin, **40**, 2146 (1967).

Experimental

Materials. The styrene and α-methylstyrene were obtained commercially. The other α-alkylstyrenes were synthesized by the Wittig reaction of alkyl phenyl ketones, much as in a previous paper.[8] By the Wittig reaction of the corresponding aldehydes, β-alkylstyrenes were prepared.[7] The *cis*- and *trans*-isomers of these styrenes were fractionated by distillation under reduced pressure, using a stainless-steel helipack column of about 30 theoretical plates. Also, the *cis*-and *trans*-α,β-dimethylstyrenes, and β,β-dimethylstyrene were obtained by the Wittig reaction. The 1,2-dihydronaphthalene was synthesized according to the literature.[9] The indene was obtained commercially. These olefines were purified by rectifications under reduced pressure and, immediately before use, were treated with lithium aluminum hydride overnight and redistilled under a high vacuum. The silver nitrate and potassium nitrate were of an analytical grade and used without further purification. The solvent for extraction, *n*-hexane, was purified in the usual way.

Measurements of the Solubility. All the experiments were carried out in the dark.

Samples of styrene derivatives (0.1—1.0 g) were added to 20 m*l* of aqueous silver nitrate solutions of varying silver ion concentrations, all the solutions containing enough potassium nitrate to maintain an ionic strength of unity. The mixtures were shaken vigorously in 50 m*l* glass-stoppered Erlenmeyer flasks for 3 hr in a constant-temperature bath at 0.00±0.05°C and 25.00±0.05°C in order to saturate the aqueous phase with styrenes. It was confirmed that one hour of shaking was sufficient for the argentation equilibrium to be reached.

TABLE 1. EXTINCTION COEFFICIENTS OF STYRENE DERIVATIVES IN HEXANE SOLUTION*

R	α-R–St		*cis*-β-R–St		*trans*-β-R–St	
	λ mμ	ε	λ mμ	ε	λ mμ	ε
H	287	3.10×10^2				
Me	285	1.40×10^2	290	1.15×10^2	293	6.30×10^2
Et	239	9.52×10^3	242	1.29×10^4	284	1.10×10^3
n-Pr	239	9.71×10^3	242	1.35×10^4	251	1.70×10^4
n-Bu	239	9.91×10^3	241	1.20×10^4	251	1.70×10^4
i-Pr	234	8.36×10^3	242	1.24×10^4	251	1.62×10^4
s-Bu	234	8.47×10^3	242	1.23×10^4	251	1.70×10^4
t-Bu	220	4.20×10^3	220	3.81×10^3	251	1.70×10^4

	λ mμ	ε
cis-α,β-Dimethyl–St	243	1.22×10^4
trans-α,β-Dimethyl–St	234	6.83×10^3
β,β-Dimethyl–St	244	1.46×10^4
Indene	281	3.02×10^2
1,2-Dihydronaphthalene	295	4.59×10^2

* Slit width 0.30 mm

9) J. von Brawn and G. Kirchbaum, *Ber.*, **54**, 604 (1921).

After the two phases had been fully separated by being kept standing (5 hr), measured volumes of the saturated aqueous phase were pipetted out and extracted with 5—10 m*l* portions of hexane by shaking in glass-stoppered flasks for one hour. The optical density of the hexane phase was measured against a hexane blank on a Hitachi Spectrophotometer (EPS-3T) at a wavelength appropriate for each styrene, the molecular extinction coefficients having been previously determined. The spectra were scanned from 210 mμ through 360 mμ to check the impurity in the solutions. It was also checked whether one extraction for one hour is sufficient for the removal of all of the styrenes, both free and complexed, from the aqueous phase. The volume of the hexane phase was adjusted to obtain the optical density readings between 0.200 and 0.800.

The total styrene concentrations of the saturated aqueous solutions were calculated from the optical density of the hexane solutions. The wavelengths (λ) and the corresponding values of the molecular extinction coefficients (ε) are given in Table 1.

Results

Argentation Constants. According to Andrews and Keefer,[1] the equilibrium reactions of styrenes (St) with the silver ion in the aqueous phase can be explained in terms of these equilibria:

$$Ag^+ + St = Ag\text{–}St^+$$
$$K_1 = [Ag\text{–}St^+]/[Ag^+][St] \quad (1)$$
$$Ag^+ + Ag\text{–}St^+ = Ag_2\text{–}St^{2+}$$
$$K_2 = [Ag_2\text{–}St^{2+}]/[Ag^+][Ag\text{–}St^+] \quad (2)$$

here, K_1 and K_2 are the equilibrium constants for the formation of the Ag-St$^+$ and Ag$_2$-St^{2+} complexes respectively.

An additional constant, K, introduced to facilitate the calculations of K_1 and K_2, is defined as:

$$K = \frac{[St]_t - [St]}{[Ag^+][St]} = K_1 + K_1K_2[Ag^+] \quad (3)$$

where $[St]_t$ and $[St]$ are the molar concentrations of all the styrene-containing species and of free styrene respectively, and where $[Ag^+]$ is the molar concentration of the free silver ion.

The solubilities were measured for styrene derivatives at 25°C, and the values of K were calculated from Eq. (3). If the equilibria (1) and (2) account for all the complexes formed, and if additional reactions do not contribute appreciably to the complex formation, the plots of K against $[Ag^+]$ should give a straight line. This was found to be the case, with reasonable accuracy, for all the styrene derivatives investigated. Figure 1 shows examples of these plots for *cis*-β-alkylstyrenes at 25°C. In such plots the ordinate intercept is K_1 and the slope is K_1K_2. The values of K_1 and K_2 thus obtained are given in Table 2. These values were determined by the method of least-squares with an error of about one percent.

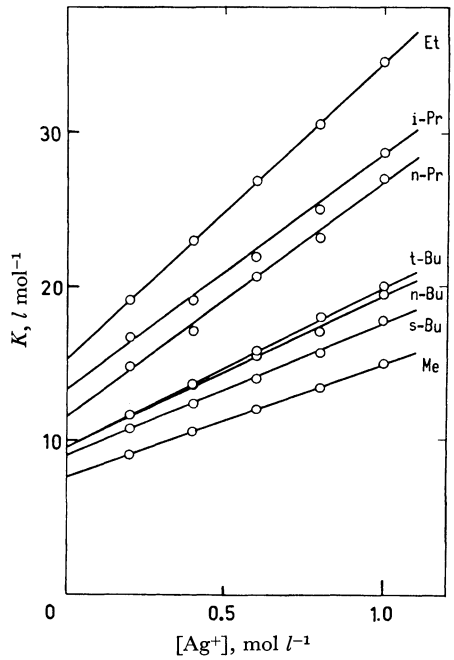

Fig. 1. Plots of K vs. [Ag+] for *cis*-β-R-styrene at 25°C.

Table 2. Argentation constants of styrene derivatives at 25°C in water

R	α-R-St		*cis*-β-R-St		*trans*-β-R-St	
	K_1 1/mol	K_2 1/mol	K_1 1/mol	K_2 1/mol	K_1 1/mol	K_2 1/mol
H	17.4	0.9				
Me	8.2	1.0	7.4	1.0	5.4	0.8
Et	11.1	1.6	15.3	1.3	8.1	1.3
n-Pr	8.2	1.7	11.6	1.3	5.5	1.7
n-Bu	6.5	1.5	8.5	1.1	2.7	1.0
i-Pr	13.6	1.4	13.8	1.1	10.5	0.9
s-Bu	7.0	1.3	8.7	1.0	5.1	0.9
t-Bu	8.6	1.2	9.3	1.1	6.6	1.4

	K_1 1/mol	K_2 1/mol
trans-α,β-Dimethyl-St	3.0	1.3
cis-α,β-Dimethyl-St	5.3	0.7
β,β-Dimethyl-St	5.0	0.8
Indene	8.5	0.9
1,2-Dihydronaphthalene	28.4	1.4

It may be noticed that the values of K_2 are appreciably smaller than the K_1 values and are insensitive to the variation in the structure of styrenes. The values of K_1 which are a measure of the stabilities of the complexes, decrease in this order for a given alkyl:

cis-β-alkylstyrene>α-alkylstyrene>*trans*-β-alkylstyrene

The K_1 value obtained for styrene in our work is in reasonable agreement with the value obtained by Andrews and Keefer.[10] However, the K_1 values for β-methylstyrenes are larger than those given in the literature.[2,5] When rectificated samples of β-alkylstyrenes without further purification were used, abnormal peaks of benzaldehyde were found in the ultraviolet spectra of the extracted hexane solutions. Since the solubility of benzaldehyde in the aqueous phase is high, while the equilibrium constant is small, the K_1 values obtained were as small as the values in the literature. Samples which were treated with lithium aluminum hydride in order to remove the benzaldehyde gave smaller solubilities in the aqueous phase and larger K_1 values.

Temperature-dependence. The argentation constants were measured at 0 and 25°C for α- and β-alkylstyrenes. At temperatures higher than 30°C the solutions became turbid and silver metal precipitated during the equilibration, thus precluding measurements.

Listed in Table 3 are the values of K_1 and K_2 obtained at 0°C from the plots described above. The values of K_1 at 0°C are greater than those at

Table 3. Argentation constants of styrene derivatives at 0°C in water

R	α-R-St		*cis*-β-R-St		*trans*-β-R-St	
	K_1 1/mol	K_2 1/mol	K_1 1/mol	K_2 1/mol	K_1 1/mol	K_2 1/mol
H	36.5	1.2				
Me	22.2	1.1	13.9	1.4	10.3	2.2
Et	18.3	2.4	22.7	2.5	14.7	2.2
n-Pr	19.0	1.7	21.0	1.8	9.7	2.5
n-Bu	13.0	1.7	15.2	1.5	6.4	1.7
i-Pr	33.0	1.3	23.5	1.8	22.6	1.8
s-Bu	13.3	1.7	15.4	1.6	10.2	0.8
t-Bu	14.7	1.8	15.4	2.1	13.0	2.3

Table 4. Thermodynamic data for argentation of styrene derivatives in water

R	α-R-St		*cis*-β-R-St		*trans*-β-R-St	
	$-\Delta H$ kcal/mol	$-\Delta S$ e.u.	$-\Delta H$ kcal/mol	$-\Delta S$ e.u.	$-\Delta H$ kcal/mol	$-\Delta S$ e.u.
H	4.9	10.6				
Me	4.9	11.6	4.0	9.2	4.3	11.1
Et	3.0	5.2	2.5	3.1	3.9	8.8
n-Pr	5.4	14.0	3.9	8.1	4.3	11.2
n-Bu	5.0	13.2	4.0	9.2	5.6	16.8
i-Pr	5.7	13.7	3.6	6.8	4.9	11.7
s-Bu	4.0	9.6	4.1	9.5	4.8	12.8
t-Bu	3.7	8.2	3.7	8.0	5.0	13.0

10) L. J. Andrews and R. M. Keefer, *J. Am. Chem. Soc.*, **72**, 5034 (1950).

25°C. These results indicate that the silver ion complexes are stable at lower temperatures.

From the K_1 values at 0 and 25°C, the thermodynamic data for the argentation in water were obtained. Table 4 gives the entropy and enthalpy changes in the argentation for α- and β-alkylstyrenes in water.

Discussion

Alkyl Substituent Effect. It has been established that, in the styrene molecule and in most styrene derivatives, the vinyl group is the center for the coordination of the silver ion.[2,10] On the basis of this consideration, it appears very likely that the K_1 values are related to the nature of the substituent about the double bond of styrenes. The effects of substituents on argentation constants may be divided into the independent contributions of the polar, resonance, and steric effects of the substituents. Thus, Taft's equation can be applied:

$$\log (K/K_0) = \rho^*\sigma^* + \delta E_s + \gamma E_\psi \qquad (4)$$

where σ^*, E_s, and E_ψ are the polar, steric, and resonance substituent constants and where ρ^*, δ, and γ are the corresponding reaction parameters. K_0 is the equilibrium constant of a standard reaction (methyl substituent). In Fig. 2, the K_1 values for

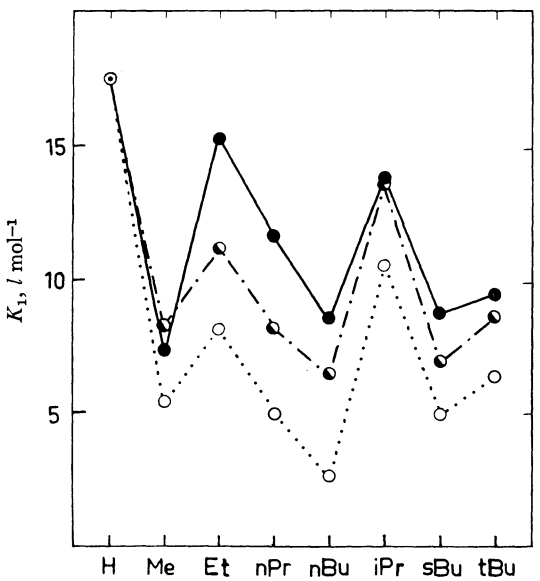

Fig. 2. Argentation constants of styrene derivatives at 25°C.
◔ α-R–St, ● *cis*-β-R–St, ○*trans*-β-R–St

α- and β-alkylstyrenes at 25°C are plotted against the alkyl substituents, which are arranged in the increasing order of E_s. The plots shows zigzag curves, although they show similar patterns for the respective series. A similar tendency is shown by the results of Muhs and Weiss[6] for alkyl-substituted ethylenes.

Table 5 collects the ultraviolet absorption spectra

TABLE 5. ULTRAVIOLET SPECTRA OF STYRENE DERIVATIVES IN HEXANE

R	α-R–St		*cis*-β-R–St		*trans*-β-R–St	
	λ_{max} mμ	log ε_{max}	λ_{max} mμ	log ε_{max}	λ_{max} mμ	log ε_{max}
H	244	4.08				
Me	243	4.04	241	4.11	249	4.16
Et	239	4.03	242	4.11	251	4.19
n-Pr	239	3.97	242	4.13	251	4.23
n-Bu	239	3.97	241	4.08	251	4.23
i-Pr	234	3.86	242	4.09	251	4.21
s-Bu	234	3.93	242	4.09	251	4.23
t-Bu	~220	3.62	~220	3.58	251	4.23

of α- and β-alkylstyrenes. It indicates that, for *cis*- and *trans*-β-alkylstyrenes, the extent of conjugation does not change appreciably within each series except for *cis*-β-*t*-butylstyrene. This means that the resonance factor varies little within each series. However, in the case of α-alkylstyrenes, the wavelengths of maximum absorption shift lower with an increase in the bulkiness of the alkyl substituents. It is generally known that an increase in the extent of conjugation causes a reduction in K_1 values. It appears, then, that the bulky alkyl groups of α-alkylstyrenes cause an increase in K_1 value as a result of the steric inhibition of conjugation. Table 5 also indicates that the resonance effect of styrene is different from those of alkylstyrenes.

Another important factor affecting the complex formation is the steric effect of the substituents neighboring the double bond. As has previously been mentioned, no correlation between K_1 and E_s can be found in Fig. 2. From Fig. 2 it appears that the K_1 values in each series can be classified into three groups according to the number of α-hydrogen atoms in the alkyl substituent. This classification suggests the effect on argentation of the hyperconjugation of the alkyl group. Therefore, we tried to separate the effects of substituents into the independent contributions of the steric substituents and the hyperconjugation effects of alkyl substituents, as represented by the equation:

$$\log (K/K_0) = \delta E_s^c + h(n - 3) \qquad (5)$$

where n is the number of α-hydrogen atoms in alkyl groups and where h is an adjustable parameter representing a measure of the hyperconjugation effect. We here used Hancock's E_s^c values[11] rather than Taft's E_s values, becuase the E_s^c values are based upon the quantitative separation of the hyperconjugation effect from Taft's steric

11) C. K. Hancock, E. A. Meyers and B. J. Yager, *J. Am. Chem. Soc.*, **83**, 4211 (1961).

substituent constants. The correlation of $\log K_1$ by Eq. (5) gave a good linearity, as is shown in Fig. 3. The h parameter was determined by trial

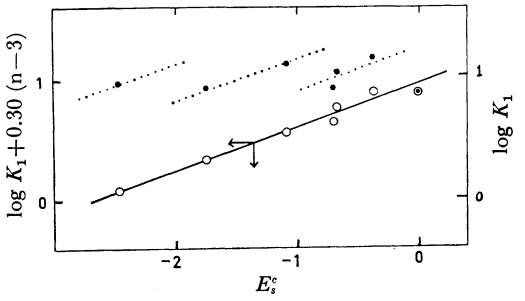

Fig. 3. Relationship between argentation constants of *cis*-β-R-styrene and E_s^c.

and error. The negative value of h in Fig. 3 indicates that the hyperconjugation effect serves to reduce the K_1 value. This is consistent with qualitative recognition that, as has already been mentioned, the conjugation between a substituent and the reaction center causes a reduction in the K_1 value.

The polar effect of substituents on the argentation of benzene derivatives was discussed by Andrews and Keefer[1] in the Hammett ρ–σ relation; they reported a reaction constant $\rho=-1.6$ for σ_m. Also, the two reaction constants $\rho=-0.766$[2] and $\rho=-5.07$[3] were reported by Fueno *et al.* for ring-substituted styrenes and vinyl compounds respectively. In our case, it is appropriate to discuss the polar effect using the reaction constant of vinyl compounds, $\rho=-5.07$, in the Hammett ρ–σ_m relation. Table 6 shows only a small difference in

Table 6. Polar and steric substituent constants of alkyl groups

R	σ_m[a]	$\rho\sigma_m$[b]	$h(n-3)$[c]	E_s^c[d]
Me	−0.069	0.35	0.00	0.00
Et	−0.07	0.35	0.30	−0.38
n-Pr			0.30	−0.67
n-Bu			0.30	−0.70
i-Pr	−0.068	0.34	0.60	−1.08
s-Bu			0.60	−1.74
t-Bu	−0.10	0.51	0.90	−2.46

a) D. H. McDaniel and H. C. Brown, *J. Org. Chem.*, **23**, 420 (1958).
b) $\rho=-5.07$ from Ref. 3.
c) $h=-0.30$ from Fig. 3.
d) Ref. 11.

the polar substituent effects $\rho\sigma_m$ of alkyl groups; therefore, the polar effect of substituents can be neglected.

It was found that Eq. (5) holds in the case of the argentation of alkenes in ethylene glycol, which has been studied by Muhs and Weiss using gas

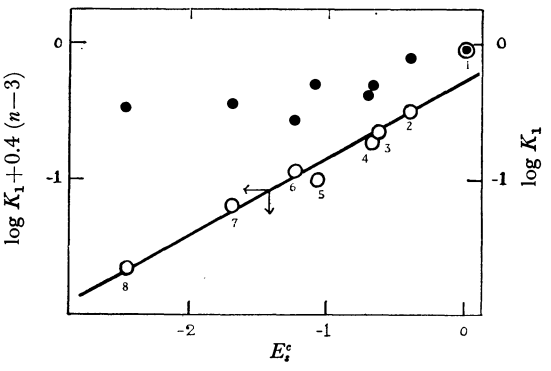

Fig. 4. Relationship between argentation constants of 1-alkene and E_s^c at 40°C.
R-CH=CH_2: 1. Me 2. Et 3. *n*-Pr 4. *n*-Bu 5. *i*-Pr 6. *i*-Bu 7. *s*-Bu 8. *t*-Bu

chromatography (Fig. 4).[6] The substituent effect of alkenyl alkyl ethers on the argentation, which was investigated by Fueno *et al.*,[4] may be interpreted in a similar manner.

The same treatment as in Fig. 3 was also applied to α- and β-alkylstyrenes; all the results are given in Fig. 5. The slope of these straight lines corre-

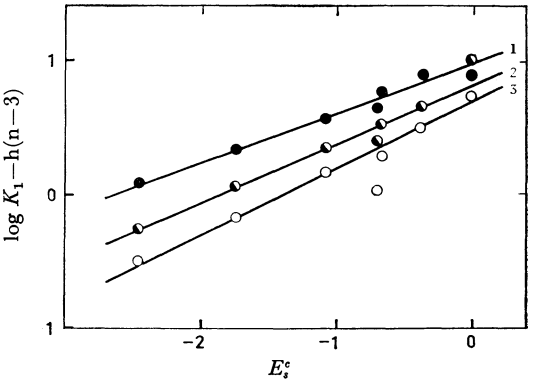

Fig. 5. Relationship between argentation constants of styrene derivatives and E_s^c.
1. *cis*-β-R–St 2. α-R–St 3. *trans*-β-R–St

sponds to the δ parameter, the steric reaction constant. Figure 5 indicates that the δ parameters of *cis*-β- and *trans*-β-alkylstyrenes are practically the same. Figure 5 also indicates that the δ parameter of the α-alkyl series is nearly equal to that of the β-alkyl series. However, since the α-alkyl groups exhibit a steric inhibition of resonance, as has been shown above, the real steric effect of the α-alkylstyrene series must be larger than the apparent value.

As has already been mentioned, Table 2 (or Fig. 5) shows a reasonable difference in the K_1 values of α-, *cis*-β-, and *trans*-β-alkylstyrenes for a given alkyl. In the previous discussion using Eq. (4), the resonance factor was assumed to be

constant within each series except the α-alkylstyrene series. When we compare the α-series, the *cis*-β-series, and the *trans*-β-series using the same equation, however, the difference in the resonance factor should be considered. The difference in the resonance factor between the three series corresponds to the large distance between the experimental lines of the α-, the *cis*-β-, and the *trans*-β-series in Fig. 5.

In order to obtain further information regarding the nature of the complexation of styrene derivatives, the thermodynamic data, ΔH and ΔS, for complexation were evaluated from the K_1 values at 0 and 25°C. No simple relation between the ΔH (or ΔS) and E_s^c values of the substituent groups was found. However, as is shown in Fig. 6, a linear correlation was found to exist between ΔH and ΔS (isokinetic relationship); the plots for α-, *cis*-β- and *trans*-β-series fell on the same line, in contrast with the case of alkenyl alkyl ethers.[4] The isokinetic temperature, 250°K, was obtained from the slope of the straight line. Since the measurements of the argentation constants were carried out above the isokinetic temperature, the entropy factor is considered to be more important than the enthalpy in this equilibrium.

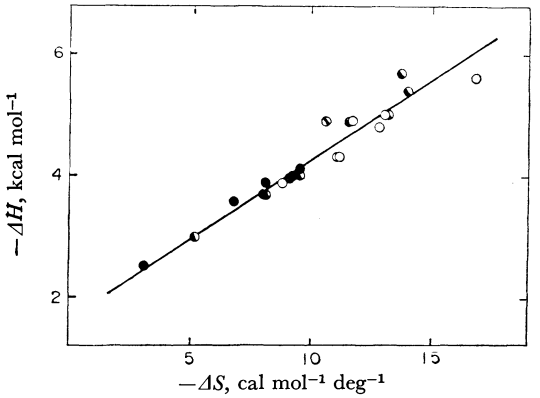

Fig. 6. Plots of ΔH *vs.* ΔS.
⊘ Styrene ◔ α-R–Styrene ● *cis*-β-R–Styrene
○ *trans*-β-R–Styrnene

Argentation Constants of the Other Styrene Derivatives. Further substitution of methyl groups at the double bond slightly influenced the K_1 values. Table 2 indicates that the K_1 values for *cis*-α,β-dimethylstyrene, and β,β-dimethylstyrene are nearly equal to the K_1 value of *trans*-β-methylstyrene, although smaller than those of α- and *cis*-β-methylstyrenes. This is considered to be due to the fact that the inhibition of conjugation between the benzene ring and the double bond is more important than the steric effect in the complex formation of those styrenes.

Considering the structure and the strain of the olefin, the K_1 value of indene is reasonable. However, the very large K_1 value of 1,2-dihydronaphthalene was unexpected from the structure of this molecule.

BULLETIN OF THE CHEMICAL SOCIETY OF JAPAN VOL. 42 2610—2614 (1969)

Synthetic Reactions by Complex Catalysts. XIII. Carbonylation of Amines by Group IB and IIB Metal Compound Catalysts*1

Takeo SAEGUSA, Shiro KOBAYASHI, Kiwami HIROTA and Yoshihiko ITO

Department of Synthetic Chemistry, Kyoto University, Sakyo-ku, Kyoto

(Received January 29, 1969)

The present investigation was undertaken in order to examine the catalytic activities of Group IB and IIB metal compounds in the carbonylation of aliphatic and aromatic amines with carbon monoxide, and in order to compare the catalyst activities with those of other metal compounds. It was found that: i) copper compounds are excellent catalysts for the carbonylation of aliphatic amines to produce the corresponding formamides; ii) the catalytic activities of copper compounds are enhanced by the addition of water; and iii) chloroauric acid catalyzes the carbonylation of aromatic amine, whereas copper compounds do not. The temperature effects on the carbonylation of morpholine were also examined.

We have preliminarily reported the copper-catalyzed carbonylation of amines; in this process primary and secondary amines are smoothly converted by carbon monoxide into the corresponding

*1 Presented in part at the 20th Annual Meeting of the Chemical Society of Japan, Tokyo, April, 1967.

formamides.[1] Now, we wish to report more detailed and more comprehensive studies of the catalytic activities of Group IB and IIB metal compounds in the carbonylation of amines.

Various catalysts have hitherto been reported for the amine-carbon monoxide reaction. Transition metals of Groups IV to VIII,[2,3] their salts,[3-6] their metal carbonyls,[7-9] and the corresponding organometallic compounds[10] catalyze this reaction to produce a mixture of formamide, urea, isocyanate, and oxamide. The alkali metal alcoholate catalyzes the carbonylation of amine to produce the corresponding formamide.[11] In addition, one patent has claimed the production of *N*-methylformamide and *N,N*-dimethylformamide from methylamine and dimethylamine respectively by a catalyst selected from the group consisting of cuprous and cupric chlorides, ammonium chloride, potassium acetate, and boron fluoride.[12]

The purpose of the present investigation is to examine the catalytic activities of Group IB and IIB metal compounds in the carbonylation of aliphatic and aromatic amines with carbon monoxide. We have found that: i) copper compounds are excellent catalysts for the carbonylation of aliphatic amines to produce the corresponding formamides; ii) the catalytic activities of copper compounds are enhanced by the addition of water, and iii) chloroauric acid catalyzes the carbonylation of aromatic amine, but copper compounds do not.

Experimental*2

Materials. All the amines were distilled before use. The copper compounds and other metal salts were commercial reagents which were used as received. The carbon monoxide was reagent-grade.

Reaction Procedures. Method A. An amine and a catalyst were placed in a 200 m*l* stainless-steel autoclave equipped with a magnetic stirrer; the autoclave was then charged with carbon monoxide up to a pressure of 60—80 kg/cm^2 at room temperature. The autoclave was closed and heated at a given temperature for a given time. Then, any catalyst precipitated was separated by filtration, and the reaction mixture was distilled or analyzed directly by glpc.

Method B. The reaction was carried out in a 50 m*l* stainless-steel pressure tube without stirring. The after-treatment of the reaction mixture was carried out by the same procedure as in Method A.

Identification and Analyses of the Prod cts. The reaction products were identified by comparing their NMR and infrared spectra and the glpc retention times with those of the respective authentic samples. The columns of glpc were PEG 6000 and Silicone DC 550. The yields of the products were determined by glpc analyses and, in some cases, by fractional distillation.

Preparations of Authentic Samples. The authentic formamide derivatives were prepared by treating the respective amines with ethyl formate. The boiling points of these authentic samples were as follows: *N*-formylpiperidine: 90—92°C/9 mmHg; *N,N*-diethylformamide: 177—178°C; *N*-formylpyrrolidine: 97—98°C/15 mmHg; *N*-2-hydroxyethylformamide: 134—136°C/0.4 mmHg; *N*-*n*-butylformamide: 142—144°C/45 mmHg; *N*-allylformamide: 120—122°C/48 mmHg; *N*-ethylformamide: 109°C/30 mmHg; *N*-formylmorpholine: 121—124°C/15 mmHg; formanilide: 90—91°C/12 mmHg, (mp 47°C), and *N*-methylformanilide: 131—133°C/25 mmHg.

The authentic samples of 1,1′-carbonyldipiperidine and 4,4′-carbonyldimorpholine were prepared by the reaction of piperidine and morpholine with phosgene; the melting points were 42°C (lit.,[13] mp 42—43°C) and and 141—142°C (lit.,[13] mp 143°C) respectively.

Results and Discussion

Carbonylation of Piperidine. The Group IB and IIB metal compounds were examined for catalyst activity in the carbonylation of piperidine. Their catalytic activities were also compared with

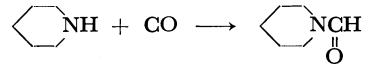

those of other metal compounds. The Group IB and IIB metal compounds, especially copper compounds, are quite active. The typical transition metal salts of the Group VIII elements, *e.g.*, Fe, Co, Ni and Pd, are less active than copper catalysts. Aluminum chloride, a strong Lewis acid, is a poor catalyst.

The catalytic behavior of the copper compounds in the amine-carbon monoxide reaction is distinguished from that of typical transition metal catalysts by the highly selective production of formamide. In the copper-catalyzed reaction, a small amount (usually only a few percent) of a *N,N′*-dialkyl derivative of urea was formed as the sole by-product.[1]

The amount of the by-product is much smaller than that in the reaction with palladium[6] and

1) T. Saegusa, S. Kobayashi, K. Hirota and Y. Ito, *Tetrahedron Letters*, **1966**, 6125.
2) W. Hieber and N. Kahler, *Chem. Ber.*, **91**, 2223 (1958).
3) W. Reppe and H. Kröper, *Ann.*, **582**, 38 (1953).
4) H. Krizikalla and E. Woldan, Ger. Pat. 863800, Jan. 19 (1953).
5) E. W. Stern and M. L. Spector, *J. Org. Chem.*, **31**, 596 (1966).
6) J. Tsuji and N. Iwamoto, *Chem. Commun.*, **1966**, 380.
7) W. Reppe, *Ann.*, **582**, 1 (1953).
8) H. Sternberg, J. Wender, R. A. Friedel and M. Orchin, *J. Am. Chem. Soc.*, **75**, 3148 (1953).
9) F. Calderazzo, *Inorg. Chem.*, **4**, 293 (1965).
10) H. J. Cragg, U. S. Pat. 3099689, July 30 (1963).
11) H. Winteller, A. Bieler and A. Guyer, *Helv. Chim. Acta*, **37**, 2370 (1954).
12) U. S. Pat. 2677706 (1954).
*2 All the temperature readings are uncorrected.
13) W. Brackman, Ger. Pat. 1105866, May 4 (1961).

Table 1. Carbonylation of piperidine in the presence of various metal compounds[a] (method B)[b]

Exp. No.	Catalyst	Reaction conditions		Yield of *N*-formylpiperidine (%)[c]
		Temp. °C	Time hr	
1	CuCl	140	15	93
2	$Cu(CN)_2$	110	15	72
3[d]	$CuCl_2$	120	14	17
4	CuCl-1.5-COD complex[e]	130	14	96
5	AgCl	140	14	25
6	$HAuCl_4 \cdot 4H_2O$	130	14	15
7	$ZnCl_2$	135	16	18
8	$Cd(OAc)_2$	140	14	15
9	$Hg(OAc)_2$	130	14	60
10	$AlCl_3$	120	15	5
11	$Fe(AA)_3$	130	14	40
12	$CoCl_2$	110	15	20
13	$NiCl_2$	110	15	7
14	$PdCl_2$	120	14	5

a) 10 ml piperidine and 1.0 g of a catalyst were used.
b) See Experimental Section.
c) Based on the initially charged piperidine.
d) Ethanol (10 ml) was used as solvent.
e) The cuprous chloride-1.5-cyclooctadiene complex was prepared according to the reference.[14]

manganese[9] catalysts. The piperidine-carbon monoxide reaction with catalysts of Ag, Au, Zn, Cd, and Hg salts also produces a trace amount of 1,1′-carbonyldipiperidine (only a few percent) as a by-product.

The coordination of carbon monoxide with cuprous salts in the presence of amine is well known.[15] It is not unreasonable to assume that carbon monoxide coordination plays an important role in the catalysis. When cupric salts are used as catalysts, they may be reduced by carbon monoxide into cuprous species which are possibly the real active species of the catalyst.

Copper compounds also catalyze the α,α-addition of the nitrogen-hydrogen bond of aliphatic amine to isocyanide.[16] It is interesting to note that the reaction with the aliphatic amine-isocyanide is similar to the reaction of the present studies, since isocyanide and carbon monoxide are isoelectronic. These two reactions caused by copper catalysts may be formulated in an analogous manner:

$$R_2NH + :C \leqq O \longrightarrow R_2NCH \overset{\|}{O}$$

$$R_2NH + :C \leqq N\text{-}R^1 \longrightarrow R_2NCH \overset{\|}{N}\text{-}R'$$

Carbonylation of Dimethylamine. Copper compounds also catalyze the dimethylamine (DMA)-carbon monoxide reaction to produce *N,N*-dimethylformamide (DMF) (Table 2). The by-product is *N,N,N′,N′*-tetramethylurea, produced only in small amounts. It is quite interesting to observe that the catalytic activity of the copper catalyst is enhanced by the addition of water. The accelerating effect of water may be closely related to the fact that CuCl-CO complexization

Table 2. Carbonylation of DMA with copper catalysts

Exp. No.	Catalyst	g	DMA ml	Method[a]	Reaction conditions		Initial rate[b] mmol/min	Yield of DMF (%)[c]
					Temp. °C	Time hr		
15	CuCl	1.0	10	B	100	13	—	73
16	$Cu(CN)_2$	1.0	10	B	100	13	—	52
17	CuCN	0.5	5	B	135	15	—	78
18	CuCl	2.0	30	A	180	28	—	96
19	None		60[d]	A	145—150	2	—	18
20	CuCN	1.0	60[d]	A	145—150	2	—	57
21	$Cu(CN)_2$	2.0	60[d]	A	120—130	10	—	85
22	CuCN	1.0	30[e]	A	175	3.0	1.2	20
23	CuCN	1.0	30[f]	A	175	3.0	5.7	84

a) See Experimental Section.
b) The rates of gas consumption during the initial 30 min are taken as a measure of the initial rate.
c) Based on DMA.
d) 40% aqueous DMA solution (60 ml) was charged.
e) Anhydrous DMA dried with potassium carbonate, was employed.
f) DMA containing 10 mol% of water was employed.

14) H. L. Haight, J. R. Doyle, N. C. Baenziger and G. F. Richards, *Inorg. Chem.*, **2**, 1301 (1963).
15) "Gmelins Handbuch der Anorganischen Chemie," System Nummer 60, Verlag Chemie GMBH, Weinheim, p. 240.
16) T. Saegusa, Y. Ito, S. Kobayashi, K. Hirota and H. Yoshioka, *Tetrahedron Letters*, **1966**, 6121.

TABLE 3. CARBONYLATION OF MISCELLANEOUS ALIPHATIC AMINES WITH COPPER CATALYSTS

Exp. No.	Amine	ml	Catalyst	g	Method[a]	Reaction conditions: Temp. °C	Reaction conditions: Time hr	Yield of formylated product (%)[b]
24	$(C_2H_5)_2NH$	50	$Cu(OAc)_2$	2.5	A	170	20	46
25		10	$Cu(CN)_2$	0.5	B	120	13	65
26	$HOCH_2CH_2NH_2$	20	$CuCl_2$	1.0	B	105	20	23
27	n-$C_4H_9NH_2$	10	CuCl	1.0	B	115	16	20
28	$C_2H_5NH_2$	10	CuCN	1.0	B	165	20	25
29	CH_2=$CHCH_2NH_2$	10	$CuCl_2$	0.5	B	120	15	15

a) See Experimental Section.
b) Based upon the charged amine.

is favored by water.[15]

The effect of a small amount of water is clearly demonstrated in the last two runs of Table 2, where the carbonylation by the CuCN catalyst was carried out both in the absence (Exp. No. 22) and in the presence of water (Exp. No. 23). The addition of 10 mol% of water increases the rate and the conversion four or five fold. Furthermore, DMA carbonylation is efficiently carried out in an aqueous system (Exp. No. 19 to No. 21, Table 2). There are two possible explanations of the effect of water. First, the water molecule is incorporated into the copper-DMA complex as a ligand, thus possibly modifying (increasing) the catalyst activity. Second, the water converts carbon monoxide to formic acid, which may then be responsible for the carbonylation reaction. In fact, it has been established that the addition of water to a reaction system without a metallic catalyst increases the rate of carbonylation, although the actual rate is quite low.[11]

Carbonylations of Miscellaneous Amines. Other aliphatic amines can also be carbonylated by means of copper-compound catalysts (Table 3). The carbonylation of secondary amines appears to be easier than that of primary amines.

The carbonylation of allylamine differentiates the copper catalyst from the cobalt carbonyl catalyst. The copper-catalyzed carbonylation of allylamine yields only *N*-allylformamide, whereas the cobalt carbonyl-catalyzed reaction gives the cyclization product, 2-pyrrolidinone.

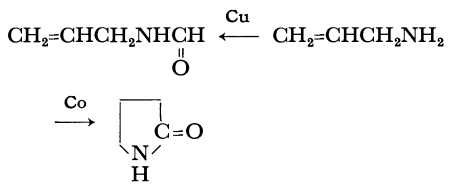

Temperature Effects on the Carbonylation of Morpholine. The rate of the carbonylation of morpholine is increased by raising the reaction temperature (Table 4). A small amount of 4,4′-carbonyldimorpholine by-product was formed at a higher reaction temperature (Exp. No. 33). The

TABLE 4. CARBONYLATION OF MORPHOLINE WITH CUPROUS CHLORIDE CATALYST AT VARIOUS TEMPERATURES

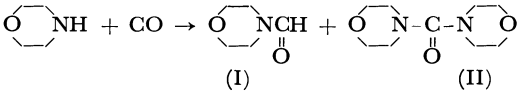

(I) (II)

Exp. No.	Temp. °C	Yield (%): I	Yield (%): II
30	80	3	—
31	115	14	trace
32	150	42	trace
33	180	76	2

Reaction conditions: morpholine 30 ml, CuCl 2.0 g as catalyst, initial CO pressure 80 kg/cm² at room temperature, with stirring for 6.5 hr.

TABLE 5. FORMYLATION OF ANILINE AND *N*-METHYLANILINE (METHOD B)[a]

Exp. No.	Amine	mmol	Catalyst	mmol	Reaction conditions: Temp., °C	Reaction conditions: Time, hr	Yield of formanilide (%)
34	$C_6H_5NH_2$	100	$HAuCl_4 \cdot 4H_2O$	1.0	180	15	17
35	$C_6H_5NH_2$	100	CuCl	1.0	180	15	0
36	$C_6H_5NH_2$	100	AgCl	1.0	180	15	0
37	$C_6H_5NHCH_3$	100	$HAuCl_4 \cdot 4H_2O$	0.8	175	40	33

a) See Experimental Section.
b) Based on the charged amine.

urea may be produced by the copper-catalyzed oxidation of morpholine with oxygen,[13] which is possibly present as a contaminant in the reaction system.

Carbonylation of Aromatic Amines. Copper compounds are inactive in the reaction of aromatic amines with carbon monoxide. On the other hand, chloroauric acid is active (Table 5).

From the isoelectronic relationship between carbon monoxide and isocyanide, it is also of interest to note that copper compounds do not work as effectively in the aromatic amine-isocyanide reaction as does chloroauric acid.[17]

17) T. Saegusa, Y. Ito, S. Kobayashi, K. Hirota and H. Yoshioka, To be published.

BULLETIN OF THE CHEMICAL SOCIETY OF JAPAN VOL. 42 2614—2617 (1969)

Intramolecular Hydrogen Bonding in α-Keto- and α-Alkoxy-carboxylic Acids. VII. Ultraviolet Spectra of Phenylglyoxylic Acid in Various Solvents

Minoru HIROTA and Fumiaki SHINOZAKI*1

Department of Applied Chemistry, Faculty of Engineering, Yokohama National University, Minami-Ku, Yokohama

(Received February 7, 1969)

The ultraviolet spectra of phenylglyoxylic acid were determined in various solvents as well as in the mixtures of solvents. A very remarkable hypsochromic shift with increase in intensity was observed when the solvent participates in the formation of hydrogen bond as a hydrogen acceptor. The measurement of the spectra in binary mixtures of the solvents shows that the hypsochromic shift is due to the formation of a 1 : 1 complex of $C_6H_5COCOOH\cdots$solvent type. This hypsochromic shift is interpreted by the destruction of the chelate ring formed by the intramolecular hydrogen bond which enforces the acid molecule to the planar conformation. This view is supported by the simple LCAO-MO calculation on this molecule.

It has been shown that the intramolecular hydrogen bonding between the carboxylic hydroxyl group and the α-oxygen containing functional groups plays an important role in the appearance of the *trans*-conformation*2 of the carboxyl group.[2-5] Thus, the α-alkoxy and α-oxo-carboxylic acids can exist as *trans*-conformers while the usual carboxylic acids take the *cis*-conformation exclusively. Phenylglyoxylic acid is an α-oxo-carboxylic acid which is capable of forming an intramolecular hydrogen bond as exemplified by Ib. We have studied it by means of infrared spectroscopy.[2] It has been also studied more extensively by Oehme *et al.*[6]

It seems certain that the acid takes a nearly planar conformation when it exists as an intramolecularly hydrogen bonded *trans*-conformer (Ib), in which both carbonyl groups are kept at a *trans* position to each other by hydrogen bond formation. The *cis* conformation of the usual carboxyl group is assumed to be about 2 kcal/mol more stable than the *trans* one,[7] but the *trans*-conformer of phenylglyoxylic acid is predominant in inert solvents because the O-H···O=C hydrogen bond energy (estimated to be about 4—5 kcal/mol) overcomes the stabilization energy of the *cis*-conformer.[8] From the measurement on the temperature dependence of the intensities of the O-H stretching absorption bands assigned to both conformations, the *trans*-conformer is shown to be more stable, and

*1 The present address: Tokyo Institute of Technology, Ookayama, Meguro-ku, Tokyo.

*2 The *cis* or *trans* implies that the oxo(O=)-group and the hydrogen of the carboxyl group are *cis* or *trans*, respectively, with respect to the C-O bond.[1]

1) C. P. Smyth, "Dielectric Behavior and Structure," McGraw Hill, New York (1955), p. 305—307.

2) M. Ōki and M. Hirota, *Nippon Kagaku Zasshi* (*J. Chem. Soc. Japan, Pure Chem. Sect.*), **81**, 856 (1960).

3) M. Ōki and M. Hirota, This Bulletin, **34**, 374, 378 (1961); *ibid.*, **36**, 290 (1963).

4) M. Ōki and M. Hirota, *Spectrochim. Acta*, **17**, 583 (1961).

5) M. Ōki and M. Hirota, *Nippon Kagaku Zasshi* (*J. Chem. Soc. Japan, Pure Chem. Sect.*), **86**, 115 (1965).

6) G. Oehme, G. Fischer and A. Schnellenberger, *Chem. Ber.*, **100**, 425 (1967).

7) T. Miyazawa and K. S. Pitzer, *J. Chem. Phys.*, **30**, 1076 (1959).

8) M. Hirota, *Kagaku To Kogyo* (*Chem. and Chem. Ind.*), **20**, 12 (1967).

the enthalpy of the conversion was determined to be 1.78 kcal/mol.

In polar solvents, the intramolecular hydrogen bond may be weakened or destroyed both by the usual polar effect and by the intermolecular association. We found a remarkable solvent effect on the ultraviolet spectrum of this acid. The acid has an absorption band at 277.8 mμ (ε, *ca.* 6000) in *n*-hexane, while the absorption in ethanol is at 252.5 mμ (ε, 12100).[9]

In order to interpret this drastic change of absorption spectra in both solvents, the spectra of phenylglyoxylic acid were measured in various solvents and also in binary mixtures of these solvents. The acid is shown to form a 1 : 1 complex with the hydrogen accepting solvent.

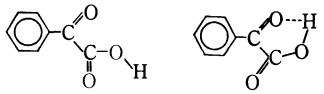

Ia Ib

Experimental

Materials. Phenylglyoxylic acid was prepared from benzoyl chloride and cuprous cyanide by the usual method.[10] Commercial spectro-grade *n*-hexane, methylene chloride and chloroform were used as solvent without further purification. Diethyl ether, ethanol and acetonitrile of commercial special grade were purified by the usual procedures.

Measurement of the Spectra. The ultraviolet spectra were measured by a Hitachi EPS-3T recording spectrophotometer. The molecular orbital calculation of the compound was carried out by a NEAC-2230 digital computer.

Results and Discussion

The ultraviolet spectra of phenylglyoxylic acid were determined in six solvents, the results of which are shown Fig. 1. Characteristic data on the absorption maxima are listed in Table 1. As shown in Table 1, the acid has an intense absorption band at about 250 mμ in ethanol, ether and acetonitrile, while it has a weaker absorption band at a longer wavelength in hexane, methylene chloride and chloroform.

The absorption bands at 250 mμ and at 280 mμ can be assigned to the solvated *cis*-conformation (Ia) and intramolecularly hydrogen bonded *trans*-conformation (Ib) of phenylglyoxylic acid, respectively. From the measurement of the O–H stretching and the C=O stretching absorption bands in the infrared region, it was concluded that the acid should take the hydrogen bonded *trans*-conformation in inert solvents which cannot participate in the formation of intermolecular hydrogen bonds to the acid. The similarity of the absorption spectra suggests a similar conformation in chloroform and methylene chloride with that in *n*-hexane. In other words, the intramolecular hydrogen bonding of the acid persists in the solvents of considerable hydrogen donating property. The absorption at about 250 mμ (ε: 12000) in hydrogen accepting solvents may be attributable to the benzoyl chromophore, because it is similar both in the location of the absorption maximum and in intensity. For example, benzaldehyde[11] has an intense absorption maximum at 242 mμ with a shoulder at 248 mμ, their intensities being 14000 and 12500, respectively. This means that the conjugation of the whole molecule is interrupted and the absorption caused by the benzoyl partial chromophore is observed in ethanol, diethyl ether and acetonitrile. These solvents are more or less basic and have hydrogen accepting ability. In these solvents, the intramolecular hydrogen bond of the acid might be destroyed and the intermolecular hydrogen

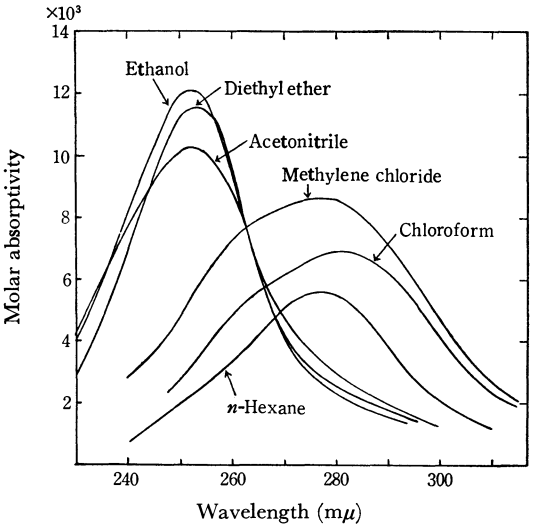

Fig. 1. The ultraviolet spectra of phenylglyoxylic acid in various solvents.

Table 1. The ultraviolet spectra of phenylglyoxylic acid in various solvents

Solvent	Wavelength (mμ)	Intensity (εmax)
n-Hexane	277.8	5930
Methylene chloride	278.9	8850
Chloroform	281.5	6900
Acetonitrile	252.8	10300
Diethyl ether	253.8	11500
Ethanol	252.5	12100

9) M. Hirota, *Kagaku no Ryoiki* (*J. Japan. Chem.*), **18**, 759 (1964).

10) "Organic Syntheses," Vol. 24, (1944), p. 14.

11) E. A. Braude and F. Sondheimer, *J. Chem. Soc.*, **1955**, 3754.

bond between the acidic O–H groups and the solvents might be formed instead. The acid is enforced to take an otherwise unfavorable *trans*-conformation by the intramolecular hydrogen bond, but it can form intermolecular hydrogen bond in the favorable *cis*-conformation. As there is no interaction between the acidic O–H and the ketonic carbonyl groups in the *cis*-form, the carboxyl group is not fixed on the plane of the benzoyl group and the rotation around the C–C bond between the carbonyl and the carboxyl carbons may occur rather freely. This may hinder the conjugation of the whole molecule and results in the appearance of the absorption band of the benzoyl chromophore in ethanol and other hydrogen accepting solvents.

It is doubtful whether the remarkable solvent dependence of the absorption spectrum is due to the electronic interaction through the hydrogen bond, and the molecule was studied from a molecular orbital theoretical point of view. The HMO calculation was carried out with phenylglyoxylic acid employing the parameters $h_{\dot{O}}=1.0$, $h_{\ddot{O}}=2.0$,

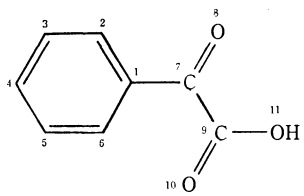

Fig. 2 (1)

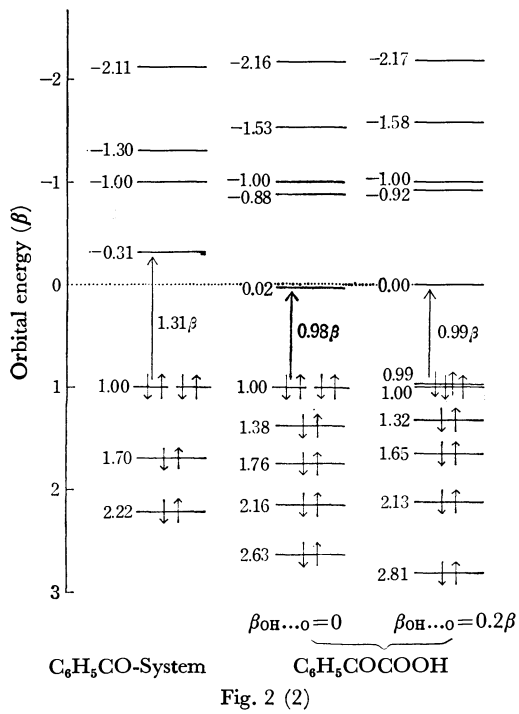

Fig. 2 (2)

Fig. 2. Simple LCAO-MO energy diagrams for phenylglyoxylic acid.

$k_{C-O}=0.8$ and $k_{C=O}=1.0$.[12] The π-electronic interaction through the hydrogen bond was considered by assuming the non-zero resonance integral ($\beta_{OH\cdots O}=0.2\beta$) between the oxygen atoms participating in the formation of hydrogen bond, but the lowest $\pi\rightarrow\pi^*$ transition energy does not change remarkably from the result obtained by neglecting the hydrogen bond effect ($\beta_{OH\cdots O}=0$).

On the other hand, the $\pi\rightarrow\pi^*$ transition energy of the benzoyl system was higher than that of phenylglyoxylic acid, so the solvent effect on its absorption spectrum is explained that the conjugate system is non-planar when the intramolecular hydrogen bond is absent. A very low double bond character of C_7–C_9 bond (bond order $p_{7,9}=0.333$) probably allows to rotate rather freely around this C–C bond. Further study on this problem is in progress, and above interpretation on the absorption spectrum agrees with the result of the Pariser-Parr-Pople MO calculation, details of which will be reported elsewhere.

In short, phenylglyoxylic acid associates with solvents which act as hydrogen acceptors in forming hydrogen bond, while it holds an intramolecularly hydrogen bonded form in the solvent with hydrogen donating ability.

In order to investigate the nature of the interaction between the acid and the solvents, the absorption spectra were measured in a binary mixture of solvents, such as methylene chloride-ethanol, *n*-hexane-diethyl ether, *etc.* The absorption spectra in binary mixture of the solvents are shown in Fig. 3. The isosbestic points were observed in all solvent systems investigated at the concentrations, at most, below 10%, and suggest the formation of only one kind of complexed species of definite composition in these concentration ranges. In order to determine the composition of the complexes, the absorption spectra of the acid in the mixture of the solvents in varying proportions were analysed by a method similar to that reported by Brealey and Kasha.[13] It was assumed that the equilibrium given by Eq. (1) exists between the solvent and solute, where r is constant throughout the range in which the isosbestic point is observed in the spectra.

$$C_6H_5COCOOH + r\cdot Solvent \rightleftarrows C_6H_5COCOOH\,(Solvent)_r \qquad (1)$$

The stability constant K and the number of solvated molecule r were calculated from the plots of $\log_{10}\{[Complex]/[C_6H_5COCOOH]\}$ against $\log_{10}$-[Solvent] shown by Fig. 3. From the definition of the formation constant expressed by Eq. (2),

12) A. Streitwieser, Jr., "Molecular Orbital Theory for Organic Chemists," John Wiley & Sons, Inc., New York (1961), p. 135.

13) G. J. Brealey and M. Kasha, *J. Am. Chem. Soc.* **77**, 4462 (1955).

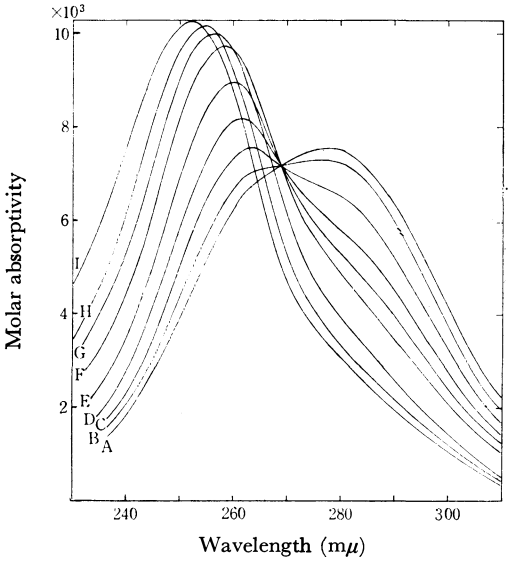

Fig. 3 (a)

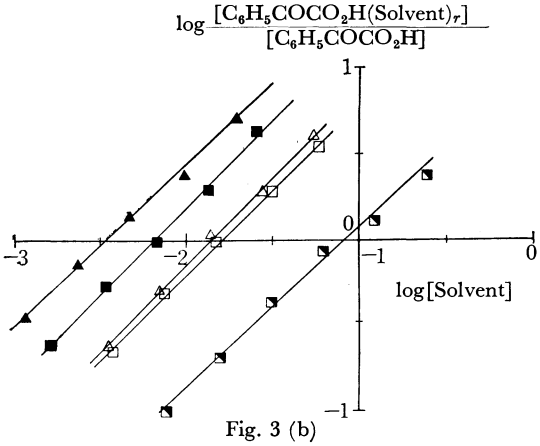

Fig. 3 (b)

Fig. 3. The ultraviolet spectra of phenylglyoxylic acid in the binary mixtures of the solvents.
(a) An example of the spectra in the binary mixtures of the hydrogen accepting solvent (ethanol) and the inert solvent (methylene chloride).
A: pure CH_2Cl_2, B: 0.4% ethanol, C: 1.6% ethanol, D: 3.2% ethanol, E: 6.4% ethanol, F: 12.8% ethanol, G: 50% ethanol, H; 80% ethanol and I: pure ethanol.
(b) Logarithm of the concentration of the hydrogen accepting solvent *versus* log $\{[C_6H_5COCOOH\cdot(Solvent)_r]/[C_6H_5COCOOH]\}$.

Eq. (3) is easily derived by taking logarithm.

$$K = [C_6H_5COCOOH\cdot(Solvent)_r]/[C_6H_5COCOOH][Solvent]^r \quad (2)$$

$$\log K = \log\{[Complex]/[C_6H_5COCOOH]\} - r\cdot\log[Solvent] \quad (3)$$

This indicates that the tangent of the log{[Complex]/[$C_6H_5COCOOH$]} *vs.* log[Solvent] plot will give the r-value and the intercept of the log[Solvent] axis will give the log$K$ value multiplied by r. The formation constants and the number of associated solvent molecule of some hydrogen bond complexes of phenylglyoxylic acid are tabulated in Table 2.

Table 2. The association constants K and the mole ratios r of the phenylglyoxylic acid-solvent complexes

Solvent system	K	r
C_6H_{14}–C_2H_5OH	219	0.95
C_6H_{14}–$(C_2H_5)_2O$	77.6	1.02
CH_2Cl_2–C_2H_5OH	178	1.03
CH_2Cl_2–$(C_2H_5)_2O$	61.7	0.98
CH_2Cl_2–CH_3CN	9.73	0.92

Formation of the 1 : 1 complex of phenylglyoxylic acid with ethanol as well as with ether and with acetonitrile, was thus confirmed from the r-values presented in the table. On the other hand, the acid does not form hydrogen bond with chloroform or methylene chloride, which can act as hydrogen donor in hydrogen bond formation. The results are in accordance with the fact that the carboxyl group is acidic and has a tendency to donate hydrogen to other molecules, while the basicity of the acid is rather low in comparison with other carbonyl compounds. The stronger hydrogen bond complex is formed when the hydrogen acceptor(solvent) has a stronger hydrogen accepting power and when the inert solvent is less polar.

In summary, the remarkable solvent shift observed in the ultraviolet spectrum of the acid is due to the 1 : 1 complex formation with hydrogen accepting solvents, which destroys the intramolecular hydrogen bonding present in inert solvents and allows the non-planar conformation of the acid.

The authors are grateful to Professor M. Ōki of the University of Tokyo and Professor H. Kakiuchi of Yokohama National University for their valuable advice throughout this investigation. The present investigation was partly supported by a Scientific Research Grant from the Ministry of Education for which the authors are grateful.

BULLETIN OF THE CHEMICAL SOCIETY OF JAPAN VOL. 42 2618—2623 (1969)

Structure Proof of Diarylmethanes Formed in the Jacobsen Reaction of Monochlorotetramethylbenzenes[1]

Hitomi Suzuki

Department of Chemistry, Faculty of Science, Kyoto University, Sakyo-ku, Kyoto

(Received February 7, 1969)

The Jacobsen reaction of monochlorotetramethylbenzenes was found to yield dichloroheptamethyldiphenylmethanes as by-product. Their indefinite structure proof was made on spectroscopy and synthesis. ^{1}H NMR spectra for a variety of polymethyldiphenylmethanes and their chlorine derivatives were determined.

In contact with concentrated sulphuric acid, monochlorotetramethylbenzenes (CTB) undergo disproportionation to give chloropentamethylbenzene (I) and 3-chloropseudocumene-5-sulphonic acid (II).[2,3] This is another phase of the Jacobsen reaction, which has long been recognized for its unique feature to orient the ring alkyl groups to vicinal positions.[4] Under suitable conditions, however, the reaction was found to yield as by-product an appreciable amount of dichloroheptamethyldiphenylmethanes.[5] When considered in connection with the recent proposal of diphenylalkane intermediate for the disproportionation of primary alkyl groups in the Friedel-Crafts reaction,[6] this result seems to provide a clue to elucidate the mode of intermolecular methyl transfer in the Jacobsen reaction. In the present work, the structures of these by-products have been definitely established.

New by-product from the Jacobsen reaction of CTB was high-melting, colourless prisms, poorly soluble in ordinary solvents. The analysis fitted the formula $C_{20}H_{24}Cl_2$ and the molecular weight determined from mass spectrum corresponded to 334 (Calcd 335). ^{1}H NMR spectrum showed the presence of one aromatic proton, two methylene protons, and twenty-one methyl protons. This composition was compatible only with dichloroheptamethyldiphenylmethane (DHD), and ruled out the other possibilities of dichloro-octamethyldiphenyl or dichlorohexamethyldiphenylethane.

Chlorodurene (IV) and chloroprehnitene (VI) mainly gave a single DHD (mp 213—215°C and mp 226—227°C, respectively), and the presence of other isomeric impurities was not so important. However, chloroisodurene (V) yielded an intimate mixture of two isomeric DHD (mp 215—216°C)[7] in the approximate ratio of 3 : 1, and several attempts for fractional crystallization proved to be fruitless, presumably due to the slight difference in their solubility in organic solvents used.

The mass spectra of these DHD showed intense fragment ion peaks at 166 ($C_{10}H_{11}Cl^+$) or 180 ($C_{11}H_{13}Cl^+$), characteristic for *o*-methyldiphenylmethanes, which arose from the ionic unimolecular rearrangement-dissociation reactions represented as below:[8]

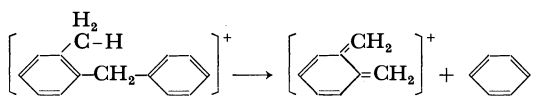

Examination of ^{1}H NMR spectra of a variety of polymethyldiphenylmethanes and their chloro derivatives (Table 2) has revealed the following correlations useful for structural assignment: 1) Aromatic protons ortho to the methylene group absorb fairly high field (3.5—4.0 τ) from meta or para protons (3.1—3.3 τ). 2) The replacement of meta or para methyl group by chlorine atom usually gives little effect to the methylene protons. However, an ortho chlorine atom deshields these protons by

1) The Reaction of Polysubstituted Aromatics. Part XIII; Part XII: This Bulletin, **42**, 851 (1969).

2) A. Töhl, *Ber.*, **25**, 1527 (1892).

3) L. I. Smith and C. L. Moyle, *J. Am. Chem. Soc.*, **58**, 1 (1936).

4) For recent reviews, *cf.* H. J. Shine, "Aromatic Rearrangements," Elsevier Publishing Company (1967), p. 23.

5) Similar formation of diarylmethanes has recently been reported in the nitration (H. Zollinger, unpublished observations) and the positive hydroxylation of certain polyalkylbenzenes (C. A. Buehler and H. Hart, *J. Am. Chem. Soc.*, **85**, 2177 (1963); H. Hart and C. A. Buehler, *J. Org. Chem.*, **29**, 2393 (1964)).

6) A. Streitwieser, Jr., and L. Reif, *J. Am. Chem. Soc.*, **86**, 1988 (1964); R. M. Roberts, A. A. Khalaf and R. N. Green, *ibid.*, **86**, 1609 (1964).

7) Smith and Molye reported the isolation of an unidentified substance, mp 209.5°C, from V.[3]

8) S. Meyerson, H. Drews and E. K. Fields, *J. Am. Chem. Soc.*, **86**, 4964 (1964).

Table 1. ^{1}H NMR and IR spectra of DHD formed in the Jacobsen reaction of CTB

DHD	Mp (°C)	^{1}H NMR spectra (in $CDCl_3$, τ) ArH	CH_2	CH_3
3′4-Dichloro-2,2′,3,4′,5,5′,6-heptamethyldiphenylmethane (XVI)	213—215	3.77	6.08	7.91 (3)* 7.71 (1) 7.61 (2) 7.52 (1)
2′,5-Dichloro-2,3,3′,4,4′,5′,6-heptamethyldiphenylmethane (XVII)	219—220	3.76	5.93	7.93 (2) 7.83 (1) 7.76 (2) 7.58 (2)
4′,5-Dichloro-2,2′,3,3′,4′,5′,6-heptamethyldiphenylmethane (XVIII)		3.76	6.08	7.79** 7.67
2′,6-Dichloro-2,3,3′,4,4′,5,5′-heptamethyldiphenylmethane (XIX)	226—227	3.74	5.74	7.92 (2) 7.84 (1) 7.78 (1) 7.72 (1) 7.60 (2)

	IR (KBr disc, cm^{-1})		Analysis C	H	Cl
XVI	767, 805, 826, 867, 941, 1003, 1081, 1155, 1178, 1209, 1229, 1387, 1445, 1460	Found Calcd	71.39 71.64	7.49 7.21	21.42 21.15
XVII	665, 714, 735, 763, 790, 834, 864, 920, 980, 1002, 1175, 1159, 1206, 1303, 1393, 1447, 1460	Found Calcd	71.80 71.64	7.27 7.21	21.45 21.15
XVIII					
XIX	741, 757, 791, 829, 866, 939, 949, 977, 1012, 1069, 1082, 1163, 1186, 1218, 1288, 1313, 1384, 1397, 1436, 1447, 1465	Found Calcd	71.41 71.64	7.30 7.21	

* Relative intensities in parentheses.
** Others are obscured by strong peaks of XVII.

Table 2. ^{1}H NMR spectra of polymethyldiphenylmethanes and their chlorine derivatives

Diphenylmethane	Mp (°C)	^{1}H NMR spectra (in CCl_4, τ) ArH	CH_2	CH_3
2,2′,3,3′,4,4′-Hexamethyl-	113—114	3.21 (*m*)* 3.49 (*o*)	6.20	7.78 (2)** 7.83 (2) 7.89 (2)
2,2′,4,4′,5,5′-Hexamethyl-	94—95	3.12 (*m*) 3.42 (*o*)	6.27	7.81 (2) 7.85 (4)
2,2′,4,4′,6,6′-Hexamethyl-	134—135	3.34 (*m*)	6.09	7.81 (2) 7.97 (4)
2,2′,3,4,4′,5,6′-Heptamethyl-	123—125	3.22 (*m*) 4.00 (*o*)	6.23	7.72 (2) 7.79 (1) 7.88 (3) 7.95 (1)
2,2′,3,4,4′,6,6′-Heptamethyl-	103—104	3.34 (*m*)	6.05	7.79 (2) 7.89 (2) 7.98 (2) 8.02 (1)
2,2′,3,4′,5,6,6′-Heptamethyl-	104—105	3.28 (*p*) 3.34 (*m*)	6.00	7.91 (3) 8.00 (4)

Table 2. (Continued)

Diphenylmethane	Mp (°C)	^{1}H NMR spectra (in CCl_4, τ)		
		ArH	CH_2	CH_3
2,2′,3,3′,4,4′,5,5′-Octamethyl-	152—153	3.53 (*o*)	6.19	7.76 (2) 7.80 (4) 7.82 (2)
2,2′,3,3′,4,4′,5,6′-Octamethyl-	165—166	3.22 (*m*) 3.99 (*o*)	6.20	7.71 (1) 7.73 (1) 7.78 (1) 7.82 (1) 7.90 (2) 7.94 (1) 7.97 (1)
2,2′,3,3′,4,5,5′,6′-Octamethyl-	201—203	3.20 (*p*) 4.01 (*o*)	6.16	7.67 (1) 7.74 (3) 7.85 (1) 7.92 (1) 7.97 (2)
2,2′,3,3′,4,4′,6,6′-Octamethyl-	116—117	3.35 (*m*)	6.01	7.80 (2) 7.92 (4) 8.04 (2)
2,2′,3,3′,5,5′,6,6′-Octamethyl-	155—157	3.30 (*p*)	5.95	7.85 (4) 8.04 (4)
2,2′,3,3′,4,4′,5,5′,6-Nonamethyl-	186—187	3.94 (*o*)	6.16	7.67 (1) 7.75 (4) 7.86 (1) 7.93 (3)
2,2′,3,3′,4,4′,5,6,6′-Nonamethyl-	139—141	3.34 (*m*)	5.93	7.77 (2) 7.79 (2) 7.83 (1) 7.92 (3) 8.01 (1)
2,2′,3,3′,4,4′,5,5′,6,6′-Decamethyl-	221—222		5.89	7.78 (2) 7.81 (4) 7.97 (4)
6-Chloro-2,2′,3,3′,4,4′,5,5′-octamethyl-	187—188	3.95 (*o*)	5.96	7.60 (1) 7.72 (2) 7.78 (2) 7.94 (3)
5-Chloro-2,2′,3,3′,4,4′,5′,6-octamethyl-	203—204	3.96 (*o*)	6.15	7.59 (1) 7.71 (1) 7.75 (1) 7.78 (2) 7.88 (1) 7.92 (1) 7.95 (1)
4-Chloro-2,2′,3,3′,4′,5,5′,6-octamethyl-	215—216	4.00 (*o*)	6.20	7.62 (2) 7.71 (1) 7.78 (1) 7.88 (1) 7.93 (3)
4-Chloro-2,2′,3,4′,5,5′,6-heptamethyl-	204—206	3.12 (*m*) 3.85 (*o*)	6.19	7.59 (2) 7.65 (1) 7.82 (1) 7.87 (2) 7.92 (1)

TABLE 2. (Continued)

Diphenylmethane	Mp (°C)	^{1}H NMR spectra (in CCl_4, τ)		
		ArH	CH_2	CH_3
3′,5-Dichloro-2,2′,3,4,4′,5′,6-heptamethyl-	205—206	3.77 (*o*)	6.08	7.53 (2) 7.65 (1) 7.76 (1) 7.83 (1) 7.95 (2)
2′,4-Dichloro-2,3,3′,4′,5,5′,6-heptamethyl-	220—221	3.86 (*o*)	6.02	7.60 (3) 7.86 (1) 7.89 (3)
5′,6-Dichloro-2,2′,3,3′,4,4′,5,6′-octamethyl-	224—225		5.70	7.62 (1) 7.65 (1) 7.77 (2) 7.82 (1) 7.91 (1) 8.00 (1) 8.23 (1)
6,6′-Dichloro-2,2′,3,3′,4,4′,5,5′-octamethyl-	221—223		5.39	7.61 (2) 7.76 (2) 7.89 (2) 8.17 (2)
5,5′-Dichloro-2,2′,3,3′,4,4′,6,6′-octamethyl-	225—226		5.86	7.62 (2) 7.78 (4) 8.01 (2)
4,4′-Dichloro-2,2′,3,3′,5,5′,6,6′-octamethyl-	232—233		5.92	7.78 (4) 7.96 (4)
3,3′,5,5′-Tetrachloro-2,2′,4,4′,6,6′-hexamethyl-	274—275		5.76	7.46 (2) 7.79 (4)

* Positions relative to methylene group.
** Relative intensities.

0.20—0.25 τ and the effect is additive. 3) A large downfield shift (0.25—0.30 τ) of the methylene protons is seen when the fourth ortho substituent group is introduced into the ring. Since the third ortho substituent gives little effect, such extra downfield shift is probably to be attributed to a combination of the steric and electronic influence enhanced by the restricted rotation of the benzene rings.

All the DHD showed a peak for ortho hydrogen atom at 3.73—3.77 τ. No chlorine atom is adjacent to the aromatic proton, otherwise the absorption will occur further downfield. The methylene protons of DHD derived from IV, V and VI absorbed at 6.08, 5.93, and 5.74 τ, respectively, indicating the presence of zero, one, and two ortho chlorine atoms. The minor component of the DHD mixture from V and the DHD from IV are supposed to possess a similar constitution in the vicinity of the methylene bridge, since both products showed the same τ - values for the aromatic and methylene protons. With these in mind and assuming no crucial rearrangement of the original hydrocarbon skeleton during the reaction, the tentative structures can readily be formulated as XVI—XIX:

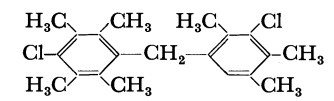
(XVI from IV)

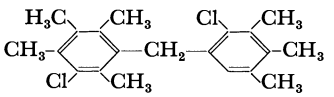
(XVII from V, major product)

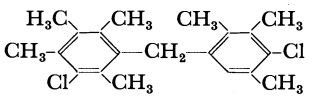
(XVIII from V, minor product)

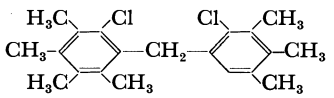
(XIX from VI)

The structural formulae proposed above were finally confirmed through unequivocal synthesis. Authentic specimens were prepared, with the exception of XVIII, according to the sequence outlined in Scheme 1 and their identity with the products was confirmed by the complete coincidence of the infrared spectra. XVIII was not accessible by the reaction of 3-chloropseudocumene with 5-chloro-2,3,4,6-tetramethylbenzyl chloride, instead 3′,5-dichloro-2,2′,3,4,4′,5′,6-heptamethyldi-

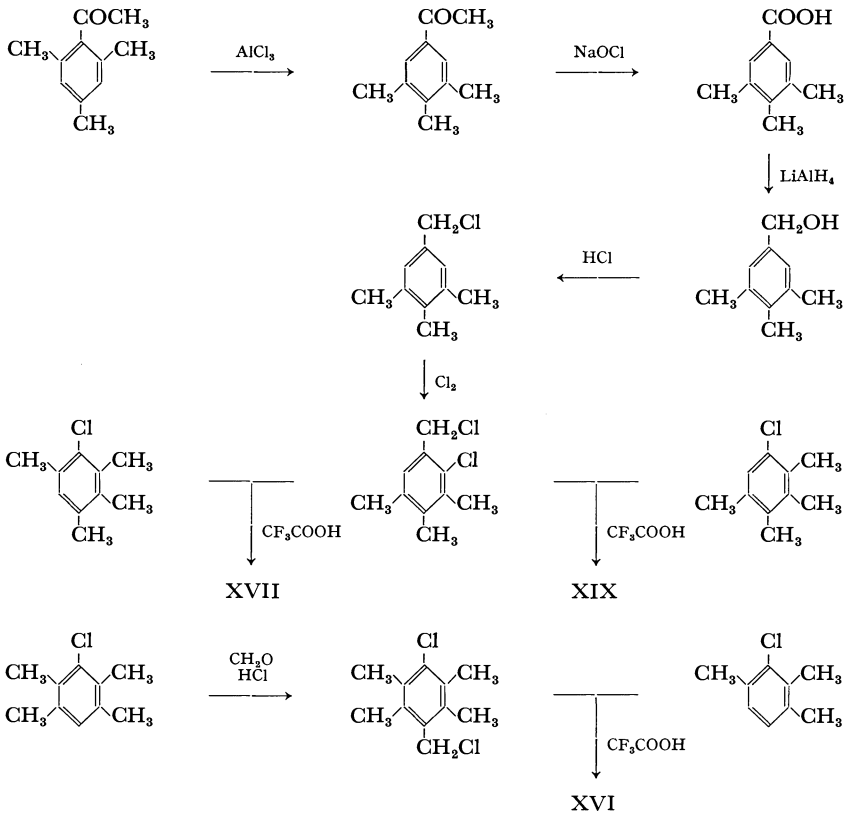

Scheme 1

phenylmethane was formed. An attempt to prepare 5,4′-dichloro-6′-iodo-2,2′,3,3′,4,5′,6-heptamethyldiphenylmethane by blocking the reactive 5-position of VII with iodine atom, and to convert this into XVIII by reductive removal of the blocking group was unsuccessful because of the failure to obtain the expected condensation. The reaction proceeded very slowly with the replacement of iodine atom by the benzyl group.

The formation of XIX from VI is rather unusual since the original prehnitene skeleton has been partly modified in the product. This anomaly may be explained by the rearrangement of the initially formed 5′,6-dichloro-2,2′,3,3′,4,4′,5-heptamethyldiphenylmethane through the 1,2-shift of the benzyl group, and may also be responsible for the partial isomerization of VI to V observed during the disproportionation.

Experimental

IR spectra were determined for KBr disc on a Jasco DS-402G spectrophotometer. ^{1}H NMR spectra were measured in carbon tetrachloride unless otherwise stated, using TMS as internal standard, on a JNM-3H spectrometer. Mass spectra were measured on an AEI MS-9 mass spectrometer at source temperature of 200°C. All mp's were determined on a hot-stage and are uncorrected.

Materials. Chlorohemimellithene (III, bp 116—117°C/33 mmHg), chlorodurene (IV, mp 47—48°C, bp 119—121°C/20 mmHg), chloroisodurene (V, bp 113—115°C/20 mmHg) and chloroprehnitene (VI, bp 126—127°C/20 mmHg) were prepared from the corresponding hydrocarbons by chlorination in chloroform.[3] 3-Chloropseudocumene (VII, bp 108—110°C/30 mmHg) was prepared from a mixture of monochloropseudocumenes as described in literature.[9]

3,4,5-Trimethylbenzoic Acid (VIII). 3,4,5-Trimethylacetophenone (58 g)[10] was added dropwise to the 10% sodium hypochlorite solution (600 ml) so as to maintain the reaction temperature at 55—60°C. The solution was then treated with a little decolourizing carbon and made acidic with dilute hydrochloric acid. White precipitate was filtered off, washed with cold water, and crystallized from 95% ethanol. Large colourless prisms, mp 220—222°C (lit.[10] 220.5—221.5°C). Yield, 39.3 g (68%).

3,4,5-Trimethylbenzyl Alcohol (IX). To a solution of lithium aluminium hydride (5 g) in dry THF (100 ml), a warm, saturated THF solution of VIII (20 g) was added with stirring. The mixture was gently refluxed for 1 hr and then concentrated to one third of the total volume. Upon pouring into excess water, the mixture separated an oil, which soon solidified to

9) "Organic Reactions," Vol. 1, John Wiley & Sons, New York (1942), p. 370.

10) D. E. Pearson and J. D. Bruton, *J. Org. Chem.*, **19**, 957 (1954).

crystalline mass and was recrystallized from light petroleum as silky fine, long needles, mp 72—74°C (lit.[11] mp 78°C). Yield, 15.5 g (85%).

3,4,5-Trimethylbenzyl Chloride (X). A solution of IX in ligroin was stirred with concentrated hydrochloric acid, and hydrogen chloride was passed to saturation. Removal of the solvent under reduced pressure, followed by several recrystallization of the residue from light petroleum gave colourless needles, mp 36—37°C. Readily soluble in ordinary solvents.

Found: C, 71.28; H, 7.91%. Calcd for $C_{10}H_{13}Cl$: C, 71.21; H, 7.77%.

2-Chloro-3,4,5-trimethylbenzyl Chloride (XI). A crystal of iodine was added to a solution of X in carbon tetrachloride, and gaseous chlorine was passed at 0°C, controlling the extent of chlorination with gas chromatograph. The solvent was removed under reduced pressure, and the residue was crystallized from light petroleum in the form of colourless needles, mp 57—58°C.

Found: C, 59.20; H, 5.85%. Calcd for $C_{10}H_{12}Cl_2$: C, 59.13; H, 5.96%.

This compound was also obtained by stirring a mixture of III (15.5 g), 36% formalin (10%) and concentrated hydrochloric acid (40 m*l*) at 80—90°C for 24 hr under the gentle introduction of hydrogen chloride. Ordinary working-up, followed by fractional distillation gave the starting material (bp 112—113°C/27 mmHg, 7.5 g) and the chloromethylated product (bp 167—168°C/27 mmHg, 8.0 g). Recrystallization of the latter from light petroleum gave white needles, mp 47—49°C, which were identified as XI by comparison with infrared spectra. Some isomeric impurities accompanying the product were difficult to remove.

5-Chloro-2,3,4,6-tetramethylbenzyl Chloride (XII). A mixture of V (13.2 g), 37% formalin (60 m*l*) and hydrochloric acid (60 m*l*) was heated at 80—90°C, and hydrogen chloride was passed with stirring for 8 hr. After cooling, the solid product was filtered off, washed with water, and pressed to remove some oily part. Repeated recrystallization from ethyl acetate gave XII as white needles, mp 111—112°C. Yield of pure product, 8.7 g (48%).

Found: C, 61.09; H, 6.52%. Calcd for $C_{11}H_{14}Cl_2$: C, 60.84; H, 6.50%.

IV and VI similarly gave *4-chloro-2,3,5,6-tetramethylbenzyl chloride (XIII)* as large plates, mp 92—93°C, and *6-chloro-2,3,4,5-tetramethylbenzyl chloride (XIV)* as needles, mp 100—101°C, respectively.

XIII: Found: C, 60.94; H, 6.67%.

XIV: Found: C, 61.00; H, 6.66%.

Calcd for $C_{11}H_{14}Cl_2$: C, 60.83; H, 6.50%.

3-Chloro-5-iodo-1,2,4-trimethylbenzene (XV). VII (15.5 g) was iodinated at 70°C by stirring with iodine (10.2 g), periodic acid dihydrate (4.56 g), and 83% acetic acid (120 m*l*) containing small amounts of sulphuric acid as catalyst.[12] The heavy oily product was distilled under 22 mmHg. The main fraction came over at 167—168°C and weighed 20.7 g (74%).

Found: C, 38.63; H, 3.45%. Calcd for $C_9H_{10}ClI$: C, 38.53; H, 3.59%.

Disproportionation of Monochlorotetramethylbenzene (CTB). A mixture of CTB (16.9 g) and sulphuric acid (98 g) was stirred vigorously in an Erlenmeyer flask fitted with a side-arm for gas exit. The content soon turned dark brown, and sulphur dioxide, accompanied by some hydrogen chloride, was slowly liberated. After 50—55 hr, the reaction was quenched by pouring the mixture onto crushed ice, and any solid products formed were filtered off, washed thoroughly with water and chromatographed on alumina using light petroleum as eluant. Some unchanged CTB and I (5.4—6.3 g) came first, and diarylmethanes (0.8—1.4 g) followed over a wide range of eluates. These diarylmethanes were best crystallized from hot ligroin. Their physical properties are given in Table 1.

Preparation of Chlorinated Polymethyldiphenylmethanes. Chlorinated polymethyldiphenylmethanes were prepared by the following three procedures: 1) Condensation of chloro-hydrocarbons with formaldehyde in hot formic acid. 2) Reaction of a benzyl chloride with hydrocarbons in trifluoroacetic acid. 3) Chlorination of polymethyldiphenylmethanes. The last method had only limited use, because the products usually contained several diarylmethanes as well as some unidentified substances, and their separation was very difficult. In some cases, extensive transbenzylation occurred during the condensation; *e. g.* an attempt to prepare 6′-chloro-2,2′,3,3′,4,4′,5,5′,6-nonamethyldiphenylmethane by condensing VI with 2,3,4,5,6-pentamethylbenzyl chloride in trifluoroacetic acid gave a mixture of three diarylmethanes.

11) H. Krömer, *Ber.*, **24**, 2413 (1891).

12) H. Suzuki, K. Nakamura and R. Goto, This Bulletin, **39**, 128 (1966).

BULLETIN OF THE CHEMICAL SOCIETY OF JAPAN VOL. 42 2624—2627 (1969)

Catalytic Activities of Salicylaldehyde Derivatives. I. Catalytic Effects of 4-Formyl-3-hydroxyphenyltrimethylammonium Bromide on the Racemization of L-Amino Acid

Makoto ANDO and Sakae EMOTO

The Institute of Physical and Chemical Research, Yamato-machi, Kitaadachi-gun, Saitama

(Received February 14, 1969)

The pyridoxal-like catalytic effects of salicylaldehyde derivatives on the racemization of amino acid in the presence of a metal ion is known to be promoted by the substitution of an electron-attracting group in the benzene ring. Of the salicylaldehyde derivatives tested thus far, 4-formyl-3-hydroxyphenyltrimethylammonium bromide shows the most effective catalytic activity of racemization at pH 10 and at 80°C; the rate constant was 11.0×10^{-3} min^{-1}. The catalytic activity of this compound was studied under various conditions; the activation energy of the racemization of L-glutamic acid at pH 10 was 14.3 kcal/mol.

In the presence of a metal ion, pyridoxal has such a catalytic effects on amino acid as racemization and transamination. The benzene analogues were studied by Snell *et al.*,[1,2] who found that 4- and 6-nitrosalicylaldehydes had catalytic effects similar to those of pyridoxal on L-amino acid.[2] Thereafter, in the studies of the racemization of amino acid, it was recognized that even salicylaldehyde showed catalytic activity in the presence of a metal ion.[3,4] Recently, Yoshikawa *et al.* found that nitro-, sulfo-, and sulfonamide-derivatives of salicylaldehyde had also catalytic effects on the racemization of L-glutamic acid in the presence of a metal ion, and observed that an electron-attracting substituent on the salicylaldehyde ring promoted the catalytic activities, among which *p*-substitution was the most effective.[5] Since, as is well known, the tetrasubstituted ammonium group is a strong electron-attracting group, the *p*-trimethylammonium derivating of salicylaldehyde may be expected to be a stronger catalyst in racemization than all others known. This paper will deal with the synthesis of 4-formyl-3-hydroxyphenyltrimethylammonium bromide and with the measurement of its catalytic effect on the racemization of L-glutamic acid in the presence of a metal ion.

Experimental

Synthesis of 4-Formyl-3-hydroxyphenyltrimethylammonium Bromide (I). To a solution of sodium hydroxide (5 g) in methyl aclohol (200 m*l*), *p*-*N*,*N*-dimethylaminosalicylaldehyde[6,7] (15 g) and methyl iodide (50 g) were added successively, and then the solution was boiled for 24 hr. After the solution had been evaporated to syrup *in vacuo*, the syrup was extracted with an equivolume mixture of water and ethyl acetate (the aqueous layer was acidic); the aqueous solution was then evaporated under diminished pressure and treated with acetone. The precipitate, a mixture of *N*-methylated and *N*,*O*-dimethylated compound, was collected on a filter paper. It was very difficult to control the reaction to give the *N*-methylated compound alone, or to separate the *N*-methylated compound from the *N*,*O*-dimethylated product. Therefore, the mixture was boiled for 1 hr with 48% hydrobromic acid (50 m*l*), and then, after the solution had been cooled and diluted with water (100 m*l*), the resinous material was filtered off with charcoal. The filtrate was concentrated to a syrup under reduced pressure and digested with methanol to crystallize it. After recrystallization from methyl alcohol, the crystalline product was shown by a study of the analytical data to be a mixture of I and a small amount of the corresponding iodide. In order to convert the iodide into I, the mixture was dissolved in water (20 m*l*) and stirred with freshly-precipitated silver bromide (prepared from silver nitrate (5 g)) at room temperature for 3 hr. The silver halide was then filtered off and the filtrate was concentrated at diminished pressure. After recrystallization from methanol, 5.3 g of I were obtained. mp 197°C dec. (uncorrected). Found: C, 46.12; H, 5.11; N, 5.61; Br, 30.79%. Calcd

1) D. E. Metzler, M. Ikawa and E. E. Snell, *J. Am. Chem. Soc.*, **76**, 648 (1954).
2) M. Ikawa and E. E. Snell, *ibid.*, **76**, 653 (1954).
3) K. Ohno, I. Sasaji and M. Hara, Japanese Pat. 295110 (1961).
4) K. Toi, Y. Izumi and S. Akabori, This Bulletin, **35**, 1422 (1962); K. Toi, *ibid.*, **36**, 739 (1963).
5) S. Yoshikawa, K. Kuga, Y. Ueda, M. Goto and H. Sugiyama, *Kogyo Kagaku Zasshi (J. Chem. Soc. Japan, Ind. Chem. Sect.)*, **70**, 331 (1967).
6) Joh. Rud. Geigy & Co., German Pat. 105103 (1901).
7) W. C. Baird, Jr., and R. L. Shriner, *J. Am. Chem. Soc.*, **86**, 3142 (1964).

for $C_{10}H_{14}O_2NBr$: C, 46.17; H, 5.43: N, 5.39: Br. 30.72 %

Preparation of Solution. *Solution of Amino Acid.* A solution of amino acid (0.1 mol) and cupric sulfate (2 mmol) in a small amount of water was adjusted to the required pH value with 2N sodium hydroxide, and then diluted with water to make a final volume of 100 ml.

Solution of Catalyst. The catalyst (2 mmol) was dissolved in 100 ml of the required Sörensen 0.05M borate buffer solution and the pH was corrected with a slight amount of 2N sodium hydroxide.

Procedure of Racemization. Unless otherwise stated, the reactions were carried out using the solutions described above. A mixed solution of amino acid (2 ml) and a catalyst (2 ml) was reacted in a tightly-stoppered test tube on a temperature-regulating water bath. When the required temperature was below room temperature, each solution was cooled for 1 hr at that temperature before mixing. After the required reaction time, the mixture was cooled under a trap and 6N hydrochloric acid (5 ml) was added immediately in order to stop the reaction. The optical rotation of the solution $[\alpha_t]$ was measured in a 10 cm tube by a Perkin-Elmer model 141 polarimeter (direct reading 0.001°) at 589 mμ. The racemization yield was calculated as follows:

$$100([\alpha_0] - [\alpha_t])/[\alpha_0]$$

Analysis of Amino Acid. After the reaction had been stopped with hydrochloric acid, the solution was diluted with water (250 fold). The amino acid content in the dilute solution (0.5 ml) was analyzed by a Mitamura Riken model II auto amino-acid analyzer.

Results and Discussion

Effect of Kind of Metal Ion Present. The effect of the kind of metal ion on the racemization was examined at 80°C at pH 10 for 3 hr. Some metal salts were not dissolved in the pH-adjusted 1M glutamic acid solution, so every metal salt was added in the solid state and reacted as it was. During the reaction, cuprous or ferrous ions might be partly turned to cupric and ferric ions respectively, but their effect was not detectable. The results are listed in Table 1. Since, of the metal ions tested, cupric, cuprous, ferric, ferrous, and aluminum ions were most effective, and since the cupric ion was the best of all, racemization was thereafter carried out in the presence of the cupric ion.

TABLE 1. COMPARISON OF METAL IONS IN RACEMIZATION OF L-GLUTAMIC ACID

Metal ion	Racemi. yield	Metal ion	Racemi. yield	Metal ion	Racemi. yield
Cu^{2+}	84.2%	Sn^{2+}	34.7%	Zn^{2+}	15.0%
Cu^{+}	81.7	Hg^{2+}	17.6	Pb^{2+}	14.3
Fe^{3+}	76.6	none	17.4	Co^{2+}	12.3
Fe^{2+}	75.0	Ba^{2+}	17.1	Ni^{2+}	10.4
Al^{3+}	71.2	Ca^{2+}	16.4	Mg^{2+}	9.8

Metal ion (0.04 mmol), catalyst (0.04 mmol), and L-glutamic acid (2 mmol) were used and reacted at 80°C for 3 hr at pH 10.

Effect of the Amounts of the Catalyst and the Cupric Ion. Racemization was carried out at pH 10 by altering the amounts of the catalyst and of the cupric ion (0—0.08 mmol) with 2 mmol of L-glutamic acid at 80°C for 1 hr. The results are shown in Fig. 1. As is shown in Fig. 1, the racemization was hastened when accompanied by an increase in the concentrations of the catalyst and of the cupric ion. However, its speed was gradually slowed when their concentrations became more than 0.04 mmol. Most reactions were undertaken in the presence of 0.04 mmol portions of the catalyst and the cupric ion. Of course, it is possible to enrich the catalyst more and more, because of its very high solubility in the reaction system.

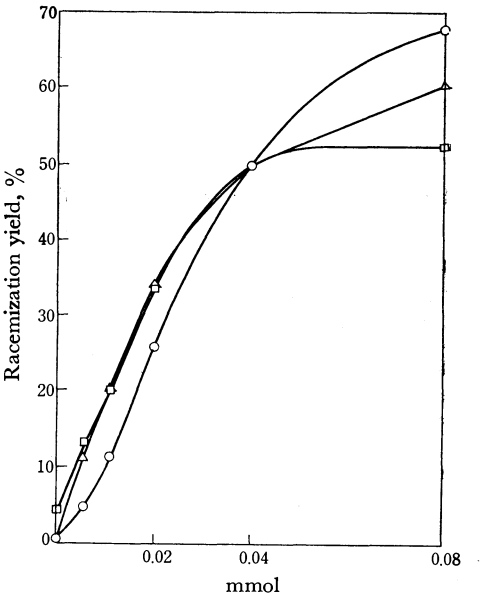

Fig. 1. Effect of the amounts of catalyst and cupric ion on racemization yield.
L-Glutamic acid (2 mmol) was used and reacted at pH 10 at 80°C for 1 hr.
○ Amounts of both catalyst and cupric ion were altered.
□ Amount of cupric ion was altered and that of catalyst was constant (0.04 mmol).
△ Amount of catalyst was altered and that of cupric ion was constant (0.04 mmol).

Effect of the Kind of Buffer Solution. Snell and Longenecker[8] have reported that in the catalytic α,β-elimination reaction of serine derivatives in the presence of pyridoxal and a metal ion, they observed the effect of the kind of buffer solution used. In order ourselves to study the effect of the kind of buffer solution, we dissolved 4-formyl-3-hydroxy-

8) J. B. Longenecker and E. E. Snell, *J. Biol. Chem.*, **225**, 409 (1957).

phenyltrimethylammonium bromide in borate, carbonate, and Britton-Robinson buffer solution (a mixture of phosphoric acid, acetic acid, boric acid, and sodium hydroxide solutions), all at pH 10. Because, at high temperatures, there was some uncertainty of this pH value being kept, the reaction was carried out at 25°C for 1 day and also for 7 days. The results are given in Table 2, which

Table 2. Comparison of kinds of buffer solutions in racemization reaction

Buffer Sol.	Racemi. yield	
	1 day	7 days
Borate	12.9%	60.5%
Carbonate	14.1	62.1
Mixed acid	14.7	64.8

Borate: 0.05M $Na_2B_4O_7$+0.1M NaOH.
Carbonate: 0.025M Na_2CO_3+0.025M $NaHCO_3$
Mixed Acid: 0.04M H_3PO_4+0.04M CH_3COOH +0.04M H_3BO_3+0.2M NaOH.
L-Glutamic acid (2 mmol), cupric sulfate (0.04 mmol), and catalyst (0.04 mmol) were used and reacted at 25°C at pH 10.

shows no serious effect of the kind of buffer solution on the racemization.

Effect of pH-Value. The effect of the pH-value on the catalytic racemization of glutamic acid was examined with or without cupric ions in a 0.05M borate buffer solution (pH 8—12) at 80°C for 1 hr; we also examined the effect on the racemization of L-alanine at pH 0—14 for 3 hr in a 0.04M Britton-Robinson buffer solution. The results are given in Fig. 2. As this figure shows, no actual racemization was observed below pH 8, and, in contrast with the case of pyridoxal,[9] no optimum pH value was observed, just as with 5-nitro- and 4-sulfo-salicylaldehydes;[5] namely, in the more alkaline solution, the faster racemization occurred in our experimental pH region. Because the racemization yields were reasonable compared with those of 5-nitro- and 4-sulfo-salicylaldehydes,[5] we can say that the zwitter ion is not formed between the ammonium group and the phenol group.

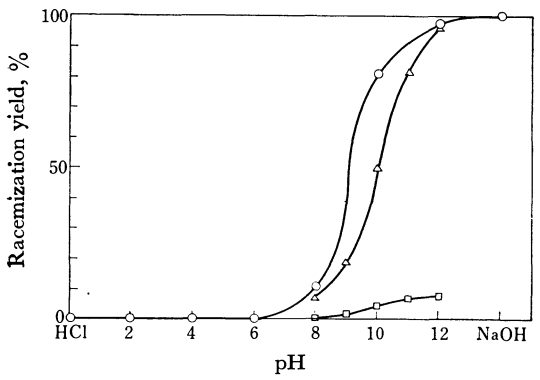

Fig. 2. Effect of pH value on racemization yield at 80°C.
△ Racemization of L-glutamic acid for 1 hr in the presence of cupric ion.
□ Racemization of L-glutamic acid for 1 hr without cupric ion.
○ Racemization of L-alanine for 3 hr in the presence of cupric ion.
HCl and NaOH mean that alanine salt is dissolved in 1N hydrochloric acid and 1N sodium hydroxide, respectively.

Effect of pH on the Rate Constant of the Racemization of L-Glutamic Acid. The racemization yield of L-glutamic acid in the presence of cupric ions at 80°C and at pH 8—12 for various periods of time was determined. The racemization should theoretically be a first-order reaction, and the relation between the rate constant, k, the time, t, and the observed rotation, $[\alpha_t]$, at t can be written as follows:

$$kt = 2.30 \times (\log[\alpha_0] - \log[\alpha_t])$$

At pH 10, in contrast with the case of pyridoxal, the activity of which decreased during the reaction,[5] 4-formyl-3-hydroxyphenyltrimethylammonium bromide indicated a first-order reaction, except at pHs 11 and 12. The plots which obeyed the first-order rate are shown in Fig. 3; the rate constants at pH 8, 9, and 10 were 1.2×10^{-3} min^{-1}, 3.3×10^{-3} min^{-1}, and 11.0×10^{-3} min^{-1} respectively. Of the salicylaldehyde derivatives tested to date, this compound was found to have the most effective activity.

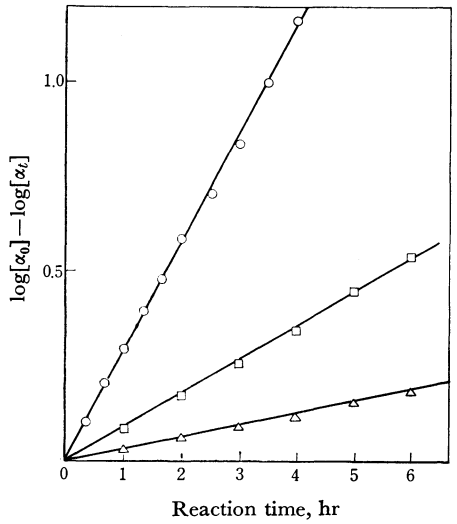

Fig. 3. Catalytic activities at pH 8, 9 and 10 in the presence of cupric ion at 80°C.
△ pH 8 □ pH 9 ○ pH 10

9) E. E. Snell, J. Olivard and D. E. Metzler, *J. Biol. Chem.*, **199**, 669 (1952)

Table 3. The rate constant k at various temperatures

Temp.	k
100°	28.9×10^{-3} min^{-1}
90	18.2
80	11.0
70	6.20
60	3.35
50	1.69
40	0.801
20	0.155

L-Glutamic acid (2 mmol), cupric sulfate (0.04 mmol), and catalyst (0.04 mmol) were used, and reacted at pH 10.

Activation Energy of the Racemization of L-Glutamic Acid. The effect of the temperature on the rate constant of the racemization of L-glutamic acid at pH 10 was also studied. The rate constants, k, at various temperatures are listed in Table 3. A linear relation between $\log k$ and $1/T$ was observed, as is shown in Fig. 4, and the activation energy was found to be 14.3 kcal/mol.

Determination of the Amount of Glutamic Acid. After the racemization reaction had been carried out at 80°C and at pH 10 for 3 hr or 6 hr, the amount of glutamic acid was changed within the limits of experimental error; although the amount of ammonia increased considerably, it was still an unmeasurable amount.

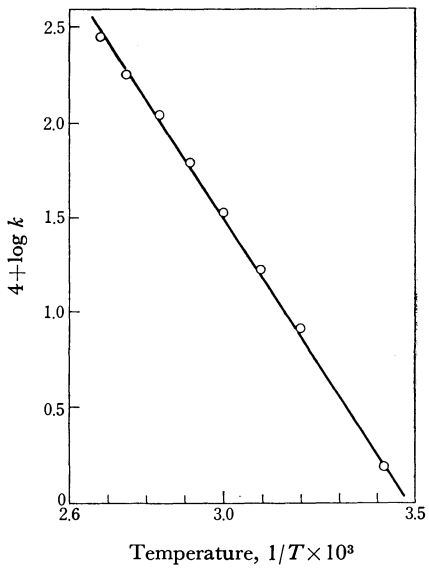

Fig. 4. Effect of temperature on rate constant at pH 10 in the presence of cupric ion.

It is easy to recover racemized free glutamic acid from the concentrated solution of a low pH, because the catalyst is very soluble in the solution.

The authors wish to express their sincere thanks to Dr. H. Homma and his co-workers of this institute for elemental analyses.

BULLETIN OF THE CHEMICAL SOCIETY OF JAPAN VOL. 42 2628—2631 (1969)

Catalytic Activities of Salicylaldehyde Derivatives. II. Kinetic Studies of the Racemization of Amino Acid

Makoto Ando and Sakae Emoto

The Institute of Physical and Chemical Research, Yamato-machi, Kitaadachi-gun, Saitama

(Received February 14, 1969)

In the racemization reaction of L-glutamic acid, catalyzed by salicylaldehyde derivatives and cupric ions, the rate constants, k, of 3-bromo-, 3-methoxy-, 3-methyl-, 3-nitro-, 4-methyl-, 5-bromo-, 5-methoxy-, 5-methyl-, and 5-nitro-salicylaldehydes and of salicylaldehyde were measured and the kinetic relation between the rate constant, k, of the salicylaldehyde derivatives and the corresponding Hammett's constant, σ, was studied. A linear relation between log k and the σ of 4- or 5-substituted salicylaldehydes and another linear relation between log k and the σ of 3-substituted salicylaldehydes were found. The activation energies of the racemizations catalyzed by pyridoxal, 3-nitro-, and 5-nitro-salicylaldehydes and by salicylaldehyde were determined, but no distinct difference between 3-nitrosalicylaldehyde and 5-nitrosalicylaldehyde was observed.

It has been reported that, in the racemization of sodium L-glutamate at pH 10 and at 80°C, 4-formyl-3-hydroxyphenyltrimethylammonium bromide, which is a salicylaldehyde derivative substituted by one of the strongest electron-attracting groups, has the most effective catalytic activity.[1] Yoshikawa *et al.*[2] have stated that the order of the racemization yield of L-glutamic acid catalyzed by nitro-, sulfo-, and sulfonamide-derivatives of salicylaldehyde agreed with the order of Hammett's constant, σ. The *p*-trimethylammonium group has a larger value based on the ionization of substituted benzoic acids than those of the corresponding nitro-, sulfo-, and sulfonamide groups.[3] This paper will deal with the kinetic relation between the catalytic activity of various salicylaldehyde derivatives and Hammett's constant, σ, of the corresponding substituents.

The activation energy of racemization catalyzed by 3-nitro- and 5-nitro-salicylaldehydes, salicylaldehyde, and pyridoxal was also studied.

Experimental

Preparation of Catalysts. 3-Bromo-,[4] 5-bromo-,[5] 4-dimethylamino-,[6] 3-methyl-,[7] 4-methyl-,[8] 5-methyl-,[9] 5-methoxy-,[10] 3-nitro-,[11] and 5-nitro-salicylaldehydes,[11] 4-formylphenyltrimethylammonium iodide,[12] 4-formyl-3-hydroxyphenyltrimethylammonium bromide,[1] and pyridoxal[13] were prepared by the method described in the literature.

Procedure of Racemization. Racemization was carried out as has been described before.[1] All the reactions were performed at pH 10 according to precedent. To 2 m*l* of a solution in a tightly-stoppered test tube containing sodium L-glutamate (2 mmol) and cupric sulfate (0.04 mmol) (pH 10), 2 m*l* of a borate buffer solution (pH 10) of a catalyst (0.04 mmol) were added; the mixture was reacted at the mentioned temperature for the mentioned time. When the required temperature was below room temperature, each solution was cooled for 1 hr at that temperature before mixing. After the required reaction time, 5 m*l* of 6N hydrochloric acid were added and the optical rotation of the solution $[\alpha_t]$ was measured by a Perkin-Elmer model 141 polarimeter (direct reading, 0.001°). The racemization yield was calculated as follows:

$$100([\alpha_0] - [\alpha_t])/[\alpha_0]$$

1) Part I of this series: M. Ando and S. Emoto, This Bulletin, **42**, 2624 (1969).

2) S. Yoshikawa, K. Kuga, Y. Ueda, M. Goto and H. Sugiyama, *Kogyo Kagaku Zasshi (J. Chem. Soc. Japan, Ind. Chem. Sect.)*, **70**, 331 (1967).

3) D. H. McDaniel and H. C. Brown, *J. Org. Chem.*, **23**, 420 (1958).

4) S. H. Dandegaonker and G. R. Revankar, *Monatsh. Chem.*, **96**, 450 (1965).

5) T. Tsumaki and H. Ohta, "Yukikagobutsu Goseiho," Vol. 12, ed. by Yukigoseikagaku Kyokai, Gihodo, Tokyo (1960), p. 83.

6) Joh. Rud. Geigy & Co., German Pat. 105103 (1901); W. C. Baird, Jr., and R. L. Shriner, *J. Am. Chem. Soc.*, **86**, 3142 (1964).

7) H. H. Hodgson and T. A. Jenkinson, *J. Chem. Soc.*, **1929**, 469.

8) T. Nakabayashi and K. Yamasaki, *Yakugaku Zasshi (J. Pharm. Soc. Japan)*, **74**, 590 (1954).

9) C. Hamada, *Nippon Kagaku Zasshi (J. Chem. Soc. Japan, Pure Chem. Sect.)*, **76**, 993 (1955).

10) H. B. Gillespie, "Biochemical Preparations," Vol. 3, ed. by E. E. Snell, John Wiley & Sons, New York (1953), p. 79.

11) C. C. Hach, L. M. Liggett and H. Diehl, *Iowa State Coll. J. Sci.*, **21**, 316 (1947); *Chem. Abstr.*, **42**, 1240 g (1948).

12) A. Zaki and W. Tadros, *J. Chem. Soc.*, **1941**, 350.

13) S. Emoto, *J. Sci. Res. Inst. (Tokyo)*, **47**, 37 (1953).

Results and Discussion

Effect of the Kind of Substituent of Benzaldehyde. The *o*-hydroxyl group in benzaldehydes must play a crucial role in the catalytic activity of racemization, and an electron-attracting substituent on the benzene ring promotes the activity.[2] In order to verify the effects of various kinds of substituents on racemization, several salicylaldehydes and benzaldehydes were carefully examined. The results are listed in Table 1, which shows

Table 1. Comparison of racemization yields by aldehydes in the presence of cupric ion

Subst. BzH				Racemi. yield
2-	3-	4-	5-	
OH	H	NMe_3Br	H	85.4%
OH	H	H	NO_2	82.7
OH	NO_2	H	H	70.6
OH	H	H	Br	62.2
OH	Br	H	H	54.9
OH	H	H	OMe	44.0
OH	OMe	H	H	40.1
OH	H	H	H	39.2
OH	H	H	Me	34.0
OH	H	Me	H	31.3
OH	Me	H	H	28.3
OH	H	OH	H	14.8
OH	H	NMe_2	H	7.5
OMe	H	H	H	7.1
H	H	NMe_2	H	3.2
H	H	NMe_3I	H	2.0
	no catalyst			2.2

Aldehyde (0.04 mmol), cupric sulfate (0.04 mmol), and L-glutamic acid (2 mmol) were used and reacted at 80°C for 3 hr.

that no benzaldehyde derivatives except *o*-methoxybenzaldehyde showed any activity of racemization. The activity of salicylaldehyde derivatives which were substituted by electron-releasing groups was weaker than that of derivatives substituted by electron-attracting groups and that of salicylaldehyde itself. Moreover, the racemization yield of 3-substituted salicylaldehyde was lower than that of the corresponding 5-isomer.

Relation between the Rate Constant, k, and Hammett's Constant, σ. The rate constant of the racemization of sodium L-glutamate in the presence of cupric ions and catalyzed by salicylaldehyde derivatives was studied. The rate constant was calculated as follows:

$$kt = 2.30 \times (\log [\alpha_0] - \log [\alpha_t])$$

where k is the rate constant, t is the time, and $[\alpha_t]$ is the observed rotation at t. The rate constant of racemization catalyzed by 4-formyl-3-hydroxyphenyltrimethylammonium bromide at 80°C has been described previously.[1] The activities of 3-bromo-, 5-bromo-, 3-methoxy-, 5-methoxy-, 3-methyl-, 4-methyl-, 5-methyl-, 3-nitro-, and 5-nitrosalicylaldehydes and salicylaldehyde were also measured at 80°C. However, within 2 or 3 hr the catalytic activity of 3-bromo-, 5-bromo-, and 3-nitro-salicylaldehydes was gradually lowered, probably because of the decomposition of these catalysts. The plots indicating the first-order reaction are shown in Fig. 1, from which rate con-

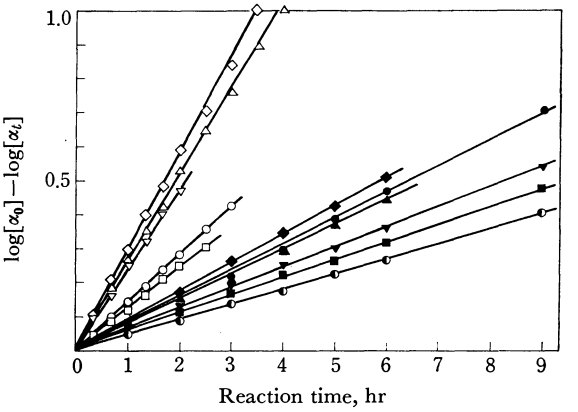

Fig. 1. Catalytic activities of salicylaldehyde derivatives at 80°C in the presence of cupric ion.
◇ 4-Trimethylammonium, △ 5-Nitro, ▽ 3-Nitro, ○ 5-Bromo, □ 3-Bromo, ◆ 5-Methoxy, ▲ 3-Methoxy, ● Salicylaldehyde, ▼ 5-Methyl, ■ 4-Methyl, ◐ 3-Methyl.

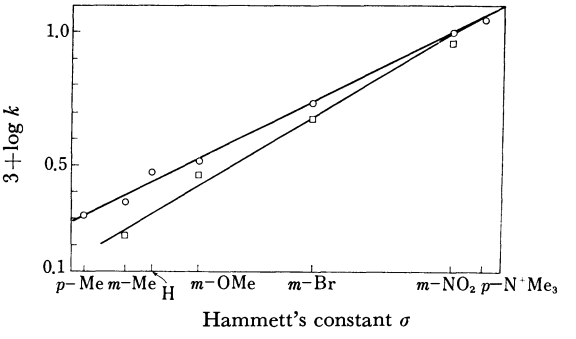

Fig. 2. Relation between rate constant k and Hammett's constant σ.
○ 4- or 5-Substituted salicylaldehydes.
□ 3-Substituted salicylaldehydes.

stants, k, were calculated. In Fig. 2 log k is plotted against Hammett's constant, σ.[3] As Fig. 2 shows, the rate constants of 5-substituted salicylaldehydes were larger than those of the corresponding 3-isomers, probably because of some ortho steric effect in the formation of the chelate ring (IV), though the structure of the chelate complex around the copper has not yet been satisfactorily clarified.

A linear relation between log k and Hammett's constant, σ, of 4- or 5-substituted salicylaldehydes, and an another linear relation between log k and the σ of 3-substituted salicylaldehydes, were observed; the reaction constants were 0.76 and 0.91 respectively.

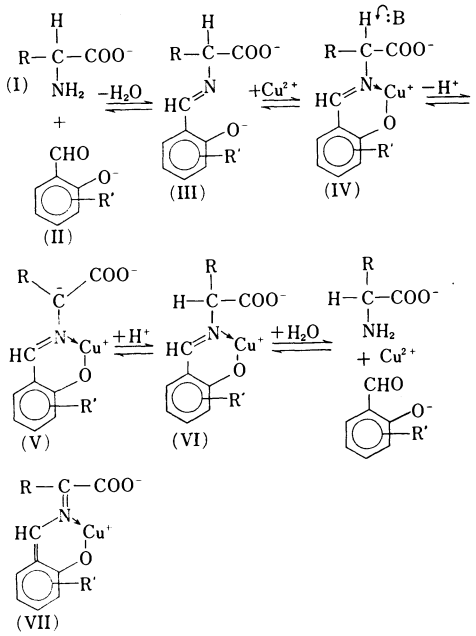

Snell[14] reported that, in a Schiff's base (III) of pyridoxal and amino acid, the α-carbon atom of amino acid was conjugated with the nitrogen atom of the pyridine ring and that consequently the α-proton of amino acid was eliminated easily and a racemization reaction occurred. However, Pullman[15] pointed that the conjugated system was only extended to the nitrogen atom of amino acid; before the transition state the α-carbon atom did not belong to the conjugated system. Yoshikawa[2] discussed how the electron-withdrawing power of the nitrogen atom of amino acid was activated by the inductive effect of the substituted benzene ring.

Since our results showed that the rate constant of the catalytic racemization by substituted salicylaldehydes obeyed Hammett's rule, the rapid formation of aldimine (III, IV) and the decrease in electron density around the nitrogen atom of the stabilized aldimine-chelate system should be caused mainly by inductive and mesomeric effects. Thus, the α-carbon of amino acid, affected by partial positively-charged aldimine nitrogen, would be readily converted to carbanion (V) by basic catalysis.

The negligible transamination together with the racemization of the glutamic acid catalyzed by 4-formyl-3-hydroxyphenyltrimethylammonium bromide[1] suggest that the p-trimethylammonium group should be unfavorable to the formation of a conjugated system with ketimine (VII)[2] from carbanion (V).

Activation Energy of Racemization, Catalyzed by 3-Nitro-, 5-Nitro-salicylaldehydes, Salicylaldehyde, and Pyridoxal Hydrochloride. Because the rate constant of 5-nitrosalicylaldehyde was larger than that of 3-nitrosalicylaldehyde, the

Table 2. The rate constants of 3-nitrosalicylaldehyde, 5-nitrosalicylaldehyde, salicylaldehyde and pyridoxal hydrochloride at various temperatures

Temp. °C	k ($\times 10^{-3}$ min^{-1})			
	3-NO_2	5-NO_2	Sal.	Pyr.
100		26.1	9.21	
90		15.8	5.44	
80	9.12	10.0	3.01	
70	5.21	5.76	1.53	
60	2.79	3.09	0.728	
50	1.45	1.55	0.351	3.92
40	0.712	0.745	0.146	2.08
30				1.04
20	0.138	0.136		0.483
0				0.0980

Aldehyde (0.04 mmol), cupric sulfate (0.04 mmol), and L-glutamic acid (2 mmol) were used.

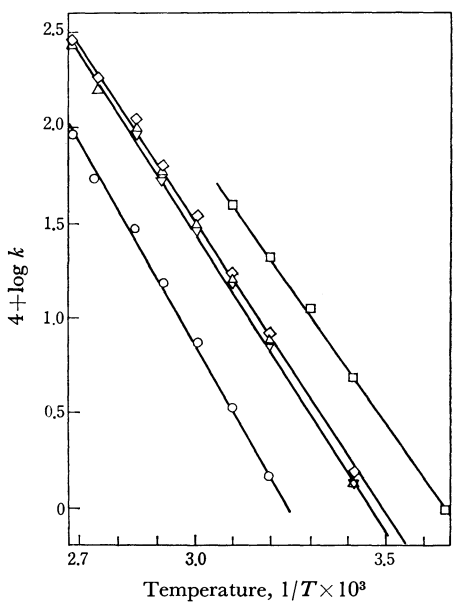

Fig. 3. Effect of temperature on rate constant.
□ Pyridoxal, ◇ 4-Formyl-3-hydroxyphenyltrimethylammonium bromide, △ 5-Nitrosalicylaldehyde, ▽ 3-Nitrosalicylaldehyde, ○ Salicylaldehyde.

14) D. E. Metzler, M. Ikawa and E. E. Snell, *J. Am. Chem. Soc.*, **76**, 648 (1954).

15) A. M. Perault, B. Pullman and C. Valdemoro, *Biochim. Biophys. Acta*, **46**, 555 (1961).

activation energies might differ from each other as a result of the ortho steric effect on the hydroxyl group. The rate constants of 3-nitro-, 5-nitrosalicylaldehydes, salicylaldehyde, and pyridoxal hydrochloride were measured at various temperatures. At 80°C pyridoxal did not satisfy the first-order reaction, as has previously been described,[1] but below 50°C our results followed the first-order reaction equation at first. At temperatures higher than 90°C, as compared with the catalytic activity of 5-nitrosalicylaldehyde, that of 3-nitrosalicylaldehyde was lowered very much as time passed, probably because of its decomposition, but the rate constant was measured only below 80°C. The rate constants are summarized in Table 2. The linear relations observed between log k and $1/T$ are shown in Fig. 3. Because the line of 3-nitrosalicylaldehyde almost overlapped with that of the 5-isomer, so that they could not be distinguished from each other, the line of the 3-isomer was omitted from Fig. 3. The activation energies of pyridoxal, 5-nitrosalicylaldehyde, 3-nitrosalicylaldehyde, and salicylaldehyde were 13.0 kcal/mol, 14.3 kcal/mol, 14.4 kcal/mol, and 16.0 kcal/mol respectively. The activation energy of 4-formyl-3-hydoxyphenyltrimethylammonium bromide was 14.3 kcal/mol.[1] Pyridoxal has the least activation energy and the largest rate constant, and it was the best catalyst for racemization, but, as has been established before, at high temperatures the catalytic activity was lowered as time passed. No distinct difference in activation energy was observed between 5-nitrosalicylaldehyde and 3-nitrosalicylaldehyde.

BULLETIN OF THE CHEMICAL SOCIETY OF JAPAN VOL. 42 2631—2635 (1969)

Sulfilimine. I. Synthesis and Formation Mechanism

Kenji TSUJIHARA, Naomichi FURUKAWA, Keiko OAE and Shigeru OAE

Department of Applied Chemistry, Faculty of Engineering, Osaka City University, Sugimoto-cho, Sumiyoshi-ku, Osaka

(Received February 18, 1969)

The kinetics of the reaction of sulfide and chloramine T was investigated. The reaction was very much affected by pH, and the rate reached the maximum at pH 5.5. The reaction was found to be facilitated by the substitution of an electron-releasing group in phenyl rings of aryl methyl sulfides. From these observations the rate-determining step appears to involve the formation of the sulfonium cation intermediate. From the mechanistic study of this reaction, an effective procedure for the synthesis of sulfilimine was devised.

N-Sulfonylsulfilimines have been known to be prepared either by treating the corresponding sulfides with *N*-sulfonyl-haloamide,[1] or by the reaction of the sulfoxides with sulfonamide[2] or sulfinylsulfonamide[3] or sulfonylisocyanate.[4] Among these, the first method is most commonly used.

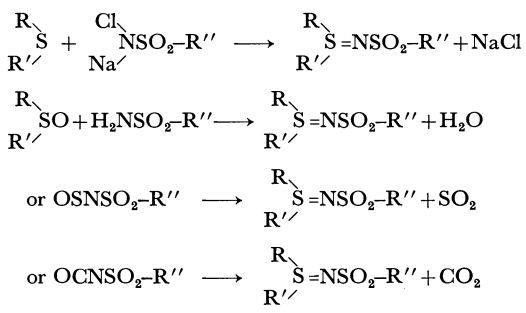

However, it is difficult to synthesize diarylsulfilimines by these methods, especially those bearing strong electron-withdrawing substituents such as halo or nitro groups. This may suggest that the formation of sulfilimine from sulfide and haloamide involves the initial slow step of halogenation of sulfide with active halogen, since the electron-withdrawing groups or substituents would hinder the formation of such a halogenated complex.

On the other hand, the similar reaction to synthesize sulfoxides from the sulfides and active halogen complex in aqueous media suggests that the initial halogenation is quite rapid and the subsequent nucleophilic attack of either acylate ion

1) F. G. Mann and W. J. Pope, *J. Chem. Soc.*, **121**, 1052 (1922).

2) D. S. Tarbell and C. Weaver, *J. Am. Chem. Soc.*, **63**, 2939 (1941).

3) G. Schulz and K. Kresze, *Angew. Chem.*, **75**, 1022 (1963).

4) C. King, *J. Org. Chem.*, **25**, 352 (1960).

or water is the slow step of the reaction.[5]

Although there have been a few works[6] which deal with mechanisms of the reaction between sulfides and chloramine T, these data are not sufficient for considering the mechanism of the reaction in detail, since the reaction systems are too complicated and hence no well-defined kinetic study has been performed.

We have carried out an extensive kinetic investigation which includes the effect of pH and the substituent effect and found out that the reaction is very much dependent on the change of pH. Thus, when a condition is set at the pH giving the largest rate of this reaction, even diarysulfilimines bearing electron-withdrawing substituents can be readily prepared. This paper will describe a detailed account of the kinetic study and the application of the results to a useful synthetic procedure.

Results and Discussion

The Mechanism of the Reaction of Aryl Methyl Sulfides with Chloramine T. Aryl methyl sulfides and chloramine T were used for the kinetic experiments. The reaction was carried out in 60% aqueous methanol solution at a constant temperature and pH. The kinetic measurements for this reaction were carried out by following the increase of the absorbance due to I_3^- at 353 mμ in the spectrum, since it is reflected in the decrease of chloramine T which can oxidize potassium iodide to give free iodine in an acidic solution. In this case, a suitable acid to acidify the solution was acetic acid and not sulfuric acid or other strong mineral acids.

The reaction was found to follow the usual second order kinetic relationship nicely over the range of 0—80% reaction (Fig. 1).

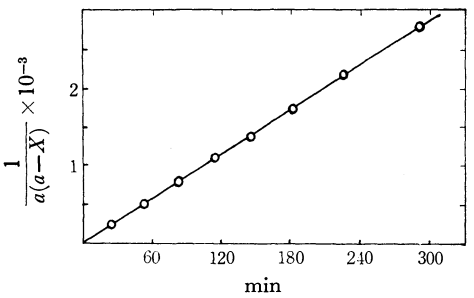

Fig. 1. Example of second order kinetics
a: the same initial concentration of methyl phenyl sulfide and chloramine T
x: a concentration of sulfilimine produced
reaction was carried out at 30°C and pH 8.61

The effect of pH on the apparent second-order rate constant K_{obs} was examined and the results are shown in Fig. 2. A plot of log K_{obs} *vs.* pH

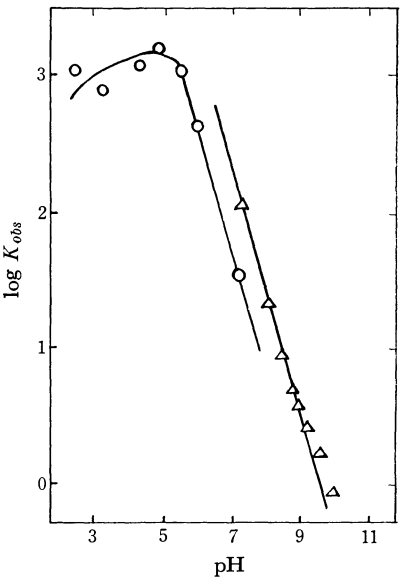

Fig. 2. The effect of pH on K_{obs}
○: at 15°C △: at 30°C

gives a straight line with a slope of −1.0 in the region between about pH 5.5 to pH 9, where the decrease of one pH unit results in the 10 fold increase of K_{obs} value.

The effects of the *p*-substituents in the phenyl ring of the sulfides upon K_{obs} are shown in Fig. 3.

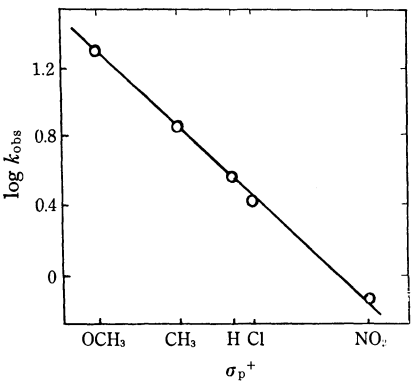

Fig. 3. The effects of the *p*-substituents in the aryl methyl sulfides on K_{obs}
temperature 30.0°C pH 9.07

A plot of log K_{obs} *vs.* σ_p^+ gives a straight line with a slope of −0.94 ($\rho = -0.94$). This seems to indicate that the formation of the chloro-sulfonium cation takes part in the rate-determining step of this reaction.

5) T. Higuchi and K.-H. Gensch, *J. Am. Chem. Soc.*, **88**, 5486 (1966); W. Tagaki, M. Ochiai and S. Oae, *Tetrahedron Letters*, **58**, 6131 (1968).

6) J. Benes, *Collection Czech. Chem. Commun.*, **28**, 1171 (1963); A. Kucsman, I. Kapovits and M. Balla, *Tetrahedron*, **18**, 75 (1962).

Based on these observations, the following mechanism may be formulated for the reaction of sulfide with chloramine T.

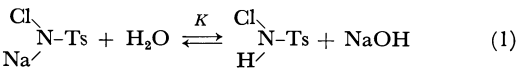

(1)

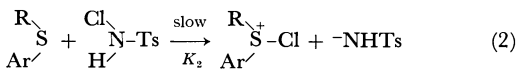

(2)

(3)

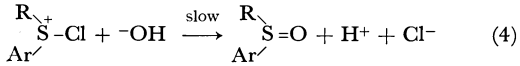

(4)

Chloramine T (I) is presumed to be in the equilibrium with its free state (II) and sulfides are considered not to react with I but with II, since the rate of this reaction is very much facilitated by the addition of a weak acid, while I is not capable to liberate free iodine from potassium iodide in alkaline solution.

Meanwhile, in the reaction shown by Eq. (2), the sulfides that possess electron-richer S atoms would react more readily with (II), namely giving minus ρ value with substituted phenyl methyl sulfides, whereas, Eq. (3) involves the chlorosulfonium cation and requires an entirely opposite electronic effect for a facile formation of sulfilimines.

The small negative ρ values (-0.94) obtained from the overall rate constants appears to suggest that the rate determining step is the second step shown by Eq. 2.

Thus, the following rate equation may be formulated.

$$d[\text{Sulfilimine}]/dt = K_2[\text{II}][\text{Sulfide}]$$

$$\text{From Eq. (1), } [\text{II}] = \frac{K[\text{I}]}{[\text{OH}^-]} = K \times 10^{14-\text{pH}}[\text{I}]$$

$$d[\text{Sulfilimine}]/dt = K_2[\text{II}][\text{Sulfide}]$$
$$= K_2 \cdot K \cdot 10^{14-\text{pH}}[\text{I}][\text{Sulfide}]$$
$$= K_{\text{obs}}[\text{I}][\text{Sulfide}]$$

The use of aqueous media for a solvent of this reaction could lead to the formation of the by-product, sulfoxide, according to Eq. (4) and hence the addition of a larger amount of water into the system could give rise to the higher ratio of sulfoxide among the products.[6]

This was not the case, however, when the reaction was conducted in the presence of a small quantity of added acid; the time required for the reaction became very short and sulfilimines were formed nearly in quantitative yields. In the conventional procedure in which no weak acid is added, a considerable portion of sulfoxide is formed in the products. This is considered to be formed by the hydrolysis of sulfilimine once formed, since the formation of sulfilimine is quite slow and sulfilimine formed would be hydrolyzed slowly under the reaction conditions. These results show that the reaction shown by Eq. (3) is considerably faster than that of sulfoxide formation (Eq. (4)).

In Fig. 2, the plateau of the curve below about pH 5 is assumed to be due to the sudden change of the rate determining step of the reaction.

p-Toluenesulfonamide anion, $^-$NHTs, formed according to Eq. (2) begins to be protonated to form the corresponding sulfonamide in a low pH region and the chlorosulfonium cation formed would react not only with the sulfonamide, but also with the aqueous solvent media. As the corollary, the sole reaction product quantitatively obtained is sulfilimine at pH 6, but at pH 2 the yield of sulfilimine became 50% while sulfoxide is formed in the same 50% yield.

The rate of sulfoxide formation (Eq. (4)) is considered to be nearly equal to, or a little smaller than that of the halosulfonium cation formation in the reaction of sulfide with halogen in aqueous media, since it is known that the rate determining step of sulfoxide formation is the reaction of the halosulfonium cation with hydroxylic species.[5]

Synthetic Application. Since it has become clear that the formation of sulfilimine becomes very facile at around pH 5, we have devised a better reaction condition for facile syntheses of sulfilimines by the addition of a small amount of a weak acid, such as acetic acid.

Sulfilimine has been prepared usually by treating sulfide with an *N*-haloamide such as chloramine T in aqueous media with either methanol, acetone or some other water miscible solvents. However, the use of water often leads to the formation of a by-product sulfoxide, and sometimes makes it difficult to dissolve the sulfides such as methyl aryl sulfides and reduces the yields of products.

In order to overcome these difficulties, we used commercial methanol as the only solvent and increased the yield of *N*-sulfonyl-sulfilimines.

In general, dialkyl and alkyl aryl sulfides readily react with chloramine T. However, diaryl sulfides do not react with chloramine T under the same reaction condition. Moreover, when an electron-withdrawing group is introduced into either one of phenyl rings of the sulfides, the reaction does not proceed. However, when the reaction was carried out by adding a small amount of a weak acid such as acetic acid, even the diarylsulfilimines having nitro and halo groups were successfully obtained in high yields.

This method is quite effective, since the acid is acting on chloramine T to liberate the free chloramine T, which supplies an active chlorine to react readily with the lone electron pair of sulfides.

The yields and mps of sulfilimines are shown in Table 1.

Table 1. Sulfilimines $R_1R_2S{:}NSO_2$–C$_6$H$_4$–Me

R_1	R_2	Mp (°C)	Yield (%)	Method		Anal. C, %	Anal. H, %	Anal. N, %
CH_3	CH_3	157—157.5	90	A				
$(CH_3)_2CH$	$(CH_3)_2CH$	117—118	95	A				
$CH_3(CH_2)_3$	$CH_3(CH_2)_3$	59—60	83	A				
$-(CH_2)_4-$		145—146	87	A				
$-(CH_2)_5-$		148—149	95	A				
CH_3	C_6H_5	129—130	90	A				
CH_3	p-$CH_3C_6H_4$	125—126	78	A				
CH_3	p-$CH_3C_6H_4$	125—126	95	B				
CH_3	p-$MeOC_6H_4$	144.5—145	74	A				
CH_3	p-ClC_6H_4	112—113	56	A	Found	51.48	4.24	4.15
					Calcd	51.30	4.27	4.27
CH_3	p-ClC_6H_4	112—113	95	B				
CH_3	p-$NO_2C_6H_4$	162—163	15[a]	A				
CH_3	p-$NO_2C_6H_4$	162—163	91	B				
CH_3CH_2	C_6H_5	97—98	82	A				
$(CH_3)_2CH$	C_6H_5	115—116	84	A				
$(CH_3)_3C$	C_6H_5	101 (decomp)	58	A				
$C_6H_5CH_2$	$C_6H_5CH_2$	190—191	80	A				
$C_6H_5CH_2$	C_6H_5	136—137	62	A				
$C_6H_5CH_2CH_2$	C_6H_5	137—138	66	A	Found	67.03	5.51	3.53
					Calcd	65.80	5.48	3.66
C_6H_5	C_6H_5	111—112	5[a]	A				
C_6H_5	C_6H_5	111—112	94	B				
C_6H_5	p-$CH_3C_6H_4$	96—98	58	B	Found	65.68	5.10	3.74
					Calcd	65.04	5.15	3.79
C_6H_5	p-ClC_6H_4	89.5—90.5	65	B	Found	58.60	3.96	3.46
					Calcd	58.54	4.11	3.59
C_6H_5	p-$NO_2C_6H_4$	148—149	59	B	Found	57.56	4.07	6.81
					Calcd	56.86	3.99	6.98
p-$CH_3OC_6H_4$	p-$CH_3OC_6H_4$	130—132	68	A				

a) The product was separated by using chromatographic technique over silica-gel.

Experimental

Kinetic Procedure of the Mechanism of the Reaction of Aryl Methyl Sulfides with Chloramine T. The kinetic experiments were carried out while maintaining both the temperature (15±0.06, 30±0.08°C) and the pH constant using the following buffer solutions in 60% aqueous methanol media. After the reaction the pH of the solution was measured. Buffer solutions:

Potassium biphthalate-HCl (below pH 4), CH_3COOH-CH_3COONa (pH 4—6.5), KH_2PO_4-Na_2HPO_4 (pH 6.5—8.5), H_3BO_3, KCl-Na_2CO_3 (pH 8.5—10.5)

Both the sulfide and the chloramine T solutions preheated to the prescribed temperature were mixed quickly and the mixture was kept at a constant temperature during the kinetic experiments. An aliquot portion (1—2 m*l*) of the reaction mixture was taken up from time to time for 5—10 times and was quenched with 2 m*l* 1N KI. Then 5 m*l* 3N AcOH aqueous solution and the water was added to the prescribed volume.

Free iodine liberated from potassium iodide by the reaction with unchanged chloramine T is in the equilibrium with triiodide ion I_3^- with absorbance at 353 mμ was followed.

The concentrations of unreacted chloramine T were obtained by the following equation.

$$\text{Chloramine T} = \frac{A}{\varepsilon}$$

A: the absorbance at 353 mμ

ε: the molar extinction coefficient which was determined for using a known amount of chloramine T under the same condition.

Syntheses. The sulfides used were prepared by the general methods and purified either by distillation or recrystallization. The bps and mps of used sulfides are following:

di-methyl bp 37—38°C di-*i*-propyl bp 119—120°C, di-*n*-butyl bp 163—164°C, tetramethylene bp 119—120°C pentamethylene bp 140—141°C, methyl phenyl bp 84—85°C/15 mmHg methyl *p*-tolyl bp 81.5—82°C/7 mmHg, methyl *p*-methoxyphenyl bp 99°C/3 mmHg, methyl *p*-chlorophenyl bp 103—104°C/12 mmHg, methyl *p*-nitrophenyl mp 67—68°C, ethyl phenyl bp 85—86°C/

12 mmHg, iso-propyl phenyl bp 92—93°C/3 mmHg, *t*-butyl phenyl bp 96—97°C/15 mmHg, di-benzyl mp 49—50°C, benzyl phenyl mp 41—42°C, 2-phenylethyl phenyl bp 189—190°C/15 mmHg, di-phenyl bp 117—118°C/2 mmHg, phenyl *p*-tolyl bp 159—160°C/8 mmHg phenyl *p*-chlorophenyl bp 167—168°C/10 mmHg, phenyl *p*-nitrophenyl mp 55—56°C, di-*p*-methoxyphenyl mp 45—46°C. Sulfilimines were prepared from the corresponding sulfides and chloramine T by the following general methods (A) and (B).

(A): To 0.01 mol of sulfide in 20 m*l* of commercial methanol was added 0.011 mol of chloramine T in 20 m*l* of methanol at room temperature. The mixture was permitted to stand at 50°C for 1—5 hr and poured into a cold dilute sodium hydroxide solution. The precipitate was filtered, washed with water and recrystallized from methanol-water or acetone-hexane mixture.

(B): In 30 m*l* of methanol were dissolved 0.01 mol of sulfide and 0.011 mol of chloramine-T. To this solution was added dropwise 1.0 m*l* of acetic acid in 5 m*l* of methanol at room temperature. The mixture was allowed to stand at 50°C for 0.2—3 hr and poured into a cold dilute sodium hydroxide solution and a precipitate formed was filtered, then washed with water, Sometimes an oily product was extracted with two 30 m*l* portions of chloroform and the chloroform layer was washed with water, dried and the solvent removed. The residue was then washed with ether. Crude products were recrystallized from either acetone-hexane or methanol-water mixture.

The Reaction at a Low pH. Into a solution of methyl phenyl sulfide (0.001 mol) dissolved in 50 m*l* of methanol and 10 m*l* of 0.5N H_2SO_4 aq. chloramine T (0.0011 mol) dissolved in 10 m*l* of methanol was added and the reaction mixture (pH was about 2) was allowed to stand for 0.5 hr at room temperature, then poured into a dil-NaOH aq. solution. The products were extracted twice with each 30 m*l* portions of chloroform and the chloroform layer was washed with water, dried and the solvent removed. The composition of the products was calculated from the NMR spectra in which CH_3 on S atom of the sulfilimine and the sulfoxide and CH_3 in *p*-tolyl group give the chemical shifts of 2.84, 2.71 and 2.35 ppm respectively. The composition was found to be 50% sulfilimine and 50% sulfoxide.

BULLETIN OF THE CHEMICAL SOCIETY OF JAPAN VOL. 42 2635—2647 (1969)

Conformational Studies of Acetonated α-L-Sorbo- and β-D-Fructopyranoses by Means of Proton Magnetic Resonance Spectroscopy[1]

Takashi MAEDA, Kazuo TORI, Shiroh SATOH and Kanji TOKUYAMA

Shionogi Research Laboratory, Shionogi & Co., Ltd., Fukushima-ku, Osaka

(Received February 19, 1969)

The favored conformations of the pyranose rings of several acetonated α-L-sorbo- and β-D-fructopyranoses have been revealed by proton magnetic resonance spectroscopy. The conformations of the rings of the pyranoses are unchanged by the introduction of 1,2-*O*- or 1,3-*O*-isopropylidene groups in α-orientation of L-sorbose, but they are affected by the introduction of the 2,3-*O*-isopropylidene group. These findings support the fact that 2,3-*O*-isopropylidene-α-L-sorbopyranose was not obtained by the acetonation of L-sorbose. The rings of diacetonated D-fructopyranoses with a *cis*-fused acetal ring adopt a distorted conformation; however, those of diacetonated L-sorbopyranoses with a *trans*-fused acetal ring are only slightly distorted from the stable 1C conformation. Angyal's anticipation of the difficult acetalation of the *trans*-glycol of a pyranose has been further experimentally supported.

Our previous studies[3] of the conformations of acetonated L-sorbofuranose rings in solutions by proton magnetic resonance (PMR) spectroscopy showed that their conformations, restricted by the ring strain of the isopropylidene ring, play an important role in the acetonation of L-sorbose. As a part of a program of research into the reaction mechanism of the acetonation,[3,4] we have investigated the conformations of the acetonated L-sorbopyranoses, which were obtained at an initial

1) Sorboses Part XVI; for Part XV, see Ref. 2.

2) T. Maeda, M. Kimoto S. Wakahara and K. Tokuyama, This Bulletin, **42**, 2021 (1969).

3) T. Maeda, K. Tori, S. Satoh and K. Tokuyama, *ibid.*, **41**, 2495 (1968).

4) a) K. Tokuyama, E. Honda and N. Hōki, *J. Org. Chem.*, **29**, 133 (1964); b) K. Tokuyama and E. Honda, This Bulletin, **37**, 591(1964); c) T. Maeda, *ibid.*, **40**, 2215 (1967).

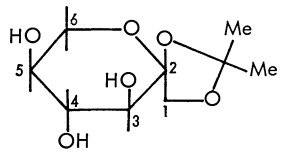

Type A

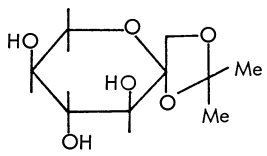

Type B

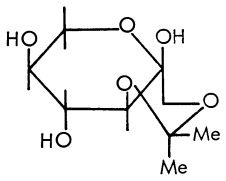

Type C

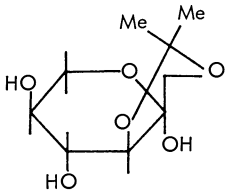

Type D

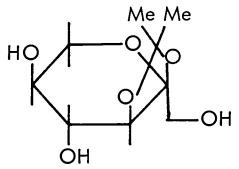

Type E

Chart 1

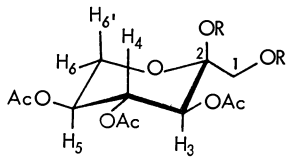

I R = Ac

II R = H

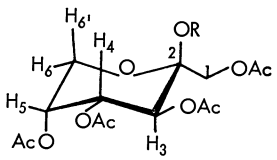

III R = Ac

IV R = H

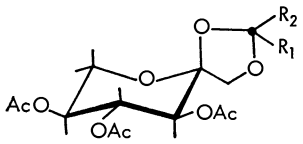

V $R_1 = R_2 = Me$

VIII $R_1 = Ph$, $R_2 = H$

IX $R_1 = Me$, $R_2 = H$

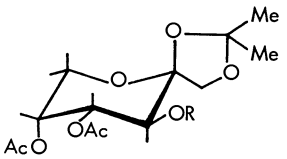

VI R = Ac

VII R = Me

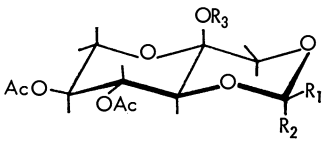

X $R_1 = R_2 = Me$, $R_3 = Et$

XI $R_1 = Ph$, $R_2 = H$, $R_3 = Me$

XII $R_1 = Me$, $R_2 = H$, $R_3 = Me$

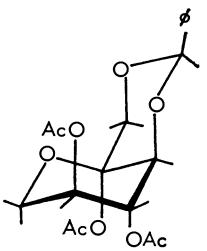

XIII

Chart 2

stage of acetonation.[4-6] In general, there are five possible monoacetonated L-sorbopyranoses; 1,2-*O*-isopropylidene-α- (type A), 1,2-*O*-isopropylidene-β- (type B), 1,3-*O*-isopropylidene-α- (type C), 1,3-*O*-isopropylidene-β- (type D), and 2,3-*O*-isopropylidene-α-L-sorbopyranoses (type E). The benzylidenation[2,7,8] and the ethylidenation[7,9] reactions yielded compounds of the types A and C, while the acetonation produced a type A compound. No compounds of the types B, D and E have yet been isolated; no formation of a type E compound is especially attractive since a derivative of this type can be formed more easily by the acetonation of D-fructose.[10]

Several workers have shown, on the basis of PMR studies, that the pyranose rings of compounds of the type E, such as 1,2-*O*-alkylidene-α-D-glucopyranose[11-14] and 1,2 : 3,4-di-*O*-isopropylidene-α-D-galacto- and β-L-arabinopyranoses (XXIII),[15] adopt distorted chair or skew conformations. In particular, 1,2-*O*-cyanoethylidene-α-D-glucopyranose has been reported to adopt a skew conformation.[11] On the other hand, Trotter and Fawcett[13] pointed out, by X-ray crystal analysis, that this compound is in a distorted, flattened Cl conformation and proposed that the PMR spectra are compatible with the conformation determined in the solid state.

This paper will deal with conformations of the pyranose rings in twelve acetonated derivatives of α-L-sorbo- and β-D-fructopyranoses by means of PMR spectroscopy. The conformations of these compounds were determined on the basis of the magnitude of their vicinal coupling constants, obtained with reference to those of 1,2,3,4,5-penta- (I), and 1,3,4,5-tetra-*O*-acetyl-α-L-sorbopyranoses (II), 1,2,3,4,5-penta- (III) and 1,3,4,5-tetra-*O*-acetyl-β-D-fructopyranoses (IV), all of which have the 1C conformation, as has previously been reported.[16]

Experimental

Measurements. All the PMR spectra were taken with a Varian HA-100 spectrometer operating at 100 MHz at an ordinary probe temperature by using about 5% (w/v) solutions in chloroform-d ($CDCl_3$), benzene-d_6(C_6D_6), pyridine-d_5(C_5D_5N), dimethylformamide-d_7 (DMF-d_7) and/or dimethyl sulfoxide-d_6 (DMSO-d_6). The charts were calibrated with direct readings of resonance frequencies using a Hewlett-Packard HP-5212 electronic counter with accuracies to within ±0.2 Hz or less. The spin-decoupling experiments were performed on the spectrometer in the frequency-swept and TMS-locked modes by using two Hewlett-Packard HP-200 ABR audio-oscillators and the HP-5212 A counter. The accuracies of the magnitudes of the chemical shifts, τ, and the coupling constants, J, are within about τ 0.02 and 0.2 Hz respectively.

The infrared (IR) spectrum of XXII was measured with a Nippon Bunko DS 402 G infrared spectrometer by using a 4.2 mg/8 m*l* (in 20 mm-cell) solution in carbon tetrachloride.

The melting points were recorded on a Kofler microstage apparatus and have been corrected. The optical rotations were measured with a Perkin-Elmer model-141 polarimeter. The concentrations were recorded in percentages.

Analysis of PMR Spectra. In the compounds reported here, the pyranose-ring protons, H_6, $H_{6'}$, H_3, H_4, and H_5, can be classified as composing an ABXYZ spin system. Therefore, it is quite certain that their signals show second-order patterns depending on the $\Delta\nu_{ij}/J_{ij}$ values, where $\Delta\nu_{ij}$ is the value of the difference in chemical shifts between H_i and H_j expressed in frequency unit. The signals of the protons H_1 and H_1' appear, in general, as an AB-type quartet. In order to determine the J values from the signal pattern with accuracies to less than 0.2 Hz, their spectra were analyzed by using the proton double resonance (PMDR) technique and by applying the solvent effects of benzene and pyridine. Since all the compounds examined here contain one or two 1,3-dioxolane rings besides hydroxyl or acetoxy groups, an alteration in the solvent from $CDCl_3$ to C_6D_6 or C_5D_5N can be expected to change their PMR spectral patterns considerably.[17] The altera-

5) H. Ohle, *Ber.*, **71**, 562 (1938).

6) a) J. R. Patil and J. L. Bose, *J. Indian Chem. Soc.*, **43**, 161 (1966); b) J. R. Patil and J. L. Bose, *Indian J. Chem.*, **5**, 598 (1967).

7) T. Maeda and K. Tokuyama, *Tetrahedron Letters*, **1968**, 3079.

8) T. Maeda, M. Kimoto, S. Wakahara and K. Tokuyama, This Bulletin, **42**, 1668 (1969).

9) T. Maeda, M. Kiyokawa and K. Tokuyama, *ibid.*, **42**, 492 (1969).

10) a) E. Fisher, *Ber.*, **28**, 1164 (1895); b) H. Ohle and I. Koller, *ibid.*, **57**, 1566 (1924); c) H. Ohle, *ibid.*, **58**, 2577 (1925); d) H. Ohle and G. Verend, *ibid.*, **60**, 1159 (1927); e) C. G. Anderson, W. Charlton, W. N. Howarth and V. S. Nicholson, *J. Chem. Soc.*, **1929**, 1337; f) M. L. Wolfrom W. L. Shilling and W. W. Binkley, *J. Am. Chem. Soc.*, **72**, 4544 (1950).

11) B. Coxon and L. D. Hall, *Tetrahedron*, **20**, 1685 (1964).

12) R. G. Ree, A. R. Tatchell and R. D. Wells, *J. Chem. Soc.*, *(C)*, **1967**, 1768.

13) J. Trotter and J. K. Fawcett, *Acta Cryst.*, **21**, 366 (1966).

14) a) R. U. Lemieux and A. R. Morgan, *Can. J. Chem.*, **42**, 2199 (1965); b) R. U. Lemieux and D. H. Detert, *ibid.*, **46**, 1039 (1968).

15) C. Cone and L. Hough, *Carbohyd. Res.*, **1**, 1 (1965).

16) K. Tokuyama, T. Maeda, K. Tori, S. Satoh and K. Kuriyama, paper presented at the 1st symposium on Structural Organic Chemistry, Tokyo, November 1968, Abstracts, p. 32.

17) a) N. S. Bhacca and D. H. Williams, *Tetrahedron Letters*, **1964**, 3127; b) D. H. Williams and N. S. Bhacca, *Tetrahedron*, **21**, 1641 (1964); c) D. H. Williams and D. A. Wilson, *J. Chem. Soc.*, *(B)*, **1966**, 144; e) K. Tori and K. Aono, *Ann. Rept. Shionogi Res. Lab.*, **14**, 136 (1964); f) J. D. Connolly and T. McCrindle. *Chem. Ind.* (London), **1965**, 2066; g) C. J. Timmons, *Chem. Commun.*, **1965**, 576.

TABLE 1. CHEMICAL SHIFT IN τ VALUE

Compound	Solvent	H_1	$H_{1'}$	H_3	H_4	H_5	H_6	$H_{6'}$	OAc	$CH_3-\overset{\vert}{C}-$	Other H	
V	$CDCl_3$	6.04,	6.12	4.98	4.57	5.02	6.13	6.23	7.93, 7.98, 7.99	8.52, 8.58		
	C_6D_6	6.10[a]		4.82	4.27	4.89	6.1	6.3[b]	8.26, 8.29, 8.37	8.62, 8.64		
VI	$CDCl_3$	6.06[a]		4.6		4.8[b]	6.22	5.92	7.88, 7.94, 8.03	8.53, 8.59		
	C_6D_6	6.00,	6.04	4.31	4.46	4.58	6.53	6.22	8.25, 8.28, 8.30	8.62 (6H)		
VII	$CDCl_3$	5.91,	5.99	6.45	4.79	4.70	6.31	5.95	7.87, 7.98	8.51, 8.58	OCH_3	7.47
	C_6D_6	5.95[a]		6.43	4.41	4.52	6.55	6.25	8.24, 8.26	8.55 (6H)		6.77
X	$CDCl_3$	6.04,	6.40	6.28	4.51	5.01	6.19	6.38	7.99 (6H)	8.56, 8.59	OCH_2CH_3	8.72[c]
XIV	$CDCl_3$	5.95,	6.01	5.88	4.42	4.77	6.03	6.21	7.89, 7.91, 7.99	8.43, 8.62		
	C_6D_6	5.54,	5.60	5.93	4.21	4.62	6.13	6.23	8.19, 8.28, 8.29	8.51, 8.73		
	DMF-d_7	5.69[a]		5.78	4.49	4.85	6.03	6.18	7.88, 7.92, 8.00	8.47, 8.62		
XVI	$CDCl_3$	5.81,	6.01	6.58	5.92	4.94	6.04	6.55	7.93	8.50, 8.55 (6H), 8.58		
	C_6D_6	5.91,	6.00	6.74	5.77	4.94	6.02	6.54	8.38	8.53, 8.62, 8.66 (6H)		
XVII	$CDCl_3$	5.91,	6.05	6.69	6.14	[b]	6.21	6.57		8.50, 8.57 (6H), 8.60	OH	7.22
XVIII	$CDCl_3$	6.05[a]		4.84	6.13	6.50	6.02	6.26	7.87	8.51, 8.56 (6H), 8.57		
XIX	$CDCl_3$	6.07,	6.17	4.90	5.7			5.9[b]	7.88	8.45, 8.52, 8.60, 8.64		
	C_6D_6	6.06,	6.10	4.62	5.72	~6.13	6.0	6.2[b]	8.27	8.45, 8.60, 8.64, 8.79		
	C_5D_5N	5.94,	5.98	4.56	5.52	~5.70	5.7	5.9[b]	7.94	8.39, 8.49, 8.53, 8.62		
XX	$CDCl_3$	5.82,	6.02	~6.33	5.8			6.0[b]		8.45, 8.46, 8.54, 8.61	OH	7.91
	C_5D_5N	5.41,	5.80	5.92	5.42	~5.70	5.75	5.9[b]		8.39, 8.44 (6H), 8.60		5.7—5.8
XI	$CDCl_3$	5.56,	5.94	5.67	5.39	5.75	6.09	6.23	7.91	8.45, 8.52, 8.59, 8.65		
XXII	$CDCl_3$	6.31,	6.35	5.66	5.37	5.77	6.09	6.24		8.45, 8.53, 8.60, 8.65	OH	7.59
	C_6D_6	5.9[d]		5.1	5.25[b]	5.70	5.91	6.15		8.41, 8.42, 8.50, 8.67		5.25
	DMSO-d_6	6.7[e]		5.72	5.43	5.80	6.25	6.47		8.55, 8.65 (6H), 8.72		6.6—6.7

a) Observed as a singlet.
b) Not exactly determined owing to overlapping signals.
c) Methylene signal of OCH_2CH_3 group appeared near at τ 6.45 as A_2 part of A_2X_3.
d) After D_2O addition, the methylene signal was appeared as an AB type quartet at τ 5.89 and 5.97.
e) After D_2O addition, the methylene signal was appeared as an AB type quartet at τ 6.66 and 6.74.

TABLE 2. COUPLING CONSTANTS J IN Hz

Compound	$J_{1,1'}$	$J_{3,4}$	$J_{4,5}$	$J_{5,6}$	$J_{5,6'}$	$J_{6,6'}$	Other J
I[a]	11.8	9.9	9.1	6.1	10.5	11.0	
II[a]	11.8	9.9	9.3	6.1	10.7	11.0	
III[a]	12.0	10.2	3.3	1.9	1.2	13.0	
IV[a]	11.6	10.2	3.2	1.9	1.2	13.0	
V	9.4	9.8	9.4	6.1	10.2	11.2	
VI	9.0	10.4	3.2	1.8	1.3	13.2	
VII	8.8	10.0	3.4	1.8	1.3	13.2	
VIII[b]	9.2	9.6	9.3—9.6	d)	d)	d)	
IX[c]	9.0	9.7	~9	d)	d)	d)	
X	12.5	10.0	9.2	6.2	10.5	11.0	$J_{CH_2CH_3}=7.0$
XI[b]	12.0	10.0	9.3	6.3	10.7	10.7	
XII[c]	12.0	9.8	~9	6.2	10.2	11.0	
XIII[e]	12.0	2	3	2	2	13	$J_{1,3}\leq 1.0$, $J_{4,6'}\leq 1.0$
XIV	11.8	3.8	3.7	5.3	6.8	12.3	$J_{4,6}=0.5$
XV[f]	—	3.15	3.15	—	9.6	—	
XVI	9.0	9.6	10.0	5.5	10.0	11.2	
XVII	9.0	9.5	10.0	5.5	10.0	11.2	$J_{5,OH}=3.5$
XVIII	g)	10.4	8.8	5.3	9.7	10.5	
XIX	9.1	7.8	~5.0	~1.8	~1.8	d)	
XX	8.2	7.8	5.0	d)	d)	d)	$J_{3,OH}$[d]
XXI	12.0	2.5	8.0	1.5	1.0	13.0	$J_{1,OH}=3.8, 9.2$
XXII	11.6	2.5	8.0	1.5	1.0	13.0	
XXIII[a]	—	2.5	8.0				

a) Reported in Ref. 16. b) Reported in Ref. 8. c) Reported in Ref. 9.
d) Obscured. e) Reported in Ref. 2. f) Reported in Ref. 12.
g) Observed as a singlet.

tion in the solvent frequently changed their signal patterns into those which can be analyzed by the first-order approximation. However, in some cases the signal patterns can be analyzed by the usual procedure.[18] The chemical shifts and J values obtained are summarized in Tables 1 and 2.

Materials. 1,2-*O*-Isopropylidene-3-*O*-methyl-4,5-di-*O*-acetyl-β-D-fructopyranose (VII). A solution of 1,2 : 4,5-di-*O*-isopropylidene-3-*O*-methyl-β-D-fructopyranose[19] (2.0 g) in 60% aq. acetic acid (10 ml) was warmed at 45°C for 4 hr. The complete removal of the solvent under reduced pressure gave a syrup; the syrup was immediately acetylated with acetic anhydride (20 ml) and pyridine (20 ml) at room temperature for 3 hr. The mixture was then poured onto crushed ice and neutralized with an excess of sodium hydrogencarbonate. The solution was extracted with chloroform; the chloroform solution was washed with water, 2N HCl, and water, and dried with anhydrous magnesium sulfate, after which the solvent was removed. The recrystallization of a residue from water and methanol gave VII in a good yield. It had a mp of 101—102°C, $[\alpha]_D^{21}$ −130.8 (*c* 1.027, acetone). Found: C, 52.96; H, 6.97%. Cacld for $C_{14}H_{22}O_8$: C, 52.82; H, 6.97%.

Ethyl 1,3-*O*-Isopropylidene-4,5-di-*O*-acetyl-α-L-sorbopyranoside (X). A mixture of ethyl α-L-sorbopyranoside[20] (0.8 g), acetone dimethylketal (15 ml) and *p*-toluenesulfonic acid (70 mg) was stirred vigorously at room temperature. A clear solution was soon obtained. After 15 min, the fine crystals which precipitated were collected by filtration. The crystals were recrystallized from ethyl acetate and then acetone. Ethyl 1,3-*O*-isopropylidene-α-L-sorbopyranoside was obtained as needles (0.46 g), mp 178—179°C, $[\alpha]_D^{22}$ −60.4 (*c* 0.998, acetone). Found: C, 53.11; H, 7.98%; mol wt, 247. Calcd for $C_{11}H_{20}O_6$: C, 53.21; H, 8.26%; mol wt, 248. The needles (1.09 g) were acetylated with acetic anhydride (1 ml) and pyridine (1 ml) for 18 hr in a refrigerator. The mixture was then poured into ice water (10 g) and made alkaline with sodium bicarbonate. The solution was extracted with chloroform, and the chloroform was washed with a 2N hydrochloric acid solution. The dried extract was evaporated to give X as a syrup (130 mg); $[\alpha]_D^{23}$ −48.6 (*c* 0.970, acetone). Found: C, 54.48; H, 7.44%. Calcd for $C_{15}H_{24}O_8$: C, 54.21; H, 7.28%.

Results and Discussion

Monoacetonated Derivatives. *i) 1,2-O-Isopropylidene Compounds (Types A and B).* Figure 1 shows the PMR spectrum of 1,2-*O*-isopropyli-

18) J. M. Emsley, J. Feeney and L. H. Sutcliffe, "High Resolution Nuclear Magnetic Resonance Spectroscopy," Pergamon Press, London (1966), Chapter 8.

19) a) J. C. Irvine and J. P. Scott, *J. Chem. Soc.*, **103**, 564 (1913); b) K. Freudenberg and A. Doser, *Ber.*, **56**, 1243 (1923).

20) R. L. Whistler and R. M. Hixon, *J. Am. Chem. Soc.*, **60**, 563 (1938).

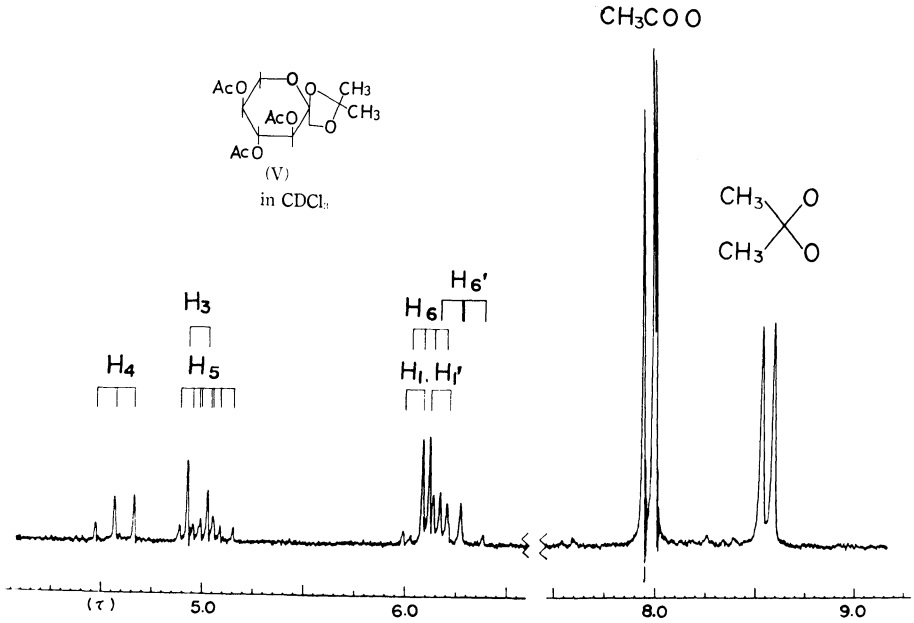

Fig. 1. PMR spectrum of V in $CDCl_3$ at 100 MHz.

dene 3,4,5-tri-*O*-acetyl-α-L-sorbopyranose (V)[4c] in $CDCl_3$ at 100 MHz. Two singlets in the high field (τ 8.52 and 8.58) are due to the isopropylidene methyls; they appear somewhat broad compared with those due to the acetoxyl methyls at τ 7.93, 7.98 and 7.99, because of the long-range coupling over 4 σ bonds.[21] The signals of H_6 and $H_{6'}$ appear as a quartet at τ 6.13 (J=(−)11.2 and 6.1 Hz) and a quartet at τ 6.23 (J=(−)11.2 and 10.2 Hz) respectively. An AB-type quartet at τ 6.04 and 6.12 (J=(−)11.8 Hz) can be assigned to H_1 and $H_{1'}$. Among the three signals arising from H_3, H_4 and H_5 at low fields, the doublet at τ 4.98 (J=9.8 Hz) should be assigned to H_3; the doublet at τ 4.57 (J=9.8 and 9.4 Hz), to H_4, and the octet at τ 5.02 (J=9.4, 6.1 and 10.2 Hz), to H_5. A similar analysis of the spectrum of V in C_6D_6 gave the results shown in Tables 1 and 2. The J values determined from the two spectra agreed well with each other. A comparison of the J values obtained with those of I and II (see Table 2) confirmed that the pyranose ring of V has the 1C conformation, in which all the secondary acetoxyl groups are equatorial. 1,2-*O*-Benzylidene- (VIII)[8] and 1,2-*O*-ethylidene-3,4,5-tri-*O*-acetyl-α-L-sorbopyranoses (IX)[9] were also believed to be in the conformation (see Table 2).

The spectrum of an analogous derivative of D-fructose, 1,2-*O*-isopropylidene-3,4,5-tri-*O*-acetyl-β-D-fructopyranose (VI),[22] whose C_5-acetoxyl group is expected to be axial, was examined in $CDCl_3$; two quartets due to H_6 and $H_{6'}$ appeared at τ 5.92 (J=(−)13.2 and 1.3 Hz) and 6.22 (J=(−)13.2 and 1.9 Hz) respectively. The signals of H_1 and $H_{1'}$ coincide as a singlet as τ 6.06. The signals due to other ring protons are too complicated to be analyzed. The spectrum in C_6D_6 shows somewhat separated signals (Fig. 2). Double irradiation at the resonance center of H_6 and $H_{6'}$ at τ 6.53 and 6.22 caused a multiplet at τ 4.58 to collapse into a doublet (J=3.2 Hz). The multiplet is clearly assignable to H_5 (Fig. 2b). The remaining doublet and quartet, at τ 4.31 (J=10.4 Hz) and τ 4.46 (J=10.4 and 3.2 Hz), should be assigned to H_3 and H_4 respectively.

To confirm the assignment of the spectra of of VI, 1,2-*O*-isopropylidene-3-*O*-methyl-4,5-di-*O*-acetyl-β-D-fructopyranose (VII) was also studied. VII was prepared from 1,2:4,5-di-*O*-isopropylidene-3-*O*-methyl-β-D-fructopyranose[19] by hydrolysis with 60% acetic acid, followed by acetylation. The spectra of VII in $CDCl_3$ and in C_6D_6 are readily analyzed. Doublets at τ 6.45 in $CDCl_3$ and at τ 6.43 in C_6D_6 (J=10.0 Hz) due to H_3; the quartets at τ 4.79 in $CDCl_3$ and τ 4.41 in C_6D_6 (J=10.0 and 3.4 Hz) due to H_4, and the octets at τ 4.70 in $CDCl_3$ and τ 4.52 in C_6D_6 to H_5 are quite distinct. The J values obtained ($J_{3,4}$=10.0—10.4 and $J_{4,5}$=3.2—3.4 Hz) from VI and VII agreed well with those obtained from III and IV, which have been established to adopt the 1C conformation.[16] The lower-field part of C_6-methylene proton signals [VI, 5.92 ($CDCl_3$) and 6.22 (C_6D_6); VII, 5.95 ($CDCl_3$) and 6.25 (C_6D_6)]

21) For example, see S. Sternhell, *Rev. Pure and Appl. Chem.*, **14**, 15 (1964).
22) E. Fisher and H. Noth, *Ber.*, **51**, 339 (1918).

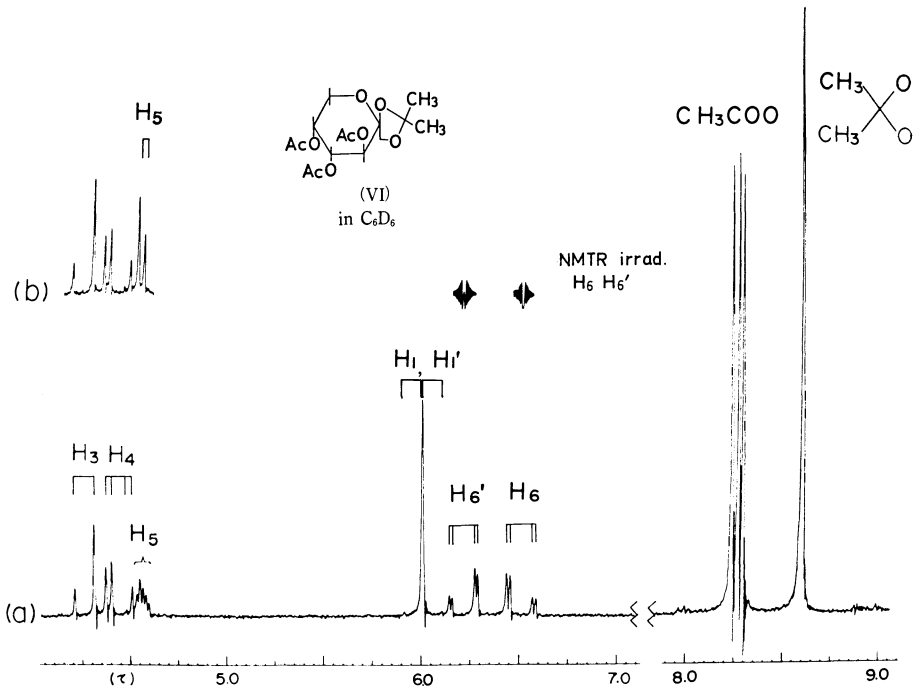

Fig. 2. PMR spectra of VI in C_6D_6 at 100 MHz.
(a) Normal spectrum (b) PMDR spectrum

can be assigned to the axial protons ($H_{6'}$) although the assignment does not obey the general rule[23] that the signal of an axial proton of a pyranose ring appears at a higher field than does that of an equatorial proton. The fact is accounted for by the long-range shielding effects of the acetoxyl group at C_5 in the *trans*-diaxial relation to $H_{6'}$.

The above-mentioned facts, that the pyranose rings of the compounds V—VII adopt 1C conformations, show that the introduction of a 1,2-*O*-isopropylidene ring causes no changes in the stable 1C conformation of the parent pyranose ring.[24] It is noteworthy that no such type B compounds such as β-anomer of V, are formed. This can be attributed to the fact that the 1,2-*O*-isopropylidene ring orients the pyranose ring in the same direction as does the influence of the anomeric effect of a methoxyl group as has been reported in the case of L-sorbofuranose.[3] The type B compounds, if they are formed, might exist in an unstable Cl chair or as a mixture of 1C and Cl forms similar to the case of methyl 1,3,4,5-tetra-*O*-acetyl-β-L-sorbopyranoside.[16]

ii) 1,3-O-Isopropylidene Compounds (Types C and D). Ethyl 1,3-*O*-isopropylidene-4,5-di-*O*-acetyl-α-L-sorbopyranoside (X) was prepared from the acetonation of ethyl α-L-sorbopyranoside,[21] followed by acetylation. The spectrum of X in $CDCl_3$ is somewhat complicated as a result of the overlapping of the signals. The signals of the methylene protons of the *O*-ethyl group constitute the A_2 part of an A_2X_3 system,[25] which partially overlaps with the higher field part of the C_1-methylene proton signals, H_3, H_6, and $H_{6'}$. The ring protons display a well resolved pattern and could be easily analyzed (Fig. 3). The J values obtained from the ring proton signals similar to those of I, II, and V show that the pyranose ring of X should have the 1C chair form. Therefore, X was confirmed to exist as a stable conformation of a *trans*-decalin type. The analogous compounds, methyl 1,3-*O*-benzylidene-(XI)[8] and 1,3-*O*-ethylidene-α-L-sorbopyranosides[9] (XII) also have conformation similar to that of X, judging from their J values. Therefore, the easy formation of 1,3-*O*-benzylidene- or 1,3-ethylidene-α-L-sorbopyranose from the acetalation of L-sorbose is reasonable. It is exceptionsl that no 1,3-*O*-isopropylidene-α-L-sorbopyranose is detected from the acetonation; its absence is probably responsible for the high instability of an axial methyl

23) L. M. Jackman, "Application of Nuclear Magnetic Resonance Spectroscopy in Organic Chemistry," Pergamon Press, London (1959), p. 115.

24) a) J. C. Jochims, G. Taigel, A. Seelinger, P. Lutz and H. E. Driesen, *Tetrahedron Letters*, **1967**, 4363; b) I. Listowsky, S. Englard and G. Avigad, *Carbohyd. Res.*, **2**, 261 (1966).

25) The complicated signal results from the hindrance of the free rotation of the ethyl group around the O-C bond; see Ref. 16.

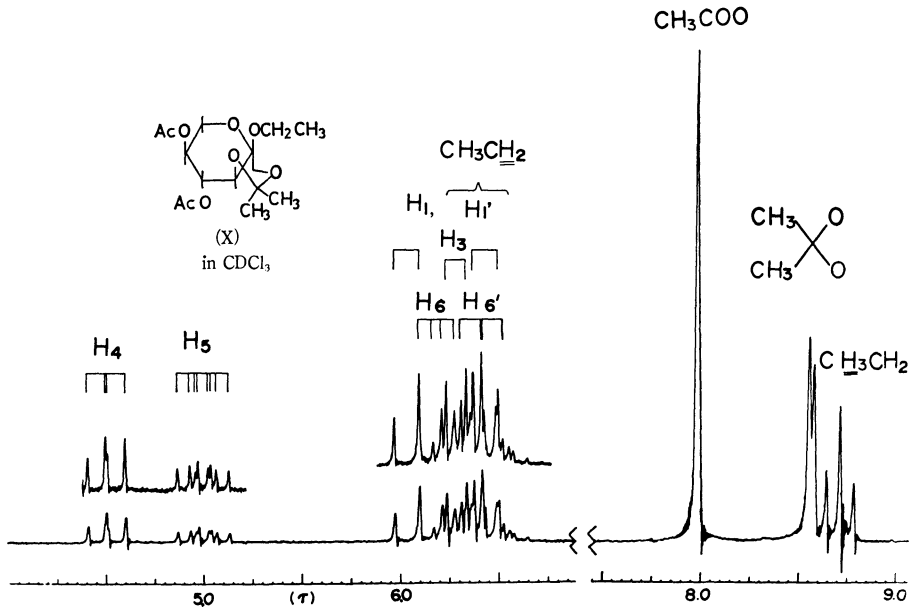

Fig. 3. PMR spectrum of X in $CDCl_3$ at 100 MHz.

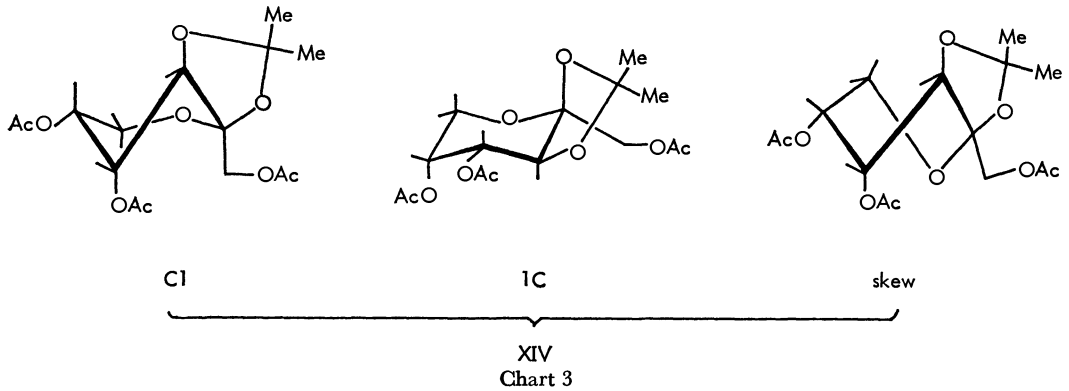

XIV
Chart 3

group at the 2-position of 1,3-dioxane.[26] This is known as the Brown-Brewster-Schechter rule.[27]

The type D compounds, the β-anomers of X—XII, have not been detected from the acetalations.[2,4,7-9] Their absence results from their stereochemical instabilities. For instance, an examination of the Dreiding models indicates that they must be in an unstable conformation of a *cis*-decalin type and of the Cl chair form. Our recent studies[2] have supported this suggestion: the pyranose ring of 1,3-*O*-benzylidene-2,4,5-tri-*O*-acetyl-β-L-sorbopyranose (XIII) has been concluded to have the conformation indicated by the models.

iii) 2,3-O-Isopropylidene Compound (Type E). The spectrum of 2,3-*O*-isopropylidene-1,4,5-tri-*O*-acetyl-β-D-fructopyranose (XIV) in $CDCl_3$ exhibits well-separated patterns; the signals were readily assigned as is shown in Fig. 4. Double irradiation at the resonance center of H_4 at τ 4.42 caused the collapse of the doublet assignable to H_3 at τ 5.88 (J=3.8 Hz) into a singlet, and that of the quartet due to H_6 at τ 6.03 (J=0.5, 5.3 and 12.3 Hz) into a sharp quartet (J=5.3 and 12.3 Hz) (Fig. 4b). Therefore, the presence of a long-range coupling between H_4 and H_6 was established.

Rees *et al.*[12] pointed out that 1,2-*O*-isopropylidene-3,4,6-tri-*O*-acetyl-α-D-glucopyranose (XV), the corresponding aldose derivative, has a distorted, flattened Cl chair conformation. Its reported J values are recorded in Table 2. The $J_{3,4}$ and $J_{4,5}$ values in XIV are not greatly different from corresponding values, $J_{2,3}$ and $J_{3,4}$, of XV.[13] Therefore, the pyranose ring of XIV seems to have a distorted, flattened 1C form. The values of the coupling constants, $J_{5,6}$ and $J_{5,6'}$, in the 1C

26) E. L. Eliel and Sr. M. C. Knoeber, *J. Am. Chem. Soc.*, **90**, 3444 (1968).

27) H. C. Brown, J. H. Brewster, and H. Schechter, *ibid.*, **76**, 467 (1954).

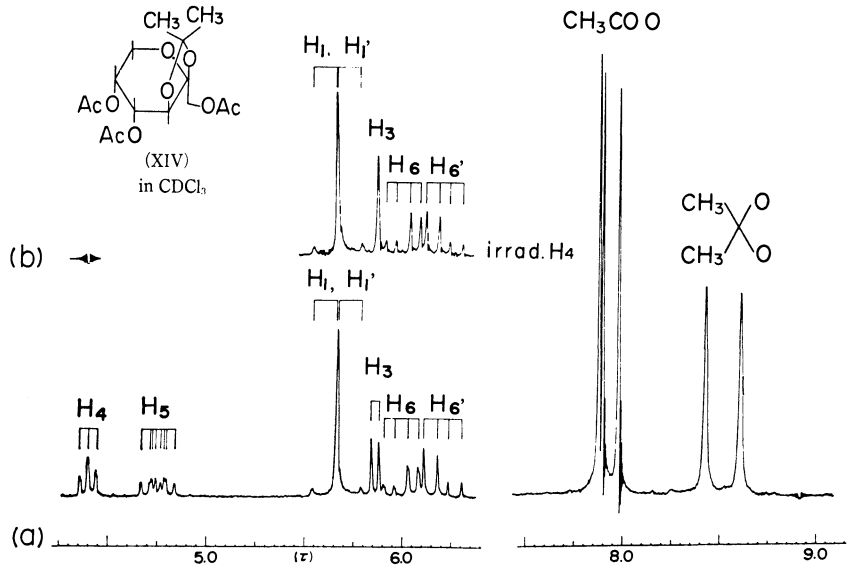

Fig. 4. PMR spectra of XIV in $CDCl_3$ at 100 MHz.
(a) Normal spectrum (b) PMDR spectrum

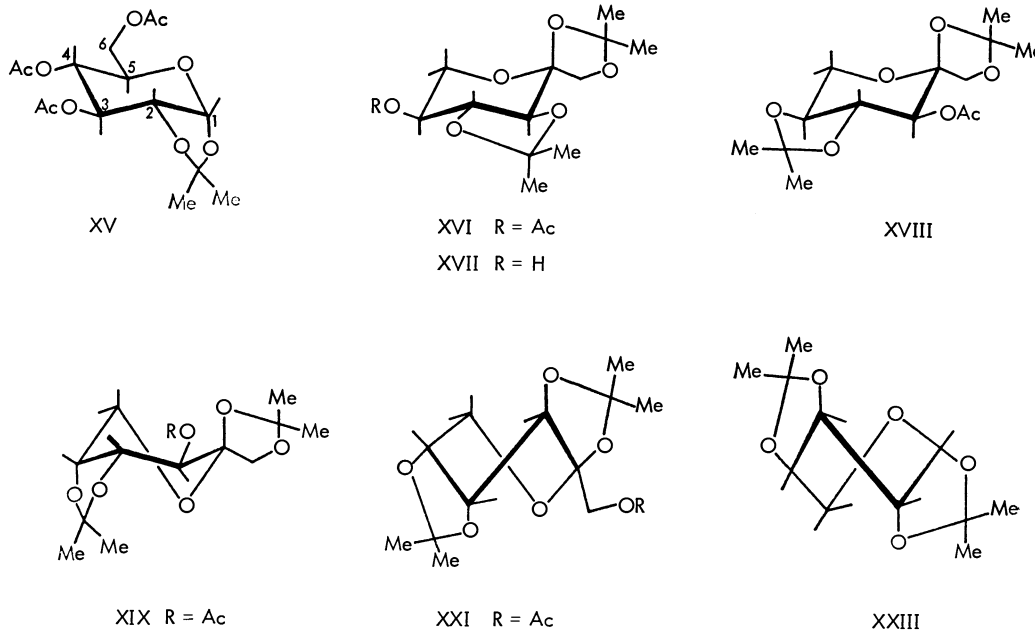

Chart 4

conformation can be expected to be about 2 Hz from the Karplus correlation,[28] since the H_5 is inevitably situated in the bisectional conformation between H_6 and $H_{6'}$. However, the values of $J_{5,6}$ (5.3 Hz) and $J_{5,6'}$ (6.8 Hz) deviate from the correlation in even a qualitative sense. Other possible skew conformations, among which one depicted in Chart 2 is the most probable, appear highly unlikely judging from the comparison of J values in 2,3 : 4,5-di-*O*-isopropylidene-β-D-fructopyranose (XXII),[10] which adopts a skew conformation, as will be described below. Therefore, the distorted Cl conformation is most likely for the pyranose ring of XIV. The presence of the long-range coupling between H_4 and H_6 also sup-

28) M. Karplus, *J. Chem. Phys.*, **30**, 11 (1959); *J. Am. Chem. Soc.*, **85**, 2870 (1963).

ported this conclusion, because it seems that H_4 and H_6 should have an equatorial conformation if we apply the "W-letter" rule.[21] As the $J_{5,6}$ value is smaller than the normal $J_{a,a}$ value, and since $J_{5,6'}$ is larger than $J_{a,e}$, the pyranose ring must be flattened. This conformation of XIV is fixed in a temperature range from 37 to 150°C in DMF-d_7 because the J values are unchanged in this temperature range.

The results show that the fused 2,3-*O*-isopropylidene group locked the pyranose ring in an unexpected direction. This is the reason why 2,3-*O*-isopropylidene-α-L-sorbopyranose is not detected in the acetonation of L-sorbose. If this compound were formed, it should adopt an unstable Cl conformation because of the ring strain of the 2,3-*O*-acetal. This unfavorable steric requirement must inhibit its formation.

Diacetonated Derivatives. It has been pointed out[29] that, in order to form the *O*-isopropylidene derivative of a vicinal glycol group of a pyranose a decrease in the projected angle in the chair form imposes little strain on the *cis*-configuration, whereas the acetonation of *trans*-glycol with acetone is impossible since a decrease in the projected angle of *trans*-one would cause severe distortion. Thus, a *trans*-fused 1,3-dioxolane formed from the acetonation with acetone dimethylketal is expected to be formed without such a distortion, that is, it should deform the pyranose ring to which it attached only slightly. We investigated 1,2 : 3,4-di-*O*-isopropylidene-α-L-sorbopyranose (XVII),[4c] its acetate (XVI),[4c] and 1,2 : 4,5-di-*O*-isopropylidene-3-*O*-acetyl-α-L-sorbopyranose (XVIII).[4c]

The spectrum of XVI in $CDCl_3$, shown in Fig. 5 exhibits well-separated signals, which were easily assigned. The assignment was further confirmed by the aid of solvent shifts in C_6D_6 and by comparison with the spectra of XVII in $CDCl_3$ and in C_6D_6. In the case of XVIII, the spectrum in $CDCl_3$ shown in Fig. 6 was rather complicated. Double irradiation at the resonance center of a doublet at τ 4.84 (J=10.4 Hz) due to H_3 caused the collapse of a quartet at τ 6.13 (J=10.4 and 8.8 Hz) assignable to H_4 into the doublet (J=8.8 Hz) (Fig. 6b). The assignment of the remaining signals are quite obvious, as is shown. The J values of XVI—XVIII for ring protons ($J_{3,4}$=9.5—10.4, $J_{4,5}$=8.8—10.0, $J_{5,6}$=5.3—5.5 and $J_{5,6'}$=9.7—10.0 Hz) indicate that their ring conformations are slightly distorted 1C forms compared with those of I, II, and V. In these conformations, and 1,3-dioxolane at the 3,4- and 4,5-positions must adopt half-chair conformations.

The conformation of a pyranose ring is not very much distorted by the introduction of a *trans*-acetal group, but it is much influenced by a *cis*-acetal group, as is confirmed below. In the spectrum of 3-*O*-acetyl-1,2:4,5-di-*O*-isopropylidene-β-D-fructopyranose (XIX)[23] in $CDCl_3$, an AB-type quartet

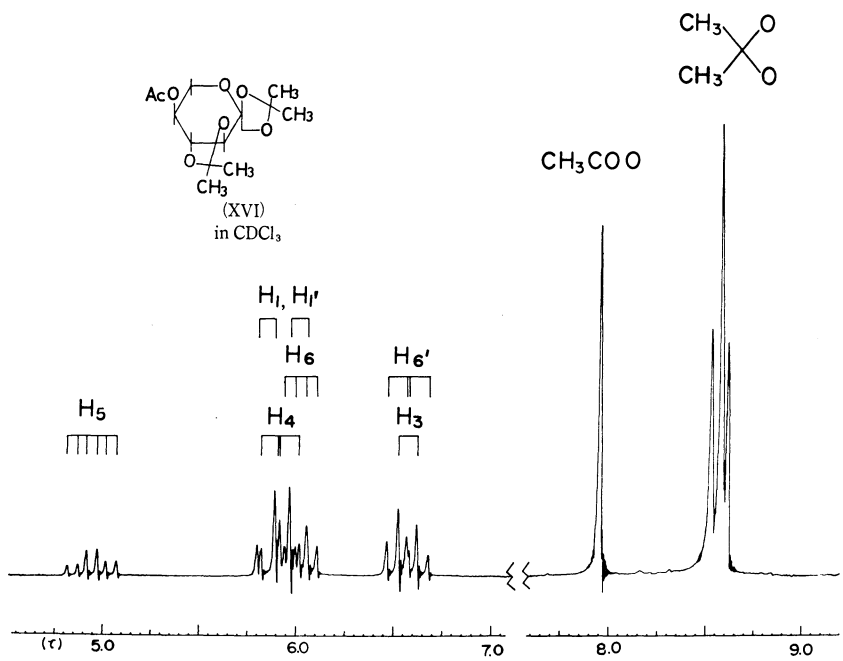

Fig. 5. PMR spectrum of XVI in $CDCl_3$ at 100 MHz.

29) a) S. J. Angyal and C. G. MacDonald, *J. Chem. Soc.*, **1952**, 686; b) R. U. Lemieux, "Molecular Rearrangements," ed. by P. De Mayo, Interscience Publishers, New York, N. Y. (1964), Chapter 12.

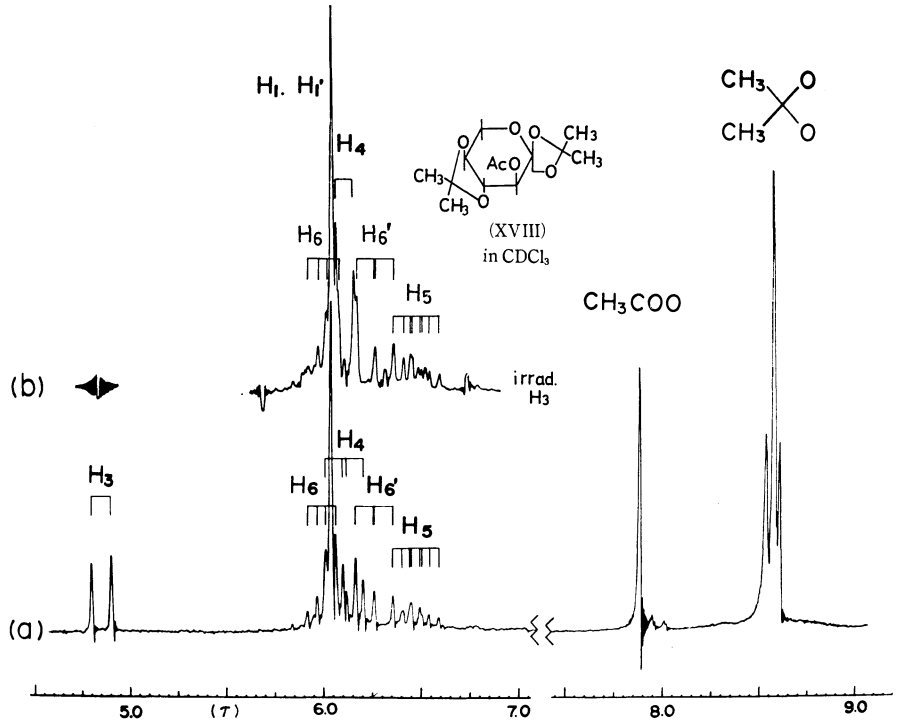

Fig. 6. PMR spectra of XVIII in $CDCl_3$ at 100 MHz.
(a) Normal spectrum (b) PMDR spectrum

assignable to H_1 and $H_{1'}$ appears at τ 6.07 and 6.17 (J=9.1 Hz). The signal due to H_3 is observed at τ 4.90 as a doublet (J=7.8 Hz). The signals of other ring protons are too close to each other to analyze in a simple way. In C_6D_6 and in C_5D_5N, the signals of the ring protons were more separated, although some of them appear as second-order patterns. The spectrum in the last solvent was assigned as is shown in Fig. 7a. Double irradiation at the resonance center of the double at τ 4.56 (J=7.8 Hz) due to H_3 causes the collapse of the multiplet assignable to H_4 around τ 5.52 into a doublet (J=5.0 Hz) (Fig. 7b). Even in these solvents, the signals due to H_5, H_6, and $H_{6'}$ are too close to each other to analyze. The analysis of the spectrum of the deacetyl derivative of XIX (XX)[10a,30] gave similar results. Judging from the J values ($J_{3,4}$=7.8 and $J_{4,5}$=5.0 Hz), the projected angles of $\phi_{3,4}$ seems to decrease, and those of $\phi_{4,5}$ to increase, as compared to the case of VI. Therefore, the conformation of the pyranose ring is more distorted by a *cis*-fused dioxolane than by a *trans*-fused one, as is to be expected.

Finally, we investigated the conformation of 2,3 : 4,5-di-*O*-isopropylidene-β-D-fructopyranose (XXII)[10] and its acetate (XXI).[10] Cone *et al.*[15]

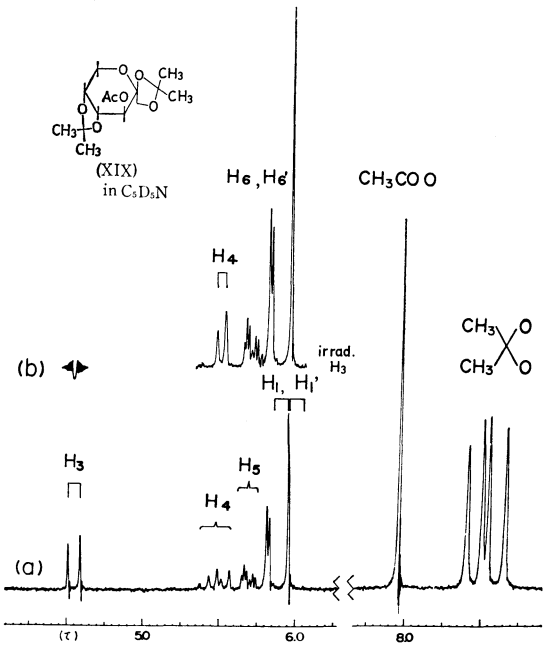

Fig. 7. PMR spectra of XIX in C_5H_5N at 100 MHz.
(a) Normal spectrum (b) PMDR spectrum

30) a) J. C. Irvine and A. Hynd, *J. Chem. Soc.*, **95**, 1220 (1909); b) J. C. Irvine and C. S. Garrett, *ibid.*, **97**, 1277 (1910); c) J. C. Irvine and J. Patterson, *ibid.*, **121**, 2146 (1922); d) H. Ohle, *Ber.*, **60**, 1168 (1927).

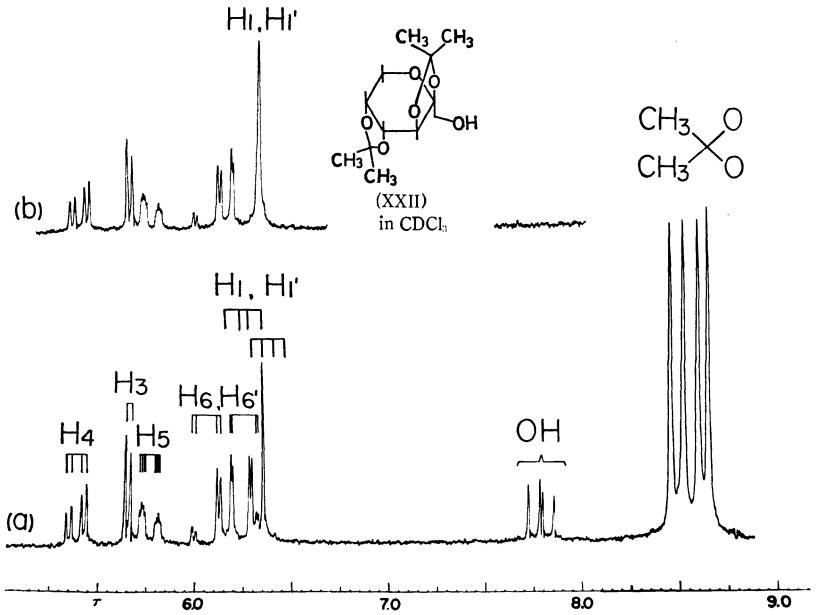

Fig. 8. PMR spectra of XXII in $CDCl_3$ at 100 MHz.
(a) Normal spectrum (b) PMDR spectrum

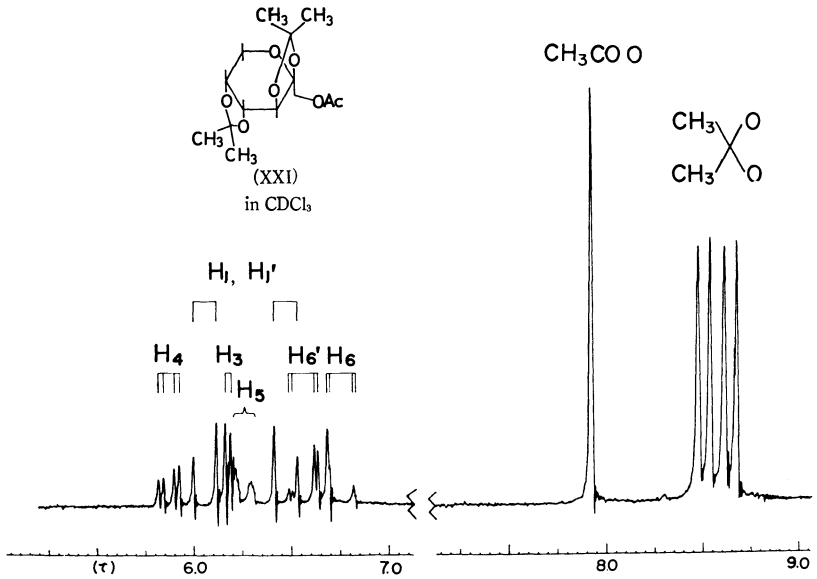

Fig. 9. PMR spectrum of XXI in $CDCl_3$ at 100 MHz.

reported that 1,2:3,4-di-*O*-isopropylidene-α-D-galacto- and β-L-arabinopyranose (XXIII) adopt a skew conformation. Our finding that XIV, the partially deacetonated derivative of XXII, adopts the Cl conformation reasonably led us to anticipate that the pyranose rings of XXI and XXII might adopt a skew conformation, much as the acetonated aldoses have the same arabino-configuration as XXI and XXII. The signals due to the ring protons of XXII are well-separated and are assigned as is shown in Fig. 8a, where the signals due to the $C\underline{H}_2O\underline{H}$ group appear as an ABX-type signal, but the addition of deuterium oxide to the solution examined changed the signal into an AB type quartet (J=12.0 Hz) (Fig. 8b). From the ABX pattern,[18] $J_{1,1'}$, $J_{1,OH}$, and $J_{1',OH}$ were calculated to be 12.0, 3.8, and 9.2 Hz respectively.

The infrared spectrum of XXII in a dilute solution of carbon tetrachloride shows the presence of two OH bands at 3518 and 3640 cm^{-1}; the

distances between OH–O have been calculated[31] to be about 1.5 and 2.34 Å respectively. The close proximity between OH–O (1.5 Å) gave valuable information concerning the conformation; an examination of the Dreiding models indicates that the intramolecular hydrogen-bonding of this OH toward C_4–O in the skew conformation depicted in Chart 2, and in other conformations, it is difficult to form the hydrogen-bonding. The latter hydrogen-bonding may exist between C_1–OH and ring-O or C_2–O in that conformation.

The spectrum of XXI in $CDCl_3$ exhibits well-separated signals and was easily analyzed; the results are shown in Fig. 9. The coupling constants obtained from the spectra of both XXI and XXII are in good agreement with those reported for those of XXIII[15] (see Table 2). Thus, the IR spectrum of XXII and the PMR spectra of XXI and XXII are uniquely compatible with the skew conformation.

In conclusion, the compounds of the types A and C have the same 1C conformation as α-L-sorbopyranose. On the other hand, the compounds of the types B, D, and E compounds have distorted conformations. Therefore, the formation of the type A and C compounds at the initial stages of the acetalations of L-sorbose[2,4,5,7–9] is reasonable. We have also established that the conformation of a pyranose is much more influenced by the introduction of a *cis*-fused acetal ring than by that of a *trans*-fused one. This fact experimentally supported Angyal's anticipation[29] of the difficult acetalation of the *trans*-glycol of a pyranose. The easy formation of the type E compound XXII from the acetalation of D-fructose[10] is very interesting, although the reasonable type A compound XX[30] appeared as the initial product. This fact can be explained in the light of the present finding in terms of the distortion of XX, which causes C_3–OH to be so close to C_2–O as to enable them to form the 1,3-dioxolane at the 2,3-position, unlike as in the parent D-fructopyranose.

The authors are deeply grateful to Professor Toshihiko Okamoto, the University of Tokyo, and Dr. Ken'ichi Takeda, Director of this laboratory, for their encouragement.

31) The distances were calculated according to Y. Matsui M. Takasuka and T. Kubota, *Ann. Rept. Shionogi Res. Lab.*, **15**, 125 (1965), and T. Kubota, M. Takasuka and Y. Matsui, *ibid.*, **16**, 63 (1966).

BULLETIN OF THE CHEMICAL SOCIETY OF JAPAN VOL. 42 2648—2655 (1969)

The Acetalation Mechanism of L-Sorbose[1-3]

Takashi MAEDA, Yoshiyuki MIICHI and Kanji TOKUYAMA

Shionogi Research Laboratory, Shionogi & Co., Ltd., Fukushima-ku, Osaka

(Received February 19, 1969)

The following reaction mechanism of the acetonation of L-sorbose is proposed:

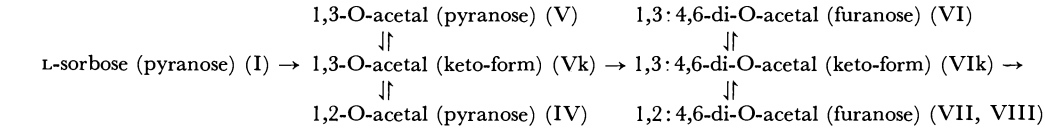

2,3:4,6-di-*O*-acetal (furanose) (II). The pyranose-to-furanose ring conversion (I→II) proceeds *via* the keto-form intermediates Vk and VIk; VIk is formed by the preferable attack of acetonating reagents on the primary hydroxyl group at the C_6 of Vk followed by cyclization with the hydroxyl group at C_4. The isolation of such keto-form intermediates as were successfully obtained from the acetalations of 1-*O*-methyl- (X) and 1,6-di-*O*-methyl-L-sorboses (XVIII) gave strong support to the above mechanism. This acetonation mechanism can also be used in the other acetalations of I; however, in the case of the benzylidenation there is a possibility that the reaction might be *via* the pathway of 1,3-*O*-acetal (pyranose)⇄1,3-*O*-acetal (furanose) (Vb)→1,3:4,6-di-*O*-acetal (furanose).

The acetonation of L-sorbose (I) is used to prepare a synthetic intermediate, 2,3:4,6-di-*O*-isopropylidene-α-L-sorbofuranose (II), for L-ascorbic acid production.[4] However, this process has not yet been subjected to systematic studies despite its relatively lower yield and longer reaction period compared with other process of L-ascorbic acid production. Without any detailed evidence, it has long been believed that the mechanism of the acetonation is that I exists as α-L-sorbofuranose, which is converted into II *via* 2,3-*O*-isopropylidene-α-L-sorbofuranose (III) (mechanism 1).[5] Recently, however, I was confirmed to exist as α-L-sorbopyranose in the 1C conformation by the analyses of the PMR spectra[6] and of the optical rotatory dispersion.[7] The pyranose-to-furanose equilibrium of I was concluded to shift far to the left, as in D-glucose and D-xylose, becuase of its xylo-configuration.[8] Accordingly, the mechanism 1 is unlikely.

A correct mechanism was necessary to improve the reaction conditions of the acetonation. We have proposed previously that the process of the acetonation with acetone in the presence of sulfuric acid should be *via* the pathway of I→1,2-*O*-isopropylidene-α-L-sorbopyranose (IV)→$(IV)_2$→II⇆III (mechanism 2).[9]

Our recent works[10,11] have shown that the acetonation with acetals of acetone affords many kinds of acetonated compounds including the above-described derivatives under controlled conditions. These compounds were 1,3:4,6-di-*O*-isopropylidene-β-L-sorbofuranose (VI) and 1,2:4,6-di-*O*-isopropylidene-α- (VII) and β-L-sorbofuranoses (VIII). Besides these types of compounds, 1,3-*O*-ethylidene-α-L-sorbopyranose (Ve)[12] and 1,3-*O*-benzylidene-

1) Sorboses, Part XVII, for Part XVI see Ref. 3.

2) Some of the results of this paper have been presented in a preliminary form in T. Maeda and K. Tokuyama, *Tetrahedron Letters*, **1968**, 3079, and at the 156th National Meeting of the American Chemical Society, Atlantic City, N. J., U. S. A., September, 1968.

3) T. Maeda, K. Tori, S. Satoh and K. Tokuyama, This Bulletin, **42**, 2635 (1969).

4) T. Reichstein and A. Grüssner, *Helv. Chim. Acta*, **17**, 311 (1934).

5) For example, see D. C. DeJoungh and K. Biemann, *J. Am. Chem. Soc.*, **86**, 67 (1964).

6) J. C. Jochims, G. Taigel, A. Seelinger, P. Lutz and H. E. Driesen, *Tetrahedron Letters*, **1967**, 4363.

7) I. Listowsky, S. Englard and G. Avigad, *Carbohyd. Res.*, **2**, 261 (1966).

8) a) R. U. Lemieux, "Molecular Rearrangements," ed. by P. de Mayo, Interscience Pub., New York (1964), Chapter 12; b) S. J. Angyal, "Conformational Analsis," ed. by E. L. Eliel, N. A. Allinger, S. J. Angyal and G. A. Morrison, John Wiley & Sons, New York (1965), Chapter 6.

9) K. Tokuyama, E. Honda and N. Hōki, *J. Org. Chem.*, **29**, 133 (1964).

10) K. Tokuyama and E. Honda, This Bulletin, **37**, 591 (1964).

11) T. Maeda, *ibid.*, **40**, 2122 (1967).

12) T. Maeda, M. Kiyokawa and K. Tokuyama, *ibid.*, **42**, 492 (1969).

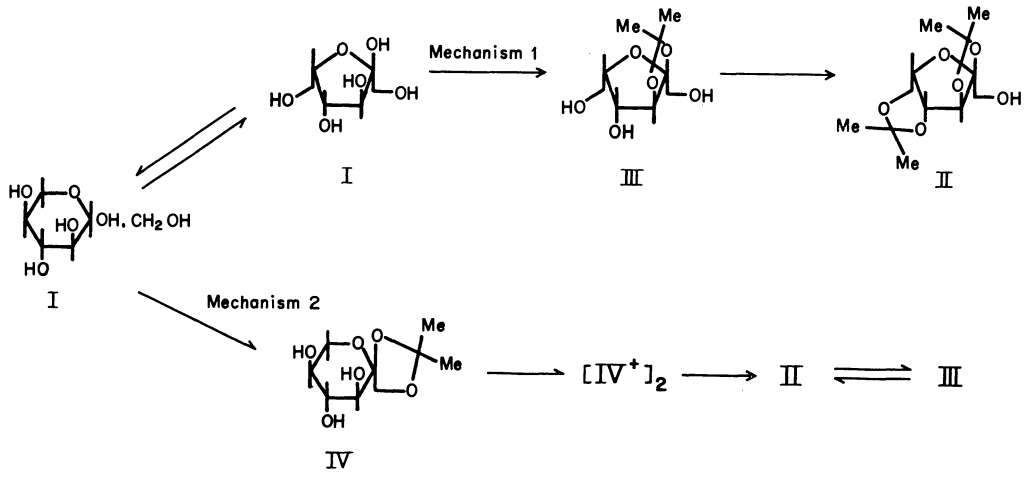

Chart 1

α-L-sorbopyranose (Vb)[13] were obtained from the ethylidenation and the benzylidenation reactions respectively.[14] Ohle[15] reported an unknown diacetonated compound; we identified it as VI by acetonating I with acetone in the presence of cupric sulfate. Patil and Bose[16] reinvestigated his reaction and isolated this unknown product. They also reported the formation of III, VII and 1,2-*O*-isopropylidene-α-L-sorbofuranose (IX).

The mechanism 2 could not explain the formation of the above-described reaction products. It was, then, found necessary to alter it, although the initial formation of IV has been unequivocally established.[9] The present paper presents a novel reaction mechanism of the acetonation, generally the acetalation, of I, a mechanism which accounts for the yielding of new intermediate products.

Results and Discussion

When slightly acidic conditions were used, the acetonation of I afforded II, VI, VII, and VIII.[10,11] On the other hand, mostly II was obtained under highly acidic conditions.[4,9] The acidic treatment of VI in the absence of acetonating reagents easily gave II as the major product and VII and VIII as the minor products, while such a treatment of VII or VIII gave II to only a limited extent. Therefore, the acetonation process must be *via* the pathway of I→(IV⇄1,3-*O*-isopropylidene-α-L-sorbopyranose (V))→VI→II⇄III. This pathway agreed well with the results of the ethylidenation[12] and the benzylidenation.[13] Although V was not obtained, the formation of Ve and Vb from other acetalations suggested its possible presence.

Formation of Monoacetonated Pyranoses (IV and V). In a preceding paper,[3] we confirmed the conformational role in the stability of the acetonated sorbopyranoses. The results can be summarized as follows: (i) the formation of β-anomers of IV and V is inhibited by their unfavorable steric factors, and (ii) that of 2,3-*O*-isopropylidene-α-L-sorbopyranose can be ruled out because of the strain of the 2,3-*O*-isopropylidene ring, which causes the pyranose ring conformation to be changed from the stable 1C chair to the unfavorable C1 form. Therefore, only IV and V can be formed.

The alcohol structure has a remarkable influence upon the acetal formation in the markedly decreasing order of primary→secondary→tertiary.[17] Among the five hydroxyl groups of the α-pyranose form of I in the 1C conformation, the axial hydroxyl group at C_2 is tertiary and is sterically hindered with axial hydrogens at C_4 and C_6; the three equatorial hydroxyl groups at C_3, C_4 and C_5 are considered to be hindered because of the steric over-crowding. The primary hydroxyl at C_1, which is sterically least hindered, is the most reactive in acetal formation. The conjugate acid of acetone or acetals of acetone reacts with the primary hydroxyl to afford a protonated form, XXI, as an intermediate; this may then be converted into stable

13) T. Maeda, M. Kimoto, S. Wakahara and K. Tokuyama, *ibid.*, **42**, 1686 (1969); *ibid.*, **42**, 2021 (1969).

14) The suffixes e and b used here mean the ethylidenated and benzylidenated analogs, respectively, corresponding to the acetonated analogs.

15) H. Ohle, *Ber.*, **71**, 562 (1938).

16) J. R. Patil and J. L. Bose, a) *J. Indian Chem. Soc.*, **43**, 161 (1966); b) *Indian J. Chem.*, **5**, 598 (1967).

17) R. H. Adkins, *J. Am. Chem. Soc.*, **49**, 2517 (1927); **55**, 299 (1933); **56**, 442 (1934).

IV and V by two possible cyclic acetal formations with hydroxyl groups at C_2 and C_3 respectively. Therefore, the formation of IV and V at the initial stages is quite reasonable. Two compounds of the type V, Ve and Vb, were easily obtained from the ethylidenation[12] and the benzylidenation,[13] however, V itself could not be isolated. This must result from the instability of the axial methyl group at the 2-position of 1,3-dioxane of V, since one of two methyl groups is inevitably axial in the chair conformation of the six-membered *O*-isopropylidene group.[18,19] Of course, the 1,3-*O*-isopropylidene derivative was easily prepared when the hydroxyl at C_2 was blocked.[3] The predominant attack of acetalating agents on the primary hydroxyl groups sterically least hindered accords well with the results of the acetalations of D-glucose and D-galactose,[20-22] which yield 4,6-*O*-acetalated compounds as the initial products. In both acetalations, the primary hydroxyl groups at C_6 are initially attacked by aldehydes or their conjugate acids.

Ring Conversion of Monoacetonated Pyranoses to Diacetonated Furanoses. The ring conversion of the pyranoses (IV and V) to the furanose (VI) is the most important step in the acetonation. We can assume the presence of a keto-form intermediate, Vk, which is an equilibrium intermediate between IV and V. The primary hydroxyl group at C_6 of Vk must be most reactive for the same reason as in the case of the α-pyranose form of I. The keto-form intermediate, Vk, reacts with acetonating reagents to afford XXII, which is then converted into VIk, the keto-form of VI, by 1,3-dioxane ring formation at the 4,6-position. Thus-formed VIk is isolated as the furanose form, VI. In this step, another intermediate, XXIII, with 1,3-dioxolane might exist, since it is well known, in the acid-catalyzed acetalations of glycerol, that the 1,3-dioxolanes form rapidly in the initial kinetic phase and that the 1,3-dioxanes are predominant at equilibrium.[23]

This idea that the pyranose-to-furanose conversion can occur through keto-form intermediates was supported by the following evidence. 1-*O*-Methyl-L-sorbose (X)[24] was prepared from 1-*O*-methyl-2,3 : 4,6-di-*O*-isopropylidene-α-L-sorbofuranose (XI)[25] by partial deacetonation with 60% acetic acid to give 1-*O*-methyl-2,3-*O*-isopropylidene-α-L-sorbofuranose (XII),[25] followed by further deacetonation with 1N hydrochloric acid at room temperature. As the acetylation of X gave 1-*O*-methyl-3,4,5-tri-*O*-acetyl-α-L-sorbopyranose (XIII) exclusively, X adopts to a pyranose form. The acetonation of X gave 1-*O*-methyl-3,4: 5,6-di-*O*-isopropylidene-L-sorbose (XIV). The IR spectrum (liquid film) of XIV showed an absorption band at 1738 cm^{-1} due to a carbonyl group. The reduction with lithium aluminum hydride in ether yielded an alcohol, which was isolated as a benzoate (XV). The structure of XV was identified as 5-*O*-benzoyl-6-*O*-methyl-1,2:3,4-di-*O*-isopropylidene-D-glucitol; it was synthesized from 6-*O*-benzoyl-1,2:3,4-di-*O*-isopropylidene-D-glucitol (XVI)[26] by the scheme as shown in Chart 2. Therefore, the structure of XIV was established. The further acetonation of X gave XI at the expense of XIV. The pyranose-to-furanose conversion (X→XI) apparently occurred through the keto-form intermediate (XIV). This result unequivocally supported the idea that the pyranose-to-furanose conversion (IV, V→VI) in the acetonation of I can occur through the keto-form intermediates.

1,6-Di-*O*-methyl-L-sorbose (XVIII) was prepared from XII *via* 1,6-di-*O*-methyl-2,3-*O*-isopropylidene-α-L-sorbofuranose (XVII) by partial methylation with methyl iodide in the presence of silver oxide, followed by the deacetonation of the 2,3-*O*-isopropylidene group with 1N hydrochloric acid at room temperature. The acetalation of XVIII was expected to afford the derivative of a furanose form, since XVIII can not adopt a pyranose form. The benzylidenation of XVIII with benzaldehyde unexpectedly gave 1,6-di-*O*-methyl-3,5-*O*-benzylidene-L-sorbose (XIX), accompanied by other two monobenzylidenated derivatives.[27] The IR spectrum (Nujol mull) of XIX showed the existence of a band due to carbonyl at 1720 cm^{-1}. The PMR spectra of the acetate of XIX (XX) in $CDCl_3$ and in C_6D_6 showed a triplet at τ 4.55 ($J_{3,4}=J_{4,5}=1.8$ Hz) assignable to the signal of the proton at C_4 bearing acetoxyl group. These spectral data supported the proposed structure. The formation of XIX suggested that even XVIII reacted as a keto-form in the acetalation, and supported the above-described idea.

Formation of the Final Product, II. Thus-formed VIk can be converted into four furanoses, VI, VII, VIII, and II. It is quite natural to assume

18) H. C. Brown, J. H. Brewster and H. Schechter, *J. Am. Chem. Soc.*, **76**, 467 (1954).
19) E. L. Eliel and Sr. M. C. Knoeber, *ibid.*, **90**, 3444 (1968).
20) T. G. Bonner, E. J. Bourne and D. Lewis, *J. Chem. Soc.*, **1965**, 7453.
21) D. H. Ball, *ibid.*, **1958**, 7905.
22) Z. G. Gros and V. Deufleu, *Chem. Ind. (London)*, **1962**, 1502.
23) a) N. Baggett, J. M. Duxbury, A. B. Foster and J. M. Webber, *Carbohyd. Res.*, **2**, 216 (1966); b) N. Baggett, K. W. Buch, A. B. Foster and J. M. Webber, *J. Chem. Soc.*, **1965**, 3401.
24) J. C. Swoden and I. I. Mao, *J. Org. Chem.*, **25**, 1461 (1960).
25) K. Tokuyama and M. Katsuhara, This Bulletin, **39**, 2728 (1966).
26) H. Mizoiri, A. Sera and R. Goto, *ibid.*, **37**, 1023 (1964).
27) Their structures were not determined.

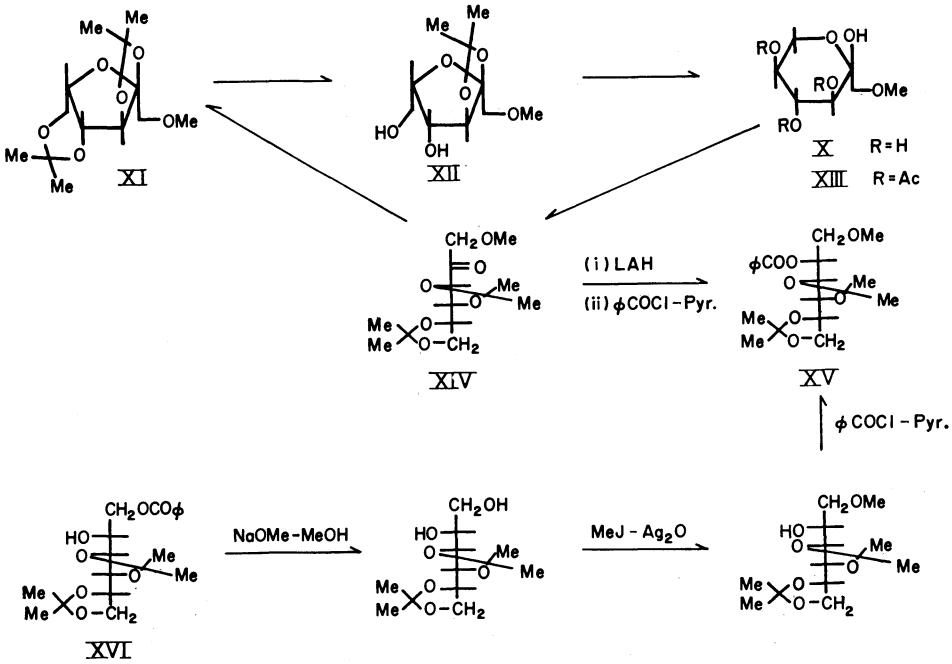

Chart 2

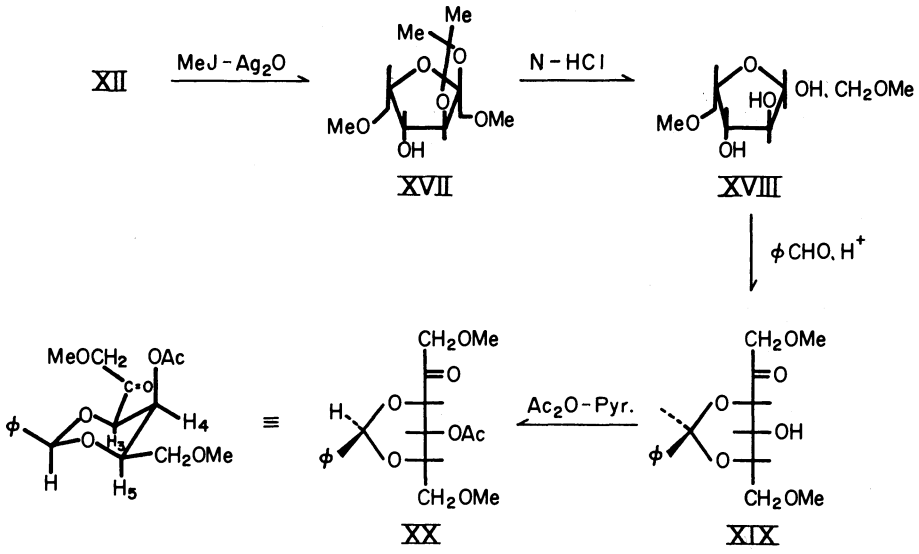

Chart 3

the existence of an equilibrium of furanoses, VII, VIII⇄VIk⇄VI, corresponding to that of pyranoses, IV⇄Vk⇄V. The stabilities of these diacetonated furanoses have been previously reported.[28] All these furanoses have a 4,6-*O*-isopropylidene group, which locks their furanose ring to the half-chair conformation of the C_3-*exo*-C_4-*endo* type. The 2,3-*O*-isopropylidene group of II and the 1,3-*O*-isopropylidene group of VI also lock the furanose ring in the same direction. Therefore, II and VI are more stable than the others. As Brown, Brewster, and Schechter pointed out,[18] a five-membered isopropylidene ring is more stable than a six-membered one. II is the most stable form among the diacetonated furanoses. Thus, VIk can be converted into II preferably.

As has been described above, it may be concluded

28) T. Maeda, K. Tori, S. Satoh and K. Tokuyama, This Bulletin, **41**, 2495 (1968).

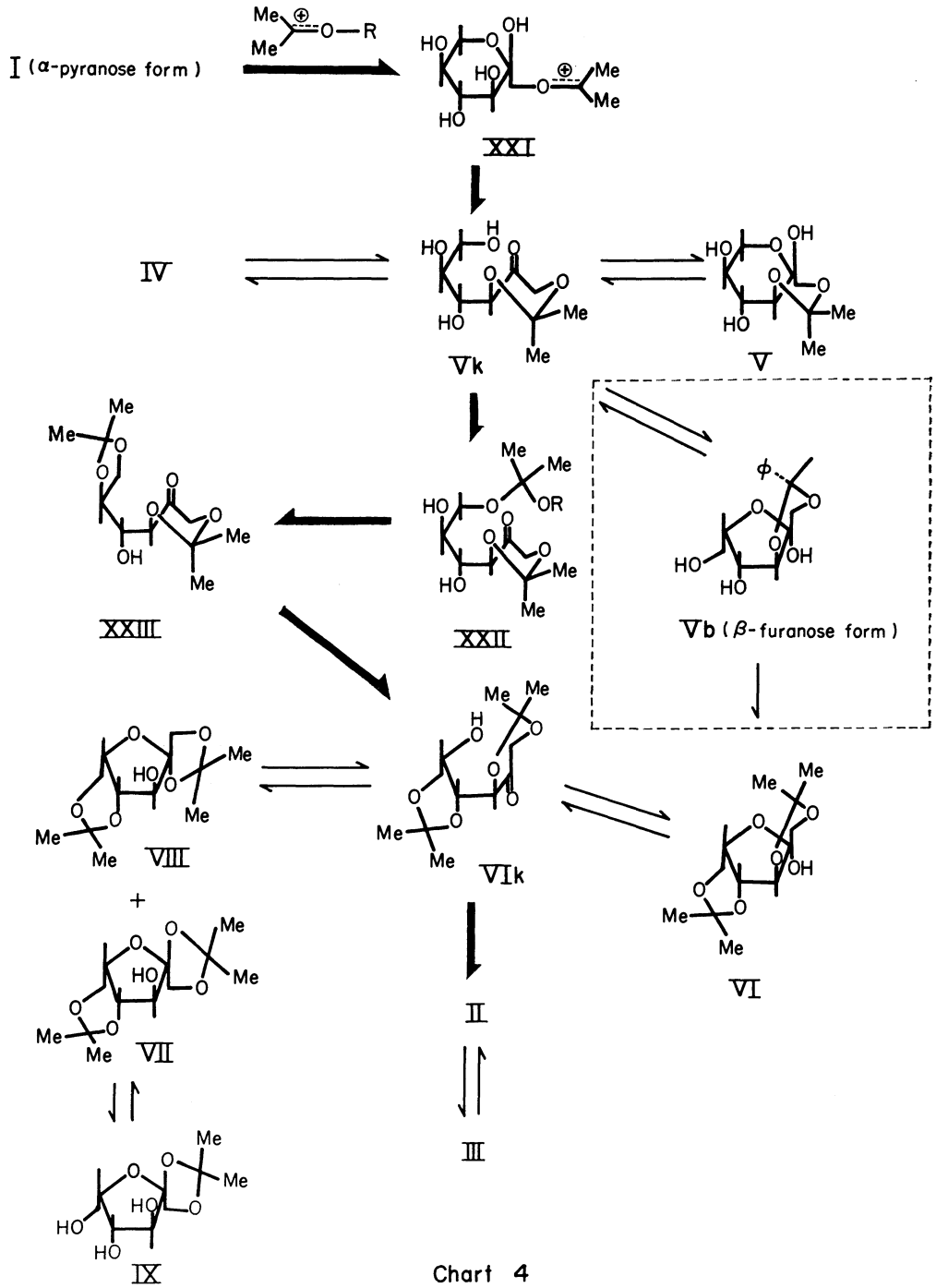

Chart 4

that the acetonation occurs *via* keto-form intermediates. The process of the acetonation proceeds *via* the pathway of

$$\begin{array}{cccc} & \text{IV} & & \text{VI} \\ & \downarrow\uparrow & & \downarrow\uparrow \\ \text{I} \rightarrow & \text{Vk} & \rightarrow \text{VIk} & \rightarrow \text{II}. \\ & \downarrow\uparrow & & \downarrow\uparrow \\ & \text{IV} & & \text{VII,VIII} \end{array}$$

The pathway is shown in detail in Chart 4, which includes minor pathways. The benzylidenation and the ethylidenation gave similar products under acidic conditions similar to those of the acetonation. Therefore, it may reasonably be concluded that the proposed mechanism for the acetonation can be generally applied to acetalations.

In the case of the benzylidenation,[13] the β-

furanose form of 1,3-*O*-benzylidene-L-sorbose (Vb) was found; the analyses of the PMR spectra and of the acetylation products of Vb clearly showed the existence of an equilibrium between the α-pyranose and the β-furanose forms.[13] The compound exists as the β-furanose form in a crystalline state and as an equilibrium mixture of the α-pyranose form, the keto-form and the β-furanose form in a solution. It is difficult to explain the preference of the β-furanose form of Vb only in the benzylidene derivative on the basis of the steric effect. Some additional polar factor of the 1,3-*O*-benzylidene ring must possibly be assumed,[13] since the acetate of the unstable β-pyranose form is abnormally obtained from the acetylation of Vb in the same proportion as that of the α-pyranose form. The existence of the β-furanose form of Vb suggests the possibility that the benzylidenation, proceeds exceptionally, *via* the β-furanose form of Vb.

We have shown that the process of the acetonation with acetone should be *via* the pathway of I→IV→$(IV)_2$→II⇄III because of the second-order reaction at the step from IV to II.[9] The intermediate IV was concluded to be acetonated with another molecule of IV, but not with acetone. The present kinetic study shows that the addition of a large amount of acetone dimethylketal to a solution of IV in acetone containing sulfuric acid changed the reaction order from the second-order to the first-order. This means that the acetals of acetone attack more easily than acetone does; the dimeric intermediate $(IV)_2$ should thus be XXII, in which the "OR" group is L-sorbose moiety. The preferable attack of the acetals must be caused by the stabilities of the intermediates XXII; the reaction with acetone gave XXII of the hemiacetal type (R=H), which should naturally be less stable than XXII of the acetal type (R=alkyl or sorbose) formed from the reaction with acetals of acetone.

It is very interesting that the reaction also proceeds when such a non-acidic catalyst as cupric sulfate was used; even in this case, however, the medium became slightly acidic because the formation of the complex of I with cupric ion freed the sulfuric acid. Therefore, it can be said that this reaction is also a kind of acid-catalyzed acetonation. Thin-layer chromatographic analyses showing the presence of the common intermediates IV—VIII supported this conclusion. Patil and Bose[16b] suggested a pathway of IV→IX→VII, which is similar to mechanism 1. Their suggestion is unlikely for the same reason that the mechanism 1 is. Further, there is no driving force to transform the pyranose IV into the furanose IX. The formation of IX might be due to the equilibrium with VII, as III is formed from II.

Experimental

All the melting points were recorded on a Kofler micro-stage apparatus and have been corrected.

The optical rotations were determined in an acetone solution unless otherwise stated, and the concentrations were recorded in percentages.

The PMR spectra were measured on a Varian A-60A spectrometer using 5% solutions of the samples in either chloroform-d ($CDCl_3$) or benzene-d_6 (C_6D_6), with TMS as the internal standard. The range of chemical shifts shown means merely that the signals occurred somewhere in the range.

Thin-layer chromatography was carried out on a silica gel plate using either acetone-chloroform (1 : 9 v/v, solvent A) or *n*-hexane-ether (2 : 1 v/v, solvent B) for both detection and preparation. The R_f values of the products were reported for II—VIII. The separated materials were located with iodine vapor of 0.2% resorcin in 10% ethanolic phosphoric acid (Seliwanoff test),[29] followed by heating on an oven. The separations of the reaction products were carried out by preparative thin-layer chromatography (PTC) unless otherwise noted. In some cases, the developed zones were extracted with acetone. The evaporation of the acetone *in vacuo* gave materials. The solvents used were removed under reduced pressure at below 40°C.

Transformation of 1,3:4,6-Di-*O*-isopropylidene-β-L-sorbofuranose (VI). i) A mixture of VI[11] (1.0 g), acetone dimethylketal (5 m*l*), chloroform (5 m*l*), and *p*-toluenesulfonic acid (TsOH) (50 mg) was stirred at room temperature for 4 hr. The solution was neutralized with methanolic sodium methoxide and then concentrated. The chloroform solution of the residue was washed, dried, and evaporated to a crystalline syrup (1.05 g). The recrystallization of the syrup from benzene gave the starting material, VI (170 mg). From the mother liquor, VI[11] (41 mg), 1,2:4,6-di-*O*-isopropylidene-α- (VII)[10,11] (71 mg) and β-L-sorbofuranoses (VIII)[11] (13 mg) were isolated.

ii) A solution of VI (1.0 g), chloroform (5 m*l*), ether (10 m*l*), and TsOH (55 mg) was stirred at 45—48°C for 3 hr and then worked up in a way similar to that described above. A syrup (1.0 g) was obtained, and from the syrup 2,3:4,6-di-*O*-isopropylidene-α-L-sorbofuranose (II)[4] (27 mg), VII (94 mg), VIII (30 mg), and VI (88 mg) were isolated.

Transformation of VII and VIII. A mixture of VII (500 mg), chloroform (3 m*l*), ether (5 m*l*), and TsOH (28 mg) was stirred at 40—45°C for 3 hr and then worked up in a way similar to that described above. A crystalline syrup was obtained. The recrystallization of the syrup gave the starting material (VII) (230 mg). From the mother liquor, a syrup (41 mg) was obtained; the thin-layer chromatogram of the syrup showed the starting material (VII) as a major spot and II and VI as minor spots. Similar results were obtained from the reaction of VIII under the same conditions.

1-*O*-Methyl-L-sorbose (X). A solution of 1-*O*-methyl-2,3:4,6-di-*O*-isopropylidene-α-L-sorbofuranose (XI) (30.5 g) in 60% aq. acetic acid (110 m*l*) was warmed at 40°C. After 3 hr, the solution was evaporated completely. The distillation of the residue gave 1-*O*-methyl-2,3-*O*-isopropylidene-α-L-sorbofuranose (XII) (26.7 g), bp 148—150°C/2 mmHg. XII (10 g) was

29) A. Anno and N. Seno, "Jikken Kagaku Kōza," Bd. 23, ed. by Chem. Soc. Japan, Maruzen, Tokyo (1957), p. 374.

hydrolyzed with 1N hydrochloric acid (100 ml) at room temperature. After 2 days, the reaction mixture was neutralized with a slight excess of Amberlite IR-45 and then evaporated to give X as a syrup (7.8 g), $[\alpha]_D^{24}$ −32.9 (*c* 0.471, water). Found: C, 43.29; H, 7.38%. Calcd for $C_7H_{14}O_6$: C, 43.29; H, 7.27%.

Acetylation of X. A mixture of X (2.0 g), acetic anhydride (10 ml), and pyridine (10 ml) was reacted in a refrigerator. After 16 hr, the solution was poured onto crushed ice and made alkaline with sodium bicarbonate. The chloroform extract was washed with 1N hydrochloric acid, and water, and then dried. The evaporation of the solvent gave crude crystals (1.8 g). The recrystallization of the crystals from ether gave 1-*O*-methyl-3,4,5-tri-*O*-acetyl-α-L-sorbopyranose (XIII) (0.98 g) as needles. It had mp 115.5—117°C, $[\alpha]_D^{24}$ −16.4 (*c* 1.026). Found: C, 49.01; H, 6.37%. Calcd for $C_{13}H_{20}O_9$: C, 48.75; H, 6.29%. PMR ($CDCl_3$)[30] τ: 7.92, 7.97 and 7.99 (OAc), 6.57 (OCH_3), 6.08 (OH), 6.6—6.7 (C_1-protons), 5.07 (H_3, doublet, $J_{3,4}$=9.5 Hz), 4.47 (H_4, doublet-doublet, $J_{4,5}$=9.5 Hz), 5.05 (H_5, multiplet), 6.1—6.3 (C_6-protons).

Acetonation of X. A mixture of X (8.7 g), acetone dimethylketal (150 ml), TsOH (260 mg), and dried chloroform (80 ml) was stirred at room temperature. After 3.5 hr, the reaction mixture was made alkaline with sodium bicarbonate and then extracted with chloroform. The dried chloroform was evaporated to give a syrup (10.3 g), which was then used; (i) for the isolation of 1-*O*-methyl-3,4:5,6-di-*O*-isopropylidene-L-sorbose (XIV), and (ii) for further acetonation. (i) The syrup (1.5 g) was separated into XIV (195 mg, R_f=0.3) and XI (240 mg, R_f=0.5) by PTC with ether-*n*-hexane (2 : 3 v/v). XIV: syrup, $[\alpha]_D^{24}$ +10.5 (*c* 1.861). Found: C, 56.63; H, 8.07%. Calcd for $C_{13}H_{22}O_6$: C, 56.92; H, 8.08%. (ii) The syrup (1.0 g) was further treated with acetone dimethylketal (15 ml) and TsOH (500 mg) at 41—42°C. No XIV was detected in the TLC. After 5.5 hr, the solution was worked up by the above-described procedure. XI (590 mg) was thus obtained.

Reduction of XIV with Lithium Aluminum Hydride. A mixture of XIV (866 mg), lithium aluminum hydride (0.45 g) and ether (30 ml) was stirred at room temperature. After 7 hr, excess lithium aluminum hydride was deactivated with ether saturated with water. The precipitates were filtered off, and then the filtrate was evaporated. The resulting syrup, dissolved in chloroform, was washed with water and dried. The evaporation of the solvent gave a syrup (726 mg), which was immediately benzoylated with benzoyl chloride (1 ml) and pyridine (15 ml), without further purification. 5-*O*-Benzoyl-6-*O*-methyl-3,4:5,6-di-*O*-isopropylidene-D-glucitol (XV) (422 mg, R_f=0.65) was isolated by PTC with benzene-ether (4 : 1 v/v) from the crude product (1.15 g). XV: syrup, $[\alpha]_D^{24}$ +13.1 (*c* 0.566). Found: C, 63.19; H, 7.48%. Calcd for $C_{20}H_{28}O_7$: C, 63.14; H, 7.42%.

Preparation of XV from 6-*O*-Benzoyl-1,2:3,4-di-*O*-isopropylidene-D-glucitol (XVI). XVI (1.0 g) was debenzoylated with methanolic sodium methoxide by the procedure of Mizoiri *et al.*[26] to give 1,2:3,4-di-*O*-isopropylidene-D-glucitol, which was methylated with methyl iodide (20 g) in the presence of silver oxide (1.0 g) under refluxing for 10 hr. The resulting 6-*O*-methyl-1,2:3,4-di-*O*-isopropylidene-D-glucitol (150 mg) was isolated as a syrup in the pure state from the reaction product (0.93 g) by PTC using the solvent A (R_f=0.50). The treatment of the syrup with bezoyl chloride and pyridine, followed by purification by PTC, gave a benzoate (88 mg) which was identified with XV by a study of its TLC and IR spectrum.

1,6-Di-*O*-methyl-L-sorbose (XVIII). A mixture of XII (10 g), methyl iodide (250 g) and silver oxide (30 g) was refluxed for 1.5 hr. Precipitates were then filtered off, and the filtrate was evaporated completely. The resulting syrup was dissolved in *n*-hexane (100 ml) and washed with water (50 ml×10). The aqueous layer was extracted with chloroform (100 ml×3), dried, and evaporated to give 1,6-di-*O*-methyl-2,3-*O*-isopropylidene-α-L-sorbofuranose (XVII) (9.5 g). XVII was hydrolyzed with 1N hydrochloric acid (110 ml) at room temperature. After 3 days, the solution was neutralized with Amberlite IR-45, washed with benzene, and then evaporated to give a syrup (5.5 g) which solidified after standing several days in a desiccator. The recrystallization from ethyl acetate gave XVIII as prisms (4.0 g), mp 78—80°C, $[\alpha]_D^{24}$ −5.3 (*c* 0.997, chloroform). Found: C, 46.15; H, 7.71%. Calcd for $C_8H_{16}O_6$: C, 46.15; H, 7.75%.

Benzylidenation of XVIII. A mixture XVIII (8.7 g), benzaldehyde (27 ml), and TsOH (47 mg) was stirred at room temperature. After 1 hr the reaction mixture was neutralized with sodium bicarbonate. The dried chloroform extract was evaporated to give a syrup (5.8 g) in which three major compounds were detected by TLC with solvent A; their R_f values were 0.50, 0.44, and 0.23 respectively. PTC with the same solvent gave needles (0.31 g, R_f 0.23) and a syrup mixture of two unknown compounds (2.28 g) (R_f 0.50 and 0.44). The recrystallization of the needles from ether gave 1,6-di-*O*-methyl-3,5-*O*-benzylidene-L-sorbose (XIX) (89 mg), mp 89—93°C, $[\alpha]_D^{20}$ −6.0 (*c* 0.329). Found: C, 60.92; H, 6.83%; mol wt 300. Calcd for $C_{15}H_{20}O_6$: C, 60.80; H, 6.80%; mol wt, 296. Unknown compounds with higher mobilities[27] were isolated by repeated PTC; a compound of R_f 0.50: syrup, 45 mg, $[\alpha]_D^{22}$ −6.9 (*c* 1.011). Found: C, 61.09; H, 6.92%; mol wt, 329. Calcd for $C_{15}H_{20}O_6$: C, 60.80; H, 6.80%; mol wt, 296; a compound of R_f 0.44: syrup, 100 mg, $[\alpha]_D^{22}$ −1.9 (*c* 0.627). Found: C, 60.78; H, 7.04%; mol wt, 305. Calcd for $C_{15}H_{20}O_6$: C, 60.80; H, 6.80%; mol wt, 296.

Acetylation of XIX. XIX (78 mg) was acetylated with acetic anhydride (1 ml) and pyridine (1 ml). The same work-up as in the acetylation of X produced a crude acetate (91 mg). The recrystallization from ether gave 1,6-di-*O*-methyl-4-*O*-acetyl-3,5-*O*-benzylidene-L-sorbose (XX) (54 mg) as needles, mp 98—99.8°C, $[\alpha]_D^{24}$ −46.9 (*c* 0.384). Found: C, 60.24; H, 6.54%. Calcd for $C_{17}H_{22}O_7$: C, 60.34; H, 6.55%. PMR ($CDCl_3$) τ: 7.93 (OAc), 6.58 and 6.64 (OCH_3), 4.32 (benzylic proton), ~6.6 (methylene protons at C_1), 5.33 (H_3, doublet, $J_{3,4}$=1.8 Hz), 4.55 (H_4, doublet-doublet, $J_{4,5}$=1.8 Hz), 5.88 (H_5, multiplet) and 6.4—6.6 (methylene protons at C_6); PMR (C_6D_6) τ: 8.35 (OAc), 6.82 and 6.88 (OCH_3), 4.72 (benzylic proton), 5.72 and 5.84 (methylene protons at C_1, $J_{1,1}$=18.3 Hz), 5.92 (H_3, doublet, $J_{3,4}$=1.8 Hz), 4.55 (H_4, doublet-doublet,

30) The *J* values supported the pyranose structure of XIII.[3]

$J_{4,5}$=1.8 Hz), 6.13 (H_5, multiplet) and 6.5—6.6 (methylene protons at C_6).

Kinetic Measurements of the Reaction of IV with Acetone Dimethylketal. Kinetic measurements were made polarimetrically[31] at 15, 25, and 35°C. A Yanagimoto Automatic Recording Polarimeter, model OR-1, was used. Acetone (5 m*l*) containing conc. sulfuric acid (45 mg) was added to a 10 m*l* solution of IV (300 mg) and acetone dimethylketal (3.00 g) in acetone at the appropriate temperature. The solution was transformed into 10 cm polarimeter cell for optical rotation determination. The data are shown in Fig. 1 and Table 1.

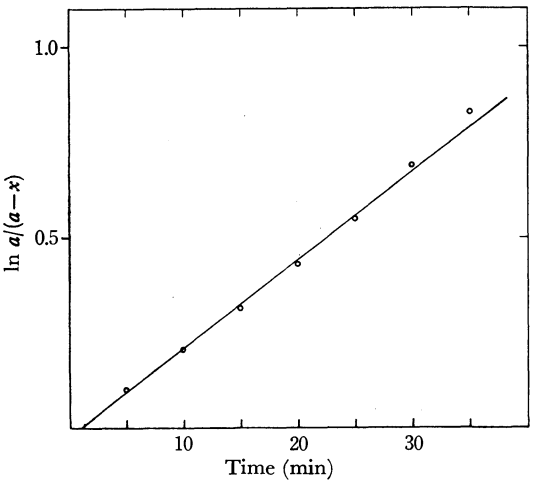

Fig. 1. Values of concentration function *vs.* time at 25°C.

Table 1. The rate constants

Reaction temp.	Rate constants $\times 10^{-4}$ (sec^{-1})
15	1.52
25	3.80
35	8.62

Acetonation of I in Acetone. A mixture of I (5.0 g), acetone (500 m*l*), and sulfuric acid (121 mg) was stirred at 30°C for 5 hr. The solution was then neutralized by a few drops of a sodium hydroxide solution. The unreacted I was filtered and washed with acetone. The combined filtrate was evaporated to give a syrup; this syrup was then dissolved in chloroform, washed with water, and dried, and the chloroform was evaporated. The recrystallization of the residual syrup (750 mg) from *n*-hexane gave VI (59.5 mg). From the mother liquor, II (53.6 mg), VII (89.4 mg), VIII (62.0 mg), and VI (42.7 mg) were isolated by repeated PTC (solvent A).

Acetonation of I in the Presence of Cupric Sulfate. A mixture of I (5.0 g), acetone (500 m*l*), and anhydrous cupric sulfate (50 g) was stirred for 8 hr at room temperature. After the cupric sulfate and the unreacted I had been removed by filtration, the neutralized solution with a few drops of a 2N sodium hydroxide solution was worked up in a way similar to the acetonation of I in acetone. II (140 mg), VII (273 mg), VIII (114 mg), and VI (114 mg) were obtained.

The authors wish to express their deep gratitude to Professor Toshihiko Okamoto, the University of Tokyo, and Dr. Ken'ichi Takeda, Director of this Laboratory, for their encouragement.

31) Under the reaction conditions employed, II as the major product and traces of 1-*O*-methoxyisopropyl-2,3:4,6-*O*-isopropylidene-α-L-sorbofuranose[11] were detected as products in the thin-layer chromatograms. The further acetonation of II under these conditions fortunately did not affect the kinetic measurements.

BULLETIN OF THE CHEMICAL SOCIETY OF JAPAN VOL. 42 2656—2662 (1969)

A Destructive Ethylation Reaction of Benzene with 3-Methylpentane-1-^{14}C

Yukio SUGAHARA,*1 Jun-ichi HAYAMI, Akira SERA and Ryozo GOTŌ

Department of Chemistry, Faculty of Science, Kyoto University, Kyoto

(Received March 10, 1969)

The destructive alkylation reaction of benzene with 3-methylpentane to give ethylbenzene in the presence of aluminum chloride was investigated. When 3-methylpentane-1-^{14}C was employed, radioactive ethylbenzene was obtained. A radioassay of radioactive ethylbenzene showed that: a) the specific radioactivity of the ethylbenzene was about one-third that of the starting 3-methylpentane-1-^{14}C, and b) more than 90% of the radioactivity of the ethylbenzene was present on the β-carbon atom of the ethyl group. These findings suggested a preceding equilibrium between 3-methylpentane and 2-methylpentane, which resulted in an equivalent localization of the radioactive label on three methyl groups of these C_6-hydrocarbons. A carbonium-ion mechanism including an intermediate ethyl cation was discussed in detail.

In 1935, Ipatieff and his co-workers[1-3] reported that the treatment of benzene with 2,2,4-trimethylpentane in the presence of an aluminum chloride-hydrogen chloride catalyst yielded *t*-butylbenzene and p-di-*t*-butylbenzene as well as isobutane. This method of preparing alkylbenzenes from arenes and alkanes was found to be affected by many kinds of Friedel-Crafts catalysts.

These reactions, examples of what Ipatieff originally termed "Destructive Alkylation,"[4] probably proceed through a carbonium-ion process. A scheme for the *t*-butylbenzene formation may be represented as is shown. The scheme involves: 1) hydride abstraction from 2,2,4-trimethylpentane by an appropriate catalytic species to give a tertiary cation, 2) which then affords a *t*-butyl cation and an isobutene molecule by β-cleavage reaction. 3) The *t*-butyl cation formed by the β-cleavage and/or formed from isobutene by the addition of a proton, alkylates benzene to give *t*-butylbenzene. 4) The *t*-butyl cation can abstract the hydride ion from 2,2,4-trimethylpentane to give isobutane and the tertiary cation.

In the destructive alkylation of the C_6-alkanes-benzene system, ethylbenzene has been reported to be the main product. Actually, in the presence of an aluminum chloride-hydrogen chloride catalyst, the destructive alkylation of benzene with 3-methylpentane afforded ethylbenzene and a small amount of an alkylbenzene mixture.[5] Most probably, the attacking species in the formation of ethylbenzene is either ethylene or ethyl cation; however, the mode of the cleavage of 3-methylpentane remains to be examined.

*1 Present address: Research Lab., Mitsubishi Chemical Industries, Ltd., Kawasaki.

1) A. V. Grosse and V. N. Ipatieff, *J. Am. Chem. Soc.*, **57**, 2415 (1935).

2) V. N. Ipatieff, V. I. Komarewsky and H. Pines, *ibid.*, **58**, 918 (1936).

3) A. V. Grosse, J. M. Mavity and V. N. Ipatieff, *J. Org. Chem.*, **3**, 137, 448 (1938).

4) For discussions of this and related reactions, see S. H. Patinkin and B. S. Friedman, "Friedel-Crafts and Related Reactions," edited by G. A. Olah, Vol. II, Interscience Publishers, New York, (1964), p. 110.

5) T. Hatsui, M. Sc. Thesis (Kyoto University, 1967).

In the present paper, the authors wish to present some experimental results which may shed light on the mechanism of the formation of ethylbenzene in a "destructive alkylation" reaction. A tracer experiment was performed using 3-methylpentane-1-^{14}C.

Results

Synthesis and Degradation of 3-Methylpentane-1-^{14}C. Carbon-14-labeled 3-methylpentane was prepared in the following way:

$$^{14}CH_3I + Ph_3P \rightarrow {}^{14}CH_3\overset{\oplus}{P}\cdot Ph_3\cdot I^{\ominus} \rightarrow$$

$$^{14}CH_3\overset{\oplus}{P}\cdot Ph_3\cdot Br^{\ominus} \rightarrow {}^{14}CH_2{=}P\cdot Ph_3$$

$$CH_3{-}CH_2{-}\underset{|}{\overset{CH_3}{\overset{|}{C}}}H{-}CHO + {}^{14}CH_2{=}P\cdot Ph_3 \rightarrow$$

$$CH_3{-}CH_2{-}\underset{|}{\overset{CH_3}{\overset{|}{C}}}H{-}CH{=}{}^{14}CH_2 \rightarrow$$

$$CH_3{-}CH_2{-}\underset{|}{\overset{CH_3}{\overset{|}{C}}}H{-}CH_2{-}{}^{14}CH_3$$

The Wittig reaction of 2-methylbutanal with methyltriphenylphosphonium bromide-methyl-^{14}C, followed by a catalytic hydrogenation, gave 3-methylpentane-1-^{14}C (5.28 μCi/mol).*2 A carrier was used where necessary. The systematic degradation of this labeled hydrocarbon was carried out as follows:

$$\underset{①}{CH_3}{-}\underset{②}{CH_2}{-}\underset{③}{\overset{④CH_3}{\overset{|}{C}}}H{-}\underset{②}{CH_2}{-}\underset{①}{CH_3} \xrightarrow[h\nu]{Br_2} CH_3{-}CH_2{-}\underset{|}{\overset{CH_3}{\overset{|}{C}}}{-}CH_2{-}CH_3$$
$$\qquad\qquad\qquad

show the important features of the "destructive ethylation" reaction. The oxidation of radioactive ethylbenzene to benzoic acid reveals that more than 90% of the radioactivity was present on the β-carbon atom of ethylbenzene. Although the origin of the radioactivity on the α-carbon atom (less than 10%) remains uncertain, this result clearly shows that no symmetric C_2-compound could be an intermediate of the reaction. Mention should be made of the specific activity of the product, ethylbenzene. The observed figure (1.53 μCi/mol) was very close to one-third of the activity of the starting material, 3-methylpentane (5.14 μCi/mol). Any mechanism that can be applicable in the present investigation should be able to give a rational explanation of the above findings.

Three pathways can be postulated for the formation of ethylbenzene in the destructive alkylation. They are: a) the reaction of ethylene with benzene; b) the formation of *t*-butylbenzene or higher alkylbenzenes by the reaction of *t*-butyl or other higher alkyl cations with benzene, followed by a sidechain demethylation to give ethylbenzene, and c) the reaction of the ethyl cation with benzene. These are summarized in the following scheme:

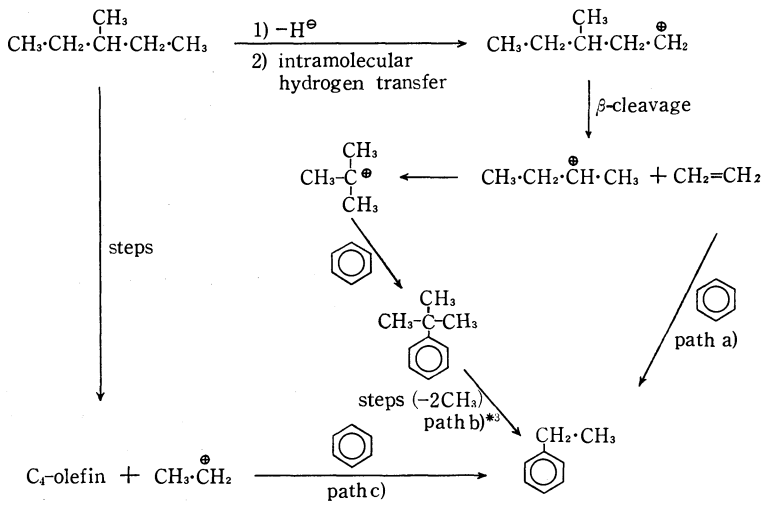

The results of the tracer experiment eliminate path a), the intervention of ethylene or other symmetric C_2-species as a direct precursor of ethylbenzene. Symmetrical intermediate(s) should incorporate an equal amount of radioactivity on both the α- and β-carbon atoms of ethylbenzene; however, this was found not to be the case.

Path b) can be ruled out by examining the fate of *t*-butylbenzene under the destructive alkylation conditions. The treatment of *t*-butylbenzene in benzene with aluminum chloride at an elevated temperature afforded not only ethylbenzene, but in addition, cumene, toluene, and *n*-propylbenzene. These four products were found to be produced in comparable amounts. One of the important features is that an appreciable amount of *t*-butylbenzene survived even after a considerable amount of alkylbenzenes had been formed. In the present instance of a destructive ethylation reaction, the ethylbenzene formed was accompanied by only small amounts of cumene and *n*-propylbenzene and by only a trace of *t*-butylbenzene. These findings suggest that the *t*-butylbenzene route (or path b) can not constitute a major part of the ethylbenzene formation under the conditions used.

Path c) remains to be examined. The intervention of the ethyl cation in the Friedel-Crafts reaction with ethyl halides is a well-known phenomenon. Roberts, Ropp, and Neville[6] reported that the reaction of ethyl-β-^{14}C chloride with benzene in the presence of aluminum chloride gave ethyl-β-^{14}C-benzene. They also found that ethyl-β-^{14}C-benzene showed little or no tendency to randomize its radioactivity even under vigorous Friedel-Crafts conditions. The results in Table 2 strongly suggest that the attacking species is the ethyl cation;*4 that is, path c) might be followed.

A reasonable explanation of the specific radioactivity of ethylbenzene may be given in terms of a

*3 Or *via* higher alkylated benzene(s).

6) R. M. Roberts, G. A. Ropp and O. K. Neville, *J. Am. Chem. Soc.*, **77**, 1764 (1955).

*4 The ethyl cation may be in a form of an aluminum chloride complex or in a tight ion pair. Interventions of the carbonium ion intermediates are thoroughly discussed in the leading references. For a detailed discussions, *cf.* G. A. Olah and M. W. Meyer, "Friedel-Crafts and Related Reactions," edited by G. A. Olah, Vol. I, Interscience Publishers, New York (1963), p. 623.

rapid equilibrium between 3-methylpentane and 2-methylpentane in the presence of aluminum chloride. Schneider and Kennedy[7] have reported an isomerization of 3-methylpentane to 2-methylpentane, and *vice versa*, catalysed by Friedel-Crafts catalysts. Evering and Waugh[8] have presented the rate constants of an aluminum chloride-catalyzed isomerization reaction. The rate constants in *n*-hexane at 100°C were 150 hr^{-1} and 65 hr^{-1} for the isomerization of 3-methylpentane to 2-methylpentane, and for the reverse reaction, respectively. In addition, Karabatsos *et al.*[9] proved that there was no mixing between terminal carbon atoms and internal carbon atoms during the isomerizations of saturated hydrocarbons under the influence of the Friedel-Crafts catalysts. A rapid interconversion of this sort gives rise to radioactive randomization; hence, the three terminal methyl groups in 2- and 3-methylpentanes become equally labeled by radioactive carbon atoms, as is shown in the following scheme:

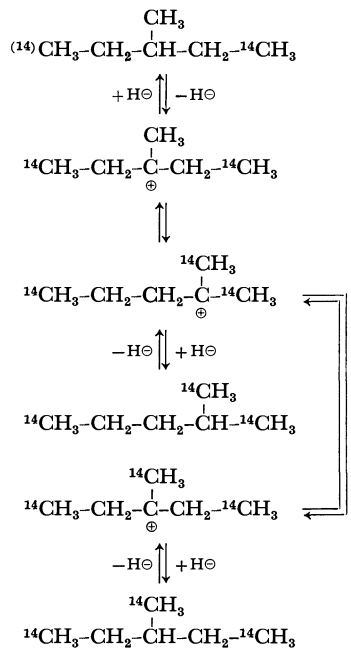

These equilibria indicate the presence of the 1,1-dimethylbutyl cation (and its conjugate acid, 2-methylpentane) in the reaction mixture. From the well-known β-cleavage rule, the precursor of the ethyl cation should be the 1,1-dimethylbutyl cation rather than the 1-methyl-1-ethylpropyl cation. The β-cleavage process now gives rise to the ethyl cation and isobutene. The presence of isobutane as the main product in the destructive alkylation of 3-methylpentane instead of isobutene shows another feature of the reaction. Isobutene can be converted into *t*-butylbenzene in the presence of benzene under Friedel-Crafts alkylation conditions. Surprisingly, in the present investigation, essentially no *t*-butylbenzene was isolated from the reaction mixture. It seemed of interest to determine the fate of *t*-butylbenzene.

In a destructive alkylation in the presence of added *t*-butylbenzene, g. l. c. analysis showed the rapid disappearance of *t*-butylbenzene, and the formation of a large amount of isobutane. The amount of ethylbenzene produced was not substantially affected by the addition of *t*-butylbenzene. From these observations, the following scheme may be suggested for the fate of *t*-butylbenzene under the present conditions:

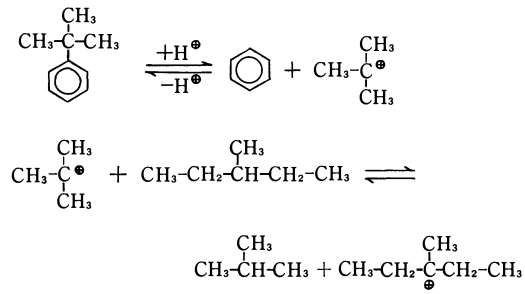

From the experimental results and from the considerations cited above, one can postulate the following reaction scheme for the destructive ethylation of benzene with 3-methylpentane in the presence of aluminum chloride at an elevated temperature. The first stage of the reaction is the initiation of the reaction by an abstraction of hydride from 3-methylpentane with a polarized catalyst complex to give the tertiary cation. The cation produced is involved in a rapid equilibrium with a tertiary cation from 2-methylpentane, which is subjected to the β-cleavage reaction to yield an ethyl cation and isobutene. The ethyl cation thus formed alkylates benzene to give ethylbenzene, and isobutene is protonated to give the *t*-butyl cation. The role of the *t*-butyl cation is either to alkylate benzene to give *t*-butylbenzene, or to abstract hydride from 3-methylpentane (or 2-methylpentane as well) to give the carbonium ion. The last sequence of the reaction would maintain the reaction cycle.

Experimental

All the melting and boiling points are uncorrected. Glc analyses were carried out by means of a Yanagimoto Gas Chromatograph G.C.G.-5DH with 5% TG-3000 on a Celite 545 (40—60 mesh) 2.25-m column, and preparative glc was achieved using Yanagimoto G.C.G.-2 with a silicon-grease DC-703 2-m column.

7) A. Schneider and R. M. Kennedy, *J. Am. Chem. Soc.*, **73**, 5013, 5017, 5024 (1951).

8) B. L. Evering and R. C. Waugh, *Ind. Eng. Chem.*, **43**, 1820 (1951).

9) G. J. Karabatsos *et al.*, *J. Am. Chem. Soc.*, **85**, 729, 733 (1963).

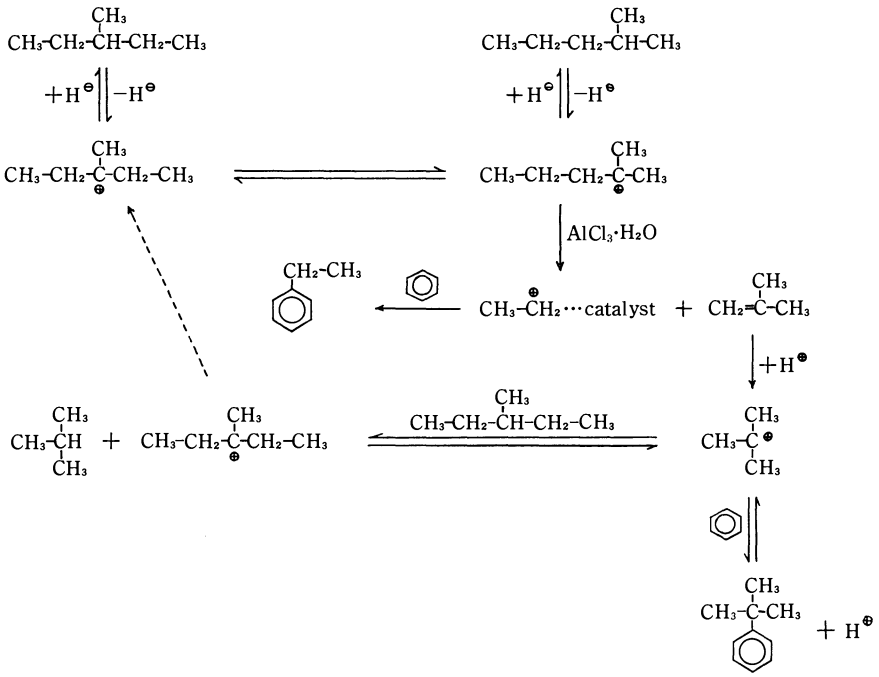

Radioactivity Assay. The radioactivity was measured by means of a Nuclear Chicago Liquid Scintillation Spectrometer 6801, using dioxane-base organic phosphor (1,4-dioxane : naphthalene : POP : POPOP=1 *l* : 120g: 7g : 0.05 g). Correction was made for the quenching using 3-methylpentane-^{14}C as the internal standard. Methyl ethyl ketone 2,4-dinitrophenylhydrazone and iodoform were converted into carbon dioxide in a Barker-type wet-combustion apparatus; carbon dioxide fixed with ethanolamine was served for assay.

Preparation of Methyltriphenylphosphonium Bromide-methyl-^{14}C. In a vacum manifold, methyl iodide-^{14}C (100 μCi, from the Radiochemical Center, Amersham) was transferred on 10-fold equivalents of triphenylphosphine by the aid of liquid nitrogen. The mixture was then warmed to 30°C and chilled again. This procedure was repeated several times, and the total system was flushed with non-radioactive methyl iodide. The methyl iodide washing was condensed on triphenylphosphine to give essentially quantitative yield of methyltriphenylphosphonium iodide-methyl-^{14}C. The crude iodide was dissolved in aqueous ethanol and was treated with freshly-prepared silver oxide. The mixture was filtered, and the precipitate was treated with non-active methyltriphenylphosphonium iodide several times. The combined filtrate and washings was acidified with hydrobromic acid, and the solution was concentrated to dryness. The residue was recrystallized from ethanol-ether to give pure methyltriphenylphosphonium bromide-methyl-^{14}C in a radioactive yield of over 90%.

Preparation of 3-Methylpentane-1-^{14}C. In a 15-m*l* centrifugal tube stoppered with a serum cap, was placed 0.26 g of sodium hydride (53% mineral oil dispersion). Two milliliters of dry light petroleum (bp 30—35°C) was then introduced into the tube through a hypodermic needle, and the suspension was centrifuged. The supernatant was drawn off and the washing was repeated with other two 2-m*l* portions of dry light petroleum. The tube was evacuated to remove the remaining light petroleum and was then flushed with dry nitrogen through hypodermic needles. Two and a half mililiters of dry dimethylsulfoxide was added through a needle, and the mixture was warmed at 70—75°C for 45 min. After the mixture had been cooled to room temperature, to this a solution of 1.79 g of methyltriphenylphosphonium bromide-methyl-^{14}C (5.0 mmol) in dry dimethylsulfoxide was added through a needle. After 10 min, 0.47 g of 2-methylbutanal*[5] (5.5 mmol) was introduced to the solution through a needle, the mixture was then allowed to react for 2 hr at room temperature. The reaction mixture was transferred into a distillation apparatus, and the reaction vessel was washed with non-radioactive 3-methylpentane (0.5 m*l*); the washings were also transferred into the distillation apparatus. Destillation was carried out to collect all of the low-boiling materials in a Dry Ice-acetone-cooled trap. The distillate was treated with a mercuric chloride-mercuric oxide mixture*[6] in ethanol for 2 hr; subsequent distillation afforded a mixture of 3-methylpent-1-ene-^{14}C, 3-methylpentane, and ethanol.

This mixture was hydrogenated using a pre-hydrogenated Adams' platinum oxide catalyst under ordinary pressure at room temperature for 24 hr. The catalyst was then filtered off and washed with non-radioactive 3-methylpentane (0.5 m*l*). To the combined filtrate and washings, a drop of cold conc. sulfuric acid was added and the mixture was stirred at ice-bath temperature. The organic layer was separated, washed with cold aqueous sodium hydrogen carbonate and water, dried over Drierite, and distilled to afford 3-methylpentane boiling at 62—63°C. The overall radioactive

*[5] Prepared from *s*-butyl magnesium bromide and ethyl orthoformate.

*[6] Mercuric chloride, made alkaline with several drops of sodium hydroxide.

yield was 30.1%.

Preparation of 3-Methyl-pentane-3-methyl-^{14}C. The Wittig reaction of pentanone-3 with methyltriphenylphosphonium bromide-methyl-^{14}C under similar conditions, followed by catalytic hydrogenation, gave the labeled hydrocarbon with a radioactive yield of better than 60%.

Degradation of 3-Methylpentane-1-^{14}C. *i) 3-Bromo-3-methylpentane-1-^{14}C.* The photochemical bromination of a 10.2 g portion of 3-methylpentane-1-^{14}C was carried out using the halogenation apparatus described by Roberts and Mazur[10] with a slight modification. Bromine was introduced into a reaction zone by means of a dry-nitrogen stream bubbling through a bottle containing bromine at room temperature. Irradiation was achieved by a high-pressure mercury lamp (HQ-400Q, Nihon Denchi). After the evolution of hydrogen bromide had ceased, a small portion of solid potassium carbonate was added. The subsequent distillation of the bromination product gave 3-bromo-3-methylpentane-1-^{14}C which boiled at 61.5—62.5°C/59 mmHg (5.63 g). No isomeric monobromides were detected.

ii) 3-Methylpent-2-ene-1-^{14}C. A mixture of 3-bromo-3-methylpentane-1-^{14}C (5.63 g) and water (25 m*l*) in a 50-m*l* flask was refluxed for 10 hr. The organic layer was separated from a cooled reaction mixture, and the aqueous layer was extracted with isooctane. The combined organic layer was dried over potassium carbonate, and distilled to give 3-methylpent-2-ene-1-^{14}C (2.34 g); bp 70.5—73.5°C.

iii) 3-Methylpentane-2,3-diol-1-^{14}C. In a three-necked 100-m*l* flask equipped with a Dimroth condenser, a thermometer, and a serum cap, were placed 18 g of 90% formic acid (0.35 mol) and 4.4 g of 30% hydrogen peroxide (0.04 mol); the mixture was stirred magnetically. A 2.1-g portion of 3-methylpent-2-ene-1-^{14}C (0.025 mol) was added, drop by drop, through a hypodermic needle while the temperature was kept below 45°C. After having been stirred for 1 hr at this temperature, the mixture was allowed to stand overnight at room temperature. Formic acid and water were distilled off under reduced pressure from the reaction flask, and to the residual viscous liquid there was added 20-g portion of sodium hydroxide in 40 m*l* of water under cooling. After stirring for 1 hr, the solution was extracted with six 10-m*l* protions of ether, and the ethereal layer was dried over magnesium sulfate. Ether was then distilled off; the subsequent distillation of the residue gave 3-methylpentane-2,3-diol-1-^{14}C (0.59 g) which boiled at 93°C/16 mmHg.

iv) Degradation of 3-Methylpentane-2,3-diol-1-^{14}C. In a 200-m*l* flask, 0.59 g of 3-methylpentane-2,3-diol-1-^{14}C (5.0 mmol) was oxidized overnight with 1.12 g of sodium metaperiodate (5.25 mmol) in 50 ml of water at room temperature. The reaction mixture was then distilled under reduced pressure, and the distillate was collected in a Dry Ice-acetone-cooled trap to give solution A. A 2-m*l* portion of the solution A was added to a solution of 50 mg of dimedone in 13 m*l* of water. A slight warming was applied, and then the solution was allowed to stand overnight at room temperature. Crystalline precitates were collected and recrystallized from aqueous methanol to afford pure acetaldehyde dimedone, mp 142—142.5°C.

To the remaining portion of the solution A, a slight excess of an aqueous potassium permanganate solution was added. After the reaction had been completed, excess permanganate was decomposed with a few drops of a sodium hydrogen sulfite solution and manganese dioxide formed was filtered off to give filtrate B. To a 10-m*l* portion of the cold filtrate B, 2 g of sodium hydroxide and an iodine-iodide solution containing 1.2 g of iodine and 2.4 g of potassium iodide were added successively. Iodoform was collected by filtration.

To the remaining portion of filtrate B, 0.53 g of 2,4-dinitrophenylhydrazine in 20 m*l* sulfuric acid-aqueous ethanol solution was added, and the precipitates were collected by filtration. Recrystallizations from ethanol afforded methyl ethyl ketone 2,4-dinitrophenylhydrazone, mp 115°C.

The above acidic filtrate was then steam distilled, and the initial 200-m*l* portion of the distillate was collected. Barium carbonate was added to this distillate, and the mixture heated for 24 hr. After cooling, excess barium carbonate was filtered off and the filtrate was evaporated to dryness. After recrystallizations from aqueous ethanol, barium acetate was dried at 120°C under reduced pressure over phosphorus pentoxide.

v) Degradation of Radioactive Barium Acetate. Barium acetate was degraded to carbon dioxide using the apparatus described by Phares.[11] Some modifications were made, however. In the present experiment, two 1N sodium hydroxide traps were used in order to absorb carbon dioxide. A stream of carbon dioxide-free nitrogen was used to convey the gas evolved. Furthermore, barium carbonate obtained was treated with perchloric acid in an evacuated Barker-type apparatus to regenerate carbon dioxide which was then again fixed with ethanolamine, and the solution was subjected to radioassay.

Destructive Alkylation. A typical experimental procedure of the destructive alkylation will be described. A mixture containing 6.15 g of 3-methylpentane (0.071 mol), 11.2 g of benzene (0.143 mol), 0.95 g of freshly-prepared anhydrous aluminum chloride (0.007 mol), and 0.064 g of water (0.0035 mol) was heated at 100°C in a glass autoclave and agitated. After an appropriate reaction period, the reaction mixture was poured into ice-water and 1 m*l* of conc. hydrochloric acid was added. The organic layer was separated, washed with cold saturated aqueous sodium hydrogen carbonate and then with cold water, and dried over anhydrous magnesium sulfate. In some experiments, *t*-butylbenzene was added in the initial reaction mixture. In this case, *t*-butylbenzene was added to the initial reaction mixture in an amount equal to that expected to be present in a destructive ethylation mixture without any added *t*-butylbenzene (here, 0.265 g).

Analysis of the reaction products by glc indicated the presence of isobutane (a large amount), 2- and 3-methylpentanes, benzene, toluene (small amounts), ethylbenzene (the main product), xylenes (small amounts), and a trace of higher alkylbenzenes. Toluene and xylenes were found to appear when reactions were carried out for 12 hr or longer, although ethylbenzene began to be produced within one hour. In the presence

10) J. D. Roberts and R. H. Mazur, *J. Am. Chem. Soc.*, **73**, 2509 (1951).

11) E. F. Phares, *Arch. Biochem. Biophys.*, **33**, 173 (1951).

of added *t*-butylbenzene, an increased amount of isobutane was detected by glc; however, no *t*-butylbenzene was present in the product.

Degradation of Radioactive Ethylbenzene. Ethylbenzene was collected by a preparative glc. Oxidation of 0.424 g of radioactive ethylbenzene (4 mmol) with 4.11 g of potassium permanganate (26 mmol) in water (20 m*l*) was performed by heating the mixture for 3 hr. Manganese dioxide was filtered out, and the filtrate and aqueous washings (3 m*l*) were combined. The solution was acidified with conc. hydrochloric acid and extracted with three 10-m*l* portions of ether. Evaporation of ether gave a residue which was recrystallized from water to afford 0.372 g of pure benzoic acid.

The authors are grateful to the staff of the Radioisotope Research Laboratory, Kyoto University, who generously allowed the authors to use the facilities for the tracer experiments.

BULLETIN OF THE CHEMICAL SOCIETY OF JAPAN VOL. 42 2662—2665 (1969)

Synthesis of 2-Amino-4-hydroxy-6-acetyl-7-methyl-7,8-dihydropteridine

Katsura SUGIURA and Miki GOTO

Department of Chemistry, Gakushuin University, Toshima-ku, Tokyo

(Received March 10, 1969)

2-Amino-4-hydroxy-6-acetyl-7-methylpteridine was synthesized by condensation of 2,4,5-triamino-6-hydroxypyrimidine and triketopentane. Reduction of this compound with sodium amalgam yielded a coloring matter, whose UV-spectra and chemical reactions strictly correspond to those of sepiapterin or isosepiapterin. On the basis of NMR spectra, the coloring matter was proved to be 7,8-dihydro-2-amino-4-hydroxy-6-acetyl-7-methylpteridine. Hence, it can be concluded that sepiapterin has the 7,8-dihydro structure as proposed by Nawa.

Sepiapterin is the main pteridine from the mutant *sepia* of the flies, *Drosophila melanogaster* and from the mutant *lemon* of the silkworms, *Bombyx mori*. This compound was proved to be 2-amino-4-hydroxy-6-lactyl-7,8-dihydropteridine by Nawa; evidence to support the 7,8-dihydro structure was obtained by demonstrating the production of dihydroxanthopterin from sepiapterin on treatment with borax solution.[1] Some additional evidences suggested also the 7,8-dihydro structure.[2-5]

The present work was undertaken in order to prove the dihydro structure more definitely by synthesizing a model compound and measuring the NMR spectrum. We have synthesized 2-amino-4-hydroxy-6-acetyl-7-methylpteridine (I) by condensation of 2,4,5-triamino-6-hydroxypyrimidine and triketopentane. Dihydro-2-amino-4-hydroxy-6-acetyl-7-methylpteridine was obtained by reduction of the compound with sodium amalgam. The UV-spectra of the dihydro compound corresponded strictly to those of sepiapterin, and the chemical reactions were similar to those reported for sepiapterin and isosepiapterin.[6,7] On the basis of NMR spectra and UV-spectral change on reduction with sodium borohydride, it was clearly demonstrated that the dihydro compound has the structure *7,8-dihydro*-2-amino-4-hydroxy-6-acetyl-7-methylpteridine. Hence, it can be now definitely concluded that sepiapterin has the 7,8-dihydro structure, as suggested by Nawa.[1]

Experimental

The NMR spectra were obtained with a Varian A-60 instrument with tetramethylsilane or sodium (ω-trimethylsilyl)trimethylenesulfonate as an internal reference. Each sample was dissolved in deuteriodimethylsulfoxide or 1N NaOD at a 10% concentration just before use. The UV-spectra were obtained using a Hitachi EPS-3 spectrophotometer.

2-Amino-4-hydroxy-6-acetyl-7-methylpteridine (I). 2,4,5-Triamino-6-hydroxypyrimidine sulfate mono-

1) S. Nawa, This Bulletin, **33**, 1555 (1960).
2) S. Kaufman, *J. Biol. Chem.*, **242**, 3934 (1967).
3) T. Fukushima and M. Akino, *Arch. Biochem. Biophys.*, **128**, 1 (1968).
4) H. S. Forrest and S. Nawa, *Nature*, **196**, 372 (1962).
5) M. Viscontini, L. Merlini and W. von Philipsborn, *Helv. Chim. Acta*, **46**, 1181 (1963).
6) H. S. Forrest, C. Van Baalen and J. Myers, *Arch. Biochem. Biophys.*, **83**, 508 (1959).
7) H. S. Forrest, D. Hatfield and C. Van Baalen, *Nature*, **183**, 1269 (1959).

hydrate (2.8 g) was dissolved in 60 m*l* of 1N hydrochloric acid at 70—90°C. Triketopentane (1.3 g) was added drop by drop and the mixture was heated for 15 min at 100°C. The solution was neutralized with 10N sodium hydroxide and left standing at room temperature. The precipitate was dissolved in 20 m*l* of 1N sodium hydroxide and filtered. Addition of a few drops of 10N sodium hydroxide gave yellow needles of the sodium salt of I, yield, 1.2 g. The salt (200 mg) was dissolved in 10 m*l* of water, acidified with acetic acid, and the resulting precipitate was filtered and washed with water, ethanol and ether. The pale yellow material was dried *in vacuo* over P_2O_5 at 120°C, yield, 160 mg, mp>250°C. NMR (1N NaOD, 40°C): τ 7.45 (3H, singlet, $-COCH_3$); UV: $\lambda_{max}^{0.1NNaOH}$ mμ (ε), 273 (1.78×10^4), 310 (7.0×10^3), 366 (1.45×10^4); $\lambda_{min}^{0.1NNaOH}$ mμ (ε), 239 (5.5×10^3), 302 (6.9×10^3), 324 (6.6×10^3); $\lambda_{max}^{0.1NHCl}$ mμ (ε), 269 (9.8×10^3), 321 (1.37×10^4), 380 (*infl.*, 1.2×10^3); $\lambda_{min}^{0.1NHCl}$ mμ (ε), 249 (6.5×10^3), 290 (5.8×10^3). Found: C, 49.02; H, 4.14; N, 31.11%. Calcd for $C_9H_9N_5O_2$: C, 49.31; H, 4.40; N, 31.95%.

2-Amino-4-hydroxy-6-(1-hydroxyethyl-7-methylpteridine (II). The sodium salt of I (482 mg) in 25 m*l* of water was added with 740 mg of sodium borohydride in 20 m*l* of 0.01N sodium hydroxide. The mixture was stirred for 6 hr at room temperature and acidified slightly with 6N hydrochloric acid. The pale brown precipitate thus obtained was crystallized from dimethylformamide and the material further purified by dissolving in 1/25N sodium hydroxide and precipitating with acetic acid. The faint yellow product (300 mg) was dried at 120°C over P_2O_5 for 6 hr, mp> 250°C. NMR (1N NaOD, 40°C): τ 8.45 (3H, doublet, J=7 cps, CH_3), 7.44 (3H, singlet, CH_3), 4.80 (1H, quartet, J=7 cps, CHOH). UV: $\lambda_{max}^{0.1NNaOH}$ mμ (ε), 253 (2.42×10^4), 358 (9.0×10^3); $\lambda_{min}^{0.1NNaOH}$ mμ (ε), 220 (9.2×10^3), 297 (1.4×10^3); $\lambda_{max}^{0.1NHCl}$ mμ (ε), 216 (2.18×10^4), 253 (1.04×10^4), 322 (1.03×10^4); $\lambda_{min}^{0.1NHCl}$ mμ (ε), 240 (8.7×10^3), 276 (2.4×10^3). Found: C, 46.88; H, 5.20; N, 30.51%. Calcd for $C_9H_{11}N_5O_2\cdot\frac{1}{2}H_2O$: C, 46.96; H, 4.81; N, 30.43%. II was also obtained by reduction of I with zinc powder in 0.5N sodium hydroxide at 40°C or by hydrogenation in 0.1N sodium hydroxide over PtO_2 (1 mole of hydrogen was absorbed per mole of I). Hydrogenation over palladised black in 0.1N sodium hydroxide did not give II.

2-Amino-4-hydroxy-6-(1-hydroxyethyl)-7-methyl-5,6,7,8-tetrahydropteridine (III). II (90 mg) was dissolved in 11 m*l* of 6N hydrochloric acid and hydrogenated over Adams' catalyst (60 mg). Hydrogenation was stopped, when 2.3 mol of hydrogen was absorbed per mole of II. The catalyst was filtered off and the solution was concentrated to dryness *in vacuo* at 40°C. Recrystallization of the product from a mixture of water, ethanol and ether (3 : 5 : 1) gave faint orange needles (hygroscopic), yield, 58 mg, mp>250°C. For analyses the material was dried *in vacuo* for 6 hr over P_2O_5 at 100°C. UV: $\lambda_{max}^{0.1NNaOH}$ mμ (ε), 255 (*infl.*, 6.3×10^3), 288 (8.5×10^3); $\lambda_{min}^{0.1NNaOH}$ mμ (ε), 235 (4.3×10^3); $\lambda_{max}^{0.1NHCl}$ mμ (ε), 218 (*infl.*, 1.20×10^4), 265.5 (1.79×10^4); $\lambda_{min}^{0.1NHCl}$ mμ (ε), 237 (5.4×10^3). Found: C, 39.98; H, 6.44; N, 26.71%. Calcd for $C_9H_{15}N_5O_2\cdot HCl\cdot\frac{1}{2}H_2O$: C, 39.93: H, 6.28; N, 25.87%.

2-Amino-4-hydroxy-6-acetyl-7-methyl-7,8-dihydropteridine (IV). The sodium salt of I (600 mg) was dissolved in 200 m*l* of 0.03N sodium hydroxide, 33 g of 4% sodium amalgam was added and the mixture was stirred for 2 hr. Mercury was removed and the mixture stirred for 2 hr at room temperature. The solution was neutralized with 6N hydrochloric acid and concentrated *in vacuo* at below 40°C. The concentrate was placed on a 7.0×24.0-cm column of Avicel (microcrystalline cellulose, FMC Corp.) and the column was eluted with 2-propanol, 1% ammonia (2 : 1). A yellow band was eluted and the eluate was acidified with acetic acid. The solution was placed on a 4.0×15.0 cm column of Florisil (100—200 mesh); the yellow compound was adsorbed at the top of the column. The column was washed well with water and then the compound was eluted with 20% aqueous acetone. The eluate was concentrated to dryness *in vacuo*, and the residue was recrystallized from water to give yellow needles (hygroscopic), yield, 102 mg, mp 200—201°C. UV- and NMR-spectra are given in Figs. 1 and 4. For analyses the sample was dried *in vacuo* over P_2O_5 at 100°C. Found: N, 29.51%. Calcd for $C_9H_{11}N_5O_2\cdot H_2O$: N, 29.28%.

Results and Discussion

The product obtained by condensation of 2,4,5-triamino-6-hydroxypyrimidine and triketopentane in acidic media was reduced with 4% sodium amalgam to give a coloring matter with a yellow fluorescence (λ_{max} 513 mμ; exciting wave length: 365 mμ). The UV-spectra of this compound is shown in Fig. 1.

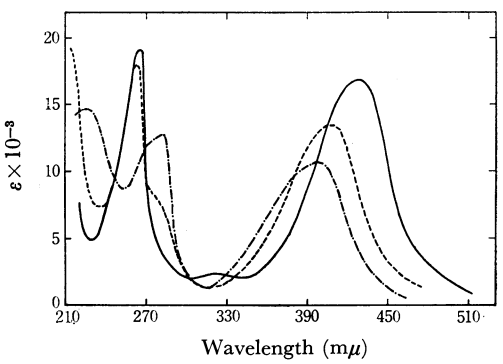

Fig. 1. UV-Absorption spectra of the coloring matter, 2-amino-4-hydroxy-6-acetyl-7-methyl-7,8-dihydropteridine.
—— in 0.1N sodium hydroxide
------ in M/30 KH_2PO_4-Na_2HPO_4 (pH 7.0)
—·— in 0.1N hydrochloric acid

The reduced product gave the following reactions:[6]

1) Oxidation with alkaline permanganate solution gave 2-amino-4-hydroxy-7-methylpteridine-6-carboxylic acid (V).[8]

2) Oxidation with hydrogen peroxide in 0.1N sodium hydroxide gave 2-amino-4,6-dihydroxy-7-

8) F. Weygand, H. Simon, K. D. Keil and H. Millauer, *Chem. Ber.*, **97**, 1002 (1964).

methylpteridine (VI).[9]

3) Treatment with excess sodium borohydride in 0.1N sodium hydroxide gave quantitatively

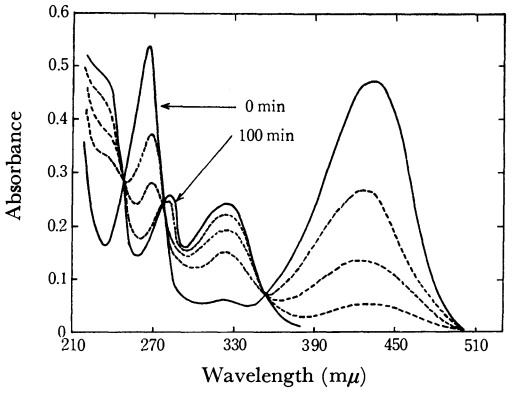

Fig. 2. UV-Spectral change of the coloring matter IV on reduction with sodium borohydride.
The compound (17 μg) was dissolved in 2.5 ml of 0.1N sodium hydroxide and 5 mg of sodium borohydride added (22°C). The UV-absorption spectra were determined before (——) and after 20, 40, 60 (------) and 100 min reduction. The spectrum at 100 min (——) remained unchanged even after 150 min.

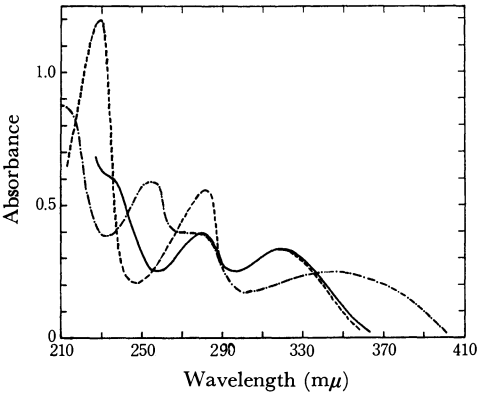

Fig. 3. UV-Spectra of the reduction ($NaBH_4$)product of the coloring matter IV.
The yellow compound IV in 0.1N sodium hydroxide was treated with excess sodium borohydride; the yellow solution became colorless. Excess sodium borohydride was destroyed with acetone. The solution was neutralized and the compound purified using a Sephadex G-25 fine column (developer: water) and an Avicel column (developer: 2-propanol, 1% ammonia=2:1). The UV-spectra of the product are quite in agreement with those of 2-amino-4-hydroxy-6-methyl-7,8-dihydropteridine.
——— in 0.1N sodium hydroxide
-------- in M/30 KH_2PO_4-Na_2HPO_4 (pH 7.0)
-·-·-· in 0.1N hydrochloric acid

9) G. B. Elion, G. H. Hitchings and P. B. Russel, *J. Am. Chem. Soc.*, **72**, 78 (1950).

2-amino-4-hydroxy-6-(1-hydroxyethyl)-7-methyl-7,8-dihydropteridine (VII), whose UV-spectra (Fig. 3) are superimposable on those of 2-amino-4-hydroxy-6-methyl-7,8-dihydropteridine;[10] UV-spectral change on reduction is given in Fig. 2. VII on heating in dilute acetic acid gave the original coloring matter (IV) and 2-amino-4-hydroxy-6-(1-hydroxyethyl)-7-methylpteridine (II).

4) Treatment with bromine in water or in 0.1N hydrochloric acid gave the original compound, 2-amino-4-hydroxy-6-acetyl-7-methylpteridine (I).

5) Reduction with sodium borohydride at pH 7.0 gave 2-amino-4-hydroxy-6-(1-hydroxyethyl)-7-methyl-5,6,7,8-tetrahydropteridine (III).

6) Action of iodine in 0.1N sodium hydroxide gave 2-amino-4-hydroxy-7-methylpteridine-6-carboxylic acid.[8]

Identification of the products described above was carried out by paper chromatographic and UV-spectral comparison with authentic materials. R_f-values of pteridines are given in Table 1.

Table 1. R_f-Values of pteridines

Compound	R_f-values			
	A	B	C	D*
I	0.54	0.48	0.55	0.50
II	0.49	0.55	0.48	0.52
V	0.14	0.27	0.29	0.58
VI	0.18	0.28	0.34	0.33
IV	0.67	0.67	0.64	0.46
IV, after $KMnO_4$ oxidation in 0.1N NaOH	0.14	0.27	0.29	0.58
IV, after H_2O_2 oxidation in 0.1N NaOH	0.18	0.28	0.34	0.33
IV, after Br_2 treatment in acidic or neutral medium	0.54	0.48	0.55	0.50
IV, after I_2 treatment in 0.1N NaOH	0.14	0.27	0.29	0.58
IV, after $NaBH_4$ reduction and reoxidation	0.49	0.55	0.48	0.52
	0.67	0.67	0.64	0.46

* Solvent: A, 2-propanol, 1% ammonia (2:1)
B, 2-propanol, 2% ammonium acetate (1:1)
C, 1-butanol, acetic acid, water (4:1:1)
D, 3% aqueous ammonium chloride

These results are in accordance with the observation for sepiapterin[1] and isosepiapterin[6] and suggest that the yellow coloring matter is a dihydropteridine with an acetyl group at the 6-position and a methyl group at the 7-position and not its isomer. Moreover, the absorption spectra of the dihydropteridine in acidit, neutral and alkaline media were superimposable on the corresponding spectra of sepiapterin and isosepiapterin; this evidence suggests that the dihydropteri-

10) W. Pfleiderer and H. Zondler, *Chem. Ber.* **99**, 3008 (1966).

dine has the same chromophore as in sepiapterin and isosepiapterin. Proof of the dihydro structure of the colored reduction product of the ketone was obtained from a study of the nuclear magnetic resonance spectrum of the coloring matter.

The following three dihydro structures come into consideration for dihydro-2-amino-4-hydroxy-6-acetyl-7-methylpteridine:

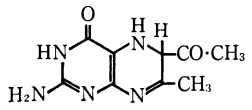

(VIII)

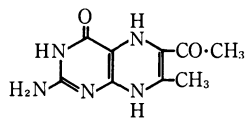

(IX)

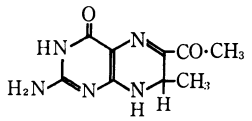

(X)

The NMR spectrum of dihydro-2-amino-4-hydroxy-6-acetyl-7-methylpteridine (Fig. 4) has a singlet at $\tau=7.66$, a doublet at $\tau=9.03$, a quartet at $\tau=5.37$ and broad singlets at $\tau=3.22$, 2.25 and -0.28; the proton ratio of each signal is 3 : 3 : 1 : 2 : 1 : 1. In comparison with NMR signals of guanosine in deuteriodimethylsulfoxide,[11] the signals $\tau=3.22$, 2.25 and -0.28 can be assigned to the amino protons at the position 2, the imino protons at the positions 8 and 3, respectively. The signal at $\tau=7.66$ is assigned to the acetyl protons at the position 6 and the doublet signal at $\tau=9.03$ to the methyl protons at the position 7. The quartet signal at $\tau=5.37$ is assigned to the proton at the position 7; this is coupling with the signal ($\tau=9.03$) of the neighboring methyl protons ($J=7$ cps) and *vice versa* ($J=7$ cps). This evidence supports the structure X for the dihydro coloring matter and the 5,6- and 5,8-dihydro structures (VIII and IX) are ruled out. It can be now definitely concluded that the dihydro-2-amino-4-hydroxy-6-acetyl-7-methylpteridine, and also, by analogy, sepiapterin has the 7,8-dihydro structure.

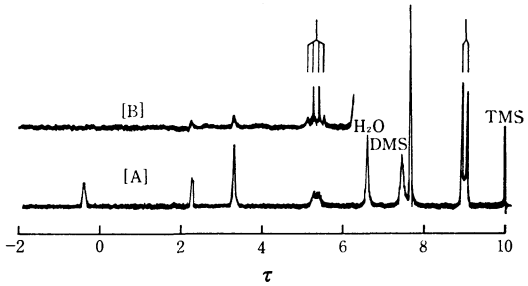

Fig. 4. NMR spectra of the yellow coloring matter IV.

The spectra were obtained with tetramethylsilane as an internal reference (60 Mc, 40°C). After spectrum A was measured in deuteriodimethylsulfoxide, a small amount of D_2O was added to exclude the interaction between the ring protons at the positions 7 and 8, and spectrum B was taken again.

The authors wish to express their thanks to Dr. M. Kondo and Mr. K. Ono, Sankyo Co., Ltd., for measuring NMR spectra and for carrying out microanalyses.

11) L. Gatlin and J. C. Davis, ibid., **84**, 4464 (1962).

BULLETIN OF THE CHEMICAL SOCIETY OF JAPAN VOL. 42 2666—2669 (1969)

Amine Derivatives of 1-(1′-Phenyl-2′-bromoethyl)-5-methyltetrazole

Akira TERADA* and Alfred HASSNER**

* *Department of Chemistry, Kyushu Institute of Technology, Tobata-ku, Kitakyushu*
** *Department of Chemistry, University of Colorado, Boulder, Colorado, U.S.A.*

(Received March 10, 1969)

As part of search for a potential new type of antimalarial, several 1-(1′-phenyl-2′-aminoethyl)-5-methyltetrazoles were prepared by the amination of 1-(1′-phenyl-2′-bromoethyl)-5-methyltetrazole using various amines, such as mono- and diamines of aliphatic and alicyclic. The reaction in the presence of a large excess of amine occurred smoothly on heating at 100—130°C, and it gave the title product without any significant by-product such as the bistetrazole compound, even though a primary amine was used.

The addition of halogens to olefins in a nitrile solvent in the presence of silver perchlorate has been shown by Hassner and his co-workers[1] to lead to nitrilium-ion intermediates. The latter reacts with azide ions, thus providing a useful method of synthesizing tetrazoles containing an additional halogen function, which can be converted to other functional groups by nucleophilic substitution. Thus, styrene reacts with bromine and silver perchlorate in acetonitrile in the presence of sodium azide to yield, in one step, 1-(1′-phenyl-2′-bromoethyl)-5-methyltetrazole (I).

A number of tetrazole derivatives have been of interest as synthetic drugs; among them, pentamethylene-tetrazole, 5-(2-dimethylaminoethoxymethyl)-1-phenyltetrazole, 4-phenyl-1-[2-(5-tetrazolyl)ethyl]piperazine, and 1-(*p*-chlorobenzyl)-5-imino-4-octyltetrazoline are especially well known.[2] An examination of the compounds that exhibit a significant therapeutic effect against malaria,[3–6] including quinine, reveals that many of them are structurally composed of a molecule forming a rigid portion, which has a high electron density and which often contains one or more N-atoms, and of a less rigid side chain, which is often an amino alkanol or a dialkylamino alkylamine.

The stability of tetrazole nuclei, the availability of such bifunctional tetrazoles as I, and the interest by one of the present authors[7] in the chemistry of styrene derivatives have led us to study amine and diamine derivatives of I as potential antimalarials. An added advantage of the members of the tetrazole system is their relatively low toxicity, as indicated by an MTD of over 0.20 mg/g in chicks.[4] Although the few tetazoles studied in the past have lacked antimalarial activity, too few were examined and none of them contained aminoalkyl or similar substituents.

The starting material, I, was prepared according to the directions previously reported.[1] Although there was no precipitation when bromine was added to an acetonitrile solution of silver perchlorate, silver bromide precipitation was rapid upon the addition of styrene to this system. This can be attributed to the formation of a three-membered-ring bromonium ion and to the concurrent trapping of the bromide ion by silver perchlorate, thus prohibiting the formation of styrene dibromide and enhancing attack by acetonitrile, all leading to the formation of a nitrilium-ion intermediate. The tetrazole I was obtained in a 48% yield[8] after the extraction of the reaction products with hot petroleum benzine. From the mother liquors of the extraction, styrene dibromide was obtained in an 11% yield. The residue of the above extraction was a crude 2-methyl-4-phenyl-2-oxazoline hydro-

1) A. Hassner, L. A. Levy and R. Gault, *Tetrahedron Letters*, **1966**, 3119.

2) a) G. M. Dyson and P. May, "May's Chemistry of Synthetic Drugs," Longmans, London (1959), p.180. b) E. R. Benson, "The Tetrazoles," in "Heterocyclic Compounds," ed. by R. C. Elderfield, Vol. 8, Wiley, New York (1967), p. 102. c) K. Tsuda and S. Yoshida, "Iyakuhin Goseikagaku (Synthetic Chemistry of Drugs)," Nankodo, Tokyo (1958), p. 317.

3) P. B. Russell in "Medical Chemistry," ed. by A. Burger, 2nd ed., Interscience Publ., New York (1960), pp. 814—845.

4) G. R. Coatney, W. C. Cooper, N. B. Eddy and J. Greenberg, "Survey of Antimalarial Agents," Public Health Monograph, No. 9 (1953), pp. 47—51, 178, 199, 255.

5) I. M. Rollo in "Pharmacological Basis of Therapeutics," ed. by C. S. Goodman and A. Gilman, 3rd ed., MacMillan Co., New York (1965), pp. 1093, 1097.

6) J. H. Williams, "Chemotherapy of Malaria," Lederle Laboratories, New York (1941—1942).

7) For the preceding paper, see A. Terada, This Bulletin, **39**, 2520 (1966).

8) Ref. 1 had reported a 35% yield.

bromide (II).[9] This oxazoline salt is formed even after the reaction products have been washed with a small amount of 20% sodium hydroxide; it must, therefore, result from the cyclization of 1-acetoamido-2-bromoethylbenzene. The latter presumably results from the reaction of some remaining nitrilium ion with water during the work-up. The instability of *N*-(2-haloethyl)-amides and the facility with which they cyclize to oxazoline salts has been recognized by Lusskin and Ritter.[10] It may, therefore, be concluded that heating during the petroleum benzine extraction results in the formation of the oxazoline salt.

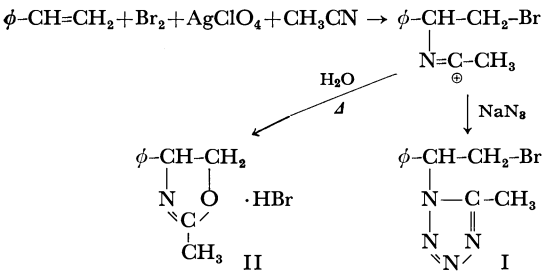

The formation of 1-(1′-phenyl-2′-aminoethyl)-5-methyltetrazoles (III) was accomplished smoothly by heating I with a large excess of amine or diamine at 100—130°C for 24 hr.

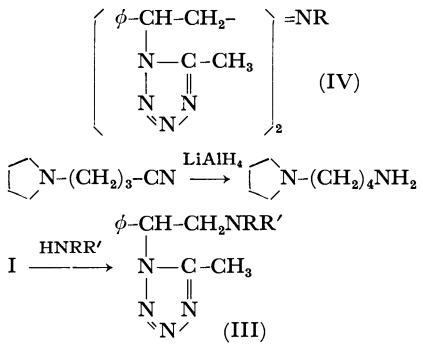

where

NRR′: $-N(CH_3)_2$ (IIIa)

: (IIIb)

: 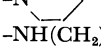 (IIIc)

: $-NH(CH_2)_3OH$ (IIId)

: 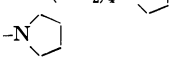 (IIIe)

: (IIIf)

: $-NHCH_2CH_2N(C_2H_5)_2$ (IIIg)

: $-NH-CH(CH_3)(CH_2)_3N(C_2H_5)_2$ (IIIh)

: $-NHCH_2CHCH_2N(C_2H_5)_2$ (IIIi)

No bistetrazole formation of the type IV was observed when the amine was primary, because at least a ten-fold excess of amine was employed. The amines used in this study were dimethylamine, morpholine, piperidine, pyrrolidine, γ-acetoxypropylamine, δ-(pyrrolidino)butylamine, 2-diethylaminoethylamine, 2-amino-5-diethylaminopentane, and 1-amino-3-diethylamino-2-propanol. The δ-(pyrrolidino)butylamine was prepared by the lithium aluminum hydride reduction of γ-(pyrrolidino)-butyronitrile. The tetrazole derivatives obtained (IIIa—i) are shown above. No significant antimalarial activity was found for these compounds in screening tests on mosquitoes A. Aegypti.[11]

Experimental

Materials. All the amines, γ-acetoxypropylamine, dimethylamine, morpholine, piperidine, and pyrrolidine were available commercially as reagent-grade substances and were used without exceptional purification. The γ-(pyrrolidino) butyronitrile was also obtained commercialy. The 2-amino-5-diethylaminopentane (bp 74°C/20 mmHg), 2-diethylaminoethylamine (bp 55—56° C/30 mmHg), and 1-amino-3-diethylamino-2-propanol were furnished by the U.S. Army, Water Reed Medical Center, and were purified by vacuum distillation.

1-(1′-Phenyl-2′-bromoethyl)-5-methyltetrazole (I). According to the directions of Gault,[9] I was prepared using acetonitrile as the only solvent of the system, while Gault used ether as the solvent in his styrene additions. A brown oil (3.612 g) was obtained from 1.17 g of styrene (0.012 mol) after the usual work-up. The repeated extraction of the oil with boiling petroleum benzine gave 1.444 g (48.3%) of I, mp 109—110°C (lit,[1] mp 109—111°C, 35% yield).

From the mother liquor, 319 mg (10.8%) of styrene dibromide were recovered, mp 69—70.5°C (lit,[12] mp 73°C). Its identity was proved by a mixed-melting-point test with an authentic sample.

The residue of the above hot-petroleum-benzine extraction was 1.758 g, which solidified on standing. Recrystallization from benzene gave white crystals of 2-methyl-4-phenyl-2-oxazoline hydrobromide; mp 163—165°C (lit,[9] 165°C, 169—170°C).

1-(1′-Phenyl-2′-dimethylaminoethyl)-5-methyl tetrazole (IIIa). A mixture of 267 mg (1 mmol) of 1-(1′-phenyl-2′-bromoethyl)-5-methyltetrazole (I) and 10 m*l* of diethylamine (25% aq. solution) was heated in a sealed glass tube in a steam bath for 24 hr. After concentration to dryness under a vacuum, the residue was dissolved in dilute hydrochloric acid and filtered. Concentration and alkalization with potassium hydroxide gave 186 mg (80.5%) of needles; mp 86—87°C. Recrystallization from benzene-petroleum benzine gave an analytical sample. This product was easily soluble in water.

Found: C, 62.41; H, 7.39%. Calcd for $C_{12}H_{17}N_5$:

9) R. Gault, M. S. Thesis, University of Colorado (1966), p. 29.

10) R. M. Lusskin and J. J. Ritter, *J. Am. Chem. Soc.*, **72**, 5577 (1950).

11) E. J. Gerberg, L. T. Richard and J. B. Poole, *Mosquito News*, **26**, 359 (1966).

12) R. H. Baundy and R. F. Boyer, "Styrene, Its Polymers, Copolymers and Derivatives," Reinhold Publ. Corp., New York (1952), p. 89.

C, 62.31; H, 7.41%.

ν_{max}^{KBr}: 3125, 3003 (phenyl); 2959, 2890 (CH_3, CH_2); 2778 (N–CH_3); 1524 (tetrazole ring); 1456, 1404, 1383; 1276, 1263, 1120, 1096, 1062, 1030, 875, 829; 730, 702 cm^{-1} (monosubstituted benzene).

1-(1′-Phenyl-2′-morpholinoethyl)-5-methyltetrazole (IIIb). A mixture of 267 mg (1 mmol) of I in 20 m*l* of mopholine was refluxed for 17 hr. Working-up as usual gave 234 mg (85%) of the product; mp 156—157°C. Recrystallization from ethanol-water raised the melting pount to 158—160°C.

Found: C, 61.34; H, 7.11%. Calcd for $C_{14}H_{19}N_5O$: C, 61.52: H, 7.01%.

ν_{max}^{KBr}: 2967, 2941, 2865 (CH_3, CH_2); 2809, 1114 (morpholino); 1520 (tetrazole ring); 1493, 1460, 1443, 1403, 1379, 1127, 1068, 1033, 1008, 913, 873, 793; 728, 701 cm^{-1} (monosubstituted benzene).

1-(1′-Phenyl-2′-piperidinoethyl)-5-methyltetrazole (IIIc). The usual procedure gave an 86% yield of the product; mp 130—130.5°C. Recrystallization from ethanol-water raised the melting point to 132—133°C.

Found: C, 66.20; H, 7.79%. Calcd for $C_{15}H_{21}N_5$: C, 66.39; H, 7.80%.

ν_{max}^{KBr}: 3049 (phenyl); 2950, 2865 (CH_3, CH_2); 2793, 2770 (piperidino); 1529 (tetrazole ring); 1497; 1453, 1445, 1403, 1381, 1309, 1279, 1167, 1124, 1111, 1098, 1044, 870, 782; 730, 701 cm^{-1} (monosubstituted benzene).

Reaction of I and γ-Acetoxypropylamine. A mixture of 267 mg (1 mmol) of I and 3 m*l* of γ-acetoxypropylamine was heated on a steam bath for 24 hr. Evaporation under reduced pressure, extraction with dil. hydrochloric acid, alkalization of the extract with sodium hydroxide, and extraction again with benzene as usual finally gave 158 mg (60.5%) of the product, a white viscous oil. The infrared spectrum showed no carbonyl peaks of acetoxyl, but there were peaks of hydroxyl; this oil was, therefore, concluded to be 1-[1′-phenyl-2′-(γ-hydroxypropylamino)ethyl]-5-methyltetrazole (IIId).

ν_{max}^{Liquid}: 3367 (NH, OH); 3058 (phenyl); 2985, 2882; 2717; 1531 (tetrazole ring); 1504, 1408, 1383; 1111 (alcohol); 749, 701 cm^{-1} (monosubstituted benzene).

All attempts to form a crystalline salt by the use of hydrobromic, hydrochloric, fumaric, sorbic, and tartaric acids were unsuccessful.

The Picrate. This was obtained as usual. Recrystallization from benzene gave yellow crystals, mp 149.5°C.

Found: C, 48.75; H, 5.66%. Calcd for $C_{19}H_{22}N_8O_8$: C, 48.50; H, 6.43%.

δ-(Pyrrolidino)butylamine. Into a solution of 4.20 g (0.1 mol as 90% purity) of lithium aluminum hydride in 200 m*l* of absolute ether under ice-cooling, 13.8 g (0.1 mol) of γ-(pyrrolidino)butylonitrile in 20 m*l* of absolute ether were stirred over a 40-min period. The reaction system was then allowed to stand overnight at room temperature. Four m*l* of water were vigorously stirred in, drop by drop, under deep cooling, and then 3 m*l* of 20% sodium hydroxide and 14 m*l* of water were added. The ether layer was separated by decantation, and the residue was washed twice with much ether. The combined ether solution was dried over potassium hydroxide pellets. On the removal of the solvent, 13.87 g of a yellow oil were obtained. This was shown to be an almost pure δ-(pyrrolidino)butylamine by the infrared spectrum determination. The yield was almost theoretical.

ν_{max}^{Liquid}: 3413, 3322, 3226, 1639 (NH_2); 2817 (*N*-alkylpyrrolidine); 1149 (tertiary amine); 1099 (primary amine); 880 cm^{-1} (amine., liquid).

Purification by vacuum distillation gave 11.35 g of a water-white liquid, bp 83—85°C/7 mmHg, whose infrared spectrum was completely identical with that of the original sample.

The Dihydrobromide. The usual method of preparation gave crystals. Recrystallization from ethanol gave an analytical sample; mp 126—127°C.

Found: C, 31.58; H, 6.74%. Calcd for $C_8H_{18}N_2 \cdot 2HBr$: C, 31.60; H, 6.63%.

1-[1′-Phenyl-2′-(δ-pyrrolidinobutylamino)ethyl]-5-methyltetrazole (IIIe). One mmol (267 mg) of I in 969 mg of the diamine obtained above was heated on a steam bath for 24 hr. After the excess amine had been removed by vacuum distillation and usual work-up, 228 mg of a yellow oil were obtained. The Beilstein reaction was negative.

ν_{max}^{Liquid}: 3356 (NH); 3058, 1499, 729, 701 (phenyl); 2809 (pyrrolidinoalkyl); 1527 (tetrazole ring); 1143, 1121 cm^{-1} (tertiary amine).

The usual salt formation with hydrochloric acid and crystallization from a solvent, an acetone-benzene-ethanol mixture, gave 318 mg (79%) of the analytical sample, dihydrochloride; mp 193—195°C.

Found: C, 53.73; H, 7.56%. Calcd for $C_{18}H_{28}N_6 \cdot 2HCl$: C, 53.86; H, 7.53%.

1-(1′-Phenyl-2′-pyrrolidinoethyl)-5-methyltetrazole (IIIf). A mixture of 167 mg (0.625 mmol) of I and 2 m*l* of pyrrolidine was refluxed for 24 hr. After work-up as usual, alkalization with conc. ammonia gave 132 mg (82%) of the product; mp 122—123°C.

Found: C, 65.44; H, 7.48%. Calcd for $C_{14}H_{19}N_5$: C, 65.34; H, 7.44%.

ν_{max}^{KBr}: 3049 (phenyl); 2994, 2959, 2841; 2778 (pyrrolidinoalkyl); 1520 (tetrazole ring); 731, 703 (monosubstituted benzene); and other spectral peaks, 1495, 1456, 1437, 1404, 1383, 1355, 1325, 1297, 1261, 1236, 1205, 1156, 1147, 1111, 1092, 1053, 1031, 952, 880, 777 cm^{-1}.

1-[1′-Phenyl-2′-(β-diethylaminoethylamino)ethyl]-5-methyltetrazole (IIIg). A sample of 534 mg (2 mmol) of I in 10 m*l* of β-diethylaminoethylamine was heated under reflux for 24 hr. After work-up as usual, 409 mg (45%) of the dihydrobromide were obtained. Recrystallization from an acetone-benzene-*n*-butanol mixture gave an analytical sample; mp 157—159°C (decomp).

Found: C, 41.70; H, 6.21%. Calcd for $C_{16}H_{26}N_6 \cdot 2HBr$: C, 41.39; H, 6.08%.

ν_{max}^{KBr}: 3521, 3436 (NH); 3030 (phenyl); 2778, 2632, 2445 (amine hydrobromide, broad); 1520 (tetrazolering); 1453, 1433, 1403, 1017; 740, 698 cm^{-1} (monosubstituted benzene).

1-[1′-Phenyl-2′-(δ-diethylamino-α-methylbutylamino)ethyl]-5-methyltetrazole (IIIh). A mixture of 534 mg (2 mmol) of I and 10 m*l* of 2-amino-5-diethylaminopentane was heated under reflux for 24 hr. After work-up as usual, the hydrobromide amorphous was obtained. This was very hygroscopic and gave a negative result on attempted crystallization. The dried sample was submitted to elemental analysis and showed the following results:

Found: C ,44.76; H, 7.53; N, 12.21%. Calcd for $C_{19}H_{32}N_6 \cdot 2HBr$: C, 45.08; H, 6.77; N, 16.60%.

ν_{max}^{KBr}: 3413 (NH); 2950, 2874 (CH_3, CH_2); 2688

(amine hydrobromide, broad); 1524 (tetrazole ring); 741 (weak), 701 (monosubstituted benzene), and other peaks, 1453, 1395, 1072, 1042, 1031 cm^{-1}.

1-[1′-Phenyl-2′-(γ-diethylamino-β-hydroxypropylamino)ethyl]-5-methyltetrazole (IIIi). A mixture of 534 mg (2 mmol) of I and 10 m*l* of 1-amino-3-diethylamino-2-propanol was refluxed for 24 hr. After work-up as usual and after the removal of the excess amine by vacuum distillation, 349m g of an oil, a free amino product, was obtained. The usual hydrobromide formation and the trituration of the oily product in acetone gave a brown powder. This decomposed at 160—163°C and was also very hygroscopic.

Found: C, 37.31; H, 6.67; N, 9.38%. Calcd for $C_{17}H_{28}N_6O \cdot 2HBr$: C, 42.69; H, 6.32; N, 17.57%.

Disagreements in these analytical results can be explained to some extent if we assume that some 1-amino-3-diethylamino-2-propanol dihydrobromide(Calcd for $C_8H_{18}N_2O \cdot 2HBr$: C, 27.27; H, 6.54; N, 9.09%) might contaminate the analytical sample. However, the excess amine had been completely removed by vacuum distillation after the reaction. The following infrared spectrum determination shows that the product was mainly an amine derivative of tetrazoe (this sample was submitted to the screening test previously described).

ν_{max}^{KBr}: 3413 (OH, NH); 2778—2353 (amine hydrobromide, broad); 1538 (tetrazole ring); 765, 703 (monosubstituted benzene), and other peaks, 1558, 1453, 1395, 1099, 1028, 826, 800 cm^{-1}.

Attempts to purify the crude products of IIIh and IIIi further by recrystallization were unsuccesful because of their high hygroscopicities and low crystallinities.

This investigation was supported by Contract DADA 17-67-C-7091 from the U.S. Army Medical Research and Development Command (Contribution No. 531 from the Army Research Program on Malaria).

BULLETIN OF THE CHEMICAL SOCIETY OF JAPAN VOL. 42 2669—2672 (1969)

Partial Asymmetric Synthesis in the Simmons-Smith Reaction. III. A Modification of the Reaction[1]

Seiji SAWADA and Yuzo INOUYE

Institute for Chemical Research, Kyoto University, Uji, Kyoto

(Received March 14, 1969)

A modification of the Simmons-Smith reaction, which involves a prior reaction of ethyl iodide with zinc copper couple followed by addition of methylene iodide and olefins, was proposed. The improved yields of cyclopropane products were obtained with various olefin substrates. It is likely that the operating species in the present modification is ethyliodomethylzinc.

Simmons and Simth[2,3] have developed a stereospecific synthesis of cyclopropanes which involves the treatment of olefins with methylene iodide and zinc copper couple. The active organozinc intermediate was generated also by Wittig[4] through the addition of diazomethane solution to zinc iodide in ether. The operating species in this reaction has been looked upon as being iodomethylzinc iodide[2,4,5] (III) or its dimer, bis-iodomethylzinc (II), although unequivocal evidence for this has not yet been presented.

Recently, Furukawa and his coworkers[6] have modified this reaction by replacing zinc copper couple with commercial diethylzinc and claimed remarkable improvement in the yield of cyclopropane compounds from olefins. This modification was featured in particular by its excellent performance even with cation-sensitive olefins such as vinyl ethers, in which with the conventional reagent, the competitive polymerization of olefins caused by the Lewis acid catalysis of zinc iodide in the medium outweighed the formation of desired cyclopropanes.

The following two organomagnesium compounds are relevant to this problem: methylene dimagnesium diiodide[7] which was prepared by the treatment

1) Previous papers of this series: a) S. Sawada and Y. Inouye, *J. Org. Chem.*, **33**, 1767 (1968); b) S. Sawada and Y. Inouye, *ibid.*, **33**, 2141 (1968).

2) H. E. Simmons and R. D. Smith, *J. Am. Chem. Soc.*, **81**, 4256 (1959); E. P. Blanchard and H. E. Simmons, *ibid.*, **86**, 1337 (1964); H. E. Simmons, E. P. Blanchard and R. D. Smith, *ibid.*, **86**, 1347 (1964).

3) See also H. Hoberg, *Ann.*, **656**, 1 (1962), *ibid.*, **695**, 1 (1965); E. LeGoff, *J. Org. Chem.*, **29**, 2048 (1964).

4) G. Wittig and K. Schwarzenbach, *Ann.*, **650**, 1 (1961); G. Wittig and F. Wingler, *Ber.*, **97**, 2139 (1964).

5) B. Rickborn and J. H. H. Chan, *J. Org. Chem.*, **32**, 3576 (1967).

6) J. Furukawa, N. Kawabata and J. Nishimura, *Tetrahedron Letters*, **1966**, 3353; *ibid.*, **1968**, 3495; *Tetrahedron*, **24**, 53 (1968).

7) D. A. Fidler, J. R. Jones, S. L. Clark and H. Stange, *J. Am. Chem. Soc.*, **77**, 6634 (1955); C. Fauveaur, Y. Gault and F. G. Gault, *Tetrahedron Letters*, **1967**, 3149.

of magnesium with methylene iodide, and α-halomethyl Grignard reagent[8] obtained by substitution of isopropylmagnesium chloride with methylene dihalide at dry-ice temperature. Although both organomagnesium compounds were inactive for methylene-transfer to olefins under the corresponding conditions, iodomethylmagnesium iodide reacted at −70°C with cyclohexene to give norcarane in the presence of equimolar zinc iodide or cadmium iodide (8 or 5% yield respectively).

Wittig[9] described recently that bis-benzoxymethylzinc, which was obtained by the exchange of iodomethyl ligands in the dimeric form of the Simmons-Smith reagent with benzoxymethyl groups having a similar nucleophilicity, successfully transferred methylene to cyclohexene to give norcarane in good yields, and this was achieved only in the presence of zinc iodide.

In connection with the above-mentioned reactions and also with our asymmetric syntheses[1] in this type of reaction, we wish to report a further modification of the Simmons-Smith reaction. The present procedure consists of the reaction of ethyl iodide with zinc copper couple which gives ethylzinc iodide probably in an equilibrium with diethylzinc plus zinc iodide,[10] and subsequent introduction of methylene iodide and olefin substrates. A mild reaction took place upon the addition of methylene iodide and olefin under stirring at room temperature and after a period of 0.5—5.0 hr, the reaction mixture was treated in the usual way[1-3] to give the corresponding cyclopropane products. In Tables 1 and 2 are summarized the yields of cyclopropane products obtained by the present procedure in comparison with those by the Simmons-Smith reagent and by the Furukawa modification.[6] The present modification offers the advantage of enabling one to eliminate explosion hazards which are so frequently encountered on handling diethylzinc and even to ensure much improved yields of cyclopropanes.

An equilibrium as schemed below is conceivable for the present system and the operating species responsible for methylene-transfer may be either ethyliodomethylzinc (I), bis-iodomethylzinc (II) or iodomethylzinc iodide (III).

$$EtZnI \rightleftarrows Et_2Zn + ZnI_2 \xrightarrow{CH_2I_2} \underset{(I)}{EtZnCH_2I} + ZnI_2 + EtI$$

$$2\,EtZnCH_2I \rightleftarrows \underset{(I)}{Et_2Zn} + \underset{(II)}{Zn(CH_2I)_2} \rightleftarrows Et_2Zn + 2\,ICH_2ZnI \quad (III)$$

Both the reactivity and reaction yield in the present modification surpassed those in the conventional Simmons-Smith reaction, and compared well with those in the Furukawa modification except that the

Table 1. Yields of cyclopropanes by the present procedure in comparison with those by the Simmons-Smith reaction and the Furukawa modification

Run	Olefin[a]	Cyclopropane product	Reaction period (hr)	% Yield by Present work	% Yield by Simmons-Smith	% Yield by Furukawa[i]
1			2	92	61[e]	79
2			1	80	65[f]	
3			3	78	32[f]	76
4			3	68	54[f]	
5			3	13		
6	[b]		3	48	18[g]	
7			3	45	17[g]	
8			3	77	70[f]	60
9			1	15		92
10	[c]		3	24	9[f]	
11			1	15	(8)[h]	
12	[d]		1	28		

a) mol ratio of olefin : CH_2I_2 : EtZnI=1 : 1 : 2 in all runs except 6,10 and 12.
b) mol rtatio=1 : 3 : 6.
c) mol ratio=1 : 2 : 2.
d) solvent composition: ether : tetrahydrofuran=1 : 1
e) Ref. 3 f) Ref. 2 g) Ref. 1
h) yield of the pyrrolidine analog. Ref. 11
i) by glpc-analysis. Ref. 6

Table 2. Yields of 1-methyl-2-hydroxymethylcyclopropane[a] by the reaction of crotyl alcohol and sodium crotylate with the present and the Simmons-Smith reagents

Run	Olefin	Mol equivalent of Simmons-Smith reagent	Mol equivalent of Present modif. (as $EtZnCH_2I$)	Reaction period (hr)	% Yield
13	crotyl alc.	1		5	8
14	crotyl alc.	2.5		5	65
15	Na crotylate	1		0.5	53
16	crotyl alc.		1	0.5	27
17	Na crotylate		1	0.5	60

a) M. Julia., S. Julia and J.A. Chaffaut, *Bull. Soc. Chim. France*, **1960**, 1735; bp 131°C, n_D^{20} 1.4284.

8) H. Normant and J. Villieras, *Compt. rend.*, **260**, 4535 (1965); J. Villieras, *ibid.*, **260**, 4137 (1965).
9) G. Wittig and M. Jautelat, *Ann.*, **702**, 24 (1966).
10) M. H. Abraham and P. H. Polfe, *Chem. Commun.*, **1965**, 325; J. Boersma and J. G. Noltes, *Tetrahedron Letters*, **1966**, 1252.

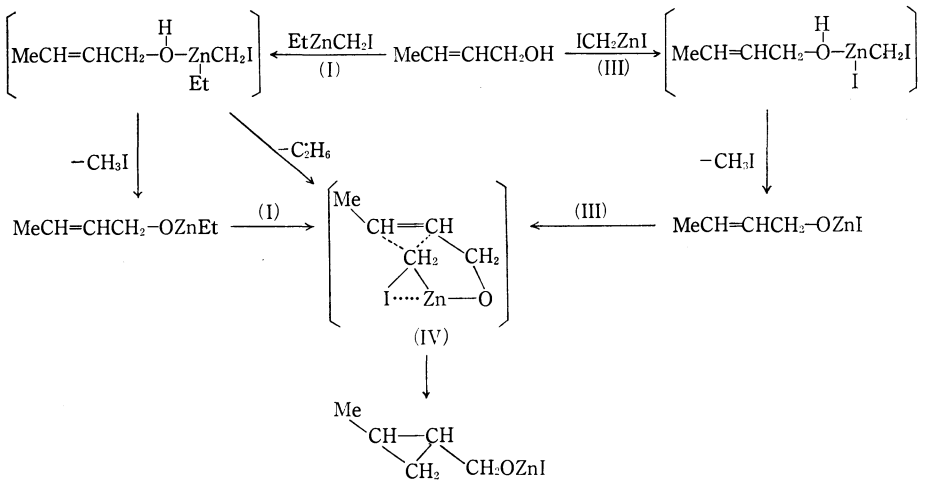

present modification was accompanied by the undesirable olefin polymerization as was also the case with the conventional procedure (runs 2, 9, 11 and 12). Accordingly, active intermediate may reasonably be looked upon as being ethyliodomethylzinc (I), and thus the reaction mechanism may be essentially the same as that in the Furukawa modification.

The behavior of the present organozinc reagent toward olefinic alcohols is worthy of note. When crotyl alcohol was allowed to react with equimolar iodomethylzinc iodide (III), 1-methyl-2-hydroxymethylcyclopropane was just sparingly produced (8%, run 13), whereas with the use of an excess of the reagent (2.5 mol equivalent, run 14) a much higher yield (65%) of the cyclopropane alcohol was obtained. A similar trend was observed in run 15 where sodium crotylate was employed instead of the free alcohol. This observation suggests that crotyl alcohol coordinates primarily with zinc atom in the reagent to form a zincate complex which in turn dissociates predominantly with elimination of methyl iodide so far as alcoholic hydrogen is available. It seems likely that crotoxyzinc iodide thus formed (or sodium crotylate in run 15) undergoes spontaneous substitution with surplus methylene-transfer reagent to form another zincate (IV), iodomethylzinc crotylate, which decomposes eventually to afford cyclopropane product. Runs 16 and 17 stand for this mechanism proposed.

The treatment of enamine (run 11) with the present organozinc reagent in ether-tetrahydrofuran (1 : 1) resulted in the formation of 1-piperidinobicyclo[4,1,0]heptane without any separation of gelatinous precipitate.[11] (−)-Menthyl crotonate and cinnamate failed to afford the corresponding cyclopropane acids when subjected to the present reaction procedure under the standard conditions.

11) E. P. Blanchard, H. E. Simmons and J. S. Taylor, *J. Org. Chem.*, **30**, 4321 (1965).

Experimental

The cyclopropane product in each run was identified by glpc, IR- and NMR-spectral comparisons with the respective authentic specimen. The yields were estimated by glpc-analysis except in runs 2, 9, 11, 12 and 14 where the products were actually isolated.

Stock Solution of Ethylzinc Iodide. Ethyl iodide (156 g, 1 mol) was allowed to react with zinc copper couple (70 g, 1 atom) in absolute ether (900 m*l*), and the mixture was stirred at room temperature overnight. The supernatant liquid was withdrawn free from sludge and stored in a stoppered flask carrying a drying tube. After storage at room temperature for a week, no precipitate was formed and the activity of the solution remained unchanged.

The cyclopropane synthesis in the present modification is exemplified by the typical run with cyclohexene to give norcarane (run 1) and essentially the same procedure except in runs 11 and 12, was followed for other runs in the mol ratio of olefin: $EtZnCH_2I = 1 : 1$.

Synthesis of Norcarane (Run 1). Methylene iodide (15 g, 0.055 mol) was added to an aliquot of the stock solution (100 m*l*) containing 2 mol equivalent of active ethylzinc iodide and the reaction mixture was stirred at 30—35°C for 1 hr. To the chilled solution, cyclohexene (4.1 g, 0.05 mol) was added and the mixture was gently refluxed under stirring and after 2 hr, *ca.* 50 m*l* of ether was distilled off. The resulting pale yellow mixture was decomposed with water and dil. HCl, and the organic layer was separated, washed with water, sodium thiosulfate solution and again with water, and dried over anhydrous $MgSO_4$. The solution which contained norcarane in a 92% yield as determined by glpc-analysis was ozonized to remove unreacted cyclohexene and washed with NaOH solution. After drying over anhydrous $MgSO_4$, the solution was distilled to give norcarane boiling at 115—117°C, n_D^{25} 1.4540. The IR- and NMR-spectra were identical with those of the authentic specimen. Yield 2.8 g. Additional amount of norcarane (1 g) was recovered by the rectification of the forerun (bp 70—115°C), totalizing the yield as 3.8 g (88%).

Synthesis of 1-(1-Piperidino)bicyclo[4.1.0]hep-

tane (Run 12). Methylene iodide (6 g, 0.02 mol) was allowed to react with ethylzinc iodide (40 m*l* of the stock solution, 0.04 mol) and 40 m*l* of absolute tetrahydrofuran was added to the solution. After 1 hr's stirring, 1-(1-piperidino)cyclohexene (bp 120°C/17 mmHg, n_D^{20} 1.5120[11]; 3 g, 0.018 mol) in 10 m*l* of THF was introduced at 30—40°C and the mixture was refluxed for an additional hr. The reaction mixture was hydrolyzed with dil. HCl and then was made alkaline with sodium carbonate. The organic layer, which exhibited a single peak of the product on glpc-analysis and indicated the absence of the parent enamine, was washed with saturated sodium chloride solution and dried over anhydrous magnesium sulfate. After removal of the solvent, the residual oil was distilled to give 1-(1-piperidino)bicyclo-[4.1.0]heptane, bp 115°C/17 mmHg, n_D^{25} 1.4889. Found: C, 80.10; H, 11.93; N, 7.66%: Calcd for $C_{12}H_{21}N$: C, 80.38; H, 11.81; N, 7.81%. Yield 0.9 g (28%).

12) Z. Eckstein and A. Sacka, *Chem. Abstr.*, **54**, 22637e (1961).

The authors are indebted to Dr. M. Ohno for his interest in this work. Partial support of this study by grant D86547 from the Ministry of Education is gratefully acknowledged (Y. I.).

BULLETIN OF THE CHEMICAL SOCIETY OF JAPAN VOL. 42 2672—2676 (1969)

Aminocyclitols. XX. Bromination of DL-*epi*-Inositol

Tetsuo SUAMI, Akira SUZUKI,* Masaru UCHIDA and Shin-ichi YANAGIDA

Department of Applied Chemistry, Faculty of Engineering, Keio University, Koganei-shi, Tokyo
** Central Research Laboratory, Kanto Denka Co., Ltd., Shibukawa, Gunma*

(Received March 19, 1969)

Bromination of DL-*epi*-inositol yielded two hitherto unknown dibromo-dideoxyinositols, along with two known bromo-deoxyinositols (DL-5-bromo-5-deoxy-*allo*-inositol and DL-1-bromo-1-deoxy-*neo*-inositol). The proton magnetic resonance spectroscopic studies of the dibromo-dideoxyinositols with the aid of spin decoupling technique established their configurations to be DL-2,4-dibromo-2,4-didoxy-*chiro*-inositol and DL-1,4-dibromo-1,4-dideoxy-*chiro*-inositol.

As a continuation of the previous paper of this series,[1] configurational studies of two hitherto unknown dibromo-dideoxyinositols which were obtained from DL-*epi*-inositol by a drastic bromination will be described in the present article.

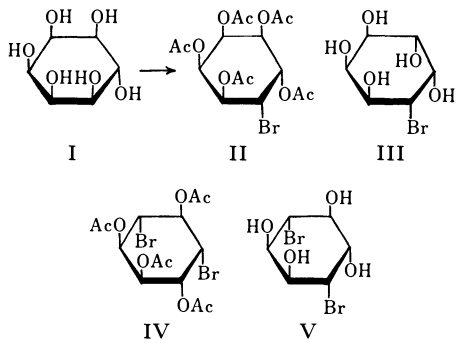

Scheme 1

When DL-*epi*-inositol (I)[2] was heated in a mixture of acetyl bromide and acetic anhydride in a sealed tube at 130—140°C for 8 hr, two new dibromo-dideoxyinositols (IV and V) were obtained, along with two known bromo-deoxyinositols (II and III).[3-5] One of the two reported bromo-deoxyinositols was DL-1,2,3,4,6-penta-*O*-acetyl-5-bromo-5-deoxy-*allo*-inositol (II) which had been described by McCasland and his co-workers in this bromination.[3] Another bromo-deoxyinositol was found to be identical with DL-1-bromo-1-deoxy-*neo*-inositol (III), which had been prepared by McCasland *et al.*[4] and Nakajima and Kurihara[5] in other preparations.

From the bromination mixture of I, II was first isolated in a yield of 25.5%, as was described by McCasland *et al.*[3] Then the tetra-*O*-acetyl-dibromo-dideoxy-inositol of mp 180—182°C (IV) was obtained in a yield of 4.2% from the mother liquor of II after a long storage in a refrigerator,

1) T. Suami, S. Ogawa, Y. Nakashima and H. Sano, This Bulletin, **40**, 2958 (1967).

2) T. Posternak, *Helv. Chim. Acta*, **19**, 1333 (1936).

3) G. E. McCasland and J. Reeves, *J. Am. Chem. Soc.*, **77**, 1812 (1955); G. E. McCasland, S. Furuta and V. Bartuska, *J. Org. Chem.*, **28**, 2096 (1963).

4) G. E. McCasland, S. Furuta, J. F. Johnson and J. N. Shoolery, *J. Am. Chem. Soc.*, **83**, 2335 (1961).

5) M. Nakajima and N. Kurihara, *Chem. Ber.*, **94**, 515 (1961).

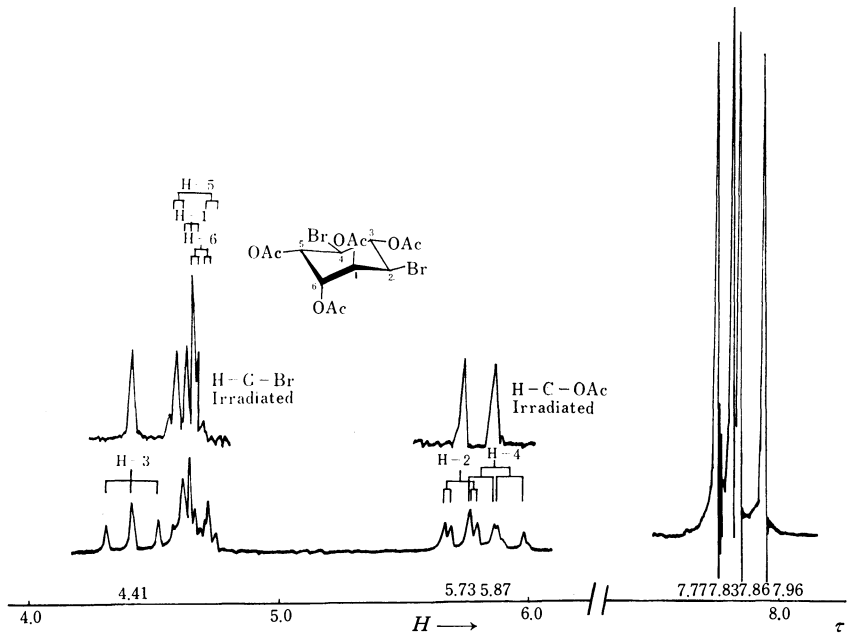

Fig. 1

and its structure was assigned to be DL-1,3,5,6-tetra-*O*-acetyl-2,4-dibromo-2,4-diedoxy-*chiro*-inositol by pmr spectroscopic studies, as will be described below.

Another dibromo-dideoxyinositol of mp 220—222°C (dec.) (V) was recovered in a 9.6% yield from the mother solution of IV after it had been hydrolyzed, and V was assigned to be DL-1,4-dibromo-1,4-dideoxy-*chiro*-inositol by pmr spectroscopic and chemical evidences.

Finally, III was obtained in a yield of 5.2% by adding ethanol to the mother liquor of V.

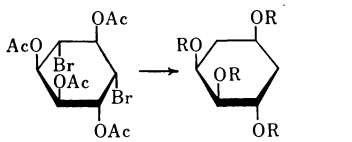

IV VII

R=CO·C$_6$H$_4$·NO$_2$

Scheme 2

In order to establish the configuration of IV, a catalytic debromination was carried out to give an oily product of tetra-*O*-acetyl-dideoxyinositol which failed to crystallize. Hydrolysis of this oily product afforded cyclohexanetetrol as a syrup, which was converted to a crystalline tetra-*O*-*p*-nitrobenzoyl-cyclohexane-tetrol (VII).

The proton magnetic resonance spectrum of IV was determined in deuteriochloroform at 100 Mc and was shown in Fig. 1 which enabled us to establish its conformation for the following reasons: 1) The four protons (H–C–OAc) showed a signal pattern at τ 4.31—4.75. In the lowest field, there was a triplet centered at τ 4.41 with a coupling constant of 10.5 Hz which revealed an axial-axial-axial arrangement of three neighboring protons. 2) The two protons (H–C–Br) exhibited the signal at τ 5.66—6.00. When these protons were irradiated, the above mentioned triplet collapsed to a singlet (Fig. 1). This fact proved that there were two bromo groups adjacent to the proton which had shown the triplet. 3) When the four protons (H–C–OAc) were irradiated simultaneously, the complex signals of the two protons (H–C–Br) collapsed to a doublet with an equal intensity (Fig. 1). This phenomenon showed that these two protons (H–C–Br) were geometrically not equivalent in their environments. Therefore, if an acetoxy group on C-1 was in an axial position, an acetoxy group on C-5 had to be in an equatorial position. 4) This arrangement of the protons was also confirmed by a coupling constant observed in the spectrum. That is, $J_{1-2}=3$ Hz, $J_{2-3}=10.5$ Hz, $J_{3-4}=10.5$ Hz and $J_{4-5}=12$ Hz, and the observed spectrum at τ 4.59—4.75 was the superposition of the three sets of a quartette. Now, the three of the four acetoxy groups occupied their proper positions, that is, there were two equatorial acetoxy groups and one axial acetoxy group. 5) The methyl protons of the four acetoxy groups showed four sharp signals at τ 7.77 (3H), 7.83 (3H), 7.86 (3H) and 7.96 (3H). The first two signals were attributed to two axial acetoxy groups and the fourth signal was ascribed to an equatorial acetoxy group.[6] Considering the fact that there was

6) F. W. Lichtenthaler and P. Emig, *Carbohyd. Res.*, **7**, 121 (1968).

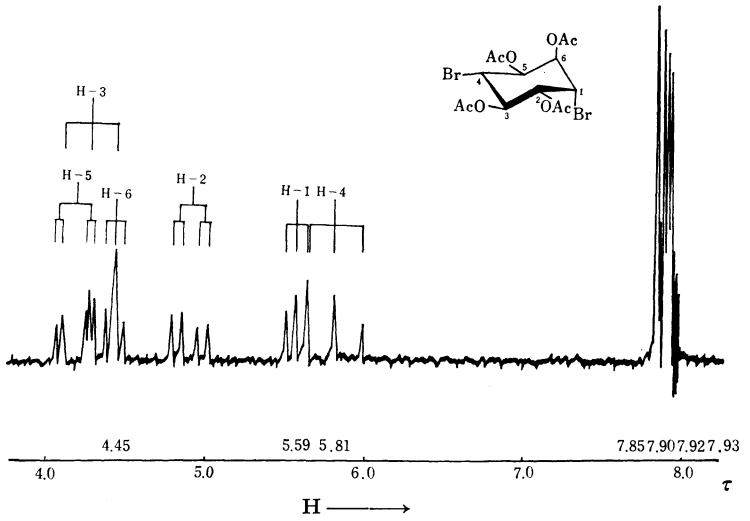

Fig. 2

one equatorial acetoxy group between two bromo groups, a signal of this type of an acetoxy group was shifted to a considerably lower field by a deshielding effect of the neighboring bromo groups. An analogous phenomenon had been observed in the pmr spectrum of DL-3-*N*-acetyl-1,5,6-tri-*O*-acetyl-2,4-dibromo-2,4-dideoxy-*chiro*-inosamine-3,[1] where a signal of an equatorial acetamido group on C-3 was shifted to a lower field by an influence of vicinal bromo groups. Therefore, the third signal (τ 7.86) was ascribed to an equatorial acetoxy group located between two bromo groups. Now, the whole conformation of IV was established to be DL-1,3,5,6-tetra-*O*-acetyl-2,4-dibromo-2,4-dideoxy-*chiro*-inositol.

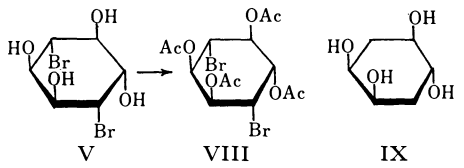

Scheme 3

The configuration of another dibromide (V) of mp 220—222°C (dec.), was studied by a catalytic hydrogenolysis and determination of pmr spectrum. A catalytic hydrogenolysis of V with Raney nickel in the presence of Amberlite IR-4B afforded cyclohexanetetrol of mp 206—208°C (IX). As judged by the melting points of its acyl derivatives, this cyclohexanetetrol was *para*-cyclohexanetetrol of (124/5).[7] Therefore, the possible configuration of V was limited to the following four structures.

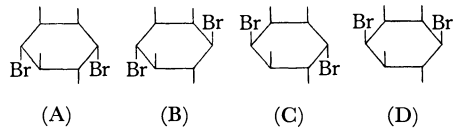

The pmr spectrum of tetra-*O*-acetyl derivative of V (VIII) in deuteriochloroform (Fig. 2) revealed four sharp signals at τ 7.85, 7.90, 7.92 and 7.93 which were attributed to the four acetoxy groups. The signals of the two protons (H–C–Br) produced a quintet (τ 5.50—6.00) which consisted of two triplets. The coupling constant of the triplet centered at τ 5.81 was 10 Hz, suggesting the existence of an axial-axial-axial arrangement of three neighboring protons. Another triplet centered at τ 5.59 had a coupling constant of 3.5 Hz, which revealed equatorial-equatorial-equatorial, an axial-equatorial-axial, an axial-equatorial-equatorial, an equatorial-axial-equatorial or an equatorial-equatorial-axial arrangement of three neighboring protons. These facts were compatible only with the structure of A and all other structures could not produce the above mentioned triplets. Also the complex pattern of the signals produced by the remaining four protons (H–C–OAc) helped to confirm the configuration. Hence VIII was reasonably assigned to be DL-2,3,5,6-tetra-*O*-acetyl-1,4-dibromo-1,4-dideoxy-*chiro*-inositol.

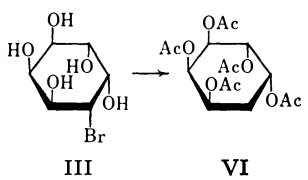

Scheme 4

7) G. E. McCasland, Stanly Furuta, L. F. Johnson and S. N. Shoolery, *J. Org. Chem.*, **28**, 894 (1963); This system for the naming of stereoisomers was proposed by G. E. McCasland: G. E. McCasland, "Advances in Carbohydrate Chemistry," Vol. 20, Academic Press Inc., London (1965), p. 13.

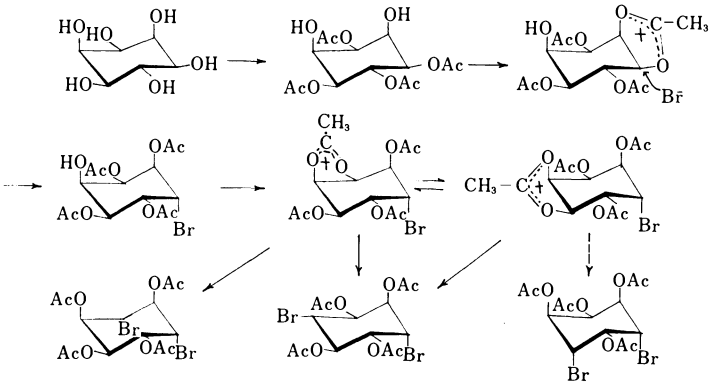

Scheme 5

The configuration of monobromide, III, was assigned to be DL-1-bromo-1-deoxy-*neo*-inositol by the following evidence. The pmr spectrum of III (mp 222—223°C) determined in deuterium oxide at 60 and 100 Mc were identical with the optically active L-1-bromo-1-deoxy-*neo*-inositol prepared by McCasland *et al.*[8] The melting point of this bromide was different from that of bromoquercitol prepared by McCasland *et al.*[8] from 1,2-anhydro-*allo*-inositol. But this could be accounted for by the fact that the present compound was racemic and McCasland's compound was levo-rotatory.

The catalytic hydrogenolysis of III yielded the previously known DL-*talo*-quercitol derivative (VI)[8] and this fact supported the above mentioned configuration of III.

The mechanism of the bromination reaction giving the dibromo-dideoxyinositols (IV and V) is proposed as follows. The monobromination of DL-*epi*-inositol occurs *via* a formation of an intermediary acetoxonium ion[9] which is then opened by a bromide ion in a manner of trans diaxial opening to give II. The second step of the bromination is likely to be a formation of another acetoxonium ion which gives E, F and G by an attack of a bromide ion. E and F are IV and V respectively, which were actually obtained in the present experiment, but G was not obtainable in this work.

Experimental

The melting points reported were determined in a liquid bath and uncorrected. The pmr spectra of the samples were recorded on Varian Associates A-60D and HA-100 spectrometers at the frequency of 60 and 100 Mc in deuteriochloroform, deuteriodimethylsulfoxide or deuterium oxide with tetramethylsilane or sodium trimethylsilylpropanesulfonate as an internal standard. The peak positions are given in τ-values.

DL-1,2,3,4,6-Penta-*O*-acetyl-5-bromo-5-deoxy-*allo*-inositol (II). Ten sealed tubes, containing a mixture of DL-*epi*-inostitol (I) (3.0 g), acetyl bromide (5.0 m*l*) and acetic anhydride (5.0 m*l*), were heated at 135—140°C for 6 hr. Then the mixture was evaporated under reduced pressure. The residue was acetylated with acetyl bromide. The reaction mixture was evaporated under reduced pressure. The oily residue was dissolved in 100 m*l* of ethanol, decolorized with active charcoal and left to settle. The crystals were collected by filtration to give 21.6 g of a crude product of mp 145—149°C. Recrystallization from ethanol afforded 17.9 g of II (25.5% yield), mp 152—153°C. (lit.[3] mp 153°C). (Found: C, 42.37; H, 4.67; Br, 17.63%).

DL-1,3,5,6-Tetra-*O*-acetyl-2,4-dibromo-2,4-dideoxy-*chiro*-inositol (IV). The mother liquor of II was left to settle in a refrigerator for a long period (two months) to give 3.4 g of a crystalline product of mp 176—180°C. The product was recrystallized from ethanol to give 3.0 g (4.2% yield) of an analytically pure sample of IV, mp 180—182°C.

Found: C, 35.79; H, 4.00; Br, 34.06%. Calcd for $C_{14}H_{18}Br_2O_8$: C, 35.44; H, 3.78; Br, 33.75%.

DL-Tetra-*O*-*p*-nitrobenzoyl-cyclohexane-1,2,3,5-tetrol (125/3) (VII). A 560 mg portion of IV was hydrogenated in 50% aqueous ethanol (20 m*l*) with Raney nickel and Amberlite IR-4B under 3.4 kg/cm^2 of hydrogen pressure for 20 hr. After the catalyst and the ion exchange resin were removed by filtration, the filtrate was evaporated giving an oily residue. The residue was heated in a mixture of 2N hydrochloric acid (15 m*l*) and ethanol (15 m*l*) for 20 hr under reflux. The hydrolyzate was evaporated *in vacuo* and an oily residue was acylated with *p*-nitrobenzoyl chloride (30 mg) in pyridine (15 m*l*). After an excess acylating reagent was removed by evaporation, the residue was crystallized from a mixture of acetone and ether to give 33 mg (3.8% yield) of needles melting at 221—223°C.

Found: C, 54.43; H, 3.61; N, 7.09%. Calcd for $C_{32}H_{24}N_4O_{16}$: C, 54.85; H, 3.25; N, 7.52%.

8) G. E. McCasland, S. Furuta, L. F. Johnson and J. N. Shoolery, *J. Am. Chem. Soc.*, **83**, 2335 (1961); G. E. McCasland, S. Furuta and V. Bartuska, *J. Org. Chem.*, **28**, 2096 (1963); The pmr spectrum of III was determined and compared with that of authentic sample of L-1-bromo-1-deoxy-*neo*-inositol by Professor G. E. McCasland.

9) R. Boshan and S. Winstein, *J. Am. Chem. Soc.*, **78**, 4921 (1956).

DL-1,4-Dibromo-1,4-dideoxy-*chiro*-inositol (V). The mother liquor of IV was mixed with 25 m*l* of 2N hydrochloric acid. The mixture was heated under reflux for 20 hr and then evaporated under reduced pressure. The residue was dissolved in 15 m*l* of water and decolorized with active charcoal. The solution was again evaporated to 5 m*l* and left to settle in a refrigerator. Then a crude products (5.1 g) of mp 202—212°C (dec.) was collected by filtration and recrystallized from 10 ml of boiling water to give 4.9 g (9.6% yield) of V, mp 220—222°C (dec.).

Found: C, 24.01; H, 3.33; Br, 58.53%. Calcd for $C_6H_{10}O_4Br_2$: C, 23.53; H, 3.27; Br, 59.29%.

DL-2,3,5,6-Tetra-*O*-acetyl-1,4-dibromo-1,4-dideoxy-*chiro*-inositol (VIII). A 535 mg portion of V was acetylated overnight with acetic anhydride (5 m*l*) in pyridine (5 m*l*) at room temperature. After an excess reagent was removed under reduced pressure, the oily product was dissolved in chloroform. The chloroform solution was washed with cold water, dried over anhydrous sodium sulfate and evaporated. The residue was crystallized from ethanol to give 325 mg of the product. The product was recrystallized from the same solvent giving 303 mg (36.8% yield) of fine crystals, mp 120—123°C.

Found: C, 35.69; H, 3.99; Br, 33.83%. Calcd for $C_{14}H_{18}Br_2O_8$: C, 35.44; H, 4.09; Br, 33.75%.

DL-Cyclohexane-1,2,4,5-tetrol (124/5) (IX). A 2.23 g portion of V was hydrogenated in 50% aqueous ethanol (30 m*l*) with Raney nickel and Amberlite IR-4B under 3.4 kg/cm² of hydrogen pressure for 20 hr. After the catalyst and the ion exchange resin were removed by filtration, the filtrate was evaporated under reduced pressure. The oily residue was crystallized from ethanol to give a crude product (203.5 mg) of mp 202—205°C. The product was recrystallized from ethanol to give 154.1 mg (14.24% yield) of an analytically pure sample, mp 206—208°C (lit.[7] mp 208—209°C). (Found: C, 48.64; H, 8.16%.).

The product was acylated with acetic anhydride in pyridine giving the tetra-*O*-acetyl derivative of mp 89—91°C (lit.[7] mp 91—93°C), and with benzoyl chloride in pyridine to yield the tetra-*O*-benzoyl derivative of mp 169—171°C (lit.[7] mp 172—173°C).

DL-1-Bromo-1-deoxy-*neo*-inositol (III). Ethanol was added to the mother liquor of V until the solution was turbid. Then the solution was left to settle in a refrigerator to give 4.2 g of a crystalline product. The crude product was collected by filtration and recrystallized from 90% ethanol to give 3.1 g (5.2% yield) of III, mp 210—213°C dec. (lit.[5] 214°C dec.). (Found: C, 29.43; H, 4.44; Br, 33.01 %).

DL-Penta-*O*-acetyl-*talo*-quercitol (VI). A 1.0 g portion of III was dissolved in 15 m*l* of water and hydrogenated in 3.4 kg/cm² of hydrogen pressure in the presence of Raney nickel catalyst (2 spatulas) and Amberlite IR-4B for 20 hr. Then the mixture was filtered, and the filtrate was evaporated under reduced pressure. The residue was acetylated by the usual procedure, and the product was recrystallized from ethanol to give 109 mg (7.1% yield) of fine crystals, mp 170—171°C (lit.[5] mp 170°C). (Found: C, 51.08; H, 6.01%).

VI was hydrolyzed in 2N hydrochloric acid and the hydrolyzate was evaporated *in vacuo*. The residue was recrystallized from aqueous ethanol to give DL-*talo*-quercitol, mp 222—225°C (dec.) (lit.[5] mp 225°C dec.). (Found: C, 44.08; H, 7.44%).

The authors wish to thank Professor G. E. McCasland for the comparison of the pmr spectra. Thanks are due also to Professor Sumio Umezawa for his helpful advice. The financial support from the Ministry of Education for this work is gratefully acknowledged.

BULLETIN OF THE CHEMICAL SOCIETY OF JAPAN VOL. 42 2677—2682 (1969)

The Rate of Penetration of Photographic Chemicals into Gelatin Layers. I. Diffusion Rate of Developing Materials

Haruhiko IWANO

Research Laboratories, Ashigara, Fuji Photo Film Co., Ltd., Minami-ashigara, Kanagawa

(Received March 8, 1969)

The rate of diffusion of various kinds of developing materials through coated gelatin layers was determined by using silver halide as a detector. *p*-Phenylenediamines have the biggest diffusion constants among materials tested. They have no pH-dependency nor concentration-dependency. *p*-Aminophenols have slightly lower diffusion constants than the corresponding *p*-phenylenediamines. The constants increase with increase in molecular sizes and also with pH. Hydroquinones have relatively low diffusion constants. They are considerably affected by variation of pH, concentration and ionic strength. These characteristics are discussed in connection with the chemical structures of developing materials.

The penetration of photographic chemicals into gelatin layers is a fundamental problem for rapid development process.

Since the measurement of dye-diffusion by Herzog and Polotzky,[1] many investigations have been reported about the diffusion of dyes and photographic chemicals in gelatin gel. Ostwald and Quast,[2] Pontius and his colaborators[3] and other investigators[4,5] determined the rate of diffusion of various dyes. Blyumberg and Davidkin[6] and Bagdanov and Polyakova[7] measured the diffusion rate of developing materials, halides and alkaline substances. Adair[8] and other investigators[9] adopted a capillary tube method to determine the diffusion rate of bromide ion in gelatin gel.

The diffusion rate in gelatin gel is different from that in a coated gelatin layer. Reckziegel[10] is the first who investigated the diffusion in coated layers.

The author made a series of investigations using gelatin coatings, and this paper deals particularly with the effect of molecular size, pH, ionic strength and temperature on the diffusion rate of various developing materials.

Experimental Procedure

The method of measurement was similar to that by Reckziegel.[10]

Test Samples. Various thickness of gelatin layers (0 to 26 μ) were coated on a silver bromo-iodide emulsion layer applied on a film support with 2.7 μ thickness which acted as a detector layer (Fig. 1).

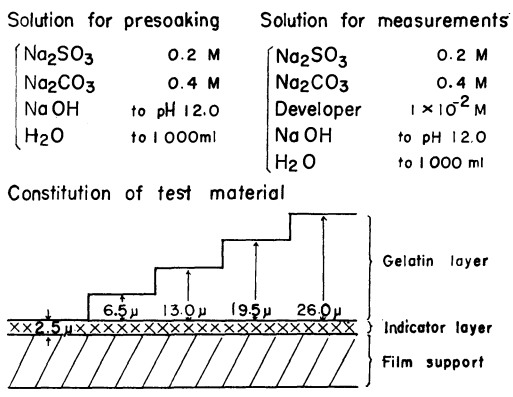

Fig. 1. Explanation of experimental procedure.

Measurement. Pre-swollen samples were dipped into a bromide-free solution containing a developing material. The developing material diffuses through gelatin to the emulsion layer at the bottom and then reduces silver halide instantaneously. The blackening indicates the time required for penetration. The solu-

1) R. O. Herzog and Polotzky, *Z. Elektrochem.*, **17**, 679 (1911); *Z. Phys. Chem.*, **87**, 449 (1914).

2) a) W. Ostwaldt and A. Quast, *Kolloid Z.*, **51**, 273 (1930); b) *ibid.*, **51**, 361 (1930); c) *ibid.*, **48**, 83 (1929).

3) a) R. B. Pontius, M. L. Kaplan and R. M. Husney, *J. Phys. Chem.*, **61**, 9 (1956); b) R. B. Pontius and J. A. Wenrich, *Phot. Sci. Engineering*, **2**, 131 (1958).

4) W. Luck, *Ber. Bunsenges. Phys. Chem.*, **69**, 255 (1965).

5) B. Vlcek and S. Vlcekova, *Zhur. Nauch. i Priklad. Foto. i Kinema.*, **5**, 187 (1960).

6) a) J. B. Blyumberg and I. M. Davidkin, *ibid.*, **8**, 3 (1963); b) *ibid.*, **8**, 81 (1963).

7) S. G. Bagdanov and N. V. Polyakova, *ibid.*, **2**, 187 (1957).

8) G. S. Adair, *Biochem. J.*, **14**, 762 (1920).

9) J. P. Stonham and A. M. Kragh, *J. Phot. Sci.*, **14**, 97 (1966).

10) R. Reckziegel, *Mitteilungen aus den Forschungslab. Agfa.*, **1**, 239 (1955).

tion used for pre-soaking to eliminate the effect of swelling had the same composition as the developer solution except that it did not contain the developing material.

Accuracy. The relative errors for measurement of layer thickness fell within ±2% by Tsugami Precision Microcator under 95% confidence limit, and that of diffusion time fell within ±5% under 95% confidence limit.

Theoretical Treatment of Diffusion Process

One dimensional expression of Fick's diffusion law may be applied to the penetration of developing materials through the gelatin layer;

$$\partial c/\partial t = K\partial^2 c/\partial x^2 \quad (1)$$

were c is the concentration of the developing material, t the time required for the developer to diffuse through the layer with thickness x and K the diffusion constant. Following Lederer,[11] Eq. (1) can be solved as follows:

$$C_i = C_a[1-(4/\pi)\cos(\pi l/2x)\exp(-ft) -(4/3\pi)\cos(2\pi l/2x)\exp(-9ft)+\cdots] \quad (2)$$

where $f = \pi^2 K/4x^2$

C_i: Concentration of the developing material at x from surface of gelatin layer.

C_a: Concentration of the developing material in bulk solution.

Supposing that the blackening of the detector layer occurs instantly when the first portion of the developing material (m) has reached through gelatin layer (x) to the detector layer, the following relation can be obtained between m and x by integrating Eq. (2).

$$m = C_a[a-(8/\pi^2)(x+a)\sin\{\pi a/(x+a)\}\exp(-ft)+\cdots] \quad (3)$$

Here, a means a hypothetical diffused length of the developing material into the detector layer to induce the first blackening.

If $h + a \gg 2a$, Eq. (3) can be simplified by approximation.

$$m = C_a a\{1-(4/\pi)\exp(-\pi^2 Kt/4x)\} \quad (4)$$

By considering the condition,

$$\lim_{x\to\infty}\{\log(C_a a/C_a a-m)\} = 0 \quad (5)$$

we can derive from simplification of Eq. (4)

$$t = (4x^2/\pi^2 K)\ln(4/\pi) \quad (6)$$

or

$$x = K't^{1/2} \quad (7)$$

where

$$K' = \pi K^{1/2}/2\{\ln(4/\pi)\}^{1/2}$$

Equation (6) or (7) means that, if penetration of the developing materials proceeds by Fick's diffusion process, the time required to penetrate through the layer will be proportional to the square of layer thickness.

Experimental Results

1. Diffusion of Various Types of Developers. The rate of diffusion was determined by a solution containing 10 mmol/l of the developing material, 0.2 mol/l of Na_2SO_3, 0.4 mol/l of Na_2CO_3 and NaOH or H_2SO_4 to adjust pH. Plots of layer thickness *vs.* square root of penetration time showed linear relation for almost all developers examined (Fig. 2). This means that the diffusion process satisfies Fick's law, so far as the equation is con-

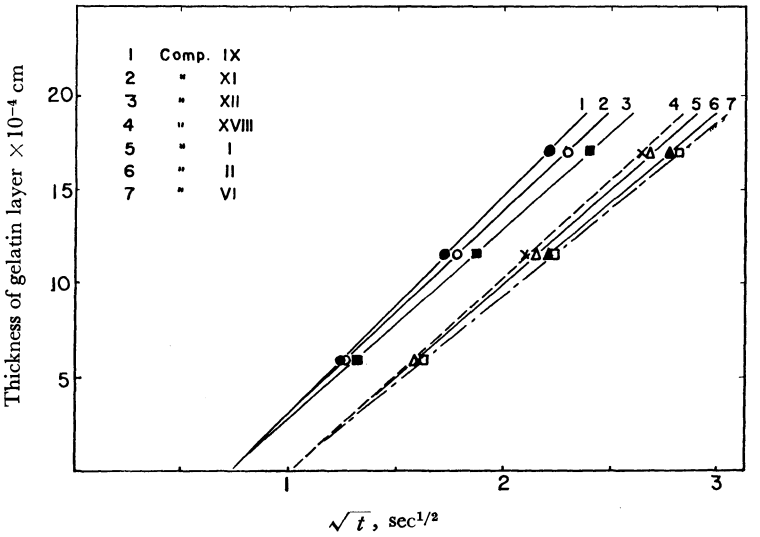

Fig. 2. Distance - time relation during diffusion process.

11) E. L. Lederer, *Kolloid Z.*, **44**, 108 (1928).

cerned. Therefore, the diffusion constant can be obtained from the tangent(K) of Fig. 2 by using Eq. (7).

The diffusion constants of various types of developers thus obtained are listed in Tables 1—3. The results showed: (1) In the series of *p*-aminophenols and *p*-phenylenediamines, diffusion constants decreased with the increase in size of substituted groups, but no distinct rule could be observed about hydroquinone derivatives. (2) The diffusion constants of *p*-phenylenediamines were generally greater than those of corresponding *p*-aminophenols and the latter were greater than those of hydroquinones.

Table 1. Diffusion constants of *p*-aminophenols

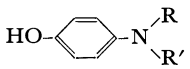

Comp.	R	R′	$D\times10^{-7}$ cm²/sec
I	-H	-H	1.69
II	-H	$-CH_3$	1.58
III	-H	$-C_2H_5$	1.20
IV	-H	$-s\text{-}C_4H_9$	1.05
V	-H	$-n\text{-}C_4H_9$	1.05
VI	-H	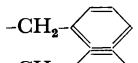	0.923
VII	-H	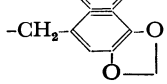	0.695
VIII	$-C_2H_5$	$-C_2H_5$	0.962

Table 2. Diffusion constants of *p*-phenylenediamines

Comp.		$D\times10^{-7}$cm²/sec
IX	*N*,*N*-Diethyl-*p*-phenylenediamine	1.85
X	3-Methyl-4-amino-*N*,*N*-diethylaniline	1.56
XI	4-Amino-*N*-ethyl-*N*-hydroxyethylaniline	1.77
XII	3-Methyl-4-amino-*N*-ethyl-*N*-hydroxyethylaniline	1.46

Table 3. Diffusion constants of hydroquinones and other developing materials

Hydroquinone and other developing material		$D\times10^{-7}$ cm²/sec
XIII	Hydroquinone	0.695
XIV	Methylhydroquinone	0.324
XV	2,5-Dihydroxyphenylamylketone	0.527
XVI	2,5-Dihydroxyphenylcetylketone	0.057
XVII	Phenylhydroquinone	0.645
XVIII	1-Phenyl-3-pyrazolidone	1.27
XIX	Amidol	1.42
XX	Pyrogallol	0.424

2. Effect of pH. The pH-dependency of the diffusion of three types of developing materials differed from each other.

A typical *p*-phenylenediamine (compound XII) showed no pH-dependency over a pH-range from 9.4 to 12.0, as shown in Fig. 3. On the other hand, *p*-aminophenols had some pH-dependency. This dependency became smaller with increase in pH. In fact, it almost disappeared over pH 10.7 in the case of metol.

In contrast to the results of *p*-aminophenols, the rate of diffusion of hydroquinones decreased with increase in pH.

3. Effect of Temperature. The temperature dependency of three types of developers also showed some difference from one another (Fig. 4).

The plots of rate *vs.* $1/T$ consists of two straight lines in case of hydroquinone. Activation energies

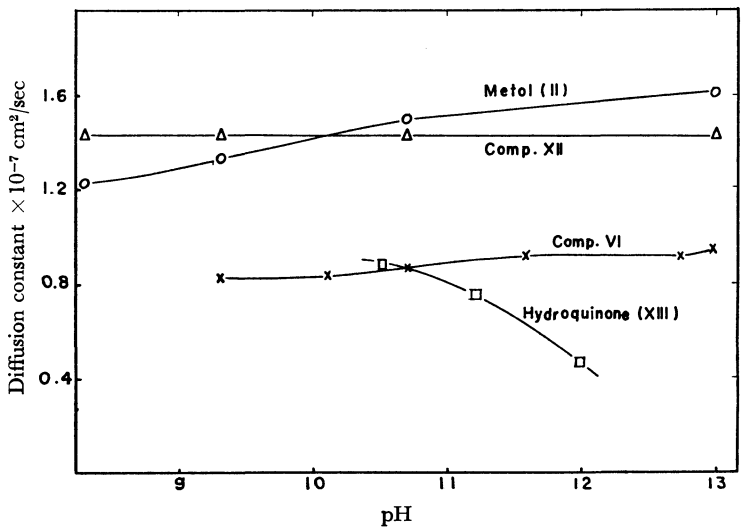

Fig. 3. Effect of pH on diffusion constant.

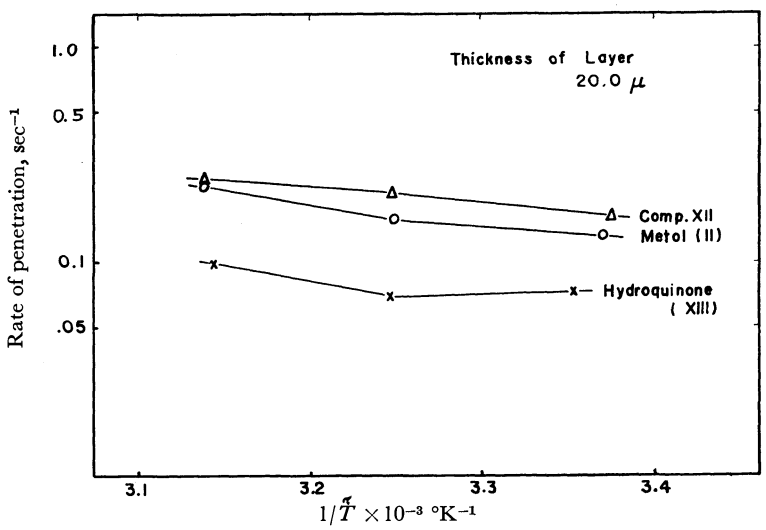

Fig. 4. Effect of temperature on penetration rate.

of diffusion obtained from the slope of the curves for the three types of developing materials are listed in Table 4.

Table 4. Activation energy of diffusion

Compound	Temperature	$E_{act.}$
II	23—35°C	2.9 kcal/mol
	35—45°C	6.5 kcal/mol
XII	23—45°C	3.1 kcal/mol
XIII	35—45°C	7.2 kcal/mol

4. Effect of Concentration of Developing Materials. The diffusion constants of *p*-aminophenols and *p*-phenylenediamines did not show any dependence on concentration except the case of extremely low concentration, but that of hydroquinone showed relatively large dependence up to the concentration of 8×10^{-2} mol/*l* (Fig. 5). The fact that the diffusion constant of metol is independent of concentration means that this process is pure physical diffusion which can be expressed by Fick's law.

5. Penetration of Developing Materials into Unswollen Layer. Measurement of penetration into the gelatin layer which had not been preswollen also gave a linear relation between the depth of penetration and the square root of penetration time (Fig. 6). Therefore, this penetration process can be simulated to diffusion, although it contains many complicated processes such as absorption of water by gelatin, swelling and hydration.

The apparent rate of penetration was independent of the types of developing materials, if the applied

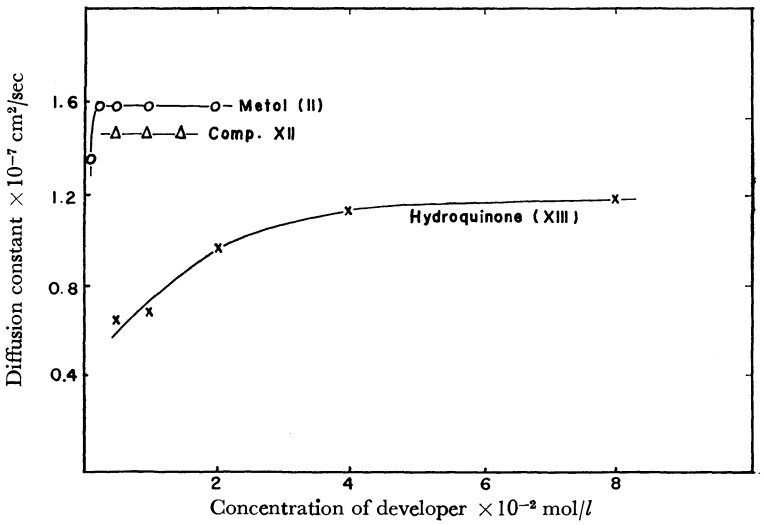

Fig. 5. Effect of developer concentration on diffusion.

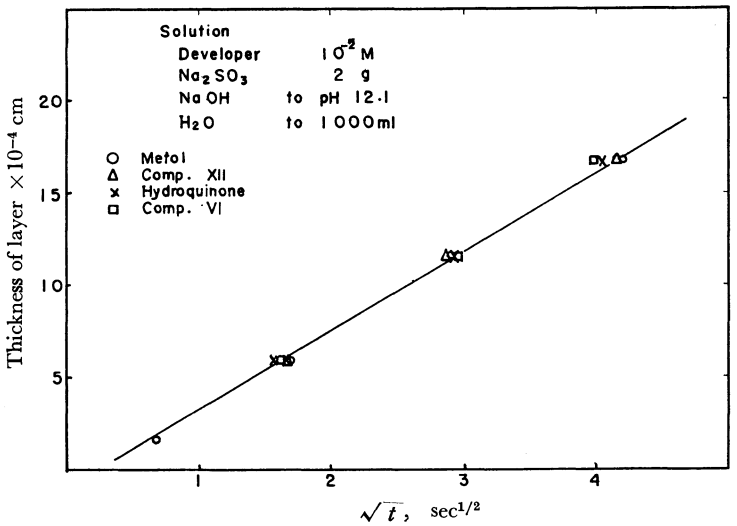

Fig. 6. Penetration of developer into unswollen layer.

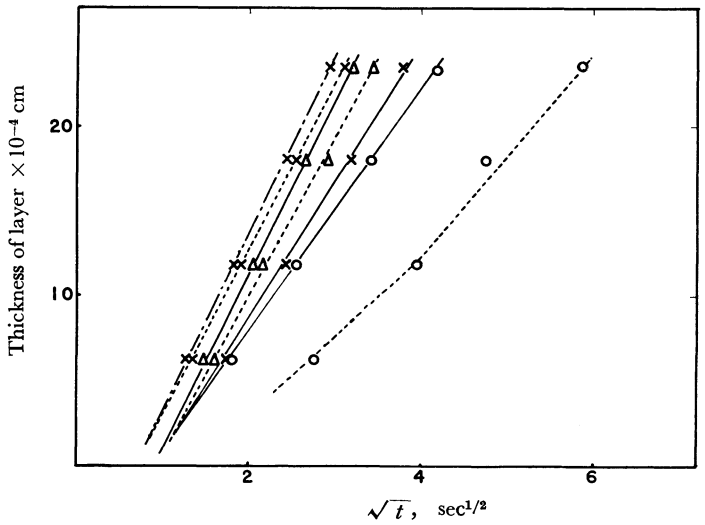

Fig. 7. Effect of salt on penetration.
△ Comp. II, × Comp. XII, ○ Comp. XIII
—— with Na_2SO_4, ----- without Na_2SO_4, —·— Na_2SO_4 soln. was applied only in pre-swelling

solution had low ionic strength or relatively low pH. This result is interpreted from the slow penetration rate of OH^- ion in these solutions which determines the initiation of blackening of detector layer. This explanation is supported by the fact that the initiation of blackening occurred about 1 sec after OH^- ion had reached the bottom layer (detector).

On the other hand, the rate of penetration from solutions of high alkalinity or of high ionic strength depended on the types of developing materials.

6. The Effect of Salt Concentration. The presence of salts such as Na_2SO_4 affected the diffusion rate in different ways according to the types of developing materials, as shown in Fig. 7. The presence of Na_2SO_4 accelerated the diffusion of hydroquinone and metol, but retarded that of a *p*-phenylenediamine derivative (compound XII). The accelerated diffusion of the compound XII, however, could also be observed, in the case Na_2SO_4 was present only in the swelling solution and not in the solution of the developing material.

Discussion

Three types of developing materials showed different characteristics with respect to diffusion.

p-Phenylenediamines have two amino groups and

no hydroxy group. They have the biggest diffusion constants, no pH-dependence or concentration dependence. Their activation energies are constant over 23—45°C. Ionic strength slightly affects the diffusion.

Hydroquinone with two hydroxy groups has just the opposite property. Its diffusion constant is the smallest and had big pH- and concentration-dependence. It varies considerably with the change of ionic strength. The apparent activation energy varies with temperature. *p*-Aminophenols have one amino and one hydroxy group. They have the characteristics intermediate between the two mentioned above.

In alkaline medium, dissociated functional groups of gelatin will interact with charged developing materials, thus affecting the rate of diffusion. Therefore, it seems that hydroquinone which dissociates with $pK_1=9.9$ and $pK_2=11.4$ has relatively large dependency on pH, concentration and ionic strength, and that non-dissociating *p*-phenylenediamines do not have such dependency.

The constancy of diffusion coefficient over a wide range of concentration of a developing material means that (1) the penetration into pre-swollen layers can be treated as pure diffusion and that (2) the condition $C_a \times a \gg m$ is satisfied to calculate K by Eq. (6).

Hydroquinone does not have a constant rate of diffusion under 8×10^{-2} mol/*l*. This means again that it has some interaction with the medium or it has relatively large m value.

The decrease in diffusion constant with increase in molecular size of substituted group in *p*-aminophenol supports the suggestion by Alburger[12] who assumed that the property of duratol having a tendency to develop surface layer selectively is due to its molecular size. But the property is more closely related to the activity of the duratol rather than its poor diffusibility.

This investigation is concerned only with the first step of development processes. Many successive steps might affect the rate of development. The effect of pre-bathing and control of swelling by addendants to the solution or to gelatin are also important in photographic development.

The author wishes to acknowledge the helpful suggestions made by Professor Dr. W. F. Berg of the Swiss Federal Institute of Technology, and the discussions with Mr. Ueda and Mr. Nakajima of this Laboratory. He also wishes to express his sincere thanks to Mr. Koseki, director of the Laboratory, for permission to write this article.

12) J. R. Alburger, *J. Soc. Motion Picture Engrs.*, **35**, 282 (1940).

NOTES

BULLETIN OF THE CHEMICAL SOCIETY OF JAPAN VOL. 42 2683—2685 (1969)

Synthetic Inorganic Ion-exchange Materials. XIII. The Mutual Separation of Alkali Metals with Three Different Antimonic Acids

Mitsuo ABE

Department of Chemistry, Tokyo Institute of Technology, Ookayama, Meguro-ku, Tokyo

(Received June 12, 1968)

The present paper will describe the use in the chromatographic separation of alkali metal ions on columns of the three different antimonic acids;[1] amorphous (S_A), glassy (S_G), and crystalline (S_C). The samples were prepared as was been described in a preceding paper,[2] and then controlled

TABLE 1. DISTRIBUTION COEFFICIENTS AND SEPARATION FACTORS (α) ON THREE DIFFERENT ANTIMONIC ACIDS

Exchanger	Solution	Li	Na	K	Rb	Cs
S_A	1×10^{-3}M MNO_3	1.0×10^2	4.1×10^2	1.5×10^3	2.8×10^3	5.8×10^3
	0.1N HNO_3	6.4	27.8	123	196	226
	(α)		4.3	4.4	1.6	1.2
	0.05M NH_4NO_3	7.7	24.8	41	41	31
	(α)		3.2	1.7	1.0	0.76
S_G	1×10^{-3}M NMO_3	2.6×10^2	7.5×10^2	2.5×10^3	6.0×10^3	9.8×10^3
	0.1N HNO_3	10.4	37.4	167	238	318
	(α)		3.6	4.4	1.4	1.3
	0.05M NH_4NO_3	12.5	37.5	55	44	37.3
	(α)		2.5	1.7	0.8	0.85
		Li	K	Cs	Rb	Na
S_C	1×10^{-3}M MNO_3	7.1×10	1.76×10^4	3.5×10^4	1.3×10^5	1.0×10^6
	0.1N HNO_3	0.9	4.5×10^2	1.4×10^3	8.1×10^3	8.3×10^4
	(α)		500	3.1	5.8	10.2
	0.05M NH_4NO_3	2.5	10.4	37.3	56.2	890
	(α)		4	3.6	1.5	15.8
		Li	Na	K	Rb	Cs
Amberlite IR-120	1×10^{-3}M MNO_3	1.6×10^3	3.1×10^3	4.2×10^3	7.8×10^3	1.3×10^4
	0.2N HNO_3	19.5	30	64	85.5	100
	(α)		1.5	2.1	1.3	1.2
Zirconium phosphate	1×10^{-3}M MNO_3	1.7×10^2	1.1×10^3	3.8×10^3	9.8×10^3	1.9×10^4
	0.1N HNO_3	15.0	41	140	390	910
	(α)		2.7	3.4	2.8	2.3

Exchanger: 0.100 g ,total volume: 25.0 m*l*, 20 ± 0.05°C, immersion; 24 hr.
S_A: amorphous antimonic acid, S_G: glassy antimonic acid, S_C: crystalline antimonic acid.
Distribution coefficient was calculated from the following equation;

$$K_d = \frac{A_0 - A_s}{A_s} \cdot \frac{ml}{g}$$

where A_0 is the concentration of alkali metal in the solution before equilibration (1×10^{-3} mol/*l*), A_s is the concentration in the solution after equilibration, m*l* is total volume of the solution in mililiters, and g is the weight of the sample in grames.

1) M. Abe and T. Ito, This Bulletin, **41**, 333 (1968).
2) M. Abe and T. Ito, *ibid.*, **41**, 2366 (1968).

in a 100—200 mesh size. The column experiments were carried out with a column ($0.8\phi \times 6.0$ cm) containing 3.0, 6.4, and 3.9 g for S_A, S_G, and S_C respectively. The concentration of alkali metals was determined flame-photometrically by using a Hitachi EPU-2A with a flame apparatus, H-2, attached.

Results and Discussion

Affinity Series for Alkali Metal Ions. Table 1 gives the values of the distribution coefficients for alkali metal ions on three different antimonic acids. The K_d values on S_C are higher than those on S_A and S_G except in the case on Li^+ adsorption, and S_A gives values almost identical with those obtained on S_G. The affinity on the S_A and S_G was found to increase in the order: $Li^+ < Na^+ < K^+ < Rb^+ < Cs^+$ in the acid solution, while the order was: $Li^+ < Na^+ \fallingdotseq Cs^+ < K^+ = Rb^+$ in the ammonium nitrate solution. The affinity series on the S_C may be written as $Li^+ < K^+ < Cs^+ < Rb^+ < Na^+$ in the acid solution and $Li^+ < K^+ < Rb^+ < Cs^+ < Na^+$ in the ammonium nitrate solution. The difference in selectivity is very large compared with those obtained for the sulfonic acid resins. In the acid solution, Rb^+ was more strongly adsorbed than Cs^+, with the separation factor of 5.8. Na^+ was more strongly adsorbed than any other alkali metal ions in the solutions of both nitric acid and ammonium nitrate. The separation factor in the pairs of lithium and other alkali metals may be compared favorably with those of other cation exchangers.

According to Lefebvre,[3] the inverse selectivity should prevail for alkali metals: $Na^+ < K^+ < NH_4^+ < Rb^+ < Cs^+$ on the polyantimonic acid.

When a large volume of a 0.1 N soultion of various alkali metal salts was passed through an S_C column, the uptake of alkali metals showed the values of 1.0, 2.8, 2.4, 1.4, and 1.2 meq/g for Li^+, Na^+, K^+, Rb^+, and Cs^+ respectively. In the solutions with a constant ionic strength of 0.1 M ($HNO_3 + MNO_3$), ion-exchange isotherms on the S_C gave ogee-sharp curves,[4] as is the case with rigid inorganic ion-exchangers (*e. g.*, zirconium phosphate, zeolites, and basic cancrinite). These results indicate that the selectivity coefficient varies strongly with the ionic composition and that the reversal of selectivity, which may be due to steric factors, arises from the course of conversion. The crystalline antimonic acid presents a fairly rigid lattice, for the volume change on conversion from the hydrogen form to the alkali forms is very small; accordingly, the lattice constants of various forms gave 10.30, 10.33, 10.37, 10.38, 10.40 and 10.47 Å for Na, Rb, Li, H, Cs, and K forms, without any change in the crystal system. The increased order in the lattice constant conforms to the inverse order in the affinity series for micro amounts of all the alkali metal ions except Li^+.

Separation of Alkali Metal Ions on the Columns of the Three Different Antimonic Acids. Small amounts of various alkali metal ions were adsorbed onto the column and then eluted with different eluants.

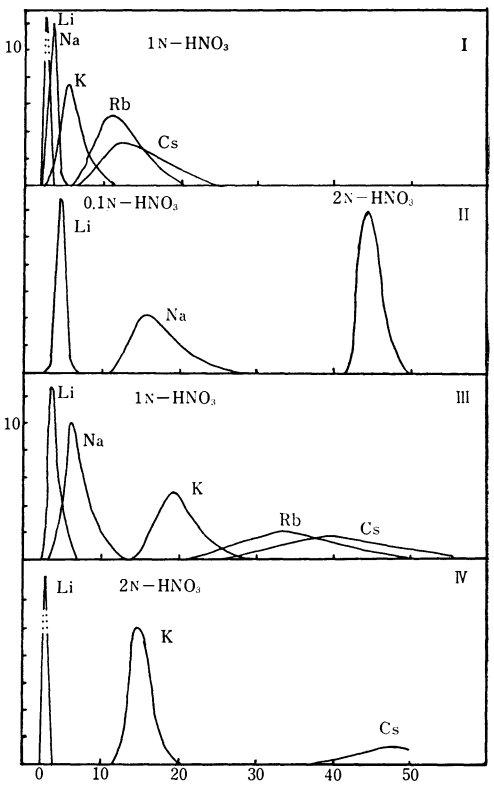

Fig. 1. The elutions of alkali metals with nitric acid of various concentrations on the three different antimonic acids.
Fraction: 5.5 m*l*, alkali metal: each 0.02 mmol, flow rate; 0.3 m*l*/min
I and II: amorphous antimonic acid, III: glassy antimonic acid, IV: crystalline antimonic acid.

Elution with Various Nitric Acid Solutions. On the S_A and S_G, all of the alkali metal ions were more easily eluted with nitric acid of a relatively dilute solution than in the case of S_C, and the elution curves were always somewhat asymmetric. Complete separation were made for Li^+, Na^+, and K^+ with an 0.1 N (S_A) or 0.2 N (S_G) and 2 N nitric acid solution. On S_C, a good separation was obtained for Li^+, K^+, and Cs^+ with a 2 N nitric acid solution, but Na^+ and Rb^+, were not eluted within 70 fractions.

3) J. Lefebvre and F. Gamard, *C. R. hebd. Seanc. Acad. Sci., Paris*, **260**, 6911 (1965).

4) M. Abe and T. Ito, Preprints for The 19th Annual Meeting of The Chemical Society of Japan (April, 1966) Vol. II, p. 292.

It has been established that, on the organic ion-exchangers, the mutual separation between Rb^+ and Cs^+ is very difficult. The separation on the S_C can be made completely with a 4N nitric acid solution. The separation factor, α_{Rb}^{Cs}, calculated from the peak volume in the elution curves showed 5.6. Sodium ions were more strongly adsorbed than any other alkali metal ions and could not be eluted by a relatively concentrated nitric acid solution within the column volume shown in Fig. 2-I. Figure 2-II shows that the order of peak

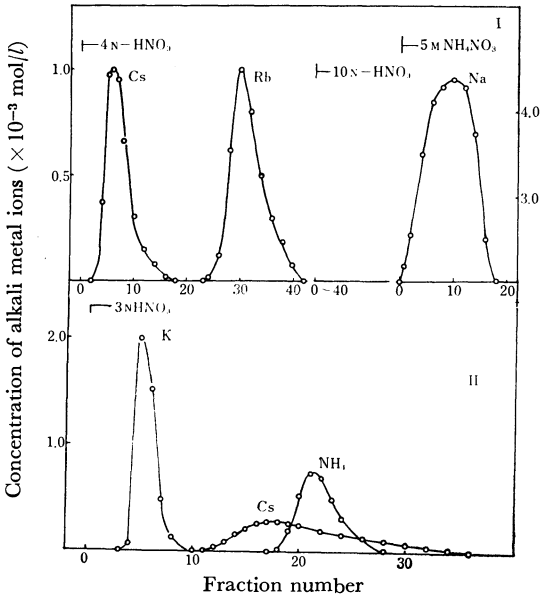

Fig. 2. The elution of alkali metals on crystalline antimonic acid
I: separation of sodium, rubidium and cesium fraction; 5.5 m*l*, Rb and Cs; each 0.04 mmol, Na; 0.1 mmol
II: elution of potassium, cesium and ammonium, ions
fraction; 5.6m*l*, K, Cs and NH_4; each 0.02mmol
Flow rate: 0.3 m*l*/min.

volume in the elution curves was $K^+ < Cs^+ < NH_4^+$ and that S_C was not for selective for ammonium and cesium ions, while there was a broader curve for cesium ions. With eluants of both nitric acid and ammonium nitrate solutions, the time required was relatively short, only about 10 hr being sufficient for a complete separation of a miligram-amount of alkali metals (Fig. 3-I).

Elutions with Various Ammonium Nitrate Solutions. On S_C, pairs of neighbouring alkali metal ions, such as Li-K, K-Rb,and Cs-Na, were

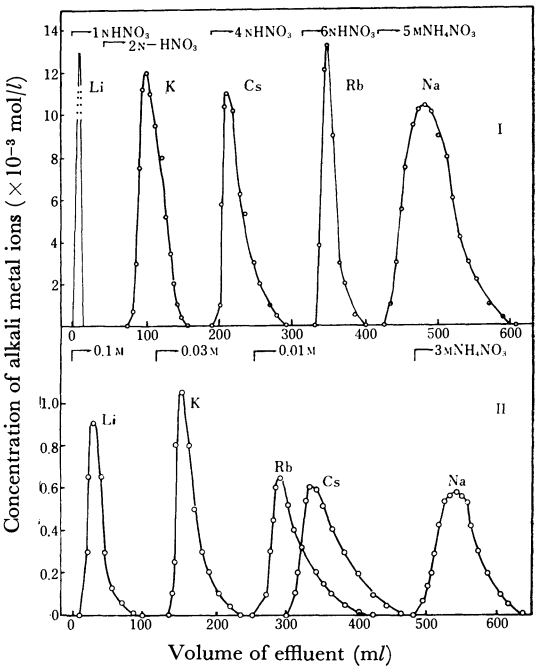

Fig. 3. The separation of alkali metal ions with nitric acid and ammonium nitrate of various concentration on the crystalline antimonic acid S_C.
Flow rate: 0.6 m*l*/min.
I: with the nitric acid and ammonium nitrate solutions, Li; 0.01 mmol, Na; 0.1 mmol, K, Rb, Cs; each 0.04 mmol
II: with the ammonium nitrate solutions, Li; 0.02 mmol, Na, K, Rb, Cs; each 0.04 mmol

easily separated in the same column length, but not the Rb-Cs pair (Fig. 3-II). On S_A and S_G, all the alkali metal ions except Li^+ were removed as a group with a 0.03M ammonium nitrate solution.

These results indicate the presence of antimonic acid of two types, with a different selectivity for alkali metal-ions adsorptions, a difference may be closely related to the disparity in the surface structure.[2] The S_G and S_C were favorable for column work because their lower solubilities and their suitable granular forms. The S_C was especially stable against almost all reagents, including concentrated acid and alkaline solutilons and oxidizing agents. The S_A was unsuitable, since it was relatively soluble in water and was gradually transformed into crystalline antimonic acid in a relatively concentrated acid solution.

The author wishes to express his thanks to Professor Takuji Ito for his valuable advice and discussions throughout this work.

BULLETIN OF THE CHEMICAL SOCIETY OF JAPAN VOL. 42 2686—2688 (1969)

Synthesis of Hypothiaminic Esters[1]

Goro TSUKAMOTO, Toshio WATANABE and Isamu UTSUMI

Pharmaceutical Research Laboratory, Tanabe Seiyaku Co., Ltd., Kashima-cho, Higashiyodogawa-ku, Osaka

(Received September 16, 1968)

In a previous paper we reported that hypothiaminic acids (I, VIII) would undergo disproportionation in methanolic hydrogen chloride to the corresponding thiolsulfonates (VII) on the basis of the formation of product (A), which was positive toward thiochrome reaction after treatment with cysteine and isolation of thiaminic acid (VI).[2]

We have made an attempt to isolate the product (A) and confirm its structure.

A solution of I in methanolic hydrogen chloride gave crystals (A), mp 110—112°C. Analogously, the same treatment in ethanolic hydrogen chloride solution of I afforded crystals (B), mp 118—120°C, which were oxidized with hydrogen peroxide to VI.

The structures of these compounds (A, B) were confirmed to be not thiolsulfonate-type compound (VII) but sulfinic esters (V) by means of NMR spectra.

The preparation of sulfinic ester by the reaction of I with diazomethane and the action of ethyl chloroformate on II in methanol gave also Va.[3]

However, sodium hypothiaminate (IX) was treated with ethyl chloroformate in chloroform to yield colorless prisms (mp 133—135°C). On the basis of spectral and analytical data, the structure of the compound was confirmed to be 1,2-oxathiolane-2-oxide derivatives (XII, hereinafter called sulfinothiamine). So far as we know, there is no report on 5-membered ring sulfinic ester.

Compound VIII was allowed to react with thionyl chloride to give sulfinyl chloride (XI) which upon the action of base cyclized to XII. XI could be prepared simply by treating X or XIV with chlorine. Similarly, the disulfide III was converted to open-chain sulfinic ester Vb by chlorine oxidation.

It was noteworthy that the bridge methylene of XII between the pyrimidine and *N*-formyl moiety showed spectrum of AB system ($J=15$ cps). The magnetic non-equivalence of the methylene seems to be due to a rotational restriction caused by the bonding between the 4-amino group and $^{+}S{=}O^{-}$ group. This might be supported by the fact that no splitting of the methylene was observed in 1,2-oxathiolane XIII, synthesized recently by Nakano and Nishimura.[4] Compound XIII was oxidized with perbenzoic acid to give XII.

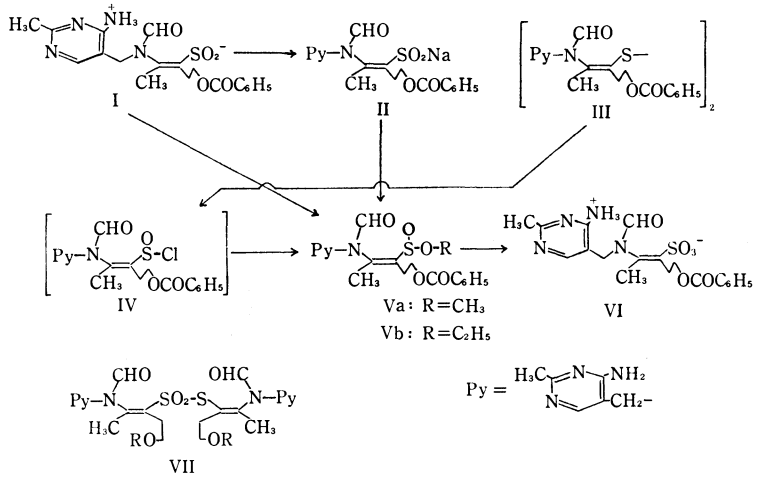

Fig. 1.

1) Part XXXIII in a series on "Studies on Thiamine Disulfide."

2) I. Utsumi, T. Watanabe, K. Harada and G. Tsukamoto, *Chem. Pharm. Bull.* (*Tokyo*), **15**, 1485 (1965).

3) Houben-Weyl, "Methoden der Organischen Chemie" 4 Auflage, Georg Tieme Verlag, **9**, 338 (1955).

4) J. Nakano and O. Nishimura, Abstracts of the 88th Annual Meeting of the Pharmaceutical Society of Japan, Tokyo, April, 1968, p. 196.

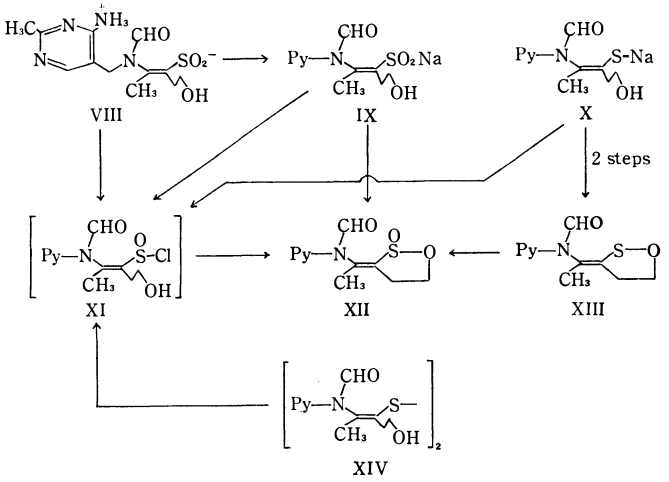

Fig. 2.

It was found that V was reduced quantitatively to thiamine with 1000 mol of cysteine per mol of Vb at pH 8.6 and 50°C for 2 hr. Accordingly, the following mechanism appears applicable:

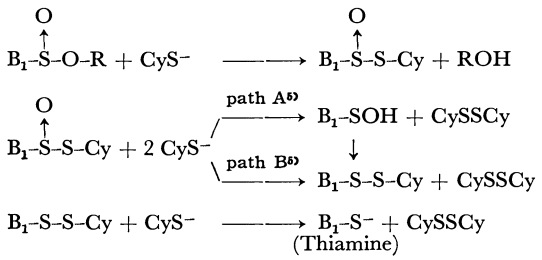

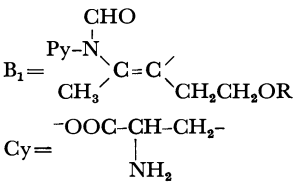

Reduction of XII to thiamine proceeds with difficulty in comparison with that of open-chain sulfinic esters (V). This might be unusual in view of the fact that the rates of hydrolysis of sultones[6] or lactones[7] are known to be very fast in comparison with the open-chain analogs. Unfortunately, there has been no data for the properties of cyclic sulfinate, even for the synthesis. A molecular model suggests a close proximity between the 4-amino group and +S=O⁻ group which would cause a strong interaction between the two groups resulting in a hindered rotation around the bridged methylene bonds as discussed for the unusual splitting of methylene protons in the NMR spectrum of XII. The same interaction might be also the cause of the resistance to the reduction, although further work is necessary in order to elucidate this interesting phenomenon.

Experimental

Methyl *O*-Benzoylhypothiaminate (Va). *i) From I.* A solution of I (840 mg) in absolute methanol (20 m*l*) containing 0.1M hydrogen chloride was warmed in a bath kept at 70° for 1 hr. The solution was concentrated *in vacuo*. After the residue dissolved in water was washed with ether, the aqueous solution, which was made alkaline with sodium bicarbonate, was extracted with chloroform. The extract, which was washed with water and dried over sodium sulfate, was concentrated *in vacuo* and to the residue was added ether to give colorless prisms (500 mg), mp 108—110°C. Recrystallization from ethanol - ether gave Va as colorless prisms, mp 110—112°C.

Found: C, 55.76; H, 5.94; N, 12.72; S, 7.16%. Calcd for $C_{20}H_{24}O_5N_4S$: C, 55.55; H, 5.59; N, 12.96; S, 7.42%.

IR ($CHCl_3$) cm^{-1}: 1713 (C=O), 1665 (NCHO), 1115 (S=O), 980 (S–O). NMR (in $CDCl_3$) τ: 5.55 (s C–CH_2–N).

The reaction of I (120 mg) in ethanol with a large quantity of diazomethane afforded Va (100 mg).

ii) From II. To a solution of II (420 mg) in methanol (15 m*l*) was added ethyl chloroformate (110 mg) under cooling with ice water. The mixture was allowed to stand at room temperature over night, concentrated *in vacuo*, and to the residue was added water and chloroform. The chloroform layer was washed with water and dried over sodium sulfate. The chloroform solution was chromatographed over alumina to afford Va (50 mg).

Ethyl *O*-Benzoylhypothiaminate (Vb). *i) From I.* The same procedure and treatment were followed as described above. The reaction between I (840 mg) and absolute ethanol (20 m*l*) containing 0.1M hydrogen chloride afforded colorless prisms (620 mg), mp 118—

5) G. Tsukamoto, T. Watanabe and I. Utsumi, This Bulletin, **42**, 2566 (1969).

6) F. G. Bordwell, C. F. Osborne and R. D. Chapman, *J. Am. Chem. Soc.*, **81**, 2698 (1959).

7) T. C. Bruice and S. J. Benkovie, "Bioorganic Mechanisms," Vol. 1, W. A. Benjamin, New York (1966), p. 21.

120°C. Recrystallization from ethanol-ether gave Vb as colorless prisms, mp 118—120°C.

Found: C, 56.26; H, 5.85; N, 12.64; S, 6.95%; mol wt (Rast), 450. Calcd for $C_{21}H_{26}O_5N_4S$: C, 56.49; H, 5.87; N, 12.55; S, 7.18%; mol wt, 446.5.

IR ($CHCl_3$) cm^{-1}; 1710 (C=O), 1665 (NCHO), 1115 (S=O), 1010 (S-O). NMR (in $CDCl_3$) τ: 5.75—6.50 (m $-\overset{O}{\overset{|}{S}}-O-CH_2-$), 5.50 (s $C-CH_2-N$).

ii) From III. A solution of III (4.36 g) dissolved in 7.2 g of acetic acid and ethanol (50 m*l*) was cooled to −10——15°C. To the mixture was added dropwise a chloroform solution (10 m*l*) containing chlorine (0.43 g), and then the mixture was titrated with a chloroform solution of dimethylamine to make it alkaline. The mixture was concentrated *in vacuo* and to the residue was added ethanol to separate crystals, which were identical in IR spectrum with III. The mother liquor was evaporated *in vacuo* and the residue dissolved in chloroform was washed with water and dried over sodium sulfate. The chloroform solution was chromatographed over alumina to yield Vb (0.60 g).

Oxidation of Vb with Hydrogen Peroxide. A solution of Vb (90 mg) dissolved in acetic acid (1 m*l*) and 30% hydrogen peroxide (0.1 m*l*) was allowed to stand at room temperature for 2 weeks. The mixture was concentrated *in vacuo*, and the residue was crystallized from 95% aqueous ethanol to yield colorless prisms (20 mg), which was identical in infrared spectrum with authentic sample (VI).

Sulfinothiamine (XII). *i) From IX.* Compound IX (1.1 g) was suspended in chloroform (10 m*l*) and ethyl chloroformate (0.35 g) was added. After the mixture was stirred for 2 hr at room temperature, it was washed with water and dried over sodium sulfate. The chloroform solution was chromatographed over alumina to afford crystals (0.13 g). Recrystallization from ethyl acetate gave colorless prisms mp 133—135°C.

Found: C, 47.94; H, 5.59; N, 18.77; S, 10.55%. Calcd for $C_{12}H_{16}O_3N_4S$: C, 48.64; H, 5.44; N, 18.91; S, 10.82%.

IR (KBr) cm^{-1}: 1110 (S=O), 990 (S-O). NMR (in $CDCl_3$) τ: 5.02 and 5.90 (q $C-CH_2-N$, $J=15$ cps), 5.00—5.50 (m $-\overset{O}{\overset{|}{S}}-O-CH_2-$).

ii) From VIII. A suspension of VIII (9.5 g) in chloroform (30 m*l*) was cooled to −3——5°C and thionyl chloride (0.38 g) was added. After the solution was stirred for 1 hr below 0°C it was alkalified under cooling by addition of a chloroform solution of triethylamine, and then allowed to stand until room temperature was reached. The mixture was washed with water and dried over magnesium sulfate. To the residue obtained by the evaporation of the solvent was added ethyl acetate to yield XII (30 mg).

iii) From XIV. A solution of XIV (3.4 g) dissolved in acetic acid (7.2 g) and chloroform (60 m*l*) was cooled to −10°C and a chloroform solution (5.5 g) containing chlorine (0.6 g) was added dropwise. The mixture was similarly treated as described above to afford XII (0.38 g).

iv) From X. A suspended solution of X (3.8 g) in chloroform (50 m*l*) was cooled to −10°C. After acetic acid (6.0 g) was added to the solution, a chloroform solution (13.0 g) containing chlorine (1.4 g) was added dropwise under cooling to −10°C. Similar treatment of the mixture to that descibed in *i)* gave XII (0.10 g).

Oxidation of XIII with Perbenzoic Acid. To a solution of XIII (280 mg, 1.0×10^{-3} mol) in chloroform (8 m*l*) was added a chloroform (2.4 m*l*) solution containing perbenzoic acid (1.2×10^{-3} mol). The mixture was allowed to stand for 30 min at room temperature, and was shaken with aqueous sodium bicarbonate solution, washed with water, and then dried over sodium sulfate. The residue obtained by the concentration of the chloroform solution was recrystallized from benzene to give XII (120 mg).

The authors wish to express their thanks to Professor S. Oae and Assistant Professor W. Tagaki of Osaka City University for their useful advice and discussion. They also thank Dr. K. Kotera for his NMR spectra determinations.

BULLETIN OF THE CHEMICAL SOCIETY OF JAPAN VOL. 42 2688—2690 (1969)

Reaction Intermediate in the Dimerization of Ethylene Catalyzed by a Palladium(II) Complex. NMR Spectral Evidence for the Formation of the π-Bonded Chloro-acetylacetonato-(1-butene)palladium(II) Complex

Keiji KAWAMOTO, Toshinobu IMANAKA and Shiichiro TERANISHI

Department of Chemical Engineering, Faculty of Engineering Science, Osaka University, Machikaneyama, Toyonaka, Osaka

(Received November 21, 1968)

In a previous paper,[1] it has been shown that bidentate ligands, such as β-diketones, have marked effects on the dimerization of ethylene to butene catalyzed by di-μ-chlorobis(ethylene)dipalladium (I), $(Pd(C_2H_4)Cl_2)_2$; that is, when bidentate ligands, especially β-diketones, are added to the ethylene-

1) K. Kawamoto, T. Imanaka and S. Teranishi, *Nippon Kagaku Zasshi (J. Chem. Soc. Japan, Pure Chem. Sect.)*, **89**, 639 (1968).

palladium(II) chloride - acetic acid system, the additive increases the rate of the dimerization besides accelerating the reduction of palladium(II) to metallic palladium. The order of the acceleration effect was as follows: acetylacetone>ethyl acetoacetate>diethyl malonate.

Though various π-allyl-acetylacetonato-palladium complexes have been isolated by Robinson and Shaw,[2] no olefin-acetylacetone-palladium complex in which the olefin is coordinated with palladium by the π-bond has ever been reported. The present paper will report the NMR spectral evidence for the formation of the π-bonded chloro-acetylacetonato(1-butene)palladium (IV), $(Pd(C_5H_7O_2)(C_2H_5CH{=}CH_2)Cl)$, which is assumed to be an intermediate in the dimerization of ethylene in the presence of an acetylacetone additive. Moreover, a possible mechanism for the dimerization with an acetylacetone additive is also discussed on the basis of the present results.

The procedure of synthesizing complex IV was similar to that described for the synthesis of di-μ-chloro-bisacetylacetonatodipalladium (II), $(Pd(C_5H_7O_2)Cl)_2$, in the previous paper.[1] Into a reaction vessel there were charged complex I and acetylacetone (an equivalent mole to palladium), plus dichloromethane as a solvent, and then ethylene was bubbled into the solution under reflux for half an hour. The resulting solution was filtered and cooled at -40°C, and the solvent was removed. After the residue had been dried under 10^{-3}—10^{-4} mmHg at -40°C, a reddish-brown complex IV was obtained. This material was very unstable, and when warmed to room temperature, changed into a brown complex which was identified as complex II,[1] with a partial precipitation of metallic palladium.

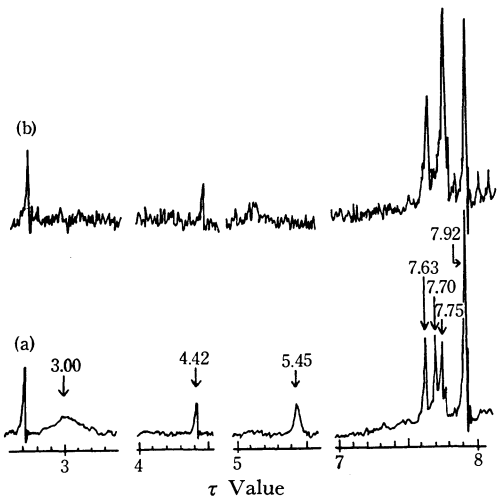

Fig. 1. NMR spectrum of complex IV.
(a) measured at -45°C in $CDCl_3$.
(b) After standing at room temperature for half an hour.

The NMR spectra*1 of the unstable reddish-brown complex IV are shown in Fig. 1, where (a) is measured at -45°C and where (b) is examined after the complex has stood at room temperature for half an hour, during which the complex IV decomposed, evolving butene gas*2 with the precipitation of metallic palladium. The assignment of the NMR spectrum is shown in Table 1. As

Table 1. Assignment of NMR spectrum

τ Value	Relative intensity -45°C	Relative intensity Room temp.	Assignment	Ref.
3.00	2	disappear	$=CH_2$ in 1-butene	2, 3
4.42	0.5		$\diagdown\!\!\diagup$C–H of acac* in complexes II and IV	2, 4, 5
5.54	1	disappear	–CH= in 1-butene	2, 3
7.63	2		$-CH_2-$ in 1-butene	2, 3
7.70	1.5	disappear	$-CH_3$ of acac* in complex IV	2, 4, 5
7.75	1.5	increase	$-CH_3$ of acac* in complex II	2, 4, 5
7.92	3	decrease	$-CH_3$ in 1-butene	2, 3

* acac=acetylacetonate group

is apparent from Table 1, the signals at τ 7.70, 7.75, and 4.42 (relative intensities 1.5 : 1.5 : 0.5) can be attributed to two methyl groups and one central methyne group respectively in the coordinated acetylacetonate group. In fact, the stable acetylacetonato-palladium complex II synthesized from acetylacetone and the ethylene-palladium complex I has NMR signals at τ 7.75 and 4.42 for the methyl and methyne groups respectively. In (b), the signal at τ 7.70 disappears with an increase in the intensity of the signal at τ 7.75; therefore, it can arise from a different methyl group besides that of complex II.

When warmed to room temperature, this complex IV evolves butene gas.*2 Therefore, the signals at τ 7.63, 3.00, 5.45, and 7.92 (relative intensities 2 : 2 : 1 : 3), which disappear or decrease at elevated temperatures were assigned to saturated methylene, olefinic methylene, olefinic methyne,

*1 NMR spectra were obtained with a JNM-4H-100 spectrometer, using tetramethylsilane as an internal standard.

*2 The composition of the gas was: *trans*-2-butene, 68 mol%; *cis*-2-butene, 27 mol%; 1-butene, 5 mol%.

2) S. D. Robinson and B. L. Shaw, *J. Chem. Soc.*, **1963**, 4806.

3) A. D. Ketley, L. P. Fisher, A. J. Berlin, C. R. Morgan, E. H. Gorman and T. R. Steadman, *Inorg. Chem.*, **6**, 657 (1967).

4) I. P. Collman, *Angew. Chem.*, **77**, 154 (1965).

5) G. Allen, J. Lewis, R. F. Long and C. Oldham, *Nature*, **202**, 589 (1964).

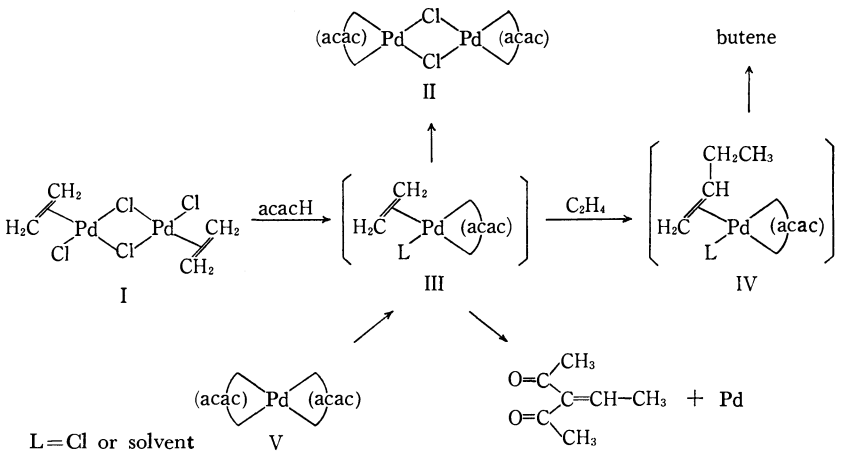

Scheme 1

and methyl groups respectively in 1-butene. However, the signals at τ 3.00 and 5.45 could also be assigned to olefinic methyne and methylene on account of these τ values. It is not clear at this time which assignment is best. The signals at τ 7.63 and 7.92 which remain in (b) might be due to a methyl group of the free acetylacetone or of the other products derived from the complex IV by decomposition, since the free acetylacetone has the signal at *ca.* τ 7.92. On the basis of these results, it could be concluded that the unstable complex obtained in the case of adding an acetylacetone was the chloro-acetylacetonato-(1-butene)palladium(IV).

Furthermore, in order to investigate the by-products of dimerization with an acetylacetone additive, acetylacetone (10 mol equivalents to palladium) was added to a solution of complex I dissolved in acetic acid, and then ethylene was bubbled into the solution for three hours. After work-up as usual, ethylideneacetylacetone was obtained in a 30% yield; it was identified through comparison with an authentic sample prepared from acetaldehyde and acetylacetone.[6] From the present results, it can be assumed that the dimerization with an acetylacetone additive proceeds *via* the two acetylacetonato-olefin-palladium complexes III and IV as is shown in Scheme 1.

Moreover, as the isomer of butene is in a nearly equilibrium composition, in which 2-butene is a main product,*[2] there might be a process of isomerization from coordinated 1-butene to free 2-butene. The intermediate complexes III and IV in the dimerization with an acetylacetone additive could not be successfully isolated, but the existence of an intermediate III could be verified from the following facts: (i) the dimerization of ethylene catalyzed by the bisacetylacetonato-palladium (V), $(Pd(C_5H_7O_2))_2$, gave butene, and also palladium metal was formed; (ii) the acetylacetonato-palladium complex II was isolated from the reaction mixture;[1] (iii) the NMR spectrum supported the idea of the formation of the intermediate complex IV, and (iv) ethylideneacetylacetone, which was the adduct of ethylene and acetylacetone, was obtained as the by-product.

6) E. Knoevenagel and W. Ruschhaupt, *Ber.*, **31**, 1028 (1898).

BULLETIN OF THE CHEMICAL SOCIETY OF JAPAN VOL. 42 2690—2692 (1969)

Reaction of 2,3-Dihydro-4-pyridone

Noboru SUGIYAMA, Makoto YAMAMOTO and Choji KASHIMA

Department of Chemistry, Tokyo Kyoiku University, Otsuka, Tokyo

(Received December 4, 1968)

In a previous paper we described the synthesis of 2,3-dihydro-4-pyridones from a Schiff base and β-diketones in the presence of excess potassium amide in liquid ammonia.[1] 2,3-Dihydro-6-methyl-1,2-diphenyl-4-pyridone (I), which was synthesized

1) N. Sugiyama, M. Yamamoto and C. Kashima This Bulletin **42**, 1357 (1969).

from acetylacetone and benzylidenaniline, is a typical enamino ketone. The reactions of 2,3-dihydro-4-pyridone have so far not been found in literature. This paper deals with the reactions of I, especially protonation, oxidation and reduction.

Protonation. Generally, β-enamino ketones can be protonated on nitrogen atom, α-carbon atom or oxygen atom.[2] Thus, the protonation of I is expected to give one of the products of three types A, B or C.

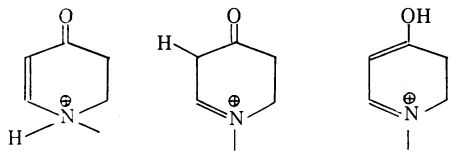

A B C

The ultraviolet absorption spectrum of the hydrochloride (II) showed the absorption maximum at 325 mμ. Compared with the absorption maximum of I at 327 mμ, the chromophore of II is the same as that of I. The methine proton signal at C-2 carbon is broad triplet in the NMR spectrum of II.

If the protonated product is type A, the methine proton of C-2 carbon is coupled to NH proton and broadened. In the infrared absorption spectrum of II, the strong absorption band appeared at 2250 cm^{-1}, which was assigned to more strongly hydrogen bonded hydroxyl group or the tertiary ammonium group. But the infrared absorption spectrum of the hydrobromide (III) showed a strong absorption band at 2420 cm^{-1}, 170 cm^{-1} apart from that of II. The results also suggest that I is protonated as shown in A.[3]

Oxidation. The dihydro heteroaromatic system containing nitrogen is known to play an important role as hydrogen donor in a biological oxidation-reduction system. By the hydrogen transfer reaction with chloranil, a typical hydrogen acceptor,[4] I gave a pyridone derivative, 6-methyl-1,2-diphenyl-4-pyridone (IV), which was synthesized by the condensation of 1-phenyl-1,3,5-hexanetrione with aniline.[5]

The treatment of I with mercuric acetate was also examined, because benzoquinolidine derivative, which has dihydropyridone neuclei, is oxidized to its hydroxypyridine derivative by mercuric acetate.[6] In this reaction IV was also produced.

On the other hand, Kehrmann reported[7] that flavanes were oxidized with iodine to flavones. When the same oxidation method was applied to I, the expected oxidation product was not produced, an unexpected product being obtained.

The ultraviolet spectrum of product V showed the absorption maximum at 360 mμ. In the NMR spectrum, similar to I, the aromatic protons, methylene protons and the methine proton appeared at τ 2.70, τ 6.78 and τ 4.99 respectively. The methyl protons appeared as a singlet at τ 7.65, and olefinic proton disappeared.

From these spectral data and the results of the elemental analyses, V was determined to be 2,3-dihydro-5-iodo-6-methyl-1,2-diphenyl-4-pyridone. In this reaction, it is supposed that iodine was added to the double bond of I and then was eliminated as hydroiodide.

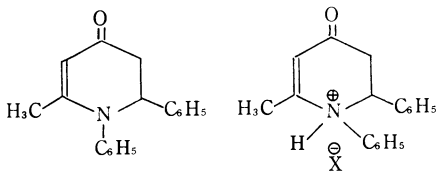

(I) (II): X=Cl, (III): X=Br

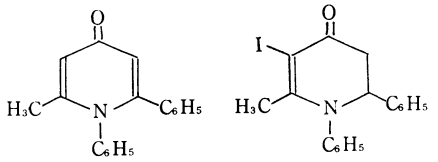

(IV) (V)

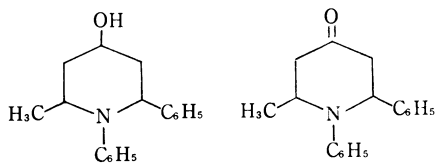

(VI) (VII)

Reduction. By treatment of I with excess sodium borohydride, 6-methyl-1,2-diphenyl-4-piperidinol (VI) was obtained. The infrared spectrum showed the hydroxyl band at 3320 cm^{-1}, but no band of carbonyl and double bond. Both 240 mμ and 327 mμ disappeared in the ultraviolet spectra of VI. From these spectral data and the results of the elemental analyses, the structure of VI was determined.

On the other hand, the hydrogenation of I in acetic acid catalyzed by platinum oxide gave two

2) H. E. A. Kramer, *Ann.*, **696**, 15 (1966).

3) E. A. V. Ebsworth and N. Sheppard, *Spectrochim. Acta*, **13**, 261 (1959).

4) E. A. Braude, J. Hannah and Sir R. Linstead, *J. Chem. Soc.*, **1960**, 3249.

5) S. Boatman, S. E. Smith, G. F. Morris, W. G. Kofron and C. R. Hauser, *J. Org. Chem.*, **32**, 3817 (1967).

6) M. von Strandtmann, M. P. Cohen and J. Shavel, Jr., *ibid.*, **31**, 797 (1966).

7) F. Kehrmann, *Ber.*, **39**, 922 (1906).

products, VI and 6-methyl-1,2-diphenyl-4-piperidone (VII). In the infrared spectrum of VII the carbonyl absorption band appeared at 1715 cm^{-1}, but the double bond band in the region of 1660—1600 cm^{-1} disappeared. In the NMR spectrum of VII, methyl protons are split to the doublet at τ 9.20. Two methylene protons appeared at τ 7.20 and 7.40, and C-2 methine proton appeared as a triplet at τ 4.10.

Under the same conditions, however, the hydrogenation of IV failed, and IV was quantitatively recovered. It is clear that the reduction of dihydropyridone is much easier than that of the corresponding pyridone.

All these reactions confirm that the dihydropyridone (I) favors the enamino ketone structure, but there exists some tautomeric iminoenol structure which is responsible for hydrogen transfer reaction.

Experimental

2,3-Dihydro-6-methyl-1,2-diphenyl-4-pyridone (I). In liquid ammonia, I was prepared by the procedure described in a previous paper,[1] mp 84—85°C.

IR(KBr): 1640, 1560 and 700 cm^{-1}. UV: λ_{max}^{EtOH} 240 mμ (ε 2180), and 327 mμ (ε 10400).

2,3-Dihydro-6-methyl-1,2-diphenyl-4-pyridone Hydrochloride (II). A mitxure of 200 mg of I and 0.1 m*l* of concentrated hydrochloric acid in 5 m*l* of ethanol was maintained for 5 min at room temperature. By the evaporation of solvent under reduced pressure, 150 mg of II was obtained, which was recrystallized from acetone to give analytical pure substance, mp 173°C (decomp).

IR (KBr): 3050, 2250, 1620, 1500, 1215, 760 and 680 cm^{-1}. UV: λ_{max}^{EtOH} 327 mμ (ε 16900).

2,3-Dihydro-6-methyl-1,2-diphenyl-4-pyridone Hydrobromide (III). III was obtained from I and hydrobromic acid by the same procedure for II, mp 153°C (decomp).

IR (KBr): 3050, 2420, 1615, 1500, 1210, 760 and 680 cm^{-1}. UV: λ_{max}^{EtOH} 327 mμ (ε 14200).

Oxidation of I by Chloranil. A solution of 120 mg of I and 120 mg of chloranil in 10 m*l* of tetrahydrofuran was refluxed for 4 hr. The reaction mixture was cooled and 50 mg of crystal was collected, mp 235°C (lit. 242°C[5]). This crystal was identified with the authentic sample, which was obtained by condensation of 1-phenyl-1,3,5-hexanetrione with aniline,[5] by means of thin layer chromatography, infrared and ultraviolet absorption spectra.

Oxidation of I by Mercuric Acetate. To a solution of 500 mg of I in 5 m*l* of acetic acid was added 640 mg of mercuric acetate. The mixture was refluxed for 2.5 hr and then mixed with 20 m*l* of water. The aqueous solution was neutralized with dilute ammonia and extracted with benzene. After removal of the solvent, the residue was identified with the sauthentic sample by means of thin layer chromatography.

2,3-Dihydro-5-iodo-6-methyl-1,2-diphenyl-4-pyridone (V). A mixture of 100 mg of I, 300 mg of iodine, 150 mg of anhydrous potassium acetate and 10 m*l* of ethanol was refluxed for 4 hr. The reaction mixture was mixed with 100 m*l* of water, made alkaline with aqueous ammonia, and extracted with ether. The ethereal solution was washed with aqueous sodium thiosulfate and water. After removal of ether, the residue was recrystallized from ethanol-water mixture to afford 100 mg of V, mp 151°C.

Found: C, 54.71, 54.77; H, 4.16, 4.15; N, 3.70, 3.51; I, 33.91%. Calcd for $C_{18}H_{16}INO$: C, 55.54; H, 4.14; N, 3.60; I, 32.61%.

IR (KBr): 3050, 1640, 1510, 1200, 730 and 710 cm^{-1}. UV: λ_{max}^{EtOH} 302 mμ (ε 3200), 352 mμ (ε 11700).

The Sodium Borohydride Reduction of I. A mixture of 130 mg of I, 36.5 mg of sodium borohydride in 10 m*l* of ethanol was stirred at room temperature. After 8 hr, the reaction mixture was acidified with hydrochloric acid and then neutraized with aqueous ammonia. This aqueous solution was extracted with ether. The ethereal layer was washed with water and dried over anhydrous sodium sulfate. After removal of the solvent, the residue was chromatographed by silica gel (Merck 7729) column with benzene-ethyl acetate (1 : 1 v/v) mixture. A fraction, which showed the R_f 0.49 on silica gel (Wako gel B-5) thin layer chromatography with benzene-ethyl acetate (1 : 1 v/v) mixture, was collected. After removal of the solvent, the residue was recrystallized from benzene, mp 84—85°C.

Found: C, 80.63; H, 8.04; N, 5.21%. Calcd for $C_{18}H_{21}NO$: C, 80.86; H, 7.92; N, 5.24%.

IR (KBr): 3320, 1600, 1370, 1020 and 695 cm^{-1}. UV: λ_{max}^{EtOH} 253 mμ (ε 1250), 259 mμ (ε 1020) and 265 mμ (ε 780).

The Catalytic Hydrogenation of I. In the presence of 14.1 mg of platinum oxide, 200 mg of I in 10 m*l* acetic acid was hydrogenated at 30°C and atmospheric pressure. After absorption of 20 m*l* of hydrogen the reaction was stopped. After the catalyst was filtered off, the filtrate was poured into water and made alkaline with aqueous ammonia, and was extracted with ether. The ethereal solution was washed with water and dried over anhydrous sodium sulfate. After removal of the solvent, the residue was separated on silical gel (Wako gel B-5) thin layer chromatograpny. The spots with the R_f 0.29 and 0.49 were identified with I and VI respectively. The product, which showed the R_f 0.71, was separated by means of silica gel (Merck 7729) column chromatography with benzene-ethyl adetate (1 : 1 v/v) mixture to give V.

IR (liquid film): 1715, 1600, 1375, 1220, 740 and 700 cm^{-1}.

NMR Spectra. NMR spectra were measured by a Hitachi H-60 high resolution Neuclear Magnetic Resonance Spectrometer. The solvent was deuterochloroform and TMS was used as the internal standard.

BULLETIN OF THE CHEMICAL SOCIETY OF JAPAN VOL. 42 2693—2694 (1969)

Infrared Absorption Bands of Benzalanilines Observed in the 1200—850 cm^{-1} Region

Katsumi TABEI and Etsurou SAITOU

Tokyo College of Pharmacy, Kashiwagi, Shinjiku-ku, Tokyo

(Received December 24, 1968)

Previous infrared studies of the azomethine derivatives have dealt with their carbon-nitrogen double-bond stretching mode, but there have been few references to the other vibration of the compounds.[1] As a part of the infrared studies of the aromatic molecule,[2] the spectra of twenty-nine kinds of *N*-(*p*-substituted-benzal)-anilines and *N*-benzal-*p*-substituted-anilines were measured; it was found that three characteristic absorption bands appear in the 1200—850 cm^{-1} region. In the present report, we wish to present the observed data and to assign them qualitatively.

In comparison with the spectra of *N*-benzylaniline, *N*-propylidenecyclohexylamine, azobenzene, acetophenoneoxime, *p*-nitrostilbene, benzalacetone, and styrene, the three absorption bands which appeared at about 1190 cm^{-1}, 975 cm^{-1}, and 880 cm^{-1} in the spectra of the present type of compounds seem to be characteristic of the benzalaniline skeleton. The wave numbers of the above observed characteristic absorption bands are listed in Table 1.

A sharp band at 1191 cm^{-1} in *N*-benzalaniline may be assigned to the aryl carbon-nitrogen (Ar-N) bond-stretching vibration, since the band is not observed in the spectra of *N*-benzylaniline; the corresponding Ar-N stretching mode of *N*-benzylaniline can be assigned to a sharp and strong absorption band at 1322 cm^{-1}.

In addition, the above reference compounds do not have an absorption band in the 1200—1170 cm^{-1} region with the exception of a few medium bands in the 1170—1100 cm^{-1} region which may be due to the aromatic C–H in-plane deformation vibration.

N-propylidenecyclohexylamine, on the other hand, has its carbon-nitrogen single-bond-stretching band at 1100 cm^{-1}.

As is listed in the table, the Ar-N stretching frequency of benzalanilines is far lower than that of aromatic amine, and also the frequencies are kept

Table 1. The characteristic absorption bands of benzalanilines

Compound	Mp (°C)	Frequencies in CCl_4 soln. (cm^{-1})		
		ν_{Ar-N}	δ_{CH} (in-plane)	δ_{CH} (out-of-plane)
X-C_6H_4-N=CH-C_6H_5				
X=-$N(CH_3)_2$	101—102	1210	965	880
-OH	182—183	1196	981	876
-OCH_3	71—71.5	1192	971	883
-OC_2H_5	72—73	1192	970	883
-CH_3	158—159**	1193	972	884
-C_6H_5*	148—149	1190	968	879
-H	52—53	1191	976	873
-Cl	63—63.5	1190	975	884
-Br	65—66	1190	974	883
-I	85—86	1192	975	880
-COOH*	191—193	1194	978	892
-$COOC_2H_5$*	47—48	1192	975	887
-$COCH_3$*	100—101	1193	975	885
-SO_2NH_2*	173—174.5	1195	956	892
C_6H_5-N=CH-C_6H_4-Y				
Y=-$N(CH_3)_2$***	99.5—100.5	1178	977	879
-OH*	191—193	1190	978	880
-OCH_3	63—64	1193	975	877
-OC_2H_5	61—62	1193	975	877
-CH_3	146—147**	1193	976	876
-H	52—53	1191	976	879
-Cl	63.5—64.5	1190	974	875
-Br	73—74	1191	974	874
-I	90—91	1189	976	880
-COOH*	224—225	1192	974	879
-$COOCH_3$***	125.5—126.5	1188	978	887
-SO_2NH_2*	176—179(d.)	1193	972	880
-NO_2***	92—93	1186	973	881
Miscellaneous				
p-C_6H_4(-N=CH-C_6H_5)$_2$*	141—141.5	1190	965	875
p-C_6H_4(-CH=N-C_6H_5)$_2$*	161.5—163	1186	973	866
O_2N-C_6H_4-CH=N-C_6H_4-$N(CH_3)_2$***	227—228	1235	950	883
C_6H_{11}-N=CH-C_2H_5	59—62****	1100	957	885

* measured in KBr disk
** bp under 3 mmHg
*** measured in $CHCl_3$ soln.
**** bp under 15 mmHg

1) E. Clougherty, J. A. Sousa and G. M. Wyman, *J. Org. Chem.*, **22**, 462 (1957); W. Kraws and C. G. J. Wagner, *Z. Naturforsch.*, **A 22** (5), 746 (1967); Yu. S. Ryabokobylko and B. M. Bolptin, *Chem. Abstr.*, **67**, 6486 (1967); G. Dudek, *J. Org. Chem.*, **32**, 882 (1967).

2) K. Tabei and C. Ito, This Bulletin, **41**, 514 (1968).

in a narrow range (1186—1196 cm^{-1}), even when a subsitutent is introduced into the para position of either the aniline or benzaldehyde ring. This fact can reasonably be understood by taking the non-planar structure of the benzalaniline molecule into account; the conjugation effect between the aniline ring and the benzalamino skeleton may be substantially interrupted, since the plane of the aniline ring is twisted from that of the benzalamino part, as is shown in Fig. 1.[3]

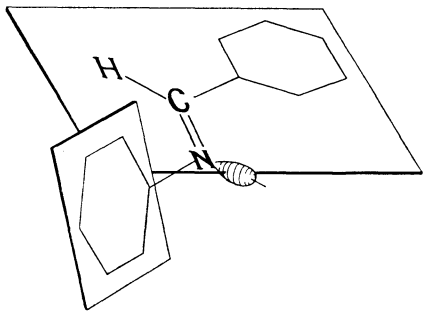

Fig. 1

That is to say, the above frequency region can safely be assigned to the stretching vibration of the non-conjugated sp^2 carbon-sp^2 nitrogen single bond which is expected to appear in the intermediate region between the C–N stretching frequency of aromatic amine and that of aliphatic amine.[4]

A strong electron-donating *p*-substituent in the aniline ring can, however, increase the Ar–N bond order by releasing an electron to the lone-pair lobe of the azomethine nitrogen, as is shown in Fig. 2. The ν_{Ar-N} of such derivative as *N*-benzal-*N'*, *N'*-dimethyl-*p*-phenylenediamine will then appear at a little higher frequency (1210 cm^{-1}). When this group is in the benzaldehyde ring, on the other hand, the ν_{Ar-N} shifts to a little lower frequency; the Ar–N stretching band of *p*-dimethylaminobenzal-aniline then appears at 1178 cm^{-1}. The above frequency shift is probably due to the fact that the electron-rich azomethine nitrogen can repel the aromatic ring of the aniline part.

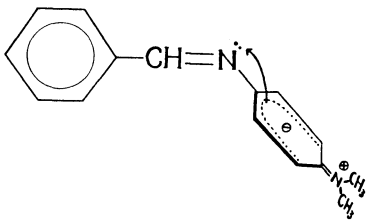

Fig. 2

It was also confirmed that the sharp absorption bands at about 972 cm^{-1} and 883 cm^{-1} give spectral information about the azomethine skeleton. The former is probably due to the C–H in-plane deformation vibration of the azomethine group, and the latter, to the C–H out-of-plane deformation mode, since the above pair of bands do not appear in the spectra of *N*-benzylaniline and other reference compounds. In the case of *N*-propylidenecyclohexylamine, the bands are observed at 956 cm^{-1} and at 845 cm^{-1} respectively. However, they have not been verified.

Experimental

Materials. Twenty-nine kinds of aromatic azomethines were prepared by usual condensation reactions between the corresponding aldehyde and amine, and were purified by recrystallization from methanol or ethanol or by distillation under reduced pressure.[5]

N-Propylidenecyclohexylamine was also prepared by the condensation of cyclohexylamine and propionaldehyde and was distilled repeatedly under reduced pressure. The purity of the materials was checked by thin-layer chromatography.

Infrared Spectra. The IR spectra of the above compounds were measured by using a JASCO DS-301 infrared spectrophotometer in a carbon tetrachloride or chloroform solution or in a disk of potassium bromide. The wave numbers determined in the present experiment are listed in Table 1, along with their physical constants.

The authors wish to express their deep gratitude to Mrs. Moriharu Nagase of the Tokyo College of Pharmacy for her helpful measurement of the infrared spectra.

3) V. A. Izmail'skii and R. A. Smirnov, *Zhur. Obshch. Khim.*, **26**, 3042 (1956); V. A. Izmail'skii and Yu. A. Fedorov, *Zh. Fiz. Khim.*, **39**, 768 (1965); N. Ebara, This Bulletin, **33**, 534, 540 (1960), **34**. 1151 (1961); M. Uehara, *Nippon Kagaku Zasshi* (*J. Chem. Soc. Japan, Pure Chem. Sect.*), **86**, 901 (1961); W. F. Smith, *Tetrahedron*, **19**, 445 (1963); V. I. Minkin, Yu. A. Zhdanov, E. A. Medyantzeva and Yu. A. Ostroumov, *ibid.*, **23**, 3651 (1967); K. Tabei and E. Saitou, This Bulletin, **42**, 1440 (1969).

4) L. J. Bellamy, "The Infra-red Spectra of Complex Molecules," John Wiley & Sons, Inc., New York (1964), p. 248.

5) H. Gilman, "Organic Syntheses," Coll. Vol. **I**, p. 80 (1956); A. Skita and C. Wulff, *Ann.*, **453**, 190 (1927).

BULLETIN OF THE CHEMICAL SOCIETY OF JAPAN VOL. 42 2695—2697 (1969)

Amino-quinoid Polymeric System. The Thermal Reaction of 2,5-Bis(*n*-butylamino)-*p*-benzoquinone

Kazuyuki SUGITA*1 and Ju KUMANOTANI

The Engineering Research Institute, Faculty of Engineering, The University of Tokyo, Yayoi, Bunkyo-ku, Tokyo

(Received January 9, 1969)

Previously we have demonstrated that the 2,5-bis(aliphatic-amino)-*p*-benzoquinone nucleus (**1**), incorporated in the polymer chain, is quite sensitive to heat and can react to give (**2**) and (**3**), through isomerization and subsequent intermolecular condensation respectively, as follows:[1]

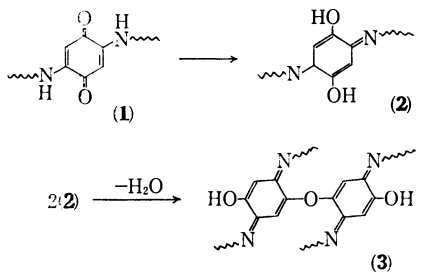

In order to elucidate the thermal reaction of (**1**) in detail, a model pyrolysis of 2,5-bis(*n*-butylamino)-*p*-benzoquinone was investigated at 195°C by means of IR spectroscopy, GLC, TLC, and pyrolytic gas chromatography. As the pyrolysis products, water, ammonia, *n*-butane and propane, 2-*n*-butylamino-*p*-benzoquinone, 2-amino-5-*n*-butylamino-*p*-benzoquinone, and 3-*n*-butylamino-7-hydroxy-9-*n*-butyl-carbazolquinone (1,4) were identified; unknown butylated butylamino-benzoquinoid and oligo-quinoid compounds were also separated.

On the basis of these results, the following reactions can be proposed for the pyrolysis reaction of 2,5-bis(*n*-butylamino)-*p*-benzoquinone: (a) the above reactions, isomerization and condensation, (b) the fission of the carbon and nitrogen bond in the alkylamino group and, (c) the migration reaction of the *n*-butylamino group. Furthermore, the distribution of the pyrolysis products and the change in the composition of the gaseous products as a function of time (see Fig. 1) show that the reactions (a) and (b) make a more significant contribution to the pyrolysis than (c), and that the reaction (a) precedes the reaction (b). This conclusion agrees well with those previously obtained for the amino-quinoid polyester system.[1]

Experimental

Materials. 2,5-Bis(*n*-butylamino)-*p*-benzoquinone (designated as Q-BuA), mp 163.5—164.5°C, was prepared by the known method[2] (Found: N, 11.19%, Calcd for $C_{14}H_{22}O_2N_2$: N, 11.16%).

Instrumental Analyses. The polarographic potential and the spectroscopic data were measured in the manner which has been described before.[3]

Pyrolysis of Q-BuA. The pyrolysis condition was established beforehand to give a major amount of the products in the minor components. Q-BuA (100 mg) in an evacuated ampoule (dia., 22 mm; length, 150 mm) fitted with a stop cock was pyrolyzed at 195°C for 3 hr in an oil bath and then cooled to room temperature.

Identification of Products. *Gaseous Products.* For IR spectroscopy the gaseous products generated in the ampoule were transferred through the cock to a cell which had previously been evacuated at 1 mmHg. The spectrum exhibits bands at 800—1200 cm^{-1} and 2880 and 2970 cm^{-1} that are characteristic of ammonia and alkanes respectively. The hydrocarbon was certified to be a mixture of *n*-butane and propane (4 : 1 in molar ratio) by the use of an Ohkura Chromatograph MS-1100 equipped with a Yanagimoto Active Alumina Column containing a tailing reducer (column temperature, 83°C; split temperature, 60°C; filament current, 120 mA; sensitivity, 1 mV; carrier gas, helium of 1.2 kg/cm^2).

Liquid Products. The liquid product that condensed on the inside wall of the ampoule was dissolved in dried methanol and submitted to GLC under conditions to be described later. The liquid product was thus revealed to be identical with water.

Solid Products. A solution of the solid products obtained from 5.00 g of Q-BuA in 200 m*l* of hot methanol was cooled to room temperature, refrigerated overnight, and filtered to give reddish crystals (4.28 g) and a mother liquor. The latter solution was concentrated to 50 m*l* at room temperature under the reduced pressure of an aspirator, refrigerated overnight, and filtered to give reddish crystals (0.40 g) and a methanol solution. The reddish crystals (4.68 g) were confirmed to be identical with Q-BuA by TLC using the same procedure

*1 Present address: Department of Graphic Engineering, Faculty of Engineering, Chiba University, Yayoi-cho, Chiba City.

1) J. Kumanotani, K. Sugita, S. Kazama and T. Yoshikawa, This Bulletin, **42**, 1130 (1969).

2) C. M. Martini and F. C. Nachod, *J. Am. Chem. Soc.*, **73**, 2953 (1951).

3) J. Kumanotani, F. Kagawa, A. Hikosaka and K. Sugita, This Bulletin, **41**, 2118 (1968).

as that described for the separation of butylamino-toluquinones.[3] The methanol solution was applied in lines on 30 plates of the silica-gel layer (1.0mm thick). The separated zones on the gel layer were scraped off and extracted with 100 m*l* of chloroform and then with 100 m*l* of methanol. The extract was evaporated to dryness at room temperature *in vacuo*. The operation by TLC was repeated three or five times in order to obtain sufficiently-isolated zones. Finally *ca.* 50 mg of each product was obtained.

Upon the identification of the mono- and di-amino-quinoid compounds, the following data were applied:[3] for monoamino-quinoid derivatives, $\nu_{max}^{CHCl_3}$ 3350 cm^{-1} (m. ν_{N-H}), 1620—1640 and 1570—1600 cm^{-1} (s. $\nu_{C=O}$); $\lambda_{max}^{CHCl_3}$ (π-π^*), 270—300 mμ; $E(1/2)$ (*vs.* SCE), −0.3—−0.35 V; for diamino-quinoid derivatives, $\nu_{max}^{CHCl_3}$ 3350 (m. ν_{N-H}), 1640 (m. $\nu_{C=C}$), 1580 (s. $\nu_{C=O}$), 1505 (s. amido II-type band) and 1460 cm^{-1} (m. δ_{C-H} in plane); $\lambda_{max}^{CHCl_3}$ (π-π^*), 330—350 mμ; $E(1/2)$ (*vs.* SCE), −0.45—−0.6 V.

The compounds identified, together with the unknown compounds, are presented below, along with their physico-chemical constants and characteristic spectral data.

2,5-Bis(*n*-butylamino)-*p*-benzoquinone: R_f, 0.20; recrystallized from chloroform as reddish crystals, mp 163.0—164.5°C (Found: N, 11.20%). This compound was found to be identical with Q-BuA by the mixed-melting-point method.

2-*n*-Butylamino-*p*-benzoquinone: R_f, 0.26; recrystallized from chloroform as reddish crystals; $E(1/2)$, −0.33 V (*vs.* SCE). IR in a KBr disk: 3350 (s. ν_{N-H}), 1665 (m. $\nu_{C=C}$), 1630 and 1590 (s. $\nu_{C=O}$), and 1505 cm^{-1} (s. amido II-type band). UV: $\lambda_{max}^{CHCl_3}$ 282 and 488 mμ.

2-Amino-5-*n*-butylamino-*p*-benzoquinone: R_f, 0.03; recrystallized from a mixed solvent of pyridine-chloroform (1 : 9 by volume) as purple-brown scales, mp 225°C (decomp.); $E(1/2)$, −0.46 V (*vs.* SCE).

Found: C, 61.68; H, 7.26; N, 14.36%: mol wt (VPO), 207. Calcd for $C_{10}H_{14}O_2N_2$: C, 61.84; H, 7.27; N, 14.42%; mol wt, 194.

IR in $CHCl_3$: 3520 and 3390 (m. ν_{N-H}), 1655 (m. $\nu_{C=C}$), 1585 and 1550 (s. $\nu_{C=O}$), and 1515 cm^{-1} (s. amido II-type band).

UV: $\lambda_{max}^{CHCl_3}$ 337 (ε 30000), 500 mμ (ε 450).

NMR in dimethyl sulfoxide: 2.3—2.9 (2H, 2(N-H), broadened), 2.8—3.2 (1H, N-H, broadened), 4.68 (1H on the quinoid ring) and 4.86τ (1H on the quinoid ring); in pyridine: 6.8—7.1 (2H, -NH-C$\underline{H}_2$-CH_2-, quartet coupled with N-H and -C$\underline{H}_2$-), 8.3—9.0 (4H, two methylene groups) and 8.8—9.3 τ (3H, one methyl group).

3-*n*-Butylamino-7-hydroxy-9-*n*-butyl-carbazolquinone (1,4): R_f, 0.04; recrystallized from chloroform, yellowish-brown powder, mp 180.7—181.5°C; $E(1/2)$, −0.48 V (*vs.* SCE) (Found: N, 8.01%). This compound was identified because it showed no drop in melting point when mixed with the authentic sample that had been previously prepared by the present authors.[4]

Butylated butylamino-benzoquinoid compound: R_f, 0.08; recrystallized from chloroform as reddish-purple plates, mp 81—84°C; $E(1/2)$, −0.14 V (*vs.* SCE).

Found: C, 66.54; H, 9.02; N, 8.64%; mol wt (VPO), 311. Calcd for $C_{18}H_{30}O_3N_2$: C, 67.05; H, 9.38; N, 8.69%; mol wt, 322.

IR in $CHCl_3$: 3385 (m. ν_{N-H}), 1660 (m. $\nu_{C=C}$), 1590 (s. $\nu_{C=O}$), 1515 cm^{-1} (s. amido II-type band).

UV: $\lambda_{max}^{CHCl_3}$ 346 (ε 9400), 495 mμ (ε 1700).

NMR in $CDCl_3$: 3.57 (1H on the quinoid ring), 4.49 (1H on the quinoid ring), 6.2—6.6 (2H, >N-C$\underline{H}_2$-CH_2-, triplet coupled with -C$\underline{H}_2$-), 6.6—7.1 (2H, -NH-C$\underline{H}_2$-CH_2-, quartet coupled with N-H and -C$\underline{H}_2$-), 7.7—8.1 (2H, -C$\underline{H}_2$- adjacent to the N, O, or quinoid ring, quartet coupled with -C$\underline{H}_2$- and another proton), 8.1—8.9 (12H, six methylene groups) and 8.8—9.3 τ (9H, three methyl groups).

From the above data, it became evident that this compound has such groups as *n*-C_4H_9-, *n*-C_4H_9-N<, and *n*-C_4H_9-NH- and a *p*-benzoquinone nucleus.

Oligo-quinoid compound: obtained from the zone of the starting line; recrystallized from chloroform as a dark brown substance, mp 120—140°C; $E(1/2)$, −0.55V (*vs.* SCE).

Found: C, 63.83; H, 7.61; N, 9.01%; mol wt (VPO), 342.

IR in $CHCl_3$: 3200—3500 (broadened, ν_{O-H}), 2850—3050 (m. ν_{C-H}), 1580 (s. $\nu_{C=O}$), 1515 (m. $\nu_{C=N}$), 1460 (m. δ_{C-H} in plane) and 1220 cm^{-1} (m. ν_{C-O-C}).

UV: $\lambda_{max}^{CHCl_3}$ 260 (ε 13000), 330 (ε 11700), 465 (ε 2220), 495 (ε 2050) and 550 mμ (ε 1230).

The above results show that the compound has the following groups: OH, -O-, >C=NH, and >C=N-C_4H_9, and the *p*-benzoquinone nucleus (cf. (3)).

Distribution of Pyrolysis Products of Q-BuA. The distribution of the products obtained from 10.0 mg of Q-BuA was examined by the extraction of the zones developed on a thin-layer chromatogram: 8.9 mg (85 mol% for the starting material) of Q-BuA, 0.6 mg (4.4 mol%) of the oligo-quinoid compound, 0.2 mg (2.5 mol%) of 2-amino-5-*n*-butylamino-*p*-benzoquinone, 0.1 mg (0.7 mol%) of the carbazolquinone, and traces of 2-*n*-butylamino-*p*-benzoquinone and the butylated butylamino-benzoquinoid compound.

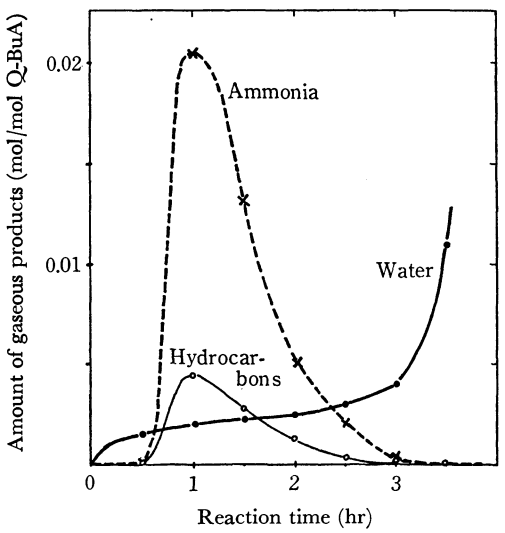

Fig. 1. The variation of the amount of gaseous products generated in the pyrolysis of Q-BuA at 195°C.

4) K. Sugita and J. Kumanotani, This Bulletin, **42**, 2043 (1969).

Pyrolytic Gas Chromatography. Its system was similar to that described by Yoshimi *et al*:[5] the pyrolytic cell was equipped with a Kotaki Super Fractioner GU-21. The column was prepared and the GLC operated in the manner reported by Amemiya.[6] Upon the pyrolytic gas chromatographic analysis, the peaks in a gas chromatogram of the products were assigned to *n*-butane, ammonia, and water. Q-BuA (100 mg) in a cell into which a stream of helium was introduced was heated in an oil bath kept at 110°C until no gas chromatographic peak of water could be detected. Then the cock was turned to close the sample cell and the cell was heated in an electric furnace kept at 195(±2)°C. The gaseous products which formed and accumulated in the cell over a 30-min period were run into the gas chromatograph with a stream of helium for a 10-sec interval by turning the cock, and then the cock was reversed in order to close the cell. The procedures of 30-min-pyrolysis and 10-sec-running of the gaseous products were repeated alternately for 3.5 hr. Thus, Fig. 1 was derived from the gas chromatograms where a normalization method was applied within a relative error of ±5%. Among the pyrolysis products, ammonia would be formed by the hydrolysis of the imino groups in the oligo-quinoid compound.

5) N. Yoshimi, T. Yamauchi, M. Yamao and N. Tanaka, *Kogyo Kagaku Zasshi* (*J. Chem. Soc. Japan, Ind. Chem. Sect.*), **65**, 1131 (1962).

6) R. Amemiya, "Gaschromatography," Kyoritsu-shuppan, Tokyo (1957), p. 76.

The authors wish to thank Mr. Masayoshi Yamao for his favor to provide the glass apparatus for the pyrolytic GLC. Thanks are also due to Associate Professor, Hiroo Tominaga of This University for the GLC measurements on the hydrocarbons.

BULLETIN OF THE CHEMICAL SOCIETY OF JAPAN VOL. 42 2697—2698 (1969)

Studies of Thin-layer Chromatography of Inorganic Salts. II. Separation of Inert Cobalt(III) Complexes by Means of Thin-layer Chromatography on Alumina[1]

Tetsuo BABA,[2] Masayuki MUTO and Hayami YONEDA[3]

Department of Chemistry, Wakayama University, Masagocho, Wakayama

(Received January 13, 1969)

We were interested in the chromatographic behavior of inert metallic complexes and wrote two papers concerning the mechanism of separation of complexes both in paper[4] and in silica gel thin-layer[5] chromatography. According to these reports, complex salts are developed separately as cations and anions on the negatively charged surface of an adsorbent, so that the R_f value of the complex increases with the decrease of its positive ionic charge and reaches nearly unity in the case of complex anions.

In order to see whether a similar separation mechanism holds in other adsorbents, we studied the chromatographic behavior of twenty-two kinds of inert cobalt(III) complexes on alumina and found interesting features characteristic of alumina thin-layer chromatography.

Experimental

As an adsorbent Merck's alumina H, prepared for thin-layer chromatography according to Stahl's method was used without further purification. The compounds studied are listed in Table 1. The development was carried out at room temperature of 22—23°C. Spots of cobalt(III) complexes were detected by spraying potassium sulfide solution.

Results and Discussion

The R_f values of the complexes are summarized in Table I. As is seen from these data, the chromatographic behavior of the complex cation on alumina is in general similar to that on silica gel. All complex cations show R_f values smaller than those of neutral complexes. This indicates that alumina is charged negatively in contact with water and adsorbs complex cations more strongly than neutral complexes. On silica gel, all complex cations including monovalent ions are strongly adsorbed and remained nearly at the origin when developed with distilled water. However, the present R_f values obtained with alumina layers are 0.5—0.8 for monovalent cations and 0.8—0.9

1) Presented at the 17th Annual Meeting of Japan Analyst Association held at the Hiroshima University, September 8, 1968.

2) On leave from the Minoshima High School, Arita-shi, Wakayama.

3) Correspondence to be addressed to this author.

4) H. Yoneda, This Bulletin, **40**, 2442 (1967).

5) T. Baba, H. Yoneda and M. Muto, *ibid.*, **41**, 1965 (1967).

Table 1. R_f values of cobalt(III) complexes developed on alumina

(The R_f value was measured at the front of the spot.)

Sample	Developer		
	Distilled water	0.5M HCOOH aq.	0.5M $(CH_3)_2NH$ aq.
$[Co(NH_3)_6](ClO_4)_3$	0.03	0.06	0.01
$[CoH_2O(NH_3)_5]Cl_3$	0.04	0.05	0.02
$[CoCH_3CO_2(NH_3)_5]$-$(ClO_4)_2$	0.09	0.20	0.09
$[CoCHCl_2CO_2(NH_3)_5]$-$(ClO_4)_2$	0.08	0.18	0.08
$[CoCCl_3CO_2(NH_3)_5]$-$(NO_3)_2$	0.06	0.14	0.05
$[CoCF_3CO_2(NH_3)_5]$-$(NO_3)_2$	0.12	0.22	0.10
$[CoCH_3CH_2CO_2$-$(NH_3)_5](NO_3)_2$	0.12	0.21	0.11
$[CoNCS(NH_3)_5](NO_3)_2$	0.05	0.13	0.05
$[CoCN(NH_3)_5]Cl_2$	0.05	0.09	0.03
$[CoCl(NH_3)_5]Cl_2$	0.06	0.15	0.08
trans-$[Co(CH_3CO_2)_2$-$(NH_3)_4]ClO_4$	0.78	0.72	0.85
cis-$[Co(CH_3CO_2)_2$-$(NH_3)_4]NO_3$	0.52	0.53	0.68
cis-$[Co(CHCl_2CO_2)_2$-$(NH_3)_4]ClO_4$	0.53	0.54	0.61
[Co ox en_2]NO_3	0.47	0.53	0.69
trans-$[Co(NCS)_2\ en_2]Cl$	0.78	0.73	0.85
trans-$[Co(NO_2)_2\ en_2]NO_3$	0.73	0.71	0.81
cis-$[Co(NO_2)_2\ en_2]NO_3$	0.60	0.64	0.78
$[Co\ gly_3]$	0.79	0.66	0.84
$[Co(NO_2)_3(NH_3)_3]$	0.88	0.75	0.89
[Co $(NO_2)_3$ den]	0.90	0.79	0.91
$Na[Co(SO_3)_2\ en_2]$	0.64	0.37	0.90
Na(Co $(NO_2)_4$ en]	0.77	0.72	0.82

for neutral complexes. Therefore it is supposed that alumina has less negative charge than that of silica gel.

While on silica gel the R_f value shows a monotonic increase in going from cations, through neutral species, to anions, a trend in R_f value variation on alumina has a maximum in neutral species and shows a decrease in anions. This suggests that the complex anion is more strongly adsorbed than the neutral complex and can be explained by assuming positively charged sites besides the negatively charged ones. We attribute this to the amphoteric nature of alumina. This idea of the coexistence of the positive and negative sites finds support from Schwab's report.[6] He showed that alumina adsorbed both NH_3 (base) and BF_3 (acid). In order to ascertain our idea, the complexes were developed with 0.5M HCOOH and 0.5M $(CH_3)_2NH$ aqueous solutions. With an acidic developer, hydrogen ions are expected to cover the negative sites of an adsorbent, so that the adsorptive power of alumina is expected to decrease towards cations and to increase towards anions, compared to those with a neutral developer. On the other hand, with a basic developer, hydroxide ions are expected to cover the positive sites, so that the adsorptive power of alumina is expected to increase towards cations and to decrease towards anions. As is seen in Fig. 1, this expectation is almost fulfilled. The R_f value varies regularly with the pH of developers. The R_f value increases in the order basic < neutral < acidic in the cases of tri- and divalent cations, and in the order acidic < neutral < basic in the case of monovalent anions.

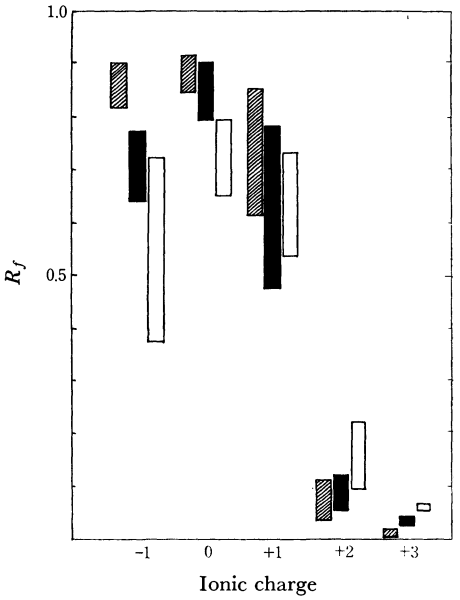

Fig. 1. pH dependency of R_f values. (Each block represents a range of R_f values.)
- developed with 0.5M HCOOH
- developed with 0.5M $(CH_3)_2NH$
- developed with distilled water

As is seen in Table 1, the cis diacido complexes show always smaller R_f values than those of the corresponding trans complexes. The trans complex has no dipole moment, while the cis complex must have a dipole moment. Therefore, this finding is acceptable if we assume that the adsorption is caused mainly by electrostatic attraction.

One of the authors, Baba, wishes to express his thanks to the Ministry of Education for a grant-in-aid for this study.

6) G. M. Schwab and H. Kral, 3rd. Internl. Congr. Catalysis (Amsterdam), 1964.

BULLETIN OF THE CHEMICAL SOCIETY OF JAPAN VOL. 42 2699—2701 (1969)

Application of a Mercury-Coated Platinum Electrode to the A.C. Stripping Analysis of a Trace Amount of Metal Ions

Mutsuo KODAMA and Tomohiko NODA

Department of Chemistry, Ibaraki University, Mito, Ibaraki

(Received January 20, 1969)

Previously,[1,2] we have studied the characteristics of a hanging mercury-drop electrode (HMDE) in alternating current (a.c.) polarography and have used this electrode for the a.c. stripping analysis of thallium(I). Although the HMDE has the advantages of a mercury electrode (high hydrogen overvoltage, reproducible surface, and suitability for multicomponent analysis), the loss of deposited metals by diffusion into the bulk of the electrode limits the application of HMDE to the stripping analysis of trace amounts of metals. In this connection, we tried to use the mercury-coated platinum electrode, which has been established not to have the above-mentioned disadvantage of a mercury-drop electrode. The preparation of mercury-coated platinum electrodes suitable for anodic stripping analysis has been reported by several authors.[3-5] In this work, we followed the continuous and simultaneous depositon procedure proposed by Bruckenstein and Nagai;[6] that is, mercury was plated by electrolysis on a platinum electrode, plated continuously and simultaneously with the deposition of the metals to be determined.

Experimental

Reagents. The way of preparing standard solutions of thallium(I), cadmium(II), lead(II), and copper(II) ions has been described in previous papers.[7,8] The standard solution of mercuric nitrate was prepared by dissolving a known amount of metallic mercury in dilute nitric acid (1+1) and by then removing the excess nitric acid by distillation under reduced pressure. All the other chemicals were of an analytical reagent grade and were used without further purification.

Apparatus and Procedure. The apparatus and the experimental procedures used were the same as those which have been described previously.[2] The platinum-base electrode to be coated with merculy was constructed by sealing a platinum wire 0.4 mm in diameter and 6 mm in length one end of a 6 mm soft-glass tube and by then bending it at right angles to the glass tube. Before use, the platinum base was treated with warm nitric acid (1+1) for 20 min and was then cathodized for 5 min in a sodium perchlorate solution containing 0.01 M $HClO_4$.

Results and Discussion

Mercury Plating. In order to prepare a mercury-coated platinum electrode suitable for a.c. anodic stripping analysis by the continuous simultaneous deposition of mercury, we first studied the current-voltage behavior of a platinum base in stirred solutions of constant pH values and ionic strengths (pH=2.0, 0.5M $NaClO_4$) but with varying concentrations of mercuric ion. Each solution was stirred by a magnetic stirring bar driven by a synchronous motor. Throughout the experiment an alternating-current potential (15 mV) was superposed on the d.c. potential; this superposition had little effect on the mercury plating or on the analysis. The a.c. base current was measured by scanning the potential of the platinum base in the anodic direction at a constnt rate (2.78 mV/sec) from the limiting-current region of the mercuric ion (−1.50 V *vs.* SCE). As the concentration of mercuric ions is increased, the a.c. base current, especially at negative potentials, decreases, whereas the a.c. peak-height due to the anodic dissolution of mercury at about +0.40 V *vs.* SCE increases. These facts clearly indicate that with an increase in the mercury-film thickness and the coverage of the platinum base with mercury, the overvoltage for the hydrogen evolution reaction is increased. At the mercuric ion concentration of 1.0×10^{-4}M, the hydrogen overvoltage almost approaches the limiting value, and in the concentration range from 1.0×10^{-4} to 1.0×10^{-3}M, a reproducible low base current could be obtained. At mercuric ion concentrations higher than 1.0×10^{-3}M, a droplet of mercury was formed.

1) M. Kodama, H. Ouchi and S. Wakui, *Nippon Kagaku Zasshi (J. Chem. Soc. Japan, Pure Chem. Sect.)*, **84**, 241 (1963).
2) M. Kodama and T. Noda, This Bulletin, **41**, 2401 (1968).
3) W. R. Matson, D. K. Roe and D. E. Carritt, *Anal. Chem.*, **37**, 1594 (1965).
4) S. P. Perone and K. K. Davenport, *J. Electroanal. Chem.*, **12**, 269 (1966).
5) A. M. Hartley, A. G. Hiebert and J. A. Cox, *ibid.*, **17**, 81 (1968).
6) S. Bruckenstein and T. Nagai, *Anal. Chem.*, **33**, 1201 (1961).
7) M. Kodama, T. Noda and M. Murata, This Bulletin, **41**, 254 (1968).
8) M. Kodama and H. Ebine, *ibid.*, **40**, 1857 (1967).

As long as the potential scanning in the anodic direction is stopped at +0.50 V *vs.* SCE, the hydrogen overvoltage increases with the number of plating-stripping cycles of mercury. At mercuric ion concentrations higher than 1×10^{-4}M, reproducible a.c. base currents were obtained on repeated runs of the plating-stripping process. On the other hand, if the electrode is oxidized at potentials more positive than +1.0 V *vs.* SCE, the electrode gives a higher base current than that at a nude platinum base. These findings agree well with those by Hartley *et al.*[5] Thus, all the above examples of current-voltage behavior can be explained in the following manner. The mercury deposited on the platinum base interacts with the platinum base and can not be removed completely by anodizing the electrode at +0.50 V *vs.* SCE. However, by anodizing the electrode at potentials more positive than +1.0 V *vs.* SCE, the mercury on the platinum base is completely removed; the resulting platinum surface behaves much as a platinized platinum. It may also be concluded that the formation of intermetallic compounds between mercury and platinum[6] is essential for the formation of mercury film with the desirable properties. Mercury plating was also studied by varying the initial potential from which the potential of platinum base was scanned in the anodic direction. Initial potentials more negative than −1.50 V *vs.* SCE resulted in vigorous hydrogen evolution and gave only the mercury-coated platinum electrode, which behaves in a less reproducible fashion.

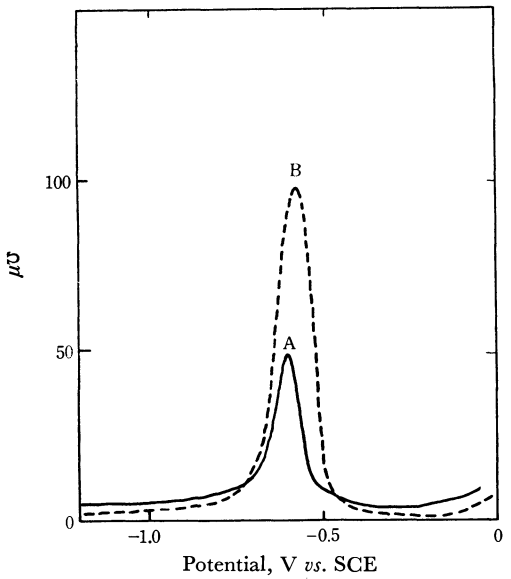

Fig. 1. A.c. polarograms of thallium(I) at a mercury-coated platinum electrode.
Concentration of mercuric ion=1.5×10^{-4}M
Concentration of thallium(I)=2.0×10^{-7}M
0.50M $NaClO_4$, pH=2.0
Scanned anodically from −1.50 V *vs.* SCE
A: Not stopped the stirring
B: Stopped the stirring at −0.65 V *vs.* SCE

A.C. Stripping Analysis of Metal Ions. A.c. polarograms of thallium(I), lead(II), and cadmium(II) ions in solution containing 1.5×10^{-4}M mercuric ions were measured by scanning the potential of a platinum base in the anodic direction from −1.50 to +0.50 V *vs.* SCE. Reproducible, well-developed a.c. polarograms were obtained on repeated potential excursions. Typical polarograms of thallium(I) are given in Fig. 1. As in the case of HMDE,[2] by stopping the stirring at potentials 70 mV negative with respect to the summit potential, a remarkable increase in sensitivity could be obtained. The a.c. peak-height of the metal was a linear function of the effective pre-electrolysis time and increased exactly with the time according to the relation (1) in Ref. (2). As Table 1 shows, the a.c. summit potentials of a metal at a mercury-coated platinum electrode are located at potentials more positive than those at a nude platinum electrode. This may

Table 1. Summit-potential of metal
0.50M sodium perchlorate
pH=2.00

Electrode	Sumitm-potential, V *vs.* SCE			
	Tl(I)	Cu(II)	Pb(II)	Cd(II)
Bright platinium electrode	−0.76	+0.05	−0.53	−0.72
Mercury-coated platinum electrode	−0.57	+0.00	−0.42	−0.64

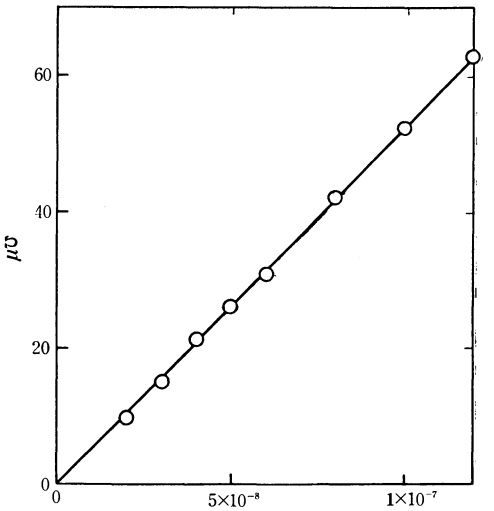

Fig. 2. The relation between thallium(I) concentration and the a.c. peak-height.
Concentration of mercuric ion=1.5×10^{-4}M
0.50M $NaClO_4$, pH=2.0
Scanned anodically from −1.50 V *vs.* SCE and stopped the stirring at −0.65 V *vs.* SCE

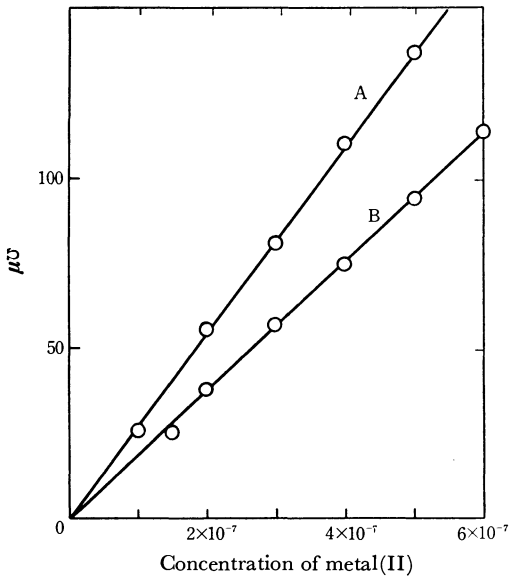

Fig. 3. The relation between metal concentration and the a.c. peak-height.
Concentration of mercuric ion=1.5×10^{-4}M
0.50M $NaClO_4$, pH=2.0
Scanned anodically from −1.50 V *vs.* SCE
A: Lead(II) system, stopped the stirring at −0.50 V *vs.* SCE
B: Cadmium(II) system, stopped the stirring at −0.70 V *vs.* SCE

indicate that the anodic dissolution process of a metal at the mercury-coated platinum electrode is much more reversible than that at the bright platinum electrode.

By employing the above experimental technique, the relation between the concentration of a metal ion and the a.c. peak-height of the anodic dissolution wave was examined. In all cases, at a given initial potential the plot of the a.c. peak-height against the concentration of metal ions gave a straight line passing the point of origin. As is shown in Figs. 2 and 3, thallium(I) ions gave the linear relation in the concentration range from 2×10^{-8} to 1×10^{-6}M, and lead(II) and cadmium(II) ions, in the concentration range from 1×10^{-7} to 3×10^{-6}M. The effect of the presence of copper(II) ions on the a.c. peak-heights of thallium, lead, and cadmium was also studied. The 2×10^{-5}M copper(II) ion had no effect on the a.c. peak-heights of the 5×10^{-8}M thallium(I) or the 2×10^{-7}M lead(II) and cadmium(II) ions.

Although the present a.c. polarographic method has the disadvantage of being restricted to use with solutions not containing anions capable of forming insoluble mercury salts, one can apply this method to the determination of thallium(I), lead(II), and cadmium(II) ions in their micromolar solutions.

The authors wish to express their thanks to the Ministry of Education for the financial support granted for this research.

BULLETIN OF THE CHEMICAL SOCIETY OF JAPAN VOL. 42 2701—2704 (1969)

The Syntheses of Centaureidin and 5,7,3′-Trihydroxy-3,8,4′-trimethoxyflavone*1

Tokunaru HORIE

Department of Applied Chemistry, Faculty of Engineering, University of Tokushima, Tokushima

(Received January 27, 1969)

Centaurein (I) was first isolated from the roots of *Centaurea jacea* L. by Bridel and Charaux.[1] The hydrolysis of I with sulfuric acid afforded an aglycone, centaureidin (5,7,3′-trihydroxy-3,6,4′-trimethoxyflavone (II)).[2] Recently, II has also been isolated from the Centaurea species by Bohlmann and Zdero.[3] A structural isomer of II, jaceidin (III), has been isolated from the same plant.[3,4] The present author and his collaborators achieved the syntheses of III,[5] axillarin (IV),[6] and two

*1 Synthetic Studies of the Flavone Derivatives. XIII. Part XII of this series: K. Fukui, M. Nakayama and T. Horie, This Bulletin, **42**, 2327 (1969). This has already been partly reported in a preliminary from: T. Horie, *Experientia*, **24**, 880 (1968).

1) M. Bridel and G. Charaux, *Compt. rend.*, **175**, 833, 1168 (1922).

2) L. Farkas, L. Hörhammer, H. Wagner, H. Rösler and R. Gurniak, *Chem. Ber.*, **97**, 1666 (1964).

3) F. Bohlmann and C. Zdero, *Tetrahedron Letters*, **1967**, 3239.

4) L. Farkes, L. Hörhammer, H. Wagner, H. Rösler and R. Gurniak, *Chem. Ber.*, **97**, 610 (1964); J. H. Bowie and D. W. Cameron, *J. Chem. Soc.*, **1965**, 5651.

5) K. Fukui, T. Matsumoto, S. Nakamura, M. Nakayama and T. Horie, *Experientia*, **24**, 108 (1968); This Bulletin, **41**, 1413 (1968).

6) K. Fukui, M. Nakayama and T. Horie, *Experientia*, **24**, 769 (1968); This Bulletin, **42**, 1649 (1969).

isomers, V[7] and VI,[6] from 3,ω-dimethoxy-2,4,6-trihydroxyacetophenone (VII).[5] The present paper is concerned with the total syntheses of II and 5,7,3′-trihydroxy-3,8,4′-trimethoxyflavone (VIII) from VII.

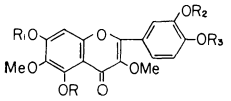

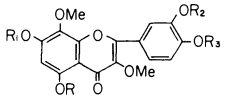

I R = R₂ = H, R₁ = Glu, R₃ = Me
II R = R₁ = R₂ = H, R₃ = Me
III R = R₁ = R₃ = H, R₂ = Me
IV R = R₁ = R₂ = R₃ = H
X R = R₁ = H, R₂ = C₆H₅CH₂, R₃ = Me
XII R = H, R₁ = Ac, R₂ = C₆H₅CH₂, R₃ = Me
XIII R = R₁ = R₂ = Ac, R₃ = Me
XIV R = R₁ = R₂ = Et, R₃ = Me

V R = R₁ = R₃ = H, R₂ = Me
VI R = R₁ = R₂ = R₃ = H
VIII R = R₁ = R₂ = H, R₃ = Me
IX R = R₁ = H, R₂ = C₆H₅CH₂, R₃ = Me
XI R = R₁ = Ac, R₂ = C₆H₅CH₂, R₃ = Me
XVI R = R₁ = R₂ = Ac, R₃ = Me
XVII R = R₁ = R₂ = Et, R₃ = Me

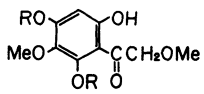

VII R = H
XV R = Et

According to the method of Allan-Robinson's flavone synthesis, the condensation of the ketone VII with *O*-benzylisovanillic anhydride and potassium *O*-benzylisovanillate, followed by treatment with alcoholic potassium hydroxide, was found to afford two isomeric cyclization products, the 3′-benzyl ether (IX) of II and 3′-benzyloxy-5,7-dihydroxy-3,8,4′-trimethoxyflavone (X). After the usual acetylation of the above mixtures, the reaction products could be separated into two crystals, A and B, by fractional crystallization from ether. The crystal A (mp 159—160°C, $C_{29}H_{26}O_{10}$) gave a negative ferric chloride reaction, and there was no band attributable to a hydroxyl group in its infrared spectrum. Further, from a comparison of the NMR spectrum (Table 1)*2 of this compound with those of 5,7,8-oxygenated flavones,[7,8] the signal at δ 6.80 (1H) (singlet) can be assigned to the C_6–H at the A ring of the flavone nucleus. Thus, the crystal A is formulated as 3′-benzyloxy-5,7-diacetoxy-3,8,4′-trimethoxyflavone (XI).

The mild hydrolysis of the crystal B gave pale yellow needles (mp 131.5—132.5°C), 7-acetoxy-3′-benzyloxy-5-hydroxy-3,6,4′-trimethoxyflavone (XII), *via* a partial acetylation. The NMR spectrum exhibits two singlets, at δ 6.78 and 12.87, due to the C_8–H of the A ring and to the hydroxyl protons respectively. The treatment of XII with dilute alkali afforded the 3′-benzyloxy-5,7-dihydroxy-compound IX. The catalytic hydrogenolysis of IX over palladium charcoal gave the desired flavone, II, which was easily converted to the triacetate, XIII. The synthetic flavone, II, and its triacetate, XIII, were found to be identical with natural centaureidin*3 and its triacetate*4 in mixed-melting-point determinations and in infrared- and ultraviolet-spectral comparisons. The triethyl ether (XIV) of II was easily obtained with diethyl sulfate in anhydrous acetone. The ether, XIV, was also prepared from 4,6-diethoxy-5,ω-dimethoxy-2-hydroxyacetophenone (XV)[5] and

TABLE 1. NMR DATA OF FLAVONES*2,5

	XI	XIII	XVI
Arom. H C-6	6.80_s		6.82_s
C-8		7.25_s	
C-2′	7.82_d	7.77_d	7.96_d
C-5′	$7.06_{d'}$	$7.03_{d'}$	$7.16_{d'}$
C-6′	7.81_q	7.98_q	8.15_q
$C_6\underline{H}_5CH_2$	7.45_{bs}(5H)		
$C_6H_5C\underline{H}_2$	5.28_s(2H)		
$C\underline{H}_3O$	4.00_s(3H)	3.89_s(3H)	4.02_s(3H)
	3.95_s(3H)	3.84_s(3H)	3.96_s(3H)
	3.65_s(3H)	3.78_s(3H)	3.86_s(3H)
$C\underline{H}_3CO$	2.45_s(3H)	2.50_s(3H)	2.47_s(6H)
	2.39_s(3H)	2.36_s(3H)	2.38_s(3H)
		2.33_s(3H)	

*5 s, singlet; bs, broad singlet; d, doublet (J_{meta}=2.5 Hz); d′, doublet (J_{ortho}=9.0 Hz); q, quartet (J_{ortho}=9.0 Hz, J_{meta}=2.5 Hz).

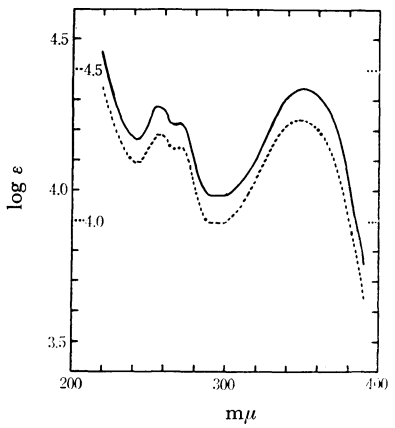

Fig. 1. Ultraviolet spectra of natural (------) and synthetic (——) centaureidin in ethanol.

*2 The NMR spectra were measured with a Hitachi R-20 spectrometer, using tetramethylsilane as the internal standerd (δ-value in $CDCl_3$).

*3 Natural centaureidin was kindly supplied by Professor F. Bohlmann, Berlin University.

*4 This compound was prepared from natural centaureidin*3 in this laboratory.

7) K. Fukui, M. Nakayama and T. Horie, *Experientia*, **24**, 417 (1968); This Bulletin, **41**, 2805 (1968).

8) a) J. Massicot and J-P. Marthe, *Bull. Soc. Chim. France*, **1962**, 1962; b) C. A. Henrick and P. R. Jefferies, *Australian J. Chem.*, **17**, 934 (1964); *Tetrahedron*, **21**, 3219 (1965); c) K. Fukui, T. Matsumoto, M. Nakayama and T. Horie, *Experientia*, **25**, 349 (1969).

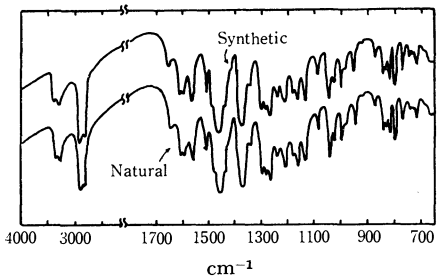

Fig. 2. Infrared spectra of natural and synthetic centaureidin in Nujol.

Table 2. Ultraviolet spectra of natural and synthetic centaureidin (II) and its 4′-benzyl ether (IX)

	λ_{max} mμ (log ε)		
	EtOH	NaOAc	$AlCl_3$
Synthetic centaureidin (II)	257 (4.29)	274(4.31)	266 (4.25)
	271 (4.22)	364(4.23)	279 (4.22)
	351 (4.35)		369 (4.29)
Natural centaureidin	256.5(4.29)	274(4.38)	266.5(4.26)
	271 (4.24)	367(4.24)	280 (4.22)
	350 (4.34)		369 (4.30)
IX	255 (4.28)	275(4.34)	261 (4.24)
	272 (4.21)	298(4.05)	366 (4.31)
	348 (4.34)	364(4.22)	

3-ethoxy-4-methoxybenzoic anhydride. The properties of the product were found to be identical with those of the above compound (XIV) by a direct comparison. The infrared and ultraviolet spectra of synthetic centaureidin superimpose on those of the natural compound (Figs. 1 and 2 and Table 2). A partial synthesis of the glucoside I[1] had been carried out earlier,[2] so the total synthesis of I is now accomplished.

On the other hand, the diacetoxy substance, XI, on treatment with dilute alkali, was easily converted to the 5,7-dihydroxyflavone, X. The catalytic debenzylation of X over palladium charcoal afforded the flavone, VIII. Its triacetate, XVI, and triethyl ether, XVII, were prepared by usual methods. The NMR spectrum of the triacetate, XVI, shows one proton signal corresponding to the C_6–H (δ 6.82) at a field higher than that of the C_8–H (δ 7.25) in the triacetate, XIII (Table I). They are in accordance with those shown in earlier reports.[8]

Experimental*5

3′-Benzyloxy-5,7-diacetoxy-3,8,4′-trimethoxyflavone (XI) and 7-Acetoxy-3′-benzyloxy-5-hydroxy-3,6,4′-trimethoxyflavone (XII). A mixture of the ketone (VII)[7] (2.0 g), *O*-benzylisovanillic anhydride (16 g), and potassium *O*-benzylisovanillate (7.5 g) was heated at 180°C under a vacuum for 10 hr. The reaction mixture was then cooled and refluxed with a solution of potassium hydroxide (10 g) in aqueous ethanol (75%; 350 m*l*) for 15 min. After the solvent had been evaporated in a vacuum, the residue was dissolved in water and saturated with carbon dioxide. The separated precipitate was collected, washed with water, and dried to give a crude flavone mixture.

A mixture of the crude flavones, acetic anhydride (10 m*l*), and anhydrous pyridine (1.0 m*l*) was heated at 110°C for 2 hr and then poured into water and extracted with ether. The ether layer (about 200 m*l*) was washed with a sodium carbonate solution and water, and allowed to stand in a refrigerator for one week. The separating crystals were collected to give the diacetate crystal B (about 0.9 g). The mother liquor was concentrated to 15—20 m*l* and then cooled at 0°C for one week. The separating crystals were corrected to give the diacetate crystal A (about 1.5 g).

The diacetate crystal A was recrystallized from methanol to give colorless needles of XI; mp 159—160°C, yield 330 mg (7%). It gave a negative ferric chloride reaction. IR: 1762, 1755, 1646 cm^{-1}. UV: λ_{max} mμ (log ε); (EtOH) 250 (4.04), 369 (4.22).

Found: C, 65.28; H, 4.82%. Calcd for $C_{29}H_{26}O_{10}$: C, 65.16; H, 4.90%

A solution of the diacetate crystal B in methanol (100 m*l*) was gently refluxed with aqueous potassium hydroxide (5%; 20 m*l*) for 3 min. After the solvent had then been evaporated under a vacuum, the resulting residue was dissolved in water and saturated with carbon dioxide. The precipitate thus separated was collected, heated with acetic anhydride-pyridine (10 : 1; 1.5 m*l*) for 2 min on a steam bath, cooled, and added to ether (10 m*l*). The crystals which separated were collected, washed with ether, and recrystallized from methanol to give pale yellow needles of XII; mp 131.5—132.5°C; yield, 210 mg(5%). It gave a dark green color with an alcoholic ferric chloride solution. IR: 1760, 1652 cm^{-1}. UV: λ_{max} mμ (log ε), (EtOH) 257 (4.64), 274_{sh} (4.50),*7 352 (4.60); ($EtOH-AlCl_3$) 259 (4.56), 360 (4.57). NMR:*2,5 12.87_{bs}(OH); 7.80_q (C-6′); 7.79_d(C-2′); 7.49_{bs}(5H, C_6H_5); $7.02_{d'}$(C-5′), 6.78_s(C-8); 5.28_s(2H, $C_6H_5CH_2$); 4.01_s, 3.96_s, 3.72_s (each 3H, CH_3O); 2.40_s(CH_3CO).

Found: C, 65.69; H, 4.66%. Calcd for $C_{27}H_{24}O_9$: C, 65.85; H, 4.91%.

3′-Benzyloxy-5,7-dihydroxy-3,6,4′-trimethoxyflavone (IX). A solution of XII (190 mg) in methanol (50 m*l*) was gently refluxed with aqueous potassium hydroxide (3%; 10 m*l*) for 2 min. The resulting solution was acidified with dilute hydrochloric acid, and the solvent was evaporated under a vacuum. The resulting precipitate was collected and recrystallized from methanol to give IX as pale yellow needles; mp 163—164°C; yield, 150 mg (86%). It gave a green color with an alcoholic ferric chloride solution. IR: 3350, 1658 cm^{-1}.

Found: C, 66.41; H, 4.90%. Calcd for $C_{25}H_{22}O_8$: C, 66.66; H, 4.92%.

Centaureidin (5,7,3′-Trihydroxy-3,6,4′-trimethoxyflavone) (II). A mixture of IX (130 mg) and Pd-C (5%: 150 mg) in methanol (70 m*l*) was shaken in an atmosphere of hydrogen until 1.1 mol of hydrogen

*5 All the melting points are uncorrected; the infrared spectra were mesured in Nujol.

*6 sh=shoulder.

had been absorbed. After the catalyst had been filtered, the filtrate was evaporated. The residue was recrystallized from aqueous methanol to give II as yellow needles; mp 196—197°C (reported[1] mp 196°C) (natural centaureidin,[*4,8] mp 196—197°C); yield, 85 mg (82%). It gave a dark green color with an alcoholic ferric chloride solution. IR: 3460, 3380, 1651 cm^{-1}. This was identified with natural centaureidin by a mixed-melting-point determination and by infrared- and ultraviolet-spectral comparisons.

Found: C, 59.79; H, 4.35%. Calcd for $C_{18}H_{16}O_8$: C, 60.00; H, 4.48%.

Centaureidin Triacetate (XIII): hot acetic anhydride-pyridine method; mp 174—175.5°C (colorless prisms from methanol) (Natural Centaureidin Triacetate,[*4] mp 174—175.5°C). IR: 1768, 1641 cm^{-1}. UV: λ_{max} mμ (log ε); (EtOH) 328 (4.00), 344 (4.06).

Found: C, 59.01; H, 4.62%. Calcd for $C_{24}H_{22}O_{11}$: C, 59.26; H, 4.56%.

Centaureidin Triethyl Ether (5,7,3′-Triethoxy-3,6,3′-trimethoxyflavone) (XIV). a) From Centaureidin (II). A mixture of synthetic centaureidin (II) (21 mg), anhydrous potassium carbonate (1.0 g), and diethyl sulfate (0.3 m*l*) in anhydrous acetone (20 m*l*) was refluxed for 20 hr, and then the reaction mixture was treated in the usual manner. Recrystallization from methanol give XIV as colorless prisms; mp 77—78°C; yield, 22 mg (85%).

After XIV had been dried at 70—80°C/0.1 mmHg for 1 hr, it had a mp of 104.5—105.5°C. IR: 1635 cm^{-1}. UV: λ_{max} mμ(log ε); 258_i(4.18),[*9] 358(4.10). NMR:[*2,5] 7.75_d (C-2′); 7.73_q (C-6′); $6.98_{d'}$ (C-5′); 6.72_s(C-8); 4.19_q (6H, J=7.0 Hz, $CH_3C\underline{H}_2O$); 3.95_s, 3.91_s, 3.84_s (each 3H, $C\underline{H}_3O$); 3.51_t (9H, J=7.0 Hz, $C\underline{H}_3H_2O$).

Found: C, 64.77; H, 6.24%. Calcd for $C_{24}H_{28}O_8$: C, 64.85; H, 6.35%.

b) From the Ketone XV. A mixture of XV[5] (1.0 g), 3-ethoxy-4-methoxybenzoic anhydride (3.0 g), and triethylamine (2 m*l*) was heated at 170°C for 8 hr. The reaction mixture was then cooled and refluxed with a solution of potassium hydroxide (1.5 g) in aqueous ethanol (80%; 100 m*l*) for 15 min. After the evaporation of the solvent under a vacuum, the residue was dissolved in water (60 m*l*). The resulting precipitate was collected and recrystallized from methanol to give colorless prisms of XIV; mp 77.5—78.5°C (after drying; mp 104.5—105.5°C); yield, 250 mg (16%). It was identical with the sample described in a).

3′-Benzyloxy-5,7-dihydroxy-3,8,4′-trimethoxyflavone (X). A mixture of XI (320 mg), methanol (10 m*l*), and aqueous potassium hydroxide (10%; 5 m*l*) was treated by a method similar to that used for IX. The crude product was recrystallized from methanol to give yellow needles of X; mp 148—149°C; yield, 230 mg (85%). It gave a green color with an alcoholic ferric chloride solution. IR: 3340, 1655 cm^{-1}. UV: λ_{max} mμ (log ε); (EtOH) 257.5 (4.30), 276 (4.27), 340 (4.20), 362_{sh}(4.20).

Found: C, 66.61; H, 4.91%. Calcd for $C_{25}H_{22}O_8$: C, 66.66; H, 4.92%.

5,7,3′-Trihydroxy-3,8,4′-trimethoxyflavone (VIII). A mixture of X (205 mg) and Pd-C (5%; 200 mg) in methanol (100 m*l*) was treated by a method similar to that used for III. The resulting precipitate was recrystallized from methanol to give yellow needles of VIII; mp 213.5—214.5°C; yield, 138 mg(84%). It gave a dark green color with an alcoholic ferric chloride solution. IR: 3400, 3300, 1648 cm^{-1}. UV: λ_{max} mμ (log ε); (EtOH) 260 (4.44), 275.5 (4.47), 360 (4.33).

Found: C, 59.91; H, 4.37%. Calcd for $C_{18}H_{16}O_8$: C, 60.00; H, 4.48%.

Triacetate (XVI): hot acetic anhydride-pyridine method; mp 144—145°C (colorless needles from methanol). IR: 1767, 1751, 1636 cm^{-1}. UV: λ_{max}mμ(log ε); (EtOH) 247_i(4.24), 351 (4.03), 360_{sh}(4.02).

Found: C, 59.16; H, 4.65%. Calcd for $C_{24}H_{22}O_{11}$: C, 59.26; H, 4.56%.

5,7,3′-Triethoxy-3,8,4′-trimethoxyflavone (XVII). A mixture of VIII (35 mg), anhydrous potassium carbonate (1.5 g), and diethyl sulfate (0.5 m*l*) in anhydrous acetone (15 m*l*) was treated in the usual manner. Recrystallization from methanol give XVII as colorless needles; mp 152.5—153°C; yield, 37 mg (76%). IR: 1633 cm^{-1}. UV: λ_{max} mμ (log ε); (EtOH) 253 (4.35), 272 (4.33), 353 (4.31). NMR:[*2,5] 7.87_q (C-6′); 7.84_d (C-2′); $7.00_{d'}$ (C-5′); 6.43_s(C-6); 4.17_q (2H), 4.23_q (4H) (each J=7.0 Hz, $CH_3C\underline{H}_2O$); 1.56_t(6H), 1.51_t (3H) (each J=7.0 Hz, $C\underline{H}_3CH_2O$).

Found: C, 65.12; H, 6.49%. Calcd for $C_{24}H_{28}O_8$: C, 64.85; H, 6.35%.

The author wishes to express his deep gratitude to Professor Kenji Fukui, Hiroshima University, for his guidance and encouragements throughout the course of this work, and also to Professor F. Bohlmann, University of Berlin, for supplying the natural centaureidin.

[*7] Natural centaureidin was measured in this laboratory.

[*8] i=inflection point.

BULLETIN OF THE CHEMICAL SOCIETY OF JAPAN VOL. 42 2705—2706 (1969)

A Synthesis of 2-(2′-Hydroxyethyl)cyclopentanone by the Barton Reaction*1

Heitaro OBARA and Hiroshi KIMURA

Department of Applied Chemistry, Faculty of Engineering, Yamagata University, Yonezawa

(Received January 31, 1969)

Previously, one of the present authors reported, during the course of his synthetic studies of aucubin,[1] the synthesis of 2-(2′-hydroxyethyl)cyclopentanone*2 (V) as an intermediate in the syntheses of five-membered cyclic ketals.

In the present investigation, we attempted the synthesis of V from 2-cyclopentylethanol (I) by the Barton reaction[2] according to the following scheme:

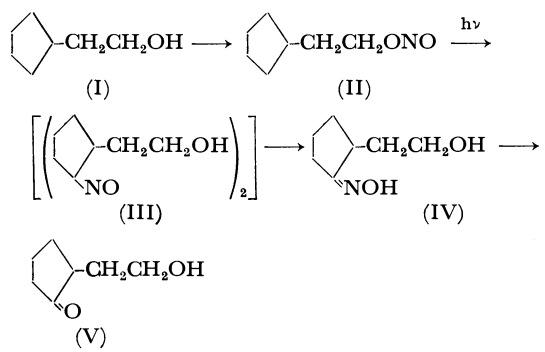

2-(2′-Hydroxyethyl)cyclopentanone oxime (IV) was obtained from 2-cyclopentylethyl nitrite (II) in a 20% yield as a white crystal, which was identified by a comparison of its IR spectrum with that of an authentic sample. A mild hydrolysis of IV with dilute hydrochloric acid gave 2-(2′-hydroxyethyl)cyclopentanone (V), which was identified by a comparison of its IR spectrum with that of the previously-synthesized specimen.[1]

Experimental

2-Cyclopentylethanol (I).[3,4] This alcohol was prepared in an 82% yield by the lithium aluminum hydride reduction of cyclopentylacetic acid.[5] Bp 180—182°C, n_D^{20} 1.4552 (lit.[3] bp 179—181°C, n_D^{20} 1.4615).

2-Cyclopentylethyl Nitrite (II). Into a suspension of 5.0 g of I and 15.0 g of sodium nitrite in 30 m*l* of water, a mixture of 2 m*l* of water and 5 m*l* of concentrated sulfuric acid was vigorously stirred, drop by drop, over a period of about 2 hr while being cooled by an ice-salt mixture.

The acid solution was then added slowly, and the temperature was kept at ±1°C. After the addition had been completed, the reaction mixture was allowed to stand in the ice-salt bath until it separated into two layers; the liquid layers were then decanted from the sodium sulfate into a separatory funnel.

The aqueous layer was removed, and the 2-cyclopentylethyl nitrite layer was washed with a 1% aqueous sodium bicarbonate solution and then with water, dried over anhydrous sodium sulfate, and evaporated to yield 4.5 g (72%) of II as a light green liquid; bp 50—51°C/15 mmHg; n_D^{18} 1.4346. IR (neat): 2940, 2860, 1643, 1603, 790 cm^{-1}.

Photolysis of 2-Cyclopentylethyl Nitrite (II). A solution of 3.07 g of II in 450 m*l* of dry benzene was irradiated by means of a 100-W high-pressure mercury arc lamp (model HLV-B, manufactured by Taika Kôgyô Co.) placed in a water-cooled quartz immersion well. The solution was slightly agitated by means of a stream of nitrogen, and the reaction temperature was kept near 25°C by regulating the temperature of the cooling water.

After 3 hr the solvent was removed *in vacuo*, and the residue was refluxed in *n*-butyl alcohol for 5 hr.*3 The solution was concentrated *in vacuo*, and the resulting viscous oil was chromatographed on a column of silica gel with ether. 2-(2′-Hydroxyethyl)cyclopentanone oxime (IV) was obtained as white crystals, which were then recrystallized from benzene. Yield, 0.625 g (20%); mp 80—82°C. This substance was found to be identical with the oxime of V which had previously been syn-

*1 Presented at the Tohoku Local Meeting of the Chemical Society of Japan, Hirosaki, October, 1967.

1) H. Obara, *Nippon Kagaku Zasshi* (*J. Chem. Soc. Japan, Pure Chem. Sect.*), **82**, 62 (1961).

*2 This compound was called 2-oxocyclopentylethanol in the previous report.[1]

2) a) M. Akhtar, "Advances in Photochemistry," Vol. 2, ed. by W. A. Noyes, G. S. Hammond and J. N. Pitts, Jr., Interscience Pub., New York, N. Y. (1964), p. 263. b) R. O. Kan, "Organic Photochemistry," McGraw-Hill, New York, N. Y. (1966), p. 233.

3) G. R. Yohe and R. Adams, *J. Am. Chem. Soc.*, **50**, 1505 (1928).

4) E. R. Shepard and J. F. Noth, *J. Org. Chem.*, **19**, 415 (1954); H. Pines, H. G. Rodenberg and V. N. Ipatieff, *J. Am. Chem. Soc.*, **76**, 771 (1954); V. N. Ipatieff, W. W. Thompson and H. Pines, *ibid.*, **73**, 555 (1951); W. Hückel and W. Gelmroth, *J. prakt. Chem.*, [2] **142**, 205 (1935).

5) E. E. Royals and A. N. Neal, *J. Org. Chem.*, **21**, 1448 (1956).

*3 It is considered that this rearrangement product exists as a dimer (III), because the oxime (IV) was not identified in the irradiation products by TLC and appeared slowly after boiling with *n*-butyl alcohol.

thesized by a comparison of their IR spectra and by a mixed-melting-point determination.

Found: C, 58.74; H, 9.34; N, 9.86%. Calcd for $C_7H_{13}O_2N$: C, 58.72; H, 9.15; N, 9.78%.

2-(2′-Hydroxyethyl)cyclopentanone (V). A mixture of 110 mg of IV and 10 m*l* of 1N hydrochloric acid was stirred at 50°C for one hour. The solution was diluted about 1.5 times with water and extracted with methylene chloride. The methylene chloride solution was washed with a 10% aqueous sodium bicarbonate solution and water, dried over anhydrous sodium sulfate, and evaporated to yield 57 mg (58%) of a colorless liquid. The IR spectrum of this liquid was identical with that of the V which had previously been synthesized.[1] 2,4-Dinitrophenylhydrazone, mp 173—174°C (lit. 177—178°C,[1] 175°C[6]).

The authors wish to acknowledge the technical assistance of Mr. Tsutomu Sato and the microanalyses of Mr. Jun-ichi Onodera and Mr. Masahiro Endo.

6) H. Booth, F. E. King, K. G. Mason, J. Parrick and R. L. St. D. Whitehead, *J. Chem. Soc.*, **1959**, 1050.

BULLETIN OF THE CHEMICAL SOCIETY OF JAPAN VOL. 42 2706—2707 (1969)

N-Alkylation of Metanilic Acid

Toshinari NAKAJIMA,[1] Nobuyuki GOTOH and Yoshio NAGAI[2]

The Institute of Industrial Science, The University of Tokyo, Roppongi, Minato-ku, Tokyo

(Received February 8, 1969)

While the alkylation reaction of amino compounds with alcohol in the presence of iodine is well known, the method does not always give satisfactory results. The present investigation was undertaken to see if a practical method could be worked out for the preparation of *N,N*-diethylmetanilic acid using iodine, red phosphorus and boric acid as a catalyst.[3]

Metanilic acid was treated with ethanol in the presence of iodine, red phosphorus and boric acid at 200—250°C for a few hours to give *N,N*-diethylmetanilic acid. The condition used in various alkylations and the yields of *N,N*-diethylmetanilic acid of individual reactions are given in Table 1.

In the reaction at 250°C, the main product was oily materials as a result of presumable desulfonation. Whereas at 210°C or below the reaction did not proceed. The best condition seemed to be heating at about 230°C (*cf.* DEM-5,10,11). An optimum reaction time was estimated to be 3 hr as a longer heating decreased the yield (*cf.* DEM-2,10). Without red phosphorus only 17.6% of metanilic acid was ethylated, and the rest was recovered unchanged. Both reactions without boric acid and without iodine and red phosphorus gave only unreacted metanilic acid. The best condition for the preparation of *N,N*-diethylmetanilic acid can be seen in run numbers DEM-10 and PE-7.

Table 1. Reaction condition and the yield of *N,N*-diethylmetanilic acid

Metanilic acid 8.88 g , Ethanol 39.4 g

Run No.	Iodine (g)	Red phosphorus (g)	Boric acid (g)	Reac. temp. (°C)	Reac. time (hr)	Yield (%)
DEM-2	0.147	0.016	0.212	230	5	68.2
DEM-3	0.224	0.045	0.278	240	5	76.6
DEM-5	0.025	0.035	0.104	240	3	79.2
DEM-8	0.072	0.004	0.093	240	3	77.2
DEM-9	0.146	0.014	0.214	240	3	69.0
DEM-10	0.129	0.019	0.215	230	3	81.8
DEM-11	0.135	0.016	0.224	210	3	—[3]
DEM-12	0.143	—	0.187	240	3	17.6
DEM-16	—	—	2.105	230	3	—[3]
DEM-18	0.129	0.018	—	230	3	—[3]
PE-2[1]	0.51	1.54	2.05	200	10	7.2
PE-7[2]	0.53	1.60	2.14	230	3	82.9
PE-9[1]	0.53	1.60	2.14	220	10	78.1
PE-10[1]	0.53	0.16	2.14	220	5	77.0
PE-11[1]	0.51	0.15	2.05	210	5	5.9

1) Metanilic acid 88.8 g, Ethanol 530 g
2) Metanilic acid 88.8 g, Ethanol 1063 g
3) The yield was negligible.

Experimental

For a typical run (DEM-10), 8.88 g (0.0513 mol) of metanilic acid, 39.4 g (50 ml, 0.85 mol) of ethanol, 0.129 g (0.000508 mol) of iodine, 0.215 g (0.00348 mol) of boric acid and 0.019 g (0.000154 mol) of red phosphorus were placed in an autoclave. The reaction

1) Present address: Ochanomizu University, Otsuka, Bunkyo-ku, Tokyo.

2) Present address: The Saitama University, Shimo-okubo, Urawa-shi.

3) Yoshio Nagai *et al.*, Japanese Pat. 177283 (1947).

mixture was heated at 230°C for 3 hr. After cooling the reaction mixture was filtered and washed with ethanol to give 10.17 g of a crude product. This product was dissolved in hot water. After removal of a hot-water-insoluble part, the filtrate was concentrated to yield 9.95 g of *N,N*-diethylmetanilic acid (84.7% of the theoretical amount). The purity of this product was estimated to be 96.5% by a functional group analysis. Thus total yield was calculated to be 81.8%.

BULLETIN OF THE CHEMICAL SOCIETY OF JAPAN VOL. 42 2707—2708 (1969)

An X-Ray Emission Spectroscopic Investigation of the Chemical Bond of Sulfur. II. The Number of Valence Electrons of the Sulfur Atom in Organic Compounds

Yoshihito TAKAHASHI, Katsumasa YABE and Toshio SATO

Goverment Industrial Development Laboratory, Hokkaido, Higashi-tsukisamu, Sapporo

(Received February 15, 1969)

We have calculated the number of valence electrons, N, of the sulfur atom in fifty compounds (or samples)[1] on the basis of this theoretical correlation; $\delta E=n(n+3)/8$,[2] where δE is the energy shift of the S$K\alpha$ line and where n is $N-6$. We also checked the reliability of the relation by using the dipole moment and structural data of several sulfur compounds.

Recently improved theoretical calculations have

TABLE 1. WAVELENGTH of S$K\alpha$ LINE AND MEAN NUMBER OF VALENCE ELECTRONNS OF SULFUR ATOM IN COMPOUNDS

Compound	Wavelength (Å)	Energy (eV)	ΔE (eV)	Mean number of valence electrons[a]
Rhombic sulfur, S_8[b]	5.37270	2307.55	0.00	6.00
$(NH_2)_2CS$[b]	7287	7.48	−0.07	6.21±0.14
$[(CH_3)_2N]_2CS$	7283	7.49	−0.06	6.18±0.12
NH_2CSCH_3	7275	7.53	−0.02	6.06±0.12
$(NH_2CS)_2$	7262	7.58	0.03	5.92±0.12
$Et_2NCSSNa$	7210	7.81	0.26	5.42±0.08
$(p\text{-}O_2NPhO)PS(OEt)_2$	7257	7.61	0.06	5.85±0.11
2-Mercaptobenzimidazole	7302	7.41	−0.14	6.44±0.16
2-Mercaptobenzoxazole	7308	7.38	−0.17	6.50±0.23
2-Thiobarbituric acid	7298	7.43	−0.12	6.36±0.15
Thiouracil	7301	7.42	−0.13	6.40±0.16
2-Methylthiobenzimidazole	7283	7.49	−0.06	6.18±0.12
Phenothiazine[b]	7275	7.53	−0.02	6.06±0.12
Methylene blue	7255	7.61	0.06	5.85±0.11
Na_2SO_3[b]	7100	8.29	0.74	4.65±0.06
$NaHSO_3$	7120	8.20	0.65	4.78±0.07
$(EtO)_2SO$	7127	8.16	0.61	4.83±0.07
$PhSO_2Na$	7107	8.25	0.70	4.70±0.06
$HOCH_2SO_2Na$[b]	7157	8.04	0.49	5.03±0.08
PhNSO	7164	8.01	0.46	5.07±0.08
$(CH_2)_4SO$	7161	8.02	0.47	5.05±0.08
$(CH_3)_2SO$[b]	7193	7.88	0.33	5.30±0.08
Cl_2SO	712	8.20	0.65	4.78±0.14
HCHO+$NaHSO_3$[c]	708	8.37	0.82	4.54±0.12
CH_3CHO+$NaHSO_3$[c]	709	8.33	0.78	4.59±0.12
$(CHO)_2\cdot 2NaHSO_3$	7053	8.48	0.93	4.39±0.06
$PhCHO\cdot NaHSO_3$	7049	8.50	0.95	4.36±0.06
$CaSO_4$[b]	6992	8.74	1.19	4.07±0.05
Na_2SO_4[b]	7002	8.70	1.15	4.12±0.05
$NaHSO_4$	6999	8.71	1.16	4.10±0.05
$PhNH_2\cdot \frac{1}{2}H_2SO_4$	7010	8.67	1.12	4.15±0.05
$(EtO)_2SO_2$	7000	8.71	1.16	4.10±0.05
$PhOSO_3K$	7012	8.66	1.11	4.16±0.05
$C_{12}H_{25}OSO_3Na$	7025	8.60	1.05	4.23±0.05
NH_2SO_3H[b]	7030	8.59	1.04	4.24±0.06
$PhSO_3H$	7047	8.51	0.96	4.34±0.06
$HOCH_2SO_3Na$	7049	8.50	0.95	4.36±0.06
$PhSO_2F$	7052	8.49	0.94	4.37±0.06
p-$EtPhSO_2Cl$[b]	7072	8.40	0.85	4.50±0.06
$PhSO_2NH_2$[b]	7070	8.41	0.86	4.48±0.06
$PhSO_2NHBu$	7054	8.48	0.93	4.38±0.06
p-$EtPhSO_2NEt_2$[d]	705	8.50	0.95	4.36±0.12
$(CH_3)_2SO_2$[b]	7095	8.30	0.75	4.64±0.06
Cl_2SO_2	704	8.54	0.99	4.30±0.12

a) Calculated by the formula, $\delta E=n(n+3)/8$.[2]
b) Refined data on previous reported compounds.[1]
c) Aqueous solution, 50%, estimated in adduct, keeping aldehyde excess.
d) Benzene solution, 50%.

1) T. Sato, Y. Takahashi and K. Yabe, This Bulletin, **40**, 298 (1967).
2) C. A. Coulson and C. Zauli, *Mol. Phys.*, **6**, 525 (1963).

been made on this problem[3,4] on the same fundamental assumption that $\delta E=f(N)$; these calculations gave results a little different from the old one. Therefore, from the experimental point of view, it is important to obtain more accurate data on δE as a basis for discussion.

In this note, we will give new data on about thirty compounds and will give refined data on some compounds previously reported on. The measurements were carried out on the same apparatus and in the same manner as in a previous work.[1] Table 1 shows the mean value of at least three measurements; the precision of the wavelength measurements was thereby improved to an extent of $\pm 0.5'$ (2θ) (± 0.0001Å). On the measurements of the liquid samples, a sample holder with a Mylar film (10 μ thick) window was used. In the cases of sulfuryl chloride and thionyl chloride, the Mylar film was replaced by polyethylene film (30 μ thick), the precision being to the extent of $\pm 1.0'$ (2θ) (± 0.0002 Å).

The structure of the methylene blue molecule has thus far been given as follows:

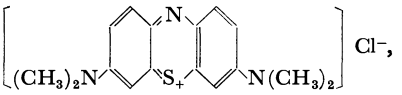

of which the sulfur atom has a plus charge. However, our measurements led to the finding that the number of valence electrons of its sulfur atom is similar to those of rhombic sulfur and phenothiazine. Consequently, the above formula for the methylene blue molecule is not proper.

The molecular structures of aldehide-bisulfite adducts and 2-mercaptobenzimidazole, *etc.*, will be discussed on the basis of the wavelength value of the S$K\alpha$ line and the shape of the S$K\beta$ band in our next paper.[5]

3) F. A. Gianturco and C. A. Coulson, *Mol. Phys.*, **14**, 223 (1968).

4) A. T. Shuvaev, *Izv. Akad. Nauk S.S.S.R., Ser. Fiz.*, **28**, 758 (1964).

5) Y. Takahashi and K. Yabe, This Bulletin, **42**, No. 11 (1969), in press.

BULLETIN OF THE CHEMICAL SOCIETY OF JAPAN VOL. 42 2708—2710 (1969)

Preparation of Some Anilinosilanes

Toshio TAKIGUCHI and Masahiro SUZUKI

Department of Synthetic Chemistry, Kiryu College of Technology, Gunma University, Tenjin-cho, Kiryu

(Received February 25, 1969)

We wish to report on the preparation of some di- and trianilinosilanes from the reaction of aniline and the corresponding organochlorosilanes by the use of triethylamine as a hydrogen chloride acceptor. Most of the products were crystalline substances and gave the corresponding silanols or siloxanes when hydrolyzed in the presence of an acidic catalyst.

The products were triphenylsiloxytrianilinosilane, bis-triphenylsiloxydianilinosilane, vinyltrianilinosilane, vinylphenyldianilinosilane, vinylbutyldianilinosilane, diphenyldianilinosilane, and phenyltrianilinosilane, the first five being new compounds.

All the products were well-defined and were characterized by their IR spectra. As for the crystalline products, the X-ray powder patterns were determined in order to identify them rapidly.

Experimental

Organochlorosilanes. The triphenylsiloxytrichlorosilane, mp 47°C, and bis-triphenylsiloxydichlorosilane, mp 141°C, were prepared according to a method previously reported.[1] The vinylphenyldichlorosilane, bp 67°C/2 mmHg, and vinylbutyldichlorosilane, bp 65—66°C/20 mmHg, were prepared by the Grignard route.[2] The vinyltrichlorosilane, diphenyldichlorosilane, and phenyltrichlorosilane were obtained from the Shin-etsu Chem. Ind. Co. and were further purified by distillation immediately before use.

Preparation of Anilinosilanes. Typical procedures will be described in detail with the preparation of bis-triphenylsiloxydianilinosilane as an example.

To a stirred mixture of freshly-distilled aniline (19.7 g; 0.21 mol), triethylamine (28.4 g; 0.28 mol), and 200 m*l* of toluene, a toluene solution of bis-triphenylsiloxydichlorosilane (57.2 g; 0.09 mol) was added drop by drop. After the addition was complete, the mixture was further stirred for 10 hr, during which period the temperature was maintained at 100°C. After standing overnight, triethylamine hydrochloride was removed by filtration and the filtrate was evaporated to about 100 m*l*.

1) T. Takiguchi, M. Abe, K. Urano and T. Sakuma, This Bulletin, **40**, 2453 (1967).

2) T. Takiguchi and M. Abe, *Kogyo Kagaku Zasshi* (*J. Chem. Soc. Japan, Ind. Chem. Sect.*), **66**, 625 (1963).

The concentrate was then combined with 100 ml of warm *n*-hexane and cooled to room temperature to give a white crystalline mass from which 37.8 g (55%) of pure *bis-triphenylsiloxydianilinosilane* as white, acicular crystlas melting at 159—160°C, was obtained by recrystallization from boiling *n*-hexane.

Found: C, 75.06; H, 5.80; N, 3.41; Si, 11.05%; mol wt, 755 (determined cryoscopically in 1,4-dioxane). Calcd for $C_{48}H_{42}N_2O_2Si_3$: C, 75.55; H, 5.56; N, 3.67; Si, 11.04%; mol wt, 763.

The hydrolysis of the anilinosilane in the presence of sulfuric acid gave quantitatively a mixture of hexaphenyltrisiloxane-3,3-diol[1] and its condensation product.

Similar procedures were applied to other chlorosilanes to give the following anilinosilanes, the mean yield being 57%: triphenylsiloxytrianilinosilane, mp 201—202°C, vinyltrianilinosilane, mp 86—87°C, vinylphenyldianilinosilane, mp 87—88°C, vinylbutyldianilinosilane, a low melting solid, bp 149—150°C/1.5 mmHg, diphenyldianilinosilane, mp 161—162°C (lit. mp 153°C,[3] 166—167°C[4]), and phenyltrianilinosilane, mp 138°C (lit. mp 134—135°C[5]). All the anilinosilanes thus obtained were readily soluble in chloroform, acetone, a dioxane, were soluble in benzene and toluene, and were barely soluble in methanol and *n*-hexane.

Triphenylsiloxytrianilinosilane. Found: C, 74.87; H, 5.83; N, 7.57; Si, 9.72%; mol wt, 576. Calcd for $C_{36}H_{23}N_3OSi_2$: C, 74.57; H, 5.74; N, 7.24; Si, 9.69%; mol wt, 580.

Vinyltrianilinosilane. Found: C, 71.33; H, 6.40; N, 12.15; Si, 8.60%; mol wt, 338. Calcd for $C_{20}H_{21}N_3Si$: C, 72.47; H, 6.39; N, 12.68; Si, 8.47%; mol wt, 332.

Vinylphenyldianilinosilane. Found: C, 75.66; H, 6.60; N, 8.57; Si, 8.90%; mol wt, 322. Calcd for $C_{20}H_{20}N_2Si$: C, 75.90; H, 6.37; N, 8.85; Si, 8.87%; mol wt, 317.

Vinylbutyldianilinosilane. Found: C, 71.77; H, 8.20; N, 9.48; Si, 9.53%; mol wt, 289. Calcd for $C_{18}H_{24}N_2Si$: C, 72.92; H, 8.16; N, 9.45; Si, 9.47%; mol wt, 297.

Diphenyldianilinosilane. Found: C, 78.82; H, 5.87; N, 7.70; Si, 7.74%; mol wt, 370. Calcd for $C_{24}H_{22}N_2Si$: C, 78.64; H, 6.05; N, 7.64; Si, 7.66%; mol wt, 367.

Phenyltrianilinosilane. Found: C, 76.33; H, 6.17; N, 10.86; Si, 7.46%; mol wt, 395. Calcd for $C_{24}H_{23}N_3Si$: C, 75.55; H, 6.08; N, 11.01; Si, 7.36%; mol wt, 382.

Infrared Absorption Spectra and X-Ray Power Diffraction Data. The absorption bands due to Si–R bonding,[2,6-7] and aromatic secondary amine attached to Si[8,9] were distinctly observed throughout all the samples. The X-ray powder patterns were also satisfactorily recorded by using Cu$K\alpha$ radiation filtered by Ni.

IR Data

$(Ph_3SiO)_2Si(NHPh)_2$ 700(S) 715(VS) 750(M) 760 (M) 800(VW) 905(M) 933(S) 1000(M) 1029(M) 1100(VS) 1120(VS) 1292(S) 1394(M) 1430(S) 1504 (M) 1605(M) 3035(W) 3380(W)

$Ph_3SiOSi(NHPh)_3$ 700(M) 710(M) 743(M) 780(W) 920(S) 1000(W) 1028(W) 1100(S) 1115(VS) 1285(S) 1383(M) 1430(W) 1504(M) 1605(M) 3045(VW) 3350(W)

$C_2H_3Si(NHPh)_3$ 695(M) 754(VS) 770(S) 823(W) 892(VS) 906(VS) 968(M) 995(S) 1011(M) 1025(M) 1076(M) 1177(M) 1230(M) 1280(VS) 1322(M) 1380(VS) 1475(VS) 1489(VS) 1598(VS) 2943(VW) 3026 (W) 3326 (M)

C_2H_3·PhSi(NHPh)$_2$ 698(S) 708(S) 738(VS) 754(VS) 770(S) 821(VW) 863(M) 900(VS) 966(S) 995(S) 1010(M) 1028(M) 1078(M) 1113(S)118 1(M) 1230(S) 1281(VS) 1323(M) 1378(VS) 1425(S) 1474(VS) 1491(VS) 1597(VS) 3024(W) 3346(W)

C_2H_3·BuSi(NHPh)$_2$ 692(S) 754(S) 890(S) 903(S) 962(M) 998(M) 1028(M) 1078(M) 1152(VW) 1170 (W) 1228(W) 1283(VS) 1382(S) 1474(S) 1494(S) 1601(S) 2850(W) 2924(M) 3036(W) 3390(M)

$Ph_2Si(NHPh)_2$ 690(S) 740(S) 754(S) 890(S) 906 (VS) 995(M) 1025(VW) 1075(VW) 1110(S) 1178 (VW) 1230(VW) 1283(VS) 1320(VW) 1378(M) 1388(M) 1424(M) 1466(S) 1484(S) 1595(VS) 3014 (VW) 3336 (W)

$PhSi(NHPh)_3$ 695(M) 740(M) 754(S) 780(W) 890(M) 910(VS) 928(S) 995(M) 1028(W) 1078 (W) 1120(M) 1170(W) 1226(W) 1278(VS) 1390(S) 1425(VW) 1478(S) 1490(S) 1599(S) 3026(VW) 3351(M)

X-Ray Data

$(Ph_3SiO)_2Si(NHPh)_2$

d, *kX*:	11.33	11.05	9.61	5.54	5.44	4.46
I/I_0:	0.40	1.00	0.13	0.13	0.10	0.51

$Ph_3SiOSi(NHPh)_3$

d, *kX*:	14.26	9.41	8.12	7.03	4.67	4.51	4.11	3.53
I/I_0:	1.00	0.16	0.70	0.13	0.54	0.51	0.13	0.18

C_2H_3·PhSi(NHPh)$_2$

d, *kX*:	9.21	9.12	8.51	8.35	5.61	5.22	4.96	4.93
	4.77	4.70	4.58	4.35	4.29	4.15	4.04	3.92
	3.77	3.38	3.31	3.10	3.05	2.95		
I/I_0:	0.81	0.14	1.00	0.35	0.19	0.24	0.35	0.38
	0.18	0.79	0.48	0.34	0.41	0.79	0.23	0.15
	0.49	0.16	0.31	0.26	0.14	0.15		

$C_2H_3Si(NHPh)_3$

d', *kX*:	10.53	8.35	7.63	7.25	6.28	5.47	5.31	5.07
	4.65	4.46	4.37	4.29	4.15	4.06	3.97	3.63
	3.60	3.52	3.27	3.22	3.09	3.01	2.96	2.87
I/I_0:	0.56	0.23	0.39	0.48	0.39	0.28	0.36	0.21
	1.00	0.80	0.32	0.56	0.31	0.23	0.49	0.53
	0.52	0.26	0.24	0.22	0.39	0.37	0.23	0.19

$Ph_2Si(NHPh)_2$

d, *kX*:	10.05	9.41	9.31	7.38	5.61	5.07	4.96	4.72
	4.67	4.51	4.44	4.27	4.00	3.66	3.38	
I/I_0:	0.12	0.27	0.21	0.23	0.17	0.11	0.11	1.00
	0.34	0.20	0.25	0.46	0.11	0.15	0.33	

$PhSi(NHPh)_3$

d, *kX*:	10.78	10.16	9.72	7.83	7.63	7.20	6.24	5.54
	5.34	5.04	4.82	4.65	4.53	4.40	4.19	4.00
	3.79	3.56	3.41	3.28	3.12	3.07	2.73	

3) H. H. Anderson, *J. Am. Chem. Soc.*, **73**, 5802 (1951).

4) W. R. Dunnavant, R. A. Markle, P. B. Stickney, J. E. Curry and J. D. Byrd, *J. Polymer Sci., A-1*, **5**, 707 (1967).

5) V. A. Prokhorova and V. O. Reikhsfel'd, *Zh. Obshch. Khim.*, **33**, 2617 (1963); *Chem. Abstr.*, **60**, 542a (1964).

6) J. G. Noltes, M. C. Henry and M. J. Janssen, *Chem. Ind.*, **1959**, 298.

7) M. C. Henry and J. G. Noltes, *J. Am. Chem. Soc.*, **82**, 555 (1960).

8) R. H. Baney and G. G. Haberland, *J. Organometal. Chem.*, **5**, 320 (1966).

9) R. M. Ismail and E. Bessler, *ibid.*, **13**, 253 (1968).

I/I_0: 0.15 0.14 0.26 0.28 0.21 0.13 0.15 0.19
0.13 0.30 0.30 0.64 0.75 1.00 0.69 0.15
0.43 0.49 0.21 0.15 0.17 0.34 0.22

The authors are grateful to the Shin-etsu Chem. Ind. Co. for the supply of the chlorosilanes used herein.

BULLETIN OF THE CHEMICAL SOCIETY OF JAPAN VOL. 42 2710—2711 (1969)

Some Remarks on the Reactions of Ferricyanide Ions with Hydrogen Atoms in Alkaline Aqueous Solutions

Akira YOKOHATA, Katsuyuki HARAKON and Satoru TSUDA

Department of Chemistry, Faculty of Engineering, Hiroshima University, Senda-machi, Hiroshima

(Received March 3, 1969)

In the radiolysis of the deaerated alkaline aqueous solutions of potassium ferricyanide, there seems to be no doubt[1-4] that aquocomplex ($Fe(CN)_5H_2O^{3-}$) is formed *via* the reactions of ferricyanide ions with the reducing species (mainly e_{aq}^-). However, the role of hydrogen atoms in the formation of aquocomplex is not well known.[5] In order to make it clear, a technique introducing hydrogen atoms generated in a microwave discharge into the alkaline aqueous solution of potassium ferricyanide was used, and the mechanism of formation of aquocomplex was successfully investigated, in relation to the concentration of hydroxyl ions.

Experimental

The apparatus consists of a conventional discharge flow system. Hydrogen atoms were produced at a moderately high pressure (13—14 mmHg*1) by 2450 Mc/sec microwave generator feeding a resonant cavity. Hydrogen (purity: >99.95%) was used without further purification. Gas flow was controlled by a needle valve to maintain their velocity at 5×10^{-5} M/min through the reaction section. The reaction section consists of the discharge tube of quartz and the reaction vessel of hard glass (Fig. 1). The gas stream was finally removed from the line with a vacuum pump.

The experimental procedure was as follows. After the system was evacuated to $<10^{-3}$ mmHg, a stream of hydrogen was passed through the system. The electrical circuit to the discharge tube was then closed. A few minutes was required for sweeping out the residual air in the system with the hydrogen stream. As soon as the red hydrogen arc appeared in the tube, the current was shut off; then 10 m*l* of the pre-deaerated sample solution was introduced into the reaction vessel by a syringe through the rubber stopper. Electric power was usually adjusted to 100 W and the reaction vessel was maintained at about 3°C by means of an ice bath.

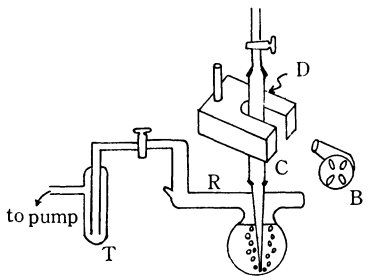

Fig. 1. Schematic diagram of apparatus.
B: blower C: cavity D: discharge tube
R: reaction vessel T: trap

Reproducible results were obtained only when the equipment was throughly cleaned before each run.

All reagents used were of research grade. Concentration of aquocomplex ($Fe(CN)_5H_2O^{3-}$) was determined spectrophotometrically by the method using NaN_3.[2,4]

Results and Discussion

A preliminary experiment of the effect of initial concentration of ferricyanide ions on the reduction yield of ferricyanide ions showed no effect in the range from 5×10^{-3}M to 5×10^{-2}M. This indicates that in this concentration range all hydrogen atoms reaching the solution are utilized to reduce ferricyanide ions. Thus, in this work the solution of 5×10^{-3}M or 1×10^{-2}M of ferricyanide ions was used.

Figure 2 shows the relation between the amount of aquocomplex formed and the duration of dis-

1) E. Masri and M. Haïssinsky, *J. Chim. Phys.*, **60**, 397 (1960).
2) S. Ohno and G. Tsuchihashi, *Radioisotopes*, **16**, 434 (1967).
3) C. E. Burchill, F. S. Dainton and D. Smithies, *Trans. Faraday Soc.*, **63**, 932 (1967).
4) A. Yokohata, This Bulletin, **42**, 658 (1969).
5) G. Navon and G. Stein, *J. Phys. Chem.*, **70**, 3630 (1966).

*1 Contains water vapor. Although the formation of OH radicals through the dissociation of water vapor can be expected, they will react with the large excess of molecular hydrogen. ($OH+H_2\rightarrow H+H_2O$): T. W. Davis, S. Gordon and E. J. Hart, *J. Am. Chem. Soc.*, **80**, 4487 (1958).

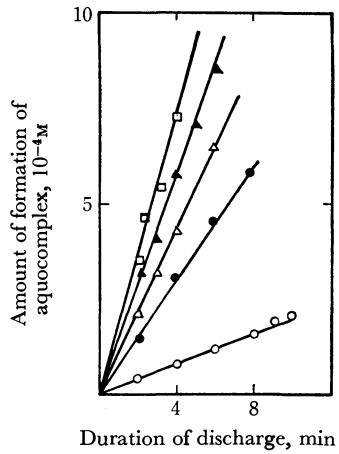

Fig. 2. Relation between the amount of formation of aquocomplex and duration of discharge.
Initial concentration: 5×10^{-3}M $Fe(CN)_6^{3-}$
○ 0.1M NaOH ● 0.5M NaOH
△ 1.0M NaOH ▲ 2.0M NaOH
□ 3.0M NaOH

charge in the concentration range of hydroxyl ions from 0.1M to 3M. The increment of aquocomplex yield with increasing concentration of hydroxyl ions has been found.

The following reaction scheme can be expected in this system.*2

$$H + Fe(CN)_6^{3-} \rightarrow Fe(CN)_6^{4-} + H^+ \quad (1)$$
$$\searrow\ Fe(CN)_5H_2O^{3-} + CN^- + H^+ \quad (2)$$
$$H + OH^- \rightarrow e_{aq}^- \quad (3)$$
$$e_{aq}^- + Fe(CN)_6^{3-} \rightarrow Fe(CN)_6^{4-} \quad (4)$$
$$\searrow\ Fe(CN)_5H_2O^{3-} + CN^- \quad (5)$$

If reaction (2) is ignored,[4] Eqs. (6) and (7) result in.*3

$$Y(-Fe(CN)_6^{3-}) = Y(H) \quad (6)$$
$$Y(Fe(CN)_5H_2O^{3-}) = Y(H)\frac{1}{1+k_1/k_3\cdot[Fe(CN)_6^{3-}]/[OH^-]}\cdot\frac{1}{1+k_4/k_5} \quad (7)$$

Equation (7) can be reformed to Eq. (8)

$$\frac{1}{Y(Fe(CN)_5H_2O^{3-})} = \frac{1+k_4/k_5}{Y(H)}\left(1+\frac{k_1[Fe(CN)_6^{3-}]}{k_3[OH^-]}\right) \quad (8)$$

A good linearity of a plot of $1/Y(Fe(CN)_5H_2O^{3-})$ against $[Fe(CN)_6^{3-}]/[OH^-]$ (Fig. 3) gives a value

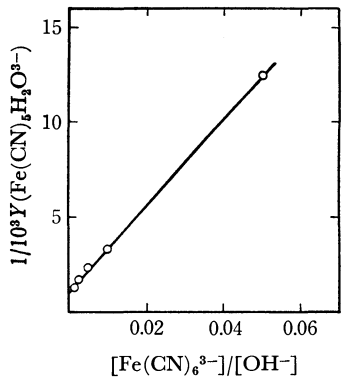

Fig. 3. A plot of $1/Fe(CN)_5H_2O^{3-}$ against $[Fe(CN)_6^{3-}]/[OH^-]$

of 230*4 for k_1/k_3 where $k_4/k_5\approx1$[4] and $Y(H)=2.0\times10^{-3}$M determined in this experiment are used. If we take $k_1=4\times10^9M^{-1}\,sec^{-1}$,[6] k_3 is estimated to be $\sim1.7\times10^7M^{-1}\,sec^{-1}$ which is almost consistent in order of magnitude with $2.3\times10^7M^{-1}\,sec^{-1}$ [7] obtained from the radiolytic experiment. In other words, these findings show that the assumption of exclusion of reaction (2) is allowable, at least in alkaline region.

It is our conclusion that (1) the increment of yield of aquocomplex with an increasing concentration of hydroxyl ions can be well interpreted in terms of the solvated electron formed *via* the reaction of hydrogen atoms with hydroxyl ions, and that (2) the contribution of hydrogen atoms themselves to the formation of aquocomplex can be ignored in alkaline region.

*2 Molecular hydrogen does not reduce ferricyanide.
*3 $Y(X)$ means the yield of product X formed during 4 min of the duration of discharge.
*4 This value can be expected to be independent of temperature, if the same activation energy (~5 kcal) for the reactions (1) and (3) is assumed, as seen in Navon's report: G. Navon and G. Stein, *J. Phys. Chem.*, **69**, 1384 (1965).

6) J. Rabani, *ibid.*, **66**, 361 (1962).
7) J. Rabani, in "Solvated Electron," R. F. Gould, Ed., Am. Chem. Soc., Washington., D. C. (1965), p. 242.

BULLETIN OF THE CHEMICAL SOCIETY OF JAPAN VOL. 42 2712—2713 (1969)

Studies of Actinium(III) in Various Solutions. III. Actinium(III) Complexes with Oxalate, Sulfate, Chloride, and Thiocyanate Ions in Perchlorate Media

Tatsuya SEKINE and Mitsuo SAKAIRI

Department of Chemistry, Science University of Tokyo, Kagurazaka Shinjuku-ku, Tokyo

(Received March 4, 1969)

In previous papers,[1-4] the stability of the complexes of lanthanum(III), europium(III), lutecium(III), and americium(III) with oxalate, sulfate, chloride, and thiocyanate ions has been determined by means of the metal chelate extraction method. The present paper studies the complex formation of actinium(III) in these aqueous systems in order to obtain further information about the stability of the complexes of trivalent lanthanides and actinides.

Experimental

All of the experiments were carried out in a thermostatted room at 25°C. The actinium-228 tracer was separated from radium-228 and purified by a solvent extraction method which was described in Paper I of this series.[5] Sodium salts of oxalate, sulfate, chloride, and thiocyanate were dissolved in water, and the concentration was analyzed by gravimetry or volumetry. The other reagents and the experimental procedures are the same as those described in Paper II of this series[6] or in other papers.[1-4]

Results and Discussion

As the statistical treatment of the experimental data was the same as in previous papers,[1-4,7] only the final form of the equations will be shown in this paper.

The stability constants for the "n-th" complex with the L^{l-} ligand are defined as;

$$\beta_n = \frac{[AcL_n^{3-nl}]}{[Ac^{3+}][L^{l-}]^n} \quad (1)$$

The net distribution ratio of the extraction with a chelating extractant, HA, in the absence of and in the presence of the complexing ligand is described as:

$$D_0 = \frac{[AcA_3]_{org}}{[Ac^{3+}]} \quad (2)$$

$$D = \frac{[AcA_3]_{org}}{[Ac^{3+}]+[AcL^{3-l}]+\cdots+[AcL_n^{3-nl}]} = \frac{D_0}{1+\beta_1[L^{l-}]+\cdots+\beta_n[L^{l-}]^n} \quad (3)$$

The extraction constant is defined as:

$$K_{ex} = D_0[H^+]^3[HA]_{org}^{-3} \quad (4)$$

When the extraction constant is determined in the absence of the complexing ligand, the stability constants are given by the following equation:

$$\frac{D[H^+]^3[HA]_{org}^{-3}}{K_{ex}} = (1+\beta_1[L^{l-}]+\cdots+\beta_n[L^{l-}]^n)^{-1} \quad (5)$$

When the $\log D[H^+]^3[HA]_{org}^{-3}K_{ex}^{-1}$ *vs.* $\log[L^{l-}]$ plot is made from the experimental data, the stability constants are determined by a curve-fitting method.[7]

The constants obtained from the experimental data are summarized in Table 1, together with the previous results on the other four ions. As the present results were analyzed by the graphic method, no range of error is included in the results.

It was reported in a previous work[6] that the extraction data of actinium(III) with TTA were reproducible only when a mixed extractant, TTA and TBP in a diluent, was used. This was confirmed in the present work. Moreover, it was also found that the formation of aqueous chelates could be prevented by the use of the mixed solvent.[8] The data on the experiments in the thiocyanate system scattered a little for some unknown reasons and so the constants for the thiocyanate complexes might be somewhat less accurate than the others.

Almost no work seems to have been done on the stabilities of the actinium(III) complexes.[9]

The results in Table 1 may be summarized as follows:

1) T. Sekine, *Acta Chem. Scand.*, **19**, 1435 (1965).
2) T. Sekine, *ibid.*, **19**, 1469 (1965).
3) T. Sekine, *ibid.*, **19**, 1477 (1965).
4) T. Sekine, *ibid.*, **19**, 1519 (1965).
5) T. Sekine, Y. Koike and M. Sakairi, *J. Nucl. Sci. Technolog.*, **4**, 308 (1967).
6) T. Sekine, Y. Koike and Y. Hasegawa, This Bulletin, **42**, 432 (1969).
7) T. Sekine, M. Sakairi and Y. Hasegawa, *ibid.*, **39**, 2141 (1966).
8) T. Sekine, M. Sakairi, F. Shimada and Y. Hasegawa, *ibid*, **38**, 847 (1965).
9) L. G. Sillén and A. E. Martell, "Stability Constants," *Spec. Pub.*, **17**, the Chemical Society, London (1964).

TABLE 1. STABILITY CONSTANTS OF COMPLEXES OF La(III), Eu(III), Lu(III), Ac(III) AND Am(III) WITH OXALATE, SULFATE, CHLORIDE AND THIOCYANATE IONS

The data of Ac(III) complexes were taken from the present work and the rests were taken from Refs. 1—4.

Ionic medium		Oxalate 1M $NaClO_4$	Sulfate 1M $NaClO_4$	Chloride 4M $NaClO_4$	Thiocyanate 5M $NaClO_4$
La^{3+}	$\log\beta_1$	4.26±0.11	1.45±0.07	−0.22±0.11	0.24±0.06
	$\log\beta_2$	7.85±0.12	2.46±0.08	−0.64±0.11	(<−0.62)
	$\log\beta_3$	10.27±0.21	—	—	−0.73±0.12
Eu^{3+}	$\log\beta_1$	4.77±0.10	1.54±0.06	−0.15±0.10	0.32±0.09
	$\log\beta_2$	8.72±0.09	2.69±0.05	−0.72±0.17	∼−0.1(<0.25)
	$\log\beta_3$	11.39±0.12	—	—	−0.36±0.15
Lu^{3+}	$\log\beta_1$	5.11±0.08	1.29±0.23	−0.35±0.07	0.45±0.09
	$\log\beta_2$	9.18±0.12	∼1.9(<2.49)	−0.57±0.05	∼−1.3(<−0.06)
	$\log\beta_3$	12.79±0.08	3.36±0.18	—	−0.14±0.23
Ac^{3+}	$\log\beta_1$	3.56[a]	1.36[a]	−0.04[b]	−0.75[c]
	$\log\beta_2$	6.16	2.68	−1.04	−0.46
	$\log\beta_3$	—	—	−1.26	—
Am^{3+}	$\log\beta_1$	4.63±0.08	1.57±0.09	−0.15±0.07	0.85±0.05
	$\log\beta_2$	8.35±0.09	2.66±0.08	−0.69±0.10	—
	$\log\beta_3$	11.15±0.07	—	—	0.55±0.15
	$\log\beta_4$	—	—	—	0.00±0.15

The range of the error is three times the standard deviation. The values in parentheses after $\log\beta_2$ give the value of $\log(\beta_2\pm3\sigma)$.

Composition of the organic phase and the extraction constant are as follows.

a) 0.03M TTA in CCl_4 with 0.2M TBP $\log K_{ex}=-5.04$

b) 0.2M TTA in CCl_4 with 0.3M TBP $\log K_{ex}=-5.55$

c) 0.015M TTA in CCl_4 with 0.1M TBP $\log K_{ex}=-5.93$

The dissociation constant of oxalic acid employed for the calculation is $pK_{a_2}=3.54$ (Ref. 2). The hydrogen ion concentration was 1×10^{-3}—3×10^{-4} except for the chloride system which contained 0.01M H^+.

(i) The actinium(III) complexes are more stable in the order: thiocyanate<chloride<sulfate<oxalate. (ii) The oxalate complexes of actinium(III) are less stable than those of the other metal ions. (iii) No very remarkable differences are observed among the sulfate or chloride complexes of actinium and those of the other ions. (iv) The thiocyanate complexes of actinium(III) are much weaker than those with the other ions.

It may be generally assumed that the actinium(III) ion forms the least stable complexes among the trivalent metal ions presented in Table 1, because it is the largest and the least basic ion. This assumption seems to hold in the oxalate complexes. However, it is not obviously true in the sulfate or chloride complexes. This may be due to the fact that the stabilities of weak complexes of analogous metal ions are influenced by many other factors, such as the hydration. Surls and Choppin[10] pointed out, on the basis of their ion-exchange data, that the trivalent actinides form more stable thiocyanate complexes than the trivalent lanthanides; this agrees with the prediction of Diamond[11] based on the assumption of f-orbital hybridization that thiocyanate ions should complex more strongly with actinides than with lanthanides. Similar results were obtained for the complexes of americium(III), as may be seen in Table 1. Actinium(III), however, forms less stable thiocyanate complexes than does lanthanum(III). One possible explanation for the lower stabilities of the actinium(III) thiocyanate complexes may be that the fourteen 5f-electrons enter the actinides beginning at thorium (or that the 5f-electrons enter beginning with thorium).[12] If so, 5f-electrons, which are connected with the fact that the stability of the thiocyanate complexes of americium(III) is greater than that of europium(III), should not contribute the formation of the actinium(III) thiocyanate complexes.

Part of this work has been carried out at the Laboratory of Nuclear Chemistry, Institute of Physical and Chemical Research. The authors are grateful to Professor Nobufusa Saito, the head of the Laboratory.

10) J. P. Surls, Jr., and G. R. Choppin, *J. Inorg. Nucl. Chem.*, **4**, 62 (1957).

11) R. M. Diamond, UCRL-1434 (1951).

12) J. J. Katz and G. T. Seaborg, "The Chemistry of the Actinide Elements," Methuen, London (1957).

BULLETIN OF THE CHEMICAL SOCIETY OF JAPAN VOL. 42 2714—2715 (1969)

Electron Spin Resonance Studies of Photo-irradiated Aroylphosphonates

Ken-ichi TERAUCHI and Hiroshi SAKURAI

The Institute of Scientific and Industrial Research, Osaka University, Suita, Osaka

(Received March 5, 1969)

In a preceding paper,[1] we have shown that *para*-substituted benzoylphosphonates have a moderately strong n–π^* transition of the carbonyl group, involving a transition with the phosphorus *d*-orbitals in the 320—390 mμ, and that the n–π^* absorption maxima of these compounds are considerably affected by the powerful electron inductive abilities of *para*-substituents, such as the methoxy and chloro functions. The present investigation was undertaken to see if the ESR spectra of irradiated aroylphosphonates exhibit the effects of *para*-substituents on the aromatic ring in the magnetic parameters.

Another point of interest was the fact that there have been very few ESR studies of the organic phosphorus compounds[2] compared to those of the inorganic phosphorus compounds; especially little has yet been done with the ESR study of the UV-irradiated organophosphorus compounds.[3] In this paper, we wish to report the results obtained by the ESR measurements of UV-irradiated *para*-substituted aroylphosphonates Ia-d, which have never before been investigated by means of the ESR technique.

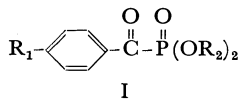

I

Ia, R_1=H; R_2=C_2H_5
b, R_1=Cl; R_2=C_2H_5
c, R_1=*t*-Bu; R_2=C_2H_5
d, R_1=CH_3O; R_2=C_2H_5

On UV-irradiation at 77°K through the filter cutting off below 3200 Å, each of the aroylphosphonates employed in this work showed unsymmetrical ESR signals. These ESR spectra have a large anisotropic doublet with a 53—128 gauss separation which is thought to be due to the interaction between an unpaired electron and the phosphorus nucleus, and a g value almost close to the free spin value. All of these spectra were quite stable at 77°K; upon a subsequent elevation of the temperature the hyperfine structure did not show any significant change except for a great decrease in the intensity during the ESR measurements. However, these signals completely vanished at 156°K. The observed g and A values in Compounds Ia—d are summarized in the Table 1.

TABLE 1. ESR RESULTS FOR THE PHOSPHORUS-CONTAINING RADICALS
(The A values are in gauss.)

Compound	$\bar{g}$	$A_\perp$	$A_{/\!/}$
Ia	2.004	127.8	5.33
b	2.005	143.4	36.9
c	2.005	125.7	52.3
d	2.005	124.6	58.6

As is obvious from the table, the *para*-substituents on the aromatic ring participate considerably in both the isotropic and anisotropic splittings of these radicals. Although such substituent effects have been extensively studied in mono- or disubstituted benzene radical anions by Bowers *et al.*,[4] it is of particular interest that similar effects have been found in the ESR spectra of irradiated aroylphosphonates.

These observations suggest that the extent of the anisotropic hyperfine interaction of substituted aroylphosphonates vary over a considerable range, depending upon the electron-withdrawing or electron-donating properties of the substituent groups on the aromatic ring. Thus, when calculating the orbital spin densities on the phosphorus atom of the observed radicals from the isotropic and anisotropic parts of the hyperfine coupling tensors, we have obtained the values of 0.30, 0.22, 0.29, and 0.32 for Ia, Ib, Ic, and Id respectively.

These results support the idea that the powerful electron-inductive abilities of the methoxy and chloro functions on the aromatic ring undoubtedly cause a change in the spin density on the phosphorus atom. Therefore, it seems interesting to compare these results with other spectroscopic data, such as the results of infrared, UV, or dipole moment measurements. Although it is recognized that ESR study, which involves excited states,

1) K. Terauchi and H. Sakurai, This Bulletin, **42**, 821 (1969).

2) F. Ramirez and S. Dershovity, *J. Am. Chem. Soc.*, **78**, 5614 (1956); E. Müller, H. Eggensperger and K. Scheffer, *Ann.*, **658**, 103 (1962); *Z. Naturforsch.*, **16b**, 764 (1961); E. A. C. Luchen, *J. Chem. Soc.*, **1963** 5123; M. W. Hanna, *J. Chem. Phys.*, **37**, 685 (1962).

3) F. J. Adrian, E. L. Cochran and V. A. Bowers, *Advan. Chem. Ser.*, **36**, 50 (1962); U. Schmidt, K. Kabitzke, K. Markau and A. Müller, *Chem. Ber.*, **99**, 1497 (1966); K. Terauchi and H. Sakurai, This Bulletin, **41**, 1736 (1968).

4) *Cf.* E. T. Kaiser and L. Kevan, "Radical Ions," Interscience Publishers, New York (1968), p. 211.

cannot normally be related to infrared or dipole moment data, which involve ground states only, the above findings are consistent with the view which has been suggested; in the dipole moment data, the values reported as 2.64D for Ib and 3.20D for Id,[5] it has been postulated that the powerful electron-inductive abilities of the methoxy and chloro functions induce a change in the electron density on the carbonyl carbon atom, and that the more the electron density on the carbonyl carbon increases, the more the lifetime of the conformation in which the carbonyl and phosphoryl groups are opposite increases. The UV and infrared data also provide evidence for the electron density on the C–P bond depending considerably upon the properties of those functions on the aromatic ring.[1] Therefore, it can be concluded that the findings of the ESR measurements are in comparatively good agreement with the other spectroscopic data.

On the other hand, these phosphorus hyperfine splittings prompt a question as to the preferred structure of the observed radicals. Since the n–π^* absorption maxima of benzoylphosphonates Ia–d show an average bathochromic shift of 50 mμ in comparison with those of the corresponding benzaldehydes, the π orbital on the carbonyl carbon atom might overlap with a vacant d orbital on phosphorus. Therefore, it may be reasonable to assume that the radicals which are produced photochemically from Compounds Ia—d contain such an extended conjugation that the electronic n–π^* excitation produces an unpaired electron, one which is probably partially delocalized over the P–O group, perhaps through the vacant d orbitals on phosphorus.

In connection with these observations, we will later report in detail on the results of our photochemical study of these compounds.

Experimental

The aroylphosphonates were synthesized by the reaction of triethylphosphite with acid chloride.[6] Repeated distillation under reduced pressure was used to purify all the compounds needed. The tests for purity were the same as those employed in a previous work.[1] A DMF solution of aroylphosphonate was pipetted into a Pyrex ESR tube; then the tube was degassed by conventional vacuum techniques before being sealed and irradiated at 77°K through a Toshiba UV-35 filter for 2 hr with a Toshiba 400-watt high-pressure mercury arc (Model HLS-4002A type). The ESR spectra were measured with a TDS Electronics Co. X-band ESR spectrometer (Model T-1000AX type), using a field modulation of 100 kc/sec and conventional elevating-temperature instruments.

5) L. G. Wesson, "Tables of Electric Dipole Moments," The Technology Press, Cambridge, Mass. (1948).

6) K. D. Berlin and H. A. Taylor, *J. Am. Chem. Soc.*, **86**, 3862 (1964).

BULLETIN OF THE CHEMICAL SOCIETY OF JAPAN VOL. 42 2715—2717 (1969)

Copper(II)-catalyzed Oxidation of Iron(II) by Molecular Oxygen in Tripolyphosphate Solution

Yoshimi KURIMURA and Keigo MURAKAMI

Chemical Laboratory, College of General Education, University of Ibaraki, Mito, Ibaraki

(Received March 6, 1969)

In a previous work on the oxygen oxidation of Fe(II) in tripolyphosphate solutions,[1] the anomalous results first obtained led us to suspect the presence of Cu(II) as an impurity. Actually the oxidation rate was subsequently proved to be markedly increased by the addition of small amounts of Cu(II). The effect of Cu(II) as a catalyst has been reported in the Fe^{2+}–O_2,[2-4] Mo(V)–O_2,[5] V(III)–Fe(III),[6] V(III)–O_2[7] and ascorbic acid-O_2[8-10] reactions. In connection with these studies,

1) Y. Kurimura and H. Kuriyama, This Bulletin, **42**, 2238 (1969).

2) M. Cher and N. Davidson, *J. Am. Chem. Soc.*, **77**, 793 (1955).

3) R. E. Huffman and N. Davidson, *ibid.*, **78**, 4836 (1956).

4) W. G. Barb, J. H. Baxendale, P. Gerorge and K. R. Hargrave, *Trans. Faraday Soc.*, **47**, 462 (1951).

5) Y. Yoshino, T. Takeuchi, H. Kinoshita and S. Uchida, This Bulletin, **41**, 765 (1968).

6) W. C. E. Higginson and A. G. Sykes, *J. Chem. Soc.*, **1962**, 2841.

7) J. B. Ramsey, R. Sugimoto and H. DeVorkin, *J. Am. Chem. Soc.*, **63**, 3480 (1941).

8) A. Weissberger, J. E. Luvalle and D. S. Thomas, Jr., *J. Am. Chem. Soc.* **65**, 1934 (1943).

9) A. Weissberger and J. E. Luvalle, *ibid.*, **66**, 700 (1944).

10) M. M. T. Khan and A. E. Martell, *ibid.*, **89**, 4176 (1967).

the effect of Cu(II) on the oxidation reaction of Fe(II) in an excess of the triphosphate solution was studied spectrophotometrically, and the results thus obtained discussed, with a view to getting some information concerning the role of Cu(II) as a reaction accelerator.

Experimental

The Cu(II) solution was prepared from reagent-grade cupric sulfate. The sodium triphosphate ($Na_5P_3O_{10}\cdot 6H_2O$) was recrystallized five times from 25% aqueous ethanol solutions. Redistilled wster was used for the preparation of all the solutions. The hydrogen ion concentration of the triphosphate solution, in which certain amounts of Cu(II) were dissolved if necessary, was adjusted by adding dilute perchloric acid or dilute sodium hydroxide. Just before each run, the Fe(II) solution was prepared by the use of reagent-grade ferrous ammonium sulfate. By mixing 20 m*l* of the triphosphate and 1 m*l* of the Fe(II) solution, the reaction was initiated. The ionic strength of each reaction mixture was kept at 0.10 M $NaClO_4$. The oxidation reaction was followed spectrophotometrically at 20°C by determining the concentrations of the Fe(III), whose molar extinction coefficient at 260 mμ is 4620 M^{-1} cm^{-1} in the pH range employed in excesses of triphosphate solutions. The method of kinetic measurement used here was virtually identical with that described before.[1] All the oxidation rates used here were obtained from the slopes of the corresponding concentration-time curves, which are essentially linear in the first stage of the reactions.

Results and Discussion

The rate laws for the oxidation reaction of the Fe(II) in excesses of triphosphate solutions at particular pH values were obtained from the results of several series of runs; in each run one of the solute concentration was varied, while all the other concentrations remained constant. The rate laws thus obtained are defined by the following expressions, from (1) to (4). At a given concentration of the Cu(II) and at pH=3.0 under 1 atm of air ($p_{O_2}=0.21$ atm), a plot of the oxidation rate against the concentration of the Fe(II), [Fe(II)], gives a straight line with a zero intercept, which accounts for the rate expression:

$$\frac{d[Fe(III)]}{dt} = k_1[Fe(II)] \quad (1)$$

From the solpe of this particular line the pseudo-first-order rate constant, k_1, is calculated. Linear variations of the rate with the Fe(II) concentration were also obtained at other pH values studied. In the 2.0—3.0 pH range, the linear dependence of the rate on the Cu(II) concentration holds well; this indicates the catalytic behavior of the Cu(II). The rate equation obtained is:

$$\frac{d[Fe(III)]}{dt} = k_2+k_2'[Cu(II)] \quad (2)$$

At pH values lower than 2, however, the rate hardly increases at all with an increase in the Cu(II) concentration, showing the saturation of the catalytic effect of the Cu(II). At pH values higher than 2, the values of the rate constants of k_2 and k_2' are calculated from the intercept and from the slope of the straight line of the rate-[Cu(II)] curve respectively. The dependence of the rate on the partial pressure of oxygen shows that the rate increases slightly with an increase in the pressure, and the relationship between these gives a straight line. The rate law at given concentrations of the Fe(II) and the Cu(II) at pH=3.0 is of the form:

$$\frac{d[Fe(III)]}{dt} = k_3+k_3'p_{O_2} \quad (3)$$

A simillar rate dependence was also obtained at other pH values studied.

The oxidation reaction of Fe(II) in excesses of triphosphate solutions in the absence of Cu(II) has been studied previously.[1] In this case the rate law at a particular pH is expressed by:

$$\frac{d[Fe(III)]}{dt} = k_a[Fe(II)]p_{O_2} \quad (4)$$

This rate expression was also confirmed in the present study in the 1.5—3.0 pH range. The values of all the apparent rate constants in the four equations, (1) to (4), at pH=3.0 are summarized in Table 1. The results obtained are consistent with the following rate equation at a particular pH (pH =2.0—3.0):

$$\frac{d[Fe(III)]}{dt} = k_a[Fe(II)]p_{O_2}+k_b[Fe(II)][Cu(II)] \quad (5)$$

where k_a is the apparent rate constant of the uncatalyzed reaction path and, k_b, that of the catalyzed path. The correlation between the appatent rate constants in Eqs. (1)—(5), which were obtained separately from several series of runs, has been established within the range of experimental error. The rate profiles for the catalyzed and uncatalyzed reaction paths are shown in Fig. 1. A reaction mechanism which accounts for Eq. (5) can be expressed by following reactions in these equations the charges of all the complex species are neglected for the sake of simplification:

$$Fe(II) + O_2 \rightarrow Fe(III) + O_2^- \quad (6)$$

$$Fe(II) + Cu(II) \rightleftarrows Fe(III) + Cu(I) \quad (7)$$

$$Cu(I) + O_2 \text{ (or } O_2 + H^+) \rightleftarrows Cu(II) + O_2^- \text{ (or } HO_2) \quad (8)$$

$$O_2^- + H^+ \rightleftarrows HO_2 \quad (pK_{HO_2} = 3.3—4.7^{11}) \quad (9)$$

The rate-determining step of the uncatalyzed path may be (6), while that of catalyzed path may be (7). Reaction (7) indicates the initiation of

11) G. Czapski and B. H. J. Bielski, *J. Phys. Chem.*, **67**, 2180 (1964).

Table 1. Apparent rate constants for the oxidation reaction of Fe(II) in excess of triphosphate solutions at 20°C
μ=0.10 ($NaClO_4$), pH=3.0

k_1[a]	k_2[b]	k_2'[b]	k_3[c]	k_3'[c]	k_a[d]
0.52 (min^{-1})	2.0×10^{-6} (M min^{-1})	6.0 (min^{-1})	3.2×10^{-5} (M min^{-1})	2.0×10^{-5} (M $min^{-1}atm^{-1}$)	4.0×10^{-2} ($min^{-1}atm^{-1}$)

a) [Cu(II)]=1.9×10^{-5}M, [TPP]=10^{-3}M, p_{O_2}=0.21 atm.
b) [Fe(II)]=2.4×10^{-4}M, [TPP]=10^{-3}M, p_{O_2}=0.21 atm.
c) [Cu(II)]=4.8×10^{-6}M, [Fe(II)]=2.4×10^{-4}M, [TPP]=10^{-3}M.
d) [TPP]=10^{-3}M, in the absence of Cu(II).

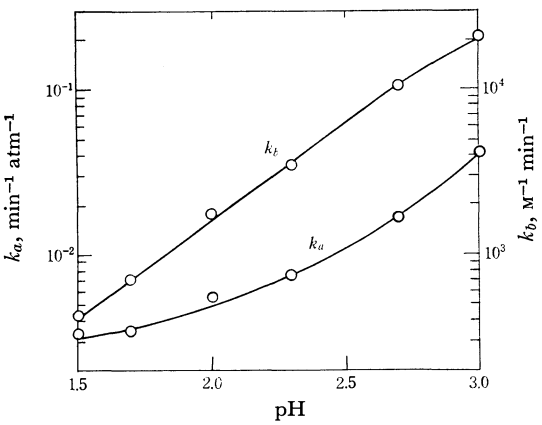

Fig. 1. Rate profile for the Cu(II) catalyzed oxidation of Fe(II) in excess of triphosphate solution at 20°C.
10^{-3}M triphosphate, μ=0.10M ($NaClO_4$)

the catalytic cycle; the resulting Cu(I) reacts rapidly with oxygen in (8).[2] The rapid back reaction in (7) was confirmed in the Cu(II)-catalyzed Fe^{2+}–O_2[2,3] and V(III)–Fe(III)[6] reactions, but this may be ignored in the initial stage of the reaction discussed here. The HO_2 and O_2^- radicals can either oxidize successively the Fe(II), as in the Weiss mechanism,[12] or react with the Cu(II) in (8).[2] The back reaction in (8) may account for the saturation of the oxidation rate as the Cu(II) concentration increases at pH values lower than 2.[2] The increase in the k_a value with an increase in the pH seems to be due to an increase in the concentration of such Fe(II)-triphosphate complexes as $Fe^{II}HL$,[1] where HL is the monoprotonated triphosphate anion ($HP_3O_{10}^{4-}$), which is oxidized more rapidly than the aquo ferrous ion by molecular oxygen. Under the present experimental conditions, the $Fe^{II}(HL)_2$ may be neglected.[1] Therefore, the main species susceptible to oxidation in (6) and (7) under the present experimental conditions may be Fe^{2+} and $Fe^{II}HL$.

12) J. Weiss, *J. Chim. Phys.*, **48**, C-6 (1951).

Though the stability constants of $Fe^{II}HL$ and $Fe^{II}(HL)_2$ have not yet been reported, this estimate also be supported by the consideration that the stability constant of $Fe^{II}HL$ may well be smaller than 10^5 since: i) the stability constant of $Cu^{II}HL$ reported[13] is $10^{5.2}$ (μ=0.1) and ii) the stability of a Fe(II) complex is generally lower than that of the corresponding Cu(II) complex (Irving-Williams order[14]).*1 The real features of the (6) reaction in the 1.5—3.0 pH range seem to be indicated by (6′) and (6″), and that of (7), by (7′), since the normal Cu(II) complex, Cu(II)L, is negligible in the pH region ($K_{Cu(II)L}=10^{7.3}$, μ=0.1[13]).*1

$$Fe^{2+} + O_2 \rightarrow Fe^{3+} + O_2^- \quad (6')$$

$$Fe^{II}HL + O_2 \rightarrow Fe^{III}HL + O_2^- \quad (6'')$$

$$\left\{\begin{matrix} Fe^{2+} \\ \uparrow\downarrow \\ Fe^{II}HL \end{matrix}\right\} + \left\{\begin{matrix} Cu^{2+} \\ \uparrow\downarrow \\ Cu^{II}HL \end{matrix}\right\} \rightleftarrows Fe(III) + Cu(I) \quad (7')$$

As the rate of (6′) may be influenced by the anions present,[2,3] and as the stability constant of $Fe^{II}HL$ is unknown, a precise analysis of the rate profiles of k_a and k_b was not undertaken at present. However, it may be suggested that the rate constant of (6″) is appreciably greater than that of (6′) since the k_a value increases markedly with an increase in the pH value. An increase in the k_b value with an increase in the pH may be attributed to the fact that the redox reaction between the Fe(II) and the Cu(II) is accelerated by the formation of the Fe(II) and Cu(II) complexes with triphosphate anions.

*1 The logarithmic K^{H}_{HjL} values of the TPP (μ=0.1) used are $H_5P_3O_{10}$, 0; $H_4P_3O_{10}^-$, 2.6; $H_3P_3O_{10}^{2-}$, 2.7; $H_2P_3O_{10}^{3-}$, 5.6; and $HP_3O_{10}^{4-}$, 7.9.[15]

13) A. Johanson and E. Wänninen, *Tranta*, **10**, 769 (1963).

14) H. Irving and R. J. P. Williams, *J. Chem. Soc.*, **1953**, 3192.

15) A. E. Martell and G. Schwarzenbach, *Helv. Chim. Acta*, **39**, 635 (1956).

BULLETIN OF THE CHEMICAL SOCIETY OF JAPAN VOL. 42 2718—2719 (1969)

The Spectrophotometric Determination of Thorium(IV) with 4-(2-Thiazolylazo)-resorcinol*1

Takayoshi SAKAI*2 and Kôichi TONOSAKI

Chemical Department, Faculty of Science, Hirosaki University, Bunkyô-chô, Hirosaki

(Received March 7, 1969)

The reagent 4-(2-thiazolylazo)-resorcinol (TAR) is an azo-dyestuff with a thiazol ring; it has a structure and properties similar to those of 1-(2-pyridylazo)-2-naphthol (PAN) and 4-(2-pyridylazo)-resorcinol (PAR), both of which have been extensively employed as metallochromic indicators and as reagents for the spectrophotometric determination of various metals. TAR has also been used for the spectrophotometric determination of nickel,[1] niobium,[2] copper and bismuth,[3] uranium(VI),[4] and palladium.[5] Nickelss and his co-workers[6] have recently reported the formation constant of TAR complexes with many metals, but not of any metals including thorium(IV).

It is found that thorium(IV) reacts with TRA in a hexamethylenetetramine buffer solution to form a stable complex. The present paper will describe the fundamental conditions for the spectrophotometric determination of thorium(IV).

Experimental

Reagents and Apparatus. *TAR Solution.* A 1×10^{-3}M TAR solution was prepared by dissolving 0.0553 g of the Dotite TAR reagent in 250 m*l* of 50% v/v methanol.

Buffer Solution. About a 10% w/v hexamethylenetetramine-potassium nitrate-nitric acid system solution was used for the pH adjustment; potassium nitrate was added in order to maintain a constant ionic strength. All the investigations were carried out at a constant ionic strength of 0.6.

The solutions of thorium(IV) and diverse ions, and the apparatus, were the same as those used in a previous work.[7]

All the measurements were made at 25 ± 0.5°C.

Procedure. To a sample solution containing up to 95 μg of thorium in a 25-m*l* volumetric flask, 2.5 m*l* of a 1×10^{-3}M TAR solution and 15 m*l* of a 10% w/v hexamethylenetetramine buffer solution with a pH of 7.4 were added; then the solution was diluted to the mark with water. The absorbance of the solution was then measured in a 1-cm cell at 615 mμ, using the reagent blank as a reference.

Results and Discussion

Absorption Curves. The carmine red Th(IV)-TAR complex formed in the pH range from 4.5 to 5.0 has the peak of its absorption curve at 525 mμ. However, a precipitate is sometimes formed. The red-violet complex with the peak at 585 mμ was formed in the pH range from 6.8 to 8.5 without any precipitate. Some of the results are shown in Fig. 1. The latter complex was recommended for the determination at 615 mμ, where the absorption of TAR was negligible.

The Effect of pH. A constant absorbance is obtained over the pH range from 6.8 to 8.5, as

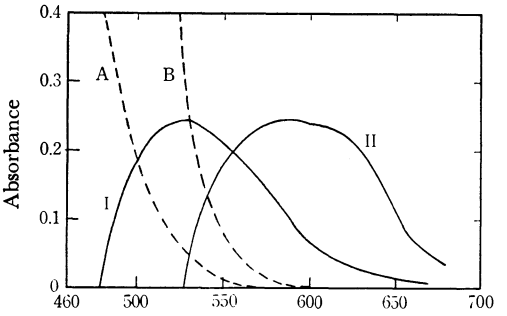

Fig. 1. Absorption curves of TAR and its thorium-(IV) complexes.
Th(IV): 46.4 μg, TAR: 4.0×10^{-5}M
TAR *vs.* water; A: pH 4.6, B: pH 7.4
Th(IV)-TAR complex *vs.* TAR; I: pH 5.0, II: pH 8.5

*1 This work was presented at the Tohoku Branch Meeting of the Chemical Society of Japan, Sendai, October, 1968.

*2 Present address: Hachinohe Technical College, Tamonoki, Hachinohe, Aomori.

1) A. Kawase, *Japan Analyst*, **12**, 810 (1963).
2) V. Patrovsky, *Talanta*, **12**, 971 (1965).
3) M. Hnilickova and L. Sommer, *ibid.*, **13**, 667 (1966).
4) L. Sommer and V. M. Ivanov, *ibid.*, **14**, 171 (1967).
5) Hui-Kai Lin, Kuang-Yi Chen, and Yen-Fan Chen, *Hua Hsueh Tung Pao*, **1966**, 365; *Chem. Abstr.*, **66**, 25818 (1967).
6) G. Nickless, (the late) F. H. Pollard and T. J. Samuelson, *Anal. Chim. Acta*, **39**, 37 (1967).
7) K. Tonosaki and T. Sakai, This Bulletin, **42**, 456 (1969).

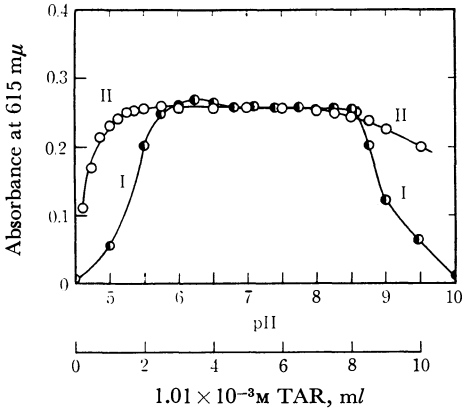

Fig. 2. Effects of pH and the amount of reagent.
Th(IV): 46.4 μg, Reference: reagent blank
I: pH, TAR: 1.01×10^{-4}M
II: Addition of TAR at pH 7.4

is shown in Fig. 2(I). The color development was, therefore, made at pH 7.4.

The Effect of the Amount of Reagent. It may be seen in Fig. 2(II) that a maximum and constant absorbance is obtained with 2 to 6 ml of a 1×10^{-3}M TAR solution. A 2.5-ml portion of the reagent was used in further experiments.

Color Stability. The absorbance of the solution containing the complex remained almost constant for at least 2 hr.

Calibration Curve. The color system follows Beer's law in the range from 2.4 to 95.2 μg of thorium in 25 ml. The molar absorptivity is 3.15×10^4. According to Sandell's notation,[8] the sensitivity of the reaction is 0.008 μg of thorium per cm^2 at 615 mμ. The reproducibility of the method was also examined. The standard deviation was calculated to be 0.003 (1.2%) in absorbance (mean of 10 determinations of 46.4 μg thorium).

The Effect of Diverse Ions. These results are listed in Table 1. Many elements interfere seriously.

A Comparison with Other Methods. Several methods have been summarized in a previous work;[7] the method proposed here is comparable with the quercetin method[9] in sensitivity and also in selectivity.

Composition of the Complex. The continuous-variation method and the mole-ratio method were used to determine the composition of the thorium-TAR complex. The results of the mole-ratio method are shown in Fig. 3. It seems that a 1 : 3*3 complex is mainly formed under the conditions investigated, although some lower complexes may also be formed when the ligand-to-metal ratio is less than three. According to the method of Harvey and Manning,[10] the apparent formation constant of the 1 : 3 complex was 7.4×10^{16} at pH 7.4.

Table 1. Effect of diverse ions on determination at pH 7.4
Thorium taken: 46.4 μg (0.20 μmol)

Ion	Tolerance limit* μmol
Sulfate	290
Chloride	250
Acetate	50
Be	20
Ag	2.5
Tl(I)	1.0
Ce(III)	0.7
Al, Cd	0.20
Zn, Sr, Ni, Mn	0.15
V(VI)	0.10
Nd, Pb	0.05
Hg, Pd, V(IV), tartrate, citrate	0.02
Bi, Co, La, Ti(IV), Y	0.01
Cr, Cu, Ga, In, Yb, Zr(IV), fluoride, phosphate, oxalate, NTA	0.005
Fe(III), EDTA	<0.005

* Value which gives less than 3% relative error

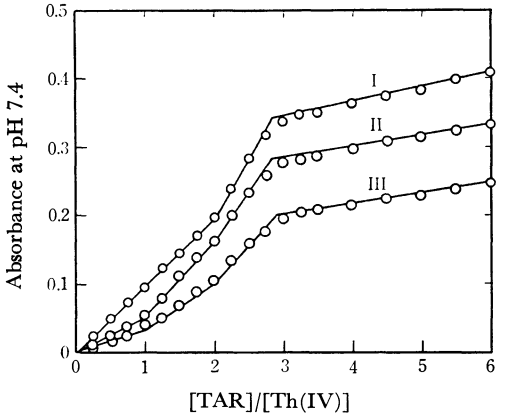

Fig. 3. Mole ratio method.
[Th(IV)]: 6.0×10^{-6}M, I: 585 mμ, II: 615 mμ, III: 635 mμ

The authors wish to express their thanks to Dr. Makoto Otomo for his discussions and Miss Fumiko Ishikura for her assistance.

8) E. B. Sandell, "Colorimetric Determination of Traces of Metals," Interscience Publishers, New York (1950), p. 49.
9) O. Menis, D. L. Manning and G. Goldstein, *Anal. Chem.*, **29**, 1426 (1957).
10) A. E. Harvey, Jr., and D. L. Manning, *J. Am. Chem. Soc.*, **72**, 4488 (1950).

*3 Studies of the mechanism of the reaction are in progress.

BULLETIN OF THE CHEMICAL SOCIETY OF JAPAN VOL. 42 2720—2722 (1969)

Studies on Hydroxy Amino Acids. II.*1 The Optical Resolution of α-Amino-β-hydroxy-γ-benzyloxybutyric Acid*2

Kenji OKAWA, Kiyotaka HORI, Katsutoshi HIROSE and Yasuo NAKAGAWA

Department of Chemistry, Faculty of Science, Kwansei Gakuin University, Nishinomiya

(Received March 8, 1969)

The optical resolution of α-amino-β-hydroxy-γ-benzyloxybutyric acid (I_{ab}) into the four stereoisomers was investigated with success as a study related to the synthesis of homoserine analogues. The synthesis and the stereochemistry of α-amino-β,γ-dihydroxybutyric acid were first investigated by Niemann[1] and by Hamel[2,3] in order to clarify the structure of Sphingosine; they succeeded in synthesizing three isomers of this amino acid, the D-erythro, L-threo, and D-threo forms, from D-mannitol. However, another isomer, the L-erythro form, could not be obtained.

The present authors prepared α-amino-β-hydroxy-γ-benzyloxybutyric acid (I_{ab}) by the condensation reaction of copper glycinate[4] with benzyloxyacetaldehyde,[5] while diastereoisomeric DL-erythro and DL-threo forms were isolated by the partial crystallization from *s*-butyl alcohol. We studied the optical resolution of both of the racemic modifications; we thus confirmed that the DL-erythro form (I_a) could be resolved by the use of Takadiastase, but the threo form (I_b) could not, though the latter could be resolved by Vogler's method[6] using the diastereoisomeric salt formation of the *N*-acyl-DL-threo amino acid (III) with L-tyrosine hydrazide (Fig. 1).

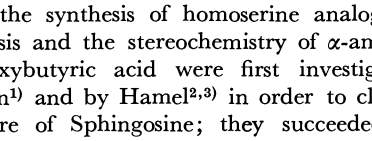

I R=$CH_2C_6H_5$, R′=H
II R=H, R′=H
III R=$CH_2C_6H_5$, R′=$COOCH_2C_6H_5$ (CHA salt)

The four stereoisomers obtained were reduced by catalytic hydrogenation to give free α-amino-β,γ-dihydroxybutyric acids (II); γ-lactone derivatives (IV) of these isomers were also obtained by treatment with dry hydrogen chloride in methanol. The melting points and specific rotations of these isomers are summarized in Tables 1 and 2.

Experimental

α-Amino-β-hydroxy-γ-benzyloxybutyric acid (I_{ab}) was prepared by the glycine - copper method in a 14% yield; mp 205—207°C.

Found: C, 58.43; H, 6.63; N, 6.07%. Calcd for $C_{11}H_{15}O_4N$: C, 58.65; H, 6.71; N, 6.22%.

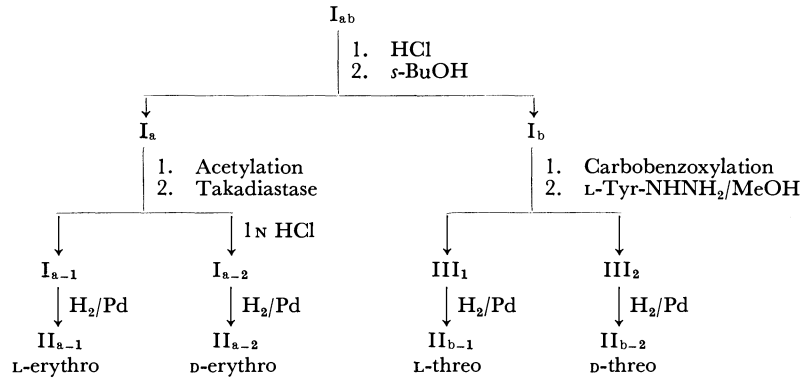

Fig. 1.

*1 Part I: K. Okawa, S. Sakai and T. Kinutani, This Bulletin, **41**, 1353 (1968).

*2 *Cf.* Original Paper: K. Okawa, K. Hori, K. Hirose and Y. Nakagawa, *Nippon Kagaku Zasshi* (*J. Chem. Soc. Japan, Pure Chem. Sect.*), **89**, 998 (1968).

1) C. Niemann and P. Nichols, *J. Biol. Chem.*, **143**, 191 (1942).

2) E. E. Hamel and E. P. Painter, *J. Am. Chem. Soc.*, **75**, 1362 (1953).

3) H. O. L. Fischer and L. Feldmann, *Helv. Chim. Acta*, **19**, 532 (1936).

4) K. Okawa and S. Akabori, This Bulletin, **30**, 937 (1957).

5) K. Okawa and H. Tani, *Nippon Kagaku Zasshi* (*J. Chem. Soc. Japan, Pure Chem. Sect.*), **75**, 1199 (1954).

6) K. Vogler and P. Lanz, *Helv. Chim. Acta*, **49**, 1348 (1966).

Table 1. Melting points and specific rotations of the four isomers of α-amino-β,γ-dihydroxybutyric acid (II)

		II_{a-1}	II_{a-2}	II_{b-1}	II_{b-2}
Author	Mp (°C)	194—195	194	214	214—215
	$[\alpha]_D^{23}$ (°)	−11.3	+11.3	−13.5	+13.6
		L-erythro	D-erythro	L-threo	D-threo
Hamel	Mp (°C)	——	193—194	214—215	214—215
	$[\alpha]_D^{23}$ (°)		+15.3	−13.6	+13.1
Niemann	Mp (°C)	——	192—194	215	——
	$[\alpha]_D^{24}$ (°)		+16.0	−13.7	

Table 2. Melting points and specific rotations of the four isomers of α-amino-β-hydroxy-γ-butyroractone hydrochloride (IV)

		IV_{a-1}	IV_{a-2}	IV_{b-1}	IV_{b-2}
Author	Mp (°C)	176	176.5—177	173—174	175—175.5
	$[\alpha]_D^{23}$ (°)	+55.6	−56.6	−26.2	+26.0
		L-erythro	D-erythro	L-threo	D-threo
Hamel	Mp (°C)	174—175	174—175	Oil	——
	$[\alpha]_D^{23}$ (°)	+50.4	−51.2		

Separation of Diastereomers. A suspended solution of I_{ab} hydrochloride (29 g) in *s*-butyl alcohol (300 m*l*) was stirred for 2 hr at 50°C. The undissolved crystals, I_a hydrochloride (19 g), were then filtered off. From the mother liquor, I_b hydrochloride (10 g) was obtained. Both of the amino acid hydrochlorides were decomposed with a pyridine-methanol solution; subsequent recrystallization from hot water gave I_a (11 g; mp 202—203°C), and I_b (6 g; mp 195—196°C).

Resolution of Racemic I_a. *N*-Acetyl-I_a was prepared in an 88% yield by the usual Schotten-Baumann method, mp 151—153°C, as CHA*3 salt. The salt obtained (7.33 g, 0.02 mol) was dissolved in 2N sodium hydroxide, and the liberated CHA was extracted with ether. After the pH of the aqueous layer had been adjusted to 6.8, the solution was incubated with Taka-diastase at 37°C for 4 days. The precipitate was then filtered off, and the filtrate was concentrated under reduced pressure until crystals appeared. The crystals of I_{a-1} were obtained in a 67% yield and were recrystallized from hot water; mp 194—195°C; $[\alpha]_D^{23}$ +21.9° (*c* 5.7, 1N HCl).

Found: C, 58.62; H, 6.75; N, 6.20%. Calcd for $C_{11}H_{15}O_4N$: C, 58.65; H, 6.71; N, 6.22%.

The mother liquor of I_{a-1} was acidified to pH 2.0 and was extracted with ethyl acetate. *N*-Acetyl-I_{a-2} was obtained from the concentrated extract as CHA salt in an 84% yield. Recrystallization from methanol-ethyl acetate gave pure crystals; mp 145—146°C; $[\alpha]_D^{23}$ −12.5° (*c* 2.5, EtOH). The partial hydrolysis of the CHA salt of *N*-acetyl-I_{a-2} with 1N hydrochloric acid gave free amino acid I_{a-2} in a 82% yield; mp 194°C; $[\alpha]_D^{23}$ −21.9° (*c* 5.5, 1N HCl).

Found: C, 58.78; H, 6.67; N, 6.25%. Calcd for $C_{11}H_{15}O_4N$: C, 58.65; H, 6.71; N, 6.22%.

***N*-Carbobenzoxy-I_b (III).** *N*-Carbobenzoxy-I_b was prepared from I_b and carbobenzoxychloride by the usual method; it was obtained as CHA salt in a 79% yield; mp 158—159°C.

L-Tyrosine Hydrazide Salt of III. The free acid (III) was obtained from CHA salt (13.7 g, 0.03 mol) by the use of 3N hydrochloric acid and by ethyl acetate extraction. L-Tyrosine hydrazide (5.86 g, 0.03 mol) was added to a solution of III in methanol (50 m*l*), and the solution was warmed at 65°C. After the removal of insolubles, the solution was concentrated; the subsequent addition of ethanol gave L-tyrosine hydrazide salt of III in a quantitative yield (16.6 g), $[\alpha]_D^{23}$ +36° (*c* 1.0, water).

Four recrystallizations of this salt (5.96 g) from methanol gave a small amount (310 mg) of optically-pure L-tyrosine hydrazide salt (V_1), mp 158.5—159°C; $[\alpha]_D^{23}$ +30.6° (*c* 1.0, water). V_1 was used as the seed of the following partial crystallization.

Resolution of Racemic III. A solution of L-tyrosine hydrazide salt of III in methanol (50 m*l*) was similarly prepared from the CHA salt of III (6.88 g, 0.015 mol). After the insolubles had been filtered off, a small amount of V_1 was seeded to the filtrate; then the mixture was stirred for 1.5 hr and kept at 25°C for 22.5 hr. The precipitated first crop (V_1) was then collected (2.12g); mp 158.5°C; $[\alpha]_D^{23}$ +30.5° (*c* 1.0, water). The mother liquor was concentrated, and the resulting crystals were dissolved in methanol (50 m*l*). After the solution had been stirred at 25°C for 4 hr and then kept at 25—17°C for 20 hr, the second crop (V_2) was obtained (2.66 g, 64%); mp 163—165°C; $[\alpha]_D^{23}$ +39.3° (*c* 1.0, water). From the filtrate of V_2, an additional crop of V_1 was obtained; the total yield of V_1 was 73%.

III_1 was obtained from V_1 by treatment with 3N hydrochloric acid; it was purified as CHA salt; mp 138.0°C; $[\alpha]_D^{23}$ +10.9° (*c* 2.0, EtOH).

Found: C, 65.61; H, 7.60; N, 6.18%. Calcd for $C_{25}H_{34}O_6N_2$: C, 65.48; H, 7.47; N, 6.11%.

The CHA salt of III_2 was obtained from V_2 in the same way; mp 137—138°C; $[\alpha]_D^{23}$ −10.3° (*c* 2.0, EtOH)

Found: C, 65.62; H, 7.57; N, 6.14%.

α-Amino-β,γ-dihydroxybutyric Acids (II). A

*3 CHA=cyclohexylamine

mixture of I_{a-1} (675 mg, 3 mmol), water (10 m*l*), palladium charcoal (160 mg), and N hydrochloric acid (3 m*l*) was stirred for 5 hr at room temperature under the bubbling of hydrogen gas. After the removal of the catalyst, the solution was neutralized and subsequently concentrated under reduced pressure. The resulting crystals were recrystallized twice from water-methanol to give II_{a-1} (305 mg, 75%); mp 194—195°C; $[\alpha]_D^{23}$ −11.3° (*c* 7.2, water).

Found: C, 35.56; H, 6.77; N, 10.30%. Calcd for $C_4H_9O_4N$: C, 35.55; H, 6.71; N, 10.37%.

II_{a-2}, II_{b-1}, and II_{b-2} were obtained from I_{a-2}, III_1, and III_2 by the catalytic hydrogenation described above.

II_{a-2}: mp 194°C; $[\alpha]_D^{23}$ +11.3° (*c* 7.0, water).
Found: C, 35.99; H, 6.91; N, 10.63%.
II_{b-1}: mp 214°C; $[\alpha]_D^{23}$ −13.5° (*c* 2.0, water).
Found: C, 35.32; H, 6.72; N, 10.21%.
II_{b-2}: mp 214—215°C; $[\alpha]_D^{23}$ +13.6° (*c* 4.8, water).
Found: C, 35.61; H, 6.74; N, 10.98%.

α-Amino-β-hydroxy-γ-butyrolactone Hydrochlorides (IV). IV_{a-1}, IV_{a-2}, IV_{b-1}, and IV_{b-2} were prepared from II_{a-1}, II_{a-2}, II_{b-1}, and II_{b-2} respectively in the way described by Hamel and Painter.[2]

IV_{a-1}: mp 176°C; $[\alpha]_D^{23}$ +55.6° (*c* 1.5, water).
Found: C, 31.31; H, 5.24; N, 9.58; Cl, 22.73%. Calcd for $C_4H_8O_3NCl$: C, 31.28; H, 5.25; N, 9.12; Cl, 23.09%.
IV_{a-2}: mp 176.5—177°C; $[\alpha]_D^{23}$ −56.6° (*c* 1.5, water).
Found: C, 31.23; H, 5.51; N, 9.18; Cl, 23.05%.
IV_{b-1}: mp 173—174°C; $[\alpha]_D^{23}$ −26.2° (*c* 1.0, water).
Found: C, 31.24; H, 5.26; N, 9.13; Cl, 23.23%.
IV_{b-2}: mp 175—175.5°C; $[\alpha]_D^{23}$ +26.0° (*c* 1.0, water).
Found: C, 31.39; H, 5.27; N, 9.13; Cl, 23.15%.

BULLETIN OF THE CHEMICAL SOCIETY OF JAPAN VOL. 42 2722—2723 (1969)

Isomerization and Hydrogenation of Dimethyl Maleate and 1,5-Cyclooctadiene by Nickel Cyanide Complex

Hiroshi SAMEJIMA, Taiichi MIZUTA, Haruhiko YAMAMOTO and Takao KWAN

Faculty of Pharmaceutical Sciences, The University of Tokyo, Hongo, Tokyo

(Received March 12, 1969)

The selective isomerization and hydrogenation of monoenes, dienes and their derivatives by nickel cyanide complex and excess sodium borohydride were the subject of our investigations,[1,2] in which it was suggested that the stability of the intermediary hydridonickel or alkylnickel complex plays a significant role in determining the distribution of products. The present work was undertaken to confirm such selectivity revealed by nickel cyanide complex for the isomerization and hydrogenation of dimethyl maleate (DMM) and of 1,5-cyclooctadiene (1,5-COD), respectively.

Nickel complexes investigated here were dicyano(1,10-phenanthroline)nickel (II), $Ni(CN)_2(phen)$, tetracyanonickelate(II), $Ni(CN)_4^{2-}$, and dicyanobis(triphenylphosphine)nickel(II), $Ni(CN)_2(P\phi_3)_2$. Previous investigation[1] revealed that hydrogenation activity increases according to the sequence: $Ni(CN)_2(P\phi_3)_2 < Ni(CN)_4^{2-} < Ni(CN)_2(phen)$ while isomerization activity is reversed.

DMM or 1,5-COD was introduced in a water-isopropanol (10 : 25) solution containing a given nickel cyanide complex and excess sodium borohydride at 0°C or 10°C. After a certain reaction interval, products were extracted with chloroform for DMM and petroleum ether for 1,5-COD respectively and analyzed by gas chromatography. The method of preparation of the nickel cyanide complexes, apparatus and experimental procedure were almost the same as those described earlier.[1]

The isomerization and hydrogenation of DMM took place rapidly with the three nickel cyanide complexes, *i. e.* more than 90% DMM was found to convert to dimethyl fumarate (DMF) and dimethyl succinate (DMS) within 30 min. However, product distribution differed with the kind of nickel cyanide employed. Typical data, obtained after 30 min, are illustrated in Table 1.

TABLE 1. PRODUCT COMPOSITION FOR THE ISOMERIZATION AND HYDROGENATION OF DIMETHYL MALEATE BY THE NICKEL CYANIDE COMPLEXES AT 10°C

	Product composition %		Substrate converted %
	DMF	DMS	DMM
$Ni(CN)_2(phen)$	28	72	90
$Ni(CN)_4^{2-}$	88	12	89
$Ni(CN)_2(P\phi_3)_2$	95	5	95

It is apparent from Table 1 that $Ni(CN)_2(phen)$ gives rise to the hydrogenation of DMM in preference to $Ni(CN)_2(P\phi_3)_2$, while the latter is quite active for the isomerization of DMM to give DMF.

1) H. Samejima, T. Mizuta and T. Kwan, *Nippon Kagaku Zasshi* (*J. Chem. Soc., Pure Chem. Sect.*), **89**, 1028 (1968).

2) T. Mizuta, H. Samejima and T. Kwan, This Bulletin, **41**, 727 (1968).

This result is in line with that of the previous report[1] which concerned the isomerization and hydrogenation of 1-butene.

The isomerization and hydrogenation of DMM would probably follow the hydride elimination-addition mechanism:

$$\mathrm{NiH(CN)(P\phi_3)_2} + \begin{matrix}\mathrm{CH_3OOCCH}\\ \|\\ \mathrm{CH_3OOCCH}\end{matrix} \text{ or } \begin{matrix}\mathrm{CHCOOCH_3}\\ \|\\ \mathrm{CH_3OOCCH}\end{matrix} \rightleftarrows$$

$$\begin{matrix}\mathrm{CH_3OOCCH_2}\\ |\\ \mathrm{CH_3OOCCH\text{-}Ni(CN)(P\phi_3)_2}\end{matrix}$$

$$\downarrow +\mathrm{H}$$

$$\begin{matrix}\mathrm{CH_3OOCCH_2}\\ |\\ \mathrm{CH_3OOCCH_2}\end{matrix} + \mathrm{NiH(CN)(P\phi_3)_2}$$

Let us investigate 1,5-COD as the substrate; 1,5-COD is expected to convert to 1,4-COD and 1,3-COD or even to cyclooctene in the presence of the nickel cyanide complex and excess sodium borohydride. Indeed, experiments indicated that 1,4-COD is formed first and then followed by 1,3-COD. No cyclooctene was detected with $Ni(CN)_2(P\phi_3)_2$. On the other hand, cyclooctene was produced more or less with the other two complexes, of which $Ni(CN)_2$(phen) gave rise to more cyclooctene. The result is again consistent with the isomerization and hydrogenation data of DMM mentioned above.

In Fig. 1 is plotted the composition of 1,4-COD and 1,3-COD produced against the degree of conversion of 1,5-COD for $Ni(CN)_2(P\phi_3)_2$ at 0°C. Assuming now that the isomerization of 1,5-COD obeys a consecutive, reversible first-order kenetics as

$$\text{1,5-COD} \underset{k_{-1}}{\overset{k_1}{\rightleftarrows}} \text{1,4-COD} \underset{k_{-2}}{\overset{k_2}{\rightleftarrows}} \text{1,3-COD},$$

rate constants were calculated according to the Runge-Kutta-Gill method.[3] That is, k_{-1}, k_2 and k_{-2} were computed so as to best fit the experimental plots of Fig. 1 with the aid of the observed value for k_1, the k_1 being evaluated from the initial rates for 1,5-COD decay. These values are shown below.

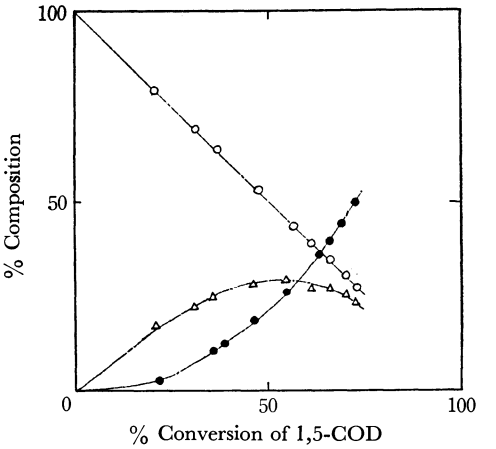

Fig. 1. Catalytic isomerization of 1,5-COD to give 1,4-COD and 1,3-COD in the presence of $Ni(CN)_2(P\phi)_2$ and excess $NaBH_4$ at 0°C.
1,5-COD: 8.3 mmol, $NaBH_4$: 2.0 mmol,
$Ni(CN)_2(P\phi_3)_2$: 0.1 mmol.
○: 1,5-COD, △: 1,4-COD, ●: 1,3-COD.

$$k_1 = 2.53\times10^{-3} \qquad k_{-1} = 4.25\times10^{-5}$$
$$k_2 = 4.25\times10^{-3} \qquad k_{-2} = 4.25\times10^{-6}\ \mathrm{sec^{-1}}$$

The solid lines of Fig. 1 refer to concentrations of substrate and products as calculated by the rate constants. Here, k_{-1} and k_{-2} should be regarded as only upper limit since lower values appeared also well suited. The validity of these values are still under investigation.

3) A. Ralton and H. S. Wilf, "Mathematical Methods for Digital Computers," John Wiley & Sons Inc., New York (1960), p. 110. A HITAC-5020 computer of The University of Tokyo was used in performing numerical calculations.

BULLETIN OF THE CHEMICAL SOCIETY OF JAPAN VOL. 42 2724—2725 (1969)

The Effect of Deuterium Exchange of Silica Gel on Dielectric Relaxation*1

Masa-aki MUROYA* and Seiichi KONDO**

* *Osaka Electro-Communication University, Neyagawa, Osaka*

** *Osaka University of Education, Tennoji, Osaka*

(Received March 14, 1969)

In a previous paper,[1] a study was made on the influence of adsorbed water and heat treatment of silica gel on its dielectirc properties with respect to surface structure. Two dielectric relaxations (Dispersion I and II) and one anomaly (Anomaly III) were found and interpreted as having close relation with the adsorbed water, the hydrogen-bond chain of surface silanol groups and free silanol groups, respectively.

This interpretation seems to have further experimental support by the dielectric investigation of deuterated silica gel shown in this paper.

Experimental

The material and the experimental procedure were the same as described.[1] The deuterium exchange of silica gel was carried out by repeating adsorption and desorption of heavy water of 99.8% purity 6 times.[2] The concentration of deuterium with respect to the original hydrogen content was estimated to be roughly 60 to 70% by assuming this concentration approximately equal to the ratio of the intensity decrease of the OH stretching vibration band at 3750 cm^{-1} to the original intensity.

Results and Discussion

The curves *a*, *b*, *c* and *d* in Fig. 1 show the relation of the values of tan δ at 1 kHz to the temperature of deuterated silica gel having 0.50 and 2.7 mmol D_2O per 1 g silica gel and heat-treated at 200°C and 500°C, respectively. The behavior of these curves seems very similar to the dotted curves *a'*, *b'*, *c'* and *d'* of ordinary silica gel having 0.56 and 2.9 mmol H_2O per 1 g silica gel (equal to 1.0 and 5.3 wt% H_2O respectively) and heat-treated at 200°C and 500°C, respectively. The tan δ anomalies of curves *a* and *b* can be considered as the dielectric relaxations (Dispersion I' and II') by the Cole-Cole arc plot calculated from these curves partly shown in Fig. 2. The shape and size of these arcs are almost similar to those of Dispersion I and II of light-water silica gel as also shown in Fig. 2. Disappearance of the higher temperature relaxation (Dispersion I') by

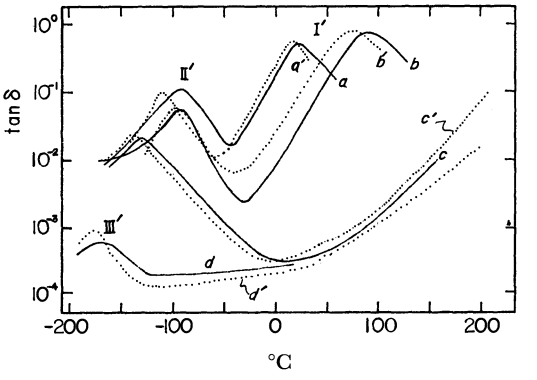

Fig. 1. The curves of tan δ *versus* temperature of deuterated and ordinary silica gel.
a and *a'*: 2.7 and 2.9 mmol D_2O and H_2O/1 g silica gel at 170°C, respectively. *b* and *b'*: 0.50 and 0.56 mmol D_2O and H_2O/1 g silica gel, respectively. *c* and *c'*: heat treatment at 200°C. *d* and *d'*: heat treatment at 500°C.

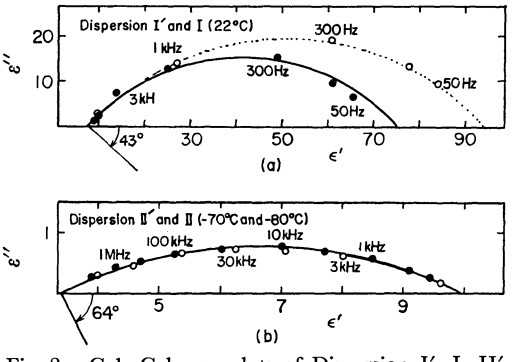

Fig. 2. Cole-Cole are plots of Dispersion I', I, II' and II of deuterated and ordinary silica gel.
(a) ●: Dispersion I' at 22°C. ○: Dispersion I at 22°C.
(b) ●: Dispersion II' at −70°C. ○: Dispersion II at −80°C.

*1 Presented at the 21st Annual Meeting of the Chemical Society of Japan, Osaka, April, 1968.

1) S. Kondo and M. Muroya, This Bulletin, **42**, 1165 (1969).

2) A. Soffer and M. Folman, *Trans. Faraday Soc.*, **62**, 3559 (1966); J. B. Peri and R. B. Hannan, *J. Phys. Chem.*, **64**, 1526 (1960).

heating at 200°C (see curve *c* in Fig. 1) shows that this relaxation originates in heavy water adsorbed, as seen analogously in the thermal behavior of Dispersion I. A similar discussion on Dispersion II′ leads to the view point that Dispersion II′ is caused by the shift of Dispersion II by deuterium exchange. The curves of ε' and ε'' versus frequency of Dispersion I′ and II′ show that these dispersions seem to be the same type as Dispersion I and II respectively. The tan δ anomaly (Anomaly III′) in curve *d* of Fig. 1 can be interpreted also as the shift of Anomaly III.

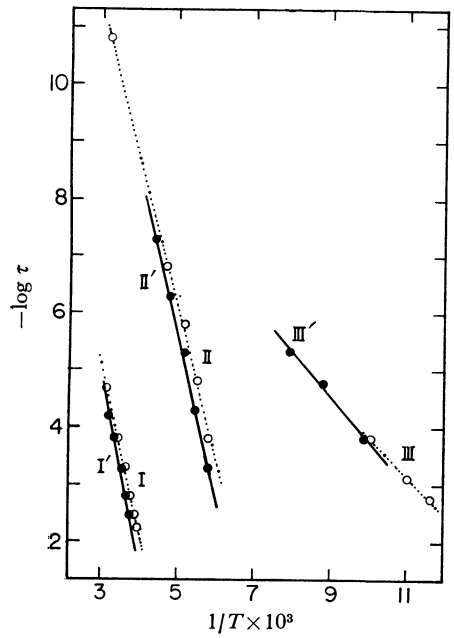

Fig. 3. The relationship of reciprocal temperature to log τ of Dispersion I′, I, II′ and II and log $\frac{1}{2}\pi f$ of Anomaly III′ and III.
●: D_2O exchange ○: H_2O-silica gel

The full lines of Fig. 3 show the relation of the relaxation times, log τ, of Dispersion I′ and II′ and the log $\frac{1}{2}\pi f$ of Anomaly III′, in which f is the frequency of ε'' maxima obtained from the ε''-temperature relation, to the reciprocal temperature $(1/T)$. The corresponding lines of light-water silica gel as shown by dotted lines in this figure are very close to the full lines. The activation energies ΔE and constants τ_0 of Dispersion I′, II′ and Anomaly III′ obtained from Fig. 3, together with those of Dispersion I, II and Anomaly III, are listed in Table 1. In reference to the effect of the amount of adsorbed water on the values of ΔE and τ_0 examined in a previous work,[1] the small difference of mol% of adsorbed water between heavy and light-water would not give an appreciable change in the values of ΔE and τ_0 of dielectric relaxation. In this table, the value of ΔE increases and τ_0 decreases by deuterium exchange. Further investigation is necessary for the more detailed discussion on the values of ΔE and τ_0 of these relaxation phenomena of deuterated silica gel.

Table 1. Activation energy ΔE and constant τ_0 of dispersion I′, I, II′, II, anomaly III′ and III of deuterated and ordinary silica gel

Dispersion	Water content or heat-treatment temperature	ΔE (kcal/mol)	τ_0 (sec)
I′	2.7 mmol D_2O/1 g SiO_2	14.8±0.2	3.3×10^{-16}
I	2.9 mmol H_2O/1 g SiO_2	13.5±0.2	2.8×10^{-19}
II′	0.50 mmol D_2O/1 g SiO_2	12.3±0.2	5.0×10^{-19}
II	0.56 mmol H_2O/1 g SiO_2	11.4±0.2	2.0×10^{-18}
III′	Heat-treated at 500°C	3.1±0.5	5×10^{-11}
III		3.0±0.5	2×10^{-10}

BULLETIN OF THE CHEMICAL SOCIETY OF JAPAN VOL. 42 2725—2728 (1969)

Chemical Studies of Minerals Containing Rarer Elements from the Far East. LXIII. Bastnaesite from Karasugawa, Fukushima Prefecture, Japan

Kin-ichi SAKURAI,* Hisanobu WAKITA,** Akira KATO* and Kozo NAGASHIMA**

* *Department of Geology, National Science Museum, Ueno Park, Tokyo*

** *Department of Chemistry, Faculty of Science, Tokyo Kyoiku University, Otsuka, Tokyo*

(Received March 18, 1969)

The chemical analysis of bastnaesite formed as an alteration product of allanite from a granite pegmatite at Karasugawa, Nashidaira, Fukushima Prefecture, gave: Rare earths 74.4, CO_2 12.8, F 6.4, $H_2O(+)$ 2.1, $H_2O(-)$ 1.5, Rem. 3.3, $-O=F$ 2.7, total 97.8%. The distribution pattern of lanthanide elements agreed well with that of the ordinary bastnaesite. The infrared absorption spectra indicate the vicarious substitution of OH^- for F^-.

Occurrence

The Karasugawa pegmatite is situated at Nashidaira, Fukushima City, and has been worked for feldspar and quartz for several years. It is in a biotite granodiorite body and is composed mainly of microcline-perthite and quartz with large tourmaline crystals. In this pegmatite β-fergusonite,[1,2] xenotime,[3] zircon, and monazite are known to occur. The present study has added bastnaesite to this list; this is the first reported occurrence of this mineral in Japan.

The bastnaesite found in the quarry dump occurs as an alteration product of allanite in microcline-perthite crystals containing quartz and muscovite, surrounding the allanite as a white, powdery crustification or replacing it. The other associated mineral is dark brown granular xenotime, with $a_0=6.91_8$Å and $c_0=6.06_0$Å, according to the X-ray powder study. Generally the allanite crystals are long and prismatic, less than one centimeter in length and two millimeters in diameter.

Table 1. X-ray powder data for bastnaesites from Birthday Claim, California and Karasugawa, Fukushima City, Japan

1.		2.				
d(Å)	I	d(Å)	I	Q_{obs}	Q_{cal}	$hkil$
4.881	42	4.89	60	0.042	0.042	0002
3.564	71	3.550	75	0.079	0.079	$11\bar{2}0$
2.879	100	2.870	100	0.1214	0.1214	$11\bar{2}2$
2.610	1	2.602	10	0.1477	0.1479	$20\bar{2}2$
2.445	9	2.438	20	0.1683	0.1683	0004
2.273	3					$10\bar{1}4$
2.238	3					$20\bar{2}3$
2.057	42	2.050	25	0.2380	0.2380	$30\bar{3}0$
2.016	42	2.009	40	0.2477	0.2476	$11\bar{2}4$
1.898	42	1.889	25	0.2804	0.2801	$30\bar{3}2$
1.783	9	1.772	5[b]	0.3186	0.3173	$22\bar{4}0$
1.674	21	1.670	15	0.3587	0.3594	$22\bar{4}2$
1.629	1					0006
1.573	15	1.571	10	0.4054	0.4063	$30\bar{3}4$
1.481	9	1.478	5	0.4581	0.4580	$11\bar{2}6$
1.439	11	1.434	10	0.4861	0.4856	$22\bar{4}4$
		1.344	5[b]	0.5534	0.5553	$41\bar{5}0$
1.298	15	1.294	10	0.5969	0.5974	$41\bar{5}2$
1.277	7					$30\bar{3}6$
$a_0=7.129$ Å		$a_0=7.10_1$ Å				
$c_0=9.774$ Å		$c_0=9.75_0$ Å				

1. Bastnaesite. Birthday Claim, Mountain Pass, California. Cu/Ni radiation. After Glass *et al.* (1958).
2. Bastnaesite. Karasugawa, Nashidaira, Fukushima City, Japan. Cu/Ni radiation. The present study.
b=broad.

X-Ray Powder Diffraction and Optical Studies

The X-ray powder study was made on hand-picked material and gave the powder data shown in Table 1, in which the data for bastnaesite from Birthday Claim, Mountain Pass, California (Glass *et al.*, 1958)[4] are also tabulated for the sake of comparison. The present data are indexed with a hexagonal symmetry, with $a_0=7.10_1$Å and $c_0=9.75_0$Å; this satisfies the extinction rule required by the $P\bar{6}2c$ space group except for $(20\bar{2}2)$.

Under the microscope, it is seen to be an aggregate of very fine grains. For this reason, the refractive indices measured are not always accurate. They are $n_1=1.72\pm0.01$ and $n_2=1.82\pm0.01$ respectively, both very close to the ω and ε of values bastnaesites hitherto studied.

Chemical Composition

The results of chemical analysis carried out on about 20 mg of hand-picked material are given in Table 2, together with those on F- and OH-bastnaesite obtained in Aleksandrov's study[5] and with those of the ideal bastnaesite with the formula of $CeFCO_3$. The H_2O content of Karasugawa bastnaesite is higher than that of natural F-bastnaesite, but lower than that of natural OH-bastnaesite,

Table 2. Chemical analysis

	$CeFCO_3$ %	F-Bastnaesite %	OH-Bastnaesite %	Karasugawa Bastnaesite %
RE_2O_3	74.90	64.10	75.20	74.4
CO_2	20.08	16.67	20.70	12.8
F	8.67	7.42	0.22	6.4
H_2O (+)		0.80	4.00	2.1
H_2O (−)		0.40	0.30	1.5
Rem.		14.56	0.30	3.3
	103.65	103.95	100.72	100.5
O=F	3.65	3.12	0.09	2.7
Total	100.00	100.83	100.63	97.8

1) K. Nagashima, A. Kato and M. Chiba, Preprints for 20th Annual Meeting of the Chemical Society of Japan (April, 1967).
2) O. Nagashima, "Chigaku-kenkyu," **17**, Nos. 10, 11, 12, p. 42 (1966) (in Japanese).
3) H. Wakita and K. Nagashima, *Kōbutsugaku Zasshi*, **9**, 92 (1968) (in Japanese).
4) J. J. Glass, H. T. Evans, Jr., M. K. Carron and F. A. Hildebrand, *Amer. Mineral.*, **43**, 460 (1958).
5) I. V. Aleksandrov, V. I. Ivanov and L. A. Sin'kova, Zap. VMO, 3rd Ser., Part XCIV, Fasc. 3(1965) (in Russian).

suggesting partial replacement of F^- ions by OH^- ions.

The Distribution Pattern of Rare Earth Elements

The distribution of lanthanum-group elements was determined by the X-ray fluorescent method; we found lanthanum, cerium, praseodymium, samarium, and gadolinium, with the maxima at lanthanum and cerium. The quantitative estimation obtained as atomic percentages including a relative error of less than 10% is plotted the *versus* atomic numbers in Fig. 1; the figure shows a fundamental coincidence between the distribution pattern of the present bastnaesite and that called the "allanite type" by Goldschmidt and Thomassen.[6]

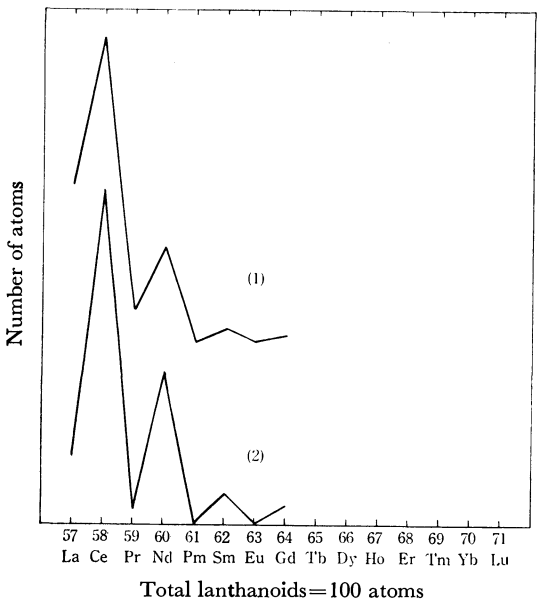

Fig. 1. Distribution of rare earth elements.
(1) Bastnaesite from Mountain Pass, Calif., U.S.A. E.I. Semenov and R.L. Barinskii, "Geochemistry," No. 4, 398 (1958)
(2) Bastnaesite from Karasugawa (this work)

Infrared Spectroscopy

The presence of OH^- ions instead of F^- in bastnaesite is very probable, as is indicated by the X-ray diffraction study showing the isostructural relation between OH-bastnaesite and F-bastnaesite, both of which belong to the same space group, D_{3h}^4. The infrared spectrum of the natural OH-bastnaesite, composed of superposed two kinds of spectra[7], involves carbonate groups with a local symmetry of C_{3h} and with less symmetrical surroundings. The former gives rise to no band splitting, whereas the latter does as a result of the presence of OH^-.

In the infrared spectra of the present heated bastnaesite, there are absorption bands of strong or medium intensities at the following frequencies: 3630, 3470, 1450, 1020, 870, 730, and 680 cm^{-1}. Basically the spectrum is determined by the vibrations of the $(CO_3)^{2-}$ group, which has D_{3h} point symmetry and C_{3h} local symmetry in the unit cell of bastnaesite. The absorption bands at 3630, and 3470 cm^{-1} are attributable to absorption by the OH group, while that at 1020 cm^{-1} may be attributed to absorption by impurities in natural bastnaesite (SiO_2, Al_2O_3). The absorption at 1660 cm^{-1} due to molecular water is not strong. The spectrum of our sample was less split than that of M.V. Akhmanova. Chemical analysis shows that Karasugawa bastnaesite has a lower H_2O content than the OH-bastnaesite in Akhmanova's

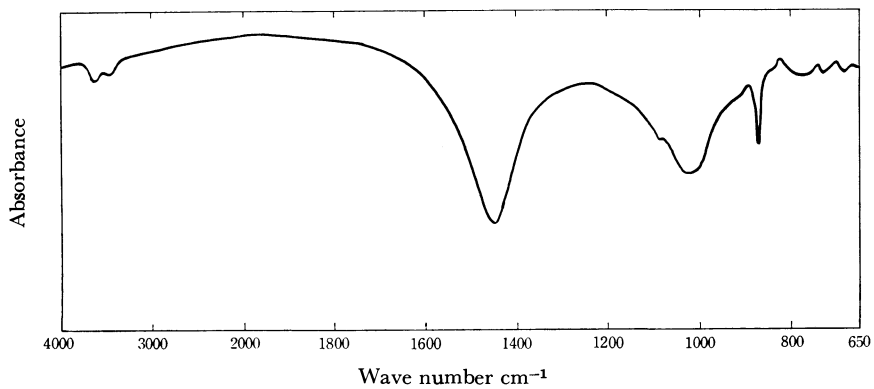

Fig.2. Infrared spectra of Karasugawa bastnaesite.
KBr disk, 110°C, 48 hr, heated

6) V. M. Goldschmidt and L. Thomassen, Vidensk. Skrifter 1. Mat.-naturv. Klasse, **1924**, No. 5.

7) M. V. Akhmanova and L. P. Orelova, *Geochemistry International*, **3**, 444 (1966).

study, so the infrared spectrum of Karasugawa bastnaesite may be less split than that of Akhmanova.

The authors wish to express their thanks to Mr. Otokichi Nagashima for his interest in this work, and for his help in collecting the materials. We also wish to thank Mr. Kyuzaburo Furuhashi for determining water and carbon dioxide contents for us.

BULLETIN OF THE CHEMICAL SOCIETY OF JAPAN VOL. 42 2728—2729 (1969)

Alternate Copolymerization of Acrylonitrile and Isobutylene

Masanobu TANIGUCHI,* Akihiro KAWASAKI* and Junji FURUKAWA**

* *Maruzen Petrochemical Co., Ltd., Ichihara, Chiba*

** *Department of Synthetic Chemistry, Faculty of Engineering, Yoshida, Kyoto*

(Received March 20, 1969)

The polymerization of isobutylene and acrylonitrile was described in a patent,[1] in which copolymerization was carried out in the presence of $ZnCl_2$ as a complexing agent together with organic peroxide as an initiator, but the structure of the copolymer has not yet been established. Gaylord *et al.*[2] assumed the copolymer to be of an alternate structure from the fact that the copolymer is always of 1:1 composition irrespective of the variation of the composition of feed monomers, but no chemical evidence for the alternate structure was afforded.

Hirooka *et al.*[3] reported the preparation of 1 : 1 copolymer from acrylonitrile and α-olefin such as styrene and propylene and concluded the alternate structure by means of IR analysis. They found $AlEtCl_2$ to be a good complexing agent, which initiates polymerization without any initiator, but neither $AlEt_3$ nor $AlCl_3$ was effective.

We have made the 1 : 1 copolymer of isobutylene and acrylonitrile in good yield in a similar way to the patent except for using $AlCl_3$ and peroxide and have established the structure of the copolymer to be alternate.

The polymerization was carried out as follows. A 25 cc glass tube was charged with 2 cc of toluene, 0.5 mmol of benzoyl peroxide, 50 mmol of acrylonitrile containing 1 mmol of $AlCl_3$ and 50 mmol of isobutylene under nitrogen atmosphere at −78°C. Subsequently the tube was sealed and was subjected to polymerization at 25°C. After 20 hr, 0.256 g of white polymer was obtained. It was completely soluble in acetone and this fact indicates that the product is a copolymer since each homopolymer is insoluble in acetone. The polymer possesses an intrinsic viscosity of 0.15 dl/g at 30°C in chloroform and contains 52 mol% of acrylonitrile unit according to an elementary analysis.

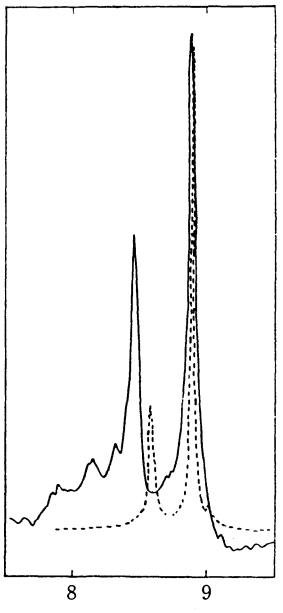

Fig. 1. NMR spectrum of alternate copolymer of acrylonitrile with isobutylene (——) and that of polyisobutylene (------).

The NMR spectrum shown in Fig. 1 was obtained in deuterated chloroform at 25°C by using TMS as a standard. The peak at 8.60 τ of methylene protons of polyisobutylene disappears completely, showing no existence of an isobutylene-isobutylene repeating unit, and a new peak appears at 8.40 τ in the spectrum of the copolymer. The strong peak at 8.85 τ corresponds to the strong peak at 8.89 τ of homopolymer of isobutylene which is ascribed

1) G. E. Serniuk and R. T. Thomas, U. S. Pat. 3183217 (1965).

2) N. G. Gaylord and A. Takahashi, paper presented at ACS Meeting, San Francisco, April 1968.

3) M. Hirooka, H. Yabuuchi, S. Morita, S. Kawasumi and K. Nakaguchi, *J. Polymer Sci., B*, **5**, 47 (1967).

to methyl protons, because the ratio of peak area at 8.40 τ of methylene protons to that at 8.85 τ of methyl protons in the copolymer is 4 : 6, whereas the area ratio of the peak at 8.60 τ to that at 8.89 τ in homopolyisobutylene is 2 : 6. Accordingly the copolymer may be a 1:1 copolymer of acrylonitrile and isobutylene and the 8.40 τ peak may be ascribed protons of the alternate copolymer. The following is the structure of the alternate copolymer.

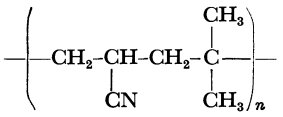

We wish to express our thanks to Nippon Electric Varian, Ltd. for their cooperation in obtaining NMR spectra.

BULLETIN OF THE CHEMICAL SOCIETY OF JAPAN VOL. 42 2729—2730 (1969)

A Convenient Method for the Preparation of Poly(Vinyl Alcohol) from Poly(*t*-Butyl Vinyl Ether)

Gentaro OHBAYASHI, Shun-ichi NOZAKURA and Shunsuke MURAHASHI

Faculty of Science, Osaka University, Toyonaka, Osaka

(Received March 29, 1969)

t-Butyl vinyl ether, like benzyl vinyl ether and trimethylsilyl vinyl ether, is known as a starting monomer for the synthesis of isotactic poly(vinyl alcohol). Poly(*t*-butyl vinyl ether) has been converted into poly(vinyl alcohol) by two methods. Fujii *et al.* converted poly(*t*-butyl vinyl ether) into ploly(vinyl acetate) by direct acetylation reaction with acetic anhydride and Lewis acid; they then saponified the resultant poly(vinyl acetate) to poly(vinyl alcohol).[1] Okamura *et al.* converted poly(*t*-butyl vinyl ether) into poly(vinyl alcohol) by the cleavage reaction of the ether bond with dry hydrogen bromide[2] in a manner similar to that used in the case of poly(benzyl vinyl ether).[3] However, since the reaction conditions are rather drastic, more or less colored poly(vinyl alcohol) specimens are usually obtained.

The present authors wish to report a more convenient method for the preparation of poly(vinyl alcohol) from poly(*t*-butyl vinyl ether) using a 46% aqueous solution of hydrogen fluoride. By this method, the procedure can be extremely simplified and colorless poly(vinyl alcohol) can be obtained.

t-Butyl vinyl ether was polymerized with $BF_3 \cdot O(C_2H_5)_2$ as an initiator in toluene at $-78°C$ under a nitrogen atmosphere. ($[M]_0=20$ vol%, $[Cat]=2\times10^{-3}$ mol/*l*). These reaction conditions are known to yield an isotactic poly(*t*-butyl vinyl ether). The resultant polymer was purified by reprecipitation into methanol from a toluene solution. The polymer thus obtained had an intrinsic viscosity $[\eta]$ of 0.356 (d*l*/g) in benzene at 30.4°C.

Found: C, 71.97; H, 12.03%. Calcd for $C_6H_{12}O$: C, 71.94; H, 12.08%.

The cleavage reaction of the polymer into poly(vinyl alcohol) was carried out in a polyethylene beaker. To 0.355 g of poly(*t*-butyl vinyl ether), 5 m*l* of a 46% aqueous solution of hydrogen fluoride was added. The reaction mixture was kept standing at room temperature and shaken occasionally. After 1 hr, the reaction mixture became homogeneous; it was kept standing for 2 more hours. The solution was then subjected to dialysis using a cellophane membrane. The dialyzate was freeze-dried to give 0.123 g of colorless poly(vinyl alcohol).

The poly(vinyl alcohol) obtained had a specific viscosity, η_{sp}, of 0.515 for a 0.905 g/d*l* aqueous solution at 30.0°C.

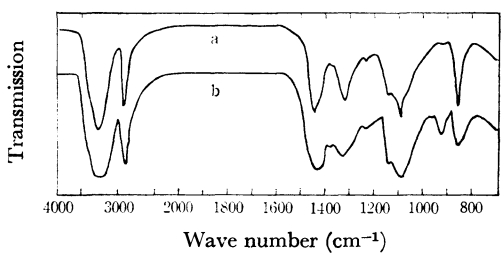

Fig. 1. Infrared spectra of isotactic (a) and atactic (b) poly (vinyl alcohol) prepared from poly(*t*-butyl vinyl ether).

1) K. Fujii and R. Mochizuki, *Kobunshi Kagaku (Chem. High Polymers, Japan)*, **19**, 124 (1962).

2) S. Okamura, T. Kodama and T. Higashimura, *Makromol. Chem.*, **53**, 180 (1962).

3) S. Murahashi, H. Yuki, T. Sano, U. Yonemura, H. Tadokoro and Y. Chatani, *J. Polymer Sci.*, **62**, 77 (1962).

Found: C, 54.26; H, 9.14%. Calcd for C_2H_4O: C, 54.53; H, 9.15%. The results of elementary analysis make it clear that pure poly(vinyl alcohol) was obtained by this method. The infrared spectrum of a film prepared from an aqueous solution of the resultant poly(vinyl alcohol) showed that the conversion was complete; it coincided with that of the isotactic poly(vinyl alcohol) obtained previously.[4]

Atactic poly(vinyl alcohol) was similarly obtained from atactic poly(*t*-butyl vinyl ether), which had itself been obtained with $BF_3 \cdot O(C_2H_5)_2$ in methylene chloride at $-78°C$ ($[M]_0=20$ vol%, $[Cat]=2\times10^{-3}$ mol/*l*).

The infrared spectra of the isotactic and atactic poly(vinyl alcohol) thus obtained are shown in Fig. 1.

4) S. Murahashi, S. Nozakura and M. Sumi, *J. Polymer Sci.*, *B*, **3**, 245 (1965).

SHORT COMMUNICATIONS

Photolytic Formation of a Ferrocenyl Radical from Iodoferrocene[1]

Takeo SATO, Shigeru SHIMADA and Kazuo HATA

Department of Chemistry, Faculty of Science, Tokyo Metropolitan University, Setagaya-ku, Tokyo

(Received July 11, 1969)

Although a number of studies have been carried out on ferrocene chemistry, not many of them deal with the generation and characterization of a ferrocenyl radical. Existence of the latter as a reactive intermediate in the reactions of metal derivatives, such as lithioferrocenes[2] and ferrocenylmercury derivatives[3] has been postulated by only a few authors.

We wish to report an attempt to generate the ferrocenyl radical by a photolytic method from iodoferrocene. Dilute solutions of iodoferrocene in appropriate solvents (*ca.* 8.5×10^{-3}M) were irradiated externally using a 100-W low-pressure (100-L) or 1-kW high-pressure lamp (1000-H). Since the ferrocene nucleus is sensitive to oxygen, especially upon illumination, all reactions have been carried out under nitrogen or using degassed solutions. Analysis of the reaction mixture was performed by gas chromatography using silicone grease on a Daichrom column.

Irradiation in cyclohexane resulted in the reductive deiodination to give ferrocene, which was obtained in 20% yield with 45 hr reaction (1000-H lamp, Pyrex filter):

$$FcI \xrightarrow{h\nu,\ C_6H_{12}} FcH$$

The rest of the material was recoverable as iodoferrocene. Irradiation in benzene produced phenylferrocene and a small amount of ferrocene:

$$FcI \xrightarrow{h\nu,\ C_6H_6} FcH + FcC_6H_5$$

The representative data are summarized in Table 1. Thus by using 253.7 mμ line (100-L), phenylferrocene was obtained in as high as 89% yield, which is far better than other methods so far described.[4] It is noteworthy that the reaction does not show any marked dependence on the wavelengths employed. A similar reaction carried out in toluene for 47 hr (1000-H lamp, quartz filter) produced ferrocene (24%) and tolylferrocenes (50%), together with bibenzyl (9%). These results are best interpreted by assuming the intermediacy of the ferrocenyl radical.

TABLE 1. PHOTOLYSES OF IODOFERROCENE IN BENZENE

Lamp	Filter	Irrad. time, hr	Products, %		
			FcH	FcC_6H_5	Recovery
100-L[a)]	Vycor	15	6	89	3
1000-H	Quartz	48	3	55	7
1000-H	Pyrex	48	13	54	15
1000-H	Glass	48	10	48	29

a) Irradiation with a 100-L lamp was performed on a degassed solution.

1) Photo-Aryl Coupling and Related Reactions. V.

2) I. J. Spilner and J. P. Pellegrini, Jr., *J. Org. Chem.*, **30**, 3800 (1965); H. Watanabe, I. Motoyama and K. Hata, This Bulletin, **39**, 790 (1966).

3) M. D. Rausch, *J. Am. Chem. Soc.*, **82**, 2080 (1960); A. N. Nesmeyanov, E. G. Rerevalova, S. P. Gubin and A. G. Kozlevskii, *J. Organometal. Chem.*, **11**, 577 (1968).

4) M. Rosenblum, "Chemistry of the Iron Group Metallocenes," Part I, John Wiley & Sons, Inc., New York, N. Y. (1965), p. 198.

New Addition Reactions of Acrylic Compounds with Fumaric Acid Esters Catalyzed by Tervalent Phosphorus Compounds

Ken-ichi MORITA and Tsuneo KOBAYASHI

The Basic Research Laboratory, Toyo Rayon Company, Kamakura

(Received April 11, 1969)

Dimerization of acrylonitrile or acrylic acid esters catalyzed by tervalent phosphorus compounds has been studied in great detail,[1,2] since the reaction furnishes industrially important products.[3] However, the study of the catalyzed reaction has been restricted only to dimerization.[4] In a previous paper,[5] we reported the reaction of acrylonitrile or acrylates with aldehydes to produce 2-(1-hydroxyalkyl)acrylonitriles or -acrylates in the presence of tertiary phosphines. This paper deals with the synthesis of 3-butene-1,2,3-tricarboxylic acid, a new tricarboxylic acid, and related compounds by the reaction of acrylic compounds with fumaric, or maleic acid esters.[6]

$$CH_2{=}CHX + ROOCCH{=}CHCOOR \xrightarrow{R_3P} \begin{matrix} CH_2{=}C(X) \\ | \\ CH(COOR) \\ | \\ CH_2(COOR) \end{matrix}$$

1 X=CO_2CH_3, R=C_2H_5
2 X=COOH, R=H
4 X=CN, R=C_4H_9

The reaction of 34.3 g (0.40 mol) of methyl acrylate, 67.0 g (0.39 mol) of diethyl fumarate and 1.5 g (5.4 mmol) of tricyclohexylphosphine in 100 m*l* of dioxane in an atmosphere of nitrogen at 70°C for 16 hr gave 95.7 g (95.5%, yield)[7] of 3-butene-1,2,3-tricarboxylic acid 1,2-diethyl-3-methyl ester (**1**) as a colorless liquid,[8] bp 101—102°C (3×10^{-3} mmHg); n_D^{20} 14502, $\lambda_{max}^{n\text{-hexane}}$ 213 mμ (ε, 5790); ν_{max}^{film} 1737 cm^{-1} (shoulder at 1721 cm^{-1}) (esters).

An acid hydrolysis of **1** gave 3-butene-1,2,3-tricarboxylic acid (**2**), mp 184—185°C: ν_{max}^{KBr} 1697, 1721 cm^{-1} (C=O); pK_1, 3.18, pK_2, 4.52, pK_3, 5.99. Catalytic hydrogenation of **1** over palladium charcoal followed by an acid hydrolysis furnished a mixture of diastereoisomers of 1,2,3-butanetricarboxylic acid (**3**), *i. e.*, a major component mp 181—182°C (lit., mp 182°C[9]; 184—185°C[10]) and a minor one, mp 147—148°C (lit.,[11] mp 146—147°C). Thermal decomposition of **2** at its melting point gave dimethylmaleic anhydride mp 94°C (lit.,[12] mp 95—96°C).

An analogous reaction of acrylonitrile with dibutyl fumarate in the presence of tricyclohexylphosphine at 100°C for 16 hr gave a mixture of dibutyl (1-cyanovinyl)succinate (**4**) and dibutyl (1-cyanoethylidene)succinate bp 128—129°C (0.1 mmHg); ν_{max}^{film} 1743 cm^{-1} (shoulder at 1723 cm^{-1}) (C=O), 2211 cm^{-1} (C≡N).

1) N. Takashima and C. C. Price [*J. Am. Chem. Soc.*, **84**, 489 (1962)] found that acrylonitrile is converted into 1,1,4,4-tetracyanoethyl-1,4-dicyano-*trans*-2-butene, in the presence of triphenylphosphine, and suggested a dimer of acrylonitrile to be probably a precursor of the hexamer.

2) Dimerization of acrylontirle to 2-methyleneglutaronitrile: a) P. Carardes, C. Grard, P. Lafont and M. Thiers (to Rhone-Poulenc), French Pat. 1336081 (1964); b) J. D. McClure (to Shell Oil Co.), U. S. Pat. 3277745 (1966); c) M. M. Baizer and H. D. Anderson, *J. Org. Chem.*, **30**, 1357 (1965); d) W. H. Dietsche, *Tetrahedron Letters*, **1966**, 6347; e) D. Wittenberg and H. Mueller (to Badische Anilin & Soda-Fabrik A. G.), French Pat. 1385883 (1963); f) J. Feldman (to National Distillers & Chem. Co.), Belg. Pat. 677175 (1966); g) J. W. Nemec and R. B. Wuchter (to Rohm & Haas Co.), Belg. Pat. 689598 (1967). The dimerization to 1,4-dicyanobutene: h) J. S. McClure (to Shell Oil Co.) U. S. Pat. 3225083 (1965); i) Badische Anilin & Soda-Fabrik A. G., Belg. Pat. 698441 (1967); j) E. I. Du Pont de Nemours Co., Belg. Pat. 697162 (1967). Dimerization of acrylates to 2-methyleneglutarates; k) M. Rauhut and H. Currier (to American Cyanamid), U. S. Pat. 3047999 (1963); l) J. D. McClure (to Shell Oil Co.), U. S. Pat. 3277745 (1966); m) J. W. Nemec and R. B. Wuchter (to Rohm & Haas Co.), French Pat. 1460427 (1966), 1438745 (1966); n) Imp. Chem. Ind., Brit. Pat. 1100350 (1968).

3) L. F. Moormeier and J. Feldman, *Hydrocarbon Process Petrol. Refiner*, **44**, 151 (1965).

4) *Cf.* a) J. D. McClure (to Shell Oil Co.), U. S. Pat. 3225082 (1965); b) A. Lantz and F. Weiss (Soc. d'Electro-Chimie, d'Electron-Metallurgie, et des Acieries Electriques D'Ugine), French Pat. 1463853 (1966).

5) K. Morita, Z. Suzuki nd H. Hirose, This Bulletin, **41**, 2815 (1968).

6) The new reaction can be called Succination.

7) A trace of dimethyl methyleneglutarate was found in the product.

8) All new compounds described here gave satisfactory elemental analyses.

9) K. Alder and H. Söll, *Ann.*, **565**, 57 (1949).

10) S. Beckmann, H. Geiger and M. Schaber-Kiechle, *Chem. Ber.*, **92**, 2419 (1959).

11) K. Alder, Herbert Söll and Hanna Söll, *Ann.*, **565**, 77 (1949).

12) W. J. Bailey, R. L. Hudson and E. T. Yates, *J. Org. Chem.*, **28**, 828 (1963).

Aromatic Benzoyloxylation with Benzoyl Peroxide - Iodine

Shizunobu HASHIMOTO, Wataro KOIKE and Masafumi YAMAMOTO

Department of Applied Chemistry, Doshisha University, Karasuma-imadegawa, Kamikyo-ku, Kyoto

(Received May 28, 1969)

Recently it was reported that the reaction products of benzoyl peroxide (BPO) with aromatic substrates could be modified by the presence of cupric chloride[1,2] or oxygen.[3] In such cases, BPO acted as an oxygenating agent on an unactivated aromatic nucleus. In 1945, Perret and Perrot[4] reported their findings on the reaction products of BPO with unsaturated compounds in the presence of iodine. With aromatic compounds, benzoic acid, the aryl benzoates, and the iodinated products were identified, but the yields of the monobenzoyloxylated products were poor. Little has been reported, however, about either the qualitative or mechanistic aspects of this reaction.

We wish here to report that aromatic compounds are benzoyloxylated in high yields by BPO in the presence of small amounts of iodine. Pure monooxygenated materials are obtained by this method of aromatic substitution; this suggests possible synthetic usefulness and also provides the possibility of a new route for aromatic oxygenation.

A toluene solution of BPO was mixed with iodine and heated at 80°C. Figure 1 shows the variation in the yields of phenyltoluenes, tolyl benzoates, and benzoic acid as a function of the initial concentration of iodine. In a control experiment with the peroxide and toluene, less than 3 mol% of the nuclear oxygenation product was found. As the initial concentration of iodine was increased, however, the formation of tolyl benzoates and benzoic acid became the major pathway. When the molar ratios of iodine to BPO are below 0.25, the amount of the oxygenation product decreased substantially. On the other hand, above this ratio the yield of tolyl benzoates and benzoic acid increased to 72—79 mol% and 80—92 mol% respectively. Small amounts of phenyltoluenes, iodobenzene, and iodotoluenes were also obtained.

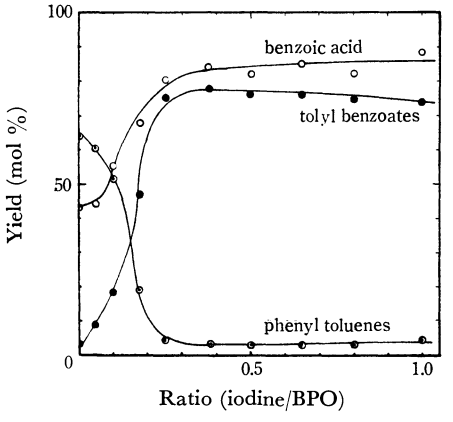

Fig. 1. Variation in iodine:BPO ratio.
BPO; 0.025 mol, Toluene; 100 ml, 80°C, 50 hr

The relative rates for this benzoyloxylation of a number of monosubstituted benzenoid compounds relative to benzene (obtained by the competitive method, using gas-liquid chromatography for the analysis of the products of the competition) were: PhOMe : PhEt : PhMe : PhPr-*i* : PhH : PhCl=6.27: 3.10 : 2.85 : 2.18 : 1 : 0.20. The isomer distribution and the partial rate factors (f) for toluene were *o*-, 53% *m*-, 16% and *p*-, 31%, and $f_o=4.53$ $f_m=1.37$ and $f_p=5.30$.

The effects of substituents on the peroxide were also examined by carrying out the reaction of *p,p'*-disubstituted benzoyl peroxide with benzene in the presence of iodine at 80°C. The mol% yields of phenyl *p*-substituted benzoate was OCH_3 : CH_3 : H : Cl : Br=86.5 : 84.0 : 75.3 : 94.6 : 95.0.

On the basis of our experimental findings, it seems that the oxidizing agent is not a polar intermediate but a benzoyloxy radical which exhibits electrophilic properties.[2] The ester could arise from the capture of **1** by iodine, an efficient radical scavenger, followed by the loss of hydrogen iodide. In the absence of iodine, the initially-formed free radical **1** is not sufficiently stable to allow the formation of the ester; hence, the benzoyloxy radical is free to undergo decarboxylation, with the resultant formation of phenylated products.

$$\mathrm{PhCOO\cdot} + \mathrm{ArH} \rightleftarrows \underset{(1)}{\mathrm{PhCOOArH\cdot}}$$

$$\mathbf{1} + \mathrm{I_2} \longrightarrow \underset{(2)}{\mathrm{PhCOOAr}\langle^{\mathrm{H}}_{\mathrm{I}} + \mathrm{I\cdot}}$$

$$\mathbf{2} \longrightarrow \mathrm{PhCOOAr} + \mathrm{HI}$$

$$\mathrm{PhCOO\cdot} + \mathrm{HI} \longrightarrow \mathrm{PhCOOH} + \mathrm{I\cdot}$$

1) P. Kovacic and M. E. Kurz, *Tetrahedron Letters*, **1966**, 2689.

2) S. Hashimoto, W. Koike and Y. Matsuda, Abstracts of Papers presented at the Symposium on Organic Reaction Mechanisms, Yamagata, October, 1968, p. 72.

3) T. Nakata, K. Tokumaru and O. Simamura, *Tetrahedron Letters*, **1967**, 3303.

4) A. Perret and R. Perrot, *Helv. Chim. Acta.*, **28**, 558 (1945).

Fluorescence Spectra of High-purity Coronene Thin Film

Takashi KAJIWARA, Koichi OHNO, Satoshi IWASHIMA and Hiroo INOKUCHI

The Institute for Solid State Physics, The University of Tokyo, Roppongi, Tokyo

(Received June 13, 1969)

Commercial and synthesized crude coronene contains perylene as an impurity, and its fluoresence spectra depend much on the degree of purification.[1]

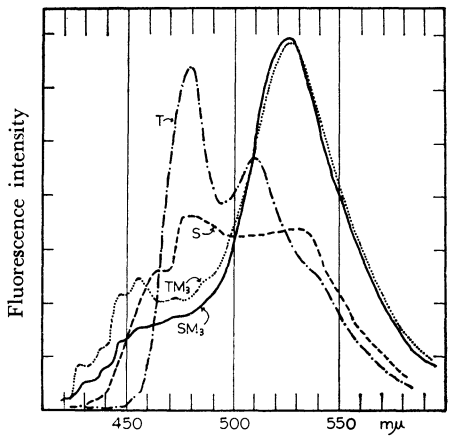

Fig. 1. The fluorescence spectra of the sublimed thin films of coronene of various degrees of purity at room temperature.
T: Commercial coronene, (crude).
S: Synthesized coronene, (crude).
TM_3: Commercial coronene purified by treatment with maleic anhydride for 3 hr (see text).
SM_3: Synthesized coronene purifide by treatment with maleic anhydride for 3 hr (see text).

Figure 1 shows the fluorescence spectra of sublimed thin films of coronene at room temperature. High-purity coronene (TM_3 and SM_3 in Fig. 1) shows a broad excimer-type fluorescence around 525 mμ, as do pyrene, α-type perylene, and benzo[*g,h,i*]perylene. The maxima around 480 mμ and 510 mμ of the fluorescence of crude coronene (T and S in Fig. 1) are due to those of perylene, because these maxima are enhanced as the concentration of perylene in the coronene matrix is increased.[2] The sample denoted as T in Fig. 1 contains about a 10^{-3} mol/mol concentration of perylene. Though benzo[*g,h,i*]perylene is also included in crude coronene, its influence on the fluorescence spectra of solid coronene is not obvious.

Figure 2 shows the temperature dependence of the fluorescence spectra of a sublimed thin film of high-purity coronene (SM_3). As the temperature decreases, the fluorescence bands around 446 mμ and 474 mμ gradually increase and the broad band around 525 mμ decreases. When the sample specimen is cooled to 4.2°K, the broad band disappears and the spectra with distinct vibrational structures appear; these spectra are similar to the fluorescence spectra in its *n*-heptane solution.[3] It is remarkable that the vibrational structures show a fairly good correspondence with the faint structures observed in the short-wavelength region (430 mμ—480 mμ) of the fluorescence spectra at room temperature. It is also interesting that the fluorescence spectra at 77°K are very different from those at 4.2°K. The measurement of the fluorescence spectra in the temperature region from 77°K to 4.2°K will now be undertaken.

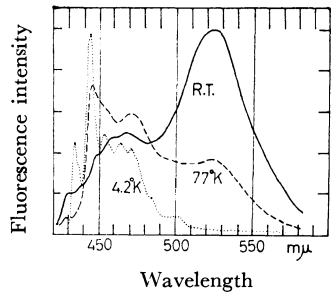

Fig. 2. Temperature dependence of the fluorescence spectra of a sublimed thin film of high purity coronene (SM^3). The relative fluorescence intensity is not corrected.
Fluorescence maxima: at 4.2°K, 434, 436, 443, 453, 464, 469, 484, and 502 mμ.

The method of purification is as follows.[4] A crude (commercial or synthesized) coronene is treated for more than 3 hr with maleic anhydride, upon which perylene and benzo[*g,h,i*]perylene change to carboxylic acid anhydride. These anhydrides are then eliminated by precipitation, making use of the fact that their solubilities in the solvent, xylene, are much less than that of coronene. Further, the coronene is purified by repeated recrystallizations and sublimations. The perylene concentration in the matrix can be decreased to less than 10^{-5} mol/mol by these procedures.

1) The same phenomena are observed in benzo[*g,h,i*]perylene. T. Kajiwara, I. Shirotani, H. Inokuchi and S. Iwashima, *J. Mol. Spectry.*, **29**, 454 (1969).

2) B. Stevens, *Spectrochim. Acta*, **18**, 436 (1962).

3) D. E. Heine and H. W. Offen, *Mol. Cryst.*, **5**, 217 (1969).

4) The details of the purification procedure are given in: S. Iwashima, K. Ohno, T. Kajiwara and J. Aoki, *Nippon Kagaku Zasshi* (*J. Chem. Soc. Japan, Pure Chem. Sect.*), **90**, 884 (1969).

The Photochromism of Evaporated Photospiran

Hajime KOBAYASHI, Isamu SHIMIZU, Mitsunobu NAKAZAWA, Hiroshi KOKADO and Eiichi INOUE

Tokyo Institute of Technology, Imaging Science and Engineering Laboratory, Ookayama, Meguro-ku, Tokyo

(Received June 26, 1969)

Photochromism in spiropyrans has been extensively investigated. We have reported the photochromic properties of 1,3,3-trimethylspiro(indoline-2,2′-benzopyran) (I) on adsorbent,[1] in solution[2] and in polymer film,[3] however, any distinct photochemical reaction of microcrystalline spiropyrans has never been reported.

We should now like to report that the thin layer of spiropyrans prepared by means of vacuum evaporation revealed a distinguished reversible photochemical reaction (photochromism).

Photospirans used are listed in Fig. 1. The samples were prepared with a hand-made vacuum evaporator. Evaporation was carried out under a pressure of about 10^{-5} mmHg and at suitable temperatures. As the base materials, glass or quartz plates were used.

In most derivatives, evaporated photospirans formed transparent and colorless uniform layers under microscopic inspection. However, in some derivatives crystallization proceeded during the course of evaporation. Evaporated photospirans, as well as those in solution, have no absorption band in visible region, but have specific absorption bands in ultraviolet region. The colorless state is transformed into corresponding colored state by irradiation with ultraviolet light (Fig. 1). The absorption spectra of the colored state are shown in Fig. 2. They have maxima near 6000Å. This behavior is similar to the solution of spiropyran in a non-polar solvent such as benzene. This indicates that there are no important intermolecular interactions between spiropyran molecules. The dark decoloration of colored species of the evaporated spiropyran proceeded according to a first order mechanism. In Table 1, the rate constants and the activation energies of dark decoloration are shown. Apparently, the colored forms of spiropyrans in evaporated state are thermally more stable than in solution or in polymer film. The photodecoloration efficiency is about the same in solution or in polymer film.

Some spiropyran such as II, crystallized during evaporation. In such circumstances photocoloration efficiency became very low and absorption spectrum was broadened. However, it was observed that such crystallization effect could be avoided by evaporation of the mixture of the compound with another derivative of spiropyran.

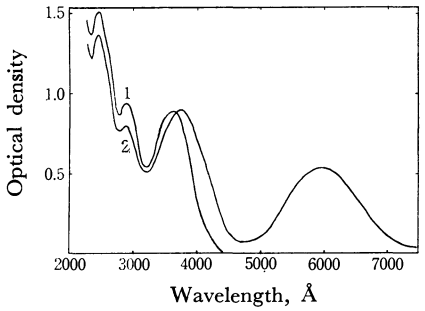

Fig. 1. Absorption spectra of evaporated spiropyran (III)
1. dark adapted 2. UV irradiated.
II 6′-NO_2 derivative of (I)
III 6′-NO_2-8′-OCH_3 IV 5-Cl-6′-NO_2
V 5-OCH_3-6′-NO_2 VI 6′-OCH_3-8′-NO_2
VII 5′-NO_2-8′-OCH_3 VIII 6′,8′-diBr

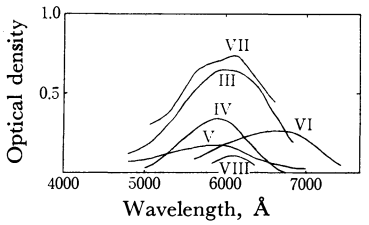

Fig. 2. Absorption spectra of the colored state of evaporated spiropyrans.

TABLE 1. KINETIC DATA EVAPORATED SPIROPYRANS

Spiropyran	Rate constant of dark decoloration at 30°C sec^{-1}	Activation energy kcal/mol
III	2.8×10^{-5}	31.8
IV	5.1×10^{-5}	36.6
VI	2.7×10^{-3}	35.2
VII	9.6×10^{-4}	24.8
VIII	6.6×10^{-3}	40.8

1) E. Inoue, H. Kokado and H. Kobayashi, *Kogyo Kagaku Zasshi* (*J. Chem. Soc. Japan, Ind. Chem. Sect.*), **71**, 1288 (1968).

2) I. Shimizu, H. Kokado and E. Inoue, This Bulletin, **42**, 1726 (1969).

3) I. Shimizu, K. Yoshida, H. Kobayashi, M. Nakazawa, H. Kokado and E. Inoue, *Kogyo Kagaku Zasshi* (*J. Chem. Soc. Japan, Ind. Chem. Sect.*), **72**, 166 (1969).

A Revised Structure of Pyrolumisantonin[1]

Tadashi SASAKI and Shoji EGUCHI

Institute of Applied Organic Chemistry, Faculty of Engineering, Nagoya University, Furo-cho, Chikusa-ku, Nagoya

(Received June 27, 1969)

The structure of pyrolumisantonin was given for the first time by Arigoni and his coworkers as IIa in 1957 on the basis of an ozonized product IV without NMR spectral evidence[2] and has been adopted again quite recently by Fisch and Richards.[3] During the course of our studies on the synthesis of some double bond derivatives of lumisantonin (I),[4] we have obtained pyrolumisantonin as a by-product, mp 127—129°C (lit.,[2] mp 126—127°C). It gave a satisfactory analysis (Found: C, 72.89; H, 7.30%. Calcd for $C_{15}H_{18}O_3$: C, 73.14; H, 7.37%) and had almost the same spectral data as those reported: $[\alpha]_D = -170°$ ($CHCl_3$, $c=0.265$, lit.,[2] $-171°$); λ_{max}^{EtOH} 219 mμ, log ε 4.06 (lit.,[2] λ_{max}^{EtOH} 220 mμ, log ε 4.07); ν_{max}^{KBr} 3090, 1843, 1635 and 920 ($C{=}CH_2$), 1769 (γ-lactone), 1705 and 1600 (cyclopentenone) cm^{-1} (the spectrum was superimposable on that reported[2]). In the NMR spectrum (Fig. 1), however, no signals due to an expected allylic methyl protons in the proposed structure IIa were observed but instead a sharp singlet signal integrated for two protons appeared at τ 4.86 which should be assigned to two *exo*-methylene protons and all other signals were compatible with the structure IIb. This led us to revise the structure of pyrolumisantonin from IIa to IIb. A double bond isomer (III) of pyrolumisantonin has been shown to isomerize to pyrolumisantonin by chromatography on alumina (neutral, grade II).[3] Our sample was treated similarly on an alumina (neutral, grade II) column using benzene as an eluent to afford needles, mp 128—130°C which showed no depression of a mixed melting point with a specimen before chromatography.

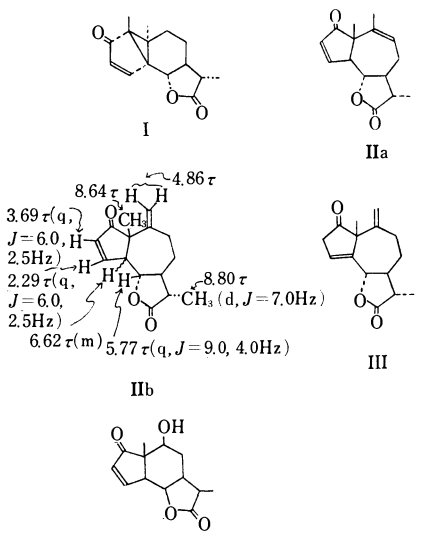

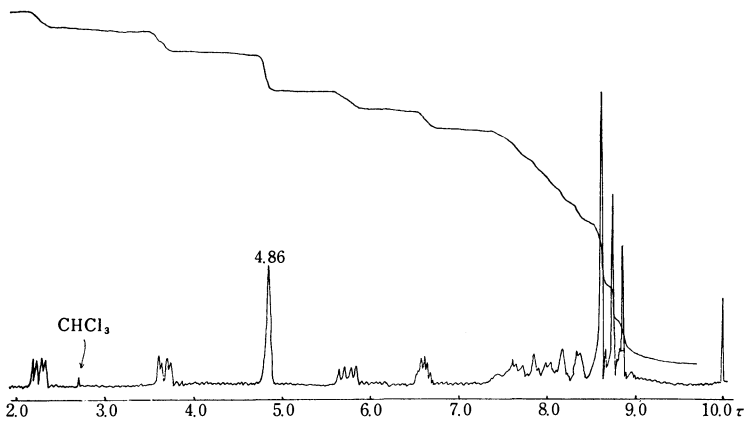

Fig. 1. NMR spectrum of pyrolumisantonin $CDCl_3$ (60 MHz).

1) Studies on Reactions of Isoprenoids. Part X. Part IX: T. Sasaki, S. Eguchi and T. Ishii, submitted to *J. Org. Chem.*

2) D. Arigoni, H. Bosshard, H. Bruderer, G. Büchi, O. Jeger and L. J. Krebaum, *Helv. Chim. Acta*, **40**, 1732 (1957).

3) M. H. Fisch and J. H. Richards, *J. Am. Chem. Soc.*, **90**, 1547, 1553 (1968).

4) T. Sasaki and S. Eguchi, *J. Org. Chem.*, **33**, 4389 (1968).

Photochemical Benzoyloxylation with Labeled Benzoyl Peroxide

Michio KOBAYASHI, Hiroshi MINATO and Yoshikuni OGI

Department of Chemistry, Tokyo Metropolitan University, Fukasawa, Setagaya-ku, Tokyo

(Received July 3, 1969)

Nakata, Tokumaru and Simamura[1] studied the photochemical decomposition of benzoyl peroxide in aromatic solvents, and explained the formation of a considerable amount of aryl benzoate under oxygen atmosphere by the following mechanism.

All the experimental results were consistent with the above mechanism.

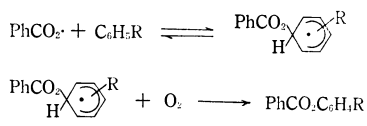

However, the mechanism of the photochemical excitation of benzoyl peroxide is not clear. On the basis of the findings that 1) very slow photolysis of benzoyl peroxide in cyclohexane was much accelerated by addition of benzene and 2) the decomposition of benzoyl peroxide was not retarded by the presence of oxygen, an effective quencher of triplet state excitation, they suggested that the decomposition of the peroxide in benzene was caused by the energy transfer from the benzene of an excited singlet state to the peroxide, followed by monomolecular decomposition of the peroxide, as shown in the following.

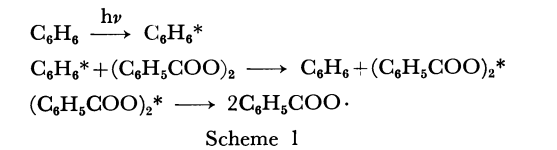

Scheme 1

Another possible mechanism is the direct attack of the excited benzene molecule upon the peroxide as shown in the following.

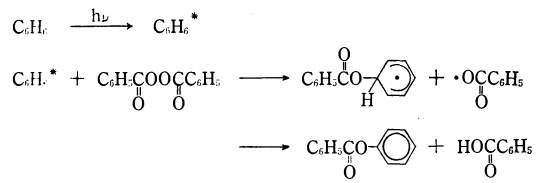

Scheme 2

By an analogy to the attack of trityl radical[2] and α-ethoxy-ethyl radical[3] upon the peroxide, the attack of the excited benzene is expected to take place on the peroxidic oxygen of the peroxide. If the benzoyl peroxide labeled with ^{18}O in the carbonyl oxygen were used, the phenyl benzoate produced *via* Scheme 1 should contain scrambled oxygen-18, whereas the phenyl benzoate produced *via* Scheme 2 should contain non-scrambled oxygen-18.

In an attempt to clarify the mechanism of the photochemical benzoyloxylation, we studied the products of decomposition of the benzoyl peroxide labeled with oxygen-18 in the carbonyl oxygen. A solution of 2.7 g of the labeled benzoyl peroxide in 500 m*l* of benzene (0.0223 mol/*l*) was irradiated with a high pressure mercury lamp either under a nitrogen atmosphere or with bubbling of oxygen gas (41 m*l*/min) at 18—20°C for 12 hr. By a separate experiment the half life of the peroxide under these conditions was found to be 55 min. After the reaction was over, the solution was evaporated to dryness, and the column-chromatographic separation of the residue gave 700 mg (in O_2) or 170 mg (in N_2) of pure phenyl benzoate. The carbonyl oxygen of phenyl benzoate or the starting peroxide was separated from alkoxy oxygen or peroxidic oxygen by the reaction with hydrazine. Benzhydrazide obtained was pyrolyzed and carbon dioxide evolved was assayed for oxygen-18 by mass spectrometry. The results are shown in Table 1.

They indicate that direct attack of excited benzene upon benzoyl peroxide does not occur to any appreciable extent. Therefore, as mechanism of the photochemical decomposition of benzoyl peroxide, Scheme 1 appears to be most probable.

TABLE 1. SPECIFICITY OF ^{18}O-LABELING

Sample	%^{18}O-Excess	%^{18}O-Calcd
Starting BPO	0.627	0.618
Its hydrazide	1.236	(1.236)
	N_2 atmosphere	
PhCOOPh*	0.606	0.618
Its hydrazide	0.535	0.618
PhCOOH*	0.612	0.618
	O_2 bubble	
PhCOOH*	0.586	0.618
Its hydrazide	0.642	0.618

* Direct products of photolyses

1) T. Nakata, K. Tokumaru and O. Simamura, *Tetrahedron Letters*, **1967**, 3303.

2) W. von E. Doering, K. Okamoto and H. Krauch, *J. Am. Chem. Soc.*, **82**, 3579 (1960).

3) D. B. Denney and G. Feig, *ibid.*, **81**, 5324 (1959).

Primary Kinetic Isotope Effect for Phenylation with Phenyl Radical[1)]

Michio KOBAYASHI, Hiroshi MINATO and Nobumasa KOBORI

Department of Chemistry, Tokyo Metropolitan University, Fukazawa, Setagaya-ku, Tokyo

(Received July 15, 1969)

Primary kinetic hydrogen isotope effect has been observed in the homolytic phenylation of aromatic compounds with the phenyl radical generated from benzoyl peroxide ($k_H/k_D=6.6$),[2)] but no primary isotope effect has been reported in the formation of biphenyls from the decomposition of phenylazotriphenylmethane or *N*-nitrosoacetanilide in deuteriobenzene. The isotope effect in the case of benzoyl peroxide has been attributed to the occurrence of disproportionation between phenylcyclohexadienyl radicals and the absence of isotope effect in the other two cases has been attributed to the non-occurrence of the disproportionation of phenylcyclohexadienyl radicals, which instead have suffered abstraction of hydrogen by triphenylmethyl radicals or phenylazooxide radicals.[3)]

TABLE 1. KINETIC ISOTOPE EFFECT FOR THE HOMOLYTIC AROMATIC PHENYLATION*

Run	Compound	k_H/k_D for the formation of substituted biphenyls		
		2-	3-	4-
1	PhC_6-d_5[a)]	1.10	1.13	1.23
2	$PhNO_2-d_5$[b)]	1.46	1.16	1.01
3	$PhNO_2-d_5$[c)]	2.3	—	1.06
		2,4-		2,6-
4	*m*-Dinitrobenzene-d_5[d)]	1.54		1.55

* All reactions were carried out at room temperature (20±3°C).

a) k_H/k_D was calculated from the partial rate factors which were determined gas-chromatographically from the competitive phenylations of C_6H_6-$C_6H_5NO_2$ and of C_6H_6 - $C_6D_5NO_2$.

b) k_H/k_D was determined by a mass spectrometer connected directly to the exit of a gas chromatograph to which nitrobiphenyl isomers obtained from the competitive phenylation of $C_6H_5NO_2$ - $C_6D_5NO_2$ were fed.

c) See text for method of determination.

d) The biphenyl isomers obtained from the competitive phenylation of *m*-dinitrobenzene - *m*-dinitrobenzene-d_4 were analyzed by the same method as that used for Run 3.

Our previous paper described the formation of phenyl radical from benzenediazonium tetrafluoroborate and sodium nitrite.[4)] We investigated the reaction with deuterated aromatics, and observed primary kinetic isotope effect in the phenylation with phenyl radical. Results are summarized in Table 1. The experimental procedure is described by use of Run 3 as an example. To a solution of nitrobenzene (40 mmol), pentadeuterionitrobenzene (40 mmol) and sodium nitrite (120 mmol) in DMSO (150 g), a solution of benzenediazonium tetrafluoroborate (34 mmol) in DMSO (70 g) was added at room temperature (20±3°C). A mixture of nitrobiphenyls obtained was separated to pure components by chromatography on an alumina column, and k_H/k_D was determined from the ratio of the parent peaks of a nitrobiphenyl and a tetradeuterionitrobiphenyl by mass spectrometry.

Quaterphenyls were not found in the product mixtures. The absence of the dimerization (and oxidation) product of phenylcyclohexadienyl radical must be due to efficient abstraction of hydrogen from phenylcyclohexadienyl radical.

The data in Table 1 may be explained on the basis of the steric effect. The larger values of k_H/k_D were observed for the formation of 2-nitrobiphenyl and 2,4- and 2,6-dinitrobiphenyls, all of which had a substituent at ortho position.

Another possible explanation is that with those substituents capable of stabilizing the intermediate phenylcyclohexadienyl radical by resonance the activation energy for the addition of phenyl radical to substituted benzene is lower and the addition step proceeds faster, and consequently the step of hydrogen abstraction makes greater contribution in the overall kinetic rate. It seems that in principle the isotope effect exists in the aromatic phenylation with phenyl radical and the isotope effect is observable only when the substituent is large enough and/or stabilizes the intermediate phenylcyclohexadienyl radical by resonance. We wish to propose the following mechanism, in which the addition of phenyl radical is reversible.

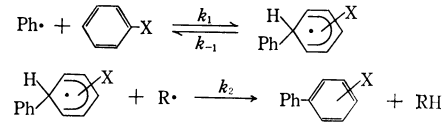

1) Aromatic Arylation with Aryl Radicals. II.

2) E. L. Eliel, Z. Welvart and S. H. Wilen, *J. Org. Chem.*, **23**, 1821 (1958); E. L. Eliel, S. Meyerson, Z. Welvart and S. H. Wilen, *J. Am. Chem. Soc.*, **82**, 2936 (1960).

3) E. L. Eliel, M. Eberhardt, O. Simamura and S. Meyerson, *Tetrahedron Letters*, **1962**, 749; E. L. Eliel, J. G. Saha and Meyerson, *J. Org. Chem.*, **30**, 2451 (1965).

4) M. Kobayashi, H. Minato, N. Kobori and E. Yamada, This Bulletin, in press.

Reactions of Hydrazinium Thiocyanate with Alcohols

Isamu ARAI, Yasuo SATOH, Ichiro MURAMATSU and Akira HAGITANI

Department of Chemistry, Faculty of Science, St. Paul's University (Rikkyo Daigaku), Toshima-ku, Tokyo

(Received July 16, 1969)

During the course of an investigation of the reactions of thiocyanogen with acylhydrazines, it was found that hydrazinium thiocyanate (I) reacted with ethanol or 2-butanol, and in both cases an interesting heterocyclic compound, 3-ethyl-3-methyl-1,2,4-triazolidine-5-thione (II), was formed.

When a mixture of the aqueous solution of I and ethanol was allowed to stand at room temperature, white needles, II mp 116°C were obtained. The elemental analysis and MS spectral data of II gave a molecular formula $C_5H_{11}N_3S$. The IR spectrum (KBr) showed absorption bands at 3130, 2960, 2920, 2850, 1520, 1400, 1225, 1180, 960, and 830 cm^{-1}. The NMR spectrum (CD_3OD) exhibited peaks at τ 9.30 (3H, methyl-protons, triplet, $J=7.0$ cps), 8.63 (3H, methyl-protons, singlet), and 8.43 (2H, methylene-protons, quartet, $J=7.0$ cps), indicating that the methyl and the ethyl groups were both attached to the same carbon atom.

From these data and the results of the hydrolysis of II, the following structure was deduced.

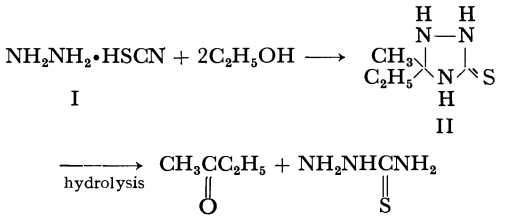

The MS spectrum also supported the structure, *viz.*, it showed the molecular peak at *m/e* 145 and peaks at *m/e* 130 (M−15) and *m/e* 116 (M−29). The *m/e* 86 peak derived from the loss of HNCS showed the presence of an –NH·CS– group in the molecule. Peaks at *m/e* 100, 96, and 82 indicated the formation of a stable triazole skeleton.

When the reaction of I with ethanol was carried out in the absence of water, another product $C_{10}H_{18}N_4S_2$ (III), mp 180°C (dec.) was isolated in a significant quantity in addition to II. Sunner[1] reported this compound (III) to be the product in the reaction of methyl ethyl ketone with I. However, when we carried out the same reaction, II was obtained in a fairly large quantity together with III.

2-Butanol reacted also with I and gave only II, both in the presence and absence of water.

This type of cyclization does not occur with the lower *n*-alcohols, except ethanol.

The triazolidine formations from ethanol, 2-butanol, and methyl ethyl ketone seem to be related to each other, and the reaction mechanisms are now being studied.

1) S. Sunner, *Svensk Kem. Tidskr.*, **67**, 361 (1955).

Nuclear Quadrupole Resonance of Nitrogen-14 in Tetracyanoethylene and 7,7′,8,8′-Tetracyanoquinodimethane

Shinzaburo ONDA, Ryuichi IKEDA, Daiyu NAKAMURA and Masaji KUBO

Department of Chemistry, Nagoya University, Chikusa, Nagoya

(Received July 29, 1969)

The pure quadrupole resonance of ^{14}N in tetracyanoethylene (TCNE), $(CN)_2C{:}C(CN)_2$, and tetracyanoquinodimethane (TCNQ), $(CN)_2C : C_6H_4 : C(CN)_2$, was observed at liquid nitrogen temperature by means of a modified Pound-Watkins type spectrometer.[1] These compounds are known to be strong π-acids and form a number of unusually stable molecular complexes.[2] In attempting to discuss the nature of these chemical properties, it is worthwhile to reveal the local electronic structure of cyano groups in these compounds.

A commercial preparation of TCNE was purified by sublimation at about 80°C in a high vacuum. Purification was repeated until two closely spaced ν^{I} lines were well resolved. Commercial TCNQ was sublimed twice at about 220°C in a high vacuum and used for the observation of quadrupole resonance. Resonance frequencies were determined by frequency modulation using a TR-5178 universal counter from Takeda Riken Company. Observed resonance lines were assigned to ν^{I} and ν^{II} by Zeeman modulation. Results are shown in Table 1.

TABLE 1. PURE QUADRUPOLE RESONANCE FREQUENCIES, ν^{I} AND ν^{II}, QUADRUPOLE COUPLING CONSTANTS, eQq, AND ASYMMETRY PARAMETERS, η, OF ^{14}N IN TCNE AND TCNQ AT LIQUID NITROGEN TEMPERATURE

Compound	ν^{I}, kHz	ν^{II}, kHz	eQq, kHz	η,%
TCNE	3213.1±1.0 3210.2±1.0	3148.3±1.0 3090.5±1.0	4331	4.4
TCNQ	3151.6±0.1 3142.9±0.1	2888.7±0.1 2879.5±0.1	4021	13.1

Both TCNE and TCNQ show two sets of ν^{I} and ν^{II} lines. The appearance of multiplet lines indicates that there are two kinds of crystallographically nonequivalent nitrogen atoms in the crystals of each compound at liquid nitrogen temperature, although four nitrogen atoms are chemically equivalent in a molecule. X-Ray analysis carried out by Trueblood *et al.*[3,4] on TCNE and TCNQ has shown that both crystals are monoclinic with two and four centrosymmetric molecules, respectively, in a unit cell and that there are two crystallographically nonequivalent nitrogen sites in each crystal. The results of quadrupole resonance agree with those of X-ray analysis, provided that no phase transition takes place between liquid nitrogen and room temperatures.

The four resonance lines observed for TCNE were very broad (about 2 kHz or more in width) even after repeated sublimation. On the other hand, TCNQ showed unexpectedly sharp lines after it was sublimed only once. Since TCNE is less stable than TCNQ, field fluctuation due to decomposition products that contaminate the crystal lattice is a possible reason for the broad signals observed for TCNE. The large asymmetry parameter of TCNQ might be responsible for the appearance of sharp signals owing to quenching of dipolar broadening.[5]

For ^{14}N with its nuclear spin equal to unity, the quadrupole coupling constant and the asymmetry parameter can be calculated from observed frequencies, ν^{I} and ν^{II}. However, for both compounds showing closely spaced doublet lines, one-to-one correspondence could not be made between ν^{I} and ν^{II}. Therefore, the frequencies of doublet lines were averaged to calculate the quadrupole coupling constant and the asymmetry parameter as shown in Table 1.

It is noteworthy that the quadrupole coupling constant of TCNE is nearly the same as that of cyanogen[6] and is very large compared with that of nitrile derivatives.[7] The large asymmetry parameter observed for TCNQ is attributable to the nonequivalence of π-electron polarization between π-orbitals parallel and perpendicular to the plane of a molecule.

1) R. Ikeda, D. Nakamura and M. Kubo, *J. Phys. Chem.*, **70**, 3626 (1966).

2) D. N. Dhar, *Chem. Rev.*, **67**, 611 (1967); D. S. Acker and W. R. Hertler, *J. Am. Chem. Soc.*, **84**, 3370 (1962).

3) D. A. Bekoe and K. N. Trueblood, *Z. Kristallogr.*, **113**, 1 (1960).

4) R. E. Long, R. A. Sparks and K. N. Trueblood, *Acta Cryst.*, **18**, 932 (1965).

5) G. W. Leppelmeier and E. L. Hahn, *Phys. Rev.*, **141**, 724 (1966).

6) P. J. Haigh and L. Guibé, *Compt. Rend.*, **261**, 2328 (1965).

7) A. Colligiani, L. Guibé, P. J. Haigh and E. A. C. Lucken, *Mol. Phys.*, **14**, 89 (1968); S. Onda, R. Ikeda, D. Nakamura and M. Kubo, This Bulletin, **42**, 1771 (1969).

BULLETIN OF THE CHEMICAL SOCIETY OF JAPAN VOL. 42 2741—2748 (1969)

Concentration Polarization Phenomena in Ion-exchange Membrane Electrodialysis. II. The Effect of the Condition of the Diffusion-boundary Layer on the Limiting-current Density and on the Relative Transport Numbers of Ions*[1]

Reiichi YAMANE, Toshikatsu SATA, Yukio MIZUTANI and Yasuharu ONOUE

Tokuyama Soda Co., Ltd., Mikage-cho, Tokuyama, Yamaguchi

(Received July 15, 1968)

The effect of the condition of the diffusion-boundary layer in the ion-exchange membrane electrodialysis on the limiting-current density and on the relative transport numbers of ionic species with the same sign was studied. The limiting-current density in the laminar flow is approximately proportional to the first power of the concentration of the solution, the one-half power of the flow velocity of the solution, and, inversely, the one-half power of the membrane length in the direction of the flow. In the natural convection, it is proportional to the five-quarters power of the concentration of the solution. These experimental results agree with the relation of the equations of the limiting-current density for the electrode process. The change in the relative transport numbers of ionic species with the same sign, such as the magnesium and sodium ions or the sulfate and chloride ions, with the flow velocity, the concentration, and the temperature of the solution, the dimension of the membrane in the direction of the flow, and the current density were observed. The results were explained in terms of the change in the condition of the diffusion-boundary layer.

On the demineralization or concentration of sea water by ion-exchange membrane electrodialysis, one of the most serious problems is the concentration polarization phenomenon. In concentrating sea water especially, it is recognized that the concentration polarization on the desalting side of the membrane-solution interfaces causes a change in the relative transport numbers of ionic species with the same sign, an increase in the electric resistance of the electrodialysis cell, and often a change in the solution pH. Industrially, these changes are very important. The increase in the electric resistance makes necessary much more electric power, and the change in the relative transport numbers influences the current efficiency of the sodium ions and may cause the precipitation of calcium sulfate in the concentrating compartment of the cell. Also, when the pH-change of the solution occurs, carbonate and hydroxide of alkali earth metals are often precipitated on the membrane surfaces.

In this work, the effect of the condition of the diffusion-boundary layer on the limiting-current density and the relative transport numbers was studied.

The limiting-current density was obtained from the current-voltage curve in electrodialysis cells; we then investigated how the limiting-current density was affected by the flow velocity, the concentration and temperature of the solution, the dimensions of the membrane, and ionic species.

Moreover, the change in the relative transport numbers of the magnesium to sodium ions and of the sulfate to chloride ions was investigated in connection with the behavior of the diffusion-boundary layer when sea water was concentrated by electrodialysis.

Theoretical

The following equation shows the limiting-current density, i_{lim}, in the ion-exchange membrane electrodialysis:

$$i_{\mathrm{lim}} = \frac{\boldsymbol{F}DC_b}{\delta(t_m - t_s)} \tag{1}$$

where $\boldsymbol{F}$ is the Faraday constant; D, the diffusion coefficient of the electrolyte in the free solution; C_b, the concentration of the bulk solution; δ, the thickness of the diffusion-boundary layer, and t_m and t_s, the transport numbers of the counterion in the membrane and in a free solution respectively.

At current densities near the limiting-current density, the transport of ions consists mainly of diffusion and convection. Levich,[1] Wilke *et al.*,[2]

*1 Studies on ion-exchange membranes. XXVIII. Presented at the 17th Meeting CITCE (Comité International de Thermodynamique et de Cinetique Electrochemiques) held in Tokyo Japan, in September, 1966.

1) B. Levich, *Discussions Faraday Soc.*, **1**, 37 (1947).

2) C. R. Wilke, M. Eisenberg and C. W. Tobias, *J. Electrochem. Soc.*, **100**, 513 (1953).

and other investigators have given relations for the thickness of the diffusion-boundary layer in the electrode process at current densities near the limiting-current density. The membrane-solution system is similar to the electrode-solution system, as an ion-exchange membrane removes ions from the solution or adds ions to the solution. Accordingly, the relations in the electrode process can be used to explain the behavior of the diffusion-boundary layer in ion-exchange-membrane electrodialysis.

The equations for the thickness are as follows: for the laminar flow:

$$\delta = K_1\left(\frac{D}{\nu}\right)^{1/3}\left(\frac{\nu x}{V}\right)^{1/2} \tag{2}$$

for the natural convection:

$$\delta = K_2\left(\frac{\nu}{D}\right)^{-1/4}\left(\frac{g\alpha'}{\nu^2}\right)^{-1/4}x^{1/4}C_b^{-1/4} \tag{3}$$

where ν is the kinematic viscosity; g, the acceleration of gravity; x, the distance from the bottom edge of a membrane; α, the specific density coefficient of the electrolyte solution $\left(=\frac{1}{\rho}\frac{d\rho}{dc},\ \rho:\right.$ specific density$\left.\right)$; V, the flow velocity of the solution in the laminar flow, and K_1 and K_2, constants.

The limiting-current density, i_{lim}, in the laminar flow is given from Eqs. (1) and (2) as the following equation:

$$i_{lim} = \frac{1}{K_1}\frac{FDC_b}{(t_m - t_s)}\left(\frac{\nu}{D}\right)^{1/3}\left(\frac{V}{x\nu}\right)^{1/2} \tag{4}$$

On the other hand from Eqs. (1) and (3) in the natural convection it is given as the following equation:

$$i_{lim} = \frac{1}{K_2}\frac{FDC_b^{5/4}}{(t_m - t_s)}\left(\frac{\nu}{D}\right)^{1/4}\left(\frac{g\alpha}{\nu^2}\right)^{1/4}x^{-1/4} \tag{5}$$

Equation (4) indicates that the limiting-current density is proportional to the first power of the concentration of the bulk solution, the one-half power of the flow velocity, and, inversely, the one-half power of the membrane length in the direction of the flow. Equation (5) indicates that the limiting-current density is proportional to the five-quarters power of the concentration of the bulk solution.

The temperature of the solution affects the limiting-current density, for the diffusion coefficient and the kinematic viscosity are functions of the temperature. If the transport numbers of the counter ion in the membrane and free solution are constant, the temperature coefficient, β, of the limiting-current density in the laminar flow can be obtained by the following method; Equation (4) is differentiated with respect to the absolute temperature, T:

$$\beta = \frac{1}{i_{lim}}\frac{di_{lim}}{dT} = \frac{2}{3}\frac{1}{D}\frac{dD}{dT} - \frac{1}{6}\frac{1}{\nu}\frac{d\nu}{dT} \tag{6}$$

Using Nernst's equation of the diffusion coefficient (8), and also Walden's equation (9), the temperature coefficient of the diffusion coefficient is obtained as follows:

$$\frac{1}{D}\frac{dD}{dT} = -\frac{1}{\nu}\frac{d\nu}{dT} + \frac{1}{T} \tag{7}$$

$$D = \frac{\lambda RT}{F^2Z} \tag{8}$$

$$\lambda\nu = \text{constant} \tag{9}$$

where λ is the equivalent conductance of the electrolyte at an infinite dilution and where Z is the valence of the ions. Accordingly, the temperature coefficient, β, is:

$$\beta = \frac{1}{i_{lim}}\frac{di_{lim}}{dT} = \frac{2}{3}\frac{1}{T} - \frac{5}{6}\frac{1}{\nu}\frac{d\nu}{dT} \tag{10}$$

The viscosity of water can be used for ν, as the concentration on the desalting side at the membrane surfaces is low at current densities near the limiting-current density.

Experimental

Membranes. Throughout this investigation commercial ion-exchange membranes prepared by the "Paste Method,"[3-5] *i. e.*, two anion-exchange membranes, NEOSEPTA AV-4T and NEOSEPTA AVS-4T, and are cation-exchange membrane, NEOSEPTA CL-2.5T, were used. The characteristics of these membranes are shown in Table 1.

Cells. Five different electrodialysis cells were used. The cells 1, 2, 3 and 4 were used for the laminar flow experiments, and the cell 5 for the natural convection experiments. In the cells 1, 2 and 3, the thickness of the compartment in which the solution flows was 1.0 cm in order to eliminate the effect of the desalting of the solution on the current-voltage curve. The characteristics of the cells are shown in Table 2.

Procedures. *The Determination of the Current-voltage Curve.* The current-voltage curve was measured with a high-impedance valve voltmeter (Tōadempa Co., Ltd., Model PM-20) connected to a pair of silver-silver chloride or calomel probe electrodes situated on the opposite sides of the membrane. Silver-silver chloride probe electrodes were put close to a membrane (about 2 mm apart in the cell 1). Calomel probe electrodes were connected to luggin capillaries (about 2mm apart from the membrane surfaces) and were used in the cells 2, 3, 4 and 5. The current-voltage curve was obtained as follows: the current was increased gradually and the voltage between the probe electrodes was measured with a valve voltmeter. The current density at which the voltage increased abruptly in the current-voltage relation was defined as the limiting-current density in the cell.

3) Y. Mizutani, R. Yamane, H. Ihara and H. Motomura, This Bulletin, **36**, 361 (1963).

4) Y. Mizutani, R. Yamane and H. Motomura, *ibid.*, **38**, 689 (1965).

5) R. Yamane, Y. Mizutani, H. Motomura and R. Izuo, *Denki Kagaku (J. Electrochem. Soc. Japan).*, **32**, 134 (1964).

TABLE 1. CHARACTERISTICS OF ION-EXCHANGE MEMBRANES

	Designation of membranes		
	NEOSEPTA*1 AV-4T	NEOSEPTA*2 AVS-4T	NEOSEPTA*3 CL-2.5T
Backing	Polyvinyl chloride	Polyvinyl chloride	Polyvinyl chloride
Thickness (mm)	0.15—0.17	0.15—0.17	0.15—0.17
Burst strength (kg/cm²)	5—7	4—6	3—4
Electric resistance ($\Omega-cm^2$)*4	3.5—4.5	3.7—4.7	2.7—3.2
Transport number*5	>0.98	>0.98	>0.98
Water content*6	0.20—0.25	0.25—0.35	0.30—0.40
Ion-exchange capacity*7	1.5—2.0	1.5—2.0	1.8—2.0

*1 Strongly basic anion-exchange membrane.
*2 Strongly basic anion-exchange membrane (univalent anion permselective).
*3 Strongly acidic cation-exchange membrane.
*4 Equilibrated with 0.5 N NaCl solution, at 25.0°C.
*5 Measured by electrodialysis in 0.5 N NaCl solution, current density: 10 mA/cm², at 25.0°C.
*6 Equilibrated with 0.5 N NaCl solution [g. H_2O/g dry membrane in Na-form (or Cl-form)].
*7 [meq./g dry membrane in Na-form (or Cl-form)].

TABLE 2. TYPES OF CELLS AND EXPERIMENTS PERFORMED

	Cells*1				
	1	2	3	4	5
Anode Cathode	Ag-AgCl	graphite iron	graphite iron	graphite iron	Ag-AgCl
Membrane (a)*1	10	40	20	20	10
Dimension (b)	20	250	variable*3	variable*4	10
Membrane*5	A or C	A and C (a pair)	A or C	A and C (a pair)	A or C
Measurement	E-I curve	1) E-I curve 2) P_B^A	E-I curve	1) E-I curve 2) P_B^A	E-I curve
B*6	10	10	10	2	30

*1 Cells except the cell 5 were used in laminar flow and the cell 5 was used in natural convection.
*2 Membrane dimension, (a) the width of the membrane, (b) the length of the membrane in the direction of the flow (mm).
*3 Lengths of the membrane are 20, 80, 250 and 400 mm.
*4 Lengths of the membrane are 250, 600 and 1200 mm.
*5 A means an anion-exchange membrane and C means a cation-exchange membrane.
*6 Thickness of the desalting compartment (mm).

The Determination of the Relative Transport Numbers of Ionic Species with the Same Sign. The relative transport numbers of ionic species with the same sign were determined by means of the concentration of sea water. The sample of the concentrated solution was taken after its composition attained an equilibrated condition (after the concentration had been carried out for about 12 hr). The chloride ions were analyzed by the Mohr method, and the magnesium and calcium ions, by the EDTA titration, while the potassium and sulfate ions were analyzed by the gravimetric method, using tetraphenyl borate and barium chloride respectively. The concentration of the sodium ions was calculated by subtracting the concentration of the magnesium, calcium and potassium ions from that of all the cations.

The relative transport numbers, P_B^A, were as follows:

$$P_B^A = \frac{(t_m^A/t_m^B)}{(C_b^A/C_b^B)}$$

where t_m^A and t_m^B are the transport numbers of the counterions, A and B, in the membrane, and C_b^A and C_b^B, the concentrations of A and B ions in the bulk solution.

Measurements. *The Effect of the Flow Velocity on the Limiting-current Density.* The measurements were made in the laminar flow at 30.0°C. The cells 1 and 2 were used for obtaining the current-voltage curve for a single membrane, NEOSEPTA AV-4T, AVS-4T or CL-2.5T, in a sodium chloride solution of 0.500 N and for a pair of membranes, NEOSEPTA AVS-4T and CL-2.5T, in diluted sea water (the concentration of chloride ions was 0.35 N) respectively.

The Effect of the Concentration of the Solution on the Limiting-current Density. Current-voltage curves in the laminar flow for NEOSEPTA AVS-4T at 30.0°C and in the natural convection for NEOSEPTA CL-2.5T at 25.0°C were measured in sodium chloride solutions of various concentrations by the use of the cells 2 and 5, respec-

tively.

The Effect of the Temperature on the Limiting-current Density. In this measurement a sodium chloride solution of 0.104 N was used in the laminar flow by the use of the cell 1. The temperatures of the measurement were 15.7, 25.0 and 35.5°C for NEOSEPTA AVS-4T, and 15.0, 25.0 and 35.0°C for NEOSEPTA CL-2.5T.

The Effect of the Membrane's Dimensions on the Limiting-current Density. The current-voltage curve was obtained by the use of the cells 3 and 4. The former cell contained a single membrane, NEOSEPTA AVS-4T or CL-2.5T, while the latter cell contained a pair of anion- and cation-exchange membranes, NEOSEPTA AVS-4T and CL-2.5T. The lengths of the membranes in the direction of the flow were 2.0, 8.0, 25.0 and 40.0 cm in the cell 3, and 25.0, 60.0 and 120.0 cm in the cell 4. Each measurement was made in a laminar flow of sea water (the concentration of chloride ions was 0.52 N) at 28.0°C.

The Effect of Ionic Species on the Limiting-current Density. Current-voltage curves in aqueous solutions of several ionic species were measured with the cell 5, containing an anion- or cation-exchange membrane, in the natural convection at 25.0°C. The ionic species were hydrogen, lithium, potassium, sodium, calcium, barium, ammonium, aluminium, ferric and cupric ions as cations, and chloride and sulfate ions as anions. All these ions had a concentration of 0.50 N.

The Change in the Relative Transport Numbers with the Condition of the Diffusion-boundary Layer. The change in the relative transport numbers of the magnesium to sodium ions or of the sulfate to chloride ions with the flow velocity, the concentration, the temperature of sea water, the dimensions of the membrane, and the current density was examined when sea water was concentrated by electrodialysis. The change in the relative transport numbers by all factors except the dimensions of the membrane was examined by concentrating sea water by the use of the cell 2. The change in the relative transport numbers by the membrane length was examined by the use of the cell 4 in which long membranes were inserted. The experimental conditions are shown in Table 3.

Results and Discussion

A typical current-voltage curve for a cation-exchange membrane, NEOSEPTA CL-2.5T, in a sodium chloride solution at 25.0°C is shown in Fig. 1. This measurement was carried out by the use of the cell 5.

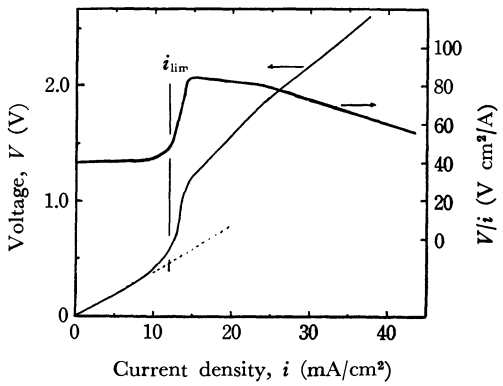

Fig. 1. An example of current-voltage curve and current $-V/i$ curve in natural convection at 25.0°C.
Membrane: CL-2.5T (with cell 5)
Solution: 0.104 N NaCl solution

The relationship between the limiting-current density and the flow velocity is shown in Fig. 2. The following relation can be found in Fig. 2.:

$$i_{lim} = mV^n \qquad (11)$$

According to Eq. (4) the constant, n, corresponds to 1/2, but the experimental values of Table 4 do not necessarily agree with 1/2. This disagreement is probably due to the difference in the structure of the cell.

If the transport numbers of counterions in the membrane and in the free solution, the diffusion coefficient, and the kinematic viscosity are nearly constant with respect to the concentration of the bulk solution, the limiting-current density is proportional to the concentration of the bulk solution. The results for an anion-exchange membrane, NEOSEPTA AVS-4T, show that the limiting-current density in the laminar flow is proportional

TABLE 3. EXPERIMENTAL CONDITIONS FOR CONCENTRATION OF SEA WATER

		Measurements				
		L (cm)	i (mA/cm²)	t (°C)	v (cm/sec)	c (N)
Effect of chloride concentration (C)	⊘	25.0	20.0	31	4	0.29—0.50
Effect of flow velocity (v)	●	25.0	20.0	20	1—16	0.52
Effect of temperature (t)	◒	25.0	>0.0	11—31	4	0.52
Effect of current density (i)	⊕	25.0	10.0—30.0	20	4	0.52
Effect of membrane length (L)	○	25.0—120.0	20.0	28	6	0.52

Marks in table are the same as those in Figs. 9 and 10.
c denotes the concentration of chloride ions of sea water.

Table 4. Empirical constants of Eq. (11)

	Membranes			
	AV-4T	AVS-4T	CL-2.5T	AVS-4T and CL-2.5T
Cell No.	1	1	1	2
m*1	100	100	66	31
n	0.3	0.5	0.4	0.5

*1 The units of the limiting-current density and the flow velocity are mA/cm² and cm/sec, respectively.

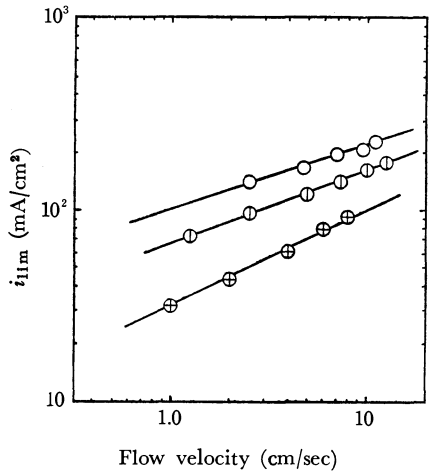

Fig. 2. The effect of the flow velocity on the limiting-current density.
cell 1: 0.500 N NaCl solution in laminar flow at 30.0°C
cell 2: diluted sea water (Cl: 0.35 N) in laminar flow at 30.0°C
○ AV-4T (with cell 1)
⦶ CL-2.5T (with cell 1)
⊕ AVS-4T and CL-2.5T

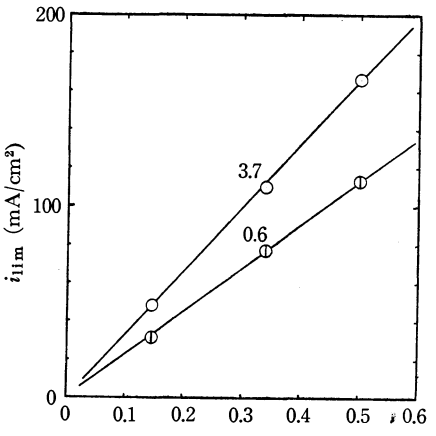

Fig. 3. The effect of the concentration on the limiting-current density in laminar flow.
Membrane: AVS-4T (with cell 1)
Solution: NaCl solution at 30.0°C
Numbers in the figure are the flow velocity of the solution (cm/sec).

to the concentration of the bulk solution, as is shown in Fig. 3. Equation (5) shows that the limiting-current density is proportional to the five-quarters power of the concentration in the natural convection. The experimental results in the natural convection agree with the theoretical value, as is shown in Fig. 4.

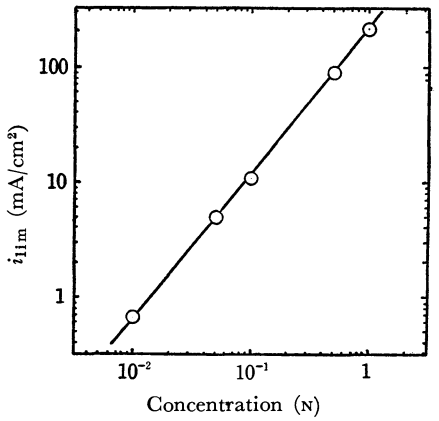

Fig. 4. The effect of the concentration on the limiting current-density in natural convection.
Membrane: CL-2.5T (with cell 5)
Solution: NaCl solution at 25.0°C

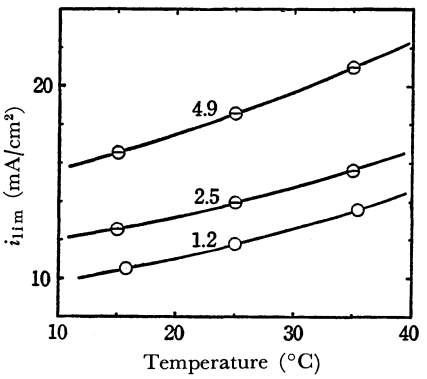

Fig. 5. The effect of the temperature on the limiting-current density.
Membrane: AVS-4T, CL-2.5T (with cell 1)
Solution: 0.104 N NaCl solution in laminar flow
Numbers in the figure are the flow velocity of the solution (cm/sec).
○ AVS-4T, ⊖ CL-2.5T

Figure 5 shows the effect of the temperature of the solution on the limiting-current density. The temperature coefficient of the limiting-current density at 25.0°C was calculated to be 2.1% from Eq. (10). However, the experimental values which were evaluated from Fig. 5 were 1.4% for the anion-exchange membrane, NEOSEPTA AVS-4T, and 1.2% for the cation-exchange membrane, NEOSEPTA CL-2.5T, at 25.0°C.

The effect on the limiting-current density of the length of a membrane in the direction of the flow is shown in Fig. 6. The concentration of the effluent decreases in comparison with that of the feed solution in the cell which contains long membranes. However, when sea water was concentrated using the cell 4 (the flow velocity of the solution was 6.0 cm/sec, the membrane length was 120 cm, and the current density was 35 mA/cm²), the concentration of the effluent decreased only about 2% in comparison with that of the feed solution. Accordingly, the effect of the desalting of the solution on the limiting-current density is negligible. Figure 7 shows current voltage curves measured at three different points from the bottom edge of a membrane 40 cm long. This figure demonstrates that the diffusion-boundary layer grows as the feed solution nears the upper edge of the membrane.

In the cell 3 the empirical equations of the limiting-current density to the length of the membrane show as follows:

for NEOSEPTA AVS-4T:

$$i_{lim} = 50L^{-0.45} \tag{12}$$

for NEOSEPTA CL-2.5T:

$$i_{lim} = 30L^{-0.45} \tag{13}$$

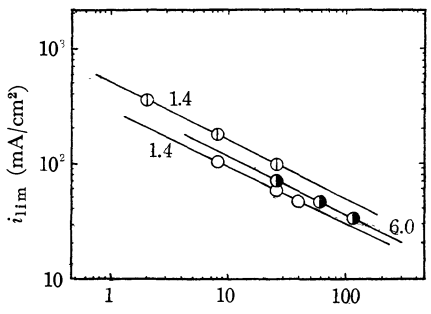

Fig. 6. The effect of a length of the membrane in the direction of flow on the limiting-current density.
Cell: cell 3 for AVS-4T or CL-2.5T
cell 4 for a pair of AVS-4T and CL-2.5T
Solution: sea water (Cl: 0.52 N) in laminar flow at 28.0°C
Numbers in the figure are the flow velocity of the solution (cm/sec).
① AVS-4T, ○ CL-2.5T,
◑ AVS-4T and CL-2.5T

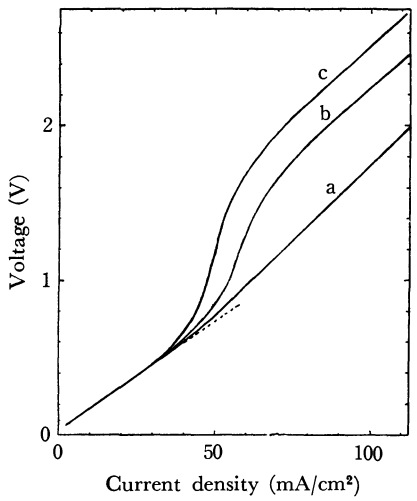

Fig. 7. Current-voltage curves measured at three different points in a membrane having a length of 40 cm in the direction of flow.
a : Measured at a distance of 2.0 cm from bottom edge of a membrane,
b : Measured at a distance of 20.0 cm from the bottom edge of a membrane,
c : Measured at a distance of 38.0 cm from the bottom edge of a membrane.
Membrane: CL-2.5T (with cell 3)
Solution: sea water (Cl: 0.52 N) in laminar flow at 28.0°C.

where L is the total length of the membrane in the direction of the flow (cm). For the cell 4 containing a pair of membranes, NEOSEPTA AVS-4T and CL-2.5T, the following equation is obtained:

$$i_{lim} = 35L^{-0.48} \tag{14}$$

These results show that the limiting-current density is approximately proportional, inversely, the one-half power of the membrane length in the laminar flow.

The concentration of the solution on both sides of the membrane was the same when the current-voltage curves were measured in the cells 1, 3 and 5. However, in practical electrodialyzers one side of the membrane is in contact with the concentrated solution, and the other, with the desalted. An electrolyte diffuses through the membrane from the concentrating compartment to the desalting. Accordingly, the effect on the limiting-current density of the diffusion of the electrolyte through the membrane must be considered in a practical electrodialyzer. If the amount of the electrolyte which diffuses through the membrane is introduced into Eq. (1), Eq. (1) is modified as follows:

$$i_{lim} = \frac{FC_b}{(t_m - t_s)\delta}\left\{D + \left(\frac{C_c}{C_b}\right)\left(\frac{D_m}{\delta_m}\right)\delta\right\} \tag{15}$$

where δ_m is the thickness of the membrane; D_m, the diffusion coefficient of the electrolyte through

the membrane, and C_c, the concentration of the concentrated solution. It was estimated from Eq. (15) that the limiting-current density increased about 4.7% in the cell 4 (the membrane length was 120 cm, the limiting-current density was 35 mA/cm², the concentration of the concentrated solution was 4.0 N, and D_m/δ_m was 2.7×10^{-6} cm/sec).

All the experiments mentioned above were performed in solutions of sodium chloride or sea water. It is apparent in Eqs. (4) and (5) that the limiting-current density changes with the ionic species as a result of the differences in the transport number and the diffusion coeffcient in the free solution, and in the viscosity of the solution. The relation of the limiting-current density in the natural convection to the diffusion coefficient and the transport numbers in various electrolytes (*e.g.*, sodium chloride, lithium chloride, potassium chloride, calcium chloride, hydrogen chloride, cupric chloride and ammonium chloride) is shown in Fig. 8; it agrees with the relation of Eq. (5).

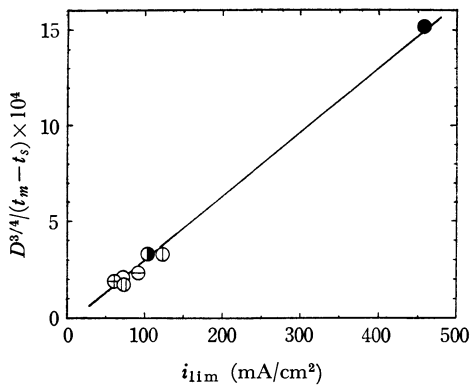

Fig. 8. The relation of the diffusion coefficient and transport numbers of the counterion in the membrane and solution to the limiting current density.
Membrane: CL-2.5T (with cell 5)
Solution: 0.5 N aqueous solution in natural convection at 25.0°C
● HCl, ⊕ LiCl, ⊖ NaCl, ⓘ KCl, ⓘ $CaCl_2$, ◑ NH_4Cl, ○ $CuCl_2$

With barium chloride, ferric chloride and aluminium chloride, the limiting-current density was not obtained because the current-voltage curve did not show any inflexion point or because their hydroxide precipitated on the surface of the membrane at a current density lower than the inflexion point.

If the current-voltage curve was measured in a solution containing two ionic species of the counterion, and if their limiting-current density differed from one another, the current-voltage curve might show two different limiting-current densities. An experiment was carried out with the anion-exchange membrane, NEOSEPTA AVS-4T, inserted in a mixed solution of sodium chloride and sodium sulfate. However, two different limiting-current densities were not observed; rather a limiting-current density was observed between the limiting-current densities observed in chloride and sulfate solutions.

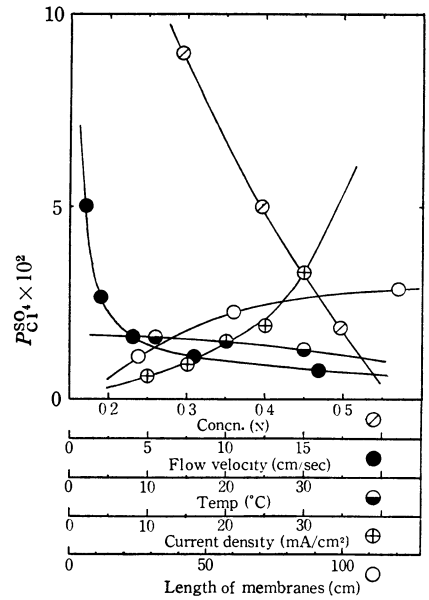

Fig. 9. The effect of conditions of the electrodialytic concentration of sea water on the relative transport numbers of SO_4^{2-} to Cl^-.
The conditions are shown in Table 3.

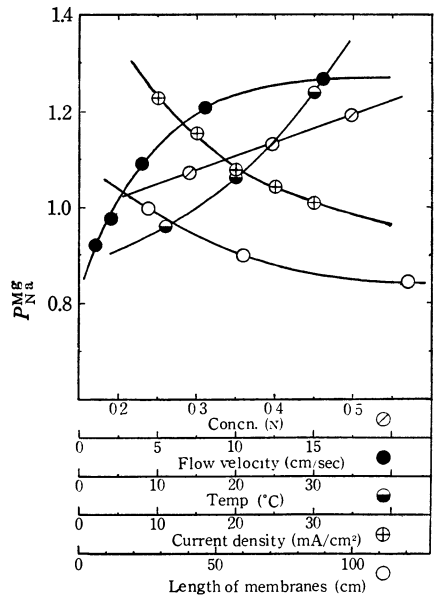

Fig. 10. The effect of conditions of the electrodialytic concentration of sea water on the relative transport numbers of Mg^{2+} to Na^+.
The conditions are shown in Table 3.

In a multiple-ionic-species system, the change in the diffusion-boundary layer causes a difference of the composition of ions at the membrane-solution interfaces from that in the bulk solution, so that the relative transport numbers between ions change. The concentration ratio at the desalting membrane-solution interface of sulfate to chloride ions, which pass through the anion-exchange membrane more easily than do sulfate ions, increases in comparison with that of the bulk solution when the electrodialysis is carried out at a low concentration, a low flow velocity, a low temperature, and a high current density and with a long membrane. Consequently, the transport number of sulfate ions increases, as is shown in Fig. 9. Inversely, the concentration ratio at the desalting membrane-solution interface of magnesium to sodium ions, which pass through the cation-exchange membrane with more difficulty than do magnesium ions, decreases in comparison with that of the bulk solution when the electrodialysis is carried out at a low concentration, a low flow velocity, a low temperature, and a high current density and with a long membrane. Consequently, the transport number of magnesium ions decreases, as is shown in Fig. 10. The condition of the diffusion-boundary layer has a remarkable influence on the relative transport numbers.

After all, the limiting-current density and the relative transport number are relative values; they vary with the condition of the diffusion-boundary layer.

The authors wish to thank Mr. S. Miyoshi for his valuable comments and advice.

BULLETIN OF THE CHEMICAL SOCIETY OF JAPAN VOL. 42 2748—2755 (1969)

A New Acidity Function, T_0, in Acid-catalyzed Reactions

Haruo TAKAYA, Naoyuki TODO and Tadasuke HOSOYA

The Government Chemical Industrial Research Institute, Tokyo, Shibuya-ku, Tokyo

(Received December 16, 1968)

In acid-catalyzed reaction systems a new acidity function, T_0, which is related to the first-order rate constant, k_1, by the equation $\log k_1 = C - T_0$ was defined by $T_0 = -\log (a_{H^+}/a_w^{h_5-h_1} f^{\neq})$ and was theoretically calculated in much the same manner as in Glueckauf's treatments on a salt solution but with the additional assumption that the character of a hydrated univalent activated complex is represented by that of a hydrated alkali metal cation. The calculated results show that T_0 in hydrochloric acid can be represented by:

$$T_0 = 2.4(3.9 - h_1 + h_5) \log a_w - \log m_a.$$

This equation shows that if the hydration number (the water molecules bound with an activated complex) of an activated complex, h_1, increases by one, the corresponding increment of T_0 becomes $-2.4 \log a_w$. It was also shown that the value of $f_{AH^+} f_B / f_A f_{BH^+}$ is not always constant, but depends on the hydration numbers of the AH^+ and BH^+ species as well as on the acid concentrations. The factors affecting the acidity function, T_0, were compared with those affecting the activity of water. The applicability of the T_0 was examined by means of the observed $\log k_1$ value reported by Bunnett.

The following mechanisms of acid-catalyzed[1] reactions in moderately concentrated acid solutions have been proposed by Bunnett,[2-5]

$$S(H_2O)h_5 + H^+(H_2O)h_2 \rightleftharpoons SH^+(H_2O)h_6 + (h_2 + h_5 - h_6)H_2O \quad (1)$$

$$SH^+(H_2O)h_6 + (h_1 - h_6)H_2O \rightleftharpoons [SH^+(H_2O)h_1]^{\neq} \xrightarrow{\text{A}} P \quad (2)$$

Adding Eq. (1) to Eq. (2) we obtain

$$S(H_2O)h_5 + H^+(H_2O)h_2 + (h_1 - h_2 - h_5)H_2O \overset{K_1}{\rightleftharpoons} [SH^+(H_2O)h_1]^{\neq} \quad (3)$$

$$[SH^+(H_2O)h_1]^{\neq} \xrightarrow{\text{A}} P \quad (4)$$

The reaction rate, v, can be expressed by Eq.(5):

$$v = km^{\neq} = \frac{kK_1 a_{H^+} f_S}{k_2 a_w^{h_5 - h_1} f^{\neq}} m_5 \quad (5)$$

where K_1, the equilibrium constant of Eq.(3), and K_2, the dissociation constant of protonated water, are given by Eq.(6) and Eq.(7) respectively:

$$K_1 = \frac{f^{\neq} m^{\neq}}{f_S m_5 a_{H^+(H_2O)h_2} a_w^{h_1 - h_2 - h_5}} \quad (6)$$

1) In this paper only strong univalent acids are considered as catalysts.

2) J. F. Bunnett, *J. Am. Chem. Soc.*, **83**, 4956 (1961).
3) J. F. Bunnett, *ibid.*, **83**, 4968 (1961).
4) J. F. Bunnett, *ibid.*, **83**, 4973 (1961).
5) J. F. Bunnett, *ibid.*, **83**, 4978 (1961).

$$K_2 = \frac{a_{H^+}}{a_{H^+(H_2O)h_2} a_w{}^{-h_2}} = 1 \quad (7)^{6)}$$

Equations (5), (6) and (7) can also be summarized by Eq.(8):

$$\log k_1 = C - T_0 \quad (8)$$

where: $k_1 = v/m_5$,[7] (9)

$$C = \log (kK_1/K_2) \quad (10)$$

and $$T_0 = -\log (a_{H^+} f_S / a_w{}^{h_5 - h_1} f^{\neq}) \quad (11)$$

we can introduce T_0 as a new acidity function, while C is constant, independent of the concentration of acid.

Hammett and Deyrup defined the acidity function, H_0, as is shown in Eq. (12):

$$H_0 = -\log \frac{a_{H^+} f_A}{f_{AH^+}} \quad (12)$$

Its value was obtained by observing m_{AH^+} and m_A:

$$\log \frac{m_{AH^+}}{m_A} = C - H_0, \quad (13)$$

where they assumed $h_2=1$ and $h_5=0$. Furthermore they mainly determined the $f_A f_{BH^+}/f_{AH^+} f_B$ values of aromatic amines in acid solutions and found that these values were constant, independent of the A and B species as well as of the concentration and the sort of acid. Zucker and Hammett[9,10] have proposed a hypothesis which is useful in distinguishing A-1 mechanisms from A-2 mechanisms.

If the reaction proceeds according to an A-1 mechanism, h_1 is zero and Eq. (14) can be derived from Eq. (8):

$$\log k_1 = C + \log \frac{a_{H^+} f_S}{f_{SH^{\neq}}}$$

$$= C + \log \frac{a_{H^+} f_A}{f_{AH^+}} + \log \frac{f_S f_{AH^+}}{f_{SH^{\neq}} f_A} \quad (14)$$

The $-\log (a_{H^+} f_A / f_{AH^+})$ term is Hammett's acidity function, and $\log (f_S f_{AH^+}/f_{SH^{\neq}} f_A)$ is constant;[11,12] hence, Eq. (14) can also be expressed by Eq. (15):

$$\log k_1 = C - H_0 \quad (15)$$

If the reaction proceeds according to an A-2 mechanism, h_1 is one; they postulated empirically that $\log k_1$ is given by Eq. (16):

$$\log k_1 = C + \log m_a \quad (16)$$

while the Zucker-Hammett hypothesis described above, though it would be useful in distinguishing A-1 from A-2 mechanisms, has been sharply criticized by several authors[2,13,14] and has not been accepted as reasonable.

The Bunnett equation (Eq. (17))[3] can also be derived from Eq. (8); Eq. (18) is thus obtained:

$$\log k_1 = C - H_0 - w \log a_w, \quad (17)$$

$$\log k_1 = C + \log \frac{a_{H^+} f_A}{f_{AH^+}} + (h_5 - h_1) \log a_w + \log \frac{f_S f_{AH^+}}{f_{SH^{\neq}} f_A} \quad (18)$$

If the term of $f_S f_{AH^+}/f_{SH^{\neq}} f_A$ is constant, the last one in Eq. (18) becomes zero; Eq. (18), therefore, becomes equivalent to Eq. (17) when we replace w and H_0 with $(h_1 - h_5)$ and $-\log (a_{H^+} f_A / f_{AH^+})$ respectively. Bunnett discussed the reaction mechanism in terms of the value of w. Its value, however, can not be considered to be the hydration number contained in an activated complex, because such large values as 7 and 8 have been obtained. Hence, the value of w must be used only as an fitting parameter for experimental data.

The main features of this study are that an activated complex is considered to be a univalent cation and that the acidity function, T_0, is theoretically derived by applying the treatment described by

6) K_2 in Eq. (7) is put to be equal to 1. This was done in view of the following facts: in Hammett's treatment of a dilute acid solution, $H_0 = -\log m_a = \mathrm{pH}$ is defined. This automatically involves the $m_a = a_{H^+}$ relation: in other words, the acid concentration, m_a, is equal to the activity of the non-hydrated proton, a_{H^+}. Also, $a_{H^+(H_2O)h_2}$ and a_w can, as usual, be defined as being equal to m_a and 1 respectively.

However, in a dilute acid solution, the species related to m_a is not H^+ but $H^+(H_2O)_{h_2}$. Therefore, as a means to definition $m_a = a_{H^+}$ seems less reasonable than $m_a = a_{H^+(H_2O)h_2}$. The more reasonable definitions of T_0 and H_0 both of which are equal to $-\log m_a$ in dilute acid solutions, are given by Eq. (11a) and Eq. (12a) respectively:

$$T_0 = -\log (a_{H^+(H_2O)h_2} f_S / a_w{}^{h_2 + h_5 - h_1} f^{\neq}) \quad (11a)$$

$$H_0 = -\log (a_{H^+(H_2O)} f_A / a_w f_{AH^+}) \quad (12a)$$

Here, if $K_2=1$, Eq. (11a) and Eq. (12a) are equal to Eq. (11) and Eq. (12) respectively.

7) In the above calculation, the first-order rate constant, k_1, was defined as the v/m_5 quantity. This is an approximation of the correct expression, $k_1 = v/(m_1 + m_5 + m_6)$. However, in the relations now under consideration, and in ordinary acid-catalyzed reactions as well, both m_1 and m_6 are negligibly small as compared with m_5; hence, this approximation is reasonable.

8) L. P. Hammett and A. J. Deyrup, *J. Am. Chem. Soc.*, **54**, 2721 (1932).

9) F. A. Long and M. A. Paul, *Chem. Revs.*, **57**, 935 (1957).

10) L. Zucker and L. P. Hammett, *J. Am. Chem. Soc.*, **61**, 2791 (1939).

11) The value of $f_{SH^{\neq}}$ is assumed to very in essentially the same way as f_{SH^+} in both Hammett's and this paper.

12) It is doubtful whether we can extend the relation in which the $\log (f_{AH^+} f_B / f_A f_{BH^+})$ of Hammett base is constant to the S substrate, for S is not a Hammett base.

J. Hine, "Physical Organic Chemistry," Second Ed., McGraw-Hill, Kogakusha, New York, San Francisco, Toronto, London, Tokyo (1956), p. 55.

13) R. W. Taft, Jr., N. C. Deno and P. S. Skell, *Ann. Rev. Phys. Chem.*, **9**, 306 (1958).

14) R. P. Bell, "The Proton in Chemistry," Cornell University Press, Ithaca, N. Y. (1959).

Glueckauf[15] and by Moriyama[16] who showed that an a thermal mixing assumed for the salt solutions led to a reasonable representation of the observed activity coefficients of salt and acids.[17] One of the features which distinguishes our treatment from Hammett's is the difference in the hydration number[18] of the proton: in Hammett's treatment, the value of the hydration number, h_2, must be 1, whereas the h_2 taken in our treatment is 3.9, a value which is widely accepted.[19] The calculated acidity function, T_0, has been represented as a function of the hydration number of an activated complex, the activity of water, and the concentration of the acid. From the calculated results it has been verified that the value of $f_A f_{BH^+}/f_{AH^+} f_B$ depends on the hydration numbers of AH^+ and BH^+ as well as on the concentrations of the acids. Our results, therefore, differ from Bunnett's because his results were obtained by assuming that the value of $f_A f_{BH^+}/f_{AH^+} f_B$ is constant, independent of the A and B species as well as of the concentration and the sort of acid.

Symbols Used

The following list gives the symbols used in this study.

h_1, h_2, h_3, h_5, h_6: hydration numbers of activated complex, proton, univalent anion, substrate, and protonated substrate respectively

$h=h_2+h_3$: hydration number of acid

a_{H^+}, $a_{H^+(H_2O)_{h_2}}$, $a_w=a_4$: activities of proton, hydrated proton, and water respectively

k, $k_1=v/m_5$: rate constant and the first-order rate constant respectively

n_1, n_2, $n_3=n_a=n_1+n_2$, n_4, $n_5=n_S$: numbers of molecules in hydrated activated complex, hydrated proton, hydrated univalent anion, free water, and hydrated substrate respectively

$m_1=m^{\neq}$, m_2, m_3, m_5, m_6: molalities of activated complex, proton, anion, substrate, and protonated substrate respectively

$m_a=m_3$: molality of acid

$n_w=n_1h_1+n_2h_2+n_3h_3+n_4+n_5h_5$: total number of water molecules

$n_R=n_1+n_5$: total number of substrates

$\bar{v}_1$, $\bar{v}_2$, $\bar{v}_3$, $\bar{v}_5$, $\bar{v}_4$: partial molar volumes of hydrated activated complex, hydrated proton, hydrated univalent anion, and hydrated substrate respectively, and that of free water. These values were treated as constant in this study.

$V=n_1\bar{v}_1+n_2\bar{v}_2+n_3\bar{v}_3+n_4\bar{v}_4+n_5\bar{v}_5$: total volume of the solution

μ_1, μ_2, μ_3, μ_5, μ_4: chemical potentials of hydrated activated complex, hydrated proton, hydrated anion, and hydrated substrate respectively, and that of free water

μ_i°: chemical potential in the standard state of ith species

$f_{SH^{\neq}}=f^{\neq}$, f_{SH^+}, f_S, f_A, f_B, f_{AH^+}, f_{BH^+}: activity coefficients of hydrated activated complex, hydrated protonated substrate, hydrated substrate, hydrated substrate A, hydrated substrate B, hydrated protonated substrate AH^+, and hydrated protonated substrate BH^+ respectively

S, A, B: substrates

SH^+, AH^+, BH^+: protonated substrates

k: Boltzmann's constant

T: absolute temperature

Theoretical

Model of the Reaction System. The acid-catalyzed reaction system consists of the following five kinds of species: hydrated activated complexes, hydrated protons, hydrated univalent anions, free water, and hydrated substrates. The Gibbs free energy of this system may be calculated in much the same manner as in Glueckauf's treatment of a salt solution, with additional assumptions. Since the structure of an activated complex is too complicated for its exact contribution to the Gibbs free energy to be evaluated, it is assumed that the character of a hydrated univalent activated complex is represented by that of a hydrated alkali metal cation. It is furthermore assumed that a substrate is neutral and that its volume[20] is that of alkali metal in solution. On the other hand, for a substrate the salting-out effect must be considered. Conway[21] theoretically calculated this effect by considering two phenomena: the hydration of ions and the change in the dielectric constant of water due to the solute present in the solution. The former is automatically taken into account in this study, because ions are always treated as

15) E. Glueckauf, *Trans. Farad. Soc.*, **51**, 1235 (1955).

16) M. Moriyama and T. Sugita, *Denki Kagaku (J. Electrochem. Soc. Japan)*, **25**, 617 (1957).

17) Bascombe theoretically derived the acidity function, H_0, by the application of Glueckauf's treatment of a salt solution, though the details of the theoretical derivation were not described.
K. N. Bascombe and R. P. Bell, *Discussions Faraday Soc.*, **24**, 158 (1957).

18) In this study the Gibbs free energy has been obtained by calculating the entropy; thus, the water molecules in hydration should be tightly bound with the ion.

19) 3.9 was taken from Ref. 12. Wicke, Eigen and Ackermann, *Z. Phys. Chem.*, **1**, 340 (1954). Th. Ackermann, *Discussion Faraday Soc.*, **24**, 180 (1957). M. Eigen and L. De Maeyer, "Article in the Structure of Electrolyte Solution," Ed. by W. J. Hamer, John Wiley and Sons, New York, N. Y. (1959).

20) In view of the co-volume effects of ions, Glueckauf obtained the activity of ions. On the other hand, the molar volume of a neutral substrate determines the dependency of its activity coefficient on the acid concentration.[24] Hence, among various physical properties belonging to a neutral substrate, the molar volume is the most predominant in the calculation of the activity.

21) B. E. Conway, J. E. Desnoyers and A. C. Smith, *Phil. Trans. Roy. Soc. London*, **256**, 389 (1964).

hydrated in the calculation of the Gibbs free energy. Therefore, only the contribution from the latter is formally introduced as $G^{s.o.}$ in the equation.

Taking the five species (four hydrated species and free water mentioned above) as the standard state in the calculation of the Gibbs free energy of the system, and subjecting them to athermal mixing, the Gibbs free energy of mixing, $\Delta G'^{mix.}$, is given by Eq. (19):

$$\Delta G'^{mix.} = \boldsymbol{k}T\sum_{i=1}^{5} n_i \ln \frac{n_i\bar{v}_i}{V}. \tag{19}$$

The fundamental equation of the total free energy of the mixing of the system can, therefore, be obtained by adding the electrostatic effect, $G^{el.}$,[22] caused by the interaction between ions, and $G^{s.o.}$ to Eq. (19):

$$\begin{aligned}\Delta G^{mix.} &= \sum_{i=1}^{5} n_1\mu_i - \sum_{i=1}^{5} n_i\mu_i^0 \\ &= \boldsymbol{k}T\sum_{i=1}^{5} n_i \ln \frac{n_i\bar{v}_i}{V} + G^{el.} + G^{s.o.}\end{aligned} \tag{20}$$

The Acidity Function, T_0. To find the equation of the acidity function, T_0, the variation in the free energy in the process of the formation of the activated complex must be evaluated. As is shown by Eq. (3), a hydrated activated complex molecule is formed by the consumption of one hydrated proton molecule and one hydrated substrate molecule, leaving free water molecules $(h_2+h_5-h_1)$. This process corresponds to the partial differentiation of the total free energy with respect to n_1 at constant n_w, n_3 and n_R values, as is shown by Eq. (21):

$$\begin{aligned}\left(\frac{\partial\Delta G^{mix.}}{\partial n_1}\right)_{n_w,\,n_3,\,n_R} &= (\mu_1-\mu_1^0) - (\mu_2-\mu_2^0) \\ &+ (h_2+h_5-h_1)(\mu_4-\mu_4^0) - (\mu_5-\mu_5^0) \\ &= \boldsymbol{k}T\left[\ln n_1 - \ln n_2 - \ln n_5 + (h_2+h_5-h_1)\ln\frac{n_4\bar{v}_4}{V}\right. \\ &+ \ln\frac{V}{\bar{v}_4} - \left(\sum_{i=1}^{5} n_i\right)\frac{(\bar{v}_1-h_1\bar{v}_4-\bar{v}_2+h_2\bar{v}_4-\bar{v}_5+h_5\bar{v}_4)}{V} \\ &\left.+ \ln\frac{\bar{v}_1\bar{v}_4}{\bar{v}_2\bar{v}_5} + (h_2+h_5-h_1) - 1\right] + \left(\frac{\partial G^{el.}}{\partial n_1}\right) \\ &+ \left(\frac{\partial G^{s.o.}}{\partial n_1}\right)\end{aligned} \tag{21}$$

From Eq. (21) the acidity function, T_0, can be derived:

$$\begin{aligned}T_0 &= -\log\frac{a_{H^+}f_S}{a_w^{h_5-h_1}f^*} \\ &= -\log m_a + (h_2+h_5-h_1)\log\frac{(1-0.018\,hm_a)}{(1+0.018\,rm_a)} \\ &+ \log(1+0.018\,rm_a) \\ &+ \frac{0.434\times0.018m_a(r+h-2)\Delta h}{1+0.018\,rm_a} \\ &+ \frac{0.434}{\boldsymbol{k}T}\left\{\left(\frac{\partial G^{el.}}{\partial n_1}\right)+\left(\frac{\partial G^{s.o.}}{\partial n_1}\right)\right\}\end{aligned} \tag{22}$$

22) The value of $G^{el.}$ takes account of the electrostatic interaction among ions in the aqueous solution when there is no neutral substrate in it.

where the term of $\ln(\bar{v}_1\bar{v}_4/\bar{v}_2\bar{v}_5)+(h_2+h_5-h_1)-\ln 0.018-\Delta h$ is omitted because this term is independent of the concentration of acid. The following six relationships were used for the sake of simplicity:

$$n_i = 0.018\,m_in_w \tag{23}$$

$$h = h_2 + h_3 \tag{24}$$

$$r\bar{v}_4 = (\bar{v}_2+\bar{v}_3) - (h_2+h_3)\bar{v}_4 \tag{25}$$

$$\Delta h\bar{v}_4 = (\bar{v}_1-h_1\bar{v}_4) - (\bar{v}_2-h_2\bar{v}_4) - (\bar{v}_5-h_5\bar{v}_4) \tag{26}$$

$$\mu_i - \mu_i^0 = \boldsymbol{k}T\ln a_i = \boldsymbol{k}T\ln f_im_i \tag{27}$$

$$m_1,\ m_5 \ll m_2 \tag{28}$$

$(0.434/\boldsymbol{k}T)(\partial G^{el.}/\partial n_1)$ in Eq. (22) corresponds to the difference in electrostatic contribution between a hydrated proton and a hydrated activated complex to the Gibbs free energy in an acid. This difference may be small because of the small difference in radius between a hydrated proton and a hydrated alkali metal cation.[23] Its approximate value can be calculated from the difference in the logarithms of the mean activity coefficients, $f_\pm^{el.}$, due to only the electrostatic effect between a hydrated proton in acid and a hydrated alkali metal cation in salt present in the solution. The value of $\log f_\pm^{el.}$ is represented as:

$$\log f_\pm^{el.} = -\frac{0.509\sqrt{I}}{1+0.329\times10^8a\sqrt{I}}$$

where I is the ionic strength and where "a" is the arbitrary parameter, which can be interpreted as the shortest distance from the center of a cation to that of an anion. We then obtain:

$$\begin{aligned}\frac{0.434}{\boldsymbol{k}T}\left(\frac{\partial G^{el.}}{\partial n_1}\right) &= -\frac{0.509\sqrt{I}}{1+0.329\times10^8a_1\sqrt{I}} \\ &+ \frac{0.509\sqrt{I}}{1+0.329\times10^8a_2\sqrt{I}}\end{aligned} \tag{29}$$

where a_1 and a_2 are arbitrary parameters of a salt and an acid respectively.

The $(0.434/\boldsymbol{k}T)(\partial G^{s.o.}/\partial n_1)$ term in Eq. (22) is neglected, for the molar volume of a neutral substrate (that of alkali metal in our model) is small.[24] Conway[21] also showed that this term was small for a small neutral substrate.

Results

Results of Calculation. For the calculation of the hydration terms in Eq. (22), the hydration numbers of Li^+, Na^+, K^+, and Rb^+ were taken from the results tabulated by Glueckauf.[15] The values of $\bar{v}_1$, $\bar{v}_2$, $\bar{v}_3$, and $\bar{v}_5$[19] were taken from the results computed by Noyes[25] and were treated as

23) R. H. Stokes and R. A. Robinson, *J. Am. Chem. Soc.*, **70**, 1870 (1948).

24) F. A. Long and W. F. McDevit, *Chem. Revs.*, **51**, 119 (1952).

25) R. M. Noyes, *J. Am. Chem. Soc.*, **86**, 971 (1964).

Table 1. T_0 calculated by Eq. (22) in the case of Li^+ in hydrochloric acid at 25°C

Molality	0.1	0.5	1.0	2.0	3.0
I	1.000	0.301	0.000	−0.301	−0.477
II	−0.002	−0.011	−0.023	−0.048	−0.075
III	0.001	0.004	0.008	0.016	0.023
IV	0.000	−0.002	−0.005	−0.009	−0.013
V	−0.001	−0.001	−0.002	−0.004	−0.004
T_0	0.998	0.291	−0.022	−0.346	−0.546

$h_1=3.4$, $\Delta h=-0.50$, $\bar{v}_5=6.9\,ml$, $r=1.00$, $h=4.8$, $h_5=0$

I, $-\log m_a$

II, $(h_2+h_5-h_1)\log(1-0.018\,hm_a)/(1+0.018\,rm_a)$

III, $\log(1+0.018\,rm_a)$

IV, $0.434\times0.018\,m_a(r+h-2)\Delta h/(1+0.018\,rm_a)$

V, $(0.434/kT)(\partial G^{el}/\partial n_1)$

Table 2. T_0 calculated by Eq. (22) in the case of Na^+ in hydrochloric acid at 25°C

Molality	0.1	0.5	1.0	2.0	3.0
I	1.000	0.301	0.000	−0.301	−0.477
II	−0.008	−0.042	−0.087	−0.182	−0.285
III	0.001	0.004	0.008	0.016	0.023
IV	−0.001	−0.006	−0.012	−0.023	−0.033
V	−0.001	−0.003	−0.006	−0.012	−0.018
T_0	0.991	0.254	−0.097	−0.502	−0.790

$h_1=2.0$, $\Delta h=-0.41$, $\bar{v}_5=11.8\,ml$, $h_5=0$

Table 3. T_0 calculated by Eq. (22) in the case of K^+ in hydrochloric acid at 25°C

Molality	0.1	0.5	1.0	2.0	3.0
I	1.000	0.301	0.000	−0.301	−0.477
II	−0.013	−0.073	−0.152	−0.317	−0.495
III	0.001	0.004	0.008	0.016	0.023
IV	−0.001	−0.003	−0.007	−0.013	−0.020
V	−0.001	−0.007	−0.013	−0.026	−0.039
T_0	0.986	0.222	−0.164	−0.641	−1.008

$h_1=0.6$, $\Delta h=-0.24$, $\bar{v}_5=13.2\,ml$, $h_5=0$

Table 4. T_0 calculated by Eq. (22) in the case of Rb^+ in hydrochloric acid at 25°C

Molality	0.1	0.5	1.0	2.0	3.0
I	1.000	0.301	0.000	−0.301	−0.477
II	−0.015	−0.086	−0.180	−0.375	−0.588
III	0.001	0.004	0.008	0.016	0.023
IV	0.000	−0.003	−0.005	−0.011	−0.016
V	−0.002	−0.009	−0.017	−0.034	−0.051
T_0	0.984	0.207	−0.194	−0.705	−1.106

$h_1=0$, $\Delta h=-0.19$, $\bar{v}_5=17.1\,ml$, $h_5=0$

constants.

The calculated values of T_0 at various concentrations of the hydrochloric acid solution for the formation of the activated complex ions are shown in Tables 1—4, where the activated complex ions are represented by Li^+, Na^+, K^+, and Rb^+. These tables show that the contribution from the hydration to T_0 is predominant, whereas that from the electrostatic is small. In Fig. 1 $-T_0$, $-H_0$, and $\log m_a$ are plotted against the acid concentration, m_a. In the case of Rb^+, the hydration number of which is zero, $-T_0$ is largest and the deviation of the T_0 from $\log m_a$ is nearly equal to H_0. On the contrary, in the case of Li^+, the hydration number of which is 3.4, $-T_0$ is small and nearly equal to $\log m_a$. In order to determine the correlation of $-T_0$ with the hydration number of the activated complex, the $-T_0$ values in a hydrochloric acid solution at a molality of 3 are plotted *versus* the hydration number in Fig. 2. Figure 2 shows that $-T_0$ increases linearly with the hydration number. Therefore, the T_0 can be represented as in Eq. (30):

$$T_0 = -0.161(3.9-h_1+h_5) - \log m_a, \qquad (30)$$

where h_2 is 3.9. Since the value of $\log a_w$ is −0.068 at the molality of hydrochloric acid of 3, Eq. (30) can be rewritten as:

$$T_0 = 2.4(3.9-h_1+h_5)\log a_w - \log m_a \qquad (31)$$

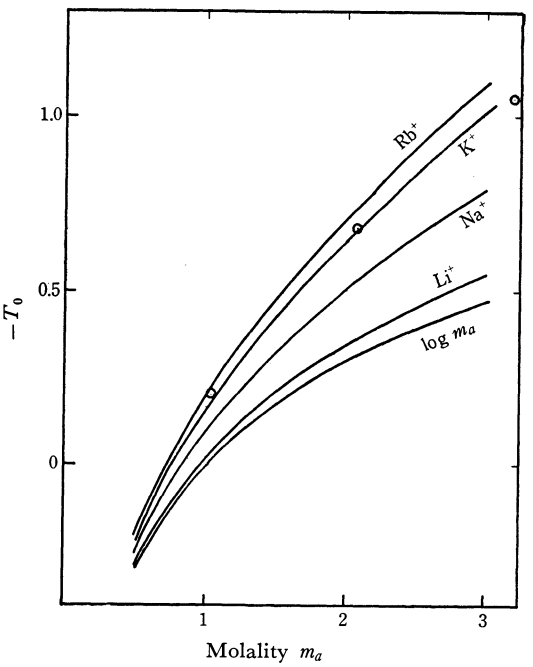

Fig. 1. $-T_0$, $-H_0$* and $\log m_a$ *versus* the molality of hydrochloric acid, m_a, at 25°C. Hydration number of Rb^+, K^+, Na^+, and Li^+ are 0, 0.6, 2.0, and 3.4 respectively.

○ observed $-H_0$

* M. A. Paul and F. A. Long, *Chem. Revs.*, **57**, 1 (1957).

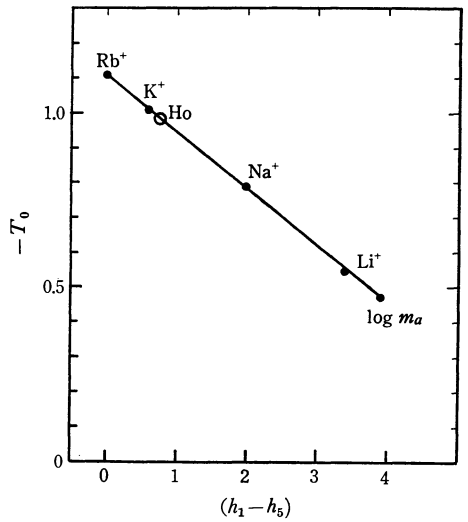

Fig. 2. $-T_0$ *versus* (h_1-h_5) at the molality of hydrochloric acid of 3 at 25°C. Since h_5, the hydration number of a substrate, can be assumed to be 0, (h_1-h_5) becomes equal to h_1, which is the number of water molecules contained in an activated complex. The hydration number of aromatic amines, which was used to determine H_0, becomes apparently 0.7 from this figure.

TABLE 5. T_0 CALCULATED BY EQ. (22) IN THE CASE OF Rb^+ IN NITRIC ACID AT 25°C

Molality	0.1	0.5	1.0	2.0	3.0
I	1.000	0.301	0.000	−0.301	−0.477
II	−0.019	−0.090	−0.179	−0.359	−0.550
III	0.002	0.008	0.014	0.026	0.038
IV	0.000	−0.003	−0.005	−0.011	−0.016
V	−0.002	−0.009	−0.017	−0.034	−0.051
T_0	0.981	0.225	−0.187	−0.679	−1.056

$r=1.68$, $h=3.9$

TABLE 6. T_0 CALCULATED BY EQ. (22) IN THE CASE OF Rb^+ IN PERCHLORIC ACID AT 25°C

Molality	0.1	0.5	1.0	2.0	3.0
I	1.000	0.301	0.000	−0.301	−0.477
II	−0.031	−0.113	−0.222	−0.425	−0.655
III	0.004	0.012	0.023	0.038	0.056
IV	−0.001	−0.003	−0.007	−0.013	−0.018
V	−0.002	−0.009	−0.017	−0.034	−0.051
T_0	0.970	0.188	−0.223	−0.735	−1.145

$r=2.51$, $h=4.2$

For nitric acid and perchloric acid, the calculated values of T_0 are shown in Tables 5 and 6 and in Fig. 3. From these results, the respective acidity

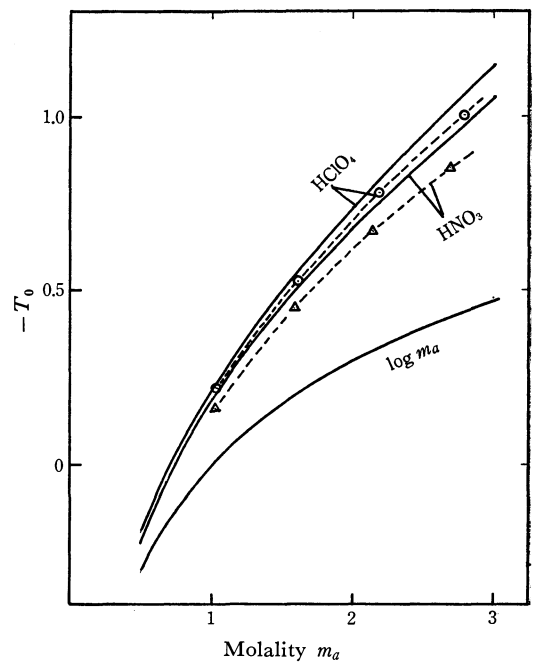

Fig. 3. $-T_0$, $-H_0$,* and $\log m_a$ *versus* the molality of nitric acid and perchloric acid, m_a at 25°C.
—— calculated $-T_0$
····· observed $-H_0$
* M. A. Paul and F. A. Long, *Chem. Revs.*, **57**, 1 (1957).

functions, T_0, for these solutions are given by Eqs. (32) and (33):
in nitric acid solutions:

$$T_0 = -0.148(3.9-h_1+h_5) - \log m_a$$
$$= 2.3(3.9-h_1+h_5)\log a_w - \log m_a \quad (32)$$

in perchloric acid solutions:

$$T_0 = -0.171(3.9-h_1+h_5) - \log m_a$$
$$= 2.3(3.9-h_1+h_5)\log a_w - \log m_a \quad (33)$$

The contribution from the electrostatic effect in these acid solutions is assumed to be the same as in hydrochloric acid solutions.

Discussion

Consideration with Respect to T_0. The most important conclusion is that if the h_1 increases by one, the corresponding increment of T_0 is $-2.4\log a_w$. If we considered only the behavior of water, however, the increment would be $-\log a_w$, because the disappearance of one molecule of free water is related to the increase of h_1 by one. In order to investigate this difference, let us compare the factors affecting the activity of water in the reaction system with those affecting the acidity function, T_0.

The activity of water can be determined from the

free-energy change due to the introduction of one molecule of water into the acid solution. The equation for this free-energy change can be obtained by differentiating Eq. (20) with respect to n_w at constant n_1, n_2, n_3, and n_5 values. The equation thus obtained is:

$$\left(\frac{\partial \Delta G^{mix.}}{\partial n_w}\right)_{n_1, n_2, n_3, n_5} = \left(\frac{\partial \Delta G^{mix.}}{\partial n_4}\right)_{n_1, n_2, n_3, n_5}$$

$$= \mu_4 - \mu_4^0 = \boldsymbol{k}T\left[\ln \frac{n_4\bar{v}_4}{V} + \left(1 - \frac{\sum_{i=1}^{5} n_i \partial V}{V\ \partial n_4}\right)\right] \quad (34)$$

The first term of Eq. (34) is the contribution due to the increase in the number of water molecules, while the second is that due to the volume increase of the solution caused by the increase in the number of water molecules. Using the relations represented by Eq. (23)—(28), we can obtain:

$$\log a_w = \log \frac{1-0.018\, hm_a}{1+0.018\, rm_a} + \frac{0.434\times 0.018(r+h-2)m_a}{1+0.018\, rm_a} \quad (35)$$

The first and second terms in Eq. (35) correspond to the second and fourth terms in Eq. (22) respectively. As is shown in Table 7, the value of each term in Eq. (35) is comparable in order to the absolute magnitude, while in Eq. (22) (see Table 4) the second term, responsible for the increase in the number of water molecules, contributes to T_0 predominantly, and the contribution of the fourth term, related to the increase in the volume of the system (which was caused by the formation of the activated complex), is small. The large increase in the volume in the calculation of water activity may be attributed to the introduction of a water molecule into the system from outside. While the small volume change in the calculation of T_0 is ascribed to the fact that the system is closed; the total numbers of the water molecule, n_w, the substrate, n_R, and acid, n_a, are constant. Since the number of water molecules freed from a hydrated proton upon the formation of an activated complex is $(h_2+h_5-h_1)$, the contribution of these water molecules to T_0 becomes $(h_2+h_5-h_1)\log a_w$. This means that the increase of h_1 by one contributes $-\log a_w$ to T_0. However, it is not enough to evaluate the small change in volume described above in the calculation of T_0 through only the value of $-\log a_w$.

Table 7. $\log a_w$ calculated by Eq. (35) in hydrochloric acid solution at 25°C

Molality	0.1	0.5	1.0	2.0	3.0
I	−0.004	−0.022	−0.046	−0.096	−0.150
II	0.003	0.014	0.028	0.056	0.082
$\log a_w$	−0.001	−0.008	−0.018	−0.040	−0.068

$r=1.00$, $h=4.8$
I, $\log(1-0.018\, hm_a)/(1+0.018\, rm_a)$
II, $0.434\times 0.018(r+h-2)m_a/(1+0.018\, rm_a)$

Consideration of the Salting-out Effects. The activity coefficient of a neutral substrate in this study can be obtained by differentiating Eq. (20) with respect to n_5, with no change of n_1, n_2, n_3, and n_4 and with $h_5=0$:

$$\log f_5 = -\log(1+0.018\, rm_a) + \frac{0.434\times 0.018(\bar{v}_5/\bar{v}_4)(r+h-2)m_a}{1+0.018\, rm_a} \quad (36)$$

The calculated values of $\log f_5$ in the case of Rb have been tabulated in Table 8. The values are small, increase linearly with the concentration of acid, and are almost independent of the sort of acids. In Table 9 the observed values of $\log f$ of hydrogen are tabulated at the molality of 1.[24] It has been known that the salting-out effects increase almost linearly with the molar volume of a substrate.[24] The value of $\log f$ of Rb represented in Table 9 were, therefore, obtained by multiplying the $\log f$ of hydrogen by 0.65, the ratio of the molar volume of Rb to that of hydrogen. Good agreements between the calculated values of Tables 8 and 9 are observed in hydrochloric acid and in nitric acid, though there is a large discrepancy in perchloric acid. This discrepancy probably results from neglecting the $(0.434/\boldsymbol{k}T)(\partial G^{s.o.}/\partial n_1)$ term. If this term could be exactly estimated, the discrepancy might be adjustable.[26]

Table 8. $\log f_5$ of Rb calculated by Eq. (36) in acid solutions at 25°C

Molality	0.1	0.5	1.0	2.0	3.0
in HCl	0.002	0.009	0.019	0.037	0.055
in HNO_3	0.001	0.006	0.013	0.024	0.035
in $HClO_4$	0.001	0.007	0.014	0.026	0.037

$\bar{v}_5=17.1$ m*l*

Table 9. $\log f$ of hydrogen observed at a molality of 1 and values of $\log f_5$ of Rb calculated by multiplying the $\log f$ of hydrogen by 0.64

	Hydrogen[24]	Rb
HCl	0.036	0.020
HNO_3	0.022	0.014
$HClO_4$	−0.030*1	−0.019

$\bar{v}_5$ of hydrogen is 26 m*l*.
*1 Calculated from the value of benzene.

26) Conway[21] calculated the salting-out effect in view of the two phenomena mentioned above; however, further phenomena such as the structure-making influence of non-polar solutes[21] must be taken into account in calculating the exact value of the salting-out effect.

The Value of $(f_A f_{BH^+}/f_{AH^+} f_B)$. As was described in the first paragraph, Hammett and Deyrup found that the value of $(f_A f_{BH^+}/f_{AH^+} f_B)$ determined with aromatic amines was constant, independent of the species, A or B, as well as of the concentrations and of the sort of acids. However, it can be shown by the following procedure that this value is not always constant. The value of the acidity function, T_0, of the "0" system is compared with that of the "1" system at the same concentration of hydrochloric acid, where the "0" system and the "1" system are defined as the systems of $(h_1-h_5)=0$ and 1 respectively. From Eq. (31) we can obtain:

$$\Delta T_0 = T_{00} - T_{01} = 2.4 \log a_w \tag{37}$$

where the $_0$ and $_1$ subscripts represent the "0" system and the "1" system respectively. From the definition of T_0, in Eq. (11):

$$\Delta T_0 = -\log \frac{a_{H^+} f_{S_0}}{f_0^{\ddagger}} + \log \frac{a_{H^+} f_{S_1}}{a_w^{-1} f_1^{\ddagger}}$$

$$= -\log \frac{f_{S_0} f_1^{\ddagger}}{f_0^{\ddagger} f_{S_1}} + \log a_w \tag{38}$$

From Eqs. (37) and (38), Eq. (39) can then be derived:

$$-\log \frac{f_{S_0} f_1^{\ddagger}}{f_0^{\ddagger} f_{S_1}} = 1.4 \log a_w \tag{39}$$

Eq. (39) shows that the values of $(f_A f_{BH^+}/f_{AH^+} f_B)$ is not always constant,[12] but depends on the hydration number of the AH^+ and BH^+ species as well as on the acid concentration.

Bunnett's equation (17) was derived by considering the relation $(f_A f_{BH^+}/f_{AH^+} f_B)$ to be constant. If the w or (h_1-h_5) is increased by one, the increment of $\log k_1$ is $\log a_w$ in his treatment, but 2.4 $\log a_w$ in our treatment.

Comparison between the Observed $\log k_1$ and the T_0. Using Eq. (8), Eq. (31), and the dependence of $\log k_1$ upon the concentration of acid, we can obtain the hydration number of an activated complex or the number of water molecules contained in an activated complex.[18] The applicability of T_0 can be examined by comparing the T_0 and the observed $\log k_1$. Bunnett reported that, for many reactions, the values of w were fairly evenly distributed from -2 to $+8$.[2] If the hydration number of an activated complex increases from 0 to 3.9 in hydrochloric acid at the molality of 3, T_0 varies from -1.106 to -0.477; also, this variation in T_0 corresponds to that in w from -1.8 to 9.2. The fact that the ranges of the distribution of w observed for many reactions agree with those of the variation in T_0 indicates that the dependence of $\log k_1$ on the concentration of acid is effected mainly through the hydration number of an activated complex, because, as is shown in Tables 1—6, the variation in T_0 can be explained mainly by the hydration effect. Also, this fact would allow us to obtain the approximate number of water molecules contained in an activated complex by the application of T_0 to $\log k_1$. The more accurate numbers must be obtained by estimating the value of the salting-out effect exactly.

The relation between H_0 and T_0 is much the same as that between T_0 and $\log k_1$. The hydration number of aromatic amines, which was used to determine H_0, apparently becomes 0.7 when we apply T_0 to H_0, as is shown in Fig. 2.

BULLETIN OF THE CHEMICAL SOCIETY OF JAPAN VOL. 42 2756—2762 (1969)

Effects of Substitution on the Phosphorescence Process of Aromatic Carbonyl Compounds

Takeshi TAKEMURA and Hiroaki BABA

Division of Chemistry, Research Institute of Applied Electricity, Hokkaido University, Sapporo

(Received December 29, 1968)

Phosphorescence and absorption spectra, phosphorescence- and excitation-polarization spectra and phosphorescence lifetimes were measured at 77°K for benzaldehyde, acetophenone and their eight derivatives with a halogen atom, or a hydroxyl, methoxyl or amino group as a substituent at the *para* position. In chloro- and bromo-derivatives, the phosphorescent triplet state is of the (n, π^*) type, and is mixed with the $^1L_a(\pi, \pi^*)$ state by direct spin-orbit interaction, as in the case of the parent carbonyls. In addition, owing to the heavy-atom effect, it gains its singlet character by the mechanism

$$^1(\sigma, \pi^*) \text{ or } ^1(\pi, \sigma^*) \overset{\text{S.O.}}{\longleftrightarrow} {}^3L_a(\pi, \pi^*) \overset{\text{Vib.}}{\longleftrightarrow} {}^3(n, \pi^*)$$

which accounts for the observation that the phosphorescence spectrum involves out-of-plane-polarized vibrational bands. Substitution of a more electron-donating hydroxyl, methoxyl, or amino group brings about a change of the phosphorescent state from the $^3(n, \pi^*)$ state to the $^3L_a(\pi, \pi^*)$. The following mechanisms are shown to be important to the $^3L_a(\pi, \pi^*)$ state:

$$^1(n, \pi^*) \overset{\text{S. O.}}{\longleftrightarrow} {}^3L_a\ (\pi, \pi^*)$$

$$\begin{array}{ccc} & ^1(n, \pi^*) & \\ \overset{\text{Vib.}}{\nearrow}\downarrow & & \overset{\text{S.O.}}{\nwarrow}\downarrow \\ ^1L_a(\pi, \pi^*) & & {}^3L_a(\pi, \pi^*) \\ \underset{\text{S.O.}}{\nwarrow}\downarrow & & \underset{\text{Vib.}}{\nearrow}\downarrow \\ & ^3(n, \pi^*) & \end{array}$$

These account for two progressions with mutually perpendicular polarizations observed in the phosphorescence spectrum. The lifetimes for the transitions from the $^3L_a(\pi, \pi^*)$ state to the ground state of the substituted carbonyls were found to be substantially shorter than the corresponding lifetimes in aromatic hydrocarbons. This fact is quantitatively interpreted as due to the presence of a low-lying $^1(n, \pi^*)$ state.

The radiative process in aromatic carbonyl compounds has been a subject of considerable interest.[1-8] In typical aromatic carbonyls such as benzophenone and acetophenone, the lowest triplet state is of (n, π^*) character, and this fact is believed to lead not only to the characteristic phosphorescence with a short lifetime but also to the high photochemical reactivity of these compounds.[9-11] Perturbation by a suitable substituent or a polar solvent may produce a change in the lowest triplet state from an (n, π^*) to a (π, π^*) type, and this change is expected to be accompanied by an essential change in both the spectral and chemical behaviors of the carbonyl compounds. Studies along these lines have recently been reported.[7-12] In particular, even for weakly perturbed acetophenones like *p*-bromo- and *p*-

1) S. K. Lower and M. A. El-Sayed, *Chem. Revs.*, **66**, 199 (1966).
2) Y. Kanda, H. Kaseda and T. Matumura, *Spectrochim. Acta*, **20**, 1387 (1964).
3) V. G. Krishna, *J. Mol. Spectry.*, **13**, 296 (1964).
4) Shimada and L. Goodman, *J. Chem. Phys.*, **43**, 2027 (1965).
5) J. Dehler and F. Dörr, *Tetrahedron Letters*, **1965**, 2155.
6) M. Akagi, Y. Amako and H. Azumi, *Nippon Kagaku Zasshi (J. Chem. Soc. Japan, Pure Chem. Sect.)*, **87**, 689 (1966).
7) D. R. Kearns and W. A. Case, *J. Am. Chem. Soc.*, **88**, 5087 (1966).
8) A. A. Lamola, *J. Chem. Phys.*, **47**, 4810 (1967).
9) G. Porter and P. Suppan, *Trans. Faraday Soc.*, **61**, 1664 (1965).
10) E. J. Baum, J. K. S. Wan and J. N. Pitts, Jr., *J. Am. Chem. Soc.*, **88**, 2652 (1966).
11) N. C. Yang, D. S. McClure, S. L. Murov, J. J. Houser and R. Dusenbery, *ibid.*, **89**, 5466 (1967).
12) H. Baba and T. Takemura, This Bulletin, **40**, 2215 (1967).

methylacetophenone, the lowest triplets were assigned to (π, π^*) states on the basis of S→T absorption spectra obtained by the phosphorescence excitation method.[7,11]

In this study the effects of substitution on the phosphorescence process of aromatic carbonyl compounds have been examined through spectroscopic analysis, polarization and lifetime measurements. Special attention was paid to the polarization of phosphorescence and excitation in relation to the mechanism of spin-orbit coupling. Several *para*-substituted benzaldehydes and acetophenones were investigated. Hydroxyl and amino derivatives display emission characteristics that are definitely ascribable to the lowest triplet state of (π, π^*) type, while the phosphorescent states of halogen derivatives appear to be of (n, π^*) from the results of polarization measurements.

An extensive polarization study was made by Shimada and Goodman[4] on carbonyl compounds including the unsubstituted benzaldehyde and acetophenone.

Experimental

Materials. All the reagents used were obtained from Wako Pure Chemical Industries, Osaka. Benzaldehyde, acetophenone and *p*-chloroacetophenone were purified by vacuum distillation, and *p*-chlorobenzaldehyde, *p*-bromobenzaldehyde and *p*-bromoacetophenone by repeated zone melting. *p*-Hydroxybenzaldehyde, *p*-hydroxyacetophenone and *p*-aminoacetophenone were recrystallized from water and from ethanol, and were further purified by vacuum sublimation. *p*-Methoxybenzaldehyde was fractionally crystallized several times.

Isopentane was refluxed over phosphorus pentoxide, and subjected to fractional distillation. Methylcyclohexane of spectroscopic quality was used without further purification. Ethyl ether was refluxed over metallic sodium, distilled, and was then passed through a freshly activated alumina column.

Apparatus and Procedure. Absorption spectra were obtained with a Hitachi EPS-3 spectrophotometer at 77°K or at room temperature. Emission and excitation spectra and their polarization were measured at 77°K with an apparatus which was constructed in our laboratory.[13] Emission spectra obtained were uncorrected for the spectral sensitivity of the detector. In polarization measurements, monochromatic light, obtained from a combination of 150-W xenon lamp and a grating monochromator (Hitachi G-3), passed through a Frank-Ritter-prism polarizer and irradiated the sample. The light emitted perpendicular to the excitation beam passed through another Frank-Ritter prism as analyzer and a quartz-prism monochromator (Hitachi EPU-2A), and it was then detected by a 1P-28 photomultiplier tube. The polarized spectra were recorded on an X-Y recorder.

The degree of polarization, P, is defined as

$$P = (I_{\parallel} - I_{\perp})/(I_{\parallel} + I_{\perp})$$

where $I_{\parallel}$ and $I_{\perp}$ are the intensities of the emitted light polarized respectively parallel and perpendicular to the exciting light which is polarized with the electric vector perpendicular to the plane formed by the excitation beam and the emission beam. The P values were corrected in the usual manner[14] for instrumental and other factors.

All the absorption and emission measurements at 77°K were carried out on rigid-glass samples in a 1-cm square quartz cell placed in a glass Dewar with quartz windows.

Phosphorescence lifetimes were measured using a Becquerel type phosphoroscope combined with a synchroscope.

Results

Figures 1—5 show absorption spectra (A), phosphorescence spectra (P), phosphorescence-polarization spectra (PP) and excitation-polarization spectra (EP) with respect to phosphorescence for benzaldehyde and its derivatives, *p*-chloro-, *p*-bromo-, *p*-hydroxy- and *p*-methoxybenzaldehyde (abbreviated to Cl-, Br-, OH- and OMe-benz-

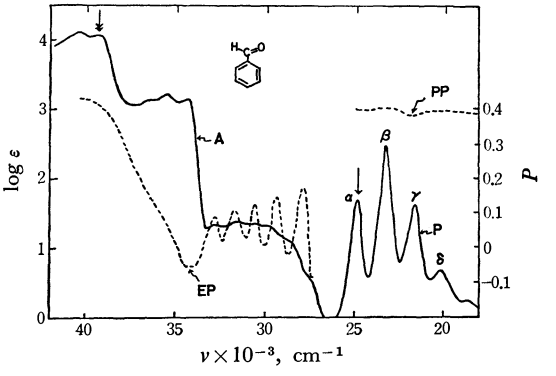

Fig. 1. Absorption, phosphorescence and polarization spectra of benzaldehyde in PME at 77°K.

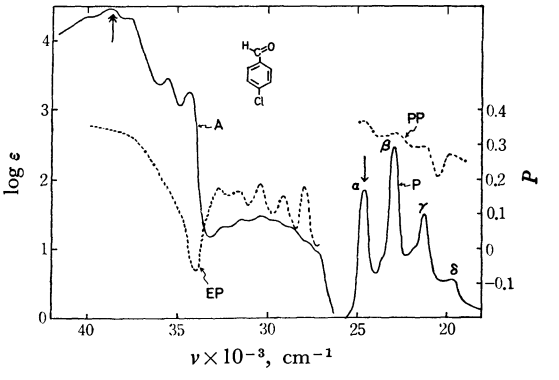

Fig. 2. Absorption, phosphorescence and polarization spectra of *p*-chlorobenzaldehyde in PME at 77°K.

13) S. Suzuki, *Bull. Res. Inst. Appl. Elec., Hokkaido Univ.*, **19**, 20 (1967).

14) T. Azumi and S. P. McGlynn, *J. Chem. Phys.*, **37**, 2413 (1962).

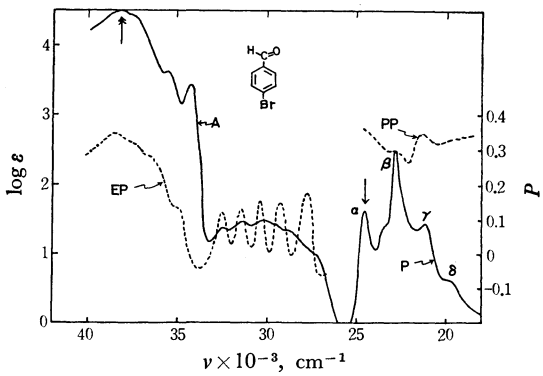

Fig. 3. Absorption, phosphorescence and polarization spectra of *p*-bromobenzaldehyde in PME at 77°K.

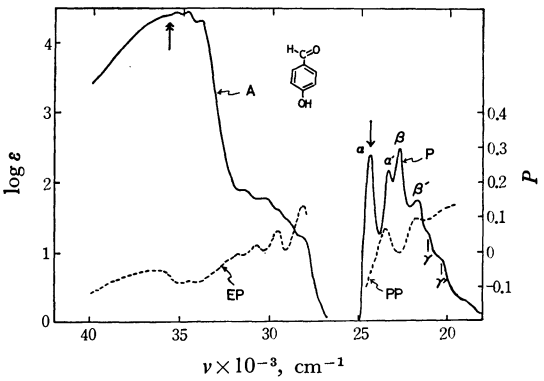

Fig. 4. Absorption, phosphorescence and polarization spectra of *p*-hydroxybenzaldehyde in PME at 77°K.

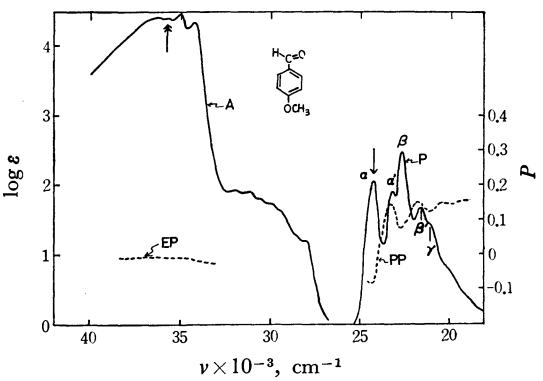

Fig. 5. Absorption, phosphorescence and polarization spectra of *p*-methoxybenzaldehyde in PME at 77°K.

aldehyde, respectively). Similar spectra are shown in Figs. 6—10 for acetophenone and its derivatives, *p*-chloro-, *p*-bromo-, *p*-hydroxy- and *p*-amino-acetophenone (abbreviated to Cl-, Br-, OH- and NH_2-acetophenone, respectively). The excitation and emission frequencies adopted in the polarization measurements are indicated by →→ and →,

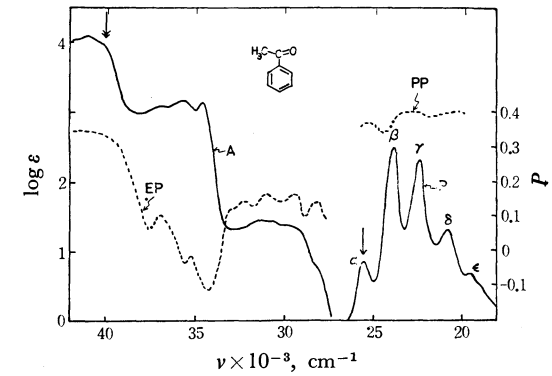

Fig. 6. Absorption, phosphorescence and polarization spectra of acetophenone in PME at 77°K.

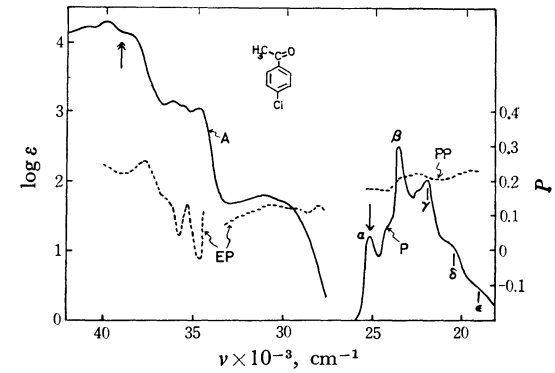

Fig. 7. Absorption, phosphorescence and polarization spectra of *p*-chloroacetophenone in PME at 77°K.

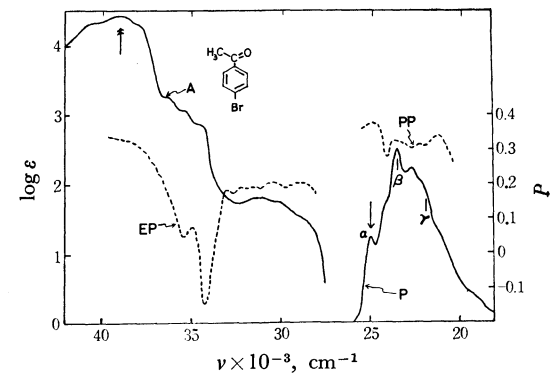

Fig. 8. Absorption, phosphorescence and polarization spectra of *p*-bromoacetophenone in PME at 77°K.

respectively.

All these spectra were measured at 77°K in an isopentane-methylcyclohexane-ether (PME) mixture (volume ratio, 7.7 : 1.3 : 1). Although it was desirable to use the hydrocarbons alone as the solvent for reducing the solvent perturbation, ether had to be added so that the solute might have the minimum solubility. Nevertheless, no well-

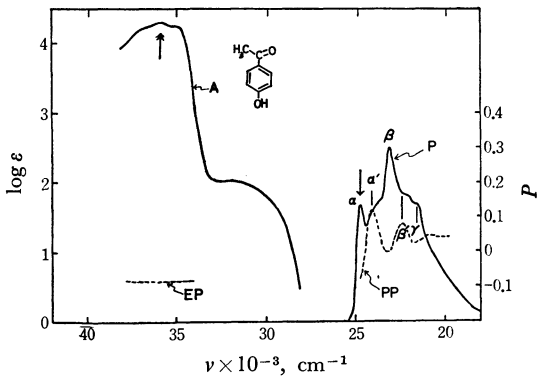

Fig. 9. Absorption, phosphorescence and polarization spectra of *p*-hydroxyacetophenone in PME at 77°K.

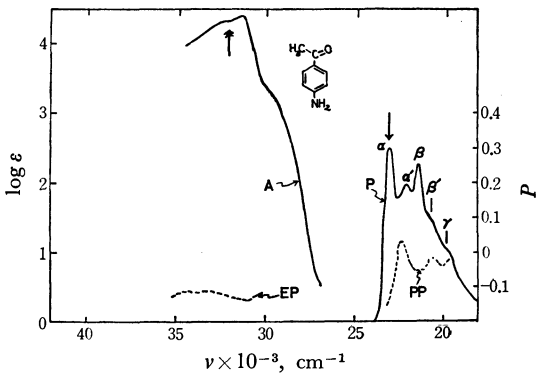

Fig. 10. Absorption, phosphorescence and polarization spectra of *p*-aminoacetophenone in PME at 77°K.

resolved absorption spectra could be obtained at 77°K in the lowest frequency ($n\rightarrow\pi^*$) region, because of the still low solubility at that temperature. However, the excitation spectra were obtained with a good resolution in the same region.

Detailed spectral data on the excitation polarization in the $n\rightarrow\pi^*$ region for two representative compounds, benzaldehyde and OH-benzaldehyde are shown in Fig. 11, together with the absorption

Table 1. Observed and calculated phosphorescence lifetimes

Compound	τ_{obs} sec	τ_{calc} sec
Benzaldehyde	0.0026	
p-Chlorobenzaldehyde	0.024	
p-Bromobenzaldehyde	0.0070	
p-Hydroxybenzaldehyde	0.14	0.15
p-Methoxybenzaldehyde	0.11	0.13
Acetophenone	0.0043	
p-Chloroacetophenone	0.060	
p-Bromoacetophenone	0.010	
p-Hydroxyacetophenone	0.50	0.28
p-Aminoacetophenone	0.86	0.58

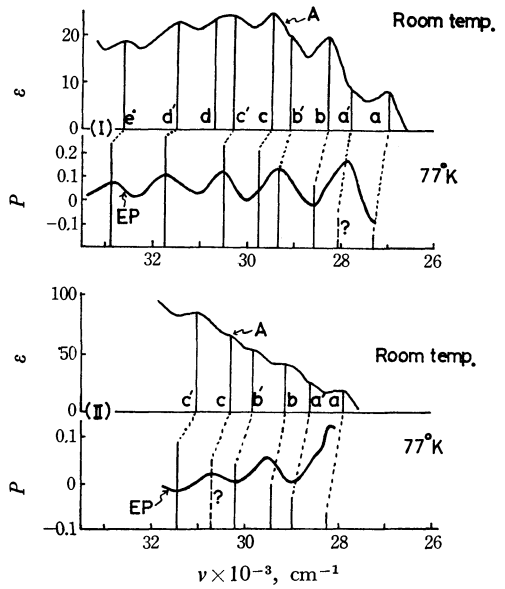

Fig. 11. Excitation-polarization spectra with respect to the phosphorescence 0-0 band in PME at 77°K and absorption spectra in PME at room temperature for benzaldehyde (I) and *p*-hydroxybenzaldehyde (II) in the region of the $n\rightarrow\pi^*$ transition. The location of absorption peaks is shown by vertical lines, the lengths of which represent the molar extinction coefficients, ε. The scale of ε values for the absorption peaks at 77°K is the same as that for the peaks at room temperature.

peaks observed at 77°K. For the sake of comparison, the absorption spectra at room temperature are also given in this figure.

The results of the polarization measurements for benzaldehyde and acetophenone are essentially the same as those reported by Shimada and Goodman,[4] although they employed EPA as the solvent.

The results of the phosphorescence lifetime measurements are recorded in Table 1.

Discussion

Spectral Changes due to Substitution. Benzaldehyde shows three electronic absorption bands in the near ultraviolet region (Fig. 1). The weak absorption band located at 30000 cm^{-1} is due to an $n\rightarrow\pi^*$ transition, and the other two to $\pi\rightarrow\pi^*$ transitions. The bands at 35000 cm^{-1} and 40000 cm^{-1} are assigned respectively to $^1A\rightarrow{}^1L_b$ and $^1A\rightarrow{}^1L_a$ (or an intramolecular charge-transfer) transitions.[4]

The ionization energies of the substituents concerned in this study are in the order $Cl\gtrsim Br> OH\gtrsim OCH_3> NH_2$.[15] The ^1L_a band is markedly

15) F. A. Matsen, "Chemical Applications of Spectroscopy," ed. by W. West, Interscience, New York (1956), p. 673.

shifted to lower frequencies with the decrease of the ionization energy of the substituent (Figs. 2—5). On the other hand, substitution produces no appreciable change in the position of the ^1L_b band, and thus in OH- and OMe-benzaldehyde the latter band is almost hidden under the stronger ^1L_a band. The substitution has no appreciable effect on the position of the $n\rightarrow\pi^*$ band. It may be noted, however, that the $n\rightarrow\pi^*$ band is slightly displaced to the red by chlorine and bromine and to the blue by OH and OMe groups.

The unsubstituted benzladehyde exhibits a phosphorescence spectrum with a well-defined and simple vibrational structure, but the structures of the phosphorescence spectra of the substituted benzaldehydes are more or less complicated.

The foregoing descriptions of the absorption and phosphorescence spectra of benzaldehyde and its derivatives apply on the whole to the spectra of acetophenone and its derivatives (Figs. 6—10).

Polarization. The polarization behaviors of the spectra of the carbonyl compounds studied can be classified into two types, one represented by benzaldehyde and the other by OH-benzaldehyde. Actually, these compounds belong to the symmetry group C_s, but their electronic structure may be discussed in terms of the structure of C_{2v} molecules. The resolution of the representations of C_{2v} into those of C_s is shown in Table 2, the coordinate axes being given in Fig. 12. It should be noted that for the carbonyl compounds concerned the lowest vacant π orbital is of b_1 type,[16] and the n orbital is of b_2 type.

Table 2. Resolution of representations

C_{2v}	C_s
$A_1(z)$	$A'(y, z, R_x)$
$A_2(R_z)$	$A''(x, R_y, R_z)$
$B_1(x, R_y)$	$A''(x, R_y, R_z)$
$B_2(y, R_x)$	$A'(y, z, R_x)$

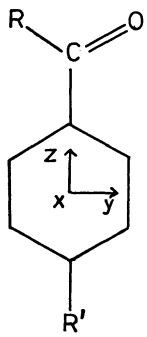

Fig. 12. Structure and coordinate axes for the carbonyl compounds. The x axis is perpendicular to the molecular plane.

16) K. Inuzuka and T. Yokota, This Bulletin, **37**, 1224 (1964).

The $^1A\rightarrow{}^1L_a$ and $^1A\rightarrow{}^1L_b$ transitions are $^1A_1\rightarrow{}^1A_1$ and $^1A_1\rightarrow{}^1B_2$ analogue transitions, respectively. The $n\rightarrow\pi^*$ band is due to a $^1A_1\rightarrow{}^1A_2$ analogue transition, which is forbidden in the C_{2v} molecules but changes to a symmetry-allowed transition $^1A'\rightarrow{}^1A''$ as a result of the lowering of symmetry from C_{2v} to C_s. Thus, in each of the two representative molecules, benzaldehyde and OH-benzaldehyde, the vibrational progression a, b, c, *etc.* (see Fig. 11) is attributable to the symmetry-allowed transition, with the band a as the 0—0 band. On the other hand, the $n\rightarrow\pi^*$ transition may steal intensity from the $^1A\rightarrow{}^1L_a$ through a vibronic interaction involving an a_2 analogue vibration.[4] This mechanism may account for the second progression a′, b′, c′, *etc.* of the $n\rightarrow\pi^*$ transitions.

To sum up, the $^1A\rightarrow{}^1L_a$ absorption and the a′-progression of the $n\rightarrow\pi^*$ absorption are polarized along the long axis (z) of the molecule and the $^1A\rightarrow{}^1L_b$ is along the short axis (y), while the a-progression of the $n\rightarrow\pi^*$ absorption should be polarized perpendicular to the molecular plane (x axis).*1

For benzaldehyde (Figs. 1 and 11), the excitation-polarization spectrum with respect to emission at the phosphorescence 0-0 band, α, is consistent with the view that the phosphorescence 0-0 band is polarized in the molecular plane and along the long axis.[4] The degree of polarization, P, of the phosphorescence with respect to excitation into the $^1A\rightarrow{}^1L_a$ absorption shows highly positive values which are nearly constant throughout the phosphorescence spectrum. This implies that the phosphorescence spectrum of benzaldehyde consists almost of a single progression, α, β, *etc.*, with the 0—0 band α as its first member.

The excitation-polarization spectra of Cl- and Br-benzaldehyde are essentially the same as that of benzaldehyde. Thus the phosphorescence 0-0 band, α, of the halo-derivatives must be polarized along the long axis. On the other hand, the phosphorescence-polarization spectra of these derivatives show distinct variations in the P value. This fact together with the features of their phosphorescence spectra suggests that the phosphorescence spectra involve a progression which differs in polarization from the main progression including the 0-0 band.

The excitation- and phosphorescence-polarization spectra of acetophenone and its chloro- and bromo-derivatives are on the whole similar to the corresponding spectra of benzaldehyde and its chloro- and bromo-derivatives, respectively. Therefore, the preceding discussions on the latter molecules are applicable to the former as well. It is to be noted, however, that in acetophenone the phosphorescence-polarization spectrum shows an

*1 The progressions starting from the bands a and a′ are called a- progression and a′-progression, respectively.

appreciable variation in the P value, which is not found in the case of benzaldehyde.

The situation is radically changed on going from benzaldehyde to OH-benzaldehyde. Thus, with respect to emission at the phosphorescence 0-0 band, α, the excitation-polarization spectrum of OH-benzaldehyde shows negative P values in the region of the $^1A \rightarrow {}^1L_a$ band and minimum values of P at the vibrational peaks of the a'-progression, whereas the P values are positive at the peaks of a-progression (Figs. 4 and 11). Further, the P values appear to be negative in the region of $^1A_1 \rightarrow {}^1L_b$ absorption, which is not clearly separated from the $^1A_1 \rightarrow {}^1L_a$ absorption. These observations lead to the conclusion that the phosphorescence 0-0 band α is polarized perpendicular to the molecular plane.

Inspection of the phosphorescence and phosphorescence-polarization spectra of OH-benzaldehyde shows that, in addition to the out-of-plane-polarized α-progression, there is an inplane-polarized progression, α', β', *etc.*, which is polarized along the long axis. The spacing between successive bands of each of the α- and α'- progressions is about 1550 cm^{-1}. The origin (band α') of the latter progression is situated about 900 cm^{-1} from the 0-0 band to the red.

The polarization characteristics and spectral features of OCH_3-benzaldehyde, and OH- and NH_2-acetophenone (Figs. 5, 9 and 10) are similar to those of OH-benzaldehyde mentioned above.

Mechanisms of Spin-Orbit Coupling and Assignment of the Phosphorescent States. The polarization data may be explained by considering the mechanisms of spin-orbit coupling in the carbonyl compounds. The following discussions are based on a few assumptions.[1] (1) The perturbation of the ground state by triplet states is negligible. (2) The first-order spin-vibronic perturbation is negligible. (3) The spin-orbit operator, H_{SO}, can be approximated as a sum of one-electron operators. According to these assumptions, spin-orbit coupling through H_{SO} occurs only between electronic states resulting from one-electron excitations which take place either from the same occupied molecular orbital or to the same vacant orbital. The phosphorescent state of benzaldehyde can be assigned to the $^3A_2(n, \pi^*)$ analogue,[4] which couples directly with the $^1A_1$ (π, π^*) state through the first order spin-orbit perturbation, $H_{SO}(R_z)$. We can write as

$$^1L_a(\pi, \pi^*) \overset{\text{S.O.}}{\longleftrightarrow} {}^3(n, \pi^*) \qquad (1)$$

The above mechanism accounts for the polarization features in the compounds of the benzaldehyde type, namely, the long-axis polarization of the α-progression, including the 0-0 band, of the phosphorescence spectra. The effective spin-orbit perturbation of the first order along with the high intensity of the $^1A \rightarrow {}^1L_a$ transition should result in very short phosphorescence lifetimes for these compounds. This is indeed the case, as seen in Table 1.

The aromatic carbonyl compounds are considered to have the $^3L_a(\pi, \pi^*)$ state close to the $^3(n, \pi^*)$ state. Because of the small energy difference between the two triplet states, an effective vibronic interaction involving an a_2 analogue vibration is expected to occur, so that the $^3(n, \pi^*)$ state will be mixed with singlet states through the second-order spin-orbit-vibronic perturbation. In most aromatic hydrocarbons, $^3(\pi, \pi^*)$ states are known to gain their singlet characters by direct coupling with $^1(\sigma, \pi^*)$ or $^1(\pi, \sigma^*)$ states.[1] Thus, in addition to mechanism (1), the following may also be responsible for the transition $^3(n, \pi^*) \rightarrow S_0$ (ground state):

$$^1(\sigma, \pi^*) \text{ or } {}^1(\pi, \sigma^*) \overset{\text{S.O.}}{\longleftrightarrow} {}^3L_a(\pi, \pi^*) \overset{\text{Vib.}}{\longleftrightarrow} {}^3(n, \pi^*) \qquad (2)$$

In the absence of a heavy atom, mechanism (2) is negligible as compared with mechanism (1). When the molecule contains a heavy atom, the spin-orbit interaction between ^3L_a and $^1(\sigma, \pi^*)$ or $^1(\pi, \sigma^*)$ will be enhanced to increase the relative importance of mechanism (2).[17] Accordingly, the $^3(n, \pi^*) \rightarrow S_0$ transition will be provided with an out-of-plane transition moment.

In the chloro- and bromo-derivatives of benzaldehyde, the phosphorescence-polarization spectra show variations in the P values; there appear minima in the positive P curves. Furthermore, the vibrational structures of the phosphorescence spectra of the halo-derivatives are more or less irregular. These observations can reasonably be explained in terms of mechanism (2).

By following the same reasoning, we can interpret the phosphorescence and phosphorescence-polarization spectra of the chloro- and bromo-derivatives of acetophenone. If this interpretation is correct, however, one problem will remain unsolved. That is, as has been pointed out, the phosphorescence-polarization spectrum of the unsubstituted acetophenone exhibits a variation. This cannot be attributed to mechanism (2), since the acetophenone molecule has no heavy atom. On the other hand, the phosphorescence spectrum itself is fairly simple as in the case of benzaldehyde. This fact suggests that the out-of-plane component should be negligible in the phosphorescence polarization of acetophenone. In any case, further studies are necessary for understanding fully the polarization behavior of the phosphorescence of acetophenone.

The radical changes in polarization produced by substitution of OH, OCH_3 and NH_2 groups can be best understood by taking account of possible

17) M. A. El-Sayed, *J. Chem. Phys.*, **43**, 2864 (1965).

changes in the phosphorescent state. Substitution of such electron-donating groups leads to a considerable lowering of the energy level of the ^1L_a state and to a slight rise of the $^1(n, \pi^*)$ level. If the ^3L_a and $^3(n, \pi^*)$ states behave similarly, the positions of the ^3L_a and $^3(n, \pi^*)$ levels are expected to be reversed, with the result that the ^3L_a state is the lowest triplet in the compounds of the OH-benzaldehyde type.

The mechanisms of the spin-orbit coupling in these molecules were examined on the assumptions mentioned before and also on the premise that the direct spin-orbit coupling between $^1(\pi, \pi^*)$ and $^3(\pi, \pi^*)$ states is vanishingly small.[1] Of the several possible mechanisms the following two seem to be most important:

$$^1(n, \pi^*) \overset{\text{S.O.}}{\longleftrightarrow} {}^3L_a(\pi, \pi^*) \tag{3}$$

$$\begin{array}{ccc} & ^1(n, \pi^*) & \\ \text{Vib.}\nearrow\swarrow & & \nwarrow\text{S.O.} \\ ^1L_a(\pi, \pi^*) & & ^3L_a(\pi, \pi^*) \\ \text{S.O.}\nwarrow\searrow & & \nearrow\swarrow\text{Vib.} \\ & ^3(n, \pi^*) & \end{array} \tag{4}$$

As will be seen later, the lifetime data show that the coupling mechanism which is important for the phosphorescent $^3(\pi, \pi^*)$ state of aromatic hydrocarbons is not operative in the carbonyl compounds in question. Thus, the direct spin-orbit interaction between $^3L_a(\pi, \pi^*)$ and $^1(\sigma, \pi^*)$ or $^1(\pi, \sigma^*)$ is not considered here.

As regards mechanism (3), the transition between the ground state and the perturbing singlet, $^1(n, \pi^*)$, is forbidden in the C_{2v} molecules, but it becomes symmetry allowed in the actual C_s molecules. On the other hand, a large absolute value is anticipated for the matrix element of H_{SO} between the $^1(n, \pi^*)$ and ^3L_a states. Thus, the mechanism (3) plays a major role in the phosphorescence transition, and it accounts for the out-of-plane polarization of the α-progression that includes the 0-0 band.

Mechanism (4) involves second-order interactions. Its importance is considered to be comparable with the importance of mechanism (3), since in the singlet $n\rightarrow\pi^*$ absorption the intensities of the a- and a'-progressions are of comparable magnitudes. Mechanism (4) results in the appearance of the α'-progression which is vibronically induced and is polarized along the long molecular axis.

Mention should be made here of the assignment of the triplet states which was made by Kearns and Case on the basis of singlet→triplet absorption spectra.[7] According to their results, the lowest triplet state is a $^3(n, \pi^*)$ state for benzaldehyde, Br-benzaldehyde and acetophenone, and is a $^3(\pi, \pi^*)$ state for OH-acetophenone, in agreement with the present assignment. As to Br-acetophenone, they assigned the lowest triplet state as a $^3(\pi, \pi^*)$ state, whereas we regard it as a $^3(n, \pi^*)$. Our assignment is based on the observation that the phosphorescence 0-0 band of Br-acetophenone is highly positively polarized with respect to excitation into the $^1A\rightarrow{}^1L_a$ absorption band. Inspection of Figs. 3 and 8 will show that there is no substantial difference in the polarization spectra between Br-benzaldehyde and Br-acetophenone, so that the latter compound should have the same type of phosphorescent state as the former, *viz.*, an (n, π^*) type of phosphorescent state. It should be noted that the discrepancy between the two assignments might result from the difference between the samples employed. (Kearns and Case used a crystalline sample of Br-acetophenone doped with naphthalene.)

Lifetimes. As seen in Table 1, the molecules with the phosphorescent triplet state of (π, π^*) type have relatively long lifetimes. However, they are still markedly shorter than the lifetimes of the $^3(\pi, \pi^*)\rightarrow S_0$ phosphorescence emissions in aromatic hydrocarbons. This problem has recently been noticed by several authors[7,12,18,19] in aromatic azines and carbonyls, and has been discussed from the viewpoint of participation of a low-lying $^1(n, \pi^*)$ state in the spin-orbit coupling.

The matrix element

$$\langle\, ^1(n, \pi^*)|\, H_{SO}\, |^3L_a(\pi, \pi^*)\,\rangle \tag{5}$$

which is associated with mechanisms (3) and (4) can be equated to

$$\langle\, ^1L_a(\pi, \pi^*)|\, H_{SO}\, |^3(n, \pi^*)\,\rangle \tag{6}$$

provided that $^1(n, \pi^*)$ and $^3(n, \pi^*)$ have the same spatial configuration.[20]

In a previous paper,[12] we assumed the matrix element (6) of OH-benzaldehyde to be approximately equal to the corresponding element for the unsubstituted benzaldehyde (*cf.* mechanism (1)), and thus calculated the phosphorescence lifetime of OH-benzaldehyde. Similar calculations were made for molecules whose phosphorescent states have been assigned to the $^3(\pi, \pi^*)$ states in this study. The calculated lifetimes, τ_{calc}, which correspond to the observed lifetimes (rather than to the natural lifetimes) were obtained by assuming that the substitution leads to no change in the phosphorescence quantum yield. This assumption is based on the observation that the phosphorescence intensity was not appreciably changed by substitution. The results are shown in Table 1. In spite of the assumptions involved, the τ_{calc} values are in good agreement with the τ_{obs} values.

18) R. M. Hochstrasser and C. Marzzacco, *J. Chem. Phys.*, **45**, 4681 (1966).
19) L. Vanquickenborne and S. P. McGlynn, *ibid.*, **45**, 4755 (1966).
20) M. A. El-Sayed, *ibid.*, **38**, 2834 (1963).

BULLETIN OF THE CHEMICAL SOCIETY OF JAPAN VOL. 42 2763—2767 (1969)

The Excited States of Acridine Dyes. I. An ESR Study of the Triplet State

Yukio KUBOTA*1 and Masaji MIURA

Department of Chemistry, Faculty of Science, Hiroshima University, Hiroshima

(Received January 8, 1969)

The lowest triplet state of acridine dyes has been studied by an ESR technique over a wide range of concentration and in various solvents. The ESR spectra of the triplet state have been observed at a resonance field of *ca.* 1550 gauss, corresponding to the $\Delta M=2$ transitions. The ESR data characteristic of the triplet state depend on the dye concentration; this has been interpreted as being due to the association of dye molecules. The values of the zero-field splitting parameter, D^*, calculated from the $\Delta M=2$ transition spectra lead to the assignment of the lowest triplet state of acridine dyes as the $(\pi-\pi^*)$ state.

Since the first observation of the ESR spectra of the phosphorescent triplet state of naphthalene molecules in a single crystalline matrix[1] and the ESR observations of the triplet state of randomly-oriented molecules in rigid glass solutions for the forbidden ($\Delta M=2$) transitions[2] and for the allowed ($\Delta M=1$) transitions,[3,4] the ESR technique has provided a powerful tool for the investigation of the triplet states of aromatic, heteroaromatic, and biological molecules. From the ESR measurements, information regarding the zero-field splitting (ZFS) parameters, D and E, the lifetime of the triplet state, and so on may be obtained.

Acridine dyes are of biological interest with regard to their photodynamic and mutagenic actions. It is of great significance to ascertain the nature of the excited states of acridine dyes, since their excited states, especially triplet states, are considered to play an important role in the primary process of photodynamic action.[5]

For this paper, the lowest triplet state of several acridine dyes, mainly acridine orange, proflavine, and acriflavine, have been investigated by the ESR technique over a wide range of concentration and in various solvents.

Experimental

Materials. The acridine orange (Tokyo Kasei) was precipitated as a free base from the aqueous solution by adding a dilute sodium hydroxide solution. The resulting precipitate was dissolved in chloroform, and then the solution was passed through an activated alumina column in chloroform.[6] The eluate containing a main band was filtered to remove any alumina particles. The free base was precipitated by evaporating chloroform under a reduced pressure and was then recrystallized three times from an ethanol-water mixture.

The proflavine (Tokyo Kasei) was also precipitated as a free base in a similar manner. The resulting free base was recrystallized twice from an ethanol-water mixture.

The acriflavine (Tokyo Kasei) was treated twice with freshly-precipitated silver hydroxide in order to remove the proflavine[7] and was then recrystallized twice from methanol.

The acridine (Tokyo Kasei) was recrystallized three times from ethanol. The acridine yellow and acridine red (Tokyo Kasei) were used without further purification. The anthracene (Tokyo Kasei) was recrystallized from ethanol, and the naphthalene (Wako Junyaku) was purified by the sublimation method.

The methanol, ethanol, ether, and ethylene glycol (EG; G. R. of Wako) were purified according to the usual methods. The glycerine (G. R. of Wako) was used without further purification.

Apparatus and Procedures. The ESR spectra were measured by using a JES-3BS-X spectrometer with a field modulation of 100 kc/sec and with a TE_{011} mode cavity; the spectrometer had been manufactured by the Japan Electron Optics Laboratory. The microwave frequency was 9100—9200 Mc/sec, and the amplitude of the modulation field was 12—20 gauss (G), peak to peak. The sample solution was kept in a quartz tube (3 mm in inner diameter) and was kept at 77°K in a quartz Dewar. Glucose glasses were made by rapid cooling after fusing an appropriate

*1 Present address: Department of Chemistry, Yamaguchi University, Yamaguchi.

1) C. A. Hutchison, Jr., and B. Mangum, *J. Chem. Phys.*, **29**, 952 (1958); *ibid.*, **34**, 908 (1961).

2) J. H. van der Waals and M. S. de Groot, *Mol. Phys.*, **2**, 333 (1959); *ibid.*, **3**, 190 (1960).

3) W. A. Yager, E. Wasserman and R. M. R. Cramer, *J. Chem. Phys.*, **37**, 1148 (1962).

4) E. Wasserman, L. C. Snyder and W. A. Yager, *ibid.*, **41**, 1763 (1964).

5) Y. Kubota and M. Miura, to be published.

6) V. Zanker, *Z. Physik. Chem. (Leipzig)*, **199**, 225 (1952).

7) M. Gailliot, *Quarterly J. Pharm. Pharmacol.*, **7**, 63 (1934).

mixture of glucose and dye; they were then kept in a desiccator with phosphorus pentoxide. Measurements were carried out at 77°K and at higher temperatures. The temperature, except at 77°K, was controlled by varying the flow rate of cold nitrogen gas through the cavity. The light sources were as follows: (1) a 750-W tungsten projector lamp with a filter (1 cm thick) containing 10% $CuSO_4$ aqueous solution, and (2) a 1-kW high-pressure mercury lamp with a filter (5 cm thick) containing a 0.1 M $NiSO_4$ aqueous solution and with two quartz lenses. The latter was used for the excitation of acridine, naphthalene, and anthracene, and the former, for the excitation of the other substances.

The absorption spectra were measured at room temperature with a Shimadzu QV-50 spectrophotometer. The phosphorescence measurements were performed at 77°K with a Hitachi MPF-2A fluorescence spectrophotometer (R-136 photomultiplier) with an attachment for the phosphorescence measurements.

Results and Discussion

The ESR spectra of the triplet state of acridine dyes were observed at a resonance field of *ca.* 1550 G corresponding to the $\Delta M=2$ transitions, which are shown in Fig. 1 for acridine orange, proflavine, and acriflavine. According to van der Waals and de Groot,[2] the position of the peak on the low-field side of the derivative spectrum (H_{min}) is related to the root-mean-square ZFS parameter, D^*, by the following equation:

$$D^* = (D^2+3E^2)^{1/2} = \sqrt{3}\,[1/4(h\nu)^2-(g\beta H_{min})^2]^{1/2}$$

where h is Plank's constant; ν, the microwave frequency; g, the spectroscopic splitting factor, and β, the Bohr magneton. The ESR results are summarized in Tables 1 and 2, where ΔH denotes the linewidth determined as the peak-to-peak distance of the derivative spectrum and where τ is the decay time of the ESR signal after the light has been extinguished; τ should be equal to the measured lifetime of phosphorescence.

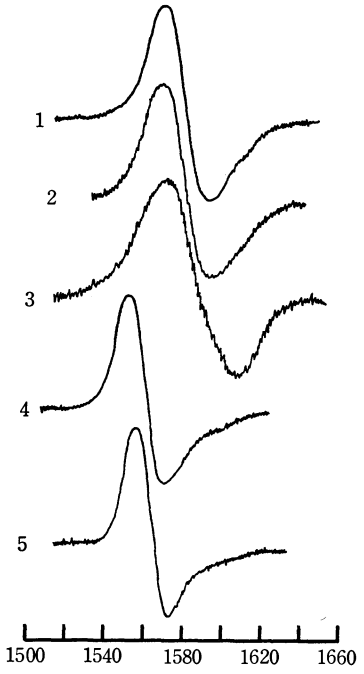

Fig. 1. ESR spectra of the triplet state of acridine dyes in glycerine at 77°K.
Microwave frequency: 9135±1 Mc/sec
(1) acridine orange: 9.7×10^{-5} M
(2) 1.3×10^{-3} M
(3) 6.5×10^{-3} M
(4) proflavine: 1.9×10^{-4} M
(5) acriflavine: 1.8×10^{-4} M

ZFS Parameters. Each D^* value for acridine dyes is constant within the range of experimental error, regardless of the dye concentration and of the kind of solvent at relatively low concentrations. At higher concentrations and in solvents containing water, however, the D^* value tends to decrease with an increase in the dye concentration. This will be discussed later. The D^* values given in Table 2 are the averages at low dye concentrations where the decrease of D^* value does not occur. These values are of the same order of magnitude as those of anthracene and naphthalene;[8] they may, therefore, make it possible to assign the lowest triplet state of acridine dyes to the $(\pi-\pi^*)$ state. For acridine, its D^* value also suggests that the lowest triplet state is the $(\pi-\pi^*)$ state.

In addition to the $\Delta M=2$ transition spectra, we could observe the $\Delta M=1$ transition spectra consisting of six lines associated with three molecular axes. The latter spectra were, however,

Table 1. The effect of concentration on ESR data of acridine dyes in glycerine at 77°K

Concn. (M)	D^* (cm^{-1})	ΔH (G)	τ (sec)
(A) Acridine orange			
9.7×10^{-5}	0.0724	25.0	1.8
1.7×10^{-4}	0.0732	25.2	
6.6×10^{-4}	0.0726	26.1	
1.3×10^{-3}	0.0723	26.5	
3.9×10^{-3}	0.0716	31.0	1.7
6.5×10^{-3}	0.0709	35.4	1.6
(B) Proflavine			
1.9×10^{-4}	0.0807	20.0	2.1
3.4×10^{-3}	0.0809	20.8	2.0
9.8×10^{-3}	0.0800	25.2	—
(C) Acriflavine			
1.8×10^{-4}	0.0786	19.0	2.2
2.2×10^{-3}	0.0790	19.5	2.2
8.1×10^{-3}	0.0783	24.8	2.1

8) B. Smaller, *J. Chem. Phys.*, **37**, 1578 (1962).

TABLE 2. ZERO-FIELD-SPLITTING PARAMETERS OF ACRIDINE DYES IN VARIOUS SOLVENTS AT 77°K

Compound	Solvent	D^* (cm^{-1})	D (cm^{-1})	E (cm^{-1})	$\bar{\nu}_p$[d] (cm^{-1})
Acridine orange	Glycerine	0.0726	0.0636	0.0159	16500
	EG	0.0728			
	EG-water (1:1)[a]	0.0718			
	Methanol	0.0723			
	Methanol-water (1:1)[a]	0.0710			
	Ethanol	0.0723			
	Glucose[b]	0.0732			
Proflavine	Glycerine	0.0807	0.0734	0.0177	17500
	EG	0.0806			
	EG-water (1:1)[a]	0.0798			
	Methanol	0.0802			
	Glucose	0.0803			
Acriflavine	Glycerine	0.0788			17300
	Glucose[c]	0.0795			
Acridine	Ether	0.0688			
Acridine yellow	Glycerine	0.0725			
Acridine red	Glycerine	0.0705			
Naphthalene	Ethanol	0.1060			
Anthracene	Ethanol	0.0773			

a) Dye concn., 10^{-3} M.
b) Measured at 88°K.
c) Measured at 91°K.
d) The 0-0 band of phosphorescence.

relatively broader and much less intense than the former spectra because of their anisotropic character. From the $\Delta M=1$ transition spectra, the values of the ZFS parameters, D and E, were calculated;[3,4] they are presented in Table 2. The D^* values obtained from these D and E values, 0.0693 and 0.0795 for acridine orange and proflavine respectively, are in fairly good agreement with those obtained from the $\Delta M=2$ transition spectra.

In order to examine the temperature dependence of the D^* value, ESR measurements of glucose glass containing acridine dyes were carried out over the temperature range from 77 to 300°K. The intensities of both the phosphorescence and the ESR signal at the $\Delta M=2$ transition decrease with an increase in the temperature. The signal-to-noise ratio at 300°K was 4 : 1 for acridine orange. For proflavine and acriflavine, no ESR signals of the triplet state were observed at room temperature; instead, another strong green luminescence (probably α-phosphorescence) was observed for these dyes. As may be seen in Fig. 2 for acridine orange and acriflavine, it was found that the D^* values decrease with a rise in the temperature; namely, the plot of D^* against the temperature in each case gives an approximately straight line with a slope of -2×10^{-5} cm^{-1} deg^{-1}. This phenomenon, similar to that of coronene in a plastic matrix,[9] seems general in the triplet state of aromatic molecules.

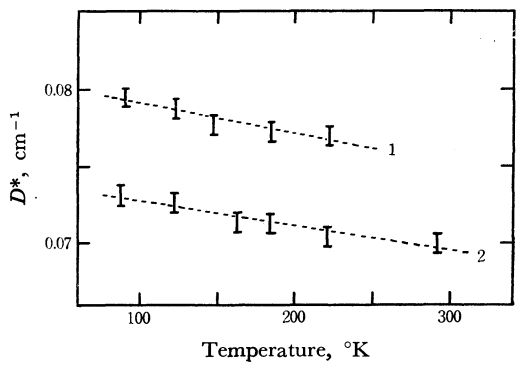

Fig. 2. Variation of D^* with temperature.
(1) Acriflavine, (2) Acridine orange

Lifetime of the Triplet State. As an example, the decay curve of the triplet state of proflavine is shown in Fig. 3 (a). The decay curve was generally exponential except for the first stage, up to 0.3 sec; this deviation may be due to the response time (0.3 sec) of the recorder. As is shown in Fig. 3(b), a plot of the logarithm of the signal intensity against the time gives a straight line; the lifetime of the triplet state can be calculated from the slope of this line. The lifetime, generally, tends to decrease with an increase in the dye concentration and is in good agreement with the results obtained from the phosphorescence measurements (see Fig. 5).

9) C. Thomson, *ibid.*, **41**, 1 (1964).

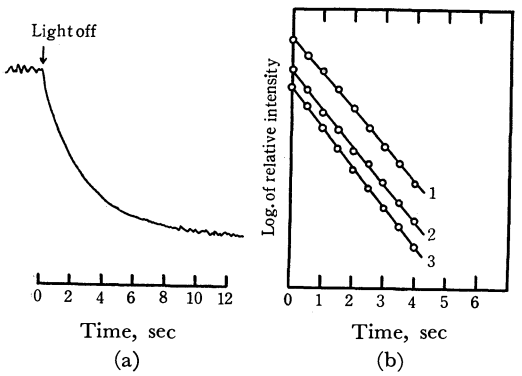

Fig. 3. Decay of the triplet state of acridine dyes in glycerine at 77°K.
(a) Proflavine: 1.9×10^{-4} M
(b) (1) Acriflvaine: 1.8×10^{-4} M
(2) Proflavine: 1.9×10^{-4} M
(3) Acridine orange: 1.7×10^{-4} M

Dependence of the ESR Data on the Dye Concentration. As may be seen from Table 1, the ESR data characteristic of the triplet state seem to depend on the dye concentration. Figure 4 shows the concentration dependence of the D^* and ΔH values in the case of acridine orange. In general, D^* decreases and ΔH increases with an increase in the dye concentration. This phenomenon, depending on the kind of solvent, was more remarkable in glycerine than in EG. As is well known,[6,10,11] acridine dyes easily form the dimer and higher aggregates at high concentrations in both water and organic solvents. First, the absorption spectra were measured at various concentrations in order to establish the associative properties of acridine dyes. These dyes were found, by the method of Zanker[10] and Mataga,[11] to exist in a monomer-dimer equilibrium in glycerine and EG.

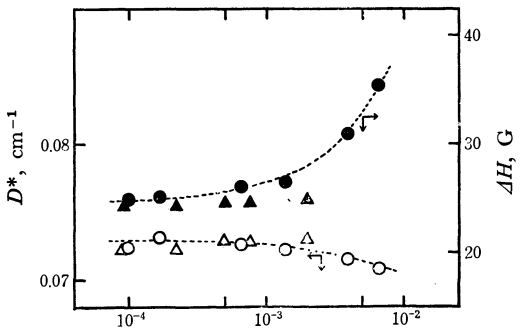

Fig. 4. Variation of D^* and ΔH with concentration of acridine orange at 77°K.
○ ●: in glycerine, △ ▲: in EG

The equilibrium constants for the dimerization of acridine orange were estimated to be about 450, 100, and 460 M^{-1} in glycerine, EG, and EG-water (1 : 1 by volume) respectively. Further, the association tendency is considerably enhanced by a drop in the temperature.[10] Second, the ΔH value was unchanged irrespective of the triplet-state concentration, which was controlled by varying the intensity of the exciting light. This fact appears to rule out the possibility that the broadening of the linewidth arises from the interaction between triplet-state molecules, even though the intermolecular distance may be expected to be shortened at a high concentration. Next, the interaction between triplet-state molecules and radicals formed during irradiation may give rise to the broadening of the linewidth. The radical concentration was, however, too low to permit the identification of the radicals, and so this effect may be disregarded. Finally, the ESR data were independent of the concentration in the case of aromatic hydrocarbons which do not tend to associate, while they were concentration-dependent in the case of acridine dyes.

In view of these facts, it seems reasonable to assume that the association of acridine dyes is responsible for the apparent decrease in the D^* value and the apparent increase in the ΔH value

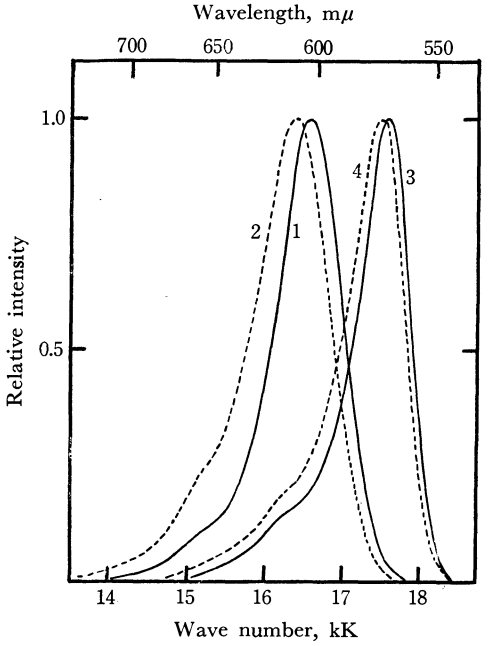

Fig. 5. Phosphorescence spectra of acridine orange and proflavine in glycerine at 77°K.
Excitation wavelength: 470 mμ for proflavine, 500 mμ for acridine orange
Acridine orange: (1) 1.05×10^{-4} M, $\tau=1.80$ sec
(2) 5.94×10^{-3} M, $\tau=1.54$ sec
Proflavine: (3) 5.86×10^{-5} M, $\tau=2.30$ sec
(4) 5.24×10^{-3} M, $\tau=2.10$ sec

10) V. Zanker, *Z. Physik. Chem. (Leipzig)*, **200**, 250 (1952).
11) N. Mataga, This Bulletin, **30**, 375 (1957).

with an increase in the dye concentration. As may be noticed from Fig. 1 for acridine orange, the ESR spectra are presumed to be made up by the superposition of the spectrum due to the triplet state of a monomer and that due to the triplet state of a dimer; the latter, having a D^* value smaller than that of the former, becomes marked with an increase in the dye concentration. In agreement with this argument, in solvents containing water, where acridine dyes form aggregates more easily than in pure organic solvents, this phenomenon is pronounced. A possible explanation for the decrease in the D^* value is the delocalization of two unpaired electrons in a dimer molecule. This theory is, of course, still speculative. If so, however, the resulting increase in the interelectronic separation (r_{12}) may lead to a decrease in the D^* value since:

$$D \propto |\langle(r_{12}^2-3z_{12}^2)/r_{12}^5\rangle| \text{ and } E \propto |(\langle y_{12}^2-x_{12}^2)/r_{12}^5\rangle|.^{12)}$$

ESR measurements clarify the nature of the triplet state itself through the magnetic dipolar interaction between unpaired spins, whereas phosphorescence measurements give information regarding the triplet-singlet transition and the energy level of the triplet state. Therefore, phosphorescence measurements have been carried out to establish further details of the triplet state of acridine dyes in connection with their association. As preliminary findings, Fig. 5 shows the phosphorescence spectra of acridine orange and proflavine. In both cases, the maximum of phosphorescence spectra shifts to a longer wavelength with an increase in the dye concentration. The phosphorescence lifetime has been found to be dependent on the dye concentration and on the wavelength (both emission and excitation). Further study is in progress and will be reported elsewhere.

12) S. A. Boorstein and M. Gouterman, *J. Chem. Phys.*, **39**, 2443 (1963).

BULLETIN OF THE CHEMICAL SOCIETY OF JAPAN VOL. 42 2767—2772 (1969)

Hybridization of Carbon and Equilibrium Distance

Tomoo MIYAZAKI and Hidehito OHBAYASHI

Department of Applied Chemistry, Faculty of Science and Engineering, Waseda University, Nishi-Ohkubo Shinjuku-ku, Tokyo

(Received February 20, 1969)

The CNDO/2 method, an approximate self-consistent molecular orbital theory, has been applied to the calculation of equilibrium distances of the carbon-hydrogen bond and the normal and hypothetical carbon-carbon single or double bonds which are usually considered te-te, tri-tri, di-di and te-tri single bonds or tri-tri and di-di double bonds between carbon hybrids. The electronic interaction energies between non-adjacent atomic orbitals for sigma system considering appropriate carbon hybrids have been estimated. From the results of these calculations, it follows that the carbon-carbon bond length of sigma system is little affected by the types of hydbridization of carbon atoms.

It is noteworthy that the CNDO/2 mthod,[1-3] the self-consistent molecular orbital method based on the neglect of differential overlap for all valence orbitals, leads to generally good agreement with experimental values for the bond lengths and bond angles of di, tri and tetra-atomic molecules. The CNDO/2 treatment satisfies the requirement that the molecular wave function and the orbital energies are invariant under orthogonal transformations of the atomic orbital basis set such as the replacement of s, p orbitals by hybrids. This type of approximation makes it possible to discuss a relationship between the lengths of single bonds in equilibrium and the types of hybridization of carbon atoms.

The carbon-carbon bond lengths for some conjugated hydrocarbons have been studied with the pi bond order (P_{pi}) - bond length (R) relationship for bonds in equilibrium.[4-6] It must be

1) J. A. Pople, D. P. Santry and G. A. Segal, *J. Chem. Phys.*, **43**, S 129 (1965).

2) J. A. Pople and G. A. Segal, *ibid.*, **43**, S 136 (1965).

3) J. A. Pople and G. A. Segal, *ibid.*, **44**, 3289 (1966).

4) H. C. Longuet-Higgins and L. Salem, *Proc. Roy. Soc. (London)*, **A251**, 172 (1959).

5) C. A. Coulson and A. Golebiewski, *ibid.*, **78**, 1310 (1961).

6) M. J. S. Dewar and H. N. Schmeising, *Tetrahedron*, **11**, 96 (1960).

remembered that the P_{pi}-R relation is based on the following two assumptions; separability of the sigma and pi energies and localization of sigma bonds formed by the overlap of two hybridized orbitals (localization of sigma electron). These assumptions are generally adopted but they will be avoided in this paper.

The relative importance of pi electron resonance and hybridization in the shortening effect for the bond lengths of conjugated hydrocarbons has been discussed by many investigators. Among others, Mulliken[7] suggested that the bond shortening effect of hybridization is of comparable magnitude to that of conjugation for butadiene C_2–C_3 bond distance, and he estimated the C–C bond length with given types of hybridization to be 1.45 Å for a di-di, 1.51 Å for a tri-tri and 1.54 Å for a te-te C–C single bond. It has been generally accepted that the shortening of the covalent radius in the C–C single bond is due to the increased *s* character in the bond orbital. The shortening of C–H distances for diagonal, trigonal and tetrahedral hybrids of the carbon atom can also be explained by this effect.[8]

However, it appeared of interest to investigate further the problem described above for the following reasons. Since little attention has so far been paid to the sigma electron delocalization effects, it was thought advisable to calculate C–C equilibrium distances for given types of hybrid by the molecular orbital method which explicitly treats sigma and pi orbitals together. The calculations were performed on several hydrocarbons; methane, ethane, propane, butane, ethylene, propylene, butadiene and acetylene. It may be concluded from the results of these calculations that the equilibrium lengths of C–C single bonds are little affected by the hybridization of carbon atoms.

Methods of Calculation

In the CNDO/2 approximation, the molecular orbitals, which are approximated as linear combination of valence atomic orbitals, and their energies can be obtained by solving the appropriate set of secular equations and the corresponding secular matrix. The elements of the SCF energy matrix are given in this method by

$$F_{\mu\mu} = H_{\mu\mu} + \left(P_{AA} - \frac{1}{2}P_{\mu\mu}\right)\gamma_{AA} + \sum_{(A\neq B)} P_{BB}\gamma_{AB}, \quad (1)$$

$$F_{\mu\nu} = H_{\mu\nu} - \frac{1}{2}P_{\mu\nu}\gamma_{AB}, \qquad (\mu \neq \nu) \quad (2)$$

$$H_{\mu\mu} = -\frac{1}{2}(I_\mu + A_\mu) - \left(Z_A - \frac{1}{2}\right)\gamma_{AA} - \sum_{A\neq B} Z_B\gamma_{AB}, \quad (3)$$

$$H_{\mu\nu} = \frac{1}{2}S_{\mu\nu}(\beta^0_A + \beta^0_B), \quad (4)$$

where $H_{\mu\nu}$ is the matrix element of the one-electron Hamiltonian which includes the kinetic energy and the electrostatic potential energy due to the core, the term $-1/2(I_\mu+A_\mu)$ is the core integral, P_{AA} and $P_{\mu\mu}$ are the atomic and orbital electron densities, respectively, $P_{\mu\nu}$ is the orbital bond order, Z_A is the core charge of atom A, γ_{AB} is the average electron-repulsion integral, β^0_A and β^0_B are empirically determined resonance integrals characteristic of atoms A and B, respectively, and $S_{\mu\nu}$ is the overlap integral between atomic orbitals μ and ν. The derivation of the method and the mathematical definitions of all quantities can be found in the original CNDO paper.[1-3] The total electronic energy of the valence electrons is

$$E_{electronic} = \frac{1}{2}\sum_{\mu,\nu} P_{\mu\nu}(H_{\mu\nu} + F_{\mu\nu}). \quad (5)$$

The total energy of the molecule is obtained by adding the repulsion energy between cores to the total electronic energy. The repulsion energy between cores is approximated by a point-charge model. The result is

$$E_{total} = E_{electronic} + \sum_{A<B}\sum Z_A Z_B/R_{AB}, \quad (6)$$

where R_{AB} is the A–B inter-nuclear distance.

The total energy and wave functions were calculated by varying the particular bonding distance considered, while the other bonds in the molecule were held fixed at their observed equilibrium distances. An equilibrium bond length was determined by minimizing the total energy with respect to the distance.

It was assumed that the hypothetical carbon-carbon equilibrium distances of molecules which include the broken pi bonds can be estimated by the following three types of calculations. The hypothetical carbon-carbon bonds are those which are usually considered to be the tri-tri, di-di and te-tri C–C single bonds or the di-di C–C double bond.

Calculation A. The contribution of pi bonding energies can be eliminated from the total energies of ethylene and acetylene in the manner

$$E^\dagger = E_{total} - \frac{1}{2}\sum_{\substack{\mu,\nu \\ (\mu\neq\nu)}}{}^{\pi} P_{\mu\nu}(H_{\mu\nu} + F_{\mu\nu}), \quad (7)$$

where the summation $\sum^\pi$ is over pi atomic orbitals. Since the summation does not include the term $\mu=\nu$, the energy $E^\dagger$ contains the energies of unpaired electrons in the pi atomic orbitals of carbons. The calculation can be performed under the condition that each pi electron density is equal to the number of atomic valence pi electrons. The treatment is confined to the calculation of ethylene and acetylene, because pi electron densities of larger conjugated hydrocarbons are non-uniformly distributed according to the CNDO/2 calculation.

7) R. S. Mulliken, *Tetrahedron*, **6**, 68 (1959).
8) "An Epistologue on Carbon Bonds," *ibid.*, **17** Nos. 3/4 (1962).

The equilibrium distances of C–C single bond are determined from the $E^{\dagger}$-R relationship.

Calculation B. Another calculation can be performed to estimate C–C single bond lengths. In the first step of calculation, the overlap integrals between pi orbitals are set equal to zero. The degenerate orbitals for pi electrons resulting from this assumption have an unpaired electron. This configuration is an open shell, but the CNDO/2 method which was designed for the closed shell configuration was used in this approximate calculation. The total energies which contain the energies of unpaired pi electrons are used to estimate the bond distances of tri-tri, di-di and te-tri C–C single bonds or di-di C–C double bond.

Calculation C. The population and energy matrices can be transformed to new matrices by the transformation

$$\boldsymbol{M}' = \boldsymbol{OMO}^{-1}, \tag{8}$$

where $\boldsymbol{M}$ is the population ($\boldsymbol{P}$) or energy ($\boldsymbol{F}$ and $\boldsymbol{H}$) matrix, $\boldsymbol{M}'$ is the matrix in the new basis, and $\boldsymbol{O}$ is an orthogonal transformation matrix.

The total electronic energy is invariant under the transformation

$$E_{\text{electronic}} = \frac{1}{2}\sum_{\mu,\nu} P_{\mu\nu}(H_{\mu\nu} + F_{\mu\nu}) = \frac{1}{2}\sum_{\mu,\nu} P'_{\mu\nu}(H'_{\mu\nu} + F'_{\mu\nu}) . \tag{9}$$

Selecting an appropriate transformation matrix, we can separate the off-diagonal matrix elements of the sigma system into two groups. The matrix elements between bonding orbitals —*e.g.* φ_1 and φ_4 in Fig. 1— form one group (group I). The matrix elements between non-bonding orbitals —*e. g.* φ_1 and φ_5—form the other group (group II). The group I matrix elements can be interpreted as representing localized bonds and the group II elements as representing non-localized bonds. In the local bond approximation in which the group II matrix elements are neglected, the total energy E^* is given by

$$E^* = \frac{1}{2}\sum\nolimits^{*}_{\mu,\nu} P'_{\mu\nu}(H'_{\mu\nu} + F'_{\mu\nu}) + \sum_{A<B}\sum Z_A Z_B / R_{AB} , \tag{10}$$

where $\sum^*$ describes the summation over the diagonal and the group I matrix elements. The equilibrium bond lengths which are determined by the E^*-R relationship are shifted in comparison with the bond lengths determined by "calculation B."

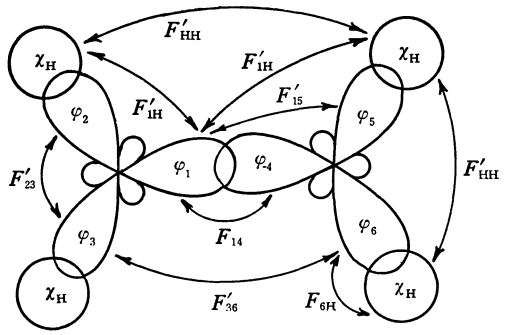

Fig. 1. Energy matrix elements of sigma systems for ethylene.
χ are atomic orbitals of hydrogens.
φ are hybridized orbitals of carbons.
$\boldsymbol{F}$ indicate the matrix elements between the bonding orbitals (group I), $\boldsymbol{F}'$ the matrix elements between the non-bonding orbital (group II).

Results and Discussion

The results of the calculations are given in Tables 1, 2 and 3. The calculated bond lengths are in reasonable agreement with their experimental values. From the calculations, the C–C single bond length is 1.476±0.006 Å, double bond length 1.317 Å, triple bond length 1.198 Å. For the C–H distances of the diagonal, trigonal and tetrahedral carbon hybrids, the agreement between the calculated and observed distances is quite satisfactory. On the basis of this set of data and the transformation properties of the CNDO method, it is felt that the CNDO/2 method is an effective approximate method for determining the relative importance of hybridization and pi electron resonance in the bond shortening effect for conjugated hydrocarbon.

The tri-tri single bond equilibrium distance of ethylene having two unpaired pi electrons was 1.475 Å by "calculation A" and "calculation B." The di-di single bond equilibrium distance of acetylene having four unpaired pi electrons was 1.476 Å. The equilibrium distances of di-di and tri-tri single bonds were longer than that of te-te single bond (ethane) by 0.005 Å and 0.004 Å.

The equilibrium distances of C_1–C_2 and C_2–C_3 single bonds of propylene were 1.487 Å and 1.480Å respectively by "calculation B" in which overlap integrals between pi orbitals were neglected. These equilibrium distances are practically in agreement with that of propane as given in Table 2. The result obtained indicates that the shortening effect for C_1–C_2 bond of propylene is only dependent upon the hyperconjugation between the double bond and the methyl group.

The equilibrium distances of C_1–C_2 and C_2–C_3 single bonds of butadiene having four unpaired pi electrons were 1.482 Å and 1.486 Å respectively by "calculation B" in which all overlap integrals between pi orbitals were set equal to zero. The equilibrium distances of C_1–C_2 and C_2–C_3 bonds of butane were 1.482 Å. The calculated shortening effect for the C_2–C_3 bond of butadiene depends little on hybridization. The results of the calculation indicate that te-te, tri-tri, di-di and te-tri C–C single bonds are substantially in agreement with one another in the range of error in the CNDO/2

Table 1. The equilibrium distances of carbon-carbon bonds between several types of carbon hybrids for C_2 hydrocarbons

Type of bond	Equilibrium distance (Å)					
	Single bond			Double bond	Triple bond	Obsd[d]
	CNDO/2	calcd C[b]	calcd C[c]	CNDO/2	CNDO/2	
te-te	1.471	1.621	1.562			1.535 (ethane)
tri-tri	1.475[a]	1.569	1.540	1.317		1.337 (ethylene)
di-di	1.476[a]	1.479	1.452	1.323[a]	1.198	1.205 (acetylene)

a) By "calculation A and B"
b) This calculation neglects the group II matrix elements except the intra-atomic (carbon) matrix elements.
c) This calculation neglects the group II matrix elements.
d) "Interatomic distances" Supplement, Special publication No. 18, The Chemical Society (London)

Table 2. Equilibrium distances of carbon-carbon bonds for C_3 and C_4 hydrocarbons

Molecule	Equilibrium distances (Å)			
	$R(C_1-C_2)$		$R(C_2-C_3)$	
	calcd	obsd[d]	calcd	obsd[d]
Propane	1.478	1.54	1.478	1.54
Propylene	1.463	1.488	1.332	1.353
$H_3\dot{C}-\dot{C}H-\dot{C}H_2$[a]	1.487		1.480	
Butane	1.482	1.539	1.482	1.539
Butadiene	1.332	1.337	1.447	1.483
$H_2\dot{C}-\dot{C}H-\dot{C}H-\dot{C}H_2$[b]	1.482		1.486	
$H_2C=CH-CH=CH_2$[c]	1.323		1.494	

a) C_2-C_3 pi overlap integral was set equal to zero. Methyl carbon was taken as C_1.
b) All overlap integrals between pi orbitals were set equal to zero.
c) C_2-C_3 pi overlap integral was set equal to zero. In the result of this calculation, pi electron densities were non-uniformly distributed.
d) See Ref. d, Table 1.

Table 3. Carbon-hydrogen equilibrium distances

Molecule	C-H Equilibrium distance (Å)			
	CNDO/2	calcd C[a]	calcd C[b]	obsd[c]
Methane	1.114	1.121	1.108	1.093
Ethane	1.117	1.114	1.085	1.093
Ethylene	1.106	1.102	1.085	1.086
Acetylene	1.088	1.085	1.067	1.058

a) This calculation neglects the group II matrix elements except the intra-atomic (carbon) matrix elements.
b) This calculation neglects the group II matrix elements.
c) See Ref. d, Table 1.

calculation.

The di-di double bond equilibrium distance of acetylene having two unpaired pi electrons was 1.323 Å by "calculation A" and "calculation B." The equilibrium distance of the C_2–C_3 bond of butadiene including two localized double bonds was 1.323 Å by "calculation B" in which the overlap integrals between pi orbitals were set equal to zero except for S_{12} and S_{34} pi overlap integrals. The equilibrium distance of di-di double bond is longer than the tri-tri double bond (ethylene) equilibrium distance by 0.006 Å. The difference is in the range of the error of CNDO calculation for bond distance.

On the basis of this calculation, it seems reasonable to assume that the carbon-carbon bond length is little affected by hybridization of the carbon atom.

From the electron densities of s and p orbitals, the types of hybridization of methane, ethane, ethylene and acetylene were essentially sp^3, sp^3, sp^2 and sp hybrids respectively as given in Table 4.

The population ($\boldsymbol{P}$) and energy ($\boldsymbol{F}$ and $\boldsymbol{H}$) matrices of methane, ethane, ethylene and acetylene were transformed to the new matrices ($\boldsymbol{P}'$, $\boldsymbol{F}'$ and $\boldsymbol{H}'$) with the hybrid basis set (sp^3 sp^2 and sp). In the new matrices, the group II matrix elements represent the electronic interaction energies between new non-bonding orbitals. These group II interaction energies were further classified into the two following types: those between neighboring atoms and those between non-neighboring atoms. The former was termed an N type interaction and the latter an N–N type interaction as given in Table 5.

The N type interaction energies between carbon hybrid and hydrogen were 0.0200 eV, 0.2574 eV, 0.3540 eV and 0.0552 eV for methane, ethane, ethylene and acetylene respectively, and those of N–N types were −0.8010 eV, −0.0332 eV and 0.5910 eV for ethane, ethylene and acetylene respectively.

The interaction energies (N type) between carbon hybrids were −4.6901 eV, −4.6725 eV and −0.8389 eV for ethane, ethylene and acetylene respectively. By minimization of total energies neglecting the group II matrix elements, the carbon-hydrogen equilibrium distances shifted from

TABLE 4. THE ORBITAL ELECTRON DENSITIES OF METHANE, ETHANE, ETHYLENE AND ACETYLENE

Molecule	Interatomic distance (Å)	Orbital electron densities				
		C_s	C_{px}	C_{py}	C_{pz}	H
Methane	1.100 (C-E)	1.0620	0.9953	0.9953	0.9953	0.9880
Ethane	1.471 (C-C)*	1.0037	1.0509	0.9719	0.9719	1.0006
Ethylene	1.320 (C-C)*	1.0485	1.0277	0.9492	1.0000	0.9873
Acetylene	1.200 (C-C)*	1.0980	0.9652	1.0000	1.0000	0.9369

* The C-H distances were held fixed at the observed equilibrium distances. X was taken as C-C sigma axis.

TABLE 5. CARBON-CARBON DISTANCES AND INTERACTION ENERGIES (sum of the group II matrix elements)

Molecule	R(C-C) (Å)	Total energies (eV)		Electronic interaction energies (eV)					
		E_{total}	$E\dagger$ [a]	C (intra)	C-C	C-H N type[b]	C-H N-N type[b]	H-H N type[b]	H-H N-N type[b]
Ethane	1.471	−511.7637		−0.0651×2	−4.6901	0.0429×6	−0.1335×6	0.0881×6	0.0021×6
	1.520	−511.6427		−0.1168×2	−3.7640	0.0263×6	−0.0971×6	0.0840×6	0.0024×6
	1.540	−511.5347		−0.1385×2	−3.4313	0.0194×6	−0.0836×6	0.0825×6	0.0024×6
	1.560	−511.3971		−0.1973×2	−3.1224	0.0126×6	−0.0708×6	0.0811×6	0.0024×6
Ethylene	1.320	−464.2028		−0.3717×2	−4.6725	0.0885×4	−0.0083×4	0.0865×4	−0.0141×4
	1.500	−462.1389	−448.8703	−0.5461×2	−1.9523	0.0303×4	0.0804×4	0.0845×4	−0.0055×4
	1.520	−461.7262	−448.8076	−0.5757×2	−1.7763	0.0235×4	0.0885×4	0.0840×4	−0.0052×4
	1.540	−461.2886	−448.7099	−0.6052×2	−1.6037	0.0167×4	0.0960×4	0.0838×4	−0.0049×4
Acetylene	1.200	−417.2808		−0.5986×2	−0.8389	0.0276×2	0.2955×2		−0.0197×2
	1.430	−412.8186	−383.7426	−0.9477×2	−0.0838	0.0014×2	0.2903×2		−0.0091×2
	1.450	−412.1451	−383.8258	−0.9792×2	−0.0698	0.0016×2	0.2876×2		−0.0087×2
	1.470	−411.4412	−383.8610	−1.0120×2	−0.0603	0.0047×2	0.2846×2		−0.0082×2

a) $E\dagger$ is defined by Eq. (7).

b) The N type interaction energies refer to the interactions between the neighboring atoms, the N-N types refer to the interactions between the non-neighboring atoms.

1.114 Å to 1.121 Å, 1.117 Å to 1.114 Å, 1.106 Å to 1.102 Å, 1.088 Å to 1.085 Å for methane, ethane, ethylene and acetylene respectively. Also, the carbon-carbon single bond equilibrium distances in a similar manner shifted from 1.471 Å to 1.621 Å 1.475 Å to 1.569 Å, 1.476 Å to 1.479 Å for ethane, ethylene and acetylene type single bonds respectively. In the calculation described above, the intra-atomic (carbon) off-diagonal elements were not neglected, because these calculations were performed to investigate the precision of the local bond approximation between specific atoms. The results of other types of calculation in which all the group II matrix elements were neglected are listed in Tables 1 and 3.

According to this approximation, the carbon-hydrogen bond distance remained unaltered, but the carbon-carbon single bond distance shifted significantly. The length of carbon-carbon single bond distance is di-di <tri-tri <te-te. The *s* character in the hybrids decreases in the same order. The result obtained neglecting the non-localized effect of the sigma electrons agrees with the usual conclusion concerning the equilibrium length of the sigma bond.

The sum total (ε) of the electronic interaction energies between non-adjacent atomic orbitals considering appropriate carbon hybrides is generally effective in stabilizing the molecule, but the effective factor in determining the equilibrium distance is the gradient of variation of the interaction energy ε with the change of the interatomic distance rather than the magnitude of its absolute value.

When the electronic interaction energy ε is neglected in the local bond approximation, the effect on the carbon-hydrogen bond length is negligible. However, for the carbon-carbon bond, the calculated distance lengthens by the neglect of the interaction energy ε because it is effective in shortening the equilibrium distance. Therefore, the idea of localized sigma bonds between pairs of atoms is not appropriate in determining the carbon-carbon bond length.

From a different point of view, however, the result of the calculation in this paper may be an example of defects which are introduced by the CNDO (complete neglect of differential overlap) approximation. If it is the case, it may be due to the following approximations of the CNDO/2 method. The arresting features about approximations of the CNDO/2 method are that the off-diagonal bonding parameters (β^0) are given the same value for resonance integrals between sigma orbitals and those between pi orbitals, the one-center exchange integrals are neglected, and the electronic interaction integrals are assumed to depend only on the atoms and not the actual type of orbital (all electron-repulsion integrals are calculated as coulomb integral involving valence *s* functions). If the calculated equilibrium distances are shifted by the introduction of one-center exchange integrals which play a crucial role in determining the electron distribution in molecule as mentioned by Cook *et al.*,[9] the problem of this paper should be re-examined by the INDO or NDDO method [1,10] which includes the one-center exchange integrals explicitly.

Conclusion

The CNDO/2 method has been applied in the present work to calculate the equilibrium interatomic distances of the hypothetical carbon-carbon single and double bonds. The equilibrium distances of the tri-tri, the di-di and also the te-tri carbon-carbon single bonds are not much different from the te-te single bond. It is also shown the di-di double bond distance is of almost the same magnitude as the tri-tri double bond distance. These results indicate that the carbon-carbon bond length of sigma system is little affected by the state of hybridization of carbon atom.

The above unexpected conclusion is largely dependent upon the validity of the CNDO/2 method employed in this calculation. It has been generally accepted that the model of localized sigma bonds is appropriate in discussing the equilibrium bond length of the sigma system. We find that this approximation is surely satisfactory for the carbon hybrid-hydrogen bond. For the bonds between carbon hybrids, however, this approximation is not reasonable because the bonds between non-adjacent atomic orbitals are appreciably effective in determining the equilibrium distances.

However, it should be emphasized that the above conclusion is obtained as a result of the CNDO/2 method under specific conditions and the result of further elaborate calculation on the problem of this paper may be a subject for future studies.

The authors wish to thank Professor K. Higasi for suggesting this problem and for his continuous interest and encouragement. They are also grateful to Professor K. Ohno (Hokkaido University) for many helpful comments and discussions regarding the manuscript. Thanks are due to Dr. J. H. Gallagher who read the manuscript and corrected the English.

9) D. B. Cook, P. C. Hollis and R. McWeeny, *Mol. Phys.*, **13**, 553 (1967).

10) J. A. Pople, D. L. Beveridge and P. A. Dobosh, *J. Chem. Phys.*, **47**, 2026 (1967).

BULLETIN OF THE CHEMICAL SOCIETY OF JAPAN VOL. 42 2773—2777 (1969)

Non-Newtonian Flow of Water-in-Oil Emulsions*[1]

Kazushige SUZUKI,* Sachio MATSUMOTO,**,*[2] Takehiko WATANABE*** and Sôzaburo ONO***

* *Research Laboratory, Nakayama Taiyodo Ltd., Naniwa-ku, Osaka*
** *College of General Education, University of Osaka Prefecture, Sakai, Osaka*
*** *Laboratory of Biophysical Chemistry, College of Agriculture, University of Osaka Prefecture, Sakai, Osaka*

(Received March 15, 1969)

In order to obtain information on the dispersion state of W/O type emulsions, the steady-flow viscosity in a wide shear range has been studied using a capillary type viscometer. Emulsions prepared by using Arlacel 83 or Arlacel 60, are classified according to the kind of hydrocarbon used as the suspending fluid, *i.e.*, benzene, cyclohexane, liquid paraffin, isopropyl myristate, and squalane systems, respectively. Although all systems show the so-called shear thinning flow, shear dependence of the viscosity is not only influenced by the disperse phase concentration and emulsifier concentration, but is also much effected by the kind of suspending fluid. Such non-Newtonian behavior is observed markedly in benzene systems. It may thus be assumed that the water droplets in benzene have a tendency to form a large aggregate not easily redispersed under shear. The formation of aggregate may be facilitated by the disturbance of the orientation of the adsorbed emulsifier molecules at the interface due to the mutual interaction between the π-electron in benzene molecule and the emulsifier molecule.

The study of rheological properties of W/O type emulsion is of utmost importance for the quality control in the fields of pharmaceutics, foods and cosmetics. However, only few reports have been presented on this subject, compared with those on O/W type.

According to Albers *et al.*[1-3] water-in-benzene emulsions, in which energy barriers between the water droplets can be calculated theoretically, are not stable against aggregation by an adsorbed layer of emulsifier and show non-Newtonian flow.

Furthermore, the relative viscosity of W/O type emulsion is found to be influenced by the species of suspending fluids, although the result was obtained by the so-called one-point method under steady shearing stress.[4] Thixotropy in the W/O type emulsion reported by Vól'fenzon[5] could not be accepted as a general phenomenon, because the sample used was a mixture of seed oil, bees wax, spermaceti and lanolin as the oil phase.

In order to observe the relationship between the rheological properties of W/O type emulsions and their components, the authors tried adjusting the W/O emulsion of different components by making various combinations of emulsifiers and oil components. The emulsions which were relatively stable were chosen to observe how their viscosity changes with the rate of shear, and how the dispersion state changes with oil composition.

Experimental

Sample. Table 1 shows emulsifiers and suspending fluids of emulsions used. In order to prevent the so-called creaming of the emulsion due to density difference between the disperse phase and continuous phase, the density of the oil phase was adjusted to that of water by addition of carbon tetrachloride. No emulsifier listed in the table, however, produced a well stabilized emulsion which has higher alcohol or cast or oil as its suspending fluid. Likewise emulsions prepared with other oil components in which emulsifiers other than sorbitan fatty acid ester were used, could not be used as a sample for viscosity measurement, because of excessive rate of coalescence of suspending droplets. Thus systems of hydrocarbon as their suspending fluid and sorbitan fatty acid ester as their emulsifier were employed for the viscosity measurements. Details of the preparation of the sample are as follows. A given quantity of oil containing the emulsifier was mixed with the specified amount of water (from 0.1 to 0.6 in its volume fraction) and then stirred at a rotational speed of 9000 rpm for 5 min by an homogenizer (manufactured by Tokushu Kika Kogyo).

Droplet size and size distribution of the system were

---

*1 Presented at the 18th Symposium of Colloid Chemistry, Matsue, Oct. 4, 1965.

*2 Present address: Laboratory of Food Chemistry, College of Agriculture, University of Osaka Prefecture, Sakai, Osaka.

1) W. Albers and J. Th. G. Overbeek, *J. Colloid Sci.*, **14**, 501 (1959).
2) W. Albers and Th. G. Overbeek, *ibid.*, **14**, 510 (1959).
3) W. Albers and J. Th. G. Overbeek, *ibid.*, **15**, 489 (1960).
4) S. Matsumoto, *Nippon Kagaku Zasshi (J. Chem. Soc. Japan, Pure Chem. Sect).*, **86**, 324 (1965).
5) I. I. Vól'fenzon, *Kolloid Zhur.*, **27**, 8 (1965).

Table 1. Emulsifiers and suspending fluids of emulsion used for their preparation

Emulsifier	
Sorbitan monostearate (Arlacel 60)*	
Sorbitan sesquioleate (Arlacel 83)*	
Glyceryl monostearate (Atmul 84)*	
Polyoxyethylene (5.5 mol) cetyl ether (Nikkol BC 5.5)**	
Polyoxyethylene (2 mol) monostearate (Nikkol MYS 2)**	
Polyoxyethylene (2 mol) monooleate (Nikkol MYO 2)**	
Trioleyl phosphate (Hostaphate KO 300)***	
Cu-laurate	
Mg-laurate	
Suspending fluid	
Cyclohexane	Castol oil
Benzene	Hexadecanol (Branched chain C_{16}
Liquid paraffin	fatty alcohol)
Squalan	Cyclohexanol
Isopropyl myristate	1-Octanol

* Kao-Atlas Co., Ltd., Japan.
** Nikko Chemicals Co., Ltd., Japan.
*** Hoechst AG., Germany.

obtained by means of microscopy.

Viscosity Measurement. Capillary viscometer of Maron-Belner type[6] was used for all viscosity measurements. By this viscometer the viscosity of a fluid in the range from a relatively high shear stress to a low stress can be obtained continuously by a single measurement. The principle and procedure of the measurement and the dimensions of the viscometer are given in a report[7] on polyvinylpyrrolidone solution.

All measurements were made at 32°C ± 0.01°C in a constant temperature bath.

The relative viscosity (η_{rel}) was calculated as the ratio between the viscosities of emulsion and suspending fluid (containing no emulsifier).

Results and Discussion

The relative viscosity of both cyclohexane and benzene systems stabilized by Arlacel 60 and Arlacel 83 is shown in Figs. 1 and 2. Non-Newtonian flow of each sample is observed throughout the range measured. It can be mentioned from the results that the dependence of viscosity on the rate of shear of the samples is noticeable in the benzene system. It is also noted that the dispersed droplets in the system form large aggregates in the low rate of shear. This fact may be responsible for the generation of a viscosity curve as represented diagramatically in broken line due to a heterogeneity of the disperse phase concentration in the capillary of viscometer. Such a tendency appears markedly in the system using Arlacel 60 as its emulsifier, where the value of maximum shear stress at which dispersed droplets form large aggregates, not entering in the capillary tube, *i.e.*, yield value, increases with increasing diperse phase concentration as indicated in Table 2.

In the emulsion using hydrocarbon other than benzene, as the suspending fluid, no large aggregates of droplets were observed, although aggregates consisting of a small amount of dispersed droplets can be detected by means of microscopy. Dependence of viscosity of the system on the rate of shear is similar to that of the cyclohexane system shown in Figs. 1 and 2. From this it may be sug-

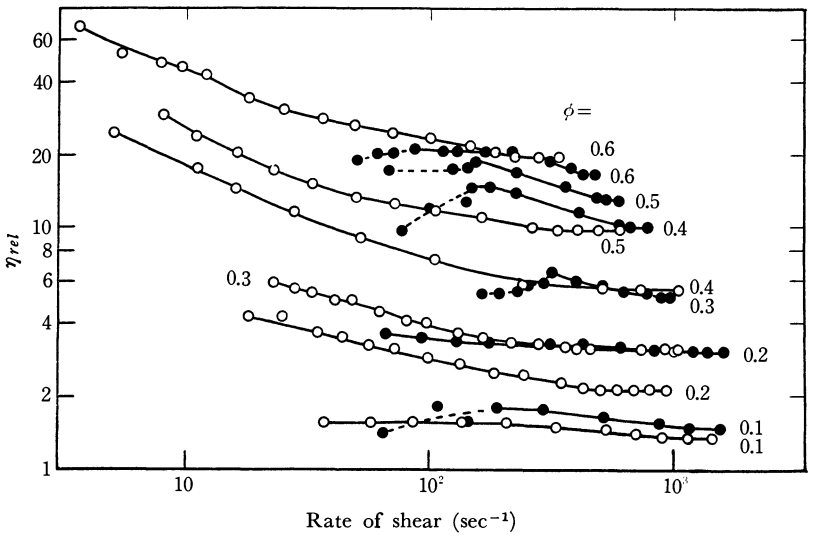

Fig. 1. Plots of relative viscosity *vs.* rate of shear for water in cyclohexane (+CCl_4) and water in benzene (+CCl_4) emulsions (ϕ=0.1—0.6) stabilized by 20 mM Arlacel 60 at 32.0°C.
○, Cyclohexane ●, Benzene

6) S. H. Maron and R. J. Belner, *J. Appl. Phys.*, **26**, 1457 (1955).

7) T. Mineshita, T. Watanabe and S. Ono, This Bulletin, **40**, 2217 (1967).

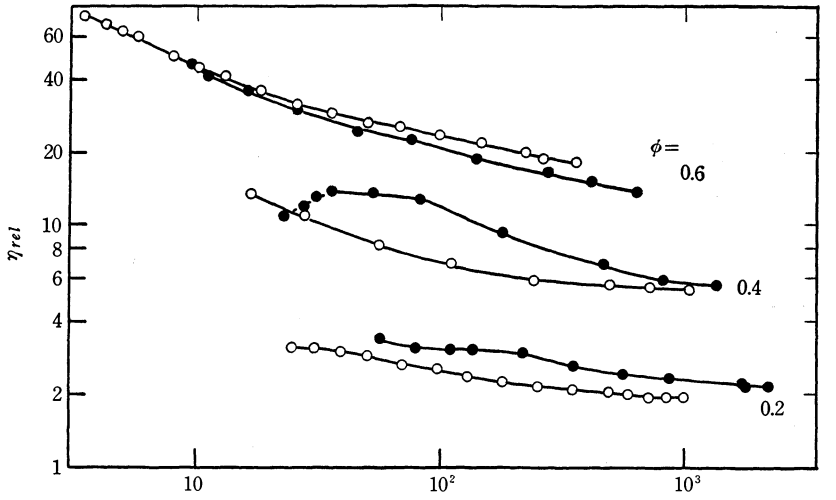

Fig. 2. Plots of relative viscosity *vs.* rate of shear for water-in-cyclohexane ($+CCl_4$) and water-in-benzene ($+CCl_4$) emulsions ($\phi=0.1-0.6$) stabilized by 20 mM Arlacel 83 at 32.0°C.
○, Cyclohexane ●, Benzene

Table 2. Concentration dependence of yield value of benzene-in-water emulsion stabilized by 20 mM Arlacel 60

Disperse phase concentration (ϕ)	0.1	0.2	0.3	0.4	0.5	0.6
Shear stress (dyne/cm²)	1.08	1.43	12.3	15.2	17.2	20.4

gested that the non-Newtonian flow shown by these W/O type emulsions is due to the variation in the number of droplets forming the aggregates of respective flow units with the rate of shear.

At a fixed disperse phase concentration, the values of relative viscosity of various samples are different as shown in Fig. 3.

The relationships between the relative viscosity and the rate of shear at different concentrations of the emulsifier, at a constant disperse phase concentration, are shown in Figs. 4 and 5 for the cyclohexane and benzene systems, respectively. In both cases, emulsifier concentration has no effect upon the dependence of relative viscosity on the rate of shear, although the value of relative viscosity in a whole range of rate of shear increases with increasing emulsifier concentration. This increase may be due to the increase of viscosity in the suspend-

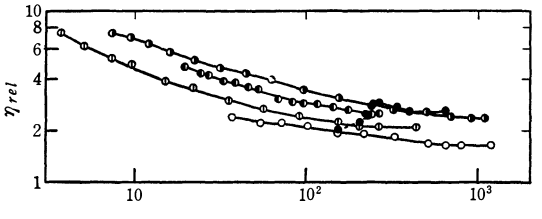

Fig. 3. Plots of relative viscosity *vs.* rate of shear for water-in-oil emulsions ($\phi=0.15$) of various suspending fluid stabilized by 27 mM Arlacel 60 at 32.0°C.
◓ Isopropylmyristate system
◑ Liquid paraffin system
○ Squalan system
◐ Benzene system
● Cyclohexane system

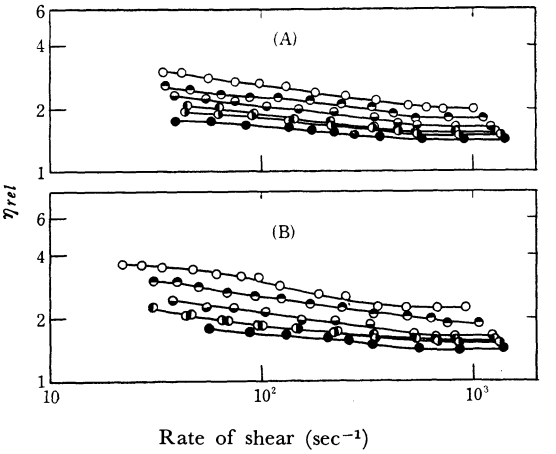

Fig. 4. Plots of relative viscosity *vs.* rate of shear for water-in-cyclohexane ($+CCl_4$) emulsions ($\phi=0.15$) stabilized by Arlacel 60 and Arlacel 83 respectively at 32.0°C.
(A) Arlacel 60 concentration are ●, 3mM; ◑, 8 mM; ◐, 14 mM; ◒, 27 mM; ◓, 55 mM; ○, 82 mM.
(B) Arlacel 83 concentration are ●, 2 mM; ◑, 6 mM; ◐, 10 mM; ◒, 21 mM; ◓, 42 mM; ○, 63 mM.

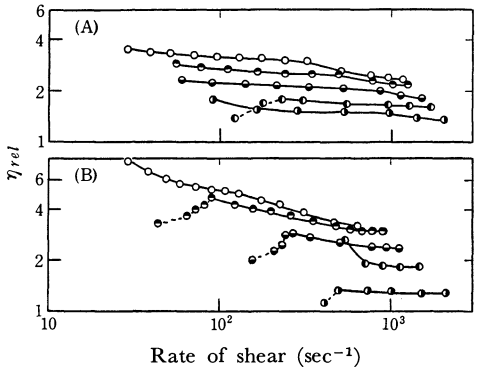

Fig. 5. Plots of relative viscosity *vs.* rate of shear for water-in-benzene ($+CCl_4$) emulsions ($\phi=0.15$) stabilized by Arlacel 60 and Arlacel 83 respectively at 32.0°C.
(A) Arlacel 60 concentration are ◑, 8 mM; ◐, 14 mM; ◒, 27 mM; ◓, 55 mM; ○, 82 mM.
(B) Arlacel 83 concentration are ◑, 6 mM; ◐, 10 mM; ◒, 21 mM; ◓, 42 mM; ○, 63 mM.

ing fluid. In the case of the benzene system stabilized by Arlacel 60, the yield value tends to become smaller with increasing emulsifier concentration as shown in Table 3. This may be brought about by the increase in the amount of the adsorbed emulsifier on the surface of the dispersed droplets with the increase of the amount of the emulsifier used. In the benzene system stabilized by Arlacel 83, the tendency to form large aggregate of droplets seems to be smaller compared with that in the system using Arlacel 60 as an emulsifier. The surface of water droplets of emulsion stabilized by Arlacel 83, containing sesquioleate chains per sorbitan molecule, is more densely covered with oleophilic chains than in the case of emulsion stabilized by Arlacel 60 containing one stearic chain per sorbitan molecule. Thus, the size of aggregate of the former emulsion could be smaller than in the case of the latter emulsion owing to the steric effect of the oleophilic group.

All viscosity measurements were made with two-day old samples. Further aging tests of sample revealed no effect upon the dependence of viscosity on the rate of shear, although a slight decrease in viscosity by aging was noted in all samples. This tendency seems more noticeable in the benzene system. This may be caused by the change in the droplet size distribution resulting from the coalescence of dispersed droplets. Microscopic examination of the size distribution of the dispersed droplets reveals the transition from mono disperse to poly disperse immediately after preparation (refer to Fig. 6 for sample with Arlacel 83 as emulsifier and Fig. 7 for sample with Arlacel 60 as emulsifier). Such transition is slightly faster in the case of the benzene system. Therefore, as a result of coalescence of the droplets, the number of droplets in an aggregate changes with time. Since any change in the dependence of the viscosity on the rate of shear could not be observed, the decrease in viscosity by aging would be brought about by the broadening of the droplet size distribution.

Table 3. Dependence on the emulsifier concentration of yield value of benzene-in-water emulsion ($\phi=0.15$) stabilized by Arlacel 60

Arlacel 60 concentration (mM)	8	14	27	55	82
Shear stress ($dyne/cm^2$)	5.82	8.52	4.69	2.53	1.31

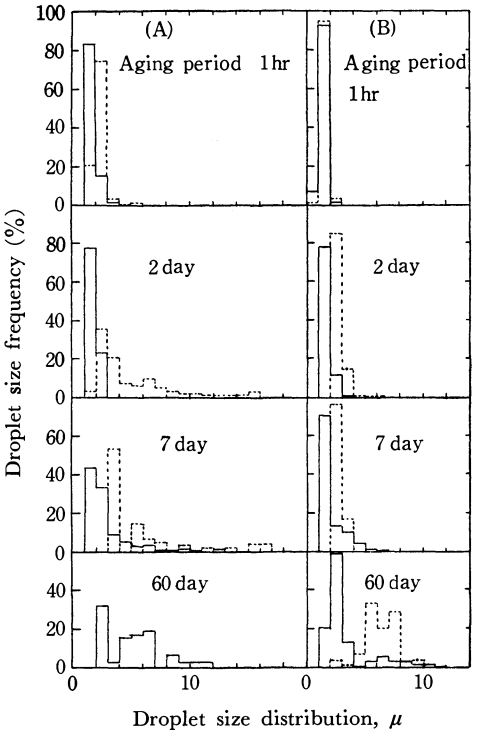

Fig. 6. Changes of droplet size distribution on aging. In the case of W/O emulsions ($\phi=0.15$) stabilized by Arlacel 83.
—— Cyclohexane system
---- Benzene system
Emulsifier concentration: (A) 6 mM; (B) 21 mM

Thus, it can be said that the benzene system shows an extraordinary characteristic in contrast to all other samples studied.

It is known that aromatic hydrocarbon indicates various affinity or peculiar solvating effects irrespective of its nonpolar character. It has been found in recent years that such an effect is due to π-electron possessed by the aromatic hydrocarbon reacting as proton acceptor of hydrogen bond, similar to lone electron-pair possessed by oxygen atom. Previously one of us (S.M.) proved that, in the case of O/W type emulsion, the dispersion state of aromatic hydrocarbon as the oil com-

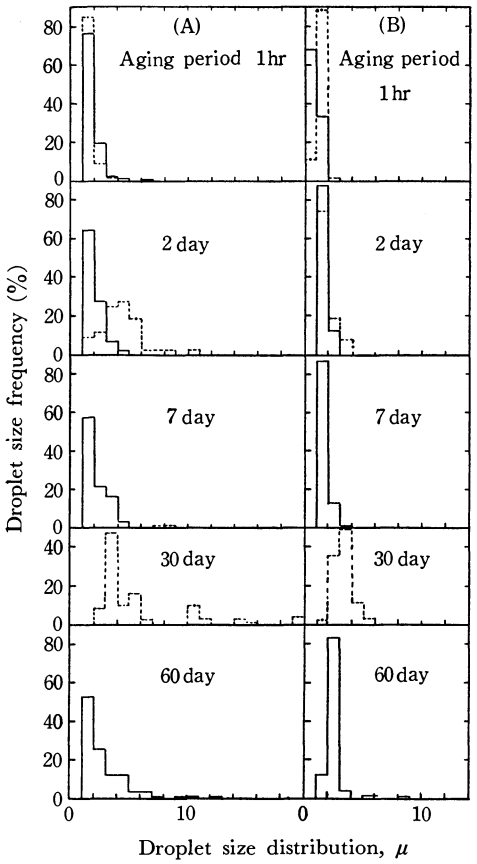

Fig. 7. Changes of droplet size distribution on aging. In the case of W/O emulsions ($\phi=0.15$) stabilized by Arlacel 60.
—— Cyclohexane system
---- Benzene system
Emulsifier concentration: (A) 8 mM; (B) 27 mM

ponent can be distinguished from that of other nonpolar oil components.[8] Although the results were obtained with O/W type emulsions, we can assume that the results thus obtained could be also

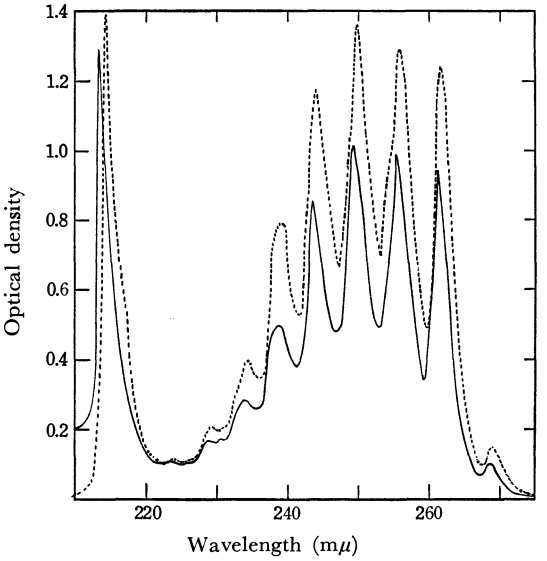

Fig. 8. UV absorption spectrum.
---- Cyclohexane : Benzene (=1000 : 1)
—— 0.5 mM Arlacel 60 in cyclohexane : Benzene (=1000 : 1)

applicable to W/O type emulsions. UV absorption spectrum of benzene shifts towards shorter wavelength by the addition of Arlacel 60 or Arlacel 83, as shown in Fig. 8. This fact suggests that there is an interaction between the hydrophilic group of the emulsifier molecules adsorbed on the surface of dispersed droplets and the π-electrons of benzene. It is probable that the orientation of emulsifier on the surface of the droplet is disturbed and the resistance to the occurence of aggregation or coalescence of the droplets in the emulsion is reduced. Thus emulsions having benzene as oil component are regarded as extraordinary.

8) S. Matsumoto, *Nippon Kagaku Zasshi (J. Chem. Soc. Japan, Pure Chem. Sect.)*, **85**, 741 (1964).

BULLETIN OF THE CHEMICAL SOCIETY OF JAPAN VOL. 42 2778—2790 (1969)

Studies of the Direct Dissolution of Metal in a β-Diketone Reagent*[1]

Kimitaka SATO and Ohiko KAMMORI

Tokyo Research Institute, Yawata Iron and Steel Co., Ltd., Ida, Kawasaki

(Received March 31, 1969)

As it was found that metallic iron is dissolved in acetylacetone (Hacac), the interaction between the solute and the solvent in the dissolution phenomena, together with the process of the dissolution of metal, were examined in detail in order to apply it to analytical techniques. The factors of the oxygen, the co-existing water, and the dissociated proton in acetylacetone were shown to be effective in the dissolution. With typical β-diketones, the exception of acetylacetone, such as trifluoroacetylacetone (HTFA), hexafluoroacetylacetone (HHFA), benzoyltrifluoroacetone (HBTA), 2-furoyltrifluoroacetone (HFTA), and 2-thenoyltrifluoroacetone (HTTA), were also employed; they were shown to have the same properties as the above one. The relationship between the solubilities of metals and the effect of adding an organic solvent, the equilibrium reactions of fluorine-containing β-diketones with water or alcohols, or the preferred enol forms of trifluorosubstituted β-diketones, were also discussed, paying attention to the accelerating effects of the solvents on the dissolution.

In general, water is employed as the solvent in the chemical analysis of iron and steel. Sometimes, however, troubles rise because of the use of an aqueous solution; for example, sometimes minute extracts float on the liquid surface in the case of separation by a centrifuge in electro-analysis. It is necessary to utilize an organic solvent effectively in solving the difficult points, so a method of electrolysis in non-aqueous solution has already been attempted.[1)]

Since β-diketone was found, in fundamental studies of the production of ultrapure iron by means of an organochemical technique in our laboratory,[2)] to have the property of dissolving metals, the present investigation was undertaken to apply the dissolution phenomena to the analysis of iron and steel. It is possible to apply the phenomena extensively to various fields of analysis. Thus, it is expected that new, simple analytical techniques can be developed by using, together with chemical analysis, gas chromatography, polarography, *etc.*[3,4)] For the above-mentioned reasons, basic problems in the phenomena were studied in detail from the point of view of analytical chemistry.

β-Diketone is well known to have the following keto-enol tautomerism[5–10)] (Eqs. (1) and (2)). Consequently, the dissociated proton is expected to have some effect on the dissolution of metal in β-diketone, as in the case of inorganic acids. On the other hand, Charles and Barnartt[11,12)] studied

*[1] A part of this study was presented: a) by O. Kammori, K. Sato, K. Takimoto and K. Arakawa at the 14th Annual Meeting of the Japan Society for Analytical Chemistry, Kyoto, November, 1965; b) by O. Kammori, K. Sato, K. Takimoto and K. Arakawa, *Japan Analyst*, **15**, 561 (1966); c) by O. Kammori, N. Yamaguchi and K. Sato, *ibid.*, **15**, 1043 (1966); d) by K. Sato, Y. Kodama and K. Arakawa, *Nippon Kagaku Zasshi (J. Chem. Soc. Japan, Pure Chem. Sect.)*, **87**, 821 (1966); e) by Y. Kodama, K. Sato and K. Arakawa, *ibid.*, **87**, 1092 (1966); f) by K. Sato and K. Arakawa, *ibid.*, **88**, 470 (1967); g) by K. Sato, Y. Kodama and K. Arakawa, *ibid.*, **88**, 968 (1967); h) by K. Sato, H. Ochi and K. Arakawa, This Bulletin, **42**, 1747 (1969), and i) by K. Sato and K. Arakawa, *Nippon Kagaku Zasshi (J. Chem. Soc. Japan, Pure Chem. Sect.)*, **89**, 1110 (1968).

1) a) O. Kammori, I. Taguchi and A. Ono, *J. Japan Inst. Metals*, **32**, 55 (1968). b) O. Kammori, I. Taguchi, K. Suzuki and A. Ono, *ibid.*, **32**, 629, 1183 (1968).

2) K. Arakawa, *Nippon Butsuri Gakkaishi (Tokyo)*, **21**, 523 (1966) (in Japanese).

3) O. Kammori, K. Sato, K. Takimoto and K. Arakawa, *Japan Analyst*, **15**, 561 (1966).

4) O. Kammori, N. Yamaguchi and K. Sato, *ibid.*, **15**, 1043 (1966).

5) J. D. Park, H. A. Brown and J. R. Lacher, *J. Am. Chem. Soc.*, **75**, 4753 (1953).

6) R. L. Belford, A. E. Martell and M. Calvin, *J. Inorg. Nucl. Chem.*, **2**, 11 (1956).

7) J. L. Burdett and M. T. Rogers, *J. Am. Chem. Soc.*, **86**, 2105 (1964).

8) K. Kondo, Y. Kondo, T. Takemoto and T. Ikegami, *Kogyo Kagaku Zasshi (J. Chem. Soc. Japan, Ind. Chem. Sect.)*, **68**, 1404 (1965).

9) Y. Kodama, K. Sato and K. Arakawa, *Nippon Kagaku Zasshi (J. Chem. Soc. Japan, Pure Chem. Sect.)*, **87**, 1092 (1966).

10) K. Sato and K. Arakawa, *ibid.*, **89**, 1110 (1968).

11) R. G. Charles and S. Barnartt, *J. Phys. Chem.*, **62**, 315 (1958).

12) S. Barnartt, R. G. Charles and L. W. Littan, *ibid.*, **62**, 763 (1958).

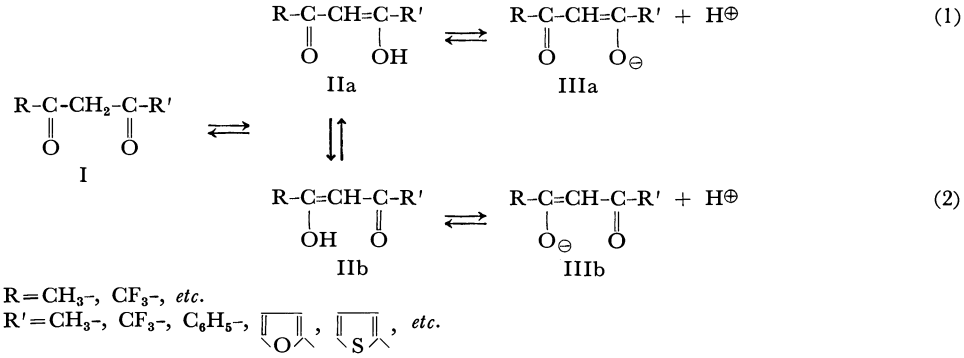

TABLE 1. STRUCTURES AND PHYSICAL PROPERTIES OF SIX β-DIKETONE REAGENTS (R·CO·CH$_2$·COR')

β-Diketone	Symbol	R	R'	Physical constant	
				mp	bp
Acetylacetone	Hacac	CH_3	CH_3	−23.2°C	137—140°C
Trifluoroacetylacetone	HTFA	CH_3	CF_3	—	107°C
Hexafluoroacetylacetone	HHFA	CF_3	CF_3	—	70.0—70.2°C
2-Furoyltrifluoroacetone	HFTA		CF_3	19—20°C	89—90°C (14 mmHg)
2-Thenoyltrifluoroacetone	HTTA		CF_3	42.5—43.5°C	103—104°C (9 mmHg)
Benzoyltrifluoroacetone	HBTA		CF_3	39—41°C	224°C

the rate theory in the reaction by concentration on the effect of oxygen in the dissolution of metals in acetylacetone. It is presumed, however, that there are other important factors in the dissolution phenomena, but the general properties have never been established in detail.

In the present paper, we will present the detailed results of an investigation made of the phenomena and the related reactivities as well as of the characteristics of β-diketone.

Experimental

Materials. The β-diketones employed are listed in Table 1. The acetylacetone was a commercial product and was also purified by distillation under reduced pressure. Hexafluoroacetylacetone obtained from the Pierce Chemical Company (U.S.A.) and the other β-diketones were used without further purification. The organic solvents and Fe(acac)$_3$ were commercially-available products of sufficient purity.

The metals were all extra-pure, commercially-available products. The metals, aluminum, beryllium, copper, manganese, molybdenum, nickel, lead, silicon, titanium, tungsten, and zinc, were sheets in shape, while the specimens of calcium and iron were granular, those of cerium, cobalt, and chromium were massive, and that of magnesium was coil-like.

Measurements. *The UV and Visible Spectra* were taken with a Cary model 14 recording spectrometer. A quartz absorption cell, 10 mm long, was used, but the measurements of absorbance in the experiment of dissolution were carried out with a Tokyo-Koden model ANA-7E colorimeter, using a glass cell of 20 mm long.

The NMR Spectra were measured at room temperature with a JNM C-60 high-resolution nuclear magnetic resonance spectrometer, using as the internal standards tetramethylsilane (TMS) in proton resonance and monofluorotrichloromethane in fluorine resonance.

Gas Chromatography was performed with a Perkin-Elmer 154 vapor fractrometer by using a column of Carbowax 1500/chromosorb W, with helium as the carrier gas.

The gas evolved in the dissolution was confirmed with a CEC 21-103C mass spectrometer.

Effective Factors in the Dissolution

When acetylacetone (Hacac) was left alone on the steel plate, a part of the iron is dissolved and red crystals appear. In order to explain the dissolution phenomena, external factors in the dissolution system and the chemical properties inside the system must be taken into consideration. We have already cited as the factors: 1) the proton dissociated in the β-diketone molecule, 2) the co-existing water in β-diketone, and 3) the oxygen dissolved in β-diketone.[3)]

Effect of Proton Dissociated in β-Diketone Molecule. β-Diketone exists as an equilibrium mixture of keto-enol tautomers. The NMR method is most favorable for determining the enol

TABLE 2. KETO-ENOL RATIO OF THE ACETYLACETONE INVOLVING WATER

Condition	Method employed	Keto form (%)	Enol form (%)	Reference
Hacac only	PMR[a]	16	84	Kammori *et al.*[c]
	PMR	15	85	Jarrett *et al.*[d]
	PMR	24	76	Bhar[e]
	PMR	18.6	81.4	Reeves *et al.*[f]
	BT[b]	24	76	Meyer *et al.*[g]
Water-saturated Hacac	PMR	19	81	Kammori *et al.*[c]
A little Hacac in water	PMR	81	19	Kammori *et al.*[c]

a) Proton magnetic resonance.
b) Bromide Titration.
c) Ref. 3.
d) H. S. Jarrett, M. S. Sadler and J. N. Shoolery, *J. Chem. Phys.*, **21**, 2092 (1953).
e) B. N. Bhar, *Arkiv. Kemi*, **10**, 223 (1956).
f) Ref. 13.
g) K. Meyer *et. al.*, *Ber.*, **44**, 2718 (1911); **45**, 2843 (1912); **47**, 826, 832 (1914).

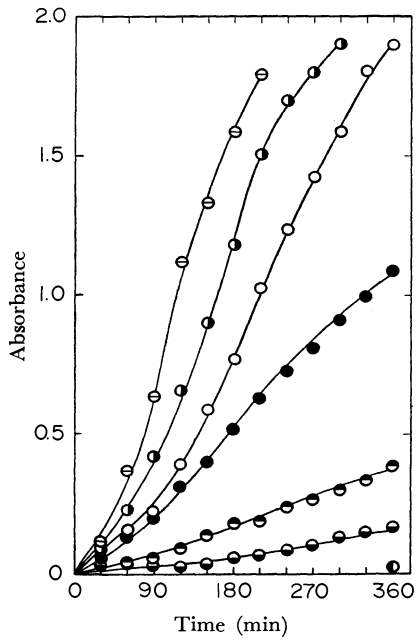

Fig. 1. Variation of solubility of iron in HTTA-methanol solution according to its concentration of HTTA.
◐, 0.0172 mol ◒, 0.0344 mol
◓, 0.0689 mol ●, 0.1379 mol
○, 0.2068 mol ◑, 0.2758 mol
⊖, 0.3448 mol (Fe: 2.0 mg)
Conditions:
Solution, 10 m*l*
Reference, methanol
Cell, glass with 20 mm long
Wavelength, 500 mμ

ratio, which was found to be 81.4% in Hacac[13] and 100% in HTFA or HHFA.[14] Moreover, the degree of the dissociation of the proton in enolized β-diketone is appraised as the acid strength, pK_a, the values of which are, respectively, 9.7 and 6.7 in Hacac and HTFA.[15] Therefore, the proton is regarded as taking part in the dissolution as in the decomposition of metal by hydrochloric acid and sulfuric acid. The keto-enol ratio of β-diketone also changes according to the kind of solvent[16] and according to the ratio of mixing with water, as is shown in Table 2.

The metals are more or less readily dissolved in solutions containing β-diketone in a greater enol ratio, but it is hard to dissolve them in a solution of β-diketone with a smaller enol ratio. The tendency of the metallic iron to dissolve was examined in HTTA-methanol solutions with different contents of HTTA, as is shown in Fig. 1. Iron is dissolved well as the concentration becomes larger. It may be concluded from the results that the proton contributes effectively to the dissolution.

Effect of Oxygen Dissolved in β-Diketone. Oxygen may be considerably dissolved in liquid β-diketone. Though the solubility of oxygen in water and typical organic solvents has already been measured, the solubility for liquid β-diketone has never been measured; however, it may be estimated to be equal to that for acetone, which is about ten times more than that of water.[17]

On the effect of oxygen, Charles and Barnartt[11] have already studied it in relation to the catalytical reaction. We investigated the same problem in

13) L. W. Reeves, *Can. J. Chem.*, **35**, 1351 (1957).
14) J. D. Park, H. A. Brown and J. R. Lacher, *J. Am. Chem. Soc.*, **75**, 4753 (1953).
15) A. E. Martell and M. Calvin, "Chemistry of the Metal Chelate Compounds," Prentice-Hall, Englewood Cliffs, N. J. (1956), p. 152.
16) J. A. Pople, W. G. Schneider and H. J. Bernstein, "High-resolution Nuclear Magnetic Resonance," McGraw-Hill Book Co., New York, Tronto, London (1959), p. 436; *cf.* also Ref. 13.
17) The Chemical Society of Japan, ed., "Kagaku Binran (New Edition)," Maruzen, Tokyo (1958), pp. 571, 576.

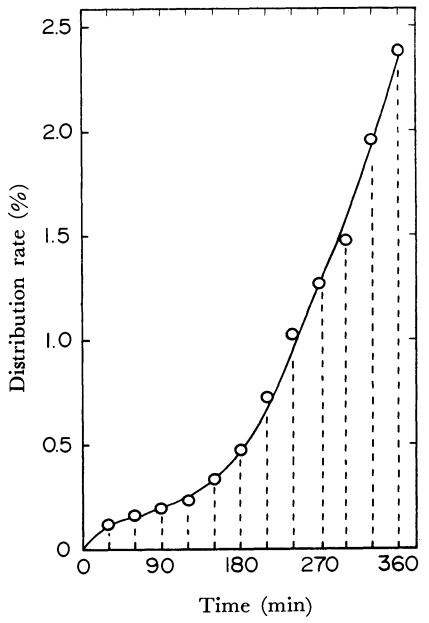

Fig. 2. Effect of oxygen on the solvency of iron in commercial acetylacetone by photometric determination.
○, Commercial Hacac (Fe: 1.700 mg)
Iron (1.787 mg) was not dissolved in deoxidated commercial Hacac for 360 min.

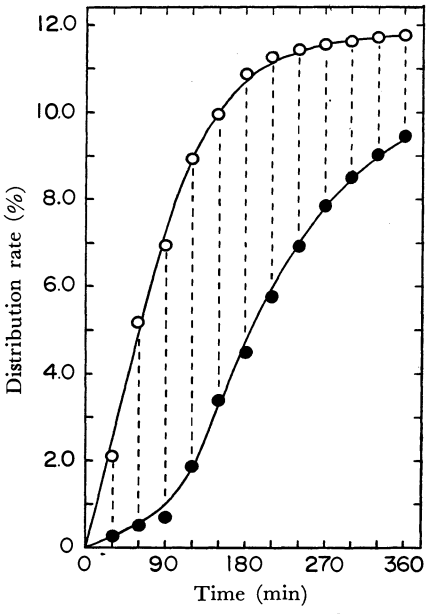

Fig. 3. Effect of oxygen on the solvency of iron in Hacac (10 m*l*) - H_2O (0.1 m*l*).
○, Hacac (10 m*l*) - H_2O (0.1 m*l*) (Fe: 1.582 mg)
●, Deoxidated (Fe: 1.660 mg)

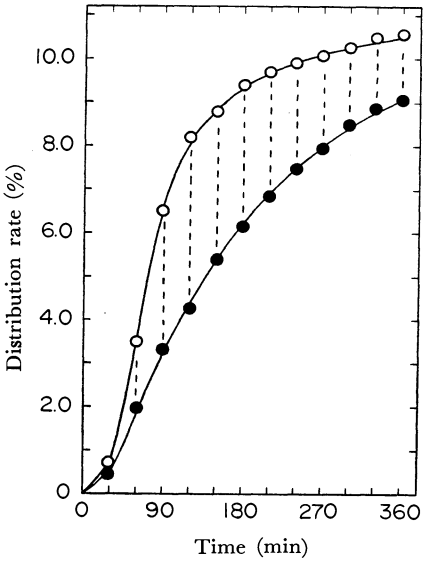

Fig. 4. Effect of oxygen on the solvency of iron in Hacac (10 m*l*) - H_2O (1 m*l*).
○, Hacac (10 m*l*) - H_2O (1 m*l*) (Fe: 1.740 mg)
●, Deoxidated (Fe: 1.596 mg)

detail from the point of view of analytical application. It was confirmed qualitatively, by the Winkler method, that considerable oxygen is dissolved in Hacac. Oxygen in 10 m*l* of liquid is removed, to the extent that no more could be detected by polarographic waves, by blowing nitrogen gas into the liquid for about 20 min. Accordingly, the effect of oxygen was investigated by blowing nitrogen gas into the solution for 30 min in order to compare the solvency of iron in the absence and presence of oxygen. Figure 2 shows the effect of oxygen in the dissolution of iron in commercial Hacac, which is expressed as the dotted line. The effects of oxygen in the case of adding 0.1 and 1.0 m*l* of water to the Hacac are shown in Figs. 3 and 4 respectively. The effect was found to become somewhat smaller when a lot of water was added. These results clearly show that oxygen is one of the important factors in the phenomena. Since it was observed that the solubility of iron increases with the quantity of water added to Hacac, as will be discussed later, the effect was further examined by adding ammonium persulfide, which acted effectively in oxidation. The correlation between the ammonium persulfide content and the dissolving time of iron obtained is shown in Fig. 5. The addition of ammonium persulfide was easily found to be more effective. Ammonium persulfide is dissolved into water as follows (Eq. (3)):

$$(NH_4)_2S_2O_8 + H_2O \rightleftarrows (NH_4)_2SO_4 + H_2SO_4 + (O) \quad (3)$$

Consequently, a lot of nascent oxygen may occur and play an effective role, together with sulfuric acid, in the dissolution of iron.

Effect of Co-existing Water in β-Diketone.

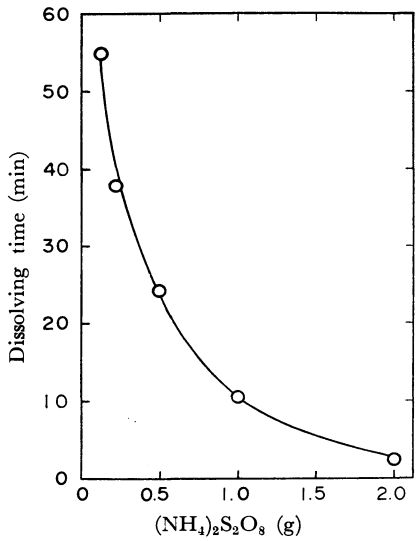

Fig. 5. Effect of addition of ammonium persulfide.
Conditions: Hacac, 10 m*l*; H_2O, 10 m*l*; Fe, 1 mg

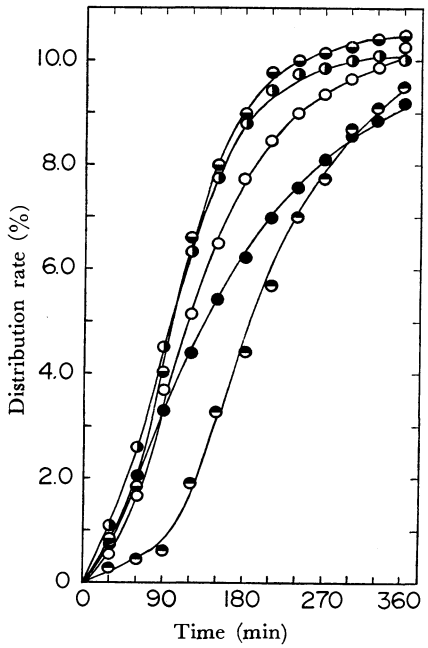

Fig. 6. Effect of water on the solvency of iron in Hacac.
Water contents in 10 m*l* of Hacac:
◓, 0.1 m*l* ◒, 0.3 m*l*
○, 0.5 m*l* ◑, 0.7 m*l*
●, 1.0 m*l* (Fe: 1.5—2.0 mg)

Since a little water is dissolved at the same time in liquid β-diketone, the influence of water on the dissolution of metal was also studied. The values of the water content in Hacac are listed in Table 3 along with those of the ratio of the area obtained in

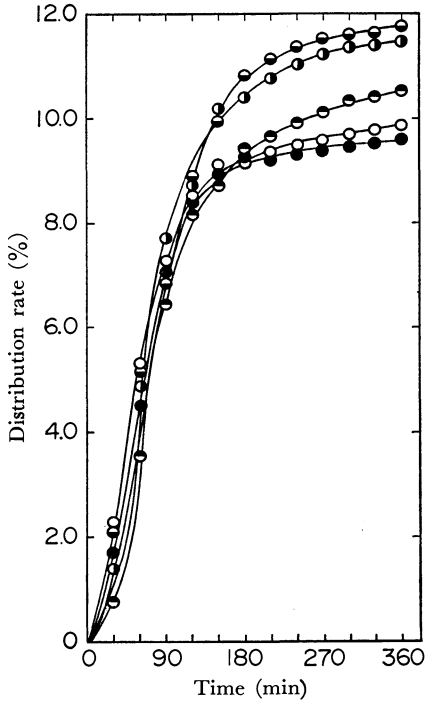

Fig. 7. Effect of water on the solvency of iron in Hacac, which is not deoxidated.
Water contents in 10 m*l* of Hacac:
◑, 0.02 m*l* ●, 0.04 m*l*
◒, 0.1 m*l* ○, 0.5 m*l*
◓, 1.0 m*l* (Fe: 1.5—2.0 mg)

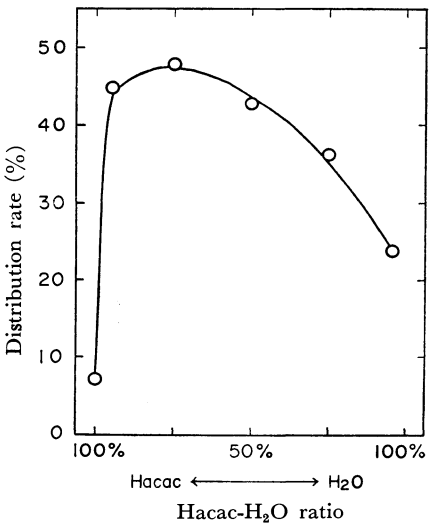

Fig. 8. Correlation between solvency of iron and Hacac-H_2O ratio.
Conditions:
Total volume of Hacac and H_2O, 20 m*l*
Fe, 1—2 mg
Treating time, 100 min

gas chromatography. A trace of water which could not easily be removed was found to be present

in the Hacac. The dissolution curve in Fig. 6 shows that only the co-exsisting water is clearly effective, even in the case of Hacac in the absence of oxygen.

Table 3. Determination of water in acetylacetone

Condition	H_2O/Hacac	H_2O in Hacac 10 m*l* (*μl*)
Commercial	1/1500	6.86
Purified	1/4800	2.08
Purified	1/8000	1.25

The tendency toward much greater solvency upon the addition of water was further examined. Figure 7 shows an example of the experimental results regarding the effect of the solvency of iron in Hacac containing 0.02—1.0 m*l* of water. Water, 0.04 m*l*, is dissolved completely into 10 m*l* of Hacac, but when there is more than 0.05 m*l* of water the solution is separated into two layers. In terms of solubility, the metal was found to be dissolved effectively in such a solution. Figure 8 shows the solvency of iron in a solution containing Hacac and water, the total quantity of which is definite. The solvency was found to be best in a solution consisting of Hacac : water=3 : 1 (vol.).

Phenomena of Dissolution

Solubilities of Various Kinds of Metals in Acetylacetone. The solubilities in Hacac were studied with 17 kinds of metals. In our experiments, the size of the metal sample was 1 cm^2 in the case of a sheet, and the sample was prepared so as the surface area became equal to that of the sheet in the cases of metals with other shapes. We attempted to initiate dissolution by agitating at 70°C in 10 m*l* of Hacac. The dissolution rate was determined by weighing insoluble metal fragments taken out at definite intervals. As is shown in Fig. 9, nine (aluminum, beryllium, cobalt, chromium, copper, molybdenum, nickel, titanium, and tungsten) of the 17 kinds of metals examined were scarcely dissolved at all in six hours. A similar experiment was made by Barnartt *et al.*[12]; their results were almost the same as ours. The tendencies toward the ionization of soluble metals in dissolution were found to be larger than that of hydrogen. Though the standard potentials of the elements in Hacac have never been measured, Strehlow[18] measured the potential of various metals in a non-aqueous solvent; the tendency he found agrees fairly well with that shown in Fig. 9.

Product of the Dissolution of Iron in Acetylacetone. The solution becomes red, when iron is dissolved in Hacac. The absorption spectra of both the above solution and the $Fe(acac)_3$-Hacac solution obtained in the visible region (340—600 m*μ*) are shown in Fig. 10. The above results show that the product of the dissolution is $Fe(acac)_3$, for the spectrum of the solution is in good agreement with that of $Fe(acac)_3$.

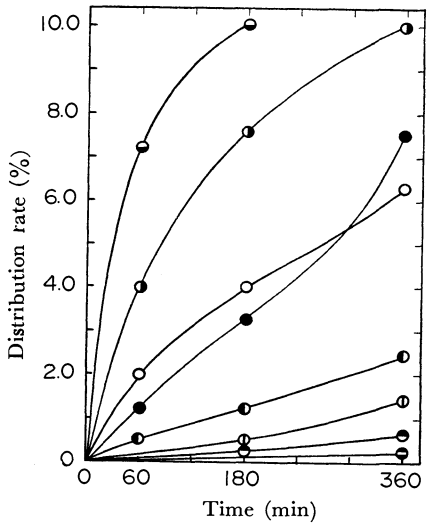

Fig. 9. Dissolution rate of various metals in Hacac.
Conditions:
Hacac, 10 m*l*
Size of metal, 10×10 mm
Temperature, 70°C
◒, Pb ◑, Mg ●, Ca ○, Zn
◐, Mn ◑, Fe ◓, Ce ◒, Si

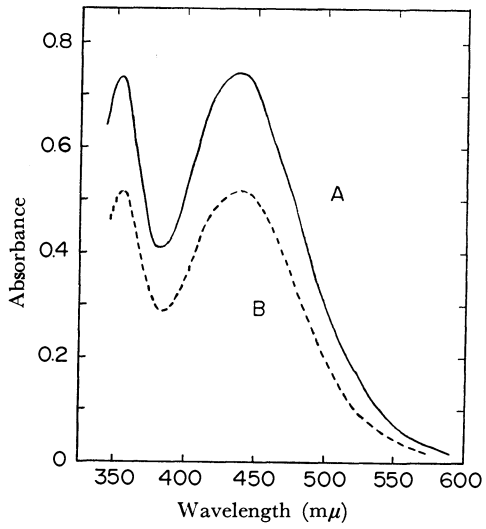

Fig. 10. Visible absorption spectra of the solution of iron in Hacac and of $Fe(acac)_3$ in Hacac.
(A) Fe: 0.0108 g/*l* Hacac
(B) $Fe(acac)_3$: 0.0487 g/*l* Hacac

18) H. Strehlow, *Z. Elektrochem., Ber., Bunsenges. Phys. Chem.*, **56**, 827 (1952).

Process of the Dissolution of Iron in Acetylacetone. The variations in the absorption spectra in the process of the dissolution of iron in Hacac are shown in Fig. 11. In the earlier steps, the absorption band at 354 mμ can not be discriminated clearly. With the passing of time, however, the absorbances at 354 and 435 mμ become larger, and at last the intensities of these two absorption bands become equal. Therefore, the spectrum may be regarded as coinciding with that of Fe(acac)$_3$.

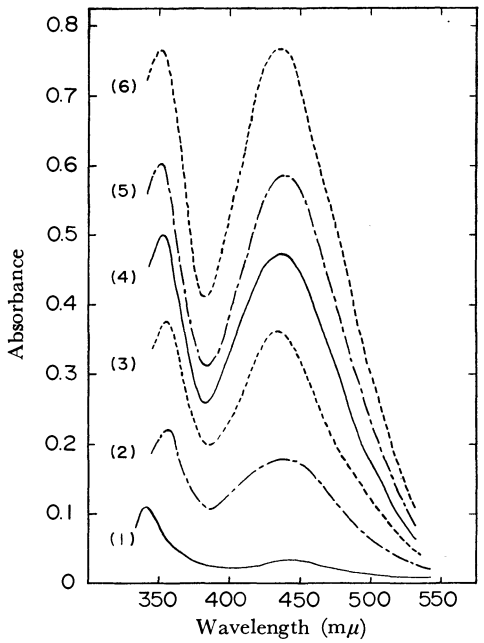

Fig. 11. Variations of the visible absorption spectrum of the solution of iron in Hacac.

On the other hand, the variations in the absorption spectra of Fe(acac)$_2$ formed from the standard iron(II) solution and Hacac are shown in Fig. 12. The behavior of the spectra shown in Fig. 12 is almost the same as that in Fig. 11. Since the Fe(acac)$_2$ with a four-coordinated-plane structure formed in the earlier step of the dissolution is stereochemically unstable, the stable form of Fe(acac)$_3$ with the octahedral six coordination is thought to be gradually formed in the solution.

In order for Fe(acac)$_2$ to be formed in a solution, it is necessary for Fe^{2+} ions to be present. Consequently, metallic iron is ionized to become Fe^{2+} ions by the action of some factor (Eq. (4)):

$$Fe \rightleftarrows Fe^{2+} + 2e^- \quad (4)$$

where the proton set free in Hacac is thought to act as follows (Eq. (5)):

$$Fe + 2H^+ \rightleftarrows Fe^{2+} + H_2 \quad (5)$$

Moreover, it was confirmed by mass spectrometry that hydrogen gas is formed during the process of

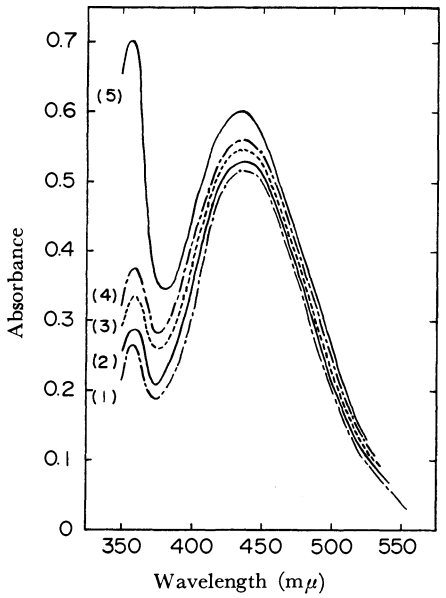

Fig. 12. Variations of the visible absorption spectrum of Fe(acac)$_2$.

the dissolution. In view of the above facts, the following reaction mechanism may be proposed for the dissolution of iron in Hacac:

$$Hacac \rightleftarrows acac^- + H^+ \quad (6)$$

$$Fe + 2H^+ \rightleftarrows Fe^{2+} + H_2$$

$$Fe^{2+} + 2acac^- \rightleftarrows Fe(acac)_2 \quad (7)$$

$$Fe(acac)_2 + acac^- \rightleftarrows Fe(acac)_3 + e^- \quad (8)$$

Dissolution of Metal in β-Diketones Except Acetylacetone. The acid strengths of β-diketones involving fluorine (HHFA, HFTA, HBTA, HTTA, *etc.*) are smaller than that of Hacac, which is 9.7.[15] Accordingly, it was thought that metal might be more readily dissolved in such fluorine-containing β-diketone solutions than in acetylacetone. Thus, its tendency in such a β-diketone solution was studied. The liquid β-diketones, such as HTFA, HHFA, and HFTA, were used in the liquid state, while the solid β-diketones, like HTTA and HBTA, were used in a solution, in which they were more enolized. The results showed that the dissolution rate of iron in a fluorine-containing β-diketone solution is ten or more times faster than that in Hacac. HHFA especially shows a powerful solubility.

On the other hand, metals were hardly dissolved at all in a solution in which a β-diketone interacted with solvents such as triethylamine and diethylamine. This fact can be explained in terms of a strong intermolecular hydrogen bond being formed between the β-diketone and the solvent.[19]

19) Ref. 16, p. 437; L. W. Reeves and W. G. Schneider, *Can. J. Chem.*, **36**, 793 (1958).

Accelerating Effect in the Dissolution

In the solvent extraction, the accelerating effect of the added ingredient is called "the synergistic effect."[20] A similar accelerating effect may be expected to appear in the dissolution of metals in a β-diketone solution.

Accelerating Effect of Adding an Organic Solvent in the Dissolution Phenomena. Figure 13 shows the synergistic effect observed in the case of adding another solvent to Hacac. The above experiment showed that carbon tetrachloride and glacial acetic acid were both effective as added solvents. The enol ratio of Hacac is 100% in triethylamine and 75—88% in the other solvents. The lack of solubility in triethylamine results from the strong intermolecular hydrogen bonding between solute and solvent, as has been mentioned above.[19] As a proton may be partially set free even in acetic acid, much as in Hacac, its effect is expected to persist in the solution. The above results clearly proved the dissolution of metal to be more effective in a solution containing an organic solvent than in an Hacac alone.

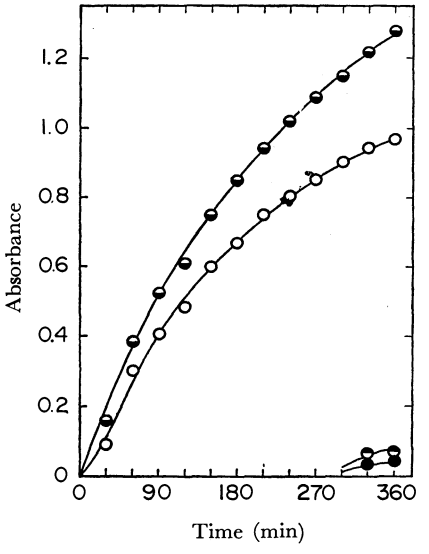

Fig. 13. Solvency of iron in Hacac solution.
◒, Hacac (5 m*l*) + acetic acid (5 m*l*) (Fe: 1.098 mg)
○, Hacac (5 m*l*) + CCl_4 (5 m*l*) (Fe: 1.020 mg)
◓, Hacac (5 m*l*) + benzene (5 m*l*) (Fe: 1.012 mg)
●, Hacac (5 m*l*) + cyclohexane (5 m*l*) (Fe: 1.011 mg)
Fe (1.155 mg) was not dissolved in Hacac (5 m*l*)-$N(C_2H_5)_3$ (5 m*l*)
Conditions:
Wavelength, 420 mμ
Reference, each solution
Cell, glass with 20 mm long

The solubility of iron in a solution containing HBTA was also examined as an example of solid β-diketones; the investigation showed that methanol was more effective than the other solvents, as is shown in Fig. 14.

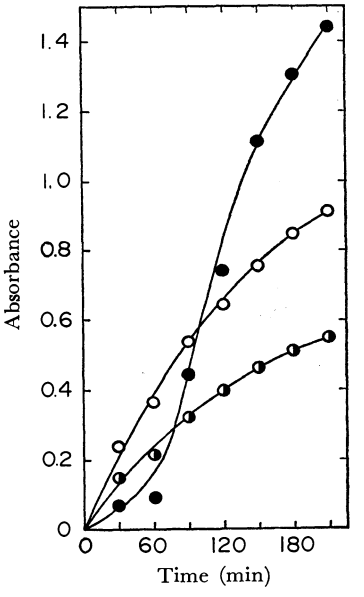

Fig. 14. Solvency of iron in HBTA solution.
●, HBTA (1 g) + Hacac (10 m*l*) (Fe: 1.187 mg)
○, HBTA (1 g) + methanol (10 m*l*) (Fe: 1.147 mg)
◑, HBTA (1 g) + CCl_4 (10 m*l*) (Fe: 1.184 mg)
Conditions:
Reference, each solution
Cell, glass with 20 mm long
Wavelength, 420 mμ

In order to ascertain the accelerating effect of alcohols, the tendency toward solubility of a metal in the solution was studied in detail. The results of the experiment in which eleven kinds of alcohols were employed as solvents are summarized in Table 4.

Equilibrium Reaction and Solubility of Metal in β-Diketone Involving the Fluorine-Alcohol System. We mentioned above that the effect is accelerated by adding water or alcohol in liquid β-diketone during the dissolution of metal. It must be noted that various chemical reactions can occur in a mixture. Such a point of view is important in discussing the accelerating effect in the phenomena.[9,21]

20) T. W. Healy, *J. Inorg. Nucl. Chem.*, **19**, 314, 328 (1961). The word "*synergism*" was first coined by Baes *et al.*; C. A. Blake, C. F. Baes, K. B. Brown, C. F. Coleman and J. C. White, Proceedings of the Second International Conference on Peaceful Uses of Atomic Energy, Geneva, 1958, 15/P/1550 (1958).

21) K. Sato, Y. Kodama and K. Arakawa, *Nippon Kagaku Zasshi (J. Chem. Soc. Japan, Pure Chem. Sect.)*, **87**, 821 (1966); **88**, 968 (1967).

TABLE 4. SOLVENCY OF IRON IN VARIOUS β-DIKETONE-ALCOHOL SOLUTIONS

Alcohol	β-Diketone				
	Hacac	HFTA	HTFA	HTTA	HBTA
Methyl alcohol	○	○	◎	◎	◎
Ethyl alcohol	○	○	◎	◎	◎
n-Propyl alcohol	○	○	◎	◎	◎
Isopropyl alcohol	○	○	◎	◎	◎
n-Butyl alcohol	○	○	◎	◎	◎
Isobutyl alcohol	×	×	○	○	○
n-Amyl alcohol	×	×	○	×	×
Isoamyl alcohol	×	×	×	○	○
4-Methyl-2-pentanol	×	×	○	○	○
4-Octyl alcohol	×	×	○	×	×
n-Octyl alcohol	×	×	○	○	×

◎: Well soluble ○: A little soluble ×: Hardly soluble

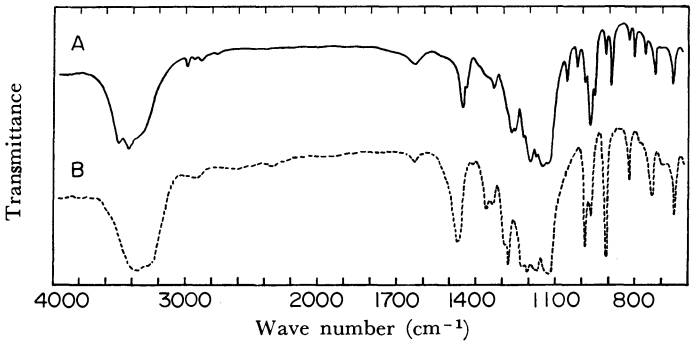

Fig. 15. Infrared spectra of the reaction product of HHFA with methanol (A) and of hexafluoroacetylacetone dihydrate (B). (KBr disk)

A white crystal was found to separate by the reaction of HHFA with water or methanol.[21] The configuration of the reaction product of HHFA with water[22] has already been studied by Schultz and Larsen,[23] who confirmed it to be hexafluoroacetylacetone dihydrate (IV), but the reaction product of HHFA with methanol has never been reported. The structure of the compound was identified on the basis of the results of elemental analysis and of the spectral investigation.

Elemental analysis showed that the compound has the formula $C_7H_{10}O_4F_6$ (Found: C, 30.77; H, 3.70%. Calcd for $C_7H_{10}O_4F_6$: C, 30.89; H, 3.57%). The IR spectrum shows absorptions at 1121 cm^{-1}(vs) due to the vibration, ν_{C-O}, of tertiary alcohol, and at 1051(w) and 1009 cm^{-1} (w) due to the ν_{C-O} of the C–O–C bond, which is illustrated in Fig. 15.

Figure 16 shows the NMR spectrum, in which signals are observed at τ 7.80, 7.66, and 4.29,

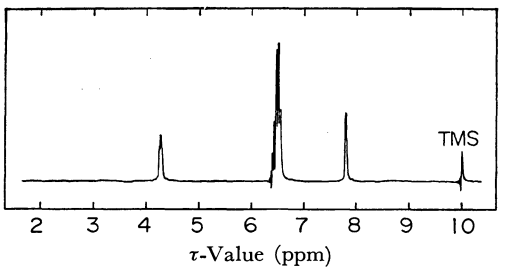

Fig. 16. Proton magnetic resonance spectrum of the reaction product of HHFA with methanol in C_2Cl_4 at 60 Mc.

with relative intensities of 1 : 3 : 1 respectively; these signals can be assigned to those due to the protons at $-CH_2-$, $-O-C_3H$, and $-OH$ respectively. The UV spectrum showed no absorptions. In view of the above facts, the most reasonable identification of the compound is as 1,1,1,5,5,5-hexafluoro-(2,4-dioxy-2,4-dimethoxy)-pentane (V).*2

22) A. L. Henne, M. S. Newman, L. L. Quill and R. A. Staniforth, *J. Am. Chem. Soc.*, **69**, 1819 (1947).
23) B. G. Schultz and E. M. Larsen, *ibid.*, **71**, 3290 (1949).

*2 Adopted later as one of the IRDC cards (No. 6777) of the Infrared Data Committee of Japan.

Table 5. Fluorine resonance data of trifluoro-substituted β-diketone solutions (φ; ppm)

β-Diketone	Water or alcohol	$CF_3C(OH)CHCOR$	$CF_3C(OH)(OR')CH_2COR$	R	R'
HTFA	H_2O	75.4	84.6	CH_3	H
HTFA	CH_3OH	75.4	80.6	CH_3	CH_3
HTFA	C_2H_5OH	75.4	80.6	CH_3	CH_3CH_2
HTFA	C_3H_7OH	75.4	80.5	CH_3	$CH_3(CH_2)_2$
HTFA	$(CH_3)_2CHOH$	75.4	81.3	CH_3	$(CH_3)_2CH$
HTFA	C_4H_9OH	75.4	80.4	CH_3	$CH_3(CH_2)_3$
HTFA	$(CH_3)_2CHCH_2OH$	75.4	80.3	CH_3	$(CH_3)_2CHCH_2$
HTFA[a)]	$ClCH_2CH_2OH$	75.8	81.5	CH_3	$ClCH_2CH_2$
HTFA[a)]	$BrCH_2CH_2OH$	75.7	81.4	CH_3	$BrCH_2CH_2$
HTFA[a)]	$CNCH_2CH_2OH$	75.8	81.6	CH_3	$CNCH_2CH_2$
HTFA[a)]	$CH_2=CHCH_2OH$	76.1	81.4	CH_3	$CH_2=CHCH_2$
HTFA[a)]	$CH\equiv CCH_2OH$	75.6	81.4	CH_3	$CH\equiv CCH_2$
HFTA	H_2O	74.5	84.3		H
HFTA	CH_3OH	74.5	80.4		CH_3
HBTA	H_2O	75.1	84.5		H
HBTA	CH_3OH	75.1	80.5		CH_3
HTTA	H_2O	74.3	84.6		H
HTTA	CH_3OH	74.3	80.4		CH_3

The concentration of each solution is 50 mol%, but 50 vol% in a) mark.

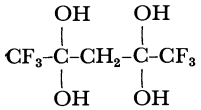

IV

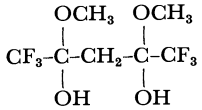

V

The equilibrium reaction of β-diketone involving fluorine with water or alcohol was also examined.[9,21] The behavior in the fluorine resonance spectra of the solution consisting of trifluoro-substituted β-diketone and water or alcohol, is summarized in Table 5. The β-diketone was clearly found to react with water or alcohol. The proton resonance spectra are shown in Figs. 17—19. A signal was observed at about δ 3 due to the methylene group, which is a singlet in water and an AB quartet in alcohol. From a consideration of the above facts, it seems most reasonable to conclude that an equilibrium reaction occurs in the solution as follows (Eq. (9)):

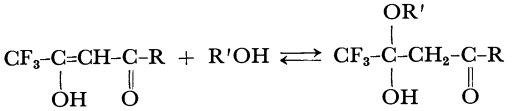

(9)

R=CH_3, , ,

R'=H, CH_3, C_2H_5, C_3H_7, $(CH_3)_2CH$, C_4H_9, $(CH_3)_2CHCH_2$, $ClCH_2CH_2$, $BrCH_2CH_2$, $CNCH_2CH_2$, $CH_2=CHCH_2$, $CH\equiv CCH_2$, $PhCH_2$

The equilibrium reaction of pivaloyltrifluoroacetone with water or alcohol has already been studied.[24]

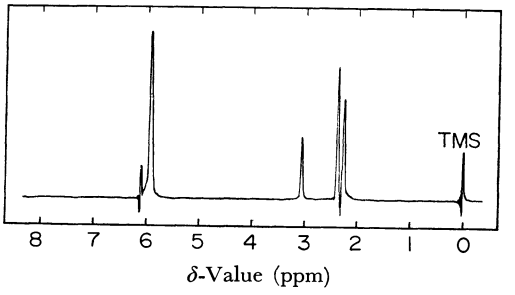

Fig. 17. Proton magnetic resonance spectrum of HTFA aqueous solution at 60 Mc.

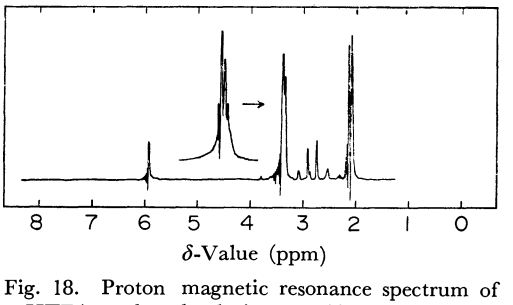

Fig. 18. Proton magnetic resonance spectrum of HTFA-methanol solution at 100 Mc.

24) K. Sato, H. Ochi and K. Arakawa, This Bulletin, **42**, 1747 (1969).

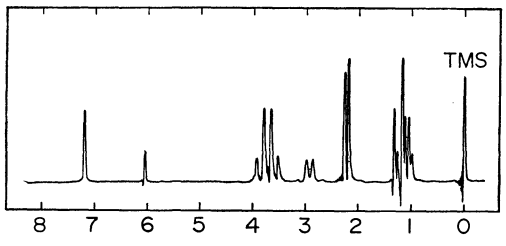

Fig. 19. Proton magnetic resonance spectrum of HTFA-ethanol solution at 60 Mc.

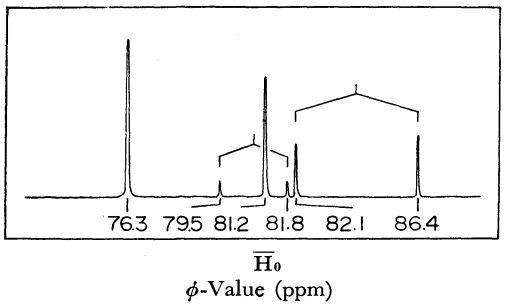

Fig. 20. Fluorine magnetic resonance spectrum of HHFA-ethylenebromohydrin solution at 56.45Mc with $CFCl_3$ as internal standard.

Equilibrium reactions different from the above results were seen with HHFA.[21] The reaction was also confirmed by NMR spectroscopy. The fluorine resonance data of the solution of HHFA obtained with alcohol are summarized in Table 6, while the existence ratio of each state is listed in Table 7. An example of these spectra is also shown in Fig. 20. The data suggest that equilibrium states with three types, states A, B, and C, exist in the course of the reaction.

The fluorine resonance spectrum clearly proved that only a reaction on the state A is preferred in an HHFA ethanol solution. The state A may be represented by Eq. (10):

$$CF_3\text{-}C(OH)=CH\text{-}C(=O)\text{-}CF_3 + 2R'OH \rightleftarrows CF_3\text{-}C(OR')(OH)\text{-}CH_2\text{-}C(OR')(OH)\text{-}CF_3 \quad (10)$$

R′ = C_2H_5, n-C_3H_7, i-C_3H_7, n-C_4H_9, $CH_3(CH_2)_6CH_2$, $BrCH_2CH_2$, $CNCH_2CH_2$, $CH_2=CHCH_2$, $CH\equiv CCH_2$, $PhCH_2$

since the signal was observed at δ 2.30 with a singlet in the proton resonance spectrum. Furthermore, the AB quartets at about δ 3.30 may be due to the following reaction (Eq. (11):

$$CF_3\text{-}C(OH)=CH\text{-}C(=O)\text{-}CF_3 + R'OH \rightleftarrows CF_3\text{-}C(OR')(OH)\text{-}CH_2\text{-}C(=O)\text{-}CF_3 \quad (11)$$

Table 6. Fluorine resonance data of hexafluoroacetylacetone solutions[a] (φ; ppm)

Solvent	R	HFA	State A	State B		State C	
Ethyl alcohol	CH_3CH_2	—	81.6	—	—	—	—
n-Propyl alcohol	$CH_3(CH_2)_2$	76.3	81.1	—	—	—	—
Isopropyl alcohol	$(CH_3)_2CH$	75.8	80.5	78.4	81.3	79.5	81.0
Ethylenebromohydrin	$BrCH_2CH_2$	76.3	81.2	79.5	81.8	82.1	86.4
Ethylenecyanohydrin	$CNCH_2CH_2$	76.1	80.8	79.1	81.1	81.4	86.4
Allyl alcohol	$CH_2=CHCH_2$	76.5	81.6	—	—	—	—
Propargyl alcohol	$CH\equiv CCH_2$	75.8	81.9	78.8	81.6	81.1	86.2

a) Each concentration is 50 vol%.

Table 7. Existence ratio of each state in the equilibrium of hexafluoroacetylacetone solution (%)

Solvent	HHFA		State A		State B		State C	
	23°C	45°C	23°C	45°C	23°C	45°C	23°C	45°C
Ethyl alcohol	—	†	100	†	—	†	—	†
n-Propyl alcohol	12	18	88	82	—	†	—	†
Isopropyl alcohol	34	45	18	15	37	30	11	10
Ethylenebromohydrin	32	†	33	†	27	†	8	†
Ethylenecyanohydrin	34	†	54	†	6	†	6	†
Allyl alcohol	20	†	80	†	—	†	—	†
Propargyl alcohol	40	41	48	41	6	†	6	9

† These values were not measured.

while the multiplet at about δ 4.70 is due to the methine group formed by the following reaction (Eq. (12)):

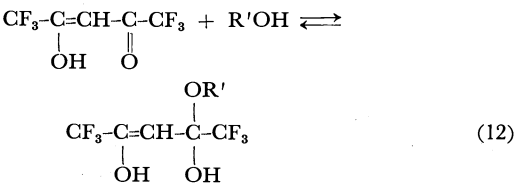

(12)

In the proton resonance spectrum of the isopropanol solution, the signal intensity at δ 3.30 with the AB quartet is greater than that at about δ 4.70. The reactions involving the states B and C were found to be due to the reactions (12) and (11) respectively. From these results, the correlation in the equilibrium of HHFA with various alcohols may be summarized as follows:

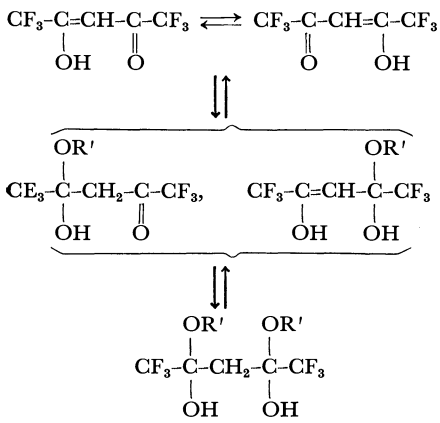

R'=C_2H_5, C_3H_7, $(CH_3)_2CH$, $BrCH_2CH_2$, $CNCH_2CH_2$, $CH_2=CHCH_2$, $CH\equiv CCH_2$, C_4H_9, C_8H_{17}, $PhCH_2$

Fluorine-containing β-diketones are generally reactive. The reactivity may be explained by considering that the carbon atom adjacent to the trifluoromethyl group is activated by the *I* effect of the functional group with the fluorine atom, which has a strong electro-negativity. The dissolution of metal in such solutions is remarkably accelerated, as has been mentioned above. The reason for this is, however, not clear; the cause may be in the acid strength of β-diketone alone or in the presence of such an equilibrium.

Preferred Enol Form of Trifluorosubstituted β-Diketone and Solubility of Metal. β-Diketones with a trifluoromethyl group are thought to take the following enol forms (Eq. (13)):[5-9]

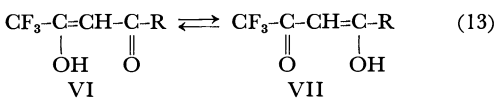

(13)

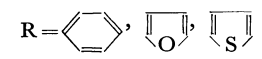

The question of which form of the above enols is preferred is an interesting problem, which has been discussed in only a few reports.[5,8,25] On the basis of the assumption that a conjugate system must be formed between the R ring and the carbonyl group in the β-diketone molecule and the UV spectrum may become remarkable due to the polarity of the solvent;[26] the investigation discussed below was undertaken in order to determine the preferred enol form.[10]

The UV spectra of HBTA and HTTA in various solvents are illustrated in Figs. 21 and 22 respectively. In view of the absorption band at about 260 mμ, the behavior of HBTA is clearly different from that of HTTA: the intensity of absorption varies in HBTA, but not in HTTA. The variations according to polar and non-polar solvents suggest that a conjugate system with a carbonyl group is formed adjacent to the aromatic ring. Accordingly, the preferred enol forms of HBTA and HTTA may be regarded as being VI and VII respectively. The results of the above studies support the theory which Pukanic *et al.*[26] derived from their study on the interaction between

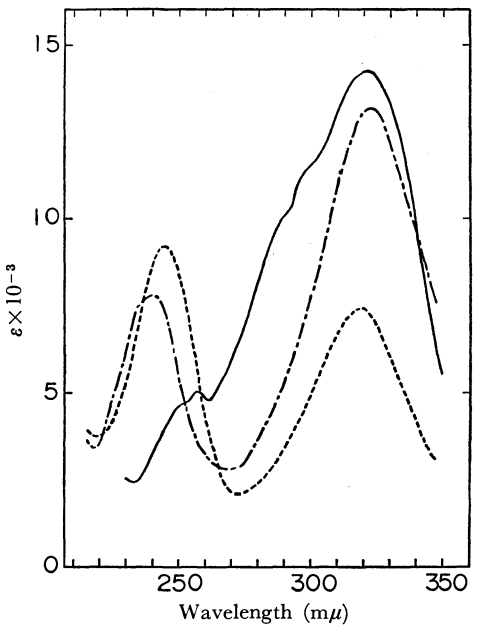

Fig. 21. UV spectrum of HBTA.
Solvent: ——, *n*-heptane
——, ethanol
----, water

25) Pukanic *et al.* have shown from the fluorine magnetic resonance frequency of enolic HTTA and HHFA in CCl_4, in the absence and in the presence of various concentrations of TBP, that the preferred enol form of HTTA is VII; G. Pukanic, N. C. Li, W. S. Brey, Jr., and G. B. Savitsky, *J. Phys. Chem.*, **70**, 2899 (1966).

26) For one of the examples, see M. Hirota, "The Interpretations of UV and Visible Spectra," Kyoritsu Shuppan, Tokyo (1967), p. 81.

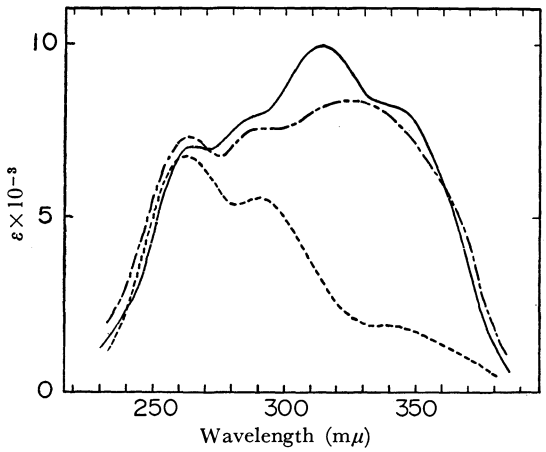

Fig. 22. UV spectrum of HTTA.
Solvents: ——, *n*-heptane
—·—, ethanol
– – –, water

HTTA and tributylphosphate (TBP) by means of the fluorine resonance spectra.

As Figs. 21 and 22 show, no special abnormalities are recognized in the so-called "*enol absorption band*" in the region with wavelengths longer than 300 mμ, so it may be concluded that the above equilibrium reaction exerts an essential influence on the molar extinction coefficient (ε). This influence must, therefore, be explained as the mutual effect of the keto-enol tautomerism with the equilibrium reaction in the solution. As the enol form of VII is preferred in the HTTA solution, the following equilibrium is also possible between HTTA and alcohol (Eq. (14)):

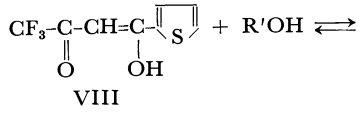

VIII

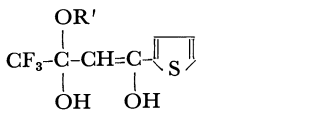

(14)

R'=H, CH_3, $(CH_3)_2CH$, $CNCH_2CH_2$, $PhCH_2$, *etc.*

However, it is conceivable that only the enol form of VIII, which is presumed, preferentially contributes to the equilibrium reaction, since the above fluorine resonance data are consistent with those of the HTFA and HBTA solutions.

Since HTTA behaves uniquely in comparison with other β-diketones, it may be interesting to discuss fundamentally the dissolution of metal in a mixed system of HTTA with Hacac.

Conclusion

Concerning the dissolution of metal in a β-diketone solution, the effective factors, the process of the dissolution, and the accelerating effect in dissolution were studied in detail. The effective factors were shown to be oxygen, co-existing water, and the dissociated proton in the solution.

The phenomena of the dissolution were expected to be applied effectively not only to the analysis of iron and steel, but also of other metals and alloys. For example, it is possible to establish new analytical methods by using these phenomena together with gas chromatography, polarography, the atomic absorption method, and so on. Part of an attempt to do so has already been reported.[27–32]

The problems related to the preferred enol forms of trifluorosubstituted β-diketones and the equilibrium reactions of fluorine-containing β-diketones with water or alcohols are interesting even in the field of organic chemistry; moreover, the solubilities of metals in these solutions must also involve a large number of significant problems.

The unique behavior of HTTA is seen not only in the dissolution of metal, but also in the solvent extraction. A thorough investigation, from a similar point of view, may be expected to establsih the cause of the series of phenomena, so the problem may be left as an interesting one for the future.

We wish to thank Professor Yojiro Tsuzuki, Science University of Tokyo, for his kind encouragement and much valuable advice. For their helpful discussions and kind encouragements, our thanks are also extended to Dr. San-ichiro Mizushima, Director of this institute, and Professor Kiichi Arakawa, Showa University.

27) K. Kishi, S. Ikeda and K. Hirota, *J. Phys. Chem.*, **71**, 4384 (1967).
28) S. Musha, T. Ishii and T. Yao, Preprint for the 16th Annual Meeting of the Japan Society for Analytical Chemistry (Chiba, October, 1967), p. B428.
29) S. Musha, T. Ishii and T. Yao, Preprints for the 21st Annual Meeting of the Chemical Society of Japan (Osaka, April, 1968), Vol. 2, p. 845.
30) S. Musha, T. Ishii and S. Sakaguchi, Preprint for the 17th Annual Meeting of the Japan Society for Analytical Chemistry (Hiroshima, October, 1968), p. B347.
31) O. Kammori and I. Taguchi, *Japan Analyst*, **15**, 1223 (1966).
32) K. Arakawa and K. Sato, *Kagaku no Ryoiki (J. Japanese Chem.)*, **22**, 230 (1968).

BULLETIN OF THE CHEMICAL SOCIETY OF JAPAN VOL. 42 2791—2796 (1969)

The Molecular and Crystal Structure of *trans*-Dinitrotetramminecobalt(III) Nitrate Monohydrate

Isao OONISHI, Fumio MUTO and Yoshimichi KOMIYAMA*1

Department of Applied Chemistry, Faculty of Engineering, Yamanashi University, Kofu, Yamanashi

(Received April 4, 1969)

The crystal structure of *trans*-dinitrotetramminecobalt(III) nitrate monohydrate $[Co(NO_2)_2(NH_3)_4]NO_3 \cdot H_2O$ has been determined from three dimensional X-ray diffraction data. The dimensions of orthorhombic unit cell are: $a=10.02$ Å, $b=6.02$ Å, $c=16.84$ Å, and $Z=4$. The space group is $P2_12_12_1$. The structure has been refined by the three dimensional Fourier and least-squares method to $R=0.103$. The complex ion has a slightly distorted octahedral coordination with six N atoms at about 1.98 Å (two are N atoms of nitro groups and the others ammonium groups). The complexes are tightly bound together by N-H···O and O-H···O interactions, constructing a three dimensional network.

Crystal structures of various nitroamminecobalt(III) complexes of the type, $[Co(NO_2)_m(NH_3)_{6-m}]^{3-m}$ have been determined, where $m=1$,[1] 3,[2] 4,[3] and 6.[4] Nitropentamminecobalt(III) salts ($m=5$) have not yet been synthesized, whereas for dinitrotetramminecobalt(III) complexes ($m=2$) *cis*- and *trans*-isomers are well known.

However, no crystal structure analysis of these salts has yet been reported. Knowledge of the crystal structures of the whole series of nitroamminecomplexes evidently is an important basis for the understanding of the stereochemistry of nitroamminecomplexes and their structural principles. We have initiated a study of the structure of dinitrotetramminecobalt(III) nitrate.

The crystal structure of the *trans* form is reported in this paper. That of the *cis* form will be described in the following paper.

Experimental

The crystals were prepared by the method of Jörgensen.[5]

Recrystallization from water containing a small amount of acetic acid yielded thin tabular or needle-like crystals, the latter being found to be twinned. The unit cell dimensions were determined from higher-order reflections of Weissenberg photographs (Ni$K\alpha$, $\lambda=1.6591$Å). The systematic absences were: $h00$ for h odd, $0k0$ for k odd and $00l$ for l odd. Hence the space group was unequivocally determined. The crystal data are listed in Table 1. Sets of multiple film equi-inclination Weissenberg photographs were taken about the b-axis (0 to 5th layers), the a- and c-axes (0th layer). Ni$K\alpha$ radiation was used throughout. The intensities were estimated visually with a standard film strip and were converted to $|Fo(hkl)|^2$ and $|Fo(hkl)|$ by applying the usual Lorentz, polarization and spot shape corrections. 998 independent reflections were observed. They are about two-thirds of those within the nickel sphere. The crystal used was a rod $0.2 \times 0.06 \times 3.0$ mm. No correction was made for absorption or extinction.

TABLE 1. CRYSTAL DATA

trans-$[Co(NO_2)_2(NH_3)_4]NO_3 \cdot H_2O$
Orthorhombic
$a = 10.02 \pm 0.02$ Å
$b = 6.02 \pm 0.01$
$c = 16.84 \pm 0.02$
$D_x = 1.84$ g·cm^{-3}
$D_m = 1.865$ g·cm^{-3}
$Z = 4$
Space group $D_2^4 - P2_12_12_1$
Linear absorption coefficient for Ni$K\alpha$, $\mu = 40.8$ cm^{-1}

Structure Analysis

At first Patterson projections $P(xz)$, $P(xy)$ were synthesized.

These led us to fix the position of Co at 0.2500, 0.0, 0.3750. Preliminary Fourier projections of electron density upon (010) and (001) were synthesized using $F(h0l)$s with $2h+l=4n$ ($n=0, 1, 2, 3, \cdots$) and $F(hk0)$s with $h+k=2n$, respectively, the signs of which were calculated from the parameter values of the cobalt atom. Approximate orientations of

*1 Deceased on Aug. 1, 1968.

1) F. A. Cotton and W. T. Edwards, *Acta Cryst.*, **B24**, 474 (1968).
2) Y. Tanito, Y. Saito and H. Kuroya, This Bulletin, **25**, 188 (1952).
3) Y. Komiyama, *ibid.*, **30**, 13 (1957).
4) M. Driel and H. J. Verweel, *Z. Krist*, **95**, 308 (1936).
5) S. M. Jörgensen, *Z. anorg. Chem.*, **17**, 477 (1898).

the complex ion could be assigned from these projections. They were in good accord with the conclusion drawn from Patterson projections $P(xz)$ and $P(xy)$. However, from the Fourier maps the atoms of nitrate ion and water molecule could not be fixed. Atomic parameters of nitrate ion were assigned by packing consideration. After inclusion of the parameters of the nitrate ion and the water oxygen atom in the structure factor calculation, considerable improvement was made in the agreement between the observed and calculated structure factors. Fourier projections of electron density upon (001) and (010) were then synthesized using all $F(hk0)$s and $F(h0l)$s, respectively, the signs of which were calculated from the parameter values of all the atoms. On the Fourier maps all the atoms were found on the expected location. At this stage the discrepancy factor R became 0.20. The structure thus obtained was refined by three dimensional difference synthesis with isotropic temperature factor to $R=0.14$, later by a block diagonal least-squares method with HBLS program written by T. Ashida.

In this least-squares method anisotropic temperature factors were introduced and four cycles of refinement were carried out.

A weighting scheme was employed:

$w = 0.2$ if $F_o \leqq F_{\min.}$ $(=4.0)$

$w = 1.0$ if $F_{\min.} < F_o \leqq F_{\max.}$ $(=100.0)$

$w = F_o/F_{\max.}$ if $F_o > F_{\max.}$

The final discrepancy factor, $R=\sum||F_o|-|F_c||/\sum|F_o|$ was 0.103 for all the reflections. Atomic scattering factors were taken from International Tables for X-ray Crystallography.[6]

Final atomic parameters and their standard deviations are summarized in Table 2. The observed and calculated structure factors are listed in Table 3.

Description of the Structure and Discussion

A perspective drawing of the complex ion, $[Co(NO_2)_2(NH_3)_4]^+$, is illustrated in Fig. 1. The bond lengths and bond angles with their e.s.d.'s calculated on the basis of the atomic parameters in Table 2 are listed in Table 4. A projection of the

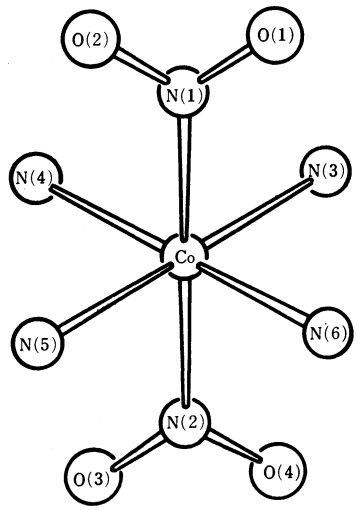

Fig. 1. A perspective drawing of the complex ion, $[Co(NO_2)_2(NH_3)_4]^+$.

Table 2. Atomic parameters and their e.s.d.'s* (10^4)

The expression of the anisotropic temperature factor is $\exp[-(h^2B_{11}+k^2B_{22}+l^2B_{33}+hkB_{12}+hlB_{13}+klB_{23})]$.

Atom	x/a	y/b	z/c	B_{11}	B_{22}	B_{33}	B_{12}	B_{13}	B_{23}
Co	2491(2)	0110(4)	3752(2)	60	207	26	−01	0	3
O(1)	3871(10)	3764(18)	4343(6)	74	188	27	−28	−31	−21
O(2)	3734(10)	3769(18)	3080(6)	69	180	28	−01	24	57
O(3)	1154(10)	−3553(18)	3149(6)	79	142	29	−70	24	41
O(4)	1211(10)	−3538(18)	4431(6)	66	204	19	−79	−10	−05
O(5)	1728(9)	3339(18)	1280(7)	7	318	34	−32	−03	14
O(6)	3450(9)	5489(16)	1281(8)	69	189	35	−29	−02	1
O(7)	3691(10)	1866(16)	1229(8)	104	197	30	19	4	30
O(8)	1221(10)	−1599(19)	1132(6)	78	273	27	23	10	−04
N(1)	3484(9)	2860(16)	3707(8)	26	98	28	−16	9	−22
N(2)	1497(9)	−2648(17)	3775(9)	25	126	30	29	−01	19
N(3)	3766(11)	−1092(19)	4518(6)	38	123	22	70	24	−34
N(4)	3601(11)	−1084(20)	2873(7)	55	117	23	50	−35	9
N(5)	1205(11)	1313(19)	2986(6)	53	70	4	8	−38	15
N(6)	1386(12)	1325(21)	4619(6)	57	145	21	53	15	−03
N(7)	2935(10)	3571(21)	1254(9)	65	274	21	29	3	−11

*e.s.d.'s in parentheses.

6) "International Tables for X-ray Crystallography," Vol. III, Kynoch Press, Birmingham (1962), p. 202

TABLE 3. CALCULATED AND OBSERVED STRUCTURE FACTORS

Columns are *l*, F_o, F_c. Unobserved merked by *

L FO FC	L FO FC	L FO FC	L FO FC	L FO FC	L FO FC	L FO FC	L FO FC	L FO FC	L FO FC
H,K= 0 0	15 17 21	17 53 45	0 150 136	0 361 348	6 112 114	11 34 33	5 27 28	7 21 19	1* 12 20
2* 4 10	16* 10 4	18 39 34	1 35 34	1 140 123	7 21 22	12 117 108	6 19 14	8 16 8	2 25 29
4 815 875	17* 9 3	19* 10 1	2 144 133	2 241 250	8 166 181	13* 14 11	7 43 48	9 26 21	3 16 18
4* 7 24	18 92 90	H,K= 1 1	3 45 45	3 76 71	9* 14 9	14 19 21	8 32 28	10 73 69	4 142 134
8 278 293	H,K= 6 0	0 246 240	4 140 123	4 196 179	10 30 28	15 31 28	9 31 25	11 16 9	5 19 16
10* 12 13	0 30 56	1 117 127	5 46 48	5 66 64	11 21 27	16 137 124	10 36 45	12 18 11	6 60 57
12 516 516	1* 12 10	2 80 92	6 148 165	6 215 231	12 123 125	17 29 32	11 31 32	13 30 32	7 23 22
14* 14 14	2* 12 15	3 84 88	7 16 11	7 30 85	13 23 22	18 19 30	12 38 35	14 121 121	8 71 82
16 263 259	3* 12 5	4 104 139	8* 15 16	8 273 275	14 114 110	H,K= 2 3	13 21 25	15* 12 7	9 16 18
18* 10 12	4 78 82	5 139 127	9 45 50	9 27 34	15* 9 6	0 164 153	14* 4 2	H,K= 4 4	10 54 64
H,K= 1 0	5 27 33	6 26 37	10 97 105	10 140 169	16 74 77	1 43 48	H,K= 8 3	0 341 350	11 30 37
1* 12 29	6 18 14	7 41 51	11 17 18	11 31 22	H,K= 7 2	2 199 183	0 75 87	1 62 53	12 34 29
2 457 471	7 29 26	8 239 231	12 16 14	12 39 42	0 93 87	3 43 46	1 35 33	2* 10 10	13* 10 12
3* 7 15	8* 14 13	9 75 75	13 19 18	13 48 63	1 30 31	4 61 52	2 184 195	3 29 36	14* 10 14
4* 9 12	9 22 26	10 87 86	14 80 81	14 97 95	2 184 190	5 55 55	3 38 40	4 68 61	H,K= 2 5
5* 10 4	10* 15 10	11 46 59	15 20 17	15 22 16	3 39 45	6 181 184	4 49 53	5* 14 21	0 70 94
6 335 272	11* 14 1	12 186 177	16 50 59	16 23 25	4 126 111	7 31 38	5 29 29	6 16 16	1 56 54
7 50 46	12* 14 12	13 37 44	H,K= 7 1	17 20 19	5 17 19	8 117 114	6 160 147	7 19 22	2 111 109
8* 12 14	13* 14 9	14 26 32	0 229 219	18 57 58	6 165 172	9 31 42	7 38 39	8 35 45	3 65 55
9* 10 16	14* 12 11	15* 15 11	1 19 20	19* 13 13	7 20 12	10 135 126	8 43 47	9 17 13	4 28 32
10 61 71	15* 10 7	16 46 51	2 70 64	H,K= 2 2	8 116 114	11 34 32	9 24 26	10 17 16	5 52 52
11 17 24	16 76 64	17 51 53	3 37 40	0 241 252	9 22 22	12 117 114	10 107 85	11* 19 19	6 109 100
12* 14 13	17* 6 7	18 44 45	4 204 218	1 55 44	10 135 129	13 35 34	11* 8 14	12 24 36	7 47 41
13 53 52	H,K= 7 0	19 17 17	5 21 18	2 644 584	11 29 22	14 85 82	12 24 36	H,K= 9 3	8 25 28
14 161 169	1 29 29	H,K= 2 1	6 79 75	3 39 38	12 36 37	15 19 22	H,K= 9 3	13 21 20	9 39 41
15 22 26	2 338 319	0 344 347	7 17 9	4 217 228	13 27 21	16 16 16	0 55 53	14* 7 9	10 53 70
16* 14 2	3 29 37	1 91 92	8 203 209	5 78 67	14 78 77	17* 14 11	1 38 44	15* 14 25	11 34 34
17 20 19	4* 14 2	2 515 466	9 22 27	6 228 202	15* 11 12	18 26 47	2* 11 18	H,K= 5 4	12 19 16
18 51 36	5 18 23	3 113 90	10 17 8	7 70 64	H,K= 8 2	H,K= 3 3	3 26 26	0* 12 14	13 23 23
19* 9 9	6 33 37	4 338 313	11* 15 11	8 152 177	0 116 118	0 251 247	4 76 75	1 70 67	14 32 54
H,K= 2 0	7* 14 1	5 95 86	12 162 149	9 36 31	1 32 35	1 65 66	5 36 38	2 162 160	H,K= 3 5
0 632 632	8* 14 19	6 348 338	13 30 10	10 41 49	2 51 48	2 28 37	6 16 13	3 36 36	0 120 122
1 47 56	9* 14 5	7 48 49	14 37 38	11* 14 15	3 22 29	3 78 77	7 31 35	4 18 25	1 32 34
2* 6 12	10 74 69	8 55 45	15* 14 19	12 123 123	4 100 104	4 268 264	8 61 52	5 37 39	2 41 59
3 20 41	11* 14 2	9 23 35	16 52 60	13* 15 15	5 36 39	5 61 43	9* 11 7	6 23 26	3 30 27
4 520 524	12* 14 14	10 241 243	H,K= 8 1	14 138 155	6 34 45	6 24 10	10* 6 9	7* 15 11	4 93 80
5 22 14	13 22 23	11 53 48	0 37 24	15* 15 7	7 20 18	7 66 68	H,K= 10 3	8 26 32	5 23 23
6* 9 10	14 148 147	12 22 17	1 23 24	16 81 78	8 98 91	8 285 270	0* 10 5	9 21 25	6 72 59
7 105 105	15* 9 14	13* 15 7	2 87 93	17* 11 7	9 34 33	9 70 63	1 24 30	10 55 65	7 32 27
8 418 407	16* 6 9	14 142 146	3 30 37	18* 9 5	10 91 84	10 83 82	2 96 94	11 27 38	8 80 84
9 25 17	H,K= 8 0	15* 15 13	4 30 26	19* 4 6	11 18 23	11 29 41	3* 14 12	12* 8 13	9 21 24
10* 12 6	0 376 394	16 95 103	5 16 16	H,K= 3 2	12 62 65	12 172 165	4 16 21	13 23 29	10 58 71
11* 14 20	1* 14 11	17 28 34	6 90 82	0 283 258	13* 8 12	13 35 32	5 26 31	14 67 80	H,K= 6 4
12 268 255	2 18 7	18 50 88	7 26 25	1 91 93	14* 4 16	14 26 17	6 113 116	H,K= 6 4	0 97 90
13 47 55	3 48 53	19* 8 10	8 37 29	2 278 296	H,K= 9 2	15 28 34	7* 13 11	1 26 28	11 43 47
14* 14 5	4 141 131	H,K= 3 1	9 37 39	3 60 59	0 116 113	16 64 55	H,K= 0 4	2 43 56	12 69 94
15* 14 0	5 30 33	0 257 307	10 137 115	4 220 181	1* 14 11	17* 13 21	0 128 123	3 19 19	13* 14 17
16 133 123	6* 14 13	1 63 67	11* 14 6	5 84 79	2 67 71	H,K= 4 3	1 42 43	4 73 66	H,K= 4 5
17* 12 9	7* 14 3	2 126 123	12* 12 8	6 217 226	3 30 38	0 75 83	2* 4 2	5 27 37	0 21 23
18* 10 3	8 25 15	3 99 85	13 19 19	7 23 28	4* 15 7	1 32 28	3 74 78	6 29 34	1 39 32
19 22 23	9* 14 17	4 293 293	14 52 50	8 241 216	5 20 27	2* 13 20	4 247 239	7 17 11	2 144 156
H,K= 3 0	10* 14 15	5 59 54	H,K= 9 1	9 34 32	6 58 61	3 28 29	5 104 118	8 89 86	3 30 24
1 76 81	11* 12 1	6 101 86	0 133 154	10 151 162	7 29 28	4 45 45	6* 9 7	9 21 21	4* 12 6
2* 15 58	12 164 156	7 30 36	1* 15 13	11 57 55	8 67 67	5 16 19	7 106 115	10 20 19	5 18 16
3 35 16	13* 9 1	8 130 138	2 48 65	12 60 60	9 20 24	6 78 81	8 329 307	11 18 18	6 76 95
4* 9 13	14* 7 16	9 37 40	3 17 19	13* 14 14	10 48 49	7 26 31	9 83 76	12 76 72	7 18 9
5 43 52	H,K= 9 0	10 39 35	4 111 104	14 121 120	11* 15 16	8 31 37	10* 12 10	13* 6 9	8* 12 10
6 599 589	1 20 15	11 32 33	5 16 10	15 43 41	12 17 26	9* 12 7	11 40 36	H,K= 7 4	9 43 44
7 45 45	2 214 207	12 104 89	6 106 91	16* 13 6	H,K= 10 2	10 122 124	12 37 29	0* 12 10	10 100 139
8* 15 31	3 33 31	13 16 9	7 19 20	17 16 11	0 81 68	11 28 27	13 23 26	1 17 13	11 19 11
9* 12 15	4* 14 8	14 33 42	8 117 104	18 69 71	1 18 19	12 26 25	14* 10 7	2 23 20	12* 8 4
10 290 269	5 18 14	15 39 35	9* 14 11	H,K= 4 2	2 60 60	13* 12 15	15* 15 7	3 38 44	H,K= 5 5
11* 14 2	6 45 45	16 146 120	10 79 75	0 369 383	3 44 54	14* 8 13	16 38 36	4 16 12	0 133 141
12* 14 26	7* 14 5	17 22 24	11* 10 11	1 49 45	4 65 61	15* 11 11	H,K= 1 4	5 34 43	1 54 56
13 55 56	8* 12 6	18 39 46	12 101 93	2 32 35	5* 11 2	16* 8 13	0* 4 4	6 161 143	2 19 17
14 37 32	9* 12 16	19 19 24	H,K= 10 1	3 49 48	6 89 87	17* 4 9	1 34 40	7 42 47	3 41 43
15* 15 18	10 145 128	H,K= 4 1	0 43 54	4 306 333	7 17 22	H,K= 5 3	2 172 144	8 17 8	4 95 86
16* 14 13	11* 9 13	0 21 13	1 21 20	5 17 23	8 51 48	0 194 198	3* 13 5	9 88 45	5 41 42
17 18 22	12* 7 4	1 26 29	2 124 116	6 30 32	9 22 29	1 61 62	4* 13 14	10 93 91	6 23 22
18 78 67	H,K= 10 0	2 371 360	3* 14 4	7 76 64	H,K= 11 2	2 31 35	5 43 38	11 18 23	7 34 29
19* 7 11	0 162 154	3 44 43	4 52 54	8 226 233	0 67 63	3 36 44	6 369 377	12* 2 9	8 104 93
H,K= 4 0	1 17 15	4 86 53	5 19 17	9 17 19	1* 8 4	4 149 159	7 43 34	H,K= 8 4	9 32 39
0 609 593	2* 12 7	5 43 41	6 70 72	10 63 68	2 32 30	5 38 41	8 19 24	0* 10 14	10 23 25
1 66 66	3 22 25	6 278 284	7 23 24	11 22 19	3 23 30	6 29 30	9 34 25	1* 10 16	11 34 45
2* 9 9	4 145 128	7 19 15	8 24 21	12 161 166	4 20 19	7 38 44	10 178 178	2* 10 20	H,K= 6 5
3 35 24	5* 12 7	8 48 50	9* 8 10	13 27 20	5* 11 15	8 157 163	11 19 16	3 31 40	0 25 18
4 110 115	6* 12 4	9 39 40	10 68 72	14* 13 13	H,K= 0 3	9 38 47	12* 10 8	4 120 122	1 21 10
5 91 84	7 25 26	10 97 90	H,K= 11 1	15* 13 18	1 88 98	10 24 30	13 18 16	5 24 17	2 124 107
6* 10 18	8 146 146	11 33 36	1* 10 6	16 109 109	2 399 421	11 23 18	14 54 56	6 26 24	3* 12 0
7 25 28	9* 9 10	12 33 27	2* 10 11	17* 9 4	3 110 93	12 115 118	15* 13 11	7 24 27	4* 12 7
8 309 306	10* 7 0	13* 15 8	3* 14 18	18* 11 14	4* 11 20	13 38 38	16* 12 13	8 169 155	5* 12 9
9 17 13	H,K= 11 0	14 121 126	4 66 60	H,K= 5 2	5 73 75	14* 9 14	H,K= 2 4	H,K= 9 4	6 107 85
10* 14 13	1* 14 24	15 22 16	5* 8 7	0 219 199	6 270 264	15 23 17	0 170 168	0* 15 17	7 19 5
11 20 18	2 87 72	16 34 21	6* 15 11	1 25 22	7 45 53	16 31 31	1 82 77	1* 14 14	8 30 26
12 45 54	3* 9 8	17 33 31	7 5 1	2 283 292	8* 13 27	H,K= 6 3	2 106 103	2 46 54	9 16 13
13 18 18	4* 9 0	18 112 115	H,K= 0 2	3 74 67	9 48 52	0 85 71	3 81 69	3 24 34	10 74 78
14* 14 14	5* 9 22	H,K= 5 1	0 35 64	4 91 78	10 120 106	1 18 6	4 203 166	4 19 21	H,K= 7 5
15* 14 2	6 167 154	0 266 284	1 62 70	5 18 25	11* 13 0	2 175 166	5 85 79	5 18 26	0 87 91
16 18 8	7* 6 2	1 17 11	2* 4 10	6 222 238	12* 14 17	3 31 25	6 51 54	6 134 137	1 38 38
17* 10 13	8* 4 10	2* 12 16	3 57 53	7 20 26	13 46 44	4 22 24	7 43 44	7 17 28	2 28 37
18* 9 11	H,K= 0 1	3 17 22	4 78 93	8 192 189	14 140 140	5 16 12	8 123 115	H,K= 0 5	3 49 50
19* 4 6	1 55 87	4 319 326	5* 8 1	9 39 40	15 26 34	6 107 97	9 49 54	1 52 55	4 111 102
H,K= 5 0	2 377 404	5 28 27	6 18 9	10 170 172	16 20 19	7* 14 11	10 26 30	2 61 60	5 36 38
1 43 40	3 84 85	6 65 78	7 93 95	11 25 26	17 16 9	8 48 57	11 29 33	3 76 68	6 16 23
2 177 166	4* 12 25	7 26 23	8 109 118	12* 14 18	18 86 104	9 23 23	12 70 78	4* 12 4	7 28 31
3 24 16	5 68 76	8 195 192	9 22 16	13* 14 3	H,K= 1 3	10 95 91	13 27 32	5 70 64	8 72 77
4* 18 15	6 308 328	9 21 24	10* 13 13	14 124 120	0 273 305	11 23 21	14 29 40	6 102 99	H,K= 8 5
5 35 40	7 61 66	10 79 84	11* 13 0	15 32 31	1 36 28	12 75 73	15 26 29	7 74 67	0 43 48
6 474 488	8* 12 32	11 34 14	12 69 75	16 18 30	2* 8 13	13* 9 17	16 54 64	8 17 6	1* 14 14
7* 12 3	9* 12 6	12 111 118	13 41 35	17* 6 10	3 58 42	14 70 62	H,K= 3 4	9 19 14	2 45 39
8* 14 12	10 398 382	13* 15 6	14* 14 11	H,K= 6 2	4 286 276	15* 14 19	0* 12 16	10 19 4	3* 8 7
9* 14 3	11 72 68	14* 15 11	15 23 18	0 219 238	5 23 14	H,K= 7 3	1 78 63	11 39 43	4 19 19
10 165 179	12 16 28	15 24 21	16 43 40	1 79 63	6 23 23	0 123 118	2 280 268	12* 14 5	5* 10 15
11 38 35	13 16 7	16 132 128	17* 11 1	2 299 271	7 26 33	1 46 52	3 35 34	13 17 8	
12* 14 11	14 148 141	17 22 24	18* 9 3	3 23 21	8 150 141	2 18 19	4 19 11	14 16 22	
13 17 17	15 16 16	18 19 28	19* 8 17	4 194 225	9 26 30	3 49 45	5 23 13	H,K= 1 5	
14 90 92	16 16 15	H,K= 6 1	H,K= 1 2	5 48 53	10 71 76	4 61 74	6 23 16	0 72 90	

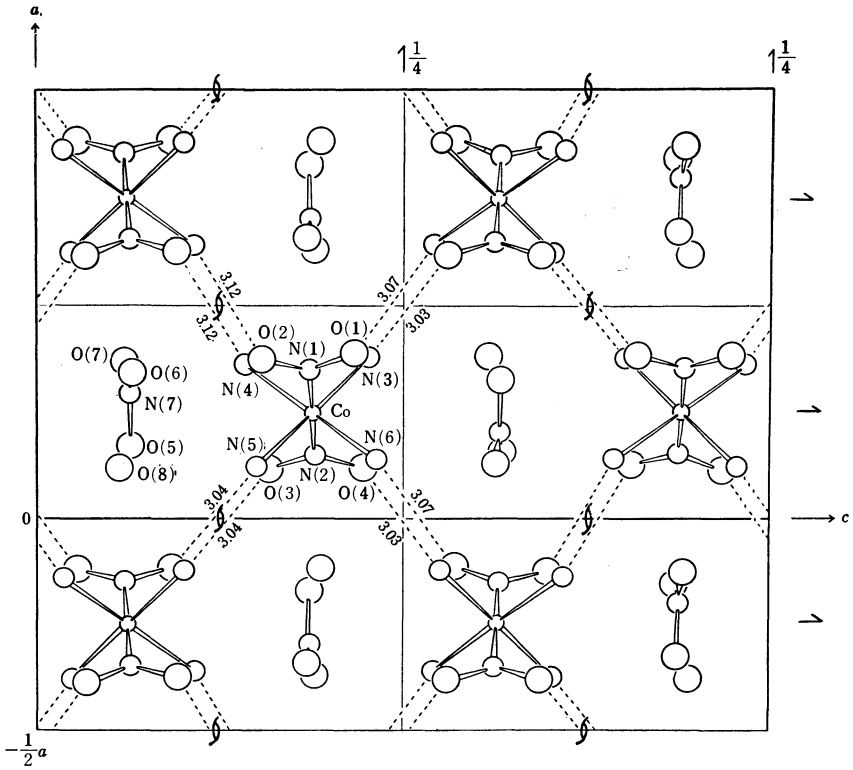

Fig. 2. Projection of the unit cell contents on the (010) plane.

Table 4. Bond distances and angles and their standard deviations

Co——N(1)	1.933(11) Å	N(1)-Co-N(3)	90.4(5)°
N(2)	1.937(11)	N(1)-Co-N(4)	89.6(5)
NH_3(3)	1.954(11)	N(1)-Co-N(5)	89.7(5)
NH_3(4)	1.986(12)	N(1)-Co-N(6)	90.0(5)
NH_3(5)	1.963(12)	N(2)-Co-N(3)	90.3(5)
NH_3(6)	1.973(12)	N(2)-Co-N(4)	89.6(5)
N(1)—O(1)	1.262(16)	N(2)-Co-N(5)	89.6(5)
O(2)	1.215(16)	N(2)-Co-N(6)	90.8(5)
N(2)—O(3)	1.235(17)	N(3)-Co-N(4)	89.5(5)
O(4)	1.260(17)	N(3)-Co-N(6)	90.9(5)
N(1)—NH_3(3)	2.758(16)	N(4)-Co-N(5)	90.6(5)
NH_3(4)	2.761(16)	N(5)-Co-N(6)	88.9(5)
NH_3(5)	2.749(15)	O(1)-N(1)-O(2)	118.7(10)
NH_3(6)	2.762(16)	Co-N(1)-O(1)	119.6(10)
N(2)—NH_3(3)	2.758(15)	Co-N(1)-O(2)	121.7(10)
NH_3(4)	2.764(16)	O(3)-N(2)-O(4)	119.8(10)
NH_3(5)	2.746(16)	Co-N(2)-O(3)	120.2(10)
NH_3(6)	2.784(16)	Co-N(2)-O(4)	120.0(10)
NH_3(3)-NH_3(4)	2.775(16)	O(5)-N(7)-O(6)	120.6(11)
NH_3(4)-NH_3(5)	2.808(16)	O(5)-N(7)-O(7)	119.9(12)
NH_3(5)-NH_3(6)	2.756(15)	O(6)-N(7)-O(7)	119.5(10)
NH_3(3)-NH_3(6)	2.798(16)		
N(7)—O(5)	1.218(14)		
O(6)	1.265(16)		
O(7)	1.277(16)		
O(5)—O(6)	2.157(14)		
O(7)	2.160(14)		
O(6)—O(7)	2.196(15)		

TABLE 5. INTERMOLECULAR CONTACTS NOT EXCEEDING 3.5 Å

N(1)—O(3) (1′)	3.315(14) Å	N(6)—O(6) (3+1″)	3.398(16) Å
O(4) (1′)	3.372(14)	O(7) (3)	3.323(16)
O(6) (4+1″)	3.388(13)	O(8) (4)	3.160(15)
N(2)—O(1) (1″)	3.352(14)	N(7)—O(2) (1)	3.180(18)
O(2) (1″)	3.323(14)	O(4) (3)	3.187(17)
O(5) (4+1″)	3.287(12)	O(8) (1′)	3.383(16)
N(3)—O(1) (1″)	3.113(16)	O(1)—O(4) (1′)	3.125(14)
O(4) (1″)	3.031(14)	O(8) (3)	3.283(15)
O(5) (3+1″)	3.298(16)	O(6) (4)	3.493(14)
O(6) (4+1″)	3.240(15)	O(7) (4)	3.222(14)
O(7) (4+1″)	3.096(15)	O(2)—O(3) (1′)	3.048(14)
O(8) (3)	3.163(15)	O(6) (1)	3.213(16)
N(4)—O(2) (1″)	3.121(16)	O(7) (1)	3.321(16)
O(2) (4+1″)	3.117(15)	O(7) (4)	3.389(14)
O(6) (1″)	3.386(16)	O(3)—O(5) (4+1″)	3.250(14)
O(6) (4+1″)	3.414(15)	O(8) (4+1″)	3.239(15)
O(7) (1″)	3.290(17)	O(4)—O(6) (3)	3.347(16)
O(7) (4+1″)	3.342(15)	O(7) (3)	3.193(16)
N(5)—O(3) (1′)	3.103(16)	O(5) (4+1″)	3.373(14)
O(3) (4)	3.041(15)	O(8) (4+1″)	3.199(14)
O(5) (1)	3.164(16)	O(5)—O(8) (1)	3.026(15)
O(8) (4)	3.114(15)	O(8) (1′)	3.099(15)
N(6)—O(1) (2)	3.068(15)	O(6)—O(8) (1′)	2.851(14)
O(4) (1′)	3.114(17)	O(7)—O(8) (1′)	3.241(14)

1) x, y, z
1′) $x, 1+y, z$
1″) $x, -1+y, z$
2) $1/2+x, 1/2-y, -z$
3) $1/2-x, -y, 1/2+z$
4) $-x, 1/2+y, 1/2-z$
e.s.d.'s in parentheses

contents of one unit cell onto the (010) plane is presented in Fig. 2, and important intermolecular contacts (*i. e.*, those$\leqq$3.5 Å) are listed in Table 5. The interatomic distances and bond angles were calculated by using program RSDA-4 written by T. Sakurai (1965).

The cobalt atoms are surrounded by nitrogen atoms of two nitro groups and of four ammonia molecules, which form a slightly distorted octahedron. Two nitrogen atoms of nitro groups are coordinated to a cobalt atom in *trans* positions.

The complex ion has an approximate symmetry *mmm*, with the first mirror containing the two nitro groups, the second containing N(3), N(4), N(5), and N(6), and the last perpendicular to the other two mirrors. In Table 6 are compared the distances between cobalt and ligand atoms and N–O distances in various complex ions. The distances are in agreement with those found in the related compounds. It is to be noted here that the Co–NO_2 distances are likely to increase with increase in number of the nitro groups. This may be partly due to the steric hindrance. Generally, the Co–N distances in Co–NH_3 seem to be longer than that in Co–NO_2.

TABLE 6. COMPARISON OF BOND LENGTHS IN VARIOUS NITROAMMINE COMPLEXES

	Co–NO_2	Co–NH_3	N–O
$[Co(NO_2)(NH_3)_5]^{2+}$ 1)	1.921 Å	1.977 Å	1.161 Å
trans-$[Co(NO_2)_2(NH_3)_4]^+$	1.935	1.969	1.243
$[Co(NO_2)_3(NH_3)_3]$ 2)	1.97	1.98	1.26
$[Co(NO_2)_4(NH_3)_2]^-$ 3)	1.96	1.98	1.23
$[Co(NO_2)_6]^{3-}$ 4)	2.03		1.11

Nitrate ion has an approximate three fold axis and N atom is 0.034 Å apart from the plane composed of three O atoms. The structure is built up of complex cations $[Co(NO_2)_2(NH_3)_4]^+$, nitrate ions and water molecules, thus being essentially ionic. The arrangement of the cobalt atoms themselves has approximately the symmetry D_{2h}^{25}-*Immm*. This characteristic feature seems to be mainly due to the presence of spatial network consisting of the complex ions. The water molecules and nitrate ions also appear to play an important role. The binding force between complex ions is mainly due to the N–H···O interactions between NH_3 and NO_2 groups. Figure 3 illustrates a network of the

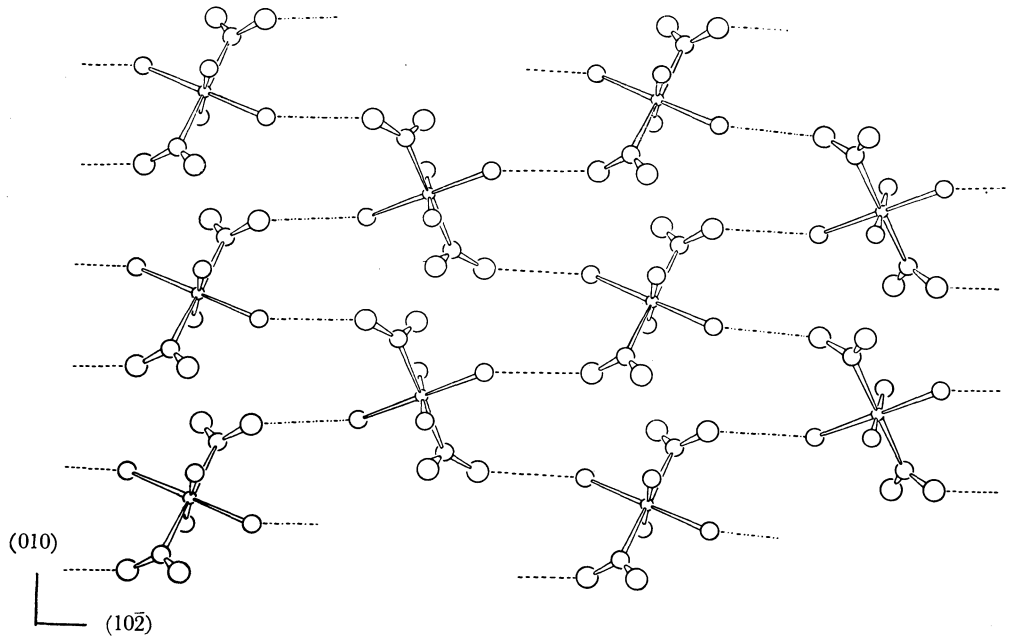

Fig. 3. Two dimensional network of complex ions found in crystal of $[Co(NO_2)_2(NH_3)_4]NO_3 \cdot H_2O$.
——: linkages of 3.041 Å; —·—: linkages of 3.068 Å; —··—: linkages of 3.031 Å

complex ions found in this structure. Each complex ion forms four N–H···O bonds with four neighboring complex ions in a similar manner to that of binding found in the structure of $[Co(NO_2)_3(NH_3)_3]$. One of the two oxygen atoms of NO_2 groups is used to form N–H···O bonds of 3.068 Å, 3.031 Å, and 3.041 Å with NH_3 of the adjacent complex ions, thus two dimensional network parallel to the plane (10$\bar{2}$) being formed. At the same time the other oxygen atom is used to form another network with N–H···O distances of 3.068 Å, 3.031 Å, and 3.117 Å in the latter, parallel to the plane (102).

Thus these layers form a three dimensional network.

The distances between two layers parallel to (10$\bar{2}$) and (102), 6.45 Å, and 6.44 Å, respectively are the same as the corresponding ones, 6.48 Å, and 6.49 Å found in the crystals of $NH_4[Co(NO_2)_4(NH_3)_2]$, but longer than that in $[Co(NO_2)_3(NH_3)_3]$ (5.10 Å). In this three dimensional network four oxygen atoms of each complex form weak N–H···O bonds with four NH_3 groups of upper and lower complex ions in the direction of the *b*-axis (3.103 Å, 3.113 Å, 3.114 Å, and 3.121 Å). This fact seems to account for the tendency for the crystal to grow along the *b*-axis. Water molecules form O–H···O hydrogen bond with oxygen of upper and lower nitrate ions in the direction of the *b*-axis (3.026 Å, and 2.851 Å). The water molecules and nitrate ions form N–H···O bond with NH_3 groups of complex ions (3.160 Å, 3.114 Å, 3.096 Å, *etc.*). These facts seem to support the conclusion drawn by Komiyama[3] that two nitro groups in *trans*-position are more likely to form N–H···O bonds than those nitro groups which are coordinated to the central cobalt atom in *trans*-positions with respect to different ligands.

The numerical calculations were carried out on the HITAC 5020 at the Computation Center, the University of Tokyo.

Part of the cost of this investigation has been defrayed by a Scientific Research Grant of the Ministry of Education, to which the authors' thanks are due.

BULLETIN OF THE CHEMICAL SOCIETY OF JAPAN VOL. 42 2797—2800 (1969)

The Adsorption of Cobaltous Ions on Glass Beads from Extremely Dilute Aqueous Solutions

Tsutomu SEIMIYA, Hisako KOZAI and Tsunetaka SASAKI

Department of Chemistry, Faculty of Science, Tokyo Metropolitan University, Setagaya-ku, Tokyo

(Received April 4, 1969)

The adsorption of cobaltous ions on fine glass beads was measured for dilute aqueous $^{60}CoCl_2$ solutions with pH values from 2 to 10 and with concentrations from 10^{-6} to 10^{-10} mol/*l*. The amount of the adsorption of cobaltous ions on glass showed a maximum at pH near 9, and it was zero at both ends of the pH region for all the initial concentrations studied. This fact is considered to confirm the theory of radiocolloid formation by the so-called adsorption method. The mechanism of radiocolloid formation was further discussed in detail. The formation of radiocolloids was explained by the adsorption of cobaltous ions on foreign particles, while the formation of insoluble cobaltous hydroxide was ruled out. It was estimated from these measurements that a very minute amount of foreign particles is sufficient to adsorb cobaltous ions and to change a large franction of the solute to radiocolloid. It was emphasized that such an estimation can be made only by the measurement of the adsorption, expressed by the unit of mol/cm^2 as in the case of the present experiment, instead of the conventional unit of cpm/g or percent adsoı ption.

Several workers have reported that the radioisotope in a very dilute aqueous solution often behaves as a colloid or a coarser dispersion rather than as a true solution. Such a disperse system, called radiocolloid by Paneth,[1] forms far below the concentration usually believed to be the solubility of the substance in question. Two possibilities have been proposed for the formation: a true colloid formation from a supersaturated solution of the radioisotope,[1] and a colloid formation by the adsorption of dissolved radioisotopes on small colloid particles of a foreign substance which are accidentally introduced into the solution as fragments of the container wall[2,3] or as impurities present in the reagent or water used.

The formation of radiocolloids has been detected by means of filtration,[4] adsorption,[5] dialysis,[1,6] electrophoresis,[1,2] diffusion,[7] precipitation,[8] and by several other methods.[9] However, considerable ambiguities are inevitably introduced in the measurement of the concentration because of the extremely low concentration at which these experiments are carried out, and because of adsorption of the solute to the wall of the container or other surfaces that might come into contact with the solution. Thus, the published reports on radiocolloids are more or less qualitative in nature; quantitative studies concerning the behavior of the main constituent of radiocolloids are few. Recently, however, a radiotracer study of manganese adsorption on glass was reported, and radiocolloid formation was inferred.[10] Nevertheless, here, as in the other reports, the amount of adsorption and the concentration of solute are expressed in relative or conventional units which are unsatisfactory for the purposes of a more quantitative discussion. The present report will deal with a study of the radiocolloidal behavior of cobaltous ions paying attention to these facts. The cobaltous ion was chosen since the radiocolloid formation of cobalt has not yet been reported in spite of the wide use of 60-Co as a radiotracer. The explanation of the radiocolloid formation of 60-Co based upon the adsorption mechanism was attemtped. For this purpose, very many small glass spheres were added to an aqueous solution of $^{60}CoCl_2$ of a known concentration, and the amount of adsorption was exactly determined in the unit of mol/cm^2 at the

1) F. Paneth, *Kolloid Z.*, **13**, 297 (1913); *Z. Elektrochem.*, **31**, 5 (1925).
2) T. Godlewski, *Le Radium*, **10**, 250 (1913); *Kolloid Z.*, **14**, 229 (1914).
3) C. Rosenblum and E. W. Kaiser, *J. Phys. Chem.*, **39**, 797 (1935).
4) G. K. Schweitzer and W. H. Jackson, *J. Chem. Educ.*, **29**, 513 (1952).
5) I. E. Starik, *Z. physik. Chem.*, **157A**, 269 (1931).
6) T. Sasaki and K. Osaka, This Bulletin, **32**, 490 (1959).
7) J. S. Anderson and K. Sassington, *J. Chem. Soc.*, **1949**, 381.
8) H. Lachs and M. Wertenstein, *Physik. Z.*, **23**, 318 (1922).
9) C. Chamie, *Compt. rend.*, **184**, 1243 (1927); *ibid.*, **192**, 1277 (1931).
10) P. Benes and A. Garba, *Radochim. Acta*, **5**, 99 (1966).

extremely dilute equilibrium concentration thus attained. These data enabled us to estimate the amount of foreign particles, which is extremely small but sufficient for adsorbing a large fraction of the cobaltous ions in a dilute solution and changing them into the radiocolloid.

Experimental

Solution. The radioisotope of cobalt was supplied by The Radiochemical Center, England, as a cobaltous chloride with a specific activity of 144 mCi/mg; it was isotopically diluted by an analytical-grade non-radioactive cobaltous chloride before use.

The water used was doubly distilled from a Hysil flask with nothing added after the reflux boiling and distillation with acid and alkaline permanganate respectively. Here, the adsorption of cobaltous ions by the wall of the container and the accidentally-introduced dust particles usually produce an error in the measurement at extremely low concentrations. To avoid this, a large quantity of carefully prepared fine glass beads was used as an adsorbent which had a far larger surface area than the surface area of the wall and of the dust particles introduced with the solvent water or reagents. The probable error due to the fine particles introduced together with the glass beads also turned out to be immaterial, as will be mentioned later. The present experiment enabled us to eliminate such an error and to attain an extremely dilute solution of a known concentration. The initial concentration was chosen in the range from 10^{-6} to 10^{-8} mol/*l*, and the equilibrium concentrations finally attained ranged from 10^{-8} to 10^{-10} mol/*l*. The concentration of cobaltous ions in the initial solution was determined by EDTA titration, using murexide as an indicator, while the amount of adsorption was determined from the change in the radioactivity of the supernatant solution due to the adsorption. Here, the loss of a solute by the adsorption on the wall of the pipet or of the container used for analysis was proved to be negligible, as will be discussed later.

Glass Beads. Beads of soda lime glass, ranging between 40 and 44 μ in diameter and with a specific surface area of about 593 cm^2/g, were used as an adsorbent. It is well known[11] that the glass surface has a considerable buffer action, and also that it often takes a fairly long time to attain the adsorption equilibrium. It was confirmed in the present study that, after the contact between the glass and the solution, a gradual change in the pH of the solution with the time was observed together with the change in the concentration of the cobaltous ions. Such a complication is not desirable for the present purpose of studying the adsorption behavior of cobaltous ions at various concentrations and pH values. For this reason, the glass beads were previously cleaned and equilibrated with the buffer solution according to the procedures shown in Fig. 1.

The pH of the buffer solution in this figure was taken to be equal to that of the solution used for the adsorption measurement. The adsorption measurement

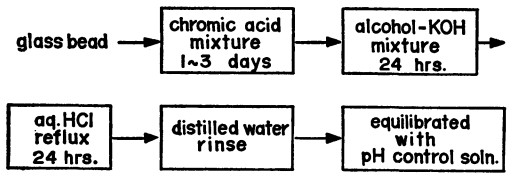

Fig. 1. Pretreatment of glass beads before adsorption.

was performed by immersing 2 g of the treated glass beads in 8 m*l* of 10^{-6} to 10^{-8} mol/*l* aqueous solution of cobaltous ions, and then by keeping it at 25±2°C with gentle stirring. At proper time intervals, the concentration of cobaltous ions of the supernatant solution was determined by radioactivity measurement using a Ten SA-100 Geiger Müller counter, the steady value of the counting rate was taken as the equilibrium. In this measurement, an aliquot of the solution was taken out by means of a constant-volume micropipet of 40 μl, placed on a circular Indian paper affixed to a glass plate, and dried completely under an infrared lamp before counting. The experiment previously performed by the present authors proved this counting technique to be satisfactory, especially for the measurement of 60-cobalt.[12] The errors due to the adsorption of cobalt on the glass surface of the pipet, errors which are unavoidable in this operation, turned out to be negligible when we compare the very slow rate of adsorption, which takes about 20 hr to attain equilibrium, with the short time of contact between pipet and solution.

Results and Discussion

The amount of the adsorption of cobaltous ions on a unit of the surface of glass, Γ, is expressed as the difference between the concentration of the solution before and after the adsorption multiplied by the volume of the solution:

$$S\Gamma = (C_i - C_e)V$$

or

$$\frac{S\Gamma}{C_i V} = 1 - \frac{C_e}{C_i} \qquad (1)$$

where S expresses the total surface area of the glass beads; C_i and C_e, the initial and equilibrium concentrations respectively of the solution used for the adsorption experiment, and V, the volume of the solution. Equation (1) expresses the linear relation between C_e and $S\Gamma/C_iV$, the latter being the ratio of the total amount of adsorption to the total amount of the solute. This linearity is shown in Fig. 2 as a straight line for the three C_i's chosen in the present experiment. With the aid of this straight line we can obtain the $S\Gamma/C_iV$ values, and therefore Γ, from the observed C_e values. In the present experiment, starting from relatively high concentrations of 10^{-6} to 10^{-8} mol/*l*, low equilibrium concentrations of 10^{-8} to 10^{-10} mol/*l* were

11) G. G. Eichholz, Ann E. Nagel and R. B. Hughes, *Anal. Chem.*, **37**, 863 (1965).

12) T. Seimiya and T. Sasaki, unpublished data.

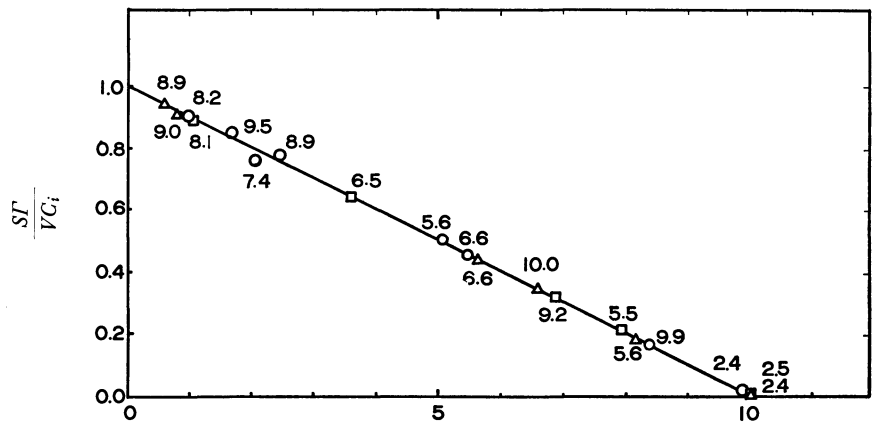

Equilibrium concentration (mol/l)

Fig. 2. Adsorption cobaltous ion on glass beads.
○ $\times 10^{-7}$ □ $\times 10^{-8}$ △ $\times 10^{-9}$

attained by adding a sufficient amount of an adsorbent. The points on the straight lines were located corresponding to the equilibrium concentrations thus obtained. The deviation of several plots from the straight line is due to the slightly different values of the corresponding C_i from those indicated in Fig. 2. The numbers indicated at the points in Fig. 2 show the pH values of the solutions at which the adsorption was equilibrated. The pH dependence of the adsorption of cobaltous ions on the glass surface is shown in Fig. 3. In this figure, the circles, squares, and triangles indicate the amounts of adsorption for the solutions of three different initial concentrations, 1×10^{-6}, 1×10^{-7}, and 1×10^{-8} mol/l respectively. The amounts of adsorption from these solutions are in the order of magnitude of 10^{-12}, 10^{-13} and 10^{-14} mol/cm^2 respectively, as is shown by the ordinate of this diagram. It may be noted that the use of glass beads as in the present experiment makes it possible to express the amount of adsorption in moles per area of glass surfaces instead of as cpm per weight of the powders or as mere percentages of the adsorption of the total solute present in the system, as has usually been done in similar studies.

As is shown in Fig. 3, all these plots can be brought near a common curve by a proper choice of the unit of the ordinate for each group of solutions with a different initial concentration. Thus, the adsorption behaviors of these solutions are quite similar towards the pH change in spite of the wide difference in initial concentrations and in the amount of adsorption. No indication of adsorption was observed at any pH lower than about 3. The adsorption increased with the pH and showed its maximum at a pH of about 9, regardless of the initial cobaltous-ion concentration. A further increase in pH sharply decreased the adsorption to zero at pH values of about 10. The amount of adsorption at its maximum is more than 90% of the total amount of solute——for instance, 95% of the cobaltous ions adsorbed from a 10^{-8} molar solution at pH values from 8 to 9, leaving a 10^{-10} molar solution in equilibrium with it. Here, we can confirm that a proportionality such as that expressed by;

$$\Gamma = kC_e \qquad (2)$$

holds as a whole at any given pH and especially well at the pH of maximum adsorption. We can further confirm, at least from the 95% adsorption at pH values of about 9, that the fine dust particles which might be introduced together with the glass beads are negligible in amount, since the dust particles of such an origin, if they existed in a considerable amount, would adsorb as many cobaltous ions and keep them in a suspended state. Such a state should markedly increase the supernatant cobaltous-ion concentration and reduce the (apparent) fraction of the amount of adsorption far below 95%. As to the radiocolloid formation of cobalt, we can take the appearance of an adsorption maximum near pH 9 as a confirmation by the so-called adsorption method. The explanation based upon the mechanism of the formation of true insoluble colloidal particles of cobaltous hydroxide was first considered, but this is unacceptable since the equilibrium concentrations studied in the present experiment (at least 10^{-10} mol/l) are far below the solubilities of cobaltous hydroxide, $10^{-5.6}$—$10^{-7.4}$ mol/l, at pH values of about 9 as calculated from its solubility product.[13,14] The formation of cobaltic hydroxide, which is far more insoluble than cobaltous hydroxide, is also unlikely

13) G. Charlot, "L'Analyse Qualitative et les Reactions en Solution," Masson et Cie., Paris (1957).

14) Landolt-Börnstein, "Physikalisch-chemische Tabellen," I. Erg., Verlag J. Springer, Berlin (1927).

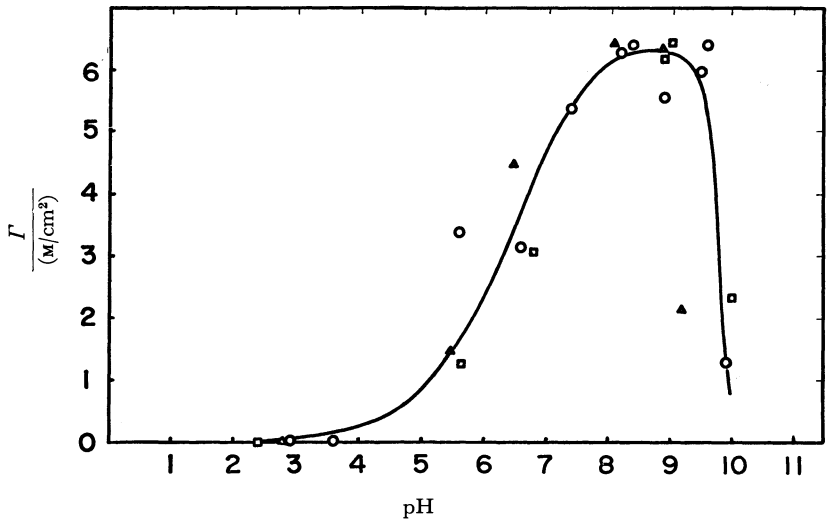

Fig. 3. Adsorption of cobaltous ion on glass beads.

	Γ	C_i
○	$\times 10^{-12}$	1.0×10^{-6}
□	$\times 10^{-13}$	1.0×10^{-7}
△	$\times 10^{-14}$	1.0×10^{-8}

considering the cobaltic-ion concentration in equilibrium with the cobaltous ion, which is calculated from the oxidation reduction potential measured for the solution used in the present experiment. Further, the electrodialysis data for the 10^{-4} molar cobaltous chloride solution which one of the present authors has formerly reported[6] showed that the colloid formation of cobaltous hydroxide is limited to the pH region slightly below the solubility of cobaltous ions calculated from the solubility product. From these facts, it can safely be concluded that true colloid of cobaltous hydroxide in any form cannot be considered to exist below the cobaltous-ion concentration of 10^{-9} mol/*l* at pH 9 and at 25°C.

On the contrary, though, we can numerically show the possibility of radiocolloid formation due to the adsorption of cobaltous ions on foreign particles. As has already been shown in the preceding section, about 95% of the solute is adsorbed by two grams of glass beads from 8 m*l* of a 10^{-8} molar aqueous solution at pH 9. Here the total area of the beads is 1186 cm². Now, simple calculation shows that as small an amount as about 6×10^{-6} g of glass particles of colloidal size (10^{-7} cm) in a 1 m*l* solution gives a 1186 cm² surface for an 8 m*l* sample solution, which just adsorbs 95% of the cobaltous ions in solution and keep them in a radiocolloidal state. It is quite conceivable that dust particles in such a small amount exist in ordinary water. Thus, the results of the above adsorption experiment with coarse glass beads indicate the possibility that the radiocolloid formation of cobalt in a dilute aqueous solution is due to the adsorption of the solute on a very small amount of foreign particles.

It should be emphasized in conclusion that the radiocolloid formation can be confirmed only by the exact measurement of the amount of adsorption expressed in the unit of moles per square centimeter and by using an adsorbent with a clearly defined total area and pH condition. Such a confirmation is impossible by the so-called adsorption method usually adopted; here the results are expressed merely by the percentage of adsorption or by the unit of moles per weight of the adsorbent, using irregular particles of an ill-defined surface area.

BULLETIN OF THE CHEMICAL SOCIETY OF JAPAN VOL. 42 2801—2807 (1969)

Effects of Cation Vacancies of the Diffusion of Nickel Ions in Defective Spinels

Goro YAMAGUCHI, Mitsuko NAKANO and Mamoru TOSAKI

Department of Industrial Chemistry, Faculty of Engineering, The University of Tokyo, Hongo, Bunkyo-ku, Tokyo

(Received April 7, 1969)

In order to clarify the influence of composition-dependent cation vacancies in defective spinels on the diffusion, the diffusion rates of Ni^{2+} in several kinds of defective spinels ($MgO \cdot xAl_2O_3$, where $x=1.1$, 1.2, 1.3, 1.4 and 1.5) and a perfect spinel ($MgO \cdot Al_2O_3$) were measured by the use of an electron probe micro-analyzer, and the diffusion coefficients were obtained. The diffusion coefficients were found to be linear to the concentrations of the composition-dependent vacancies. The so-called activation energies which were calculated from the Arrhenius plot were about 70 kcal/mol for the defective spinels and 106 kcal/mol for the perfect spinel. It may be concluded that composition-dependent cation vacancies govern the diffusion of cations in the defective spinel, while temperature-dependent vacancies probably predominate in the perfect spinel.

The diffusion in ionic crystals has been well investigated with regard to sodium chloride.[1] It has been shown that there are two ranges in the Arrhenius plot of the self-diffusion coefficients of Na^+ in sodium chloride. This phenomenon may be explained as follows: in the lower temperature range the concentration of the vacancies which are caused by impurities and which govern the diffusion is much larger than that of the temperature-dependent vacancies, while in the higher temperature range the temperature-dependent vacancies predominate. The same phenomenon was found with regard to the self-diffusion of O^{2-} in aluminum oxide,[2] and it is thought that the vacancies caused by impurities contribute to the diffusion in the case of oxide as well.

As for the effect of impurities, the influence of impurities (Fe_2O_3, Cr_2O_3 and CoO) on the diffusion of Ni^{2+} in magnesium oxide has been reported.[3] It was found that when Fe_2O_3 or Cr_2O_3 was added to MgO the diffusion of Ni^{2+} in MgO was promoted. The phenomenon can be explained by the fact that, when Mg^{2+} is replaced with Fe^{3+} or Cr^{3+}, the difference in the valence causes cation vacancies which then contribute to the diffusion.

The no-cation sites in oxide crystals may be classified into the three groups: the structural no-cation sites, the temperature-dependent vacancies, and the composition-dependent vacancies. An example of a structural no-cation site is the no-Al octahedral site in alpha-Al_2O_3. The vacancies caused by impurities belong to the composition-dependent vacancy, and the temperature-dependent vacancy is thermally formed. Composition-dependent vacancies can be intentionally realized and controlled in a complex oxide with a fairly wide solid-solution range such as spinel. Such vacancies caused by structural nonstoichiometry are expected to contribute to the diffusion, but no study of this problem has yet been reported. This paper will report the results of an experiment investigating the influence on the diffusion of cation vacancies occuring in a spinel solid solution.

The $MgAl_2O_4$-Al_2O_3 system has a large region of a

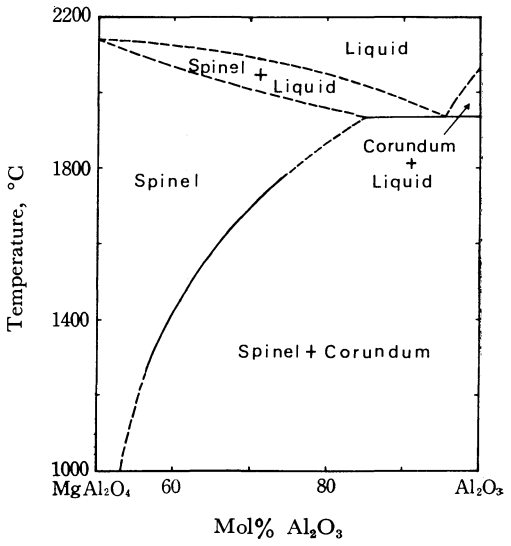

Fig. 1. Phase diagram for the system $MgAl_2O_4$-Al_2O_3.[4]

1) D. Mapother, H. N. Crooks and R. Maurer, *J. Chem. Phys.*, **18**, 1231 (1950).

2) Y. Oishi and W. D. Kingery, *ibid.*, **33**, 480 (1960).

3) G. Yamaguchi and T. Tokuda, *J. Ceram. Assoc. Japan*, **76**, 350 (1968).

solid solution on the side of spinel, as may be observed in the phase diagram[4] (Fig. 1). In this report this solid solution will be called the "defective spinel,"[5] while the spinel with a perfect spinel structure will be called the "perfect spinel." It is thought that excessive oxygen causes cation vacancies with an increase in the Al_2O_3 concentration in the defective spinel[6] and that they are composition-dependent vacancies. Because of the wide range of solubility, the concentration of composition-dependent vacancies can be much larger than that of temperature-dependent defects. Since the concentration gradient was found in the spinel layer at the time of practical formation from magnesium oxide and aluminum oxide,[7] the defective spinel whose composition varies continuously is thought to constitute the product layer. The material transport through the product layer controls the reaction rate in a solid state reaction such as spinel formation. Accordingly, it is important in the study of the solid state reaction to examine the influence on the diffusion of cation vacancies present in the defective spinels.

In this report the diffusion rates of Ni^{2+} in several kinds of defective spinels ($MgO \cdot xAl_2O_3$, where $x=1.1$, 1.2, 1.3, 1.4 and 1.5) and the perfect spinel are investigated using an electron probe micro-analyzer, and the influence on the diffusion of composition-dependent cation vacancies in defective spinels is clarified. Spinels also have many structural no-cation sites, such as no-Al sites in alpha-Al_2O_3; this experiment might be able to suggest the nature of the effect of those no-cation sites on the cation diffusion.

Experimental

Preparation of Specimens. The spinels whose compositions are listed in Table 1 were synthesized from basic magnesium carbonate, basic nickel carbonate, and gibbsite. Ten per cent of the Mg^{2+} of the spinels designated as M1, M2, M3, M4, M5, and M6 were replaced with Ni^{2+}; these spinels were designated as N1, N2, N3, N4, N5, and N6 respectively. The degrees of defectiveness or the concentrations of the composition-dependent cation vacancies of Nj may be expected to be equal to that of Mj, where $j=1$, 2, 3, 4, 5, and 6. The calculated concentrations of such vacancies are shown in Table 1.

Mg^{2+} and Ni^{2+} are similar in valence, ionic radius, and chemical property, and the concentrations of Ni^{2+} in the spinels of the N series are not large. Therefore, the properties of the spinels of the N series are thought to be very similar to those of the M series. Therefore, when M1 and N1, M2 and N2, and so on are paired as

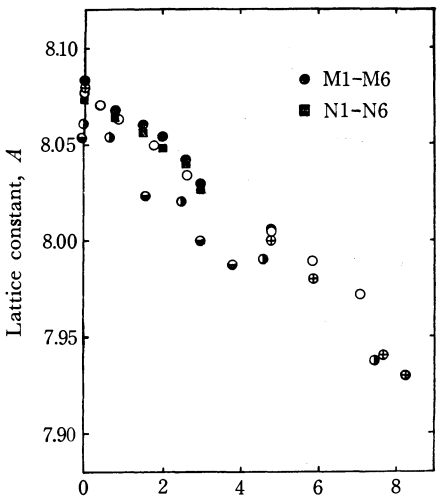

Fig. 2. Lattice constants of spinels *vs.* calculated concentrations of composition-dependent cation vacancies.
● and, ■ this experiment; ○, I. I. Visknerskii and V. N. Skripak; ◑, D. M. Roy, R. Roy and E. F. Osborn; ◐, P. T. Sarjeant and R. Roy; ◒, G. Hägg and G. Söderholm; ⊕, G. Yamaguchi

TABLE 1. COMPOSITIONS OF SPECIMENS AND THE CALCULATED CONCENTRATIONS OF COMPOSITION-DEPENDENT CATION VACANCIES*

Designation	Composition	Designation	Composition	Concn. of cation vacancies (cation site %)
M1	$MgO \cdot Al_2O_3$	N1	$(Mg_{0.9}Ni_{0.1})O \cdot Al_2O_3$	0.0
M2	$MgO \cdot 1.1Al_2O_3$	N2	$(Mg_{0.9}Ni_{0.1})O \cdot 1.1Al_2O_3$	0.78
M3	$MgO \cdot 1.2Al_2O_3$	N3	$(Mg_{0.9}Ni_{0.1})O \cdot 1.2Al_2O_3$	1.45
M4	$MgO \cdot 1.3Al_2O_3$	N4	$(Mg_{0.9}Ni_{0.1})O \cdot 1.3Al_2O_3$	2.04
M5	$MgO \cdot 1.4Al_2O_3$	N5	$(Mg_{0.9}Ni_{0.1})O \cdot 1.4Al_2O_3$	2.57
M6	$MgO \cdot 1.5Al_2O_3$	N6	$(Mg_{0.9}Ni_{0.1})O \cdot 1.5Al_2O_3$	3.03

* Porosities of specimens are within the range of 1 to 3%.

4) D. M. Roy and E. F. Osborn, *J. Am. Ceram. Soc.*, **36**, 147 (1953).
5) G. Yamaguchi, This Bulletin, **26**, 204 (1953).
6) G. Hägg and G. Söderholm, *Z. Physik. Chem.*, **B29**, 88 (1935).
7) G. Yamaguchi and T. Tokuda, This Bulletin, **40**, 843 (1967).

diffusion couples, the degree of defectiveness does not vary at the time of diffusion treatment and Ni^{2+} ions may be expected to diffuse with the same diffusion coefficient on both sides of the diffusion interface. These spinels were pressed into pellets and heated at 1650°C for several hours. Specimens were sintered densely so that they had less than 5% of porosity to avoid its influence as much as possible. The lattice constants of these spinels were measured accurately by an X-ray diffractometer. The measured values are shown in Fig. 2, along with the lattice constants previously reported.[6,8-11] It was found that the lattice constants varied linearly with the compositions in both series, M and N, so that the spinels whose cation-vacancy concentrations are equal to the calculated value may be supposed to have been synthesized. These pellets were polished with silicon carbide grains and diamond paste. Magnesium aluminum spinels were paired with spinels containing Ni^{2+} whose cation-vacancy concentrations were equal to the former, such as M1-N1. Their polished faces were placed in contact, and they were pressed perpendicularly to the contact face under a pressure of about 3 kg/cm² for 15 min at the temperature of 1500°C. After this treatment, the pellets were stuck together.

The specimens prepared as mentioned above were polycrystalline and contained grain boundaries. In order to estimate the influence of grain boundaries on the cation diffusion, two kinds of single crystal spinels were treated in the same way as the sintered specimens. The compositions of these single crystals were $MgO \cdot Al_2O_3$ and $MgO \cdot 1.5Al_2O_3$; they were designated as M1(S) and M6(S) respectively. M1(S) was paired with N1, and M6(S) with N6, and they were jointed in the same way as the other couples.

Heat Treatment for Diffusion. The six couples prepared as described above were heated in a controlled electric furnace for from 48 to 216 hr. The heat-treating temperatures were 1305±10, 1372±10, 1477±10, and 1527±10°C.

Analyzing Method. Each specimen was buried in resin after the heat treatment and cut perpendicularly to the diffusion interface with a diamond cutter. The cut surface was polished carefully with silicon carbide grains and diamond paste, and then coated with beryllium by vacuum spattering in order to get the electric conductivity. Specimens were mounted on the sample holder and analyzed by the electron probe micro-analyzer. At the time of measurement specimens were moved perpendicularly to the diffusion interface at a velocity of 20 μ/min, while the electron beam was fixed; then the intensity profile of the characteristic X-rays of Ni was obtained.

For the standard samples the spinels whose compositions are described as $(Mg_{1-x}Ni_x)O \cdot Al_2O_3$, where $x=0.0$, 0.01, 0.02, and 0.05, were synthesized. They were sintered, polished, and coated with beryllium in the same way as in the case of diffusion couples. With these standard samples, the intensities of the Ni$K\alpha$ rays were measured by the electron probe micro-analyzer. It was found that the plot of the intensities of the Ni$K\alpha$ rays against the concentrations of Ni^{2+} was almost linear, as is shown in Fig. 3. Therefore, it might be supposed that the intensity profile of Ni$K\alpha$ rays obtained

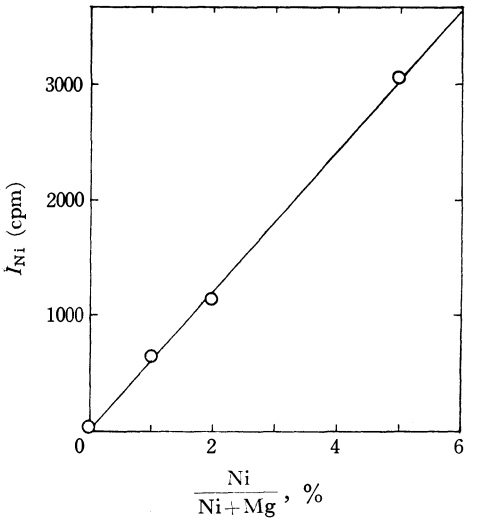

Fig. 3. Plot of Ni$K\alpha$ intensities *vs.* concentrations of Ni^{2+}.

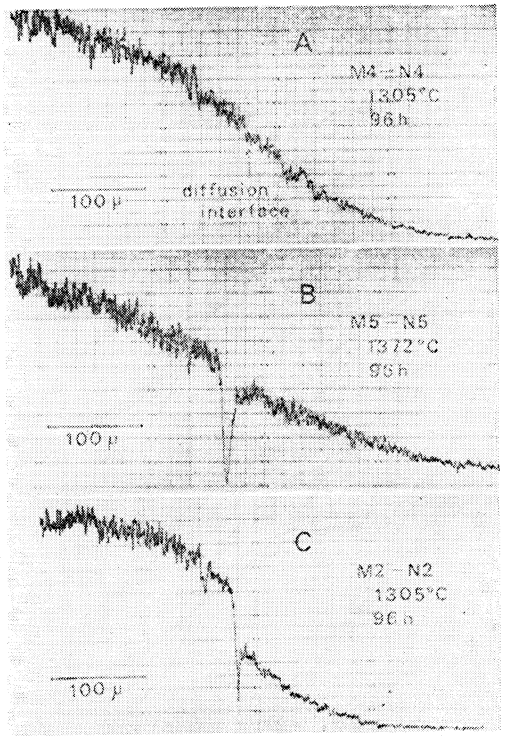

Fig. 4. The typical profiles belonging to the three classes represented by the adhesive sign A, B and C.

8) G. Yamaguchi, *J. Ceram. Assoc. Japan*, **61**, 594 (1953).
9) I. I. Visknerskii and V. N. Shripk, *Soviet Phys.-Solid State*, **7**, 2374 (1966).
10) D. M. Roy, R. Roy and E. F. Osborn, *Am. J. Sci.*, **251**, 337 (1953).
11) P. T. Sarjeant and R. Roy, *J. Appl. Phys.*, **38**, 4540 (1967).

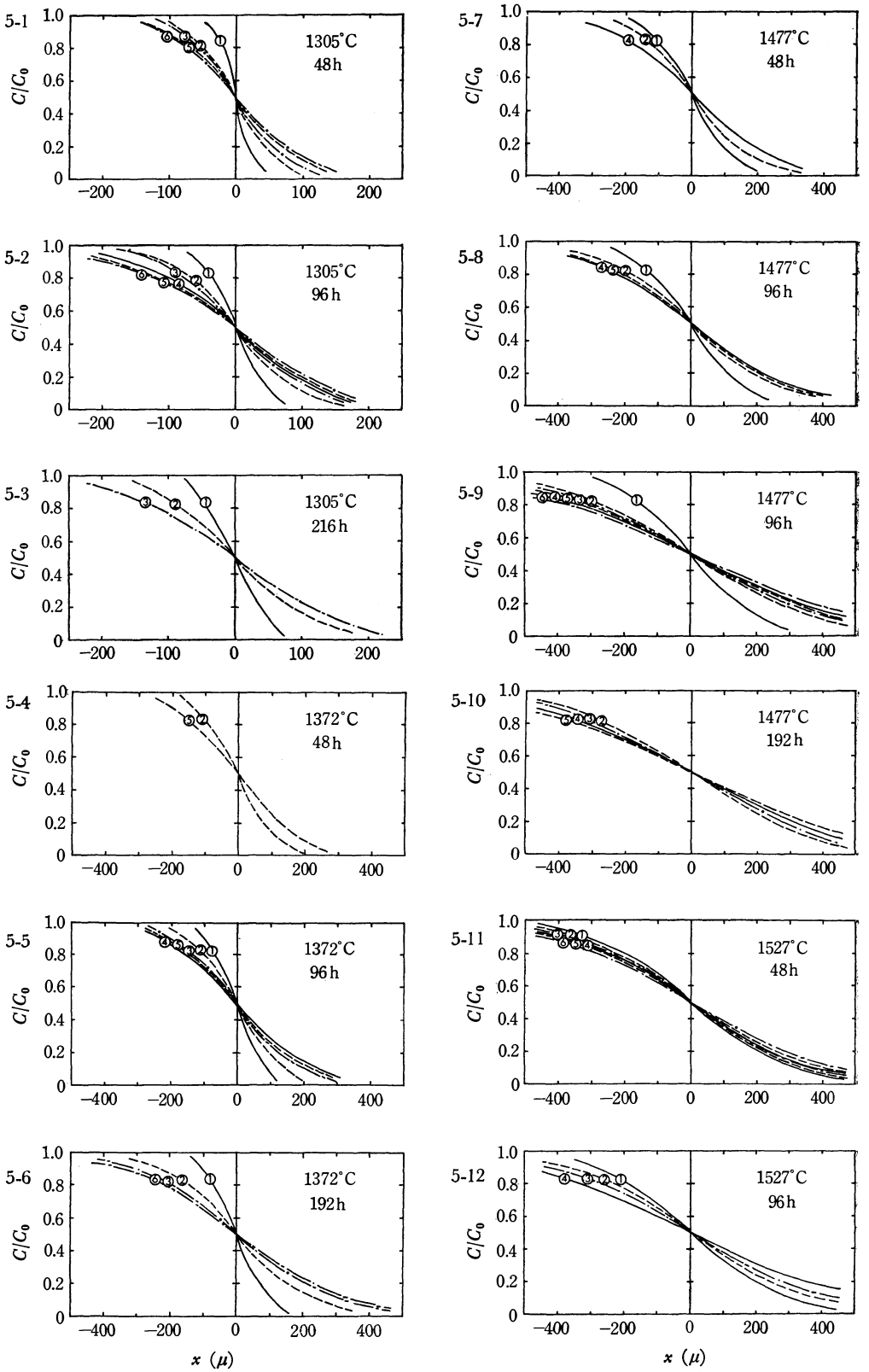

Fig. 5. Concentration distributions of Ni^{2+} in the diffusion couples.
—①—, M1-N1; --②--, M2-N2; —③—, M3-N3; —④—, M4-N4; --⑤--, M5-N5; —⑥—, M6-N6

by the measurement about the diffusion couple represents the concentration distribution of Ni^{2+} as it really is.

Results and Calculation of Diffusion Coefficients

The intensity profiles of Ni$K\alpha$ rays measured by the electron probe micro-analyzer can be grouped into the following three classes on the basis of the features of the diffusion interface and its neighborhood. The first class consists of the profiles which have no clear falling of intensity at the position of the diffusion interface. In the couples of this group the pellets are thought to be stuck very fast; such an adhesive condition is represented by the sign A. The second class consists of the profiles which have clear fallings of intensity at the position of the diffusion interface, but in which the Ni$K\alpha$ intensities on both sides are nearly equal. In this case the pellets are thought to be stuck quite fast; such an adhesive condition is represented by the sign B. The third class consists of the profiles which have clear fallings at the position of the diffusion interface and in which there are gaps of Ni$K\alpha$ intensities on both sides of the diffusion interface. Such an adhesive condition is represented by the sign C. Examples of the original profiles belonging to all three classes recorded by the electron probe micro-analyzer are shown in Fig. 4. The experiments whose results have the profiles represented by the adhesive signs A and B were thought to be established well enough, and so the results were used as data for the calculation of the diffusion coefficients. The results of the experiments belonging to the class represented by the adhesive sign C were not used, however, because in this case the adhesive condition was thought to be not so good.

The intensity profile was smoothed so as to average the statistical fluctuations; it can now be thought of as a smoothed profile to represent the concentration distribution of Ni^{2+} in the diffusion couple as it really is. The concentration distribution curves of Ni^{2+} in the diffusion couples which are thought to be well establsihed are shown in

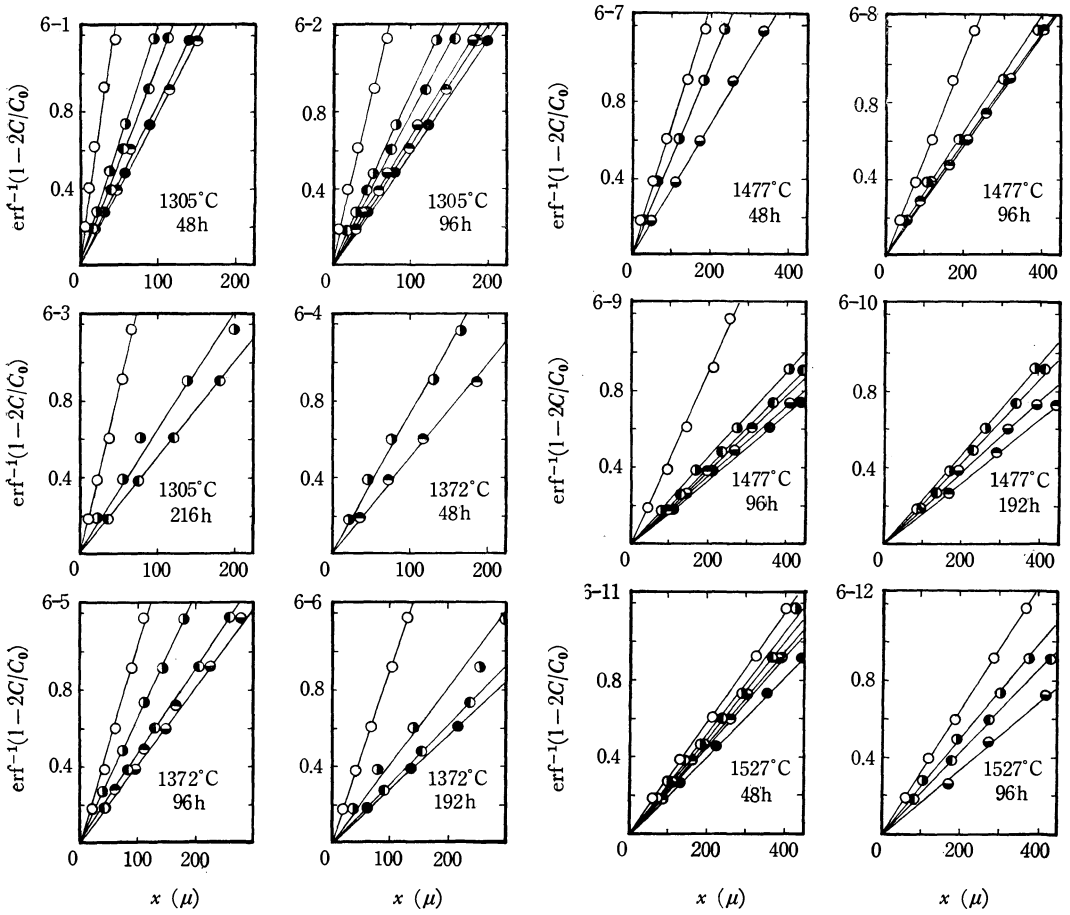

Fig. 6. Plots of $\mathrm{erf}^{-1}(1-2C/C_0)$ *vs.* x.

○, M1-N1; ◑, M2-N2; ◐, M3-N3; ◒, M4-N4; ◓, M5-N5; ●, M6-N6

Figs. 5-1 to 5-12. The shapes of the curves are symmetrical, as is shown in Figs. 5-1 to 5-12; on both sides of the diffusion interface the equal values of the diffusion coefficient of Ni^{2+} were calculated by the method to be described below.

In obtaining the diffusion coefficients, it was assumed that the diffusion follows Fick's law. Considering the initial state, the concentration, C, of Ni^{2+} at a certain distance, x, from the diffusion interface after time t is given by:

$$C = C_0/2 \cdot \{1-\mathrm{erf}(x/2\sqrt{Dt})\}$$

Therfore,

$$\mathrm{erf}^{-1}(1-2C/C_0) = x/2\sqrt{Dt},$$

where D is the diffusion coefficient of Ni^{2+}, C_0 is the initial concentration of Ni^{2+} at $x<0$, $\mathrm{erf}(\xi)$ is Gauss' error function, and $\mathrm{erf}^{-1}(\zeta)$ is the inverse function of Gauss' error function. Plots of $\mathrm{erf}^{-1}(1-2C/C_0)$ against x based on the results shown in Figs. 5-1 to 5-12 are shown in Figs. 6-1 to 6-12. In every plot good straight lines are obtained; from the slope of these lines, that is $1/2\sqrt{Dt}$, the diffusion coefficients can be calculated. The diffusion coefficients of Ni^{2+} obtained in the way described above were arranged for every couple and every heat-treatment temperature; the results are shown in Table 2. In order to estimate the influence of grain boundaries, the diffusion coefficients were calculated from the measurements of M1(S)-N1 and M6(S)-N6; it was found that they were nearly equal to the values obtained from M1-N1 and M6-N6 respectively. The plots of $\mathrm{erf}^{-1}(1-2C/C_0)$ *vs.* x for M1(S)-N1 and M6(S)-N6 are shown in Fig. 7, along with the plots about M1-N1 and M6-N6. Accordingly, it seems that there is no influence of grain boundaries on the diffusion in such an experiment using a sintered specimen fired at a temperature above 1650°C.

TABLE 2. DIFFUSION COEFFICIENTS OF Ni^{2+} IN DEFECTIVE SPINELS

Couple of specimens	$D\times10^{10}$ (cm²/sec) 1305°C	1372°C	1477°C	1527°C
M1-N1	0.16±0.07	0.63±0.16	3.6±0.5	12±3
M2-N2	0.77±0.15	2.0±0.7	8.2±4.5	15±3
M3-N3	1.2±0.2	3.2±0.9	12±5	18±2
M4-N4	1.6±0.5	3.6±1.2	14±5	24±5
M5-N5	2.0±0.4	4.1±1.3	16±4	26±7
M6-N6	2.2±0.3	5.1±1.0	21±4	32±8

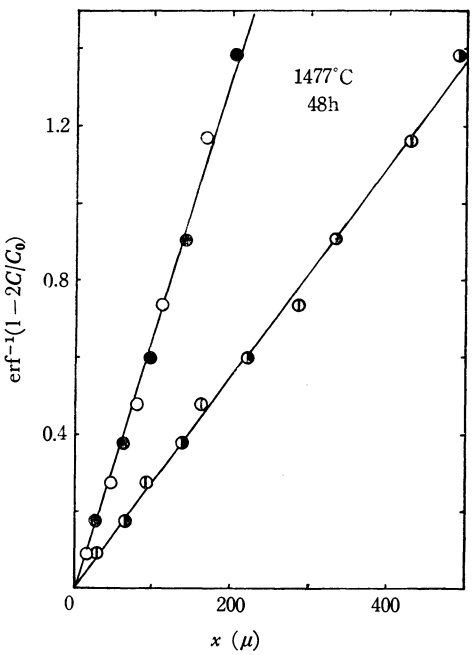

Fig. 7. The plot of $\mathrm{erf}^{-1}(1-2C/C_0)$ *vs.* x about M1-N1, M1(S)-N1, M6-N6 and M6(S)-N6.
○, M1-N1; ●, M1(S)-N1; ⓘ, M6-N6; ◑, M6(S)-N6

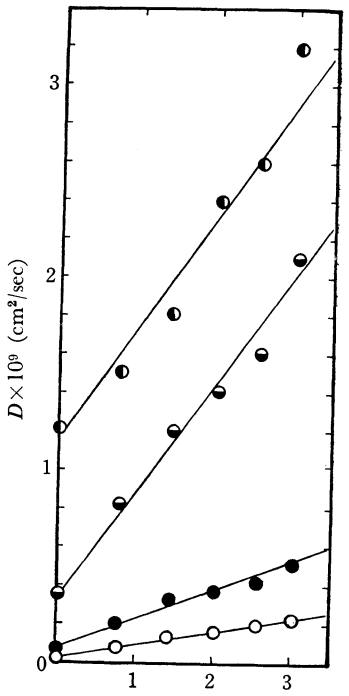

Fig. 8. Plots of diffusion coefficients *vs.* concn. of composition-dependent cation vacancies.
◐, 1527°C; ◒, 1477°C; ●, 1372°C; ○, 1305°C

Discussion

The plots of the diffusion coefficients of Ni^{2+} *vs.* the concentrations of the composition-dependent vacancies are shown in Fig. 8. The figure shows that the diffusion coefficients of Ni^{2+} are linear to

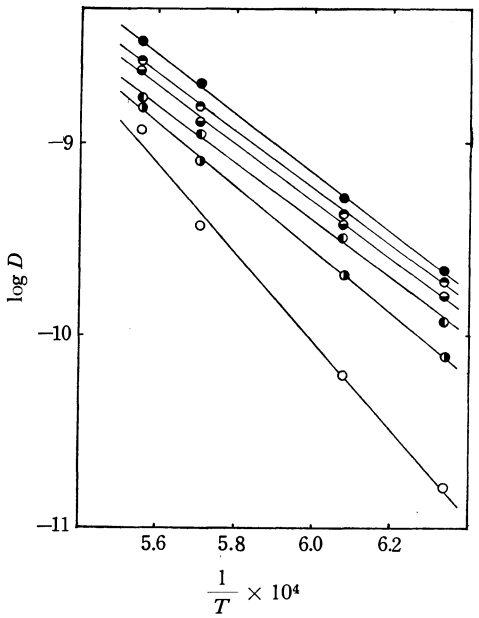

Fig. 9. Arrhenius plot of the diffusion coefficient.
○, M1-N1; ◑, M2-N2; ◐, M3-N3;
◒, M4-N4; ◓, M5-N5; ●, M6-N6

the concentrations of the composition-dependent vacancy. The Arrhenius plot for each couple is shown in Fig. 9. The so-called activation energies obtained from the Arrhenius plots are listed in Table 3. The activation energy is 106 kcal/mol for the M1-N1 couple with a perfect spinel structure, while it is about 70 kcal/mol for the couples containing composition-dependent vacancies, M2-N2, M3-N3, M4-N4, M5-N5, and M6-N6. Therefore, it was confirmed that the composition-dependent vacancies contribute to the cation diffusion in the defective spinel. In the perfect spinel the temperature-dependent vacancy or the structural no-cation site is thought to contribute to the cation diffusion. The fact that the diffusion

Table 3. The temperature dependence of the diffusion coefficients
(the so-called activation energy)

Couple of specimens	So-called activation energy (kcal/mol)
M1-N1	106
M2-N2	75
M3-N3	69
M4-N4	68
M5-N5	67
M6-N6	69

constants of Ni^{2+} in the perfect spinel are fairly small compared with the values in the defective spinels suggests that, if there exists a diffusion caused by the structural no-cation sites, the contribution of those no-cation sites to the diffusion will seem small. However, the effects of the temperature-dependent vacancies and the strucutral no-cation sites could not be discriminated in this experiment. Therefore, according to the genral interpretation, it was assumed that the diffusion in the perfect spinel was caused by the temperature-dependent vacancies. The diffusion coefficient D in M1-N1 can, then, be represented as follows:

$$D = D_0 \exp\left(-\frac{U+E}{RT}\right)$$

where U is the energy necessary for the movement of Ni^{2+} and where E is the energy necessary to form the temperature-dependent vacancy contributing to the diffusion. The so-called activation energy for the perfect spinel, $U+E$, is 106 kcal/mol, as is shown in Table 3. In defective spinels the diffusion coefficient, D, is represented as follows:

$$D = D_0' \exp\left(-\frac{U}{RT}\right)$$

where U is the energy necessary for the movement of Ni^{2+}. The so-called activation energy is about 70 kcal/mol for the defective spinel, as is shown in Table 3. Therefore, the tentative values of $U=70$ kcal/mol and $E=36$ kcal/mol were obtained. This value of E is about 1.6 times larger than the value reported for Na^+ in NaCl, that is, 23 kcal/mol,[1] this ratio does not seem unreasonable. In the case of the diffusion of Ni^{2+} in MgO containing Cr_2O_3, 70 kcal/mol was obtained as the extrinsic activation energy;[3] this is almost equal to the value found in the present investigation.

Conclusion

The diffusion of Ni^{2+} in several kinds of defective spinels and the perfect spinel were investigated using an electron probe micro-analyzer. It was found that the diffusion coefficient of Ni^{2+} in the defective spinel increased linearly with the increase in the concentration of the composition-dependent cation vacancies. The so-called activation energy calculated from the Arrhenius plot for the defective spinel was different from that for the perfect spinel; the difference between them was 36 kcal/mol. The results support the suggestions that the composition-dependent cation vacancies govern the cation diffusion in the defective spinel, while the temperature-dependent vacancies predominate in the perfect spinel.

BULLETIN OF THE CHEMICAL SOCIETY OF JAPAN VOL. 42 2808—2814 (1969)

ESR Studies of the Negative Ions of Biphenyl Derivatives. III. Restricted Rotation of Alkyl Group in Some *ortho* or *para* Higher Alkylated Biphenyl Anion Radicals*[1]

Kazuhiko Ishizu,* Kazuo Mukai,* Hideo Hasegawa,** Koichi Kubo,** Hiroaki Nishiguchi*** and Yasuo Deguchi***

* *Department of Chemistry, Faculty of Science, Ehime University, Bunkyo-cho, Matsuyama*
** *Japan Electron Optics Laboratory, Akishima-shi, Tokyo*
*** *Department of Chemistry, Faculty of Science, Kyoto University, Sakyo-ku, Kyoto*

(Received April 9, 1969)

The electron spin resonance has been observed for the anion radicals of 4,4′-diethyl biphenyl, 4,4′-diisopropyl biphenyl, 4,4′-dicyclohexyl biphenyl, 2,2′-diethyl biphenyl, and 2,2′-diisopropyl biphenyl. Both of the β- and γ-proton coupling constants of alkyl groups have been precisely determined, and the positive temperature dependence has been verified for the β-proton coupling constant of 4,4′-dialkyl biphenyls. The ratio (R) of β-proton coupling constant of the other alkyls to the methyl proton coupling constant has been derived, and the evidence of the restricted rotation has been widely established for each derivative based on the angular dependence of the β-proton coupling constant, which can be expressed as follows:

$$a_i^{\beta} = \rho_{\pi} < Q >, \quad Q = B_0 + B\cos^2\theta$$

The minimum R value obtained for 2,2′-diethyl biphenyl enabled us to assume that a rotation of the alkyl group would be tightly locked at the *ortho* position. The R value of 2,2′-diisopropyl biphenyl revealed that the isopropyl β-proton would lie on the biphenyl aromatic plane. The anomalous R values associated with the *ortho*-alkylated biphenyls can be well understood as resulting from the facts that anion radicals have a more dominant character than do neutral molecules to reduce a twisting angle between the two phenyls, and that the free rotation of the alkyl group is strongly restrained by the steric hindrance between the alkyl group and the closely-oriented *ortho*-ring proton.

The theory of hyperconjugation has been widely accepted for numerous radicals based on the ESR observation of the methyl-proton splitting.

In many cases the observed methyl splitting has been successfully explained in terms of McLachlan's splitting parameter[1] on the assumption that a methyl group is freely rotating. In the case of the other alkyl derivatives, however, it has been established that the quantities of the β-*[2] proton splitting for alkyl groups differ from molecule to molecule because of the restricted rotation of the alkyl group.

In this study, ESR observations are made of anion radicals of 4,4′-diethyl biphenyl, 4,4′-diisopropyl biphenyl, 4,4′-dicyclohexyl biphenyl, 2,2′-diethyl biphenyl, and 2,2′-diisopropyl biphenyl.

The coupling constants of both the β- and the γ-*[2] proton in each alkyl group are determined, and the temperature dependence of the β-proton coupling constant is studied, in order to establish the relation between the preferred conformation of the alkyl groups and their proton splitting in these radicals. Our investigation of *ortho* derivatives is continuing, and we are likely to demonstrate that the rotation of the alkyl group can be strongly hindered at the *ortho* position. The general structure of a biphenyl ring is:

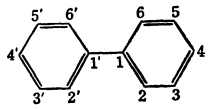

Experimental

The *ortho*- or *para*-alkylated biphenyls were made by an Ullman reaction on either *ortho* or *para* iodo alkyl

*[1] A part of this work was presented at 17 th Annual Meeting of the Chemical Society of Japan, Tokyo, April, 1964 and at the 18th Annual Meeting, Osaka, April, 1965.

*[2] The hydrogen atoms bonded to the sp^3 hybridized carbon atom at either the β- or γ-position are described as β-protons or γ-protons, as is shown in the illustration. The coupling constants are denoted as a_i^{β} and a_i^{γ}.

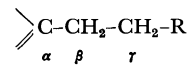

1) A. D. McLachlan, *Mol. Phys.*, **1**, 233 (1958).

benzene, according to the following process. The iodo compound (0.04 mol) was heated with 0.22 mol of activated copper powder in a bath kept at *ca.* 230—280°C for 15 hr. The organic product was extracted with *n*-hexane. After the removal of the solvent, the residue was fractionated under reduced pressure or recrystallized from ethyl alcohol. The materials thus obtained were all purified by silica gel chromatography, using *n*-hexane as the solvent. The physical constants[2,3] of the materials are listed below:

4,4′-diethyl biphenyl, mp 82.5°C; 4,4′-diisopropyl biphenyl, 64.8°C; 4,4′-dicyclohexyl biphenyl, mp 199°C; 2,2′-diethyl biphenyl, bp 110.5—111.2°C/7 mmHg, n_D^{21} =15649; 2,2′-diisopropyl biphenyl, mp 68°C.

The anion radicals were prepared in a solution of dimethoxyethane by reduction with potassium metal held in an acetone - dry ice bath.

The ESR spectrometer employed here and its operating conditions have been described in a previous paper.[4]

Results and Discussion

4,4′-Diethyl Biphenyl. In Fig. 1(a), we show the ESR spectrum of the 4,4′-diethyl biphenyl anion measured at 0°C. The observed hyperfine structures were adequately analyzed, and the hyperfine coupling constants of the ring protons, a_i^H, and the alkyl proton, a_4^β, were determined in the manner described before,[4] that is:

$a_4^\beta = 3.99$, $a_2^H = 2.68$ and $a_3^H = 0.51$ gauss.

The analyzed spectrum given in Fig. 1(b) is in good accordance with the observed spectrum.

With a depression in the temperature, the spectrum changed the hyperfine structures; Fig. 1(c) was recorded at −50°C. Both the a_i^H and a_4^β values were confirmed by the reconstruction of

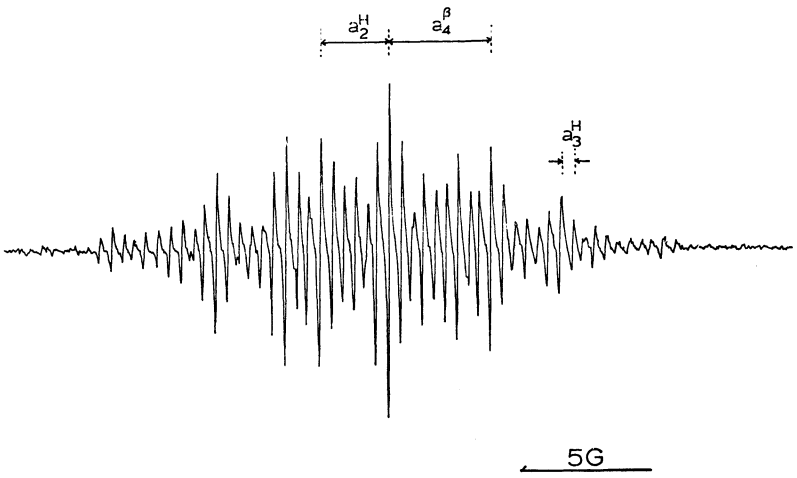

Fig. 1(a)

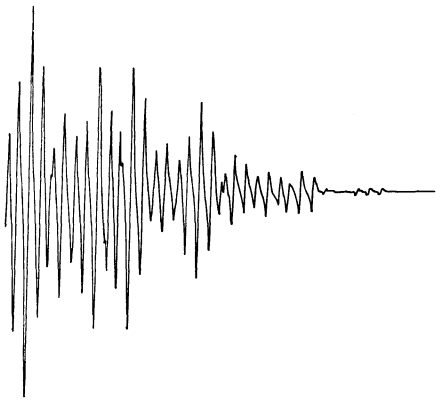

Fig. 1(b)

2) M. E. Pauline, D. M. Hall and E. E. Turner, *J. Chem. Soc.*, **1956**, 2286.

3) Bun-Hoi and P. Cagruiant, *Compt. rend.*, **216**, 381 (1943).

4) K. Ishizu, This Bulletin, **36**, 938 (1963).

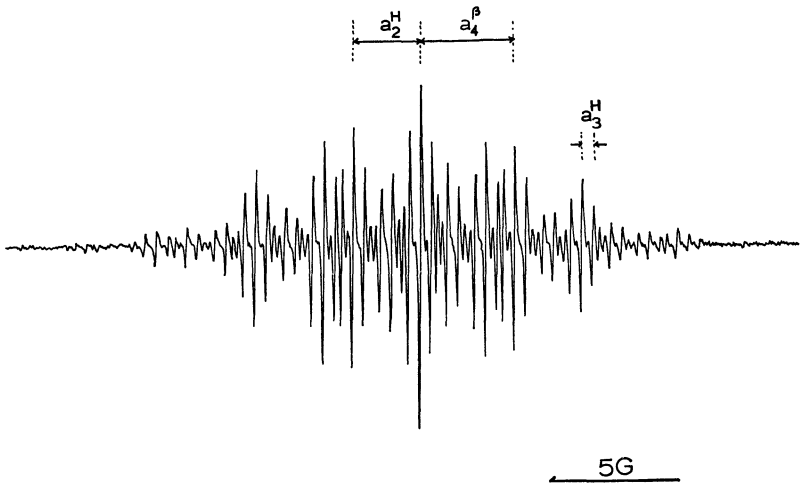

Fig. 1(c)

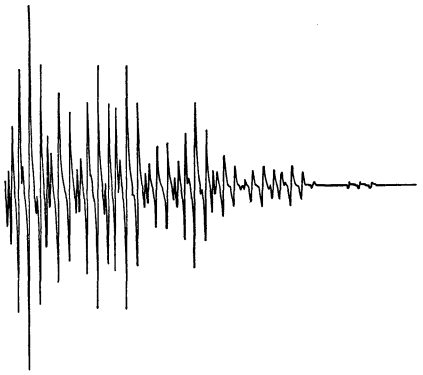

Fig. 1(d)

Fig. 1. 4,4'-Diethyl biphenyl.

(a) ESR spectrum recorded at 0°C. (b) A part of simulated spectrum of (a).
(c) ESR spectrum recorded at −50°C. (d) A part of simulated spectrum of (c).
A line shape is respectively assumed to be as a Lorentzian with the line width of 0.175G (b) and 0.100G (d).

the spectrum, as is shown in Fig. 1(d).

$a_4^\beta = 3.76$, $a_2^H = 2.65$ and $a_3^H = 0.42$ gauss.

In the present experiments, the γ-proton splitting of the ethyl group could never be detected.

On the basis of a comparison of the hyperfine coupling constants obtained in the two cases, one may say that the modified hyperfine structures are caused by a diminution of the value for a_4^β with a lowering of the temperature, whereas either a_2^H or a_3^H remains constant or has only a minor change.

4,4'-Diisopropyl Biphenyl. The spectrum measured at −30°C is given in Fig. 2(a), in which one may see that the smallest splitting (0.09 gauss) resulted from the isopropyl γ-proton. The spectrum consists of seven groups, whose relative intensity ratios are 1:6:15:20:15:6:1; the separation between the neighboring groups is about 2.6 gauss. This means that the a_4^β of isopropyl groups has the closing quantity of a_2^H, the *ortho* proton coupling constant.

The coupling constants deduced by the trial-and-error calculation of the line intensity are given as follows:

$a_4^\beta = 2.85$, $a_4^\gamma = 0.09$, $a_2^H = 2.66$
and $a_3^H = 0.45$ gauss.

When the observation temperature was lowered to −50°C, a reduction of the value for a_4^β was again noted and the hyperfine structures of the spectrum varied as is shown in Fig. 2(b). There is probably a smaller variation in the value for a_4^γ at the same

time, but we had failed to detect any important change in the value for a_4^{γ} anywhere. The hyperfine coupling constants determined at $-50°C$ are:

$$a_4^{\beta} = 2.66,\ a_4^{\gamma} = 0.09,\ a_2^{H} = 2.66$$
$$\text{and } a_3^{H} = 0.47 \text{ gauss.}$$

4,4′-Dicyclohexyl Biphenyl. In Fig. 3, we give the observed spectrum of the 4,4′-dicyclohexyl biphenyl anion recorded at room temperature. Except for a_4^{γ}, the other hyperfine coupling constants, a_4^{β}, a_2^{H}, and a_3^{H}, were very similar to those for 4,4′-diisopropyl biphenyl; that is,

$$a_4^{\beta} = 2.92,\ a_4^{\gamma} = 0.24\ a_2^{H} = 2.60$$
$$\text{and } a_3^{H} = 0.47 \text{ gauss.}$$

The value of a_4^{γ} is interesting, for it is much larger than that of 4,4′-diisopropyl biphenyl. The large value of a_4^{γ} for 4,4′-dicyclohexyl biphenyl can probably be attributed to the fact that the methylene groups are tightly locked in the cyclohexyl ring, although it freely rotates in the case of isopropyl groups.

2,2′-Diethyl Biphenyl. The ESR measurement was carried out at $-70°C$, as is shown in Fig. 4. The ethyl proton splitting, a_2^{β}, was easily estimated from the quintet splitting of 1.02 gauss. The other four sets of triplet splitting (4.97, 2.19, 0.59 and 0.18 gauss) assumed here were found to be very close to those for *o,o′*-bitolyl already studied;[5] the values for a_4^{H}, a_6^{H}, a_5^{H}, and a_3^{H} were determined to be as follows:

$$a_4^{H} = 4.97,\ a_2^{\beta} = 1.02,\ a_6^{H} = 2.19,$$
$$a_5^{H} = 0.59 \text{ and } a_3^{H} = 0.18 \text{ gauss.}$$

2,2′-Diisopropyl Biphenyl. In Fig. 5, we show the spectrum of the 2,2′-diisopropyl biphenyl anion radical observed at $-70°C$. In this case, one may specify two sets of triplet splitting (5.41 and 2.17 gauss) which are close to those of a_4^{H} and a_6^{H} for *o,o′*-bitolyl on the one hand. On the other hand, in the terminal group of the spectrum, one may see eleven lines equally spaced at 0.28 gauss, and the splitting has the relative intensity ratio of 1 : 2 : 5 : 8 : 10 : 12 : 10 : 8 : 5 : 2 : 1. This suggests that either a_2^{β} or a_5^{H} is equal to 0.58 gauss and that a_3^{H} is nearly half the value of a_5^{H}.

The hyperfine coupling constants thus estimated are:

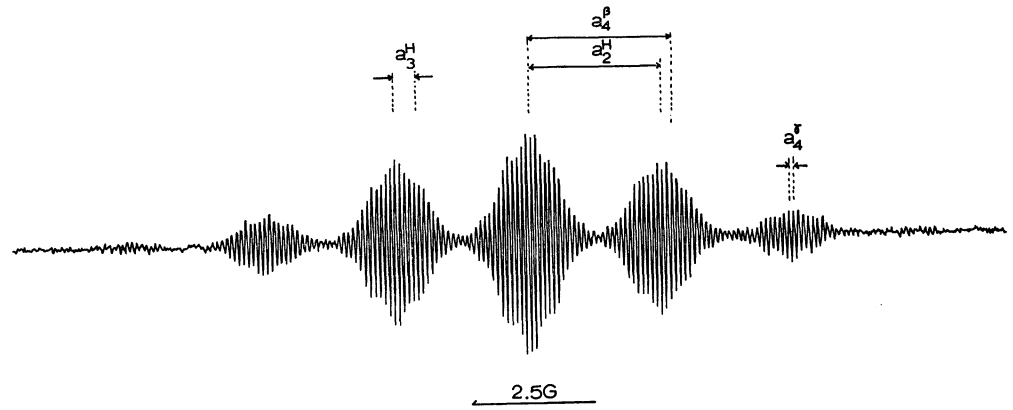

Fig. 2(a)

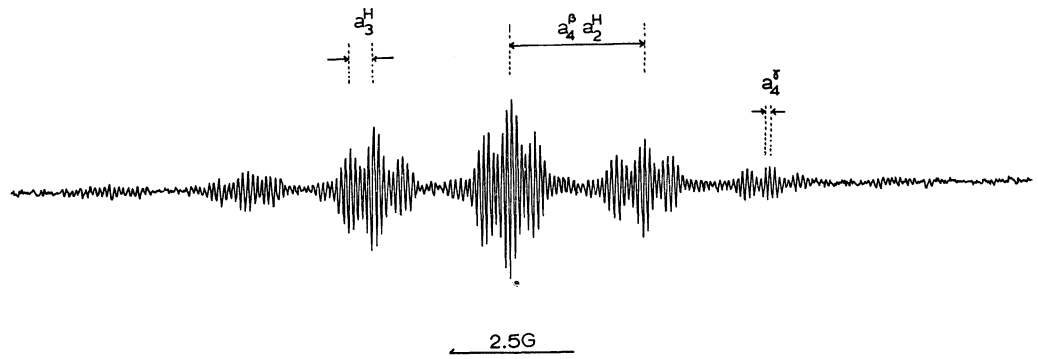

Fig. 2(b)

Fig. 2. 4,4′-Diisopropyl biphenyl.
(a) ESR spectrum recorded at $-30°C$. (b) ESR spectrum recorded at $-50°C$.

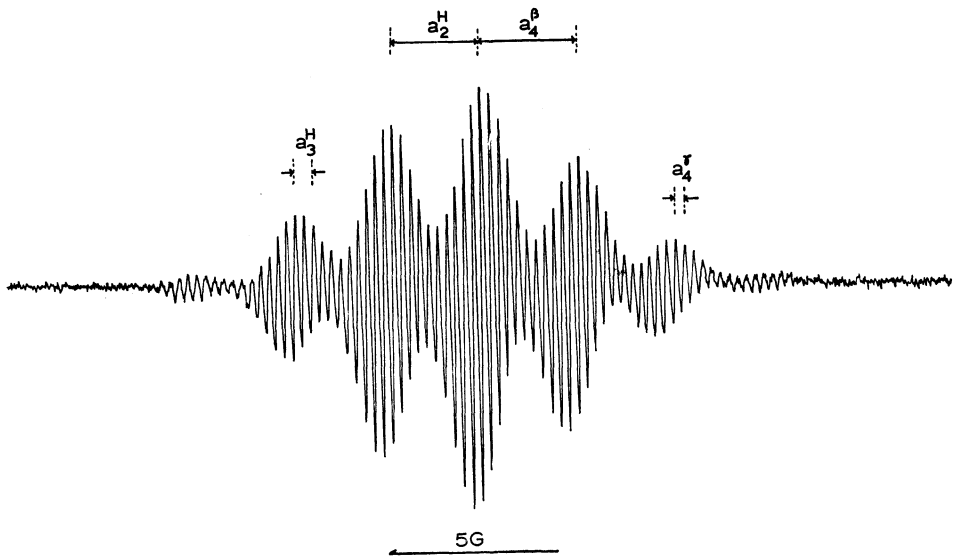

Fig. 3. 4,4'-Dicyclohexyl biphenyl.

$a_4^H = 5.14$, $a_6^H = 2.17$, $a_5^H = a_2^\beta{}_4 = 0.85$ and $a_3^H = 0.28$ gauss.

The observed proton splittings for alkylated biphenyl anion radicals are summarized in Table 1.

Ring-proton Splitting. A small perturbation is usually caused in the unpaired π distribution by an alkyl substitution into an aromatic ring. Indeed, as is shown in Table 1, this is also true for all the alkyl derivatives studied in the present work. In the case of *ortho* derivatives, however, it should be particularly noticed that the same magnitude of the ring-proton splitting can be observed regardless of the alkyl substitution; this is because the magnitude of the ring-proton splitting for *ortho* derivatives is a measure of not only an inductive effect due to the alkyl group, but also of the degree of steric hindrance between the two phenyl groups. The relation between the HMO spin density on the biphenyl π orbital and the steric hindrance between the two phenyls has already been established, and the ring-proton splitting ratios, a_4^H/a_6^H, have been taken as a parameter for estimating the degree of steric hindrance in the twisted biphenyls.[5]

Table 1. Proton coupling constants of alkyl biphenyl anion radicals (gauss)

4,4'-Dialkyl biphenyl

	a_2^H	a_3^H	a_4^β	a_4^γ	$\frac{a_4^\beta}{a_4^{CH_3}}$
p,p'-Bitolyl[a]	2.66	0.51	5.63	—	—
4,4'-Diethyl	2.68	0.51	3.99	—	0.71
4,4'-Diisopropyl	2.66	0.45	2.85	0.09	0.51
4,4'-Dicyclohexyl	2.60	0.47	2.92	0.24	0.52

2,2'-Dialkyl biphenyl

	a_2^β	a_3^H	a_4^H	a_5^H	a_6^H	$\frac{a_2^\beta}{a_2^{CH_3}}$
o,o'-Bitolyl[b]	2.20	0.28	5.12	0.56	2.20	—
2,2'-Diethyl	1.02	0.18	4.97	0.59	2.19	0.46
2,2'-Diisopropyl	0.58	0.28	5.14	0.58	2.17	0.26

Observation temperatures: a) room temperature, b) −15°C

Compared with the a_4^H/a_6^H ratio for *o,o'*-bitolyl (2.32) and those for 2,2'-diethyl biphenyl (2.27) and 2,2'-diisopropyl biphenyl (2.37), one may speculate that the biphenyl ring in the present anion radicals has a conformation which more or less resembles that for *o,o'*-bitolyl, in which two phenyls are twisted by 30—45°. From this point of view, our present results may be accepted as additional evidence to support the previous proposal that the anion radicals have a more greater tendency than do the neutral molecules to hold the biphenyl ring in a coplanar conformation.[6] Furthermore, the present results establish a base for a direct discussion of alkyl proton splitting with relation to the restricted rotation of an alkyl group.

Alkyl-proton Splitting. It has been pointed out that the β-proton coupling constant can be expressed by the following equation:[7]

$$a_i^\beta = <Q>\rho_\pi \quad (1)$$

$$Q = B_0 + B\cos^2\theta \quad (2)$$

where θ is the angle between the carbon-hydrogen

5) K. Ishizu, This Bulletin, **37**, 1093 (1964).

6) K. Ishizu, H. Hasegawa, H. Chikaki, H. Nishiguchi and Y. Deguchi, *Kogyo Kagaku Zasshi (J. Chem. Soc. Japan, Ind. Chem. Sect.)*, **68**, 1522 (1965).

7) C. Heller and H. M. McConnel, *J. Chem. Phys.*, **32**, 1535 (1960).

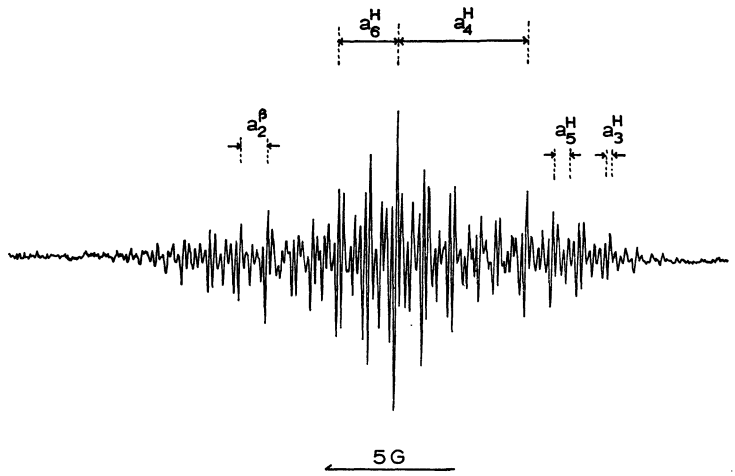

Fig. 4. 2,2'-Diethyl biphenyl.

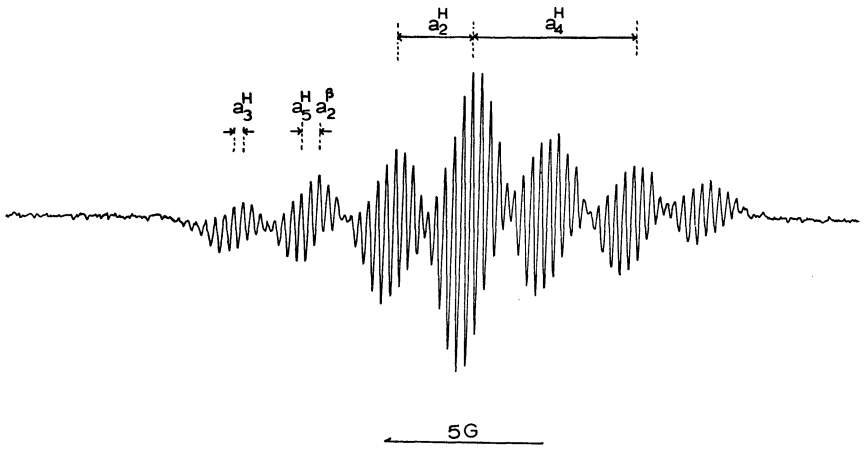

Fig. 5. 2,2'-Diisopropyl biphenyl.

bond and axis of the ring carbon $2p_z$ orbital; $<Q>$, the average quantity in Eq. (2), and ρ_π, the π electron spin density on the atom to which the alkyl group is bonded. The splitting parameter, B_0, defining a contribution from spin polarization is regarded as small in comparison with B, the parameter for hyperconjugation.[8] The methyl group in a radical has been thought to be freely rotating; thus, $<Q>$ becomes $B/2 \approx 25$ gauss, since $<\cos^2\theta> = 1/2$.

If the other alkyl groups were freely rotating, their β-proton splitting would have the same quantity for the methyl proton splitting. A large discrepancy has, however, been observed between the β-proton splitting of a methyl and those of the other alkyl groups; this has been discussed in terms of a preferred conformation of alkyl groups resulting from restricted rotation.[9]

For ease of comparison, the ratio, R, of the β-proton coupling constant to the methyl-proton coupling constant has been tabulated in Table 1.

The observed R value for 4,4'-diethyl biphenyl has been found to be close to those for such *para*-substituted benzene derivatives as 4-ethyl nitrobenzene ($R=0.74$) and 4-ethyl phenoxyl ($R=0.85$).[10]

According to this model, the theoretical R value for the ethyl group should be equal to either 0.5 or 1.50 if it is rigidly locked in the conformation illustrated in Fig. 6(a) and (b). The present R value (0.71) for 4,4'-diethyl biphenyl suggests

8) J. P. Colpa and E. de Boer, *Mol. Phys.*, **10**, 233 (1966).

9) D. H. Geske, "Progress in Physical Organic Chemistry," Vol. 4, Interscience Publishers, New York, N. Y. (1967), p. 182.

10) T. J. Stone and W. A. Waters, *J. Chem. Soc.*, **213** (1964).

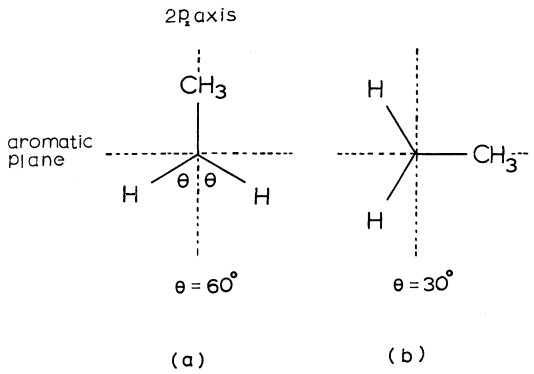

Fig. 6. Equilibrium confomation of a rotating ethyl group.

that alkyl groups more likely take the position of Fig. 6(a) rather than that of Fig. 6(b), but retain some residual rotation about their equilibrium positions.

From this assumption, the positive temperature dependence of a_4^β can be well understood as resulting from the thermal acceleration of a rotation. A similar temperature dependence has been reported for the hexaethyl benzene cation radical.[11] The β-proton coupling constant for either 4,4′-diisopropyl or 4,4′-dicyclohexyl biphenyl indicates that the β-proton would be oriented at $\theta=60°$, as calculated by Eqs. (1) and (2). These observed R values are nearly equal to those for the 4-isopropyl nitrobenzene anion ($R=0.56$)[9] and 4-isopropyl phenoxyl ($R=0.50$).[10]

In the case of 2,2′-diethyl biphenyl, the observed R value is much like those of ethyl cyclooctatetraene ($R=0.49$),[12] the 9-ethyl anthracene ($R=0.58$)[13] anion radical, and the hexaethyl benzene cation radical[11] ($R=0.46$), in which the rotation of the ethyl group has been considered to be strictly restrained, forcing it to take the preferential conformation illustrated in Fig. 6(a). The large diminution in the observed R value for 2,2′-diisopropyl biphenyl in comparison with the value for 4,4′-diisopropyl biphenyl indicates that the isopropyl β-proton is closer to the aromatic plane of biphenyl.

A molecular model is set up for 2,2′-diisopropyl biphenyl; it shows that the isopropyl free rotation is greatly restricted, when the two phenyls are twisted by about 45° taking account of the results for hindered methyl biphenyls.[5,6]

One may see that the isopropyl β-proton comes into contact with the 2′-*ortho* proton and nearly falls on the aromatic plane, as is illustrated in Fig. 7.

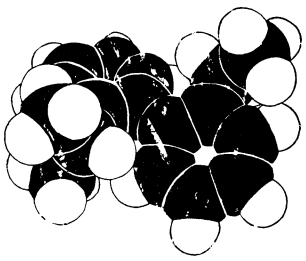

Fig. 7. A Stuart model of 2,2′-diisopropyl biphenyl anion radical.

The anomalous decrease in R values obtained for the present *ortho* derivatives can thus be attributed to the fact that the free rotation of the alkyl group is greatly restricted by the steric hindrance at the *ortho* position, where the alkyl groups are assumed to behave as torsional oscillators rather than rotators. The present results for the *ortho* alkyl proton-splitting also provide new experimental evidence to justify the previous proposal concerning hindered methyl biphenyls.

The authors wish to thank Professor Hideo Takaki for his encouragement through the course of this work. They are also indebted to Mrs. Ikuyo Higuchi for her assistance in the preparation of the samples.

11) M. K. Carter and G. Vincow, *J. Chem. Phys.*, **47**, 302 (1967).
12) A. Carrington and P. F. Todd, *Mol. Phys.*, **8**, 299 (1964).
13) D. Bachmann, *Z. Phys. Chem.*, **43**, 198 (1964).

BULLETIN OF THE CHEMICAL SOCIETY OF JAPAN VOL. 42 1815—1820 (1969)

Vapor Pressure of Carbon Monoxide in Condensed Phases*[1]

Takako SHINODA

Government Chemical Industrial Research Institute, Tokyo, Shibuya-ku, Tokyo

(Received April 11, 1969)

A theoretical vapor pressure equation of the form $\log P+(3/2)\log T=a+b/T$ for a diatomic molecule was applied to carbon monoxide in condensed phases. The two parameters in the equation determined from experimental vapor pressure data were used to obtain values of the static lattice energy E_0, the zero point energy E_Z, the geometric mean frequency ω_g and the mean frequency of molecular rotation ω_R in the respective phases by the information of lattice vibrations at low temperatures. From the mean values of molecular rotation frequencies, the hights of the potential barrier for hindered rotations were estimated to be 360, 230±10 and 110 cal/mol respectively.

Molecular rotations in the condensed phases of carbon monoxide have been theoretically and experimentally investigated by several authors.[1-5] However, there is little quantitative information about the state of hindered molecular rotation. Calorimetric studies showed that crystalline CO undergoes phase transition at 61.57°K and melts at 68.15°K.[6,7] The low- and high-temperature phases are denoted by α and β, respectively.

We have measured vapor pressures[7] of CO in two crystalline phases and liquid in the vicinity of the melting point. We will analyze these experimental vapor pressure data in terms of the quasi-harmonic theory of molecular vibrations, in which the normal modes of vibration are assumed to be harmonic, but have frequencies dependent upon the volumes of the solid and liquid. Values of the static lattice energy E_0 and the geometric mean frequency of the lattice vibrations ω_g in the respective phases of CO might be obtained from the analysis of vapor pressure. We will estimate the zero point energy E_Z and the mean frequency of molecular rotation ω_R or the height of the hindering potential V_0 by making use of the results of numerical calculation[8] of lattice vibrations for solid carbon monoxide at low temperatures.

Vapor Pressure Equation for Carbon Monoxide

The theory of the vapor pressure of a diatomic crystal was derived by Salter[9] along with monoatomic crystals, and applied to alkali halides by Leadbetter and Newsham.[10] According to their results, the vapor pressure of a diatomic crystal at high temperatures can be related to the temperature by an equation of the form

$$\ln P + (3/2)\ln T = a + b/T \qquad (1)$$

The measurement for the vapor pressure of CO was made in the region 55° to 72°K as previously reported,[7] and the results are listed in Table 1. An attempt has been made to find coefficients a and b which would make Eq. (1) fit these observed values in the α, β and liquid phases. The final equations are given in the following:

i) 55°K $< T <$ transition point

$$\log_{10}P + (3/2)\log_{10}T = -439.66/T + 11.27820, \qquad (2)$$

ii) transition point $< T <$ triple point

$$\log_{10}P + (3/2)\log_{10}T = -426.03/T + 11.06503, \qquad (3)$$

iii) $T >$ triplet point

$$\log_{10}P + (3/2)\log_{10}T = -384.90/T + 10.46265. \qquad (4)$$

At temperatures near melting point the contribution by the formation of lattice vacancies must be considered. Unfortunately no information on vacancy formation for CO crystal has been obtained

*1 Presented at the 22nd Annual Meeting of the Chemical Society of Japan, Tokyo, April 1969.

1) G. E. Ewing, *J. Chem. Phys.*, **37**, 2250 (1962); G. E. Ewing and G. C. Pimentel, *ibid.*, **35**, 925 (1961).

2) B. C. Kohin, *ibid.*, **33**, 882 (1960).

3) L. Jansen, A. Michels and J. M. Lupton, *Physica*, **20**, 1235 (1954); *ibid.*, **20**, 1244 (1954).

4) M. W. Melhuish and R. L. Scott, *J. Phys. Chem.*, **68**, 2301 (1964).

5) R. F. Curl, Jr., H. P. Hopkins, Jr., and K. S. Pitzer, *J. Chem. Phys.*, **48**, 4064 (1968).

6) J. O. Clayton and W. F. Giauque, *J. Am. Chem. Soc.*, **54**, 2610 (1932).

7) T. Shinoda, T. Atake, H. Chihara, Y. Mashiko and S. Seki, *Kogyo Kagaku Zasshi (J. Chem. Soc. Japan, Ind. Chem. Sect.)*, **69**, 1619 (1966).

8) T. Shinoda and H. Enokido, *J. Phys. Soc. Japan*, **26**, 1353 (1969).

9) L. Salter, *Trans. Faraday Soc.*, **59**, 657 (1963).

10) A. J. Leadbetter and D. M. T. Newsham, *ibid.*, **61**, 1646 (1965).

TABLE 1. VAPOR PRESSURE OF SOLID AND LIQUID CO

T (°K)	P (Torr)	$P-P$ (Eqs. (2), (3) and (4)) (Torr)
Solid (α-form)		
54.779	4.54	+0.13
55.363	5.22	−0.05
55.926	6.21	−0.03
56.476	7.30	−0.04
57.017	8.54	−0.03
57.549	9.91	−0.05
58.068	11.36	−0.14
58.577	13.12	−0.09
59.125	15.21	−0.08
59.930	18.93	+0.07
60.488	21.92	+0.19
61.028	25.15	+0.28
Solid (β-form)		
61.871	31.08	+0.03
61.934	31.54	+0.04
62.319	34.40	−0.02
62.755	37.97	−0.03
63.571	45.60	+0.05
64.299	53.22	−0.11
65.020	61.99	−0.12
65.657	70.84	−0.02
66.287	80.60	+0.09
66.916	91.30	+0.08
67.462	101.61	+0.14
67.171	95.79	−0.10
67.708	106.38	−0.01
*67.999	112.71	+0.24
*67.985	112.52	+0.35
*68.074	114.32	+0.24
Liquid		
68.292	118.93	+0.08
68.296	118.83	−0.11
68.681	126.87	+0.04
69.590	147.18	0.00
70.490	169.82	−0.05
71.523	199.33	+0.03

* These data were omitted on analysis.

from analysis of the thermal properties at high temperatures, because the transition point for CO crystal is considerably close to its triple point. We have, therefore, omitted the vapor pressure data at temperatures right below the melting point. The deviation of the calculated values(horizontal line), using Eqs. (2), (3) and (4), from the observed ones is shown by open circles in Fig. 1.

Quasi-harmonic Analysis

The constants a and b of Eq. (1) give values of the static lattice energy E_0 and the geometric mean frequency for the translational and rotational lattice modes ω_g (ω_{gT} and ω_{gR}) on the basis of the theory for ideal gas, liquid and crystal, as follows:

$$\left.\begin{aligned} a &= 3\ln\omega_{gT} + 2\ln\omega_{gR} \\ &\quad + \tfrac{1}{2}\ln[(m/(2\pi))^3(1/\boldsymbol{k})] + \ln[(2\boldsymbol{I})/\boldsymbol{k}], \\ b &= E_0/(\boldsymbol{N}\boldsymbol{k}). \end{aligned}\right\} \quad (5)$$

Here m is the molecular mass, $\boldsymbol{k}$ Boltzmann's constant, $\boldsymbol{I}$ its moment of inertia and $\boldsymbol{N}$ Avogadro's number. As the quantities E_0 and ω_g are temperature dependent, the values obtained by Eqs. (1) and (5) correspond to a certain mean temperature T_m in the respective phases. If we use the quasi-harmonic approximation, the effects of the change in volume of solid and liquid must be considered, but their variation over the respective temperature range of the analysis will be small. For the translational part of lattice vibrations we may expect the quasi-harmonic approximation to be adequate, because the most important parts in the translational motions of molecules are the spherical attractive dispersion and repulsive force between molecules.[8]

We first calculated the static lattice energy $E_0(V_0)$ referring to the 0°K volume V_0 in terms of the same molecular interaction potential[8] as used in the calculation of lattice vibrations for solid CO. The geometric mean frequency for the translational lattice modes $\omega_{gT}(0)$, and the translational and rotational zero point energies $E_{ZT}(V_0)$ and $E_{ZR}(V_0)$ referring to the 0°K volume have been estimated from frequency distributions in the harmonic approximation[8] as is shown in Fig. 2.

On the other hand, the heat of sublimation of CO crystal at 0°K, $\Delta H_0(V_0)$, was calculated from experimental data on thermodynamic properties.[6,7] The result is summarized in Table 2. The $E_0(V_0)$ can also be obtained from the relation

$$-E_0(V_T) = \Delta H_0(V_T) + E_{ZT}(V_T) + E_{ZR}(V_T), \quad (6)$$

where V_T is the volume at T°K. The values of $E_0(V_0)$ calculated are −2337 cal/mol and −2423 cal/mol. The discrepancy between them is probably due to the uncertainty on the rotational potential energy of molecular interaction. We have therefore used the mean value of these values, −2380 cal/mol, as the value of $E_0(V_0)$, and then the difference, 43 cal/mol, has been subtracted from the value of the zero point energy due to rotation of molecules

TABLE 2. CALCULATION OF HEAT OF SUBLIMATION AT 0°K (in units of cal/mol)

$\int_0^{bp} c_p(\text{solid})\mathrm{d}T$	1003
Heat of vaporization (at bp)	1444
$\int_0^{bp} C_p(\text{gas})\mathrm{d}T$	−568
Correction for gas imperfection	17
Heat of sublimation at 0°K, $\Delta H_0(V)$	1896

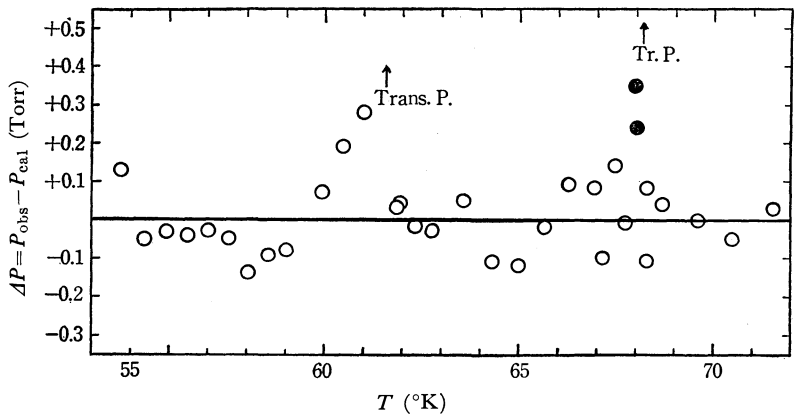

Fig. 1. Deviation of observed vapor pressure of CO from the calculated one by using Eqs. (2), (3) and (4). The black circles are data excluded on analysis.

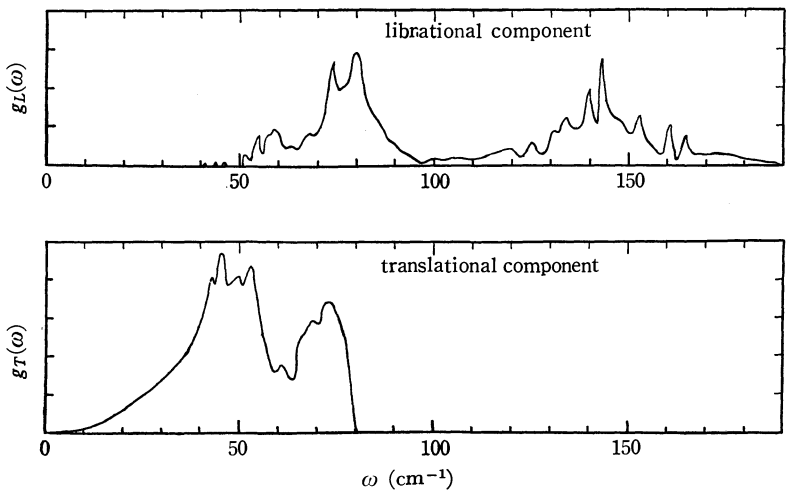

Fig. 2. The separated "translational" and "librational" distributions for CO crystal at 0°K, taken from Fig. 3 of Ref. 8.

$E_{ZR}(V_0)$ obtained by frequency distributions to make it consistent with other quantities.

To check the validity of the method adopted to estimate $E_0(V_0)$, $E_Z(V_0)$ and $\omega_g(0)$, the shape of the curve of the $\nu_D(n)$ function

$$\left.\begin{aligned} \nu_D(n) &= [(1/3)(n+3)\mu_n]^{1/n}, \\ \mu_n &= (1/5N)\int_0^\infty \omega^n g(\omega)\mathrm{d}\omega, \end{aligned}\right\} \tag{7}$$

where μ_n is the nth moment, has been established against n as is shown in Fig. 3 through use of the lattice frequency distributions in solid CO, since the $\nu_D(n)$ curve should be smooth, and $\nu_D(-3)$, $\nu_D(0)$ and $\nu_D(1)$ can be related to θ_0, ω_g and $E_Z(V_0)$ respectively, where θ_0 is the Debye characteristic temperature at 0°K and can be obtained from analyses of low temperature heat capacity data.[6,7]

The values of $E_0(V_0)$, $\omega_{gT}(V_0)$ and $E_Z(V_0)$ given above, have been used to analyze the vapor pressure for CO in the respective phases as fixed reference

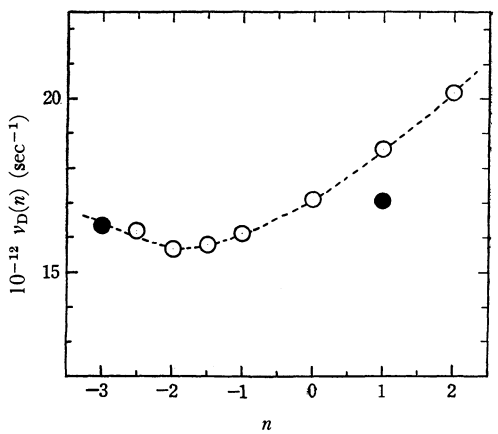

Fig. 3. The function $\nu_D(n)=[(1/3)(n+3)\mu_n]^{1/n}$ for CO. The open circles have been obtained from calculations and the black circles by analysis of the thermodynamic properties.

values.

The α-form; (54.8—61.0°K, T_m=57.9°K). The value of static lattice energy $E_0(V_{T_m})$ referring to the volume V_{T_m} at T_m in harmonic librational case has been estimated in the same way as for $E_0(V_0)$. In the quasi-harmonic approximation we may assume that the volume dependence of the static lattice energy is described by that of the zero point energy (*i.e.*, $\partial E_0/\partial V \simeq \partial E_Z/\partial V$). We may therefore estimate the zero point energy due to harmonic translation and libration of molecules corresponding to the mean temperature T_m, $E_Z(V_{T_m})(=E_{ZT}(V_{T_m})+E_{ZR}(V_{T_m}))$, by the approximate formula

$$E_0(V_{T_m})/E_0(V_0) \simeq E_Z(V_{T_m})/E_Z(V_0). \quad (8)$$

We may also obtain $\Delta H_0(V_{T_m})$ as the difference between $|E_0(V_{T_m})|$ and $E_Z(V_{T_m})$ values from Eq. (6).

The deviation of the value of static lattice energy $E_0(V_{T_m})$ in harmonic libration from that derived directly by the constant a of Eq. (2), might be interpreted as CO molecules being in the state of not harmonic but anharmonic libration (or hindered rotation) at the mean temperature T_m. Thus, the difference between the two $E_0(V_{T_m})$ values has been treated as the decrease in the rotational zero point energy $E_{ZR}(V_{T_m})$. The general treatment for the anharmonic contribution to the lattice vibration has not been given. Barron[11] suggested that as a first approximation the anharmonic effects may be represented by a frequency shift in the quasi-harmonic expression. We have calculated $\omega_R(T_m)$, which can be replaced by the sum of the harmonic librational frequency plus the anharmonic frequency shift, using the resultant value of $E_{ZR}(V_{T_m})$ on the basis of the Einstein model of lattice vibration.

The geometric mean frequency for the rotational lattice modes $\omega_{gR}(T_m)$, has been obtained from the coefficient b in Eq. (2) using Eq. (5). We have assumed that the translational modes of lattice vibrations are harmonic but with frequencies dependent upon the volume, and the effect of the change in volume is expressed by that of the zero point energy due to translation of molecules. If we assume that

$$\omega(0)/\omega_g(0) \simeq \omega_R(T_m)/\omega_{gR}(T_m), \quad (9)$$

where $\omega(T)=(1/5N)\int_0^\infty \omega g(\omega)d\omega$, then the resultant value of $\omega_{gR}(T_m)$ can give the value of $\omega_R(T_m)$. This value, 29.3 cm^{-1}, is in excellent agreement with the value of $\omega_R(T_m)$ obtained from $E_{ZR}(V_{T_m})$, 29.4 cm^{-1}.

The β-form; (61.9—67.7°K, T_m=65.0°K). If the rotation of CO molecules in the β-phase is free, then the zero point energy due to rotation $E_{ZR}(V_{T_m})$ is zero and the translational lattice vibrations still possess the zero point energy $E_{ZT}(V_{T_m})$. The structure of CO crystal was studied by Vegard.[12] The molecular centers are located in face-centered cubic lattice sites in the α-phase, and in hexagonal close packed sites in the β-phase. The face-centered cubic and the hexagonal close-packed structures may be regarded as equivalent arrangement, as illustrated in Fig. 4. The β-phase crystal may therefore be taken as the face-centered cubic lattice which has the same density as the actual crystal at T_m. Since the major forces of interaction potential for the translational motion of molecules are the spherical dispersion and repulsive forces.[8] We may assume that the change in $E_{ZT}(V_{T_m})$ due to the α–β-phase transition is the only effect corresponding to the volume change. In the case of free rotation the static lattice energy $E_0(V_{T_m})$ can be calculated using $E_0(V_0)$ in free rotation at 0°K as the reference value, where $|E_0(V_0)|$ is equal to the sum of $\Delta H_0(V_0)$ plus $E_{ZT}(V_0)$. The difference between the value of static energy $E_0(V_{T_m})$ obtained from the slope a of vapor pressure Eq. (3) and that in the case of free rotation is equivalent to the zero point energy $E_{ZR}(V_{T_m})$ due to rotation of molecules in the β-phase. By the treatment described in analysis for the α-form, this value of $E_{ZR}(V_{T_m})$ gives the rotational frequency $\omega_R(T_m)$ of 22.0 cm^{-1}. Estimate of the value of $\omega_R(T_m)$ using the geometric mean frequency for the rotationals modes $\omega_{gR}(T_m)$ in the β-phase, which has been derived from the intercept b of Eq. (3), gives the resultant value of 23.7 cm^{-1}.

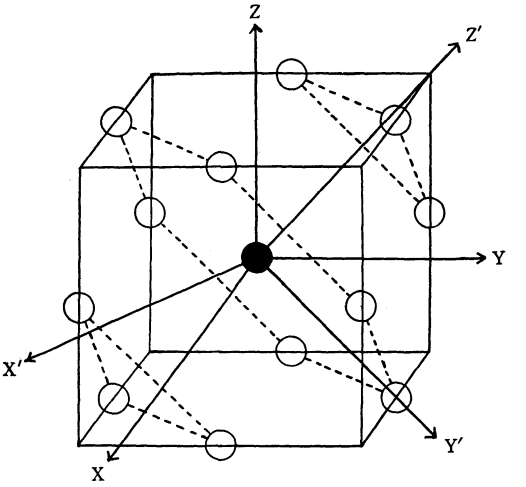

Fig. 4. The spatial arrangement of molecular centers in the face-centered cubic and the hexagonal close-packed lattices.

11) T. H. K. Barron, "Proceedings of the 1963 International Conference on Lattice Dynamics," ed. by R. F. Wallis, Pergamon Press, Inc., New York (1965), p. 247.

12) L. Vegard, *Z. Physik.*, **61**, 185 (1930).

TABLE 3. RESULTS OF ANALYSIS OF THE VAPOR RRESSURE DATA FOR CO

	α-Form			β-Form		Liquid		
	Harmonic libration	Harmonic libration	α-CO	Free rotation	β-CO	Harmonic libration	Free rotation	Liquid CO
Mean temperature (T_m)	0°K	57.9°K	57.9°K	65.0°K	65.0°K	69.9°K	69.9°K	69.9°K
Density	1.04	0.95	0.95	0.929	0.929	0.846	0.846	0.846
Lattice constant	5.63A	5.81A	5.81A	—	—	—	—	—
Spherical dispersion	−2903	−2403	—	—	—	−1971	—	—
Spherical repulsion	+1792	+1228	—	—	—	+845	—	—
Quadrupole interaction	−811	−693	—	—	—	−585	—	—
Anisotropic repulsion	−430	−277	—	—	—	−179	—	—
Anisotropic dispersion	+20	+17	—	—	—	+14	—	—
Dipole interaction	−5	0	—	—	—	0	—	—
Total (cal/mol)	−2337	−2128	—	—	—	−1876	—	—
$E_0(V_{Tm})$ (cal/mol)	−2380	−2167	−2012	−1886	−1951±2	−1911	−1719	−1761
$\Delta H_0(V_{Tm})$ (cal/mol)	1896	1726	1726	1688±2	1688±2	1541	1541	1541
$E_{ZT}(V_{Tm})$ (cal/mol)	222	202	202	198	198	178	178	178
$E_{ZR}(V_{Tm})$ (cal/mol)	262(305)	239	84	0	65±2	192	0	42
$\omega_R(T_m)$ (cm^{-1})	—	—	{29.4 {29.3	—	{22.0 {23.7	—	—	{14.7 {13.9
$\omega_g(T_m)$ (cm^{-1})	65.1	—	35.9	—	32.5	—	—	24.6

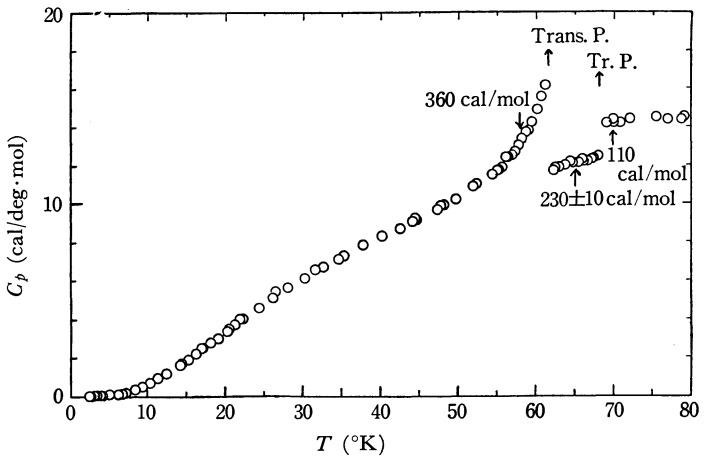

Fig. 5. The hindering potential barriers in the condensed phases, together with the experimental heat capacity curve of CO.

The Liquid in the Vicinity of the Melting Point; (T_m=69.9°K). We have adopted the cluster model for the liquid CO in the vicinity of its melting point. It may be assumed that the liquid consists of clusters containing 13 molecules,*2 and that the spatial arrangement of molecular centers in each cluster is the same as in a hypothetical solid, which has the density value at T_m determined by the extrapolation from the observed values. This is an approximation, which may be justified by the fact that only a continuous change in infrared spectral characteristic of CO occurs during the transition from liquid to solid.[1] In such liquids at least four different distances between the nearest neighboring molecules R_S, R_L, (R_L+R_{L-S}) and (R_L+2R_{L-S}) may be taken into consideration, where R_S is the nearest neighbor distance in a lattice having the density of a hypothetical solid, R_L in a lattice having the observed density of liquid CO at T_m, and R_{L-S} is the difference between R_S and R_L. We have assumed that all molecules in liquid are arranged with the statistical weights of these nearest neighbor distances of 6/13, 4/13, 2/13 and 1/13, respectively. The values of $E_0(V_{Tm})$, $E_{ZT}(V_{Tm})$ and $\Delta H_0(V_{Tm})$ in both harmonic libration and free rotation have been evaluated by the same treatment as was used in the solid phases. The value of $E_{ZT}(V_{Tm})$ evaluated as the difference between

*2 This is equal to the number of nearest neighbor molecules in addition to the one at center in face-centered cubic lattice.

$E_0(V_{Tm})$ obtained from the constant a in Eq. (4) and that in free rotation, leads to $\omega_R(T_m)=$ 14.7 cm^{-1}. This value is compared with the value of 13.9 cm^{-1} for $\omega_R(T_m)$ obtained from the constant b in Eq. (4).

Results and Analysis

Results of calculations are summarized in Table 3.

Discussion

Analysis of experimental vapor pressure data for CO has given us useful information about molecular motions in condensed phases. The values of $\omega_R(T_m)$ obtained in the respective phases may give the corresponding potential barriers, V_0, in which molecules are understood as the double-minimum two-dimensional rotators in a potential field of the type

$$V = (1/2)V_0(1 - \cos 2\theta). \tag{10}$$

The Schrödinger equation for the rotational motion is

$$-(\hbar^2/2I)\left(\frac{1}{\sin\theta}\frac{\partial}{\partial\theta}\sin\theta\frac{\partial\psi}{\partial\theta}+\frac{1}{\sin^2\theta}\frac{\partial^2\psi}{\partial\phi^2}\right) + (1/2)V_0(1 - \cos 2\theta)\psi = E\psi. \tag{11}$$

Curl *et al.* have recently solved this problem and given a table of its energy levels.[13] If the above $\omega_R(T_m)$ corresponds to the separation of the two lowest levels, the values of the hindering potential, V_0, can be calculated by the help of Pitzer's table. The results are given in Fig. 5, together with the experimental heat capacity curve of CO.[6,7] There are no values available in literature to compare with the $\omega_R(T_m)$ or V_0 values derived here except for the V_0 in the region 10—30°K and in liquid, which were estimated to be 1.7 kcal/mol and 120 cal/mol by Curl *et al.*[13] and Ewing[1] from the low temperature heat capacity data and the band intensity of infrared spectra for liquid. The present values of V_0 are not unreasonable for the respective phases.

Although we have analyzed in terms of quasi-harmonic lattice theory, the static lattice energy, the geometric mean frequency, the zero point energy and the molecular rotational frequency (or hindering potential barrier) may serve to investigate molecular rotational state in the condensed phases for CO when the treatment of anharmonic effects is not clear. However, it must be noted that the derived values all correspond to some mean values over whole molecules in crystal and liquid CO at some mean temperature T_m over the temperature range of analysis. Much more exact treatment will be made by analysis of heat capacity data shown in Fig. 5 on the basis of the statistical theory taking into account cooperative phenomena in the condensed phases, in which adjacent molecules appear to rotate together like meshed gears.

13) R. F. Curl, Jr., H. P. Hopkins, Jr., and K. S. Pitzer, *J. Chem. Phys.*, **48**, 4064 (1968).

BULLETIN OF THE CHEMICAL SOCIETY OF JAPAN VOL. 42 2820—2827 (1969)

Electrophotographic Properties of Titanium-Dioxide Resin Dispersion Layers

Takeaki IIDA and Hiroshi NOZAKI

The Institute of Industrial Science, The University of Tokyo, Roppongi, Minato-ku, Tokyo

(Received April 15, 1969)

The electrophotographic properties of titanium dioxide-polymer dispersion layers were studied. The titanium dioxide powder of the rutile type and three well-known polymers, polyvinyl acetate, polyvinyl chloride, and polystyrene, were used. The measurements were done on the corona-charging properties, *e. g.*, the resistivity and the capacitance of the layer, the rising gradient of the surface potential, and the fatigue effect of pre-illumination. The results make it clear that the analysis of an equivalent circuit can be applied to the interpretation of the rising gradient of the surface potential and to that of the dark decay to some extent. Moreover, it is found that the logarithm of the potential of the dark decay decreases proportionally to the cube root of the time at the initial step, while, at the next following step, it decays proportionally to the square root of the time. The mechanism of the dark decay of the surface potential is also discussed.

Titanium dioxide is famous as a white pigment, and it is one of the compounds of the transition elements. Therefore, this material has many interesting properties; for example, titanium dioxide ceramics have a high dielectric constant (114), and titanium dioxide has a photoconductivity at the wavelength of around 410 mμ.[1] At first we used this material as a photoconductor. Then we

have developed an Electrofax method,[2] in which titanium dioxide was used as a photoconductor instead of zinc oxide; we have obtained many good results with this method. Moreover, the image quality could thus be improved to the same quality as that of the zinc-oxide paper.

On the other hand, in the Electrostatic Recording method, a quite new application has recently been discovered;[3] that is, the addition of titanium dioxide to the recording paper improves the image quality of the electrostatic recording process, in which a pin tube is used as the recording head.[4] It is considered that the electrical capacity of the recording layer is increased by the addition of titanium dioxide; the real impedance of the layer against a pulse signal is then decreased. It results that an electron beam emitted from the pin head can easily pass through the recording paper, and the tailing phenomenon of a signal,[5] which is caused by the residual potential at the pin head, decreases greatly. Then the signal-to-noise ratio of the image is increased and the image quality is improved. The electrostatic recording methods have been applied in many fields, *e. g.*, in making of the facsimiles of newspapers, in the recording method of an electronic computer,[6] in the recording of TV images,[7] and in the use of an electrostatic printer.[8]

In view of these points, it is very important to study the electrophotographic properties of the dispersion layer of titanium dioxide. The electrophotographic properties of the zinc oxide-resin dispersion layer were studied by Inoue[9] and by Tashiro *et al.*,[10] and the mechanism of the corona charging was discussed by Amick[11] to some extent. Therefore, we investigated the electrophotographic properties of the titanium dioxide-resin dispersion layer on various titanium-dioxide contents. We believe that these studies will contribute as fundamental data to the industrial applications of the Electrostatic Recording technique.

Experimental

Sample. *Titanium Dioxide.* Titanium dioxide powder of the rutile type was produced by the hydrolysis of titanium tetrachloride.[12] The purity of this powder corresponded to spectro grade. The major impurities detected by chemical analysis were as follows: Fe, less than 0.005%, As, less than 0.0005%, and Pb, less than 0.002%. The average crystal size of this powder was from 0.2 to 0.7μ. The specific surface area of this powder, as determined by the B.E.T. method, was 1.57 m^2/g.

Organic Polymers. These were used as a powder's binder. In order to make an experiment on a definite

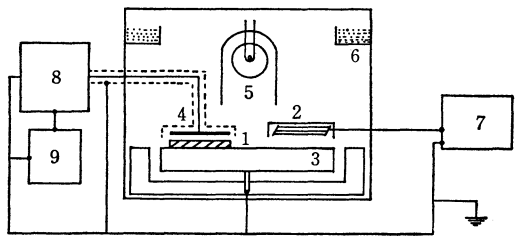

Fig. 1. The block diagram of the experimental equipment.
(1) dispersion layer, (2) steel wand for corona discharge, (3) turn-table, (4) detector, (5) tungsten light, (6) silicagel powder, (7) electric source of high voltage, (8) surface potentialmeter of chopper type, (9) electrical recorder.

Table 1. The properties of the polymers

Polymer	Mean degree of polymerization	Mean molecular weight	Dielectric constant (at 1 kc)	Dipole moment (Debye unit, at 20°C)
Polyvinyl acetate (P. V. Ac.)	1400	100000	5.2	1.68[13]
Polyvinyl chloride (P. V. C.)	1300	80000	4.5	1.62[14]
Polystyrene (P. S.)	1400	130000	2.4	0.26[15]

1) T. Iida and H. Nozaki, This Bulletin, **42**, 929 (1969).
2) H. Nozaki, Manuscrips for 1st International Congress on Reprography, Köln (1963); H. Nozaki and T. Iida, Manuscrips for 2nd International Congress on Reprography, Köln (1967).
3) S. Matsui and Y. Higaki, Manuscrips for 22nd Congress of Electrophotographic Soc. Japan, 1968.
4) S. Matsui, *Electrophotography*, **7**, 94 (1967).
5) S. Matsui, Manuscrips for 20th Congress of Electrophotographic Soc. Japan, 1967.
6) J. Hojo, *Electrophotography*, **7**, 117 (1967).
7) S. Kineri and Y. Okajima, *ibid.*, **7**, 151 (1967).
8) K. Kobayashi, H. Ohta, Y. Okajima and S. Nanba, *ibid.*, **7**, 105 (1967).
9) E. Inoue, H. Kokado, T. Yamaguchi, S. Nagashima and K. Takahashi, *ibid.*, **1**, 27 (1959).
10) I. Tashiro, T. Kimura, M. Kuwahara and G. Ohno, *ibid.*, **8**, 3 (1967).
11) J. A. Amick, *RCA Rev.*, *Dec.*, 753, 770 (1959).
12) T. Iida and H. Nozaki, *Kogyo Kagaku Zasshi (J. Chem. Soc. Japan, Ind. Chem. Sect.)*, **69**, 2087 (1966).
13) A. Kodera, *Kagaku*, **10**, 81 (1955).
14) P. Debye and F. Bueche, *J. Chem. Phys.*, **19**, 589 (1951).
15) O. Broen and F. H. Muller, *Kolloid-Z.*, **140**, 121 (1955); *ibid.*, **141**, 20 (1956).

system, pure polymers were used. The properties of these polymers are shown in Table 1.

Solvents. Solvents purified by repeated distillations were used; ethyl acetate was used for polyvinyl acetate; cyclohexanone, for polyvinyl chloride, and benzene, for polystyrene.

Procedures for Making the Dispersion Layer. The powder of titanium dioxide and the polymer solution were mixed in a blender for ten hours. The suspension of these materials was coated uniformly on a domestic aluminium foil (7 cm × 10 cm) by means of a film applicator of the Baker type. These specimens were dried at 110°C for two hours, and then they were preserved in a dark chamber for 48 hr or more; the relative humidity was controlled at about 20%, and the temperature was between 15 and 25°C. The thickness of the coated layer was between 15 and 20 microns. The weight of the titanium dioxide against the weight of the polymer changed between 0% and 90%.

The Measurement of the Electrical Resistivity and the Electrostatic Capacity of the Disperison Layer. At first silver metal was evaporated with a vacuum evaporator on the layer surface. This specimen was fixed in a dark chamber in which the relative humidity was controlled with a silica gel powder. An electrode of stainless steel was put on the sample surface. The weight of the electrode was 10.0 g/cm^2. The electrical resistivity was directly measured with a Keithley electrometer of the 610-B type. The electrostatic capacity was measured with a Wheatstone's bridge, applying an alternative current of 1 kc.

The Measurement of the Corona-charging Potential. The measurement was done by the turn-table method. A block diagram of the experimental equipment is shown in Fig. 1.

All the measurements were done at room temperature in air with a relative humidity of about 20%. The table was rotated at a speed of 78 rpm; the surface potential was measured with a surface potentialmeter of the chopper type, and the corona discharge was done with three steel wands, 0.1 mm in diameter, which were fixed 5 mm above the turn-table. The conditions of the corona discharge were as follows: the discharge voltages were −6.0 kV and 6.5 kV at the negative and at the positive corona discharge respectively; the current of the corona discharge was maintained at a constant current of 4.2×10^{-5} A and the corona discharge was done for one minute. After the dark decay had been observed for one minute, the tungsten light of 200 lux at the sample surface was lighted until the surface potential disappeared. In the case of the measurement of the light-fatigue effect, the sample was irradiated with a tungsten light of 1200 lux for two minutes, and then, the above measurements were made. The potential change was recorded with an electrical recorder, as is shown in Fig. 1. One of the examples of the potential change against the time is shown in Fig. 2. The full line corresponds to the surface potential on fresh layers, and the dotted line, to the surface potential measured after irradiation with a light of 1200 lux for two minutes as a pre-illumination.

The notations of the electrophotographic properties are shown in Table 2.

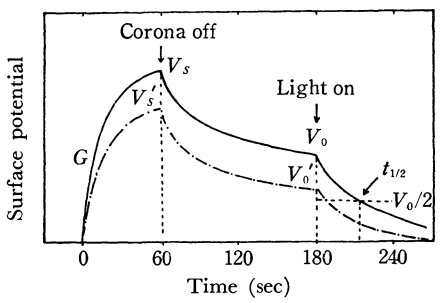

Fig. 2. The time dependence of the surface potential of the corona charging.

TABLE 2. SYMBOLS

Notation	Unit	Meaning
V_s	volt	saturation surface potential
E_s	volt/μ	saturation potential per one micron thickness
V_0	volt	initial surface potential
G	volt/sec	rising gradient of surface potential
$t_{1/2}$	sec	half-time of light decay
V_0/V_s	—	quantity of dark decay
V'_s/V_s	—	quantity of fatigue effect by pre-illumination

Results

The specific resistivity of the dispersion layer decreases with an increase in the titanium-dioxide contents, as is shown in Fig. 3. The resistivity of these dispersion layers is situated between 10^{13} and 10^{15} Ω cm. The polystyrene dispersion layer has the highest resistivity, while the polyvinyl acetate layer has the lowest resistivity. Each curve has a minimum resistivity at around 50% of the titanium-dioxide contents.

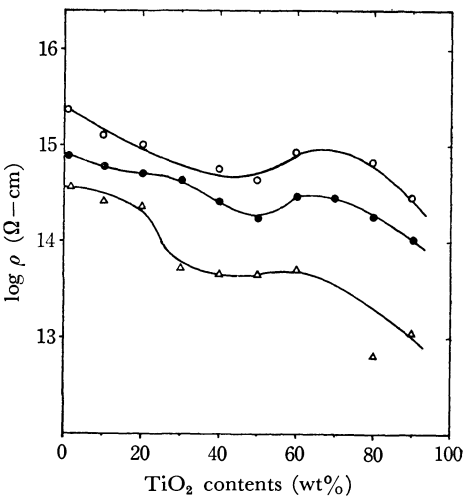

Fig. 3. Relations between the specific resistivity of the dispersion layer and the titanium-dioxide contents.
○ P. S. ● P. V. C. △ P. V. Ac.

The electrostatic capacities of the dispersion layer are plotted against the contents of titanium dioxide. The capacity was calculated with the normalization of a unit area of 1 cm^2 and of a unit thickness of one micron. As can be seen in Fig. 4, the capacity of the plyvinyl acetate layer is the highest, while that of the polyvinyl chloride layer is slightly lower than that of the polyvinyl acetate layer. The capacity of the polystyrene layer has the lowest value of the three. The dielectric constants of the rutile ceramics is 114, but that of these dispersion layers of the titanium-dioxide contents of between 80% and 90% takes a value as small as between 30 and 40. The dielectric constants gradually decreases with a decrease in the titanium-dioxide contents.

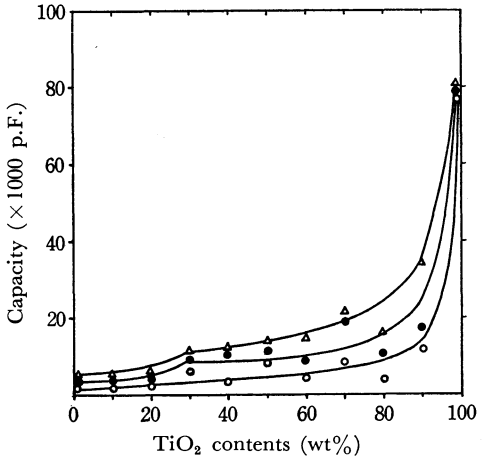

Fig. 4. Relations between the electrostatic capacity of the dispersion layer and the titanium-dioxide contents.
△ P. V. Ac. ● P. V. C. ○ P. S.

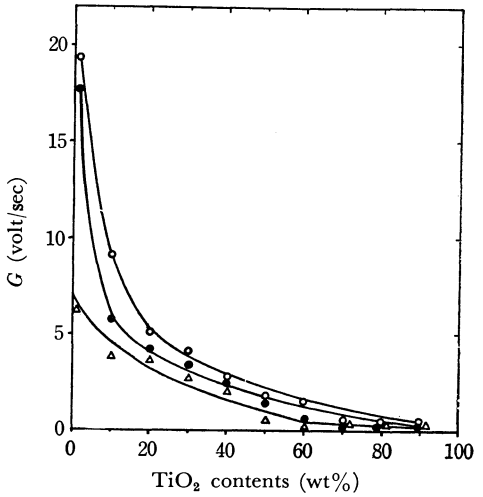

Fig. 5. The rising gradients of the surface potential plotted against the titanium-dioxide contents.
○ P. S. ● P. V. C. △ P. V. Ac.

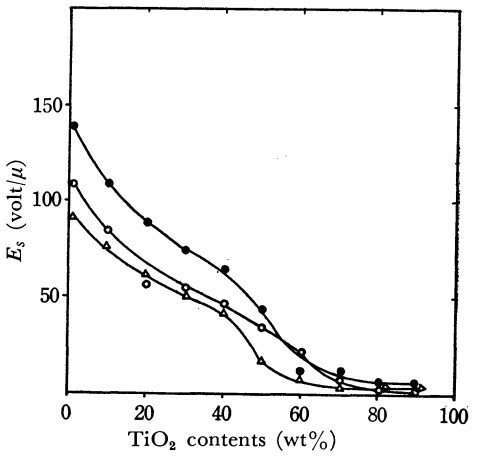

Fig. 6. The relations between the saturation potential per one micron thickness and the titanium-dioxide contens.
● P. V. C. ○ P. S. △ P. V.

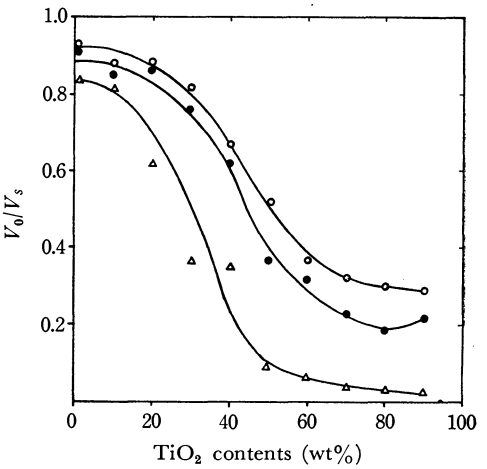

Fig. 7. The quantity of the dark decay measured one minute after the turn off of the corona discharge.
○ P. S. ● P. V. C. △ P. V. Ac.

The corona charging was done with both the negative and the positive corona discharging, but in the case of the titanium-dioxide dispersion layer, the potential of the positive corona charging can hardly be observed. Therefore, all the following results are the properties of the negative corona charging.

The rising gradients of the surface potential in the negative corona charging decrease with an increase in the titanium-dioxide contents. The rising gradients of the surface potential are plotted against the titanium-dioxide contents in Fig. 5. The order of the rising gradients of these dispersion layers is as follows: the polystyrene dispersion layer>the polyvinyl chloride dispersion layer>the polyvinyl acetate dispersion layer.

The relations between the saturation potential of the negative corona charging per micron of thickness and the titanium-dioxide contents are shown in Fig. 6. The saturation potential decreases with an increase in the titanium-dioxide contents. The polyvinyl chloride layer takes the value of the highest potential; the next is the polystyrene layer, and the polyvinyl acetate layer takes the smallest potential.

The quantities of the dark decay, measured one minute after the turn-off of the corona discharge, are shown in Fig. 7. The dark decay increases with an increase in the titanium-dioxide contents. The polystyrene layer has the slowest decay, and the polyvinyl acetate has the quickest.

The half-time of the light decay decreases with an increase in the titanium-dioxide contents, as is shown in Fig. 8. At the lower contents of titanium dioxide of between 0% and 30%, the order of the speed of the light decay is as follows: the polystyrene dispersion layer > the polyvinyl acetate dispersion layer > the polyvinyl chloride dispersion layer. At high contents of titanium dioxide (between 40% and 90%), no clear differences in the light decay are detected among these dispersion layers.

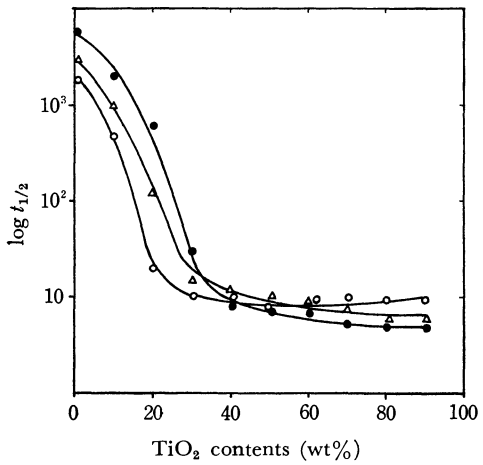

Fig. 8. The logarithm of the half-time of the light decay plotted against the titanium-dioxide contents.
○ P. S. △ P. V. Ac. ● P. V. C.

The quantities of the fatigue effect produced by pre-illumination are shown in Fig. 9. As can be seen in the figure, the fatigue effects of the polyvinyl acetate layer and the polyvinyl chloride layer increase with an increase in the titanium-dioxide contents, reaching a maximum at contents of around 80%. However, the fatigue effect of the polystyrene layer is somewhat different from the former two binders; it has its maximum at contents of around 40%.

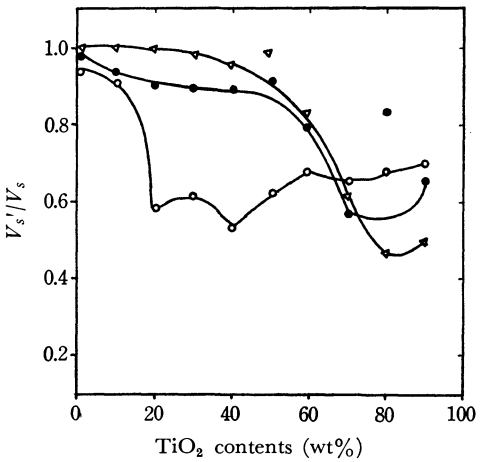

Fig. 9. The quantity of the fatigue effect by a pre-illumination.
△ P. V. Ac. ● P. V. C. ○ P. S.

The relations between the logarithm of the surface potential in the dark decay and the square root of the time, which were measured in the case of 0% contents of titanium dioxide, are shown in Fig. 10. In the region from 1 min to 9 min, the surface potential does not decay proportionally to the square root of the time, but in the region from 9 min to 80 min the surface potential does decay so. The decay gradient of $-\mathrm{d}\log V/\mathrm{d}t^{1/2}$ are evaluated as follows: the polyvinyl chloride layer is 0.216, the polystyrene layer is 0.316, and the polyvinyl acetate layer is 0.533.

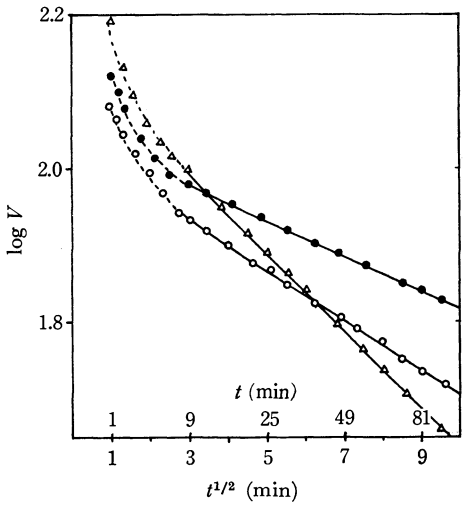

Fig. 10. The relations between the logarithm of the dark decay potential on the polymer layer of 0% titanium-dioxide contents and the square root of the time.
Polymer 100% ● P. V. C.
○ P. S.
△ P. V. Ac.

The same measurements were made on the dispersion layers of 30% contents of titanium dioxide. the results are shown in Fig. 11. In this case the proportionality between the logarithm of the surface potential in the dark decay and the square root of the time starts about six minutes after the turn-off of the corona discharge.

As has been mentioned above in discussing the results of Fig. 10, the logarithm of the surface potential does not decay proportionally to the square root of the time in the region from 1 min to 9 min. Therefore, we tried to plot the logarithm of the potential decay of this region against the cube root of the time. The results are shown in Fig. 12. As can be seen in the figure, the logarithm of the surface potential does indeed decay proportionally to the cube root of the time.

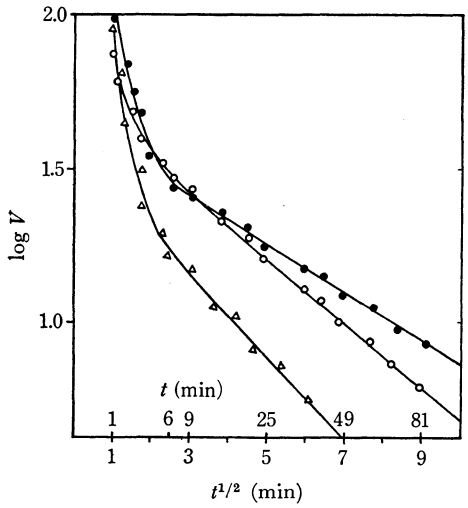

Fig. 11. The relations between the logarithm of the dark decay potential on the dispersion layer of 30% titanium-dioxide contents and the square root of the time.
● P. V. C.
TiO_2 30% ○ P. S.
△ P. V. Ac.

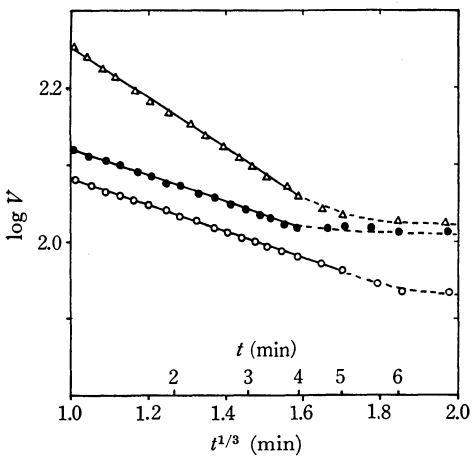

Fig. 12. The relations between the logarithm of the dark decay potential at the initial step and the cube root of the time.
Polymer 100% △ P. V. Ac.
● P. V. C.
○ P. S.

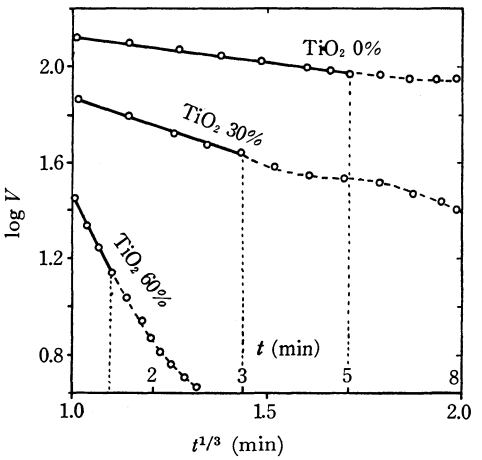

Fig. 13. The relations between the logarithm of the dark decay potential at the initial step on the polystyrene dispersion layer of the various titanium dioxide contents and the cube root of the time.

The period for which the proportionality of the relation between log V and $t^{1/3}$ is retained depends on the contents of titanium dioxide. As an example, the relations between the log V and $t^{1/3}$ of the polystyrene layer at various titanium-dioxide contents are shown in Fig. 13. The polystyrene layer of 0% contents of titanium dioxide retains the proportionality for 5.0 min, that of 30% contents of titanium dioxide does so for 3.0 min, and that of 60% contents of titanium dioxide does so for 1.5 min. Therefore, it is found that the period of the proportionality decreases with an increase in the titanium-dioxide contents.

Discussion

The charging properties were studied by the use of three different polymers, and it was found that the charging properties depend considerably on the polymer used as a binder. As is shown in Table 1, the mean degrees of polymerization and the molecular weights of these polymers are not very different, but the dielectric constants and the dipole moments of these polymers are quite different. A polymer which has a high dipole moment generally has a high dielectric constant. It is quite reasonable that a layer's capacity, as measured by direct measurements, increases with an increase in the dielectric constant of the polymer, as is shown in Fig. 4. Moreover, the resistivity of the layers is

shown in Fig. 3. We can, therefore, see the resistivity and the capacity of the layer. It is reasonable to explain these charging properties qualitatively with the use of an equivalent circuit, which is shown in Fig. 14.

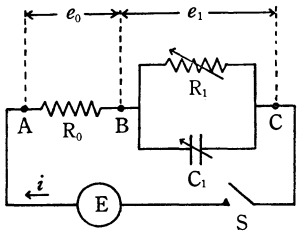

Fig. 14. The equivalent circuit of the dispersion layer in the corona charging process.
e_0: potential difference between A and B
e_1: potential difference between B and C
R_0: resistance of the circuit
R_1: variable resistance which corresponds to the resistance of the layer
C_1: variable capacity which corresponds to the capacity of the layer
E: electric source
S: switch

When the switch, S, is turned on, and a voltage, E, is applied to the circuit, the change in the potential between B and C is derived as the following equation:

$$e_1 = \frac{ER_1}{R_0 + R_1}\left[1 - \exp\left\{-\frac{1}{C_1}\left(\frac{1}{R_0} + \frac{1}{R_1}\right)t\right\}\right] \quad (1)$$

When e_1 is differentiated by the time, the rising gradient of the potential between B and C is obtained:

$$G = \frac{de_1}{dt} = \frac{ER_1^2C_1R_0}{(R_0 + R_1)^2} \exp\left\{-\frac{1}{C_1}\left(\frac{1}{R_0} + \frac{1}{R_1}\right)t\right\} \quad (2)$$

From Eq. (2) it can be deduced that G decreases with an increase in C_1, if R_1 is kept as a constant value. It can also be deduced from Eq. (2) that G decreases with an increase in R_1 if C_1 is kept as a constant value. As is shown in Fig. 5, the order of G is as follows: the polystyrene dispersion layer> the polyvinyl chloride dispersion layer>the polyvinyl acetate dispersion layer. This means that the rising gradient of the corona charging decreases with an increase in the capacity of the layer. Therefore, it can be clarified that the rising gradient of the corona charging depends greatly on the capacitance of the layer.

In the case of the discharging process, when the switch is turned off the potential between B and C decreases, because the discharging current flows through the resistance of R_1. Therefore, the speed of the dark decay of the surface potential depends greatly on the resistance of R_1. Figure 7 shows that the speed of the dark decay of the dispersion layer which has the low resistance is high, while that of the dispersion layer which has the high resistance is low; therefore, it is evident that the dark decay depends greatly on the resistance of the layer.

The saturation potential of the layer can not be explained directly from Eq. (1), for the measurements were done by the turn-table method and so the corona discharge was applied on the layer intermittently. Another reason is that the surface potential depends on many complex factors, *i. e.*, the charge density of the corona ions, which are chemisorbed on the layer surface,[16] the injection of electrons from corona ions into the layer, and the orientation of the dipole moment of the binder. Therefore, it is not possible to explain this property from this equivalent circuit model.

The differences in the light decay and in the fatigue effect upon pre-illumination among these polymers' layers can not easily be explained from this model. The only thing we can describe is the experimental results. However, we assume that the photo-phenomena on the surface of titanium dioxide[16] can be explained to some extent by analogy to the case of the zinc-oxide dispersion layer.[17]

The results show that the surface potential of the dark decay decreases proportionally to the square root of the time in the region from 9 min to 80 min. It is impossible to derive the equation in which the surface potential of the dark decay depends on the squre root of the time with the use of the equivalent circuit shown in Fig. 14. Moreover, it is quite significant that this phenomenon appears not only in the dispersion layer, but also in the polymer layer which does not contain titanium dioxide. Inoue proposed an experimental equation in which the decay decreases proportionally to the square root of the time in the zinc-oxide dispersion layer.[9] However, the theoretical meaning of this equation has not yet been clarified. We are now studying the theoretical reason for this time dependency from various viewpoints, but we assume that the diffusion of the corona ions through the layer plays an important role in this phenomenon.

Moreover, it is found in the titanium-dioxide dispersion layer that the logarithm of the surface potential in the dark decay decreases proportionally to the cube root of the time, that it is retained for 4—6 min, and that the period of the proportionality of $\log V$ to $t^{1/3}$ depends on the titanium-dioxide content. These phenomena have not been found in the zinc-oxide dispersion layer. It is first time to find such phenomena in the dark decay as electrophotographic properties.

16) T. Iida and H. Nozaki, This Bulletin, **42**, 243 (1969).
17) E. Inoue and T. Yamaguchi, *Electrophotography* **5**, 65 (1964).

These phenomena can not be analyzed easily by the simple model, so we can only describe the experimental results. However, it can be ascribed that there are two different steps in the process of the dark decay of the titanium-dioxide dispersion layer.

The gradient of the dark decay is quite small in the case of the polyvinyl chloride dispersion layer, as is shown in Fig. 10. Therefore, it can be said that polyvinyl chloride is the best material for the electrostatic recording.

At any rate, the corona-charging phenomena of the dispersion layer are quite complicated. We think that the major factors which govern the corona-charging properties are given as follows: (1) the degree of the dispersion between titanium dioxide powder and the polymer, (2) the covering power of the polymer over the surface of titanium dioxide, (3) the chemisorption of corona ions on the layer, (4) the injection of electrons from corona ions into the layer, and (5) the orientation of the dipole moment of the polymer. Therefore, in the future we should study these factors in detail in order to clarify the mechanism of the corona-charging phenomena of the dispersion layer.

BULLETIN OF THE CHEMICAL SOCIETY OF JAPAN VOL. 42 2827—2830 (1969)

Radical Conversions in γ-Irradiated 3-Methylpentane-Isobutene Systems

Kozo Tsuji*1 and Seizo Okamura

Department of Polymer Chemistry, Faculty of Engineering, Kyoto University, Kyoto

(Received May 1, 1969)

Radical conversions in γ-irradiated 3-methylpentane-isobutene systems were observed by means of the electron spin resonance method after keeping the sample at -196°C for a few days, or by subjecting it to ultraviolet irradiation. One of the changes was caused by hydrogen atom abstraction from neighboring molecules by original free radicals. The other change was attributed to dissociation of the free radicals from 3-methylpentane by ultraviolet irradiation.

There have been several studies on photoinduced radical conversions. Among them the photoinduced dissociations of alcohol radicals are well known.[1,2] Recently several authors reported photoinduced conversions of hydrocarbon radicals; photoinduced conversions of allyl radicals to alkyl radicals in γ-irradiated polyethylene by Ohnishi *et al.*,[3] isomerization of *t*-butyl radicals to isobutyl radicals in γ-irradiated isobutyl bromide,[4] a similar isomerization in γ-irradiated polypropylene by Iwasaki *et al.*,[5] and the photoinduced conversion of allylic radicals to other allylic radicals in γ-irradiated 2-methylpentene-1 (2MP-1) by Smith and Pieroni.[6] Smith *et al.*[7] also observed radical conversions in a γ-irradiated 3-methylpentane (3MP)-2MP-1 (15 mol%) mixture by storing the sample for 24 hr at -196°C and ultraviolet irradiation. After receiving a 1 Mrad dose from Co-60 γ-rays, the 3MP-2MP-1 mixture became blue and the ESR spectrum consisted of a narrow intense singlet superimposed on the central line of the spectrum of the 3-methylpentyl radical $CH_3CH_2\dot{C}(CH_3)CH_2$-$CH_3$. The ESR singlet and blue color were easily eliminated by visible light illumination. After keeping the sample for 24 hr at -196°C, the spectrum converted to that of an allylic radical. Upon subsequent UV photolysis, the ESR spectrum changed to that which has been attributed to the 3-methylpentyl radical.[8] It was concluded[7] that ultraviolet light induces the allylic radical from 2MP-1 in 3MP to abstract a hydrogen atom from a neighboring 3MP molecule.

We have reported[9] that $\dot{C}(CH_3)_2$-CH_2-R radicals with two different conformations and relatively

*1 Present address: Central Research Laboratory, Sumitomo Chemical Company, Ltd., Takatsuki, Osaka, Japan.

1) R. S. Alger, T. H. Anderson and L. A. Webb, *J. Chem. Phys.*, **30**, 695 (1959).
2) R. H. Johnsen, *J. Phys. Chem.*, **65**, 2144 (1961).
3) S. Ohnishi, S. Sugimoto and I. Nitta, *J. Chem. Phys.*, **39**, 2647 (1963).
4) M. Iwasaki and K. Toriyama, *ibid.*, **46**, 2852 (1967).
5) M. Iwasaki, T. Ichikawa and K. Toriyama, *J. Polymer Sci.*, **B5**, 423 (1967).
6) D. R. Smith and J. J. Pieroni, *J. Phys. Chem.*, **70**, 2379 (1966).
7) D. R. Smith, F. Okenka and J. J. Pieroni, *Can. J. Chem.*, **45**, 833 (1967).
8) S. Aditya and J. E. Willard, *J. Am. Chem. Soc.*, **88**, 229 (1966).

stable trapped electrons were observed in γ-irradiated 3MP-isobutene (IB) systems. The latter was easily bleached out by visible light illumination, and only neutral free radicals remained. In the present investigation we report that these neutral free radicals convert to other ones by keeping the sample at -196°C for a few days or by ultraviolet irradiation as in the 3MP-2MP-1 mixtures.[7]

Experimental

Commercial 3-methylpentane was distilled over sodium after passing through activated alumina. It was dried four times with Na-K alloy. Isobutene was dried with Na-K alloy after passing through potassium hydroxide.

Samples were made in ESR sample tubes by vacuum distillation and sealed off after evacuating to about 10^{-4} mmHg. Irradiation was carried out by γ rays from Co-60 (6×10^5 R/hr). Ultraviolet photolysis was carried out at -196°C with a high pressure mercury lamp (Toshiba Electric Company, Ltd., H-400-p, 400W).

A conventional X band ESR spectrometer was used with 100 Kc field modulation. Microwave power was less than 1 mW. γ-Irradiations and ESR measurements were carried out at -196°C in the dark.

Results

A mixture of 3MP-IB (2.4 mol%) forms a transparent colorless glass at -196°C. When it was irradiated to a dose of 2×10^5 R in the dark at -196°C, it turned blue and gave the ESR spectrum shown in Fig. 1a, which consists of an eight-line spectrum with a hyperfine separation of 23 gauss and a sharp singlet spectrum at the center. The former is attributed probably to the free radical $R\text{-}CH_2\text{-}\dot{C}(CH_3)_2$ with a certain conformation.[9] The sharp singlet spectrum and blue color were easily bleached out by visible light illumination, and they were attributed to trapped electrons.[9] The intensities of both the singlet and eight-line spectra are proportional to dose up to 3×10^5R. After photolysis with visible light, only the eight-line spectrum (Fig. 1a dotted line) remained, and after 7 days, this converted at -196°C to the other spectrum shown in Fig. 1b, where the five-line spectrum with a coupling constant of about 13 gauss due to allylic radicals (arrow marks) and another spectrum (maybe 6 lines) were observed. This spectrum further changed by subsequent ultraviolet irradiation into the spectrum shown in Fig. 1c without any decrease of radical concentration; both six- and four(arrow marks)-line spectra were observed, and the latter decayed out at -168°C as shown in Fig. 1d. The coupling constant of the six-line spectrum is about 22 gauss, and the

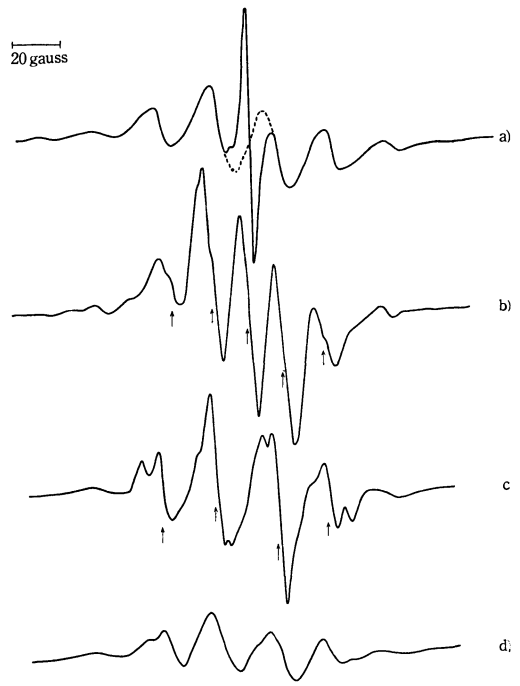

Fig. 1. ESR spectra of 3MP-IB (2.4 mol%) irradiated to a dose of 2×10^5 R at -196°C.
a) immediately after γ-irradiation (solid line); after bleaching with visible light (dotted line).
b) after keeping the sample at -196°C for 7 days; arrow marks represent a five-line spectrum due to allylic radicals.
c) after subsequent ultraviolet irradiation of the sample b) for 45 min. Arrow marks represent a four line spectrum due to methyl radicals.
d) same sample as c) measured at -168°C.

spectrum is the same as that produced by γ-irradiation of 3MP. Thus this spectrum is attributed to the free radicals produced from 3MP($CH_3\text{–}CH_2\text{–}\dot{C}(R)\text{–}CH_2\text{–}CH_3$, R=H or CH_3). The four-line spectrum is attributed to methyl radicals because of its coupling constant (23 gauss) and intensity ratio (1 : 3 : 3 : 1). Methyl radical production, however, was slow and methyl radical concentration seemed to saturate at a certain ratio to that of 3MP radicals.

A mixture of 3MP-IB (61 mol%) made an apparent transparent glass at -196°C. After γ-irradiation, only a fifteen-line spectrum was obtained, and neither a sharp singlet nor blue color were observed. The fifteen-line spectrum shown in Fig. 2a has been attributed to the free radicals $\cdot C(CH_3)_2\text{–}CH_2\text{–}R$ formed with two conformations.[9] This spectrum did not change by keeping the sample at -196°C for a few days, but converted

9) K. Tsuji, H. Yoshida, K. Hayashi and S. Okamura, *J. Polymer Sci.*, **B5**, 313 (1967).

to the five-line spectrum due to allylic radicals by subsequent ultraviolet irradiation as shown in Fig. 2b. The intensity of the allylic radicals decreased with the increase of the time of irradiation,

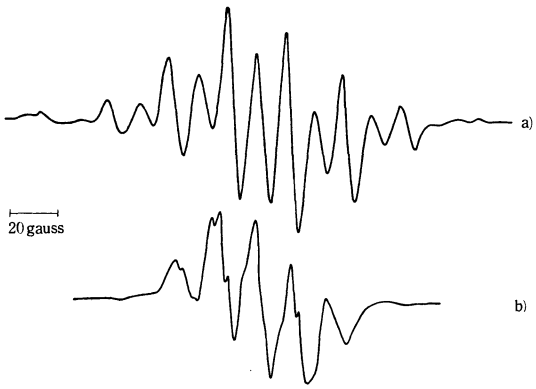

Fig. 2. ESR spectra of 3MP-IB (61 mol%) irradiated to a dose of 2×10^5R at -196°C.
a) immediately after γ-irradiation.
b) after subsequent ultraviolet irradiation for 15 min.

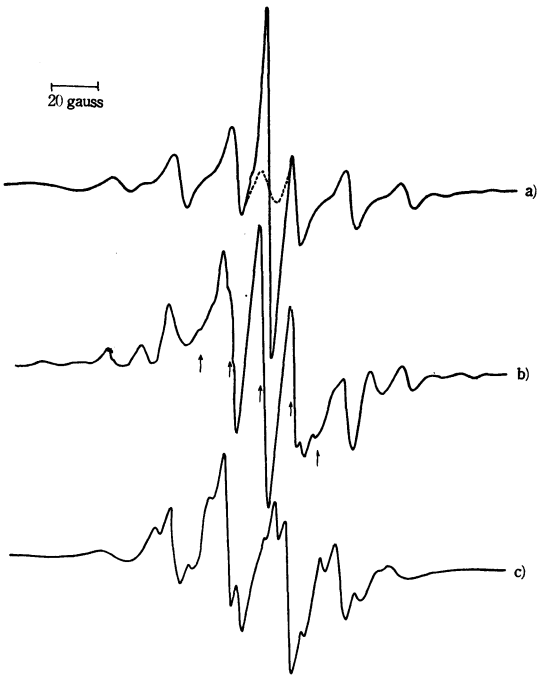

Fig. 3. ESR spectra of 3MP-IB (12 mol%) irradiated to a dose of 2×10^5 R at -196°C.
a) immediately after γ-irradiation (solid line); after bleaching with visible light (dotted line).
b) after keeping the sample at -196°C for two days; arrow marks represent a five-line spectrum due to allylic radicals.
c) after subsequent ultraviolet irradiation for 45 min.

but no methyl radicals were observed.

For an intermediate case 3MP-IB (12 mol%), an eight-line spectrum and a sharp singlet were initially observed after γ-irradiation as shown in Fig. 3a. The sharp singlet at the center was removed by visible-light illumination (Fig. 3a dotted line), but the eight-line spectrum remained unchanged. After keeping the sample at -196°C for a few days, however, the eight-line spectrum changed into the superposition of 15 lines observed for 3MP-IB (61 mol%) and five lines (arrow marks) due to allylic radicals as shown in Fig. 3b. By subsequent ultraviolet irradiation, the spectrum converted to the same one as observed for 3MP-IB (2.4 mol%), the radical concentration remaining constant.

Discussion

We observed two kinds of radical conversions. One proceeds by keeping the sample at -196°C for a few days, and the other by subsequent ultraviolet irradiation. They could be explained by intermolecular reactions with original free radicals and by dissociation of the free radicals.

When IB concentration in 3MP is low (2.4 mol%), radical conversions were observed at -196°C without UV irradiation, and the five-line spectrum due to allylic radicals and the other spectrum which seemed to be attributed to the free radicals from 3MP were obtained. This could be explained in terms of hydrogen atom abstraction by the original free radicals from both neighboring IB and 3MP molecules.

$$\left.\begin{array}{l} \mathrm{CH_3} \\ \cdot\mathrm{C}-\mathrm{CH_2}-\mathrm{R} \\ \mathrm{CH_3} \end{array}\right\} \begin{cases} + \text{ IB} \rightarrow \mathrm{CH(CH_3)_2\text{-}CH_2R} \\ \qquad + \mathrm{CH_2{=}\overset{\mathrm{CH_3}}{\overset{|}{C}}\text{-}\dot{C}H_2} \qquad (1) \\ + \text{ 3MP} \rightarrow \mathrm{CH(CH_3)_2\text{-}CH_2R} \\ \qquad + \mathrm{CH_3\text{-}CH_2\text{-}\overset{\mathrm{R'}}{\overset{|}{\dot{C}}}\text{-}CH_2\text{-}CH_3} \\ \qquad (\mathrm{R'{=}H \text{ or } CH_3}) \qquad (2) \end{cases}$$

These reactions might be caused by the mobility of free radicals in the glass. Reaction (1) is very similar to that observed in the 3MP-2MP-1 system,[7] although the original free radicals were 3-methylpentyl radicals in this case. It seems reasonable to conclude that a hydrogen atom is abstracted more readily from IB than from 3MP, since even at low concentrations of IB, allylic radicals were produced and at higher concentration only allylic radicals were produced. This might be caused by the stability of allylic radicals.

Methyl radicals were produced by subsequent ultraviolet irradiation. Since 3MP does not absorb UV light, any reactions through an excited 3MP molecule can be ruled out. In fact although unirradiated 3MP gave methyl radicals and other free

radicals by ultraviolet irradiation under the same conditions employed for the γ-irradiated 3MP-IB systems, the intensity was negligible compared with the present intensity. Methyl radical production is thought to be caused by dissociation of the free radical from 3MP(CH_3–CH_2–$\dot{C}$(R)–CH_2–CH_3), since the same change was observed for γ-irradiated 3MP.[10]

$$CH_3\text{–}CH_2\text{–}\dot{C}(R)\text{–}CH_2\text{–}CH_3 \rightarrow CH_3\text{–}CH_2\text{–}C(R)=CH_2 + \cdot CH_3 \quad (3)$$

Allylic radicals disappeared by ultraviolet irradiation and new alkyl radicals (CH_3–CH_2–$\dot{C}$(R)–CH_2–CH_3) were observed, besides methyl radicals. This result is consistent with that reported for 3MP-2MP-1 systems,[7] and could be explained in terms of intermolecular hydrogen abstraction by allylic radicals from neighboring 3MP molecules. In the case of irradiated polyethylene, allyl radicals converted to alkyl radicals by UV irradiation. This was, however, explained by intramolecular hydrogen atom shift.[3] But it may also occur by an intermolecular hydrogen atom abstraction mechanism.

Some of the free radicals CH_3CH_2–$\dot{C}$(R)–CH_2CH_3 produced in the course of UV photolysis of allylic radicals would be photolyzed to produce methyl radicals by the mechanism (3). The concentration of methyl radicals, however, was not so large and no significant increase was observed with longer time of irradiation. This might be caused by the recombination of methyl radicals.

When IB concentration was high (61 mol%), no change in the spectrum was observed by keeping the sample at -196°C for a few days in contrast to the systems with lower IB concentration (2.4 mol%). This seems to be due to a smaller mobility of free radicals as the glass of this mixture is close to the polycrystalline state, as could be supposed from the fact that no trapped electrons were observed.[11]

A spectrum change was observed by subsequent ultraviolet irradiation, and only allylic radicals were observed. This is caused by hydrogen atom abstraction only from an IB molecule. It is reasonable to expect that hydrogen atom abstraction by UV irradiation proceeds only from IB molecules as IB molecules are present close to the parent free radicals because of high IB concentration, and because IB is more reactive than 3MP for hydrogen abstraction.

It should be noted that the eight-line spectrum gradually converted to the fifteen line spectrum when the sample with intermediate IB concentration (12 mol%) was stored at -196°C for a few days. According to our tentative interpretation,[9] this is caused by changes in the conformations of the free radicals. Therefore the conversion from the eight-lines to the fifteen lines seems to be a kind of relaxation process. On the other hand, if the two conformations have an intimate relation with the chain length,[9] a spectrum change could be caused by the propagation of post-polymerization at -196°C.

The authors wish to thank Professor I. Sakurada for his kindness in permitting them to carry out the work at Osaka Laboratories, Japanese Association for Radiation Research on Polymers (now Osaka Laboratories for Radiation Chemistry, Japan Atomic Energy Research Institute). Thanks are also due to Professor K. Hayashi, Dr. H. Yoshida, and Mr. H. Kamiyama for their helpful discussions, and to Professor F. Williams for reading the manuscript.

10) K. Tsuji, H. Yoshida, K. Hayashi and S. Okamura, *Ann. Rept. of Japanese Association for Radiation Research on Polymers*, **7**, 119 (1965—1966).

11) M. A. Bonin, J. Lin, K. Tsuji and F. Williams, *Advances in Chemistry Series*, **82**, 269 (1968).

BULLETIN OF THE CHEMICAL SOCIETY OF JAPAN VOL. 42 2831—2835 (1969)

Separation and Identification of Chlorocomplexes of Technetium(IV) formed in Hydrochloric Acid Solutions

Yoshihiko KANCHIKU*1

Faculty of Science, Kyoto University, Sakyo-ku, Kyoto

(Received November 2, 1968)

The chemical behavior of $TcCl_6^{2-}$ in HCl solutions of different concentrations has been investigated. It was confirmed that $TcCl_6^{2-}$ is sensitive to ultraviolet and visual light, giving a series of aquated species the quantities of which depend on the HCl concentration. Those technetium(IV) chlorocomplexes were isolated by means of ion-exchange and paper electrophoresis, and the composition of each species was determined by measuring the Cl/Tc ratio and the charge per species. The absorption spectra of isolated species were also measured.

A number of compounds of technetium are known for the valency states from +7 to −1.[1-3] In the field of the solution chemistry of technetium, the chemical behavior of pertechnetate(VII) ion has been investigated more extensively than the chemical species of any other valency state.

The lower oxidation states of technetium which result from the pertechnetate ion by the reduction have not been quantitatively investigated except for their reactions with special analytical reagents[4] and their magnetic properties.[5] The pertechnetate ion is gradually reduced to lower valency states by halides in acidic solution.[1] Lederer *et al.* have qualitatively investigated the reduction products of pertechnetate by chloride and bromide by separating them by means of paper chromatography.[6] In a previous communication[7] it was pointed out, on the basis of an analysis of the change of its absorption spectra, that hexachlorotechnetate(IV) underwent a photochemical aquation associated with a small quantity of oxidation in hydrochloric acid solution.

The present work will deal with the quantitative details of technetium(IV) chlorocomplex formation in hydrochloric acid solution. K_2TcCl_6 obtained by reducing the pertechnetate ion was dissolved in hydrochloric acid solutions of various concentrations. The experiments have proved that several new technetium chlorocomplexes are formed, step by step, during the aquation. These complexes were separated from each other by means of ion exchange, and the ratios of technetium to chloride were determined by analysing them. The electrical charges of the complex ions were determined by the ion-exchange equilibrium method.[8,9]

From the results obtained, the photo-aquation of $TcCl_6^{2-}$(1) is regarded as the main sequence in the formation of a variety of aquo-chlorocomplexes:

$$TcCl_6^{2-} + xH_2O \rightleftarrows TcCl_{6-x}(H_2O)_x^{(2-x)-} + xCl^- \quad (1)$$

The effects of light absorption were interpreted in terms of an equilibrium condition among the technetium chlorocomplex species in hydrochloric acid.

Experimental

Apparatus. All the absorption spectra were measured on a Shimadzu Recording Spectrophotometer, Model SV-50A, using quartz cells.

The radioactivities of technetium-99 were measured by a Osaka Dempa GM-Counter, Model GM-2.

Reagents. The technetium-99 had been obtained from Oak Ridge National Laboratory (U. S. A.). The chemical form was NH_4TcO_4 solution. The solution was standardized by gravimetry, using tetraphenylarsonium chloride as the precipitant.

The hydrochloric acid was a Koso Chemicals special grade reagent in which no impurities absorbing the

*1 Present address: Research Laboratory, Mitsubishi Rayon Co., Ltd., Otake, Hiroshima.

1) J. W. Cobble, "Treatise on Analytical Chemistry," Part II, ed. by I. M. Kolthoff *et al.*, Interscience Co., New York (1964), Section A, p. 408.

2) E. Anders, "The Radiochemistry of Technetium," U. S. A. Energy Comm., NAS-NS, 3021 (1960).

3) R. Cotton, J. Dalzeil, W. P. Griffith and G. Wilkinson, *J. Chem. Soc.*, **1960**, 71.

4) F. Jasim, R. J. Magee and C. L. Wilson, *Talanta*, **2**, 93 (1959).

5) C. M. Nelson, G. E. Boyd and W. T. Smith, Jr., *J. Am. Chem. Soc.*, **76**, 348 (1954).

6) L. Ossicini, E. Saracino and M. Lederer, *J. Chromatog.*, **16**, 524 (1964).

7) T. Fujinaga, M. Koyama and Y. Kanchiku, This Bulletin, **40**, 2970 (1967).

8) T. Ishimori and R. Hirota, "Jikken Kagaku Koza, Zoku," Vol. 6, ed. by Y. Kondo and H. Okuno, Maruzen Co., Tokyo (1965), p. 50.

9) H. H. Cady and R. E. Connick, *J. Am. Chem. Soc.*, **80**, 2646 (1958).

UV light were detected.

K_2TcCl_6: Ammonium pertechnetate (100 mg) was mixed with 0.2 g of KCl and 10 m*l* of concentrated hydrochloric acid, and then the mixture was heated on a water bath while being refluxed for 20 hr. After evaporation to near dryness, the technetium residue was dissolved in concentrated hydrochloric acid. The absorption spectrum of the solution was identical with that of the K_2TcCl_6 solution obtained by the KI reduction of NH_4TcO_4.[10]

Formation of Other Chlorocomplexes of Technetium. K_2TcCl_6 was dissolved in 12 M, 8 M, 6 M, 3 M, 1 M, and 0.1 M HCl. One group of acid solutions was kept at room temperature in the dark, while another group was irradiated by luminescent lamps (Toshiba 10w×4) at 20°C in a thermostat. The absorption spectra of the two groups were measured at regular intervals.

In spite of the varied concentrations of the acid, the group kept in the dark showed the absorption spectrum of $TcCl_6^{2-}$ constantly, while the group irradiated with the luminescent lamps showed different absorption spectra according to the acid concentrations. This variation seemed to be caused by the formation of aquo-chlorocomplexes of technetium. Their spectra reached equilibria after two weeks under the experimental conditions.

Isolation of the Complexes by Ion-exchange Resin. Samples which had been irradiated for two weeks and had already been in equilibrium were subjected to ion-exchange separation.

The sample solutions were first passed through an anion exchange column (Dowex 2×8, 50—100 mesh, R-ClO_4 type, 15ϕ×200mm) in order to remove any anionic species. The cationic and neutral species were thoroughly washed with pure water and 0.1 M $HClO_4$.

The eluted fractions, containing cationic and neutral species, were again passed through a cationic exchanger column (Dowex 50×8, 100—200 mesh, R-H type, 15ϕ×200 mm). From the cation exchanger column, the neutral species was readily removed by 0.1 M $HClO_4$, while the cationic species were eluted by 1 M $HClO_4$. These species were eluted in discrete bands that could be detected by measuring their characteristic absorption spectra.

Analysis of Technetium. The technetium in the effluent was distilled as pertechnetate with concentrated sulfuric acid and was spectrophotometrically determined by measuring the absorbance at 244 mμ[1]; a molar extinction coefficient of 6220 was used for pertechnetate at this wavelength. It was also determined by the diphenylcarbazide method.[11]

Analysis of Chloride. The chloride of the eluted species was analyzed by titration with mercuric ion, using diphenylcarbazone as an indicator.[12] Prior to the titration, the complexes had been hydrolyzed by making the solution alkaline with the addition of potassium hydroxide and had been boiled for five minutes in order to liberate the chloride ion.

Measurement of Charge per Species. The charge per species was measured according to the method of Connick and Cady.[9]

The technetium distribution was obtained by measuring the radioactivities of ^{99}Tc. Before these measurements, the solutions were neutralized with NH_4OH in order to avoid the vaporization of pertechnetate as Tc_2O_7 and were dried up in glass counting dishes.

Separation of the Species by Paper Electrophoresis. The species, spotted on paper strips (Toyo No. 53, 40×2 cm) which had been immersed in an electrolytic solution (0.1 M $NaClO_4$+0.1 M HCl), were separated by high voltage (500 V). The heat generated during electrophoresis was removed by cooling the strips through a glass vessel filled with ice water. Electrophoretic patterns were obtained by autoradiography.

Results and Discussion

When K_2TcCl_6 was dissolved in hydrochloric acid and the solutions were irradiated with visible or UV light, the absorption spectra of the solutions changed and reached equilibria depending on the hydrochloric acid concentrations and the intensity of light. The spectrum of the 12 M HCl solution, however, did not change upon photo-irradiation, and so it was identified as the original species.

The spectra of the solution equilibrated by photolysis are shown in Fig. 1, where the 12 M, 8 M, 6 M, and 3 M HCl solutions show two isosbestic points at 311 mμ and 362 mμ. The isosbestic points can be employed to determine the total amount of technetium(IV) in the solution.

From the hydrochloric acid solutions, two anionic, one neutral, and one cationic species of technetium chlorocomplex were isolated by the ion-exchange method.

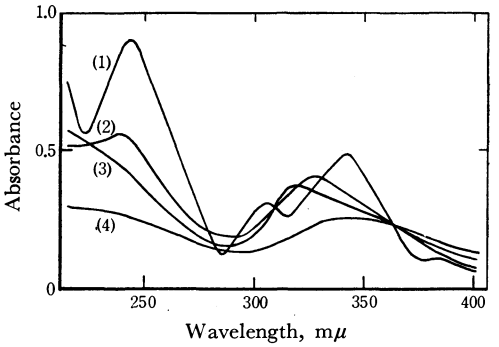

Fig. 1. Absorption spectra of Tc-chlorocomplexes in HCl.
(1) in 12 M HCl equilibrated after irradiation for 2 weeks
(2) in 6M HCl equilibrated after irradiation for 2 weeks
(3) in 3M HCl equilibrated after irradiation for 2 weeks
(4) in 1M HCl equilibrated after irradiation for 2 weeks

10) C. M. Nelson, G. E. Boyd and Wm. T. Smith, Jr., *J. Phys. Chem.*, **76**, 348 (1954).
11) T. Fujinaga, M. Koyama and Y. Kanchiku, *Nippon Kagaku Zasshi (J. Chem. Soc. Japan, Pure Chem. Sect.)*, **87**, 1243 (1966).
12) F. K. Clarke, *Anal. Chem.*, **22**, 553 (1950).

Prior to the following experiments, the stability of the separated species in perchloric acid solution was examined. From the fact that the absorption spectra remain unchanged for several days, the separated species seems to be stable in the elutant, perchloric acid, if they are kept in the dark. The degradation of the complexes during the spectrophotometric procedure is too small to be detected.

The distribution of the anionic and cationic species between ion-exchange resins and aqueous perchloric acid are shown in Figs. 2 and 3, these data can be used in calculation the values of the charge per ion.

The ratios of technetium to chloride for two anionic species are shown in Table 1, along with the charge per species. The ratios for the cationic and neutral species could not be determined by analysing technetium and chloride, because it was impossible to separate the two forms of technetium from chloride by either the ion-exchange or precipitation method without any destruction of the complexes in question. For the neutral species, however, it is reasonable to assume that the ratio of Tc to Cl is 1 : 4.

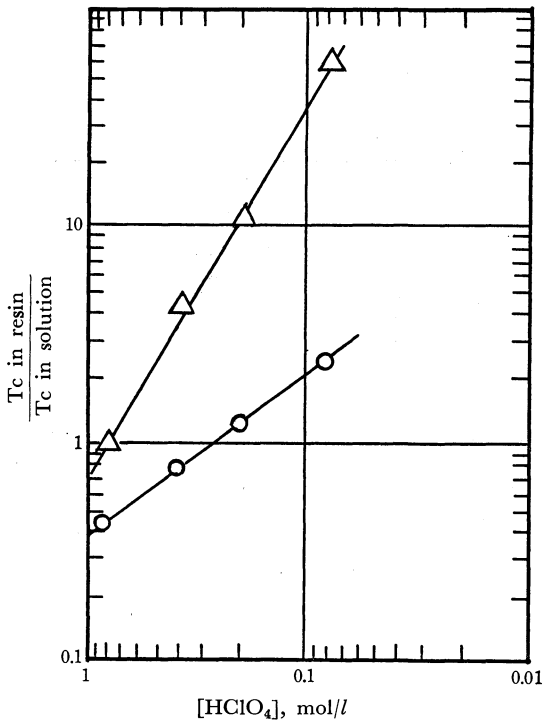

Fig. 2. Relative distribution ratios of anionic complexes between Dowex 1×8 and $HClO_4$.
○ anionic species (−1)
△ anionic species (−2)

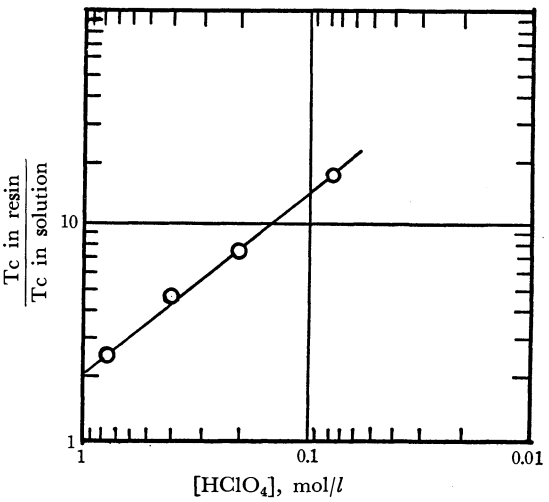

Fig. 3. Relative distribution ratios of cationic complex between Dowex 50×8 and $HClO_4$.

Table 1. Identification of isolated complexes

Fraction	Mole ratio Cl : Tc	Charge/ Species	Complex
Anionic (−2)	5.98 6.05	−1.7	$[TcCl_6]^{2-}$
Anionic (−1)	5.27 5.23	−0.73	$[TcCl_5(H_2O)]^-$
Neutral (0)	—	0	$[TcCl_4(H_2O)_2]$
Cationic (+1)	—	+0.81	$[TcCl_3(H_2O)_3]^+$

Table 2. Spectral characteristics of Tc-chloro-complexes

Complex	λ_{max}	ε_{max}
$[TcCl_6]^{2-}$	234 mμ	19200
$[TcCl_5(H_2O)]^-$	235 mμ	11100
$[TcCl_4(H_2O)_2]$	354 mμ	5500
$[TcCl_3(H_2O)_3]^+$	342 mμ	—

λ_{max}: Wavelength of absorption maximum.
ε_{max}: Molar extinction coefficient at the absorption maximum.

Isosbestic points	λ	ε
of $[TcCl_6]^{2-}$ and	311 mμ	6000
$[TcCl_5(H_2O)]^-$	362 mμ	3500

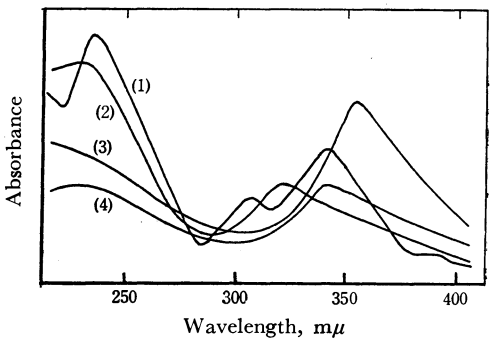

Fig. 4. Absorption spectra of Tc-chlorocomplexes separated by ion exchange.
(1) $[TcCl_6]^{2-}$ (3) $[TcCl_4(H_2O)_2]$
(2) $[TcCl_5(H_2O)]^-$ (4) $[TcCl_3(H_2O)_3]^+$

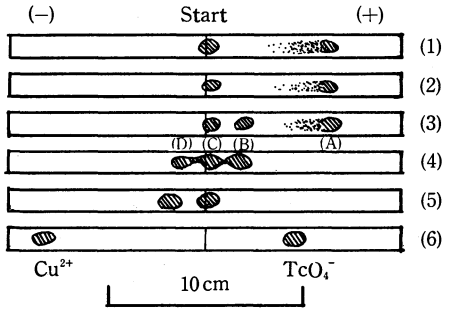

Fig. 5. Electrophoretic patterns of Tc-chlorocomplexes in HCl electrolytic solution.
0.05 M $NaClO_4$ 500 V 40 min
0.05 M $HClO_4$
Tc-chlorocomplexes
(1) in 12 M HCl
(2) in 8 M HCl
(3) in 6 M HCl
(4) in 3 M HCl
(5) in 1 M HCl
(6) reference Cu^{2+}, TcO_4^-

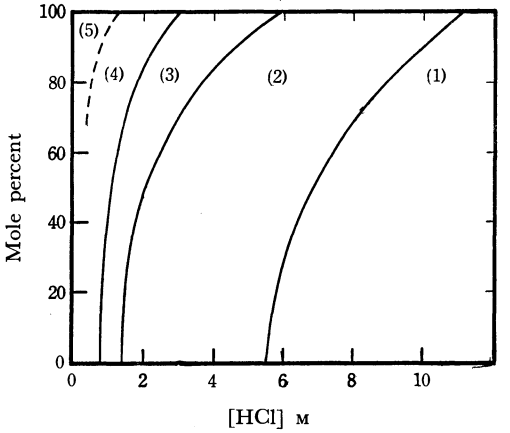

Fig. 6. Approximate compositions of Tc-chlorocomplexes at different concentration of HCl under the experimental conditions.
(1) $[TcCl_6]^{2-}$
(2) $[TcCl_5(H_2O)]^-$
(3) $[TcCl_4(H_2O)_2]$
(4) $[TcCl_3(H_2O)_3]^+$
(5) TcO_4^- and TcO_2

The spectra of the four isolated technetium complex species are shown in Fig. 4, while their wave lengths of maximum absorption and extinction coefficients are tabulated in Table 2. From these results, it can be quantitatively explained that the change in the absorption spectra of $TcCl_6^{2-}$ solution upon irradiation is due to the aquation of the complex in question.

Figure 5 presents electrophoretic patterns which give evidence of the isolation of four different species.

Four main spots, A, B, C, and D, appear in the figure. From their mobilities, it is probable that these spots correspond to the following species:

A-anionic species (−2)
B-anionic species (−1)
C-neutral species (0) and precipitated TcO_2
D-cationic species (+1)

The species could not, however, be assigned definitely because the interaction between the paper and each species is not always the same. The pertechnetate and cupric ions which were used as pilot ions gave clear spots and did not have any tailing.

The spots at the original points appeared in the electrophoretic patterns of the samples of 12 M, 8 M, and 6 M HCl solutions where no zero-charge species were detected by means of the ion-exchange method. The reason for this is not clear, but it is assumed that complexes partly hydrolyze during the electrophoresis as a result of the local heating at the original point. The electrophoresis, however, provides a qualitative figure of the species in the solutions.

In Fig. 6, the abundances of the species are plotted against the hydrochloric acid concentrations. It shows the distribution of complexes found in the solution by the ion-exchange method. It seems that TcO_4^- is formed in the dilute hydrochloric acid by the photochemical formation of the Tc(IV) complex and its subsequent disproportionation reactions. This figure, however, represents only the distribution of technetium complexes under the experimental conditions employed here, as will be discussed later.

As has been mentioned previously, this experiment was performed in order to identify the species of technetium(IV) chlorocomplexes in hydrochloric acid solution.

The photochemical reaction was used to produce different chlorocomplexes in solution. By taking into account the experimental results of electrical charges and the Cl/Tc ratios of complexes, it may be concluded that the main reaction induced by the irradiation is not reduction but the step-by-step substitution of chloride with water molecules. Therefore, the four isolated species can be assigned to the group of chemical forms indicated in Table 1. Furthermore, it is confirmed that the backward reaction (1) proceeds almost quantitatively without any influence of photons; this supports the theory that the reaction taking place is not a redox type reaction but a substitution reaction.

However, the charge-transfer reaction in the primary step of the reaction sequence can not be excluded, for the technetate ion is detected in 0.1 M and 1 M HCl solutions in which the backward reaction can practically be ruled out.

It should be noted that the reaction system used here does not provide a thermodynamic equilibrium, but a transient one. The rates of the forward and backward reactions of the first step in Eq. (1) are expressed as follows:

$$R_f = K_f[TcCl_6^{2-}] \quad (2)$$

$$K_f = K_{df} + f \cdot q \quad (3)$$

$$R_b = K_b[TcCl_5^-][Cl^-] \quad (4)$$

where R_f: rate of forward reaction,
R_b: rate of backward reaction,
K_f: forward reaction constant,
K_{df}: forward reaction constant in the dark,
K_b: backward reaction constant,
f: flux of photon,
q: quantum yield

at the apparent equilibria:

$$R_f = R_b. \quad (5)$$

Therefore,

$$(K_{df} + f \cdot q)[TcCl_6^{2-}] = K_b[TcCl_5(H_2O)^-][Cl^-] \quad (6)$$

$$\frac{[TcCl_5(H_2O)^-]}{[TcCl_6^{2-}]} = \left(\frac{K_{df}}{K_b} + \frac{f \cdot q}{K_b}\right) \Big/ [Cl^-] \quad (7)$$

From Eq. (7), it is clear that the $[TcCl_5(H_2O)^-]/[TcCl_6^{2-}]$ ratio in a given solution is proportional to the light flux irradiated and also inversely proportional to the concentration of chloride in the solution.

To elucidate the reaction mechanism and also to determine the thermodynamic constants, more quantitative experiments from the kinetic point of view are necessary.

The author wishes to express his hearty thanks to Professor Taitiro Fujinaga and Dr. Mutsuo Koyama for their helpful advice and encouragement throughout this work.

BULLETIN OF THE CHEMICAL SOCIETY OF JAPAN VOL. 42 2835—2840 (1969)

The Chromium(III) Complexes with β-Aminoethylsulfonic-*N*,*N*-diacetic Acid and Aspartic-*N*,*N*-diacetic Acid*[1]

Akira UEHARA, Eishin KYUNO and Ryokichi TSUCHIYA

Department of Chemistry, Faculty of Science, Kanazawa University, Kanazawa

(Received January 31, 1969)

The following chromium(III) complexes with the β-aminoethylsulfonic-*N*,*N*-diacetic acid (AEDA) and aspartic-*N*,*N*-diacetic acid (ASDA) were newly prepared; $K_3[Cr(aeda)_2]\cdot 4H_2O$ (pale red) (I), $[Cr(OH)(Haeda)(o\text{-phen})]\cdot 2H_2O$ (orange) (II) and $[Cr(Hasda)(H_2O)_2]\cdot H_2O$ (reddish purple) (III). From the results of spectral measurments, it was found that AEDA acts as a quadridentate ligand as well as a terdentate one in an aqueous solution, but only as a terdentate ligand in a crystal state, and that the coordinating ability of the oxygen atom of sulfonic radical in AEDA is weaker than that of carboxylic radical in ammoniapropionicdiacetic acid (APDA). In Complex III, ASDA behaved as a quadridentate ligand rather than as a quinquedentate. Complexes II and III showed some interesting thermal decomposition processes. The former lost one mole of water at 110°C from the hydrogen atom in free sulfonic acid radical and the coordinated OH group, accompanied with the increase of coordination number of AEDA from 3 to 4. In the latter, one mole of crystalline water was lost first, and then the carboxylic acid bound to the methylene group at β-position in the ligand was decomposed to liberate carbon dioxide, and the coordinated asda was changed into apda.

Preparations and properties of chromium(III) complexes with ammoniatriacetic acid (ATA),[1] ammoniapropionicdiacetic acid (APDA) and ammoniaisopropionicdiacetic acid (AIPDA)[2] have already been reported. These ligands have one nitrogen and three oxygen atoms capable of coordinating. Thus their maximum coordination number is commonly four. But it has often been pointed out that their coordinating behaviors are somewhat different from each other because of the differences in their structures and in their chemical properties such as acid dissociation constants.[1,2]

Although the complexes of (A) and (B) types in Fig. 1, which shows the possible structures of complexes, were obtained in an aqueous solution with all three ligands, the crystals of (A) type were obtained only with APDA. One reason for this may be due to the small solubility of APDA complex. The (B) type complex containing ATA or AIPDA instantly changed to (C) type when they were dissolved in water, but the (C) type complex could not be obtained in the case of APDA. This sug-

*1 Presented in part at the 18th Symposium on Coordination Compounds, Kyoto, October (1968).

1) A. Uehara, E. Kyuno and R. Tsuchiya, This Bulletin, **40**, 2317, 2322 (1967).

2) A. Uehara, E. Kyuno and R. Tsuchiya, *ibid.*, **41**, 2385, 2393 (1968).

gests that the complex containing 5-, 5- and 6-membered chelate rings with ligand such as APDA is more stable than that having three five-membered rings with ligand such as ATA or AIPDA. The complex assigned to (D) type could not be obtained only with AIPDA. This suggests that some steric hindrance due to a methyl group exists in the case of AIPDA.[2]

β-Aminoethylsulfonic-*N,N*-diacetic acid and aspartic-*N,N*-diacetic acid (abbreviated as AEDA and ASDA, respectively) were selected as the related ligand to ATA, APDA and AIPDA in the present work. Rational formulas of these ligands are shown in Fig. 2.

This study was undertaken (1) to investigate how AEDA and ASDA behave toward metal in these complexes, (2) to prepare various complexes containing these ligands and (3) to compare the complexing properties of AEDA and ASDA with those of ATA, APDA or AIPDA.

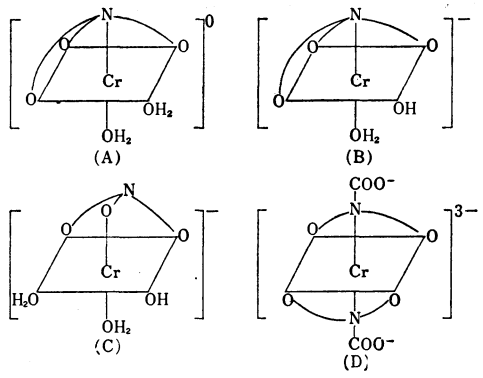

Fig. 1. Structures of the complexes.

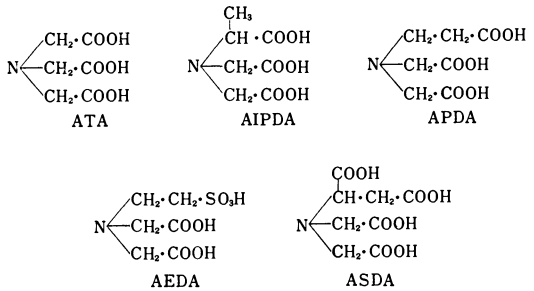

Fig. 2. Rational formulas of the ligands.

Experimental

Preparation of Ligands. *β-Aminoethylsulfonic-N,N-diacetic Acid Dihydrate*: $C_6H_{11}O_7NS \cdot 2H_2O$. The method described here is the modified one reported by Schwarzenbach *et al.*[3] Twenty five grams of taurin were neutralized with 100 m*l* of water containing about 8 g of sodium hydroxide. Thirty-nine grams of monochloroacetic acid were dissolved in 200 m*l* of water and 34 g of sodium bicarbonate was gradually added to it. The two solutions were mixed, the mixture was heated on a water bath up to about 70°C, and 16 g of sodium hydroxide in 50 m*l* of water was added. Heating was continued about one hour. After cooling, gradual addition of concentrated hydrochloric acid and scrubbing by a glass rod, produced white powdered crystals. Recrystallization was achieved from water. Yield about 15 g.

Found: N, 4.96; C, 25.78; H, 5.38%. Calcd for $C_6H_{11}O_7NS \cdot 2H_2O$: N, 5.05; C, 25.99, H; 5.45%.

Aspartic-N,N-diacetic Acid: $C_8H_{11}O_8N$. Twenty six grams of aspartic acid were suspended in about 200 m*l* of water, and 35 g of sodium bicarbonate was added little by little under magnetic stirring. Thirty eight grams of monochloroacetic acid were neutralized with about 200 m*l* of water containing 35 g of sodium bicarbonate. After the two solutions were mixed, the mixture was heated on a water bath at 70—80°C, and then 50 m*l* of water containing 15 g of sodium hydroxide was added. Heating was continued for 1 hr in order to complete the reaction. After cooling, the solution was made acidic with concentrated hydrochloric acid, and then evaporated to a half volume. The sodium chloride was filtered off whenever it was separated out. After the filtrate was concentrated up to syrupy state, a small amount of acetone was added, and the solution was kept for several days in a refrigerator. White powdered crystals were obtained. The crude products were recrystallized from an acetone-water (1 : 1) mixture. Yield about 3 g.

Found: N, 5.49; C, 38.22; H, 4.37%. Calcd for $C_8H_{11}O_8N$: N, 5.62; C, 38.56; H, 4.44%.

Preparation of Complexes. *Potassium Bis(β-aminoethylsulfonic-N,N-diacetato)chromate(III) Tetrahydrate*: $K_3[Cr(aceda)_2] \cdot 4H_2O$ (I). Two and a half grams of chromium chloride hexahydrate were dissolved in 200 m*l* of water and then 2.5 g of AEDA was added. The mixture was heated on a water bath. The color of the solution changed from green to purple as the reaction proceeded. Two and a half grams of AEDA and 3 g of potassium bicarbonate were added and the solution was heated. When the color of the solution became red, the pH was adjusted to *ca.* 6. The pale red crystals were obtained from the cooled solution. The crude products were recrystallized from water. Yield about 1 g. The use of ammonium carbonate instead of potassium bicarbonate gave the ammonium salt.

Found: N, 3.81; C, 20.06; H, 3.25%. Calcd for $K_3[Cr(aeda)_2] \cdot 4H_2O$: N, 3.90; C, 20.07; H, 3.37%.

Hydroxohydrogen-β-aminoethylsulfonic-N,N-diacetato-o-phenanthrolinechromium(III) Dihydrate: [Cr(OH)(Haeda)-(*o*-phen)]·$2H_2O$ (II). The procedure was the same as mentioned above until the purple solution was obtained. To the resulting solution, 2 g of *o*-phenanthroline was added. The pH of the solution was adjusted to 4—5 by adding an appropriate amount of potassium bicarbonate. Orange crystals were obtained from the cooled resulting solution. Recrystallization was achieved from an aqueous solution. Yield about 1.5 g.

Found: N, 8.32; C, 41.25; H, 4.14%. Calcd for [Cr(OH)(Haeda)(*o*-phen)]·$2H_2O$: N, 8.01; C, 41.22; H, 4.23%.

3) G. Schwarzenbach, H. Ackermann and P. Ruckstull, *Helv. Chim. Acta*, **32**, 1175 (1949).

Hydrogenaspartic-N,N-diacetatodiaquochromium(III) Monohydrate: $[Cr(Hasda)(H_2O)_2]\cdot H_2O$ (III). The mixture of five grams of ASDA and an appropriate amount of chromium hydroxide was suspended in water, and was heated on a water bath almost to dryness. The residue was dissolved in a small amount of water, and the reddish purple filtrate was concentrated. The resulting solution was adjusted to pH 2, and after adding a small amount of acetone, it was kept in a refrigerator for a few days. Reddish purple crystals were obtained. Recrystallization was carried out from water-acetone (70 : 30) mixture. Yield about 0.5 g.

Found: N, 3.81; C, 27.59; H, 3.83%. Calcd for $[Cr(Hasda)(H_2O)_2]\cdot H_2O$: N, 3.97; C, 27.28; H, 3.99%

Instruments. The instruments used in this work were the same as described previously.[2]

Results and Discussion

Observation on Thermal Decomposition Processes by using a Derivatograph and an IR Spectrometer. Some interesting thermal decomposition processes were observed by using a derivatograph and an IR spectrometer. Their derivatograms measured in a nitrogen stream with a heating rate of *ca.* 1°C/min are shown in Fig. 3. About 500 mg of the sample was used for each run. Figures 4 and 5 give the IR spectra of these complexes and of the samples taken out at several heating steps.

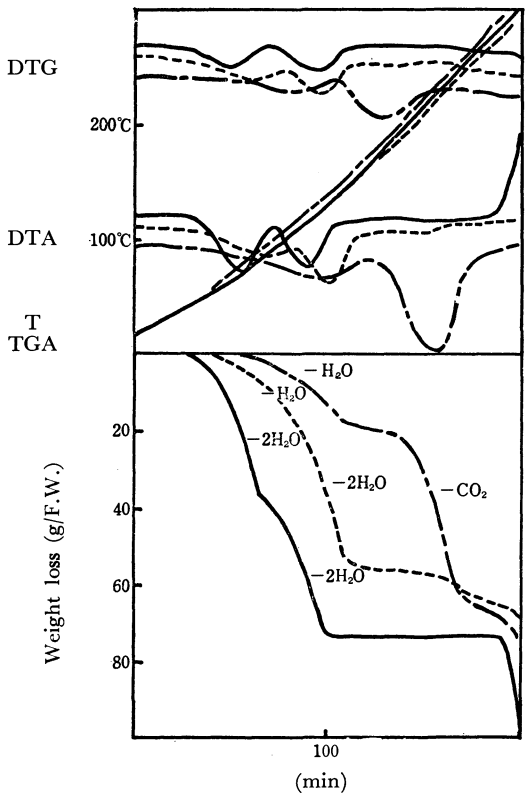

Fig. 3. Derivatograms for I (——), II (----) and III (—·—).

As shown in Fig. 3, Complex I lost 4 mol of crystalline water in two distinct steps: the first two moles were removed at *ca.* 80°C and the last two, at 135°C. A violent decomposition started at *ca.* 280°C.

For Complex II, though TGA curve shows the weight loss corresponding to 3 mol of water from 65 to 150°C, both DTA and DTG curves indicate the split peaks below and over *ca.* 110°C. The corresponding difference could also be detected in IR spectra, which is shown in Fig. 4. The split bands at *ca.* 1200 cm^{-1} probably assigned to sulfonate ion changed to one peak when the complex was heated at 110°C, and the band due to H_2O (3400—3200 cm^{-1}) disappeared at 150°C. These facts combined with the TGA curve mean that the weight loss at the first step until 110°C is due to the evolution of one mole of water from the hydrogen ion of free sulfonic acid and the hydroxyl group and that at the second step over 110°C corresponds to the liberation of two moles of the crystalline water.

From Complex III, the weight loss corresponding to the liberation of one mole of water and to that of one mole of carbon dioxide can be observed at 75—155°C and 180—250°C on TGA curve in Fig. 3, respectively. As shown in IR spectral features in Fig. 5, both the bands at 1730 and at 1610 cm^{-1} could be detected in the sample before heating; the former has been assigned to non- and the latter, to coordinated carboxylic acid.[4]

The sample at 155°C shows the same pattern, but the band at 1730 cm^{-1} disappears at 250°C. Nevertheless, the band at 3500 cm^{-1} due to the OH stretching vibration can be seen in all these samples. The results suggest that the crystalline water is lost first, and then the free carboxylic acid attached to the methylene group at β-position in the ligand is decomposed to produce carbon dioxide without losing any coordinated water, and the coordinated asda is changed into apda.

Visible and UV Absorption Spectra. All the measurements of absorption spectra were carried out in aqueous solutions. In Fig. 6, the spectrum of Complex I and that of the corresponding ATA complex are shown. The spectra of the purple solution obtained by the reaction of $CrCl_3\cdot 6H_2O$ with AEDA and of the solution of $[Cr(ata)(H_2O)_2]$ are shown in the figure. Figure 7 gives the spectra of Complex II and Complex III. The numerical data of their absorption maxima are summarized in Table 1, together with those measured in Complex III by a diffuse-reflectance method. As seen in Fig. 6, the spectrum of Complex I is quite similar to that of the corresponding ATA complex, indicating that they may have the analogous structure. Although it is known that the gradual

4) D. H. Busch and J. C. Bailar, Jr., *J. Am. Chem. Soc.*, **75**, 4574 (1953).

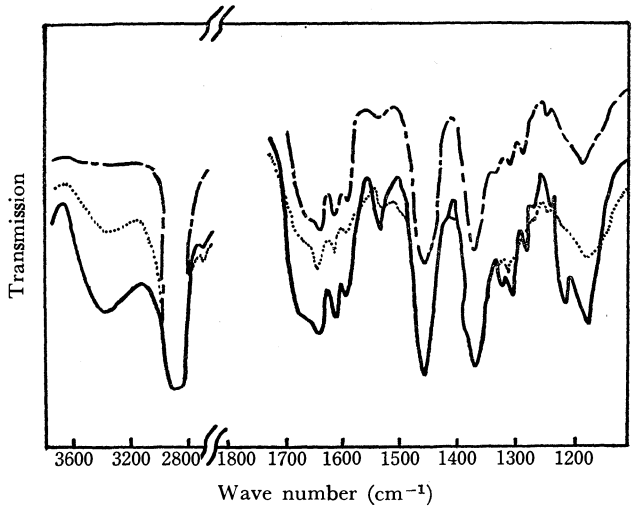

Fig. 4. Infrared spectra for II. (room temp.: ——, 110°C: – – –, 150°C: —·—)

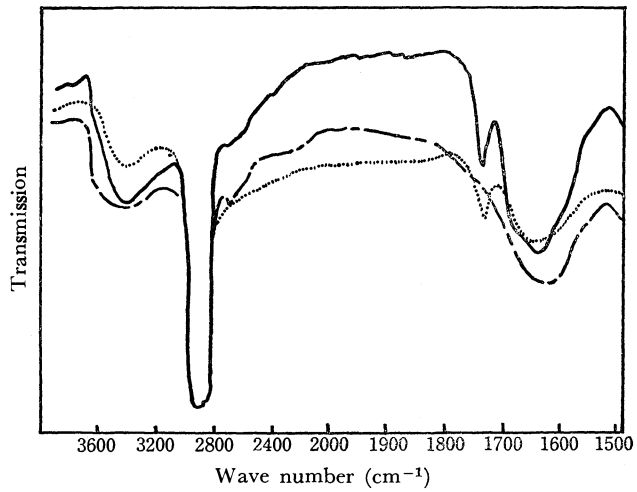

Fig. 5. Infrared spectra for III. (room temp.: ——, 155°C: – – –, 250°C: —·—)

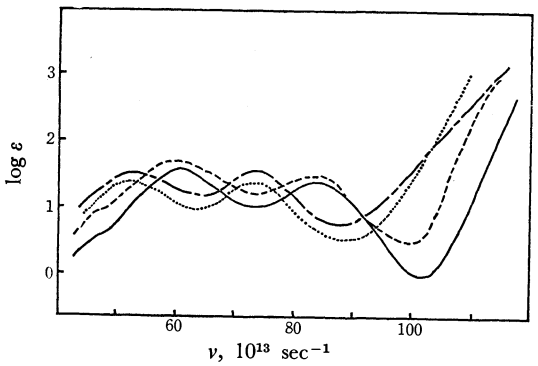

Fig. 6. Electronic Spectra for I (——), $K_3[Cr(ata)_2]\cdot 4H_2O$ (– – –), $[Cr(ata)(H_2O)_2]$ (—·—) and purple solution produced by the reaction of $CrCl_3\cdot 6H_2O$ with AEDA (·····).

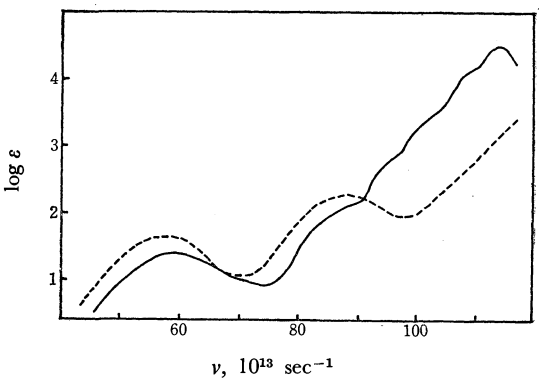

Fig. 7. Electronic spectra for II (——) and III (– – –).

Table 1. Absorption maxima

Complex	$\nu_1(10^{13}/\text{sec})$ (log ε_1)	$\nu_2(10^{13}/\text{sec})$ (log ε_2)
Purple solution of $[Cr(aeda)(H_2O)_2]$	54.1 (1.89)	74.4 (2.01)
Purple solution of $[Cr(ata)(H_2O)_2]$	54.9 (1.91)	74.1 (2.03)
I	60.0 (1.54)	83.3 (1.39)
$K_3[Cr(ata)_2]\cdot 4H_2O$[1]	60.1 (1.65)	83.6 (1.48)
II	59.0 (1.51)	88.2 (2.02)
III	58.4 (1.64)	86.9 (2.25)
III*	54.5	75.0

* This absorption maximum was measured by a diffuse-reflectance method.

decomposition from $[Cr(ata)_2]^{3-}$ to $[Cr(OH)(ata)(H_2O_2)]^-$ proceeds in an aqueous solution even at room temperature,[1] no change in the spectrum could be observed even in the solution kept for a few days in the case of Complex I.

The spectrum for the purple solution of AEDA is very similar to that of $[Cr(ata)(H_2O)_2]$, showing that they may have an analogous structure, and that AEDA acts as a quadridentate ligand in an aqueous solution only in this complex.

As shown in Fig. 7, Complex II gives a rather complicated spectrum due to the coordinated *o*-phenanthroline. The spectrum of Complex III in an aqueous solution has the maxima at 58.4 and 86.9×10^{13}/sec, whereas that in a solid state measured by a diffuse-reflectance method shows the maxima at 54.5 and 75.0×10^{13}/sec. This considerable deviation may indicate that Complex III has a different structure in an aqueous solution and in a solid state. The numerical data given in Table 1 show that the bands in a solid state of Complex III are very close to that of $[Cr(ata)(H_2O)_2]$. In other words, Complex III will have a coordinating structure similar to that of $[Cr(ata)(H_2O)_2]$ in a solid state. In an aqueous solution, however, the coordinating structure is still unkown.

Molar Conductivities and pH Values. In Table 2, the values of molar conductivities and pH were listed together with the behaviors toward ion exchangers. The sign + means the adsorption of the complex by ion exchangers, and −, the reverse. All three complexes in solution were adsorbed by Cl-form anion exchangers. For Complex I, the pH value and molar conductivity were 6.8 and 383.1 mho cm^{-1}, respectively, showing that it is a 1 : 3 type electrolyte.

The solution of Complex II was acidic (pH 3.4) and molar conductivity was 161.3 mho cm^{-1}. It suggests that the hydrogen ion is partly dissociated from Haeda in an aqueous solution.

For Complex III, the values of considerably low pH (pH 1.8) and of the higher conductivity (481.2 mho cm^{-1}) were observed, which may indicate that the strong dissociation of hydrogen ion in free carboxylic acid takes place in an aqueous solution.

Table 2. Some properties of the complexes

Complex	Adsorption to the ion exchanger		Molar conductivity* (mho cm^{-1})	pH**
	Na-form	Cl-form		
I	−	+	383.1	6.8
II	−	+	161.3	3.4
III	−	+	481.2	1.8

* 1.0×10^{-3} mol/*l* aqueous solution was used.
** 1.0×10^{-2} mol/*l* aqueous solution was used.

Possible Structures of the Complexes. From the results, the possible structures proposed are depicted in Fig. 8. The purple solution formed from the reaction of chromium chloride hexahydrate with AEDA may have (a) type structure, in which AEDA acts as a quadridentate ligand. For Complex I, (b) type may be assigned, where the sulfonic acid is not coordinated. The (c) type structure having some interaction between the hydrogen atom in the sulfonic acid and the oxygen atom in the coordinated hydroxyl group seems to be reasonable for Complex II.

When ASDA acts as a quadridentate ligand, two kinds of characteristic coordinating structures are expected. One makes three five-membered chelate rings, and the other two five- and one six-membered chelate rings. However, as it has already been reported,[2,5] the latter case makes a more stable complex formation than the former, so that the preferable structure for Complex III is the (d) type.

Comparisons among AEDA-, ATA-, AIPDA-, and APDA-Complexes. As the structure of AEDA resembles that of APDA, it was expected that AEDA forms a stable complex in which AEDA acts as a quadridentate ligand. However, this was proved not to be the case by the following results. Firstly, the complex in which AEDA acts as a quadridentate ligand was formed in an aqueous

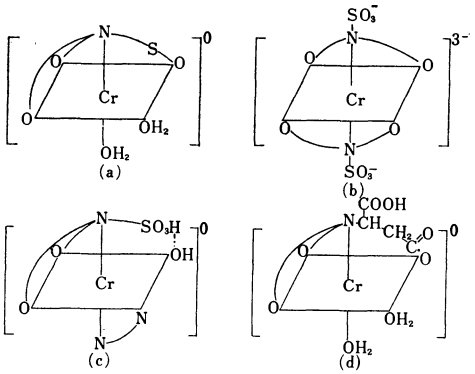

Fig. 8. Possible structures.

5) E. Martell and S. Chaberek, Jr., *J. Am. Chem. Soc.*, **75**, 2888 (1953).

solution, but not in a crystal state. Secondly, in the mixed complexes, ATA, AIPDA and APDA behaved only as a quadridentate ligand, whereas AEDA acts as a terdentate ligand owing to the non-coordination of the sulfonic acid. Thirdly, although the ATA and APDA complexes gradually decomposed in an aqueous solution from $[Cr(ata)_2]^{3-}$ and $[Cr(apda)_2]^{3-}$ to $[Cr(OH)(ata)(H_2O)_2]^-$ and $[Cr(OH)(apda)(H_2O)]^-$ respectively, the coordinating AEDA complex I underwent no change in an aqueous solution. These facts suggest that the coordinating ability of the oxygen atom of sulfonic acid in AEDA is smaller than that of carboxylic acid in APDA. They are in good agreement with the result that APDA has larger stability constants than AEDA in the bivalent metal complexes.[6]

Possible Thermal Decomposition Processes. The possible thermal decomposition processes for Complexes II and III are described schematicaly in Fig. 9. Complex II lost one mole of water at 110°C from the hydrogen atom in free sulfonic acid and the coordinated hydroxyl group, resulting in the increase of coordination number of AEDA from 3 to 4. Such phenomena have also been observed in APDA complex, $[Cr(OH)(Hapda)(H_2O)_2]$.[2] On the other hand, for Complex III, one mole of crystalline water is first lost and then

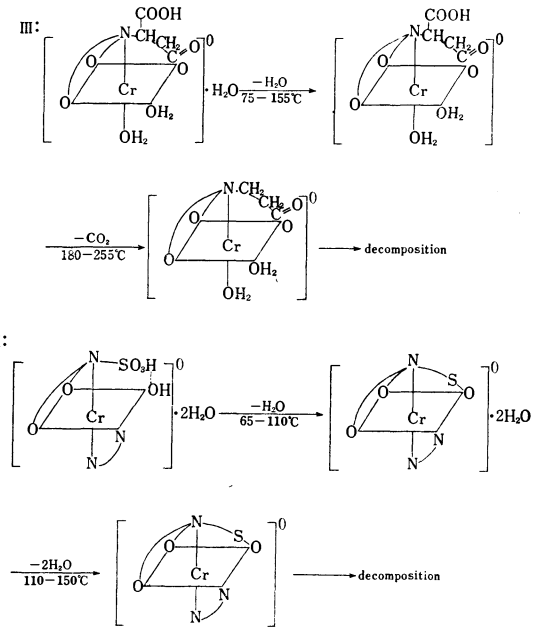

Fig. 9. Possible thermal decomposition schemes for II and III.

the carboxylic acid attached to the carbon atom at β-position in the ligand may be decomposed into carbon dioxide, and the coordinated asda is changed into apda.

6) H. Ackermann and G. Schwarzenbach, *Helv. Chim. Acta*, **32**, 1543 (1949).

BULLETIN OF THE CHEMICAL SOCIETY OF JAPAN VOL. 42 2841—2843 (1969)

The Kinetics of the Ligand-substitution Reactions of Nitrilotriacetatoniccolate(II) Complexes with *trans*-1,2-Cyclohexanediaminetetraacetate Ions

Masaru KIMURA*1

Department of Applied Chemistry, Yamagata University, Jonan, Yonezawa-shi

(Received February 3, 1969)

The kinetics of the ligand-substitution reactions of the nitrilotriacetatoniccolate(II) complexes with *trans*-1,2-cyclohexanediaminetetraacetate (CyDTA) ions were studied polarographically from pH 4.8 to 5.8 at an ionic strength of 0.2 and at 25°C. The reactions were found to proceed only through the dissociation reactions of the nitrilotriacetatoniccolate(II) complexes. The rate constants of the dissociation reactions were also determined. In contrast to the reactions of the same complex with ethylenediaminetetraacetate (EDTA) ions and *N*-2-hydroxyethylenediaminetriacetate (HEDTA) ions, there were no direct reactions of the nitrilotriacetatoniccolate(II) complexes with CyDTA ions. The reaction was of the first order in respect to the concentration of the nickel-complex and independent of the CyDTA concentration; the reaction of the complex with CyDTA ions was found to have the different mechanisms from the similar reaction with EDTA and HEDTA, and to be due to the steric effect of the cyclohexane ring in the CyDTA molecule.

In a previous paper[1] the kinetics of the ligand-substitution reactions of nickel(II)-nitrilotriacetate (NTA) complexes with EDTA ions and HEDTA ions were dealt with. Both reactions were found to proceed through four reaction paths, involving two paths of the dissociation reactions of Ni(II)-NTA complexes. Recently, it has been reported that the reactions of copper(II) ion with Ni(II)-CyDTA complexes,[2] and those of cadmium(II) ion with Ca(II)-CyDTA complexes,[3] behave different kinetically from the similar reactions with EDTA complexes.[3-5] These phenomena could be explained by the fact that the cyclohexane ring in CyDTA prevents the free rotation about the ethylenic bond between the two nitrogen atoms; with this steric restriction it is impossible to bond a different metal ion to each iminodiacetate segment of CyDTA, although such reaction intermediates are possible with EDTA.[2,3] It seems to be important and also interesting to examine whether a similar kinetic behavior holds in the case of the ligand-substitution reaction, particularly in the case of the reaction using CyDTA as the entering ligand. Thus, the ligand-substitution reactions of Ni(II)-NTA complexes with CyDTA ions have been investigated in the present study. The reaction mechanisms have been compared with those of the similar reactions with EDTA and HEDTA, and also with the metal-substitution reactions described above.

Experimental

The solutions of dipotassium nitrilotriacetate and dipotassium *trans*-1,2-cyclohexanediaminetetraacetate were prepared from commercial nitrilotriacetic acid (DOTITE NTA) and *trans*-1,2-cyclohexanediaminetetraacetic acid (DOTITE CyDTA) respectively, and were standardized against a standard solution of nickel(II) nitrate by amperometric titration. The standard solution of nickel(II) nitrate was prepared by dissolving an appropriate amount of pure nickel metal in reagent-grade nitric acid. The concentration of the nickel(II) solution was determined by the conventional gravimetric method, using dimethylglyoxime.[6] Commercial guaranteed reagents were used for acetate buffer solution and supporting electrolytes without further purification.

The rate of the reaction of nickel(II)-NTA complex with CyDTA was determined by measuring the decrease of the polarographic anodic diffusion-limiting currents of CyDTA ions with time.

Current-time curves were obtained with a Yanagimoto-PA-102 pen-recording polarograph. The dropping-mercury electrode had an m value of 1.9 mg/sec and a drop time, t_d, of 4.3 sec in an air-free solution contain-

*1 Correspondence to be addressed to: c/o Prof. Kolthoff, Dept. of Chem., Univ. of Minn., Minneapolis, Minn. 55455, U.S.A.

1) M. Kimura, *Nippon Kagaku Zasshi (J. Chem. Soc. Japan, Pure Chem. Sect.)*, **89**, 1209 (1968).

2) D. W. Margerum and T. J. Bydalek, *Inorg. Chem.*, **2**, 683 (1963).

3) J. R. Kuempel and W. B. Schaap, *ibid.*, **7**, 2435 (1968).

4) T. J. Bydalek and S. W. Margerum, *J. Am. Chem. Soc.*, **83**, 4326 (1961).

5) D. W. Margerum and T. J. Bydalek, *Inorg. Chem.*, **1**, 582 (1962).

6) F. P. Treadwell and W. T. Hall, "Analytical Chemistry," Vol. 2, John Wiley & Sons, New York (1951), p. 193.

ing 0.2 M potassium nitrate at 25°C and at −0.5 V *vs.* SCE.

Measurements were made at 25°C in an acetate buffer solution containing 0.04 M acetate ion. The ionic strength of the solution was adjusted to 0.2 with potassium nitrate. Gelatin (0.005% in concentration) was added as a maximum suppressor. The pH of the solution was measured after the polarographic measurements with a Hitachi-Horiba Model F-5 pH meter equipped with a glass electrode.

Results and Discussion

The overall ligand-substitution reactions between nickel(II)-NTA complexes and CyDTA ions can apparently be expressed by:

$$NiX^- + \left\{\begin{matrix} Z^{4-} \\ \downarrow\uparrow \\ \vdots \\ \downarrow\uparrow \\ H_4Z \end{matrix}\right\} \overset{V_i^+}{\rightleftharpoons} NiZ^{2-} + \left\{\begin{matrix} X^{3-} \\ \downarrow\uparrow \\ \vdots \\ \downarrow\uparrow \\ H_3X \end{matrix}\right\} \quad (1)$$

Where X^{3-} and Z^{4-} denote a tervalent NTA anion and a tetravalent CyDTA anion respectively.

The concentrations that can be determined polarographically, [CyDTA] are given by:

$$[CyDTA] = \sum_{j=0}^{4} [H_jZ^{(4-j)-}]$$

Under the present experimental conditions, the rate of the reaction given by Eq. (1) was so slow that the initial rate of the forward reaction, $-\Delta[CyDTA]_i/\Delta t$, could be determined accurately. The subscript i indicates the initial state.

Table 1 shows the characteristics of the reaction of Ni(II)-NTA complexes with CyDTA ions, which were obtained from the preliminary measurements of the initial rate under varied conditions.

Judging from these characteristics, the reaction mechanism of the ligand-substitution reaction between Ni(II)-NTA complex and CyDTA ions may be considered to be as follows:

$$NiX^- \underset{k_a^-}{\overset{k_{NiX}}{\rightleftharpoons}} Ni^{2+} + X^{3-} \quad (2)$$

$$NiX^- + H^+ \underset{k_b^-}{\overset{k^H_{NiX}}{\rightleftharpoons}} Ni^{2+} + HX^{2-} \quad (3)$$

$$Ni^{2+} + \left\{\begin{matrix} Z^{4-} \\ \downarrow\uparrow \\ \vdots \\ \downarrow\uparrow \\ H_jZ^{(4-j)-} \end{matrix}\right\} \overset{k_j^+}{\rightleftharpoons} NiZ^{2-} + jH^+ \quad (4)$$

Consequently, it was found that the relations of:

$$\sum_{j=0}^{4} k_j^+[H_jZ^{(4-j)-}] \gg k_a^-[X^{3-}] + k_b^-[HX^{2-}]$$

are satisfactorily fulfilled under the present experimental conditions from the series No. 3 in Table 1, and that there are no paths of the direct reaction of CyDTA ions with the complex from the series No. 4 in Table 1. Therefore, the overall reaction rate for the reaction the (1) is expressed by:

$$-\Delta[CyDTA]_i/\Delta t \equiv V_i^+ = [NiX^-]_i\{k_{NiX} + k^H_{NiX}[H^+]\} \quad (5)$$

Determination of the Rate Constant. The initial rate of the reaction (1), $-\Delta[CyDTA]_i/\Delta t$, was determined under the conditions given by series No. 1 in Table 1. The values of $V_i^+/[NiX^-]_i$ were plotted against $[H^+]$ according to Eq. (5). These plots gave straight lines, as shown in Fig. 1, from which the values of the rate constants in Eq. (5) were determined. The rate constants obtained are given in Table 2, together with the values previously reported.[1)]

In Table 2 it can be seen that the values obtained in the present study are in good agreement with those obtained from the other reaction systems. The

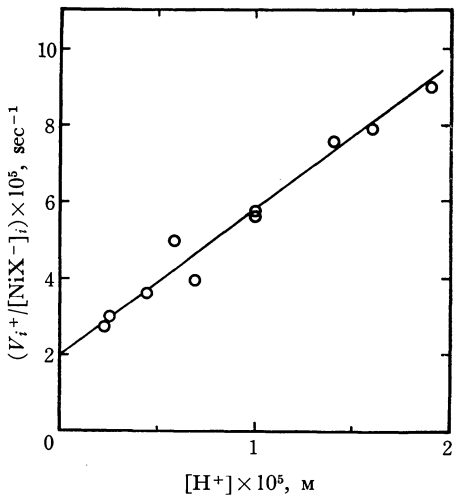

Fig. 1. $V_i^+/[NiX^-]_i$ as a function of the hydrogen ion concentration in acetate buffer-potassium nitrate solutions of ionic strength 0.2 at 25°C. Initial concentrations are $[NiX^-]_i = 2.02\times10^{-3}$ M and $[CyDTA]_i = 4.49\times10^{-4}$ M. Concentration of uncomplexed NTA is $[NTA]_f = 2.6\times10^{-4}$ M.

TABLE 1. CHARACTERISTICS OF THE REACTION OF NI(II)-NTA COMPLEX WITH CyDTA IONS

Series No.	$[H^+]$	$[NiX^-]_i$	$[NTA]_f$*	$[CyDTA]_i$	Initial rate (V_i^+)
1	varied	const.	—	—	first-order for $[H^+]$
2	const.	varied	—	—	proportional to $[NiX^-]_i$
3	const.	const.	varied	—	independent of $[NTA]_f$
4	const.	const.	—	varied	independent of $[CyDTA]_i$

* $[NTA]_f$ indicates the concentration of uncomplexed NTA.

TABLE 2. RATE CONSTANTS OF THE DISSOCIATION REACTION AT THE IONIC STRENGTH OF 0.2 AT 25°C

Reaction system	k_{NiX} (sec^{-1})	k^{H}_{NiX} ($M^{-1}\,sec^{-1}$)	Investigator
NiX-EDTA	3.0×10^{-5}	3.7	M. Kimura[1]
NiX-HEDTA	3.4×10^{-5}	3.7	M. Kimura[1]
NiX-CyDTA	2.0×10^{-5}	3.8	This study

reactions of Ni(II)-NTA complex with EDTA and HEDTA were of the first-order in the concentrations of EDTA and HEDTA.[1] However, the reaction of the same complex with CyDTA was independent of the concentration of CyDTA. Experimental examples of this behavior are shown in Fig. 2. Margerum and Bydalek[2] reported that the metal-substitution reaction of copper(II) ion with Ni(II)-CyDTA complex does not include copper ion attack of Ni(II)-CyDTA complex; the absence of any copper dependence may be attributed to the inability of the copper(II) ion to form binuclear intermediates such as [Ni-CyDTA-Cu] because of hindered rotation and steric blocking due to the cyclohexane ring. Recently, Kuempel and Schaap[3] reported similar behavior in the reaction of the cadmium(II) ion with Ca(II)-CyDTA complex. The results obtained in the present study on the ligand-substitution reaction, using CyDTA as an entering ligand molecule, may be consistent with those of the two previous papers on metal-substitution reactions involving CyDTA.

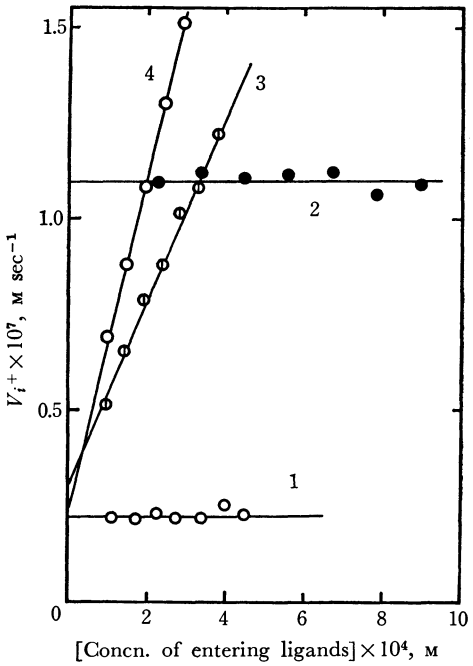

Fig. 2. V_i^+ as a function of the concentrations of the entering ligands. The conditions are the same as for Fig. 1. The entering ligands are CyDTA (1 and 2), EDTA (3) and HEDTA (4). The initial concentrations of complexes, $[NiX^-]_i$ are 0.81 mM (1), 2.02 mM (2) and 0.40 mM (3 and 4). The pH values of the solutions are 5.70 (1), 5.10 (2), 5.00 (3) and 5.26 (4).

The author wishes to thank the Ministry of Education for the financial support granted for this research.

BULLETIN OF THE CHEMICAL SOCIETY OF JAPAN VOL. 42 2844—2848 (1969)

The Kinetics of the Ligand-substitution Reactions of Nitrilo(diacetic)-propionato- and Nitrilo(diacetic)isopropionatoniccolate(II) Ions with EDTA, and of Taurin-*N*-diacetatoniccolate(II) Ions with EDTA and CyDTA

Masaru KIMURA*1

Department of Applied Chemistry, Yamagata University, Jonan, Yonezawa-shi

(Received February 24, 1969)

The kinetics of the reactions of nickel(II)-nitrilo(diacetic)propionate (NDAP) and nickel(II)-nitrilo(diacetic)isopropionate (NDAIP) complexes with ethylenediaminetetraacetate (EDTA) ions, and those of the nickel(II)-taurin-*N*-diacetate (TDA) complex with EDTA and *trans*-1,2-cyclohexanediaminetetraacetate (CyDTA) ions, have been studied polarographically in solutions with pH 4.8—6.0 at 25°C and at an ionic strength of 0.2. All the reactions except those with CyDTA proceeded through four reaction paths, and the rate constants for the reaction paths were determined. The reaction of the nickel(II)-TDA complex with CyDTA was found to proceed only through the complete dissociation of the Ni(II)-TDA complex. There was not a direct reaction of the complex with CyDTA. Consequently, the overall reaction with CyDTA became much slower than that of the same complex with EDTA. The rate constants obtained were compared with those of the similar reactions of the nickel(II)-nitrilotriacetate (NTA) complex with EDTA and CyTDA which had been reported previously. The rate of the dissociation reaction of nickel(II) complexes increased in the order: NDAIP≦NDAP<NTA<TDA. Especially, the rate of the Ni(II)-TDA complex was about 30 times that of Ni(II)-NTA complex.

The metal-chelating tendencies of the chelating agents, nitrilo(diacetic)propionic acid (NDAP) and taurin-*N*-diacetic acid (TDA), which are resulted from the substitution of one acetate group in nitrilotriacetic acid (NTA) have been extensively investigated.[1-3] Recently, a new agent, nitrilo(diacetic)-isopropionic acid (NDAIP) was synthesized by Uehara *et al.*[3] In previous studies,[4,5] the kinetics of the reaction of the nickel(II)-NTA complex with ethylenediaminetetraacetate (EDTA) ions, *N*-hydroxyethylethylenediaminetriacetate(HEDTA) ions, and *trans*-1,2-cyclohexanediaminetetraacetate (CyDTA) ions were dealt with. Since it seems important and necessary to extend the study to the investigation of the effect of various ligands on the reaction rate and the mechanism, the reactions of several nickel(II) complexes with EDTA and/or CyDTA were carried out in the present study. The rate constants of the dissociation of the nickel(II) complexes were compared with the metal-chelating tendencies of the chelating agents.

The reaction of the nickel(II)-TDA complex with CyDTA was run for the purpose of determining the rate constant of the dissociation reaction of the nickel complex; this study aimed to determine the rate constants of the ligand-substitution reactions and also those of the dissociation reactions of the nickel complexes. In a previous paper,[4] the kinetics of the reaction of the nickel(II)-NTA complex with CyDTA were dealt with and compared with those of the reaction of the same complex with EDTA. Changes in the reaction mechanism and a large decrease in the overall rate were observed when EDTA was replaced by CyDTA. The reasons for this were discussed in the previous paper.[4]

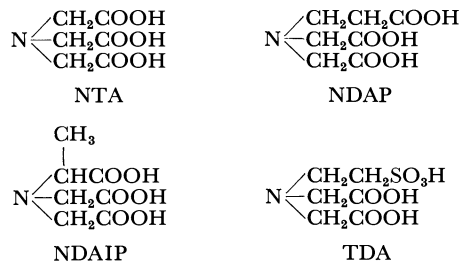

Fig. 1. Structural formulas of the chelating agents.

*1 Correspondence to be addressed to: c/o Prof. Kolthoff, Dept. of Chem., Univ. of Minn., Minneapolis, Minn. 55455, U.S.A.

1) G. Schwarzenbach, H. Ackermann and P. Ruckstuhl, *Helv. Chim. Acta*, **42**, 1175 (1949).

2) S. Chaberek, Jr., and A. E. Martell, *J. Am. Chem. Soc.*, **75**, 2888 (1953).

3) A. Uehara, E. Kyuno and R. Tsuchiya, This Bulletin, **41**, 2393 (1968).

4) M. Kimura, *ibid.*, **42**, 2841 (1969).

5) M. Kimura, *Nippon Kagaku Zasshi (J. Chem. Soc. Japan, Pure Chem. Sect.)*, **89**, 1209 (1968).

Experimental

The chelating agents, NDAIP,[3] NDAP[6] and TDA,[7] were prepared by the procedures reported by Uehara *et al.* Uehara's method for the syntheses of NDAP and TDA was a modification of Schwarzenbach's.[1] All the other chemicals and the apparatus used were the same as had been described in previous papers.[4,5] The rate of the reaction was measured by a method which was, in principle, the same as that employed in previous studies.[4,5] The temperature was maintained at 25°C. The ionic strength was adjusted to 0.2 with potassium nitrate.

Results

The overall reaction of Ni(II)-NDAP, Ni(II)-NDAIP, and Ni(II)-TDA complexes with EDTA or CyDTA may be expressed as:

$$\left\{\begin{matrix}NiX^{-}\\ \downarrow\uparrow\\ NiHX\end{matrix}\right\}+\left\{\begin{matrix}Y^{4-}\\ \downarrow\uparrow\\ \vdots\\ \downarrow\uparrow\\ H_4Y\end{matrix}\right\}\overset{V_i^{+}}{\rightleftharpoons}\left\{\begin{matrix}NiY^{2-}\\ \downarrow\uparrow\\ NiHY^{-}\end{matrix}\right\}+\left\{\begin{matrix}X^{3-}\\ \downarrow\uparrow\\ \vdots\\ \downarrow\uparrow\\ H_3X\end{matrix}\right\} \qquad (1)$$

Where X^{3-} indicates *ndap*$^{3-}$, *ndaip*$^{3-}$ and *tda*$^{3-}$, which are tervalent anions of NDAP, NDAIP, and TDA respectively, and where Y^{4-} indicates edta^{4-} and cydta^{4-}, which are tetravalent anions of EDTA and CyDTA respectively. The concentrations of EDTA and CyDTA that can be determined polarographically are those of the uncomplexed EDTA and CyDTA, which are given by the equation:

$$[\text{EDTA}]=\sum_{j=0}^{4}[H_jY^{(4-j)-}] \qquad (2)$$

(or [CyDTA])

Under the present experimental conditions, all the reactions of Eq. (1) except that of the Ni(II)-TDA complex with EDTA were so sluggish that the initial rate, $-\Delta[\text{EDTA}]_i/\Delta t$ or $-\Delta[\text{CyDTA}]_i/\Delta t$ could be measured accurately (the subscript i indicates the initial state). Two experimental examples of the current-time curve of the reaction of the Ni(II)-TDA complex with EDTA and CyDTA are given in Fig. 2. The initial rates (V_i^+) were obtained under various experimental conditions. The initial rates of the reactions of nickel(II)-NDAP and nickel(II)-NDAIP complexes with EDTA were: (1) independent of the concentration of uncomplexed NDAP or NDAIP (see Table 1); (2) proportional to the initial concentration of the complex, [Ni *ndap*$^{-}$]$_i$ or [Ni *ndaip*$^{-}$]$_i$; (3) linear to the initial concentration of the entering

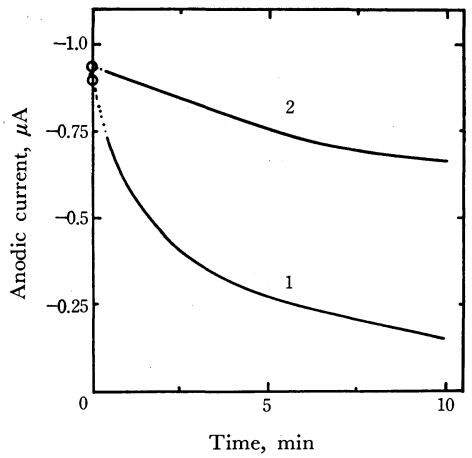

Fig. 2. Limiting current - time relation (at +0.2 V *vs.* SCE at 25°C in acetate buffer - potassium nitrate solution containing 0.04 M acetate and 0.005% gelatin).
Curve 1: the reaction of Ni(II)-TDA complex with EDTA
Curve 2: the reaction of Ni(II)-TDA complex with CyDTA
Initial concentrations are [Ni *tda*$^{-}$]$_i$=2.06×10^{-4} M and [EDTA]$_i$=1.90×10^{-4} M for curve 1, and [Ni *tda*$^{-}$]$_i$=1.03×10^{-4} M and [CyDTA]$_i$=2.26×10^{-4} M for curve 2. The pH's of the solutions are (1) pH 5.10 and (2) pH 5.14.

Table 1. Initial rates (V_i^+) at various concentrations of uncomplexed NDAP and NDAIP (μ=0.2, 25°C)*

i) Ni(II)-NDAP reaction system:
Initial concentrations are [Ni *ndap*$^{-}$]$_i$=3.09×10^{-4} M and [EDTA]$_i$=1.89×10^{-4} M. pH 5.08.

[NDAP]$_f$×10^4, M	V_i^+×10^8, M sec^{-1}
0.46	3.56
1.88	3.68
1.30	3.71
4.72	3.67
6.14	3.58
7.56	3.55

ii) Ni(II)-NDAIP reaction system:
Initial concentrations are [Ni *ndaip*$^{-}$]$_i$=2.06×10^{-4} M and [EDTA]$_i$=1.89×10^{-4} M. pH 5.10.

[NDAIP]$_f$×10^4, M	V_i^+×10^8, M sec^{-1}
0.16	1.80
1.05	1.87
1.95	1.77
2.83	1.80
3.71	2.10
5.49	1.81
7.26	1.92

* [NDAP]$_f$ and [NDAIP]$_f$ mean the concentrations of uncomplexed NDAP and NDAIP, respectively.

6) A. Uehara, E. Kyuno and R. Tsuchiya, This Bulletin, **41**, 2385 (1968).

7) A. Uehara, E. Kyuno and R. Tsuchiya, presented at the 18th Symposium on Coordination Compounds, Kyoto, Japan, Oct. 1968.

ligand, $[EDTA]_i$ and $[edta^{4-}]_i$ (see Figs. 3,4 and 5), and (4) in a first- and second-order relation to the hydrogen-ion concentration (see Eq. (8), Figs. 6 and 7). On the basis of these results, the reaction mechanism of the ligand-substitution reactions of nickel(II)-NDAP, -NDAIP, and -TDA complexes with EDTA was assumed to be as follows:

$$NiX^- + HY^{3-} \overset{k_{NiX}^{HY}}{\rightleftharpoons} \begin{Bmatrix} NiY^{2-} \\ \downarrow\uparrow \\ NiHY^- \end{Bmatrix} + HX^{2-} \quad (3)$$

$$NiX^- + H_2Y^{2-} \overset{k_{NiX}^{H_2Y}}{\rightleftharpoons} \begin{Bmatrix} NiY^{2-} \\ \downarrow\uparrow \\ NiHY^- \end{Bmatrix} + H_2X^- \quad (4)$$

$$NiX^- \underset{k_a^-}{\overset{k_{NiX}}{\rightleftharpoons}} Ni^{2+} + X^{3-} \quad (5)$$

$$NiX^- + H^+ \underset{k_b^-}{\overset{k_{NiX}^H}{\rightleftharpoons}} Ni^{2+} + HX^{2-} \quad (6)$$

$$Ni^{2+} + \begin{Bmatrix} Y^{4-} \\ \downarrow\uparrow \\ \vdots \\ \downarrow\uparrow \\ H_4Y \end{Bmatrix} \overset{k_j^+}{\rightleftharpoons} \begin{Bmatrix} NiY^{2-} \\ \downarrow\uparrow \\ NiHY^- \end{Bmatrix} + jH^+ \quad (7)$$

On the other hand, the initial rate of the reaction of the nickel(II)-TDA complex with CyDTA was: (1) independent of the concentration of uncomplexed TDA and also of the initial concentration of CyDTA (see Fig. 3); (2) proportional to the initial concentration of the Ni(II)-TDA complex, and (3) linear to the hydrogen-ion concentration (see Fig. 8). These results indicate that the reaction of the nickel(II)-TDA complex with CyDTA proceeds only through the complete dissociation of the Ni(II)-TDA complex, as is shown in Eqs. (5)—(7). The relation of $\sum_{j=0}^{4} k_j^+[H_jY^{(4-j)-}] \gg k_a^-[X^{3-}]+k_b^-[HX^{2-}]$, was fulfilled because the initial rate was independent of the concentrations of uncomplexed NDAP, NDAIP, and TDA. Judging from the equilibrium constant,[8] the protonated complex, NiHX, in Eq. (1) was not expected to be present in any appreciable concentration under the present experimental conditions.

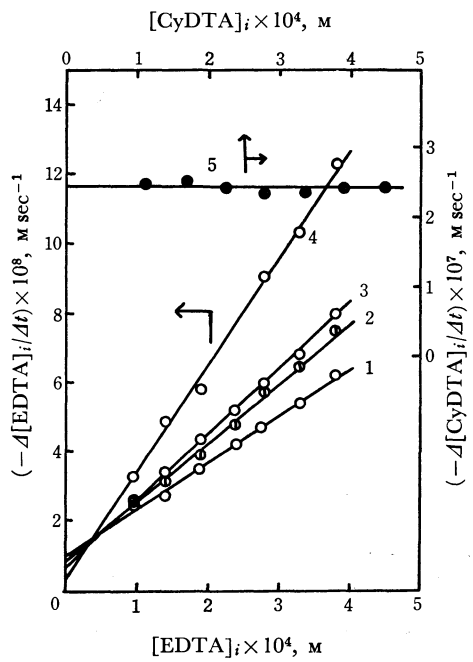

Fig. 3. Initial rates (V_i^+) as a function of the concentrations of entering ligands ($[EDTA]_i$ and $[CyDTA]_i$) in acetate buffer-potassium nitrate solutions of ionic strength 0.2 at 25°C. Initial concentrations of Ni(II)-NDAP and Ni(II)-TDA complexes are 3.09×10^{-4} M (curves 1, 2, 3 and 4) and 2.06×10^{-4} M (curve 5) respectively. The pH's of the solutions are (1) pH 5.08, (2) pH 5.30, (3) pH 5.46, (4) pH 5.81 and (5) pH 5.52.

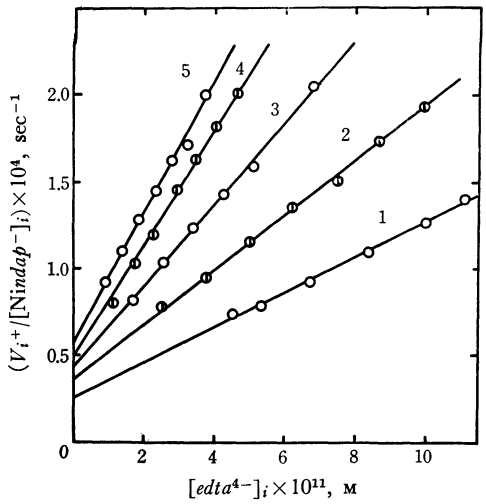

Fig. 4. $V_i^+/[Ni\,ndap^-]_i$ as a function of $[edta^{4-}]_i$ in acetate buffer-potassium nitrate solutions of ionic strength 0.2 at 25°C. Initial concentration of Ni(II)-NDAP complex is 6.18×10^{-4} M. The pH's of the solutions are (1) pH 5.17, (2) pH 5.04, (3) pH 4.95, (4) pH 4.88 and (5) pH 4.82.

From the reaction mechanism, the expressions for the rates of decrease from the initial concentration, $[EDTA]_i$ and $[CyDTA]_i$, can be derived as:

$$-\Delta[EDTA]_i/\Delta t = [NiX^-]_i\{k_{NiX} + k_{NiX}^H[H^+] + (k_1[H^+]+k_2[H^+]^2)[Y^{4-}]_i\} \quad (8)$$

where

$$k_1 = k_{NiX}^{HY}/K_{HY},\ k_2 = k_{NiX}^{H_2Y}/(K_{HY}K_{H_2Y}),$$

$$[Y^{4-}]_i = [EDTA]_i/\alpha_H$$

$$\alpha_H = 1 + [H^+]/K_{HY} + [H^+]^2/(K_{HX}K_{H_2Y}) + [H^+]^3/(K_{HY}K_{H_2Y}K_{H_3Y}) + [H^+]^4/(K_{HY}K_{H_2Y}K_{H_3Y}K_{H_4Y}) \quad (8')$$

and

8) N. Tanaka and M. Kimura, *Sci. Repts. Tohoku Univ. Ser. I*, **50**, 203 (1967).

$$-\Delta[\mathrm{CyDTA}]_i/\Delta t = [\mathrm{NiX}^-]_i(k_{\mathrm{NiX}} + k^{\mathrm{H}}_{\mathrm{NiX}}[\mathrm{H}^+]) \quad (9)$$

In these equations, the initial concentrations, $[\mathrm{EDTA}]_i$, $[\mathrm{NiX}^-]_i$ and $[\mathrm{CyDTA}]_i$, are substituted for [EDTA], [NiX$^-$], and [CyDTA] respectively. The changes in their concentrations during the period of the measurement of the initial rate of the reaction were considered to be negligibly small under the present conditions. Equation (8) indicates that if the values of $V_i^+/[\mathrm{NiX}^-]_i$ are plotted against $[\mathrm{Y}^{4-}]_i$ (or $[\mathrm{EDTA}]_i$) when all quantities but $[\mathrm{EDTA}]_i$ are kept constant, a straight line should be obtained with an intercept at $[\mathrm{Y}^{4-}]_i=0$ given by:

$$(\mathrm{Intercept}) = k_{\mathrm{NiX}} + k^{\mathrm{H}}_{\mathrm{NiX}}[\mathrm{H}^+] \quad (10)$$

and a slope given by:

$$(\mathrm{Slope}) = k_1[\mathrm{H}^+] + k_2[\mathrm{H}^+]^2 \quad (11)$$

Therefore, if the values of the intercept and the slope obtained at various concentrations of hydrogen ion are plotted against the hydrogen-ion concentrations, the values of the rate constants in Eq. (8) can be determined. In the case of the reaction of the nickel(II)-TDA complex with CyDTA, the $V_i^+/[\mathrm{NiX}^-]_i$ obtained from Eq. (9) corresponds to Eq. (10) itself.

Determination of the Rate Constants of the Reactions of Ni(II)-NDAP and Ni(II)-NDAIP Complexes with EDTA. The initial rate (V_i^+) was measured for the reactions of nickel(II)-NDAP and -NDAIP complexes with varied concentrations of EDTA, but a constant concentration of other species present and at constant pH. Several examples of the plots of V_i^+ *vs.* $[\mathrm{EDTA}]_i$ and $V_i^+/[\mathrm{NiX}^-]_i$ *vs.* $[\mathrm{Y}^{4-}]_i$ are given in Figs. 3, 4, and 5 (Fig. 3 shows one example of V^+ *vs.* $[\mathrm{CyDTA}]_i$ together with the plots of V_i^+ *vs.* $[\mathrm{EDTA}]_i$).

The intercepts and the slopes of the plots, $V_i^+/[\mathrm{NiX}^-]_i$ *vs.* $[\mathrm{Y}^{4-}]_i$, correspond to Eqs. (10) and (11) respectively. The intercepts and the slopes were also plotted against the hydrogen-ion concentrations according to Eqs. (10) and (11). These plots are shown in Figs. 6 and 7, from which the values of the rate constants in Eq. (8) were determined.

The rate constants for reactions (3) and (4) were calculated from the relations given in Eq. (8′). The results are shown in Table 2.

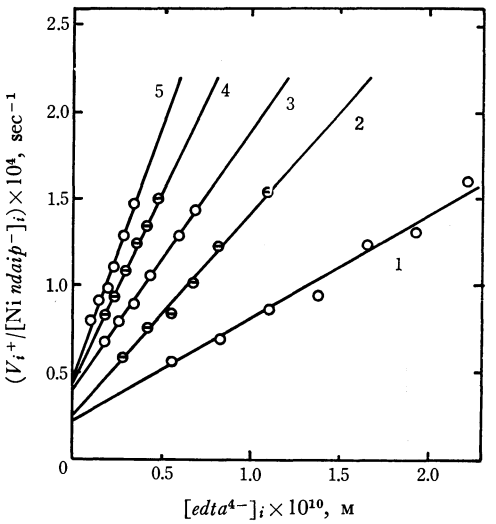

Fig. 5. $V_i^+/[\mathrm{Ni}\ ndaip^-]_i$ as a function of $[edta^{4-}]_i$ in acetate buffer-potassium nitrate solutions of ionic strength 0.2 at 25°C. Initial concentration of Ni(II)-NDAIP complex is 6.18×10^{-4} M. The pH's of the solutions are (1) pH 5.22, (2) pH 5.08, (3) pH 4.94, (4) pH 4.86 and (5) pH 4.82.

The acid dissociation constants of EDTA, K_{HY}, $K_{\mathrm{H_2Y}}$, $K_{\mathrm{H_3Y}}$, and $K_{\mathrm{H_4Y}}$, which were used in the calculation of $k^{\mathrm{HY}}_{\mathrm{NiX}}$, $k^{\mathrm{H_2Y}}_{\mathrm{NiX}}$, and α_{H} are the same values as those employed in a previous study.[5]

Determination of the Rate Constants of the Reaction of the Ni(II)-TDA Complex with CyDTA. The initial rate, $-\Delta[\mathrm{CyDTA}]_i/\Delta t$, was measured at varied concentrations of hydrogen ion and at two different concentrations of $[\mathrm{Ni}\ tda^-]_i$ and $[\mathrm{CyDTA}]_i$. The values of $(-\Delta[\mathrm{CyDTA}]_i/\Delta t)/[\mathrm{Ni}\ tda^-]_i$ were then plotted against the hydrogen-ion concentrations. The results are given in Fig. 8. The rate constants of the dissociation reactions, (5) and (6), were obtained from the intercept and the slope in Fig. 8. The results are given in Table 2, together with the rate constants obtained from the other reaction systems.

Table 2. Rate constants at ionic strength 0.2 and 25°C

Reaction system	Rate constants*						Ref.
	k_{NiX}	$k^{\mathrm{H}}_{\mathrm{NiX}}$	$k^{\mathrm{HY}}_{\mathrm{NiX}}$	$k^{\mathrm{H_2Y}}_{\mathrm{NiX}}$	k_1	k_2	
Ni(*nta*)-HEDTA	3.4×10^{-5}	3.7	1.96	4.27×10^{-1}	1.45×10^{10}	6.3×10^{14}	5)
Ni(*nta*)-EDTA	3.0×10^{-5}	3.7	4.14	4.43×10^{-1}	6.7×10^{10}	1.2×10^{16}	5)
Ni(*nta*)-CyDTA	2.0×10^{-5}	3.8					4)
Ni(*ndap*)-EDTA	1.0×10^{-5}	2.4	3.27	3.89×10^{-1}	5.3×10^{10}	7.9×10^{15}	Thit study
Ni(*ndaip*)-EDTA	0.4×10^{-5}	2.5	1.73	2.84×10^{-1}	2.8×10^{10}	5.5×10^{15}	This study
Ni(*tda*)-CyDTA	8×10^{-4}	8.8×10					This study

* Units of rate constants: sec^{-1} for k_{NiX}; $l\ \mathrm{mol}^{-1}\ \mathrm{sec}^{-1}$ for $k^{\mathrm{H}}_{\mathrm{NiX}}$, $k^{\mathrm{HY}}_{\mathrm{NiX}}$ and $k^{\mathrm{H_2Y}}_{\mathrm{NiX}}$; $l^2\ \mathrm{mol}^{-2}\ \mathrm{sec}^{-1}$ for k_1; $l^3\ \mathrm{mol}^{-3}\ \mathrm{sec}^{-1}$ for k_2.

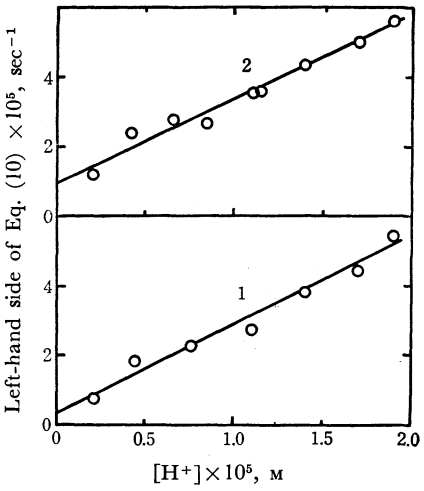

Fig. 6. Eq. (10) as a function of the hydrogen ion concentrations. Reaction systems are Ni *ndaip*-EDTA (curve 1) and Ni *ndap*-EDTA (curve 2). The conditions are the same as for Figs. 3, 4 and 5.

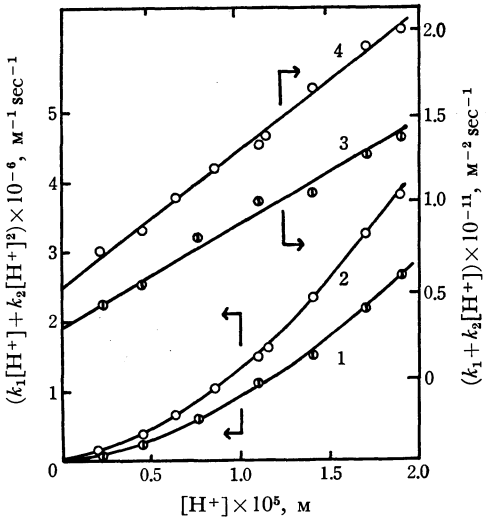

Fig. 7. Eq. (11) and Eq. (11)/[H⁺] as the functions of the hydrogen ion concentrations. Reaction systems are Ni *ndaip*-EDTA (curves 1 and 3) and Ni *ndap*-EDTA (curves 2 and 4). The conditions are the same as for Figs. 3, 4 and 5.

Discussion

Eigen[9,10] reported that, with most of the divalent transition metal ions in the first series, the rate of a complex-forming reaction of a metal ion with a ligand is independent of the nature of the ligand. If this assumption is satisfied, the rate of the dissociation reaction of a metal complex is expected to be dependent on the stability of the complex. The rate constants of the dissociation reactions of

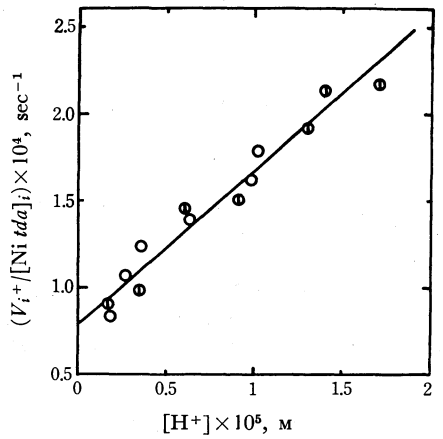

Fig. 8. $(-\Delta[\text{CyDTA}]_i/\Delta t)/[\text{Ni } tda^-]_i$ as a function of the hydrogen ion concentrations in acetate solutions of ionic strength 0.2 at 25°C. Initical oncentrations are $[\text{Ni } tda^-]_i = 2.06\times10^{-4}$ M (○) and 1.03×10^{-4} M (◑), and $[\text{CyDTA}]_i = 4.49\times10^{-4}$ M (○) and 2.25×10^{-4} M (◑). The concentrations of uncompleyed TDA are $[\text{TDA}]_f = 2\times10^{-5}$ M (○) and 1×10^{-5} M (◑).

nickel complexes in Table 2 indicate that the reaction becomes fast in the order of: NDAIP≦NDAP<NTA<TDA, which seems to be opposite to the order of the stability of the complex. Schwarzenbach *et al.*[1] reported that the third acid dissociation constant of TDA ($pK_{\text{H}tda}=8.16$) was larger than that of NTA ($pK_{\text{H}nta}=9.73$), and that the formation constants of the alkaline earth metal complexes with TDA were smaller than those of the corresponding complexes with NTA. These facts are consistent with the fact that the dissociation reaction of the TDA complex is faster than that of the NTA complex. The segment groups, CH_3 | $-CHCOOH$ in NDAIP and $-CH_2CH_2COOH$ in NDAP, seem to bond more strongly than any acetate group in NTA. This fact may be consistent with the statements by Chaberek and Martell,[2] and by Uehara *et al.*[3,6] that there is a considerable strain on the nitrogen atom in NTA coordinated with three five-membered rings, while a formation with one six-membered ring reduces the strain in NDAP, giving a more stable complex.

The author wishes to thank Professor N. Tanaka of Tohoku University for affording facilities for the elementary analysis and infrared measurements. He is also grateful to Drs. E. Kyuno and A. Uehara, Kanazawa University, for their kind advice concerning the syntheses of the chelating agents.

9) M. Eigen, "Advances in the Chemistry of Coordination Compounds," ed. by S. Kirschner, Macmillan, New York (1961), p. 371.
10) M. Eigen, *Pure Appl. Chem.*, **6**, 97 (1963).

BULLETIN OF THE CHEMICAL SOCIETY OF JAPAN VOL. 42 2849—2853 (1969)

Spectroscopic Studies of the Mixture of Dialkylaluminum 2-Aminoethoxide $(AlR_2OCH_2CH_2NR'_2)_2$ and Trialkylaluminum $(AlR''_3)_2$*1

Hideo SATO, Ryokichi TARAO and Hiromi HIGASHI

The Central Research Laboratories, Chisso Co., Ltd., Kamariya, Kanazawa-ku, Yokohama

(Received March 10, 1969)

The proton magnetic resonance and infrared spectra of the mixtures of dialkylaluminum 2-aminoethoxide $(AlR_2OCH_2CH_2NR'_2)_2$ and trialkylaluminum $(AlR''_3)_2$ were measured. Special attention was paid to the infrared frequencies of the NH_2 stretching and scissors bands and to the chemical shifts of the methyl groups attached to the aluminum and nitrogen atoms. From the results it was concluded that $(AlR''_3)_2$ reacts with $(AlR_2OCH_2CH_2NR'_2)_2$ to form a 1 : 1 coordination compound $AlR_2OCH_2CH_2NR'_2 \rightarrow AlR''_3$ quantitatively. At the same time, the redistribution and exchange reactions of the alkyl groups were observed.

It is known that trialkylaluminums $(AR''_3)_2$ such as $(AlMe_3)_2$ and $(AlEt_3)_2$ are associated to dimers and that rapid inter- and intramolecular exchanges of alkyl groups take place.[1,2] These exchange reactions are due to the weak bonding between aluminum atom and carbon atom of the bridged alkyls. $(AlR''_3)_2$ also forms 1 : 1 coordination compounds with ethers and amines. Although the bonding between aluminum atom and electron donors seems to be stronger than that between aluminum atom and carbon atom of the bridged alkyls, the alkyl group exchange is still observed in the mixture of such a coordination compound and $(AlR''_3)_2$.[3-5]

One of us obtained the crystals of the dimers of diethylaluminum 2-aminoethoxides $(AlEt_2OCH_2CH_2NRR')_2$ by reacting $(AlEt_3)_2$ with several aminoethanols $HOCH_2CH_2NRR'$; R,R'=H, alkyl, cycloalkyl, and/or aryl groups.[6] We investigated the structures of these comopunds spectroscopically and concluded that their structures could reasonably be repoesented by formula I with two NRR' $\rightarrow$Al coordination bonds.[7]

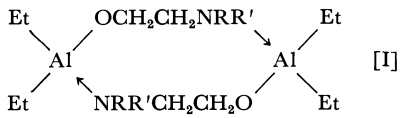

[I]

The behaviors of the mixture of $(AlR_2OCH_2CH_2NR'_2)_2$ and $(AlR''_3)_2$ seemed to be very interesting in comparison with the mixture of two trialkylaluminums——$(AlR_3)_2+(AlR'_3)_2$——and the mixture of trialkylaluminum and an electron donor, because $(AlR_2OCH_2CH_2NR'_2)_2$ may act as an electron donor ($-NR'_2$ group) and as an electron acceptor ($-AlR_2$ group) simultaneously. Therefore the mixture was studied by IR and NMR spectroscopically.

Experimental

Preparation of the Samples. $(AlEt_2OCH_2CH_2NH_2)_2$ and $(AlEt_2OCH_2CH_2NMe_2)_2$ were prepared by the reaction of $(AlEt_3)_2$ with the corresponding alkanolamine following the synthetic methods described previously.[7] $(AlMe_2OCH_2CH_2NMe_2)_2$ was obtained by the reaction of $(AlMe_3)_2$ with dimethylaminoethanol $HOCH_2CH_2NMe_2$ as white crystals (mp 116.5°C—118.5°C; Found: Al, 18.48%; mol wt, 304.7. Calcd for $Al_2C_{12}H_{32}O_2N_2$: Al, 18.58%; mol wt, 290.4). $(AlEt_3)_2$ and $(AlMe_3)_2$ were purchased from Ethyl Corp. and fractionally distilled before use.

Measurements of IR and NMR Spectra. The IR spectra of the dilute benzene solutions of the samples (the concentrations of the solutions were 1.10 g/100 m*l*) were measured in the 4000—420 cm^{-1} region by using KRS-5 liquid fixed cell of 0.5 mm thickness. A Japan Spectroscopic Co. Model DS-402G infrared spectrophotometer was used.

The NMR spectra were run on a Varian A-60A high resolution NMR spectrometer equipped with variable temperature accessories. About 0.5 m*l* of the solution of the sample (10% weight/volume solution) was injected into the sample tube by a hypodermic syringe under nitrogen atmosphere and sealed. Benzene was used as solvent for room temperature measurements

*1 Presented at the Symposium on Organometallic Compounds, Tokyo, October 1968.

1) N. Muller and D. E. Prichard, *J. Am. Chem. Soc.*, **82**, 248 (1960).

2) E. G. Hoffmann, *Trans. Faraday Soc.*, **58**, 642 (1962).

3) T. Mole, *Aust. J. Chem.*, **16**, 801 (1963).

4) T. Mole, *Chem. Ind. (London)*, **1964**, 281.

5) M. Kawai, T. Ogawa and K. Hirota, This Bulletin, **37**, 1302 (1964).

6) H. Higashi and S. Namikawa, *Kogyo Kagaku Zasshi (J. Chem. Soc. Japan, Ind. Chem. Sect.)*, **70**, 93, 368 (1976).

7) H. Sato, R. Tarao and H. Higashi, This Bulletin, **42**, 1588 (1969).

and toluene for high temperature measurements. The solvents were also used as internal references. The signal intensities were usually measured by an integrator.

Results and Discussion

The IR Spectra of the System $(AlEt_2OCH_2CH_2NH_2)_2+(AlEt_3)_2$. The IR spectrum of the benzene solution of $(AlEt_2OCH_2CH_2NH_2)_2$ is shown in Fig. 1a. The spectra of the mixtures of $(AlEt_2OCH_2CH_2NH_2)_2$ and $(AlEt_3)_2$ are shown in Figs. 1b, 1c and 1d together with the spectrum of triethylaluminum-*n*-propylamine $AlEt_3\cdot n\text{-}PrNH_2$ in Fig. 1e. For $(AlEt_2OCH_2CH_2NH_2)_2$, the bands at 3375 and 3309 cm^{-1} have been assigned to the NH_2 antisymmetric and symmetric stretching vibration and a sharp band at 1590 cm^{-1} to the NH_2 scissors respectively in a previous paper.[7]

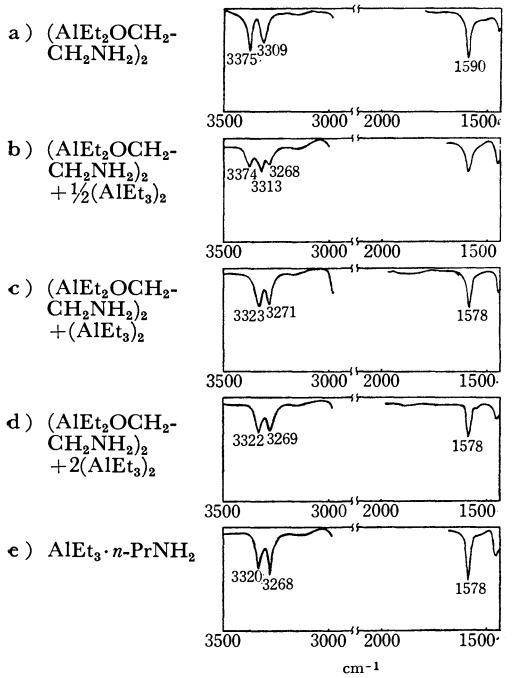

Fig. 1. The IR spectra of the systems $(AlEt_2OCH_2CH_2NH_2)_2+(AlEt_3)_2$.

The spectrum of the 1 : 1 mixture of $(AlEt_2OCH_2CH_2NH_2)_2$ and $(AlEt_3)_2$, Fig. 1c, shows the bands of the NH_2 stretching vibrations at 3323 and 3271 cm^{-1}, and the NH_2 scissors at 1578 cm^{-1}. These frequencies are almost equal to the values of the corresponding bands of $AlEt_3\cdot n\text{-}PrNH_2$, Fig. 1e, 3320, 3268 and 1578 cm^{-1} respectively. This fact is reasonably interpreted by the assumption that the NH_2 group in $(AlEt_2OCH_2CH_2NH_2)_2$ coordinates to the Al atom of $(AlEt_3)_2$. The NH_2 stretching vibrations of the 1 : 0.5 mixture, Fig. 1b, are clearly a superposition of those of Figs. 1a and 1c. The spectrum of the 1 : 2 mixture, Fig. 1d, shows the bands of NH_2 stretching vibrations at the same frequencies as those of the 1 : 1 mixture shown in Fig. 1c.

These observations lead to the conclusion that $(AlEt_3)_2$ forms a 1 : 1 coordination compound with $(AlEt_2OCH_2CH_2NH_2)_2$ quantitatively.

The NMR Spectra of the System $(AlMe_2OCH_2CH_2NMe_2)_2+(AlMe_3)_2$. The NMR spectra of the benzene solutions of the mixtures of $(AlR_2OCH_2CH_2NR'_2)_2$ and $(AlR''_3)_2$ (R=Me, Et, R'=H, Me, Et, R''=Me, Et) support the above conclusion obtained from the IR spectra. The result for the particular case where R, R' and R'' are methyl group will be described in detail, although similar conclusions are reached for all other cases. In Fig. 2a, the spectrum of the benzene solution of $(AlMe_2OCH_2CH_2NMe_2)_2$ is given. The 7.83 and the 5.28 ppm peaks are due to the methyl group attached to the Al atom and the N atom (hereafter abbreviated as the Al–Me group and the N–Me group) respectively. Two triplets at 5.14 and 3.67 ppm are assigned to the N-methylene group and O-methylene group respectively by taking the assignments given in Ref. 7 into consideration.

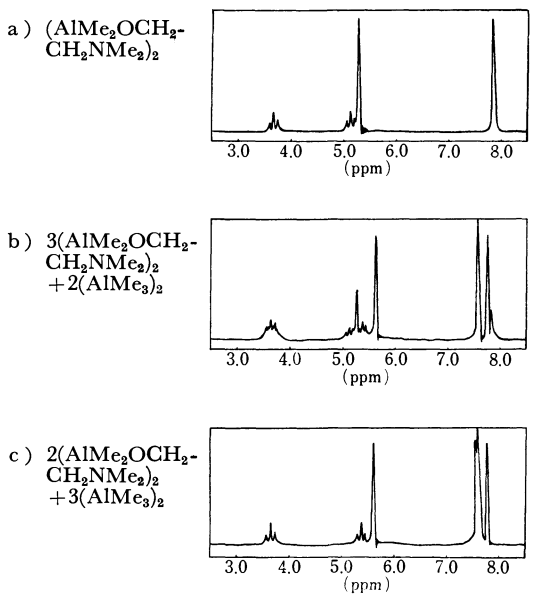

Fig. 2. The NMR spectra of the mixtures of $(AlMe_2OCH_2CH_2NMe_2)_2$ and $(AlMe_3)_2$.

The NMR spectrum of the 3 : 2 mixture of $(AlMe_2OCH_2CH_2NMe_2)_2$ and $(AlMe_3)_2$ is shown in Fig. 2b. There appear two new peaks due to the Al–Me group at 7.77 and 7.56 ppm, and also one new peak due to the N–Me group at 5.63 ppm.

The areas of the 7.77 ppm and the 5.63 ppm peaks are equal and the ratio of the areas of the 7.77 ppm and the 7.56 ppm peaks is 2 : 3. Thus the 7.56 ppm peak is assigned to the Al–Me group of $(AlMe_3)_2$ which is coordinated by the N atom in $(AlMe_2OCH_2CH_2NMe_2)_2$. The spectrum of

the 2 : 3 mixture is shown in Fig. 2c. The 7.83 ppm peak due to the Al–Me group and the 5.28 ppm peak due to the N–Me group of $(AlMe_2OCH_2CH_2NMe_2)_2$ disappear and excess $(AlMe_3)_2$ gives the peak at 7.53 ppm.

These observations support the conclusion that $(AlMe_2OCH_2CH_2NMe_2)_2$ and $(AlMe_3)_2$ form a 1 : 1 coordination compound quantitatively.

The Molecular Weight of the 1 : 1 Coordination Compound of $(AlMe_2OCH_2CH_2NMe_2)_2$ and $(AlMe_3)_2$. As to the structure of this coordination compound, there are two possible formulas II (monomeric) and III (dimeric).

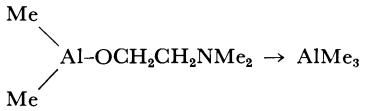

[II]

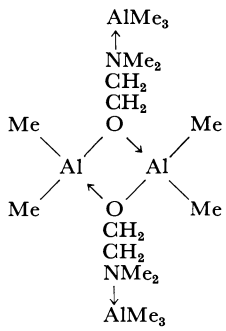

[III]

In order to determine which formula is preferable, the freezing point depression of the benzene solution of the 1 : 1 mixture of $(AlMe_2OCH_2CH_2NMe_2)_2$ and $(AlMe_3)_2$ was measured. The results are shown in Fig. 3. The molecular weight obtained by extrapolation to the infinite dilution is a little larger than the value calculated by assuming the monomeric formula II. If the coordination compound is a mixture of species represented by formulas II and III, two triplets due to the *O*-methylene group should be expected, but only one triplet is observed. Therefore the coordination compound might exist in an equilibrium represented by Eq. (1) in the benzene solution.

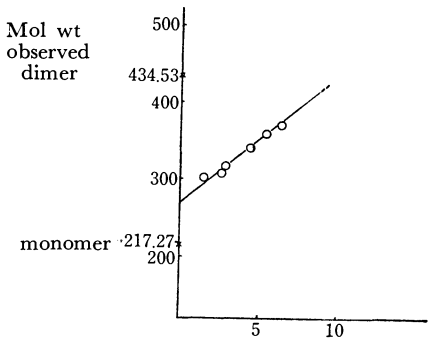

$AlMe_2OCH_2CH_2NMe_2 \rightarrow AlMe_3$ wt%
$(AlMe_2OCH_2CH_2NMe_2\ 50\pm2$ mol%)

Fig. 3. Concentration dependence of molecular weight of the coordination compound $AlMe_2OCH_2CH_2NMe_2 \rightarrow AlMe_3$.

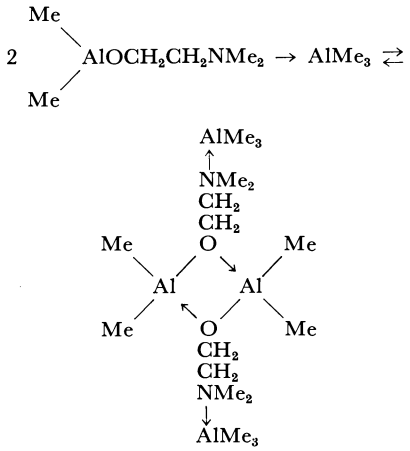

(1)

Although the possibility of the existence of the dimeric species could not be completely excluded, the molecular weight extrapolated to infinite dilution apparently suggests the predominance of monomeric species; so, in the following discussion, the structure of the coordination compound will be considered as given by formula II (monomeric).

The Redistribution Reactions of the Alkyl Groups. As described previously, there exist the following species in the mixture of $(AlR_2OCH_2CH_2NR'_2)_2$ and $(AlR''_3)_2$ depending on the molar ratio.

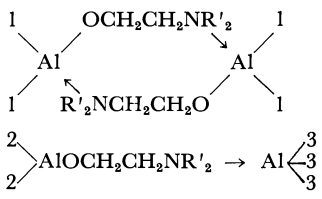

when $(AlR_2OCH_2CH_2NR'_2)_2$ is in excess

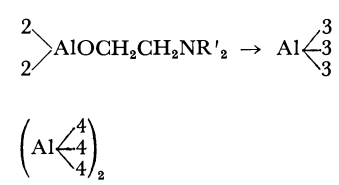

when $(AlR''_3)_2$ is in excess

(The numbers 1, 2, 3 and 4 mean the sites to be occupied by the Al–R groups. For example, the methyl group at site 1 will be hereafter abbreviated as 1-Me.)

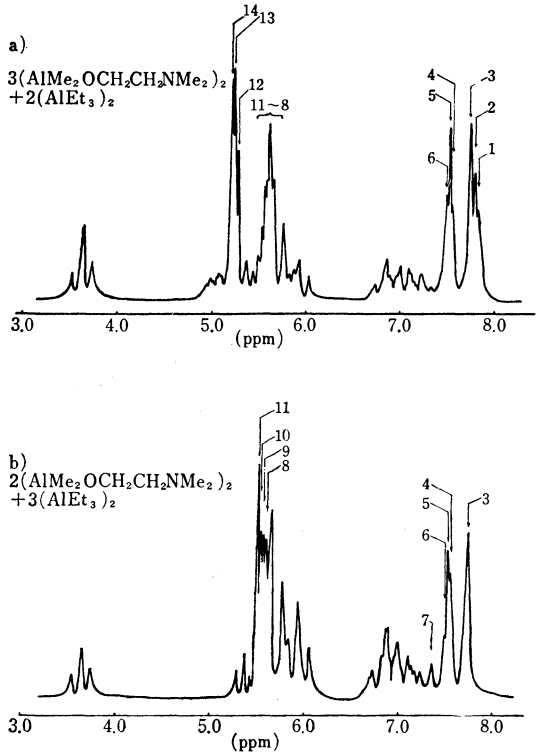

Fig. 4. The NMR spectra of the mixtures of $(AlMe_2OCH_2CH_2NMe_2)_2$ and $(AlEt_3)_2$.

When R differs from R″, the redistribution of the alkyl groups is observed in the NMR spectra. The NMR spectra of the benzene solutions of the mixtures of $(AlMe_2OCH_2CH_2NMe_2)_2$ and $(AlEt_3)_2$ are shown in Figs. 4a and 4b. If the redistribution of the alkyl groups does not take place, 3-Me peak would not be observed. In Figs. 4a and 4b, however, the 7.56 ppm peak is reasonably assigned to the 3-Me by taking the assignments of the spectrum of the mixture of $(AlMe_2OCH_2CH_2NMe_2)_2$ and $(AlMe_3)_2$ into consideration. These observations show clearly the existence of the redistribution of the Al-R groups.

The 3-Me group gives a fine structure of three peaks corresponding to the following formulas respectively as the result of the redistribution of

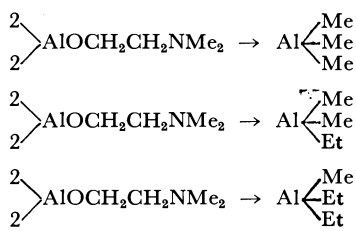

the alkyl groups. Also, the 5.28 ppm peak due to the N-Me group in $(AlRR'OCH_2CH_2NMe_2)_2$ gives a fine structure of three peaks corresponding to the following formulas respectively.

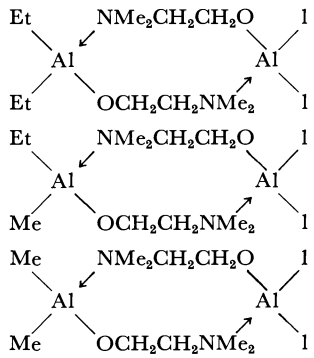

These fine structures of the N-Me group owing to the redistribution of the Al-R groups provide a strong evidence that N atom in $(AlR_2OCH_2CH_2NR'_2)_2$ coordinates to the Al atom and supports the conclusion reported as to the structures of these compounds in Ref. 7. The assignments of the N-Me and Al-Me groups in Figs. 4a and 4b are summarized in Table 1.

Table 1. The assignments of the Al-Me and N-Me peaks in the NMR spectra of the mixtures of $(AlMe_2OCH_2CH_2NMe_2)_2$ and $(AlEt_3)_2$

No. of peak	Assignment	Chemical shift*
1	1-Me ($AlEtMe$)	7.85
2	1-Me ($AlMe_2$)	7.83
3	2-Me ($AlMe_2$+$AlEtMe$)	7.77
4	3-Me ($AlEt_2Me$)	7.58
5	3-Me ($AlEtMe_2$)	7.57
6	3-Me ($AlMe_3$)	7.56
7	4-Me	7.38
8	N-Me (NMe_2 → $AlMe_3$)	5.63
9	N-Me (NMe_2 → $AlEtMe_2$)	5.60
10	N-Me (NMe_2 → $AlEt_2Me$)	5.58
11	N-Me (NMe_2 → $AlEt_3$)	5.55
12	N-Me (NMe_2 → $AlMe_2O$-)	5.28
13	N-Me (NMe_2 → $AlEtMeO$-)	5.26
14	N-Me (NMe_2 → $AlEt_2O$-)	5.24

* ppm from benzene peak.

In the mixture of $(AlMe_3)_2$ and $(AlEt_3)_2$, a rapid exchange of the alkyl groups is observed, and it has been shown that the methyl group prefers to occupy the bridge position from six to seven times as much as the ethyl group.[8] In the system under investigation, there are four sites to be occupied by the alkyl groups. To see if such a selectivity exists among the four sites as observed in the system of $(AlMe_3)_2$ and $(AlEt_3)_2$, the distribution of the methyl group among the four sites was measured. The results are shown in Figs. 5a and 5b. The dotted lines are theoretical curves obtained by as-

8) O. Yamamoto and K. Hayamizu, *J. Phys. Chem.*, **72**, 822 (1968).

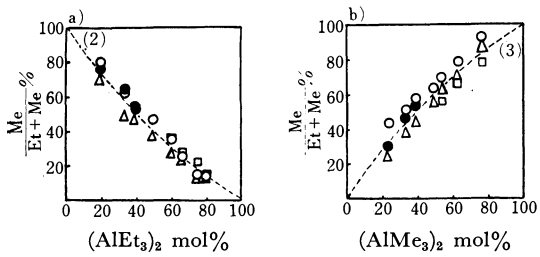

Fig. 5. The distribution of the methyl group.
a) $(AlMe_2OCH_2CH_2NMe_2)_2+(AlEt_3)_2$
b) $(AlEt_2OCH_2CH_2NMe_2)_2+(AlMe_3)_2$
● 1-Me ○ 2-Me △ 3-Me □ 4-Me

suming that the methyl and ethyl groups distribute to the four sites at random and expressed by the following equations. We have for the mixture of $(AlMe_2OCH_2CH_2NMe_2)_2$ and $(AlEt_3)_2$

$$y = \frac{200x}{300-x}, \tag{2}$$

and for the mixture of $(AlEt_2OCH_2CH_2NMe_2)_2$ and $(AlMe_3)_2$

$$y = \frac{300(100-x)}{300-x}, \tag{3}$$

where x is molar ratio (per cent) of $(AlR_2OCH_2CH_2NMe_2)_2$ and y is the ratio (per cent) of the methyl group. The agreement of the experimental data with the theoretical curves (Fig. 5) shows that the methyl and ethyl groups distribute to the four sites at random.

The Exchange Reactions of the Alkyl Groups. After the redistribution reaction took place, the rapid exchange of the alkyl group is not observed at room temperature except for the 4-alkyl group. Chemical shifts of the 4-Me signals in the mixture of $(AlR_2OCH_2CH_2NMe_2)_2$ and $(AlR''_3)_2$ are shown in Fig. 6. These tendencies observed in Fig. 6 could be explained according to the fact that the methyl group prefers to occupy the bridge position from six to seven times as much as the ethyl group in the mixture of $(AlMe_3)_2$ and $(AlEt_3)_2$.

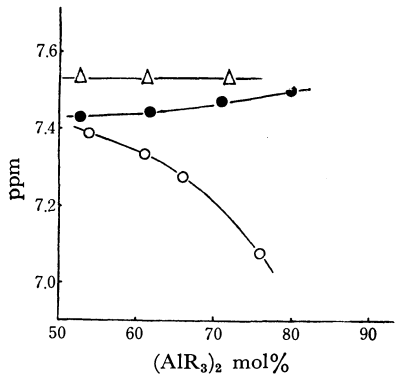

Fig. 6. Chemical shifts of the 4-Me signals in the mixture of $(AlR_2OCH_2CH_2NMe_2)_2$ and $(AlR''_3)_2$.
△ $(AlMe_2OCH_2CH_2NMe)_2+(AlMe_3)_2$
● $(AlEt_2OCH_2CH_2NMe_2)_2+(AlMe_3)_2$
○ $(AlMe_2OCH_2CH_2NMe_2)_2+(AlEt_3)_2$

When the temperature of the system is raised to 100°C, the rapid exchanges of the alkyl groups are observed except for the 1-alkyl group. The NMR spectra of the Al-Me group of the mixtures of $(AlMe_2OCH_2CH_2NMe_2)_2$ and $(AlMe_3)_2$ are shown in Figs. 7a and 7b. In Fig. 7a, the 2-Me

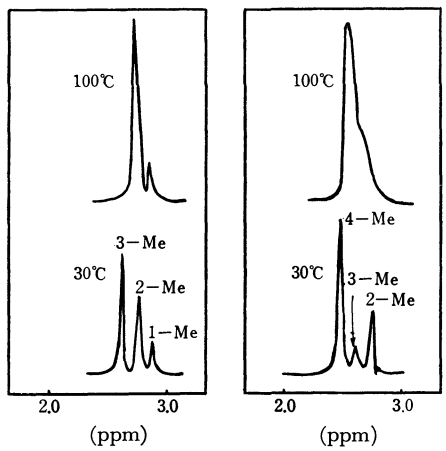

a) $3(AlMe_2OCH_2CH_2NMe_2)_2 + 2(AlMe_3)_2$
b) $(AlMe_2OCH_2CH_2NMe_2)_2 + 4(AlMe_3)_2$

Fig. 7. Temperature dependence of signal shape of the Al-Me group in the system of $(AlMe_2OCH_2CH_2NMe_2)_2$ and $(AlMe_3)_2$.

and the 3-Me peaks coalesce into a single peak, while the 1-Me peak only broadens slightly. This fact suggests that the 1-alkyl group is less mobile than the alkyl groups at any other site.

The authors are indebted to Dr. Osamu Yamamoto and Miss Kikuko Hayamizu of the Government Chemical Industrial Research Institute, Tokyo, and to Professors Takehiko Shimanouchi and Ichiro Nakagawa of the University of Tokyo for valuable discussions.

They would also like to express their thanks to Mr. Tsutomu Kinoshita for his continued interest in this work.

BULLETIN OF THE CHEMICAL SOCIETY OF JAPAN VOL. 42 2854—2857 (1969)

Thermal Decomposion Reactions of Chromium(III) Complexes. Hexammine, Chloropentammine and *cis*-Dichlorotetrammine Complexes

Nobuyuki TANAKA

Department of Chemistry, Faculty of Science, Tohoku University, Katahira-cho, Sendai

and Kenzo NAGASE

Department of Chemistry, College of General Education, Tohoku University, Kawauchi, Sendai

(Received March 14, 1969)

The thermal decomposition reactions of $[Cr(NH_3)_6]Cl_3$, $[CrCl(NH_3)_5]Cl_2$ and *cis*-$[CrCl_2(NH_3)_4]Cl$ in solid state were studied by the manometric, infrared spectroscopic and reflectance spectroscopic methods. The decomposition of these complexes in vacuum was initiated by substitution of an outer-sphere chloride ion for a coordinated ammonia. The rate constants, activation energies and activation entropies of these substitution reactions were obtained and the possible reaction processes were discussed. The products *cis,cis*-$[CrCl_3(NH_3)_3]$ and *cis,trans*-$[CrCl_3(NH_3)_3]$ were obtained on the heating of *cis*-$[CrCl_2(NH_3)_4]Cl$.

The thermal decomposition of ammine complexes of chromium(III) has been extensively investigated. Generally, these complexes were found to lose ammonia upon heating and to form non-electrolytes. Schlesinger *et al.*[1,2] obtained a green insoluble product $[CrCl_3(NH_3)_3]$ on the heating of $[CrCl(NH_3)_5]Cl_2$ in an atmosphere of dry hydrogen chloride but its structure has not been proposed. The complex of the same composition, $[CrCl_3(NH_3)_3]$, had been prepared by Werner and Halben[3] from an aqueous solution, but it was described as a blue-green solid.

Wendlandt and Chou[4] studied the thermal properties of several hexamminechromium(III) complexes by means of thermogravimetric analysis, differential thermal analysis and reflectance spectroscopy. They reported that the decomposition took place according to the equations

$$[Cr(NH_3)_6]X_3 \rightarrow [CrX(NX_3)_5]X_2 + NH_3 \quad (1)$$

$$[CrX(NH_3)_5]X_2 \rightarrow [CrX_3(NH_3)_3] + 2NH_3 \quad (2)$$

$$4[CrX_3(NH_3)_3] \rightarrow 3CrX_3 + CrN + 3NH_4X + 8NH_3 \quad (3)$$

where X represents Cl or Br.

Stembridge[5] prepared the triammine intermediate in an atmosphere of hydrogen chloride, ammonia and nitrogen, and reported that each preparation gave an identical compound as determined by X-ray diffraction and differential thermal analysis.

In the present paper, the kinetic studies of the substitution reaction between a coordinated ammonia and an outer-sphere chloride ion are presented. The formation of the blue and the green type of $[CrCl_3(NH_3)_3]$ on the heating of *cis*-$[CrCl_2(NH_3)_4]Cl$ is described, and their infrared and reflectance spectra are demonstrated.

Experimental

Apparatus and Procedure. Pressure-time curves of amminechromium(III) complexes were obtained with the apparatus reported in a previous paper.[6] The temperature of the furnace was kept within $\pm 0.5°C$. The pressure was measured with an accuracy of 1/100 mmHg by means of a mercury manometer and a microscope. The samples which were smaller than 200 mesh in size weighed 2 to 10 mg in each measurement.

The sample in a small crucible of about 1 m*l* in volume was placed in the reaction tube. The system of about 300 m*l* in volume was evacuated by a rotary pump for 1 hr. Then, the system was closed by operating a cock and the temperature of the furnace was rapidly elevated to that at which the reaction was to be investigated. After the temperature of the sample reached that of the furnace (about 20 min), the change of pressure with time was measured.

1) H. I. Schlesinger and R. K. Worner, *J. Am. Chem. Soc.*, **51**, 3520 (1929).

2) H. I. Schlesinger and D. N. Rickles, *ibid.*, **51**, 3523 (1929).

3) A. Werner and J. Halben, *Ber.*, **39**, 2668 (1906).

4) W. W. Wendlandt and C. Y. Chou, *J. Inorg. Nucl. Chem.*, **26**, 943 (1964).

5) W. W. Wendlandt and J. P. Smith, "The Thermal Properties of Transition-Metal Ammine Complexes," Elsevier, Amsterdam (1967), p. 109.

6) N. Tanaka and K. Nagase, This Bulletin, **40**, 546 (1967).

Results

$[Cr(NH_3)_6]Cl_3$. Figure 1 shows pressure-time curves which were obtained with various amounts of $[Cr(NH_3)_6]Cl_3$. The initial rate was found to increase linearly with the increase of the sample amount. A series of kinetic runs for $[Cr(NH_3)_6]Cl_3$ in a temperature range from 174°C to 210°C are given in Fig. 2, where the term α means the mole fraction of liberated ammonia to chromium(III) complex. The results in Fig. 2 suggest that $[Cr(NH_3)_6]Cl_3$ liberates one mole of ammonia below 190°C, but three moles of ammonia at higher temperatures. The infrared spectra of the product obtained at 190°C were identical with those of $[CrCl(NH_3)_5]Cl_2$. The product obtained at 210°C was green in color as reported by Schlesinger,[1,2] but was found to be accompanied by a small amount of ammonium chloride. The analytical data of the green compound after being washed with cold water agreed with the calculated values for $[CrCl_3(NH_3)_3]$. These results support the processes of Eqs. (1) and (2) which were reported by Wendlandt.[4] The first-order rate constants for the reaction of Eq. (1) were calculated from the plots given in Fig. 3.

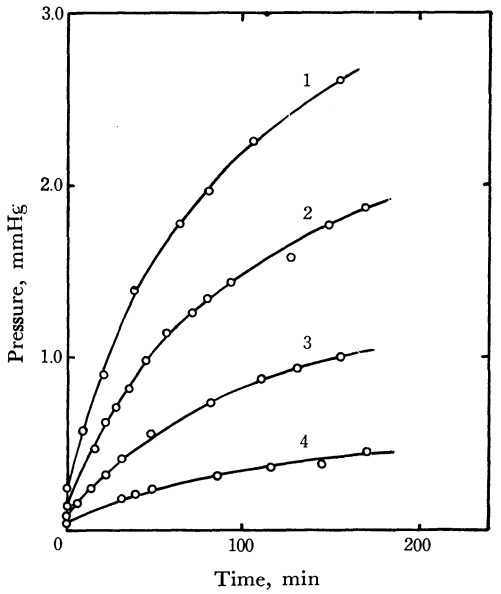

Fig. 1. Reaction rates with various sample amounts for $[Cr(NH_3)_6]Cl_3$ at 178°C.
(1) 15.2, (2) 10.1, (3) 5.0 and (4) 2.2 mg

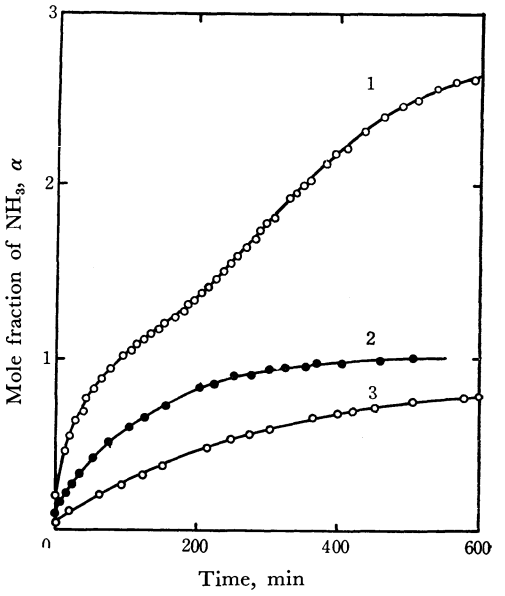

Fig. 2. Fractional decomposition curves of $[Cr(NH_3)_6]Cl_3$ at (1) 210, (2) 190 and (3) 174°C.

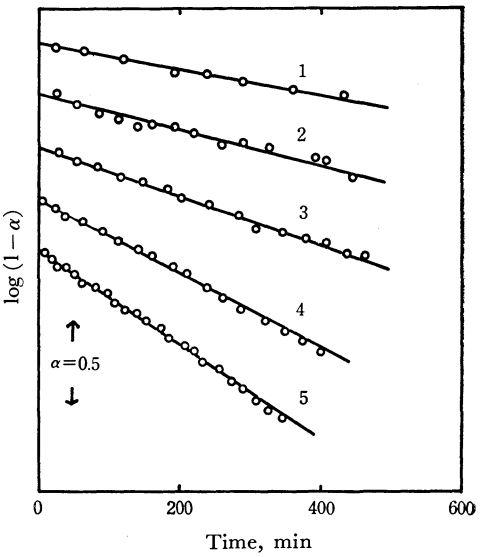

Fig. 3. Plots of the first-order rate function for $[Cr(NH_3)_6]Cl_3$ at (1) 170, (2) 174, (3) 177, (4) 183 and (5) 188°C.

$[CrCl(NH_3)_5]Cl_2$. In Fig. 4 are shown fractional decomposition curves of $[CrCl(NH_3)_5]Cl_2$ measured at various temperatures. The curve at 222°C indicates that $[CrCl(NH_3)_5]Cl_2$ liberates about two moles of ammonia. The product was green and its infrared spectra agreed with those of the product obtained from $[Cr(NH_3)_6]Cl_3$. On the curve at 210°C, however, the inflection point was observed, which suggests that an intermediate such as $[CrCl_2(NH_3)_4]Cl$ exists. In order to detect the intermediate, $[CrCl(NH_3)_5]Cl_2$ was heated at 220°C for 5 hr in a sealed tube. A green product was formed, and when it was treated with cold water, part of it was dissolved to give a green solution, suggesting the formation of *trans*-$[CrCl_2(NH_3)_4]Cl$.

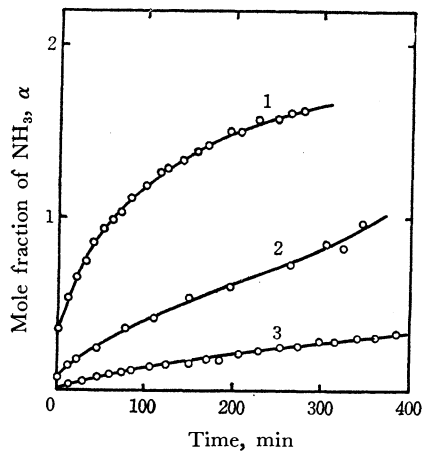

Fig. 4. Fractional decomposition curves of $[CrCl(NH_3)_5]Cl_2$ at (1) 222, (2) 210 and (3) 191°C.

***cis*-$[CrCl_2(NH_3)_4]Cl$.** In Fig. 5 are shown fractional decomposition curves of *cis*-$[CrCl_2(NH_3)_4]Cl$ measured at various temperatures. One mole of ammonia was liberated from *cis*-$[CrCl_2(NH_3)_4]Cl$. The product which was obtained by treating at 153°C for 3 hr was blue and its analytical data agreed with the calculated values for $[CrCl_3(NH_3)_3]$. When this blue compound was heated at 153°C for 3 days, the blue color gradually changed into green without any decomposition. The infrared spectra of both compounds are shown in Fig. 6. The blue compound gives symmetric deformation bands at 1280 and 1255 cm^{-1} and the NH_3 rocking bands at 780, 735 and 700 cm^{-1}, whereas the green compound gives the corresponding bands at 1280 and 735 cm^{-1}, respectively.

The reflectance spectra of both compounds are shown in Fig. 7. The blue compound in solid state has two absorptions at 17200 (the first band) and 23300 cm^{-1} (the second band), whereas the

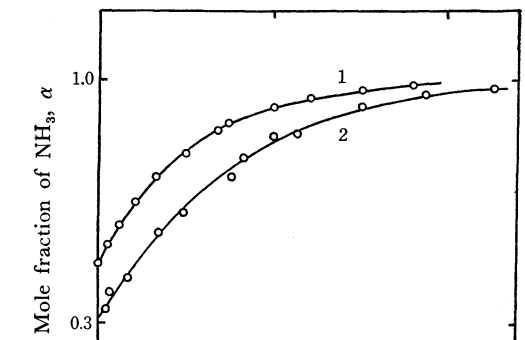

Fig. 5. Fractional decomposition curves of *cis*-$[CrCl_2(NH_3)_4]Cl$ at (1) 142 and (2) 136°C.

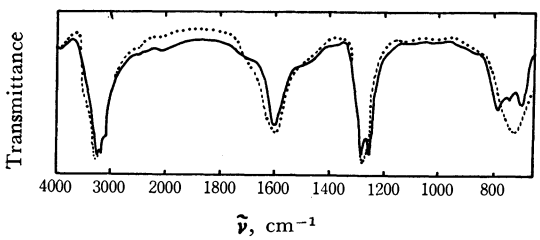

Fig. 6. Infrared absorption spectra of blue (solid line) and green (broken line) compounds in KBr disk.

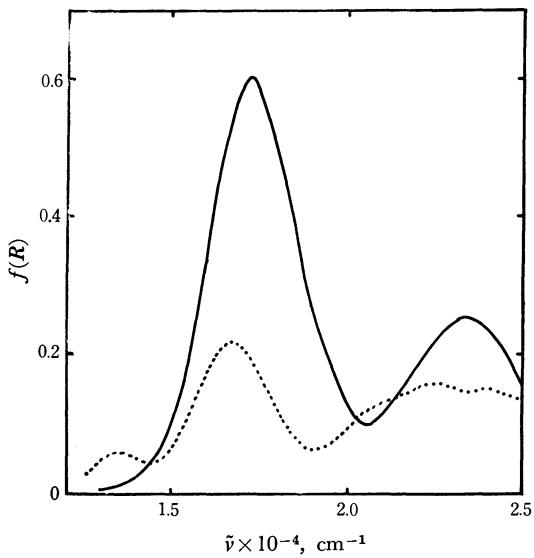

Fig. 7. Reflectance spectra of blue (solid line) and green (broken line) compounds. The spectra were plotted used the Kubelka-Munk function $f(R)=(1-R)^2/2R$, where R is the reflectance.

TABLE 1. X-RAY DIFFRACTION PATTERN OF $[CrCl_3(NH_3)_3]$ (CuK_α, $\lambda=1.5418$ Å)

Blue compound		Green compound	
d	*i*	*d*	*i*
5.609	m	5.644	m
5.539	s	5.574	s
5.215	f	5.277	m
4.901	m	5.126	m
4.796	f	4.928	m
3.739	m	3.969	m
3.708	m	3.900	f
3.132	f	3.770	f
2.979	m	2.849	m
2.867	f	2.831	f
2.747	m	2.763	m
2.557	s	2.747	m
2.398	f	2.730	m

s, strong; m, medium; f, fine

green compound has three absorptions. The weak absorption in a low energy region (13400 cm^{-1}) may be due to the spin-forbidden transition ($^4A_{2g} \rightarrow {}^2E_g$). The absorptions in the region of the second band split into three parts. The X-ray diffraction pattern of the blue compound was different from that of the green compound as shown in Table 1.

When *cis*-$[CrCl_2(NH_3)_4]Cl$ was heated at 165°C for 10 days in a sealed tube, a product which was partly dissolved in cold water to give a green solution was obtained. This fact suggests that the product contained an electrolyte such as *trans*-$[CrCl_2(NH_3)_4]Cl$.

Discussion

The kinetic parameters of the substitution reactions in solid state are given in Table 2. The order of increasing rates of reaction was as follows:

$$[CrCl(NH_3)_5]Cl_2 < [Cr(NH_3)_6]Cl_3 < cis\text{-}[CrCl_2(NH_3)_4]Cl$$

Table 2. Kinetic parameters for the substitution reaction of some chromium(III) complexes in solid state

Complex	$k \times 10^5$, sec^{-1} (Temp, °C)	E_a kcal/mol	ΔS^* e.u.
$[Cr(NH_3)_6]Cl_3$	4.0(174), 8.5(183)	30	−12
$[CrCl(NH_3)_5]Cl_2$	2.8(198), 7.7(210)	39	1.4
cis-$[CrCl_2(NH_3)_4]Cl$	11 (136), 16 (142)	31	−2.3

From the standpoint of a steric hindrance, *cis*-$[CrCl_2(NH_3)_4]Cl$ may most easily lose ammonia coordinated at the *cis*-position to both chloride ions. This led to the conclusion that trichlorotriammine complex obtained by heating of *cis*-$[CrCl_2(NH_3)_4]Cl$ must have a *cis,cis*-configuration. The *cis,cis*-configuration, however, is less stable than the *cis,trans*-configuration, if a steric hindrance is considered. Therefore, *cis,cis*-$[CrCl_3(NH_3)_3]$ will convert to *cis,trans*-$[CrCl_3(NH_3)_3]$ by heating for a long time.

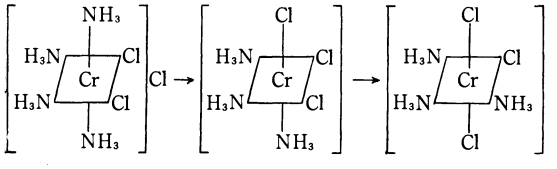

These considerations suggest that the blue and the green compounds obtained in the present study correspond to *cis,cis*-$[CrCl_3(NH_3)_3]$ and *cis,trans*-$[CrCl_3(NH_3)_3]$, respectively. The reflectance spectra shown in Fig. 7 also support the above consideration, *i. e.*, the absorption bands of the blue compound are symmetrical and their maxima are at higher frequencies than those of the absorption bands of the green compound.

Hexamminechromium(III) chloride had a small activation entropy, which suggests the possibility of a seven-coordinated activated complex. If the substitution reactions of hexammine complexes take place through a seven-coordinated state, kinetic parameters must be strongly influenced by an outer-sphere ion. Actually, the results obtained with $[Cr(NH_3)_6]Cl_3$ greatly differed from those obtained with $[Cr(NH_3)_6]Br_3$. The kinetic parameters for $[Cr(NH_3)_6]Br_3$ are:

$$k = 2.2 \times 10^{-5}\ sec^{-1} \text{ at } 192°C,$$
$$E_a = 43\ kcal/mol$$
and $$\Delta S^* = 12\ e.u.$$

From the above results and consideration, possible reaction processes of ammine chromium(III) complexes could be represented as follows:

$$[Cr(NH_3)_6]Cl_3 \xrightarrow{-NH_3} [CrCl(NH_3)_5]Cl_2 \xrightarrow{-NH_3}$$

$$\underset{\text{cis,trans-}[CrCl_3(NH_3)_3]}{\text{trans-}[CrCl_2(NH_3)_4]Cl} \xrightarrow[-NH_3]{\text{isomerization}} \underset{\text{cis,cis-}[CrCl_3(NH_3)_3]}{\text{cis-}[CrCl_2(NH_3)_4]Cl}$$

(A) (B)

However, the formation of *trans*-$[CrCl_2(NH_3)_4]Cl$ is not yet confirmed. As the process (B) was strongly depressed by the pressure of ammonia, *cis,cis*-$[CrCl_3(NH_3)_3]$ was obtained only by heating in vacuum. Therefore, the process (A) takes place to a considerable extent when *cis*-$[CrCl_2(NH_3)_4]Cl$ is heated under the pressure of ammonia.

The authors wish to express their thanks to Mr. Yoroshi Tsuda in the arrangement of the apparatus. They also thank the Ministry of Education for financial support.

BULLETIN OF THE CHEMICAL SOCIETY OF JAPAN VOL. 42 2858—2862 (1969)

Nitrosyl Complexes of Bis(acetylacetone)-, and Bis(benzoylacetone)-ethylenediimine Cobalt(II)

Motonori TAMAKI, Isao MASUDA and Koichiro SHINRA

Department of Applied Chemistry, Faculty of Engineering, Osaka University, Yamada, Suita, Osaka

(Received March 27, 1969)

Square, planar bis(acetylacetone)-, and bis(benzoylacetone)-etylenediimine-Co(II) chelates with a low-spin d^7 electron structure yield nitrosyl complexes with the chelate : NO molar ratio of 1 : 1. On the basis of the IR spectra and the NMR spectra, and on the basis of molecular-weight determinations, these nitrosyls have been considered as being penta-coordinate cobalt complexes with square-pyramidal configuration. The nitrosyls are diamagnetic, indicating an electron-pairing bond between the central Co(II) and the NO molecule. The NO groups in these nitrosyls have been postulated to be predominantly neutral. In the electronic spectra, these penta-coordinate, diamagnetic Co(II) complexes show a characteristic absorption band at 18—20×10^3 cm^{-1} with $\log\varepsilon\fallingdotseq3$.

The transition metal complexes of the bis(acetylacetone)-ethylenediimine Schiff base are considered to undergo two types of reaction with nitric oxide: i) at γ-carbon atoms in the chelate rings, and ii) at the central metal atom. The nickel(II) and palladium(II) complexes, in which the central metal ion has a spin-paired, d^7 electron structure, have already been shown to react with nitric oxide to produce oxime-type complexes such as are shown in Fig. 1.[1] This type of complex may be regarded as a product of i reaction.

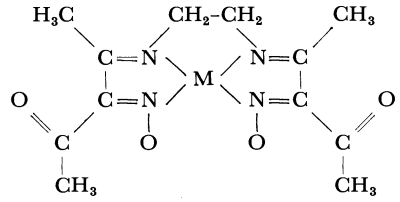

Fig. 1. M=Ni(II), Pd(II), Cu(II)

In the present work, divalent, low-spin cobalt(II) complexes with one unpaired electron will be shown to react with nitric oxide to form nitrosyl complexes, which are regarded as products of the ii reaction. These nitrosyl complexes are diamagnetic, and they are supposed to be penta-coordinate, square-pyramidal Co(II) complexes (Fig. 4) where the Co-NO bonding is essentially a σ-bond formed by one unpaired electron of NO and one of Co(II).

A copper(II) chelate with bis(acetylacetone)-ethylenediimine possessing one unpaired electron on the central metal ion yields either nitrosyl- or oxime-type complexes, depending on the experimental conditions.[1,2]

1) I. Masuda, M. Tamaki and K. Shinra, This Bulletin, **42**, 157 (1969).

Experimental

Materials. *The bis(acetylacetone)ethylenediimine*, AEH_2 *and bis(benzoylacetone)ethylenediimine*, BEH_2*[1] were prepared according to the method of the literatures.[3,4] AEH_2; recrystallized from water, mp 110—110.7°C. BEH_2; recrystallized from ethanol, mp 179.5—180.5°C.

Bis(acetylacetone)ethylenediimino-Co(II),[3] CoAE; purified by recrystallization from hot ether and then dried at 100°C *in vacuo* over P_2O_5; reddish yellow crystals.

Bis(benzoylacetone)ethylenediimino-Co(II),[4] CoBE; recrystallized from an acetone or benzene solution, and dried *in vacuo* over P_2O_5, at room temperature.

The nitric oxide was generated and purified by the method reported previously.[1]

Preparations of Nitrosyl Complexes. *Bis(acetylacetone)ethylenediimino-nitrosyl-cobalt(II)*, $Co^{II}AENO$.*[1] The complex can be prepared by the following three methods:

A) 2.8 g (0.01 mol) of CoAE were dissolved in 50 m*l* of dichloromethane. Nitric oxide was bubbled through this solution with ice cooling for about half an hour, by which time the solution had turned from reddish yellow to brown. Then, the nitric oxide in the solution was expelled with nitrogen gas. The addition of 250 m*l* of petroleum ether to the solution gave a precipitate of brownish-black compounds, which were then purified by recrystallization from a large volume of ether to give black crystals (complex I). The complex I is insoluble in water, and soluble in such

2) M. Tamaki, Y. Nigo, I. Masuda and K. Shinra, presented at the 21th Annual Meeting of the Chemical Society of Japan, Osaka, April, 1968.

*1 AEH_2 and BEH_2 represent bis(acetylacetone)-ethylenediimine and bis(benzoylacetone)ethylenediimine, respectively.

3) G. Morgan and J. Smith, *J. Chem. Soc.*, **1925**, 2030.

4) P. J. McCarthy, R. J. Hovey, K. Ueno and A. E. Martell, *J. Am. Chem. Soc.*, **77**, 5820 (1955).

Table 1. Elementary analyses of the complexes

Complex		Calcd %				Found %			
		Co	C	H	N	Co	C	H	N
I*	$CoC_{12}H_{18}N_3O_3$	18.97	46.30	5.78	13.50	19.14	46.29	5.99	13.46
I**	$CoC_{12}H_{18}N_3O_3$	18.97	46.30	5.78	13.50		45.27	5.62	13.68
II	$CoC_{22}H_{22}N_3O_3$	13.53	60.69	5.10	9.65	13.47	60.43	4.95	9.62

* Prepared by method A
** Prepared by method C

common organic solvents as ether, chloroform, dimethylformamide, and dimethyl sulfoxide. The results of the elementary analysis given in Table 1 correspond to that of the formula shown in Fig. 4.

B) CoAE, in the solid state, absorbs nitric oxide and yields the nitrosyl complex. Crystalline CoAE was allowed to stand in a nitric oxide atmosphere under a pressure of 760 mmHg, and at room temperature. The CoAE thereupon took up the nitric oxide and turned brownish-black. The recrystallization of this product from ether gave black crystals. Elementary analyses and a study of the IR spectrum indicated that the black compound obtained was identical with the complex I prepared by the method A.

C) The complex I was most expeditiously prepared by the following procedure. 2.5 g (0.01 mol) of cobaltaous acetate tetrahydrate were dissolved in 50 m*l* of methanol, and the air was expelled from the solution and reaction flask by flushing with nitrogen. Then the solution, with ice cooling, was saturated with nitric oxide until it had turned from a reddish violet to a dark violet. Then AEH_2 (2.3 g, 0.01 mol) dissolved in 50 m*l* of acetone was stirred into this dark-violet solution, drop by drop. The solution thereupon turned black. The nitric oxide in the solution was then driven off by nitrogen. The addition of petroleum ether to the solution gave a black precipitate of the crystalline, nitrosyl complex. The complex was proved by elementary analyses and by a study of the IR spectral data to be identical with the complex I.

Bis(benzoylacetone)ethylenediimino-nitrosyl-cobalt(II), Co^{II}-BENO.*[1] This complex was prepared according to the method C. In this case, however, because of the poor solubility of BEH_2, 3.5 g (0.01 mol) of it were suspended in 50 m*l* of acetone; then the mixture was saturated with nitric oxide, followed by the addition of 2.5 g (0.01 mol) of cobaltous acetate tetrahydrate in 50 m*l* of methanol. The black precipitate was recrystallized from acetone to give 2 g of black needles (complex II). The elementary analyses agreed with the formula shown in Fig. 4. The complex II is insoluble in water and soluble in common organic solvents, but it is, unlike the complex I, insoluble in ether.

Bis(salicylaldehyde)enthylenediimino - nitrosyl - cobalt(II), Co^{II}(Salen)NO.*[2] This complex has already been presented by Earnshaw *et al.*[5] In the present study it was prepared according to the method C. The complex obtained showed, in its IR spectrum, the same characteristic frequencies as those reported by Earnshaw,[5] and the analysis of the complex agreed with the structure written above.

Measurements and Results

Molecular weight was determined in chloroform solution at 25°C, with a Mechrolab vapor pressure osmometer 302. The results are listed in Table 2.

The magnetic measurements were carried out at room temperature by the Gouy method, using an aqueous nickel(II) chloride solution as the standard. The magnetic susceptibilities obtained at 20°C for solid samples were; -0.42×10^{-6} emu/g for the complex I, and -0.39×10^{-6} emu/g for the complex II. These values indicate that the complexes are diamagnetic.

Table 2. Molecular weight in $CHCl_3$

	Calcd*	Found
Complex I	311	303
Complex II	435	429

* Calculated on the basis of the formula shown in Fig. 4.

The thermogravimetric analysis (TGA) and the differential thermal analysis (DTA) were carried out by using a Rigakudenki thermobalance at a heating rate of about 2°C/min. The curves thus obtained are shown in Figs. 2 and 3. In the TGA curve of the complex I, the weight loss of

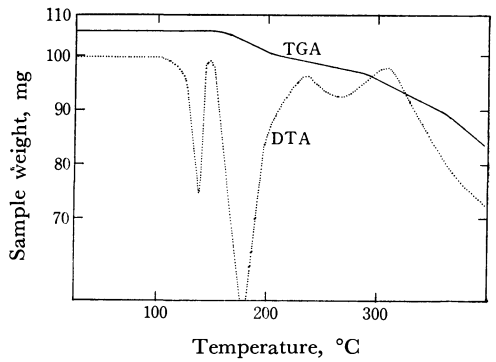

Fig. 2. DTA and TGA curves of complex I.

*2 $SalenH_2$ represents bis(salicylaldehyde)ethylenediimine.

5) A. Earnshaw, P. C. Hewlett and L. F. Larkworthy, *J. Chem. Soc.*, **1965**, 4718.

about 9% observed between 160°C—200°C corresponds to the calculated value of 9.7%; the weight loss is assumed to be caused by the loss of the nitric oxide in the complex (Fig. 4). In the case of the complex II, no weight loss was observed below 200°C, as is shown in Fig. 3, indicating that the complex II is more stable than the complex I.

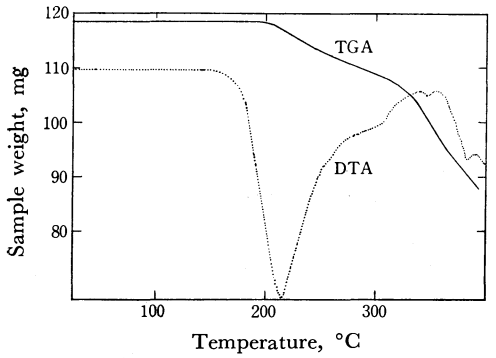

Fig. 3. DTA and TGA curves of complex II.

The NMR spectra were obtained with a Japan Electron Optics JNM-3H-60 spectrometer, at 60 Mc/sec, using tetramethylsilan (TMS) as the internal reference. The NMR spectrum of complex I in a 5 wt% $CDCl_3$ solution is, in Fig. 5, compared to the spectrum of the NiAE complex.

The IR spectra were measured in Nujol or in hexachlorobutadiene, using a Hitachi EPI-2G spectrometer for the 4000—650 cm^{-1} region. The IR spectra obtained for the complex I and II are shown in Figs. 6 and 7. The electronic absorption spectra of the complexes I and II, which were determined in chloroform using a Hitachi EPS-3 spectrophotometer, are shown in Fig. 8.

Discussion

The elementary analyses for the complexes I and II agreed well with those of the mono-nitrosyl derivatives of CoAE and CoBE respectively, as is shown in Fig. 4. The molecular weight, determined in chloroform, is consistent with this formula:

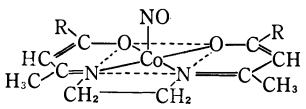

Fig. 4. Complex I: $R=CH_3$
Complex II: $R=C_6H_5$

NMR and IR Spectra. The above formulation of the complexes was examined further by the following considerations of the NMR and IR spectral evidence. As may be seen in Fig. 5, the NMR spectra of the complex I in $CDCl_3$ shows four peaks, at τ; 5.1, 6.5, 7.8, and 7.95, with an integral

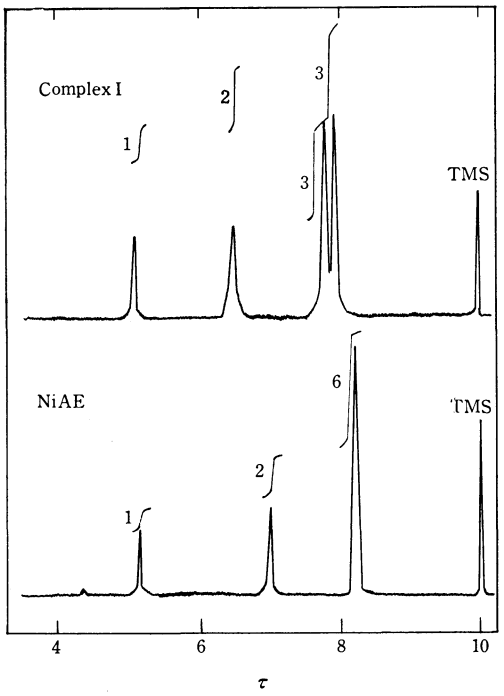

Fig. 5. NMR spectra of complex I and NiAE.

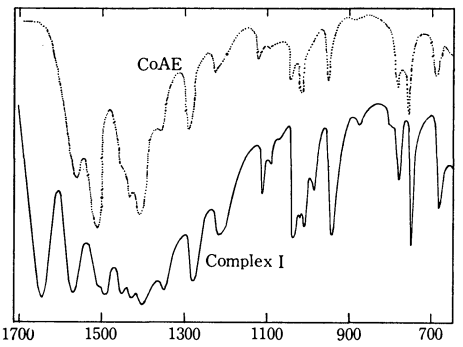

Fig. 6. IR spectra of complex I and CoAE.

ratio of 1 : 2 : 3 : 3 from the lower-side field. The features of this spectrum are quite similar to those of NiAE or $[CoAE(NH_3)_2]Cl$;[6] the above four resonances may, therefore, be assigned to the CH group, to the CH_2CH_2 group, and to two types of CH_3 groups of the complex (Fig. 4, $R=CH_3$) respectively.

A comparison of the IR spectrum of the complex I in the 1700—700 cm^{-1} range with that of the CoAE indicates that, as is shown in Fig. 6, the complex I has essentially the same pattern of frequencies as the CoAE, with the exception of a

6) H. Yoneda and Y. Morimoto, This Bulletin **41**, 2544 (1968); P. J. McCarthy and A. E. Martell, *Inorg. Chem.*, **6**, 781 (1967).

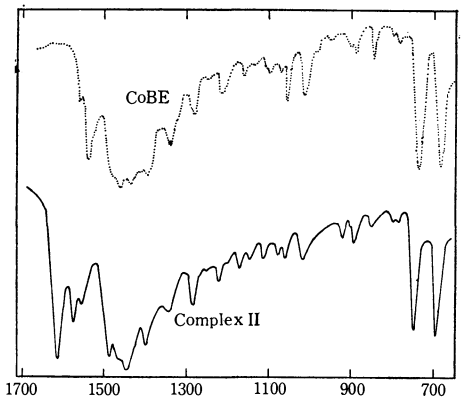

Fig. 7. IR spectra of complex II and CoBE.

new frequency at 1654 cm^{-1}. Similarly, the complex II shows the same frequencies as those of the CoBE except for a new frequency at 1635 cm^{-1}, as may be seen in Fig. 7. The new frequencies will be discussed later as being due to the nitric oxide group in the complexes (Fig. 4).

Thus, from the above-described NMR and IR spectral evidences and from the analytical results, we may assume such a nitrosyl structure for the two complexes, I and II, as is shown in Fig. 4, where the cobalt atom in the planar chelate is bound to a nitric oxide group to form a penta-coordinate, square pyramidal configuration. The nitrosyl complexes are monomeric in chloroform and contain, in the solid state, no solvent, as is indicated by the TGA curves (Figs. 2 and 3).

Most of the nitrosyl complexes have so far been characterized by a strong, nitrosyl-stretching frequency. Lewis *et al.*[7] have surveyed numerous nitrosyl complexes of transition metals on the basis of the nitrosyl frequencies in the IR spectra. In general, the position of the nitrosyl frequency is susceptible to the electronic structure of the nitrosyl group in the complex and to the nature of the central metal ion. For example, the NO frquency is observed at 1626 cm^{-1} for $\{(CH_3)_2NCS_2\}_2CoNO$, at 1673 cm^{-1} for $\{(C_2H_5)_2NCS_2\}_2FeNO$, and at 1845 cm^{-1} for $\{(CH_3)_2NCS_2\}_3RuNO$.[7] Hecne, it would be more appropriate to take into account analogous nitrosyl complexes containing the same metal ion when the nitrosyl frequency is taken as an indication of the structure of the complex. Table 3 lists the cobalt-nitrosyl complexes, along with the positions of their NO stretching frequencies. As can be seen in this table, most of these nitrosyl complexes, which are apparently penta-coordinate and diamagnetic, show the characteristic NO frequency in the 1623—1705 cm^{-1} range. As has been described before, the complexes I and II, which are penta-coordinate and diamagnetic, show new absorption bands at 1654 and 1635 cm^{-1} respectively. These new bands can reasonably be assigned to the NO stretching frequency on the basis of the facts presented in Table 3.

Lewis *et al.*[7] postulated two types of NO groups existing in complexes; the $(NO)^-$ anion which shows a $(NO)^-$ stretching frequency at around 1200 cm^{-1}, exemplified by $[Co(8\text{-aminoquinoline})_2NO]Cl_2$ (Table 3), and the $(NO)^+$ cation which is said to show a characteristic frequency over the

Table 3. IR characteristic frequencies and magnetic properties of nitrosyl complexes

Nitrosyl complex	NO str., cm^{-1}	Mag. property***	Ref.
Co{bis(acetylacetone)ethylenediimine}NO*	1654	d.m	present work
Co{bis(benzoylacetone)ethylenediimine}NO**	1635	d.m	present work
$Co(acetylacetonate)_2NO$	1675	d.m	8
Co{bis(salicylaldehyde)ethylenediimine}NO	1624	d.m	5
Co(*N,N'*-diethyldiselenocarbamate)$_2$NO	1623		9
Co(*N,N'*-dimethyldithiocarbamate)$_2$NO	1626	d.m	10, 11
Co(phthalocyanine)NO	1705		12
$[Co(ethylenediamine)_2NO](NO_3)_2$	1645	d.m	13
$[Co(8\text{-aminoquinoline})_2NO]Cl_2$	1170	3.45 B.M	14
$Na_2[Co(NO_2)_4(OH)NO]$	1740		7

* complex I ** complex II *** d.m, diamagnetic; B.M, Bohr Magneton

7) J. Lewis, R. J. Irving and G. Wilkinson, *J. Inorg. Nucl. Chem.*, **7**, 32 (1958); W. P. Griffith, J. Lewis and G. Wilkinson, *ibid.*, **7**, 38 (1958).
8) R. Nast and H. Bier, *Chem. Ber.*, **92**, 1958 (1959).
9) K. A. Jensen and V. Karishnan, *Acta Chem. Scand.*, **21**, 2904 (1967).
10) F. A. Miller and C. H. Wilkins, *Anal. Chem.*, **24**, 1253 (1952).
11) R. L. Carlin, F. Canziani and W. K. Bratton, *J. Inorg. Nucl. Chem.*, **26**, 898 (1964).
12) C. Ercolani, C. Neri and G. Sartori, *J. Chem. Soc.*, **A 1968**, 2123.
13) T. B. Jackson, M. J. Baker, J. O. Edwards and D. Tutas, *Inorg. Chem.*, **5**, 2046 (1966).
14) R. Nast, H. Bier and J. Gremm, *Chem. Ber.*, **94**, 1185 (1961).

wide range from 1626 to 1938 cm^{-1}.[7] Accepting their point of view, the complexes I and II should contain $(NO)^+$ and, consequently, Co(I). However, the complexes are actually more stable than Co(I) complexes might be expected to be. The polarographic behavior*3 indicated that these complexes contained neutral NO and Co(II). Thus, it seems more probable to ascribe the new bands observed at 1654 or 1635 cm^{-1} in the present complexes to the stretching frequency of predominantly neutral NO. The NO molecule shows the stretching frequency at 1878 cm^{-1},[15] and one would expect a shift towards the lower-wave number region upon complexation. On the other hand, the nitrosonium ion $(NO)^+$ is known to show the frequency at $\sim$2220 cm^{-1}.[16] Therefore, in the case of the nitrosyl complexes that shown the NO frequency in the wave number region higher than 1878 cm^{-1}, the NO group may be regarded as being $(NO)^+$, as is seen in $[Fe^{II}(CN)_5(NO)]^{2+}$ (1938 cm^{-1}).[7] As far as cobalt-nitrosyls are concerned, there are but a few examples which show NO frequencies in a wave number region higher than 1800 cm^{-1}.[7]

Electronic Spectra. It has been well established that the electronic absorption spectra in the near-infrared region of Co(II) complexes are informative of the structure of the complexes. Nishikawa and Yamada[17] established that the square-planar Co(II) complexes with one unpaired electron exhibit a sharp peak at about 8.3×10^3 cm^{-1} ($\log\varepsilon\fallingdotseq1.3$). As may be expected from the above fact, the CoBE shows a sharp peak at 8.7×10^3 cm^{-1} ($\log\varepsilon\fallingdotseq1.3$), as is shown in Fig. 8. On the contrary, a similar absorption band is not

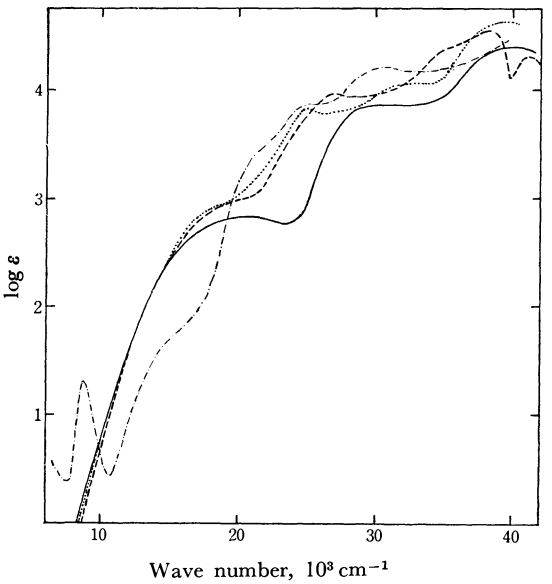

Fig. 8. Electronic spectra of complex I, complex II, Co(Salen)NO and CoBE.

——— Complex I ----- Complex II
..... Co(Salen)NO —·—· CoBE

observed for either complex, I or II (Fig. 8), suggesting that the complexes have a symmetry different from that of the planar configuration of the parent complexes. This is consistent with the anticipation from the diamagnetic properties of the complexes I and II. As to the Co(Salen)NO*2, an absorption band representative of square-planar, low spin Co^{II}(Salen)[17] was not observed either. In the case of these nitrosyl complexes, an absorption band with $\log\varepsilon\fallingdotseq2.8$ appeared at 18—20×10^3 cm^{-1}; this may be considered to be characteristic of the diamagnetic Co(II) complexes with square-pyramidal configuration. It is of interest to note that penta-coordinate alkyl derivatives of bis(acetylacetone)ethylenediimine cobalt complexes with a square-pyramidal configuration are reported to show absorption maxima at about 15×10^3 cm^{-1} ($\log\varepsilon\fallingdotseq2.9$).[18]

*3 The polarogram of the CoBE in DMF gave a one-step reduction wave at -1.46 V (applied potential), whereas the complex II gave a two-step reduction wave, one step at -1.04 V which can be ascribed to the reduction of NO in the complex and one at -1.43 V that is almost equal to that (-1.46 V) of CoBE and which can be ascribed to the reduction of Co(II) in the complex. The details will be published later.

15) E. L. Saier and A. Pozefsky, *Anal. Chem.*, **26**, 1079 (1954).

16) D. J. Millen and D. Watson, *J. Chem. Soc.*, **1957**, 1369.

17) H. Nishikawa and S. Yamada, This Bulletin, **37**, 8 (1964).

18) G. Costa, G. Mestroni, G. Tauzher and L. Stefani, *J. Organometal. Chem.*, **6**, 181 (1966); G. Costa, G. Mestroni and L. Stefani, *ibid.*, **7**, 493 (1967).

BULLETIN OF THE CHEMICAL SOCIETY OF JAPAN VOL. 42 2863—2869 (1969)

Absorption Spectra and Circular Dichroisms of Metal Complexes. IV.*1 Dichloro-diamine Type Complexes of Platinum(II) and Palladium(II)

Haruko Ito, Junnosuke Fujita and Kazuo Saito

Department of Chemistry, Faculty of Science, Tohoku University, Katahira-cho, Sendai

(Received April 3, 1969)

Absorption (AB) spectra of dichloro(*l*-tetrahydrogenpropylenediaminetetraacetato)platinum-(II) and palladium(II) and dichloro(*d*-hydrogendiaminopropionato)platinum(II) and palladium(II) were interpreted on the basis of a comparison of their circular dichroism (CD) spectra with those of dichloro(*l*-propylenediamine)platinum(II) and palladium(II). The *d-d* bands of $edtaH_4$ and *l*-$pdtaH_4$ complexes shifted to longer wavelength as compared with those of *l*-pn complexes. The shift was discussed, based on the effects of the weaker ligand field strength and apical interaction of the acetato groups of these ligands.

In the first paper of this series,[1] we examined the absorption spectra of dichloro(*l*-propylenediamine)-platinum(II) and palladium(II)*2 and found that the analysis of ciruclar dichroism spectra gave useful information about the assignment of the absorption bands of these metal complexes. Bailar and Busch[2] prepared dichloro(tetrahydrogen-ethylenediaminetetraacetato) platinum(II) and palladium(II) pentahydrate, $[PtCl_2(edtaH_4)]\cdot 5H_2O$ and $[PdCl_2(edtaH_4)]\cdot 5H_2O$, and predicted that ethylenediaminetetraacetic acid coordinated to the metal ions as a bidentate ligand. The structure was recently confirmed by X-ray analysis for the palladium compound.[3] However, no spectroscopic study of such complexes has been reported. In this paper AB and CD spectra of $[PtCl_2(l\text{-}pdtaH_4)]\cdot 5H_2O$ and $[PdCl_2(edtaH_4)]\cdot 5H_2O$ are interpreted by comparing them with those of dichloro-diamine complexes of platinum(II) and palladium(II).

Experimental

Ligands. *l*-Propylenediamine was obtained by resolving its commercial racemate.[4] *l*-Propylenediaminetetraacetic acid and *d*-diaminopropionic acid were prepared according to Dwyer's[5] and Karrer's[6] method, respectively.

Preparations of the Complexes. *(1) Dichloro-(l-tetrahydrogenpropylenediaminetetraacetato) platinum(II) pentahydrate*, $[PtCl_2(l\text{-}pdtaH_4)]\cdot 5H_2O$ and *dichloro (l-tetrahydrogenpropylenediaminetetraacetato)palladium(II) pentahydrate*, $[PdCl_2(l\text{-}pdtaH_4)]\cdot 5H_2O$ were prepared by Busch and Bailer's method[2] for the corresponding $edtaH_4$ complexes.

Found: C, 19.94; H, 4.69; N, 4.02%. Calcd for $C_{11}H_{28}N_2O_{13}Cl_2Pt$: C, 19.95; H, 4.26; N, 4.88%.

Found: C, 22.42; H, 5.32; N, 5,12%. Calcd for $C_{11}H_{28}N_2O_{13}Cl_2Pd$: C, 23.03; H, 4.92; N, 4.88%.

(2) Dibromo(l-tetrahydrogenpropylenediaminetetraaceta-to)platinum(II), $[PtBr_2(l\text{-}pdtaH_4)]$, was obtained by recrystallizing $[PtCl_2(l\text{-}pdtaH_4)]$ twice from hot 3 M hydrobromic acid.

Found: C, 19.86; H, 3.44; N, 3.95%. Calcd for $C_{11}H_{18}N_2O_8Br_2Pt$: C, 19.98; H, 2.74; N, 4.24%.

(3) Dichloro(d-hydrogendiaminopropionato)platinum(II) $[PtCl_2(d\text{-}dampH)]$. A mixture of 1 g of $K_2[PtCl_4]$, 0.34 g of *d*-diaminopropionic acid monohydrochloride and 0.33 g of K_2CO_3 in 30 ml of water was heated on a water bath at 80°C for two hours and then cooled to room temperature. Purple crystals of Magnus type salt produced during the reaction were filtered off and the filtrate was evaporated to dryness on a water bath. The residue was dissolved in a minimum amount of hot water and filtered. To the filtrate were added a few drops of concentrated hydrochloric acid. Yellow crystals were formed on cooling. They were recrystallized from 2 M hydrochloric acid.

Found: C, 9.83; H, 2.52; N, 7.50%. Calcd for $C_3H_8N_2O_2Cl_2Pt$: C, 9.74; H, 2.18; N, 7.57%.

(4) Dichloro(d-hydrogendiaminopropionato)palladium(II), $[PdCl_2(d\text{-}dampH)]$. Five hundred milligrams of

*1 Part III, H. Ito, J. Fujita and K. Saito, This Bulletin, **42**, 1286 (1969).

*2 Following abbreviations were used in this paper; *l*-pn=D-(−)D-propylenediamine, *d*-dampH=L-(+)D-diaminopropionic acid, *l*-$pdtaH_4$=D-(−)D-propylene-diaminetetraacetic acid, *l*-$pdtaH_3$=unianion of D-(−)D-propylenediaminetetraacetic acid, $eddaH_2$=ethylene-diamine-*N,N'*-diacetic acid, *NN'*-Meen=*N,N'*-dimethyl-ethylenediamine, *NN'*-MeenH=unication of *N,N'*-di-methylethylenediamine, *NN*-Eten=*N,N*-diethylethyl-enediamine, Me_4en=*N,N,N',N'*-tetramethylethylene-diamine.

1) H. Ito, J. Fujita and K. Saito, This Bulletin, **40**, 2584 (1967).

2) D. H. Busch and J. C. Bailar, Jr., *J. Am. Chem. Soc.*, **78**, 716 (1956).

3) D. J. Robinson, and C. H. Kennard, *Chem. Commun.*, **1967**, 1236.

4) F. P. Dwyer, F. L. Garvan and A. Shulman, *J. Am. Chem. Soc.*, **81**, 290 (1959).

5) F. P. Dwyer and F. L. Garvan, *ibid.*, **81**, 2955 (1959).

6) P. Karrer and A. Schlosser, *Helv. Chim. Acta*, **6**, 415 (1913).

$K_2[PdCl_4]$ was dissolved in a small amount of water, and then 0.25 g of *d*-diaminopropionic acid monohydrochloride in 5 m*l* of water was added dropwise with stirring. A gelatinous substance appeared, and crystallized gradually. The product was filtered off, washed with cold water, ethanol and ether.

Found: C, 13.25; H, 3.05; N, 9.68%. Calcd for $C_3H_8N_2O_2Cl_2Pd$: C, 12.80; H, 2.80; N, 9.95%.

(5) Dichloro(dihydrogenethylenediaminediacetato)palladium(II), $[PdCl_2(eddaH_2)]$. An aqueous solution containing 1 g of $K_2[PdCl_4]$ and 0.54 g of ethylenediaminediacetic acid was heated on a water bath (about 80°C) for half an hour and cooled. Orange yellow precipitate was filtered off, dissolved in hot water, cooled to room temperature rapidly, and treated with several drops of concentrated hydrochloric acid, the wall of the vessel being scratched to induce crystallization. The crystals were filtered off, and washed with cold water, ethanol and ether.

Found: C, 20.83; H, 3.49; N, 7.79%. Calcd for $C_6H_{12}N_2O_4$: C, 20.39; H, 3.42; N, 7.93%.

(6) Dichloro(N, N'-dimethylethylenediamine)palladium(II), $[PdCl_2(NN'\text{-Meen})]$. One gram of $[Pd(NN'\text{-Meen})_2]Cl_2$, which was obtained by a similar method to that described for $[Pd(en)_2]Cl_2$, was dissolved in 3 m*l* of water, and treated with 3 m*l* of concentrated hydrochloric acid under cooling in an ice bath. The solution was filtered to remove a small amount of unknown product, and then ethanol was added to the filtrate. Orange yellow precipitate was filtered off. Chemical analysis of the product shows the following compound, $[PdCl_2(NN'\text{-MeenH})_2]Cl_2$. Found: C, 22.59; H, 5.77; N, 13.22%. Calcd for $C_8H_{24}N_4Cl_4Pd$: C, 22.74; H, 5.25; N, 13.26%. This was dissolved in a small amount of hot water and cooled to room temperature, and treated with 6 M hydrochloric acid to produce 0.5 M hydrochloric acid solution. Orange yellow crystals precipitated on cooling. They were filtered off, and washed with water, ethanol and ether.

Found: C, 18.60; H, 4.39; N, 10.58%. Calcd for $C_4H_{12}N_2Cl_2Pd$: C, 18.24; H, 3.83; N, 10.63%.

Other complexes were prepared according to the methods described in literature.[1,7,8]

Measurements. Visible and ultraviolet absorption spectra were obtained with a Hitachi 124 recording spectrophotometer. The CD curves were recorded with a Model ORD/UV-5 spectrophotometer of Japan Spectroscopic Co. with its CD attachment. The diffuse reflectance spectra were measured with a Hitachi EPU-2A spectrophotometer with appropriate attachment. All the measurements were made at room temperature.

To avoid the aquation of coordinated halides, dichlorodiamine platinum(II) complexes were dissolved in 2 M hydrochloric acid, $[PtBr_2(l\text{-pn})]$ in 2 M hydrobromic acid, $[PtBr_2(l\text{-pdtaH}_4)]$ in 3 M hydrobromic acid and dichloro-diamine palladium(II) complex in 0.2 M potassium chloride solution, unless otherwise stated.

Proton magnetic resonance (PMR) spectra were measured with a Varian A-60 spectrometer in deuterated methanol, with tetramethylsilane (TMS) as internal reference. For the PMR measurement, the complex $[PtCl_2(edtaH_4)]\cdot 5H_2O$ and $[PdCl_2(edtaH_4)]\cdot 5H_2O$ were dehydrated at 60°C *in vacuo*.

Results and Discussion

The AB and CD spectra of the complexes are shown in Figs. 1—6. Numerical data are summarized in Tables 1—3.

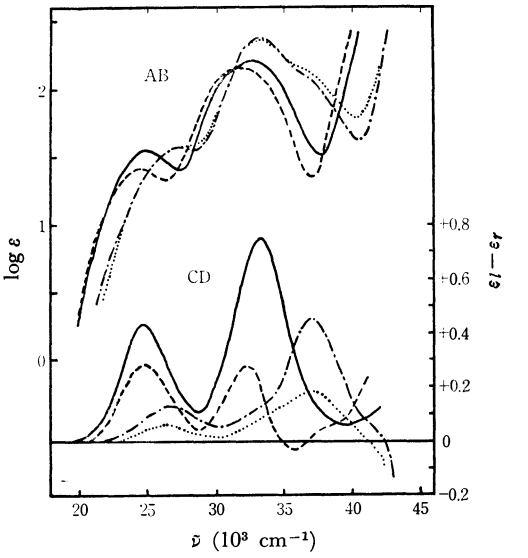

Fig. 1. AB and CD spectra of $[PtCl_2(l\text{-pn})]$ (—·—), $[PtCl_2(d\text{-dampH})]$ (·····), in 2M hydrochloric acid, and $[PtCl_2(l\text{-pdtaH}_4)]\cdot 5H_2O$ in 6 M hydrochloric acid (——) and in ethanol (– – –).

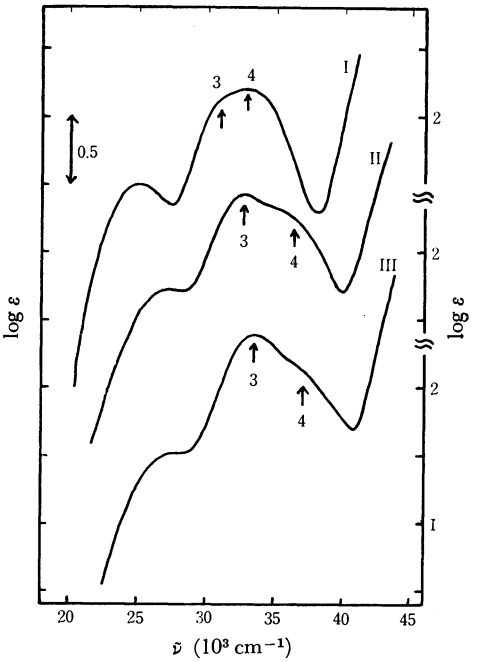

Fig. 2. AB spectra of $[PtCl_2(en)]$ (I), $[PtCl_2(eddaH_2)]$ (II), in 2M hydrochloric acid and $[PtCl_2(edtaH_4)]$(III), in 6 M hydrochloric acid.

7) S. P. Tanner, F. Basolo and R. G. Pearson, *Inorg. Chem.*, **6**, 1089 (1967).

8) G. W. Watt and D. G. Upchurch, *J. Am. Chem. Soc.*, **89**, 177 (1967).

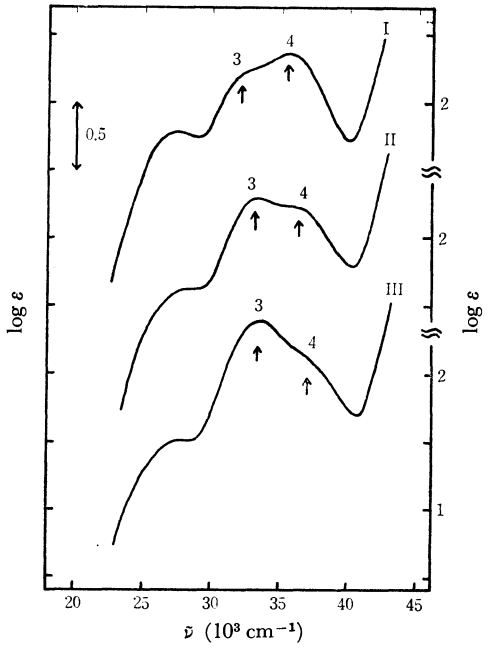

Fig. 3. AB spectra of $[PtCl_2(en)]$ (I), $[PtCl_2(NN'\text{-Meen})]$ (II) and $[PtCl_2(Me_4en)]$ (III) in 2 M hydrochloric acid.

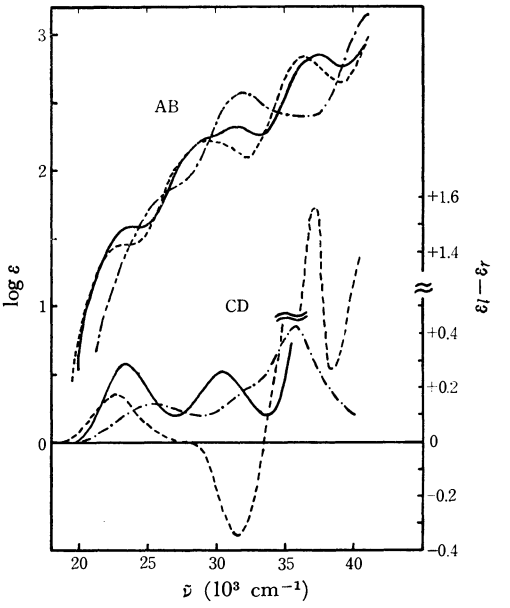

Fig. 5. AB and CD spectra of $[PtBr_2(l\text{-pn})]$ in 2 M hydrobromic acid (—·—), $[PtBr_2(l\text{-pdtaH}_4)]$ in 3 M hydrobromic acid (——) and in ethanol (----).

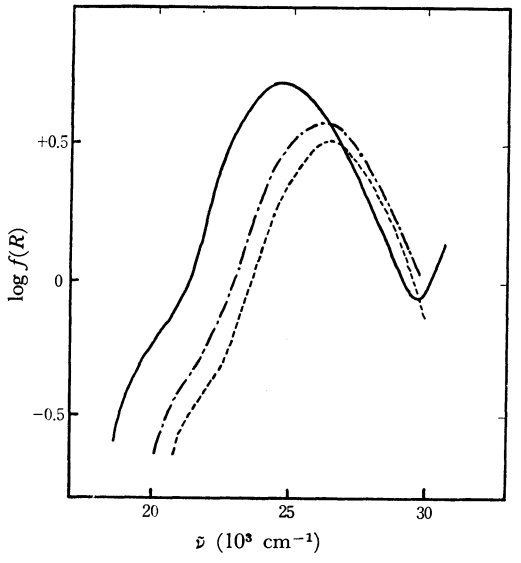

Fig. 4. Diffuse reflectance spectra of $[PdCl_2(l\text{-pdtaH}_4)]\cdot 5H_2O$ (——), $[PdCl_2(eddaH_2)]$ (—·—) and $[PdCl_2(l\text{-pn})]$ (----).

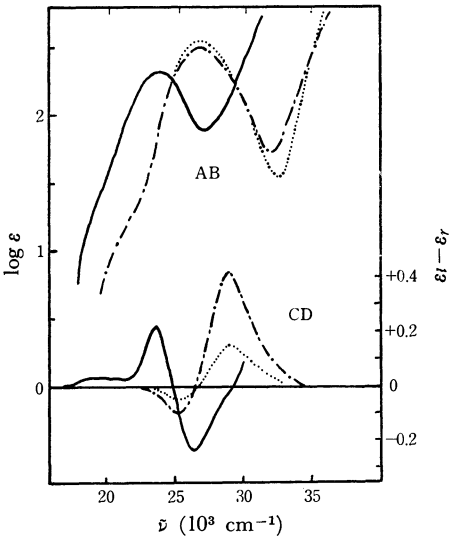

Fig. 6. AB and CD spectra of $[PdCl_2(l\text{-pdtaH}_4)]\cdot 5H_2O$ in ethanol - conc. hydrochloric acid (99:1) mixed solvent (——), $[PdCl_2(l\text{-pn})]$ (—·—) and $[PdCl_2(d\text{-dampH})]$ (·····) in 0.2 M KCl soln.

Complexes Containing *d*-Diaminopropionic Acid. The infrared absorption spectra indicate that the *d*-diaminopropionic acid of $[PtCl_2(d\text{-dampH})]$ and $[PdCl_2(d\text{-dampH})]$ coordinates through two amino groups, though it is a potential terdentate ligand with two amino groups and a carboxyl group;[9] the band at 1754 cm^{-1} must correspond to antisymmetric stretching frequency of uncoordinated carboxylic acid.

The absolute configuration of this ligand is compared with that of D-(−)$_D$-propylenediamine in Fig. 7. Recent conformational analysis on the

9) W. A. Freeman and C. F. Liu, *Inorg. Chem.*, **7**, 764 (1968).

Table 1. AB data of platinum(II) complexes, $\tilde{\nu}$ in 10^3 cm^{-1}

	Solvent	$\tilde{\nu}_{max}$ (log ε)	$\tilde{\nu}_{max}$ (log ε)	$\tilde{\nu}_{max}$ (log ε)
[$PtCl_2$(en)]	a	*ca.* 27.0 (1.4)	33.2 (2.40)	*ca.* 37 (2.1)
[$PtCl_2$(*l*-pn)]	a	*ca.* 27.3 (1.5)	33.1 (2.37)	*ca.* 37 (2.1)
[$PtCl_2$(*d*-dampH)]	a	*ca.* 27.0 (1.5)	33.0 (2.35)	*ca.* 37 (2.2)
[$PtCl_2$(*NN'*-Meen)]	a	*ca.* 27.5 (1.6)	33.2 (2.34)	*ca.* 36 (2.2)
[$PtCl_2$(Me_4en)]	a	27.0 (1.77)	*ca.* 32.3 (2.2)	35.5 (2.37)
[$PtCl_2$(*NN*-Eten)]	a	27.4 (1.62)	32.8 (2.39)	*ca.* 36 (2.2)
	b	26.7 (1.56)	32.3 (2.36)	*ca.* 35.7 (2.1)
[$PtCl_2$(eddaH_2)]	a	*ca.* 27.0 (1.7)	32.5 (2.43)	*ca.* 36 (2.3)
[$PtCl_2$(edtaH_4)]	c	25.0 (1.51)	*ca.* 31 (2.1)	32.8 (2.22)
[$PtCl_2$(*l*-pdtaH_4)]	c	24.8 (1.50)	*ca.* 31 (2.1)	32.7 (2.19)
	b	24.4 (1.40)	*ca.* 30 (2.0)	32.1 (2.15)
	d	24.4 (1.40)	*ca.* 30.2 (2.05)	32.0 (2.07)
[$PtBr_2$(*l*-pn)]†	e	*ca.* 26.5 (1.8)	31.8 (2.57)	*ca.* 36 (2.4)
[$PtBr_2$(*l*-pdtaH_4)]††	f	*ca.* 23.5 (1.6)	*ca.* 29 (2.25)	31.0 (2.33)
	b	*ca.* 23.0 (1.48)	*ca.* 28.5 (2.2)	29.7 (2.24)

† Another band appears at 37300 cm^{-1} (log ε=2.87), †† another band appears at 36400 cm^{-1} (log ε=2.86)
a, 2 M HCl; b, ethanol; c, 6 M HCl; d, tetrahydrofuran; e, 2 M HBr; f, 3 M HBr

Table 2. CD data of platinum(II) complexes, $\tilde{\nu}$ in 10^3 cm^{-1}

	Solvent	$\tilde{\nu}_{max}$ ($\varepsilon_l-\varepsilon_r$)	$\tilde{\nu}_{max}$ ($\varepsilon_l-\varepsilon_r$)	$\tilde{\nu}_{max}$ ($\varepsilon_l-\varepsilon_r$)	$\tilde{\nu}_{max}$ ($\varepsilon_l-\varepsilon_r$)
[$PtCl_2$(*l*-pn)]	a	26.3 (+0.13)		37.0 (+0.45)	
[$PtCl_2$(*d*-dampH)]	a	26.3 (+0.07)		37.0 (+0.19)	
[$PtCl_2$(*l*-pdtaH_4)]	c	24.7 (+0.43)		33.3 (+0.75)	
	b	24.3 (+0.29)		31.7 (+0.28)	35.2 (−0.02)
	d	24.0 (+0.31)		31.0 (+0.15)	34.2 (−0.16)
[$PtBr_2$(*l*-pn)]	e	25.3 (+0.14)	*ca.* 32 (*ca.* +0.15)	35.7 (+0.42)	
[$PtBr_2$(*l*-pdtaH_4)]	f	23.3 (+0.30)		30.3 (+0.27)	
	b†	22.8 (+0.18)			31.7 (−0.34)

† Another band was observed at 37100 cm^{-1} ($\varepsilon_l-\varepsilon_r$=+1.56).
a, 2 M HCl; b, ethanol; c, 6 M HCl; d, tetrahydrofuran; e, 2 M HBr; f, 3 M HBr

Table 3. AB and CD data of palladium(II) complexes, $\tilde{\nu}$ in 10^3 cm^{-1}

	AB	CD		Measurement
	$\tilde{\nu}_{max}$ (log ε)	$\tilde{\nu}_{max}$ ($\varepsilon_l-\varepsilon_r$)	$\tilde{\nu}_{max}$ ($\varepsilon_l-\varepsilon_r$)	
[$PdCl_2$(*l*-pn)]	27.0 (2.54)	25.3 (−0.10)	28.7 (+0.43)	a
	26.3			b
[$PdCl_2$(*d*-dampH)]	27.0 (2.56)	25.3 (−0.06)	29.2 (+0.25)	a
[$PdCl_2$(*NN'*-Meen)]	26.7 (2.57)			a
[$PdCl_2$(Me_4en)]	26.0 (2.51)			a
[$PdCl_2$(eddaH_2)]	26.3			b
[$PdCl_2$(*l*-pdtaH_4)]	24.1 (2.32)	23.5 (+0.19)	26.3 (−0.20)	c
	24.6			b

a, in 0.2M KCl solution; b, diffuse reflectance spectrum; c, in a mixed solution (ethanol: conc. HCl= 99 : 1 v/v)

basis of PMR study[10] has shown that in diamagnetic cobalt(III), palladium(II) and platinum(II) complexes, the *l*-propylenediamine coordinates to the metal ions to form a fixed λ-gauche chelate with the methyl group equatorial direction to the chelate ring even in an aqueous solution at room temperature. If the carboxyl group of *d*-diaminopropionic acid also required such an equatorial conformation, the gauche form of the chelate in its platinum(II) and palladium(II) complex should also be of λ-type. The CD spectra of these complexes shown in Figs. 1 and 6 are quite similar to those of *l*-pn complexes, though the intensities are smaller, to

10) S. Yano, H. Ito, Y. Koike, J. Fujita and K. Saito, *Chem. Commun.*, **1969**, 460.

indicate that the chelate ring of *d*-dampH is of λ-gauche form.

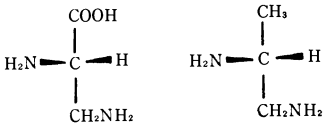

Fig. 7. Absolute configurations of D-(−)D-propylenediamine and L-(+)D-diaminopropionic acid.

Complexes Containing *l*-Propylenediaminetetraacetic Acid. Recent kinetic study[7] has shown that acetato groups participate in the elimination reaction of the chloride ions from $[PtCl_2(eddaH_2)]$. Such participation of a neighboring group and anchimeric assistance is expected to be more remarkable in platinum(II) and palladium(II) complexes containing $edtaH_4$ and *l*-$pdtaH_4$. For example, the spectrum of $[PtCl_2(l\text{-}pdtaH_4)]$ in 0.1 M hydrochloric acid is subject to a rapid change to reach a constant curve after about 80 min at room temperature. During the reaction isosbestic points appear at 345, 320 and 250 mμ

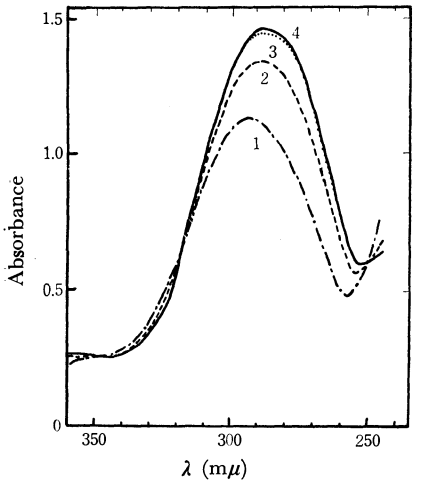

Fig. 8. Change in the spectrum of $[PtCl_2(l\text{-}pdtaH_4)]\cdot 5H_2O$ in 0.1 M hydrochloric acid with time. After (1), 10 min; (2), 20 min; (3), 30 min; (4), after equilibrium is reached.

and the absorption peak shifts to 288 mμ, as shown in Fig. 8. The spectral change may correspond to the following equilibrium shift.

$$[PtCl_2(l\text{-}pdtaH_4)] \rightarrow [PtCl(l\text{-}pdtaH_3)] + H^+ + Cl^-$$

Thus, the spectrum of $[PtCl_2(l\text{-}pdtaH_4)]$ was measured in 6 M hydrochloric acid.

The spectra of the complexes $[PtCl_{4-n}(NH_3)_n]^{(n-2)+}$ in the *d-d* band region consist of four bands, which are denoted as band 1, band 2, band 3 and band 4 from longer to shorter wavelength.[11] They were assigned to triplets of $d_{xy} \rightarrow d_{x^2-y^2}$ and d_{xz}, $d_{yz} \rightarrow d_{x^2-y^2}$, and singlets of $d_{xy} \rightarrow d_{x^2-y^2}$ and d_{xz}, $d_{yz} \rightarrow d_{x^2-y^2}$, respectively.[1,11] As in the case of *cis*-$[PtCl_2(NH_3)_2]$, $[PtCl_2(l\text{-pn})]$ gives a peak at 33100 cm^{-1} (band 3) and a shoulder at about 37000 cm^{-1} (band 4), while $[PtCl_2(l\text{-}pdtaH_4)]$ gives a peak at 32700 cm^{-1} and presumably a shoulder band at the longer wavelength side (at about 31000 cm^{-1}). The energy difference of these two neighboring bands are 3900 and about 2000 cm^{-1} for $[PtCl_2(l\text{-pn})]$ and $[PtCl_2(l\text{-}pdtaH_4)]$, respectively.

When the *l*-$pdtaH_4$ coordinates to the metal with the methyl group equatorial, the structure of chelate ring should be of λ -type, which is the same as that of the chelated *l*-pn. Therefore, the CD spectra of *l*-$pdtaH_4$ and *l*-pn complex should have the same sign in a corresponding transition band. Figure 1 suggests that the positive peak at 33300 cm^{-1} of $[PtCl_2(l\text{-}pdtaH_4)]$ corresponds to the positive peak of $[PtCl_2(l\text{-pn})]$ at 37000 cm^{-1} (band 4).

In order to examine the large difference in the spectral shape and the transition energy of the band 4 between *l*-pn and *l*-$pdtaH_4$ complex, the absorption spectra of a series of $[PtCl_2(en)]$, $[PtCl_2(NN'\text{-Meen})]$ and $[PtCl_2(Me_4en)]$ and a series of $[PtCl_2(en)]$, $[PtCl_2(eddaH_2)]$ and $[PtCl_2(edtaH_4)]$ are compared in Figs. 2 and 3. The trend of change in spectra is similar in the two series: (1) The intensity of band 4 relative to that of band 3 increases with increase in the number of the substituents on the nitrogen atoms.

(2) The absorption maxima of the bands 3 and 4 of *N,N,N',N'*-tetrasubstituted ethylenediamines shift to a longer wavelength as compared with those of *N,N'*-disubstituted and non-substituted compounds. This phenomenon is also observed for palladium(II) complexes in 0.2 M potassium chloride solution (Table 3).

These results further support the fact that the positive CD peak at 33300 cm^{-1} of $[PtCl_2(l\text{-}pdtaH_4)]$ corresponds to band 4 and the absorption shoulder at about 31000 cm^{-1} to band 3. Such an assignment leads to the conclusion that the ligand field strength of $pdtaH_4$ and $edtaH_4$ is considerably weaker than that of the other diamines, because the energy of band 3 ($d_{xy} \rightarrow d_{x^2-y^2}$) corresponds approximately to the so-called 10 *Dq*. It is known that the treatment of $[PtCl_2(en)]$ and $[PtCl_2(eddaH_2)]$[12] with aqueous ammonia produces $[Pt(NH_3)_2(en)]Cl_2$ and $[Pt(NH_3)_2(eddaH_2)]Cl_2$, respectively. For $[PtCl_2(l\text{-}pdtaH_4)]$, however, the same treatment gave $[Pt(NH_3)_4]^{2+}$. Such a difference in chemical reaction suggests a weaker bond between platinum(II) and nitrogens of $edtaH_4$ and *l*-$pdtaH_4$. In the diffuse reflectance spectra

11) J. Chatt, G. A. Gamlen and L. E. Orgel, *J. Chem. Soc.*, **1958**, 486.

12) C. F. Liu, *Inorg. Chem.*, **3**, 680 (1964).

shown in Fig. 4, the absorption peak of $[PdCl_2(l\text{-}pdtaH_4)]\cdot 5H_2O$ is also shifted to longer wavelength as compared with those of $[PdCl_2(l\text{-}pn)]$ and $[PdCl_2(eddaH_2)]$.

The shift of band 4 to longer wavelength in $edtaH_4$ and l-$pdtaH_4$ complexes seems to be abnormally large. According to the X-ray analysis of $[PdCl_2(edtaH_4)]\cdot 5H_2O$, two oxygen atoms of the acetato groups on each nitrogen atom are present above and below the palladium atom (distance 3.04 Å). Such a structure may also cause the spectra red shift. If two acetato groups were coordinated weakly to form a distorted octahedral complex, chemical environment of two acetato groups on one nitrogen atom would be non-equivalent and would give PMR spectrum with two different methylene signals. However, the PMR spectrum of $[PdCl_2(edtaH_4)]$ in deuterated water reported by Aochi and Sawyer,[13] and that of $[PtCl_2(edtaH_4)]$ in 6 M deuterium chloride solution reported by Erickson *et al.*[14] indicate no such difference. We also measured the spectra of these complexes in deuterated methanol as shown in Fig. 9. No difference between the four acetato groups were observed either; the singlets at 3.39 ppm of the palladium complex and 3.58 ppm of the platinum complex, and the qualtets centered at 4.31 ppm (J= 17.7 Hz) of the palladium complex and 4.43

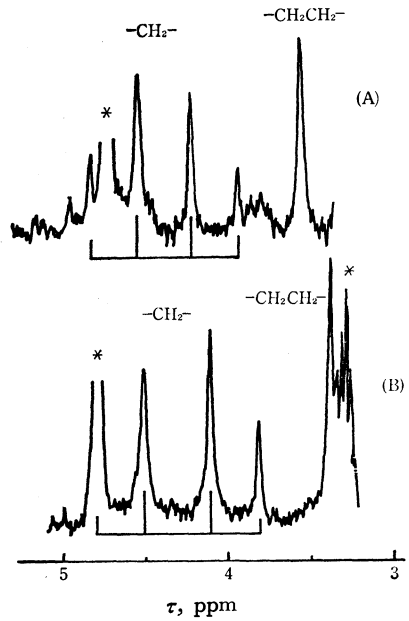

Fig. 9. PMR spectra of $[PtCl_2(edtaH_4)]$ (A) and $[PdCl_2(edtaH_4)]$ (B) in deuterated methanol, TMS as internal reference. (* indicates signals of solvent)

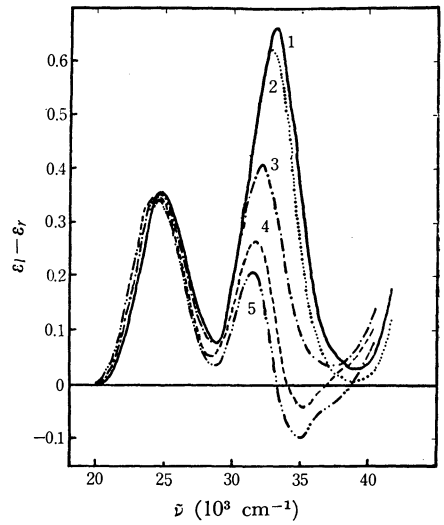

Fig. 10. CD spectra of $[PtCl_2(l\text{-}pdtaH_4)]\cdot 5H_2O$ in mixtures of ethanol and water containing abont 2 mol/l of hydrogen chloride: (1), 10%; (2), 55%; (3), 82%; (4), 100% ethanol.

ppm (J=17.3 Hz) of the platinum complex were assigned to signals of the ethylene and the methylene protons, respectively. Such an equivalence for the four acetato groups may not necessarily reject the electrical perturbation from apical positions to cause spectral red shift. Whenever one acetato oxygen parts from palladium or platinum, oxygen of the other acetato group on the same nitrogen atom can occupy the site in its place. This may be reflected in the rapid elimination reaction of the chloride ions in the complex, $[PtCl_2(l\text{-}pdtaH_4)]$, as stated before. The signals at about 3.8 ppm of the platinum complex may be due to the satellites corresponding to ^{195}Pt.

As mentioned before, bands 3 and 4 were assigned to $d_{xy} \rightarrow d_{x^2-y^2}$ and $d_{xz}, d_{yz} \rightarrow d_{x^2-y^2}$, respectively, therefore the spectral red shift is considered to be larger for band 4 than that for band 3, since the presence of very weakly attracted dipolar molecules in the apical positions destabilizes d_{z^2}, d_{xz} and d_{yz} orbitals to a greater extent than d_{xy} and $d_{x^2-y^2}$ orbitals. In fact the energy difference between bands 3 and 4 is smaller for $[PtCl_2(l\text{-}pdtaH_4)]$ (about 2000 cm^{-1}) than that for $[PtCl_2(l\text{-}pn)]$ (3900 cm^{-1}).

The absorption spectrum of $[PtCl_2(l\text{-}pdtaH_4)]$ in ethanol solution shifts to longer wavelength as a whole as compared with that in hydrochloric acid (Fig. 1). Such a shift was also observed for $[PtCl_2(NN\text{-Eten})]$ in hydrochloric acid and ethanol (Table 1). On the other hand, the shape of the CD spectrum in ethanol is quite different from that in hydrochloric acid (Fig. 1). A negative CD peak (35200 cm^{-1}) appears at shorter wavelength side of a positive CD peak (31700 cm^{-1}) in ethanol, which corresponds to the positive one at 33300 cm^{-1}

13) Y. O. Aochi and D. T. Sawyer, *ibid.*, **5**, 2085 (1966).

14) L. E. Erickson, J. W. McDonald, J. K. Howie and R. P. Clow, *J. Am. Chem. Soc.*, **90**, 6371 (1968).

in hydrochloric acid. The CD spectra in methanol, dioxane and tetrahydrofuran are quite similar to that in ethanol. Figure 10 shows the CD spectra in mixtures of water and ethanol containing about 2 M hydrogen chloride. With increase in the intensity of the negative CD component, the positive CD peak shifts to longer wavelength and its intensity decreases.

In Fig. 5 the AB and CD spectrum of [$PtBr_2$-(*l*-pn)] in 2 M hydrobromic acid, and those of [$PtBr_2$-(*l*-pdtaH_4)] in 3 M hydrobromic acid and in ethanol are shown. The spectrum of [$PtBr_2$(*l*-pn)] is quite similar to that of [$PtCl_2$(*l*-pn)] in acid solution except that the corresponding bands appear at longer wavelengths for the dibromo complex. In AB spectrum of [$PtBr_2$(*l*-pdtaH_4)] in hydrobromic acid, apparently four absorption bands are observed at about 23500, 29000, 31000 and 37300 cm^{-1}. The AB and CD spectra are compared to those of the corresponding dichloro complex, and the band at 23500 cm^{-1} can be assigned to the spin forbidden band (band 2) and the bands at 29000 and 31000 cm^{-1} to bands 3 and 4, respectively. The band at 37300 cm^{-1} may be due either to $d_{z^2} \rightarrow d_{z^2-y^2}$ transition or a charge transfer transition. A fairly strong positive CD appears in this region (in ethanol). Since $d_{z^2} \rightarrow d_{x^2-y^2}$ transition is magnetic dipole forbidden, the CD strength of the band corresponding to $d_{z^2} \rightarrow d_{x^2-y^2}$ transition should be weak. Therefore, this absorption peak can be assigned to a charge transfer band involving *p* orbitals of the bromide and $d_{x^2-y^2}$ orbital of the platinum(II).*[1,1] The location of the band corresponding to $d_{z^2} \rightarrow d_{x^2-y^2}$ transition remains uncertain.

The difference of the CD spectra of [$PtBr_2$(*l*-pdtaH_4)] in the band 4 region between hydrobromic acid and ethanol solution is striking; the signs of CD in the two solvents are different (Fig. 5). Considering that the AB and CD peaks of chloro- and bromo-platinum(II) complexes in ethanol appear at longer wavelengths than those in hydrochloric or hydrobromic acid, the negative CD band of the bromo-complex at 31700 cm^{-1} in ethanol seems to correspond to the negative CD band (35200 cm^{-1}) of [$PtCl_2$(*l*-pdtaH_4)] in ethanol. In the bromo-complex, the positive component around band 4 may be canceled by the adjacent strong negative component with unknown nature. Such a remarkable CD difference in the two solvents is not clear at present.

The AB and CD spectra of [$PdCl_2$(*l*-pdtaH_4)] in a mixed solution (ethanol : conc. HCl=99 : 1 v/v) are shown in Fig. 6. Corresponding to the absorption peak at 24100 cm^{-1}, a positive and a negative CD appear at 23700 and 26300 cm^{-1}. The positive CD component at longer wavelength can be assigned to spin forbidden transition. The CD spectrum seems to be similar to that of the corresponding platinum complex in ethanol. The complex decomposed rapidly in 1 M hydrochloric acid to give $[PdCl_4]^{2-}$. Beer's law did not hold even in dehydrated ethanol. The CD spectrum of a solution 4.07×10^{-3} mol/*l* in ethanol is quite similar to that in the mixed solvent. However, in a very dilute solution, the absorption peak corresponding to [PdCl(*l*-pdtaH_3)] was observed.

We thank the Ministry of Education for financial support granted to this research.

BULLETIN OF THE CHEMICAL SOCIETY OF JAPAN VOL. 42 2870—2873 (1969)

Pyrolysis-Gas Chromatographic Determination of Chlorine in Chlorine-Containing Synthetic Polymers

Shin TSUGE, Tadaoki OKUMOTO and Tsugio TAKEUCHI

Department of Synthetic Chemistry, Faculty of Engineering, Nagoya University, Chikusa-ku, Nagoya

(Received April 10, 1969)

A new, simple and rapid method for determining chlorine in chlorine-containing polymers was investigated by means of pyrolysis-gas chromatography. Hydrogen chloride evolved during the thermal degradation of the polymers was eliminated by a NaOH precut column, and only the organic compounds sensitive to flame ionization detector were separated to record the pyrograms. Chlorine content of the polymers was calculated from the relative yield of the degradation products using a theoretical equation deduced from the degradation mechanisms of the polymers. This unique method permits very rapid determination of chlorine with the use of about 0.1 mg of the sample without either the use of calibration curves or weighing of the samples.

Various kinds of chlorine-containing polymers with C–C bond in the backbone chains are now available. The routine determination of chlorine in the polymers is carries out by means of either ordinary chemical method or elemental analysis. Although these methods are excellent for accuracy, they are troublesome and time-consuming.

Recently, we have presented a series of studies[1–4] on polymers by pyrolysis-gas chromatography (PGC), in which we proposed a method to obtain characteristic and reproducible pyrograms with the use of an improved pyrolyzer,[1] and successfully characterized the microstructures of such chlorine-containing polymers as vinyl chloride-vinylidene chloride copolymers[2], chlorinated polyethylene[3] and chlorinated polyvinylchlorides[4].

The present work describes a new method for the simple and rapid determination of chlorine in various kinds of chlorine-containing polymers by means of PGC.

Experimental

Materials. Four kinds of chlorine-containing polymers were prepared. Chlorinated polyethylenes (CPE) were obtained by chlorination of polyethylene with the use of CCl_4-solution method proposed by Campbell and Lyman.[5] Chlorinated polybutadienes (CPB) and chlorinated polyvinylchlorides (CPVC) were synthesized by chlorination of polybutadiene and polyvinylchloride, respectively, utilizing the $CHCl_3$-solution method.

Vinyl chloride-vinylidene chloride copolymers were prepared by suspension polymerization using azobisisobutyronitrile as a catalyst.

Apparatus. A furnace type pyrolyzer was used to decompose the polymers. Figure 1 shows a schematic diagram of the pyrolyzer. It was directly attached to the inlet port of the gas chromatograph, Yanagimoto Model GCG-550F with dual flame ionization detectors. The sample holder of the pyrolyzer was so modified as to obtain characteristic and reproducible pyrograms by reducing its heat capacity.[1] Hydrogen chloride evolved during the thermal decomposition of the polymers was eliminated by a NaOH precut column whose temperature was maintained at about 200°C. To minimize the change of the pyrolysis temperature, which influences the reproducibility of the results, a voltage-stabilizer was used for the pyrolyzer. A sample weighing about 0.1—0.3 mg was pyrolyzed under a flow of carrier gas (N_2) at fixed pyrolysis temperatures for 1 min which was sufficient for complete pyrolysis.

Gas Chromatographic Conditions. Gas chromatographic conditions and the method of identification of the peaks appearing on the pyrograms are the same as described previously.[2–4] Separation columns (3 mm i.d. ×2 m) containing 10 wt% of Carbowax 6000 coated on Diasolid L (80—100 mesh) were used. The column temperature was first programed from 50 to 210°C at a rate of 16°C/min, and then operated isothermally at 210°C. The flow rate of carrier gas (N_2) was maintained at 40 ml/min at 50°C. Hydrogen flame was made by means of 40 ml/min of H_2 and 700 ml/min of air. As the flame ionization detector responds nearly to the number of carbon atoms in the component, the relative yield (wt%) of the degradation products was calculated from the relative peak area on the pyrogram by making weight sensitivity corrections of each component for the flame ionization detector.

1) S. Tsuge, T. Okumoto and T. Takeuchi, *Kogyo Kagaku Zasshi (J. Chem. Soc. Japan, Ind. Chem. Sect.)*, **71** 1634 (1968).

2) S. Tsuge, T. Okumoto and T. Takeuchi, *Makromol. Chem.*, **123**, 123 (1969).

3) S. Tsuge, T. Okumoto and T. Takeuchi, *Macromolecules*, **2**, 200 (1969).

4) S. Tsuge, T. Okumoto and T. Takeuchi, *ibid.*, **2**, 277 (1969).

5) T. W. Campbell and J. Lyman, *J. Polymer Sci.*, **55**, 169 (1961).

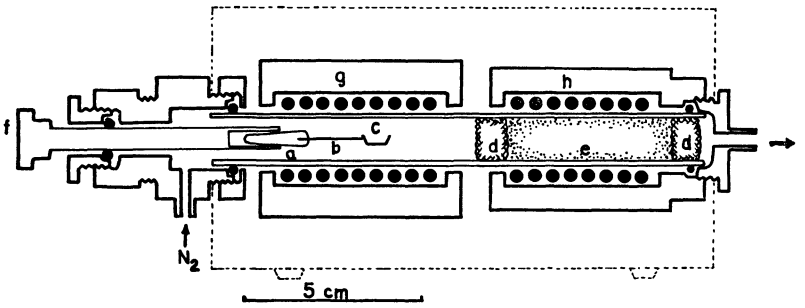

Fig. 1. Pyrolyzer: a, glass rod; b, needle; c, sample holder(Ag); d, glass wool; e, NaOH coated on Diasolid H; f, sample charging rod; g, pyrolysis heater; h, precut heater.

Results and Discussion

In order to obtain characteristic, reproducible and sharp pyrograms, the optimum pyrolysis temperatures were decided experimentally; 400°C for P(VC-VDC) and CPVC, 490°C for CPB and 660°C for CPE. The relatively high pyrolysis temperature of 660°C reflects a fairly good thermal stability of CPE.

Figure 2 shows typical pyrograms of CPE, CPB, P(VC-VDC) and CPVC. The degradation products appearing on the pyrograms can be divided into two classes. The first consists of the products formed mainly by simple thermal scissions of the polymer chains; lower hydrocarbons (C_1-C_6) and vinylidene chloride. For example:

$$-CH_2-CH_2-CH_2-CCl_2- \rightarrow CH_2=CH_2 + CH_2=CCl_2$$

The second consists of those formed by dehydrochlorination followed by cyclization; aromatic hydrocarbons and some chlorine-substituted benzenes. For example:

dehydrochlorination

$$-CH_2-CHCl-CHCl-CHCl-CH_2-CHCl- \rightarrow -CH=CH-CH=CCl-CH=CH- + 3HCl$$

cyclization

$$-CH=CH-CH=CCl-CH=CH- \rightarrow$$

In this case, it is assumed that the dehydrochlorination reaction occurs to form the conjugated polyene-structures along the chain of the polymers. Consequently, to make the latter type of degradation products correspond to the original structures of the polymer, we have to consider the products together with the eliminated 3 mol of hydrogen chloride. For the sake of simplicity, lower hydrocarbons were regarded as mono-olefines, and a small amount of toluene, styrene and naphthalene was converted into benzene in the calculation and added to the observed yield of benzene.

From these degradation mechanisms of the polymers, we obtain a calculation table (Table 1) and the following equation for the determination of chlorine in the polymers:

$$\text{Cl wt\%} = \frac{\sum_{i=2}^{7} \frac{C_i Y_i D_i}{A_i}}{\sum_{i=2}^{7} \frac{C_i Y_i}{A_i} + Y_1} \qquad (1)$$

where A is the molecular weight of the degradation product, C is the molecular weight of the original structure before dehydrochlorination, D is chlorine content (wt%) in C, Y is the observed yield (wt%) of the degradation product and the suffix i designates the component number in Table 1.

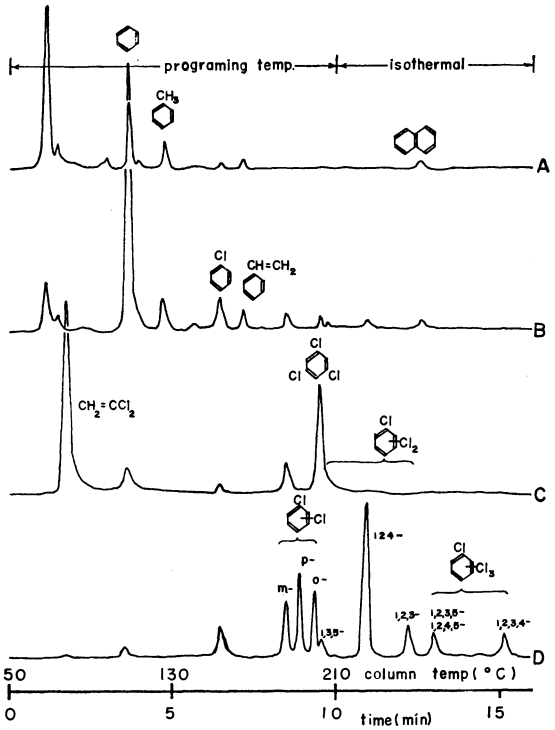

Fig. 2. Typical pyrograms of chlorine-containing polymers.
A; CPE(Cl: 28.8 wt%) at 660°C, B; CPB(Cl: 54.5 wt%) at 490°C, C; P(VC-VDC)(Cl: 68.6 wt%), D; CPVC(Cl: 73.2 wt%) at 460°C

Table 1. Calculation table for the determination of chlorine content

No. (i)	Degradation product P	Molecular weight of P A	Eliminated HCl (mol) from C B	Molecular weight of the original structure $C=(A+B)$	Cl-content in C (wt%) D	Observed yield of P Y
1	Lower hydrocarbons	—	0	—	0	Y_1
2	Vinylidenechloride	97.0	0	97.0	73.2	Y_2
3	Benzene	78.0	3	187.5	56.8	Y_3
4	Chlorobenzene	112.5	3	222.0	64.0	Y_4
5	Dichlorobenzenes[a]	147.0	3	256.5	69.2	Y_5
6	Trichlorobenzenes[b]	181.5	3	291.0	73.2	Y_6
7	Tetrachlorobenzenes[c]	216.0	3	325.5	76.4	Y_7

a) Total of *o*-, *m*- and *p*-dichlorobenzene.
b) Total of 1,2,3-, 1,2,4- and 1,3,5-trichlorobenzene.
c) Total of 1,2,3,4-, 1,2,3,5- and 1,2,4,5-tetrachlorobenzene.

Table 2. Data of reproducibility and accuracy

Degradation product	Observed relative yield of the degradation product (wt %)											
	CPE			CPB			P(VC-VDC)			CPVC		
	Cl: 28.8 wt %[a]			Cl: 54.5 wt %[a]			Cl: 68.6 wt %[a]			Cl: 73.2 wt %[a]		
Lower hydrocarbon	73.6	74.0	73.0	18.9	19.6	16.9	—	—	—	—	—	—
Vinylidenechloride	—	—	—	—	—	—	27.1	35.6	20.4	—	—	—
Benzene	26.4	26.0	27.0	67.7	66.6	69.2	1.6	1.6	1.9	0.4	0.3	0.3
Chlorobenzene	—	—	—	8.9	8.8	8.3	13.9	11.3	15.9	3.7	4.6	3.5
Dichlorobenzenes[b]	—	—	—	3.6	3.8	4.5	43.2	37.6	45.9	30.3	29.7	29.2
Trichlorobenzenes	—	—	—	0.9	1.2	1.1	14.2	13.9	15.9	46.6	44.4	44.5
Tetrachlorobenzenes[d]	—	—	—	—	—	—	—	—	—	19.0	21.0	22.5
Cl-content (wt %)[e]	26.3	26.0	26.7	52.7	52.5	53.4	69.2	69.7	68.8	72.0	71.9	72.2
Mean (wt %)[f]	26.3			52.9			69.3			72.0		
Std. deviation	0.34			0.46			0.45			0.15		
Rel. std. dev. (%)	1.27			0.87			0.65			0.21		
Abs. dev. (f−a wt %)	−2.5			−1.6			+0.6			−1.2		

a) Determined chemically.
b, c, d) Refer to Table 1.
e) Calculated from Eq. (1).

Figure 3 shows the analytical results obtained by PGC against those by chemical analysis. The relatively good linearity of the calibration curve may support the assumptions implicit in this method. Statisticaly evaluation of the method is presented in Table 2. Three observations were made with each polymer sample. As might be expected from the small relative standard deviations, the reproducibility of the method is good, but not the accuracy data expressed as absolute deviations. This method tends to give a lower chlorine content than that obtained chemically except in the case of P(VC-VDC). This tendency is especially conspicuous with CPE. This phenomenon is related to the thermal stability and the relatively high pyrolysis temperature of the polymer. With pyrolysis temperature lower than 660°C, however, CPE did not decompose to give quantitative results. As shown in Table 2, it is possible to determine the chlorine content of CPB, P(VC-VDC) and CPVC,

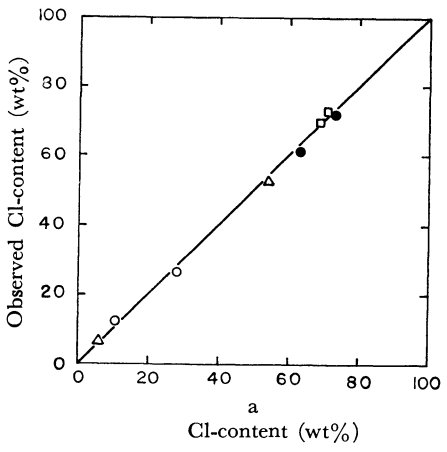

Fig. 3. Calibration curve for chlorine-containing polymers.
○, CPE; △, CPB; □, P(VC-VDC); ●, CPVC; *a*, chlorine content obtained chemically

whose optimum pyrolysis temperatures lie between 460 and 490°C, within 1% of relative standard deviation. To attain good reproducibility, the pyrolysis temperatures must be regulated by the voltage-stabilizer for the pyrolyzer.

This technique is very simple and rapid, and needs neither calibration curves nor weighing of the sample. Moreover, a very small amount of the polymer sample (0.1—0.3 mg) is sufficient.

The authors thank Professor Yuya Yamashita of Nagoya University for his supply of the copolymers (P(VC-VDC)). One of the authors (S.T.) wishes to thank the Sakkokai Foundation.

BULLETIN OF THE CHEMICAL SOCIETY OF JAPAN VOL. 42 2873—2877 (1969)

Preparation and Properties of the Mixed Dinitro Complexes of Cobalt(III) with the Carbonato or Oxalato Ligand*1

Hiroyasu ICHIKAWA and Muraji SHIBATA

Department of Chemistry, Faculty of Science, Kanazawa University, Kanazawa

(Received May 10, 1969)

Three new tervalent dinitro complexes of cobalt(III) have been prepared by the use of a tricarbonatocobaltate(III) solution or a similar solution as the starting material. These complexes, $[Co(NO_2)_2(CO_3)_3]^{3-}$, $[Co(NO_2)_2(OX)_2]^{3-}$ and $[Co(NO_2)_2CO_3OX]^{3-}$ are characterized by their absorption spectra in solution. The geometrical structures of these complexes have been determined as of the *cis*-form on the basis of their IR spectra. The compounds were not stable against decomposition in aqueous solutions: the bis(oxalato) compound was most unstable against the decomposition to the Co(II) state. The stability has been discussed in connection with the specific absorption band of the coordinated NO_2^- ligand.

A number of mixed dinitro complexes of cobalt(III) have already been prepared. The tetraammine-type and bis(ethylenediamine)-type[1] complexes are quite familiar and are typical univalent cationic complexes. For these complexes, *cis* and *trans* isomers are known. On the other hand, as the univalent anionic complexes the bis(acetylacetonato)[2-4] and the bis(glycinato)[5] complexes are known in only the *trans*-form and in only the *cis*-form respectively. Furthermore, the oxalato (or carbonato)diammine(or ethylenediamine)-type complexes[6,7] have also been reported, and a none-electrolyte complex *cis*-dinitroglycinatoethylenediaminecobalt(III)[5] has been prepared.

In the present work, the preparation of tervalent anionic dinitrocomplexes containing carbonato or oxalato ligands, or both, was undertaken. The complex $[Co(NO_2)_2(CO_3)_2]^{3-}$ was obtained from a reaction mixture of potassium tricarbonato cobaltate(III)[8] and potassium nitrite. The complexes $[Co(NO_2)_2(OX)_2]^{3-}$ and $[Co(NO_2)_2CO_3OX]^{3-}$ were obtained by the reaction of potassium nitrite with a green solution produced by oxidizing the Co^{2+} ion with hydrogen peroxide in the presence of potassium oxalate and bicarbonate. The geometrical structures of these complexes were determined as of the *cis*-form on the basis of the IR spectra.

Experimental

Preparation. *1) Potassium Dinitrodicarbonatocobaltate(III) Monohydrate*, $K_3[Co(NO_2)_2(CO_3)_2]\cdot H_2O$. To a green solution of tricarbonatocobaltate(III) ($CoCl_2\cdot 6H_2O$ 10 g scale, 0.048 mol), which had been prepared by the usual method,[8] 13 g (0.15 mol) of potassium nitrite was added. The reaction mixture was then stirred under an iced condition for 3—4 hr. A large amount (100 ml) of ethanol was added to the resulting red solution, and the whole was kept in a refrigerator for a day to precipitate the crude product. The precipitates was recrystallized by dissolving them in a minimum amount of cold water and by then adding

*1 Presented at the 18th Symposium on Coordination Chemistry, Kyoto, Oct., 1968.

1) F. Basolo, *J. Am. Chem. Soc.*, **72**, 4393 (1950).

2) A. Rosenheim and A. Garfunkel, *Ber. Dtsch. Chem. Ges.*, **44**, 1865 (1911).

3) L. J. Boucher and J. C. Bailar, Jr., *J. Inorg. Nucl. Chem.*, **27**, 1093 (1965).

4) R. O. Archer and B. P. Cotsoradis, *Inorg. Chem.*, **4**, 1584 (1965).

5) N. Matsuoka, J. Hidaka and Y. Shimura, This Bulletin, **39**, 1257 (1966).

6) E. Kyuno, *Nippon Kagaku Zasshi (J. Chem. Soc. Japan, Pure Chem. Sect.)*, **80**, 987 (1959).

7) E. Kyuno, *ibid.*, **81**, 724 (1960).

8) M. Shibata, *ibid.*, **87**, 771 (1966).

ethanol. The complex was violet-red needle-shaped crystals. The yield was about 3 g.

Found: C, 6.21; N, 6.95; H, 0.55%. Calcd for $K_3[Co(NO_2)_2(CO_3)_2]\cdot H_2O$: C, 5.91; N, 6.90; H, 0.50%.

2) Potassium Dinitrobis(oxalato)cobaltate(III) Monohydrate, $K_3[Co(NO_2)_2(OX)_2]\cdot H_2O$. Twenty-seven grams (0.15 mol) of potassium oxalate monohydrate and 5 g (0.05 mol) of potassium bicarbonate were dissolved in a minimum amount of hot water (50°C). Separately, 10 g (0.042 mol) of cobalt chloride hexahydrate were dissolved in a minimum amount of hot water. After cooling, 15 m*l* of hydrogen peroxide (30%) were added. This latter solution was added, drop by drop to the 40—50°C warmed oxalate-bicarbonate solution. To the resulting green solution there were added 9 g (0.10 mol) of potassium nitrite; the mixture was stirred at 40—50°C for 2—3 hr, whereupon the solution turned red. On the ice cooling of the solution, the desired complex was precipitated. This was filtered, washed with methanol, and then dried in air. On the other hand, the filtrate was used for another complex of 3). The product was needle-shaped crystals; the yield was about 7 g. Found: C, 10.45; N, 6.27; H, 0.55%. Calcd for $K_3[Co(NO_2)_2(OX)_2]\cdot H_2O$: C, 10.39; N, 6.08; H, 0.44%. The complex was not recrystallized from water because of its rapid decomposition to cobalt(II) oxalate.

3) Potassium Dinitrocarbonatooxalatocobaltate(III), $K_3[Co(NO_2)_2CO_3OX]$. To the filtrate of 2), ethanol (*ca.* 20 m*l*), was added, and the whole was kept in a refrigerator for a few hours in order to precipitate some of the bis(oxalato) complex and potassium oxalate. After the removal of these precipitated salts, an additional 50 m*l* portion of ethanol was added to the filtrate and the whole was kept in a refrigerator for a day. The red crystals thus precipitated were purified twice by dissolving them in a minimum amount of cold water and by adding ethanol. The final product was red stick-form crystals. The yield was about 4 g.

Found: C, 8.62; N, 6.80%. Calcd for $K_3[Co(NO_2)_2CO_3C_2O_4]$: C, 8.65; N, 6.73%.

Measurements. The infrared absorption spectra in the 4000—650 cm^{-1} region were measured as KBr disks using a Japan Spectroscopic Co., DS-301 infrared spectrometer. The visible and near-ultraviolet absorption spectra were measured with a Hitachi Perkin-Elmer 139 UV-VIS spectrophotometer, using a 0.10 M potassium bicarbonate aqueous solution as the solvent for the dicarbonato complex, a 0.10 M potassium oxalate aqueous solution for the bis(oxalato) complex, and a 0.05 M bicarbonate - 0.05 M oxalate mixed aqueous solution for the carbonatooxalato complex.

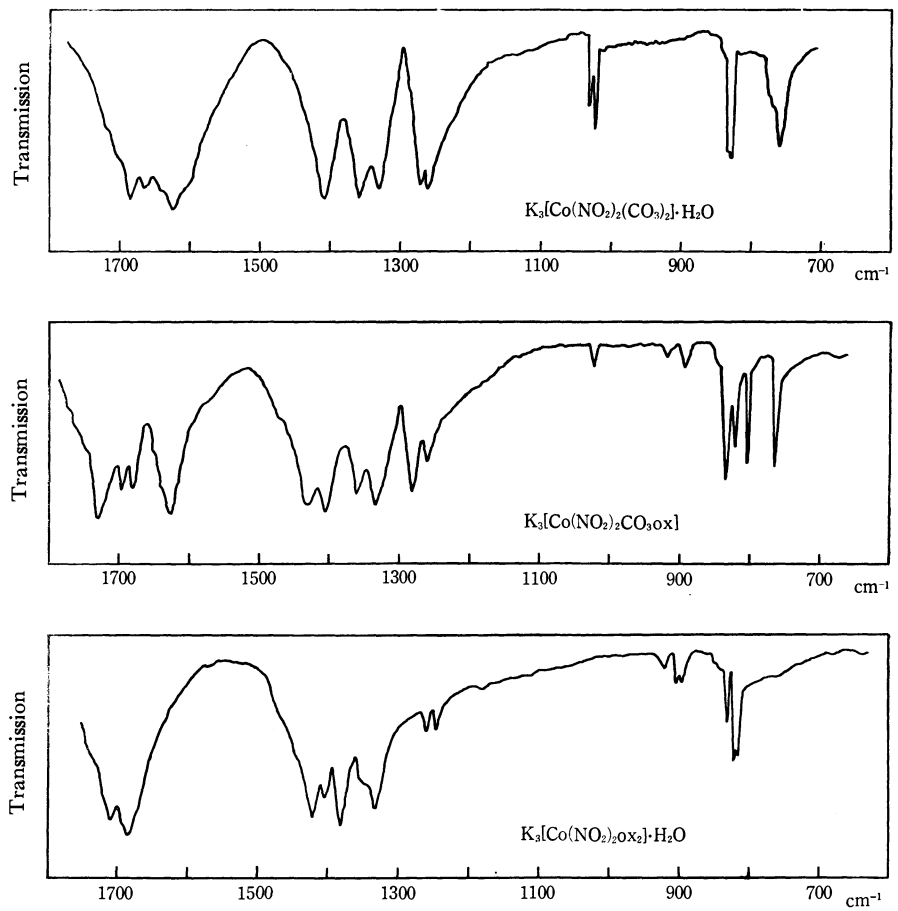

Fig. 1. Infrared absorption spectra of the *cis*-$K_3[Co(NO_2)_2(CO_3)_2]\cdot H_2O$, *cis*-$K_3[Co(NO_2)_2CO_3OX]$, and *cis*-$K_3[Co(NO_2)_2(OX)_2]\cdot H_2O$.

Table 1. IR data of the dinitro and related complexes (cm^{-1})

	NO_2^-			CO_3^{2-}					$C_2O_4^{2-}$						
	asym.	sym.	sym.	asym.	sym.	sym.	out of plane	sym.	asym.		sym.		sym.	asym.	Ref.
	ν(NO)	ν(NO)	δ(ONO)	ν(CO)	ν(CO)	ν(CO)	(OCC)	δ(OCO)	ν(CO)	ν(CO)	ν(CO)	ν(CO)	ν(CC)	δ(OCO)	
$K_3[Co(NO_2)_2(CO_3)_2]\cdot H_2O$	1403	1360 1323	833[a] 830	1685 1623	1272 1260	1030 1024	833	759 772 sh							*
$K_3[Co(NO_2)_2CO_3OX]$	1405	1360 1332	833[b] 820	1680 1623	1282	1022	833	764	1730	1695	1430	1257	920 894	802	*
$K_3[Co(NO_2)_2(OX)_2]\cdot H_2O$	1402	1380 1346 sh 1337	838 824[c]						1707	1684	1420	1255 1248	902 892	824 818	*
$K_3[Co(CO_3)_3]\cdot 3H_2O$				1527	1330	1037	851	—							8
$K_3[Co(C_2O_4)_3]\cdot 3H_2O$									1710	1658	1389	1257	900	824 810	8
$K_3[Co(NO_2)_6]$	1386	1332	827												21
cis $[Co(NO_2)_2\,en_2]Cl$	1422	1344 1312	837 819												
trans $[Co(NO_2)_2\,en_2]Cl$	1414	1325 1312 sh	819												17
cis $[Co(NO_2)_2(NH_3)_4]Cl$	1406	1374 1357	825 822												
trans $[Co(NO_2)_2(NH_3)_4]Cl$	1407	1361	828 819												**
$Na[Co(NO_2)_2(acac)_2]$	1425	1308	827												4

* Present work.

a) Overlap sym. δ(ONO) and out of plane (OCO) for $K_3[Co(NO_2)_2(CO_3)_2]\cdot H_2O$.

b) Overlap sym. δ(ONO) and out of plane (OCO) for $K_3[Co(NO_2)_2CO_3OX]$.

c) Overlap sym. δ(ONO) and sym. δ(OCO) for $K_3[Co(NO_2)_2(OX)_2]\cdot H_2O$.

** I. R. Beatlie and H. J. V. Tyrrell, *J. Chem. Soc.*, **1956**, 2849.

Table 2. Absorption data for the new dinitro complexes

	ν_1	ν_{sp}	ν_3	$\nu_{sp}-\nu_1$
	$10^{13}\,sec^{-1}$ ($\log\varepsilon$)			
$K_3[Co(NO_2)_2OX_2]\cdot H_2O$	57.32(2.13)	81.02(3.60)	110.22(4.19)	23.70
$K_3[Co(NO_2)_2CO_3OX]$	56.00(2.26)	85.85(3.55)	113.80(4.38)	29.85
$K_3[Co(NO_2)_2(CO_3)_2]\cdot H_2O$	54.80(2.24)	87.15(3.47)	113.80(4.31)	32.35

Results and Discussion

Preparation. The green solution which is used for the preparation of the bis(oxalato) and carbonatooxalato complexes is prepared in the same way as the tricarbonatocobaltate(III) solution.[8] The attempt to isolate the complexes from the green solution failed because of the high solubility of the complex species, but the absorption spectrum of the solution suggested the formation of such mixed complexes as $[Co(CO_3)_n(OX)_{3-n}]^{3-}$ ($n=1, 2$). When a cold solution of $CoCl_2$ containing H_2O_2 was added not to a warmed but to an ice-cold solution of potassium oxalate and bicarbonate, a large quantity of the Durrant's salt,[9,10] $K_4[(C_2O_4)_2Co\langle^{OH}_{OH}\rangle Co(C_2O_4)_2]\cdot 4H_2O$, was precipitated. Furthermore, when H_2O_2 was added toan ice-cold oxalate-bicarbonate solution which had previously mixed with a $CoCl_2$ solution, the Durrant's salt was almost quantitatively precipitated. When the reaction was carried out at 40—50°C, tris(oxalato)cobaltate(III) was precominantly formed.

IR Spectra. The IR spectra of three new complexes are shown in Fig. 1, while the numerical data are given in Table 1 with the related complexes. In the spectra of the dicarbonato and carbonatooxalato complexes, the key bands indicating the existence of the coordinated carbonate ion are observed as one or two sharp bands attributable to the CO symmetrical stretching vibration in the 1050—1020 cm^{-1} region——at 1033 and 1024 cm^{-1} for the dicarbonato complex and at 1022 cm^{-1} for the monocarbonato complex. If the carbonate ion is acting as a monodentate ligand, the corresponding CO vibration will appear in a higher-wave-number region.[11] The key bands indicating the existence of the coordinated oxalate ion are the C–C symmetrical stretching vibrations appearing in the 900 cm^{-1} region; the monooxalato complex has two distinct bands at 920 and 894 cm^{-1}, and the bis(oxalato) complex, at 902 and 892 cm^{-1}. If the oxalate ion is acting as a monodentate ligand, the corresponding C–C stretching vibration will appear in a higher-wave-number region.[11,12] Although the nitrite anion can coordinate to a central atom through the N- or O-atom, the present three complexes are coordinated through the N-atom, because of the absence of a nitrito characteristic band at 1050 cm^{-1}.[13,14] The absorption peaks appearing at 833, at 833 and at 824 cm^{-1} for the dicarbonato, carbonatooxalato, and bis(oxalato) complexes respectively, are undoubtedly due to the overlapping of the absorptions due to the oxalato, carbonato, and nitro ligands.

Several methods have been employed to distinguish between *cis* and *trans* isomers of dinitro complexes of cobalt(III).[3,15–18] It is said that the *cis* isomer gives a more complicated spectrum than the corresponding *trans* isomer because of the lower symmetry of the former.[15–18] For example, the IR spectrum of *trans*-$[Co(NO_2)_2(NH_3)_4]^+$ shows one band attributable to the NO_2^- symmetrical stretching vibration, whereas the spectrum of the *cis* isomer shows two bands.[15,18] The spectrum of *trans*-$[Co(NO_2)_2en_2]^+$ also shows one band attributable to the NO_2^- bending mode, whereas the *cis* isomer shows two bands.[16] Furthermore, *trans*-$[Co(NO_2)_2(acac)_2]^-$ exhibits one band each attributable to the NO_2^- symmetrical stretching and bending vibrations.[3] Each of the present complexes has two clear bands attributable to the NO_2^- symmetrical stretching vibration; the dicarbonato complex has them at 1360 and 1323 cm^{-1}; the carbonatooxalato one, at 1360 and 1332 cm^{-1}, and the bis(oxalato) one, at 1386 and 1327 cm^{-1} (with a 1346 cm^{-1} shoulder). From this evidence, it may be concluded that the present new complexes have *cis* structures.

UV Spectra. The absorption spectra in solution are shown in Fig. 2, while the numerical data are listed in Table 2. The maximum values of the first absorption bands (ν_1) for the present

9) R. G. Durrant, *J. Chem. Soc.*, **1905**, 1784.
10) E. Percival and W. Wardlaw, *ibid.*, **1929**, 2628.
11) K. Nakamoto, J. Fujita, S. Tanaka and M. Kobayashi, *J. Am. Chem. Soc.*, **79**, 4904 (1957).
12) J. Fujita, K. Nakamoto and M. Kobayashi, *J. Phys. Chem.*, **61**, 1014 (1957).
13) K. Nakamoto, J. Fujita and H. Murato, *J. Am. Chem. Soc.*, **80**, 4817 (1958); *J. Chem. Soc.*, **1959**, 4073.
14) R. B. Perland, T. J. Lane and J. V. Quagliano, *J. Am. Chem. Soc.*, **78**, 883 (1962).
15) J. P. Faust and J. V. Quagliano, *ibid.*, **76**, 5346 (1954).
16) B. M. Gathehouse, *J. Inorg. Nucl. Chem.*, **8**, 79 (1958).
17) M. L. Morris and D. H. Busch, *J. Am. Chem. Soc.*, **82**, 1521 (1960).
18) M. Lepostollec, J. P. Mathieu and H. Poulet, *J. Chim. Phys.*, **60**, 1319 (1963).

complexes are regularly shifted to a higher frequency in order of the dicarbonato, carbonatooxalato, and bis(oxalato) complexes, with 1.2—1.3$\times 10^{13}$ sec^{-1} intervals. Those of *cis*-dicarbonato, carbonatooxalato, and bis(oxalato)diamminecobalt(III) complexes are also shifted to a higher frequency in the same order with regular intervals (0.9×10^{13} sec^{-1}).[8] These regularities can be expected from "the spectrochemical series."[19] However, the maximum values for these complexes themselves differ considerably from those calculated on the basis of "the rule of average environment";[20] calcd maxima, 53.8 for $[Co(NO_2)_2(OX)_2]^{3-}$; 52.8 for $[Co(NO_2)_2CO_3OX]^{3-}$; 51.7 for $[Co(NO_2)_2(CO_3)_2]^{3-}$. Perhaps the reason for this poor agreement is the value (62.0×10^{13} sec^{-1})[21] for the hexanitro complex, which is much lower than the expected value from "the spectrochemical series." On the other hand, the maximum frequencies (ν_{sp}) of the specific band of coordinated NO_2^- are shifted lower from the dicarbonato complex to the bis(oxalato) complex. In other words, the maximum positions of the first and specific bands move in an opposite direction from the dicarbonato to bis(oxalato) complexes. Accordingly, the values of $\nu_{sp}-\nu_1$ are calculated as a measure of the shifts; they are given in Table 2. The value for the dicarbonato complex is the largest one (32.35×10^{13} sec^{-1}) in the reported dinitro complexes. This fact seems to be interesting.

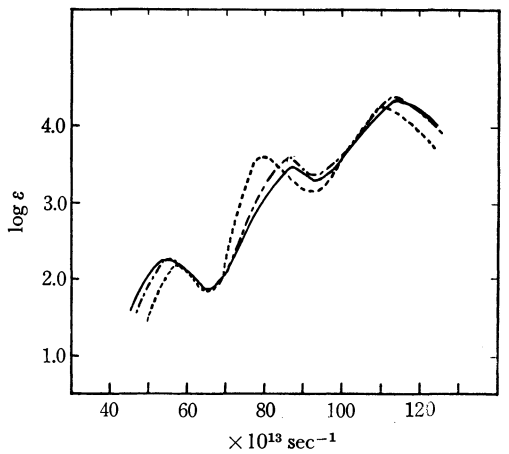

Fig. 2. Absorption spectra of the *cis* dinitro complexes.
(1) $K_3[Co(NO_2)_2(CO_3)_2]\cdot H_2O$ ——
(2) $K_3[Co(NO_2)_2CO_3OX]$ —·—
(3) $K_3[Co(NO_2)_2OX_2]\cdot H_2O$ – – –

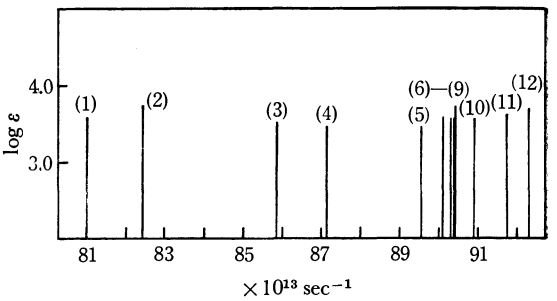

Fig. 3. The position of specific absorption band of *cis*-dinitro complexes of cobalt(III).
(1) $[Co(NO_2)_2OX_2]^{3-}$
(2) $[Co(NO_2)_6]^{3-}$
(3) $[Co(NO_2)_2CO_3OX]^{3-}$
(4) $[Co(NO_2)_2(CO_2)_2]^{3-}$
(5) γ-$[Co(NO_2)_2CO_3(NH_3)_2]^-$
(6) $[Co(NO_2)_2OX(NH_3)_2]^-$
(7) $[Co(NO_2)_2\,gly_2]^-$
(8) $[Co(NO_2)_2CO_3\,en]^-$
(9) $[Co(NO_2)_2\,edda]^-$
(10) $[Co(NO_2)_2OX\,en]^-$
(11) $[Co(NO_2)_2(NH_3)_4]^+$
(12) $[Co(NO_2)_2\,en_2]^+$

The frequency values of a number of dinitro complexes were inspected; they are diagrammatically represented in Fig. 3. From this inspection it was found that the maxima of the specific bands for the dinitro complexes shift to a lower frequency with the order of the ligands; en, NH_3 edda gly, CO_3^{2-}, NO_2^- and OX^{2-}. Since this order differs from that in the spectrochemical series, we can not discuss the stability of dinitro complexes in terms of the ligand-field theory.[22] However, as far as the present three complexes are concerned, they are less stable than the tris(oxalato)cobaltate(III) complex in their aqueous solutions and rapidly decompose to the cobalt(II) state. Among the three complexes, the dicarbonato complex is the most stable and the bis(oxalato) complex is the least stable. It is well known that the hexanitrocobaltate(III) complex is not stable in solution. Considering these facts, the order of CO_3^{2-}, NO_2^-, and OX^{2-} ligands seems to represent the stability of the dinitro complexes against decomposition to the cobalt(II) state. Furthermore, if these decompositions depend upon the photochemical reaction, it can be said that these dinitro complexes will sensitively react to light in the 80.0—83.0$\times 10^{13}$ sec^{-1} region.

In addition, it is interesting that in the dicarbonato or bis(oxalato) complex only the *cis* isomer is known in the case of present complexes as well as in the case of the diammine complexes.[8]

19) Y. Shimura and R. Tsuchida, This Bulletin, **29**, 311 (1956).
20) C. K. Jørgensen, "Absorption Spectra and Chemical Bonding in Complexes," Pergamon Press, New York and London (1961).
21) R. Tsuchida, *Nippon Kwagaku Kwaishi (J. Chem. Soc. Japan)*, **59**, 586 (1938).
22) C. J. Ballhausen, "Introduction to Ligand Field Theory," McGraw-Hill Book Company, Inc., New York (1962).

BULLETIN OF THE CHEMICAL SOCIETY OF JAPAN VOL. 42 2878—2881 (1969)

Reaction of Titanium Tetrahalides with Phenylhydrazones

R. C. AGGARWAL and S. K. SINGH

Chemistry Department, Lucknow University, Lucknow, India

(Received October 22, 1968)

Titanium tetrafluoride reacts with benzaldehyde phenylhydrazone to yield 1 : 1 adduct and with benzophenone phenylhydrazone 1 : 2 as well as 2 : 1 adducts, while other tetrahalides form 1 : 1 adducts with both the phenylhydrazones. All these complexes are coloured and stable at room temperature. The infrared spectral studies of phenylhydrazones and their titanium (IV) complexes have been made in the 4000—200 cm^{-1} region.

Snyder and Smith[1] have investigated the reactions of boron trifluoride with a number of phenylhydrazones containing α-methylene group and they showed that these reactions lead to the formation of indoles presumably through the intermediate formation of 1 : 1 adducts.

Recently Aggarwal and Makhija[2] in this laboratory prepared 1 : 1 adducts of tin tetrachloride with benzaldehyde phenylhydrazone and studied their structures from infrared spectral measurements. This work has now been extended to the reactions of titanium tetrahalides and the results obtained are described in the present communication.

Experimental

Titanium tetrahalides and organic solvents were purified and made anhydrous by standard literature methods. Benzaldehyde phenylhydrazone[3] and benzophenone phenylhydrazone[4] were prepared as described in literature and recrystallized from methanol (mp 157°C) and ethanol (mp 105°C) respectively.

Preparation of Complexes. *i) Titanium Tetrafluoride - Benzaldehyde Phenylhydrazone Complex.* 1—5% tetrahydrofuran solutions of TiF_4 and phenylhydrazone were mixed together and shaken vigorously. The reaction mixture was refluxed for 30 min and excess of solvent removed. The greenish-yellow solid mass thus obtained was washed repeatedly to remove excess of the base, and dried *in vacuo*.

ii) Titanium Tetrafluoride - Benzophenone Phenylhydrazone Complexes. Greenish-brown titanium tetrafluoride-benzophenone phenylhydrazone complex was prepared in a similar way as described above. Another complex (brown) was isolated from the filtrate of the above complex by the removal of excess of the solvent and washing the residual solid with a mixture of chloroform and tetrahydrofuran.

iii) Titanium Tetrachloride - Phenylhydrazone Complexes. On adding dropwise (1—5%) solution of phenylhydrazone in chloroform to a solution of titanium tetrachloride in the same solvent, coloured precipitate was obtained which was allowed to settle for several hours, filtered, washed and dried under reduced pressure.

iv) Titanium Tetrabromide - Phenylhydrazone Complexes. These complexes were prepared just like the titanium tetrachloride complexes.

No definite complexes of titanium tetraiodide with phenylhydrazones could be isolated from reactions carried out in chloroform and benzene solutions.

Complexes thus prepared were analysed for titanium, halogen, and nitrogen. Analytical results and general behaviour of the complexes are given in Table 1.

Infrared spectra measurements were carried out on a Beckman infrared spectrophotometer, Model IR-8. The spectra were recorded in Nujol mulls using sodium chloride plates. The far infrared spectra were taken on a Perkin Elmer-621 spectrophotometer in Nujol mulls using cesium iodide cells. The results obtained are included in Tables 2 and 3.

Discussion

Titanium tetrafluoride reacts with benzaldehyde phenylhydrazone to yield 1 : 1 adduct and with benzophenone phenylhydrazone 1 : 2 as well as 2 : 1 adducts, while other tetrahalides form 1 : 1 adducts with both the phenylhydrazones.

Titanium tetrahalides produce intense coloration with phenylhydrazones. The appearance of colour probably may be due to the existence of an equilibrium between the colourless phenylhydrazone and coloured phenylazo tautomer depicted below as titanium tetrahalide adducts:

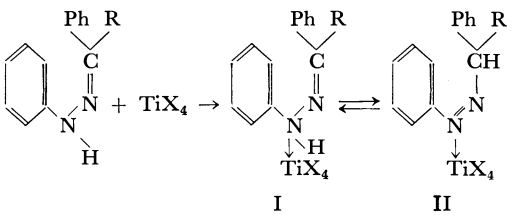

I II

1) H. R. Snyder and Curtis W. Smith, *J. Am. Chem. Soc.*, **65**, 2452 (1943).

2) R. C. Makhija, "A study of some silicon and tin tetrahalides with hydrazine and its derivatives," Ph. D. thesis, Univ. of Lucknow (1966).

3) F. G. Mann and B. S. Saunders "Practical Organic Chemistry," Longman, Green & Co., Ltd., 4th Edition, London (1960), p. 227.

4) F. G. Mann and B. S. Saunders, *ibid.*, p. 343.

TABLE 1. ANALYTICAL DATA AND GENERAL BEHAVIOUR OF COMPLEXES

Molar ratio TiX_4 : Base taken for reaction	Composition of the reaction product formed	% Found			% Calcd			Appearance and solubility	Temperature of decomposition (°C)	Magnetic behaviour
		Ti	Halogen	N	Ti	Halogen	N			
1 : 2	$TiF_4 \cdot C_6H_5CH{=}NNHC_6H_5$	15.3	23.8	9.0	15.00	23.50	8.75	greenish yellow solid, hygroscopic, s in $CHCl_3$, CCl_4, C_6H_6, $C_6H_5NO_2$	turns green at 130	diamagnetic
1 : 2	$(TiF_4)_2 \cdot (C_6H_5)_2C{=}NNHC_6H_5$	18.5	27.9	—	18.46	29.23	—	greenish brown solid, sensitive to moisture, s in THF, $C_6H_5NO_2$, i. in $CHCl_3$, CCl_4	turns dark brown at 144	diamagnetic
1 : 2	$TiF_4 \cdot 2(C_6H_5)_2C{=}NNHC_6H_5$	6.4	9.9	8.55	7.18	11.37	8.38	brown solid, sensitive to moisture, s in THF, $C_6H_5NO_2$, i in $CHCl_3$, CCl_4, C_6H_6	melts at 125 with change in colour	diamagnetic
1 : 2	$TiCl_4 \cdot C_6H_5CH{=}NNHC_6H_5$	12.7	37.0	—	12.44	36.75	—	brown solid, hygroscopic and fuming, i in $CHCl_3$, CCl_4, C_6H_6	turns black at 125	diamagnetic
1 : 2	$TiCl_4 \cdot (C_6H_5)_2C{=}NNHC_6H_5$	10.9	30.7	—	10.39	30.70	—	violet solid, hygroscopic i in $CHCl_3$, CCl_4, C_6H_6	—	diamagnetic
1 : 2	$TiBr_4 \cdot C_6H_5CH{=}NNHC_6H_5$	8.8	56.5	—	8.51	56.88	—	red solid, hygroscopic and fuming, i in $CHCl_3$, CCl_4, C_6H_6, dissolves in THF giving green solution.	turns black at 105	diamagnetic
1 : 2	$TiBr_4 \cdot (C_6H_5)_2C{=}NNHC_6H_5$	7.8	50.5	—	7.50	49.97	—	dark brown solid, i in $CHCl_3$, CCl_4, C_6H_6	turns black at 88	diamagnetic

Abbreviations: THF, tetrahydrofuran; s, soluble, i; insoluble.

Table 2. Assignment of important bands in the spectra of phenylhydrazones and their titanium tetrahalide complexes

Compound	ν(N–H) (cm^{-1})	ν(C=N) (cm^{-1})	Aromatic ring vibration and/or ν(N=N) (cm^{-1})	ν(C–N) (cm^{-1})	ν(N–N) (cm^{-1})
$C_6H_5CH{=}NNHC_6H_5$	3290 m, 3090 m	1652 w, 1635 w	1600 s, 1588 s, 1562 s	1298 m, 1285 m, 1258 s	928 m, 878 w
$TiF_4 \cdot C_6H_5CH{=}NNHC_6H_5$	3290 m, 3150 s	1652 w, 1635 w, 1612 m	1598 m, 1578 m, 1570 m, 1565 m	1300 m, 1262 m	920 m, 885 m, b
$TiCl_4 \cdot C_6H_5CH{=}NNHC_6H_5$	—	1650 w, 1632 w, 1612 m	1590 m, 1572 m, 1565 m	1292 w	—
$TiBr_4C_6H_5CH{=}NNC_6H_5$	—	1658 vw, 1638 vw	1560 m, b	—	—
$(C_6H_5)_2C{=}NNHC_6H_5$	3310 m, 3110 m	1650 w, 1632 w	1595 s, 1572 m,	1305 w, 1275 w	960 m, 880 m
$(TiF_4)_2 \cdot (C_6H_5)_2C{=}NNHC_6H_5$	3290 m, b 3138 m	1620 w	1598 w, 1572 w, 1568 w	1305 w, 1290 w	955 m, 890 m
$TiF_4 \cdot 2(C_6H_5)_2C{=}NNHC_6H_5$	3310 m	—	1585 m	1302 w, 1285 w	955 m
$TiCl_4 \cdot (C_6H_5)_2C{=}NNHC_6H_5$	—	1650 w, 1632 w, 1615 w	1585 w, 1572 w, 1568 w	1285 w	—
$TiBr_4 \cdot (C_6H_5)_2C{=}NNHC_6H_5$	—	—	1595 s, b	—	—

Table 3. Far infrared spectral results of phenylhydrazones and their titanium tetrahalide complexes

Compound	ν(Ti–X) (cm^{-1})	ν(Ti–N) (cm^{-1})	Ligand bands, (cm^{-1})
$C_6H_5CH{=}NNHC_6H_5$	—	—	685 s, 662 w, 638 m, 628 m, 608 m, 500 s, 438 m, 388 m, 345 w, 318 w, 285 w, 258 m
$TiF_4 \cdot C_6H_5CH{=}NNHC_6H_5$	630 s, 575 s, b	515 s	695 s, 280 s, 268 s, 258 s
$TiCl_4 \cdot C_6H_5CH{=}NNHC_6H_5$	395 m, 298 m	570 w	675 m, b, 325 m, b, 272 m, 242 m
$TiBr_4 \cdot C_6H_5CH{=}NNHC_6H_5$	320 m,	513 w	690 s, b, 372 m, b
$(C_6H_5)_2C{=}NNHC_6H_5$	—	—	652 m, 652 m, 560 w, 502 w, 435 m, 370 w, 345 w, 322 w, 261 m, 250 m, 242 m
$TiF_4 \cdot 2(C_6H_5)_2C{=}NNHC_6H_5$	658 m, 560 m	508 m	440 m
$(TiF_4)_2 \cdot (C_6H_5)_2C{=}NNHC_6H_5$	660 m, 552 m	515 m	695 m, 685 m, 350 w, 270 w, 240 w
$TiCl_4 \cdot (C_6H_5)_2C{=}NNHC_6H_5$	385 m	565 m, b	375 w, 365 w
$TiBr_4 \cdot (C_6H_5)_2C{=}NNHC_6H_5$	315 m	515 w	678 s, b, 555 m, 382 w, 275 w.

The adducts are intractable, insoluble in common organic solvents and do not possess sharp melting points.

There are two sites for coordination in phenylhydrazones *viz.*, N^I and N^{II} as shown below:

$$R_1R_2C{=}N^{II}{-}N^IHC_6H_5 \rightleftharpoons R_1R_2CHN^{II}{=}N^IC_6H_5$$
(I) (II)

In titanium tetrahalide complexes of phenylhydrazones, one would expect changes in N–H, N–N, C=N and /or N=N and Ti-X stretching frequencies as compared with the location of these bands in the parent bases and Lewis acids, and appearance of new band characteristic of ν(Ti-N).

N–H Stretching Bands. Spectra of benzaldehyde and benzophenone phenylhydrazones recorded in the present work contain two bands at 3290, 3090 cm^{-1} and 3310, 3110 cm^{-1} respectively assigned to N-H stretching modes.[5,6]

A negative shift in ν(N–H) would be expected if coordination takes place through N^I of the isomer-I. An intramolecular change in phenylhydrazones would yield isomer-II containing no >NH group and hence the infrared spectra of this isomer and its complexes should show no absorptions characteristic of >NH group.

The presence of N–H stretching bands in the spectra of $TiF_4{\cdot}C_6H_5CH{=}NNHC_6H_5$, $(TiF_4)_2{\cdot}(C_6H_5)_2C{=}NNHC_6H_5$, and $TiF_4{\cdot}2(C_6H_5)_2C{=}NNHC_6H_5$, therefore, indicates that the adducts are formed mainly with tautomeric form-I.

In the infrared spectra of titanium tetrachloride and tetrabromide complexes of phenylhydrazones, the N–H stretching bands almost disappear. This indicates that the adduct formation takes place mainly with phenylazo tautomeric form-II.

C=N, N=N and N–N Stretching Frequencies. Weak bands observed in the spectra of the phenylhydrazones in 1620—1652 cm^{-1} region are assigned to ν(C=N).[7-10]

A tautomeric change in phenylhydrazones would be expected to give a new band corresponding to N=N stretching vibration. The specific assignment of the N=N stretching modes in aromatic azo compounds is difficult due to the interference of C=C ring vibrations.[8]

The N–N stretching modes are absent in the titanium tetrachloride and tetrabromide complexes, further supporting the adduct formation with isomer-II. The presence of N–N stretching bands of medium intensity in titanium tetrafluoride complexes supports the existence of the phenylhydrazones mainly in the isomeric form-I in these complexes.

Ti–N and Ti–X Stretching Bands. The new bands occurring in 570—513 cm^{-1} region in the complexes are tentatively assigned to ν(Ti-N).[11,12] The magnitude of the ν(Ti-N) is in good agreement with the thermal stability of complexes.

The occurrence of ν(Ti-X) modes in the octahedral region in the spectra of the complexes shows that they have octahedral geometry.[13,14]

The authors are grateful to the Council of Scientific and Industrial Research, New Delhi (India), for the award of Junior Research Fellowship to one of them (S.K.S.), and to Dr. M. Onyszchuk, McGill University, Montreal (Canada), for his kind help in the form of chemicals and equipment.

5) D. Hadzi and J. Jan, *Spectrochim. Acta,* **23** A, 571 (1967).
6) D. Hadzi and J. Jan, *Rev. Roumaine Chim.,* **10**, 1183 (1965).
7) J. Fabian, M. Legrand and P. Poirier, *Bull. Soc. Chim. France,* **1956** 1499.
8) L. J. Bellamy, "The Infrared Spectra of Complex Molecules," John Wiley & Sons, Inc., New York (1960), pp. 267—271.
9) L. D. Frederickson, *Anal. Chem.,* **36**, 1349 (1964).
10) J. Fabian and M. Legrand, *Bull. Soc. Chim. France,* **1956**, 1461.
11) R. T. Cowdell, G. W. A. Fowles and R. A. Welton, *J. Less-Common Metals,* **5**, 386 (1963).
12) S. C. Jain and R. Rivest, *Can. J. Chem.,* **45**, 139 (1967).
13) I. R. Beattie and M. Webster, *J. Chem. Soc.,* **1964**, 3507.
14) R. J. H. Clark and W. Errington, *ibid.,* (A), **1967**, 258.

BULLETIN OF THE CHEMICAL SOCIETY OF JAPAN VOL. 42 2882—2885 (1969)

Configuration of 1,3-Dipolar Cycloaddition Products of Nitrones with *N*-Phenylmaleimide

Yoshio IWAKURA, Keikichi UNO and Tatsuhiko HONGU

Department of Synthetic Chemistry, Faculty of Engineering, The University of Tokyo, Hongo, Bunkyo-ku, Tokyo

(Received October 30, 1968)

1,3-Dipolar cycloaddition reaction of aldonitrones such as *C*-2-furyl-*N*-phenyl-, *C,N*-diphenyl-, and *C*-2-thienyl-*N*-phenylnitrone with *N*-phenylmaleimide was carried out. The product was separated into two stereo isomers, *cis* and *trans* isoxazolidines with respect to H_3 and H_4, which were identified by NMR spectra. Spin-spin coupling of protons on C_3 and C_4 of isoxazolidine ring was found to be 8.4—9.0 cps for *cis* isomers and to be zero for *trans* isomers.

In a series of studies on the synthesis of new polymers, we have reported syntheses of polymers through 1,3-dipolar cycloaddition reaction.[1] As a basic study of these polymer formation reaction, the reaction of nitrones with *N*-phenylmaleimide was examined. There are some reports on the synthesis of isoxazolidines by 1,3-dipolar cycloaddition reaction of nitrones with C–C double bond.[2-6] However, few studies were carried out from a structural viewpoint. Recently, Huisgen reported the reaction of nitrones with norbornene, and two stereo isomers were isolated in the reaction of *C,N*-diphenylnitrone with norbornene.[7]

We found that *C,N*-diphenylnitrone, *C*-2-furyl- and *C*-2-thienyl-*N*-phenylnitrone gave two kinds of stero isomers, *cis*- and *trans*-isoxazolidines, in each reaction with *N*-phenylmaleimide. NMR spectra of these compounds confirmed their configurations. Details are described in this paper.

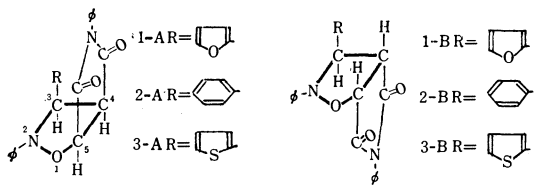

A *cis* B *trans*

Scheme 1

Results and Discussion

Two configurations, *syn* and *anti* forms, are expected for the structure of nitrone.

anti form *syn* form

However, only an *anti* form has been shown to actually exist for aldonitrone by UV and NMR spectroscopy by Hamer and Macaluso.[4] Analytical and physical data of nitrones used are shown in Table 1.

Only one signal was observed as a methine proton in the NMR spectrum of each nitrone. The nitrones used in the present study can therefore be considered to be pure and their configurations *anti* according to Hamer and Macaluso.

The reaction of nitrones with *N*-phenylmaleimide was carried out by heating a mixture of both reagents in anhydrous tetrahydrofuran (THF). The results, analytical and physical data of these products are summarized in Table 2.

Elemental analysis for the paired products gave the same values in spite of their different melting points. Therefore, it is reasonable that these paired compounds are isomers with each other. The ratio of the isomers was determined by comparing the weight of the separated product, and the value obtained was in good agreement with the ratio determined by NMR. Some NMR spectra are shown in Figs. 1 and 2.

Signals observed in lower magnetic fields than $\tau 3$ were assigned to protons on benzene and hetero-

1) Y. Iwakura, M. Akiyama and S. Shiraishi, This Bulletin, **38**, 335 (1965); *ibid.*, **38**, 513 (1965).

2) Y. Iwakura, K. Uno, S. Shiraishi and T. Hongu, The 20th Annual Meeting of the Chemical Society of Japan, April, 1967, Tokyo.

3) R. Huisgen, R. Grashey and J. Sauer, "Cycloaddition Reaction of Alkenes," in "The Chemistry of Alkenes," ed. by S. Patai, Interscience Publishers, New York, N. Y. (1946), p. 739.

4) J. Hamer and Macaluso, *Chem. Revs.*, **64**, 473 (1964).

5) G. H. Delpierre and M. Lamchen, *Quart. Revs. (London)*, **19**, 329 (1965).

6) Y. Nomura, F. Furusaki and Y. Takeuchi, This Bulletin, **40**, 1740 (1967).

7) R. Huisgen, R. Grashey, H. Hauch and H. Seidl, *Chem. Ber.*, **101**, 2043 (1968).

TABLE 1. PHYSICAL DATA OF NITRONES

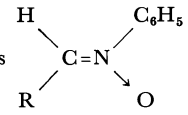

R	Mp °C	Yield %	Recrystal.	NMR* Methine proton (τ)	NMR* Proton ratio aromatic : methine	Anal. (Calcd) C%	H%	N%
	89	63	Petroleum ether	1.02 (singlet)	8 : 1	70.58 (70.58	4.95 4.85	7.52 7.48)
	111—112	95	Benzene-*n*-hexane	1.43 (singlet)	10 : 1	80.01 (79.16	5.58 5.62	7.21 7.10)
	90	87	Petroleum ether	0.85 (singlet)	8 : 1	64.99 (65.05	4.49 4.47	6.39 6.59)

* NMR spectra were observed in 10 wt% DMSO-d_6 solution at 26°C.

TABLE 2. PHYSICAL DATA OF PRODUCTS

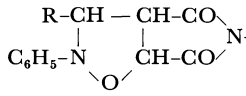

: A (*cis*) AND B (*trans*)

	Mp °C	NMR Chemical shift (τ) H_3	H_5	H_4	NMR Coupling constant (cps) J_{3-4}	J_{4-5}	Solvent	Anal. (Calcd) C%	H%	N%
1-A	185—186	5.14(d)	4.65(d)	5.95(q)	8.4**	7.2**	DMSO-d_6	69.80 (69.99	4.61 4.48	7.72 7.77)
2-A	197—199	4.96(d)	4.57(d)	5.84(q)	9.0**	7.2**	DMSO-d_6	74.30 (74.59	4.48 4.96	7.44 7.56)
3-A	171.5	4.35(d) 4.95(d)	4.45(d) 4.85(d)	5.73(q) 6.16(q)	9.0** 9.0**	7.2** 7.2**	DMSO-d_6 $CDCl_3$	66.93 (67.01	4.21 4.29	7.71 7.44)
1-B	140—141	4.43(s)	4.86(d)	5.87(d)	0	7.2	$CDCl_3$	69.77	4.45	7.75
2-B	153—155	4.32(s) 4.07(s)	5.08(d) 4.54(d)	6.31(d) 5.84(d)	0 0	7.2 7.2	$CDCl_3$ DMSO-d_6	75.01	5.08	7.75
3-B	174—175	3.88(s)	4.66(d)	5.84(d)	0	7.2	DMSO-d_6	67.11	4.32	7.50

* NMR spectra were observed in 10 wt% solution at 26°C.
** Values were obtained by first order analysis.
s: singlet, d: doublet, q: quartet.

aromatic rings. Signals of protons on isoxazolidine ring were observed as three groups in a field from τ4 to 6. The ratios of the integrated intensities of signals of protons on aromatic rings and those of isoxazolidine rings were 13/3 for 1-A, 13/3 for 1-B, 15/3 for 2-A, 15/3 for 2-B, 13/3 for 3-A, and 13/3 for 3-B. These values were the same as theoretical values 13/3, 15/3, and 13/3 for compounds 1, 2, and 3, respectively.

Signals observed around τ6 could be assigned to the protons on C_4 of isoxazolidine ring as the atoms of both sides of C_4 are carbon. It is generally accepted that the spin-spin coupling of protons in *cis* position is larger than that in *trans*. In oxazolidine obtained here, the relative position of protons on C_4 and C_5 is to be *cis* position because C_4 and C_5 are also ring members of succinimide at the same time. Therefore, it is reasonable to consider that coupling constants of protons on C_4 and C_5 are comparatively large, and their values are the same independent of the position and kind of substituent on the isoxazolidine ring.

As shown in Table 2 and Fig. 1, compounds obtained could be divided into two groups by the figure of the signal (H_3) of isoxazolidine which was observed in the lowest magnetic field. Compounds 1-B, 2-B, and 3-B belong to group B only, in which signals (H_3) appear as a singlet. On the other hand, compounds 1-A, 2-A, and 3-A form another group A in which signals (H_3) are observed as a doublet.

In group B, signals (H_3) were assigned to those of protons on C_3, because protons on C_4 and C_5 should be *cis* and give doublet signals. Signals (H_4) observed around τ6 were assigned to those of protons on C_4 on the assumption described above,

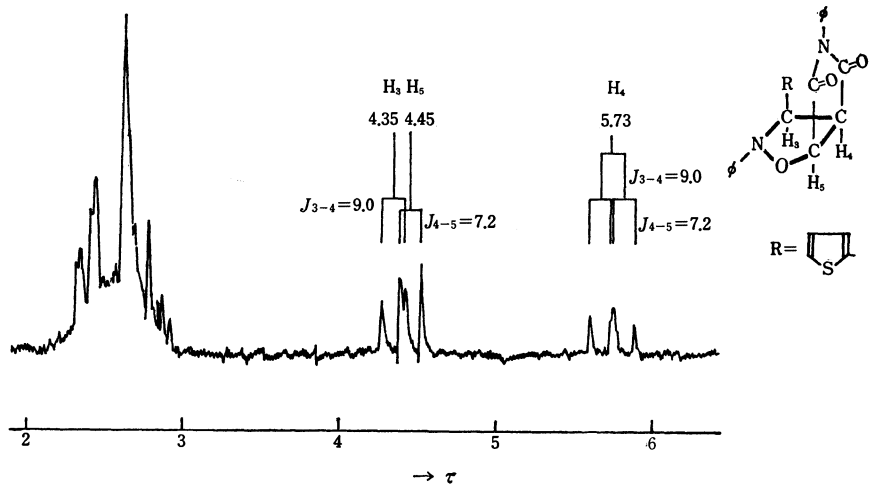

Fig. 1. NMR spectrum of cycloadduct 3-A in DMSO-d_6 by 60 Mc.

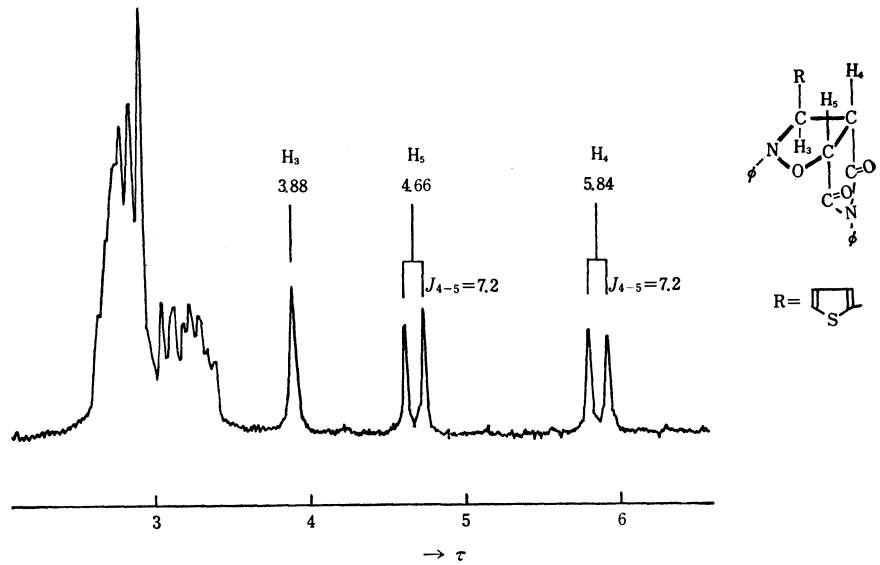

Fig. 2. NMR spectrum of cycloadduct 3-B in DMSO-d_6 by 60 Mc.

and were observed as doublets with spacing of 7.2 cps. The residual signals (H_5) which were observed around τ4.5 were assigned to those of protons on C_5 and were observed as doublets with spacing of 7.2 cps. The same spacing (7.2 cps) of H_4 and H_5 appeared to confirm the above consideration. As the protons on C_4 and C_5 are in *cis*-position, the coupling constants of 7.2 cps are reasonable for the structure. Thus the configuration of compounds in group B was concluded to be *trans* as shown in Scheme I.

In group A, the signals of the protons on isoxazolidine ring were observed as three groups, two doublets and a quartet, as shown in Table 2 and Fig. 2. Coupling constants of these protons were found to be large. Therefore, the relative position of these protons on a ring seems to be *cis*-position. Assignment of the signals in the highest magnetic field to the proton on C_4 may be reasonable because the signals are quartet.

If we assume that the relative position of the protons on C_4 and C_5 is the same, then the coupling constant of the protons on C_4 and C_5 will be independent of the position and the kind of substituent on isoxazolidine ring. Therefore, coupling constants 7.2 cps, which were concluded as that of the protons on C_4 and C_5 in group B may be attributed to the protons on C_4 and C_5 in group A. As shown in Table 2, little variation in values of the chemical shifts of H_5 and H_4 was observed. However, a large variation appeared in the chemical sihft of H_3.

The proton on C_5 is always placed on the opposite side of carbonyl group and far from other groups. Therefore, the difference in relative position between the proton and other groups gave a weak effect on the chemical shift of the proton. On the other hand, the proton on C_3 is located very near the carbonyl group in the compounds of group B, but the distance between the proton and the carbonyl group is great in the compounds of group A. The variation of the distance and relative position between the proton and carbonyl group is known to influence the chemical shift of the proton. Accordingly, the chemical shift of the proton on C_3 was expected to be different according to whether the compound belongs to group A or B. The results obtained were interpreted well by the configuration in Scheme 1.

Experimental

Nitrones. A typical example of the reaction of *C*-2-furyl-*N*-phenylnitrone is as follows. To 150 m*l* of ethanol 22 g (0.23 mol) of 2-furfural and 30 g (0.275 mol) of phenylhydroxylamine were added. The mixture was allowed to react at room temperature over night. The product was obtained by removing the solvent. Recrystallization three times from petroleum ether gave 27 g (63%) of needles, mp 89°C.

1,3-Dipolar Cycloaddition Reaction. The reaction was carried out in a closed tube. To a 30 m*l* of anhydrous THF, 3 g (0.015 mol) of *C*-2-furyl-*N*-phenylnitrone and 2.19 g (0.015 mol) of *N*-phenylmaleimide were dissolved in the presence of a small amount of *β*-naphthylamine which is an inhibitor of radical polymerization. The tube was sealed and heated at 100°C, for 10 hr. The solvent evaporated under reduced pressure to give white mass. It was recrystallized from benzene - hexane to yield white crystals, mp 142—167°C. The crystals were extracted with hot ethanol, and the ethanol solution was cooled to give white needles, mp 142—150°C, which were recrystallized twice from benzene - *n*-hexane to give B, mp 142—144°C. The fraction insoluble in ethanol was recrystallized twice from benzene - *n*-hexane to give A, mp 185—186°C. The reaction of *C*,*N*-diphenylnitrone or *C*-2-thienyl-*N*-phenylnitrone with *N*-phenylmaleimide was carried out by a similar procedure.

NMR Spectra Measurements. The NMR spectra were taken with a Japan Electron Optics C-60 spectrometer at a frequency of 60 Mc using about 10% solution of the sample in $CDCl_3$ or DMSO-d_6 with tetramethylsilane as an internal standard.

BULLETIN OF THE CHEMICAL SOCIETY OF JAPAN VOL. 42 2885—2894 (1969)

Configuration and Conformation of So-called Bis(alkylidenearylamines)

Masuo FUNABASHI, Masaharu IWAKAWA and Juji YOSHIMURA

Laboratory of Chemistry for Natural Products, Faculty of Science, Tokyo Institute of Technology, Meguro-ku, Tokyo

(Received November 27, 1968)

The proposed structures of the dimeric products obtained from aliphatic aldehydes and arylamines were reexamined by IR and NMR spectra. The 1,2,3,4-tetrahydroquinoline structure was ascertained in the case of acetaldehyde or propionaldehyde, and aldolic structure was confirmed in the case of *n*-butyraldehyde. It was observed that the latter readily isomerizes to the former type in the presence of acetic acid. Conformational analysis of a racemic pair of the former (IIIa—c: 2,4-disubstituted, IIId- 2,3,4-trisubstituted) indicated that two isomers of IIIa—c (one has 2-equatorial, 4-quasi-equatorial and the other 2-equatorial, 4-quasi-axial substituents) have a flattened half-chair conformation and two isomers of IIId (one has 2,3-diequatorial, 4-quasi-equatorial, and the other 2-equatorial, 3-axial, 4-quasi-axial substituents) have a more remarkably flattened half-chair, *i. e.* a nearly plane structure. The acylation of ring nitrogen enhanced this tendency, and one of the 1-acetyl derivatives of III was deduced to have a twist half-boat conformation.

On the structure of so-called bis(alkylidene-arylamines) which have been regarded as one of the key-intermediates[1] in the Doebner-von Miller synthesis of quinolines from arylamines and aliphatic aldehydes, the following three formulas have been proposed; the acyclic structure of the aldol type (I), the enamine structure due to the isomerization of I (II) and the cyclic structure having 1,2,3,4-tetrahydroquinoline skelton (III).

1) N. Campbell, R. E. Fairbairn, E. Hoggarth, J. D. Loudon and T. S. Stevens, "Chemistry of Carbon Compounds," Vol. IV, ed. by E. H. Rodd and S. Coffey, Elsevier Publishing Company, Amsterdam, London, New York (1957), p. 588.

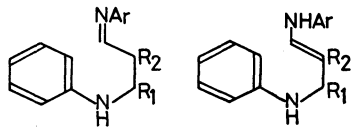

I II

$R_1 = CH_2CH_2CH_3$
$R_2 = CH_2CH_3$
Ar = C_6H_5

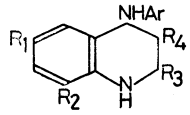

III

	R_1	R_2	R_3	R_4	Ar
a)	H	H	CH_3	H	C_6H_5
b)	CH_3	H	CH_3	H	4-Tolyl
c)	CH_3	CH_3	CH_3	H	2,4-Xylyl
d)	H	H	C_2H_5	CH_3	C_6H_5
e)	H	H	n-C_3H_7	C_2H_5	C_6H_5

Scheme 1

For a long time, structure I has been accepted without any definite evidences.[2] However, Minkin and Tumakoba[3] have recently proposed that, on the basis of IR and UV spectral investigation, both bis(ethylideneaniline) and bis(propylideneaniline) are of structure III, and bis(butylideneaniline), to which Kharasch *et al.*,[4] had given structure I, is of structure II.

In a previous paper,[5] the authors have reported the easy dimerization of *N*-phenyl-acetone-D-glyceraldimine to 4-anilino-1,2,3,4-tetrahydroquinoline derivatives in the presence of catalytic amount of acetic acid, and the determination of their partial absolute configuration by chemical degradation and spectral measurements.

These results stimulated us to determine the configuration and conformation of general bis(alkylidenearylamines) and their isomers by IR and NMR spectral studies, in connection with the mechanism of Doebner-von Miller reaction. The results obtained are discussed in this paper.

Results and Discussion

Configuration of Bis(alkylidenearylamines). The structures I, II, and III would be easily distinguished by the presence or absence of a characteristic absorption of C=C and C=N bonds in IR spectra, and azomethine and olefinic proton signals in NMR spectra. The results obtained indicated that bis(ethylideneaniline)[2] (IIIa), bis(ethylidene *p*-toluidine)[6] (IIIb), bis(ethylidene *m*-xylidine)[7] (IIIc) and bis(propylideneaniline)[2] (IIId) have structure III, because they showed the absence of C=C and C=N absorption band in IR spectra and the absence of azomethine and olefinic proton signals in NMR spectra, and furthermore, their monoacyl derivatives still showed the presence of NH absorption band at *ca.* 3300 cm^{-1}. The NMR spectra of these compounds will be shown and discussed in the next paragraph.

Contrary to Minkin's findings, NMR spectrum of bis(butylideneaniline) (I) shown in Fig. 1 indicated that it has aldol type structure. Irradiation of Ha caused Hc to collapse to a quartet, and reversal irradiation of Hc caused Ha to collapse to a seemingly narrow triplet with a long range coupling. Therefore, the quintet at τ 7.43, the quartet at τ 6.3 and the doublet at τ 2.2 (J=6.25) can be assigned to Hc, Hb and Ha, respectively.

The chemical shift of Ha is too low for that of olefinic proton and moreover, the coupling constants, which remained unchanged by addition of deuterium oxide, are too large to expect a long range coupling of the olefinic proton in structure II. The following examples of the chemical shifts of azomethine protons may also support the above conclusion; τ 1.65 in benzylideneaniline,[8] τ 2.37 in ethylidenepropylamine,[8] τ 2.56—3.16 in acetoaldoxime.[9] On the other hand, 2-ethylhexylideneaniline (IV), which is partially analogous to I and obtained from aniline and 2-ethylhexaldehyde, showed the presence of azomethine proton signal at τ 2.4 (J=6.5).

It has thus become clear that acetaldehyde or propionaldehyde give type III in the condensation with arylamines even in the absence of an acid catalyst, and a higher aldehyde such as *n*-butyraldehyde gives acyclic type I. In order to clarify such an effect of acid catalyst as was observed in a previous study[5] and the relationship between I and III, a catalytic amount of acetic acid was added to a solution of I in $CDCl_3$ (Fig. 2). The azomethine proton signal (Ha) disappeared promptly and a ring proton signal of 1,2,3,4-tetrahydroquinoline appeared at τ 5.62. This fact suggests the conversion of I to III, whose structure was also ascertained by UV (λ_{max} 251, 302 mμ) and IR (the disappearence of the absorption

2) W. v. Miller, J. Plöchl and F. Eckstein, *Ber.*, **25**, 1241, 2020 (1892); W. v. Miller and J. Plöchl, *ibid.*, **27**, 1299 (1894).

3) V. I. Minkin and Z. A. Tumakoba, *Zh. Obschch. Khim.*, **33**, 642 (1963); *ibid.*, **34**, 357 (1964).

4) M. S. Kharasch, J. Richlin and F. R. Mayo, *J. Am. Chem. Soc.*, **62**, 494 (1940).

5) M. Funabashi and J. Yoshimura, This Bulletin, **41**, 2735 (1968).

6) M. G. Edward, R. E. Garrod and H. O. Jones, *J. Chem. Soc.*, **1912**, 1383.

7) H. O. Jones and E. J. White, *ibid.*, **1910**, 632.

8) J. F. King and T. Durst, *Can. J. Chem.*, **40**, 882 (1962).

9) Varian's "NMR Spectra Catalog," Vol. 2.

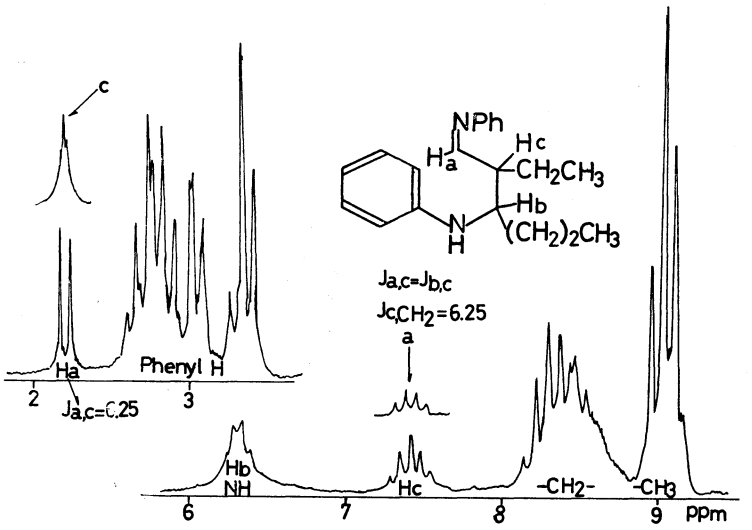

Fig. 1. NMR spectra of bis(butylideneaniline) (I) (100 Mc, CDC_3l).

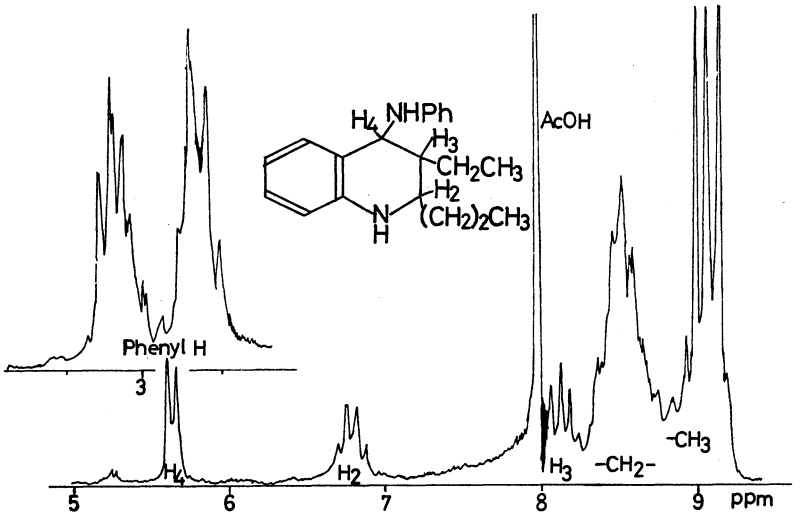

Fig. 2. NMR spectra of the isomerised compound (IIIe) of I in the presence of acetic acid (100 Mc, $CDCl_3$).

band of C=N and the increase of the intensity of the absorption band of NH), and moreover, by the fact that 1-tosyl derivative of IIIe still showed NH absorption band at 3300 cm^{-1}. Besides, distillation of I caused the β-elimination of aniline to give 2-ethyl-2-hexenylideneaniline (V). Such a phenomenon is characteristic for structure I, but not for III.

The Doebner-von Miller synthesis of quinolines from arylamines and lower aliphatic aldehydes has been done in a strongly acidic condition at a high temperature, and two reaction mechanisms[1] have been postulated for it; one includes the formation of α,β-unsaturated aldehydes due to the aldol condensation, the β-addition of arylamines and cyclization similar to that of the Skraup synthesis, and the other the intermediate such as I formed by the aldolic addition of alkylidenearylamines. The results described above seem to be closely related to the latter mechanism, and more detailed work is being undertaken.

Conformation of Bis(ethylidenearylamines) and Bis(propylidenearylamines). It is known that there are usually two isomers in bis-(ethylideneaniline). Some workers[10] considered them to be a pair of geometric isomers of structure II. However, it is now obvious that they should be the diastereomer of substituted 1,2,3,4-tetrahydroquinolines. Minkin and Gorelob[11] distinguished them from

10) A. Eibner, *Ann.*, **318**, 58 (1901).

11) V. I. Minkin and M. I. Gorelob, *Zh. Obschch. Khim.*, **33**, 647 (1963); *Chem. Abstr.*, **59**, 2624f (1963).

their dipole moment, but the results are doubtful becasse of fundamental misunderstanding of stereochemistry. Therefore, the authors attempted to analyse the conformation of known and some new tetrahydroquinolines with NMR technique.

It has been concluded by X-ray analysis[12] that the cyclohexene molecule preferentially exists as a half-chair conformation, and the result has been applied to the conformational analysis of 1,2,3,4-tetrahydroquinolines,[13] glucal triacetate,[14] shikimic acid[15] and 1,2,3,4-tetrahydroisoquinolines.[16]

a) Conformation of Bis(ethylidenearylamines). Theoretically, there are two *cis* and two *trans* racemic stereoisomers, respectively in bis(ethylidenearylamines), *i.e.*, 1,2,3,4-tetrahydro-2,4-disubstituted-quinolines. Two substituents at C_2 and C_4 are equatorial and quasi-equatorial, or axial and quasi-axial in the case of *cis*-1 and *cis*-2, and equatorial and quasi-axial, or axial and quasiequatorial*1 in the case of *trans*-1 and *trans*-2, respectively.

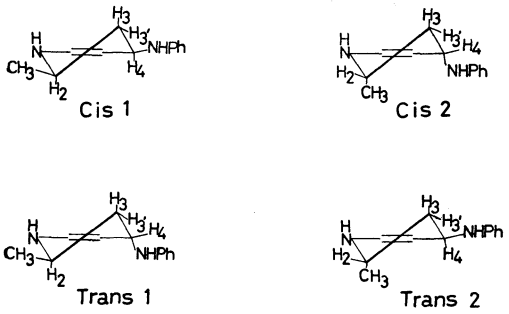

Scheme 2

The order of the stability of four conformation will be empirically given as follows; *cis*-1, *trans*-1, *trans*-2 and *cis*-2. As has been pointed out by Booth[13] that the methyl group of 1,2,3,4-tetrahydro-2-methylquinoline prefers an equatorial orientation, it is probable that the favoured conformations of two known isomers of bis(ethylideneaniline) should be *cis*-1 and *trans*-1. The coupling constants of each ring protons, which can be calculated from the angle parameters of cyclohexene[17] and are listed in Table 1, make it possible to distinguish them. The order of the chemical shifts (τ) of ring protons will be given; H_3 (a), H_3' (e), H_2 and H_4 from higher to lower field.

Table 1. The expected dihedral angles[a] for 2,4-disubstituted 1,2,3,4-tetrahydroquinolines and the corresponding coupling constants[b]

	(H_2, H_3)	(H_2, $H_{3'}$)	($H_{3'}$, H_4)	(H_3, H_4)
cis-1	178°	62°	45°	165°
J	14.2	2.7	6.2	13.4
	(11.0)	(3.0)	(7.1)	(10.0)
trans-1	178°	62°	75°	45°
J	14.2	2.7	0.83	6.2
	(11.0)	(3.0)	(0.77)	(7.1)
cis-2	62°	58°	75°	45°
J	2.7	2.8	0.83	6.2
	(3.0)	(3.0)	(0.77)	(7.1)
trans-2	62°	58°	45°	165°
J	2.7	2.8	6.2	13.4
	(3.0)	(3.2)	(7.1)	(10.3)

a) obtained from Bucourt's parameters
b) calculated from Abraham's equation[18] (Lemieux's equation[19])

The NMR spectrum of the one isomer of 1,2,3,4-tetrahydro-4-anilino-2-methylquinoline ($IIIa_1$, mp 126°C) is shown in Fig. 3. Inspection of this chart indicates that the $\delta\nu/J$ is sufficiently large to allow a first-order analysis. The quartet at τ 8.50, which is partly superimposed on the methyl proton signal, the octet at τ 7.67, the multiplet at τ 6.4, and the quartet at τ 5.2 are easily assigned to H_3 ($J_{3,3'}=J_{3,2}=J_{3,4}=11.5$ Hz), $H_{3'}$ ($J_{3',4}=5.0$, $J_{3',2}=2.5$ Hz), H_2 and H_4 respectively. Comparison of the above data with that of Table 1 clearly demonstrated that $IIIa_1$ belongs to *cis*-1 conformation. The dihedral angles of $IIIa_1$ are estimated from the equation of Abraham[18] as follows; (H_2, H_3)=(H_3, H_4)=155°, (H_2, $H_{3'}$)=63° and ($H_{3'}$, H_4)=51°.

The NMR spectrum of another isomer ($IIIa_2$, mp 86°C) is shown in Fig. 4. In this case, the sextet at τ 8.57 and τ 7.93, the multiplet at τ 6.63 and the quartet at τ 5.58 are assigned to H_3 ($J_{3,3'}=J_{2,3}=11.3$, $J_{3,4}=3.75$ Hz), $H_{3'}$ ($J_{2,3'}=J_{2',4}=2.5$ Hz), H_2 ($J_{2,CH_3}=6.5$ Hz) and H_4, respectively. The results indicate that $IIIa_2$ belongs to *trans*-1 conformation, and the dihedral angles are estimated in the similar manner: (H_2, H_3)=152°, (H_2, $H_{3'}$)=($H_{3'}$, H_4)=63° and (H_3, H_4)=58°.

The analytic data of IIIa, IIIb, IIIc and their 1-acyl derivatives, and 1,2,3,4-tetrahydro-2,6-dimethyl-4-hydroxyquinoline[2] (III'a; *trans*), 1,2,3,4-tetrahydro-1-acetyl-4-acetoxy-2,6-dimethylquinoline[2] (III'b; *cis*) and 1,2,3,4-tetrahydro-1-acetyl-4-ethoxy-2-phenylquinoline (III'c; *cis*) are summarized in Table 2. The ratio of the formation

*1 Axial, equatorial, quasi-axial and quasi-equatorial are abbreviated to a, e, qa and qe, respectively.

12) J. M. Lindsay and W. H. Barnes, *Acta Cryst.*, **8**, 227 (1955).
13) H. Booth, *J. Chem. Soc.*, **1964**, 1841.
14) L. D. Hall and L. F. Johnson, *Tetrahedron*, **20**, 883 (1968).
15) R. McCrindle, K. H. Overton and R. A. Baphael, *Tetrahedron Letters*, **1968**, 1847.
16) G. Grethe, M. Uskovic, T. Williams and A. Brossi, *Helv. Chim. Acta*, **50**, 2397 (1967).
17) R. Bucourt, *Bull. Soc. Chim. France*, **1964**, 2080; R. Bucourt and D. Hainaut, *ibid.*, **1965**, 1366.
18) R. J. Abraham, *Mol. Phys.*, **5**, 513 (1962).
19) R. U. Lemieux and W. J. Lown, *Can. J. Chem.*, **42**, 893 (1964).

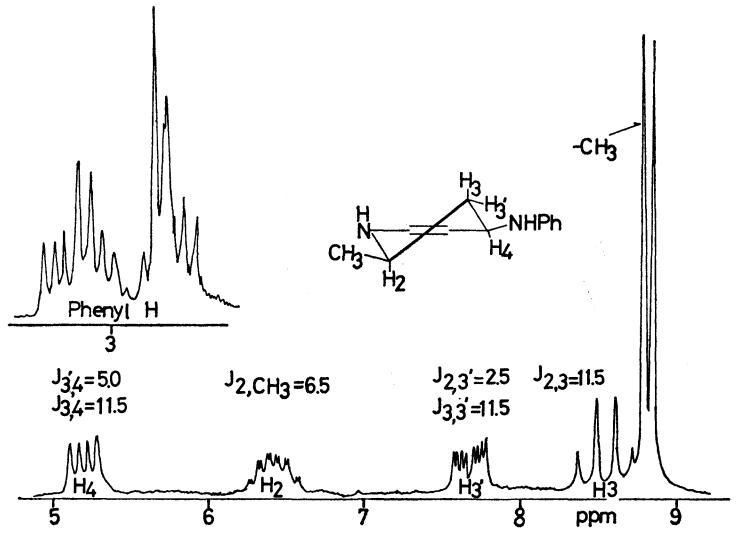

Fig. 3. NMR spectrum of 1,2,3,4-tetrahydro-4-anilino-2-methylquinoline ($IIIa_1$) [bis(ethylideneaniline):*cis*] (100 Mc, $CDCl_3$).

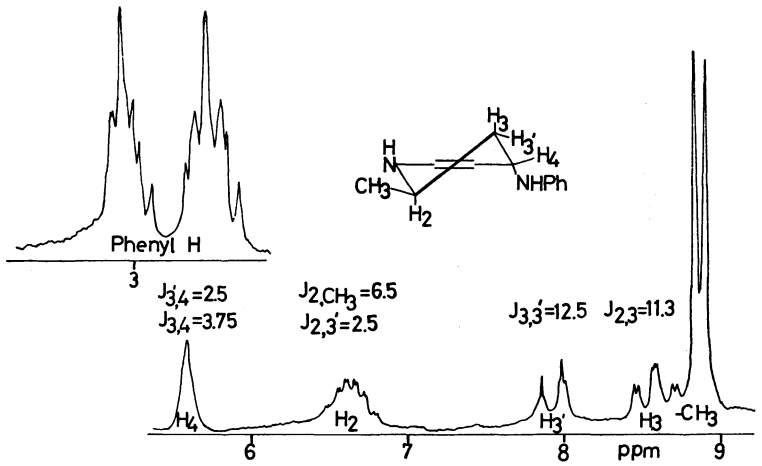

Fig. 4. NMR spectrum of 1,2,3,4-tetrahydro-4-anilino-2-methylquinoline ($IIIa_2$) [bis(ethylideneaniline):*trans*] (100 Mc, $CDCl_3$).

of $IIIa_1$ and $IIIa_2$ in the crude product was estimated from the intensity of each H_4 proton signal, to be 1 : 1, whereas, in the case of IIIc, *trans*-1 type was preferentially formed. The latter case will be probably due to the allylic strain[20] between the carbon atom at C_5 and *m*-xylidine residue at C_4 bulkier than phenyl.

The phenomenon that the spiltting number of the methylene proton in 4-ethoxy group of III'c is not a quartet, but a double quartet, suggests the presence of such a hindrance.

The fact that the dihedral angles (H_2, H_3) and (H_3, H_4) are less than that of cyclohexene indicates a considerable flattening of the typical half-chair conformation. A more remarkable tendency to flatten the conformation has been observed in the case of 1-acyl derivatives of IIIa, IIIb and IIIc, in which the coupling constants between H_2 and H_3 are generally smaller than those of the parent compounds. For example the coupling constant: $J_{2,3}$ (7.5 Hz) of 1-acetyl derivative of IIIc indicates the decrease of the angle from 156° to 136°. This change will be attribuable to the 1,2-skew interaction of acetyl group at C_1 and methyl group at C_2, and also to the allylic strain between acetyl group and methyl group at C_8.

As a general tendency of the NMR data (see Table 2), H_4 proton (qa) of 1-acyl derivatives of *cis*-1 type shifts to a higher magnetic field than H_4 proton of the parent compounds free of acyl group.

20) F. Johnson, *Chem. Revs.*, **68**, 378 (1968).

However, it is scarcely changed in the case of *trans*-1 type. H_3 proton also indicates a similar tendency. The former case is consistent with the report of Lambert[21] *et al.*, in which they indicated that the anticoplanarity between H_γ proton and axial lone pair electron of nitrogen atom in the *N*-substituted piperidine ring causes the chemical shift of H_γ (τ) to a higher magnetic field.

b) Conformation of Bis(propylidenearylamines). In the case of bis(propylidenearylamines), *i. e.*, 1,2,3,4-tetrahydro-4-anilino-2-ethyl-3-methylquinoline, eight half-chair conformations of racemic diastereoisomers are theoretically possible, and among them, the most favored ones will be the two having C_2-e, C_3-e, C_4-qe or C_2-e, C_3-e, C_4-qa substituents. Miller *et al.*[2] have found only one isomer ($IIId_1$; mp 103°C). However, another one should exist as in the case of bis(ethylidene-aniline), and in fact, we have succeeded in isolating one ($IIId_2$) as a syrup from the mother liquor of $IIId_1$. The IR spectrum of $IIId_2$, which is very similar to that of $IIId_1$, showed absence of C=C or C=N absorption band, and that of 1-acyl derivative of $IIId_2$ still showed NH absorption band at 3320 cm^{-1}.

In the NMR spectrum of $IIId_1$ shown in Fig. 5,

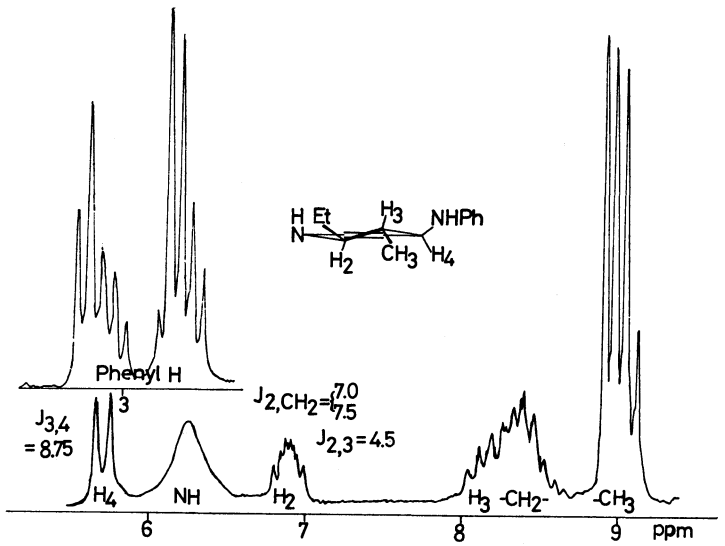

Fig. 5. NMR spectrum of 1,2,3,4-tetrahydro-4-anilino-2-ethyl-3-methylquinoline ($IIId_1$) [bis(propylideneaniline): 2,4-*cis*] (100 Mc, $CDCl_3$).

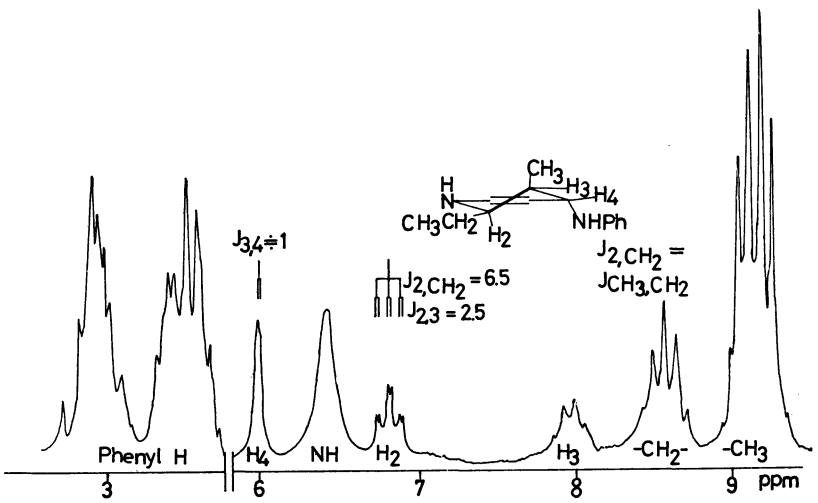

Fig. 6. NMR spectrum of 1,2,3,4-tetrahydro-4-anilino-2-ethyl-3-methylquinoline ($IIId_2$) [bis(propylideneaniline): 2,4-*trans*] (100 Mc, $CDCl_3$).

21) J. B. Lambert, R. G. Keste, R. E. Carhart and A. P. Javanovich, *J. Am. Chem. Soc.*, **89**, 3761 (1967).

TABLE 2. FIRST-ORDER ANALYSIS OF NMR SPECTRA OF 2,4-DISUBSTITUTED 1,2,3,4-TETRAHYDROQUINOLINES

	Chemical shifts (τ)						Coupling constants (Hz) (dihedral angles)					
	H_2	$H_{3'}$	H_3	H_4	CH_3	$=NCOCH_3$	$J_{2,3}$	$J_{2,3'}$	$J_{3,3'}$	$J_{3,4}$	$J_{3,4}$	J_{2,CH_3}
IIIa$_1$	6.30	7.67	8.55	5.20	8.82	—	11.5	2.5	11.5	5.0	11.5	6.5
(*cis*)	m*	o	q	q	d		(155°)	(63°)		(51°)	(155°)	
IIIa$_2$	6.50	7.86	8.49	5.45	8.80	—	11.3	2.5	12.5	2.5	3.75	6.5
(*trans*)	m	dt	o	q	d		(152°)	(63°)		(63°)	(58°)	
1-acetyl	5.04	7.33	ca. 8.7	5.75	8.83	7.80	7.0	8.75	12.5	4.5	12.5	7.0
of IIIa$_1$	m	o	s	q	d		(134°)	(33°)		(53°)	(159°)	
1-benzoyl	5.12	7.23	8.64	5.56	8.73	—	8.0	9.2	12.5	5.0	11.3	6.5
of IIIa$_1$	m	dt	dt	t	d		(139°)	(30°)		(51°)	(152°)	
1-benzoyl	5.19	7.58	8.1	5.33	8.72	—	6.5	6.5	12.5	5.0	5.0	7.0
of IIIa$_2$	m	dt	dt	t	d		(132°)	(43°)		(51°)	(51°)	
IIIb	6.45	7.60	8.55	5.25	8.83	—	11.3	—	11.3	5.0	11.3	6.0
(*cis*)	m	o	q	q	d		(152°)			(51°)	(152°)	
1-acetyl	5.19	7.38	ca. 8.8	5.89	8.90	7.92	11.3	—	12.5	4.0	11.5	6.5
of IIIb	m	o	s	q	d		(152°)			(56°)	(155°)	
IIIc	6.50	—	8.50	5.45	8.76	—	12.0	—	12.0	2.5	3.5	6.3
(*trans*)	m		o	q	d		(157°)			(63°)	(58°)	
1-acetyl	4.85	7.31	8.61	5.52	8.94	7.80	7.5	7.5	12.5	2.5	4.0	7.5
of IIIc	s	o	o	q	d		(136°)	(38°)		(63°)	(56°)	
III'a**	6.57	8.07	8.55	5.39	8.83	—	12.0	2.5	13.7	2.5	3.5	6.25
(*trans*)	m	dt	dt	q	d		(157°)	(54°)		(63°)	(58°)	
III'b	5.08	7.40	8.52	4.28	8.83	7.62	7.0	7.0	12.5	5.0	10.0	6.0
(*cis*)	m	o	o	q	d		(134°)	(41°)		(51°)	(147°)	
III'c	4.30	7.06	8.36	5.65	—	7.87	10.0	10.0	12.0	3.75	12.0	—
(*cis*)	m	o	dt	q			(147°)	(26°)		(58°)	(157°)	

* d=doublet, dt=double triplet, m=multiplet, o=octet, q=quartet, s=sextet, t=triplet. ** IIIa'; 1,2,3,4-tetrahydro-2,6-dimethyl-4-hydroxyquinoline, IIIb'; 1,2,3,4-tetrahydro-4-acetoxy-1-acetyl-2,6-dimethylquinoline, IIIc'; 1,2,3,4-tetrahydro-1-acetyl-4-ethoxy-2-phenylquinoline.

TABLE 3. FIRST-ORDER ANALYSIS OF NMR SPECTRA OF 2,3,4-TRISUBSTITUTED 1,2,3,4-TETRAHYDROQUINOLINES

	Chemical shifts (τ)							Coupling constants (Hz) (dihedral angles)				
	H_2	H_3	H_4	CH_3-C_3	$C\underline{H}_2$-CH_3	$CH_2C\underline{H}_3$	$=NCOCH_3$	$J_{2,3}$	$J_{3,4}$	J_{2,CH_2}	J_{3,CH_3}	$J_{CH_2-CH_3}$
IIId$_1$	6.90	8.17	5.72	8.95	8.40	9.06		4.5	8.75	7.0	6.3	7.0
	o	m	d	d	m	t		(124°)	(142°)	7.5		
IIId$_2$	6.80	7.97	5.95	9.07	8.57	9.18		2.5	ca. 1	6.5	5.0	6.5
	dt	m	d	d	m	t		(63°)	(74°)			
1-acetyl	5.39	8.5	6.07	8.73	ca. 8.5	9.15	7.80	7.0	9.0	—	6.5	7.0
of IIId$_1$	m	m	d	d	m	t		(134°)	(143°)			
1-aectyl	5.29	8.37	5.65	8.87	ca. 8.7	9.10	7.72	3.5	11.3	7.0	7.50	7.0
of IIId$_2$	m	m	d	d	m	t		(58°)	(17°)			

the multiplet at *ca.* τ 8.2, which is partly superimposed on C_3 methyl proton signal, the octet at τ 6.90 and the doublet at τ 5.72 are assigned to H_3 ($J_{2,3}=4.5$ Hz), H_2 ($J_{2,CH_2}=7.0$, 7.5 Hz) and H_4 ($J_{3,4}=8.75$), respectively. The irradiation of H_3 caused H_4 proton signal to collapse to a singlet. The coupling constants mentioned above roughly support the fact that the substituents of $IIId_1$ at C_2, C_3 and C_4 are e, e and qe. The dihedral angles of ring protons; (H_2, H_3)=124° and (H_3,H_4) =141° indicate a more remarkably flattened half-chair (rather plane) conformation than that of IIIa.

In the NMR spectrum of the other isomer ($IIId_2$) shown in Fig. 6, a multiplet centered at τ 7.97, a triplet doublet at τ 6.80 and a narrow doublet at τ 5.95 are assigned to H_3, ($J_{2,3}=2.5$ Hz), H_2 ($J_{2,CH_2}=6.5$ Hz) and H_4 ($J_{3,4}=ca.$ 1 Hz), respectively. The dihedral angles are similarly estimated to be (H_2, H_3)=114° or 64° and (H_3, H_4)=105° or 74°. The most profitable conformation to be justified by these angles is a flattened half-chair having C_2-e, C_3-a and C_4-qa substituents or a rather contracted half-boat conformation having C_2-e, C_3-e and C_4-qa substituents, but not a half-chair having C_2-e, C_3-e and C_4-qa which was mentioned above as a stable one. Among the two probable conformations, however, the latter is not adoptable because of the instability factor due to the constraction strain. Therefore, the former is preferable to $IIId_2$.

This conclusion will be supported by the following considerations. If $IIId_1$ and $IIId_2$ can be formed through the structure of type I, as in the case in which I cyclizes to IIIe, racemic *threo* and *erythro* isomers of type I should exist in the intermediate step. The *threo* isomer will preferentially cyclize to the conformation having C_2-e and C_3-e substituents. However, the *erythro* isomer should give a half-chair conformation having C_2-a or C_3-a substituent. Though C_4 configuration can not be estimated unless the transition state of such a cyclization is clarified, we can understand that $IIId_1$ is preferentially formed, so far as stability is concerned. However, in the case of *erythro*, two stable conformations are equally possible from the standpoint of the nonbonded interaction. The following consideration may be allowed: there are four possible conformations to be formed by the cyclization of the *erythro* intermediate;

A) C_2-a, C_3-e and C_4-qe, B) C_2-a, C_3-e and C_4-qa, C) C_2-e, C_3-a and C_4-qe, D) C_2-e, C_3-a and C_4-qa. The instability factor of the substituents can be roughly estimated as follows: A; 3 skews (C_2-a and C_3-e, C_2-a and C_3-C_4 bond, C_3-e and C_4-e), B; 4 skews (C_2-a and C_3-e, C_2-a and C_3-C_4 bond, C_4-a and C_3-e, C_4-a and C_2-C_3 bond) and 1,3-diaxial interaction (C_2-a and C_4-a), C; 4 skews (C_3-a and C_2-e, C_3-a and C_2-N bond, C_3-a and C_4-e, C_3-a and C_4-$C_{benzene}$), and D; 4 skews (C_3-a and C_2-e, C_3-a and C_4-$C_{benzene}$, C_3-a and C_2-N bond, C_4-a and C_2-C_3 bond), respectively. Among these skew interactions, C_2-a and C_3-C_4 bond, C_3-e and C_4-e, C_3-a and C_2-N bond, C_3-a and C_4-$C_{benzene}$, C_4-a and C_2-C_3 bond interactions will be weakened by flattening of half-chair conformation (enlargement of the dihedral angles), and others will be enhanced because of the eclipse effect of the substituents. Therefore, both A and D conformations are almost equivalent with respect to the instability factor. The A conformation, however, is rejected so far as NMR is concerned, because the coupling constant ($J_{3,4}$) of $IIId_2$ is too small (*ca.* 1 Hz) for that of A conformation (H_3 and H_4; *trans*-diaxial). Accordingly, D conformation is preferable to $IIId_2$.

The formation ratio of $IIId_1$ (*threo*) and $IIId_2$ (*erythro*) was measured from the intensity of each H_4 protons in the crude mixture to be 55 : 45. The coupling constants of ring protons of acetyl derivatives of $IIId_1$ and $IIId_2$ shown in Table 3 indicate that the conformation of $IIId_1$ remained almost unchanged. However, $J_{3,4}$ value of $IIId_2$ changed remarkably from *ca.* 1 to 11.3. This change may be explained by the conversion of the conformation from half-chair to a twisted half-boat or by the conversion to A conformation, in order to avoid 1,2-interaction between acetyl and ethyl group.

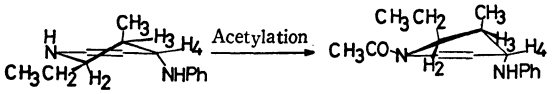

$IIId_2$

Scheme 3

On the other hand, the NMR data in Table 3 indicate that H_4 proton of 1-acetyl derivative of $IIId_1$ (2,4-*cis*) shifts to a higher magnetic field than that of $IIId_1$ as in the case of IIIa or IIIb. This phenomenon may be of use for the conformational analysis of 4-, or 2,4- or 2,3,4-substituted 1,2,3,4-tetrahydroquinolines and others.

A general conclusion may be given for the conformation of the substituted 1,2,3,4-tetrahydroquinolines that; 1) 2,4-disubstituted 1,2,3,4-tetrahydroquinolines have a flattened half-chair conformation (C_2-e, C_4-qe or C_2-e, C_4-qa). 2) 2,3,4-Trisubstituted 1,2,3,4-tetrahydroquinolines have a remarkably flattened half-chair or twisted half-boat conformation (C_2-e, C_3-e and C_4-qe or C_2-e, C_3-a and C_4-qa). 3) 1-Acyl derivatives of the substituted 1,2,3,4-tetrahydroquinolines have a more flattened half-chair than the acyl free derivatives.

Experimental

All the aliphatic aldehydes and arylamines were purified before use by distillation of the commercial

products. The melting points were uncorrected. The measurements of NMR spectra were effected with JEOL JNM-4H-100 in deuteriochloroform by using TMS as an internal reference. IR spectra were measured with Hitachi EPI-G2. UV spectra were measured with Hitachi EPS-3T in methanol solution. TLC was carried out on layers of silica gel (WAKO-GEL B-Q) on glass plates, using benzene (system A) or benzene-ligroin (3 : 1, system B) as developers and 2% aqueous potassium permanganate-sodium carbonate or chromic-sulfuric acid (5%-$K_2Cr_2O_7$ in 40% H_2SO_4) as spray reagents. R_a value is the rate of movement of the 1,2,3,4-tetrahydroquinolines relative to aniline.

Bis(butylideneaniline) (I : 3-anilino - 2 - ethylhexylideneaniline). Equimolar amount of freshly distilled aniline and *n*-butyraldehyde was mixed and allowed to stand at room temperature for 24 hr according to the method of Kharasch *et al.*[4] White crystals were obtained in a yield of 55%. Mp 92°C (lit, 92.5°C). I in an alcoholic solution gradually isomerized to 1,2,3,4-tetrahydro-4-aniline-3-ethyl-2-propylquinoline (IIIe) and the yield decreased.

1,2,3,4-Tetrahydro-4-anilino-3-ethyl -2- propylquinoline (IIIe). To a solution of bis(butylideneaniline) (I: 2.94 g, 10 mmol) dissolved in chloroform (10 m*l*) was added two drops of acetic acid and the solution was allowed to stand at room temperature overnight, neutralized with an aqueous sodium hydrogene carbonate, washed with water and dried over Na_2SO_4. Evaporation of chloroform gave a pale yellow syrup (2.9 g), which shows no absorption band of imine at *ca.* 1650 cm^{-1}. UV: λ_{max}^{MeOH} 251 mμ (log ε=4.43), 302 mμ (log ε=3.87).

1-Tosyl Derivative of IIIe. IIIe was tosylated with *p*-toluenesulfonyl chloride (1.2 times mole of IIIe) in pyridine in an usual manner to give 1,2,3,4-tetrahydro-4-anilino-3-ethyl-2-propyl-1-tosylquinoline in a yield of 22% (crystals). Mp 210—211°C (recrystallized from acetone). IR; 3400 cm^{-1} (NH), 1340, 1162cm^{-1} (*N*-tosyl).

Found: C, 72.04; H, 7.33; N, 6.50; S, 7.42%. Calcd for $C_{27}H_{32}O_2N_2S$ (448): C, 72.29; H, 7.19; N, 6.29; S, 7.15%.

2-Ethyl-1-hexylideneaniline (IV). 2-Ethylhexaldehyde (12.8 g, 0.1 mol) was added to aniline (9.3 g, 0.1 mol) with cooling in an ice-water and the mixture was allowed to stand at room temperature overnight. After drying over Na_2SO_4, distillation of the reaction product was effected under 1 mmHg to give a pale yellow oil (15.8 g, 77.6%). Bp 92—95°C/1 mmHg.

Found: C, 82.75; H, 10.19; N, 6.76%. Calcd for $C_{14}H_{21}N$: C, 82.70; H, 10.41; N, 6.89%.

Pyrolysis of Bis(butylideneaniline)(I) to 2-Ethyl-2-hexenylideneaniline (V). I (3 g, 10.2 mmol) was filled in a sealed tube and heated in an oil bath at 120—140°C for 12 hr. Distillation of the reaction product *in vacuo* gave an oil (V) (1.5 g, 74%) having bp 142—147°C/11 mmHg (lit,[4] 146—148°C/15 mmHg). Refluxing of the acidic ethanol solution of V with 2,4-dinitrophenylhydrazine for 2 hr gave 2,4-dinitrophenylhydrazone (red crystals). Mp 118°C (lit,[4] 119—120°C).

Bis(ethylideneaniline) (1,2,3,4 - Tetrahydro - 4 - anilino-2-methylquinoline: $IIIa_1$ and $IIIa_2$). $IIIa_1$ (*cis*) and $IIIa_2$ (*trans*) were prepared from aniline (0.1 mol) and acetaldehyde (0.1 mol) in a mixture of ethanol (150 m*l*) and water (100 m*l*) in a yield of 20% ($IIIa_1$) and 22% ($IIIa_2$), respectively, by the Method of Minikin and Tumakoba.

$IIIa_1$: mp 121—124°C (lit,[2] 126°), R_a 1.64 (system A).

$IIIa_2$: syrup (lit,[2] 85.5°), R_a 2.07 (system A).

(Found of $IIIa_2$: C, 80.45: H, 7.92; N, 11.40%. Calcd for $C_{16}H_{18}N_2$: C, 80.63; H, 7.61; N, 11.78%).

1-Acetyl derivative of $IIIa_1$. To a solution of $IIIa_1$ (0.3 g, 1.26 mmol) in pyridine (2 m*l*), acetic anhydride (1 g, 10 mmol) was added and the mixture was allowed to stand at room temperature for 2 days, and then poured into ice-water. The precipitated crystalline products were filtered, washed with water, dried and recrystallized from ethanol. Yield, 0.3 g (84.6%). Mp 110.5—111°C.

Found: C, 77.40; H, 6.92; N, 9.52%. Calcd for $C_{18}H_{20}N_2O$: C, 77.11; H, 7.19; N, 9.99%.

1-Benzoyl derivative of $IIIa_1$: mp 216—217°C (lit,[2] 218°C).

1-Benzoyl derivative of $IIIa_2$: mp 156—157°C (lit,[2] 186°C).

Bis(ethylidene *p*-toluidine) [1,2,3,4-Tetrahydro-2,6-dimethyl-4-(*p*-toluidino)quinoline: IIIb]. IIIb (*cis*) was prepared by the method of Jones *et al.*[6] in a yield of 43%. Mp 113—114°C (lit, 114—116°C).

1-Acetyl derivative of IIIb; mp 141—143°C, yield 57.5%.

Found: C, 77.38; H, 7.65; N, 8.74%. Calcd for $C_{20}H_{24}N_2O$: C, 77.88; H, 7.85; N, 9.08%.

Bis(ethylidene *m*-xylidine) [1,2,3,4-Tetrahydro-2,6,8 - trimethyl - 4 - (*m*-xylidino)quinoline: IIIc]. IIIc was prepared by the method of white *et al.*[9] in a yield of 97%. Mp 141—143°C (lit, 145°C). 1-acetylation was difficult probably because of the steric hindrance due to the 8-methyl group. Yield, 15%. Mp 142—143°C (lit, 145°C).

1,2,3,4-Tetrahydro-4-hydroxy-2,6-dimethylquinoline (III'a : *trans*): mp 107.5—110°C (lit,[2] 108—110°C).

1,2,3,4-Tetrahydro-4-acetoxy -1- acetyl-2,6 - dimethylquinoline (III'b : *cis*): mp 119—119.5°C (lit,[2] 117—119°C).

1,2,3,4-Tetrahydro -1- acetyl -4- ethoxy -2- phenylquinoline (III'c : *cis*). A mixture of 1,2,3-4-tetrahydro-4-ethoxy-2-phenylquinoline[22] (1 g, 3.93 mmol), acetic anhydride (10 m*l*) and pyridine (1 m*l*) was refluxed for 15 min, allowed to stand at room temperature for 2 hr and then poured into ice-water. Precipitated oil was extracted with chloroform, and organic layer was neutralized with aqueous $NaHCO_3$, washed with water and dried over Na_2SO_4. Evaporation of chloroform gave a syrup, which was purified with a silica gel column (WAKO-GEL Q-50). From the fraction of benzene and benzene-acetone (10:1), crystalline product was obtained in a yield of 53%. Mp 120—121°C.

Found: C, 76.89; H, 6.83; N, 4.57%. Calcd for $C_{19}H_{21}NO_2$: C, 77.26; H, 7.17; N, 4.74%.

Bis(propylideneaniline) (1,2,3,4 - Tetrahydro - 4 - anilino-2-ethyl-3-methylquinoline: $IIId_1$ and $IIId_2$). To a cold solution of aniline (9.3 g, 0.1 mol) in ethanol (25 m*l*), propionaldehyde (5.8 g, 0.1 mol) was added and

22) V. I. Grigos, L. S. Povarov and B. M. Mikhailov, *Izv. Akad. Nauk. SSSR, Ser. Khim.*, **1965**, 2163; *Chem. Abstr.*, **64**, 9680c (1966).

the reaction solution was allowed to stand in a refrigerator for 2 days. The white crystalline mass was filtered and the crude product ($IIId_1$, 4.8 g) was recrystallized from ethanol. Mp 104—105°C (lit,[2] 103°C), R_a 2.46 (system B). The mother liquor, scarcely containing any $IIId_1$, was evaporated *in vacuo* to a syrup ($IIId_2$, 5.2 g) and the small amount of remaining aniline was distilled off. R_a 2.88 (system B).

Found: C, 80.99; H, 8.31; N, 11.42%. Calcd for $C_{18}H_{22}N_2$: C, 81.16; H, 8.33; N, 10.52%.

Acetylation of $IIId_1$ and $IIId_2$ with acetic anhydride and pyridine gave 1-acetyl derivatives respectively in good yields.

1-Acetyl derivative of $IIId_1$: mp 135—136°C.

Found: C, 78.09; H, 7.86; N, 8.73%. Calcd for $C_{20}H_{24}N_2O$: C, 77.88; H, 7.84; N, 9.08%.

1-Acetyl derivative of $IIId_2$: mp 175—175.5°C.

Found: C, 78.12; H, 8.10; N, 9.27%. Calcd for $C_{20}H_{24}N_2O$: C, 77.88; H, 7.84; N, 9.08%.

BULLETIN OF THE CHEMICAL SOCIETY OF JAPAN VOL. 42 2894—2898 (1969)

Reaction of *p*-Nitrophenyl Benzenesulfonates with Thiophenoxides

Waichiro TAGAKI, Takehiko KURUSU and Shigeru OAE

Department of Applied Chemistry, Faculty of Engineering, Osaka City University, Sumiyoshi-ku, Osaka

(Received December 29, 1968)

The reaction of *p*-nitrophenyl benzenesulfonates has been investigated in dioxane-water solvent. The overall rate constant, k_A, was separated into two composite rate constants, k_{Ar}, and k_{SO_2}, corresponding to the cleavage of C–O and S–O bonds respectively. The reactivities of hydroxide and thiophenoxide in this reaction were compared. The overall rate constant was found to be several times larger with OH^- than with PhS^-. The reactivity of OH^- was largely due to its higher reactivity toward sulfur, while its reactivity toward carbon atom was comparable to that of PhS^-. Substituent effect of the nucleophile, thiophenoxide and of the substrate shed some light on the mechanism of this reaction.

The nucleophilic substitution reaction of sulfonic acid esters is well known. The attacking site of the ester is either the sulfur atom (S–O bond cleavage) or the phenolic or alcoholic carbon atom (C–O bond cleavage), or both, depending on the type of the ester, nucleophiles and reaction conditions. For the substitution reaction on sulfur, there are two possible mechanisms. One is the S_N2 type synchronous mechanism and the other is the two step mechanism, *i.e.* addition and elimination, using a low energy 3*d*-orbital of sulfur atom. The latter possibility, however, has been ruled out for the alkaline hydrolysis of phenyl benzenesulfonate on the basis of our ^{18}O tracer study,[1] and the former S_N2 type substitution has been found to be the main reaction pathway. The C–O bond cleavage is well known in aliphatic compounds. However, for unsubstituted phenyl benzenesulfonate, such C–O bond cleavage is not important, and becomes significant only with *p*-nitrophenyl benzenesulfonte. In an extreme case, Bunnett[2] has shown that 2,4-dinitrophenyl benzenesulfonate undergoes exclusive C–O bond cleavage when thiophenoxide is used as the nucleophile, while such C–O bond cleavage become less significant, when phenoxide is used as the nucleophile. Meanwhile the nucleophilic substitution reaction of 4-nitrohalobenzene has been investigated rather extensively.[3] The most reasonable mechanism for this reaction seems to be the two step mechanism, *i.e.* addition of a nucleophile to the benzene ring (bond forming) followed by the cleavage of the group (bond breaking) to be substituted. According to Bunnett[4] the bond forming step is the rate limiting for most of the substrates and nucleophiles.

During the course of our studies on the mechanism of the nucleophilic reduction of sulfur atom in sulfate and sulfonate by thiol compounds, we became interested in the reaction of *p*-nitrophenyl benzenesulfonate with thiophenol. We began the present study to investigate the following questions: the reactivities of hydroxide and thiophenoxide anions, the relative rate of the reactions on

1) D. R. Christmann and S. Oae, *Chem. & Ind.*, **1959**, 1251.

2) J. F. Bunnett and J. Y. Bassett, Jr., *J. Am. Chem. Soc.*, **81**, 2104 (1959).

3) a) A. J. Parker, "Organic Sulfur Compounds," ed. by N. Kharasch, Vol. I (1961), p. 103. b) T. C. Bruice, S. J. Benkovic, "Bioorganic Mechanism," Vol. I, (1966), p. 45; J. F. Bunnett and R. E. Zahler, *Chem. Revs.*, **49**, 297 (1951).

4) J. F. Bunnett, *Quart. Revs.*, **12**, 1 (1958).

sulfur and carbon, and the relative importance of bond forming and bond breaking steps. Another purpose was to compare this reaction with the alkaline hydrolysis of thiolsulfinate and thiolsulfonate as described in the preceding two papers.[5]

Results and Discussion

Products. The major reaction pathways can be formulated as in the Eqs. (1)—(3). The product analysis was carried out for the reaction of *p*-nitrophenyl *p*-toluenesulfonate (X=CH_3) with thiophenoxide (Y=H).

All the possible products shown in Eqs. (1)—(3) except thiolsulfonate III, were identified (Table 1); the tabulated yields are the total yields.

The relative rate of the initial two reactions, k_{SO_2} and k_{Ar} could be judged from the relative yield of *p*-nitrophenol IV, and *p*-nitrophenyl *p*-tolyl sulfide VI, respectively. Although quantitative sepatation of IV and VI was not attempted, it was possible to estimate the amounts of IV and VI and found to be comparable from the measurement of optical density of the UV absorption of the reaction mixture at around 340 mμ. The rate of the reaction of thiolsulfonate III (Eq. (3)) is presumably

Table 1. Product analysis of the reaction of *p*-nitrophenyl *p*-toluenesulfonate and sodium thiophenoxide (Eqs. (1)—(3))[a]

Product		Yield[b] (%)
p-Nitrophenyl phenyl sulfide Diphenyl disulfide	(VI) (VIII)	70
p-Nitrophenol	(IV)	37
p-Toluenesulfonic acid *p*-Toluenesulfonic acid	(V) (VII)	90

a) In 80% dioxane-water, 50°C, 12 hr, in sealed tube under nitrogen atmosphere.
b) Based on the ester used.

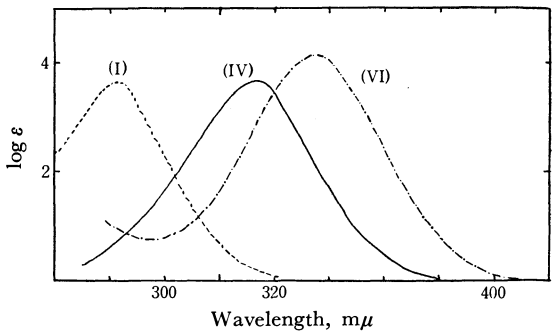

Fig. 1. UV spectra of *p*-nitrophenyl *p*-toluenesulfonate (I); ----, *p*-nitrophenol (IV); ——, and phenyl *p*-nitrophenyl sulfide (VI); —·—, in 0.01 N HCl-ethanol.

greater than that of I in view of the fact that III undergoes rapid alkaline hydrolysis.[6] The relative amounts of sulfonic acid salt V and sulfinic acid salt VII, were not determined. However, their amounts should be the same as those of IV and VI.

Kinetics and Substituent Effects. The UV spectra of the starting ester and the two products, *p*-nitrophenol IV and *p*-nitrophenyl *p*-tolyl sulfide VI, are shown in Fig. 1. Their spectral shapes and the extinction coefficients were nearly the same as for the other substituted compounds.[5] The spectra of the other products, salts V and VII and disulfide VIII, are found in the same spectrum region of the ester, but are different from those of IV and VI. Therefore the rate of the reaction could be followed easily by observing the increase of the optical density near 320 mμ due to the formation of IV and VI (as the total) where the absorption by the ester is negligible. A typical example of the plot of optical density change against the reaction time is shown in Fig. 2. In order to

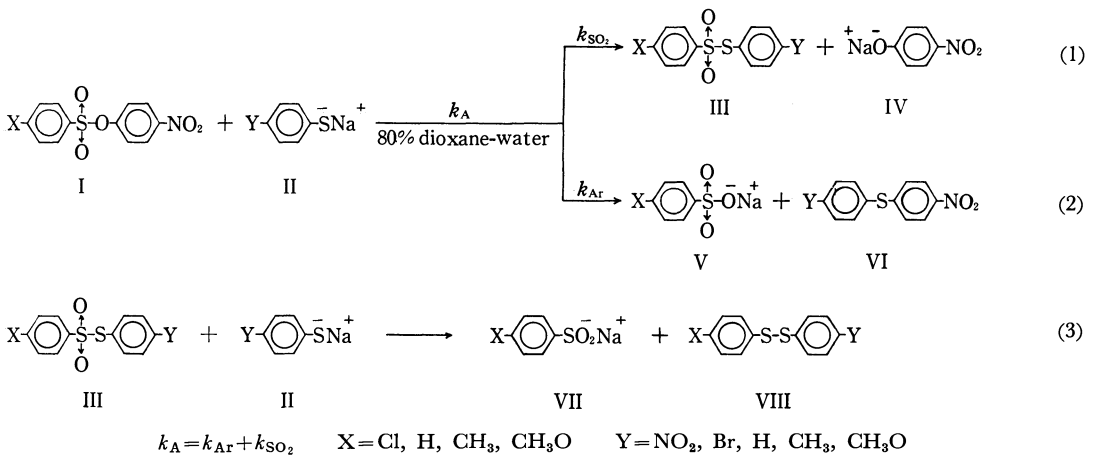

5) See for example: A. Mangini, R. Passerini and S. Serra, *Gazz. Chim. Ital.*, **84**, 47 (1954).

6) S. Oae, W. Tagaki, R. Nomura and Y. Yohsikawa, This Bulletin, accompanying papers.

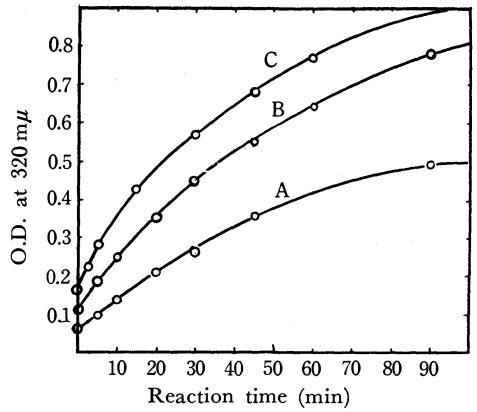

Fig. 2. Plot of optical density *vs.* reaction time, $(RS^-)_0$; 0.01M, $(E)_0$; A, 0.005 M, B, 0.010 M, C, 0.015 M, at 70°C.

avoid complication from the rest of the reactions shown in Eq. (3), only the initial rate was used for the calculation of the rate constant using Eq. (4).

$$\text{Initial rate} = k_A\,(RS^-)_0\,(\text{Ester})_0 \qquad (4)$$

$k_A = k_{Ar} + k_{SO_2}$

$(RS^-)_0$ = Initial concentration of thiophenoxide

$(\text{Ester})_0$ = Initial concentration of the ester

Details of the kinetic procedures and the modification of Eq. (4) for the actual calculation are described in the experimental part. In Eq. (4), one needs to know the initial concentration of thiophenoxide anion, $(RS^-)_0$, which is not necessarily the same as that of added salt, sodium thiophenoxide II. In order to calculate the concentration of thiophenoxide ion, the apparent pK_a of unsubstituted thiophenol was determined spectrophotometrically as a function of solvent composition in dioxane-water mixture. The pK_a of thiophenol thus obtained increased substantially as the dioxane content increased: water, 6.65 : 40% dioxane-water (v/v), 7.78; 60% dioxane-water, 8.70. From these values, one can obtain the concentration of the anion when one knows the pH of the reaction mixture. It is also possible to observe the change of the ratio of $(PhS^-)/(PhSH)$ as a function of the concentration of added salt (PhS^-Na^+). These two methods indicate that the added salt exists essentially as dissociated anion even in 80% dioxane-water, provided that the concentration of the added salt is kept around 0.005—0.015 M.

The effect of the composition of dioxane-water mixture on the rate has been examined as shown in Table 2. Although the rate increased as the solvent polarity increased, the effect was rather small. Therefore, the rates were determined for comparison in 80% dioxane-water, in which organic substrates can be readily dissolved.

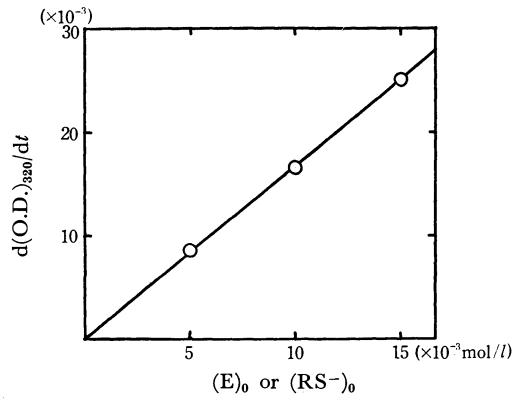

Fig. 3. Plot of initial slope of optical density change against the intial concentration of ester or thiophenoxide in 80% dioxane-water at 70°C.

TABLE 2. EFFECTS OF SOLVENT COMPOSITION OF DIOXANE-WATER MIXTURE ON THE RATE OF THE REACTION OF *p*-NITROPHENYL *p*-TOLUENESULFONATE WITH THIOPHENOXIDE AT 60°C

Dioxane vol. %	$k_A \times 10^3$ *l*/mol sec
50	9.83
60	7.53
70	6.66
80	5.50

The rate constants thus obtained are the overall rate constants including both that of the C–O bond cleavage, k_{Ar}, and that of the S–O bond cleavage, k_{SO_2}. The separation of the two rates was next attempted. The value of k_{Ar} was calculated using the change of optical density at 360 mμ where the absorption by the ester is negligible and that by IV is small compared to that by VI. The rate constant, k_{SO_2}, was then computed by substracting k_{Ar} from the overall rate constant, k_A. Although the reproducibility of k_A was quite satisfactory, high accuracy of the subsequent separation may not be expected, since the absorption at 360 mμ is not

TABLE 3. THE REACTION OF *p*-NITROPHENYL *p*-TOLUENESULFONATE WITH *p*-SUBSTITUTED THIOPHENOXIDE IN 80% DIOXANE-WATER AT 50°C

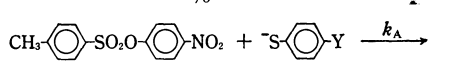

Y	$\times 10^3$ *l*/mol sec			k_{SO_2}/k_{Ar}
	k_A	k_{Ar}	k_{SO_2}	
CH_3O	10.0	7.05	2.95	0.42
CH_3	4.5	3.12	1.38	0.44
H[a)]	3.5	1.28	2.20	1.72
Br	2.5	0.58	1.92	3.32

a) $k_A = 1.12 \times 10^{-3}$ *l*/mol sec^{-1} (40°C), 5.5×10^{-3} *l*/mol sec^{-1} (60°C).
$E_a = 16$ kcal/mol $\Delta S^{\neq} = -20$ e.u. (50°C).

at λ_{max} but at a declinging slope. In spite of this limitation, the results were quite reproducible.

The rate constants observed for the reaction of *p*-nitrophenyl *p*-toluenesulfonate with four different thiophenoxides are shown in Table 3. The rate constants for the reaction of *p*-nitrophenyl *p*-substituted - benzenesulfonate with thiophenoxide are shown in Table 4. The correlation of these rate constants with Hammett σ constants are shown in Figs. 4 and 5.

Table 3 and Fig. 4 indicate that an electron donating substituent at the *p*-position of nucleophile increased the overall rate (k_A), giving Hammett ρ value $= -0.63$. The separation of k_A into k_{Ar} and k_{SO_2} revealed that the overall rate change is

Table 4. The reaction of *p*-nitrophenyl *p*-substituted - benzensulfonate with thiophenoxide in 80% dioxane-water at 50°C

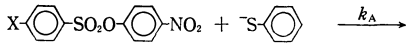

X	$\times 10^3$ *l*/mol sec			k_{SO_2}/k_{Ar}
	k_A	k_{Ar}	k_{SO_2}	
CH_3	3.50	1.28	2.20	1.72
H	5.47	2.50	2.97	1.19
Cl	10.4	2.73	7.68	2.28
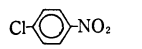	—	2.43	—	

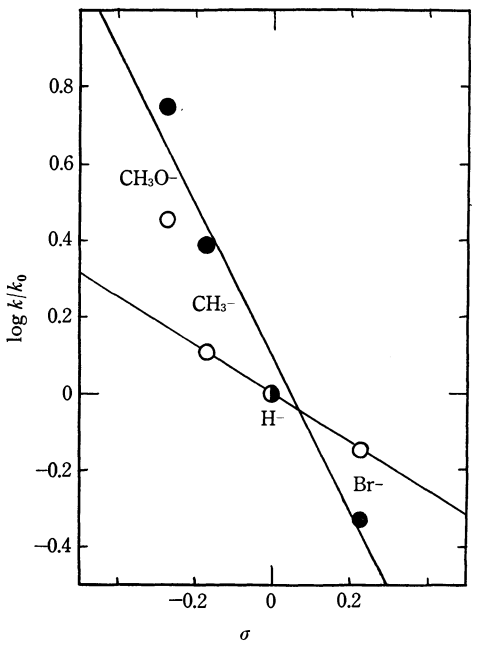

Fig. 4. Hammett plot for the reaction of *p*-substituted thiophenoxides with *p*-nitrophenyl *p*-toluenesulfonate in 80% dioxane-water at 50°C.
○ $\rho = -0.63$ (k_A, the overall rate)
● $\rho = -2.11$ (k_{Ar}, C–O bond cleavage)

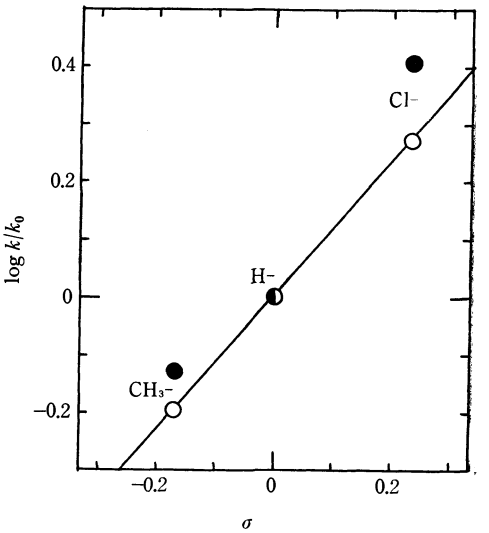

Fig. 5. Hammett plot for the reaction of *p*-nitrophenyl *p*-substituted - benzenesulfonates with thiophenoxide in 80% dioxane-water at 50°C.
○ $\rho = 1.18$ (k_A, the overall rate)
● $\rho = 1.38$ (k_{SO_2}, S–O bond cleavage)

caused mainly by the change of k_{Ar} ($\rho = -2.11$). That is, the C–O bond cleavage is more susceptible to the change of nucleophile than the S–O bond cleavage, and the C–O bond cleavage appears to increase with increasing nucleophilicity of the nucleophile. The results in Table 4 and Fig. 5 indicate that the effect of substituent X is larger for the S–O bond cleavage than for the C–O bond cleavage.

In nucleophilic substitution reactions of *p*-substituted nitrobenzene derivatives, one of the criteria for the rate limiting step is the effect of the leaving group.[3,4] The rate limiting step would be the bond formation (the addition of nucleophile to the benzene ring), if the reaction is insensitive to the leaving group. According to this criteria, the rate limiting step of this reaction would be also the addition of thiophenoxide anion to the benzene ring in line with the results in Table 4. The bond forming step also seems to be more important in the nucleophilic reaction on the sulfur atom, as the k_{SO_2} increases with an increasing electron withdrawing group (Table 4), although the effect of the nucleophile (Table 3) is not in line with this argument. The reaction of *p*-chloronitrobenzene was also carried out under the same condition. The results (Table 4) indicate that the abilities of chloride and sulfonate anion are comparable with those of the leaving group, suggesting also the indifference of this reaction to the nature of the leaving group.

In Table 5, the rates of the alkaline hydrolysis and the reaction with thiophenoxide are compared. The overall rate of the alkaline hydrolysis is about

3—4 times higher than that of the reaction with thiophenoxide ($X=CH_3$). The separation of the overall rate (from ^{18}O data) then revealed that in alkaline hydrolysis the rate is largely due to the cleavage of the S–O bond, while in the reaction of thiophenoxide the rates of both the C–O and the S–O bond cleavage are of a comparable magnitude.

TABLE 5. REACTION OF HYDROXIDE AND THIOPHENOXIDE TOWARD *p*-NITROPHENYL *p*-TOLUENESULFONATE ($X=CH_3$) AND *p*-NITROPHENYL BENZENESULFONATE ($X=H$), 50°C, 80% DIOXANE-WATER

X	Nucleophile	$\times 10^3$ *l*/mol sec			Ref.
		k_A	k_{Ar}	k_{SO_2}	
CH_3	OH^-	11.5			c)
	PhS^-	3.5	1.28	2.20	c)
H	OH^-	78.6[a]	16[b]	63[b]	8)
	PhS^-	5.47	2.5	2.97	c)

a) 49.5°C; b) Based on the ^{18}O tracer data, 20% C–O bond cleavage in 1% KOH solution;[8] c) Present work.

Experimental

Material. Substituted *p*-nitrophenyl benzenesulfonate was prepared by the reaction of *p*-nitrophenol with substituted benzenesulfonyl chloride in pyridine. The produced esters were recrystallized from ethanol: *p*-$XC_6H_4SO_2OC_4H_4NO_2$-*p*; X=H, mp 87°C (lit, 88—89°C) *p*-CH_3, mp 95—96°C (lit, 97°C); *p*-Cl, mp 112—113°C (lit, 110°C). Dioxane was purified just before use by treating with hydrochloric acid and metallic sodium under N_2 gas.[7]

***p*-Substituted Sodium Thiophenoxide.** Thiophenol was dissolved in benzene and to this was added a slightly less amount of sodium hydroxide than that required in order to avoid inclusion of any excess sodium hydroxide in the product. The mixture was refluxed for 3 hr under stirring. The water formed was distilled off with benzene and the resulting white powder was collected by filtration and washed with benzene and dried.

Product Analysis. Reaction of *p*-Toluenesulfonate with Sodium Thiophenoxide in 80% Dioxane-Water. *p*-Nitrophenyl *p*-toluenesulfonate (0.2 g) and thiophenoxide (0.2 g) were dissolved in 80% dioxane-water (10 m*l*) in an ampoule. The ampoule was sealed under N_2 atmosphere and then kept at 50°C for 12 hr. The reaction mixture was made slightly acidic and extracted with ether. Treatment of the ether layer gave 0.21 g of the mixture of *p*-nitrophenol, phenyl *p*-nitrophenyl sulfide and diphenyl disulfide. The water layer gave a mixture of sodium *p*-toluenesulfonate and *p*-toluenesulfinate (0.18 g). The yield of *p*-nitrophenol could also be measured spectrophotometrically in an alkaline solution.

Kinetic Experiment. Solution of both *p*-nitrophenyl benzenesulfonate (0.01—0.02 M), 10 m*l*, and thiophenoxide (0.01—0.02 M) in dioxane-water were kept separately in a constant temperature bath for over 10 min. Then 10 m*l* of thiophenoxide solution was added to the ester solution, and 1 m*l* aliquots of this reaction mixture were pipetted out at suitable time intervals and quenched with 0.01 N HCl - ethanol solution in 50 m*l* volumetric flask to give an assay solution. Thus the concentration of this assay solution was 1/50 of that of the reaction mixture.

Since the reactions were not simple (Eqs. (1)—(3)), only the UV absorption due to the formation of both *p*-nitrophenol (IV) and phenyl *p*-nitrophenyl sulfide (VI) was followed. Figure 1 indicates that both IV and VI give the same molar extinction coefficient at 320 mμ in acidic solution. Therefore the initial change of the optical density of the above assay solution at 320 mμ should be proportional to the change of the total concentration of IV and VI which should then be proportional to the initial concentrations of the ester and thiophenoxide as formulated in

$$\frac{\mathrm{d(O.D.\ at\ 320\,m\mu)}}{\mathrm{d}t} = \frac{\varepsilon_0}{\alpha}\frac{\mathrm{d((IV)+(VI))}}{\mathrm{d}t} \quad (5)$$

$$\frac{\mathrm{d((IV)+(VI))}}{\mathrm{d}t} = \frac{\alpha}{\varepsilon_0}\frac{\mathrm{d(O.D.)}}{\mathrm{d}t} = k_A\,(RS^-)_0(E)_0 \quad (6)$$

where $(E)_0$=initial concentration of the ester, $(RS^-)_0$=initial concentration of the thiophenoxide, ε_0=molar extinction coefficient at 320 mμ, α=dilution factor of the reaction mixture for recording of optical density, and k_A=the overall second order rate constant.

A typical example of the plot of optical density change against reaction time is shown in Fig. 2. A plot of the initial slope of optical density change as a function of the initial concentration of ester gives a straight line as shown in Fig. 3, from which one can obtain k_A.

The above k_A is the overall rate constant including both of the C–O and S–O bond cleavages. Their separation was then attempted by recording the absorbance change at 360 mμ which corresponded to the formation of V.

The applicability of the absorption above 320 and 360 mμ for these kinetics was checked for several known mixtures of IV and V at the same total concentrations, and it was confirmed that Beer's law holds and the accuracy is satisfactory. The error involved in the graphical reading of the slope (Fig. 2) sometimes amounted to ±5%. However, the rate constants (k_{obs}) shown in Fig. 3 were surprisingly reproducible; the deviation was generally within ±3%.

The alkaline hydrolysis was also carried out by the same method. The results are shown in Tables 3, 4 and 5.

pK_a of Thiophenol in Dioxane-Water of Different Composition. Undissociated thiophenol has an absorption maximum at around 240 mμ (ε=7425) and the dissociated anion at around 270 mμ (ε=14500). Based on these absorptions the pK_a value of thiophenol was determined spectrophotometrically using phosphate buffer in three different dioxane-water mixtures at 25°C: water, 6.65; 40% dioxane-water (v/v), 7.78; 60% dioxane-water, 8.70.

7) L. F. Fieser, "Experiments in Organic Chemistry," D. C. Heath and Co. (1957).

8) S. Oae and R. Kiritani, This Bulletin, **38**, 765 (1965).

BULLETIN OF THE CHEMICAL SOCIETY OF JAPAN VOL. 42 2899—2903 (1969)

Alkaline Hydrolysis of Aryl Benzenethiolsulfinates

Shigeru OAE, Yoichiro YOSHIKAWA and Waichiro TAGAKI

Department of Applied Chemistry, Faculty of Engineering, Osaka City University, Sumiyoshi-ku, Osaka

(Received December 29, 1968)

The alkaline hydrolysis of substituted phenyl benzenethiolsulfinates has been kinetically investigated. The rates were correlated with the second order kinetic equation, first order with respect to each of the hydroxide and the ester concentration. The second order rate constant for the unsubstituted ester was found to be 3.17×10^3 *l*/mol sec (water, 30°C). The Hammett ρ values were found to be $\rho_{X,Y=H}=2.4$ and $\rho_{Y,X=H}=1.6$ for Y- 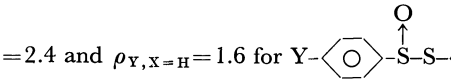 -X respectively.

Bond forming and scission of sulfur-sulfur linkage are important not only in industrial chemistry but also in biochemistry since the disulfide bridge is most frequently involved in the building up structures of proteins and enzymes and its formation and cleavage play an important role in controlling protein structures and the catalytic activities of enzymes.[1] The compounds which have S-S linkage undergo various reactions and may be classified into the following types (I—VI).[2] These compounds are involved in such reactions as hydrolysis, oxidation reaction and disproportionation of various organosulfur compounds. For

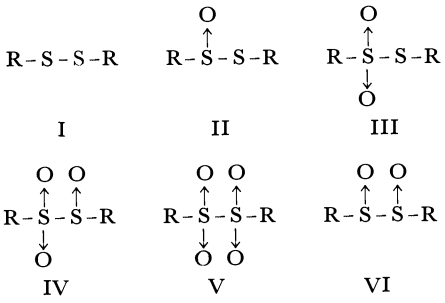

I II III

IV V VI

example, in the alkaline hydrolysis of diphenyl thiolsulfonate, the following consecutive reaction steps seem to be involved.

$$Ph\text{-}SO_2\text{-}S\text{-}Ph + OH^- \xrightarrow{-H^+} PhSO_2^- + PhSO^- \quad (1)$$

$$2PhSO^- \xrightarrow{+2H^+} Ph\text{-}\overset{\overset{O}{\uparrow}}{S}\text{-}S\text{-}Ph + H_2O \quad (2)$$

$$Ph\text{-}\overset{\overset{O}{\uparrow}}{S}\text{-}S\text{-}Ph + OH^- \xrightarrow{-H^+} PhSO_2^- + PhS^- \quad (3)$$

$$Ph\text{-}SO_2S\text{-}Ph + PhS^- \longrightarrow PhSO_2^- + PhSSPh \quad (4)$$

$$Ph\text{-}\overset{\overset{O}{\uparrow}}{S}\text{-}S\text{-}Ph + PhS^- \xrightarrow[etc.]{} PhSO^- + PhSSPh \quad (5)$$

The product analysis and the qualitative rough kinetic estimation of the rates of the nucleophilic substitution of these compounds, particularly with hydroxide ion, have been subjects of continued investigation.[3] Recently Kice has reviewed the chemistry involved in the cleavage of S-S linkage in the substitution reactions of various sulfur compounds whose central sulfur atoms are S^{II}, S^{III}, S^{IV}, *etc.*

It is believed that thiolsulfinate (II) and thiolsulfonate (III) are substantially more reactive than the corresponding disulfide (I) toward common nucleophile. However, no rate of alkaline hydrolysis of thiolsulfinate (II) or thiolsulfonate (III) has ever been determined.

From our interest in organic sulfur compounds and their biological significance, we have investigated the alkaline hydrolyses of II and III together with a related reaction of phenyl benzenesulfonate with thiophenoxide which gives III as the intermediate.

This paper describes the results for substituted phenyl benzenethiolsulfinate (II). The other two papers[4] will describe the results for substituted phenyl benzenethiolsulfonate (III) and aryl

1) R. Cecil, "The Proteins," ed. by H. Neurath, Vol. I, Academic Press, New York (1964), p. 379.

2) J. L. Kice, *Accounts of Chemical Research*, **1**, 58 (1968).

3) See the review; a) A. J. Parker and N. Kharasch, *Chem. Revs.*, **59**, 583 (1958); b) O. Foss, "Organic Sulfur Compounds", ed. by N. Kharasch, Vol. I, Cap. 8, Pergamon Press (1961), p. 75; c) R. E. Davis, "Survey of Progress in Chemistry," Vol. II, Academic Press, New York (1964), p. 189; d) W. A. Pryor, "Mechanism of Sulfur Reactions," McGraw Hill, New York (1962).

4) S. Oae, R. Nomura, Y. Yoshikawa and W. Tagaki, This Bulletin, **42**, 2903 (1969); W. Tagaki, S. Oae and T. Kurusu, *ibid.*, **42**, 2894 (1969).

benzenesulfonate, respectively.

Results and Discussions

Products. According to Vinkler and Klivenyi,[5] the products of alkaline hydrolysis of aryl benzenethiolsulfinate are arenesulfinic acid and diaryl disulfide. We confirmed their result. However, it is difficult to visualize how these products are formed. Presumably a part or all of the reactions shown in Eqs. (1)—(5) (and more) take place in a competitive manner to result in the products. Thus the overall reaction appears rather complicated. However, as for the very initial reaction there are only two possibilities, the attack of hydroxide ion on sulfinyl sulfur, Eq. (3)[6] and that on the divalent sulfur atom Eq. (6). Of the two, Eq. (3) is certainly more important than, Eq. (6),

$$\mathrm{Ph\text{-}\overset{\uparrow}{\underset{\mathrm{O}}{S}}\text{-}S\text{-}Ph} + OH^- \xrightarrow{-H^+} \mathrm{Ph\text{-}\overset{\uparrow}{\underset{\mathrm{O}}{S}}\text{-}O^-} + PhS^- \qquad (3)$$

$$\mathrm{Ph\text{-}\overset{\uparrow}{\underset{\mathrm{O}}{S}}\text{-}S\text{-}Ph} + OH^- \xrightarrow{-H^+} 2\,\mathrm{Ph\text{-}S\text{-}O^-} \qquad (6)$$

since hydroxide being a hard base, would preferentially attack the harder acidic sulfinyl sulfur than the sulfenyl sulfur atom[7] and moreover the sulfenate anion formed would regenerate the starting ester according to Eq. (2).[8] Therefore the initial rate of this hydrolysis can be taken as the rate of the displacement of thiophenoxide ion by the attack of hydroxide ion on the sulfinyl sulfur. This is the basic assumption for the present kinetics.

Kinetics for the Phenyl Benzenethiolsulfinate. The rates of alkaline hydrolyses of all the compounds examined were found to be very great. The kinetic experiments were therefore carried out in a pH-controlled buffer solution, the concentration of the ester being kept around 10^{-4} M. The buffer chosen was *N*-ethylmorpholine *N*-ethylmorpholine sulfate which was advantageous in view of its inertness to the reaction system, and its fair solubility in 60% ethanol-water solvent (no precipitation).

The kinetic measurement was carried out by observing the disappearance of a characteristic UV absorption band of a strating ester (*e.g.* 282 mμ for phenyl benzenethiolsulfinate) spectrophotometrically, and the initial rate was then determined graphically (Fig. 1). The initial rate should be proportional to the initial concentrations of both the ester and hydroxide ion as expressed by

$$-\frac{d(\mathrm{Ester})}{dt} = k_{obs}(E)_0 = [k_0 + k_{OH^-}(OH^-)_0](E)_0 \qquad (7)$$

where k_0 and k_{OH^-} are the rate constants for spontaneous and alkaline hydrolyses, respectively, and $(OH^-)_0$ and $(E)_0$ the initial concentrations of hydroxide and the ester, respectively. Since the hydrolysis was not observed in 60% ethanol-water solvent (pH≈5) without buffer, the contribution of k_0 must be small.

The first order dependence of the rate on the initial concentration of the ester is shown in Fig. 2. The first order dependence of the k_{obs}, obtained from the slope in Fig. 2, on the hydroxide ion concentration is shown in Fig. 3. The error involved in the graphical reading of the initial slope was within ±3% for duplicate or triplicate runs and the deviation of the rate constants was generally within ±3%.

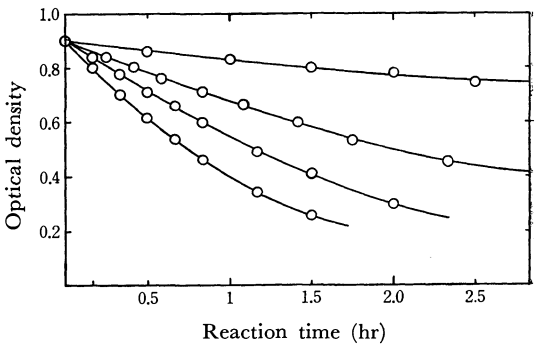

Fig. 1. Typical plots of optical density *vs.* reaction time.

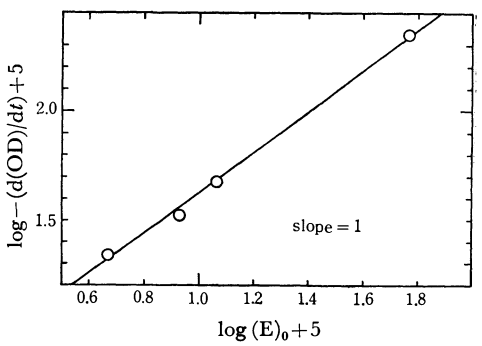

Fig. 2. Plot of initial rate of hydrolysis *vs.* the initial concentrations of ester; ester, PhS(O)SPh; solvent, 60% ethanol-water; 20°C pH=7.6 in 60% ethanol-water.

5) a) E. Vinkler and F. Klivebyi, *Acta Chemica Acad. Sci. Hung.*, **11**, 15 (1957); *Chem. Abstr.*, **52**, 6242 (1958); b) E. Vinkler, *Acta Chemica Hung.*, **22**, 345 (1960).

6) W. E. Savige and J. A. Maclaren, "Org. Sulfur Compounds," Vol. II, ed. by N. Kharasch, Pergamon Press, London (1966), p. 367.

7) a) J. L. Kice, "3rd Organosulfur Symposium," Caen, France, May, 1968; b) J. L. Kice and G. B. Large, *J. Am. Chem. Soc.*, **90**, 4069 (1969).

8) Benzenesulfenic acid has never been isolated, and hence must be a very unstable compound. In the hydrolysis of benzenesulfenyl chloride, the products are known to be sufinic acid and disulfide, where the initial intermediate must be sulfenic acid.

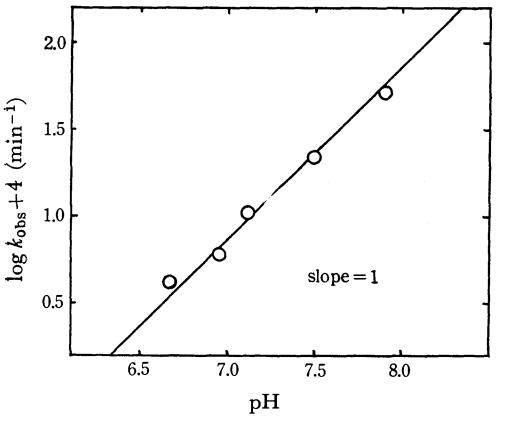

Fig. 3. Plot of log k_{obs} *vs.* pH; ester, PhS(O)SPh; solvent, 60% ethanol-water; 30°C $(E)_0 = 1.10 \times 10^{-4}$ M.

The intercept gives the value of log k_{OH^-} K'_w based on:

$$\log k_{obs} = \log k_{OH^-}(OH^-)_0 = \log k_{OH^-}K'_w + pH \quad (8)$$

In order to determine k_{OH^-} one has to know the ion product, K'_w in 60% ethanol-water solvent. Meanwhile it is possible to extrapolate the k_{obs} found in 60% ethanol-water solvent to that in water by changing the solvent composition, using the same buffer ratio and concentration.[9] Figure 4 shows that such an extrapolation gives k_{obs} in water and permits the calculation of k_{OH^-} in water using $pK_w = 13.83$ (30°C).[10]

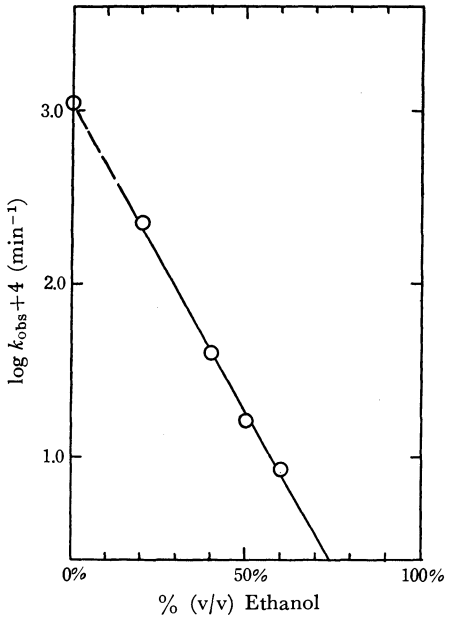

Fig. 4. Plot of log k_{obs} *vs.* percent of ethanol in the solvent; ester, PhS(O)SPh; 30°C pH=7.59 in water.

The k_{OH^-} value thus obtained for unsubstituted phenyl benzenethiolsulfinate is 3.17×10^3 *l*/mol sec at 30°C. From the Arrhenius plot shown in Fig. 5, E_a and $\Delta S^{\neq}$ were calculated to be 13 kcal/mol and −3 e.u. (at 30°C), respectively, for the unsubstituted phenyl benzenethiolsulfinate.

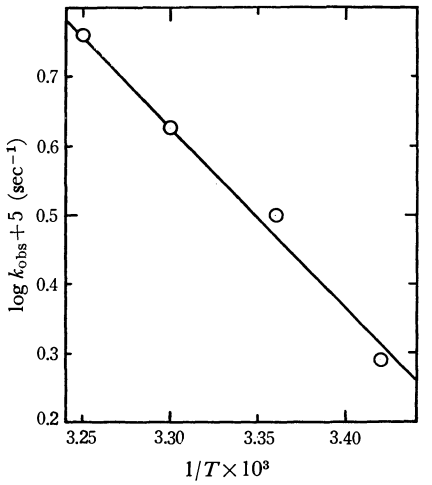

Fig. 5. Arrhenius plot; ester, PhS(O)SPh; solvent, 60% ethanol-water; pH=7.5 in 60% ethanol-water.

Substituent Effect. As shown in Fig. 6, introduction of an electron-withdrawing substituent into *p*-position of either one of the two benzene rings of the thiolsulfinate accelerated the rate, while an electron-releasing substituent retarded, giving Hammett ρ values of $\rho_{X,Y=H} = 2.4$ and $\rho_{Y,X=H} = 1.6$ respectively.

As discussed already, the above rates are those of the reaction 3, *i. e.*, the reaction on sulfinyl sulfur. A question may arise whether the reaction proceeds in one step mechanism (a) or through a pre-equilibrium formation of an unstable addition complex involving sulfur 3*d*-orbital (b). The observed substituent effect unfortunately does not answer these questions.

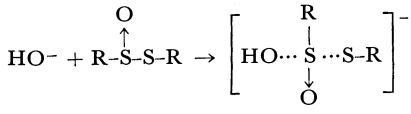

$$\xrightarrow{-H^+} RSO_2^- + RS^- \quad (a)$$

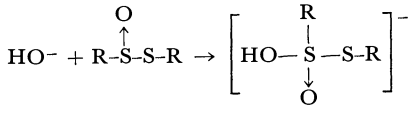

$$\xrightarrow{-H^+} RSO_2^- + RS^- \quad (b)$$

9) E. T. Kaiser, *J. Am. Chem. Soc.*, **89**, 1393 (1967).

10) H. S. Harned and B. B. Owen, "The Physical Chemistry of Electrolytic Solutions," Reinhold, New York (1950).

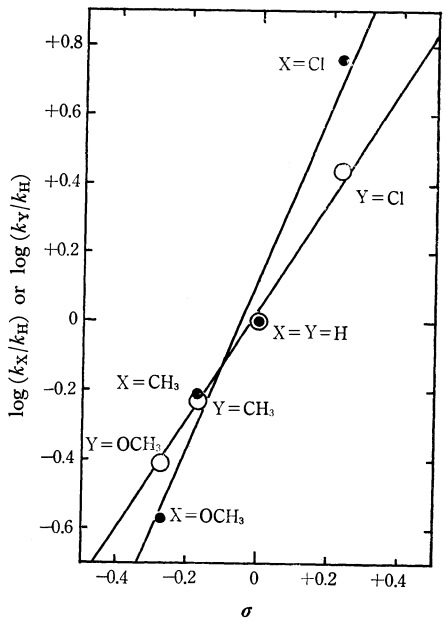

Fig. 6. Hammett plot; plot of log (k_X/k_H) or log-(k_Y/k_H) for alkaline hydrolysis of *p*-substituted phenyl benzenethilosulfinates in 60% ethanol-water at pH 7.5 and 30°C *vs.* σ.
● $\rho_X=2.4$, ○ $\rho_Y=1.6$

Thiolsufinates are known to be rather unstable. They undergo thermal disproportionation at relatively low temperatures,[11] and are very susceptible to the acid catalyzed nucleophilic reactions.[2] This unstable nature of the thiolsulfinates is partly responsible for its unusually high reactivity, $k_{OH^-}=3.17\times10^3$ M^{-1} sec^{-1} (30°C) and the relatively low activation energy ($E_a=13$ kcal/mol).[12]

Experimental

Materials. *Substituted Phenyl Benzenethiolsulfinates* were prepared by the reaction of benzenesulfinyl chloride with thiophenol in the presence of pyridine according to the method of Backer and Kloosterziel.[13] The products were recrystallized from petroleum ether-chloroform mixed solvent. Their properties are listed in Table 1.

N-Ethylmorpholine. Commercial sample (Nakarai Co.) was distilled, bp 135—136°C/760 mmHg.

Ethanol. Commercial sample was treated with calcium oxide and rectified.

Buffer Solutions. Stock solutions of *N*-ethylmorpholine *N*-ethylmorpholinesulfate buffer, 0.1 M, were made by mixing 0.2 M solution of *N*-ethylmorpholine with 0.2 N sulfuric acid in several buffer ratios, log-(BH$^+$)/(B) = −0.955—+0.477.

Kinetic Experiment. A solution of 1 m*l* of phenyl benzenethiolsulfinate (5×10^{-3} M) in absolute ethanol was added to the mixture of 29 m*l* of ethanol and 20 m*l* of the above buffer stock solution, the latter mixture being kept in a constant temperature bath prior to the addition of ester. Aliquots of this reaction mixture were withdrawn and recorded for the optical density near 280 mμ, using Hitachi 124 double beam spectrophotometer.[14] The change of optical density was plotted against reaction time. The initial slope obtained graphically was proportional to the initial rate of the reaction with proportionality constant, ε, the molar extinction coefficient of the ester at the wavelength, near 280 mμ, as shown in Eq. (7′). A typical

Table 1. Properties of the substituted phenyl benzeneethiolsulfinates

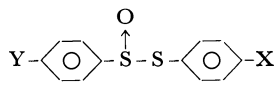

X	Y	Mp, °C	Lit[13]	UV (in 60 v/v % ethanol-water) λ_{max}, mμ	ε
CH_3O	H	76—77	(75—77)	292—3	11200
CH_3	H	83—84[a]	(70—71)	285	9350
H	H	69—70	(69—70)	282	7900
Cl	H	62	(61—62)	286	9100
H	CH_3O	59—60	(61—62)	295	10000
H	CH_3	68	(70—71)	287	9200
H	Cl	68	b	285—286	10900

a) Found: C, 62.58; H, 4.89%. Calcd for $C_6H_5S(O)\cdot S\cdot C_6H_4\cdot CH_3$: C, 62.90; H, 4.84%.
b) Indentified by IR, UV and elemental analysis.
Found: C, 53.52; H, 3.41%. Calcd for $Cl\cdot C_6H_4\cdot S(O)\cdot S\cdot C_6H_5$: C, 53.55; H, 3.35%.

11) a) Ref. 5, p. 369; b) P. Koch and A. Fava, *J. Am. Chem. Soc.*, **90**, 3867 (1968); c) in our preliminary experiment, the rate of thermal disproportionation of PhS(O)SPh was found to be 1.8×10^{-5} sec^{-1} in toluene at 80°C.

12) See discussion in the accompanying paper, S. Oae, R. Nomura, Y. Yoshikawa and W. Tagaki, This Bulletin, **42**, 2903 (1969).

13) a) H. J. Backer, and H. Kloosterziel, *Rec. Trav. Chim.*, **73**, 129 (1954); b) D. Barnard, *J. Chem. Soc.*, **1957**, 4675.

14) The absorption by the products sulfinic acid and disulfide could be neglected near 280 mμ.

example of the optical density change *vs.* reaction time is shown in Fig. 1. Plot of the rate against the initial concentration of the ester gave a straight line as shown in Fig. 2.

$$-\frac{d(\text{Ester})}{dt} = -\frac{1}{\varepsilon} \cdot \frac{d(\text{O.D})}{dt} = k_{OH^-}(OH^-)_0(E)_0 \quad (7')$$

Plot of k_{obs} against pH also gave a straight line as shown in Fig. 3.

Effect of Temperature. The data shown in Fig. 5, were as follows:
$k=1.2\times10^{-3}$ (20°C), 1.9×10^{-3} (25°C), 2.5×10^{-3} (30°C), 3.5×10^{-3} (35°C) min^{-1}, pH=7.5.

Substituent Effect. The rate constants (k_{obs}) for substituted esters shown in Fig. 6. were as follows at pH 7.1; For Ph-S(O)-S-Ph-X-*p*; X=Cl, 7.4×10^{-3} min^{-1}; H, 1.30×10^{-3}; CH_3, 7.9×10^{-4}; CH_3O, 3.5×10^{-4}. For *p*-Y-Ph-S(O)-S-Ph; Y=Cl, 3.6×10^{-3} min^{-1}; CH_3, 7.6×10^{-4}; CH_3O, 5.1×10^{-4}.

BULLETIN OF THE CHEMICAL SOCIETY OF JAPAN VOL. 42 2903—2906 (1969)

Alkaline Hydrolysis of Aryl Benzenethiolsulfonates

Shigeru OAE, Ryuichi NOMURA, Yoichiro YOSHIKAWA and Waichiro TAGAKI

Department of Applied Chemistry, Faculty of Engineering, Osaka City University, Sumiyoshi-ku, Osaka

(Received December 29, 1968)

The alkaline hydrolysis of substituted phenyl benzenethiolsulfonates has been investigated. The rate was found to be first order with respect to both hydroxide and ester. The second order rate constant for the unsubstituted ester was found to be 3.2×10^3 M^{-1} sec^{-1} (water 45°C). The Hammett ρ values were found to be $\rho_{X,Y=H}=2.1$ and $\rho_{Y,X=H}=1.1$ for 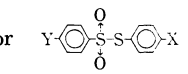 respectively. The reactivities of three esters, *i. e.* phenyl benzenethiolsulfonate, -thiolsulfonate and -sulfonate were compared.

The bond forming and breaking of sulfur-sulfur linkage are very important in biochemistry as well as in organic syntheses. However, the substitution reactions on S^{II}, S^{III}, S^{IV} are relatively unexplored.[1]

In a previous paper, we have shown that the alkaline hydrolysis of substituted phenyl benzenethiolsulfinate (I) is very rapid and proceeds mainly by the attack of hydroxide ion on the sulfinyl sulfur to give sulfinic acid and disulfide.[2] A compound closely related to I is phenyl benzenethiolsulfonate (II) which is known also to give sulfinic acid and disulfide in alkaline hydrolysis.[3] However, there is an important difference between the two esters. While II appears thermally more stable than I, the attacking site of hydroxide is

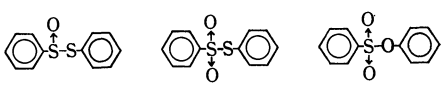

I II III

considered to be the sulfenyl sulfur atom in the case of II, unlike the case of I[3] although detailed features of these chemistries are yet to be clarified.

The present investigation has been undertaken to disclose the nature of the alkaline hydrolysis of the substituted derivatives of II, by means of the kinetic determination of the rates and a comparison with those of I and the related compound III.

Results and Discussion

Product. Phenyl benzenethiolsulfonate (II) was found to give 1.7 mol of benzenesulfinic acid and a small amount of diphenyl disulfide from one mole of the ester in the reaction with an excess amount of sodium hydroxide in 96% ethanol.

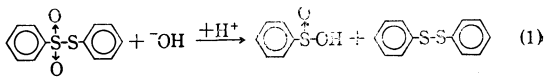

(1)

1 mol excess 1.7 mol detected

Attempts to confirm the possible formation of the corresponding sulfonic acid have failed as was the case with other workers.[3] The formation of more than equimolar amount of the sulfinic acid from the ester used may be rationalized if one assumes the following consecutive reactions.

$$PhSO_2SPh + OH^- \xrightarrow{-H^+} PhSO_2^- + PhSO^- \quad (2)$$

1) J. L. Kice, *Accounts of Chemical Research*, **1**, 58 (1968).

2) S. Oae, Y. Yoshikawa and W. Tagaki, This Bulletin, **42**, 2899, (1969).

3) R. Otto and A. Rossing, *Ber.*, **19**, 1235 (1886).

$$2PhSO^- \xrightarrow{+2H^+} PhS(O)SPh + H_2O \quad (3)$$

$$PhS(O)SPh + OH^- \xrightarrow{-H^+} PhSO_2^- + PhS^- \quad (4)$$

$$PhSO_2SPh + PhS^- \longrightarrow PhSO_2^- + PhSSPh \quad (5)$$

Kinetics. From product analysis, the attacking site of hydroxide ion is most likely the sulfenyl sulfur atom. (Eq. (2)). However, there still remains a question as to sulfenic acid. The rates of the alkaline hydrolyses of all the compounds examined were also found to be very rapid. Therefore the kinetic measurements were carried out in a pH-controlled buffer solution. The buffer used was *N*-ethylmorpholine *N*-ethylmorpholine sulfate which did not react with the ester under the same reaction condition and did not precipitate in 60% ethanol-water solution.

The kinetic rates were followed by observing the amounts of disappearance of the starting ester (see experimental). Since the reaction was expected to be complicated as illustrated in Eqs. (2)—(5), only the initial rate was used for the calculation of the rate constants based on

$$\frac{-d(Ester)}{dt} = k_{obs}(E)_0 = [k_0 + k_{OH^-}(OH)_0](E)_0 \quad (6)$$

where k_0 and k_{OH^-} are the rate constants for both spontaneous and alkaline hydrolyses respectively, and $(OH^-)_0$ and $(E)_0$ are the initial concentrations of hydroxide and the ester, respectively.

The first order dependence of the rate on the initial concentration of II and on pH was observed to be similar to that in the hydrolysis of the corresponding sulfinate.[2] In order to obtain an extrapolated value of the rate in water, k_{obs} was plotted against ethanol concentration in the solvent under the same buffer ratio to give a straight line, as shown in Fig. 1.

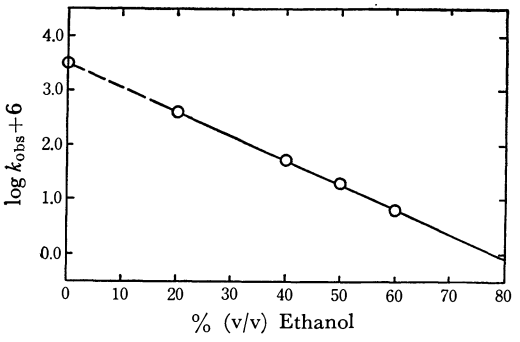

Fig. 1. Plot of pseudo first-order rate constants k_{obs} *vs.* percent of ethanol in the solvent; ester, $PhSO_2SPh$; $(E)_0 = 3.60 \times 10^{-3}$; 45°C; pH=7.5 in 60% ethanol-water.

From Fig. 1 the second order rate constant of the alkaline hydrolysis of II in water was calculated to be 3.2×10^3 *l*/mol sec at 45°C. Meanwhile the Arrhenius plot gave E_a and $\Delta S^{\neq}$ values to be 10 kcal/mol and −13 e.u. (at 45°C), respectively, in 60% ethanol-water. The error involved in the rate constant was within, +5% *i. e.*, the same order of magnitude as in the previous paper.

Substituent Effect. Introduction of an electron-withdrawing substituent at *p*-position of either one of the two benzene rings of the ester accelerated the rate while that of an electron-releasing substituent retarded. The results are shown in Table 1 and their Hammett plot is shown in Fig. 2. From Fig. 2 Hammett ρ values were calculated to be $\rho_X = 2.1$ and $\rho_Y = 1.1$.

Although the results so far described are not sufficient to allow any detailed discussion on the mechanism of the overall hydrolysis reaction, it is interesting to compare the initial rate of the hydrolysis of the following three closely related esters which are summarized in Table 2.

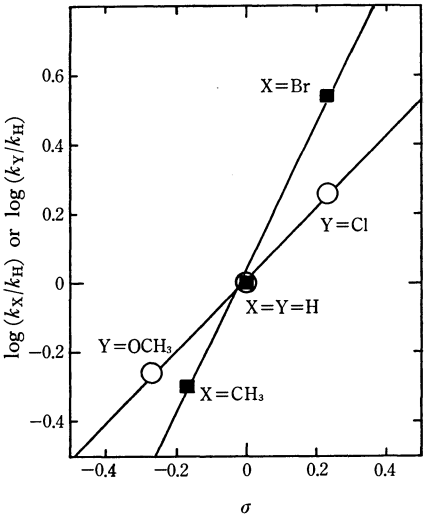

Fig. 2. Hammett plot; plot of $\log(k_X/k_H)$ or $\log(k_Y/k_H)$ for hydrolysis of *p*-substituted phenyl-benzenethiolsulfonates in 60% ethanol-water at pH 7.5 and 45°C *vs.* σ.
■ $\rho_X = 2.1$, ○ $\rho_Y = 1.1$

TABLE 1. ALKALINE HYDROLYSIS OF SUBSTITUTED PHENYL BENZENETHIOLSULFONATES

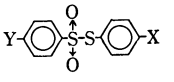

X	Y	10^5 k_{obs} (45°C)
CH_3	H	1.0
H	H	2.1
Br	H	7.3
NO_2	H	1.3*
H	CH_3	1.2
H	Cl	3.8

* pH=6.9
60% (v/v) Ethanol-water, pH=7.5

TABLE 2. THE DATA FOR THE ALKALINE HYDROLYSIS OF PHENYL BENZENETHIOLSULFINATE (I), THIOLSULFONATE (II) AND SULFONATE (III)

Compound[a]	k_{OH^-} rel. (50°)[b]	ρ (Y)	ρ (X)	E_a kcal/mol[b]	ΔS^*, e. u.[b]	Ref.
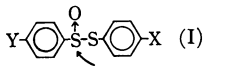 (I)	10^6 [c]	1.6	2.4	13	−3 (30°C)	2
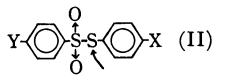 (II)	10^5 [c]	1.1	2.1	10	−13 (45°C)	e
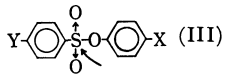 (III)	1[d]	2.4	3.0	18	−21 (50°C)	4

a) Arrow indicates the attacking site of hydroxide
b) for X=Y=H
c) In 60% (v/v) ethanol-water
d) In 70% (v/v) dioxane-water
e) This work

In order to correlate the rates and the substituent effects, it is necessary to know the attacking site of hydroxide ion for each of the esters. In the case of sulfonate (III), the attacking site is known to be exclusively the sulfonyl sulfur atom from the ^{18}O tracer study, except for the ester bearing $X=NO_2$ which undergoes significant C–O bond cleavage (about 20%) by the attack of hydroxide ion on the benzenoid carbon of phenolic part.[5]

For the other two esters, I and II, the assignment of the attacking site is by no means clear, since in both cases the reactions appear to be so complicated that the product analysis alone cannot give a conclusive answer. However, the assignement is possible if one limits the discussion to only the very initial stage of the reactions. Since no sulfonic acid was detected in the hydrolysis of II, the rate of its initial reaction must be that of the initial attack of hydroxide on the sulfenyl sulfur, whereas in the case of I, the reaction is either an exclusive attack on the sulfinyl sulfur or a competitive attack on both the sulfinyl and the sulfenyl sulfur. Since the hydrolysis products of I are benzenesulfinic acid and diphenyl disulfide, the attack on the sulfenyl sulfur to give the sulfenic acid must be followed by other succeeding reactions. The probable reaction of the sulfenic acid in neutral or acidic media is self-condensation to regenerate the starting ester, I (Eq. (3)). Therefore, the rate of the hydrolysis of I becomes the same as that of the initial attack of hydroxide ion on the sulfinyl sulfur. The ρ_X values are identical for all the three esters in spite of the wide range of their reactivities, while the ρ_Y values vary somewhat more widely. The fact that both ρ_X and ρ_Y are almost the same for sulfonates (III) appears to be in line with the one step S_N2 mechanism which has been suggested from our previous ^{18}O tracer study.[6] The same mechanism might also be applied in the hydrolysis of I and II although the ρ_Y is smaller than ρ_X. A smaller ρ_Y for II could be due to the difference in the attacking site, and the effect of ρ_Y may be weakened by the presence of sulfonyl group inserted between the reaction centers.

The most important finding is an enormous rate difference between the sulfonate and the other two sulfur analogs. Both the heat and entropy of activation seem to be responsible for this rate difference. Unfortunately the data for substituted phenyl benzenesulfinates are not yet available for a comparison with those of thiolsulfinate (I). Both thiolsulfonate (II) and sulfonate (III) are presumed to be stabilized by the following type of resonance that involves an extra π-bond formation with the central sulfur atoms.

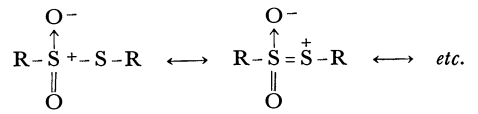

II

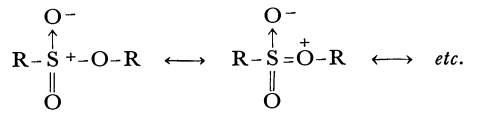

III

Generally, however, the electron donating conjugation of sulfur is smaller than that of oxygen.[7]

4) a) R. V. Vizgert, *Zhur Obshch. Khim.*, **28**, 1873 (1958). b) R. V. Vizgert and E. K. Savchuk, *ibid.*, **26**, 2268 (1956).

5) S. Oae, T. Fukumoto and R. Kiritani, This Bulletin, **36**, 346 (1963).

6) D. R. Christman and S. Oae, *Chem. & Ind.*, **1959**, 1251.

7) C. C. Price and S. Oae, "Sulfur Bonding," Donald Press, New York (1962).

Therefore the S–O bond in III would be stronger than the S–S bond in II, thus resulting in a large rate difference of the rates of the hydrolyses. Sulfonamides are also known to be very stable toward alkali. The higher stability of sulfonamide linkage is also due mainly to the stronger electron donating ability of nitrogen than oxygen and sulfur. In addition to the difference of the bond strengths, the approach of hydroxide anion to the attacking site should be much easier in I and II than in III because of the smaller electrostatic repulsion between sulfonyl oxygen and the hydroxide anion (in II), and also because of the electron accepting ability of the sulfur atom using one of its vacant 3*d*-orbitals.

Experimental

Materal. Substituted phenyl benzenethiolsulfonates were prepared by the reaction of benzenesulfenyl chloride with sulfinic acid in dry ether.[8] The products were recrystallized from methanol or ethanol: *p*-$XC_6H_4SSO_2C_6H_5$; X=H, mp 44—45°C (lit[9] 44—45°C); CH_3, 54°C (52—54°C); Br, 85°C; NO_2, 103—105°C (104—105°C).
p-$YC_6H_4SO_2SC_6H_5$: Y=CH_3, 78°C (77—78°C): Cl, 82—82.5°C (81°C), OCH_3, 54°C (54—55°C).

N-Ethylmorpholine buffer and the solvent ethanol were described in the preceding paper.[2]

Product. Unsubstituted ester (2.5 g, 0.01 mol) and potassium hydroxide (1.2 g, 0.2 mol) were dissolved in 50 m*l* of 96% ethanol-water solvent and the mixture was refluxed for 5 hr. Ethanol was removed from the reaction mixture and the residue was dissolved in ether and extracted with water. A part of the water extract was used for the detection of sulfonic acid by converting it to the thiuronium salt.

But no thiuronium salt was formed. The water extract was also titrated with 0.2 N sodium nitrite and the formation of 0.017 mol of sulfinic acid was observed. From the ether layer was isolated 300 mg of diphenyl disulfide which accounted for 14% of the total sulfur, while 0.017 mol of sulfinic acid accounted for 85% of the total sulfur in the starting ester. Thiophenol was not detected in any significant amount either in water or the ether layer. These results clearly indicated that the reaction leads to the quantitative formation of sulfinic acid and disulfide, and the formation of the sulfonic acid was negligible if none at all.

Kinetics. A solution of the thiolsulfonate (3×10^{-3} M) in 30 m*l* of 60% ethanol-water (v/v) and 30 m*l* of the *N*-ethylmorpholine buffer, in 60% ethanol-water were mixed after temperature equilibration in a constant temperature bath. Aliquot (5 m*l*) of this reaction mixture was added to a separating funnel containing 20 m*l* of chloroform and 25 m*l* of acidic water. The chloroform layer was washed and the upper water layer was removed by suction. Two more washings with 25 m*l* each of water were repeated. The optical density of this chloroform solution of the UV absorptions at 270 mμ was recorded and plotted against reaction time. The initial rate was then obtained graphically. The other methods for the treatment of the kinetic data were essentially the same as described in the preceding paper.[2]

8) a) F. Klivenyi, *Magyan Kem. Folyoivat*, **64**, 121 (1958); *Chem. Abstr.*, **54**, 16416 (1960). b) G. Kresze and W. Kort, *Chem. Ber.*, **94**, 2624 (1961).

BULLETIN OF THE CHEMICAL SOCIETY OF JAPAN VOL. 42 2906—2911 (1969)

Reactive Species in the Explosion of Silver Acetylide. I. Reaction with Saturated Hydrocarbon

KO TAKI

The Institute of Physical and Chemical Research, Yamato-machi, Saitama

(Received February 5, 1969)

The reactive species produced by the explosion of silver acetylide were found to react with hydrocarbon and to give acetylene and ethylene as the main products. The reactive species must be carbon oligomers. Since, in the reactions with higher hydrocarbons, acetylene and ethylene are also produced, their formation process may be the decomposition of the adduct of the reactive species. From the product distributions, the phase dependence of the ratio of ethylene to acetylene, and the effect of such moderator as carbon dioxide and inert gas, the reactive species are considered to be not only the monoatomic carbon (C_1) but also the diatomic carbon (C_2). The effect of a NO radical scavenger in the reactions of both ethane and propane is also described.

Thermally-unstable materials, especially solid explosives, usually decompose with the generation of gaseous products, but silver acetylide yields only solid decomposition products. The decomposition is represented by the following equation:

$$Ag_2C_2 \rightarrow 2Ag(s) + 2C(s) \qquad \Delta H = -83 \text{ kcal}^{1)}$$

A few studies[2,3] of the explosions of silver acetylide

(Ag_2C_2) have been reported recently. McCowan showed[2] that the activation energy of explosions of silver acetylide was 41 kcal/mol and that it decomposed also upon exposure to light. Some detailed studies have been performed by several workers,[4,5] but no work has been reported about the reaction of the reactive species produced by the explosion of silver acetylide.

Recently there have been intensive investigations of the reaction of hydrocarbons with free carbon atoms produced by the nuclear recoil reaction,[6,7] the photoreaction,[8] the vaporization of carbon (carbon arc),[9] and the laser-induced reaction.[10] In the reaction of these carbon atoms with hydrocarbons, however, the products and their distributions vary greatly from case to case. In this paper the reactions of the carbon species which are formed by the explosion of silver acetylide will be investigated, and some comparisons of the carbon atoms produced by the other methods cited above will be made.

Experimental

1) Preparation of Silver Acetylide. Silver acetylide was prepared by passing acetylene into an ammoniacal solution of silver perchlorate (Junsei Co.). The precipitate of silver acetylide thus obtained was washed with water containing acetylene and finally with methanol. Then it was spread out on a filter paper (it should not be filtered off because it often explodes when it is pulverized to a fine powder) and dried in a dark room. Irradiation by light darkens the surface of silver acetylide very quickly. The very fine powder, when it was irradiated, turned black within a few minutes, but it was still explosive after several days' exposure.

2) Apparatus for the Explosion of Silver Acetylide. In the gas-phase and solid-phase reactions, the explosion of silver acetylide was performed in a specially-designed flask such as is shown in Figs. 1 and 2.

In the solid-phase (cold-film) reaction, about 0.1—

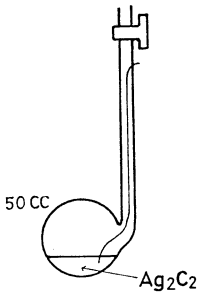

Fig. 1. Explosion vessel for gas-phase reaction.

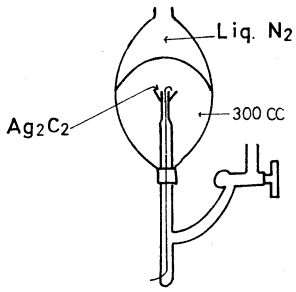

Fig. 2. Explosion vessel for solid-phase reaction.

0.3 g of silver acetylide was placed on the top of the gas inlet tube, as is shown in Fig. 2; the substrate was then introduced as cold film on the glass wall cooled by liquid nitrogen under a pressure of less than 10^{-3} Torr. The explosion was started by the use of a Tesla coil. In the explosion technique described here, 0.1 g of Ag_2C_2 can be exploded perfectly safely in this flask at a pressure of 500 Torr.

When neopentane was condensed on the bottom of the flask, as is shown in Fig. 3, no products were detected. In this reaction vessel the reactive species can not collide with the substrate. Therefore, the direct collision of the reactive species with the substrate is necessary for the formation of the products.

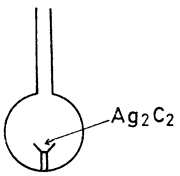

Fig. 3

3) Analyses. The products were analyzed by gas chromatography using silica gel and squalane columns. Quantitative analyses were performed by the internal-standard system, using neopentane as the standard.

4) Ageing of Silver Acetylide. In order to examine the ageing effect of silver acetylide, neopentane ($2.1—2.5\times10^{-4}$ mol) was used as the substrate in the solid-phase reaction. The gases produced by explosion were mainly acetylene and methane. The yields of acetylene and methane from aged silver acetylide (0.10 g) were as follows:

1) F. R. Bichowsky and F. D. Rossini, "The Thermochemistry and Chemical Substances," Reinhold Pub. Co. (1951), p. 79.

2) J. D. McCowan, *Trans. Faraday Soc.*, **59**, 1860 (1963).

3) V. D. Hogan and S. Gordon, U. S. Dept. Com. Office Tech. Serv. A. D. 419625, 15 pp. (1960).

4) W. E. Baker and F. Hoese, *Chem. Eng. News*, **43** (49), 46, 48 (1965).

5) Y. Tanaka and Y. Mizushima, *Kogyo Kagaku Kyokaishi*, **24**, 206 (1963).

6) M. Marshall, C. MacKay and R. Wolfgang, *J. Am. Chem. Soc.*, **86**, 4741 (1964).

7) H. J. Ache and A. P. Wolf, *ibid.*, **88**, 888 (1966).

8) K. D. Bayes, *ibid.*, **84**, 4077 (1962).

9) P. S. Skell and R. R. Engel, *ibid.*, **88**, 3749 (1966).

10) K. Taki, P. H. Kim and S. Namba, This Bulletin, **42**, 823 (1969).

Ageing time	1d	4d	6d	10d
Yield of C_2H_2 ($\times 10^{-5}$ mol)	0.7	1.2	1.1	1.4
Yield of CH_4 ($\times 10^{-5}$ mol)	0.8	1.6	1.8	1.8

From the above results, it can be said that the explosion of silver acetylide will give reproducible results within 10 days (after preparation).

Results

1) Impurities in Silver Acetylide. In the explosion of the above silver acetylide, 2—5 mol% of gases were produced. Mass spectrometrical analyses showed that the gases were 30% hydrogen, 50—60% nitrogen, and 10—20% carbon monooxide, plus a small amount of hydrocarbons (methane and ethane). They must be the decomposition products from the impurities in Ag_2C_2.

2) Reaction with Na Film. Silver acetylide (0.2 g) was exploded under a 10^{-4} Torr pressure in a 50-cc flask (Fig. 1) with walls coated with sodium film. After the decomposition of the reaction products with Na film by the use of water, ethylene and a small amount of acetylene were found. These experiments show that some carbon species produced by the explosion of silver acetylide react with sodium film to make sodium carbide, which in turn produces acetylene during decomposition by water. Ethylene will be formed by the hydrogenation of acetylene according to the following reaction sequence:

$$Ag_2C_2 \rightarrow 2Ag + 2C$$

$$2Na + 2C \rightarrow Na_2C_2$$

$$Na_2C_2 + 2H_2O \rightarrow C_2H_2 + 2NaOH$$

$$2Na + 2H_2O \rightarrow 2H + 2NaOH$$

$$C_2H_2 + 2H \rightarrow C_2H_4$$

3) Reaction of the Reactive Species Produced by the Explosion of Silver Acetylide with Hydrogen Sulfide. In the solid-phase reaction of the reactive species with hydrogen sulfide, the principal products were methane and acetylene, as is shown in Fig. 4. The detection of other sulfide compounds were not performed. Carbon species gave acetylene with H_2S.

Caution: Avoid the contact of hydrogen sulfide with silver acetylide, because silver acetylide explodes in a hydrogen sulfide atmosphere.

Discussion

Judging from the facts that, in the reaction with sodium film, sodium carbide was produced and that acetylene was produced by the reaction with hydrogen sulfide, carbon oligomers (C_1, C_2, C_3,$\cdots$) must be reactive species. As has been shown in 2) of the Experimental section, the reaction products are obtained only by the direct collision of reactive species with the substrate. In the reactions with hydrocarbons as the substrate in both the gas and solid phases, acetylene and ethylene were produced as the principal products. The ratio of ethylene to acetylene was larger in the solid phase than in the gas phase. Since the reactive species did not react with carbon dioxide, the reaction was also carried out in a carbon dioxide matrix.[11] The main products here were also ethylene and acetylene, but the ratio of ethylene to acetylene was lower in the CO_2 matrix than in the solid phase. The results are listed in Tables 1 and 2.

These results were compared with the results of the reaction of a free carbon atom produced by a nuclear reaction which is apparently the reaction of monoatomic carbon.

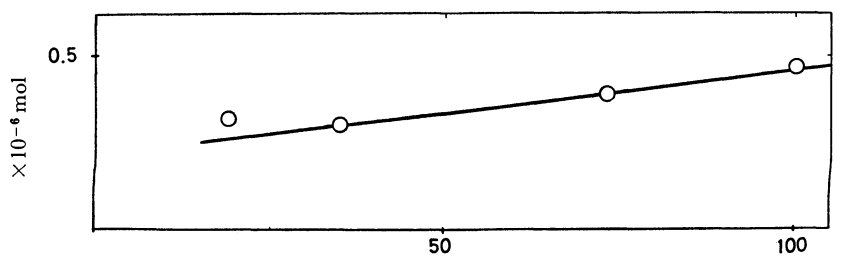

Reaction with H_2S
Ag_2C_2 0.10 g
H_2S 2.2×10^{-4} moles

Products
CH_4 0.056×10^{-6} mol
C_2H_4 0.048×10^{-6} mol
C_2H_2 0.47×10^{-6} mol

Fig. 4. Acetylene yield plotted as a function of the amounts of Ag_2C_2 in the reaction with hydrogen sulfide.

11) W. Weltner, Jr., and McLeod, Jr., *J. Chem. Phys.*, **45**, 3096 (1966).

Table 1. Reaction products for various hydrocarbons in solid-phase
Ag_2C_2 0.10 g, Substrate 2.0—2.3×10⁻⁴ mol

Substrate	Product ($\times 10^{-5}$ mol)						
	CH_4	C_2H_6	C_2H_4	C_2H_2	Propane	Propylene	C_4
Methane	—	0.3	0.6	0.2	—	0.02	—
Ethane	3.9	—	5.4	2.0	—	0.8	0.07
Propane	4.2	0.5	5.5	2.2	—	0.4	0.1
n-Butane	3.0	0.5	5.6	1.1	0.1	1.0	—
Isobutane	4.4	0.6	2.1	1.1	—	2.3	—
Cyclopropane	3.8	0.05	2.4	3.6	—	4.5	0.1
Neopentane	1.3	0.05	0.3	0.5	—	—	—

Table 2. Product yields in CO_2 matrix

Product	Substrate ($\times 10^{-5}$ mol)							
	Ethane		Propane		*n*-Butane		Isobutane	
	a	b	a	b	a	b	a	b
CH_4	3.9	2.9	4.2	4.2	3.0	1.5	4.4	3.4
C_2H_4	5.4	2.6	5.5	4.3	5.6	1.9	2.1	1.2
C_2H_2	2.2	2.0	2.2	2.6	1.0	1.5	1.1	1.5
$\frac{C_2H_4}{C_2H_4}$	2.5	1.3	2.5	1.6	5.6	1.3	1.9	0.85

a = Solid, b = CO_2 Matrix

Table 3. Reaction of carbon atom[12,13] produced by $^{12}C(\gamma,n)^{11}C$

Substrate	Product	
	C_2H_2 %	C_2H_4 %
CH_4	30.0	28.0
C_2H_6	32.7	19.5
C_3H_8	29.5	12.1
c-C_3H_6	65.5	0

Product %	Ethane phase		Propane phase		
	Gas	Liq.	Gas	Liq.	Solid
CH_4	2.1	3.7	2.9	3.4	4.7
C_2H_2	31.2	17.4	25.0	18.2	11.2
C_2H_4	23.7	15.7	17.9	12.7	8.9
$\frac{C_2H_4}{C_2H_2}$	0.76	0.90	0.71	0.70	0.80

In the hot-atom reaction, the reaction of the carbon atom with methane, ethane, and propane produces mainly acetylene and ethylene, as is shown in Table 3.[12,13] By the fact that methane also gives acetylene, the most primary process has been considered to be the decomposition of the excited insertion intermediate (the energy-rich complex) of the carbon atom to acetylene and ethylene according to this scheme: $CH_4+C\rightarrow CH_3-\dot{C}-H\rightarrow CH_2=CH_2$ or $CH\equiv CH+H_2$. These acetylene and ethylene formation processes have also been confirmed by the evidence that the yields of acetylene and ethylene decrease with the change in phase from gas to solid and that, in the moderation of the carbon atom by an inert gas mixture,[14] the ratio of ethylene to acetylene increases with the change in phase from gas to solid. The formation mechanism[15] of ethylene in the hot atom reaction has also been considered to be the hydrogen abstraction of the vinyl radical or the reaction of the CH radical as follows:

$$R-CH_2-\dot{C}-H \rightarrow R\cdot + CH_2=\dot{C}H \rightarrow C_2H_4$$

$$CH + R-CH_3 \rightarrow R-CH_2-\dot{C}H_2 \rightarrow C_2H_4$$

These formation mechanisms of acetylene and ethylene do not conflict with the above experimental results (Table 3).

Since the phase dependence of the yield of ethylene relative to that of acetylene in this explosion reaction was in qualitative agreement with that in hot-atom chemistry, the formation processes of acetylene and ethylene might be considered to be the reaction of monoatomic carbon, as in the hot-atom reaction. However, the results with the CO_2 matrix conflicted with those of the monoatomic reaction, as has previously been described.

12) C. Mackay and R. Wolfgang, *J. Am. Chem. Soc.*, **83**, 2399 (1961).
13) G. Stöcklin and R. Wolfgang, *ibid.*, **85**, 229 (1963).
14) J. E. Nicholas, C. MacKay and R. Wolfgang, *ibid.*, **88**, 1610 (1966).
15) J. Dubrin, C. MacKay and R. Wolfgang, *ibid.*, **86**, 959 (1964).

If monoatmoic carbon is the only reactive species, the moderation of the carbon atom should show an increase in the C_2H_4/C_2H_2 ratio. Moreover, in the gas-phase reaction, the pressure dependence of the C_2H_4/C_2C_2 and CH_4/C_2H_4 ratios in the presence of ethane or helium was not observed, as Tables 4 and 5 show. It seems that the moderation of reactive species is not sufficient. Therefore, helium gas was used as the moderator in the solid-phase reaction. The results showed the decrease in the C_2H_4/C_2H_2 ratio shown in Table 6. These results also conflict with those for the reaction of the free carbon atom.

In order to examine the lifetime of the species, the CH_4/C_2H_4 and C_2H_4/C_2H_2 ratios were plotted as functions of the distance from the explosion position to the solid substrate, as is shown in Fig. 5.

Table 4. Pressure dependence for ethane in gas-phase reaction

Ag_2C_2 0.10 g

Product ($\times 10^{-5}$ mol)	Ethane pressure (Torr) 50	100	200	300	400
CH_4	4.2	6.7	7.2	7.3	4.9
C_2H_4	6.1	11.7	11.7	10.8	8.0
C_2H_2	3.0	5.7	5.3	5.4	7.5
$\frac{C_2H_4}{C_2H_4}$	2.0	2.1	2.2	2.0	2.3
$\frac{CH_4}{C_2H_4}$	1.4	1.2	1.4	1.4	1.4

Table 5. Pressure dependence for ethane by helium in gas-phase reaction

Ethane (Torr) / He (Torr)	50 / 0	50 / 50	50 / 150	50 / 250
$\frac{CH_4}{C_2H_2}$	1.4	1.1	1.0	1.0
$\frac{C_2H_4}{C_2H_2}$	2.0	1.6	1.4	1.9

Table 6. Pressure dependence for ethane in solid-phase reaction

Ag_2C_2 0.10 g
Ethane 2.22×10^{-4} mol

Products ($\times 10^{-5}$ mol)	He pressure (Torr) 0	100	300
CH_4	3.9	0.9	0.6
C_2H_4	5.4	1.3	0.8
C_2H_2	2.0	1.6	0.3
C_3	1.0	0.06	0.05
C_4	0.1	—	—
$\frac{C_2H_4}{C_2H_2}$	2.7	2.2	2.5
$\frac{CH_4}{C_2H_4}$	0.7	0.7	0.75

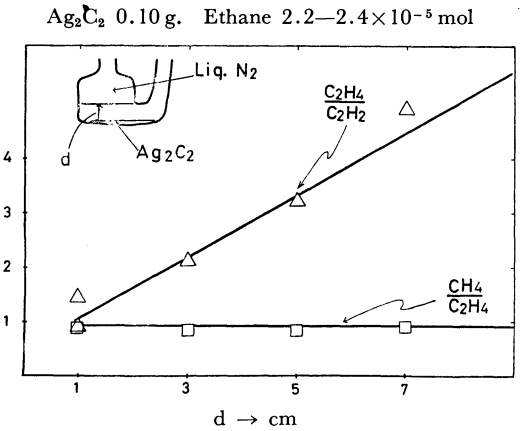

Fig. 5. C_2H_4/C_2H_2 and CH_4/C_2H_2 ratios plotted as a function of distance from explosion position.

Naturally the yields of products decreased with an increase in the distance, but the ratio of ethylene to acetylene increased and the ratio of methane to ethylene was constant, as was previously shown in helium moderation.

The constancy of the CH_4/C_2H_4 ratio and the increase in the C_2H_4/C_2H_2 ratio suggest that both methane and ethylene are formed from a common precursor, but that at least a part of the acetylene is formed from a different precursor. Moreover, the lifetime of the acetylene precursor is considered to be shorter than that of methane and ethylene precursor. Similar results were also observed in the reactions with propane and neopentane.

In comparison with the reactions of the carbon arc,[16] the product distributions are quite different. In the carbon arc reaction, it is considered that monoatomic carbon is also the reactive species and that products are formed by the further reaction of the carbon-atom-insertion intermediates, but acetylene is not detected.

Reaction with Cyclopropane. The reaction of the reactive species with cyclopropane gave ethylene, acetylene, and propylene as the main products. The ratio of ethylene to acetylene was 0.5 in the solid phase and 0.7 in the CO_2 matrix. The yield of ethylene was smaller than that of acetylene.

The reaction of a free carbon atom-^{11}C produced by nuclear reaction with cyclopropane[12] has been known to give a 65% yield of acetylene. This result was explained by the mechanism in which the insertion intermediate ($\triangle$-$^{11}\dot{C}$-H)[17] decomposes to almost an equivalent amount of radioactive acetylene-^{11}C and nonradioactive ethylene.

If the monoatomic carbon is the reactive

16) P. S. Skell and R. R. Engel, *J. Am. Chem. Soc.*, **88**, 4883 (1966).
17) P. B. Shevlin and A. P. Wolf, *ibid.*, **88**, 4735 (1966).

species in this work, ethylene may be expected to be formed in a yield almost equivalent to that of acetylene. The experimental result was, however, quite different from that expectation. From these results it seems that the reaction species involve not only monoatomic carbon (C_1) but another polyatomic carbon, such as diatomic carbon (C_2), which abstracts the hydrogen atom from hydrocarbon to produce acetylene.

Effect of Scavenger. The nitric oxide radical scavenger did not inhibit the formation of the ethylene and acetylene; rather, it promoted it in the gas-phase and solid-phase reactions of ethane, as is shown in Table 7.

Table 7. The effect of NO in gas and solid ethane

Ag_2C_2 0.10 g
Ethane 2.5×10^{-4} mol (100 Torr)

Product ($\times10^{-5}$ mol)	Gas Phase NO %		
	0	7.3	18.1
C_2H_4	10.4	10.8	8.3
C_2H_2	4.4	4.7	4.7
C_3 products	0.3	0.2	0.1
Butadiene	0.02	0.02	0

Product ($\times10^{-5}$ mol)	Cold Surface −196°C NO %				
	0	14.8	20.8	24.0	34.6
C_2H_4	5.4	8.2	7.1	7.1	7.0
C_2H_2	2.0	2.2	3.6	3.3	1.8
C_3 products	1.06	0.20	0.16	—	0.14
Butadiene	0.10	—	0.004	—	—

These observations indicate that the elimination of the radicals causes an increase in the yields of acetylene and ethylene.

On the basis of these results, it can be said that acetylene and ethylene may be produced by molecular processes, while C_3 products and butadiene may be formed by radical processes inhibited by the NO scavenger. Similar facts were also observed in the reaction with propane. The data are listed in Table 8.

Emission Spectrum. Since the emission spectrum in the explosion of silver acetylide showed a continuous band from 4000 to 6500 Å, C_2 Swan bands[18] were not detected. Unfortunately, the presence of C_2 was not confirmed spectroscopically.

Table 8. The effect of NO in propane

Ag_2C_2 0.10 g
Propane 2.5×10^{-4} mol (100 Torr)

Product ($\times10^{-5}$ mol)	Gas Phase NO %		
	0	6.9	13.5
CH_4	5.5	5.2	6.3
C_2H_6	0.82	0.95	0.40
C_2H_4	7.6	8.80	7.3
C_2H_2	2.4	3.0	2.8
Propylene	1.4	1.8	1.4
Butadiene	0.13	0.14	0.11

From the above observations, it may be concluded that the explosion of silver acetylide involves the formation of two kinds of reactive species, probably mono and diatomic carbons. The reaction products are mainly ethylene and acetylene, the formation of which is not inhibited by the NO radical scavenger.

The reaction of the C_2 diatomic carbon produced by the photolysis of diacetylene was reported by Pontrelli[19] to give triacetylene in the insertion process with diacetylene, while the reaction of C_2 produced by laser-induced reaction[10] with hydrocarbon gave acetylene and ethylene. Moreover, the reaction of carbon vapor produced by carbon arc with methanol, propanol, and *t*-butyl chloride gave acetylene and ethylene. By the technique[20] employing carbon electrodes enriched in ^{14}C, the presence of a C_2 reaction to form acetylene and ethylene has been confirmed.

The presence of a diatomic carbon reaction in this explosion reaction was confirmed by other experimental evidence that the reaction with 1,3-butadiene gave benzene. The details will be described in a second paper.

The author wishes to thank Professor S. Murahashi for his useful discussions and suggestions and Miss K. Motegi for the valuable assistance with this work, as well as to express his appreciation to Mr. S. Satooka for the mass spectrometrical analyses and to Dr. P. H. Kim for the spectroscopic analyses of the explosion emission of silver acetylide.

18) L. J. Stief, V. J. Decarlo and R. J. Mafaloni, *J. Chem. Phys.*, **42**, 3113 (1965).
19) G. J. Pontrelli, *ibid.*, **43**, 2571 (1965).
20) P. S. Skell and R. F. Harris, *J. Am. Chem. Soc.*, **88**, 5933, (1966).

BULLETIN OF THE CHEMICAL SOCIETY OF JAPAN VOL. 42 2912—2917 (1969)

A Structural Study of the Catalytic Activity in Formaldehyde Polymerization in Liquid Carbon Dioxide

Tsutomu KAGIYA and Kōzō NARITA

Faculty of Engineering, Kyoto University, Sakyo-ku, Kyoto

(Received February 17, 1969)

The catalytic activities of various acids, bases, and salts in formaldehyde polymerization in a liquid carbon dioxide solution were studied in connection with the structures of the catalysts. The activity of the catalysts increased with decreases in the pK_a of Brönsted acids and in the ion-dissociation energy of alkyl acetates, and with increases in the pK_a' of organic compounds containing a nitrogen or oxygen atom, such as triethylamine or diethyl ether, and in the pK_a of the conjugated acids of sodium salts. The activity of the salts obtained from a strong acid with various bases increased with a decrease in the pK_a' of the bases, while that of the salts from weak acids with weak bases decreased with an increase in the summation of the pK_a values of acids and the pK_a' values of bases, reaching a minimum point and then increasing. The activity of various salts decreased with an increase in the pH in an aqueous solution, reached a minimum point at pH 6, then increased.

It has been established that formaldehyde easily forms polymers with various catalysts.[1] Yokota *et al.* reported[2] that a high polymer of formaldehyde was obtained in liquid carbon dioxide. The present authors reported[3] previously that the formaldehyde polymerization in liquid carbon dioxide was initiated by the formic acid produced by the pyrolysis of α-polyoxymethylene or paraformaldehyde, and no polymer was obtained with the monomer removed from the formic acid.

The purpose of this paper is to determine quantitatively the relationship between the catalytic activity and the structure and thermodynamic nature of the catalyst, and to discuss the mechanism of polymerization on the basis of an energetic study of the catalytic activity in ionic polymerization.[4]

Experimental

Materials. Formaldehyde in liquid carbon dioxide was prepared by means of a two-step method reported previously.[3] Eighteen hundred grams (paraform), 1000 g of polyethylene glycol (degree of polymerization of about 10) (PEG), and 1.8 mol of calcium carbonate were put into a 3000 m*l* decomposer and heated at 110 to 160°C under a carbon dioxide stream (flow rate: 160 m*l*/min). The polyethylene glycol hemiformal (PEGH) was prepared by bubbling the mixed gas thus obtained into a 3000 m*l* absorber (95—110°C) containing 2000 g of PEG. Eight hundred grams of PEGH were placed in a 1000 m*l* decomposer and pyrolyzed at 130 to 180°C under a carbon dioxide stream (flow rate: 160 m*l*/min). The mixture of formaldehyde and carbon dioxide was passed through a tube cooled at −20°C and then liquefied in the monomer reservoir at −78°C. The alkyl acetates (commercial) were dried over calcium chloride and distilled before use. The Brönsted acids and bases (commercial) were purified in the usual ways. The sodium borate was dehydrated by heating before use. The other sodium compounds were used without further purification. *N*-Phenylethylenimine was prepared according to the method of the literature[5] from β-bromoethylaniline hydrobromide, it was dried over sodium sulfate and fractionated twice before use (bp 70—70.5°C/13 mmHg). The salts (commercial) were recrystallized from ethanol, methanol, or ethyl acetate. Triethanolamine nitrate was prepared by the reaction[6] of potassium nitrate with triethanolammonium borofluoride, and was recrystallized from ethanol (mp 99°C). Aniline trichloroacetate was prepared by the neutralization of aniline with trichloroacetic acid in ethanol, and was recrystallized from ethanol (mp 147°C). The other solid salts, which were not obtained commercially, were prepared by the same method as was triethanolamine nitrate. The aniline salt of methanol, nitroethane, or nitromethane (liquid) was used as an equimolar mixture of aniline and methanol (nitromethane or nitroethane). The dimethyl ether acetate was prepared by

1) J. C. Bevington and R. G. W. Norrish, *Proc. Roy. Soc. (London)*, **A205**, 516 (1951); R. N. MacDonald, U. S. Pat. 2768994 (1956), 2828286 (1958).

2) H. Yokota, M. Kondo, T. Kagiya and K. Fukui, *J. Polymer Sci.*, **A-1**, **6**, 425 (1968).

3) T. Kagiya, M. Kondo, K. Narita and K. Fukui, This Bulletin, **42**, 1688 (1969).

4) T. Kagiya, Y. Sumida and T. Nakata, *ibid.*, **41**, 2239 (1968); *ibid.*, **41**, 2247 (1968).

5) H. W. Heine, B. L. Kapur and C. S. Milch, *J. Am. Chem. Soc.*, **76**, 1173 (1954).

6) H. J. Emeleus and H. G. Heal, *J. Chem. Soc.*, **1946**, 1126.

the reaction[7] of monochloromethyl ether with potassium acetate, and was purified by distillation (bp 117—118°C).

Polymerization Procedure. A stainless-steel autoclave with a capacity of 30 m*l* (16 mm×150 mm) was used as the reaction vessel. Into the vessel, which had been degassed *in vacuo* and cooled with liquid nitrogen, 0.22 mmol of the catalyst and 10 m*l* of a carbon dioxide solution of formaldehyde were introduced, after which the mixture was maintained at 20±1°C for one hour. After the polymerization, the unreacted monomer and carbon dioxide gas were purged out. The white powdery polymer thus obtained was sufficiently washed with cooled diethyl ether, dried *in vacuo* at room temperature, and then weighed. The catalytic activity of the catalyst is defined as the value of the ratio of conversion (%) to the reaction time (hr) under definite conditions.

Analysis. The number-average degree of polymerization of the polymer was measured in a manner which has been described previously.[3] The melting point of the polymer was visually determined under a nitrogen atmosphere in an electric heater. The infrared spectrum was obtained by using the potassium bromide pellet technique on a Japan Spectroscopic infrared spectrophotometer, Model DS-402G. The pH of the salt in an aqueous or ethanol solution with a 0.1 g equivalent/*l* was determined on a Hitachi Horiba pH meter, type M-4.

Results and Discussion

The Catalytic Activity of Brönsted Acids. The catalytic activities of various Brönsted acids in the polymerization in a liquid carbon dioxide solution were determined under definite conditions. As is shown in Fig. 1, the acids whose pK_a values are over 15 show little catalytic activity, while the activities of the acids with less than that value increased with a decreased with a decrease in pK_a.*1 It has previously been reported[8] that this polymerization system belongs to a group of no-termination polymerizations with rapid initiations.

It is observed that the catalytic activity of the Brönsted acid (HB) is proportional to the rate of the propagation of the initiating species ($HOCH_2B$)

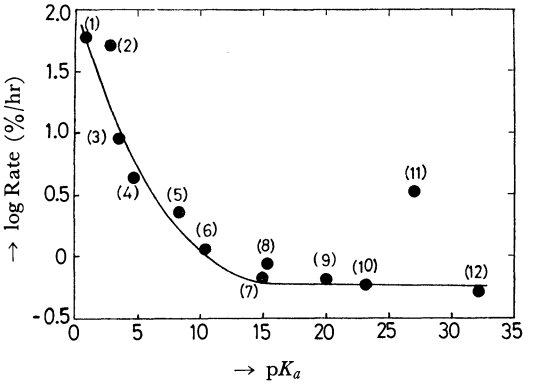

Fig. 1. Catalytic activity and pK_a of Brönsted acids: temp., 20°C; time, 60 min; monomer, 6 g; carbon dioxide, 4 g; additive/monomer (mole ratio), 1/1000; reaction vessel, 30 m*l*-autoclave.
(1) trichloroacetic acid (2) chloroacetic acid (3) formic acid (4) acetic acid (5) nitroethane (6) nitromethane (7) acetamide (8) methanol (9) acetone (10) diphenylamine (11) aniline (12) benzene

produced by the reaction of formaldehyde with the acid. The propagation rate increased with a decrease in the ion-dissociation energy of the initiating species, which may be proportional to the pK_a value of the Brönsted acid. The results shown in Fig. 1 are in accordance with this theory.

The Catalytic Activity of Alkyl Acetates. Methyl acetate has little catalytic activity, while the dimethyl ether acetate produced by the reaction of methyl acetate with formaldehyde has a high catalytic activity,[9] one 20 times that of methyl acetate (Table 1). Moreover, the infrared spectrum of the polymer produced with a large quantity of benzyl acetate as a catalyst indicated the characteristic peaks of both the phenyl group (1500 (shoulder), 755, 703 cm^{-1}) and the carbonyl group (1740 cm^{-1}) (Fig. 2). These results indicate that, in this polymerization, the initiating species is

Table 1. The catalytic activity of dimethylether acetate

Additive	Polymer yield (g)	Yield percent (wt%)	Degree of polymerization	Mp (°C)
Dimethyl ether acetate	3.42	57.0	1900	174—175
t-Butyl acetate	1.40	21.6	270	174
Methyl acetate	0.17	2.8	200	168—172
No additive	0.16	2.6	230	171—172

polymerization temperature: 20°C, time: 60 min, monomer: 6 g, carbon dioxide: 4 g, additive/monomer (mol ratio): 1/1000

7) Deutschen Chemischen Gesellschaft, "*Beilsteins Handbuch der Organischen Chemie*," Band III, J. Springer, Berlin, (1921), p. 236.

*1 The values of pK_a (25°C) are taken from "Ionization Constants of Acids and Bases, A Laboratory Manual," ed. by A. Albert and E. P. Serjeant, Methuen & Co., Great Britain (1962), p. 115.

8) H. Yokota, K. Kondo, T. Kagiya and K. Fukui, *J. Polymer Sci., A-1*, **6**, 435 (1968).

9) H. Yokota, M. Kondo and T. Kagiya, *ibid.*, **A-1**, **6**, 425 (1968).

methyl alkyl ether acetate ($ROCH_2OOCCH_3$), and that the reaction of alkyl acetate ($ROOCCH_3$) with the monomer to produce the initiating species is the rate-determining step.

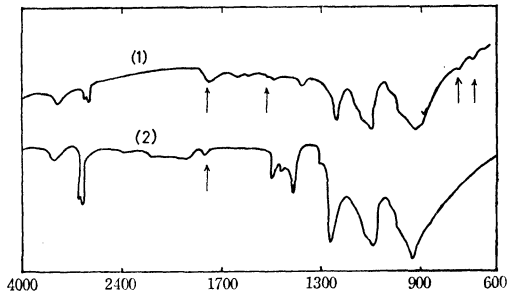

Fig. 2. The infrared spectrum of the polyoxymethylene obtained by the catalysts of both benzyl acetate and acetic acid.
(1) the polymer obtained by benzyl acetate catalyst: temp., 50°C; time, 30 min; additive/monomer (mole ratio), 1/6; (2) the polymer obtained by acetic acid catalyst: temp., 20°C; time, 60 min; additive/monomer (mole ratio), 1/1000

The catalytic activities of various alkyl acetates increased with a decrease in the ion-dissociation energy of alkyl chloride ($D(R^+,Cl^-)$) (Fig. 3). In view of the fact that the ion-dissociation energy of alkyl acetate is proportional to that of alkyl chloride,*2 it may be concluded that the rate of initiation reaction increases with a decrease in the ion-dissociation energy of alkyl acetate.

The Catalytic Activity of Organic Compounds Containing a Nitrogen or Oxygen Atom. As has been described previously (Fig. 1), aniline has a strong catalytic activity, though its pK_a value is large (27). In order to clarify the role of aniline, the catalytic activities of various organic compounds containing a nitrogen or oxygen atom, such as amines, ethers, ketones, or amides were studied. As is shown in Fig. 4, those substances with values less than the zero of pK_a',*3 such as diethyl ether, have little catalytic activity, while the activities of those with values more than 0 increased with an increase in pK_a'.

On the other hand, it is known that the shift of

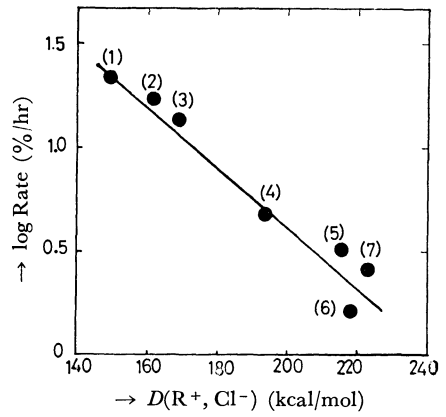

Fig. 3. Catalytic activity of alkyl acetates and ion-dissociation energy of alkyl chlorides: the condition is the same as described in Fig. 1.
(1) *t*-butyl acetate (2) alkyl acetate
(3) isopropyl acetate (4) ethyl acetate
(5) phenyl acetate (6) vinyl acetate
(7) methyl acetate

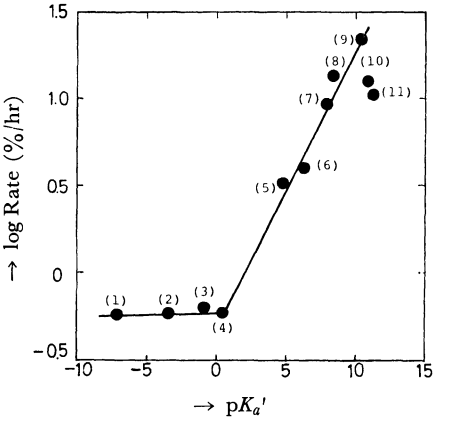

Fig. 4. Catalytic activity and pK_a' of organic compounds containing a nitro en or oxy en atom: the condition is the same as described in Fig. 1.
(1) acetone (2) diethyl ether (3) acetamide
(4) diphenylamine (5) aniline (6) pyridine
(7) *N*-phenyl ethylenimine (8) ethylenimine
(9) *n*-butyl amine (10) triethylamine
(11) diethylamine

the O–D vibrational band of methanol-D in liquid organic compounds increases with an increase in the pK_a values of the compounds.[10] In view of the facts presented above, it can be suggested that, in the polymerization by a basic substance (B) such as amine or ether, the initiating species

*2 The ion dissociation energy of organic compound (RX) is expressed as $D(R^+, X^-)=D(R\cdot, X\cdot)+I_p(R\cdot)-E_a(X\cdot)$, where $D(R\cdot, X\cdot)$ is the dissociation energy of RX; $I_p(R\cdot)$, the ionization potential of the alkyl radical, and $E_a(X\cdot)$, the electron affinity of the X radical Therefore, the ion-dissociation energy of alkyl acetate ($D(R^+, {}^-OOCH_2)$) is expressed as $D(R^+, {}^-OOCH_3)=D(R^+, Cl^-)+\{D(R\cdot, CH_3COO\cdot)-D(R\cdot, Cl\cdot)\}-\{E_a(CH_3COO\cdot)-E_a(Cl\cdot)\}$, The difference between $D(R\cdot, CH_3COO\cdot)$ and $D(R\cdot, Cl\cdot)$ is about 7—9 kcal/mol, while the value of $D(R^+, Cl^-)$ is 150—225 kcal/mol.

10) T. Kagiya, Y. Sumida and T. Inoue, This Bulletin, **41**, 773 (1968).

*3 The pK_a' is the negative logarithm of the ion-dissociation constant of the reaction: $BH^+ \overset{K_a'}{\rightleftharpoons} H^+ + B$. Moreover, the pK_a' values of bases plotted in the figure were obtained as the values in water (25°C) according to the following equation: $pK_a'=14.17-pK_b$.

($HOCH_2OHB$) is produced by the reaction of the water in the system, the monomer, and the basic substance:

$$H_2O + CH_2O + B \rightleftarrows HOCH_2OB$$

As is suggested by the mechanism of the polymerization by Brönsted acids, the rate of the initiation reaction by amine or ether may be much larger than that of the propagation. Since the structure of the propagating species depends on the kind of basic substance, the catalytic activities of amines or ethers are proportional to the propagation rate, and increase with a decrease in the ion-dissociation energy of the initiating species, which itself may increase proportionally with a decrease in the pK_a' of amines or ethers.

The Catalytic Activity of Salts. The catalytic activity of sodium salts obtained from a strong base (sodium hydroxide) with various acids, hydrochloride salts from a strong acid (hydrochloric acid) with various bases (amines), acetate or nitrate from weak acids (acetic acid or nitric acid) with various bases (amines), and aniline salts with various acids were observed under definite condition.

a) The Activity of Sodium Salts. As is shown in Fig. 5, the activity of sodium salts increased with an increase in pK_a the in an aqueous solution of the conjugated acids of sodium salts. In the polymerization by sodium salt (NaB), two mechanisms of the initiation reaction may be proposed. One of them involves the polymerization by the initiating species (BCH_2ONa) produced by the reaction of sodium salt with monomer. The other involves that by the initiating species ($HOCH_2ONa$) formed by the reaction of the monomer with the sodium hydroxide produced by the hydrolysis of sodium salt with water in the system.

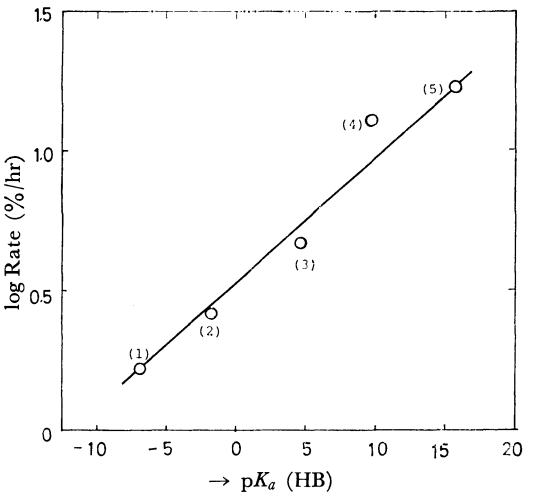

Fig. 5. Catalytic activity and pK_a of the conjugated acids of sodium salts: the condition is the same as in Fig. 1.
(1) sodium chloride (2) sodium nitrate
(3) sodium acetate (4) sodium borate
(5) sodium methoxide

The infrared spectrum of the polymer obtained with a large amount of the sodium acetate catalyst did not show the characteristic peak at 1750 cm^{-1} of the carbonyl group, but that at 3640 cm^{-1} of the hydroxy group. Therefore, it may be concluded that this polymerization proceeds by means of the initiating species of $HOCH_2ONa$. If this polymerization proceeds by the initiating species ($HOCH_2ONa$), the structure of the end group of the propagation species is the same in the polymerization with sodium salt. Furthermore, the catalytic activity of sodium hydroxide was 1.6 times that of sodium methoxide. On the basis of these facts, the formation of the initiating species may be considered to be the rate-determining step.

The rate of the formation of the initiating species may be proportional to the concentration of the hydroxy anion. On the other hand, in the hydrolysis of sodium salt, the logarithm of the concentration of the hydroxy anion is proportional to the pK_a (in an aqueous solution) of the conjugated acid of the salt.*4 These considerations lead to the conclusion that the catalytic activity of sodium salts increases with an increase in the pK_a of the conjugated acid of the sodium salt.

b) The Catalytic Activity of the Hydrochloride Salts. The activities of the salts obtained from hydrochloric acid with various amines increased with a decrease in the pK_a' values of the amines

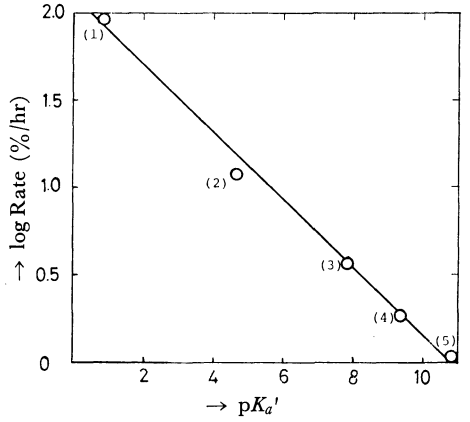

Fig. 6. Catalytic activity of hydrochloride salts and pK_a' of amines: the condition is the same as described in Fig. 1.
(1) diphenylamine hydrochloride
(2) aniline hydrochloride
(3) triethanolamine hydrochloride
(4) ammonium hydrochloride
(5) triethylamine hydrochloride

*4 In the reaction of $NaB+H_2O \rightleftharpoons Na^+ + OH^- + HB$, the concentration of the hydroxy anion (OH^-) is expressed as: $\sqrt{K_w(H_2O)(B^-)/K_{HB}}$, where K_w is the ionic product of water.

(Fig. 6). The salt obtained from hydrochloric acid with an amine such as R_3NHB may produce a proton and a counter anion (B^-) by hydrolysis.*5 Moreover, the initiating species ($HOCH_2B$) is considered to be produced by the reaction of a proton with a monomer in this polymerization. Just as in the polymerization by sodium salt, the formation reaction of the initiating species may be also the rate-determining step. Moreover, the rate of initiation is proportional to the concentration of the proton which increases proportionally with a decrease in the pK_a' values of the amines. This consideration is in accordance with the results shown in Fig. 6.

c) The Catalytic Activity of the Salts Obtained from Weak Acids with Various Amines. As is shown in Fig. 7, the activity of the acetate or nitrate salts decreased with an increase in the summation of the pK_a values of the acids and the pK_a' of the amines (pK_a+pK_a'), reached a minimum at *ca.* 7, and then increased with an increase to values larger than 7. Further, as is shown in Fig. 8, the activity of aniline salts also showed the same tendency as that of the acetate or nitrate salts, that is, a folded line with a minimum point.

Just as in polymerization by the sodium salts or hydrochloride salts, the formation of the initiating species may be also the rate-determining step in this polymerization.

On the other hand, it is known that the hydrolysis

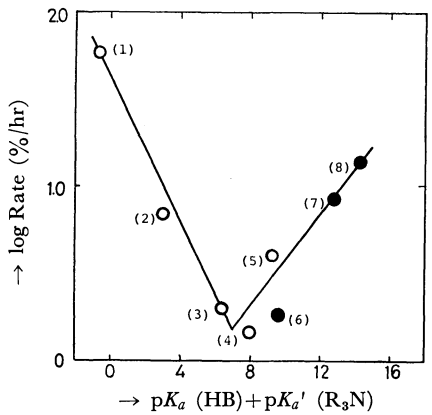

Fig. 7. Catalytic activity of acetate or nitrate salts and the summation of pK_a of acid and pK_a' of base: the condition is the same as described in Fig. 1.
(1) diphenylamine nitrate (2) aniline nitrate (3) triethanolamine nitrate (4) ammonium nitrate (5) triethylamine nitrate (6) aniline acetate (7) triethanolamine acetate (8) ammonium acetate

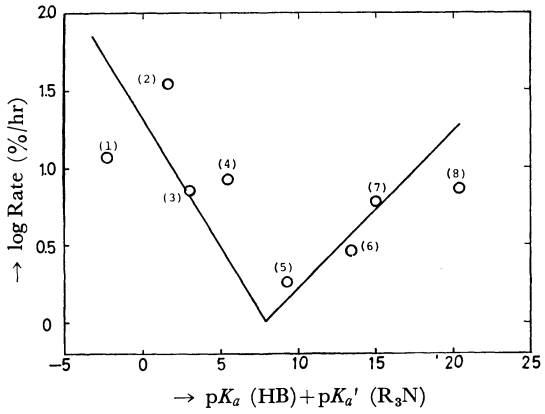

Fig. 8. Catalytic activity of aniline salts and the summation of pK_a of acid and pK_a' of base: the condition is the same as described in Fig. 1.
(1) aniline hydrochloride (2) aniline sulfate (3) aniline nitrate (4) aniline trichloroacetate (5) aniline acetate (6) aniline-nitroethane (7) anilinenitromethane (8) aniline-methanol

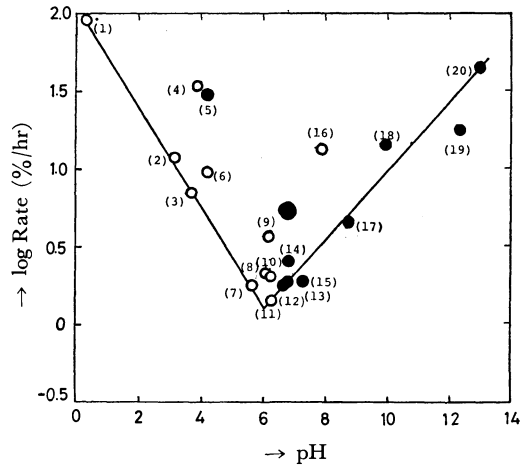

Fig. 9. Catalytic activity and pH of various salts: the condition of polymerization is the same as described in Fig. 1 the measurement of pH is carried out at 20°C with 0.1 mol/*l* aqueous (ethanol) solution.
(1) diphenylamine hydrochloride (2) aniline hydrochloride (3) aniline trichloroacetate (4) aniline sulfate (5) sodium dichloroacetate (6) triethylamine hydrochloride (7) aniline acetate (8) ammonium hydrochloride (9) triethanolamine hydrochloride (10) triethanolamine nitrate (11) ammonium nitrate (12) sodium chloride (13) tetraethylammonium iodide (14) sodium nitrate (15) tetraethylammonium bromide (16) ammonium acetate (17) sodium acetate (18) sodium borate (19) sodium ethylate (20) tetraethylammonium hydroxide

of the salt obtained from the weak acid (HB) with a weak base (NR_3) is in equilibrium:

$$R_3NHB + H_2O \rightleftharpoons R_3NHOH + HB$$

Therefore, it may be considered that this poly-

*5 The hydrolysis reaction of the salt obtained from a strong acid with various amines is:

$$R_3NHB + H_2O \rightleftharpoons H^+ + B^- + R_3NHOH$$

The concentration of the proton is expressed as $\sqrt{K_a'/C}$, where C is the concentration of the salt.

merization proceeds by means of the initiating species ($HOCH_2B$ or $HOCH_2OHNR_3$) produced by the reaction of the monomer with the proton or the hydroxy anion, and that the activities of the salts depend upon the quantity of protons or hydroxy anions produced by the reaction of the salt with the water present in the system.

The proton concentration is considered to be equal to the $K_{a(HX)}^{1/2} \cdot K_{a}'^{1/2}_{(NR_3)}$ value, and that of the hydroxy anion, to $K_w \cdot K_{a(HX)}^{-1/2} \cdot K_{a}'^{-1/2}_{(NR_3)}$. The reactions shown in Figs. 7 and 8 are in good accordance with these considerations.

The relationship between the activity and the pH[*6] in aqueous solutions of various salts are shown in Fig. 9. From this finding, it may be concluded that, in the range of pH values lower than 6, the polymerization proceeds by means of the initiating species ($HOCH_2B$) produced by the reaction of proton with the monomer, while in the range of pH values higher than 6, it proceeds by means the initiating species ($HOCH_2OHNR_3$) from the hydroxy anion and the monomer.

*6 The pH values were determined at 20°C by using 0.1 mol/l of an aqueous or ethanol solution of salts.

The authors are grateful to Professor Kenichi Fukui for his valuable suggestions and to Mr. Masatsune Kondō for his helpful discussions. They also wish to express their gratitude to Mr. Hiroshi Hatta for his technical assistance in carrying out the experiments.

BULLETIN OF THE CHEMICAL SOCIETY OF JAPAN VOL. 42 2917—2920 (1969)

The Mechanism of the Base-Promoted Rearrangement of *N,N*-Dichlorocyclohexylamine to 2-Aminocyclohexanone and the Deaminative Diazotization of 2-Aminocyclohexanone

Mamoru NAKAI,*1 Naomichi FURUKAWA and Shigeru OAE

Department of Applied Chemistry, Faculty of Engineering, Osaka City University, Sugimoto-cho, Sumiyoshi-ku, Osaka

(Received February 21, 1969)

N,N-Dichlorocyclohexylamine-1-^{14}C has been treated with sodium methoxide in methanol and then with hydrochloric acid to yield ^{14}C-labeled 2-aminocyclohexanone hydrochloride. Successive degradations have revealed that practically all the ^{14}C activity was found in the carbonyl carbon of the original aminoketone. From the ^{14}C distribution, it has been concluded that the reaction is essentially the same as that proposed for the Neber rearrangement. As a part of the degradation of 2-aminocyclohexanone, deaminative diazotization was employed to obtain cyclopentanecarboxylic acid together with other minor products. The ^{14}C tracer work revealed that the carbonyl group of the acid is originated from the carbonyl group of the 2-amino-ketone.

Baumgarten and his coworkers[1] reported that when *N,N*-dichlorocyclohexylamine is reacted with sodium methoxide and then treated with aqueous hydrochloric acid 2-aminocyclohexanone hydrochloride is formed, analogous to the Neber rearrangement of the corresponding oxime tosylate.[2,3] They have extended this reaction to other various *N,N*-dichloro-*s*-alkylamines.[4] A similar rearrangement of *N,N*-dichlorocyclohexylamine to 2-aminocyclohexanone hydrochloride has also been recently reported.[5] Meanwhile the rearrangement of *N,N*-dichlorodiphenylethylamine to desylamine was investigated by us using ^{14}C-labeled compound and revealed to proceed according to the mechanism similar to the Neber rearrangement as shown below[6] (Fig. 1).

Although the same mechanism may hold for the reaction of *N,N*-dichlorocyclohexylamine with sodium methoxide, the reaction could proceed *via* other mechanistic routes, since the Neber type rearrangement involves a very highly strained bicyclic azirine bearing a double bond at the bridge-head position, and other possibilities such as that involving the prior *gem*-dichlorination followed by hydrolysis could occur (Fig. 2). Thus

*1 Ube Industries Ltd., Ube, Yamaguchi.

1) H. E. Baumgarten and F. A. Bower, *J. Am. Chem. Soc.*, **76**, 4561 (1954).

2) D. J. Cram and M. S. Hatch, *ibid.*, **75**, 33 (1953).

3) M. S. Hatch and D. J. Cram, *ibid.*, **75**, 38 (1953).

4) H. E. Baumgarten and J. M. Petersen, *ibid.*, **82**, 459 (1960).

5) G. H. Alt and W. S. Knowles, *J. Org. Chem.*, **25**, 2047 (1960).

6) S. Oae and N. Furukawa, This Bulletin, **38**, 62 (1965).

a similar ^{14}C tracer work is quite desirable. However, the same degradative procedure gave rather obscure results. Hence other better degradative methods have been tried. Among a few methods employed, a degradative diazotization of 2-aminocyclohexanone has been proved to be very promising since it gives the rearranged cyclopentanecarboxylic acid in yields always exceeding 35%. However, this degradative procedure must be examined at first, because it is not known whether or not this procedure changes the sequence of carbon skeleton, nor has it been clarified that the carbon dioxide formed during the rearrangement originates from the carbonyl carbon of 2-aminocyclohexanone.

We have accumulated data of the ^{14}C tracer experiments on these reactions. This paper will describe the results in detail.

N,N-dichlorocyclohexylamine-1-^{14}C has been synthesized, and a series of successive degradation has been carried out.

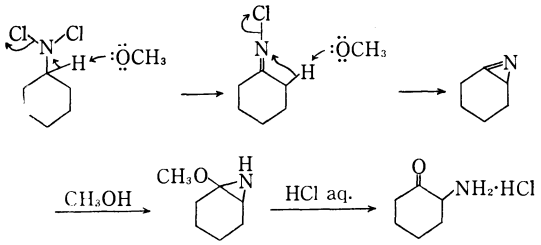

Fig. 1

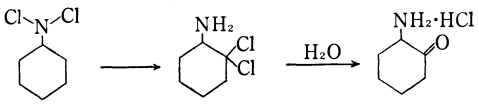

Fig. 2

Synthetic Method

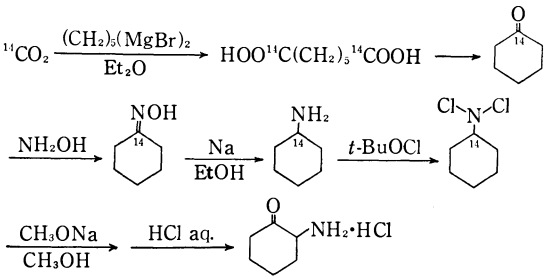

Degradative Mothod

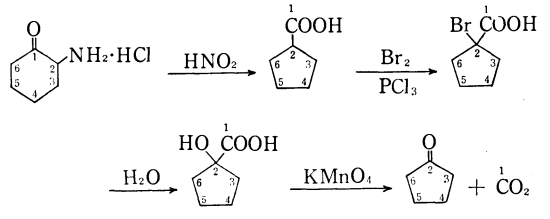

Fig. 3

Both the synthetic and degradative procedures are shown below (Fig. 3).

Experimental

Preparation of *N,N*-Dichlorocyclohexylamine-1-^{14}C. Pimeric acid-1,7-^{14}C was obtained by the carbonation of pentamethylene magnesium bromide which was prepared from 0.9 g of magnesium and 4.0 g of pentamethylene dibromide, with $^{14}CO_2$ generated from 7.0 g (1 mCi) of barium carbonate. The crude product was recrystallized from benzene; yield 2.0 g (70%), mp 104°C.

A mixture of 1.8 g of pimeric acid-1,7-^{14}C and 0.1 g of barium carbonate was gradually heated in a metallic bath up to about 320°C and the distillate was collected. The crude cyclohexanone-1-^{14}C (0.9 g) was purified by distillation (bp 155°C).

The above cyclohexanone-1-^{14}C (2.5 g) was added to a solution containing 2.2 g of hydroxylamine hydrochloride in 5 m*l* of water, into which a solution containing 1.7 g of sodium carbonate in 5 m*l* of water was added. The mixture was filtered to collect the precipitate which was then washed with cold water and recrystallized from 50% ethanol. The yield of cyclohexanone oxime-1-^{14}C was 1.9 g in 75%; mp 91°C.

Strips of sodium (6 g) were added to a solution of cyclohexanone oxime-1-^{14}C (2.0 g) in 60 m*l* of absolute ethanol. From the reaction mixture, cyclohexylamine-1-^{14}C (1.3 g) was obtained in 75% yield; bp 132°C.

Cyclohexylamine-1-^{14}C (6.5 g) was chlorinated with 15 g of *t*-butyl hypochlorite in anhydrous benzene. *N,N*-Dichlorocyclohexylamine-1-^{14}C thus obtained was not isolated; the solution was used directly for the preparation of 2-aminocyclohexanone hydrochloride-*x*-^{14}C, as in the experiments of previous workers.[4]

Rearrangement of *N,N*-Dichlorocyclohexylamine-1-^{14}C. The rearrangement of *N,N*-dichlorocyclohexylamine-1-^{14}C was carried out by the following procedure used previously;[4] the benzene solution of *N,N*-dichlorocyclohexylamine-1-^{14}C prepared from 6.5 g of cyclohexylamine was treated with a methanolic sodium methoxide prepared from 4.8 g of sodium and 50 m*l* of methanol. The reaction mixture became very dark when the reaction ended. The aqueous acid extract was tan to red-brown, but most of the color could be removed by repeated treatments with active charcoal. The resulting, crude 2-amino-cyclohexanone hydrochloride-*x*-^{14}C was recrystallized from absolute methanol, then washed with a mixture of isopropanol and methanol to give a pure substance; yield 4.6 g (47%), nearly colorless crystals, mp 158°C.

Degradation of 2-Aminocyclohexanone Hydrochloride-*x*-^{14}C. Deamination of 2-aminocyclohexanone hydrochloride was reported by Edwards and Lesage,[7] who revealed that the reaction affords cyclopentanecarboxylic acid, bicyclo[3,1,0]hexane-2-one and 2-methyl-2-cyclopentene-1-one as the products from 2-aminocyclohexanone.

We also carried out the deaminative diazotization in a similar way. 2-Aminocyclohexanone hydrochloride-*x*-^{14}C (1.60 g) was dissolved in 9 m*l* of 6 N hydrochloric acid, and to this solution cooled in an ice-salt bath was

7) O. E. Edwards and M. Lesage, *Can. J. Chem.*, **41**, 1592 (1963).

added a solution of 3.6 g of sodium nitrite in 9 m*l* of water dropwise with stirring. The reaction mixture turned to blue. After the addition was complete the contents of the flask was stirred for 1 hr while keeping the temperature below 0°C, and then for 1 hr at room temperature, followed by heating for 1/2 hr at 50°C. It was then made alkaline with sodium carbonate and extracted with ether to remove neutral and acidic substances. The aqueous solution was acidified with hydrochloric acid and extracted with ether. This etheral solution was dried over anhydrous sodium sulfate and distilled, affording 0.8 g of acidic materials, *i. e.*, cyclopentanecarboxylic and adipic acids which were identified by comparing their infrared spectra with those of authentic samples. The latter acid was further confirmed by the mixed melting point determination with the authentic sample of adipic acid. Thus cyclopentanecarboxylic acid-*x*-^{14}C was obtained in about 35% yield based on the data of the isotopic dilution method; bp 103—105°C/8 mmHg.

The method of Loftfield was used to degradate cyclopentanecarboxylic acid-*x*-^{14}C[8]. This acid (2.3 g), bromine (1.1 m*l*) and phosphorus trichloride (0.15 m*l*) were heated to 100°C for one hour in a sealed tube. 1-Bromocyclopentanecarboxylic acid-*x*-^{14}C was dissolved in a mixture of 30 m*l* of acetone, 30 m*l* of water, 2.5 m*l* of acetic acid and 2 g of sodium acetate and then allowed to stand for 16 hr at room temperature. The resulting 1-hydroxycyclopentanecarboxylic acid-*x*-^{14}C (1.0 g) was obtained in 38% yield; mp 103°C.

In a distillation flask, a solution of 0.2 g of the hydroxy acid-*x*-^{14}C and 0.12 g of potassium permanganate in 30 m*l* of water was gradually heated to boiling. A stream of nitrogen was bubbled through the solution and the carbon dioxide released was introduced into a barium hydroxide trap. From the distillate (6.5 m*l*) was obtained cyclopentanone; the conversion was about 60%. One-third of this distillate was used to prepare cyclopentanone semicarbazone which was recrystallized from water; mp 207°C.

Measurement of the Activities. The activities of the samples were measured with a JRC Aloka 2π-gas flow G-M counter using Q gas. 1-Hydroxycyclopentanecarboxylic acid-*x*-^{14}C was used as the standard sample of the total activity. An aliquot of a sample was thoroughly oxidized by the Van Slyke-Folch Method, and all the carbon dioxide formed was converted to a barium carbonate tablet which was then subjected to ^{14}C counting.

The counting data obtained are shown in Table 1.

Table 1. The ^{14}C counting data

	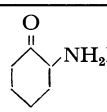	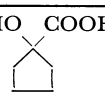	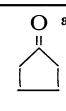 a)
Run 1	1240 cpm	278 cpm (100%)	7±3 cpm (~2.5%)
Run 2	17200 cpm	3650 cpm (100%)	63 cpm (1.7%)

a) Assayed as semicarbazone.

8) R. B. Loftfield, *J. Am. Chem. Soc.*, **73**, 4707 (1951).

Results and Discussion

1-Hydroxycyclopentanecarboxylic acid was used as the standard sample of 2-aminocyclohexanone, and the ^{14}C total activities were counted. The value which substracts the ^{14}C activity of cyclopentanone from that of 1-hydroxycyclopentanecarboxylic acid may be regarded as the ^{14}C activity of carbonyl carbon of original 2-aminocyclohexanone. Thus semicarbazone of cyclopentanone obtained can be counted for the activity of all the positions except carbonyl carbon of aminoketone. As shown in Table 1, the ^{14}C activity (1.7%) of cyclopentanone carries only a very small portion of the original activity of 2-aminocyclohexanone. Therefore, carbonyl carbon of the original aminoketone carries essentially all the ^{14}C activity.

All the synthetic procedures used for the ^{14}C compounds are quite common ones that have often been tested in the past, and it is known that no rearrangement is involved in any step of the total synthesis of *N,N*-dichlorocyclohexylamine-1-^{14}C. Meanwhile the degradation of cyclopentanecarboxylic acid has also been carried out by a well-known procedure involving no skeletal rearrangement. A serious problem lies, however, in the step of deaminative diazotization of 2-aminocyclohexanone, since it involves the rearrangement of the carbon skeleton. However, since nearly all the carbon-14 activity was found to be concentrated at the resulting carboxyl group of cyclopentanecarboxylic acid, the formation of cyclopentanecarboxylic acid from 2-aminocyclohexanone appears to proceed through a simple Wagner-Meerwein type rearrangement as shown below.

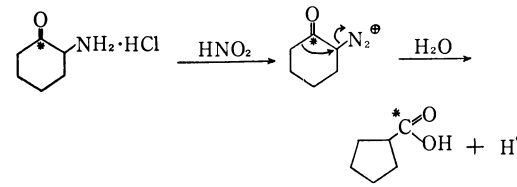

Thus, other possible routes such as that analogous to the one involved in the hydrolysis of α-halocyclohexanone,[9] shown below are excluded.

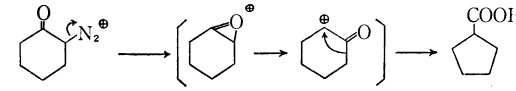

Although degradation was not performed for the other two products, namely 2-methyl-2-cyclopentene-1-one and bicyclo[3.1.0]hexane-2-one,[7] these are undoubtedly formed by the initial 1,2-shift from 4-position as shown below.

9) T. Masuike, N. Furukawa and S. Oae, unpublished.

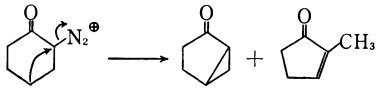

The formation of a substantial amount of cyclopentanecarboxylic acid (35%) is interesting in connection with the highly energy-recoiled carbonium ion formed by the deaminative diazotization. Here again, the migration of the carbon-skeleton took place rather indiscriminately regardless of the electronic nature of β-methylene groups which undergo 1,2-shift.

The results of the degradation revealed that nearly all the ^{14}C activity originally placed at 1-position of *N,N*-dichlorocyclohexylamine was found in the carbonyl carbon of 2-aminocyclohexanone formed, similar to the previous case with *N,N*-dichlorodiphenylethylamine.

Therefore, the plausible mechanism for this reaction is that suggested previously by Banmgarten *et al.*; this is essentially the same as that proposed originally by Cram and Hatch for the Neber rearrangement.

BULLETIN OF THE CHEMICAL SOCIETY OF JAPAN VOL. 42 2920—2924 (1969)

The Reaction of Cobalt Hydrocarbonyl with Vinylacetate, Crotonate, Styrene, and Acrylates*[1]

Sohei SUGA, Hiromitsu MASADA and Haruki SUDA

Department of Industrial Chemistry, Faculty of Technology, Kanazawa University, Kanazawa

and Yoshihisa WATANABE and Yoshinobu TAKEGAMI

Department of Hydrocarbon Chemistry, Faculty of Engineering, Kyoto University, Kyoto

(Received February 27, 1969)

Ethyl vinylacetate and ethyl crotonate reacted with cobalt hydrocarbonyl at 25°C to give three isomeric acylcobalt carbonyls, α- and γ-carbethoxy-butyrylcobalt carbonyls and β-carbethoxy-isobutyrylcobalt carbonyl. The distribution of these complexes depends greatly on the reaction time (0.5—20 hr). In both cases the β-isomer predominates at shorter reaction times (0.5—1.5 hr), while the γ-isomer predominates at longer reaction times. This shows that isomerization occurs among the complexes and that the equilibrium is very favorable to the γ-isomer. Acrylates and styrene react with cobalt hydrocarbonyl to give two isomeric acylcobalt carbonyls. The isomerization of the acylcobalt complex with a branched structure to that with a straight-chain structure is much promoted by the phenyl and ester groups. The promoting effect of the ester groups is the highest in benzyl, followed by allyl, and ethyl, isopropyl, butyl, and cyclohexyl. Such a promoting effect can reasonably be attributed to the $-I$ effect of these groups.

Some of the present authors have previously shown that acylcobalt carbonyls isomerize under relatively mild conditions.[1-4] In the reaction of cobalt hydrocarbonyl with ethyl acrylate, the α-carbon was selectively carbonylated to give α-carbethoxypropionylcobalt carbonyl.[2] This fact shows that the ester group in the acrylate has a significant effect on the addition of cobalt hydrocarbonyl to the carbon-carbon double bond of the acrylate. The α-isomer, however, isomerized to β-isomer much more readily in non-polar solvents. On the other hand, *n*- and isobutyrylcobalt carbonyls isomerized with difficulty in non-polar solvents. Thus, the ester group adjacent to the acylcobalt carbonyl group has a promoting effect on the isomerization.

The present study will be concerned with the reaction of cobalt hydrocarbonyl with ethyl crotonate, ethyl vinylacetate, and different acrylates. From the former two olefins, three isomeric acylcobalt carbonyls are possible as reaction products. The effects of the ester groups on the distribution of these complexes and on the isomerization of the

*1 Presented in part at the Annual Meeting of the Chemical Society of Japan, Osaka, April, 1968.

1) Y. Takegami, C. Yokokawa, Y. Watanabe and Y. Okuda, This Bulletin, **37**, 181 (1964).

2) Y. Takegami, C. Yokokawa, Y. Watanabe, H. Masada and Y. Okuda, *ibid.*, **37**, 1190 (1964).

3) Y. Takegami, C. Yokokawa, Y. Watanabe, H. Masada and Y. Okuda, *ibid.*, **38**, 787 (1965).

4) Y. Takegami, Y. Watanabe, H. Masada, Y. Okuda, K. Kubo and C. Yokokawa, *ibid.*, **39**, 1495 (1966).

comlexes will be examined. The reaction behavior of different acrylates and styrene will also be examined and compared.

Experimental

Reaction Procedure. The reaction was carried out in the way described in a previous paper, using 50 m*l* of a 0.09 M cobalt hydrocarbonyl solution in hexane in each run.[2]

Analytical Procedure. The solution of crude products was treated with iodine and ethyl alcohol, and then the excess iodine was removed with crystalline sodium thiosulfate. After the solution had been concentrated, the products were gas-chromatographed on a column, three meters long, 3 mm in diameter, and filled with Apiezon L or Carbowax on Cerite, at 130—220 °C and at the carrier-gas (helium) flow rate of 70 ml/min. The infrared spectra were recorded on a Nippon Bunko Model DS-301 spectrophotometer.

Materials. The ethyl acrylate, ethyl crotonate, styrene, ethylmalonate, methylsuccinate, glutarate, succinates, α- and β-phenylpropionates, and methylmalonates were commercial products. The following acrylates were synthesized by the usual ester exchange method: benzyl, allyl, isopropyl, and cyclohexyl acrylates. They have been proved to be sufficiently pure by gas chromatography. The cobalt hydrocarbonyl was prepared in the way described previously.[1] The ethyl vinylacetate was prepared from allyl chloride.[5]

Results and Discussion

The Reaction of Ethyl Vinylacetate and Ethyl Crotonate with Cobalt Hydrocarbonyl. The results of the reaction are summarized in Table 1. All of the reactions were carried out in hexane under an atmosphere of carbon monoxide.

The vinylacetate reacted with cobalt hydrocarbonyl at 25°C, with a carbon monoxide absorption, to give three isomeric acylcobalt carbonyls, α- and γ-carbethoxybutyrylcobalt carbonyls and β-carbethoxy-isobutyrylcobalt carbonyl, which then gave the corresponding esters, diethyl ethylmalonate, diethyl methylsuccinate, and diethyl glutarate, upon treatment with an alcoholic iodine solution. The distribution of these complexes depended greatly on the reaction time (Exps. 1—5). When the reaction time was only 0.5 hr, the β-isomer, the methylsuccinate, was predominant (Exp. 1). The percentage of the β-isomer decreased with an increase in the reaction time, but that of the γ-isomer, the glutarate, increased reversely. When the reaction time was more than 1.5 hr, the γ-isomer was predominant and the percentage of the γ-isomer amounted to more than 90%. These facts show that the β-carbon of the vinylacetate is readily carbonylated with cobalt hydrocarbonyl to give the β-carbethoxy-isobutyrylcobalt carbonyl as the major product, then the β-isomer is readily isomerized to the γ-isomer under the conditions employed, and that the equilibrium among the complexes is very favorable to the γ-isomer. On the other hand, such 1-olefins as 1-pentene reacted with cobalt hydrocarbonyl to give *n*-caproylcobalt carbonyl as the major product and also α-methylvalerylcobalt carbonyl,[6] these complexes were isomerized with much difficulty under the conditions described above.[4] The results obtained here show that the ester group in the vinylacetate has a great

Table 1. The reaction of cobalt hydrocarbonyl with ethyl vinylacetate and ethyl crotonate

Exp. No.	Reaction conditions* Time (hr)	CO Absorbed mol/mol-$HCo(CO)_4$	Yield of esters** mol/mol-$HCo(CO)_4$	Distribution of esters (%) Ethyl-malonate	Methyl-succinate	Glutarate
1a	**Ethyl vinylacetate**					
1	0.5	0	0.05	7	56	37
2	1.5	0.07	0.14	11	30	59
3	3	0.14	0.16	9	26	65
4	4.5	0.20	0.15	3	12	85
5***	5	0.30	0.30	1	7	92
1b	**Ethyl crotonate**					
6	0.5	0	0.02	29	71	0
7	1.5	—	0.07	7	85	8
8	3	—	0.08	12	30	58
9***	5	0.20	0.21	9	30	61
10***	20	0.20	0.15	2	9	89

* Under an atmosphere of carbon monoxide at 25°C. The olefins: 1.5 mol/mol-$HCo(CO)_4$
** Diethyl ethylmalonate, diethyl methylsuccinate and diethyl glutarate
*** The olefins: 3 mol/mol-$HCo(CO)_4$

5) E. Rietz, "Organic Syntheses," Coll. Vol. III, p. 851 (1955).

6) R. F. Heck and D. S. Breslow, *J. Am. Chem. Soc.*, **83**, 4023 (1961).

effect on the addition of cobalt hydrocarbonyl to the double bond and on the isomerization of the acylcobalt carbonyls: the ester group promotes the carbonylation of the carbon of the double bond more adjacent to the ester group, while on the contrary, the ester group promotes the isomerization of the acylcobalt carbonyls to that which has an acylcobalt group further from the ester group.

In this reaction, the α-isomer, the ethylmalonate, was obtained in a considerable yield. For the formation of this complex, two routes are possible: one from ethyl crotonate, and the other from the β-isomer. Under the conditions employed, the vinylacetate did not isomerize to ethylcrotonate. Thus, it is safe to conclude that the α-isomer is formed *via* the β-isomer by the isomerization.

On the basis of these results, the reaction seems to follow this reaction scheme:

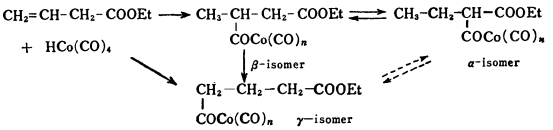

Ethyl crotonate also gave the three isomeric acylcobalt carbonyls as the reaction products (Exps. 6—10). The distribution of the complexes depended on the reaction time. Longer reaction times were more favorable to the γ-isomer. The percentage of the α- and β-isomers decreased to less than 10%. When the reaction time was only 0.5 hr, the percentage of the α-isomer amounted to about 30%, indicating that, at the initial step of the reaction, the α-carbon of the crotonate was carbonylated relatively readily. The reaction of the crotonate was very slow. At 25°C, after even 20 hr, the yield of the products was only 0.2 mol/mol-$HCo(CO)_4$. On the contrary, the isomerization among the complexes, especially from the α-isomer to the β-isomer, appears to occur more readily. In the light of these results, the reaction of the crotonate may be considered to proceed typically as follows:

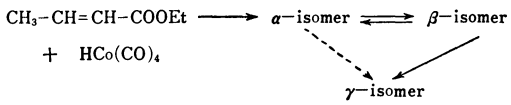

The Reaction of Cobalt Hydrocarbonyl with Styrene and Different Acrylates. The results of the reaction are summarized in Tables 2 and 3 and in Fig. 1. All of the reactions under an atmosphere of carbon monoxide were carried out in hexane in two stages: at first for 3 hr at 0°C, and then at 25°C for 0.5—6 hr. The gas absorption ceased completely within 3 hr at 0°C. As we have previously reported in detail, the rate of cobalt hydrocarbonyl consumption may be estimated by means of the rate of carbon monoxide absorption in the system.[2] At a low temperature

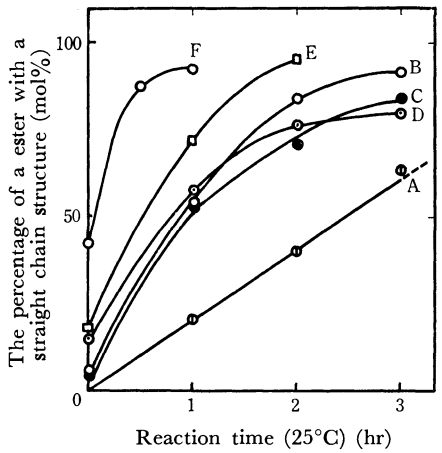

Fig. 1. The percentage of a ester with a straight chain structure *vs.* time plots for the reaction of cobalt hydrocarbonyl with styrene and acrylates.

All of the reaction were carried out in two stages: At 0°C for 3 hr and then at 25°C for 0.5—3 hr.

A: Styrene
B: Ethyl acrylate
C: Isopropyl acrylate
D: Cyclohexyl acrylate
E: Allyl acrylate
F: Benzyl acrylate

the acylcobalt carbonyls with a branched-chain structure were almost selectively formed by the direct addition of cobalt hydrocarbonyl to the olefins, while higher temperatures promoted the isomerization of these complexes to those with a straight-chain structure. The complexes were finally converted to the corresponding esters upon treatment with an alcoholic iodine solution. The effects of the structures on the isomerization were examined by means of the distribution of the esters.

A large excess of the olefin was used in order that the cobalt hydrocarbonyl used might be consumed completely and in order that acyl cobalt carbonyls might not be converted to aldehydes. The amount of aldehydes formed was negligible.

Styrene. As Table 2 shows, styrene gave selectively, α-phenylpropionylcobalt carbonyl at 0°C, while at 25°C this isomerized gradually to β-phenylpropionylcobalt carbonyl. The isomerization was slower than that in the case of acrylates (*cf.* Fig. 1). These facts show that the phenyl group activates the α-carbon of the styrene for the carbonylation and that it also promotes the isomerization. On the other hand, in the case of 1-pentene, caproyl- and α-methylvalerylcobalt carbonyls were formed in a 3 : 1 ratio at 0—25°C in non-polar solvents; these complexes were isomerized with much difficulty under these conditions.[4,6] This apparent discrepancy is due to some difference between the effects of the phenyl and propyl groups (CH_2=CH–R, R=Ph and Pr). Two effects appear to operate here. The first,

Table 2. The reaction cobalt hydrocarbonyl with styrene

Exp. No.	Reaction conditions* Temp. (°C)	Time (hr)	CO Absorbed mol/mol-$HCo(CO)_4$	Yield of esters** mol/mol-$HCo(CO)_4$	The percentage of β-phenylpropionate (mol%)
11	0	3	0.47	0.51	0
12***	0—25	3+1	0.50	0.40	21
13	0—25	3+2	0.46	0.40	40
14	0—25	3+3	0.47	0.35	64
15	0—25	3+6	0.46	0.35	88

* Under an atmosphere of carbon monoxide. Styrene: 3 mol/mol-$HCo(CO)_4$
** α- and β-Phenylpropionates
*** The reaction was carried out in two stages: at first at 0°C for 3 hr and then at 25°C for 1 hr

Table 3. The reaction of cobalt hydrocarbonyl with acrylates

Exp. No.	Reaction conditions* Temp. (°C)	Time (hr)	CO Absorbed	Yield of esters**	The percentage of succinate (mol%)
3a	**Ethyl acrylate**				
16	0	3	0.47	0.57	3
17	0—25	3+1	0.49	0.60	54
18	0—25	3+2	0.51	0.58	84
19	0—25	3+3	0.48	0.59	91
3b	**Cyclohexyl acrylate**				
20	0	3	0.33	0.25	15
21	0—25	3+1	0.35	0.64	56
22	0—25	3+2	0.35	0.73	76
23	0—25	3+3	0.33	0.74	80
3c	**Isopropyl acrylate**				
24	0	3	0.40	0.50	3
25	0—25	3+1	0.44	0.58	54
26	0—25	3+2	0.47	0.61	70
27	0—25	3+3	0.48	0.64	84
3d	**Benzyl acrylate**				
28	0	3	0.33	0.18	42
29	−5	5	0.41	0.10	45
30	0—25	3+0.5	0.36	0.29	87
31	0—25	3+1	0.35	0.45	92
3e	**Allyl acrylate**				
32	0	3	0.47	0.51	17
33	0—25	3+1	0.54	0.56	71
34	0—25	3+2	0.55	0.50	95

* Under an atmosphere of carbon monoxide. Acrylate: 3 mol/mol-$HCo(CO)_4$
** Succinate and methylmalonate

and probably the most important, is an electronic effect. The electron-attracting effect, the $-I$ effect, of the phenyl group is stronger than that of the propyl, and the phenyl group also has a conjugation effect. A second effect concerns a steric factor. The steric effect of the phenyl, however, seems to be almost comparable to that of the propyl. Thus, the large difference in reaction behavior between these groups may be attributed to the electronic effect.

In the α-phenylpropionylcobalt carbonyl, the $-I$ effect of the phenyl group probably decreases the electron density on the cobalt atom; this, in turn, reduces the thermal stability of this complex. This consideration is strongly supported by the fact that acylcobalt carbonyls are safely separated as more stable triphenylphosphine derivatives,[6] in which a stronger basicity of the phosphine increases the electron density on the cobalt atom.[7]

7) E. R. Tucci, *Ind. Eng. Chem., Product Research and Development*, **7**, 32 (1968).

Accordingly, it is safe to conclude that the promoting effect of the phenyl on the isomerization of the α-phenylpropionylcobalt carbonyl to the β-isomer is due to the $-I$ effect.

Acrylates. As Table 3 shows, different acrylates were used. All of them behave similarly in this reaction. At first at 0°C, acylcobalt carbonyls with a branched-chain structure predominated, and then at 25°C they were isomerized readily to those with a straight-chain structure.

As Fig. 1 shows, the isomerization rate was the highest in benzyl acrylate, followed by allyl and by ethyl, isopropyl, and cyclohexyl acrylates. It is well known that the ester groups have the $-I$ effect. Thus, the promoting effect of the ester groups on the isomerization can be explained by the argument employed in the case of styrene. The fact that even α-carbethoxypropionylcobalt carbonyl triphenylphospine is too unstable to be separated[6] indicates that the ester group greatly reduces the thermal stability of this type of complex. Moreover, the largest promoting effect of the benzyl and allyl ester groups may be attributed to the larger $-I$ effect of the benzyl and allyl groups. The effects of such saturated alkyl groups as ethyl and isopropyl seem to be almost comparable (*cf.* Fig. 1).

BULLETIN OF THE CHEMICAL SOCIETY OF JAPAN VOL. 42 2924—2930 (1969)

Studies on *s*-Triazines. I. Cotrimerization of Trichloroacetonitrile with Other Nitriles*[1]

Ko WAKABAYASHI, Masaru TSUNODA and Yasushi SUZUKI

Research Laboratory, Mitsubishi Chemical Industries Ltd., Mizonokuchi, Kawasaki, Kanagawa

(Received March 7, 1969)

2-Substituted 4,6-bis(trichloromethyl)-*s*-triazines have been prepared by the cotrimerization of CCl_3CN with some nitriles. The reaction proceeds, in general, smoothly at ordinary pressure in the presence of hydrogen halide or Friedel-Crafts catalyst-hydrogen halide complex. An improved method was developed for the nitriles such as propionitrile with which CCl_3CN did not easily cotrimerize under above mentioned conditions.

2-Substituted 4,6-bis(trichloromethyl)-*s*-triazines and their derivatives, such as 2-substituted 4-amino-6-trichloromethyl-*s*-triazines, are highly effective as herbicides,[1,2] fungicides,[3,4] nitrification inhibitors,[5-10] in soil and antimalarials.[11]

Starting material, CCl_3CN, is easily obtained by the chlorination[12-16] of CH_3CN which is a by-product in SOHIO acrylonitrile process. This led us to investigate the cotrimerization of CCl_3CN with other nitriles.

*1 Taken in part from the dissertation presented by K. Wakabayashi to the University of Tokyo, 1969.

1) R. Yamamoto, I. Yamamoto and H. Honda, Japanese Pat. 17796 (1965).
2) M. Okuzu, K. Wakabayashi and T. Okada, Japanese Pat. 6825 (1967).
3) K. Matsui, H. Kasugai, K. Wakabayashi and S. Motojima, Japanese Appl. 74210 (1967).
4) O. Weiberg, German Pat. 1117131 (1961).
5) T. Nishihara, *Tsuchi to Biseibutsu (Soil and Microbe)*, **7**, 28 (1965).
6) M. Okuzu, K. Wakabayashi and T. Okada, Japanese Pat. 15889 (1967).
7) M. Okuzu, K. Wakabayashi and T. Okada, Japanese Pat. 25170 (1967).
8) Y. Yokoi, K. Wakabayashi, Y. Suzuki and M. Tsuda, Japanese Pat. 5752 (1968).
9) M. Okuzu, K. Wakabayashi and T. Okada, Japanese Appl. 30187 (1965).
10) M. Okuzu, R. Hayashi, K. Wakabayashi and Y. Suzuki, Japanese Appl. 52006 (1967).
11) S. Birtwell and W. Hepworth, Brit. Pat. 767848 (1957).
12) K. Dachlauer, German Pat. 694479 (1942); D. R. P. *Org. Chem.*, **6**, 1384; Brit. Pat. 522835 (1940).
13) F. N. Stepanov and N. I. Shirokova, *Zhur. Obshch. Khim.*, **25**, 941 (1955).
14) G. Käbisch, U. S. Pat. 2745868 (1956); Brit. Pat. 750712 (1956).
15) J. J. Gray and F. Burgess, U. S. Pat. 2426091 (1947).
16) R. T. Foster, U. S. Pat. 2375545 (1945).
17) A. Weddige, *J. prakt. Chem.*, (2), **33**, 76 (1886).
18) N. Tscherwen-Iwanow, *ibid.*, (2), **46**, 142 (1892).
19) K. Dachlauer, German Pat. 699493 (1940); D. R. P. *Org. Chem.*, **6**, 2621.
20) E. McBee, O. Pierce and R. Bolt, *Ind. Eng. Chem.*, **39**, 391 (1947).

Table 1.* The effect of combined catalyst for trimerization of CCl_3CN

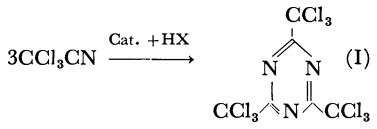

Combined catalyst		Starting material	Product (I)	Yield	Mp
Catalyst	HX	(g)	(g)	(%)	°C
None	HCl	32.0	0.5	1.6	93
None	HBr	32.0	11.0	34.0	93
AlF_3	HCl	32.0	21.5	67.2	93
$AlCl_3$	HCl	32.0	11.5	35.9	92—93
$AlBr_3$	HCl	32.0	30.5	95.3	93
$AlBr_3$	HBr	32.0	30.5	95.3	92—93
BF_3-acetate	HCl	32.0	20.3	62.5	92—93
BF_3-etherate	HCl	32.0	30.1	93.8	93
$FeCl_3$	HCl	32.0	14.0	43.8	93
$ZnCl_2$	HCl	32.0	13.4	42.2	93
$SnCl_4$	HCl	32.0	16.4	51.6	92—93
$SbCl_3$	HCl	32.0	15.1	46.9	93
$TiCl_4$	HCl	40.0	16.2	40.5	92—93
$TiBr_4$	HCl	40.0	24.9	62.3	92—93

All samples in Table 1 were identified by a mixed melting point with an authentic sample[21] and IR spectra analyses.

* Reaction condition; See Experimental A).

Several authors[17-33] observed the formation of the *s*-triazines from α-chlorinated nitriles.

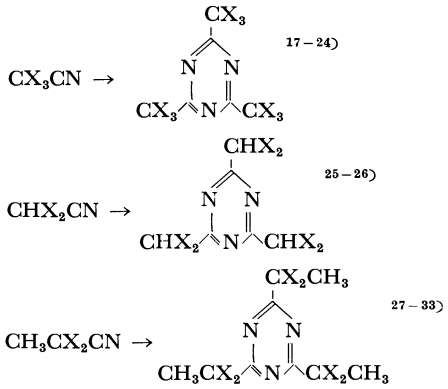

Scheme 1. (X: halogen)

Trimerization of nitriles has been effected with both basic and acidic catalysts. The basic catalysts, such as sodium,[34,35] potassium methoxide,[36] diethylzinc,[37,38] sodium hydride[38] and *N*-sodium methylaniline[38] give, in general, dimers[39] or pyrimidines[36] as main products. Acid catalyzed trimerization of nitriles [17-21,23-33] affords *s*-triazines in good yields. The reaction [19-21] was carried out in a closed system. $AlBr_3$-HCl (Norton's catalyst) is so effective that it can afford excellent yield under ordinary pressure in trimerization of CCl_3CN.[21]

The cotrimerization of CCl_3CN with other nitriles, RCN (R: methyl,[25,40-42,44] phenyl,[25,40,41] 2-

21) T. Norton, *J. Am. Chem. Soc.*, **72**, 3527 (1950).
22) L. Reilly and H. C. Brown, *J. Org. Chem.*, **22**, 698 (1957).
23) C. Broche, *J. prakt. Chem.*, (2), **47**, 304 (1893).
24) C. Broche, *ibid.*, (2), **50**, 97 (1894).
25) C. Grundmann, G. Weisse and S. Seide, *Liebigs Ann. Chem.*, **577**, 77 (1952).
26) E. Ghigi, *Gazz. chim. ital.*, **71**, 641 (1941).
27) R. Otto, *Liebigs Ann. Chem.*, **116**, 195 (1860).
28) R. Otto, *ibid.*, **132**, 181 (1864).
29) H. Beckurts and R. Otto, *Ber.*, **9**, 1593 (1876).
30) H. Beckurts and R. Otto, *ibid.*, **10**, 2040 (1877).
31) R. Otto, *Ber.*, **23**, 836 (1890).
32) R. Otto and K. Voigt, *J. prakt. Chem.*, (2), **36**, 78 (1887).
33) J. Tröger, *ibid.*, (2), **46**, 353 (1892).
34) A. Hofmann, *Ber.*, **1**, 194 (1868).
35) A. Lottermoser, *J. prakt. Chem.*, (2), **54**, 113 (1896).
36) A. R. Ronzio and W. B. Cook, "Organic Syntheses," Coll. Vol. III, p. 71 (1955).
37) E. Frankland and J. C. Evans, *J. Chem. Soc.*, **37**, 563 (1880).
38) F. Swamer, G. Reynolds and C. Hauser, *J. Org. Chem.*, **16**, 43 (1951).
39) H. Adkins and G. M. Whitman, *J. Am. Chem. Soc.*, **64**, 150 (1942).
40) K. Dachlauer, German Pat. 682391 (1939); D. R. P. *Org. Chem.*, **6**, 2619.
41) C. Grundmann and A. Kreutzberger, U. S. Pat. 2858310 (1958).
42) G. I. Braz, G. V. Myasnikova, A. Ya. Yakubovich, V. P. Bazov and K. I. Sakodynskii, *Zhur. Obshchei Khim.*, **33**, 1939 (1963).

Table 2.* The effect of combined catalyst for cotrimerization of CCl_3CN with CH_3CN

$$2CCl_3CN + CH_3CN \xrightarrow{\text{Cat. }+HX} \text{(II)}$$

Combined catalyst: Catalyst (g)		Combined catalyst: HX	Reaction time (hr)	Product (II) yield (%)	Mp °C
AlF_3	3.0	HCl	8.0	95	96—97
$AlCl_3$	3.0	HCl	12.0	85	96—97
$AlBr_3$	3.0	HCl	3.0	95	96—97
$AlBr_3$	3.0		96.0	0	
BF_3-acetate	5.0	HCl	3.0	95	96—97
BF_3-etherate	5.0	HCl	4.0	95	96—97
BBr_3	3.0	HCl	5.0	88	96
$FeCl_3$	3.0	HCl	16.0	83	96
$ZnCl_2$	4.0	HCl	16.0	78	96
$SnCl_4$	4.0	HCl	16.0	83	96—97
$SbCl_5$	4.0	HCl	24.0	76	96—97
$TiCl_4$	3.0	HCl	3.0	90	96
$TiBr_4$	3.0	HCl	3.0	90	96
$CuCl_2$	10.0	HCl	48.0	58	96
$MgCl_2$	10.0	HCl	48.0	50	96—97
None		HBr	48.0	87	96
None		HCl	96.0	85	96—97

* Reaction condition; See experimental B-a).

naphthyl,[40] 2-chloroethyl[43] and 2-bromoethyl[43]), has also been reported, although the reaction is exceedingly slow.

We wish to report the results of reexamination and development of Norton's catalyst and also results of cotrimerization of CCl_3CN with other nitriles to give *s*-triazines.

Results and Discussion

Trimerization of CCl_3CN was undertaken to find out a new effective catalyst.

As shown in Table 1, it is clear that the use of combined catalysts to trimerize CCl_3CN (Friedel-Crafts catalysts-hydrogen halides) produces a good result, especially with $AlBr_3$-HCl, $AlBr_3$-HBr and BF_3 etherate-HCl. But the use of HCl only produces 1.6% yield of I.

Under a similar condition the use of combined catalysts to cotrimerize CCl_3CN with CH_3CN was investigated. These results are listed in Table 2. It is evident that the use of hydrogen halides only as well as that of the combined catalysts were effective, although the reaction was slow.

The parent peaks in mass spectrum of I and II are *m/e* 429(P_1) and *m/e* 327(P_2). Peaks at mass *m/e* 394(P_1-35), 292(P_2-35); 359($P_1-35\times2$), 257($P_2-35\times2$); 324($P_1-35\times3$), 222($P_2-35\times3$) are results from the loss of one, two and three chlorine atom(s) respectively. There are also large peaks at mass *m/e* 117($^+CCl_3$) and 108($^+CCl_2$-CN) in both spectra. Intensities of isotope peaks of I relative to the parent peak for chlorines (Cl_9) are as follows: P_1, 100% (100%), (Calcd (Found)); P_1+2, 287 (294); P_1+4, 366 (368); P_1+6, 273 (276); P_1+8, 130 (134); P_1+10, 42 (43). Similarly, intensities of isotope peaks of II relative to the parent peak for chlorines (Cl_6) are P_2, 100 (100); P_2+2, 190 (192); P_2+4, 153 (152); P_2+6, 65 (69).

The structure of all samples, (II), was identified by the consideration of Mass, IR, UV and NMR spectra with an authentic sample.[25,40]

The data in Table 2 indicate that the combined catalyst, $AlBr_3$-HCl, are most effective and economical.[44] This particular catalyst was used to investigate the distribution of the products by changing the molar ratio of CCl_3CN and CH_3CN. Table 3 shows the results.

We see that the best result was obtained in molar ratio, *n*: 1.5 or 2.0, in the cotrimerization of CCl_3CN with CH_3CN. GLC's relative R_t values are (I)=1.00, (II)=0.38 (based on (I)=1.00). These values were the same as those of authentic samples.

43) Z. N. Pazenko and T. N. Lebedeva, *Ukr. Khim. Zhur.*, **29**, 1192 (1963).

44) M. Okuzu, K. Wakabayashi and T. Okada, Japanese Pat. 11750 (1967).

Table 3.* The effect of molar ratio for cotrimerization of CCl_3CN with CH_3CN

$n\,CCl_3CN + CH_3CN \rightarrow I + II$

CCl_3CN/CH_3CN Molar ratio (n)	Yield** of II (%)	Selectivity I	Selectivity II
1.0	97		100
1.5	97		100
2.0	95	0.5	99.5
3.0		23.5	76.5
4.0		38.8	61.2

* Experiment was carried out in the same reaction condition as Experimental B-a) in the presence of $AlBr_3$ (3g), using 41 g (1 mol) of CH_3CN.

** Based on CCl_3CN.

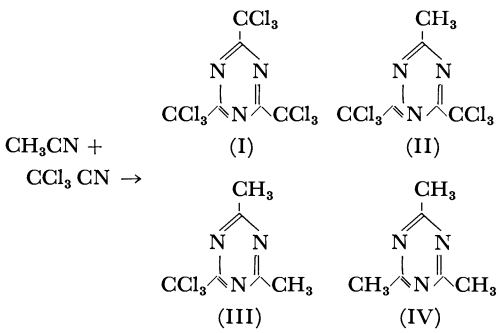

Scheme 2

Although the values of relative R_t of III and IV synthesized from another route were 0.16 and 0.08, no peak was found when the sample prepared from cotrimerization of CCl_3CN with CH_3CN was inspected.

Several other nitriles as well as CH_3CN were cotrimerized with CCl_3CN, using HCl-catalyst only. As shown in Table 4, several 2-substituted 4,6-bis(trichloromethyl)-*s*-triazines were obtained.

Some aliphatic nitriles which have more than 3 carbon atoms did not cotrimerize until a new improved method[45,46] was developed.

That is to say, 2-alkyl*2-4,6-bis(trichloromethyl)-*s*-triazines were prepared from cotrimerization of 2 mol CCl_3CN and 1 mol aliphatic nitriles in good yield when anhydrous HCl was introduced into the mixture and then heated strongly. The use of a combined catalyst also promoted this reaction. But it was not necessarily required, because the use of HCl only gave good results.

Table 5 shows the compounds obtained from the above mentioned method.

The following two experiments were carried out to observe some aspects of the mechanism about HCl-catalysed cotrimerization of CCl_3CN with CH_3CN. This mechanism may explain the cotrimerization of CCl_3CN with other nitriles also.

a) Addition of 1 mol CH_3CN to the adduct*3 of 2 mol of CCl_3CN and 1 mol HCl.

b) Addition of 1 mol CH_3CN that has already absorbed 1 mol HCl to the adduct of 2 mol of CCl_3CN and 1 mol HCl.

Like Grundmann *et al.*[25] we could hardly obtain the (co)trimerized product under the condition of a). However, the reaction proceeded readily to afford in a good yield under the condition of b).

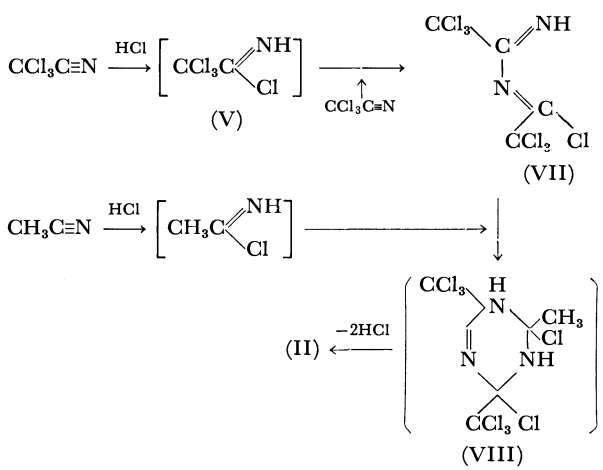

Scheme 3

45) K. Matsui, K. Wakabayashi, M. Tsunoda, Y. Suzuki, M. Tsuda and M. Nakazawa, Japanese Appl. 79006 (1967).

46) K. Matsui, K. Wakabayashi, M. Tsunoda, Y. Suzuki, M. Tsuda and M. Nakazawa, Japanese Appl. 79470 (1967).

*2 Alkyl having more than C_2 in Table 5

*3 The adduct was identified in the form of $(CCl_3CO)_2NH$ (lit. 25).

Table 4.*1 Cotrimerization of CCl_3CN with other nitriles

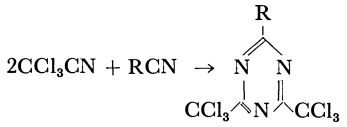

R	Yield %	Mp*2 °C	UV $\lambda_{max}^{CH_3OH}$ mμ(ε)	IR*3 cm^{-1}	Molecular formula		Anal., % C	H	N	Cl
CH_3	95	96—97*4	219(1920) 280(950)	1543						
C_6H_5†	94	97—98*4	282(23210)	1514 1548						
2-ClC_6H_4	91	120—122		1510 1548	$C_{11}H_4N_3Cl_7$	Calcd Found	30.99 31.04	0.95 1.11	9.86 9.57	58.21 58.50
3-ClC_6H_4	93	125—127		1512 1548	$C_{11}H_4N_3Cl_7$	Calcd Found	30.99 30.86	0.95 0.99	9.86 10.03	58.21 58.19
4-ClC_6H_4	92	158—159*5		1510 1548						
2,4-$Cl_2C_6H_3$	88	143—145	216(22690) 283(2600)	1510 1550	$C_{11}H_3N_3Cl_8$	Calcd Found	28.67 28.34	0.66 0.87	9.12 9.36	61.55 61.38
3,4-$Cl_2C_6H_3$	90	139—140		1510 1548	$C_{11}H_3N_3Cl_8$	Calcd Found	28.67 28.61	0.66 0.74	9.12 8.96	61.55 61.41
2,4,5-$Cl_3C_6H_2$	85	153—155		1510 1550	$C_{11}H_2N_3Cl_9$	Calcd Found	26.68 26.52	0.41 0.53	8.49 8.50	64.43 64.72
4-BrC_6H_4	92	161—163		1512 1548	$C_{11}H_4N_3Cl_6Br$	Calcd Found	28.06 27.99	0.86 0.72	8.93 8.76	62.15*6 62.22
4-$CH_3C_6H_4$	95	122—123*5		1512 1546						
3-$NO_2C_6H_4$	74	103—104*5		1510 1538						
4-$CH_3OC_6H_4$†	90	144—145*5	240(7930) 328(22580)	1512 1546						
1-Naphthyl	83	216—218		1545	$C_{15}H_7N_3Cl_6$	Calcd Found	40.76 40.52	1.60 1.86	9.50 9.43	48.13 48.46
2-Naphthyl	78	210—212*4		1545						

*1 Cotrimerization was carried out in the same reaction condition as Experimental B-a) in the presence of $AlBr_3$ (3 g), using 2 moles of CCl_3CN and 1 mole of RCN. *2 Recrystallized from ethanol. *3 Characteristic absorption of *s*-triazine system. *4 K. Dachlauer, German Pat. 682391 (1939). *5 H. G. Schmelzer *et al.*, U. S. Pat. 3277091 (1966); German Pat. 1200314 (1965). *6 Calcd Value: Cl+Br.

† NMR ($CDCl_3$) 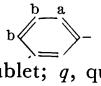 τ 1.38 (*d*, 2H), a; 2.41 (*q*, 3H), b. 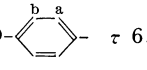 τ 6.10 (*s*, 3H), c; 2.97 (*d*, 2H), b; 1.36 (*d*, 2H), a.
(*s*, singlet; *d*, doublet; *q*, quartet)

Table 5.† Cotrimerization of CCl_3CN with aliphatic nitriles

$$2CCl_3CN + RCN \rightarrow$$ 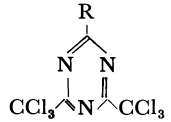

R	Yield %	Bp, °C/mmHg Mp, °C (From solvent)	UV $\lambda_{max}^{CH_3OH}$ mμ (ε)	IR*1 cm⁻¹	NMR*2 τ	Molecular formula		Anal., % C	H	N	Cl
C_2H_5	92	165—166/11*3 34—36	221(1770) 278(570)	1525 1543	8.64(*t*, 3H) 6.79(*q*, 2H)						
n-C_3H_7	93	136—138/2	220(1820) 278(660)	1528 1548	8.92(*t*, 3H) 8.01(*h*, 2H) 6.82(*t*, 2H)	$C_8H_7N_3Cl_6$	Calcd Found	26.85 26.70	1.97 1.82	11.74 11.75	59.44 59.62
i-C_3H_7	87	170—175/14	214(3220) 265(580)	1522 1545	8.55(*d*, 6H) 6.60(*m*, H)	$C_8H_7N_3Cl_6$	Calcd Found	26.85 26.49	1.97 1.89	11.74 11.83	59.44 60.11
n-C_4H_9	90	157—159/3		1528 1545		$C_9H_9N_3Cl_6$	Calcd Found	29.06 28.88	2.44 2.39	11.30 11.34	57.20 57.36
i-C_4H_9	82	154—156/3	216(3840) 281(730)	1528 1545	8.97(*d*, 6H) 7.58(*m*, H) 6.94(*d*, 2H)	$C_9H_9N_3Cl_6$	Calcd Found	29.06 28.96	2.44 2.34	11.30 11.48	57.20 57.43
s-C_4H_9	81	142—146/3	222(1910) 276(600)	1528 1548	9.04(*t*, 3H) 8.56(*d*, 3H) 8.17(*qi* 2H) 6.80(*m*, H)	$C_9H_9N_3Cl_6$	Calcd Found	29.06 29.20	2.44 2.56	11.30 11.21	57.20 57.34
t-C_4H_9	56	154—157/8 68—70	224(2220) 283(610)	1525 1543	8.50(*s*)	$C_9H_9N_3Cl_6$	Calcd Found	29.06 29.17	2.44 2.62	11.30 11.42	57.20 57.08
n-C_5H_{11}	95	175—177/5	216(3500) 280(650)	1528 1548	9.08(*t*, 3H) 7.93—8.72(*m*, 6H) 6.83(*t*, 2H)	$C_{10}H_{11}N_3Cl_6$	Calcd Found	31.12 31.03	2.87 2.74	10.89 10.73	55.12 55.08
n-C_9H_{19}	78	192—194/5*4	216(2320) 262(450)	1525 1548	9.12(*t*, 3H) 7.42—8.46(*m*, 14H) 6.84(*t*, 2H)	$C_{14}H_{19}N_3Cl_6$	Calcd Found	38.04 37.95	4.33 4.18	9.50 9.55	48.12 48.34
n-$C_{17}H_{35}$	92	210—215/4*5		1520 1548		$C_{22}H_{35}N_3Cl_6$	Calcd Found	47.67 47.54	6.36 6.30	7.58 7.52	37.38 37.51
CH_2ClCH_2 a b	69	65—67*6 (EtOH)	244(3320)	1528	6.36(*t*, 2H),[b] 5.88(*t*, 2H),[a]						
CH_2ClCCl_2	87	47—48 (EtOH)	223(2330) 285(770)	1548	518(*s*)	$C_7H_2N_3Cl_9$	Calcd Found	18.10 18.72	0.45 0.38	9.40 9.43	71.35 71.54

† Reaction conditions; See Experimental B-b).

*1 Characteristic absorption of *s*-triazine system. *2 *s*, singlet; *d*, doublet; *t*, triplet; *q*, quartet; *qi*, quintet; *h*, heptet; *m*, multiplet. *3 H. G. Schmelzer *et al.*, German Pat. 1200314 (1965). *4 n_D^{28} 1.4746. *5 n_D^{28} 1.4850. *6 Z. H. Pazenko *et al.*, *Ukr. Khim. Zh.*, **29**, (11), 1192 (1963). It was reported that this compound was obtained without strong heating.

The mechanism may be explained as follows. The dimer (VII) (formed from 2 molecules CCl_3CN and 1 molecule HCl) and acetimidoyl chloride (VI) (formed from 1 molecule CH_3CN and 1 molecule HCl) may produce the adduct (VIII) by Diels-Alder type reaction. VIII may be changed into resonance-stabilised *s*-triazine, II, by the loss of 2 molecules HCl.

It may be explained that the intermediates (VIII) from the nitriles in Table 4 are converted smoothly into *s*-triazine by the loss of 2 molecules HCl at room temperature, but the intermediates (VIII) from the nitriles in Table 5 are not converted without strong heating.

Experimental

All the boiling points and melting points are uncorrected. Gas-liquid chromatography was performed with a Shimadzu GC-2C fitted with a flame ionization detecter, with 25 ml/min of nitrogen, using a 2 m×4 mm column containing 4% SE-30 on Gaschrom. P. IR spectra were obtained with a JASCO model IR-S spectrometer. UV spectra were obtained with a Perkin-Elmer model 202 spectrometer. NMR spectra were determined at 60 Mc with a Varian A-60 spectrometer, using TMS as the internal standard. Mass spectra were obtained with a Hitachi RMU-6C spectrometer.

Materials. *Nitriles.* CH_2ClCH_2CN[47] was prepared from acrylonitrile. CCl_3CN[12] was prepared by the chlorination of acetonitrile and CH_2ClCCl_2CN[48] by the chlorination of acrylonitrile. *i*-C_4H_9CN, *s*-C_4H_9CN, *t*-C_4H_9CN, *n*-$C_9H_{19}CN$, 2-ClC_6H_4CN, 3-ClC_6H_4CN, 4-BrC_6H_4CN, 2,4-$Cl_2C_6H_3CN$, 3,4-$Cl_2C_6H_3CN$ and 2,4,5-$Cl_3C_6H_2CN$ were prepared by the dehydration of corresponding amide with P_2O_5. Acetonitrile and acrylonitrile were supplied from Kasei Mizushima Ltd. Other nitriles were obtained from Tokyo Kasei Kogyo Co., Ltd.

Metal Halides. All reagents were obtained from Wako Pure Chemical Industries Ltd.

A) Trimerization of CCl_3CN. *2,4,6-Tris(trichloromethyl)-s-triazine (I).* 32 g (0.22 mol) of CCl_3CN and 0.5 g of a catalyst were placed into a 300 ml flask. The mixture was saturated with anhydrous HCl at −10—0°C with stirring. The reaction mixture was kept at room temperature for 12 hr to complete trimerization. The contents of the flask was melted by heating at 100—110°C and poured into a large quantity of water to wash out HCl and catalyst. The mixture was cooled to let the product solidify again. The solid product was filtered, dried in air and recrystallized from ethanol (Table 1). Analysis example; using $AlBr_3$-HCl as the catalyst.

Found: C, 16.60; N, 9.49; Cl, 73.90%. Calcd for $C_6N_3Cl_9$: C, 16.64; N, 9.70; Cl, 73.66%.

IR absorption; 1545, 1341 cm^{-1} (*s*-triazine ring).

UV absorption; $\lambda_{max}^{CH_3OH}$ 219 mμ (ε 2590); 287 mμ (ε 790).

B) Cotrimerization of CCl_3CN. *a) 2-Methyl-4,6-bis(trichloromethyl)-s-triazine (II).* 289 g (2 mol) of CCl_3CN and 50 g (1.2 mol) of CH_3CN and a catalyst were placed into a 500 ml flask. The mixture was saturated with anhydrous HCl at −20—0°C with stirring, which was continued at the same temperature for 2—3 hr. At the end of the reaction time the contents of the flask solidified. After the reaction mixture was kept at room temperature to complete cotrimerization, the product was melted by heating at 100—110°C and poured into a large quantity of water to wash out HCl and the catalyst. After being cooled to room temperature, the separated solid was collected, dried in air and then recrystallized from ethanol. (Table 2).

Analysis example; using $AlBr_3$-HCl as the catalyst.

Found: C, 21.99; H, 1.00; N, 12.69; Cl, 64.48%. Calcd for $C_6H_3N_3Cl_6$: C, 21.84; H, 0.92; N, 12.74; Cl, 64.49%.

IR absorption; 1543, 1339 cm^{-1} (*s*-triazine ring).

UV absorption; $\lambda_{max}^{CH_3OH}$ 219 mμ (ε 1920); 280 mμ (ε 950).

NMR spectrum ($CDCl_3$); τ 7.02 (CH_3).

b) 2-Alkyl[2]-4,6-bis(trichloromethyl)-s-triazine.* The mixed solution of 289 g (2 mol) of CCl_3CN and 1.2 mol of RCN was saturated with anhydrous HCl at −30—−15°C by cooling with dry ice-methanol bath for 2 hr with stirring, which was continued at −10—0°C for 2—3 hr. The reaction mixture was kept overnight at room temperature. Then HCl gas was removed under reduced pressure by a water pump, gradually heating the reaction mixture at 150—200°C to complete cotrimerization. The residue is fractionated under reduced pressure. Thus 2-alkyl-4,6-bis(trichloromethyl)-*s*-triazine was obtained (Table 5).

C) The Preparation of Authentic Samples. *a) 2,4-Dimethyl-6-trichloromethyl-s-triazine (III).* III was prepared from acetic anhydride and *N*-(acetimidoyl) trichloroacetamidine which was prepared from CCl_3CN and acetamidine.[49] Yield 55%. Mp 72—73°C (lit[49] mp 69—71°C).

IR absorption; 1540 cm^{-1} (*s*-triazine ring).

UV absorption; $\lambda_{max}^{CH_3OH}$ 234 mμ (ε 2020); 260 mμ (ε 890).

NMR spectrum ($CDCl_3$); τ 7.26 (CH_3).

b) 2,4,6-Trimethyl-s-triazine (IV). IV was prepared by the method of Schaefer[50] from ethyl acetimidate. Yield 90%. Mp 60°C. Bp 150—155°C (lit[50] bp 155°C).

IR absorption; 1536 cm^{-1} (*s*-triazine ring).

UV absorption; $\lambda_{max}^{CH_3OH}$ 228 mμ (ε 270); 257 mμ (ε 390).

NMR spectrum ($CDCl_3$); τ 7.42 (CH_3).

D) Experiments to Elucidate HCl-catalysed Cotrimerization of CCl_3CN with CH_3CN. *a) The Reaction of CH_3CN and the Adduct (VII) of CCl_3CN and HCl.* 18 g (0.5 mol) of anhydrous HCl was absorbed into 144.5 g (1 mol) of CCl_3CN at −10—0°C for 0.5 hr. Then 20.5 g (0.5 mol) of CH_3CN was added to this solution with stirring. The mixture was allowed to stand for 90 hr at room temperature. The product was distilled under reduced pressure by a water pump.

47) R. Stewart and R. H. Clark, *J. Am. Chem. Soc.*, **69**, 714 (1947).

48) N. B. Lorette, *J. Org. Chem.*, **26**, 2324 (1961).

49) American Cyanamid Co., Brit. Pat. 912112 (1962).

50) F. C. Schaefer and G. A. Peters, *J. Org. Chem.*, **26**, 2778 (1961).

The distillate was a mixture of CH_3CN and CCl_3CN. A small amount of residue was obtained. This compound was found out to be a mixture of II and unidentified substance by GLC and IR analyses.

b) The Reaction of the Adduct (VI) of CH_3CN and HCl, and the Adduct (VII) of CCl_3CN and HCl. 18 g (0.5 mol) of anhydrous HCl was absorbed into 144.5 g (1 mol) of CCl_3CN at −10—0°C for 0.5 hr. 18 g of anhydrous HCl was also absorbed into 20 .5g (0.5 mol) of CH_3CN under the same condition. Then two solutions were mixed at 0—10°C with stirring. The mixture was allowed to stand for 90 hr at room temperature. At the end of the reaction, the reaction mixture almost solidified which was then poured into water. The crude product was filtered and air-dried to yield 140 g (85%). Mp 90—93°C. This compound was identified II by GLC and IR analyses.

The authors are indebted to the Mitsubishi Chemical Industries Ltd. for their generous support of this publication. They also wish to express their thanks to Mr. Y. Takigawa for obtaining and interpreting the spectra which were of great assistance in this work and Mr. K. Suzuki for the microanalyses. Valuable technical assistance was also provided by Mr. M. Tsuda and Mr. M. Nakazawa.

BULLETIN OF THE CHEMICAL SOCIETY OF JAPAN VOL. 42 2931—2937 (1969)

Studies on *s*-Triazines. II. Cotrimerization of Trichloroacetonitrile with Thiocyanates[1),*1]

Ko WAKABAYASHI, Masaru TSUNODA and Yasushi SUZUKI

Research Laboratory, Mitsubishi Chemical Industries Ltd., Mizonokuchi, Kawasaki, Kanagawa

(Received April 11, 1969)

2-Substituted thio-4,6-bis(trichloromethyl)-*s*-triazines, a new class of *s*-triazine derivatives, were obtained by the cotrimerization of CCl_3CN with a wide variety of thiocyanates. Generally, the reaction proceeded smoothly at ordinary pressure in the presence of hydrogen chloride or the combined catalyst, Friedel-Crafts catalyst-hydrogen chloride.

Literature[2–4] has revealed that attempts to prepare 2-substituted thio-4,6-bis(trichloromethyl)-*s*-triazines have mostly met with failure.

Kober[5] reported that the reaction of 2,4,6-tris-(trichloromethyl)-*s*-triazine (I) with alcohols, in the presence of tertiary amines, led to the stepwise replacement of the CCl_3-groups with the alkoxyl groups, depending upon the reaction condition. Then Kober further attempted to determine whether the reaction of I with alkanethiols, instead of alcohols, would react in the presence of tertiary amines resulting in the formation of 2-alkylthio-4,6-bis(trichloromethyl)-*s*-triazines. His results, however, indicated that the reaction of I with

TABLE 1. ISOTOPE ABUNDANCES FOR CHLORINES AND SULFUR OF V

			P	P+2	P+4	P+6	P+8
M^+	387	Calcd	100	196	161	72	18
		Found	100	203	174	74	21
M^+-CH_3	372	Calcd	100	196	161	72	
		Found	100	199	150	75	
M^+-Cl	352	Calcd	100	164	109	37	
		Found	100	152	111	46	

Calculation based on $^{35}Cl : {}^{37}Cl = 75.53 : 24.47$
$^{32}S : {}^{34}S = 95.77 : 4.23$

*1 Taken in part from the dissertation presented by K. Wakabayashi to the University of Tokyo, January 1969.

1) Previous paper of this series, K. Wakabayashi, M. Tsunoda and Y. Suzuki, This Bulletin, **42**, 2924 (1969).

2) E. Kober, *J. Org. Chem.*, **26**, 2270 (1961).

3) H. G. Schmelzer, G. Dankert, E. Degener and H. Holtschmidt, German Pat. 1200314 (1965); U.S. Pat. 3277091 (1966); Japanese Pat. 3178 (1966).

4) H. G. Schmelzer, E. Degener and H. Holtschmidt, *Angew. Chem.*, **78**, 982 (1966).

5) E. Kober, *J. Org. Chem.*, **25**, 1728 (1960).

TABLE 2. COTRIMERIZATION OF

$CCl_3CN + RSCN \rightarrow$

R	Yield (%)	Physical property Bp, °C/mmHg	Mp, °C	UV $\lambda_{max}^{CH_3OH}$ mμ(ε)	IR*1 cm^{-1}	NMR τ*2) (Sol. $CDCl_3$)
CH_3*3a,*4	93	160—165/0.65	71—72	217 (3340) 272 (15060)	1550 1498	7.27 (*s*, SCH_3)cf.)
C_2H_5*3b	94	170—171/1.0		221 (2850) 274 (13530)	1550 1505	8.51 (*t*, 3H, CH_3)cf.) 6.68 (*q*, 2H, SCH_2)
n-C_3H_7	88	188—190/2.0		215 (3500) 274 (13100)	1550 1503	8.88 (*t*, 3H, CH_3) 8.24 (*h*, 2H, CH_2) 6.73 (*t*, 2H, SCH_2)
i-C_3H_7	95	185—187/4.0	58—60	215 (3600) 274 (13840)	1548 1498	8.47 (*d*, 6H, CH_3) 5.88 (*m*, H, SCH)
n-C_4H_9	86	189—193/3.0		221 (2890) 275 (13690)	1550 1503	9.00 (*t*, 3H, CH_3) 7.92—8.73 (*m*, 4H, CH_2) 6.67 (*t*, 2H, SCH_2)
i-C_4H_9	95	180—183/2.0		220 (2960) 274 (14250)	1550 1505	8.87 (*t*, 6H, CH_3) 7.67—8.34 (*m*, H, CH) 6.77 (*d*, 2H, SCH_2)
n-C_5H_{11}	95	192—194/2.0		221 (2890) 275 (13690)	1550 1505	9.03 (*t*, 3H, CH_3) 7.98—8.82 (*m*, 6H, CH_2) 6.68 (*t*, 2H, SCH_2)
n-C_6H_{13}	90	195—200/1.0		218 (2590) 275 (14040)	1548 1504	9.05 (*t*, 3H, CH_3) 7.90—8.73 (*m*, 8H, CH_2) 6.68 (*t*, 2H, SCH_2)
n-$C_{12}H_{25}$*5	85	230—235/0.2		214 (2670) 274 (13490)	1542 1504	9.12 (*t*, 3H, CH_3) 8.04—8.96 (*m*, 20H, CH_2) 6.93 (*t*, 2H, SCH_2)
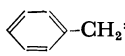 *3c	72	186—189/1.0	84—85	231 (2420) 277 (13780)	1543 1504	5.43 (*s*, 2H, CH_2) 2.35—2.70 (*m*, 5H, Aro.)
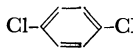	68		91—93	232 (3600) 279 (15200)	1542	
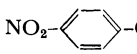	74		121—122	295 (20400)	1535	
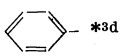 *3d	95	210—214/2.0	65—67	271 (9710)	1537 1504	2.20—2.60 (*m*, 5H, Aro.)
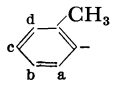	95	185—187/1.0	47—48	270 (9680)	1532 1503	7.56 (*s*, 3H, CH_3) 2.50—2.70 (*m*, 3H, b+c+d) 2.41 (*d*, H, a)
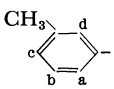	93		74—75	270 (9720)	1545 1504	7.55 (*s*, 3H, CH_3) 2.69 (*m*, 2H, b+c) 2.41 (*m*, 2H, a+d)
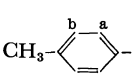	95		82—85	269 (10240)	1546 1504	7.53 (*s*, 3H, CH_3) 2.74 (*d*, 2H, b) 2.42 (d, 2H, a)
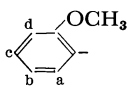	83		98—101	272 (11020)	1542 1508	6.18 (*s*, 3H, CH_3) 2.50—3.10 (*m*, 3H, b+c+d) 2.40 (*d*, H, a)
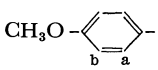	86		100—103	271 (11000)	1545 1508	6.23 (*s*, 3H, CH_3) 3.13 (*d*, 2H, b) 2.61 (*d*, 2H, a)
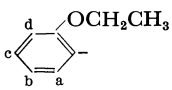	88		45—48	213 (19000) 282 (9030)	1534 1504	8.56 (*t*, 3H, CH_3) 5.84 (*q*, 2H, CH_2) 2.60—3.10 (*m*, 3H, b+c+d) 2.45 (*d*, H, a)

CCl_3CN WITH THIOCYANATES

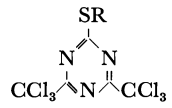

Method		Molecular formula		Anal., %				
A or B	Solvent			C	H	N	S	Cl
A		$C_6H_3N_3SCl_6$	Calcd	19.91	0.83	11.61	8.86	58.78
			Found	19.86	0.91	11.35	8.88	58.58
A		$C_7H_5N_3SCl_6$	Calcd	22.37	1.34	11.18	8.53	56.59
			Found	22.52	1.38	11.10	8.63	56.61
A		$C_8H_7N_3SCl_6$	Calcd	24.64	1.81	10.78	8.22	54.55
			Found	24.69	1.85	10.76	8.07	54.65
A		$C_8H_7N_3SCl_6$	Calcd	24.64	1.81	10.78	8.22	54.55
			Found	24.51	1.88	10.51	7.90	54.98
A		$C_9H_9N_3SCl_6$	Calcd	26.76	2.25	10.40	7.94	52.66
			Found	26.66	2.24	10.29	8.02	52.81
A		$C_9H_9N_3SCl_6$	Calcd	26.76	2.25	10.40	7.94	52.66
			Found	26.85	2.35	10.16	8.06	52.77
A		$C_{10}H_{11}N_3SCl_6$	Calcd	28.73	2.65	10.05	7.67	50.89
			Found	28.86	2.62	9.83	7.55	50.93
A	Ether	$C_{11}H_{13}N_3SCl_6$	Calcd	30.58	3.03	9.73	7.42	49.24
			Found	30.72	3.11	9.67	7.50	49.40
A	Ether	$C_{17}H_{25}N_3SCl_6$	Calcd	39.55	4.88	8.14	6.21	41.21
			Found	39.41	5.02	8.33	6.29	41.32
A	Ether	$C_{12}H_7N_3SCl_6$	Calcd	32.91	1.61	9.59	7.32	48.57
			Found	32.68	1.86	9.48	7.35	48.81
B	Ether	$C_{12}H_6N_3SCl_7$	Calcd	30.51	1.28	8.89	6.79	52.53
			Found	30.62	1.43	9.02	6.65	52.48
B	Ether	$C_{12}H_6N_4O_2SCl_6$	Calcd	29.84	1.25	11.60	6.64	44.04
			Found	30.01	1.36	11.45	6.55	44.12
A	Ether	$C_{11}H_5N_3SCl_6$	Calcd	31.16	1.19	9.91	7.56	50.17
			Found	31.38	1.41	9.73	7.48	49.97
A	Ether	$C_{12}H_7N_3SCl_6$	Calcd	32.91	1.61	9.59	7.32	48.57
			Found	32.88	1.81	9.63	7.53	48.67
B	Ether	$C_{12}H_7N_3SCl_6$	Calcd	32.91	1.61	9.59	7.32	48.57
			Found	32.76	1.58	9.72	7.47	48.49
B	Ether	$C_{12}H_7N_3SCl_6$	Calcd	32.91	1.61	9.59	7.32	48.57
			Found	33.19	1.77	9.31	7.31	48.66
B	Ether	$C_{12}H_7N_3OSCl_6$	Calcd	31.75	1.55	9.26	7.06	46.86
			Found	31.70	1.44	9.06	7.24	46.51
B	Ether	$C_{12}H_7N_3OSCl_6$	Calcd	31.75	1.55	9.26	7.06	46.86
			Found	31.65	1.61	9.33	7.16	46.53
B	Ether	$C_{13}H_9N_3OSCl_6$	Calcd	33.36	1.94	8.98	6.85	45.45
			Found	33.55	2.02	9.11	6.79	45.51

TABLE 2.

R	Yield (%)	Physical property Bp, °C/mmHg	Mp, °C	UV $\lambda_{max}^{CH_3OH}$ mμ(ε)	IR*1 cm^{-1}	NMR τ*2 (Sol. $CDCl_3$)
CH_3CH_2O-(b a)	81		54—56	212 (15190) 283 (11830)	1542 1503	8.55 (*t*, 3H, CH_3) 5.92 (*q*, 2H, CH_2) 3.02 (*d*, 2H, b) 2.47 (*d*, 2H, a)
Cl-(a)	92		58—60	210 (15680) 270 (10150)	1532 1510	2.18—2.80 (*m*, 4H, Aro.)
Cl(a)-(d c b)	93		57—58	213 (17780) 270 (10910)	1540 1510	2.50 (*m*, 3H, b+c+d) 2.27 (*s*, H, a)
Cl-(b a)	95	224—226/1.0	68—70	210 (19070) 268 (10900)	1548 1504	2.46 (*d*, 4H, a+b)
Cl(a)-Cl-(b c)	86	230—240/2.0	68—70	213 (21090) 267 13090)	1545 1512	2.55 (*d*, H, c) 2.36 (*d*, H, b) 2.23 (*s*, H, a)
Cl(a)-Cl-(c b)	90	245—248/2.0	85—87	212 (23840) 271 (9170)	1540 1512	2.47 (*d*, 2H, b+c) 2.18 (*s*, H, a)
Cl(a)-Cl-Cl(b)	83		97—99	213 (23730) 266 (7070)	1538 1516	2.29 (*s*, H, b) 2.14 (*s*, H, a)
Br-	83		60—62	215 (17500) 270 (10650)	1540 1510	
CH_3(b)-Cl-(a c)	87		75—76	270 (10770)	1540 1508	7.58 (*s*, 3H, CH_3) 2.52 (*m*, 2H, b+c) 2.45 (*d* H, a)
NO_2-(a b)	61		93—95	288 (16320)	1520	2.30 (*d*, 2H, b) 1.66 (*d*, 2H, a)
NO_2(a)-Cl-(c b)	83		65—66	263 (11080)	1540 1512	2.25 (*d*, 2H, b+c) 1.75 (*s*, H, a)
NO_2-(a c)-OCH_3(b)	64		65—67	286 (9980)	1526	5.93 (*s*, 3H, CH_3) 2.20 (*m*, 2H, b+c) 2.08 (*d*, H, a)

*1 Characteristic absorption of *s*-triazine system.

*2 *s*, singlet; *d*, doublet; *t*, triplet; *q*, quartet; *qi*, quintet; *h*, heptet; *m*, multiplet.

*3 H. G. Schmelzer *et al.*, U. S. Pat. 3347859 (1967) a) mp 63°C; b) bp 154—157°C/0.4 mmHg; c) mp 83—84°C; d) mp 68—70°C.

*4 H. G. Schmelzer *et al.*, German Pat. 1200314 (1965).

*5 n_D^{28} 1.5710

Continued

Method		Molecular formula		Anal., %				
A or B	Solvent			C	H	N	S	Cl
B	Ether	$C_{13}H_9N_3OSCl_6$	Calcd	33.36	1.94	8.98	6.85	45.45
			Found	33.41	2.04	8.90	6.72	45.25
B	Ether	$C_{11}H_4N_3SCl_7$	Calcd	28.82	0.88	9.17	7.00	54.14
			Found	28.61	0.92	8.99	6.97	54.25
B	Ether	$C_{11}H_4N_3SCl_7$	Calcd	28.82	0.88	9.17	7.00	54.14
			Found	29.03	0.93	8.97	7.09	53.92
A	Ether	$C_{11}H_4N_3SCl_7$	Calcd	28.82	0.88	9.17	7.00	54.14
			Found	28.96	0.92	9.06	7.01	53.96
A	Ether	$C_{11}H_3N_3SCl_8$	Calcd	26.81	0.61	8.53	6.51	57.55
			Found	26.66	0.63	8.44	6.41	57.31
A	Ether	$C_{11}H_3N_3SCl_8$	Calcd	26.81	0.61	8.53	6.51	57.55
			Found	26.82	0.73	8.31	6.27	57.65
B	Ether	$C_{11}H_2N_3SCl_9$	Calcd	25.05	0.38	7.97	6.08	60.51
			Found	25.37	0.63	8.05	5.83	60.73
B	Ether	$C_{11}H_4N_3SBrCl_6$	Calcd	26.27	0.80	8.36	6.38	58.19[*6]
			Found	26.34	0.96	8.45	6.43	58.24
B	Ether	$C_{12}H_6N_3SCl_7$	Calcd	30.51	1.28	8.89	6.79	52.53
			Found	30.69	1.40	8.69	6.66	52.47
B	Ether	$C_{11}H_4N_4O_2SCl_6$	Calcd	28.17	0.86	11.95	6.84	45.36
			Found	28.34	1.01	12.13	6.76	45.51
B	Ether	$C_{11}H_3N_4O_2SCl_7$	Calcd	26.24	0.60	11.13	6.37	49.30
			Found	26.35	0.81	10.85	6.34	49.19
B	Ether	$C_{12}H_6N_4O_3SCl_6$	Calcd	28.88	1.21	11.23	6.43	42.63
			Found	29.01	1.45	11.36	6.53	42.55

[*6] Calcd value: Cl+Br

cf. NMR ($CDCl_3$)

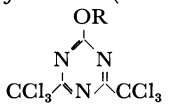

R=CH_3CH_2- τ: 8.44 (*t*, 3H, CH_3); 5.26 (*q*, 2H, CH_2)

R=CH_3- τ: 5.72 (*s*, 3H, CH_3)

alkanethiols in the presence of tertiary amines took an entirely different course as compared with the reaction of I with alcohols. Instead of being replaced with the alkylthio groups, the CCl_3-groups were converted into $CHCl_2$-groups and resulted in 2,4,6-tris(dichloromethyl)-*s*-triazine (II).[2]

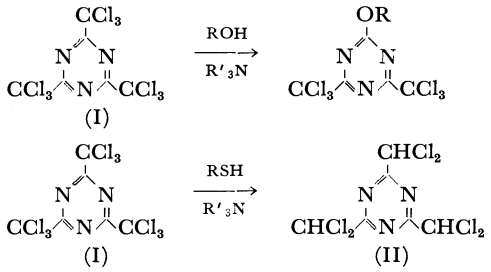

Scheme 1

The only type of these *s*-triazines hitherto known, is 2-methylthio-4,6-bis(trichloromethyl)-*s*-triazine[3] (III) which was obtained from the reaction of *S*-methyl isothiourea with *N*-pentachloroethyl-trichloroacetimidoyl chloride (IV). The following Scheme 2 shows this method to be successful.

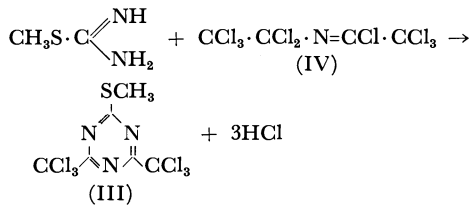

Scheme 2

While the *S*-methyl isothiourea is derived readily from thiourea,[6] IV has been only obtained by high temperature (250—300°C) chlorination reaction of $(C_2H_5)_2NH$[7] or of *N*-ethyl-trichloroacetimidoyl chloride[8] under UV irradiation. Many side reactions may occur, if the reaction is not carried out carefully in this chlorination process. Because of such conditions, the method mentioned above is not readily applicable to the preparation of the desired compounds.

The authors have also investigated the preparation of 2-substituted thio-4,6-bis(trichloromethyl)-*s*-triazines, in order to evaluate these *s*-triazines as fungicides[9] or nitrification inhibitors[10] in soil. Accordingly, the extention of the cotrimerization reaction[1] of CCl_3CN with other nitriles to that of CCl_3CN with RSCN, have been examined as a method in the preparation of these types of *s*-triazines. The results show that 2-substituted thio-4,6-bis(trichloromethyl)-*s*-triazines can be prepared in high yield by a less costly and moderate reaction condition involving the simple cotrimerization of CCl_3CN with RSCN at atmospheric pressure.

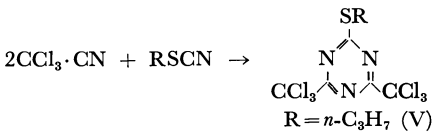

Scheme 3

Cotrimerization reaction was done by introducing HCl gas into the mixture of 2 mol of CCl_3CN and 1 mol of RSCN and a small amount of Friedel-Crafts catalyst.[11] The strong heating treatment was

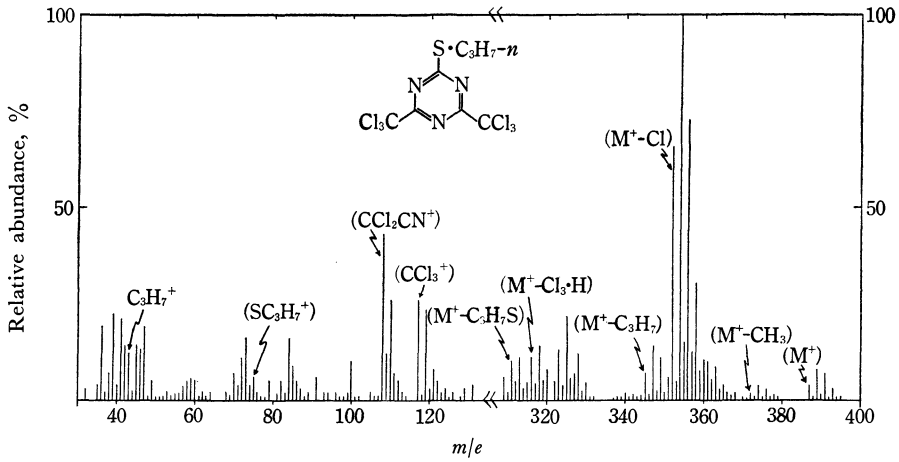

Fig. 1. Mass spectrum of V.

6) P. R. Shildneck and Wallace Windus, "Organic Syntheses," Coll. Vol. II, p. 411 (1943).

7) W. Zecher, H. Tarnow and H. Holtschmidt, German Pat. 1222918 (1966); Netherland Appl. 6516622 (1966).

8) H. Holtschmidt, E. Degener and H. G. Schmelzer, *Liebigs Ann. Chem.*, **701**, 107 (1967).

9) K. Matsui, H. Kasugai, K. Wakabayashi, S. Motojima and M. Tsuda, Japanese Appl. 67973 (1968).

10) M. Okuzu, K. Wakabayashi, M. Tsunoda, S. Fujita and M. Tsuda, Japanese Appl. 86933 (1968).

11) H. G. Schmelzer and E. Degener, U. S. Pat. 3347859 (1967).

We came across this patent a few days after we carried out our experiment. $ZnCl_2$-HCl is used in the patented reaction instead of our combined catalyst, $AlBr_3$-HCl.

necessary to cotrimerize completely CCl_3CN with RSCN as well as the cotrimerization of CCl_3CN with aliphatic nitriles.[1] The reaction time was shortened by using Friedel-Crafts catalyst, which was not necessarily required to achieve this reaction.

In several cases the authors did not use solvents. When RSCN was not dissolved completely in CCl_3CN, suitable solvents such as ether, chloroform, carbon tetrachloride, *etc.*, could be used.

The following information shows that the product from CCl_3CN and n-C_3H_7SCN was to be a 2 : 1 cotrimer of them. The product has a strong infrared absorption at 1550 and 1503 cm^{-1} (*s*-triazine ring). Figure 1 shows the result of mass spectrum analysis.

As shown in Fig. 1, the molecular peak (M^+), *m/e* 387, corresponds to the calculated molecular weight of 2-(*n*-propylthio)-4,6-bis(trichloromethyl)-*s*-triazine (V). *m/e* 352 and 317 register the exact weight of M^+-35(atomic weight of chlorine) and $M^+-2\times35$, respectively. Also as shown in Table 1, the isotope abundances are the same as those calculated, and the NMR spectrum of the product shows the existence of the n-C_3H_7 group.

Judging from these results, we can state that the product from CCl_3CN and n-C_3H_7SCN is the 2 : 1 cotrimer of them, V.

Table 2 shows 2-substituted thio-4,6-bis(trichloromethyl)-*s*-triazines obtained from the cotrimerization of CCl_3CN with RSCN.

The authors also attempted Kober's methods,[2] making I react with methanethiol in the presence of $(C_2H_5)_3N$, but could not obtain the desired III.

II and 2,4-bis(dichloromethyl)-6-bis(methylthio)-methyl-*s*-triazine were confirmed by IR and NMR to be the products in this reaction.

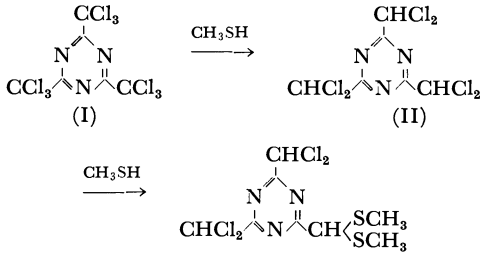

Scheme 4

Experimental

All boiling points and melting points are uncorrected. IR spectra were obtained with a JASCO model IR-S spectrometer. UV spectra were obtained with a Perkin-Elmer model 202 spectrometer. NMR spectra were determined at 60 Mc with a Varian A-60 spectrometer using TMS as the internal standard. Mass spectra were obtained with a Hitachi RMU-6C spectrometer.

Procedure of the Method. *2-Substituted Thio-4,6-bis(trichloromethyl)-s-triazine.* 290 g (2 mol) of CCl_3CN and thiocyanate*[2] (1 mol) and 3 g of $AlBr_3$ were placed in a 500 m*l* flask (if necessary, the solvent should be added). Anhydrous hydrogen chloride (*ca.* 150 g) was introduced into the mixed solution at −40—−20°C with stirring. The reaction mixture was kept at −10—0°C for 12 hr and then at room temperature for the next 24 hr. Hydrogen chloride gas was then removed under reduced pressure (20—30 mmHg) by use of a water pump from the reaction mixture, gradually heating it to 150—200°C to complete cotrimerization. The residue was fractionated under reduced pressure (Method A) or recrystallized from ethyl acetate (Method B). 2-Substituted thio-4,6-bis(trichloromethyl)-*s*-triazines obtained were shown in Table 2.

2,4,6-Tris(dichloromethyl)-s-triazine[2] (*II*). To the mixed solution of 21 g (0.2 mol) of $(C_2H_5)_3N$ and 96 g (2 mol) of CH_3SH was added 43.3 g (0.1 mol) of 2,4,6-tris-(trichloromethyl)-*s*-triazine by small portion at −20—−30°C with stirring. After adding, 200 m*l* of ether was added to this solution and the excess CH_3SH was removed below room temperature. The separated $(C_2H_5)_3N$-HCl salt was filtered and the filtrate was concentrated to remove ether and CH_3SSCH_3. The resulting oily residue was fractionated to give 24.7 g (75% yield) of 2,4,6-tris(dichloromethyl)-*s*-triazine, bp 150—60°C/0.5 mmHg, mp 62—65°C. Recrystallization from petroleum ether raised the melting point to 67—70°C. Found: C, 21.95; H, 1.03; N, 12.66; Cl, 64.52%. Calcd for $C_6H_3N_3Cl_6$: C, 21.84; H, 0.92; N, 12.74; Cl, 64.49%. IR absorption (KBr): 1552 cm^{-1} (characteristic absorption of *s*-triazine system). NMR spectrum ($CDCl_3$): τ 3.27 (singlet, $CHCl_2$).

2,4-Bis(dichloromethyl)-6-bis(methylthio)methyl-s-triazine. Using 50 g (0.5 mol) of $(C_2H_5)_3N$ and 96 g (2 mol) of CH_3SH and 43.3 g (0.1 mol) of 2,4,6-tris(trichloromethyl)-*s*-triazine, the reaction was carried out in the same way as in the preparation of II. The major product, 23 g (65% yield), bp 125—128°C/0.01 mmHg, n_D^{23} 1.5572, was 2,4-bis(dichloromethyl)-6-bis(methylthio)methyl-*s*-triazine.

Found: C, 27.35; H, 2.46; N, 12.01; Cl, 39.96; S, 18.34%. Calcd for $C_8H_9N_3Cl_4S_2$: C, 27.21; H, 2.57; N, 11.90; Cl, 40.16; S, 18.16%.

IR absorption (Film): 1548 cm^{-1} (characteristic absorption of *s*-triazine system).

NMR spectrum ($CDCl_3$): τ 7.73 (singlet, 6H, SCH_3); 6.12 (singlet, H, $-CH\langle^{S}_{S}$); 3.35 (singlet, 2H, $CHCl_2$).

The authors are indebted to the Mitsubishi Chemical Industries Ltd. for their generous support of this work. They also wish to thank Mr. Y. Takigawa for kindly assisting in interpreting the spectra. Valuable technical assistance was also provided by Mr. M. Tsuda and Mr. M. Nakazawa.

*2 Materials. Alkyl thiocyanates were prepared from KSCN and the corresponding alkyl halides and aryl thiocyanates from the corresponding anilines.

BULLETIN OF THE CHEMICAL SOCIETY OF JAPAN VOL. 42 2938—2944 (1969)

Reactions of Diazoketones in the Presence of Metal Chelates. II. Reactions with Olefinic Compounds*[1]

Matsuji TAKEBAYASHI, Toshikazu IBATA, Hideki KOHARA and Kozaburo UEDA

Department of Chemistry, College of General Education, Osaka University, Toyonaka, Osaka

(Received March 10, 1969)

The reaction of α-diazoacetophenone with olefinic compounds, such as vinyl acetate, *cis*- and *trans*-stilbenes and cyclohexene, has been studied in the presence of bis(acetylacetonato)copper-(II). The reaction gave the corresponding cyclopropane derivatives, the addition products of benzoylcarbene to the double bond of olefinic compounds in good yields, accompanied by *cis*- and *trans*-dibenzoylethylenes, dibenzoylethane or dilactone. Addition of carbene was found to be stereospecific in the cases of *cis*- and *trans*-stilbenes. A mechanism has been advanced in which a ketocarbene-metal chelate complex is included as an intermediate of the reaction.

In a previous paper[1] we reported that the reaction of α-diazoacetophenone (I) with alcohols in the presence of metal chelates, such as bis(acetylacetonato)copper(II) and bis(acetylacetonato)-nickel(II), gives the corresponding alkoxyacetophenones(II), and that the tertiary amines such as triethylamine, pyridine and quinoline, suppress the formation of the alkoxyacetophenones (II) and promote that of alkyl phenylacetates (IV) in proportion to the increase in the amount of amines added. The mechanism of the reaction has been explained as follows by assuming the intermediacy of a ketocarbene-metal chelate complex (III).

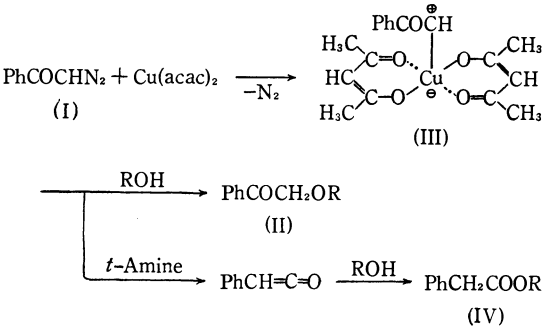

This paper deals with the reaction of the ketocarbene-metal complex with olefinic compounds. Stork and Ficini[2] have studied the copper-catalyzed decomposition of 1-diazo-6-hepten-2-one, and obtained bicyclo[4.1.0]heptanone-2 as an intramolecular cyclo-addition product of olefinic ketocarbene. Thereafter, the intramolecular cycloaddition of olefinic ketocarbenes has been utilized for the formation of strained bicyclo- and tricyclo-compounds.[3,4] On the other hand, studies of the intermolecular addition of ketocarbenes to carbon-carbon double bonds have recently been reported.[5,6]

We studied the reaction of α-diazoacetophenone with olefinic compounds in the presence of bis(acetylacetonato)copper(II) in order to gain further insight on the carbenoid mechanism of copper-chelate-catalyzed decomposition of diazoketones.[1]

Results and Discussion

Reaction of α-Diazoacetophenone with Vinyl Acetate. The bis(acetylacetonato)copper-catalyzed decomposition of α-diazoacetophenone (I) was carried out in a large excess of vinyl acetate under a homogeneous condition. Exothermic reaction took place and an evolution of almost theoretical amount of nitrogen was observed. The reaction product was separated into two fractions by vacuum distillation.

By means of elemental analyses and IR and NMR spectra, the lower boiling fraction was confirmed to be a mixture of *cis*- and *trans*-1-benzoyl-2-acetoxy-cyclopropanes (V) (1 : 6), the addition products of benzoylcarbene to vinyl acetate. The NMR spectra of the components are different from each other as shown in Figs. 1 and 2.

*1 Part of this work was presented at the "Symposium of Organic Reaction Mechanism," Toyama, October, 1965.

1) M. Takebayashi, T. Ibata, H. Kohara and Bu Hong Kim, This Bulletin, **40**, 2392 (1967).

2) G. Stork and J. Ficini, *J. Am. Chem. Soc.*, **83**, 4678 (1961).

3) M. M. Fawzi and C. D. Gutsche, *J. Org. Chem.*, **31**, 1390 (1966), and references cited.

4) S. Masamune, *J. Am. Chem. Soc.*, **86**, 735 (1964).

5) W. Kirmse, "Carbene Chemistry," Academic Press, New York (1964), p. 132.

6) D. O. Cowan, M. Couch, K. R. Kopecky and G. S. Hammond, *J. Org. Chem.*, **29**, 1922 (1964).

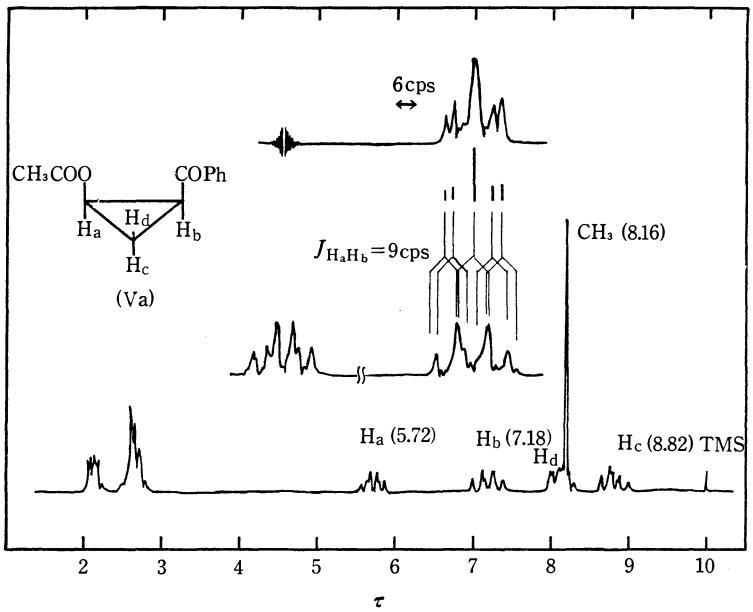

Fig. 1. NMR spectrum of Va.

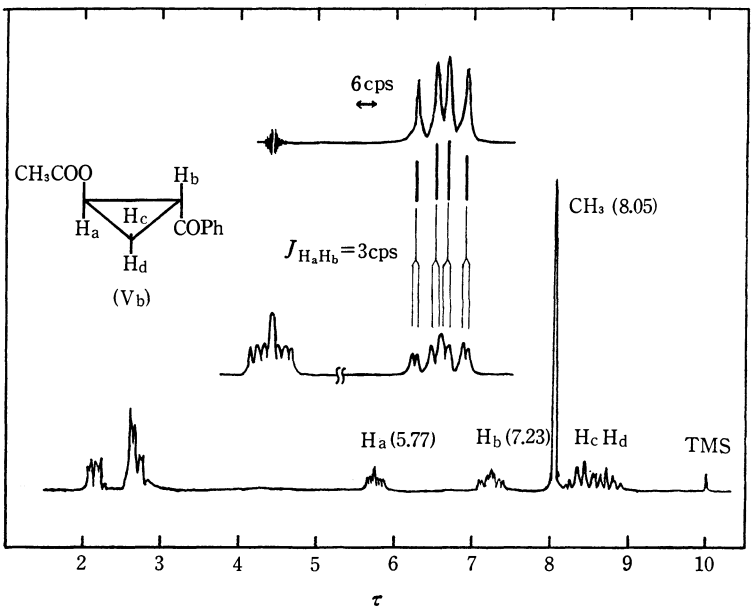

Fig. 2. NMR spectrum of Vb.

One component is identified as *cis*-1-benzoyl-2-acetoxy-cyclopropane (Va) and the other as *trans*-isomer (Vb) by the observation of their NMR spectra. The singlet signal of acetoxy proton of Va appears at higher field (8.16 τ) than that of Vb (8.05 τ), and the J_{HaHb} coupling constant of Va (9 cps) is larger than that of Vb (2.3 cps).*2 The

*2 The coupling constants were measured by the spin-decoupling method. The *cis*-coupling constant of vicinal protons of cyclopropane ring is generally larger than the *trans*-coupling constant. The *trans*-coupling constant (J_{HaHb}) of Vb was observed to be abnormally smaller than usual.[7] The other coupling constants between protons of Va and Vb will be reported elsewhere in detail.

*3 Decomposition of I in a large excess of vinyl acetate in the presence of catalytic amount of nickelocene was carried out and the same results as shown in the case of $Cu(acac)_2$ were observed, affording a mixture of Va and Vb in 44% yield.

yield of this isomeric mixture was 58 per cent of the theoretical amount calculated from I.*3 The vpc analysis of the lower boiling fraction showed a very small peak at the retention time of 9.5 min, which became larger with the addition of authentic acetophenone. Further investigation of the presence of acetophenone in this fraction was not carried out.

The higher boiling fraction was a mixture of *trans*-1,2-dibenzoylethylene (VIb)[8] (5% yield) and a trace of 1,2-dibenzoylethane (VII).[9] The structure of VIb and VII was confirmed by the comparison of the melting points and IR spectra with those of the authentic samples.

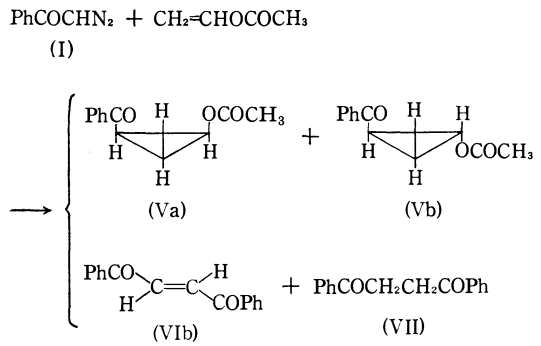

Reaction of α-Diazoacetophenone with Cyclohexene. The reaction of I with cyclohexene in the presence of copper-salts to give 7-benzoylnorcarane (VIII) has been reported by Cowan *et al.*[6] The decomposition of I in a large excess of cyclohexene at 75°C in the presence of $Cu(acac)_2$ gave a small amount (5%) of VII in addition to the main product VIII (51%). Product VIII was also found to be a mixture of *syn*- and *anti*-isomers by elemental analyses, melting point test and IR absorption spectra of their 2,4-dinitrophenylhydrazones, although Cowan *et al.* had reported only one hydrazone of VIII.[6]

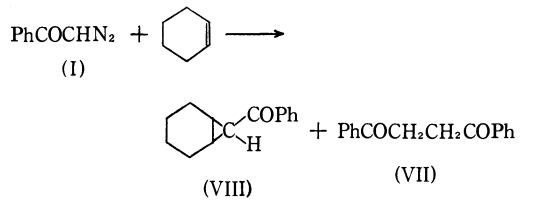

Reaction of α-Diazoacetophenone with Stilbene and Diphenylacetylene. In the cases of the reactions of I with *cis*- and *trans*-stilbenes and diphenylacetylene, the "dropwise addition method" was applied in order to avoid the formation of dimers of benzoylcarbene. In the case of *cis*-stilbene, the cyclopropane derivative (IXa) was obtained in 19% yield, accompanied with dilactone (X)[10] and VII in 3.2 and 2.4% yield, respectively. The structure of X was assigned by the comparison of IR spectrum with that of the authentic sample obtained by the photolysis of I in a benzene solution.[11]

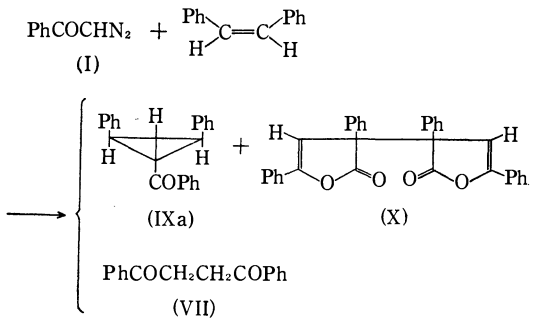

The structural assignment of IXa was established by the IR and NMR spectra. The NMR spectrum of IXa has quasi-doublet signal of Ha at 6.74 τ and quasi-triplet signal of Hb at 6.48 τ in 2 : 1 area ratio as shown in Fig. 3.

This NMR pattern of cyclopropane ring protons agreed with that of calculated AB_2 type having coupling constant of 2.0 cps and chemical shift difference of 6.0 cps.[12] The coupling constant of cyclopropane ring protons Ha and Hb of IXa, J_{HaHb}=5 cps, has a normal value compared with those of usual *trans*-protons in cyclopropane derivatives.[9]

The reaction of I with *trans*-stilbene gave an adduct (IXb), in 5 per cent yield besides the recovered *trans*-stilbene and X (1.5%).

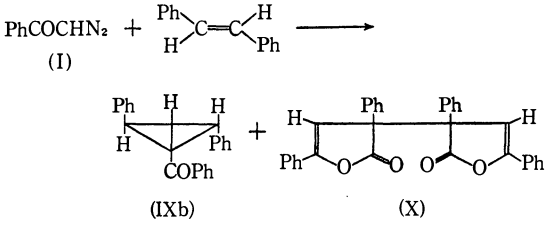

The structure of IXb was established by means of

7) F. A. Bovey, "NMR Data Tables for Organic Compounds," Vol. 1, Interscience, New York (1967), p. 3822.

8) C. Grundmann and H. Trischmann, *Ann.*, **536**, 29 (1938).

9) Ad. Claus, *Ber.*, **20**, 1375 (1887).

10) P. Yates and J. J. Clark, *Tetrahedron Letters*, **1961**, 435.

11) M. Takebayashi, T. Ibata, H. Kohara and M. Hamaguchi, *Sci. Rept., Coll. Gen. Ed. Osaka Univ.*, **17**, 7 (1968).

12) K. B. Wiberg and B. J. Nist, "Interpretation of NMR Spectra," W. A. Benjamin, Inc., New York (1962), p. 15.

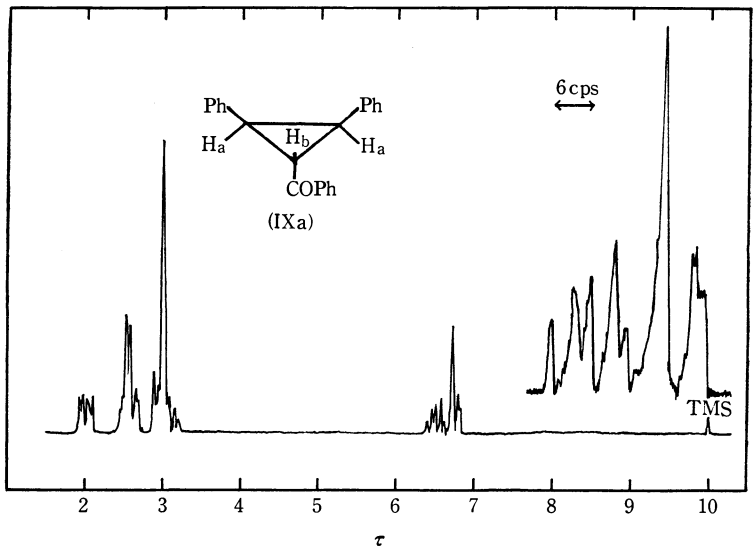

Fig. 3. NMR spectrum of IXa.

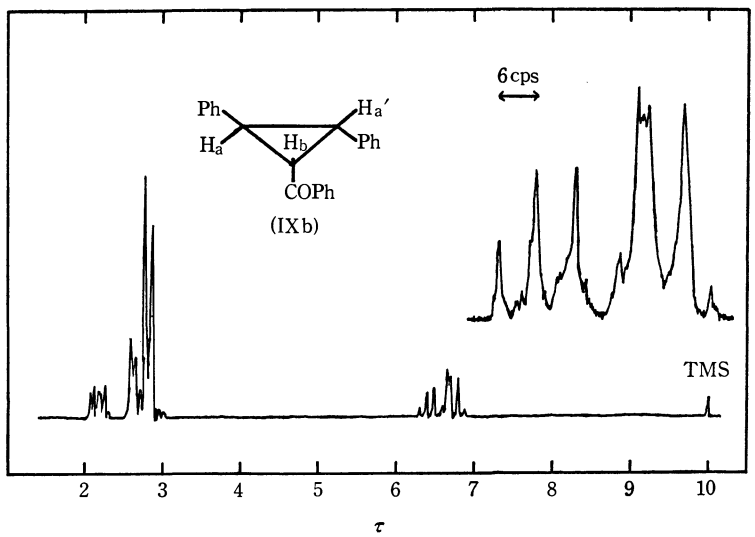

Fig. 4. NMR spectrum of IXb.

elemental analysis and IR and NMR spectra (Fig. 4).

The sharp melting points of IXa and IXb and their thin-layer chromatograms suggest that they are not contaminated with each other and are chemically pure. The NMR spectrum of IXa has a singlet signal at 3.00 τ corresponding to ten protons of two phenyl groups bonding directly to cyclopropane ring. On the other hand, the NMR spectrum of IXb has two singlet signals at 2.78 and 2.87 τ attributed to two phenyl groups which are in a different magnetic state, and quasitriplet of one proton at 6.42 τ and also quasi-doublet of two protons at 6.74 τ of ABB′ type. The *ortho*-proton signal of benzoyl group of IXb appears at higher field than that of IXa.

These results indicate that the addition of this carbene complex (III) to stilbene proceeds stereospecifically.

While the reaction of I with diphenylacetylene in a benzene solution gave no adduct of carbene to carbon-carbon triple bond, small amounts of VII and X (4.5%) were obtained.

Decomposition of α-Diazoacetophenone in Inert Solvents. When the catalytic decomposition of I was carried out by the "mixed method" in a benzene solution at 48°C, the adduct of carbene to benzene, *viz.*, a norcaradiene derivative, was not detected. However, *cis*- and *trans*-1,2-dibenzoylethylenes (VIa and VIb), the formal dimers of

benzoyl-carbene, were obtained in the yields of 11.3 and 13.6 per cent, respectively.

In a chloroform solution, I also gave VIa and VIb in the yields 13.0 and 0.06 per cent, respectively, contrary to the result of Grundmann and Trischmann[8] who obtained neither of these products.

In methyl benzoate, 57.0 per cent yield of VIa and 2.9 per cent yield of VIb were obtained by the "mixed method," while only a polymer of benzoylcarbene was produced by the "dropwise addition method."[13]

Mechanism. From the results mentioned above, the catalytic reaction of α-diazoacetophenone with olefinic compound is also reasonably explained by assuming the copper-carbenoid intermediate (III) as well as the metal-chelate-catalyzed decomposition of I in alcohols.[1] Since no addition products to diphenylacetylene[14] and to benzene were obtained, the reactivity of this carbenoid intermediate seems to be not so large.

The *cis*- and *trans*-1,2-dibenzoylethylenes (VI) may be formed by the reaction of I with carbenoid (III) in the case of "mixed method" where no substrate having enough reactivity to the carbenoid is present except I in the reaction system. Grundmann and Trischmann[8] have reported that the copper-powder-catalyzed decomposition of I in various solvents gives *trans*-1,2-dibenzoylethylene (VIa). However, the isolation of *cis*-isomer has not been accomplished yet by the catalytic decomposition of α-diazoketones. The ratio of *cis*- and *trans*-isomers largely depends upon the nature of the solvents.

On the other hand, dilactone (X) was observed in the reaction of I with *cis*- and *trans*-stilbenes and diphenylacetylene, which have no large reactivity toward III. In these cases, the concentration of substrate reacting with III is so small that a part of carbenoid (III) releases benzoylcarbene, which leads to phenylketene (XI) by concerted phenyl migration. The phenylketene reacts with I and finally affords dilactone as reported in the case of photolysis of I.[11] The release of benzoylcarbene from carbenoid (III) seems to be rather slow, since the yield of X is small (1.5—4%). This may be supported by the fact that the formation of esters, produced from phenylketene, is accelerated in alcohols by the addition of tertiary amines.[1] The formation of 1,2-dibenzoylethane (VII) is explained by the dimerization of relatively stable phenacyl radical, which is formed by the hydrogen abstraction of the carbenoid from the solvents or substrates.

The mechanism of the formation of products obtained is summarized as follows:

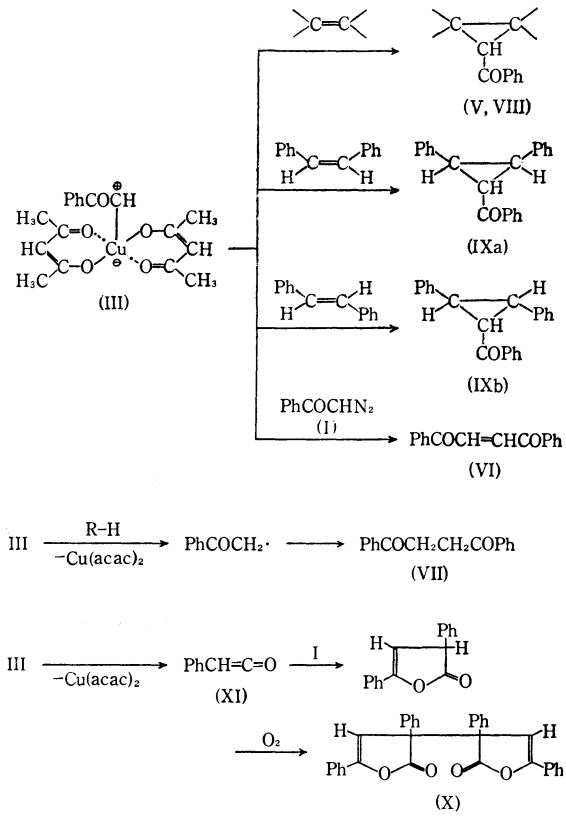

Experimental

All melting and boiling points described in this paper were not corrected. The IR spectra were determined in potassium bromide disks for crystals or in liquid film for liquid samples, respectively, on a Hitachi Infrared Spectrophotometer, model EPI-S2. The NMR spectra were recorded at 60 Mc with a Hitachi High Resolution NMR Spectrometer, model R-20, using tetramethylsilane as an internal standard.

Materials. *α-Diazoacetophenone* was prepared from benzoyl chloride and diazomethane according to the method of Newman and Beal,[15] and recrystallized several times from *n*-hexane, mp 47.5—48.0°C.

Bis(acetylacetonato)copper(II) was prepared according to published directions.[16]

cis-Stilbene was prepared by the decarboxylation[17] of α-phenylcinnamic acid in the presence of copper chromite in a quinoline solution, and purified by distillation, bp 108—110°C/5 mmHg.

trans-Stilbene was obtained by the reduction of benzoin[18] by zinc amalgam and hydrochloric acid, and was recrystallized from 95% ethanol, mp 123.5—124.0°C.

Diphenylacetylene was prepared by the oxidation of

13) M. Takebayashi, T. Ibata and K. Ueda, unpublished data.

14) N. Obata and I. Moritani, This Bulletin, **39**, 1975 (1966).

15) M. S. Newman and P. F. Beal, *J. Am. Chem. Soc.*, **71**, 1506 (1949).

16) H. S. Booth, "Inorganic Syntheses," Vol. 2, McGraw-Hill, New York (1949), p. 14.

17) "Organic Syntheses," Coll. Vol. 4, p. 857 (1963).

18) *Ibid*, Coll. Vol. 3, p. 786 (1955).

benzil dihydrazone using yellow mercuric oxide,[19] mp 60—61°C.

Cyclohexene was obtained by dehydration of cyclohexanol in the presence of catalytic amount of sulfuric acid,[20] and dried over calcium chloride and purified by distillation before use.

Vinyl Acetate, Benzene and Chloroform. Commercial products were purified by distillation before use.

vinyl acetate	bp 71.5—72.0°C
benzene	bp 79.5—80.0°C
chloroform	bp 61.0—61.2°C

Reaction of α-Diazoacetophenone (I) with Vinyl Acetate in the Presence of Cu(acac)$_2$. A solution of 5.0 g (0.034 mol) of I and 0.1 g (3.8×10^{-4} mol) of Cu(acac)$_2$ in 150 m*l* of vinyl acetate was warmed gradually under an atmosphere of nitrogen. The evolution of nitrogen was observed at 48°C, and then the temperature rose to 55—56°C by exothermic reaction. Within 20 min an almost theoretical amount of nitrogen was evolved and the color of the mixture turned to dark-green with the evolution of nitrogen. After leaving the reaction mixture to stand for two hours more at 50°C, unreacted vinyl acetate was removed by distillation under ordinary pressure. The residue was fractionally distilled under reduced pressure and two fractions were obtained; bp 115—125°C/1 mmHg, and bp 160—172°C/1 mmHg.

The lower boiling fraction was further purified by distillation, bp 114—116°C/1 mmHg.

Found: C, 70.63; H, 6.09%. Calcd for $C_{12}H_{12}O_3$: C, 70.57; H, 5.92%.

IR (neat); 3050, 1750(ester), 1665(benzoyl), 1450 and 1230 cm^{-1}.

The gas chromatogram*4 of this fraction showed two main peaks of retention time 17.5 and 22.5 min in the area ratio of about 1 : 6. The former indicates *cis*-isomer (Va) and the latter *trans*-isomer (Vb).

The higher boiling fraction crystallized on standing at room temperature. The fractional recrystallization from light petroleum gave two substance. One was 0.24 g (5%) of yellow crystals and the other was a trace of colorless crystals. The yellow compound of melting point 107—109°C was identified as *trans*-1,2-dibenzoylethylene (VIb) in good agreement with the IR spectrum and the melting point (mp 110°C) with the authentic sample[8] prepared by the copper-bronze catalyzed decomposition of I.[11] The colorless crystalline compound, mp 147—148°C (from ethanol), was identified as 1,2-dibenzoylethane (VII) in agreement with elemental analysis data with $C_{16}H_{14}O_2$, and IR (KBr disk); 3025, 2900, 1675, 1590, 1220, 990, 775, 740 and 695 cm^{-1}.

Reaction of I with Cyclohexene in the Presence of Cu(acac)$_2$. A solution of 5.0 g (0.34 mol) of I in 150 m*l* of cyclohexene was decomposed at 75°C until nitrogen evolution was complete in the presence of 0.1 g (3.8×10^{-4} mol) of Cu(acac)$_2$ by the method described above. The reaction mixture was distilled under reduced pressure after removal of cyclohexene, and 3.5 g of distillates was obtained, bp 124—140°C/1 mmHg. The elemental analysis data of this compound agreed with the calculated one for 7-benzoylnorcarane, $C_{14}H_{16}O$, after further distillation. IR (neat); 3050, 3020, 1450, 760, 700 cm^{-1} (phenyl), 2940 2860, 1420 cm^{-1} (aliphatic C-H) and 1675 cm^{-1} (C=O). NMR (in CCl_4); 2.05—2.17 τ, (m), 2H, *o*-H in phenyl group: 2.5—2.75 τ, (m), 3H, *m*- and *p*-H in phenyl group: 7.55—7.70 τ, (m), 1H, methyne-H adjacent to benzoyl group: 7.9—8.4 τ, (broad d), 6H: 8.55—8.80 τ, (broad s), 4H.

The IR and NMR spectra showed no olefinic absorption bands. From these results this compound was identified as VIII. The 2,4-dinitrophenylhydrazone of VIII was derived from 1.0 g of VIII and 1.1 g of 2,4-dinitrophenylhydrazine in the presence of sulfuric acid in aqueous alcoholic solution. The hydrazone obtained was fractionally recrystallized from ethyl acetate and two hydrazones were obtained; one was cubic orange crystals, mp 210—211°C. Found: C, 63.25; H, 5.21; N, 14.87%. Calcd for $C_{20}H_{20}N_4O_4$: C, 63.15; H, 5.30; N, 14.73%. The other was orange needles, mp 188.5—189.0°C (easily soluble in ethyl acetate). Found: C, 63.34; H, 5.16; N, 14.40%.

The distillation residue was further distilled at higher temperature, and 0.20 g (5%) of 1,2-dibenzoylethane was obtained mp 147.0—148.0°C (from ethanol).

Reaction of I with *cis*-Stilbene in the Presence of Cu(acac)$_2$ (by Dropwise Addition Method). The 50 m*l* of benzene solution of 5.0 g (0.034 mol) of I was added drop by drop to the 100 m*l* of benzene solution of 6.2 g (0.036 mol) of *cis*-stilbene and 0.1 g (3.8×10^{-4} mol) of Cu(acac)$_2$ at 80°C under stirring. After the evolution of nitrogen was observed and the reaction was complete, the reaction mixture was allowed to stand for one hour at 80°C and then overnight at room temperature. The white substance precipitated was separated by filtration, and washed several times by a small amount of benzene. This precipitate did not dissolve in the usual organic solvents at room temperature. It melted at 250—255°C (lit[6] 290—292°C) but its IR spectrum was completely superimposable with that of dilactone (X) prepared by the photolysis of I in a benzene solution.[11] The yield of X was 0.12 g (3.2%). Benzene was removed by distillation from the filtrate and the residue was distilled under reduced pressure. Unreacted *cis*-stilbene was removed by distillation at 108°C/1 mmHg, 5.0 g (80%). The fraction boiling at 150—170°C/1 mmHg crystallized at room temperature, and was left to recrystallize four times from ethanol and twice from light petroleum, mp 93.0—94.5°C.

Found: C, 88.80; H, 6.15%. Calcd for $C_{22}H_{18}O$: C, 88.56; H, 6.08%. IR (KBr disk); 3050, 1655, 750 and 700 cm^{-1}.

From the distillation residue, 0.10 g (2.4%) of VII was isolated by the distillation at higher temperature and recrystallized from ethanol, mp 147—148°C (lit[8] 140°C).

Reaction of I with *trans*-Stilbene (by Dropwise Addition Method). The reaction of 3.3 g (0.023 mol) of I and 4.0 g (0.022 mol) of *trans*-stilbene was carried out by the "dropwise addition method" at the reflux temperature of benzene in the presence of 0.1 g of Cu(acac)$_2$. 0.06 g (1.5%) of X was obtained as an insoluble precipitate. A part of the residue crystallized

19) *Ibid.*, Coll. Vol. 4, p. 377 (1963).
20) *Ibid.*, Coll. Vol. 2, p. 14 (1950).

*4 Gas chromatographic measurement was carried out with a Yanagimoto Gas Chromatograph, model GCG-3DH, using a 3 m column packed with Apiezon Grease M. Temp. : 195°C; carrier gas: H_2, 80 cc/min.

by the removal of benzene under reduced pressure. The crystals, 2.6 g (65%), were identified as the recovered *trans*-stilbene by comparison of IR spectrum with that of the authentic sample, and by the mixed melting point test, mp 127—128°C. The liquid part crystallized on standing in the refrigerator for several days, and was purified by repeated recrystallization from *n*-hexane, mp 155.5—156.5°C.

Found: C, 88.84; H, 5.95%. Calcd for $C_{22}H_{18}O$: C, 88.56; H, 6.08%.

Reaction of I with Diphenylacetylene. The reaction of I (5.0 g, 0.034 mol) and diphenylacetylene (6.1 g, 0.034 mol) was carried out by the "dropwise addition method" in benzene at 80°C in the presence of $Cu(acac)_2$ (0.1 g). By a similar treatment of the reaction mixture, 0.2 g (4.5%) of X and a trace of VII (mp 143—145°C) were obtained besides the recovered diphenylacetylene. No other detectable compound was isolated.

Reaction of I in Inert Solvents. The $Cu(acac)_2$ catalyzed decomposition of I (5.0 g, 0.034 mol) was performed in benzene or chloroform by "mixed method" at 48—80°C. Solvent was removed *in vacuo* from the reaction mixture, and residue was fractionally recrystallized into two compounds from *n*-hexane. One was identified as *trans*-1,2-dibenzoylethylene. The other was identified as *cis*-1,2-dibenzoylethylene by elemental analyses and IR and NMR spectra, white needles from *n*-hexane, mp 135.5—136.5°C (Found: C, 81.43; H, 5.37%).

NMR (in $CDCl_3$); 2.89 τ, (s), 2H, olefinic-H: 2.4—2.7 τ, (m), 6H, *m*- and *p*-H in phenyl: 1.95—2.25 τ, (m), 4H, *o*-H in phenyl.

The authors express their cordial thanks to Dr. Takashi Ando and Mr. Yoshio Takai of Osaka University for their suggestion on the assignment of NMR spectra, and also to the Ministry of Education for a grant-in-aid for Scientific Research.

BULLETIN OF THE CHEMICAL SOCIETY OF JAPAN VOL. 42 2944—2947 (1969)

Conformation and S=O Stretching Absorptions of Simple Sulfoxides

Michinori Ōki, Isao Oka and Katsushiro Sakaguchi

Department of Chemistry, Faculty of Science, The University of Tokyo, Hongo, Bunkyo-ku, Tokyo

(Received March 12, 1969)

The infrared S=O stretching absorptions of several simple sulfoxides have been measured. Some sulfoxides show one absorption maximum, whereas others show two. These results may be attributed to the rotational isomerism about the S–C axis. Convincing evidence for this conclusion has been obtained by the measurement of the spectra of methyl isopropyl sulfoxide at various temperatures.

The conformation of thian oxide has been discussed on the basis of various pieces of evidence. An X-ray diffraction study of *trans*-1,4-dithian 1,4-dioxide has led to the conclusion that the S=O axial conformation is present in the crystals.[1] The nuclear magnetic resonance spectrum of the same compound also supports the idea that the stable conformation is the S=O axial form.[2] On the other hand, it has been claimed from the thermal equilibration of thian 1-oxide that the stable form of the compound is the S=O axial chair (2).[3] Since the axially-substituted isomer of cyclohexane is well known to be less stable than the equatorial, there must be some force operating to stabilize the axial form of the thian oxide or to destabilize the equatorial form.[1] Their stereochemical interest in the thian oxide derivatives has led the present authors to examine the infrared spectra of several simple sulfoxides.

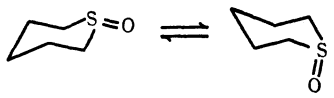

(1) (2)

During the course of this study, Cairns *et al.* reported that the multiplicity of the S=O stretching absorption of sulfoxides could be explained by the Fermi resonance.[4] The data accumulated in this laboratory agree with those obtained by Cairns and his co-workers in the sense that sulfoxides sometimes give multiple absorption bands in the region of 1100—1000 cm^{-1}, but not on the origin of this phenomenon. The purpose of this communication is to present the basis upon which the authors would like to ascribe the phenomenon to

1) H. M. M. Shearer, *J. Chem. Soc.*, **1959**, 1394.
2) C.-Y. Chen and R. J. W. LeFevre, *Austr. J. Chem.*, **16**, 917 (1963).
3) C. R. Johnson and D. McCants, Jr., *J. Am. Chem. Soc.*, **86**, 2935 (1964); *ibid.*, **87**, 1109 (1965).
4) T. Cairns, G. Eglinton and D. T. Gibson, *Spectrochim. Acta*, **20**, 31 (1964).

the presence of the rotamers about the C–S bonds.

Experimental

The infrared spectra were measured on a Perkin-Elmer 112 G grating spectrophotometer (slit width: 1.6 cm^{-1}) and a Japan Optics Co., Ltd., 402 G spectrometer. In every case the agreement of the data of the two instruments was good. The samples were dissolved in carbon disulfide or carbon tetrachloride to make up *ca.* 0.05 mol/*l* solution unless otherwise mentioned. The temperature dependence of the spectra was determined using liquid cells consisting of a Hg-Sn amalgam spacer and KBr discs at 0.03 mol/*l* concentration in carbon disulfide.

The spectra were scanned in the region of 1100—1000 cm^{-1} and were compared with those of the parent sulfide in order to eliminate absorptions due to skeletal vibrations. This technique, together with the operation to form an intermolecular hydrogen bond, removed the difficulty in assigning the S=O stretching absorption band.

Materials were prepared and purified according to the literature, and the physical constants were measured in order to check the purity. Special care was taken to avoid moisture during the handling of the lower homologs.

Results and Discussion

Some of the sulfoxides show single absorption bands and others, doublet absorption bands. In order to clarify the origin of these bands, two techniques were used. One was the comparison of the spectra measured in carbon tetrachloride or carbon disulfide with those obtained in chloroform. The other was the comparison of the spectra of the sulfoxide obtained in carbon tetrachloride with those obtained by adding phenol to carbon tetrachloride. In every case, the bands observed in a carbon tetrachloride solution diminish in intensity when measured in chloroform or when phenol is added, and new bands are observed at *ca.* 1020 cm^{-1} and at a frequency lower than the original by *ca.* 20 cm^{-1}. Although it was not possible to erase completely the bands at 1070—1040 cm^{-1} by these techniques, the results mentioned above are good evidence that there is an equilibrium, such as is shown by Eq. (1), because the reduced intensity corresponds to the decreased population of the free sulfoxide and the new band

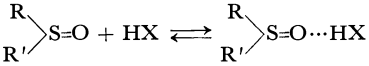

(1)

at a lower frequency is an indication of the formation of the hydrogen bond. Thus, one or two bands of sulfoxide in the 1070—1040 cm^{-1} region can be assigned to S=O stretching vibrations. These facts, together with the findings that some symmetrical sulfoxides have only one absorption, whereas the unsymmetrical sulfoxides usually have two, are not in agreement with the postulation by Cairns *et al.*[4]

Other possible causes for the appearance of multiple absorptions for the S=O stretching vibration are: 1) solute-solvent interactions, 2) solute-solute interactions, 3) the coupling of vibrations, and 4) equilibrium among rotational isomers. The possibility of 1) can be disregarded because multiple absorption is observed even in carbon tetrachloride and carbon disulfide solutions, in which no significant solute-solvent interactions are to be expected. There is a possibility that monomer-dimer equilibrium (Eq. (2)) is a cause of the doublet nature of the bands, but the dependency of the absorption upon the concentration of the solute (to be discussed below), together with the fact that this possibility cannot be the reason why some sulfoxides give one band while others give two, are good indications that it is not really the case.

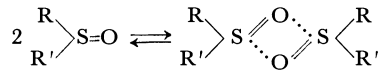

(2)

The S=O stretching absorptions of dimethyl sulfoxide and methyl isopropyl sulfoxide in carbon disulfide were measured in solutions from 3 to 0.0003 mol/*l*. The results indicate that when the concentration is higher than *ca.* 0.5 mol/*l* the shape of the spectra changes, but it does not in solutions of less than 0.1 mol/*l* concentration. Thus, Beer's law is applicable to the absorption when the concentration is less than 0.1 mol/*l*.*1

With the above discussions in mind, it seems attractive to consider that the origin of the multiplicity of the S=O stretching bands is the rotational isomerism. Two C–S bonds must be considered when one discusses the isomerism of sulfoxides. Projection through one of the C–S axes may be given as I—III.*2 I is the conformation in which S=O oxygen staggers between two hydrogens.

*1 The authors prefer, in this connection, to say that the association of sulfoxide occurs according to Eq. (2) when the concentration is higher than 0.5 mol/*l*. This opinion conflicts with the report[5] by Mislow *et al.* that a sulfoxide forms a dimer in the concentration range of 0.02—0.06 mol/*l*, but it is almost unbelievable that the dimer survives even at the concentration of 0.0003 mol/*l*, where no change of spectra was observed. The matter is still to be explored. However, the following discussions are not affected whether the sulfoxide is a monomer or a dimer unless significant populations of monomers and dimers are present due to equilibration.

5) K. Mislow, M. G. Green, P. Laur and D. R. Chisholm, *J. Am. Chem. Soc.*, **87**, 665 (1965); see also R. F. Watson and J. F. Eastham, *ibid.*, **87**, 664 (1965).

*2 The present authors adopt this classification mainly because of the success of similar classification in alcohols; primary, secondary, and tertiary alcohols were shown to possess O–H stretching absorptions according to their classes.[6]

6) M. Ōki and H. Iwamura, This Bulletin **32**, 950 (1959).

Table 1. Absorption of dialkyl sulfoxides due to S=O stretching (*ca.* 0.1 mol/*l* solution in carbon tetrachloride) (RSOR')

R	R'	Conformations	ν_{max} (cm^{-1})	ε[a]
CH_3	CH_3	I+I	1069	385
CH_3	C_2H_5	I+I, I+II	1065	186
CH_3	$(CH_3)_2CH$	I+II, I+III	1065 1054	268 245
CH_3	$(CH_3)_3C$	I+III	1058	356
C_2H_5	C_2H_5	I+I, I+II, II+II	1065 1058	250 (210)
C_2H_5	$(CH_3)_2CH$	I+II, I+III, II+II, I+III	1065 1056	178 245
C_2H_5	$(CH_3)_3C$	I+III, II+III	1056 1045	315 244
$(CH_3)_2CH$	$(CH_3)_2CH$	II+II, II+III, III+III	1058	312
$(CH_3)_2CH$	$(CH_3)_3C$	II+III, III+III	1050 1040	300 (160)
$(CH_3)_3C$	$(CH_3)_3C$	III+III	1040	412

[a] The numbers in parentheses involve considerable uncertainty because these bands are observed as shoulders.

Similarly, S=O oxygen staggers between methyl and hydrogen and between two methyls in the II and III conformations respectively.

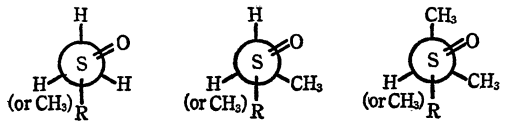

(I) (II) (III)

Looking at the results listed in Table 1, it is rather striking that the data fit in well with the idea of rotational isomerism. Thus, dimethyl sulfoxide can assume only one conformation (a combination of I and I; *i.e.*, Newman projections written through two C–S axes can be presented by I) whatever potential minima are taken, as long as the ethane-like potentials are postulated; indeed, it has only one absorption. Likewise, di-*t*-butyl sulfoxide (a combination of III and III) and methyl *t*-butyl sulfoxide (a combination of I and III) can take only one stable conformation and give only one absorption band. Column 3 of Table 1 lists all the possible conformations of sulfoxides. It is noticeable that some are able to take more conformations than the number of absorption bands, but no compound has more absorption bands than the number of conformations possible for the sulfoxides. The exact reason for the apparent lack of conformity between the number of conformations and that of absorptions is not known, but, it may be attributed to the scarce population of certain rotamers due to steric and/or thermodynamical reasons or to the poor resolution of the instrument.

It is tempting, from the data, to postulate that a conformation gives rise to a characteristic absorption in a certain range; the classification may be summarized as is shown in Table 2. The reason

Table 2. Correlation between the conformations of sulfoxide and S=O stretching absorptions

Conformation (combination of)	$\nu_{S=O}$ (cm^{-1})
I and I	1069
I and II	1065
I and III II and II	1058—1054
II and III	1051—1045
III and III	1040

for the effect of alkyl branching (the shift to a lower frequency) is not quite understood at present, but it may be either the inductive effect of the alkyl group and/or a possible interaction between C–H and S=O groups, as will be discussed later.

Simpler examples are alkyl aryl sulfoxides, whose S=O stretching absorption data and their conformations are given in Table 3. In these cases the rotation about the C_{Ar}–S bond can be neglected, because a single conformation is so favored that its contribution is overwhelming as long as the phenyl ring is substituted symmetrically.*3

It will be noted that *p*-tolyl methyl sulfoxide gives only one band because only one conformation is possible. The same reason can be given for the

*3 In this respect, it is interesting to note that *o*-tolyl methyl sulfoxide gives three bands in the S=O stretching region, 1073, 1060 and 1040 cm^{-1}, all of which are diminished in intensity when dissolved in chloroform; after a dissolution, also, a new band is observed at 1032 cm^{-1}.

TABLE 3. S=O STRETCHING ABSORPTION DATA OF ALKYL ARYL SULFOXIDES IN CARBON DISULFIDE (ArSOR)

Ar	R	Conformations*			$\nu_{S=O}$ (cm^{-1})
p-$CH_3C_6H_4$	CH_3	IV			1062
C_6H_5	C_2H_5	IV	V		1056, 1048
C_6H_5	$(CH_3)_2CH$		V	VI	1052, 1047
C_6H_5	$(CH_3)_3C$			VI	1048

* Conformations may be represented as follows.

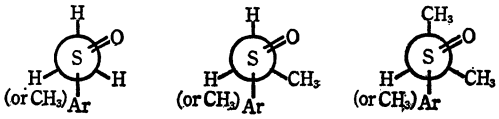

(IV) (V) (VI)

presence of one band in phenyl t-butyl sulfoxide. Phenyl isopropyl sulfoxide and phenyl ethyl sulfoxide can have two stable conformations and possess two S=O stretching absorptions. Thus, it may be said that the IV conformation gives rise to a band at 1065—1055 cm^{-1}. Similarly, the V and VI conformations give bands at 1055—1050 and 1048 cm^{-1} respectively.

The possibility of a coupling of vibrations can not be ruled out completely because the lower frequency region has not been extensively studied, but the possibility of rotational isomerism is so great, as has been discussed above, that the coupling is less likely.

The most convincing evidence for the idea that the multiplicity of the S=O stretching absorptions is attributable to the rotational isomerism is obtained by measuring the spectra at various temperatures. Methyl isopropyl sulfoxide was selected as an example to study the temperature dependence of the spectra because this compound shows a distinctly two-peaked band and possesses only two possible classes of rotational isomers. The results are shown in Fig. 1.

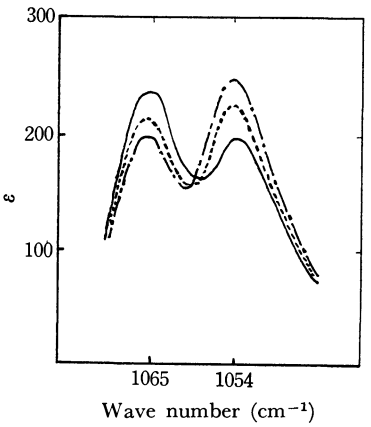

Fig. 1. Temperature dependence of S=O stretching absorptions of methyl isopropyl sulfoxide: room temperature (——), −10——20°C (·····), and −50——80°C (—·—).

It is apparent that the intensity at the lower frequency increases at the expense of the other band when the temperature is lowered, the results lending firm support to the idea of rotational isomerism.

It is not thermodynamically possible for a stable isomer to be less populated at any temperature. Therefore, if it is assumed that the absorption intensity per molecule is the same for any kind of rotamer, the observed change in intensity seems to contradict the thermodynamical considerations. The apparent contradiction can, however, be overcome when the statistical factor is considered; namely, there are two conformations (VII and VIII) which give rise to the absorption at a higher frequency, whereas there is only one conformation which corresponds to the absorption at a lower frequency (IX).*4

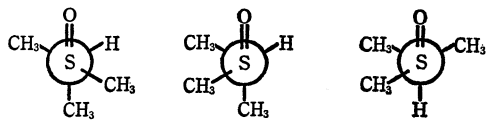

(VII) (VIII) (IX)

These considerations inevitably lead to the conclusion that the IX conformation is more stable than VII and VIII. No convincing evidence accounting for the stability of IX has yet been obtained, but two items are worthy of note. The first is the assumption that the steric bulkiness of the oxygen atom in sulfoxide is less than that of the lone-pair electrons, and the second is the possibility of the existence of a hydrogen bond between the methyl group and the oxygen atom of sulfoxide. The first possibility arises in connection with the fact that the S=O axial form is more stable than the equatorial in thian 1-oxide, but the same reasoning may also be used in favor of the second possibility. Work is now in progress attempting to distinguish these possibilities.

*4 The mirror images of rotamers, VII, VIII, and IX, are neglected in these discussions, because each enantiomer should exist in an equal quantity.

BULLETIN OF THE CHEMICAL SOCIETY OF JAPAN VOL. 42 2948—2951 (1969)

A Partial Asymmetric Synthesis *via* a Cyclic Oxyphosphorane[1)]

Motoo Muroi, Yuzo Inouye[2)] and Minoru Ohno

Institute for Chemical Research, Kyoto University, Uji, Kyoto

(Received March 14, 1969)

A partial asymmetric synthesis was achieved in the carbon-carbon condensation which involved the reaction of (−)-menthyl pyruvate with trimethyl phosphite, followed by alkaline hydrolysis of the intermediate cyclic oxyphosphorane to yield (−)-(S:S)-2,3-dimethyltartaric acid. With knowledge of absolute configurations of both the chiral center and the predominant enantiomer of the product, an *ex post facto* interpretation of the steric course was made on the basis of relative steric stability of transition state conformations of the addition step of III to I.

It has been known that a dicarbonyl compound reacts with trialkyl phosphite to give a cyclic oxyphosphorane (1 : 1 adduct), which can further react with another molecule of the same or of other dicarbonyl compound to yield diastereomeric forms of saturated oxyphosphorane (2:1 adduct).[3)]

In the case of methyl pyruvate and trimethyl phosphite,[3c)] the intermediate 1 : 1 adduct was not an isolable 2,2,2-trimethoxy-1,3,2-dioxaphospholene (II) containing new P–O bonds but exclusively an open dipolar species (III) presumably in a rapid equilibrium with a 1 : 1 adduct having a P–C bond (IV), and the quite reactive dipolar intermediate underwent nucleophilic addition to a second molecule of pyruvate with formation of a mixture of stable diastereomeric 1,3,2-dioxaphospholanes (V). Upon alkaline hydrolysis, the resulting cyclic oxyphosphoranes yielded a mixture of *meso* and racemic 2,3-dimethyltartaric acids (VI).

The new carbon-carbon condensation of this type seems to be interesting from the viewpoint of asymmetric synthesis. Should asymmetric synthesis be obtained by this process, two asymmetric carbon atoms would be simultaneously created in the *threo*-form, and furthermore, this might provide the means of preparing optically active hydroxy-acids of biochemical interest and of assigning absolute configurations thereof. Since pyruvic acid has both a suitably activated prochiral carbonyl function (reaction center) and an adequate "handle" (carboxyl group) through which a chiral reagent (asymmetric center) may be properly accommodated, the present system fulfils the requirements for practice of asymmetric synthesis.

As expected, the asymmetric reaction of (−)-menthyl pyruvate with trimethyl phosphite followed by alkaline hydrolysis of the resulting diastereomeric oxyphosphorane mixture gave 2,3-dimethyltartaric acid of a levorotation. The present asymmetric system produced exclusively the *racemic* form of 2,3-dimethyltartaric acid, in contrast to the corresponding non-dissymmetric reaction.[3c)] This may be attributed to the bulkiness effect of carbomenthoxy groups in the intermediate oxyphosphoranes.

The geometry of the two possible optically inactive forms of 2,3-dimethyltartaric acid was determined by the unambiguous stereospecific routes of synthesis: dimethylfumaric acid[4)] was oxidized with hydrogen peroxide in the presence of WO_3 to give the corresponding dihydroxy-acid, mp 178—180°C. As generally accepted,[5)] the WO_3-catalyzed hydroxylation proceeds in a *trans*-fashion, so that the *trans*-addition of hydroxyl groups to *trans*-olefin should lead to *meso*-modification. Thus, the *meso*-configuration can be safely assigned to this form. In a similar way, the hydroxylation of dimethyl dimethylfumarate with permanganate in ethanol at −40°C gave another isomer melting at 186—186.5°C. The *racemic* configuration can be deduced to this form, for the permanganate hydroxylation is a well-established *cis*-addition.[5)] This deduction is in agreement with that from optical resolvability criterion[6)] and from the IR-spectral study of calcium and barium salts of the two optically inactive modifications.[7)]

1) Taken in part from the dissertation submitted by M. M. to Kyoto University.

2) To whom inquiries should be addressed.

3) F. Ramirez *et al.*, a) *J. Am. Chem. Soc.*, **82**, 2651 (1960); b) *J. Org. Chem.*, **26**, 3041 (1961); c) *Tetrahedron Letters*, **1963**, 323; d) *J. Org. Chem.*, **31**, 3159 (1966); e) *Bull. Soc. Chim. France*, **1966**, 2443.

4) E. Ott, *Ber.*, **61**, 2124 (1928).

5) F. D. Gunstone, in "Advances in Organic Chemistry," Vol. 1, Interscience Publishers, New York (1960), p. 103.

6) Y. Izumi, S. Tatsumi, M. Imaida, Y. Fukuda and S. Akabori, This Bulletin, **39**, 361 (1966).

7) S. Tatsumi, *ibid.*, **39**, 2202 (1966).

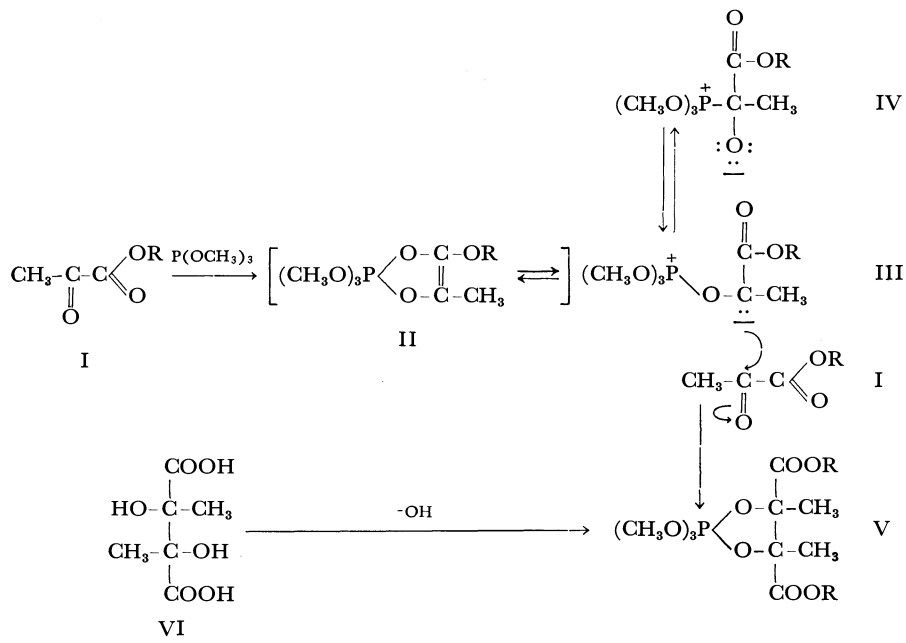

R=CH_3- or (−)-menthyl

Scheme 1

The absolute configuration of the chiral form of this acid has not yet been established, without the knowledge of which the steric course of the present asymmetric reaction can not be successfully elucidated. It is hazardous to compare the optical activities of homologous α-hydroxy-acids such as lactic, malic, tartaric and mandelic acids of the well-defined configurations and to extrapolate the correlation as such to the present acid, since the steric environment of the α-carbon atom is substantially changed by replacement of a hydrogen atom with a methyl group. This replacement changes neither configurational series of the conventional DL-system nor notation of configuration based on the RS-system since the sequence of ligands on the chiral α-carbon is not inverted by this process. However, the order of bulkiness of the ligands does alter as one traverses from hydrogen to methyl, the latter being obviously bulkier than hydroxyl. Thus, the characterization of absolute configuration based on both the RS- and DL-systems does not allow unequivocal correlation with sign of the optical activities. Citramalic acid whose absolute configuration has been determined[8] seems to be adequate for configurational correlation with 2,3-dimethyltartaric acid. The stereochemical environments of the α-carbon atom in both acids are closely similar, since the order of priority (sequence rule) parallels that of bulkiness of ligands. The Cotton effect in 200—230 mμ region due to the optically active carboxyl chromophore was observed with both chiral acids. It was found that (+)-(S)-citramalic acid and (−)-2,3-dimethyltartaric acid exhibited a negative Cotton effect in this region, so that the (S:S)-configuration may be tentatively assigned to (−)-2,3-dimethyltartaric acid. The Brewster atomic asymmetry rule[9] also predicts a levorotation for the (S:S)-configuration of this acid.*1

We can now discuss the steric course of the present asymmetric synthesis, having the necessary information on absolute configuration of both the asymmetric center and the final product. The stereochemical-determining step in the present system is the nucleophilic addition of the open dipolar species (III) to a second molecule of (−)-menthyl pyruvate (I) leading to diastereomeric dioxaphospholanes (V). Since it has been shown that, under those conditions (20°C), the condensation is irreversible and there is no detectable equilibration among diastereomers once they are formed[3d], this step must be kinetically controlled. The conformation of the open dipolar **III** may well be assumed to be coplanar as implicit in the figure, since the lateral overlap of 3d-p-p-p(-p)-p orbitals of $\overset{+}{P}$–O–C–$\overset{-}{C}$(=O)–O concerned may be maximal in this conformation and stabilize the system. The transoidal coplanar topology may reasonably be

8) D. A. Stadler, A. J. Frey and A. Hofmann, *Helv. Chim. Acta*, **46**, 2300 (1963).

9) J. Brewster, *J. Am. Chem. Soc.*, **81**, 5475 (1959).

*1 Other experimental evidence for this assignment will be presented in a future publication.

postulated also for (−)-menthyl pyruvate (I) because this conformation with the minimum dipole-dipole and steric interactions has been invoked by Prelog with some measure of success in his asymmetric reactions involving the nucleophilic addition of Grignard reagent to α-keto esters of chiral alcohols.

A priori, the prime consideration being that all nonbonded repulsive interactions should be minimized in the transition state, the nucleophilic addition of III to I should take place in staggered orientations of substituents of both prochiral carbons and with the carbonyl-oxygen (in I) oriented closer to the phosphorus atom (in II) so as to permit a concerted process in which a new P–O bond concomitantly forms as the new C–C bond does. Under these propositions, four transition state conformations may be possible, if one takes into consideration the diastereotopic faces of both prochiral sp^2-carbanionic carbon in III and carbonyl carbon in I. Of the four, the *re-si* and *si-re* combinations *i.e.* the nucleophilic attack of III with its front side to the rear side of I and the reverse, equally lead to the same and identical transition state conformation, which eventually should afford the *meso*- end product. As can be seen, accumulated *gauche* (*cis*) interactions between substituents, in particular between the two bulkier carbomenthoxy groupings, would make this transition state kinetically unfavorable and this may account for the lack of the *meso*-form in the reaction product. In contrast, the two bulkier carbomenthoxy groups in the *re-re* and *si-si* transition state conformations, which would lead to R:R and S:S enantiomers respectively, are disposed to be *anti* to each other. These transition states are sterically more favored and are thus expected to be energetically more stable than the *meso*-counterpart. Inspection of the scale models reveals that, of these two, the *si-si* transition state conformation is sterically more favored than the *re-re* competitor, since the former is less crowded with respect to the two chiral moieties than the latter. The chemical consequence of this situation is the predominant formation of the (−)-(S : S)-2,3-dimethyltartaric acid in the present asymmetric synthesis. The above-mentioned argument on the steric course combined with its reaction mechanism of the present asymmetric system is in good agreement with what has been found experimentally. This furnishes another example of "double induction"—the discrimination between diastereotopic faces of a chiral compound by another chiral reagent.

Experimental

Asymmetric Synthesis of Dimethyl 2,3-Dimethyltartrate. (−)-Menthyl pyruvate (bp 106—108°C/4 mmHg, n_D^{15} 1.4522, $[\alpha]_D^{25}$ −75.3° (*c* 20.2, methanol);

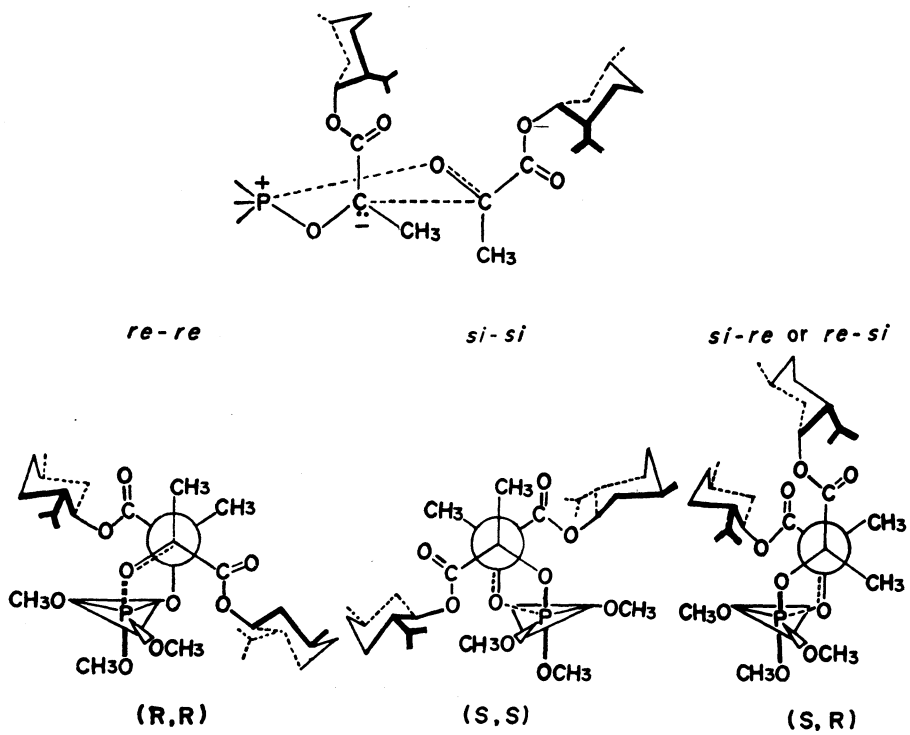

Fig. 1

22.6 g, 0.1 mol) was slowly added to trimethyl phosphite (12.4 g, 0.1 mol) with stirring and external cooling. The mixture was kept at 0°C for 1 hr and at 20°C for 8 hr. The excess of phosphite was removed *in vacuo*, the residue (26.3 g) was poured into water (11 m*l*) and the strongly acidic solution was treated with one equivalent of 2 N NaOH solution. The solution was refluxed for 7 hr and was neutralized with 2 N NaOH and extracted with ether. After removal of ether, the residue (13.8 g) was saponified with an excess of KOH in aqueous methanol for 40 hr. Methanol was evaporated and the liberated menthol was thoroughly extracted with ether. The resulting solution was acidified with dil. sulfuric acid and evaporated to dryness. Ethereal solution of diazomethane was added to the residue and the organic layer was distilled under reduced pressure to give dimethyl 2,3-dimethyltartrate, bp 80—85°C/0.09 mmHg, n_D^{15} 1.4510. The IR-spectrum was identical in every respect with that of the authentic dimethyl (+)-2,3-dimethyltartrate. Yield 2.2 g (35.1%). $[\alpha]_D^{15}$ −1.39° (*c* 9.46, methanol), optical yield 7.06% based on the maximum rotation 19.7° (*vide infra*).

***meso*-2,3-Dimethyltartaric Acid.** Tungstic oxide (150 mg) was dissolved in 30% hydrogen peroxide (10 m*l*) and water (15 m*l*) and to this solution was added dimethylfumaric acid[4] (4.8 g). The mixture was stirred at 70°C for 5 hr and then dried up to give a crystalline product (0.7 g), which was recrystallized from nitromethane to yield *meso*-2,3-dimethyltartaric acid, mp 179—180°C.[6,7] Yield 0.2 g (3.4%).

***racemic* 2,3-Dimethyltartaric Acid.** To a chilled (−40°C) solution of dimethyl dimethylfumarate (5.5 g) in ethanol (180 m*l*) was added a solution of potassium permanganate (5 g) and magnesium sulfate heptahydrate (4.5 g) in water (150 m*l*) during 6 hr. The mixture was set aside at room temperature for 12 hr and then filtered. The combined filtrate and washings were concentrated under reduced pressure to about 30 m*l*-volume and was thoroughly extracted with chloroform. The extract was distilled to give dimethyl 2,3-dimethyltartrate boiling at 91—93°C/0.2 mmHg (3.1 g). The dimethyl ester was saponified with KOH (1.3 g) in boiling methanol and the solvent was removed, acidified with 2 N HCl and extracted with ethyl acetate. Removal of ethyl acetate yielded a crystalline product (2.1 g), which was recrystallized from nitromethane to give *racemic* 2,3-dimethyltartaric acid, mp 185—186°C. Found: C, 40.60; H, 5.64%. Calcd for $C_6H_{10}O_6$: C, C, 40.45; H, 5.66%. Yield 1.2 g (18.2%).

Resolution of *racemic* 2,3-Dimethyltartaric Acid. The racemic acid (7 g) and (−)-ephedrine (6.5 g) were dissolved in hot ethyl acetate (300 m*l*) and the solution was allowed to stand overnight at room temperature, when the ephedrine salt (10.5 g) crystallized out. After triangular fractional recrystallization from acetone, the salt was decomposed with ammonia to afford, after acidification and usual work-up, the optically active acid of the constant rotation (0.7 g). Mp 161—162°C, $[\alpha]_D^{25}$ 13.6° (*c* 0.99, water).

The active acid was converted by the standard method with diazomethane into the dimethyl ester. bp 81—83°C/0.1 mmHg, n_D^{25} 1.4485, $[\alpha]_D^{25}$ 19.7° (*c* 2.65, methanol).

Synthesis and Resolution of Citramalic Acid. According to the method in literature,[11] (±)-citramalic acid, mp 116—117°C, was prepared and resolved through the brucine salt to afford optically pure (+)-acid, mp 112°C, $[\alpha]_D^{25}$ 23.6° (*c* 3.0, water).

Optical rotatory dispersion curves were measured on a Yanagimoto Model ORD-185A recording spectropolarimeter using a 0.5 cm cell at 20°C in 0.1 N HCl solution.

(+)-Dimethyltartaric acid $[\phi]_{589}$ +24.2° (*c* 1.53): ORD (*c* 0.055) $[\phi]_{350}$ +120°, $[\phi]_{229}$ +3170° (1st extremum), $[\phi]_{218}$ 0°, $[\phi]_{208}$ −4530°! (shoulder). (*a*) +77!.

(+)-Citramalic acid $[\phi]_{589}$ +35.8° (*c* 2.31): ORD (*c* 0.196) $[\phi]_{350}$ +94°, $[\phi]_{240}$ 0°, $[\phi]_{228}$ −197° (1st extremum), $[\phi]_{222}$ 0°, $[\phi]_{212}$ +1290°! (shoulder). (*a*) −14!.

Partial support of this study by grant D86547 from the Ministry of Education is gratefully acknowledged (Y. I.). The authors are indebted also to the referee for his valuable suggestions.

10) *Biochem. Prepns.*, **9**, 25 (1962).

BULLETIN OF THE CHEMICAL SOCIETY OF JAPAN VOL. 42 2952—2956 (1969)

Base-catalyzed Condensation of *o*-Nitroacetophenone. IV. Structure of Dehydro-derivative of Compound A, a Condensation Product

Takeo SAKAN, Kousuke KUSUDA[1] and Toshio MIWA

Faculty of Science, Osaka City University, Sumiyoshi-ku, Osaka

(Received March 22, 1969)

The alkaline hydrogen peroxide oxidation of compound A, $C_{17}H_{14}O_5N_2$, a base-catalyzed condensation product of *o*-nitroacetophenone, gave a dehydro compound, $C_{17}H_{12}O_5N_2$. The structure of the dehydro compound was deduced from the spectral data of its derivatives to be a (*o*-nitrobenzoyl)-1-hydroxycarbostyril. The forced hydrogenation of the dehydro compound gave 3-(*o*-aminobenzoyl)-4-methylcarbostyril, which was synthesized by the condensation of *o*-aminoacetophenone and ethyl *o*-nitrobenzoylacetate followed by reduction. Therefore, the dehydro compound proved to be 1-hydroxy-4-methyl-3-(*o*-nitrobenzoyl)carbostyril. On the other hand, the alkaline hydrogen peroxide oxidation of compound A methyl ether gave *o*-nitrobenzoic acid and 1-methoxy-3-methyldioxindole along with *o*-nitroacetophenone. These facts are explained by assuming a transition state which would be controlled by the presence of a hydrogen bonding.

In the first paper of this series,[2] the alkaline hydrogen peroxide oxidation of compound A(I),[3] $C_{17}H_{14}O_5N_2$, a base-catalyzed condensation product of *o*-nitroacetophenone, was reported to give dehydro-compound A, $C_{17}H_{12}O_5N_2$, with a loss of two atoms of hydrogen. A striking change of the ultraviolet absorption of compound A by the dehydrogenation implied that the compound had undergone a major reaction during the transformation.

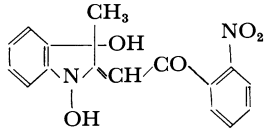

I

Dehydro-compound A is a weak acid similar to compound A and has a broad band at 3145 cm^{-1} in its infrared spectrum. In contrast to the latter, the dehydro compound shows carbonyl stretching absorptions at 1675 and 1600 cm^{-1}.

Methylation of dehydro-compound A with dimethyl sulfate and potassium carbonate gave a methyl ether, which lost both acidity and the 3145 cm^{-1} band of the original compound. The 1600 cm^{-1} carbonyl band of dehydro-compound A was shifted to 1647 cm^{-1} during methylation.

On hydrogenation over palladium-on-carbon, dehydro compound A methyl ether absorbed three moles of hydrogen to yield a yellow amine, $C_{18}H_{16}O_3N_2$, melting at 220—222°C. This amine has a C-methyl group and a methoxyl group. Its ultraviolet spectrum has a new band at 384 mμ. Acetylation of the amine with acetic anhydride led to a monoacetyl derivative, $C_{20}H_{18}O_4N_2$, mp 202—203°C. In the ultraviolet spectrum of this compound, the 380 mμ band of the amine shifted by 40 mμ to a shorter wavelength (Fig. 1). Such a characteristic hypsochromic shift indicates that the original amine contains an *o*-aminobenzoyl

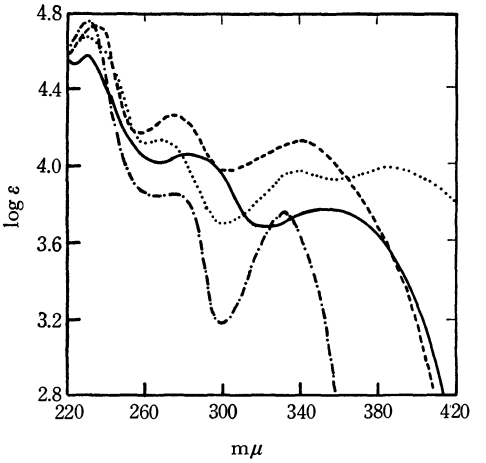

Fig. 1. UV spectra of dehydro-compound A methyl ether (II, OMe for OH) (——), amine VIII (·····), amide IX (----) and its $NaBH_4$ reduction product (X) (-·-).

1) Present address: Research Institute of Atomic Energy, Osaka City University, Sumiyoshi-ku, Osaka.

2) T. Sakan, K. Kusuda and T. Miwa, This Bulletin, **37**, 1678 (1964).

3) T. Sakan, K. Kusuda and T. Miwa, *ibid.*, **38**, 18 (1965).

group;[4] therefore, dehydro-compound A should be an o-nitrophenyl ketone.

Reduction of the acetamido derivative with sodium borohydride gave a compound decomposing at 141—143°C. This compound was difficult to purify, but its infrared spectrum showed that the keto function of the o-acetamidobenzoyl group was reduced. All the compounds derived from dehydro-compound A have a set of triple absorption maxima (near 230, 280 and 340 mμ) as shown in Fig. 1. The spectral feature is characteristic of the carbostyril derivative;[5] consequently, dehydro-compound A was assumed to be an α-quinolone derivative. The carbonyl band (1647 cm^{-1}) of its methyl ether is in good accord with those (1661—1650 cm^{-1}) of α-quinolones.[5,6]

Providing that the carbostyril system still possesses a hydroxyl group on the nitrogen atom as proposed for compound A (I), dehydro-compound A would be a cyclic hydroxamic acid; the weak acidity as well as the carbonyl band (1600 cm^{-1}) of longer wavelength than those of usual α-quinolones may be attributed to the hydroxamic function.

These facts suggest structure II or III for dehydro-compound A. Of these structures, the former appears to be more plausible, if the carbostyril ring is formed by the C_α-C_β ring fission of the indoline nucleus[7] with a β-methyl group in compound A (I).

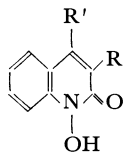

II: R=o-Nitrobenzoyl, R'=CH_3
III: R=CH_3, R'=o-Nitrobenzoyl

In order to derive dehydro-compound A to a readily available compound, attempts were made to remove the hydroxyl group attached to the cyclic nitrogen atom. The methoxyl group of an *N*-methoxycarbostyril was reported to be removed by reduction with zinc and hydrochloric acid.[8] No reduction was carried out with the yellow amine, $C_{18}H_{16}O_3N_2$, derived from dehydro-compound A methyl ether. Catalytic hydrogenation over Raney nickel seemed promising, because such a hydrogenolysis of a 1-methoxyoxindole led to an oxindole;[3] however, this also failed with dehydro-compound A methyl ether. Forced hydrogenation of dehydro-compound A over Raney nickel at a hydrogen pressure of 80 atm and at a temperature of 115°C yielded a deoxy compound. Being difficult to purify, the product was acetylated immediately to produce a monoacetyl derivative, $C_{19}H_{16}O_3N_2$, mp 279—280°C, and a diacetyl derivative, $C_{21}H_{18}O_4N_2$, mp 218—220°C. Both of the acetyl derivatives on hydrolysis gave the same bright yellow amine, $C_{17}H_{14}O_2N_2$, decomposing at 277—279°C. Thus ultraviolet absorption spectra of the amine and its acetyl derivatives indicate the survival of the o-aminobenzoyl system through the hydrogenation process. The amine would be represented by formula V on the basis of the assumed preferential structure II for dehydro-compound A. This was proved to be the fact by the following synthesis of the amine.

Heating o-aminoacetophenone with ethyl o-nitrobenzoylacetate afforded 4-methyl-3-(o-nitrobenzoyl)carbostyril IV, which in turn was hydrogenated to the corresponding amine V. This amine was spectroscopically identical with the amine obtained by the high-pressure hydrogenation of dehydro-compound A. Acetylation of V gave a monoacetyl derivative VI, which was identified with the monoacetyl compound, $C_{19}H_{16}O_3N_2$, by a mixed melting point determination; consequently, the diacetyl compound, $C_{21}H_{18}O_4N_2$, was assumed to have the structure VII because of the absence of the amide II band in its infrared spectrum.

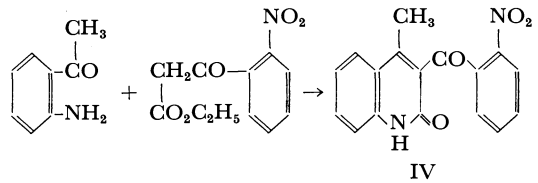

IV

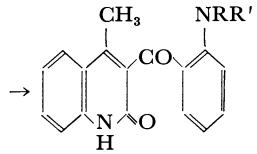

V : R, R'=H
VI : R=H, R'=$COCH_3$
VII: R, R'=$COCH_3$

The establishment of the structure of amine V excluded structure III for dehydro-compound A and evidently confirmed that dehydro-compound A is 1-hydroxy-4-methyl-3-(o-nitrobenzoyl)-2-quinolone. As a corollary, the C_{18}-amine derived from dehydro-compound A methyl ether, its acetyl derivative, and the sodium borohydride reduction product of the latter were assigned structures VIII,

4) The ultraviolet absorption maximum at 385 mμ of o-aminobenzophenone is shifted to 325 mμ by acetylation: P. Grammaticakis, *Bull. Soc. Chim. France*, **1953**, 93.

5) B. Witkop, J. B. Patrick and M. Rosenblum, *J. Am. Chem. Soc.*, **73**, 2641 (1951).

6) M. F. Grundon, N. J. McCorkindale and M. N. Rodger, *J. Chem. Soc.*, **1955**, 4284.

7) Example of the ring enlargement of indoline nucleus through such a ring fission is found in literature.[4]

8) F. A. Arndt, C. Ergener and O. Kutlu, *Chem. Ber.*, **86**, 962 (1953).

IX, and X, respectively.

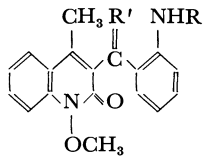

VIII: R=H, R'=O
IX : R=Ac, R'=O
X : R=Ac, R'=H, OH

Formation of the dehydro compound from compound A may be explained as shown in Chart 1.

The oxidation of α,β-unsaturated ketones with alkaline hydrogen peroxide is a familiar reaction leading to epoxy ketones.[9] The reaction was proposed to be stereoselective and to proceed through a transition state controlled by the overlap of the pi-orbitals of the enolate anion.[10] In this case, the transition state is presumed to involve the overlap of p (or pi)-orbital on the α-carbon atom with the vacant orbital which is developing in the S_N2 reaction on the peroxide oxygen atom.[11] The hydrogen bondings shown in XII would force the transition state to assume a conformation where the overlap required for the formation of the epoxide ring is apparently impossible (Fig. 2-a). Therefore, another alternative nucleophilic substitution shown in XII may occur at the β-carbon atom of the indoline nucleus, if we assume a transition state shown in Fig. 2-b which leads to the formation of a cyclopropane ring in XIII.

The importance of the hydrogen bonding in the above rearrangement was substantiated by the alkaline hydrogen peroxide oxidation of the methyl

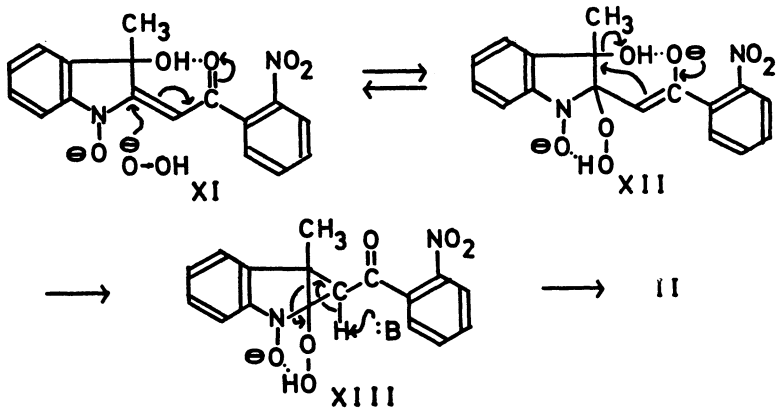

Chart 1

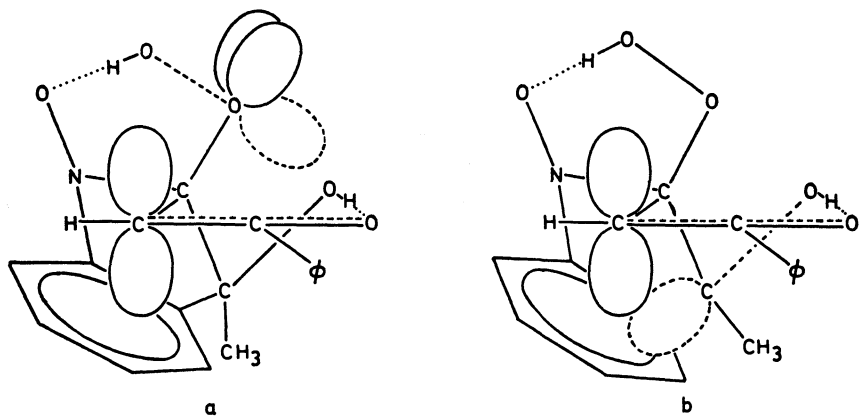

Fig. 2. Transition state for the reaction of XII. Overlapping of the orbitals is inhibited (a) or allowed (b).

9) *E. g.*, H. O. House, "Modern Synthetic Reactions," Benjamin, New York (1965), p. 117.

10) H. E. Zimmerman, L. Singer and B. S. Thyagarajan, *J. Am. Chem. Soc.*, **81**, 108 (1959).

11) In the nucleophilic substitution of the peroxide, the nucleophile is assumed to approach the peroxides along the line formed by the two peroxide oxygens. (J. O. Edwards, "Peroxide Reaction Mechanisms," ed. by J. O. Edwards, Interscience Publishers, New York (1962), p. 69).

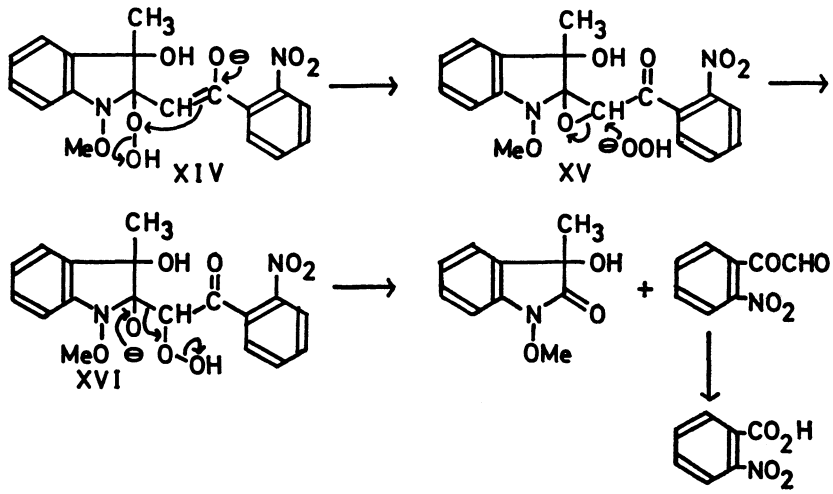

Chart 2

ether of compound A. The reaction of compound A methyl ether with alkaline hydrogen peroxide in dioxane followed quite a different course from that of compound A, leading to 1-methoxy-3-methyldioxindole, which was previously obtained by the ozonolysis of the methyl ether,[3] and *o*-nitrobenzoic acid, along with a small amount of *o*-nitroacetophenone. The difference is not due to the solvent effect since the oxidation of compound A under the same condition as the methyl ether gave dehydro-compound A as a sole product. A mechanism shown in Chart 2 may be proposed for the oxidation of the methyl ether.

In the transition state of the oxidation of the methyl ether, however, the hydrogen bond would be too weak to prevent the overlap of the p-orbital of the α-carbon atom with the vacant orbital on the oxygen atom in the peroxide group. The epoxide may be attacked by another hydroperoxide ion at the electron-defficient site to produce an open-chain alkoxide ion XVI, which will give the dioxindole and *o*-nitrophenylglyoxal, the latter being further oxidized into *o*-nitrobenzoic acid.

o-Nitroacetophenone was formed apparently by the oxidation of the dioxindole, because it was formed in some quantity even when *o*-nitrobenzoic acid was formed almost quantitatively.

Experimental

Hydrogenation of Dehydro-compound A Methyl Ether. 3-(*o*-Aminobenzoyl)-1-methoxy-4-methyl-2-quinolone (VIII). A solution of 2.8 g of dehydro-compound A methyl ether in 80 cc of ethanol was hydrogenated at atmospheric pressure using 1.4 g of 5% palladium-on-carbon to absorb 530 cc (20°C) of hydrogen. During the hydrogenation greenish yellow crystals separated. The catalyst was removed by filtration from the hot solution and washed well with hot ethanol. Evaporation of the ethanol left 2.5 g of yellow amine, which, after recrystallization from ethanol, melted at 220—222°C. λ_{max}^{EtOH} mμ (log ε): 230 (4.68), 266—270 (4.14), 336 (3.98), 384 (4.00). λ_{max}^{Nujol} cm^{-1}: 3425, 3310 (NH), 1645, 1613 (C=O).

Found: C, 70.15; H, 5.69; N, 9.20%. C-Methyl group (Kuhn-Roth):[12] 0.52. Calcd for $C_{18}H_{16}O_3N_2$: C, 70.11; H, 5.23; N, 9.09%. C-Methyl group: 1.00.

***N*-Acetyl Derivative (IX)** was obtained by treatment of 0.7 g of the amine with 10.5 cc of boiling acetic anhydride for 5 min. Excess of the anhydride was decomposed with water and the product was recrystallized from methanol, mp 202—203°C. λ_{max}^{EtOH} mμ (log ε): 232 (4.74), 275 (4.27), 340 (4.13). ν_{max}^{Nujol} cm^{-1}: 3290 (NH), 1698, 1650, 1634 (C=O), 1520 (amide II).

Found: C, 68.63; H, 5.26; N, 8.32%. Calcd for $C_{20}H_{18}O_4N_2$: C, 68.56; H, 5.18; N, 8.00%.

Sodium Borohydride Reduction of the *N*-Acetyl Derivative was effected in methanol at room temperature. After being allowed to stand overnight, the reduction mixture was diluted with water and evaporated to remove methanol. Extraction with benzene gave crystals, which, after recrystallization from benzene-ligroin, decomposed at 141—143°C. λ_{max}^{EtOH} mμ (log ε): 230 (4.77), 276 (3.86), 331 (3.76). λ_{max}^{Nujol} cm^{-1}: 3345 (OH and NH), 1695, 1637 (C=O), 1522 (amide II).

High Pressure Hydrogenation of Dehydro-compound A. 3-(*o*-Aminobenzoyl)-4-methyl-2-quinolone (V). Hydrogenation of 1.4 g of dehydro-compound A was effected in ethanol over 0.8 g of Raney nickel at a hydrogen pressure of 80 atm and at a temperature of 115°C for 16 hr. Without removal of the catalyst, the solvent was distilled off under reduced pressure. The resulting residue was heated with acetic anhydride under reflux for one hour. After removal of the catalyst, work-up in usual way gave crystals, which were recrystallized repeatedly from methanol. From the less soluble fraction, the monoacetyl derivative VI was obtained as leaflets, mp 274—276°C.

12) E. J. Eisenbraun, S. M. McElvain and B. F. Aycock, *J. Am. Chem. Soc.*, **76**, 607 (1954).

λ_{max}^{EtOH} mμ (log ε): 230 (4.68), 270 (4.28), 328—332 (4.08). ν_{max}^{Nujol} cm^{-1}: 3248 (NH), 1692, 1658, 1631 (C=O), 1520 (amide II).

Found: C, 70.56; H, 5.08; N, 8.93%. Calcd for $C_{19}H_{16}O_3N_2$: C, 71.24; H, 5.03; N, 8.75%.

The monoacetyl derivative was identified with the independently synthesized amide VI (see below) by a mixed melting point determination.

The more soluble fraction gave the diacetyl derivative VII as leaflets melting at 218—220°C. λ_{max}^{EtOH}: 328 mμ (log ε 3.82). ν_{max}^{Nujol} cm^{-1}: 1706, 1672, 1637 (C=O).

Found: C, 69.84; H, 5.16; N, 8.02%. Calcd for $C_{21}H_{18}O_4N_2$: C, 69.60; H, 5.00; N, 7.73%.

A mixture of 35 mg of the monoacetyl derivative and 1 cc of concentrated hydrochloric acid was heated on a water bath for 3 hr. Evaporation of the hydrochloric acid *in vacuo* followed by recrystallization from 90% acetic acid gave bright yellow prisms decomposing at 272—275°C. Hydrolysis of the diacetyl derivative in a similar way afforded a base decomposing at 277—279°C, which showed no depression by a mixed melting point determination with the product from the monoacetyl derivative. λ_{max}^{EtOH} mμ (log ε): 229—230 (4.62), 270 (4.08), 335 (3.87), 350 (3.88), 378—382 (3.89). ν_{max}^{Nujol} cm^{-1}: 3400, 3290 (NH), 1647, 1626 (C=O).

Found: C, 73.10; H, 5.26; N, 9.97%. Calcd for $C_{17}H_{14}O_2N_2$: C, 73.36; H, 5.07; N, 10.07%.

The amine was identified with the authentic specimen (see below) by ultraviolet and infrared spectroscopy.

4-Methyl-3-(*o*-nitrobenzoyl)-2-quinolone (IV). A mixture of 0.55 g of *o*-aminoacetophenone and 0.95 g of ethyl *o*-nitrobenzoylacetate was heated in a sealed tube at 170—200°C for 4 hr. The mixture was treated with benzene and the resulting precipitate was recrystallized from methanol to give leaflets, mp 238—240°C. λ_{max}^{EtOH} mμ (log ε): 231 (4.51), 284 (3.95), 351 (3.75). ν_{max}^{Nujol} cm^{-1}: 1681, 1621 (C=O), 1531, 1351, 860 (NO_2).

Found: C, 66.42; H, 4.13; N, 9.20%. Calcd for $C_{17}H_{12}O_4N_2$: C, 66.23; H, 3.92; N, 9.09%.

3-(*o*-Aminobenzoyl)-4-methyl-2-quinolone (V). A solution of 48 mg of the nitro compound IV in 1 cc of ethanol was hydrogenated in the presence of 40 mg of 5% palladium-on-carbon to give amine V decomposing at 275—277°C.

3-(*o*-Acetamidobenzoyl)-4-methyl-2-quinolone (VI). Acetylation was accomplished by heating 36 mg of the amine IV in 3 cc of acetic anhydride under reflux. Work-up in the usual way and recrystallization from methanol gave 31 mg of crystals melting at 282—284°C.

Alkaline Hydrogen Peroxide Oxidation of Compound A Methyl Ether. To a solution of 690 mg of compound A methyl ether in 5 cc of dioxane was added 2 cc of 10% methanolic potassium hydroxide, followed by the addition of 5 cc of 30% hydrogen peroxide with cooling. After removal of half of the solvent under reduced pressure, the residue was made acidic with 20% hydrochloric acid. The resulting mixture was extracted with a mixture of benzene and ether, and the extract was washed with aqueous sodium hydrogencarbonate solution. Acidification of the aqueous solution gave 329 mg (96.5%) of *o*-nitrobenzoic acid. The neutral fraction (190 mg) was chromatographed on active alumina "Wako" as a benzene solution. The first band was eluted with benzene to give 48 mg of an oil; it was characterized as a 2,4-dinitrophenylhydrazone, mp 170—174°C, which was identified with that of *o*-nitroacetophenone by infrared spectroscopy. The second band, eluted with a mixture of 300 cc of benzene and 5 drops of ethanol gave 130 mg of crystals, which, after recrystallization from benzene-ligroin, melted at 134—135°C, and which was identified with 1-methoxy-3-methyldioxindole[3] by infrared spectroscopy.

Alkaline Hydrogen Peroxide Oxidation of Compound A in Dioxane. A solution of 347 mg of compound A in 3 cc of dioxane was treated with 1.5 cc of 10% methanolic potassium hydroxide and 1.5 cc of 30% hydrogen peroxide. After being stirred overnight, the mixture was acidified with saturated sulfur dioxide solution. Concentration of the mixture, followed by filtration of the resulting precipitate gave 258 mg of crude dehydro-compound A, which, after recrystallization from methanol, was identified with the authentic sample[2] by infrared spectroscopy.

BULLETIN OF THE CHEMICAL SOCIETY OF JAPAN VOL. 42 2957—2961 (1969)

Asymmetric Reactions. III. Stereoselectivity Difference between Grignard and Alkyllithium Reactions with 2,3-*O*-Substituted-D-glyceraldehydes

Yoshiaki OHGO, Juji YOSHIMURA, Masami KONO and Tetsuo SATO

Laboratory of Organic Chemistry, Tokyo Institute of Technology, Ookayama, Meguro-ku, Tokyo

(Received March 24, 1969)

Stereoselectivity has been investigated in addition reactions of 2,3-*O*-isopropylidene-D-glyceraldehyde (I) or 2,3-di-*O*-benzyl-D-glyceraldehyde (II) with phenylmagnesium bromide or phenyllithium. Stereoselectivity difference between the Grignard and phenyllithium reactions occurred in the case of compound (I): the phenyllithium reaction gives *threo* and the Grignard reaction *erythro* products predominantly. On the other hand, no difference in stereoselectivity has been observed between the reactions with 2,3-di-*O*-benzyl-D-glyceraldehyde (II): both reactions gave *threo* product predominantly.

In a previous paper,[1] it has been reported that the asymmetric induction of *N*-substituted 2,3-*O*-isopropylidene-D-glyceraldimines with alkyllithium produced *threo* compound, and that with the Grignard reagent gave *erythro* product predominantly.

The steric direction of the alkyllithium reaction can be explained by Cram's rigid model.[2] Stereoselectivity of the Grignard reaction which was incompatible with the Cram's model was explained by assuming a coordinative interaction between C_3-oxygen and magnesium.

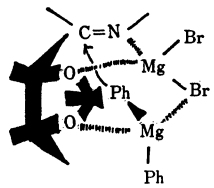

A

This paper reports that the same steric difference was observed in the reaction with 2,3-*O*-isopropylidene-D-glyceraldehyde and the fixation of oxygen atoms at 2- and 3-position by ketal ring is an essential factor for the occurrence of the stereoselectivity difference between the Grignard and alkyllithium reactions.

Materials

2,3-*O*-Isopropylidene-D-glyceraldehyde was prepared according to the method established by Baer and Fisher.[3] Freshly distilled material was used in each experiment.

2,3-*O*-Benzyl-D-glyceraldehyde was synthesized as follows.

Benzylation of 3,4-*O*-isopropylidene-D-mannitol with benzyl chloride and sodium hydride in dimethyl sulfoxide afforded 1,2;5,6-tetrabenzyl-3,4-*O*-isopropylidene-D-mannitol which was subjected to acid hydrolysis to give 1,2;5,6-tetra-*O*-benzyl-D-mannitol. Oxidative scission of the tetrabenzyl derivative with lead tetraacetate in benzene solution gave 2,3-di-*O*-benzyl-D-glyceraldehyde (bp 143—144°C/0.004 mmHg, $[\alpha]_{578}=+52°$) in a comparatively high yield (see experimental part). The structure was confirmed by means of IR data and microanalysis.

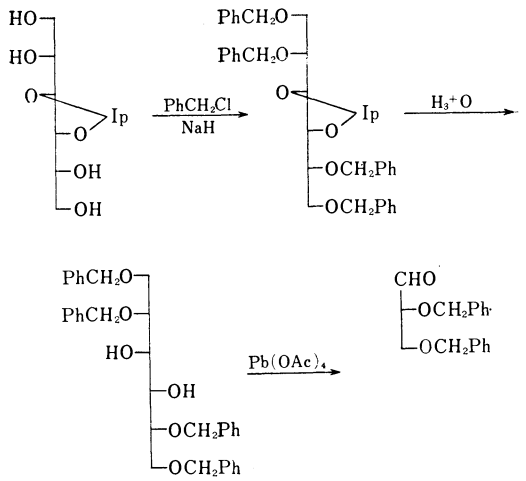

Scheme 1

1) a) J. Yoshimura, Y. Ohgo and T. Sato, *J. Am. Chem. Soc.*, **86**, 3858 (1964). b) Y. Ohgo, J. Yoshimura and T. Sato, This Bulletin, **42**, 728 (1969).

2) D. J. Cram and K. R. Kopecky, *J. Am. Chem. Soc.*, **81**, 2737 (1959).

3) E. Baer and H. O. L. Fischer, *J. Biol. Chem.*, **128**, 463 (1939).

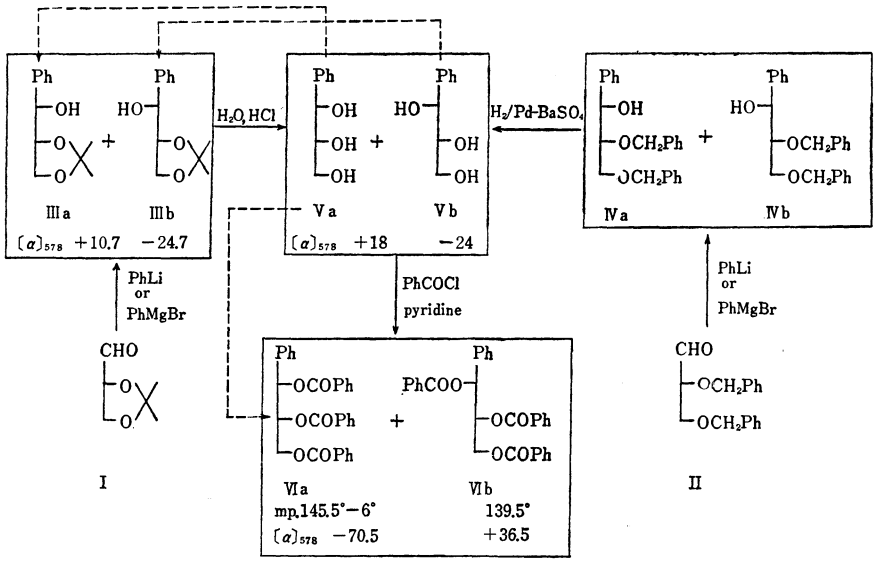

Scheme II

—— Sequence of asymmetric induction experiment.
---- Process carried out in order to establish stereochemical correlation.

Results and Discussion

2,3-*O*-Isopropylidene-D-glyceraldehyde (I)[3] or 2,3-di-*O*-benzyl-D-glyceraldehyde (II) was treated with 3 mol of phenyllithium or phenylmagnesium bromide in ether. The reaction mixture was decomposed with ice water, and from the ether layer a diastereomeric mixture of the corresponding addition products was obtained (IIIa, IIIb or IVa, IVb).

III and IV were respectively converted to a diastereomeric mixture of crystalline 1-*C*-phenyl-1,2,3-tri-*O*-benzoyl-glycerols (VIa and b) by acid hydrolysis of III or by catalytic hydrogenation of IV followed by benzoylation. The optical rotations and analytical results of the mixture are shown in Table 1. From the diastereomeric mixture two crystalline compounds were obtained by fractional crystallization, *i. e.*, mp 145.5—146°C, $[\alpha]_{578}$ −70.5°; mp 139.5°C, $[\alpha]_{578}$ +36.5°.

The isomer with mp 145.5—146°C has been reported by Tiffeneau and Neuberg.[4] However, no assignment of configuration was made.

The above diastereomers should have D-*threo* or D-*erythro* configuration. The configuration will be assigned as follows.

The de-acetonated product (Va+Vb) was distilled at 150—153°C/0.09 mmHg. It crystallized partially and the crystals with mp 103—105°C (Va) were separated from syrup (Vb). On the other hand, IIIa and IIIb were derived from Va and Vb by acetonation, respectively. The configuration of IIIa, IIIb, Va and Vb was presumed from comparison of optical rotational strength and sign with those of analogous compounds 1-*C*-phenyl-glycitols and their isopropylidene derivatives.[5,6]

The isomer bearing oxygen right in the Fischer Projection seems to have more positive rotation than the one bearing oxygen left. The analgous relation has been observed in the case of α-aminonitrile and 1-*C*-phenyl-1-alkylamino-1-deoxy-D-glycerols.[7,1a] Since Va and IIIa have positive values (+18° and +10.2°) [Vb and IIIb have negative (−24° and −24.7°)], it can be inferred that Va and IIIa have D-*erythro* configuration, and Vb and IIIb D-*threo*.

Their configurations are also deduced from comparison of the IR spectra of dilute solution of IIIa and IIIb (which were derived from Va and Vb by acetonation). The ratio of the bonded and free hydroxy stretching frequency (at 3630—3580 region) of IIIb is much greater than that of IIIa in dilute solution (see experimental). This implies that IIIb has *threo* configuration whose hydrogen bonding is stable.[8] The same conclusion may be derived from NMR spectra. Stable conformation of the *erythro* and the *threo* compound (IIIa,b)

4) M. Tiffeneau and I. Neuberg, *Compt. rend.*, **198**, 2174 (1934).

5) W. A. Bonner, *J. Am. Chem. Soc.*, **73**, 3126 (1951).

6) J. English, Jr., and P. H. Griswald, Jr., *ibid.*, **67**, 2039 (1945); *ibid.*, **70**, 1390 (1948).

7) J. Yoshimura, Y. Ohgo and T. Sato, This Bulletin, **34**, 1197 (1961).

8) W. A. Mosher and N. D. Heindel, *J. Org. Chem.*, **28**, 2154 (1963).

will be regulated by the balance of attractive force due to O_1H–O_2 hydrogen bonding and the repulsion between non-bonded groups. Most stable conformations of the *erythro* and *threo* may be represented by B and C respectively in which phenyl group

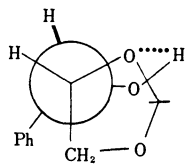

B

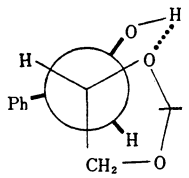

C

is located in such a way that the non-bonded interaction may be minimized within the range making hydrogen bonding possible. If so, it can be expected from Karplus equations[9] that $J_{H_1H_2}$ of *threo* is larger than that of the *erythro* compound. In the case of IIIa, signal at 5.15 due to H_1 splits in quartet (J=5 cps and 2.5 cps). By addition of H^+ the quartet changes to doublet with J=5 cps which is ascribed to $J_{H_1H_2}$. The coupling constant ($J_{H_1H_2}$) of IIIb is 8 cps. This fact is consistent with the above assumption.

On the other hand, Va was correlated with VIa (mp 145.5°C) by benzoylation of the former. In consequence, series a (IIIa, Va, VIa) belongs to D-erythro type, and series b (IIIb, Vb, VIb) to D-threo type.[10]

The produced diastereomer ratio was calculated from optical rotations of *erythro* (VIa), *threo* (VIb) and the diastereomeric mixture produced in the reaction. The results are shown in Table 1.

As expected, the difference in stereoselectivity between the Grignard and phenyllithium reactions occurred with 2,3-*O*-isopropylidene-D-glyceraldehyde; the phenyllithium reaction gives *threo* and Grignard reaction *erythro* products predominantly.

On the other hand, the same reaction with 2,3-di-*O*-benzyl-D-glyceraldehyde gives no difference in stereoselectivity between the two reactions; *threo* product is predominant in both reactions. This may imply that C_3–O must be fixed in a certain steric position suitable to interaction with the reagent for the Grignard reaction to give *erythro* product.

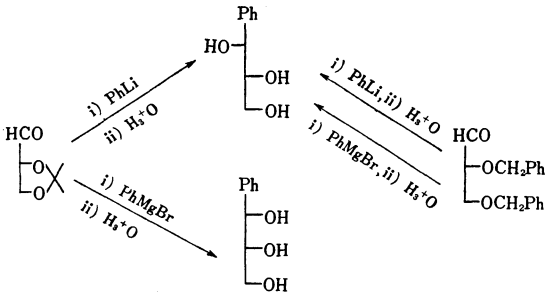

Scheme 3

Experimental

The NMR spectrum was taken in deuteriochloroform solution with a JNM-4H-100 Spectrometer (Japan Electron Optics Laboratory Co., Ltd.) at 100 Mc/sec, using tetramethylsilane as an internal standard.

The hydrogen bonding measurements were performed in dilute CCl_4 solution on a Perkin-Elmer 125

Table 1

Run	Substrate	Reagent	Products: Optical rotation $[\alpha]_{546}$	Optical rotation $[\alpha]_{578}$	Analysis C	Analysis H	Ratio *threo*	Ratio *erythro*
1	I	PhLi	−3.0	−3.6	74.99	5.25	63	37
2	I	PhMgBr	−20.0	−23.0	74.07	6.13	47*	53*
3	I	PhMgBr	−18.2	−21.7	74.79	5.12	48	52
4	II	PhLi	+0.5	−1.0	76.38	5.99	65	35
5	II	PhLi	−6.4	−7.4	75.71	5.50	60	40
6	II	PhMgBr	−6.5	−8	74.84	5.27	60	40
7	II	PhMgBr	−4.0	−4.5	75.73	5.61	62	38

* During the course of preparation of our article, a similar study was reported by M. H. Delton and G. U. Yuen [*J. Org. Chem.*, **33**, 2473 (1968)]. According to their report, the Grignard reaction gives *threo* products in 58% and *erythro* in 42% yield. The difference between their results and ours may be due to the difference in experimental methods, particularly in measurements. Delton and Yuen determined the diastereomeric ratio by gas chromatography, while we carried it out by optical rotation. In view of this, further experiments are now in progress and the results will be published later.

9) M. Karplus, *J. Chem. Phys.*, **30**, 11 (1959).

10) This assignment was confirmed by preliminary experiment deriving IIIa and IIIb to L(+) and D(−)-1-methoxyphenylacetaldehyde[5] respectively. More precise experiments are under investigation and will be published later.

grating spectrophotometer. The optical rotations were measured on a Carl Zeis Photoelectric Precision Polarimeter (0.005°).

Addition Reaction of 2,3-*O*-Isopropylidene-D-glyceraldehyde with Phenylmagnesium Bromide. A solution of 14 g of 2,3-*O*-isopropylidene-D-glyceraldehyde in 20 m*l* of ether was slowly added to a well-stirred solution of phenylmagnesium bromide prepared from 51 g (0.32 mol) of bromobenzene and 7.93 g. of magnesium in 170 m*l* of ether. The mixture was stirred for 1 hr at 0—5°C and for four hours at reflux-temperature of the ether solution. The reaction mixture was poured into ice-water containing ammonium chloride. The ether layer was separated, and washed with water. The solution was dried and concentrated under reduced pressure to give a syrup (16.5 g, yield 74%, $[\alpha]_{578}$ −4.77). The syrup was dissolved in 300 m*l* of ethanol and to the solution was added 4.4 m*l* of concentrated hydrochloric acid and 142 m*l* of water. The mixture was refluxed for 2 hr. The reaction mixture was neutralized by potassium carbonate solution and concentrated under reduced pressure. The residue was extracted twice with 100 m*l* of ethyl acetate. The combined ethyl acetate solution was concentrated *in vacuo* to give 6.5 g of syrup (yield 49%).

The diastereomeric mixture (5 g) of 1-*C*-phenyl-D-*threo*- and D-*erythro*-glycerol was treated with benzoyl chloride (14.2 g) and pyridine (8 g) in chloroform (40 m*l*) at room temperature. The mixture was allowed to stand overnight and then poured into ice-water. The chloroform layer was separated and washed with water repeatedly until the layer became neutral. The chloroform layer was dried and concentrated under about 15 mmHg and then under 0.001 mmHg at 80—100°C for 5 hr to give colorless crystals (14 g, yield 98%). Analytical data agreed with those of the 1,2,3-tri-*O*-benzoyl-1-*C*-phenyl-D-glycerol (see Table 1). Optical rotation was measured ($c=2.00$, $l=0.5$, benzene). Fractional crystallization from an ethanol-benzene mixture gave two diastereomers; VIa (1,2,3-tri-*O*-benzoyl-1-*C*-phenyl-*erythro*-D-glycerol) mp 145.5—146°C; $[\alpha]_{578}$ −70.5, $[\alpha]_{546}$ −81 ($c=2.00$, $l=0.5$, benzene); VIb (1,2,3-tri-*O*-benzoyl-1-*C*-phenyl-*threo*-D-glycerol) mp 139.5°C, $[\alpha]_{578}$ +36.5 ($c=2.028$, $l=0.5$, benzene), $[\alpha]_{546}$ +41.5. Found: C, 74.57; H, 5.08%. Calcd for $C_{30}H_{24}O_6$: C, 74.99; H, 5.03%.

Addition Reaction of I with Phenyllithium. A solution of 14 g of 2,3-*O*-isopropylidene-D-glyceraldehyde in 20 m*l* of ether was slowly added to a well-stirred solution of phenyllithium prepared from 51 g (0.32 mol) of bromobenzene and 4.48 g of lithium in 170 m*l* of ether. The same procedure as in the Grignard reaction gave a diastereomeric mixture of 1,2,3-tri-*O*-benzoyl-1-*C*-phenyl-*threo*-D- and *erythro*-D-glycerols in total yield of about 50%.

1-*C*-Phenyl-2,3-*O*-isopropylidene-*erythro*-D-glycerol (IIIa). 1-*C*-Phenyl-*erythro*-D-glycerol (Va) (12 g) was treated with 250 m*l* of acetone containing 19.3 g of zinc chloride at room temperature for 2 days. The reaction mixture was poured with stirring into a solution of K_2CO_3 (26 g) in 26 m*l* of water covered with 300 m*l* of ether. The acetone-ether solution was dried over potassium carbonate and then concentrated *in vacuo* to give 16 g of syrup. The syrup was distilled at 175—176°C/30 mmHg. Yield, 10 g, (67%). $[\alpha]_{578}$ +10.7, $[\alpha]_{546}$ +12.2 ($c=2.052$, ethanol).

Found: C, 69.22; H, 7.89%. Calcd for $C_{12}H_{16}O_3$: C, 69.21; H, 7.74%.

The infrared measurement was carried out in 0.013 molar carbon tetrachloride solution. The infrared spectrum shows free and bonded OH stretching vibrations at 3619 cm^{-1} and 3578 cm^{-1} respectively. The ratio of bonded OH to free OH absorption is about 2—2.5. NMR spectrum: CH_3, 8.55, 8.66; OH, 7.35 (doublet, $J=2.5$ cps, this doublet disappeared on addition of trifluoroacetic acid); H_3 and H_3', 6.15τ (multiplet); H_2, 5.72τ (multiplet); H_1, 5.15τ (quartet, $J_{H_1H_2}=5$ cps, $J_{H_1OH}=2.5$ cps); phenyl, 2.65τ.

1-*C*-Phenyl-2,3-*O*-isopropylidene-*threo*-D-glycerol (IIIb). Vb was converted to IIIb by the same procedure as above (Va to IIIa) (yield; 56%). $[\alpha]_{578}=-24.7$ ($c=1.06$, $l=0.5$, ethanol), $[\alpha]_{546}=-27.5$ ($c=1.06$, $l=0.5$, ethanol).

Found: C, 68.85; H, 7.89%. Calcd for $C_{12}H_{16}O_3$: C, 69.21; H, 7.74%.

The infrared measurement was carried out in 0.0125 M carbon tetrachloride solution. The infrared spectrum shows bonded OH stretching vibration at 3600 cm^{-1} but no substantial absorption at higher frequency region. NMR spectrum: CH_3, 8.5 and 8.46τ; H_3 and H_3', 6.2τ (unresolved multiplet); H_2, 5.75τ (multiplet); H_1, 5.5τ (doublet, $J_{H_1H_2}=8$ cps).

1-*C*-Phenyl-*erythro* and *threo*-D-glycerols (Va and Vb). The reaction of phenylmagnesium bromide (prepared from 17 g of magnesium and 7.35 m*l* of bromobenzene) in ether (350 m*l*) with an ether solution of 2,3-*O*-isopropylidene-D-glyceraldehyde followed by acid hydrolysis [with a mixture of ethanol (560 m*l*), water (270 m*l*) and 12 N HCl (20 m*l*)] gave a syrup (30 g) of a diastereomeric mixture of 1-*C*-phenyl-*erythro* and *threo*-D-glycerols. From the syrup 9.4 g of a crystalline compound was obtained: mp 103—105°C, $[\alpha]_{587}$ +18, $[\alpha]_{546}$ +20 ($c=2$, $l=0.5$, ethanol).

When the residual syrup was distilled at 150—153°C/0.09 mmHg and left standing at room temperature additional crystals (3 g) were obtained. Total yield of crystalline isomer is 12.4 g. The residual syrup weighed 12.7 g. The rotation of the residual syrup; $[\alpha]_{578}$ −24, $[\alpha]_{546}$ −28 ($c=1.01$, $l=0.5$, ethanol).

Addition Reaction of 2,3-Di-*O*-benzyl-D-glyceraldehyde with Phenylmagnesium Bromide. A solution of 10 g (0.037 mol) of 2,3-di-*O*-benzyl-D-glyceraldehyde in 20 m*l* ether was added slowly into a stirred solution of phenylmagnesium bromide prepared from 17.5 g (0.11 mol) of bromobenzene and 2.7 g of magnesium in 100 m*l* ether at 0—5°C.

The same procedure as in the case of addition reaction of I with organometallic reagents gave 11.5 g of syrup (yield 89%) of addition products. The syrup (7.2 g) obtained above was hydrogenated with 10 g of palladium-barium sulfate catalyst in 260 m*l* of ethanol containing concd. hydrochloric acid (2.6 m*l*). The reaction mixture was neutralized with a 2 N sodium hydroxide solution and concentrated under reduced pressure. The residue was extracted with ethyl acetate. The ethyl acetate solution was concentrated to a syrup (3.7 g). 3.7 g of the diastereomeric mixture of 1-*C*-phenyl-D-glycerols was benzoylated with the same procedure as described before to give 10 g of the tribenzoate (100%). Fractional crystallization from a mixture of ethanol and benzene afforded two crystalline compounds of mp 145—146°C and mp 138—139°C. These com-

pounds were identified with VIa and VIb (mixed melting point).

Addition Reaction of 2,3-Di-*O*-benzyl-D-glyceraldehyde (II) with Phenyllithium. A solution of 10 g of II in 20 m*l* ether was added slowly to a well-stirred solution of phenyllithium prepared from 17.5 g of bromobenzene and 1.54 g of lithium at 0—5°C. The same procedure as in the Grignard reaction gave a diastereomeric mixture of 1,2,3-tri-*O*-benzoyl-1-*C*-phenyl-D-*threo* and D-*erythro* glycerol. Analytical results and optical rotations of diastereomeric mixtures are shown in Table 1.

2,3-Di-*O*-benzyl-D-glyceraldehyde. To a solution of 40 g of 3,4-*O*-isopropylidene-D-mannitol in 400 m*l* of dimethyl sulfoxide was slowly added 50 g of 50% sodium hydride and then 220 m*l* of benzyl chloride with vigorous stirring. The mixture was heated on a water bath for 30 min and left standing overnight. The reaction mixture was poured into ice-water, extracted with benzene, benzene layer was washed with water, dried over sodium sulfate and concentrated *in vacuo*. Last traces of benzyl chloride and dimethyl sulfoxide were removed in a high vacuum. The syrup thus obtained has no absorption due to OH stretching vibration. Yield; 90 g.

A suspension of 90 g of 1,2;5,6-tetra-*O*-benzyl-3,4-*O*-isopropylidene-D-mannitol in 200 m*l* of ethanol, 70 m*l* of water and 36 m*l* of concentrated hydrochloric acid was refluxed for 2 hr, and concentrated under reduced pressure to about 100 m*l* and extracted with benzene (400 m*l*). The benzene layer was washed first with a potassium carbonate solution and then water. The benzene layer was concentrated to a syrup. The syrup was washed with petroleum ether and dried *in vacuo*. Yield, 67 g (70%).

To a vigorously stirred solution of 40 g of 1,2;5,6-tetra-*O*-benzyl-D-mannitol in 500 m*l* of benzene was added 34 g of lead tetraacetate. The reaction mixture was stirred at room temperature for 3 hr. The resulting precipitate was filtered off. The mother liquor was dried over sodium sulfate and concentrated under reduced pressure to give a syrup. The syrup was distilled at 143—144°C/0.003 mmHg. $[\alpha]_{578}$ +52, $[\alpha]_{546}$ +58 (c=2.00, l=0.5, benzene). Yield, 20 g.

Found: C, 75.59; H, 7.04%. Calcd for $C_{17}H_{18}O_3$: C, 75.53; H, 6.71%.

The distillate has no substantial absorption in the OH region but has a remarkable absorption at about 1715 cm^{-1} which is due to aldehydic carbonyl stretching vibration.

The authors express their cordial thanks to Mr. K. Fukukawa for measurements of NMR spectra.

BULLETIN OF THE CHEMICAL SOCIETY OF JAPAN VOL. 42 2961—2965 (1969)

Synthetic Studies of Cobalt Carbonyl by Noble Metal Catalysts. I.*[1] The Effects of the Form of Cobalt Feed and Noble Metal Catalysts

Seiji USAMI, Takayoshi KONDO, Kotaro NISHIMURA and Yuzo KOGA

Central Research Laboratory, Toa Nenryo K. K., Oi-cho, Iruma-gun, Saitama

(Received March 24, 1969)

A novel method of synthesizing cobalt carbonyl was investigated by using noble metal catalysts. It has been observed that the materials containing palladium, *i. e.*, palladium black, palladium chloride, palladium acetylacetonate, bistriphenylphosphine dichloropalladium, and palladium-on-carriers, have a catalytic effect on the cobalt carbonylation reaction, and that palladium-on-carbon (Pd-C) is the most active catalyst. The reactivity of cobalt compounds in the cobalt carbonylation reaction catalyzed by noble metals increases in this order: $CoSO_4 \ll CoO \lesssim Co(OAc)_2 \lesssim$ Co-oleate $< Co(OH)_2$. When the Pd-C catalyst is used, cobalt hydroxide reacts with synthesis gas of 150 kg/cm^2 to give cobalt carbonyl almost quantitatively, even at from 50 to 55°C. The catalytic activities of noble metals were shown to be, in the order of decreasing activity: Pd > Au > Pt $\gg$ Ag. The effect of the catalyst concentration and the activity of noble-metal catalysts were also compared with those in the case of dicobalt octacarbonyl, as an auto-catalyst.

Cobalt carbonyl has been used in various organic synthetic reactions, *e. g.*, in hydroformylation, oligomerization, and the synthesis of acetic acid from methanol, and as a metal source for the synthesis of many organo-metal complexes. Many methods of synthesizing cobalt carbonyl have been proposed.

Making a general classification, the methods of synthesizing cobalt carbonyl may be divided into

*1 Presented partly at the 21st Annual Meeting of the Chemical Society of Japan, Osaka, April, 1968.

main methods, *i. e.*, with or without an autocatalyst. In the method without an autocatalyst, the cobalt carbonyl is prepared from inorganic cobalt salt and carbon monoxide in the presence of an alkaline substance,[1] or from cobaltous salts of weak acids under a high pressure of carbon monoxide[2] or synthesis gas.[3] On the other hand, the cobalt carbonyl is also prepared by using dicobalt octacarbonyl as an autocatalyst.[4] However, no synthetic method using any catalyst other than the autocatalyst has ever been reported.

In the present investigation, the promoting ability of several noble metals, *i. e.*, palladium, platinum, gold, and silver, which have been known to form the corresponding simple metal carbonyls only with difficulty, has been studied in connection with the cobalt carbonylation reaction.

Experimental

Reaction Procedures. The experimental method will be explained in terms of a typical run. An autoclave (500 m*l*), made of stainless steel and equipped with a magnetic stirrer, was used. *n*-Butyl alcohol (190 m*l*), 0.241 mol of a cobaltous compound, and 2.36 atom% of palladium-on-cobalt were placed in the autoclave. After the air in the autoclave had been replaced with synthesis gas ($H_2/CO=1.2$), the synthesis gas was introduced up to 150 kg/cm^2.

The autoclave was heated rapidly until 40°C and then at a rate of 0.6°C per minute until the gauge pressure began to decline. The temperature when the pressure began to drop was defined as the initiation temperature of the reaction, as is illustrated in Fig. 1, and the initiation temperature was used as one of the scales for measuring the reaction activity of cobalt salts and the promoting ability of the materials added. The autoclave was then kept at the initiation temperature for 60 min. Thereafter, the autoclave was rapidly cooled and depressured, and the cobalt carbonyl produced was taken out and analyzed.

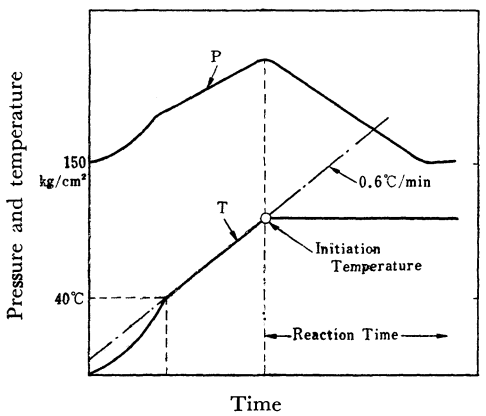

Fig. 1. Definition of the initiation temperature of reaction.

Analytical Procedures. The gasometric method reported by Wender *et al.*[5] was employed to determine the content of cobalt carbonyl in the carbonylation products. The crystals obtained from the products were identified as dicobalt octacarbonyl by the gasometric method, by infrared spectrometry, and by cobalt-metal analysis.

The cobalt and palladium were analyzed by the flame-photometric method.

Materials. The cobalt compounds and solvents were commercially available and were proved to be sufficiently pure. Materials containing palladium, *e. g.*, palladium chloride, palladium acetylacetonate, and palladium black, were purchased, but bis-triphenylphosphine dichloropalladium was prepared according to the method of Chatt.[6] The palladium-, platinum-, gold-, silver-, and copper-on-carbon (300 mesh up) containing 5 wt% metal were also commercially-available materials.

Results and Discussion

The Promoting Abilities of Materials Containing Palladium. The promoting abilities of various materials containing palladium were investigated in connection with the cobalt-carbonylation reaction. The results are summarized in Table 1. As Table 1 shows, in the absence of palladium, there was an induction period of about 10 min before the initiation of the cobalt carbonylation reaction even at high temperatures, from 213 to 220°C. However, the reaction occurred without any induction period even at extremely low temperatures when a catalytic amount of palladium was present. When the amount of palladium added was fixed at 2 atom%, the initiation temperatures were 155, 103, and 50—55°C for palladium black, palladium chloride, and palladium-on-carbon respectively.

The palladium complexes containing organic ligands, *i. e.*, palladium acetylacetonate and bis-triphenylphosphine dichloropalladium, were less active than the above palladium compounds. These findings seem to indicate that the most efficient form of materials containing palladium is the metal supported on a carrier.

When we compare the activity of dicobalt octacarbonyl as an autocatalyst with the materials containing palladium, we find that the autocatalyst is remarkably inferior to palladium-on-carbon.

1) P. Gilmont and A. A. Blanchard, "Inorganic Syntheses," Vol. II, ed. by W. C. Fernelius (Editor-in-Chief), McGraw-Hill Book Company, New York (1946), p. 238.

2) R. H. Hasek, U. S. Pat. 2865716 (1958).

3) I. Wender, H. W. Sternberg, S. Meltin and M. Orchin, "Inorganic Syntheses," Vol. V, ed. by T. Moeller (Editor-in-Chief), McGraw-Hill Book Co., New York (1957), p. 190.

4) J. Kato, H. Wakamatsu and H. Iwanara, Japanese Pat. 265091 (1960).

5) H. W. Sternberg, I. Wender and M. Orchin, *Anal. Chem.*, **24**(1), 174 (1952).

6) J. Chatt, *J. Chem. Soc.*, **1939**, 1631.

Table 1. The activities of various palladium promoters*1

Catalyst	None	Pd black	Pd-*3 C	$PdCl_2 \cdot 2H_2O$	Pd $(acac)_2$	$PdCl_2(ph_3P)_2$	$Co_2(CO)_8$*4
Initiation temp. °C	213—220*2	155	50—55	103	159	189	83

*1 Reaction conditions: cobalt hydroxide, 0.241 mol; materials containing palladium (2.36 atom%) on cobalt and *n*-butyl alcohol (190 m*l*); initial pressure 150 atm; H_2/CO ratio of synthesis gas, 1:2.
*2 An induction period of 9 min was observed.
*3 Palladium on carbon; 300 mesh up; Pd contents 5%.
*4 2.36 atom% on cobalt hydroxide feed was added.

Table 2. The effects of the carriers*1

Carrier	Carbon	Zeolite	γ-Alumina	Titania	Black*3
SA,*2 m^2/g	1200	69	170	10	89
Particle size, mesh	300	100	300	200—300	—
Pd contents,*4 %	5	7.5	3	3	99.9
Initiation temp. °C	50—55	67	124	138	155

*1 The reactions were carried out under the same conditions as are presented in Table 1.
*2 The specific surface area of Pd on a carrier catalyst measured by the BET method using nitrogen.
*3 Palladium black, referential data.
*4 Pd concentration is fixed at 2.36 mol% on cobalt in each case.

Table 3. The reactivities of various cobalt compounds*1

No.	Cobalt compound	Solvent	Initiation temp. °C	Yield of cobalt carbonyl (mol%)
1	Cobalt metal powder*2	*n*-butyl alcohol	78	18.2
2	Cobalt oleate	*n*-butyl alcohol	76	73.9
3	$Co(CH_3COO)_2 \cdot 4H_2O$	*n*-butyl alcohol	75	72.8
4	$CoSO_4 \cdot 7H_2O$	*n*-butyl alcohol	220	no reaction
5	$Co(OH)_2$	*n*-butyl alcohol	50—55	62.2
6	$Co(OH)_2$	mixed solvent*3	60	97.0

*1 Reaction conditions: Feed, 0.241 mol (No. 1 to 5), 0.059 mol (No. 6); Pd on carbon (Pd content 5 wt%), 2.36 atom% on feed (No. 1 to 5), 2.41 atom% (No. 6); Solvent, 190 m*l*. Synthesis gas (H_2/CO 1.2) 150 kg/cm^2; Reaction time, 60 min. No carbon monoxide was supplied after the initiation of the reactions in the runs No. 1 to No. 5 but the reaction in No. 6 was carried out under a constant pressure by supplying carbon monoxide.
*2 Commercially-available material: cobalt content 96.5 wt%, CoO 15.86%.
3* 100 m*l* of *n*-butyl alcohol and 90 m*l* of toluene.

This fact is important in considering the reaction mechanism of cobalt carbonylation in the presence of palladium.

The Effect of the Carrier. The effect of the carrier of the materials containing palladium on the initiation temperature was also examined.

As Table 2 shows, the carrier remarkably affects the activity of the materials containing palladium. The palladium supported on a carrier is relatively more active than palladium black, which includes no carrier, palladium-on-carbon is the most active material among the palladiums supported on carriers. These results indicate the specific incorporation of palladium and carrier. The relation between the activity of the palladium-on-carrier and the physical properties, *i. e.*, the surface area and the particle size, was also investigated. However, the reactivity seems to be due to key factors other than those properties.

The Reactivities of Various Cobalt Compounds. The reactivities of various cobalt compounds in the cobalt-carbonylation reaction were examined in the presence of palladium-on-carbon; the results are shown in Table 3.

When commercially-available cobalt metal powder (300 mesh up) containing 96.5 per cent of cobalt was used, the carbonylation reaction was initiated at 78°C. Afterwards, it was revealed by X-ray analysis that the remarkable activity of cobalt metal powder was due to the cobalt monoxide which was formed on the surface of the cobalt metal powder rather than to the cobalt metal itself. Cobalt acetate and oleate showed similar initiation temperatures of from 75 to 76°C, while cobalt hydroxide showed much lower initiation temperatures between 50 and 55°C. The reactions

of those cobalt compounds were carried out at each initiation temperature for 60 min, the yields of cobalt carbonyl were about 60 to 70 mole per cent in each case.

These reaction conditions were unfit for determining the yield at complete conversion because of the following reasons. First, no excess of carbon monoxide was supplied. Second, the accurate analysis of the product was difficult, because large amounts of crystalline dicobalt octacarbonyl were precipitated from the reaction mixture and mingled with the powdery palladium-on-carbon. To determine accurately the yield at complete conversion for the reaction system using cobalt hydroxide, palladium-on-carbon, and butyl alcohol as solvents, the reaction with a lower concentration in cobalt hydroxide by supplying carbon monoxide was carried out in a solvent mixture of butyl alcohol and toluene, which is a good solvent system for the dicobalt octacarbonyl. Cobalt carbonyl was thus obtained in a 97% yield when these was a reaction at 60°C for 60 min, as is shown in Table 3. Moreover, no crystalline cobalt carbonyl was found in the reaction product. In the case of using cobalt sulfate, no reaction occurred until 220°C. These results may be understood easily by considering that the following equilibrium between the formation and the decomposition of cobalt carbonyl is partial to the left side:

$$2CoSO_4 + 8CO + 2H_2 \rightleftarrows Co_2(CO)_8 + 2H_2SO_4$$

The Effect of the Palladium Concentration. The effect of the palladium concentration in the reaction zone on the initiation temperature was investigated by using *n*-butyl alcohol as the solvent. The results are shown in Fig. 2.

The plot of the initiation temperature against the ratio of the promoter metal to the cobalt concentration indicates that the initiation temperature significantly decreases, with only a small increase (less than 1 atom percent on cobalt) in the concentration of palladium, and that less than 5 per cent of the palladium concentration gives rise to an adequate efficiency.

By comparing the effect of the palladium concentration on the initiation temperature with that of dicobalt octacarbonyl as an autocatalyst, as is shown in Fig. 2, the strong promoting activity of palladium-on-carbon is easily evaluated. In addition, no dissolved palladium was detected in the solution of the reaction product by careful analysis using a "Plane Grating Spectrograph Model GE 340." The behavior of palladium in the reaction mentioned above may be considered to suggest that palladium operates catalytically in the cobalt carbonylation reaction.

Catalytic Activity of Other Noble Metals. The other metals which are found in the neighborhood of palladium in the periodic table and which are generally considered to form simple metal carbonyls by themselves only with difficulty have also been investigated to see if they promote the cobalt carbonylation reaction.

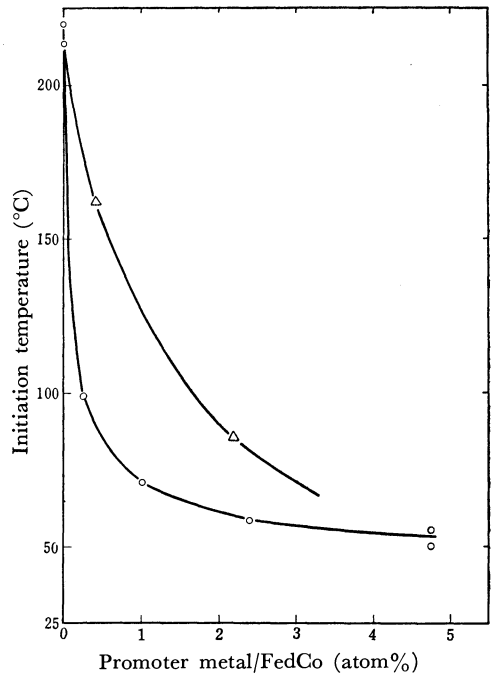

Fig. 2. Effects of the concentrations of promoters on the initiation temperature.
$Co(OH)_2$ 0.241 mol, Synthesis gas (H_2 : CO= 1.2 : 1) 150 kg/cm², *n*-BuOH 190 ml
⊙ Pd-C (H_2O (7.9 volume% on *n*-BuOH) was added in this series.)
△ $Co_2(CO)_8$

The experiments with the palladium catalyst showed that metal-on-carbon was the most active form. Platinum, gold, silver, and copper were tested as the metal-on-carbon for each metal. The results are shown in Fig. 3.

The initiation temperature in the reaction using the platinum-on-carbon catalyst fell sharply to 100°C when the concentration of platinum was increased to 0.723 atom%. However, little additional effect occurred over 1 atom%.

On the other hand, with gold-on-carbon, the initiation temperature fell gradually along the curve with the platinum catalyst in the low-concentration region, but over 1 atom% it fell dramatically, as was the case with palladium. At the Au/Co ratio of 4.5 atom%, gold-on-carbon can initiate the reaction at temperatures as low as 55°C. Silver-on-carbon showed only a poor activity, and copper-on-carbon had practically no effect on the cobalt-carbonylation reaction.

Thus, the relative activities of carbon-supported metals in the cobalt carbonylation are as follows: Pd> Au> Pt≫Ag≫Cu.

It is clear from the available data that platinum- and gold-on-carbon are excellent alternative cata-

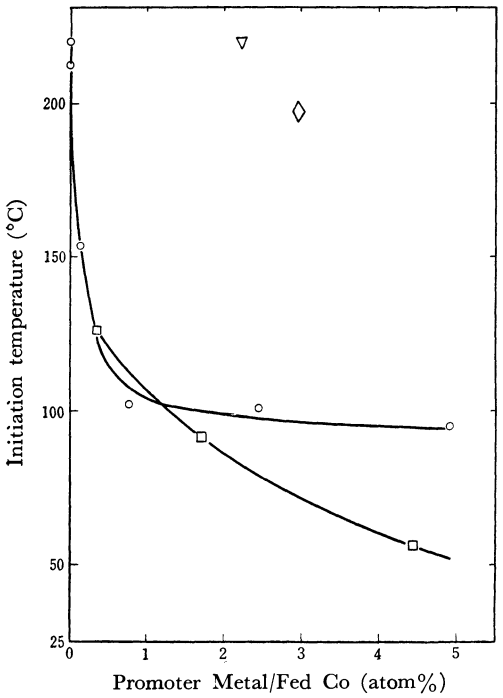

Fig. 3. Promoting activities of various metals in the cobalt carbonylation reaction.
$Co(OH)_2$ 0.241 mol, Synthesis Gas $H_2 : CO = 1.2 : 1$, 150 kg/cm², *n*-BuOH 190 m*l*
○ Pt-C (5%Pt), □ Au-C (5%Au), ◇ Ag-C (5%Ag), ▽ Cu—C (5%Cu)

lysts, and that palladium-on-carbon is still the best among the five materials examined here.

Summary

Cobalt carbonyl synthesis with noble metals as promoters has been investigated by using the initiation temperature of the reaction as a measure. The results of this study are as follows.

(1) It has been observed that materials containing palladium, platinum, gold, and silver have promoting effects on the cobalt-carbonylation reaction. The form of the materials containing metal significantly affects the promoting activity. Metal supported on active carbon exhibits an activity superior to that of the corresponding salts or complexes. The promoting activities of the noble metals supported on carbon examined here are in the order of: $Pd > Au > Pt \gg Ag$.

(2) From the plots of the promoter concentration against the initiation temperature, it has been revealed that by adding a small amount of noble metal promoters the initiation temperature of the reaction is markedly lowered; with an increase in the concentration, Pd and Au serve to lower the initiation temperature whereas Pt gives a constant initiation temperature above a certain concentration. Dicobalt octacarbonyl as an autocatalyst shows a concentration effect similar to those of Pd and Au, but the activity is much inferior to theirs.

(3) A cobalt-carbonylation reaction with a Pd-C promoter is also affected by the kind of cobalt compound as in the conventional case. The reactivities are in the order: $Co(OH)_2 >$ Co oleate $\simeq Co(oAc)_2 \simeq CoO \gg CoSO_4$.

Cobalt hydroxide, then, reacts at temperatures as low as from 50 to 55°C.

(4) It has been shown by a careful analysis that no dissolved palladium is present in the product solution. This and other data suggest that noble-metal promoters operate catalytically in the cobalt-carbonylation reaction.

BULLETIN OF THE CHEMICAL SOCIETY OF JAPAN VOL. 42 2966—2970 (1969)

Synthetic Studies of Cobalt Carbonyl by Noble Metal Catalysts. II.*1 The Investigation of Reaction Conditions

Seiji USAMI, Kotaro NISHIMURA, Takeo KOYAMA and Saburo FUKUSHI

Central Research Laboratory, Toa Nenryo Kogyo K. K., Tsurugaoka, Oi-cho, Iruma-gun, Saitama

(Received March 24, 1969)

The reaction conditions of cobalt carbonylation catalyzed by palladium have been investigated. Polar solvents have, with some exceptions, been shown to be superior to nonpolar solvents. The fact that the total pressure of synthesis gas and the partial pressure of hydrogen, especially the latter, have a great effect on the initiation temperature of reaction suggests that the presence of hydrogen is very important in the present reaction. The low reactivity and poor yield in the reactions of Raney cobalt indicate that a low-valency intermediate in the course of the cobalt-carbonylation reaction of cobaltous compounds may be somewhat different from the Raney-type Co(0). The initial step of the reaction seems to be affected only a little by various additives *e. g.*, water, triphenyl phosphine, lead naphthenate, and sodium hydroxide. The data previously available suggest that a palladium catalyst may primarily promote the reduction of Co(II) to Co(0) by activating hydrogen. The test of the lifetime of a palladium-on-carbon catalyst for a month indicates that there is no apparent decrease in the catalytic activity within this period.

Previous work[1] in our laboratory has shown that material containing palladium, platinum, gold, or silver, especially metals supported on active carbon, catalytically promotes the cobalt-carbonylation reaction.

In the present program, the effects of solvent, pressure, and additives on cobalt-carbonylation reactions catalyzed by palladium have been investigated.

Furthermore, in order to elucidate the behavior of palladium-on-carbon catalysts, the reaction of Raney cobalt has been studied. On the basis of these data, the role of the palladium catalyst will be briefly discussed.

Experimental

General Procedures. The experiments and the analysis of the reaction products were carried out in the way described in a previous paper.[1] The initiation temperature of the reaction, which was defined in the previous paper,[1] was also used here as one of scales measuring the reactivities of cobalt compounds and of the materials added.

Materials. Cobalt compounds, solvents, and other chemicals which were proved to be sufficiently pure were commercially available materials and were used without further purification. Palladium-on-carbon (300 mesh up) containing 5 wt% of palladium metal was purchased from the Kawaken Fine Chemicals Co., Ltd.

Raney Cobalt Feed. Thirty grams of Al-Co (1 : 1) alloy were added, drop by drop, to a 10% excess of an aqueous sodium hydroxide solution in open air or in a nitrogen atmosphere. After the addition has been completed, the developed Raney cobalt was decanted, washed with distilled water, and exchanged by acetone and finally by 190 m*l* of *n*-butanol. The freshly prepared suspension was used for the carbonylation reaction. After the reaction, the insoluble materials, *i. e.*, unreacted Raney cobalt and the catalyst, were filtered out and the cobalt carbonyl in the filtrate was analyzed as usual. The yield of cobalt carbonyl was calculated on the basis of the filtered solution of the reaction mixture in order to avoid any overestimation of the yield caused by adsorption gas on the surface of the Raney cobalt and the Pd-on-carbon.

Results and Discussion

The Effects of Solvents. The effects of solvents on the initiation temperature in the cobalt-carbonylation reaction promoted by palladium-on-carbon were studied, they are summarized in Table 1. The reaction was initiated at lower temperatures in such polar solvents as *n*-butanol, diethyl ether, isobutyraldehyde, and pyridine than in the nonpolar solvent, *n*-hexane. With isobutyraldehyde, however, the initiation temperature was somewhat higher compared to those of the polar solvents examined. Such a superior property of polar solvents has also been found in conventional cobalt-carbonylation reactions.[2,3] In any case, since the reaction catalyzed by palla-

*1 Presented in part at the 21st Annual Meeting of the Chemical Society of Japan, Osaka, April, 1968.

1) S. Usami, T. Kondo, K. Nishimura and Y. Koga, This Bulletin, **42**, 2961 (1969).

2) J. Kato, H. Wakamatsu and R. Iwanaga, Japanese Pat. 265091 (1960).

3) F. Calderazzo, R. Ercoli and G. Natta, "Organic Syntheses *via* Metal Carbonyls," Interscience Publishers, ed. by I. Wender and P. Pino, New York (1968), p. 20.

Table 1. Effects of solvents on the initiation temperature of the reaction

Solvent used	Initiation temperature °C
Diethyl ether	53
Pyridine	54.5
n-butanol	50—55
Isobutyraldehyde	61
n-Hexane	80

Reaction conditions: $Co(OH)_2$ 0.241 mol
Pd-C (5 wt% Pd; 300 mesh up): Pd/Fed Co 2.36 atom%
Solvent 190 m*l*, Synthesis gas (H_2/CO 1.2) 150 kg/cm²

dium proceeds smoothly at low temperatures in either solvent, it is possible to select a solvent according to whether the desired form of cobalt carbonyl is crystalline dicobalt octacarbonyl or another. However, care must be taken to use such solvents as pyridine or isobutyraldehyde, because the following reactions occur in these solvents to form the complex (I) or the trimer (II).

The isobutyraldehyde trimer (II) was identified by means of its molecular weight, elemental analysis, its melting point, and its IR spectra.

$$Co^{2+} + \text{Pyridine} \longrightarrow Co(Py)_6[Co(CO)_4]_2 \quad \text{(I)}$$

$$3(CH_3)_2CHCHO \xrightarrow{HCo(CO)_4} \text{2,4,6-triisopropyl-1,3,5-trioxane} \quad \text{(II)}$$

For experimental convenience, *n*-butanol was used as the solvent in the subsequent experimental runs unless otherwise noted.

The Effect of the Total Pressure. The influence of the total pressure of the synthesis gas on the initiation temperature was examined at a fixed ratio (1 : 3) of hydrogen to carbon monoxide. As Table 2 shows, the initiation temperature becomes higher with a decrease in the total pressure.

In these runs, the partial pressures of carbon monoxide were larger than the equilibrium pressures

Table 2. Effect of total pressure

Total press (kg/cm²)	Partial press (kg/cm²) H_2	Partial press (kg/cm²) CO	Equil. press P_{CO}* (kg/cm²)	Initiation temp. (°C)
142	77.5	64.5	0.7	50—55
72	39.3	32.7	1.7	72
26	14.8	11.2	2.8	82

* Calculated from Rudkovskii's equation.

of carbon monoxide at each temperature, while dicobalt octacarbonyl began to decompose thermally. The equilibrium pressure was calculated from the following equation, proposed by Rudkovskii:[4]

$$Co_2(CO)_8 \rightleftarrows 2Co + 8CO$$

$$\log P_{CO} = 7.94 - 2660/T$$

where P_{CO} and T are the partial pressure of CO (kg/cm²) and the absolute temperature (°K) respectively. From this and other data to be presented in the next section, it seems more likely that the upward tendency of the initiation temperature with a decrease in the total pressure is to be attributed to the effective concentration of gases, particularly hydrogen, in the liquid phase rather than to the equilibrium pressure of carbon monoxide.

In order to ascertain the yield of cobalt carbonyl in the reaction under a low pressure, the experiments were carried out with 58 mmol of cobalt hydroxide and 2.45 atom% of a palladium catalyst on cobalt in 190 m*l* of *n*-butanol. The results are shown in Table 3.

The pressure was kept at 80 kg/cm² by adding carbon monoxide; two experimental runs were carried out, one at 80°C for 100 min and one at 100°C for 60 min. Under those sets of conditions cobalt carbonyl was obtained in 79 and 88% yields, respectively. However, these yields were considered to be minimum values because of the analytical difficulty caused by the precipitation of crystalline $Co_2(CO)_8$. For comparison, the results at 150 kg/cm² of synthesis gas are also shown in the table, within the range of experimental error, a quantitative yield of cobalt carbonyl was attained even at temperatures as low as 60°C.

Table 3. Cobalt carbonyl synthesis under low pressure

Run No.	React. temp. (°C)	React. press. (kg/cm²)	React. time (min)	Cobalt carbonyl yield (mole %)	Note
1	80	80	100	79<	ppt of cryst. $Co_2(CO)_8$
2	100	80	60	88<	ppt of cryst. $Co_2(CO)_8$
3	60	150	60	97.0	no ppt of cryst. $Co_2(CO)_8$

$Co(OH)_2$ 0.0580 mol, Pd/Co 2.45 atom%, H_2/CO=1, Solvent *n*-BuOH 190 m*l*
In No. 1 and No. 2 runs, a conspicuous gas absorption stopped after 15 and 27 min respectively.
In No. 3 run, mixed solvent of *n*-BuOH 90 m*l* and benzene 100 m*l* was used.

4) a) D. P. Krinkin and D. M. Rudkovskii, *Zh. Prikl. Khim.* **38**(8), 1670 (1965). b) V. Yu. Gankin, D. P. Krinkin and D. M. Rudkovskii, *Zh. Fiz. Khim.* **40**(1), 215 (1966).

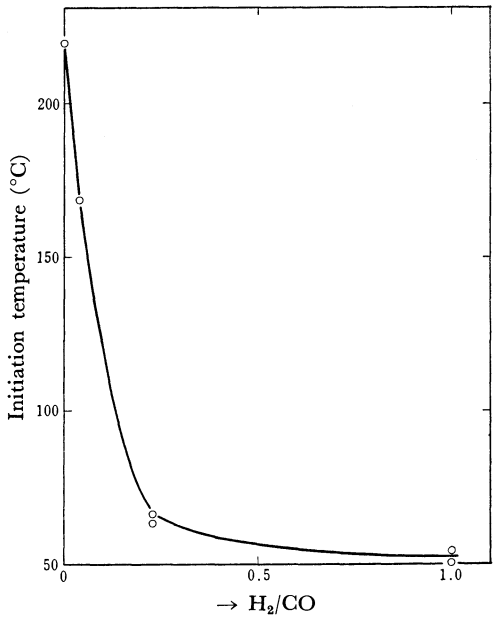

Fig. 1. Effect of H_2/CO ratio.
$Co(OH)_2$ 0.241 mol, Pd/Co 2.36 atom% *n*-BuOH 190 m*l*, Synthesis Gas. 150 kg/cm²

The Effect of the Partial Pressure. Reactions were conducted at a fixed total pressure of 150 kg/cm² but with various ratios of hydrogen to carbon monoxide. The results are shown in Fig. 1 as a plot of the ratio of hydrogen to carbon monoxide against the initiation temperature. In the absence of hydrogen, no decline in the gauge pressure was found until 220°C. However, after the reactor has been cooled, the gauge pressure became a little lower than the initial pressure, and about 10% of cobalt carbonyl was formed.

These facts suggest that the reaction rate under the above conditions is too slow for the pressure decline to be detected. It was interesting that, in the reaction under a carbon monoxide atmosphere, a dehydrogenation reaction of the solvent, *n*-butanol, occurred. Small amounts of *n*-butyraldehyde, 1,1-dibutoxy-*n*-butane, 2-ethylhex-2-en-1-al, and 2-ethylhexanol-1 were detected by gas chromatography. When *n*-butanol was treated with palladium-on-carbon under carbon monoxide pressure at 170°C for 7 hr, no dehydrogenation product was detected.

Therefore, hydrogen appears to be abstracted from *n*-butanol by cobalt. However, the above data are insufficient for us to conclude which is the immediate acceptor of hydrogen, cobalt or palladium, at 220°C, or how the hydrogen thus abstracted acts in the reaction. On the contrary, the cobalt-carbonylation reaction occurred at much lower temperatures when hydrogen was added. With a total pressure of 150 kg/cm² and otherwise identical conditions except that the partial pressures of hydrogen were 5.8, 28.0, and 81.8 kg/cm², the initiation temperatures were 170, 65, and 55°C respectively. These marked effects of added hydrogen on the initiation temperature are of great importance in considering the role of palladium catalysts.

Cobalt Carbonylation of Raney Cobalt. Experiments were carried out to see whether palladium catalysts participate on the step of the addition of carbon monoxide to a low-valent cobalt intermediate in the course of the cobalt-carbonylation reaction. Raney cobalt was selected on the assumption that the intermediate has zero valence and was very similar to Raney cobalt. The results are summarized in Table 4.

Table 4. Cobalt carbonylation of Raney cobalt

Pd/Co (atom %)	H_2/CO (V/V)	Atmosphere for develop. of Al-Co alloy	Reaction initiation temp. (°C)	Co carbonyl yield (mol%)
0	0	Air	200<	3.2
0	1	Air	185	1.2
2.22	0	Air	200<	6.3
2.22	1	Air	163	2.2
0	0	N_2	200<	2.8
0	1	N_2	183	1.4
2.22	0	N_2	200<	3.2
2.22	1	N_2	178	1.7

Raney Co 15.0 g, *n*-BuOH 190 m*l*, Total press. 150 kg/cm² Pd-C (5 wt% Pd; 300 mesh up), Reaction time 60 min.

With 150 kg/cm² of carbon monoxide, no decline in the pressure was observed up to 200°C even in the presence of a palladium catalyst. On the other hand, a slow but apparent decline of the pressure was observed from 170 to 185°C in the reaction under 150 kg/cm² of synthesis gas, irrespective of the presence of a palladium catalyst. However, equally poor yields of cobalt carbonyl were obtained in both reactions under carbon monoxide and in the pressure of synthesis gas. A similar low yield in the conventional cobalt carbonylation with Raney cobalt has also been disclosed in the literature.[5]

According to a German patent,[6] cobalt carbonylation with reduced cobalt is strongly inhibited by a small amount of oxygen. In the present study, however, this factor may be excluded because the reactions of Raney cobalt developed in nitrogen and in an open atmosphere give very similar results. The results obtained here indicate that the reaction rate with Raney cobalt is much slower than that with cobalt hydroxide. In conclusion, it

5) Ref. 3, p. 19.
6) I. G. Farben A. G., Brit. Pat. 307112 (1927); *Chem. Abstr.*, **23**, 5281 (1929).

seems reasonable to consider that the low-valent intermediate in the course of the cobalt carbonylation of a cobaltous compound, cobalt hydroxide, for example, is somewhat different from the Raney-type cobalt, Co(0), Therefore, the role of the palladium catalyst in this step is still obscure.

The Effects of Additives. In order to characterize the reaction in more detail, various materials, *i. e.*, dicobalt octacarbonyl, water, triphenyl phosphine, pyridine, dihexyl sulfide, lead naphthenate, and sodium hydroxide, were added to the reaction system. The results are listed in Table 5. The

Table 5. Effect of various additives

Additive	Additive/Pd (mol%)	H_2O/*n*BuOH (wt%)	Reaction initiation temp. (°C)
$Co_2(CO)_8$	26.0	—	51
none	—	—	50—55
none	—	7.9	58
Ph_3P	10.8	7.9	58
Pyridine	38.2	7.9	64
$(C_6H_{13})_2S$	10.8	—	55
Pb-Naph.	10.8	—	63
NaOH	10.8	—	61

reaction where dicobalt octacarbonyl coexisted with a palladium catalyst gave essentially the same initiation temperature as the case without dicobalt octacarbonyl as an additive. Such organic ligands as triphenyl phosphine and pyridine also had little effect on the initiation temperature. These results may be understood from the consideration that the examined materials probably react with cobalt carbonyl once formed and do not participiate in the step of cobalt-carbonyl formation. The addition of sulfur compounds such as dihexyl sulfide and heavy metals such as lead naphthenate, which are regarded as strong poisons for a usual hydrogenation reaction, showed no significant retarding effect. Sodium hydroxide, which seems to be a retarder of autocatalysis by cobalt hydrocarbonyl, also exerted the same retardation as lead soap. It is noteworthy that the initial step of cobalt carbonylation catalyzed by palladium-on-carbon is affected only a little by various additives. This phenomenon is considered to be very closely related to the characteristic mode of cobalt carbonylation where cobalt is reduced by hydrogen, even in the presence of such a strong poison as carbon monoxide in the general hydrogenation reaction.

The Role of the Palladium-on-carbon Catalyst. The reaction of cobalt carbonylation is schematically shown in Fig. 2. The first step (I) is the reduction of cobaltous cobalt to a low-valent intermediate; the second (II), is the coordination of carbon monoxide to the reduced cobalt intermediate, and the final step (III) is the reaction of the dicobalt octacarbonyl thus formed with hydrogen to produce cobalt hydrocarbonyl.

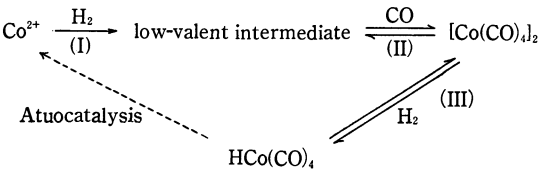

Fig. 2. Schematic reaction path of cobalt carbonylation.

Of these three steps, the contribution of hydrogen must be considered in I and III. If neither dicobalt octacarbonyl nor cobalt hydrocarbonyl is initially added as an autocatalyst, the contribution of hydrogen in III can be disregarded, at least at the beginning of the reaction. The following facts have been pointed out above:

1) The cobalt-carbonylation reaction is very slow under the pressure of only carbon monoxide, even in the presence of a palladium catalyst.

2) Even in the presence of hydrogen, when no palladium-on-carbon catalyst is used, a high initiation temperature is needed.

3) The reaction is promoted very much by the coexistence of hydrogen and a palladium catalyst.

In view of the above facts, the most reasonable conclusion to be drawn from the available data is that the role of a palladium-on-carbon catalyst consists in reducing Co(II) to a low-valent intermediate by activating hydrogen in I. From the observed difficulty in the cobalt carbonylation of Raney cobalt compared with that of cobalt hydroxide, a low-valent intermediate may be somewhat different from the Raney-type Co(0).

According to the equation presented by Rudkovskii,[4b] the equilibrium constant of Step III is calculated to be 3.37×10^{-5} at 52.5°C.

On the other hand, Iwanaga[7] has reported that the rate of (III) at 100°C under 100 to 200 kg/cm² of synthesis gas (H_2/CO; 1) is 1.7 mol%/min. Judging from these data, the contribution of an autocatalyst to the cobalt-carbonylation reaction with a palladium catalyst at a low temperature (55—55°C) is suspected to be very small.

Test of Catalyst Life. In order to ascertain the lifetime of a palladium-on-carbon catalyst, a flow test run was conducted for one month by using cobalt oleate at 120°C under a synthesis-gas (H_2/CO; 1.2) pressure of 200 kg/cm². No tendency of the catalytic activity to decrease could be observed within that period.

7) R. Iwanaga, This Bulletin, **35**, 774 (1962).

Summary

Following the preceding experiment, the reaction conditions of cobalt carbonylation catalyzed by palladium-on-carbon have been investigated. The experimental results obtained here indicate the following:

1) Such polar solvents as *n*-butanol, diethyl ether, isobutyraldehyde, and pyridine show excellent properties compared with the nonpolar solvent, *n*-hexane. In an ether solvent, the reaction proceeds smoothly at lower temperatures. Isobutyraldehyde and pyridine are not suitable for simple cobalt-carbonyl synthesis, since they easily react under the present reaction conditions.

2) With a decrease in the total pressure below 100 kg/cm^2, the initiation temperature of the reaction becomes higher. On the other hand, a marked lowering of the initiation temperature upon the addition of a small volume of hydrogen to the carbon monoxide atmosphere was observed. These data indicate that the presence of hydrogen is very important for the reaction.

A high yield of cobalt carbonyl can be obtained even at low pressure by adding carbon monoxide.

3) It is difficult for Raney cobalt to give cobalt carbonyl under a synthesis gas even in the presence of a palladium catalyst. Therefore, the low-valency intermediate in the course of cobalt carbonylation from a cobaltous compound may be somewhat different from the Raney-type Co(0).

4) The initiation temperature of the reaction is not affected significantly by such additives as water, dicobalt octacarbonyl, triphenyl phosphine, pyridine, dihexyl sulfide, lead naphthenate, and NaOH. This fact indicates that at least the initial step of the reaction is affected only a little by the above additives.

5) The available data suggest that the role of a palladium catalyst consists in reducing Co(II) to Co(0) by activating hydrogen.

6) The test of lifetime of a palladium-on-carbon catalyst for a one-month period gives no proof of a decrease in catalytic activity.

BULLETIN OF THE CHEMICAL SOCIETY OF JAPAN VOL. 42 2970—2973 (1969)

Photoinduced Reactions. XXXIII. Photochemical Reaction of a *para*-Quinone Methide[1]

Teruo MATSUURA and Katsuyuki OGURA

Department of Synthetic Chemistry, Faculty of Engineering, Kyoto University, Sakyo-ku, Kyoto

(Received March 28, 1969)

The photochemistry of a quinone methide (Ia) was investigated. Ia was unchanged on photolysis of an alcoholic solution (0.0064 M) with a high-pressure mercury lamp (Pyrex filter). However irradiation of a highly dilute solution of Ia or a sensitized reaction (acetophenone) gave an alcohol adduct (IIe in methanol and IIf in isopropyl alcohol) which might be formed *via* triplet excited state(s) of Ia. The methanol adduct IIe was also formed by the irradiation of Ia in methanol with a low-pressure mercury lamp through quartz. In this case the formation of IIe appears to be initiated by photochemical decomposition of methanol.

Photolysis of quinone methides is of interest in connection with the photochemical discoloration of xanthene dyes and the photorearrangement of 2,5-cyclohexadienones. We investigated the photochemistry of a quinone methide (Ia). During the course of our study, two papers on the photochemical reaction of quinone methides have appeared. Becker[2] found the quinone methide Ia to convert a phenol (IIa) by the photolysis of a highly dilute solution in isopropyl alcohol or by the acetophenone-sensitized photolysis. Recently, Krull and Schuster[3] showed that a quinone methide (Ib) in ethyl ether or cyclohexadiene afforded photochemically the corresponding solvent-adduct IIb or IIc, respectively, together with a small amount of a reduction product (IId). These papers prompted us to report the results obtained in our investigation on photolysis of the quinone methide Ia.

On photolysis of a methanol solution (0.0064 M) with a high-pressure mercury lamp (Pyrex filter) Ia was entirely unchanged. However, a methanol adduct IIe and a reduction product IIa were formed in the presence of acetophenone in 74 and 7% yields,

1) Part XXXII: T. Matsuura, K. Omura and A. Nishinaga, *Chem. Commun.*, **1969**, 366.

2) H.-D. Becker, *J. Org. Chem.*, **32** 2115 (1967).

3) I. S. Krull and D. I. Schuster, *Tetrahedron Letters*, **1968**, 135.

respectively. The structure of the adduct IIe was assigned from the NMR spectra of the adduct and of its acetate (see Experimental Section). The methanol adduct IIe was also formed as a main product in 50% yield by irradiation of a dilute methanol solution of Ia. The formation of IIe in the photolysis of a highly dilute solution of Ia or a sensitized reaction was perfectly quenched by air-bubbling. Therefore, it should be reasonable to presume that the adduct IIe was formed *via* the triplet excited state(s) of Ia. On the other hand, photolysis of a highly dilute solution of Ia in isopropyl alcohol with a high-pressure mercury lamp afforded not only the reduction product IIa (63% yield), as reported by Becker,[2] but also an isopropyl alcohol adduct (IIf) in 11% yield. The structure of the isopropyl alcohol adduct IIf was also deduced from its NMR spectrum.

It should be noted that the adduct IIe (44% yield) was also formed by the irradiation of Ia in methanol with a low-pressure mercury lamp (quartz filter) under bubbling nitrogen. On the other hand, in isopropyl alcohol the reduction product IIa was formed in 54% yield in addition to the adduct IIf (11%). In contrast to the photolysis of Ia with a high-pressure mercury lamp, the adduct IIe was also obtained in the presence of air, although in a low yield (14%), and 2,6-di-*t*-butyl-*p*-benzoquinone was obtained in 16% yield. When a low-pressure lamp with a Vycor filter was used for the photolysis of Ia in methanol, the formation of the adduct IIe was completely depressed. This is obviously due to the fact that a Vycor filter cuts off the 185-mμ line responsible for the photodecomposition of methanol to the hydroxymethyl radical as reported by Yang *et al.*[4] In fact, methanol was photochemically decomposed to afford ethylene glycol (80 mg per hour) with the low-pressure mercury lamp (quartz filer). These facts confirm that the formation of the adduct IIe in the photolysis of Ia with a low-pressure mercury lamp using a quartz filter resulted from the addition of the hydroxymethyl radicals, formed by the photochemical decomposition of methanol, to the quinone methide Ia as shown in Scheme I, rather than the excitation of Ia. The formation of IIe at high dilution or in the acetophenone-sensitized photolysis may be initiated by hydrogen abstraction of the triplet state(s) of Ia as described in Scheme II.

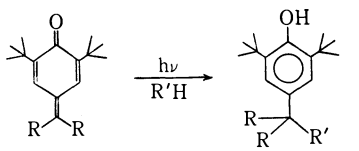

Ia R=Ph
Ib R=H

IIa R=Ph, R'=H
b R=H, R'=-CHOC$_2$H$_5$ (CH$_3$)
c R=H, R'=
d R=R'=H
e R=Ph, R'=-CH$_2$OH
f R=Ph, R'=-C(CH$_3$)$_2$OH

4) N. C. Yang, D. P. C. Tang, D. Thap S. and J. Sallo, *J. Am. Chem. Soc.*, **88**, 2851 (1966).

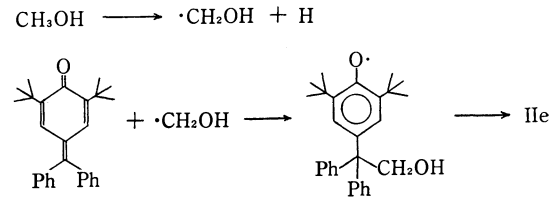

Scheme I

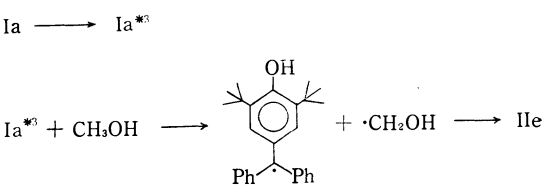

Scheme II

Experimental

Photolysis of Ia in Methanol. *(a) With a Low-pressure Mercury Arc Lamp.* A solution containing 1.00 g of the quinone methide Ia in 720 m*l* of methanol was irradiated for 15.5 hr with a 40 W low-pressure mercury arc lamp surrounded by a quartz filter under bubbling nitrogen. After removal of the solvent under reduced pressure, the residue was chromatographed on 40 g of silica gel. Elution with 75 m*l* of benzene yielded 120 mg of a yellow oil which was shown by a tlc analysis to contain a small amount of IIa. Further elution with 160 m*l* of benzene gave 482 mg of pale yellow crystals which were recrystallized from petroleum ether to afford the adduct IIe as colorless crystals, mp 119—120°C. NMR (in $CDCl_3$); τ 2.78 (10H, singlet, 2C_6H_5), 3.08 (2H, singlet, two aromatic protons), 4.88 (1H, singlet, a phenolic OH), 5.42 (2H, singlet, CH_2O-), 8.41 (1H, singlet, OH), and 8.66 (18H, singlet, two *t*-butyl groups).

Found: C, 83.30; H, 8.58%. Calcd for $C_{28}H_{34}O_2$: C, 83.54; H, 8.51%.

The acetate of the adduct IIe was prepared as usual (acetic anhydride and pyridine). Recrystallization from methanol gave colorless crystals, mp 124—126°C. NMR (in $CDCl_3$): τ 2.78 (10 H, a difused singlet, two phenyl). 3.11 (2H, singlet, two aromatic protons), 4.88 (1H, singlet, a phenolic OH), 4.92 (2H, singlet, CH_2O-), 8.12 (3H, singlet, CH_3COO), and 8.67 (18H, singlet, two *t*-butyl groups).

Found: C, 81.22; H, 8.32%. Calcd for $C_{30}H_{36}O_3$: C, 81.04; H, 8.16%.

(b) With a Low-pressure Mercury Arc Lamp under Air. A solution containing 500 mg of Ia in 250 m*l* of meth-

anol was irradiated for 16.5 hr with a 40 W low-pressure mercury arc lamp (quartz filter) under bubbling air. After removal of the solvent under reduced pressure, the residue was chromatographed on 40 g of silica gel. Elution with 200 m*l* of petroleum ether-benzene (1 : 1) gave 31 mg of a yellow oil which was shown by a vpc analysis to contain a trace of benzophenone. Further elution with 170 m*l* of the same solvent yielded 46 mg of yellow crystals, mp 59—60°C, which were identified as 2,6-di-*t*-butyl-*p*-benzoquinone (by infrared spectrum and mixture mp). Elution with 200 m*l* of benzene afforded 11mg of yellow oil which was not further investigated. Elution with 100 m*l* of benzene gave 84 mg of yellow crystals which were identified as the adduct IIe (by infrared spectrum).

(c) A Sensitized Reaction. A solution containing 500 mg of Ia and 6.67 g of acetophenone in 90 m*l* of methanol was irradiated for 17 hr with 100-W a high-pressure mercury arc lamp (Ushio UM 102) surrounded by a Pyrex cooling jacket under bubbling nitrogen. After the solvent had been removed under reduced pressure, the residue was chromatographed on 200 g of silica gel. Elution with 5 m*l* of benzene yielded 33 mg of yellow crystals. Recrystallization from methanol afforded 14 mg of pale yellow crystals which were identified as IIa (by infrared spectrum). Further elution with 20 m*l* of benzene gave 60 mg of a yellow oil which was not further investigated. Elution with 110 m*l* of benzene yielded 400 mg of yellow crystals. Recrystallization from petroleum ether gave 206 mg of colorless crystals, mp 118—120°C, which were identified as IIe (by infrared spectrum and mixture mp).

(d) With High Dilution. A solution containing *ca.* 15 mg of Ia in 1000 m*l* of methanol was irradiated with a 450-W high-pressure mercury arc lamp (Ushio UM 450) surrounded by a Pyrex cooling jacket under bubbling nitrogen until the yellow color discolored (50 min). Further *ca.* 15 mg of Ia was added and irradiated. This operation was repeated eight times and the total amount of the quinone methide Ia irradiated was 125 mg. After removal of the solvent under reduced pressure, the residue was chromatographed on 5 g of silica gel. Elution with 10 m*l* of benzene yielded 45 mg of a yellow oil which was shown by a tlc analysis to contain Ia and IIa. Further elution with 40 m*l* of benzene gave 68 mg of pale yellow crystals. Recrystallization from petroleum ether afforded pale yellow crystals, mp 119—120°C, which were identified as the adduct IIe (by infrared spectrum and mixture mp).

Photolysis of Ia in Isopropyl Alcohol. *(a) With a Low-pressure Mercury Arc Lamp.* A solution containing 500 mg of Ia in 200 m*l* of isopropanol was irradiated for 6 hr with a 40-W low-pressure mercury arc lamp surrounded a quartz filter under bubbling nitrogen. After removal of the solvent under reduced pressure, the residue was crystallized from petroleum ether to give 87 mg of pale yellow crystals, which were identified as IIa (by infrared spectrum). The mother liquor was chromatographed on 20 g of silica gel. Elution with 25 m*l* of petroleum ether - benzene (1 : 1) afforded 184 mg of pale yellow crystals, which were identified as IIa (by infrared spectrum). Further elution with 165 m*l* of petroleum ether - benzene (1 : 1) yielded 44 mg of a yellow oil which was not further investigated. Elution with 150 m*l* of petroleum ether - benzene (1 : 1) gave 66 mg of pale yellow crystals, which, on recrystallization from petroleum ether, afforded the adduct as chloroless crystals, mp 155.5—156.5°C. NMR (in $CDCl_3$); τ 2.81 (12H, a difiused singlet, two phenyl and two aromatic protons), 4.93 (1H, singlet, a phenolic OH), 8.44 (1H, singlet, OH), and 8.52 (6H, difused singlet, 2 CH_3), and 8.69 (18 H, singlet, two *t*-butyl groups).

Found: C, 83.71; H, 9.19%. Calcd for $C_{30}H_{38}O_2$: C, 83.67; H, 8.90%.

(b) With High Dilution. The procedure analogous to that performed in the photolysis of Ia in methanol was used. The total amount of the quinone methide Ia which was irradiated in a period of 28 hr was 330 mg. After removal of the solvent under reduced pressure, the residue was chromatographed on 15 g of silica gel. Elution with 100 m*l* of petroleum ether-benzene (1 : 1) gave 207 mg of yellow crystals which were identified as IIa (by infrared spectrum). Further elution with 50 m*l* of petroleum ether - benzene (1 : 1) afforded 13 mg of a yellow oil which was not investigated. Elution with 250 m*l* of 32 mg of yellow crystals, which were identified as IIf (by infrared spectrum).

One of the authors (K.O.) is indebted to Fuji Film Co. for a financial support.

BULLETIN OF THE CHEMICAL SOCIETY OF JAPAN VOL. 42 2973—2975 (1969)

Photoinduced Reactions. XXXIV. Photosensitized Oxygenation of 2,4,5-Triphenylthiazole[1]

Teruo MATSUURA and Isao SAITO

Department of Synthetic Chemistry, Faculty of Engineering, Kyoto University, Sakyo-ku, Kyoto

(Received March 28, 1969)

In connection with the photodynamic action of the biological systems, photosensitized oxygenation of a thiazole was investigated. Photooxidation of 2,4,5-triphenylthiazole in methanol in the presence of rose bengal resulted in the formation of benzil and benzamide. On the other hand, photooxidation of 2,4,5-triphenylthiazole in chloroform containing methylene blue as a sensitizer gave *N,N*-dibenzoylthiobenzamide in good yield. Possible mechanisms for these reactions, involving an *endo*-peroxide or a zwitterionic peroxide, are discussed.

Recently much attention has been drawn to the photosensitized oxygenation of five-membered heterocyclic bases in relation to the photodynamic action of the biological systems.[2] Although the photosensitized oxygenation of imidazoles,[3] pyrroles,[4] oxazoles,[5] indoles[6] and purines[7] has been studied extensively, the photooxidation of thiazole, which is an important part of thiamine, has never been investigated. In this paper, the photosensitized oxygenation of 2,4,5-triphenylthiazole is described. The results provide further information regarding the structure of the peroxide intermediate and the manner of its decomposition in the photosensitized oxygenation of five-membered heterocyclic compounds.

When a methanol solution of 2,4,5-triphenylthiazole (I) was subjected to photosensitized oxygenation in the presence of rose bengal, 0.45 mol equivalent of oxygen was consumed and benzil (II) and benzamide (III) were obtained in 11 and 18% yield, respectively.

On the other hand, when photosensitized oxygenation was carried out in chloroform using methylene blue as sensitizer, I afforded a different product. Thus, I gave, after consumption of 0.9 mol equivalent of oxygen, a red-colored compound $C_{21}H_{15}NO_2S$, an oxygen adduct of I, in 30% yield. The IR spectrum showed a broad carbonyl absorption band at 1700 cm^{-1}. In its UV spectrum a weak absorption maximum was observed at 500 mμ. Treatment of the adduct with boiling methanol gave thiobenzamide (V) in 50% yield. The adduct gave tribenzamide (VI) in aqueous silver nitrate solution in 10% yield. These reactions and spectral data are known to be generally found in the case of *N*-acylthiobenzamides.[8] The above results led us to assign structure IV to the adduct.

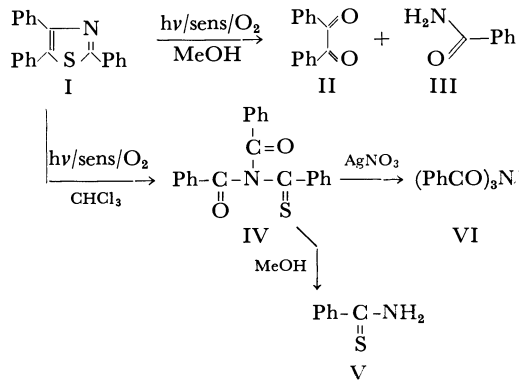

In the absence of the sensitizer, I did not consume oxygen and the starting material remained unchanged. This indicates that the presence of a sensitizer is a necessary condition for the present photooxygenation.

1) Part XXXIII. T. Matsuura and K. Ogura, This Bulletin, **42**, 2971 (1969).

2) M. I. Simon, "Comprehensive Biochemistry," Vol. 27, ed. by M. Florkin and E. H. Stotz, Elsevier Publishing Company, Amsterdam (1967), p. 137; D. Schugar and A. D. McLaren, "Photochemistry of Proteins and Nucleic Acids," Pergamon Press Inc., New York (1964).

3) H. H. Wasserman, K. Stiller and M. B. Floyd, *Tetrahedron Letters*, **1968**, 3277; M. Tomita, M. Irie and T. Ukita, *ibid.*, **1968**, 4933; T. Matsuura and M. Ikari, *Kogyo Kagaku Zassi (J. Chem. Soc. Japan, Ind. Chem. Sect.)*, **72**, 179 (1969) and references cited therein.

4) G. Rio, A. Ranhon, and O. Pouchot, *Compt. rend.*, **263**, 634 (1966) and references cited therein.

5) H. H. Wasserman and M. B. Floyd, *Tetrahedron*, Suppl. No. 7, 441 (1966).

6) Z. Yoshida and M. Kato, *J. Am. Chem. Soc.*, **76**, 311 (1954); *Nippon Kagaku Zassi (J. Chem. Soc. Japan, Pure Chem. Sect.)*, **75**, 112 (1954).

7) T. Matsuura and I. Saito, *Tetrahedron Letters*, **1968**, 3273; *Tetrahedron*, **24**, 6609 (1968); **25**, 541, 549, 557 (1969) and references cited therein.

8) J. Goerdeler and H. Horstmann, *Chem. Ber.*, **93**, 663 (1960).

The formation of benzil (II) and benzamide (III) in the photosensitized oxygenation of I in methanol is well rationalized by a pathway involving a cyclic peroxide VII (Scheme 1). Such a cyclic peroxide is commonly recognized as an intermediate in the photosensitized oxygenation of five-membered heterocycles, *i. e.*, imidazoles,[3] pyrroles,[4] oxazoles,[5] isoindoles[9] and isobenzothiophenes.[10] The initially formed peroxide VII could undergo rearrangement to form a Schiff base VIII, which is hydrolysed to give II and III. The loss of a sulfur atom from VII has analogy in the photosensitized oxygenation of 1,3-diphenylisobenzothiophene leading to the *o*-dibenzoylbenzene.[10]

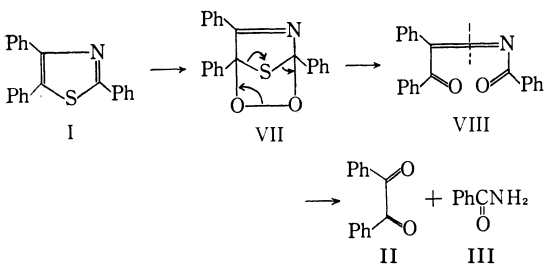

Scheme 1

In inert solvents such as chloroform, the photosensitized oxygenation of I takes a different course. Such a solvent effect on photooxidation has also been observed in the cases of purines[7] and oxazoles.[11] Two mechanisms seem to account for the formation of IV from I. In this case a zwitterionic peroxide IXa or IXb[3,7,12] is proposed for the first step intermediate. As shown in Scheme 2, IX could be rearranged to a four-membered cyclic peroxide X (path a), which undergoes ring cleavage to give *N*-benzoyl-*S*-benzoylisothiobenzamide (XI). Such a photooxidative cleavage of C=C double bond is analogous to the photooxidation of 1,2,3,4-tetraphenylpyrrole leading to α-*N*-benzoylamino-α'-benzoylstilbene.[13] The isothiobenzamide (XI) would then undergo further intramolecular rearrangement to give IV. Such a type of rearrangement has been proposed in the reaction of acyl chloride with thiobenzamide (Eq. (1))[8] and *N*-phenylthiobenzamide (Eq. (2)).[14] *S*-Benzoylisothiobenzamide (a) in the former and *N*-phenyl-*S*-benzoylisothiobenzamide (b) in the latter case are considered to be an intermediate.

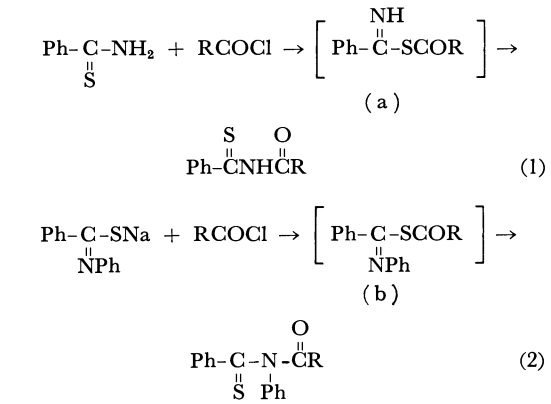

An alternative pathway (path b) involving a cyclic peroxide VII, which is analogous to the photosensitized oxygenation of oxazole,[5] may also account for the formation of IV. The peroxide VII could be rearranged to give XII, which undergoes an intramolecular rearrangement, analogous to *N*-benzoylisoimide, to give IV.[5] The formation of the *endo*-peroxide VII may occur either directly from I or stepwise *via* the zwitterionic peroxide IXa.

Although the above two modes of the formation of IV cannot be distinguished from the available results, path a seems to be more favorable considering the reaction of Eq. (2).

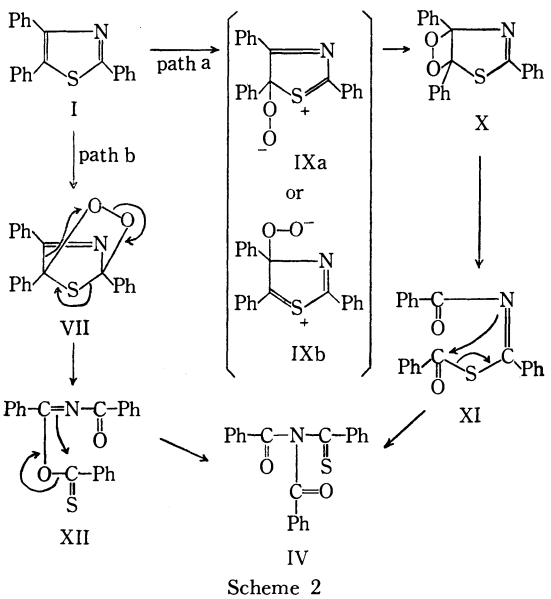

Scheme 2

Experimental

Photosensitized Oxygenation of 2,4,5-Triphenylthiazole (I). A. In Methanol. A solution of 2,4,5-

9) W. Theilacker and W. Schmidt, *Ann.*, **605**, 43 (1957).

10) C. Dufraisse and S. Ecary, *Compt. Red.*, **223**, 735 (1946); A. Mustafa, *J. Chem. Soc.*, **1949**, 256.

11) H. H. Wasserman and E. Druckrey, *J. Am. Chem. Soc.*, **90**, 2440 (1968).

12) C. S. Foote and J. W. P. Lin, *Tetrahedron Letters*, **1968**, 3267.

13) H. H. Wasserman and A. Liberles, *J. Am. Chem. Soc.*, **82**, 2086 (1960).

14) C. S. Jamieson, *ibid.*, **26**, 177 (1904).

triphenylthiazole[15] (I) (2.8 g. 9 mmol) in methanol (300 ml) containing rose bengal (50 mg) was irradiated at room temperature by a 100 W high-pressure mercury lamp through a Pyrex cooling jacket. During irradiation oxygen was bubbled by means of a circulating pump through a sintered-glass joint which was attached to the bottom of the reaction vessel. Oxygen consumption was manometrically followed. Oxygen absorption ceased after oxygen (105 ml, 4.2 mmol) had been taken up for 24 hr. After removal of the solvent *in vacuo*, the residue was chromatographed on a neutral alumina column (50 g). Elution with chloroform (400 ml) gave unchanged starting material (I) (0.95 g, 34% recovery). Further elution with chloroform (*ca.* 600 ml) gave benzil (II) (135 mg, 11% based on the reacted starting material). Recrystallization from ethanol gave yellow prisms, mp 93—94°C, which were identical with an authentic sample by comparison of their IR spectra. Chloroform (1000 ml) eluted benzamide (III) (95 mg, 18% based on reacted I). Recrystallization from ethanol gave crystals, mp 128°C.

B. In Chloroform. A solution of 2,4,5-triphenylthiazole (I) (2.4 g, 7.7 mmol) in dry chloroform (200 ml) containing methylene blue (50 mg) was irradiated by a 100 W high-pressure mercury lamp for 10 hr as described above, until oxygen (170 ml, 6.8 mmol) was consumed. The solvent was removed *in vacuo*, and the residue was dissolved in ether (100 ml). The ethereal solution was treated with Norit. After removal of the solvent, the residue was crystallized from ether to give *N,N*-dibenzoylthiobenzamide (IV) (0.78 g, 30%). Recrystallization from ether (5 ml) gave red-colored crystals, mp 102—103°C. $\lambda_{max}^{cyclohexane}$ 224 mμ (ε 29000), 233 (25000), and 500 (150); ν_{max}^{Nujol} 1700, 1600, and 1300—1200 cm^{-1}.

Found: C, 73.43; H, 4.47; N, 4.08; S, 9.24%. Calcd for $C_{21}H_{15}NO_2S$: C, 73.04; H, 4.63; N, 4.06; S, 9.28%.

Reactions of *N,N*-Dibenzoylthiobenzamide (IV). A. With Methanol. A solution of IV (100 mg) in methanol (40 ml) was boiled for 10 min. A thin layer chromatographic analysis (silica gel, chloroform-ethanol (20 : 1)) of the mixture showed that it consisted of at least five compounds among which thiobenzamide (V), (20 mg, 50%) was isolated by preparative thin layer chromatography.

B. With Silver Nitrate. To a suspension of IV (100 mg) in the mixture of methanol (10 ml) and water (10 ml) silver nitrate (400 mg) was added, according to the procedure of Goerdeler and Horstmen.[8] The solution was acidified, diluted with water (50 ml), and then extracted with ether (100 ml). After removal of ether, ethanol was added to the residue. The ethanol-insoluble solid was collected by filtration and was crystallized from boiling ethanol (*ca.* 80 ml) to give tribenzamide (VI) (10 mg, 10%), mp 198—200°C (lit,[16] mp 201—202°C), which was identical with the authentic sample prepared according to the method of Curtius[16] (by IR).

The authors wish to thank the Ministry of Education for a research grant.

15) K. Hubacher, *Ann.*, **259**, 245 (1890).

16) T. Curtius, *Ber.*, **23**, 3041 (1890).

BULLETIN OF THE CHEMICAL SOCIETY OF JAPAN VOL. 42 2975—2981 (1969)

Reactions of Diarylphosphines, Their Oxides and Sulfides with Isothiocyanates and Thiocyanic Acid

Iwao OJIMA, Kin-ya AKIBA and Naoki INAMOTO

Department of Chemistry, Faculty of Science, The University of Tokyo, Hongo, Bunkyo-ku, Tokyo

(Received April 10, 1969)

N-Substituted thiocarbamoyldiarylphosphine oxides and sulfides were prepared by the addition reaction of diarylphosphine oxides and diphenylphosphine sulfide with isothiocyanates. Diarylphosphine oxides and diphenylphosphine reacted with ammonium thiocyanate under hydrogen chloride stream to produce diarylphosphinyl- and diarylthiophosphinyl-substituted bis(iminomethyl) sulfides, which are a new type of sulfide. Diphenylphosphine also reacted with thiocyanic acid in ether to give thiocarbamoyldiphenylphosphine and bis(diphenylphosphinyliminomethyl) sulfide. Mechanisms for formation of these bis(iminomethyl) sulfides have been discussed.

In recent years, some attempts have been made to introduce the carbamoyl or thiocarbamoyl group to phosphines and phosphites.[1-3] Issleib and Harzfeld[3] prepared *N*-substituted thiocarbamoylphosphines by reactions of phosphines or their metal salts with isothiocyanates. *N*-Substituted thiocarbamoylphosphine oxides and sulfides were prepared by the reaction of the corresponding *N*-

1) T. Reetz, D. H. Chadwick, E. E. Hardy and S. Kaufman, *J. Am. Chem. Soc.*, **77**, 3813 (1955).

2) R. C. Schulz and H. Hartmann, *Monatsh. Chem.*, **93**, 905 (1962).

3) K. Issleib and G. Harzfeld, *Chem. Ber.*, **97**, 3430 (1964); *Z. anorg. allg. Chem.*, **351**, 18 (1967).

substituted thiocarbamoylphosphines with oxygen and sulfur, respectively.

We found that diarylphosphine oxides (I) and diphenylphosphine sulfide (I′, R=C_6H_5) as well as phosphines reacted with isothiocyanates in the presence of a few drops of triethylamine[4] at 70—80°C to give *N*-substituted thiocarbamoyldiarylphosphine oxides (II) and sulfides (II′) in good yields, respectively. These results are summarized in Table 1. The elemental analyses and spectral data of these compounds support the structures (see Tables 2 and 3).

$$R_2PH + R'NCS \xrightarrow{Et_3N} R_2PCSNHR'$$

$$\begin{matrix} R_2P(=X)H & & R_2P(=X)CSNHR' \end{matrix}$$

I : X=O II : X=O
I′: X=S II′: X=S

As shown in Table 3, the UV spectra of II and II′ in ethyl alcohol displayed an intense band in the 290—350 mμ region, which presumably arises from the π–π^* transition in the C=S group. The n–π^* transition band appeared in the 390—450 mμ region.

Table 1. *N*-Substituted thiocarbamoyldiarylphosphine oxides (II) and sulfides (II′)

	R	R′	Mp (°C) (lit)	Yield (%)
IIa	C_6H_5	CH_3	190—191 (194)[3]	87
IIb*	C_6H_5	CH_2=$CHCH_2$	119—122	80
IIc*	C_6H_5	α-$C_{10}H_7$	181—183	67
IId*	C_6H_5	C_6H_5	163.5—164.5	75
IIe*	p-$CH_3C_6H_4$	C_6H_5	163—164	68.5
IIf*	p-$CH_3OC_6H_4$	C_6H_5	138—140	65
IIg*	p-ClC_6H_4	CH_3	225—226	90
IIh*	p-ClC_6H_4	α-$C_{10}H_7$	157—160	50
II′a*	C_6H_5	C_6H_5	126—128	75
II′b	C_6H_5	CH_3	98—100 (103)[3]	60
II′c*	C_6H_5	α-$C_{10}H_7$	128—130	95

* New compound

Table 2. Analytical data for II and II′

	R	R′	Elemental analyses* (%)				
			C	H	N	S	Cl
IIa	C_6H_5	CH_3	60.92 (61.09)	5.32 (5.09)	4.86 (5.09)	11.97 (11.64)	
IIb	C_6H_5	CH_2=$CHCH_2$	63.59 (63.79)	5.75 (5.32)	4.57 (4.65)	10.63 (10.63)	
IIc	C_6H_5	α-$C_{10}H_7$	71.12 (71.32)	4.86 (4.65)	3.70 (3.62)	8.45 (8.27)	
IId	C_6H_5	C_6H_5	67.69 (67.66)	5.01 (4.75)	4.24 (4.15)	9.52 (9.49)	
IIe	p-$CH_3C_6H_4$	C_6H_5	68.72 (69.04)	5.61 (5.48)	3.88 (3.84)	8.78 (8.76)	
IIf	p-$CH_3OC_6H_4$	C_6H_5	63.54 (63.48)	5.31 (5.04)	3.34 (3.52)	8.27 (8.06)	
IIg	p-ClC_6H_4	CH_3	48.77 (48.86)	3.73 (3.51)	4.22 (4.07)	9.32 (9.31)	20.60 (20.49)
IIh	p-ClC_6H_4	α-$C_{10}H_7$	60.68 (60.53)	3.45 (3.51)	3.29 (3.07)	7.11 (7.02)	15.32 (15.57)
II′a	C_6H_5	C_6H_5	64.50 (64.59)	4.60 (4.53)	4.22 (3.97)	18.41 (18.13)	
II′b	C_6H_5	CH_3	57.87 (57.73)	4.93 (4.81)	4.86 (4.81)	22.06 (21.99)	
II′c	C_6H_5	α-$C_{10}H_7$	68.34 (68.49)	4.39 (4.47)	3.38 (3.48)	15.88 (15.88)	

* Values in parentheses show the calculated values.

4) R. B. Fox and D. L. Venezky, *J. Am. Chem. Soc.*, **78**, 1661 (1956).

Table 3. UV and IR spectra of II and II'

	λ_{max}^{EtOH} (mμ)		ν^{Nujol}		
	π–π* (ε)	n–π* (ε)	ν_{N-H}	"Amide II"	$\nu_{P=O}$
IIa	291 (6970)	395 (83)	3160	1520	1190
IIb	292 (7970)	401 (84)	3150	1515	1185
IIc	343 (6930)	436 s (154)	3060*	1480	1180
IId	330 (13000)	443 (120)	3060*	1530	1180
IIe	329 (12000)	441 (150)	3050*	1495	1170
IIf	328 (12900)	442 (115)	3070*	1490	1165
IIg	290 (7190)	394 (80)	3150	1520	1190
IIh	335 (5780)	388 s (67)	3050*	1490	1190
II'a	333 (11300)	447 (101)	3150 3100	1530	
II'b	280 (7500)	400 (68)	3230 3180	1515	
II'c	352 (7340)	446 s (127)	3180*	1500	

* In hexachlorobutadiene

Lately, Vaughan and Lindsey, Jr., reported[5] that carbamoyldiphenylphosphine was prepared by the addition reaction of diphenylphosphine with isocyanic acid in benzene. Papp and Buckler also prepared it by the addition of aqueous potassium cyanate to the mixture of diphenylphosphine and acetic acid.[6]

We extended the addition reaction of I and I' with isothiocyanates to the syntheses of thiocarbamoyldiphenylphosphine (IIIa) and its oxide (IIIb) by the reaction of diphenylphosphine and its oxide with thiocyanic acid. First, thiocyanic acid was generated *in situ* from the reaction of ammonium thiocyanate with dry hydrogen chloride analogously to the synthesis of diphenylthiourea from diphenylamine.[7]

Diphenylphosphine was allowed to react with ammonium thiocyanate and dry hydrogen chloride in chlorobenzene under nitrogen atmosphere at 80—85°C. However, bis(diphenylthiophosphinyliminomethyl) sulfide (IVa), which is a new type of sulfide, was obtained in 20% yield, instead of the expected IIIa. In benzene at 50°C, the corresponding phosphinyl compound(IVb) was obtained in 20% yield. The oxygen atoms in IVb might

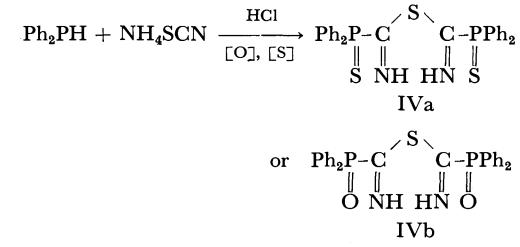

be taken in during column chromatography on alumina, and the sulfur atoms in IVa might be taken in from some sulfur compound during the reaction. These reactions have not been known in the case of secondary amines.

A similar reaction of diphenylphosphine oxide in refluxing benzene gave the bis(iminomethyl) sulfides, IVb and IVc, in 28% and 13% yields, respectively. However, in chlorobenzene at 100°C, only IVc was obtained in 25% yield. In some cases, diphenylthiophosphinyl isothiocyanate (V) and diphenylthiophosphinic anhydride (VI) were obtained in 3—10% yield. A similar reaction of di-*p*-tolylphosphine oxide gave IVd (analogous to IVc) in 7—10% yield.

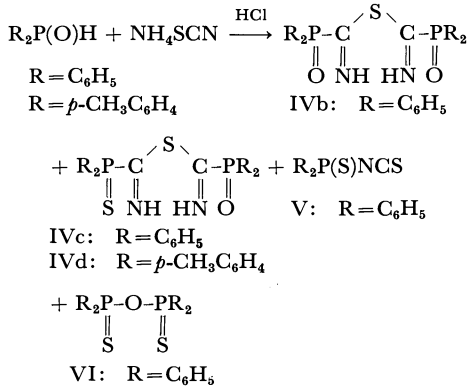

The structures of IVa, IVb, IVc, IVd, V and VI were supported by elemental analyses, IR, NMR and mass spectra. These data, however, can not exclude the possibility of structures VII or VIII, which are isomers of IV. II and II' are yellow

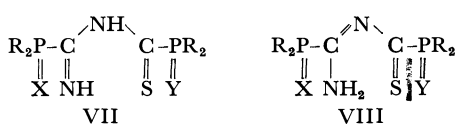

5) L. G. Vaughan and R. V. Lindsey, Jr., *J. Org. Chem.*, **33**, 3088 (1968).

6) G. P. Papp and S. A. Buckler, *ibid.*, **31**, 588 (1966).

7) H. Passing, *J. prakt. Chem.*, **153**, 1 (1939).

Table 4. UV and IR spectra of IIIa, IIIb and IIIc

	λ_{max}^{EtOH} (mμ)				ν^{Nujol} (cm^{-1})		
	π-π* (ε)		n-π* (ε)		ν_{N-H}	"Amide II"	$\nu_{P=O}$
IIIa	292	(8720)	376	(135)	3300 3260 s 3130	1605	
IIIb	295	(5770)	406	(38)	3260 3170 s 3030*	1640	1160
IIIc	290	(5940)	412	(41)	3250 3200 s 3100*	1590	

* In hexachlorobutadiene

crystals and display the intense π–π* and n–π* transition bands which arise from C=S group in their UV spectra(Table 3). However, compounds IVa—d are colorless and their UV spectra did not show any peaks due to π–π* and n–π* transitions of C=S group (see Experimental). Therefore, the structures of these compounds were determined to be IVa—d, which do not contain C=S group. Possible pathways for the formation of V and VI might be as follows, from separate experimental results (see Experimental).

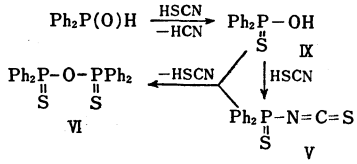

The formation of IVc or IVd from diarylphosphine oxide, ammonium thiocyanate and hydrogen chloride may be attributed to an oxygen-sulfur exchange reaction in P=O bond by thiocyanic acid during the course.

The compounds IVa, IVb and IVc were presumed to be formed by the condensation of IIIa or its oxide (IIIb) in the presence of hydrogen chloride. With this in mind, we let diphenylphosphine react with thiocyanic acid in ether[8] without hydrogen chloride under nitrogen atmosphere at room temperature for a week, and obtained IIIa (57%) and IVb (10%). The oxygen atoms in IVb might be taken in during column chromatography on silica gel. Thiocarbamoyldiphenylphosphine oxide (IIIb) and sulfide (IIIc) were prepared by the reaction of IIIa with oxygen and sulfur in 62% and 70% yields, respectively. These spectral data are listed in Table 4.

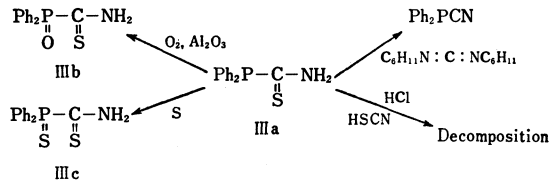

The condensation reaction of IIIa to IVa—c was attempted with hydrogen chloride or/and thiocyanic acid under various conditions. The expected condensation products (IVa—c) were not obtained, but only diphenylphosphine oxide and inorganic compounds (ammonium chloride or/and thiocyanate, from IR, respectively) were isolated. Namely, III decomposed in the presence of strong acid. This fact explains that no III could be obtained in the reactions of diphenylphosphine or diarylphosphine oxide with ammonium thiocyanate under hydrogen chloride at 50—100°C. This fact also made it certain that IV was not formed by the condensation of III.

Though the path of the formation of IV is not clear, one of possible paths is the addition of diphenylphosphine to a trimer (XI)*1 of thiocyanic acid which is assumed to be present analogously to cyamelide form,[9] as shown below.

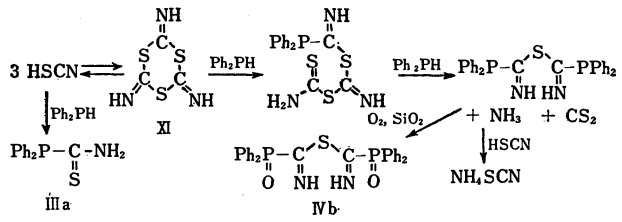

8) R. Klason, *J. prakt. Chem.*, **35**, 407 (1887).

The reaction of IIIa with *N,N'*-dicyclohexylcarbodiimide as condensation reagent gave only diphenylcyanophosphine (X) in 71% yield, without any intermolecular condensation product, IV.

Experimental*2

Materials. Diphenylphosphine was prepared by the reduction of diphenylchlorophosphine with lithium aluminum hydride.[11] Bp 100—110°C/0.8—1.0 mmHg (lit 100—102°C/1.5 mmHg). Diphenylphosphine oxide was prepared by the hydrolysis of diphenylchlorophosphine.[12] Diarylphosphine oxides were prepared according to the directions of Grayson, Farley and Streuli.[13,14] $R_2P(O)H$: R=C_6H_5, mp 51—54°C (lit[12] 51—54°C); R=*p*-$CH_3C_6H_4$, mp 98—100°C (lit[14] 102—103°C); R=*p*-$CH_3OC_6H_4$, mp 121—124°C (lit[14] 125—126°C); R=*p*-ClC_6H_4, mp 130—133°C (lit[14] 131—133°C). Diphenylphosphine sulfide was prepared by the reaction of diphenylphosphine with sulfur.[15] Mp 96—97°C (lit[15] 95—97°C).

Reaction of Diarylphosphine Oxides and Diphenylphosphine Sulfide with Isothiocyanates. A typical procedure is described for the reaction of diphenylphosphine oxide with phenyl isothiocyanate. A mixture of diphenylphosphine oxide (2.0 g, 10 mmol) and phenyl isothiocyanate (1.35 g, 10 mmol) was heated without solvent in the presence of a few drops of triethylamine for 5 hr at 70—80°C. The crystalline product obtained was recrystallized from ethanol to afford 2.52 g (7.5 mmol, 75%) of *N*-phenylthiocarbamoyldiphenylphosphine oxide (IId), mp 163.5—164.5°C.

Physical properties and analytical data are shown in Tables 1—3.

Reaction of Diphenylphosphine with Ammonium Thiocyanate and Hydrogen Chloride. *a) In Chlorobenzene.* A solution of 18 g (89 mmol) of diphenylphosphine in 50 m*l* of chlorobenzene was vigorously stirred with 9 g (118 mmol) of dried ammonium thiocyanate powder under nitrogen atmosphere, and dry hydrogen chloride was passed through the mixture. After the initial exothermic reaction subsided, the reaction mixture was heated at 80—85°C for 1.5 hr. After removal of solvent under reduced pressure, the residue was chromatographed on alumina. Bis(diphenylthiophosphinyliminomethyl) sulfide (IVa) (4.2 g, 8.04 mmol, 20%) was eluted with dichloromethane and recrystallized from *n*-butyl alcohol; colorless needles, mp 221—222°C (dec.). IR(Nujol): 3370, 3230, 3150 (sh) (ν_{NH}), and 1525 cm^{-1} ($\nu_{C=N}$). $\lambda_{max}^{CH_3CN}$: 257(sh)mμ (ε=16000). NMR(DMSO): δ 8.16 (NH, doublet, J_{PCNH}=10.5 Hz). Mass spectrum (significant peaks): *m/e*=520 (M^+, 0.08), 488 (M^+-32, 14), 218 (Ph_2PSH^+, 86.5), 217 (Ph_2PS^+, 100), 185 (Ph_2P^+, 73), 140 ($PhPS^+$, 54.5), 108 (PhP^+, 50), 77 (Ph^+, 45.5), and 63 (PS^+, 50).

Found: C, 60.01; H, 4.34; N, 5.35; S, 18.47%. Calcd for $C_{26}H_{22}N_2P_2S_3$: C, 60.00; H, 4.23; N, 5.38; S, 18.46%.

b) In Benzene. When this reaction was carried out in benzene at 50°C for 2hr, the corresponding phosphinyl compound (IVb) was obtained in 20% yield by a similar treatment. Mp 228—229°C (dec.). The IR spectrum was identical with that of the product obtained from the reaction of diphenylphosphine oxide (described below).

Reaction of Diphenylphosphine Oxide with Ammonium Thiocyanate and Hydrogen Chloride. *a) In Benzene.* A solution of 10 g (49.5 mmol) of diphenylphosphine oxide in 100 m*l* of benzene was vigorously stirred with 3.5 g (46 mmol) of ammonium thiocyanate under dry hydrogen chloride stream. After the initial exothermic reaction subsided, the reaction mixture was heated under reflux for 5 hr and then chromatographed on alumina. Diphenylphosphine oxide (3.5 g, 35%) was recovered from a benzene eluate. Elution with ether afforded diphenylphosphinyliminomethyl diphenylthiophosphinyliminomethyl sulfide (IVc) (500 mg, 0.99 mmol. 13.4%), colorless prisms from isobutyl alcohol, mp 230—231°C (dec.). IR(Nujol): 3450, 3280, 3150(sh) (ν_{NH}), 1545 ($\nu_{C=N}$) and 1180 cm^{-1} ($\nu_{P=O}$). λ_{max}^{EtOH}: 253 (sh) mμ (ε=19700) and two weak shoulders in 260—275 mμ region. NMR(DMSO): δ 8.30 (NH, doublet, J_{PCNH}=10.5 Hz). Mass spectrum (significant peaks): *m/e*=504 (M^+, 3), 488 (M^+-16, 27), 472 (M^+-32, 3.3), 218 (Ph_2PSH^+, 61), 217 (Ph_2PS^+, 100), 202 (Ph_2POH^+, 23), 201 (Ph_2PO^+, 77), 185 (Ph_2P^+, 57) 140 ($PhPS^+$, 16), 124 ($PhPO^+$, 14), 108 (PhP^+, 25), 77 (Ph^+, 66), 63 (PS^+, 31), and 47 (PO^+, 20).

Found: C, 61.82; H, 4.72; N, 5.58; S, 12.65%. Calcd for $C_{26}H_{22}N_2OP_2S_2$: C, 61.90; H, 4.36; N, 5.58; S, 12.75%.

Elution with ethyl acetate - ethyl alcohol (1 : 1) gave bis(diphenylphosphinyliminomethyl) sulfide (IVb) (2.0 g, 4.1 mmol, 27.6%), colorless prisms from isobutyl alcohol, mp 229—229.5°C (dec.). IR (Nujol): 3475(sh), 3250, 3150 (ν_{NH}), 1550 ($\nu_{C=N}$), and 1170 cm^{-1} ($\nu_{P=O}$) λ_{max}^{EtOH}: 253(sh) (ε=18300), 265(sh) (14800), and 272 (sh) mμ (11800). NMR($CDCl_3$): δ 9.93 (NH, doublet, J_{PCNH}=10.5 Hz). Mass spectrum (significant peaks):

*1 Thiocyanic acid reversibly polymerizes to trimer or hexamer,[10] whose structures are not clear. Although we assumed the existence of "thiocyamelide"(XI), in

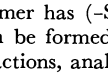

so far as the polymer has (-S-C-)$_n$ structure, III, IV, NH_3 and CS_2 can be formed through ring opening or chain cleavage reactions, analogously to the case of XI.

9) E. A. Werner and W. R. Fearon, *J. Chem. Soc.*, **117**, 1356 (1920); A. Senier and T. Walsh, *ibid.*, **81**, 290 (1902).

10) L. Birckenbach and E. Büchner, *Ber.*, **73**, 1153 (1940).

*2 IR spectra were recorded on a grating spectrometer HITACHI Model EPI-G2. The NMR spectra were recorded on a JEOL Model JNM-C-60H using TMS as an internal standard. UV spectra were measured on a HITACHI Model EPS-3. Mass spectra were measured on a HITACHI Model RMU-6D. The melting and boiling points are not corrected.

11) W. Kuchen and H. Buchwald, *Chem. Ber.*, **91**, 2871 (1958).

12) L. D. Quin and R. Montgomery, *J. Org. Chem.*, **28**, 3315 (1963); R. C. Miller, *ibid.*, **24**, 2013 (1959).

13) R. H. Williams and L. A. Hamilton, *J. Am. Chem. Soc.*, **74**, 5418 (1952).

14) M. Grayson, C. E. Farley and C. A. Streuli, *Tetrahedron*, **23**, 1065 (1967).

15) G. Peters, *J. Am. Chem. Soc.*, **82**, 4751 (1960).

m/e=488 (M^+, 2), 472 (M^+-16, 16), 202 (Ph_2POH^+, 60), 201 (Ph_2PO^+, 100), 185 (Ph_2P^+, 18), 124($PhPO^+$, 10), 108 (PhP^+, 7), 77 (Ph^+, 56), and 47 (PO^+, 28).

Found: C, 63.72; H, 4.78; N, 5.70; S, 6.77%. Calcd for $C_{26}H_{22}O_2P_2S$: C, 63.93; H, 4.51; N, 5.74; S, 6.56%.

b) In Chlorobenzene. When diphenylphosphine oxide (25 g, 124 mmol) was allowed to react with ammonium thiocyanate (11 g, 145 mmol) in 100 m*l* of chlorobenzene at 100°C for 1.5 hr under hydrogen chloride stream, only IVc was obtained in 25% yield. Mp 230—231°C (dec.). The IR and mass spectra were identical with those obtained by the reaction mentioned above.

Diphenylthiophosphinyl isothiocyanate (V), mp 48—49°C (lit[16] 48°C), and diphenylthiophosphinic anhydride (VI), mp 198—199°C (lit[17] 197—198°C), were often obtained in 3—10% yield in these reactions.

Reactions of Diphenylthiophosphinic Acid (IX) with Thiocyanic Acid and Diphenylthiophosphinyl Isothiocyanate (V). Diphenylthiophosphinic acid (IX) was prepared conveniently from diphenylphosphine oxide and sulfur in the presence of hydrogen chloride in refluxing benzene for 1.5 hr. The precipitated needles were washed once with carbon disulfide. Yield: 70%. Mp 142—144°C (lit[18] 143—144°C). IR(Nujol): 895 cm^{-1} (ν_{P-OH}). Two grams (8.6 mmol) of IX was allowed to react with 1.0 g (13.2 mmol) of ammonium thiocyanate and hydrogen chloride in chlorobenzene at 100—110°C for 1.5 hr. After the solvent was removed, the IR spectrum of the residue showed a strong band at 1960 cm^{-1} ($\nu_{N=C=S}$), which is identical with that of V. Diphenylthiophosphinyl isothiocyanate (V) (1.0 g, 4.0 mmol) and IX (0.5 g, 2.14 mmol) were mixed without solvent and heated at 90—96°C for 3 hr and the IR spectrum of the reaction mixture was measured. There appeared[16] strong new peaks at 940(sh), 925, and 915 cm^{-1} (ν_{P-O-P}) which is identical with that of VI.

Reaction of Di-*p*-tolylphosphine Oxide with Ammonium Thiocyanate under Hydrogen Chloride. Di-*p*-tolylphosphine oxide (10 g, 43.5 mmol) was reacted with ammonium thiocyanate (3.3 g, 43.5 mmol) in 100 m*l* of chlorobenzene under hydrogen chloride stream at 100—105°C for 1.5 hr. Treatment similar to that for the reaction of diphenylphosphine oxide gave di-*p*-tolylphosphinyliminomethyl di-*p*-tolylthiophosphinyliminomethyl sulfide (IVd) (7—10%), colorless prisms, mp 226—227°C (dec.). IR (Nujol): 3460, 3260, 3150 (sh) (ν_{NH}), 1540($\nu_{C=N}$), and 1175 cm^{-1} ($\nu_{P=O}$). NMR(DMSO): δ 8.15 (NH, doublet, J_{PCNH}=10.5 Hz). Mass spectrum (significant peaks): m/e=560 (M^+, 2.5), 544 (M^+-16, 90), 528 (M^+-32, 10), 246 (T_2PSH^+, 90), 245 (T_2PS^+, 100), 230 (T_2POH^+, 85), 229 (T_2PO^+, 95), 213 (T_2P^+, 85), 154 (TPS^+, 65), 138 (TPO^+, 50), 122 (TP^+, 80), 91 (T^+, 90), 63 (PS^+, 45), and 47 (PO^+, 25), where T represents *p*-$CH_3C_6H_4$.

Found: C, 63.83; H, 5.64; N, 4.96; S, 11.16%. Calcd for $C_{30}H_{30}N_2OP_2S_2$: C, 64.29; H, 5.36; N, 5.00; S, 11.43%.

IR spectrum, 1965 cm^{-1} ($\nu_{N=C=S}$), of a benzene eluate by column chromatography on alumina showed formation of isothiocyanate, which might be the *p*-tolyl derivative of V, but was not isolated in pure state. When this reaction was carried out in benzene under reflux for 2 hr, IVd, mp 226—227°C (dec.), was also obtained in 7% yield.

Reaction of Diphenylphosphine with Thiocyanic Acid. To ammonium thiocyanate (6.9 g, 91 mmol) in 7.0 g of water was added concd. sulfuric acid (4.5 g) in 9.0 g of water, and the aqueous solution was shaken twice with 50 m*l* of ether. According to Klason,[8] 95% of thiocyanic acid generated is extracted by ether. The ethereal solution of thiocyanic acid was added dropwise to 15.0 g (81 mmol) of diphenylphosphine in ether (20 m*l*) under nitrogen atmosphere and then the mixture was allowed to stand at room temperature for a week with stirring. The residue after concentration was chromatographed on silica gel (Davison No. 922). Unreacted diphenylphosphine was oxidized during chromatography and 5.0 g of diphenylphosphine oxide was eluted with benzene. Thiocarbamoyldiphenylphosphine (IIIa) was eluted with benzene-chloroform and recrystallized from isobutyl alcohol as colorless needles, mp 114—116°C. Yield: 7.8 g (31.8 mmol, 57%). Mass spectrum (significant peaks): m/e=245 (M^+, 90), 211 (M^+-34, 60), 186 (Ph_2PH^+, 95), 185 (Ph_2P^+, 35), 108 (PhP^+, 100), 77 (Ph^+, 30), and 60 ($CSNH_2^+$, 40).

Found: C, 63.85; H, 5.08; N, 5.57; S, 13.18%. Calcd for $C_{13}H_{12}NPS$: C, 63.67; H, 4.90; N, 5.72; S, 13.06%.

Bis(iminomethyl) sulfide (IVb) was also eluted with ethyl acetate and recrystallized from isobutyl alcohol. Yield: 1.35 g (5.6 mmol, 10.0%). Mp 228—229°C.

Preparation of Thiocarbamoyldiphenylphosphine Oxide (IIIb). Thiocarbamoyldiphenylphosphine (IIIa) (489 mg, 2.00 mmol) was dissolved in 50 m*l* of ethyl alcohol, and 3.0 g of alumina was suspended and oxygen was passed through the mixture under reflux for 2 hr. After removal of alumina and the solvent, the residue was recrystallized from isobutyl alcohol to give 325 mg (1.25 mmol, 62.3%) of pure IIIb, mp 205°C (dec.). Mass spectrum (significant peaks): m/e=261 (M^+, 11), 227 (M^+-34, 28), 202 (Ph_2POH^+, 100), 201 (Ph_2PO^+, 56), 185 (Ph_2P^+, 22), 124 ($PhPO^+$, 17), 108 (PhP^+, 17), 77 (Ph^+, 95), 60 ($CSNH_2^+$, 39), and 47 (PO^+, 95).

Found: C, 60.00; H, 4.68; N, 5.59; S, 12.74%. Calcd for $C_{13}H_{12}NOPS$: C, 59.77; H, 4.60; N, 5.37; S, 12.26%.

Preparation of Thiocarbamoyldiphenylphosphine Sulfide (IIIc). Sulfur (73 mg, 2.28 g atom) and IIIa (503 mg, 2.05 mmol) were dissolved in 50 m*l* of benzene, and the mixture was heated under reflux for 2 hr. After the solvent was removed, the residue was recrystallized from isobutyl alcohol. Yellow prisms thus obtained were washed once with 5 m*l* of carbon disulfide to afford 397 mg (1.43 mmol, 70%) of pure IIIc, mp 132—135°C. Mass spectrum (significant peaks): m/e=277 (M^+, 23), 243 (M^+-34, 10), 218 (Ph_2PSH^+, 100), 217 (Ph_2PS^+, 30), 185 (Ph_2P^+, 53), 140 ($PhPS^+$, 53), 108 (PhP^+, 47), 77 (Ph^+, 63), and 63 (PS^+, 77).

Found: C, 56.48; H, 4.09; N, 5.05; S, 22.98%. Calcd for $C_{13}H_{12}NPS_2$: C, 56.32; H, 4.33; N, 5.05; S, 23.10%.

Reaction of Thiocarbamoyldiphenylphosphine

16) A. Schmidpeter and H. Groeger, *Chem. Ber.*, **100**, 3052 (1967).

17) T. R. Hopkins and P. W. Vogel, *J. Am. Chem. Soc.*, **78**, 4447 (1956).

18) F. Knotz, *Monatsh. Chem.*, **87**, 359 (1956).

(IIIa) with Dicyclohexylcarbodiimide. Dicyclohexylcarbodiimide (813 mg, 3.95 mmol) and IIIa (1.003 g, 4.09 mmol) were heated in 20 m*l* of benzene under reflux for 6 hr. Then the reaction mixture was cooled and 754 mg (3.14 mmol, 80%) of *N,N'*-dicyclohexylthiourea thus obtained, mp 179—181°C (lit[19] 180—181°C), was filtered off. The filtrate was chromatographed on silica gel (Davison No. 922). Diphenylcyanophosphine (X)[20] (596 mg, 2.82 mmol) was eluted with benzene as colorless oil in 71% yield. (Found: C, 73.24; H, 5.12; N, 6.39%). IR: 2180 cm^{-1} ($\nu_{C\equiv N}$, weak).

19) A. Skita and H. Rolfes, *Ber.*, **53**, 1247 (1920).
20) I. B. Johns and H. R. DiPietro, *J. Org. Chem.*, **29**, 1970 (1964).

BULLETIN OF THE CHEMICAL SOCIETY OF JAPAN VOL. 42 2981—2983 (1969)

Photolysis of Aromatic Oxime Benzoates

Taiichi OKADA, Mituyosi KAWANISI and Hitoshi NOZAKI

Department of Industrial Chemistry, Kyoto University, Sakyo-ku, Kyoto

(Received May 1, 1969)

Irradiation of aromatic oxime benzoates, $R^1R^2C{=}N{-}OCOPh$, in benzene solution gives the corresponding azines, $(R^1R^2C{=}N{-})_2$, and ketones, $R^1R^2C{=}O$, along with $PhCO_2NH_4$. $PhCO_2H$ and Ph_2 are also obtained in all cases. The reaction course can be explained by assuming a radical fission of excited $R^1R^2C{=}N{-}OCOPh$ which gives radicals $R^1R^2C{=}N\cdot$ and $\cdot OCOPh$ in the initial step. Sensitization experiment establishes the fact that a triplet state of the oxime benzoate is involved as a chemically reactive species.

Considerable interest has been focused on the photochemical rearrangement of enol esters, in which the acyl group migrates from oxygen to the vinylic carbon atom.[1] In continuation of our recent investigation on the photochemistry of *N*-acylketimine as an aza-analog of α,β-enone system,[2] we have studied the photochemical reaction of certain oxime benzoates,[*1,*2] which may be regarded as an aza-analog of enol benzoate and expected to rearrange photochemically in analogous manner. Actually, however, the reaction took place quite differently as described below.

Irradiation of a benzene solution of acetophenone oxime benzoate (Ia) was effected by means of 300 W high pressure mercury arc (Pyrex jacket) under N_2 atmosphere at room temperature. Chromatographic separation on silica gel column afforded acetophenone azine (IIa) (49%), acetophenone (IIIa) (30%), benzoic acid (9%) and diphenyl (11%). Ammonium benzoate (IV) (9%) deposited on the wall during the irradiation.

Irradiation of other oxime benzoates (Ib—d) was effected in the same way. The possible reaction sequences are given in Scheme 1 and the products isolated are summarized in Table 1. Ammonium benzoate (IV) was obtained in the photolysis of *p*-methylacetophenone oxime benzoate (Id) as well, which indicated that this had arisen from the benzoyloxy group of the original oxime benzoates.

Inspection of Table 1 leads to the conclusion that the photochemical primary step is the cleavage of N–O bond and all the products isolated may be ascribed to the imino radical (V) and benzoyloxy radical (VI). Recombination of radicals V yields azine II and abstraction of hydrogen even from benzene[5] gives the ketimine of the type $R^1R^2C{=}NH$ (VII), which possibly produces the corre-

*1 Photochemistry of oximes presents several interesting points. For details, see Ref. 3.

*2 As the *syn-anti* isomerization of the parent oximes has been reported to occur by the effect of ultraviolet illumination,[4] the same behavior could be expected in the present system. No attempt has been made to observe this kind of isomerization, as irradiation was conducted up to the complete disappearance of the strating I.

1) a) R. A. Finnegan and A. W. Hagen, *Tetrahedron Letters*, **1963**, 365. b) M. Feldkimel-Gorodetsky and Y. Mazur, *ibid.*, **1963**, 369. c) A. Yogev, M. Gorodetsky and Y. Mazur, *J. Am. Chem. Soc.*, **86**, 5208 (1964). d) M. Gorodetsky and Y. Mazur, *ibid.*, **86**, 5213 (1964). e) M. Gorodetsky and Y. Mazur, *Tetrahedron*, **22**, 3607 (1966). f) V. I. Stenberg, "Advances in Organic Photochemistry," ed. by O. L. Champan, Vol. 1, Marcel-Dekkar, New York (1967), p. 141.

2) T. Okada, M. Kawanisi, H. Nozaki, N. Toshima and H. Hirai, *Tetrahedron Letters*, **1969**, 927.

3) a) T. Oine and T. Mukai, *ibid.*, **1969**, 157. b) G. Just and L. S. Ng, *Can. J. Chem.*, **46**, 3381 (1968). c) H. Izawa, P. de Mayo and T. Tabata, *ibid.*, **47**, 51 (1969).

4) G. Ciamician and P. Silber, *Ber.*, **36**, 4268 (1903).

5) S. S. Hirsch, *J. Org. Chem.*, **32**, 2433 (1967).

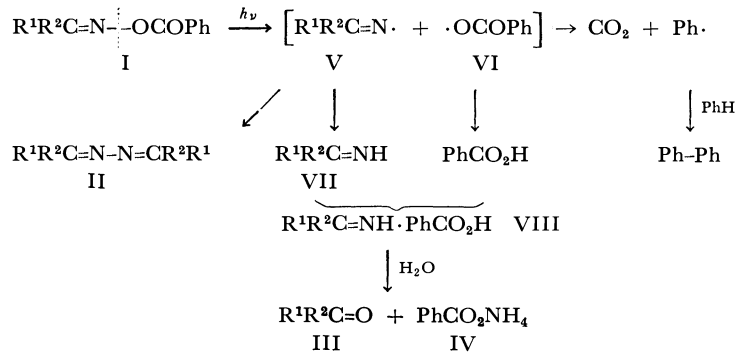

Table 1. Yields in mole % of products of the photolysis of oxime benzoates

Oxime benzoate	R^1	R^2	Azine[a]		Ketone		$PhCO_2NH_4$	$PhCO_2H$	Ph_2
Ia[b]	Ph	Me[c]	IIa[d]	49	IIIa	30	13	9	11
Ib[e]	Ph	Ph[f]	IIb[g]	43	IIIb	33	9	4	21
Ic[h]	Ph	H	IIc	tr[i]	—	—[k]	12	25	20
Id[l]	*p*-Me-C_6H_4	Me	IId[m]	50	IIId	27	10	14	13
Ia[n]	Ph	Me	IIa[d]	49	IIIa	26	15	20	12

a) Authentic samples were prepared by treatment of the corresponding carbonyl compounds with hydrazine sulfate in the presence of equimolar amount of alkali according to the published method.[d,g,j,m] Photoproducts were identical with the authentic ones with respects to mps, IR spectra and R_f values in TLC.

b) Mp 98—99°C (from ethanol) (lit, 98—100°C; K. von Auwers and H. Müller, *J. prakt. Chem.*, **137**, 81 (1933)).

c) Trace amount of benzonitrile was detected by vpc. Carbon dioxide was detected by aqueous calcium hydroxide.

d) Mp 122—123°C (from ethanol) (lit, 124°C; G. Knopfer, *Monats. Chem.*, **30**, 29 (1909)).

e) Mp 99—100°C (from ethanol) (lit, 98—99°C; A. W. Chapman and C. C. Howis, *J. Chem. Soc.*, **1933**, 806.

f) Benzanilide (18%) was also obtained.

g) Mp 160—161°C (from ethanol) (lit, 162°C; T. Curtius and F. Rauterberg, *J. prakt. Chem.*, (N)**44**, 192 (1891)).

h) Mp 99—100°C (from ethanol) (lit, 101—102°C; G. Minnuni and G. Corselli, *Gazz. chim. ital.*, **22**, 164 (1892); *Chem. Zentr.*, **63**, 905 (1892)).

i) A spot of same R_f value (0.80) with the authentic sample[j] was visualized in TLC.

j) Mp 92—93°C (from ethanal) (lit, 93°C; T. Curtius and R. Ray, *J. prakt. Chem.*, (N)**39**, 27 (1889)).

k) Benzoic acid would partly originate from benzaldehyde which is oxidized during the work-up.

l) Mp 88—89°C (from ethanol) (Found: C, 75.8; H, 5.9; N, 5.3. Calcd for $C_{16}H_{15}NO_2$: C, 75.9; H, 6.0; N, 5.5%).

m) Mp 132—133°C (from ethanol) (lit, 136°C; T. Curtius and K. Kopf, *J. prakt. Chem.*, (N)**86**, 113 (1912)).

n) Benzophenone-sensitized reaction by means of light of wavelength longer than 350 nm using 10% $CuSO_4$ aq. as a filter solution.

sponding ketone III during chromatography on silica gel column.[6],*3 Radical VI decomposes to carbon dioxide and phenyl radical[8] which attacks the solvent benzene to give diphenyl.[8] An alternative reaction of radical VI is the hydrogen abstraction to form benzoic acid.[9]

Under anhydrous condition an equimolar mixture of benzoic acid and VII ($R^1=R^2=Ph$) is reported to form a salt, *viz.*, diphenylketimine benzoate (VIII).[10] Ammonium benzoate (IV) is explained by the reaction of benzoic acid with ammonia which is generated by hydrolysis of VII or alternatively by the hydrolysis of VIII during irradiation and subsequent treatment. The assumption is

6) P. A. S. Smith, "Open-chain Nitrogen Compounds," W. A. Benjamin, Inc., New York (1965), p. 297.

*3 Silica gel contains 7% free water physically absorbed. See Ref. 7.

7) K. R. Lenge, *Chem. & Ind.* (London), **1968**, 441.

8) W. A. Pryor, "Free Radicals," McGraw-Hill, Inc., New York (1966), p. 253.

9) *Ibid.*, p. 91.

10) D. F. Lynch and J. D. Reid, *J. Am. Chem. Soc.*, **55**, 2515 (1933).

supported by the fact that the intended addition of a small amount of water into an equimolar mixture of benzoic acid and VII ($R^1=R^2=Ph$) in a benzene solution afforded IV and IIIb in a quantitative yield after standing overnight. Photolysis of Ib gave benzanilide in an 18% yield besides the normal products, but the origin is not certain yet.

A priori photocleavage of enol benzoates (IX) can proceed on both C–O bonds at *a* and *b*, but fission occurs exclusively at *b* to afford X through recombination in a solvent cage.[1] The present system

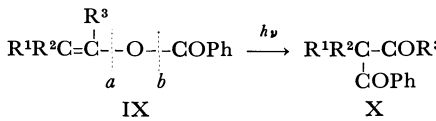

IX X

as an aza-analog of IX is characterized by the absence of participation of benzoyl radical, the fission exclusively occuring at the N–O bond. This is not surprising in view of the bond energies of N–O and C–O bonds calculated as 53 and 85.5 kcal/mol, respectively.[11] The preference of rupture at N–O bond can be considered as prevailing in the photochemical reaction of compounds containing >C=N–O– system, such as isoxazoles,[12] benzisoxazoles,[13] oxadiazoles[14] and anthranils.[15]

The benzophenone-sensitized reaction of Ia was induced by the light of wavelength longer than 350 nm*4 to afford the same products in almost same product distributions as in the case of direct photolysis (Table 1). This strongly suggests that a triplet state acts as a chemically reactive species in the photochemical reaction of the oxime benzoates I.

Experimental

All melting points were taken in capillaries and were uncorrected. The TLC was performed on silica gel G using benzene-ethyl acetate (10 : 1) as an eluent and the spots were visualized with iodine vapor. The UV spectra were obtained in ethanol on a Hitachi EPS-2 recording spectrophotometer.

Materials. Oxime benzoates (Ia—d) were prepared by benzoylation of the corresponding oximes by means of benzoyl chloride in the presence of excess pyridine. All the oxime benzoates were recrystallized several times from ethanol and had the same melting points as reported in the literature cited in the footnotes of Table 1.

General Procedure for Irradiation. Unless otherwise stated, experiments were conducted with the solutions of I (10 mmol) in benzene (300 m*l*) by means of immersion-type 300 W high pressure mercury arc (Pyrex jacket for water-cooling) under N_2 atmosphere at room temperature. The progress of the reaction was monitored by TLC analysis of the aliquots. After the starting materials had been completely consumed (*ca.* 50 hr) and the depositing solid was removed by filtration, the filtrate was concentrated *in vacuo* and the residue was chromatographed on silica gel. The products isolated are listed in Table 1.

Irradiation of Ia in the Presence of Benzophenone. A solution of Ia (2.40 g, 10 mmol) in benzene (200 m*l*) containing benzophenone (0.90 g, 5 mmol) was irradiated by light of wavelength longer than 350 nm (10% $CuSO_4$ aq. as a filter solution) under N_2 atmosphere at room temperature for 20 hr. Only benzophenone absorbs the incident light, as Ia has no absorption in this region. The reaction mixture was concentrated *in vacuo* and chromatographed on silica gel column. The products isolated are shown in Table 1. Unchanged benzophenone was recovered quantitatively.

A solution of Ia in benzene was also irradiated in the same manner as a reference. TLC examination of the reaction mixture indicated the complete recovery of Ia.

The Reaction of Benzoic Acid and Diphenylketimine in the Presence of Water. A solution of benzoic acid (1.22 g, 10 mmol) and diphenylketimine[16] (1.81 g, 10 mmol) in benzene (100 m*l*) was added with water (2 m*l*) under vigorous stirring and allowed to stand overnight. Ammonium benzoate IV (1.30 g, 95%) separated as a crystalline mass, which was collected by filtration and the filtrate was dried (Na_2SO_4) and evaporated. The residue was distilled at 120°C/2 mmHg to afford benzophenone.

The authors are grateful to Professor Keiiti Sisido for help and encouragement.

11) J. D. Roberts and M. C. Caserio, "Basic Principles of Organic Chemistry," W. A. Benjamin, Inc., New York (1964), p. 77.

12) a) E. F. Ullman and B. Singh, *J. Am. Chem. Soc.*, **88**, 1844 (1966). b) D. W. Kurtz and C. H. Schechter, *Chem. Commun.*, **1966**, 689. c) H. Göth, A. R. Gagneux, C. H. Eugster and H. Schmid, *Helv. Chim. Acta*, **19**, 137 (1967).

13) H. Göth and H. Schmid, *Chimia*, **20**, 148 (1966).

14) H. Newman, *Tetrahedron Letters*, **1968**, 2417, 2421.

15) M. Ogata, H. Kano and H. Matsumoto, *Chem. Commun.*, **1968**, 397.

*4 The oxime benzoates had no absorption above 350 nm, but exhibited the following absorptions:

Ia: λ_{max} (EtOH) 254 nm (log ε 4.33) and λ 280 nm (log ε 3.83).

Ib: λ_{max} (EtOH) 263 nm (log ε 4.32) and λ 280 nm (log ε 4.15).

Ic: λ_{max} (EtOH) 261 nm (log ε 4.42) and λ 280 nm (log ε 4.09).

Id: λ_{max} (EtOH) 262 nm (log ε 4.46) and λ 280 nm (log ε 4.21).

16) P. L. Pickard and T. L. Tobbert, "Organic Syntheses," Vol. 44, p. 51 (1964).

BULLETIN OF THE CHEMICAL SOCIETY OF JAPAN VOL. 42 2984—2988 (1969)

Studies on Hydrogenolysis. LIV.[1] Catalytic Hydrogenolysis of Optically Active 2-Methyl-2-phenylaziridine*[1]

Yoshihiro SUGI and Sekio MITSUI

Department of Applied Science, Faculty of Engineering, Tohoku University, Sendai

(Received May 9, 1969)

In order to obtain further information about the catalytic hydrogenolysis of benzyl-type compounds, the hydrogenolysis of optically active 2-methyl-2-phenylaziridine (I) over several group VIII transition metal catalysts was investigated in ethanol under ordinary pressure and at room temperature. 2-Phenylpropylamine (II) was obtained as the main product over all the catalysts. The configuration of II was inverted over the palladium catalyst. However, the hydrogenolysis over the platinum catalyst occurred with a significant retention of the configuration. Further, in the case of Raney nickel and Raney cobalt catalysts, the configurations of II were retained with the low stereoselectivities, and a small amount of 2-phenyl-2-propylamine (III) was also produced in addition to II. These results are attributable to the free-energy difference at the transition states to form π-benzyl intermediates, which depends on the affinity of these metals for the nitrogen lone-pair, the catalyst hindrance, and other factors. The S_N2-type reaction is favored over the palladium catalyst. On the other hand, the S_Ni-type reaction is favored over platinum, Raney nickel, and Raney cobalt catalysts, where the radical-cleavage reaction will participate in addition to the S_Ni-type reaction over the latter two catalysts. The differences in behavior between styrene imines and styrene oxides on the catalyst surface were also discussed.

The catalytic hydrogenolysis of benzyl-type compounds is an important method for investigating the mechanism of heterogenous catalysis. For several decades, much attention has been paid to the stereochemical courses of this reaction.[1–18] Some of the factors which affect the courses of the reaction are the structure of the compound,[1–9] the catalyst,[1–3,5,8–15] the additive,[13,16,17] and the medium.[16–18] Mitsui and his co-workers[1–3] suggested that the stereoselectivity of this reaction could be ascribed to the free-energy difference at the transition states to form π-benzyl intermediates. However, the corresponding stereoselectivity of benzylamine derivatives has been studied in detail by only Mitsui and Sato.[5] In this paper, we will describe the stereoselectivity of the catalytic hydrogenolysis of optically active 2-methyl-2-phenylaziridine, which has reactive carbon-nitrogen bonds. Moreover, the differences in behavior between styrene imines and styrene oxides on the catalyst surface are studied.

The hydrogenolysis of 2-methyl-2-phenylaziridine (I) in ethanol was carried out under ordinary pressure and at room temperature. The reaction mixtures were analyzed quantitatively by gas

1) Part LIII: S. Mitsui, S. Imaizumi and Y. Esashi, This Bulletin, to be published.

*1 This work has previously been reported in a preliminary form: S. Mitsui and Y. Sugi, *Tetrahedron Letters*, **1969**, 1287.

2) S. Mitsui and S. Imaizumi, *Nippon Kagaku Zasshi (J. Chem. Soc. Japan, Pure Chem. Sect.)*, **77**, 1516 (1956); This Bulletin, **34**, 774 (1961), **36**, 855 (1963).

3) S. Mitsui, M. Fujimoto, Y. Nagahisa and T. Sukegawa, *Chem. & Ind. (London)*, **1969**, 241.

4) S. Imaizumi, *Nippon Kagaku Zasshi (J. Chem. Soc. Japan, Pure Chem. Sect.)*, **77**, 1511 (1956); **81**, 627, 631, 633 (1960); **82**, 245 (1961).

5) S. Mitsui and E. Sato, *ibid.*, **86**, 416 (1965).

6) W. A. Bonner, *J. Am. Chem. Soc.*, **74**, 1034, 5086 (1952).

7) W. A. Bonner, J. A. Zderic and G. A. Caseletto, *ibid.*, **74**, 5089 (1952).

8) E. W. Garbisch, Jr., L. Schreader and J. J. Frankel, *ibid.*, **89**, 4233 (1967).

9) A. M. Khan, F. J. McQuillin and I. Jardine, *J. Chem. Soc., C*, **1967**, 136.

10) S. Mitsui, Y. Senda and K. Konno, *Chem. & Ind. (London)*, **1963**, 1354.

11) S. Mitsui, K. Iijima and T. Masuko, *Nippon Kagaku Zasshi (J. Chem. Soc. Japan, Pure Chem. Sect.)*, **84**, 833 (1963).

12) S. Mitsui and K. Iijima, *ibid.*, **84**, 682 (1964).

13) S. Mitsui and S. Imaizumi, *ibid.*, **86**, 219 (1965).

14) S. Mitsui, Y. Kudo and M. Kobayashi, *Tetrahedron*, **25**, 1921 (1969).

15) J. H. Brewster and W. E. Braden, Jr., *Chem. & Ind. (London)*, **1964**, 1759.

16) K. Iijima and S. Mitsui, *Nippon Kagaku Zasshi (J. Chem. Soc. Japan, Pure Chem. Sect.)*, **85**, 687 (1964).

17) S. Mitsui and Y. Sugi, *Tetrahedron Letters*, **1969**, 1291.

18) R. A. Grimm and W. A. Bonner, *J. Org. Chem.*, **32**, 3470 (1967).

chromatography. The results are summarized in Table 1. 2-Phenylpropylamine (II) was the main product over all the catalysts, but the following compounds were also obtained: 2-Phenyl-2-propylamine (III) over Raney nickel and Raney cobalt catalysts, 2-phenylpropane and 2-cyclohexylpropylamine over the platinum catalysts, and 2-phenylpropene over the Raney cobalt catalyst.

(+)-I has the S configuration, as will be described in the Experimental section. (−)-II also has the S configuration.[19,20] Therefore, when (+)-II is obtained from (+)-I, the reaction occurs with a retention of the configuration. On the basis of these relationships, the stereochemical consequences of the hydrogenolysis of I are found to be listed as in Table 1. The maintained optical activities and the configurations of II varied with the catalysts. The hydrogenolysis proceeded with a predominant inversion of the configuration over the palladium catalysts; the maintained optical activities were 50—70%. The configurations of II were retained significantly over platinum catalysts, but the maintained optical activity with platinum oxide was higher than that with platinum black. Further, the hydrogenolysis occurred with a predominant retention of the configuration over Raney nickel and Raney cobalt catalysts, but the maintained optical activities were only 10—20%. Since II was racemized only slowly under these conditions, the above results may be considered to exhibit the stereoselectivities of the hydrogenolysis of I.

It has previously been proposed that the catalytic hydrogenolysis of benzyl-type compounds proceeds *via* paths (1) and (2) unless the substituent X has a very strong affinity for the catalyst.[1-3] The configuration of the product is determined by the free-energy difference at the transition states **4** and **5** to form the π-benzyl intermediates **6** and **7**, respectively. When X is an electron-withdrawing group and has a relatively weak affinity for the catalyst, the stereoelectronic effect is operative, so path (1) becomes more probable than path (2). Consequently, the hydrogenolysis proceeds with a predominant inversion of the configuration. However, when X is not so bulky and has a relatively strong affinity for the catalyst, the strong chemisorption of X makes it so prone to the hydrogenolysis as to overcome the unfavorable stereoelectronic situation. Therefore, the free-energy level of the transition state **5** becomes lower than that of **4**, and the configuration of the product is retained predominantly. Further, when X has a very strong affinity for the catalyst, path (3) as well as path (2) participates in this reaction. The benzyl carbon-X bond cleaves into two radicals **8** and ·X, on the catalyst because of the strong chemisorption of X and the phenyl group. Consequently, the racemic product is obtained. In summary, the catalytic hydrogenolysis of benzyl-type compounds occurs competitively *via* paths (1), (2), and (3), and the configuration of the product is determined at the moment of forming π-benzyl intermediates.

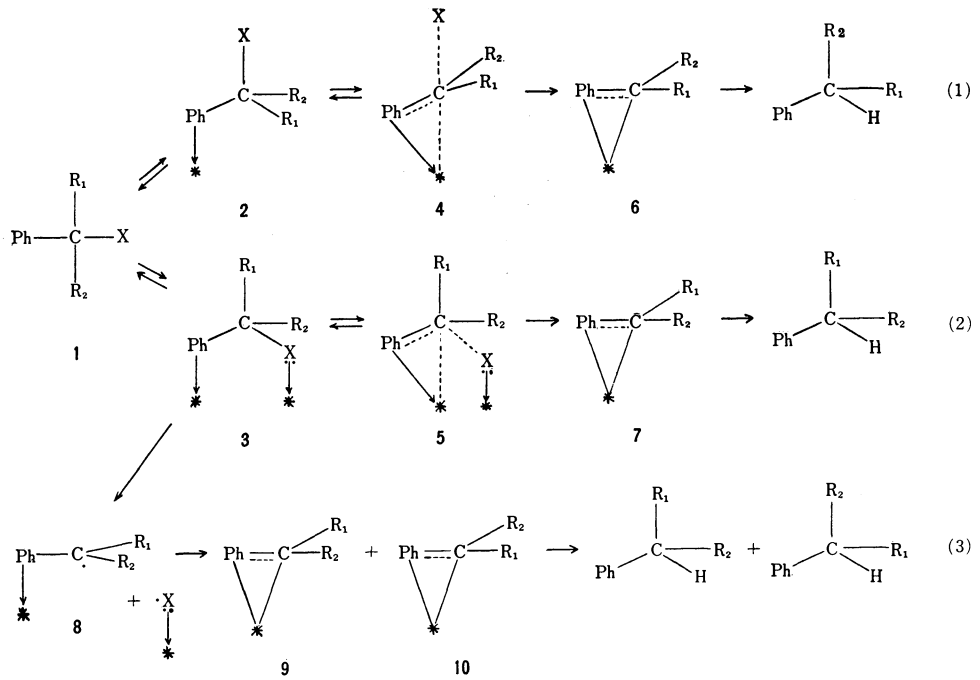

19) P. A. Levene, L. A. Mikeska and K. Passoth, *J. Biol. Chem.*, **88**, 27 (1930).

20) E. L. Eliel and J. P. Freeman, *J. Am. Chem. Soc.*, **74**, 923 (1952).

The mechanism of the hydrogenolysis of I will now be discussed on the basis of the above considerations.

In spite of the low reactivity of benzylamine derivatives, not only 2-phenylaziridines, as reported in this paper, but also 2-alkylaziridines undergo catalytic hydrogenolysis even under ordinary pressure and at room temperature.[21] These high reactivities is attributable to the high strain of the aziridine ring.

Because of the tetrahedral character of the nitrogen of aziridine, I will favorably be adsorbed edgewise on the catalyst as **11**, which corresponds to **3**. Since palladium has not such a strong affinity

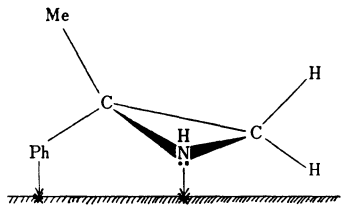

11

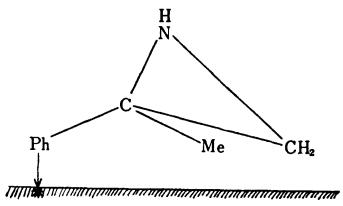

12

for the nitrogen lone-pair, the benzyl carbon in **11** does not bear a sufficiently large positive charge and can not approach so closely to the catalyst as that in **12**, which corresponds to **2**. Moreover, the stereoelectronic requirement at the transition state to form the π-benzyl intermediate is fulfilled *via* the latter state. Therefore, the hydrogenolysis *via* **12** is more probable than that *via* **11**, and the configuration of II will predominantly be inverted over the palladium catalyst. Mitsui and Sato,[5] however, estimated that the hydrogenolysis of ethyl 2-amino-2-phenylpropionate (IV) over a palladium catalyst occurred with a predominant retention of the configuration on the basis of the assumption of the configuration of IV by Cram and his co-workers.[22] This estimation has been confirmed to be correct, for Mizuno and his co-workers[23] reported that (+)-IV has the S configuration. These differences in I and IV suggest the following considerations. The benzyl carbon of I in **11** can not approach so closely to the catalyst as that in **12**, as has been mentioned above, whereas the benzyl carbon of IV can approach to the catalyst at two states, those corresponding to **2** and **3**. Therefore, path (2) is more probable than path (1) in the hydrogenolysis of IV over the palladium catalyst in contrast with that of I.

In order to investigate the possibility of the addition of hydrogen from the top of π-benzyl intermediates, the hydrogenolysis of I was carried out with occluded hydrogen in palladium under a helium atmosphere. Similar results were obtained under both hydrogen and helium atmospheres. Kowaka[24] reported that the occluded hydrogen in palladium is more reactive than molecular or physically-adsorbed hydrogen in the catalytic hydrogenation of ethylene. From these evidences, the hydrogenolysis of I may be said to occur by means of chemisorbed hydrogen from the bottom of the adsorbed molecule on the catalyst surface. These considerations are supported also by the hydrogenolysis of 1-phenylcyclohexane-1,2-diol derivatives[3] and the hydrogenation of 1-phenylcyclohexene derivatives.[25]

The hydrogenolysis of styrene oxide derivatives over the palladium catalysts occurred predominantly with an inversion of the configuration similar to that of I, because of the small affinity of palladium for the oxygen.[13]

Several workers have reported the anchor effect of the nitrogen lone-pair for the platinum catalyst.[26-28] Platinum is less sensitive to the catalyst hindrance than palladium and nickel.[25] Therefore, path (2) is more probable than path (1) in the hydrogenolysis of I over the platinum catalysts, and the configuration of II will be retained predominantly. The maintained optical activity with platinum oxide was higher than that with platinum black, which was prepared by the hydrogen reduction of platinum oxide and by washing with water. This is the effect of alkaline substances contained in platinum oxide.[17] The hydrogenolysis of styrene oxide derivatives over platinum catalysts, however, occurs with an inversion of the configuration.[13] This difference may be ascribed to the differences in the electronegativity and in the affinity for platinum between nitrogen and oxygen.

Nickel and cobalt have stronger affinities for the nitrogen lone-pair than platinum and palladium.

21) S. Mitsui, Y. Sugi and M. Nagata, unpublished work.

22) D. J. Cram, L. K. Gaston and H. Jäger, *J. Am. Chem. Soc.*, **83**, 2183 (1961).

23) H. Mizuno, S. Terashima, K. Achiwa and S. Yamada, *Chem. Pharm. Bull.* (*Tokyo*), **25**, 1747 (1967).

24) M. Kowaka, *Shokubai* (*Catalyst*), **2**, 197 (1960).

25) S. Mitsui, Y. Nagahisa, K. Tomomura and M. Shionoya, *ibid.*, **10**, Preprint for the 23th Symposium on Catalysis, Chem. Soc. Japan, 75 P. (1968).

26) H. Kugita and E. L. May, *J. Org. Chem.*, **26**, 1954 (1961).

27) H. O. House, H. C. Müller, C. G. Pitt and P. P. Wickham, *ibid.*, **28**, 2407 (1963).

28) C. P. Rader, G. W. Wichs, Jr., R. L. Young, Jr., and H. S. Aaron, *ibid.*, **29**, 2252 (1964).

Therefore, the hydrogenolysis occurs *via* **11**. Both benzyl and homobenzyl carbons approach closely to the catalyst and bear positive charges because of the strong chemisorption of the phenyl group and the nitrogen. Therefore, hydrogen will attack nucleophilically not only the benzyl but also the homobenzyl carbons; consequently, II and a small amount of III will be obtained.*2 However, some of I will cleave to the radical because of the high strain of aziridine and the strong chemisorption of the phenyl group and the nitrogen. In this case, the attack of the electron on the radical will be retarded, so the radical will come to have a life long enough to be racemized almost completely. Therefore, the hydrogenolysis of I over Raney nickel and Raney cobalt catalysts will occur competitively *via* paths(2) andand(3), the low maintained optical activities may be attributed to the radical-cleavage reaction.

The hydrogenolysis of styrene oxide derivatives occurred predominantly with a retention of the configuration over Raney nickel and Raney cobalt catalysts, similar to the case of I.[13,29] However, α-phenetylalcohols were not obtained; this is in contrast with the case of I. This suggests the following considerations. The oxygen atom in oxirane has two lone-pairs. Therefore, styrene oxides will more probably be hydrogenolysed *via* **13**. The homobenzyl carbon in **13** is not so approachable to the catalyst surface and scarcely any attack on this carbon will occur. Further,

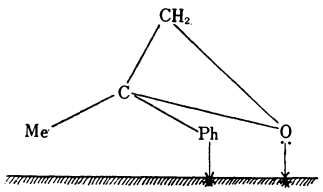

13

styrene oxide derivatives gave the corresponding hydrocarbons in addition to β-phenetylalcohols in the hydrogenolysis over Raney nickel and Raney cobalt catalysts.[29] Mitsui and his co-workers[29] confirmed these hydrocarbons to be formed *via* olefins and proposed a possible mechanism. Because oxygen has a strong affinity for nickel, the styrene oxide derivative **15** cleaves to the radical **16** in addition to nucleophilic reactions *via* paths (1) and (2). This radical follows competitively paths (4) and (5), and the alcohol and the hydrocarbon

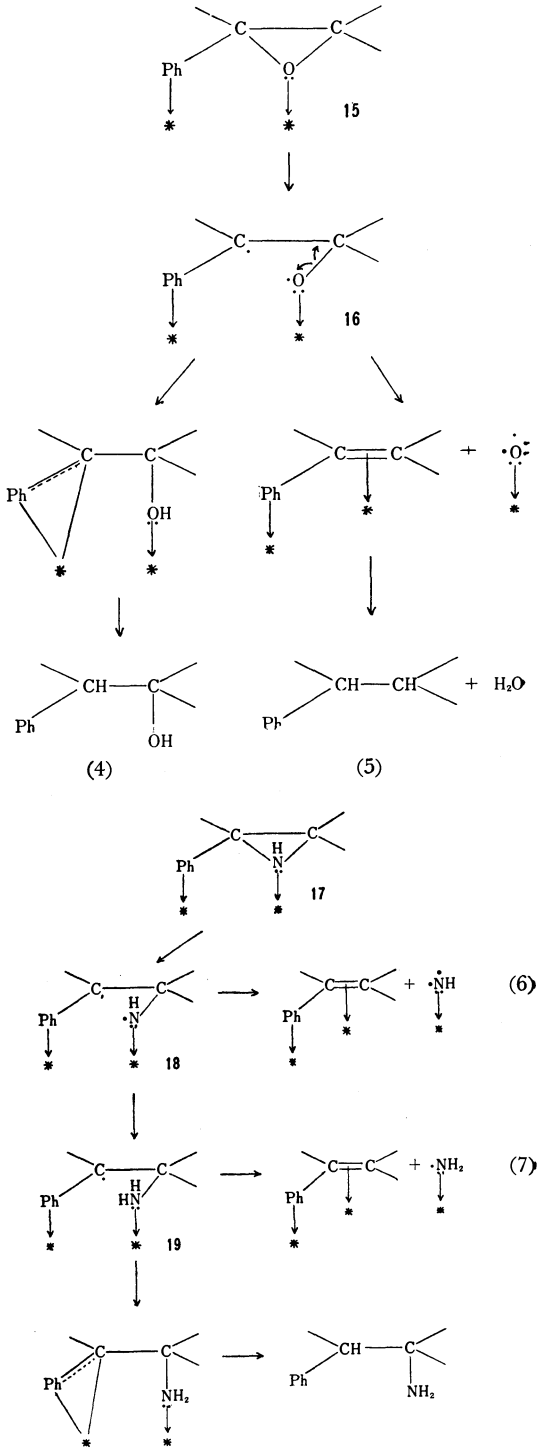

are formed respectively. However, I, gave little hydrocarbon with the Raney nickel catalyst. This suggests that nickel can not stabilize ·NH and/or ·NH_2, which are formed according to paths (6) and (7), respectively. On the other hand, 2-phenyl pro-

*2 It suggests also an importance of the distances between the carbon and the catalyst surface that the less-substituted carbon-nitrogen bond cleaved selectively in the hydrogenolysis of 2-alkyl- and 2,2-dialkylaziridines over the Raney nickel catalyst.[21]

29) S. Mitsui, S. Imaizumi, M. Hisashige, M. Fujimoto, T. Sukegawa, M. Yokozawa and K. Okamura, unpublished work.

Table 1. The catalytic hydrogenolysis of 2-methyl-2-phenylaziridine (I)

Exp. No.	Catalyst (g)	Optical purity of I*1	Products			II			
			II	III	HC*6	$[\alpha]_D$	Optical purity*2	Maintained optical activity	Configuration
1	$Pd(OH)_2$ 0.05	R 43.6	100	—	trace	+ 9.28	31	72	Inversion
2	Pd(H)*3 5.0	R 43.6	100	—	trace	+ 6.08	21	47	Inversion
3	Pd(H)*4 5.0	R 43.6	100	—	trace	+ 7.08	24	55	Inversion
4	PtO_2 0.1	R 43.6	88(6*5)	—	6	−10.60	36	83	Retention
5	PtO_2 0.1	R 37.3	92(4*5)	—	4	−10.36	35	95	Retention
6	Pt-black 0.1	R 43.6	89(3*5)	—	8	− 7.65	26	70	Retention
7	Pt-black 0.1	S 91.0	94(3*5)	—	3	+19.60	67	73	Retention
8	Ra-Ni 1(wet)	S 91.0	93	7	trace	+ 6.26	21	23	Retention
9	Ra-Co 4 (alloy)	S 91.0	92	3	5*7	+ 3.76	13	14	Retention

I, 1.33 g; Solvent: Ethanol, 20 m*l*; Under ordinary pressure and at room temperature.
*1 optically pure $[\alpha]_D^{22}$ +33.3° (*c* 9.22, ethanol). *2 optically pure $[\alpha]_D$ +29.5° (ethanol). *3 Under a hydrogen atmosphere. *4 Under a helium atmosphere. *5 2-Cyclohexylpropylamine. *6 2-Phenylpropane. *7 2-Phenylpropene.

pene was obtained from I with the Raney cobalt catalyst. The stabilizing ability of cobalt for $\cdot\dot{N}H$ and/or $\cdot\ddot{N}H_2$ is greater than that of nickel, because cobalt has a stronger affinity for the nitrogen.

In conclusion, the variations in the configuration and in the maintained optical activity of II in the hydrogenolysis of I are attributable to the free-energy difference at the transition states to form π-benzyl intermediates, which depends on the affinity of catalysts for the nitrogen, the catalyst hindrance, and other factors.

Experimental

S(+)- and R(−)-Ethyl 2-Amino-2-phenylpropionates (IV). 2-Amino-2-phenylpropionic acid was prepared according to the procedure of Steiger[30] and was converted into IV.[31] IV was resolved by the fractional recrystallization of its tartrate from ethanol. The resulting salt (mp 175.5—176.0°C, $[\alpha]_D^{20}$ +45.57° (*c* 8.91, water)) afforded S(+)-IV; bp 137—139°C/15 mmHg, α_D^{18} +10.80° (neat), $[\alpha]_D^{18}$ +25.02° (*c* 9.43, ethanol). R(−)-IV: $\alpha_D^{23.5}$ −5.00° (neat) was also obtained from mother liquor. For the rotation of optically pure IV, we adopted the greatest value (α_D^{24} +12.14° (neat))[22] hitherto reported for the ester.

S(+)-2-Amino-2-phenylpropanol (V). The amino-alcohol V was obtained according to the procedure of Tsuboyama[32] for the preparation of isoleucinol. S(+)-IV (38.6 g α_D^{20} +11.01° (neat), 90.2% optically pure) in ether (100 m*l*) was added dropwise with stirring to lithium aluminum hydride (8.0 g) in ether (100 m*l*), and the resulting mixture was heated under reflux for 2 hr. After cooling, water (30 m*l*) was added with vigorously stirring, and the ethereal layer was decanted from the precipitates. The resulting precipitates were dissolved with aqueous sodium hydroxide, and then the aqueous solution was continuously extracted with ether for 24 hr, the combined ethereal solution was dried over anhydrous sodium sulfate. After the evaporation of the ether, the oily residue was distilled under a nitrogen stream to give 23.0 g of S(+)-V; bp 116—118°C/0.4 mmHg, $[\alpha]_D^{22}$ +17.16° (*c* 9.39, benzene).

Found: C, 71.40; H, 8.72; N, 9.11%. Calcd for $C_9H_{13}NO$: C, 71.49; H, 8.66; N, 9.26%.

S(+)-2-Methyl-2-phenylaziridine (I). The imine I was prepared by the procedure of Brois[33] with slight modifications. A cold mixture of sulfuric acid (16.8 g) and water (50 m*l*) was added, with shaking, to a solution of (+)-V (23.0 g, $[\alpha]_D^{22}$ +17.16° (*c* 9.39, benzene) and water (50 m*l*). The water was removed by heating at 15—20 mmHg and finally at 0.5—1 mmHg below 140°C for 20 hr. A cold solution of 40% sodium hydroxide was added to the solidified product, and then the mixture was slowly heated in an oil bath. The basic material was steam-distilled into a cooled receiver and saturated with sodium hydroxide. The imine product was extracted with ether and dried over sodium hydroxide pellets. The evaporation of the ether and subsequent distillation under a nitrogen stream afforded 16.2 g of S(+)-I; bp 94—95°C/14 mmHg, α_D^{22} +45.60° (neat), $[\alpha]_D^{22}$ +30.04° (*c* 9.22, ethanol).

Found: C, 80.89; H, 8.47; N, 10.19%. Calcd for $C_9H_{11}N$: C, 81.15; H, 8.33; N, 10.52%.

Catalysts. The Raney nickel and Raney cobalt were prepared by the method used for W-4[34] and were stored in ethanol. The palladium hydroxide ($Pd(OH)_2$) was obtained by the method of Takagi *et al.*[35] The palladium hydride (Pd(H)) was prepared as has previously been described.[1] The platinum oxide was purchased from the Wako Junyaku Co., Ltd., Osaka. The platinum black was prepared by the hydrogen reduction of platinum oxide and was washed well with water.

Catalytic Hydrogenolysis. The following general

30) R. E. Steiger, "Organic Syntheses," Coll. Vol. III, p. 88 (1955).
31) A. McKenzie and J. Hyles, *Ber.*, **65**, 309 (1932).
32) S. Tsuboyama, This Bulletin, **35**, 1004 (1962).
33) S. J. Brois, *J. Org. Chem.*, **27**, 3532 (1963).
34) H. Adkins and A. A. Pavlic, *J. Am. Chem. Soc.*, **69**, 3039 (1947).
35) Y. Takagi, T. Naito and S. Nishimura, This Bulletin, **38**, 2119 (1965).

procedure was used. After a definite amount of catalyst in ethanol had been agitated under a hydrogen atmosphere for 1 hr, 1.33 g (0.01 mol) of I in ethanol was added; the resulting suspension was agitated with hydrogen under ordinary pressure and at room temperature. After the theoretical amount of hydrogen had been absorbed, the catalyst was filtered off, and the mixture was analyzed by gas chromatography (polyethylene glycol 4000 and potassium hydroxide dispersed on firebrick at 150—180°C using helium-carrier gas). After the evaporation of the ethanol, the oily residue was distilled under reduced pressure to give II; 78—82°C/17 mmHg. When the unreacted imine was involved, the oily residue was treated with dilute hydrochloric acid. After standing for several hours, the hydrochloride solution was made basic with aqueous ammonia. The resulting suspension was extracted with ether, and the etheral solution was dried over anhydrous sodium sulfate. The evaporation of ether and subsequent distillation afforded II. Moreover, when the reaction mixture involved substances other than II, II was purified by preparative gas chromatography. The rotation of II was measured in ethanol at *c* 9.0—10.0. For the rotation of optically pure II, we adopted $[\alpha]_D$ 29.5° (ethanol), a value which was calculated from the values given by Levene *et al.*[24] and by Eliel and Freeman.[25]

The authors are grateful to the Takeda Science Foundation for its financial support.

NOTES

BULLETIN OF THE CHEMICAL SOCIETY OF JAPAN VOL. 42 2989—2991 (1969)

The Claisen-Schmidt Condensation of Acetonitrile with Aromatic Carbonyl Compounds

Akira UCHIDA, Satoshi SAITO and Sumio MATSUDA

Faculty of Engineering, Osaka University, Suita, Osaka

(Received May 20, 1968)

The reaction of acetonitrile with aromatic carbonyl compounds in ether, using sodium amide as the catalyst, are known[1] to form the derivatives of 3-hydroxypropionitrile. This paper will deal with the same reactions in acetonitrile, using sodium as the catalyst.

It has been established that methane, sodium cyanide, and diacetonitrile are formed when sodium is dissolved in acetonitrile. Diacetonitrile is the addition product of cyanomethylsodium to acetonitrile[2] and is known to add to the aromatic carbonyl compounds.[3] Therefore, if some aromatic carbonyl compounds are added to a solution prepared by dissolving sodium in acetonitrile, the following reactions are expected to occur: the addition reactions of cyanomethylsodium to the carbonyl compounds (addition a), the addition reaction of cyanomethylsodium to acetonitrile (addition b), the addition reaction of diacetonitrile to the carbonyl compound, and the reaction of the carbonyl compound with the carbonyl compound (reaction c). These reactions might be competing reactions. If the addition a is faster than the addition b or the reaction c, the adducts of cyanomethylsodium to the carbonyl compounds must be formed. The reactions of benzaldehyde, acetophenone, or benzophenone with cyanomethylsodium in acetonitrile have been attempted in order to clarify this possibility.

When benzaldehyde or acetophenone was added to a solution which has been prepared by dissolving sodium in acetonitrile (solution I), 3-hydroxy-3-phenylpropionitrile or 3-hydroxy-3-phenylpropionitrile was isolated from the reaction products. This fact suggests that cyanomethylsodium in acetonitrile dose not react with acetonitrile as rapidly as anticipated.

When benzaldehyde is stirred into solution I

1) a) H. Lettré, G. Meiners and H. Wickmann, *Naturwissenschaften*, **33**, 158 (1946). b) While the present authors were preparing the manuscript of this paper, E. M. Kaiser *et al.* reported that 3-hydroxy-3,3-diphenylpropionitrile can be formed by the reaction of acetonitrile with benzophenone in the presence of *n*-butyl lithium. They obtained *β*-phenylcinnamonitrile, not as the reaction product, but only through the dehydration of 3-hydroxy-3,3-diphenylpropionitrile with mineral acid; *J. Org. Chem.*, **33**, 3402 (1968).

2) R. Holtzwart, *J. prakt. Chem.*, [2] **39**, 230.

3) E. Mohr, *ibid.*, [2] **56**, 125.

at room temperature, benzyl alcohol, 3-hydroxy-3-phenylpropionitrile, and a small amount of cinnamonitrile are formed. Although benzoic acid was not isolated, benzyl alcohol might be formed by the Cannizzaro reaction of benzaldehyde and cinnamonitrile might be formed by the Claisen-Schmidt condensation of acetonitrile with benzaldehyde.

In the case of acetophenone, 3-hydroxypropionitrile was isolated from the product when the reaction was carried out at room temperature, while β-methylcinnamonitrile, the product of the Claisen-Schmidt condensation of acetonitrile with acetophenone, was formed when the reaction mixture was refluxed for 3 hr.

When a solution of benzophenone in the solution I was stirred for 17 hr at room temperature, the product isolated was not the derivative of hydroxypropionitrile but β-phenylcinnamonitrile, the product of the Claisen-Schmidt condensation of acetonitrile with benzophenone. The yield of β-phenylcinnamonitrile increased markedly when the reaction mixture was heated under reflux for 9 hr.[4]

The formation of the derivatives of dicyanovinylidene by the reaction of malonitrile with ketones are well known,[5] but the formation of the derivatives of cinnamonitrile by the one-step reaction with aromatic carbonyl compounds has not been found. This reaction will serve as a convenient method for preparing β-phenylcinnamonitrile.

Experimental

All the mps are corrected, while the bps are not corrected. The NMR spectra were taken on a JNM-3H-60 (60 Mc) NMR Spectrometer, with tetramethylsilane as the internal standard. The chemical shifts (ppm) were followed by splitting patterns (s, singlet; d, doublet; t, triplet; q, quartet; m, multiplet) and relative strengths. The IR spectra were recorded on a Hitachi EPI-G2-type Grating Infrared Spectrophotometer. The molecular weight was determined on a vapor-pressure osmometer in a benzene solution.

The acetonitrile was dried over phosphorus pentoxide and was distilled before use. The benzaldehyde and acetophenone were distilled before use, while the benzophenone was used without purification.

The solution I was prepared by dissolving 4.6 g (0.2 g atom) of sodium in 150 m*l* of acetonitrile. The flask which contained the solution I was flushed with nitrogen, and the aromatic carbonyl compounds were added from a dropping funnel (benzaldehyde or acetophenone) or directly (benzophenone).

Reaction of Acetonitrile with Benzaldehyde. A mixture of 21.1 g (0.2 mol) of benzaldehyde in solution I was stirred for 5 hr at room temperature. The reaction mixture was then neutralized, and the precipitates were removed by filtration. The filtrate was dried over anhydrous magnesium sulfate, concentrated, and distilled *in vacuo* to give the following fractions: *fraction 1*, 1.5 g (7%) of benzyl alcohol (I); bp 61—67°C/1.5 mmHg; $n_D^{13.6}$ 1.5396 (lit[6] n_D^{20} 1.5403); IR (neat) 3300, 1370, 1010 cm^{-1} (OH); NMR ($CDCl_3$) τ 2.9 (s, 5), 5.6 (s, 2), 5.9 (s, 1); *fraction 2*, 2.0 g of a mixture of I, 3-hydroxy-3-phenylpropionitrile (II), and cinnamonitrile (III); bp 67—129°C/0.002 mmHg; NMR ($CDCl_3$) τ 2.9 (I+II), 4.2, 4.5 (III), 5.3 (II), 5.6 (I+II), 7.5 (II); *fraction 3*, 5.2 g (18%) of II; bp 127—131°C/0.002 mmHg; $n_D^{13.0}$ 1.5447; IR (neat) 3400, 1320, 1050 cm^{-1} (OH), 2230 cm^{-1} (CN); NMR ($CDCl_3$) τ 2.8 (s, 5), 5.3 (t, 1, J=6 cps, -C**H**(OH)-), 5.5 (s, 1, O**H**), 7.6 (d, 2, J=6 cps, -C**H**$_2$-); mol wt, Found: 146, Calcd for C_9H_9NO: 147; and *a residue*, 13.1 g of unknown compound.

When an ethanol solution of the fraction 3 was treated with hydrogen peroxide under alkaline conditions, white crystals were obtained; 3-hydroxy-3-phenylpropionamide, mp 124°C; Found: C, 65.71; H, 6.68; N, 8.90%; Calcd for $C_9H_{11}O_2N$: C, 65.44; H, 6.71; N, 8.48%.

The presence of I and II in the fraction 2 was confirmed by a study of NMR spectrum. Besides the resonance signals of I and II, there were other signals at τ 4.2 and 4.5. These signals were presumed to be signals of *cis*- and *trans*-III, because the following fraction was isolated from the reaction product which was obtained under similar reaction conditions: bp 81—84°C/4 mmHg; IR (neat) 2200 cm^{-1} (CN), 960 cm^{-1} (C=C); NMR ($CDCl_3$) τ 2.3—2.8 (m, 6), 4.3—4.9 (q, 1). When an ethanol solution of the fraction was treated with hydrogen peroxide under alkaline conditions, white crystals were formed; cinnamamide, mp 145—147°C; Found: C, 74.00; H, 6.16; N, 9.51%; Calcd for C_9H_9ON: C, 73.49; H, 6.16; N, 9.52%.

Reaction of Acetonitrile with Acetophenone. *1) Reaction at Room Temperature* A mixture of 24.0 g (0.2 mol) of acetophenone and solution I was allowed to stand at room temperature. The reaction product was then worked up to give the following fractions: *fraction 1*, 10.2 g (44%) of acetophenone; bp below 66°C/2 mmHg; $n_D^{13.3}$ 1.5342 (lit[6] n_D^{20} 1.5337); The IR was identical with that of acetophenone except for the weak absorption at 2180 cm^{-1} (perhaps from an impurity); *fraction 2*, 1.9 g of an unknown compound; bp 66—120°C/2 mmHg; *fraction 3*, 3.9 g of crude 3-hydroxy-3-methyl-3-phenylpropionitrile (VI); bp 120—129°C/2 mmHg; IR (neat) 3450, 1380, 1020 cm^{-1} (OH), 2185 cm^{-1} (CN), 1740 cm^{-1} (perhaps from an impurity); NMR ($CDCl_3$) τ 2.6 (m, 5), 6.5 (s, 1, -O**H**), 7.3 (s, 2, -C**H**$_2$-),

4) According to Holtzwart,[2] half of the sodium used was consumed in the formation of cyanomethylsodium by the following equation:

$$2CH_3CN + 2Na = CH_4 + NaCN + CH_2NaCN.$$

When a mixture of benzophenone (0.1 mol) and cyanomethylsodium in acetonitrile (0.2 g atom of Na in 150 m*l* of acetonitrile) was refluxed for 9 hr, the yield of β-phenylcinnamonitrile reached 88% (based on benzophenone). This suggested that 88% of the cyanomethylsodium formed was trapped by benzophenone and not by acetonitrile.

5) T. Metler, A. Uchida and S. I. Miller, *Tetrahedron*, **24**, 4290 (1968).

6) W. Foerst, "Ullmanns Enzyklopädie der technischen Chemie," 9. Band, Urban & Schwarzenberg, München-Berlin (1957), p. 559.

8.3 (s, 3, $-CH_3$) and small signals at τ 7.5 and 8.1 (perhaps from impurities), and *fraction 4*, 8.3 g (26%) of VI; bp 110—125°C/0.005 mmHg; mp 61—63°C (benzene); Found: C, 74.49; H, 7.65; N, 8.82%; mol wt, 157; Calcd for $C_{10}H_{11}ON$: C, 74.51; H, 6.88; N, 8.69%; mol wt, 161; (KBr Disk) 3430, 1378, 1028 cm^{-1} (OH), 2250 cm^{-1} (CN); NMR ($CDCl_3$) τ 2.7 (m, 5), 7.1 (s, 2, $-CH_2-$), 8.3 (s, 3, $-CH_3$).

2) Reaction under Reflux. A mixture of 24.0 g (0.2 mol) of acetophenone and solution I was refluxed for 3 hr. The reaction product was worked up to give the following fractions: *fraction 1*, 4.2 g (*ca.* 18%) of crude acetophenone; bp 61—91°C/3 mmHg; *fraction 2*, 7.0 g (25%) of β-methylcinnamonitrile (VII); bp 91—93 C/3 mmHg; $n_D^{25.0}$ 1.5836; IR (neat) 2210 cm^{-1} (CN), 830 cm^{-1} (C=C); NMR (neat) 2.7 (s, 5), 4.5, 4.6 (both q, total 1, J=*ca.* 1.5 cps, $-CH_3$); *fraction 3*, 0.8 g of a mixture of VI and VII; bp 140—170°C/0.001 mmHg; NMR (neat) τ 2.6 (m), 7.3 (s), 8.3 (s) which were the signals of VI and 2.7 (m), 4.5 (q), 7.7 (d) which were the signals of VII, and *a residue*, 15.5 g of an unknown compound.

Reaction of Acetonitrile with Benzophenone. A mixture of 18.2 g (0.1 mol) of benzophenone and solution I was refluxed for 9 hr. The reaction product was worked up to give the following fractions: *fraction 1*, 1.3 g of an unknown compound; bp below 160°C/1.5 mmHg; *fraction 2*, 18.1 g (88%) of β-phenylcinnamonitrile; bp 160—200°C/1.5 mmHg; mp 47—48°C (benzene-ethanol); Found: C, 88.28; H, 5.18; N, 6.79%; mol wt, 198; Calcd for $C_{15}H_{11}N$: C, 87.77; H, 5.40; N, 6.82%; mol wt, 205; NMR ($CDCl_3$) τ 2.7 (d, 10), 4.3 (s, 1, $-CH=C=$); IR (KBr Disk) 2200 cm^{-1} (CN), 840 cm^{-1} (C=C), and *a residue*, 3.0 g of an unknown compound.

When a mixture of 18.2 g of benzophenone and cyanomethylsodium (0.1 g atom of sodium in 100 m*l* of acetonitrile) was stirred for 17 hr at room temperature, 71% of benzophenone was recovered and 9% of the β-phenylcinnamonitrile was obtained. When the same reactants were refluxed for 6 hr, 35% of the benzophenone was recovered and 37% of the β-phenylcinnamonitrile was obtained.

BULLETIN OF THE CHEMICAL SOCIETY OF JAPAN VOL. 41 2991—2993 (1969)

Reactions of Organometallic Compounds with Conjugated Enol Ethers: Synthesis of β-Arylacrylates, Diarylmethylmalonates and Analogous Compounds

D. P. NABAR and S. V. SUNTHANKAR

Department of Chemical Technology, University of Bombay, Bombay, India

(Received July 17, 1968)

It has been reported earlier that the addition of enol ether such as ethoxymethylenemalonic ester (EMME) to aryl Grignard reagents at the ether reflux temperature leads to the formation of symmetrical diarylmethylmalonates in good yields. In order to get the mono-conjugate addition products, *i. e.*, the corresponding acrylates, the Grignard reaction was studied at lower temperatures, and the desired acrylates were obtained, as expected.

The temperature effect was studied by using 1-naphthylmagnesium bromide as the organometallic compound. At −50 to −60°C as well as at −10 to −14°C, diethyl 1-naphthylmethylenemalonate was obtained in 31.5% and 26.6% yield respectively. However, at 8 to 10°C both the acrylate as well as the second conjugate addition product were isolated indicating that higher temperatures promote the second conjugate addition. Phenyllithium when reacted with EMME at −50 to −60°C also gave the acrylate in 22.2% yield. The analogous compounds *i. e.* ethoxymethyleneacetoacetate and ethoxymethyleneacetylacetone, when reacted with Grignard reagents gave even at ether reflux temperature only the respective acrylates and not the double conjugate addition products.

In contrast to aryl Grignard reagents, benzylmagnesium chloride gave both the addition compounds at ether reflux temperature. The acrylate when further reacted with phenylmagnesium bromide at 0°C gave 1,2-diphenylethylmalonate, a product of second conjugate addition which was hydrolysed to a known acid.[1] The reaction of benzylmagnesium chloride with ethoxymethylenecyanoacetate and ethoxymethylenemalononitrile gave only the second conjugate addition products in over 50% yield and not the acrylates as in the above case.

Thus the conjugate addition reaction seems to depend on the structure of both organometallic compound as well as the conjugated enol ether.

Experimental

The reactions of Grignard reagents with these enol ethers were carried out by the normal procedure[2]

1) S. D. Gupte and S. V. Sunthankar, *J. Org. Chem.*, **24**, 1334 (1959).

2) E. Knoevenagel, *Ber.*, **31**, 31 (1898).

Table 1. Products of the reaction of Grignard reagents with conjugated enol ethers

Grignard reagent (Reaction temp.)	Enol ether $EtOCH=CR^1R^2$	Product $R^3CH=CR^1R^2$ ($R^3R^4CH-CHR^1R^2$)	Molecular formula	Yield %	Bp °C/mmHg (Mp °C) (Crystn. Solv.)	Anal. C% Found (Calcd)	Anal. H% Found (Calcd)	Anal. N% Found (Calcd)	Anal. Cl% Found (Calcd)
PhMgBr (−50 to −60°C)	$R^1=R^2=COOEt$	$R^1=R^2=COOEt$ $R^3=Ph$	$C_{14}H_{16}O_4$	50.5	105—110/0.0125 lit.*1 163—170/5	67.90 (67.73)	7.00 (6.50)		
α-Naph.MgBr (−50 to −60°C)	$R^1=R^2=COOEt$	$R^3=\alpha$-Naph.	$C_{18}H_{18}O_4$	31.5	140—145/0.004 lit.*2 203—205/2	71.90 (72.46)	7.42 (6.08)		
(−10−14°C)		$R^3=\alpha$-Naph.		26.6					
(8 to 10°C)		$R^3=\alpha$-Naph.		21.9					
		($R^3=R^4=\alpha$-Naph)	$C_{28}H_{26}O_4$	28.2	(112—113) (lit.*2 113—114)	78.30 (78.85)	5.90 (6.14)		
At ether reflux temp									
$PhCH_2MgCl$	$R^1=R^2=COOEt$	$R^3=PhCH_2$	$C_{15}H_{18}O_4$	19.4	110—115/0.003	68.20 (68.68)	6.70 (6.92)		
		($R^3=R^4=PhCH_2$)	$C_{22}H_{26}O_4$	57.7	150—155/0.006	74.30 (74.55)	7.10 (7.40)		
o-$ClC_6H_4CH_2$-Mg Br	$R^1=R^2=COOEt$	$R^3=o$-$ClC_6H_4CH_2$	$C_{15}H_{17}O_4Cl$	31	120—125/0.01	60.50 (60.71)	6.10 (5.73)		12.60 (11.98)
		($R^3=R^4=o$-Cl $C_6H_4CH_2$)	$C_{22}H_{24}O_4Cl_2$	57	160—165/0.02	62.20 (62.41)	6.00 (5.67)		17.00 (16.78)
p-ClC_6H_4-CH_2MgBr	$R^1=R^2=COOEt$	$R^3=p$-$ClC_6H_4CH_2$	$C_{15}H_{17}O_4Cl$	22	125—130/0.009	61.20 (60.71)	5.90 (5.73)		12.80 (11.98)
		($R^3=R^4=p$-Cl $C_6H_4CH_2$)	$C_{22}H_{24}O_4Cl_2$	62	(52—53) (methanol)	62.30 (62.41)	5.50 (5.67)		17.10 (16.78)
PhMgBr	$R^1=COCH_3$ $R^2=COOEt$	$R^1=COCH_3$ $R^2=COOEt$ $R^3=Ph$	$C_{13}H_{14}O_3$	39.4	90— 95/0.025 lit.*3 189—191/15	71.00 (71.54)	6.92 (6.47)		
$PhCH_2MgCl$	$R^1=COCH_3$ $R^2=COOEt$	$R^3=PhCH_2$	$C_{14}H_{16}O_3$	47.2	95—100/0.02	72.70 (72.39)	7.20 (6.94)		
α-Naph.MgBr	$R^1=COCH_3$ $R^2=COOEt$	$R^3=\alpha$-Naph.	$C_{17}H_{16}O_3$	38.7	135—140/0.007	76.70 (76.10)	5.80 (6.01)		
C_6H_5MgBr	$R^1=R^2=COCH_3$	$R_3=Ph$	$C_{12}H_{12}O_2$	10.1	90— 95/0.002 lit.*4 180—185/15	76.10 (76.57)	6.60 (6.43)		
$PhCH_2MgCl$	$R^1=COOEt$ $R^2=CN$	($R^1=COOEt$ $R^2=CN$) $R^3=R^4=PhCH_2$	$C_{20}OH_{21}NO_2$	58.8	155—160/0.002	78.50 (78.14)	6.82 (6.89)		
$PhCH_2MgCl$	$R^1=R^2=CN$	($R^1=R^2=CN$ $R^3=R^4=PhCH_2$)	$C_{18}H_{16}N_2$	53.8	(111) (ethanol)	83.10 (83.04)	6.13 (6.20)		
o-$ClC_6H_4CH_2$-MgBr	$R^1=R^2=CN$	($R^1=R^2=CN$ $R^3=R^4=o$-$ClC_6H_4CH_2$)-	$C_{18}H_{14}N_2Cl_2$	52	(122—3) (ethanol)	65.20 (65.65)	4.10 (4.25)	8.10 (8.51)	

*1 El. Ahmadi, I. Heiba and C. Anderson, *J. Am. Chem. Soc.*, **81**. 1119 (1959).
*2 M. S. Newman and D. Lednicer, *ibid.*, **78**, 4765 (1956).
*3 G. Casimir, *Ann. Chim.* (*Paris*), **7**, 807, (1962).
*4 E. Knoevenagel and R. Werner, *Liebig's Ann.*, **281**, (1894).

at suitable temperatures. The experiment given below will serve as an example.

Diethyl (1,2-Diphenylethyl)-malonate. To a filtered solution of phenylmagnesium bromide (from magnesium 0.7 g and bromobenzene 3.925 g) cooled in ice bath was added a solution of diethyl benzylmethylenemalonate (5.24 g) in ether (25 m*l*). The reaction mixture was stirred for 3 hr. After the usual work up the product was purified by fractional distillation at temperature 140—150°C/0.004 mmHg.

Found: C, 74.50; H, 7.50%. Calcd for $C_{21}H_{24}O_4$: C, 74.09; H, 7.11%.

We are grateful to Messrs Kay-Fries Chemicals, Inc., West Haverstraw; N. Y. (U. S. A.) for their generous gift of ethoxymethylenemalonate and analogous enol ethers used in this work.

BULLETIN OF THE CHEMICAL SOCIETY OF JAPAN VOL. 42 2993—2995 (1969)

The Reaction of Alcohols and Hydrocarbons in a Silent Electric Discharge. II. The Reaction of 2-Propanol with Ethylene— The Effects of the Reaction Conditions*1

Teruo HIRAKI

Institute of Commodities, Faculty of Economics, Kagawa University, Takamatsu-shi

(Received August 18, 1968)

It has been established that the α-C-alkylations of primary and secondary alcohols result from their peroxide-,[1] light-,[2] and gamma-rays-induced[3] reactions with olefins. However, no detailed study of the reaction of alcohol with olefin under a silent discharge has been reported.

A previous study[4] of the decomposition of 2-propanol under a silent discharge showed that an α-hydrogen atom in 2-propanol is replaced by alkyl groups. The present study was undertaken to ascertain whether or not a chain telomerization occurs in the reaction of 2-propanol and ethylene by a silent discharge, and to establish the difference in the chemical behavior of 2-propanol between that in the presence of ethylene and that in its absence. The author wishes to report some observations on the ethylene effects on the reaction of 2-propanol, and to report that no 2-methyl-2-hexanol (1 : 2 telomer) or higher telomers, derived from a 2-propanol-ethylene mixture excited by light, peroxide or γ-rays, were formed by the silent discharge.

Experimental

Materials. The 2-propanol was purified and the packing material was prepared by the methods described in a previous paper.[4] Commercial ethylene was used without purification. No impurity was found in either reagent by gas chromatography using columns of PEG-6000 and of activated charcoal respectively.

Apparatus and Procedure. The apparatus and the procedure were similar to those previously reported,[4] except that the reaction was carried out in the presence of ethylene. All the experiments were performed using a flow system. Ethylene coming from a reservoir was passed through a solid sodium hydroxide tube in order to remove any water, and was then introduced into a discharge tube with gaseous 2-propanol. The ethylene flow rate was measured by a calibrated flowmeter.

The reaction products coming through the tube were separated into a condensable part and non-condensable gases by three traps cooled at 0°C. The voltage was stepped up by a transformer (capacity: 15 kV) to give the required value.

Analyses. The non-condensable gases were identified by comparing their retention times on a gas chromatogram with those of authentic samples (Columns of activated charcoal, hexamethylphosphoramide, and molecular sieve-13X were used). The condensable products were identified by gas chromatography (column, tricresyl phosphate, PEG-6000 and silicone DC-550 at 120°C; carrier gas, He) as well as by derivatization.[5]

*1 The major part of these research results were presented at the 20th Annual Meeting of the Chemical Society of Japan, Tokyo, April, 1967.

1) W. H. Urry, F. W. Stacey, E. S. Huyser and O. O. Juveland, *J. Am. Chem. Soc.*, **76**, 450 (1954); E. V. Kirkland, *Ind. Eng. Chem.*, **52**, 397 (1960).

2) W. H. Urry, F. W. Stacey, O. O. Juveland and C. H. McDonnell, *J. Am. Chem. Soc.*, **75**, 250 (1953).

3) K. Hirota and M. Hatada, This Bulletin, **34**, 1644 (1961); T. Kurihara and H. Hotta, *ibid.*, **37**, 1448 (1964).

4) T. Hiraki, *ibid.*, **42**, 470 (1969).

5) The 3,5-dinitrobenzoates of 2-methyl-2-butanol and *dl*-2-pentanol were prepared according to the procedure of Shriner *et al.*; R. L. Shriner, R. C. Fuson and D. Y. Curtin, "The Systematic Identification of Organic Compounds," 4th Ed., John Wiley & Sons, New York (1956), p. 212.

TABLE 1. INFLUENCE OF ETHYLENE ADDITION ON THE DISCHARGE REACTION OF 2-PROPANOL

Run No.	1	2	3	4	12	13
Packing	None*				$Cu(OH)_2$**	
Second. voltage, kV	15	15	15	13.5	15	15
Second. current, mA	3.0	2.8	4.9	4.7	1.2	0.9
Temp. of discharge tube, °C	85	85	32	32	85	85
Residence time, hr	6	4.5	6	9	5	4
Materials						
2-Propanol amount, g	38.63	36.99	39.24	38.78	38.95	38.56
2-Propanol velocity, g/hr	6.44	8.22	6.54	4.31	7.79	9.65
Ethylene volume, *l*	13.32	0	13.20	0	13.10	0
Ethylene velocity, *l*/hr	2.22	0	2.20	0	2.62	0
Molar ratio (C_2H_4/*i*-PrOH)	0.93	0	0.90	0	0.89	0
Amount of liquid products, g	1.72	2.10	0.12	0.20	1.31	1.68
Conversion, %***	4.46	5.68	0.31	0.52	3.36	4.36
Composition of liquid products, %****						
Acetone	23.4	50.6	10.9	24.3	83.5	29.9
Acetaldehyde	17.7	16.7	2.2	0.3	4.3	5.9
2-Methyl-2-butanol	9.6	0.6	18.8	2.2	2.1	0.3
2-Methyl-2-propanol	2.4	2.0	7.8	9.3	1.1	4.5
dl-2-Butanol	7.2	6.9	10.5	3.7	0.8	3.0
dl-2-Pentanol	6.4	1.2	0	0	0.9	0.4
Methyl vinyl ketone	2.8	2.8	4.4	1.2	1.7	9.6
Hydrocarbons	23.9	13.9	7.4	53.0	4.8	43.9
The others	6.6	5.3	38.0	6.0	0.8	2.5

* Siemens ozonizer was used.
** A 5 g of $Cu(OH)_2$ was filled in a glass filter.
*** The conversion efficiency was given by (grams of reaction product per grams of 2-propanol used) × 100.
**** The yields of each compound produced were given by (grams of each compound per grams of total reaction product) × 100.

Results and Discussion

Influence of Ethylene Addition on the Discharge Reaction of 2-Propanol. *a) With a Siemens Tube.* The main liquid products of the reaction in the Siemens ozonizer were acetone, acetaldehyde, 2-methyl-2-butanol, *dl*-2-butanol, *dl*-2-pentanol, and hydrocarbons (Run No. 1). The percentage compositions of these products shown in the tables are the averages of three experiments; the fluctuations in the yields of these compounds were less than 1%. The gaseous products were C_1-C_4-hydrocarbons, carbon monoxide, and hydrogen; they were not determined quantitatively. An unidentified brown solid was deposited on the glass wall.

All the compounds, except the deposit, had also been formed in the silent discharge-induced reaction of 2-propanol without ethylene.[4] However, the distribution of the products was different from that in the reaction without ethylene: (1) The acetone yield decreased greatly in the presence of ethylene, while the yields of 2-methyl-2-butanol, *dl*-2-pentanol, and hydrocarbons increased. These findings suggest that there is a close relationship between the formations of acetone and of these alcohols.

The radicals from 2-propanol in the silent discharge are mainly $(CH_3)_2\dot{C}OH$, $CH_3CHOH\dot{C}H_2$ and $\dot{C}H_3$, as has been described in the previous paper.[4] Acetone can be formed by the elimination of a hydrogen atom from the $(CH_3)_2\dot{C}OH$ and CH_3-$CHOH\dot{C}H_2$ radicals, while 2-methyl-2-butanol and *dl*-2-pentanol can be formed by adding these radicals to ethylene. Thus, the decrease in acetone in the presence of ethylene seems to be due to the latter addition reaction. A similar mechanism has also been observed in the light-[2] and γ-ray-induced[3] reactions.

The possible combination reaction of the $(CH_3)_2$-$\dot{C}OH$ radical with the $\dot{C}_2H_5$ radical which might explain 2-methyl-2-butanol has been discarded, since little or no *n*-butane, which would indicate the presence of $\dot{C}_2H_5$ radicals, was observed.

(2) The yield of *dl*-2-butanol was scarcely affected by the presence of ethylene. Possible ways of this production are thought to be as follows:

TABLE 2. TEMPERATURE DEPENDENCE OF THE YIELD

Run No.	10	11	12	14
Packing		$Cu(OH)_2$**		
Second. voltage, kV	0	15	15	15
Second. current, mA	0	1.4	1.2	1.0
Temp. of discharge tube, °C	150	150	85	28
Residence time, hr	5	5	5	5
Materials				
2-Propanol amount, g	39.02	37.55	38.95	39.21
2-Propanol velocity, g/hr	7.80	7.51	7.79	7.84
Ethylene volume, *l*	14.00	12.20	13.10	13.68
Ethylene velocity, *l*/hr	2.80	2.44	2.62	2.74
Molar ratio (C_2H_4/*i*-PrOH)	0.96	0.87	0.89	0.93
Amount of liquid products, g	11.30	7.67	1.31	0.02
Conversion, %***	28.96	20.42	3.36	0.05
Composition of liquid products, %****				
Acetone	97.0	83.7	83.5	43.6
Acetaldehyde	0	1.7	4.3	5.1
2-Methyl-2-butanol	0	0.5	2.1	10.3
2-Methyl-2-propanol	0	0	1.1	Trace
dl-2-Butanol	0	0.1	0.8	Trace
dl-2-Pentanol	0	0	0.9	7.7
Methyl vinyl ketone	0	0	1.7	0
Hydrocarbons	1.3	13.5	4.8	7.7
The others	1.7	0.5	0.8	25.6

$$CH_3\dot{C}HOH + CH_2{=}CH_2 \rightarrow CH_3CHOH\dot{C}_2H_4$$
$$\xrightarrow[i\text{-PrOH}]{} CH_3CHOHC_2H_5 \quad (A)$$
$$CH_3CHOH\dot{C}H_2 + \dot{C}H_3 \rightarrow CH_3CHOHC_2H_5 \quad (B)$$

Thus, reaction B may be thought to be retarded in the presence of ethylene and reaction A, to be facilitated, because ethylene may act as a free radical scavenger; the reverse is the production of *dl*-2-butanol in the reaction without ethylene.

b) With a Special Tube. When the reaction of 2-propanol with ethylene was carried out in a special discharge tube filled with $Cu(OH)_2$ (Run No. 12), as compared with the reaction without ethylene (Run No. 13), the following differences were noticed in the liquid products: (1) the acetone yield increased remarkably, and (2) the yields of 2-methyl-2-propanol, methyl vinyl ketone, and hydrocarbons decreased. A similar tendency was observed when a reduced copper tube[4] was used.

Thomas *et al.*[6] showed that, in the decomposition of ethylene under a silent discharge, the products most frequently identified were hydrogen, acetylene, and a liquid.

In the present work the hydrogen thus produced may turn $Cu(OH)_2$ into some effective catalyst for the dehydrogenation of 2-propanol.[7] For this reason, the acetone yield might increase in the presence of ethylene.

Thomas *et al.*[6] have also shown that acetylene and hydrogen are formed through the vinyl radical, and that the radical could give 1-butene and 1,3-butadiene. These C_4-hydrocarbons were observed little in the reaction of 2-propanol with ethylene (Run No. 12), though some were obtained in the reaction without ethylene (Run No. 13). Thus, it is thought that most of the vinyl radicals produced decompose immediately to form C_2H_2 and H_2 when there is a high flow rate of ethylene in the presence of $Cu(OH)_2$. For this reason, the methyl vinyl ketone yield might decrease in the reaction with ethylene.

Temperature Dependence of the Yield. As may be seen from Run No. 10 in Table 2, the reaction of 2-propanol with ethylene at 150°C without an electrical field afforded a great quantity of acetone. Similar results were also observed in the silent-discharge-induced reaction at 150°C (Run No. 11). Thus, at such a high temperature, it may be said that the dehydrogenation to give acetone occurred preferably to an interaction of 2-propanol and ethylene induced by the discharge.

The author wishes to express his thanks to Professor Tamon Matsuura, Hiroshima University, and to Professor Kazuaki Kawamoto, Kagawa University, for their kind advice.

6) C. L. Thomas, G. Egloff and J. C. Morrell, *Chem. Revs.*, **28**, 1 (1941).

7) Sabatier showed that $Cu(OH)_2$ treated with hydrogen was an effective catalyst for the dehydrogenation of alcohols; P. Sabatier, *Compt. rend.*, **172**, 733 (1921).

BULLETIN OF THE CHEMICAL SOCIETY OF JAPAN VOL. 42 2996—2997 (1969)

Antituberclous Compounds. XXVII. Synthesis of 7,8-Dihydropyrido-[2.3-*d*]pyridazin-(6*H*)-one[1]

Shichiro KAKIMOTO and Shuichi TONOOKA

Research Institute for Tuberculosis, Hokkaido University, Sapporo

(Received December 29, 1968)

In a previous paper,[2] it was reported that attempts to prepare some derivatives of dihydropyrido[2.3-*d*]pyridazine in order to study relationship between chemical constitution and tuberclostatic activity were not successful. In this paper, two different synthetic methods of 7,8-dihydropyrido[2.3-*d*]pyridazin-5(6*H*)-one will be reported; the synthesis of this substance was attempted previously.

Hurst and Wibberley[3] prepared ethyl 2-bromomethylnicotinate by the bromination of ethyl 2-methylnicotinate with *N*-bromosuccinimide (NBS). By the same method, its hydrobromide (I) was obtained directly in a pure state. When the compound was treated with hydrazine hydrate, two new compounds, (II), mp 213—215°C, and (III), mp 195—197°C, were obtained in good yields. The ratio of their yields was about 4 : 1. By treatment with alkali, III was converted to II, which was also obtained by the reduction of pyrido[2.3-*d*]pyridazin-5(6*H*)-on-thiol[4] (VI) with amalgamated aluminum. The IR spectrum of II has absorption bands at 3270 cm^{-1} (amino group) and at 1660 cm^{-1} (carbonyl group). The NMR spectrum indicates that it has three protons of the pyridine ring in an AMX-type arrangement and shows a 2-proton singlet of the methylene group at τ 6.45. The compound was oxidized to pyrido[2.3-*d*]pyridazin-5(6*H*)-one[2] (IV) by chromic acid anhydride in acetic acid or by aeration in the presence of peroxide. It was, therefore, concluded that II is 7,8-dihydropyrido[2.3-*d*]-pyridazin-5(6*H*)-one.

The behavior of the pyridine ring is different from that of the benzene ring. Methyl 2-bromomethyl benzoate was treated with hydrazine hydrate in the same way. Only phthalazin-1(2*H*)-one was produced, not 3,4-dihydrophthalazin-1(2*H*)-one. It is certain that the latter is easily oxidized during preparation. Hirsch *et al.*[5] found that some 4-substituted 3,4-dihydrophthalazine derivatives were oxidized to the corresponding phthalazinone by aeration without peroxide.

The IR spectrum of compound III has two bands, at 3330 cm^{-1} and 3270 cm^{-1} indicating an amino group, and one band, at 1690 cm^{-1}, indicating a carbonyl group. The NMR spectrum shows three 1-proton doublet-doublets due to the three protons of the pyridine ring, at τ 1.25, 1.90, and 2.60; a 2-proton singlet at τ 5.40 due to a methylene group, and a 2-proton broad peak at τ 5.65 due to an amino group. The amino group was acetylated with acetic anhydride. It is clear that III is 2-amino-dihydropyrrolo[3.4-*b*]pyridin-1-one.

Experimental[6]

Ethyl 2-Bromomethylnicotinate Hydrobromide (I). Ethyl 2-methylnicotinate (5g) was brominated with NBS in carbon tetrachrolide as usual. Dried hydrobromic acid was introduced into the reaction mixture, and then hydrobromide was separated from the mixture as a yellow crystalline substance. Recrystallization from ethanol - ligroin afforded 4.4 g of I, mp 157—159°C (decomp.). NMR (D_2O) τ: 4.93 ($-CH_2Br$, singlet). Found: C, 33.17; H, 3.62%. Calcd for $C_9H_{10}O_2NBr \cdot HBr$: C, 33.26; H, 3.41%.

7,8-Dihydropyrido[2.3-*d*]pyridazin-5(6*H*)-one (II). i) To a solution of 0.95 g of I in 20 m*l* of ethanol there was added 0.7 m*l* of hydrazine hydrate, and then the mixture was refluxed for 2.5 hr. After evaporation to a small volume, it was cooled to afford 320 mg of II, mp 213—215°C.

ii) A mixture of 0.5 g of VI, 0.5 g of amalgamated aluminum, and 100 m*l* of 50% ethanol was refluxed for 10 hr. The filtrate of the reaction mixture was then evaporated to dryness. The residue was extracted with water, and the aqueous solution was evaporated to give a crystalline product. Recrystallization from water afforded 0.1 g of II, mp 213—215°C, as needles with one mole of the water of crystallization.

IR: ν_{max} 3270, 3210 (NH), 1660 cm^{-1} (CO). NMR

1) Presented at the 21th Annual Meeting of the Chemical Society of Japan, Osaka, April, 1968.

2) S. Kakimoto and S. Tonooka, This Bulletin, **40** 153 (1967).

3) J. Hurst and D. G. Wibberley, *J. Chem. Soc.*, **1962**, 120.

4) S. Kakimoto, H. Shintani and K. Yamamoto, Annual Report of Research Institute for Tuberculosis, Hokkaido University, **27**, 1 (1966).

5) A. Hirsch and D. G. Orphanos, *J. Heterocyclic Chem.*, **3**, 38 (1966).

6) All the melting points are uncorrected; the IR spectra were measured in Nujol, while the NMR spectra were determined on a Japan Electron Optics 3H-60 high resolution NMR spectrometer, using TMS or DSS as the internal reference.

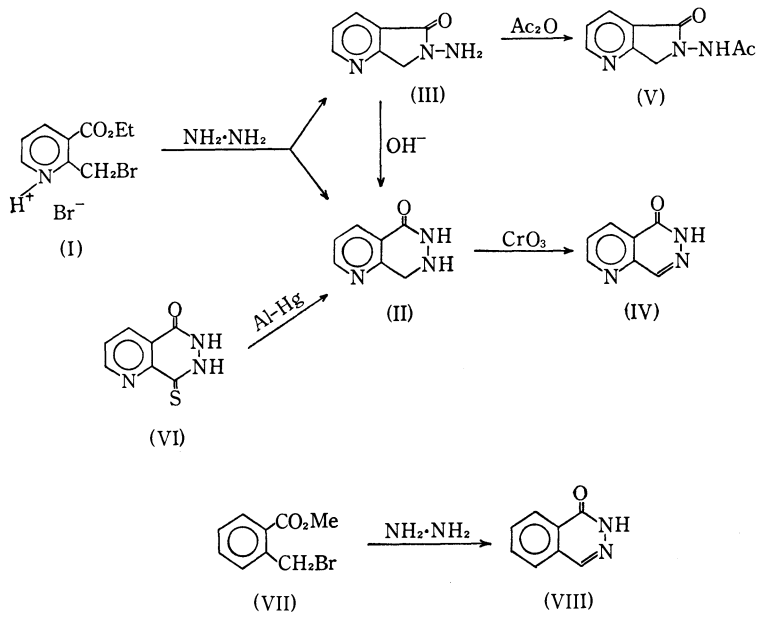

(D_2O) τ: 2.20 (H_α of pyridine-ring, doublet-doublet), 2.45 (H_γ of pyridine-ring, doublet-doublet), 3.40 (H_β of pyridine-ring, doublet-doublet), $J_{\alpha\beta}=5.0$, $J_{\beta\gamma}=8.0$, $J_{\alpha\gamma}=2.0$ cps. 6.45 ($-CH_2-$, singlet) Found: C, 50.29; H, 5.38; H_2O, 10.88%. Calcd for $C_7H_7ON_3\cdot H_2O$: C, 50.29; H, 5.43; H_2O, 10.77%.

Oxidation of II to IV. i) To a mixture of 0.1 g of II and 2 m*l* of acetic acid these were added 10 m*l* of a 1/5 N chromic oxide solution in acetic acid; the mixture was then allowed to stand for 1 hr. After the evaporation of the acetic acid under reduced pressure, the residue was recrystallized from water to give 0.1 g of white needles. Its identity as IV was established by a study of the IR spectra and melting points.

ii) A solution of 0.1 g of II in 5 m*l* of ethanol, along with several mg of benzoyl peroxide, was aerated at 50—60°C for 24 hr. During aeration the total volume was kept at about 5 m*l* by the addition of ethanol from time to time. After the ethanol had then been removed, the residue was recrystallized from ethanol-ligroin to give 35 mg of white needles. Its identity as IV was confirmed by a study of the IR spectra and melting points.

2-Aminodihydropyrrolo[3.4-*b*]pyridin-1-one (III). The mother liquor of II was evaporated to dryness and the residue was recrystallized from ethanol-ligroin to give 85 mg of III as white crystalline plates, mp 195—197°C. IR: ν_{max} 3330, 3270 (NH), 1690 cm^{-1} (CO). NMR ($CDCl_3$) τ: 1.25 (H_α of pyridine-ring, doublet-doublet), 1.90 (H_γ of pyridine-ring, doublet-doublet), 2.60 (H_β of pyridine-ring, doublet-doublet), $J_{\alpha\beta}=4.5$, $J_{\beta\gamma}=8.0$, $J_{\alpha\gamma}=1.5$ cps. 5.40 (methylene-group, singlet), 5.65 (amino-group, broad peak). Found: C, 56.37; H, 4.75%. Calcd for $C_7H_7ON_3$: C, 56.37; H, 4.73%.

2-Acetamidodihydropyrrolo[3.4-*b*]pyridin-1-one (V). III (60 mg) was dissolved in 5 m*l* of acetic anhydride, and the mixture was warmed on a steam bath for 4 hr. After the removal of the excess acetic anhydride under reduced pressure, the residue was recrystallized from ethanol-ligroin to give 25 mg of an acetyl compound, V, mp 173—175°C. IR: ν_{max} 3230 (NH), 1720 ($COCH_3$), 1690 cm^{-1} (CO). Found: C, 51.65; H, 5.35; H_2O, 8.99%. Calcd for $C_9H_9O_2N_3\cdot H_2O$: C, 51.67; H, 5.30; H_2O, 9.23%.

III to II. III (53 mg) was heated in a dilute potassium hydroxide solution on a steam bath for 1 hr. After neutralization with dilute hydrochloric acid, the solution was evaporated to dryness under reduced pressure, and the residue was extracted with ethanol. After the ethanol had then been removed under reduced pressure, the residue was recrystallized from ethanol-ligroin to give 20 mg of white needles. Its identity as II was established by a study of the IR spectra and melting points.

Phthalazin-1(2*H*)-one (VIII). Methyl 2-methyl benzoate was treated with NBS in carbon tetrachloride in the manner used to cause I to afford VII. Its NMR spectrum showed four protons of benzene at τ 2.0—2.6, a 2-proton singlet at τ 5.05, and a 3-proton singlet at τ 6.10. VII (2 g) was treated with hydrazine hydrate in the same manner as has been described for II to give 0.35 g of VIII, mp 181—183°C. Its identity with an authentic sample[7] was confirmed by a study of the IR spectra and a mixed-melting-point determination.

7) Paul, *Ber.*, **32**, 2020 (1899).

BULLETIN OF THE CHEMICAL SOCIETY OF JAPAN VOL. 42 2998—3000 (1969)

The Spectrophotometric Determination of Beryllium with Chromal Blue G

Katsuya UESUGI

Laboratory of Chemistry, Himeji Institute of Technology, Himeji

(Received January 16, 1969)

The present author and his co-workers[1-5] have studied the methods of the spectrophotometric determination of several metals using dyes of the triphenylmethane series, and have previously reported[5] a spectrophotometric determination of scandium with chromal blue G (sodium-2''-chloro-4''-nitro-4'-hydroxy-3,3'-dimethylfuchsone-5,5'-dicarboxylate, color index 43835), and found that a very small amount of beryllium also reacts with this reagent in a weakly acidic medium to form a complex. This paper will describe a spectrophotometric determination of beryllium using this reagent. The proposed method is not selective, like other reagents for beryllium, but it is more sensitive than the methods using chromazurol S,[6] eriochrome cyanine R,[7] or xylenol orange,[8] which have structures similar to that of this reagent.

Experimental

Reagents and Apparatus. *Standard Beryllium Solution.* A standard beryllium solution was prepared by dissolving 1.964 g of beryllium sulfate tetrahydrate (Mitsuwa Chemicals) in distilled water, then adding 10 m*l* of hydrochloric acid and diluting the solution to 1 *l*. The solution contained 100 μg of beryllium per milliliter. This standard stock solution was then further diluted to 10 ppm with distilled water.

Chromal Blue G Solution. The chromal blue G (Geigy Chemicals, New York, U. S. A.) was purified by recrystallization from ethanol before use, and then 0.1 g of it was dissolved in 100 m*l* of 95% ethanol. This solution was stable for at least a month.

All the other reagents and the apparatus used were the same as those reported previously.[5]

The Standard Procedure for Beryllium Determination. To a sample solution containing from 1 to 8 μg of beryllium, add 2 m*l* of the chromal blue G solution, then add 10 m*l* of an acetate buffer solution (pH 6.0), mix well, and make up to 25 m*l* with distilled water. Determine the absorbance at 610 mμ against a reagent blank solution treated in a similar manner. From the measured absorbance, determine the beryllium concentration of the sample solution by the use of a calibration curve.

Results and Discussion

Absorption Curves. The absorption curves of chromal blue G have been presented in a previous paper;[5] the maximum absorption is at 480 mμ below pH 4.0, at 430 mμ over the pH range from 5.5 to 10.0, and at 590 mμ above pH 10.5. The absorption curves of the beryllium-chromal blue G complex at various pH values are shown in Fig. 1. These curves were obtained by measuring the absorbance of the solution containing 0.12 ppm of beryllium and 80 ppm of chromal blue G at various pH values against a reagent blank solution. Above pH 5.0, the solutions give essentially identical absorption curves, with an absorption maximum

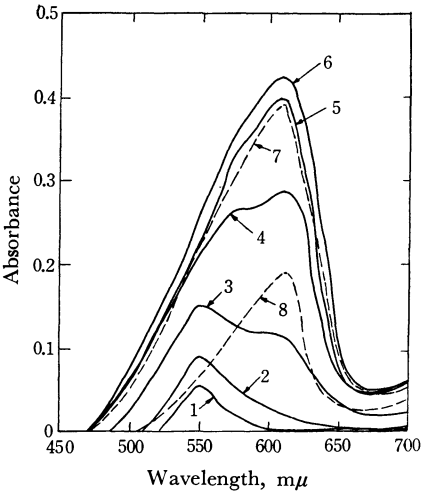

Fig. 1. Absorption spectra of beryllium complex at various pH.
Be 0.12 ppm, Reagent 80 ppm, Reference: Reagent blank
pH 1 : 3.5, 2 : 4.0, 3 : 4.5, 4 : 5.0, 5 : 5.5, 6 : 6.0—6.3, 7 : 7.0, 8 : 8.0

1) Y. Katsube, K. Uesugi and J. H. Yoe, This Bulletin, **34**, 72 (1961).
2) Y. Katsube, K. Uesugi and J. H. Yoe, *ibid.*, **34**, 829 (1961).
3) K. Uesugi, Y. Katsube and J. H. Yoe, *ibid.*, **35**, 516 (1962).
4) T. Shigematsu, K. Uesugi and M. Tabushi, *Bunseki Kagaku (Japan Analyst)*, **12**, 267 (1963).
5) K. Uesugi, This Bulletin, **42**, 2051 (1969).
6) L. Silverman and M. E. Shideler, *Anal. Chem.*, **31**, 152 (1959).
7) U. T. Hill, *ibid.*, **30**, 521 (1958).
8) M. Otomo, This Bulletin, **38**, 730 (1965).

at 610 mμ. However, the reagent solution has a slight absorption at this wavelength in the pH range from 5.5 to 7.5. Below pH 4.5, the position of the maximum absorption shifts to 570 mμ. The curve obtained at pH 5.0 has a shoulder at about 580 mμ.

Effect of pH. The effect of pH on the color development of the complex was examined by measuring, at 610 mμ, the absorbance of a solution containing 0.12 ppm of beryllium and 80 ppm of the reagent at different pH values from 4.5 to 9.0. The results are shown in Fig. 2, from which it can be seen that the maximum absorbance of the beryllium complex occurs in the pH range from 5.8 to 6.4. The amount of the buffer solution (pH 6.0 and 0.2 M in acetate) was found to have no effect on the absorbance over the range from 5 to 10 ml per 25 ml of the solution.

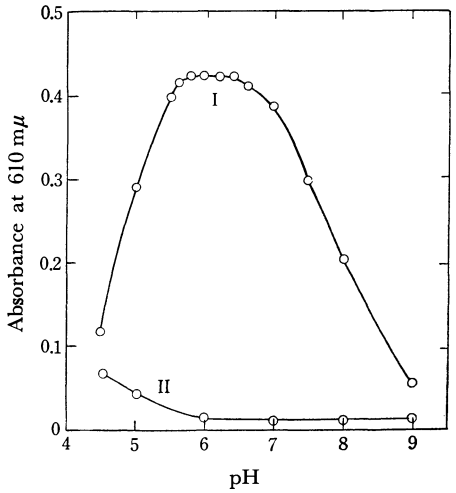

Fig. 2. Effect of pH on color development.
I: Be 0.12+Reagent 80 ppm (Reference: Reagent blank)
II: Reagent 80 ppm (Reference: Water)

Stability of Color. The color development between beryllium and the reagent occurs instantaneously at room temperature. The color intensity of the solution remains almost constant for at least 2 hr after preparation when measured against a reagent blank.

Effect of Reagent Concentration. The effect of the chromal blue G concentration on the color development was examined by varying the concentration of the reagent at a constant beryllium concentration. The absorbance of the beryllium complex at 610 mμ gradually increases at higher reagent concentrations. However, above 1.0 ml of a 0.1% reagent solution, the rate of the increase of the absorbance is relatively small. On the basis of these data, 2.0 ml of 0.1% reagent solution was chosen as the fixed quantity to be added. Two milliliters of a 0.1% chromal blue G solution for 25 ml of the solution was found to be a sufficient amount for less than 0.3 ppm of beryllium.

Effect of Temperature. The effect of the temperature on the color development was examined by measuring the absorbance of colored solutions kept at various temperatures for 20 min after preparation. There was no variation in the absorbance of the colored complex over the temperature range from 10 to 40°C. At temperatures over 40°C, however, the color intensity decreased.

Beer's Law and Sensitivity. The linearity between the absorbance of the beryllium-chromal blue G complex and the beryllium concentration was examined by varying the beryllium concentration and by measuring the absorbance at a wavelength of 610 mμ and at pH 6.0. The beryllium complex was found to follow Beer's law up to a beryllium concentration of at least 0.3 ppm. The molar absorptivity is 31000 at 610 mμ. The spectrophotometric sensitivity[9] is estimated to be 3×10^{-4} μg of beryllium per cm², corresponding to $\log I_0/I=0.001$.

Effect of Diverse Ions. A study was made of the effect of several cations and anions. The most commonly-encountered ions were added individually to a solution containing 10 μg of beryllium. From the results, it can be concluded that copper(II), aluminum, iron(III), nickel, scandium, yttrium, and rare earth elements interfere seriously with the determination of beryllium.

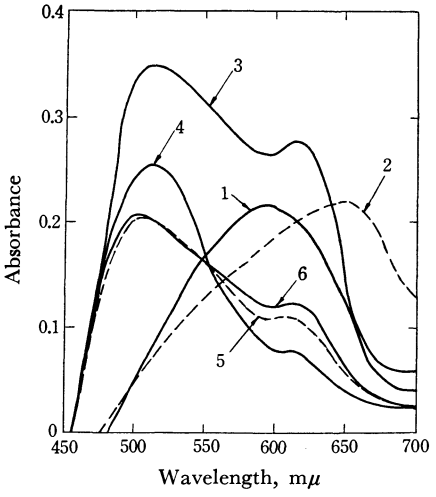

Fig. 3. Absorption spectra of aluminum, iron(III), yttrium, lanthanum, gadolinium, and erbium complexes at pH 6.0.
Reagent 80 ppm, Reference: Reagent blank
1 : Al 0.13 ppm, 2 : Fe(III) 0.26 ppm, 3 : Y 1.5 ppm, 4 : La 1.5 ppm, 5 : Gd 1.5 ppm, 6 : Er 1.5 ppm

9) E. B. Sandell, "Colorimetric Determination of Traces of Metals," 3rd Ed., Interscience Publishers, New York (1959), p. 83.

Sulfate, chloride, nitrate, and acetate ions, on the other hand, do not interfere. Oxalate, fluoride, citrate, phosphate, and EDTA bleach the complex.

The absorption curves of the complexes of aluminum, iron(III), yttrium, and some of the rare earth elements at pH 6.0 are shown in Fig. 3. The maximum absorption of the aluminum complex is at 590 mμ, much like that of the scandium complex,[5] while that of the iron(III) complex is shifted toward a longer wavelength. The complexes of yttrium, lanthanum, gadolinium, and erbium at pH 6.0 have two absorption maxima, as is shown in Fig. 3.

Complex Formation. The composition of the beryllium-chromal blue G complex was established by the continuous variation method.[10] The results are shown in Fig. 4, which indicates that a 1-to-2 complex is formed between beryllium and chromal blue G at pH 6.0. Similar relations were also observed for scandium and the chromal blue G complex.[5] In order to estimate the composition of the complex formed below pH 4.5, the method of continuous variation was employed. The results indicated that the combining ratio of beryllium and chromal blue G is 1 to 1. These results were confirmed by the mole ratio method.

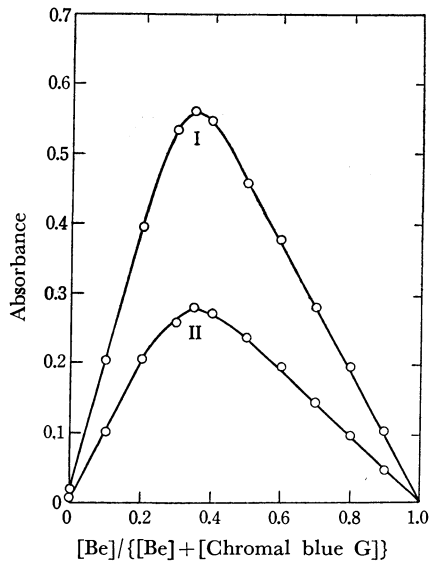

Fig. 4. Continuous variation method.
pH 6.0, Wavelength: 610 mμ
I: [Be]+[Chromal blue G]=8.52×10^{-5} M
II: [Be]+[Chromal blue G]=4.26×10^{-5} M

10) P. Job, *Ann. Chim.*, **9**, 113 (1928).

The formation constant of the beryllium complex was determined spectrophotometrically by the method used in a previous paper.[5] The conditional formation constant for the complex at pH 6.0 and 20°C was calculated, from the curves of the continuous variation, to be 4.3×10^{10}.

The proposed method was compared with the methods using some other reagents with structures similar to that of this reagent. The results are listed in Table 1. The proposed method using chromal blue G has some advantages: the sensitivity is very high, the solution is stable and the calibration curve is very reproducible, and the procedure is simple.

Table 1. Comparisone with other method

Method	Molar absorptivity [Sensitivity]	Precision
Aluminon[11]	*2.6×10^3 (535 mμ)	$\sigma=12\%$
Eriochrome cyanine R[7]	*2×10^4 (512 mμ)	
Chromazurol S[6]	*1.55×10^4 (575 mμ)	*$\sigma=1.15\%$
Naphthochrome green G[12]	3.88×10^4 (652 mμ)	Error$\leqq$3%
Xylenol orange[8]	*1.5×10^4 (495 mμ) [6×10^{-4} μg/cm^2]	
Pontachrome azure blue B[1]	4.5×10^4 (570 mμ)	$\sigma=1.8\%$
Chromal blue G	3.1×10^4 (610 mμ) [4×10^{-4} μg/cm^2]	$\sigma=0.65\%$

* Calculated from the reference
σ : Relative standard deviation

The author wishes to express his hearty thanks to Professor Tsunenobu Shigematsu of the Institute for Chemical Research, Kyoto University, for his kind guidance.

11) G. E. Kosel and W. F. Neuman, *Anal. Chem.*, **22**, 936 (1950).

12) T. Fujinaga, T. Kuwamoto, K. Kuwabara and S. Ikezawa, *Bunseki Kagaku (Japan Analyst)*, **12**, 1213 (1964).

BULLETIN OF THE CHEMICAL SOCIETY OF JAPAN VOL. 42 3001—3002 (1969)

Reaction of α-Phenethyl Radical in Liquid Sulfur Dioxide

Masashi IINO,*1 Tsutomu ENOMOTO and Niichiro TOKURA

Department of Applied Chemistry, Faculty of Engineering, Osaka University, Suita-shi, Osaka

(Received January 21, 1969)

Squire and Waters found that in the reaction of phenyl radical with sulfur dioxide diphenyl disulfone was formed by coupling reaction of benzene sulfonyl radicals, but diphenyl sulfone could not be obtained.[1] On the other hand, in the reaction of methyl radical with sulfur dioxide both dimethyl disulfone and dimethyl sulfone were formed.[2]

We have investigated the reaction of sulfur dioxide with α-phenethyl radical formed by the decomposition of 1,1′-azo-bis-1-phenylethane or by the abstraction of α-hydrogen atom from ethyl benzene.

We obtained neither disulfone ($CH_3CH(C_6H_5)$-$SO_2SO_2CH(C_6H_5)CH_3$) nor monosulfone (CH_3CH-$(C_6H_5)SO_2CH(C_6H_5)CH_3$) in thermal or photochemical decomposition reaction of 1,1′-azo-bis-1-phenylethane in liquid sulfur dioxide, although 2,3-diphenylbutane, the coupling product of α-phenethyl radicals, was obtained. The same results as described above have been obtained in the reaction of ethylbenzene and benzoyl peroxide in the presence of sulfur dioxide.

These results are interesting, contrasting with those of reactions of methyl and phenyl radical. It is reasonable to consider that α-phenylethane sulfonyl radical is formed in these reactions, and has little reactivity toward coupling reaction, because in the radical copolymerization of styrene and sulfur dioxide[3] styrene polysulfone ($-CH_2CH$-$(C_6H_5)SO_2-$) is formed and a substituted α-phenylethane sulfonyl radical ($-CH_2CH(C_6H_5)$-$SO_2\cdot$) seems to be one of the chain carriers. At present, however, the reason why we have obtained neither disulfone nor monosulfone is not clear.

Experimental

Materials. 1,1′-Azo-bis-1-phenylethane was prepared from acetophenone.[4,5] 1,1′-Azo-bis-1-phenylethane obtained was recrystallized three times from 99% ethanol. Found: C, 79.93; H, 7.24; N, 12.22%. Calcd for $C_{16}H_{18}N_2$: C, 80.67; H, 7.56; N, 12.22%. mp 70.2—73.0°C (lit[5] 72.3—72.9°C), λ_{max} 355—357 mμ.

Liquid sulfur dioxide was dehydrated with phosphorus pentoxide and distilled. Ethylbenzene was washed with concentrated sulfuric acid and water successively, dried with anhydrous magnesium sulfate, and then distilled. Commercial benzoyl peroxide was used without further purification.

Reaction of 1,1′-Azo-bis-1-phenylethane with Sulfur Dioxide (Thermal Decomposition of 1,1′-Azo-bis-1-phenylethane in Liquid Sulfur Dioxide). Into a glass pressure vessel (about 300 m*l* capacity)[6] charged with 1,1′-azo-bis-1-phenylethane (3 g), liquid sulfur dioxide (45 g) was introduced by using a pressure resistant buret[6] after the replacement of oxygen in the vessel by nitrogen stream. This reaction vessel was then immersed in boiling water (95—97°C) and kept for eight hours. Sulfur dioxide in the vessel was then evaporated under reduced pressure. Extraction with petroleum ether from the residue (3.2 g) and removal of the solvent from the extract (petroleum ether-soluble part) gave a viscous oil (2.1 g). This oil was then dissolved in about 10 m*l* of petroleum ether and chromatographed on an alumina column. Elution with petroleum ether gave colorless crystals of 2,3-diphenylbutane (0.1 g), which were recrystallized from methanol. Found: C, 91.44; H, 8.56%. Calcd for $C_{16}H_{18}$: C, 91.37; H, 8.63%. mp 123.5—124.5°C (lit[5] 125.3—125.9°C). Elution with benzene gave yellow crystals of acetophenone-azine (1.0 g), mp 122—123°C (recrystallized from ethanol) (lit[5] 122.2—123.0°C), which showed no depression of melting point by mixing with an authentic specimen. Further elution with benzene gave a yellow liquid of actophenone (small amount) which was identified by its transformation into 2,4-dinitrophenylhydrazone.

As the petroleum ether-insoluble part was found to be acidic, about 30 m*l* of water was added into the substance and the resulting solution was neutralized by aqueous sodium hydroxide solution. The solution was then extracted with diethyl ether. Acetophenone (0.3 g) was obtained from the ethereal solution by evaporating ether and then distilling the residue under reduced pressure. Addition of aqueous barium chloride solution to water layer gave 0.3 g of barium sulfate.

Neither disulfone nor monosulfone could not be identified, and IR spectra of petroleum ether-soluble and insoluble parts did not show their presence.

On the other hand, acetophenone and sulfate ion obtained from the petroleum ether-insoluble part are considered to be formed by the decomposition of petro-

*1 Present address: Chemical Research Institute of Non-Aqueous Solutions, Tohoku University, Sendai.

1) J. M. Squire and W. A. Waters, *J. Chem. Soc.*, **1962**, 2068.

2) A. Good and J. C. J. Thyne, *Trans. Faraday Soc.*, **63**, 2708, 2720 (1960).

3) W. G. Barb, *J. Polymer Sci.*, **10**, 49 (1953).

4) S. G. Cohen, S. J. Groszos and D. B. Sparrow, *J. Am. Chem. Soc.*, **72**, 3947 (1950).

5) S. Seltzer, *ibid.*, **83**, 2625 (1961).

6) N. Tokura and M. Matsuda, *Kogyo Kagaku Zasshi (J. Chem. Soc. Japan, Ind. Chem. Sect.)*, **64**, 501 (1961).

Table 1. Thermal reaction of 1,1'-azo-bis-1-phenylethane (APE) with sulfur dioxide

Reactant (g)		Solvent (g) ethyl-benzene	Reaction temp. (°C)	Reaction time (hr)	Product (mol%)*			
APE	SO_2				2,2-diphenyl-butane	acetophenone azine	aceto-** phenone	SO_4^{2-} **
1.0		43	95—97	8	24.0			
3.0	47		70	72	3.0	12.4	6.6	9.1
3.0	45		95—97	8	3.0	35.0	11.6	11.6
3.0	15	78	95—97	8	9.4	7.4	19.6	6.8
3.0	30	69	95—97	8	8.3	2.1	16.5	7.5

* This value was calculated from the molar ratio of product *vs.* APE.
** Sulfate ion and probably a part of acetophenone was formed from the decomposition of an unidentified product by water.

Table 2. Photochemical reaction of 1,1'-azo-bis-1-phenylethane (APE) with sulfur dioxide

Reactant (g)		Solvent (g) ethyl-benzene	Reaction temp. (°C)	Reaction time (hr)	Product (mol%)*			
APE	SO_2				2,3-diphenyl-butane	acetophenone azine	aceto-** phenone	SO_4^{2-} **
2.9	45		room temp.	24	5.7	trace	19.8	16.3
3.0	15	82	room temp.	24	20.4	12.1	16.5	9.5

* This value was calculated from the molar ratio of product *vs.* APE.
** Sulfate ion and probably a part of acetophenone was formed from the decomposition of an unidentified product by water.

leum ether-insoluble product by water. This materials was at first a white solid and then turned into a yellow and sticky solid on exposure to air, and had the absorption near 2600 cm^{-1} (broad) and 1200 cm^{-1} which disappeared after the addition of water. Although the structure of the product is not yet established, it is considered to be neither disulfone nor monosulfone from its chemical behavior.

Similar experiments were carried out at different reaction temperatures, or by using solvents. The results are summarized in Table 1. Table 1 also shows that the decomposition of 1,1'-azo-bis-1-phenylethane in ethyl benzene gave 2,3-diphenylbutane. No reaction occurred at room temperature in the 1,1'-azo-bis-1-phenylethane - sulfur dioxide system, although mixing of the two reactants exhibited a yellow coloration due, probably, to the formation of a charge-transfer complex.

Reaction of 1,1'-Azo-bis-1-phenylethane with Sulfur Dioxide under Irradiation of Ultraviolet Light. 1,1'-Azo-bis-1-phenylethane has a strong absorption in the region of 320 mμ to 400 mμ (λ_{max} 355—357 mμ). The reaction vessel was a quartz cylindrical vessel equipped with a stainless steel joint connected by a stopcock[6] to a pressure-resistant buret.[6] The reaction was carried out under irradiation by using a 300 W mercury lamp. Other details of the experimental procedure were the same as described in the case of the thermal decomposition of 1,1'-azo-bis-1-phenylethane in liquid sulfur dioxide and the results obtained are summarized in Table 2.

Table 2 shows that the same products as listed in Table 1 were obtained and no sulfone could be detected.

Reaction of Ethylbenzene and Benzoyl Peroxide in the Presence of Sulfur Dioxide. A Solution of benzoyl peroxide (30 g) in ethylbenzene (300 m*l*) in a 1 *l* round-bottomed flask was heated at 70°C under a reflux condenser, and sulfur dioxide was passed into slowly through an inlet glass tube extending to the bottom of the flask. Passage of sulfur dioxide was continued for 42 hr. The treatment of the reaction mixture afforded 14.2 g of benzoic acid, 0.4 g of 2,3-diphenylbutane and 4.5 g of low molecular-weight styrene-polysulfone, but no sulfone having α-phenethyl group could be obtained.

The authors wish to thank the Seitetsu Kagaku K. K. for the donation of liquid sulfur dioxide.

BULLETIN OF THE CHEMICAL SOCIETY OF JAPAN VOL. 42 3003—3004 (1969)

Preparation and Ion-exchange Behavior of Potassium Zinc Ferrocyanide

Shoichi KAWAMURA, Katsumi KUROTAKI and Masami IZAWA

Chemistry Division, National Institute of Radiological Sciences, Anagawa, Chiba-shi

(Received January 22, 1969)

Since the early work of Miller[1] in 1896, a number of compounds containing potassium, zinc and ferrocyanide have been prepared and their compositions investigated mainly for the study of volumetric determination of zinc ion or of ferrocyanide ion.[2-7] During the past few years, considerable interest has been shown in the ion-exchange property of zinc ferrocyanide.[8-12]

In an attempt to elucidate this property of the ferrocyanides, the authors tried to prepare zinc ferrocyanide $Zn_2Fe(CN)_6$, according to the procedure described by Kohn.[13] The resulting product was found to be potassium zinc ferrocyanide $K_2Zn_3[Fe(CN)_6]_2$, but not zinc ferrocyanide. This paper describes some ion-exchange properties and X-ray diffraction data concerning potassium zinc ferrocyanide and zinc ferrocyanide.

Experimental

Preparation by the Kohn Method.[13] Into 300 m*l* of 0.1 M $K_3Fe(CN)_6$, 630 m*l* of 0.1 M $ZnSO_4$, 180 m*l* of 15% sodium acetate and 300 m*l* of 3% hydrogen peroxide were added little by little in this order. On continuous stirring, the slurry was heated on a boiling water bath until its color changed from yellow to white. It was then poured into cold water, tenfold in volume of the slurry, allowed to stand for 24 hr, filtered, washed thoroughly and dried at 60°C for 24 hr.

Zinc Ferrocyanide.[10,11] Zinc ferrocyanide was prepared by mixing 300 m*l* of 0.1 M $Na_4Fe(CN)_6$, and 900 m*l* of 0.1 M $Zn(NO_3)_2$. The white slurry was obtained by dropping the solutions little by little simultaneously into a beaker for 30 min under stirring. It was heated with stirring on a boiling water bath for 2 hr, allowed to stand for 24 hr, filtered, washed thoroughly and dried at 60°C for 24 hr. The ferrocyanides thus prepared were compressed into pills under a pressure of about 300 kg/cm^2, allowed to break down in water for several days, air dried, and sieved into 200—300 mesh.

Analyses. The ferrocyanides were dissolved with a minimum amount of 0.1 M EDTA-ammonium solution, followed by dilution with water to a given volume, to be subjected to the determination of potassium, zinc and ferrocyanide. Zinc and ferrocyanide were determined by volumetric analysis, and potassium by atomic absorption spectroscopy.

Distribution Coefficient. Distribution coefficients (ml/g) for cesium were determined by equilibrating 0.1 g of the ferrocyanides with 5 m*l* of NH_4NO_3 solutions (3×10^{-2}—3.5 M) containing 5×10^{-2} mmol of $CsNO_3$ tagged with ^{137}Cs, followed by centrifugation at 1000 g for 15 min. The radioactivity of the supernatant was measured by a well type scintillation counter.

Results and Discussion

The product prepared by the Kohn method[13] was analyzed, the result of which is shown in Table 1. The stoichiometrical composition is best represented by $K_2Zn_3[Fe(CN)_6]_2$. The same compound can be prepared by adding 0.1 M potassium ferrocyanide to 0.1 M zinc nitrate in the mole proportion of 1 : 1.5, followed by the same treatment as with zinc ferrocyanide. Adsorption rates of cesium ion on potassium zinc ferrocyanide and zinc ferrocyanide[10,11] were determined. Figure 1

TABLE 1. ANALYTICAL RESULTS OF THE PRODUCT OBTAINED BY THE KOHN METHOD

Percent			Ratio			Composition
K	Zn	$Fe(CN)_6$	K	Zn	$Fe(CN)_6$	
8.5	21.5	46.4	2.0	3.0	2	$K_2Zn_3[Fe(CN)_6]_2$

1) E. H. Miller, *J. Am. Chem. Soc.*, **18**, 1100 (1896).
2) G. C. Stone and D. A. Van Ingen, *ibid.*, **19**, 542 (1897).
3) E. H. Miller and J. A. Mathews, *ibid.*, **19**, 547 (1897).
4) E. H. Miller and J. L. Danziger, *ibid.*, **24**, 823 (1902).
5) W. G. Waring, *ibid.*, **26**, 4 (1904).
6) E. H. Miller and M. J. Falk, *ibid.*, **26**, 956 (1904).
7) W. M. Cumming and W. Good, *J. Chem. Soc.*, **1926**, 1927.
8) B. Barton, J. L. Hepworth, E. D. McClanhan, Jr., R. L. Moore and H. H. Van Tuyl, *Ind. Eng. Chem., Anal. Ed.*, **50**, 212 (1958).
9) N. Mishio, A. Kamoshida, S. Kadoya and T. Ishihara, *J. At. Energy Soc. Japan (in Japanese)*, **6**, 2 (1964).
10) V. Kouřim, J. Rais and B. Million, *J. Inorg. Nucl. Chem.*, **26**, 1111 (1964).
11) V. Kouřim and B. Million, *Collection Czech. Chem. Commun.*, **30**, 2848 (1965).
12) S. Kawamura, K. Kurotaki, H. Kuraku and M. Izawa, *J. Chromatog.*, **26**, 557 (1967).
13) M. Kohn, *Anal. Chim. Acta*, **3**, 38 (1949).
14) V. Veselý and V. Pekárek, *J. Inorg. Nucl. Chem.*, **27**, 1419 (1965).

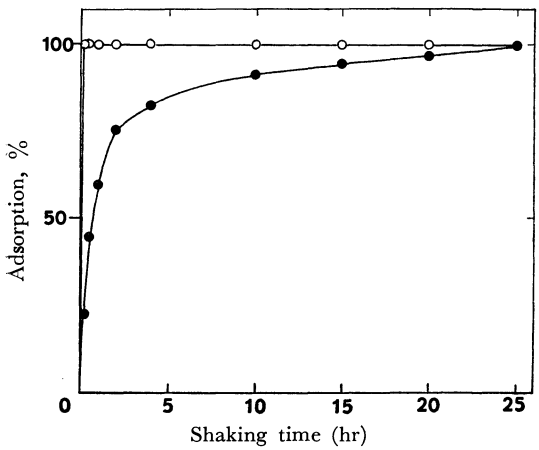

Fig. 1. Relative adsorption rate for Cs on $K_2Zn_3[Fe(CN)_6]_2$ and $Zn_2Fe(CN)_6$.
-○- $K_2Zn_3[Fe(CN)_6]_2$ -●- $Zn_2Fe(CN)_6$
Adsorbed percent was determined by shaking 0.1 g of adsorbents with 5 m*l* of 0.01 M $CsNO_3$ tagged with ^{137}Cs.

TABLE 2. X-RAY DIFFRACTION DATA

Potassium zinc ferrocyanide		Zinc ferrocyanide	
d(Å)	I/I_0	d(Å)	I/I_0
6.49	0.10		
6.33	0.09		
5.45	0.79		
4.52	0.43	4.33	0.85
4.09	1.00		
3.79	0.08	3.80	1.00
3.69	0.22		
3.63	0.40		
3.43	0.13	3.29	0.19
3.14	0.09	3.16	0.08
3.10	0.31		
2.99	0.13	2.86	0.33
2.71	0.15		
2.68	0.09	2.64	0.21
2.54	0.12		
2.52	0.14	2.29	0.41

X-ray powder patterns were taken on an apparatus from Rigaku Denki Co., Ltd., Tokyo, Japan, using filtered CuK_α radiation (1.5418Å).

shows that the adsorption rate of potassium zinc ferrocyanide is significantly higher than that of zinc ferrocyanide.

Comparison of these ferrocyanides was made by means of X-ray diffraction. Table 2 shows that the X-ray diffraction patterns of potassium zinc ferrocyanide are quite different from those of zinc ferrocyanide. The discrepancy of X-ray data, *viz.*, the difference in crystal structure, may be comparable to the difference of the adsorption rate.

Ion-exchange behaviors of both ferrocyanides were studied in ammonium nitrate solutions. The relations of the log K_d *versus* log[NH_4] showed a straight line of slope -1. Further experiments showed that, in the batch equilibration in the concentration <0.01 M Cs, potassium ions in the potassium zinc ferrocyanide are equivalently replaced by the adsorption of cesium ion in the external solution and zinc ions in the zinc ferrocyanide by the adsorption of cesium ion in the external solution. Therefore, the precipitation mechanism reported by Veseleý and Pekárek[14] was not observed in either ferrocyanide.

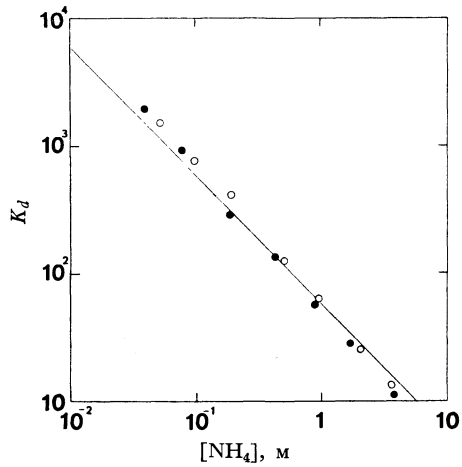

Fig. 2. Relationship between distribution coefficient for Cs and ammonium ion concentration.
-●- $Zn_2Fe(CN)_6$ -○- $Na_2Zn_3[Fe(CN)_6]_2$

These results indicate that the reaction is an ion-exchange ruled by the mass action law. The ferrocyanides were unfavorable for column work, since both were relatively fine powder and broken down slightly in aqueous suspension. However, the powdery characters were suitable as an adsorbent in thin layer chromatography. Potassium zinc ferrocyanide could advantageously be applied to a rapid separation of sodium, potassium, rubidium and cesium by thin layer chromatography.[12] This might be attributed to its rapid adsorption rate.

BULLETIN OF THE CHEMICAL SOCIETY OF JAPAN VOL. 42 3005—3007 (1969)

Photoreaction of 2,6-Diphenyl-4*H*-thiopyran-4-one

Noboru SUGIYAMA, Yoshiaki SATO, Hiroshi KATAOKA, Choji KASHIMA and Kazutoshi YAMADA

Department of Chemistry, Tokyo Kyoiku University, Otsuka, Bunkyo-ku, Tokyo

(Received March 17, 1969)

Although numerous reports on the photoreaction of nonbenzenoid aromatic compounds have been published,[1] there has been only one report on the photochemistry of a γ-pyrone-type compound, *i. e.*, 2,6-dimethyl-4*H*-pyran-4-one.[2] This paper will be concerned with the photoreaction of 2,6-diphenyl-4*H*-thiopyran-4-one(I).

The irradiation of I in a benzene solution (0.3 mol/*l*) by a high-pressure mercury lamp gave pale yellow crystals (II), mp 160—161°C, in a 25% yield. When the benzene solution of I was irradiated by a high-pressure mercury lamp with a Pyrex filter or a low-pressure mercury lamp with a quartz filter, the yield of II decreased to 8 or 2% respectively. When a solution of I in ether, methylene chloride, or ethanol was irradiated, hardly any formation of II detected. By the irradiation of I in the solid state, only an oily substance was produced. It was observed that a conversion of II to I of several per cent took two weeks to proceed at room temperature, but it occurred quantiatively at the melting point of II in only five minutes. In the boiling benzene, this conversion occurred with a half-life of five hours.

The structure of II was determined as follows. The NMR spectrum of II showed a singlet signal at τ 5.50 whose intensity was equivalent to that of a vinyl proton at τ 3.41. The IR spectrum of I showed a carbonyl band at 1600 cm^{-1}, but that of II showed it at 1640 cm^{-1}. The thermal formation of I from II and the NMR and IR spectra of II suggested that the structure of II was a dimer of I containing a cyclobutane ring.

For this type of dimer, four isomers are possible. However, their NMR spectra would show their cyclobutane methine protons as singlets in each case, for the environments of both methine protons would be equivalent. In order to distinguish the two protons, II was converted to a monobromo-derivative (III) by treating with a half mole of bromine. In its IR spectrum III showed carbonyl bands at 1657 and 1640 cm^{-1}. This fact indicates that the substitution with bromine occurred at the α-position of one enone system. This was also supported by the UV spectrum of III, which showed at 339 nm(ε 11200) the absorption maximum which was observed at 335 nm(ε 13200) in II. In the NMR spectrum of III, two singlet signals, at τ 5.31 and 5.28, show that both methine protons are situated at 1,3-positions in the cyclobutane ring. If both the protons are situated at 1,2-positions, they should have the coupling constant of 2.7—11 Hz.[3] Thus, the structure of II was

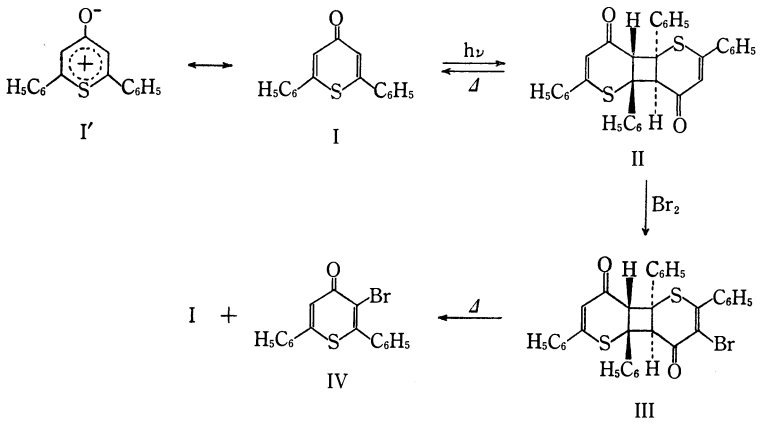

Fig. 1

1) *E. g.*, T. Tezuka, Y. Akasaki and T. Mukai, *Tetrahedron Letters*, **1967**, 5003.

2) P. Yates and M. J. Jorgenson, *J. Am. Chem. Soc.*, **85**, 2956 (1963); P. Yates and J. W. J. Still, *ibid.*, **85**, 1208 (1963).

3) I. Fleming and D. H. Williams, *Tetrahedron*,, **23**, 2747 (1967).

determined to be a head-to-tail dimer.

Moreover, the chemical shift of the vinyl proton of III is exactly the same as that of II. This fact indicates that the vinyl proton of III is not affected by the substitution with the bromine atom, though the chemical shifts of two methine protons of III are moved to a lower field. Therefore, the anti type is the preferable structure.

When III was heated at the melting point, both I and IV were quantitatively obtained. IV was identified with the authentic sample, which was synthesized from 2,6-diphenyl-tetrahydro-4*H*-thiopyran-4-one (V).

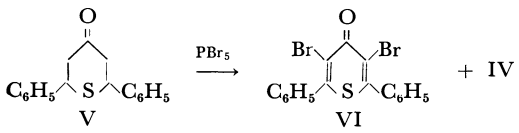

Fig. 2

In conclusion, it was proved that an anti, head-to-tail dimer was produced by the irradiation of I. This result indicates that the behavior of I in the excited state is similar to that of the enone system[4] in spite of its aromaticity. In the case of the irradiation of I in polar solvents, there was no product of II. This result seems to be attributable to the readier π-electron decrease (I') in its ring in the polar solvent, which gives rise to its aromaticity. This theory may be supported by the UV and NMR spectra of I in various solvents, shown in the Experimental section.

Experimental

Preparation of 2,6-Diphenyl-4*H*-thiopyran-4-one (I). I was synthesized by Arndt's method.[5] Mp 131—132°C (lit 132—133°C).

UV: $\lambda_{max}^{Benzene}$ nm(ε), 278(22500)
λ_{max}^{Ether} nm(ε), 276(22600)
$\lambda_{max}^{CH_2Cl_2}$ nm(ε), 266(26800), 300(15700)
λ_{max}^{EtOH} nm(ε), 265(19000), 304(21400)
IR: ν_{max}^{KBr} cm^{-1}, 1600
NMR: (τ in CCl_4), 2.2—2.7(m. 10H), 3.01(s.2H)
(τ in Ether), 2.2—2.7(m.10H), 2.97(s. 2H)
(τ in CH_2Cl_2), 2.2—2.7(m.10H), 2.85(s. 2H)
(τ in $CDCl_3$), 2.2—2.6(m.10H), 2.80(s. 2H)

Irradiation of I. On the irradiation of a benzene solution of I (0.3 mol/*l*) with a high-pressure mercury lamp under a nitrogen atmosphere for a week, pale yellow crystals (II) were produced on the wall of the reaction vessel in a 25% yield. These crystals were collected, chromatographed on silica gel with chloroform, and recrystallized from benzene or a chloroform-*n*-hexane mixture.

UV: $\lambda_{max}^{CHCl_3}$ nm(ε), 283(23700), 335(13200)
IR: ν_{max}^{KBr} cm^{-1}, 1640, 1560

a) Recrystallization from Benzene. Upon recrystallization from benzene, II gave pale yellow prisms. Mp 160—161°C. Found: C, 79.78; H, 5.29%. Calcd for $C_{34}H_{24}O_2S_2 \cdot C_6H_6$: C, 79.19; H, 4.98%.
NMR: (τ in $CDCl_3$) 2.4—2.8(m.26H), 3.41(s.2H), 5.50(s.2H).

b) Recrystallization from Chloroform-n-Hexane. This recrystallization of II gave pale yellow leaflets; mp 159—160°C. Found: C, 70.38; H, 4.17%. Calcd for $C_{34}H_{24}O_2S_2 \cdot 1/2CHCl_3$: C, 70.35; H, 4.32%.
NMR: (τ in $CDCl_3$) 2.4—2.8(m.20H), 3.41(s.2H), 5.50(s.2H). From these data of elemental analyses and NMR spectra, it can be said that II, which was recrystallized from benzene or chloroform-*n*-hexane, contains the solvents of crystallization. These solvents were not removed by heating under reduced pressure because of the instability of II described above.

When a high-pressure mercury lamp with a Pyrex filter or a low-pressure mercury lamp with a quartz filter was used under the same conditions, the yield of II was decreased to 8 or 3% respectively. By the irradiation of I in ether (0.1 mol/*l*) or in benzene (0.03 mol/*l*), only a trace of II was detected. However, on the irradiation of I in methylene chloride (0.3 mol/*l*) or in ethanol (0.1 mol/*l*), II was not detected at all. From the irradiated solutions, I was mainly recovered.

Irradiation in the solid state with a high-pressure mercury lamp produced an oily substance.

Preparation of the Monobromo-substituted Dimer (III). To an ice-cooled chloroform (5 m*l*) solution of II (80 mg) there was added a chloroform (2 m*l*) solution of bromine (24 mg). After the solution had been stirred for half an hour, the solvent was evaporated. The residue was chromatographed on silica gel with chloroform. As the main product, III (40 mg) was obtained; it was recrystallized from chloroform-*n*-hexane to afford colorless crystals; mp 170—171°C.

Found: C, 66.47; H, 3.95%. Calcd for $C_{34}H_{23}O_2S_2Br$ C, 67.21; H, 3.79%.
UV: $\lambda_{max}^{CHCl_3}$ nm(ε), 281 (21900), 339(11200).
IR: ν_{max}^{KBr} cm^{-1}, 1657, 1640, 1555.
NMR: (τ in $CDCl_3$) 2.3—2.8(m.20H), 3.41(s.1H), 5.28(s.1H), 5.31(s.1H).

Preparation of 3-Bromo-2,6-diphenyl-4*H*-thiopyran-4-one(IV) and 3,5-Dibromo-2,6-diphenyl-4*H*-thiopyran-4-one(VI). A benzene solution (10 m*l*) of 2,6-diphenyl-tetrahydro-4*H*-thiopyran-4-one (V) (530 mg) was refluxed with phosphorus pentabromide (3 g) for 5 hr. To the reaction mixture a saturated aqueous sodium thiosulfate solution (50 m*l*) was then added, and the mixture was extracted with benzene. The benzene solution was washed with water and dried over sodium sulfate. After the removal of the solvent, the residue was chromatographed on silica gel with benzene and benzene-ethyl acetate (19 : 1). VI (60 mg) and IV (30 mg) were obtained from the former and the latter respectively. The structure of VI was supported by its IR, UV and NMR spectra. The recrystallization of IV from carbon tetrachloride gave colorless needles; mp 121—123°C.

Found: C, 59.37; H, 3.27%. Calcd for $C_{17}H_{11}OSBr$: C, 59.42; H, 3.21%.
UV: $\lambda_{max}^{CHCl_3}$ nm(ε), 273(23300), 308(16800).
IR: ν_{max}^{KBr} cm^{-1}, 1603.
NMR: (τ in CCl_4) 2.60 (s. 10H), 2.94(s. 1H).

4) *E. g.*, P. E. Eaton, *J. Am. Chem. Soc.*, **84**, 2344 (1962).

5) F. Arndt, P. Nachtwey and J. Pusch, *Ber.*, **58**, 1633 (1925).

Recrystallization of VI from methanol afforded yellow needles; mp 163.5—164.5°C.
Found: C, 48.32; H, 3.13%. Calcd for $C_{17}H_{10}SOBr_2$: C, 48.34; H, 2.37%.

UV: $\lambda_{max}^{CHCl_3}$ nm(ε), 273 (21800), 317(14600).
IR: ν_{max}^{KBr} cm^{-1}, 161.
NMR: (τ in CCl_4) 2.60(s.).

BULLETIN OF THE CHEMICAL SOCIETY OF JAPAN VOL. 42 3007—3008 (1969)

The Effects of Outer Sphere Cations and Halide Ions on Infrared Spectra of Pentahalogenonitrosylruthenium(III) Complexes

Eiichi MIKI, Tatsujiro ISHIMORI, Hideo YAMATERA* and Hisateru OKUNO

Department of Chemistry, College of Science, St. Paul's (Rikkyo) University, Nishi-Ikebukuro, Toshima-ku, Tokyo
**Department of Chemistry, Faculty of Science, The University of Nagoya, Chikusa-ku, Nagoya*

(Received March 20, 1969)

On the infrared spectra of alkali metal salts of nitrosylruthenium(III) complex anions, studies have been made on the effects of outer sphere cations and coordinated halide ions. The wave number of the N–O stretching vibration decreases in the order of K^+, NH_4^+, Rb^+ and Cs^+ for $M_2[RuCl_5(NO)]$ (M=K, NH_4, Rb and Cs)[1] and in the order of NH_3, Cl^-, Br^- and OH^- for $[RuX(NH_3)_4(NO)]^{n+}$ ion (X=NH_3, Cl, Br and OH *trans* to NO group).[2] Sinitsyn and Petrov have reported that, for $M_2[RuX_5(NO)]$ (M=Na, K, Rb and Cs; X=Cl, Br and I), the wave number of the Ru-N stretching as well as the N–O stretching vibration increases in the order of I, Br and Cl for a given alkali metal salt.[3] However, a distinction between the two skeletal vibrations of the RuNO group does not seem to have been fully made. Recently, we have made a clear assignment on the skeletal vibrations of the RuNO group of $K_2[RuX_5(NO)]$ (X=Cl and Br).[4,5]

We studied the infrared spectra of $M_2[RuX_5(NO)]$ (M=K, Rb and Cs; X=Cl, Br and I) and measured the wave numbers of the N–O stretching, Ru–N stretching, RuNO bending and Ru–X stretching vibrations. This report presents interesting observations on the shifts of the wave numbers of the vibrations by the replacement of the outer sphere cations and the halide ions.

In Table 1 are shown the wave numbers of the vibrations measured for $M_2[RuX_5(NO)]$.

For these compounds, the effects caused by the replacement of the outer sphere cations were observed on the Ru–N stretching and especially on the Ru–X (X *cis* to NO) stretching vibrations as well as on the N–O stretching vibration, but hardly any on the RuNO bending vibration. The wave

TABLE 1. INFRARED SPECTRA OF $M_2[RuX_5(NO)]$ (M=K, Rb and Cs; X=Cl, Br and I)

Compounds	N–O str. (A_1)		Ru–N str. (A_1)	RuNO bend. (E)	Ru–X str. (E)		Ru–X str. (A_1)
$K_2[RuCl_5(NO)]$	1915 vs	1904 vs	606 w	588 s	336 vs	327 vs	286 vs
$K_2[RuBr_5(NO)]$	1888 vs	1880 vs	606 w	573 s	260 vs	252 vs	221 vs
$K_2[RuI_5(NO)]$	1865 sh	1854 vs	600 m	554 s	214 vs		174 vs
$Rb_2[RuCl_5(NO)]$	1900 sh	1888 vs	600 w	587 s	326 vs		281 vs
$Rb_2[RuBr_5(NO)]$	1872 vs		602 m	579 m	260 vs	250 vs	218 vs
$Rb_2[RuI_5(NO)]$	1840 vs		600 w	556 s	210 vs		—
$Cs_2[RuCl_5(NO)]$	1873 vs		596 w	588 s	320 vs		277 vs
$Cs_2[RuBr_5(NO)]$	1855 vs		597 m	576 s	250 vs		220 vs
$Cs_2[RuI_5(NO)]$	1824 vs		594 m	557 s	205 vs		—

Abbreviations: str=stretching; bend=bending; vs=very strong; s=strong; m=medium; w=weak; sh=shoulder.

1) N. M. Sinitsyn and O. E. Zvyagintsev, *Zh. Neorg. Khim.*, **8**, 234 (1963).
2) N. M. Sinitsyn and O. E. Zvyagintsev, *Dokl. Acad. Nauk SSSR*, **145**, 109 (1962).
3) N. M. Sinitsyn and K. I. Petrov, *Zh. Struk. Khim.*, **9**, 45 (1968).
4) E. Miki, T. Ishimori, H. Yamatera and H. Okuno, *Nippon Kagaku Zasshi (J. Chem. Soc. Japan, Pure Chem. Sect.)*, **87**, 703 (1966).
5) E. Miki, This Bulletin, **41**, 1835 (1968).

numbers of the N–O, the Ru–N and the Ru–X (X *cis* to NO) stretching vibrations decreased regularly in the order of M=K, Rb and Cs.

On the other hand, the shifts caused by the replacement of the halide ions were observed on the N–O stretching and especially on the RuNO bending vibrations, but hardly any on the Ru–N stretching vibration; replacing Cl^- with Br^- and I^-, the wave numbers of the N–O stretching and the RuNO bending vibrations decreased regularly in the order of X=Cl, Br and I. Although the N–O stretching and the RuNO bending vibrations shifted, the wave numbers of the Ru–N stretching vibration hardly changed at all by the replacement of the halide ions. This seems to be due to the fact that the RuNO bending vibration (E) is nearer the Ru–X (X *cis* to NO) stretching vibration (E) than the Ru–N stretching vibration (A_1) is to the Ru–X (X *trans* to NO) stretching vibration (A_1).

The effect on the vibrations caused by the replacement of the outer sphere cations and the halide ions can be qualitatively explained by the difference in electronegativities of the outer sphere cations and halide ions as suggested by Sinitsyn *et al.*[1-3] Although the positions of the cations in the crystals have not been determined yet, it should be noted that the outer sphere cations have an appreciable effect on the N–O, the Ru–N and the Ru–X (*cis* to NO) stretching vibrations.

BULLETIN OF THE CHEMICAL SOCIETY OF JAPAN VOL. 42 3008—3010 (1969)

Studies of Heteroaromaticity. XXXI.[1] New Reactions of Aromatic Amidoximes with Diketene

Tadashi SASAKI and Toshiyuki YOSHIOKA

Institute of Applied Organic Chemistry, Faculty of Engineering, Nagoya University, Chikusa-ku, Nagoya

(Received March 22, 1969)

While diketene is known to react with thiourea, amidines and guanidines affording uraciles,[2-4] no report has been given on the reactions with amidoximes. As a continuation of the previous papers[1,5] concerning the reactivity of aromatic amidoximes, this note deals with their new reactions with diketene.

Treatment of *p*-nitrobenzamidoxime (Ia) with a small excess amount of diketene in refluxing toluene afforded a quantitative yield of colorless product (IIIa); the infrared spectrum in a potassium bromide pellet showed a strong carbonyl absorption at 1720 cm^{-1} and the NMR spectrum in deuteriochloroform exhibited chemical shifts at 1.70 τ (singlet, 4 H, *p*-substituted phenyl protons), 5.81 (singlet, 2 H, methylene) and 7.60 (singlet, 3 H, methyl). From these data and microanalysis, compound IIIa was concluded as 3-(*p*-nitrophenyl)-5-acetonyl-1,2,4-oxadiazole. This result is of interest, when compared with our previous report[6] that 3-(5-nitro-2-furyl)-5-methylisoxazole was prepared by the reaction of diketene with 5-nitro-2-furhydroxamoyl chloride. Similarly, the products, IIIb and IIIc, were obtained from *m*-nitrobenzamidoxime (Ib) and 5-nitro-2-furamidoxime (Ic) respectively. These results are summarized in Table 1.

When treated with diketene in acetic acid or in pyridine at room temperature, Ic afforded a quantitative yield of 5-nitro-2-furamidoxime *O*-acetoacetate (IIc), a ring-opened product of IIIc, as thin yellow crystals of mp 136—138°C, which was readily cyclized to IIIc by refluxing in toluene. This provides good evidence that the formation of IIIc from Ic might proceeds *via* an intermediate IIc and that this reaction is initiated by the nucleophilic attack of diketene to the hydrogen of hydroxime, not to that of amine.[7] When diketene was replaced by ethylene carbonate, phenyl glycidyl ether or β-propiolactone in the above reactions, no reactions could be observed.

When the *N*-phenyl- (IVc) or the *N*-methylamidoxime (IVc') was treated with diketene instead of Ic under the reaction conditions similar

1) Part XXX of this series: T. Sasaki and T. Yoshioka, This Bulletin, **42**, 556 (1969).

2) R. Lacy, *J. Chem. Soc.*, **1954**, 839.

3) Y. Iwakura and K. Nakakubo, *Nippon Kagaku Zasshi (J. Chem. Soc. Japan, Pure Chem. Sect.)*, **57**, 947 (1951).

4) N. Khromov-Borisov and R. Karlinskaya, *Zhur. Obschchei Khim.*, **26**, 1728 (1956).

5) T. Sasaki and T. Yoshioka, *Yuki Gosei Kagaku Kyokai-shi (J. Soc. Org. Synth. Chem. Japan)*, **25**, 665 (1967).

6) T. Sasaki and T. Yoshioka, This Bulletin, **42**, 258 (1969).

7) T. Kato, *Yuki Gosei Kagaku Kyokai-shi (J. Soc. Org. Synth. Chem. Japan)*, **26**, 311 (1968).

TABLE 1. OXADIAZOLES

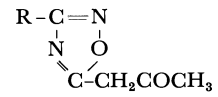

III

R	Product	Mp °C	Yield %	Found (Calcd) C%	H%	N%	UV λ_{max}^{EtOH} mμ ($\varepsilon \times 10^{-4}$)
p-NO_2-C_6H_4-	IIIa	143—144	95	53.15 (53.44	3.61 3.67	16.67 17.00)	274 (1.4)
m-NO_2-C_6H_4-	IIIb	150—151	95	53.68 (53.44	3.80 3.67	16.75 17.00)	262 (1.0)
5-NO_2-2-C_4H_2O-	IIIc	108—110	85	45.58 (45.57	2.95 2.98	17.94 17.72)	310 (1.3)

TABLE 2. OXADIAZOLINES

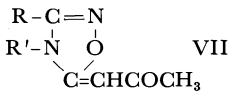

VII

R	R′	Product	Mp °C	Yield %	Found (Calcd) C%	H%	N%	UV λ_{max}^{EtOH} mμ ($\varepsilon \times 10^{-4}$)
p-NO_2-C_6H_4-	C_6H_5-	VIIa	220—222	95	63.47 (63.15	4.55 4.65	12.74 13.00)	292 (3.7) 250 (1.2)
p-NO_2-C_6H_4-	CH_3-	VIIa′	221—223	95	54.98 (55.17	3.97 4.24	15.75 16.09)	294 (3.6) 246 (1.2)
5-NO_2-2-C_4H_2O-	C_6H_5-	VIIc	235—237	90	57.63 (57.51	3.58 3.54	13.57 13.42)	304 (3.5)
5-NO_2-2-C_4H_2O-	CH_3-	VIIc′	195—196	90	47.97 (47.81	3.64 3.61	16.21 16.21)	

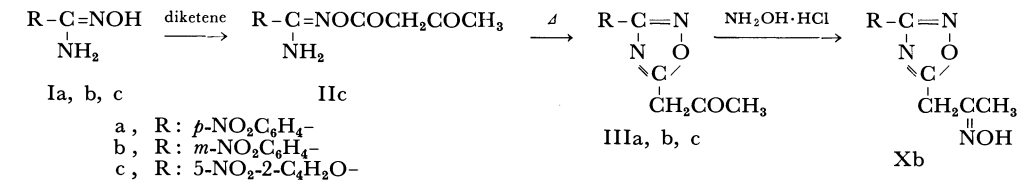

Ia, b, c — IIc — IIIa, b, c — Xb

a, R: *p*-$NO_2C_6H_4$-
b, R: *m*-$NO_2C_6H_4$-
c, R: 5-NO_2-2-C_4H_2O-

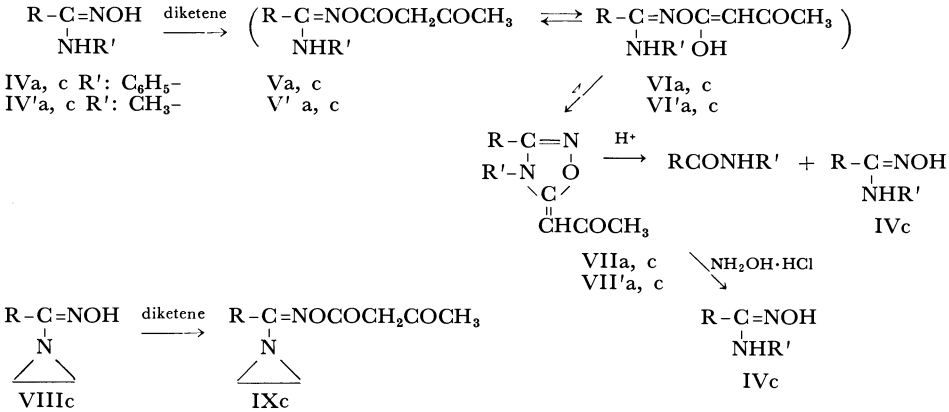

IVa, c R′: C_6H_5- — Va, c — VIa, c
IV′a, c R′: CH_3- — V′a, c — VI′a, c

VIIa, c
VII′a, c

IVc

VIIIc — IXc — IVc

to those of *N*-non-substituted amidoximes, the product, VIIc or VIIc′, showed a different UV-spectral pattern, as seen by comparing Tables 1 and 2. The NMR spectrum of the product VIIa′ from *N*-methyl *p*-nitrobenzamidoxime (IVa′) and diketene showed a methine signal at 4.92τ, in addition to those at 7.88 (singlet, 3 H, methyl), 6.78 (singlet, 3 H, methyl), and 2.04 (quartet, 4H, J=9 cps, *p*-nitrophenyl protons). Similarly, the NMR spectrum of the product VIIa from the *N*-phenyl amidoxime (IVa) and diketene showed a methine signal at 5.45τ, in addition to those at 7.91 (singlet, 3 H, methyl), 2.40 (singlet, 5 H, *N*-phenyl protons) and 2.0 (quartet, 4 H, J=9 cps, *p*-nitrophenyl protons). Acidic hydrolysis of VIIc afforded a 50% yield of 5-nitro-2-furanilide, mp

171—173°C[8] together with a 30% yield of IVc, which was also produced directly from VIIc and hydroxylamine hydrochloride in boiling ethanol, though IIIb afforded the corresponding ketoxime (Xb) under similar reaction conditions. The mechanism for the formation of VII from IV might be explained similarly by the intermediate formation of a simple adduct (V) which is in tautomeric equilibrium with its enol form (VI), and VI is cyclized to VII after removal of water. In fact, an oily product obtained from IVc and diketene in acetic acid at room temperature was thermally converted to VIIc.

Similar treatment of 1-(5-nitro-2-furoyl)aziridine oxime (VIIIc) with diketene afforded a simple addition product (IXc); this structure was confirmed on the basis of analytical and spectral data.

As previously reported about VIIIc,[1] IXc remained also unchanged upon treatment with sodium iodide in boiling acetone.

Experimental

NMR spectra were measured by a Varian A-60 spectrometer at 60 Mc using tetramethylsilane as an internal standard and DMSO-d_6 as a solvent, unless otherwise stated. The chemical shifts were expressed in τ-values.

3-(*p*-Nitrophenyl) - 5 - acetonyl - 1,2,4 - oxadiazole (IIIa). A mixture of Ia (0.5 g) and diketene (1 m*l*) was refluxed in toluene (20 m*l*) for 10 hr. After removing toluene under reduced pressure from the reaction mixture, water was added to the residue and extraction was carried out with ether. The ether layer was washed with dilute hydrochloric acid. The residue obtained after removing ether was recrystallized from a mixture of ethanol and petroleum ether to afford IIIa. Similar treatment of Ib and Ic afforded the corresponding oxadiazoles, IIIb and IIIc, respectively. All the results are summarized in Table 1.

5-Nitro-2-furamidoxime *O*-Acetoacetate (IIc). A mixture of Ic (0.5 g) and diketene (0.5 m*l*) was dissolved in acetic acid (10 m*l*) and the solution was stirred for 2 hr at room temperature. The precipitated crystals were collected and recrystallized from a mixture of ethanol and benzene to afford 0.35 g of IIc. Further 0.3 g of IIc were obtained from the filtrate. The total yield was over 90%. Mp 136—138°C. ν_{max}^{KBr} 3570, 3400 (NH), 1770 (OCO), 1720 (CO) cm^{-1}.

Found: C, 42.47; H, 3.46; N, 16.25%. Calcd for $C_9H_9O_6N_3$: C, 42.36; H, 3.56; N, 16.47%.

When the same procedure was applied to Ic in pyridine instead of acetic acid, a quantitative yield of IIc was also obtained.

The Thermal Conversion of IIc to IIIc. IIc (0.4 g) was dissolved in toluene (25 m*l*) and the solution was refluxed for ten days. The precipitates were filtered after cooling and recrystallized from a mixture of ethanol and benzene to afford 0.1 g (30%) of Ic, which was identified by IR-spectral comparison with a specimen prepared by the above method. The filtrate was condensed under reduced pressure and the residue was recrystallized from a mixture of benzene and petroleum ether to afford 0.2 g (50%) of IIIc. When this thermal conversion was carried out in the presence of diketene, IIIc was obtained almost quantitatively.

3-(5-Nitro-2-furyl)- methyl- 5 -acetonylidene - 1,2, 4-oxadiazoline (VIIc). A mixture of IVc (0.5 g) and diketene (1 m*l*) was dissolved in toluene (20 m*l*) and the solution was refluxed for 11 hr. The reaction mixture was condensed and ethanol was added to the residue. The resulting crystals were filtered and recrystallized from ethanol several times to give 0.6 g (90%) of thin yellow needles, VIIc, having a mp 195—196°C (decomp.). ν_{max}^{KBr} 1660 (CO) cm^{-1}. The results are given in Table 2.

Acidic Hydrolysis of VIIc. VIIc (0.4 g) was added to a mixture of concd. hydrochloric acid (0.6 m*l*) and water (20 m*l*) and the mixture was stirred at 85—90°C for 7 hr. The crystals precipitated after cooling were collected and recrystallized from a mixture of benzene and petroleum ether to give 0.24 g (50%) of 5-nitro-2-furanilide.[8] The filtrate was made alkaline with sodium carbonate and the resulting crystals were collected and characterized as *N*-phenyl 5-nitro-2-furamidoxime IVc by IR-spectral comparison with a specimen prepared by another method.[5] The yield was 30% (0.2 g).

1-(5-Nitro-2-furyl)aziridine Oxime *O*-Acetoacetate (IXc). VIIIc (0.46 g) and diketene (1 m*l*) were dissolved in toluene (20 m*l*) and the solution was refluxed for 10 hr. After removing toluene under reduced pressure, the residual oil was recrystallized from ethanol to give 0.6 g (90%) of IXc, mp 195—196°C (decomp.). ν_{max}^{EtOH} ($\varepsilon \times 10^{-4}$) 320 (1.4), 245 (1.1) m$\mu$. ν_{max}^{KBr} 1775 (OCO), 1710 (CO) cm^{-1}.

Found: C, 46.71; H, 3.89; N, 14.96%. Calcd for $C_{11}H_{11}O_6N_3$: C, 46.98; H, 3.94; N, 14.94%.

8) R. Marquis, *Ann. Chim.*, (8), **4**, 196 (1905).

BULLETIN OF THE CHEMICAL SOCIETY OF JAPAN VOL. 42 3011—3013 (1969)

Synthesis of 2-Methoxycarbonyl-5-methyl-7-methoxy-8-isopropyl-tetrahydronaphthalen-1-one and Rearrangement of Isopropyl Group of γ-(5-Isopropyl-4-methoxy-2-methylphenyl)-butyric Acid in Polyphosphoric Acid Cyclization

Kiyoyuki YAMADA, Susumu TAKADA, Yoshihiro HAYAKAWA and Yoshimasa HIRATA

Department of Chemistry, Faculty of Science, Nagoya University, Chikusa-ku, Nagoya

(Received March 24, 1969)

This paper describes the synthesis of the title compound, a tetralone derivative (II) which is regarded as an important intermediate in our synthetic project of sesquiterpenes. Rearrangement of the isopropyl group in γ-(5-isopropyl-4-methoxy-2-methylphenyl)-butyric acid (I) occurred during the cyclization by polyphosphoric acid (PPA). In the course of the preparation of II, a tetralone (III) was required. It was previously reported that tetralone (III) was prepared by a Friedel-Crafts reaction of the acid chloride of I, employing stannic chloride.[1] We attempted to prepare tetralone (III) in a single step by cyclizing butyric acid (I) with PPA.

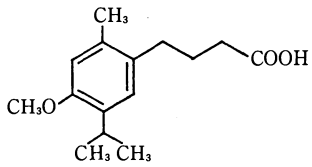

I

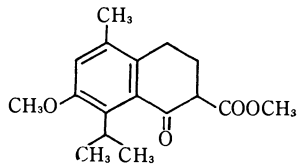

II

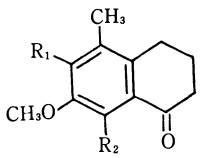

III: R_1=H, R_2=*i*-C_3H_7
IV: R_1=R_2=H
V: R_1=*i*-C_3H_7, R_2=H

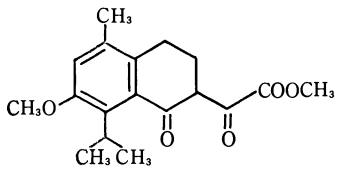

VI

When acid (I) was treated with PPA (77% as P_2O_5), a mixture of three compounds, A, B, and C was obtained in the ratio of 3 : 68 : 29 (determined by gas chromatography). The minor product A, obtained in a crystalline form was found to be the expected tetralone (III) by comparison with authentic III prepared by the unambiguous route.[1] The major product B was a desisopropyl tetralone (IV), which was identified with the authentic specimen[2] prepared from *m*-cresol methylether. Though elimination of alkyl groups (usually *t*-butyl group) on a benzene ring is a recognized feature in certain Friedel-Crafts reactions, very few cases of dealkylations have been recorded for the intramolecular ring closure reactions.[3,4]

The third product C was isomeric with tetralone (III). The NMR spectral patterns of C were similar to those of tetralone (III) except for two signals. The signal (7.31 ppm) due to an aromatic proton in product C appeared at a significantly lower field than the corresponding signal (6.71 ppm) in tetralone (III), and the reverse relationship was observed with the signal due to a methine proton of the isopropyl group (3.40 ppm in C and 3.82 ppm in III) (Fig. 1 and Fig. 2). These differences were ascribed to the anisotropic effect of the carbonyl group and structure V was assigned to product C. Formation of tetralone (V) evidently indicated that a rearrangement of the isopropyl group occurred during cyclization of I. In order to determine whether or not the rearrangement took place after cyclization, tetralone (III) was

1) P. B. Talukdar, *J. Org. Chem.*, **21**, 506 (1956).
2) L. Ruzicka and L. Sternbach, *Helv. Chim. Acta*, **23**, 355 (1940); R. B. Woodward and T. Singh, *J. Am. Chem. Soc.*, **72**, 494 (1950); A. S. Dreiding and W. J. Pummer, *ibid.*, **75**, 3162 (1953); P. Cagniant and Mme. P. Cagniant, *Bull. soc. chim. France*, **1956**, 1152.
3) N. P. Buu-Hoi and P. Cagniant, *Bull. soc. chim. France*, **11**, 349 (1944).
4) B. A. Nagasampagi, S. Dev, C. Rai and K. L. Murthy, *Tetrahedron*, **22**, 1949 (1966).

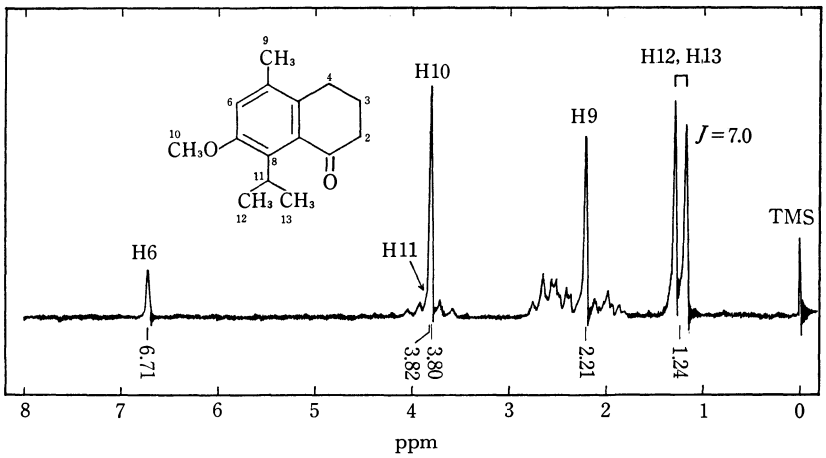

Fig. 1. NMR spectrum of III (CCl_4).

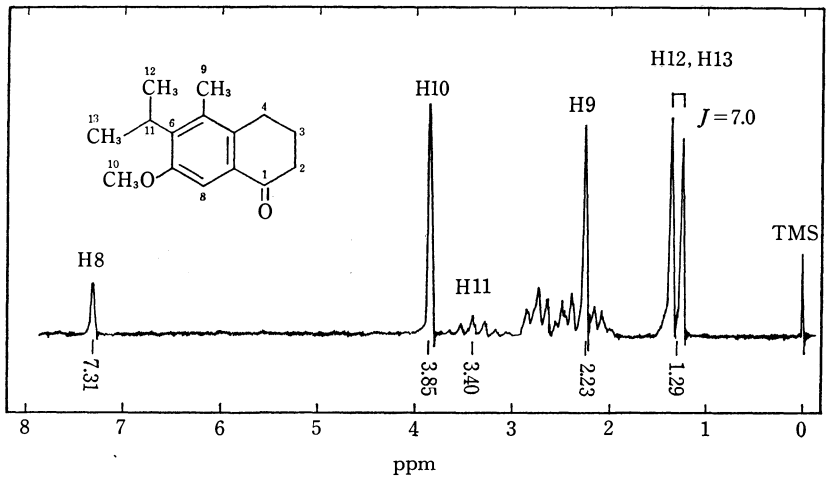

Fig. 2. NMR spectrum of V (CCl_4).

treated with PPA under the same conditions as employed for cyclization of I, affording IV and V. The result indicated that elimination and rearrangement of the isopropyl group occurred after cyclization.

It is of interest that on treatment of tetralone (IV) with PPA in the presence of isopropyl alcohol tetralones (III) and (V) were formed in an almost equal amount after a short period of time, while tetralone (V) was a sole product after a long reaction time. From the findings described above it was deduced that the rearrangement of isopropyl group observed in PPA cyclization of butyric acid (I) was an intermolecular one, the process of which would be as follows. Butyric acid (I) was initially transformed into a normal product, tetralone (III), which underwent elimination of the isopropyl group to give tetralone (IV); some IV further reacted with isopropyl carboium ion which resulted from the reaction, III→IV, at the C-6 position to afford tetralone (V).

Attempts were made to introduce a carboxyl function in the C-2 position of III for the preparation of tetralone (II) having a cadalene skeleton. Among the reactions examined the following sequence of reactions was found to be satisfactory.

Tetralone (III), when treated with dimethyl oxalate in the presence of sodium methoxide, afforded a product (VI), which was decarbonylated by heating with powdered glass to give a crystalline product (II). The spectral data obtained for this compound were in complete agreement with the assigned structure.

Experimental

Melting points and boiling points were uncorrected. The IR spectra were measured on a JASCO IR-S spectrophotometer and the UV spectra (ethanol as solvent) on a Beckman DK-2 spectrophotometer. The NMR spectra (carbon tetrachloride as solvent) were

recorded on a Varian A-60 spectrometer: only prominent peaks are cited; chemical shifts are given in ppm relative to internal tetramethylsilane (TMS); s, singlet; d, doublet; m, multiplet; coupling constants are given in cps. Mass spectra were obtained on a Hitachi RMU-6D mass spectrometer equipped with an all glass inlet system. The gas chromatographic analysis was performed on a Hitachi K-52 instrument. Thin layer chromatography (TLC) was carried out on silica gel G, (E. Merck, A. G., Germany) and column chromatography on silicic acid (100 mesh, Mallinckrodt, U. S. A.).

Polyphosphoric Acid Cyclization of Butyric Acid (I). A solution of acid (I) (3 g) in PPA (70 g: 77% as P_2O_5) was kept at 70°C for 7 hr and left at room temperature overnight. The resulting reddish solution was poured into ice-water. The mixture was extracted with three 30 m*l* portions of ether. The ethereal extract was washed with water, a 5% sodium hydroxide solution (20 m*l*), water (twice) and a saturated sodium chloride solution, and dried over sodium sulfate. On acidification of the sodium hydroxide solution (I) (240 mg) was obtained. The ethereal solution was concentrated to afford a neutral oil (2.2 g), GLC analysis (2 m column, SE-30 on Chromosorb W, 210°) of which showed three peaks, III, IV, and V in the ratio of 3 : 68 : 29. The oily mixture was distilled under reduced pressure (bp 141—144°C/ 2 mmHg) to give an almost colorless liquid, which solidified on standing. The solid mixture was dissolved in hot ethanol and after cooling a crystalline precipitate of IV appeared, which was filtered (0.5 g). The filtrate was concentrated and the residue was chromatographed on silicic acid with ethyl acetate - *n*-hexane (v/v 1 : 25): early fractions afforded crystalline III (40 mg), which was recrystalized from *n*-hexane, and from later fractions a colorless liquid (*ca.* 0.7 g) was obtained, which was distilled to give pure V (*ca.* 330 mg; analytical sample was obtained by preparative GLC); elution with ethyl acetate - *n*-hexane (v/v 1 : 10) gave IV (430 mg), which was recrystallized from *n*-hexane. Spectral and analytical data of III, IV, and V were as follows.

III: mp 88—89°C (lit[1] 88°C); IR (CCl_4), 1685, 1590 (weak) cm^{-1}; UV, 325 mμ (ε, 2400), 259 (6100), 220 (19000); NMR (see Fig. 1).

Found: C, 77.87; H, 8.62%. Calcd for $C_{15}H_{20}O_2$: C, 77.55; H, 8.68%.

IV: mp 57—58°C (lit[2] 57—57.5°C); IR (KBr), 1680, 1605 (medium), 1580 (shoulder) cm^{-1}; UV, 321 mμ (ε, 3200), 257 (8400), 218 (20000); NMR, 2.23 (3H, s, aromatic CH_3), 3.77 (3H, s, OCH_3), 6.79 (1H, d, J=3.0, meta coupling, aromatic H), 7.24 (1H, d, J=3.0, meta coupling, aromatic H).

Found: C, 75.73; H, 7.37%. Calcd for $C_{12}H_{14}O_2$: C, 75.76; H, 7.42%.

V: bp 156—157°C / 2 mmHg; IR (CCl_4), 1685, 1590 (weak) cm^{-1}; UV, 323 mμ (ε, 4000), 269 (12000), 224 (20000); NMR (see Fig. 2); Mass, M^+ 232.

Found: C, 77.20; H, 8.55%. Calcd for $C_{15}H_{20}O_2$: C, 77.55; H, 8.68%.

Action of Polyphosphoric Acid on III. A stirred solution of III (50 mg) in PPA (2 m*l*) was kept at 70°C for 8 hr and at room temperature for 2 days. The solution was carefully diluted with ice-water and extracted with ether. The ethereal extract was washed with water, a saturated sodium bicarbonate solution, water and a saturated sodium chloride solution, and dried over sodium sulfate. On removal of ether there remained an oil, GLC analysis of which showed formation of IV and V in the ratio of 88 : 12.

Action of Polyphosphoric Acid on V. A stirred solution of V (50 mg) in PPA (2 m*l*) was kept at 70°C for 7 hr and at room temperature overnight. After usual work-up the liquid product (47 mg) was obtained, which was shown to be V.

Action of Polyphosphoric Acid on IV in the Presence of Isopropyl Alcohol. a) A solution of IV (50 mg) in PPA (5 m*l* : 77% as P_2O_5) containing isopropyl alcohol (0.4 m*l*) was heated at 70 for 1 hr. The mixture was diluted with ice-water and extracted with three 10 m*l* portions of ether. The ethereal extract was washed with a 5% sodium hydroxide solution (5 m*l*), water and a saturated sodium chloride solution and dried over sodium sulfate. On removal of ether there remained a colorless oily mixture (*ca.* 50 mg), which consisted of V, III and IV in the ratio of 13 : 17 : 70 (GLC analysis).

b) The experiment in a) was repeated except that the reaction time was extended to 10 hr. GLC analysis of the resulting mixture showed the presence of V and IV in the ratio of 48 : 52.

Tetralone (VI). To a stirred solution of dimethyl oxalate (472 mg) and sodium methoxide (220 mg) in benzene (3 m*l*) was added dropwise a solution of III (455 mg) in benzene (3 m*l*) under ice-bath cooling. The operation was carried out under nitrogen. On standing at room temperature overnight the gray mixture partly solidified, to which 2 N hydrochloric acid was gradually added under cooling. The resulting mixture was extracted with ether repeatedly and the reddish ethereal extract was washed with water and a saturated sodium chloride solution, and dried over sodium sulfate. On removal of ether and excess dimethyl oxalate there remained a crystalline solid (*ca.* 500 mg), which was recrystallized from benzene to give pale yellow needles, VI; mp 133—134°C; IR (KBr), 1735, 1610, 1585 cm^{-1}; UV, 330 mμ (ε, 12000); NMR, 1.30 (6H, d, J=7.0, $\underline{CH_3}$-CH-$\underline{CH_3}$), 2.25 (3H, s, aromatic CH_3), *ca.* 2.7 (4H, m, $-CH_2-CH_2-$), 3.77 (1H, m, $CH_3-\underline{CH}-CH_3$), 3.82 (3H, s, OCH_3 or $COOCH_3$), 3.85 (3H, s, OCH_3 or $COOCH_3$), 6.77 (1H, s, aromatic H), 15.50 (1H, s, enolic OH due to β-diketone).

Found: C, 67.98; H, 7.11%. Calcd for $C_{18}H_{22}O_5$: C, 67.91; H, 6.97%.

Tetralone (II). Powdered glass was added to melted tetralone (VI) (100 mg) in a flask kept at 160°C. Gas was evolved for several minutes. After cooling the residue was extracted with benzene and the benzene extract was concentrated to give a solid. Recrystallization from methanol and from *n*-hexane afforded pure II (60 mg); mp 77—78°C; IR (KBr), 1745, 1685, 1595 (weak) cm^{-1}; UV, 328 mμ (ε, 2900), 262 (7000); NMR, 1.24 (3H, d, J=7.0, $\underline{CH_3}$-CH-CH_3), 1.27 (3H, d, J=7.0, $CH_3-\underline{CH}-\underline{CH_3}$), 2.21 (3H, s, aromatic CH_3), 3.65 (1H, m, $CH_3-\underline{CH}-CH_3$), 3.68 (3H, s, OCH_3 or $COOCH_3$), 3.80 (3H, s, OCH_3 or $COOCH_3$), 6.73 (1H, s, aromatic H); Mass, M^+ 290.

Found: C, 70.46; H, 7.95%. Calcd for $C_{17}H_{22}O_4$: C, 70.32; H, 7.64%.

BULLETIN OF THE CHEMICAL SOCIETY OF JAPAN VOL. 42 3014—3015 (1969)

The Chemiluminescence of Indole Accompanying Oxidation by Perbenzoic Acid

Yoshimori OMOTE, Hiroshi YAMAMOTO, Kazushige FUNASAKI, Masamoto AKUTAGAWA and Noboru SUGIYAMA

Department of Chemistry, Tokyo Kyoiku University, Otsuka, Bunkyo-ku, Tokyo

(Received March 26, 1969)

Previously we[1] investigated the chemiluminescence of indoles using two types of reaction: *A*, the indoles in alkaline ethanol, to which a mixture of 3% hydrogen peroxide and 3% potassium ferricyanide has been added, and *B*, the indoles in DMSO, to which a 5 N potassium hydroxide aqueous solution has been added. We[2] also proposed the mechanism of chemiluminescence in the system B, a mechanism which is in accord with the report by McCapra *et al.*[3]

The previous papers[1-5] on the chemiluminescence of indoles have dealt almost exclusively with the reaction in a basic solution. Now we have found a chemiluminescent reaction of indoles which proceeds in a chloroform solution by means of perbenzoic acid. This is a new chemiluminescence of indoles in that it takes place in the absence of a base.

Results and Discussion

Indole (I), 3-methylindole (II), and 3-phenylindole (III) were chosen as typical indole compounds. The compound II is suitable for the investigation of the inductive effect of a 3-substituent on the indole nucleus, and compound III, for a study of the mesomeric effect.

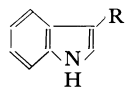

I R=H
II R=CH_3
III R=C_6H_5

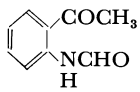

IV

Witkop and Fielder[6] reported that II gave *o*-formamidoacetophenone (IV) by perbenzoic acid oxidation. We observed the emission of light in this reaction. Thus we measured the chemiluminescence of indoles which accompanied the oxidation reaction caused by perbenzoic acid in chloroform. The relative intensities of the chemiluminescence of I, II, and III are summarized in Table 1. As a comparison, the relative intensities in the two systems, A and B, are also quoted from our previous report.[1]

Table 1. Relative intensities of chemiluminescence of indoles

Indoles (10^{-2} mol/*l*)	Perbenzoic acid (10^{-2})	Perbenzoic acid (10^{-1})	A	B
Indole (I)	0.6	9.6	1	1
3-Methylindole (II)	8.2	71	0.5	13
3-Phenylindole (III)	0.1	1.5	90	0

A: EtOH-KOH-H_2O_2-$K_3Fe(CN)_6$
B: DMSO-KOH-O_2

The intensity of chemiluminescence by perbenzoic acid decreases in the order: II> I> III, while that in the system A decreases in the order: III> I> II, and that in the system B: II> I> III. The order in each system is considered to depend on the substituents on the 3-position. The change in the order between the reaction systems suggests a difference in the reaction mechanism. It is probable that the mechanism of chemiluminescence in the system A involves the formation of a hydroperoxy radical, a process which can be expressed by the equation: $H_2O_2+Fe^{3+}\rightarrow HOO\cdot+Fe^{2+}+H^+$. The system B involves a cyclic peroxide intermediate.[2,3] As the order in the perbenzoic acid oxidation system is similar to that in the system B rather than to that in the system A, the mechanism of the chemiluminescence of oxidation by perbenzoic acid seems to be analogous to that of the chemiluminescence with a base and oxygen in DMSO.

After the chemiluminescent reaction of II by perbenzoic acid, the ultraviolet absorption maxima of II at 275 and 291 nm change to 260 and 320 nm and the fluorescence maximum, 465 nm,

1) N. Sugiyama, M. Akutagawa, T. Gasha, Y. Saiga and H. Yamamoto, This Bulletin, **40**, 347 (1967).
2) N. Sugiyama and M. Akutagawa, *ibid.*, **40**, 240 (1967); N. Sugiyama, M. Akutagawa and H. Yamamoto, *ibid.*, **41**, 936 (1968); N. Sugiyama, H. Yamamoto, Y. Omote and M. Akutagawa, *ibid.*, **41**, 1917 (1968).
3) F. McCapra and Y. C. Chang, *Chem. Commun.*, **1966**, 522.
4) G. E. Philbrook, J. B. Ayer, J. F. Garst and J. R. Totter, *Photochem. Photobiol.*, **4**, 869 (1965).
5) A. W. Berger, J. N. Driscoll and J. A. Pirog, *ibid.*, **4**, 1123 (1965).
6) B. Witkop and H. Fielder, *Ann.*, **558**, 91 (1947).

changes to 497 nm. These facts shown that the indole chromophore changes into another one. The spectral data of II are summarized in Table 2.

Table 2. Fluorescence and chemiluminescence maxima of 3-methylindole (nm) in $CHCl_3$

	Fluorescence	Chemiluminescence
3-Methylindole(II)	465 (497) (495)*	weak 495*
o-Formamidoacetophenone (IV)	525 495*	
Perbenzoic acid	470	
Benzoic acid	no	

* in DMSO-alkali condition
( ) fluorescence after chemiluminescent reaction

The presence of benzoic acid or perbenzoic acid was not proved to have any influence upon the chemiluminescence. The chemiluminescent spectrum of II by perbenzoic acid in chloroform could not be measured because of the weakness of the emission and the short life-time of the emitter. However, it was proved that 40% of the IV was produced from the chemiluminescent reaction in chloroform by perbenzoic acid. The product was identified with an authentic sample by TLC and by a study of the spectral data.

The spectrum of the chemiluminescence of II in DMSO in the presence of oxygen and a base (type B) was also measured (Table 2); from its reaction mixture, 15% of the IV was obtained, along with some unreacted II. From the facts that the chemiluminescence maximum is in accord with the fluorescence maximum after the chemiluminescent reaction in the DMSO-oxygen-base system, we propose the following reaction mechanism for the chemiluminescence of II in a basic solution.

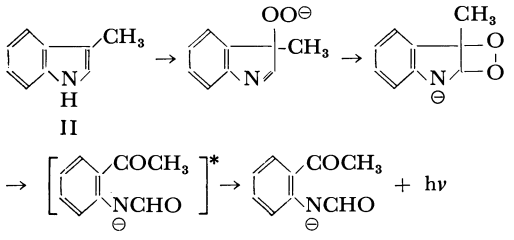

Scheme

It is clear that the emitter in a basic solution is the singlet excited state of the *o*-formamidoacetophenone anion (V). However, the excited state of V cannot be the emitter in the chemiluminescence by perbenzoic acid because the fluorescence maximum of IV in chloroform is different from that after the chemiluminescent reaction of II. Therefore, we tentatively suggest that the emitter of this chemiluminescence is different from the anion of IV, but it might be IV itself. The difference in the fluorescence maxima might result from the fluorescence of the unreacted indole or the peracid.

Experimental

Materials. The commercial indole (I) was recrystallized from ligroin and sublimed *in vacuo*. Mp 52°C. The commercial 3-methylindole (II) was also purified in the same way; mp 95°C. The 3-phenylindole (III) was synthesized by a modification of the procedure of Fischer;[7] mp 88.8°C. The *o*-formamidoacetophenone (IV)[8] was prepared from *o*-aminoacetophenone;[9] mp 78.2—78.5°C. The perbenzoic acid[10] was freshly prepared before the oxidation experiment.

Chemiluminescence Intensity. One milliliter of a indole chloroform solution (10^{-2} mol/*l*) was mixed with 1 m*l* of a perbenzoic acid chloroform solution (10^{-1} mol/*l*) in a glass tube (10 mm × 70 mm). Moreover, the light intensity was measured by a modified Model 139 Hitachi Photometer.

Spectra. The chemiluminescent spectrum was measured by means of a EPS-2 Hitachi Spectrophotometer into which 5 m*l* of a 3-methylindole DMSO solution (10^{-1} mol/*l*) and 2 g of solid potassium hydroxide were bubbled by an oxygen stream. The fluorescence spectrum was measured by the same photometer equipped with a high-pressure mercury lamp (365 nm line for excitation).

Separation and Identification of Products. Ten milliliters of a 3-methylindole solution (10^{-2} mol/*l*) were mixed with 10 m*l* of a perbenzoic acid chloroform solution (10^{-2} mol/*l*). The evaporation residue showed a main spot with R_f 0.60 (Wakogel B-5) upon TLC with a benzene-ether (1 : 1 v/v) mixture. The product was purified by means of a silica-gel column (Wakogel C-200) with benzene. The ultraviolet absorption spectrum of this product was identical with that of *o*-formamidoacetophenone.

7) E. Fisher and T. Schmidt, *Ber.*, **21**, 1811 (1887).
8) R. Camps, *ibid.*, **34**, 2703 (1901).
9) H. G. Walker and C. R. Hauser, *J. Am. Chem. Soc.*, **68**, 1386 (1946).
10) G. Brown, C. R. Noller and P. Liang, "Organic Synthesis," Coll. Vol. I, p. 431 (1956).

BULLETIN OF THE CHEMICAL SOCIETY OF JAPAN VOL. 42 3016—3017 (1969)

Synthesis of 5-Chloro-6-Methoxy-*N*-Methylisatin

Yoshimori OMOTE, Hinako TAZAWA, Yoshimori FUJINUMA and Noboru SUGIYAMA

Department of Chemistry, Tokyo Kyoiku University, Otsuka, Bunkyo-ku, Tokyo

(Received March 27, 1969)

In connection with the investigation of melanin precursors, we have reported the synthesis of the DOPA dimer[1] and pipataline.[2] These substances are interesting as model compounds of melanin precursors. This paper will be concerned with the synthesis of 5-chloro-6-methoxy-*N*-methylisatin (IV), which would make a black pigment upon oxidative polymerization. The compound has been identified with a metabolite of *Micromonospora carbonacea* reported by Reimann and Jaret.[3]

Compound IV was prepared as follows. The chlorination of the diazonium salt obtained from 5-nitro-*o*-anisidine gave 2-chloro-5-nitroanisole (I) in the presence of cuprous chloride. The reduction of I with stannous chloride and hydrochloric acid afforded the corresponding amine; the amine was then converted to 4-chloro-3-methoxyisonitrosoacetanilide (II). After the cyclization of II into 5-chloro-6-methoxyisatin (III), it was methylated with methyl iodide to give IV. The spectral data (IR, UV, and NMR) of the synthetic substance are in good agreement with those of the natural substance, but the melting point of the synthetic substance is lower than that of the natural one.

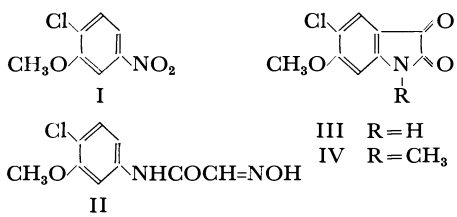

Experimental

All the melting points are uncorrected.

2-Chloro-5-nitroanisole (I). 5-nitro-*o*-anisidine (20 g), suspended in concentrated hydrochloric acid (50 m*l*) and water (40 m*l*), was diazotized at 0—6°C with sodium nitrite (9 g) in water (50 m*l*). Then the cold diazonium solution was rapidly stirred into an ice-cooled cuprous chloride solution. As the commercial cuprous chloride considerably diminished the yield, it was freshly prepared.*1 The reaction proceeded very vigorously, with the release of nitrogen gas and the separation of the precipitates. The mixture was stirred for 1.5 hr at room temperature, warmed for 30 min at 50—60°C, and then heated to 80°C for 15 min to decompose the addition product completely. By the steam distillation of the reaction mixture, 2-chloro-5-nitroanisole (19 g, yield 85%) was obtained; mp 84—85°C (lit[4] mp 83°C).

4-Chloro-3-methoxyisonitrosoacetanilide (II). *a) Reduction of 2-Chloro-5-nitroanisole.* A solution of I (20 g) in glacial acetic acid (50 m*l*) was boiled. The heat was removed from the solution of I, to which stannous chloride (104 g) dissolved in concentrated hydrochloric acid was gradually added. A stannic chloride compound of the amine then began to crystallize. After the addition of the stannous chloride solution, the mixture was heated gently for 30 min and then cooled with ice water. The separated crystals were filtered and dried. The yield was 33 g.

b) 4-Chloro-3-methoxyisonitrosoacetanilide. To a solution of chloral hydrate (17 g) in water (200 m*l*), there were added, in order: crystallized sodium sulfate (240 g), a solution of the amine obtained above (32 g) in water (200 m*l*), and finally a solution of hydroxylamine hydrochloride (21 g) in water (90 m*l*). While the mixture was gently boiled for 1.5 hr, the precipitates of the isonitrosoacetanilide separated. After cooling with water, the precipitates were filtered, dried, and extracted with ethyl acetate. The removal of the solvent gave the crude isonitrosoacetanilide (17 .2g), which was reprecipitated from ethanol-water; mp 185°C.

Found: C, 47.40; H, 3.98; N, 12.32%. Calcd for $C_9H_9O_3N_2Cl$: C, 47.27; H, 3.97; N, 12.25%. UV λ_{max}^{EtOH} nm (ε) 215—220 (17800, sh), 290 (9600, sh), and 300 (10000). IR ν^{KBr} cm^{-1} 3305, 2860, 1620, 1603, 1549, 1289, 1257, and 1066.

5-Chloro-6-methoxyisatin (III). According to the method of the literature,[5] II (15 g) was treated with concentrated sulfuric acid (50 m*l*) to produce the corresponding isatin. The crude product was then purified by dissolving it in aqueous sodium hydroxide and by then slowly adding dilute hydrochloric acid. The

*1 A solution of cuprous chloride was prepared from crystallized copper sulfate (13 g), copper powder (7 g), sodium chloride (6 g) and concentrated hydrochloric acid (40 m*l*).

1) a) Y. Omote, Y. Fujinuma and N. Sugiyama, *Chem. Commun.*, **1968**, 190. b) Y. Omote, Y. Fujinuma and N. Sugiyama, This Bulletin, **42**, 1752 (1969).

2) Y. Omote, H. Tazawa, Y. Fujinuma and N. Sugiyama, This Bulletin, **42**, 569 (1969).

3) H. Reimann and R. Jaret, *Chem. & Ind.*, **1967**, 2173.

4) E. L. Holmes and C. K. Ingold, *J. Chem. Soc.*, **1926**, 1684.

5) C. S. Marvel and G. S. Hiers, "Organic Syntheses," Coll. Vol. I, p. 327 (1956).

yellow precipitates that separated at first were filtered at once. The pale orange filtrate was acidified to congo red paper with hydrochloric acid. The solution was then cooled, and the isatin (III) which separated (2.3 g) was collected by filtration; mp 278°C.

Found: C, 50.16; H, 3.02; N, 6.96%. Calcd for $C_9H_6O_3NCl$: C, 51.09; H, 2.86; N, 6.62%.
UV λ_{max}^{EtOH} nm (ε) 220 (16500), 267 (25800), 273 (25100), 317 (7400), and 418 (110). IR ν^{KBr} cm^{-1} 3235, 1764, 1614, 1488, 1447, and 1038. This compound produced a black pigment when it was treated with hydrobromic acid.

5-Chloro-6-methoxy-*N*-methylisatin (IV). To a suspension of III (0.3 g) in methanol (3 m*l*) there was added a solution of sodium methoxide (0.12 g) in methanol (3 m*l*). After the mixture had been stirred for 10 min, the sodium salt precipitated was collected. The sodium salt suspended in methyl iodide (6 m*l*) was heated at 100°C for 2 hr in a sealed tube. After the removal of the excess methyl iodide under reduced pressure, the residue was purified in the manner described for the preparation of III. The yield was 0.08 g; mp 242—243°C.

Found: C, 52.92; H, 3.68; N, 6.13%. Calcd for $C_{10}H_8O_3NCl$: C, 53.24; H, 3.57; N, 6.21%.
UV λ_{max}^{EtOH} nm (ε) 221 (17400), 270 (27200), 276 (26400), 319 (6900), and 430 (800). IR ν^{KBr} cm^{-1} 3100, 1745, 1613, 1587, 1493, and 1248.
NMR δ (d_6-DMSO) 3.15 (s, $ArNCH_3$), 4.02 (s, $ArOCH_3$), 6.88 (s, ArH), and 7.52 (s, ArH).

BULLETIN OF THE CHEMICAL SOCIETY OF JAPAN VOL. 42 3017—3018 (1969)

The Cation-exchange Separation of Copper and Iron in Ammoniacal Pyrophosphate Media

Toshio NISHIIDO

Department of Chemistry, Faculty of Science, Tokyo Metropolitan University, Setagaya-ku, Tokyo

(Received March 31, 1969)

Kharin and Soraka[1] and Marczenko[2] have reported the separation of copper and iron using cation exchange resin in the ammonium form, with sodium pyrophosphate as the eluting agent. In their method, however, much sodium pyrophosphate seems to prevent an ion exchange of copper because sodium ions also exchange with ammonium ions. However, their method merits further study.

The purposes of the present study are to establish a cation-exchange method for the separation of copper from iron using ammonium pyrophosphate instead of sodium pyrophosphate, and to apply it to the determination of copper in hot spring waters. This method is based on the difference in stability[3] between copper and iron pyrophosphate complexes. The separation of copper and iron with cation-exchange resin is affected by the pH and by the concentrations of pyrophosphate and ammonia.

Experimental

Reagent and Apparatus. *Pyrophosphate Solution.* 72 g of pyrophosphoric acid were dissolved in 100 m*l* of distilled water. The solution was adjusted to pH 5 with ammonia and then diluted to 200 m*l*. Copper and other impurities were removed from the solution by extraction with a dithizone carbon tetrachloride solution.

Ammonia Solution. 50 g of ammonium nitrate were dissolved in 50 m*l* of distilled water. Copper and other elements were removed as has been described above. The solution was diluted to 100 m*l* after 36 m*l* of 10 M distilled ammonia had been added. The final solution showed pH 10 and 10 M in ammonia, $NH_3+NH_4^+$.

Washing Solution. This solution was made by mixing 0.5 m*l* of the pyrophosphate and 10 m*l* of the ammonia solution and by then diluting to 100 m*l* with distilled water.

Resin and Column. Dowex 50×8 (50—100 mesh) was converted to the ammonium form with 1 M ammonium chloride. The ion-exchange column was 10 mm in diameter and 100 mm long.

Determination of Copper and Iron. The copper was determined colorimetrically using either cuprferazone[4] or dithizone.[5] The iron was determined by the *o*-phenanthroline method.[5] In order to promote color development, solutions were kept at 40°C after adding reagents, and the transmittance was measured at 500 mμ.

Procedure. To a solution containing 50 μg of copper and 500 μg of iron, 0.25 m*l* of the pyrophosphate and 5 m*l* of the ammonia solution were added. The solution was then diluted to 50 m*l* with distilled water and passed through the column at a flow rate of 1.0 to 1.2 m*l*/min. The column was washed with 50 m*l* of the washing solution. The effluent obtained was used to determine the iron. Then, the column was treated

1) A. H. Kharin and N. N. Soraka, *Zh. Prikl. Khim.*, **37**, 672 (1964).

2) Z. Marczenko, *Chemia Analityczma*, **1**, 263 (1956); *Anal. Abstr.*, **4**, Abstract 3569 (1957).

3) A. Ringbom, "Complexation in Analytical Chemistry," Interscience Publishers, New York (1963).

4) T. R. Williams and R. R. T. Morgen, *Chem. Ind. (London)*, **1954**, 461.

5) E. B. Sandell, "Colorimetric Determination of Traces of Metals," 3rd Ed., Interscience Publishers, New York (1959), pp. 453, 537.

Table 1. Major components and copper contents of the samples

Sample	pH	mg/l								μg/l
		Na	K	Mg	Ca	Al	Fe	Cl	SO_4	Cu
Synthetic solution	0.9	250	200	100	250	800	70	12000	1300	0
Tateyama-jigokudani hot spring*	0.7	244	191	88	248	840	68.6	12340	1314	7
Kankō Hotel spring in Narugo**	2.3	173	15.1	—	—	—	35.3	108	—	5
Karabuki spring in Manza***	1.8	565	105	245	78	56	32.4	966	4170	2

* Analyst: M. Imahashi; ** Analyst: H. Miyazawa; *** Analyst: R. Nakagawa

with 50 m*l* of 2 N hydrochloric acid. This effluent was then used to determine the copper.

Results

The Effect of pH on Separation of Copper and Iron. The pH of the solutions was adjusted to between 8 to 11 with either nitric acid or sodium hydroxide. Iron passed through the column at any pH. The copper was entirely retained in the column at pH 9 to 10, but it was partly lost below pH 9. It was best to separate the copper and iron at pHs from 9 to 10; the recoveries were found to be 99% for copper and 100% for iron.

The Effect of the Concentration of Ammonia, $NH_3+NH_4^+$. The experiments were made on solutions containing up to 2 M of ammonia at pH 9.5. The results showed that the separation of copper and iron was favorable between 1 to 2 M in ammonia, but it was not suitable below 0.5 M because the copper partly passed through the column.

The Effect of the Concentration of Pyrophosphate. The effect of the concentration of pyrophosphate on the separation of copper and iron was examined using sodium, potassium, and ammonium pyrophosphate. The results showed that above 0.05 M sodium and potassium pyrophosphate disturbed the ion exchange of copper because sodium and potassium ions were exchangeable with ammonium ions in the column. On the other hand, ammonium pyrophosphate did not disturb the ion exchange of copper up to 0.5 M in pyrophosphate.

Application

The above method was used in the determination of copper in synthetic samples and hot spring waters.

Table 2. Determination of copper in synthetic solution*

Cu added (μg)	Cu found (μg)
0.0	0.0, 0.0, 0.1
1.0	1.0, 0.9, 0.9
2.0	2.2, 1.9

* Synthetic solution was prepared by dissolving chemical reagent.

The components of these samples are shown in Table 1.

A 50-m*l* portion of the sample was placed in a beaker, and then 10 m*l* of the pyrophosphate and 20 m*l* of the ammonia solutions were stirred in.*1 The solution was diluted to 100 m*l* and passed through the column. The column was washed with 30 m*l* of the washing solution. Then, copper was eluted with 50 m*l* of 2 N hydrochloric acid and determined by the dithizone method.[5] The results are shown in Tables 1 and 2. Though traces of copper and a great quantity of iron were found, the error involved in this method was not significant. Moreover, the copper contents in hot spring waters determined by the present method were in good agreement with those reported by Ichikuni.[6]

The author wishes to thank Professor K. Noguchi and Dr. M. Ichikuni for their helpful discussions during this work.

*1 When much aluminum exists in the sample, aluminum hydroxide is gradually formed in the solution. In that case, the precipitate was separated from the solution with a centrifuge and was later dissolved in the elute containing copper.

6) M. Ichikuni, *Geochim. et Cosmochim. Acta*, **23**, 305 (1959).

BULLETIN OF THE CHEMICAL SOCIETY OF JAPAN VOL. 42 3019—3021 (1969)

Organische Metallkomplexe. VII.*1 Darstellung und Eigenschaften der Kupfer(II)chelate einiger *N*-Alkyliden-*N'*-alkanoyl-hydrazine*2

Hiroshi OHTA, Jun-ichi MATSUOKA, Toshihide ADACHI, Ken-ichiro YOSHIDA und Akio TAKUWA

Institut für Organische Chemie, Shimane Universität, Matsue

(Eingegangen am 3. April, 1969)

In der vorliegenden Arbeit werden die bisherigen Untersuchungen von einem von uns über die Metallchelate der *N*-Alkyliden-*N'*-benzoyl-hydrazine[1] weitergeführt und die Kupfer(II)chelate einiger *N*-Alkyliden-*N'*-alkanoyl-hydrazine dargestellt.

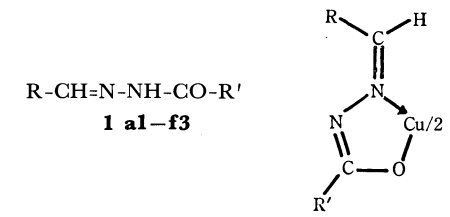

	R	R'
a1	CH_3-$(CH_2)_7$-	CH_3-
a2	CH_3-$(CH_2)_8$-	CH_3-
b1	CH_3-$(CH_2)_5$-	CH_3-CH_2-
b2	CH_3-$(CH_2)_6$-	CH_3-CH_2-
b3	CH_3-$(CH_2)_7$-	CH_3-CH_2-
b4	CH_3-$(CH_2)_8$-	CH_3-CH_2-
c1	CH_3-$(CH_2)_4$-	CH_3-$(CH_2)_2$-
c2	CH_3-$(CH_2)_5$-	CH_3-$(CH_2)_2$-
c3	CH_3-$(CH_2)_6$-	CH_3-$(CH_2)_2$-
c4	CH_3-$(CH_2)_7$-	CH_3-$(CH_2)_2$-
c5	CH_3-$(CH_2)_8$-	CH_3-$(CH_2)_2$-
d1	CH_3-$(CH_2)_4$-	CH_3-$(CH_2)_3$-
d2	CH_3-$(CH_2)_6$-	CH_3-$(CH_2)_3$-
d3	CH_3-$(CH_2)_8$-	CH_3-$(CH_2)_3$-
e1	CH_3-$(CH_2)_4$-	CH_3-$(CH_2)_4$-
e2	CH_3-$(CH_2)_6$-	CH_2-$(CH_2)_4$-
e3	CH_3-$(CH_2)_8$-	CH_2-$(CH_2)_4$-
f1	CH_3	C_6H_5-CH_2-
f2	CH_3-$(CH_2)_3$-	C_6H_5-CH_2-
f3	CH_3-$(CH_2)_8$-	C_6H_5-CH_2-

Als Ausgangsstoffe für die Komplexdarstellung haben wir **1 a1—f3** und die Metallacetate herangezogen. Im Gegensatz zu den beständigen Kupfer-(II)-(rötlich-violett) und Nickel(II)chelaten (orange-rot) der *N*-Alkyliden-*N'*-benzoyl-hydrazine, die leicht dargestellt und auf übliche Weise umkristallisiert werden können, sind diejenigen der *N*-Alkyliden-*N'*-alkanoyl-hydrazine ziemlich unbeständig, und trotz der verschiedenen Versuche wurden nur die Kupfer(II)chelate erhalten; die Darstellung der Nickel(II)chelate ist uns bisher nicht gelungen.

Wir fanden, daß die Kupfer(II)chelate bequem in Kristallen zugänglich sind, indem man nach dem Vermischen beider Komponente in Äthanol so viel Wasser bei Zimmertemperatur sorgfältig hinzufügt, bis die Lösung trüb wird, und die

TABELLE 1. *N*-ALKYLIDEN-*N'*-ALKANOYL-HYDRAZINE (**1**)

Nr.	Summenformel	Schmp. (°C)	Analysendaten Ber.	Gef.
a1	$C_{11}H_{22}N_2O$	65—67	C 66.62	C 66.81
			H 11.18	H 11.25
			N 14.13	N 13.56
a2	$C_{12}H_{24}N_2O$	77—78	N 13.19	N 12.90
b1	$C_{10}H_{20}N_2O$	49—51	N 15.20	N 15.49
b2	$C_{11}H_{22}N_2O$	57—58	N 14.13	N 13.89
b3	$C_{12}H_{24}N_2O$	57—58	N 13.19	N 13.01
b4	$C_{13}H_{26}N_2O$	58—59	N 12.38	N 12.28
c1	$C_{10}H_{20}N_2O$	53—54	N 15.20	N 15.35
c2	$C_{11}H_{22}N_2O$	44—46	N 14.13	N 14.16
c3	$C_{12}H_{24}N_2O$	60—61	N 13.19	N 13.19
c4	$C_{13}H_{26}N_2O$	54—56	N 12.38	N 12.31
c5	$C_{14}H_{28}N_2O$	67—68	N 11.65	N 11.49
d1	$C_{11}H_{22}N_2O$	54—56	N 14.13	N 14.18
d2	$C_{13}H_{26}N_2O$	44—45	N 12.38	N 12.10
d3	$C_{15}H_{30}N_2O$	63—64.5	N 11.01	N 11.09
e1	$C_{12}H_{24}N_2O$	62—65	N 13.19	N 13.44
e2	$C_{14}H_{28}N_2O$	63—64	N 11.65	N 11.90
e3	$C_{16}H_{32}N_2O$	69—71	N 10.44	N 10.23
f1	$C_{10}H_{12}N_2O$	144—145	N 15.90	N 15.97
f2	$C_{13}H_{18}N_2O$	104—105	N 12.83	N 12.93
f3	$C_{18}H_{28}N_2O$	108—109	N 9.71	N 9.65

*1 VI. Mitteilung: H. Ohta, *Mem. Faculty Sci., Kyushu Univ., Ser. Chem.*, **4**, 129 (1961).

*2 Vorgetragen in Tokushima auf der Generaltagung der Chugoku-, Shikoku- und Kyushu-Zweiganstalten der Japanischen Chemischen Gesellschaft, am 8. Nov., 1968.

1) H. Ohta, Dieses Bulletin, **33**, 1337 (1960).

trübe Lösung dann lange Zeit bei etwa 0°C stehen läßt. Die Chelate können folgenderweise umkristallisiert werden; sie werden in möglichst wenig Äthanol oder Methanol bei Zimmertemperatur schnell gelöst und längere Zeit bei etwa 0°C stehen gelassen. Ausnahmsweise ist das Bis-(*N*-äthyliden-*N'*-phenylacetyl-hydrazinato)kupfer(II) (**2 f1**) beständig und in kaltem Äthanol schwer löslich; es kann nur in üblicher Weise aus heißem Äthanol umkristallisiert werden.

Die Kupfer(II)chelate in Tabelle 3 sind in den meisten organischen Lösungsmitteln leicht löslich und zeigen bestimmte Schmelzpunkte auf Grund der längeren aliphatischen Ketten.[1,2] In reinem, trockenem Zustand sind sie ziemlich beständig, in Lösung aber, außer bei niedriger Temperature sind sie unbeständig. Die Instabilität dieser Chelate im Vergleich mit denjenigen der *N*-Alkyliden-*N'*-benzoyl-hydrazine würde auf die Alkyl-Reste in den Acylgruppen zurückzuführen sein. Aus einigen niedrigeren *N*-Alkyliden-*N'*-alkanoyl-hydrazinen konnten wir sogar die Kupfer(II)-chelate nicht erhalten.

Beschreibung der Versuche

Die Schmelzpunkte sind nicht korrigiert.

Allgemeine Vorschrift zur Darstellung der Bis(*N*-alkyliden-*N'*-alkanoyl-hydrazinato)kupfer-(II). (Tab. 2). Bei Zimmertemperatur gibt man zur Lösung von *a* mg **1 a1—f3** in *b* ccm Äthanol eine Lösung von *c* mg Kupfer(II)acetat in *d* ccm Äthanol, und darauf *e* ccm Wasser. Die trübe Lösung läßt man bei etwa 0°C stehen.

Die Ausgangshydrazine und die dargestellten Kupfer-(II)chelate sind in den Tabellen 1 und 3 zusammengefaßt.

Tabelle 2. Einzeldaten über die Darstellung der Kupfer(II)chelate

	Ausgangs-hydrazine **1** *a* mg	Äthanol *b* ccm	$(CH_3COO)_2Cu \cdot H_2O$ *c* mg	Äthanol *d* ccm	Zugefügtes Wasser *e* ccm
a1	400	5	200	25	30
a2	425	5	200	25	25
b1	370	5	200	20	40
b2	400	5	200	20	35
b3	425	5	200	20	30
b4	455	5	200	20	40
c1	370	5	200	20	25
c2	400	5	200	20	25
c3	425	5	200	20	25
c4	455	5	200	20	25
c5	480	5	200	20	40
d1	400	5	200	20	25
d2	452	5	200	20	20
d3	515	5	200	20	20
e1	425	5	200	20	15
e2	480	5	200	20	10
e3	545	5	200	20	10
f1	350	5	200	20	40
f2	440	5	200	20	20
f3	577	10	200	20	12

Tabelle 3. Dargestellte Kupfer(II)chelate

Chelate **2**	Umkrist. aus (Aussehen)	Summenformel (Mol.-Gew.)	Schmp. °C	Analysendaten Ber.	Gef.
a1	Äthanol (Rötlichviolette Nädelchen)	$C_{22}H_{42}N_4O_2Cu$ (458.15)	83—85	C 57.68 H 9.24 N 12.23 Cu 13.87	C 57.80 H 9.36 N 11.95 Cu 14.00
a2	Methanol (Violette Nadeln)	$C_{24}H_{46}N_4O_2Cu$ (486.20)	84—85	N 11.52 Cu 13.07	N 11.50 Cu 12.87
b1	Äthanol (Violette Nädelchen)	$C_{20}H_{38}N_4O_2Cu$ (430.10)	68—69†	N 13.03 Cu 14.77	N 13.11 Cu 14.95

2) T. Tsumaki und Mitarbb., *Nippon Kagaku Zasshi (J. Chem. Soc. Japan, Pure Chem. Sect.)*, **78**, 1086 (1957).

Chelate **2**	Umkrist. aus (Aussehen)	Summenformel (Mol.-Gew.)	Schmp. °C	Analysendaten Ber.	Gef.
b2	Äthanol (Violette Nädelchen)	$C_{22}H_{42}N_4O_2Cu$ (458.15)	69—70†	N 12.23 Cu 13.87	N 12.25 Cu 13.82
b3	Äthanol (Violette Nädelchen)	$C_{24}H_{46}N_4O_2Cu$ (486.20)	68—69	N 11.52 Cu 13.07	N 11.50 Cu 13.20
b4	Äthanol (Violette Nädelchen)	$C_{26}H_{50}N_4O_2Cu$ (514.26)	70—71	N 10.89 Cu 12.36	N 11.02 Cu 12.41
c1	Äthanol (Violette Nädelchen)	$C_{20}H_{38}N_4O_2Cu$ (430.10)	78—80	N 13.03 Cu 14.77	N 13.06 Cu 14.57
c2	Äthanol (Violette Nädelchen)	$C_{22}H_{42}N_4O_2Cu$ (458.15)	70—71	N 12.23 Cu 13.87	N 12.14 Cu 13.82
c3	Äthanol (Violette Nädelchen)	$C_{24}H_{46}N_4O_2Cu$ (486.20)	88—90†	N 11.52 Cu 13.07	N 11.56 Cu 13.31
c4	Äthanol (Violette Nädelchen)	$C_{26}H_{50}N_4O_2Cu$ (514.26)	65—66	N 10.89 Cu 12.36	N 10.83 Cu 12.38
c5	Äthanol (Rötlichviolette Nadeln)	$C_{28}H_{54}N_4O_2Cu$ (542.31)	68—69	N 10.33 Cu 11.72	N 10.39 Cu 11.76
d1*	Äthanol (Rötlichviolette Nädelchen)	$C_{22}H_{42}N_4O_2Cu$ (458.15)	54—56	N 12.23 Cu 13.87	N 12.21 Cu 13.99
d2*	Äthanol (Rötlichviolette Nädelchen)	$C_{26}H_{50}N_4O_2Cu$ (514.26)	72—73	N 10.89 Cu 12.36	N 10.91 Cu 12.30
d3*	Äthanol (Violette Nädelchen)	$C_{30}H_{58}N_4O_2Cu$ (570.37)	69—72	N 9.82 Cu 11.32	N 9.95 Cu 11.13
e1*	Äthanol (Hellviolette Nädelchen)	$C_{24}H_{46}N_4O_2Cu$ (486.20)	62—65	N 11.52 Cu 13.07	N 11.81 Cu 13.31
e2*	Äthanol (Rötlichviolette Nädelchen)	$C_{28}H_{54}N_4O_2Cu$ (542.31)	79—81	N 10.33 Cu 11.72	N 10.48 Cu 11.88
e3*	Äthanol (Rötlichviolette Nädelchen)	$C_{32}H_{62}N_4O_2Cu$ (598.42)	81—82	N 9.36 Cu 10.62	N 9.30 Cu 10.88
f1	heißem Äthanol (Rötlichviolette Nädelchen)	$C_{20}H_{22}N_4O_2Cu$ (413.97)	168—169	N 13.53 Cu 15.35	N 13.33 Cu 15.38
f2	Äthanol (Rötlichviolette Nadeln)	$C_{36}H_{34}N_4O_2Cu$ (498.13)	101—102	N 11.25 Cu 12.76	N 11.06 Cu 12.88
f3	Äthanol (Hellviolette Nadeln)	$C_{26}H_{54}N_4O_2Cu$ (638.40)	76—77	N 8.78 Cu 9.95	N 8.90 Cu 9.86

† **2 b1** sintert bei 62—63°C, **2 b2** bei 62—63°C, **2 c3** bei 83—85°C. Die mit * versehenen Chelate kann man auch aus heißem Äthanol analysenrein umkristallisieren, wenn man schnell arbeitet.

BULLETIN OF THE CHEMICAL SOCIETY OF JAPAN VOL. 42 3021—3022 (1969)

Rotational Isomers in Two Crystalline Phases of *N*-Methylchloroacetamide

Tatsuo MIYAZAWA

Institute for Protein Research, Osaka University, Kita-ku, Osaka

(Received April 4, 1969)

In a previous investigation by Mizushima *et al.*[1] the internal rotation about the CH_2-CO bond was studied for *N*-methylchloroacetamide, $ClCH_2$-$CONHCH_3$, a model molecule of polypeptide chains. The infrared and Raman spectra and dipole moments were measured and the *trans* and *gauche* isomers (see Fig. 1 of Ref. 1) were found to coexist in the liquid phase.

1) S. Mizushima, T. Shimanouchi, I. Ichishima, T. Miyazawa, I. Nakagawa and T. Araki, *J. Am. Chem. Soc.*, **78**, 2038 (1956).

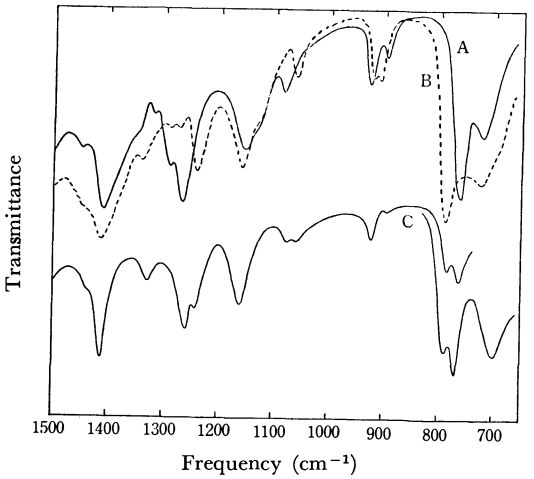

Fig. 1. Infrared spectra of solid films (at 20°C), (A) slowly cooled from the melt, (B) rapidly cooled from the melt, and liquid film (C) at 60°C. A Baird Infrared Spectrophotometer was used for absorption measurements.

In the present infrared study, however, two different spectra were obtained, one (A) for the solid film slowly cooled from the melt and the other one (B) for the solid film rapidly cooled from the melt (C). As seen in Fig. 1, these solid films A and B exhibit the infrared bands of the *gauche* (763 cm^{-1}) and *trans* isomer (786 cm^{-1}), respectively, of *N*-methylchloroacetamide. Apparently, the solid film A (with the *gauche* isomer) is stable at room temperature, while the solid film B (with the *trans* isomer) is metastable after being quenched.

The temperature effect on the infrared absorption of *N*-methylchloroacetamide was carefully observed; a narrow spectral region 950—870 cm^{-1} was repeatedly scanned while the sample temperature was lowered from 65°C down to 9°C in 75 min and subsequently was raised back to 63°C in 65 min. Reversible spectral changes (C)⇌(B)⇌(A) were observed and the transition point was found at about 38°C between the high-temperature phase (with the *trans* isomer) and the low-temperature phase (with the *gauche* isomer). Thus, *N*-methylchloroacetamide exhibits a new type of phase transition that is accompanied with the internal-rotation transition (*trans*↔*gauche*) of constituent molecules. The presence of the *gauche* molecules in the low-temperature phase was recently confirmed by an X-ray analysis of the crystal structure.[2)]

2) Y. Koyama, T. Shimanouchi and Y. Iitaka, Preprints for the 22nd Annual Meeting of the Chemical Society of Japan (Tokyo, April, 1969), 01602.

BULLETIN OF THE CHEMICAL SOCIETY OF JAPAN VOL. 42 3022—3023 (1969)

Preparation of Ethyl 19-Bromononadecanoate by a Mixed Coupling Reaction

Yasuo SUHARA and Shoji MIYAZAKI

Government Chemical Industrial Research Institute, Tokyo, Shibuya-ku, Tokyo

(Received April 10, 1969)

Woolford *et al.*[1] prepared several long-chain ω-bromofatty esters from mixtures of ω-bromofatty acids and methyl hydrogen esters by a mixed coupling reaction. However, the yields of the desired cross-coupling products were generally low, and it was difficult to separate the coupling products by distillation. Therefore, two modifications of the procedure were attempted in this investigation: A) the ethyl hydrogen ester[2] was used instead of the methyl hydrogen ester and B) the coupling products were separated by column chromatography, not by distillation.

In the present investigation, 5: 1 to 1 : 5 mixtures of 11-bromoundecanoic acid (I) and ethyl hydrogen sebacate (II) were used for the electrolysis. By the electrolysis, ethyl 19-bromononadecanoate (III), 1,20-dibromoeicosane (IV), and diethyl octadecanedioate (V) were obtained as the coupling products. The coupling products were successfully separated by column chromatography on silica gel.

The lowest yield of III (29%) was given by an equimolar mixture of I and II, but the yield was increased when an excess of I or II was employed. The best yield in the present experiments was 54%; it was obtained from a 1 : 5 mixture of I and II. The largest amount of III, however, was given by an equimolar mixture of I and II.

For the identification of the coupling products, TLC on silca gel was preferable to GLC. Their R_f-values were as follows: IV, 0.80; III, 0.47; V, 0.25 (methyl ethyl sebacate, 0.37; methyl 11-bromoundecanoate, 0.15).

1) R. G. Woolford, W. Arbic and A. Rosser, *Can. J. Chem.*, **42**, 1788 (1964).

2) H. Agata and A. Tanaka, *Yakugaku Zasshi (J. Pharm. Soc. Japan)*, **76**, 960 (1956).

The IR spectrum of III showed bands at 1740 cm^{-1} (ester carbonyl group) and 645 cm^{-1} (C–Br linkage[3]). The NMR spectrum of III showed chemical shifts at 5.96 τ (F), 6.68 τ (A), 7.81 τ (E), 8.19 τ (B), 8.46 τ (D), 8.73 τ (C), and 8.77 τ (G).

$$\underset{A}{Br}\underset{B}{CH_2}\underset{C}{CH_2}(\underset{D}{CH_2})_{14}\underset{E}{CH_2}\underset{F}{CH_2}\underset{G}{COOCH_2CH_3}$$

Experimental

TLC was conducted on a silica-gel plate (0.25 mm, Merck, G, No. 7731), with ligroin (bp 85—115°C)-acetone (50 : 1, v/v) as the solvent. For the detection of the spots, the plate was sprayed with a 10% phosphomolybdic acid-ethanol solution and then heated at 140°C.

The IR spectra were recorded with a Perkin-Elmer 337 Grating Infrared Spectrophotometer in a KBr disk.

The NMR spectra were recorded with a Varian 100-HA Spectrometer for a 10% carbon tetrachloride solution, with tetramethylsilane as the internal reference.

Materials. The I was prepared from 10-undecenoic acid.[4] Mp, 52°C (50°C[4]). The II was obtained from sebacic acid and diethyl sebacate.[5] Bp, 150—154°C/1 mmHg (bp 183—187°C/6 mmHg[5]); mp 35.5—36.5°C (34—36°C[5]).

The IV was prepared from I by electrolysis,[6] and the crude product was recrystallized from ligroin with small amounts of silica gel for decolorization. Mp, 68.5—69°C (67.4—68°C[7]). The V was prepared from II by electrolysis. The crude product was distilled *in vacuo*, and a fraction boiling at 192—194°C at 1 mmHg was recrystallized from ethanol. Mp, 47—47.5°C (46.9—47.8°C[8]).

Procedures. The cell used was a 500 m*l* measuring cylinder fitted with a thermometer and two parallel platinum plates electrodes (4×3 cm) placed about 2 mm apart. The cell was surrounded with ice water to maintain the internal temperature within the range of 40—45°C.

Three and eithteen hundredth grams of I (0.012 mol), 13.82 g of II (0.06 mol), and 0.16 g of sodium (0.007 atom) were dissolved in 176 m*l* of methanol. A current of about 1.5 A was passed through for three times the theoretical time while the mixture was being stirred with a magnetic stirrer.

After the unreacted materials had been removed by washing with 5% potassium bicarbonate solution, the product mixture was distilled *in vacuo* to separate the non-coupling products as the distillate. The coupling products remaining as a residue (9.2 g) were separated by column chromatography on silica gel (110 g), with ligroin as the solvent.

The first fraction, melting at 65—68°C, was recrystallized from ligroin; white plate crystals were thus obtained. The crystals, which melted at 68.5—69°C, were shown to be IV by a study of their TLC, IR, and NMR spectra. The yield was 8% based on the moles of I employed. A mixed-melting-point determination with an authentic sample showed no depression.

The second fraction, melting at 47—49°C was recrystallized from ethanol; white flaky crystals were thus obtained. The crystals, which melted at 49.5—50°C, were shown to be III by elemental analysis, and by a study of their TLC, IR, and NMR spectra. The yield was 54% based on the moles of I employed.

Found: C, 62.40; H, 10.26; Br, 19.55%. Calcd for $C_{21}H_{41}O_2Br$: C, 62.21; H, 10.19; Br, 19.71%.

The third fraction, melting at 43—46°C, was distilled *in vacuo*; the distillate was recrystallized from ethanol to obtain white large flaky crystals. The crystals, which melted at 47—47.5°C, were shown to be V by a study of their TLC, IR, and NMR spectra. The yield was 57% based on the moles of II employed. A mixed-melting-point determination with an authentic sample showed no depression.

We are grateful to Mr. Masaru Yanagisawa for recording the NMR spectra, to Dr. Osamu Yamamoto for his helpful comments on the NMR spectra, and to Kajio Matsuoka and Sukehide Tsuchiya for their assistance in our experimental work.

3) L. J. Bellamy, "The Infra-red Spectra of Complex Molecules," Methuen & Co., Ltd., London (1958), p. 331.

4) R. Ashton and J. C. Smith, *J. Chem. Soc.*, **1934**, 435.

5) Y. Iwakura and K. Uno, "Yuki-kagobutsu Gosei-ho (Organic Syntheses, Japan)," Vol. 10, Giho-do, Tokyo (1958), p. 47.

6) R. G. Woolford, *Can. J. Chem.*, **40**, 1846 (1962).

7) H. Korshing, *Chem. Ber.*, **86**, 943 (1953).

8) V. N. Belov, E. K. Smol'yaninova, E. A. Ogordnikova, V. M. Rodionov, N. P. Solov'eva, G. E. Svadkovskaya and N. N. Shevyakova, *Trudy Vsesoyuz. Nauch.-Issledovatel. Inst. Sintet. i Natural. Dushistykh Veshchestv*, **1958**, No. 4, 3; *Chem. Abstr.*, **53**, 15969a (1959).

BULLETIN OF THE CHEMICAL SOCIETY OF JAPAN VOL. 42 3024—3026 (1969)

Studies on Heterocyclic Chemistry. IV.[1] Preparation of Several Trifluoromethyl-substituted Heterocyclic Compounds and Observation of Metastable Ion in the Mass Spectra of Trifluoromethyl-pyrazoles

Tarozaemon NISHIWAKI

Department of Chemistry, Faculty of Arts and Sciences, Yamaguchi University, Yamaguchi

(Received April 11, 1969)

From a continued interest in mass spectrometry of heterocyclic compounds,[2,3] the preparation of trifluoromethyl-substituted heterocyclic compounds and determination of their mass spectra were considered. As it is known that trifluoromethyl-substituted benzene compounds eliminate CF_2 radical during a series of their electron-impact-induced decompositions,[4] it seemed interesting to see if this behaviour also holds for heterocyclic compounds.

Trifluoromethyl-pyrimidines (I, II, IV, V, VI) and trifluoromethyl-pyrazoles*1 (VII, IX, X) were prepared by standard procedures. New β-diketones (XI, XII) which are their precursors were obtained according to Reid and Calvin.[5] Fluorine analysis of XII was not sufficient to be recorded here, but its authenticity is established by its transformation into VI and IX.

Contrary to expectation, the spectra of the examined compounds (I, II, IV, VII, IX, X), where the molecular ion (M^+) is the base peak, have not the $(M-CF_2)^+$ ion at all, which is in line with the observation on trifluoromethylpyridines.[6]

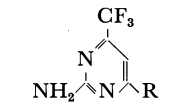

I R=Me
II R=Ph
III R=C_6D_5
IV R=2-Thienyl
V R=2-Furyl
VI R=C_6H_4Me-*p*

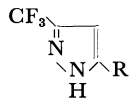

VII R=Ph
VIII R=C_6D_5
IX R=C_6H_4Me-*p*
X R=2-Thienyl

$RCOCH_2COCF_3$ XI R=C_6D_5; XII R=C_6H_4Me-*p*

It appears that loss of CF_2 radical from M^+ or its fragment ions takes place only in the benzene compounds. All of them have ions $(M-F)^+$, $(M-CF_3)^+$, and CF_3^+ as expected, and the fragmentation of the present pyrimidines can be nicely explained after the established patterns,[2,7] namely, loss of F and HF from M^+ competing with the elimination of HCN for I, or elimination of HF occurring after the loss of H from M^+ for II*2 and IV as supported by an appropriate metastable ion.

However, the pyrazole compounds (VII and X) have an interesting ion at (M-48) (Table). A low-intensity metastable ion observed in both spectra (*ca. m/e* 127 for VII and *ca. m/e* 132.5 for X) suggests that this might be generated in one step. An *m/e* 164 ion observed for VII shifts to *m/e* 169 for its pentadeuteriated analogue (VIII), where a metastable ion can be seen at *ca. m/e* 131.5, revealing no participation of benzene hydrogens in the lost 48 masses, and, further, retention of a phenyl group in the (M–48). Among several possible ion compositions to fulfill the *m/e* 48, N_2HF is the only rational one to agree with the observed labeling data. Further, exact mass measurements could establish the lost entity to be solely N_2HF for X. A metastable ion correspond-

1) Part III, T. Nishiwaki, *Tetrahedron Letters*, **1969**, 2049.

2) T. Nishiwaki, *Tetrahedron*, **23**, 1153 (1967).

3) T. Nishiwaki, *ibid.*, **25**, 747 (1969).

4) H. Budzikiewicz, C. Djerassi and D. H. Williams, "Mass Spectrometry of Organic Compounds," Holden-Day, San Francisco (1967), p. 441.

*1 Structures of the pyrazoles are written without implication on tautomerism.

5) J. Reid and M. Calvin, *J. Am. Chem. Soc.*, **72**, 2948 (1950).

6) Y. Kobayashi, F. Nakano and E. Chinen, *Chem. Pharm. Bull. (Tokyo)*, **15**, 1901 (1967).

7) J. M. Rice, G. O. Dudek and M. Barber, *J. Am. Chem. Soc.*, **87**, 4569 (1965).

*2 As previously shown,[2] labeling data can establish that the lost hydrogen from M^+ originates from the benzene hydrogens. But the structure of the resulting ion is not considered to be as simple as that suggested for the (M–1) of phenylphthalazine.[8] The fact that 2-amino-4-phenyl-6-methylpyrimidine shows a very intense(M–1),[2] while 4-phenyl-6-methylpyrimidine does not,[9] suggests this fragmentation to be closely associated with the presence of a functional group, at which the collapse of M^+ starts. It is likely that the pyrimidine ring has already lost its identity in the (M–1) ion.

8) J. H. Bowie, T. G. Cooks, P. F. Donaghue, J. A. Halleday and H. J. Rodda, *Aust. J. Chem.*, **20**, 2677 (1967).

9) T. Kato, H. Yamanaka, T. Chiba, K. Ichikawa, S. Sasaki and E. Abe, Abstracts of the 4th Symposium on the Mass Spectrometry of Organic Compounds, Nagoya (1968), p. 51.

Table 1. Partial mass spectra of I, II, IV, VII, IX, and X[a)]

	M-F	$M-CF_3$	CF_3	$M-N_2HF$	$M-N_2H$
I	10	22	12	—	—
II	6	3	4	—	—
IV	7	2	13	—	—
VII	8	34	7	22	6
IX[b)]	45	62	—[c)]	23[d)]	17[e)]
X	7	8	19	28	3[g)]

a) Intensity is relative to the base peak. b) The spectrum (70 eV) was taken with a CEC-110-B spectrometer by a direct insertion procedure. c) Omitted from tabulation. d) Found: 178.059. Calcd for $C_{11}H_3F_2$: 178.060. e) Found: 197.058. Calcd for $C_{11}H_3F_3$: 197.058. f) Found: 169.996. Calcd for $C_8H_4F_2S$: 170.000. g) Found: 188.997. Calcd for $C_8H_4F_3S$: 188.999.

ing to the process $M^+ \rightarrow (M-48)^+$ was not well discerned in the spectrum of IX, which is probably due to its being recorded on a photographic plate, but the *m/e* 178 was exactly $(M-N_2HF)^+$.

One step loss of N_2HF from M^+, which does not exist as a structural entity in the original molecule, is rather surprising unless there operates a fluorine migration to a remote N_2H group. Fluorine shift can not necessarily be ruled out.[10] However, the $(M-F)^+$ and $(M-N_2H)^+$ ions are found in all spectra of VII, IX, and X, although metastable ions for the process $(M-F)^+ \rightarrow (M-N_2HF)^+$ and $(M-N_2H)^+ \rightarrow (M-N_2HF)^+$ are entirely absent. The most reasonable explanation is that loss of F and N_2H from M^+ is a slow step, both of the resulting ions $(M-F)^+$ and $(M-N_2H)^+$ rapidly lead to the $(M-N_2HF)^+$. The overall result thus appears to be one-step elimination of N_2HF with an accompanying metastable ion. Similar observations have been described recently.[11-13]

Experimental

Mass spectra were determined with a Hitachi RMU 6D mass spectrometer fitted with an all glass inlet system: ionization energy, 80 eV; total ion currents, 80 μA; ion source and inlet system temperature, 200°C. Exact mass measurements were carried out with a CEC-110-B spectrometer at 70 eV on a photographic plate. d_6-Benzene (99% isotopic purity) was purchased from Chiba Product.

Preparation of the Pyrimidines. The preparation of II is given as an example. Benzoyltrifluoroacetone (1.08 g) and guanidine carbonate (0.5 g) were melted in an oil bath (140—150°C) for 1 hr. After cooling a solid (0.80 g) was obtained and recrystallized from *n*-heptane as colorless needles, mp 133—133.5°C.

Found: C, 55.22; H, 3.42; N, 17.30%. Calcd for $C_{11}H_8F_3N_3$: C, 55.23; 3.37; N, 17.57%.

The following compounds were prepared by a similar procedure. I, mp 129°C (from cyclohexane), (Found: C, 40.83; H, 3.77; N, 23.59%. Calcd for $C_6H_6F_3N_3$: C, 40.68; H, 3.41; N, 23.73%); IV, mp 160—160.5°C (from cyclohexane), (Found: C, 44.37; H, 2.60; N, 16.90%. Calcd for $C_9H_6F_3N_3S$: C, 44.08; H, 2.45; N, 17.14%); V, mp 148°C (from *n*-heptane), (Found: N, 18.50%. Calcd for $C_9H_6F_3N_3O$: N, 18.34%); VI, mp 171—172°C (from petroleum ether), (Found: N, 16.37%. Calcd for $C_{12}H_{10}F_3N_3$: N, 16.60%).

Preparation of the Pyrazoles. The preparation of VII is given as an example. Benzoyltrifluoroacetone (0.30 g) and hydrazine hydrate (0.8 m*l*) were heated in water (1 m*l*) for 1 hr in a boiling water bath. Precipitates (0.23 g) were recrystallized from cyclohexane as colorless rectangular plates, mp 121—123°C.

Found: N, 13.13%. Calcd for $C_{10}H_7F_3N_2$: N, 13.21%.

The following compounds were prepared by a similar procedure. IX, mp 165—166°C (from cyclohexane), (Found: N, 12.39%. Calcd for $C_{11}H_9F_3N_2$: N, 12.44%); X, mp 118—120°C (from petroleum ether), (Found: N, 12.83%. Calcd for $C_8H_5F_3N_2S$: N, 12.84%).

Compound XI. To a stirred solution of d_6-benzene (4.0 g) in carbon disulfide (20 m*l*) anhydrous aluminum chloride (15.0 g) was added, and into the gently refluxing mixture acetic anhydride (4.1 g) was added and reflux was continued for 1 hr. After removing the solvent the residue was poured into a mixture of ice and hydrochloric acid and the organic matter was extracted with ether. The ethereal solution was washed with water, 10% aqueous sodium hydroxide, and water, dried ($CaCl_2$) and distilled (bp 50—54°C/1 mmHg) to give d_5-acetophenone, 1.8 g. To a stirred mixture of sodium methoxide (0.82 g) in anhydrous ether (15 m*l*) ethyl trifluoroacetate (2.1 g) was added. Homogeneous solution resulted, into which the above acetophenone (1.8 g) was added and stirred for 2 hr at room temperature. The following day any volatile material was removed *in vacuo* and the residue was acidified with 10% sulfuric acid. Precipitates were dried under reduced pressure to give almost pure β-diketone, mp 39—41°C, 2.0 g. Undeuteriated compound had mp 39—40.5°C.[5] Isotopic purity was d_5, 63%; d_4, 26%; d_3, 8%; d_2, 3% neglecting a small (M-1) (R.I. 2%) observed in the undeuteriated compound, where the base peak was CF_3^+. This β-diketone was condensed with hydrazine hydrate to VIII, mp 120—121°C (d_5, 68%; d_4, 27%; d_3, 4%; d_2, 1%) and

10) P. Brown and C. Djerassi, *Angew. Chem.*, **79**, 481 (1967).
11) Ref. 4, p. 29
12) E. Caspi, J. Wicha and A. Mandelbaum, *Chem. Commun.*, **1967**, 1161.
13) F. G. Holliman, R. A. W. Johnstone and B. J. Millard, *J. Chem. Soc., C*, **1967**, 2351.

guanidine carbonate to III, mp 131°C.

p-Toluoyltrifluoroacetone (XII) was prepared by a similar procedure and had bp 96—100°C/2 mmHg, mp 43—44.5°C. Analysis indicated the presence of impurity.

I wish to thank Mr. Nobuhide Wasada, the Government Institute of Technology, Tokyo, for his help in high resolution mass spectrometry.

BULLETIN OF THE CHEMICAL SOCIETY OF JAPAN VOL. 42 3026—3028 (1969)

Monoterpene Constituents of the Essential Oil of Mitsuba (*Cryptotaenia japonica* Hassk.)

Shûichi HAYASHI, Toshiko OKUDA and Tamon MATSUURA

Department of Chemistry, Faculty of Science, Hiroshima University, Higashisenda-machi, Hiroshima

(Received April 17, 1969)

Mitsuba, *Cryptotaenia japonica* Hassk., which is an herb of the Umbelliferae family, is cultivated as a vegetable in Japan for its fresh flavor. The chemical constituents of the essential oil of mitsuba have been investigated by Hirao[1] in fairly long ago; he characterized the main component of the monoterpene fraction as a new terpene compound with a structure of 2-methylnonatriene, and he gave it the name "Cryptotaenene." However, its structure still has not been completely established.

The essential oil was obtained in a 0.013% yield by the steam distillation of the whole herb; it was then separated into a monoterpene fraction (26%) and a sesquiterpene fraction (40%).

A gas chromatogram of the monoterpene fraction is shown in Fig. 1.

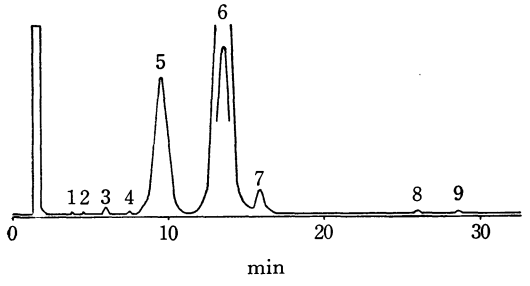

Fig. 1. Gas chromatogram of mitsuba oil at 65°C on Carbowax-6000 - Diasolid L.

The main component of the monoterpene fraction, Peak 6 in Fig. 1, was isolated by preparative gas chromatography as a colorless, oily compound with a characteristic odor. The compound had a molecular formula of $C_{10}H_{16}$ (M^+, m/e 136). Its IR spectrum indicated the presence of a terminal methylene group (890—910 cm^{-1}) and a conjugated diene system (1596 cm^{-1}), and its NMR spectrum showed the presence of two allylic methyl groups (1.59 and 1.67 ppm, each 3H), a vinyl group attributable to an ABX-type split (6.36, 1H, q, J=18, 11; 5.19, 1H, q, J=18, 1.2; 5.00 ppm, 1H, q, J=11 and 1.2 cps), and a terminal methylene group (4.96 ppm, 2H, s). These IR and NMR spectra and its mass spectrum were in good agreement with those[2,3] of β-myrcene.

An adduct of this compound with maleic anhydride and its free acid were found to be identical with those of β-myrcene by a mixed-melting-point determination; moreover, a bromide which was obtained by the reduction of this monoterpene with sodium and alcohol, followed by bromination, showed a melting point corresponding to that of tetrabromide of dihydromyrcene. Thus, it is certain that the main component is β-myrcene.

The components of the 3, 5, and 7 peaks were isolated and identified as α-pinene, (+)-β-pinene, and (−)-limonene respectively on the basis of the measurement of the IR and the mass spectra; the minor components of the 4 and 8 peaks were also identified as camphene and p-cymene by means of gas-chromatographic comparison with authentic specimens. In addition, α-thujene and sabinene were found to be included in Peak 3 or 5 in the gas chromatogram of Carbowax-6000 (Fig. 1).

The relative composition of this essential oil was calculated to be as shown in Table 1 from the peak areas in the gas chromatogram as measured by Carbowax-6000 at 65°C. The main components of the essential oil of *Cryptotaenia japonica* were β-myrcene and (+)-β-pinene.

Hirao's *cyrptotaenene*, which was separated by

1) N. Hirao, *Kogyo Kagaku Zasshi (J. Chem. Soc. Japan, Ind. Chem. Sect.)*, **29**, 48 (1926).

2) G. Ohloff, J. Seibl and E. sz. Kovâts, *Ann. Chem.*, **675**, 83 (1964); B. M. Mitzner, E. T. Theimer, L. Steinbach and J. Walt, *J. Org. Chem.*, **30**, 646 (1965).

3) A. F. Thomas and B. Willhalm, *Helv. Chim. Acta*, **47**, 475 (1964); R. Ryhage and E. von Sydow, *Acta Chem. Scand.*, **17**, 2025 (1963).

Table 1. Monoterpene hydrocarbons of the essential oil of *Cryptotaenia japonica*

No. of peak in Fig. 1	Compound identified	Retention time*		Relative content (%)
		Apiezon L	β,β'-Hydroxydipropionitrile	
1	unidentified	—	—	trace
2	unidentified	—	—	trace
3	α-pinene	7.80	5.20	1.5
	α-thujene	6.90	5.95	trace
4	camphene	8.95	7.15	0.1
5	(+)-β-pinene	10.50	8.80	34.9
	sabinene	9.35	11.65	trace
6	β-myrcene	9.10	15.10	56.9
7	(−)-limonene	14.30	15.10	56.9
8	p-cymene	13.35	35.70	trace
9	unidentified	—	—	trace

* Operating condition. Apiezon L: 110°C, N_2 17 ml/min; β,β'-hydroxydipropionitrile: 60°C, N_2 15 ml/min.

fractional distillation only and which was characterized as a new terpene hydrocarbon on the basis of the difference of its physical properties from those of β-myrcene, seems to be β-myrcene contaminated with a small amount of (+)-β-pinene; this conclusion is based on the closeness of the boiling points of β-myrcene and β-pinene. This view is also supported by a comparison of the physical constants of cryptotaenene, bp 67—68°C/15 mmHg, $[\alpha]_D^{19.8}$ +2.66°, d_4^{25} 0.8128, n_D^{25} 1.47476, with those of β-myrcene and β-pinene.

Experimental

For the measurement of the gas chromatograms, a Shimadzu GC-2B apparatus equipped with a hydrogen-flame-ionization detector was used in combination with three kinds of separation columns (4 mm×3 m): Carbowax-6000 on Diasolid L (3%), Apiezon L on Gas-Chrom P (4.6%), and β,β'-hydroxydipropionitrile on Diasolid H (10%). Preparative gas chromatography was carried out by using Carbowax-6000 on Celite (20%) (8 mm×3 m). The NMR spectrum was measured in a $CDCl_3$ solution.

Steam Distillation of the Essential Oil. Mitsuba (1323 kg) cultivated in the suburbs of Hiroshima City was harvested, together with its roots, in May, 1966, by which time it had grown to a height of 40—50 cm. It was air-dried in the shade for several hours and then distilled with steam. In addition to an oil (I) (104 g, d_4^{25} 0.8637, $[\alpha]_D^{25}$ +52.44°, n_D^{25} 1.4888) floating upon the distilled water, an oil (II) (68 g, d_4^{25} 1.1101, n_D^{25} 1.4831) was obtained by extracting the distilled water with ether and chloroform. In the present experiment, the oil (I) (100 g) was fractionated into thirty-four fractions *in vacuo*; the monoterpene fractions (Fr. 1—11), bp 82—140°C/50 mmHg, totaled 26.46 g, and the sesquiterpene fractions (Fr. 12—34), bp 84.5—168.0°C/3 mmHg, 40.30 g.

α-Pinene and α-Thujene (Peak 3). The hydrocarbon, $C_{10}H_{16}$ (M^+, *m/e* 136), was isolated by the preparative gas chromatography of Fr. 2 (4.1 g, $[\alpha]_D^{18}$ +13.5°, 9% content of α-pinene). Its IR and mass spectra were in good agreement with those of α-pinene;[3,4] its identity was also confirmed by gas-chromatographic comparison with an authentic specimen, a comparison which was carried out by the use of three separation columns.

When the isolated hydrocarbon was re-gaschromatographed with Apiezon L or β,β'-hydroxydipropionitrile, it showed a small peak in addition to the main peak of α-pinene (*cf.* the third and fourth columns in Table 1). This small peak was assigned to α-thujene on the basis of a comparison with an authentic specimen.

(+)-β-Pinene and Sabinene (Peak 5). The hydrocarbon, $C_{10}H_{16}$ (M^+, *m/e* 136), was isolated from Fr. 2. Its IR and mass spectra and gas chromatogram were in good agreement with those of β-pinene.[3,4] In gas chromatography using Apiezon L or β,β'-hydroxydipropionitrile, this isolated hydrocarbon exhibited a small peak in addition to the main peak of β-pinene; this small peak was assigned to sabinene by using an authentic specimen.

The β-pinene in the essential oil was classified as *d*-form on the basis of the positive optical rotation of Fr. 3 containing 66% of β-pinene ($[\alpha]_D^{18}$ +14.7°).

β-Myrcene (Peak 6). The component was separated from Fr. 7 (3.7 g, $[\alpha]_D^{18}$ −1.4°). Its IR ν_{max}: 3080, 1792, 1633, 1596, 1378, 1104, 989, 902, 890 and 820 cm^{-1}. Its mass spectrum: *m/e* 136 (M^+, 3.9%), 93 (82.8), 69 (64.5) and 41 (100).

Maleic Anhydride Adduct and Its Dibasic Acid. To 2.5 g of Fr. 6 containing 85% of Peak 6, 1.7 g of maleic anhydride was added; the mixture, after having been allowed to stand for two days at room temperature in a tightly-corked tube, was distilled to obtain a maleic anhydride adduct (bp 158—164°C/2 mmHg, 2.86 g), mp 28—30°C.[5] Its IR ν_{max}: 1835 and 1772 cm^{-1}. This adduct, after being dissolved in ether, was treated with 3% aqueous solution of sodium hydroxide in order to convert it into free acid (1.24 g), which was obtained as white needles, mp 122—123°C, in recrystallization from acetone. No depression was observed in a mixed-

4) L. Friedmann and A. P. Wolf, *J. Am. Chem. Soc.*, **80**, 2424 (1958).

5) L. Ruzick, *Helv. Chim. Acta*, **19**, 423 (1936).

melting-point determination with an authentic specimen; mp 122—123°C.[5]

Tetrabromodihydromyrcene. 2.0 g of Fr. 7 containing 96% of Peak 6 was reduced with sodium (1.3 g) in absolute ethanol (15 m*l*) to obtain an oily product (bp 83—84°C/5 mmHg, 1.79 g). Its IR ν_{max}: 1660 and 823 cm^{-1}. The bromination of the product furnished a light yellow mass which showed a mp of 91.0—91.5°C[6] after being recrystallized from ethanol and ether. Its IR ν_{max}: 1370 and 1363 cm^{-1}.

(−)-Limonene (Peak 7). The hydrocarbon was isolated as an unreacted oil in the maleic anhydride-treatment of Fr. 10 (0.6 g, $[\alpha]_D^{18}$ −58.56°), which was contaminated with 10% of *β*-myrcene. It was gas-chromatographically identical with limonene; its IR and mass spectra also coincided with those of limonene.[3,4]

Camphene and *p*-Cymene. Although no attempt was made to isolate these compounds because of their minor components, the 4 and 8 peaks were identified as camphene and *p*-cymene respectively by comparison with authentic specimens in gas chromatography using the three separation columns.

The authors are deeply indebted to Professor Shô Itô of Tohoku University for his kind measurement of the NMR spectrum.

6) F. W. Semmler, *Ber.*, **34**, 3126 (1901).

BULLETIN OF THE CHEMICAL SOCIETY OF JAPAN VOL. 42 3028—3029 (1969)

The NMR Study of Poly-L-Prolines I and II

Rume SAKAI,*1 Hirofumi OKABAYASHI and Toshizo ISEMURA

Division of Physical Chemistry, Institute for Protein Research, Osaka University, Kita-ku, Osaka

(Received April 22, 1969)

As is well known, poly-L-proline (PLP) takes two different helical structures, the so-called I and II forms, which were established by the X-ray diffraction method; one is a right-handed helix and the peptide bonds are in a *cis* configuration,[1] whereas the other is left-handed, with the peptide bonds *trans*.[2]

The rotation about the Cα–N bond of L-proline is severely restricted because the Cα–N bond participates in a pyrrolidine ring. The rotation about the Cα–CO bond of PLP is also definitely restricted by the steric hindrance, as can be verified by using atomic models.[3] According to Steinberg *et al.*[3] the hydrogen atom attached to the alpha carbon is restricted to the *cis* or the *trans* position in relation to the C–O bond, although the configurations have some rotational freedom around the Cα–CO bond.

Both helices of the poly-L-prolines take nearly the *trans* configuration about this bond. The *cis* configuration, in regard to the bond of PLP, is expected to exist only in a concentrated salt solution of lithium bromide[3] or calcium chloride.[4]

On the other hand, the conformation and the transconformation of PLP in solutions[5] have been studied by using its optical-active properties, such as ORD[6] or CD,[7] and its hydrodynamic property.[3] The results have shown that the poly-L-proline takes the PLP-I and II-helices in solutions, unlike the homo-polypeptides of the other α, L-amino acid. Moreover, it has been also reported that poly-L-α, amino acids show different nuclear magnetic resonance spectra because of their conformations.[8] Therefore, the study of PLP by the NMR method is interesting in that the confromational characteristics of PLP should be reflected in the NMR spectrum. The NMR method may also give us additional information on the property of PLP in solutions.

This communication will describe how poly-L-prolines have different NMR spectra according to their conformations. The poly-L-proline has the I-helical form immediately after the sample was dissolved in acetic acid. However, it changed into the II-helix within two weeks after dissolution when kept at 25°C. The value of $[\alpha]_{546}^{25}$ was

*1 Present address: Graduate Department of Biochemistry, Brandeis University, Waltham, Mass., U. S. A.

1) W. Traub and U. Shmueli, "Aspects of Protein Structure," ed. by G. N. Ramachandran, Academic Press, New York (1963), p. 81.

2) P. Cowan and S. McGavin, *Nature*, **176**, 501 (1955).

3) I. Z. Steinberg, W. F. Harrington, A. Berger, M. Sela and E. Katchalski, *J. Am. Chem. Soc.*, **82**, 5263 (1960).

4) M. L. Tiffany and S. Krimm, *Biopolymers*, **6**, 1767 (1968).

5) E. Katchalski, A. Berger and J. Kurtz, "Aspects of Protein Structure," ed. by G. N. Ramachandran, Academic Press, New York (1963), p. 205.

6) F. A. Bovey and F. P. Hood, *J. Am. Chem. Soc.*, **88**, 2326 (1966).

7) F. A. Bovey and F. P. Hood, *Biopolymers*, **5**, 325 (1967).

8) F. A. Bovey, G. V. D. Tiers and G. Filipovich, *J. Polymer Sci.*, **38**, 73 (1959); W. E. Stewart, L. Mandelkern and R. E. Glick, *Biochemistry*, **6**, 143 (1967); J. A. Ferretti, *Chem. Commun.*, **1967**, 1030.

ca. +50°C for the I-helix and *ca.* −550° for the II-helix.[9] The conformation of PLP in the mixed solvent (CD_3COOD : $CDCl_3$=1 : 8) is considered to be a PLP-I-like helix, in which the value of $[\alpha]_{546}$ is +30°C and invariable. The NMR spectrum of the PLP-I-helical structure is shown in Fig. 1. A PLP solution which had a value of $[\alpha]_{546}$=−560° after the sample had been dissolved in an acetic acid and kept for two weeks was used for measuring the NMR spectrum of the PLP-II-helical structure, as is also shown in Fig. 1. The peak assignments were made from the ratios of the areas of the peaks; they are also shown in Fig. 1.

The magnetic shielding values of the hydrogen atoms a), b)-c), and d) for the poly-L-proline which has the PLP-I-helix were 5.5, 7.8—8.0, and 6.3_{ppm} respectively. The values for the PLP-II-helix were 5.2_3, 7.9_{ppm}, and 6.2_5 respectively.

The values for the peaks of the hydrogen atoms b)-c) and d) depend little on their conformations. However, the value of the hydrogen atom a) for the I-helix was in a field up by 0.3_{ppm} from that for the II-helix. The chemical shift of the αCH in the NMR spectra of the two poly-L-prolines seems to be influenced more by the configuration of the peptide group on the imino side than that on the carbonyl side; in both helices of the poly-L-prolines the hydrogen atom a) is nearly in the *trans* position relative to the C=O, where the chemical shift of αCH peaks is assumed to be decided by the relative position of the preceding or the following carbonyl group.

The difference between the magnetic shielding values of the αCH in the *cis* and *trans* configurations of the peptide groups is similar to that found for the N-CH_3 of *N*-methylformamide[10] in benzene,

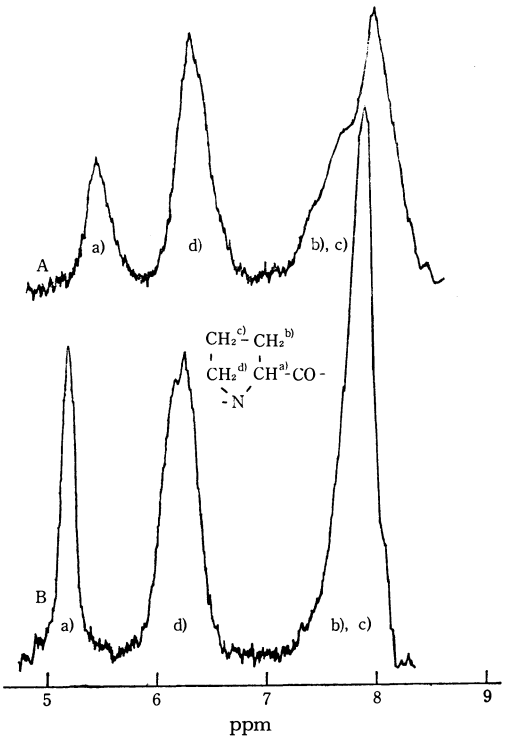

Fig. 1. The NMR spectra of poly-L-prolines I and II.
A: poly-L-proline I (solvent, $CDCl_3$: CD_3COOD =8 : 1).
B: poly-L-proline II (solvent, CD_3COOD).
Reference; TMS.
a), b), c) and d) show the assignment of the hydrogen atoms of pyrrolidine ring.

where the solvent-solute interaction is involved. The difference in the shielding values of the αCH peaks of the two poly-L-prolines can be used in the study of the *trans*-conformation of PLP.

It should also be mentioned that, during the I ⇌ II transition of the poly-L-prolines, two αCH peaks were observed at 5.2 and 5.5_{ppm}; the ratios of the areas of the two peaks changed with time.

9) T. Isemura, S. Ikeda and O. Maeda, *Nippon Kagaku Zasshi (J. Chem. Soc. Japan, Pure Chem. Sect.)*, **88**, 421 (1967).

10) D. G. de Kowalewski and V. J. Kowalewski, *Arkiv. for Kemi.*, **16**, 373 (1960).

BULLETIN OF THE CHEMICAL SOCIETY OF JAPAN VOL. 42 3030—3032 (1969)

Quenching of Rubicene Fluorescence by Amines

Akira NAKAJIMA*1 and Hideo AKAMATU

Department of Chemistry, Faculty of Science, The University of Tokyo, Hongo, Bunkyo-ku, Tokyo

(Received May 6, 1969)

In a previous paper,[1] the charge transfer (CT) interaction between an excited fluorescer and a quencher was shown to play a significant part in the mechanism of fluorescence quenching on the basis of the correlation between the quenching constants and the electron affinities of quenchers. A study was made on quenching of fluorescence of anthracene and pyrene by electron-accepting substances. With the purpose of clarifying further the inner quenching mechanism, the present work was carried out for the systems of rubicene and various amines, where excited rubicene may be considered as an electron-acceptor and amines as electron-donors. Amines have been known to be effective quenchers, and if their large quenching abilities can be attributed to their strong electron-donating powers, it will be expected that in combinations of a given fluorescer and a series of amines their effective quenching radii are related to their ionization potentials.

The advantage in dealing with these systems is that rubicene fluoresces at a relatively long wavelength (553 mμ) and the amines employed scarecely absorb the exciting light (436 mμ), so that the possibility of the trivial "quenching" caused by the inner filter effect and the waste of exciting light can be excluded to permit one to make a more reliable discussion.

Experimental

Rubicene was synthesized from fluorenone[2] and recrystallized several times from toluene. The absorption spectrum of this sample agreed with that given in literature.[3] The liquid amines were fractionally distilled in a nitrogen atmosphere under reduced pressure after being dried with potassium hydroxide, and the crystalline amines were recrystallized and sublimed in a vacuum. Such amines as are very apt to be colored were purified by repeated distillations or sublimations in a vacuum until they became colorless. Toluene was distilled once from a G. R. grade reagent and used as a solvent for the measurement of fluorescence. For the observation of CT bands, spectro-grade carbon tetrachloride was used as a solvent and purified chloranil was employed as an electron-acceptor.

The apparatus and the procedure were almost the same as described in the previous paper.[1] The excitation wavelength was selected at 4358Å Hg line with a Bausch & Lomb grating monochromator. The concentration of rubicene was 4.96×10^{-5} mol/*l*.

Results and Discussion

The ionization potentials of the amines were estimated by making use of the CT absorption bands of chloranil complexes with these amines. It is well known that for a given electron-acceptor the CT absorption maximum, $h\nu_{CT}$, can be related to the ionization potential of a donor, I_p, as follows:[4]

$$h\nu_{CT} = aI_p + b$$

where a and b are the constants to be determined experimentally. Since the interaction between an aliphatic amine and chloranil (n–π interaction) may be different from that between an aromatic amine and chloranil (π–π interaction), the two cases should be treated separately.[4] Using those amines whose ionization potentials had been measured directly,[5] the following relations were obtained by the method of least squares:

$$h\nu_{CT} = 0.60\, I_p - 2.58 \text{ (eV)} \quad \text{(aliphatic)}$$

$$h\nu_{CT} = 0.45\, I_p - 1.32 \text{ (eV)} \quad \text{(aromatic)}$$

From these the ionization potentials of the other amines were estimated.[6] The I_p-values thus obtained as well as the positions of the CT bands observed are given in Table 1.

The quenching constants were evaluated from the Stern-Volmer equation:[7]

*1 Present address: Research Institute of Applied Electricity, Hokkaido University, Sapporo.

1) A. Nakajima and H. Akamatu, This Bulletin, **41**, 1961 (1968).

2) E. Clar, "Aromatische Kohlenwasserstoffe," Springer, Berlin (1952).

3) R. A. Friedel and M. Orchin, "Ultraviolet Spectra of Aromatic Compounds," John Wiley & Sons, New York (1951).

4) G. Briegleb, "Elektronen-Donator-Acceptor-Komplexe," Springer, Berlin (1961); J. Rose, "Molecular Complexes," Pergamon, London (1967).

5) V. I. Vedeneyev, L. V. Gurvich, V. N. Kondrat'yev, V. A. Medvedev and Ye. L. Frankevich, "Bond Energies, Ionization Potentials and Electron Affinities," Edward Arnold, London (1966); A. Terenin and F. Vilessov, "Adv. in Photochem.," Vol. 2, ed. by W. A. Noyes *et al.*, Interscience, New York (1964), p. 385.

6) G. Briegleb, *Angew. Chem.*, **76**, 326 (1964); P. Farrell, *J. Phys. Chem.*, **69**, 3506 (1965).

7) Th. Förster, "Fluoreszenz Organischer Verbindungen," Vandenhoeck und Ruprecht, Göttingen (1951).

TABLE 1. THE POSITION OF CT BANDS, THE IONIZATION POTENTIALS, THE QUENCHING CONSTANTS AND THE EFFECTIVE QUENCHING RADII FOR THE AMINES

No.	Compound	Position of CT-band (mμ)	Position of CT-band (eV)	I_p (eV)	k (l/mol)	(γR) (Å)
1	*N,N,N',N'*-Tetramethyl-*p*-phenylenediamine	890	1.39	5.97	121	82.5
2	*N,N,N',N'*-Tetramethylbenzidine	848	1.46	6.12	96	74.1
3	*N,N*-Dimethyl-*p*-phenylenediamine	868	1.42	6.04	109	69.1
4	*p*-Phenylenediamine	760	1.64	6.52	108	61.1
5	Benzidine	690	1.82	6.87	77	53.6
6	*N,N*-Dimethyl-β-naphthylamine	750	1.65	6.54	62	42.3
7	*o*-Phenylenediamine	620	1.99	7.29	58	32.8
8	*N,N*-Diethylaniline	725	1.71	6.67*	46.7	31.7
9	*N,N*-Dimethylaniline	641	1.93	7.14*	51	31.3
10	α-Naphthylamine	646	1.92	7.30*	46.8	29.1
11	*m*-Phenylenediamine	630	1.97	7.26	50	28.3
12	*N*-Methylaniline	600	2.07	7.34*	47	27.2
13	*N,N'*-Diphenylethylenediamine	608	2.03	7.38	32.2	23.6
14	*N*-Phenyl-β-naphthylamine	710	1.75	6.76	32.7	23.4
15	*p*-Toluidine	584	2.12	7.50*	40	23.1
16	*o*-Anisidine	584	2.12	7.57	37.2	22.0
17	*N*-Phenyl-α-naphthylamine	701	1.76	6.78	30.2	21.6
18	Diphenylamine	653	1.90	7.25*	13.7	9.3
19	Tri-*n*-butylamine	711	1.74	7.22	11.8	8.9
20	Triethylamine	660	1.87	7.85*	12.6	7.7
21	Aniline	570	2.18	7.70*	8.8	4.9
22	Diethylenetriamine	530	2.34	8.23	2.4	1.4
23	*N,N*-Dimethylbenzylamine	500	2.48	8.45	1.7	1.1
24	Triphenylamine	710	1.74	6.68*	0.8	0.6
	Diethylamine	558	2.22	8.01*	—	—

* Directly measured ionization potentials taken from Ref. 5, used for determining the values of a and b.

$$I_0/I = 1 + k[Q]$$

where I_0 and I are the fluorescence intensities respectively in the absence and presence of the quencher. The slopes of the plots of $(I_0-I)/I$ against [Q], the concentration of quencher, give the quenching constants, k, which are listed in Table 1.

Since the absorption spectrum of rubicene was not affected by the addition of an amine, it may be considered that a dynamical quenching process is predominant and the interaction of rubicene in the ground state with an amine is very small, but in the excited state, quite large.

For dynamical quenching, the quenching constant is approximated by the following formula:[7,8]

$$k = 4\pi N'\tau D(\gamma R)$$

where τ is the fluorescence life-time of rubicene in the absence of a quencher, N' is the number of the fluorescent molecules per millimol, *i. e.*, 6.02×10^{20}, D is the relative diffusion constant in toluene, *i. e.*, the sum of the diffusion constants for rubicene and a quencher, and (γR) represents the effective quenching radius. τ was estimated by the relation $\tau=\tau_0\phi$,[*2] where τ_0 is the natural life-time evaluated from the absorption spectrum of rubicene, and ϕ_0 is the fluorescence quantum yield of rubicene determined by comparing it with that of perylene in a degassed benzene solution.[9] The diffusion constants of the fluorescer and the quenchers were estimated by the method of Othmer and Thaker.[10] The (γR)-values obtained from the above formula are also listed in Table 1.

Since the effective quenching radius of a quencher can be reasonably taken as a measure for its quenching ability, it is of great interest to plot the effective quenching radii, (γR), against the ionization potentials, I_p, which is shown in Fig. 1.

As is seen from the figure, a good correlation can be recognized between (γR) and I_p; that is, the lower the ionization potential of an amine, the larger its effective quenching radius. This fact suggests that the charge transfer or electron trans-

8) A. Weller, *Z. physik. Chem., N. F.*, **13**, 335 (1957).

*2 Our values were: $\phi=0.18$, $\tau_0=7.05\times 10^{-9}$ sec; therefore, $\tau=1.27\times 10^{-9}$ sec.

9) J. B. Birks, *Proc. Roy. Soc.*, **A275**, 135 (1963).

10) D. F. Othmer and M. S. Thaker, *Ind. Eng. Chem.*, **45**, 589 (1953).

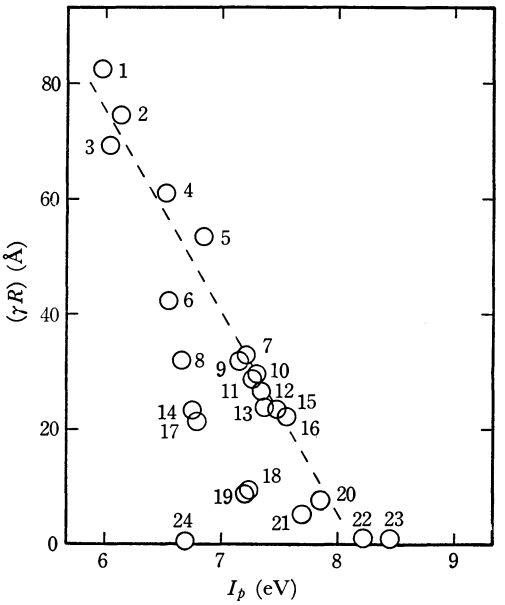

Fig. 1. Relation between the ionization potentials and the effective quenching radii of the amines. Numerals refer to the respective numbers of the compounds in Table 1. The broken curve is drawn tentatively.

fer mechanism[11] is especiallyi mportant for fluorescence quenching.

Because the absorption spectra of the amines and the fluorescence spectrum of rubicene do not overlap at all, the energy transfer mechanism,[12] in which excited rubicene is an energy-donor and amines are energy-acceptors, can be left out of account. The trend observed can not be explained by the mechanism of external heavy-atom effect, in which rubicene in the singlet excited state is converted into the triplet state.

As one can see from Fig. 1, the (γR)-values for some *N*-substituted amines*3 are considerably smaller than those expected from their I_p-values. This may be interpreted in terms of a kind of steric effect; *e. g.*, the steric effect of the massive groups attached to the nitrogen atom. A remarkable example is found in triphenylamine, whose molecular structure may be unfavorable for an interaction.

The relationship between (γR) and I_p will be useful for estimating the ionization potential of an amine from its (γR)-value.

The authors wish to thank Professor Hiroaki Baba for some valuable advice in preparing the manuscript.

11) H. Leonhardt and A. Weller, "Luminescence of Organic and Inorganic Materials," ed. by H. Kallman and G. Spruch, John Wiley & Sons, New York (1962). p. 74.

12) Th. Förster, *Discussions Faraday Soc.*, **27**, 7 (1959).

*3 Those compounds (Nos. 8, 14, 17, 18, 19, 24) that lie extraordinarily lower than the tentatively drawn curve in Fig. 1.

BULLETIN OF THE CHEMICAL SOCIETY OF JAPAN VOL. 42 3032—3034 (1969)

Electronic Absorption Spectra of Cation Radicals of *p*-Dialkoxybenzenes in Concentrated Sulfuric Acid

Katsumi KIMURA*[1] and Hikoichiro YAMADA

Department of Chemistry, Faculty of Engineering Science, Osaka University, Toyonaka, Osaka

(Received May 6, 1969)

The cation radicals of *p*-dialkoxybenzenes produced by different methods of oxidation have been studied mainly with ESR technique:[1-4] Oxidations have been performed with concentrated sulfuric acid,[1] lead tetra-acetate-boron trifluoride in dichloromethane,[2] aluminum chloride in nitromethane[3] and polarographically.[4]

This note is concerned with the electronic absorption spectra of cation radicals formed from several *p*-dialkoxybenzenes (hydroquinone, *p*-methoxyphenol, *p*-dimethoxybenzene, *p*-ethoxyphenol, *p*-

*1 Present address: Physical Chemistry Laboratory, Research Institute of Applied Electricity, Hokkaido University, Sapporo.

1) W. F. Forbes and P. D. Sullivan, *Can. J. Chem.*, **44**, 1501 (1966); A. B. Barabas, W. F. Forbes and P. D. Sullivan, *ibid.*, **45**, 267 (1967); P. D. Sullivan and J. R. Bolton, *J. Am. Chem. Soc.*, **90**, 5366 (1968).

2) D. L. Allara, B. C. Gilbert and R. O. C. Norman, *Chem. Commun.*, **1965**, 319.

3) W. F. Forbes and P. D. Sullivan, *J. Am. Chem. Soc.*, **88**, 2862 (1966); W. F. Forbes, P. D. Sullivan and H. M. Wang, *ibid.*, **89**, 2705 (1967); P. D. Sullivan, *ibid.*, **89**, 4294 (1967).

4) A. Zweig, W. G. Hodgson and W. H. Jura, *ibid.*, **86**, 4124 (1964).

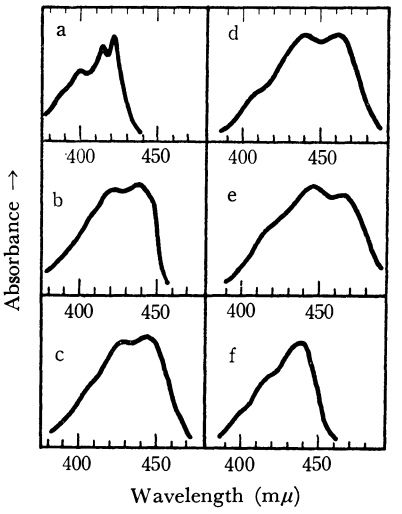

Fig. 1. Electronic absorption bands of the cation radicals of various *p*-dialkoxybenzenes in concentrated sulfuric acid at room temperature.
a) [hydroquinone]$^+$, b) [*p*-methoxyphenol]$^+$, c) [*p*-ethoxyphenol]$^+$, d) [*p*-dimethoxybenzene]$^+$, e) [*p*-diethoxybenzene]$^+$ and f) [2,3,5-trimethylhydroquinone]$^+$.

diethoxybenzene and 2,3,5-trimethylhydroquinone) in concentrated sulfuric acid. The electronic absorption bands of the cation redicals of these compounds in concentrated sulfuric acid were first measured (Fig. 1). These spectra may be ascribed to the cation radicals of the *p*-dialkyoxybenzenes, since the solution of hydroquinone gives an ESR spectrum identical to that already assigned to the cation.[1)]

In order to confirm the existence of the cation radicals, the absorption band obtained by the oxidation with concentrated sulfuric acid (Method 1) from *p*-dimethoxybenzene was compared with the absorption spectra which were obtained by other methods of oxidation: oxidation with $SbCl_5$ in acetonitrile at room temperature (Method 2), and photo-oxidation in a deaerated transparent rigid matrix of the mixture of concentrated sulfuric acid and glacial acetic acid at 77°K (Method 3). It was found that the electronic absorption bands around 450 mμ obtained by these three kinds of oxidation are very similar to one another. The absorption band obtained through photo-oxidation (Method 3) has been reported.[5)] However, in the present work, the photo-oxidation study has been carried out by means of optical absorption as well as ESR technique. The photolyzed solution was confirmed to have the ESR spectrum with the same hyperfine structure as that reported,[1)] when the photolyzed rigid solution is warmed up to room temperature.

It is interesting to note that when a concentrated sulfuric-acid solution of *p*-dimethoxybenzene was bubbled with nitrogen gas in order to remove oxygen, neither electronic absorption in the visible region nor the ESR spectrum of the cation was detected. This indicates that the oxygen molecule participates in the oxidation of the compound in concentrated sulfuric acid.

The cations of the compounds studied here are iso-electronic to one another, as well as to Würster's cations. Thus it seems that the absorption bands obtained herewith are similar to the long wavelength bands of Würster's cations. Electronic spectra of the cations of several aminophenols have been studied by Kimura *et al.*,[6)] and shifts in wavelength of the absorption spectrum from the absorption spectrum of the *p*-phenylenediamine cation were interpreted in terms of ionization-potential differences of the substituents by using a first-order perturbation theory. The same situation may occur in the case of the cations of *p*-dialkoxybenzenes. Let us consider how the ionization potential of a substituent affects the transition energy of the hydroquinone cation. Expressing its MO's with linear combinations of $2p\pi$ AO's ($\varphi_i=\sum_\mu c_{i\mu}\phi_i$), energies of the MO's may be given by $\varepsilon_i=\sum_{\mu\nu}c_{i\mu}c_{i\nu}F_{\mu\nu}$, where $F_{\mu\nu}$'s are Fock-Hamiltonian elements. Assuming the same molecular orbitals for all these cations to

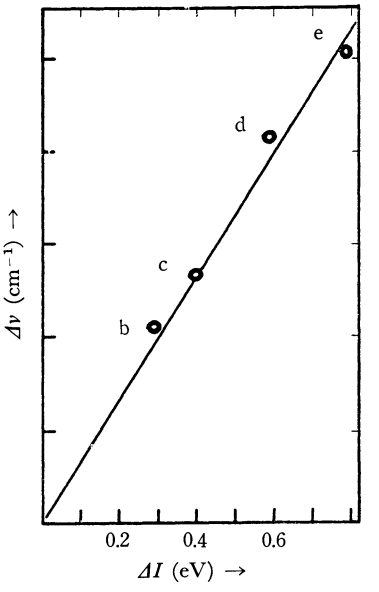

Fig. 2. The shifts of the longest absorption bands of the several cations from that of the hydroquinone cation are plotted against the ionization-potential differences of substituents.
b) [*p*-methoxyphenol]$^+$, c) [*p*-ethoxyphenol]$^+$, d) [*p*-dimethoxybenzene]$^+$ and e) [*p*-diethoxybenzene]$^+$.

5) H. Tsubomura, K. Kimura, H. Yamada and M. Kato, *Tetrahedron Letters*, **47**, 4217 (1965).

6) K. Kimura, K. Yoshinaga and H. Tsubomura, *J. Phys. Chem.*, **71**, 4485 (1967).

the first approximation and taking only the differences ΔI_1 and ΔI_2 in the valence-state ionization potentials of two substituents at the *para* position into account, we find that the resulting differences in transition energy may be proportional to $\Delta I_1 + \Delta I_2$. This means that the effect of two substituents at the *para* position can be expressed as the sum of the ionization potentials of the substituents. In Fig. 2, the shifts ($\Delta\nu$ in cm^{-1} units) of the longest absorption bands of the several cations from that of the hydroquinone cation are plotted against the ionization-potential differences of the substituents (ΔI in eV units). In this calculation, values for ionization potentials of the hydroxy, methoxy and ethoxy groups were taken from those used in the previous calculations of phenol, anisole and phenetole.[7] It is seen from Fig. 2 that a good linearity is obtained between the band shift and the ionization potential difference.

Experimental

Commercial materials of the compounds studied; *e. g.*, hydroquinone, *p*-methoxyphenol, *p*-dimethoxybenzene, *p*-ethoxyphenol, *p*-diethoxybenzene and 2,3,5-trimethylhydroquinone were purified by vacuum sublimation. Commercial $SbCl_5$, sulfuric acid (95%), and glacial acetic acid of G. R. grade were used without further purification. Acetonitrile was distilled after reflux and dehydration on P_2O_5.

Measurement of electronic absorption spectra was carried out with a Cary spectrophotometer Model 15. ESR spectra were measured by a JES-3BX ESR spectrometer at 100 kc/s modulation.

We are grateful to Professor H. Tsubomura for his valuable discussion.

7) K. Kimura and S. Nagakura, *Mol. Phys.*, **9**, 117 (1965).

BULLETIN OF THE CHEMICAL SOCIETY OF JAPAN VOL. 42 3034—3035 (1969)

Nuclear Quadrupole Resonance in *syn*- and *anti*-7-Chloronorbornene

Hideaki CHIHARA and Nobuo NAKAMURA

Department of Chemistry, Faculty of Science, Osaka University, Toyonaka, Osaka

and Tadashi IRIE

Shionogi Research Laboratory, Shionogi and Co., Ltd., Fukushima-ku, Osaka

(Received May 14, 1969)

Norbornenyl halides and other derivatives show unusual rate effects in their solvolysis reactions:[1] *syn*-7-chloronorbornene (II) and its saturated analog (I) solvolyze in aqueous ethanol at comparable rates, whereas the *anti*-isomer (III) solvolyzes some 10^5 faster than I and II under the same conditions.[2] These and other large variations in the reaction rate in norbornenyl systems have been interpreted in terms either of the "*participation*" of the neighboring π-bond electrons in the initial carbonium ion formation or of some modification of the bridgehead molecular structure due to steric effects of the large substituents.[1]

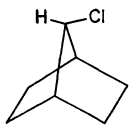

I

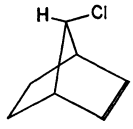

II

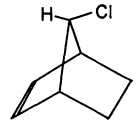

III

To examine if such isomeric rate effect is associated with the nature of the C–Cl bonds or the valence state of carbon atom, we have measured the nuclear quadrupole resonance frequencies of ^{35}Cl in II and III. The details of the experimental procedures have been reported.[3]

The experimental results are given in Table 1, from which we recognize that two crystallographically nonequivalent molecules exist in each of the compounds II and III. The mean value of the resonance frequencies in II is some 860 kHz larger than that of III but their absolute values fall in the range generally found in compounds of the type $(CH_3)_nCH_{3-n}Cl$.[4] This means that the C–Cl bonds in II and III themselves are not unusual. On the other hand, the difference in the resonance frequencies in II and III seems to be significant,

1) H. Tanida, *Accounts of Chemical Research*, **1**, 239 (1968) and the references therein.

2) W. G. Woods, R. A. Carboni and J. D. Roberts, *J. Am. Chem. Soc.*, **78**, 5653 (1956).

3) H. Chihara, N. Nakamura, H. Ōkuma and S. Seki, This Bulletin, **41**, 1809 (1968).

4) E. I. Fedin and G. K. Semin, "Use of Nuclear Quadrupole Resonance in Chemical Crystallography II," in "The Mössbauer Effect and its Applications in Chemistry," Consultants Bureau Enterprises, Inc., New York (1964).

Table 1. The nuclear quadrupole resonance frequencies of ^{35}Cl at liquid nitrogen temperature

Substance	Resonance frequency (kHz)
syn-7-Chloronorbornene (II)	33016.3±0.2 33026.2±0.1
anti-7-Chloronorbornene (III)	32125.2±0.1 32191.4±0.1

because the intermolecular contributions to the NQR frequencies of chlorine bonded to carbon atoms are relatively small and vary regularly from compound to compound.[5]

The difference between the mean resonance frequencies of II and III may be attributed to a change in the hybridization of the C–Cl bond. Thus, in the case of simple molecules such as $CH_{4-n}X_n$ and $(CH_3)_nCH_{3-n}X$ (X=Cl, Br or I), it can easily be confirmed from $J(^{13}C\text{–}H)$ data[6] or from molecular geometry that the halogen nuclear quadrupole coupling constant in C–X bond increases with an increase in the *s*-character of the carbon atomic orbital bonded to the halogen atom.[7] On applying this relation to the case of the compounds II and III, we see that the *s*-character of the carbon atomic orbital in the C–Cl bond in II is larger than that in III and this trend agrees qualitatively with the direction of the shift of $J(^{13}C\text{–}H)$ observed in these two compounds[8] and in some similar compounds.[9] Such a difference in the carbon *s*-character is probably due to distortion of the C–Cl bond originating from the repulsion between the bulky chlorine atom and the carbon π-orbital in II although some delocalization of the π-electrons in III cannot be entirely excluded.[9]

Although both the NQR frequencies and $J(^{13}C\text{–}H)$ data can be explained consistently by the change in the carbon hybridization as mentioned above, the question of how the large reaction rate effect in 7-norbornenyl system can be interpreted by such a mechanism remains unclarified.

Another explanation for the difference of the NQR frequencies is to assume that a weak hydrogen bond is operating between the bridge carbon and the π-electrons. This makes the chlorine in III more electronegative than in II *via* the inductive effect between the hydrogen and the chlorine. In other words the chlorine in III is more ionic than in II and is more susceptible to solvolysis. Actually these two alternative explanations are compatible and are probably both correct. Though their relative significance is unknown, they complement each other in making the chlorine resonance displaced to a lower frequency in III.

The authors wish to thank Drs. K. Tori and H. Tanida of the Shionogi Research Laboratory for their helpful discussion.

5) See, for example, D. Biedenkapp and A. Weiss, *Ber. Bunsenges. Physik. Chem.*, **70**, 788 (1966); W. J. Considine, *J. Chem. Phys.*, **44**, 4036 (1966).

6) The *s*-character of the carbon hybrid orbital involved in the C–H bond is proportional to $J(^{13}C\text{–}H)$; see C. Juan and H. S. Gutowsky, *J. Chem. Phys.*, **37**, 2198 (1962).

7) A qualitative account for the relation between the carbon *s*-character and the NQR frequencies is as follows: From the point of view of Jaffe's electronegativity scheme (J. Hinze *et al.*, *J. Am. Chem. Soc.*, **84**, 540 (1962); *ibid.*, **85**, 148 (1963)), the increase in the *s*-character of the carbon orbital tends to increase the carbon orbital electronegativity. Therefore, the amount of the electron transfer, necessary for matching the orbital electronegativities, from the carbon hybrid orbital to the chlorine orbital may decrease and so the number of the unbalanced *p*-electrons at the chlorine increases, with the result of a higher NQR frequency.

8) M. Ueyama and K. Tori, private communication. The coupling constants, $J(^{13}C\text{–}H)$'s, between the bridge carbon and the hydrogen bonded to it were determined to be 156.5±1 Hz and 164.2±1 Hz for II and III, respectively.

9) K. Tori, S. Sato, T. Tsushima and H. Tanida, Abstract for the 6th Conference on Nuclear Magnetic Resonance, Kyoto (1967).

BULLETIN OF THE CHEMICAL SOCIETY OF JAPAN VOL. 42 3036—3037 (1969)

Dissociation Pressure of Ferric Oxide

Kumasaburo KODERA, Isao KUSUNOKI and Minoru WATANABE*1

Department of Chemistry, Faculty of Science, Kyoto University, Sakyo-ku, Kyoto

(Received May 20, 1969)

The dissociation pressure of various oxides was measured in a high vacuum, and the results were found to be in good agreement with the values calculated from standard free energy data.[1] However, it was also found that all metallic oxides evolved a large amount of carbon monoxide and carbon dioxide at lower temperatures.

Direct measurement of the oxygen dissociation pressure of ferric oxide at high temperatures is desirable. It is of interest to study the evolution of gases during the course of the reduction of ferric oxide by vacuum heat teratment.[2]

In the present experiment, the equilibrium pressures of ferric oxide and the desorbed gases have been measured with a McLeod gauge and the percentage compositions of the gases have been investigated by means of an omegatron mass spectrometer.

Experimental

The apparatus was similar to that described previously.[1] The sample of ferric oxide (α-type, diamagnetic) was a Merk reagent of extra pure grade (Germany) and was used without further purification.

Measurements were carried out under various initial conditions of the samples. In the first run, a freshly powdered sample of about 500 mg was placed in the decomposition cell and evacuated for a day in a high vacuum at room temperature. The sample was then heated to 300°C. The equilibrium pressure of the evolved gases was measured by a McLeod gauge and analyzed by an omegatron mass spectrometer. A similar procedure was repeated at temperatures from 300 to 1200°C. The sample which was heated to 1200°C in the first run was cooled in a vacuum and used again in the second run. The same procedure was repeated in the second run. Replacing the sample with a new one, the measurement was repeated several times.

Results and Discussion

Carbon dioxide, methane, and water were evolved from the new samples below 600°C and in some cases total pressure of these gases amounted to 10^{-3} Torr. However, the evolution of these gases decreased after the first vacuum heat treatment, and the reproducibility of the equilibrium pressures could not be obtained in different runs. On the other hand, the amount of carbon monoxide increased with the oxygen evolution at higher temperature and reproducible equilibrium pressure was attained ($P_{CO}=2\times10^{-2}$ Torr at 1150°C).

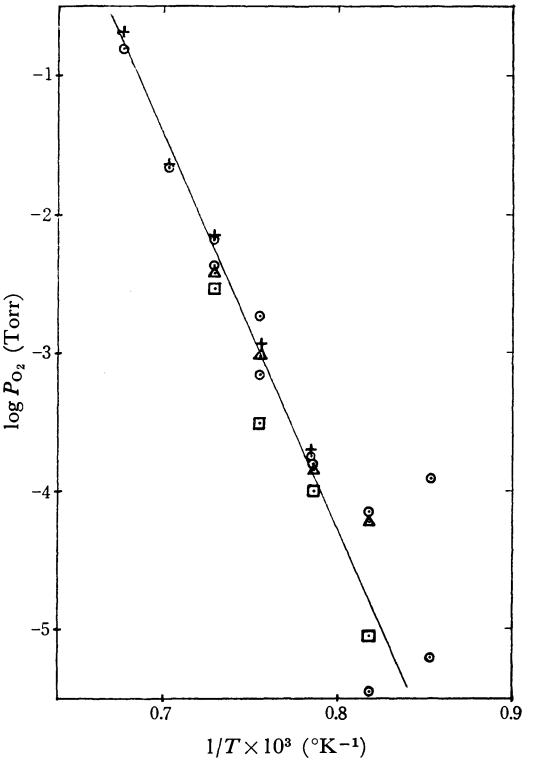

Fig. 1. Dissociation pressure of ferric oxide *vs.* $1/T$.
The values of different symbols show different runs.

Oxygen gas resulting from thermal decomposition can be observed above 900°C. In Fig. 1 the equilibrium pressures of oxygen are plotted against the reciprocal of the absolute temperatures. The straight line obtained in Fig. 1 can be represented by the following equation.

$$\log P_{O_2}\ (\text{Torr}) = -\frac{28.5}{T}\times10^3 + 18.5 \qquad (1)$$

*1 Present address: Tokyo Shibaura Electric Co.

1) K. Kodera, I. Kusunoki and S. Shimizu, This Bulletin, **41**, 1039 (1968); *Nippon Kagaku Zasshi (J. Chem. Soc. Japan, Pure Chem. Sect.)*, **86**, 814 (1965).

2) M. Onchi and I. Kusunoki, *Nippon Kagaku Zasshi (J. Chem. Soc. Japan, Pure Chem. Sect.)*, **85**, 612, 619 (1964).

The sample treated in the second run was analyzed by means of X-ray diffraction and confirmed to be a mixture of oxides Fe_2O_3 and Fe_3O_4. On the other hand, it was confirmed by X-ray analysis that the sample evacuated in vacuum at 1200°C for a day transformed into magnetite (Fe_3O_4, ferromagnetic). The sample did not evolve oxygen gas further at 1200°C. This result is consistent with the report[3] in which the preparation of Fe_3O_4 by heating Fe_2O_3 up to 1300°C in a vacuum was described.

Thus the reaction in the present experiment may be written as

$$6Fe_2O_3(s) \rightleftarrows 4Fe_3O_4(s) + O_2, \quad (2)$$

and the standard free energy change, $\Delta G°$, for the reaction may be given by

$$\Delta G°(\text{cal}) = 130600 - 71.51T. \quad (3)$$

On the other hand, the value obtained by Richardson and Jefes[4] is shown as

$$\Delta G°(\text{cal}) = 119240 - 67.24T. \quad (4)$$

These values are in good agreement in the temperature range of measurement.

3) L. Brewer and D. Mastick, *J. Chem. Phys.*, **19**, 834 (1951).

4) F. D. Richardson and J. H. E. Jefes, *J. Iron Steel Inst.*, **160**, 261 (1948); **163**, 397 (1947).

SHORT COMMUNICATIONS

A New Alkaloid from *Aconitum sachalinense* Fr. Schmidt

Yoshiyuki ICHINOHE and Makiko YAMAGUCHI

Department of Chemistry, Faculty of Science and Engineering, Nihon University, Narashinodai, Funabashi, Chiba

(Received July 17, 1969)

It has been known that the roots of *Aconitum sachalinense* Fr. Schmidt, which is found throughout southern Sakhalin, contain two alkaloids, jesaconitine $C_{35}H_{49}O_{12}N$ (I) and kobusine $C_{20}H_{27}O_2N$ (II).[1]

This paper will report on the isolation of a further new toxic alkaloid, III, belonging to the group having a aconitine-type skeleton, from the same plant and from *Aconitum sachalinense* Fr. Schmidt var.*1

The III alkaloid was crystallized as its perchlorate (IV) mp 254—256°C (dec.), $[\alpha]_D$ −12° (Found: C, 52.49; H, 6.59%. Calcd for $C_{34}H_{47}O_{12}N\cdot HClO_4$: C, 52.26; H, 6.34%, from the mother liquor after the isolation of I and II. The hydrolysis of the amorphous base III with methanolic potassium hydroxide gave anisic acid, acetic acid (characterized as the silver salt), and an amorphous alkamine, V. V gave the crystalline hydrochloride (VI) (mp 174—179°C) and also the crystalline pentaacetyl derivative (VII), mp 240.5—241.5°C (Found: C, 58.62, 58.64; H, 7.01, 7.02%. Calcd for $C_{34}H_{49}O_{14}N$: C, 58.69; H, 7.09%), on acetylation with acetyl chloride.

From the above experiments, eight out of twelve oxygen atoms in the new alkaloid, III, have been shown to be present in the form of an acetyl group, an anisoyl group, and three free hydroxyl groups. In general, alkaloids with toxic aconitine-type skeletons have several methoxyl groups. The presence of four methoxyl groups in the V alkamine has been confirmed by the micro-Zeisel determination. The permanganate oxidation of anisoyltetraacetylalkamine (VIII) (mp 198—202°C), obtained by the acetylation of III with acetyl chloride, gave formaldehyde (characterized as the dimedone derivative), as in mesaconitine (IX)[2] or hypaconitine (X)[3]. This suggests the presence of an *N*-methyl group in III.

The above evidence shows that the formula of III may be extended as follows:

$$C_{19}H_{19}\begin{cases}(OCH_3)_4\\(OH)_3\\OCOCH_3\\OCOC_6H_4OCH_3(p)\\N\text{-}CH_3\end{cases}$$

As with other alkaloids in the aconitine group, the pyrolytic reaction of the new base, III, gave a pyro-base upon the elimination of the acetic acid. Although the molecular formula and the functional groups of the V alkamine corresponded to those of mesaconine, the alkamine from mesaconitine IX, VII and pentaacetylmesaconine were found to be different by comparisons of their IR spectra and melting points. It is very likely the new alkaloid, III, is an epimer with regard to a secondary hydroxyl or a methoxyl group of mesaconine.

The structural study of the new alkaloid, III, is now in progress.

1) H. Suginome and S. Imato, *J. Fac. Sci., Hokkaido Univ. Ser. III Chem.*, **4**, 35 (1950).

*1 This species is distributed over northern Hokkaido. It contains jesaconitine, kobusine, *etc.*, as does the original species.

2) K. Tamura, *Ann.*, **533**, 183 (1938).

3) R. Majima and K. Tamura, *ibid.*, **526**, 116 (1936).

Bi- and Tri-Nuclear Copper(II) Complexes Derived from Bi- and Tetra-dentate Schiff-base Complexes

Michinobu KATO,* Yoneichiro MUTO,** Hans B. JONASSEN,*** Kyoko IMAI,* Michio KONDO,** Kazuko KATSUKI** and Seishi IKEGAMI**

* *Aichi Prefectural University, Mizuho-ku, Nagoya*

** *Department of Chemistry, Saga University, Saga*

*** *Department of Chemistry, Tulane University, New Orleans, La., U. S. A.*

(Received April 5, 1969)

As an extension of a previous study,[1] we have prepared a large number of copper(II) complexes with bidentate or tetradentate salicylideneimines and the appropriate anions. Tow types of complexes were prepared; the first (Group A), by the reaction of $Cu(Sal\cdot N\text{–}R)_2$ and cupric chloride or nitrate in hot ethanol, where $Sal\cdot N{=}{=}\cdot\overset{1}{O}\cdot C_6H_4\cdot\overset{2}{C}H{=}N\cdot$ and R = various alkyl or substituted phenyl groups; the second (Group B), from the reaction of $Cu(Sal\cdot N\text{–}CH_2CH_2\text{–}N\cdot Sal)$ with cupric chloride, nitrate, or perchlorate under similar conditions. Nearly all of these complexes have subnormal magnetic moments, suggesting the presence of a strong intramolecular spin-spin interaction. Most of them seem to be binuclear, $[Cu(Sal\cdot N\text{–}R)Cl]_2$; however, some complexes of the group B were found to be trinuclear when cupric perchlorate was used.

One of the most significant features of the chloro-complexes of the group A is the existence of a linear relation between the d–d band positions, $\bar{\nu}_{max}$ (cm^{-1}, kK), and the magnetic moments, $\mu_{eff}^{25°C}$ (B.M.), "lower moments——higher energies of d–d bands," where R = alkyl(10—14 kK, 1.5—0.9 B.M.) and substituted phenyl groups (11—12.5 kK, 1.5—1.1 B.M.), which is the same relation as that observed for the binuclear copper(II) halide complexes with substituted pyridine *N*-oxides (9—13.5 kK, 1.2—0.2 B.M.).[1] For *N*-phenyl-complexes *ortho*-substituents in the *N*-phenyl group increase the energies of the singlet-triplet separation and the d–d bands, irrespective of the polar nature of the substituents (CH_3, Cl, and NO_2). This same shielding effect of *ortho*-substituents was found previously for the pyridine *N*-oxide complexes. The chloro-complexes of Group A are mostly dark brown in color; a few, however, are orange with a broad band at longer wavelengths (9—11 kK). The orange complexes do not obey the above linear relation, suggesting a different structure even though they have the same composition as the binuclear complexes, $Cu(Sal\cdot N\text{–}R)Cl$. They also have the lowest moments of the two groups; for example, when $R=CH_3$ (0.90 B.M. orange; 1.5 B.M. brown) and $R=CH_2CH_2CH_2OH$ (1.06 B.M.), *o*- and *p*-NO_2-phenyl (1.06 and 0.97 B.M.), and $Cu(5\text{-}Cl\text{–}Sal\cdot N\text{–}CH_3)Cl$ (0.95 B.M.).

The nitrato-complexes of Group A are, in general, green with the d–d bands at much shorter wavelengths (13.5—15.5 kK) than those of the corresponding chloro-complexes (10—14 kK). They seem to have a phenolic oxygen-bridged binuclear structure; this is based on the observed chemical formula, $Cu(Sal\cdot N\text{–}R)NO_3$, the molecular-weight determination by osmotic pressure measurement, the observation of a bridging phenolic C–O band at 1550—1560 cm^{-1},[2,3] and the low magnetic moments, 1.1—1.4 B.M. Some nitrato-complexes with R = 3-CH_3– and 3-Cl-phenyl (green) or *t*-butyl group (greenish brown) have normal magnetic moments, 1.7—1.8 B.M. These complexes show a non-bridging phenolic C–O band at *ca.* 1530 cm^{-1}, suggesting a monomeric structure.[2,3] However, when R = isopropyl, a trinuclear complex, $2Cu(Sal\cdot N\text{–}R)_2\cdot Cu(NO_3)_2$, was produced, with a normal moment (1.84 B.M. at 19°C). The nitrato-complexes with subnormal magnetic moments did not show the linear relation between $\mu_{eff}^{25°C}$ and $\bar{\nu}_{max}$ which was observed for the corresponding chloro-complexes. This suggests that the dimeric structure of nitrato-complexes differs from that of chloro-complexes.

The binuclear chloro- and nitrato-complexes produced by reaction (2) (Group B) revealed two bands, at 18.5—19.5 kK and 10—11.5 kK, indicating that the environment of the two copper atoms in the molecule is greatly different. However, the bands of the chloro-complexes appeared at longer wavelengths than those of the corresponding nitrato-complexes, and the former exhibited a smaller magnetic interaction (1.5 B.M.) than the latter (1.2—1.3 B.M.). This is essentially the same trend as the linear relation observed for the chloro-complexes of Group A.

1) Y. Muto, M. Kato, H. B. Jonassen and L. C. Cusachs, This Bulletin, **42**, 417 (1969).

2) S. J. Gruber, C. M. Harris and E. Sinn, *J. Inorg. Nucl. Chem.*, **30**, 1805 (1968).

3) C. M. Harris and E. Sinn, *ibid.*, **30**, 2723 (1968).

The Behaviour of Chemisorbed Species under the Reaction Conditions and the Mechanism of the Water-gas Shift Reaction on ZnO and MgO

Akifumi UENO, Toshiki YAMAMOTO, Takaharu ONISHI and Kenzi TAMARU

Department of Chemistry, The University of Tokyo, Hongo, Bunkyo-ku, Tokyo

(Received June 3, 1969)

The importance of adsorption measurements during surface catalysis has previously been emphasized by one of the present authors.[1] The mechanism of the water-gas shift reaction on ZnO and MgO was studied by means of infrared techniques during the course of the reaction. It was found that a surface formate is formed on both of the catalysts as the reaction intermediate. The rate-determining step of this reaction was the decomposition of the surface formate.

When carbon dioxide and hydrogen were conducted onto ZnO at 150°C, the surface formate could be observed by infrared spectroscopy. The isotope shift of the C–H (and C–D) stretching vibration band was observed by employing deuterium gas. It was, however, difficult to find the surface formate in a mixture of carbon monoxide and water vapour on ZnO, though the surface OH group and CO(a) were found to be formed at a considerable rate. The dependence of the optical density of the infrared spectrum of the surface formate upon its coverage was obtained from a comparison of the spectroscopic and volmetric measurements on the adsorption of formic acid. The coverage of the surface formate during the overall reaction was obtained from the optical density.

The rate of the decomposition of the surface formate (v) was examined by means of infrared spectroscopy at the reaction temperature (230°C), forming the surface formate by introducing a known amount of formic acid vapour. Then the rate of the dehydration decomposition (v') was oatained by the following equation; $v'=v\times s$, where s is the selectivity, ([CO]/[CO]+[CO_2]), of the decomposition of the surface formate. It was then compared with the rate of the overall reaction ($H_2+CO_2 \rightarrow CO+H_2O$), v'', as measured by gas chromatographic analysis for the carbon monoxide produced. The two rates were in reasonable agreement within the limits of experimental error, provided the coverage was the same, which leads us to the conclusion that the surface formate is the reaction intermediate of the water-gas shift reaction and that its dehydration decomposition, step (2) in the following scheme, is the rate-determining step.

Run	Rate of overall reaction (v'') cc/g·hr	Rate of dehydration (v') cc/g·hr	Coverage
1	0.023	0.022	0.35
2	0.028	0.025	0.35
3	0.030	0.029	0.41

$$\left.\begin{array}{l} H_2(g) \rightleftarrows 2H(a) \\ CO_2(g) \rightleftarrows CO_2(a) \end{array}\right\} \overset{1)}{\rightleftarrows} HCOO(a) \overset{2)}{\rightleftarrows} H(a)$$

$$\left\{\begin{array}{l} OH(a) \rightleftarrows H_2O(g) \\ CO(a) \rightleftarrows CO(g) \end{array}\right.$$

When a mixture of carbon monoxide and water vapour was introduced over MgO, we confirmed the formation of a surface formate on the catalyst by means of infrared spectroscopy in a manner similar to that used in ZnO, as has been found by Scholten.[2] However, it was found that the surface formate could not be easily observed from a mixture of carbon dioxide and hydrogen on MgO.

We measured the rate of the dehydrogenation decomposition of the surface formate by infrared spectroscopy at 280°C in order to compare it with the overall reaction rate, as measured by gas-chromatographic analysis, for the carbon dioxide produced. As was the case over ZnO, the two rates were in reasonable agreement within the limits of experimental error if the adsorption of surface formate was the reaction intermediate of the reaction on MgO; the rate-determining step was the step of the dehydrogenation decomposition of the surface formate, step (1).

In the water-gas shift reaction over both ZnO and MgO, the change in the adsorptions of water, carbon dioxide, carbon monoxide, and hydrogen did not considerably influence the rate of the decomposition of surface formate under the reaction conditions employed.

1) K. Tamaru, "Adv. Catalysis", Vol. 15 Academic Press, Inc., New York (1964) p. 65; *Nippon Kagaku Zasshi (J. Chem. Soc. Japan, Pure Chem. Sect.)*, **87**, 1007 (1966).

2) J. J. F. Scholten, P. Mars, P. G. Menon and R. van Hardeveld, Proc. 3rd. Int. Congr. Catalysis, Amsterdam, 881 (1964).

Polymerization by the Active Species Produced from the Charge Transfer Complex. IV. Phototerpolymerization of *N*-Vinylpyrrolidone, Maleic Anhydride and Methyl Methacrylate

Hajime TAMURA, Makoto TANAKA and Niro MURATA

Department of Applied Chemistry, College of Engineering, University of Osaka Prefecture, Sakai, Osaka

(Peceived July 19, 1969)

It was found by us that the photo and thermal polymerizations of methyl methacrylate (MMA) were largely accelerated in the presence of both amide and maleic anhydride (MAH) and the acceleration was more effective in air than *in vacuo*. Besides, it was assumed that the radical species initiating the polymerization of MMA was produced *via* the complex between amide and MAH.[1)]

As *N*-vinylpyrrolidone (VPD) is an amide concontaining a vinyl group, it probably interacts with MAH, as a result the complex may participate in polymerization as a monomer unit. Therefore, it is expected that the terpolymerization of VPD, MAH, and MMA is induced by the VPD-MAH complex.

The mixture of VPD and MAH turned yellowish and then pink or scarlet upon UV irradiation. The spectra of the solutions of VPD and MAH in 1,2-dichloroethane are shown in Fig. 1. The results suggest a complex formation between VPD and MAH.

The composition of the VPD-MAH complex was determined by the continuous-variation method,

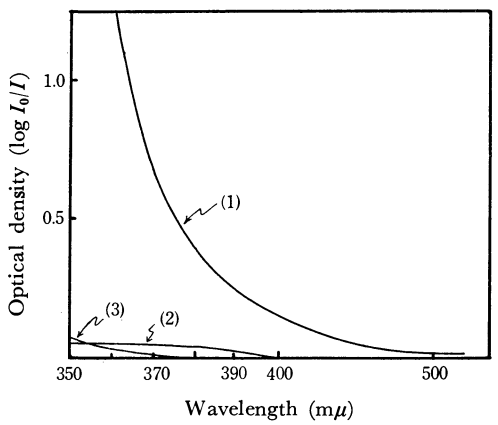

Fig. 1. Absorption spectra of the complex between VPD and MAH.
(1) VPD 1.185 mol/*l* + MAH 0.069 mol/*l*
(2) VPD 1.185 mol/*l*
(3) MAH 0.069 mol/*l*
(solvents, 1,2-dichloroethane)

1) H. Tamura, M. Tanaka and N. Murata, to be published.

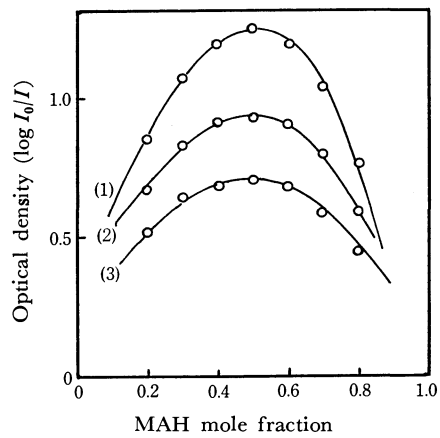

Fig. 2. The continuous variation method of VPD-MAH complex. VPD 0.404 mol/l, MAH 0.400 mol (solvent, chloroform)
(1) 360 mμ (2) 365 mμ (3) 370 mμ

TABLE 1. PHOTOPOLYMERIZATION OF VPD, MAH, AND MMA AT 30°C IN AIR
(polymerization time, 3 hr)

Experimental number	VPD (mol/*l*)	MAH (mol/*l*)	MMA (mol/*l*)	Polymer yield (g)
1	3.75	0.41	5.62	0.421***
*2	3.75	0.41	0	0.120
3	3.75	0	5.62	0.047
*4	0	0.41	5.62	0
**5	3.75	0.41	5.62	0.290

* The total volume was maintained at 5 m*l* by employing benzene instead of MMA or VPD.
** Polymerization was carried out for 2 hr using AIBN (2×10^{-2} mol/*l*) as the initiator.
*** The polymerization in the dark was almost negligible.

the results shown in Fig. 2 were obtained. The curves reached a maximum at the 0.5 mol fraction of MAH, and it was estimated that a 1 : 1 complex was formed between VPD and MAH.

The polymerization of the VPD-MAH-MMA system was induced, in fact, without any initiator, the results of the photopolymerization are shown in Table 1.

Polymerization by the Active Species Produced from the Charge Transfer Complex. V. The Thermal Copolymerization of *N*-Vinyl-pyrrolidone and Methyl Methacrylate

Hajime TAMURA, Makoto TANAKA and Niro MURATA

Department of Applied Chemistry, College of Engineering, University of Osaka Prefecture, Sakai, Osaka

(Received July 31, 1969)

It was previously reported by us[1] that the polymerization of the *N*-vinylpyrrolidone (VPD)-maleic anhydride(MAH)-methyl methacrylate(MMA) ternary system was induced photochemically in air at 30°C without any initiator and that the active species was presumably produced *via* the 1 : 1 complex between VPD and MAH. Furthermore, their polymerizations occurred thermally in air at 70°C.

In the photochemical polymerization, the lack of any one component remarkably lowered the polymer yield, but in the thermal polymerization it was found that the spontaneous copolymerization of VPD and MMA took place simultaneously in air after some induction period and that the copolymerization rate was quite fast, though it was somewhat smaller than that of the ternary system.

Therefore, the following experiments were carried out. The copolymerization of VPD and MMA did not occur at all *in vacuo*. This suggests that oxygen may participate in the reaction of the production of the active species. The copolymers were obtained from mixtures with various ratios of VPD and MMA, and the copolymerization rate was remarkably accelerated by adding a small amount of $ZnCl_2$. Neither VPD nor MMA alone was polymerized under the experimental conditions employed here. The results are shown in Table 1.

TABLE 1. THE SPONTANEOUS COPOLYMERIZATION OF VPD AND MMA AT 70°C

VPD (mol/*l*)	MMA (mol/*l*)	Polymer yield (g)	
		In air (%)*	*In vacuo*
7.50	1.87	0.272 (5.3)	0
6.56	2.81	0.217 (4.3)	0
5.62	3.74	0.419 (8.4)	0
4.68	4.68	0.391 (7.9)	0
**4.68	4.68	2.727 (55.2)	—
3.75	5.62	0.524 (10.7)	0
2.81	6.55	0.221 (4.6)	0
1.87	7.49	0.123 (2.6)	0
***3.75	0	0	—
***0	5.62	0	—

* Weight %-conversion to the total monomer concentration.

** About 0.2 g of $ZnCl_2$ was added to the mixture of VPD and MMA.

*** The total volume was maintained at 5 m*l* employing benzene.

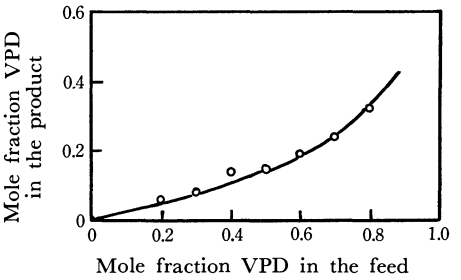

Fig. 1. Composition curve for the VPD-MMA copolymer (in air at 70°C).

It is known that the positive *e*-value of such monomers as MMA and acrylonitrile is elevated by the addition of a Lewis acid such as $ZnCl_2$.[2] Although there is no spectroscopic evidence for thr existence of the VPD-MMA complex, it is possible, judging from these results, that the active species is formed by the reaction of the VPD-MMA complex and oxygen.

The compositions of the copolymers were determined by elemental analysis, while the composition curve for the VPD-MMA copolymer was obtained as is sown in Fig. 1.

The monomer reactivity ratio (M_1=MMA, M_2=VPD) were decided from the Mayo-Lewis plots to be the following: $r_1=4.6\pm0.4$, $r_2=0.02\pm0.02$. The copolymerization of VPD and MMA by a radical initiator (AIBN) at 50°C has already been reported by Bork and Coleman,[3] who obtained the following values: $r_1=4.7\pm0.5$, $r_2=0.005\pm0.05$.

The results we have obtained here are quite consistent with theirs. This suggests that the spontaneous copolymerization of VPD and MMA proceeds by way of a radical mechanism. The details of the study will be reported later.

1) H. Tamura, M. Tanaka and N. Murata, This Bulletin, **42**, 3041 (1969).

2) M. Imoto, T. Otsu and Y. Harada, *Makrmol. Chem.*, **65**, 180 (1963).

3) J. F. Bork and L. E. Coleman, *J. Polymer Sci.*, **43**, 413 (1960).

Hydrogen-Deuterium Exchange of Several Optically Active Complexes of Cobalt(III) in D_2O Solutions

Hideo YAMATERA and Miho FUJITA

Department of Chemistry, Nagoya University, Chikusa-ku, Nagoya

(Received July 28, 1969)

The rates of hydrogen isotope exchange were measured for several optically-active cationic cobalt complexes dissolved in D_2O containing an optically-active anionic species. The rate constant was obtained from the plot of $-\log(1-A_t/A_\infty)$ *vs.* t,[1] where A_t is the observed absorbance at 6000 cm^{-1} (due to HDO) at time t and where A_∞ is the equilibrium value. A Carl-Zeiss spectrophotometer PMQII was used for the measurements.

The rates of amino-hydrogen exchange for *d*- and *l*-$[Co(en)_3]^{3+}$ were measured in the presence of *d*-tartrate.*1 The results are given in Table 1. The conditions were practically the same within each pair of runs, except that different optical isomers of the complex were used. In the pair of runs, D-0 and L-0, where the solution contained no tartrate, but instead an acetate buffer, the rates of hydrogen exchange were very similar. In the presence of *d*-tartrate, however, the rate constants were appreciably smaller for *d*-$[Co(en)_3]^{3+}$ than for the *l*-isomer. This seems to imply that

TABLE 1. RATE CONSTANTS FOR THE HYDROGEN EXCHANGE OF *d*- AND *l*-$[Co(en)_3]^{3+}$ (25°C)

Sample No.	Complex $\times 10^2$M	*d*-tartrate $\times 10^2$M	pH**	k $\times 10^4$ sec^{-1}
D-0**	*d* 3.02	0.00	4.75	6.70
L-0**	*l* 3.00	0.00	4.75	6.69
D-1	*d* 3.28	3.06	4.77	4.70
L-1	l 3.21	3.13	4.81	5.24
D-2	*d* 3.07	3.10	4.79	4.82
L-2	*l* 3.02	3.10	4.79	5.04
D-3	*d* 2.93	5.11	5.38	15.1
L-3	*l* 2.90	5.11	5.38	17.0
D-4	*d* 2.94	6.95	5.21	8.47
L-4	*l* 2.90	6.95	5.21	10.9
D-5	*d* 2.92	9.93	5.37	9.61
L-5	*l* 2.90	9.93	5.37	10.8

* Values given are apparent pH values measured with a usual pH meter in D_2O solution.

** The run was carried out in an acetate buffer solution.

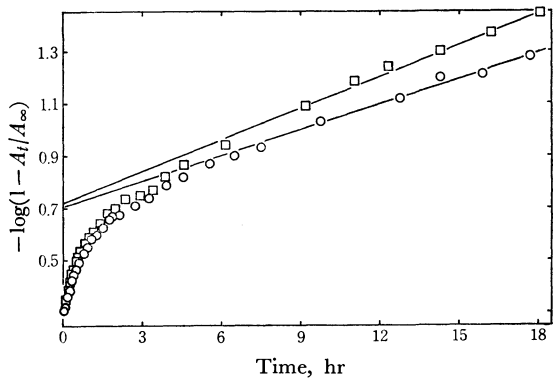

Fig. 1. Hydrogen exchange for *d*- (○) and *l*-$[Co(NO_2)_2(en)_2]^+$ (□) in the presence of *l*-[Co(EDTA)]$^-$.

TABLE 2. RATE CONSTANTS FOR THE HYDROGEN EXCHANGE OF *d*- AND *l*-$[Co(NO_2)_2(en)_2]^+$ (25°C)

Sample No.	Complex $\times 10^2$M	*l*-[CoY]$^-$ *** $\times 10^2$M	pH*	k $\times 10^5$ sec^{-1}
D-0**	*d* 3.90	0.00	6.29	12.0
L-0**	*l* 3.87	0.00	6.29	12.0
D-1	*d* 3.88	3.49	6.07	1.93
L-1	*l* 3.90	3.49	6.07	2.25

*, ** See corresponding reference in Table 1.

*** Y=EDTA

there is some stereoselective interaction in the solution between the isomers of $[Co(en)_3]^{3+}$ and the *d*-tartrate ion. In this connection, it is interesting to note that Ogino and Saito obtained a higher association constant for the pair consisting of *d*-$[Co(en)_3]^{3+}$ and *d*-tartrate.[2]

Similar results were obtained for *d*- and *l*-$[Co(NO_2)_2(en)_2]^+$ in the presence of *l*-[Co(EDTA)]$^-$, as is shown in Fig. 1 and Table 2. In this case, the amino groups are not equivalent and *at least* two exchange rates may be expected.[3] Table 2 gives data for the smallest rate constant, which is probably due to amino groups *cis* to nitro groups.

Further results and a more detailed discussion will be given elsewhere.

1) See, *e.g.*, H. A. C. McKay, *Nature*, **142**, 997 (1938).

*1 The notations *d* and *l* in this communication mean, as usual, that the compound is dextrorotatory or levorotatory respectively at the sodium D line.

2) K. Ogino and U. Saito, This Bulletin, **40**, 826 (1967).

3) J. W. Palmer and F. Basolo, *J. Phys. Chem.*, **64**, 778 (1960).

Optical and ESR Studies on Triphenylimidazolyl Radicals Produced by Photolysis and Radiolysis at Low Temperature*[1]

Tadamasa SHIDA, Koko MAEDA* and Taro HAYASHI

The Institute of Physical and Chemical Research, Yamatomachi, Kitaadachi-gun, Saitama

** Department of Chemistry, Faculty of Science, Ochanomizu University, Bunkyo-ku, Tokyo*

(Received July 29, 1969)

In a previous paper[1] we reported that UV-illumination of the photochromic dimer of triphenylimidazolyl (photo-dimer, abbreviated as R_2) in EPA at −196°C induced a coloration which was attributed to the formation of a radical cation of the dimer.[1] We wish to report here that the coloration should be associated with the formation of triphenylimidazolyl radical R·, as in the case of photolysis of the dimer at room temperature.[2]

When a colorless solution of photo-dimer in methyltetrahydrofuran (MTHF) in a thin quartz cell was exposed at −196°C to UV-light (λ= 240—400 mμ), an absorption with λ_{max} 350, 556 mμ appeared which was almost the same as that of R· in MTHF at room temperature. The ESR spectrum of the solution at −196°C showed a broad doublet which is unambiguously attributable to the fine structure due to the close-lying two radicals. From these observations it is concluded that photo-dimer in MTHF at −196°C dissociates homolytically upon UV-illumination. When the same solution was radiolyzed at −196°C with γ-rays from a ^{60}Co source, an absorption spectrum very similar to that of the photolyzed solution appeared (λ_{max} 347, 552 mμ) indicating the formation of R·. The ESR spectrum of the radiolyzed solution, however, showed no sign of the doublet due to the radical pair but a sharp singlet of ΔH_{msl}=8.1 gauss. The line width is close to that of the monomeric R· in solutions photolyzed at room temperature. In the radiolysis of the rigid solution, R· is apparently formed not as a geminate radical pair but as a single isolated radical by the reaction $R_2+e^- \rightarrow R\cdot+R^-$. The reaction is consistent with the ESR result as well as several other observations.

When both photolyzed and radiolyzed solutions at −196°C were carefully warmed, a subtle color change was noticed just before the solution thawed. The warmed solution, when quickly dipped again in liquid nitrogen, exhibited another spectrum similar to the original, but with a significant red shift (λ_{max} 354, 566 mμ). In addition to the red shift the absorption bands became narrower and the band structure was more manifested. It is assumed that the newly appearing spectrum is associated with triphenylimidazolyl radical whose phenyl groups are more or less coplanar with the plane of the imidazole ring. The spectrum reported previously as the cation radical of R_2 might have been the spectrum of this conformational isomer of the radical.

We obtained quite analogous results in the studies on tetraphenylpyrryl radical produced by oxidation of tetraphenylpyrrole.

---

*[1] Presented at the Symposium on Photochemistry of the Chemical Society of Japan (T. Shida, K. Maeda and T. Hayashi; Oct., 1968, Sendai).

1) T. Hayashi and K. Maeda, This Bulletin, **40**, 2990 (1967).

2) T. Hayashi, K. Maeda and K. Morinaga, *ibid.*, **37**, 1563 (1964).

Acidity of Methine Hydrogen in Cyclopropyl Ketone—*Cis-Trans* Rearrangement of 1-Acetyl-2-phenylcyclopropane with Base

Katsuhiko ICHIKAWA, Osamu ITOH and Nobuyuki YAMAMOTO

Department of Hydrocarbon Chemistry, Faculty of Engineering, Kyoto University, Sakyo-ku, Kyoto

(Received August 5, 1969)

Acidity of methine hydrogen in cyclopropyl ketone is of current interest. Dessy *et al.* reported that the base catalyzed isotopic exchange of the methine hydrogen in cyclopropyl phenyl ketone proceeded 14 times faster than the methine hydrogen in isobutyrophenone in D_2O-DMF solution because of the *s*-character of the carbon orbital of cyclopropane.[1] Recent reinvestigation of the same reaction, however, has shown that the exchange in D_2O-DMF containing NaOD (0.17 M) underwent resistance in 14 hr at 60°C,[2] and accordingly the above conclusion should be modified.

Rappe and Sachs reported also that the exchange of cyclopropyl methine proton is much slower than that of isopropyl methine proton in the same system.[3] Van der Maeden *et al.*, however, gave results which suggest that the opposite may be the case.[4] It is clear that further investigations are required on the acidity of cyclopropyl methine hydrogen. We wish to report our results on this question.

cis-1-Acetyl-2-phenylcyclopropane rearranges to *trans* isomer readily in 75% ethanol solution containing potassium hydroxide. The rates of the reaction were followed by gas chromatographical method. The results showed that the reaction follows first-order rate law at various base concentrations at 40 and 60°C. Constant values of k_1/[KOH] were obtained at both temperatures (Table 1).

TABLE 1. KINETICAL DATA OF REARRANGEMENT OF *cis*-1-ACETYL-2-PHENYLCYCLOPROPANE TO *trans*-ISOMER IN 75% ETHANOL

React. temp. °C	Initial concn. of *cis*-isomer (mol/*l*)	KOH concn. (mol/*l*)	$k_1 \cdot 10^5$ sec^{-1}	$\frac{k_1}{[KOH]} \cdot 10^4$
40.0	0.100	0.100	2.7	2.7
	0.100	0.196	5.2	2.7
	0.194	0.194	5.7	2.9
	0.200	0.388	10.8	2.8
60.0	0.0997	0.102	18	17
	0.0989	0.204	33	16
	0.194	0.204	32	16

Activation energy, 18 kcal/mol.

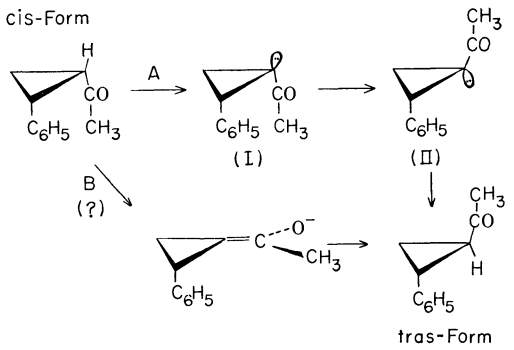

Fig. 1. Possible pathways for the rearrangement.

Two possible pathways of the reaction can be described (A and B in Fig. 1). Pathway B, however, appears to be unlikely, since enolization in this system is repressed because of steric inhibition.[2] The most probable mechanism A involves proton abstraction from cyclopropyl methine system to form carbanion. The rate determining step appears to be the proton abstraction, since no plausible reason for the stability of carbanion I can be found in this system. Large k_1 values obtained here make sharp contrast with those by isotopic exchange method. The reason for the disagreement might be found in the effect of the phenyl group attached to the cyclopropane ring. Assuming this to be the case, a pronounced effect through the ring is expected. Experiments along the line are under progress.

cis-1-Acetyl-2-phenylcyclopropane was prepared by alkaline deacetylation of 1,1-diacetyl-2-phenylcyclopropane[5] in 75% ethanol containing potassium hydroxide at 0°C. *Cis*- and *trans*-isomers were separated by column chromatography using WAKO GEL C-200 and hexane - ethyl acetate (90 : 10).

1) By R. Dessy, Y. Okuzumi and A. Chen in H. Shechter and M. J. Collins and R. Dessy, Y. Okuzumi and A. Chen, *J. Am. Chem. Soc.*, **84**, 2905 (1962).

2) H. W. Amburn, K. C. Kauffman and H. Shechter, *ibid.*, **91**, 530 (1969).

3) C. Rappe and W. H. Sachs, *Tetrahedron*, **24**, 6287 (1968).

4) F. P. B. van der Maeden, H. Steinberg and Th. J. de Boer, *Tetrahedron Letters*, **1967**, 4521.

5) To be published shortly.

A New Pair of Isomers of a Schiff Base Nickel(II) Complex

Akira TAKEUCHI and Shoichiro YAMADA

Institute of Chemistry, College of General Education, Osaka University, Toyonaka, Osaka

(Received August 8, 1969)

It is well known that the bis(*N*-alkyl- or bis(*N*-aryl-salicylideneiminato)nickel(II) complex (abbreviated as Ni(X-SAL·R)$_2$, Fig. 1) in non-donor solvents exists as an equilibrium mixture consisting of the planar, tetrahedral and polymeric species. The equilibrium depends upon the nature of X and R, as well as upon concentration and temperature.[1,2] From the solutions, however, only one component is usually obtained as crystals. Two forms of crystals consisting of complexes with different configurations have so far been isolated for only a few sets of X and R.[3,4] For the complexes with R=*iso*-C_3H_7, where there is remarkable steric hindrance, either the planar or the tetrahedral form was isolated as crystals, depending upon the nature of X. No pair of isomers has ever been isolated for any substituent X. The present communication deals with successful isolation of two isomers of Ni(3-CH_3O-SAL·*iso*-C_3H_7)$_2$.

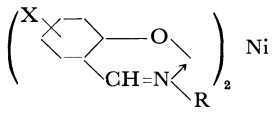

Fig. 1. Ni(X-SAL·R)$_2$

Isopropyl amine (0.04 mol) was added to a suspension of bis(3-methoxysalicylaldehydato)-nickel(II) dihydrate (0.02 mol) in methanol (100 m*l*), and the resulting solution was heated on a water-bath at about 40°C for one hour. A brown crystalline precipitate separated out from the brown solution. Recrystallization of the precipitate from methanol yielded brown crystals (Form I) of the desirable complex, Ni(3-CH_3O-SAL·*iso*-C_3H_7)$_2$. Spontaneous evaporation of a green solution of the precipitate in ethyl ether-methanol or ethyl ether - chloroform (20:1) yielded green crystals (Form II) of the same complex. Elemental analysis of both Form I and Form II agree with the formula Ni(3-CH_3O-SAL·*iso*-C_3H_7)$_2$. Both forms, when dissolved in the same solvents, show the same electronic spectra which are also dependent upon the concentration, solvents and temperature.

Since Form II is diamagnetic, it is considered to consist of uninuclear, planar complexes. The conclusion is supported by the electronic spectrum in the solid state, which is typical of the planar nickel(II) complex of this series. Form I is paramagnetic with a magnetic moment of 3.32 B. M. at room temperature, showing that this form does not consist of the planar species. The electronic spectrum of Form I in the solid state is typical of the tetrahedral nickel(II) complex, and is indeed quite similar to that of Ni(H-SAL·*iso*-C_3H_7)$_2$,[5] which was previously concluded to consist of the tetrahedral nickel(II) species.[6] So far as we know, this is the first isomeric pair of tetrahedral and planar nickel(II) complexes with the Schiff base to be isolated as crystals.

It is also interesting to note that on raising the temperature, Form II is transformed at 157—158°C into Form I, eventually showing the same behaviour as Form I, which melts at 187—188°C after sintering at 169—170°C.

The details of the work will be published elsewhere.

1) L. Sacconi, "Essays in Coordination Chemistry," ed. by W. Schneider, G. Anderegg and R. Gut, Birkhäuser Verlag, Basel (1964), p. 148.

2) R. H. Holm, G. W. Everett, Jr., and A. Chakravorty, "Progress in Inorganic Chemistry," ed. by F. A. Cotton, Vol. VII, Interscience Publishers, New York, N. Y. (1966), p. 83.

3) L. Sacconi, P. Paoletti and R. Cini, *J. Am. Chem. Soc.*, **80**, 3583 (1958); C. M. Harris, S. L. Lenzer and R. L. Martin, *Austral. J. Chem.*, **11**, 331 (1958).

4) S. Yamada, K. Iwasaki and A. Takeuchi, *Inorg. Chim. Acta*, **2**, 382 (1968).

5) S. Yamada and H. Nishikawa, This Bulletin, **36**, 755 (1963); L. Sacconi, P. Paoletti and M. Ciampolini, *J. Am. Chem. Soc.*, **85**, 411 (1963).

6) M. R. Fox, E. C. Lingafelter, P. L. Orioli and L. Sacconi, *Nature*, **197**, 1104 (1963).

Rotational Raman Spectrum of Oxygen

Koichi ABE and Takehiko SHIMANOUCHI

Department of Chemistry, Faculty of Science, The University of Tokyo, Hongo, Bunkyo-ku, Tokyo

(Received August 14, 1969)

We have measured the Raman spectrum of oxygen at one atmospheric pressure, using a JEOL argon ion laser as the exciting source and a Nalumi Raman spectrometer. The monochromator is equipped with a 300 line/mm Bausch and Lomb 35—53—32—45 echelle grating. The focal length is 2m ($F=11$) and the twelfth order diffraction gives the linear dispersion of 2.4 cm^{-1}/mm at 5000A. Eastman Kodak 103-aF film was used and the exposure time was 5—24 hr. The Raman cell was placed in the laser cavity and the beam was focused at the Raman cell.

We have found that the lowest frequency Raman lines corresponding to the $N=1\rightarrow N=3$, $N=3\rightarrow N=5$ and $N=5\rightarrow N=7$ transitions have satellites on both sides of the main lines. The multiplicity is interpreted to be caused by the spin-spin coupling in the $^3\sum_g^-$ ground state of oxygen. The main line and the satellites are assigned to the $\Delta J=2$ and 0 and $\Delta J=1$, respectively, except for the $N=1\rightarrow N=3$ transition, where the case of $J=0\rightarrow J=2$ is included in the higher frequency satellite.

In the course of the study we were informed that Renschler, Hunt, McCubbin and Polo measured the same phenomena in the spectra excited in the cavity of the He-Ne laser (1). Since independent observation by the argon ion laser completely eliminates the possibility of ghosts, the result is reported here.

The microphotometer reproduction of the spectrum is shown in Fig. 1 with the assignments, confirming the interpretation given by Renschler *et al.*

We are grateful to Professor McCubbin for communicating the result before publication.

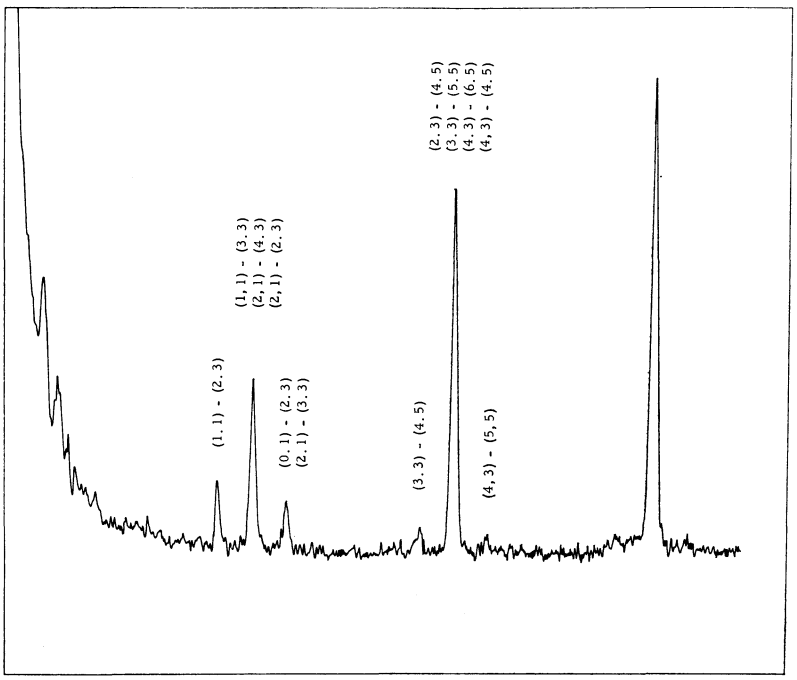

Fig. 1. Stokes lines with satellites. Assignments are shown as (J'', N'')-(J', N'). The Rayleigh line has the Stokes and Antistokes satellites corresponding to the $\Delta N=0$ and $\Delta J=1$ transition. However, it is accompanied also with ghost lines and the assignments are not definite.

1) D. L. Renschler, J. L. Hunt, T. K. McCubbin, Jr., and S. R. Polo, *J. Mol. Spectry.*, **31**, 173 (1969).

An ESR Study of 1:1 Adducts of Bis-salicylaldehyde-imine-cobalt(II) Complexes with Oxygen in Solutions

Akira MISONO and Seiichiro KODA

Department of Industrial Chemistry, Faculty of Engineering, The University of Tokyo, Hongo, Bunkyo-ku, Tokyo

(Received August 18, 1969)

The present authors have already reported[1] that oxygen coordinates reversibly in the ratio of 1 : 1 with bis-salicylaldehyde-imine-cobalt complexes supported on poly-4-vinylpyridine. In the present communication, they wish to report on the observation of the ESR spectra of 1 : 1 adducts of bis-salicylaldehyde-imine-cobalt(II) complexes with oxygen, which may exist equilibrially in solutions.

When a pyridine solution of *N,N'*-ethylene-bis(3-methoxysalicylideneiminato)cobalt(II) (Co 3-MeOsalen) was exposed to oxygen, there appeared an ESR signal in which hf structures caused by a cobalt nucleus were observed (eight lines, I (^{59}Co)= 7/2). This signal decreased when the solution was exposed to nitrogen and increased again when the solution was again exposed to oxygen. Similar spectra could be observed in substituted pyridines, *N,N*-dimethylformamide, and dimethyl sulfoxide used as solvents. Moreover, *N,N'*-ethylene-bis-(salicylideneiminato)cobalt(II) (Co salen) showed a similar spectrum in pyridine under oxygen.

These observations prove that there may be some amounts of a 1 : 1 adduct of bis-salicyl-aldehyde-imine-cobalt(II) complexes with oxygen in some solutions. The observed ESR spectra may be caused by the 1 : 1 adducts, for the existence of eight resolved lines in the spectra clearly shows that the adducts intrinsically contain only one cobalt atom. In fact, the observed ESR spectra closely resemble those of superoxocobalamin ($Co/O_2=1/1$).[2] Moreover, recently the preparation of the adduct, (Co 3-MeOsalen)·py·O_2 has been reported.[3]

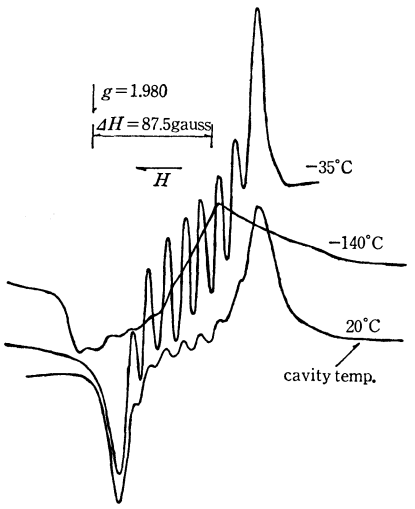

Fig. 1. ESR Spectra of Co 3-MeOsalen in pyridine under oxygen (1 atm).
complex concn. = 1.4×10^{-2} mol/*l*

The small A_{Co} values (A_{Co} is the mean interval of two adjacent lines among the eight lines) may mean that little of the unpaired spin is at the cobalt atom; if so, the adducts can be regarded as essentially superoxide cobalt(III) complexes. The explanation of the solvent effect is difficult, but it is reasonable that a solvent molecule coordinates to a cobalt complex in the *trans* position against oxygen and affects the electron distribution on the coordinated oxygen molecule.

TABLE 1. ESR CHARACTERS OF THE ADDUCTS

Complex	Solvent (complex concn., 10^{-2} mol/*l*)	*g*	A_{Co} (gauss)	Cavity temp. (°C)
Co 3-MeOsalen	Pyridine(1.4)	2.023	12.8	−35
Co 3-MeOsalen	Pyridine(1.8)	2.022*	—	20
Co 3-MeOsalen	4-Methylpyridine(1.7)	2.022*	13*	20
Co 3-MeOsalen	4-Ethylpyridine(1.7)	2.022	12.8	−10
Co 3-MeOsalen	DMF(1.4)	2.028	17.0	−15
Co 3-MeOsalen	DMSO(1.7)	2.028	17.3	20
Co 3-MeOsalen	DMF+Pyridine (1/1 vol)(0.9)	2.023	12.8	−10
Co salen	Pyridide(1.1)	2.022*	13*	20

* The spectrum is not well resolved. oxygen pressure = 1 atm

1) A. Misono, S. Koda and Y. Uchida, This Bulletin, **42**, 580 (1969); *ibid.*, No. 12 (1969).
2) J. H. Bayston, N. K. King, F. D. Looney and M. E. Winfield, *J. Am. Chem. Soc.*, **91**, 2775 (1969)
3) C. Floriani and F. Calderazzo, *J. Chem. Soc.*, *A* **1969**, 946.

New Type Acetylene Compexes with Mixed Transition Metals

Katsutoshi YASUFUKU and Hiroshi YAMAZAKI

The Institute of Physical and Chemical Research, Yamato-machi, Saitama

(Received August 26, 1969)

At an early stage of acetylene complex chemistry, an assumed structure (I) was proposed for the complexes $RC_2R'Co_2(CO)_6$ by Sternberg *et al.*[1] Afterwards, X-ray diffraction study[2] verified that the structure is II which has been recognized as a general structure of the coordinated acetylenes in the acetylene complexes.

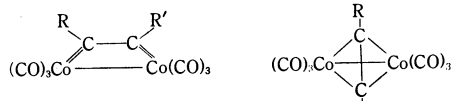

(I) (II)

In this communication, we wish to report the preparation of new type acetylene complexes in which the acetylene attaches to nickel and iron with the structure proposed by Sternberg.

Tolan and μ-diphenylphosphido-π-cyclopentadienyltetracarbonylironnickel(III)[3] were heated for six hours under reflux in benzene. After evaporation of the solvent, the residue was subjected to chromatography on alumina with hexane-methylene chloride mixture as an eluant. Concentration of the eluate gave air-stable brown crystals (IVa). (Yield 85%, mp 215—220°C (with decomp). Found: C, 65.02; H, 4.19%. Calcd for $C_{34}H_{25}O_3PFeNi$: C, 65.13; H, 4.00%.)

IR spectrum (KBr disk) showed bands of terminal carbonyls at 2010, 1960, and 1948 cm^{-1} (ν_{CO}). NMR spectrum (in $CDCl_3$) indicated phenyl protons at 2.0—3.2 τ and π-cyclopentadienyl protons at 4.93 τ. Mass spectrum showed a parent peak at *m/e* 626 corresponding to the formula $C_{34}H_{25}O_3P^{56}Fe^{58}Ni$. Peaks due to the successive loss of three carbonyl groups and tolan were also found at *m/e* 598, 570, 542, and 364.

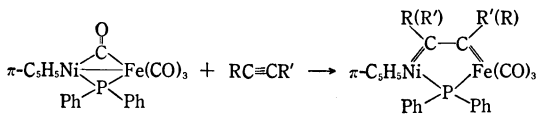

(III) (IV)

a : R, R′=Ph
b : R, R′=CO_2CH_3
c : R=Ph, R′=CO_2CH_3
d : R=Ph, R′=CH_3

Following similar procedures, the complexes of dimethyl acetylenedicarboxylate (IVb), methyl phenylacetylenecarboxylate (IVc), and methylphenylacetylene (IVd) were obtained, in which IVc and IVd consist of two isomers respectively.

IVb: Yield 37%, mp 128—133°C. NMR: 1.9—2.9 τ (C_6H_5), 4.82 τ (C_5H_5), 6.11 τ (one CH_3), and 6.43 τ (another CH_3). M(*m/e*) 590.

IVc_1: (formerly eluted isomer): Yield 36%, mp 178—179°C. NMR: 1.9—2.9 τ (C_6H_5), 4.84 τ (C_5H_5), and 6.60 τ (CH_3). M(*m/e*) 608.

IVc_2: (lately eluted isomer): Yield 24%, mp 159—161°C. NMR: 2.0—3.0 τ (C_6H_5), 4.93 τ (C_5H_5), and 6.14 τ (CH_3). M(*m/e*) 608.

IVd_1: Yield 20%, brown oil. NMR: 2.1—3.0 τ (C_6H_5), 5.02 τ (C_5H_5), and 6.88 τ (CH_3, doublet, $J_{P-M=C-CH}$=4.8 cps). M(*m/e*) 565.

IVd_2: Yield 21%, mp 169—170°C. NMR: 2.1—2.9 τ (C_6H_5), 4.95 τ (C_5H_5), and 8.46 τ (CH_3, doublet, $J_{P-M=C-CH}$=13.2 cps). M(*m/e*) 565.

We suggest structure IV for these complexes. A relatively large coupling constant of CH_3 in IVd_1 and in IVd_2 with ^{31}P nucleus seems to give effective support.

Presence of dissimilar methyl groups in IVb and the presence of isomers in IVc and in IVd eliminate structure V. Another probable structure VI might be excluded from the absence of $\nu_{C=C}$ band in the IR spectra, and from steric consideration.

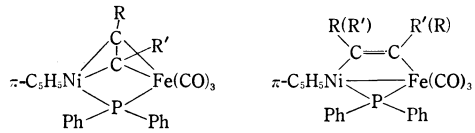

(V) (VI)

The complexes are new compounds for the following reasons: (1) They are the first complexes in which acetylene coordinates on two different transition metals, and (2) they are considered to coordinate on metals with the dicarbene structure. The configurations of the isomers have not been determined as yet. Detailed study of these complexes is now in progress.

1) H. W. Sternberg, H. Greenfield, R. A. Fiedel, J. Wotiz, R. Markby and I. Wender, *J. Am. Chem. Soc.*, **76**, 1457 (1954).

2) W. G. Sly, *ibid.*, **81**, 18 (1959).

3) III was obtained in the reaction of $HPh_2PFe(CO)_4$ with $(C_5H_5)_2Ni$, which was an extention of the method by Benson *et al.* (*Chem. Commun.*, **1968**, 1506).

New Red-pentamminenitrosylcobalt(III) Complexes

Eiichi MIKI, Tatsujiro ISHIMORI and Hisateru OKUNO

Department of Chemistry, College of Science, St. Paul's (Rikkyo) University, Nishi-Ikebukuro, Toshima-ku, Tokyo

(Received September 16, 1969)

The black and red series of the compounds with the composition of $Co(NH_3)_5(NO)X_2$ have been extensively studied ever since they were originally prepared by Sand and Genssler.[1] The red series (Red salt I) are binuclear, and the two cobalt atoms are bridged through a hyponitrite ion.[2]

Recently, the present authors prepared the new "red-pentamminenitrosylcobalt(III) chloride and nitrate" (Red salt II) by the use of a procedure similar to that for the red series reported by Odell *et al.*[3] To a cobalt(II) chloride or nitrate solution (5 g of $CoCl_2 \cdot 6H_2O$ or $Co(NO_3)_2 \cdot 6H_2O$/20 m*l* H_2O), enough ammonia water was added to give about 5 mol/*l*; the solution was then exposed to air for more than 20 hr at room temperature. The solution was placed in a reaction apparatus which had been outgassed with nitrogen gas. When nitric oxide gas was passed into the solution cooled with an ice-water bath, the red precipitate was yielded. Red salt II (nitrate) obtained could be recrystallized only from dimethylsulfoxide, but not from an aqueous solution.

Found: Co, 21.5; N, 30.84; H, 5.42; NH_3, 32.0; Cl, 25.2%. Calcd for $[Co_2(NH_3)_{10}(NO)_2]Cl_4 \cdot 4H_2O$: Co, 20.97; N, 29.90; H, 6.81; NH_3, 30.30; Cl, 25.23%. Found: Co, 18.9; N, 33.63; H, 4.62; NH_3, 27.2%. Calcd for $[Co_2(NH_3)_{10}(NO_2)](NO_3)_4 \cdot 2H_2O$: Co, 18.64; N, 35.44; H, 5.42; NH_3, 26.94%.

The molar conductivities of Red salt II in aqueous and dimethylsulfoxide solutions were examined by the method of Feltham and Hayter[4]; the relations between the conductivities and the square root of the concentrations for these salts coincided with those for Red salt I. It was suggested that Red salt II was a 4 : 1-type electrolyte.

The infrared spectra of Red salt II were similar to those of Red salt I. For Red salt I, the shifts of three absorption bands on the ^{15}NO-substitution were observed (from 1137, 1048, and 930 cm^{-1} to 1112, 1027, and 916 cm^{-1}). These shifts coincide with those reported by Mercer *et al.*[5] On the other hand, for the chloride of Red salt II the absorptions at 1481, 1278, 1020 and 804 cm^{-1} shifted to 1450, 1259, 1019 and 783 cm^{-1} respectively.

The gaseous products obtained by the decomposition of Red salt I and II were detected by the use of an infrared spectrophotometer. The ^{15}NO-complex of Red salt II (chloride) was decomposed by the addition of 6 M H_2SO_4 to give $^{15}NOCl$ and a small amount of $^{15}N^{15}NO$, while only $^{15}N^{15}NO$ was derived from the ^{15}NO-complex of Red salt I (nitrate). In the thermal decomposition *in vacuo*, for Red salt II (chloride and nitrate) $^{14}N^{14}NO$ and $^{14}N^{15}NO$ were derived from both the ^{15}NO-complex and the mixture of the ^{14}NO- and ^{15}NO-complex (1 : 1), while for Red salt I (nitrate) $^{14}N^{14}NO$ and $^{15}N^{15}NO$ were derived from both the ^{15}NO-complex and the mixture of the ^{14}NO- and ^{15}NO-complex (1 : 1). A part of the N_2O was formed as a by-product in the thermal decomposition; it contained two nitrogen atoms which came from the nitrogen of ammines in the complex. The ^{15}NO-Red salt II yielded $^{15}N^{15}NO$ upon mild decomposition by an acid, and $^{14}N^{15}NO$ upon thermal decomposition *in vacuo*.

Thus, the chloride and nitrate of Red salt II may be represented as $[Co_2(NH_3)_{10}(NO)_2]Cl_4 \cdot 4H_2O$ and $[Co_2(NH_3)_{10}(NO)_2](NO_3)_4 \cdot 2H_2O$ respectively. Furthermore, it is considered that the two cobalt atoms are bridged through a hyponitrite ion in Red salt II and that the N–N bond strength in the hyponitrite bridge may be weaker than that for Red salt I. Crystal X-ray study has determined that, in Red salt I, one cobalt atom is bound to an oxygen atom and the other to a nitrogen atom.[2] Red salt II may be considered to be the linkage isomer of Red salt I with respect to the hyponitrite bridge.

The details of this study will be published later.

1) J. Sand and O. Genssler, *Ber.*, **36**, 2083 (1903).
2) B. F. Hoskins, F. D. Whillans, D. H. Dale and Dorothy Crowfoot Hodgkin, O. M., *Chem. Commun.*, **1969**, 69.
3) A. L. Odell, R. W. Olliff and A. A. Taggart, *J. Chem. Soc.*, **1965**, 6024.
4) R. D. Feltham and R. G. Hayter, *ibid.*, **1964**, 4587.
5) E. E. Mercer, W. A. McAllister and J. R. Durig, *Inorg. Chem.*, **6**, 1816 (1967).

BULLETIN OF THE CHEMICAL SOCIETY OF JAPAN VOL. 42 3051—3055 (1969)

Magnetic and Optical Properties of Aromatic Hydrocarbon Cation Radical Salts

Yoichiro SATO, Minoru KINOSHITA, Mizuka SANO*1 and Hideo AKAMATU

Department of Chemistry, Faculty of Science, The University of Tokyo, Hongo, Bunkyo-ku, Tokyo

(Received September 29, 1968)

Stable cation radical salts were prepared by oxidation of perylene, 9,10-diphenylanthracene, 9,10-dimethylanthracene, and 9,10-dichloranthracene with antimony pentachloride. Perylene perchlorate was also obtained in a stable form. From the temperature variations of their paramagnetic susceptibilities, the exchange coupling constants for these salts were found to increase in the sequence of above listing ranging from ~ 0 to 8.5×10^{-2} eV. The absorption spectra of these solid compounds were compared with those observed with solutions. While the absorption bands of each salt in the visible region were found to correspond to those of the solution spectrum of the respective compound, an extra absorption band was observed in the near-infrared region for compounds with larger exchange coupling constants. The appearance of the new absorption band was reasonably ascribed to charge-transfer interaction between the radicals. These observations are considered to support further our previous suggestion that the magnitude of the exchange coupling constant obtained through magnetic measurements is basically determined by the stabilization energy due to the charger-transfer configurational interaction.

In the magnetic behaviors of organic radicals, when they are formed into solid, a deviation from the Curie or Curie-Weiss law has often been found in a commonly avaiable temperature range. The anomaly of paramagnestim is caused by the interaction between radicals, and has been interpreted in terms of an exchange-coupled linear chain model.[1-6] The model has been applied to various organic radical crystals and their magnetic behaviors have been characterized by an empirical parameter, that is by the exchange coupling constant (J). It should be noted that, if the parameter could be explained on the basis of molecular wavefunctions, the interaction in organic radical crystals would be better understood through such a parameter.

We have suggested the importance of charge-transfer interaction in the observed exchange coupling constant, based on the correlation found between the exchange coupling constants and the charge-transfer absorption bands for phenothiazine, *N*-methylphenothiazine and thianthrene cation radical salts.[7] The present work is intended to confirm the contribution of charge-transfer interaction to magnetic behaviors of organic radical crystals by the measurements of paramagnetic susceptiblities and charge-transfer absorption bands for aromatic hydrocarbon radical salts.

Lewis and Singer[8] have prepared a number of aromatic hydrocarbon cations in solution with a skillful technique, and observed their ESR hyperfine structures. We have tried extensively to obtain crystalline radical salts from a variety of aromatic hydrocarbons treated with antimony pentachloride. So far tested, perylene (P) and anthracene derivatives substituted at 9 and 10 positions, *i. e.*, 9,10-diphenylanthracene (DPA), 9,10-dimethylanthracene (DMA) and 9,10-dichloranthracene (DCA) have formed stable monopositive ion radical salts at room temperature. Another stable cation radical salt has been prepared from perylene as perchlorate.

Experimental

Preparation. Stable cation radical salts were prepared by the following procedures and the compositions of the solid salts were determined by elementary analysis of carbon, hydrogen and chlorine. No appreciable chlorination of the hydrocarbons was observed,

*1 Present address: Department of Materials Science, The University of Electro-Communications, Chofu, Tokyo.

1) Y. Sato, M. Kinoshita, M. Sano and H. Akamatu, This Bulletin, **40**, 2539 (1967).

2) H. Nishiguchi, *ibid.*, **40**, 1587 (1967).

3) R. G. Kepler, *J. Chem. Phys.*, **39**, 3528 (1963).

4) W. Duffy, Jr., and D. L. Strandburg, *ibid.*, **46**, 456 (1967).

5) A. S. Edelstein, *ibid.*, **40**, 488 (1964).

6) Z. G. Soos, *ibid.*, **43**, 1121 (1965).

7) Y. Sato, M. Kinoshita, M. Sano and H. Akamatu, This Bulletin, **42**, 548 (1969).

8) I. C. Lewis and L. S. Singer, *J. Chem. Phys.*, **43**, 2712 (1965).

which was checked by elementary analysis of the hydrocarbons recovered from the salts by hydrolysis. X-Ray diffraction of the powdered samples of all the salts gave distinct, crystalline patterns.

DPA·$SbCl_6$: To a solution of 9,10-diphenylanthracene in dichloromethane was added a dichloromethane solution of $SbCl_5$ in an excess amount (2 to 3 equivs.). Dark blue crystalline powder precipitated, the composition of which was determined to be $C_{26}H_{18}\cdot SbCl_6$. This salt was found to be the most stable among the salts of aromatic hydrocarbons prepared here.

P·$SbCl_5$: Dark green powder with the composition of $C_{20}H_{12}\cdot SbCl_5$ was obtained by adding a dichloromethane solution of $SbCl_5$ to a solution of perylene.

DMA·$SbCl_5$: The greenish product of $C_{16}H_{14}\cdot SbCl_5$ was obtained from 9,10-dimethylanthracene by a similar procedure. The addition of a nearly equivalent amount of $SbCl_5$ seemed preferable for the preparation.

DCA·$SbCl_5$: The greenish product of $C_{14}H_8Cl_2\cdot SbCl_5$ was obtained when 9,10-dichloranthracene was used in place of 9,10-dimethylanthracene.

P·ClO_4: To a nearly saturated solution of 1 mmol perylene in dichloromethane, 1 mmol $AgClO_4$ dissolved in a very small amount of acetonitrile was added, and then mixed thoroughly. When a dichloromethane solution of 0.4 mmol iodine was poured into the solution with stirring, color characteristic of perylene monopositive ion appeared immediately, and then dark green powder precipitated. No noticeable oxidation of perylene occurred by the addition of either $AgClO_4$ or iodine only. An elementary analysis indicated the composition to be $C_{20}H_{12}ClO_4\cdot AgI$ with high reproducibility. An X-ray diffraction pattern of the product revealed the inclusion of silver and iodine in the form of AgI. From these observations, the product was found to be a homogeneous mixture of P·ClO_4 and AgI in an equivalent amount, which was formed as follows,

$$P + AgClO_4 + \frac{1}{2}I_2 \longrightarrow P^+ + ClO_4^- + AgI$$

Measurements. In the same manner as described in a previous paper,[1] the static susceptibilities of the salts were measured with a Faraday-type susceptibility microbalance in the temperature range from 77 to 296°K. The measurement was made at three different field strengths up to 15 k gauss in order to check ferromagnetic impurities. The susceptibility balance was calibrated by referring to distilled oxygen-free water, for which the susceptibility was taken to be -0.720×10^{-6} emu/g at room temperature.

The absorption spectra of solid radical salts dispersed in liquid paraffin were measured in the range from 340 to 2500 mμ at room temperature. The solution spectra were observed by using dichloromethane as a solvent.

Results

Magnetic Susceptibilities. The salts formed by the reaction with $SbCl_5$ were found to be strongly paramagnetic at room temperature. As the temperature was lowered, the paramagnetic susceptibilities of DPA·$SbCl_6$ and P·$SbCl_5$ continued to increase, while those of DMA·$SbCl_5$ and DCA·$SbCl_5$ reached a maximum at about 80°K. Perylene perchlorate was found to be diamagnetic and showed a little change in susceptibility with temperature.

Diamagnetic contribution was estimated from the value of diamagnetic susceptibility of each component. The experimentally determined value of diamagnetic susceptibility for a neutral organic molecule was used in place of the value for the molecular ion, *i.e.*, -167×10^{-6} for perylene, -234×10^{-6} for 9,10-diphenylanthracene, -146×10^{-6} for 9,10-dimethylanthracene, and -167×10^{-6} emu/mol for 9,10-dichloranthracene. The values for $SbCl_5^-$ and $SbCl_6^-$ were taken to be -124×10^{-6}, and -139×10^{-6} emu/mol, respectively, following Kainer and Hausser.[9] The diamagnetic susceptibilities calculated from these values are given in Table 1, together with the observed susceptibilities at 296°K and the paramagnetic susceptibilities χ_p estimated by subtracting the diamagnetic contribution.

The paramagnetic susceptibility of P·$SbCl_5$ was found to obey the Curie-Weiss law, while that of DPA·$SbCl_6$ obeyed the Curie law. The values of the Curie constant and the Weiss constant were determined by plotting the inverse paramagnetic susceptibility $1/\chi_p$ against temperature, as shown

TABLE 1. MAGNETIC SUSCEPTIBILITIES AND EXCHANGE COUPLING CONSTANTS

Substance	Observed susceptibility at 296°K $\times10^6$ (emu/mol)	Diamagnetic susceptibility $\times10^6$ (emu/mol)	Paramagnetic susceptibility at 296°K $\times10^6$ (emu/mol)	Weiss constant θ (°K)	Radical concentration (%)	Exchange coupling constant J (eV)
DPA·$SbCl_6$	752	−373	1125	0 ± 4	89	~0
P·$SbCl_5$	707	−291	998	-4 ± 4	80	3.4×10^{-4}*
DMA·$SbCl_5$	467	−270	737		(74—89)	6.9×10^{-3}*
DCA·$SbCl_5$	234	−291	525		(52—63)	6.9×10^{-3}*
P·ClO_4	−195	−209	14			8.5×10^{-2}**

* The value calculated according to the linear Ising model.
** The value calculated according to the singlet-triplet model.

9) H. Kainer and K. H. Hausser, *Chem. Ber.*, **86**, 1563 (1953).

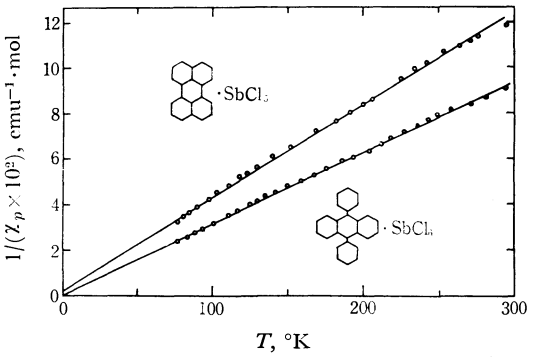

Fig. 1. The inverse paramagnetic susceptibilities of DPA·$SbCl_6$ and P·$SbCl_5$ as a function of temperature.

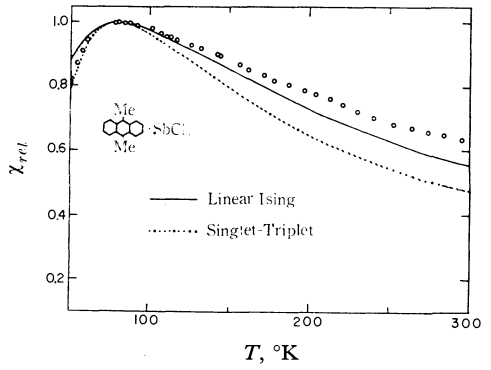

Fig. 2. The relative paramagnetic susceptibility of DMA·$SbCl_5$ as a function of temperature. The experimental plot and the theoretical curves are normalized at T_{max}=80°K.

in Fig. 1, and then the radical concentration was estimated from the Curie constant. DPA·$SbCl_6$ exhibited the highest radical concentration, which was consistent with its remarkable stability.

The paramagnetic susceptibility of DMA·$SbCl_5$ showed a broad maximum at approximately 80°K, when the measurement was made down to 50°K, as shown in Fig. 2. The reliable determination of both the Curie constant and the Weiss constant was not feasible, since the deviation from the Curie-Weiss law was appreciable even at high temperatures. DCA·$SbCl_5$ showed a quite similar behavior in susceptibility, though its radical concentration was lower. The relative paramagnetic susceptibilities for these two salts were found to coincide fairly closely with each other in a wide temperature range.

The apparent susceptibility of perylene perchlorate was found to be diamagnetic, after the correction was made for the susceptibility for AgI, which was taken to be -87×10^{-6} emu/mol. As shown in Fig. 3a, the apparent susceptibility showed a minimum around 200°K. The rise in susceptibility in the lower temperature region seems to

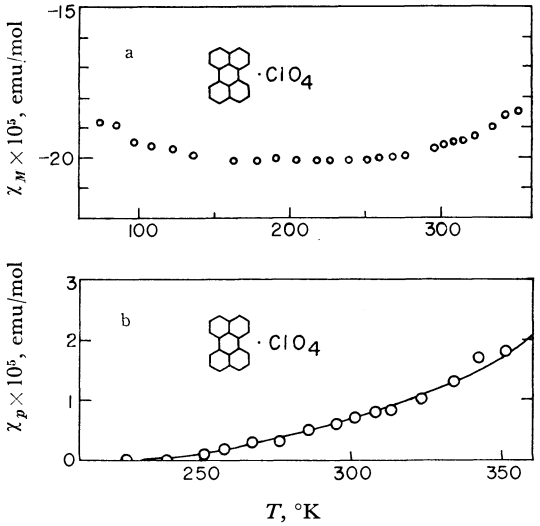

Fig. 3. The susceptibility of P·ClO_4 as a function of temperature. a, The observed susceptibility. b, The intrinsic paramagnetic susceptibility. The solid curve indicates the susceptibility calculated according to the singlet-triplet model for J= 0.085 eV.

indicate the presence of a small amount of paramagnetic impurities. Assuming that the susceptibility variation in the lower temperature region was dominated by the impurity paramagnetism which obeyed the Curie law, the diamagnetic susceptibility of the salt was estimated to be -209×10^{-6} emu/mol. After the correction was made for the diamagnetism and the impurity paramagnetism thus evaluated, the intrinsic paramagnetic susceptibility for the salt was obtained as a function of temperature. It increased with the increase in temperature, as shown in Fig. 3b.

Determination of Exchange Coupling Constant. The exchange coupling constant (J) was determined by the comparison between experimental and theoretical values. The paramagnetic susceptibility is expressed analytically as a function of temperature for two extreme cases of an exchange-coupled linear chain model. As it was discussed in a previous paper,[1] we will summarize the results only, for convenience of discussion. For the singlet-triplet case, the paramagnetic susceptibility is given by

$$\chi_p = (2N'g^2\beta^2/kT)[3+\exp(2J/kT)]^{-1} \quad (1)$$

where $2J$ corresponds to the singlet-triplet energy separation, and N' is the number of spin pairs. In a low temperature region, *i. e.*, $T \ll 2J/k$, Eq. (1) reduces to a simple form,

$$\chi_p = (2N'g^2\beta^2/kT)\exp(-2J/kT) \quad (2)$$

For the linear Ising case, the paramagnetic susceptibility is expressed by

$$\chi_p = (Ng^2\beta^2/4kT)\exp(-J/kT) \quad (3)$$

in the temperature range discussed.

We could find a relation between the exchange coupling constant J and the temperature T_{max} at which the susceptibility reaches its maximum value. The ratio, kT_{max}/J is 1.25 for the singlet-triplet model, 1.00 for the linear Ising model, and 1.28 for the regular chain Heisenberg model.[10]

In a high temperature region, *i. e.*, $T \gg J/k$, however, the paramagnetic susceptibility obeys the Curie-Weiss law,

$$\chi_p = C/(T-\theta) \quad (4)$$

where C is the Curie constant, and θ is the Weiss constant. The exchange coupling constant could also be evaluated from the Weiss constant. The relation, $J=-2k\theta$ holds for the singlet-triplet model, and $J=-k\theta$ for the linear Ising model.

The exchange coupling constant for P·$SbCl_5$ was estimated from the Weiss constant of -4°K to be 6.9×10^{-4} eV in the case of the singlet-triplet model, or 3.4×10^{-4} eV in the case of the linear Ising model. The coupling constant for DMA·$SbCl_5$ was evaluated from the temperature T_{max} of 80°K to be 6.9×10^{-3} eV according to the linear Ising model. The radical concentration for this salt was not known accurately, so that the relative paramagnetic susceptibility is shown in Fig. 2. It is compared with the theoretical curves for the singlet-triplet and the linear Ising models, which are normalized at the temperature T_{max}.

The exchange coupling constant for P·ClO_4 could be evaluated either from Eq. (1) or (2). As shown in Fig. 3b, the observed values fitted closely to the curve calculated from the singlet-triplet model with the exchange coupling constant of 0.085 eV. According to Eq. (2), a plot of $\log \chi_p \cdot T$ against $1/T$ gives a straight line, the slope of which corresponds to $-2J/k$. The slope is not affected by the change in radical concentration, so that this analytical method is useful in the case that radical concentration is unknown. The exchange coupling constant thus estimated was 0.09 eV for P·ClO_4.

Absorption Spectra. The absorption spectrum of solid DPA·$SbCl_6$ was found to greatly resemble the spectrum of the salt in solution, as shown in Fig. 4a. The spectrum was in agreement with that reported for 9,10-diphenylanthracene mono-positive ion by Shida and Hamill.[11] The spectrum of solid P·$SbCl_5$ was also found to correspond with that of the salt in dichloromethane, as shown in Fig. 5a. No extra absorption band could be detected in the near-infrared region. These solution and solid spectra of perylene ion are in good agree-

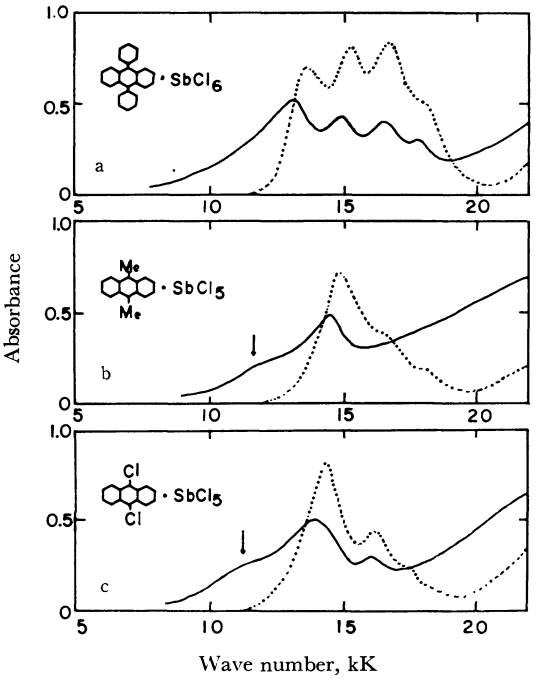

Fig. 4. The absorption spectra of the mono-positive ion radical salts of the anthracene derivatives: a, DPA·$SbCl_6$; b, DMA·$SbCl_5$; c, DCA·$SbCl_5$. The full lines indicate the solid spectra and the broken lines indicate the spectra of the salts in dichloromethane solution. The arrows indicate the charge-transfer bands.

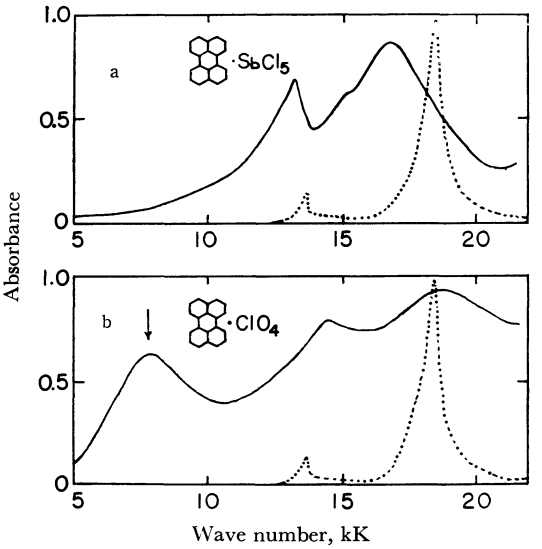

Fig. 5. The absorption spectra of the mono-positive ion radical salts of perylene: a, P·$SbCl_5$; b, P·ClO_4. The full lines indicate the solid spectra and the broken lines indicate the spectra of the salts in dichloromethane solution. The arrow indicates the charge-transfer band.

10) J. C. Bonner and M. E. Fisher, *Phys. Rev.*, **135**, A640 (1964).

11) T. Shida and W. H. Hamill, *J. Chem. Phys.*, **44**, 4372 (1966).

ment with those observed by other investigators.[12,13]

In contrast with P·$SbCl_5$, solid P·ClO_4 showed broad absorption bands, and in addition, a new absorption band was observed at approximately 7700 cm^{-1} as shown in Fig. 5b. The spectra for solid DMA·$SbCl_5$ and DCA·$SbCl_5$ showed a shoulder at longer wavelengths, besides the absorption bands which corresponded to those in the solution spectrum, as shown in Figs. 4b and 4c.

Discussion

The high radical concentration in the salts studied here indicates that one unpaired electron is associated with each formula unit. An ESR measurement revealed that the aromatic hydrocarbon radical salts showed a single exchange-narrowed line with a *g*-value between 2.002 and 2.003, which was characteristic of aromatic hydrocarbon radicals.[14] It is, therefore, reasonable to ascribe the unpaired electron to the mono-positive ion radicals produced by oxidation of the aromatic hydrocarbons with $SbCl_5$.

The new absorption bands in the near-infrared region observed for solid P·ClO_4, DMA·$SbCl_5$ and DCA·$SbCl_5$ is reasonably explained by the charge-transfer interaction between aromatic ion radicals caused upon the formation of an aggregate state. An appearance of a similar absorption band for a number of organic radicals has been ascribed to the charge-transfer interaction between radicals. For example, a quite similar spectrum to that observed with solid P·ClO_4 has been reported in a previous paper for a solution of perylene mono-positive ions in a solvent of low dielectric constant.[15] We have attributed it to perylene ions in an associated state, and the absorption band in the near-infrared region has been suggested to originate from the charge-transfer interaction between perylene ions. Hausser and Murrell have also suggested charge-transfer between radical molecules for the appearance of a new absorption band in the solution spectra of Wurster's blue perchlorate and *N*-ethylphenazyl at low temperatures.[16]

The appearance of a charge-transfer band in a solid spectrum is noted to correlate to the deviation of paramagnetism from the Curie law or, equivalently, the magnitude of an exchange coupling constant. Solid P·ClO_4 shows the large values both in an exchange coupling constant and an intensity of a charge-transfer band, which indicates the presence of strong interaction between perylene ions. Solid DPA·$SbCl_6$ and P·$SbCl_5$, on the other hand, exhibit nearly free nature of their aromatic ions, which is reflected on the negligible value of exchange coupling constant and the absence of charge-transfer band. DMA·$SbCl_5$ and DCA·$SbCl_5$ are an intermediate case with respect to the intermolecular interaction.

It is likely that the correlation between the magnetic and optical properties holds generally for a variety of crystalline radicals. From the observations so far made, the following qualitative features have been derived: 1) The apparent susceptibility of a radical solid which shows an intense charge-transfer band is diamagnetic, or at most weakly paramagnetic at room temperature. The exchange coupling constant for such a solid is usually found to be larger than 0.05 eV. 2) The crystalline radicals with the exchange coupling constant $J \lesssim 0.02$ eV exhibit a fairly weak charge-transfer band, which is thus usually observed as a shoulder. 3) The charge-transfer band for the solid with $J < 10^{-3}$ eV is usually undetectable.

The parallelism found between the exchange coupling constant and the charge-transfer band is, therefore, considered to support strongly our previous suggestion that the value of exchange coupling constant obtained through magnetic measurements is basically determined by the stabilization energy due to the charge-transfer configurational interaction associated with the crystalline state of radical molecules.

12) W. I. Aalbersberg, G. J. Hoijtink, E. L. Mackor and W. P. Weijland, *J. Chem. Soc.*, **1959**, 3055.

13) G. E. Blomgren and J. Kommandeur, *J. Chem. Phys.*, **35**, 1636 (1961).

14) A. J. Stone, *Mol. Phys.*, **6**, 509 (1963); B. G. Segal, M. Kaplan and G. K. Fraenkel, *J. Chem. Phys.*, **43**, 4191 (1965).

15) H. Kuroda, T. Sakurai and H. Akamatu, This Bulletin, **39**, 1893 (1966).

16) K. H. Hausser and J. N. Murrell, *J. Chem. Phys.*, **27**, 500 (1957).

BULLETIN OF THE CHEMICAL SOCIETY OF JAPAN VOL. 42 3056—3064 (1969)

The Effect of Organic Additives on the Autoxidation of Benzene and Toluene in the Aqueous Phase and the Kinetic Analysis*1

Hiroshi HOTTA, Nobutake SUZUKI and Kazuo ISODA

Japan Atomic Energy Research Institute, Takasaki-shi, Gunma

(Received November 6, 1968)

The effect of organic additives on the autoxidations of benzene and toluene was studied at 180°C in a ferrous sulfate aqueous solution. The additives were benzene, toluene, ethylbenzene, cumene, cyclohexene, cyclohexane, *n*-hexane, *t*-butyl alcohol, isopropyl alcohol, and ethyl alcohol. The yields of the phenol and benzaldehyde produced were measured as functions of the initial volume fraction of the additive. The yields decreased with the addition of a trace of the additive, and the yields increased still more with further addition. In order to interpret these results, the general expression for the yield of the main product was derived by the Gale-Wagner method and was analyzed numerically by using the IBM 7044. The mole fraction of the additive, corresponding to the maximum yield, can give information regarding the relative reactivity of the additive as compared with the results of the above numerical analysis. It is concluded from the present study that the experiment of the flow system for the autoxidation of toluene containing various additives is necessary to get exact kinetic information concerning these additives by using the present numerical analysis, because the equation is derived on the assumption that the concentration of the additive is constant.

It had been noted in a previous study that the yield of phenol from the autoxidation of benzene in an aqueous solution is considerably affected by impurities in benzene.[1] In the present paper, the effect of organic additives on the autoxidations of benzene and toluene is investigated in considerable detail and analyzed on the basis of the numerical analysis of the equation for the yield of the product as a function of the fraction of an additive, obtained as a result of the kinetic analysis of the binary autoxidation in the aqueous phase on the assumption of the reaction scheme previously established in our laboratory.[1-5]

Experimental

As in the previous study,[1] 1 cc of an organic mixture with benzene or toluene was put on 15 cc of a 0.01M ferrous sulfate aqueous solution in a hard-glass tube in a 50 cc stainless-steel reactor under an oxygen pressure of 30 atm. Then, this system was heated at 180°C for 30 min by means of a controlled heater. After cooling, the phenol from benzene was analyzed by the measurement of the optical absorbance in ether,[5] while the benzaldehyde from toluene was analyzed gas-chromatographically by using a column of PEG 6000.[3] These methods were described in detail in the previous papers.

The composition of the organic mexture is represented by the volume fractions of the additives, which were ethylbenzene, cumene, cyclohexene, cyclohexane, *n*-hexane, *t*-butyl alcohol, isopropyl alcohol, and ethyl alcohol. The autoxidation was carried out by using mixtures containing these additives in fractions of 0.0002, 0.001, 0.005, 0.01, and more than 0.01. The benzene was purified by the previous method,[1] and the toluene was of the spectro-grade, Merck. The additives were used without further purification.

Results

The Yields of Phenol and Benzaldehyde. The amounts of phenol and benzaldehyde produced from the mixture of benzene and toluene are plotted against the volume fraction of toluene in the original organic mixture in Fig. 1. The results for the systems containing benzene or toluene of less than a 0.05 fraction are shown in detail in Figs. 2(A) and 3(A).

The yields of phenol from the benzene mixtures and of benzaldehyde from the toluene mixtures are represented by the relative yield, namely, by the ratios of the amounts produced from these mixtures to those produced from the pure benzene or toluene, in Figs. 2 and 3. The additives are

*1 The Autoxidation of Aromatic Hydrocarbons in Aqueous Solutions. XIII.

1) N. Suzuki and H. Hotta, This Bulletin, **37**, 244 (1964).
2) H. Hotta, N. Suzuki and T. Abe, *ibid.*, **39**, 417 (1966).
3) N. Suzuki and H. Hotta, *ibid.*, **40**, 1361 (1967).
4) H. Hotta and N. Suzuki, *ibid.*, **41**, 1537 (1968).
5) H. Hotta, A. Terakawa, K. Shimada and N. Suzuki, *ibid.*, **36**, 721 (1963).

represented in Figs. 2 and 3 by the following symbols: a) benzene, b) toluene, c) ethylbenzene, d) cumene, e) cyclohexene, f) cyclohexane, g) *n*-hexane, h) *t*-butyl alcohol, i) isopropyl alcohol and j) ethyl alcohol.

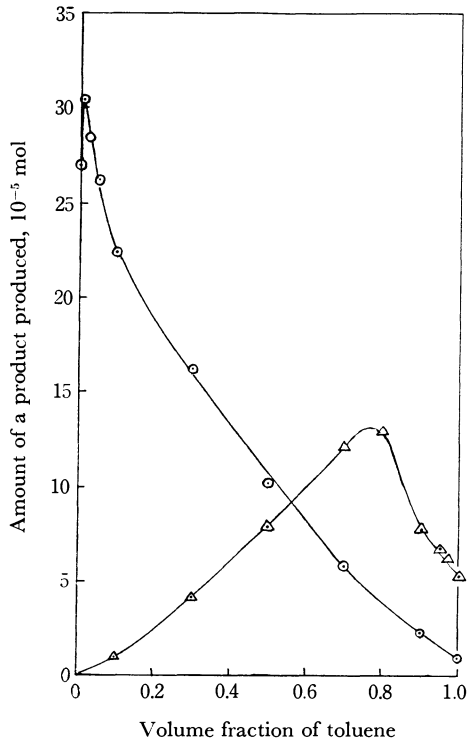

Fig. 1. Amounts of phenol (⊙) and benzaldehyde (△) produced from the mixture of benzene and toluene against the volume fraction of toluene.

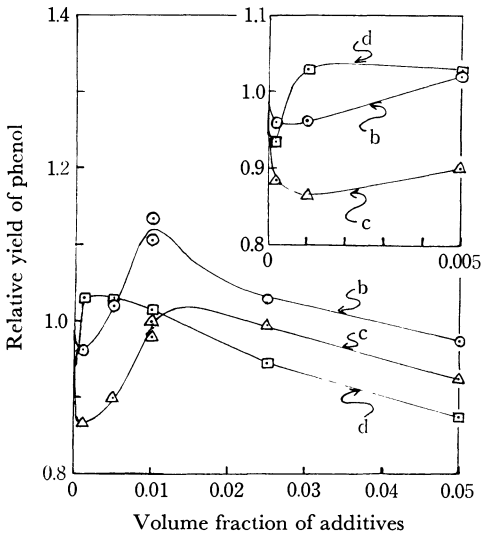

Fig. 2(A). Relative yields of phenol produced from the benzene mixture with various additives; b) toluene (⊙), c) ethylbenzene (△), and d) cumene (⊡).

In Fig. 1, the yield of benzaldehyde from the pure toluene is one-fifth as large as the yield of phenol from the pure benzene in spite of the fact that the dissociation energy of the $PhCH_2$–H bond is lower than that of the Ph–H bond, as has been pointed out in previous papers.[3,4] This may be partly attributed to the difference in the number of hydrogen atoms available for reaction. However,

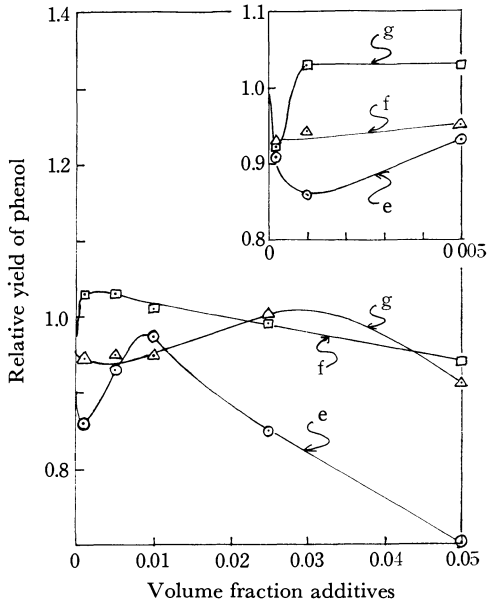

Fig. 2(B)
e) Cyclohexene (⊙), f) cyclohexane (△), and g) *n*-hexane (⊡).

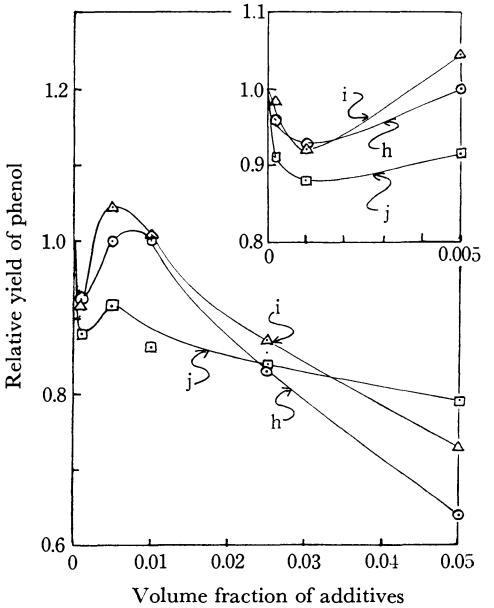

Fig. 2(C)
h) *t*-Butyl alcohol (⊙), i) isopropyl alcohol (△), and j) ethyl alcohol (⊡).

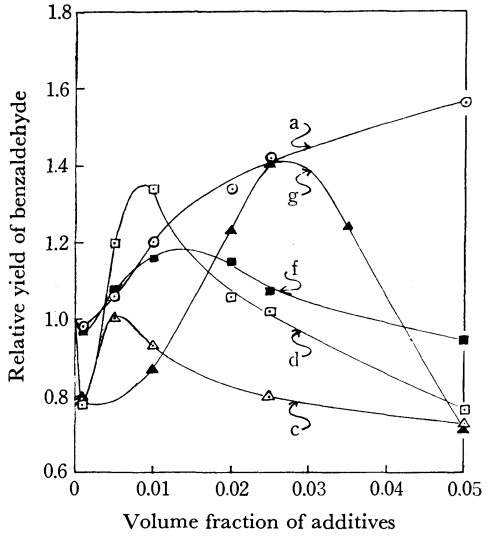

Fig. 3(A). Relative yields of benzaldehyde from the toluene mixture with various additives; a) benzene (⊙), c) ethylbenzene (△), d) cumene (▣), f) cyclohexane (▲), and g) *n*-hexane (■).

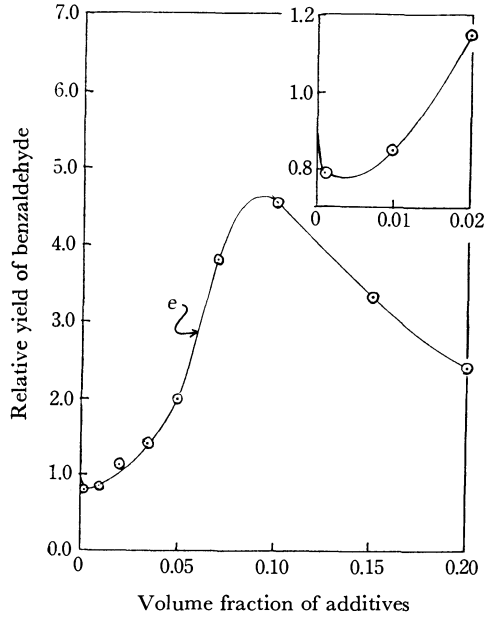

Fig. 3(B)
e) Cyclohexene (⊙).

recently, the solubility of benzene and toluene in water was measured between 100°C and 200°C.[6] According to these results, the main reason for the difference of their yield can be attributed to the difference in their solubility in water, which will be discussed in the following section.

The Relative Solubility in Water. Although the abscissas of the yield curves in Figs. 1, 2, and

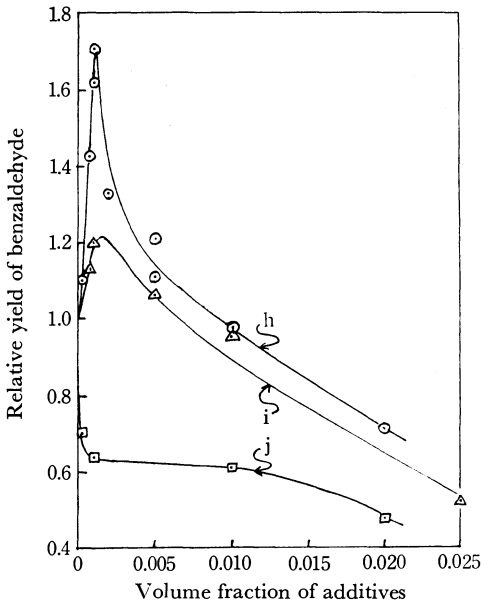

Fig. 3(C)
h) *t*-Butyl alcohol (⊙), i) isopropyl alcohol (△), and j) ethyl alcohol (▣).

3 represent the initial volume fractions of additives in the oil phase, v_B, it is necessary to know the mole fraction of additives to the total of the organic reactants in the aqueous phase, x_B, in order to make a kinetic analysis of these results. Although the measurement of the solubility at 180°C is not so easy, the x_B can be estimated by means of the following equation;

$$x_B = \frac{(BH)_{aq}}{(AH)_{aq} + (BH)_{aq}} \quad (1)$$

$$= \frac{y_B}{y_B + \frac{s_A}{s_B}(1 - y_B)} \quad (2)$$

where AH (or A) and BH (or B) represent a host reactant (benzene or toluene) and an additive respectively, and where s is the solubility of the pure AH or BH in water. If y_B, the mole fraction of an additive in the oil phase in equilibrium with x_B, is assumed to be equal to the initial one in the oil phase, it can easily be related to v_B. Furthermore, it is assumed in Eq. (2) that the ratio of the molar solubility, s_A/s_B, at 180°C is equal to that at room temperature; the figures for the latter are cited in Table 1 from the data of McAuliffe[7] except in the case of cyclohexene.[8] The solubility of benzene or toluene, measured in our laboratory, is 0.224M or 0.058M respectively at 180°C.[6] This ratio (3.86) is in good agreement with that at room temperature (3.90) shown in Table 1. For alcohols, since the values of v_B are very low, it is assumed

6) H. Hotta, M. Ito and H. Murashima, unpublished.

7) C. McAuliffe, *Nature*, **200**, 1093 (1963).

8) E. J. Farkas, *Anal. Chem.*, **37**, 1173 (1965).

Table 1. Ratio of molar solubility at room temperature

Benzene	3.90
Toluene	1.00
Cyclohexene	0.303
Ethylbenzene	0.256
Cyclohexane	0.112
Cumene	0.0758
n-Hexane	0.0190

that all the alcohols added in the oil phase are dissolved in the aqueous phase at 180°C.

Discussion

The Reaction Scheme and the Kinetic Analysis. According to the previous studies,[1-5] the reaction scheme of the co-oxidation of AH and BH in an oxygenated aqueous solution containing metal ions (M^+ and M^{2+}) can be assumed to be as follows:

$$H_2O \xrightarrow{M^+ + O_2} \cdot OH \quad (3)$$

$$AH + \cdot OH \rightarrow A\cdot + H_2O \quad (4a)$$

$$BH + \cdot OH \rightarrow B\cdot + H_2O \quad (4b)$$

$$A\cdot + O_2 \rightarrow AOO\cdot \quad (5a)$$

$$B\cdot + O_2 \rightarrow BOO\cdot \quad (5b)$$

$$AOO\cdot + AH \rightarrow AOOH + A\cdot \quad (6aa)$$

$$AOO\cdot + BH \rightarrow AOOH + B\cdot \quad (6ab)$$

$$BOO\cdot + AH \rightarrow BOOH + A\cdot \quad (6ba)$$

$$BOO\cdot + BH \rightarrow BOOH + B\cdot \quad (6bb)$$

$$AOOH + M^+ \rightarrow AO\cdot + OH^- + M^{2+} \quad (7a)$$

$$AOOH + M^{2+} \rightarrow AOO\cdot + H^+ + M^+ \quad (8a)$$

$$BOOH + M^+ \rightarrow BO\cdot + OH^- + M^{2+} \quad (7b)$$

$$BOOH + M^{2+} \rightarrow BOO\cdot + H^+ + M^+ \quad (8b)$$

$$AO\cdot \rightarrow \text{Product A} \quad (9a)$$

$$BO\cdot \rightarrow \text{Product B} \quad (9b)$$

and partly:

$$AOO\cdot + AOO\cdot \rightarrow \text{Inactive products} \quad (10aa)$$

$$AOO\cdot + BOO\cdot \rightarrow \text{Inactive products} \quad (10ab)$$

$$BOO\cdot + BOO\cdot \rightarrow \text{Inactive products} \quad (10bb)$$

where M^+ and M^{2+} represent ferrous and ferric ions respectively for the present experiment. The rate constants of the respective reactions are represented by the subscript k; for example, k_{4a} indicates that for reaction (4a). The general expression for the yield of the product from such a chain process can be derived in the following manner by the Gale-Wagner method.[9,10]

When the yield of the hydroxyl radical from reaction (3) is represented by $Y(OH)$, the yield of A· or B· from reaction (4) is expressed in the form:

$$(A)_0 = a_0 Y(OH) \quad (11a)$$

$$(B)_0 = (1-a_0) Y(OH) \quad (11b)$$

where:

$$a_0 = \frac{k_{4a}(AH)}{k_{4a}(AH) + k_{4b}(BH)} \quad (12)$$

It is assumed in the derivation of Eq. (11) that the contribution of reaction (4 m)

$$M^+ + \cdot OH = M^2 + OH^- \quad (4m)$$

can be ignored because the hydroxyl radical usually reacts faster with organic reactants than with inorganic reactants.

After these radicals, A· and B·, are oxidized instantaneously to the peroxides by reaction (5), they give the hydroperoxides, AOOH or BOOH, and the equimolar radicals, A· or B·, by reaction (6). The relative reactivity of peroxy radicals (ROO·) toward hydrocarbons is fairly independent of the structure of R.[11] Recently, the dependence on the structure of R is illustrated rather finely.[12] When it is assumed in the present analysis that:

$$\frac{k_{4b}}{k_{4a}} = \frac{k_{6ab}}{k_{6aa}} = \frac{k_{6bb}}{k_{6ba}} = R_{b/a} \quad (13)$$

the yield of the products from reaction (6) is expressed in the forms:

$$(AOOH) = (A) = \frac{k_{6aa}(AH)}{k_{6aa}(AH)+k_{6ab}(BH)} \times a_0 Y(OH)$$
$$= a_0^2 Y(OH) \quad (14aa)$$

$$(AOOH) = (B) = \frac{k_{6ab}(BH)}{k_{6aa}(AH)+k_{6ab}(BH)} \times a_0 Y(OH)$$
$$= a_0(1-a_0) Y(OH) \quad (14ab)$$

$$(BOOH) = (A) = \frac{k_{6ba}(AH)}{k_{6ba}(AH)+k_{6bb}(BH)} \times (1-a_0) Y(OH)$$
$$= a_0(1-a_0) Y(OH) \quad (14ba)$$

$$(BOOH) = (B) = \frac{k_{6bb}(BH)}{k_{6ba}(AH)+k_{6bb}(BH)} \times (1-a_0) Y(OH)$$
$$= (1-a_0)^2 Y(OH) \quad (14bb)$$

because, on the assumption of Eq. (13),

$$a_0 = \frac{k_{4a}(AH)}{k_{4a}(AH) + k_{4b}(BH)} = \frac{k_{6aa}(AH)}{k_{6aa}(AH)+k_{6ab}(BH)} = \frac{k_{6ba}(AH)}{k_{6ba}(AH)+k_{6bb}(BH)} = \frac{1}{1+R_{b/a}\frac{(BH)}{(AH)}} \quad (15)$$

9) L. H. Gale and C. D. Wagner, *J. Am. Chem. Soc.*, **86**, 4531 (1964).

10) H. Kurihara and H. Hotta, This Bulletin, **40**, 719 (1967).

11) G. A. Russell and R. C. Williams, Jr., *J. Am. Chem. Soc.*, **86**, 2364 (1964).

12) B. S. Middleton and K. U. Ingold, *Can. J. Chem.*, **45**, 191 (1967).

The subscripts of Eq. (14) correspond to those or reaction (6). Therefore, the total yields of the hydroperoxides from reaction (6) are:

$$(\mathrm{AOOH})_1 = a_0 Y(\mathrm{OH}) \tag{16a}$$

$$(\mathrm{BOOH})_1 = (1-a_0) Y(\mathrm{OH}) \tag{16b}$$

Since these hydroperoxides are decomposed by reactions (7) and (8), the amounts of the products from them by these reactions are given by:

$$(\mathrm{AO})_1 = \frac{k_{7a}(\mathrm{M}^+)}{k_{7a}(\mathrm{M}^+)+k_{8a}(\mathrm{M}^{2+})} \times a_0 Y(\mathrm{OH})$$

$$= a_0 m_a Y(\mathrm{OH}) \tag{17a}$$

$$(\mathrm{AOO}) = \frac{k_{8a}(\mathrm{M}^{2+})}{k_{7a}(\mathrm{M}^+)+k_{8a}(\mathrm{M}^{2+})} \times a_0 Y(\mathrm{OH})$$

$$= a_0(1-m_a) Y(\mathrm{OH}) \tag{18a}$$

$$(\mathrm{BO})_1 = \frac{k_{7b}(\mathrm{M}^+)}{k_{7b}(\mathrm{M}^+)+k_{8b}(\mathrm{M}^{2+})} \times (1-a_0) Y(\mathrm{OH})$$

$$= (1-a_0) m_b Y(\mathrm{OH}) \tag{17b}$$

$$(\mathrm{BOO}) = \frac{k_{8b}(\mathrm{M}^{2+})}{k_{7b}(\mathrm{M}^+)+k_{8b}(\mathrm{M}^{2+})} \times (1-a_0) Y(\mathrm{OH})$$

$$= (1-a_0)(1-m_b) Y(\mathrm{OH}) \tag{18b}$$

where:

$$m_a = \frac{k_{7a}(\mathrm{M}^+)}{k_{7a}(\mathrm{M}^+)+k_{8a}(\mathrm{M}^{2+})}$$

$$m_b = \frac{k_{7b}(\mathrm{M}^+)}{k_{7b}(\mathrm{M}^+)+k_{8b}(\mathrm{M}^{2+})}$$

Equations (17) and (18) correspond to reactions (7) and (8) respectively.

The oxyradicals, given by Eq. (17), become the final products by means of reaction (9), while the peroxides regenerate the new peroxides and oxyradicals through the same cycle. When the above cycle, starting from the primary hydroxyl radical, is named the first cycle, the cycle started by these peroxides of Eq. (18) can be called the second cycles. Since the radicals, A· and B·, of Eq. (14) are oxidized instantaneously to the peroxides by reaction (5) the total yield of the peroxides formed during the first cycle or of the starting peroxides for the second cycle is given as the sum of Eqs. (14) and(18);

$$(\mathrm{AOO}) = a_0(2-m_a) Y(\mathrm{OH}) \tag{19a}$$

$$(\mathrm{BOO}) = (1-a_0)(2-m_b) Y(\mathrm{OH}) \tag{19b}$$

However, since some of them are terminated by reaction (10), the correction coefficient, c, must be multiplied to Eq. (19) as a measure of the fraction of the peroxides carrying the chain process to the next cycle without termination reactions like:

$$(\mathrm{AOO})_1 = a_0(2-m_a)c_a Y(\mathrm{OH})$$

$$= a_1 Y(\mathrm{OH}) \tag{20a}$$

$$(\mathrm{BOO})_1 = (1-a_0)(2-m_b)c_b Y(\mathrm{OH})$$

$$= b_1 Y(\mathrm{OH}) \tag{20b}$$

The yields of the products formed during the second cycle are expressed similarly with the first cycle as follows;

$$(\mathrm{AOOH})_2 = a_1 Y(\mathrm{OH})$$

$$(\mathrm{AOO})_2 = (\alpha a_1 + a_0 b_1) c_a Y(\mathrm{OH})$$

$$= a_2 Y(\mathrm{OH})$$

$$(\mathrm{AO})_2 = a_1 m_a Y(\mathrm{OH})$$

$$(\mathrm{BOOH})_2 = b_1 Y(\mathrm{OH})$$

$$(\mathrm{BOO})_2 = [\beta b_1 + (1-a_0) a_1] c_b Y(\mathrm{OH})$$

$$= b_2 Y(\mathrm{OH})$$

$$(\mathrm{BO})_2 = b_1 m_b Y(\mathrm{OH})$$

where;

$$\alpha = 1 - m_a + a_0 \tag{21a}$$

$$\beta = 2 - m_b - a_0 \tag{21b}$$

Generally, the yields of the products formed during the nth cycle are expressed in the forms;

$$(\mathrm{AOOH})_n = a_{n-1} Y(\mathrm{OH}) \tag{22a}$$

$$(\mathrm{AOO})_n = (\alpha a_{n-1} + a_0 b_{n-1}) c_a Y(\mathrm{OH})$$

$$= a_n Y(\mathrm{OH}) \tag{23a}$$

$$(\mathrm{AO})_n = a_{n-1} m_a Y(\mathrm{OH}) \tag{24a}$$

$$(\mathrm{BOOH})_n = b_{n-1} Y(\mathrm{OH}) \tag{22b}$$

$$(\mathrm{BOO})_n = [\beta b_{n-1} + (1-a_0) a_{n-1}] c_b Y(\mathrm{OH})$$

$$= b_n Y(\mathrm{OH}) \tag{23b}$$

$$(\mathrm{BO})_n = b_{n-1} m_b Y(\mathrm{OH}) \tag{24b}$$

Since Product A is formed from AO· by reaction (9), the total yield of product A over all the cycles can be estimated in the following manner:

$$Y(\text{Product A}) = \sum_n (\mathrm{AO})_n$$

$$= m_a Y(\mathrm{OH}) \left(\sum_n a_n\right) \tag{25}$$

$$= m_a Y(\mathrm{OH})(a_0 + F) \tag{26}$$

where:

$$F = \left[1 + \frac{c_a c_b a_0 (1-a_0)}{(1-c_a\alpha)(1-c_b\beta)}\right] \times \left[\frac{c_a a_0 (1-m_a)}{(1-c_a\alpha)} + \frac{c_a c_b a_0 (1-a_0)(1-m_b)}{(1-c_a\alpha)(1-c_b\beta)} + \frac{c_a a_0}{(1-c_a\alpha)}\left(1 + \frac{c_b(1-a_0)}{(1-c_b\beta)}\right)\right] \tag{27}$$

Reaction (10) might give AO··. When it is assumed that all the termination processes (reaction (10)) are the same type with the following reaction (28);

$$2\mathrm{ROO}\cdot \rightarrow 2\mathrm{RO}\cdot + \mathrm{O}_2 \tag{28}$$

the factor, $(1-c_a)/c_a m_a$, must be multiplied to Eq. (26).

Although α and β are not always less than unity, according to the definition of Eq. (21), the termination reaction (10), *i.e.*, the correction coefficient, c, controls the chain process like:

$$1 > c_a\alpha > 0 \text{ or } 1 > c_b\beta > 0 \tag{29}$$

It is assumed for the summation of Eq. (25) that c, $(M^+)/(M^{2+})$, and (BH)/(AH) are constant for all the cycles, but they may be at least somewhat different in a few cycles at the beginning from in the later cycles.

Numerical Analysis of Eq. (27). Equation (27) was analyzed numerically by means of the IBM 7044 against the mole fraction of BH, namely, x_B, as defined by Eq. (1), for all the combinations of $R_{b/a}$ (which was 0.1, 0.3, 1.0, 3.0, or 10.0), m_a and m_b (which were 0.8, 0.7, or 0.6), and c_a and c_b (which were 0.90, 0.85, 0.80, 0.75, 0.70, 0.65, or 0.60). Some examples are shown in Figs. 4—7 to illustrate the relationships between the yield of the product and these factors. In these figures, the value of F relative to F_0, which is for $x_B=0$, is plotted as F_{rel}. The F_{max} and x_{max} values in the following discussion mean, respectively, the maximum value of F_{rel} and the value of x_B, which gives F_{max} for certain conditions.

The F_{rel}-x_B curve against various $R_{b/a}$ values is shown in Fig. 4 for $m_a=m_b=c_a=c_b=0.7$. This figure indicates that F_{max} is almost independent of $R_{b/a}$ for a certain combination of other factors, while x_{max} decreases with an increase in $R_{b/a}$.

The F_{rel}-x_B curve against various m_a values is shown in Fig. 5 for $R_{b/a}=3.0$ and $m_b=c_a=c_b=0.7$. This figure indicates that F_{max} decreases with an increase in m_a, while x_{max} does not so vary with m_a. The curve becomes concave with a decrease in m_a in spite of an increase in F_{max}. The value of F_{rel} was not so affected by m_b, as numerical analysis showed.

The F_{rel}-x_B curve against various c_a values is shown in Fig. 6 for $R_{b/a}=3.0$ and $m_a=m_b=c_b=0.7$. This figure indicates that F_{max} decreases with a decrease in c_a, while x_{max} does not so vary with c_a. The curve becomes concave with an increase in c_a in spite of the increase in F_{max}.

The F_{rel}-x_B curve against various c_b values is

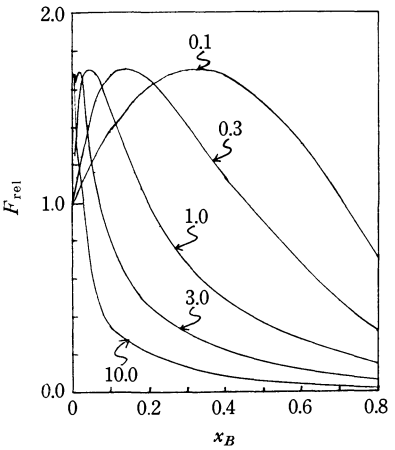

Fig. 4. The value of as F_{rel} the function of x_B for various $R_{b/a}$ ($m_a=m_b=c_a=c_b=0.7$).

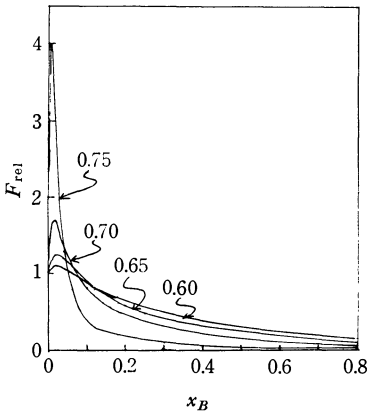

Fig. 6. The value of F_{rel} as the function of x_B for various c_a ($R_{b/a}=3.0$, $m_a=m_b=c_b=0.7$).

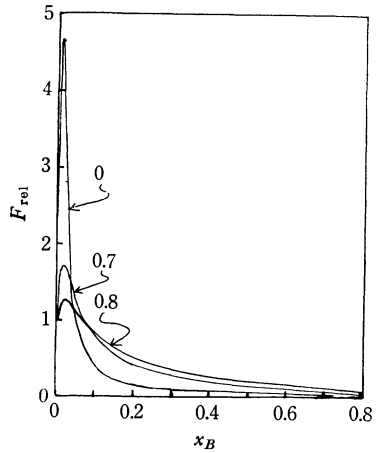

Fig. 5. The value of F_{rel} as the function of x_B for various m_a ($R_{b/a}=3.0$, $m_b=c_a=c_b=0.7$).

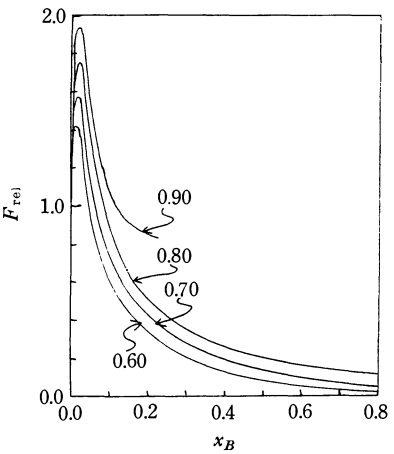

Fig. 7. The value of F_{rel} as the function of x_B for various c_b ($R_{b/a}=3.0$, $m_a=m_b=0.8$, $c_a=0.75$).

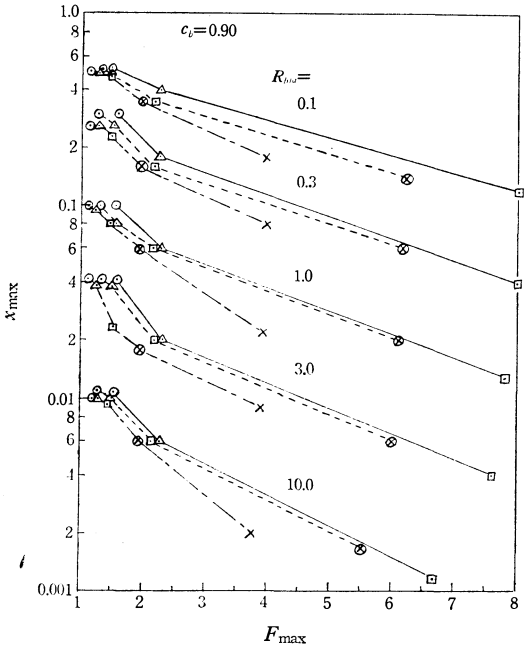

Fig. 8. Conditions for the relative peak height of the yield curve at c_b=0.90. Figures give the value of $R_{b/a}$. —— for m_a=0.6, ------ for m_a=0.7, —·— for m_a=0.8, × for c_a=0.80, ⊗ for c_a=0.75, ⊡ for c_a=0.70, △ for c_a=0.65 and ⊙ for c_a=0.60.

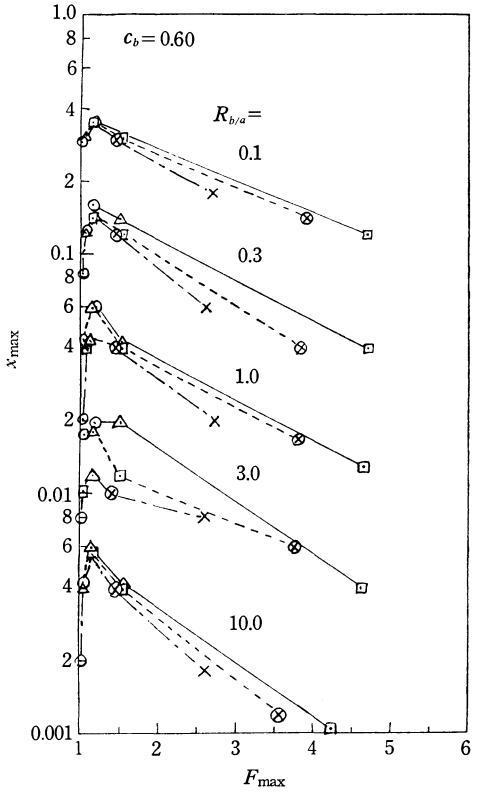

Fig. 9. Conditions for the relative peak height of the yield curve at c_b=0.60. Figures give the value of $R_{b/a}$. Marks are the same as in Fig. 8.

shown in Fig. 7 for $R_{b/a}$=3.0, $m_a=m_b$=0.8, and c_a=0.75. This figure indicates that F_{max} decreases with a decrease in c_b, while x_{max} and the shape of the curve do not so vary with c_b.

These relationships are summarized in Fig. 8 for c_b=0.90 and in Fig. 9 for c_b=0.60. Although the two figures are separated so as not to confuse the plottings, they should be overlapped in order to make the dependence on c_b clear. The F_{max} values are plotted against log x_{max} for various conditions. Since the points for the respective $R_{b/a}$ values are in a group, the value of $R_{b/a}$ is indicated above the group. They are classified by the m_a value in the group, that is, by solid lines for m_a=0.60, by dotted lines for m_a=0.70, and by broken lines for m_a=0.80. The values of c_a are indicated by the marks explained in Fig. 8.

The patterns of the points for the respective $R_{b/a}$ values differ a little. Since the values of F were computed from point to point for x_B, the patterns are similar between the $R_{b/a}$ groups in a close computation, as may be expected from Fig. 4. The larger $R_{b/a}$ gives the smaller x_{max} for the same F_{max}, and the smaller c_a gives the smaller F_{max}, as may be seen clearly in Figs. 8 and 9.

As may be seen in Figs. 5 and 6, the concavity or shape of the F_{rel}-x_B curve also gives kinetic information. Therefore, the values of x_B, giving F_{rel}=1 after passing F_{max}, may be classified as in Figs. 8 and 9. Although this figure is omitted in the present paper, is shown a regularity similar to that of Figs. 8 and 9.

Oxidation of Toluene Mixtures. As may be seen in Fig. 3, the yield of benzaldehyde decreases at first with the addition of a trace of the additive, but the further addition of it causes the yield to to increase to a maximum yield. The minimum or maximum relative yields ($Y(A)_{min}$ or $Y(A)_{max}$), the values of v_B, corresponding to them in Fig. 3, (v_{min} or v_{max}), and the values of x_{min} or x_{max}, as estimated from these v values by means of Eq. (2) on the assumption presented above, are listed in Table 2, in which the additives are listed in the order of x_{max}. Similar values for the yield of phenol from benzene, obtained from Fig. 2, are also listed in Table 2.

When the x_{max} and $Y(A)_{max}$ for hydrocarbons added in Table 2 B) are applied to the diagram in Figs. 8 and 9, which indicate the relationship between x_{max} and F_{max} ($Y(A)_{max}$) as the function of $R_{b/a}$, the reactivities of these hydrocarbons for the reaction of the type:

$$ROO\cdot + RH \rightarrow ROOH + R\cdot \qquad (30)$$

are in the order of:

benzene<cyclohexene<toluene[13,14]<cyclohexane[14]
<ethylbenzene[13]<cumene[13]<n-hexane (31)

Table 2. The minimum or maximum relative yields and the corresponding compositions of additives

Additives	Minimum condition			Maximum condition		
	v_{min}	x_{min}	$Y(A)_{min}$	v_{max}	x_{max}	$Y(A)_{max}$
A) Oxidation of Benzene						
Toluene	0.001	2×10^{-4}	0.96	0.01	2×10^{-3}	1.12
Cyclohexane	0.005	1×10^{-4}	0.94	0.03	7×10^{-4}	1.01
Ethylbenzene	0.001	5×10^{-5}	0.87	0.015	7×10^{-4}	1.02
Cyclohexene	0.001	7×10^{-5}	0.86	0.01	7×10^{-4}	0.97
Cumene	1×10^{-4}	1×10^{-6}	0.94	0.001	1×10^{-5}	1.03
n-Hexane	1×10^{-4}	3×10^{-7}	0.92	0.001	3×10^{-6}	1.03
t-Butyl alcohol	0.001	3×10^{-3}	0.92	0.007	2×10^{-2}	1.01
Isopropyl alcohol	0.001	4×10^{-3}	0.92	0.005	2×10^{-2}	1.05
Ethyl alcohol	0.001	5×10^{-3}	0.86	0.005	2×10^{-2}	0.92
B) Oxidation of Toluene						
Benzene	0.001	4×10^{-3}	0.99	0.2	0.54	2.6
Cyclohexene	0.001	3×10^{-4}	0.79	0.1	0.04	4.7
Cyclohexane	0.001	1×10^{-4}	0.78	0.027	3×10^{-3}	1.44
Ethylbenzene	0.001	2×10^{-4}	0.78	0.005	1×10^{-3}	1.00
Cumene	0.001	6×10^{-5}	0.79	0.01	6×10^{-4}	1.34
n-Hexane	0.001	2×10^{-5}	0.97	0.015	3×10^{-4}	1.08
t-Butyl alcohol	n.d.	—	n.d.	0.001	0.01	1.7
Isopropyl alcohol	n.d.	—	n.d.	0.001	0.015	1.2
Ethyl alcohol	n.d.	—	n.d.	n.d.	—	n.d.

"n.d." means "not detected."

When $R_{b/a}$ is defined as in Eq. (13). The order between toluene, cyclohexane, ethylbenzene, and cumene has been cofirmed by other investigators.[13-15] However, cyclohexene has been expected to be more reactive than cumene.[15]

The present computation of Eq. (27) gave no curve with both the minimum and maximum seen in Figs. 2 and 3 for any combination of various parameters; rather it gave a curve which has only the maximum seen in Figs. 4—7 or a curve which decreases monotonously. Since Eq. (27) is derived on the assumption that (BH)/(AH) is constant throughout the cycles, another equation was derived by the same procedure on the assumption that all amount of an additive added is consumed by the fourth cycle. This equation gave a monotonously decreasing curve for the numerical analysis over the same range of parameters as with Eq. (27), except for the combination, $m_a=0.8$, $m_b=0.6$, and $c_a=c_b=0.8$, which gives both the minimum and the maximum. In the light of these results, the present curves in Figs. 2 and 3 suggest that, when x_B is very small, all of the additive is consumed within a few cycles at the beginning in a batch system like the present reactor.

Cyclohexene is fairly soluble in water, as may be seen in Table 1, and it would be very reactive for reaction (30).[15] In fact, the oil phase after the reaction was greatly colored only in the case of cyclohexene. Therefore, the irregularity of cyclohexene in the series 31 may be concluded to be due to the shift in the maximum in Fig. 3(B), because if cyclohexene is present in the later cycles without such consumption, the value of x_{max} would be even smaller.

Since *n*-hexane is very insoluble in water, as may be seen in Table 1, there is no trouble with the consumption, as has been mentioned above. Supporting this conclusion, the $Y(A)_{min}$ of *n*-hexane is nearly equal to unity. Therefore, although there has been no report about the relative reactivity of *n*-haxane for reaction (30), the x_{max} value of *n*-hexane in Fig. 3(A) is the most reliable.

The v_{max} values of the other additives are more or less shifted to larger values due to the consumption of the smaller x_B. Therefore, an experiment on the flow system, for which (BH)/(AH) can be kept constant, is necessary for the useful application of the diagram in Figs. 8 and 9. Furthermore, the direct measurement of the solubility without the use of Eq. (2) is necessary in order to get exact information from it. Toluene is the most suitable as the host reactant (AH), for the reaction scheme (reactions (3)—(10)) is correct for it.[3,4]

Another problem is that the x_{max} value as esti-

13) G. A. Russell, *J. Am. Chem. Soc.*, **78**, 1047 (1956).
14) D. J. Carlson and K. U. Ingold, *ibid.*, **89**, 4891 (1967).
15) J. A. Howard and K. U. Ingold, *Can. J. Chem.*, **45**, 793 (1967).

mated by Eq. (2), is too small, for the value of $R_{b\,a}$ obtained from it by using Figs. 8 and 9 is too large compared with the data provided by the other methods at lower temperatures.[13-15] It is not clear whether this discrepancy is due to reaction temperature, a characteristic of the aqueous phase, or some approximation for the derivation of Eq. (26).

The values of $Y(\mathrm{A})_{max}$ for alcohols are in the order of:

$$t\text{-butyl} > \text{isopropyl} > \text{ethyl} \qquad (32)$$

In the diagram of Figs. 8 and 9, the larger $Y(\mathrm{A})_{max}$ or F_{max} value corresponds to the larger c_a value. This means that reaction (10) for toluene is suppressed by alcohol, which has a more complex structure or is more oxidable.

Oxidation of Benzene Mixtures. According to the previous studies, the autoxidation of benzene is initiated by reaction (4) with impurities in benzene, which are more reactive than benzene.[1] Even though the hydroxyl radical reacts with benzene, reaction (4) may involve addition. Furthermore, more than one half of the phenol produced is formed not through $C_6H_5O\cdot$ but through $C_6H_5^+$.[4] Therefore, Eq. (25) must be modified for benzene to the form:

$$Y(\text{Phenol}) = \sum[(1-i)m_a + if]a_{n-1} + \sum ifb_{n-1} \qquad (33)$$

where i is the fraction of phenol produced through $C_6H_5^+$, which can be determined by using oxygen-18, as has been seen in a previous study,[4] and where f, which is not necessarily equal to a_0 as defined by Eq. (12) for the case of benzene, is defined in the form:

$$f = \frac{k_{6aa}(\mathrm{AH})}{k_{6aa}(\mathrm{AH}) + k_{6ab}(\mathrm{BH})} = \frac{k_{6ba}(\mathrm{AH})}{k_{6ba}(\mathrm{AH}) + k_{6bb}(\mathrm{BH})} \qquad (34)$$

instead of Eq. (15).

The order of the x_{max} values in Table 2A is not always the same as in series 31. This is due to the difference between benzene and toluene in the reaction mechanism, as has been mentioned above. Since the mechanism for benzene is rather complex, benzene is not a suitable standard reactant (AH) for a study of the relative reactivity using the present method. The value of x_{max} for toluene (0.002) suggests that toluene is more reactive than benzene in the series 31 in spite of the fact that the yield of phenol is larger than that of benzaldehyde in Fig. 1. This subject has already been discussed in the section on the yields of benzaldehyde in "Results."

BULLETIN OF THE CHEMICAL SOCIETY OF JAPAN VOL. 42 3064—3072 (1969)

An X-Ray Emission Spectroscopic Investigation of the Chemical Bond of Sulfur. III. The Profile of S$K\beta$ Band in Sulfur Compounds

Yoshihito TAKAHASHI and Katsumasa YABE

Government Industrial Development Laboratory, Hokkaido, Higashi-tsukisamu, Sapporo

(Received February 15, 1969)

The profile of the S$K\beta$ band in various sulfur compounds, including many organic compounds, was separated into peaks, and the wavelength values and the intensities of the separated peaks were discussed in relation to the chemical bonding. The band of sulfone and sulfoxide consists of three or four peaks. We named the peaks A, B, C (the strongest), and D, beginning from the longer-wavelength side. The relative intensity of the peak A (generally named $K\beta'$) increases as the number of valence electrons of the sulfur atom decreases. The peak B may be attributed to the non-polar single bond of sulfur in sulfone and sulfoxide. The clear peak, D, appears only in the band of sulfite and sulfoxide. The band of the compounds of thiourea type consists of two peaks. Using the results of the above study, the chemical structures of aldehyde-bisulfite adducts and 2-mercaptobenzimidazole, *etc.*, were discussed.

In a previous paper,[1] we reported a study of the number of valence electrons of the sulfur atom in compounds in relation to the shifts of the S$K\alpha$ wavelength. However, the S$K\alpha$ line has no direct relation to the valence electrons which are con-

1) T. Sato, Y. Takahashi and K. Yabe, This Bulletin, **40**, 298 (1967).

nected with the chemical bond, for the S$K\alpha$ line arises from the inner-shell electron transition (2p→1s). On the contrary, the S$K\beta$ band arises from the transition of the valence electron (valence level→1s), so the structure of the S$K\beta$ spectrum is greatly influenced by the chemical state of the attributed compounds.

Faessler and Schmid has reported that the S$K\beta$ band spectra of sulfates have peculiar structures, unlike the bands of sulfides and rhombic sulfur.[2] Schnell studied the structures of the $K\beta$ band spectra, together with the relative intensity of $K\beta$ to $K\alpha$, in the elements of sulfur, phosphor, silicon, and aluminum in various compounds.[3] Also, Wilbur and Gofman studied the S$K\beta$ spectra of comparatively many materials, stressing the intensity.[4] Besides, the SL bands (valence level→2p) of various compounds were investigated by Fischer and Baun.[5] However, no sufficiently systematic investigation of the S$K\beta$ spectra of various organic compounds and liquid samples has yet been made. Moreover, no separation of the S$K\beta$ band spectrum into its component peaks has ever been attempted.

Our purpose was to make clearer the relationship between the character of the chemical bond and the S$K\beta$ band structure.

Experimental

The spectra were obtained on the improved Rigaku-Denki K-3 Fluorescent X-ray Spectrograph. Its details have been presented in the previous paper.[1] However, the glancing angle, α (the take-off angle of the X-ray), was changed to 35°. A flat sodium chloride crystal ($2d$: 5.6396 Å) was used as the analyzing crystal. Two Soller slits were inserted into the light path; the one situated between the sample and the crystal was 10 cm long, with 0.15 mm spacing, while the other, between the crystal and the detector, was 5 cm long and had 0.10 mm spacing. The helium path was maintained using a flow of 2 l/min. The Machlett OEG-50S chromium target X-ray tube was usually operated at 40 kV, 30 mA.

In the measurements of most of the liquid samples, a liquid sample holder with a Mylar-film window (10 μ thick) was employed, but in the cases of concentrated sulfuric acid, sulfuryl chloride, and thionyl chloride, the Mylar-film window was replaced by a polyethylene film window (30 μ thick).

The band profile was obtained as follows: the X-ray intensities were measured for a minute at each 3′(2θ) stage, and then these intensities, each measured maximum intensity having been made the same values, were plotted against the wavelength. The background was measured at 129°00′(2θ) (5.0902 Å), on the longer-wavelength side of the S$K\beta$ band, because, on the the shorter-wavelength side of the S$K\beta$ band, the absorption edge is near the band and, moreover, its position varies with the kind of compound.

The wavelength of the band was determined within an accuracy of ±0.0008 Å by referring to the third-order reflection lines of Ni$K\alpha_1$ (4.97352 Å) and Ni$K\alpha_2$ (4.98507 Å). On the measurement of the half-peakwidth, the half-linewidth of third-order reflection line of Ni$K\alpha_1$, 16.0′(2θ) (2.8 eV), was chosen as the standard.

Most of the sample materials were guaranteed or extra pure reagents. The materials which we prepared in our laboratory were confirmed by X-ray diffraction or infrared analysis. The surface temperatures of the samples were 30—40°C while the measurements were being carried out.

Results

The profiles of the S$K\beta$ band are related to the various bonding forms of the sulfur atom. We may divide them roughly into five classes according to the bonding form. The profiles of the S$K\beta$ band on several materials of each class are shown in Figs. 1—5, while the wavelength values, half-peakwidths, relative integrated intensities, and other data on the peaks of the S$K\beta$ band spectrum are listed in Tables 1—5.

1) Inorganic Sulfide. Except for cuprous sulfide, the S$K\beta$ spectra of ten inorganic sulfides

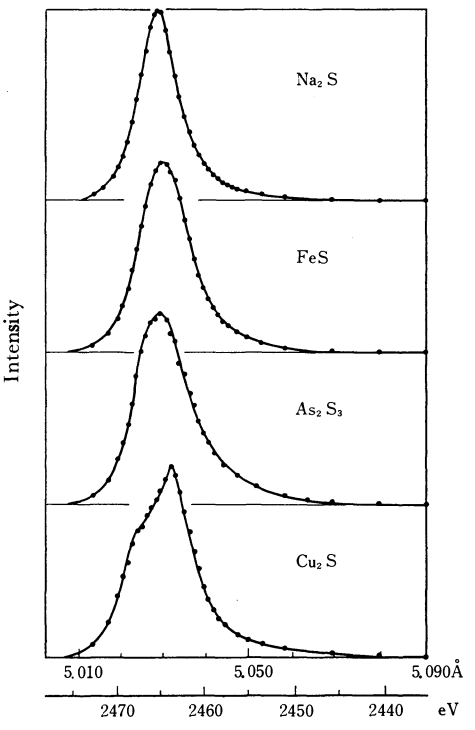

Fig. 1. S$K\beta$ spectra of inorganic sulfides.

2) A. Faessler and E. D. Schmid, *Z. Physik*, **138**, 71 (1954).

3) E. Schnell, *Monatsh. Chem.*, **94**, 703 (1963).

4) D. W. Wilbur and J. W. Gofman, "Advances in X-Ray Analysis," Vol. 9, ed. by Mallett, Fay, and Mueller, Plenum Press, New York (1965) p. 354.

5) D. W. Fischer and W. L. Baun, *ibid.*, Vol. 9, p. 329.

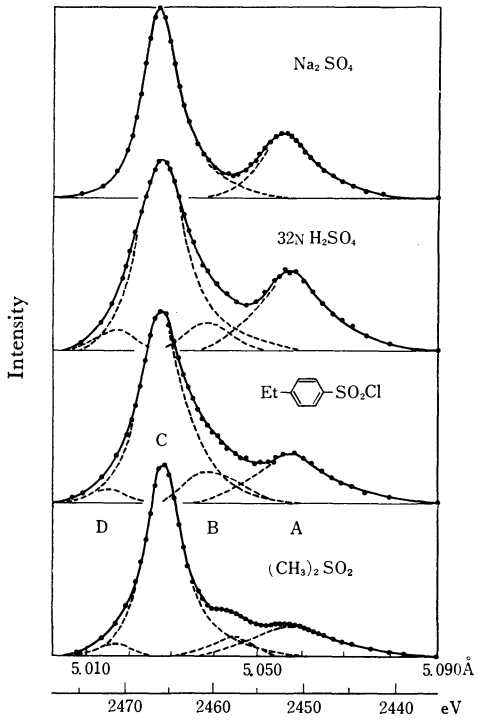

Fig. 2. S$K\beta$ spectra of sulfates and sulfones.

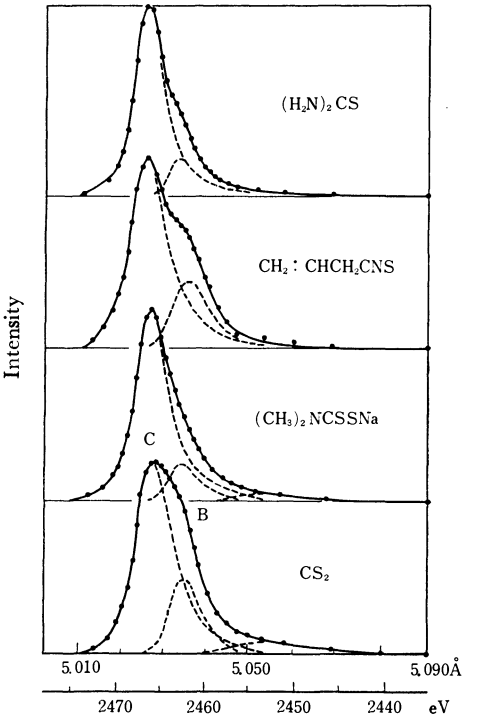

Fig. 4. S$K\beta$ spectra of thiourea, carbon disulfide, *etc.*

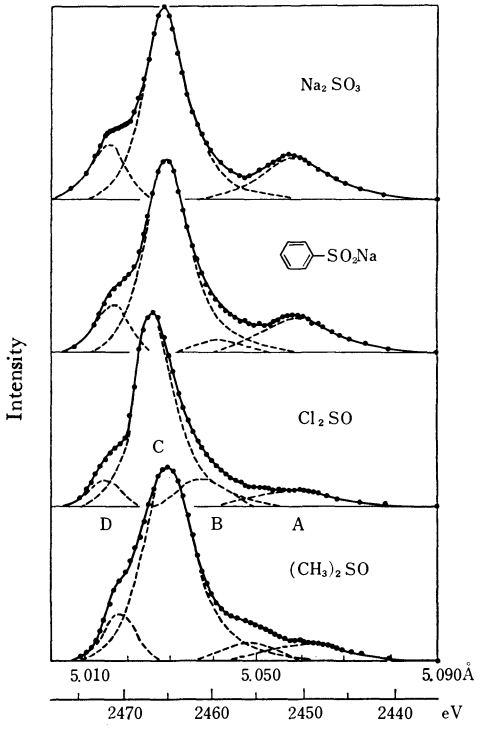

Fig. 3. S$K\beta$ spectra of sulfites and sulfoxides.

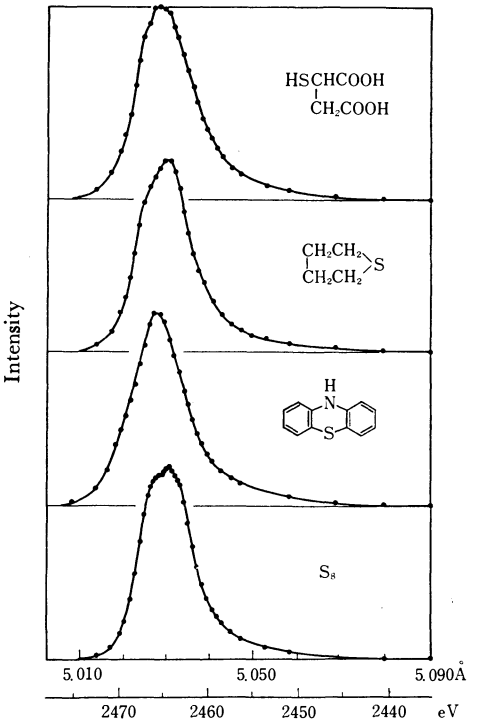

Fig. 5. S$K\beta$ spectra of thiol, organic sulfides and rhombic sulfur.

Table 1. Wavelengths half-widths and asymmetry indexes of peak in S$K\beta$ spectra of inorganic sulfides

Compound	Coordination number*	Wavelength (Å)	Width (1/2)	Asymmetry index
Na_2S	8	5.0293	2.01	1.07
CaS	6	299	2.20	1.05
Cr_2S_3	6	297	2.33	1.06
α-MnS	6	295	2.60	1.07
ZnS	4	289	2.42	1.10
CdS	4	289	2.27	1.11
FeS**	6	304	2.54	1.05
NiS	6	304	2.58	1.05
Sb_2S_3		285	2.68	1.15
As_2S_3		285	2.79	1.20
Cu_2S**		32	2.9	
Error		±0.0008	±0.10	±0.03

* The number related to sulfur atom.
** Lack in sulfur content is an extent of about 1.0 wt %.

are almost identical in shape, but they slightly differ in position and in the width of the band. From their simple profiles, it can be assumed that the S$K\beta$ spectrum of inorganic sulfide consists of only one peak. The peaks of sulfides in which the coordination number of sulfur atom is six show a little longer-wavelength values and smaller asymmetry indexes than those of the other sulfides.

2) Sulfate and Sulfone. In Figs. 2—4, the dotted lines show the results obtained by the separation into peaks, using the profile of the S$K\beta$ band of sodium sulfide (shown in Fig. 1) as the standard shape of a single peak. A peak profile of an arbitrary size was made by lengthening or shortening the standard single peak in the direction of the ordinate or abscissa, while keeping the degree of asymmetry unchanged. Each of their spectra consists of two, three, or four peaks, which are named as A, B, C, and D beginning from the longer-wavelength side.

3) Sulfite and Sulfoxide. A feature of this class is the appearance of a remarkable peak D. The relative intensities of the peak A in this class generally take smaller values than those in the

Table 2. Wavelengths half-widths and relative intensities of peaks in S$K\beta$ spectra of sulfates and sulfones

Compound	Wavelength (Å)				Width (½)		Intensity			
	A	B	C	D	A	C	A	B	C	D
Na_2SO_4	5.055		5.0262		2.6	1.9	0.30		0.70	
2M Na_2SO_4	5.055	5.038	5.0266	5.012	2.8	2.3	0.29	0.01	0.69	0.01
8N H_2SO_4	55	35	260	13	2.8	1.9	0.30	0.03	0.66	0.01
32N H_2SO_4	56	34	262	15	3.0	2.5	0.30	0.06	0.62	0.02
$NaHSO_4$	55	35	260		2.7	2.0	0.29	0.03	0.68	
$CaSO_4$	55		265		2.8	1.8	0.32		0.68	
$(NH_4)_2SO_4$	55	35	258		2.8	1.9	0.28	0.02	0.70	
$PhNH_2 \cdot ½H_2SO_4$	55	34	258		2.9	2.0	0.31	0.03	0.66	
$(EtO)_2SO_2$	56	37	264	16	3.3	2.5	0.30	0.05	0.61	0.04
$C_{12}H_{25}OSO_3Na$	56	35	259	14	3.2	2.2	0.31	0.02	0.66	0.01
$PhOSO_3K$	55	34	255		3.1	1.9	0.31	0.05	0.64	
H_2NSO_3H	55	34	262		2.8	1.9	0.29	0.03	0.68	
$HOCH_2SO_3Na$	57	41	270	12	3.2	2.0	0.27	0.03	0.67	0.03
$PhSO_3H$	56	38	268	16	3.3	2.3	0.26	0.05	0.66	0.03
$PhSO_2NH_2$	55	36	270	14	3.9	2.2	0.24	0.04	0.70	0.02
$PhSO_2NHBu$	55	38	270	14	3.3	2.3	0.24	0.09	0.65	0.03
p-$EtPhSO_2NEt_2$*	57	38	268	16	3.0	2.3	0.21	0.12	0.66	0.01
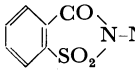	55	38	277	16	4.0	2.4	0.24	0.06	0.65	0.05
Cl_2SO_2	55	35	257	12	3.7	2.0	0.27	0.07	0.65	0.01
p-$EtPhSO_2Cl$	56	38	264	14	3.8	2.2	0.24	0.10	0.63	0.03
$PhSO_2F$	56	37	266	16	3.8	2.6	0.24	0.08	0.64	0.04
$(CH_3)_2SO_2$	56	43	268	16	4.0	2.0	0.20	0.05	0.72	0.03
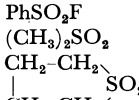	57	41	274	16	3.8	2.3	0.19	0.08	0.68	0.05
Ph_2SO_2	57	40	274	16	3.7	2.2	0.21	0.08	0.68	0.03
Error	±0.001	±0.001	±0.0008	±0.002	±0.2	±0.1	±0.02	±0.03	±0.02	±0.03

* Benzene solution, 50%.

TABLE 3. WAVELENGTHS, HALF-WIDTH AND RELATIVE INTENSITIES OF PEAKS IN $SK\beta$ SPECTRA OF SULFITES AND SULFOXIDES

Compound	Wavelength (Å)				Width (1/2)		Intensity			
	A	B	C	D	A	C	A	B	C	D
Na_2SO_3	5.058		5.0288	5.016	3.3	2.2	0.20		0.66	0.14
$NaHSO_3$	5.059	5.039	5.0288	5.016	3.7	2.2	0.21	0.03	0.67	0.09
$(EtO)_2SO$	59	40	277	16	3.7	2.6	0.18	0.06	0.68	0.06
$HOCH_2SO_2Na$	58	41	283	16	3.4	2.3	0.16	0.02	0.75	0.07
$PhSO_2Na$	57	40	280	15	3.5	2.3	0.18	0.03	0.69	0.10
PhNSO	58	38	288	18	4.0	2.3	0.17	0.04	0.70	0.09
Cl_2SO	58	36	260	14	3.8	2.0	0.15	0.08	0.72	0.05
$(CH_3)_2SO$	60	47	280	17	4.0	2.6	0.09	0.05	0.75	0.11
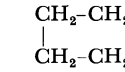	57	42	278	17	3.8	2.2	0.14	0.05	0.74	0.07
Error	±0.001	±0.001	±0.0008	±0.002	±0.2	±0.1	±0.02	±0.03	±0.02	±0.03

TABLE 4. WAVELENGTHS, HALF-WIDTHS AND RELATIVE INTENSITIES OF PEAKS IN $SK\beta$ SPECTRA OF ISOTHIOCYANATES, THIOUREA, *etc.*

Compound	Wavelength (Å)		Width (1/2)		Intensity	
	B	C	B	C	B	C
CH_2:$CHCH_2NCS$	5.036	5.0255	1.8	1.9	0.23	0.77
PhNCS	36	260	1.6	1.9	0.16	0.84
$(H_2N)_2CS$	33	255	1.3	1.5	0.14	0.86
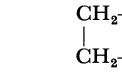	34	262	1.5	1.5	0.15	0.85
$(PhHN)_2CS$	34	265	1.7	1.5	0.23	0.77
$[(H_3C)_2N]_2CS$	34	267	1.5	1.5	0.18	0.82
$[(H_3C)_2NPh]_2CS$	34	272	1.9	1.9	0.21	0.79
$(H_3C)(H_2N)CS$	34	270	1.7	1.5	0.17	0.83
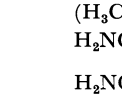	33	265	2.0	1.8	0.25	0.75
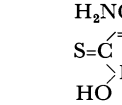	32	255	2.0	1.8	0.25	0.75
CS_2	33	262	1.6	2.0	0.23	0.77
KSCN	34	253	2.0	1.5	0.26	0.74
$Et_2NCSSNa$	33	260	1.9	1.6	0.17	0.83
$(O_2NPhO)(EtO)_2PS$*	36	288	2.0	2.0	0.17	0.83
Error	±0.001	±0.0008	±0.2	±0.1	±0.02	±0.02

* Kerosene solution, 50%.

sulfate and sulfone class.

4) Thiourea Derivatives, Thiocyanates, Isothiocyanates, and Monothiophosphate (Abbr.: Thiourea Class). Each of their spectra consists of two main peaks, but in certain cases, as when a large tail exists on the longer-wavelength side, there seems to be another very weak peak.

5) Organic Sulfide, Thiol and Rhombic Sulfur. All of their spectra have broader bands. As with thiophene and phenothiazine, the spectrum of the compounds with a sulfur atom in unsaturated ring shows a prominent inflection on the shorter-wavelength side of the band.

Discussion

Inorganic Sulfide. The relationship between the $SK\beta$ bandwidth and the ionic character of the

Table 5. Wavelengths of peaks in $SK\beta$ spectra of organic sulfides, thiols and rhombic sulfur

Compound	Wavelength (Å)
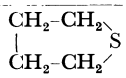	5.0285
	285
$[CH_2(OH)CH_2]_2S$	274
Ph_2S	282
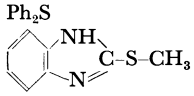	275
$PhCH_2-S-C(NH_2)NH$	265
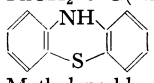	270
Methylene blue	280
$HS-CH_2COONa$	275
HS-Ph	285
o-HS-PhCOOH	280
$HS-(CH_2)_{15}CH_3$	301
HS-CH(COOH)CH_2COOH	270
	280
$(PhCH_2S-)_2$	265
$(ClS-)_2$	285
$(-CH_2S-)_3$	270
S_8	295
Error	0.0008

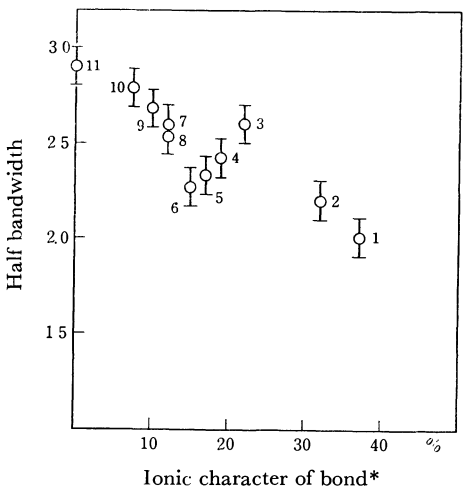

Fig. 6. Relationship between bandwidth of $SK\beta$ and ionic character of bond.

1 Na_2S, 2 CaS, 3 α-MnS, 4 ZnS, 5 Cr_2S_3, 6 CdS, 7 NiS, 8 FeS, 9 Sb_2S_3, 10 As_2S_3, 11 $HS-CH_2COONa$

* Ionic characters were calculated by the following equation,[6]

Ionic character (%) $= 16|X_a-X_b| + 3.5|X_a-X_b|^2$, X_a, X_b: electronegativity of element.

6) N. B. Hannay and C. P. Smyth, *J. Am. Chem. Soc.*, **68**, 171 (1946).

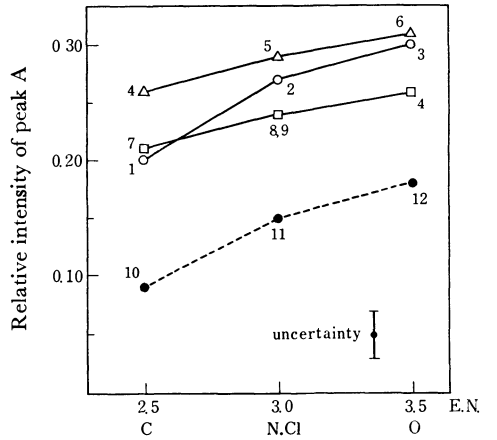

Fig. 7. Relationship between relative intensity of peak A and kind of atom combined with sulfonyl and sulfinyl group.

1 $(CH_3)_2SO_2$, 2 Cl_2SO_2, 3 $(EtO)_2SO_2$, 4 $PhSO_3H$, 5 H_2NSO_3H, 6 $C_{12}H_{25}OSO_3Na$, 7 Ph_2SO_2, 8 *p*-$EtPhSO_2Cl$, 9 $PhSO_2NH_2$, 10 $(CH_3)_2SO$, 11 Cl_2SO, 12 $(EtO)_2SO$

—— sulfone ------ sulfoxide

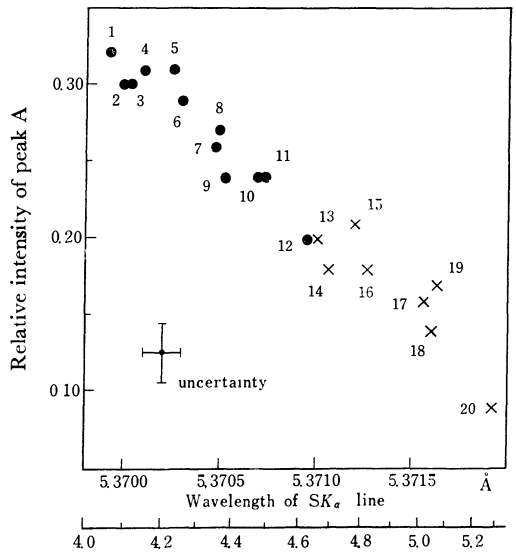

Fig. 8. Relationshop between relative intensity of peak A and number of valence electrons of sulfur atom.

1 $CaSO_4$, 2 $(EtO)_2SO_2$, 3 Na_2SO_4, 4 $PhNH_2 \cdot \frac{1}{2}H_2SO_4$, 5 $C_{12}H_{25}OSO_3Na$, 6 H_2NSO_3H, 7 $PhSO_3H$, 8 $HOCH_2SO_3Na$, 9 $PhSO_2F$, 10 $PhSO_2NH_2$, 11 *p*-$EtPhSO_2Cl$, 12 $(CH_3)_2SO_2$, 13 Na_2SO_3, 14 $PhSO_2Na$, 15 $NaHSO_3$, 16 $(EtO)_2SO$, 17 $HOCH_2SO_2Na$, 18 $(CH_2)_4SO$, 19 PhNSO, 20 $(CH_3)_2SO$

● sulfone, × sulfoxide.

Wavelength values of $SK\alpha$ line were refered from Ref. 7.

bond is shown in Fig. 6. As the ionic character of the bond increases, the bandwidth becomes narrower. On rhombic sulfur and organic sulfide, taken for reference, their S$K\beta$ bandwidths show the values to be expected from Fig. 6.

The S$K\beta$ band of cuprous sulfide takes a unique shape (see Fig. 1). It may be that its prominent shoulder on the shorter-wavelength side of the main peak is caused by the conduction electrons. Cuprous sulfide exhibits a highly electronic conductivity.

Sulfate, Sulfone, Sulfite and Sulfoxide. Concerning the energy differences between the peaks A and C in the S$K\beta$ band spectrum, no noticeable distinction can be found among the sulfates, sulfones, sulfites, and sulfoxides measured at about 14 eV. Since no peak corresponding to A can be found in the S$K\beta$ spectrum of sulfur compounds except for oxocompounds of sulfur, and since the energy difference varies almost not at all with the compound, the peak A may be attributed to the SO bond.

Figure 7 shows that the relative intensity of the peak A increases as the electronegativity value of the atom that is combined with the sulfonyl or sulfinyl group increases. In other words, as the plus charge on the sulfur atom increases, the intensity of the peak A increases. Figure 8 shows the relationship between the relative intensity of the peak A and the effective charges of the sulfur atom in sulfone and sulfoxide.[1] In Fig. 7, with regard to the relative intensity of the peak A of the sulfones and sulfoxides which have the same functional group (for example, $(EtO)_2SO_2$ and $(EtO)_2SO$, Cl_2SO_2 and Cl_2SO, $(CH_3)_2SO_2$ and $(CH_3)_2SO$, *etc.*), the former have values about twice as large as the latter. This fact shows that the increase in the relative intensity of the peak A is mainly influenced by the oxygen atom in the double bond. Therefore, with regard to the relative intensity of the peak A, comparing alkyl sulfate with alkyl sulfone and alkyl sulfite with alkyl sulfoxide, diethyl sulfate has twice as many oxygen atoms in a molecule as dimethyl sulfone, but the relative intensity of diethyl sulfate is considerably smaller than twice the value of dimethyl sulfone; moreover, though diethyl sulfite has three times as many oxygen atoms in a molecule as dimethyl sulfoxide, the relative intensity of the former is considerably smaller than three times the value of the latter. These facts show that, in the contribution to the increase in the relative intensity of the peak A, the oxygen atom in the single bond is smaller than that in the double bond. Assuming that the alkyl group scarcely contributes at all to the electron transfer, the above facts can be explained in terms of the concept that the inductive effect of the oxygen atom in the double bond is much larger than that of the oxygen atom in the single bond.

Most sulfones and sulfoxides have the peak B between the peaks A and C in the S$K\beta$ spectra. The sulfone combined with the same two functional groups has a symmetrical peak B in the spectrum. On the other hand, the sulfone combined with two different groups has a partly asymmetrical peak B, which might consist of two peaks. Figure 9 shows

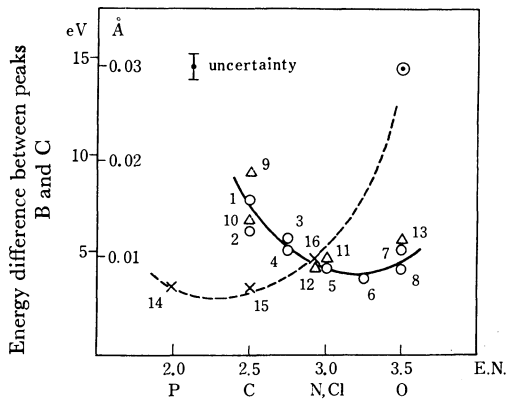

Fig. 9. Behavior of peak B.

1 $(CH_3)_2SO_2$, 2 Ph_2SO_2, 3 *p*-$EtPhSO_2Cl$, 4 $PhSO_2NH_2$, 5 Cl_2SO_2, 6 H_2NSO_3H, 7 $(EtO)_2SO_2$, 8 $C_{12}H_{25}OSO_3Na$, 9 $(CH_3)_2SO$, 10 $(CH_2)_4SO$, 11 Cl_2SO, 12 PhNSO, 13 $(EtO)_2SO$
○ sulfone, △ sulfoxide.

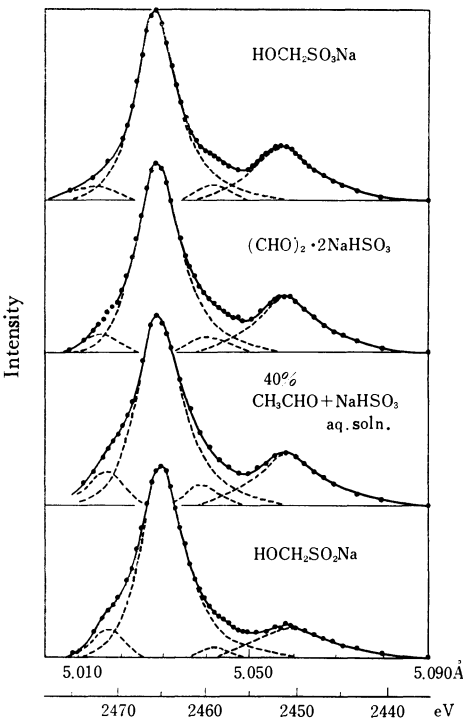

Fig. 10. Comparison of S$K\beta$ spectra of aldehyde-bisulfite adducts with sulfone and sulfoxide.

Table 6. Comparison of S$K\beta$ spectra of aldehyde-bisulfite adducts with sulfones and sulfoxides

Compound	S$K\alpha$ Wavelength (Å)*	S$K\beta$ Wavelength (Å)		S$K\beta$ Intensity	
		A	C	A	D
$NaHSO_4$	5.36999	5.055	5.0260	0.29	
$HOCH_2SO_3Na$	7049	57	270	0.27	0.03
$HCHO+NaHSO_3$**	708	57	272	0.25	0.05
$CH_3CHO+NaHSO_3$**	709	57	275	0.24	0.07
$(CHO)_2\cdot 2NaHSO_3$	7053	57	272	0.26	0.03
$PhCHO\cdot NaHSO_3$	7049	57	280	0.27	0.05
$HOCH_2SO_2Na$	7157	58	283	0.16	0.07
$NaHSO_3$	7120	59	288	0.21	0.09
Error	±0.0001	±0.001	±0.0008	±0.02	±0.03

* Ref. 7.
** Aquous solution, 50%, estimated in adduct, keeping aldehyde excess.

the relationship of the energy difference between the peaks B and C to the kind of atom combined with the sulfonyl and sulfinyl groups. There is no clear distinction in the energy difference among the elements of chlorine, nitrogen, and oxygen, but on carbon the peak B appears further apart from the peak C than in the cases of the other elements. In the compounds combined with amino or hydroxyl groups, the reltive intensity of the peak B is generally small (see Tables 2 and 3). The hydrogen atom in an amino or hydroxyl group is rather dissociable. A more dissociable group, such as –ONa, contributes very little to the intensity of the peak B. In sulfonamides, the relative intensity of the peak B is larger in the order: tertiary, secondary, and primary amino groups. This order is the reverse of the order of the number of dissociable hydrogen atoms in the amino group. These facts suggest that the evolution of the peak B is more affected by the non-polar single bond of sulfur in sulfone and sulfoxide.

In the spectrum of sodium bisulfite (see Fig. 3), a weak peak B is observed, so its hydroxyl group seems not to be very dissociable.

In the spectrum of concentrated sulfuric acid, the peak B is also observed; the peakwidth and the relative intensity of the peak are similar to those of diethyl sulfate rather than to those of diluted sulfuric acid or sodium sulfate (see Table 2). Consequently, the hydroxyl groups of concentrated sulfuric acid seem to be rather undissociable.

The appearance of the peak D is clear only in the spectra of sulfites and sulfoxides. But then, the peak corresponding to the peak D of sulfur compounds has been observed in the B$K\alpha$ band spectra of boric oxide $(B_2O_3)_n$ and boric nitride $(BN)_n$.[5] The boron atom in their compounds has a sp^2 hybrid orbital, analogous with the sulfur atom in a sulfite ion. Therefore, the peak D may result from the presence of the sp^2 hybrid orbital. In the spectra of some sulfones, a very weak peak like D was separated by the separation into peaks.

The S$K\beta$ spectra of aldehyde-bisulfite adducts are shown in Fig. 10. Their peak C shifts about 0.001 Å to the shorter-wavelength side from the position of bisulfite salt or sodium formaldehyde sulfoxylate ($HOCH_2SO_2Na$), and the relative intensities of the peak A are larger, and those of the peak D are smaller, than those of sulfites and sulfoxides (see Table 6). These take values rather closer to those of such sulfones as hydroxymethansulfonate ($HOCH_2SO_3Na$). Moreover, the wavelength of the S$K\alpha$ line of the adducts take values closer to those of sulfones. Two structural formulas in the equilibrium state may be given for the aldehyde-bisulfite adduct;

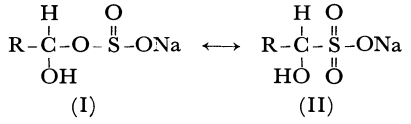

(I) (II)

According to this fact, a considerable portion of the materials have sulfone-type structures (II). This conclusion is supported by the results of the X-ray structural analysis.[8]

Thiourea Class. The values of the energy differences between the peaks B and C range from 3 to 5 eV, much as with those of sulfones. However, it cannot be asserted that this peak B has virtually the same quality as those of sulfones because the two bonding forms which seem to be attributable to the peak B are different; that is, in sulfnones,

7) Y. Takahashi, K. Yabe and T. Sato, This Bulletin, **42**, 2707 (1969).

8) T. Kuroda, T. Ashida, Y. Sasada and M. Kakudo, *ibid.*, **40**, 1377 (1967).

TABLE 7. COMPARISON OF S*Kβ* SPECTRA OF 2-MERCAPTOBENZIMIDAZOLE AND ITS HOMOLOGS WITH THIOUREA AND THIOLS

Compound	S*Kα* Wavelength (Å)	S*Kβ* Wavelength (Å)		S*Kβ* Width (1/2)		S*Kβ* Intensity
		B	C	B	C	B
2-Mercaptobenzimidazole	5.37302*	5.034	5.0262	1.6	1.4	0.19
2-Mercaptobenzimidazole pyridine soln., 40%	*	34	258	1.5	1.3	0.17
2-Mercaptobenzoxazole	7308*	34	258	1.7	1.4	0.19
2-Thiobarbituric aicd	7298*	34	258	1.7	1.5	0.21
2-Thiouracil	7301*	34	258	1.3	1.5	0.19
$(H_2N)_2CS$	7287*	33	255	1.3	1.5	0.14
$(PhHN)_2CS$	731**	34	265	1.7	1.5	0.23
o-HS-PhCOOH	728**		280		2.7	
$HS-CH_2COONa$	728**		275		2.9	
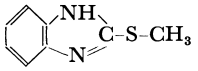	7283*		275		2.7	
Error	±0.0001	±0.001	±0.0008	±0.2	±0.1	±0.02

* Ref. 7. ** Ref. 1.

there is a single bond, and in the thiourea class, a double bond.

On 2-mercaptobenzimidazole, 2-mercaptobenzoxazole, 2-thiouracil, and 2-thiobarbituric acid, we can assume two structural formulas, *i. e.*, thiol and thiocarbonyl forms. For example, 2-mercaptobenzimidazole may have the following two forms:

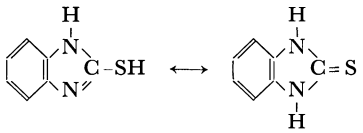

(III) (IV)

However, in the solid state and in a pyridine solution, its S*Kβ* spectrum differs from those of thiols and is similar to those of thiocarbonyl-type compounds, as is shown in Fig. 11. Furthermore, the wavelengths of the S*Kα* lines also have values closer to that of thiourea. Consequently, they may be said to have thiocarbonyl forms (IV) in the solid state and in a pyridine solution at room temperature.

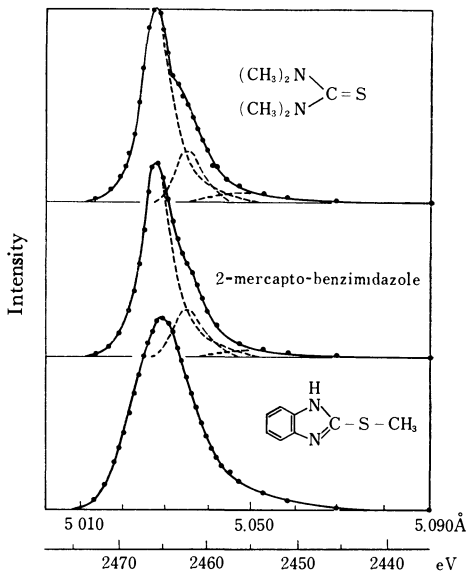

Fig. 11. Comparison of S*Kβ* spectra of 2-mercaptobenzimidazole with thiourea and 2-methylthiobenzimidazole.

Conclusion

In this study, we found that S*Kβ* spectra give appreciable information relating not only to the kind of bonding but also to the kind of atom combined with the sulfur atom in compounds. Especially, we have obtained much information on sulfones and sulfoxides. If the separation into peaks were more accurate, a more detailed discussion could be made with respect to the peaks B and D, thus making the analysis of the bonding state feasible, even in a mixture.

The authors wish to thank Dr. T. Sato, Dr. E. Asada, Professor T. Sagawa, and Dr. Y. Gohshi for their helpfull advice.

BULLETIN OF THE CHEMICAL SOCIETY OF JAPAN VOL. 42 3073—3075 (1969)

Energy Transfer between Benzene and Toluene in the Singlet States at 90°K

Akihiko NAKAHARA, Motohiko KOYANAGI, Yoshio MURAKAMI, Takao EDAMURA and Yoshiya KANDA

Department of Chemistry, Faculty of Science, Kyushu University, Fukuoka

(Received March 11, 1969)

The fluorescence spectrum of toluene in benzene has been photographed at 90°K and analyzed accurately. Systematic studies of concentrations made it possible to estimate the efficiency of energy transfer from the singlet state of the host molecule to that of the guest molecule. The fluorescence spectrum of pure benzene has also been studied at 4.2°K and 90°K for comparison, and the effect of toluene as an impurity in the benzene spectra has been discussed.

Leach, Lopez-Campillo and Lopez-Delgado[1] studied the effect of occluded gas and the thermal treatment of a sample on the probability of electronic-energy transfer between benzene and toluene at 80°K. We have also studied electronic-energy transfer in the lowest excited singlet states of benzene and toluene and estimated the rate of energy transfer in the system.

Experimental

The benzene was purified by the way described in a previous paper.[2] Commercial benzene often contains toluene as an impurity at a concentration of about 10^{-2}—10^{-3} mol/*l*. The purification was repeated until no toluene bands in the fluorescence spectrum could be detected within the experimental limits employed in this work.

The toluene was purified according to the method of Schwalbe.[3] A gaseous mixture of nitric and nitrous oxide was introduced into toluene, and then 2% of sulfuric acid was added 2 or 3 hr later. The toluene was stirred for 5 min and then left standing for 15 min. The lower layer was removed. This operation was repeated three times. When the acid part became faint yellow, the toluene was washed with a dilute caustic soda solution until no color change was detected in the solution. It was then dried over calcium oxide and distilled.

The optical setup was exactly the same as that described previously.[2] A super-high-pressure Hg lamp (ORA CHM-12) was used as a light source, and the Hg 2537 Å was projected on a sample through a filter system. The sample solutions employed were 10^{-5}, 10^{-4}, 5×10^{-4}, 10^{-3}, 5×10^{-4}, 10^{-2}, 10^{-1}, and 1 mol/*l* of toluene in benzene. For comparison a solution of 10^{-3} mol/*l* of toluene in cyclohexane was also studied. A sample solution was cooled rapidly by liquid air. While it was being frozen in a cell, the cell was pumped so that all occluded gas in the solution was removed.

The fluorescence spectrum of toluene in benzene was photographed with a Shimadzu quartz spectrograph, QM-60. The exposure time was fixed as 1 hr with a slit width of 50 μ, and Eastman-Kodak 103 a-O plates were used.

Results and Discussion

The fluorescence spectrum of the benzene crystal and the spectrum of toluene in benzene at various concentrations were studied. The microphotometer tracing curves are shown in Fig. 1. The spectral data of toluene in benzene and in cyclohexane are given in Tables 1 and 2 respectively. The spectrum of toluene increases in intensity with an increase in the concentration. It is, therefore, possible to make a quantitative analysis of toluene in benzene. Commercial benzene often contains toluene as an impurity the concentration of which can be estimated by, for example, comparing the height of a band 0—623 of toluene with that of a band, 0—992, of benzene of the tracing curves assumed as intensity (since the spectrum of toluene overlaps that of benzene so extensively that it is impossible to integrate a band intensity). By the way, the 0–0 band of the benzene crystal was not photographed under these experimental conditions, its spectral position was determined with plates subjected to prolonged exopsure.

At a concentration of 10^{-5} mol/*l*, no toluene fluorescence, but rather benzene fluorescence, was observed under the present experimental conditions and only toluene fluorescence was photographed at concentrations of more than 10^{-1} mol/*l* of toluene in benzene. The fluorescence of benzene disappeared at concentrations between 3×10^{-2} and 4×10^{-2} mol/*l* of toluene.

1) S. Leach, A. Lopez-Campillo, R. Lopez-Delgado and Maria-Clandina Tomas-Magos, *Compt. rend.*, **263**, 1230 (1966).
2) Y. Murakami and Y. Kanda, to be published.
3) C. Schwalbe, *Chem. Zentr.*, **1905**, 1, 360.

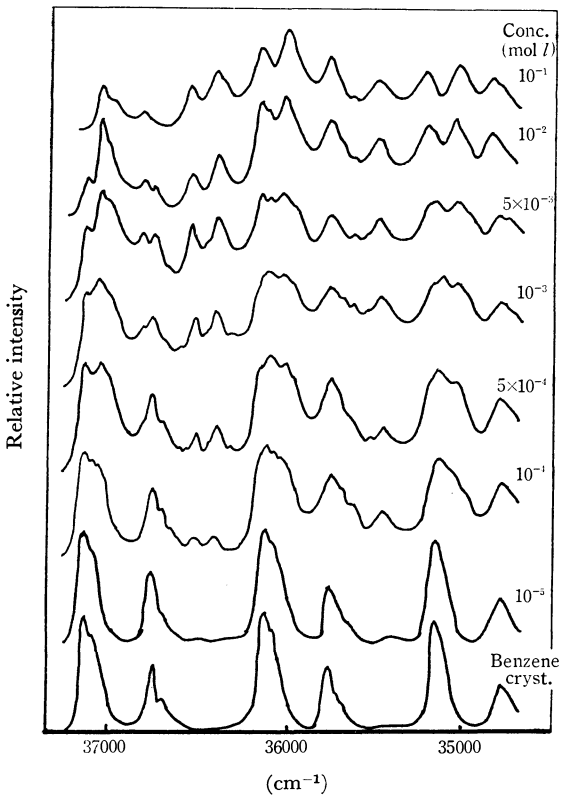

Fig. 1. Fluorescence spectra of toluene in benzene at various concentrations.

If there is no energy transfer from benzene to toluene, the ratio of the fluorescence intensity of toluene to that of benzene should be equal to the ratio of the molar fractions of toluene and benzene molecules, provided that the absorption coefficients of toluene and benzene at the wavelength of the excitation are the same and that the quantum

TABLE 1. FLUORESCENCE SPECTRA OF TOLUENE IN CYCLOHEXANE AT 77°K

No.	Wave number (cm^{-1})	$\Delta\nu$ (cm^{-1})	Assignment	Rel. Int.
1	37140	0	0-0.	5
2	36930	210	0-0.-220	2
3	36625	515	0-0.-520	6
4	36530	610	0-0.-623	8
5	36350	790	0-0.-788	10
6	36150	990	0-0.-1005	10
7	35930	1210	0-0.-1217	8
8	35775	1365	0-0.-1380	5
9	35735	1405	0-0.-623-788	5
10	35620	1520	0-0.-520-1005	6
11	35535	1605	0-0.-623-1005	7
12	35475	1665		6s*
13	35335	1805	0-0.-788-1005	8
14	35135	2005	0-0.-1005-1005	8
15	34940	2200	0-0.-1217-1005	6

* shoulder

TABLE 2. FLUORESCENCE SPECTRA OF TOLUENE AND BENZENE IN A MIXED SYSTEM AT 90°K

No.	Assignment (cm^{-1})			Relative intensity at various concentrations of tolunene (mol/l)							
				0,	10^{-5},	10^{-4},	5×10^{-4},	10^{-3},	5×10^{-3},	10^{-2},	10^{-1}
1	37826	0-0.*	(B)**	—	—	—	—	—	—	—	—
2	37220	0-0.-606	(B)	9	9	9	9	8	7	3	—
3	37100	0-0.	(T)	—	—	7s	9	9	10	7	4
4	36875	0-0.-220	(T)	—	—	—	—	5s	7	3	—
5	36835	0-0.-992	(B)	6	6	6	7	6	7	2	—
6	36575	0-0.-520	(T)	—	—	2	3	6	7	3	4
7	36475	0-0.-623	(T)	—	—	2	3	7	7	5	6
8	36305	0-0.-788	(T)	—	—	7s	8s	8s	10	9	8
9	36215	0-0.-606-992	(B)	10	10	10	10	10	9s	9s	—
10	36100	0-0.-1005	(T)	—	—	7s	9s	9	10	10	10
11	35885	0-0.-1217	(T)	—	—	—	—	8	8	8	8
12	35845	0-0.-2×992	(B)	5	4	8	8	—	—	—	—
13	35560	0-0.-520-1005	(T)	—	—	—	—	5s	6s	3s	4s
14	35480	0-0.-623-1005	(T)	—	—	5	3	7	7	6	5
15	35295	0-0.-788-1005	(T)	—	—	7s	8s	8s	9	7	6
16	35230	0-0.-606-2×992	(B)	9	9	8	9	9	—	—	—
17	35090	0-0.-2×1005	(T)	—	—	7s	8s	8s	9	7	6

s shoulder
* 37200 + 606 = 37826
** (B) and (T) are attributed to the bands of benzene and toluene, respectively.

yields of toluene and benzene are also the same. However, the numbers of benzene molecules are much greater than those of toluene molecules at the various concentrations employed here. This suggests that a considerable amount of energy transfer takes place from benzene to toluene.

The rate of energy transfer between toluene and benzene can now be calculated. Let us assume the following processes:

$$B + h\nu \longrightarrow B^* \qquad \alpha I \qquad (1)$$
$$B^* \longrightarrow B + h\nu'_F \qquad k_1[B^*] \qquad (2)$$
$$B^* \longrightarrow B \qquad k_2[B^*] \qquad (3)$$
$$B^* + T \longrightarrow B + T^* \qquad k_3[B^*][T] \qquad (4)$$
$$T + h\nu \longrightarrow T^* \qquad \beta I \qquad (5)$$
$$T^* \longrightarrow T + h\nu''_F \qquad k_4[T^*] \qquad (6)$$
$$T^* \longrightarrow T \qquad k_5[T^*] \qquad (7)$$

where I means the intensity of excitation absorbed by molecules per unit time and where α and β are the fractions of the absorption of benzene and toluene respectively. Namely, $\alpha=\varepsilon_B[B]/(\varepsilon_T[T]+\varepsilon_B[B])$ and $\beta=\varepsilon_T[T]/(\varepsilon_T[T]+\varepsilon_B[B])$, where ε stands for the absorption coefficient.

If the excitation is of a constant intensity and if the whole system is in equilibrium, we obtain:

$$[B^*] = \alpha I/(k_1+k_2+k_3[T]).$$

From Eq. (2) the fluorescence intensity per unit time of benzene is expressed as follows:

$$F_B = k_1[B^*] = k_1\alpha I/(k_1+k_2+k_3[T]) = Q_B\alpha I/(1+K[T]).$$

Q_B and K are defined by the following relations;

$$Q_B = k_1/(k_1+k_2) \text{ and } K = k_3/(k_1+k_2).$$

Similarly, we obtain for toluene:

$$F_T = k_4[T^*] = Q_T I\{\beta+K[T](\alpha+\beta)\}/(1+K[T]).$$

If $\varepsilon_T \approx \varepsilon_B$ and $Q_T \approx Q_B$, we obtain:

$$F_T/F_B = Q_T(\beta+K[T])/\alpha Q_B = \{[T]+K[T]([T]+[B])\}/[B].$$

Therefore, we obtain:

$$K = (F_T/F_B)[B]/[T]([T]+[B]) - 1/([T]+[B]).$$

According to Robinson and Frosch,[4]

$$k_1 = 1.5 \times 10^6 \text{ sec}^{-1},$$

we obtain from this definition:

$$k_2/k_1 = (1-Q_B)/Q_B.$$

According to Lim,[5]

$$Q_B = 0.2 \text{ in EPA at } 77^\circ\text{K}.$$

If we use his data in our case, we obtain:

$$k_1 + k_2 = 5k_1 = 7.5 \times 10^6 \text{ sec}^{-1}.$$

The F_T/F_B ratio was estimated from the total fluorescence intensities of toluene and benzene, which were themselves derived from the fractional intensities of the key bands, of 0—623 of toluene and 0—992 of benzene, relative to the total intensities of toluene and benzene respectively. The results are shown in Table 3.

Table 3. Rate of energy transfer from benzene to toluene at various concentrations

Toluene in benzene (mol/l)	F_T/F_B	k_3 (mol^{-1} sec^{-1})
10^{-4}	5.4×10^{-1}	4.1×10^{10}
5×10^{-4}	1.3	2.0×10^{10}
10^{-3}	2.1	1.6×10^{10}
5×10^{-3}	2.7	4.1×10^{9}
10^{-2}	9.5	7.1×10^{9}

Colson, Kopelman, and Robinson[6] studied the selection rules of the Frenkel exciton for the $k=0$ transition in molecular crystal. They assumed the $g\leftrightarrow u$ selection rule. We photographed the fluorescence spectrum of the benzene crystal at 90°K and found the very weak 0-404 band at 37400 cm^{-1}. It is believed that this experimental evidence provides important information for discussing the intermolecular interactions of the molecular crystal.

Pesteil and Zmerli[7] reported two phosphorescence spectra from benzene crystal at 20°K and ascribed them to the 1st and 2nd triplet–ground state transitions. We checked their spectra in detail and assumed that their spectra might be due to some impurity in benzene since the analysis looked too artificial to be understood. They placed the 0–0 bands at unobserved positions at 30574 cm^{-1} and 38724 cm^{-1} and analyzed the spectra of the 1st and 2nd transitions respectively. We studied the phosphorescence and fluorescence spectra of toluene of 10^{-3} mol/l in benzene at 4.2°K and 77°K and found that they coincided with the spectra of the 1st and 2nd transitions respectively, as established by Pesteil and Zmerli. The phosphorescence spectrum of toluene in benzene was observed at 4.2°K, but it could not be observed at 77°K.

The band at 28985 cm^{-1} was taken as the 0–0 band, and vibrational frequencies of 225, 226, 450, 622, 699, 795, 988, 1174, 1586, and 1609 cm^{-1} were found. They corresponded to the Raman frequencies[8] of 216(b_2), 216×2, 623(b_1), 695(b_2), 786(a_1), 1004(a_1), 1177(a_1), 1585(b_1), and 1604(a_1) cm^{-1} respectively. The fluorescence spectrum was observed even at 77°K and 90°K, as has been described previously. Pesteil[9] has also published a paper concerning Wannier exciton bands. The absorption band at 37112 cm^{-1} of the benzene crystal in his Fig. 4 must be ascribed to the 0–0 band of toluene. By the way, a similar explanation may be given for the band at 31061 cm^{-1} of the naphthalene crystal in his Fig. 6, which is to be ascribed to the 0–0 band of β-methylnaphthalene.

4) G. W. Robinson and R. P. Frosch, *J. Chem. Phys.*, **38**, 1187 (1963).
5) E. C. Lim, *ibid.*, **36**, 3497 (1962).
6) S. D. Colson, R. Kopelman and G. W. Robinson, *ibid.*, **47**, 27 (1967).
7) P. Pesteil and A. Zmerli, *Ann. Phys.*, **10**, 1079 (1955).
8) Catalog of API, NSS, No. 2.
9) P. Pesteil, *J. Chem. Phys.*, **58**, 661 (1961).

BULLETIN OF THE CHEMICAL SOCIETY OF JAPAN VOL. 42 3076—3083 (1969)

The Intensity of the n–π^* Absorption Bands of Several Aliphatic Carbonyl Compounds

Kayoko Ozeki,[*1] Masaji Inagaki[2*] and Jiro Tanaka

Department of Chemistry, Nagoya University, Chikusa-ku, Nagoya

(Received April 15, 1969)

The mechanism of the intensity gain of the n–π^* transition has been investigated in several carbonyl compounds; (1) cyclohexane-1,4-dione, (2) *d*-α-bromocamphor, (3) bromonoranisatinone, (4) *d*-α-cyanocamphor, and (5) spiradine A methiodide. The results on the polarized absorption spectra of single crystals at room temperature have revealed that several mechanisms are involved in the appearance of the carbonyl n–π^* band. These mechanisms, (1) the vibronic coupling, (2) the lowering of the symmetry properties of the n and π orbitals by the substituent perturbations, and (3) the charge transfer from the substituents, are discussed theoretically and compared with the experimental results. It is shown that the in-plane components, either parallel or perpendicular to the carbonyl axis, are predominant as the source of the band intensity. The ratio of intensities parallel and perpendicular to the carbonyl axis is estimated by the use of the polarization results.

Since McMurry[1] first discussed the nature of the n–π^* transitions of the carbonyl compounds, there have appeared many experimental and theoretical studies of the mechanism of the intensity gain of the n–π^* electronic transitions.[2] The intensities of the symmetry-forbidden transitions can be observed by vibrational or other kinds of perturbations; the detailed mechanism of these transitions are important in elucidating the origin of the optical activity of the carbonyl compounds.[3] Pople and Sidman[4] studied the vibronic coupling in formaldehyde, considering especially the mixing of the A_2-type n–π^* excited state with the B_1 and B_2-type excited states. Their conclusions were in agreement with those of the classical experimental work of Dieke and Kistiakowsky,[5] who had decided that the transition is allowed along the direction in plane and perpendicular to the carbonyl axis. Cookson and his group[6] noticed the intensification of the n–π^* transition in the β,γ-unsaturated carbonyl compounds; Labhart and Wagniere[7] explained it by the charge-transfer mechanism. Vala and Tanaka[8] have demonstrated that the direction of the n–π^* transition moment of 4,4′-dichlorobenzophenone is parallel to the carbonyl axis and have discussed the mechanism of the intensity gain. In the present paper we will present results on the polarized absorption spectra of several compounds containing carbonyl groups.

The results of the low-temperature spectral studies of cyclohexane-1,4-dione, which are consistent with the present results, will be presented in a separate paper.

The optical activity of the carbonyl compounds have attracted much attention from the organic chemical point of view,[9] and the "octant-rule" has been establisehd[10] and discussed in many papers.[11] The direction of the n–π^* transition moment is definitely important in clarifying the mechanism of the octant rule.[12] The present results will provide fundamental information con-

*1 Present address: Government Industrial Research Institute, Nagoya, Hiratemachi, Kita-ku, Nagoya.

*2 Present address: Dainippon Ink and Chemicals, Inc., Urawa, Saitama.

1) H. L. McMurry, *J. Chem. Phys.*, **9**, 231, 241 (1941).

2) J. W. Sidman, *Chem. Revs.*, **58**, 689 (1958); V. G. Krishna and L. Goodman, *J. Chem. Phys.*, **36**, 2217 (1962); R. Shimada and L. Goodman, *ibid.*, **43**, 2027 (1965).

3) S. F. Mason, *Quart. Rev.*, **17**, 20 (1963).

4) J. A. Pople and J. Sidman, *J. Chem. Phys.*, **27**, 1270 (1957).

5) C. H. Dieke and G. B. Kistiakowsky, *Phys. Rev.*, **45**, 4 (1934).

6) R. C. Cookson and N. S. Wariyar, *J. Chem. Soc.*, **1956**, 2302.

7) H. Labhart and G. Wagniere, *Helv. Chim. Acta*, **42**, 2219 (1959).

8) M. Vala and J. Tanaka, *J. Chem. Phys.*, **49**, 5222 (1968).

9) C. Djerassi, "Optical Rotatory Dispersion; Application to Organic Chemistry," McGraw-Hill, New York (1960).

10) W. Moffitt, R. B. Woodward, A. Moscowitz, W. Klyne and C. Djerassi, *J. Am. Chem. Soc.*, **83**, 4013 (1961).

11) A. Moscowitz, *Advan. Chem. Phys.*, **4**, 67 (1962); J. A. Schellman and P. Oriel, *J. Chem. Phys.*, **37**, 2114 (1962); G. Wagniere, *J. Am. Chem. Soc.*, **88**, 3937 (1966); O. E. Weigang, Jr., *J. Chem. Phys.*, **43**, 3609 (1963).

12) S. F. Mason, *Mol. Phys.*, **5**, 343 (1963).

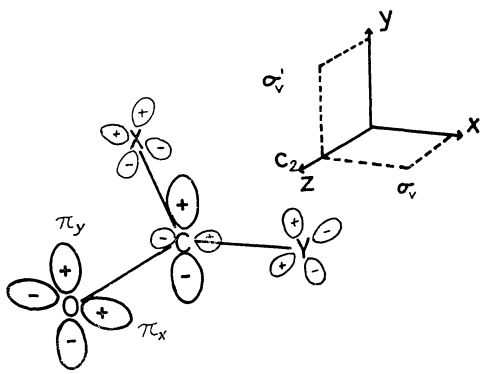

Fig. 1. The perturbing orbitals of all substituents are schematically shown at X and Y. The coordinates for the carbonyl group are shown together, the z is the direction of the carbonyl axis, x is in the plane and perpendicular to the axis, and y is in the direction out of the plane.

cerning the origin of the optical rotatory power of the carbonyl compounds.

Theoretical Considerations

The origin of the electronic transition of formaldehyde is shown to be intensity borrowing by the vibronic interactions. The theory of Pople and and Sidman,[4] confirmed by several experiments,[13] is that the transition moment is along the x axis, as is shown in Fig. 1. However, a little component is found along the carbonyl axis, though it is not big enough to explain the optical activity of the asymmetric ketones.[14] The vibronically-perturbed n-π^* excited states for the C_{2v} symmetry system may be given by:

$$\Phi(n\text{-}\pi^*) = \varphi_{A_2}(n\text{-}\pi^*) + \sum_a \frac{\langle \varphi_{A_2}(n\text{-}\pi^*) | \left(\frac{\partial H}{\partial q_a}\right) q_a | \varphi_{B_1}(n\text{-}\sigma^*) \rangle}{\varepsilon_{A_2}(n\pi^*) - \varepsilon_{B_1}(n\sigma^*)} \varphi_{B_1}(n\text{-}\sigma^*) + \sum_b \frac{\langle \varphi_{A_2}(n\text{-}\pi^*) | \left(\frac{\partial H}{\partial q_b}\right) q_b | \varphi_{B_2}(\sigma\text{-}\pi^*) \rangle}{\varepsilon_{A_2}(n\pi^*) - \varepsilon_{B_2}(\sigma\pi^*)} \varphi_{B_2}(\sigma\text{-}\pi^*) + \sum_c \frac{\langle \varphi_{A_2}(n\text{-}\pi^*) | \left(\frac{\partial H}{\partial q_c}\right) q_c | \varphi_{A_1}(\pi\text{-}\pi^*) \rangle}{\varepsilon_{A_2}(n\pi^*) - \varepsilon_{A_1}(\pi\pi^*)} \varphi_{A_1}(\pi\text{-}\pi^*) \quad (1)$$

where q_a, q_b, and q_c refer to the normal coordinates of the b_1, b_2 and a_1-type vibrational motions. The mixing with higher excited states will allow the n-π^* transition to appear along the x, y, and z axes respectively. A quantitative calculation of these terms is difficult for complex molecules; however, the selection rules can be confirmed by the polarized absorption measurements.

In β,γ-unsaturated ketones the intensity of the n-π^* transition is greatly enhanced, as is shown in Table 1. Labhart and Wagniere[7] suggested that the configurational interaction with the charge-transfer state is the major source of the intensity enhancement. The mixing of the charge transfer in the n-π^* state may be described by:

$$\Phi(n\text{-}\pi^*) = \varphi_{A_2}(n\text{-}\pi^*) + \frac{\langle \varphi_{A_2}(n\text{-}\pi^*) | \mathbf{H} | \varphi_{CT} \rangle}{\varepsilon_{A_2}(n\pi^*) - \varepsilon_{CT}} \varphi_{CT} \quad (2)$$

Where φ_{CT} indicates the charge-transfer state from the β,γ-unsaturated bond to the carbonyl group. The other charge-transfer configuration, one which involves the transfer of the nonbonding electron of the carbonyl group to the unsaturated bond, will have a higher energy because of the large ionization potential of the nonbonding electron

Table 1. The energies and intensities of the n-π^* transitions

	Crystal		Solution			
	ν_{max}	ratio $I_x : I_z$	ν_{max}	ε_{max}	$f \times 10^3$	$\Delta(\varepsilon_l - \varepsilon_r)$
Cyclohexane-1,4-dione	35.5	74 : 26	35.0	58	1.50	
d-Camphor			35.1	36	0.80	1.30
d-α-Cyanocamphor	35.0	80 : 20	34.7	42	1.00	0.64
d-α-Bromocamphor	32.0	57 : 43	32.8	107	2.11	1.81
Bromonoranisatinone	32.5	56 : 44				
Dihydrospiradine A			33.3	35	0.65	3.50
Spiradine A			32.8	194	3.18	2.30
Spiradine A methiodide	33.0	0 : 100?				

Here ν_{max} is the frequency of the absorption maximum in the crystalline state and in solutions.
The ratio is that of two components x and z by assuming that the polarization of the transition moment is in the plane of the carbonyl group (see Fig. 1).
ε_{max} is the maximum molar extinction coefficient.

13) J. C. D. Brand, *J. Chem. Soc.*, **1956**, 858.

14) J. Tanaka and K. Ozeki, to be published.

and small matrix elements; therefore, it will be neglected in further discussions. The transition moment induced by the charge-transfer configuration will have the direction inherent in the charge-transfer transition. Although Labhart and Wagniere[7] have not discussed the direction of the induced n–π^* transition, it is along the line connecting the centers of the electron donor and the acceptor groups. Another source of the intensities of the n–π^* transition is the deformation of the nonbonding and π orbitals by the perturbation of the adjacent conjugated systems.

The symmetry properties of the n and π molecular orbitals of the carbonyl group are destroyed when the substituents are located asymmetrically to the plane of the carbonyl group. For instance, the vacant π^* orbital involves not only the $2p\pi_y$ a.o., but also the $2p\pi_x$ a.o. of the carbon and oxygen atoms, because the maximum stabilization of the energy is obtained after the mixing of the orbitals of asymmetric substituents with all the orbitals of the carbonyl group. If we denote the asymmetric substituents by X and Y, as is shown in Fig. 1, the wavefunction of the carbonyl group will be given by:

$$\varphi_n = a_O\pi_x(O) + a_C\pi_x(C) + a_O'\pi_y(O) + a_C'\pi_y(C) + a_X\pi_x(X) + a_Y\pi_x(Y) + a_X'\pi_y(X) + a_Y'\pi_y(Y)$$

$$\varphi_\pi = b_O\pi_y(O) + b_C\pi_y(C) + b_O'\pi_x(O) + b_C'\pi_x(C) + b_X\pi_y(X) + b_Y\pi_y(Y) + b_X'\pi_x(X) + b_Y'\pi_x(Y)$$

$$\varphi_{\pi^*} = c_O\pi_y(O) + c_C\pi_y(C) + c_O'\pi_x(O) + c_C'\pi_x(C) + c_X\pi_y(X) + c_Y\pi_y(Y) + c_X'\pi_x(X) + c_Y'\pi_x(Y)$$

The electronically-allowed component of the n–π^* transition will be given by the transition matrix elements of the type;

$$\langle \sum_I a_I\pi_x(I) | \mathbf{r} | \sum_I c_I'\pi_x(I) \rangle$$

and

$$\langle \sum_I a_I'\pi_y(I) | \mathbf{r} | \sum_I c_I\pi_y(I) \rangle$$

both of which are polarized along the z-axis. The coefficients a_X, b_X,$\cdots$ will be large when the X and Y groups have pronounced substituent effects. However, they will be zero for the strict C_{2v} symmetry system.

A semiquantitative discussion of the mixing of n, π, and π^* orbitals has been presented by Allinger and Tai.[15]

Since the polarization properties of the n–π^* transition produced by these mechanisms are different, it is important to determine the direction of the electronic transition moment with several kinds of carbonyl compounds in order to clarify which mechanism is predominant as the source of the n–π^* intensity.

15) N. L. Allinger and J. C. Tai, *J. Am. Chem. Soc.*, **88**, 2179 (1966).

Experimental

The electronic absorption spectra of the following compounds; (1) cyclohexane-1,4-dione, (2) *d*-α-bromocamphor, (3) bromonoranisatinone, (4) *d*-α-cyanocamphor, and (5) spiradine A methiodide were measured in ethanol or EPA solutions and in the crystalline states. The polarized crystalline absorption spectra were measured by means of an ultraviolet microspectrophotometer described previously.[16] The materials used were recrystallized from ethanol or ligroin. The bromonoranisatinone and spiradine A were gifts from Professor Hirata of our department. The crystalline axes of these crystals were confirmed by the X-ray method before the measurement of the crystalline absorptions.

Results

1) Cyclohexane-1,4-dione. The crystal structure of cyclohexane-1,4-dione has been determined by Mossel and Romers,[17] and by Groth and Hassel.[18] The crystal is monoclinic, with a space group of $P2_1$ with two molecules in a unit cell. The projection of the molecules in the unit cell on the $(10\bar{1})$ plane, which is the most frequently developed face, is shown in Fig. 2. The crystalline spectra of cyclohexane-1,4-dione at room temperature are shown in Fig. 3. The spectrum in an EPA solution at room temperature is also shown there; its maximum is observed at 35500 cm^{-1}, with a molar extinction coefficient of 60. The crystalline absorption bands were observed

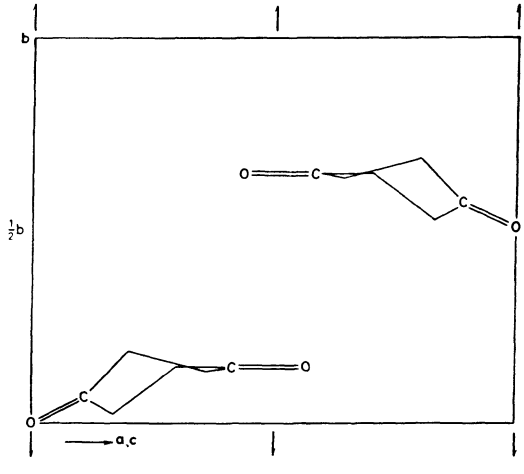

Fig. 2. Projected view of cyclohexane-1,4-dione on to the $(10\bar{1})$ plane according to the X-ray results.

16) J. Tanaka and M. Shibata, This Bulletin, **41**, 34 (1968).

17) A. Mossel and C. Romers, *Acta Cryst.*, **17**, 1217 (1964).

18) P. Groth and O. Hassel, *Acta Chem. Scand.*, **18**, 923 (1964).

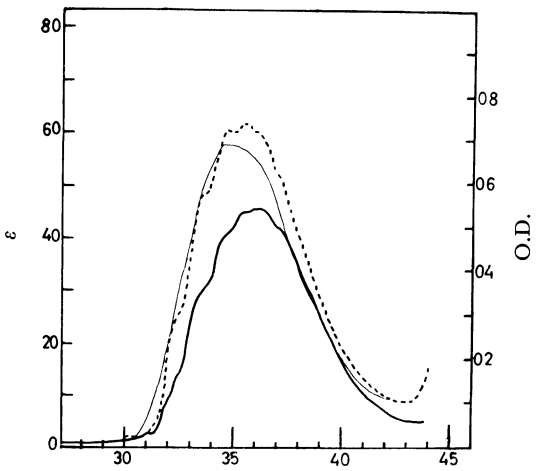

Fig. 3. The spectrum of cyclohexane-1,4-dione in EPA solution at room temperature (fine line) and the absorption of cyclohexane-1,4-dione crystal taken with the (10$\bar{1}$) plane.

—— The light is polarized parallel to the b axis. (bold line).

------ The light is polarized parallel to the [10$\bar{1}$] axis

Ordinate: left, the molar extinction coefficient for the spectrum of the solution.
right, the optical density for the crystal spectra.

Abscissa: frequency (in 10^3 cm^{-1} unit)

—— in EPA ------ I_{ac} —— I_b

in the same region; they show intervals of 1100 cm^{-1}. The dichroic intensity ratio parallel to and perpendicular to the b axis ($I_b : I_{ac}$) is 1.0 : 1.3. Since the absorption intensities are weak and since the strong transitions are located in the higher-energy region, it is safe to use the oriented gas intensity ratio in discussing the direction of the transition moment. If the transition were allowed along the y axis in Fig. 1, the absorption intensity would be far stronger along the b axis than along the [10$\bar{1}$] direction. The experimental results are contrary to this presumption; therefore, we may disregard the possibility of the y axis polarization for the n–π^* transition in this compound. Although Brand[19] discovered an out-of-plane component in some α,β-conjugated carbonyls, none of the present results showed any evidence for an out-of-plane component, at least in the saturated ketones. If we restrict the polarization in the plane of the carbonyl group, neither x nor the z axis polarization alone can explain the observed intensity ratio. Therefore, the whole band may be considered to consist of two components, x and z; the ratio of the components has been determined to be $I_x : I_z =$ 0.74 : 0.26. This result indicates that more than two different mechanisms are operative in the present molecule. The low-temperature spectra, which will be presented in the succeeding paper, support this idea by showing the details of the vibrational progressions of this band.

2) d-α-Bromocamphor. The crystal structure analysis of d-α-bromocamphor and d-α-cyanocamphor has been made by Wiebenga and Krom.[20]

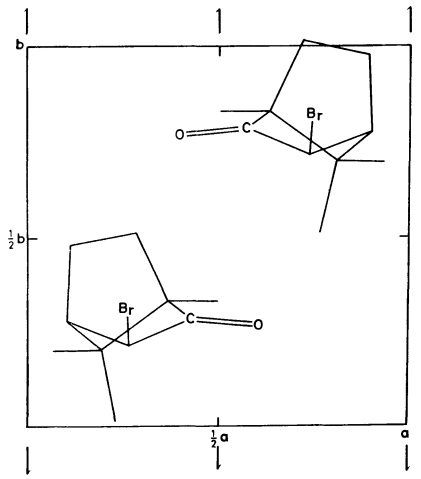

Fig. 4. Projection of the d-α-bromocamphor on to the (001) plane by the X-ray results.
The projection of cyanocamphor is nearly the same except that the bromine atom is replaced by the cyano group.

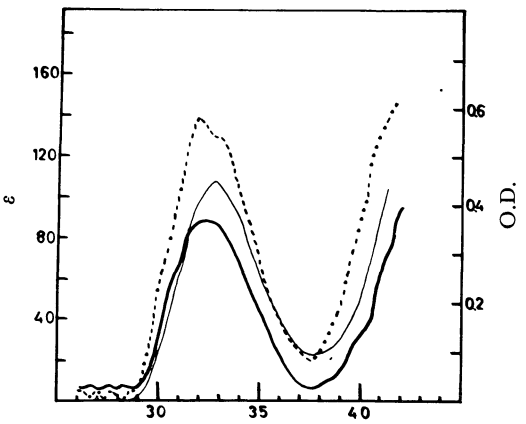

Fig. 5. The spectrum of d-α-bromocamphor in the ethanol solution (fine line) and absorption spectra of the crystal.

—— The light is polarized parallel to the b axis (bold line).

------ The light is polarized parallel to the a axis.

Ordinate: left, the molar extinction coefficient for the spectra of the solution.
right, the optical density for the crystal spectra.

Abscissa: frequency (in 10^3 cm^{-1}).

—— in ethanol ------ I_a —— I_b

19) J. C. D. Brand, J. G. Callomon and J. K. G. Watson, *Discussions Faracay Soc.*, **35**, 175 (1963); J. C. D. Brand and G. D. Williamson, *ibid.*, **35**, 184 (1963).

These two compounds are isomorphous. They belong to a monoclinic system, the space group being $P2_1$; two molecules are contained in the unit cell. The crystals develop (001) faces. The projection of the molecules is shown for *d*-α-bromocamphor in Fig. 4, while the spectrum in the ethanol solution is shown in Fig. 5. The maximum of the absorption is shifted about 2300 cm^{-1} to the red and intensity is increased to about three times that of *d*-camphor. This shift was explained by Allinger, Tai and Miller[21] as being due to the effect of the σ^*(C-Br) orbital at the axial position, but the enhancement of the intensity was qualitatively shown and it was not enough to account for the large value observed. The direction of the transition moment was not discussed by these investigators.

The crystalline absorption spectra for the (001) plane are shown in Fig. 5; the dichroic intensity ratio is $I_a : I_b = 1.5 : 1.0$. The out-of-plane component is again neglected with this molecule, since otherwise the *b*-axis spectrum would be much stronger. If the increase in the intensity is produced by the $n\sigma^*$ mixing, the charge-transfer component from the n to σ^* orbital may be expected. Another possible mechanism is the symmetry breakdown of n and π^* orbitals by the axial bromine atom; it would produce the transition along the z axis. The analysis all of the band intensities into the x and z components yielded the value of $I_x : I_z = 0.57 : 0.43$. The direction of the n-σ^* transition nearly coincides with the z axis on this crystalline plane; therefore the increase in the z component may be attributed to either the inherent moment increased along the z axis or to the charge-transfer moment of the n-σ^* type transition. This point will be discussed below.

3) Bromonoranisatinone. Anisatine is a toxic terpenoid separated from seeds of *Illicium Religiosum Siebold et Zuccarini* (Japanese star anise). The crystal structure of bromonoranisatinone was analyzed by Furusaki, Tomiie, Nitta, Sakabe, and Hirata.[22] It has one carbonyl group and two ester groups. The ester groups absorb in the 50000 cm^{-1} region; therefore, we will consider only the carbonyl group in the 33000 cm^{-1} region. The carbonyl is adjacent to the bromine atom at the α position; this conformation can be explained as an intermediate of the axial and equatorial positions. The substituent effect is found to shift the band by just the same order or magnitude as in the case of *d*-α-bromocamphor. The projection of the molecules onto the developed (100) plane is shown in Fig. 6, while the crystalline absorption spectra are shown in Fig. 7. The dichroic ratio was $I_b : I_c = 1.0 : 2.0$. The separation of the band intensities along the x and z components of the carbonyl group showed that the ratio is $I_x : I_z = 0.56 : 0.44$. This finding is very close to that with *d*-α-bromocamphor. The enhancement along the z axis may be originated by a mechanism similar to that of *d*-α-bromocamphor; it will be discussed in the last section.

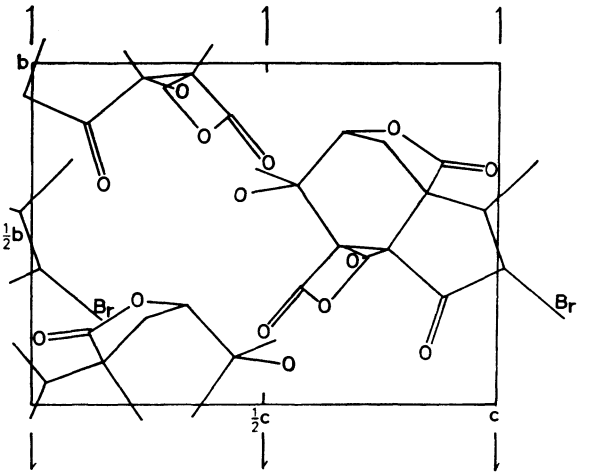

Fig. 6. Projection of bromonoranisatinone on to the (100) plane by the X-ray results.

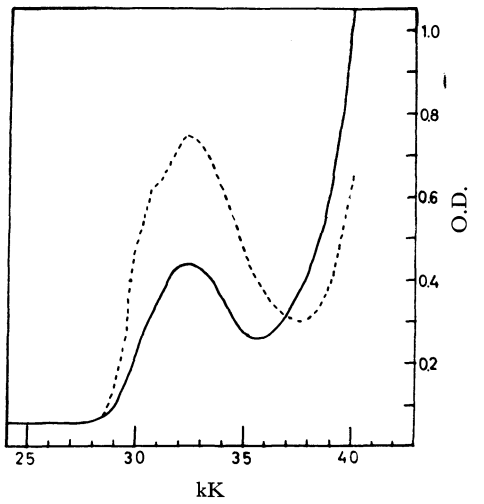

Fig. 7. Absorption spectra of bromonoranisatinone crystal.
—— The light is polarized parallel to the *b* axis (bold line).
------ The light is polarized parallel to the *c* axis.
Ordinate: optical density for the crystal.
Abscissa: frequency (in 10^3 cm^{-1} unit)
—— I_b ------ I_c

4) *d*-α-Cyanocamphor. The projection of *d*-α-cyanocamphor is almost the same as that of

20) E. H. Wiebenga and C. J. Krom, *Rec. Trav. Chim.*, **65**, 663 (1946).
21) N. L. Allinger, J. C. Tai and M. A. Miller, *J. Am. Chem. Soc.*, **88**, 4495 (1966).
22) N. Sakabe, Y. Hirata, A. Furusaki, Y. Tomiie and I. Nitta, *Tetrahedron Letters*, **52**, 4795 (1965).

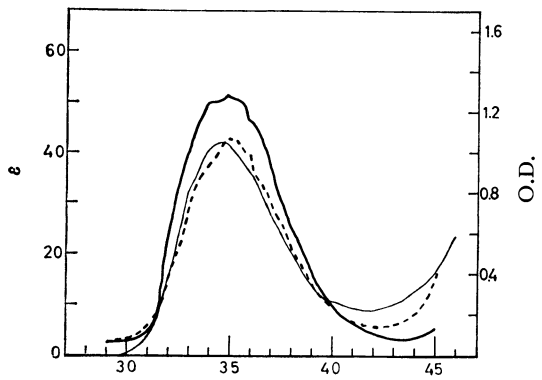

Fig. 8. The spectrum of *d*-α-cyanocamphor in the ethanol solution (fine line) and the absorption spectra of *d*-α-cyanocamphor crystal.
—— The light is polarized parallel to the *b* axis (bold line).
------ The light is polarized parallel to the *a* axis.
Ordinate: left, the molar extinction coefficient for the spectra of the solution.
right, the optical density for the crystal.
Asbcissa: frequency (in 10^3 cm^{-1}).
—— in ethanol ------ I_a —— I_b

d-α-bromocamphor except that the bromine atom is replaced by the cyano group. The spectrum in the ethanol solution is shown in Fig. 8, together with the crystalline spectra. The maximum of the absorption was observed at 33000 cm^{-1}, while the molar extinction coefficient was 42. The integrated intensity ratio for the light polarized parallel to the *b* and *a* axes was $I_b : I_a = 1.0 : 0.74$.

As has been found in the cases of cyclohexane-1,4-dione and *d*-α-bromocamphor, the out-of-plane (y aixs) component is negligible; otherwise, the *b*-axis polarized band would be much stronger.

The total band intensity was divided into the x and z components; the ratio was then obtained as $I_x : I_z = 0.80 : 0.20$. The effect of the cyano group at the axial β,γ-position is not very prominent, except that the intensity is slightly increased. The donor property of the cyano group is very poor, and the overlapping of cyano π orbitals with the n and π orbitals of the carbonyl group is not very large; therefore, few charge transfer effects may be anticipated. Another reason for this may be that the cyano group does not have a strong π-π^* transition in the ultraviolet region; therefore the perturbation is correspondingly small.

5) Spiradine A Methiodide. Spiradine A methiodide, an alkaloid botained from *spiraea japonica*,[23] has an ethylenic bond at the β,γ-position. The absorption intensity for spiradine A in the ethanol solution is $\varepsilon = 194$ at 32800 cm^{-1}, about six times that of the dihydro spiradine A, which has $\varepsilon = 35$ at 33300 cm^{-1}. This increase in the intensity is typical of β,γ-unsaturated ketones. The crystalline structure analysis was made by Sakabe, Sasaki and Hirata,[24] the molecule is projected onto the developed crystalline plane in Fig. 9. The crystalline absorption spectra are presented in Fig. 10. The measurement of the absorption intensities showed that $I_b : I_c = 1.0 : 1.75$. This result may be explained by the direction of the transition moment, which is parallel to either the carbonyl axis or the ethylenic bond. The charge-transfer mechanism produces the moment along the line connecting the donor and acceptor groups the ethylenic and the carbonyl groups. Therefore, the present results show that the charge-transfer contribution is not a major source of the intensity and

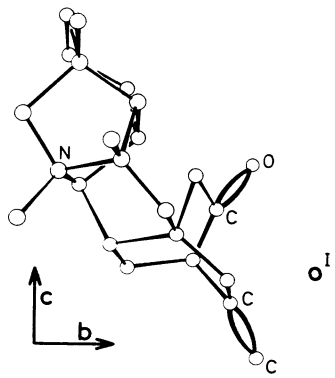

Fig. 9. Projection of spiradine A methiodide onto the (100) plane according to the X-ray results. Eight molecules are contained in a unit cell, but they are related with the two-fold screw axis symmetry operation. (space group $P2_12_12_1$)

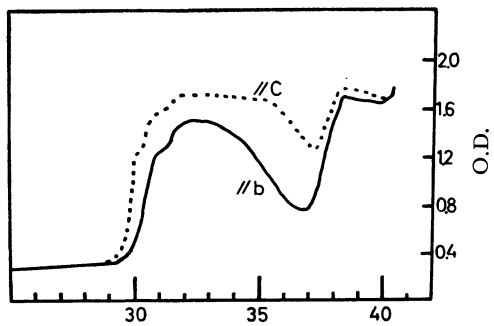

Fig. 10. Absorption spectra of spiradine A methiodide crystal.
—— The light is polarized parallel to the *b* axis (bold line).
------ The light is polarized parallel to the *c* axis.
Ordinate: optical density for the crystal
Abscissa: frequency (in 10^3 cm^{-1} unit)

23) V. I. Frova, A. I. Bankowskii, A. D. Kuzorvkov and M. M. Molodozhnikov, *Med. Prom. S.S.S.R.*, **18**, 19 (1964).

24) G. Goto, K. Sasaki, N. Sakabe and Y. Hirata, *Tetrahedron Letters*, **1968**, 1369.

that the x component also contributes little. Accordingly the origin of the intensity enhancement may be ascribed to either of two reasons; either the symmetry of the carbonyl group is broken by the adjacent double-bond or the ethylenic π-π^* transition moment is mixed in the n-π^* transition of the carbonyl group by the perturbation of the dipole-dipole interaction. The question which of these two alternative mechanisms is predominant can not be answered from the present results only. In addition, the mixing of these two states is not conceivable, since in that case the direction of the transition moment would deviate from the confirmed direction. Further experiments on other β,γ-unsaturated carbonyl compounds are desirable in order to clarify these ambiguities.

Discussion

The findings on spectral data are summarized in Table 1. Cyclohexane-1,4-dione and d-α-cyanocamphor show large x components, 74 and 80%, with the absorption maximam at 35500 and 34700 cm^{-1}, respectively. Pople and Sidman[4] stated that the n-π^* transition induced by the vibrational interaction gives the main component in the x direction in formaldehyde. Although these molecules have heavier atoms attached to the carbonyl group, most of the intensity gain seems to be the same in origin as that of formaldehyde. However, a certain amount of the intensity is found along the z axis; this has significance for the quantitative estimate of the optical activity of asymmetric ketones. This point will be discussed in the succeeding paper.

The maximum frequencies of the absorption spectra for d-camphor, d-α-cyanocamphor, and d-α-bromocamphor in the solution of ethanol are at 35100, 34700 and 32800 cm^{-1} respectively. The effects of the substituents are slightly different; there is a little blue shift for the cyano group and a large red shift for the bromine atom. The maximum molar extinction coefficients are 36, 42, and 107, indicating a typical bathochromic effect, particularly in the bromine atom. According to Allinger, Tai and Miller,[21] the interaction between the σ^* orbital of the C–Br bond and the π^* orbital depresses the transition energy of d-α-bromcaomphor. Mixing of this type induces the transition moment along the line connecting the centers of the σ^* and π^* orbitals. Another possibility is the deformation of the n and π^* orbitals, which would give a transition moment parallel to the carbonyl axis. If the direction of the transition moment could be determined exactly, the contribution of these alternative mechanisms would be elucidated.

Both bromonoranisatinone and d-α-bromocamphor have a bromine atom in the α-position relative to the carbonyl group; the former has its in the position intermediate between the equatorial and axial axes, while the latter has its in the axial axis. Bromonoranisatione shows its absorption maximum at 32500 cm^{-1}; the similar red shift indicates the bathochromic effect of the substituent bromine atom, even for the intermediate geometry. In d-α-bromocamphor the direction of the transition moment could not be conclusively determined, for the carbonyl axis and n-to-σ^* orbital directions are nearly parallel on the measured crystalline plane. Bromonoranisatinone shows a crystalline plane in which the directions of the π-π^* and n-σ^* (C–Br) transitions are different; therefore, these different mechanisms could be distinguished by the polarization measurements. The observed results show that the z component is 43%; this value is exactly the same as that of d-α-bromocamphor. This means that the n-σ^* transition moment contributes little to the enhancement of the overall transition moment; the assumed deformation of π, π^*, and n orbitals seems to be more attractive.

In the n-π^* transitions of the carbonyl group, the magnetic transition moment has a component in the z-axis direction, so if there is to be optical activity there must be an electronic transition moment parallel to the z-axis direction. The optical rotational strength of d-α-bromocamphor is three times those of d-camphor and d-α-cyanocamphor. This may mean that the z component of the transition moment is about three or more times larger in d-bromocamphor than in d-camphor and d-α-cyanocamphor. This would agree with the present findings regarding the crystal spectra; the increase in the z component is established in d-α-bromocamphor and bromonoranisatinone.

The absorption spectra of spiradine A (β,γ-unsaturated ketone), dihydro spiradine A and spiradine A methiodide were investigated in an ethanol solution. The maximum wave numbers differ only slightly, but the maximum molar extinction coefficient increases drastically for β,γ-unsaturated ketone. The β, γ double bond has a great effect on the intensification of the n-π^* transition. Although the mixing of the charge-transfer state was suggested by Labhart and Wagniere, the crystal spectrum gives rather negative evidence for the contribution of the CT transition moment.

The wavefunction for the perturbed n-π^* state of β,γ-unsaturated ketone may be given by:

$$\Phi(n\pi^*) = a\varphi_z(n\pi^*) + b\varphi(\pi\pi^*;\ \text{C=O}) + c\varphi(\text{CT}) + d\varphi(\pi\pi^*;\ \text{C=C}) \qquad (3)$$

$$c = \frac{\langle\varphi_{n\pi}{}^*|\mathbf{H}|\varphi_{\text{CT}}\rangle}{E_{n\pi}{}^* - E_{\text{CT}}}$$

$$d = \frac{\langle\varphi_{n\pi}{}^*|\mathbf{H}|\varphi_{\pi\pi}{}^*;\ \text{C=C}\rangle}{E_{n\pi}{}^* - E_{\pi\pi}{}^*;\ \text{C=C}}$$

The appearance of the b term is mainly due to the deformation of the π and n orbitals, as has been

discussed previously, or to the second-order perturbations. The first term, which includes the vibronic mechansisms, is not significant for the whole transition moment, the second will give a component along the carbonyl axis, and the last one, one along the unsaturated carbon-carbon bond. The experiment indicates that either the second or the last one is most important for the present system. Conclusive proof on this point must, however, await some more experiments on other crystalline systems. However, recent results by Kearns, Marsh and Schaffner[25] seemingly show that in α,β-unsaturated ketone the 0-0 transition of the $n-\pi^*$ band is allowed electronically. Further effort along these lines is desirable for the elucidation of the source of the $n-\pi^*$ intensity of the unsaturated ketone.

Our thanks are due to Professor Yoshimasa Hirata of our department for his gift of samples.

25) D. R. Kearns, G. Marsh and K. Schaffner, *J. Chem. Phys.*, **49**, 3316 (1968).

BULLETIN OF THE CHEMICAL SOCIETY OF JAPAN VOL. 42 3083—3087 (1969)

The Radiolysis of Liquid Nitrogen Containing Hydrocarbons. I. Ethylene and Propylene

Takefumi OKA, Yoshikazu SUDA and Shin SATO

Department of Applied Physics, Tokyo Institute of Technology, Ookayama, Meguro-ku, Tokyo

(Received April 22, 1969)

The γ-radiolysis of liquid nitrogen containing ethylene and propylene has been investigated. As the nitrogenous products, hydrogen cyanide (0.18) and acetonitrile (0.04) were observed in the case of ethylene, and acetonitrile (0.12), in the case of propylene. The values in the parentheses are the *G*-values estimated on the basis of the energy absorbed by liquid nitrogen. In order to elucidate the mechanism of the reaction between nitrogen atoms and propylene, the mixture of C_3H_6 and C_3D_6 and the $CD_3CH=CHD$ compound have also been used as solutes. The acetonitrile obtained was mainly CH_3CN and CD_3CN in the former case, and CD_3CN in the latter. These results suggest that a nitrogen atom produced in the system attacks the carbon atom in the middle of propylene and produces acetonitrile, leaving a methyl radical, the carbon atom in which was originally attached to the double bond.

As an important branch of reaction kinetics, numerous investigations have been made of reactions between simple atoms and hydrocarbons.[1] Among them, the reaction between nitrogen atoms and hydrocarbons has been the most annoying one to investigators, because the reaction mechanism has to be formulated on the basis only of the measurement of a fragmentation product, hydrogen cyanide.[2] This compound is always observed as the principal product of the reaction between active nitrogen and hydrocarbons in the gas phase. Several researchers have reported that some other nitrogenous compounds, such as ammonia, acetonitrile,[3] and pyrrole,[4] are formed in the reaction between active nitrogen and hydrocarbons. However, the yields of these products are always too small compared with hydrogen cyanide to help to elucidate the reaction mechanism. Recently, though, Safrany and Jaster proposed a new approach to the reaction between active nitrogen and hydrocarbons;[5] they think that hydrogen cyanide obtained is not formed in the direct reaction between nitrogen atoms and hydrocarbons, but in the reaction between nitrogen atoms and the hydrocarbon radicals eventually formed in the reaction system.

With these things in mind, we have examined the γ-radiolysis of liquid nitrogen containing several hydrocarbons, and have found that hydrogen cyanide is not necessarily the principal nitrogenous product. For example, when propylene is used as the solute, the formation of hydrogen cyanide is not observed, but acetonitrile is formed. The

1) "Progress in Reaction Kinetics," Vols. 1, 2, 3 and 4 ed. by G. Porter, Pergamon Press, Oxford (1961—1967).

2) G. G. Mannella, *Chem. Revs.*, **63**, 1 (1963).

3) Y. Shinozaki, R. Shaw and N. N. Lichtin, *J. Am. Chem. Soc.*, **86**, 341 (1964).

4) A. Tsukamoto and N. N. Lichtin, *ibid.*, **84**, 1601 (1962).

5) D. R. Safrany and W. Jaster, *J. Phys. Chem.*, **72**, 518 (1968).

preliminary results with several hydrocarbons have been previously reported in a short communication.[6] These results suggest that the γ-radiolysis of a liquid nitrogen solution of hydrocarbons is a promising method for the study of the reactions between nitrogen atoms and hydrocarbons. In the present paper, we will report the details of the experimental method and procedure along with the results obtained with ethylene and propylene.

Experimental

Nitrogen gas of a high purity purchased from the Takachiho Trading Co. was bubbled through sulfuric acid before use. The gas-chromatographic analysis showed that the contamination of oxygen did not exceed 0.01%. All the hydrocarbons except the deuterated ones were of a pure grade purchased from the Takachiho Trading Co. The deuterated propylenes (C_3D_6 and $CD_3CH{=}CHD$) were synthesized from methylacetylene-d_4 by a method already reported.[7]

The vessel for γ-irradiation consisted of a simple Pyrex tube connected with a high-pressure stopcock through a joint held by a small spring. When the pressure in the tube rose over 2 atm, the spring was disengaged so as to avoid an explosion. The tube was graduated from the bottom in m*l*. To prepare the irradiation sample, a certain amount of a hydrocarbon volumetrically measured in advance was first condensed in the tube by means of liquid nitrogen. Then, nitrogen gas of a high purity was introduced under a pressure of about 1.5 atm. The gas was easily liquefied at the bottom of the tube. After a certain amount (usually 3 m*l*) of liquid nitrogen had been liquefied, the stopcock was closed and the tube was taken off the apparatus and shaken to dissolve the hydrocarbon in the liquid nitrogen. This sample tube was then irradiated with ^{60}Co-γ rays in a liquid-nitrogen Dewar flask. The exposure-dose rate used was 1.0×10^6 R/hr, and the irradiation time was usually 3 hr.

After the irradiation, the sample tube was evacuated at 77°K and the condensable product was analyzed by gas chromatography. For the analysis of acetonitrile, a 2.5-m column packed with polyethylene glycol-on-celite was used, while for hydrogen cyanide, a 2-m column of dioctyl phthalate was used. To detect the presence of ammonia, the irradiation product was treated with a Nessler reagent and the solution was analyzed spectrophotometrically at 430 mμ. The hydrocarbons were usually analyzed with a 4-m column of active alumina at a temperature of 40—60°C. To identify the nitriles, use was made of infrared and mass spectrometers.

Since the solubilities of hydrocarbons in liquid nitrogen could not be found in the literature, a rough estimate was made as follows. An excess amount of a hydrocarbon and a certain amount of liquid nitrogen were introduced into a sample tube which had a second thimble. After the ingredients had been mixed well, the solution was decantated into the second thimble, which was then evacuated at 77°K and fused. Then, the amount of the hydrocarbon remaining in the other thimble was measured volumetrically. Table 1 shows the results thus obtained. The numerical values should not be taken strictly, however.

Table 1. Solubilities of ethylene and propylene in liquid nitrogen

Hydrocarbons	Solubility (mole fraction)
Ethylene	1×10^{-3}
Propylene	3×10^{-4}

Results

γ-Radiolysis of Liquid Nitrogen Containing Ethylene. The observed products were acetylene, hydrogen cyanide, acetonitrile, ethane, propane, *n*-butane, 1-butene, C_6-hydrocarbons, a trace of ammonia, and the polymer. Figure 1 shows the amount of hydrogen cyanide produced as a function of the irradiation time using two concentrations of ethylene. Figures 2 and 3 show the *G*-values

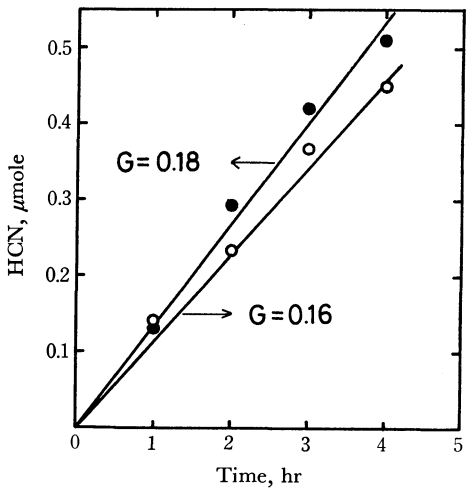

Fig. 1. Irradiation time dependence of HCN formation in ethylene-liquid nitrogen solution.
● C_2H_4, 2×10^{-4} in the mole fraction
○ C_2H_4, 1×10^{-4} in the mole fraction

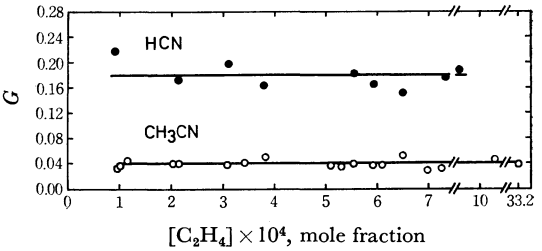

Fig. 2. *G*-values of CH_3CN and HCN from the ethylene-liquid nitrogen solution.

6) T. Oka and S. Sato, This Bulletin, **42**, 582 (1969).

7) Y. Hatano, S. Shida and S. Sato, *ibid.*, **41**, 1120 (1968).

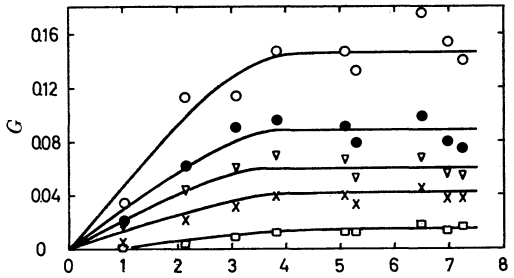

Fig. 3. *G*-values of hydrocarbon products from the ethylene-liquid nitrogen solution.

○ C_2H_6, ● $C_2H_2 \times 1/10$, ▽ C_3H_8, × n-C_4H_{10}, □ 1-C_4H_8.

of the observed products as a function of the amount of ethylene introduced into the 3-m*l* portion of liquid nitrogen. The irradiation time was 3 hr at the dose rate of 1.0×10^6 R/hr. Obviously, nitrogenous products and hydrocarbons are different in their dependency upon the amount of ethylene introduced. The *G*-values of acetonitrile and hydrogen cyanide are practically constant over the range of mole fractions investigated, while the *G*-values of hydrocarbons increased initially and then leveled off over the mole fraction of 4×10^{-4}. When the liquid nitrogen was contaminated by oxygen, no products other than acetylene were observed and sometimes light emission and explosion occurred when the condensable product was warmed up for analysis.

γ-Radiolysis of Liquid Nitrogen Containing Propylene. The observed products were acetonitrile, propane, ethylene, ethane, isobutane and/or allene, 1,5-hexadiene, 4-methylpentene-1 and/or, 2,3-dimethylbutane, a trace of ammonia, and the polymer. The dose dependence of the formation of acetonitrile is shown in Fig. 4. The *G*-values of the observed products are shown in Figs. 5 and 6 as a function of the amount of propylene introduced. The dependences of the *G*-values of

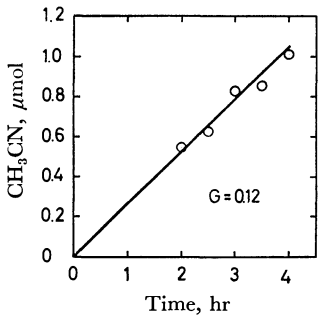

Fig. 4. Irradiation time dependence of CH_3CN formation in propylene-liquid nitrogen solution.

C_3H_6, 1.3×10^{-4} in the mole fraction

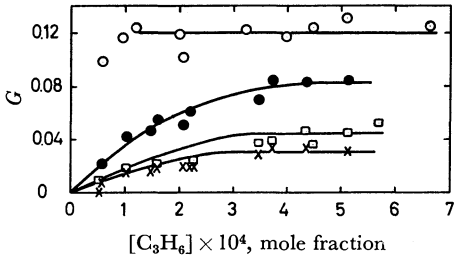

Fig. 5. *G*-values of products from the propylene-liquid nitrogen solution.

○ CH_3CN ● C_3H_8

□ 4-methylpentene-1 and/or 2,3-dimethylbutane

× isobutane and/or allene.

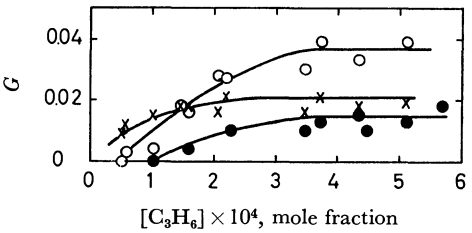

Fig. 6. *G*-values of products from the propylene-liquid nitrogen solution.

○ C_2H_4, × C_2H_6, ● 1,5-hexadiene.

Table 2. Isotopic distribution of acetonitriles produced in the γ-radiolysis of liquid nitrogen containing propylene

Propylene	Acetonitrile			
	d_3	d_2	d_1	d_0
$C_3H_6+C_3D_6$ (1:1)	72	15	8	100
$CD_3CH=CHD$	100	18	18	4

the products upon the amount of propylene are similar to those obtained with ethylene. Here, it should be noted that the formation of hydrogen cyanide is not observed.

To elucidate the mechanism of the formation of acetonitrile, deuterated propylenes were used as solutes. Table 2 shows the distributions of the isotopic acetonitriles obtained with a partially-deuterated propylene ($CD_3CH=CHD$) and a 1 : 1 mixture of C_3H_6 and C_3D_6. Obviously, the main process of the formation of acetonitrile does not involve radical reactions. If it did, the d_1- and d_2-acetonitriles would be comparable in the amount with the d_0- and d_3-acetonitriles. The *G*-value of acetonitrile from a deuterated propylene solution was smaller than that from a usual propylene solution, although it was not measured quantitatively.

The Polymer Formation. Although the amount of the polymer formed was not measured in either radiolysis, its formation was detected as

follows. After the analysis of the volatile products, the tube was heated in the air; thereby small black particles, probably carbon, were obtained on the inside wall.

Discussion

As has been stated above, ethylene and propylene are soluble in liquid nitrogen, although their amounts are very small. Moreover, as has been reported in a short communication,[6] hydrocarbons with high melting points gave no nitrogenous products.*1 This is probably due to the small solubilities of these hydrocarbons in liquid nitrogen. From these facts, it may be concluded that the nitrogenous compounds observed are formed in homogeneous reactions in liquid nitrogen.

The initial reactions occurring in a γ-irradiated liquid nitrogen solution may be described as follows:

$$N_2 \text{ -}\!\!\sim\!\!\rightarrow [N_2^+ + e] \quad (1)$$

$$\text{-}\!\!\sim\!\!\rightarrow N_2^* \quad (2)$$

$$\text{-}\!\!\sim\!\!\rightarrow [N^+ + N + e] \quad (3)$$

Here, brackets denote spurs. For the estimation of the G values of free ions, the $\exp(-r_c/r)$ factor is known to be important; it corresponds to the probability that a thermalized electron at the distance, r, from its parent positive ion can escape from the Coulombic field. Here, r_c stands for the Onsager length ($e^2/\varepsilon kT$).[8] Since the dielectric constant of liquid nitrogen, ε, is close to 1.45, the Onsager length in liquid nitrogen is very much larger than that in a hydrocarbon liquid, for example, cyclohexane, at room temperature.[9] The G-values of free ions in cyclohexane are known to be about 0.1.[10] Therefore, the G values of free ions in liquid nitrogen will be much smaller than 0.1.

Since the concentration of the solute in the present experiment does not exceed 10^{-3} in the mole fraction, the reaction between the solute molecules and the ions in spurs may be ignored.*2 In other words, almost all the electrons produced in the reactions (1) and (3) return to their respective ions and are neutralized, leaving an excited nitrogen molecule in the reaction (1) and two nitrogen atoms in the reaction (3).

In the gas-phase experiments, a long-lived excited state of the nitrogen molecule is known to be $N_2(A\ ^3\Sigma_u^+)$.[12] This excited state is not easily quenched by nitrogen molecules, and the life-time is estimated to be more than 10^{-2} sec. The active species responsible for the successive reactions in the liquid nitrogen solution, therefore, are probably nitrogen atoms and the excited molecules, $N_2(A\ ^3\Sigma_u^+)$. In many reports on the reactions of active nitrogen, it seems to have been established that the nitrogenous compounds observed are produced in the reaction of nitrogen atoms, but not in that of excited nitrogen molecules. Accordingly, the hydrogen cyanide and acetonitrile obtained in the present experiment may have been produced in the reactions of nitrogen atoms.

In the system of ethylene and liquid nitrogen, the formation of both hydrogen cyanide and acetonitrile has been observed. The reactions may be written as follows:

$$C_2H_4 + N \longrightarrow HCN + CH_3 \quad (4)$$

$$\searrow\ CH_3CN + H \quad (5)$$

This mechanism contradicts that recently proposed by Safrany and Jaster.[5] According to them, hydrogen cyanide is mainly produced in the reaction between nitrogen atoms and such alkyl radicals as C_2H_5. However, the γ-radiolysis of the liquid nitrogen solution containing ethane gives more acetonitrile than hydrogen cyanide as the nitrogenous product.[13] This suggests that, even if it occurs, the reaction between ethyl radicals (this radical most probably exists in the present system) and nitrogen atoms gives mainly acetonitrile.

$$C_2H_5 + N \longrightarrow CH_3CN + H_2 \text{ (or 2H)} \quad (6)$$

Reaction (5) has not been proposed in the gas-phase experiment. If ethyl radicals are produced in the system of ethylene and liquid nitrogen, as

*1 In the short communication, we have classified hydrocarbons into two groups, I and II. The group I involves ethylene, propylene, propane, allene, and 1-butene, which give nitrogenous products in the γ-radiolysis of the liquid nitrogen solution and which have melting points lower than -130°C, while those of the group II (acetylene, *trans*-2-butene, and 1,3-butadiene) do not give nitrogenous products and have melting points higher than the group I.

*2 The time taken for the geminate recombination after the ionization is estimated to be $10^{-10\pm1}$ sec.[9] On the other hand, the average time between two successive collisions of an ion A, with the solute, B, is estimated by means of this equation:[11]

$$t=\{4\pi(D_A+D_B)(R_A+R_B)n\}^{-1} \quad (I)$$

Here, D is the diffusion constant, R is the collision radius, and n is the concentration of the solute, B. By assuming $D_{N_2^+}=10^{-5}$ cm^2/sec, $D_{C_2H_4}=5.3\times10^{-5}$ cm^2/sec, $R_{N_2^+}=2.4$ Å, $R_{C_2H_4}=1.9$ Å, and $t=10^{-10}$ sec, n is calculated to be 2.9×10^{20} molecules/cc, which corresponds to 1.7×10^{-2} in the mole fraction. This value is about 10^2 times the solute concentration in the present experiment.

8) L. Onsager, *Phys. Rev.*, **54**, 554 (1938).
9) F. Williams, *J. Am. Chem. Soc.*, **86**, 3954 (1964).
10) W. F. Schmidt and A. O. Allen, *J. Phys. Chem.*, **72**, 3730 (1968).
11) N. V. Klassen, *ibid.*, **71**, 2409 (1967).
12) J. F. Noxon, *J. Chem. Phys.*, **36**, 926 (1962); H. B. Dunford, *J. Phys. Chem.*, **67**, 258 (1963).
13) T. Oka and S. Sato, to be published.

will be discussed later, the reaction (6) might be the only source of acetonitrile.

In the system of propylene and liquid nitrogen, the nitrogenous product was acetonitrile. The reaction may be written as follows:

$$C_3H_6 + N \longrightarrow CH_3CN + CH_3 \quad (7)$$
$$\searrow X \text{ (unknown)} \quad (8)$$

The reaction (8) has to be involved because, in the case of ethylene, the total G-value of the nitrogenous products was 0.22, while that obtained with propylene was 0.12. The difference may be attributed to the formation of unknown products. A more thorough investigation of the products is obviously needed.

The results shown in Table 2 are very suggestive as to the details of the reaction (7). If the formation of acetonitrile is mainly due to the reaction between nitrogen atoms and some radicals, the acetonitrile obtained with the 1 : 1 mixture of C_3H_6 and C_3D_6 should contain many more d_1- and d_2-compounds than those shown in Table 2. Moreover, the results obtained with a partially-deuterated propylene ($CD_3CH{=}CHD$) clearly show that most of the methyl radical in propylene remains, as it is, in the acetonitrile produced. The bond cleavage in the intermediate, if it is produced, may be visualized as follows:

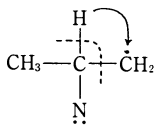

The reaction between nitrogen atoms and alkyl radicals, however, cannot be entirely ignored, because the formation of the d_1- and d_2- compounds has been observed with the 1 : 1 mixture.

In a previous note[14] on the γ-radiolysis of nitrogen gas, we have estimated the G-values of nitrogen atoms to be 0.8. This value is more than three times the G-value (0.22) of the nitrogenous products formed in the system of ethylene and liquid nitrogen. Since the cage effect has to be considered in the liquid, the value of 0.22 may not be far from the G-value of nitrogen atoms in liquid nitrogen.

The reaction of $N_2(A\,^3\Sigma_u^+)$ with ethylene may be written as follows:[15]

$$N_2(A^3\Sigma_u^+) + C_2H_4 \longrightarrow N_2 + C_2H_4^*$$
$$C_2H_4^* \longrightarrow C_2H_2 + H_2 \text{ (or } 2H)$$
$$\searrow C_2H_3 + H$$

These reactions will be followed by such radical reactions as:

$$H + C_2H_4 \longrightarrow C_2H_5$$
$$C_2H_3 + C_2H_4 \longrightarrow C_4H_7$$

This is consistent with the finding that, in the presence of oxygen, the only product observed was acetylene. In the case of propylene, a similar reaction mechanism can easily be constructed.

The amount of each hydrocarbon observed in both radiolyses leveled off over the mole fraction of 4×10^{-4}. If this is due to the complete quenching of excited nitrogen molecules, the life-time of excited nitrogen molecules in liquid nitrogen can be estimated by using Eq. (I). The obtained value is about 10^{-8} sec. This is very much smaller than that estimated as the life-time in the gas phase. This is obviously another subject which needs to be investigated.

14) T. Oka, R. Kato, S. Sato and S. Shida, This Bulletin, **41**, 2192 (1968).

15) D. D. Stedman, J. A. Meyer and D. W. Setser, *J. Am. Chem. Soc.*, **90**, 6856 (1968).

BULLETIN OF THE CHEMICAL SOCIETY OF JAPAN VOL. 42 3088—3092 (1969)

Radiolysis of Methylcyclohexane. II. The Effect of Cumene on Hydrogen Formation from γ-Irradiated Methylcyclohexane

Toyoaki KIMURA Kenji FUEKI and Zen-ichiro KURI

Department of Synthetic Chemistry, Faculty of Engineering, Nagoya University, Chikusa-ku, Nagoya

(Received May 1, 1969)

The effect of cumene on the hydrogen yields from methylcyclohexane γ-irradiated at 100, 20, -72, -120 and -196°C has been investigated. Cumene did not compete with N_2O for capturing electrons in methylcyclohexane and the yield of thermal H atoms in methylcyclohexane, determined by use of ethylene as an H atom scavenger, was smaller than the decrease in hydrogen yield in methylcyclohexane-cumene systems. Therefore, the decrease in hydrogen yield in methylcyclohexane-cumene systems can be ascribed mainly to positive charge transfer from methylcyclohexane to cumene. Further, the evidence of charge transfer from methylcyclohexane to cumene was found by the optical absorption method. The effect of cumene on the hydrogen yield from methylcyclohexane was similar in the temperature range from 100 to -196°C, especially at high cumene concentration. The effect of an electron scavenger at high concentrations was also examined with *n*-butyl chloride. In the present work, we have found that although the effect of a positive ion scavenger on the hydrogen yield from methylcyclohexane in the liquid state differs little from that in the glassy state, the effect of electron scavengers on the former differs considerably from that on the latter.

In a previous paper[1] we have reported the effects of temperature and electron scavengers on the hydrogen yield from γ-irradiated methylcyclohexane. We have shown that both in the liquid and glassy states the neutralization of a positive ion and an electron leads to the formation of a hydrogen molecule,

$$MCH \text{ -}\!\!\wwarrow\!\!\rightarrow MCH^+ + e^- \quad (1)$$

$$MCH^+ + e^- \longrightarrow H_2 \quad (2)$$

and that the efficiency of electron scavenging by solutes in the glassy state differs considerably from that in the liquid state. Some workers[2,3] showed that the yields of scavengable electrons in hydrocarbon glasses were lower than those in liquid hydrocarbons, and that they are at most 1.6 (G unit).[2] At present, the reason for this is not clear, but the following reasons may be considered; (1) the separation distances of positive ions and thermalized electrons in glasses are shorter than those in liquids, (2) positive ions may play a part in neutralization processes, for instance, in glasses charge transfer from positive ions to neutral molecules occurs rapidly and initial charge recombination is increased. Therefore it is of interest to know the behavior of positive ions both in liquid and glassy hydrocarbons.

Hitherto, studies of positive ions have been undertaken in several ways; observation of optical absorption spectra,[4] measurements of HD formed from solutions containing deuterated compounds such as ND_3 and C_2H_5OD as proton acceptors,[5,6] measurements of methane produced from solutions containing neopentane,[7] and observation of changes in product distribution by addition of ammonia.[8] These methods, however, are not necessarily useful for our purpose, because we can observe only positive ions surviving after a large fraction of ion pairs have neutralized, and both deuterated ammonia and deuterated ethanol are not sufficiently soluble in methylcyclohexane glass at -196°C for a major fraction of positive ions to be scavenged. Also, neopentane cannot be used to scavenge a large fraction of positive ions, since ionization potential of neopentane (10.35 eV) is higher than that of methylcyclohexane (9.85 eV).

1) T. Kimura, T. Miyazaki, K. Fueki and Z. Kuri, This Bulletin, **41**, 2861 (1968).

2) T. Wakayama, T. Kimura, T. Miyazaki, K. Fueki and Z. Kuri, presented at 22nd Annual Meeting of the Chemical Society of Japan, Apr., 1969, Tokyo.

3) M. Shirom and J. E. Willard, *J. Phys. Chem.*, **72**, 1702 (1968).

4) W. H. Hamill, "Radical Ions," ed. by E. T. Kaiser and L. Kevan, John Wiley & Sons, Inc., New York (1968).

5) F. Williams, *J. Am. Chem. Soc.*, **86**, 3954 (1964).

6) J. W. Buchanan and F. Williams, *J. Chem. Phys.*, **44**, 4377 (1966).

7) J. A. Stone, *Chem. Commun.*, **1968**, 1677.

8) K. Tanno, S. Shida and T. Miyazaki, *J. Phys. Chem.*, **72**, 3496 (1968).

In this work we have used cumene as a positive ion scavenger. The reasons are that cumene is soluble at any concentration in the methylcyclohexane glass at −196°C, the hydrogen yield from cumene is low (described later), and the ionization potential of cumene (8.69 eV) is lower than that of methylcyclohexane. Positive charge transfer from alkanes to olefins and aromatics and the subsequent decrease in hydrogen yields have been reported.[9,10] Thus it can be expected that cumene will scavenge the methylcyclohexane positive ion and suppress hydrogen formation.

$$MCH^+ + \text{Cumene} \longrightarrow MCH + \text{Cumene}^+ \quad (3)$$

$$\text{Cumene}^+ + e^- \longrightarrow H_2 \text{ (low yield)} \quad (4)$$

Here we report the thermal H atom yield from γ-irradiated methylcyclohexane in the liquid and glassy states, determined by use of ethylene as an H atom scavenger, and the effect of cumene on the hydrogen yield at various temperatures. In addition to these results we will show evidence for positive charge transfer from methylcyclohexane to cumene by the optical absorption method and discuss primary processes in the radiolysis of methylcyclohexane in the liquid and glassy states.

Experimental

The experimental procedure was almost the same as that described earlier.[1] Cumene was Nakarai guaranteed reagent and purified by distillation prior to use. *s*-Butyl chloride was Tokyo Kasei guaranteed reagent and was passed through a silica gel column after distillation. Tokyo Kasei guaranteed *n*-butyl chloride was passed through a silica gel column and fractionally distilled through 1.2 m long column filled with small cylindrical hollow glass packing. The purity of *n*-butyl chloride thus obtained was 99.8%. In the methylcyclohexane-cumene system, γ-irradiations were performed at 100, 20, −72, −120, and −196°C. Irradiations of samples at 100°C were performed in a Dewar filled with boiling water. In measurements of optical absorption spectra, samples were degassed in a glass tube and transferred in a rectangular quarz cell (10 mm × 5 mm), and sealed off. Irradiations were carried out at −196°C in the dark. The dose was usually 1.19×10^{19} eV/g. Optical absorption measurements were made on a Hitachi EPU-2 spectrophotometer.

Results

The hydrogen yields from pure methylcyclohexane, cumene, and *n*-butyl chloride irradiated at various temperatures and irradiation doses are listed in Table 1. The hydrogen yields from methylcyclohexane-ethylene systems irradiated at 20 and −196°C are shown in Fig. 1. The decrease in hydrogen yield is about 1.0 G in the liquid state and 0.5 G in the glassy state.

Table 1. Hydrogen yields from pure methylcyclohexane (MCH), cumene, and *n*-butyl chloride (*n*-BuCl) at various temperatures and doses

Sample	Irradiation temp. °C	$G(H_2)$	Dose eV/g
MCH	100	5.4	6.51×10^{19}
MCH	20	4.9	2.93×10^{20}
MCH	−72	4.5	2.60×10^{20}
MCH	−120	4.5	6.51×10^{19}
MCH	−196	4.4	2.60×10^{20}
Cumene	100	0.19	6.51×10^{19}
Cumene	20	0.19	2.93×10^{20}
Cumene	−196	0.11	2.60×10^{20}
n-BuCl	−196	0.92	2.60×10^{20}

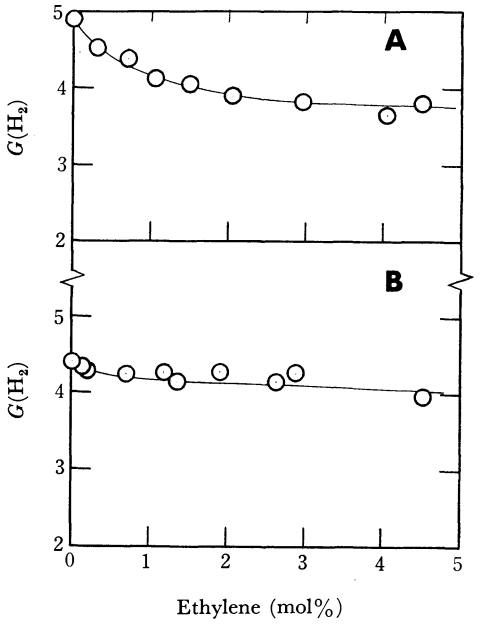

Fig. 1. Hydrogen yields from γ-irradiated methylcyclohexane-ethylene systems. (A), at 20°C; (B), at −196°C
Dose = 2.93×10^{20} eV/g

To see whether cumene scavenges an electron to form cumene anion, we have examined the nitrogen and hydrogen yields from methylcyclohexane solutions containing 3 mol % of N_2O together with various concentrations of cumene. These results are shown in Fig. 2. Though the experimental data are somewhat scattered because of the variation in the volume above the liquid surface in irradiation cells, the nitrogen yield is not affected by the presence of cumene. Moreover, it was found in γ-irradiated 3MP glasses containing biphenyl at −196°C, the yield of biphenyl anions was not affected by the

9) G. R. Freeman, *J. Chem. Phys.*, **36**, 1542 (1962).
10) L. A. Raibenbach and U. Kaldor, *ibid.*, **47**, 242 (1967).

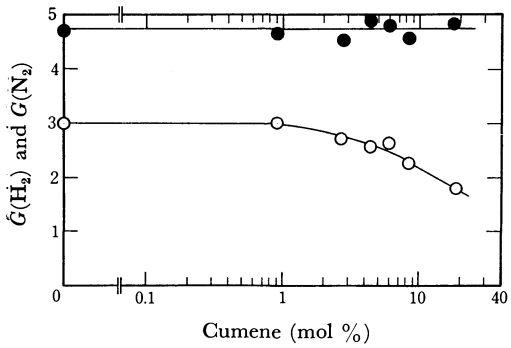

Fig. 2. The effect of cumene on hydrogen and nitrogen yields from methylcyclohexane containing 3 mol % N_2O irradiated at 20°C.
○ $G(H_2)$ ● $G(N_2)$
Dose=2.93×10^{20} eV/g

presence of cumene in much higher concentrations than that of biphenyl.[11] Therefore it is concluded that cumene does not scavenge electrons.

The hydrogen yields from methylcyclohexane-cumene systems irradiated at 100, 20, −72, −120, and −196°C are shown in Fig. 3.

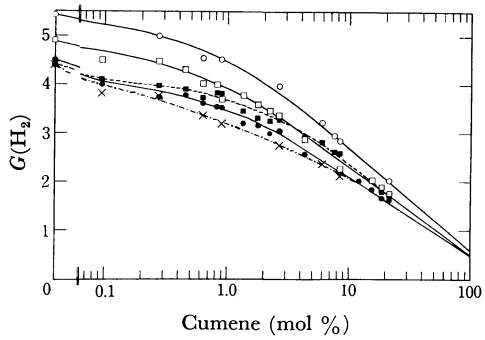

Fig. 3. Hydrogen yields from methylcyclohexane-cumene systems.
(a) —○— irradiated at 100°C (Dose=6.51×10^{19} eV/g)
(b) —□— irradiated at 20°C (Dose=2.93×10^{20} eV/g)
(c) —●— irradiated at −72°C (Dose=2.60×10^{20} eV/g)
(d) ---×--- irradiated at −120°C (Dose=6.51×10^{19} eV/g)
(e) ---■--- irradiated at −196°C (Dose=2.60×10^{20} eV/g)

These G values were obtained based on the energy absorbed only in methylcyclohexane. It can be seen from the data in Table 1 that the contribution of hydrogen formation from cumene by the direct effect of radiation is at most ~1% of the total hydrogen even at the highest cumene concentration studied, 21.5 mol 1%. Comparing the hydrogen yields from methylcyclohexane-cumene systems (Fig. 3) with those from methylcyclohexane-ethylene systems (Fig. 1), we see that the decrease in hydrogen yield in the former cannot be explained only by H atom scavenging by cumene because H atom scavenging is a minor process for the suppression of hydrogen formation, especially in the glassy state at −196°C, as shown in Fig. 1. The experimental curves (Fig. 3) which represent the hydrogen yield *vs.* cumene concentration are very similar to each other, practically at high cumene concentrations. The hydrogen yields at −72 and −120°C (Fig. 3. c and d) are somewhat lower than those at 20 and −196°C (Fig. 3. b and e). This may be partly due to inaccuracy in the evaluation of the energy absorbed in cooling agents.

Though the effect of cumene on the hydrogen yields in the liquid state at 20°C is practically the same as that in the glassy state at −196°C (Fig. 3. b and e), the effect of electron scavengers on the former is considerably different from that on the latter.[1] Therefore, in the present work we have extended the study of the effect of electron scavengers in the glassy state to higher concentrations than before.[1] For this purpose we have examined the hydrogen yield from methylcyclohexane glass with *n*-butyl chloride as an electron scavenger, since it has been found that *n*-butyl chloride is soluble at any concentration in methylcyclohexane glass at −196°C. The results are shown in Fig. 4 together with the previous data[1] for comparison. The values were obtained based on the energy absorbed only in methylcyclohexane. The observed hydrogen yield at the highest concentration of *n*-butyl chloride (26.8 mol %) is 2.8 G, which contains the hydrogen yield from *n*-butyl chloride by 0.33. Since the observed decrease in hydrogen yield at the highest concentration of *n*-butyl chloride is 1.6 G,

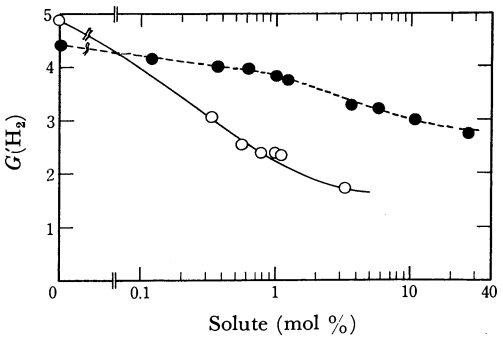

Fig. 4. Hydrogen yields from methylcyclohexane solutions.
—○— $G(H_2)$ from methylcyclohexane-iodobenzene systems irradiated at 20°C (Dose=3.06×10^{20} eV/g)[1]
---●--- $G(H_2)$ from methylcyclohexane *n*-butyl chloride systems irradiated at −196°C (Dose=2.60×10^{20} eV/g)

11) N. Kato, K. Fueki and Z. Kuri, unpublished results.

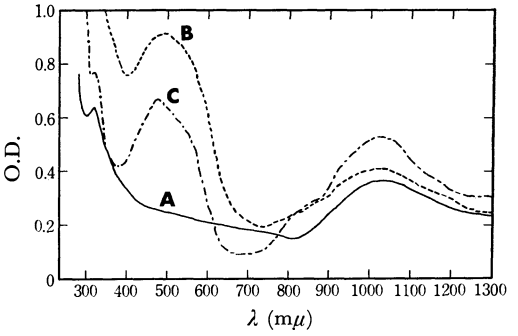

Fig. 5. Optical absorption spectra of (A) methyl cyclohexane containing 3 mol % N_2O and 3.5 mol % cumene after γ-irradiation (Dose$=1.19\times10^{19}$ eV/g); of (B) *s*-butyl chloride containing 7.9 mol % cumene after γ-irradiation (Dose$=2.38\times10^{19}$ eV/g); of (C) the same sample as (B) after photobleaching with visible light from a tungsten lamp at -196°C.

the corrected decrease, that is the scavenged electron yield, is estimated to be 1.9 G.

The optical absorption spectra of γ-irradiated methylcyclohexane glass containing cumene and N_2O, and of γ-irradiated *s*-butyl chloride glass containing cumene are shown in Fig. 5. The spectrum of methylcyclohexane glass containing 3 mol % of N_2O and 3.5 mol % of cumene has an absorption maximum at 1050 mμ (Spectrum A), which resembles that of toluene cation.[4] The spectrum of *s*-butyl chloride containing 7.9 mol % of cumene also has an absorption maximum at 1050 mμ. When γ-irradiated *s*-butyl chloride-cumene sample is photobleached with visible light from a tungsten lamp, the absorption spectrum changes from spectrum (B) to spectrum (C) and the 1050 mμ band increases in intensity. Thus, the 1050 mμ band can be assigned to the cumene cation. The dependence of the optical density at 1050 mμ on the cumene concentration in methylcyclohexane is shown in Fig. 6. The result is similar to that on toluene in 3MP glass[4] and indicates that the cumene cation is produced by charge transfer from methylcyclohexane to cumene.

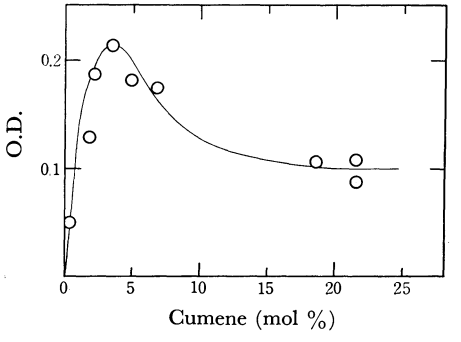

Fig. 6. Optical density *vs.* the concentration of cumene in methylcyclohexane glasses containing 3 mol % N_2O.
Dose$=1.19\times10^{19}$ eV/g.

Discussion

The decreased hydrogen yield in methylcyclohexane-ethylene systems can be ascribed to thermal H atom scavenging by ethylene.[12] The decrease in hydrogen yield in the liquid state (1.0 G) is twice that in the glassy state (0.5 G), as shown in Fig. 1. It should be noted that the difference between the hydrogen yields of pure liquid methylcyclohexane irradiated at 20°C and of pure glassy methylcyclohexane at -196°C is 0.5 G. As we reported previously,[1] these results seem to suggest the following mechanism:

at room temperature

$$H_{thermal} + MCH \longrightarrow H_2 + MCH\cdot \quad (1.0G) \quad (5)$$

at -196°C

$$H_{thermal} + MCH \not\longrightarrow H_2 + MCH\cdot \quad (6)$$

$$H_{thermal} + H_{thermal} \longrightarrow H_2 \quad (0.5G) \quad (7)$$

Thermal H atoms abstract H atoms from solvent molecules to produce hydrogen molecules (1.0 G), but they are unable to abstract H atoms at -196°C and recombine with one another to produce hydrogen molecules (0.5 G).

Since cumene does not compete with N_2O for capturing electrons (Fig. 2), the decrease in hydrogen yield in methylcyclohexane systems (Fig. 3) cannot be attributed to electron scavenging by cumene. *s*-Butyl chloride matrix is widely used for trapping cation species.[4] Photobleaching of γ-irradiated *s*-butyl chloride-cumene glass causes the intensity of the 1050 mμ band to increase. This phenomenon is interpreted in terms of positive charge transfer from *s*-butyl chloride to cumene. It is known that the *s*-butyl chloride cation has an absorption maximum at 540 mμ[13] and can be excited by visible light to migrate over many molecules by resonant charge transfer.[14] The optical absorption measurements clearly demonstrate the formation of cumene cations in methylcyclohexane-cumene systems. It can also be seen from Fig. 6 that cumene cations are not produced by the direct ionization of cumene, but by charge transfer from methylcyclohexane to cumene. Thus, it may be said that the decrease in hydrogen yield in methylcyclohexane-cumene systems is mainly due to charge transfer from methylcyclohexane to cumene and partly due to thermal H atom scavenging by cumene.

Extrapolation of the curves in Fig. 3 to 100% cumene concentration gives hypothetical *G* values

12) W. A. Cramer and G. J. Piet, *Trans. Faraday Soc.*, **63**, 1402 (1967).
13) T. Shida and W. H. Hamill, *J. Chem. Phys.*, **44**, 2375 (1966).
14) W. F. Louwrier and W. H. Hamill, *J. Phys. Chem.*, **72**, 3878 (1968).

for hydrogen formation based on the energy absorbed only in methylcyclohexane, where all the effects of cumene on the radiolysis of methylcyclohexane are assumed to be completed. It should be noted that (1) the curves are very close to each other, and (2) the hypothetical hydrogen yields at 100% cumene are approximately the same (0.5—0.7 G). To interpret the results, two different effects of cumene are considered: H atom addition to cumene at low cumene concentrations and charge transfer to cumene at high concentrations.[9] Thus at high cumene concentrations the curves are interpreted to indicate positive ion scavenging curves at each irradiation temperature. One of the most notable features in the curves is that they differ little from each other in the temperature range from 100°C to −196°C. It is certain that in the glassy state at −196°C the mechanism of charge migration is resonant charge transfer. Since the curve of positive ion scavenging in the liquid state differs little from that in the glassy state, charge transfer in the liquid state may possibly be resonant. According to Freeman's calculation,[15] more than 10 mol % of scavenger is required to scavenge positive ion completely. Assuming the number of molecules surrounding a positive ion is six, it is shown that 13 mol % of scavenger is required for scavenger molecule to be adjacent to a positive ion. Therefore, it is difficult to discern between charge transfer by resonance and that by diffusional collision. Further study is needed to establish the charge transfer mechanism in liquid.

The hypothetical hydrogen yields at 100% cumene do not coincide with the hydrogen yields from pure cumene, as is seen from Table 1, and are tentatively considered to be the hydrogen yields from directly excited methylcyclohexane molecules:

$$MCH \rightsquigarrow MCH^* \longrightarrow H_2 \qquad (6)$$

The decrease in hydrogen yields in Fig. 4 is assumed to be equal to the yields of scavenged electrons. This interpretation is reasonable especially in the case of methylcyclohexane. It has been proposed by many workers that Eq. (2) holds in the radiolysis of liquid hydrocarbons, but some workers have shown by ESR studies that charge neutralization does not lead to decomposition of hydrocarbon lgasses at −196°C,[3] although others have shown by product analysis studies that Eq. (2) holds even in the glassy state at −196°C.[1,16] In the previous work on methylcyclohexane,[1] we have shown that the scavenged electron yield is equal to the decrease in hydrogen yield at −196°C as well as 20°C. Further, the hydrogen yield from pure methylcyclohexane irradiated at 20°C is not so different from that at −196°C. Thus, Eq. (2) seems to be valid at −196°C as well as 20°C, and we could evaluate by the decrease in hydrogen yield both the scavenged electron and the scavenged positive ion yield in methylcyclohexane.

As already described, the efficiency of electron scavenging in liquids differs considerably from that in glasses at −196°C (Fig. 4), though the efficiency of positive ion scavenging in liquids scarcely differs from that in glasses at −196°C (Fig 3). Further, the yield of scavenged electrons in methylcyclohexane-*n*-butyl chloride glasses at −196°C is at most 1.9 G at the highest concentration of *n*-butyl chloride where a *n*-butyl chloride molecule exists adjacent to a positive ion. Therefore, assuming the total ion-pair yield of methylcyclohexane is ~4, we can say that more than half of the electrons canont be scavenged at such a high solute concentration. To explain these experimental facts, we are forced to state as follows; a significant fraction of charge transfer in glasses will be completed before electrons ejected from molecules by radiation are thermalized. Since molecules in a glass at −196°C are not allowed for translational motions, charge transfer must be resonant. Hamill has suggested that resonant charge transfer is a very fast process.[14] Our results are consistent with the following mechanism: positive ions transfer their charge to solute molecules or trapping sites of the matrix before ejected electrons are thermalized, and then thermalized electrons return to positive ions or are scavenged by electron scavengers. One of the causes for the scavenged electron yield in glasses to be less than half of the total ejected electrons may be the shorter separation distances between trapped positive ions and thermalized electrons in glasses. However, it is not so easy to give a theoretical explanation for this reasoning.

We have found that the scavengable electron yield in glasses is ~2G. If this value is used in the previous calculation of electron scavenging in methylcyclohexane-iodobenzene glasses,[1] the experimental points fit well in the calculated curve without the assumption of aggregation of iodobenzene molecules at −196°C. Since positive ions do not move after electrons are thermalized, the previous calculation will be valid except for uncertainty in the initial ion-pair yield assumed in glasses.

15) G. R. Freeman, *J. Chem. Phys.*, **46**, 2282 (1967).
16) N. H. Sagert, *Can. J. Chem.*, **46**, 89 (1968).

BULLETIN OF THE CHEMICAL SOCIETY OF JAPAN VOL. 42 3093—3099 (1969)

A Study of the Properties of Dilute Polymer Solutions by the Archibald Ultracentrifugal Method*1

Akira KOTERA, Hideomi MATSUDA*2 and Yuji MIYAZAWA*3

Department of Chemistry, Faculty of Science, Tokyo Kyoiku University, Otsuka, Bunkyo-ku, Tokyo

and Etsuo JOKO

The Tokyo Metropolitan Technical College, Higashioi, Shinagawa-ku, Tokyo

(Received May 1, 1969)

A modification of the Archibald method for determining the molecular weight of a polydisperse sample in ideal and non-ideal solutions is developed in this paper. A reliable value of the weight-average molecular weight is obtained from the plot of an apparent weight-average molecular weight against the centrifugal time rather than against the amount of the solute sedimented from the meniscus. This fact is explained on the assumption of a fractionation effect of the solute caused by the centrifugal potential.

The sedimentation equilibrium method, one of the most reliable procedures for the molecular-weight determination of a polymer, is based on the strict thermodynamical treatment, but the time required for the attainment of the equilibrium is, in general, very long.

Archibald[1] has suggested that the molecular weight of a polymer can be determined from the data obtained during the approach to the sedimentation equilibrium for a monodisperse sample in an ideal solution.

For the system of a monodisperse sample in a non-ideal solution, Fujita and Inagaki[2,3] have derived a relationship according to which the apparent weight-average molecular weight of the solute at the meniscus at a given time is corrected to the value of that at zero time.

For a polydisperse sample in ideal and non-ideal solutions a weight-average molecular weight can be, in principle, determined in the same way, but the apparent weight-average molecular weight calculated at a given time must be extrapolated to zero time for the determination of the weight-average molecular weight of the sample.[1] It was shown in the experiments for the polydisperse sample in non-ideal solutions that the value of the apparent weight-average molecular weight of the sample at each centrifugal time at the meniscus, $M_{(app)}(t)$, does not change linearly with time, but that the extrapolated value at the meniscus to zero time is usually larger than that at the bottom of the cell.[4-7] According to the other reports, the values of $M_{(app)}(t)$ at the meniscus and the bottom of the cell vary approximately linearly with time for some cases of polydisperse samples in non-ideal solutions, and these values give the same intercept at zero time.[2,8,9] The purpose of this paper is to find out, experimentally, a suitable procedure for the extrapolation of the $M_{(app)}(t)$ of a polydisperse sample to the starting condition, and to obtain a reliable value for the molecular weight.

Experimental

Materials. Poly-α-methylstyrene 17*4 (PαMST-17, $\bar{M}_w = 37 \times 10^4$), poly-α-methylstyrene 18*4 (PαMST-18,

*1 Parts of this work were presented at the 15th Annual Meeting of the Society of Polymer Science, Japan (Nagoya University, May 22, 1966), and at the 16th Polymer Symposium in Japan (Kyushu University, October 21, 1967).

*2 Present address: Department of Chemical Engineering, Faculty of Textile Science, Shinshu University, Ueda, Nagano.

*3 Present address: Department of Chemistry, Faculty of Science, Science University of Tokyo, Kagurazaka, Shinjuku-ku, Tokyo.

1) W. J. Archibald, *J. Phys. Chem.*, **51**, 1204 (1947).

2) H. Fujita, H. Inagaki, T. Kotaka and H. Utiyama, *J. Phys. Chem.*, **66**, 4 (1962).

3) A. Nakazawa and H. Inagaki, *Nippon Kagaku Zasshi (J. Chem. Soc. Japan, Pure Chem. Sect.)*, **87**, 1049 (1966).

4) A. Ginsburg, P. Appel and H. K. Schachman, *Arch. Biochem. Biophys.*, **65**, 545 (1956).

5) H.-G. Elias, *Angew. Chem.*, **73**, 209 (1961).

6) H. A. Swenson, A. J. Morak and S. Kurath, *J. Polymer Sci.*, **51**, 231 (1961).

7) A. Kotera, N. Iso, K. Umezawa and Y. Miyazawa, This Bulletin, **35**, 699 (1962).

8) H. Inagaki, S. Kawai and A. Nakazawa, *J. Polymer Sci., Part A*, **1**, 3303 (1963).

9) H. Inagaki, A. Nakazawa and T. Kotaka, *Bull. Inst. Chem. Res., Kyoto Univ.*, **43**, 135 (1965).

*4 Polymerized anionically in the laboratory of Professor M. Nagasawa, Nagoya University.

$\bar{M}=59\times10^4$), and polystyrene NBS705*5(PST-NBS705, $\bar{M}=19\times10^4$) were used as samples with a narrow molecular-weight distribution. PαMST-mixt, which is a 1 : 1 mixture in weight of PαMST-17 and PαMST-18, and polystyrene SM1*6 (PST-SM1, $\bar{M}_w=30\times10^4$) were used as the polydisperse samples.

Solvents. Cyclohexane was repeatedly washed with a sodium hydroxide solution and with water after being treated with a mixture of sulfuric acid and nitric acid; then it was distilled twice and fractionally distilled after being dried over calcium chloride and metallic sodium. The physical constants were as follows: bp 80.8°C, n_D^{20} 1.4264, d^{38} 0.7619 g/ml.

Toluene was repeatedly washed with sodium hydroxide and water after being treated with sulfuric acid. It was dried over calcium chloride and then distilled fractionally. The physical constants were as follows: bp 110.8°C, d^{30} 0.8579 g/ml.

Butanone was distilled after being treated with potassium permanganate; then it was distilled fractionally after being dried over sodium sulfate. The physical constants were as follows: bp 79.4°C, d^{25} 0.7986 g/ml.

Ultracentrifugation. The measurements were made with a Hitachi Analytical Ultracentrifuge, UCA-1, equipped with a schlieren optical system. A double-sector cell was used. The experimental conditions in this study are summarized in Table 1. The values of the partial specific volume, $\bar{v}$, the density of the solvent, ρ, and the refractive index increment, dn/dC, used in this experiment are also listed in Table 1. The concentration in the cell was determined in accordance with the Klainer and Kegeles method.[10]

Results and Discussion

Determination of $M(t)$. $M(t)$, a weight-average molecular weight at each centrifugal time, was calculated by the following equation:[1]

$$M(t) = \{RT/(1-\bar{v}\rho)\omega^2\}(1/C_m x_m)(dC/dx)_m \qquad (1)$$

where R is the gas constant, T is the absolute temperature, $\bar{v}$ is the partial specific volume of the solute, ρ is the density of the solvent, ω is the angular velocity of the rotation, x_m is the distance from the axis of rotation to the meniscus or to the bottom of the cell, C_m is the concentration of the solute at the meniscus or the bottom, and $(dC/dx)_m$ is the concentration gradient at the meniscus or the bottom.

The schlieren pattern at the bottom of the cell was so indistinct that it was impossible to determine the concentration gradient. Therefore, only the results obtained at the meniscus will be discussed in this report.

In the calculation of $M(t)$ at the meniscus by Eq. (1), the value of $(1/C_m x_m)(dC/dx)_m$ was obtained by extrapolating a plot of log $(1/Cx)(dC/dx)$ against a given point in the cell, x, to the meniscus.[2]

The values of $M(t)$ obtained were plotted against time, t; the value extrapolated to $t=0$ gives the weight-average molecular weight of the solute at zero time, $M(t=0)$. The centrifugal time was calculated as follows; one-third of the time before the rotor attained its final speed was added to the time which elapsed after the operational speed was reached.[19]

The Results for Ideal Systems. The results of experiments for ideal systems are summarized in Table 2, where the value of $\Delta M(t)/\Delta t$ shows the

TABLE 1. THE EXPERIMENTAL CONDITIONS AND THE VALUES OF THE PHYSICAL CONSTANT USED IN THE SEDIMENTATION MEASUREMENTS

Sample	Solvent	Temp. (°C)	$\bar{v}$ (ml/g)	ρ (g/ml)	dn/dC (ml/g) (546 mμ)
PαMST-17	Cyclohexane	38.0 (θ)	0.865[11]	0.761[11]	0.201[11]
PαMST-18	Cyclohexane				
PαMST-mixt	Cyclohexane				
PαMST-18	Toluene	30.0	0.726[12]	0.8579[12]	0.1287[12]
PST-SM 1	Cyclohexane	35.0 (θ)	0.940[13]	0.7650[14]	0.173[15]
	Butanone	25.0	0.925[12]	0.7986[12]	0.221[16]
	Toluene	30.0	0.913[17]	0.8579[12]	0.109[18]
PST-NBS705	Toluene				

(θ): θ-temperature for the polymer solution

*5 A standard sample distributed by the National Bureau of Standards.

*6 A sample distributed by the Committee on Molecular Weight and Molecular Weight Distribution of the Society of Polymer Science, Japan.

10) S. M. Klainer and G. Kegeles, *J. Phys. Chem.*, **59**, 952 (1955).
11) C. Hosoi, Thesis, Tokyo Kyoiku University, 1964.
12) C. Hosoi, unpublished data, 1965.
13) B. Rosen, *J. Polymer Sci.*, **17**, 559 (1955).
14) International Critical Tables, Vol. 3, 1st Ed., pp. 27, 29 (1928).
15) W. R. Krigbaum and D. K. Carpenter, *J. Phys. Chem.*, **59**, 1166 (1955).
16) I.U.P.A.C., *J. Polymer Sci.*, **10**, 129 (1953).
17) W. Heller and A. C. Thompson, *J. Colloid Sci.*, **6**, 57 (1951).
18) H. P. Frank and H. F. Mark, *J. Polymer Sci.*, **17**, 1 (1955).
19) E. G. Pickels, "Ultracentrifugation," in "Methods in Medical Research," Vol. 5, ed. by A. C. Corcoran, Year Book Publishers, Chicago (1953), p. 123.

TABLE 2. THE VALUES OF $\Delta M(t)/\Delta t$, AND M FOR IDEAL SYSTEM

Sample	Solvent and Temp.	Initial concn. (g/dl)	Rotor speed (rpm)	$\Delta M(t)/\Delta t \times 10^{-4}$ (min^{-1})	$M \times 10^{-14}$
PαMST-17 (monodisperse)	Cyclohexane 38.0°C (θ)	0.211	7640	-0.17_5	$37._0$
		0.325	7640	-0.18_7	$39._8$
		0.459	8270	-0.17_7	$36._1$
		0.541	8950	-0.21_1	$41._1$
		0.661	8270	-0.18_5	$38._3$
PαMST-18 (monodisperse)	Cyclohexane 38.0°C (θ)	0.203	7060	-0.24_4	$58._0$
		0.286	7060	-0.24_2	$57._0$
		0.406	7060	-0.26_8	$56._3$
		0.557	7060	-0.31_9	$55._8$
		0.667	7060	-0.31_2	$55._6$
PαMST-mixt (polydisperse)	Cyclohexane 38.0°C (θ)	0.224	7060	-0.28_9	$48._7$
		0.411	7060	-0.35_7	$50._3$
		0.601	7060	-0.35_3	$49._0$
		0.795	7060	-0.35_5	$50._3$
		0.979	7640	-0.38_0	$48._3$
PST-SM 1 (polydisperse)	Cyclohexane 35.0°C (θ)	0.136	8270	-0.16_0	$29._0$
		0.209	8950	-0.14_8	$31._3$
		0.568	9690	-0.18_2	$31._8$
		0.699	8270	-0.13_1	$31._6$

$\Delta M(t)/\Delta t$: the magnitude of the slope of the plot $M(t)$ against t
M: the molecular weight of sample

TABLE 3. THE VALUES OF $\Delta M_{(app)}(t)/\Delta t$, AND $M_{(app)}$ FOR NON-IDEAL SYSTEM

Sample	Solvent and Temp.	Initial concn. (g/dl)	Rotor speed (rpm)	$\Delta M_{(app)}(t)/\Delta t \times 10^{-4}$ (min^{-1})	$M_{(app)} \times 10^{-4}$
PαMST-18 (monodisperse)	Toluene 30.0°C	0.202	7060	$+0.12_9$	$33._0$
		0.311	8270	$+0.02_6$	$26._8$
		0.408	10490	-0.05_3	$21._3$
		0.515	10490	-0.04_8	$19._1$
		0.614	10490	-0.02_7	$17._0$
PST-NBS705 (monodisperse)	Toluene 30.0°C	0.480	10490	$+0.04_4$	$12._9$
		0.648	11350	$+0.02_8$	$11._4$
		0.821	13310	$+0.01_3$	$10._3$
PST-SM1 (polydisperse)	Butanone 25.0°C	0.101	10490	-0.15_0	$26._2$
		0.338	10490	-0.11_9	$22._2$
		0.515	10490	-0.13_0	$17._8$
		0.649	10490	-0.09_4	$14._4$
		1.084	10490	-0.06_2	$12._2$
	Toluene 30.0°C	0.346	10490	-0.02_4	$23._5$
		0.446	11350	-0.02_7	$21._8$
		0.487	11350	-0.02_5	$19._9$
		0.711	13310	-0.03_8	$15._8$

$\Delta M_{(app)}(t)/\Delta t$: the magnitude of the slope of the plot $M_{(app)}(t)$ against t
$M_{(app)}$: the apparent molecular weight of the solute depending on the initial concentration

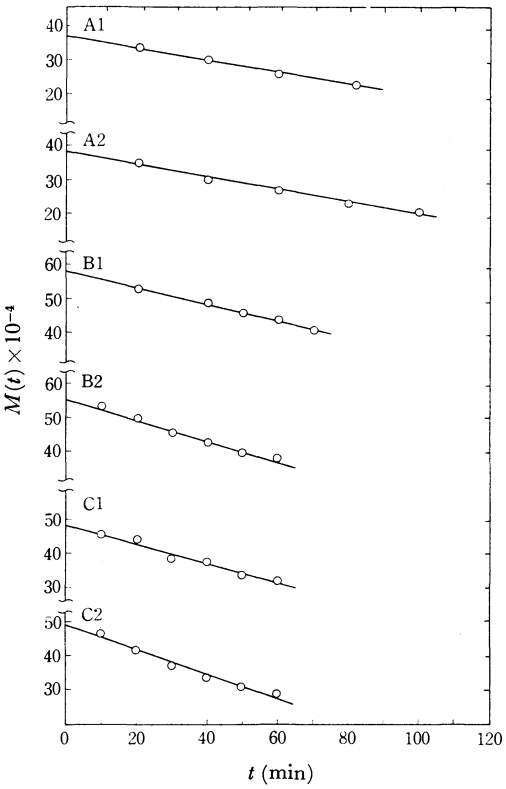

Fig. 1. Plots of $M(t)$ against t for PαMST in cyclohexane at 38°C.

PαMST-17: (A1) C_0=0.211 g/dl
rotor speed=7640 rpm
(A2) C_0=0.661 g/dl, 8270 rpm
PαMST-18: (B1) C_0=0.203 g/dl, 7060 rpm
(B2) C_0=0.667 g/dl, 7060 rpm
PαMST-mixt: (C1) C_0=0.224 g/dl, 7060 rpm
(C2) C_0=0.601 g/dl, 7060 rpm
$M(t)$: Molecular weight of the solute at each centrifugal time t
C_0: Initial concentration of the solute

magnitude of the slope in the plot of $M(t)$ against t. A typical plot of $M(t)$ against t is shown in Fig. 1 for three samples of PαMST in the theta solvent.

The data for ideal systems in Table 2 and Fig. 1 show that: (1) the values of $M(t)$ vary linearly with the time (though it has no theoretical basis), and (2) the plots have a negative slope.

The measured value of the molecular weight, at the meniscus, of a monodisperse solute in an ideal solution should be independent of the centrifugal time. When the time dependence of $M(t)$ observed in the sample of an ideal system is supposed to be caused by the sedimentational fractionation of the solute molecules at the meniscus, the more heterogeneous the solute is, the more negative the time dependence to be expected for $M(t)$. In the present study, it is consistent with the above expectation that $M(t)$ for PαMST-mixt in the theta solvent shows a negative time dependence, and that

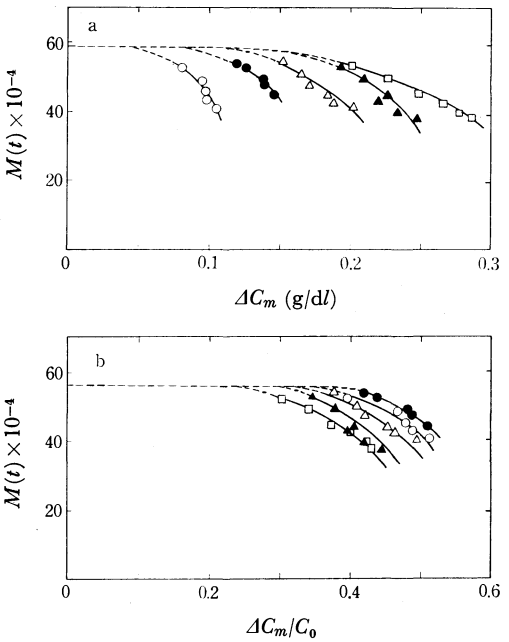

Fig. 2. (a) Plots of $M(t)$ against ΔC_m for PαMST-18 in cyclohexane at 38°C.
(b) Plots of $M(t)$ against $\Delta C_m/C_0$ for PαMST-18 in cyclohexane at 38°C.

(○) C_0=0.203 g/dl (●) C_0=0.286 g/dl
(△) C_0=0.406 g/dl (▲) C_0=0.557 g/dl
(□) C_0=0.667 g/dl
The measurements were carried out at 7060 rpm.
$M(t)$: Molecular weight of the solute at each centrifugal time t
ΔC_m: Amount of the solute sedimented from the meniscus
C_0: Initial concentration of the solute

the magnitude of its time dependence is larger than that of either PαMST-17 or PαMST-18 in the theta solvent. A distinct negative time dependence of PαMST-17 and PαMST-18 in an ideal solution, whose molecular-weight distribution is fairly narrow, suggests the strong sensitivity of this method to sample heterogeneity. The larger gradient of the plot of $M(t)$ against t for PαMST-18 in cyclohexane than that for PαMST-17 in cyclohexane is concluded on the basis of a comparison of the sedimentation patterns for the two samples. Both samples show the schlieren pattern with a leading minor peak of the second component; the area under the minor peak in PαMST-18 in cyclohexane is a little larger than that in PαMST-17 in cyclohexane.[12]

It seems appropriate to use amounts of the solute sedimented from the meniscus, ΔC_m and $\Delta C_m/C_0$, as variables in the analysis of $M(t)$ to obtain $M(t=0)$. A typical plot of $M(t)$ against ΔC_m is shown in Fig. 2-a for PαMST-18 in the theta solvent. The plot shows a downward-curving line for a solution of a given initial concentration. When the

fractionation of the solute by the sedimentation is independent of C_0, the plots of $M(t)$ against $\Delta C_m/C_0$ for the different values of C_0 will fall on a master curve because the molecular-weight distributions of the solute at the meniscus for the different concentrations may be expected to be identical for the same value of $\Delta C_m/C_0$. Figure 2-b shows a typical plot of $M(t)$ against $\Delta C_m/C_0$ for PαMST-18 in the theta solvent. This plot also gives curved lines for each C_0 value, though the lines are close to each other. It might be reasonable to assume that the fractionation of the solute at the meniscus does not always proceed regularly in the order of the molecular weight, but that the hydrodynamic interactions between the solute molecules are influenced by the initial concentration of the solute under the conditions used in this experiment.

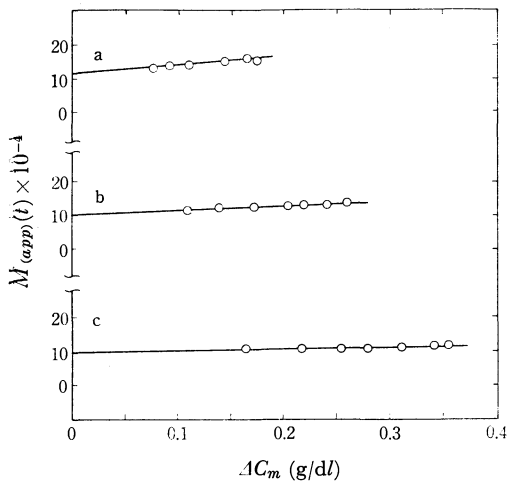

Fig. 3. Plots of $M_{(app)}(t)$ against ΔC_m for PST-NBS705 in toluene at 30°C.

(a) C_0=0.480 g/dl, rotor speed=10490 rpm
(b) C_0=0.648 g/dl, 11350 rpm
(c) C_0=0.821 g/dl, 13310 rpm
$M_{(app)}(t)$: Molecular weight of the solute at each centrifugal time t
ΔC_m: Amount of the solute sedimented from the meniscus
C_0: Initial concentration of the solute

The Results for Non-ideal Systems. For a non-ideal system the value of $M(t)$ calculated from Eq. (1) is an apparent weight-average molecular weight, $M_{(app)}(t)$, because the value depends on C_0. The results for non-ideal systems are summarized in Table 3. The gradient of the plot of $M_{(app)}(t)$ against t decreases slightly with an increase in C_0 at the same rotor speed, as is shown in the systems of PαMST-18 in toluene, PST-SM1 in butanone, and PST-SM1 in toluene. All of the plots for PST-SM1 show negative slopes; moreover, the slopes become small in magnitude in the order of the cyclohexane, the butanone, and the toluene solutions. The plot of $M_{(app)}(t)$ against t for PST-NBS705 in toluene shows a positive slope, while that for PαMST-18 in toluene shows either a positive slope or a negative one. A positive time dependence in a non-ideal system, such as PST-NBS705 in toluene and PαMST-18 in toluene, is expected from the theory of Fujita and Inagaki[2] for the sample of a sufficiently narrow molecular-weight distribution. It may be concluded from the results in this study that the time dependence of $M_{(app)}(t)$ in a non-ideal system becomes smaller with an increase in C_0. This result shows that the fractionation effect of the solute during sedimentation is superposed on the thermodynamic non-ideality of the solution.

For a monodisperse sample in a non-ideal solution, the following equation was given by Fujita and Inagaki:[2]

$$M_{(app)}(t) = M_{(app)} + M^2\{B_{11}+(\bar{v}/M)\}\Delta C_m + (\text{higher terms in } \Delta C_m) \quad (2)$$

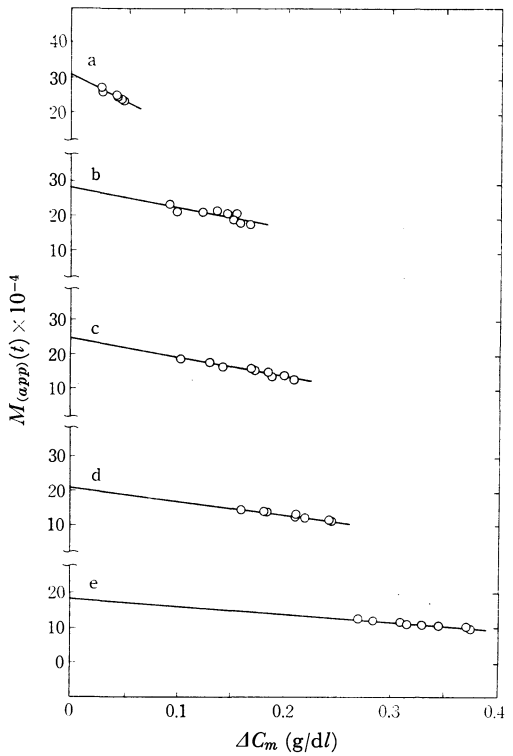

Fig. 4. Plots of $M_{(app)}(t)$ against ΔC_m for PST-SM1 in butanone at 25°C.

(a) C_0=0.101 g/dl (b) C_0=0.338 g/dl
(c) C_0=0.515 g/dl (d) C_0=0.649 g/dl
(e) C_0=1.084 g/dl
The measurements were carried out at 10490 rpm.
$M_{(app)}(t)$: Molecular weight of the solute at each centrifugal time t
ΔC_m: Amount of the solute sedimented from the meniscus
C_0: Initial concentration of the solute

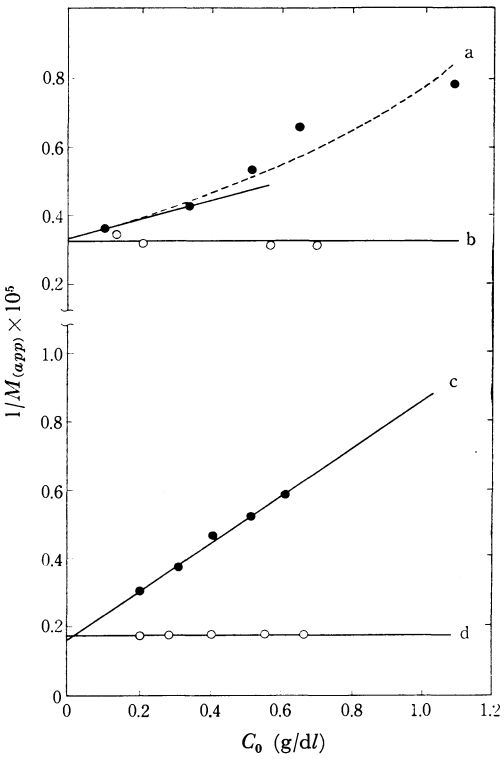

Fig. 5. Plots of $1/M_{(app)}$ against C_0.

(a): (●) PST-SM1 in butanone at 25°C
(b): (○) PST-SM1 in cyclohexane at 35°C (θ)
(c): (●) PαMST-18 in toluene at 30°C
(d): (○) PαMST-18 in cyclohexane at 38°C(θ)
The solid line in (a) is the initial tangent of the plot.
$M_{(app)}$: Apparent molecular weight of the solute
C_0: Initial concentration of the solute

where $M_{(app)}$ is the apparent molecular weight of the solute (it is independent of time), M is the molecular weight of the solute, B_{11} is the parameter for thermodynamic interaction between the solutes, and $\bar{v}$ is the partial specific volume of the solute. Generally speaking, the value of ΔC_m depends on time and takes a positive value. Equation (2) suggests a linear relation between $M_{(app)}(t)$ and ΔC_m for a monodisperse solute by neglecting the higher terms. Nakazawa and Inagaki[3] reported that the plot of $M_{(app)}(t)$ against ΔC_m has a linear relation for a monodisperse solute in a non-ideal solution, as is to be expected from Eq. (2), and concluded that the effect of the rotor speed on the plot of $M_{(app)}(t)$ against t can be eliminated by the plot of $M_{(app)}(t)$ against ΔC_m. Consequently, $M_{(app)}$ is obtained more satisfactorily when $M_{(app)}(t)$ is extrapolated to $\Delta C_m=0$ than when it is extrapolated to $t=0$. The plot of $M_{(app)}(t)$ against ΔC_m for PST-NBS705 in toluene is shown in Fig. 3, where it shows a positive slope and a straight line,

Table 4. Weight-average molecular weight $\bar{M}_w$

Sample	Solvent Temp. (°C)	$\bar{M}_w \times 10^{-4}$ This method	$\bar{M}_w \times 10^{-4}$ Literature values
PαMST-17	Cyclohexane 38.0 (θ)	38.5	40.7(SE)[12] 40.0(LS)[21]
PαMST-18	Cyclohexane 38.0 (θ)	56.5	60.6(LS)[21]
	Toluene 30.0	60.6	
PαMST-mixt	Cyclohexane 38.0 (θ)	49.3 (48.6)*	
PST-SM 1	Cyclohexane 35.0 (θ)	30.9	28.9(LS)[20] 28.2(A)[20]
	Butanone 25.0	28.4	27.9(LS)[20] 28.2(A)[20]
	Toluene 30.0	31.7	
PST-NBS705	Toluene 30.0	20.7	17.9(LS)[22] 19.0(SE)[22]

Asterisk (*): Calculated from $\bar{M}_w$ of PαMST-17 and PαMST-18
SE: Sedimentation equilibrium method
LS: Light scattering method
A: Archibald method

as may be expected from Eq. (2). However, the value of B_{11} obtained from the slope depends on the initial concentration and the rotor speed; this finding suggests that the effect of the fractionation of the solute is fairly large, even on this sample with a narrow molecular-weight distribution.

The plot of $M_{(app)}(t)$ against ΔC_m for PST-SM1 in butanone is shown as a typical example for a non-ideal polydisperse system in Fig. 4. The plot is approximately a straight line showing a negative slope. However, the observed values of $M_{(app)}(t)$ were localized in a limited range of ΔC_m, so the values of $M_{(app)}$ obtained by the extrapolation might be considered to be more ambiguous than that shown on the plot of $M_{(app)}(t)$ against t.

The weight-average molecular weight of the sample is determined from the intercept on the plot of $1/M_{(app)}$ against C_0, where $M_{(app)}$ is the value obtained by the plot of $M_{(app)}(t)$ against t. Figure 5 shows typical plots of $1/M_{(app)}$ against C_0. For an ideal system the reciprocals of M obtained by the extrapolation of the plot of $M(t)$ against t are independent of C_0 as was expected. The reciprocals of $M_{(app)}$ for a polydisperse solute in a non-ideal solution, such as PST-SM1 in butanone and PST-SM1 in toluene, show a dependence on C_0 with an upward curvature; this finding agrees with that reported by Toyoshima and Fujita.[20] On the

20) Y. Toyoshima and H. Fujita, *J. Phys. Chem.*, **68**, 1378 (1964).
21) A. Wada, Thesis, Tokyo Kyoiku University, 1964.
22) National Bureau of Standards, Certificate.

other hand, the plot of $M_{(app)}$ against C_0 for the sample of a narrow molecular-weight distribution in a non-ideal solution shows that the contribution of a third term to the virial expansion of Eq. (2) can be neglected. The values of M_w obtained by this method are summarized in Table 4; the values agree with those in literature.

The authors wish to express their hearty thanks to Professor Mitsuru Nagasawa of Nagoya University for his kind help in supplying the samples. They also wish to express their hearty thanks to Dr. Takahide Saito of Tokyo Kyoiku University for his many helpful discussions, and to Miss Yasuko Nishibe and Miss Makiko Muraki for their assistance in the experimental work.

BULLETIN OF THE CHEMICAL SOCIETY OF JAPAN VOL. 42 3099—3105 (1969)

The Crystal and Molecular Structure of the Sodium Salt of Xanthine

Hiroshi MIZUNO, Takaji FUJIWARA and Ken-ichi TOMITA

Faculty of Pharmaceutical Sciences, Osaka University, Toyonaka, Osaka

(Received May 6, 1969)

The crystals of sodium salt of xanthine, $C_5H_3N_4O_2Na \cdot 4H_2O$, are monoclinic with four molecules in a unit cell of dimensions; $a=7.31$, $b=19.52$, $c=7.17$ Å, $\beta=100.0°$, space group $P2_1/c$. The structure has been determined by application of the sign relationship $S(hkl)S(h'k'l') \sim S(h+h', k+k', l+l')$ from $(hk0)$ intensity data and refined by three-dimensional least-squares methods. The positions of the hydrogen atoms were determined by a three-dimensional difference Fourier analysis, and it was confirmed that deprotonation took place at the position of the imino N(3)H of the xanthine molecule. Each Na^+ cation is surrounded by six water molecules and each xanthine anion participates in ten hydrogen bonds, forming a close-packed system.

Xanthine, 2,6-dioxypurine, is well known as a

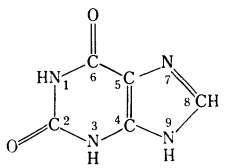

metabolic intermediate related to the common bases in nucleic acids. In man, the end product of purine metabolism is uric acid, and xanthine oxydase, an enzyme found in the liver, is capable of oxydizing xanthine to uric acid. Xanthine is a purine base which is not common in ribonucleic acid or deoxyribonucleic acid, but the deamination of guanine results in xanthine base, and this base is still able to pair with cytosine by two hydrogen bonds. Therefore the deamination of guanine by nitrous acid cannot be mutagenic, while adenine or cytosine deaminated by nitrous acid is lethal.

Its sodium salt was crystallized as the tetrahydrate from a ethanol-water solution, and this crystal structure was investigated by X-ray method. It is of particular interest to study the nature of the hydrogen bond between xanthine and water molecules, to determine the predominant resonance forms of the xanthine anion and also to investigate the environment around the sodium ion.

Experimental

The sample of the sodium salt of xanthine was purchased from the Nakarai Chemicals Ltd. (Kyoto), and recrystallized by slow evaporation of a ethanol-water solution at room temperature. The obtained crystals were in the form of colorless needles elongated along the c axis. Weissenberg photographs around the c axis demonstrated that the crystals were twins consisting of two components, in which only the a axis has different directions rotating 20.0° about the b axis, and which are united about a twin plane (100). Crystallographic data obtained from measurements of rotation, Weissenberg and precession photographs around the c axis are listed in Table 1.

Partial three-dimensional intensity data ($l=0$ to 5) with Ni-filtered Cu$K\alpha$ radiation were collected by the multiple film method using the equi-inclination Weissenberg camera. A needle-shaped crystal about 0.15×0.15 mm in cross-section was used. The crystals being twins as mentioned above, the reflection of each component was easily separable from that of the other, and the intensity was estimated by visual comparison with a caribrated scale. 1516 reflections were recorded, 1175 of which had measurable intensities. Lorentz and

TABLE 1. CRYSTAL DATA

$C_5H_3N_4O_2Na \cdot 4H_2O$
Monoclinic
$P2_1/c$
$a=7.31\pm0.02$ Å
$b=19.52\pm0.04$ Å
$c=7.17\pm0.02$ Å
$\beta=100.0\pm0.5°$
$Z=4$
μ (for Cu$K\alpha$) $=18.0$ cm^{-1}
$D_m=1.64$ g/cm^3
$D_c=1.62$ g/cm^3

polarization corrections were applied, but no further corrections were made to the intensities, which were then converted to the absolute scale by means of the usual averaging process.

Structure Determination

For the reflections of appropriately large unitary structure factors (U) in centrosymmetric space groups, the sign relations

$$S(hkl)S(h'k'l') = S(h+h',\ k+k',\ l+l') \quad (1)$$

$$S(hkl) = S\{\sum_{h'k'l'} S(h'k'l')S(h+h',\ k+k',\ l+l') \quad (2)$$

are applicable, where $S(hkl)$ is the sign of $U(hkl)$.[1-3] The root-mean-square value (σ) for the unitary structure factors of this crystal was equal to

$$\sigma = \{\sum_j Z_j^2/(\sum_j Z_j)^2\}^{1/2} = 0.116$$

where Z_j is the number of electrons in the jth atom. This value seems to be suitable for the application of a direct method described by Zachariasen.[3]

A sharpened Patterson synthesis was previously calculated with the three-dimensional data. Many peaks on the Patterson sections at $W=0$ and $W=1/4$, and the two strongest reflections, (002) and (004), indicated that the xanthine anions were approximately parallel to the (001) plane. It was, therefore, to be expected that the approximate crystal structure might be revealed by the Fourier projection on (001) with only the signs of large structure factors.

For those reflections which lie within the range of $|U(hk0)|\geq 1.5\sigma=0.174$, Eq. (1) was used to determine the signs. 17 out of 132 reflections fell in this category, where the signs of two structure factors were chosen arbitrarily in order to fix the origin. The signs of remaining structure factors for $|U(hk0)|\geq 0.100$, were determined by Eq. (2). Thus the signs of 44 reflections were finally determined from Eqs. (1) and (2), but of which 7 reflections, all with the low magnitude of U, were later shown to be incorrect.

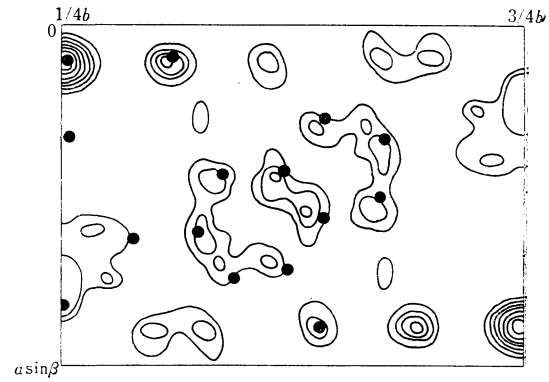

Fig. 1. First Fourier projection on (001) calculated with the signs of 44 reflections which were determined by the direct method. The black circles show the final atomic positions. One of the water oxygen atom is hidden by another one ($x=0.11$, $y=0.37$).

The first electron density projection on (001) calculated with the signs of 44 reflections is shown in Fig. 1, and there appeared significant peaks to be the purine ring atoms across a center of symmetry. Using the phases based on these peak positions, a second electron density map was calculated with all the observed ($hk0$) data, which showed the peaks of two carbonyl oxygen atoms and water oxygen atoms.

Succesive Fourier approximations by superimposing two water oxygen atoms O(5) and O(6) at $x=0.11, y=0.37$ along the c axis indicated a reasonable agreement between the observed and calculated amplitudes. At this stage the discrepancy factors, $R=\Sigma||F_o|-|F_c||/\Sigma|F_o|$, was 0.30 for ($hk0$) reflections. Because of the overlap, however, no further refinement of the structure on the projection was attempted.

An initial set of z coordinates was derived by considering the packing of the xanthine anions. Thus a three-dimensional Fourier synthesis was carried out with signs based on the phases of the xanthine ring atoms, and five peaks were newly and immediately identified; one peak was supposed to be the sodium ion in view of the peak height, and the others to be the water oxygen atoms. The second three-dimensional Fourier map calculated with the phases of all the non-hydrogen atoms showed the whole structure more clearly, and R-factor was now dropped to 0.26.

The positional parameters thus obtained, together with isotropic temperature factors, initially set to $B=3.0$ Å^2, were used as starting parameters for five cycles of block-diagonal least-squares refinement, and at the end of these cycles, the R-factor was

1) W. Cochran, *Acta Cryst.*, **5**, 65 (1952).
2) D. Sayre, *ibid.*, **5**, 60 (1952).
3) W. H. Zachariasen, *ibid.*, **5**, 69 (1952).

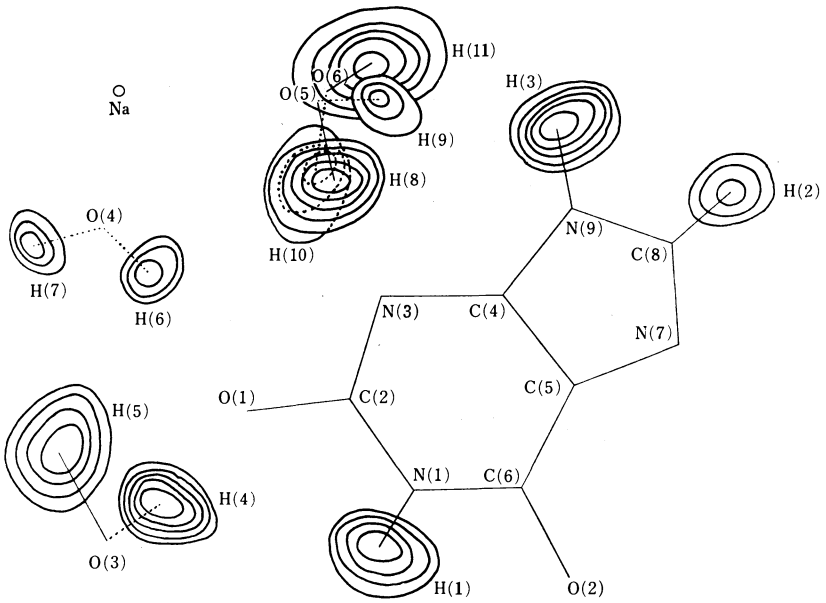

Fig. 2. A projection along the c axis of sections of a difference Fourier map for the location of hydrogen atoms. Contours are at interval of 0.1 e.Å^{-3}, starting with the 0.2 e.Å^{-3} contour.

reduced to 0.13. Anisotropic temperature factors in the form of

$$\exp[-(B_{11}h^2+B_{22}k^2+B_{33}l^2+B_{12}hk+B_{13}hl+B_{23}kl)]$$

were now used for all the non-hydrogen atoms. In the last few cycles, the contribution of the hydrogen atoms except H(7) were introduced to the calculation, and the coordinate of each hydrogen atom was located assuming the C–H, N–H and O–H distances to be 1.08, 1.03 and 1.00 Å, respectively, and also each hydrogen atom was given a temperature factor equal to the final isotropic value of the covalently bonded carbon, nitrogen or oxygen atom, but none of these parameters was refined. The R-factor at the end of the refinement was 0.11 for all observed reflections.

A three-dimensional difference Fourier synthesis was then calculated, where only H(7) was excluded for structure factor calculation. As illustrated in Fig. 2, locations of all the hydrogen atoms are clearly shown.

The final atomic coordinates and thermal parameters are listed in Tables 2 and 3. The observed and calculated structure factors are listed in Table 4. Some discrepancies between F_0 and F_c of low-order reflections may be due to absorption and

Table 2. The atomic coordinates and their standard deviations

	x/a	$\sigma(x)$	y/b	$\sigma(y)$	z/c	$\sigma(z)$
Na	0.1019	0.003	0.2452	0.003	0.4859	0.004
C(2)	0.6024	0.008	0.3876	0.008	0.3112	0.009
C(4)	0.4310	0.007	0.4843	0.008	0.2565	0.008
C(5)	0.5771	0.007	0.5260	0.008	0.2381	0.008
C(6)	0.7563	0.007	0.4970	0.008	0.2632	0.008
C(8)	0.3424	0.008	0.5898	0.008	0.1961	0.010
N(1)	0.7567	0.006	0.4270	0.006	0.2976	0.007
N(3)	0.4350	0.006	0.4161	0.006	0.2933	0.007
N(7)	0.5199	0.006	0.5941	0.007	0.2009	0.007
N(9)	0.2792	0.006	0.5255	0.007	0.2290	0.007
O(1)	0.6306	0.006	0.3249	0.006	0.3454	0.007
O(2)	0.9068	0.005	0.5274	0.005	0.2575	0.006
O(3)	0.8507	0.006	0.2402	0.006	0.1634	0.007
O(4)	0.3252	0.006	0.2357	0.006	0.2797	0.007
O(5)	0.1148	0.005	0.3669	0.005	0.4605	0.007
O(6)	0.1022	0.006	0.3720	0.006	0.0264	0.007

Table 3. The thermal parameters and their standard deviations ($\times 10^4$)

	B_{11}	σ	B_{22}	σ	B_{33}	σ	B_{12}	σ	B_{13}	σ	B_{23}	σ
Na	147	6	16	1	150	11	5	4	90	12	3	5
C(2)	118	16	15	2	99	24	−15	9	26	28	−18	11
C(4)	82	13	21	2	15	21	1	9	32	23	−2	10
C(5)	129	15	19	2	−14	21	0	9	28	24	2	10
C(6)	112	15	18	2	46	22	11	9	50	25	7	10
C(8)	113	15	17	2	153	27	20	10	57	29	18	12
N(1)	107	12	16	2	56	19	8	7	51	21	3	8
N(3)	101	13	14	2	102	20	−16	7	22	23	−9	9
N(7)	119	13	16	2	102	20	3	8	52	23	1	9
N(9)	88	12	22	2	88	20	8	8	71	22	4	9
O(1)	133	12	13	2	237	20	−2	7	33	23	5	9
O(2)	90	10	16	2	171	18	3	7	59	19	17	8
O(3)	144	12	21	2	166	20	−3	8	49	23	−20	9
O(4)	109	11	23	2	196	20	−15	7	79	22	−13	9
O(5)	129	11	15	2	164	18	−7	7	60	21	2	8
O(6)	173	11	17	2	142	19	−19	8	22	23	9	8

TABLE 4. OBSERVED AND CALCULATED STRUCTURE FACTORS

K	FO	FC
H,L=	0	0
2	33	49
4	45	47
6	55	-70
8	84	107
10	8	-8
12	44	46
14	33	-31
16	10	10
18	32	-32
20	15	-15
24	5	6
H,L=	1	0
0	41	-25
1	12	-8
2	51	-61
3	26	24
4	25	25
5	2	1
7	33	34
8	58	57
9	54	-53
10	58	-59
11	6	-6
12	27	-24
13	10	9
15	5	5
16	29	28
17	10	-10
18	10	-12
19	10	10
20	5	3
22	6	-6
24	6	4
H,L=	2	0
0	5	-7
1	50	-55
2	7	8
3	51	-49
4	37	-37
5	59	58
6	6	-7
7	3	3
8	4	5
9	27	-30
10	9	9
11	10	-11
12	7	-6
14	13	-14
15	22	24
16	11	-10
17	8	-10
18	7	-8
21	5	5
23	6	6
H,L=	3	0
0	22	-24
1	53	-54
2	5	-4
3	51	-49
4	5	2
5	55	-58
6	22	21
8	28	-28
9	46	-50
10	7	6
11	10	-8
13	16	-14
14	8	-5
15	19	-19
16	8	-6
17	32	-32
18	10	10
19	5	6
20	7	-6
21	4	5
23	8	7
H,L=	4	0
0	54	-63
1	27	-29
2	50	50
3	43	46
5	8	-8
6	8	8
7	31	29
8	36	-36
9	33	-31
10	25	28
11	13	14
12	5	2
13	10	9
14	25	24
15	23	24
16	11	-12
18	9	9
19	6	5
21	6	-4
H,L=	5	0
0	36	-42
1	11	-11
2	15	14
3	7	-8
4	15	-14
6	19	20
8	30	-31
9	8	9
10	20	21
13	23	-22
14	8	7
17	5	3
18	18	17
19	4	4
H,L=	6	0
0	36	-35
1	29	28
2	31	-30
3	11	11
4	10	-9
6	11	-12
7	11	+12
8	11	+13
12	5	3
13	7	7
16	6	-6
17	6	6
18	8	7
H,L=	7	0
K	FO	FC
0	5	4
2	8	8
3	5	-5
4	10	10
5	7	7
6	10	-9
7	19	18
H,L=	8	0
0	10	8
1	15	15
4	8	-8
5	8	8
7	10	-9
8	18	17
0	1	9
1	12	11
2	21	24
3	16	-17
4	21	-25
5	7	7
6	48	-54
7	5	4
8	8	-9
9	14	-17
10	55	-57
11	8	9
12	9	-7
14	26	-30
15	7	6
16	7	7
17	9	11
18	7	-6
19	9	8
20	18	17
21	4	-4
22	6	-6
23	3	4
24	7	5
H,L=	1	1
1	26	-26
2	4	3
3	12	13
4	9	-8
5	25	-26
6	7	-8
7	6	5
8	24	-28
9	5	3
11	8	-8
12	13	-14
13	4	-4
14	7	7
15	27	-29
16	5	4
17	5	-4
18	7	-7
19	21	21
20	8	-8
21	12	-10
22	3	-2
23	6	-6
H,L=	4	1
1	5	-6
2	15	-13
3	13	11
4	21	19
5	46	15
6	19	21
7	16	-17
8	19	1
9	8	9
10	28	28
11	9	-9
12	9	-9
13	18	18
14	7	8
15	6	6
16	7	8
17	7	5
18	6	6
19	8	-8
H,L=	5	1
1	16	16
2	21	24
3	3	2
4	16	7
5	10	10
6	16	16
7	6	-6
8	10	10
9	10	9
10	5	6
11	14	14
12	32	-29
13	18	17
14	6	5
15	3	3
16	13	14
17	4	3
18	5	4
19	6	6
20	13	12
21	6	-6
22	4	-3
23	8	8
H,L=	6	1
1	15	-15
2	11	-11
3	9	-8
K	FO	FC
6	5	5
8	29	32
10	7	6
11	7	-7
12	11	10
13	12	-10
14	12	-10
15	5	2
16	14	13
17	6	6
18	2	2
19	8	8
20	13	12
21	6	-6
22	2	-3
23	2	2
H,L=	7	1
1	16	16
2	7	5
3	7	5
4	10	10
5	11	10
6	104	-121
7	3	2
8	3	3
9	6	-6
10	4	-4
11	10	-11
12	32	-29
13	18	17
14	6	5
15	3	-2
16	2	2
17	5	6
18	1	1
19	2	2
20	10	9
21	6	-6
22	4	-3
23	8	8
H,L=	1	2
0	68	111
1	52	-88
2	40	-41
3	42	-45
4	7	9
6	55	-60
7	33	37
8	67	67
10	16	-16
11	10	9
12	15	15
13	18	-18
14	9	-8
15	10	10
16	10	9
17	12	-13
18	8	8
19	6	6
20	6	-6
21	6	-6
22	4	-3
23	8	8
H,L=	2	2
0	61	61
1	57	-59
2	44	-43
3	23	25
4	22	22
5	24	-24
6	4	4
7	37	40
8	23	22
9	40	-43
10	23	-23
11	24	24
12	18	17
13	7	-6
15	7	6
16	21	24
17	24	-26
H,L=	3	2
0	10	-9
1	7	-8
2	30	30
3	27	25
4	10	11
5	39	42
6	13	-13
7	48	55
8	10	-11
9	6	-7
10	9	8
11	15	15
12	12	11
13	22	25
14	12	13
15	24	28
16	7	-7
18	6	-6
H,L=	4	2
0	38	-41
1	18	-17
2	8	-5
3	21	-21
4	6	5
5	11	12
6	11	14
7	9	-10
8	13	-16
10	7	4
11	7	-7
12	12	-12
13	12	-13
14	12	-13
15	22	25
16	12	13
17	24	28
18	5	4
19	8	8
H,L=	5	2
0	19	-19
1	9	8
2	18	18
3	15	15
4	7	-7
5	7	6
6	10	13
7	7	7
8	24	-27
9	6	6
10	12	-12
11	15	15
12	32	-29
13	12	12
14	6	-6
15	2	2
16	6	-6
17	11	11
18	7	8
19	4	-4
H,L=	6	2
0	68	111
1	52	-88
2	40	-41
3	42	-45
4	7	9
6	55	-60
7	33	37
8	67	67
10	16	-16
11	10	9
12	15	15
13	18	-18
14	9	-8
15	10	10
16	10	9
17	12	-13
18	8	8
19	6	6
20	6	-6
21	6	-6
22	4	-3
23	8	8
H,L=	3	2
0	10	-9
1	7	-8
2	30	30
3	27	25
4	10	11
5	39	42
6	13	-13
7	48	55
8	10	-11
9	6	-7
10	9	8
11	15	15
12	12	11
13	22	25
14	12	13
15	24	28
16	7	-7
18	6	-6
H,L=	4	2
0	38	-41
1	18	-17
2	8	-5
3	21	-21
4	6	5
5	11	12
6	11	14
7	9	-10
8	13	-16
10	7	4
11	7	-7
12	12	-12
13	22	25
14	12	13
15	24	28
16	7	-7
18	6	-6
H,L=	5	2
0	19	-19
1	9	8
2	18	18
3	15	15
4	7	-7
5	7	6
6	10	13
7	7	7
8	24	-27
9	6	6
10	12	-12
11	15	15
12	32	-29
13	12	12
14	6	-6
15	2	2
16	6	-6
17	11	11
18	7	8
19	4	-4
H,L=	6	2
0	68	111
1	52	-88
2	40	-41
3	42	-45
4	7	9
6	55	-60
7	33	37
8	67	67
10	16	-16
11	10	9
12	15	15
13	18	-18
14	9	-8
15	10	10
16	10	9
17	12	-13
18	8	8
19	6	6
20	6	-6
21	6	-6
22	4	-3
23	8	8
H,L=	4	2
0	10	-9
1	7	-8
2	30	30
3	27	25
4	10	11
5	39	42
6	13	-13
7	48	55
8	10	-11
9	6	-7
10	9	8
11	15	15
12	12	11
13	22	25
14	12	13
15	24	28
16	7	-7
18	6	-6
H,L=	5	2
0	19	-19
1	9	8
2	18	18
3	15	15
4	7	-7
5	7	6
6	10	13
7	7	7
8	24	-27
9	6	6
10	12	-12
11	15	15
12	32	-29
13	12	12
14	6	-6
15	2	2
16	6	-6
17	11	11
18	7	8
19	4	-4
H,L=	6	2
0	68	111
1	52	-88
2	40	-41
3	42	-45
4	7	9
6	55	-60
7	33	37
8	67	67
10	16	-16
11	10	9
12	15	15
13	18	-18
14	9	-8
15	10	10
16	10	9
17	12	-13
18	8	8
19	6	6
20	6	-6
21	6	-6
22	4	-3
23	8	8
H,L=	5	2
0	10	-9
1	7	-8
2	30	30
3	27	25
4	10	11
5	39	42
6	13	-13
7	48	55
8	10	-11
9	6	-7
10	9	8
11	15	15
12	12	11
13	22	25
14	12	13
15	24	28
16	7	-7
18	6	-6
H,L=	6	2
0	10	-9
1	7	-8
2	30	30
3	27	25
4	10	11
5	39	42
6	13	-13
7	48	55
8	10	-11
9	6	-7
10	9	8
11	15	15
12	12	11
13	22	25
14	12	13
15	24	28
16	7	-7
18	6	-6
H,L=	7	2
0	10	-9
1	7	-8
2	30	30
3	27	25
4	10	11
5	39	42
6	13	-13
7	48	55
8	10	-11
9	6	-7
10	9	8
11	15	15
12	12	11
13	22	25
14	12	13
15	24	28
16	7	-7
18	6	-6
H,L=	8	2
0	10	-9
1	7	-8
2	30	30
3	27	25
4	10	11
5	39	42
6	13	-13
7	48	55
8	10	-11
9	6	-7
10	9	8
11	15	15
12	12	11
13	22	25
14	12	13
15	24	28
16	7	-7
18	6	-6
H,L=	9	2
0	10	-9
1	7	-8
2	30	30
3	27	25
4	10	11
5	39	42
6	13	-13
7	48	55
8	10	-11
9	6	-7
10	9	8
11	15	15
12	12	11
13	22	25
14	12	13
15	24	28
16	7	-7
18	6	-6
H,L=	10	2
0	10	-9
1	7	-8
2	30	30
3	27	25
4	10	11
5	39	42
6	13	-13
7	48	55
8	10	-11
9	6	-7
10	9	8
11	15	15
12	12	11
13	22	25
14	12	13
15	24	28
16	7	-7
18	6	-6
H,L=	11	2
0	10	-9
1	7	-8
2	30	30
3	27	25
4	10	11
5	39	42
6	13	-13
7	48	55
8	10	-11
9	6	-7
10	9	8
11	15	15
12	12	11
13	22	25
14	12	13
15	24	28
16	7	-7
18	6	-6
H,L=	12	2
0	10	-9
1	7	-8
2	30	30
3	27	25
4	10	11
5	39	42
6	13	-13
7	48	55
8	10	-11
9	6	-7
10	9	8
11	15	15
12	12	11
13	22	25
14	12	13
15	24	28
16	7	-7
18	6	-6
H,L=	13	2
0	10	-9
1	7	-8
2	30	30
3	27	25
4	10	11
5	39	42
6	13	-13
7	48	55
8	10	-11
9	6	-7
10	9	8
11	15	15
12	12	11
13	22	25
14	12	13
15	24	28
16	7	-7
18	6	-6
H,L=	14	2
0	10	-9
1	7	-8
2	30	30
3	27	25
4	10	11
5	39	42
6	13	-13
7	48	55
8	10	-11
9	6	-7
10	9	8
11	15	15
12	12	11
13	22	25
14	12	13
15	24	28
16	7	-7
18	6	-6
H,L=	15	2
0	10	-9
1	7	-8
2	30	30
3	27	25
4	10	11
5	39	42
6	13	-13
7	48	55
8	10	-11
9	6	-7
10	9	8
11	15	15
12	12	11
13	22	25
14	12	13
15	24	28
16	7	-7
18	6	-6
H,L=	16	2
0	10	-9
1	7	-8
2	30	30
3	27	25
4	10	11
5	39	42
6	13	-13
7	48	55
8	10	-11
9	6	-7
10	9	8
11	15	15
12	12	11
13	22	25
14	12	13
15	24	28
16	7	-7
18	6	-6
H,L=	17	2
0	10	-9
1	7	-8
2	30	30
3	27	25
4	10	11
5	39	42
6	13	-13
7	48	55
8	10	-11
9	6	-7
10	9	8
11	15	15
12	12	11
13	22	25
14	12	13
15	24	28
16	7	-7
18	6	-6
H,L=	18	2
0	10	-9
1	7	-8
2	30	30
3	27	25
4	10	11
5	39	42
6	13	-13
7	48	55
8	10	-11
9	6	-7
10	9	8
11	15	15
12	12	11
13	22	25
14	12	13
15	24	28
16	7	-7
18	6	-6
H,L=	19	2
0	10	-9
1	7	-8
2	30	30
3	27	25
4	10	11
5	39	42
6	13	-13
7	48	55
8	10	-11
9	6	-7
10	9	8
11	15	15
12	12	11
13	22	25
14	12	13
15	24	28
16	7	-7
18	6	-6
H,L=	20	2
0	10	-9
1	7	-8
2	30	30
3	27	25
4	10	11
5	39	42
6	13	-13
7	48	55
8	10	-11
9	6	-7
10	9	8
11	15	15
12	12	11
13	22	25
14	12	13
15	24	28
16	7	-7
18	6	-6
H,L=	21	2
0	10	-9
1	7	-8
2	30	30
3	27	25
4	10	11
5	39	42
6	13	-13
7	48	55
8	10	-11
9	6	-7
10	9	8
11	15	15
12	12	11
13	22	25
14	12	13
15	24	28
16	7	-7
18	6	-6
H,L=	22	2
0	10	-9
1	7	-8
2	30	30
3	27	25
4	10	11
5	39	42
6	13	-13
7	48	55
8	10	-11
9	6	-7
10	9	8
11	15	15
12	12	11
13	22	25
14	12	13
15	24	28
16	7	-7
18	6	-6
H,L=	23	2
0	10	-9
1	7	-8
2	30	30
3	27	25
4	10	11
5	39	42
6	13	-13
7	48	55
8	10	-11
9	6	-7
10	9	8
11	15	15
12	12	11
13	22	25
14	12	13
15	24	28
16	7	-7
18	6	-6
H,L=	24	2
0	10	-9
1	7	-8
2	30	30
3	27	25
4	10	11
5	39	42
6	13	-13
7	48	55
8	10	-11
9	6	-7
10	9	8
11	15	15
12	12	11
13	22	25
14	12	13
15	24	28
16	7	-7
18	6	-6
H,L=	25	2
0	10	-9
1	7	-8
2	30	30
3	27	25
4	10	11
5	39	42
6	13	-13
7	48	55
8	10	-11
9	6	-7
10	9	8
11	15	15
12	12	11
13	22	25
14	12	13
15	24	28
16	7	-7
18	6	-6
H,L=	26	2
0	10	-9
1	7	-8
2	30	30
3	27	25
4	10	11
5	39	42
6	13	-13
7	48	55
8	10	-11
9	6	-7
10	9	8
11	15	15
12	12	11
13	22	25
14	12	13
15	24	28
16	7	-7
18	6	-6
H,L=	27	2
0	10	-9
1	7	-8
2	30	30
3	27	25
4	10	11
5	39	42
6	13	-13
7	48	55
8	10	-11
9	6	-7
10	9	8
11	15	15
12	12	11
13	22	25
14	12	13
15	24	28
16	7	-7
18	6	-6
H,L=	28	2
0	10	-9
1	7	-8
2	30	30
3	27	25
4	10	11
5	39	42
6	13	-13
7	48	55
8	10	-11
9	6	-7
10	9	8
11	15	15
12	12	11
13	22	25
14	12	13
15	24	28
16	7	-7
18	6	-6
H,L=	29	2
0	10	-9
1	7	-8
2	30	30
3	27	25
4	10	11
5	39	42
6	13	-13
7	48	55
8	10	-11
9	6	-7
10	9	8
11	15	15
12	12	11
13	22	25
14	12	13
15	24	28
16	7	-7
18	6	-6
H,L=	30	2
0	10	-9
1	7	-8
2	30	30
3	27	25
4	10	11
5	39	42
6	13	-13
7	48	55
8	10	-11
9	6	-7
10	9	8
11	15	15
12	12	11
13	22	25
14	12	13
15	24	28
16	7	-7
18	6	-6
H,L=	31	2
0	10	-9
1	7	-8
2	30	30
3	27	25
4	10	11
5	39	42
6	13	-13
7	48	55
8	10	-11
9	6	-7
10	9	8
11	15	15
12	12	11
13	22	25
14	12	13
15	24	28
16	7	-7
18	6	-6
H,L=	32	2
0	10	-9
1	7	-8
2	30	30
3	27	25
4	10	11
5	39	42
6	13	-13
7	48	55
8	10	-11
9	6	-7
10	9	8
11	15	15
12	12	11
13	22	25
14	12	13
15	24	28
16	7	-7
18	6	-6
H,L=	33	2
0	10	-9
1	7	-8
2	30	30
3	27	25
4	10	11
5	39	42
6	13	-13
7	48	55
8	10	-11
9	6	-7
10	9	8
11	15	15
12	12	11
13	22	25
14	12	13
15	24	28
16	7	-7
18	6	-6
H,L=	34	2
0	10	-9
1	7	-8
2	30	30
3	27	25
4	10	11
5	39	42
6	13	-13
7	48	55
8	10	-11
9	6	-7
10	9	8
11	15	15
12	12	11
13	22	25
14	12	13
15	24	28
16	7	-7
18	6	-6
H,L=	35	2
0	10	-9
1	7	-8
2	30	30
3	27	25
4	10	11
5	39	42
6	13	-13
7	48	55
8	10	-11
9	6	-7
10	9	8
11	15	15
12

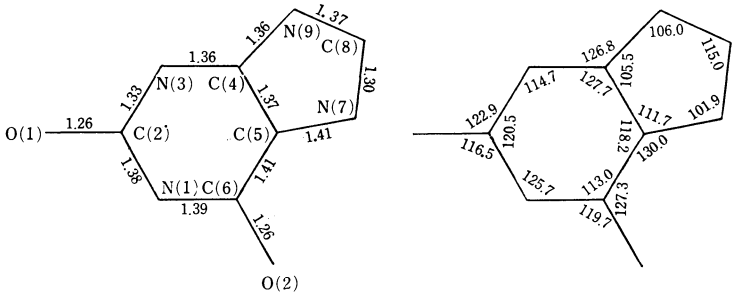

Fig. 3. Bond lengths and angles of xanthine anion.

extinction effects.

All the numerical computations were carried out on the NEAC 2203, NEAC 2206 and the NEAC 2200-model 500 Computors in the Computation Center of Osaka University. The used programs are SFFR for the three-dimensional Fourier synthesis, HBLS IV for the least-squares and DAPH for the bond lengths and angles written by Tamaichi Ashida, and the others by the authors.

Description of the Structure and Discussion

The intramolecular bond lengths and angles are listed in Table 5 and also shown in Fig. 3. The angle C(2)-N(3)-C(4)=114.7°, suggests that a hydrogen atom is not attached to N(3) in the six-membered ring, since Singh's survey[4] has shown that when an extra-annular hydrogen is attached to a nitrogen atom in a six-membered ring, the internal ring angle is 125.3°, whereas it is 116.3° when there is no hydrogen atom attached to the nitrogen atom. It may, of course, be expected that a lone pair electron of nitrogen atom gives rise to a stronger repulsion than a bonding pair. The fact that the difference Fourier map (Fig. 2) reveals no hydrogen peak at the N(3) position supports the compatibility of this empirical rule.

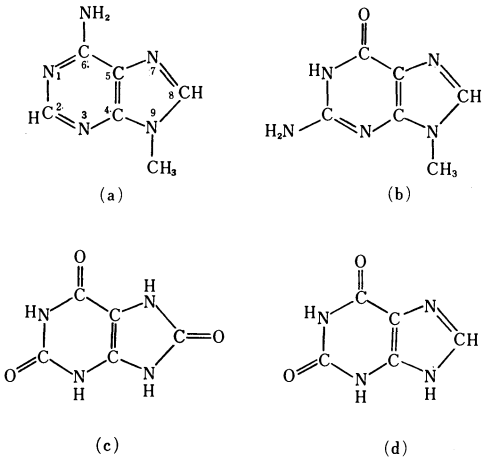

Fig. 4. Purine derivatives.

It is also probable that the reasonable position of the imidazole hydrogen atom is at the N(9) rather than at the N(7) in consideration of the hydrogen H(3) peak position on the difference Fourier map (see Fig. 2).

The C(2)-N(3) bond of 1.33 Å is in good agreement with the C(2)-N(3) bond distances of 1.322 Å found in 9-methyladenine[5] and 1.33 Å in 9-methylguanine hydrobromide;[6] however it is shorter than that of 1.382 Å found in uric acid,[7] indicating that this bond has double bond character as shown in 9-methyladenine(a) or in 9-methylguanine hydrobromide(b) rather than single bond character in uric acid(c), though the essential difference in structure between xanthine(d) and uric acid is the only atom attached to C(8), a hydrogen atom in the former and a carbonyl oxygen atom in the latter (see Fig. 4).

The C(2)-O(1) and C(6)-O(2) bond distances are both equal to 1.26 Å and are significantly longer than the standard double bond distance of 1.20 Å. These results suggest the resonance forms (I), (II) and (III) in Fig. 5 as predominant. These three resonance forms have a common feature, that is, the negatively charged O(1), O(2) or N(3) forms two or three hydrogen bonds (as seen in Fig. 6a) to the surrounding water molecules which have the induced dipolar character, suggesting that resonance forms (I), (II) and (III) contribute extra electrostatic energy to these hydrogen bonds in this crystal structure. It is of considerable interest that the nitrogen N(3) acting as hydrogen acceptor participates in two hydrogen bonds with water molecules as clearly seen in Figs. 6a and 6b.

The best plane through the xanthine ring atoms, as calculated by the least-squares method, is defined by the equation

$$0.04230x-0.18440y-0.98194z-3.39443=0.$$

4) C. Singh, *Acta Cryst.*, **19**, 861 (1965).

5) R. F. Stewart and L. H. Jensen, *J. Chem. Phys.*, **40**, 2071 (1964).

6) H. M. Sobell and K. Tomita, *Acta Cryst.*, **17**, 126 (1964).

7) H. Ringertz, *ibid.*, **20**, 397 (1966).

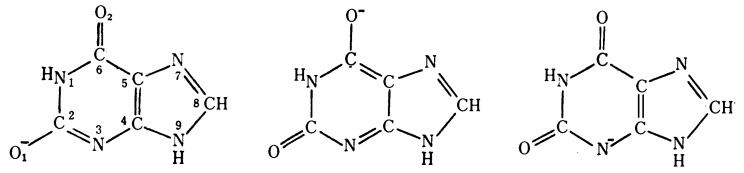

(I) (II) (III)

Fig. 5. Resonance forms.

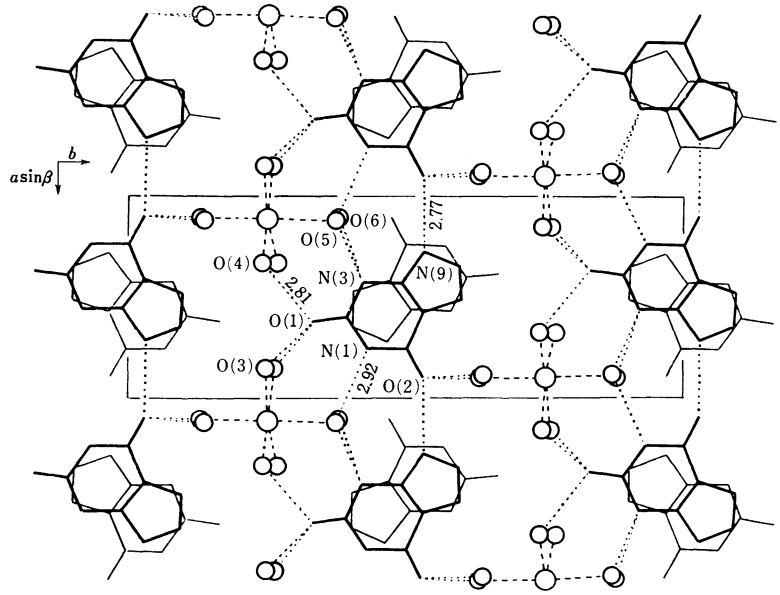

Fig. 6a. The crystal structure viewed down the *c* axis.

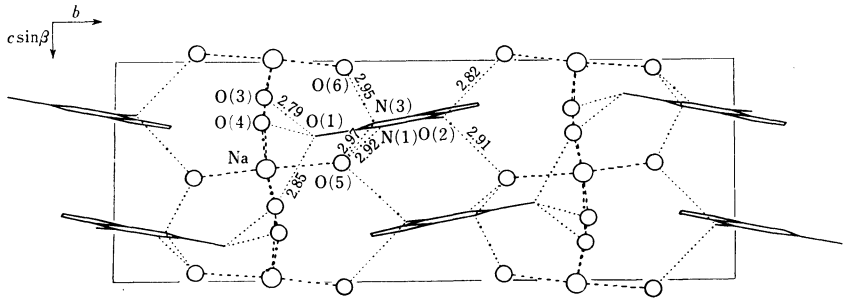

Fig. 6b. The crystal structure viewed down the *a* axis.

The average deviation of the eleven atoms from the plane is 0.01 Å which is within the errors in atomic positions. The molecular plane is inclined at an angle of 11° to the (001) plane. The van der Waals distances between adjacent molecular planes related by the center of symmetry are all nearly 3.5 Å.

A sodium ion is coordinated to six water oxygen atoms: O(3′), O(3″), O(4), O(4′), O(5) and O(6′). The O-Na-O angles range from 84.5 to 97.0°, and the Na-O distances range from 2.31 to 2.69 Å with a mean value of 2.45 Å, forming an approximately regular octahedron (see Table 6). These data are in good agreement with those of an earlier report for six-coordinate sodium compounds.[8]

The sodium-oxygen coordination polyhedrons are joined together by the shared edges O(3′)-O(3″) and O(4)-O(4′), forming a polymer-like chain parallel to the *c* axis by the continuous octahedron repeat. On the other hand, xanthine anions are stacked parallel to the *c* axis, and surrounded by these polymer-like chains.

8) "International Table for X-Ray Crystallography," Vol. III, p. 258 (1962).

TABLE 5. BOND DISTANCES AND ANGLES AND THEIR STANDARD DEVIATIONS

N(1)-C(2)	1.38 (0.012) Å	C(6)-N(1)-C(2)	125.7 (0.7) °
C(2)-N(3)	1.33 (0.012)	N(1)-C(2)-N(3)	120.5 (0.8)
N(3)-C(4)	1.36 (0.011)	N(1)-C(2)-O(1)	116.5 (0.8)
C(4)-C(5)	1.37 (0.011)	N(3)-C(2)-O(1)	122.9 (0.9)
C(5)-C(6)	1.41 (0.011)	C(2)-N(3)-C(4)	114.7 (0.7)
C(6)-N(1)	1.39 (0.011)	N(3)-C(4)-C(5)	127.7 (0.7)
C(4)-N(9)	1.36 (0.011)	C(5)-C(4)-N(9)	105.5 (0.7)
N(9)-C(8)	1.37 (0.012)	N(3)-C(4)-N(9)	126.8 (0.7)
C(8)-N(7)	1.30 (0.013)	C(4)-C(5)-C(6)	118.2 (0.7)
C(5)-N(7)	1.41 (0.011)	C(4)-C(5)-N(7)	111.7 (0.7)
C(2)-O(1)	1.26 (0.012)	C(6)-C(5)-N(7)	130.0 (0.7)
C(6)-O(2)	1.26 (0.011)	C(5)-C(6)-N(1)	113.0 (0.7)
		N(1)-C(6)-O(2)	119.7 (0.8)
		C(5)-C(6)-O(2)	127.3 (0.8)
		C(5)-N(7)-C(8)	101.9 (0.7)
		N(7)-C(8)-N(9)	115.0 (0.9)
		C(4)-N(9)-C(8)	106.0 (0.7)

The standard deviations are shown in parentheses.

TABLE 6. BOND LENGTHS AND ANGLES IN THE ENVIRONMENT OF SODIUM ION

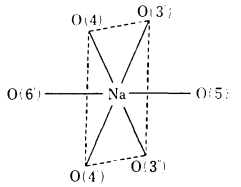

O(3')-Na-O(3'')	89.4°	Na-O(3')	2.69Å
O(3')-Na-O(4)	84.5	Na-O(3'')	2.43
O(3'')-Na-O(4')	89.0	Na-O(4)	2.39
O(4)-Na-O(4')	96.8	Na-O(4')	2.46
O(5)-Na-O(3')	90.1	Na-O(5)	2.39
O(5)-Na-O(3'')	88.1	Na-O(6')	2.31
O(5)-Na-O(4)	89.4		
O(5)-Na-O(4')	83.4		
O(6')-Na-O(3')	93.3		
O(6')-Na-O(3'')	92.0		
O(6')-Na-O(4)	90.8		
O(6')-Na-O(4')	93.3		
O(3')-Na-O(4')	173.3		
O(4)-Na-O(3'')	173.4		
O(5)-Na-O(6')	176.7		

TABLE 7. HYDROGEN BONDS

N(1)---O(5)	2.92 Å
N(3)---O(5)	2.97
N(3)---O(6)	2.95
N(9)---O(2')	2.77
O(1)---O(3)	2.79
O(1)---O(3')	2.85
O(1)---O(4)	2.81
O(2)---O(5')	2.91
O(2)---O(6')	2.82

The possible twinning operation of this compound is now presumable from its molecular arrangement in crystal as shown in Fig. 6a. The contact distances between molecules at the twinning boundary are reasonable, provided the additional *b*-glide plane perpendicular to *a**-axis is considered to be the symmetry operation of the space group $P2_1/c$.

All the water molecules may stabilize the crystal lattice in two ways, that is, by coordinating to the sodium ion as above mentioned, and by linking xanthine anion through hydrogen bonds. The lengths and arrangement of hydrogen bonds can be seen in Fig. 6 and Table 7. Seven out of the eight water hydrogen atoms form hydrogen bonds, but only the remaining hydrogen H(7) does not participate in any hydrogen bonds as occasionally seen in crystalline hydrates, for example in $MgSO_4 \cdot 4H_2O$.[9]

All the water molecules lie in the electrostatic fields of the surrounding ions; the positively charged Na^+, and the negatively charged O(1), O(2) and N(3) of xanthine anion. Therefore it seems that the orientation of each water molecule depends mainly upon the electrostatic interactions between the induced dipole of water molecule and the surrounding ions, and in this case, the hydrogen bonds are essentially electrostatic.

We wish to express our thanks to the staff of the Computation Center of Osaka University. Thanks are also due to Dr. Tamaichi Ashida for permission to use the computor programs. Finally, the authors are grateful to emeritus Prof. Tokunosuke Watanabé and Prof. Shuzo Seki for their valuable advice and discussion throughout the course of this work.

9) W. H. Baur, *Acta Cryst.*, **17**, 863 (1964).

BULLETIN OF THE CHEMICAL SOCIETY OF JAPAN VOL. 42 3106—3108 (1969)

The Structure-Stability Relationship of the Metal Ion Complexes of Unsaturated Compounds. V. Stabilities of the Silver-Ion Complexes of Some *cis*-Stable Olefins

Tadashi OKUYAMA and Takayuki FUENO

Faculty of Engineering Science, Osaka University, Toyonaka, Osaka

and Junji FURUKAWA

Department of Synthetic Chemistry, Kyoto University, Sakyo-ku, Kyoto

(Received May 6, 1969)

The silver-ion complexation equilibria of a few *cis*-stable olefins have been investigated in an aqueous phase at 25°C. The *trans* isomers of β-chlorovinyl ethyl ether and 1,2-dichloroethylene were found to have greater equilibrium constants than the corresponding *cis* isomers. It was concluded that the relative stabilities of parent olefin isomers play an exclusive role determining their relative complexation abilities.

The stability of the silver ion-olefin complexes in relation to the structure of the olefins has been investigated by several groups of workers[1-9] and discussed in terms of steric, strain, and electronic effects. The electronic effect was examined from the influence of substituents on the argentation equilibria of benzene,[2b] styrene,[7] and ethylene.[8] As for the steric and strain effects, various aliphatic[1,5,6] and alicyclic olefins[3,5] as well as some alkynes[4,5] have been investigated.

Some of the above investigations include several geometrical isomer pairs of alkenes, in which the greater complexation abilities of *cis* isomers have been interpreted in terms of the effects of steric hindrance and strain relief.[1d,5,6] We have previously studied similar complexations of a variety of *cis*- and *trans*-alkenyl alkyl ethers and found that the *cis* isomers form more stable complexes with the silver ion than do the corresponding *trans* isomers.[9] It was suggested that the greater complexation abilities of the *cis* isomers be due to their relative instability at the ground state. Although the origin of this is rather ambiguous as yet, it may be conceivable that, in cases where the instability is ascribable to the steric strain of the crowded *cis* substituents, the relief of strain on complexation would be a factor responsible for the greater stability of the complexes of *cis* isomers. However, such an interpretation of the effects of geometrical isomerism seems to be biased because all the olefins treated so far have been those that are known to be more stable in the *trans* form.

The present study will treat the silver-ion complexation of a few *cis*-stable olefins with particular interest in the relative stabilities of the complexes formed from *cis* and *trans* isomers. The *trans* isomers have proved to form more stable complexes in the present cases. This finding provides a favorable counterpart to the previous interpretation and supports the concept that the ground-state stability of the olefins is a major factor governing the effect of geometrical structure of olefins on stabilities of their silver-ion complexes.

1) a) S. Winstein and H. J. Lucas, *J. Am. Chem. Soc.*, **60**, 863 (1938); b) H. J. Lucas, R. S. Moore and D. Pressman, *ibid.*, **65**, 227 (1943); c) H. J. Lucas, F. W. Billmeyer and D. Pressman, *ibid.*, **65**, 230 (1943); d) F. R. Hepner, K. N. Trueblood and H. J. Lucas, *ibid.*, **74**, 1333 (1952); e) K. N. Trueblood and H. J. Lucas, *ibid.*, **74**, 1338 (1952).

2) a) L. J. Andrews and R. M. Keefer, *ibid.*, **71**, 3644 (1949); b) L. J. Andrews and R. M. Keefer, *ibid.*, **72**, 3113 (1950); c) L. J. Andrews and R. M. Keefer, *ibid.*, **72**, 5034 (1950); d) R. M. Keefer and L. J. Andrews, *ibid.*, **74**, 640 (1952); e) N. Ogimachi, L. J. Andrews and R. M. Keefer, *ibid.*, **78**, 2210 (1956).

3) a) J. G. Traynham and M. F. Sehnert, *ibid.*, **78**, 4024 (1956); b) J. G. Traynham and J. R. Olechowski, *ibid.*, **81**, 571 (1959).

4) a) W. S. Dorsey and H. J. Lucas, *ibid.*, **78**, 1665 (1956); b) G. K. Helmkamp, F. L. Carter and H. J. Lucas, *ibid.*, **79**, 1306 (1957); c) A. E. Comyns and H. J. Lucas, *ibid.*, **79**, 4341 (1957).

5) M. A. Muhs and F. T. Weiss, *ibid.*, **84**, 4697 (1962).

6) R. J. Cvetanović, F. J. Duncan, W. E. Falconer and R. S. Irwin, *ibid.*, **87**, 1872 (1965).

7) T. Fueno, T. Okuyama, T. Deguchi and J. Furukawa, *ibid.*, **87**, 170 (1965).

8) T. Fueno, O. Kajimoto and J. Furukawa, This Bulletin, **41**, 782 (1968).

9) T. Fueno, O. Kajimoto, T. Okuyama, and J. Furukawa, *ibid.*, **41**, 785 (1968). Part IV of this Series.

Experimental

Materials. *cis*- and *trans*-β-chlorovinyl ethyl ethers (CVE) were obtained as described previously.[10] *cis*- and *trans*-1, 2-dichloro- (DCE) and 1,2-dibromoethylenes (DBE) were purchased and distilled. Cyclohexane, toluene, silver nitrate and potassium nitrate were of the best commercial grade.

Procedure. The equilibrium constants, K, for the formation of the silver-ion complexes in the aqueous phase

$$Ag^+ + M \rightleftarrows AgM^+, \quad K = [AgM^+]/[Ag^+][M] \quad (1)$$

were measured at 25°C by the solubility method in the same manner as described previously.[7] The volumes of the olefins and the aqueous phase were 1 and 10 m*l*, respectively.

The concentrations of olefins in the aqueous phase were determined by gas chromatography after extraction with cyclohexane. Five-hour shaking of an aqueous phase (5 m*l*) with cyclohexane (1 m*l*) was sufficient to complete the extraction of an olefin.[7] Cyclohexane used here contained 2 vol% toluene as an internal standard for the gas-chromatographic determination. A Shimadzu model GC-2C gas chromatograph was used with a column packed with polyethylene glycol (for DCE and DBE) or apiezon grease L (for CVE). It was found by calibration that the half-height width method fully sufficed for linearly correlating the obtained peak area to the olefin concentration.

Results

Solubility experiments were undertaken in the dark, and during that time no appreciable side reaction was observed. The solubilities of the isomeric pairs of β-chlorovinyl ethyl ether (CVE), 1,2-dichloroethylene (DCE) and 1,2-dibromoethylene (DBE) in aqueous $AgNO_3$-KNO_3 solutions are listed in Table 1. The experiments for DBE and CVE were conducted with the mixture of isomers, and the concentrations of respective isomers were determined separately. It was confirmed that such an expedience introduced no serious error into the K-values.[11] The composition of isomers in the organic phase was assumed to be invariant during the equilibrium experiments, as the amount of the substrate transferring from the organic to the aqueous phase was only of the order of 1% of the total olefin used.

The equilibrium constants, K, were calculated by the least squares treatment of the solubility data according to the equation[7]

$$K = ([M]-[M]_0)/[Ag^+][M]_0 \quad (2)$$

where $[M]_0$ is the olefin concentration in the aqueous phase at $[Ag^+]=0$. The equilibrium leading to the formation of the 2 : 1 complex, Ag_2M^{2+}, was ignored since its contribution was immaterially small.

The equilibrium constants, K, calculated from Eq. (2) for the isomeric olefins are given in Table 2, together with the related data available in the literature. Although the K values for the disubstituted polar olefins studied here are very small, the differences between the respective geometrical isomers are certainly significant. The *trans* isomers of CVE and DCE have greater K values than their *cis* isomers (**1** and **2**). This finding is the

Table 1. Solubilities[a] of olefins in aqueous $AgNO_3$-KNO_3 solutions[b] at 25°C

$[Ag^+]$, mol/*l*	$[M] \times 10^2$, mol/*l*	
	cis	*trans*
	$ClCH=CHOC_2H_5$[c]	
0.00	0.421	0.914
0.60	0.502	1.244
1.00	0.552	1.454
	ClCH=CHCl[d]	
0.00	5.78	3.45
0.60	6.55	4.20
1.00	7.56	4.96
	BrCH=CHBr[e]	
0.00	1.096	0.560
0.20	1.229	0.632
0.60	1.527	0.756
1.00	1.844	0.878

a) Averages of three or four independent measurements. Accurate to within ±6%
b) Ionic strength $\mu=1.00$
c) Isomeric composition: *cis*/*trans*=11.5/88.5
d) Isomeric purities: *cis*, 97.8%; *trans*, 97.6%
e) Isomeric composition: *cis*/*trans*=56.9/43.1

Table 2. The equilibrium constants for argentation of some 1,2-disubstituted ethylenes, $R_1CH=CHR_2$, at 25°C

No.	Substituent		*K*, *l*/mol		Stable isomer
	R_1	R_2	*cis*	*trans*	
1	Cl	OC_2H_5	0.32	0.59	*cis*[c]
2	Cl	Cl	0.25	0.40	*cis*[d]
3	Br	Br	0.68	0.56	*cis*≃*trans*[e]
4	CH_3	CH_3	62.3[a]	24.6[a]	*trans*[d]
5	CH_3	OC_2H_5	3.13[b]	0.54[b]	*trans*[c]

a) Ref. 1d.
b) Ref. 9, in ethylene glycol at 20°C.
c) Ref. 12.
d) Ref. 13.
e) R. M. Noyes and R. G. Dickinson, *J. Am. Chem. Soc.*, **65**, 1427 (1943).

10) T. Okuyama, T. Fueno, and J. Furukawa, *J. Polymer Sci. A*-1, in press.

11) The solubilities of pure *cis*-CVE were 3.63, 4.34 and 5.06×10^{-2} mol/*l* for the silver ion concentrations of 0.00, 0.60 and 1.00 mol/*l*, respectively. These data lead to the equilibrium constant $K=0.39$ *l*/mol, which is in fair agreement with $K=0.32$ *l*/mol obtained from the experiments with the mixture of *cis*- and *trans*-CVE.

first demonstration that *trans* isomers of some α,β-disubstituted ethylenes can form more stable silver-ion complexes than the corresponding *cis* isomers. On the other hand, the K value of *trans*-DBE is comparable in magnitude with that of the corresponding *cis* isomer (**3**).

Discussion

The different abilities of geometrical isomers in forming complexes with the silver ion have already been reported for several alkenes[1d,5,6] and alkenyl alkyl ethers.[9] In all these cases, the *cis* isomers have greater equilibrium constants than the corresponding *trans* isomers, as shown in Table 2 (**4** and **5**). Such effects of the geometrical isomerism on the stabilities of the complexes have been interpreted in terms of strain effects.[1d,5,6] That is, the strain due to the group repulsions present in the *cis* isomers may be relieved on the formation of the complexes, which largely contributes to the stability of the complexes of *cis* isomers.

However, the concept of the strain relief effect is clearly inapplicable to the *cis*-stable olefins, because such a strain, if present, should be of minor importance. In fact, *cis* isomers of CVE and DCE, which were found to be more stable than the respective *trans* isomers,[12,13] have proved to form less stable complexes than do their *trans* isomers. On the other hand, all of the previous studies reporting the greater complexation abilities of *cis* isomers have been confined to the *trans*-stable olefins, where the strain may destabilize the *cis* isomers. In the case of DBE (**3**), in which both isomers are known to have nearly equal stabilities at the ground state, the K value of the *cis* isomer is only a little greater than that of the *trans* isomer. This result also accords with the expectation from the stability of the parent isomeric olefins. Thus, a more generalized idea might be that the isomers of lesser stability in the ground state lead to the more stable complexes. In other words, any structural difference between *cis* and *trans* isomers is relieved by the loosening of the olefinic double bonds on complexation, and hence the ground-state stability determines the stability of the complexes formed. In this sense, therefore, the term "stabilization effect" would be of more general use than the customary term "strain effect."

In conclusion, the relative stabilities of the silver-ion complexes of geometrical isomers are determined primarily by the relative stabilities of parent isomeric olefins. The less stable isomers, whether they are *cis* or *trans* and whatever the origin of their relative stabilities may be, have greater ability for the silver-ion complexation than their isomeric partners which are more stable.

12) T. Okuyama, T. Fueno and J. Furukawa, *Tetrahedron*, in press.

13) E. L. Eliel, "Stereochemistry of Carbon Compounds," McGraw-Hill Book Co., Inc., New York, N. Y. (1962), Chapter 12.

BULLETIN OF THE CHEMICAL SOCIETY OF JAPAN VOL. 42 3109—3115 (1969)

Group Interactions in Polyelectrolytes. II. Kinetics of Alkaline Hydrolysis of Polymethyl Acrylate

Hiroshi KAWABE and Masaya YANAGITA

The Institute of Physical and Chemical Research, Yamato-machi, Saitama

(Received May 9, 1969)

The second-order rate constant of the alkaline hydrolysis of polymethyl acrylate in an aqueous acetone solution decreases as the reaction proceeds. The plot of the logarithmic term of the second-order rate equation against the reaction time is divided into four lines; this suggests that the reaction proceeds in four steps. The rate equation of the reaction can be derived by assuming that the reactivity of ester groups is electrically affected mainly by a few neighboring hydrolyzed groups. The kinetic behavior is compared with the titration data of polyacrylic acid; the sets of data can be correlated through a simple equation containg two constants, k_0, the intrinsic rate constant, and pK_0, the intrinsic ionization constant.

Kawabe and Yanagita[1] studied the kinetics of the reaction of chloromethylated polystyrene with *n*-butylamine and di-*n*-butylamine in dioxane; they found that the apparent rate constant computed by the simple second-order rate equation decreased continuosly as the reaction proceeded, and that the plot of the logarithmic term in the equation against the reaction time was divided into two straight lines. The kinetics could be expressed by the rate equation of a two-step reaction derived by assuming two distinct reactivities of chloromethyl groups, depending on their environments.

In the present study, the above procedure of plotting the logarithmic term against the time has been applied to the published kinetic data of the alkaline hydrolysis of polymethyl acrylate;[2] it has been thus revealed that the reaction in a 29% (v/v) aqueous acetone solution proceeds in four steps. The rate equation for this reaction has been derived by assuming that the reactivity of the ester group on the macromolecule is electrostatically affected mainly by a few already-hydrolyzed groups situated within relatively short distance. The derived equation has first been examined in the alkaline hydrolysis of model compounds, such as dimethyl succinate and triethyl citrate. The results obtained by the application of the equation to polymethyl acrylate has then been discussed in relation to the titration data of polyacrylic acid.

Experimental

Materials. The polyacrylic acid used for the titration was prepared by the alkaline hydrolysis of polymethyl acrylate. One hundred grams of methyl acrylate containing 3 g of benzoyl peroxide were added, drop by drop, to boiling methyl ethyl ketone over the period of an hour, and then the solution was stirred for five hours. The solution was then poured into petroleum ether to precipitate polymethyl acrylate, which was dried in a vacuum oven, dissolved in acetone, and again precipitated in water. The purified polymer was hydrolyzed with sodium hydroxide in an aqueous acetone solution according to the procedure described in the literature.[2] The dry sodium salt of polyacrylic acid was dissolved in water and converted to polyacrylic acid by passing the solution through a column of Dowex-50 (X-8) in hydrogen form.

Titration of Polyacrylic Acid. An aqueous solution of polyacrylic acid (0.05 equiv/*l*) was titrated with a 0.1N sodium hydroxide solution at 25°C; the pH of the solution was measured by means of a Beckman Model G pH meter.

Alkaline Hydrolysis of Dimethyl Succinate and Triethyl Citrate. Alkaline hydrolyses of dimethyl succinate and teiethyl citrate were carried out in water and in a 32% (v/v) aqueous ethanol solution respectively, both containing a slight excess of sodium hydroxide. During the course of this reaction, the temperature was kept constant to ±0.1°C. The rate of hydrolysis was followed, according to the usual method, by the removal of aliqots at appropriate intervals of time, pouring them into water containing an excess of hydrochloric acid, and titrating them with 0.1N sodium hydroxide.

When a large excess of sodium hydroxide (about ten times as much as the moles of the ester group) was used as a hydrolyzing agent, it interfered with the precise determination of the percentage of hydrolysis in the usual method. Sodium ions in the solution, however, could be effectively removed by the use of Dowex-50. It was ascertained by preliminary tests that sodium ions in an aqueous solution containing succinic acid or citric acid, and also excess sodium hydroxide, could be removed practically at once and completely

1) H. Kawabe and M. Yanagita, This Bulletin, **41**, 1518 (1968).

2) I. Sakurada, Y. Sakaguchi and S. Fukui, *Kobunshi Kagaku (Chem. High Polymers Japan)*, **13**, 355, 361, 408 (1956).

within 45 sec by stirring the solution in the presence of Dowex-50 (X-8, 50—100 mesh) in hydrogen form, and also that the esters were not hydrolyzed, at least during the first 10 min. In the kinetic runs in which a large excess sodium hydroxide was used, portions of the reaction mixture were poured into water containing Dowex-50, which had previously been half neutralized, and the mixture was stirred for a few minutes. After the resin had then been removed, the solution was titrated with 0.1N sodium hydroxide. This method was tentatively applied to a run in which accurate determination by the usual method was possible; both methods produced the same results.

Rate Equations

The rate equation for a polymer reaction which proceeds in two steps has already been derived, in a previous paper,[1] by assuming two distinct reactivities of reactive groups, depending on their environments, and by rearranging the polymer reaction for a reaction between a low-molecular compound with two reactive groups and a reagent. If it is assumed, in a polymer reaction which proceeds in more than two steps, that any step of the reaction is controlled by two reactivities, the rate equation of the reaction can be similarly derived by considering the reaction of a low-molecular compound with a few reactive groups and a reagent, as is illustrated below:

$$\underset{(\mu_{n-1})}{X_{n-1}Y_{\sigma-(n-1)}} \xrightarrow{k_n} \underset{(\mu_n)}{X_nY_{\sigma-n}} \xrightarrow{k_{n+1}} \underset{(\mu_{n+1})}{X_{n+1}Y_{\sigma-(n+1)}}$$

where X represents a changed group in a compound, and Y, an unchanged one; the suffix indicates the number of the group, in which σ is the total number of the group. The relationship among the concentrations are:

$$\mu_0 = M - x_1 = (b/\sigma) - x_1 \quad (1)$$

$$\mu_n = x_n - x_{n+1} \quad (2)$$

where M is the initial concentration of the compound; μ_0 and μ_n, the concentrations of the unchanged compound and the partially-changed one, n groups of which have been changed at time t; b, the initial concentration of the group, and x_1 and x_n, the concentrations of the first and nth changed groups respectively at time t.

By assuming the bimolecular mechanism for the individual reaction of each group, the over-all rate of the above reaction with σ rate constants is given by:

$$dx/dt = \sum_{n=1}^{\sigma} dx_n/dt = (a-x)\sum_{n=1}^{\sigma}(\sigma-n+1)k_n\mu_{n-1} \quad (3)$$

where a is the initial concentration of a reagent and where x is the change in the concentration of a reagent or the concentration of the changed group at time t; k_n is the rate constant of the elementary reaction, *i.e.*, the reaction of the nth group. When it is assumed in any step of the reaction that its main part is practically composed of two elementary reactions at most, the rate can be formulated for the nth step by introducing $\mu_{n-2}\simeq 0$ and $\mu_{n+1}\simeq 0$ into Eq. (3) and by then combining Eq. (3) with Eq. (4):

$$x_{n-1} \simeq b/\sigma, \quad x_n \simeq x - b(n-1)/\sigma \quad (4)$$

Thus, Eq. (3) becomes:

$$dx/dt = (a-x)[\{(\sigma-n+1)nk_n-(\sigma-n)(n-1)k_{n+1}\}b/\sigma - \{(\sigma-n+1)k_n-(\sigma-n)k_{n+1}\}x] \quad (5)$$

Upon integration, Eq. (5) yields:

$$k_n = \frac{\ln[(1-\alpha)/(1-A\beta/B)] - \ln[(1-\chi_{n-1}/a)/(1-A\chi_{n-1}/Bb)]}{(Aa-Bb)(t-\tau_{n-1})} \quad (6)$$

where τ_{n-1} is the time and χ_{n-1} is the value of x at a point where $x_{n-1}\simeq b/\sigma$; $\alpha(=x/a)$ is a fractional conversion of a reagent, and $\beta(=x/b)$ is that of the reactive group. A and B are:

$$\begin{cases} A = (\sigma-n+1) - (\sigma-n)k_{n+1}/k_n \\ B = [(\sigma-n+1)n - (\sigma-n)(n-1)k_{n+1}/k_n]/\sigma \end{cases}$$

When $\sigma=2$, k_1 and k_2 are given as follows:

$$k_1 = \frac{1}{[(2-k_2/k_1)a-b]} \ln \frac{1-\alpha}{1-(2-k_2/k_1)\beta} \quad (7)$$

$$k_2 = \frac{1}{(a-b)(t-\tau_1)}\left(\ln\frac{1-\alpha}{1-\beta} - \ln\frac{1-\chi_1/a}{1-\chi_1/b}\right) \quad (8)$$

These equations are the same as those which have been derived directly for the two-step reaction in the previous paper,[1] in which the over-all course of the reaction with a large excess of reagent was also expressed by the equation:

$$\beta = 1 - \frac{k_1-k_2}{2k_1-k_2}e^{-2k_1at} - \frac{k_1}{2k_1-k_2}e^{-k_2at} \quad (9)$$

When $\sigma=3$, Eq. (6) also yields three equations to determine k_1, k_2, and k_3. In the case with a large excess of reagent, the over-all kinetics can be expressed by a combination of two simple rate equations, each of which is derived on the assumption that the rate is cotrolled mainly by two rate constants in some range of β. If the reaction in the range of β, *i.e.*, 0—2/3, is assumed to be controlled by k_1 and k_2, Eq. (3) is simplified to:

$$dx/dt = a[k_1b - (3k_1-4k_2)x_1 - 2k_2x] \quad (10)$$

and x_1 is given by:

$$x_1 = -(1-e^{-3k_1at})b/3 \quad (11)$$

Upon integration, Eq. (10) becomes:

$$\beta = \frac{2}{3} - \frac{(3k_1-4k_2)}{3(3k_1-2k_2)}e^{-3ak_1t} - \frac{k_1}{3k_1-2k_2}e^{-2ak_2t} \quad (12)$$

Similarly, in the 1/3—1 range of β, the following equations can be derived:

$$dx/dt = a[(2k_2+k_3)b/3 - 2(k_2-k_3)x_2 - k_3x] \quad (13)$$

$$x_2 = (1-e^{-2k_2a(t-t_{1/3})})b/3 \quad (14)$$

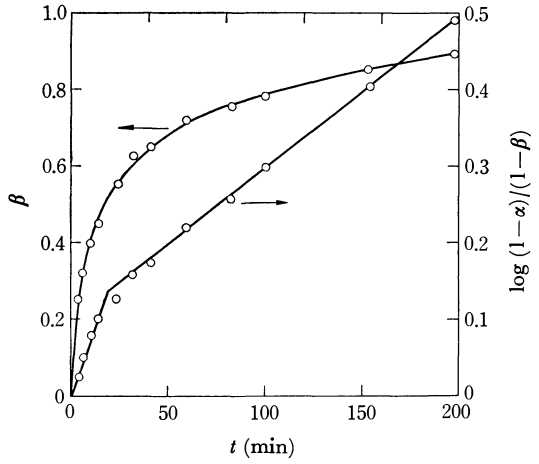

Fig. 1. Alkaline hydrolysis of dimethyl succinate in water at 10°C. (Run A)

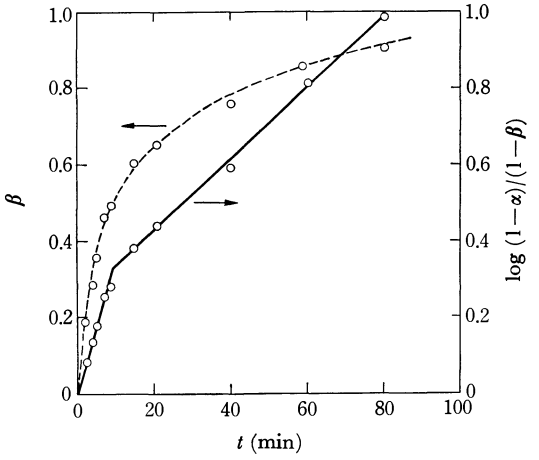

Fig. 2. Alkaline hydrolysis of dimethyl succinate in water containing a large excess of sodium hydroxide at 4.5°C. (Run B)

Upon integration, Eq. (13) then yields:

$$\beta = 1 - \frac{2(k_2-k_3)}{3(2k_2-k_3)}e^{-2k_2a(t-t_{1/3})} - \frac{2k_2}{3(2k_2-k_3)}e^{-k_3a(t-t_{1/3})} \quad (15)$$

where $t_{1/3}$ is the time, when β is 1/3.

Results and Discussion

Alkaline Hydrolysis of Dimethyl Succinate. The results obtained in the alkaline hydrolysis of dimethyl succinate in an aqueous solution are shown in Figs. 1 and 2. The apparent rate constant, k_{app}, computed by Eq. (16) decreases as the reaction proceeds:

$$k_{app} = \frac{1}{(a-b)t}\ln\frac{b(a-x)}{a(b-x)} = \frac{2.303}{(a-b)t}\log\frac{1-\alpha}{1-\beta} \quad (16)$$

Table 1. Rate constants of alkaline hydrolysis of dimethyl succinate

Run	Temp. °C	Concn. (10^{-2} mol/l) a	Concn. (10^{-2} mol/l) b	k_1 l/mol min	k_2 l/mol min	$\log(k_1/k_2)$
A	10	1.93	1.41	4.92	0.880	0.75
B	4.5	3.38	0.26	3.63	0.684	0.73

where a and b are the initial concentrations of sodium hydroxide and the ester group, and where α and β are their fractional conversions, respectively. Plots of the logarithmic term of Eq. (16) against the time, which are shown in the figures, consist of two straight lines which intersect nearly at $\beta=0.5$, in accordance with the two-step reaction mechanism. The rate constants calculated by means of Eqs. (7) and (8) are shown in Table 1. Since a large excess of sodium hydroxide was used for the run B, the over-all course of reaction can be expressed by Eq. (9), using k_1 and k_2 values listed in Table 1. The calculated values are in good agreement with the observed values, as may be seen in Fig. 2, where the dotted line and the circles show the calculated and the observed values respectively.

Since the numerical difference between k_1 and k_2 is based on the electrostatic effect of the first hydrolyzed group in the reaction of the second group, the electrostatic free energy of activation, $\Delta F_{el}^{\neq}$, is given by:

$$\Delta F_{el}^{\neq} = 2.303\boldsymbol{R}T\log(k_1/k_2) \quad (17)$$

where T is the temperature of the reaction. On the other hand, the electrostatic free energy of ionization, ΔF_{el}^{i}, of succinic acid is given by:

$$\Delta F_{el}^{i} = 2.303\boldsymbol{R}T'(pK_2-pK_1-\log 4) \quad (18)$$

$$\Delta F_{el}^{i} = \boldsymbol{N}e^2/Dr \quad (19)$$

where T' is the temperature of the titration; pK_1 and pK_2 are negative logalithms of the ionization constants at the first and second ionization steps respectively; D is the effective dielectric constant, and r is the distance between the two ionizable groups. If the two electrostatic free energies are equal, a simple correlation between the titration and kinetic data may be established; the distance between the groups may also be estimated on the basis of the kinetic data by means of the above equations. On the basis of the dissociation constant data,[3] the pK_1 and pK_2 values of succinic acid at 10°C are found to be 4.246 and 5.649 respectively. By the use of Eqs. (17) and (18), $\log(k_1/k_2)$ is calculated to be 0.80; this is quite close to the kinetically-obtained values, which are given in Table 1. Furthermore, if D is assumed to

3) R. A. Robinson and R. H. Stokes, "Electrolyte Solutions," Butterworths, London (1955), p. 521.

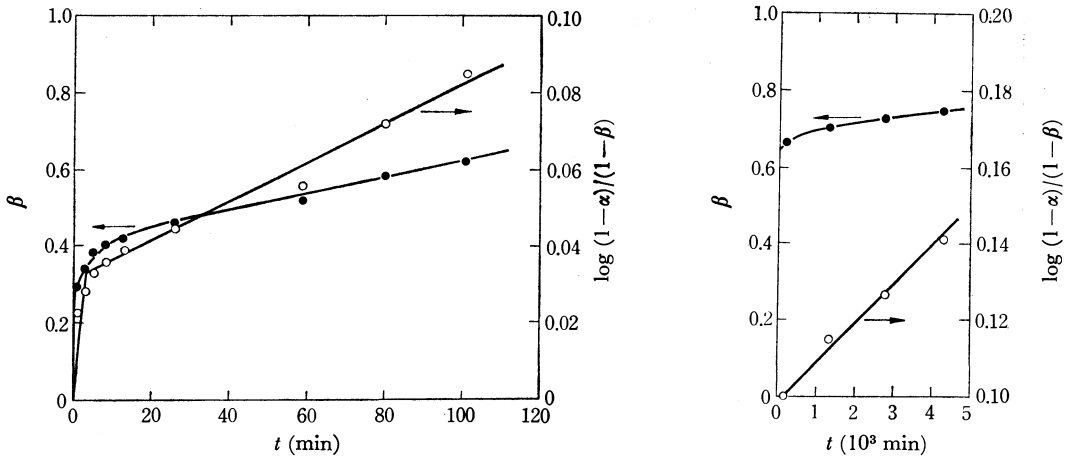

Fig. 3. Alkaline hydrolysis of triethyl citrate in 32% aqueous ethanol solution at 10°C. (Run D)

TABLE 2. RATE CONSTANTS OF ALKALINE HYDROLYSIS OF TRIETHYL CITRATE

Run		C	D	E	F
Concn., l/mol min	a	1.32×10^{-2}	2.97×10^{-2}	7.26×10^{-2}	2.95×10^{-1}
	b	1.34×10^{-2}	2.59×10^{-2}	6.70×10^{-2}	2.58×10^{-1}
k_n', l/mol min	k_1'	6.48	(5.46)		
	k_2'	(2.31×10^{-1})	3.10×10^{-1}	4.11×10^{-1}	
	k_3'		(5.90×10^{-3})	6.46×10^{-3}	6.47×10^{-3}
k_n, l/mol min	k_1	7.93			
	k_2		5.66×10^{-1}	6.43×10^{-1}	
	k_3			6.46×10^{-3}	6.47×10^{-3}

( ) shows less accurate measurement.

be 81, a reasonable value of 4.4 Å can be calculated for r by the use of Eqs. (17) and (19).

Alkaline Hydrolysis of Triethyl Citrate. The alkaline hydrolysis of triethyl citrate in a 32% aqueous ethanol solution was carried out at 10°C; an example of the kinetic runs is graphically shown in Fig. 3. The plot of the logarithmic term of Eq. (16) against the time is divided into three lines, which intersect nearly at $\beta=1/3$ and $\beta=2/3$; this indicates that the reaction proceeds in three steps. The experimental results are summarized in Table 2, where k_n' is the approximate value of the rate constant of the nth step, estimated by:

$$k_n' = [2.303/(a-b)]\times[\Delta\log\{(1-\alpha)/(1-\beta)\}/\Delta t] \quad (20)$$

The corrected value of the rate constant, k_n, has been calculated according to Eq. (6), assuming $\sigma=3$. An average value of k_2, 6.05×10^{-1} l/mol·min, is used for the calculation of k_1.

The reaction was also carried our by using a large excess of sodium hydroxide and the observed values were compared with those calculated by means of Eqs. (12) and (15). In Fig. 4 the circles represent the observed values, while the full and dotted lines are obtained by means of Eqs. (12) and

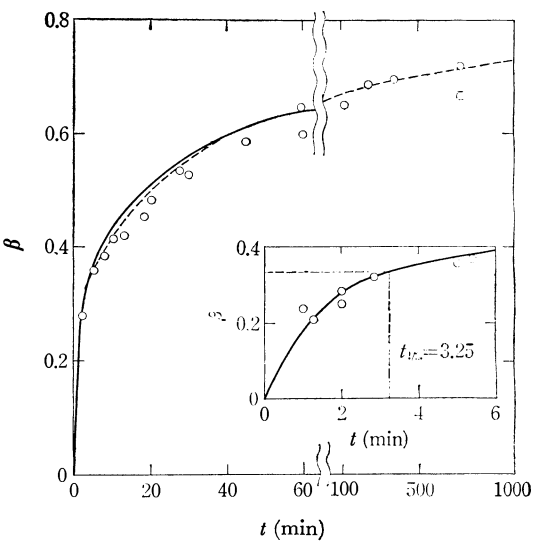

Fig. 4. Alkaline hydrolysis of triethyl citrate in 32% aqueous ethanol solution containing a large excess of sodium hydroxide at 10°C. ($a=3.38\times10^{-2}$, $b=3.04\times10^{-3}$ mol/l)

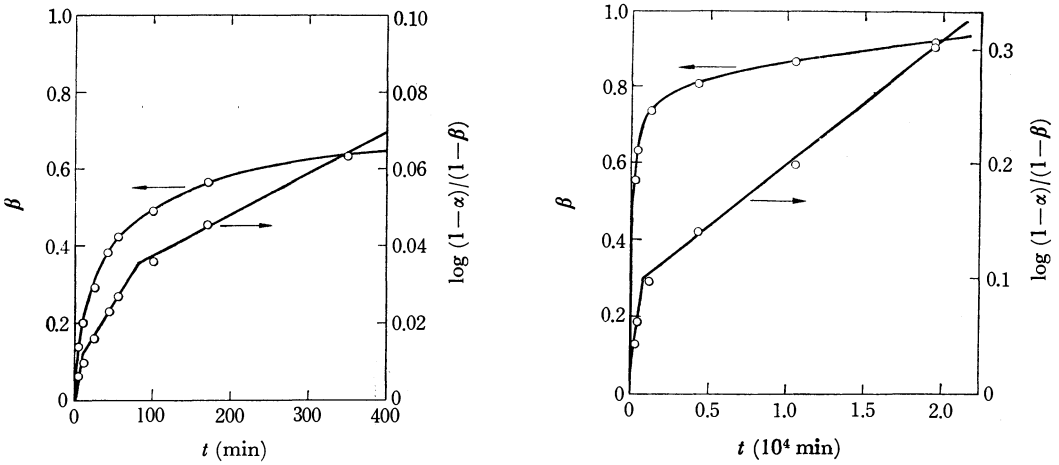

Fig. 5. Alkaline hydrolysis of polymethyl acrylate in 29% aqueous acetone solution at 55°C.[2] ($a=8.22\times10^{-2}$, $b=7.41\times10^{-2}$ mol/l)

(15) respectively, where the rate constants are: $k_1=7.93$, $k_2=6.05\times10^{-1}$, and $k_3=6.46\times10^{-3}$ l/mol·min. The fairly good agreement between the two values in the figure may show the correctness of the application of the rate equations to a reaction which proceeds in more than two steps.

Application of the Rate Equations to the Alkaline Hydrolysis of Polymethyl Acrylate. When an ester of polymeric acid is hydrolyzed in an alkaline solution, the apparent rate constant computed by Eq. (16) decreases as the reaction proceeds[2,4] as a result of the electrostatic effect of the hydrolyzed groups fixed on the macromolecule. If the reactivity of the ester group is mainly affected by a few hydrolyzed groups situated a relatively short distance apart, the k_n' given by Eq. (20) will remain almost constant over a relatively wide range, forming a step of the reaction, because it is expected that the environment of the reactive group will remain unchanged for some time and that the reaction will proceed discontinuously.

The value of $\log[(1-\alpha)/(1-\beta)]$, calculated on the basis of the kinetic data of the alkaline hydrolysis of polymethyl acrylate[2] in a 29% aqueous acetone solution, are plotted aginst the reaction time in Fig. 5. The four straight lines in this figure, which intersect nearly at $\beta=1/4$, 2/4, and 3/4, suggest that the reaction proceeds in four steps. The corresponding four rate constants have been calculated by Eq. (6), assuming $\sigma=4$. The results are summarized in Table 3, where k_n' is the approximate value of the rate constant estimated by means of Eq. (20).

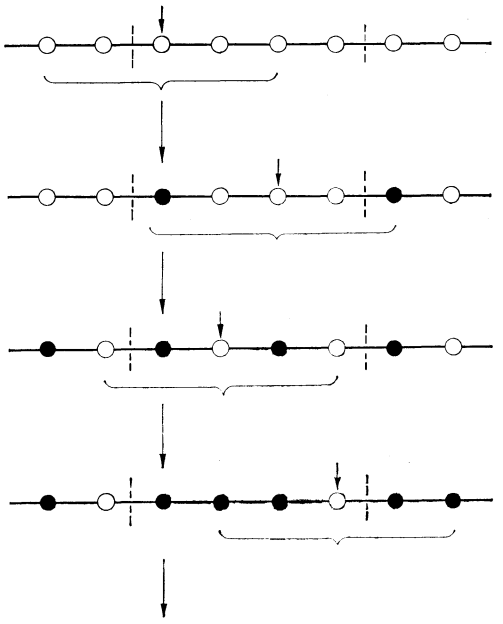

Fig. 6. Illustration of the four-step hydrolysis of polymethyl acrylate.

Table 3. Rate constnts of alkaline hydrolysis of polymethyl acrylate

n	k_n' l/mol min	k_n l/mol min	$\log(k_0/k_n)$
1	3.99×10^{-1}	8.02×10^{-1}	0.405
2	1.40×10^{-1}	1.66×10^{-1}	1.09
3	3.07×10^{-2}	4.04×10^{-2}	1.70
4	3.31×10^{-3}	3.31×10^{-3}	2.79

If it is assumed that the hydrolysis of the ester group is mainly affected by the electrical charge of the first and second neighboring groups, the electrical environment of the reactive group is considered to change in the four steps illustrated in Fig. 6, where the white and black circles represent ester and hydrolyzed groups respectively and where

4) A. Katchalsky and J. Feitelson, *J. Polymer Sci.*, **13**, 385 (1954).

the arrows indicate reacting groups. The electrostatic free energy of the activation of the nth reaction is given by:

$$(\Delta F_{el}^{*})_n = 2.303\boldsymbol{R}T\log(k_0/k_n) \quad (21)$$

where k_0 is the intrinsic rate constant. Since this energy is also given, on the basis of the above assumption, by summing up that shown in Eq. (19), the following relation is obtained:

$$\log(k_0/k_n) = (\boldsymbol{N}e^2/2.303\boldsymbol{R}TD)\sum_i(z_i/\bar{r}_i) \quad (22)$$

where z_i is the number of the electrical charge in the ith group apart from the reacting group (z_i= 0, 1 or 2, i=1 and 2) and where $\bar{r}_i$ is the average distance between the reacting group and the ith group, which is defined by:

$$1/\bar{r}_i = \sum_j(X_{i,j}/r_{i,j}) \quad (23)$$

where j is related to the steric configuration of the ith group and where X is the mole fraction ($\sum_j X_{i,j}$= 1). On the basis of the assumption illustrated in Fig. 6, three equations can be obtained:

$$\begin{cases} \log(k_0/k_2) = A(1/\bar{r}_2) \\ \log(k_0/k_3) = A(1/\bar{r}_1) \\ \log(k_0/k_4) = A(1/\bar{r}_1+1/\bar{r}_2) \end{cases}$$

where $A=2\boldsymbol{N}e^2/2.303\boldsymbol{R}TD=5.53$ (T=328, D= 80). By using the value of the rate constant in Table 3, the equations are solved to give:

$\bar{r}_1$=3.23 Å, r_2 = 5.07 Å, k_0 = 2.04 l/mol min

As the alkaline hydrolysis of polymethyl acrylate proceeds, the polymer chain stretches as a result of the charges formed on the polymer; the partly-hydrolyzed polymer may exhibit a planar zigzag structure, at least in the vicinity of reacting group. On the basis of the above assumption, two kinds of j (in Eq. (23)) may be defined; firstly, j=1, when both groups are situated sterically on the same side of the plane of zigzag, and secondly, j=2, on the opposite side. Then $X_{1,2}=1-X_{1,1}$. By introducing the two values $r_{1,1}$=2.6Å and $r_{1,2}$=4.3Å, which are estimated on the basis of the length and angles of the bonds, and the kinetically-determined value, $\bar{r}_1$=3.25Å, into Eq. (23), $X_{1,1}$ is found to be 0.5_0; this suggests that an atactic polymethyl acrylate exhibits a sterically random struture.

The relation given in Eq. (18) may be generalized in the formula given by Eq. (24) provided that a polybasic acid with σ carboxylic acid groups ionized in σ steps:

$$(\Delta F_{el}^{i})_n = 2.303\boldsymbol{R}T'[\mathrm{p}K'-\mathrm{p}K_0-\log(n/\sigma-n+1)] \quad (24)$$

where $(\Delta F_{el}^{i})n$ represents the electrostatic free energy at the nth step of ionization; K_0, the intrinsic dissociation constant of the acidic group, and K_n', the dissociation constant of the group at the nth step. If it is assumed, by analogy to the alkaline hydrolysis of polymethyl acrylate, that the ionization of polyacrylic acid is mainly affected by a few ionized groups on the polymer, $(\Delta F_{el}^{i})n$ is also given by $(\boldsymbol{N}e^2/D)\sum_i(z_i/\bar{r}_i)$. The comparison of Eq. (21) with Eq. (24) leads to the relation:

$$\log(k_0/k_n)=(T'/T)[\mathrm{p}K_n'-\mathrm{p}K_0-\log\{n/(\sigma-n+1)\}] \quad (25)$$

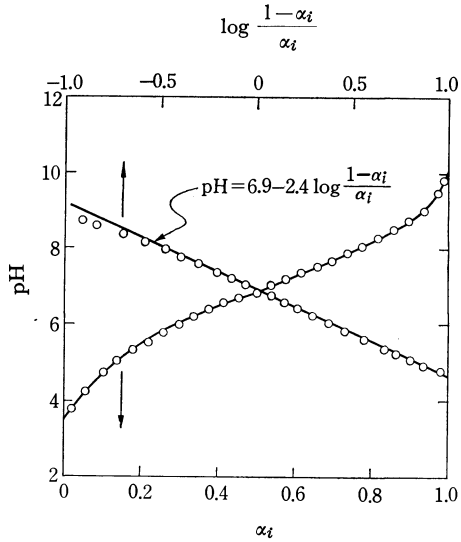

Fig. 7. Titration of polyacrylic acid with sodium hydroxide in the absence of salt.

TABLE 4. $\mathrm{p}K_0$ OF POLYACRYLIC ACID CALCULATED BY THE KINETIC DATA

n	$\mathrm{p}K_n'$	$\log[n/(5-n)]$	$(T/T')\log(k_0/k_n)$	$\mathrm{p}K_0$
2	6.40	−0.18	1.20	5.38
3	7.39	0.18	1.87	5.34
4	8.61	0.60	3.07	4.93

An aqueous solution of polyacrylic acid was titrated with a sodium hydroxide solution in the absence of added salt; the titrated data are represented in Fig. 7, in which the straight line represents the modified Henderson-Hasselbach relation,[5] $\mathrm{pH}=\mathrm{p}K_a-n'\log[(1-\alpha_i)/\alpha_i]$, where α_i is the degree of ionization. These data are in accordance with those given by Gregor and Frederic.[6] By assuming a four-step ionization for polyacrylic acid, $\mathrm{p}K_0$ may be estimated by using Eq. (25) in terms of the kinetic data. The results of the calculation are given in Table 4, where the pH values at α_i=3/8, 5/8, and 7/8 are used as the $\mathrm{p}K_n'$ values, because $\mathrm{p}K_n'$ is, by definition, equal to pH at the half-ionization point in each ionization step.

The fairly good constancy of the calculated value of $\mathrm{p}K_0$ suggests that both the alkaline hydrolysis of

5) A. Katchalsky and P. Spitnik, *J. Polymer Sci.*, **2**, 432 (1947).

6) H. P. Gregor and M. Frederic, *ibid.*, **32**, 451 (1957).

polymethyl acrylate in an aqueous solution and the ionization of polyacrylic acid are controlled by the same electrostatic effect of the charged group on the polymer, and that the ionization of polyacrylic acid can be explained approximately in terms of the four-step ionization concept.

The authors wish to express their thanks to Mr. T. Katayama for his helpful assistance in carrying out the measurements.

BULLETIN OF THE CHEMICAL SOCIETY OF JAPAN VOL. 42 3115—3118 (1969)

Measurement of Negative Ions Formed by Electron Impact. V. Negative Ion Mass Spectra and Ionization Efficiency Curves of Negative Ions of *m/e* 16, 25 and 41 from Tetrahydrofuran

Satoru TSUDA, Akira YOKOHATA and Michihiro KAWAI

Department of Chemistry, Faculty of Engineering, Hiroshima University, Senda-machi, Hiroshima

(Received May 19, 1969)

The negative ion mass spectra of tetrahydrofuran, with an emphasis on their relative abundances to the positive ions under 80 eV and 40 eV electron energies, and the ionization efficiency (IE) curves of *m/e* 16(O^-), *m/e* 25(C_2H^-) and *m/e* 41(C_2HO^-) ions to the extent of 40 eV electron energies were measured. The electron impacts of 80 eV and 40 eV gave almost the same distribution of *m/e* for negative ion mass spectra. The relatively strong peaks were observed at *m/e* 24(C_2^-) ions for 80 eV and *m/e* 14(CH_2^-) ions for 40 eV, besides the commonly strong peaks of *m/e* 25(C_2H^-), *m/e* 16(O^-) and *m/e* 41(C_2HO^-) ions. The comparison of the yield of C_2H^- ions with that of $C_3H_6^+$ gave the values 9.4×10^3 and 2.7×10^4 for $C_3H_6^+/C_2H^-$ at 80 eV and 40 eV electron energies, respectively. The reaction schemes expected to occur at each onset observed in the IE curves were also discussed. It is of interest to note that C_2H^- ions are not obtained in the range of low energy of electrons, but become observable at ~23.5 eV.

Recently, several studies have been reported on the measurement of negative ion mass spectra by the electron impact method.[1-6] However, they were made for a limited number of compounds, and data for the ionization efficiency curves of negative ions are very limited.[7-9] The role of negative ions is attracting increasing attention in the field of radiation chemistry. Compounds containing oxygen atom are of special interest. Warman,[10] Rzad[11] and Henz[12] have pointed out the occurrence of the negative ion-molecule reactions containing O^- ions.

This work was extended to tetrahydrofuran (C_4H_8O). Recently, the importance[13] of negative ions was suggested on the radiolysis of tetrahydrofuran-nitrous oxide system, but we haven't any informations about negative ions from tetrahydrofuran. In this paper negative ion mass spectra from tetrahydrofuran, with emphasis on their relative abundances to the positive ions, and the ionization efficiency (IE) curves of *m/e* 16 (O^-), *m/e* 25 (C_2H^-) and *m/e* 41 (C_2HO^-) ions are reported. There seem to be few papers so far on this subject.

1) C. E. Melton, "Mass Spectrometry of Organic Ions," ed. by F. W. McLafferty, Academic Press, New York, N. Y. (1963), p. 163.
2) E. W. McDaniel, "Collision Phenomena in Ionized Gases," John Wiley & Sons Inc., New York (1964), p. 368.
3) F. Fiquat-Fayard, *Actions Chim. Biol. Radiations.*, **8**, 31 (1965).
4) R. T. Aplin, H. Budzikieweiz and C. Djerassi, *J. Am. Chem. Soc.*, **87**, 3180 (1965).
5) C. E. Melton and P. S. Rudolf, *J. Chem. Phys.*, **47**, 1771 (1967).
6) D. F. Munro, J. E. Ahnell and W. S. Koski, *J. Phys. Chem.*, **72**, 2682 (1968).
7) L. G. Christophorou, R. N. Compton, G. S. Hurst and P. W. Reinhardt, *J. Chem. Phys.*, **45**, 536 (1966).
8) L. G. Christophorou and R. N. Compton, *Health Physics*, **13**, 1277 (1967).
9) T. Sugiura, T. Seguchi and K. Arakawa, This Bulletin, **40**, 2992 (1967).
10) J. M. Warman, *Nature*, **213**, 382 (1967), *J. Phys. Chem.*, **72**, 52 (1968).
11) S. J. Rzad and J. M. Warman, *ibid.*, **72**, 3013 (1968).
12) R. R. Henz and S. J. Rzad, *ibid.*, **72**, 1027 (1968).
13) M. Matsui, T. Karasawa, H. Seki and M. Imamura, Preprints for the 11th Conference of Radiation Chemistry, Tokyo (Sept., 1968).

Experimentals

Experiments were performed on a Hitachi RMU-6D mass spectrometer equipped with T-2M ion source having a rhenium filament. The ion detection circuit consisted of a ten stage electron multiplier and of a Faraday collector. The experimental condition was as follows: total emission=20 μA, accelerating voltage =3.6 kV and electron multiplier voltage=2.5 kV. The correction method of electron energy scale was the same as that used previously.[14] The sample was of reagent grade.

Results and Discussion

Negative Ion Mass Spectra. Table 1 shows the relative abundances of negative ions at 80 eV and 40 eV electron energies. The electron impacts of 80 eV and 40 eV gave almost the same distribution of *m/e* for negative ion mass spectra. The spectra obtained are shown as follows; *m/e* 12 (C^-), *m/e* 13 (CH^-), *m/e* 14 (CH_2^-), *m/e* 15 (CH_3^-), *m/e* 16 (O^-), *m/e* 17 (OH^-), *m/e* 24 (C_2^-), *m/e* 25 (C_2H^-), *m/e* 26 ($C_2H_2^-$), *m/e* 29 ($C_2H_5^-$), *m/e* 36 (C_3^-), *m/e* 37 (C_3H^-), *m/e* 38 ($C_3H_2^-$), *m/e* 40 (C_2O^-),*1 *m/e* 41 (C_2HO^-),*1 *m/e* 42 ($C_2H_2O^-$) and *m/e* 43 ($C_2H_3O^-$), in which parent ion ($C_4H_8O^-$) was not detected. Since their data were taken at a pressure of 10^{-6} mmHg in the source, the possibility of ions induced by ion-molecule reactions would be ruled out.

Table 1. Relative abundances of negative ions (normalized to $[C_2H^-]=100$)

m/e	Probable negative ion	Relative abundances 80 eV	40 eV
12	C	3.0	1.0
13	CH	14.8	15.0
14	CH_2	10.9	28.3
15	CH_3	trace	—
16	O	55.5	63.4
17	OH	4.2	12.7
24	C_2	29.9	8.4
25	C_2H	100.0	100.0
26	C_2H_2	2.4	4.3
29	C_2H_5	0.7	2.3
36	C_3	8.8	3.3
37	C_3H	4.5	3.3
38	C_3H_2	1.9	8.3
40	C_2O	6.6	14.0
41	C_2HO	27.7	86.7
42	C_2H_2O	trace	2.3
43	C_2H_3O	5.39	21.7

The relatively strong peaks were observed at *m/e* 24 (C_2^-) ions for 80 eV and *m/e* 14 (CH_2^-) ions for 40 eV, besides the commonly strong peaks of *m/e* 25 (C_2H^-), *m/e* 16 (O^-) and *m/e* 41 (C_2HO^-) ions.

The reason for the absence of fragment ions such as $x=4$ at CH_x^-, $x=3$, 4 and 6 at $C_2H_x^-$, $x=3$—8 at $C_3H_x^-$, $y=4$ at C_y^-, $z=1$, 3 and 4 at C_2O^-, $u=1$—4 at CH_uO^-, $u=4$ at $C_2H_uO^-$, $u=1$—6 at $C_3H_uO^-$, and $u=1$—8 at $C_4H_uO^-$ is not well known. As described by MacNeil and Thynne,[15] however, they may be explained from the size, symmetry and bonding of the molecule, or the electron affinity of each radical. Ferguson *et al.*[16] reported the geometrical considerations for

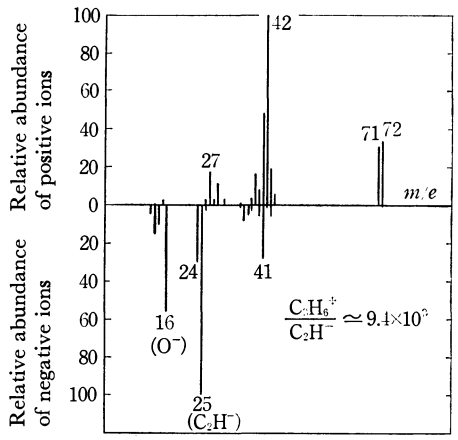

Fig. 1a

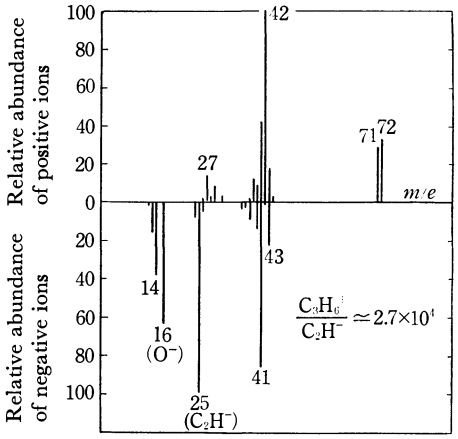

Fig. 1b

Fig. 1. Positive and negative ion mass spectra of tetrahydrofuran (source pressure; $\sim 10^{-6}$ mmHg).
a 80 eV b 40 eV

14) S. Tsuda, A. Yokohata and M. Kawai, This Bulletin, **42**, 614 (1969).

*1 Since no formation of $C_3H_4^-$ (*m/e* 40) and $C_3H_5^-$ (*m/e* 41) ions from butane,[1] nitropropane[14] and propylalcohol[1,20] was observed, these ions might be ruled out.

15) K. A. G. MacNeil and J. C. J. Thynne, *Trans, Faraday Soc.*, **64**, 2112 (1968).

16) E. E. Ferguson, F. C. Fehsenfeld and A. L. Schmeltekopf, *J. Chem. Phys.*, **47**, 3085 (1967).

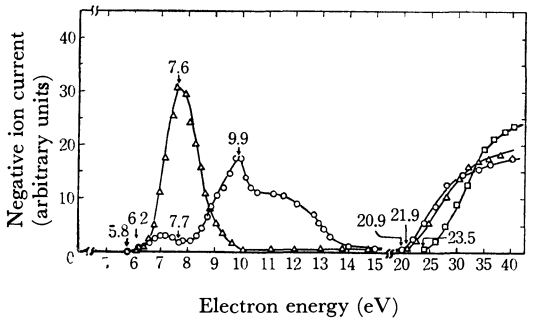

Fig. 2. Ionization efficiency curves of negative ions of *m/e* 16, 25 and 41 obtained from tetrahydrofuran.
○ *m/e* 16 (O^-) □ *m/e* 25 (C_2H^-)
△ *m/e* 41 (C_2HO^-)

negative ion processes but their discussions are only made for a few simple molecules.

The most intense peak was observed at C_2H^- ions. The situation is quite similar to acetylene, ethane, *n*-butane and *n*-butyl alcohol.[1] This finding seems to show that C_2H^- ion is relatively stable and its electron affinity is relatively high.

A relatively large change in their relative abundances with electron energies (80→40 eV) was found at C^-, CH_2^-, OH^-, C_2^-, $C_2H_5^-$, C_3^-, $C_3H_2^-$, C_2HO^- and $C_2H_3O^-$ ions. This would be interpreted by electron energy dependency of cross section of the reaction (ion pair formation) which governs the formation of each ion.

Figure 1 shows the negative ions mass spectra at 80 eV and 40 eV electron energies, in relation to the positive ion mass spectra.

The comparison of the yield of C_2H^- ions with that of $C_3H_6^+$ ions (the most intense peak among the positive ions) gave $C_3H_6^+/C_2H^- \simeq 9.4\times10^3$ and 2.7×10^4 at 80 eV and 40 eV electron energies, respectively.

IE Curves. Figure 2 shows the IE curves of O^-, C_2H^- and C_2HO^- ions to the extent of 40 eV.

O^- Ions. It can be understood that three processes contribute to their formation. The first process appears at ~5.8 eV, the second process at ~7.7 eV*[2] and the third process at ~20.9 eV. The shape of IE curves suggests the dissociative capture process and ion pair formation.

The onset of ~5.8 eV would be interpreted with reaction (1), because it gives a reasonable value of ~3.64 eV[17] for D(RC–O),*[3] by combining 5.8 eV with EA(O)=1.47 eV.[18]

$$C_4H_8O + e^- \rightarrow C_4H_8 + O^- \quad (1)$$

Then, $\Delta H_f(C_4H_8O) = -2.2$ eV[19] and $\Delta H_f(O^-) = 1.09$ eV[20] result in $\Delta H_f(C_4H_8) \simeq 2.51$ eV.*[4]

For the second and third processes, the following reactions may be assigned.

$$C_4H_8O + e^- \rightarrow C_4H_8^* + O^- \quad (2)$$

$$C_4H_8O + e^- \rightarrow C_4H_7 + H + O^- \quad (3)$$

$$C_4H_8O + e^- \rightarrow C_4H_7^+ + H + O^- + e^- \quad (4)$$

However, the appearance potential (~5.8 eV) of reaction (1) and C–H bond energy (4.3 eV[15]) would give a value of ~10.1 eV for the appearance of reaction (3) which is inconsistent with ~7.7 eV. Thus, reaction (3) is excluded. Although speculative because of unknown value of C_4H_8,* reaction (2) appears to fit the second process.

On the other hand, the formation of reaction (4) requires a higher energy than reaction (3)—energy to be required for at least ionizing C_4H_7. The appearance potential of ~20.9 eV gives $IP(C_4H_7) \approx$ 10.8 eV, which seems a little too large to be accepted.[21] However, a small allowance of the kinetic energy of fragment ions at AP≈20.9 eV acts for $IP(C_4H_7)$ toward its decrement. Hence, the assignment of reaction (4) for the third process would be reasonable.

C_2H^- Ions. It is characteristic that C_2H^- ions are not obtained in the range of low energy and become observable at electron energy of ~23.5 eV. Probably, ion pair formation would responsible for this onset value.

C_2HO^- Ions. These ions show the typical dissociative electron capture process in the range of electron energies from ~6.2 to ~10 eV. Appearance potential of ~21.9 eV seems to correspond to ion pair formation.

For each onset value of these ions the reactions (5), (6) and (7) may be expected.*[5] However, their exact determination is difficult, because of difficulty of the assignment of ΔH_f values which is due to the unknown structure of negative ions and radicals produced.

For C_2H^- ions;

$$C_4H_8O + e^- \rightarrow C_2H^- + C_2H_4O^+ + H_2 + H + e^- \quad (5)$$

*2 Since the tailing due to the 1st process might be overlapped with the appearance of the 2nd process, the exact determination of appearance potential of the 2nd process is difficult. In this work, the minimum values in the IE curves have been discussed as by Schulz (G. J. Schulz, *Phys. Rev.*, **113**, 816 (1959)).

17) T. L. Cottrell, "The Strengths of Chemical Bonds," Butterworths, London (1958), p. 275.

*3 Tetrahydrofuran contains two C–O bonds. D(RC–O) means the average value of C–O bond energy.

18) B. Edlen, *J. Chem. Phys.*, **33**, 98 (1960).

19) R. C. Cass, S. E. Fletcher, C. T. Moltimer, H. D. Springall and C. T. White, *J. Chem. Soc.*, **1958**, 1406.

20) S. Tsuda, A. Yokohata and M. Kawai, to be published.

*4 The structure of C_4H_8 shown in reaction (1) is not well known. It is probably in the form of tetramethylene.

21) R. R. Bernecker and F. A. Long, *J. Phys. Chem.*, **65**, 1565 (1961).

*5 There are other possibilities too.

For C_2HO^- ions;

$$C_4H_8O + e^- \rightarrow C_2HO^- + C_2H_5 + H_2 \quad (6)$$

$$\rightarrow C_2HO^- + C_2H_4^+ + H + H_2 + e^- \quad (7)$$

It should be emphasized that the main negative ionic species to be considered on the radiolysis of tetrahydrofuran are not parent ions but *m/e* 25 (C_2H^-), *m/e* 41 (C_2HO^-) and *m/e* 16 (O^-) ions.

The authors are indebted to Drs. M. Imamura and M. Matsui, the Institute of Physical and Chemical Research, for the sample.

BULLETIN OF THE CHEMICAL SOCIETY OF JAPAN VOL. 42 3118—3123 (1969)

The Electronic Structures of Glycine in the Isolated State and in Water

Akira IMAMURA, Hiroko FUJITA and Chikayoshi NAGATA

Biophysics Division, National Cancer Center Research Institute, Tsukiji, Chuo-ku, Tokyo

(Received May 20, 1969)

The electronic structures of glycine have been calculated for the dipolar-ion form and the neutral form by means of the CNDO method. The relative stability of both the dipolar-ion form and the neutral form in the gas state was reproduced by our calculation. The geometry of the glycine was also reproduced by the CNDO method, indicating the validity of our calculation. In addition, the relative stability of the two tautomeric forms of glycine was proved to be independent of its geometrical modifications. The experimental fact that the dipolar-ion form is more stable than the neutral form in an aqueous solution was well explained by the calculation of the interaction energy between the solute and the solvent.

Glycine is the simplest α-amino acid and constitutes the backbone of the protein, namely, polypeptide. Therefore, the electronic structure of glycine is of interest since the general features of the electronic structures of the amino acid and the backbone of protein can be derived from that of glycine.

Glycine is well known to exist as a dipolar ion in water and crystal, and, on the other hand, to exist in the neutral form in the isolated state.[1] Therefore, the interaction between glycine and water makes the dipolar-ion form more stable than the neutral form.

The electronic structures of various α-amino acids have already been calculated by Del Re's method;[2] a good parallelism between the electron densities of the proton and the NMR chemical shift[3] was found. Moreover, the dissociation constants of α-amino acids were found to be correlated with the calculated energy differences between the dissociated and non-dissociated forms.[4] Recently, the CNDO method was developed by Pople *et al.*;[5,6] it has proved to be very useful for the prediction of the electronic structures of many organic molecules, especially polar molecules, in the ground state.[7,8]

In the present paper, the total electronic energies of glycine in its neutral and dipolar-ion forms were calculated by the CNDO method.[5,6] The most stable geometry of glycine obtained by the calculations agrees well with the results of X-ray diffraction.[9,10] Moreover, the relative stabilities of the neutral form and of the dipolar-ion form were calculated in water and in gas, and the solvent effect considered.

1) K. Biemann, J. Seibl and F. Gapp, *J. Am. Chem. Soc.*, **83**, 3795 (1961); G. Junk and H. Sevec, *ibid.*, **85**, 839 (1963); J. P. Greenstein and M. Winitz, "Chemistry of the Amino Acids," Vol. 1, John Wiley & Sons, New York (1961), Chap. 4.

2) G. Del Re, *J. Chem. Soc.*, **1958**, 4031.

3) G. Del Re, B. Pullman and T. Yonezawa, *Biochim, Biophys. Acta*, **75**, 153 (1963).

4) T. Yonezawa, G. Del Re and B. Pullman, This Bulletin, **37**, 985 (1964).

5) J. A. Pople, D. P. Santry and G. A. Segal, *J. Chem. Phys.*, **43**, s 129 (1965); J. A. Pople and G. A. Segal, *ibid.*, **43**, s135 (1965).

6) J. A. Pople and G. A. Segal, *ibid.*, **44**, 3289 (1966).

7) J. A. Pople and M. Gordon, *J. Am. Chem. Soc.*, **89**, 4253 (1967).

8) J. E. Bloor and D. L. Breen, *ibid.*, **89**, 6835 (1967).

9) G. Albrecht and R. B. Corey, *ibid.*, **61**, 1087 (1939).

10) R. E. Marsh, *Acta Cryst.*, **11**, 654 (1958); Y. Iitaka, *ibid.*, **11**, 225 (1958).

TABLE 1. THE PARAMETERS USED IN THE CALCULATION

Atom	H	C	N	O
Extended Hückel method				
$Z_{eff.}$	1.2	3.25	3.90	4.55
I_p[a] s orbital	−13.6	−21.43	−27.50	−35.30
p orbital		−11.42	−14.49	−17.76
CNDO method				
$Z_{eff.}$	1.2	3.25	3.90	4.55
$\frac{1}{2}(I+A)$[a] s orbital	− 7.176	−14.051	−19.316	−25.390
p orbital		− 5.572	− 7.275	− 9.111
β[a]	− 9.0	−21.0	−25.0	−31.0

a) in eV.

Methods

The calculations were carried out in the framework of the extended Hückel method developed by Hoffmann[11] and the CNDO/2 method developed by Pople *et al.*[5,6] All the parameters included in these methods are collected in Table 1; these values are the same as those usually employed. In the CNDO method the total energy is the sum of the total electronic and core-repulsion energies. The core-repulsion energy was calculated by the following equation:

$$E_{\text{core rep.}} = \frac{1}{2}\sum_{A}\sum_{\substack{B \\ (\neq A)}} \frac{Z_A Z_B e^2}{R_{AB}} \qquad (1)$$

where R_{AB} is the distance between the atoms A and B and where Z_A is the effective nuclear charge on the atom A. In order to carry out the population analysis by the CNDO method, the molecular orbitals on the CNDO basis were transformed to those on the Slater function basis by using the overlap matrix. Then the new set of the molecular orbitals thus obtained was employed to calculate the total electron densities using the population analysis[12] which was also employed in the extended Hückel method.

The convergency of the iteration procedure in the CNDO method was checked against the total electronic energy; that is, if the ratio of the total electronic energy to the energy difference between the former iteration and the present one was less than 10^{-6}, the convergency was considered to be accomplished. The usual number of the iteration was eight or nine.

Results and Discussions

The Electronic Structures of Glycine in the Neutral and the Dipolar-ion Forms. The electronic structures of glycine in the neutral and the dipolar-ion forms were calculated by the extended Hückel[11] and CNDO/2 methods.[5,6] The geometries of glycine assumed[9,10] are indicated in Fig. 1, while the total energies obtained are listed in Table 2. As is shown in Table 2, the extended Hückel method predicts that the dipolar-ion form will be more stable than the neutral form, in

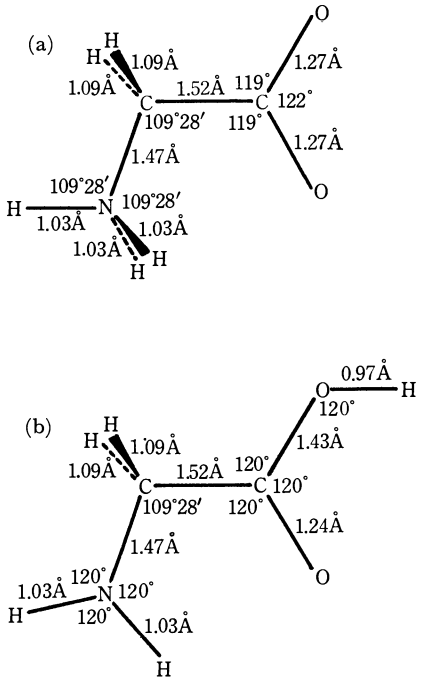

Fig. 1. The geometry of glycine used for calculations.
(a) the dipolar ion form
(b) the neutral form

TABLE 2. THE TOTAL ENERGY OF GLYCINE CALCULATED BY THE EXTENDED HÜCKEL AND CNDO METHODS (in eV)

	Extended Hückel	CNDO
Neutral form	−630.81	−1807.58
Dipolar ion form	−632.36	−1804.44

11) R. Hoffmann, *J. Chem. Phys.*, **39**, 1397 (1963).
12) R. S. Mulliken, *ibid.*, **23**, 1833, 1841, 2338, 2343 (1955).

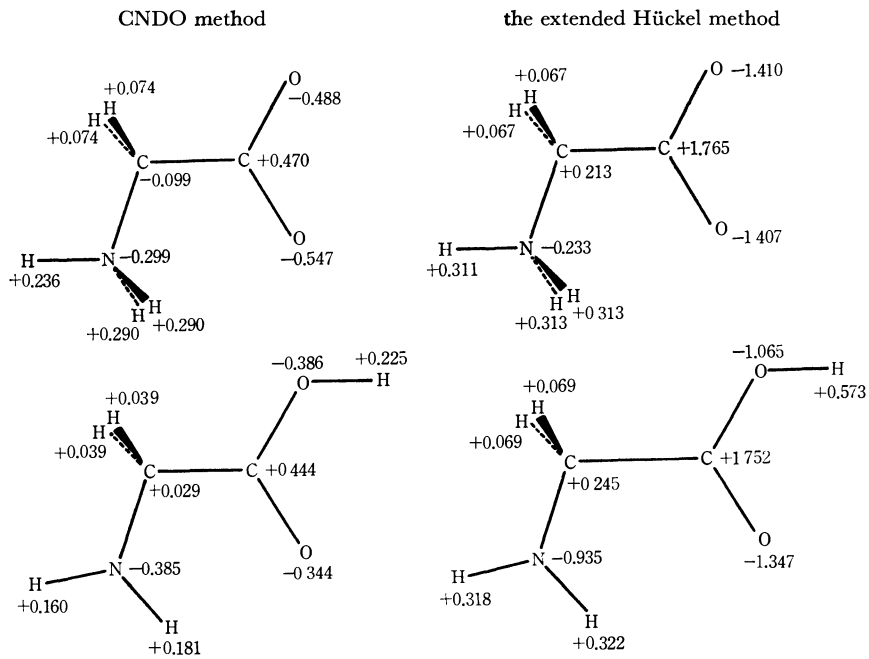

Fig. 2. The electron distribution of glycine calculated by CNDO and the extended Hückel methods.

agreement with the previous calculation;[13] on the contrary, the neutral form is indicated to be more stable by the CNDO method. This discrepancy between the two methods may be attributable to the explicit neglect of the electron-electron repulsion in the extended Hückel method. The above-mentioned inference was supported by the electron distributions of glycine calculated by the two methods; that is, the electron distributions calculated by the extended Hückel method deviate from neutral more than those calculated by the CNDO method, as is shown in Fig. 2. In other words, the electron densities of glycine calculated by the extended Hückel method exaggerate its polar nature too much; for example, the oxygen net negative charges in glycine exceed one, and the net positive charge of one of the carbons is approximately two, because of the neglect of the explicit effect of electron-electron repulsion. Glycine in water or in the solid state is well known to exist as a dipolar ion.[1] However, glycine in the isolated state, namely, in the gas state, is in the neutral form;[1] this is in accordance with the results calculated by the CNDO method.

The Geometry of Glycine in the Dipolar-ion Form. In order to investigate the validity of the CNDO method for such a polar molecule as glycine and estimate the variation in the total energy with the bond lengths and the bond angles, the calculations were carried out for various geometries of the molecule in order to establish the energy minimum. First of all, the energy dependences upon the C–C and C–N bond lengths were investigated, with the other geometrical parameters fixed as indicated in Fig. 1. The calculated results are listed in Table 3. In Table 3-A, the C–C bond length is fixed at 1.52 Å, while the C–N bond lengths range from 1.20 to 1.60 Å. Thus we obtain the energy minimum at 1.43 Å. Therefore, in Table 3-B the C–N bond length is fixed at three points, namely at 1.39, 1.43, and 1.47 Å, and the energy dependences upon the change in the C–C bond length was investigated. In the table, the energy minimum was found at the C–C bond length of 1.48 Å for all C–N bond lengths. That is to say, equilibrium C–C and C–N bond lengths were determined independently of each other. The equilibrium bond lengths calculated were approximately in accordance with the data obtained by X-ray diffraction analysis; that is, from X-ray diffraction analysis the C–C bond length was determined as 1.52 Å,[9,10] and for the C–N bond two different values, of 1.47[10] and 1.39 Å,[9] have been given by different authors. With regard to the bond angle, the energy variation with the angle between the C–C and C–N bonds was calculated, fixing the C–C bond at 1.48 Å and the C–N bond at 1.43 Å. In this case, the bond angle between the two C–H bonds was changed in harmony with the alteration of the CCN bond angle; that is, the directions of the four bonds were determined in order to construct four orthonormally-hybridized

13) T. Yonezawa, "Seitai Ryôshi Kagaku" (Biological Quantum Chemistry), ed. by K. Fukui, Kyoritsu, Tokyo (1967), p. 29.

Table 3. The energy dependence on the change of the bond length[a)]

(A)	C–C bond length = 1.52 Å			
C–N bond length (Å)	1.20	1.30	1.39	1.43
Total energy (eV)	−1800.03	−1803.21	−1804.36	−1804.50
C–N bond length (Å)	1.47	1.51	1.55	1.60
Total energy (eV)	−1804.45	−1804.25	−1803.95	−1803.45
(B)	C–N bond length = 1.39 Å			
C–C bond length (Å)	1.44	1.48	1.52	
Total energy (eV)	−1804.29	−1804.40	−1804.36	
	C–N bond length = 1.43 Å			
C–C bond length (Å)	1.44	1.48	1.52	
Total energy (eV)	−1804.46	−1804.55	−1804.50	
	C–N bond length = 1.47 Å			
C–C bond length (Å)	1.44	1.48	1.52	
Total energy (eV)	−1804.41	−1804.50	−1804.44	

a) Observed C–C bond length = 1.52 Å[9,10]
Observed C–N bond length = 1.39 Å[9] or 1.47 Å[10]

Table 4. The energy dependence on the NCC angle[a)]

NCC angle	106°	109°28′	112°	115°	118°
Total energy (eV)	-1804.51_7	-1804.52_4	-1804.51_7	−1804.47	−1804.41

a) Observed = 112°[9] or 118.8°[10]

Table 5. The energy dependence on the rotational angle around the C–C bond[a)]

Rotational angle	0°	30°	60°	90°
Total energy (eV)	−1804.55	−1804.48	−1804.35	−1804.30

a) Observed $\fallingdotseq$20°[10]

orbitals for any values of the bond angle. The total energies calculated at various angles between the C–C and C–N bonds are listed in Table 4. The energy minimum was found at the tetrahedral configuration, which agrees fairly well with the experimental data of 112°[9] and 118.8°.[10] Moreover, the variation in the energy with the change in the angle is so small that the determination of the equilibrium bond angle is probably very difficult. Judging from this fact, the small discrepancy between the calculated bond angle and the observed one is possibly not serious. The last geometrical parameter investigated was the rotational angle around the C–C bond, with the C–C bond length of 1.48, with the C–N bond length of 1.43 Å, and with a tetrahedral configuration of the central carbon. The results in Table 5 indicate that the planar configuration is most stable. From X-ray diffraction analysis, glycine has been shown to deviate slightly from the planar configuration.[9,10] On the whole, the geometry of glycine predicted by means of the CNDO method is in good agreement with the experimental results. In addition, the energy change of the molecule with the alterations in the geometry is rather small. Therefore, it is quite impossible to expect the reversion of the relative stability of the neutral and the dipolar-ion forms by means of the variation in the geometry.

The Electronic Structure of Glycine in Water. As has already been mentioned, glycine exists in the dipolar-ion form in water, but in the neutral form in gas.[1] These facts suggest that the interaction between glycine and water stabilizes the dipolar-ion form more than the neutral form. The exact calculation of the interaction energy between the solute and the solvent is quite impossible because of the diversity of the relative conformations of glycine and water in solution. The interaction energy can be estimated roughly, however, by such a simple model as the cavity in a dielectric solution.[14] The alternative approach is treatment by

14) For example, H. Fröhlich, "Theory of Dielectrics," The Clarendon Press, Oxford (1958), Chap. 2.

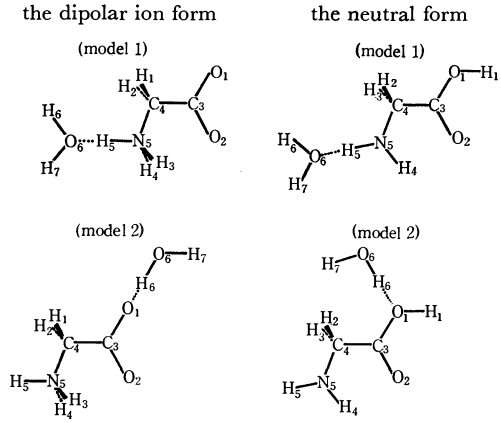

Fig. 3. The models of the hydrogen bond between glycine and water.

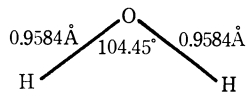

Fig. 4. The geometry of water.

the molecular orbital theory, in which the representative relative conformations of the solute and the solvent are tentatively assumed and in which the calculation is carried out for the conformation thus assumed. In this method, however, only a part of the interaction energy can be obtained; in other words, the molecular orbital approach can be used only to estimate the order of magnitude of the interaction energy. From this point of view, it is of interest to calculate the stabilization energies of the hydrogen bonds between water and glycine in the dipolar-ion form or in the neutral form in order to estimate the magnitude of the solvent effect. Although the stabilization energy by the hydrogen-bond formation is a part of the interaction energy, its contribution to the energy may reasonably be the main one; thus, this treatment can be employed for the rough estimation of the interaction energy. The models of hydrogen bonds calculated are shown in Fig. 3. The model 1 in Fig. 3 had already been accepted for the study of the protolysis kinetics of amino acid analogs.[15] The geometry of water is shown in Fig. 4. The total energies calculated by the CNDO method are listed in Table 6 for the model system of the hydrogen bonds with various intermolecular distances. For any models, the energy minimum was obtained between the intermolecular distances of 2.4 and 2.7 Å; this is in good agreement with the results obtained by means of the X-ray diffraction method used on usual hydrogen bonds. It is noteworthy that the stabilization energies by hydrogen-bond formation in the dipolar-ion form are greater than those in the neutral form by about 0.3 eV. Since many hydrogen-bond formations and other types of interaction between glycine and water can be expected in a water solution, the differences in the stabilization energies calculated are large enough to change the relative stability of the neutral and the dipolar-ion forms of glycine. In other words, the dipolar-ion form of glycine is more stable than the neutral form in water, probably because of such a solute-solvent interaction as the hydrogen bonds.

Table 6. The stabilization energy of the hydrogen bonds between glycine and water

N-O distance (model 1) O-O distance (model 2)	Total energy (eV) Model 1	Model 2
Dipolar ion form		
2.0	−2341.79	−2343.44
2.3	−2345.39	−2345.59
2.4	−2345.61	−2345.67
2.5	−2345.65	−2345.63
2.75	−2345.54	−2345.46
3.0	−2345.37	−2345.31
3.5	−2345.21	−2345.17
∞	−2345.09	−2345.09
Stabilization energy	0.56	0.54
Neutral form		
2.0	−2343.85	−2345.49
2.4	−2348.14	−2348.33
2.5	−2348.29	−2348.39
2.6	−2348.34	−2348.38
2.7	−2348.34	−2348.35
3.0	−2348.26	−2348.24
3.5	−2348.17	−2348.16
∞	−2348.12	−2348.12
Stabilization energy	0.22	0.27

The electron densities obtained by the population analysis for various intermolecular distances are listed in Table 7. From this table, the charge transfer between water and glycine in the dipolar-ion form may be found to be larger than those in the neutral form, corresponding to the relative magnitudes of the stabilization energies. More remarkable is the fact that the charge redistribution by the hydrogen-bond formation occurs predominantly not between molecules, but within molecules; this is in good agreement with the non-empirical calculation of the hydrogen bond between water molecules[16] and the CNDO calculation of the dimer of the formic acids.[17] Moreover, when hydrogen bonds are formed, the proton-accepting

15) M. Sheinblatt, *J. Chem. Phys.*, **36**, 3103 (1962).

16) K. Morokuma and L. Pedersen, *ibid.*, **48**, 3275 (1968).

17) A. Ocvirk, H. Ažman and D. Hadži, *Theoret. Chim. Acta*, **10**, 187 (1968); A. Pullman and H. Berthod, *ibid.*, **10**, 461 (1968).

TABLE 7. THE CHARGE DISTRIBUTION FOR VARIOUS HYDROGEN BOND SYSTEMS

(A) Dipolar ion form—model 1[a]

N_5–O_6 distance	Atomic population					
	H_1	H_3	H_5	H_6	H_7	CT[b]
2.0	0.970	0.765	0.462	0.700	0.708	−0.069
2.5	0.941	0.726	0.683	0.755	0.761	−0.033
3.0	0.931	0.713	0.741	0.780	0.784	−0.007
3.5	0.928	0.710	0.755	0.789	0.793	−0.001
∞	0.927	0.707	0.767	0.804	0.804	0.0

N_5–O_6 distance	Atomic population					
	O_1	O_2	C_3	C_4	N_5	O_6
2.0	6.525	6.556	3.527	4.065	5.461	6.523
2.5	6.502	6.555	3.528	4.084	5.345	6.451
3.0	6.505	6.548	3.525	4.090	5.309	6.429
3.5	6.493	6.553	3.527	4.093	5.302	6.417
∞	6.491	6.552	3.527	4.095	5.298	6.392

a) The numbering of the atoms is shown in Fig. 3.
b) The charge transfer quantity from water to glycine.

(B) Dipolar ion form—model 2[a]

O_1–O_6 distance	Atomic population					
	H_1	H_3	H_5	H_6	H_7	CT[b]
2.0	0.910	0.703	0.755	0.526	0.905	−0.020
2.5	0.921	0.706	0.762	0.709	0.842	−0.018
3.0	0.925	0.707	0.765	0.760	0.820	−0.004
3.5	0.927	0.707	0.766	0.778	0.813	−0.001
∞	0.927	0.707	0.767	0.804	0.804	0.0

O_1–O_6 distance	Atomic population					
	O_1	O_2	C_3	C_4	N_5	O_6
2.0	6.576	6.516	3.504	4.097	5.303	6.589
2.5	6.518	6.537	3.514	4.096	5.299	6.467
3.0	6.511	6.543	3.519	4.094	5.298	6.424
3.5	6.507	6.545	3.522	4.094	5.298	6.410
∞	6.491	6.552	3.527	4.095	5.298	6.392

a) The numbering of the atoms is shown in Fig. 3.
b) The charge transfer quantity from glycine to water.

(C) Neutral form—model 1[a]

N_5–O_6 distance	Atomic population						
	H_1	H_2	H_4	H_5	H_6	H_7	CT[b]
2.0	0.787	0.995	0.872	0.540	0.767	0.767	0.007
2.5	0.778	0.972	0.835	0.761	0.789	0.788	−0.011
3.0	0.776	0.964	0.824	0.810	0.799	0.799	−0.003
3.5	0.775	0.962	0.821	0.830	0.802	0.802	−0.001
∞	0.775	0.961	0.819	0.840	0.804	0.804	0.0

N_5–O_6 distance	Atomic population					
	O_1	O_2	C_3	C_4	N_5	O_6
2.0	6.400	6.343	3.571	3.962	5.529	6.473
2.5	6.393	6.338	3.566	3.968	5.425	6.412
3.0	6.391	6.337	3.564	3.972	5.394	6.399
3.5	6.390	6.336	3.564	3.973	5.387	6.395
∞	6.386	6.344	3.556	3.971	5.385	6.392

a) The numbering of the atoms is shown in Fig. 3.
b) The charge transfer quantity from water to glycine.

(D) Neutral form—model 2[a]

O_1–O_6 distance	Atomic population						
	H_1	H_2	H_4	H_5	H_6	H_7	CT[b]
2.0	0.756	0.949	0.817	0.832	0.578	0.882	0.006
2.5	0.764	0.959	0.817	0.837	0.750	0.829	−0.009
3.0	0.770	0.962	0.818	0.839	0.790	0.812	−0.002
3.5	0.773	0.963	0.818	0.839	0.799	0.808	0.0
∞	0.775	0.961	0.819	0.840	0.804	0.804	0.0

O_1–O_6 distance	Atomic population					
	O_1	O_2	C_3	C_4	N_5	O_6
2.0	6.467	6.332	3.550	3.970	5.385	6.535
2.5	6.407	6.342	3.549	3.971	5.385	6.430
3.0	6.394	6.346	3.551	3.970	5.385	6.400
3.5	6.390	6.347	3.552	3.971	5.385	6.393
∞	6.386	6.344	3.556	3.971	5.385	6.392

a) The numbering of the atoms is shown in Fig. 3.
b) The charge transfer quantity from glycine to water.

oxygen becomes more negative, and the hydrogen-bonding proton, more positive; this is in contrast with the other atoms, the charge of which does not change considerably except in the case of a few atoms adjacent to the hydrogen bond. Therefore, the mutual electrostatic interaction can be considered to determine predominantly the charge redistribution of the molecule by the hydrogen-bond formation. The electronic structures at the intermolecular distance of 2.0 Å show a characteristic feature; that is, the charge distribution of the molecules at 2.0 Å is quite different from that at 2.5 Å because of the strong solute-solvent interaction; this is parallel with the sudden increase in the total energy indicated in Table 6.

The authors are grateful to Miss Fumiko Kitazumi for her assistance in the programming.

BULLETIN OF THE CHEMICAL SOCIETY OF JAPAN VOL. 42 3124—3130 (1969)

Effect of Halogens and Oxygen on the Emission of Thermal Positive Ions from the Tungsten Surface*1

Kumasaburo KODERA, Yoshifumi KITA,*2 Isao KUSUNOKI, Hiroshi KISHI and Atsuhiro SAKIYAMA

Department of Chemistry, Faculty of Science, Kyoto University, Sakyo-ku, Kyoto

(Received May 20, 1969)

The effect of chlorine, bromine, and oxygen on the emission of thermal positive ions from tungsten filaments has been studied. When a tungsten filament is heated in a vacuum, positive ion emission is always observed, and it cannot be removed completely by flashing the filament at high temperatures. This background ion emission increases greatly in halogen or oxygen. Main positive ions are K^+ and Na^+. The increase cannot be explained by the increase of the work function of tungsten by the formation of adsorbed layer of halogen or oxygen atoms. It is ascertained that the tungsten surface reacts with these gases and the reaction products evaporate as neutral particles. As the reaction proceeds, tungsten surface is removed successively and alkali metal atoms in the bulk are exposed to the surface and contribute to the positive ion emission.

For the measurement of the intensity of an alkali metal beam, surface ionization on a hot tungsten filament is usually utilized. This is an excellent method for the measurement of the alkali metal beam, because, in spite of the high ionization efficiency, it does not ionize residual gases in the vacuum system. However, even after the filament is flashed for a long time, background positive ion emission cannot be removed completely. The background positive ion emission increases markedly when halogen or halide molecules strike the filament. Sometimes this increase amounts to more than a hundred times the original background emission, and causes serious trouble in an experiment with halogen or halide crossed beam. Birely, Wilson, and Herschbach[1] have alluded to this phenomenon, but so far no detailed study has been published.

Hendrick, Phipps, and Copley[2] have studied the effect of halogens on the ionization of alkali metal atoms on a tungsten surface. They studied the ionization of potassium halide molecular beams on a tungsten filament and discussed the presence of potassium halide or halogen layer on the surface. Metlay and Kimball[3] studied the effect of fluorine molecules on the surface ionization of alkali metals on a tungsten surface and concluded that a stable fluorine layer was formed which increased the work function of the tungsten. Zmbov[4] found the increase of ionization efficiency of Mg and Al atomic beams on the tungsten surface when the filament was exposed to a stream of halogen molecules, and explained the fact by the increase of the work function of the tungsten. However, nothing is stated in his paper on the increase of the background ion emission. As a mass spectrometer was used for the detection of the ions, even if the background emission increased, it would not give any trouble so far as the background ions were different from Mg or Al.

In all these papers the increase of the ionization efficiency of the atoms hitting the surface was described, and the increase of the work function of the tungsten by the formation of an adsorbed layer of the halogen or alkali halide was assumed to be the cause of the increase. For the ionization of potassium, instead of Mg or Al in the case of Zmbov, the work function of even a clean tungsten surface is higher than the ionization potential of potassium. Therefore, according to the Saha-Langmuir equation, considerable part of potassium atoms which hit a tungsten surface should be ionized, and the large increase of the positive ion emission could not be expected.

The present study was undertaken to clarify the cause of the increase of the positive ion emission from the tungsten surface in halogen or oxygen atmosphere.

*1 This paper was presented to the 16th Annual Conference of Mass Spectrometry and Allid Topics, 1968, at Pittsburgh, held under the auspices of ASTM E-14.

*2 Present address: Faculty of Engineering, Osaka University, Suita-shi, Osaka.

1) J. H. Birely, R. R. Herm, K. R. Wilson and D. R. Herschbach, *J. Chem. Phys.*, **47**, 993 (1967).

2) J. O. Hendricks, T. E. Phipps and M. J. Copley, *ibid.*, **5**, 868 (1937).

3) M. Metlay and G. E. Kimball, *ibid.*, **16**, 776 (1948).

4) K. F. Zmbov, *Adv. Mass Spectrometry*, **3**, 765 (1966).

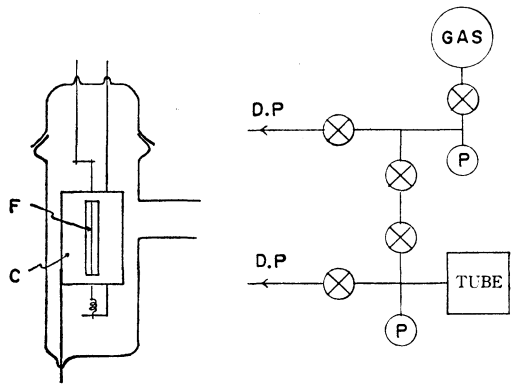

Fig. 1. Diode tube for the measurement of total positive emission and gas inlet system. F, filament; C, ion collector; P, Pirani gauge; D. P., diffusion pump.

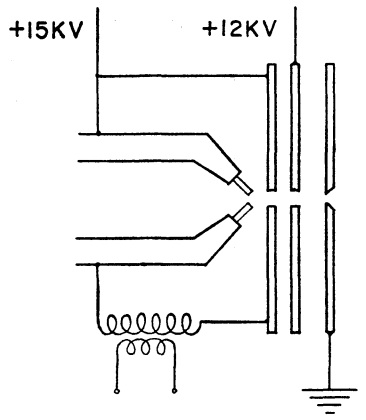

Spark lonization source

Fig. 2. Spark ion source.

Experimental

A diode tube shown in Fig. 1 was used to measure the increase of the total positive ion emission from a tungsten filament in halogen gas.

A Mattauch-Herzog type double focussing mass spectroscope was used for the analysis of impurities in tungsten filaments and for the identification of thermally emitted positive ions and neutral particles evaporated from the tungsten surface. Ilford Q-2 plates were used for the detection of the ions, and relative intensity of the ions was determined from the density of the lines on the plate by means of a microdensitometer.

For the analysis of the tungsten filament, bundles of about ten pieces of the filament each were fixed to the sample holder electrodes as shown in Fig. 2, and intermittent radio frequency voltage was applied between the electrodes for spark discharge ionization.

For the identification of thermal ions, the tungsten filament was fixed between the electrodes and heated by electric current. Halogen gases were introduced into the ion source through a glass tube from the outside. The end of the glass tube was drawn into a nozzle and placed just behind the filament as shown in Fig. 3 (a). Negative ions were also detected by reversing both the acceleration potential and the magnetic field.

To analyze neutral particles which evaporate from the filament, electron impact ionization by electrons emitted from the sample filament itself was utilized. 75 V was applied between the filament and the first slit to accelerate the electrons to ionize the neutral particles. The ions produced were accelerated and drawn into the analyzer by the negative potential applied on the second and the third slits as shown in Fig. 3 (b).

Two different samples of tungsten filament were used for the experiments, one of them was an ordinary doped filament of 0.13 mm diameter, and the other was a 0.18 mm diameter filament not doped with alkali. The latter was supplied from Matsushita Electronics Corporation.

The chemicals for the experiments were used without any treatment: Cl_2 and O_2, Takachiho Chemical Industry, pure: Br_2, Nakarai Chemicals, extra pure: K, Merck, extra pure.

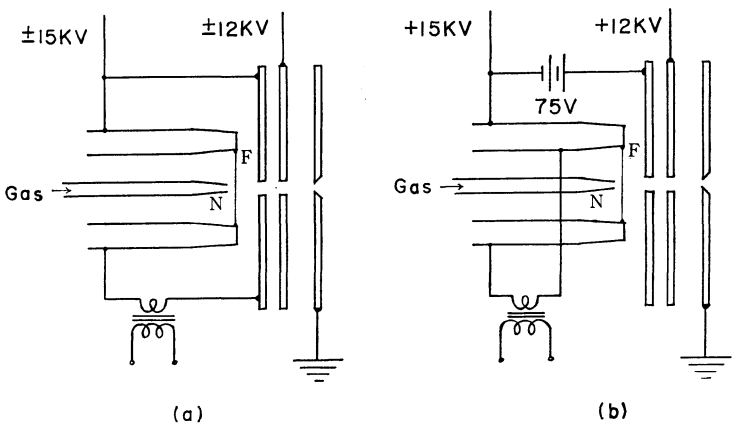

Fig. 3. (a) Surface ionization source with gas inlet nozzle, (b) electron bombardment source with gas inlet nozzle.

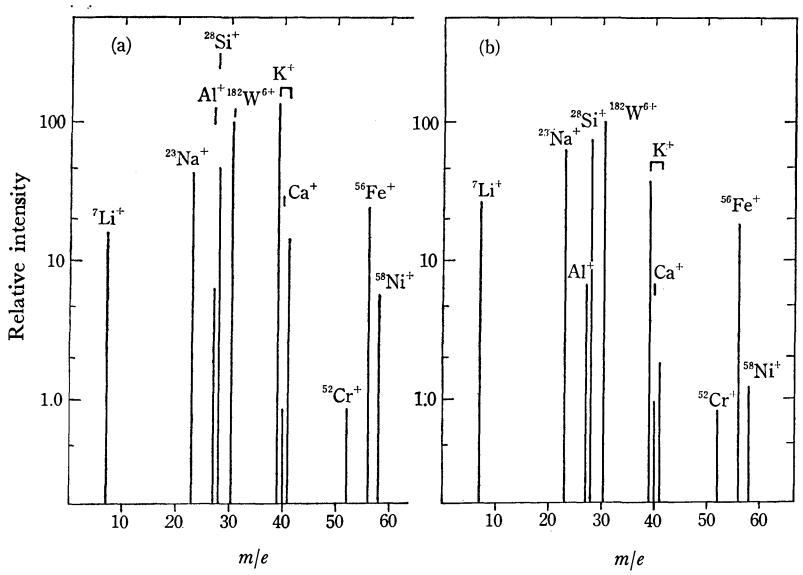

Fig. 4. Impurity spectra of tungsten filaments, (a) doped filamement, (b) undoped filament.

Results

Analysis of Impurities in the Tungsten Filaments. Mass spectra obtained by the spark discharge are shown in Fig. 4. (a) shows the result with the doped filament, and (b) shows that of the undoped filament. Both filaments contain K, Na, Li, Al, Si, Ca, Fe, Ni, and Cr as impurities. There is some difference in the quantitative distribution of these impurities between the two samples, but the difference is not remarkable. Therefore, it was found that unless a filament is manufactured particularly free of alkali metals, even an undoped filament contains some amount of alkali metal. As no precaution to remove surface contamination was taken before analysis, the impurities may include the surface contamination. Although a large difference of impurities was not observed between both filaments, after flashing, the background positive ion emission from the undoped filament was smaller than that of the doped one.

Total Positive Ion Emission. The total positive ion emission from the heated filament in vacuum and in halogen gas was measured by the diode tube shown in Fig. 1. The tungsten filament used here was the doped one. Before the measurement, the filament was flashed at about 2000°C for 30 min in a vacuum of 1×10^{-6} Torr. After the positive ion emission attained a constant value at a certain temperature, chlorine was introduced about 5×10^{-3} Torr by Pirani gauge, and then pumped out after a few minutes. The total positive ion emission during the procedure is shown in Fig. 5.

At the instant of introduction of chlorine, the positive ion emission increased for a moment and then decreased rapidly, but the final amount was greater than that before the introduction of the chlorine. When the chlorine was pumped out, the positive ion emission again decreased rapidly until it reached a value which was smaller than that before the introduction.

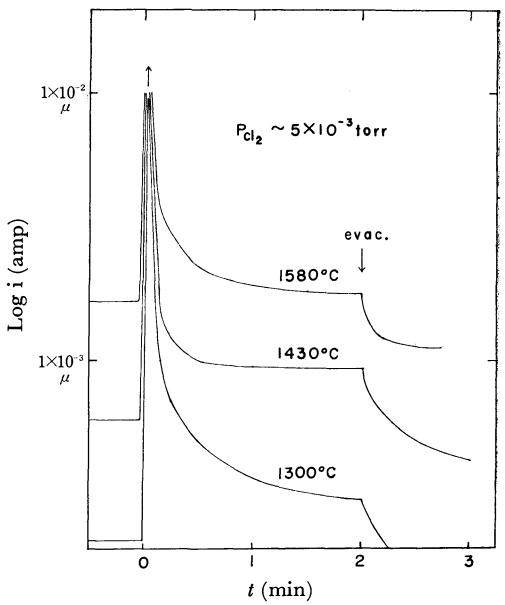

Fig. 5. Behavior of total positive ion emission in chlorine.

From these results, it was concluded that the positive ion emission in the chlorine is greater than that before the introduction and the increased background emission is greater at higher filament temperature.

Mass Spectroscopic Analysis of Thermally Emitted Ions. The thermally emitted ions from the tungsten filament were mass analyzed using the ion source shown in Fig. 3 (a). The doped filament was used for this purpose. Main ions observed were K^+ and Na^+. Quantity of the total ions measured by a monitor electrode of the mass spectroscope was larger by a hundred times in chlorine than in a vacuum.

Figures 6, 7, 8, and 9 show mass spectra of emitted positive ions. Figure 6 shows the spectra with and without chlorine under the same exposure time. In chlorine, intensity of K^+ increased greatly, and Cr^+, Ca^+, Fe^+, Cl^+ and Cl_2^+ were also observed. In Fig. 7, the effect of bromine for the same exposure is given. In bromine, emission of K^+ and Na^+ increased, and Al^+, Si^+, Cr^+, Mn^+, Fe^+, Co^+, Ni^+, Br^+, and Br^{2+} were observed.

Negative ions formed by surface ionization were also examined, but only Cl^- and Br^- were detected.

In Fig. 8, the emission from the doped filament in oxygen and in a vaccum is compared. In oxygen, emission of K^+ and Na^+ increased greatly as in chlorine and bromine. Difference in the

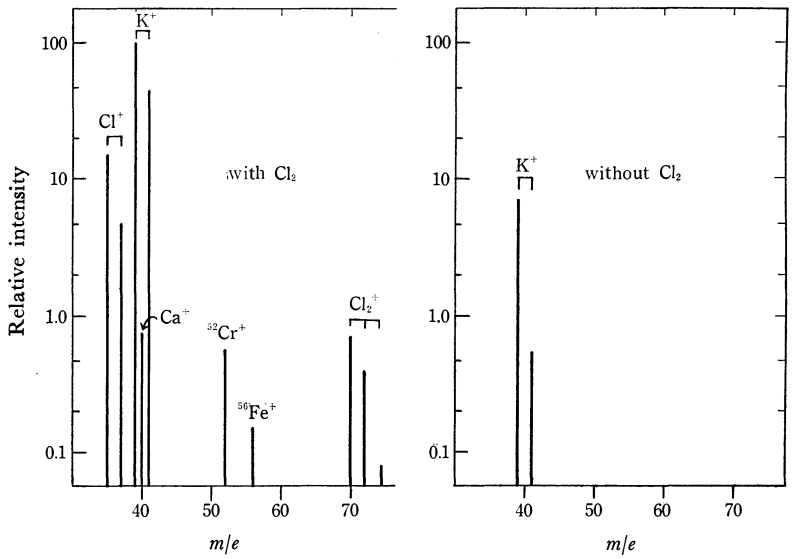

Fig. 6. Surface ionized ions from a doped filament, (a) in chlorine, (b) without chlorine.

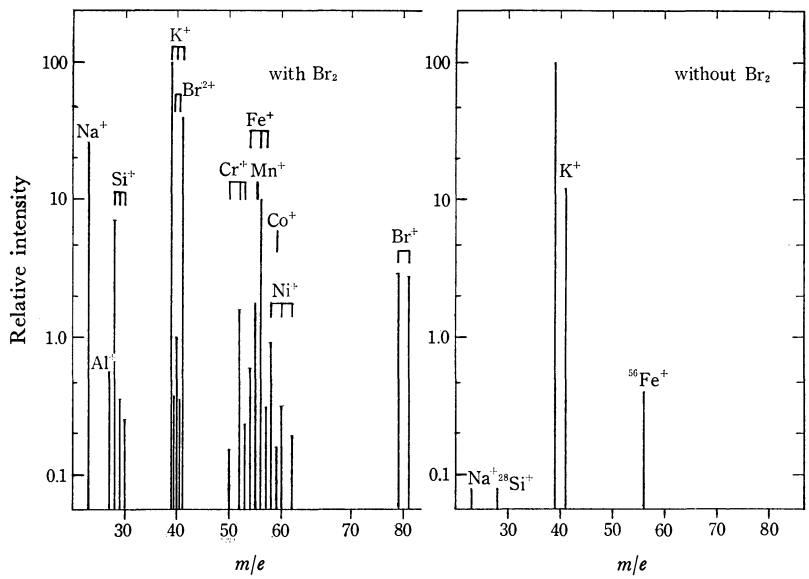

Fig. 7. Surface ionized ions from a doped filament, (a) in bromine, (b) without bromine.

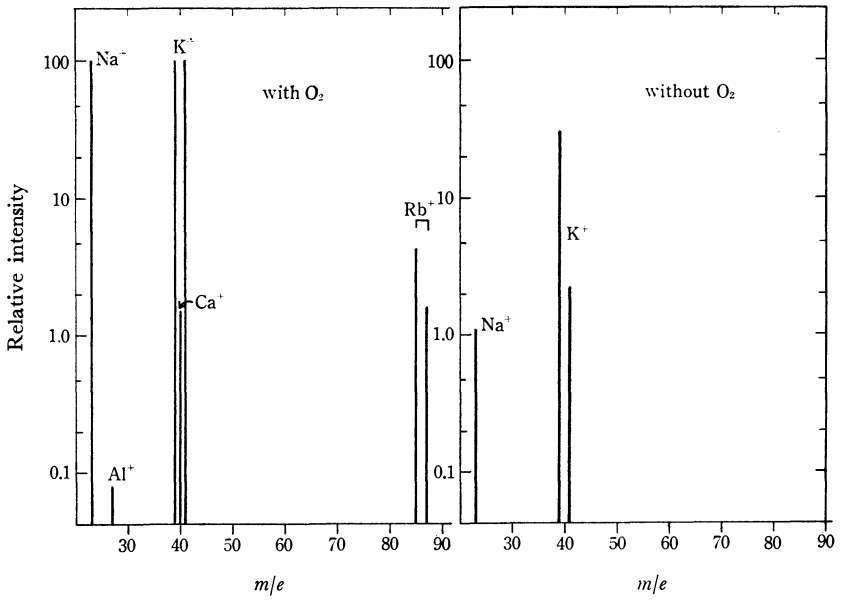

Fig. 8. Surface ionized ions from a doped filament, (a) in oxygen (b) without oxygen.

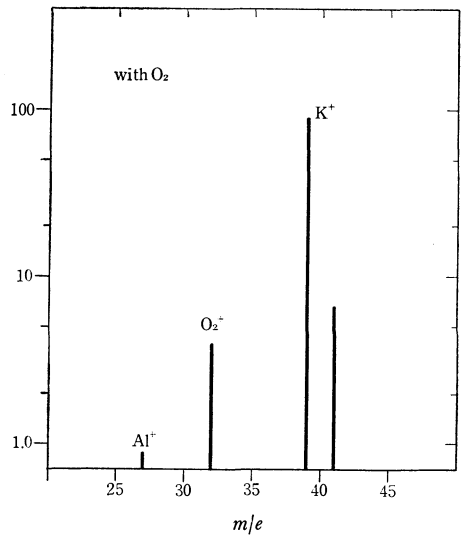

Fig. 9. Surface ionized ions from an undoped filament in oxygen.

emission in oxygen and in halogen is that no metal ions other than a small amount of Al^+ was observed in case of the former. With doped filament shown in Fig. 9, O_2^+ was detected. In both cases O^+ was out of the range of detection, and it is not certain that this ion was emitted or not. In some cases Rb^+ was found in oxygen but it was not possible to conclude under what condition Rb^+ emission could be detected, because the number of runs in oxygen was not enough. In runs with chlorine and bromine, Rb^+ was out of the range of detection.

In the above experiments, no ion of the reaction product of tungsten and halogen or oxygen were found. Therefor, it is expected that tungsten halides or oxides formed evaporate as neutral particles.

Identification of Neutral Particles by Mass Spectroscopy. Mass spectrum of neutral particles formed in chlorine is shown in Fig. 10. Ions of tungsten atoms, tungsten oxides, tungsten chlorides, and tungsten oxychlorides were observed. The detected species are W^+, WO^+, WOH^+, WO_2^+, WCl^+, WO_2Cl^+, WCl_2^+, $WOCl_2^+$, $WO_2Cl_2^+$, WCl_3^+, $WOCl_3^+$, ($WO_2Cl_3^+$), WCl_4^+, and WCl_5^+. Thus, it is confirmed that the chlorine reacted with the tungsten filament and products formed evaporated as neutral particles.

In Fig. 11, neutral particles formed in oxygen are shown. WO^+ and WO_2^+ were found in addition to W^+, but not WO_3^+.

Discussion

By the experiment of the thermal emission, Cl^+, Br^+, Cl_2^+, Br^{2+}, and O_2^- were found. As these atoms or molecules have higher ionization potentials than the electron affinity of tungsten or oxidized tungsten, it is impossible to assume that these ions were formed by the surface ionization from the standpoint of the Saha-Langmuir equation. A more probable explanation is that these ions were formed by the ion impact of chlorine, bromine or oxygen molecules around the filament, because increased positive ions (mainly alkali metal ions) could be accelerated sufficiently by the ion acceleration potential of 15 keV to ionize these molecules.

In the neutral particles evaporated from the

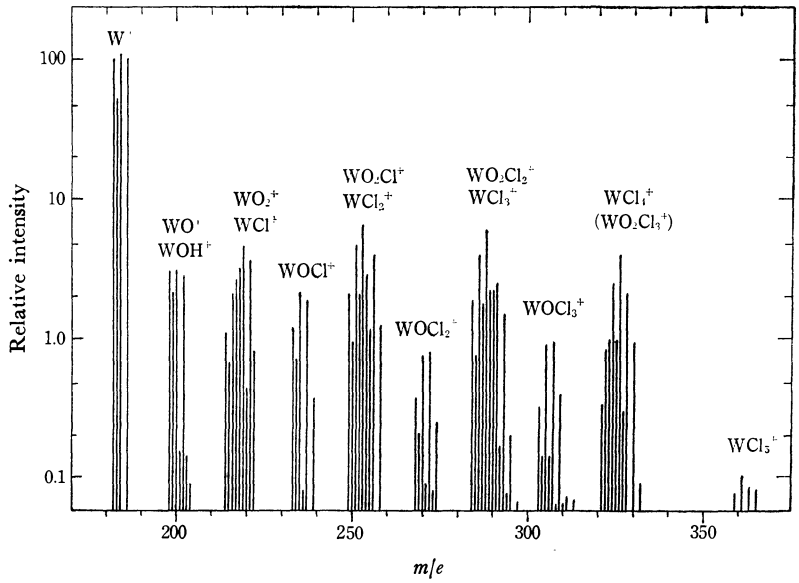

Fig. 10. Mass spectrum of neutral particles from a doped filament in chlorine.

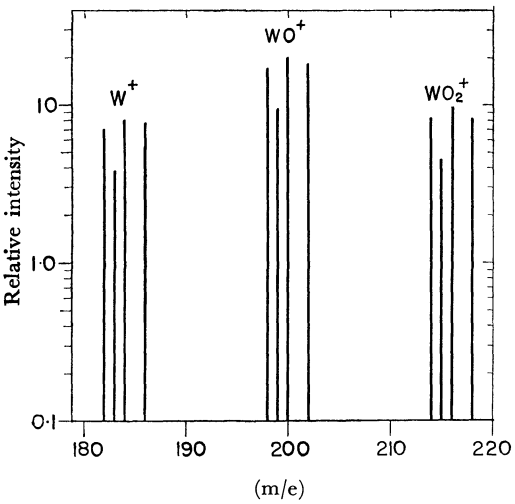

Fig. 11. Mass spectrum of neutral particles from a doped filament in oxygen.

filament in chlorine, many oxygen containing compounds were found. The origin of the oxygen should be traced. Probable sources of oxygen are the residual oxygen or water vapor in the ion source chamber, impurity in the chlorine, and the oxygen contained in the tungsten filament.

During the runs, vacuum in the ion source chamber was about 3×10^{-6} Torr and the amount of oxygen in the compounds was comparable with that of chlorine, so it is difficult to attribute the source of the oxygen entirely to the residual gas. However, there might be some contribution of the water vapor, because some hydroxy compound was seen in the mass spectrum. Impurity in the chlorine is not probable either, bacause pure sample was used and gas inlet system was evacuated carefull before the introduction of chlorine.

During the process of manufacture of tungsten filament, there are many chances that oxides are mixed. For this experiment, doped filament was used. In the process of doping, K, Na, Si, and Al are added to the tungsten powder in the form of salts. These salts are converted into oxides during the manufacturing procedure. Since the filament contains oxygen and impurities in approximately equivalent amount, it may be considered the most probable source of the oxygen.

In oxygen, W^+, WO^+, and WO_2^+ were observed as mentioned above. Berkowitz-Mattuck *et al.*[5] studied the reaction of oxygen with heated tungsten surface. They heated a piece of tungsten plate from the back by thermal radiation and electron bombardment from a W-Re filament placed behind it. A stream of oxygen from a nozzle was applied against the heated surface and neutral particles evaporated from the surface was introduced into the ion source of a mass spectrometer before any collision had occurred in the gas phase and were ionized by electron impact and mass analyzed. Oxides produced at the temperature region of 1500—2600° K were studied. Main oxides found were WO_2 and WO_3. At high temperatures WO_2 was more abundant than WO_3, but no WO was found. They proved that WO_2 was not a fragmentation product of WO_3. In a run under oxygen pressure of 7.2×10^{-4} Torr, the amount of WO_3 was

5) J. B. Berkowitz-Mattuck, A. Büchler, J. L. Engelke and S. N. Goldstein, *J. Chem. Phys.*, **39**, 2722 (1963).

maximum at 1875° K and that of WO_2 was maximum at 2200° K. At 2600° K, almost no WO_3 was seen.

As the sample filament was used as an electron emitter in the present experiment, the filament temperature was considerably high. The filament temperature could not be measured, but it might be considerably higher than 2600° K considering from the heating current. At this temperature, existence of lower oxides WO may be probable. Existence of WO^+ has been observed by Bennighoven[6] and Rybalko, Kalot, and Fogel',[7] although their experiments were somewhat different from the present ones. In these studies, oxidized tungsten surface was bombarded by Ar^+. W^+, WO^+, WO_2^+, and WO_3^+ were found by Benninghoven, and in addition ot these oxides, many other oxides were found by Rybalko *et al.*

It should be noticed that the ions observed under the electron bombardment might come from the first slit surface where the tungsten compounds might deposit while the filament was heated in the gases. But the existence of the deposit also indicates that some neutral tungsten compounds were evaporated from the filament.

It is difficult to attribute the unusual increase of positive ion emission from the heated tungsten surface in chlorine, bromine, and oxygen to the increase of the work function of tungsten by adsorbed halogen or oxygen, because, as mentioned above, the ionization efficiency of potassium on clean tungsten surface should be high and no great increase of the positive ion emission can be expected. However, for the emission of metal ions other than alkali metals, the increase of the work function may be responsible. Therefore, an entirely different mechanism should be considered.

When halogen is introduced around the tungsten filament, it reacts with the tungsten surface and tungsten halides and oxyhalides will evaporate as the reaction products. By the evaporation of these products, alkali metal atoms contained in the bulk of the tungsten are exposed to the surface and emitted as positive ions. In Fig. 5, it is seen that, when chlorine is introduced, the positive ion emission increased for the moment and decreased rapidly again. This means there is a concentrated layer of alkali metal atoms at the filament surface, and removal of the surface by the reaction causes the sudden increase of the positive ion emission. When the filament is heated at high temperatures, alkali metal atoms inside the bulk diffuse towards the surface and evaporate. The difference between the diffusion rate and the evaporation rate will build a concentrated layer of alkali metal atoms just under the surface. After the concentrated layer of alkali metal atoms are removed by the reaction, rate of the emission of the positive ions is controlled by the corrosion rate of the tungsten by chlorine. But without chlorine, the emission rate is controlled by the diffusion rate of alkali metal atoms in the bulk of the tungsten.

6) A. Benninghoven, *Z. Physik*, **220**, 159 (1969).

7) U. F. Rybalko, V. Ja. Kolot and Ja. M. Fogel' will be presented to the International Conf. on Mass Spectrometry, Kyoto (1969).

BULLETIN OF THE CHEMICAL SOCIETY OF JAPAN VOL. 42 3131—3134 (1969)

On the Viscosity of Liquid Oligotrifluorochloroethylene

Naosato Yoshida, Shuichi Hamada and Toshiaki Shirai

Department of Chemistry, Faculty of Science, Science University of Tokyo, Kagurazaka, Shinjuku-ku, Tokyo

(Received May 22, 1969)

The viscosities and densities of liquid oligotrifluorochloroethylene were measured over a molecular-weight range from 820 to 1090 at temperatures from 40°C to 100°C. The temperature-dependences of the viscosities did not show an Arrhenius-type variation, but were extremely adaptable in the WLF equation; *i. e.*, a viscoelastic behavior was shown under the present experimental conditions. The apparent activation energies, ΔH_a, for the viscous flow of the liquid samples were comparatively large and increased with an increase in the number-average molecular weight. The logarithm of the viscosity, $\log \eta$, varied linearly with the logarithm of the number-average molecular weight, $\log \eta = A \log M_n + B$. The slopes, A, of the linear relationships were estimated to be 11.0, 10.4, 9.3, and 8.4 at 50, 60, 70, and 80°C respectively. The values of the slopes, A, were very much larger than unity in the case of usual organic polymers below the critical values of the molecular weight, and they decreased with an increase in the temperature.

Polytrifluorochloroethylene is a chain polymer with only fluorine and chlorine atoms on the side of the carbon chain, and so the lone-pair electrons surrounding the chain molecules may be expected to have effects on their physical properties. In many respects, polytrifluorochloroethylene has peculiar properties compared with those of usual organic polymers; for example, its thermal and chemical stabilities are unusual. Though a highly-polymerized trifluorochloroethylene is a rigid plastic material and is insoluble in many solvents,[1] the trifluorochloroethylene oligomers are oily, grease-like, and wax-like at room temperature, and they are soluble in various solvents. In this work, the properties of the liquid oligomers will be studied in order to establish those of polytrifluorochloroethylene.

Experimental

Materials. The Daifloil No. 20 and No. 50, which were obtained from the Daikin Kogyo Company, were used as the samples of oligotrifluorochloroethylene.

The precipitation method was employed to fractionate the oligotrifluorochloroethylene using an acetone and water as the solvent and the precipitant respectively. A suitable quantity of water was added to an acetone solution of the sample, and the mixture was stirred at about 30°C. The precipitates were dissolved by again heating the mixture about 55°C, and then the mixture was allowed to stand for about 5 hr at 30°C. The fractionated precipitates were separated, and then a great quantity of methanol was added to them in order to separate the precipitates easily. The precipitates were decanted repeatedly with methanol and were dried at 30°C *in vacuo*. The number-average molecular weights of the fractionated oligotrifluorochloroethylene were estimated to be from 820 to 1090 by the cryoscopic method, using a benzene as the solvent.

Procedure. The viscosities and the densities of the liquid samples were measured at temperatures from 40°C to 100°C in the manner described in a previous paper.[2]

The viscosity, η_θ, at the tilting angle, θ, of the Ubbelohde-type viscometer was calculated by the following equation:

$$\eta_\theta = A_\theta \rho t$$

where A_θ, ρ, and t are the parameter of the viscometer, the density of the liquid sample, and the efflux time respectively. The parameter, A_θ, of the viscometer was estimated by measuring the efflux time of the standard liquid of a known viscosity at 30°C and at various tilting angles, θ. The viscosities, η_θ, of the liquid samples were measured at several tilting angles. The densities of the liquid samples were measured with the U-type densimeter described in a previous paper.[2] The viscosities and densities of the liquid samples were measured at specified temperatures within an accuracy of ± 0.01°C in thermostated baths of silicone oil and water.

The linear expansion coefficient of the densimeter was 7.95×10^{-7}°C^{-1} over the temperature range from 30°C to 50°C, while those of the liquid oligotrifluorochloroethylene were calculated to be about 3×10^{-4}°C^{-1} over the temperature range from 40°C to 100°C. Therefore, the expansion of the densimeter was negligible compared with that found with the liquid samples.

Results

The thermal degradation of the oligotrifluorochloroethylene was considered to result from heating

1) H. T. Hall, *J. Am. Chem. Soc.*, **74**, 68 (1952).

2) S. Hamada, N. Yoshida and T. Shirai, This Bulletin, **42**, 1025 (1969).

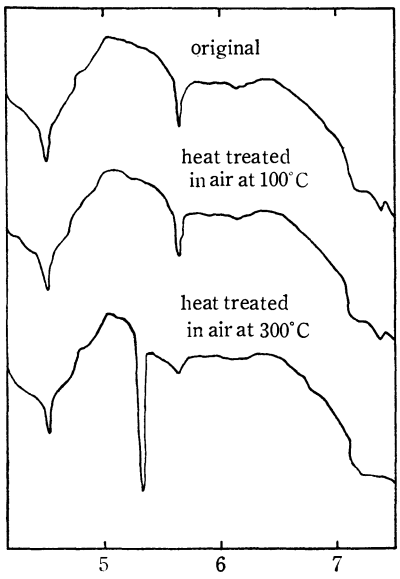

Fig. 1. IR spectra of original and heat-treated samples.

in the atmosphere.[3] Figure 1 shows the IR spectra of the sample with the molecular weight of 1090. A sharp absorption band assigned to an acid fluoride group at 5.31 μ coming from the thermal degradation was not observed in the sample heated at 100°C for 10 hr, as is shown in Fig. 1. Therefore, the measurements were carried out below 100°C, since the influence of the thermal degradation was considered to be negligible under these conditions.

The Viscosities of the Liquid Oligotrifluorochloroethylene. The viscosities, η_θ, of the liquid samples at several tilting angles were measured at temperatures from 40°C to 100°C. Table 1 shows the viscosities, η_θ, of the fractionated sample with the number-average molecular weight of 1090 at 70, 85, and 100°C, and at several tilting angles, θ_n.

The tilting angles, θ_n, represent the relative angles of the capillary of the viscometer to the vertical line, and they increase with an increase in the subscript, n; the difference between θ_5 and θ_1 is 45°. The viscosities, η_θ, were nearly constant regardless of the variation in θ_n, *i. e.*, the variation in the rate of shear. The viscosities of the other fractionated liquid samples showed the same appearance as that of the sample, $M_n=1090$. Therefore, liquid oligotrifluorochloroethylene are considered to behave as a Newtonian liquid under these experimental conditions.

Table 1. Dependence of viscosities on tilting angles

Tilting angle, θ_n	Viscosities, η_θ, poise		
	70°C	85°C	90°C
θ_1	11.8_1	4.03_1	
θ_2	11.8_0	4.03_1	1.61_0
θ_3	11.8_1	4.03_9	1.60_9
θ_4		4.03_0	
θ_5	11.8_0	4.02_9	

Table 2. Viscosities of oligotrifluorochloroethylene

Molecular weight, M_n	Viscosities, η, poise						
	40°C	50°C	60°C	70°C	80°C	90°C	100°C
820	6.43	3.04	1.51				
860	10.78	4.73	2.33	1.42	0.717		
870	15.81	6.65	3.15	1.88	0.916		
890	22.39	9.18	4.23	2.13	1.17	0.698	
1010		29.53	12.61	5.90	2.98	1.63	
1030		40.52	16.60	7.52	3.77	2.01	1.14
1050		55.90	21.62	9.49	4.61	2.44	1.36
1070			23.20	10.31	5.03	2.63	1.51
1090			27.45	11.81	5.64	2.94	1.61

The viscosities of the fractionated liquid samples are given in Table 2.

The Temperature-dependences of the Viscosities. The temperature-dependences of the viscosities, η, did not show an Arrhenius-type variation under these conditions. Therefore, the temperature-dependences of the viscosities, η were treated with the WLF equation, $\log a_T=-C_1^0(T-T_0)/(C_2^0+T-T_0)$.[4]

Figure 2 shows the relationships between $(T-T_0)$ and $(T-T_0)/\log a_T$. The shift factors, a_T, which were expressed to be $\rho_0\eta T_0/\rho\eta_0 T$, were calculated

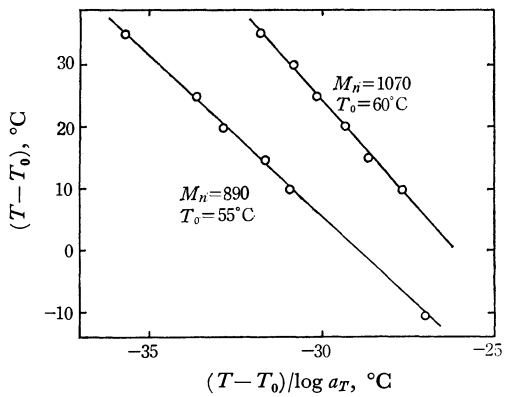

Fig. 2. Relationship between $(T-T_0)$ and $(T-T_0)/\log a_T$.

3) M. Iwasaki, M. Aoki and R. Kojima, *J. Polymer Sci.*, **25**, 377 (1957).

4) M. L. Williams, R. F. Landel and J. D. Ferry, *J. Am. Chem. Soc.*, **77**, 3701 (1955).

on the basis of a voluntary fixed temperature, T_0, because the glass-transition temperatures, T_g, of the fractionated samples were not known. The linear relationship shown in Fig. 2 makes it obvious that the temperature-dependences of the viscosities were extremely adaptable in the WLF equation. Therefore, the viscoelastic behavior was shown in the viscous flow of the liquid samples over the temperature range from 40°C to 100°C. The WLF parameters, C_1^0 and C_2^0, were estimated on the basis of T_0 from the linear relationships in Fig. 2, while the apparent activation energies, ΔH_a, for the viscous flow were estimated from the following equation:

$$\Delta H_a = 2.303 R C_1^0 C_2^0 T^2/(C_2^0 + T - T_0)^2$$

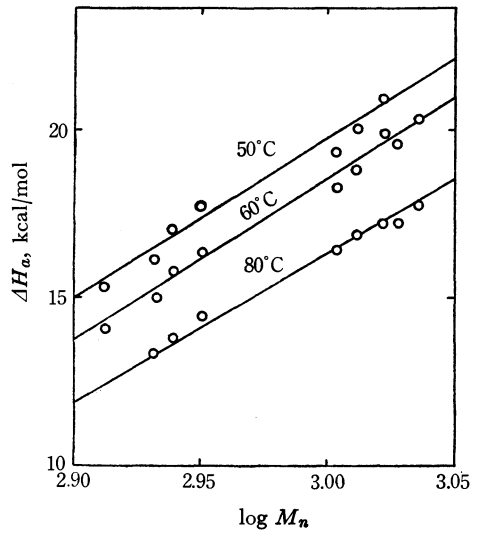

Fig. 3. Dependence of apparent activation energy for viscous flow on log M_n.

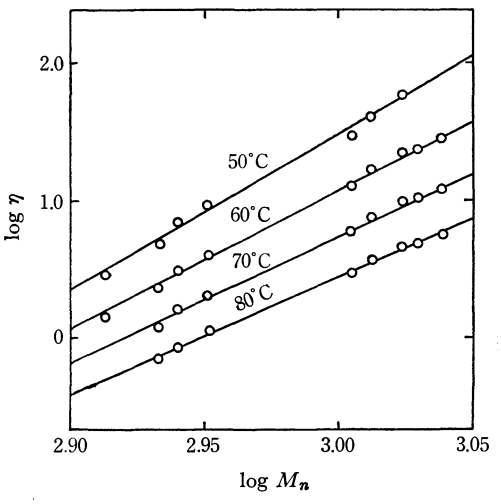

Fig. 4. Dependence of log η on log M_n.

Figure 3 shows the dependence of ΔH_a on the molecular weight. The apparent activation energy, ΔH_a, for the viscous flow increased linearly with an increase in the logarithm of the molecular weight, log M_n.

The Molecular-weight Dependences of the Viscosities. The dependences of the viscosities on the molecular weight are shown in Fig. 4. The logarithm of the viscosity, log η, varied linearly with the logarithm of the number-average molecular weight, log M_n. The linear relationships at the specified temperatures could be expressed as follows:

$$\log \eta = A \log M_n + B^{5)}$$

The slopes, A, of the linear relationships were very much larger than unity at lower temperatures, unlike the case of usual organic-polymers below the critical values of the molecular weights, and they decreased with an increase in the temperature, as is shown in Table 3.

Table 3. Slopes, A, of linear relationships

Temp., °C	50	60	70	80
A	11.0	10.4	9.3	8.4

Discussion

The relationship between the viscosity and the free volume is satisfactorily described by the Doolittle equation:[6,7]

$$\ln \eta = \ln P + Q(v - v_f)/v_f$$
$$= \ln P + Q/f$$

where P and Q are the empirical constants; v, the specific volume; v_f, the free volume, and f, the fraction of the free volume. The fraction of the free volume, f, at T is expressed as follows:

$$f = f_g + \alpha_f (T - T_g)$$

where f_g is the fraction of the free volume at T_g, and α_f, the thermal expansion coefficient of the free volume. All the oligotrifluorochloroethylenes used in the study are quite small in number-average molecular weight; $M_n \leq 1090$. In general, the melting points of the lower-molecular-weight oligomers rise remarkably with an increase in the molecular weight; also, their glass-transition temperatures, T_g, are considered to show a tendency similar.[8] Particularly the glass-transition temperatures of the oligotrifluorochloroethylene rise remark-

5) T. G. Fox and P. J. Flory, *J. Chem. Phys.*, **55**, 221 (1951).

6) A. K. Doolittle, *J. Appl. Phys.*, **22**, 1471 (1951); *ibid.*, **23**, 236 (1952).

7) A. K. Doolittle and D. B. Doolittle, *J. Appl. Phys.*, **28**, 901 (1957).

8) T. G. Fox and P. J. Flory, *J. Appl. Phys.*, **21**, 581 (1950).

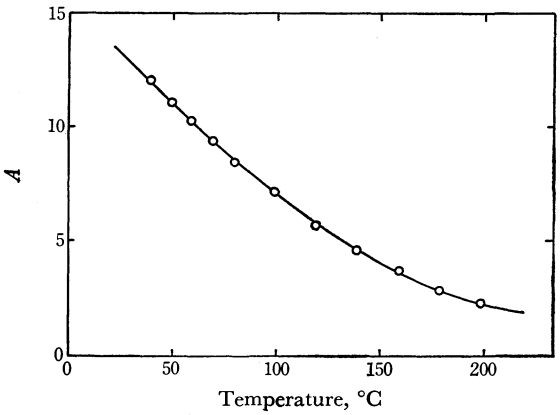

Fig. 5. Temperature dependence of slope, A, of linear relationship.

ably as the molecular weights increase; in fact, the states of the samples at room temperature depend notably on the molecular weight. They are all oily, grease-like, and wax-like, in spite of the small range of molecular weight (from 820 to 1090).

Thus, since a large dependence of the fraction of the free volume, f, on the molecular weight at specified temperatures may be expected, the viscosity will rise remarkably with an increase in the glass-transition temperature in the lower-molecular-weight range. The slopes, A, of the linear relationships in Table 3, which indicated the dependences of the viscosities on the molecular weights, show large values at lower temperatures. The large values of A are caused by the large dependence of the fraction of the free volume on the molecular weight. Though the slopes, A, were very much larger than unity at the lower temperatures, they gradually decreased as the temperature was elevated; they were considered finally to approach a certain value, A_0, as is shown in Fig. 5. The values, A, above 100°C were calculated from the WLF equation. The decrease of A with an increase in the temperature is caused by the decrease in the dependence of the fraction of the free volume on the molecular weight as the temperature is elevated.

Large dependences of the viscosities on the molecular weights have also been reported for the oligostyrene and oligoisobutylene.[5,9] For example, the A values of the oligoisobutylene over the molecular-weight range from 530 to 2190 were estimated to be 5.45, 3.08, and 1.75 at 0, 30, and 217°C respectively.

The liquid organic-chain polymers, in general, show comparatively small values of the apparent activation energies for the viscous flow, though they increase with an increase in the bulk of the side chains.[10] The comparatively large values of ΔH_a for oligotrifluorochloroethylene, with no branched chain, are considered to be caused by a high rotational barrier about carbon-carbon bonds which is to be attributed to the lone-pair electrons of fluorine and chlorine atoms.

9) T. G. Fox and P. J. Flory, *J. Polymer Sci.*, **13**, 315 (1954).

10) H. Schott, *J. Appl. Polymer Sci.*, **6**, S29 (1962).

BULLETIN OF THE CHEMICAL SOCIETY OF JAPAN VOL. 42 3135—3140 (1969)

Infrared Study of Rotational Isomers of *meso*- and *racemic*-2,3-Dibromobutane

Kazuyoshi IIMURA

Department of Chemistry, Faculty of Science, Science University of Tokyo, Kagurazaka, Shinjuku-ku, Tokyo

(Received June 4, 1969)

The infrared spectra of *meso*- and *racemic*-2,3-dibromobutanes in solution and in gaseous states were obtained in the study of the rotational isomers. The occurrence of three rotational isomers was confirmed for both *meso*- and *racemic*-isomers. The quantitative estimation of the equilibrium concentrations of the rotational isomers was also made in various solvents. The energy difference between the rotational isomers was determined by measuring the temperature-dependence of the absorption intensities of ν(C–Br) vibrations.

In our infrared investigation of *meso*- and *racemic*-2,3-dichlorobutanes,[1] it has been shown that three rotational isomers exist for both *meso*- and *racemic*-isomers, and that the equilibrium concentrations change depending upon the solvent dielectric constants.

In the present study the infrared spectra of *meso*- and *racemic*-2,3-dibromobutanes, the molecular structures of which are analogous to those of *meso*- and *racemic*-2,3-dichlorobutanes, will be observed, and the conformational equilibria of the rotational isomers in solvents of different dielectric constants and the energy difference between the rotational isomers in the gaseous state will be investigated.

The existence of three rotational isomers for both *meso*- and *racemic*-isomers has been established by studies of the Raman spectra[2] and of the nuclear magnetic resonance (NMR).[3,4] However, in these investigations, no quantitative spectroscopic estimation of the conformational equilibria in various solvents, or of the difference in energy between the rotational isomers were made. In the recent NMR investigation of *meso*-2,3-dibromobutane reported by Deb,[5] the energy difference between the rotational isomers was determined to be 1.0 kcal/mol. However, this value seems too small compared with that of 1,2-dibromoethane.

Experimental

The *meso*- and *racemic*-2,3-dibromobutanes (hereafter abbreviated as *meso*- and *racemic*-DBB respectively) were prepared by the addition of bromine to *trans*- and *cis*-butene-2 (Matheson Co.; purity, 99.8%) at −15—−18°C. The materials were distilled, and the fractions with boiling points of 73.0—75.0°C/55 mmHg for the *meso* isomer and of 77.0—79.0°C/60 mmHg for the *racemic* isomer were collected (reported boiling points: *meso*, 74—74.2°C/50 mmHg; *racemic*, 75.6°C/50 mmHg[6]). The NMR spectra of the materials were completely identical with those observed by Bothner-By and Naar-Colin[3] and by Anet.[4] A gas-chromatographic analysis indicated also that the purity is more than 99% for both isomers. The infrared spectra were recorded mainly for the region of 800—400 cm^{-1} using a Hitachi EPI-2 double-beam spectrophotomer with a KBr prism. Spectral observation was also made in the region of the NaCl prism for reference. In measuring the solution spectra, the absorption due to the solvent was compensated for by a variable-thickenss cell filled with the solvent. The gas-phase spectra were obtained using a gas cell with an optical path-length of 7 cm and with a heating device.

Results and Discussion

ν(C-Br) Bands and Rotational Isomers. As Fig. 1 shows, it is possible for three rotational isomers to exist in both *meso*- and *racemic*-DBB. The conformations of the rotational isomers are designated by T, G, or G′, indicating whether the carbon chains are located *trans* or *gauche*. As for the *meso*-isomer, MG and MG′ are mirror images of each other and are not different in their infrared spectra.*1

The ν(C–Br) vibrations for bromine attached to the secondary carbon atom are usually observed in the region of 620—520 cm^{-1}; they appear at different frequencies depending upon the conformational

1) K. Iimura, M. Kawakami and M. Takeda, This Bulletin **42**, 2091 (1969).

2) N. J. Taufen, M. J. Murray and F. F. Cleaveland, *J. Am. Chem. Soc.*, **65**, 1130 (1943).

3) A. A. Bothner-By and C. Naar-Colin, *ibid.*, **84**, 743 (1962).

4) A. L. Anet, *ibid.*, **84**, 747 (1962).

5) K. K. Deb, *J. Phys. Chem.*, **71**, 3095 (1967).

6) S. Winstein and H. J. Lucas, *J. Am. Chem. Soc.*, **61**, 1577 (1939).

*1 Hereafter the term MG will be used to represent two *gauche* forms, MG and MG′.

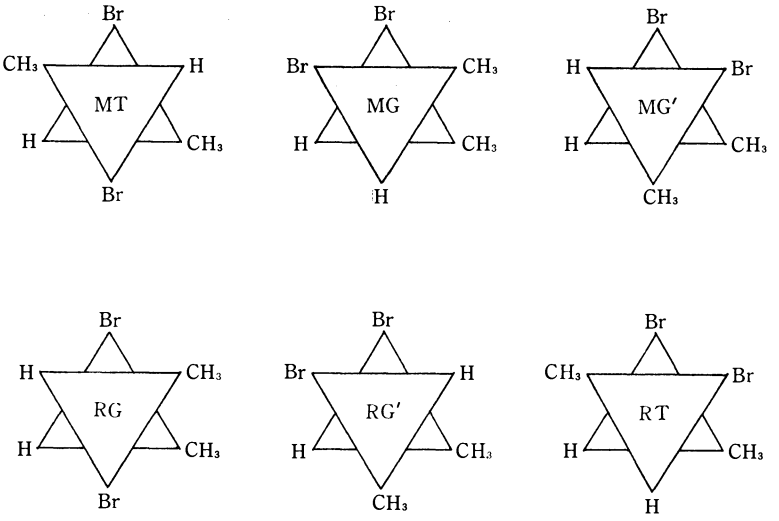

Fig. 1. The posible conformations of rotational isomers.

structures of the rotational isomers.[7,8] Figure 2 shows the infrared spectra of *meso*- and *racemic*-DBB in the pure liquid state. The strong band at 552 cm^{-1} and the weaker band at 600 cm^{-1} of *meso*-DBB, and the two strong bands at 561 and 543 cm^{-1} of *racemic*-DBB, can be assigned to the ν(C-Br) vibrations. The absorption band at 635 cm^{-1} of *meso*-DBB and those at 648 and 632 cm^{-1} of *racemic*-DBB are found somewhat apart from the ν(C-Br) region. However, these absorption bands can safely be assigned to the ν(C-Br) vibrations, because the infrared spectra in the NaCl region of *meso*- and *racemic*-DBB correspond fully to those of *meso*- and *racemic*-2,3-dichlorobutanes respectively[9] and because the frequencies of these absorption bands are too low to be assigned to the CH_3 rocking vibrations. The frequencies associated with the skeletal bending modes occur, in general, below 500 cm^{-1}. The bands at 466 cm^{-1} of *meso*-DBB and at 444 cm^{-1} of *racemic*-DBB are assigned to these modes. The weak band at 502 cm^{-1} of *racemic*-DBB is perhaps due to the skeletal bending mode.

We have calculated the dipole moment of the rotational isomers by means of the method proposed by Miyagawa.[10] The values thus calculated are listed in Table 1. In accounting for the difference in dipole moment, it can be said that the population of the rotational isomers in solution changes because it is affected by a reaction field induced by the solvent molecules.[11] The assignment of ν(C-Br) bands to each of the rotational isomers, therefore, becomes possible if we measure the intensity change of these bands in a different solvent, because a

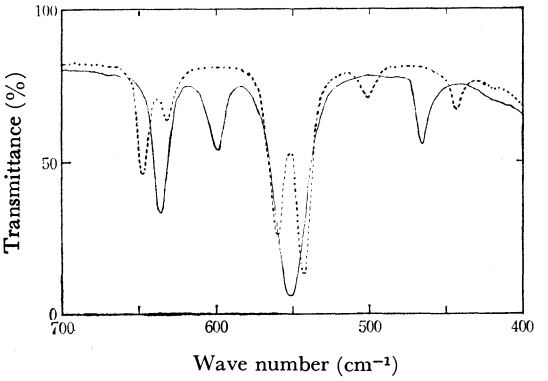

Fig. 2. Infrared spectra in liquid state.
Full line;*meso*-DBB, broken line; *racemic*-DBB.

TABLE 1. CALCULATED DIPOLE MOMENTS (in D. U.) FOR *meso*- AND *racemic*-2,3-DIBROMOBUTANES

Isomer	Chain conformation	Dipole moment
meso-DBB	MT	0
	MG	2.78
	MG'	2.78
racemic-DBB	RG	1.08
	RT	2.24
	RG'	3.30

7) K. Nakamura, *Nippon Kagaku Zasshi (J. Chem. Soc. Japan, Pure Chem. Sect.)*, **78**, 1164 (1957).
8) F. F. Bentley and N. T. McDevitt, *Spectrochim. Acta*, **20**, 105 (1964).
9) K. Iimura, M. Kawakami and M. Takeda, unpublished data.
10) I. Miyagawa, *Nippon Kagaku Zasshi (J. Chem. Soc. Japan, Pure Chem. Sect.)*, **75**, 1165 (1954).
11) I. Watanabe, S. Mizushima and Y. Mashiko, *ibid.*, **64**, 962 (1943).

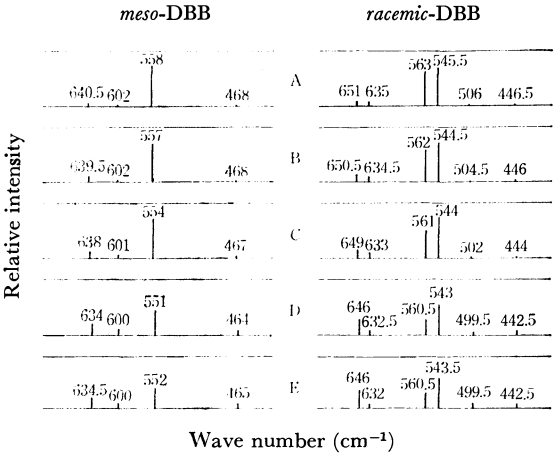

Fig. 3. Infrared spectra in various solvents.
A, *n*-hexane; B, cyclohexane; C, carbon disulfide, D, cyclohexanone; E, acetonitrile.
Temperature, 29°C, Concentration, 0.50—0.85 mol/*l*; Cell-thickness, 0.047—0.054 cm

change in the intensity will result from a change in the population. Figure 3 gives the solvent-effect for the intensity of the ν(C-Br) bands.

In the solution spectra of *meso*-DBB, the intensities of the bands at 635 and 600 cm^{-1} increase, and that of the band at 552 cm^{-1} decreases, as the dielectric constant of the solvent increases from 1.89 (*n*-hexane) to 37.5 (acetonitrile). At the same time it is noted that the positions of the ν(C-Br) bands shift downward in their frequencies by *ca.* 2—6 cm^{-1}.*2 According to Watanabe *et al.*,[11] when a molecule of the dipole moment, μ, in the gaseous state is transferred from the vacuum into the solvent medium of a dielectric constant, ε, the potential energy is lowered by:

$$Er = (\varepsilon-1)\mu^2/(2\varepsilon+1)a^3 \quad (1)$$

where a is the radius of the solute molecule. In view of the above findings, the population of the polar rotational isomer may be expected to become dominant in the solvent of the larger dielectric constant, since the values of a can be considered to be not very different for each rotational isomer. The two bands at 635 and 600 cm^{-1} can, therefore, be assigned to the ν(C-Br) vibrations arising from the polar MG, and the band at 552 cm^{-1}, to that arising from the nonpolar MT, the population of which would be expected to decrease in the polar solvent. As MT has a center of symmetry, only one ν(C-Br) vibration is possible in an infrared absorption; this is related to the antisymmetric stretching vibration of the C-Br bonds. The band at 552 cm^{-1} must be due to the antisymmetric ν(C-Br) vibration.

*2 A downward shift of absorption frequencies is also noted for *racemic*-DBB; hence, hereafter for convenience the frequencies of the absorption bands will be given by those observed in the pure liquid spectra.

On the other hand, two ν(C-Br) vibrations may be expected from MG, since this conformation has no center of symmetry. The two bands at 635 and 600 cm^{-1} correspond exactly to these vibrations. In the Raman spectrum of liquid *meso*-DBB,[2] an intense band at 632 cm^{-1} and a weaker band at 600 cm^{-1} are found in the ν(C-Br) region. Since the ν(C-Br) vibrations of MG are active for both Raman and infrared spectra, these two bands, the frequencies of which coincide exactly with those of the infrared bands, are considered to have arisen from MG. However, the intense Raman band at 632 cm^{-1} possibly involves the Raman active symmetric ν(C-Br) vibration of MT. It is very probable that no Raman band is found near 550 cm^{-1} because the infrared band at 552 cm^{-1} is a Raman-inactive antisymmetric ν(C-Br) vibration.

As is evident from Fig. 3, the intensity change in the ν(C-Br) band of *racemic*-DBB depending with the solvent is also remarkable. Two ν(C-Br) vibrations are possible in the infrared absorption for each of the three rotational isomers of *racemic*-DBB, which have no center of symmetry. The bands at 632 and 561 cm^{-1}, the intensities of which decrease with an increase in the solvent dielectric constant, can be assigned to the ν(C-Br) vibrations of the less polar RG. On the other hand, the 648 and 543 cm^{-1} bands may be ascribed to the ν(C-Br) vibrations of polar RG′ or RT, since their intensities increase as the dielectric constant of solvent increases. It is noted, however, that the solvent-effect on the intensity change of the 648 cm^{-1} band is different from that on that of 543 cm^{-1} band; that is, the increase in the relative intensity of the 648 cm^{-1} band in the polar solvent is remarkable in comparison with that of the 543 cm^{-1} band. By taking account of the facts that the potential energies of RG′ and RT in the gaseous state are almost the same order in magnitude, and that both are higher than that of RG by approximately 1.5 kcal/mol, as will be described below, the population of the most polar RG′ may be expected to become dominant in the acetonitrile solvent over that of RT. Therefore, the bands at 648 and 543 cm^{-1} may be considered to arise from RG′ and RT respectively. This assignment is also in accord with the experimental finding that the position of the ν(C-Br) vibration *trans* to a C-C bond appears usually at a frequency higher than that *trans* to a C-H bond.[7,8] Although a residual ν(C-Br) vibration must be expected for both RG′ and RT, no bands except the 648 and 543 cm^{-1} bands are found in the ν(C-Br) region. The absence of bands cannot be explained at present.

Taufene *et al.*[2] have found three Raman bands, at 633, 563, and 540 cm^{-1}, for *racemic*-DBB in the liquid state; they have ascribed them to RG, RG′, and RT respectively. The assignment of the former two bands is the reverse of our interpretation. It

can be seen, however, that the most intense band is found at 567 cm^{-1} in the infrared spectrum of *racemic*-DBB in the gaseous state (see Fig. 4). Judging from the electron diffraction investigation by Stevenson and Schomaker,[12] where they have shown that the *trans* conformation for the bromine atoms predominates in the gaseous state, the very intense 567 cm^{-1} band, which corresponds to the 563 cm^{-1} band in the Raman spectrum, must be assigned to the ν(C-Br) vibration arising from RG. The weaker bands at 651 and 547 cm^{-1} appearing in the infrared spectrum of the gaseous state may be ascribed to RG′ and RT respectively, both of which are relatively small in population.

Energy Difference between the Rotational Isomers in the Gaseous State. As Fig. 4 shows, the bands appearing at 646, 607, and 559 cm^{-1} of *meso*-DBB correspond to those at 635, 600, and 552 cm^{-1} respectively in the liquid state. For the gaseous *racemic*-DBB, the bands corresponding to those at 648, 561 and 543 cm^{-1} of the liquid state are observed at 651, 567, and 547 cm^{-1} respectively.

As Fig. 5 shows the relations of the logarithmic values of the intensity ratios for the ν(C-Br) bands in the gaseous state against 1/T were found to be linear. From the slope of the straight lines, the energy differences in the gaseous state are found to be:

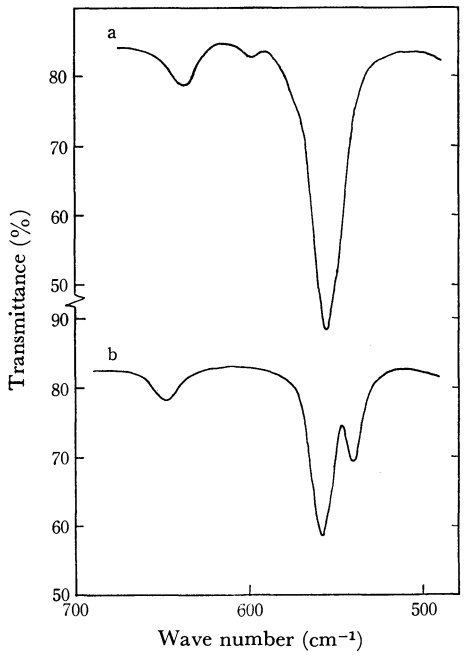

Fig. 4. Infrared spectra in gaseous state.
a, *meso*-DBB (at 96°C); b, *racemic*-DBB (at 98°C)

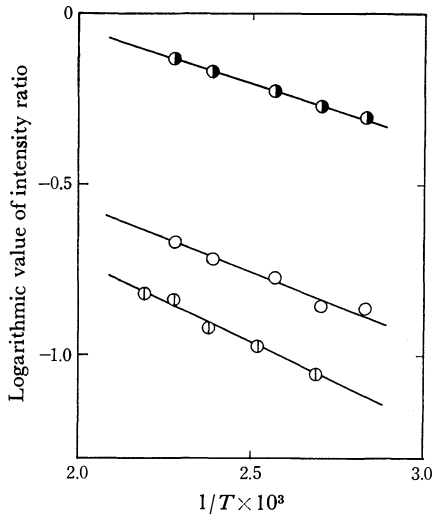

Fig. 5. Relations of the intensity ratio of ν(C-Br) bands against $1/T$ in the gaseous state.
◑: log (D_{547}/D_{567}) of *racemic*-DBB
○: log (D_{651}/D_{567}) of *racemic*-DBB
◫: log (D_{646}/D_{559}) of *meso*-DBB

$$\Delta E^{gas}_{MG\text{-}MT} = 2.2 \text{ kcal/mol}$$

$$\Delta E^{gas}_{RG'\text{-}RG} = 1.7 \text{ kcal/mol}$$

and;

$$\Delta E^{gas}_{RT\text{-}RG} = 1.5 \text{ kcal/mol}$$

by means of a previously-reported method.[1] It may be noted that the observed values of ΔE^{gas} are higher by approximately 0.5 kcal/mol than those corresponding ΔE^{gas} values for *meso*- and *racemic*-2,3-dichlorobutanes.[1] The relative behavior of chlorine and bromine substituents for ΔE^{gas}, in these cases, is in harmony with the findings for 1,2-dihalogenoethanes; *i. e.*, the values of ΔE^{gas} between the *gauche* and *trans* forms have been determined to be 1.45—1.70 kcal/mol for 1,2-dibromoethane and 1.0—1.1 kcal/mol for 1,2-dichloroethane respectively.[13,14]

The energy difference for *meso*-DBB, however, can be determined by an independent method, *e. g.*, by studing the solvent effect upon the intensity of the ν(C-Br) band. Since the MT-form has no dipole moment, its potential energy may be not subjected to any influence from the solvent dielectric constant (see Eq. (1)). The lowering in the potential energy of MG, *Er*, in the solvent of the dielectric constant, ε, can, therefore, be represented with reference to the energy differences between MG and MT in the gaseous state, ΔE^{gas}, and that in solution, ΔE^{soln}, as follows:

12) D. P. Stevenson and V. Schomaker, *J. Am. Chem. Soc.*, **61**, 3173 (1939).

13) T. Shimanouchi, H. Tsuruta and S. Mizushima, *Sci. Pap. Inst. Phys. Chem. Res. Tokyo*, **42**, 51 (1944).

14) K. Kuratani, T. Miyazawa and S. Mizushima, *J. Chem. Phys.*, **21**, 1411 (1953).

$$Er = \Delta E^{gas} - \Delta E^{soln} = (\mu^2/a^3)[(\varepsilon-1)/(2\varepsilon+1)] \quad (2)$$

In the solution, on the other hand, the ratio of the optical density of the ν(C-Br) bands can be written with reference to ΔE^{soln} as follows:

$$D_{MG}/D_{MT} = (2k_{MG}f_{MG}/k_{MT}f_{MT}) \exp(-\Delta E^{soln}/RT) \quad (3)$$

where k is the absorption coefficient and f, the partition function. Combining Eqs. (2) and (3), we thus obtain:

$$\log(D_{MG}/D_{MT}) = \log(2k_{MG}f_{MG}/k_{MT}f_{MT}) - \Delta E^{gas}/2.303RT + (\mu^2/2.303RTa^3)[(\varepsilon-1)/(2\varepsilon+1)] \quad (4)$$

At a constant temperature, the log (D_{MG}/D_{MT}) should be a linear function with $(\varepsilon-1)/(2\varepsilon+1)$. Taking the 635 cm^{-1} band to MG, and the 552 cm^{-1} band to MT, as in Fig. 6, the relation of $\log(D_{635}/D_{552})$ to $(\varepsilon-1)/(2\varepsilon+1)$ at the constant temperature of 29°C is found to be linear. This result agrees satisfactorily Eq. (4). The value of the first two terms of the right-hand equation gives -1.34 as the value of $\log(D_{635}/D_{552})$ at $(\varepsilon-1)/(2\varepsilon+1)=0$, where ε is extraporated to 1. We then have:

$$\log(2k_{MG}f_{MG}/k_{MT}f_{MT}) - \Delta E^{gas}/2.303RT = -1.34 \quad (5)$$

Assuming $f_{MG}/f_{MT}=1$,[1] and into Eq. (5) putting the value of k_{MG}/k_{MT}, which has been determined to be 0.534, as will be described below, we have found the value of ΔE^{gas} to be 1.9 kcal/mol. The value of ΔE^{gas} thus obtained is approximately the same as that obtained by measuring the temperature-change in the absorption intensity in the gaseous state.

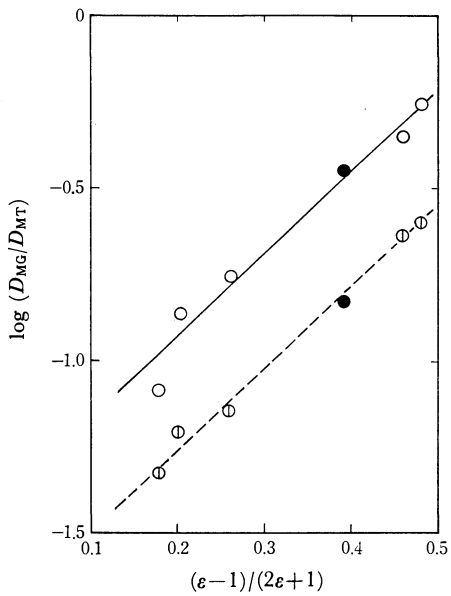

Fig. 6. Relations of log (D_{MG}/D_{MT}) against $(\varepsilon-1)/(2\varepsilon+1)$ at 29°C.
○: $D_{MG}/D_{MT}=D_{635}/D_{552}$
◑: $D_{MG}/D_{MT}=D_{600}/D_{552}$
Black circles: data for the pure liquid.

As is presented in Fig. 6, it should also be noted that the origin of the 600 cm^{-1} band seems to be same as that of the 635 cm^{-1} band, since the two lines are parallel in direction. This result gives a basis for the assignment of the 635 and 600 cm^{-1} bands to MG.

From his NMR study of *meso*-DBB, Deb[5] has found the value of ΔE^{gas} to be 1.0 kcal/mol. This value of ΔE^{gas}, however, seems to be too small as compared with the energy difference between the *gauche* and *trans* forms of 1,2-dibromoethane, for which the value of ΔE^{gas} was found to be 1.45—1.70 kcal/mol.[13,14] Since, on going from MT to MG, the number of *gauche* interactions between bulky groups, Br and CH_3, is increased from two to three, the difference in steric potential between the MG of *meso*-DBB and the corresponding *gauche* form of 1,2-dibromoethane may be larger than that between the *trans* forms of these two substances. In this case, a contribution of the electrostatic repulsion between the bromine atoms to ΔE^{gas} is considered to be approximately the same for the corresponding *gauche* and *trans* forms of these two substances. The values of ΔE^{gas} between the MG and MT may, therefore, be expected to exceed that between the *gauche* and *trans* forms of 1,2-dibromoethane.

For the gaseous *racemic*-DBB, it may be noted that the potential energies of RG′ and RT are almost the same in magnitude and that both are higher than that of RG. The same situation has been found for *racemic*-2,3-dichlorobutane, as has been reported in our previous paper.[1]

The Equilibrium Concentrations of Rotational Isomers in Various Solvents. The equilibrium concentrations of rotational isomers in various solvents were determined by measuring the intensity ratio of the ν(C-Br) bands. The ratio of the concentrations of the two rotational isomers, I and II, C_I/C_{II}, can be represented with reference to the optical densities of the ν(C-Br) bands belonging to these rotational isomers as follows:

$$C_I/C_{II} = (k_{II}/k_I)(D_I/D_{II}) \quad (7)$$

where D is the optical density and k, the absorption coefficient. In general, the determination of the k_{II}/k_I value is a little more difficult. Fortunately, in the case of liquid *meso*-DBB, the ratio of the concentration of MG to MT, C_{MG}/C_{MT}, can be calculated to be 0.667 from the observed dielectric constant and the density of the liquid.*3 Putting into Eq. (7) the C_{MG}/C_{MT}, and the observed value of D_{MG}/D_{MT}, 0.356, for the pure liquid *meso*-DBB at room temperature, we have then

*3 The value of C_{MT}/C_{MG} was calculated by a method reported in our previous paper.[1] The observed data of the dielectric constant ($\varepsilon=6.245$), the density ($d=1.7747$), and the refractive index ($n=1.5091$) at 25°C were taken from the paper of Winstein and Wood.[15]

15) S. Winstein and R. E. Wood, *J. Am. Chem. Soc.*, **62**, 548 (1960).

Table 2. Equilibrium concentrations of the rotational isomers in *meso*-2,3-dibromobutane

Solvent	D_{635}/D_{552}	C_{MT} %[a]	$J_{AA'}$ (cps)[b]	C_{MT} %[a,c]
n-Hexane (1.89)	0.081	87	9.00	80—78
Cyclohexane (2.02)	0.141	79	8.93	80—78
Carbon disulfide (2.64)	0.175	75	8.69	77—74
Pure liquid (6.245)	0.356	60		
Cyclohexanone (18.3)	0.461	54		
Acetonitrile (37.5)	0.566	49	6.55	56—51
Carbon disulfide[d]			8.81	*ca.* 80
Pure liquid[d]			7.81	70—66

a) Composition of MG, C_{MG} %, is given by 100-C_{MT}.
b) Data by Deb.[5]
c) Calculated from the values of $J_{AA'}$ by Deb assuming $J_T=11$ cps and $J_G=1$—2 cps.[3,4,16]
d) NMR data from the paper of Bothner-By and Naar-Colin.[3]

found the value of k_{MT}/k_{MG} to be 1.87. Using this value, the equilibrium concentrations at room temperature for *meso*-DBB in various solvents have been determined from Eq. (7), they are listed in Table 2.*4

Deb observed the NMR spectra of *meso*-DBB in various solvents and found that the vicinal coupling constant, $J_{AA'}$, between two methine protons changes depending upon the solvents.[5] From these observed $J_{AA'}$ values, we have calculated the equilibrium concentration, C_{MT}, assuming *trans* and *gauche* coupling constants of two methine protons, to be $J_T=11$ cps and $J_G=1$—2 cps respectively.[3,4,16] The agreement between the equilibrium concentrations obtained by the two different methods is satisfactory.

Table 3 gives the equilibrium concentrations of the rotational isomers of *racemic*-DBB in solution; these concentrations have been obtained by means of the method[1] we previously applied to *racemic*-2,3-dichlorobutane.*5 It may be seen that the data for the pure liquid state are in accord with those reported in the NMR investigation by Bothner-By and Naar-Colins.[3] That the increase in the population of RG′ is remarkable in the polar solvents in spite of the small effect of the solvent on the population of RT can be explained by the fact that the loss in the potential energy of RG′ under the influence of an electrostatic interaction of the solvent dipole is approximately twice that of RT.*6 A certain increase in the populations of RT may be expected in the polar solvent; at present, however, we have no good explanation for the small effect of the solvent on RT shown in Table 3.

Table 3. Equilibrium concentrations of the rotational isomers in *racemic*-2,3-dibromobutane

Solvent	D_{648}/D_{561}	D_{543}/D_{561}	$C_{RG'}$ %	C_{RG} %	C_{RT} %
n-Hexane (1.89)	0.140	1.102	6	75	19
Cyclohexane (2.02)	0.225	1.202	10	71	19
Carbon disulfide (2.64)	0.314	1.574	13	64	23
Pure liquid (5.758)	0.499	1.618	19	59	22
Cyclohexanone (18.3)	0.958	1.922	30	49	21
Acetonitrile (37.5)	1.174	1.944	34	46	20
Pure liquid[a]			20	60	20

a) NMR data from the paper of Bothner-By and Naar-Colin.[3]

The author wishes to express his hearty thanks to Professor M. Takeda of Science University of Tokyo and Professor T. Shimanouchi of The University of Tokyo for their encouragement during the progress of the work, and to M. Kawakami for his assistance.

*1 In this case we have taken the 635 cm^{-1} band to MG and the 552 cm^{-1} band to MT. When the remaining band at 600 cm^{-1} is taken to MG, the value of k_{552}/k_{600} becomes 4.48. If either band at 635 or at 600 cm^{-1} is taken for MG, the result is the same as those obtained in the determination of the equilibrium concentrations in various solvents.

16) S. Kondo, E. Tagami, K. Iimura and M. Takeda, This Bulletin, **41**, 790 (1968).

*5 The existing ratios of the rotational isomers at 80°C, $C_{RG'}/C_{RG}$ and C_{RT}/C_{RG}, were calculated from the observed energy differences, $\Delta E^{gas}_{RG'-RG}=1.7$ kcal/mol and $\Delta E^{gas}_{RT-RG}=1.5$ kcal/mol; they were found to be 0.089 and 0.118 respectively. Putting these values and the observed ratios of the optical densities at 80°C, $D_{RG'}/D_{RG}=0.139$ and $D_{RT}/D_{RG}=0.510$, into Eq. (7), the values of $k_{RG'}/k_{RG}$ and k_{RT}/k_{RG} were determined to be 1.56 and 4.32 respectively. The equilibrium concentrations were then calculated using these ratios of the absorption coefficients.

*6 Using Eq. (1), the losses in potential energies in the acetonitrile solvent ($\varepsilon=37.5$), for instance, are calculated to be 1.6 kcal/mol for RG′, 0.7 kcal/mol for RT, and 0.2 kcal/mol for RG; hence, the energy differences between the rotational isomers in the solvent become $\Delta E_{RG'-RG}=0.3$ kcal/mol and $\Delta E_{RT-RG}=1.0$ kcal/mol. In this calculation, the value of the density, 1.7836, was taken from the paper of Winstein and Wood.[15]

BULLETIN OF THE CHEMICAL SOCIETY OF JAPAN VOL. 42 3141—3147 (1969)

Kinetics of Reactions of Amines with Alkene Oxides

P. K. SUNDARAM and M. M. SHARMA

Department of Chemical Technology, University of Bombay, Bombay 19, India

(Received August 10, 1968)

A variety of amines such as piperazine, pyrrolidine, morpholine, dialkyl amines, alkanolamines *etc.* were reacted with ethylene-, propylene-, and 1,2-butylene oxides in aqueous medium. Most of the experiments were made at 20°C. For some typical amines kinetic runs were made over a wide temperature range to obtain values of activation energy. Theoretical aspects of the reaction are discussed. It is shown that the method suggested by Swain and Scott could be used to correlate the rate constants. A close relationship exists between the relative rates of reaction of amines with CO_2, COS, CS_2 and alkene oxides.

The reaction of an amine with an alkene oxide results in the formation of an alkanolamine. The first addition to the epoxide is followed by one or more secondary additions of the epoxide to the reaction products. The reactions are:

$$R_1\text{-}\underset{\backslash O /}{CH\text{-}CH_2} + RNH_2 \rightarrow R_1CH(OH)CH_2NHR \quad (1)$$

$$R_1\text{-}\underset{\backslash O /}{CH\text{-}CH_2} + R_1CH(OH)CH_2NHR \rightarrow [R_1CH(OH)CH_2]_2NR \quad (2)$$

which may be followed by

$$R_1\text{-}\underset{\backslash O /}{CH\text{-}CH_2} + [R_1CH(OH)CH_2]_2NR + H^+ \rightarrow [R_1CH(OH)CH_2]_3N^+R \quad (3)$$

which occurs very slowly at a very late stage in the reaction.

Sharma[1] and Kothari and Sharma[2] have studied the kinetics of reactions between a variety of primary and secondary amines and CO_2, COS and CS_2 and have found close relationships in their rates of reactions *e.g.*:

$$\log_{10} k_{Am\text{-}CS_2} \approx \log_{10} k_{Am\text{-}CO_2} - 4.3 \quad (4)$$

where k is the second order rate constant. It is likely that there also exists a close relationship between the rates of reactions of amines with CO_2, COS, CS_2 and alkene oxides.

Experimental Methods, Analytical Techniques and Theoretical Aspects

Many methods have been reported in the literature for following the amine-alkene oxide reactions: the distillation method, conductivity method, dialatometric method, polarimetric method and the gas chromatographic method. Hansson[3] in his extensive series of reactions between amines and alkene oxides had adopted the "distillation method," which does not appear to be sound. Here an aliquot of the reaction mixture was taken at appropriate times and was subjected to vacuum. *n*-Octadecyl alcohol was added to the flask in which the aliquot of the reaction mixture was taken to reduce foaming on application of vacuum. It was supposed by Hansson that on application of vacuum to the aliquot of the reaction mixture, none of the reaction product (that is, the alkanolamine which was thought to be non-volatile) was lost and what was distilled off was only the relatively more volatile reactants in the reaction mixture. The material left in the flask after application of vacuum for sufficient length of time was titrated directly with a standard mineral acid. The supposition that no reaction product distilled off is not valid. Hansson had realized that some alkanolamine is likely to be lost and he therefore, applied a 'correction' factor. His method of correcting for the loss of the alkanolamine is theoretically unsound.

Known and appropriate amounts of freshly estimated epoxide[4] and amine[5] were taken separately in two 250 m*l* iodination flasks and brought to the experimental temperature in a thermostatic bath where the temperature could be controlled to ±0.05°C of the desired temperature. The reactants were mixed at a known time and aliquots of the reaction mixture were withdrawn at known intervals of time and added to sufficient quantity of dilute sulphuric acid taken in a 100 m*l* conical flask to arrest the reaction. The volatile epoxide (*i.e.* ethylene- or propylene oxide) was removed by the application of vacuum. In the case of 1,2-butylene oxide the reaction sample withdrawn was analysed immediately after adding it to sulphuric acid with the minimum lapse of time——this being necessitated due to its relative nonvolatility (bp 63.2°C/760 mmHg)

1) M. M. Sharma, *Trans. Faraday Soc.*, **61**, 681 (1965).
2) P. J. Kothari and M. M. Sharma, *Chem. Engng. Sci.*, **21**, 391 (1966).
3) J. Hansson, *Sevensk Kem. Tidskr.*, **67**, No. 5, 263 (1955).
4) W. C. J. Ross, *J. Chem. Soc.*, **1950**, 2257.
5) S. Siggia, "Quantitative Organic Analysis *via* Functional Groups," III Ed., John Wiley & Sons Inc., New York (1963), p. 423.

and the difficulty in removing it by the application of vacuum. In this case the analysis was carried out quickly so as to reduce to a minimum any possibility of reaction of the protonated amine with the epoxide.

Most of the reactions were studied at 20°C in aqueous medium. However, in some typical cases, experiments were made upto 40°C to obtain values of activation energy.

In most of the cases secondary amines were reacted with an epoxide and in a few cases when primary amine-epoxide reactions were studied, the relative amine concentration in the reaction mixture was taken at least four times that of the epoxide so that the secondary reactions are either obviated or reduced to a minimum. Similarly when a secondary amine is reacted with an epoxide the product of the reaction is a tertiary amine and the complications due to its reaction with another molecule of the epoxide to form a tetra-alkyl ammonium hydroxide (in the presence of a hydrogen ion from the solvent) are insignificant.

Analytical Techniques

Primary Amine-Epoxide Reactions. The analysis involving the separation of the primary amine and the product (a secondary amine) was effected by the Schiff's reaction of salicylaldehyde in 1:1 ethylene glycol, isopropanol solvent with the primary amine and the potentiometric titration of the unreacted secondary amine with hydrochloric acid in the same prescribed solvent:[6,7] The method depends upon the fact that salicylaldehyde reacts quantitatively with primary amines to form compounds of decreased basicity capable of being differentiated from the secondary amine in a non-aqueous potentiometric titration.[7]

It was found that the above method was suitable only for studying the reactions between alkene oxides and amines like cyclohexyl-, and benzylamines, the products of reactions of which had steric resistance and were likely to react sluggishly, if at all, with salicylaldehyde under normal conditons. However, this method failed to differentiate between simple amines like *n*-butylamine and its product with ethylene oxide-butylaminoethanol or that with propylene oxide, butylaminoisopropanol.

Secondary Amine-Epoxide Reactions. This involved an estimation of the secondary amine in the presence of the tertiary amine. An aliquot of the reaction mixture withdrawn in an excess of sulphuric acid was subjected to vacuum to remove the volatile epoxide. The solution was then neutralized with alkali using thymolphthalein indicator after running in 30—40 m*l* of isopropanol. An excess of CS_2 was then added to convert the secondary amine to the dithiocarbamic acid which was only 90—95 per cent complete. It was forced to completion by a standard sodium hydroxide titrant to a first blue or blue green end point. The amount of the standard sodium hydroxide titrant gave a direct measure of the secondary amine present. The reactions involved are:

$$R_2NH + CS_2 \rightarrow R_2N\overset{\overset{S}{\|}}{C}\text{-}S^- + H^+ \qquad (6a)$$

and $$OH^- + H^+ \rightarrow H_2O \qquad (6b)$$

This method of the estimation of secondary amine[8] is specific as only the secondary amine can react with carbon disulphide; the tertiary amine does not have a labile hydrogen atom to react with carbon disulphide. In this method only amines that are highly branched in the 2-position, like diisopropylamine, tertiary butylamine, *etc.* do not react quantitatively with CS_2 under the conditions used.

Materials

All the chemicals used were, in general, technical grade. The materials were purified whenever necessary and estimated before using them for experimental work.

Propylene- and 1,2-butylene oxides were obtained as liquids and were sufficiently pure to be used as such without further purification. Ethylene oxide was available in cylinders and an aqueous solution was prepared for reactions immediately prior to use. All the three epoxides were estimated prior to use in aqueous solution by Ross method[4]——by estimating the total amount of hydroxide ion liberated in the reaction between the epoxide and an excess of thio-sulphate anion in a 50 per cent aqueous acetone solution, by using a standard acetic acid solution.

Methylaminoethanol, ethylaminoethanol, butylaminoethanol and methylaminoisopropanol were synthesized by reacting the relevant epoxide and the amine; the amount of the amine being at least five times the concentration of the epoxide. The alkanolamines were recovered in aqueous solutions from the synthetic mixture (after allowing it to stand for sufficient length of time) by removing the relatively more volatile amine used, by application of vacuum.

Discussion of the Reactions

The primary reactions are:

$$R_1\text{-}\underset{\diagdown O \diagup}{CH}\text{-}CH_2 + RNH_2 \begin{cases} \nearrow R_1CH(OH)\text{-}CH_2NHR & (1) \\ \searrow R_1\underset{\displaystyle NHR}{\underset{|}{CH}}\text{-}CH_2OH & (7) \end{cases}$$

which can give rise to one or both possible isomers, with the exception of ethylene oxide or symmetrically substituted alkene oxides. In accordance with the general practice and also the rule summarized from the work of Krassusky[9] product obtained through Eq. (1) will be termed "Normal" and the one obtained through Eq. (7) as "Abnormal."

The literature pertaining to the direction of the cleavage of the substituted epoxide ring is extensive and various hypotheses to explain the observed isomer distribution have been considered by various workers. It may be summarized that the reactions between amines and alkene oxides

6) Ref. 5, p. 450.

7) C. D. Wagner, R. H. Brown and E. D. Peters, *J. Am. Chem. Soc.*, **69**, 2661 (1947).

8) F. E. Critchfield and J. B. Johnson, *Anal. Chem.*, **28**, 430 (1956).

9) K. A. Krassusky and V. D. Kutzenos, *Ukrain Khem. Zhur. Sci.*, Pt. 4, 75 (1929) cited from *Chem. Abstr.*, **24**, 1083 (1930).

give predominantly the "Normal" isomer under neutral or basic conditions. Since the reactions studied here are all under basic conditions reaction (7) could be neglected.

When primary amine reactions are studied complications arise due to the consecutive and competitive reaction of the product amine with the epoxide. The same could be avoided or reduced to a minimum by taking high ratios of the amine to the alkene oxide as pointed out earlier. In the case of secondary amine the reactions become reasonably free of complications as the reaction rate of the tertiary amine product will be very small compared to the secondary amine used due to the steric inhibition.

Another important factor to be considered is the solvolysis of the epoxide. In the case of water (and even alcohol) the solvolysis does not disturb the main reaction of addition of amine to the alkene oxide as the solvolysis rates are of no significance till almost the very end of the reaction. This becomes important however, when rather slow reactions, as those between sterically hindered amines and epoxides are studied as the rate constant for the primary reactions may be affected appreciably due to the side reaction.

Results

The reactions between amines and alkene oxides were found to follow a second order rate equation:

$$\frac{dx}{dt} = k(a-x)(b-x) \tag{8}$$

giving,

$$\log_{10}\frac{(a-x)}{(b-x)} = \frac{k_2(a-b)}{2.303}t - \log_{10}\frac{b}{a} \tag{9}$$

where,

a=the initial concentration of the epoxide
and b=the initial concentration of the amine.

The values of the second order rate constants k_2 were obtained graphically by plotting $\log_{10}\frac{(a-x)}{(b-x)}$ against t, the slope of the line being $\frac{k_2(a-b)}{2.303}$. The points fell on good straight lines. A good portion usually 5—75 per cent of the reaction was followed and all the runs were done at least in duplicate. There was always a good agreement between the duplicate runs.

The rate constants for the reactions between amines and alkene oxide in water at 20°C are presented in Table 1.

In Tables 2 and 3 are presented the rate constants for the reactions of some typical amines with propylene oxide and ethylen oxide, respectively, at different temperatures along with the values of the activation energies evaluated from the slopes of the Arrhenius plots.

Table 1. Rate constants for the reactions between amines and alkene oxides in water

Temperature=20°C k_2 in l mol^{-1}min^{-1}

No.	Amine	Ethylene oxide	Propylene oxide	1,2-Butylene oxide
	Group I			
1	Piperazine	0.215	0.141	—
2	Pyrrolidine	0.146	0.103	0.094
3	Piperidine	0.157	0.110	0.073
4	Morpholine	0.068	0.051	0.031
	Group II			
5	Dimethyl-	0.207	0.134	—
6	Diethyl-	0.042	0.021	0.014
7	Di-*n*-butyl-	0.033	0.018	—
8	Di-*n*-propyl-	0.031	0.016	—
	Group III			
9	Methylaminoethanol	0.103	—	—
10	Ethylaminoethanol	0.032	—	—
11	Butylaminoethanol	0.027	—	—
12	Methylaminoisopropanol	—	0.047	—
13	Diethanol-,	0.015	0.011	—
	Group IV			
14	Benzyl-	0.037	0.015	—
15	Cyclohexyl-	0.028	0.031	—

Table 2. Reaction rates and the energies of activation for the reaction of some typical amines with propylene oxide

k_2 in l mol^{-1} min^{-1}

No.	Amine	20°C	30°C	35°C	40°C	E kcal/gmol
1	Piperazine	0.141	0.275	—	—	12.18
2	Piperidine	0.110	0.222	0.328	0.432	12.43
3	Morpholine	0.051	0.103	—	—	13.22
4	Di-*n*-propyl	0.016	0.036	—	0.079	14.76

Table 3. Reaction rates and the energies of activation for the reaction of piperidine and diethylamine with ethylene oxide

k_2 in l mol^{-1} min^{-1}

No.	Amine	20°C	30°C	35°C	39.6°C	E kcal/gmol
1	Piperidine	0.157	0.345	0.489	—	13.75
2	Diethyl	0.042	0.097	—	0.204	14.55

Discussion

The reactions of amines with alkene oxides follow a second order rate equation and follow the S_N2 mechanism, the rate being proportional to the

concentration of both the nucleophilic reagent and the substrate.[10]

The rates of the reactions of amines with the alkene oxides (see Table 1) show a close relationship. A plot of logarithms of the rate constants of the amines for one epoxide say ethylene oxide with the same parameter for another epoxide say propylene oxide shows a linear free energy relationship (see Figs. 1 and 2). The relationships are:

$$\log_{10} k_{\text{Am-Propylene oxide}} \approx \log_{10} k_{\text{Am-Ethylene oxide}} - 0.17 \quad (10)$$

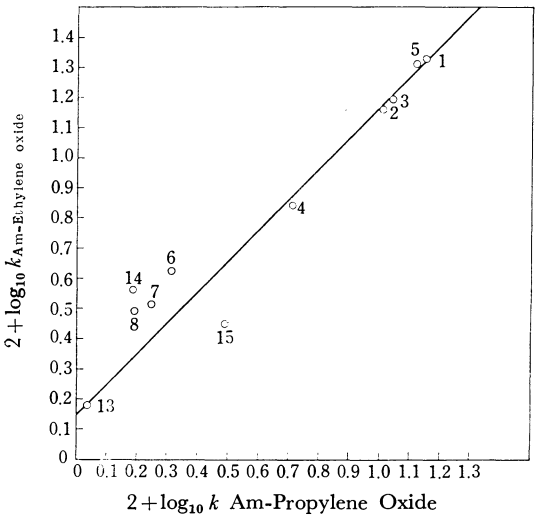

Fig. 1. Plot of rate constans of amines with ethylene oxide against rate constants for propylene oxide.

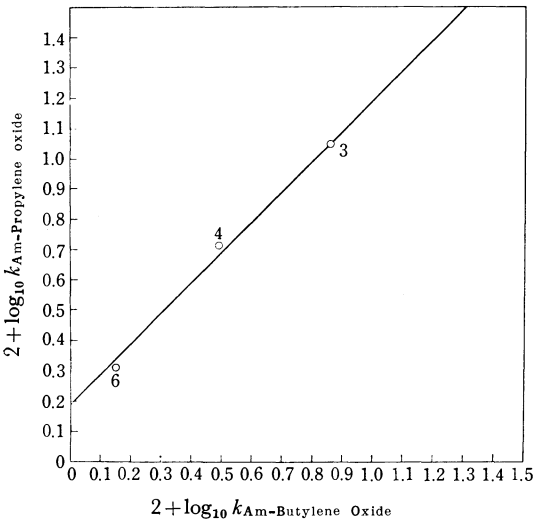

Fig. 2. Plot of rate constants of amines with propylene oxide against rate constants for 1,2-butylene oxide.

10) L. F. Fieser and M. Fieser, "Organic Chemistry," III Ed., Reinhold Publishing Corp., New York (1958), p. 337.

$$\log_{10} k_{\text{Am-Butylene oxide}} \approx \log_{10} k_{\text{Am-Propylene oxide}} - 0.19 \quad (11)$$

so that with the same amine on passing from ethylene-, propylene-, to 1,2-butylene oxide the rate goes on decreasing approximately in the ratio 1 : 0.67 : 0.44.

A similar trend has been observed in the results obtained by Hansson[11] and other workers,[12] where ethylene oxide was found to react faster than propylene oxide and epichlorohydrin even faster than ethylene oxide. This behaviour could be understood by considering the transition state

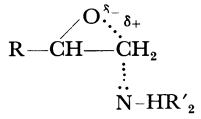

(I)

supposed to involve the attack of the nucleophile on the methylene group of the epoxide ring, with a simultaneous displacement of the ring oxygen atom in the opposite direction.[13]

The presence of the substituent R in the epoxide acts as an impediment for the approach of the reactant and hence the reaction will be slower the larger the size of this substituent R. Thus the increasing size of the alkyl substituent group in propylene oxide ($R=CH_3$) and 1,2-butylene oxide ($R=CH_3CH_2$), explains the decreasing rate of reaction.

However, if the positive inductive effect of the alkyl groups is considered simultaneously, the transition state could be represented by:

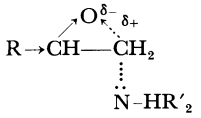

(II)

The density of electrons at the CH-carbon atom will increase due to the presence of the electron repelling group R.[14] Consequently, the demand for the electron shift from the methylene carbon atom (CH_2 carbon) will be lowered resulting in a smaller positive charge on it and a lower reaction rate. Thus the dual effect of the alkyl groups, one steric and the other polar (with a positive inductive effect) act in the same direction as to inhibit the reaction.

Similar reasoning accounts for the much higher reactivity of epichlorohydrin[12] when compared to the other epoxides. In this instance it appears

11) J. Hansson, "A Kinetic Study of the Addition of Amines to Propylene Oxide," Lindstedts. Lund (1955), and earlier papers.

12) L. Smith, S. Mattsson and S. Andersson, Lunds Univ. Arsskr., Nr. 7, 1 (N. F.) (1946).

13) R. E. Parker, N. B. Chapman and N. S. Issaacs, *J. Chem. Soc.*, **1959**, 1925.

14) D. Swern, G. N. Billen and H. B. Knight, *J. Am. Chem. Soc.*, **71**, 1152 (1949).

that the increased size of the substituent in the epoxide from CH_3 (in propylene oxide) to $ClCH_2$ (in epichlorohydrin) does not have as much effect in retarding the reaction rate as the acceleration of the rate due to the negative inductive character of the chloromethyl group.

Normal and Abnormal Reactions. The attack of the epoxide by the nucleophile on the terminal methylene carbon atom (CH_2) bearing a positive charge and having less steric hindrance is much easier than the attack on the CH carbon atom. Moreover the secondary amines themselves show appreciable primary steric effects. All these factors contribute to the preferential formation of the normal rather than the abnormal products of the reactions considered.

Conformational Analysis. Conformational analysis as to the relative stabilities of the normal isomer (a) and the abnormal isomer (b) (see Fig. 3) also favours the formation of the former rather than the latter.

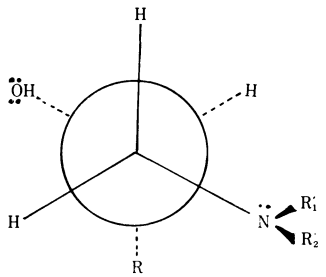

Normal isomer R-CH(OH)-CH_2-N$\begin{matrix}R'_1\\R'_2\end{matrix}$

(a)

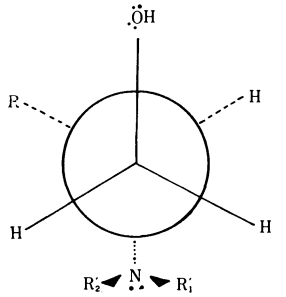

Abnormal isomer R-CH-CH_2OH

N$\begin{matrix}R'_1\\R'_2\end{matrix}$

(b)

Fig. 3. Projection formulae of normal and abnormal Isomers

Of the various rotational isomers possible for the normal and the abnormal isomers (a) and (b) represent the most stable conformation in each set. The relative stabilities of the above two structures will determine as to which isomer is formed predominantly, if at all. In the formula (b) the groups R'_1 and R'_2 are situated very close to the hydrogen atoms and the conformation though not exactly, is similar to an eclipsed one. These two "almost eclipsed" interactions combined with the strong skew interaction between groups R and $\ddot{O}H$ and the probable R–R'_2 interaction make the molecule very constrained and of much higher energy content than (a) where there are two mild interactions between $\ddot{O}H$ and H, R'_1 and H, and R and $\ddot{N}$. But the sum of these interactions should be much smaller than that of (b). These indicate that the isomer (b) is under great strain and of higher energy content and hence the predominance, if not the exclusive formation of the isomer (a), in most of the reactions.

In view of the above considerations, it may be inferred that the greater the size of the alkyl group R and also the greater the branching of the chains present in the alkyl groups R'_1 and R'_2, the more difficult should be the formation of the isomer (b).

Reactivities of Heterocyclic Amines. The heterocyclic amines pyrrolidine, piperidine, *etc.* (See Table 1) react markedly faster compared to most of the amines listed. Pyrrolidine reacts with ethylene oxide about 3.5 times as fast as diethylamine and about 5 times as fast with propylene oxide. Similarly, the reactivity of morpholine (pK_a at 25°C[15]=8.36) is about 4—5 times that of diethanolamine (pK_a at 25°C[16]=8.88) though the former is the weaker base.

The structures of pyrrolidine and morpholine could be obtained from those of diethyl- and diethanolamines respectively with a little distortion and this results in the high increase in the reaction rates.

The relative rates of reactions of morpholine and diethanolamine with CO_2 and COS are about 13.5 and 20 respectively as shown by the work of Sharma.[1] Pyrrolidine reacts about 5 times as fast as diethylamine with COS.[1] The rate of reactions with CS_2 also follow a similar trend—pyrrolidine reacting about 6 times as fast as diethylamine and morpholine about 10 times as fast as diethanolamine.[2] Further at 25°C, pyrrolidine and morpholine react with 4-nitrofluoro-benzene[17] about 90 times as fast as diethylamine and diethanolamine respectively. The increased reactivity of the heterocyclic amines is due to the restriction of the free play of the alkyl groups about the nitrogen atom about the ring.

If the same analogy is applied in the case of dimethylamine and ethylenimine, it would be con-

15) H. K. Hall, Jr., *J. Am. Chem. Soc.*, **79**, 5441 (1957).
16) V. E. Bower, R. A. Robinson and R. G. Bates, *J. Res. Nat. Bur. Stand.*, **A66**, 71 (1962).
17) H. Suhr, *Ann. Chem.*, **689**, 109 (1965).

cluded that ethylenimine should be a very highly reacting species as even dimethylamine is a fast reacting compound. Some preliminary experiments showed that ethylenimine was reacting so slow as to be termed "almost inert" when compared to the other amines listed. In agreement with the above observation, the reactivity of dimethylamine with 4-nitrofluoro-benzene is seen to be 156 times as great as that of ethylenimine.[17] The "inert" character of ethylenimine is probably due to the aromaticity or electron delocalization of the three membered ring.[18] The fact that ethylenimine is a base (pK_a at 25°C[19]=8.04) even weaker than ammonia (pK_a at 25°C[15]=9.21) is also due to the same reason.

Steric and Inductive Effects. The relative rates of reactions of dimethyl-, diethyl-, di-*n*-propyl-, and di-*n*-butylamines with propylene oxide are seen to be 8.60 : 1.32 : 1.00 : 1.13. The same order of reactivity is maintained in their reactions with ethylene oxide, with a minimum in the rate in case of di-*n*-propylamine. But then to di-*n*-butylamine there is a slight but a definite increase in the rate. This may be explained by considering the simultaneous operation of two effects——the rate decreasing steric effect and the rate increasing positive inductive character of the alkyl groups attached to the amino nitrogen.

It appears that from dimethyl-, to di-*n*-propylamine the steric effect outweighs the inductive effect but from di-*n*-propyl- to di-*n*-butylamine, the effect of the increase in the inductive character is a little more than that of the increase in the size of the alkyl groups, giving rise to the observed minimum at the di-*n*-propylamine.

Amine Reactivities and pK_a Values. No correlation between the reactivities of amines with the epoxides, with the pK_a values of the amines is found.

It may be that the steric arrangements of the amines are such that the different groups attached to the amino nitrogen are not effective in preventing a hydrogen ion in combining with it in the equilibrium reaction:

$$RNH_2 + H^+ \rightleftarrows RNH_3^+ \qquad (12)$$

on which the basicity of the amine depends, but offering strong resistance to the transition state formation with a bulkier substrate like an epoxide.

The non-dependence of the basicities of the substituted ammonium ions on the steric factors is reflected in the fact that *n*-, *s*-, and *t*-butylamines have practically the same basicities (pK_a's 10.5 at 25°C[15]).

The importance of steric and inductive factors is evident from the following examples in the reactions of amines with ethylene oxide:

1) piperazine (pK_{a_1}=9.81[20]) and dimethylamine (pK_a=10.64[15]) react almost with the same velocity.

2) dimethylamine (pK_a=10.64[15]) reacts more than six times as fast as di-*n*-butylamine (pK_a=11.25[15])

3) methylaminoethanol (pK_a=9.70[21]) reacts more than three times as fast as ethylaminoethanol (pK_a=9.80[21]) and

4) morpholine (pK_a=8.36[15]) reacts more than four times as fast as diethanolamine (pK_a=8.80[16]).

Similarly with CO_2, *n*-butylamine and isobutylamine (pK_a=10.42 at 25°C[22]) show practically the same rate of reaction, but *s*-butylamine reacts at one third this rate; *t*-butylamine, where the steric factors are likely to be most important, reacts at about only a tenth of that for *n*- and isobutylamine.[1]

Similarity of Structures and Reactivities. The rate constant in the case of ethylaminoethanol (containing one ethyl and one hydroxy-ethyl groups) is about the mean of the rate constants of diethylamine (containing two ethyl groups) and diethanolamine (containing two hydroxyethyl groups). A similar relation in the case of methylaminoethanol with that of dimethyl- and diethanolamines is also seen to exist.

In the above case, the groups mentioned are similarly linked with the reaction centre both in the compounds considered for isolating the combined contribution of the polar and steric effects of each group and also in the compounds for which the estimations of the rates are made in addition to the mechanism of the reactions as well as the substrate being the same in all the cases. However, it is unlikely that general group contribution values could be assigned to various functional groups.

Swain-Scott Correlation. Plots of the values of *n*[23] the nucleophilic constants of the amines against their respective logarithms of rate constants with alkene oxides are found to give approximate linear plots (Fig. 4) showing that the nucleophilic reactivities of aliphatic amines towards varied substrates can be correlated by the four parameter equation proposed by Swain and Scott.[24] The correlation of course is not exact as indicated by the scatter of the points.

18) P. E. Fanta, "Heterocyclic Compounds," Vol. 19, ed. by A. Weissberger, Interscience Publishers, New York (1964), p. 527.

19) S. Searles, M. Tamres, F. Block and L. A. Quarterman, *J. Am. Chem. Soc.*, **78**, 4917 (1956).

20) N. A. Lange, "Handbook of Chemistry," McGraw Hill Book Co., Inc., New York (1961), X Ed., 1204.

21) Union Carbide Co., (Chemical Division, 8, Grafton St., London, W. 1) "Bulletin on Alkanolamines and Morpholines."

22) H. K. Hall, Jr., *J. Physical Chem.*, **60**, 63 (1956).

23) H. K. Hall, Jr., *J. Org. Chem.*, **29**, 3539 (1964).

24) C. G. Swain and C. B. Scott, *J. Am. Chem. Soc.*, **75**, 141 (1953).

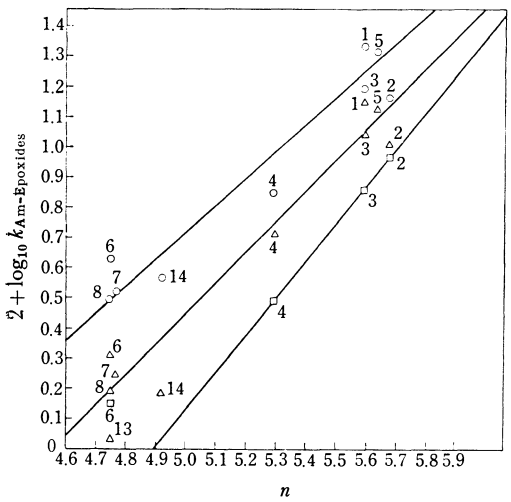

Fig. 4. Plot of logarithms of the rate constants of amines with alkene oxides against the nucleophilic constant, *n*, of the amines.
○ Ethylene oxide, △ Propylene oxide, □ 1,2-Butylene oxide

The values of *n* are found to be higher for the faster reacting amines and *vice-versa*. Thus the values of *n* are found to give the quantitative measures for the reactivities of different nucleophiles.

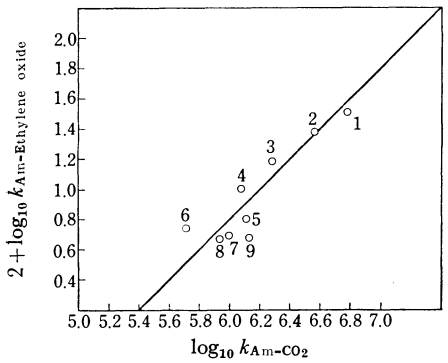

Fig. 5. Plot of rate constants of amines with ethylene oxide against rate constants for CO_2.

Linear Free Energy Relationship. An attempt was made to see whether a linear free energy relationship exists between the reactions of a variety of amines with ethylene oxide and CO_2. The values of the logarithms of the rate constants of amines with ethylene oxide at 25°C (obtained from the respective rates at 20°C using a value of activation energy of 14 kcal/g mol) were plotted against the logarithms of the rate constants of the amines with CO_2[1] at 25°C (Fig. 5). Although there is some scatter of data, the following relation is likely to hold:

$$\log_{10} k_{\text{Am-Ethylene oxide}} \approx \log_{10} k_{\text{Am-CO}_2} - 7.20 \qquad (13)$$

Conclusions

1) The rate constant for a given reaction is found to be a function of (i) steric and (ii) polar factors: (i) For a specified amine, the rate constant for ethylene oxide is significantly greater than that for propylene- and 1,2-butylene oxides; (ii) In the case of dialkylamines the rate constant decreases from dimethyl- to di-*n*-propylamine and then there is a nominal increase in the rate when higher di-*n*-alkylamines are used.

2) The "Normal" addition of amines to epoxides could be explained on the basis of conformational analysis.

3) Heterocyclic amines react faster than the other related amines probably due to structural factors.

4) For all classes of amines there is no general relationship between their basicities and rate constants.

5) In general, the rate constants for a variety of amines can be correlated by the Swain-Scott equation.

6) Linear free energy relationships exist between the rates of reactions of a variety of amines with ethylene-, propylene-, 1,2-butylene oxides, CO_2, *etc.*

One of us (P.K.S.) wishes to thank the University Grants Commission for an award of Scholarship which enabled this work to be carried out.

BULLETIN OF THE CHEMICAL SOCIETY OF JAPAN VOL. 42 3148—3154 (1969)

Investigations on the Kinetics and Mechanism of the Reduction of Mercuric Chloride by Malic Acid, Induced by Potassium Peroxodisulphate

Krishna KUMAR and L. K. SAXENA

Chemical Laboratories, Agra College, Agra, India

(Received August 22, 1968)

The $S_2O_8^{2-}$ induced reduction of mercuric chloride by malic acid has been studied by estimating the precipitated calomel. Kinetic measurements reveal the reduction rate to be independent of the acid concenıration and first order in peroxodisulphate, but only to up an optimum concentration, whereafter further increase in inductor concentration decreases the reduction rate. A fractional order dependence in mercuric chloride concentration is encountered. The reaction is characterized by an initial of period induction. The initial rapid consumption of the acid results in lowering of the rate beyond a particular stage of the reaction. Increase of temperature and concentration of reactants is found to effect the period of induction. H^+ ions and oxygen inhibit the reduction rate. Products identified are mainly calomel, carbon dioxide and malonic acid. A chain mechanism in which radical ion chain carriers participate, has been suggested.

Induced reduction of mercuric chloride by certain organic acids was first observed by Dhar.[1] The role of the inductor (normally an oxidizing agent) in activating the acid was later investigated by Cartledge,[2] Weiss,[3] and others.[4] Kinetic investigations undertaken by Weiss led him to propose a chain mechanism based on free radical formation. Mathur and Bansal,[5] employing MnO_4^- as the inducing ion, have kinetically investigated the reduction of mercuric chloride by certain organic acids.[6] They have based the mechanisms, in the respective cases, on the formation of an intermediate complex which on decomposition furnishes the reducing radical. Mechanisms for aqueous decomposition of such manganic complexes have been cited as evidence for free radical generation in the reactant solutions.[7]

The reduction of mercuric chloride to the mercurous state by oxalic acid[8] and tartaric acid[9] induced by $S_2O_8^{2-}$ ion has also been studied kinetically by one of the authors. Kinetic measurements conducted to determine the exponents in the rate law

$$d(Hg_2Cl_2)/dt = k(HgCl_2)^x(C_2O_4^{2-})^y(S_2O_8^{2-})^z$$

showed that $x=0.5$ to 1, $y=0$, and $z=1$.
With tartaric acid the reduction was found to obey a second order rate.

From the references cited above, it is clear that the reduction of mercuric chloride employing peroxodisulphate as the inducing ion, has been investigated only in cases of oxalic and tartaric acids. However, $S_2O_8^{2-}$ induced reduction of mercuric chloride by malic acid remains hitherto uninvestigated from the viewpiont of kinetics and mechanism.

Investigations have revealed that the mechanism, consistent with the observations on induced reduction of mercuric chloride by organic acids, were mainly dependent on the acid-inductor reaction mechanism. Therefore, observations incorporated in this paper were preceded by kinetic studies on the reaction between malic acid and potassium peroxodisulphate so as to ascertain the mechanism involved therein.[10] The paper includes our results on kinetic investigations undertaken to uncover the mechanism of peroxodisulphate induced reduction of mercuric chloride by malic acid.

Experimental

The chemicals employed were of A.R. quality and the solutions contained in pyrex conical flasks were

1) N. R. Dhar, *J. Chem. Soc.*, **111**, 690 (1917).
2) G. H. Cartledge, *J. Am. Chem. Soc.*, **63**, 906 (1941).
3) J. Weiss, *Trans. Faraday Soc.*, **188**, 2 (1947).
4) E. Abel, *Z. Electro. Chem.*, **43**, 629 (1937).
5) P. C. Mathur, Ph. D. dissertation, Agra Univ. (1966).
6) P. C. Mathur and O. P. Bansal, *J. Ind. Chem. Soc.*, **42**, 863 (1965), *ibid.*, **42**, 235 (1965); *ibid.*, **43**, 215 (1966).
7) W. A. Waters, *J. Chem. Soc.*, **1955**, 217, *ibid.*, **1964**, 1192.
8) L. K. Saxena and C. P. Singhal, *J. Ind. Chem. Soc.*, **37**, 405 (1960); *ibid.*, **38**, 863 (1961).
9) L.K. Saxena, Ph.D. dissertation, Agra Univ. (1961).
10) K. Kumar and L. K. Saxena, *J. Ind. Chem. Soc.*, **44**, 612 (1967).

placed in a thermostat maintained at desired temperature. For a single kinetic run the reaction was allowed to progress for different intervals of time in different conical flasks under identical conditions of temperature and concentrations of the reactants. The kinetics was followed by estimating the amount of calomel precipitated in each flasks at desired intervals of time.

Estimation of Calomel. Calomel precipitated was filtered off through a double-walled funnel containing ice-cold water in between its walls. With this technique further reduction of mercuric chloride is prevented even during filtration. The precipitate was then washed and estimated by a standard potassium iodate solution.[11]

Estimation of Peroxodisulphate. Peroxodisulphate was also estimated during a kinetic run. Aliquot portions of the solution, usually 10 m*l* were withdrawn at intervals with a pipette plugged with wool to avoid calomel and analyzed for residual peroxodisulphate by the usual method.[12] Excess of potassium iodide removed mercuric chloride in solution, as complex. Experiments showed that the presence of this complex caused no error.

The apparent first and second order rate constants (k_1 and k_2 respectively) in mercuric chloride were calculated by the established relations. The average rate of mercuric chloride reduction between successive time intervals was calculated by the expression dx/dt, where dx is the amount of mercurous chloride (in mol l^{-1}) formed during an interval dt. Average C signifies the mean concentration of mercuric chloride, between two successive time intervals, calculated in terms of the equivalent titre volume of KIO_3 in m*l*.

Results of Rate Measurements

Preliminary experiments showed that the induced reduction of mercuric chloride by malic acid proceeds with measurable speed at 60°C and with 0.2M initial concentration of the acid. A typical set of results is shown in Table 1.

TABLE 1

Malic acid=0.2M, $HgCl_2$=0.02M,
$K_2S_2O_8$=0.02M, Temp. 60°C.
Period of induction=3 min 30 sec

t min	KIO_3 m*l*	Average C m*l*	Hg_2Cl_2 mol/*l* $\times 10^{-3}$	$10^5(dx/dt)$	10^3k_1	$10k_2$
0	0.0	40.0	—	—	—	—
30	1.7	39.15	0.425	1.416	1.451	1.479
60	4.9	36.70	1.225	2.666	2.168	2.324
120	8.7	33.20	2.175	1.580	2.044	2.316
180	11.0	30.15	2.750	0.958	1.787	2.106
240	12.7	28.15	3.175	0.708	1.592	1.938
300	14.2	26.55	3.550	0.625	1.462	1.835
360	15.6	25.10	3.900	0.583	1.374	1.776
420	16.8	23.80	4.200	0.500	1.297	1.724
480	17.9	22.65	4.475	0.458	1.234	1.689
540	18.8	21.65	4.700	0.375	1.179	1.643
600	19.6	20.80	4.900	0.333	1.122	1.602

The data in Table 1 shows that reduction of mercuric chloride commences after an initial period of induc- tion (3.5 min) and proceeds to about 50% in 10 hr. Figure 1 reveals that the reaction is autocatalytic for a comparatively short period of 60 min, whereafter the rate decreases continuously with time.

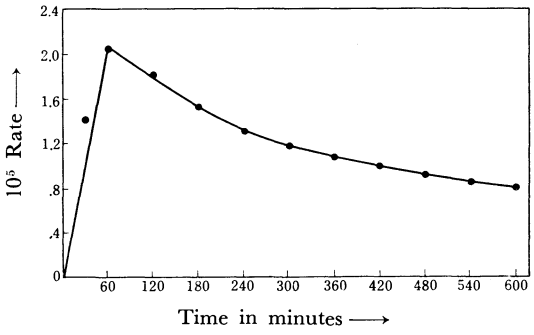

Fig. 1
Malic acid=0.2 M, $HgCl_2$=0.02 M,
$K_2S_2O_8$=0.02 M, Temp.=60°C

First and second order kinetic plots in mercuric chloride revealed marked deviations from linearity; the downward curvatures in each plot signifying the rapid fall in concentration of one of the reactants.[13] Since the reduction of mercuric chloride proceeds only to 50% and is also rapid during the initial few hours, it leads one to suspect that the acid concentration falls much below that of mercuric chloride. This could happen only if the acid is consumed rapidly during the initial stages of the run. It could also be possible that peroxodisulphate concentration may fall much below the acid concentration. But, as will be seen later, this does not happen.

In view of these observations it seems obvious that one is dealing with a complex system wherein, because of the initial rapid consumption of the acid, the reduction does not exceed 50%. This conclusion finds further confirmation from kinetic measurements with initially high acid concentration, which reveal the acid consumption to follow a similar trend. Despite the ratio (Acid)/($HgCl_2$) being kept 50 in certain experiments, we have not been able to obtain reduction of mercuric chloride beyond 50—60% in a period of 10 hr.

Dependence of the Reduction Rate on the Initial Concentration of Reactants. Table 2 records the results of a series of experiments showing the influence of the initial concentration of inductor ($K_2S_2O_8$), actor (malic acid) and acceptor ($HgCl_2$)

11) A. Vogel, "Text book of Quantitative Inorganic Analysis," Longmans, Green & Co., Ltd. New York (1961), p. 361.

12) L. K. Saxena and C. P. Singhal, *Z. Physik. Chem.*, **161**, 211 (1959).

13) A. Weissberger, "Rates and Mechanisms of Reactions," Interscience Publishers, Inc., New York (1961), pp. 191—192.

Table 2

Temp.=60°C

(a) $HgCl_2$=0.01M, $K_2S_2O_8$=0.02M		(b) Acid=0.1M, $K_2S_2O_8$=0.02M			(c) $HgCl_2$=0.01M, Acid=0.1M		
$(Acid)_0$ M	$IR\times10^5$	$(HgCl_2)_0$ M	$IR\times10^5$	$\frac{IR\times10^5}{(HgCl_2)_0^{0.3}}$	$(K_2S_2O_8)_0$ M	$IR\times10^5$	$\frac{IR\times10^2}{(K_2S_2O_8)_0}$
0.15	1.33	0.005	0.89	4.33	0.01	0.58	0.058
0.20	1.41	0.010	1.14	4.55	0.02	1.14	0.057
0.25	1.46	0.015	1.19	4.18	0.03	1.70	0.056
0.30	1.48	0.020	1.36	4.37	0.04	1.60	0.040
0.40	1.54	0.025	1.50	4.53	0.05	1.52	0.030
		0.030	1.62	4.65	0.06	1.50	0.025

on the rate of mercuric chloride reduction. In each experiment the concentrations of two reactants were kept constant and the third was varied as noted in the columns. Since the overall reduction rate changes with time (as shown in Fig. 1), the initial rate (IR) at each concentration was calculated for 120 min from the x–t curves.

The initial reduction rate is not appreciably affected over a range of 0.15M to 0.40M acid concentration which suggests the rate law to be zero order in (malic acid) (Table 2a), and the variation of rate with respect to mercuric chloride concentration can be expressed as $d(Hg_2Cl_2)/dt=k(HgCl_2)^{0.3}$ (Table 2b, Fig. 2).

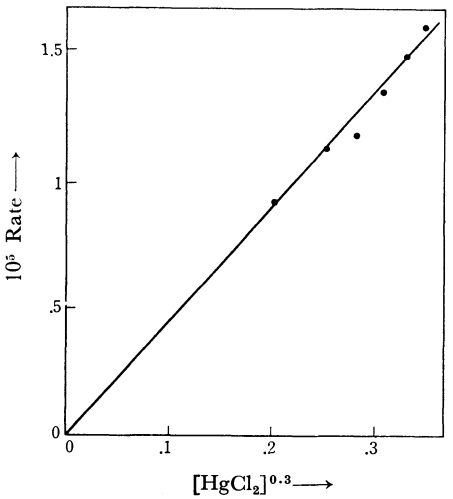

Fig. 2

Malic acid=0.1 M, $K_2S_2O_8$=0.02 M, Temp.=60°C

Scrutiny of results in Table 2(c) shows the reduction rate to be strictly of first order with respect to peroxodisulphate up to 0.03M concentration of the inductor. However, further increase in the initial concentration decreases the reduction rate.

Temperature Dependence. From Fig. 3 it can be seen that increase of temperature increases the overall reaction velocity. The mean energy and

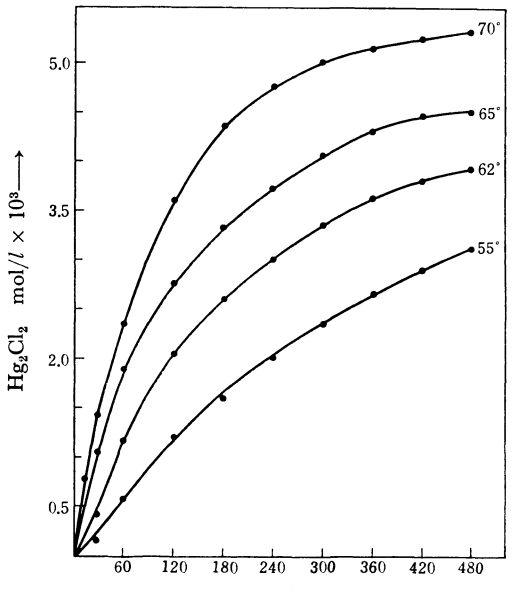

Fig. 3

Malic acid=0.1 M, $HgCl_2$=0.02 M, $K_2S_2O_8$=0.02 M

entropy of activation for the range 55—65°C were found to be 18 kcal/mol and −16 e.u., respectively. It may be pointed out that these values are merely qualitative in nature since they have been calculated from average values of the rate constants from regions exhibiting fair amount of constancy; nevertheless, their order and magnitude helps to evaluate the mechanism of the reaction.

Influence of Gases. Influence of gaseous atmosphere on the reduction rate is represented graphically in Fig. 4. In nitrogen and carbon dioxide atmospheres the reduction rate is faster; the effect of nitrogen being more than carbon dioxide under comparable conditions. Oxygen is found to exert a strong inhibitive influence.

Influence of Acids and Salts. The influence of some acids and their salts was studied to ascertain the role of specific ions on the reduction rate. The percentage reduction of mercuric chloride, in each

TABLE 3

Malic acid=0.05M, $HgCl_2$=0.01M, $K_2S_2O_8$=0.02M, Temp. 60°C

Time	Titre volume of KIO_3 in m*l*					
	Nil.	0.05M HCl	0.05M H_2SO_4	0.05M KCl	0.05M K_2SO_4	0.10M CH_3COONa
0 min	0.0	0.0	0.0	0.0	0.0	0.0
120 min	4.2	0.0	3.4	0.3	4.0	9.7
% Reduction	21.0	0.0	17.0	1.5	20.0	48.5

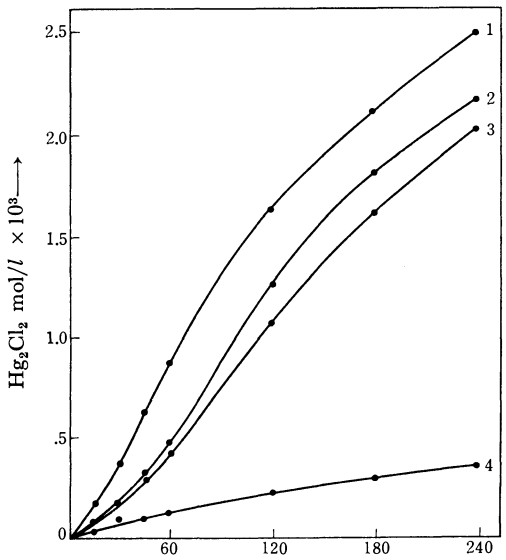

Fig. 4

1. Nitrogen atmosphere
2. Carbon dioxide atmosphere
3. Air atmosphere
4. Oxygen atmosphere

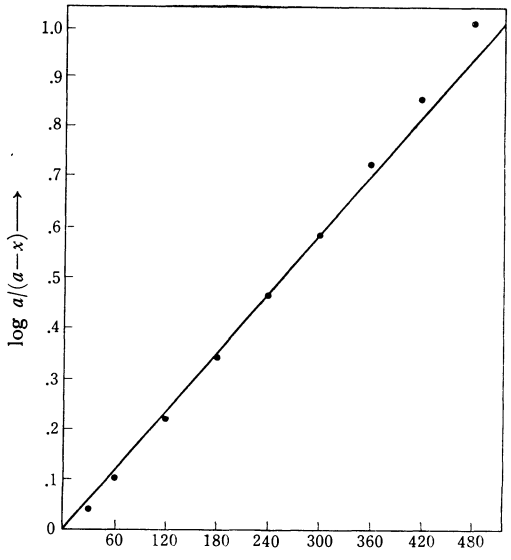

Fig. 5

Malic acid=0.1 M, $HgCl_2$=0.01 M, $K_2S_2O_8$=0.02 M. Temp.=60°C
Slope=0.0019 $k_1=4.3767\times10^{-3}$

case, was calculated as follows:

$$\% = \frac{\text{Titre vol. of } KIO_3 \text{ in m}l}{20\ \text{m}l} \times 100$$

where 20 m*l* KIO_3 volume corresponds to the amount of Hg_2Cl_2 formed on complete reduction of 0.01M $HgCl_2$ in the reaction mixture.

From the foregoing data it may be concluded that H^+ and Cl^- ions inhibit the reduction of mercuric chloride. It appears that Cl^- ion exerts a very strong inhibitive influence. The % reduction is observed to be maximum in the presence of sodium acetate.

Rate of Peroxodisulphate Decomposition. As already mentioned in the experimental part, peroxodisulphate was also estimated. The first order plot at 0.02M concentration of the inductor, is a straight line with a slope giving, $k=4.37\times10^{-3}$ min^{-1}. It can be seen that almost 8 hr are required for the complete decomposition of peroxodisulphate.

The Period of Induction. When peroxodisulphate was added to a solution containing mercuric chloride and malic acid, the reduction of mercuric chloride to the mercurous state did not start immediately. The reduction was observed to begin after a certain time interval after the mixing of the reactants. This time interval has been termed as the period of induction.

Investigations on the induction period were divided into two parts: its dependence on (i) temperature, and (ii) reactant concentration. Results obtained showed that increase in concentration of any of the reactants decreased the period of induction. It was further observed that increase of temperature also decreased this period. Hence, it may be concluded that the induction period depends upon the concentrations of the reactants as well as on the temperature of the reaction. In view of these findings it appears that the induction period is related with the mechanism of the reduction of mercuric chloride.

Discussion

Prolonged oxidation of malic acid by peroxodisul-

phate involves its degradation to malonic acid and carbon dioxide, as revealed by our investigations described earlier.[10] The stoichiometric equation of the reaction verified by us approximates as follows:

$$2K_2S_2O_8 + \begin{matrix}CH_2COOH\\|\\CHOHCOOH\end{matrix} + H_2O$$

$$= CH_2\begin{matrix}COOH\\\diagup\\\diagdown\\COOH\end{matrix} + 4KHSO_4 + CO_2$$

(found: 2 equiv. $S_2O_8^{2-}$: 1 equiv. acid.)

When mercuric chloride is added, the evolution of carbon dioxide sets in immediately, indicative of the degradation of malic acid in this case as well. Products that have been identified are mainly mercurous chloride, malonic acid,[14] carbon dioxide and sulphuric acid. A steady decrease in pH is observed, as the induced reduction of mercuric chloride proceeds, signifying the increase in acidity of the system. Under such conditions the stoichiometry may be represented as follows:

$$2HgCl_2 + \begin{matrix}CH_2COOH\\|\\CHOHCOOH\end{matrix} + K_2S_2O_8 + H_2O$$

$$= Hg_2Cl_2 + CH_2\begin{matrix}COOH\\\diagup\\\diagdown\\COOH\end{matrix} + 2KCl + CO_2 + 2H_2SO_4$$

Malic acid alone, like oxalic and tartaric acids, does not reduce mercuric chloride even on boiling. However, addition of small amounts of peroxodisulphate activates the acid to reduce it. This clearly suggests that as a result of the interaction of malic acid and the inductor, some active substance is produced which reduces Hg^{2+} to Hg^+ state. The mere fact that the reduction commences after an initial period of induction, further lends support to this view. Evidently, the nature of this active species is related to the product of oxidation of malic acid by peroxodisulphate.

At this point it would be pertinent to refer to our investigations carried out earlier on the reaction between $S_2O_8^{2-}$ and malic acid (loc. cit.). The proposed mechanism consistent with the rate data, involves chain sequences with transient products SO_4^- and CO_2^- radicals. It has been our contention that these active transients act as chain carriers and control the mechanism of the process of reduction of mercuric chloride,[15] as has been suggested for oxalic and tartaric acid (loc. cit.).

We believe this reaction to be a free radical chain reaction for the following reasons:

1) It progresses through various successive zones;

2) Fractional order dependence in mercuric chloride concentration is encountered (Fig. 2, Table 2b);

3) The marked inhibition by oxygen implicates CO_2^- as a reactive intermediate, since oxygen is known to inhibit certain chain reactions involving CO_2^- radical;[16,17]

4) Peroxodisulphate-malate reaction is a chain reaction in itself.

A reasonable mechanism, similar to that proposed for oxalic and tartaric acids (loc.cit.) may have the gross features as given below:

Chain Initiating Sequence:

1. $S_2O_8^{2-} = 2SO_4^-$ slow

Chain Propagating Sequences:

2. $SO_4^- + \begin{matrix}CH_2COO^{2-}\\|\\CHOHCOO\end{matrix} = SO_4^{2-} + \begin{matrix}CH_2COO^-\\|\\CHOHCOO\\(\text{unstable})\end{matrix}$ fast

$$\xrightarrow{2OH} CH_2\begin{matrix}COOH\\\diagup\\\diagdown\\COOH\end{matrix} + CO_2^- + H_2O$$

3. $CO_2^- + S_2O_8^{2-} = SO_4^{2-} + SO_4^- + CO_2$ fast

Chain Terminating Sequences:

4. $CO_2^- + Hg^{2+} = Hg^+ + CO_2$ faster than 3

5. $SO_4^- + H_2O = HSO_4^- + OH$ slow

$2OH = H_2O + \frac{1}{2}O_2$ fast

6. $CO_2^- + O_2 = CO_2 + O_2^-$ slow

7. $O_2^- + H^+ = HO_2$ leading to H_2O_2 (3)

8. $CO_2^- + SO_4^- = CO_2 + SO_4^{2-}$ slow at low concs.

The primary step is characteristic of peroxodisulphate decomposition and sequences 2 and 3 have been postulated as the mechanism for the reaction between peroxodisulphate and malic acid (loc.cit.).

The chain initiation is caused by the thermal decomposition of peroxodisulphate ion which undergoes a fission on the weak O–O bond with formation of two sulphate radical ions.[18] In a recent review Wilmarth[19] has discussed at length the role of this active species. He maintains SO_4^- to be energetically capable of reacting with the organic substrate and with the solvent, though with unequal efficiencies. Accordingly, in the beginning step 2 would predominate, producing CO_2^- radical and malonic acid.

14) F. Feigl, "Spot Tests," Elsevier Publishing Co., New York (1960).

15) K. Kumar and L. K. Saxena, *J. Ind. Chem. Soc.*, **43**, 669 (1966).

16) E. Ben Zvi and T. L. Allen, *J. Am. Chem. Soc.*, **83**, 4352 (1961).

17) A. J. Kalb and T. L. Allen, *ibid.*, **86**, 5107 (1964).

18) D. A. House, *Chem. Revs.*, **62**, 185 (1962).

19) W. K. Wilmarth and A. Haim, Peroxide reaction mechanisms, Conference, Rhode Island, 1960.

CO_2^- being a reactive species reacts with peroxodisulphate ion, thereby regenerating SO_4^-. This could lead to a two pronged attack on malate ions (as long as steps 2 and 3 are equally fast). Our results conform to this initial rapid consumption of the acid.

CO_2^- radical also reacts with Hg^{2+} ion resulting in the precipitation of calomel by step 4. Accordingly, the initial period of induction is the time required for the thermal activation of the $S_2O_8^{2-}$ ion so as to break into SO_4^- radicals which produce CO_2^- responsible for the reduction of mercuric chloride. Increase of temperature increases the velocity of the chain initiating process, resulting in the decrease of period of induction. Similarly, increase in the concentration of either malate or $S_2O_8^{2-}$ increases the rate of SO_4^- production by step 1 or by step 2, respectively, thereby decreasing the period of induction. These conclusions are supported by our observations.

The initial auto-catalytic nature of the reduction reaction probably is a result of chain sequences 2 and 3. Due to the two pronged attack on malic acid the rate of CO_2^- production increases. This results in the reaction becoming autocatalytic in the initial stages (Fig. 1). With the progress of the reaction, however, the accumulated acid would inhibit the rate of reduction since it has been observed that H^+ ions inhibit the reduction of mercuric chloride (Table 3) by catalyzing the chain terminating sequence 5 as follows:

9. $SO_4^- + H^+ = HSO_4$

10. $HSO_4 + H_2O = HSO_4^- + OH + H^+$

$$SO_4^- + H_2O = HSO_4^- + OH \qquad (18)$$

This increases the contribution of sequence 5 to the overall chain termination, resulting in the observed rate drop after the induction period (Table 1). Sodium acetate removes H^+ ions, thereby stabilizing SO_4^- with the result that the chains are elongated (Table 3).

The proposed mechanism also accounts for the independence of the reduction rate on malic acid concentration, since step 4 of the mechanism, which governs the reduction of mercuric chloride, involves free radical CO_2^-. Its rate of production is governed by peroxodisulphate concentration. This further explains the first order dependence in peroxodisulphate in low concentration range (Table 2c). With increase in the initial peroxodisulphate concentration, the oxygen content of the system increase, making sequence 11 quite effective:

11. $O_2 + Hg^+ = Hg^{2+} + O_2^-$

Inhibition by oxygen could also occur through reaction with CO_2^- radical (seq. 6) followed by chain termination, as observed by Allen.[17] This finds support from the enhanced rate obtained by the authors working with nitrogen and carbon dioxide atmospheres which might dispel the accumulated oxygen (Fig. 4).

Appendix

$$d(Hg_2Cl_2)/dt = k_4(CO_2^-)(Hg^{2+}) \qquad (1)$$

In the stationary state of chains:

$$d(CO_2^-)/dt = k_2(SO_4^-)(Mal^{2-}) - k_3(CO_2^-)(S_2O_8^{2-}) - k_4(CO_2^-)(Hg^{2+}) - k_6(CO_2^-)(O_2) - k_8(CO_2^-)(SO_4^-) = 0 \qquad (2)$$

and

$$d(SO_4^-)/dt = 2k_1(S_2O_8^{2-}) + k_3(CO_2^-)(S_2O_8^{2-}) - k_2(SO_4^-)(Mal^{2-}) - k_5(SO_4^-) - k_8(CO_2^-)(SO_4^-) = 0 \qquad (3)$$

from 2 and 3 we have:

$$2k_1(S_2O_8^{2-}) = k_5(SO_4^-) + 2k_8(CO_2^-)(SO_4^-) + k_4(CO_2^-)(Hg^{2+}) + k_6(CO_2^-)(O_2) \qquad (4)$$

Consideration of all the termination steps 5—8 would involve a complicated rate term with various limiting-forms. It is not unlikely that one or two of these steps may be most important of all and a consideration of these would lead to a simple rate expression conforming of the experimental facts. The possibility of other steps becoming important under changed conditions is also not ruled out. However, our results can be best explained by assuming steps 6 and 8 to be insignificantly operative in the initial stages of the reaction and therefore considered negligible as compared to the propagating sequences of the proposed mechanism.
Therefore,

$$2k_1(S_2O_8^{2-}) = k_5(SO_4^-) + k_4(CO_2^-)(Hg^{2+}) \qquad (5)$$

Under these conditions, the steady-state concentration

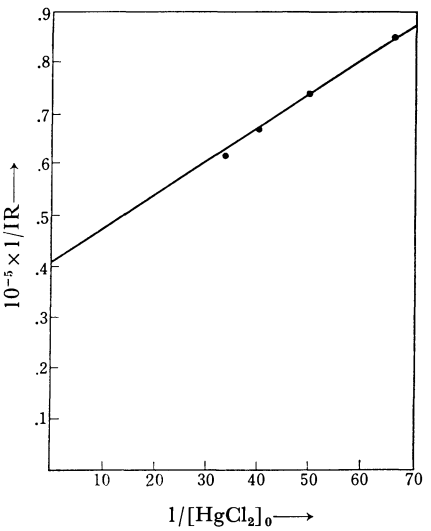

Fig. 6. Dependence of reaction rate on $HgCl_2$ concentration.
Intercept. $= 0.41 \times 10^5$ Slope $= 650$

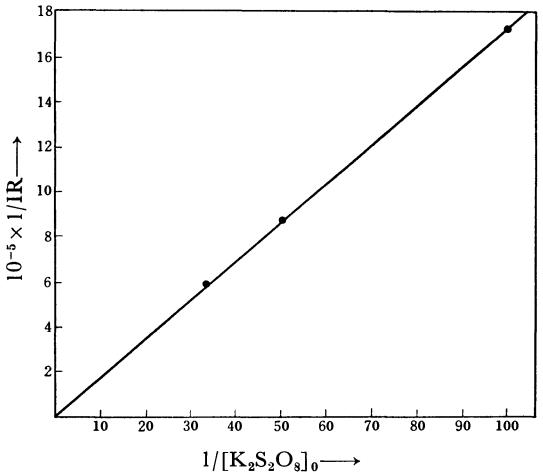

Fig. 7. Dependence of reaction rate on $K_2S_2O_8$ in low concentration range.
Slope = 1745

of SO_4^- as derived from Eq. (2) is:

$$(SO_4^-) = \frac{k_3(S_2O_8^{2-}) + k_4(Hg^{2+})}{k_2(Mal^{2-})}(CO_2^-)$$

Substituting this expression into Eq. (5), we get

$$(CO_2^-) = \frac{2k_1k_2(S_2O_8^{2-})(Mal^{2-})}{k_3k_5(S_2O_8^{2-}) + k_4k_5(Hg^{2+}) + k_2k_4(Mal^{2-})(Hg^{2+})}$$

and

$$\text{rate} = k_4(CO_2^-)(Hg^{2+}) = \frac{2k_1k_2k_4(S_2O_8^{2-})(Mal^{2-})(Hg^{2+})}{k_3k_5(S_2O_8^{2-}) + k_4k_5(Hg^{2+}) + k_2k_4(Mal^{2-})(Hg^{2+})} \quad (A)$$

On the other hand, at the outset of reaction when the stationary state is not yet attained, the rate is given by:

$$\text{rate} = 2k_1(S_2O_8^{2-})\frac{k_4(Hg^{2+})}{k_3(S_2O_8^{2-}) + k_4(Hg^{2+})} \quad (B)$$

In either case the experimental data should fit linear plots of the type

$$1/\text{rate} = a + [b/(\text{reagent})],$$

intercept and slopes of these straight lines giving the constants a and b.

Figures 6 and 7 are such plots of the data in Table 2 and the following tables record the values of rate as obtained by the use of Eq. (B):

TABLE 4. DEPENDENCE OF THE REACTION RATE ON $HgCl_2$ CONCENTRATION
(conditions same as in Table 2)

$(HgCl_2)(mol\,l^{-1})$	0.01	0.015	0.02	0.025	0.03
$10^5(min^{-1})$(obsd)	1.14	1.19	1.36	1.50	1.62
$10^5(min^{-1})$(calcd)*	0.96	1.18	1.36	1.51	1.60

* IR calculated from the relation
$1/\text{rate} = 0.41 \times 10^5 + [650/(Hg^{2+})]$

TABLE 5. DEPENDENCE OF THE REACTION RATE ON $K_2S_2O_8$ IN LOW CONCENTRATION RANGE
(conditions same as in Table 2)

$(K_2S_2O_8)(mol\,l^{-1})$	0.01	0.02	0.03
$10^5(min^{-1})$(obsd)	0.58	1.14	1.70
$10^5(min^{-1})$(calcd)*	0.57	1.14	1.71

* IR calculated from the relation
$1/\text{rate} = O + 1754/(S_2O_8^{2-})$

The observed rates compare reasonably well with those calculated from Eq. (B) (after appropriate choice of values for a and b), thus justifying the proposed reaction scheme and the rate equations derived therefrom.

The authors wish to thank Drs. C. P. Singhal and O. P. Bansal for their interest and encouragement. Thanks are due to Professor P. N. Sharma for his valuable discussion and advice given to the authors. Financial support by the U. G. C. is gratefully acknowledged.

BULLETIN OF THE CHEMICAL SOCIETY OF JAPAN VOL. 42 3155—3158 (1969)

Oscillopolarographic Behaviour of Lanthanide Ions in Potassium Iodide Solutions

Akio IWASE and Chieko YOKOYAMA

Department of Chemistry, Faculty of Science, Yamagata University, Koshirakawa-cho, Yamagata

(Received November 8, 1968)

The oscillopolarographic depolarization effect of lanthanide ions in KI solutions was investigated using dropping (DME) and hanging-drop (HME) mercury electrodes. The lanthanide-ion incision depth in the $dE/dt=f(E)$ curve, measured in a 1M KI solution (pH 3.65) with a DME, was found to be much deeper than that in a 1M KCl solution. The temperature coefficient was negative for the La and Sm incision depths in the temperature range from 25° to 50°C. The incision depths of the La (pH 4.0) and Sm (pH 4.5) ions in a solution with an ionic strength of 0.7 (KCl added) were found to depend on the I^- concentration. These facts seem to show that I^- is adsorbed on DME, and that the adsorbed I^- (at -1.4 V) promotes the electrode reaction of lanthanide ions.

Treindl[1] has reported a study of the oscillopolarographic behaviour of La, Pr, Nd, and Sm ions in KI solutions. He has pointed out that, in a 0.2—1M KI (pH 6.4—6.8) solution, the position of the Q incision quotient of the $dE/dt=f(E)$ curves are 0.66, and that a reversible incision is observed. However, no systematic study of the lanthanide ions has been reported. The present authors have noted previously that the lanthanide-ion incision[2] depth measured in such supporting electrolytes as $NaClO_4$, KCl, KBr, and KSCN depends on the first ionization potential and the basicity of the lanthanides. In this study we investigated the oscillopolarographic behaviour of lanthanide ions in KI solutions; we found that their incision depths are much deeper than those in KCl solutions. This seems to indicate that the deeper incision depth is due to the I^- adsorption on the DME.

Experimental

The preparation of 0.01M lanthanide-ion solutions has been described previously.[2] All the other materials were of a reagent grade and were used without further purification. The KI solutions were prepared just before use. The pH values of the electrolyte solutions were adjusted by adding either a 0.01N HCl or 0.01N NaOH solution. All the experiments except for those shown in Figs. 6 and 7 were carried out in a constant temperature bath at 25 ± 0.1°C. Dissolved oxygen was removed by passing nitrogen gas through.

The curves, $dE/dt=f(E)$, were recorded by a manual Heyrovsky-Forejt-type oscillopolarograph, as has been described previously.[2] DME or HME was used as the polarizable electrode. The characteristics of the DME and the HME were as follows. The value of m with a mercury height of 57.6 cm was 0.936 mg/sec; the dropping time was 1.7 sec (in the 1M KI solution), and the weight of a mercury drop was 0.0058 g. An alternating-current source provided 150 V at 50 cps; a 0.23 mA current (0.12 mA for the experiment in Fig. 2) was passed through the cell. The oscillopolarogram in Fig. 1 was photographically recorded by a Polaroid-Land camera using an Iwasaki UP-7 photo-oscilloscope unit. The incision positions and the depths of the $dE/dt=f(E)$ curves were measured directly on the oscilloscope just before the mercury dropped. The values obtained are the averages of three measurements. The vertical-deflection sensitivity of the oscilloscope was 10.0 mV/cm.

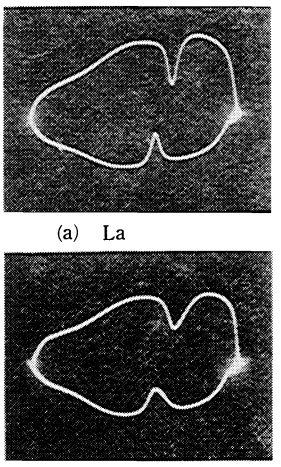

(a) La

(b) Sm

Fig. 1. Typical curves of the $dE/dt=f(E)$ of the lanthanum and samarium ions in a deaerated M KI solution at pH 3.65. The concentration of lanthanide was 0.5 mM and the curves were obtained with a DME.

1) L. Treindl, *Chem. Listy*, **50**, 154 (1956).

2) A. Iwase and C. Yokoyama, This Bulletin, **42**, 2243 (1969).

when the DME was used and 5.5 mV/cm when the HME was used. The horizontal deflection sensitivity was 25 mV/mm.

Results and Discussion

The $dE/dt=f(E)$ curves of La^{3+} and Sm^{3+} are shown in Fig. 1. The solutions contained 5×10^{-4}M La^{3+} (Curve a) or 5×10^{-4}M Sm^{3+} (curve b) in M KI(pH=3.65±0.05). The Q values of the cathodic and anodic incisions were 0.67 and 0.61 respectively. The values are shifted from the Q value, 0.66, of the reversible incision. The Q values for other lanthanide ions were the same as with the lanthanum. Figure 2 shows the incision

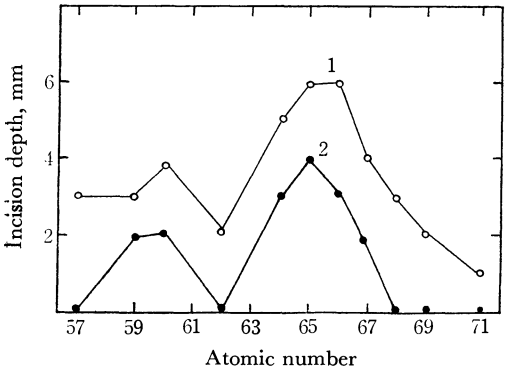

Fig. 2. Variation of the cathodic incision depth with the lanthanides in M (1) KI and (2) KCl solutions at pH 3.65±0.05. The concentration of lanthanides was 0.5 mM.

depth of the 5×10^{-4}M lanthanide solution measured in M KI (curve 1) and in M KCl (curve 2) at pH 3.65 plotted against the atomic number of the lanthanides. The vertical deflection sensitivity was 10 mV/cm for curve 1 and 2.5 mV/cm for curve 2. Curve 1 shows a deeper incision depth than does curve 2. Note that such ions as La^{3+}, Sm^{3+}, Er^{3+}, Tm^{3+}, and Lu^{3+}, which do not give any incision in M KCl (pH 3.65), show a sharp incision in M KI (pH 3.65). The difference between curves 1 and 2 can be difinitely attributed to the presence of I^-.

Therefore, the depth of this incision depends on the concentration and a.c. frequency according to the following formula:[3]

$$h = kc/(kc+4C'\omega^{1/2})$$
$$k = n^2F^2D^{1/2}/RT$$

where C' denotes the differential capacity of the mercury, and ω, the angular frequency. Moreover, the capacity-potential curves reported by Grahame[4]

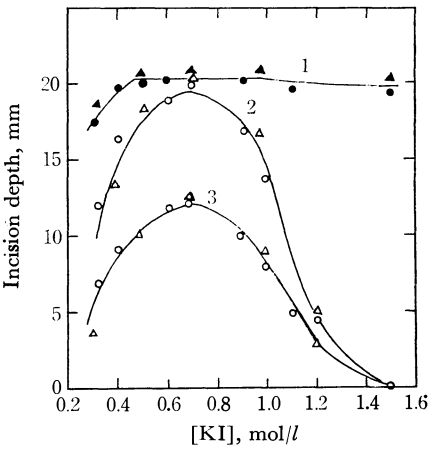

Fig. 3. Effect of potassium iodide concentration on incision depth of the lanthanum and samarium ions. The ploarizable electrode used was a DME for (2) and (3) and a HME for (1).

were the same for mercury in KI and KCl (concentrations not stated) solutions except at potentials markedly were positive than the incision potential for the lanthanide ions. Consequently, it seems that the depth of incision in Fig. 2 is mainly a function of the electrode reaction rate.

The effect of the KI concentration on the electrode reaction of the La^{3+} and Sm^{3+} ions was investigated. Figure 3 shows the incision depths of a 5×10^{-4}M lanthanide (La or Sm) solution of pH 3.65 with KI concentrations from 0.3 to 1.5 M. In this figure, curve 1 is a plot of the cathodic incision depth obtained using HME, while curves 2 and 3 are the plots of the cathodic and anodic incision depths respectively. In curve 1, the incision depth is almost constant over the KI concentration range from 0.4 to 1.0M. However, in curves 2 and 3, the incision depths show a maximum when the KI concentration is about 0.7M, and at a KI concentration of 1.5M, no incision depth was observed. On the contrary, at the KI concentrations, 1.5 and 0.7M, the incision depths in curve 1 are almost the same. It seems that KI promotes or retards the electrode reaction when the concentration is either lower or higher than 0.7M respectively. We interpret this as follows. In a 0.3—0.7M KI solution, the amount of I^- adsorbed on the electrode in the positively-polarized branch with respect to the electro-capillary maximum point, e.c.m., increases with an increase in the I^- concentration in the solution bulk. This results in an increase in the I^- remaining on the electrode surface in the desorption process in the negative polarization region, and it promotes the electrode reaction. In a 0.7—1.5M KI solution the electrode reaction rate decreases as the KI concentration increases. This effect may be attributed to the change in the potential,

3) P. Zuman and I. M. Kolthoff, "Progress in Polarography," Vol. 2, Interscience Publishers, New York (1952), p. 453.

4) P. Delahay, "Double Layer and Electrode Kinetics," Interscience Publishers, New York (1966), p. 123.

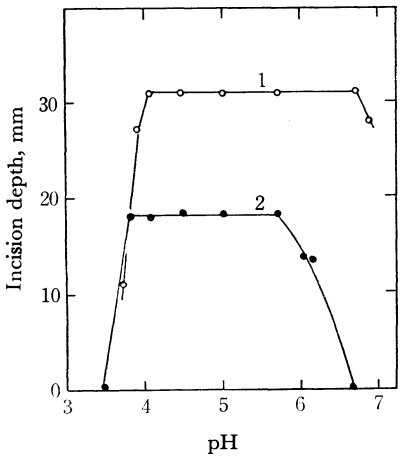

Fig. 4. Effect of pH on incision depth of (1) lanthanum and (2) samarium ions in M KI solution.

ϕ_2*1 (which becomes less negative). A similar phenomenon has been observed with Zn.[5]

Figure 4 shows the effect of the pH on the incision depths of La^{3+} and Sm^{3+} ions. Both curves 1 (La) and 2 (Sm) were measured in solutions containing M KI and 5×10^{-4}M lanthanide ions, with pH values between 3.5 and 6.8. The incision depth was independent of the pH in the region between pH 4.0 and 6.7 for La^{3+} and between pH 3.8 and 5.7 for Sm^{3+}. At higher pH values the incision depth decreased due to the hydrolysis of La^{3+} and Sm^{3+} ions, and with a decrease in pH values in the lower pH region the incision depth decreased, eventually reaching zero at pH values of about 3.5. However, at pH 3.5, a fairly deep incision was observed with the HME. It seems that the cathodic incision of lanthanides is attributable to the reduction of H^+ in hydrated water molecules[6] and that the anodic incision is attributable to the oxidation of lanthanide-halogeno hydride complexes,[7] which are formed by the hydride ions produced at the cathode. Consequently, the increase in the hydrogen-ion concentration on the electrode surface might suppress the formation of lanthanide-halogeno hydride complexes. The ratio of the incision depths of curves 1 and 2 at the plateaus is 1.7, and the depth is greater for La^{3+} than for Sm^{3+}. It is probably true that the larger the ionic size, the less the concentration of the ions in the Helmholtz layers, since the Stokes radius[8] of a Sm^{3+} ion is larger than that of a La^{3+} ion.

Figure 5 shows the relation between the incision depth and the concentrations of La^{3+} and Sm^{3+} ions. Curves 1 and 2 were measured using DME, while curves 3 and 4 were measured using HME in M KI solutions at pH 4.5. Curve 1 is linear in the range of La^{3+} concentrations ranging from 0.5 to 3×10^{-3}M, and curve 2 is linear in throughout the range measured. However, the plot of the ion concentration *versus* the incision depth shows

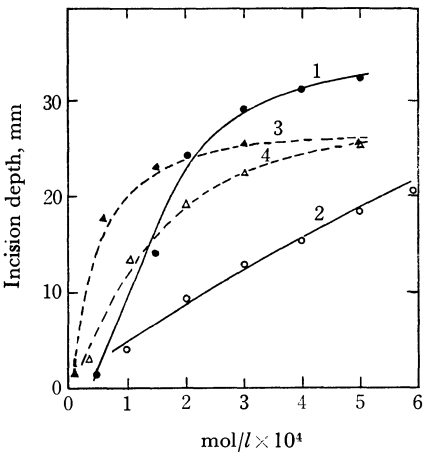

Fig. 5. Calibration curves of lanthanum and samarium ions in M KI solution at pH 4.5. The polarizable electrode used was a DME for 1 (La) and 2 (Sm) and a HME for 3 (La) and 4 (Sm).

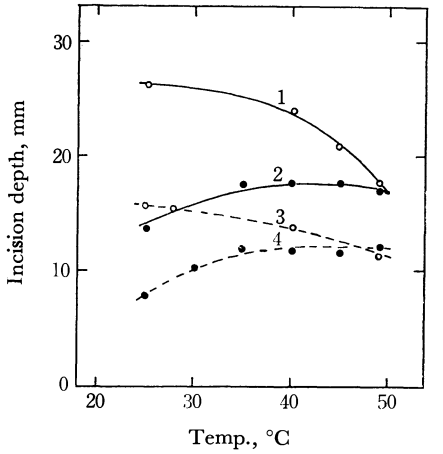

Fig. 6. Temperature dependence of incision depth of the lanthanum ion in KCl plus KI and KCl solutions at pH 4.4 (ionic strength, 0.7). Supporting electrolyte: curve 1 (cathodic) and 3 (anodic), 0.5M KI plus 0.2M KCl; curve 2 (cathodic) and 4 (anodic), 0.7M KCl.

*1 Potential in outer plane of closest approach referred to the potential in the bulk of the solution outside the double layer.

5) T. Fujinaga and M. Maruyama, "Polarography," Vol. 3, Nankodo, Tokyo (1965), p. 201.

6) S. Misumi and Y. Ide, *Mem. Faculty Sci., Kyushu Univ., Ser. C, Chem.*, **3**, No. 3, 205 (1961).

7) J. Heyrovsky and R. Kalvoda, "Oszillographische Polarographie mit Wechselstrom," Akademie-Verlag, Berlin (1960), p. 106.

8) A. Iwase and T. Ito, This Bulletin, **42**, 2064 (1969).

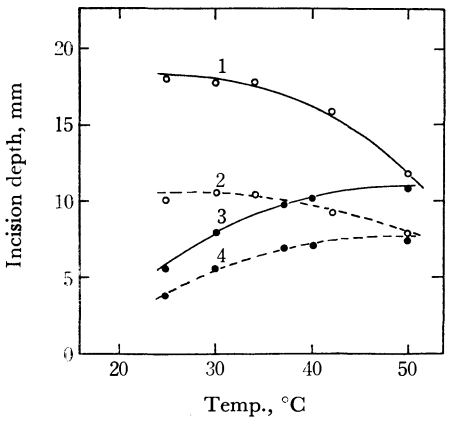

Fig. 7. Temperature dependence of incision depth of the samarium ion in KCl plus KI and KCl solutions at pH 4.4 (ionic strength, 0.7). Supporting electrolyte: curve 1 (cathodic) and 2 (anodic), 0.5M KI plus 0.2M KCl; curve 3 (cathodic) and 4 (anodic), 0.7M KCl.

saturated curves for La^{3+} and Sm^{3+} when the HME is used.

The characteristic behaviour of KI, compared with that of other supporting electrolytes such as KCl or KBr, seems to be due to the adsorption of I^- on the electrode. Accordingly, we investigated the relative temperature dependence of La^{3+} and Sm^{3+}-ion incisions in the KCl and KI solutions. The results are shown in Figs. 6 (La^{3+}) and 7 (Sm^{3+}). In Fig. 6, curve 1 and curve 3 are the cathodic and anodic incisions, respectively, in 0.5M KI plus 0.2M KCl solutions, while curves 2 and 4 are the cathodic and anodic incisions respectively, in 0.7M KCl solutions. All the measurements shown in Fig. 6 were carried out at pH 4.4 in the temperature range from 25° to 50°C and with a 5×10^{-4}M La^{3+} solution. The temperature coefficient of the incision depth in the KI solutions was found to be negative, whereas it was positive in the KCl solutions. The same result was obtained for Sm^{3+} ions (Fig. 7). The concentration dependence of the incision depth was further investigated at I^- concentrations from

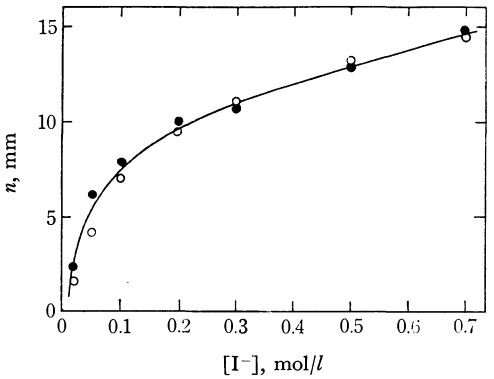

Fig. 8. Relation between the cathodic incision depth of La (pH 4.0) and Sm (pH 4.5) ions and the iodide concentration (ionic strength, 0.7).

0.02 to 0.7M, with the ionic strength kept at 0.7 with KCl. The results are shown in Fig. 8. In this figure, n is the increase in incision depth (in mm) on the addition of iodide ions. The n value increases sharply in the KI concentration range from 0.02 to 0.1M, and then it tends to slope gently above 0.1M. It may be supposed that the ionic adsorption of the I^- on the electrodes has a large effect on the electrode reaction of lanthanide ions, and that, therefore, the iodide complex is formed at the electrode surface. This assumption is also supported by the evidence of curve 1 in Fig. 2, which shows the dependence of the incision depth on the first ionization potential of lanthanides.

The incision depth of lanthanide ions increases with the following order of supporting electrolyte anions:

$$ClO_4^- < Cl^- = Br^- = SCN^- < I^-$$

There is no experimental evidence that Cl^-, Br^-, and SCN^- ions remain on the electrode surface at a negative voltage (−1.4 V). However, since these anions become strongly adsorbed at positive voltages, as is indicated by the above relation, some may remain as a lanthanide complex in the Helmholtz layer.

BULLETIN OF THE CHEMICAL SOCIETY OF JAPAN VOL. 42 3159—3165 (1969)

Polarographic Study of Metal Complexes. VIII.[1] Dicyanobis-(ethylenediamine)cobalt(III) Complex with a *cis*-Configuration[2]

Nobufumi MAKI, Kouei YAMAMOTO, Hiroshi SUNAHARA*1 and Shukichi SAKURABA

Department of Chemistry, Faculty of Engineering, Shizuoka University, Johoku, Hamamatsu

(Received November 12, 1968)

In an aqueous solution containing an excess of ethylenediamine, *i. e.*, under the conditions where the aquation is prevented, the dicyano-cobalt(III) complex, *cis*-$[Co(CN)_2en_2]NO_3$, has been found to be reduced in three steps at the dropping mercury electrode (DME). The first step, corresponding to the acceptance of one electron, represents the reduction from the cobalt(III) to the cobalt(II) state, while the second and the third step were interpreted as being due to the reduction of two kinds of the cobalt(II) species formed by the overall rearrangement of ligands in solution. One such kind of cobalt species is the binuclear tetracyanocobaltate(II) complex, $[Co(CN)_4\text{-en-}Co(CN)_4]^{4-}$, which is reduced to the metal through the cobaltate(I) complex, while the other is the cobalt(II) complexes with ethylenediamines in an equilibrium state, which are reduced directly to the metal at the DME. Namely, the second step represents the reduction from the cobalt(II) complex of the former to the cobalt(I) state, while the third step, denoting the reduction to the metal, was observed only on the dE/dt-E curve of the oscillopolarogram, but not on the current-potential curve due to the maximum wave. In the non-aqueous solution of dimethyl sulfoxide, the dicyano-cobalt(III) complex, *cis*-$[Co(CN)_2en_2]ClO_4$, undergoes the step-by-step reduction of Co(III)→Co(II)→Co(I)→Co(0), as it were, at the DME. Neither aquation nor rearrangements of ligands take place throughout reductions under these experimental conditions, that is, even in lower oxidation states of the cobalt.

The ammine and amine cobalt(III) complexes have hitherto been well known to be reduced to the metal through the hexaquocobalt(II) ions at the dropping mercury electrode (DME). Namely, this kind of reduction type is regarded as belonging to the group of the "*inert-labile*" type according to the classification of Vlček.[3]

On the other hand, the cyano-cobalt(III) complexes in general exhibit a reduction of the "*inert-inert*" type from the view-point of the lability of the complex. For example, the pentacyanocobaltate(III) complexes are reduced to the cobaltate(I) complex in one or two steps at the DME.[4,5]

The polarography of the tetracyano complexes, $Na_5[Co(CN)_4(SO_3)_2]$ and $K[Co(CN)_4en]\cdot H_2O$, proves that the tetracyanocobaltate(I) complexes can exist stably in solution during reduction when such labile ligands as ethylenediamine and SO_3^{2-} ions are present in solution in an overwhelmingly large excess.[6] The net electrode processes of the tetracyanocobaltate(III) complexes are thus simplified under these conditions.[1,6]

As for the dicyano-cobalt(III) complexes, however, the aquation and the overall rearrangement of ligands are both involved in the electrode processes. Accordingly, in the presence of an excess of ethylenediamine, only the latter appears to take place through the electrode reduction. In the present work, most of our effort was devoted to elucidating the effects of the overall rearrangement of ligands on the current-potential curves.

On the other hand, the electrode processes are ultimately simplified in dimethyl sulfoxide (DMSO), since the dicyano-cobalt(II) and cobalt(I) complexes are regarded as "*inert*"-type complexes in such a non-aqueous solvent. Hence, the polarographic behavior in DMSO will be dealt with here briefly for the sake of comparison, because such simplified processes of the electrode reaction may serve to

1) Previous paper of this series: N. Maki and K. Okawa, *J. Electroanal. Chem.*, **8**, 262 (1964).

2) Presented at the 21st Annual Meeting of the Chem. Soc. Japan, held at Osaka, April 2, 1968.

*1 H. S., Present address: Government Industrial Research Institute, Hirate-machi, Kita-ku, Nagoya.

3) A. A. Vlček, *Collection Czechoslov. Chem. Commun.*, **24**, 3572 (1959).

4) D. N. Hume and I. M. Kolthoff, *J. Am. Chem. Soc.*, **71**, 867 (1949).

5) N. Maki, J. Fujita and R. Tsuchida, *Nature*, **183**, 458 (1959); N. Maki, *ibid.*, **195**, 682 (1960).

6) N. Maki and R. Tsuchida, This Bulletin, **34**, 891 (1961).

provide information which can then be used in interpreting more complicated processes of the polarographic reduction in an aqueous solution.

In the present paper, however, the polarographic reduction of the dicyano-cobalt(III) complex, *cis*-$[Co(CN)_2en_2]NO_3$, was dealt with mainly in an aqueous solution containing ethylenediamine.

Experimental

Apparatus. The experimental details of the measurements have been described previously.[1] The current-potential curves of the cobalt(II) complex in the presence of ethylenediamine were determined in a stream of nitrogen which had previously been passed through the same supporting electrolyte containing ethylenediamine. The current-time (t) curves were recorded on a Yanagimoto Polarovision model PE 20 equipped with a National X-Y recorder, model VR 301. The potential (E) - dE/dt curves were photographed on a Polaroscope P 576 of Kovo, Inc. The characteristics of the capillary used were as follows: m=1.81 mg/sec and t=4.43 sec (both of which values were measured in a 0.5M Na_2SO_4 solution containing 1M en), and m=1.69 mg/sec and t=4.42 sec in a 0.5M Na_2SO_4 aqueous solution only.

Materials. Twenty grams of *trans*-$[CoCl_2en_2]NO_3$,[7] were suspended in 700 m*l* of distilled water, mixed with 20 g of AgCN, and then heated on a water bath (90°C) for three hours. The color of the solution changed from green to yellow. The solution was then filtered, and the filtrate was concentrated by evaporation to one-third its former volume. When the solution was allowed to stand, silky-yellow crystals separated from the solution; these were filtered and washed with cold water, ethanol, and ether. The crude product was recrystallized from hot water.[8] Found: Co, 19.98; C, 24.49; N, 33.49; H, 5.63%. Calcd for $[Co(CN)_2en_2]NO_3$: Co, 20.10; C, 24.58; N, 33.44; H, 5.50%. The absorption spectrum in the visible and ultraviolet regions agrees with that reported by Ohkawa *et al.*[9]

The perchlorate of the complex was analogously obtained by treating *trans*-$[CoCl_2en_2]ClO_4$ (20 g) with 22 g of AgCN instead of the nitrate of the praseo salt. Found: Co, 17.90; C, 21.78; N, 25.34; H, 4.90%. Calcd for $[Co(CN)_2en_2]ClO_4$ (anhydrous): Co, 17.83; C, 21.80; N, 25.42; H, 4.88%. For making polarographic measurements in DMSO, the perchlorate of the complex is suitable; it was used since its solubility in DMSO is considerably larger than that of the corresponding nitrate.

The binuclear complex of potassium μ-ethylenediamine-bis{tetracyanocobaltate(II)} monohydrate was prepared according to the directions of Ripân *et al.*[10] Found: Co, 20.98; C, 21.22; N, 24.86; H, 1.91%. Calcd for $K_4[Co(CN)_4\text{-en-}Co(CN)_4]\cdot H_2O$: Co, 21.03; C, 21.43; N, 24.99; H, 1.80%.

Results and Discussion

The *cis*-$[Co^{III}(CN)_2en_2]^+$ ion behaves quite differently polarographically, depending upon the experimental conditions, especially on whether or not the supporting electrolyte contains an excess of ethylenediamine (en) and cyanide ions. Therefore, the electrode processes were studied and discussed in these four cases: (1) in an aqueous solution of 0.5M Na_2SO_4 only; (2) in a water solution containing 1M en and 0.5M Na_2SO_4; (3) in a water solution containing 1M en, 0.1M KCN and 0.45M Na_2SO_4, and (4) in dimethyl sulfoxide (100%) containing 0.1M $[(C_2H_5)_4N]ClO_4$.

1) In an Aqueous Solution of 0.5M Na_2SO_4 Containing No Ethylenediamine. Here the *cis*-$[Co(CN)_2en_2]^+$ ion gives rise to waves of two steps at the DME. The ratio of the height of the first wave to that of the second is approximately 1 : 2. The electrode process of the first step is of the *"inert-labile"* type and is considered to be quite similar to that of the usual ammine cobalt(III) complexes. That is, the resulting cobalt(II) complex of the *"labile"* type is broken up into several kinds of aquocobalt(II) species, which are subsequently reduced to the metal at the DME:

$$\underset{inert}{cis\text{-}[Co^{III}(CN)_2en_2]^+} \xrightarrow{e} \underset{labile}{cis\text{-}[Co^{II}(CN)_2en_2]}$$

$$\downarrow$$

$$[Co^{II}(CN)_2(OH_2)_4],\ etc. + 2en$$

$$\downarrow 2e$$

$$Co(metal) + 2CN^-.$$

2) In an 0.5M Na_2SO_4 Aqueous Solution Containing 1M Ethylenediamine. Here the *cis*-$[Co(CN)_2en_2]^+$ ion gives rise to the well-defined waves of two steps at the DME. The third or the last step is not distinct in conventional polarography,

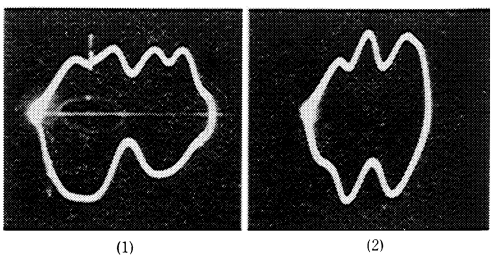

(1) (2)

Fig. 1. The oscillopolarograms of dE/dt - E curves of the *cis*-$[Co(CN)_2en_2]^+$ ion (10^{-3}M) obtained; (1) in the 0.5M Na_2SO_4 aqueous solution containing 1M ethylenediamine; (2) in the 0.5M Na_2SO_4 solution only.

7) S. M. Jørgensen, *J. Pr. Chem.*, **41**, 252 (1890); *Gmelins Handbuch der anorganischen Chemie.* Nr. 58, Teil B Kobalt, Verlag Chemie, GmbH, Berlin (1930), p. 239.

8) Briefly reported: N. Maki, T. Hamazaki and S. Sakuraba, This Bulletin, **41**, 1735 (1968); N. Maki and S. Sakuraba, *ibid.*, **42**, 1908 (1969).

9) K. Ohkawa, J. Fujita and Y. Shimura, *ibid.*, **38**, 66 (1965).

10) R. Ripân, A. Farcăs and O. Piringer, *Z. anorg. u. allgem. Chem.*, **346**, 211 (1966).

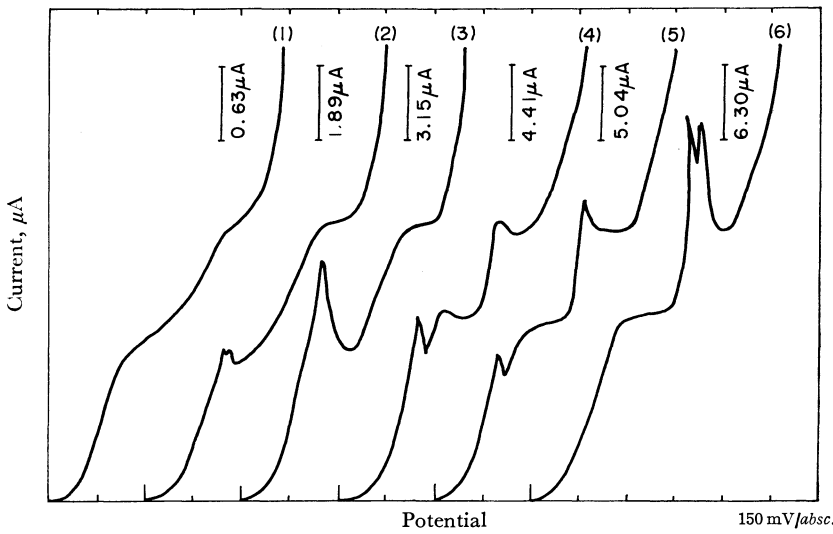

Fig. 2. The dependence of the current-potential curves on the concentration of the complex: (1) 10^{-3}; (2) $3\cdot10^{-3}$; (3) $5\cdot10^{-3}$; (4) $7\cdot10^{-3}$; (5) $8\cdot10^{-3}$; (6) 10^{-2}M (25°C).
Supporting electrolyte: 0.5M Na_2SO_4 + 1M en
Recorded from −0.60 V *vs.* SCE.

but it was seen to exist in the oscillopolarogram of the Heyrovský-Forejt type: indeed, the last step was covered completely with the large maximum, which could not be suppressed with a usual surface-active agent, such as Triton X 100*2 or gelatin.

Figure 1 shows the dE/dt - E (potential) curves photographed in the presence and the absence of excess ethylenediamine. In the former case three cuts were observed on the cathodic branch of the curve: the first two cuts correspond to the reduction waves of two steps in the classical d. c. polarogram, while the last cut may correspond to the last step of the maximum, which probably represents the reduction to the metallic cobalt, since only a cut ($Co \rightarrow Co^{II}$) was noticed on the anodic branch of the curve.

On the other hand, in the latter case two cuts were seen to exist on the cathodic branch of the curve; these cuts correspond to the reductions of Co(III)→Co(II) and of Co(II)→Co(*metal*) respectively.

The limiting current of the first and the second wave is linearly related to the concentration of the complex in the range between $4\cdot10^{-4}$ and $2\cdot10^{-2}$M. The ratio of the height of the first wave to that of the second is approximately 1 : 0.5. The limiting current of each step was found to be proportional to the square root of the height of the mercury reservoir, as is shown in Table 1. The values of $i_1/\sqrt{h_{corr.}}$ are independent of the increase in mercury pressure. Accordingly, the

Table 1. The relationship between the current and height of the mercury reservoir (25°C)

h_{corr}	i_1(μA)	i_2(μA)	$i/\sqrt{h_{corr}}$	$i_2/\sqrt{h_{corr}}$
91.4	11.2	5.3	1.17	0.55
86.4	10.8	5.0	1.16	0.54
81.4	10.3	4.9	1.14	0.54
76.4	9.9	4.8	1.13	0.55
71.4	9.5	4.6	1.12	0.54
66.4	9.2	4.4	1.13	0.54
61.4	8.8	4.1	1.12	0.52

The concentration of the complex: $7\cdot10^{-3}$M;
Supporting electrolyte: 0.5M Na_2SO_4 + 1M en
In the presence of 0.0021% Triton X 100

*2 Triton X 100=Alkyl-aryl-polyether alcohol.

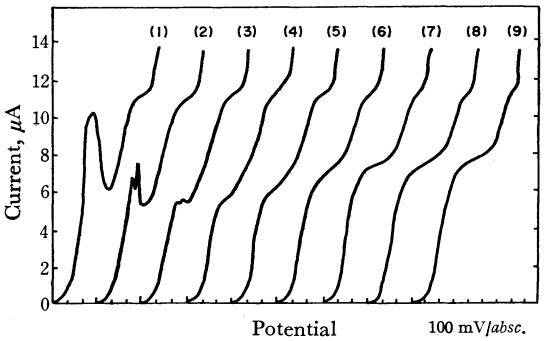

Fig. 3. The effect of Triton X 100 on the current-potential curves (25°C).
The concentration of Triton X 100: (1) 0; (2) 0.00042%; (3) 0.00084%; (4) 0.00126%; (5) 0.00168%; (6) 0.00210%; (7) 0.00252%; (8) 0.00294%; (9) 0.00336%.
Supporting electrolyte: 0.5M Na_2SO_4+1M en
Concn. of the complex: $5\cdot10^{-3}$M
Recorded from −0.70 V *vs.* SCE

limiting current of both the waves is diffusion-controlled. This conclusion was also supported by the results of the analyses of *i-t* curves coupled with the temperature-dependence of the limiting currents, as will be discussed hereafter.

Figure 2 shows the dependence of the current-potential curve on the concentration of the complex. In the figure, the current scale was individually curtailed, lest the current scale should change with the concentration of the complex. The two maxima observed at higher concentrations are considered to be due to the adsorption of the complex on the DME, judging from the electrocapillary curves measured. The maxima could be suppressed in the presence of Triton X 100 more than 0.0025%, as is shown in Fig. 3.

Figures 4 and 5 show the effect of Trition X 100 on the diffusion currents of both the waves obtained at the concentration of the complex of 10^{-3} and $5\cdot10^{-3}$M. In the figure, at the steady state, *i. e.*, when Triton X 100 suppresses the maxima to exclude the adsorption of the complex on the DME, the height of the second wave is seen to become nearly a half of that of the first wave.

Figure 6 shows the effect of an excess of ethylenediamine on the current-potential curve at the 10^{-3}M complex ion. At concentrations higher than 0.007M, the single wave is seen to split into the double wave. This fact suggests that the cobalt(II) complexes formed at the first step of the reduction react with each other in the presence of excess ethylenediamine to produce two kinds of stable new species. One of the species might be the binuclear tetracyanocobaltate(II) complex, $[Co(CN)_4\text{-en-}Co(CN)_4]^{4-}$, formed partly as a result of the overall rearrangement of ligands in solution, which is reduced in two steps to the metal through the cobaltate(I) complex; the other of the cabalt(II) species is a mixture of the aquocobalt(II) complexes with ethylenediamines in an equilibrium state, with all the elements being reduced directly to the metal at the DME. That is, the reduction of the former to a cobalt(I) state takes place at -1.18 V *vs.* SCE, while the reduction of the latter to the metal is not observed because of the maximum. In short, the former is polarographically active, but the latter is apparently inactive. Consequently, the fact that the wave-height of the second step, corresponding to an apparently 1/2 electron reduction, is always a half of that of the first step can be explained in terms of the following processes of the electrode reaction:

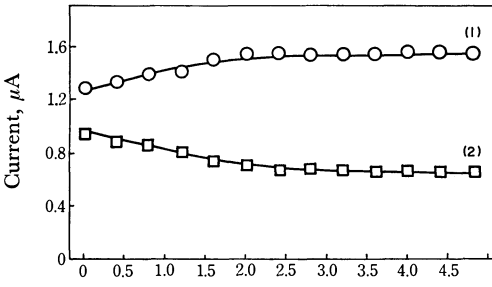

Fig. 4. The effect of Triton X 100 on the limiting currents of the first and the second wave obtained at 10^{-3}M complex ion: (1) 1st wave; (2) 2nd wave.
Supporting electrolyte: 0.5M Na_2SO_4 + 1M en (25°C)

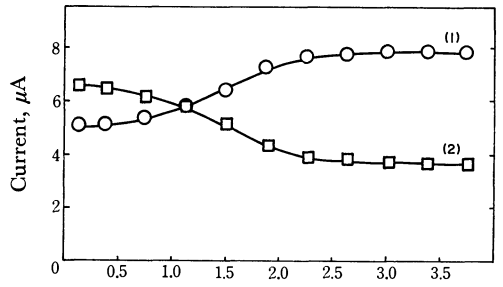

Fig. 5. The effect of Triton X 100 on the limiting currents of the first and the second wave obtained at $5\cdot10^{-3}$M complex ion: (1) 1st wave; (2) 2nd wave.
Supporting electrolyte: 0.5M Na_2SO_4 + 1M en (25°C).

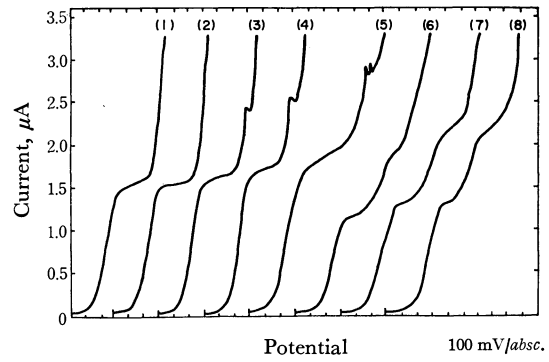

Fig. 6. The effect of the ethylenediamine on the current-potential curves obtained at 10^{-3}M complex ion in the 0.5M Na_2SO_4 solution (25°C).
The concentration of ethylenediamine: (1) 0.00; (2)0.01; (3) 0.03; (4) 0.05; (5) 0.06; (6) 0.07; (7) 0.09; (8) 0.10M
Recorded from -0.60 V *vs.* SCE

$$4\,cis\text{-}[Co^{III}(CN)_2en_2]^+ \xrightarrow{4e} 4\,cis\text{-}[Co^{II}(CN)_2en_2]$$
inert → *labile*

$$[Co^{II}(CN)_4\text{-en-}Co^{II}(CN)_4]^{4-} \qquad 2\,[Co^{II}(OH_2)_n en_m]^{2+}$$

$$\downarrow 2e \qquad \downarrow 2e$$

$$2\,[Co^{I}(CN)_4en]^{3-} \qquad 2\,Co(metal)$$

$$\downarrow 2e$$

$$2\,[Co^{0}(CN)_4]^{4-}$$

$$\downarrow$$

$$2\,Co(metal)$$

In the previous paper,[1] the tetracyanocobaltate(I) complex, $[Co^{I}(CN)_4en]^{3-}$, was speculated to be present stably in a solution containing ethylenediamine. Furthermore, Watt *et al.*[11,12] have reported isolating two complexes, $K_3[Co^{I}(CN)_4]$ and $K_4[Co^{0}(CN)_4]$, as solids by the reduction of $K_3[Co(CN)_6]$ in liquid ammonia with metallic potassium. Therefore, it would not be out of the way to assume that such tetracyanocobaltate(I) and cobaltate(0) complexes are present in solution as intermediates in the reduction process.

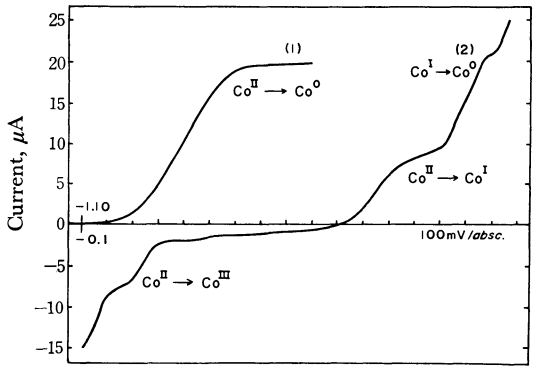

Fig. 7. The current-potential curves of the cobalt(II) complexes: (1) $[Co(OH_2)_6]^{2+}$ ion (10^{-2}M) in 0.5M Na_2SO_4 solution; Recorded from −1.10 V *vs.* SCE. (2) $K_4[Co(CN)_4\text{-en-}Co(CN)_4]\cdot H_2O$ ($5\cdot10^{-3}$M) in 0.5M Na_2SO_4 solution containing 1.5M ethylenediamine (25°C); Recorded from −0.10 V *vs.* SCE in a stream of nitrogen.

Figure 7 shows the current-potential curve for $K_4[Co(CN)_4\text{-en-}Co(CN)_4]\cdot H_2O$ obtained in a stream of nitrogen. For comparison, the two-electron reduction wave of the hexaquocobalt(II) ion is also shown in the figure. Both the curves were obtained at the same concentration of the cobalt(II). The $[Co(CN)_4\text{-en-}Co(CN)_4]^{4-}$ ion gave rise to waves of two steps: the first and the second wave, corresponding to a gain of one electron,

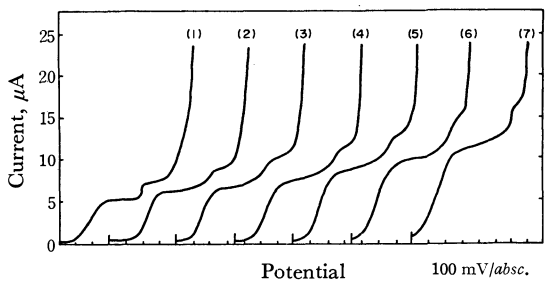

Fig. 8. The dependence of the current-potential curves upon the temperatures obtained at the concentration of the complex, $5\cdot10^{-3}$M, in the 0.5M Na_2SO_4 solution containing 1M ethylenediamine. The temperature of the electrolyte: (1) 0°C; (2) 10°C; (3) 20°C; (4) 30°C; (5) 40°C; (6) 50°C; (7) 60°C.
Recorded from −0.70 V *vs.* SCE

Table 2. The half-wave potentials of the waves for the mixed cyano cobalt(III) and cobalt(II) complexes (25°C)

Compound	1st wave	2nd wave	3rd wave	Supporting electrolyte
cis-$[Co(CN)_2en_2]NO_3$	−0.95 ($Co^{III}\rightarrow Co^{II}$)		−1.38 ($Co^{II}\rightarrow Co^{0}$)	0.5M Na_2SO_4 aq. soln.
	−0.86 ($Co^{III}\rightarrow Co^{II}$)	−1.18 ($Co^{II}\rightarrow Co^{I}$)	—* ($Co^{II}\rightarrow Co^{0}$)	0.5M Na_2SO_4+1M en 0.00084% Triton X 100
	−0.78 ($Co^{III}\rightarrow Co^{II}$)	−1.33 ($Co^{II}\rightarrow Co^{I}$)	—* ($Co^{I}\rightarrow Co^{0}$)	0.45M Na_2SO_4+1M en +0.1M KCN
cis-$[Co(CN)_2en_2]ClO_4$	−0.95 ($Co^{III}\rightarrow Co^{II}$)	−1.48 ($Co^{II}\rightarrow Co^{I}$)	−1.99 ($Co^{I}\rightarrow Co^{0}$)	DMSO(100%)+0.1M $(C_2H_5)_4NClO_4$
trans-$[Co(CN)_2en_2]NO_3$	−0.87 ($Co^{III}\rightarrow Co^{II}$)	−1.20 ($Co^{II}\rightarrow Co^{I}$)	—* ($Co^{II}\rightarrow Co^{0}$)	0.5M Na_2SO_4+1M en
	−0.78 ($Co^{III}\rightarrow Co^{II}$)	−1.31 ($Co^{II}\rightarrow Co^{I}$)	—* ($Co^{I}\rightarrow Co^{0}$)	0.45M Na_2SO_4+1M en +0.1M KCN
trans-$[Co(CN)_2en_2]ClO_4$	−0.97	−1.52	−1.99	DMSO(100%)+0.1M $(C_2H_5)_4NClO_4$
cis-$[Co(CN)_2dip_2]NO_3\cdot 7H_2O$	−0.43 ($Co^{III}\rightarrow Co^{II}$)	−0.87 ($Co^{II}\rightarrow Co^{I}$)	−1.23 ($Co^{II}\rightarrow Co^{0}$)	0.5M Na_2SO_4 aq. soln.
cis-$[Co(CN)_2phen_2]NO_3\cdot 6H_2O$	−0.42 ($Co^{III}\rightarrow Co^{II}$)	−0.86 ($Co^{II}\rightarrow Co^{I}$)	−1.22 ($Co^{II}\rightarrow Co^{0}$)	0.5M Na_2SO_4 aq. soln.
$K_4[Co(CN)_4\text{-en-}Co(CN)_4]\cdot H_2O$	−0.32 ($Co^{II}\rightarrow Co^{III}$)	−1.23 ($Co^{II}\rightarrow Co^{I}$)	−1.57 ($Co^{I}\rightarrow Co^{0}$)	0.5M Na_2SO_4+1.5M en 0.00084% Triton X 100
$K[Co(CN)_4en]\cdot H_2O$[1]	−1.36 ($Co^{III}\rightarrow Co^{I}$)	−1.51 ($Co^{I}\rightarrow Co^{0}$)		0.5M Na_2SO_4+2M en 0.0078% Triton X 100

Voltage unit: volt *vs.* SCE * The maximum wave

11) G. W. Watt and R. J. Thompson, *J. Inorg. Nucl. Chem.*, **9**, 311 (1959).

12) G. W. Watt, J. L. Hall, G. R. Choppin and P. S. Gentile, *J. Am. Chem. Soc.*, **76**, 373 (1954); W. Hieber and C. Bartenstein, *Naturwissenschaften*, **13**, 300 (1952).

represent the step-by-step reduction of Co(II)→Co(I) and of Co(I)→Co(0) respectively. The half-wave potential (−1.23 V *vs.* SCE) of the first step ($Co^{II}\rightarrow Co^{I}$) is near that of the second wave for the *cis*-$[Co(CN)_2en_2]^+$ ion, as Table 2 shows. Therefore, the second step for the *cis*-$[Co(CN)_2en_2]^+$ ion may be concluded to represent the overall reduction from the binuclear tetracyanocobaltate(II) to the cobaltate(I) complex at the DME.

Figure 8 shows the temperature-dependence of the current-potential curves. The diffusion currents are linearly related with the temperature; the tangents of the lines for the first and the second wave-heights are 1.25 and 1.23% at 25°C respectively. The shape of the second wave at higher temperatures becomes more obvious than that at lower temperatures.

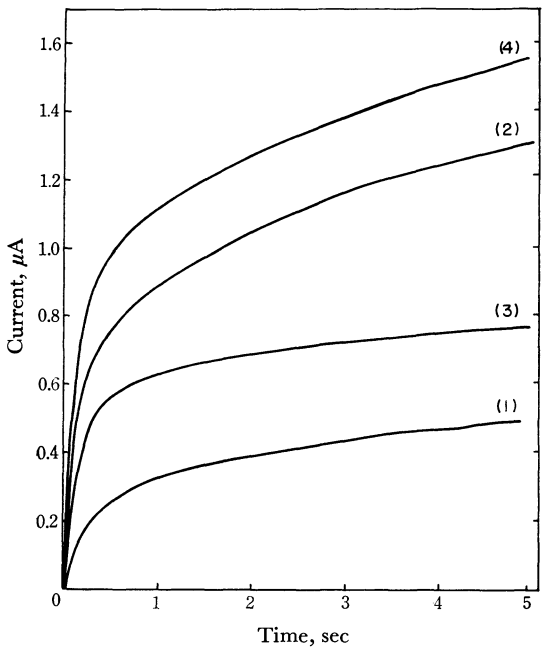

Fig. 9. The current-time curves of the *cis*-$[Co(CN)_2en_2]^+$ ion recorded during one drop growth of DME at the potentials: (1) −0.85; (2) −1.00; (3) −1.18; (4) −1.35 V *vs.* SCE.
Supporting electrolyte: 0.5M Na_2SO_4 + 1M en (25°C)

Figure 9 shows the current-time curves during a one-drop growth of DME obtained at a constant potential. The current varies with time to the powers of 0.17 and 0.19 at the potentials at which the first and the second step respectively exhibit the limiting currents. This result, combined with the above-mentioned finding in relation to the effect of the mercury head, supports the conclusion regarding the diffusion-controlled features of both the waves in a supporting electrolyte of this sort.

3) In a 0.45M Na_2SO_4 Aqueous Solution Containing 0.1M KCN and 1M Ethylenediamine. Here the *cis*-$[Co(CN)_2en_2]^+$ ion similarly gave rise to well-defined waves of two steps at the DME. The second wave-height, however, increases twice as much as that in a solution containing no excess cyanide ions, that is, in a solution containing only excess ethylenediamine. More exactly, the ratio of the wave-heights of the first and the second waves was 1 : 1.03 which had been corrected for the drop time. Undoubtedly, the cyanide ions in excess are available for producing the binuclear tetracyanocobaltate(II) complex through the rearrangement of ligands in solution.

The limiting currents of the two steps were found to be proportional to the square root of the mercury pressure on the DME; the limiting currents exhibit the diffusion-controlled feature.

In addition to these results, the d. c. polarogram of two steps for the $K_4[Co(CN)_4\text{-en-}Co(CN)_4]\cdot H_2O$ (a pale yellow crystal) dissolved in a 0.45M Na_2SO_4 solution containing both 0.1M KCN and 1M ethylenediamine agrees quite well with that of the hexaquocobalt(II) chloride dissolved in the same supporting electrolyte in the shape of the waves and in the half-wave potentials (see Table 2).

The presence of ethylenediamine in excess is essential for the existence of the $[Co(CN)_4\text{-en-}Co(CN)_4]^{4-}$ ion in water solution, but the cyanide ions in excess are not necessary; the binuclear tetracyanocobaltate(II) complex should be regarded as "*partly-labile.*"

Accordingly, the net processes of the electrode reaction presented below may be considered to be the most plausible:

$$2\ cis\text{-}[Co^{III}(CN)_2en_2]^+ \xrightarrow{2e} 2\ cis\text{-}[Co^{II}(CN)_2en_2]$$
$$\downarrow$$
$$[Co^{II}(CN)_4\text{-en-}Co^{II}(CN)_4]^{4-}$$
$$\downarrow 2e$$
$$2\ [Co^{I}(CN)_4en]^{3-}$$
$$\downarrow 2e$$
$$2\ [Co^{0}(CN)_4]^{4-}$$
$$\downarrow$$
$$2\ Co(metal)$$

in the presence of both CN^- ions and en.

Thus, all the resulting cobalt(II) species of the $[Co^{II}(CN)_2en_2]$ complex are presumed to be totally subject to the rearrangement of ligands to produce a binuclear tetracyanocobaltate(II) complex in solution; this is then reduced to the metal through the cobaltate(I) complex at the DME. Under these experimental conditions, no aquation occurs, and only the rearrangement of ligands is discerned to take place in solution.

4) In Dimethyl Sulfoxide (100%) Con-

taining 0.1M $[(C_2H_5)_4N]ClO_4$. Here the complex, *cis*-$[Co(CN)_2en_2]ClO_4$, gave rise to waves of three steps at the DME. The limiting current of each step is strictly diffusion-controlled. The diffusion currents of the first, the second, and the third wave, named from positive to negative potentials, are proportional to the concentration of the complex in the range between $5\cdot10^{-4}$ and $5\cdot10^{-3}$M. The first, the second, and the third wave, corresponding to an acceptance of one electron, represent the step-by-step reductions of Co(III)→Co(II), Co(II)→Co(I), and of Co(I)→Co(*metal*) respectively. The following processes of the electrode reaction seem to be the most plausible:[13]

$$\underset{inert}{cis\text{-}[Co^{III}(CN)_2en_2]^+} \xrightarrow{e} \underset{inert}{cis\text{-}[Co^{II}(CN)_2en_2]} \downarrow e \; \underset{inert}{[Co^{I}(CN)_2en_2]^-} \downarrow e \; Co(metal)$$

Thus, the dicyano-cobalt(III) complex is considered not to undergo any structural changes throughout the reductions and to undergo the step-by-step reductions, as it were, without disrupting the complex. In other words, neither the aquation nor the rearrangement of ligands takes place during the reductions.

Figure 10 shows the current-potential curves obtained in the four kinds of supporting electrolytes mentioned above. In the figure, the limiting currents of only three waves in a DMSO are relatively depressed to some extent compared with those of the other curves.

As far as the processes of the electrode reaction in these solutions are concerned, the processes in a DMSO are most simplified and can be best understood, an understanding of them evidently serves to provide information for interpreting more complicated processes in water solutions, since the polarographic reductions are regarded as of the "*inert-inert*" type in such a DMSO.

On the other hand, it is evident from the above-mentioned results that the dicyano-cobalt(II) complex in itself tends to be broken up and to turn into the more stable species of the tetracyanocobaltate(II) complex as a result of the overall rearrangement of ligands in a water solution containing excess ethylenediamine. The rearrangement of ligands was also observed for the other dicyanocobalt(III) complexes; for example, *cis*-$[Co(CN)_2dip_2]NO_3\cdot7H_2O$, *cis*-$[Co(CN)_2phen_2]NO_3\cdot6H_2O$, *trans*-$[Co(CN)_2en_2]NO_3$, and *trans*-$[Co(CN)_2(NH_3)_4]NO_3\cdot H_2O$. In a DMSO, even the $[Co^I(CN)_2(NH_3)_4]^-$ ion was found to be able to exist stably without disrupting the complex.

The merit of adopting a non-aqueous solvent lies not only in such a simplification of the electrode processes, but also in the stabilization of the lower oxidation states of the central metal ion from the point of view of the other side.

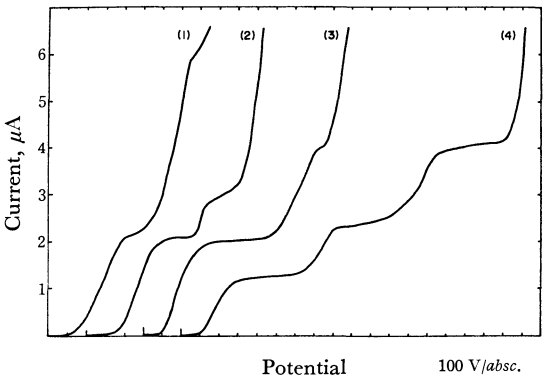

Fig. 10. The current-potential curves of the *cis*-$[Co(CN)_2en_2]^+$ ion measured at the concentration of the complex, 10^{-3}M, in the various kinds of the supporting electrolytes: (1) in 0.5M Na_2SO_4 aqueous solution only; (2) in 0.5M Na_2SO_4 aqueous solution containing 1M ethylenediamine; (3) in 0.45M Na_2SO_4 aqueous solution containing 0.1M KCN and 1M ethylenediamine; (4) in dimethyl sulfoxide (100%) containing 0.1M $[(C_2H_5)_4N]ClO_4$ (25°C). The curves, (1), (2), and (3), were recorded from −0.60 V *vs.* SCE, while the curve of (4) was recorded from −0.80 V *vs.* SCE.

13) More details in a non-aqueous solution are to be reported in the next paper of this series.

The authors wish to thank the Ministry of Education for the financial support granted this investigation.

BULLETIN OF THE CHEMICAL SOCIETY OF JAPAN VOL. 42 3166—3171 (1969)

Polarographic Study of Metal Complexes. IX.[1] Halogeno- and Aquo-bis(dimethylglyoximato)amminecobalt(III) Complexes[2]

Nobufumi MAKI, Yukio ISHIUCHI and Shukichi SAKURABA

Department of Chemistry, Faculty of Engineering, Shizuoka University, Johoku, Hamamatsu

(Received January 13, 1969)

The halogeno- and aquo-bis(dimethylglyoximato)amminecobalt(III) complexes of the *trans*-[$Co^{III}X\ dg_2(NH_3)$]-type have been found to be reduced to the metal through the cobalt(I) state in a 0.5M Na_2SO_4 aqueous solution at the dropping mercury electrode (DME), where the ligand, X, denotes the ion, Cl^-, Br^-, or I^-, or the molecule, OH_2. The aquation of the halogeno complexes is found to take place more rapidly in solution in this order: $Cl^- < Br^- < I^-$. The diaquobis(dimethylglyoximato)cobalt(III) ion, $[Co(OH_2)_2dg_2]^+$, has also been ascertained to undergo a step-by-step reduction to the metal through the cobalt(I) state at the DME.

In previous papers,[3-5] the dicyanobis(dimethylglyoximato)cobaltate(III) complex, *trans*-$K[Co(CN)_2dg_2]\cdot\frac{3}{2}H_2O$, was found to be reduced down to the cobaltate(I) complex in a 0.5M Na_2SO_4 solution at the dropping mercury electrode (DME). The resulting cobaltate(I) complex was isolated as an almost black soid *in vacuo* by the reduction of a 3% sodium amalgam. The aqueous solution of the cobaltate(I) complex assumed a deep blue color.

The bis(dimethylglyoximato)diamminecobalt(III) complex, $[Codg_2(NH_3)_2]Cl\cdot 5H_2O$ (efflorescent crystals), has been reported to undergo the step-by-step reduction of Co(III)→Co(II)→Co(I)→Co(0) at the DME in a neutral Na_2SO_4 solution.[3] In connection with these complexes, the cyanobis(dimethylglyoximato)amminecobalt(III), *trans*-$[Co(CN)dg_2(NH_3)]\cdot\frac{1}{2}H_2O$,[5] has also been found to be reduced to a cobalt(0) complex through the cobalt(I) state in the same supporting electrolyte. It is of interest that this complex, with both the cyanide ion and an ammonia ion, has a configuration similar to that of cyanocobalamine (vitamin B_{12})[6] in the coordination sphere around the cobalt.

The stabilization of such lower oxidation states of the central cobalt can be interpreted as being due to the strong π-bonding character, *i. e.*, the "back donation" in the coordinate-bonds of the cyanide ions and of a pair of dimethylglyoximes with two hydrogen bonds.

The purpose of this study is to determine if the oxidation state of a cobalt(I) can be detected in a solution or not for the halogeno- and aquo-ammine complexes, in which the contribution of the π-bonding character at the fifth and the sixth ligands is regarded as being absent.

Experimental

The experimental details of the measurements have been described previously.[7] The current-time curves were recorded on a Yanagimoto Polarovision, Model PE 20, equipped with a National X-Y recorder, Model VR 301. The characteristics of the capillary used were as follows: $m=1.42$ mg/sec, $t=4.80$ sec, both measured at an open circuit in a 0.5M Na_2SO_4 water solution.

Materials. The chloro-ammine complex, $[CoCldg_2(NH_3)]$ (anhydrous) was prepared according to the directions of Tschugaeff.[8] Found: Co, 17.28; C, 28.03; N, 20.39; H, 5.21%. Calcd for $[CoCldg_2(NH_3)]$: Co, 17.25; C, 28.13; N, 20.50; H, 5.02%.

Preparation of *trans*-[Co Br $dg_2(NH_3)$]. The bromo- and iodo-bis(dimethylglyoximato)amminecobalt(III) complexes were prepared analogously to the method of Tschugaeff.[8]

Twenty grams of $[CoBr(NH_3)_5]Br_2$[9] dissolved in 400 ml of water were heated on a water bath for two hours with 12.1 g of dimethylglyoxime and 50 g of ammonium acetate. During the reaction, 15 ml of

1) Previous paper of this series: N. Maki, K. Yamamoto, H. Sunahara and S. Sakuraba, This Bulletin, **42**, 3159 (1969).

2) Presented at the 14th Symposium on Polarography, held at Hiroshima, October 8, 1968.

3) N. Maki, "Proceedings of the 3rd International Congress of Polarography", ed. by G. J. Hills, Vol. 1, Macmillan & Co., London (1966), p. 505.

4) N. Maki, This Bulletin, **38**, 2013 (1965).

5) N. Maki, T. Itoh and S. Sakuraba, *ibid.*, **41**, 529 (1968).

6) M. Brezina and P. Zuman, "Polarography in Medicine, Biochemistry and Pharmacy", Interscience Publ. Inc., New York, N. Y. (1958), pp. 397—401.

7) N. Maki and K. Okawa, *J. Electroanal. Chem.*, **8**, 262 (1964).

8) L. Tschugaeff, *Ber.*, **39**, 2694 (1906); *ibid.*, **40**, 3499 (1907).

9) S. M. Jφrgensen, *J. prakt. Chem.*, 2 **19**, 49 (1879); *Z. Anorg. Allgem. Chem.*, **17**, 463 (1898).

glacial acetic acid were added to the solution in small portions. The reaction took place, evolving ammonia, to yield a brown solution. When the temperature of the solution went down, lustrous brown crystals were deposited from the solution, these were filtered and washed with cold water, ethanol and ether. The crude product was recrystallized from hot water containing acetic acid. Found: Co, 15.37; C, 24.99; N, 18.04; H, 4.64%. Calcd for [Co Br $dg_2(NH_3)$]: Co, 15.26; C, 24.89; N, 18.14; H, 4.44%.

Preparation of *trans*-[CoIdg$_2$(NH$_3$)].[10] Twenty grams of $[CoI(NH_3)_5](NO_3)_2$[11] and 50 g of ammonium acetate were dissolved in 400 m*l* of water, and the mixture was heated on a water bath with 9.5 g of dimethylglyoxime. During the reaction, 15 m*l* of acetic acid were stirred into the solution. After the solution had then been allowed to stand overnight, dark brown crystals were separated from the solution; they were filtered and washed with water, ethanol, and ether. The crude product was purified by recrystallization from hot water containing acetic acid. Found: Co, 13.54; C, 22.09; N, 16.02; H, 4.16%. Calcd for [CoIdg$_2$(NH$_3$)]: Co, 13.61; C, 22.19; N, 16.17; H, 3.96%.

Preparation of *trans*-[Co(OH$_2$)dg$_2$(NH$_3$)]OCOCH$_3$. Ten grams of [CoCldg$_2$(NH$_3$)][8] and about 6 g of wet Ag_2O were well mixed together in 50 m*l* of distilled water under ice cooling, then the mixture was allowed to stand for three hours below 0°C. The exothermic reaction took place gently to yield the hydroxo complex, [Co(OH)dg$_2$(NH$_3$)]. No smell of ammonia could be discerned during the reaction. The suspension was filtered, and the filtrate was concentrated to one-fifth its volume by evaporation *in vacuo* with a rotatory evaporator after 15 m*l* of acetic acid had been added to it. On cooling, bright yellow crystals separated from the solution; they were filtered and washed with ethanol and ether. Recrystallizations were carried out from hot water containing acetic acid. The yield was 48% of theory. The complex has no water of crystallization. Found: Co, 15.21; C, 31.11; N, 18.28; H, 5.85%. Calcd for [Co(OH$_2$)dg$_2$(NH$_3$)]OCOCH$_3$: Co, 15.38; C, 31.34; N, 18.27; H, 5.79%. The complex is soluble in water, while the corresponding salt of nitrate, [Co(OH$_2$)dg$_2$(NH$_3$)]NO_3, is insoluble in water. The absorption spectra of this and the diammine complex in the visible and ultraviolet regions are shown in Fig. 1. The first spin-allowed band is located at a longer wavelength than that of the corresponding diammine cobalt(III) complex, [Codg$_2$(NH$_3$)$_2$]Cl·5H$_2$O, though the first d–d band is hidden by the foot of the charge-transfer bands of dimethylglyoximes.

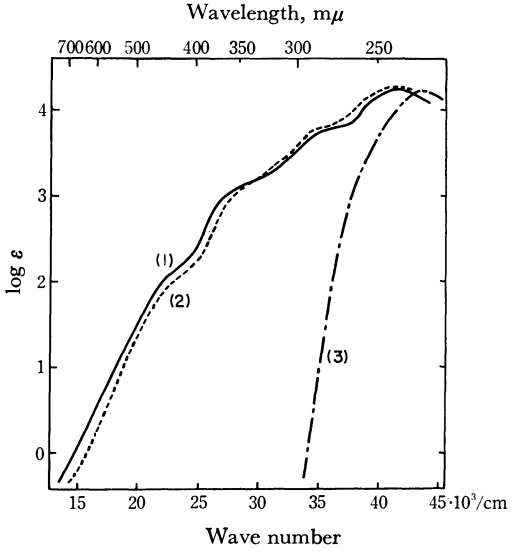

Fig. 1. The absorption spectra of the aquo-ammine and the diammine cobalt (III) complexes obtained in water.
(1) —— *trans*-[Co(OH$_2$)dg$_2$(NH$_3$)]OCOCH$_3$ (a new compouund)
(2) ------ *trans*-[Co dg$_2$(NH$_3$)$_2$]Cl·5H$_2$O
(3) —·— dimethylglyoxime (dgH) in methanol

Results and Discussion

The halogenobis(dimethylglyoximato)ammineco-balt(III) complexes, [Co^{III}Xdg$_2$(NH$_3$)], gave rise to four step waves in a 0.5M Na_2SO_4 aqueous solution at the DME, where the ligand, X, is the ion, Cl^-, Br^-, or I^-. The first two steps, corresponding to a total acceptance of one electron, represent the reductions from the cobalt(III) and the aquated cobalt(III) species to a cobalt(II) state, while the following two steps represent the reduction of $Co^{II} \rightarrow Co^{I}$ and of $Co^{II} \rightarrow Co^{0}$ respectively. The waves of the second, the third, and the fourth step for halogeno complexes agree completely with those of the aquo-complex, [Co(OH$_2$)dg$_2$(NH$_3$)]OCOCH$_3$. Therefore, the aquation of the halide ligands is considered to be almost completely finished in lower oxidation states. Judging from the wave-height of the first wave, it can be said that the aquation proceeds more rapidly in a solution according to this order of the ligands: Cl<Br<I.

Figure 2 shows the current-potential curves of the halogeno- and the aquo-ammine complexes under the same experimental conditions. The two-electron reduction wave of *trans*-K[Co(CN)$_2$dg$_2$]·$\frac{3}{2}$H$_2$O under the same conditions is given for the sake of comparison. It may be seen that the total height of the first and the second steps for halogeno complexes is approximately equal to that of the first step for the aquo-complex. The ratio of the wave-heights corrected for drop time is given in Table 1.

Each of the limiting currents of the waves was proportional to the concentration of the complex in the range of $2.5 \cdot 10^{-3}$—$5 \cdot 10^{-4}$M for halogeno complexes and in the ragne of 10^{-2}—$5 \cdot 10^{-4}$M for

10) *Cf.* "Gmelins Handbuch der anorganischen Chemie," Nr. 58, Teil B Kobalt-Ergänzungsband, Verlag Chemie, GmbH, Berlin (1964), p. 724.

11) J. Sand and G. Böckman, *Ber.*, **40**, 4497 (1907); "Gmelins Handbuch der anorgenischen Chemie," Nr. 58, Teil B Kobalt, Verlag Chemie, GmbH, Berlin (1930), p. 179.

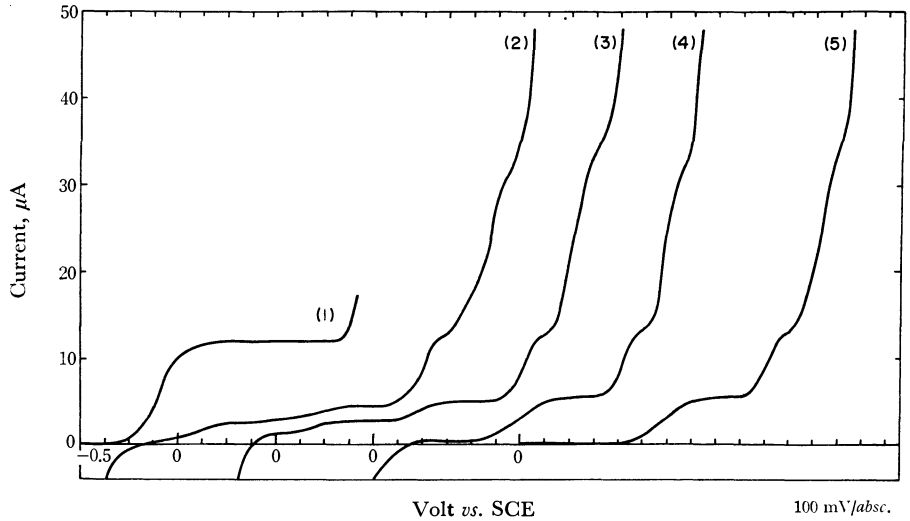

Fig. 2. The current-potential curves of the bis(dimethylglyoximato)cobalt(III) complexes obtained at the concentration of the complex, $2.0 \cdot 10^{-3}$M in 0.5M Na_2SO_4 under the same experimental conditions.
(1) *trans*-$K[Co(CN)_2dg_2] \cdot \frac{3}{2}H_2O$ (the two-electron reduction wave); (2) *trans*-$[CoCldg_2(NH_3)]$ (anhydrous); (3) *trans*-$[CoBrdg_2(NH_3)]$; (4) *trans*-$[CoIdg_2(NH_3)]$; (5) *trans*-$[Co(OH_2)dg_2(NH_3)]OCOCH_3$; recorded from 0 V (*vs.* SCE) for the halogeno- and aquo-complexes, (2)—(5), and from −0.50 V (*vs.* SCE) for the dicyano complex, (1).

TABLE I. THE RATIO OF THE WAVE-HEIGHTS OBTAINED FOR THE HALOGENO- AND AQUO-BIS(DIMETHYLGLYOXIMATO)COBALT(III) COMPLEXES (25°C)

Compound	1st Wave	2nd Wave	3rd Wave	4th Wave
trans-$[CoCldg_2(NH_3)]$	0.41	0.59	1.10	2.44
trans-$[CoBrdg_2(NH_3)]$	0.38	0.62	1.14	2.53
trans-$[CoIdg_2(NH_3)]$	0.09	0.91	1.20	2.57
trans-$[Co(OH_2)dg_2(NH_3)]OCOCH_3$	1		1.15	2.18

The wave-heights corrected for drop time were measured at the concentration of $2 \cdot 10^{-3}$M in 0.5M Na_2SO_4 solution.

the aquo-ammine complex, $[Co(OH_2)dg_2(NH_3)]OCOCH_3$.

The limiting currents of the first, the second, and the third steps (named from positive to negative potentials) were found to be proportional to the square root of the mercury pressure on the DME, whereas that of the fourth step was not proportional for all the halogeno complexes, the value of $i_{1(4)}/\sqrt{h_{corr.}}$ becoming smaller with the increase in the mercury pressure. Table 2 shows the dependence of the limiting currents on the mercury pressure obtained for the chloro-ammine complex. The results for the aquo-ammine complex quite agree with the above results obtained for the waves following the second step of the halogeno-ammine complexes. Accordingly, hereafter the polarographic data for the halogeno complexes only will be described, unless otherwise stated, since the three waves following the second step of the halogeno complexes coincide completely with those of the aquo-ammine complex.

TABLE 2. THE RELATIONSHIP BETWEEN THE LIMITING CURRENT AND THE HEIGHT OF THE MERCURY RESERVOIR (25°C)

$h_{corr.}$	i_1 (μA)	i_2 (μA)	i_3 (μA)	i_4 (μA)	$i_1/\sqrt{h_{corr.}}$	$i_2/\sqrt{h_{corr.}}$	$i_3/\sqrt{h_{corr.}}$	$i_4/\sqrt{h_{corr.}}$
90.0	0.89	3.60	6.26	13.00	0.09	0.38	0.66	1.37
83.0	0.82	3.56	6.19	12.90	0.09	0.38	0.68	1.42
76.0	0.78	3.31	6.18	12.00	0.09	0.38	0.71	1.38
69.0	0.75	3.15	6.06	11.70	0.09	0.38	0.73	1.41
62.0	0.79	3.00	5.76	10.30	0.10	0.38	0.73	1.30
55.0	0.74	2.73	5.62	9.80	0.10	0.37	0.76	1.33

For the iodo-ammine complex, $[CoIdg_2(NH_3)]$: $2.5 \cdot 10^{-3}$M in 0.5M Na_2SO_4 containing $2.3 \cdot 10^{-3}$ % of Triton X 100.

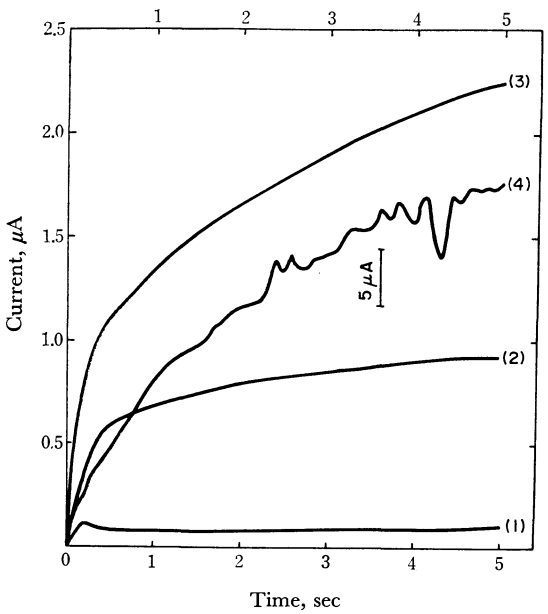

Fig. 3. The current-time curves obtained at the constant potentials.
(1) −0.40; (2) −0.85; (3) −1.15; (4) −1.33 V *vs.* SCE. Concn. of the complex: $1\cdot10^{-3}$M; Supporting electrolyte: 0.5M Na_2SO_4 soln. The current scale of the curve (4) only is curtailed, as indicated in the figure.

The temperature coefficients of the first, the second, the third, and the fourth steps were 1.2, 1.5, 2.4, and 2.5%/deg respectively at 25°C for all the halogeno complexes, and 1.5, 2.4, and 2.4%/deg respectively at 25°C for the aquo-ammine complex (in this case, the first step is absent).

Figure 3 shows the current-time curves observed during the life of a mercury drop at various potentials for the iodo-ammine complex. At the potentials of −0.85 and −1.15 V (*vs.* SCE), at which the current reaches the limiting plateaus of the second and third steps, the exponents (τ) of the drop time (t) in the Ilkovič equation, $i_d=kt^{\tau}$, were 0.21 and 0.33 respectively (25°C); the value of the former falls within 0.16—0.22, a range characteristic of diffusion-controlled values, but the value of the latter did not because of the disruption of the resulting cobalt(I) complex in solution. At the potentials of −0.40 and −1.33 V (*vs.* SCE), at which the current reaches the limiting plateaus of the first and fourth steps, the current-time curves show an abnormal shape. At the former potential, the current is quenched with time to some extent, this distinctive quenching may be attributed to the adsorption of the halogeno complex at the DME. The electrocapillary curve also indicated that the adsorption was taking place and so supported this interpretation. At the latter potential, the oscillations observed on the abnormal curve are undoubtedly connected with the time involved in the formation and adherence of the disruption species of dimethylglyoximes insoluble in an aqueous solution at the DME. In a 40% methanolic solution containing 1M LiCl, no oscillations were observed.

Thus, the limiting current of the second step only may be concluded to be strictly diffusion-controlled, whereas those of the other three steps involve, more or less, a kinetic character, though the polarographic data of the others presented above indicate the rate-determining step of the first three steps to be by diffusion.

The half-wave potentials of each of the steps for halogeno- and their related complexes are summarized in Table 3. The half-wave potentials of the waves following the second step for halogeno complexes agree approximately with those of the aquo-complex $[Co(OH_2)dg_2(NH_3)]^+$ and do not coincide with those of the diaquo-complex $[Co(OH_2)dg_2(OH_2)]^+$. Therefore, the ammonia ligand for the halogeno- and aquo-ammine complexes may be concluded not to aquate in the lower oxidation states of the cobalt in a solution.

On the other hand, Figs. 4 and 5 show the dependences of the current-potential curves on the concentration of excess ammonia in a solution for the aquo-ammine and the diammine cobalt(III)

Table 3. The half-wave potentials of the waves for the bis(dimethylglyoximato)cobalt(III) complexes (25°C)

Compound	1st Wave $Co^{III}\rightarrow Co^{II}$	2nd Wave $Co^{III}\rightarrow Co^{II}$	3rd Wave $Co^{II}\rightarrow Co^{I}$	4th Wave $Co^{I}\rightarrow Co^{0}$	Supporting electrolyte
trans-$[CoCldg_2(NH_3)]$	+	−0.58	−1.03	−1.20	0.5M Na_2SO_4
trans-$[CoBrdg_2(NH_3)]$	+	−0.58	−1.03	−1.20	0.5M Na_2SO_4
trans-$[CoIdg_2(NH_3)]$	+	−0.59	−1.01	−1.23	0.5M Na_2SO_4
trans-$[Co(OH_2)dg_2(NH_3)]OCOCH_3$		−0.58	−1.03	−1.22	0.5M Na_2SO_4
		−0.78	−0.94	−1.25	0.5M Na_2SO_4+1M NH_3
trans-$[Co(NH_3)dg_2(NH_3)]Cl\cdot5H_2O$		−0.60	−1.03	−1.23	0.5M Na_2SO_4
		−0.78	−0.94	−1.27	0.5M Na_2SO_4+1M NH_3
trans-$[Co(OH_2)dg_2(OH_2)]^+$		+	−0.75	−0.99	0.5M Na_2SO_4

Voltage unit: volt *vs.* the saturated calomel electrode (SCE)

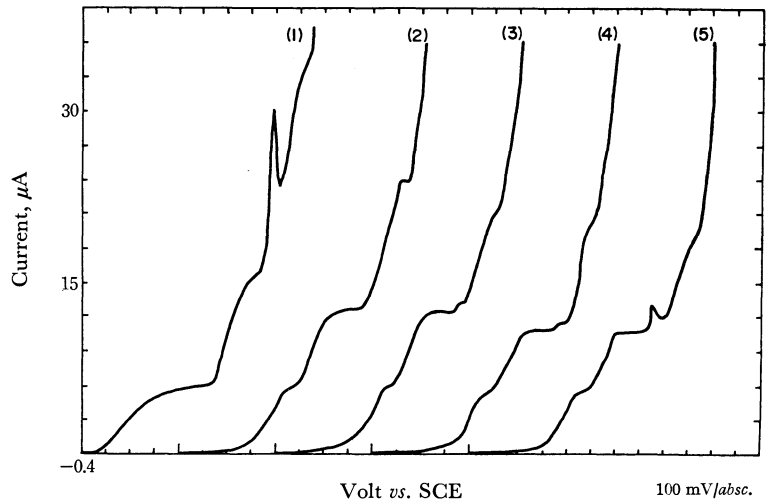

Fig. 4. The dependence of the current-potential curves upon the concentration of excess ammonia in a solution.
(1) 0; (2) 0.1; (3) 0.5; (4) 1.0; (5) 1.5M; obtained for the complex, *trans*-$[Co(OH_2)dg_2(NH_3)]OCOCH_3$, at the concentration of the complex, $2.5 \cdot 10^{-3}$M in 0.5M Na_2SO_4 (25°C).

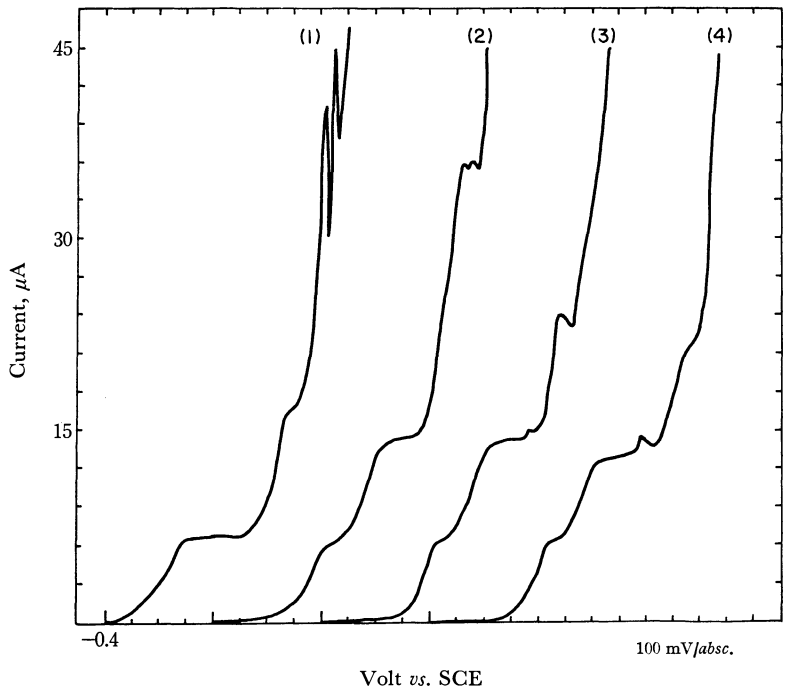

Fig. 5. The dependence of the current-potential curves upon the concentration of excess ammonia in a solution.
(1) 0; (2) 0.1; (3) 0.5; (4) 1.0M; obtained for the complex, *trans*-$[Codg_2(NH_3)_2]Cl \cdot 5H_2O$, at the concn. of the complex, $2.5 \cdot 10^{-3}$M in 0.5M Na_2SO_4 (25°C).

complexes respectively. In Figs. 4 and 5, the shapes of the waves for the aquo-ammine and the diammine complexes are seen to come to resemble each other with the increase in the concentration of ammonia, especially in the shapes of the last steps. This suggests that the ammine complexes tend to aquate in a solution in the absence of excess ammonia, especially in the last step of reduction

($Co^{I} \rightarrow Co^{0}$). Nevertheless, the fifth ligand of ammonia or, at least, one of ammonia ligands is not replaced with a water molecule in a neutral Na_2SO_4 solution throughout the reductions, taking account of the half-wave potentials for the diaquo-complex (see Table 3).

Accordingly, the overall processes of the electrode reaction given below may be considered to be the most plausible:

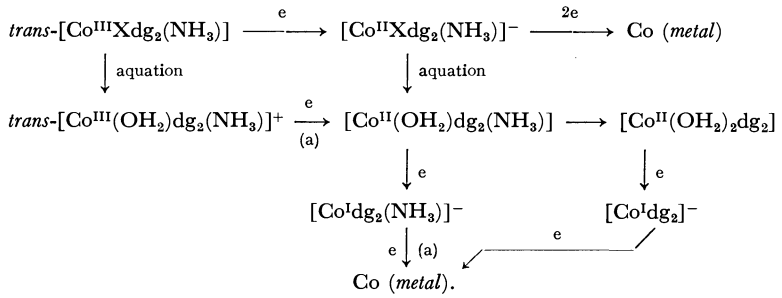

The electrode reaction in a 0.5M Na_2SO_4 solution is considered to proceed mainly along the (a) path rather than along the other paths. The contribution of the other paths, accompanied by the disruption of the cobalt(I) complexes, is considered to be one of the reasons why the limiting currents of the last two steps exhibit some kinetic character. From the view point of the electronic structure, the cobalt(I) complex might have the tetra-coordinate formula, $[Co^{I}dg_2]^-$, even in solutions.

The authors wish to thank the Ministry of Education for the financial support granted for this research.

BULLETIN OF THE CHEMICAL SOCIETY OF JAPAN VOL. 42 3172—3177 (1969)

Copper(II) Complexes of Ethylenediaminemonoacetic Acid (EDMA). A Polarographic Study of the Solution Equilibria between the Copper(II) Ion and EDMA and the Preparation of Copper(II)-EDMA Complexes

Yuki Fujii and Mutsuo Kodama

Department of Chemistry, Ibaraki University, Bunkyo-cho, Mito

(Received April 2, 1969)

In the present paper, the solution equilibria between the copper(II) ion and ethylenediaminemonoacetic acid (EDMA) were determined polarographically and, then copper(II)-EDMA complexes were prepared and characterized using ion-exchange chromatography and the visible and infrared absorption spectra. Since copper(II) ions in an EDMA solution behave reversibly in a polarographic electrolysis, the composition and the stability constants of copper(II)-EDMA complexes were determined from the dependence of the half-wave potential on the concentration of uncomplexed EDMA by employing a modification of the Deford-Hume method. The copper(II) ion was found to form complexes of 1-to-1 and 1-to-2 compositions with EDMA. Their successive formation constants, K_1 and K_2, were $2.5_2\times10^{13}$ and 1.10×10^{8} respectively. The copper(II)-EDMA complex with a 1-to-1 composition was easily isolated from an aqueous solution of pH 3.0—4.0. On the other hand, the complex with a 1-to-2 composition could be isolated in a low yield by adding ethanol from a solution containing an excess amount of EDMA in the pH range from 10.0 to 11.0. From the infrared spectra and the ion-exchange chromatographic behavior, the ethylenediaminemonoacetate ion in the complexes was concluded to function as a tridentate ligand.

The metal complexes of ethylenediamine and aminopolycarboxylic acids which derived from ethylenediamine have been studied in various aspects, but the investigations of the complexes with ethylenediaminemonoacetic acid (EDMA) as the ligand have been quite limited. In this connection, in order to understand the detailed properties of EDMA as the ligand in the complex formation reaction, it seemed that it would be worthwhile to study thermodynamically the complex formation reaction involving EDMA and to prepare and characterize the metal complexes of EDMA. In this paper, the polarographic determination of the solution equilibria between the copper(II) ion and EDMA and the preparation of copper(II) complexes of EDMA from an aqueous solution will be described. The participation of the acetate group in the complex formation was demonstrated by studying the infrared absorption spectra and by ion-exchange chromatography.

Experimental

Reagents. The ways of preparing and standardizing a standard copper(II) perchlorate solution were given previously.[1] The preparation and purification of EDMA dihydrochloride were also described in a previous paper.[2] Its purity was checked by means of C.H.N. analysis. All the other chemicals used in the polarographic measurements were of an analytical reagent grade.

Apparatus and Experimental Procedures. All the d. c. current-voltage curves were measured by using a manual polarograph similar to that of Kolthoff and Lingane.[3] The rate of the flow of mercury, m, and the drop time, t_d, of the dropping mercury electrode (DME) were 0.839 mg/sec and 3.92 sec respectively, as measured in an air-free 0.10M acetate buffer solution of pH 5.00 with an open-circuit and 70.0 cm of a mercury column at 25°C. A saturated calomel electrode used as the reference electrode has also been described previously.[4] The pH value of the solution was measured with a glass electrode pH meter (Hitachi-Horiba Model M-5). In the pH titration, a semimicroburet with a capacity of 10 ml was used. All the experimental procedures in the polarography were given previously.[4,5] Under the present experimental conditions, the maximum

1) M. Kodama and H. Ebine, This Bulletin, **40**, 1857 (1967).

2) Y. Fujii, E. Kyuno and R. Tsuchiya, *ibid.*, to be published.

3) I. M. Kolthoff and J. J. Lingane, "Polarography," Vol. 1, Interscience, New York (1952), p. 297.

4) M. Kodama and A. Kimura, This Bulletin, **40**, 1639 (1967).

5) M. Kodama, S. Naito and M. Ebine, *Nippon Kagaku Zasshi (J. Chem. Soc. Japan, Pure Chem. Sect.)*, **84**, 576 (1963).

of the first kind appeared in the reduction wave of the copper(II) ion in an EDMA solution. Therefore, 6×10^{-6}M LEO (polyoxyethylene lauryl ether) was added to the sample solution in order to surpress it.

All the visible absorption spectra were recorded on a Hitachi EPS-3 pen-recording spectrophotometer using water as a solvent. The infrared absorption spectra were taken on Nujol mulls between sodium chloride plates or potassium bromide disks, using a Hitachi EPI-S2 spectrometer. The magnetic susceptibility was determined by the Gouy method using powdered samples at 24°C.

Methods of Analysis. The carbon, hydrogen, and nitrogen analyses of the solid complexes were performed by the conventional combustion method using a Yanagimoto C.H.N. Corder MT-1. The copper was determined polarographically by measuring the wave-height of the copper(II) ion in an acetate buffer solution of pH 5.0 containing 20.0 mM EDMA.

Results and Discussion

Polarographic Determination of Solution Equilibria between Copper(II) Ions and EDMA. In the theoretical analysis of the polarographic data, accurate pK values of EDMA are necessary. Therefore, the pK values of EDMA were first determined by the potentiometric acid-base titration. Titration was carried out on oxygen-free sample solutions in a beaker-type cell with a water-jacket thermostatted at 25°C. The titration curve of an EDMA with a carbonate-free sodium hydroxide exhibited sharp inflections corresponding to the successive stages of neutralization (Fig. 1). The pK_2 value corresponding to the following dissociation reaction was estimated to be 6.65 from the pH value at the half-titration point.

$$H_2X^+ \overset{pK_2}{\rightleftharpoons} HX + H^+$$

The pK_1 and pK_3 values were then calculated by using the pH values at the first and second inflection points with the aid of the well-known relation (1):[6]

$$pH_i = \frac{(pK_2+pK_j)}{2} \quad (1)$$

where pH$_i$ denotes the pH at the first or second inflection point, and pK_j, the pK_1 or pK_3 value corresponding to the following proton dissociation equilibria. The estimated pK_1 and pK_3 were 2.15 and 10.15 respectively.

$$H_3X^{2+} \overset{pK_1}{\rightleftharpoons} H_2X^+ + H^+$$

$$HX \overset{pK_3}{\rightleftharpoons} X^- + H^+$$

The copper(II) ion in an EDMA solution invariably gave a single well-defined polarographic wave (Fig. 2). Its wave-height was exactly proportional to the square-root of the effective mercury pressure on the DME and to the bulk concentration of the

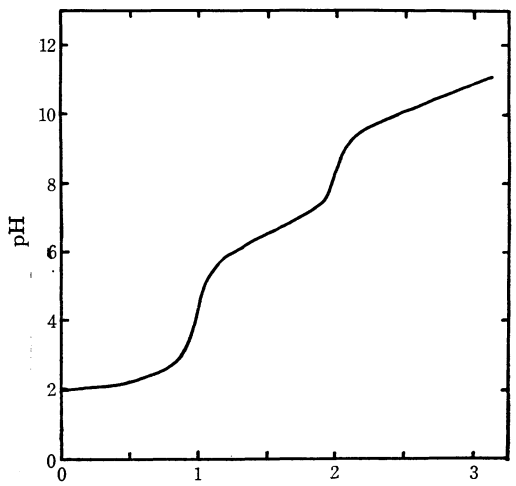

Fig. 1. The pH titration of EDMA with sodium hydroxide solution.
Initial concentration of EDMA dihydrochloride =5.0 mM
Volume of EDMA dihydrochloride solution =100 ml
Concentration of sodium hydroxide solution =0.914M
25°C, μ=0.20

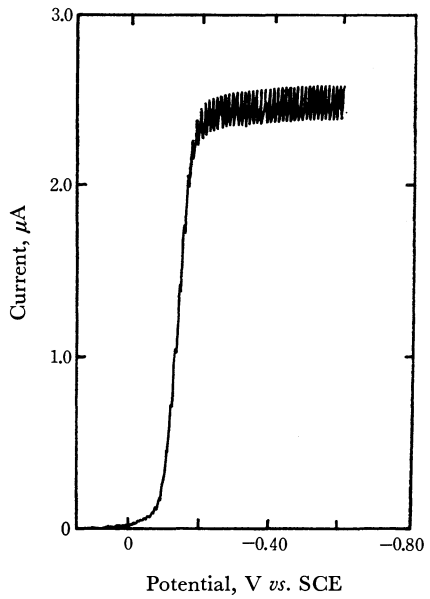

Fig. 2. D.c. polarogram of copper(II) ion in the EDMA solution.
Concentration of copper(II) ion=0.686 mM
Concentration of uncomplexed EDMA=20.0 mM
Concentration of acetate ion=0.10M
Concentration of LEO=6×10^{-6}M
μ=0.20, pH=5.03

6) J. J. Lingane, "Electroanalytical Chemistry," Interscience, New York (1953).

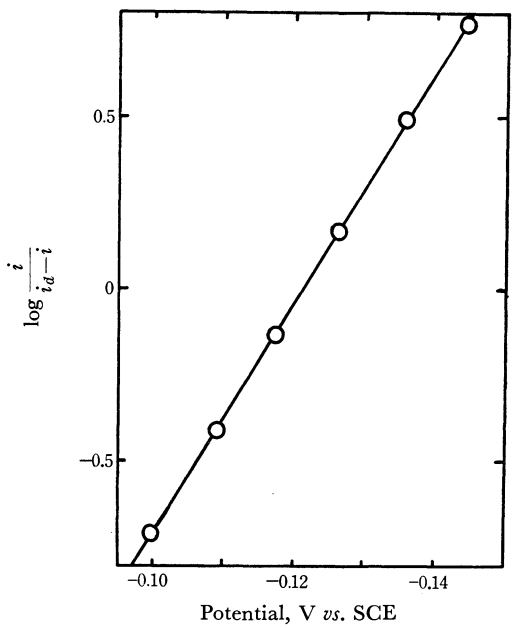

Fig. 3. Log-plot examination.
Concentration of copper(II) ion=0.686 mM
Concentration of uncomplexed EDMA=20.0 mM
Concentration of acetate ion=0.10M
Concentration of LEO=6×10^{-6}M
μ=0.20, pH=5.03

copper(II) ion. At pH's lower than 7.0, the log-plot analysis of the polarogram has a linear relation with a reciprocal slope falling in the range from 33 to 35 mV. A typical example is shown in Fig. 3. Therefore, it can be concluded that the copper(II) ion in the EDMA solution undergoes a two-electron reversible reduction at the mercury electrode. Consequently, the solution equilibria between the copper(II) ion an EDMA can be successfully determined by the conventional polarographic method. Since and EDMA anion has two nitrogen groups and one acetate group, it may act as a tridentate ligand. Therefore, the copper(II) ion may be expected to form the complexes with 1-to-1 and 1-to-2 compositions. If both 1-to-1 and 1-to-2 complexes are formed, the electrode reaction of the copper(II) ion at the mercury electrode can be assumed to be:

$$\begin{array}{l} CuX^{+} + nH^{+} + Hg + 2e^{-} \rightleftharpoons Cu(Hg) + H_nX^{n-1} \\ \quad\quad \uparrow\downarrow \\ \quad\quad CuX_2 \end{array}$$

where CuX^{+} and CuX_2 are copper(II)-EDMA complexes of 1-to-1 and 1-to-2 compositions and where H_nX^{n-1} means the protonated EDMA ion. Hence, the shift of the half-wave potential of the copper(II) ion due to the complex formation can be derived thermodynamically as:

$$\Delta E_{1/2} = (E_{1/2})_{Cu} - (E_{1/2})_{CuX}$$

$$= 0.0296\left[\log\left(\frac{K_1\cdot[X]_f}{(\alpha_H)_X} + \frac{K_1\cdot K_2\cdot[X]^2_f}{(\alpha_H)^2_X}\right) + \log\frac{k_{CuX}}{k_{Cu^{2+}}}\right] \quad (3)$$

where $(E_{1/2})_{Cu}$, $(E_{1/2})_{CuX}$, k_{CuX}, and $k_{Cu^{2+}}$ have their usual meanings[7] and where $(\alpha_H)_X$ and $[X]_f$ denote the (α_H) value of EDMA and the concentration of uncomplexed EDMA respectively. K_1 and K_2 are the successive formation constants of copper(II)-EDMA complexes.

Equation (3) clearly indicates that when the solution pH is kept constant, the plot of (antilog $[\Delta E_{1/2}/0.0296+\log k_{Cu^{2+}}/k_{CuX}])/[X]_f$ against $[X]_f$ will give the linear relation, the slope and the intercept of which correspond to $K_1\cdot K_2/(\alpha_H)^2_X$ and $K_1/(\alpha_H)_X$ respectively. On the other hand, if only the complex with a 1-to-1 composition is formed, the plot of antilog $[\Delta E_{1/2}/0.0296+\log k_{Cu^{2+}}/k_{CuX}]$ against $[X]_f$ should give the linear relation. These relations were examined at pH 5.0. Experiments were carried out on acetate buffer solutions containing an uncomplexed EDMA, because at this pH the system containing only uncomplexed EDMA does not have enough buffer capacity to keep the solution pH constant during the electrolysis. The linear relation shown in Fig. 4 clearly indicates that the copper(II) ion forms complexes of 1-to-1 and 1-to-2 compositions under the present experimental conditions. From the intercept and the slope of the linear relation, the K_1 and K_2 values were estimated to be $2.5_2\times10^{13}$ and 1.10×10^{8} respectively.

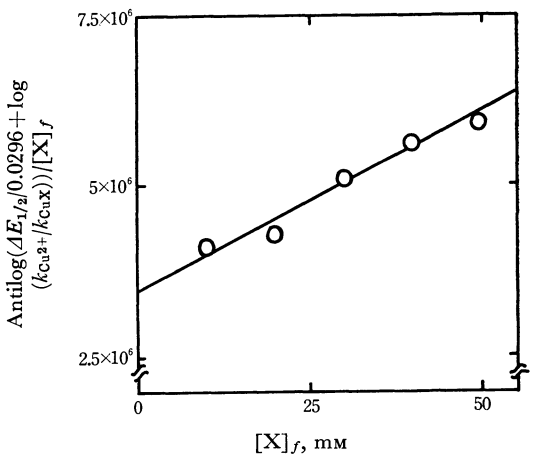

Fig. 4. Determination of successive formation constants of copper(II)-EDMA complexes.
Concentration of copper(II) ion=0.686mM
Concentration of acetate ion=0.10M
Concentration of LEO=6×10^{-6}M
μ=0.20, pH=5.00, 25°C

7) M. Kodama and Y. Tominaga, This Bulletin, **42**, 394 (1969).

Table 1. The effect of acetate or chloride ion on the half-wave potential

μ=0.20, 25°C
Concentration of copper(II) ion=0.686 mM
Concentration of uncomplexed EDMA=20.0 mM

A: Chloride ion effect*

Concentration of chloride ion, M	Half-wave potential V *vs.* SCE
0.040	−0.322
0.187	−0.321

B: Acetate ion effect**

Concentration of Acetate ion, M	Half-wave potential V *vs.* SCE
0.05	−0.126
0.14	−0.124

* pH=7.00, 25°C
No buffer reagent was used because uncomplexed EDMA can serve as a buffer reagent at this pH.
** pH=5.00, 18°C

Table 2. The effect of pH on the half-wave potential

μ=0.20, 25°C
Concentration of copper(II) ion=0.686 mM
Concentration of uncomplexed EDMA=20.0 mM
Concentration of acetate ion=0.10 M

A: Acid medium

pH	Half-wave potential V *vs.* SCE	$\Delta E_{1/2}$, mV obsd	$\Delta E_{1/2}$, mV calcd
5.03	−0.122	0	0
5.59	−0.171	−49	−53.4
6.13	−0.229	−107	−105.9

B: Neutral or weak alkaline medium*

pH	Half-wave potential V *vs.* SCE	$\Delta E_{1/2}$, mV obsd	$\Delta E_{1/2}$, mV calcd
6.90	−0.309	+44	+40.6
7.11	−0.324	+29	+24.7
7.48	−0.353	0	0
7.83	−0.384	−31	−24.0
8.01	−0.397	−44	−35.1

* No buffer reagent was used because uncomplexed EDMA can serve as a buffer reagent in this pH range.

The possible formation of a mixed ligand complex involving acetate or chloride ions could be ruled out by the fact that the half-wave potential was independent of the concentration of acetate or chloride ions, provided that the solution pH and EDMA concentration were kept constant (Table 1). If the above conclusion is correct, the dependence of the half-wave potential on the solution pH must be explained satisfactorily by using the K_1 and K_2 values thus determined. The pH dependence of the half-wave potential was calculated with the aid of Eq. (3) and compared with the observed data. The results are shown in Table 2. In acid and neutral media, the calculated values agreed well with the observed values. In a weak alkaline medium, however, the observed values are slightly larger than the calculated ones. This can be ascribed to the fact that the reversibility of the electrode reaction in a weak alkaline medium is not so complete as in acid and neutral media. This explanation could be confirmed by the value of the reciprocal slope (45 mV).

From all the above results and discussion, it can be concluded that the pK values of EDMA and K_1 and K_2 values of copper(II)-EDMA complexes thus determined are reasonable.

Characterization of Copper(II)-EDMA Complexes. Since the formation of copper(II)-EDMA complexes of 1-to-1 and 1-to-2 compositions was confirmed polarographically, we tried to prepare and characterize these complexes. Although, because of kinetic, solubility and other limitations, the predominant species in the solution can not always be separated selectively from the equilibrium mixture, for the successful preparation of metal complexes, it seems that its formation reaction in solution had better to be complete in a thermodynamic sense. Therefore, in order to find the optimum conditions for the preparation, we first calculated the fraction of the copper(II) ion present in each species of the copper(II)-EDMA complex using the pK values of EDMA and the formation constants of copper(II)-EDMA complexes with the aid of the following relations:

$$[\mathrm{Cu}]_t = [\mathrm{Cu}^{2+}] + [\mathrm{CuX}^+] + [\mathrm{CuX}_2]$$

$$[\mathrm{X}]_t = [\mathrm{X}]_f + [\mathrm{CuX}^+] + 2\cdot[\mathrm{CuX}_2]$$

$$\frac{K_1}{(\alpha_H)_X} = \frac{[\mathrm{CuX}^+]}{[\mathrm{Cu}^{2+}]\cdot[\mathrm{X}]_f}, \quad \frac{K_2}{(\alpha_H)_X} = \frac{[\mathrm{CuX}_2]}{[\mathrm{CuX}^+]\cdot[\mathrm{X}]_f}$$

Table 3. The fraction of copper(II) ion presents as each species of copper(II)-EDMA complex
Total concentration of copper(II)=0.80 M

pH	Total concentration of EDMA, M	Fraction Cu^{2+}	CuX^+	CuX_2
3.0	0.80	5.8×10^{-2}	9.41×10^{-1}	6.6×10^{-4}
4.0	0.80	2.0×10^{-3}	9.96×10^{-1}	2.0×10^{-3}
10.0	3.20	3.6×10^{-22}	9.1×10^{-9}	1.00
11.0	3.20	8.2×10^{-23}	4.3×10^{-9}	1.00

where $[Cu]_t$ and $[X]_t$ mean the total concentrations of copper(II) and EDMA respectively, and $[CuX^+]$ and $[CuX_2]$, the concentrations of copper(II)-EDMA complexes of 1-to-1 and 1-to-2 compositions. The results summarized in Table 3 clearly indicate that the copper(II) ion in the solution of pH 3.0—4.0, which is 0.80M with respect to copper(II) and 0.80M with respect to EDMA, exists predominantly in the form of CuX^+ and that the copper(II) ion in the solution of pH 10.0—11.0 containing 0.80M copper(II) and 3.20M EDMA exists only in the form of CuX_2. On the basis of the above thermodynamic information, we tried to prepare the copper(II)-EDMA complexes. The complex with a 1-to-1 composition could be prepared and isolated from the solution of pH 3.0—4.0, and that with a 1-to-2 composition, from the solution of pH 10.0—11.0 containing an excess of EDMA, as will be described below.

Preparation of Ethylenediaminemonoacetatoaquocopper(II) Chloride Monohydrate. To 50 m*l* of an aqueous solution containing 3.4 g (0.02 mol) copper(II) chloride dihydrate, about 4.2 g (0.02 mol) of EDMA·2HCl·H_2O were added. After adjusting the solution pH to 3.0—4.0 by adding a 6N sodium hydroxide solution, the mixture solution was heated on a water bath until its volume was reduced to 25 m*l*. When the resulting solution was cooled to 0°C, light blue crystals were deposited and filtered off. This crude product was then recrystallized from a 50% ethanol solution. The yield was 1.5 g (approximately 30%). Found: Cu, 24.6; C, 18.78; H, 4.87; N, 11.14%. Calcd for $[Cu(EDMA)(H_2O)]Cl\cdot H_2O$: Cu, 25.2; C, 19.04; H, 5.21; N, 11.11%.

Preparation of Bis(ethylenediaminemonoacetato)copper(II) Tetrahydrate. To 50 m*l* of an aqueous solution containing 3.4 g (0.02 mol) copper(II) chloride dihydrate, about 16.0 g (0.08 mol) EDMA·2HCl·H_2O were added. After the resulting mixture had been heated on a water bath for ten minutes, the solution pH was adjusted to 10.0—11.0 by adding a 6N sodium hydroxide solution. The mixture solution was then evaporated naturally to about 10 m*l*, whereby the sodium chloride thus deposited was filtered off. At this point, ethanol (80—100 m*l*) was added to the solution. The resulting mixture was then cooled to 0°C and allowed to stand in a refrigerator for 2—3 weeks. Dark blue crystals were obtained. The yield was about 10%. Found: Cu, 16.6; C, 26.01; H, 6.65; N, 15.41%. Calcd for $[Cu(EDMA)_2]\cdot 4H_2O$: Cu, 17.2; C, 25.97; H, 7.10; N, 15.15%.

Table 4. The visible and IR spectra of the copper(II)-EDMA complexes

Compound	λ_{max} (c/s) $\times 10^{-13}$	log ε	Carboxylate asym. str., cm^{-1}
$[Cu(H_2O)_6^{2+}]$	36.5	1.09	—
$[Cu(EDMA)(H_2O)]Cl\cdot H_2O$	44.4	1.62	1600
$[Cu(EDMA)_2]\cdot 4H_2O$	49.2	1.86	1626
EDMA·2HCl·H_2O	—	—	1730

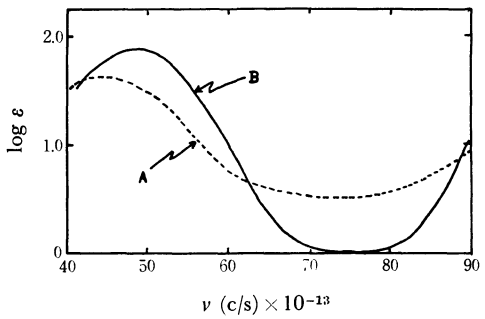

Fig. 5. Visible absorption spectra of copper(II)-EDMA complexes.
Concentration of uncomplexed EDMA = 10.0 mM
A: pH=4.0, Acetate buffer solution (0.10M), the complex with 1-to-1 composition
B: pH=7.0, The complex with 1-to-2 composition

As is shown by the visible absorption spectra in Fig. 5, the copper(II)-EDMA complexes of 1-to-1 and 1-to-2 compositions gave absorption maxima at 44.4×10^{13} and 49.2×10^{13} sec^{-1} respectively. The maxima can be regarded as the peaks due to the d–d transition. The large shift of the absorption curve to the higher energies may be a strong indication that the nitrogen groups of EDMA are coordinated to the copper(II) ion[8,9] (Table 4). Since the visible absorption study can not give any confirmative information about the participation of the acetate group in the coordination bond formation, the infrared (IR) study was carried out. The IR absorption spectrum of dark blue crystal was measured in a potassium bromide disk, but that of light blue crystal, in a Nujol-mull state. Because, in the case of light blue crystal, the color of the potassium bromide disk changed from light blue to yellow. This can be ascribed to the formation of a mixed ligand complex involving the bromide ion. As the spectral data in Table 4 show, the light blue and dark blue crystals show the strong bands of the carboxylate group at 1600 and 1626 cm^{-1} respectively. Generally, the uncoordinated $-COO^-$ group of aminopolycarboxylic acid has been observed to exhibit its characteristic band in the range from 1610 to 1580 cm^{-1}, and the –COOH group, from 1750 to 1690 cm^{-1}.[10] Therefore, the above two bands of copper(II)-EDMA

8) T. Dreisch and W. Trommer, *Z. Phys. Chem.*, **37**, 37 (1937).
9) M. Kubota, *Nippon Kagaku Zasshi (J. Chem. Soc. Japan, Pure Chem. Sect.)*, **62**, 509 (1941).
10) T. Sakaguchi and K. Ueno, "Metal Chelates," Vol. II, Nankodo, Tokyo (1963), p. 43.

complexes can probably be ascribed to the coordinated carboxylate group.

The ion-exchange chromatographic study also supports the above interpretation. In the aqueous solution of the light blue crystal (pH=4.0; concentration of uncomplexed EDMA=10.0 mM), the cation exchange regin (Dowex 50W-X8, 100—200 mesh) in the Na^+ form could capture the copper(II) ion effectively, but the anion exchange regin (Dowex 1-X8, 100—200 mesh) in the Cl^- form could not. On the other hand, in the case of the solution containing the dark blue crystal (pH=7.0; concentration of uncomplexed EDMA=10.0 mM), neither ion-exchange resin could capture the copper(II) ion. These facts clearly indicate that the copper(II) ion in the former solution exists as a positively-charged species, but in the latter solution, as a zero-charged species, suggesting the participation of the carboxylate group in the complex formation.

The possibility of the formation of the dimer structure in the crystal state could be ruled out by the magnetic susceptibility measurements (1.75 B.M. for the light blue crystal and 1.92 B.M. for the dark blue crystal).[11]

From the above results and discussion, we have concluded that the light blue crystal isolated from an acid solution is $[Cu(EDMA)(H_2O)]Cl \cdot H_2O$, corresponding to the square planar structure, and that the dark blue crystal obtained from the alkaline medium is $[Cu(EDMA)_2] \cdot 4H_2O$, corresponding to the octahydral structure.

The authors wish to thank Professor Ryokichi Tsuchiya and Dr. Eishin Kyuno of Kanazawa University and Professor Katsumi Yamamoto of Ibaraki University for their helpful suggestions. The authors also wish to thank to Professor S. Ito and his coworkers of Tohoku University for their kind help in Elemental Analyses.

11) K. Gora, E. Kyuno and R. Tsuchiya, This Bulletin, **41**, 2624 (1968).

BULLETIN OF THE CHEMICAL SOCIETY OF JAPAN VOL. 42 3177—3184 (1969)

The Ion Exchange of a Mixture of Er and Tm with HEDTA

Zenzi HAGIWARA and Hideo ŌKI

Faculty of Engineering, Tohoku University, Katahira-cho, Sendai

(Received April 18, 1969)

Under experimental conditions similar to those in the elution system of the rare earth with a dilute HEDTA eluant, the Er-Tm separation factor has been found in the system of HEDTA and Dowex 50W, X-8, 50—100 mesh. The values for this pair, 1.57 at 25°C and 1.63 at 60°C were in agreement with the values calculated from the stability constants of the rare earth-HEDTA chelates. Further, an equimolar mixture of Er and Tm has been eluted with a 0.015M HEDTA solution buffered with ammonium hydroxide. Under the present experimental conditions, the adsorption band of each rare earth reached a steady state after it had moved down through the hydrogen-retaining bed to a distance several times the initial band length. Several series of experimental data were used for analyses of the adsorption band from the point of view of rate theory. It was concluded that the present ion-exchange process with a HEDTA eluant was controlled by film diffusion as the rate-determining step. The plate-height values were also found to be functions of the flow rate.

In the ion-exchange separation of the rare-earth series on a commercial scale, EDTA[1] (ethylenediamine-*N,N,N',N'*-tetraacetic acid, H_4Y) and HEDTA[2] [*N'*-(2-hydroxyethyl)-ethylenediamine-*N,N,N'*-triacetic acid, H_3Ch] eluants buffered with ammonium hydroxide has been employed with marked success. In order to make a theoretical treatment of the elution system of the rare earth by HEDTA complexation, it is necessary to find an accurate separation factor for adjacent rare-earth pairs and to understand the mechanism of the separation of the rare-earth group under steady-state conditions.

In connection with the above ion-exchange

1) J. E. Powell and F. H. Spedding, *Trans. Met. Soc. AIME*, **215**, 457 (1959).

2) J. R. Morton and D. B. James, *J. Inorg. Nucl. Chem.*, **29**, 2997 (1967).

system, the formation of the H_5Ch^{2+}-band[3] during elution was studied; the adsorption isotherm was also discussed in detail. Theoretical treatments[4] of the ion-exchange column involving the rare-earth band with dilute HEDTA were made in order to clarify the elution mechanism of the rare-earth species. Further, one of the present authors previously reported the separation factors[5] for adjacent rare-earth pairs, such as Er-Tm, Dy-Ho, Y-Dy, Tb-Y, Eu-Gd and Sm-Nd, in the presence of EDTA, significant differences were then found in them between the values calculated from the stability constants of the rare earth-EDTA chelates and the measured values. Thus we arrived at the conclusion that, except in special cases, the separation factor should be measured experimentally under conditions similar to those in a practical elution system containing a mixture of rare earths.

One of the purposes in this work is to find the Er-Tm separation factor in the presence of HEDTA at different temperatures, and to use these values for analyzing the elution system involving the Er-Tm pair. Another purpose is to analyze the elution system of a rare-earth mixture under steady-state conditions so that a comparison of both dilute and concentrated eluants can be made.

Separation Factor for the Er-Tm Pair in the Presence of HEDTA

The separation factor (α) of an adjacent rare-earth pair (Ln_1-Ln_2) in the presence of a chelating agent, such as EDTA (H_4Y) or HEDTA (H_3Ch), can be estimated using the values of the stability constants of the Ln-chelates.

In the ion-exchange system involving adjacent rare-earths and HEDTA, the main exchange reaction is written by:

$$\overline{Ln_1}^{3+} + Ln_2Ch \rightleftarrows \overline{Ln_2}^{3+} + Ln_1Ch$$

where the barred symbols refer to the resin phase, and the unbarred symbols, the aqueous phase. The exchange quotient (or selectivity coefficient) is expressed by:

$$K' = \frac{[\overline{Ln_2}^{3+}][Ln_1Ch]}{[\overline{Ln_1}^{3+}][Ln_2Ch]} \tag{1}$$

where the brackets represent the concentrations of related species. In the elution system with a dilute eluant of HEDTA buffered with ammonium hydroxide, the following species are present in the aqueous phase of the rare-earth band:

$LnCh^0$, Ln^{3+}, NH_3^+, H^+, H_3Ch, H_2Ch^-, HCh^{2-}, Ch^{3-}.

Whether a chelating agent is present in the system or not, $\alpha^{Ln_1}_{Ln_2}$ is defined as the concentration ratio of the two elements:

$$\alpha^{Ln_1}_{Ln_2} = \frac{[\overline{Ln_{1T}}][Ln_{2T}]}{[\overline{Ln_{2T}}][Ln_{1T}]} \tag{2}$$

where the T's indicate the total concentrations of indicated rare earths in both phases. Since the rare earth is present as the tripositive ion in the resin, Eq. (2) is expressed in this form:

$$\alpha^{Ln_1}_{Ln_2} = \frac{[\overline{Ln_1}^{3+}][Ln_{2T}]}{[\overline{Ln_2}^{3+}][Ln_{1T}]} \tag{3}$$

Considering the presence of Ln^{3+} and $LnCh^0$ as the Ln-species, we have:

$$\alpha^{Ln_1}_{Ln_2} = \frac{[\overline{Ln_1}^{3+}]\{[Ln_2^{3+}]+[Ln_2Ch]\}}{[\overline{Ln_2}^{3+}]\{[Ln_1^{3+}]+[Ln_1Ch]\}} \tag{4}$$

Introducing $[LnCh]=K_{LnCh}[Ln^{3+}][Ch^{3-}]$ into (4), we have:

$$\alpha^{Ln_1}_{Ln_2} = \frac{[\overline{Ln_1}^{3+}][Ln_2^{3+}]\{1+K_{Ln_2Ch}[Ch^{3-}]\}}{[\overline{Ln_2}^{3+}][Ln_1^{3+}]\{1+K_{Ln_1Ch}[Ch^{3-}]\}} \tag{5}$$

In the above expressions, K_{LnCh} indicates the stability constant of LnCh and the brackets represent the molarities of the indicated species. As $[Ln^{3+}]$ is very small compared with [LnCh], we have:

$$\alpha^{Ln_1}_{Ln_2} = \frac{[\overline{Ln_1}^{3+}][Ln_2^{3+}]K_{Ln_2Ch}}{[\overline{Ln_2}^{3+}][Ln_1^{3+}]K_{Ln_1Ch}} = K^{Ln_1}_{Ln_2}\frac{K_{Ln_2Ch}}{K_{Ln_1Ch}} \tag{6}$$

When the exchange quotient, $K^{Ln_1}_{Ln_2}$, is almost equal to unity, one obtains the following approximation:

$$\alpha^{Ln_1}_{Ln_2} \cong \frac{K_{Ln_2Ch}}{K_{Ln_1Ch}} \tag{7}$$

Surls and Choppin[6] studied the ion-exchange equilibrium between Ln^{3+} and the hydrogen form of Dowex 50 using radioactive Ln-nuclides and perchloric acid; they observed no difference in the distribution coefficient ($K_d=[\overline{Ln^{3+}}]/[Ln^{3+}]$) between the adjacent rare earths. Consequently, $K^{Ln_1}_{Ln_2}$ is approximately equal to unity. According to their study, the mean K_d-values of 2.20×10^5 and 2.22×10^5 were obtained for the Er-H and Tm-H systems respectively. It can be decided from these data that K^{Er}_{Tm} is approximately equal to unity.

In the presence of HEDTA, the Er-Tm separation factor is expressed by Relation (7):

$$\alpha^{Er}_{Tm} \cong \frac{K_{TmCh}}{K_{ErCh}} \tag{8}$$

It may be said qualitatively that $\alpha^{Ln_1}_{Ln_2}$ in the system containing a chelating agent is independent of the composition of the aqueous and resin phases and

3) Z. Hagiwara and H. Ōki, This Bulletin, to be published.

4) Z. Hagiwara, *J. Inorg. Nucl. Chem.*, **31**, 2933 (1969)

5) M. Noguchi, A. Yoshifuji and Z. Hagiwara, This Bulletin, **42**, 2286 (1969).

6) J. P. Surls, Jr., and G. R. Choppin, *J. Am. Chem. Soc.*, **79**, 855 (1957).

of the type of exchanger, and that the $\alpha^{Ln_1}_{Ln_2}$-value is decided only by the ratio of the stability constants of the Ln-chelates. However, it is recommended the α-values should be measured directly, for the reason described in the previous paper.[5] In the present work, the α-values were measured at 25 and 60°C using the batch method and their temperature dependency was investigated.

Experimental

1) Experimental Method for Determining the Separation Factor. *Preparation of Aqueous Phase.* Erbium and thulium were eluted separately using a 0.015M HEDTA eluant buffered with ammonium hydroxide (pH=7.5) and using a hydrogen-retaining bed with Dowex 50W, X-8, 100—200 mesh. The elution conditions were the same as those in Exp. No. 12 and 13 in the previous paper;[7] the rare-earth eluates from the exchange column were employed as the aqueous phase in the equilibrium experiments. As the composition of the Er-eluate obtained by this elution was almost identical with that of the Tm-eluate, it was very easy to prepare aqueous solutions having different ratios of Er to Tm but without any other notable change in constituents.

Preparation of the Rare Earth and Ammonium Types of Resins. By passing the load solutions, such as $ErCl_3$, $TmCl_3$ and NH_4Cl, into an ion-exchange column containing Dowex 50W, X-8, 50—100 mesh in the hydrogen form, the erbium, thulium, and ammonium types of resins were prepared.

Equilibrium Experiment. A total of about 5 g of the prepared resins was taken; for weighing, the ammonium and Ln-types of resin were taken into the required portions, so that the constituents in the resin phase would become a 0.8 equivalent fraction of the sum of $\overline{Er^{3+}}$ and $\overline{Tm^{3+}}$ and a 0.2 equivalent fraction of $\overline{NH_4^+}$. Further, the ratio*1 of Er to Tm in the resin was adjusted to give a α^{Er}_{Tm}-value of approximately 1.6, as was to be expected from the α^{Er}_{Tm}-values in Table 3. After the resin mixture (5 g) had been equilibrated with a total volume of 300 m*l* of the erbium and thulium eluates at a constant temperature of either 25°C or 60°C for 48 hr in a thermostat, the two phases were separated and analyzed.

Analytical Method. The analytical methods employed for the determination of the various species present in the two phases were the same as those given in the literature,[4] while the rare-earth mixtures were determined spectrophotometrically using a Shimadzu QR-50 spectrophotometer and a 1.00-cm cell. The samples of the rare-earth oxides obtained from the two phases were placed in a volumetric flask and dissolved with a slight excess of 1M $HClO_4$ under heating. After dilution to a definite volume, the resulting solutions were analyzed at the following wavelengths:

Rare earth	λ (mμ)	Slit width (mm)	Molecular absorption coefficient (l/mol·cm)
$ErClO_4$	379.0	0.0240	6.55
$TmClO_4$	683.0	0.0135	2.50

A 1.00-cm quartz cell was used.

2) Experimental Method of the Elution of the Er-Tm Mixture. As the experimental method[4] for the elution at 60°C has already been reported, only the outline will be given here. In the experiments, 22-mm I.D. columns made of Pyrex glass jacketed with 60-mm-I.D. columns were used. At the bottom of each column, a sintered glass disk was fixed in order to support the resin bed containing Dowex 50W, X-8, 50—100 mesh. The column was kept at a certain temperature by circulating water through the jacket columns from the thermostat. The jacket column with an equimolar mixture of Er and Tm was connected to the main column containing the hydrogen form of Dowex 50W, X-8, 50—100 mesh. The connection was made by the aid of a vinyl tube, whose outside was covered with shielding material. In elution, the HEDTA eluant (0.015M) was first passed through the pre-heater equipped with a stirrer; here the solution temperature was raised in order to remove any dissolved air. Then the eluant entered the top of the rare-earth adsorption column. The eluate from the retaining column was cooled through the condenser and collected into small fractions by means of a fraction collector. The experimental apparatus is represented in Fig. 1.

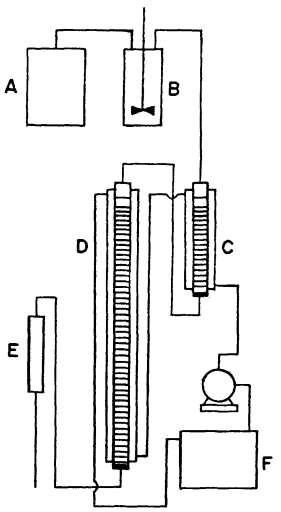

A Eluant
B Preheater
C R.E. Adsorption column
D Retaining column
E Cooler
F Thermostat

Fig. 1. Schematic representation of apparatus.

Results and Discussion

Separation Factor for the Er-Tm Pair. The compositions of the two phases at equilibrium

7) Z. Hagiwara and H. Ōki, *J. Inorg. Nucl. Chem.*, to be published.

*1 If the composition of the aqueous phase employed for the equilibrium experiment is known, the ratio of Er to Tm in the resin can be determined on the assumption that $\alpha^{Er}_{Tm} \cong 1.6$ (see Table 3).

TABLE 1. COMPOSITION OF THE AQUEOUS AND RESIN PHASES AT EQUILIBRIUM (25°C)

Exp. No.	Aqueous phase (mmol/l)						Resin phase (eq. fraction)					α^{Er}_{Tm}
	Er_T	Tm_T	(Er_T+Tm_T)	NH_{4T}	Ch_T	pH	$\overline{Er^{3+}}$	$\overline{Tm^{3+}}$	$(\overline{Er^{3+}}+\overline{Tm^{3+}})$	$\overline{NH_4^+}$	$\overline{H^+}$	
E-3-1	0.96	7.83	8.79	4.92	15.20	3.29	0.1094	0.6551	0.7645	0.1741	0.0614	1.36
E-3-2	1.95	6.81	8.76	5.03	15.11	3.29	0.2418	0.5216	0.7634	0.1739	0.0627	1.62
E-3-3	3.28	5.40	8.68	5.09	15.02	3.30	0.3805	0.3805	0.7610	0.1752	0.0637	1.65
E-3-4	5.01	3.71	8.72	5.03	15.07	3.31	0.5206	0.2409	0.7615	0.1732	0.0653	1.60
E-3-5	6.76	1.98	8.74	5.29	15.14	3.33	0.6424	0.1160	0.7584	0.1749	0.0668	1.62

Ave.: 1.57

TABLE 2. COMPOSITION OF THE AQUEOUS AND RESIN PHASES AT EQUILIBRIUM (60°C)

Exp. No.	Aqueous phase (mmol/l)						Resin phase (eq. fraction)					α^{Er}_{Tm}
	Er_T	Tm_T	(Er_T+Tm_T)	NH_{4T}	Ch_T	pH	$\overline{Er^{3+}}$	$\overline{Tm^{3+}}$	$(\overline{Er^{3+}}+\overline{Tm^{3+}})$	$\overline{NH_4^+}$	$\overline{H^+}$	
E-4-1	0.99	8.10	9.09	4.72	15.35	3.25	0.1021	0.6428	0.7449	0.1812	0.0740	1.30
E-4-2	1.95	7.12	9.07	4.72	15.34	3.24	0.2371	0.4922	0.7293	0.1791	0.0916	1.76
E-4-3	3.30	5.71	9.01	4.72	15.29	3.25	0.3802	0.3737	0.7539	0.1817	0.0643	1.76
E-4-4	4.95	4.00	8.95	4.73	15.23	3.25	0.5225	0.2325	0.7550	0.1853	0.0597	1.82
E-4-5	6.93	1.97	8.90	4.75	15.19	3.30	0.6451	0.1199	0.7650	0.1806	0.0544	1.53

Resin: Dowex 50W, X-8, 50—100 mesh

Ave.: 1.63

are listed in Tables 1 and 2. The α^{Er}_{Tm}-values were calculated by the use of Eq.(2):

$$\alpha^{Er}_{Tm} = [\overline{Er_T}][Tm_T]/[\overline{Tm_T}][Er_T]$$

Table 1 and 2 indicate that when the total composition of rare earths in the resin and aqueous phases shows an almost constant value [see (Er_T+Tm_T) and $(\overline{Er^{3+}}+\overline{Tm^{3+}})$], the variation in α with the Er/Tm ratio and temperature is not remarkable. The average α^{Er}_{Tm} -values were 1.57 at 25°C and 1.63 at 60°C. The stability constants of the Ln-HEDTA chelates have been found by several investigators. Introducing these data into Eq.(8), the Er-Tm separation factors were calculated as tabulated in Table 3, in which the agreement is excellent with the α^{Er}_{Tm}-values calculated from the data of Spedd-

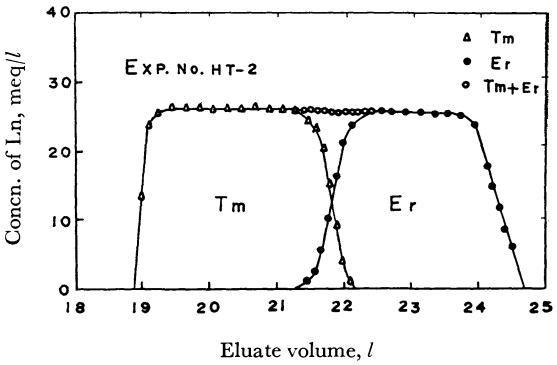

Fig. 2. Elution curve of the Er-Tm pair under a steady state condition.

TABLE 3. CALCULATED VALUES OF THE Er-Tm SEPARATION FACTOR IN THE PRESENCE OF HEDTA

Investigator	Method	Measured condition		log K_{ErCh}	log K_{TmCh}	$\alpha^{Er}_{Tm}=\frac{K_{TmCh}}{K_{ErCh}}$
Spedding et al.[8]	pH-titration	μ=0.1	(25°C)	15.17	15.38	1.62
	polarograph	μ=0.1	(25°C)	15.4	15.5	1.3
Moeller and Ferrus[9]	pH-titration	μ=0.1	(15°C)	15.45	15.66	1.62
			(20°C)	15.45	15.64	1.58
			(25°C)	15.42	15.59	1.48
			(30°C)	15.41	15.62	1.62
			(35°C)	15.46	15.72	1.82
			(40°C)	15.42	15.69	1.86
Powell and Mackey[10]	Hg-electrode	μ=0.1	(20°C)	15.61	16.00	2.45

Table 4. Experimental conditions used for the elutions of equimolar mixture of Er and Tm

Exp. No.	Composition of eluant			Elution temp. °C	Flow rate cm/min	Dimention of bed		Band length*
	$\widetilde{Ch}_T$ mol/l	$\widetilde{NH_4}_T$ mol/l	pH			Rare Earth bed cm	Retaining bed cm	
HT-2	0.01502	0.03096	7.44	60	0.53	2.2×18.0	2.2×85.2	4.7
HT-4	0.01500	0.03092	7.44	60	1.58	2.2×18.0	2.2×85.9	4.8
HT-5	0.01500	0.03050	7.43	60	2.11	2.2×18.0	2.2×85.9	4.8
HT-6	0.01500	0.03075	7.47	60	2.63	2.2×18.0	2.2×85.9	4.8
HT-9	0.01500	0.04248	9.04	60	1.58	2.2×17.3	2.2×85.9	5.0
RT-1	0.01500	0.03076	7.43	25	1.05	2.2×17.6	2.2×85.5	4.9

* Band length=length of retaining bed used/length of rare earth bed
Resin: Dowex 50W, X-8, 50—100 mesh
I.D.-22 mm-column

ing[8] and Moeller.[9] The α-value calculated from the data of Powell and Mackey[10] seems, however, to be too large. In spite of measurements at different ionic strengths, the α_{Tm}^{Er}-value observed at 25°C is in good agreement with that calculated Spedding's data.[8]

Elution Results. After the break-through of rare earth, the total concentration of the rare earth in the eluate was plotted against the eluate volume. As may be seen in Fig. 2 (Exp. No. HT-2), the total amount of Er and Tm in the eluate was kept almost constant; an elution curve with a flat top for each element was obtained over a fairly wide range of eluate volume. After the rare-earth band had been moved down the hydrogen-retaining bed a distance corresponding to about 5 band lengths,*2

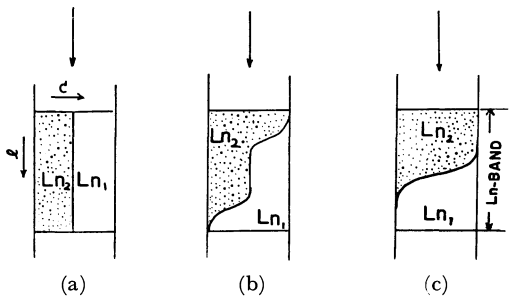

Fig. 3. Change in the composition of rare earth during the ion exchange process.

a steady state was reached. In such a steady state, the mixed rare-earth boundary with Er and Tm has a pattern with a definite gradient of composition; further progress in the separation of these species can not be expected by increasing the elution distance. The elution curves obtained under different flow rates did not differ from the elution curve shown in Fig. 2. However, tailing and channelling were increased to some degree with the increase in the flow rate.

When the rare-earth-saturated band containing equimolar adjacent rare earths (Fig. 3-a) is displaced down the hydrogen-retaining bed with the HEDTA eluant buffered with ammonium hydroxide in the beginning of the elution step, ammonium and hydrogen ions in the eluant leak through the rare-earth band until the band expands to its equilibrium band length. During this early step, Ln_1 and Ln_2 begin to be separated at the boundary, the degree of separation is gradually increased, as Fig. 3-b shows. However, the analysis of the exchange system on the basis of the rate theory seems to be difficult in this step, because complicated phenomena are still occurring in the rare-earth band, with Ln, NH_4, H, and HEDTA species included in both phases. With further progress in elution, a steady state is finally attained, as may be seen in Fig. 3-c, in which the composition of the Ln_1-Ln_2 boundary has been fixed to a definite gradeint, as has been mentioned above. Under steady-state conditions (Fig. 3-c), all the other species except the rare earths are considered to be distributed homogenously over the entire range of the band. This may be explained by the fact that, after the attainment of a steady state, the exchange system is finally fixed by the composition of the eluant itself, as has been illustrated in a previous paper.[7] In other words, when the composition of the eluant and the exchange constants related to the system are known, all the constituents in the resin and aqueous phases of each pure rare-earth band formed during elution can be calculated as functions of the eluant composition on the assumption of a true equilibrium for the ion-exchange

8) F. H. Spedding, J. E. Powell and E. J. Wheelwright, *J. Am. Chem. Soc.*, **78**, 34 (1956).

9) T. Moellor and R. Ferrus, *J. Inorg. Nucl. Chem.*, **20**, 261 (1961).

10) J. E. Powell and J. L. Mackey, *Inorg. Chem.*, **1**, 418 (1962).

*2 The minimum number of displacements (v) of the mixed rare-earth band needed to carry out separation is about 2.1 using the relation of $v=(1+\varepsilon N_0)/\varepsilon$, where N_0 is the mole fraction of Er in the mixture of Er and Tm being separated, and where N_0 and ε are 0.5 and 0.63 respectively in this run. Therefore, the value of *ca.* 5 band lengths (see Table 4) is enough to realize a steady-state elution.

process. The effective separation of rare earths by ion exchange is based mainly on differences in K_{LnCh} between the lanthanons. However, these differences are not very large between the adjacent rare-earth pairs. Further, significant differences in such exchange constants as $K^{Ln}_{NH_4}$ and K^{Ln}_{H} cannot be expected between the adjacent pairs. Considering only the presence of rare earth as the cationic species in the rare-earth band, and taking only the reaction of Eq. (1) as important, the Ln_1-band can be assumed to be displaced by Ln_2(see Fig. 3-c; Ln_1=Tm and Ln_2=Er in this study).

Analysis of the Ion-Exchange System by the Rate Theory. For an elution system involving the rare earths under steady-state conditions, the analysis on the basis of the rate theory[4,11,12] is possible using the experimental data related to the mixed region with adjacent rare earths.

In the ion-exchange process, the rate of particle and film-diffusion may be expressed by the following relation.[13] For particle-diffusion control, we have:

$$\left(\frac{\partial \bar{X}_i}{\partial t}\right)_Z = \frac{\bar{D}}{0.071 r_0^2}(\bar{X}_i^* - \bar{X}_i) \tag{9}$$

and for film-diffusion control:

$$\left(\frac{\partial \bar{X}_i}{\partial t}\right)_Z = \frac{3D}{2\delta r_0}(C_i - C_i^*) \tag{10}$$

The r_0 and δ symbols indicate the radius of the resin particle and the film thickness respectively, while $\bar{D}$ and D express the self-diffusion or interdiffusion coefficient in the resin and aqueous phases. The symbol C_i represents the concentration of species i in the interstitial solution, and $\bar{X}_i$, the amount of species i in the resin per unit volume of the resin bed. The asterisks refer to equilibrium; for example, C_i^* denotes the concentration of the interstitial solution in equilibrium with $\bar{X}_i$. The symbol Z represents the distance from a reference point in the column.

From Eqs. (9) and (10), the following relations can finally be deduced. When particle diffusion is the rate-limiting step, one obtains:

$$Z(x_{Ln_2}) = H_p\left\{-\frac{1}{\alpha-1}\ln x_{Ln_2} + \frac{\alpha}{\alpha-1}\ln(1-x_{Ln_2}) + 1\right\} \tag{11}$$

where:

$$H_p = v_b r_0^2/14\bar{D}$$

For film-diffusion control, one obtains:

$$Z(x_{Ln_2}) = H_f\left\{-\frac{\alpha}{\alpha-1}\ln x_{Ln_2} + \frac{1}{\alpha-1}\ln(1-x_{Ln_2}) - 1\right\} \tag{12}$$

where:

$$H_f = 2\delta r_0 v_b \bar{X}/3DC$$

In Eqs. (11) and (12), $Z(x_{Ln_2})$ indicates the distance of the plane with a concentration of x_{Ln_2} from the gravity center of a rare-earth boundary containing Ln_1 and Ln_2, and α is the separation factor. The symbol v_b represents the linear velocity for the movement of the rare-earth band; $\bar{X}$, the total amount of species in the resin phase per unit volume of bed, and C, the total concentration of counter ions. Further, H_p and H_f indicate the plate height due to particle diffusion and film diffusion. Using Eqs. (11) and (12), the plots of x_{Ln_2} with respect to Z give the shape of the boundary in a steady state.

In particle-diffusion control, the shapes of the boundary with Ln_1 and Ln_2 are represented in Fig. 4, in which some relationships between x_{Ln_2} and Z may be seen at the α-values of 1.2, 1.5, 2, and 3 on the assumption that H_p=0.5 cm. For film-diffusion control, similar relations are represented

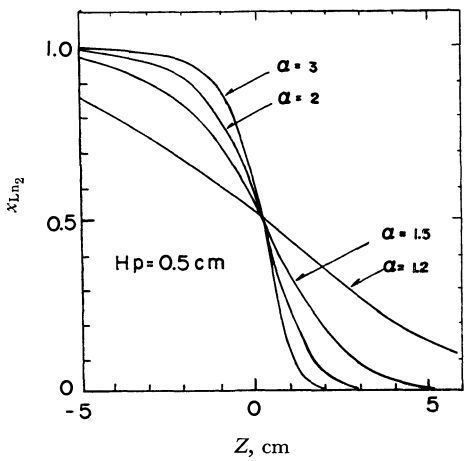

Fig. 4. Relationship between x_{Ln_2} and Z in particle-diffusion control.

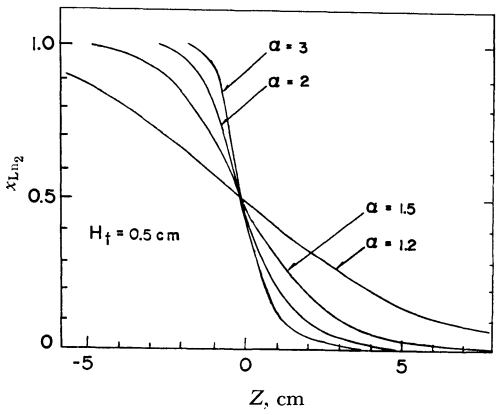

Fig. 5. Relationship between x_{Ln_2} and Z in film-diffusion control.

11) Z. Hagiwara and A. Kamei, *J. Inorg. Nucl. Chem.*, to be published.

12) Z. Hagiwara, *J. Phys. Chem.*, **73**, 3102 (1969).

13) F. Helfferich, *Angew. Chem. Intern. Ed.*, **1**, 440 (1962).

in Fig. 5. As may be clear from the above figures, under steady-state conditions, the concentration gradient of the mixed region is decided by the value of either H_p or H_f as well as by the α-value, and a sharp boundary can be expected if we decrease the plate height. In general, some leakage of Ln_2 is observed in film-diffusion control and some tailing of Ln_1 in particle-diffusion control.

Employing the experimental data obtained in the elution of the Er-Tm mixture, the analysis of the overlap region in a steady state was performed on the basis of the rate theory. The following values were used as the Er-Tm separation factors in a system with HEDTA:

$$\alpha_{Tm}^{Er} = 1.57 \text{ at } 25°C;\ \alpha_{Tm}^{Er} = 1.63 \text{ at } 60°C$$

Introducing them into Eq. (12), we obtain the following equations:

for 25°C-elution:

$$Z(x_{Er}) = H_f\{-6.34 \log x_{Er} + 4.04 \log (1-x_{Er}) - 1\} \quad (13)$$

and for 60°C-elution:

$$Z(x_{Er}) = H_f\{-5.96 \log x_{Er} + 3.66 \log (1-x_{Er}) - 1\} \quad (14)$$

where $Z(x_{Er})$ indicates the distance of the plane with a concentration of x_{Er} from the gravity center of the Er-Tm overlap region. The dimensions of x_{Er} and Z are expressed in the equivalent fraction and in centimeters respectively. Further, the separation factor is assumed to be constant throughout the Er-Tm overlap zone. The plate-height contribution due to film-diffusion can be found from the cruve-fitting method using Eqs. (13) and (14); the experimental data are represented graphically in Figs. 6 and 7. As the figures show, most of the experimental data fall on the theoretical line. On the contrary, the elution results in this study cannot be explained with the aid of Eq. (11). It is obvious that the elution system of the rare earth with a dilute HEDTA, such as 0.015M as the total anionic species of HEDTA ($\widetilde{Ch}_T$) and with

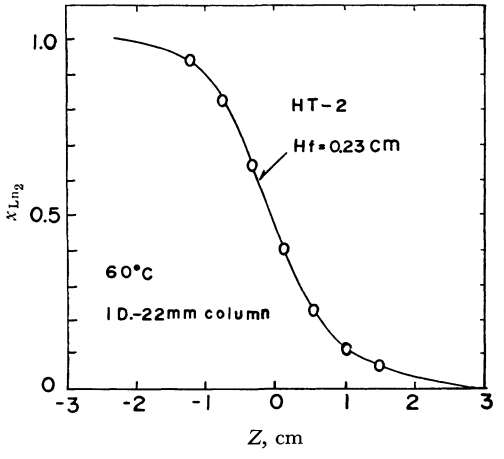

Fig. 6. Relation between x_{Er} and Z in film-diffusion control.

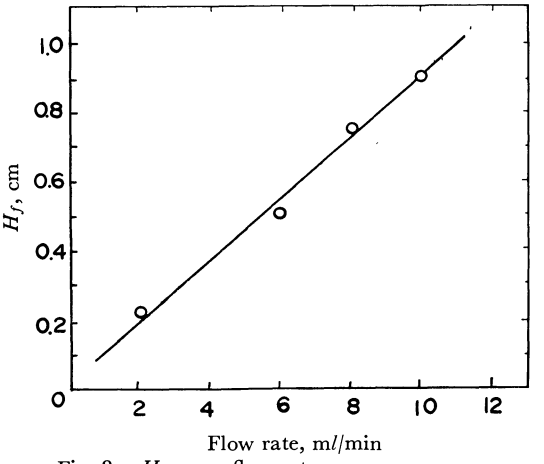

Fig. 8. H_f *versus* flow rate.
temp. 60°C I.D.-22 mm jacket column

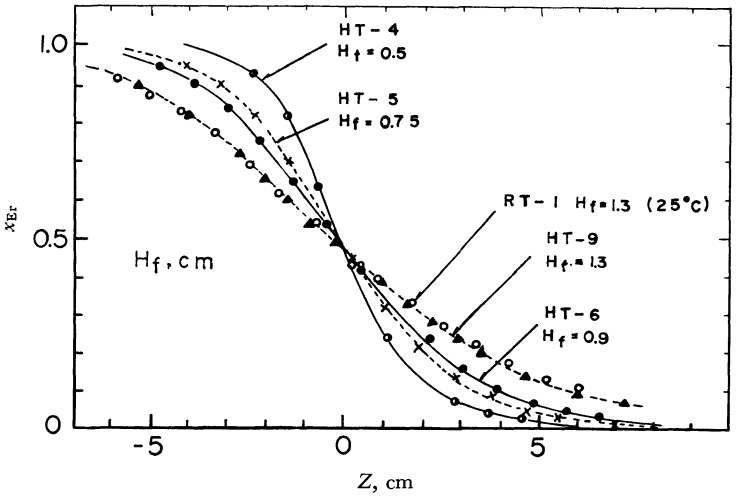

Fig. 7. x_{Er} *versus* Z in film-diffusion control.

Table 5. H_f-Values as a function of flow rate

Exp. No.	Elution temp. (°C)	Flow rate* ml/min	H_f cm
HT-2	60	2.0	0.23
HT-4	60	6.0	0.50
HT-5	60	8.0	0.75
HT-6	60	10.0	0.90
HT-9	60	6.0	1.30
RT-1	25	4.0	1.25

* I.D. 22 mm-Jacket column
Eluant composition:
$\widetilde{Ch}_T$=0.015 mol/l; $\widetilde{NH}_{4T}$=0.031 mol/l.
except for HT-9
$\widetilde{Ch}_T$=0.015 mol/l; $\widetilde{NH}_{4T}$=0.042 mol/l.
for HT-9.

a moderate crosslinked resin (X-8) is mainly controlled by film-diffusion as the rate-determining step. The plots of H_f *versus* the flow rate are shown in Fig. 8, where a linear relation may be observed. Also, the detailed values of H_f obtained in the elution at 25° and 60°C are tabulated in Table 5. The elution temperature affects the plate-height value as well as the separation factor. Since a smaller value of the plate height is obtained with an increase in the temperature, the separation efficiency in the ion-exchange process is improved by elution at high temperatures. Generally, film diffusion, particle diffusion, and particle size all contribute to the plate height. The contribution of the last two is, however, very small in the present exchange system, and film-diffusion plays the most important role for the rate-determining step. As may be seen in Table 5, the plate-height value by film diffusion at 60°C becomes smaller than that at 25°C; this is because the diffusion rates of various species in the Nernst film layer increase with a rise in the temperature.

Summary

1) The separation factors for the Er-Tm pair were found to be 1.57 at 25°C and 1.63 at 60°C in the system with HEDTA and Dowex 50W, X-8.

2) Under various experimental conditions, elutions of an equimolar mixture of Er and Tm were carried out at 25° and 60°C using a 0.015M HEDTA eluant buffered with ammonium hydroxide; a steady state was established through the rare-earth band.

3) The elution system of the rare earth under steady-state conditions was analyzed on the basis of the rate theory; the present exchange system was thereby confirmed to be controlled by film-diffusion the rate-determining step.

4) By raising the elution temperature, the separation efficiency was increased; this was because of the decrease in the plate-height value as well as because of the increase in the separation factor itself.

BULLETIN OF THE CHEMICAL SOCIETY OF JAPAN VOL. 42 3184—3189 (1969)

Nuclear Magnetic Resonance Study of Metal Complexes. I. A Conformational Analysis of D-(*l*)-Propylenediamine Chelate Rings of Diamagnetic Cobalt(III), Palladium(II) and Platinum(II) Complexes

Shigenobu YANO, Haruko ITO, Yoshio KOIKE,*1 Junnosuke FUJITA and Kazuo SAITO

Department of Chemistry, Faculty of Science, Tohoku University, Katahira-cho, Sendai

(Received May 26, 1969)

Proton magnetic resonance (PMR) spectra of tetracyano-*l*-propylenediamine cobalt(III) ion and bis(*l*-propylenediamine) platinum(II) and palladium(II) ion have been measured in deuterated water and analyzed according to Castellano and Waugh's exact analysis. The values of coupling constants clearly indicate that the *l*-propylenediamine chelate rings in these diamagnetic complexes have fixed *λ-gauche* form in aqueous solutions at room temperature.

Recent researches have shown that high resolution proton magnetic resonance spectroscopy provides useful information on the structure of a variety of organic compounds in solution, but only a few papers have reported on its application to metal

*1 Present address: Faculty of Engineering, Kanagawa University, Kanagawa-ku, Yokohama.

complexes.[1] It is known that ethylenediamine (en) and propylenediamine (pn) coordinate to various metal ions to form nonplanar *gauche* chelates. Spees *et al.*[2] measured proton magnetic resonance (PMR) spectra of various metal complexes containing ethylenediamine and propylenediamine, and showed that the ethylenediamine chelate changes its conformation rapidly from λ- to δ-*gauche* form (IUPAC, 1966) and *vice versa* in an aqueous solution at room temperature. No clear experimental evidence has been given, however, concerning the chelate conformation of propylenediamine ring in solution.

Propylenediamine chelate ring was considered to be less labile to such conformational change, because the preference for the methyl group to be equatorial to the chelate ring would make one of the conformers more stable. The energy difference between the conformers with the methyl group in the axial and the equatorial direction was estimated to be about 2 kcal/mol, and it was supposed that about ninetyfive per cent of the ligand has the methyl group equatorial even in a solution at room temperature.[3]

We have measured PMR spectra of the diamagnetic complexes, $K[Co(CN)_4(l\text{-pn})]$, $[Pt(l\text{-pn})_2]Cl_2$ and $[Pd(l\text{-pn})_2]Cl_2$ and obtained significant information on the conformation of the *l*-propylenediamine chelate ring.

Experimental

Preparation of the Complexes. *Potassium Tetracyano-l-propylenediamine Cobalt(III) Dihydrate* $K[Co(CN)_4(l\text{-pn})]\cdot 2H_2O$. A mixture containing 5.0 g of $K_3[CoI(CN)_5]$[4] and 1.5 g of *l*-propylenediamine in 50 m*l* of water was warmed on a water bath at 80°C until the color changed to yellow. The solution was cooled, filtered, and evaporated to almost dryness under reduced pressure at 60°C. The residue was treated with 100 m*l* of absolute methanol and filtered. The crude complex was precipitated by adding 95% ethanol to the filtrate, filtered off, washed with absolute ethanol and ether. The product was recrystallized from methanol solution by adding 95% ethanol.

Found: C, 27.62; H, 4.60; N, 26.44%. Calcd for $C_6H_{12}N_6O_2KCo$. C, 26.91; H, 4.52; N, 26.90%.

Other complexes used in this work were the lots prepared in our previous work.[5]

Measurements. Proton magnetic resonance spectra of $K[Co(CN)_4(l\text{-pn})]$, $[Pt(l\text{-pn})_2]Cl_2$ and $[Pd(l\text{-pn})_2]Cl_2$ were recorded with Varian A-60, T-60 and HA-100 spectrometers. The spectra of $K[Co(CN)_4(l\text{-pn})]$ and $[Pt(l\text{-pn})_2]Cl_2$ were obtained in deuterated water and in a mixture of pyridine and deuterated water. The spectra of $[Pd(l\text{-pn})_2]Cl_2$ were measured in deuterated water. Sodium trimethylsilylpropanesulfonate (Na-TMS) was used as an internal reference. In all the solvents, hydrogen atoms of the amino groups were deuterated rapidly and only the C–H resonance was observed. Diamagnetic contributions of the complex and the solvent on the chemical shifts have not been corrected. To facilitate the analysis of spectra, nuclear magnetic double resonance technique was used; *i.e.* the methyl signal was decoupled to give a simpler ABC pattern with HA-100 spectrometer. All the measurements were made at about 39°C.

The coupling constants, the chemical shifts and the intensities were calculated with a HITAC 5020 electronic computer at the University of Tokyo. The Fortran program for Castellano and Waugh's[6] exact analysis was kindly supplied by Dr. J. Cavanaugh at Research Department, Socony Mobil Oil Company, Inc., Paulsboro, New Jersey, U.S.A. to whom our sincere thanks are due.

Results and Discussion

The spectra of $K[Co(CN)_4(l\text{-pn})]$ in deuterated water are shown in Fig. 1. Whenever amino group hydrogens are deuterated, propylenediamine $ND_2CH(CH_3)CH_2ND_2$ should give an $ABCX_3$ pattern. One sharp doublet and one triplet were observed at about 1.25 and 2.38 ppm, respectively. That the splitting (J=6.0 cps for the doublet and 12.3 cps for the triplet) is not affected by the outer magnetic field strength indicates that these splittings are brought about by the spin-spin coupling. The doublet is safely assigned to the methyl signal, and its integrated intensity is three times as large as that of the triplet. In the lower field, complicated signals appear in the region from 2.80 to

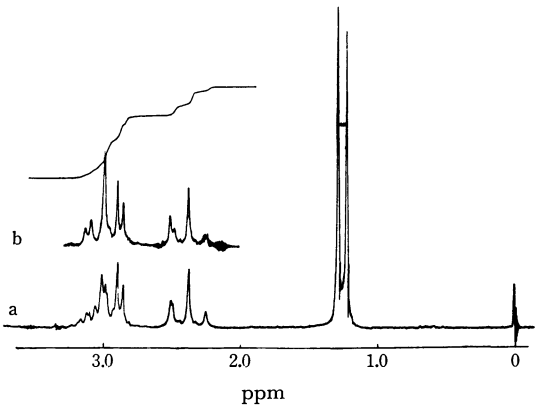

Fig. 1. 100 MHz PMR spectrum of $K[Co(CN)_4(l\text{-pn})]$ in D_2O (a) and the double resonance spectrum irradiated on the methyl signal (b).

1) L. E. Erickson, J. W. McDonald, J. K. Howie and R. P. Clow, *J. Am. Chem. Soc.*, **90**, 6371 (1968).

2) S. T. Spees, Jr., L. J. Durham and A. M. Sargeson, *Inorg. Chem.*, **5**, 2103 (1966).

3) E. J. Corey and J. C. Bailar, Jr., *J. Am. Chem. Soc.*, **81**, 2620 (1959).

4) A. W. Adamson, *ibid.*, **78**, 4260 (1956).

5) H. Ito, J. Fujita and K. Saito, This Bulletin, **40**, 2584 (1967).

6) S. Castellano and J. S. Waugh, *J. Chem. Phys.*, **34**, 295 (1961).

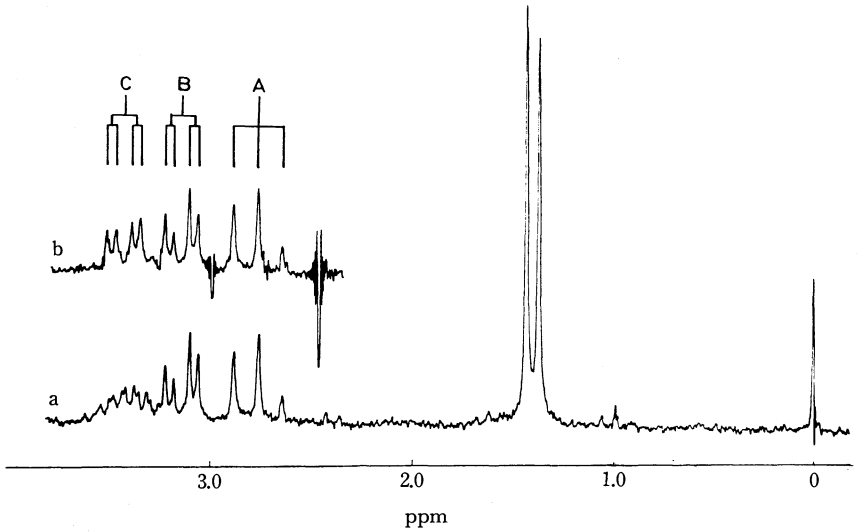

Fig. 2. 100 MHz PMR spectrum of K[Co(CN)$_4$(*l*-pn)] in pyridine-D_2O mixed solvent (a) and the double resonance spectrum irradiated on the methyl signal (b).

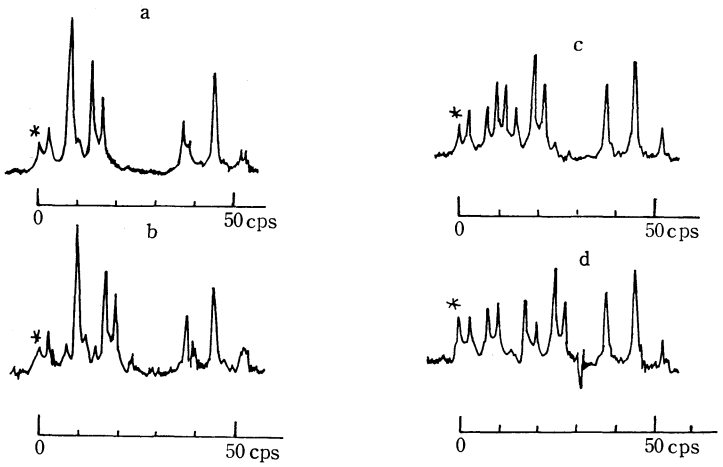

Fig. 3. The methine and methylene part of 100 MHz PMR double resonance spectra irradiated on the methyl signal of K[Co(CN)$_4$(*l*-pn)] in pyridine-D_2O mixed solvents (Chemical shifts from * peak). Approximate ratios (by volume) of pyridine to water are as follows; (a) 0, (b) 0.231, (c) 0.455 and (d) 0.600

3.20 ppm. The integrated intensity ratio of these signals to that of the doublet is two thirds. Although the signal of methine proton appears usually at a lower field than those of methylene protons, the spectra are too complicated to be analyzed further. Thus we used the nuclear magnetic double resonance technique. Irradiation at 1.25 ppm (the region of the methyl signal) made the signals from 2.80 to 3.20 ppm region less complicated, as shown in Fig. 1-b. Conversely, irradiation at the lower region of the complicated signals (3.10 ppm) converted the methyl doublet into a single sharp peak. This indicates that the signals at the lower region of the complicated part correspond to the methine proton. The double resonance spectrum obtained on irradiation at the methyl region should consist of ABC or ABB′ pattern, which gives rise to fifteen lines including three combination bands. However, the signals arising from methylene and methine group overlap with each other to make the analysis of spectrum still difficult.

The PMR spectra of K[Co(CN)$_4$(*l*-pn)] in pyridine-D_2O mixed solvents irradiated in the methyl signal region are shown in Fig. 2. With increase in the amount of pyridine, the whole signal shift to a lower field and the complicated part splits into two quartets as shown in Fig. 3. The higher field quartet is shifted to a lower field to a

less extent as compared with the other quartet. The extent of splitting of these groups of signals remains unchanged with the change in molar ratio of pyridine to water. Since coupling constants are not affected by changing solvents, these quartets were considered to be brought about by the spin-spin coupling. We denote tentatively the triplet, the higher quartet and the lower quartet A, B and C, respectively. Their integrated intensities are equal.

All the experiments described above lead to the assignment that A and B are due to protons of CH_2 group and C to that of CH group (Fig. 2). On the basis of these eleven lines of the spectra in aqueous pyridine solutions, we have calculated the coupling constants, the chemical shifts and the intensities, according to Castellano and Waugh's exact analysis[6] (Tables 1 and 2).

Two possible conformers can exist when *l*-propylenediamine coordinates to a metal, *λ-gauche* and *δ-gauche* form with the methyl group equatorial and axial to the chelate ring, respectively (Fig. 4). The *λ-gauche* form can provide three kinds of coupling: a *geminal*, a *trans* and a *gauche*. On the other hand, the *δ-gauche* form gives two different kinds of coupling: one *geminal* and two *gauche*. Karplus,[7] Lemieux and Lown,[8] and Abraham and Mclauchlan[9] calculated theoretical values of vicinal coupling

Table 1. Chemical shifts and spin-spin coupling constants (in cycle/sec) of $K[Co(CN)_4(l\text{-pn})]$ in pyridine-deuterated water mixed solvents

Pyridine D_2O	Chemical shifts			Coupling constants		
	C	B	A	AB	BC	AC
0.600	−30.9	−2.1	33.0	−12.4	4.4	12.4
0.455	−28.2	−8.1	36.2	−12.5	4.4	12.4
0.23	−26.2	−10.5	36.6	−12.8	4.4	12.7

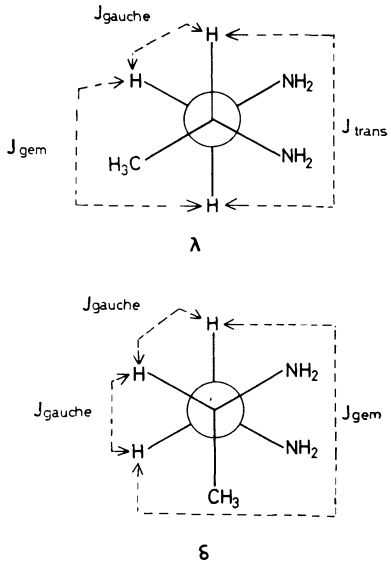

Fig. 4. The schematic diagram of spin-spin couplings for λ-and *δ-gauche* conformer.

Table 2. Calculated and observed intensities

$K[Co(CN)_4(l\text{-pn})]$			$[Pd(l\text{-pn})_2]Cl_2$			$[Pt(l\text{-pn})_2]Cl_2$*		
Position (cps)	obsd	calcd	Position (cps)	obsd	calcd	Position (cps)	obsd	calcd
−69.28		0.0	−61.76		0.0	−64.20		0.0
−39.97	0.9	0.7	−40.84	0.8	0.8	−37.90	0.9	0.7
−35.67	0.9	0.9	−36.54	1.0	0.9	−33.60	0.7	0.9
−27.67	1.1	1.0	−31.04	1.0	1.0	−27.90	1.1	1.0
−23.37	1.1	1.4	−26.74	1.2	1.3	−23.60	1.2	1.3
−11.27	1.0	0.8	−5.82		0.0	−9.60	0.9	0.7
−6.97	0.7	0.6	−5.44	0.6	0.6	−5.30	0.6	0.5
1.03	1.4	1.5	−1.14	0.5	0.5	2.60	1.4	1.6
5.33	1.0	1.1	6.96	1.7	1.6	2.70		0.0
5.94		0.0	11.26	1.5	1.3	6.90	1.2	1.2
22.34	1.5	1.6	19.78	1.6	1.7	21.00	1.2	1.6
34.64	1.9	1.1	29.58	1.1	1.2	31.00	1.1	1.1
34.64		1.0	32.18	0.8	0.6	33.20	1.1	0.7
46.94	0.6	0.6	41.98	0.5	0.5	43.20	0.6	0.5
63.34		0.0	67.38		0.0	61.50		0.0

* The influence of the satellites due to ^{195}Pt ($I=1/2$) was ignored.

7) M. Karplus, *J. Chem. Phys.*, **30**, 11 (1959).
8) R. V. Lemieux and J. W. Lown, *Can. J. Chem.*, **42**, 893 (1964).
9) R. J. Abraham and K. A. Mclauchlan, *Mol. Phys.*, **5**, 513 (1962).

TABLE 3. THEORETICAL AND CALCULATED VALUES OF SPIN-SPIN COUPLING CONSTANTS (in cycle/sec) OF K[Co(CN)$_4$(*l*-pn)]

	Experimental	Theoretical	
J_{trans} (CA)	12.4	11.0	16.1
J_{gauche} (BC)	4.4	2.0	4.0
J_{gem} (AB)	−12.4	13.2	13.4

constants, which are dependent on the dihedral angle between two vicinal CH bonds. Barfield and Grant[10] calculated the *geminal* coupling constants for methane derivatives on the basis of the valence bond approach. These values are shown in Table 3.

The coupling constant J_{AB}(−12.4 cps) is undoubtedly for *geminal*, because A and B are the signals of methylene protons. The constants J_{BC} and J_{AC} are, therefore, of vicinal coupling. Of these, J_{BC} (4.4 cps) is in good agreement with the theoretical value of the *gauche* coupling constant.

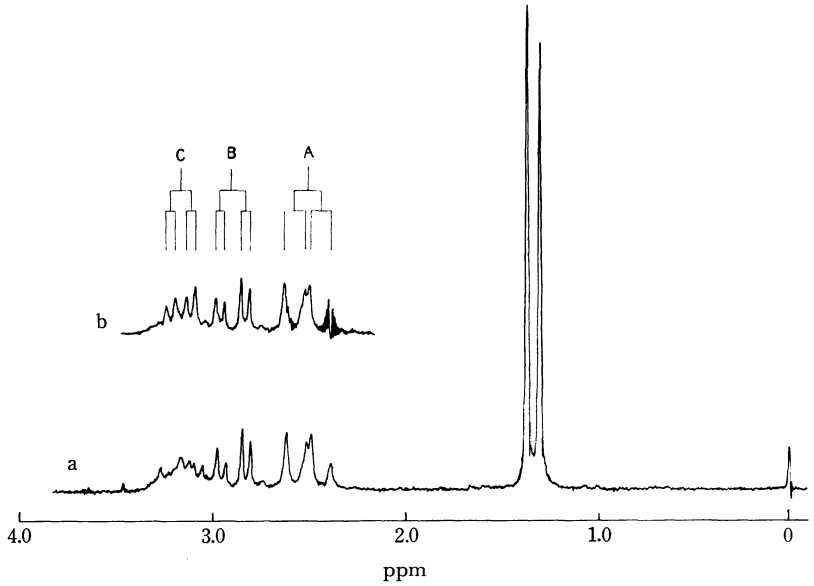

Fig. 5. 100 MHz PMR spectrum of [Pt(*l*-pn)$_2$]Cl$_2$ in D$_2$O (a) and the double resonance spectrum irradiated on the methyl signal (b).

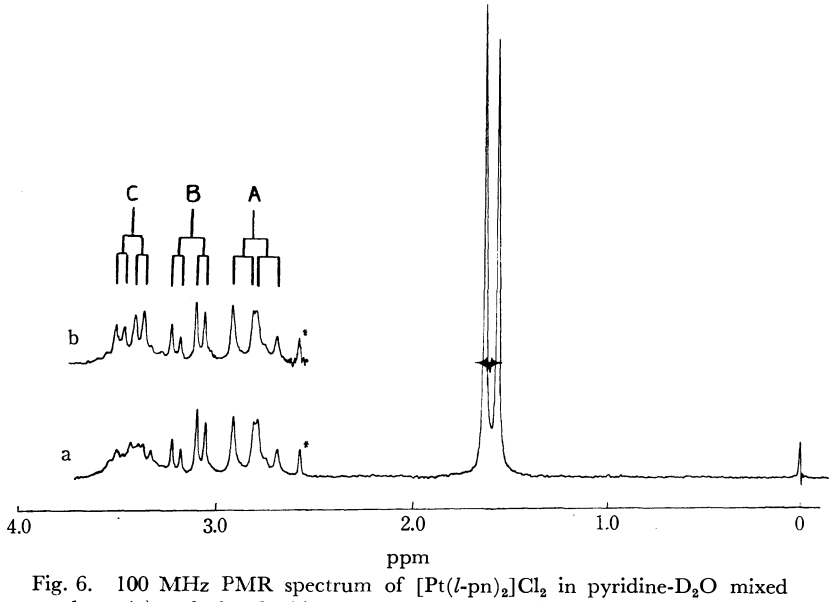

Fig. 6. 100 MHz PMR spectrum of [Pt(*l*-pn)$_2$]Cl$_2$ in pyridine-D$_2$O mixed solvent (a) and the double resonance spectrum irradiated on the methyl signal (b).

10) M. Barfield and D. M. Grant, *J. Chem. Phys.*, **36**, 3054 (1962).

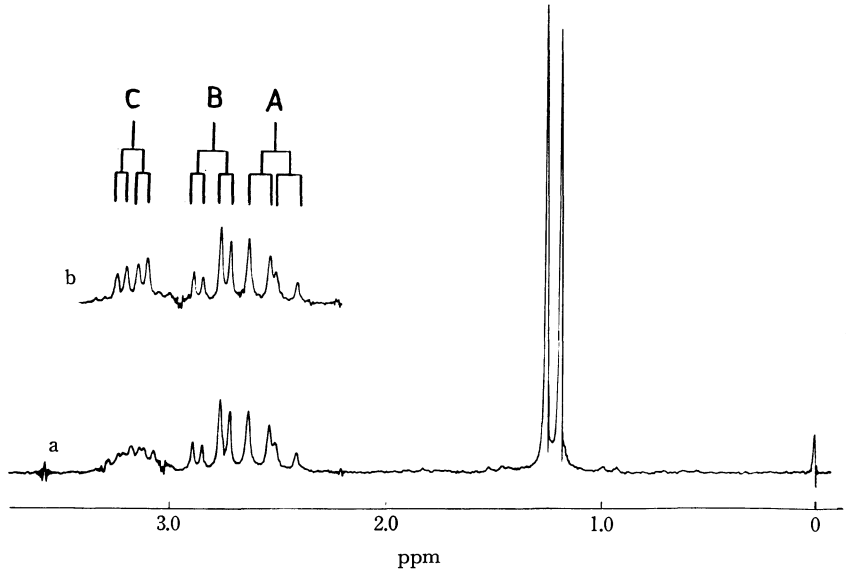

Fig. 7. 100 MHz PMR spectrum of $[Pd(l\text{-pn})_2]Cl_2$ in D_2O (a) and the double resonance spectrum irradiated on the methyl signal (b).

TABLE 4. CALCULATED CHEMICAL SHIFTS AND SPIN-SPIN COUPLING CONSTANTS (in cycle/sec) OF $[Pd(l\text{-pn})_2]Cl_2$ IN DEUTERATED WATER AND $[Pt(l\text{-pn})_2]Cl_2$ IN PYRIDINE-DEUTERATED WATER

	Chemical shifts			Coupling constants		
	C	B	A	AB	BC	CA
$[Pd(l\text{-pn})_2]Cl_2$	−33.3	4.3	29.0	−12.5	4.2	9.9
$[Pt(l\text{-pn})_2]Cl_2$	−30.2	−0.3	30.5	−12.3	4.3	10.0

The constant J_{AC} is 12.4 cps and agrees well also with the theoretical *trans* coupling constant. These results indicate that the *l*-propylenediamine chelate ring has a *λ-gauche* form, and that A and B are due to the axial and the equatorial proton, respectively. The coupling constants J_{AC} and J_{AB} must have accidentally coincided with each other.

The large difference of the chemical shifts between the methylene protons may also support fixed *λ-gauche* form of the *l*-propylenediamine chelate ring. On the basis of the above assignment the axial proton gives a signal at a higher field than the equatorial proton does. This is consistent with the observation for substituted cyclohexanes.[11]

The PMR spectra of $[Pt(l\text{-pn})_2]Cl_2$ in deuterated water and in a mixture of pyridine and deuterated water, and $[Pd(l\text{-pn})_2]Cl_2$ in deuterated water are shown in Figs. 5, 6 and 7. These spectra are not significantly different from that of $K[Co(CN)_4(l\text{-pn})]$, except that the difference of the chemical shift between B and C protons is large enough to be distinguished without use of the solvent effect. In these cases twelve lines are observed and all the coupling constants J_{AB}, and J_{BC} and J_{AC} have different values as shown in Table 4. On these results, we conclude that the *l*-propylenediamine chelate rings in these complexes have also fixed *λ-gauche* form under the given conditions.

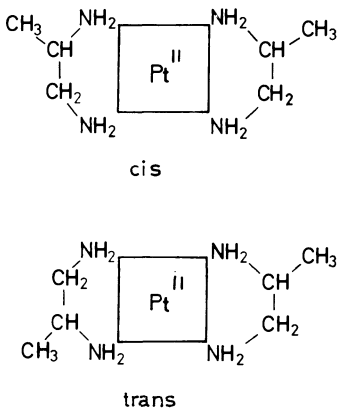

Fig. 8. Two geometrical isomers for square planar $[Pt(l\text{-pn})_2]^{2+}$ ion.

Two geometrical isomers are possible for bis-*l*-propylenediamine complex of a planar type shown in Fig. 8. The chemical environment for protons should be different between these two isomers. Such a difference, however, would be too small[1] to be detected by the present spectrometer.

In Table 2 are listed the values of observed and calculated intensities. They seem to agree with each other satisfactorily, to support our assignments.

The authors thank the Ministry of Education for Grant in aid.

11) J. A. Pople, W. G. Schneider and H. J. Bernstein, "High Resolution Nuclear Magnetic Resonance," McGraw-Hill, New York (1959), p. 392.

BULLETIN OF THE CHEMICAL SOCIETY OF JAPAN VOL. 42 3190—3194 (1969)

Tautomerism in 3-Substituted-2,4-pentanediones and Their Copper Chelates

Minoru TANAKA, Toshiyuki SHONO and Koichiro SHINRA

Department of Chemical Technology, Faculty of Engineering, Osaka University, Yamadakami, Suita

(Received may 29, 1969)

Seventeen 3-substituted-2,4-pentanediones were synthesized. The effect of substituents in the position 3 on the tautomeric equilibria, *i. e.*, keto-, *cis*-enol- and *trans*-enol-forms, has been investigated by nuclear magnetic resonance spectroscopy. It has been found that the percentage of each tautomer depends upon the electronic and steric effects of the substituents. The relative intensity of intramolecular hydrogen bonds in these compounds was evaluated from both the NMR and IR data. It has been found from the half-wave potential data of polarographic reduction and the Cu–O stretching frequencies of 16 copper chelates of 3-substituted-2,4-pentanediones that the relative stability of the chelate decreases with an increase in the electron-withdrawing effect of the substituents.

In recent years, NMR spectroscopy has been frequently used for the study of β-dicarbonyls, especially for keto-enol tautomerism and hydrogen bonding. Burdett and Rogers examined the NMR spectra of β-diketones and β-keto esters, determined their equilibrium constants[1] and discussed the solvent effect[2] on the chemical shifts and on the tautomeric equilibrium. Lowe and Ferugson[3] studied the direction and the percentage of the enolization of several substituted benzoylacetones by infrared, ultraviolet, and NMR spectroscopy and found that the benzoylacetones were enolized toward the carbonyl close to the phenyl group. Lintvedt and Holtzclaw studied the position of the methylene proton and enolic proton resonance peaks of several substituted 1,3-diketones with respect to the electronic effects[4] of the groups substituted in the position 1 or 3 and the correlation between the position of this enolic proton resonance peak and the thermodynamic formation constants[5] of the 1,3-diketone metal chelates. They reported that, with a greater electron-releasing effect of the substituents, the hydrogen bond became stronger as the electron density on the oxygen increased. The enolic proton resonance peak was shifted toward a lower field, and the stability of the chelates was increased.

In a previous paper the tautomeric equilibria of six 3-alkylated-2,4-pentanediones[6] were reported; they had been studied using NMR spectroscopy. In this paper seventeen 3-substituted-2,4-pentanediones will be investigated in order to establish the substituent effect on the tautomerism and on the intramolecular hydrogen bond. The relative stability of these sixteen copper chelates was, further, checked by infrared spectroscopy and by polarography.

Experimental

Preparation of 3-Substituted-2,4-pentanediones and Copper Chelates. The 3-substituted-2,4-pentanediones were prepared by the established methods, references for which are listed in Table 1. The copper chelates were prepared by adding an ethanol solution of 3-substituted-2,4-pentanedione to an excess aqueous solution of cupric acetate, except in the case of bis[3-nitro-2,4-pentanediono]copper. The analytical data are shown in Table 2.

NMR Spectroscopy. The NMR spectra were obtained on a JNM-3H-60 spectrometer at 60 Mcps. All the samples were run in carbon tetrachloride. The sample concentration was 2 mol/*l*. The chemical shift values are reported in cps from internal tetramethylsilane.

Polarography. The polarograms for copper chelates were recorded using a Yanagimoto Model P-8 polarograph. Each sample solution was 10^{-3} mol/*l* with respect to the chelate, 0.1 mol/*l* with respect to potassium nitrate as the supporting electrolyte, and 1.6 g/*l* with respect to Tween-80 as the maximum suppressor. The chelate, supporting electrolyte and maximum suppressol-

1) J. L. Burdett and M. T. Rogers, *J. Am. Chem. Soc.*, **86**, 2105 (1964).

2) M. T. Rogers and J. L. Burdett, *Can. J. Chem.*, **43**, 1516 (1965).

3) J. U. Lowe, Jr., and L. N. Ferugson, *J. Org. Chem.*, **30**, 3000 (1965).

4) R. L. Lintvedt and H. F. Holtzclaw, Jr., *J. Am. Chem. Soc.*, **88**, 2713 (1966).

5) R. L. Lintvedt and H. F. Holtzclaw, Jr., *Inorg. Chem.*, **5**, 239 (1966).

6) T. Shono, M. Tanaka, Y. Murotani and K. Shinra, *Nippon Kagaku Zasshi (J. Chem. Soc. Japan, Pure Chem. Sect.)*, **88**, 1068 (1967).

Table 1. Preparation of 3-substituted-2,4-pentanediones

3-Substituent	Bp (°C)	Pressure (mmHg)	Ref.
CH_3	60—62	18	6
C_2H_5	68—70	12	6
n-C_3H_7	75—77	12	6
i-C_3H_7	74—76	17	6
n-C_4H_9	114—115	35	6
i-C_4H_9	79—80	11	6
s-C_4H_9	88—89	14	6
Cl	154—156	760	b)
$COOC_2H_5$	95—98	12	7
$CH_2COOC_2H_5$	141—143	22	6
$CH_2CH_2COOC_2H_5$	151—153	14	6
$OCOCH_3$	101—102	17	8
C_6H_5	56—58[a]	—	5
CN	54—55[a]	—	7
OCH_3	57—58	15	7
COC_6H_5	30—31[a]	—	9
$CH(C_6H_5)CH_3$	49—50[a]	—	6

a) Melting point is shown.
b) This compound was prepared by adding sulfuryl chloride (67.5 g) to acetylacetone (50 g) at 0—5°C over 2 hr, pouring the mixture into water (100 m*l*) and extracting with ether.

were dissolved in aqueous 75% dioxane. The cell temperature was maintained at 25.0±0.1°C, and oxygen-free nitrogen was bubbled through each solution for 20 min to remove dissolved oxygen before measurement.

Infrared Spectroscopy. The infrared spectra in the 4000—650 cm^{-1} region were recorded on a Hitachi Model EPI-S2 spectrometer, while those in the 700—250 cm^{-1} region were recorded on a Hitachi Model EPI-L spectrometer using Nujol mulls.

Results and Discussion

Keto-Enol Tautomeric Equilibria. In general there are three possible tautomeric isomers for 3-substituted-2,4-pentanediones; they are shown

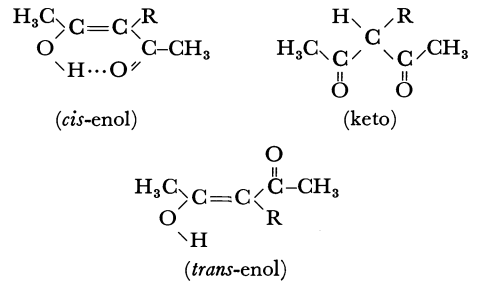

below. As has previously been reported, 2,4-pentanediones substituted in the position 3 with

Table 2. Analytical data for 3-substituted-2,4-pentanedione copper chelates

Code	3-Substituent	Analyses, % C Found	C Calcd	H Found	H Calcd	N Found	N Calcd
1	CH_3	49.22	49.74	6.69	6.26		
2	C_2H_5	52.75	52.91	6.88	6.98		
3	n-C_3H_7	55.28	55.56	7.62	7.57		
4	i-C_3H_7	67.71	67.58	9.95	9.92[a]		
5	n-C_4H_9	57.54	57.82	8.02	8.09		
6	i-C_4H_9	57.74	57.82	8.28	8.09		
7	s-C_4H_9	69.31	69.20	10.29	10.32[a]		
8	Cl	36.30	36.33	3.73	3.66		
9	$COOC_2H_5$	47.28	47.35	5.43	5.46		
10	$CH_2COOC_2H_5$	49.85	49.82	5.85	6.04		
11	$CH_2CH_2COOC_2H_5$	51.54	52.00	6.18	6.55		
12	$OCOCH_3$	44.36	44.51	5.15	4.80		
13	C_6H_5	63.40	63.84	5.12	5.36		
14	CN	45.43	46.29	3.97	3.88	8.81	8.95
15	OCH_3	44.19	44.79	5.79	5.64		
16	COC_6H_5	61.59	61.34	5.02	4.72		
17	$CH(C_6H_5)CH_3$	76.92	76.44	7.91	7.90[a]		
18	NO_2[7]	34.24	34.15	3.29	3.44	7.90	7.96
19	H						

a) Analyzed as 3-substituted-2,4-pentanedione as they formed no chelates.

7) J. P. Fackler, Jr., and F. A. Cotton, *Inorg. Chem.*, **2**, 102 (1963).
8) H. Bähm and H. Schneider, *Chem. Ber.*, **91**, 1100 (1958).
9) M. M. Coombs and R. P. Houghton, *J. Chem. Soc.*, **1961**, 5015.

TABLE 3. TAUTOMERIC EQUILIBRIA OF 3-SUBSTITUTED-2,4-PENTANEDIONES

Code	3-Substituent	Proton chemical shifts, cps			Percentage of tautomer, %		
		cis-enol OH	*trans*-enol OH	3-methine H	*cis*-enol	*trans*-enol	keto
1	CH_3	979	—	218 (Q)	36	0	64
2	C_2H_5	993	—	210 (T)	25	0	75
3	*n*-C_3H_7	998	325	219 (M)	22.2	11.1	66.7
4	*i*-C_3H_7	—	323	201 (D)	0	24	76
5	*n*-C_4H_9	989	324	212 (T)	22	5.5	72.5
6	*i*-C_4H_9	1001	324	216 (T)	40	10	50
7	*s*-C_4H_9	—	325	208 (D)	0	52.6	47.4
8	Cl	920	—	279	91	0	9
9	$COOC_2H_5$	1081	—	206	96	0	4
10	$CH_2COOC_2H_5$	1002	—	246[a]	33[d]	0	67[d]
11	$CH_2CH_2COOC_2H_5$	999	—	222 (T)	26	0	74
12	$COOCH_3$	861	—	321	20	0	80
13	C_6H_5	996	—	—	100	0	0
14	CN	1002	—	—	100	0	0
15	OCH_3	845	—	b)	c)	0	c)
16	COC_6H_5	1017	—	—	100	0	0
17	$CH(C_6H_5)CH_3$	—	—	236 (D)	0	0	100
19	H	915	—	210	93	0	7

D=doublet, T=triplet, Q=quartet and M=multiplet.

a) This signal overlaps CH_2 signal of $CH_2COOCH_2CH_3$.

b) It is impossible to find the signal because this material cannot be purified.

c) Signal intensity at 845 cps is very low.

d) Determined using CH_2 proton signal intensity of $CH_2COOC_2H_5$.

isopropyl and *s*-butyl groups have no *cis*-enol form. In the case of a methyl substituent, *cis*-enol and keto forms have been found. Substitution with *n*-propyl, *n*-butyl, and isobutyl groups showed *cis*- and *trans*-enol forms and the keto form. Substituents with an inductive effect different from alkyl groups as well as bulky substituents were introduced. Table 3 summarizes the chemical shift values of the enolic proton and the methine proton in the keto form, and the percentage of each tautomer obtained from the corresponding signal intensity. Table 3 shows that the substitution of carbethoxy, cyano, or benzoyl groups in the position 3 of 2,4-pentanedione results in a considerable increase in the *cis*-enol tautomer, while in the case of alkyl, acetoxy, and methoxy substituents, an increase of

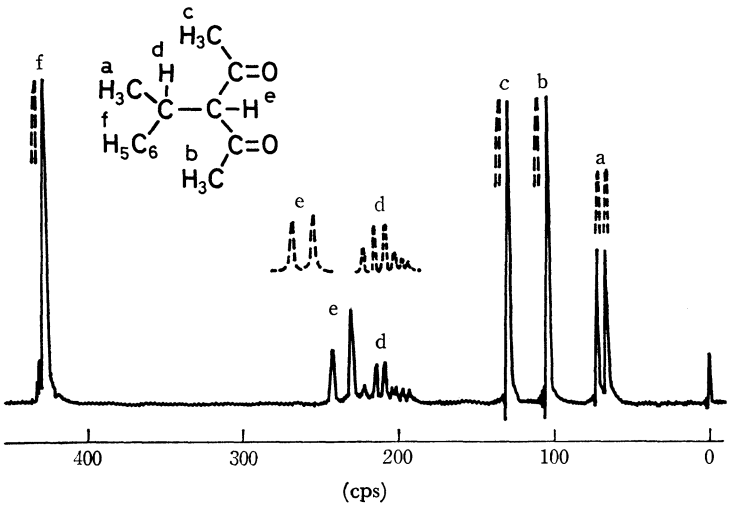

Fig. 1. NMR spectra for 3-(α-phenylethyl)-2,4-pentanedione in CCl_4 (solid line) and in *d*-DMSO (broken line).

the keto tautomer is found. Though many factors influence the keto-enol tautomeric equilibrium, the results in Table 3 can be qualitatively explained in terms of both the electronic and steric factors of the substituent. The electron density in the vicinity of the methine proton must be decreased by the substitution of electronegative groups in the position 3. The enol tautomer will, then, be more stabilized. Among keto-, *cis*-enol-, and *trans*-enol-forms, the steric hindrance between acetyl methyl groups and the 3-substituent is the largest in the *cis*-enol tautomer. The percentage of the *cis*-enol tautomer was found to decrease with an increase in the bulkiness of the substituent in the position 3. In the absence of steric hindrance, the *cis*-enol tautomer is more stabilized than the *trans*-enol tautomer by an intramolecular hydrogen bond.[1,10] The combination of the electronic and steric effects mentioned presumably influences the tautomeric equilibrium. In fact, substitution with electron-withdrawing groups, such as carbethoxy, cyano, and benzoyl groups, results in a considerable increase in the *cis*-enol tautomer. In the case of electron-releasing groups, such as alkyl, acetoxy, and methoxy, the keto tautomer increases reversely. It should be sterically impossible for 2,4-pentanediones substituted with isopropyl anb *s*-butyl groups to take the *cis*-enol form. The presence of only small amounts of the *trans*-enol form in the cases of *n*-propyl, *n*-butyl, and isobutyl substituents is presumably the result of steric hindrance, which is even larger in isopropyl and *s*-butyl groups (see Table 3). The α-phenylethyl group, which is bulkier than the isopropyl and *s*-butyl groups, was introduced in the position 3. The NMR spectrum of 3-(α-phenylethyl)-2,4-pentanedione is shown in Fig. 1. In the case of the carbon tetrachloride solution (see Fig. 1, solid line), three signals, corresponding to three protons, appear at 69 cps as a doublet, and at 104 cps and 130 cps as a singlet. Phenyl proton resonance occurs at 428 cps. The signals corresponding to the two methine protons appear in the 210—236 cps region. Using *d*-dimethyl sulfoxide as the solvent, these signals can be separated into two signals with the same intensity (*cf.* the broken line) *i.e.*, the multiplet centered at 210 cps and the doublet, at 263 cps. An examination of this spectrum leads to the conclusion that this compound has only the keto form, and no *cis*- and *trans*-enol forms, because of its great bulky substituent. The same results have been reported in the case of 3-(*t*-butyl)-2,4-pentanedione.[11]

Intramolecular Hydrogen Bond. As Table 3 shows, the *cis*-enol OH protons show considerable variations in chemical shift and all are at a very low applied magnetic field, indicating the presence of intramolecular hydrogen bonds in these compounds. With an increase in the strength of this hydrogen bond, the carbonyl stretching vibration is shifted to a lower frequency.[12,13] The *cis*-enol OH proton chemical shift values are plotted *vs.* the carbonyl stretching frequencies in Fig. 2. It is

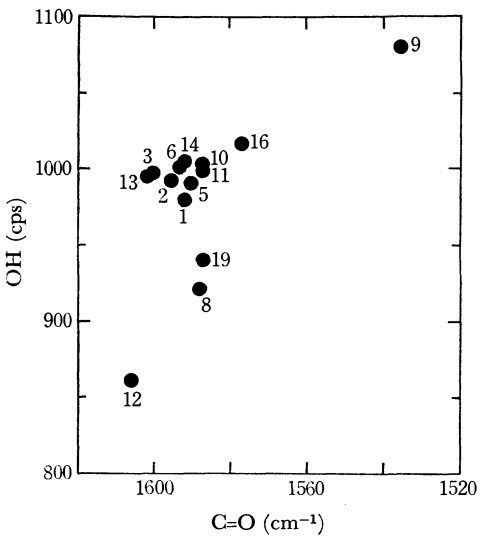

Fig. 2. Chemical shift of *cis*-enol OH proton *vs.* carbonyl stretching frequency.
(Code numbers refer to compounds of Table 3)

Table 4. Polarographic and infrared spectral data for copper chelates

Code	3-Substituent	Half-wave potential (V)	Cu–O stretching frequency (cm^{-1})	C=O stretching frequency (cm^{-1})
1	CH_3	−0.87	468	1577
2	C_2H_5	−0.92	468	1570
3	*n*-C_3H_7	−0.90	467	1576
5	*n*-C_4H_9	−0.89	468	1575
6	*i*-C_4H_9	−0.94	468	1575
8	Cl	−0.65	467	1574
9	$COOC_2H_5$	−0.63	462	1582
10	$CH_2COOC_2H_5$	−0.85	465	1572
11	$CH_2CH_2COOC_2H_5$	−0.92	468	1577
12	$OCOCH_3$	−0.86	462	1587
13	C_6H_5	−0.82	471	1572
14	CN	−0.37	450	1592
15	OCH_3	−0.82	457	1579
16	COC_6H_5	−0.52	450	1583
18	NO_2	−0.29	448	1590
19	H	−0.81	455	1577

10) G. W. Wheland, "Advanced Organic Chemistry," 3rd Ed., John Wiley & Sons, Inc., New York (1960).

11) P. Bolat and H. Militzer, *Tetrahedron Letters*, **1966**, 3599.

12) S. Forsen and M. Nilsson, *Acta Chem. Scand.*, **13**, 1383 (1959).

13) S. Forsen and M. Nilsson, *ibid.*, **14**, 1333 (1960).

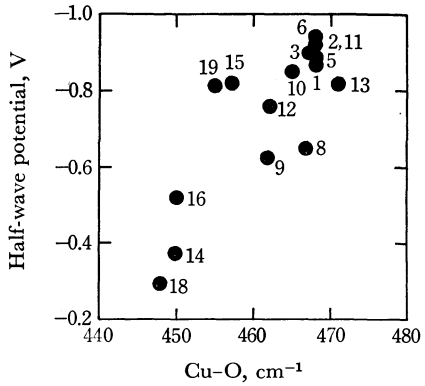

Fig. 3. Half-wave potential *vs.* copper-oxygen stretching frequency of copper chelates.
(Code numbers refer to compounds of Table 4)

found that, with an increase in the strength of the hydrogen bond, the *cis*-enol OH proton resonance signal is shifted toward a lower field.

Copper Chelates of 3-Substituted-2,4-pentanediones. The polarograms and infrared spectra of sixteen 3-substituted-2,4-pentanedione copper chelates were recorded in order to investigate their relative stability. Lintvedt *et al.*[14] reported that the reduction potential should be a function of the electronic density on and around the copper atom. The reduction potential becomes more negative as the chelate becomes more stable, because the stability of the chelate increases with an increase in the electron density near the copper ion. Much information concerning the nature of coordinate bonds and chelate rings has been obtained from the infrared spectroscopy of 2,4-pentanedione metal chelates.[15,16] Especially, the metal-oxygen stretching modes appearing in the 700—250 cm^{-1} region may directly provide information on the relative strength of coordinate bonds. Table 4 shows the half-wave potential data of the polarographic reduction, the copper-oxygen stretching frequencies, and the carbonyl stretching frequencies of copper chelates. A plot of the half-wave potentials *vs.* the copper-oxygen stretching frequencies (Fig. 3) shows that the chelate with a more negative half-wave potential tends to show a higher copper-oxygen stretching frequency. Namely, in the case of copper chelates reduced more easily when substituted with electron-withdrawing substituents, such as nitro, cyano, and benzoyl groups, coordinate bonds become weaker because the electron density near the copper atom decreases. The chelates with a higher frequency of the copper-oxygen stretching vibration also tend to show a lower carbonyl stretching frequency. The electronic effect of the substituent thus affects the electron density on the copper atom. This proves the delocalization of π-electrons in the chelate ring. Murakami *et al.*[17] have studied the delocalization of π-electrons for 2,4-pentanedione metal chelates substituted in the position 3 with phenyl and benzyl derivatives.

14) R. L. Lintvedt, H. D. Russel and H. F. Holtzclaw, Jr., *Inorg. Chem.*, **5**, 1603 (1966).

15) M. Mikami, I. Nakagawa and T. Shimanouchi, *Spectrochimica Acta*, **23A**, 1037 (1967).

16) G. T. Behnke and K. Nakamoto, *Inorg. Chem.*, **6**, 433 (1967).

17) Y. Murakami, K. Nakamura, H. Uchida and Y. Kanaoka, *Inorg. Chim. Acta*, **2**, 133 (1968).

BULLETIN OF THE CHEMICAL SOCIETY OF JAPAN VOL. 42 3195—3198 (1969)

A New Monoclinic Phase of Cerium Orthovanadate ($CeVO_4$)

Masahiro YOSHIMURA and Toshiyuki SATA

Research Laboratory of Engineering Materials, Tokyo Institute of Technology, Ookayama, Meguro-Ku, Tokyo

(Received June 2, 1969)

A new monoclinic phase of cerium orthovanadate, $CeVO_4$(H), was found during the course of oxidation of pseudo-perovskite $CeVO_3$ below 400°C. It has been confirmed to crystallize in the huttonite-type structure (C_{2h}^5—$P2_1/n$), that of $LaVO_4$. The lattice parameters were determined to be:

$$a_0 = 6.98\text{Å},\ b_0 = 7.22\ \text{Å},\ c_0 = 6.76\ \text{Å},\ \beta = 105°02',\ V = 328\ \text{Å}^3 \text{ and } Z = 4.$$

This phase was metastable, and exothermally transformed into a known stable $CeVO_4$ (tetragonal zircon-type, D_{4h}^{19}-$I4_1/amd$) above 400°C, releasing a small amount of oxygen. From magnetic, chemical and thermogravimetric analyses, the valences of cerium ion and vanadium ion in $CeVO_4$-(H) seem to be tripositive and pentapositive respectively, but V^{4+} ion is mixed in zircon-type $CeVO_4$; $CeVO_4$(Z).

It has been reported[1-7] that all rare earth (except La) orthovanadates are isostructural with xenotime which has the tetragonal zircon-type structure (D_{4h}^{19}-$I4_1/amd$), while $LaVO_4$ is isostructural with monazite, the monoclinic huttonite-type structure (C_{2h}^5-$P2_1/n$). The polymorphism of $LnMO_4$ (Ln= lanthanide, M=P, As, V, Nb, Ta, *etc.*) was studied in view of crystallographic interest. Stubican and Roy[3] investigated the phase transition of rare earth vanadates and arsenates under high pressure, but gave no description on the polymorphism of $CeVO_4$.

Several researchers[5-7] reported that zircon-type $CeVO_4$, represented as $CeVO_4$(Z), was prepared by the reaction between Ce^{3+} salts or oxide and V_2O_5 in an inert atmosphere taking the instability of Ce^{3+} into consideration. However, this consideration seems unnecessary.

During the course of study on the valence states of ions in cerium vanadium double-oxides, a new monoclinic huttonite-type phase of $CeVO_4$, represented as $CeVO_4$(H), was found as a metastable phase. In this paper, the formation of $CeVO_4$(H) and its characteristic properties are presented in relation to those of $CeVO_4$(Z).

Experimental

Materials are ceria for optical use (CeO_2 contents 99.99%) and a guaranteed grade NH_4VO_3 or V_2O_5 which was obtained by decomposition of NH_4VO_3 at 500°C for 12 hr in air. The reaction processes were traced by the ordinary TGA and DTA methods programmed 5°C/min under various atmospheres. The reaction products were identified by means of powder X-ray diffraction ($CuK\alpha_1$=1.5405 Å).

Samples for X-ray powder diffraction were obtained as follows: $CeVO_4$(H), prepared by oxidation of $CeVO_3$ at 370°C for 8 hr in air. $LaVO_4$ and $CeVO_4$(Z) prepared by heating equimolar mixtures of V_2O_5 and La_2O_3 or CeO_2 at 800°C for 4 hr.

Their magnetic susceptibilities were measured with a torsion-type magnetobalance (Shimadzu MB-II) at temperatures between 77 and 1000°K.

Results and Discussion

Contrary to expectation, the formation of $CeVO_4$ from component salts is represented by the equation,[8]

$$CeO_2 + \tfrac{1}{2}V_2O_5 \longrightarrow CeVO_4 + \tfrac{1}{4}O_2, \qquad (1)$$

*1 A part of this study was presented at the 21th Annual Meeting of the Chemical Society of Japan, April, 1968. Proceedings II, p. 1340.

1) M. K. Carron, M. E. Mrose and K. J. Murata, *Am. Mineralogist*, **43** (9—10), 985 (1958).

2) H. Schwarz, *Z. anorg. allgem. Chem.*, **323**, 44 (1963).

3) V. S. Stubican and Rustum Roy, *Z. Kristallographie*, **119**, 90 (1963).

4) A. Durif, *Acta Cryst.*, **9**, 471 (1956).

5) ASTM No. 12-757, *Nat. Bur. Standards(U.S.) Mono*, **25**, sect. 1, (1961).

6) V. A. Nautov, *Zhur. Strukt. Khim.*, **3** (5), 608 (1962).

7) L. H. Brixner and E. Abramson, *J. Electrochem. Soc.*, **112**, 70 (1965).

8) T. Sata and M. Yoshimura, Preprints for the 20th Annual Meeting of Chem. Soc. Japan, Tokyo (April, 1967), II, p. 127.

because CeO_2, instead of Ce_2O_3, is obtained by the thermal decomposition of Ce(III) salts under usual conditions.[9] This reaction is different from those of the formation of other lanthanide orthovanadates:

$$\frac{1}{2}Ln_2O_3 + \frac{1}{2}V_2O_5 \longrightarrow LnVO_4. \quad (2)$$

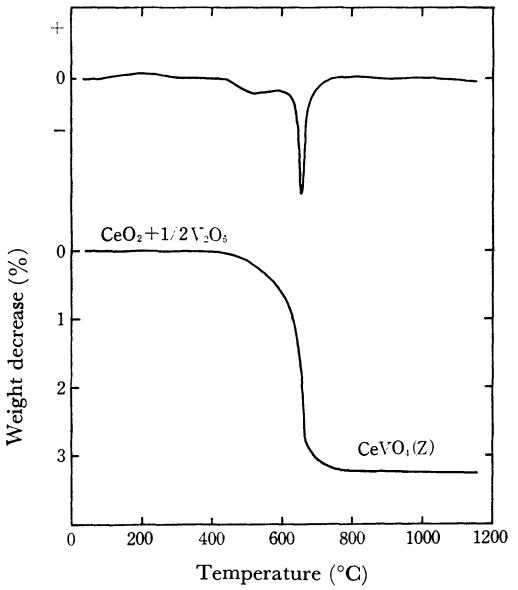

Fig. 1. DTA and TGA curves for the reaction (1).

TGA and DTA curves for the reaction (1) in air are shown in Fig. 1. The same results were also obtained in argon atmosphere. As shown in Fig. 1, the reaction starts above 400°C releasing oxygen, and is completed at about 800°C. The sharp endothermic peak at 655°C near the eutectic temperature[10] of V_2O_5 and YVO_4 suggests that the reaction is accelerated by the formation of liquid phase. The reaction product was dark purplish brown and identified to be the tetragonal zircon-type $CeVO_4$ by means of X-ray analysis. The lattice parameters were calculated to be $a_0=$ 7.400 Å and $c_0=6.497$ Å. The observed weight decrease (3.230%) was larger than the calculated value (3.041%) according to raection (1). This indicates that the real composition of $CeVO_4$(Z) is not stoichiometric $CeVO_{4.000}$ but $CeVO_{3.968}$. A further discussion on $CeVO_4$(Z) will be presented in a next paper.[11]

$CeVO_4$ was also obtained by the oxidation of $CeVO_3$ which has a pseudo-perovskite structure.[12] This reaction is given by the following equation:

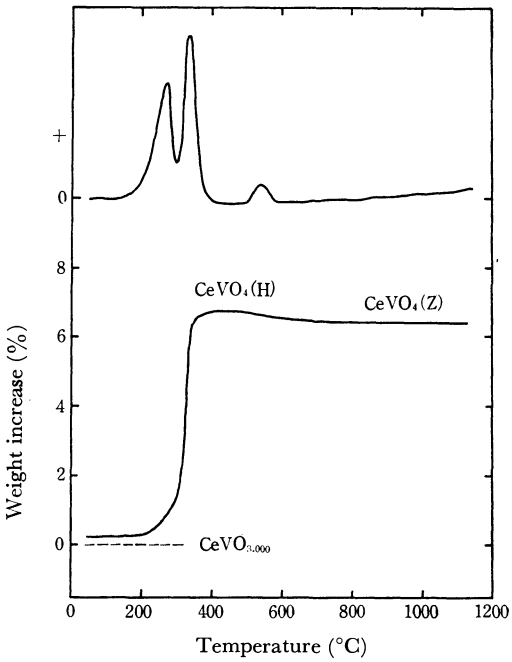

Fig. 2. DTA and TGA curves for the reaction (3). Starting compound, $CeVO_{3.030}$, was prepared by the reaction that equimolar mixture of component oxides was heated at 1200°C for 10 hr in hydrogen atmosphere.

$$CeVO_3 + \frac{1}{2}O_2 \longrightarrow CeVO_4. \quad (3)$$

The TGA and DTA results of this reaction are given in Fig. 2. Two exothermic peaks at 280°C and 330°C seems to be caused by the oxidation of $CeVO_3$. However, no intermediate compound such as $Ce_2V_2O_7$ was found. The same behavior was observed in the case of the oxidation of perovskite $LaVO_3$ into $LaVO_4$. Thus it is reasonable that the valency of cerium ion remained trivalent and only that of vanadium ion changed from trivalent to pentavalent during the course of this reaction. When the oxidation of $CeVO_3$ took place below 400°C, $CeVO_4$(H) was obtained. It was brownish yellow and identified to be isostructural with $LaVO_4$, huttonite-type (C_{2h}^5-$P2_1/n$). X-Ray powder data of $CeVO_4$(H) are given in Table 1 in comparison with $LaVO_4$. The difference in the cell volume corresponds to that in ionic radii; $Ce^{3+}=1.07$ Å, $La^{3+}=1.14$ Å.

The transition of $CeVO_4$(H) to $CeVO_4$(Z) was exothermic, gradually releasing oxygen gas, as shown in Fig. 3. This gives rise to the increase of lattice symmetry and cell volume. The third peak at about 540°C in Fig. 2 corresponds to this transition.

Magnetic studies on $CeVO_4$ (Fig. 4) demonstrate

9) O. K. Srivastava and A. R. Vasudeva Murthy, *J. Sci. Ind. Research (India)*, **20B**, 96 (1961).

10) E. M. Levin, *J. Am. Ceram. Soc.*, **50**, 381 (1967).

11) M. Yoshimura and T. Sata, This Bulletin, to be published.

12) T. Sata and M. Yoshimura, Preprints for the 5th Basic Ceramic Science Symposium, Tokyo (Jan., 1967), pp. 156—159.

Table 1. X-ray powder diffraction data for $CeVO_4$(H) and $LaVO_4$

$CeVO_4$(H) d (obsd.)	$CeVO_4$(H) I/I_0	$LaVO_4$ d (obsd.)	$LaVO_4$ I/I_0	hkl
5.41	10	5.46	10	$\bar{1}01$
4.85	14	4.85	14	110, 011
4.35	20	4.36	18	$\bar{1}11$
—	—	4.19	6	101
3.598	24	3.637	24	111, 020
3.371	60	3.404	60	200
3.181	100	3.210	100	120
3.051	10	3.081	18	210
2.947	72	2.974 2.968	80	$\bar{1}12$ 012
2.711	18	2.727	20	$\bar{2}02$
2.539	18	2.567	30	$\bar{2}12$
—	—	2.518	10	112
—	—	2.336	6	301
2.259	16	2.272	18	031
2.220	20	2.235	20	$\bar{1}03$
2.170	12	2.191	14	221, $\bar{1}31$
1.996	24	2.015	40	212, $\bar{3}12$
—	—	1.973	12	$\bar{2}31$
1.939	24	1.950	40	103, $\bar{1}32$
1.907	22	1.925	22	311, 320
—	—	1.842	22	$\bar{3}22$
1.801	10	1.817	16	231, $\bar{2}22$
1.779	18	1.799	28	132
1.740	10	1.759	16	140, $\bar{3}21$
—	—	1.700	12	400
1.658	8	—	—	$\bar{4}02$
1.642	8	1.656	18	410, $\bar{2}04$
—	—	1.626	8	312
1.593	12	1.603	18	214

$a_0=6.98$ Å	$a_0=7.05$ Å
$b_0=7.22$ Å	$b_0=7.26$ Å
$c_0=6.76$ Å	$c_0=6.75$ Å
$\beta=105°02'$	$\beta=104°56'$
$V=a_0b_0c_0\sin\beta=328$ Å^3	$V=334$ Å^3
$Z=4$	$Z=4$

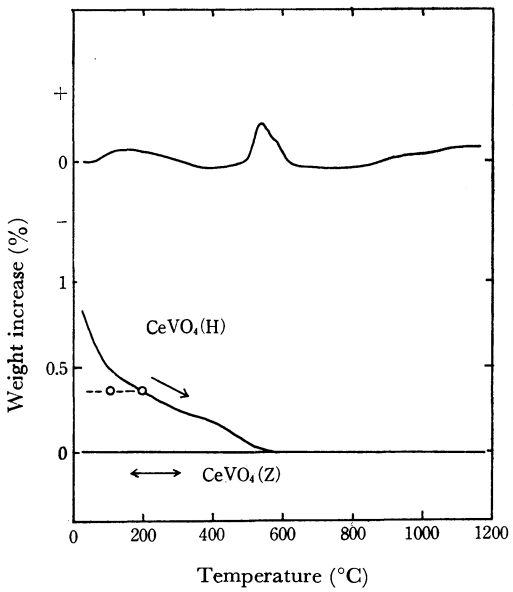

Fig. 3. DTA and TGA curves for the transition from $CeVO_4$(H) to $CeVO_4$(Z); $CeVO_4$(H) was moist. ---○---: after keeping for 2hr at this temp.

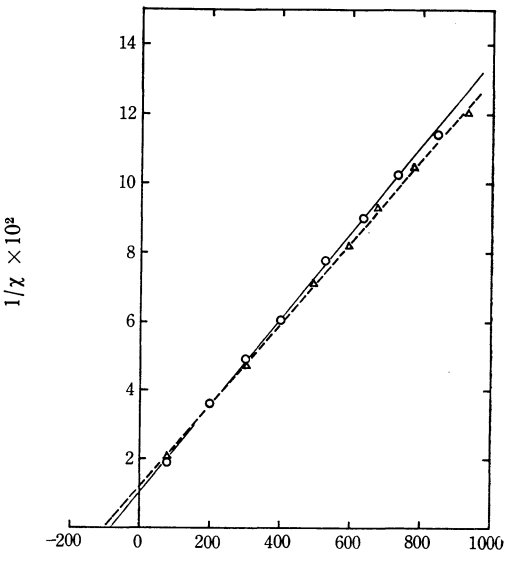

Fig. 4. Reciprocal susceptibility *vs.* temperature of $CeVO_4$. $H=10500$ Oe.
——○—— $CeVO_4$(H)
——△—— $CeVO_4$(Z)

that both $CeVO_4$(H) and $CeVO_4$(Z) showed paramagnetic behavior following the Curie-Weiss law, $\chi=C/(T+\theta)$, above 100°K, where χ is molar magnetic susceptibility, C, the Curie constant, T, the absolute temperature, and θ, the Weiss constant. The correction of diamagnetism was made using the value given by Selwood.[13]

Some results of magnetic and chemical analyses for $CeVO_4$(H) and $CeVO_4$(Z) are summerized in Table 2. The effective magnetic moment, 2.51 μ_B for $CeVO_4$(H), indicates that the valence states are almost tripositive for cerium ion and pentapositive for vanadium ion respectively, since this value is fairly smaller than the theoretical value of 2.54 μ_B for free Ce^{3+} ion. On the contrary, the value of 2.58 μ_B would indicate that a small quantity of V^{4+} coexists with V^{5+} in $CeVO_4$(Z) and the magnetic moment obtained is caused by both Ce^{3+} and V^{4+}. TGA, chemical analysis and color support the results.

13) P. W. Selwood, "Magnetochemistry," Interscience Publishers, New York (1956), 2nd Ed., p. 78.

Table 2. Magnetic and chemical analyses for $CeVO_4$(H) and $CeVO_4$(Z)

	$CeVO_4$(H)	$CeVO_4$(Z)
Composition	$CeVO_{4.024}$	$CeVO_{3.968}$
Curie const. (C)	0.789	0.830
Effective moment	2.51 μ_B	2.58 μ_B
Weiss const. (θ)	−82°K	−103°K
Body color	brownish yellow	dark purplish brown

$CeVO_4$(H) could not be detected during the course of the reaction (1). It was observed that $CeVO_4$(H) transformed into $CeVO_4$(Z) after being kept at 400°C for 20 hr or at 450°C for 8 hr. The reverse transition, $CeVO_4$(Z)→$CeVO_4$(H), could not be observed. Even treatments under high-pressure oxygen (P_{O_2}=500—1000 atm, temperature 350—500°C, 2—40 hr) gave no change on $CeVO_4$(Z). From these results, it seems that $CeVO_4$(H) is a metastable phase and $CeVO_4$(Z) a stable phase.

The authors wish to thank Mr. Y. Shibazaki, Professor M. Koizumi and Assistant Professor S. Kume of the Osaka University, Osaka, for experiments and comments on the high-pressure oxygen treatments.

BULLETIN OF THE CHEMICAL SOCIETY OF JAPAN VOL. 42 3198—3203 (1969)

Chemical and Spectral Study of 6- and 7-Nitro-2-Methyl, 2-Benzyl, 2-Styryl and 2-(1-Phenylstyryl)-3*H*-4-Ketoquinazolines and Their 3-Me and 3-Ph Derivatives

R. K. THAKKAR and S. R. PATEL

Department of Chemistry, Sardar Patel University, Vallabh Vidyanagar, Gujarat State, India

(Received September 5, 1968)

6- and 7-Nitro-2-benzyl-3*H*-4-ketoquinazolines and their 3-Me and 3-Ph derivatives were prepared by condensing the 6-nitro (III) and 7-nitro (XII) derivatives of -4*H*-3,1-benzoxazin-4-one with ammonia, methylamine and aniline, respectively. The compounds III and XII were formed on refluxing 5- and 4-nitro-*N*-phenylacetylanthranilic acids with acetic anhydride. 6- and 7-Nitro-2-benzyl-3*H*-4-ketoquinazolines (IV and XIII) were also prepared by condensing 5- and 4-nitro-*N*-phenylacetylanthranilic acids with formamide, respectively, in very low yields. The compounds IV and XIII yielded the corresponding 2-benzoyl derivatives on oxidation and the corresponding 2-(1-phenylstyryl) derivatives on reaction with benzaldehyde. 6- and 7-Nitro-2-styryl and 2-(1-phenylstyryl)-3*H*-4-ketoquinazolines were not oxidized by alkaline permanganate. UV spectra of these compounds have been studied.

Quinazoline has proved to be a very stable ring-system. Unlike quinoline and isoquinoline, a quinazoline does not undergo a ring-cleavage when subjected to an oxidation reaction which normally brings about such a cleavage. Simple quinazoline yields 4-ketoquinazoline on oxidation.[1] 2-Methyl-3-phenyl-3,4-dihydroquinazoline affords 2-methyl-3-phenyl-4-ketoquinazoline on oxidation with alkaline permanganate.[2] 2-Methyl-3*H*-4-keto-quinazoline remains unchanged on treatment with this reagent.[1]

Patel and coworkers have reported that 2-benzyl and 2-(1-phenylstyryl)-3*H*-4-ketoquinazolines on oxidation yield 2-benzoyl-3*H*-4-ketoquinazoline, but 2-styryl-3*H*-4-ketoquinazoline remains uneffected.[3] 2-(1-Phenylstyryl)-3*H*-4-ketoquinazoline was formed on condensing 2-benzyl-3*H*-4-ketoquinazoline with benzaldehyde.[4] In continuation of this, the syntheses and the study of the oxidation reactions of various 6- and 7-nitro-2-R-3*H*-4-ketoquinazoline derivatives were undertaken. UV spectra of these compounds have been studied with a view to studying the spectra-structure correlation. Because of the interesting aspect of the tautomeric behaviour of 6- and 7-nitro-3*H*-4-ketoquinazolines, their

1) H. Yamanaka, *Chem. and Pharm. Bull.* (Tokyo), **7**, 152 (1959); *Chem. Abstr.*, **54**, 22672 (1960).

2) C. Paal and Krecke, *Ber.*, **23**, 2634 (1890).

3) V. K. Mehta, Ph. D. thesis, Gujarat University, Ahmedabad (1965).

4) M. T. Bogert and R. A. Gortner, *J. Am. Chem. Soc.*, **32**, 1657 (1910); **57**, 729 (1935).

spectra were compared with those of the corresponding 3-methyl and 3-phenyl derivatives which have fixed amide-structures. With this aim in view, the 3-methyl and 3-phenyl derivatives of 6- and 7-nitro 2-benzyl-3*H*-4-ketoquinazolines were also prepared.

5-Nitro-*N*-phenylacetylanthranilic acid (II) was formed on reaction of 5-nitroanthranilic acid (I) with phenylacetyl chloride. 6-Nitro-2-benzyl-4*H*-3,1-benzoxazin-4-one (III), synthesized by refluxing II with acetic anhydride, afforded 6-nitro-2-benzyl-3*H*-4-ketoquinazoline (IV) on reaction with liquid ammonia at 100°C. The compound IV was also synthesized in about 15% yield by condensing II with formamide following the modified Niementowski 4-ketoquinazoline synthesis.[5] Patel has reported that condensation of 5-nitro-*N*-acetylanthranilic acid with formamide yields a mixture of 6-nitro-3*H*-4-ketoquinazoline and its 2-methyl derivative, while its condensation with acetamide affords pure 6-nitro-2-methyl-3*H*-4-ketoquinazoline.[6] The condensation of 6-nitro-2-benzyl-4*H*-3,1-benzoxazin-4-one III with methylamine and with aniline at 100°C afforded 6-nitro-2-benzyl-3-methyl and 3-phenyl-4-ketoquinazolines (V and VI) respectively.

6-Nitro-2-methyl-3*H*-4-ketoquinazoline was not oxidized on treatment with alkaline permanganate at 100°C. 6-Nitro-2-benzyl-3*H*-4-ketoquinazoline (IV) on oxidation with alkaline potassium permanganate at 100°C afforded 6-nitro-2-benzoyl-3*H*-4-ketoquinazoline (VII) in very low yield.

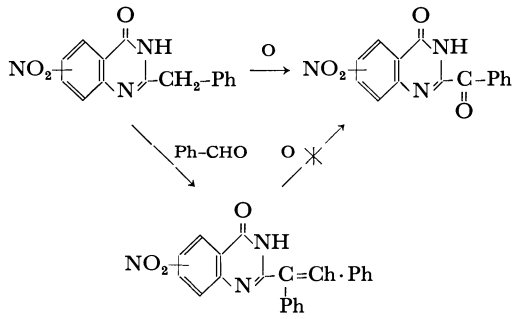

Chart

Most of the original compound (IV) was recovered unchanged. The same product (VII) was also formed in good yield when the oxidation of IV was carried out with selenium dioxide in isoamyl alcohol. The oxidation reaction of IV leading to the formation of a ketone is a characteristic property of a benzylic methylene group. Selenium dioxide has been reported to be a specific oxidizing agent for an alkyl group attached to an *ortho* or a *para* position to ring-nitrogen of a heterocyclic system.[7] 6-Nitro-2-methyl-3*H*-4-ketoquinazoline (VIII) on reaction with benzaldehyde afforded the corresponding 2-styryl derivative (IX). Compound IV likewise afforded 6-nitro-2-(1-phenylstyryl)-3*H*-4-ketoquinazoline (X) on reaction with benzaldehyde. Both 2-styryl (IX) and 2-(1-phenylstyryl) (X) derivatives did not undergo oxidation reaction when treated with alkaline permanganate solution at 100°C even on prolonged heating with excess of the reagent. As indicated previously, 2-(1-phenylstyryl)-3*H*-4-ketoquinazoline is reported to be oxidized to the corresponding 2-benzoyl derivative on treatment with permanganate in acetone solution in cold.

7-Nitro-2-benzyl-4*H*-3,1-benzoxazin-4-one (XII), formed on treating 4-nitro-*N*-phenylacetylanthranilic acid (XI) with boiling acetic anhydride, afforded 7-nitro-2-benzyl-3*H*-4-ketoquinazoline (XIII) and their 3-methyl (XVIII) and 3-phenyl (XIX) derivatives on reaction with ammonia, methylamine and aniline solutions, respectively. The compound (XIII) was also formed on condensing 4-nitro-*N*-phenyl acetylanthranilic acid (XI) with formamide in about 23% yield. Compound XIII was oxidized by heating it with a large excess of alkaline permanganate solution at 100°C for twenty four hours to 7-nitro-2-benzoyl-3*H*-4-ketoquinazoline (XIV) in very poor yield. Most of compound XIII was recovered from precipitated manganese dioxide on extracting it with boiling acetone. Compound XIV was formed in very good yield on oxidation of XIII with selenium dioxide in isoamyl alcohol solution. 7-Nitro-2-methyl-3*H*-4-ketoquinazoline (XV) and its 2-benzyl analog (XIII) on reaction with benzaldehyde afforded 7-nitro-2-styryl-3*H*-4-ketoquinazoline (XVI), and 7-nitro-2-(1-phenylstyryl)-3*H*-4-ketoquinazoline (XVII). Both these 2-styryl (XVI) and 2-(1-phenylstyryl) (XVII) derivatives were not oxidized on treatment with alkaline permanganate solution at 100°C. Even 7-nitro-2-methyl-3*H*-4-ketoquinazoline was not oxidized by the same reagent.

These results suggest that owing to the presence of the nitro group, the permanganate oxidation reaction of nitro-substituted 2-benzyl-3*H*-4-ketoquinazolines becomes difficult and that of the correspondingly substituted 2-(1-phenylstyryl)-3*H*-4-ketoquinazoline is completely prevented. The fact that the presence of a nitro group makes oxidation reaction of so-substituted compound difficult is well known.[8]

5) V. S. Patel and S. R. Patel, *J. Indian Chem. Soc.*, **42**, 531 (1965); **45**, 167 (1968).

6) V. S. Patel, Ph. D. thesis, Sarder Patel University, Vallabh Vidyanagar (1967).

7) a) W. Borsche and W. Doeller, *Ann.*, **39**, 537 (1938); *Ber.*, **76**, 1176 (1944); A. Kjaer, *Acta. Chem. Scand.*, **2**, 455 (1948). b) H. D. Law and F. M. Perkin, *J. Chem. Soc.*, **93**, 1633 (1908); Weiler, *Ber.*, **32**, 1050 (1899).

8) M. J. S. Dewar and P. M. Maitlis, *J. Chem. Soc.*, **1957**, 2521.

TABLE 1. ULTRAVIOLET SPECTRAL DATA FOR 6- AND 7-NITRO-(2-R-3-R′-)-4-KETOQUINAZOLINES

NO_2	R	R′	β-Band		*Para*-band	
			mμ	log ε	mμ	log ε
6	$-CH_3$	H	255 (i)	4.02	320	4.01
6	$-CH_2-Ph$	H	260 (s)	3.90	325	4.01
6	-CO-Ph	H	258	4.41	325 (i)	3.86
					370	4.06
6	-CH=CH-Ph	H	255 (i)	4.12	360 (i)	4.2
			310 (i)	4.14		(Broad band)
6	$-C(H)=C(Ph)-Ph$	H	260	4.30	305 (i)	4.20
					375	4.17
6	$-CH_2-Ph$	$-CH_3$	260 (s)	4.00	335	4.14
6	$-CH_2-Ph$	$-C_6H_5$	260 (i)	4.06	320	4.21
7	$-CH_3$	H	255	4.34	340	3.47
7	$-CH_2-Ph$	H	253	4.44	350	3.47
7	-CO-Ph	H	258	4.43	320 (i)	3.68
					340 (i)	
7	-CH=CH-Ph	H	*210 to 323	*4.7 to 4.29	*323—380	*4.29—3.7
7	$-C(H)=C(Ph)-Ph$	H	216	4.59	323	4.23
			256	4.16		
7	$-CH_2-Ph$	$-CH_3$	248	4.38	326	3.56
7	$-CH_2-Ph$	$-C_6H_5$	250	4.55	320	3.53
					345	3.59

* Indicates a change in log ε value over the indicated range of spectrum.
(i) = Inflexion; (s) = Shoulder.

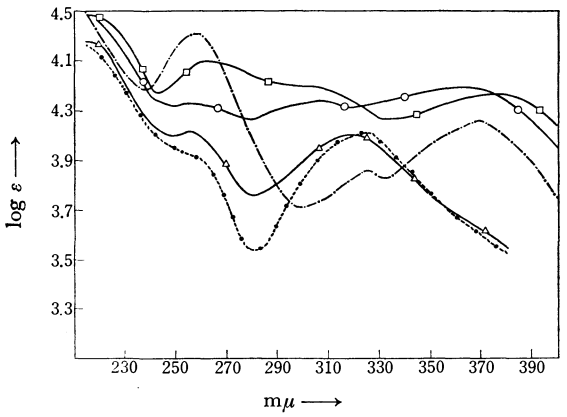

Fig. 1

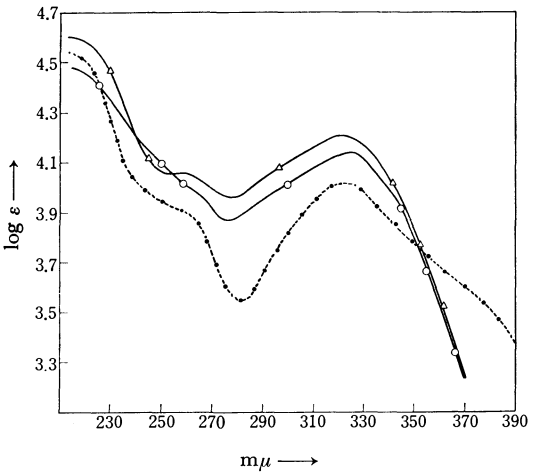

Fig. 2

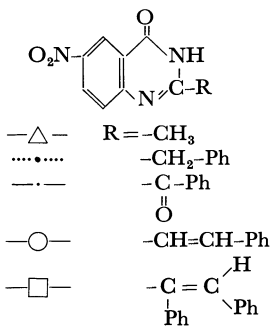

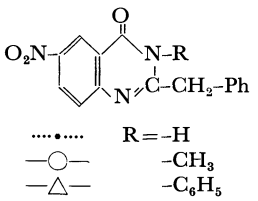

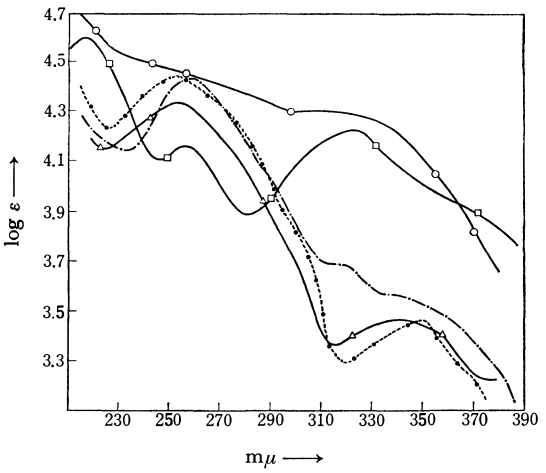

Fig. 3

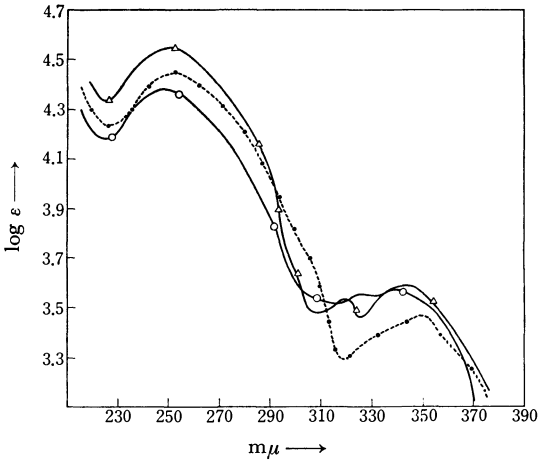

Fig. 4

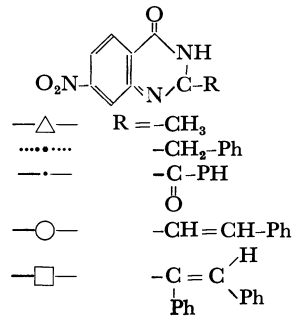

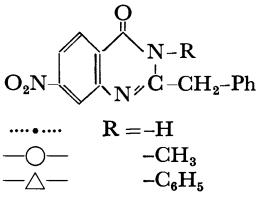

The ultraviolet spectra of the compounds described in this communication have been studied on Beckmann DU Spectrophotometer in ethanol solution. The sepctral data have been reported in Table 1 and the spectral curves have been shown in Figs. 1—4. 2-Alkyl-3*H*-4-ketoquinazoline normally exhibits a three band spectrum characteristic of a bicyclic aromatic hydrocarbon with the only difference that the long wavelength band does not show a much finer structure.[9] The spectra of all the 2,3-disubstituted 6- and 7-nitro-4-ketoquinazolines described in the present communication comprise only two bands. They have been designated as β and *para* bands.[10] The disappearance of the long wave length α band in the spectrum of the nitrosubstituted 2-alkyl-3*H*-4-ketoquinazoline seems most probably due to the presnece of the nitro group which is known to be a very strong chromophore.

The β and *para* bands in the spectrum of 6-nitro-2-methyl-3*H*-4-ketoquinazoline appear at 255 mμ (log ε=4.02) and 320 mμ (log ε=4.01) (Fig. 1). The corresponding bands appear at relatively longer wavelengths ($\Delta\lambda\approx+5$ mμ) in the spectrum of 6-nitro-2-benzyl-3*H*-4-ketoquinazoline (IV). In the spcctrum of 6-nitro-2-benzoyl-3*H*-4-ketoquinazoline (VII) the β band is much more intense (log ε=4.41) and the *para* band appears at a much longer wavelength, 370 mμ (log ε=4.06), than the corresponding bands in the spectrum of its parent compound, 6-nitro-2-benzyl-3*H*-4-ketoquinazoline (IV). This seems to be due to the -C-Ph group acting as a strong chromophore.
O

Attachment of a styryl group in 2-position increases the length of the conjugated system. This is reflected in the spectrum of 6-nitro-2-styryl-3*H*-4-ketoquinazoline (IX) which exhibits a strong absorption over the whole of the spectrum range with the value of log ε ranging around the value of 4.0. In the spectrum of 6-nitro-2(1-phenylstyryl)-3*H*-4-ketoquinazoline (X) the short wavelength β band is slightly stronger probably owing to an extra phenyl group while the long wavelength *para* band is somewhat weaker than the corresponding band in the spectrum of its 2-styryl compound (IX). Similar differences in the spectral trends have been observed in the spectra of stilbene and α-phenylstibene by Suzuki.[11] According to this author, the difference in the spectral trend is due to the fact that all the three phenyl groups in α-phenylstilbene are not accomodated in a strain-free planar configuration around the ethylenic bond, but have

9) J. B. Koepfli, J. F. Mead and J. A. Brockman, *J. Am. Chem. Soc.*, **71**, 1048 (1949).

10) E. Clar, "Aromatische Kohlenwasserstoffe," 2. Auflage., Julius Springer, Berlin (1952).

11) H. Suzuki, This Bulletin, **33**, 389 (1960).

been possibly tilted slightly away from the main plane. By analogy 6-nitro-2-(1-phenylstyryl)-3*H*-4-ketoquinazoline (X) may be supposed to have a similar configuration for the quinazolone moiety and the two phenyl groups around the styryl double bond. Had only the α-phenyl group been tilted away from the main plane and the other two groups left remaining in the same plane, the spectra of 2-(1-phenylstyryl) and 2-styryl compounds would have probably been almost exactly the same in the long wavelength part of their spectra. The spectra of 6-nitro-2-benzyl-3*H*-4-ketoquinazoline (IV), and its 3-methyl and 3-phenyl derivatives (V and VI) exhibit mainly the same trends (Fig. 2). The β and *para* bands in the spectra of both the 3-methyl and 3-phenyl compounds (V and VI) appear respectively at almost the same positions as, but more intense than, the corresponding bands in the spectrum of their parent 3*H* compound (IV). The spectral similarity is an indication of the fact that compound IV exists mostly in the amide-form like its 3-methyl and 3-phenyl derivatives (V and VI) which have fixed keto-structures.

The ultraviolet spectra of 7-nitro-2-methyl-3*H*-4-ketoquinazoline (XV) and its 2-benzylanalog (XIII) comprise only two bands (Fig. 3). The β band appears near about 255 mμ but is more intense in the spectrum of XIII than that in the spectrum of XV; the *para* band appears round about 350 mμ in the spectra of both these compounds. The spectrum of the 7-nitro-2-benzoyl compound (XIV) also comprises two bands; its long wavelength *para* band is almost featureless and is more intense than the corresponding band in the spectrum of XIII in the region beyond 310 mμ as expected, owing to the presence of the 2-benzoyl group acting as a stronger chromophore. The UV spectrum of 7-nitro-2-styryl 3*H*-4-ketoquinazoline (XVI) exhibits a strong absorption over a range from 210 to 323 mμ with log ε value decreasing slowly from 4.7 to 4.2; the only feature in the spectrum of XVI seems to be a broad shoulder near about 323 mμ, beyond which the intensity of absorption decreases comparatively more rapidly. The broadening, the increased intensity and the disappearance of the fine structure of the constituent bands are the usual effects of increased conjugation which in this case is due to the presence of styryl group in 2-position. The spectrum of 7-nitro-2(1-phenylstyryl)-3*H*-4-ketoquinazoline (XVII) exhibits an arm at 261 mμ (log ε=4.59) and a peak at 256 mμ (log ε=4.16) and a broad band at 256 mμ (log ε=4.16) and a broad band at about 323 mμ (log ε=4.23). However the intensity of all the bands in the spectrum of the 7-nitro-2-(1-phenylstyryl) compound (XVII) is less than that of the corresponding bands in the spectrum of its parent compound (XVI) almost over the whole spectral range. It seems to be due to the steric effect exerted by the α-phenyl group which would not allow all the three groups to remain in a strain-free planar configuration. The spectra of 7-nitro-2-benzyl-3-methyl and phenyl (XVIII and XIX) derivatives are very closely similar to that of their parent compound (XIII) (Fig. 4), indicating that XIII exists mostly in the keto-form.

Experimental

5-Nitro-*N*-phenylacetylanthranilic Acid (II). The compound was prepared by heating 5-nitroanthranilic acid (2.58 g) with phenylacetyl chloride (4.2 g) in dry benzene (20 m*l*) containing a drop of pyridine for two hours. Excess of benzene was removed by steam distillation and the residual solid product was collected, washed with hot water and crystallized from a mixture of chloroform and benzene (2 : 1) in white long needles, mp 187—189°C. Yield: 2.5 g.

Found: N, 9.40%. Calcd for $C_{15}H_{12}O_5N_2$: N, 9.33%.

4-Nitro-*N*-phenylacetylanthranilic Acid (XI). The compound was prepared as described above from 4-nitroanthranilic acid and crystallized from aqueous ethanol in white needles, mp 206—208°C.

Found: N, 9.28%. Calcd for $C_{15}H_{12}O_5N_2$: N, 9.33%.

6-Nitro-2-benzyl-4*H*-3,1-benzoxazin-4-one (III). A mixture of 5-nitro-*N*-phenylacetylanthranilic acid (0.660 g) and acetic anhydride (1.5 m*l*) was refluxed for forty five minutes. The solution was clarifide with activated charcoal, filtered hot and cooled to room temperature to give yellowish crystalline solid. It was filtered and washed with dry petroleum ether, mp 177—179°C. Yield: 0.550 g.

Found: N, 9.85%. Calcd for $C_{15}H_{10}O_4N_2$: N, 9.92%.

7-Nitro-2-benzyl-4*H*-3,1-benzoxazin-4-one (XII). The compound was synthesised from 4-nitrophenylacetylanthranilic acid (0.5 g) and acetic anhydride as described above in the form of yellowish white needles, mp 125—126°C. Yield: 0.390 g.

Found: N, 9.82%. Calcd for $C_{15}H_{10}O_4N_2$: N, 9.92%.

6-Nitro-2-benzyl-3*H*-4-ketoquinazoline (IV). 6-Nitro-2-benzyl-4*H*-3,1-benzoxazin-4-one (0.550 g) was suspended in liquid ammonia and heated for three hours at 100°C. The reaction mixture was acidified and the solid product was stirred in dilute bicarbonate solution. The residual solid was then filtered, washed and crystallized from glacial acetic acid (carbon) in pale yellow crystalline solid, mp 258—260°C. Yield: 0.405 g.

Found: N, 15.02%. Calcd for $C_{15}H_{11}O_3N_3$: N, 14.95%.

7-Nitro-2-benzyl-3*H*-4-ketoquinazoline (XIII). The compound was prepared as described above from 7-nitro-2-benzyl-4*H*-3,1-benzoxazin-4-one (0.380 g). It was crystallized from ethanol (carbon) in white cottony needles, mp 262—264°C. Yield: 0.315 g.

Found: N, 14.85%. Calcd for $C_{15}H_{11}O_3N_3$: N, 14.95%.

6-Nitro and 7-Nitro-2-benzyl-3*H*-4-ketoquinazolines (IV and XIII) by Modified Niementowski Method. A mixture of 4- or 5-nitro-*N*-phenylacetylanthranilic acid (1.3 g) and formamide (2.0 g) was heated to 160—165°C for two hours. The solid product was powdered and stirred in bicarbonate solution,

filtered, and washed with water. It was crystallized from glacial acetic acid. Yield 22.9% for the 7-nitro isomer and 15.5% for 6-nitro isomer, respectively. They were compared (mixed mp) with corresponding products prepared by an alternate method describeed earlier.

6-Nitro-2-benzyl-3-methyl-4-ketoquinazoline (V). The compound was formed on heating a suspension of 6-nitro-4*H*-3,1-benzoxazin-4-one (0.350 g) and methylamine (2.0 m*l*; 10%) for an hour on a water bath. The dark orange coloured solution was decomposed with dilute hydrochloric acid (10 m*l*) and the solid product was collected, washed with bicarbonate solution and crystallized from ethanol (carbon) in white amorphous powder, mp 180—182°C. Yield: 0.275 g.

Found: N, 14.13%. Calcd for $C_{16}H_{13}O_3N_3$: N, 14.25%.

7-Nitro-2-benzyl-3-methyl-4-ketoquinazoline (XVIII). The compound was prepared from 7-nitro-2-benzyl-4*H*-3,1-benzoxazin-4-one (0.4 g) and methylamine and was crystallized from ethanol (carbon) in light amorphous powder, mp 155—158°C. Yield: 0.330 g.

Found: N, 13.78%. Calcd for $C_{16}H_{13}O_3N_3$: N, 14.25%.

6-Nitro-2-benzyl-3-phenyl-4-ketoquinazoline (VI). The compound was prepared by reacting 6-nitro-2-benzyl-4*H*-3,1-benzoxazin-4-one (0.4 g) with 20% alcoholic solution of aniline (3.0 m*l*). It was crystallized from glacial acetic acid in yellowish white plates, mp 231—233°C. Yield: 0.365 g.

Found: N, 11.92%. Calcd for $C_{21}H_{15}O_3N_3$: N, 11.76%.

7-Nitro-2-benzyl-3-phenyl-4-ketoquinazoline (XIX). The compound was synthesised from 7-nitro-2-benzyl-4*H*-3,1-benzoxazin-4-one (0.5 g) and aniline. The product was crystallized from ethanol (carbon) in silvery plates, mp 171—173°C. Yield: 0.420 g.

Found: N, 11.69%. Calcd for $C_{21}H_{15}O_3N_3$: N, 11.76%.

6-Nitro-2-styryl-3*H*-4-ketoquinazoline (IX). A suspension of 6-nitro-2-methyl-3*H*-4-ketoquinazoline (0.3 g) in freshly distilled benzaldehyde (2 m*l*) was heated for an hour at 180°C. The reaction mixture was steam distilled to remove excess benzaldehyde. The brownish orange product was collected, treated with bicarbonate solution and crystallized (carobn) from glacial acetic acid in orange yellow powder, mp 322—323°C. Yield: 0.405 g.

Found: N, 14.20%. Calcd for $C_{16}H_{11}O_3N_3$: N, 14.33%.

7-Nitro-2-styryl-3*H*-4-ketoquinazoline (XVI). The compound was synthesised from 7-nitro-2-methyl-3*H*-4-ketoquinazoline (0.420 g) and benzaldehyde (2.0 m*l*). The product was crystallized from glacial acetic acid in light yellow powder, mp 298—300°C. Yield: 0.575 g.

Found: N, 13.96%. Calcd for $C_{16}H_{11}O_3N_3$: N, 14.33%.

6-Nitro-2-(1-phenylstyryl)-3*H*-4-ketoquinazoline (X). The compound was prepared from 6-nitro-2-benzyl-3*H*-4-ketoquinazoline (0.570 g). The product was crystallized from glacial acetic acid in yellowish short needles, mp 274—276°. Yield: 0.600 g.

Found: N, 11.59% Calcd for $C_{22}H_{14}O_3N_3$: N, 11.41%.

7-Nitro-2-(1-phenylstyryl)-3*H*-4-ketoquinazoline (XVII). The compound was prepared from 7-nitro-2-benzyl-3*H*-4-ketoquinazoline and benzaldehyde. The brownish sticky mass was dissolved in a minimum amount of acetone and the acetone extract was poured in dilute bicarbonate solution and left overnight at room temperature. The solid product was collected, washed and crystallized from aqueous ethanol in light yellow short needles, mp 242—244°C. Yield: 98.5%.

Found: N, 11.18%. Calcd for $C_{22}H_{14}O_3N_3$: N, 11.41%.

7-Nitro-2-benzoyl-3*H*-4-ketoquinazoline (XIV). The compound was formed on, oxidation of 7-nitro-2-benzyl-3*H*-4-ketoquinazoline by the following two methods.

a) Oxidation with Alkaline Permanganate. 6-Nitro-2-benzyl-3*H*-4-ketoquinazoline (1.0 g) was suspended in a mixture of sodium hydroxide solution (5.0 m*l*; 4%) and potassium permanganate solution (50.0 m*l*; 2%). The reaction mixture was heated on a boiling water bath for six hours with continuous stirring. As the violet colour disappeared, extra permanganate (1.0 g) was added and heating was continued for two more hours. Excess permanganate was destoryed by adding required amount of ethanol to the hot reaction mixture. The latter was then filtered hot and the precipitates were washed with boiling water. The combined filtrate was concentrated and acidified with acetic acid. The product which separated was collected and crystallized from ethanol in pale yellow short needles, mp 235—237°C. The precipitated manganese dioxide was extracted with boiling acetone. Acetone was evaporated to dryness to give a major portion of the unreacting original compound (XIII).

Found: 13.96%. Calcd for $C_{15}H_9O_4N_3$: N, 14.23%.

b) Oxidation with Selenium Dioxide. A mixture of 7-nitro-2-benzyl-3*H*-4-ketoquinazoline (0.6 g) and selenium dioxide (0.6 g) in isoamyl alcohol (15.0 m*l*) was refluxed for fifteen hours. The yellowish brown solution was filtered hot and the residual solid was washed with a minimum amount of hot isoamyl alcohol. The combined filtrate was steam distilled to remove isoamyl alcohol. The residual brownish yellow product was collected, washed and crystallized from ethanol (charcoal) in light yellow short needles, mp 235—237°C.

Found: N, 14.12%. Calcd for $C_{15}H_9O_4N_3$: N, 14.23%.

6-Nitro-2-benzoyl-3*H*-4-ketoquinazoline (VII). The compound was formed on oxidation of 6-nitro-2-benzyl-3*H*-4-ketoquinazoline by the two methods described above. In the permanganate oxidation reaction major part of the starting substance (IV) was recovered unchanged. The product was crystallized from ethanol in yellowish white tiny needles, mp 230—233°C.

Found: N, 14.15%. Calcd for $C_{15}H_9O_4N_3$: N, 14.23%.

BULLETIN OF THE CHEMICAL SOCIETY OF JAPAN VOL. 42 3204—3207 (1969)

Imidazoles. II.[1] A General Synthesis for 1-Hydroxyimidazoles

Katsuo AKAGANE,[2] F. J. ALLAN, G. G. ALLAN,[3] T. FRIBERG, S. Ó MUIRCHEARTAIGH and J. B. THOMSON

Institute of Forest Products, College of Forest Resources, University of Washington, Seattle, Washington 98105 *U.S.A.*
Chemistry Department, Paisley Technical College, Paisley, Scotland
Department of Chemistry, University College, Dublin, Eire

(Received October 14, 1968)

The reaction of α-dione monoximes with aldehydes and ammonia affords a general and facile synthetic route to 1-hydroxyimidazoles. By selection of the starting materials substituents can be readily introduced into the 2,4 and/or 5 positions of the imidazole ring which is formed *via* the intermediacy of a *gem*-aminoalcohol. The reactions of the *N*-hydroxyl function are discussed.

In a study of cellulosic fiber-polymer interactions[4,5] we have been concerned with the synthesis of imidazoles[6–9] and other polyaza heterocycles suitable for the attachment of vinylic moieties having differing reactivity ratios.[10] Thus, although 4(5)-vinylimidazole has been described,[11–15] the procedure is not amenable to facile variation and this alkene does not readily copolymerize with a wide range of monomers.[13] Our attention was thus directed to the fact that almost exactly half a century ago Diels discovered[15] that when aldehydes (RCHO) and butane-2,3-dione monoxime (I) are shaken with aqueous ammonia, a clan of compounds is formed by the elimination of two moles of water. Their reductive conversion into trisubstituted imidazoles (III) and their reversible hydrolysis to products considered to be the diols (IV) led[16] to their formulation as II.

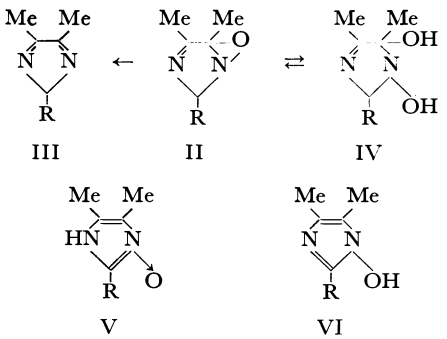

III II IV

V VI

Although the synthesis of the somewhat labile oxaziridine ring system has been achieved[17,18] by several, usually oxidative, procedures, its generally limited stability in alkaline solutions and its apparent ease of formation in this alkaline condensation suggested that a re-examination of this group of products was merited.

Repetition of the prescribed procedure smoothly afforded II in good yield. Examination of this compound then disclosed (for R=Ph) that IV is a simple hydrate of II and that the transformations

1) Part I, F. J. Allan and G. G. Allan, *Chem. & Ind.*, **1964**, 1837.
2) Present address, Kansai Paint Co., 27-5 Chome, Fushimi-cho, Higashi-ku, Osaka, Japan.
3) To whom inquiries should be addressed.
4) G. G. Allan, M. D. Desert, P. Mauranen and W. M. Reif, *Paperi Puu*, **50**, 529 (1968).
5) G. G. Allan, A. Lacitis, J-h. Lee, F-m. Liu and P. Mauranen, *Holzforschung*, **23**, (1969).
6) K. Hofmann, "Imidazole and Its Derivatives," Part I, Interscience Publishers, Inc., New York (1953). pp. (a) 3, (b) 13.
7) W. Schaeg, H. Finger and H. Niemann, *Biochim. Biophys. Acta*, **126**, 168 (1966).
8) S. M. Wang and N. C. Li, *J. Am. Chem. Soc.*, **88**, 4592 (1966).
9) D. M. W. Anderson, J. L. Duncan and F. T. C. Rosotti, *J. Chem. Soc.*, **1961**, 2165.
10) J. Brandrup and E. H. Immergut, "*Polymer Handbook*," Interscience Publishers, John Wiley & Sons, New York (1966), p. II-141.
11) C. Pasini and A. Vercellone, *Gazz. Chim. Ital.*, **85**, 349 (1955).
12) K. Masuda, *J. Pharm. Soc. Japan*, **76**, 325 (1956).
13) C. G. Overberger and N. Vorchheimer, *J. Am. Chem. Soc.*, **85**, 951 (1963).
14) C. G. Overberger, T. St. Pierre, C. Yaroslavsky and S. Yaroslavsky, *J. Am. Chem. Soc.*, **88**, 1184 (1966).
15) O. Diels, *Ber.*, **51**, 965 (1918).
16) O. Diels and C. Salomon, *ibid.*, **52**, 43 (1919).
17) W. D. Emmons, in "The Chemistry of Heterocyclic Compounds," Vol. 19, "Heterocyclic Compounds with Three- and Four-Membered Rings." Part I. ed. by A. Weissberger. Interscience Publishers, John Wiley & Sons, Inc., New York (1964), p. 624.
18) M. Schulz, A. Rieche and D. Becker, *Chem. Ber.*, **99**, 3233 (1966).

of IV into II and II into IV can readily be effected by crystallization from anhydrous and aqueous solvents respectively. The transition IV→II can also be realized by melting. The representational inadequacies of the general formula II were further underscored by the ultraviolet absorption spectrum of the congener (II, R=Me) originating from acetaldehyde which exhibited an absorption maximum at 2240 Å (ε=8800). This is indicative of the di-unsaturation of an imidazole ring and further clarification of the alleged structure II (with R=Me) resulted from a scrutiny of its nuclear magnetic resonance spectrum in chloroform solution. This contained three singlets (τ= 8.02, 7.77 and −3.33 ppm) corresponding to a pair of closely similar methyl groups, a single different methyl group and a very polar proton. These facts are in accord with a general hydroxylamine formulation (VI) and its hydrate as the corrected versions of the structure of these condensation products previously represented as II and IV respectively. A more recently suggested formulation of these products as *N*-oxides (V) and their hydrates[19] could be discounted in favor of the hydroxylamine representation because the condensation product, with R=phenyl, is amphoteric (pK_A 9.41, pK_B 9.36) and because its derived benzoate forms a well defined hydrochloride salt which of course requires the presence of a basic center. Final definitive chemical evidence eliminating the *N*-oxide alternative (V) was secured by replacing butane-2,3-dione monoxime (I) in the condensation reaction with its *O*-benzoate (VII).[20] The product isolated was also a benzoate (VIII) and was identical with that afforded by direct benzoylation of the condensation product originating from butane-2,3-dione monoxime itself. The moderate yield of VIII provided by the *O*-benzoate (VII) can be attributed to the diminution in the nucleophilic character of the oxime nitrogen occasioned by the attached benzoyloxy group.

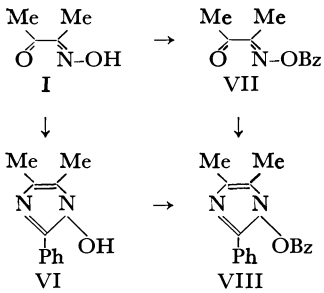

With structure VI established, many of the previously recorded transformations of these compounds are obviously inadequately formulated and this situation is remedied by the clarifications summarized in Table 1. The evolution of carbon dioxide and the isolation of diphenylurea from the reaction of phenyl isocyanate with IV[16] is further substantiation of the hydrate structure. It is to be emphasized that the hydrates are the usual reaction products isolated and these can easily be mistaken[24] for the parent hydroxylamine.

Table 1. Reformulated derivatives of 1-hydroxy-2-phenyl-4,5-dimethylimidazoles originally prepared by Diels and Salomon[15]

Derivatizing reagent	Formula	Reaction product mp °C	Structure
EtOOCNCO	$C_{15}H_{17}N_3O_4$	80	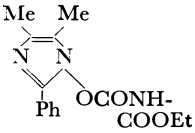
PhNCO	$C_{18}H_{17}N_3O_2$	140	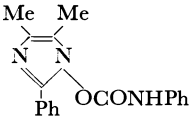
CH_3COCl	$C_{13}H_{15}N_2O_2Cl$	148	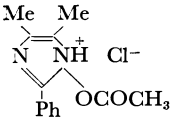
EtNCO	$C_{14}H_{17}N_3O_2$	116	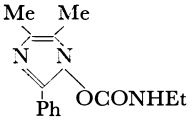
PhCOCl	$C_{18}H_{17}N_2O_2Cl$	162	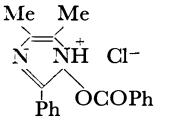

Another objective of this research was to begin an assessment of the generality and scope of this synthetic route to 1-hydroxyimidazoles, a class of compounds not previously explicitly recognized although the corresponding 1-hydroxybenzimidazoles[21] are known and noted for their physiological action and the closely related *N*-oxides have been described.[22–28]

19) J. W. Cornforth and H. T. Huang, *J. Chem. Soc.*, **1948**, 731.

20) G. de Stevens, A. B. Brown, D. Roe, H. I. Chernov and A. J. Plummer, *J. Med. Chem.*, **10**, 211 (1967).

21) O. Diels and M. Stern, *Ber.*, **40**, 1631 (1907).

22) A. T. Balaban, P. J. Halls and A. R. Katritzky, *Chem. & Ind.*, **1968**, 651.

23) A. T. Boulton, A. C. Gripper Gray and A. R. Katritzky, *J. Chem. Soc.*, B, **1967**, 911.

24) K. Volkamer, H. Bäumgartel and H. Zimmerman, *Angew. Chem. Intern. Ed.*, **6**, 947 (1967).

25) J. B. Wright, *J. Org. Chem.*, **29**, 1620 (1964).

26) G. La Parola, *Gazz. Chim. Ital.*, **75**, 216 (1945).

27) K. Bodendorf and H. Towliati, *Arch. Pharm.*, **298**, 293 (1965).

28) G. Heinning and H. Zimmerman, *Ber. Bunsenges. Phys. Chem.*, **72**, 630 (1968).

TABLE 2. PROPERTIES OF 1-HYDROXYIMIDAZOLES

Compound*	Crystalline form**	mp °C	Yield %	Formula	% Nitrogen Calcd	Found
1-Hydroxy-2,4,5-trimethylimidazole	Light tan needles[b]	62—63	77	$C_6H_{10}N_2O$	22.2	22.4
1-Hydroxy-2-ethyl-4,5-dimethylimidazole	White needles[a]	53—53.5	55	$C_7H_{12}N_2O$	20.0	20.3
1-Hydroxy-2-*iso*propyl-4,5-dimethylimidazole	White plates[a]	141—141.5	25	$C_8H_{14}N_2O$	18.1	17.7
1-Hydroxy-2-methoxymethyl-4,5-dimethylimidazole	White needles[c]	234—236	10	$C_7H_{12}N_2O_2$	17.9	18.1
1-Hydroxy-2-(1-methyl-*n*-butyl)-4,5-dimethylimidazole	White needles[a]	125—127	25	$C_{10}H_{18}N_2O$	15.4	15.0
1-Hydroxy-2-(1-ethyl-1-*n*-butyl-4-methyl-penta-2,3-dienyl)-4,5-dimethylimidazole	Colorless rhomboids[a]	206—208	8	$C_{17}H_{28}N_2O$	10.1	9.8
1-Hydroxy-2-vinyl-4,5-dimethylimidazole	White needles[a]	90—94	14	$C_7H_{10}N_2O$	20.3	20.5
1-Hydroxy-2-trichloromethyl-4,5-dimethylimidazole	White needles[a,d]	175—180(d)	18	$C_6H_7N_2OCl_3$	12.2	12.1
1-Hydroxy-2-vinyl-4,5-diphenylimidazole	Tan needles[c]	180—184	15	$C_{17}H_{14}N_2O$	10.7	10.6
1-Hydroxy-4,5-diphenylimidazole	White plates[a,d]	210—211	8	$C_{15}H_{12}N_2O$	11.9	12.0
1-Hydroxy-2-(2-ethyl-*n*-pentyl)-4,5-diphenylimidazole	White needles[c]	234—235	85	$C_{22}H_{26}N_2O$	8.4	8.9
1-Hydroxy-2-methyl-4,5-diphenylimidazole	Pinkish white rhomboids[c]	247—248	20	$C_{16}H_{14}N_2O$	11.2	10.7
1-Hydroxy-2-phenylphenanthrimidazole***	Colorless needles[c,e]	280—282	34	$C_{21}H_{14}N_2O$	9.0	8.9

* The 13 compounds appearing in this Table were similarly prepared and were dehydrated before crystallization from anhydrous solvents.

** Crystallization solvents: [a] acetone, [b] dioxan, [c] ethanol, [d] hexane, [e] dimethylformamide.

*** The hydrate[24] has mp 235—238°C.

Since the formation of these 1-hydroxyimidazoles probably requires the genesis of an aldehyde-ammonia intermediate as the initial step, a wide variety of aldehydes should be capable of participation in this cyclization with butane-2,3-dione monoxime. This is indeed the case and the properties of the 2-substituted 1-hydroxyimidazoles obtained from various aldehydes are collected in Table 2. The participation of the aldehyde ammonia intermediate was confirmed by the formation of the same 1-hydroxyimidazole (IX) from trichloroacetaldehyde (X) and also directly from 1-amino-2,2,2-trichloroethanol (XI)[29] without the use of aqueous ammonia.

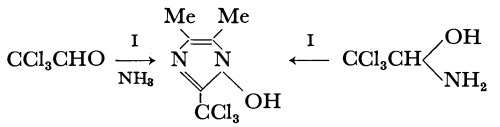

X IX XI

The versatility of this synthetic route to 1-hydroxyimidazoles can also be further extended by replacement of the aliphatic α-dione monoxime (I) with the monoximes of aromatic diketones such as benzil or *o*-phenanthraquinone. These variations permit the introduction of polymerizable moieties of various types in positions 2, 4 and 5 of the imidazole ring.

Experimental

General Preparation of 1-Hydroxyimidazoles. An equimolecular solution of the aldehyde and the dione monoxime in the minimum amount of ethanol (95%) or dioxan was treated at room temperature with aqueous ammonia (*d*, 0.88; 80 m*l*/mol of dione monoxime) when an exotherm was usually noted. The temperature was not allowed to rise above 60°C and the reaction mixture was allowed to stand overnight before collecting and crystallizing the product which had separated.

1-Benzoyloxy-2-phenyl-4,5-dimethylimidazole (VIII). a) A solution of 1-hydroxy-2-phenyl-4,5-dimethylimidazole (0.859 g, 3.4 mmol) in dioxan (200 m*l*) was heated with benzoyl chloride (0.63 g, 5 mmol) at 80—100°C for 10 min. After the addition of a suspension of sodium bicarbonate (0.34 g) in dioxan (100 m*l*) the reaction mixture was shaken for 10 min, allowed to stand for 5 days at room temperature, warmed to 50°C for 10 min and filtered. The cooled filtrate deposited needles (1.0 g) which were recrystallized from dioxan to give the benzoate (VIII) as needles (0.79 g), mp 163—165°C, which showed an IR absorption maximum at 1730 cm^{-1}.

Found: N, 9.2%. Calcd for $C_{18}H_{16}N_2O_2$: N, 9.6%.

b) A mixture of benzaldehyde (3.8 g, 0.036 mol) and aqueous ammonia (*d*, 0.88; 1.8 g, 0.03 mol) in dioxan (200 m*l*) was treated with butane-2,3-dione monoxime benzoate[20] (6.8 g, 0.04 mol, mp 111—113°C) and allowed to stand overnight. The material which had separated was crystallized from dioxan to afford the product as needles (0.5 g), mp 163—165°C, which showed no mp depression when mixed with VIII prepared in a). IR spectra of the two products were superimposable.

Found: N, 9.2%. Calcd for $C_{18}H_{16}N_2O_2$: N, 9.6%.

1-Hydroxy-2-trichloromethyl-4,5-dimethylimidazole (IX). a) A solution of trichloroacetaldehyde (2.94 g,

29) R. Schiff, *Ber.*, **10**, 167 (1877).

0.02 mol) and butane-2,3-dione monoxime (2.02 g, 0.02 mol) in dioxan (6 m*l*) was treated at room temperature with aqueous ammonia (*d*, 0.88, 1.6 m*l*) and allowed to stand overnight. Recrystallization of the separated material from acetone-hexane afforded the product as white needles (0.89 g, 18% yield), mp 175—180°C (dec).

Found: N, 12.10%. Calcd for: $C_6H_7N_2OCl_3$: N, 12.20%.

b) A solution of 1-amino-2,2,2-trichloroethanol (1.64 g, 0.01 mol) and butane-2,3-dione monoxime (1.01 g, 0.01 mol) in ethanol-dioxan (1 : 1, 4 m*l*) was allowed to stand overnight, the material which had separated was recrystallized from acetone-hexane to yield white needles (0.6 g, 14% yield), mp 178—182°C (dec.). This product showed no mp depression when mixed with IX prepared in a). IR spectra of the two products were superimposable.

Found: N, 12.15%. Calcd for $C_6H_7N_2OCl_3$: N, 12.20%.

Financial aid (to T.F.) was provided by the Undergraduate Research Participation Program of the National Science Foundation. One of us (K.A.) thanks the Kansai Paint Co. for support during a study leave.

BULLETIN OF THE CHEMICAL SOCIETY OF JAPAN VOL. 42 3207—3210 (1969)

The Polymerizations and Copolymerizations of α-Methoxyacrylonitrile and Methyl α-Methoxyacrylate

Takayuki Otsu, Bunichiro Yamada and Hiroshi Yoneno

Department of Applied Chemistry, Faculty of Engineering, Osaka City University, Sugimoto-cho, Sumiyoshi-ku, Osaka

(Received December 12, 1968)

A study of the polymerizations and copolymerizations of α-methoxyacrylonitrile(MeOAN) and methyl α-methoxyacrylate(MeOA) has been made. These monomers were homopolymerized with a radical initiator at 60°C, but did not give any polymer with such ionic catalysts as $BF_3O(C_2H_5)_2$ and C_6H_5MgBr at 0°C. From the radical copolymerizasions of these monomers with styrene at 60°C, their Q and e values were determined to be as follows:

$Q = 0.72$, $e = 0.40$ for MeOAN

$Q = 0.47$, $e = 0.04$ for MeOA

These monomers were also copolymerized with acrylonitrile, and the copolymerization parameters were determined.

In previous papers, it was pointed out that some α-substituted acrylate monomers, such as methyl α-cyanoacrylate[1] and alkyl α-phenylacrylate,[2] showed remarkably higher copolymerization reactivities than the respective unsubstituted monomers, such as methyl acrylate, acrylonitrile, and styrene. Similar enhanced reactivities of the monomers upon the introduction of some α-substituents have also been observed in the reported copolymerization data.[3]

By using these copolymerization data, we recently found that α-substituents of acrylonitrile and acrylic esters contributed additively to the values of e and $\log Q$ in the following equations, (1) and (2):[4]

$$e_{CH_2=C\langle^{X}_{Y}} = e_{CH_2=C\langle^{H}_{Y}} + 2.4\sigma_X = e_{CH_2=C\langle^{X}_{H}} + 2.4\sigma_Y \quad (1)$$

$$\log Q_{CH_2=C\langle^{X}_{Y}} = \log Q_{CH_2=C\langle^{H}_{Y}} + (\log Q_{CH_2=C\langle^{X}_{H}} - \log Q_{CH_2=CH_2}) = \log Q_{CH_2=C\langle^{H}_{Y}} + \Delta\log Q_X$$

or

$$\log Q_{CH_2=C\langle^{X}_{Y}} = \log Q_{CH_2=C\langle^{X}_{H}} + (\log Q_{CH_2=C\langle^{H}_{Y}} - \log Q_{CH_2=CH_2}) = \log Q_{CH_2=C\langle^{X}_{H}} + \Delta\log Q_Y \quad (2)$$

where X represents the methoxy, methyl, hydrogen, chloro, bromo, acetoxy, carboalkoxy, and cyano groups, and Y cyano and carboalkoxy groups.

1) T. Otsu and B. Yamada, *Makromol. Chem.*, **110**, 297 (1967).

2) T. Otsu, B. Yamada and T. Nozaki, *Kogyo Kagaku Zasshi (J. Chem. Soc. Japan, Ind. Chem. Sect.)*, **70**, 1941 (1967).

3) H. Mark, B. Immergut, E. H. Immergut and L.J. Young, "Copolymerization," ed. by G. E. Ham, Interscience (1964), p. 695.

4) B. Yamada and T. Otsu, *J. Macromol. Sci.-Chem.*, ***A3***, 1551 (1969).

In the course of studying the effect of the α-substituents of vinyl monomers on their radical reactivities, α-methoxy acrylonitrile (MeOAN) and methyl α-methoxyacrylate (MeOA) were prepared and copolymerized with styrene and acrylonitrile. The present paper will describe the results thus obtained. Since it has been generally known that some 1,1-disubstituted ethylenic monomers, especially α-substituted styrenes, have low ceiling temperatures,[5] the homopolymerizabilities of these monomers will also be described in this study.

Experimental

Preparations of Monomers. The MeOAN monomer was prepared by the method described by Baker[6] through the following reaction path:

$$CH_3CHO + CH_3OH + HCl \longrightarrow CH_2CHOCH_3 \quad (Cl)$$

$$\xrightarrow{Br_2} CH_2(Br)\text{-}CH(Br)OCH_3 \xrightarrow{CuCN} CH_2(Br)\text{-}C(CN)\text{-}OCH_3$$

$$\xrightarrow{\text{Pyridine}} CH_2{=}C(CN)COCH_3 \text{ (MeOAN)}$$

The resulting MeOAN monomer was purified by fractional distillations under reduced pressure: bp 32—33°C/22 mmHg. (lit,[6] 32.5°C/23 mmHg), n_D^{20} 1.4155, d_4^{15} 0.942.

Found: C, 58.23; H, 6.13%. Calcd for C_4H_5NO: C, 57.83; H, 6.07%.

The MeOA monomer was also obtained as follows:

$$CH_2(Br)\text{-}CH(CN)OCH_3 \xrightarrow[HCl]{CH_3OH} CH_2(Br)\text{-}CH(OCH_3)\text{-}C(OCH_3){=}NH\cdot HCl \xrightarrow{H_2O}$$

$$CH_2(Br)\text{-}CH(COOCH_3)OCH_3 \xrightarrow{\text{Piperidine}} CH_2{=}C(COOCH_3)COCH_3 \text{ (MeOA)}$$

The resulting MeOA monomer was also purified by fractional distillation: bp 52.5—53.0°C/11 mmHg. (lit,[6] 51.5—52.0°C/11 mmHg), n_D^{20} 1.4347 (lit,[6] 1.4316), d_4^{15} 1.068.

Found: C, 51.65; H, 6.98%. Calcd for $C_5H_8O_3$: C, 51.72; H, 6.90%.

Other Reagents. The styrene and acrylonitrile were purified by ordinary methods and were distilled under reduced pressure before use. The α,α'-azobisisobutyronitrile(AIBN) was recrystallized from ethanol. The benzene, methylene chloride, and toluene were used after purification by ordinary methods.

Radical Polymerizations and Copolymerizations. The required amounts of the monomer, AIBN, and the solvent were charged into a polymerization ampoule. After it had then been degassed by a freezing and thawing method, the ampoule was sealed off under a vacuum.

The polymerizations and copolymerizations were carried out at 60°C under shaking. After polymerization for a given time, the content of the ampoule was poured into a large amount of mehanol (the homopolymer of MeOAN and copolymers) or diethyl ether (the homopolymer of MeOA) to precipitate the polymer. The resulting copolymers with styrene and with acrylonitrile were purified by the reprecipitation method from benzene-methanol and dimethylformamide-methanol systems respectively.

The compositions of the copolymers were calculated from their carbon or nitrogen content, and the monomer reactivity ratios were determined by the Fineman-Ross[7] and curve-fitting methods.

Ionic Polymerizations. The cationic polymerizations of these monomers were carried out by the use of boron trifluoride diethyl etherate in methylene chloride at 0°C. The anionic polymerizations were performed with phenylmagnesium bromide in toluene at 0°C. After a given polymerization time, the reaction mixture was poured into a large excess of methanol or diethyl ether.

Results and Discussion

Homopolymerizations of MeOAN and MeOA. The results of the homopolymerizations of MeOAN and MeOA monomers with radical and ionic initiators are shown in Table 1.

From Table 1, it can be seen that these monomers were homopolymerized only by the AIBN initiator

Table 1. Homopolymerizations of MeOAN and MeOA monomers

Monomer	(ml)	Initiator (g)	Solvent (ml)	Temp. (°C)	Time (hr)	Yield (%)
MeOAN	0.6	AIBN, 0.0023	C_6H_6, 1.0	60	150	8.9
	0.5	$BF_3O(C_2H_5)_2$, 0.009	CH_3Cl_2, 0.5	0	24	0
	1.0	C_6H_5MgBr*	$C_6H_5CH_3$, 1.0	0	24	0
MeOA	1.0	AIBN, 0.0022	C_6H_6, 1.5	60	150	25.7**
	0.5	$BF_3O(C_2H_5)_2$, 0.009	CH_2Cl_2, 0.5	0	24	0
	1.0	C_6H_5MgBr*	$C_6H_5CH_3$, 1.0	0	24	0

* Used 1 ml of its tetrahydrofuran solution prepared from 13.5 g of bromobenzene and 2 g of magnesium in 55 ml of tetrahydrofuran.

** Specific viscosity (η_{sp}/c) of this polymer was 0.197 (c=1.05 g/100 ml benzene).

5) H. Lüssi, *Chimia*, **20**, 379 (1966).
6) J. W. Baker, *J. Chem. Soc.*, **1942**, 520.
7) M. Finneman and S. D. Ross, *J. Polymer Sci.*, **5**, 269 (1950).

Table 2. Copolymerizations of MeOAN and MeOA (M_1) with styrene (M_2) at 60°C

$([M_1]+[M_2]) = 8$ mol/l in benzene.*

M_1	$[M_1]$ in comonomer (mol%)	Time (hr)	Conversion (%)	Copolymer obtained N (%)	C (%)	$[M_1]$ (mol%)
MeOAN	16.0	10.2	8.3	3.04	—	21.6
	30.0	10.5	4.1	4.90	—	33.9
	43.1	27.2	10.2	6.22	—	42.3
	53.4	28.0	8.1	7.12	—	47.8
	63.2	53.0	10.0	8.39	—	55.5
	75.4	53.5	8.0	9.55	—	61.5
	83.9	61.5	6.0	11.36	—	72.3
MeOA	13.6	4.0	6.8	—	86.81	12.0
	26.1	5.5	7.9	—	82.80	21.5
	37.9	5.5	7.1	—	78.24	32.2
	49.7	6.5	7.1	—	74.33	41.6
	61.3	6.25	6.3	—	70.70	50.5
	75.0	8.0	5.3	—	64.80	65.3
	84.1	9.33	6.4	—	60.53	76.4

* In the copolymericaztions of MeOAN and MeOA, the concentrations of AIBN were kept constant at 4.63×10^{-3} and 5.06×10^{-3} mol/l, respectively.

under the present conditions. However, their rates were quite low compared with those of the respective unsubstituted monomers, acrylonitrile and methyl acrylate. Between the two monomers, the homopolymerizability of MeOA was larger than that of MeOAN. This tendency was identical to that observed in the radical homopolymerizabilities for α-methyl substituted monomers, such as methacrylonitrile and methyl methacrylate. It was also obvious that these monomers have ceiling temperatures higher than 60°C.

Although these monomers have both an electron-donating methoxy substituent and an electron-withdrawing cyano or carbomethoxy substituent, they were not found to give any homopolymer with cationic and anionic catalysts ($BF_3O(C_2H_5)_2$ and C_6H_5MgBr respectively) at 0°C.

Copolymerizations of MeOAN and MeOA with Styrene. Table 2 shows the results of the radical copolymerizations of MeOAN and MeOA (M_1) with styrene (M_2) at 60°C.

From Table 2, the rate of copolymerization was found to decrease with an increase in the concentration of MeOAN or MeOA in the feed-monomer mixture. The monomer-copolymer composition curves are shown in Fig. 1.

The copolymerization parameters (r_1, r_2, Q_1 and e_1) were determined to be as follows:

for MeOAN (M_1)-styrene (M_2):
$r_1 = 0.35$, $r_2 = 0.53$, $Q_1 = 0.72$, $e_1 = 0.40$

for MeOA (M_1)-styrene (M_2):
$r_1 = 0.51$, $r_2 = 1.10$, $Q_1 = 0.47$, $e_1 = 0.04$

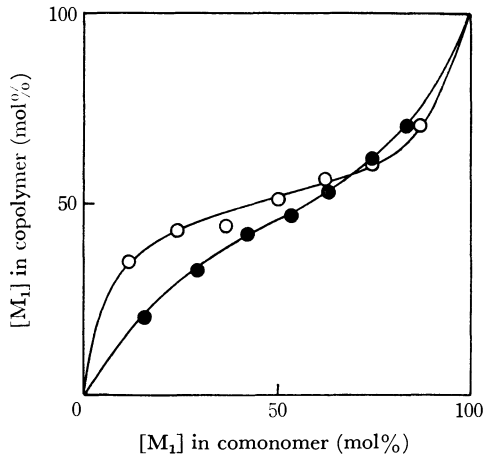

Fig. 1. Monomer-copolymer composition curves for MeOAN (M_1)-styrene(M_2) (○) and MeOA(M_1)-styrene(M_2) (●) at 60°.

where the Q_1 and e_1 values were calculated by assuming that the Q_2 and e_2 values were 1.0 and −0.80 respectively.

The values of e_1 and Q_1 obtained for MeOAN and MeOA were then compared with those calculated from Eqs. (1) and (2). When the values of e and log Q for acrylonitrile and methyl acrylate used were $e=1.20$ and log $Q=-0.22$, and $e=0.60$ and log $Q=-0.38$ from the literature,[3] and when those of Δ log Q and σ for the methoxy substituent used were 0.06 and −0.27, as reported in a previous paper,[4] the following values of Q_1 and e_1 were obtained:

for MeONA: $Q_1 = 0.69$, $e_1 = 0.49$

for MeOA: $Q_1 = 0.48$, $e_1 = -0.11$

It was clear that the Q_1 and e_1 values calculated from Eqs. (1) and (2) were in agreement with those obtained in this experiment; the validity of the above equations was thus confirmed.

Copolymerizations of MeOAN and MeOA with Acrylonitrile. The results of the radical copolymerizations of these monomers (M_1) with acrylonitrile (M_2) are shown in Table 3, while the resulting copolymer composition curves are indicated in Fig. 2.

The following copolymerization parameters were obtained:

for MeOAN (M_1)-acrylonitrile (M_2):
$r_1 = 1.93$, $r_2 = 0.37$, $Q_1 = 0.83$, $e_1 = 0.61$

for MeOA (M_1)-acrylonitrile (M_2):
$r_1 = 0.30$, $r_2 = 0.15$, $Q_1 = 0.48$, $e_1 = -0.56$

where the Q_1 and e_1 values were calculated by assuming that $e_2 = 1.20$ and $Q_2=0.60$ for acrylonitrile.

Contrary to the results of the copolymerizations with styrene, the relative reactivities ($1/r_2$) of these monomers toward a polyacrylonitrile radical were

Table 3. Copolymerizations of MeOAN and MeOA (M_1) with acrylonitrile (M_2) at 60°C

$([M_1]+[M_2]) = 8.00$ mol/l in benzene*

M_1	$[M_1]$ in comonomer (mol%)	Time (hr)	Conversion (%)	Copolymers obtained	
				N (%)	$[M_1]$ (mol%)
MeOAN	12.0	5.6	17.3	23.01	25.4
	25.0	31	8.4	21.00	43.9
	37.0	31	5.7	19.81	57.0
	50.0	31	3.5	18.84	68.5
	63.0	70	6.8	18.27	75.9
	75.0	106	6.7	17.50	86.2
	87.0	134	5.8	17.05	93.0
MeOA	12.0	5	12.9	11.81	36.1
	25.0	5	15.0	10.08	42.6
	37.0	5	15.1	8.83	44.3
	50.0	5	13.7	7.75	52.4
	63.0	5	11.6	6.39	58.9
	75.0	5	8.8	5.53	63.3
	87.0	5	5.4	3.83	72.9

* In the copolymerizations of MeOAN and MeOA, the concentrations of AIBN were kept constant at 5.47×10^{-3} and 5.00×10^{-3} mol/l, respectively.

found to be greater than those of the respective unsubstituted monomers of acrylonitrile and methyl acrylate, probably because of the electron-donating nature of the methoxy group. It was also noted that the e_1 value for MeOA obtained from the copolymerization with acrylonitrile was not in agreement with that obtained with styrene.

Although the Q and e values for α-substituted acrylonitriles and acrylic esters obtained from the copolymerizations with styrene were in agreement with those calculated from Eqs. (1) and (2), those

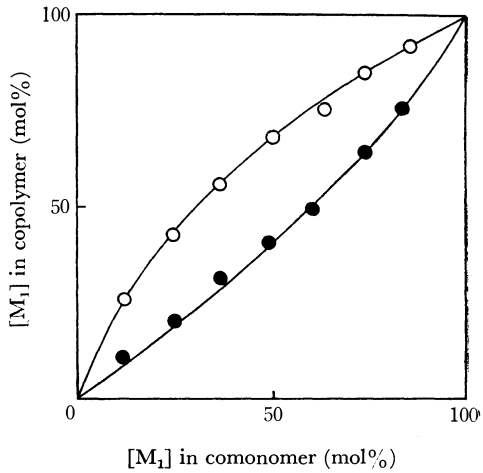

Fig. 2. Monomer-copolymer composition curves for MeOAN(M_1)-acrylonitrile(M_2)(○)and MeOA (M_1)-acrylonitrile(M_2) (●) at 60°C.

obtained from the copolymerizations with acrylonitrile did not agree. In Table 4, the Q_1 and e_1 values of several α-substituted acrylonitriles and acrylic esters calculated from the copolymerizations with styrene and with acrylonitrile are summarized. In this table, the negative e_1 values of α-substituted acrylic esters carrying the electron-donating methyl and methoxy groups are noted; their e_1 values are not those with would be predicted from Eq. (1). However, no such abnormal behavior was found in the copolymerizations of α-substituted acrylonitriles, and Eqs. (1) and (2) were valid for the copolymerization with acrylonitrile.

The effects of electron-donating α-substituents on the relative reactivities of α-substituted vinyl monomers toward a polyacrylonitrile radical will be discussed in detail in a subsequent paper.

Table 4. The values of Q_1 and e_1 of α-substituted acrylonitriles and α-substituted acrylic esters (M_1) determined from the copolymerizations with acrylonitrile and with styrene (M_2) at 60°C

M_1	M_2: Acrylonitrile		M_2: Styrene		Ref.
	Q_1	e_1	Q_1	e_1	
α-Methoxyacrylonitrile	0.83	0.62	0.72	0.40	This work
Methacrylonitrile	1.45	0.63	1.12	0.81	3
α-Acetoxyacrylonitrile	1.18	1.10	1.17	1.06	8
Methyl α-methoxyacrylate	0.48	−0.56	0.47	0.04	This work
Methyl methacrylate	0.84	−0.12	0.74	0.40	3
Ethyl α-acetoxyacrylate	0.41	0.12	0.54	0.67	3, 4
Methyl acrylate	0.55	0.79	0.42	0.60	3

8) T. Oota, M. Kobayashi and H. Ogawa, *Kogyo Kagaku Zasshi (J. Chem. Soc. Japan, Ind. Chem. Sect.)*, **71**, 1542 (1968).

BULLETIN OF THE CHEMICAL SOCIETY OF JAPAN VOL. 42 3211—3215 (1969)

Crystalline Terpolymer of Formaldehyde, Carbon Dioxide, and *N*-Phenylethylenimine

Tsutomu KAGIYA and Kōzō NARITA
Faculty of Engineering, Kyoto University, Sakyo-ku, Kyoto

and Masatsune KONDO
Sumitomo Chemical Co., Ltd., Takatsuki

(Received March 14, 1969)

Formaldehyde, carbon dioxide, and *N*-phenylethylenimine were allowed to terpolymerize by means of dimethyl ether acetate to give a crystalline solid terpolymer, melting at 178—265°C, with the composition of: CH_2O: 70—95, CO_2: 0.5—5, C_8H_9N: 5—25 mol%. The content of *N*-phenylethylenimine in the terpolymer thus obtained increased with the content of the imine in the feed, and that of carbon dioxide in the terpolymer, with the content of the imine in the feed, the lowering of the polymerization temperature, and the polymerization time. The infrared spectrum of the terpolymer showed the characteristic peaks of $-(-CH_2OCH_2O-)-$, $-(-\overset{\overset{O}{\|}}{OCO}-)-$ and $-(-\underset{\underset{C_6H_5}{|}}{N}CH_2CH_2-)-$. The mechanism of the terpolymerization was proposed on the basis of these results.

Recently, the copolymerizations[1] of formaldehyde with olefins or with various aldehydes have been studied. No paper on the copolymerization of carbon dioxide as a monomer has, however, been reported.

The present authors have previously studied formaldehyde polymerization in a liquid carbon dioxide solution.[2] During the course of their study, the authors found that the crystalline terpolymers of formaldehyde, carbon dioxide, and *N*-phenylethylenimine were produced by dimethyl ether acetate.

In this paper, the sturcture and the physical properties of the terpolymer will be determined, and the mechanism of the terpolymerization will be discussed.

Experimental

Materials. The formaldehyde in liquid carbon dioxide was prepared by means of the two-step method reported previously.[2] Eighteen hundred grams of paraformaldehyde, 1000 g of polyethylene glycol (a degree of polymerization of about 10), and 1.8 mol of calcium carbonate were put into a 3000 m*l* decomposer, and then the mixture was heated at from 110 to 160°C under a carbon dioxide stream (flow rate: 160 m*l*/min). The mixture of formaldehyde and carbon dioxide was passed through two tubes cooled at −20°C and then liquefied in the monomer reservoir at −78°C. The *N*-phenylethylenimine was prepared according to the method of the literature[3] from *β*-bromoethylaniline hydrobromide; it was dried over sodium sulfate and fractionated twice before use (bp 70—70.5°C/13 mmHg). Commercial carbon dioxide was dried through two drying tubes packed with phosphorus pentoxide. The dimethyl ether acetate was prepared by the reaction[4] of monochloromethyl ether with potassium acetate; it was then purified by distillation (bp 117—118°C). The toluene, acetonitrile, and formic acid were purified in the usual way.

Polymerization Procedure. A 30 m*l* stainless steel autoclave or a 20 m*l* glass ampule was used as the reaction vessel. The vessel was degassed *in vacuo* and cooled at −198°C. Then, measured quantities of the catalyst and *N*-phenylethylenimine were put into the autoclave, and then a carbon dioxide solution of formaldehyde (about 60 wt%) or liquid formaldehyde was introduced. In the experiment using the glass ampule, a measured quantity of the organic solvent containing the catalyst, *N*-phenylethylenimine, and liquid formaldehyde was put into the ampule. The vessel was kept standing for the definite time at a constant temperature. After the reaction, the unreacted formaldehyde

1) C. Chachaty, *Compt. rend.*, **251**, 385 (1960); U.S. Pat. 2373561.

2) T. Kagiya, M. Kondo, K. Narita and K. Fukui, This Bulletin, **42**, 1688 (1969); T. Kagiya and K. Narita, *ibid.*, **42**, 2912 (1969).

3) H. W. Heine, B. L. Kapur and C. S. Match, *J. Am. Chem. Soc.*, **76**, 1173 (1954).

4) "Beilsteins Handbuch der Organischen Chemie," Band III, Deutschen Chemischen Gesellschaft, Julius Springer, Berlin (1921), p. 236.

TABLE 1. TERPOLYMERIZATION OF FORMALDEHYDE, CARBON DIOXIDE, AND *N*-PHENYLETHYLENIMINE

Expt. No.	Monomer (g, mol)			Polymerization condition*		Yield (g)	η_{sp}/c (dl/g)	Mp (°C)	Terpolymer composition (mol%)		
	CH_2O	CO_2	C_8H_9N	Temp. (°C)	Time (min)				CH_2O	CO_2	C_8H_9N
1	3.0 (0.10)	2.0 (0.045)	0.4 (0.0034)	10	60	1.77	8.38	178	95.0	0.5	4.5
2	6.0 (0.20)	4.0 (0.090)	1.2 (0.0100)	10	60	3.09	0.20	227	92.4	1.1	6.5
3	5.1 (0.170)	3.4 (0.077)	1.2 (0.0100)	10	1 day	3.25	1.60	206	87.0	3.3	9.7
4	6.6 (0.220)	4.4 (0.099)	1.2 (0.0100)	−20	60	2.31	0.20	269	89.7	3.6	6.9
5	5.1 (0.170)	3.4 (0.077)	1.2 (0.0100)	−78	60	0.56	0.19	270	80.0	4.3	15.7
6	4.8 (0.160)	3.2 (0.160)	3.1 (0.0260)	10	60	2.73	0.84	218	83.2	1.3	15.5
7	2.4 (0.080)	1.6 (0.036)	2.4 (0.0201)	10	60	2.16	0.16	225	73.9	2.5	23.6
8	0.6 (0.020)	0.4 (0.009)	4.8 (0.0402)	10	1 day	0.581	0.10	262	70.3	4.9	24.8

* Catalyst, dimethyl ether acetate 0.2 mmol.

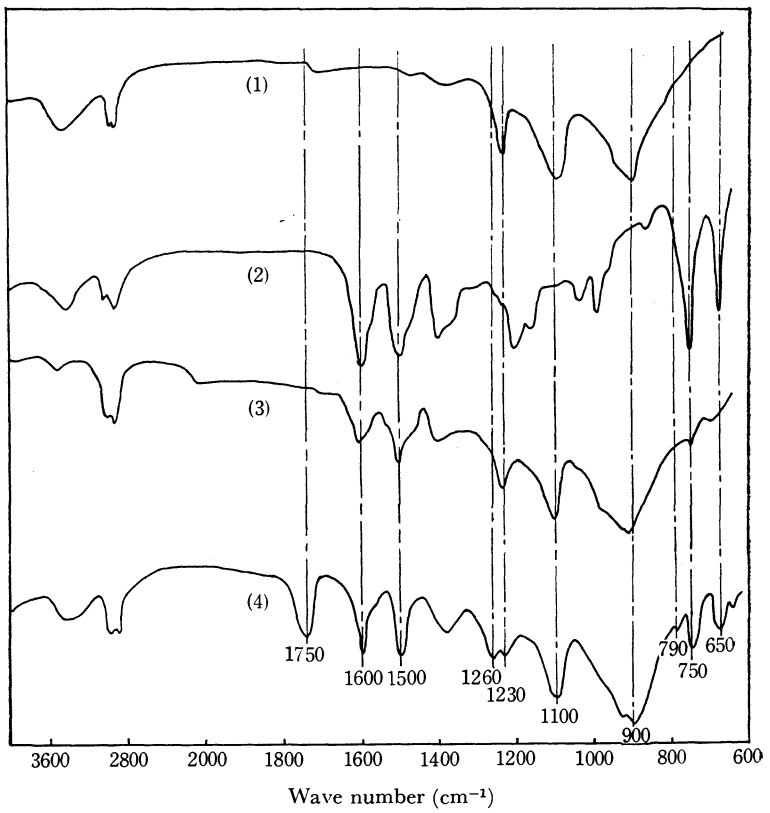

Fig. 1. Infrared spectra of: (1) poly-formaldehyde; (2) poly-*N*-phenylethylenimine; (3) copolymer of formaldehyde and *N*-phenylethylenimine; (4) terpolymer of formaldehyde, carbon dioxide, and *N*-phenylethylenimine.

and carbon dioxide were purged out, and the polymer was washed with cooled diethyl ether, dried *in vacuo* at room temperature, and weighed.

Analysis. The composition of the terpolymer was determined by elementary analysis. The specific viscosity measurement of the solution containing 0.5 g of the polymer in 100 m*l* of *p*-chlorophenol containing 2% α-pinene was carried out with the aid of an Ostwald viscometer at 60°C. The melting point of the polymer was visually determined in a nitrogen atmosphere in an electric heater. The infrared spectrum was obtained by using the potassium bromide pellet technique on a Japan Spectroscopic infrared spectrometer, Model DS-402G, with a sodium chloride prism. The X-ray diffraction diagram was recorded with a powder camera on a Shimadzu X-ray difractometer, Model GX-3B, employing Ni-filtered CuK_α radiation and standard techniques. The differential thermograms were obtained by using sandwiches with α-alumina powder as a diluent under an argon atmosphere on a Shimadzu differential thermal apparatus, Model DT-10, equipped with a platinum cell.

Results and Discussion

Terpolymerization of Formaldehyde, Carbon Dioxide, and *N*-Phenylethylenimine. The results of the terpolymerization of formaldehyde, carbon dioxide, and *N*-phenylethylenimine are shown in Table 1. Formaldehyde, being unable to copolymerize with carbon dioxide, was allowed to terpolymerize with carbon dioxide and *N*-phenylethylenimine in the presence of dimethyl ether acetate to give a white powdery polymer, which was soluble in *p*-chlorophenol, *m*-cresol, and dimethylformamide, and insoluble in diethyl ether, acetone, ethanol, chloroform, and toluene. The melting points of the terpolymers were 178°C to 265°C, between those of poly-*N*-phenylethylenimine (285—292°C) and poly-formaldehyde (*ca.* 170°C).

As is shown in Table 1, the *N*-phenylethylenimine content of the terpolymer increased with the imine content of the feed, and that of carbon dioxide in the terpolymer increased with the imine content of the feed, the lowering of polymerization temperature, and the polymerization time. The yield of the terpolymer increased with a rize in the reaction temperature.

Structure of the Terpolymer. The infrared spectrum of the resulting polymer showed the characteristic absorptions at 1230, 1100, and 900 cm^{-1} based on the acetal linkage (formaldehyde unit); at 1600, 1500, 750, and 690 cm^{-1} based on the benzene nucleus (*N*-phenylethylenimine unit), and at 1750, 1260, 1040, and 790 cm^{-1} based on the carbonate linkage (carbon dioxide unit) (Fig. 1). In addition, the infrared spectra of the polymers obtained by the polymerization of formaldehyde or *N*-phenylethylenimine in the presence of carbon dioxide and the copolymer of formaldehyde and *N*-phenylethylenimine in the absence of carbon dioxide are shown in Fig. 1. It is found that none of these polymers has the structure of the carbonate group -(-OCO-)-.

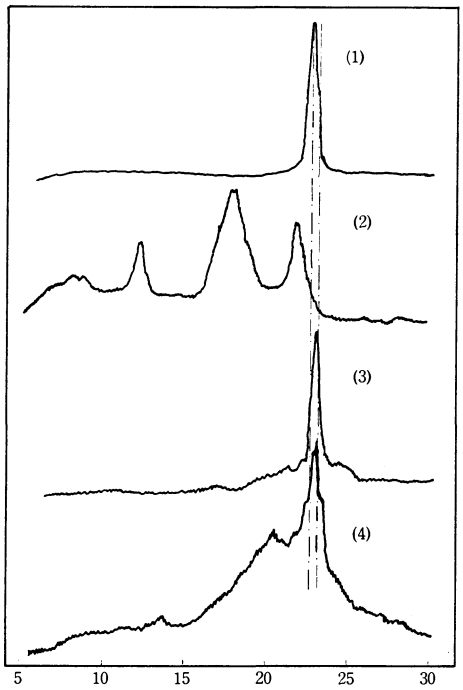

Fig. 2. X-Ray diffraction diagrams of: (1) poly-formaldehyde; (2) poly-*N*-phenylethylenimine; (3) copolymer of formaldehyde and *N*-phenylethylenimine; (4) terpolymer of formaldehyde, carbon dioxide, and *N*-phenylethylenimine.

Table 2. Characteristic peaks of X-ray diffraction diagrams of the polymers

	2θ (°)
Poly-formaldehyde	22.6
Poly-*N*-phenylethylenimine	8.3(s), 12.0, 18.0, 21.8
Copolymer of formaldehyde and *N*-phenylethylenimine	23.0, 24.2(s)
Terpolymer	13.5(s), 20.8(b), 23.0

(s) means small peak. (b) means broad peak.

X-Ray diffraction diagrams of the terpolymer (carbon dioxide 2.5 mol%, *N*-phenylethylenimine 23.6 mol%), the poly-*N*-phenylethylenimine, and poly-formaldehyde are shown in Fig. 2. The characteristic peaks (2θ) of these polymers are listed in Table 2. The X-ray diffraction diagram of the terpolymer displayed the main characteristic peak and a broad shoulder. The main characteristic peak of the terpolymer is the same as that of the copolymers of *N*-phenylethylenimine and formaldehyde, but a little different from the characteristic peaks of poly-formaldehyde and poly-*N*-phenyl-

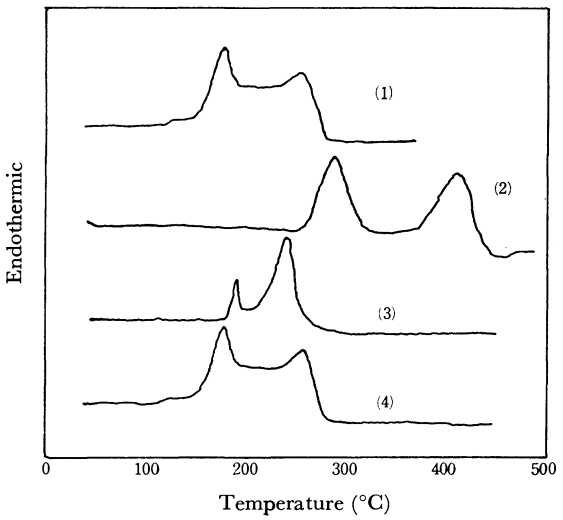

Fig. 3. Differential thermograms of: (1) polyformaldehyde; (2) poly-*N*-phenylethylenimine; (3) copolymer of formaldehyde and *N*-phenylethylenimine; (4) terpolymer of formaldehyde, carbon dioxide, and *N*-phenylethylenimine.

ethylenimine. On the other hand, the broad shoulder of the terpolymer is not different from the characteristic peaks of the above three polymers. It follows that the X-ray diagram indicates that the polymer from the three components contains a part of the block of the characteristic sequence of the terpolymer. In view of the relative half-value width, it may be concluded that the terpolymer is partially crystalline. Figure 3 shows a differential thermogram of the terpolymer (carbon dioxide 3.6 mol%, *N*-phenylethylenimine 6.7 mol%) in comparison with those of both homopolymers and those copolymers. The endothermic peak corresponds to the melting point of neither homopolymer, but a new peak of the terpolymer was observed.

Mechanism of the Terpolymerization. On the basis of the results shown in Table 1 and 3, the following reaction mechanism of the terpolymerization of formaldehyde, carbon dioxide, and *N*-phenylethylenimine by dimethyl ether acetate can be proposed.

Since formaldehyde was homopolymerized in the presence of carbon dioxide (Expt. No. 1 in Table 3), the reaction of formaldehyde with the propagating species of $-OCH_2^{\delta+}-OOCCH_3^{\delta-}$ (Eq. (1)) really occurs. On the other hand, from the fact that *N*-phenylethylenimine was hardly allowed to polymerize at all by dimethyl ether eacetate (Expt. No. 2 in Table 3), the reaction of *N*-phenylethylenimine with the propagating species of $-NCH_2CH_2^{\delta+}-OOCCH_3^{\delta-}$ (C_6H_5) is negligible in this polymerization.

On the other hand, formaldehyde was allowed to copolymerize with *N*-phenylethylenimine in

Table 3. Copolymerization of formaldehyde and *N*-phenylethylenimine

Expt. No.	Monomer (g, mol) CO_2	Monomer (g, mol) CH_2O	Monomer (g, mol) C_8H_9N	Catalyst (mol × 10^4)	Solvent[a]	Yield (g)	η_{sp}/c (dl/g)	Mp (°C)	The structures in the polymer obtained -(-CH_2O-)-	-(-NC_2H_4-)- (C_6H_5)	-(-OCO-)- (O)
1[c]	4.0 (0.090)	6.0 (0.200)	—	Dimethyl ether acetate 2	—	3.42	3.13	174	◎	—	—
2[c]	8.0 (0.108)	—	2.4 (0.0201)	Dimethyl ether acetate 2	—	0.03	—	—	—	◎	—
3[d]	—	—	1.2 (0.0100)	Formic acid 2	Acetonitrile	0.96	0.46[b]	285	—	◎	—
4[d]	—	1.7 (0.057)	0.6 (0.0050)	Dimethyl ether acetate 1	Toluene	0.52	3.32	180	◎	◎	—
5[d]	—	3.1 (0.103)	4.8 (0.0402)	Dimethyl ether acetate 1	Toluene	1.38	1.12	173	◎	◎	—
6[d]	—	1.1 (0.037)	0.6 (0.0050)	Dimethyl ether acetate 1	Acetonitrile	0.80	0.40	175	◎	◎	—
7[c]	—	3.6 (0.120)	3.2 (0.0402)	Dimethyl ether acetate 1	Toluene	2.85	0.82	172	◎	◎	—

The polymerization temperature, 20°C; The polymerization time, 60 min.

a) Solvent, 5 m*l*.

b) The viscosity was measured with 100 m*l* of the formic acid solution containing 0.5 g of the polymer.

c) Reaction was carried out in a stainless steel autoclave.

d) Reaction was carried out in a glass ampule.

organic solvents by dimethyl ether acetate (Expts. No. 4, 5, 6, and 7 in Table 3). Therefore, both the reactions of *N*-phenylethylenimine with the propagating species of $-OCH_2{}^{\delta+\delta-}OOCCH_3$ (Eq. (2)) and of formaldehyde with the propagating species of 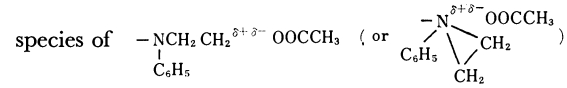 (Eq. (3)) may occur. From the results of both Expt. No. 2 in Table 1 and Expt. No. 1 in Table 3, it may be supposed that the rate of the propagation of reaction (1) is larger than that of reaction (2). On the basis of these results, the following elementary reactions may be proposed:

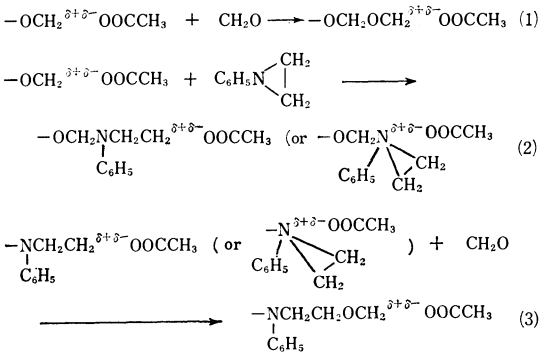

Further, carbon dioxide was allowed by dimethyl ether acetate to react only with formaldehyde in the presence of *N*-phenylethylenimine to give a terpolymer. The infrared spectrum of the terpolymer showed the existence of $-(-OCH_2OCH_2-)-$, $-(-NCH_2CH_2-)-$, and $-(-OCO-)-$. Therefore, it may be considered that the existence of carbon dioxide in this terpolymer is caused by the attack of the complex of formaldehyde, carbon dioxide, and *N*-phenylethylenimine on the propagating species of $-CH_2{}^{\delta+\delta-}OOCCH_3$ as follows:

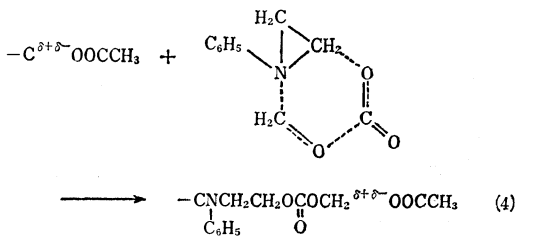

The low carbon dioxide content (0.5—5 mol%) in the terpolymer indicates that the equilibrium constant of the reaction (4) is very small. This quantitative mechanism is consistent with the experimental results. A detailed study of the mechanism of this type of terpolymerization is now being carried out and will be reported on in a subsequent paper.

The authors wish to express their gratitude to Professor Kenichi Fukui for his helpful suggestions and to Mr. Hiroshi Hatta for his assistance in carrying out the experiments.

BULLETIN OF THE CHEMICAL SOCIETY OF JAPAN VOL. 42 3216—3220 (1969)

The Reaction of Carboxylic Acids and Hydrocarbons in a Silent Electric Discharge. II. The Reactions of Ethylene with Methyl Acetate and with Acetic Anhydride*1

Teruo HIRAKI

Institute of Commodities, Faculty of Economics, Kagawa University, Takamatsu

(Received March 19, 1969)

The present study was undertaken in order to ascertain the difference, if any, in the chemical behavior of methyl acetate and acetic anhydride submitted to a silent discharge between that in the presence and that in the absence of ethylene. (1) In the reaction of methyl acetate without ethylene, the main products were methanol, diacetyl, liquid hydrocarbons, formaldehyde, methane, carbon dioxide, carbon monoxide, and hydrogen. Although the methanol yield was almost the same, regardless of the presence or absence of ethylene, the yields of the hydrocarbons, all the carbonyl compounds, and of *n*-butyl acetate increased in the presence of ethylene. The great quantity of methanol produced might indicate that C–OCH_3-bond breaking in the methyl acetate occurs preferably upon the discharge. (2) With acetic anhydride, on the other hand, acetaldehyde, acetone, ethyl acetate, ethyl methyl ketone, diacetyl, hydrocarbons, carbon monoxide, carbon dioxide, and hydrogen were obtained as the main products. The yields of acetone and diacetyl decreased remarkably in the presence of ethylene, while the yields of hydrocarbons, ethyl methyl ketone, *n*-butyl methyl ketone, and of *n*-butyl acetate increased. The $CH_3COO\cdot$ and $CH_3CO\cdot$ radicals are thought to be the main intermediates in this reaction. The formation of *n*-butyl acetate and of *n*-butyl methyl ketone in the presence of ethylene can be explained on the basis of the telomerization of ethylene initiated by these radicals.

In the previous paper,[1] the reaction between acetic acid and ethylene by a silent discharge was studied. The α-C-alkylation which has been known to take place in the reaction[2,3] of a saturated organic acid with ethylene in the presence of benzoyl peroxide at 70—80°C did not occur when there was the discharge. Instead, the formations of ethyl and *n*-butyl acetates and of carbonyl compounds (acetone, ethyl methyl ketone, *etc.*) were observed in the discharge reaction. These observations were explained in terms of the telomerization of ethylene initiated by the $CH_3COO\cdot$ and $CH_3CO\cdot$ radicals which were formed from CH_3COOH under the discharge.

One of the purposes of the present study was to ascertain whether the $CH_3COO\cdot$ and $CH_3CO\cdot$ radicals are formed as the main intermediate also in the decompositions of methyl acetate and acetic anhydride under a silent discharge, and to check whether or not a similar telomerization occurs under the present reaction conditions.

*1 The major part of these research results were presented at the 21st Annual Meeting of the Chemical Society of Japan, Osaka, April, 1968.

1) T. Hiraki, This Bulletin, **42**, 1981 (1969).

2) J. R. Roland and J. Harmon, U. S. Pat. 2433015 (1947); *Chem. Abstr.*, **42**, 2268 (1948).

3) D. D. Coffman, U. S. Pat. 2433016 (1947); *Chem. Abstr.*, **42**, 2456 (1948).

Experimental

Materials. The methyl acetate was purified by washing it with a 10% sodium chloride solution three times, refluxing it over quick lime, and then distilling it through a column. The acetic anhydride was purified by column distillation *in vacuo* after it had been allowed to stand for 2—3 days with a small amount of sodium. Commercial ethylene was used without purification. No impurity was found in these reagents by gas-chromatographical analysis. For the analyses of methyl acetate and acetic anhydride and of ethylene, a 3-m column of DEGS (diethylenglycol succinate) and a 3-m column of activated charcoal respectively were used at 100°C.

Apparatus and Procedure. All the experiments were performed in a flow system. The apparatus and the procedure were similar to those previously reported.[1]

Analysis of the Products. The non-condensable gases produced were identified by comparing their retention times on gas chromatography with those of authentic samples. (Columns of activated charcoal, hexamethylphosphoramide, and molecular sieve-13X were used.) The gaseous products were not determined quantitatively.

The condensable products were confirmed not only by gas chromatography (columns; tricresyl phosphate, DEGS, PEG-6000, and silicon DC-550 at 120°C; carrier gas: He), but also by the formation of their derivatives. Thus, ethyl methyl ketone, obtained as a fraction boiling at 80—82°C, and acetone (bp 56—

57°C) were converted into their semicarbazones,*[2] the melting points of the derivatives being 146—146.5°C and 186.5—187°C respectively. They showed no depression in their melting points when mixed with authentic specimens. The quantitative analysis of the liquid products was performed by gas chromatography (column: a 3-m column of PEG-6000 and a 3-m column of DEGS, at 120°C).

Results and Discussion

When the discharge reactions of methyl acetate or acetic anhydride with ethylene were carried out in a Pyrex tube of the Siemen type under the conditions shown in Table 1 (helium was used in the case of the reaction without ethylene), a large number of compounds were obtained in every run. Among these, the identified compounds are summarized in Table 2. The percentage compositions of products shown in this table are the averages of three experiments; the fluctuations in the yields of these compounds were less than 1%.

I. The Reaction of Methyl Acetate. *Influence of Ethylene on the Discharge Reaction of Methyl Acetate.* As may be seen from Experiments No. 21 and 22 in Table 2, a large number of compounds were formed along with methanol, the major product in the reaction of methyl acetate with ethylene; acetaldehyde, diacetyl, ethyl methyl and methyl vinyl and *n*-butyl methyl ketones, *n*-propyl and *n*-butyl acetates, liquid hydrocarbons, formaldehyde, C_1—C_4-hydrocarbons, carbon dioxide, carbon monoxide, and hydrogen were all detected.

Most of these compounds were also formed in the silent discharge-induced reaction of methyl acetate without ethylene (Exp. No. 20). However, the distribution of the products was different from that in the reaction without ethylene: (1) While the methanol yield was scarcely affected at all by the presence of ethylene, the yields of all the carbonyl compounds and acetates increased in the presence of ethylene. (2) The propylene, *n*-butane, 1-butene, and 1,3-butadiene in the gaseous products were formed only in the presence of ethylene. (3) Influences of the molar ratio of ethylene to methyl acetate on the conversion efficiency (percentage of grams of the reaction product per grams of methyl acetate used) and the products pattern were not recognized in the region of the ratios from 0.6 : 1 to 0.9 : 1.

The increase in methyl vinyl ketone in the presence of ethylene may be due to the combination of a $CH_3CO\cdot$ radical with a vinyl radical, which has been reported to be formed from ethylene in the electrical discharge.[4] The formation of acetylene, 1-butene, and 1,3-butadiene also supports the idea of the formation of the intermediate vinyl radical. On the other hand, the formation of *n*-butyl methyl ketone and *n*-butyl acetate in the presence of ethylene suggests telomerization of ethylene involving the $CH_3CO\cdot$ and $CH_3COO\cdot$ radicals.

The Assumed Radicals and the Reaction Scheme. It is believed that most of the products in the discharge-induced reaction can be explained on the basis of known free redical processes. Since many

Table 1. Conditions of the reactions of ethylene with methyl acetate, and with acetic anhydride in a silent discharge

Reaction system		Methyl acetate			Acetic anhydride		
Experiment No.		20	21	22	30	31	32
Materials used							
a) AcOMe or Ac_2O	Amount, g	46.60	46.28	47.16	45.05	45.82	53.60
	Velocity, g/hr	7.8	7.7	7.9	7.5	7.6	8.9
b) Ethylene*	Volume, *l*	0	8.35	12.55	0	7.35	11.70
	Velocity, *l*/hr	—	1.39	2.09	—	1.22	1.92
Molar ratio (b/a)		0	0.6	0.9	0	0.4	0.6
Second. voltage, kV		11.6	11.6	11.6	11.6	11.6	11.6
Second. current, mA		0.2	2.5	2.7	3.2	2.0	2.0
Temp. of discharge tube							
Inside, °C		80	88	87	86	88	88
Outside, °C		84	85	80	82	81	84
Discharge time, hr		6	6	6	6	6	6

* Exp. Nos. 20 and 30 were carried out in a stream of helium (velocity, 1.33 and 1.26 *l*/hr respectively) instead of ethylene.

*[2] The semicarbazones of ethyl methyl ketone and acetone were prepared according to the procedure of R. L. Shriner, R. C. Fuson and D. Y. Curtin, "The Systematic Identification of Organic Compounds," 4th ed., John Wiley & Sons, New York (1956), p. 218.

4) C. L. Thomas, G. Egloff and J. C. Morrell, *Chem. Revs.*, **28**, 1 (1941).

TABLE 2. THE REACTION PRODUCTS

Experiment No.	20	21	22	30	31	32
Amount of liquid products, g	6.22	6.15	5.81	1.63	1.51	1.57
Conversion, %*	10.99	13.29	12.32	3.62	3.29	2.92
Composition of liquid products, %**						
Methanol	94.6	81.1	81.9	—	—	—
Acetaldehyde	0.3	1.1	0.9	6.9	7.4	7.1
Acetone	—	—	—	50.9	27.3	12.5
Ethyl methyl ketone	0.5	0.7	0.8	14.3	17.1	25.5
n-Butyl methyl ketone	—	0.1	0.1	—	3.3	2.8
Methyl vinyl ketone	1.0	4.1	3.0	—	—	—
Diacetyl	1.6	1.0	1.1	12.4	5.6	7.1
Ethyl acetate	***	***	***	6.5	7.7	6.8
n-Propyl acetate	—	1.3	1.1	—	—	—
n-Butyl acetate	—	0.1	0.3	—	4.5	5.7
Hydrocarbons	1.5	7.2	8.1	7.2	27.1	32.5
The others	0.5	3.3	2.7	1.8	—	—

Gaseous products****: Methane, Ethane, Acetylene, Propane, Propylene, Butane, 1-Butene, 1,3-Butadiene, Carbon monoxide, Carbon dioxide, Hydrogen, and Formaldehyde.

* The conversion efficiency was given by (grams of reaction product per grams of methyl acetate or acetic anhydride used) × 100.

** The yields of each compound produced were given by (grams of each compound per grams of total liquid product) × 100.

*** Ethyl acetate might has been produced, but this product could not be identified because of interference by a large peak of methanol.

**** Formaldehyde was only obtained in the reaction of methyl acetate, and also hydrocarbons higher than C_3 were not obtained in Exp. Nos. 20 and 30.

workers[5] have reported that the extent of the formation of ionized molecules in the discharge reaction is very small, the possible ion-molecule reactions which might explain the products will not be considered in this discussion.

Primary Processes. The possible homolytic cleavage of methyl acetate can be shown as follows:

$$CH_3COOCH_3^* \rightarrow CH_3CO\cdot + \cdot OCH_3 \quad (I)$$

$$\rightarrow \cdot CH_2COOCH_3 + H\cdot \quad (II)$$

$$\rightarrow CH_3\dot{C}OOCH_2 + H\cdot \quad (III)$$

$$\rightarrow CH_3COO\cdot + \cdot CH_3 \quad (IV)$$

$$\rightarrow \cdot CH_3 + \cdot COOCH_3 \quad (V)$$

$$\rightarrow 2\cdot CH_3 + CO_2 \quad (VI)$$

where $CH_3COOCH_3^*$ denotes a methyl acetate excited by the discharge.

The high yield of methanol in the reaction of methyl acetate without ethylene by the silent discharge indicates that Step I is the most probable primary process. This cleavage has been proposed as a major process in the radiolysis of methyl acetate also.[6]

Rust *et al.*[7] have shown that the dissociation of the $\cdot OCH_3$ radicals formed in the vapor-phase decomposition of methyl *t*-butyl peroxide ($Me_3C\cdot O\cdot O\cdot Me$) in the presence of cyclohexene was no more than 0.2%; 99.8% of the radical produced was converted into methanol. Evidence for the stability of $\cdot OCH_3$ radicals has also been reported by Shteen *et al.*[8] On the other hand, the presence of carbon monoxide in the gaseous products indicates that another radical in Step I, $CH_3CO\cdot$, immediately decomposed, as has been proposed to be the case in photolysis[9] and radiolysis.[6] As a result, the yields of carbonyl compounds may be low. Thus, at least to some extent, process I may be written:

$$CH_3COOCH_3^* \rightarrow \cdot CH_3 + CO + \cdot OCH_3$$

Although the presence of hydrogen in the gaseous products may be good evidence for the occurrence of processes II and III, the formation of the $\cdot CH_2COOCH_3$ radical (process II) is apparently of minor importance in view of the fact that no

5) S. C. Lind and G. R. Schultz, *J. Phys. Chem.*, **42**, 547 (1938); H. Wiener and M. Burton, *J. Am. Chem. Soc.*, **75**, 5815 (1953); J. C. Devins and M. Burton, *ibid.*, **76**, 2618 (1954); E. Inoue, *Denki Kagaku (J. Electrochem. Soc. Japan)*, **23**, 76 (1955).

6) P. Ausloos and C. N. Trumbore, *J. Am. Chem. Soc.*, **81**, 3866 (1959).

7) F. F. Rust, F. H. Seibold and W. E. Vaughan, *ibid.*, **72**, 338 (1950).

8) Shteen *et al.* have shown that the stability of $\cdot OCH_3$ radicals may be due to the geometrical configuration of H and O in the radical and to the endothermic dissociation process of the radicals; N. YA Shteen, N. YA Chernyak, V. L. Antonovskii and A. F. Revzin, *Zh. Fiz. Khim.*, **28**, 240 (1954).

methyl propionate and butyrate were obtained.

It can be thought that carbon dioxide, ethane, and methane are formed *via* three processes, IV, V, and VI. The IV and V processes have previously been proposed in radiolysis.[6]

Secondary Reactions. The possible ways of the production of methanol are thought to be as follows:

$$\cdot OCH_3 + CH_3COOCH_3 \rightarrow CH_3OH + R\cdot \quad (1)$$

$$2\cdot OCH_3 \rightarrow CH_3OH + HCHO \quad (2)$$

Wijnen has reported that methanol production *via* reaction (1) occurs mainly in the photolysis of CH_3COOCH_3 over the temperature range from 29 to 217°C,[9] and that a similar tendency is observed also in the photolysis of i-$C_3H_7OOCC_2H_5$ at 29—65°C.[10] From the above data, most of the methanol here can be thought to be formed through reaction (1).

The methanol yield was almost the same both in the presence and in the absence of ethylene. This might indicate that most of the methoxy radicals abstract the hydrogen atom from methyl acetate rather than add to the ethylene (little or no ethyl methyl ether or butyl methyl ether was obtained). Rust *et al.*[7] have also shown that $\cdot OCH_3$ radicals add to cyclohexene scarcely at all.

The formations of methyl vinyl ketone and n-butyl acetate in the presence of ethylene are thought to occur *via* the following reactions:

$$CH_3CO\cdot + \cdot CH{=}CH_2 \rightarrow CH_3COCH{=}CH_2 \quad (3)$$

$$CH_3COO\cdot + CH_2{=}CH_2 \rightarrow CH_3COOCH_2\dot{C}H_2 \quad (4)$$

$$CH_3COOCH_2\dot{C}H_2 + CH_2{=}CH_2 \rightarrow CH_3COO\dot{C}_4H_8 \quad (5)$$

$$CH_3COO\dot{C}_4H_8 + CH_3COOCH_3 \rightarrow CH_3COOC_4H_9 + R\cdot \quad (6)$$

Some of the $CH_3CO\cdot$ or $CH_3COO\cdot$ radicals (though most of these radicals may decompose immediately) may react on a vinyl radical and/or ethylene. The possibility that these reactions occur in a silent discharge has been discussed in connection with the reaction of acetic acid with ethylene previously studied.[1]

Comparison with Radiolysis. The products that were obtained in the decomposition of the methyl acetate excited by the silent discharge were similar to those obtained in the rediolysis;[6] Ausloos and Trumbore have shown that the G-values of the gaseous products are 2.14 (H_2), 1.76 (CH_4), 0.43 (C_2H_6), 2.68 (CO), 1.10 (CO_2), and 0.034 (CH_3OCH_3), and that methanol is the major liquid product.

Interestingly, however, the γ-ray-induced reaction of methyl formate with ethylene[11] has been found to produce the esters, $H(CH_2CH_2)_n COOCH_3$ (n=6.9 on the average), which were not formed by the discharge reaction.

II. The Reaction of Acetic Anhydride. *Influence of Ethylene Addition on the Discharge Reaction of Acetic Anhydride.* As may be seen from Experiments No. 31 and 32 in Table 2, the main liquid products in the silent discharge-induced reaction of acetic anhydride with ethylene were acetaldehyde, acetone, ethyl methyl and n-butyl methyl ketones, diacetyl, and ethyl, n-propyl and n-butyl acetates. The gaseous products were C_1—C_4-hydrocarbons, carbon dioxide and monoxide, and hydrogen.

Most of these compounds were also obtained in the reaction without ethylene (Exp. No. 30), but the distribution of the products was different from that in the reaction without ethylene; also, it was influenced by the molar ratio of the reactants: (1) The highest yields of acetone and diacetyl were in the absence of ethylene; the yields of these products decreased almost linearly with a rise in the ratio of the ethylene to the acetic anhydride concentration. Especially, the acetone yield decreased remarkably at a high ratio. (2) In the presence of ethylene, the yield of ethyl methyl ketone increased. Further, n-butyl acetate and n-butyl methyl ketone, which were not formed in the reaction without ethylene, were obtained; their yields increased slightly with an increase in the ratio of the ethylene to the acetic anhydride concentration.

These results suggest that, in the presence of ethylene, most of the $CH_3CO\cdot$ radicals which did not decompose add to ethylene rather than recombine with the methyl radical. The production of n-butyl acetate in the presence of ethylene may be good evidence for the formation of the $CH_3COO\cdot$ radical as an intermediate.

The Reaction Occurring in the Silent Discharge. The discharge-induced reaction of acetic anhydride is presumed to be chiefly a radical reaction, also. Thus, on the basis of the products, the assumed radicals and a part of the postulated reaction scheme may be formulated as follows:

$$(CH_3CO)_2O^* \rightarrow CH_3CO\cdot(A) + CH_3COO\cdot(B) \quad (7)$$

$$\rightarrow 2\cdot CH_3(C) + CO_2 + CO \quad (\text{or } C_2H_6 + CO_2 + CO) \quad (8)$$

$$\rightarrow 2\,CH_3CO\cdot + \cdot O\cdot(D) \quad (9)$$

where $(CH_3CO)_2O^*$ represents the acetic anhydride excited by the discharge.

The evidence for the occurrence of the A and B radicals in this reaction system has been already

9) M. H. J. Wijnen, *J. Chem. Phys.*, **27**, 710 (1957); *ibid.*, **28**, 271 (1958).

10) M. H. J. Wijnen, *J. Am. Chem. Soc.*, **82**, 1847 (1960).

11) A. D. Petrov, G. I. Nikisin and V. D. Vorob'ev, *Fette u. Seifen*, **59**, 1023 (1957); *Chem. Abstr.*, **52**, 7141 (1958).

discussed. Moreover, the presence of carbon monoxide and dioxide in the gaseous products may be clear evidence of the production of the excited $CH_3CO\cdot$ and $CH_3COO\cdot$ radicals, which decompose before taking part in any reactions. It has been demonstrated by many workers[9,12,13] that these radicals are rather unstable. Thus, the reactions (7) and (8) are thought to be the most probable primary processes.

The Mechanisms of the Formations of n-Butyl Acetate and n-Butyl Methyl Ketone. The one-to-two adducts, such as *n*-butyl acetate and *n*-butyl methyl ketone, were obtained in the reaction of acetic anhydride with ethylene under the silent discharge. The formation of these telomers may be presented as follows:

$$R\cdot + CH_2{=}CH_2 \rightarrow RCH_2\dot{C}H_2 \quad (10)$$

$$RCH_2\dot{C}H_2 + CH_2{=}CH_2 \rightarrow R(CH_2)_3\dot{C}H_2 \quad (11)$$

$$R(CH_2)_3\dot{C}H_2 + AH \rightarrow R(CH_2)_3CH_3 + A\cdot \quad (12)$$

where R· represents a $CH_3COO\cdot$ or $CH_3CO\cdot$ radical and where AH is any hydrogen donor (most AH's are probably the hydrocarbons produced).

Comparison with Pyrolysis. Szwarc and Murawski[14] have shown that the thermal decomposition of acetic anhydride is not a radical reaction, but a "molecular" process, because equimolecular amounts of ketene and acetic acid are obtained in the pyrolysis of acetic anhydride in a stream of toluene vapor. However, the possibility of this process is not thought to be important in the present study because such products were not obtained.

This difference in reaction paths is not surprising. It has been proposed by Thomas *et al.*[4] that there are essential differences between thermal activation and electrical activation. In the former energy must be put into the entire aggregation of molecules, but in the latter the electron collides with the bonding electrons.

The author wishes to express his thanks to Professor Tamon Matsuura, Hiroshima University, and to Professor Kazuaki Kawamoto, Kagawa University, for their kind advice.

12) R. W. Hummel, *Trans. Faraday Soc.*, **56**, 234 (1960).

13) L. Jaffe, E. J. Prosen and M. Szwarc, *J. Chem. Phys.*, **27**, 416 (1957); P. Ausloos, *Can. J. Chem.*, **36** 383 (1958); W. A. Pryor, "Introduction to Free Radical Chemistry," Prentice-Hall, New Jersey (1966), p. 23.

14) M. Szwarc and J. Murawski, *Trans. Faraday Soc.*, **47**, 269 (1951).

BULLETIN OF THE CHEMICAL SOCIETY OF JAPAN VOL. 42 3220—3223 (1969)

Solvent Effects in the Oxidation of Hydrocarbons. I. Chain Initiation by Azobisisobutyronitrile

Etsuo NIKI, Yoshio KAMIYA and Nobuto OHTA

Department of Fuel Engineering, The University of Tokyo, Hongo, Bunkyo-ku, Tokyo

(Received March 26, 1969)

The effects of solvents on the rate of decomposition and the efficiency of radical production by AIBN were studied by measuring the rate of evolution of nitrogen from AIBN and the inhibition time in the oxidation of tetralin. The rates of decomposition of AIBN were larger in aromatic solvents than in aliphatic solvents. The efficiency of AIBN was found to depend more on the viscosity of the medium than on the polarity of the solvents. The requirements for the determination of the inhibition time are discussed.

Azobisisobutyronitrile (AIBN) is one of the most widely used initiators for the radical reactions such as autoxidation and polymerization. The mechanism for the initiation by AIBN has been thoroughly studied by numerous investigators and confirmed to proceed by the following equations, where brackets indicate pairs of radicals which have not been separated by diffusion.[1)]

$$\mathrm{AIBN} \xrightarrow{k_i} [2(CH_3)_2(CN)C\cdot] + N_2 \quad (1)$$

$$[2(CH_3)_2(CN)C\cdot] \xrightarrow{k_c} (CH_3)_2C(CN)-C(CN)(CH_3)_2 + \text{disproportionation products} \quad (2)$$

1) C. E. Boozer, G. S. Hammond, C. E. Hamilton and J. N. Sen, *J. Am. Chem. Soc.*, **77**, 3233 (1955).

$$[2(CH_3)_2(CN)C\cdot] \xrightarrow{k_d} 2(CH_3)_2(CN)C\cdot \xrightarrow{O_2} \text{initiate chains} \quad (3)$$

It is known that the efficiency of the radical production by the thermal decomposition of AIBN, which can be expressed as $e=k_d/(k_c+k_d)$, is smaller than unity. This phenomenon has been explained as being due to the geminate recombination of demethylcyanomethyl radical in the solvent cage to from tetramethylsuccinonitrile and the disproportionation product, ketenimine. The solvent effects on the decomposition of AIBN have been studied by several investigators,[2] but a definite conclusion has not yet been obtained. In the course of our study on the solvent effects in the autoxidation of hydrocarbons, the effects of solvents in the initiation step by AIBN had to be elucidated. The rate of decomposition and the efficiency of radical production of AIBN were studied in the various solvents.

Theoretical

The mechanism of the autoxidation of hydrocarbons in the liquid phase at moderate temperature under sufficient oxygen pressure is represented as follows.

$$RH \rightarrow R\cdot \qquad R_i = 2ek_i[AIBN] \quad (4)$$

$$R\cdot + O_2 \rightarrow RO_2\cdot \quad (5)$$

$$RO_2\cdot + RH \xrightarrow{k_p} ROOH + R\cdot \quad (6)$$

$$RO_2\cdot + RO_2\cdot \xrightarrow{k_t} \text{non-radical products} + O_2 \quad (7)$$

When the inhibitor IH is added to the system, the following fast termination step replaces the normal termination reaction (7).

$$RO_2\cdot + IH \xrightarrow{k_{inh}} ROOH + I\cdot \quad (8)$$

$$RO_2\cdot + I \xrightarrow{\text{fast}} ROOI\cdot \quad (9)$$

In this case, the values of ek_i can be obtained by measuring the inhibition time, t_{inh}, using the equation[1]

$$t_{inh} = n[IH]/R_i = n[IH]/2ek_i[AIBN], \quad (10)$$

where n represents the number of peroxy radicals which are scavenged by each inhibitor molecule.

This inhibition method is useful not only for determination of the rate or efficiency of intiation but also for comparing the activities of various inhibitors for polymers, oils, *etc.* It is important to confirm the validity and accuracy of this technique. The two reactions (7) and (8) are competitive and Eq. (10) is applicable only when reactions (8) and (9) replace completely reaction (7). The ratio of the rate of reaction (8) to that of (7) is given by

$$\frac{V_8}{V_7} = \frac{k_{inh}[IH][RO_2\cdot]}{2k_t[RO_2\cdot]^2} = \frac{k_{inh}[IH]}{2k_t[RO_2\cdot]} \quad (11)$$

where V_8 and V_7 represent the rates of reactions (8) and (7) respectively. The steady state treatment for the elementary steps (4), (5), (6), (7), (8) and (9) gives the concentration of the peroxy radical as

$$[RO_2\cdot] = \{-k_{inh}[IH] + (k_{inh}^2[IH]^2 + 2k_tR_i)^{1/2}\}/2k_t \quad (12)$$

Substitution of Eq. (12) into Eq. (11) yields

$$\frac{V_8}{V_7} = \frac{1}{-1+\{1+4ek_ik_t[AIBN]/k_{inh}^2[IH]^2\}^{1/2}} \quad (13)$$

Therefore, the importance of reactions (8) and (7) in the specific reaction system is determined by the value of $[AIBN]/[IH]^2$, and the contribution of reaction (8) decreases with the increase in this value.

Table 1. Contribution of the two termination steps in the oxidation of tetralin at 70°C with 1.00×10^{-2}M AIBN

[IH] M	[AIBN]/[IH]	$[AIBN]/[IH]^2$ M^{-1}	V_8/V_7	Percent of reaction (8)
5.00×10^{-3}	2.0	4.0×10^2	292	99.7
2.00×10^{-3}	5.0	2.5×10^3	48.3	98.0
1.00×10^{-3}	10	1.0×10^4	12.3	92.5
5.00×10^{-4}	20	4.0×10^4	3.40	77.3
2.00×10^{-4}	50	2.5×10^5	0.782	43.9
1.00×10^{-4}	100	1.0×10^6	0.311	23.7
1.00×10^{-5}	1000	1.0×10^8	0.0250	2.45

IH: 2,6-di-*t*-butyl-4-methylphenol

In Table 1 are summarized the calculated values of V_8/V_7 for the oxidation of tetralin at 70° with 1.00×10^{-2}M of AIBN at various concentrations of 2,6-di-*t*-butyl-4-methylphenol (BMP), a well known inhibitor. n was assumed to be 2.0.[3] The value of k_t was taken as 8.0×10^6 *l*/mol/sec, k_{inh} as 7.0×10^3 *l*/mol/sec, e as 0.65, and k_i as 3.96×10^{-5} sec^{-1}, respectively, from literature values.[4] Table 1 shows how the relative contribution of the termination reaction (8) decreases with the decreases in the concentration of the inhibitor. When the relative importance of the termination reaction (7) is not small enough, Eq. (10) is not applied and the value of ek_i thus measured may be unreliable.

2) a) L. M. Andronof and G. E. Zaikov, *Kinetika i Kataliz*, **8**, 270 (1967); b) O. Yamamoto, J. Yamashita and H. Hashimoto, *Kogyo Kagaku Zasshi (J. Chem. Soc. Japan, Ind. Chem. Sect.)*, **71**, 223 (1968), and the papers cited therein.

3) E. C. Horswill and K. U. Ingold, *Can. J. Chem.*, **44**, 263, 269, 985 (1966).

4) E. Niki, Y. Kamiya and N. Ohta, This Bulletin, in press.

TABLE 2. REQUIRED CONCENTRATIONS OF THE INHIBITOR IN THE OXIDATION OF TETRALIN, α-METHYLSTYRENE AND CUMENE AT 70°C, $V_8/V_7 \geqq 40$

[AIBN] M	[IH]≧, M ([AIBN]/[IH]≦) Tetralin	α-Methylstyrene	Cumene
1.00×10^{-1}	5.74×10^{-3} (17.4)	3.04×10^{-3} (32.9)	5.28×10^{-4} (189)
4.00×10^{-2}	3.63×10^{-3} (11.0)	1.92×10^{-3} (20.8)	3.33×10^{-4} (120)
2.00×10^{-2}	2.57×10^{-3} (7.78)	1.36×10^{-3} (14.7)	2.36×10^{-4} (84.7)
1.00×10^{-2}	1.81×10^{-3} (5.52)	9.62×10^{-4} (10.4)	1.67×10^{-4} (59.9)
1.00×10^{-3}	5.74×10^{-4} (1.74)	3.04×10^{-4} (3.29)	5.28×10^{-5} (18.9)

IH: 2,6-*t*-butyl-4-methylphenol

As is clear from Eq. (13), the relative importance of reaction (8) depends also on the value of k_t, *i. e.*, on the hydrocarbons. In Table 2 are shown the calculated concentrations of the inhibitor required to make the value of V_8/V_7 larger than 40, corresponding to 97.5% termination by inhibitor, in the oxidation of tetralin ($k_t=8.0\times10^6$ *l*/mol/sec), α-methylstyrene ($k_t=1.0\times10^6$ *l*/mol/sec), and cumene ($k_t=3.0\times10^4$ *l*/mol/sec) at 70°C with various concentrations of AIBN. The values of k_{inh} for the oxidation of α-methylstyrene and cumene were taken as 4.7×10^3 and 1.6×10^3 *l*/mol/sec, respectively, from the fact that the relative reactivities of tetralylperoxy, α-methylstyrylperoxy and cumylperoxy radicals are in the ratios of 4.5 : 3.0 : 1.0.[4] Table 2 suggests that the required concentration of the inhibitor is largely dependent on the hydrocarbons and the concentration of the initiator.

As described above, the concentrations of AIBN and the inhibitor used in the determination of the inhibition time should be carefully chosen in order to satisfy the above requirements and to obtain accurate and reasonable data. These important conditions seem to have been overlooked until now, and the inhibition time has been determined with an insufficient amount of inhibitor.

Results and Discussion

The rate constant for the unimolecular decomposition of AIBN was determined by measuring the rate of nitrogen evolution. The inhibition time was measured in the oxidation of tetralin using 2,6-di-*t*-butyl-4-methylphenol (BMP) as an inhibitor assuming that 2 radicals reacted with one molecule of inhibitor.[3]

Equation (10) suggests that the inhibition time is proportional to the concentration of the inhibitor and inversely proportional to the concentration of AIBN. Figure 1 shows that the inhibition time in

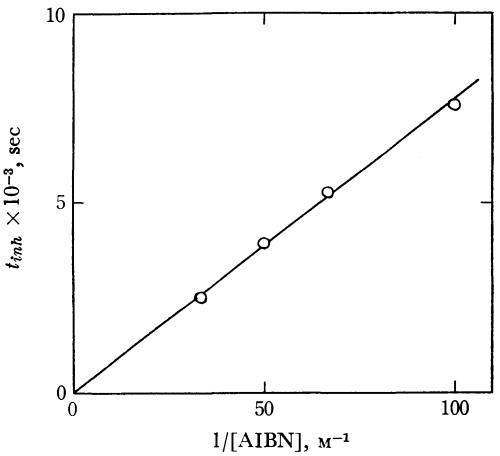

Fig. 1. Inhibition time in the oxidation of tetralin in chlorobenzene at 70°C.
[Tetralin]=1.47M, [BMP]=2.00×10^{-3}M

TABLE 3. INHIBITION TIME IN THE OXIDATION OF TETRALIN IN CHLOROBENZENE AT 70°C, [tetralin]=1.47 M

[AIBN]$\times10^2$ M	[BMP]$\times10^3$ M	t_{inh} sec	t_{inh}/([IH]/[AIBN]) $\times10^{-4}$, sec
10.0	6.04	2140	3.54
4.00	3.67	3280	3.57
3.00	2.00	2350	3.53
2.00	2.00	3730	3.73
1.50	2.00	5100	3.82
1.00	2.00	7360	3.68

TABLE 4. INHIBITION TIME, RATE CONSTANT FOR DECOMPOSITION AND EFFICIENCY OF AIBN IN THE OXIDATION OF TETRALIN IN THE VARIOUS SOLVENTS AT 70°C, [tetralin]=1.47M

Solvent	D[a]	η[b] centipoise	t_{inh}[c] sec	$ek_i\times10^5$ sec^{-1}	$k_i\times10^5$ sec^{-1}	e
Chloro-benzene	4.440	0.5568	2140	2.82	4.10	0.688
Anisole	3.651	0.6232	2350	2.55	3.89	0.656
Nitro-benzene	21.10	0.9694	2200	2.73	4.70	0.581
Acetophe-none	11.21	0.8958	2390	2.51	4.41	0.569
Butyric acid	2.937	0.8232	2920	2.05	3.64	0.563
n-Decane	2.069	0.5633	3790	1.58	3.05	0.518
Diethyl maleate	5.811	1.211	3370	1.78	3.64	0.489
Tetralin[d]	2.657	0.9869	2935	2.02	4.22	0.483
Butyl stearate	2.857	2.337	5020	1.20	3.67	0.327

a) Dielectric constant of the solution measured at 70°C.
b) Viscosity of the solution measured at 70°C.
c) Inhibition time measured at 70°C in the presence of 0.100M AIBN and 66.00×10^{-3}M BMP.
d) Pure tetralin.

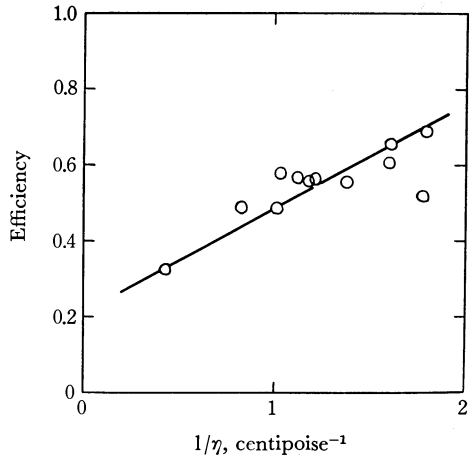

Fig. 2. Plots of efficiency of AIBN as a function of viscosity of the solution.

the oxidation of tetralin in chlorobenzene solvent is inversely proportional to the concentration of AIBN. In addition, Table 3 indicates that the inhibition time is proportional to [IH]/[AIBN]. Since all the solvents used in this study were found to be really inert under the reaction conditions employed here and since sufficient amount of inhibitor was used in the measurement, it may be said that Eq. (10) applies for solvents other than chlorobenzene.

The inhibition time in the oxidations of tetralin in various solvents with added AIBN and BMP is summarized in Table 4. The values of ek_i calculated from Eq. (10), the measured rate constant for the decomposition of AIBN, and calculated efficiency of chain initiation are also included in Table 4. Both k_i and e were reproducible within an experimental error of about 5%. The results indicate that both k_i and e are dependent on the reaction medium. The rate of decomposition of AIBN differs by a factor of 1.54, and is a little higher in an aromatic than in an aliphatic solvent. The efficiency of initiation differs by a factor of 2.10 ranging from 0.33 to 0.69. It depends mostly on the viscosity of the oxidizing solution and is a nearly linear function of the reciprocal of the viscosity, as shown in Fig. 2. Such a correlation has been observed in other systems.[5] However, there is also some contribution to this efficiency from the dielectric constant of the solution: the three solvents that give the greatest positive deviations from the indicated line, nitrobenzene, acetophenone, and diethyl maleate, also have the highest dielectric constants, and in the same order. *n*-Decane, which gives the greatest negative deviation, has the lowest dielectric constant.

Table 5. Inhibition time, rate constant for decomposition and efficiency of AIBN in the oxidation of tetralin in chlorobenzene at 70°C, [AIBN]=0.100M, [BMP]=6.00×10^{-3}M

[Tetralin] M	D	η centipoise	t_{inh} sec	$ek_i\times10^5$ sec^{-1}	$k_i\times10^5$ sec^{-1}	e
7.35	2.657	0.9869	2935	2.02	4.22	0.483
5.88	3.086	0.8424	2650	2.26	4.04	0.559
4.41	3.509	0.7238	2410	2.49	4.47	0.557
2.94	4.017	0.6257	2290	2.62	4.33	0.605
1.47	4.440	0.5568	2140	2.82	4.10	0.668

The effect of dilution by chlorobenzene was also studied. As shown in Table 5, the effect of medium change on k_i is less than the experimental error, and e is approximately a linear function of the reciprocal of the viscosity (Fig. 2).

Experimental

Tetralin and various solvents used were the same as in the previous paper.[6] AIBN and 2,6-di-*t*-butyl-4-methylphenol were recrystallized from methanol several times.

The inhibition time was determined by performing the oxidation of tetralin in a variety of solvents with added inhibitor under atmospheric pressure of oxygen in a constant pressure closed system. The rates of decomposition of AIBN in the various solvents were determined by measuring the rate of nitrogen evolution using a buret connected to the constant closed system under atmospheric pressure of nitrogen. Oxygen which might possibly interfere with the accurate measurement of the nitrogen evolution was carefully eliminated from the system. The viscosity was measured at 70°C with a modified Ostwald viscometer.

5) O. Dobis, J. M. Pearson and M. Szwarc, *J. Am. Chem. Soc.*, **90**, 278 (1968).

6) E. Niki, Y. Kamiya and N. Ohta, This Bulletin, in contribution.

BULLETIN OF THE CHEMICAL SOCIETY OF JAPAN VOL. 42 3224—3229 (1969)

Solvent Effects in the Oxidation of Hydrocarbons. II. Oxidations of Tetralin in Various Solvents

Etsuo NIKI, Yoshio KAMIYA and Nobuto OHTA

Department of Fuel Engineering, The University of Tokyo, Hongo, Bunkyo-ku, Tokyo

(Received March 26, 1969)

The rates of oxidation of 1.47M tetralin in a variety of solvents at 70°C in the presence of 1.00×10^{-2}M AIBN varied by a factor of 2.9, ranging from 6.39×10^{-6} mol/*l*/sec in *n*-decane to 1.84×10^{-5} mol/*l*/sec in nitromethane. The rate of oxidation was dependent on the composition of the solution as well as the kinds of solvents. It was found that the solvents affected the initiation step approximately as much as they affected the propagation and/or temination step. The rate of initiation by AIBN was mainly dependent on the viscosity of the medium, while that of propagation and termination was mainly determined by the dielectric constant of the medium. The correlation between log $(k_p/(2k_t)^{1/2})$ and $(D-1)/(2D+1)$ was discussed, where k_p and k_t are the rate constants for propagation and termination steps, respectively, and D is the dielectric constant of the medium, under conditions where the complication caused by the selective solvation could be excluded.

Although it was once accepted that the solvent effects in the reactions of free radicals and atoms are small in contrast to the ionic reactions, it is known nowadays that the solvent affects both the rate and the course of the free radical reactions.[1,2] The solvent effects in the autoxidation of hydrocarbons, a typical example of the reaction by a free radical mechanism, have been studied by several investigators. Zaikov[3-6] studied the oxidation of methyl ethyl ketone in benzene and acetic acid solutions by varying the compositions of the reactant and the solvents, and found that the rates of oxidation and the rate constants could be well correlated with Kirkwood equation[7]

$$\log(\text{rate or rate constant}) = a(D-1)/(2D+1)+b \quad (1)$$

where D is the dielectric constant of the medium, and a and b are constants. Hendry and Russell,[8] and Howard and Ingold[9] studied the oxidation of several hydrocarbons in a number of solvents and found that the rates of oxidation increased with the increase in the dielectric constants of the solvents. They suggested that the dipolar transition state was involved in the propagation step and the contribution of the solvation at this stage enhanced the rates of propagation and oxidation. They also suggested that the solvation is greater at the ground state than at the transition state in the termination step, which decreased the rate of termination and increased the rate of oxidation.[8]

Since then, several papers concerning the solvent effects on the autoxidation of hydrocarbons have been presented and the correlation between the rates of oxidation and the dielectric function, $(D-1)/(2D+1)$, has been discussed.[10-12]

However, two important problems have been overlooked. One is the variation of the dielectric constant with temperature and the other is the difference between the bulk dielectric constant and the microscopic dielectric constant. In particular, the microscopic dielectric constant in the immediate vicinity of a reactant particle and the existence, extent, and nature of selective solvation have received little attention. This paper deals with the study on the solvent effects in the oxidation of tetralin taking the problems mentioned above into consideration. Tetralin was chosen as the oxidant since its oxidation mechanism is now well established,

1) G. A. Russell, *J. Am. Chem. Soc.*, **79**, 2977 (1957), and the subsequent papers.
2) E. S. Huyser, "Advances in Free-Radical Chemistry," Vol. I, ed. by G. H. Williams, Logos Press, London (1965), Chap. 3.
3) G. E. Zaikov, *Neftekhimiya*, **3**, 381 (1963).
4) G. E. Zaikov and Z. K. Maizus, *Dokl. Akad. Nauk SSSR*, **150**, 116 (1963).
5) G. E. Zaikov and Z. K. Maizus, Advances in Chemistry Series, **75**, Am. Chem. Soc., Washington D. C. (1968), p. 150.
6) G. E. Zaikov, *Kinetika i Kataliz*, **9**, 511 (1968).
7) J. G. Kirkwood, *J. Chem. Phys.*, **2**, 351 (1934).
8) D. G. Hendry and G. A. Russell, *J. Am. Chem. Soc.*, **86**, 2368 (1964).
9) J. A. Howard and K. U. Ingold, *Can. J. Chem.*, **42**, 1044, 1250 (1964); **44**, 1119 (1966).
10) Y. Kamiya, This Bulletin, **38**, 2156 (1965).
11) J. Yamashita, O. Yamamoto, K. Shimizu and H. Hashimoto, *Kogyo Kagaku Zasshi (J. Chem. Soc. Japan, Ind. Chem. Sect.)*, **71**, 225 (1968).
12) H. Masuda, K. Kobayashi and N. Ohta, *ibid.*, **71**, 994 (1968).

and in addition its oxidation rate is greater than those of other hydrocarbons. This is advantageous for studying the oxidation of dilute solutions.

Results and Discussion

The autoxidation of tetralin in a variety of solvents at 70°C initiated by azobisisobutyronitrile (AIBN) were carried out in order to estimate the solvent effects on the rates of oxidation. The results are summarized in Table 1. The observed rates of oxygen absorption were corrected for nitrogen evolved from AIBN and for oxygen absorbed and evolved in the initiation and termination steps respectively, the correction factor being $R_i(1/e-1)/2$ where R_i is the rate of initiation and e is the efficiency of AIBN for radical production.[13] Table 1 indicates that the rates of oxidation of 1.47M tetralin in 35 solvents studied differ by a factor of 2.9, ranging from 6.39×10^{-6} mol/l/sec in n-decane to 1.84×10^{-5} mol/l/sec in nitromethane.

Table 1. Rates of oxidation of tetralin in various solvents 70°C
[AIBN] = 1.00×10^{-2}M, [tetralin] = 1.47M

No.	Solvent	$-dO_2/dt$, mol/l/sec
	(i) Aromatic hydrocarbon	
1	t-Butylbenzene	0.779×10^{-5}
2	m-Dichlorobenzene	0.946
3	Bromobenzene	0.999
4	1-Chloronaphthalene	1.00
5	Chlorobenzene	1.05
6	Nitrobenzene	1.34
	(ii) Alphatic hydrocarbon	
7	n-Decane	0.639
8	n-Nonane	0.662
9	n-Octane	0.666
10	Tetrachloroethylene	0.743
11	2-Nitropropane	1.36
12	1-Nitropropane	1.42
13	Nitroethane	1.54
14	Nitromethane	1.84
	(iii) Fatty acid	
15	Isovaleric acid	0.798
16	Valeric acid	0.814
17	Butyric acid	0.909
18	Acetic acid	1.21
	(iv) Alcohol	
19	1-Propanol	0.671
20	1-Pentanol	0.704
21	1-Octanol	0.790
	(v) Ketone	
22	Acetophenone	0.998
	(vi) Ether	
23	Anisole	1.04
	(vii) Ester	
24	Butyl stearate	0.664
25	Dibutyl sebacate	0.729
26	Dibutyl phthalate	0.875
27	Amyl acetate	0.878
28	Diethyl maleate	0.996
29	Ethyl cinnamate	1.00
30	Butyl acetate	1.01
31	Ethyl benzoate	1.04
32	Methyl benzoate	1.04
33	Ethyl propionate	1.06
34	Propyl acetate	1.07
35	Diethyl malonate	1.12

The rates of oxidation are dependent on the composition of the solutions as well. The effects of dilution on the rates of oxidation of tetralin in eight inert solvents, n-decane, butyl stearate, butyric acid, anisole, chlorobenzene, diethyl maleate, acetophenone and nitrobenzene, are summarized in Table 2. The rate of oxidation of tetralin is

Table 2. Effects of dilution in the oxidation of tetrlin in various solvents[a]
70°C, [AIBN] = 1.00×10^{-2}M

Tetralin, M	6.61	5.88	4.41	2.94	1.47	0.668
Solvent		$-dO_2/dt\times10^5$, mol/l/sec				
n-Decane		2.98	2.11	1.35	0.639	0.297
Butyl stearate		3.01	2.08	1.27	0.664	0.295
Butyric acid		3.32	2.60	1.77	0.909	0.404
Anisole		3.48	2.79	1.98	1.04	0.494
Chloro-benzene	3.91	3.55	2.84	1.95	1.05	0.486
Diethyl maleate		3.51	2.81	1.91	0.996	0.494
Acetophenone		3.58	2.93	1.99	1.01	0.464
Nitrobenzene	4.16	4.02	3.19	2.45	1.34	0.614

a) The rate of oxidation of pure tetralin under the same reaction conditions was 3.95×10^{-5} mol/l/sec.

given by the following equation:

$$-dO_2/dt = k_p(2k_t)^{-1/2}[RH]R_i^{1/2} = k_p(ek_i/k_t)^{1/2}[RH][AIBN]^{1/2} \quad (2)$$

where k_i is the rate constant for the unimolecular decomposition of AIBN, and k_p and k_t are the rate constants for the following propagation and termination steps respectively.

$$RO_2\cdot + RH \xrightarrow{k_p} ROOH + R\cdot$$

$$RO_2\cdot + RO_2\cdot \xrightarrow{k_t} \text{tetralone} + \text{tetralol} + O_2$$

Equation (2) implys that the rate of oxidation of tetralin is strictly first with respect to tetralin concentration at a constant initiator concentration. However, plots of the rates of oxidation in Table 2 as a function of tetralin concentration always show some curvature and, as shown in Fig. 1, the values of $k_p(ek_i/k_t)^{1/2}$ calculated from Eq. (2) varies monotonously with the tetralin concentration.

13) E. Niki, M. Kuwata, Y. Kamiya and N. Ohta, *ibid.*, **70**, 1679 (1967).

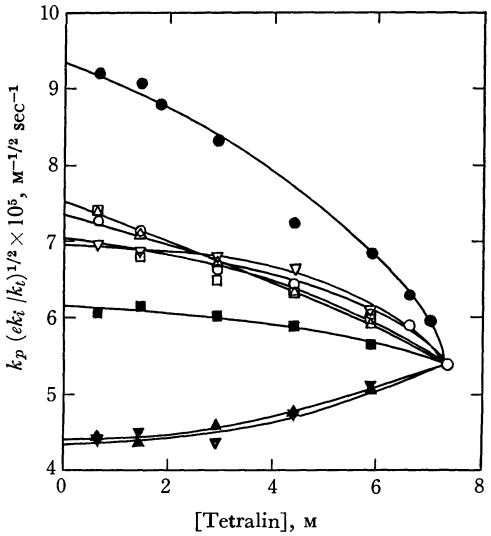

Fig. 1. Plots of $k_p(ek_i/k_t)^{1/2}$ as a function of tetralin concentration.
70°C, [AIBN]$=1.00\times10^{-2}$M
▲ *n*-Decane ▼ Butyl stearate
■ Butyric acid △ Anisole
○ Chlorobenzene □ Diethyl maleate
▽ Acetophenone ● Nitrobenzene

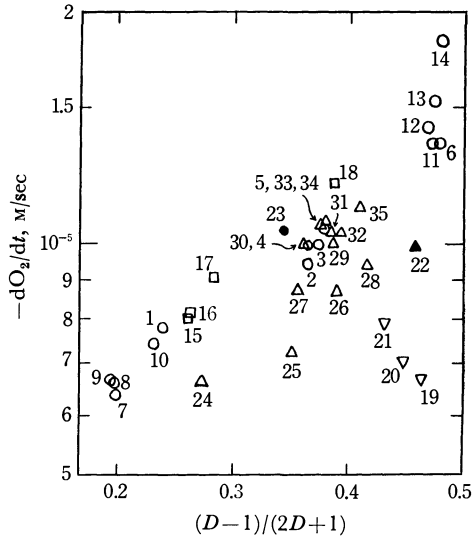

Fig. 3. Plots of the rates of oxidations of tetralin in various solvents as a function of dielectric function.
70°C, [AIBN]$=1.00\times10^{-2}$M, [tetralin]$=1.47$M
○ Hydrocarbon ▲ Ketone
□ Acid ● Ether
▽ Alcohol △ Ester

That the rates of oxidation of tetralin are dependent on the nature of the solvents is more clearly established by oxidation in the binary inert solvents media. The rates of oxidation of tetralin in the binary solvents are shown in Fig. 2. A deviation from linearity is again observed for each system, and it is interesting that the curves in nitrobenzene - *n*-decane and nitrobenzene - chlorobenzene systems are convex upward, while that in nitrobenzene-acetophenone system convex downward.

Data in literature and in this work indicate that the rate of oxidation of hydrocarbon increases, as a whole, with the increase in the dielectric constant of the medium. However, with regard to the correlation between the rate of oxidation and the dielectric function, $(D-1)/(2D+1)$, some are satisfactory but others are not. In Fig. 3 are shown the plots of the rates of oxidation of tetralin in Table 1 against the dielectric function of the solvents. Fugure 3 shows that the solvents evidently affect the rates of oxidation but the correlation predicted from Eq. (1) is not applicable.

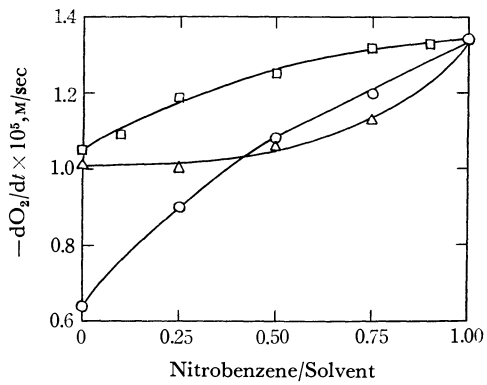

Fig. 2. Rates of oxidation of tetralin in binary solvents.
70°C, [AIBN]$=1.00\times10^{-2}$M, [tetralin]$=1.47$M
○ Nitrobenzene+*n*-decane
□ Nitrobenzene+chlorobenzene
△ Nitrobenzene+acetophenone

As shown in Eq. (2), the rate of oxidation is determined by k_p, k_t, e, and k_i at constant concentration of hydrocarbon and initiator. The solvent may affect some or, more probably, all of the above mentioned four constants. The kinetic data for the oxidation of 1.47M tetralin in the various solvents are summarized in Table 3 together with the physical properties of the media measured at 70°C.[14,15] As shown in Table 3, the values of $k_p(ek_i/k_t)^{1/2}$, $(ek_t)^{1/2}$, and $k_p/(2k_t)^{1/2}$ range from 4.35×10^{-5} to 9.12×10^{-5} $l^{1/2}$/mol$^{1/2}$/sec (by a factor of 2.1), from 3.46×10^{-3} to 5.31×10^{-3} sec$^{-1/2}$ (by a factor of 1.5), and from 7.73×10^{-3} to 1.23×10^{-2} $(l$/mol/sec$)^{1/2}$ (by a factor of 1.6), respectively. Thus, in the oxidation of tetralin initiated by AIBN, the solvents give an effect about as much in the initiation step as in the propagation and/or termination step. As discussed in the preceding paper,[15] the

14) E. Niki, Y. Kamiya and N. Ohta, This Bulletin, in contribution.

15) E. Niki, Y. Kamiya and N. Ohta, *ibid.*, in contribution.

Table 3. Oxidation of 1.47M tetralin in various solvents at 70°C, [AIBN]$=1.00\times10^{-2}$M

Solvent	D[b]	$\frac{(D-1)}{(2D+1)}$	η[c] centi-poise	d[d]	M[e]	$-dO_2/dt$ $\times10^5$ M/sec	$k_p(ek_i/k_t)^{1/2}$ $\times10^5$ $M^{-1/2}sec^{-1}$	k_i $\times10^5$ sec^{-1}	e	ek_i $\times10^5$ sec^{-1}	$(ek_i)^{1/2}$ $\times10^3$ $sec^{-1/2}$	$k_p/(2k_t)^{1/2}$ $\times10^3$ $(M\,sec)^{-1/2}$
n-Decane	2.069	0.208	0.5633	0.6921	142.3	0.639	4.35	3.05	0.518	1.58	3.98	7.73
Tetralin[a]	2.657	0.260	0.9869	0.9302	132.2	3.95	5.38	4.22	0.483	2.04	4.52	8.44
Butyl stearate	2.857	0.277	2.337	0.8189	340.6	0.664	4.52	3.67	0.327	1.20	3.46	9.29
Butyric acid	2.937	0.282	0.8232	0.9083	88.1	0.909	6.18	3.64	0.563	2.05	4.53	9.65
Anisole	3.651	0.319	0.6232	0.9470	108.1	1.04	7.07	3.89	0.656	2.55	5.05	9.93
Chlorobenzene	4.440	0.348	0.5568	1.0523	112.6	1.05	7.14	4.10	0.688	2.82	5.31	9.50
Diethyl maleate	5.811	0.381	1.211	1.0187	172.2	0.996	6.78	3.64	0.489	1.78	4.22	11.4
Acetophenone	11.21	0.436	0.8958	0.9853	120.1	1.01	6.87	4.41	0.569	2.51	5.01	9.72
Nitrobenzene	21.10	0.465	0.9694	1.1538	123.1	1.34	9.12	4.70	0.581	2.73	5.23	12.3

a) Pure tetralin.
b) Dielectric constant of the solution containing 20 vol% tetralin and 80 vol% solvent measured at 70°C.[14]
c) Viscosity of the solution measured at 70°C.[15]
d) Density of the pure solvent at 70°C.
e) Molecular weight of the solvent.

value of k_i was larger in the aromatic solvent than in the aliphatic solvent and that of e was dependent more on the viscosity of the solution rather than its polarity. But the solvent affected e more than k_i and the rate of initiation by AIBN was mainly dependent on the viscosity of the medium.

Before discussing the correlation between $\log(k_p/((2k_t)^{1/2})$ and $(D-1)/(2D+1)$, the error involved in the measurement should be examined. The rates of oxidation of tetralin in various solvents were fairly good in reproducibility. The largest negative and positive deviations from the lines in Fig. 1 are those for the oxidation of 4.41M tetralin in nitrobenzene and 0.668M tetralin in diethyl maleate, the deviations being about 6%. It may be said that the experimental error involved in most of the measurements is within 5%. On the other hand, the values of e and k_i were reproducible within an experimental error of 5%. The physical constants determined for the media may be more accurate. Thus we could say that the results obtained in this work are accurate within an experimental error of 5% and 10% for the worst.

Now we should like to discuss the correlation between $k_p/k_t^{1/2}$ and the dielectric function. If the solvent effects on the propagation and termination[16] steps may be attributed to the solvation of the solvents at the transition state and/or ground state as proposed by Hendry and Russell,[8] and Howard and Ingold,[9] and if both k_p and k_t are expressed in terms of the dielectric function, $(D-1)/(2D+1)$, as in Eq. (1), then logarithm of $k_p/k_t^{1/2}$ should be proportional to $(D-1)/(2D+1)$. In the meantime, tetralin acts not only as a reactant but also as a solvent. The solution has been regarded as a medium of uniform dielectric constant. However, this assumption is not valid when one of the solvents solvates more preferentially than the others. Such a preferential, or selective, solvation has been observed in some cases.[18] In this case, the bulk dielectric constant of the medium is not important, but the microscopic dielectric constant in the immediate vicinity of a reactant particle may be the more important factor in determining the extent of solvation. Although the bulk dielectric constant can be measured, the microscopic dielectric constant can not be measured easily, and the extent of the selective solvation is hard to evaluate from the

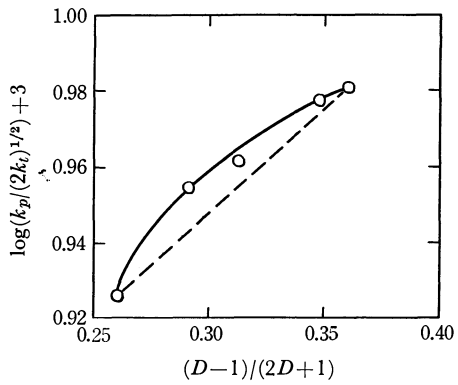

Fig. 4. Plots of $\log(k_p/(2k_t)^{1/2})$in the oxidation of tetralin in chlorobenzene against the dielectric function, 70°C.

16) It is known that the viscosity of the medium has significant effect on the bimolecular interaction of the tertiary peroxy radicals.[17] However, the bimolecular interaction of the tetralylperoxy radicals at 70°C may be all terminating and no free tetraloxy radical should be produced. Therefore, the viscosity of the solution may have little effect on the termination step in the oxidation of tetralin.

17) R. Hiatt and T. G. Traylor, *J. Am. Chem. Soc.*, **87**, 3766 (1965).

18) N. Tokura, *Yukigosei Kagaku Kyokaishi (J. Soc. Org. Synth. Chem. Japan)*, **25**, 1084 (1967).

conventional kinetic study. If the selective solvation does exist, then the plot of $\log(k_p/(2k_t)^{1/2})$ as a function of $(D-1)/(2D+1)$ should give a curve convex upward. In Fig. 4 is shown the plot of $\log(k_p/(2k_t)^{1/2})$ in the oxidation of tetralin in chlorobenzene, calculated from $k_p(ek_i/k_t)^{1/2}$ and ek_i measured for each mixture,[15] against the dielectric function calculated from the measured dielectric constants of the media at 70°C.[14] The curve is indeed convex upward, but the curvature is small and it is difficult to measure the extent of selective solvation. Although the problem of selective solvation is interesting and important itself, it complicates the situation and it is desirable to disregard the problem discussing the correlation between the rate constant and the dielectric function. One possible approach so as to reduce the effect of selective solvation may be the oxidation of the very dilute reactant in a large excess of solvent. However, the lower the concentration, the smaller the rate of oxidation and the shorter the kinetic chain length, and the radical produced from the initiator may also participate in the terminating reactions, complicating the over-all kinetics.[19] The most suitable method may be the extrapolation to the infinite dilution of the reactant by the solvent. In Fig. 5 is shown the plot of $\log(k_p/(2k_t)^{1/2})$, calculated from $k_p(ek_i/k_t)^{1/2}$ and ek_i extrapolated to the infinite dilution, against the dielectric function of the neat solvent at 70°C. A fairly good linear correlation between the two functions is observed, although $\log(k_p/(2k_t)^{1/2})$ for the aromatic solvents, especially for acetophenone, is somewhat smaller than expected.

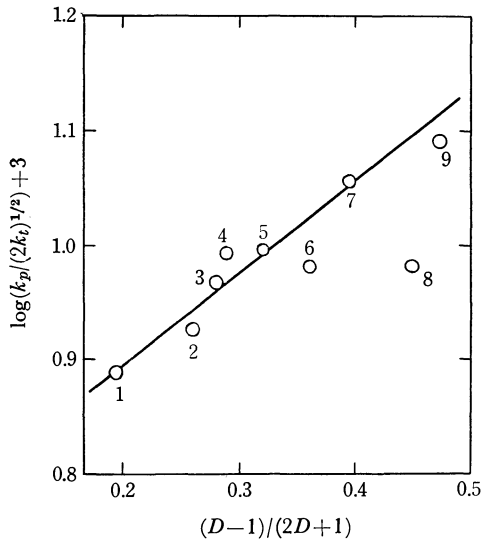

Fig. 5. Plots of $\log(k_p/(2k_t)^{1/2})$ at the infinite dilution as a function of the dielectric function.

1: *n*-Decane
2: Tetralin
3: Butyl stearate
4: Butyric acid
5: Anisole
6: Chlorobenzene
7: Diethyl maleate
8: Acetophenone
9: Nitrobenzene

Powling and Bernstein[20] introduced the function of $d(D-1)/M(2D+1)$, where d and M are density and molecular weight of the solvent respectively, on the study of the heats of tautomerization of several substances in a variety of solvents on the assumption that the radii of the reactants and the transition state are dependent on the molar volume of the solvent. The plot of $\log(k_p/(2k_t)^{1/2})$ at the infinite dilution against $d(D-1)/M(2D+1)$, however, gave a poorer correlation than that against $(D-1)/(2D+1)$.

In addition to the general dielectric effect some specific interactions between the solute and the solvent such as hydrogen bonding, π-complex and charge transfer complex formations may also participate, to some extent, in the solvent effects. It has been known that the peroxy radical forms hydrogen bonding with the hydroxy group such as water, acid and alcohol. Hendry and Russell[8] observed that the rates of oxidation of cyclohexene and cumene in acetic acid were smaller than anticipated, and they interpreted this as being due to the decrease in the reactivity of the hydrogen-bonded peroxy radical. In the present study, however, the rates of oxidation of tetralin in fatty acids were not small. This might be because although such a hydrogen bonding, if any, would decrease the rate of propagation, it would also decrease the rate of termination. Such a phenomenon was observed experimentally by Zaikov.[5] The formation of π-complex was observed for chlorine atom and alkoxy radical,[1] but this π-complexing may not be so important for the peroxy radical since the electron affinity of the peroxy radical may be smaller than chlorine atom and alkoxy radical.[21] In any event, if the peroxy radical forms complex with the solvent and desolvation is necessary for both propagation and termination steps, both k_p and k_t values are expected to decrease and the effect of complex formation on the over-all rate or on $k_p/(2k_t)^{1/2}$ may in part be cancelled.

In summary, in the oxidation of tetralin initiated

19) C. Gadelle and G. Clement, *Bull. Soc. Chim. France*, **1967**, 1175.

20) J. Powling and H. J. Bernstein, *J. Am. Chem. Soc.*, **73**, 1815, 4353 (1951).

21) The speculation that the π-complex formation between the tetralylperoxy radical and the aromatic solvents should give smaller values for $k_p/(2k_t)^{1/2}$ than expected in Fig. 5 may be ruled out. Because, if so, the decrease should be in the order, anisole>chlorobenzene>nitrobenzene>acetophenone, as predicted by the electron density at the aromatic ring. However, this is not the case as is clear from Fig. 5. This does not necessarily deny the π-complex formation of the peroxy radical, and the information on this complex formation may be obtained by studying the products distribution in the various solvents.

by AIBN the solvents affect approximately as much the initiation step as the propagation and/or termination step. The effects of solvents on the initiation step are mainly determined by the viscosity of the medium, while those on the propagation and/or termination step are mainly dependent on the dielectric constant of the medium.

Experimental

Materials used were the same as in the preceding papers.[14,15] All of the solvents were found to be oxidation resistant under the experimental conditions employed here. Oxidation was performed under atmospheric pressure of oxygen and the oxygen uptake was measured periodically in a constant pressure closed system. Satisfactory and reproducible straight line was obtained.

BULLETIN OF THE CHEMICAL SOCIETY OF JAPAN VOL. 42 3229—3233 (1969)

On the Oxidation of Guaiazulene*1,*2

Kazuko KOHARA

Kōnan Chemical Industry Co., Ltd., Nakagawachō, Takatsuki, Osaka

(Received March 26, 1969)

Guaiazulene was oxidized with potassium permanganate and with selenium dioxide according to the Treibs procedure. An acidic and a neutral crystalline compounds obtained from the permanganate oxidation in acetone were identified by means of UV, IR, and NMR spectrum measurements as 4-methyl-7-isopropylazulene-1-carboxylic acid and 1-formyl-4-methyl-7-isopropylazulene respectively. It was also confirmed that the selenium dioxide oxidation of guaiazulene in acetone gave 3-formylguaiazulene and 3,3′-diguaiazulenylacetone, the chemical structure of which had already been established by Treibs.

In 1957, Treibs[1] reported that guaiazulene (GA) was oxidized in acetone with pulverized potassium permanganate to yield small amounts of an acidic compound, A, and also that the oxidation with selenium dioxide gave compounds B and C. According to the results of the elemental analyses and the visible absorption spectrum measurements, he proposed the structural formula; 2,3-dihydroxyguaiazulene (I), 1-formyl-4-methyl-7-isopropylazulene (II), and 3,3′-diguaiazulenylacetone (III)[2] for the compounds A, B, and C respectively.

In the present work the oxidation of GA was carried out by Treibs procedure in order to prepare these three compounds as reference substances for the thin-layer chromatographic study of the photooxidation of GA.[3] By the selenium dioxide oxidation of GA, compounds B and C were obtained as has been described by Treibs;[1,2] in the case of permanganate oxidation, another neutral compound, D, was obtained together with an acidic compound,

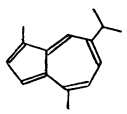

GA

$GuCH_2COCH_2Gu$
(Gu: 3-guaiazulenyl group)
III

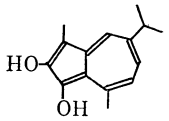

I

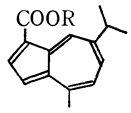

IV R: H
VI R: Me

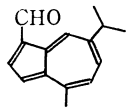

II

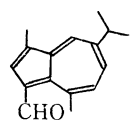

V

Fig. 1.

*1 Studies of the Azulenes. Part II. Part I: N. Sakota and K. Kohara, *Nippon Kagaku Zasshi (J. Chem. Soc. Japan, Pure Chem. Sect.)*, **86**, 747 (1965).

*2 Presented at 10th Symposium on the Chemistry of Terpenes, Essential Oils and Aromatics, Tokyo, 1966.

1) W. Treibs, *Ber.*, **90**, 761 (1957).

2) W. Treibs and R. Vogt, *ibid.*, **94**, 1739 (1961).

3) K. Kohara, Y. Otani and N. Sakota, Preprints for the 9th Symposium on the Chemistry of Terpenes, Essential Oils and Aromatics (Sendai, 1965), p. 147.

A. The present results of the IR and NMR spectra measurements of these compounds revealed that compounds A, B, and D should correspond to the structures 4-methyl-7-isopropylazulene-1-carboxylic acid (IV), 3-formylguaiazulene (V) and 1-formyl-4-methyl-7-isopropylazulene (II) respectively, and that compound C is III, as was determined by Treibs and Vogt.

Experimental

Measurements. The NMR data were obtained on a Japan Optics Lab. JNM-3H-60 spectrometer using tetramethylsilane as an internal standard. The infrared absorption spectra were recorded on a Shimadzu model IR-27 infrared spectrophotometer. The ultraviolet and visible absorption measurements were carried on a Jasco model ORD/UV-5 recording spectrophotometer.

The plates for thin-layer chromatography were prepared with silica gel G (Merck) and developed with ethyl acetate - *n*-hexane (15 : 85).

Oxidation of GA with Potassium Permanganate. To a solution of 10.0 g of GA in 1000 m*l* of acetone containing 60 m*l* of water, 25 g of powdered potassium permanganate were added in small portions at room temperature. The reaction mixture was then filtered to separate manganese dioxide. By evaporating off the acetone from the filtrate under reduced pressure, a blue, oily product was obtained.

Purification of 4-Methyl-7-isopropylazulene-1-carboxylic Acid (IV). The ether solution of the blue, oily product was extracted with a 2% sodium hydroxide solution, and the alkaline layer was then acidified with hydrochloric acid and extracted again with ether. The deep-red-colored ether extract was washed with a dilute sodium bicarbonate solution and then with water, and dried. The evaporation of ether gave 0.3 g of the acidic compound, A, as red needle crystals, mp 169°C. It was recrystallized from petroleum ether, mp 171°C, and was identified as IV, as will be shown later. Found: C, 78.03; H, 7.18%. Calcd for $C_{15}H_{16}O_2$: C, 78.92; H, 7.07%. Visible: λ_{max} 532, 565, 620 mμ. IR: 1628 cm^{-1} for C=O, 2550 cm^{-1} for O-H (Nujol). Tlc: R_f=0.15 (red).

Methyl 4-Methyl-7-isopropylazulene-1-carboxylate (VI). A tenth of a gram of IV was dissolved in 2 m*l* of anhydrous methanol containing a small amount of sodium. To this solution 0.4 g of methyl sulfate was added, drop by drop, under cooling with ice. The mixture was then poured into water and extracted with ether. The ether solution was dried on sodium sulfate and evaporated to give a red oil. The red oil was purified by chromatography through a silica gel column (Wako gel C-200) with ethyl acetate - *n*-hexane (15 : 85). Found: C, 78.99; H, 7.61%. Calcd for $C_{16}H_{18}O_2$: C, 79.31; H, 7.49%. Visible: λ_{max} 536, 574, 627 mμ. IR: 1692 cm^{-1} for C=O (CCl_4). Tlc: R_f=0.46 (red).

Isolation of 1-Formyl-4-methyl-7-isopropylazulene (II). A neutral oil obtained by the permanganate oxidation was chromatographed on silica gel. About 5.5 g of unreacted GA was eluted with petroleum ether, while several kinds of colored compounds (red, yellowish-green, blue, *etc.*) remained on the column. They could be eluted separately with ethyl acetate - *n*-hexane (15 : 85). A tenth of a gram of the red compound, D, which spotted at R_f=0.52 on a thin-layer was purified by repeated elution chromatography with ethyl acetate - *n*-hexane (15 : 85) on a silica-gel column. Thus, 0.05 g of dark red crystals, mp 60—61°C, was obtained. Found: C, 84.44 H, 7.67%. Calcd for $C_{15}H_{16}O$: C, 84.87; H, 7.60%. Visible: λ_{max} 535, 580 (shoulder), 630 mμ. IR: 1645 cm^{-1} for C=O, 2790, 2700 cm^{-1} for aldehydic C-H (CCl_4). Tlc: R_f=0.52 (red). 2,4-DNP, mp 265—266°C. Found: C, 64.49; H, 5.03; N, 14.20%. Calcd for $C_{21}H_{20}O_4N_4$: C, 64.27; H, 5.14; N, 14.28%.

Oxidation of GA with Selenium Dioxide. A solution of 7 g of SeO_2 in 50 m*l* of water was added, drop by drop, to a solution of 15 g of GA in 1000 m*l* of acetone under ice cooling; the mixture was allowed to stand for 24 hr at room temperature. Meanwhile, the solution changed green from blue. After the neutralization of the mixture with solid sodium carbonate, the solvent was distilled off and the residue was extracted with cyclohexane. A carbonyl compound, C, and a small quantity of an aldehyde, B, were obtained by repeated chromatography with benzene on a silica gel column. Only a small amount of GA was recovered at that time.

3-Formylguaiazulene (V). Compound B (0.1 g) was recrystallized from ethanol as brownish-red crystals, mp 84—86°C. Found: C, 85.14; H, 7.94%. Calcd for $C_{16}H_{18}O$: C, 84.92; H, 8.02%. Visible: λ_{max} 568 mμ IR: 1630 cm^{-1} for C=O, 2680 cm^{-1} for aldehydic C-H (CCl_4). Tlc: R_f=0.28 (brownish-red). 2,4-DNP, mp 181°C. Found: C, 64.82; H, 5.32; N, 13.88%. Calcd for $C_{22}H_{22}O_4N_4$: C, 65.01; H, 5.46; N, 13.79%.

3,3'-Diguaiazulenylacetone (III). Compound C (3.8 g) was recrystallized from *n*-hexane as blue needle crystals, mp 196°C. Found: C, 88.13; H, 8.32%. Calcd for $C_{33}H_{38}O$: C, 87.95; H, 8.50%. Visible: λ_{max} 622, 675 mμ. IR: 1705 cm^{-1} for C=O (Nujol). Tlc: R_f=0.59 (blue).

Results and Discussion

Structure of Acidic Compound A. Treibs[1] proposed the structure I for an acidic compound, A, in view of the position of the visible absorption maximum of compound A and the formation of guaiazulene dimethyl ether-2,3 (compound E) by treating compound A with methyl sulfate.

In the present work, however, a broad absorption of ν_{O-H} near 2550 cm^{-1} (Nujol) and an intense absorption of a hydrogen-bonded carbonyl at 1628 cm^{-1} were found in the infrared spectrum of compound A. Furthermore, the treatment of compound A with methyl sulfate led to the disappearance of the ν_{O-H} absorption and the shift of the $\nu_{C=O}$ absorption to a higher frequency in CCl_4. Moreover, compounds A and E were found to have the visible absorption maximum at 532 and 536 mμ in *n*-hexane respectively (Fig. 2). Hence, it was deduced that the acidic compound, A, should be a carboxylic acid and that compound E should be the methyl ester of compound A.

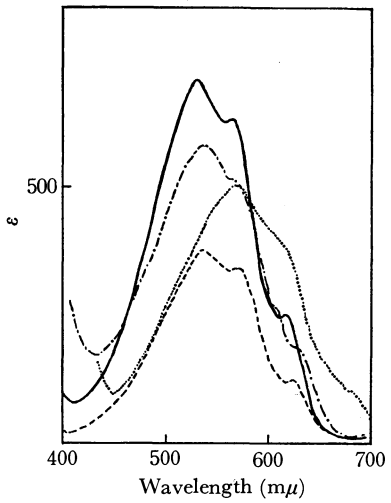

Fig. 2. The visible absorption spectra of compound A(IV)(——), B(V)(·····), D(II)(·-·-) and E(VI)(------) in *n*-hexane.

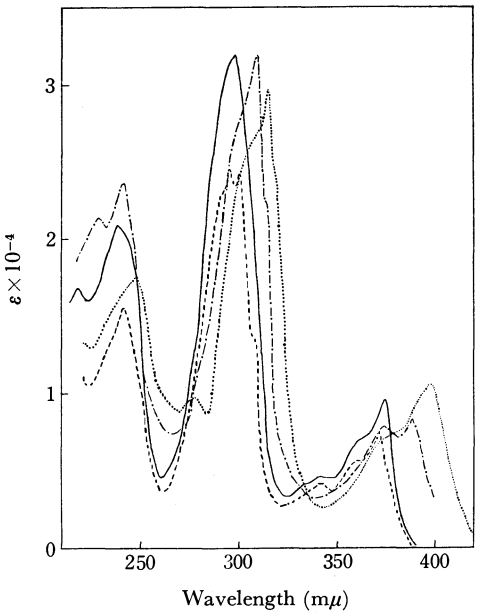

Fig. 3. The ultraviolet absorption spectra of compound A(IV)(——), B(V)(·····), D(II)(·-·-) and E(VI)(------) in *n*-hexane.

The NMR spectra of compounds A and E are shown in Fig. 4. In comparison with the assignment of the NMR spectrum of GA, which had already been reported,[4] it was found that the signal corresponding to one of the two methyl groups of GA disappeared in the spectrum of compound A and that the two signals due to ring protons, H_2 and H_8, shifted considerably to a lower magnetic field compared with those of GA. Those results have lead the present author to conclude that the methyl group in the 1-position was oxidized to a carboxyl group. The signals of ring protons can be assigned as is shown in Fig. 4-a. As the signal at 7.14 ppm, which was not assigned to the ring proton, remains unchanged upon deuterium exchange, it may be assigned to the peak of a proton of $CHCl_3$ in the solvent $CDCl_3$. The signal to be assigned to an acidic proton was not found in Fig. 4-a; this is presumably because of the disappearance of the signal by shifting to a lower magnetic field or by a spectral broadening of the peak. The NMR spectrum of compound E indicated the

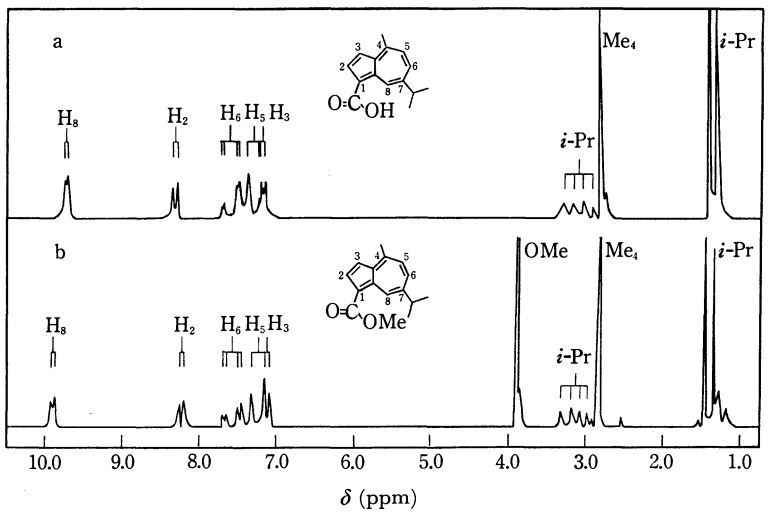

Fig. 4. The NMR spectra of two compounds at 60 Mc.
a, compound A in $CDCl_3$. b, compound E in CCl_4.

4) D. Meuche, B. B. Molloy, D. H. Reid and E. Heilbronner, *Helv. Chim. Acta*, **46**, 2483 (1963).

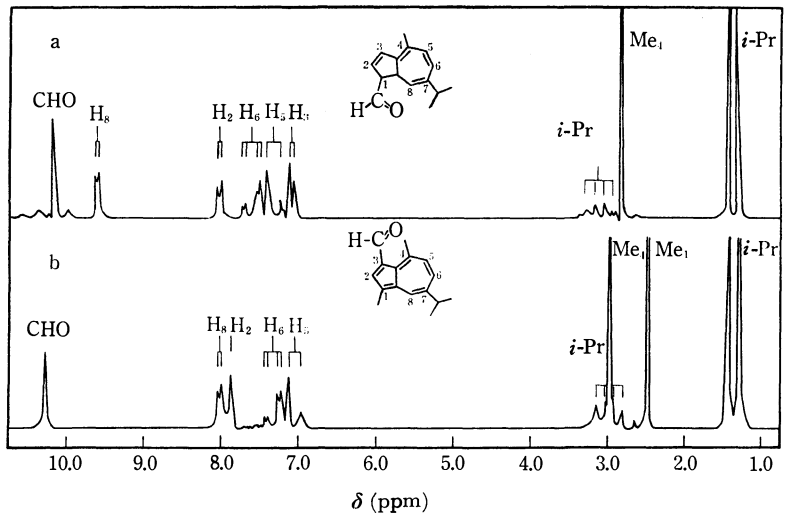

Fig. 5. The NMR spectra of azulene aldehydes at 60 Mc.
a, compound D in CCl_4. b, compound B in CCl_4.

presence of an ester methyl (3.89 ppm), a ring methyl (2.84 ppm), and five ring protons which are in just the same positions as those of the carboxylic acid, A. Besides, the chemical shifts of the ester methyl and ring protons (H_2 and H_3) in compound E are in good agreement with those of the methyl 4-methylazulene-1-carboxylate isolated by Meuche *et al.*[5] from natural Moose. From the results above mentioned, it may be deduced that the structures of compounds A and E should correspond to 4-methyl-7-isopropylazulene-1-carboxylic acid (IV) and methyl 4-methyl-7-isopropylazulene-1-carboxylate (VI) respectively. The absorption maxima in the visible region of these compounds satisfy the Plattner rule.[6]

Structure of Compound D. The dark red crystal (mp 60—61°C) obtained from a neutral portion of the reaction mixture in the permanganate oxidation is a new substance which had not been isolated by Treibs or by others. The visible absorption spectrum of compound D showed a maximum at 535 mμ, which shifted by 70 mμ to a shorter wavelength as compared with that of GA at 605 mμ. The UV spectrum of compound D (Fig. 3) showed a maximum at 390 mμ corresponding to carbonyl. The infrared spectrum of compound D also indicates a strong $\nu_{C=O}$ absorption at 1645 cm^{-1} and ν_{C-H} (aldehydic) absorptions at 2790 and 2700 cm^{-1} (CCl_4). In the NMR spectrum of compound D (Fig. 5-a), a methyl proton signal in the 1-position of GA vanished and an aldehydic proton[7,8] appeared at 10.12 ppm. The ring protons are assigned as indicated in the figure from the coupling constants. From these results, it may be concluded that compound D is 1-formyl-4-methyl-7-isopropylazulene (II). It has also been clarified by thin-layer chromatography that this aldehyde is gradually oxidized in CCl_4 to give a carboxylic acid (IV). This structure is also supported by the fact that the absorption maxima of the compound D at 535, 580, and 630 mμ are closely similar to those of lactaroviolin[9—12] at 538, 577, and 633 mμ.

Structure of Compound B. Treibs has reported that an aldehyde, mp 88.5—89.5°C, obtained by the selenium dioxide oxidation of GA corresponds to formula II. As is shown in Fig. 5-b, however, the NMR spectrum of this aldehyde, mp 84—86°C, obtained by the present author showed that two methyl groups and one isopropyl group remained as they were in GA. An aldehydic proton signal[7,8] was found at 10.34 ppm. The formyl group should be situated in the 3-position of the azulene ring, since four ring protons were assigned to H_2, H_5, H_6, and H_8, as is indicated in Fig. 5-b. The R_f value of tlc and the UV, visible, IR, and NMR spectra of compound B were in good agreement with those of 3-formylguaiazulene obtained by means of the formylation of GA,[13] and

5) D. Meuche and S. Huneck, *Ber.*, **99**, 2669 (1966).
6) E. Heilbronner, "Non-Benzenoid Aromatic Compounds," ed. by D. Ginsburg, Interscience, New York (1959), p. 171.
7) D. Meuche, D. Dreyer, K. Hafner and E. Heilbronner, *Helv. Chim. Acta*, **50**, 1178 (1967).
8) A. J. Fry, B. W. Bowen and P. A. Leermakers, *J. Org. Chem.*, **32**, 1970 (1967).
9) H. Willstaedt, *Ber.*, **68**, 333 (1935).
10) P. Karrer, H. Ruckstuhl and E. Zbinden, *Helv. Chim. Acta*, **28**, 1177 (1945).
11) E. Heilbronner and R. W. Schmidt, *ibid.*, **37**, 2018 (1954).
12) K. Hafner and C. Bernhard, *Angew. Chem.*, **69**, 533 (1957).
13) K. Hafner and C. Bernhard, *Ann.*, **625**, 108 (1959).

the melting point of compound B was not depressed when it was mixed with the latter. From these results, it may be concluded that the aldehyde B is not II but 3-formylguaiazulene (V).

The author wishes to thank Professor Naokazu Sakota of Ehime University for the valuable advice he has given throughout this study and Dr. Akio Ishizawa of Kyoto University for his measurements of the NMR spectra.

BULLETIN OF THE CHEMICAL SOCIETY OF JAPAN VOL. 42 3233—3237 (1969)

The Reaction of Carbon Suboxide with Alicyclic Diketones and with Phenols. Formation and Structure of Pyrone Derivatives

Akira Omori, Noboru Sonoda, Yuzo Uchida and Shigeru Tsutsumi

Department of Chemical Technology, Faculty of Engineering, Osaka University, Suita, Osaka

(Received April 7, 1969)

The reactions of carbon suboxide with alicyclic diketones and with phenols were found to give various pyrone derivatives. From the reaction of 5,5-dimethyl-1,3-cyclohexanedione, 4-hydroxy-7,7-dimethyl-5,6,7,8-tetrahydro-2*H*-benzo[*b*]pyran-2,5-dione (II) was produced in the presence of a sulfuric acid catalyst. However, the reaction with 1,2-cyclohexanedione gave the malonic acid diester (III), and the formation of corresponding pyrone was not observed. The reaction of phenols with carbon suboxide gave only esters of malonic acid in the presence of the sulfuric acid catalyst, whereas cyclization to coumarin derivatives occurred on the presence of aluminum trichloride, in addition to the formation of the esters. The structure of the pyrone derivatives and the possible reaction mechanism were discussed.

The reaction of carbonyl compounds with carbon suboxide has been reported by several workers.[1-3] The reaction between carbon suboxide and benzaldehyde was reported to give the benzalmalonic acid benzylidenester,[1] whereas the reaction of carbon suboxide with some ketones produced dipyrone derivatives.[2,3]

In a recent publication,[4] we have reported the reaction of carbon suboxide with acetylacetone in the presence of a sulfuric acid catalyst to produce 3-acetyl-6-hydroxy-2-methyl-4-pyrone (I), (1) while the reaction with aliphatic-1,3-diketones affords dipyrone derivatives.

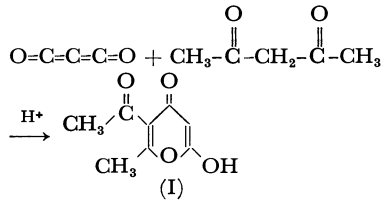

(1)

(I)

In the present paper, we wish to report on the reaction for the formation of various pyrone derivatives by the reaction of carbon suboxide with alicyclic diketones and with phenols, which have an enol functional group(>C=C(OH)–) in their molecular structure.

Results and Discussion

Reaction of Cyclohexanedione Derivatives. Pyrone (II) was prepared in a 44% yield by the reaction of carbon suboxide with 5,5-dimethyl-1,3-cyclohexanedione at 0—5°C in the presence of a catalytic amount of sulfuric acid (2). However, by the reaction with 1,2-cyclohexanedione, only the malonic acid diester (III) was isolated in a 41% yield under similar conditions (3). In the reaction of 1,4-cyclohexanedione, the dione was recovered almost completely.

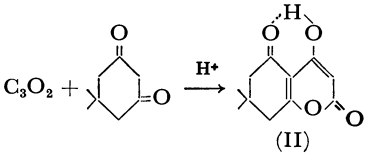

(2)

(II)

1) H. Hopff and G. Hegar, *Helv. Chim. Acta*, **44**, 2016 (1961).
2) E. Ziegler and H. Bieman, *Monatsh. Chem.*, **93**, 34 (1962).
3) F. Haadetzky and E. Ziegler, *Monatsh. Chem.*, **97**, 398 (1966).
4) A. Omori, N. Sonoda, S. Okano and S. Tsutsumi, *Tetrahedron Letters*, **1968**, 3647.

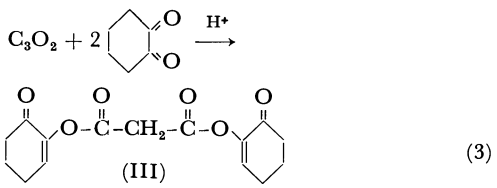

(3)

The pyrone structure of II was confirmed by a study of infrared, ultraviolet, and NMR spectra. The ultraviolet spectrum of II showed two bands, at 232 mμ (log ε, 4.27) and 270 mμ (log ε, 4.13), which were closely similar to those of 5-acetyl-4-hydroxy-6-methyl-2-pyrone (Ia) [225 mμ (log ε, 4.00) and 261 mμ (log ε, 3.91)],[4] characteristic absorptions of the pyrone ring. The infrared spectrum of II in both KBr and a chloroform solution showed a band at 3000 cm^{-1} which suggested the presence of hydrogen bonding, and one at 1742 cm^{-1} due to the carbonyl stretch of α-pyrone. However, the infrared spectrum[4] of I in KBr showed bands at 2600 cm^{-1} (strong hydrogen-bonded ν-OH) and at 1660 cm^{-1} (νC=O of γ-pyrone), but in a chloroform solution they were at 3000 cm^{-1} (hydrogen-bonded ν-OH) and 1739 cm^{-1} (νC=O of α-pyrone). Therefore, I is considered to have a γ-pyrone structure (I) in the solid phase and α-pyrone structure (Ia) in the liquid phase.

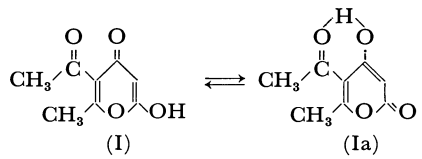

Additionally, the hydroxy proton shifts of the NMR spectrum of II in a deuteriochloroform solution were independent of the concentration, as is shown in Table 1.

Table 1. Influence of concentrtion on OH shifts*

Concentration	τ Value of OH-proton
1.1%	−1.58
2.5	−1.60
4.5	−1.62

* In $CDCl_3$ Solution at 25°C.

In contrast with the pyrone (I) from acetylacetone, this evidence suggested the α-pyrone structure for the pyrone (II), which had a strong intramolecular hydrogen bond, in both the solid phase and the liquid phase. The structure of III was established by analyses of the infrared, ultraviolet, and NMR spectra. The ultraviolet spectrum of III showed bands at 230 mμ (log ε, 4.27) and 304 mμ (log ε, 2.57) which were similar to the characteristic absorption bands reported for α,β-unsaturated ketone. The infrared and NMR spectra were consistent with those of the malonic acid diester (III).

Two pathways for the formation of the pyrone (II) may be worthy of consideration. The first of these may be C-acylation of the enol of dione with protonated carbon suboxide; the alternative pathway may involve the O-acylation as the initial step (Scheme I). However, in the case of 1,2-cyclohexanedione, the formation of the diester(III) of malonic acid indicates that O-acylation occurred preferentially (Scheme II). Therefore, in the case of 1,3-cyclohexanedione, the reaction path may also include O-acylation mainly rather than C-acylation.

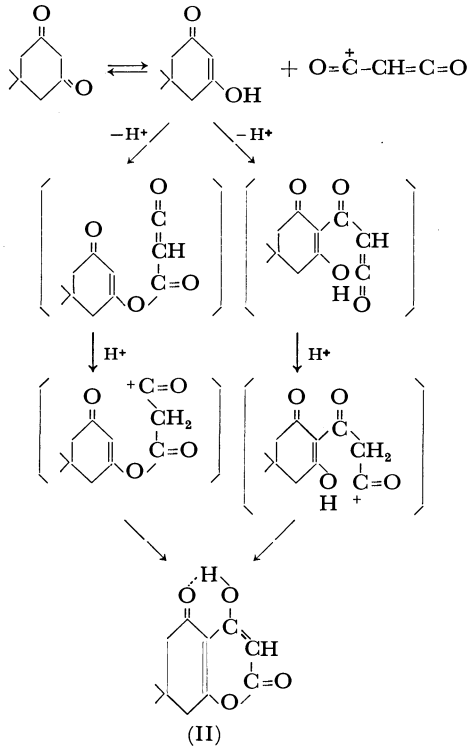

Scheme I

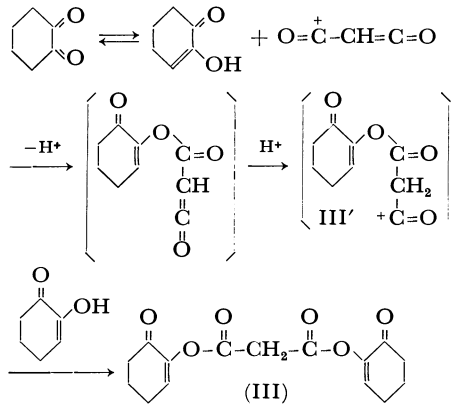

Scheme II

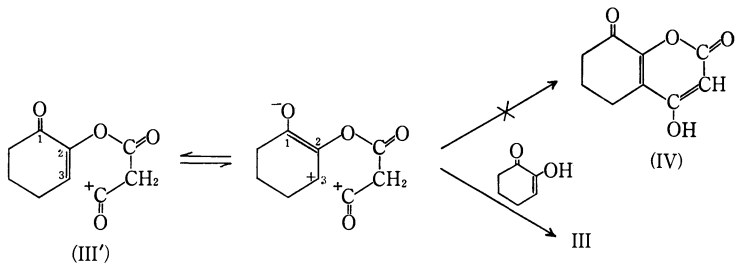

(4)

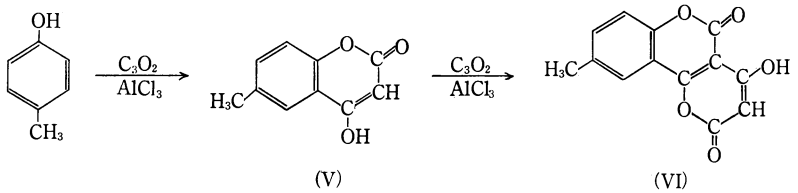

(5)

To account for the formation of pyrone(II), a reaction process is proposed which involves an electrophilic attack on the C-2 position by the acyl cation (Scheme I). In the case of the reaction with 1,2-dione, the presence of an electron-withdrawing carbonyl group at the C-1 position in the intermediate (III′) would deactivate the C-3 position toward electrophilic attack (4); consequently, the cyclization to pyrone (IV) is not likely.

Reaction of Phenols. The reaction of carbon suboxide with phenols in the presence of a sulfuric acid catalyst gave only diphenyl malonate derivatives, and no cyclization to coumarin derivatives was observed. However, it was confirmed that, in the presence of aluminum trichloride, the reaction of phenols produced coumarins to some extent at low temperatures. In the case of *p*-cresol, 4-hydroxy-6-methyl-coumarin (V) was obtained in an 8.5% yield in tetrachloroethane plus traces of 4-hydroxy-9-methyl-2*H*,5*H*-pyrano[3,2-*c*]benzo[*b*]-pyran-2,5-dione (VI) and di-*p*-tolyl malonate (5).

The structure of V and VI was confirmed by comparison with an authentic sample or by analyses of the infrared and ultraviolet spectral data. The ultraviolet spectrum of VI showed two bands, at 261 mμ (log ε, 4.16) and 351 mμ (log ε, 4.02), which were closely similar to those reported for 4-hydroxy-7-methyl-2*H*,5*H*-pyrano[3,2-*c*]pyran-2,5-dione[4] [270 mμ (log ε, 3.81) and 330 mμ (log ε, 3.76)], while the infrared spectrum of VI showed bands at 3150 cm^{-1} (-OH), 1745, 1695 cm^{-1} (C=O of lactone, and 1520 cm^{-1} (C=C of dipyrone).

m-Cresol reacted with carbon suboxide to give two isomers, 4-hydroxy-7-methyl-coumarin (VII) and 4-hydroxy-5-methyl-coumarin (VIII); the ratio of the two isomers was determined by the ultraviolet spectrum analysis. The results obtained by the reaction of phenols are shown in Table 2.

The table shows that tetrachloroethane is a better solvent than nitrobenzene for the formation of 4-hydroxy-coumarins. The reaction process for the formation of 4-hydroxy-coumarins may include cyclization to 4-hydroxy-coumarins through an intermediate (A); the further reaction of 4-hydroxy-coumarins with carbon suboxide yielded the pyrono-coumarins (Scheme III).

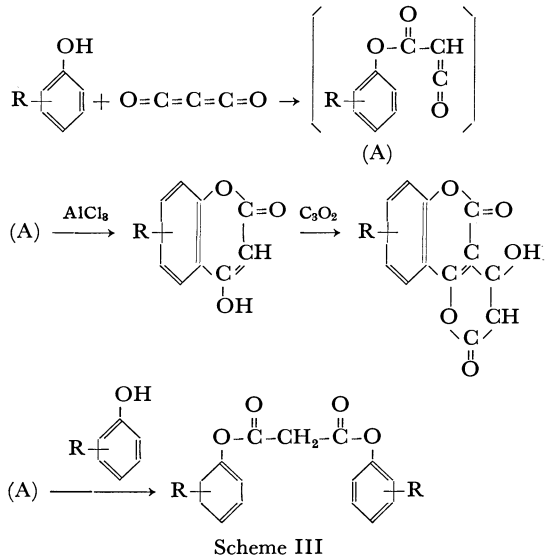

Scheme III

Experimental

Preparation of Carbon Suboxide. Carbon suboxide was prepared by the pyrolysis[5] of diacetyltartaric anhydride at about 700°C; it was trapped at −78°C in a bath of dry ice-methanol and purified by distillation from trap to trap. The identification of carbon suboxide was established by the preparation of malonanilide by the reaction of carbon suboxide with aniline.

4-Hydroxy-7,7-dimethyl-5,6,7,8-tetrahydro-2*H*-benzo[*b*]pyran-2,5-dione (II). To a solution of carbon suboxide (1.65 g, 0.024 mol) in dry ether (60 m*l*)

5) E. Ott, *Ber.*, **47**, 2388 (1914).

Table 2

Reactant	Solvent	Product (Yield* %) Coumarin	Product (Yield* %) Diester
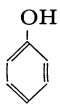	$CHCl_2CHCl_2$	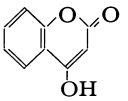 0.2	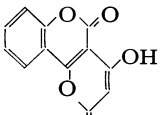 0.9	28
	$C_6H_5NO_2$		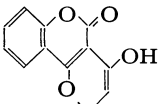 0.7	36
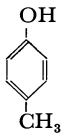	$CHCl_2CHCl_2$	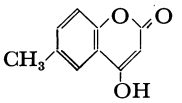 8.4	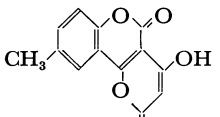 0.5	16
	$C_6H_5NO_2$		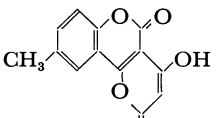 0.5	31
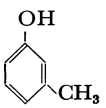	$CHCl_2CHCl_2$	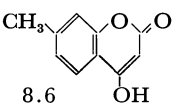 8.6 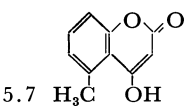 5.7	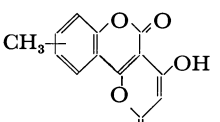 0.5	34
	$C_6H_5NO_2$	———		35
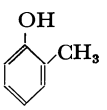	$CHCl_2CHCl_2$	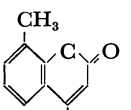 8.6	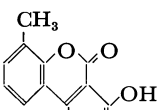 0.2	18
	$C_6H_5NO_2$	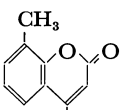 3.0 1.1	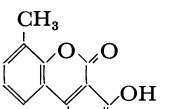 1.1	22

* The yield was based on used phenol or cresol.

and THF (75 m*l*), 5,5-dimethyl-1,3-cyclohexanedione (3.75 g, 0.024 mol) and conc. sulfuric acid (0.02 m*l*) were added at −78°C. The reaction mixture was maintained at 0—5°C for 7 days. The solids (2.4 g, 44%) were then separated on a filter; subsequent recrystallization from ethyl acetate gave the compound II; mp 138—139°C; ν_{max} (KBr and $CHCl_3$) 3000 (broad ν-OH), 1742 (C=O), 1670 (C=O), 1570 (C=C) cm^{-1}; λ_{max}^{EtOH} 232 (log ε, 4.27), 270 (log ε, 4.13) mμ: NMR ($CDCl_3$) τ 8.81 (s, 6H, $-CH_3$), 7.52 (s, 2H, $-CH_2-$), 7.28 (s, 2H, $-CH_2-$), 4.49 (s, H, >C=CH-); enolic -OH group (by $FeCl_3$ test). Found: C, 63.66; H, 5.90%; mol wt ($CHCl_3$ osmotic method), 203. Calcd for $C_{11}H_{12}O_4$: C, 63.45; H, 5.81; mol wt, 208.2.

Bis(6-oxo-1-cyclohexenyl) Malonate (III). To a solution of carbon suboxide (1.2 g, 0.018 mol) in dry ether (100 m*l*), 1,2-cyclohexanedione (4.2 g, 0.038 mol) and conc. sulfuric acid (0.05 m*l* were added at −78°C. The reaction mixture was maintained at 25°C for 1 day. The solids (2.1 g, 41%) were then separated on

a filter; subsequent recrystallization from ethanol gave the compound II; mp 80—81°C; ν_{max}^{KBr} 1760 (C=O), 1685 (C=O), 1650 (C=C) cm^{-1}; λ_{max}^{EtOH} 230 (log ε, 4.27), 304 (log ε, 2.57) mμ; NMR ($CDCl_3$) τ 7.9 (m, 4H, $-CH_2-$), 7.5 (m, 8H, $-CH_2-$), 6.3 (s, 2H, $-\overset{O}{\overset{\|}{C}}-CH_2-\overset{O}{\overset{\|}{C}}-$), 3.4 (t, 2H, $-CH=C\langle$). Found: C, 62.40; H, 5.34%; mol wt (benzene cryoscopic method), 298. Calcd for $C_{15}H_{16}O_6$: C, 61.64; H, 5.52%; mol wt, 292.

4-Hydroxy-coumarin and 4-Hydroxy-2*H*,5*H*-pyrano[3,2-*c*]benzo[*b*]-pyran-2,5-dione. To a solution of phenol (6.1 g, 0.06 mol) in tetrachloroethane (130 m*l*) we added a solution of carbon suboxide (4.4 g, 0.06 mol) in carbon disulfide (20 m*l*) at −44°C under nitrogen; then a solution of $AlCl_3$ (17.3 g, 0.12 mol) in tetrachloroethane (140 m*l*) was stirred into this reaction mixture drop by drop over a period of 2 hr. The reaction mixture was maintained at −44——30°C for 9 hr, at 0°C for 10 hr, and at 25°C for 12 hr, and was then poured into ice water. A solid thus deposited was extracted with a saturated sodium bicarbonate solution, and the solution was acidified. From the non-soluble materials thus separated were isolated ethanol-soluble crystals and non-soluble crystals. The recrystallization of the former from ethanol gave 4-hydroxy-coumarin (0.02 g, 0.2%); mp 203—205°C. From ethanol-non-soluble crystals, 4-hydroxy-2*H*,5*H*-pyrano[3,2-*c*]benzo-[*b*]pyran-2,5-dione (0.13 g, 0.9%) was isolated by crystallization from acetone; mp 241—243°C (decomp.); ν_{max}^{KBr} 3250 (-OH), 1750 (C=O), 1695 (C=O), 1550 (C=C) cm^{-1}; λ_{max}^{EtOH} 260.5 (log ε, 4.19), 339 (log ε, 4.03) mμ; enolic -OH group (by $FeCl_3$ test). Found: C, 62.52; H, 2.71%. Calcd for $C_{12}H_6O_5$: C, 62.62; H, 2.63%. From the tetrachloroethane layer, diphenyl malonate (164—168°C/3.5 mmHg) was obtained; yield 2.3 g (28%).

4-Hydroxy-6-methyl-coumarin (V) and 4-Hydroxy-9-methyl-2*H*,5*H*-pyrano[3,2-*c*]benzo[*b*]pyran-2,5-dione (VI). To a solution of *p*-cresol (8.7 g, 0.08 mol) in tetrachloroethane (150 m*l*) there was added a solution of carbon suboxide (5.5 g, 0.08 mol) in carbon disulfide (20 m*l*) at −44°C under nitrogen; a solution of $AlCl_3$ (21.6 g, 0.16 mol) in tetrachloroethane (130 m*l*) was then stirred into this reaction mixture drop by drop over a period of 2 hr. By treating the reaction mixture as has been described above for the case of phenol, 4-hydroxy-6-methyl-coumarin (V) (1.2 g, 8.4%; mp 247—249°C) and VI (0.1 g, 0.5%; mp 241—243°C (decomp.)) were obtained; ν_{max}^{KBr} 3160 (OH), 1740 (C=O), 1695 (C=O), 1570 (C=C) cm^{-1}; λ_{max}^{EtOH} 261(log ε, 4.16), 351 (log ε, 4.02) mμ. Found: C, 63.90; H, 3.25%. Calcd for $C_{13}H_8O_5$: C, 63.94; H, 3.30%. From a similar organic layer, 1.87 g (16%) of di-*p*-tolyl malonate (181—185°C/3.0 mmHg) was obtained.

4-Hydroxy-8-methyl-coumarin and 4-Hydroxy-7-methyl-2*H*,5*H*-pyrano[3,2-*c*]benzo[*b*]pyran-2,5-dione. To a solution of *o*-cresol (7.0 g, 0.06 mol) in tetrachloroethane (150 m*l*) there was a solution of carbon suboxide (4.4 g, 0.06 mol)in carbon disulfide (20 m*l*) at −44°C under nitrogen; then a solution of $AlCl_3$ (17.3 g, 0.12 mol) in tetrachloroethane (130 m*l*) was stirred into this reaction mixture drop by drop over a period of 2 hr. By treating the reaction mixture as has been described above for the case of phenol, 4-hydroxy-8-methyl-coumarin (0.98 g, 8.6%; mp 231—233°C) and 4-hydroxy-7-methyl-2*H*,5*H*-pyrano[3,2-*c*]-benzo[*b*]pyran-2,5-dione (0.04 g, 0.2%; mp 229—231°C) were obtained; ν_{max}^{KBr} 3220 (-OH), 1740 (C=O), 1715 (C=O), 1570 (C=C) cm^{-1}; λ_{max}^{EtOH} 264 (log ε, 4.23), 348 (log ε, 4.05); Found: C, 64.46; H, 3.19%. Calcd for $C_{13}H_8O_5$: C, 63.94; H, 3.30%. From a similar organic layer, 1.66 g (18%) of di-*o*-tolyl malonate (180—190°C/4.5 mmHg) were obtained.

4-Hydroxy-7-methyl-coumarin (VII) and 4-Hydroxy-5-methyl coumarin (VIII) and 4-Hydroxy-8-methyl- or 4-Hydroxy-10-methyl-2*H*,5*H*-pyrano-[3,2-*c*]benzo[*b*]pyran-2,5-dione (IX). To a solution of *m*-cresol (8.7 g, 0.08 mol) in tetrachloroethane (150 m*l*) there was added a solution of carbon suboxide (5.5 g, 0.08 mol) in carbon disulfide (20 m*l*) at −44°C under nitrogen; then a solution of $AlCl_3$ (21.6 g, 0.16 mol) in tetrachloroethane (170 m*l*) was stirred into this reaction mixture drop by drop over a period of 2 hr. By treating the reaction mixture as has been described above for phenol, VII (1.2 g, 8.6%; mp 214—216°C) and VIII (0.8 g, 5.7%; mp 221—223°C) were obtained. The ratio of the two isomers was determined by the UV spectrum analysis. IX (0.1 g, 0.5%.) was obtained in addition to the two isomers; mp 218—220°C; ν_{max}^{KBr} 3090 (-OH), 1755 (C=O), 1690 (C=O), 1565 (C=C)cm^{-1}; λ_{max}^{EtOH} 266 (log ε, 4.15), 339 (log ε, 4.10) mμ. Found: C, 64.22; H, 3.33%. Calcd for $C_{13}H_8O_5$: C, 63.94; H, 3.30%. From a similar organic layer, 3.91 g (34%) of di-*m*-tolyl malonate (180°C/4.0 mmHg) were obtained.

BULLETIN OF THE CHEMICAL SOCIETY OF JAPAN VOL. 42 3238—3242 (1969)

Characterization and Some Reactions of Peroxy-*trans*-crotonic Acid[1a)]

Ryo Yoshizawa and Takashi Inukai[1b)]

The Central Research Laboratories, Chisso Corporation, Kamariya, Kanazawa-ku, Yokohama

(Received April 14, 1969)

Peroxy-*trans*-crotonic acid was prepared from dicrotonyl peroxide by alkaline cleavage and isolated for the first time in a crystalline state, mp 41—42°C. It was characterized by NMR and IR spectra, and its stability briefly tested. Reaction with dimethyl sulfide gave a quantitative yield of crotonic acid. Its pK_a in water at 25°C was 8.2. Second order rate constants of reaction with crotonaldehyde in benzene (Table 4) were measured: E_a, 13.3 kcal/mol; log A(l/mol sec), 5.3; $\Delta S^{\neq}$, −36 eu/mol. Detection of a possible intermediate, a peracid-aldehyde complex X, was attempted by means of NMR but evidence for it was not obtained.

Peroxycrotonic acid, first prepared by Fichter and Rosenzweig[2)] in an impure liquid form, has remained unidentified, although it has been reasonably assumed to be identical with, and appeared in chemical literature as, the peroxidic intermediate of vapor phase[3)] and liquid phase[4)] autoxidation of crotonaldehyde. Recently some infrared absorption bands were ascribed to the peroxycrotonic acid that was believed to be formed transiently in the course of autoxidation of crotonaldehyde.[5)]

We wish to describe the preparation, characterization, and some reactions of peroxy-*trans*-crotonic acid.

Results and Discussion

Peroxycrotonic acid was prepared from dicrotonyl peroxide by cleavage with sodium methoxide. It is necessary to handle the alkaline solution of the peracid quickly and in the cold, as in the preparation of peroxybenzoic acid,[6,7)] in order to get satisfactory results. Peroxycrotonic acid forms colorless needle crystals which melt at 41—42°C with slow decomposition and flash vividly in free flames. The crystals are stable against fairly strong mechanical shock. In crystalline state the peracid could be stored for longer than one year at −70°C without appreciable deterioration, while at 0—5°C the loss of peroxidic oxygen amounted to 0.5, 4.9, and 14% after periods of 38, 55, and 82 days, respectively. In benzene solution (0.45M) at 30°C the decrease of the iodometric titre was about 1.7% per day in the first week, indicating that its stability is greater[8)] than that of peroxybenzoic acid[7)] under the same conditions.

Table 1. NMR Parameters of crotonic acid derivatives

$CH_3(c)\diagdown \quad \diagup H(a)$
$\quad\quad C=C$
$H(b)\diagup \quad \diagdown COO-$

	Peroxycrotonic acid[a)]	Dicrotonyl peroxide[a)]	Crotonic acid[b)]
τ_a	4.15	4.13	4.17
τ_b	2.88	2.89	2.90
τ_c	8.03	8.03	8.10
τ_d[c)]	−0.67	—	−2.18
J_{ab}	16 cps	15.5 cps	15.5 cps
J_{bc}	7	7	7
J_{ac}	1.5	1.6	1.6

a) 10 wt % solution in carbon tetrachloride containing tetramethylsilane as internal standard.
b) In $CDCl_3$, quoted from Varian NMR Spectra Catalog, Varian Associates, Palo Alto, Calif., 1962, Spectrum No. 61.
c) The chemical shift of acidic protons.

1) a) Peroxyacid. I. Presented in part at the 21st Annual Meeting of the Chemical Society of Japan, Suita, Osaka, April 1968; Abstract, p. 1630. b) To whom inquiries should be addressed.

2) F. Fichter and J. Rosenzweig, *Helv. Chim. Acta*, **18**, 238 (1935).

3) J. Cartlidge and C. F. Tipper, *Anal. Chim. Acta*, **22**, 106 (1960).

4) Kirk-Othmer, "Encyclopedia of Chemical Technology," Vol. 6, 2nd ed., Interscience Publishers, New York, N. Y. (1965), p. 466.

5) X. Deglise and J. Lemaire, *J. Chim. Phys.*, **64**, 1768 (1967).

6) G. Braun, "Organic Syntheses," Coll. Vol. I, 2nd Ed., p. 431 (1948).

7) I. M. Kolthoff, T. S. Lee and M. A. Mairs, *J. Polymer Sci.*, **2**, 199 (1947).

8) The comparison is only tentative since peracid stability is easily influenced by contamination of metallic impurities.

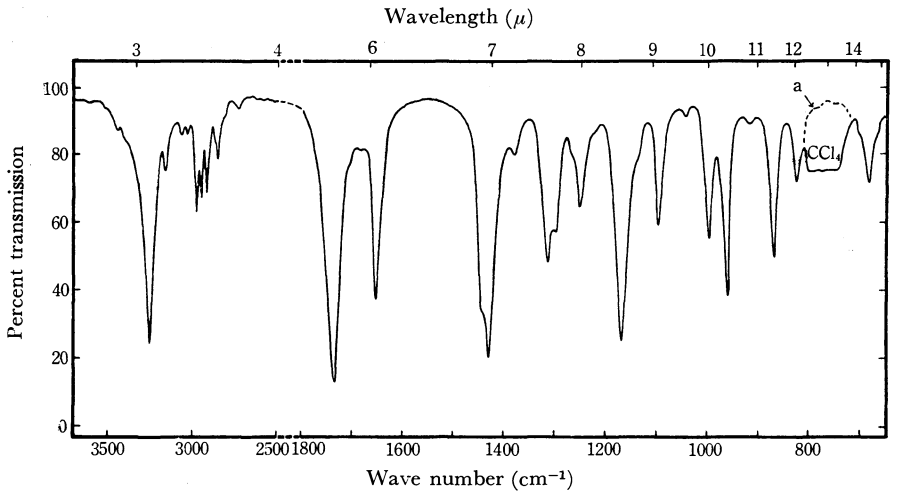

Fig. 1. Infrared absorption spectrum of peroxy-*trans*-crotonic acid in CCl_4: 650—2000 cm^{-1}, 1.0 mol/*l*, 0.025 mm optical length: 2000—4000 cm^{-1}, 0.25 mol/*l*, 0.1 mm optical length. Solvent absorptions are compensated, except in the region 720—810 cm^{-1} where the peracid has no absorption bands in CS_2 solution (curve a), by adjusting the optical length of CCl_4 reference.

Peroxycrotonic acid can be identified by the following observations, 1) the wt% of its peroxidic oxygen agrees with the calculated value, 2) it is quantitatively converted to crotonic acid by reduction with dimethyl sulfide, and 3) its NMR and IR spectra are consistent with the assigned structure.

The NMR parameters are listed, together with those for dicrotonyl peroxide and crotonic acid as authentic references, in Table 1.

The infrared absorption spectrum and the tentative assignment[9] of the principal bands are shown in Fig. 1 and Table 2, respectively. Many of the absorption bands agree with those reported by Deglise and Lemaire[5] for the peroxycrotonic acid intermediate of the autoxidation of crotonaldehyde (Table 2), supporting identity of the substance.

The pK_a of peroxycrotonic acid in water at 25°C (pH of half neutralization) was found to be 8.15. When correction for ionic strength was made, it was calculated to be 8.21. However, it should be noted that pK_a determination of peroxyacids by the acidimetric titration method cannot be accurate since the compounds are unstable.[10] As an example of the present determinations, 15% of the initial peroxidic activity had been lost when pH determination at half neutralization point was finished (in about 15 min at 25°C). Although the pK_a value should be taken as approximate, it is comparable with those of some other peracids as shown in Table 3. The difference in acid strength of a peroxyacid and the parent carboxylic acid is around 3.4 in pK_a units on the average.[11]

The rate of reaction of peroxycrotonic acid with crotonaldehyde in benzene solution forming two moles*1 of crotonic acid was measured by iodometric determination of the remaining peracid. The rate followed the second order kinetics, first order in both reactants, with no induction period within experimental error (Fig. 2). The decrease of the rate caused by the addition of 1,3,5-trinitrobenzene, a stronger inhibitor of radical chain reaction,[12] was real, but to an extent that would permit us to neglect the induced decomposition of the peracid in evaluation of the rate data (Table 4). The least-squares treatment of the Arrhenius equation afforded the following parameters of activation: E_a, 13.3±0.5 kcal/mol; log A (*l*/mol sec), 5.3±0.5

9) For the basis of the assignment see Ref. 5, as well as W. V. F. Brooks and C. M. Haas, *J. Phys. Chem.*, **71**, 650 (1967); D. Swern and L. S. Silbert, *Anal. Chem.*, **35**, 880 (1963); and R. Kavcic, B. Plesnicar and D. Hadzi, *Spectrochim. Acta*, **23A**, 2483 (1967).

10) a) J. F. Goodman, P. Robson and E. R. Wilson, *Trans. Faraday Soc.*, **58**, 1846 (1962). b) E. Koubek, M. L. Haggett, C. J. Battaglia, K. M. Ibne-Rasa, H.Y. Ryun and J. O. Edward, *J. Am. Chem. Soc.*, **85**, 2263 (1963). c) K. Akiba and O. Simamura, *Chem. Ind. (London)*, **1964**, 705.

11) This relation was used in estimation of pK_a of peroxytrifluoroacetic acid; W. D. Emmons and P. S. Pagona, *J. Am. Chem. Soc.*, **77**, 89 (1955).

*1 Over 90% yield of crotonic acid based on reacted crotonaldehyde is obtained by autoxidation of crotonaldehyde at 40% conversion (unpublished work); see also H. Inoue, H. Ito, and K. Takahashi, *Kogyo Kagaku Zasshi, (J. Chem. Soc. Japan, Ind. Chem. Sect.)*, **71**, 1862 (1968). This shows that the intermediate peroxycrotonic acid reacts with crotonaldehyde to give two moles of crotonic acid in an almost quantitative yield, with practical exclusion of formation of 1-propenyl formate.

12) C. G. Swain, W. H. Stockmayer and J. T. Clarke, *J. Am. Chem. Soc.*, **72**, 5428 (1950).

Table 2. Assignment of infrared absorption bands of peroxy-*trans*-crotonic acid

Observed (cm^{-1})	Assignment	by Ref. 5
3266	ν_{O-H}	3262
1736	$\nu_{C=O}$	1730
1656	$\nu_{C=C}$	1656
1443	δ_{CH_3} asym.	—
1434	δ_{O-H} in plane	1431
1382	δ_{CH_3} sym.	—
1311	δ_{C-H} (sp^2) in plane	1308
1297		—
1252	ν_{C-O}	1260
1170		—
1098		1103
994	δ_{C-H} (sp^2) out of plane	990
965	δ_{O-H} out of plane	—
871	ν_{O-O}	873

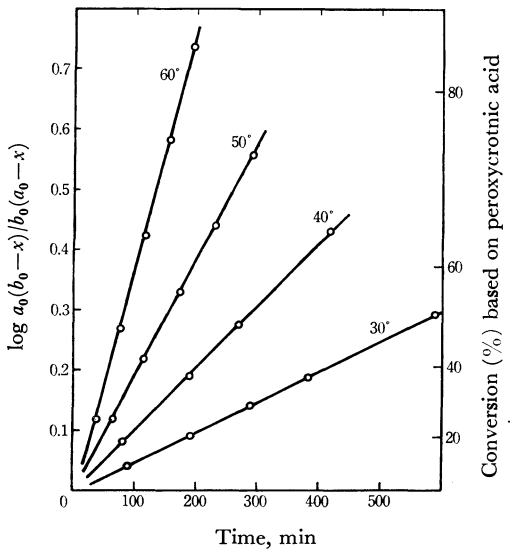

Fig. 2. Representative kinetic runs.

(in the absence of trinitrobenzene): and E_a, 13.5± 0.1 kcal/mol; log A (l/mol sec), 5.4±0.1 (in the presence of trinitrobenzene).[13]

From these results we could regard the reaction as a simple bimolecular reaction, where a highly ordered alignment of the reactants in the transition state is implied by the small pre-exponential factor A ($\Delta S^{\neq} = -36$ eu/mol) comparable to that of the Diels-Alder reactions.

Further considerations as to the course of the reaction seem to be required. It is known that peracetic acid and acetaldehyde react to form an isolable complex, "AMP" (X: R=CH_3),[14] which

13) The attached ranges are limits of 95% confidence of the regression analysis.

14) B. Phillips, F. C. Frostic, Jr., and P. S. Starcher, *J. Am. Chem. Soc.*, **79**, 5982 (1957).

Table 3. pK_a values of some peroxyacids and the parent carboxylic acids in water[a)]

	Temp. °C	pK_a Peroxyacid	pK_a Acid	ΔpK_a
Formic	20	7.1	3.75	3.3
Acetic	20	8.2	4.76	3.4
Chloroacetic	25	7.2[b)]	2.87	4.3
Propionic	23	8.1	4.88	3.2
n-Butyric	21.5	8.2	4.81	3.4
Crotonic	25	8.2[c)]	4.66	3.5
Benzoic	25	7.78[d)]	4.20	3.6

a) *cf.* "Landolt-Börnstein, Zahlenwerte und Funktionen," 6th ed, Springer-Verlag, Berlin (1960), Vol. 2, Part 7, p. 847 for the unannotated figures.
b) E. Koubek and J. O. Edward, *J. Org. Chem.*, **28**, 2157 (1963).
c) The present work.
d) J. F. Goodman, P. Robson and E. R. Wilson, *Trans. Faraday Soc.*, **58**, 1846 (1962).

Table 4. Rate constants of reaction of peroxycrotonic acid with crotonaldehyde

Temp. °C	a_0[a)] mol/l	b_0[b)] mol/l	TNB[c)] mol/l	k (l/mol sec) $\times 10^4$
30	0.0532	0.504	0	0.432
	0.0489	0.254	0	0.415
	0.0563	0.506	0	0.436
	0.0489	0.509	0.0175	0.407
40	0.0457	0.505	0	0.872
	0.0457	0.505	0.0176	0.832
50	0.0505	0.498	0	1.68
	0.0505	0.498	0.0176	1.63
60	0.0568	0.507	0	3.28
	0.0492	0.507	0.0173	3.08

a) Initial concentration of peroxycrotonic acid.
b) Initial concentration of crotonaldehyde.
c) 1,3,5-Trinitrobenzene added.

eventually transforms to two moles of acetic acid. Similar intermediates have been shown spectrometrically in the peroxyheptanoic acid - heptaldehyde[15] and peroxycrotonic acid - heptaldehyde[5] cases. In the cases of peroxybenzoic acid - benzaldehyde and peroxycrotonic acid - crotonaldehyde pairs, however, direct search by infrared spectrometry for the intermediate, X, turned out to be negative,[5,15,16] although X (R=phenyl) was assumed as an intermediate from kinetic studies.[17] Whether

15) J. C. André, J. F. Large, X. Deglise, J. Lemaire and M. Niclause, *Rev. Inst. Fr. Petrole Ann. Combust. Liquides*, **23**, 219 (1968).

16) C. R. Dick and R. F. Hanna, *J. Org. Chem.*, **29**, 1218 (1964).

17) Y. Ogata, I. Tabushi and H. Akimoto, *ibid.*, **26**, 4803 (1961).

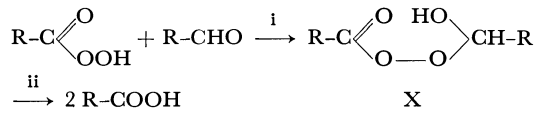

X can accumulate to a detectable concentration or not depends evidently on the ratio of rates of steps i and ii of the particular system under investigation. In an extreme case the structure X can be a representation of the transition state of a single step reaction.

An attempt to detect X (R=CH_3CH=CH–) by NMR was made. As an example, a solution of peroxycrotonic acid (2M) and crotonaldehyde (2M) in methyl acetate was stored at 0°C for 76 hr to accomplish a half conversion of the reactants and the NMR spectrum was taken. No extra absorption, other than those from the reactants and crotonic acid, were observed. A critical examination of the spectrum in order to find an upper limit of the steady state concentration of X did not give a definite conclusion, but it seems that X very probably does not exist in a considerable concentration. This result is in accord with the conclusion by Deglise and Lemaire[5] based on infrared spectroscopic studies.

The contrast between the behavior of saturated aldehydes and the α,β-unsaturated and aromatic aldehydes with regard to the intermediacy of X is ascribed partly to the reduced rate of step i in the latter, because of the loss of conjugative stabilization of the carbonyl group in transforming into hemi-acetal structure X. The effect of unsaturation to the rate of step ii cannot be predicted. From failure to detect X it is inferred that step i is slower than step ii, if X is an unstable intermediate in contrast to the transition state. However, the possibility that a rapid equilibrium between the reactants and X, together with step ii, may give an undetectable steady state concentration of X, cannot be ruled out.[18]

Experimental[19]

Dicrotonyl peroxide was prepared by the method of Tuerck[20] and was purified by recrystallization from petroleum ether; mp 41.3—42.3°C, lit mp 40—41°C,[20] mp 41°C.[2] The peroxidic oxygen as determined by the iodometric titration for dibenzoyl peroxide[6] was 97.9% of the theoretical.

Preparation of Peroxycrotonic Acid. A solution of 17.0 g (0.10 mol) of dicrotonyl peroxide in 70 m*l* of chloroform was placed in a round bottomed flask equipped with a loosely fitted thermometer, and was cooled in a dry ice-acetone bath. To this solution (at *ca.* −65°C) was added an ice cold methanolic sodium methoxide solution, prepared from 2.4 g (0.105 g atom) of sodium and 20 m*l* of absolute methanol, in less than 1 min with swirling. The flask was vigorously shaken in the bath for several seconds and was transferred into an ice-salt bath (−5°C) in which it was vigorously shaken for 4 min.[21] The solution was immediately poured onto 250 g of water containing chopped ice in a separatory funnel, the sodium peroxycrotonate extracted quickly into the aqueous layer, and the chloroform discarded. After washing with two successive 50 m*l* portions of cold chloroform, the aqueous solution was admixed with 50 m*l* of chloroform and 120 g of 5% aqueous sulfuric acid, and the peroxycrotonic acid was extracted with three further 50 m*l* portions of cold chloroform. The combined chloroform extracts were washed twice with water, dried with anhydrous sodium sulfate, and the chloroform was evaporated in a vacuum by a water aspirator to obtain 10 g of white solid of crude peroxyacid as residue. The solid was recrystallized from 100 m*l* of petroleum ether, bp 40—60°C, to obtain fine needles. After storing overnight in a refrigerator, the crystals, 4.5 g, were collected by suction filtration under dry atmosphere: mp 41—42°C. Further crops, 1.4 g, were obtained from the filtrate: total yield, 57.8% of the theory. When the petroleum ether suspension of the peroxyacid is stored in a refrigerator for a week, massive crystals which are easier to handle are obtained.

In a run of smaller scale (0.02 mol) the alkaline cleavage reaction was carried out in an ice bath with similar yield of the product.

The purity of the specimen was determined to be nearly 100% by the iodometric titration or the wt % of the peroxidic oxygen was found to be 15.57%: Calcd for $C_4H_6O_3$, 15.67%.

Reaction with Dimethyl Sulfide. Dimethyl sulfide, 1.0 m*l*, was added dropwise to 1 m*l* of ethyl acetate solution of 0.0450 g of peroxycrotonic acid in a dry ice-acetone bath. After standing in a refrigerator for 1 hr the solution was treated with a slight excess of ethereal diazomethane at −70°C, and was kept overnight at this temperature. The methyl crotonate formed was determined to be 96—99% of theory by quantitative glpc analysis using ethylbenzene as the internal standard. Esterification with diazomethane at 0°C gave erratic results presumably because of the pyrazoline formation.[22]

Kinetic Measurements.[23] A 200 m*l* two-mouthed

18) When this mechanism is adopted the net forward rate of step i should mean the rate of step i of the foregoing description.

19) Melting points are corrected. NMR spectra were taken using a Varian A-60A spectrometer. IR spectra were recorded on a Nihon Bunko Model DS-402G double-beam grating spectrophotometer. A Hitachi-Horiba glass electrode pH meter type M-5, calibrated with pH standard solutions, was used for pH determinations.

20) K. H. W. Tuerck, U. S. Pat. 2379390 (1945); *Chem. Abstr.*, **39**, 4620 (1945).

21) In a few runs in which this procedure was allowed to continue for about 10 min, very poor results were obtained.

22) a) A. Ledwith and D. Parry, *J. Chem. Soc.*, *C*, **1966**, 1408. b) T. V. Van Auken and K. L. Rinehard, Jr., *J. Am. Chem. Soc.*, **84**, 3736 (1962).

23) Commercial crotonaldehyde was dried with anhydrous calcium sulfate and rectified under nitrogen stream; bp 42°C/83 mmHg. Benzene was purified by treatment with concentrated sulfuric acid, dried with calcium chloride, and was distilled from sodium wire.

flask, fitted with a gas-inlet and a stopper, was flushed with dry nitrogen and 50 m*l* of a benzene solution of crotonaldehyde was added and thermostated. While a slow stream of nitrogen, saturated with benzene vapor, was bubbled through the solution, a 50 m*l* benzene solution of peroxycrotonic acid was added to start the reaction, and the system was stoppered under a slight pressure of nitrogen. After appropriate time intervals an aliquot of 10 m*l* was taken out into a flask containing 2 g of potassium iodide, 45 m*l* of water, 5 m*l* of acetic acid, 10 m*l* of chloroform, and a few pieces of dry ice. The liberated iodine was immediately titrated with a standard sodium thiosulfate solution: the end-point was sharp.

BULLETIN OF THE CHEMICAL SOCIETY OF JAPAN VOL. 42 3242—3244 (1969)

Homolytic Chlorination of Aliphatic Compounds. II.[1] Photochlorination of Aliphatic Nitriles

Masanori Kosugi, Kohji Takeuchi and Toshihiko Migita

Department of Chemistry, Gunma University, Kiryu, Gunma

(Received April 16, 1969)

Acetonitrile, propionitrile, *n*-butyronitrile and pivalonitrile were photochlorinated competitively at 40°C in the presence of an appropriate chlorinated ethane, and relative amounts of the chlorinated products were determined by v.p.c. From the results the relative reactivities of C-H bonds toward hydrogen abstraction by chlorine atom were estimated. A linear free energy relationship was observed between σ^* value of X and the reactivity of CH_3–X toward chlorination (X: –CN, $-CH_2CN$, $-CH_2CH_2CN$, $-CMe_2CN$). This indicates that cyano group will affect the reactivities of these C-H bond through its inductive effect.

Orientation of photochlorination of saturated aliphatic nitriles has been studied by Bruylants *et al.*[2] In order to investigate the effect of cyano group on the reactivities of aliphatic chains toward chlorination, we have estimated relative reactivities of acetonitrile, propionitrile, *n*-butyronitrile and pivalonitrile.

Nitriles and the standard substrate were competitively photochlorinated in carbon tetrachloride. The reaction mixture were analyzed for chlorinated products by v.p.c. method. Since a large excess of the substrate was used, the relative reactivities of R_1H and R_2H can be calculated from the molar ratio of R_1Cl and R_2Cl by the equation

$$\frac{k_2}{k_1} = \frac{[R_2Cl]}{[R_1Cl]} \times \frac{[R_1H]_0}{[R_2H]_0},$$

where k_2/k_1 is the ratio of the rate constants for R_2H and R_1H, $[R_2H]_0$ and $[R_1H]_0$ are the initial concentrations of the substrates, and $[R_2Cl]$ and $[R_1Cl]$ are the molar amounts of the chlorinated products. The relative reactivities of C–H bonds were calculated by correcting the relative rate constants for the statistic factors. Unit reactivity was assigned to one of the six available hydrogen atoms of 2,2-dichloropropane. Results are summarized in Table 1.

Table 1. Relative reactivities* of nitriles at 40°C

CH_3——CN			
0.02			
CH_3——CH_2——CN			
1.4	0.98		
CH_3——CH_2——CH_2——CN			
3.7	7.7	0.39	
CH_3——CMe_2CN			
2.7			

* The values are relative to the raeactivity of a C-H bond of 2,2-dichloropropane and average of four runs.

The relative reactivity of acetonitrile toward photochlorination reported by Russell[3] is ten times higher than that we obtained. However, our value is considered to be more plausible. Russell estimated the relative reactivities from the amounts of substrates consumed by competitive reactions. In this technique, considerably high conversions are required. In such circumstances, acetonitrile seems to undergo consecutive chlorination and triazine derivatives formation as shown in the

1) Part I: T. Migita, M. Kosugi and Y. Nagai, This Bulletin, **40**, 920 (1967).

2) A. Bruylants, M. Tits, C. Dieu and R. Gauthier, *Bull. Soc. Chim. Belges*, **61**, 366 (1952).

3) G. A. Russell, *J. Am. Chem. Soc.*, **80**, 4997 (1958).

following equations.[4,5]

$$CH_3CN + Cl_2 \xrightarrow{slow} (CH_2ClCN)HCl$$

$$(CH_2ClCN)HCl + Cl_2 \xrightarrow{fast} (CHCl_2CN)HCl + HCl$$

$$(CHCl_2CN)HCl + Cl_2 \xrightarrow{fast} (CCl_3CN)HCl + HCl$$

$$CH_3CN + 2\,CCl_3CN \xrightarrow{HCl}$$

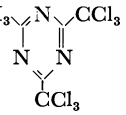

We obtained a considerable amount of 2-methyl-4,6-di-trichloromethyl-1,3,5-triazine in the photo-induced chlorination of acetonitrile at a high conversion. Since acetonitrile is consumed not only by chlorination but also by triazine formation, it would be possible that the relative reactivity obtained from the amount of acetonitrile consumed gives an overestimated value. In our method, such consecutive chlorination might lead us to underestimate the reactivity of acetonitrile, since relative reactivities were derived from the relative amounts of the monochlorinated products. However, the conversion was so small (less than 10%) that the possibility of underestimation due to the consecutive reaction may be negligible.

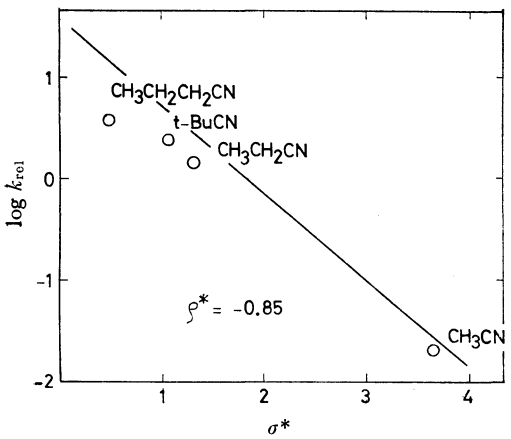

Fig. 1. Hammett plot for CH_3–X. 40°C.

Table 2. Polar substituent constants

Substituennt	σ^*
CH_3	0.000
CH_2Cl	1.050
$CHCl_2$	1.940
CCl_3	2.65
CH_2CMe_3	−0.165
CH_2CH_2Cl	0.385
CH_2CHCl_2	0.693*
CH_2CCl_3	0.946*
CMe_3	−0.300
CMe_2Cl	0.851*
$CMeCl_2$	1.890*
H	0.490
CN	3.64*
CH_2CN	1.300
CH_2CH_2CN	0.464*
CMe_2CN	1.100*

* Estimated by the following relations:
$\sigma^*(CH_2CHCl_2) = 1/2.8\,\sigma^*(CHCl_2)$
$\sigma^*(CMeCl_2) = \sigma^*(CHCl_2) + \sigma^*(Et)$.
Ref. 7, p. 592.

The orientation patterns of chlorination of propionitrile and *n*-butyronitrile were in good agreement with those obtained by Bruylants *et al.*,[2] except for α-position of *n*-butyronitrile. In our experiments formation of α-chloro-*n*-butyronitrile (at least 3—4% of total chlorinated products) was recognized. The structure of the product was derived from its NMR spectra.

As previously reported,[1,6] a linear free energy relationship was found to exist between the reactivities of methyl hydrogen of CH_3–X and Taft's σ^* constants[7] for the substituents X (X: CH_3, CH_2Cl, $CHCl_2$, CCl_3, CH_2CMe_3, CH_2CH_2Cl, CH_2CHCl_2, CH_2CCl_3, CMe_3, CMe_2Cl, $CMeCl_2$). The straight line in Fig. 1 represents Hammett's relationship we obtained previously,[6] ρ^* value being −0.85. As shown in Fig. 1, the same relationship can approximately hold for the chlorina-

Table 3. NMR Spectra of chlorinated nitriles (τ Values)

α-Chloropropionitrile	$CH_3{}^1CH_2{}^2ClCN$	8.15 (H^1 doublet)	5.45 (H^2 quartet)	
β-Chloropropionitrile[9]	$CH_2{}^1ClCH_2{}^2CN$	6.25 (H^1 triplet)	7.10 (H^2 triplet)	
α-Chlorobutyronitrile	$CH_3{}^1CH_2{}^2CH^3ClCN$	8.80 (H^1 triplet)	7.90 (H^2 multiplet)	5.63 (H^3 triplet)
β-Chlorobutyronitrile	$CH_3{}^1CH^2ClCH_2{}^3CN$	8.35 (H^1 doublet)	5.80 (H^2 sextet)	7.25 (H^3 doublet)
γ-Chlorobutyronitrile	$CH_2{}^1ClCH_2{}^2CH_2{}^3CN$	6.37 (H^1 triplet)	7.90 (H^2 multiplet)	7.50 (H^3 triplet)
Chloropivalonitrile[10]	$(CH_3{}^1)_2CH_2{}^2ClCCN$	8.55 (H^1 singlet)	6.48 (H^2 singlet)	

4) F. N. Stepanov and N. J. Shirokova, *J. Gen. Chem. U. S. S. R.* **25**, 905 (1955).

5) G. I. Braz, G. V. Myasnikova, A. Y. Yakubovich, V. P. Bazov and K. I. Sakodyaskii, *Zh. Obshch. Khim.*, **33**, 1939 (1963).

6) T. Migita, M. Kosugi, Y. Tanaka and Y. Nagai, *Yukigosei kagaku kyohaishi (J. Soc. Org. Synth. Chem. Japan)*, **25**, 908 (1967). Similar tendency was observed in gas phase chlorination of chloroethanes. C. Cillien, P. Coldfinger, G. Huybrechts and G. Martens, *Trans. Faraday Soc.*, **63**, 1631 (1967); W. Mack, *Tetrahedron Letters*, **1967**, 4993.

7) M. S. Newman, "Steric Effects in Organic Chemistry," Wiley, New York (1956), p. 619.

tion of the nitriles, when σ^* constants noted in Table 2 are used.

It is quite reasonable that reactivities of β- or γ-C–H bonds of nitriles are represented by Hammett's equation, since a cyano group will affect the reactivities of these C–H bonds through its inductive effect. However, it is noteworthy that the relationship holds even in reactivities of α-C–H bonds. This may indicate that resonance stabilizing effect of a cyano group on an intermediate radical $\dot{R}CHCN$ hardly enhances the reactivity of α-C–H bonds of RCH_2CN.

$$R\text{-}\dot{C}H\text{-}C{\equiv}\overline{N} \longleftrightarrow R\text{-}CH{=}C{=}\overline{\dot{N}}\cdot$$

Experimental

Materials. Acetonitrile and propionitrile (commercial materials) were treated with activated silica gel chromatographically and refluxed over phosphorus pentoxide and then rectified through a Vigreux column. The boiling points were 81°C and 97°C, respectively. *n*-Butyronitrile and pivalonitile were prepared by the dehydration of the corresponding acid amide.[8] The boiling points were 118°C and 105°C, respectively. All the materials were shown by v.p.c. analysis to be pure.

Reaction Products. Monochlorinated products were collected by v.p.c. method and their structures were derived from their NMR spectra. The NMR data are given in Table 3.

2-Methyl-4,6-di-trichloromethyl-1,3,5-triazine was isolated from the chlorination mixture of acetonitrile.[5] Mp 94—95°C. NMR 7.0 (H singlet). Found: C, 22.28; H, 1.18%. Calcd for $C_6H_3N_3Cl_6$: C, 21.84; H, 0.92%.

Competitive Chlorination Procedure. The chlorination procedure has already been described.[1] Analysis of the chlorination products were performed by v.p.c. method employing a 1.5 m Carbowax 20M 25% column. Competitive experiments were carried out on the mixtures of nitriles with an appropriate chloroethanes in carbon tetrachloride solution. The reactivities of C–H bonds of nitriles relative to that of 2,2-dichloropropane were calculated from the data thus obtained on the basis of the reactivity values of chloroethanes.[1]

Since acetonitrile has much lower reactivity than 2,2-dichloropropane, competitive experiments with 2,2-dichloropropane have difficulties in gas chromatographical analysis for determination of reliable relative rates. Acetonitrile was made to compete with 1,1,1-trichloroethane. The rate factor was calculated as,

$$f\left(\frac{MeCN}{MeCCl_2Me}\right) = f\left(\frac{MeCN}{MeCCl_3}\right) \times f\left(\frac{MeCCl_3}{MeCCl_2Me}\right).$$

The results of competitive experiments are shown in Table 4.

Table 4. Competitive chlorination of nitriles

1. Acetonitrile, 40°C, in 2 m*l* of CCl_4

$\frac{MeCN}{MeCCl_3}$	Molar ratio of products $\frac{CH_2ClCN}{ClCH_2CCl_3}$	Rel. reactivities* CH_3–
3.54	0.717	0.20
3.54	0.663	0.19
3.54	0.635	0.18
3.54	0.650	0.18
	average	0.19

2. Propionitrile, 40°C, in 2 m*l* of CCl_4

$\frac{CH_3CH_2CN}{CHCl_2CHCl_2}$	Molar ratio of products $\frac{CH_2Cl\text{-}CH_2CN}{CCl_3\text{-}CHCl_2}$	$\frac{CH_3CHCl\text{-}CN}{CCl_3\text{-}CHCl_2}$	Rel. reactivities* CH_3–	$-CH_2$–
0.444	2.43	0.969	3.65	2.18
0.444	2.21	1.11	3.32	2.50
0.444	2.05	0.933	3.08	2.10
0.444	2.25	1.03	3.36	2.22
		average	3.36	2.28

3. *n*-Butyronitrile, 40°C, in 2 m*l* of CCl_4

n-Butyronitrile was chlorinated in carbon tetrachloride at 40°C. Intramolecular reactivity pattern was found to be:

CH_3—CH_2—CH_2—CN

0.48 1 0.05

Competitive chlorination with 1,1,2-trichloroethane was carried out to find relative reactivity of β-position of *n*-butyronitrile.

$\frac{CH_3CH_2CH_2CN}{CH_2ClCHCl_2}$	Molar ratio of products $\frac{CH_3CHClCH_2CN}{(CHCl_2)_2}$	Rel. reactivities* $-CH_2$–
0.229	3.60	15.1
0.239	4.65	19.5
0.239	3.71	15.5
0.229	3.63	15.2
	average	16.3

4. Pivalonitrile, 40°C, in 2m*l* of CCl_4

$\frac{t\text{-}BuCN}{CH_2ClCH_2Cl}$	Molar ratio of products $\frac{Me_2CH_2ClCCN}{CHCl_2CH_2Cl}$	Rel. reactivities* CH_3–
0.480	0.977	0.91
0.480	1.01	0.93
0.480	0.958	0.88
0.480	0.941	0.86
	average	0.90

* Relative to a C–H bond of the corresponding chloroethanes.

We are deeply grateful to Professor Y. Nagai for numerous suggestions and discussions concerning assay problems.

8) R. E. Kent and S. M. McElvain, "Org. Synth.," Coll. Vol. III. p. 493 (1955).

9) β-Chloropropionitrile was prepared by addition of hydrogen chloride to acrylonitrile.[11]

10) Found: Cl, 29.09%. Calcd for C_5H_8NCl: Cl, 30.16%.

11) R. Stewart and R. H. Clark, *J. Am. Chem. Soc.*, **69**, 713 (1941).

BULLETIN OF THE CHEMICAL SOCIETY OF JAPAN VOL. 42 3245—3248 (1969)

Sugars Containing a Carbon-phosphorus Bond. I. Photochemical Addition of Diethyl Thiophosphonate to Unsaturated Sugars

Kazuo KUMAMOTO, Hiroshi YOSHIDA, Tsuyoshi OGATA and Saburo INOKAWA*1

Department of Synthetic Chemistry, Faculty of Engineering, Shizuoka University, Johoku, Hamamatsu

(Received April 26, 1969)

Sugars containing a carbon-phosphorus bond were synthesized by the photochemical addition of diethyl thiophosphonate to unsaturated sugars. By UV illumination from a high-pressure mercury lamp in the presence of diethyl thiophosphonate, D-glucal gave 1,5-anhydro-2-deoxy-2-(diethyl thiophosphonate)-D-glucit; 3-deoxy-1,2;5,6-di-*O*-isopropylidene-α-D-*erythro*-hex-3-enose gave 1,2;5,6-di-*O*-isopropylidene-3-deoxy-3-(diethyl thiophosphonate)-α-D-glucofuranose and 1,2;5,6-di-*O*-isopropylidene-3-deoxy-3-(diethyl thiophosphonate)-α-D-galactofuranose (4:1 mol ratio); 6-*O*-benzyl-5-deoxy-1,2-*O*-isopropylidene-α-D-*xylo*-hexofuran-5-enose gave 6-*O*-benzyl-5-deoxy-5-(diethyl thiophosphonate)-1,2-*O*-isopropylidene-α-D-glucofuranose and 6-*O*-benzyl-5-deoxy-5-(diethyl thiophosphonate)-1,2-*O*-isopropylidene-α-L-idofuranose (2:5 or 5:2 mol ratio), and 5-deoxy-1,2-*O*-isopropylidene-3-*O*-methyl-α-D-xylofuranose-4-ene gave 5-deoxy-5-(diethyl thiophosphonate)-1,2-*O*-isopropylidene-3-*O*-methyl-α-D-xylofuranose.

Recently, a large number of sugars with sulfur and nitrogen atoms directly connected to the carbon chain have been synthesized and investigated not only with regard to their chemical properties, but also with regard to their biological activities. These sugars represent a potentially important area of sugar chemistry.[1] However, sugars with a phosphorus atom connected to the carbon chain are little-known. Exploration of the phosphorus sugars may be expected to provide information leading to another important new area of sugar chemistry.

In order to prepare the phosphorus sugars,[2] an investigation of the addition of diethyl thiophosphonate (DETP) to unsaturated sugars was undertaken. The results will be reported here. As the unsaturated sugars, D-glucal [1], 3-deoxy-1,2; 5,6-di-*O*-isopropylidene-α-D-*erythro*-hex-3-enose [2], 6-*O*-benzyl-5-deoxy-1,2-*O*-isopropylidene-α-D-xylo-hexofuran-5-enose [3], and 5-deoxy-1,2-*O*-isopropylidene-3-*O*-methyl-α-D-xylofuranose-4-ene [4] were used. The structures of the products were determined by studying the NMR spectra and by elementary analyses. The stereoselectivity of the radical addition will also be described.

Experimental

The infrared spectra were measured on a Hitachi-Perkin-Elmer 337 spectrophotometer. The nuclear magnetic resonance spectra were at 60 Mc on a Hitachi-Perkin-Elmer R-20 spectrometer, using tetramethylsilane as the internal reference. The thin-layer chromatograms were run on a silica-layer G[3] using various mixtures of ethyl acetate and petroleum ether, and phosphorus compounds were detected by spraying the plates with a cobalt chloride solution[4] and then heating them. The gas chromatograms were run on Yanagimoto GCG-3D gas chromatograph with a stainless column (2 mm×2 m) packed with Apiezon Grease M[5] (20 wt % on Celite 545 of 40—60 mesh, using H_2 as the carrier gas (100 ml/min) at 200°C. The UV source was a 100-W Halos PIH-100 (high-pressure mercury lamp). Periodic sampling and examination by thin-layer chromatography permitted the determination of the most suitable irradiation times for the preparative runs.

Materials. The D-glucal [1] was prepared by the method of Roth and Pigman;[6] mp 57—59°C. The 3-deoxy-1,2;5,6-di-*O*-isopropylidene-α-D-*erythro*-hex-3-enose [2] was prepared by the method of Schmidt;[7] mp 108—110°C. The 6-*O*-benzyl-1,2-*O*-isopropylidene-α-D-*xylo*-hexofuran-5-enose [3] was prepared by the

*1 This work was presented at the 22nd Annual Meeting of the Chemical Society of Japan, Tokyo, April 2, 1969.

1) H. Paulsen and K. Todt, "Advances in Carbohydrate Chemistry," Vol. 23 ed. by M. L. Wolfrom and R. S. Tipson, Academic Press, New York and London (1968), p. 116.

2) *Cf.* R. L. Whistler, C.-C. Wang, and S. Inokawa, *J. Org. Chem.*, **33**, 2495 (1968).

3) Nakarai Chemicals Ltd., Kyoto.

4) R. Donner and K. Lohs, *J. Chromatog.*, **17**, 349 (1965).

5) Nishi Kogyo Co., Ltd., Tokyo.

6) W. Roth and W. Pigman, "Methods in Carbohydrate Chemistry," Vol. II, ed. by R. L. Whistler and M. L. Wolfrom, Academic Press, New York and London (1963), p. 221.

7) O. T. Schmidt, *ibid.*, p. 318.

method of Gramera and Whistler[8]; mp 113°C. The 5-deoxy-1,2-*O*-isopropylidene-3-*O*-methyl-α-D-xylofuranose-4-ene [4] was prepared by the method of Inokawa *et al.*;[9] bp 80°C/7 mmHg. The diethyl thiophosphonate [DETP] was prepared by the method of Krawiechi and Michalski;[10] bp 73—75°C/14 mmHg, λ_{max} 252 mμ, ε_{max} 162.

1,5-Anhydro-2-deoxy-2-(diethyl thiophosphonate)-D-glucit [5]. A solution of 5 g of [1] and 10 m*l* of DETP in 70 m*l* of dioxane in a reaction vessel was irradiated internally for 10 hr with a high-pressure mercury UV lamp (100 W) under a nitrogen atmosphere with stirring. The solution was then concentrated *in vacuo*; the residue was washed with petroleum ether and recrystallized from ethanol-petroleum ether to give, in a 90% yield(9.5 g), colorless needles of [5]; mp 93—95°C, $[\alpha]_D^{16}$ +23.4° (*c* 10, chloroform).

Found: C, 39.74; H, 7.04%. Calcd for $C_{10}H_{21}O_6PS$: C, 39.99; H, 7.06%.

The acetate; mp 93—95°C (from petroleum ether), $[\alpha]_D^{16}$ +62.5 (*c* 10, chloroform). The ^{1}H NMR data (carbon tetrachloride) were as follows: τ 4.50 (one-proton quartet, $J_{2,3}$=9.0 Hz, $J_{3,4}$=9.0 Hz, $J_{3,P}$=15 Hz, H_3), 5.06 (one-proton triplet, $J_{3,4}$=9.0 Hz, H_4), 5.4—6.7 [nine-proton multiplets, $H_{1,1',5,6'}$, (P-O-CH_2-)$_2$], 6.35 (one-proton multiplet, $J_{1,2}$=4.0 Hz, $J_{1',2}$=9.0 Hz, $J_{2,P}$=25 Hz, H_2), 7.8—7.9 [nine-proton singlets, (CH_3CO)$_3$], and 8.7 [six-proton triplets, (P-O-C-CH_3)$_2$].

1,2;5,6-Di-*O*-isopropylidene-3-deoxy-3-(diethyl thiophosphonate)-α-D-glucofuranose [6] and 1,2;5,6-di-*O*-isopropylidene-3-deoxy-3-(diethyl thiophosphonate)-α-D-galactofuranose [7]. A mixture of 3 g of [2], 6 m*l* of DETP, and 6 m*l* of dioxane in a quartz tube was irradiated for 15 hr from a high-pressure mercury UV lamp (100 W) at a distance of about 3 cm under a nitrogen atmosphere. The mixture was then concentrated *in vacuo*; the residue was dissolved in ether, washed with water, dried over magnesium sulfate, and concentrated *in vacuo* to give an oil. The fractional vacuum distillation of the resulting oil gave, in a 42% yield (2.0 g), a pale yellow oil, a mixture of [6] and [7]; bp 175—177°C/2 mmHg.

Found: C, 48.74; H, 7.61%. Calcd for $C_{16}H_{29}O_7PS$: C, 48.46; H, 7.38%.

This mixture was separated into [6] and [7] by gas chromatography. The mol ratio of [6] and [7] in the mixture was 4 to 1. The product (retention time, 62 min) gave [6], $[\alpha]_D^{16}$ −4.6° (*c* 21, chloroform). The ^{1}H NMR data (carbon tetrachloride) were as follows: τ 4.4 (one-proton doublet, $J_{1,2}$=4.0 Hz, H_1), 5.2 (one-proton multiplet, $J_{3,4}$=2.8 Hz, $J_{4,5}$=4.9 Hz, $J_{4,P}$=14.0 Hz, H_4), 5.5—6.3 [eight-proton multiplets, $H_{2,5,6,6'}$, (P-O-CH_2-)$_2$], 7.3 (one-proton multiplet, $J_{2,3}$=7.0 Hz, $J_{3,4}$=2.8 Hz, $J_{3,P}$=16.0 Hz, H_3), and 8.4—8.9 [eighteen-proton multiplets, C(CH_3)$_2$, (P-O-C-CH_3)$_2$]. The product (retention time, 78 min) gave [7]; $[\alpha]_D^{16}$ −9.3° (*c* 6, chloroform). The ^{1}H NMR data (carbon tetrachloride) were as follows: τ 4.3 (one-proton doublet, $J_{1,2}$=4.0 Hz, H_1), 5.1 (one-proton quartet, $J_{4,5}$=3.5 Hz, $J_{4,P}$=9.0 Hz, H_4), 5.4—6.4 [eight-proton multiplets, $H_{2,5,6,6'}$, (P-O-CH_2-)$_2$], 7.3 (one-proton quartet, $J_{2,3}$=5.0 Hz, $J_{3,P}$=16.0 Hz, H_3], and 8.5—8.8 [eighteen-proton triplets, C(CH_3)$_2$, (P-O-C-CH_3)$_2$].

6-*O*-Benzyl-5-deoxy-5-(diethyl thiophosphonate)-1,2-*O*-isopropylidene-α-D-glucofuranose [8] and 6-*O*-benzyl-5-deoxy-5-(diethyl thiophosphonate)-1,2-*O*-isopropylidene-α-L-idofuranose [9]. A mixture of 1.8 g of [3], 2 m*l* of DETP, and 4 m*l* of dioxane in a quartz tube was irradiated for 5 hr from a high-pressure mercury UV lamp (100 W) at a distance of about 3 cm under a nitrogen atmosphere. The solution was then concentrated *in vacuo*; the residue was dissolved in ether, washed with water, dried over magnesium sulfate, and concentrated *in vacuo* to give an oil. The high-vacuum distillation of the resulting oil gave, in a 55% yield (1.6 g), a pale yellow oil, a mixture of [8] and [9], bp 120—125°C/10^{-3}—10^{-4} mmHg, in company with small amounts of impurities. The mixture was separated into [8] and [9] by thin-layer chromatography using a solvent of ethyl acetate and petroleum ether (1 : 1 v/v). The mol ratio of [8] and [9] in the mixture was 2 to 5 or 5 to 2. The product of R_f 0.6 showed $[\alpha]_D^{16}$ +32° (*c* 17, chloroform). The ^{1}H NMR data (carbon tetrachloride) were as follows: τ 2.7 (five-proton singlet, C_6H_5), 4.2 (one-proton doublet, $J_{1,2}$=4.0 Hz, H_1), 5.5 (two-proton singlet, CH_2Ph), 5.5—6.5 [nine-proton multiplets, $H_{2,3,4,6,6'}$, (P-O-CH_2-)$_2$], 6.8 (one-proton singlet, OH), 7.6 (one-proton multiplet, H_5), and 8.5—9.0 [twelve-proton multiplets, C(CH_3)$_2$, (P-O-C-CH_3)$_2$]. The product of R_f 0.5 showed $[\alpha]_D^{16}$ −13° (*c* 17, chloroform). The ^{1}H NMR data (carbon tetrachloride) were as follows: τ 2.8 (five-proton singlet, C_6H_5), 4.3 (one-proton doublet, $J_{1,2}$=4.0 Hz, H_1), 5.6 (two-proton singlet, CH_2Ph), 5.6—6.5 [nine-proton multiplets, $H_{2,3,4,6,6'}$, (P-O-CH_2-)$_2$], 6.7 (one-proton singlet, OH), 7.5 (one-proton multiplet, H_5), and 8.5—8.8 [twelve-proton multiplets, C(CH_3)$_2$, (P-O-C-CH_3)$_2$].

5-Deoxy-5-(diethyl thiophosphonate)-1,2-*O*-isopropylidene-3-*O*-methyl-α-D-xylofuranose [10]. A mixture of 2.5 g of [4], 5 m*l* of DETP, and 5 m*l* of dioxane in a quartz tube was irradiated for 40 hr from a high-pressure mercury UV lamp (100 W) at a distance of about 3 cm under a nitrogen atmosphere. The mixture was then concentrated *in vacuo*; the residue was dissolved in ether, washed with water, dried over magnesium sulfate, and concentrated *in vacuo* to give an oil. The vacuum distillation of the resulting oil gave, in a 95% yield, a colorless oil; bp 149°C/2 mmHg, $[\alpha]_D^{20}$ −23.2° (*c* 10, carbon tetrachloride).

Found: C, 45.86; H, 7.51%. Calcd for $C_{14}H_{25}O_6PS$: C, 45.88; H, 7.36%. The ^{1}H NMR data (carbon tetrachloride) were as follows: τ 4.3 (one-proton quartet, $J_{1,2}$=4.0 Hz, H_1), 5.6 (one-proton doublet, partially overlapping with H_4; H_2), 4.5—6.2 [five-proton multiplets, partially overlapping with H_3; H_4, (P-O-CH_2-)$_2$], 8.2 (one-proton doublet, partially overlapping with (P-O-CH_2-)$_2$; $J_{3,4}$=1.6 Hz, H_3), 7.6 (two-proton quartet, $J_{4,P}$=16 Hz, H_4), 8.5, 8.8 [six-proton singlets, overlapping with (P-O-C-CH_3); C(CH_3)$_2$], and 8.7 [six-proton triplets, overlapping with C(CH_3)$_2$; (P-O-C-CH_3)$_2$].

8) R. E. Gramera and R. L. Whistler, *J. Org. Chem.*, **29**, 878 (1965).

9) S. Inokawa, H. Yoshida, C.-C. Wang, and R. L. Whistler, This Bulletin, **41**, 1472 (1968).

10) Cz. Krawiechi and V. Michalski, *Chem. & Ind.*, **1957**, 1323.

Results and Discussion

According to Pudovik and Konovalova,[11] the radical addition of diethyl thiophosphonate (DETP) to olefins affords a carbon-phosphorus bond. Also, Lehmann has made it clear that the radical addition to an enolic sugar derivative occurs at the β-position[12] to a hydroxyl group. When [1] is exposed to UV radiation in the presence of DETP, a reaction takes place, with the formation of one major product, as is indicated by thin-layer chromatography. The concentration on the solution gave, in a good yield, a solid residue. After recrystallization from ether-petroleum ether, this product was identified as 1,5-anhydro-2-deoxy-2-(diethyl thiophosphonate)-D-glucit [5]. The structure of this product was established by elementary analysis and by a study of the NMR spectrum of its acetate. The coupling constants,[13] $J_{1,2}=4.0$ Hz, $J_{1',2}=9.0$ Hz, and $J_{2,3}=9.0$ Hz, show that a diethyl thiophosphonate group is in an equatorial conformation.

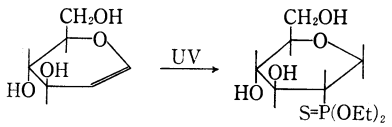

[1] [5]

The compound [2] was exposed to UV radiation in the presence of DETP: the solution was then concentrated *in vacuo* to give, in a good yield, an oil, a mixture of two major products. After purification by vacuum distillation and separation by gas chromatography, they were identified as 1,2; 5,6-di-*O*-isopropylidene-3-deoxy-3-(diethyl thiophosphonate)-α-D-glucofuranose [6] and 1,2; 5,6-di-*O*-isopropylidene-3-deoxy-3-(diethyl thiophosphonate)-α-D-galactofuranose [7]. The structures of these two products were established by elementary analyses and by studies of the NMR specta. It was generally accepted[14] that the *endo*-side of [2] was sterically strongly hindered by the 1,2-*O*-isopropylidene group. Therefore, the diethyl thiophosphonate group should be on the *exo*-side at the C-3 position. The fact that, in these NMR spectra, the coupling constant,[15] $J_{3,4}$, is 2.8 Hz for [6] and practically zero for [7] shows that [6] has the configuration of 1,2-*O*-isopropylidene-α-D-glucofuranose, while [7] has that of 1,2-*O*-isopropylidene-α-D-galactose. The mol ratio of [6] and [7] in the product was 4 to 1.

The compound [3] was exposed to UV radiation in the presence of DETP; the solution was then concentrated *in vacuo* to give an oil containing two major products, as indicated by thin-layer chromatography. After purification by high-vacuum distillation and separation by thin-layer chromatography, these products were identified as 6-*O*-benzyl-5-deoxy-5-(diethyl thiophosphonate)-1,2-*O*-isopropylidene-α-D-glucofuranose [8]*2 and 6-*O*-benzyl-5-deoxy-5-(diethyl thiophosphonate)-1,2-*O*-isopropylidene-α-L-idofuranose [9].*2 The structure of these products were established by a study of the NMR spectra. The NMR spectra of these two products are very similar and shown that the number of hydrogen atoms at the carbon-bearing phosphorus is one. The optical rotations differed by $+32°$ and $-13°$ respectively. However, from the present results, it seems to be difficult to identify either of the two products as [8] or [9]. The mol ratio of the two products was 5 to 2.

The compound [4] was exposed to UV radiation in the presence of DETP; the solution was then concentrated *in vacuo* to give, in an almost quantitative yield, an oil containing one product, as indicated by thin-layer chromatography. After vacuum distillation, this product was identified as 5-deoxy-

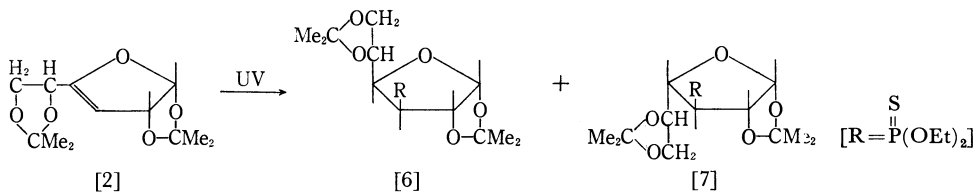

[2] [6] [7]

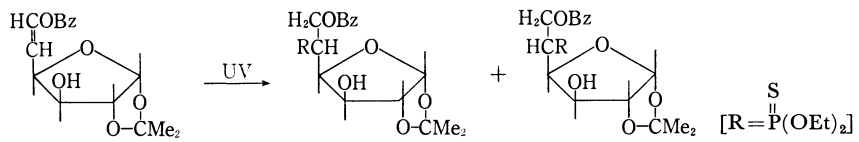

[3] [8] or [9] [9] or [8]

11) A. N. Pudovik and I. V. Konovalova, *Zh. Obshch. Khim.*, **30**, 2348 (1960).
12) J. Lehmann, *Carbohydrate Res.*, **2**, 486 (1966).
13) J. Lehmann, *ibid.*, **2**, 499 (1966).
14) H. Paulsen, *ibid.*, **2**, 80 (1966); L. Lehmann, *ibid.*, **2**, 1 (1966), and so on.
15) R. J. Abraham, L. D. Hall, L. Hough and K. A. McLauchlan, *J. Chem. Soc.*, **1962**, 3699.

*2 The product still contained a small amount of impurities.

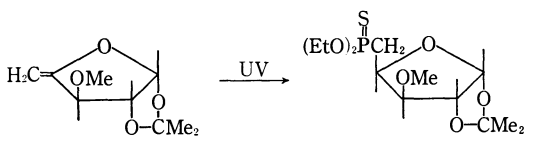

[4] [10]

5-(diethyl thiophosphonate)-1,2-*O*-isopropylidene-3-*O*-methyl-α-D-xylofuranose [10]. The structure of this product was established by elementary analysis and by a study of the NMR spectrum. The coupling constant, $J_{3,4}=1.6$ Hz, in the NMR spectrum and the finding that the photochemical addition of benzyl mercaptan to [4] gave only one product, 5-benzylthio-5-deoxy-1,2-*O*-isopropylidene-3-*O*-methyl-α-D-xylofuranose,[9] show that [10] has the configuration of xylofuranose.

The results described above are summarized in Table 1.

The authors express their sincere thanks to Professor R. L. Whistler of Purdue University for his continued interest in this work and to Professor S. Kunichika of Kyoto University for carrying out elementary analyses. They are also grateful to Hashimoto Kaseikogyo, Ltd. for supplying them silver fluoride.

TABLE 1. THE FORMATION OF SUGARS CONTAINING A CARBON-PHOSPHORUS BOND BY THE PHOTOCHEMICAL ADDITION OF DIETHYL THIOPHOSPHONATE TO UNSATURATED SUGARS

Unsaturated sugars	Products	Mol ratios of products	Mp or bp	$[\alpha]_D^{16}$ ($CHCl_3$)
[1]	[5]	—	mp 114°C	+23.4° (*c* 10)
[2]	[6]	4	bp 175—177°C/2 mmHg	− 4.6° (*c* 21)
	[7]	1		− 9.3° (*c* 6)
[3]	[8]	2 or 5	bp 120—125°C/10^{-3}—10^{-4} mmHg	+32° (*c* 17)
	[9]	5 2		−13° (*c* 17)
[4]	[10]	—	bp 149°C/2 mmHg	−23.2° (*c* 10)*

* $[\alpha]_D^{20}$ (CCl_4)

BULLETIN OF THE CHEMICAL SOCIETY OF JAPAN VOL. 42 3249—3254 (1969)

One-Electron Reduction of Carbonium Ions. II. Reduction of the Tropylium Ion and the Triphenylmethyl Cation with Metallic Powders and Metallic Ions*1

Kunio OKAMOTO, Kôichi KOMATSU and Haruo SHINGU

Department of Hydrocarbon Chemistry, Faculty of Engineering, Kyoto University, Yoshida, Sakyo-ku, Kyoto

(Received April 28, 1969)

The reaction of tropylium fluoroborate in an aqueous solution has been carried out at room temperature with powders of various metals (Mg, Al, Mn, Zn, Cr, Fe, Cd, Co, Ni, Sn, Pb, Sb, Cu, Hg, and Ag) under heterogeneous conditions and with several metallic ions (Cr(II), Ti(III), Sn(II), Cu(I), Fe(II), Fe(III), Hg(I), Hg(II), and Ag(I)) in a homogeneous solution. All these reagents, except Ag, Fe(III), Hg(I), Hg(II), and Ag(I), reduce with ease the tropylium ion to give the tropyl radical, which then rapidly couples to bitropyl; their reducing powers, estimated by comparing the yields of bitropyl under the same reaction conditions, correlate with their oxidation electrode potentials and oxidation-reduction potentials. The ferric ion, the mercurous ion, the mercuric ion, and the silver ion afforded no bitropyl, but only an oxidation product of the tropylium ion, *i.e.*, benzaldehyde. Silver powder gives neither a reduction nor an oxidation product under these reaction conditions. The reduction has also been carried out in an acetonitrile solution, and the reducibility of tropylium fluoroborate with powders of Zn, Fe, Ni, Sb, Cu, and Ag has been compared with that of triphenylmethyl fluoroborate under heterogeneous conditions. Both the tropylium ion and the triphenylmethyl cation are smoothly reduced by Zn, Fe, Ni, Sb, and Cu in this solvent. The tropylium ion, however, is not reduced by silver powder, while the triphenylmethyl cation is reduced to the triphenylmethyl radical. This greater reducibility of the triphenylmethyl cation is consistent with what could be anticipated from the data of half-wave potentials, ionization potentials, and H.M.O. calculation reported with respect to these two carbonium ions.

Although the reactivity scale of carbonium ions in a one-electron reduction in the gaseous phase has araised much theoretical interest in association with the ionization potential of organic radicals to carbonium ions,[1] relatively little attention has been devoted to the reducibility scale in solutions, and the range of carbonium-ion structures investigated is quite small. Heretofore, the tropylium ion[2] and the triarylcyclopropenyl[3] and polyarylmethyl cations[2c-4] have been reported to be carbonium ions whose reducibilities in the liquid phase have been determined by a polarographical method[2,3] and by the measurement of the reversible-electrode reduction potentials of the solutions of carbonium ions and the corresponding redicals.[4] Thus, a systematic investigation into the reducibility scale in solution for other carbonium ions with a wide range of structures should be of considerable interest. However, preliminary to a systematic scrutiny of the carbonium-ion structure, the exploration of simple reducing agents with a wide range of applicability is needed because of the restricted applicability of the electrochemical measurements.[2-4]

As for the reducing agents of the carbonium ions, Conant and his collaborators[5] first demonstrated that the vanadous ion reduces serveal stable polyarylmethyl cations. There have since been employed such reductants as the chromous ion,[6] zinc,[7]

*1 Part I: K. Okamoto, Y. Matsui and H. Shingu, This Bulletin, **38**, 153 (1965).

1) For a review, see K. Okamoto, *Kogyo Kagaku Zasshi (J. Chem. Soc. Japan, Ind. Chem. Sect.)*, **69**, 825 (1966).

2) a) M. E. Vol'pin, S. I. Zhdanov and D. N. Kursanov, *Dokl. Acad. Nauk SSSR*, **112**, 264 (1957); *Chem. Abstr.*, **51**, 12057e (1957). b) P. Zuman, J. Chodkowski, H. Potesilova and F. Santavy, *Nature*, **182**, 1535 (1958). c) M. I. James and P. H. Plesch, *Chem. Commun.*, **1967**, 508.

3) R. Breslow, W. Bahary and W. Reinmuth, *J. Am. Chem. Soc.*, **83**, 1763 (1961).

4) E. D. Jenson and R. W. Taft, *ibid.*, **86**, 116 (1964).

5) a) J. B. Conant and A. W. Sloan, *J. Am. Chem. Soc.*, **45**, 2466 (1923). b) J. B. Conant and A. W. Sloan, *ibid.*, **47**, 572 (1925). c) J. B. Conant, L. F. Small and B. S. Tayler, *ibid.*, **47**, 1959 (1925). d) J. B. Conant and L. F. Small, *ibid.*, **47**, 3068 (1925). e) J. B. Conant, L. F. Small and A. W. Sloan, *ibid.*, **48**, 1743 (1926).

6) K. Ziegler, F. A. Fries and F. Sälzer, *Ann.*, **448**, 249 (1926).

7) W. von E. Doering and L. H. Knox, *J. Am. Chem. Soc.*, **79**, 352 (1957).

ferrocene,[8] tetraphenyl-*p*-xylylene,[9] the dinegative ion of cyclooctatetraene,[10] carbazole,[11] phenylenediamine,[11] the triphenylmethyl radical,[12] and others.[13] Among these reducing agents we chose various metals and low-valent metallic ions with the idea that these reducing agents would show various degrees of reducing power, which would correlate with their oxidation electrode potentials and oxidation-reduction potentials, and that a spectrum of the percentage yields of the reduction products would reflect the intrinsic reducibility of the carbonium ion concerned. In this paper we will report on the results of the reduction of the tropylium ion and of the triphenylmethyl cation with these reductants in aqueous and in acetonitrile solutions and will discuss the applicability of the spectrum of the radical yields as a measure for estimating the reducibility of the respective stable carbonium ions.

Reduction of the Tropylium Ion in an Aqueous Solution with Metallic Powders. A 0.1N solution of tropylium fluoroborate in 0.1N hydrochloric acid[14] was treated with various metallic powders at room temperature for ten minutes. As Doering and Knox[7] found in zinc-dust reduction, most of the metals examined (see Table 1) were found to reduce the tropylium ion to bitropyl readily. As Table 1 shows, magnesium, aluminum, manganese, zinc, iron, cadmium, cobalt, tin, lead, and antimony afforded bitropyl in fairly good yields, whereas the yield of bitropyl was poor in the cases of chromium (1%), nickel (0.4%), copper (0.2%), and mercury (0.03%). In each reduction only the unchanged tropylium ion was identified as an organic compound other than bitropyl, and a good material balance (>94%) was obtained. Since these reductions were carried out under heterogeneous conditions and with metals of various grain sizes, the percentage yields of bitropyl might not exactly reflect the intrinsic reducing powers of these metals. However, an examination of the standard oxidation electrode potentials of these metals reveals that there exists a correlation between the spectra of the values of the bitropyl yield and of the oxidation electrode potentials of these metals; that is, under these reduction conditions the reducibility of the tropylium ion seems to correspond to the values of the oxidation electrode potential between those of mercury and silver, *i. e.*, −0.789 and −0.799 V.

Table 1. The reduction of the tropylium ion in the aqueous solution with metallic powders at 21—31°C[a]

Metal (mesh)	Oxidation potential[b] (V)	Bitropyl Yield (%)	Tropylium ion, unchanged[e] (%)
Mg (200—250)	2.37	92	3.2
Al (200—250)	1.66	99	0.0
Mn (>400)	1.18	98	1.8
Zn (>400)	0.763	100	0.0
Cr (200—250)	0.74	1.0	99
Fe (200—250)	0.440	20	79
Cd (>200)	0.403	26	73
Co (>250)	0.277	94	0.0
Ni (>400)	0.250	0.4[d]	95
Sn (>400)	0.136	100	0.0
Pb (200—250)	0.126	60	41
Sb (200—250)	−0.212	5.4	94
Cu (200—250)	−0.521	0.2[d]	95
Hg (liq.)[c]	−0.789	0.03[d]	99
Ag (≷200)	−0.799	0.0[d]	99

a) Except when otherwise noted, all reactions were conducted with about 15 molar equivalents of metallic powder under an atomosphere of nitrogen for ten minutes, aqueous hydrochloric acid (0.1N) being used as the solvent. Initial concentration of tropylium fluoroborate was 0.100N.
b) W. M. Latimer, "Oxidation Potentials," Prentice-Hall (1952).
c) The reaction was carried out for 30 min with 50 molar equivalents of mercury, aqueous nitric acid (0.1N) being used as the solvent.
d) Estimated by t.l.c. analysis.
e) Determined by UV spectrophotometry.

Reduction of the Tropylium Ion in an Aqueous Solution with Low-Valent Metallic Ions. An aqueous 0.1N hydrochloric acid solution of tropylium fluoroborate (0.1N) was treated with about three equivalents of various metallic ions at room temperature under an atmosphere of nitrogen. As is shown in Table 2, bitropyl was readily obtained as the sole product in the reductions with chromous[15] and titanous ions, whereas it was obtained in poor yields in the reduction with stannous, cuprous, and ferrous ions. However, the mercurous ion, which oxidation-reduction potential is the lowest among the ions examined,

8) M. F. Hawthorne, *J. Org. Chem.*, **21**, 363 (1956).
9) a) E. Weitz and F. Schmidt, *Ber.*, **75**, 1921 (1942). b) H. Hart, J. S. F. Flemming and J. L. Dye, *J. Am. Chem. Soc.*, **86**, 2079 (1964).
10) a) K. Conrow and P. C. Radlick, *J. Org. Chem.*, **26**, 2260 (1961). b) R. W. Murray and M. L. Kaplan, *ibid.*, **31**, 962 (1966).
11) A. Ledwith and M. Sambhi, *Chem. Commun.*, **1965**, 64.
12) J. W. Lown, *Proc. Chem. Soc.*, **1963**, 283.
13) J. E. Leffler, *J. Am. Chem. Soc.*, **75**, 3598 (1953).
14) The degree of hydrolysis of the tropylium ion in this solution was calculated to be 1.8×10^{-2}%, using the value of the equilibrium constant measured by Doering and Knox (W. von E. Doering and L. H. Knox, *J. Am. Chem. Soc.*, **76**, 3203 (1954)).
15) The reduction rate of the tropylium ion by the chromous ion has been measured by a flow method. The details of the experiment will be reported elsewhere.

TABLE 2. THE REACTION OF THE TROPYLIUM ION IN THE AQUEOUS SOLUTION WITH METALLIC IONS AT 18—28°C[a)]

Ion	Oxidation potential[b)] (V)	Reaction time (hr)	Bitropyl yield (%)	Benzaldehyde yield (%)	Tropylium ion unchanged[e)] (%)
Cr(II)[c)]	0.41	0.01	100	0.0	0.0
Ti(III)	−0.1	0.17	18	0.0	84
Sn(II)	−0.15	2	0.2[f)]	0.0	97
Cu(I)	−0.153	2	0.02[f)]	0.0	101
Fe(II)	−0.771	2	0.6[f)]	~0.1	102
Hg(I)[d)]	−0.920	2	0.0[f)]	35	0.0
Fe(III)		2	0.0[f)]	9.3	65
Hg(II)		2	0.0[f)]	46	0.0
Ag(I)		2	0.0[f)]	~1	100

a) Except when otherwise noted, all reactions were conducted with three molar equivalents of metal chloride under an atmosphere of nitrogen, and aqueous hydrochloric acid (0.1N) was used as the solvent. Initial concentration of tropylium fluoroborate was 0.100N.
b) W. M. Latimer, "Oxidation Potentials," Prentice-Hall (1952).
c) Chromous sulfate was used.
d) Mercurous nitrate was used, along with 0.02N nitric acid as the solvent.
e) Determined by UV spectrophotometry.
f) Estimated by t.l.c. analysis.

afforded no detectable amounts of bitropyl, but an oxidation product of the tropylium ion, *i. e.*, benzaldehyde,[16,17)] in the 35% yield. Furthermore, in this reaction the mercurous ion was reduced to metallic mercury by the tropylium ion. The formation of benzaldehyde due to the oxidation of the tropylium ion was also observed in the reaction with mercuric, ferric, and silver ions in yields of 46, 9.3, and ~1% respectively (Table 2). Thus, as in the case of metallic powder reduction under heterogeneous conditions, the correlation between the reducing power of low-valent metallic ions, as measured by the use of the yields of bitropyl, and of the oxidation-reduction potential of these metallic ions seems to be fairly good; in Table 2 it is clearly demonstrated that the tropylium ion in an aqueous solution can be reduced by the ions with oxidation-reduction potentials with values higher than that of the ferrous ion, and that under these reaction conditions the oxidation-reduction potential of the tropylium ion seems to be just between those of ferrous and mercurous ions, *i. e.*, −0.771 and −0.920 V.

Reduction of the Tropylium Ion and the Triphenylmethyl Cation in an Acetonitrile Solution with Metallic Powders. Since it has been demonstrated for the tropylium ion that its reducibility can be estimated by the use of a spectrum of bitropyl yields in the reduction with various metallic powders, the reducibility of the other carbonium ion was examined by the use of this method. Among the other carbonium ions the triphenylmethyl cation was chosen as a representative carbonium ion, which is stable in an acetonitrile solution. For purposes of comparison, the tropylium ion was reduced also in an acetonitrile solution. In each reduction the respective carbonium ions were allowed to react with 15 molar equivalents of various metallic powders under exactly the same reaction conditions as those employed in the experiments with the tropylium ion in an aqueous solution.

The spectrum of the yields of the reduction product is shown in Table 3, along with the values for the oxidation-electrode potentials of metals and the half-wave potentials of the respective metallic ions in an acetonitrile solution.

In an acetonitrile solution the triphenylmethyl cation was smoothly reduced by zinc dust to the triphenylmethyl radical, which was identified as triphenylmethyl peroxide and a minor amount of benzophenone after its oxidation by air. Similarly, the tropylium ion in acetonitrile was readily reduced by zinc dust to bitropyl, as was observed in an aqueous solution. Iron powder and copper powder also reduced each carbonium ion with ease. It is of interest to note that the yield of bitropyl in copper reduction increased from 0.2% in an aqueous solution (Table 1) to 100% in acetonitrile (Table 3). This dramatic increase in the yield may be a reflection of an intrinsic increase in the reducing power of copper in acetonitrile, as is shown by the relatively higher values of the oxidation-electrode potential of the metal and the half-wave potential of the ion (Table 3), values which

16) It is reported that the tropylium ion is oxidized to benzaldehyde by bromine in absolute alcohol,[17)] by dilute aqueous permanganate,[17)] by chromic acid in acetic acid,[7)] and by silver oxide in water.[7)]
17) M. J. S. Dewar and R. Pettit, *J. Chem. Soc.*, **1956**, 2026.

Table 3. The reduction of the tropylium ion and the triphenylmethyl cation in the acetonitrile solution with metallic powders at 14—24°C[a)]

Metal (mesh)	Zn (>400)	Fe (150—250)	Ni (>400)	Sb (200—250)	Cu (>400)	Ag (≳200)
Reduction of tropylium ion:						
Bitropyl, yield (%)	100	48	0.1[c)]	2.3	100	0.0[b,c)]
Tropylium ion, unchanged (%)[d)]	0.0	—	94	—	0.0	82
Reduction of triphenylmethyl cation:						
Triphenylmethyl radical, yield (%)[e)]	73	69	0.6	1.7	63	43
Triphenylmethyl cation, unchanged (%)[f)]	19	29	98	100	27	51
$-E_{1/2}$ in acetonitrile[g)] (Hg electrode) (V)	0.70	1.00	0.33	—	0.36	−0.32
Oxidation electrode pot.[h)] in acetonitrile (V)	0.74	—	—	—	0.38	−0.23

a) All reactions were conducted with about 15 molar equivalents of metallic powder under an atmosphere of nitrogen for ten minutes. Initial concentrations of tropylium ion and of triphenylmethyl cation were 0.100N.
b) Tropone (15% yield), identified by the superimposability of the IR spectrum, was obtained as a reaction product.
c) Estimated by t.l.c. analysis.
d) Determined by UV spectrophotometry.
e) The sum of the yields of triphenylmethyl peroxide and of benzophenone. The yields of benzophenone were *ca.* 1% for Zn, *ca.* 4% for Cu, and *ca.* 2% for Ag. No benzophenone was produced in the reactions with Fe, Ni and Sb powders.
f) Isolated as triphenylcarbinol.
g) The half-wave potentials of the corresponding metallic ions, measured *vs.* aqueous SCE; I. M. Kolthoff and J. F. Coetzee, *J. Am. Chem. Soc.*, **79**, 870, 1852 (1957).
h) W. A. Plaeskow, *Zh. Fiz. Khim.*, **22**, 351 (1948).

are closely related to the stabilization of the cuprous ion caused by the strong solvation by the acetonitrile molecules (see the references cited in Table 3).

As has been shown in an aqueous solution, nickel and antimony, which have relatively lower oxidation-electrode potentials, were found to have low reducing powers in acetonitrile for each carbonium ion, this being shown in the low yields of the reduction product from each carbonium ion (Table 3).

Silver did not show any reducing power to the tropylium ion under these reaction conditions; this is a result similar to that observed in an aqueous solution (Tables 1 and 3). In contrast to this, the triphenylmethyl cation was easily reduced by silver powder, indicating that this cation is more reducible than the tropylium ion (Table 3).

The ready reducibility of the triphenylmethyl cation observed in these experiments is consistent with the following reactivity sequence of these two cations: (a) the half-wave potentials of the tropylium ion and the triphenylmethyl cation, measured in methylene dichloride by direct-current polarography, are estimated to be −0.45 and −0.135 V respectively,[2c)] showing the ready reducibility of the latter cation; (b) the ionization potentials of tropyl and triphenylmethyl radicals in the gaseous phase are determined to be 6.60 and 7.25 eV[18)] respectively, indicating that the former radical is more easily transformed into the tropylium ion (in other words, the tropylium ion is less reducible). The loss of delocalization energy resulting when the tropylium ion is converted to the tropyl radical is calculated to be $-0.45\,\beta$ (from the simple H.M.O. theory),[19)] whereas between the triphenylmethyl cation and radical there exists no difference in delocalization energy. When we assume that the reducibility of the cation is governed by the difference in the electronic stabilization (delocalization) energy between the carbonium ion and the corresponding radical, this reslut of calculation is also consistent with the ready reducibility of the triphenylmethyl cation.

18) Cited in Ref. 2c.

Experimental[20)]

Materials. Tropylium fluoroborate was prepared from tropilidene according to the method of Conrow,[21)] that is, by hydride abstraction with phosphorus pentachloride and by the subsequent addition of aqueous

19) A. Streitwieser, Jr., and J. I. Brauman, "Supplemental Tables of Molecular Orbital Calculations," Pergamon Press, London (1965).

20) The infrared and the ultraviolet spectra were obtained from Shimadzu models, an IR-27 spectrometer and a UV-50M spectrometer respectively.

fluoroboric acid. Tropilidene was prepared by the reaction of a large excess of benzene with diazomethane in the presence of cuprous bromide as a catalyst, according to the method of Müller and Fricke.[22] Triphenylmethyl fluoroborate was prepared by the reaction of triphenylcarbinol with aqueous fluoroboric acid in propionic anhydride, according to the method of Dauben *et al.*[23] Acetonitrile was refluxed over phosphorus pentoxide and distilled; bp 80.8—81.2°C. For all the inorganic reagents, except silver powder, commercial materials were used as received. Metallic silver was prepared by the reduction of silver nitrate with saccharose, as has been described by Brauer,[24] while metallic copper employed was the electrolytically-prepared material supplied by the E. Merck Co.

The Reduction of the Tropylium Ion in an Aqueous Solution with Metallic Powders. The results are shown in Table 1; the details of the procedure are illustrated in the following description of a representative run with metallic iron.

The Reduction of the Tropylium Ion in an Aqueous Solution with Iron. In a 50-m*l*, round-bottomed flask equipped with a magnetic stirring bar, a thermometer, and a nitrogen inlet and outlet, 0.399 g of tropylium fluoroborate (2.24 mmol) was dissolved in 22.4 m*l* of 0.1N aqueous hydrochloric acid to give a clear, colorless solution. To the stirred solution of the tropylium ion there was then added a 1.865-g portion of iron powder (200—250 mesh) (33.4 mg atom) under an atmosphere of nitrogen at 30.8°C. The reaction temperature immediately rose by 1.1°C and remained almost constant for 10 min. The reaction mixture was then filtered and washed with three 5-m*l* portions of 0.1N aqueous hydrochloric acid and with five 10-m*l* portions of ether. The amount of the unchanged tropylium ion in the aqueous layer was estimated from the ultraviolet absorbance of the tropylium ion ($\lambda_{max}^{0.1NHCl}$ 219 and 275 mμ); 79.4% of the charged ion. The organic layer was washed once with 40 m*l* of 5% aqueous sodium carbonate and twice with 40 m*l* of 10% aqueous sodium chloride, dried over magnesium sulfate, concentrated by distillation, and evaporated *in vacuo* to give 0.0407 g of bitropyl (0.224 mmol, 20.0% yield), identified by the superimposability of the infrared spectrum on that of the authentic sample.

The Reduction of the Tropylium Ion in an Aqueous Solution with Low-Valent Metallic Ions. The results are shown in Table 2; the details of the procedure are illustrated in the following description of a run which affords a small amount (<1% yield) of the reduction product.

The Reduction of the Tropylium Ion in an Aqueous Solution with Ferrous Chloride. In a 50-m*l*, round-bottomed flask equipped with a magnetic stirring bar, a thermometer, a rubber serum bottle cap, and a nitrogen inlet and outlet, 0.322 g of tropylium fluoroborate (1.81 mmol) was dissolved in 6.0 m*l* of 0.1N aqueous hydrochloric acid and then kept under an atmosphere of nitrogen. The aqueous solution of ferrous chloride was prepared by dissolving 1.067 g of $FeCl_2 \cdot 4H_2O$ (5.37 mmol) in 12.1 m*l* of 0.1N aqueous hydrochloric acid. The ferrous chloride solution was added with a syringe through the rubber serum cap to a stirred solution of tropylium fluoroborate. A specific change in neither the color nor reaction temperature was observed. The solution was stirred under nitrogen at 18.0—20.0°C for two hours and then extracted with three 20-m*l* portions of ether. The amount of the unchanged tropylium ion was determined from the ultraviolet absorbance (*vide supra*) of the aqueous layer (102% of the charged tropylium ion). The organic layer was washed with a 40-m*l* portion of 5% aqueous sodium carbonate and with two 50-m*l* portions of 10% aqueous sodium chloride, and was then dried over magnesium sulfate. The dried ethereal solution was concentrated and evaporated *in vacuo* to give 0.0027 g of a colorless oil, which was shown to be a mixture of bitropyl, benzaldehyde, and other minor components by a study of the infrared spectrum. The t.l.c. analysis of the oily product with the authentic bitropyl showed that the bitropyl content was *ca.* 38 wt% of the oil; 0.0055 mmol, 0.6% yield, based on the charged tropylium ion.

The Reduction of the Tropylium Ion and the Triphenylmethyl Cation in an Acetonitrile Solution with Metallic Powders. The results are shown in Table 3; the reaction of the tropylium ion with the metallic powder was carried out at room temperature for 10 min under nitrogen and worked up in a manner similar to that described above. The details of the procedure in the reaction of the triphenylmethyl cation are illustrated in the following description of a representative run with metallic iron.

The Reduction of the Triphenylmethyl Cation in an Acetonitrile Solution with Iron. In a 50-m*l*, round-bottomed flask equipped with a magnetic stirrer, a thermometer, and a nitrogen inlet and outlet there was placed a 0.504-g portion of triphenylmethyl fluoroborate (1.53 mmol). In a stream of nitrogen 15.3 m*l* of acetonitrile was added, and a clear, orange colored solution was obtained by magnetic stirring; the initial concentration of the triphenylmethyl cation was 0.100N. To the stirred solution there was then added a 1.299-g portion of iron powder (150—250 mesh) (23.3 mg atom) under an atmosphere of nitrogen at 20.5°C. The reaction temperature rose by 4.1°C within two minutes and remained almost constant for the rest of the reaction time. With the increase in the temperature, it was observed that a white precipitate appeared and was dispersed throughout the reaction vessel. After the reaction time of 10 min, 10-m*l* portions of water and ether were added to the reaction mixture with continuous stirring in order to stop the reaction by the hydrolysis of the unchanged cation. The reaction mixture was filtered and washed with three 10-m*l* portions of ether in a stream of nitrogen. Air was then bubbled into the pale yellow organic layer. A white precipitate was formed with the simultaneous disappearance of the yellow color of the solution. This precipitate was filtered, washed with ether, and dried at 60°C under reduced pressure (5 mmHg) to give 0.272 g of white, powdery crystals, identified as triphenylmethyl peroxide by the superimposability of the infrared spectrum; 0.524 mmol, 68.6% yield. The organic layer of the

21) K. Conrow, "Organic Syntheses," Vol. 43, p. 101 (1963).
22) E. Müller and H. Fricke, *Ann.*, **661**, 38 (1963).
23) H. J. Dauben, Jr., L. R. Honnen and K. M. Harmon, *J. Org. Chem.*, **25**, 1442 (1960).
24) G. Brauer, "Handbuch der Präparativen Anorganischen Chemie," Ferdinand Enke Verlag, Stuttgart (1954), p. 765.

filtrate was separated, washed with a 80-m*l* portion of 5% aqueous sodium carbonate and with two 80-m*l* portions of 10% aqueous sodium chloride, and dried over magnesium sulfate. The dried ethereal solution was concentrated by distillation and evaporated *in vacuo* to give 0.117 g of white crystals; the crystals were identified as triphenylcarbinol by a study of the infrared spectrum; 0.448 mmol, 29.3% yield.

The authors wish to thank Professor W. von E. Doering of Harvard University for his encouragement and interest.

BULLETIN OF THE CHEMICAL SOCIETY OF JAPAN VOL. 42 3254—3258 (1969)

Intermolecular Hydrogen Bond Involving a π Base as the Proton Acceptor. VI. Hydrogen Bonding of Phenols and Naphthols to Aromatic Hydrocarbons. Entropy Anomaly and the Role of Charge-Transfer

Zen-ichi Yoshida and Nobuyuki Ishibe*

Department of Synthetic Chemistry, Kyoto University, Yoshida, Sakyo-ku, Kyoto

(Received April 30, 1969)

Using a series of alkylphenols and naphthols as the proton donors, the hydrogen bond shifts and the association constants of hydrogen-bonded complexes involving methyl benzenes, naphthalene, and phenanthrene as the proton acceptors have been determined from the infrared spectra in carbon tetrachloride. The frequency shifts ($\Delta\nu$) of the hydroxyl stretching vibration and the free energy changes ($-\Delta F$) for complex formation increase with decreasing pK_a of the proton donors. Linear correlation between $-\Delta F$ and $\Delta\nu$ are obtained for each proton donor interacting with methyl benzenes. The entropy anomaly discovered previously was confirmed. Charge-transfer arguments of Basila and co-workers are reconsidered for the hydrogen-bonded systems involving a π base as the proton acceptor.

Recently, there has been increasing evidence for hydrogen bond formation involving olefins and aromatics as the proton acceptors,[1,2] and this has been quantitatively studied by several investigators.[3–5] A good linear correlation of pK_a *vs.* the hydrogen-bonded frequency shift exists for many compounds of entirely different functional types.[1] Recently we have developed such a correlation for the hydrogen bonding of 4-substituted-2,6-xylenols to mesitylene.[6]

The purpose of this paper is to confirm (A) the existence of this correlation through methyl benzenes, naphthalene, and phenanthrene as the proton acceptor and (B) the correlation between the association constants and $\Delta\nu$. Another objective is to show the importance of charge-transfer type contributions[7] to hydrogen bond which are revealed from the results of infrared spectroscopic measurements.

Experimental

The OH stretching absorption spectra were scanned on a Shimadzu IR 600 (high precision grating spectrophotometer) with spectral slit width 1.5 cm^{-1} in the region of 3 μ. The cells had an optical path length of 0.2 cm, and were equipped with NaCl windows. The

*1 Present address: Department of Chemistry, University of Illinois at Chicago Circle, Chicago, Illinois 60680, U.S.A.

1) For a review, see E. M. Arnett, "Progress in Physical Organic Chemistry," ed. by S. G. Cohen, A. Streitwieser, Jr., and R. W. Taft, Vol. 1, Interscience Publ., New York (1963), p. 259.

2) a) L. P. Kuhn and R. E. Bowman, *Spectrochim. Acta*, **23A**, 189 (1967). b) R. J. Oullette, D. L. Marks and D. Miller, *J. Am. Chem. Soc.*, **89**, 913 (1967). c) M. R. Basila, E. L. Saier and L. R. Cousins, *ibid.*, **87**, 1665 (1965). d) C. J. Collins, *ibid.*, **89**, 1652 (1967).

3) M. Ōki and H. Iwamura, *J. Am. Chem. Soc.*, **89**, 567 (1967) and the preceding papers.

4) L. Joris, P. v. R. Schleyer and R. Gleiter, *ibid.*, **90**, 327 (1968) and the preceding papers.

5) a) Z. Yoshida and E. Ōsawa, *J. Am. Chem. Soc.*, **87**, 1467 (1965). b) Z. Yoshida and E. Ōsawa, *ibid.*, **88**, 4019 (1966). c) Z. Yoshida and N. Ishibe, *ibid.*, **91**, (1969), in press.

6) Z. Yoshida and N. Ishibe, to be published.

7) For a review, see S. Bratoz, "Advances in Quantum Chemistry," ed. by L. O. Lowdin, Vol. 3, Academic Press, New York (1967), p. 209.

TABLE 1. HYDROGEN BOND SHIFT $\Delta\nu_{OH}$ AND FREE ENERGY CHANGE $-\Delta F$ DUE TO 1:1 HYDROGEN BONDED COMPLEX FORMATION AND APPARENT INTEGRATED MOLAR ABSORPTION COEFFICIENT OF BONDED OH BAND A^b IN CCl_4 AT 26°C

(A) $\Delta\nu_{OH}$ (cm^{-1})

Proton donor	nil (ν_f)	π-Base 1 Benzene	2 Toluene	3 *m*-Xylene	4 *o*-Xylene	5 *p*-Xylene	6 Mesitylene	7 Hexamethyl-benzene	8 Naphthalene	9 Phenanthrene
α-Naphthol	3608.0±0.4	51.9±0.8	58.9±0.8	69.3±0.8	69.4±0.8	70.0±0.8	80.0±0.6	108.7±0.5	47.0±0.8	48.1±0.7
β-Naphthol	3609.2±0.4	50.2±0.8	57.5±0.8	68.0±0.8	68.5±0.8	69.5±0.7	79.1±0.7	105.1±0.5	46.5±0.9	46.8±0.8
Phenol[a)]	3610.0±0.4	49.2±0.8	57.0±0.8	66.5±0.7	66.5±0.7	69.0±0.7	77.0±0.6	104.8±0.5	46.2±0.8	46.8±0.8
m-Cresol	3611.0±0.5	48.0±0.7	55.0±0.8	65.0±0.8	66.5±0.8	67.0±0.7	76.0±0.6	103.0±0.6	44.3±0.7	46.2±0.7
p-Cresol	3611.8±0.4	47.3±0.7	54.6±0.8	63.5±0.7	65.0±0.7	66.0±0.8	74.8±0.7	102.0±0.6	43.0±0.8	45.5±0.8
o-Cresol	3612.5±0.5	46.5±0.8	53.5±0.8	63.2±0.8	65.0±0.7	65.5±0.8	74.2±0.7	102.0±0.5	43.0±0.9	45.3±0.7
p-*t*-Butylphenol	3613.0±0.5	46.5±0.8	53.3±0.8	62.7±0.8	64.2±0.8	64.0±0.8	74.0±0.6	101.0±0.6	43.0±0.9	45.2±0.8

(B) $-\Delta F$ (kcal/mol)

Proton donor	π-Base 1 Benzene	2 Toluene	3 *m*-Xylene	4 *o*-Xylene	5 *p*-Xylene	6 Mesitylene	7 Hexamethyl-benzene	8 Naphthalene	9 Phenanthrene
α-Naphthol	−0.69±0.03	−0.58±0.02	−0.45±0.03	−0.44±0.04	−0.40±0.04	−0.26±0.02	0.11±0.03	−0.26±0.02	−0.22±0.06
β-Naphthol	−0.71±0.02	−0.62±0.03	−0.47±0.06	−0.46±0.03	−0.43±0.03	−0.28±0.02	0.10±0.02	−0.27±0.01	−0.23±0.02
Phenol[a)]	−0.73±0.03	−0.62±0.02	−0.51±0.01	−0.47±0.03	−0.45±0.02	−0.30±0.03	0.03±0.03	−0.27±0.04	−0.23±0.03
m-Cresol	−0.75±0.01	−0.65±0.03	−0.51±0.04	−0.50±0.04	−0.47±0.03	−0.35±0.02	0.01±0.01	−0.28±0.03	−0.25±0.04
p-Cresol	−0.78±0.01	−0.69±0.01	−0.54±0.02	−0.53±0.02	−0.49±0.02	−0.39±0.01	−0.04±0.02	−0.30±0.03	−0.27±0.03
o-Cresol	−0.81±0.05	−0.71±0.02	−0.58±0.03	−0.56±0.01	−0.53±0.02	−0.41±0.02	−0.10±0.01	−0.31±0.04	−0.26±0.05
p-*t*-Butylphenol	−0.80±0.02	−0.73±0.03	−0.60±0.04	−0.59±0.03	−0.54±0.04	−0.45±0.02	−0.13±0.04	−0.31±0.05	−0.26±0.05

(C) A^b ($l\cdot mol^{-1}\cdot cm^{-1}\times 10^{-4}$) (In part)

Proton donor	π-Base 1 Benzene	2 Toluene	3 *m*-Xylene	4 *o*-Xylene	5 *p*-Xylene	6 Mesitylene	7 Hexamethyl-benzene	8 Naphthalene	9 Phenanthrene
α-Naphthol	1.97±0.33	1.99±0.20	2.44±0.02	2.24±0.14	2.50±0.20	2.64±0.21	2.79±0.32	2.26±0.37	2.50±0.14
Phenol	1.95±0.20	2.16±0.13	2.27±0.10	2.43±0.20	2.54±0.10	2.71±0.16	3.03±0.18	2.09±0.21	2.29±0.30
p-*t*-Butylphenol	1.46±0.10	1.55±0.15	1.77±0.13	1.94±0.14	1.82±0.09	2.05±0.16	2.21±0.13	1.69±0.11	1.82±0.21

a) Literature values are summarized in Ref. 5a and 5b.

concentration of phenols and naphthols in carbon tetrachloride was kept below 0.015—0.010 mol/*l* to avoid self-association of the proton donor. Concentration of π bases ranged from 0.2 to 4 mol/*l*. All measurements were carried out at average room temperature of 26°C. Two peaks were observed on all spectra, as is well-known in hydrogen-bonded systems.[8] A previously described procedure was employed for calculating the equilibrium constants and the apparent integrated molar absorption intensities of the OH···π complexes and for analyzing the infrared spectra to obtain the hydrogen-bonded frequency shifts.[5a]

All materials used were commerciall products and purified by the usual methods.

Results

In the presence of aromatic hydrocarbons, the spectra of the hydroxyl stretching vibration of alkylphenols and naphthols in carbon tetrachloride were seen as doublets. Table 1 summarizes: (A) Shifts of ν_{OH} of alkylphenols and naphthols due to interaction with the added π base ($\Delta\nu$); (B) free energy change, $-\Delta F$, due to 1 : 1 hydrogen bond complex formation; and (C) apparent integrated molar absorption coefficient, A^b, of the bonded OH bond.

Discussion

Effect of the pK_a of proton donors on $\Delta\nu$ and $-\Delta F$: The previous works with *t*-BuOH,[2c] pyrrole,[9] and phenol[5a,10] as proton donors showed

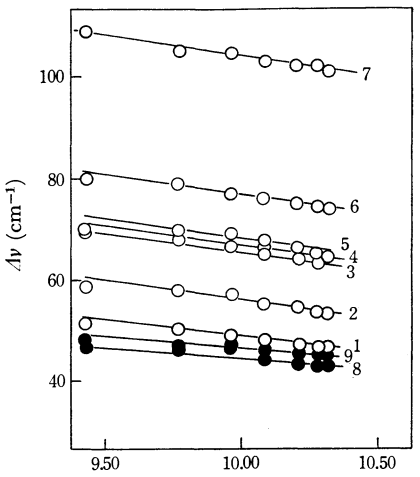

Fig. 1. Relationship between $\Delta\nu$ and pK_a of the proton donors. Numbers correspond to the π bases listed in Table 1.

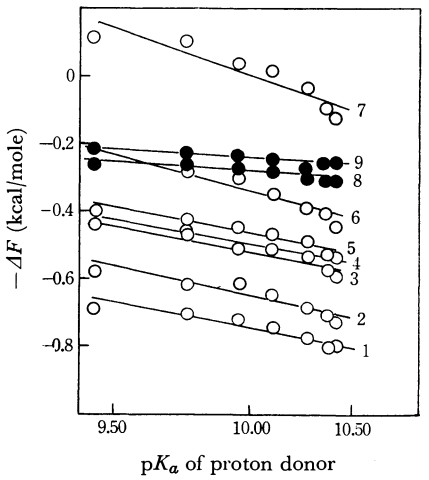

Fig. 2. Plots of $-\Delta F$ *vs.* pK_a of the proton donors. Numbers correspond to the π bases listed in Table 1.

a regular increase of $\Delta\nu$ with a number of methyl groups on the benzene ring. We have observed a similar increase using different proton donors. The linear correlation between $\Delta\nu$ and the pK_a of proton donors[11] (Fig. 1) is in agreement with the relation observed for ordinary hydrogen bonds involving lone pair electrons on oxygen and nitrogen atoms.[12,13] The slopes of all lines in Fig. 1 are virtually the same. The pK_a in aqueous solution of the proton donors includes both the enthalpy and entropy terms. The linear relationships, therefore, indicate that the proton donors used in this study have the same effect on $\Delta\nu$ when each infrared frequency shifts are measured in a solvent (CCl_4) different from water; consequently, one might conclude that the base strength of a series of π bases can be obtained by using a proton donor as reference. The "$\Delta\nu$" becomes a convenient measure for the base strength, as pointed out by Arnett.[1]

As shown in Fig. 2, when the free energy changes of hydrogen bond formation ($-\Delta F$) are plotted against the pK_a values of the proton donors, linear correlations are obtained for each π base except *p*-*t*-butylphenol (pK_a 10.31 at 26°C) and α-naphthol (pK_a 9.43 at 26°C) as the proton donor. While

8) G. C. Pimentel and A. L. McClellan, "The Hydrogen Bond," Freeman and Co., San Francisco (1960), p. 67.

9) N. Fuson, P. Pineau and M. I. Josien, *J. Chim. Phys.*, **55**, 464 (1958).

10) R. West, *J. Am. Chem. Soc.*, **81**, 1614 (1959).

11) The titration curve of various proton donors in water was obtained by using the automatic potentiometric titration method at 26°C. The slopes of observed curves were so steep that the break point in the curve could not be determined precisely as in the case of carboxylic acids. The dissociation constants were, therefore, determined at the point where the observed curve meets the theoretical one.

12) Ref. 1, p. 256.

13) R. Denger, A. Gilchirst, J. Pegg, J. Smith, T. Thompson and L. Sutton, *J. Chem. Soc.*, **1955**, 3889; J. Gordon, *J. Org. Chem.*, **26**, 738 (1961).

the slope of the lines for methyl benzenes increases with basicity ($-\Delta F$) of the proton acceptors,[14] the slopes for phenanthrene and naphthalene are very small, in spite of the high $-\Delta F$ values. In contrast, the dependence of $\Delta\nu$ on the pK_a values of the proton donor is essentially the same for these polycyclic compounds as it is for the methyl benzenes (Fig. 1). This observation can be interpreted by assuming a large entropy effect. By comparing the $\Delta\nu$- and $-\Delta F$-values for each of the proton donors, a larger entropy effect with the polycyclic compounds than with the methyl benzenes is confirmed. This entropy anomaly has been reported in the hydrogen bonding of phenol with aromatic π base.[5a,15]

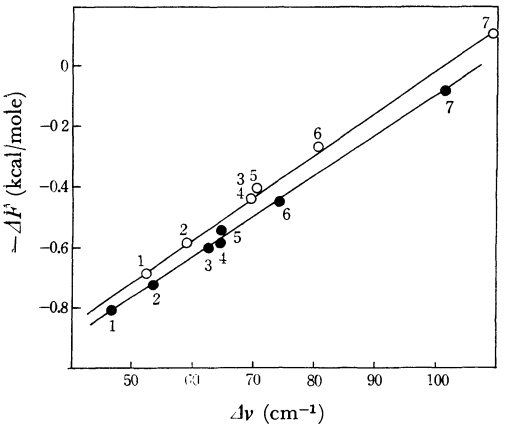

Fig. 3. Plots of $-\Delta F$ *vs.* $\Delta\nu$ for the α-naphthol- and *p-t*-butylphenol-methylbenzene systems. ○ : α-Naphthol, ● : *p-t*-Butylphenol. Numbers correspond to the π bases listed in Table 1.

Linear correlations between $-\Delta F$ and $\Delta\nu$ were obtained for each proton donor (even for *p-t*-butylphenol and α-naphthol as shown in Fig. 3) interacting with methyl benzenes. The value of the slopes was 0.014 ± 0.001 kcal/mol·cm^{-1}. This value agrees with the one obtained by Joesten and Drago[16] for thermodynamic measurements of the phenol adducts.

On the role of charge transfer: The possibility of detecting experimentally the role of charge-transfer involving π electrons from the proton acceptor to the proton donors has been anticipated.[17] The arguments of Basila, Saier, and Cousins[2c] is based on quantitative infrared spectroscopic studies of *t*-butyl alcohol-methyl benzene complexes. Their observed deviations for benzene, ethyl benzene, and mesitylene, when compared with other π bases, were not well explained. Although they consider 1 : 2 as well as 1 : 1 complexes involving these three π bases, the reexamination of their experiments proved that the deviations were due to the use of cells which were too long (15 mm).[5b] For these reasons, it seems best to reconsider their arguments.

The first argument for the importance of charge-transfer in hydrogen bonding is the linear relationship between ionization potential of the proton acceptor, I_D, and the frequency function, $\nu^f/\Delta\nu$:

$$I_D = C_1 \times (\nu^f/\Delta\nu)^{1/2} + C_2$$

where ν^f is the stretching frequency of the free OH. According to the Puranik-Kumar equation,[18] based on Mulliken's second-order perturbation theory for loose 1 : 1 complexes,[19] the plot of I_D *vs.* $(\nu^f/\Delta\nu)^{1/2}$ should be a straight line for a series of related proton acceptors with a given proton donor. Figure 4 shows the plots for phenol-aromatic hydrocarbon complexes as well as those for phenol-olefin complexes.[20] The methyl benzenes

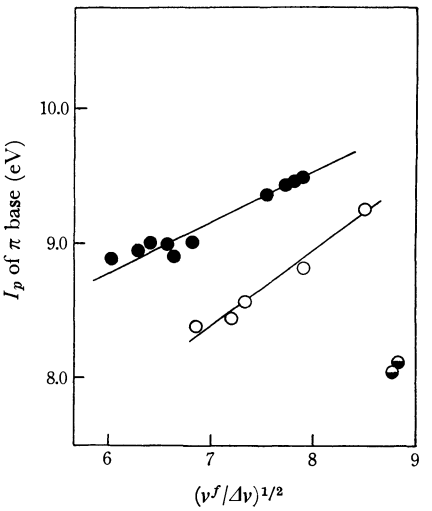

Fig. 4. Correlation between the ionization potential of π bases and $(\nu^f/\Delta\nu)^{1/2}$. ●, olefins; ○, Methylbenzene; ◒, Polyacenes.

fit the straight line. The same relations were obtained with other proton donor-aromatic hydrocarbon complexes. A linear correlation was also obtained for phenol-olefin complexes, although

14) This trend has been observed in the ordinary hydrogen bond: S. Nagakura, *J. Am. Chem. Soc.*, **76**, 3070 (1954).

15) R. West, International Symposium on Molecular Structure and Spectroscopy, Tokyo, 1962, D-117.

16) M. D. Joesten and R. S. Drago, *J. Am. Chem. Soc.*, **84**, 3817 (1962).

17) L. N. Ferguson, "The Modern Structural Theory of Organic Chemistry," Prentice-Hall, Inc., Englewood Cliffs, N. J. (1963), p. 134.

18) P. G. Puranik and V. Kumar, *Proc. Indian Acad. Sci., Sec. A*, **58**, 29 (1963).

19) R. S. Mulliken, *J. Am. Chem. Soc.*, **74**, 811 (1952); *J. Phys. Chem.*, **56**, 80 (1952).

20) Z. Yoshida and N. Ishibe, to be published.

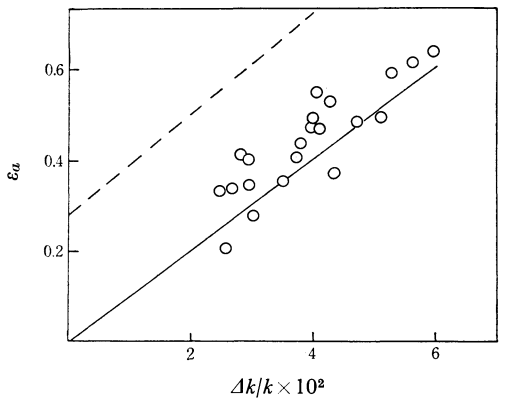

Fig. 5. Plots of the added effective nuclear change ε_a *vs.* the relative change in force constant $\Delta k/k$. The solid line is the one expected from the model discussed in the text and the dashed one is the one reported by Person *et al.* Ref. 23).

some of the ionization potentials of the olefins[21] used in this plot were not determined experimentally.[22] Naphthalene and phenanthrene both show large deviations from the correlation line found for the methyl benzenes; this implies that the polycondensed aromatics fit another line. This could be expected from the fact that the parameters C_1 and C_2 involve terms such as (1) overlap integral between the molecular orbital of the proton acceptor molecule and that of the negative ion of the proton donor molecule, and (2) polarity of the proton donor orbital.

The second argument of Basila and co-workers[2c] is based on the linear relation between ε_a, the added effective charge on the oxygen atom of the OH group due to the hydrogen bonding, and $\Delta k/k$, the relative change of the force constant of the OH stretching vibration due to hydrogen bonding. This correlation, proposed by Person and co-workes,[23] is based on the "van der Waals interaction-charge-transfer" resonance model, (a)↔(b),

for some charge-transfer complexes. Figure 5 shows the result of this plot for complexes with

$$\underset{\text{(a)}}{\text{A–H}\cdots\cdots\text{B}} \longleftrightarrow \underset{\text{(b)}}{\text{A}^-\cdots\cdots(\text{H–B})^+}$$

α-naphthol, phenol, and *p-t*-butylphenol. It should be noted that the plots are between the line obtained by Person *et al.* and the theoretical line obtained by assuming that the structures (a) and (b) would be equally important (*i. e* $\Delta k/k=0.50$, $\varepsilon_a=4.8$).

As additional evidence, Fig. 6 shows the plots of $\Delta\nu$ *vs.* the increment of the apparent absorption coefficient of the OH stretching band due to hydrogen bond formation, ΔA, for complexes where β-naphthol, phenol, and *p-t*-butylphenol are the proton donors. In the hydrogen bonding with lone-pair electrons Huggins and Pimentel[24] found a much larger ratio of $\Delta A/\Delta\nu$ (dashed line in Fig. 6). Since ΔA is a measure of the increased polarity of the OH group due to hydrogen bonding, Fig. 6 suggests that not only electrostatic interactoins but also charge-transfer interactions are important.

The results of three different treatments lead to the same conclusion, that is, charge-transfer from the proton acceptor to the vacant antibonding orbital of the proton donor plays an important role in the hydrogen bonding with π electrons.

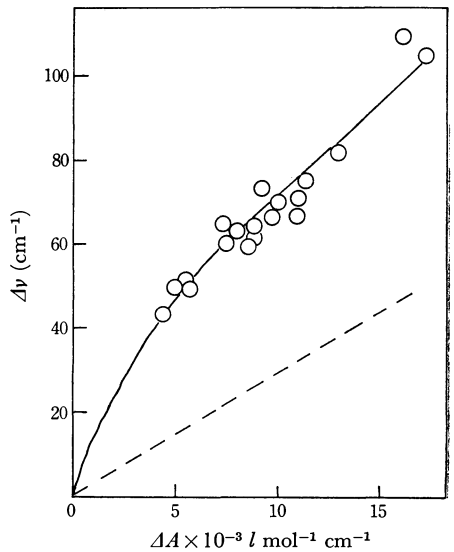

Fig. 6. Plots of $\Delta\nu$ *vs.* the difference between the integrated molar absorption intensity of the hydrogen bonded OH band and that of the free one. The dashed line is the one obtained by Huggins and Pimentel (Ref. 24).

21) a) K. Watanabe, T. Kayama and J. Mottl, "Final Report on Ionization Potentials of Molecules by a Photoionization Method," Department of Army No. 5B-99-01-004, ORD TB 2-0001-00R-1624 (1959). b) K. Watanabe, *J. Chem. Phys.*, **26**, 542 (1957).

22) Ionization potentials of some olefins were calculated from the relation described by Turner. D. W. Turner, "Determination of Organic Structure by Physical Methods," ed. by F. C. Nachod and W. D. Phillips, Vol. 2, Academic Press, New York (1962), p. 354.

23) W. B. Person, R. H. Humphrey, W. A. Deskin and A. J. Popov, *J. Am. Chem. Soc.*, **80**, 2049 (1958); W. B. Person, R. H. Humphrey and A. I. Popov, *ibid.*, **81**, 273 (1959); W. B. Person, R. E. Erickson and R. E. Buckles, *ibid.*, **82**, 29 (1960).

24) C. M. Huggins and G. C. Pimentel, *J. Phys. Chem.*, **60**, 1615 (1956).

BULLETIN OF THE CHEMICAL SOCIETY OF JAPAN VOL. 42 3259—3262 (1969)

Intermolecular Hydrogen Bond Involving a π Base as the Proton Acceptor. VII. Substituents and Steric Effects in the Hydrogen Bonding of 2,6-Xylenols to Mesitylene

Zen-ichi YOSHIDA, and Nobuyuki ISHIBE*1

Department of Synthetic Chemistry, Kyoto University, Yoshida, Sakyo-ku, Kyoto

(Received April 30, 1969)

Hydrogen bonding of 4-substituted-2,6-xylenols to mesitylene has been investigated by measurement of the hydroxyl stretching vibration. A linear relationship between the electronic effects of *para* substituents (Hammett σ_p constant) and the frequency shifts of the hydroxyl stretching vibration was obtained. A similar correlation was also observed with the free energy change associated with the formation of the hydrogen-bonded complex. The thermodynamic sutdies on the hydrogen bonding of 2,6-xylenol and phenol with both mesitylene and acetonitrile demonstrated the steric effect of 2- and 6-methyl groups on hydrogen bond formation. The free energy change for hydrogen bond formation with 2,6-xylenols as the proton donor was lower than with phenol. This is explained in terms of both entropy and enthalpy factors.

Many workers have investigated the substituent effects of proton donors such as phenols on the intramolecular hydrogen bond[1] and reported that usually there was a correlation between the electronic effects of substituents and the frequency shifts of hydroxyl stretching vibration due to hydrogen bond formation. Recent studies of the substitutent effects on the intermolecular hydrogen bond[2] show that the proton donors having typical substituents auch as nitro, acetyl, or alkoxyl groups are subject to self association.[3] This phenomenon is explained in terms of the proton accepting ability of these substituentents. In order to resolve this experimental difficulty, the sterically hindered phenols were used as the proton donor[2] because they are less associated than the simple hydroxyl compounds.[4-6]

Singh and Rao[2a] reported that in the hydrogen bonding of *para* substutited-2,6-di-*t*-butylphenols with tetrahydrofuran neither the equilibrium constantsnor the values of frequency shifts show a linear relationship with the Hammett σ_p constants. Both values of pK_a[7] and OH stretching vibration[8,9] in the infrared are, however, correlated with σ_p. The substituent effects of the proton donor on weak hydrogen bonding involving benzenes as a π base have not been investigated. We report the effect in the system of the 4-substituted-2,6-xylenols and mesitylene by measurement of the stretching frequencies of the OH group. In order to reveal whether the decrease of the equilibrium constant is due to the steric effect of 2- and 6-methyl groups on the enthalpy change and/or on the entropy change, the thermodynamic measurements of hydrogen bonding of phenol and 2,6-xylenol with both mesitylene and acetonitrile were carried out. These experiments are important because there is some discrepancy in the explanation of the smaller frequency shifts and free energy changes in hydrogen bonding of the hindered phenols to various proton acceptors involving a lone pair electron.[2a,5]

*1 Present address: Department of Chemistry, University of Illinois at Chicago Circle, Chicago, Illinois 60680, U.S.A.

1) L. L. Ingraham, J. Corse, G. F. Bailey and F. Stiff, *J. Am. Chem. Soc.*, **74**, 2297 (1952); M. Ōki and H. Iwamura, This Bulletin, **32**, 955 (1959); *ibid.*, **34**, 1395 (1961); C. K. Hancock and A. D. H. Clague, *J. Am. Chem. Soc.*, **86**, 4942 (1964); Z. Yoshida and M. Haruta, *Tetrahedron Letters*, **1964**, 263; *ibid.*, **1965**, 3745.

2) a) S. Singh and C. N. R. Rao, *J. Am. Chem. Soc.*, **88**, 2142 (1966). b) S. Singh, A. S. M. Murth and C. N. R. Rao, *Trans. Faraday Soc.*, **62**, 1056 (1966).

3) P. J. Stone and H. W. Thompson, *Spectrochim. Acta*, **10**, 17 (1957).

4) a) B. G. Somers and H. S. Gutowsky, *J. Am. Chem. Soc.*, **85**, 3065 (1963). b) I. Yamaguchi, This Bulletin, **34**, 744 (1961).

5) F. Takahashi and N. C. Li, *J. Phys. Chem.*, **69**, 1622 (1965).

6) a) W. Heinen, *Rec. Trav. Chim.*, **82**, 859 (1963). b) L. J. Bellamy, G. Eglinton and J. F. Morman, *J. Chem. Soc.*, **1961**, 4762; L. J. Bellamy and R. L. Williams, *Proc. Roy. Soc. (London)*, A**254**, 119 (1960).

7) L. A. Cohen and W. M. Jones, *J. Am. Chem. Soc.*, **85**, 3402 (1963).

8) K. U. Ingold, *Can. J. Chem.*, **38**, 1092 (1960).

9) Z. Yoshida, N. Ishibe and K. Shobatake, *Kogyo Kagaku Zasshi (J. Chem. Soc. Japan, Ind. Chem. Sect.)*, **68**, 808 (1965).

Experimental

Materials. Carbon tetrachloride as a solvent, mesitylene and acetonitrile as the proton acceptors, and phenol as a proton donor were purified by known methods.[10] 4-Substituted-2,6-xylenols were prepared by known methods.[9] The details of the preparative method were reported previously.[9]

Determination and Analysis of Spectra. All spectra of the hydroxyl stretching vibration, ν_{OH}, were obtained with a double pass grating infrared spectrophotometer JASCO DS-402G. The scanning conditions for determination of the spectra were the same as in the previous report.[11] Two liquid cells of 2 and 10 mm thickness (window material: NaCl), were used. Concentration ranged from 0.001 to 0.04 mol/*l* for the proton donors and from 1.5 to 4 mol/*l* for mesitylene. The cells were placed in a thermostated air-bath[12] to adjust the sample to an appropriate temperature. Analysis of the spectra and calculation of the equilibrium constants have been described previously.[13]

When thermodynamic values were estimated from a linear plot of log K *vs.* $1/T$, concentrations of free phenol and 2,6-xylenol were corrected. This was necessary because the integrated absorption intensities of phenol[14] and 2,6-xylenol in the absence of base depend not only on their concentration but also on temperature. In the range of -10 to 50° C the integrated molar absorption intensities of phenol[14] and 2,6-xylenol (A_p and A_x, *l*/mol cm) (whose band shape are assumed to be represented by Lorentzian function) correlate with the sample temperature (T) as follows:

$$A_p = 18200 - 26.50 \times T$$

$$A_x = 13700 - 18.09 \times T$$

Results

The OH stretching frequency of 4-substituted-2,6-xylenols (ν^f), the frequency shifts ($\Delta\nu$), the relative frequency shifts ($\Delta\nu/\nu^f$), and the free energy changes for hydrogen bonding between 4-substituted-2,6-xylenols and mesitylene are summarized in Table 1. The thermodynamic values of hydrogen bonding of phenol and 2,6-xylenol to both mesitylene and acetonitrile are given in Table 2. The values of frequency shifts in the hydrogen bond involving mesitylene remain constant with the change of concentration of π base and the temperature. In the case of acetonitrile, however, they depend not only on the concentration of acetonitrile[15] but also on the temperature. The frequency shifts decrease with increase of temperature.[14] This behavior could be explained as a specific solvent effect (dipole-dipole interaction).[16]

Table 1. Frequency shifts and free energy changes for the hydrogen bond between 4-substituted-2,6-xylenols and mesitylene

Substituent	ν^f [a] (cm^{-1})	$\Delta\nu$ [b] (cm^{-1})	$\Delta\nu/\nu^f$ ($\times 10^3$)	$-\Delta F$ [c] (kcal/mol)	σ [d]
t-C_4H_9	3623.3	42.6	11.7_5	−1.04	−0.197
CH_3	3623.6	42.8	11.8_1	−0.99	−0.170
C_2H_5	3623.4	43.1	11.8_9	−0.94	−0.151
i-C_3H_7	3624.3	42.9	11.8_3	−0.95	−0.151
Cyclo-C_6H_{11}	3623.2	42.8	11.8_1	−0.94	—
H	3622.5	44.0	12.1_4	−0.92	0
Cl	3620.1	47.0	12.9_7	−0.80	0.227
Br	3619.9	47.3	13.0_7	−0.74	0.232
I	3617.9	47.9	13.2_3	−0.72	0.276
CH_3CO	3611.9	50.8	14.0_6	−0.54	0.87
NO_2	3606.5	53.4	14.8_0	−0.41	1.27

a) ν_{OH} in dilute solution of carbon tetrachloride.
b) The maximum error is within ± 0.5 cm^{-1}.
c) The maximum error is within ± 0.07 kcal/mol.
d) See Ref. 23.

Discussion

Steric Effects on Hydrogen Bonding. A linear relationship was obtained in a plot of pK_a values of unhindered phenols (alkylphenols and naphthols) *vs.* the free energy changes for hydrogen bond of these phenols to mesitylene.[17] If this correlation also holds in the hydrogen-bonded system involving 2,6-xylenol as the proton donor, the value for $-\Delta F$ is expected to be -0.60 kcal/mol when the pK_a of 2,6-xylenol is 10.58.[18] This value is much larger than the observed one of -0.94 kcal/mol. Introduction of alkyl groups to the 2 and 6 positions of phenol causes a decrease of the equilibrium constant in the hydrogen bond with a lone pair electron in amides,[5] ethers,[2a,4a] ketones,[2a,6a] nitro compounds,[2a] and other compounds.[2a] A similar decrease ($-\Delta F$) was also found in the hydrogen bond interaction with the delocalized π electrons of mesitylene. Introduction of the methyl groups (into phenol) causes a decrease of $-\Delta F$ value, which is larger in the hydrogen bond with acetone and acetonitrile than with mesitylene. The differences in $-\Delta F$ are about 0.8 kcal/mol with mesitylene (Table 2). Table 2 shows that the hydro-

10) A. Weissberger, "Technique of Organic Chemistry," Vol. 7, Organic Solvent, Interscience Publ., New York (1955).
11) Z. Yoshida and E. Ōsawa, *J. Am. Chem. Soc.*, **88**, 4019 (1966).
12) Z. Yoshida and N. Ishibe, unpublished result.
13) Z. Yoshida and E. Ōsawa, *J. Am. Chem. Soc.*, **87**, 1467 (1965).
14) Z. Yoshida adn N. Ishibe, *Spectrochim. Acta*, **24A**, 893 (1968).
15) S. S. Mitra, *J. Chem. Phys.*, **36**, 3286 (1962).
16) E. Ōsawa and Z. Yoshida *Spectrochim. Acta*, **23A**, 2029 (1967).
17) Z. Yoshida and N. Ishibe, unpublished result.
18) G. W. Wheland, R. M. Brownell and E. C. Mays, *J. Am. Chem. Soc.*, **70**, 2492 (1948).

TABLE 2. FREQUENCY SHIFTS AND THERMODYNAMIC VALUES OF HYDROGEN BOND FORMATION

Proton Donors	Proton Acceptor	$\Delta\nu$ (cm^{-1})	$-\Delta H$ (kcal/mol)	$-\Delta F°$ (kcal/mol)	$-\Delta S°$ (e.u.)
Phenol	Mesitylene	73	1.92±0.16	−0.38	7.8
	Acetonitrile	154[a]	4.74±0.08	1.12	12.2
	Acetone[b]			1.47	
2,6-Xylenol	Mesitylene	44	1.26±0.20	−0.92	7.3
	Acetonitrile	112[a]	2.88±0.10	0.33	8.6
	Acetone[b]			0.66	
p-Cresol	Mesitylene	74.8		−0.39	
	Acetone[b]			1.35	
2,4,6-Trimethylphenol	Mesitylene	42.8		−0.99	
	Acetone[b]			0.53	

a) These values are measured at 25°C.
b) Ref. 6a. These values were obtained at 23°C.

gen bond energy and the frequency shift are much smaller in hydrogen bond of acetonitrile with 2,6-xylenol than with phenol, but the entropy change ($\Delta S°$) increases with introduction of methyl substituents into phenol. Mesitylene behaves in a similar way, although the entropy changes for these proton donors are nearly equal.

Our results are consistent with those of Takahashi and Li[5] who studied hydrogen bonding in amides. However, our results are not consistent with those of Singh and Rao[2a] who reported that the enthalpies of hydrogen bonding are nearly equal for both phenols and hindered phenols. The thermodynamic values reported here should be more accurate than those of Singh and Rao,[2a] because the dependence of the intensity of ν_{OH} of the free phenol on the sample temperature was considered in the calculation of the equilibrium constant. These authors[2a] stated that the increase in barrier height in the double minimum potential with increasing bulkiness of the substituent could be used to explain both the invariance of the enthalpies and the decrease of the frequency shifts in the hydrogen-bonded system involving the hindered phenols. They assumed there is little or no variation of the distance, $R_{x\cdots y}$, in the hydrogen bond X–H···Y. A more reasonable explanation is that $R_{x\cdots y}$ increases with the bulkiness of the alkyl substituents of the proton donors; therefore, the enthalpies decrease with introduction of the methyl substituents to 2 and 6 positions of phenol. As expected from this consideration, the frequency shift of the hydrogen bond between 2,6-xylenol and mesitylene is less than the values calculated from the $\Delta\nu - pK_a$ relationship,[17] where the steric effects were not detected. This decrease is, therefore, explained by the larger distance $R_{x\cdots y}$ and the higher OH stretching frequency of 2,6-xylenol.[9] Qualitatively this could be supported by the correlation between the frequency shift and the X···Y bond distance in the hydrogen-bonded solid.[19] The values of entropy changes support these considerations; the steric effect of the methyl substituent causes an increase of $R_{x\cdots y}$ in the hydrogen-bonded complex so that to some extent the rotational and vibrational movement of the complex is less restricted. The same trend apparently occurs in the complex involving acetonitrile as the proton acceptor. For mesitylene the entropy change in both phenol and 2,6-xylenol are nearly equal. $R_{x\cdots y}$ in the hydrogen-bonding of phenol with acetonitrile may be shorter than in the case of phenol with mesitylene. When the methyl groups are introduced into phenol, there seemingly occurs a greater increase of $R_{x\cdots y}$ with acetonitrile than with mesitylene, resulting in the differences in entropy changes mentioned above. It should be noted that the entropy anomaly observed in the hydrogen bonding of phenol with aromatic hydrocarbons[13] was obtained in the hydrogen-bonded system involving the hindered phenols.

From these considerations, steric effects on hydrogen bonding could influence not only the enthalpy but also the entropy changes associated with the formation of the hydrogen-bonded complex. Although a large steric effect was not observed in hydrogen bonding of phenol with di-*t*-butyl ether and di-*t*-butyl sulfide,[20] it is interesting that introduction of bulky groups into the proton donor causes a steric effect.

Substituent effects on hydrogen bonding: From Table 1 it is clear that both the frequency shifts and the free energy changes increase with enhance-

19) G. C. Pimentel and A. L. McClellan, "The Hydrogen Bond," W. H. Freeman and Co., San Francisco and London (1960), p. 85; W. C. Hamiton and J. A. Iber, "Hydrogen Bonding in Solids," W. A. Benjamin, New York (1968), p. 85.

20) R. West, D. L. Powell, M. K. T. Lee and L. S. Whatley, *J. Am. Chem. Soc.*, **86**, 3227 (1964).

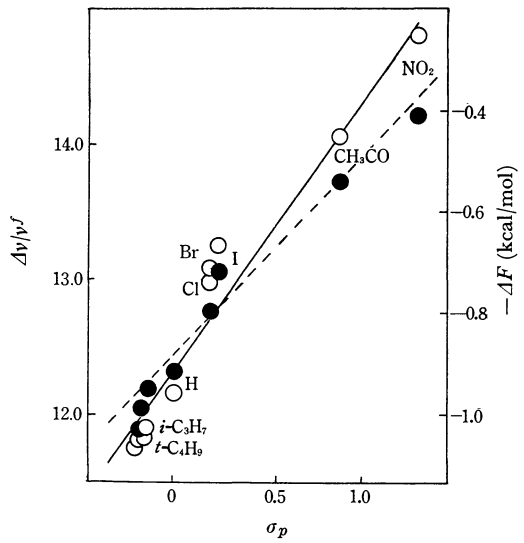

Fig. 1. $\Delta\nu/\nu^f$ and $-\Delta F$ *vs.* Hammett σ_p plots in hydrogen bonding of 2,6-xylenol with mesitylene. (—○— $\Delta\nu/\nu^f$ *vs.* σ_p, ---●--- $-\Delta F$ *vs.* σ_p)

ment of the proton donating ability of the 4-substituents in 2,6-xylenols. A similar trend was also observed in some other hydrogen bonded systems, *e.g.* alkyl phenols-aromatic hydrocarbons,[17] alcohols-diethyl amine or -ethyl ether.[21] As shown in Fig. 1, both the relative frequency shift, $\Delta\nu/\nu^f$,[22] and the free energy change vary linearly with the Hammett σ_p constants.[23] In these plots the best linear relationship was obtained when σ_p[23] was used for the substituent constants of nitro and acetyl groups. This suggests the coplanarity of the OH group of 2,6-xylenols with the benzene ring in the hydrogen-bonded complexes, as well as in free 2,6-xylenols.[9] In the hydrogen bond between *para* substituted-2,6-di-*t*-butylphenols and tetrahydrofuran, however, neither the equilibrium constants nor the frequency shifts vary linearly with the Hammett σ constants.[28] This discrepancy cannot be explained adequately, but in the latter system, steric interaction of the *t*-butyl groups with the hydrogen atom of tetrahydrofuran causes bending of the OH group out of the plane of the benzene ring.

The slope of $\Delta\nu/\nu$ *vs.* pK_a for the hydrogen bonding of 2,6-xylenols with mesitylene is smaller than that of phenols with mesitylene.[17] The slope of $\Delta\nu/\nu$ *vs.* Hammett σ constant for the hydrogen bonding of 2,6-xylenols with mesitylene is larger than that of the intramolecular hydrogen bonding of 2-hydroxylbiphenyl derivatives.[24] The OH stretching frequencies of 4-substituted-2,6-xylenols are higher than those of the corresponding phenols,[17] so that the transmission of electronic effects of *para* substituents to the reaction center becomes more difficult in the hydrogen-bonded complexes with 4-substituted-2,6-xylenols than those with phenols. In the intramolecular hydrogen bonding of 4 (or 5)-substituted-2-hydroxylbiphenyls, the electronic effects of the substituent transmit the the reaction center not only through the benzene ring involving the OH group but also through the other ring because of conjugation between the two aromatic nuclei. The substituent effects on the OH group, therefore, cancel each other, thereby reducing the slope in the relationship $\Delta\nu/\nu^f$ *vs.* Hammett σ constants.

It is concluded that investigation of the hydrogen bond involving the hindered phenols might present interesting information about the transition states involving the hydrogen bond.

21) G. Barrow, *J. Phys. Chem.*, **59**, 1129 (1954); J. Hine and M. Hine, *J. Am. Chem. Soc.*, **74**, 5266 (1952).

22) L. J. Bellamy and R. L. Williams, *Trans. Faraday Soc.*, **55**, 14 (1959).

23) R. W. Taft, Jr., "Steric Effects in Organic Chemistry," ed. by M. S. Newman, Chapter 13, John Wiley & Sons, New York (1956); H. H. Jaffé, *Chem. Revs.*, **53**, 191 (1953).

24) M. Ōki and H. Iwamura, This Bulletin, **32**, 955 (1959).

BULLETIN OF THE CHEMICAL SOCIETY OF JAPAN VOL. 42 3263—3266 (1969)

Intermolecular Hydrogen Bond Involving a π Base as the Proton Acceptor. IX. Hydrogen Bonding of Phenol to Monoolefins

Zen-ichi YOSHIDA and Nobuyuki ISHIBE

Department of Synthetic Chemistry, Faculty of Engineering, Kyoto University, Yoshida, Sakyo-ku, Kyoto

(Received April 30, 1969)

The π hydrogen bonding between phenol and monoolefins has been studied by examining the OH stretching vibration spectra of phenol in the presence of monoolefins. From comparison of the hydrogen bond shifts, it has been shown that the basicity of the aliphatic olefins toward phenol increases with the increasing alkylsubstitution on the double bond carbon. The endocyclic olefins are more basic than $RCH{=}CH_2$ and $RCH{=}CHR'$ where R and R′ represent alkyl groups. The equilibrium constants for complex formation with olefins were smaller than those with aromatic hydrocarbons. The steric effects on the hydrogen bond complex with aliphatic and endocyclic olefins have been discussed.

In relation to the various proposed conformations of olefin carbonium ions[1] the investigation of the hydrogen bonds involving olefins as the base is of interest, since hydrogen bonding could be the first step of the proton transfer.[2] Several examples are found in literatures.[3-6] The effect of structure (but not of strain) of base upon hydrogen bonding has been studied by West[5] and Kuhn and Bowman.[6] However, the influences of structure and strain of base on the hydrogen bonding have not been studied so far. The present paper describes the infrared data on hydrogen bonding of phenol with straight, branched and cycloolefins. The frequency shifts of the hydroxyl stretching vibration of phenol and the free energy changes due to complex formation were found to be strongly affected by the structure of the olefins. These variations are explained in terms of steric strain and electronic effects.

Experimental

Materials. 1-Olefins were prepared by pyrolysis of the methyl esters of the corresponding alcohols at 470—515°C under nitrogen atmosphere.[7,8] Cyclopentene and cycloheptene were prepared by dehydration[9,10] of the cycloalcohols obtained by hydrogenation[11] of the ketones.[12,13] The other materials were commerical products and purified by the usual methods, special care being taken to remove all traces of water. Their purity was confirmed by gas chromatography, using Apiezon L or β,β'-bispropionitrile ether columns.

Measurements and Analysis of Spectra. Hydroxyl stretching vibration spectra of phenol were recorded on a Double Pass High Precision Spectrophotometer of Japan Spectroscopic Co. A pair of 0.10 cm cells equipped with NaCl windows were used for double path operations. The concentration of olefins were 1—7 mol/*l* and that of phenol 0.01—0.02 mol/*l* in carbon tetrachloride. The detailed conditions for measuring the ν_{OH} spectra of phenol have been described previously.[14] The analysis of the observed spectra was carried out by use of the Lorentz equation[15] as mentioned in previous papers.[14-16] The equilibrium constants were calculated according to a previous paper.[14]

1) a) "The Transition State," Special Publication No. 16, The Chemical Society, London (1962). b) R. Hoffmann, *J. Chem. Phys.*, **40**, 2480 (1964).
2) a) B. C. Challis and F. A. Long, *Discussions Faraday Soc.*, **39**, 67 (1965), V. Gold and M. A. Kessick, *ibid.*, **39**, 84 (1965). b) R. F. W. Badger, *Can. J. Chem.*, **42**, 1822 (1964).
3) H. C. Brown and T. D. Brady, *J. Am. Chem. Soc.*, **71**, 3573 (1949); **74**, 3570 (1952).
4) D. Cook, Y. Lupien and W. G. Schneider, *Can. J. Chem.*, **34**, 957 (1956).
5) R. West, *J. Am. Chem. Soc.*, **81**, 1614 (1959).
6) L. P. Kuhn and R. E. Bowman, *Spectrochim. Acta*, **23A** 189 (1967).
7) J. A. van Pelt, Jr., *Rec. trav. chim.*, **57**, 1055 (1938); **60**, 55 (1941).
8) H. Geldof and J. P. Wibaut, *ibid.*, **67**, 110 (1948).
9) H. Waldmann and F. Petru, *Chem. Ber.*, **83**, 287 (1950).
10) E. P. Khohler, M. Tischler, H. Potter and H. W. Thompson, *J. Am. Chem. Soc.*, **61**, 1057 (1939).
11) C. P. Noller and R. Adams, *ibid.*, **48**, 1084 (1926).
12) J. F. Thorpe and G. A. R. Kon, "Organic Syntheses" Coll. Vol. 1, p. 192 (1941).
13) H. J. Dauben, Jr., H. J. Ringold, R. W. Wabe, D. I. Pearson and A. G. Anderson, Jr., *ibid.*, **34**, 19 (1954).
14) Z. Yoshida and E. Ōsawa, *J. Am. Chem. Soc.*, **88**, 4019 (1966).
15) D. A. Ramsay, *ibid.*, **74**, 72 (1952).
16) Z. Yoshida and E. Ōsawa, *ibid.*, **87**, 1467 (1965).

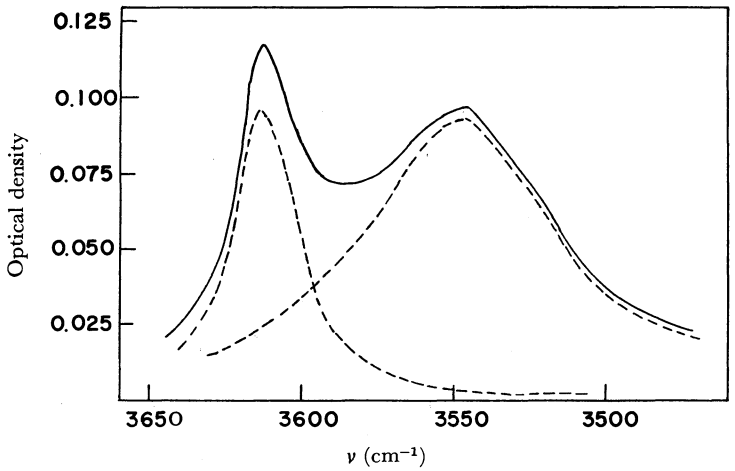

Fig. 1. OH strecthing absorption spectrum of 0.0174M phenol in the presence of 6.97M 1-pentene in CCl_4. Broken lines are analyzed component curves according to the Lorentz equation.

Results and Discussion

The hydroxyl stretching vibration spectra of phenol in the presence of olefins were all doublets as shown in Fig. 1 for the system of phenol-1-pentene. The hydrogen bond shifts, $\Delta\nu$, and the free energy changes for the complex formation, $-\Delta F$, are summarized in Table 1. Generally the half width of the bonded OH band for olefins was larger than that for aromatic hydrocarbons[14] with similar frequency shifts. For example, the hydrogen bond shifts are nearly equal for 1-octene and *m*-xylene, but the half widths of the bonded OH band were 73 cm^{-1} and 39 cm^{-1}, respectively.

From Table 1 it is apparent that for a given type of olefin, such as a monosubstituted ethylene, the hydrogen bond shifts are nearly constant, but they are strongly affected by the number and the position of alkyl groups attached to the double bond carbon, in the order $RCH{=}CH_2(A) < RCH{=}CHR'$ (B) $< \begin{matrix} R \\ R' \end{matrix}\!\!>C{=}CH_2(C)$, where R and R′ are alkyl groups. This trend is interpreted in terms of an increase in the electron density of the double bond with an increase in the total inductive effect due to alkyl-substitution as ascertained in the case of phenol-alkylsubstituted benzenes system.[16] Since the frequency shift is a good measure of the base strength of the proton acceptor,[17-19] the result obtained for aliphatic olefins means that alkyl-substitution at the double bond carbon increases its base strength toward the phenolic proton. This order corresponds well with West's results,[5] but the frequency shift (particularly for 1-olefins) in our investigation was about 1—13 cm^{-1} smaller than those of West. The effect of alkyl substitution on the frequency shift is also expected from the ionization potentials of olefins, the ionization potential of branched aliphatic olefins being smaller

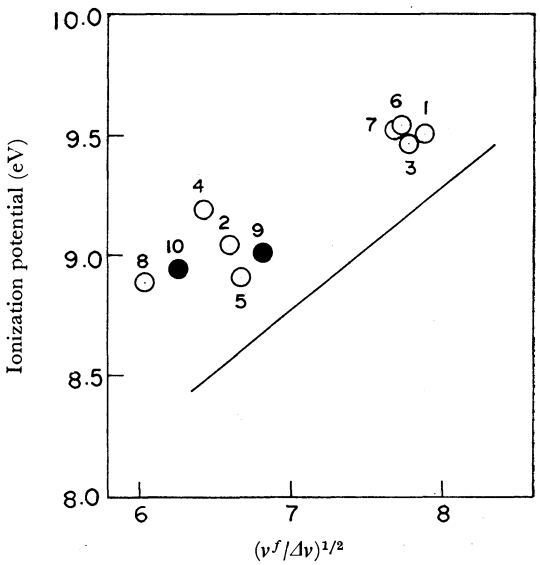

Fig. 2. Correlation between ionization potential of olefins and $(\nu^f/\Delta\nu)^{1/2}$.
○, aliphatic olefins; ●, cycloolefins. The numbers correspond to those listed in Table 1. Solid line is the correlation for phenol-methylbenzenes.

17) E. M. Arnett, "Progress in Physical Organic Chemistry," ed. by S. G. Cohen, A. Streitwieser, Jr., and R. W. Taft, Vol. 1. Interscience Pub., New York and London (1963), p. 221.

18) L. J. Bellamy, G. Englinton and J. F. Mormen, *J. Chem. Soc.*, **1961**, 4762; J. E. Gordon, *J. Org. Chem.*, **26**, 738 (1961).

19) Z. Yoshida and N. Ishibe, to be published.

Table 1. Frequency shifts and change of free energy (29°) in π hydrogen bonding of phenol with monoolefins[f]

No.	Olefins	$\Delta\nu$ (cm^{-1})	$-\Delta F$ (kcal/mol)	Ionization potential of the proton acceptors (eV)
1	1-Pentene	58±1[a]	−1.16±0.05[a]	9.50[b]
2	2-Pentene	82±1.5	−1.01±0.07	9.06[c]
3	1-Hexene	59.5±1	−1.46±0.05	9.46[b]
4	2-Methyl-1-pentene	87±1	−1.04±0.03	9.20[c]
5	4-Methyl-2-pentene	81±1.5	−1.03±0.08	8.89[c]
6	1-Heptene	60±1	−1.37±0.03	9.54[c]
7	1-Octene	61±1	−1.47±0.02	9.52[c]
8	2-Ethyl-1-hexene	100±1.5	−0.79±0.05	8.88[d]
9	Cyclopentene	77.5±1	−1.40±0.07	9.01[e]
10	Cyclohexene	92±2	−0.93±0.09	8.945[b]
11	4-Methyl-cyclohexene	93±1.5	−0.93±0.07	
12	Cycloheptene	87.5±1	−1.05±0.06	
13	*cis*-Cyclooctene	88.5±1	−1.19±0.06	
14	Benzene	49±1	−0.66±0.05	
15	Toluene	58±1	−0.56±0.07	
16	*m*-Xylene	69±1	−0.53±0.04	
17	Mesitylene	78±1	−0.34±0.04	
18	Durene	85±1	−0.31±0.05	
19	Hexamethylbenzene	106±1	−0.28±0.03	

a) Mean deviation from the average.
b) Refs. 20 and 21.
c) J. Collin and F. P. Lossing, *J. Am. Chem. Soc.*, **81**, 2064 (1959).
d) This value was calculated from the relation described by Turner (D. W. Turner, "Determination of Organic Structure by Physical Methods," ed. by F. C. Nachod and W. D. Phillips, Vol. 2, Academic Press, New York and London (1962), p. 354).
e) K. Watanabe, T. Kayama and J. Motl, "Final Report on Ionization Potenitials of Molecules by Photoionization Method," 1959, Dept. Army No. 5B-99-01-004, ORD TB 2-0001-OOR1624.
f) The data for methyl substituted benzenes were taken from a previous paper (Ref. 14).

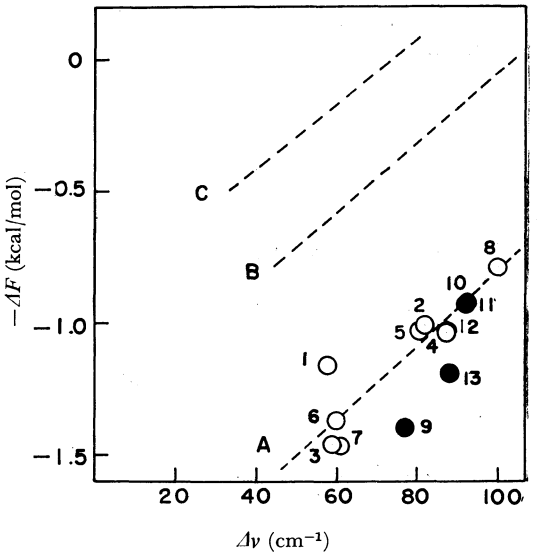

Fig. 3. $-\Delta F$ *vs.* $\Delta\nu$ plot with phenol-olefin complexes. Numbers correspond to those listed in Table 1. ○, aliphatic olefins; ●, cyclic olefins. (A) olefin line, (B) alkylbenzene line, (C) polyacene line.

than those of the linear ones.[20,21] The importance of charge-transfer in hydrogen bond interaction has been suggested by many workers,[22] and it has been demonstrated[19,23] that a linear correlation between the ionization potential of the aromatic donor and $(\nu_f/\Delta\nu)^{1/2}$ is observed. Such correlation was also obtained for phenol and olefins system as shown in Fig. 2.

Table 1 shows that the free energy change, $-\Delta F$, in π hydrogen bond formation increases with the frequency shifts. Accordingly, the more basic the proton acceptor, the easier the complex formation. In contrast, these $-\Delta F$ values are smaller than those obtained for aromatic hydrocarbons as the proton acceptors. For example, while the frequency shifts for mesitylene and 4-methyl-2-pentene are about the same, $-\Delta F$ for the latter (−1.03 kcal/mol) is much (*i. e.* −0.30 kcal/mol) smaller than that for the former. The plot of $-\Delta F$ *vs.* $\Delta\nu$ (Fig. 3) shows that $-\Delta F$ depends strongly on the type of the π base; monoolefins behave as a distinct group from polycondensed aromatics and alkylbenzenes. According to our previous considerations,[14,16] the entropy decrease for the phenol monoolefin interactions is the largest. In charge-transfer complexes involving alkylbenzenes and olefins as the electron donor, however, the formation constants as well as the entropy changes are nearly equal.[24] This suggests that degrees of freedom of movement of the electron acceptor molecule should be much smaller in the case of π hydrogen bond interactions involving

20) C. D. Isaacs, W. C. Price and R. G. Ridley, "The Threshold of Space," ed. by M. Zelikoff, Pergamon Press, London (1957), p. 143.
21) K. Watanabe, *J. Chem. Phys.*, **26**, 542 (1957).
22) G. C. Pimentel and A. L. McClellan, "The Hydrogen Bond," W. H. Freeman and Co. New York, N. Y. (1960), p. 229.
23) P. G. Puranik and V. Kumar, *Proc. Indian Acad. Sci., Sect. A*, **58**, 29 (1963); M. B. Basila, E. L. Saier and L. R. Cousins, *J. Am. Chem. Soc.*, **87**, 1665 (1965).
24) G. Briegleb, "Elektronen-Donator-Acceptor-Komplexe," Springer-Verlag, Berlin (1961), s. 124, 128.

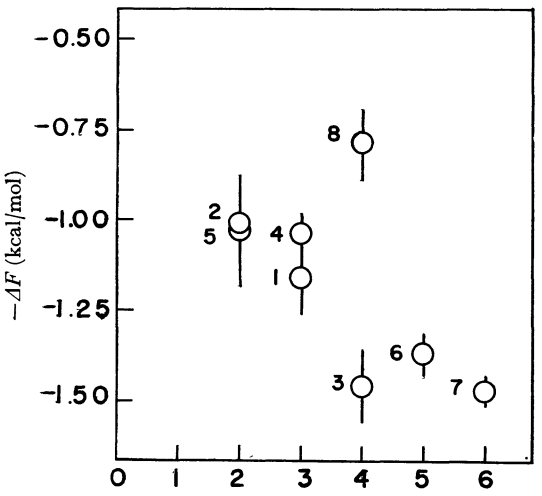

Fig. 4. Dependence of lenght of the carbon chain adjacent to olefinic double bond on $-\Delta F$. Numbers correspond to those listed in Table 1.

olefins as the electron donor than in the case of typical charge-transfer complexes. It can be seen from Table 1 that the increasing length of the alkyl group attached to the double bond carbon causes a decrease of $-\Delta F$. This trend is significant in the α-olefin series, where $-\Delta F$ decreases with the increasing length of the alkyl group while the frequency shifts being nearly constant (See Fig. 4). This could be due to steric hindrance. The steric hindrance has also been observed in the Ag^+-olefin complex formation.[25]

From a comparison of $-\Delta F$ values of the hydrogen bonded complexes with those of the Ag^+-olefin complexes it is shown that the branched olefins give more stable complexes for the hydrogen bond formation, and less stable complexes for the argentation than in the case of α-olefins. This opposite relation of basicity of the alkyl-substituted olefins toward phenolic proton and Ag^+ might be explained in terms of π (for the π hydrogen bonding) and σ complex-formations (for the argentation). If this is correct, the phenolic proton approaches the π electron cloud of olefin along the z axis, assuming that the olefin molecule lies on the xy plane with the y axis passing through the carbon atom of the double bond.[1b] The steric hindrance (Fig. 4) in such configuration of the π hydrogen bond complex could be explained as follows. The carbon chain of the alkyl groups adjacent to the double bond could freely rotate in solution. Since the aliphatic olefins used in this work have *trans*-form, judging from their boiling points, the saturated carbon chain has a considerable rotational freedom around the carbon-carbon single bonds. Accordingly, the length of the alkyl group would control the stability of π hydrogen bonded complex.

Table 2 shows that endocyclic olefins are more basic than RCH=CHR′ where R and R′ are alkyl groups, though the ring size of the endocyclic olefins has an effect on the value of $\Delta\nu$. The decreasing order of $\Delta\nu$ and $-\Delta F$ is the following: cyclohexene>cycloheptene≈*cis*-cyclooctene>cyclopentene. This result differs from the order of the equilibrium constants for Ag^+-complexes involving the endocyclic olefins as the electron donor.[26] If the linear Badger-Bauer relationship[27] between $-\Delta H$ and $\Delta\nu$ is correct, the effects of variations in ring size on $-\Delta F$ may be attributed to differences in ring strain, resulting from deformations and hydrogen-hydrogen repulsion with the endocyclic olefins. If we assume that the steric strain of cycloolefins is correlated with the distortion of the C=C–C bond angle, the differences in $\nu_{C=C}$ for cyclohexene and other cycloolefins will be a measure of the steric strain.[28] Table 2 shows that the smaller the $\Delta\nu_{C=C}$ value, the easier the formation of π hydrogen bond complexes. Namely, in π hydrogen bond ring strain does not appear to lead or facilitate deformation strain of the π orbital for complex formation as observed in the argentation of the cycloolefins.[26] This would suggest that the hydrogen bonded complexes are π complexes, while the Ag^+-complexes would be of the σ type.

Table 2. Stretching frequency of carbon-carbon double bond $\nu_{C=C}$ for cycloolefins, and change of free energy in the phenol-cycloolefins system

Cycloolefin	$\nu_{C=C}$[a] (cm^{-1})	$\Delta\nu_{C=C}$ (cm^{-1})	$-\Delta F$ (kcal/mol)
Cyclopentene	1611	35	−1.40
Cyclohexene	1646	0	−0.93
Cycloheptene	1651	5	−1.05
Cyclooctene	1673	27	−1.19

a) Ref. 28

25) S. Winstein and H. J. Lucas, *J. Am. Chem. Soc.*, **60**, 836 (1938); M. A. Muhs and F. T. Weiss, *ibid.*, **84**, 4697 (1962).

26) J. G. Traynham and M. F. Sehnert, *ibid.*, **78**, 4024 (1956).

27) M. D. Joesten and R. S. Drago, *ibid.*, **84**, 3817 (1962).

28) R. Lord and R. W. Walker, *ibid.*, **76**, 2518 (1954); C. F. W. Icox, Jr., and R. R. Craig, *ibid.*, **83**, 3866 (1961).

BULLETIN OF THE CHEMICAL SOCIETY OF JAPAN VOL. 42 3267—3269 (1969)

Nitroalkenylferrocene. III.[1] Condensation Reaction of Acetylferrocene Using Lewis Acid and Cyclic Amine

Hiromichi KONO, Mikio SHIGA, Izumi MOTYOAMA and Kazuo HATA

Department of Chemistry, Faculty of Science, Tokyo Metropolitan University, Setagaya-ku, Tokyo

(Received May 9, 1969)

Acetylferrocene reacted with nitromethane and morpholine in the presence of titanium(IV) chloride to give a Mannich base, 2-ferrocenyl-2-morpholino-1-nitropropane (**7**), whose sodium salt (**8**) was then converted to 2-ferrocenyl-1-nitropropene (**9**) by acidifying it with hydrochloric acid. In the presence of aluminum chloride in place of titanium(IV) chloride, acetylferrocene as well as 1,1′-diacetylferrocene dimerized to form α,β-unsaturated ketone, (**10**) or (**11**).

In a previous paper[2] it has been reported that a condensation reaction of formylferrocene with nitroalkane and cyclic amine gave a Mannich base through an intermediacy involving an immonium ion-carbonium ion resonance[3] participated with ferrocene nuclei.

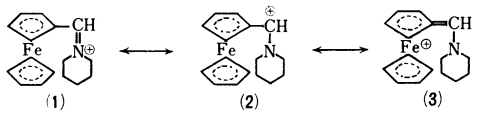

(1) (2) (3)

The fact that the Mannich base was the main product indicates that the carbonium-ion structure (**2**) is the most favorable and that it is predominantly attacked by a carbanion generated from nitroalkane.

However, neither acetylferrocene nor benzoylferrocene reacted under similar conditions. In these cases it can be assumed that the methyl or phenyl group on a carbonyl carbon may sterically prevent the formation of enamine. The procedure reported by White and Weingarten[4] for the preparation of enamines from sterically-hindered ketones in the presence of Lewis acid was applied to the condensation of acylferrocene with nitroalkane, using titanium(IV) chloride as the condensing agent. By this procedure, acetylferrocene reacted with morpholine to give an enamine when a solution of titanium(IV) chloride in benzene was added to a benzene solution of acetylferrocene and an excess of morpholine. A part of the enamine thus formed was isolated as a perchlorate, which then crystallized in fine, dark red scales. In the IR spectrum of the perchlorate, a characteristic absorption band of the $-C=\overset{+}{N}-$group was observed at 1613 cm^{-1}.[5] When nitromethane was added to the reaction mixture containing the enamine, 2-

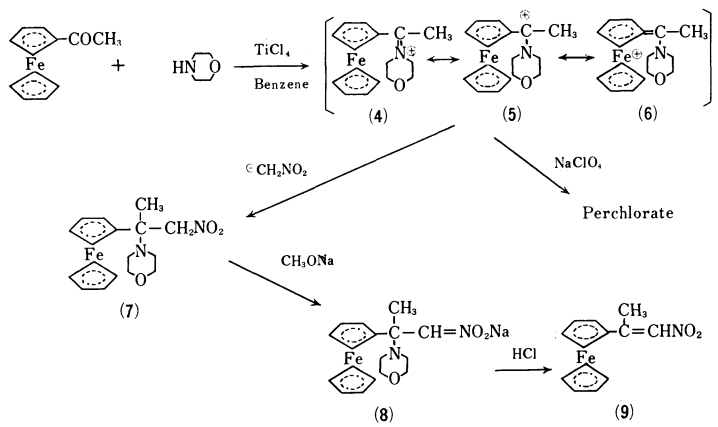

1) Part II: M. Shiga, H. Kono, I. Motoyama and K. Hata, This Bulletin, **42**, 798 (1969).

2) M. Shiga, H. Kono, I. Motoyama and K. Hata, *ibid.*, **41**, 1897 (1968).

3) R. Oda, *Chemistry (Kagaku)*, **18**, 127 (1963).

4) W. A. White and H. Weingarten, *J. Org. Chem.*, **32**, 213 (1967).

5) M. Sato, H. Kono, M. Shiga, I. Motoyama and K. Hata, This Bulletin, **41**, 252 (1968).

TABLE 1. THE SELF-CONDENSATION OF ACETYLFERROCENE

Reaction temp.: room temperature (15°C).
Solvent: benzene.

Exp. No.	$FcCOCH_3$	Morpholine	$AlCl_3$	Reaction time	Yield of condensation product	Recovery of $FcCOCH_3$
1	1.0 g	5.0 g	0.5 g	5 hr	0.3 g (31.2%)	0.42 g (42%)
2	11.4	22.0	8.3	20	4.3 (39.2)	4.5 (39.4)
3	2.0	5.0	—	5	—	1.9 (95.0)
4	1.0	—	0.5	5	—	0.75 (75.0)
5*1	2.2	10.0	1.5	5	1.2 (56.7)	0.55 (25.0)
6*2	2.2	10.0	1.5	20	1.3 (61.3)	0.58 (26.0)

*1 2.0 g of acetic acid was added after the condensation reaction had been over.
*2 15 g of acetic anhydride was added after the condensation reaction had been over.

ferrocenyl-2-morpholino-1-nitropropane (**7**), mp 156—158°C, was obtained as orange crystals. When the Mannich base (**7**) was converted into its sodium salt (**8**) by sodium methoxide and then acidified with dilute hydrochloric acid, 2-ferrocenyl-1-nitropropene (**9**) was almost quantitatively obtained as violet crystals, mp 120—122°C.

The formation of an enamine from benzoylferrocene by a similar procedure was also proved by the isolation of its perchlorate. Nevertheless, no product was isolated from the reaction of the enamine with nitromethane. It is considered that the enamine from benzoylferrocene is far less reactive than that from acetylferrocene because of both the electronical stabilization and the steric hindrance by a phenyl group on it. Probably, a positive charge on the carbon atom bonded with a nitrogen atom in the enamine will be largely delocalized by the aid of the phenyl group attached to the carbonium ion; hence, the electrophilic nature of the enamine will be much reduced.

The IR spectrum of the nitroolefin (**9**) has an olefinic absorption band at 1606 cm^{-1} and characteristic asymmetric and symmetric nitro-stretching bands at 1508 cm^{-1} and 1320 cm^{-1} respectively. It is very interesting that the olefinic absorption band of 2-ferrocenyl-1-nitropropene (**9**) is 22 cm^{-1} lower than that of 2-ferrocenyl-1-nitroethylene, while that of 1-ferrocenyl-2-nitropropene, which is an isomer of **9**, is 24 cm^{-1} higher than that of 2-ferrocenyl-1-nitroethylene.[1] This observation suggests that the ethylenic bond of 2-ferrocenyl-1-nitroethylene may be much polarized *in situ*.

The NMR spectrum of **9** shows a singlet peak for methyl protons at τ 7.47, two singlet peaks at τ 5.82 and τ 5.48 for unsubstituted and substituted ferrocene ring protons respectively, and a singlet for vinyl proton at τ 2.69.

When aluminum chloride was used as a catalyst instead of titanium(IV) chloride, acetylferrocene dimerized in the presence of morpholine to form a self-condensation product, 1,3-diferrocenyl-2-buten-1-one (**10**), which had previously been reported to be formed from acetylferrocene by the reaction with potassium *t*-butoxide or sodium hydride.[6,7] By a similar reaction, 1,1′-diacetylferrocene also gave 1,3-bis(1′-acetylferrocenyl)-2-buten-1-one (**11**) in a moderate yield. Such a self-condensation reaction never occurs when only morpholine or aluminum chloride is used alone. The reaction conditions and the yields are listed in Table 1.

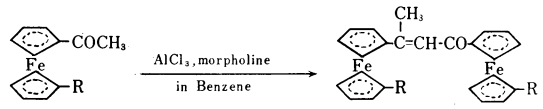

(**10**) R=H; (**11**) R=$COCH_3$

The reaction seems to proceed through an aldol condensation-type mechanism, and aluminum chloride may promote the polarization of the carbonyl group of acetylferrocene and facilitate the attack of a nucleophile on it. The yield of **10** increased upon the addition of acetic acid, acetic anhydride, or acetyl chloride after the primary condensation reaction was over. The acid was expected to be effective at the stage of the elimination of water molecule from the aldol-type condensation product[8] (Table 1, Exps. No. 5 and 6).

The IR spectrum of **11** has two kinds of carbonyl absorption bands, at 1664 cm^{-1} (acetyl group) and at 1644 cm^{-1} (α,β-unsaturated ketone), and an olefinic absorption band at 1597 cm^{-1}. The NMR spectra of the unsaturated ketones, (**10**) and (**11**), are presented in Table 2. The NMR spectrum of **10** shows the presence of three kinds of peaks for the substituted ferrocene ring protons, at τ 5.19, 5.40, and 5.54, with the relative intensities of 2, 2, and 4 respectively. The signals at τ 5.19 and 5.40

6) P. L. Pauson and W. E. Watts, *J. Chem. Soc.*, **1962**, 3880.
7) K. L. Rinehart, Jr., R. J. Curby, D. H. Gustafson, K. G. Harrison, R. E. Bozak and D. E. Bublitz, *J. Am. Chem. Soc.*, **84**, 3263 (1962).
8) A. C. Cope, *ibid.*, **59**, 2327 (1937).

Table 2. The NMR spectra of α,β-unsaturated ketones (τ-value, in $CDCl_3$)

	1,3-Diferrocenyl-2-buten-1-one (**10**)		1,3-Bis(1′-acetylferrocenyl)-2-buten-1-one (**11**)	
	τ-Value	Relative intensities	τ-Value	Relative intensities
Ferrocene ring protons				
Unsubstituted	5.81 (s)	5		
	5.84 (s)	5		
Substituted	5.19 (t)	2	5.23 (m)	6
	5.40 (t)	2	5.24 (m)	2
	5.54 (m)	4	5.50 (t)	8
Vinyl proton	3.27 (s)	1	3.38 (s)	1
Allylic methyl protons	7.44 (m)	3	7.49 (s)	3
Acetyl methyl protons			7.64 (s)	6

were assigned to α-protons to the carbonyl and olefinic substituents on the ferrocene rings respectively, and the signal at τ 5.54, to β-protons on the substituted ring. In the NMR spectrum of **11**, the signals at τ 5.23 and 5.34 were assigned to α-protons to the carbonyl and olefinic substituents respectively, and the signal at τ 5.50, to β-protons on the ferrocene ring.

Experimental

2-Ferrocenyl-2-morpholino-1-nitropropane (7). A solution of titanium(IV) chloride (3.5 g) in benzene (10 m*l*) was added, drop by drop, to a stirred solution of acetylferrocene (4.4 g) and morpholine (10 g) in benzene (20 m*l*) which had previously been cooled in an ice bath. In a little while, a yellowish-brown solid appeared to form a suspension in the reaction mixture. The suspension was stirred for 4 hr at room temperature, and then nitromethane (5 g) was added. After the reaction mixture had been stirred for another 16 hr, it was filtered and the residue on the filter was repeatedly washed with ether. The filtrate and the washing were combined and concentrated under reduced pressure at room temperature. From the concentrated solution 2-ferrocenyl-2-morpholino-1-nitropropane (**7**) was obtained as orange needles (0.58 g, 8.4%); mp 156—158°C. IR (KBr): 2850—3000 ($-CH_2-$), 1557 (NO_2) and 1105 cm^{-1} (C–O–C).

Found: C, 57.41; H, 6.42; N, 7.63%. Calcd for $C_{17}H_{22}N_2O_3Fe$: C, 57.03; H, 6.14; N, 7.82%.

A part of the yellowish-brown solid which separated in the initial reaction was dissolved in water to give a deep red solution. On the treatment of the aqueous solution with $NaClO_4$, dark red crystals of perchlorate were isolated. IR spectrum: 1613 cm^{-1} ($-C=\overset{+}{N}-$ group).

2-Ferrocenyl-1-nitropropene (9). Following the procedure described in a previous report,[1] 2-ferrocenyl-2-morpholino-1-nitropropane (0.13 g) was treated with sodium ethoxide in ethanol and then with dilute hydrochloric acid to afford 2-ferrocenyl-1-nitropropene (**9**), mp 120—122°C. The chromatographic purification of the nitroolefin (**9**) was carefully done because of its instability on alumina. IR (CCl_4): 1606 (C=C), 1508 (asym. NO_2) and 1319 cm^{-1} (sym. NO_2). NMR (in $CDCl_3$): τ 7.47 (singlet, 3H), 5.82 (singlet, 5H), 5.48 (singlet, 4H), 2.69 (singlet, 1H).

Found: C, 58.29; H, 5.08; N, 5.17%. Calcd for $C_{13}H_{13}NO_2Fe$: C, 57.59; H, 4.79; N, 5.16%.

1,3-Diferrocenyl-2-buten-1-one (10). (a) To a stirred mixture of 8.3 g (0.06 mol) of aluminum chloride and 50 m*l* of anhydrous benzene cooled in an ice bath there was added, drop by drop, a solution of 11.4 g (0.05 mol) of acetylferrocene and 22 g (0.25 mol) of morpholine in 70 m*l* of anhydrous benzene under an atmosphere of nitrogen. After the addition had been completed, the mixture was stirred for another 20 hr at room temperature. At the end of the reaction, the deep red reaction mixture was poured into water and the aqueous layer was extracted with benzene. The organic layer thus obtained was washed thoroughly with water and dried over anhydrous magnesium sulfate. The removal of the solvent left 8.8 g of an oil, which was then chromatographed on alumina with *n*-hexane-benzene (1 : 1). The first fraction gave 4.5 g of acetylferrocene, and the second fraction gave 4.3 g (39.2%) of 1,3-diferrocenyl-2-buten-1-one (**10**), which was recrystallized from methanol to yield fine, deep red crystals; mp 122—124°C (lit 123—124°C[7]). IR (KBr): 1638 (C=O) and 1585 cm^{-1} (C=C).

(b) A mixture of acetylferrocene (2.2 g, 0.01 mol), morpholine (10 g, 0.11 mol), and aluminum chloride (1.5 g, 0.01 mol) in anhydrous benzene (30 m*l*) was treated similarly. After it had been stirred for 18 hr at room temperature, 15 g (0.15 mol) of acetic anhydride was added, drop by drop, to the reaction mixture under ice cooling; the resulting reaction mixture was stirred for another 2 hr at room temperature. The treatment of the reaction mixture much as in the procedure (a) gave 0.58 g of acetylferrocene and 1.3 g (61.3%) of 1,3-diferrocenyl-2-buten-1-one (**10**).

1,3-Bis(1′-acetylferrocenyl)-2-buten-1-one (11). A reaction was carried out in the same way as has been described in the case of the procedure (a) above by using 1,1′-diacetylferrocene (1.20 g, 0.005 mol), morpholine (7.0 g, 0.08 mol), aluminum chloride (1.2 g, 0.001 mol), and anhydrous benzene (40 m*l*). After it had been stirred for 20 hr, the reaction mixture was poured into ice water and the aqueous layer was extracted with benzene. The organic layer was washed with water and dried over anhydrous magnesium sulfate. After the solvent had been removed by a rotatory evaporator, the deep red oily residue was carefully chromatographed on alumina with *n*-hexane, benzene and chloroform successively as the elution solvents. The first fraction, eluted with *n*-hexane-benzene, gave diacetylferrocene (0.7 g), while the second fraction, eluted with chloroform, gave a deep red oil which was then rechromatographed with *n*-hexane-benzene (1 : 2) to give 0.2 g (17%) of 1,3-bis(1′-acetylferrocenyl)-2-buten-1-one (**11**) as an oil. An analytical sample of **11** was obtained by repeated chromatography of the oily product on alumina. IR (liquid film): 1664 and 1644 (C=O), 1576 cm^{-1} (C=C).

Found: C, 63.94; H, 5.18%. Calcd for $C_{28}H_{26}O_3Fe$: C, 64.45; H, 4.98%.

The authors are indebted to Mr. Kisaburo Yamazaki and his group of the Central Research Laboratory, Yamanouchi Pharmaceutical Co., Ltd., for their measurement of the NMR spectra.

BULLETIN OF THE CHEMICAL SOCIETY OF JAPAN VOL. 42 3270—3273 (1969)

Nitroalkenylferrocene. IV.[1] Preparation of 1-Ferrocenyl-2-iodo-2-nitroethylene and Configurations of Several Nitroalkenylferrocenes

Hiromichi KONO, Mikio SHIGA, Izumi MOTOYAMA and Kazuo HATA

Department of Chemistry, Faculty of Science, Tokyo Metropolitan University, Setagaya-ku, Tokyo

(Received May 19, 1969)

A new method of synthesizing 1-ferrocenyl-2-iodo-2-nitroethylene (**6**) was presented, whereas 1-ferrocenyl-2-halo-2-nitroethylene could not be prepared by the usual method, involving the direct halogenation of the nitroolefin. The iodonitroethylene (**6**) was prepared by the reaction of the sodium salt of 1-ferrocenyl-2-nitroethylene with iodine or with potassium iodide. This procedure proved to be useful for introducing various groups on the α-carbon of the nitroethylene. The stereochemistry of nitroalkenylferrocenes, including some previously reported ones, was discussed on the basis of their spectral data.

In the course of study of the reactions of nitroalkenyl-ferrocenes, it has been found that a sodium salt (**5**) which was obtained when 1-ferrocenyl-2-nitroethylene (**4**) was treated with sodium methoxide reacted directly with iodine to give 1-ferrocenyl-2-iodo-2-nitroethylene (**6**). The usual method[2] for the synthesis of α-halonitroethylene (**3**) from α-nitroethylene (**1**) through dibromide (**2**) was found to be unsuccessful when applied to 1-ferrocenyl-2-nitroethylene (**4**). The reaction of **4** with bromine gave no dibromide, but the ferrocene nuclei was largely decomposed, even at −65°C in the presence of bromine.

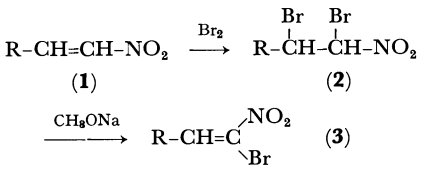

On the other hand, 1-ferrocenyl-2-iodo-2-nitroethylene (**6**) was easily obtained in a 30% yield when the sodium salt (**5**) was treated with iodine in dry ether under an atmosphere of nitrogen and then treated with aqueous sodium thiosulfate. The sodium salt (**5**) also reacted with mercury(II) chloride in the presence of excess sodium methoxide to give a brownish sodium salt (**7**). The brownish salt (**7**), on treatment with dilute hydrochloric acid, was easily converted into 1-ferrocenyl-2-chloromercuri-2-nitroethylene (**8**), which separated as a blue solid. The structure of **8** was assumed on the basis of its IR spectrum: an olefinic absorption band at 1588 cm^{-1}, an asymmetrical NO_2 stretching band at 1480 cm^{-1}, and a pair of symmetrical NO_2 stretching bands at 1290 cm^{-1} and 1282 cm^{-1}. The results of elemental analyses also support the structure.

When **8** was stirred with iodine and potassium

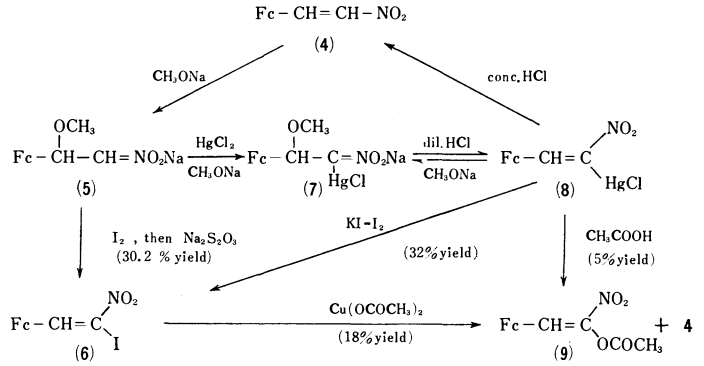

1) Part III: H. Kono, M. Shiga, I. Motoyama and K. Hata, This Bulletin, **42**, 3267 (1969).

2) B. Priebs, *Ann.*, **225**, 342 (1884); W. E. Parham and J. L. Bleasdale, *J. Am. Chem. Soc.*, **73**, 4664 (1951).

iodide in dioxane containing a trace of water, 1-ferrocenyl-2-iodo-2-nitroethylene (**6**) was obtained in a 32% yield after the treatment of the crude product with aqueous sodium thiosulfate. The reaction of **8** with iodine was carried out in several kinds of solvents; the results are summarized in Table 1. The chloromercuri compound (**8**) was easily decomposed to the nitroolefin (**4**) and mercury(II) chloride by the action of concentrated hydrochloric acid. The identity of the decomposition product with the starting nitroolefin (**4**), which has been prepared by the condensation of formylferrocene with nitromethane using a base catalyst,[3] was proved by the coincidence of their IR spectra.

Table 1. Iodination of 1-ferrocenyl-2-chloromercuri-2-nitroethylene (**8**) (at 0°C)

8 (g)	**8** (mol)	Iodinating reagent	(g)	Solvent	Reaction time (hr)	Yield of **6** (%)
15	0.03	I_2	11.1	THF (200 m*l*)	20	19
15	0.03	I_2	11.1	CH_2Cl_2 (200 m*l*)	20	24
15	0.03	I_2	11.1	CCl_4 (200 m*l*)	20	26
15	0.03	I_2 KI	11.1 5	Dioxane (200 m*l*) H_2O (2 drops)	20	32

When **8** was stirred in acetic acid, a small amount of violet oil was obtained, together with the nitroolefin (**4**) as the main product. The minor product was too unstable to be thoroughly purified, and it easily decomposed into formylferrocene. The IR spectrum indicated the presence of acetoxy group (1758 cm^{-1} and 1200 cm^{-1}), as well as nitro group (1502 cm^{-1} (asym. NO_2) and 1325 cm^{-1} (sym. NO_2)). Accordingly, 1-ferrocenyl-2-acetoxy-2-nitroethylene (**9**) was tentatively proposed as the structure of this compound. The same compound (**9**) was also obtained by the reaction of **6** with copper(II) acetate.

Infrared Spectra and Configuration of Nitroalkenylferrocenes. Although various nitroalkenylferrocenes have been synthesized in our laboratory,[1,3,4] no discussion of the geometric relationship between nitro and ferrocenyl groups has yet been undertaken becasue of the difficulty of isolating their geometric counterparts. Recently, however, Watarai *et al.*[5] have shown that the geometric relationship between nitro and phenyl groups in nitrostyrene and the related compounds could be determined by means of their IR spectra. According to their rule, the absorbance of the symmetrical NO_2 stretching absorption band is smaller than that of the asymmetrical one in the case of the cis isomer, while the former is equal to or larger than the latter in the case of the trans isomer. Because of the close structural resemblance of 1-ferrocenyl-2-nitroethylene to β-nitrostyrene, it is quite reasonable to assume that this empirical rule would be applicable to the system of 1-ferrocenyl-2-nitroethylene and would give a strong suggestion regarding its stereochemistry. Thus, the IR spectra of several 1-ferrocenyl-2-nitroalkenes were measured in CCl_4. All the results are summarized in Table 2. By comparing the absorbances of the symmetrical and asymmetrical NO_2 stretching absorption bands with each other, it is evident that the absorbance of the former band considerably exceeds that of the latter in all the compounds listed in Table 2. Therefore, the configuration of these nitroalkenes can be concluded to be trans, according to the Watarai rule.

Table 2. IR spectra of nitroalkenylferrocenes (cm^{-1}, in CCl_4)

Compound	C=C (ε)	Asym. NO_2 (ε)	Sym. NO_2 (ε)
Fc-CH=CH-NO_2*1 (**4**)	1628 (388)	1518 (285)	1343 (350) 1331 (649)
Fc-CH=C(CH_3)NO_2*1	1652 (283)	1512 (496)	1324 (386) 1313 (1038)
Fc-CH=C(C_2H_5)NO_2*1	1645 (331)	1512 (457)	1323 (512) 1303 (328)
Fc-CH=CINO_2 (**6**)	1596 (492)	1523 (371)	1302 (1294) 1287 (552)
Fc-C(CH_3)=CH-NO_2*2	1606 (332)	1508 (476)	1344 (291) 1320 (980)

*1 Ref. 3 *2 Ref. 1

A similar conclusion can be derived from the results of the NMR spectra of these compounds. The $J_{\alpha\beta}$-value of the olefinic protons in **4** (12.5 cps) corresponds to that of *trans*-olefin, and the chemical shifts of the olefinic β-protons in the other nitroolefins[3,4] were almost the same as that of 1-ferrocenyl-2-nitroethylene (**4**).

Jensen *et al.*[6,7] have reported that mercuri-

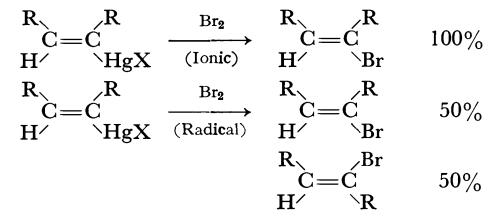

3) M. Shiga, H. Kono, I. Motoyama and K. Hata, This Bulletin, **41**, 1897 (1968).

4) M. Shiga, H. Kono, I. Motoyama and K. Hata, *ibid.*, **42**, 798 (1969).

5) S. Watarai, K. Yamaura and T. Kinugasa, *ibid.*, **40**, 1448 (1967).

6) F. R. Jensen and L. H. Gale, *J. Am. Chem. Soc.*, **78**, 2597 (1956); *ibid.*, **82**, 148 (1960).

7) S. Winstein and T. G. Traylor, *ibid.*, **78**, 2597 (1956).

olefins are replaced by a cationoid reagent with the retention of the configuration, but not by a radical reagent.

1-Ferrocenyl-2-chloromercuri-2-nitroethylene (**8**) was easily converted to *trans*-1-ferrocenyl-2-nitroethylene (**4**) by the action of hydrochloric acid. According to Jensen's observation, the compound **8** is considered to have a trans configuration with respect to ferrocenyl and nitro groups. A similar consideration can be applied to the compound **6**, which was prepared by the reaction of **8** with iodine and potassium iodide.

Careful examination of the stereochemistry using a molecular structure model reveals that the cis form may bring about a considerable steric strain in the molecule because of a steric interaction between nitro and ferrocenyl groups.

As was expected from this consideration, *cis*-1-ferrocenyl-2-iodo-2-nitroethylene could be obtained neither from the reaction of 1-ferrocenyl-2-chloromercuri-2-nitroethylene with iodine under radical conditions nor from the attempted isomerization of the trans isomer by UV irradiation in CCl_4.

Some interesting phenomena have been observed in the symmetrical NO_2 stretching absorption bands of the nitroalkenylferrocenes. All the nitroolefins studied here have doubly-split absorption bands in the range of 1287—1343 cm^{-1}. The positions and the relative intensities of the split bands depend on the substituents on the double bond of nitroolefin, as well as on the state in which the IR spectra were observed, as is shown in Fig. 1 and Table 2. Such splitting in the symmetrical NO_2 stretching absorption band has never been observed in the benzene analogs. Therefore, it seems to be attributable to a certain influence of the ferrocenyl group on the nitro group. However, no simple explanation of the splitting is possible at present.

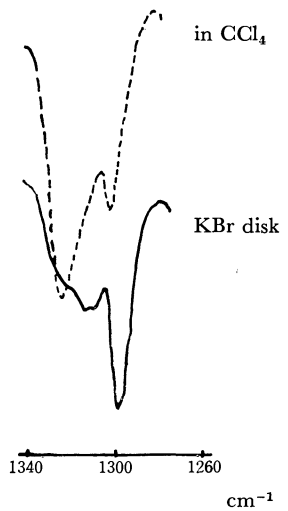

Fig. 1. The symmetrical NO_2 stretching absorption bands of $FcCH=C(C_2H_5)NO_2$.

Experimental

1-Ferrocenyl-2-chloromercuri-2-nitroethylene (8). To 10.8 g (0.041 mol) of finely-powdered 1-ferrocenyl-2-nitroethylene in 20 m*l* of absolute methanol, there were slowly added, at 0°C, 10.8 g (0.2 mol) of sodium methoxide which had been freshly prepared from absolute methanol and sodium metal. Subsequently, 20.2 g (0.075 mol) of finely-powdered mercury(II) chloride were added to the mixture with stirring. In a little while, the sodium salt of the chloromercuri compound (**7**) precipitated as a brown solid. An additional 5.4-g portion (0.1 mol) of sodium methoxide was added, and the reaction mixture was stirred for a while. Then, the mixture was poured into 500 m*l* of 20% hydrochloric acid and stirred for half an hour. A blue solid was collected on a filter, washed three times with methanol, and dried in a desiccator under reduced pressure. The finely-powdered material was then stirred in 100 m*l* of chloroform for half an hour in order to remove the unreacted starting material. After filtration, 19.5 g (96% yield) of **8** were obtained as a pale blue solid.

Found: C, 25.26; H, 2.31; N, 2.56%. Calcd for $C_{12}H_{10}FeNO_2HgCl$: C, 29.26; H, 2.03; N, 2.84%.

Repeated elemental analyses failed to give good results owing to the difficulty of purification.

1-Ferrocenyl-2-iodo-2-nitroethylene (6). (a) Into 15 g (0.03 mol) of 1-ferrocenyl-2-chloromercuri-2-nitroethylene (**8**) in 200 m*l* of dioxane, a solution of iodine (11.1 g) and potassium iodide (5 g) in 200 m*l* of dioxane containing two drops of water was slowly added with stirring at 0°C. After having been stirred for 20 hr, the reaction mixture was poured into a solution of 30 g of sodium thiosulfate in 200 m*l* of water; then the mixture was stirred for another hour. Subsequently, the mixture was extracted with ether, and the solution was washed with aqueous sodium thiosulfate and dried over anhydrous magnesium sulfate. After the removal of the solvent, the residue was chromatographed on Florisil using a mixture of benzene and *n*-hexane (1 : 3) as the solvent. The first fraction gave blue needles of 1-ferrocenyl-2-iodo-2-nitroethylene (**6**) (3.7 g, 32% yield), mp 139—141°C, after recrystallization from methanol. NMR spectra (in $CDCl_3$): τ 5.70 (5H, unsubstituted ring H, singlet), 5.28 (2H, substituted ring H, triplet), 4.91 (2H, substituted ring H, triplet), and 1.22 (1H, vinyl H, singlet).

Found: C, 37.02; H, 2.49; N, 3.62%. Calcd for $C_{12}H_{10}FeNO_2I$: C, 37.59; H, 2.61; N, 3.65%.

(b) To a solution of 5.14 g (0.02 mol) of 1-ferrocenyl-2-nitroethylene in 100 m*l* of dry ether, 3 g (0.05 mol) of sodium methoxide were added at 0°C under an atmosphere of nitrogen. After the reaction mixture had been decolored, a solution of 13 g (0.05 mol) of iodine in 200 m*l* of dry ether was added, drop by drop, to the stirred mixture within an hour. After it had then been stirred for 2 hr, the solution was let stand overnight. Then the reaction mixture was treated in the way described for the procedure (a). After the removal of the solvent from the dried ethereal solution thus obtained, the residue was repeatedly extracted with a mixture of benzene and *n*-hexane (1 : 1). The residue, obtained from the extracts by the removal of the solvent, was chromatographed on Florisil using a mixture of

benzene and *n*-hexane (1 : 3). The first fraction gave 2.3 g (30.2% yield) of **6**.

1-Ferrocenyl-2-acetoxy-2-nitroethylene (9). (a) 1-Ferrocenyl-2-iodo-2-nitroethylene (**6**) (0.5 g, 0.002 mol) dissolved in 3 m*l* of dioxane was added to a mixture of 20 m*l* of ethanol and 20 m*l* of water containing 1.5 g of copper(II) acetate, and then the mixture was heated at 90°C for 4 hr. At the end of the reaction, the hot reaction mixture was poured into 100 g of ice water and the product was extracted with ether. The extracts were shaken with 5% hydrochloric acid, and then washed with water and dried over anhydrous magnesium sulfate. After the removal of the solvent, the residue was chromatographed on Florisil with benzene to afford 1-ferrocenyl-2-nitroethylene (**4**). Further elution with chloroform afforded crude **9** (90.1 mg, 18% yield) as a blue violet oil which contained a small amount of formylferrocene. Formylferrocene is considered to be produced by the decomposition of the unstable product (**9**) during elution, although the chromatographic column was covered with aluminum foil in order to prevent the decomposition of the product by light.

(b) 1-Ferrocenyl-2-chloromercuri-2-nitroethylene (**8**) (10 g) was added to 20 m*l* glacial acetic acid, and the mixture was heated at 95°C for 3 hr. At the end of the reaction, the reaction mixture was poured into 200 m*l* of water. The precipitate was collected by filtration and washed with water. The product was then dissolved in 30 m*l* of benzene and dried over anhydrous magnesium sulfate. The benzene solution, treated much as in the procedure (a), afforded 0.3 g (5% yield) of **9**.

Spectral Measurements. The infrared spectra were measured in carbon tetrachloride using a 0.52-mm rock salt cell on a Hitachi EPI-G2 grating infrared spectrometer.

BULLETIN OF THE CHEMICAL SOCIETY OF JAPAN VOL. 42 3273—3277 (1969)

β-Ferrocenyl-α,β-unsaturated Ketones. I. Condensation Reactions of Formylferrocene with Ketones

Hiromichi KONO, Mikio SHIGA, Izumi MOTOYAMA and Kazuo HATA

Department of Chemistry, Faculty of Science, Tokyo Metropolitan University, Setagaya-ku, Tokyo

(Received May 19, 1969)

The condensation reaction of formylferrocene with simple aliphatic and alicyclic ketones, as acetone, ethyl methyl ketone, isobutyl methyl ketone, and cyclohexanone, in the presence of piperidine as a condensing agent afforded seven kinds of β-ferrocenyl-α,β-unsaturated ketones. The geometric configurations of the unsaturated ketones were discussed on the basis of their NMR spectra, and the influences of the ferrocenyl group on the π-π* transition bands in their UV spectra were also discussed.

It is widely known[1] that formylferrocene, like aromatic aldehydes, undergoes a variety of condensation reactions and thereby serves as an important starting material for the syntheses of many ferrocene derivatives. A Knoevenagel-type or aldol-type condensation[2] with a compound having a reactive methylene group under the influence of a base catalyst affords a ferrocene derivative with an unsaturated group conjugated with the ferrocene nucleus. Base-catalyzed condensations of formylferrocene or 1,1′-diformylferrocene with acetone have been reported by Boichard *et al.*[3] and by Osgerby and Pauson.[4] However, little has been reported on the condensation of formylferrocene with other simple aliphatic ketones.

A cyclic amine proved to be a very useful catalyst for the condensation of formylferrocene with nitroalkane.[5] In the present investigation, seven kinds of β-ferrocenyl-α,β-unsaturated ketones were prepared by the condensation of formylferrocene with various ketones, such as acetone, cyclohexanone, ethyl methyl ketone, and isobutyl methyl ketone, in the presence of piperidine, which was also found to be the most effective catalyst for such condensations.

1) M. Rosenblum, "Chemistry of the Iron Group Metallocenes," Part 1, John Wiley & Sons, New York, N. Y. (1965), p. 80.

2) G. D. Broadhead, J. M. Osgerby and P. L. Pauson, *J. Chem. Soc.*, **1965**, 650; K. Schlögl, *Monatsh. Chem.*, **88**, 601 (1957); C. R. Hauser and J. K. Lindsey, *J. Org. Chem.*, **22**, 906 (1957); P. J. Graham, R. V. Lindsey, G. W. Parshal, M. L. Peterson and G. M. Whitman, *J. Am. Chem. Soc.*, **79**, 3416 (1957).

3) J. Boichard, J. P. Monin and J. Tirouflet, *Bull. Soc. Chim. France*, **1963**, 851.

4) J. M. Osgerby and P. L. Pauson, *J. Chem. Soc.*, **1961**, 4604.

5) M. Shiga, H. Kono, I. Motoyama and K. Hata, This Bulletin, **41**, 1897 (1968).

Results and Discussion

The α,β-unsaturated ketones obtained in the present study were five 1 : 1 adducts (from 1 mol of formylferrocene and 1 mol of ketone) (**1a–d**) and two 2 : 1 adducts (from 2 mol of the aldehyde and 1 mol of ketone) (**2a,b**).

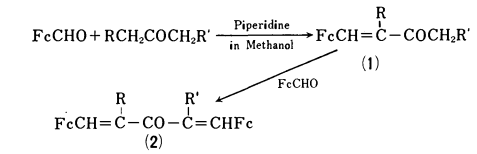

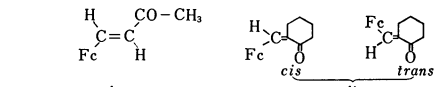

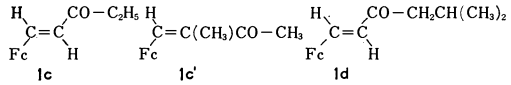

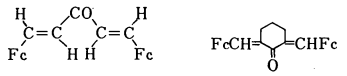

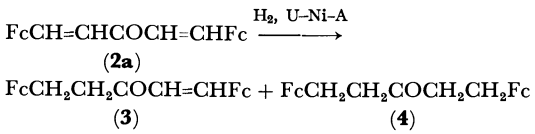

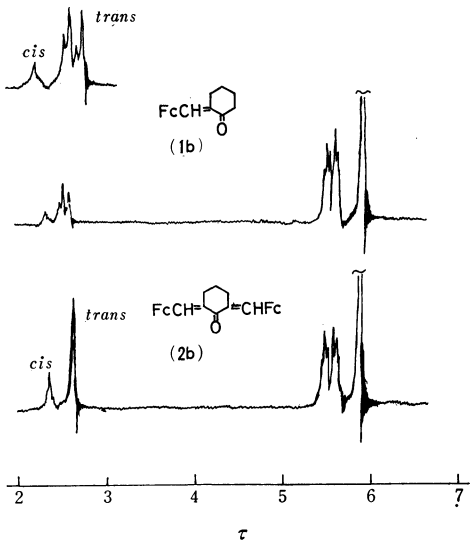

Fig. 1. NMR spectra of **1b** and **2b** in $CDCl_3$ (60 Mc).

The hydrogenation of 1,5-diferrocenyl-1,4-pentadien-3-one (**2a**) with Urushibara nickel A[6] proceeded step-by-step and afforded 1,5-diferrocenyl-1-penten-3-one (**3**) and 1,5-diferrocenyl-3-pentanone (**4**).

The NMR spectral data of the β-ferrocenyl-α,β-unsaturated ketones obtained here are listed in Table 1, together with those of vinylferrocene.

Table 1. The NMR spectra of β-ferrocenyl-α,β-unsaturated ketones and vinylferrocene (τ-value, in $CDCl_3$)

Compound	MP (°C)	Configuration	Cyclopentadienyl ring protons (unsubst.)	Cyclopentadienyl ring protons (subst.)	Vinyl protons β	Vinyl protons α	Alkyl protons
$FcCH=CH_2$*			5.90(s)	5.80(t) 5.65(t)	3.48(q)	4.67(q) 4.97(q) (J=11, 17, 1.5 cps)	
1a	84—85	*trans*	5.84(s)	5.50(s)	2.56(d) (J=16 cps)	3.68(d)	7.73(s, CH_3)
1b	110—112	mixture (*trans*/*cis*=*ca.* 8)	5.87(s)	5.58(t) 5.48(t)	2.52(q, *trans*) (J=1.5 cps) 2.30(s, *cis*)		7.13—8.30 (broad, CH_2)
1c	101—102	*trans*	5.84(s)	5.52(s)	2.53(d) (J=16 cps)	3.66(d)	7.41(q, CH_2) 8.84(t, CH_3)
1d	31—32	*trans*	5.87(s)	5.52(s)	2.57(d) (J=16 cps)	3.68(d)	7.63(CH_2) 7.96(CH) 9.02(d, CH_3) (J=6.2 cps)
3	113—114	*trans*	5.85(s)	5.88(m) 5.52(s)	2.49(d) (J=16 cps)	3.65(d)	7.25 (s, CH_2CH_2)**
2a	203—204	*trans-trans*	5.85(s)	5.55(t) 5.45(t)	2.38(d) (J=15.5 cps)	3.43(d)	
2b	163—165	mixture	5.82(s)	5.56(t) 5.45(t)	2.59(s, *trans*) 2.33(s, *cis*)		7.26, 8.17 (broad CH_2)

* These data were in accord with those reported by Rausch *et al.*, (*J. Organometal. Chem.*, **11**, 317 (1968)).
** This signal did not show A_2B_2 type coupling.

6) Y. Urushibara and S. Nishimura, This Bulletin, **28**, 466 (1955).

Table 2. The UV spectra data of β-ferrocenyl-α,β-unsaturated ketones* and other ferrocene derivatives**

Compound	Transition bands λ_{max} mμ (ε_{max})				
			π–π*	d–d type	
FcCH=CHCOCH$_3$ (**1a**)	210 (15900)	258 (9860)	305 (14300)	369 (2150)	486 (1750)
FcCH=CHCOC$_2$H$_5$ (**1c**)	211 (26150)	258 (9500)	305 (24400)	371 (1950)	486 (1600)
FcCH=C(CH$_3$)COCH$_3$ (**1c′**)	218 (6386)	256 (4959)	308 (5710)	357 (1277)	479 (864)
FcCH=CHCOCH=CHFc (**2a**)	207 (35940)	—	340 (17870)	402 (4140)	527 (5080)
FcCH=CHCOC$_6$H$_5$**				387 (3120)	490 (2970)
FcCOCH=CHC$_6$H$_5$**				383 (1960)	484 (1660)

* Ethanol was used as solvent.
** R.T. Lundiquist and M. Cais, *J. Org. Chem.*, **27**, 1167 (1962).

Representative NMR spectra of **1b** and **2b** are shown in Fig. 1. The UV spectra of some of these unsaturated ketones are listed in Table 2, together with those of the related compounds.

When symmetrical ketones, such as acetone and cyclohexanone, were employed, considerable quantities of 2 : 1 adducts (**2a** and **2b**) were obtained as by-products besides the 1 : 1 adducts (**1a** and **1b**). On the other hand, unsymmetrical ketones, such as ethyl methyl ketone and isobutyl methyl ketone, gave 1 : 1 adducts (**1c**, **1c′**, and **1d**) exclusively.

A well-known reaction of this type is the Claisen-Schmidt condensation[7] with aromatic aldehydes. Benzaldehyde condenses with acetone under acidic conditions to form dibenzylideneacetone predominantly, whereas under basic conditions the main product is benzylideneacetone, accompanied by dibenzylideneacetone as a minor product.

It is known that ethyl methyl ketone suffers an enolization-controlled reaction mainly on the methyl side rather than on the ethyl side under basic conditions.[8] The same tendency was observed in the present experiments. Ethyl methyl ketone condensed with formylferrocene to afford **1c** as the main product and **1c′** as a minor product, while isobutyl methyl ketone afforded **1d** as the sole product. These observations indicate that steric hindrance against an electrophilic attack on the α-carbon to the carbonyl group of the ketone is apparently an important factor in the orientation of these condensation reactions.

Assignment of the Geometrical Configuration of the α,β-Unsaturated Ketone. The geometrical configurations of the α,β-unsaturated ketones were determined in terms of the coupling constants between the vinyl protons. As is shown in Table 1, α- and β-protons of the vinyl group gave respective doublet peaks, corresponding to an AB pattern. The coupling constant of the vinyl protons was 16 cps in the cases of **1a**, **1c**, and **1d**, and 15.5 cps for **2a**. The magnitude of the coupling constant reveals these α,β-unsaturated ketones to have trans configurations, in which ferrocenyl and carbonyl groups are on opposite sides of the double bond.[9] In this connection, it has been pointed out that the coupling constant of trans vinyl protons is 17 cps for vinylferrocene itself and 12.5 cps for *trans*-1-ferrocenyl-2-nitroethylene.[5]

The compound **1b** gave complex signals due to the β-vinyl proton in the range from τ 2.26 to 2.60, as is shown in Fig. 1. In the trans isomer of this compound, in which the ferrocenyl group is on the side opposite to that of the carbonyl group, a signal of the vinyl proton is expected to appear in a higher field, because of an anisotropic effect of the carbonyl group on the same side, than that of the cis isomer. Further, the splitting of the former is expected, considering a long-range coupling with a methylene group situated trans to the vinyl proton. Therefore, a quartet in the higher field, centered at about τ 2.52, was assigned to the vinyl proton of the trans isomer, whereas a broad signal centered at about τ 2.30 was assigned to that of the cis isomer. On the basis of the relative intensities of these signals, the trans : cis ratio in **1b** was determined to be about 8 : 1.

The compound **2b**, which contains two exo-double bonds in the molecule, showed the signals of the vinyl protons at τ 2.59 and 2.33 as two singlets. The former, in the higher field, was assigned to the trans vinyl proton for the same reason as has been described for **1b**, and the latter was assigned to the cis. No such long-range coupling as was observed in *trans*-**1b** was observed in *trans*-**2b**, probably because of a conformational change in the cyclohexanone ring caused by the two exo-double bonds.

Ultraviolet Spectra. The UV spectra of **1a**, **1c**, **1c′**, and **2a** were observed in 95% ethanol and

7) L. F. Fieser and M. Fieser, "Advanced Organic Chemistry," Reinhold Pub. Co., New York, N. Y. (1961), p. 467.

8) E. S. Gould, "Mechanism and Structure in Organic Chemistry," Henry Holt and Company, New York, N. Y. (1959), p. 383.

9) L. M. Jackman, "Applications of Nuclear Magnetic Resonance Spectroscopy in Organic Chemistry," Pergamon Press, London (1959), p. 85.

are summarized in Table 2, together with those of some related ferrocene derivatives. The strongest absorption bands, at 305—308 mμ, in the spectra of **1a**, **1c**, and **1c'** can be assigned to the π–π* transition band of the α,β-unsaturated ketone conjugated with the ferrocene nucleus, while the corresponding absorption bands of nitroalkenylferrocenes appear at about 325 mμ.[10] As the π–π* transition band of methyl vinyl ketone has been reported to appear at 219 mμ (ε=3600),[11] the replacement of a vinyl hydrogen by a ferrocenyl group causes a remarkable shift of this band to a longer wavelength (305 mμ). Such a large bathochromic shift (85 mμ) by a ferrocenyl group has also been observed in the nitroalkene series.[10]

The UV spectrum of ferrocene has been discussed in detail by Scott and Becker,[12] who assigned the two long wavelength bands at 325 and 440 mμ to *d–d* type transitions, with some mixing with ring orbitals. In the cases of **1a**, **1c**, and **1c'**, both of these long wavelength bands, due to the *d–d* type transitions, appeared in the longer-wavelength region, namely, at about 370 and 480 mμ respectively.

In the spectrum of **2a**, the π–π* and *d–d* type transition bands exhibited larger bathochromic shifts and appeared at 340, 402, and 527 mμ respectively.

However, such a large bathochromic shift as that observed in the π–π* transition band cannot simply be explained in terms of conjugation of the α,β-unsaturated ketone with the ferrocene ring. It will be necessary to consider the interaction of the non-bonding *d*-orbitals of the metal in the ferrocene nucleus with the π-orbital of the side chain on the ferrocene ring.

Further work on this subject is now in progress, and a more detailed discussion will be presented in the near future.

Experimental

General Procedure for the Preparation of β-Ferrocenyl-α,β-unsaturated Ketones. A solution of formylferrocene (1 mol) and a ketone (2 mol) in methanol was left to stand for 2—4 days in the presence of piperidine (2 mol) at room temperature. After the subsequent removal of the solvent under reduced pressure, a deep red residue was dissolved in benzene; then the benzene solution was washed repeatedly with water and dried over anhydrous magnesium sulfate. The benzene solution was concentrated under reduced pressure and then chromatographed on alumina using a mixture of benzene-hexane (1 : 1) as a sovlent. The isolated products were identified by means of the NMR, IR, and UV spectra and elemental analyses.

4-Ferrocenyl-3-buten-2-one (1a) and 1,5-Diferrocenyl-1,4-pentadien-3-one (2a). The condensation product from the reaction of formylferrocene and acetone was chromatographed on alumina. The first fraction gave **1a** in a 78.9% yield. The product was recrystallized from petroleum ether to afford a deep red powder, mp 84—85°C (lit mp 86°C[3]). IR (in CCl_4): 3100, 1689, 1666, 1619, 1601, 1359, 1251, 1186, 1108, 1043, 1028, 998 and 964 cm^{-1}.

Found: C, 67.25; H, 5.70%. Calcd for $C_{14}H_{14}OFe$: C, 66.18; H, 5.52%.

The second fraction gave **2a** in a 4.3% yield; it was recrystallized from benzene-hexane (1 : 1) to afford reddish-orange leaflets, mp 203—204°C. IR (in CCl_4): 3100, 1665, 1649, 1614, 1104, 1090, 1037, 1024 and 995 cm^{-1}.

Found: C, 65.89; H, 4.81%. Calcd for $C_{25}H_{22}OFe_2$: C, 66.71; H, 4.89%.

2-(Ferrocenylmethylene)cyclohexanone (1b) and 2,6-Bis(ferrocenylmethylene)cyclohexanone (2b). The condensation product from formylferrocene and cyclohexanone was chromatographed on alumina. From the first fraction, **1b** was obtained, on recrystallization from benzene-hexane (1 : 1), as deep red powder, mp 110—112°C, in a 70.4% yield. IR (in CCl_4): 3080, 2920, 1677, 1585, 1309, 1239, 1137, 1100, 1040 and 991 cm^{-1}.

Found: C, 69.79; H, 6.16%. Calcd for $C_{17}H_{18}OFe$: C, 69.35; 6.11%.

The second fraction gave **2b**; it was then recrystallized from petroleum ether-benzene (1 : 1) to give deep red needles, mp 163—165°C, in a 12% yield. IR (in CCl_4): 3100, 2940, 1666, 1604, 1304, 1273, 1240, 1158, 1136, 1101, 1037 and 991 cm^{-1}.

Found: C, 69.20; H, 5.55%. Calcd for $C_{28}H_{26}OFe_2$: C, 68.60; H, 5.30%.

1-Ferrocenyl-1-penten-3-one (1c) and 4-Ferrocenyl-3-methyl-3-buten-2-one (1c'). 1-Ferrocenyl-1-penten-3-one (**1c**) was obtained as a first fraction from the chromatographic separation of the crude product, which had been obtained by the reaction of formylferrocene and ethyl methyl ketone. The recrystallization of **1c** from petroleum ether gave a deep red powder, mp 101—102°C, in a 41.2% yield. IR (in CCl_4): 3100, 2900, 1688, 1665, 1621, 1606, 1350, 1100 and 1025 cm^{-1}.

Found: C, 68.00; H, 6.20%. Calcd for $C_{15}H_{16}OFe$: C, 67.20; H, 5.95%.

A small amount of another product was isolated from the second fraction as reddish-orange needles, mp 162—164°C. It was found to be 4-ferrocenyl-3-methyl-3-buten-2-one (**1c'**) by means of a study of the IR, UV, and NMR spectra and by elemental analysis. IR (in CCl_4): 3110, 2900, 1682, 1658, 1604, 1107, 1038 and 1000 cm^{-1}. NMR (in $CDCl_3$): τ 8.45—8.80 (methyl), 5.82 (unsubstituted ring), 5.40—5.60 (substituted ring) and 2.53 (vinyl).

Found: C, 67.83; H, 6.64%. Calcd for $C_{15}H_{16}OFe$: C, 67.20; H, 5.95%.

1-Ferrocenyl-5-methyl-1-hexen-3-one (1d). The repeated chromatographic purification of the crude product from isobutyl methyl ketone afforded **1d**. Recrystallization from *n*-hexane gave reddish orange needles, mp 31—32°C, in a 54.2% yield. IR (in CCl_4):

10) Unpublished data.
11) L. K. Evans and A. E. Gillam, *J. Chem. Soc.*, **1941**, 815.
12) D. R. Scott and R. S. Becker, *J. Chem. Phys.*, **35**, 516, 2246 (1962); D. R. Scott and R. S. Becker, *J. Organometal. Chem.*, **4**, 409 (1965).

3140, 2950, 2800, 1685, 1656, 1619, 1602, 1472, 1363, 1290, 1170, 1109, 1058, 1040, 997 and 960 cm^{-1}.

Found: C, 69.00; H, 7.04%. Calcd for $C_{17}H_{20}OFe$: C, 68.96; H, 6.76%.

Catalytic Hydrogenation of 1,5-Diferrocenyl-1,4-pentadien-3-one (2a). Dienone **2a** (1.1 g) dissolved in 10 m*l* of dioxane was placed in a hydrogenating vessel together with 0.5 g of Urushibara nickel A and vigorously shaken with hydrogen for 7 hr at atmospheric pressure and at 24°C. After the catalyst had been removed by filtration, the filtrate was poured into water; the aqueous layer thus obtained was extracted with ether. The extract was washed with water and dried over anhydrous magnesium sulfate. The removal of the solvent under reduced pressure gave 1.2 g of a red oil; this oil was then subjected to chromatographic separation on alumina using benzene-hexane (1 : 1). The first fraction afforded 0.4 g of a yellow solid which was recrystallized from *n*-hexane to give 1,5-diferrocenyl-3-pentanone (**4**) as greenish-yellow needles, mp 110—111°C. IR (in CCl_4): 3100, 2900, 1710, 1475, 1440, 1413, 1362, 1110, 1090, 1043, 1027 and 1003 cm^{-1}. NMR (in $CDCl_3$): τ 7.39 (methylene), 5.94 (substituted ring), 5.89 (unsubstituted ring).

Found: C, 65.62; H, 5.44%. Calcd for $C_{25}H_{26}OFe_2$: C, 66.12; H, 5.73%.

From the second fraction, 0.2 g of a solid was obtained. Recrystallization from benzene afforded 1,5-diferrocenyl-1-penten-3-one (**3**) as reddish-orange plates, mp 113—114°C. IR (in CCl_4): 3100, 1690, 1660, 1621, 1604, 1355, 1215, 1180, 1107, 1093, 1045, 1030 and 1000 cm^{-1}.

Found: C, 66.02; H, 5.30%. Calcd for $C_{25}H_{24}OFe_2$: C, 66.41; H, 5.31%.

The authors wish to express their thanks to Professor Michio Kobayashi, Tokyo Metropolitan University, for his kind advice regarding the identification of the geometrical configuration. Thanks are also due to Mr. Kisaburo Yamazaki and his group of the Central Research Laboratory, Yamanouchi Pharmaceutical Co., Ltd., for the measurement of the NMR spectra and to Mr. Takeo Akiyama, Sophia University, for the measurement of the UV spectra.

BULLETIN OF THE CHEMICAL SOCIETY OF JAPAN VOL. 42 3277—3284 (1969)

Reactions of Alkyltropylium Ions with a Base[1]

Tetsuo NOZOE,[2] Kazuko TAKAHASHI and Hiroshi YAMAMOTO[3]

Department of Chemistry, Faculty of Science, Tohoku University, Katahira-cho Sendai

(Received May 13, 1969)

On the reaction with a base (*e.g.*, aqueous sodium hydroxide), isopropyl- and methyl-tropylium ions afforded cycloheptatrienyl polymers with an alkylene bridge, such as IIIa and IIIb, while the *t*-butyltropylium ion gave a mixture of 3- and 4-*t*-butyltropone, which was then transformed to 4- and 5-*t*-butyltropolone (VIIIa and IX). The bromination of VIIIa with 3 mol of bromine in methanol gave 3,7-dibromo-4-*t*-butyl-2-methoxy-2,3-dihydrotropolone (XIIa). On the heating of the adduct (XIIa) at 130°C, 7-bromo-4-*t*-butyltropolone (XIa) was formed.

It has been reported that the tropylium ion reacts with phenols,[4] aromatic amines,[5] and arylmagnesium halides[6] to give arylcycloheptatrienes, the dehydrogenation products of which, aryltropylium ions, are very stable in an aqueous solution or in the solid state. Upon the treatment of aryl-(such as phenyl- or *p*-methoxyphenyl)-tropylium ions with alkali, followed by the disproportionation reaction,[7,8] aryltropones have been

1) Partially presented at the 17th Annual Meeting of the Chemical Society of Japan, Tokyo, March, 1964.

2) Present address: No. 811, 2-5-1, Kamiyoga, Setagaya-ku, Tokyo.

3) Present address: Department of Chemistry, Faculty of Science, Okayama University, Okayama.

4) a) T. Nozoe and K. Kitahara, *Chem. & Ind.*, **1962**, 1192; b) R. van Helden, A. P. ter Borg and A. F. Bickel, *Rec. Trav. Chim.*, **81**, 599 (1962); c) P. Bladon, P. L. Pauson, G. R. Proctor and W. J. Rodger, *J. Chem. Soc.* **1966**, (*C*), 926; d) K. Takahashi, This Bulletin, **40**, 1462 (1967); e) J. J. Looker, *J. Org. Chem.*, **32**, 2941 (1967).

5) a) J. J. Looker, *J. Org. Chem.*, **30**, 4180 (1965); b) T. Nozoe, K. Kitahara and H. Susumago, to be published; c) T. Nozoe, K. Takahashi and H. Susumago, to be published.

6) C. Yutz and F. Voithenleitner, *Chem. Ber.*, **97**, 29 (1964).

7) T. Ikemi, T. Nozoe and H. Sugiyama, *Chem. & Ind.* **1960**, 932.

8) A. P. ter Borg, R. van Helden, A. F. Bickel, W. Renold and A. S. Dreiding, *Helv. Chim. Acta*, **43**, 457 (1960).

Table 1. NMR spectra

Compounds	τ-Values† for protons[a]								
	H (7)	H (1)	H (2)	H (3)	H (4)	H (5)	H (6)	Substitutents	
Cycloheptatrienes									
Ia	8.84 m	4.85 dd *J* 9.5, 6.0	3.89 m	3.44 m	3.44 m	3.89 m	4.85 dd	8.99 d, *J* 6.0	8.23 dsep *J* 8.5, 6.0
Ib	8.5 m	4.49 dd *J* 8.5, 5.0	3.93 m	3.42 m	3.42 m	3.93 m	4.49 dd	8.69 dbr *J* 6.0	
Ic	8.87 t *J* 6.0	4.77 dd *J* 9.5, 6.0	3.88 m	3.41 tm *J* 3, 0.7	3.41 tm	3.88 m	4.77 dd	8.97 s	
3[b]-(VIa)	7.85 t *J* 6.8	4.78 dt *J* 9.0, 6.8	3.90 d *J* 9.0	—	3.66 d *J* 6.0	3.94 dd *J* 9.0, 6.0	4.78 dt *J* 9.0, 6.8	8.88 d, *J* 6.5	7.2—8.0 m
3-(VIb)	7.82 t *J* 6.8	4.75 dt *J* 9.0, 6.8	4.10 d *J* 9.0	—	3.68 d *J* 6.0	4.00 dd *J* 9.0, 6.0	4.79 dt *J* 9.0, 6.8	7.97 s	
3-(VIc)	7.88 t *J* 6.8	*		—				8.82 s	
1-(VIa)	7.79 d *J* 6.6	—						8.92 d, *J* 6.5	7.3—8.2 m
1-(VIb)	7.77 d *J* 6.8	—	4.17 d *J* 3.0	3.69 tt *J* 3.0, 0.7	3.69 tt	4.07 dd *J* 9.0, 0.7	4.80 dt *J* 9.0, 6.8	8.06 sbr	
1-(VIc)	7.78 d *J* 6.8	—						8.87 s	
2-(VIc)	7.91 t *J* 6.8		—					8.90 s	

Compounds	τ-Values† for protons[a]						
	OH (2)	H (3)	H (4)	H (5)	H (6)	H (7)	Substituents
Tropolones							
VIIIa	0.90 s	2.61 d *J* 1.5	—	2.90 m	2.90 m	2.90	8.65 s
IX	1.67	2.47 *J* 11.0	2.66 *J* 11.0, 1.2	—	2.66 *J* 11.0, 1.2	2.47 *J* 11.0	8.67 s
XIa	0 99 s	2.55 d *J* 2.0	—	3.14 dd *J* 11.0, 2.0	2.00 d *J* 11.0	—	8.63 s
XIIa	4 94 m	5.30 d *J* 1.7	—	4.15 dd *J* 9.5, 1.7	2.65 d *J* 9.5	—	8.77 s (*t*-Bu) 6.96 s (OMe)
XIIb	4.91 m	5.27 d *J* 1.7	—	4.12 dd *J* 9.0, 1.7	2.62 d *J* 9.0	—	8.76 s (*t*-Bu) 8.96 t, 6.75 q (OEt) *J* 6.0

Compounds	ppm-Values for protones[c]	
	seven-membered ring	substituents
Alkyl cycloheptatrienium ions		
IIb	9.10	3.24 s
IIa	9.24	3.73 m, 1.60 d *J* 6.8
IIc	9.33	1.71 s

a) In carbon tetrachloride as solvent, except for IX (deuteriochloroform).
b) The initial number denotes the position of the substituent on the cycloheptatriene ring.
c) In trifluoroacetic acid as solvent.
† br, Broad; s, singlet; d, doublet; dd, double doublet; t, triplet; dt, double triplet; sep, septet; m, multiplet; *J* in Hz.
* The spectrum is too complicated to determine the chemical shift remained blank.

obtained. Tropylium ions carrying alkyl side chains have also been studied to some extent.[9,10] However, a more detailed investigation of alkyltropylium ions would be desirable, because the ions could be precursors of alkyltropones and alkyltropolones,[7,8,11] which mostly cannot be prepared

9) H. J. Dauben, F. A. Gadecki, K. M. Harmon and D. L. Pearson, *J. Am. Chem. Soc.*, **79**, 4557 (1957).
10) D. N. Kursanov and M. E. Vol'pin, *Doklady Akad. Nauk S.S.S.R.*, **113**, 339 (1957).
11) M. E. Vol'pin, Z. N. Parnes and D. N. Kursanov, *Izvest. Akad. Nauk S.S.S.R., Otdel, Khim. Nauk*, **1960**, 950.

by the direct alkylation of tropone or tropolone. In view of these points, our intense interest was focused on the reaction of alkyltropylium ions with the base.

7-Isopropylcycoheptatriene[12] (Ia), prepared in a good yield by the reaction of ethoxycycloheptatriene with isopropylmagnesium bromide, was kept at 175°C for 1.5 hr in order to cause a thermal isomerization of the double bonds.[13-15] The intramolecular 1—5 H shift of Ia gave an isomeric mixture of 3-, 1- and 7-isopropylcycloheptatriene in the ratio of 6 : 3 : 1. The positions of the isopropyl group and the ratio of the products were determined on the basis of the NMR spectral data (*cf.* Table 1). The mixture was treated with phosphorus pentachloride to afford the isopropyltropylium ion (IIa) ($X=\frac{1}{2}PtCl_6$). The spectral data of IIa, recorded in the Experimental section, were consistent with the structure. Although the cation (IIa) was very stable in an acidic medium, it changed to a colorless amorphous powder on treatment with a base such as aqueous sodium hydroxide or sodium bicarbonate, and no isopropyltropyl alcohol or isopropyltropone (IVa) was detected. The powder contained virtually no oxygen atoms (on the evidence of elemental analysis), and the infrared (IR) spectrum showed no hydroxy, carbonyl, or ether bands. The NMR spectrum (in CCl_4) had three, very broad signals at τ 3.55, 4.15, and 4.90 typical of a cycloheptatrienyl system and two broad signals at 8.5 and 8.8. The ratio of the intensities of the down- and the up-field signals was approximately 5 : 7. These spectral data, together with the unusual broadness of the signals and the possible modes of formation of the compound (see below), suggested that it was a polymer and that it most likely had the structure IIIa.

When 7-methylcycloheptatriene[9] (Ib) was heated at 170°C for 3.5 hr, a mixture of 3- and 1-methylcycloheptatriene was obtained in the ratio of 1 : 2 (from the NMR spectrum). The treatment of the mixture with phosphorus pentachloride gave the methyltropylium ion[9] (IIb) ($X=\frac{1}{2}PtCl_6$), which was very stable in the solid state and in a strongly acidic aqueous solution. However, a weakly acidic (pH 3—5) or neutral solution of IIb gradually turned orange and finally yielded a colorless, amorphous powder. The formation of the material was also demonstrated, but in a better yield, when an aqueous solution of IIb was treated with sodium

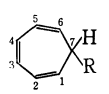

I

a: R=*i*-C_3H_7
b: R=CH_3
c: R=*t*-C_4H_9

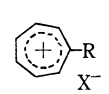

II

a: R=*i*-C_3H_7
b: R=CH_3
c: R=*t*-C_4H_9

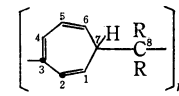

III

a: R=CH_3
b: R=H

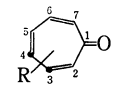

IV

a: R=*i*-C_3H_7
b: R=CH_3
c: R=*t*-C_4H_9

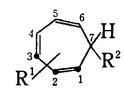

V

a: R^1=*i*-C_3H_7, R^2=$N(CH_3)_2$
b: R^1=*i*-C_3H_7, R^2=$NHCH_3$
c: R^1=*t*-C_4H_9, R^2=OCH_3

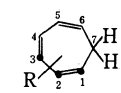

VI

a: R=*i*-C_3H_7
b: R=CH_3
c: R=*t*-C_4H_9

hydroxide, but the reaction was accompanied by the formation of a trace (1%) of methyltropone[16] (IVb) as the by-product (ν_{max} 1630, 1590 cm^{-1}). The main product was shown by the IR spectrum to possess methine, methylene, and cycloheptatriene groups, but no hydroxy nor carbonyl group, although all bands were very broad (*cf.* Experimental section). The spectral evidence presumably verifies the structure IIIb for the compound.

The formation of the poylmers IIIa and IIIb could reasonably be explained in terms of the attack of a hydroxide anion on the α-hydrogen atom, H_A, in the formula A, rather than on the seven-membered ring; thus, the heptafulvene-type compound B could be formed as an intermediate. It is at present uncertain on which site of the cycloheptatriene ring the polymerization reaction takes place, but the products are considered to be a mixture of the alkylated cycloheptratiene polymers with an alkylene bridge at the 3,7 and 2,7 positions, assuming that the negatively-charged carbon (C-8) in the formula B, instead of a hydroxide anion,[17] attacks the 4- or 3-position of the seven-membered ring of another molecule (a steric repulsion would prevent the 2—8 polymerization). The fact that the methyltropylium ion (IIb) required a stronger acidic medium than IIa to keep the cation stable indicated that the stability of the two alkyltropylium ions, IIa and IIb, dependend on the acidity of the medium. A similar phenomenon had been observed in aliphatic alkenyl cation systems.[18]

12) W. von E. Doering and L. H. Knox, *J. Am. Chem. Soc.*, **75**, 297 (1953).

13) A. P. ter Borg, H. Kloosterziel and N. van Meurs, *Rec. Trav. Chim.*, **82**, 717 (1963); A. P. ter Borg and K. Kloosterziel, *ibid.*, **82**, 741 (1963).

14) K. W. Egger, *J. Am. Chem. Soc.*, **89**, 3688 (1967).

15) T. Nozoe and K. Takahashi, This Bulletin, **38**, 665 (1965).

16) The position of the methyl group is uncertain. The product would be a mixture of 4-, 3- and 2-methyltropone.

17) It has been reported that a hydroxy anion attacks the 3- or 4-position of aryltropylium ions, giving 3- or 4-aryltropones. See Refs. 4 and 7.

18) N. C. Deno, H. G. Rickey, Jr., N. Friedman, J. D. Hodge, J. J. Houser and C. U. Pittman, Jr., *J. Am. Chem. Soc.*, **85**, 2991 (1963).

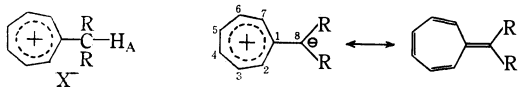

A B

When the isopropyltropylium ion (IIa) was allowed to react with dimethylamine, a mixture of 1-, 2- and 3-isopropyl-7-dimethylaminocycloheptatriene (Va) was formed. By the same reaction with monomethylamine, a mixture of 1-, 2-, and 3-isopropyl-7-methylaminocycloheptatriene (Vb) was obtained. Although the methyltropylium ion (IIb) gave no clear substance, it was noteworthy that, upon treatment with alkylamines, the cation IIa did not undergo a polymerization reaction but instead afforded the *N*-alkylaminocycloheptatriene derivatives. A similar treatment of IIa with methanolic sodium bicarbonate, however, mostly afforded the polymer IIIa.

These observations led us to a further study of the *t*-butylcycloheptatrienium ion (IIc) which has no acidic hydrogen atom at the α-position of the substituent. Upon the heating of 7-*t*-butylcycloheptatriene (Ic), prepared in a good yield by the reaction of 7-ethoxycycloheptatriene with *t*-butyl magnesium chloride, at 175°C for 2 hr, a mixture of 7-, 3-, 1- and 2-*t*-butylcycloheptatriene was obtained in the ratio of 1 : 2.2 : 10 : 2 (from NMR). The subsequent dehydrogenation of the mixture with phosphorus pentachloride in carbon tetrachloride gave the stable cation, IIc ($X=\frac{1}{2}PtCl_6$). A considerable amount of 7- and 1-*t*-butylcycloheptatriene was recovered unchanged in the above reaction, indicating that the hydride abstraction from the sterically-hindered 7-position of the cycloheptatriene seemed to be relatively difficult. The treatment of the cation IIc with sodium hydroxide afforded an oily stuff, di-(*t*-butyl-cycloheptatrienyl) ether, which was then converted with a trace of acid into the tropone (IVc) and the cycloheptatriene (VIc). The IR band of IVc observed at 1623 cm^{-1} was attributed to the carbonyl group. A broad peak due to the ring protons appeared at τ 3.1 in the NMR spectrum (in CCl_4). Although IVc showed a sharp singlet due to the *t*-butyl group at τ 8.72 and gave one 2,4-dinitrophenylhydrazone, mp 182—184°C it was assumed to be a mixture of 3- and 4-*t*-butyltropone, because two spots (R_f 0.7, 0.6) appeared on an alumina thin-layer plate in a ratio of *ca.* 2 : 1 (benzene-ethyl acetate, 20 : 1, as the solvent). The moiety, VIc, was concluded to be a nearly equivalent amount of a mixture of 1-, 2-, and 3-*t*-butylcycloheptatriene, considering the presence of three methylene signals at τ 7.78 (d), 7.88 (t), and 7.91 (t), and three singlets of approximately the same intensities due to *t*-butyl groups at 8.83, 8.87, and 8.90 in the NMR spectrum (in CCl_4). The treatment of a methanolic solution of IIc with sodium bicarbonate gave a 1 : 1 mixture of 2- and 3-*t*-butyl-7-methoxycycloheptatriene (Vc), the structures of which were derived from the NMR spectrum (see Experimental section). No polymerized hydrocarbon similar to IIIa and IIIb was produced on the treatment of the cation IIc with the base.

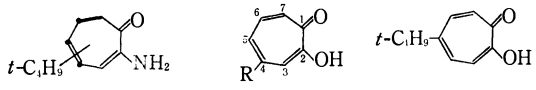

VII VIII IX

a: R = *t*-C_4H_9
b: R = *i*-C_3H_7

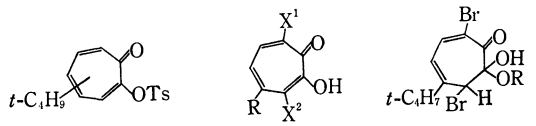

X XI XII

a: R = *t*-C_4H_9, X^1 = Br, X^2 = H
b: R = *i*-C_3H_7, $X^1 = X^2$ = Br
[c: R = *t*-C_4H_9, $X^1 = X^2$ = Br]

a: R = CH_3
b: R = C_2H_5

The two *t*-butyltropolones, VIIIa and IX, were successfully synthesized by treating the tropone (IVc) with hydrazine hydrate, followed by the hydrolysis of the resulting aminotropone mixture (VII) with alcoholic potassium hydroxide. The tropolone (VIIIa) readily gave the sodium salt as yellow crystals with aqueous sodium carbonate, while the tropolone (IX) formed hardly any salt under the same conditions. Thus, IX could be extracted from the above basic layer with chloroform or ether; the separation and purification of VIIIa and IX from the crude mixture were effectively achieved by repetition of the above procedure. The yields of VIIIa and IX from the tropone mixture (IVc) were 40 and 1% respectively. The IR spectrum of VIIIa showed absorption bands at 3226 and 1610 cm^{-1} typical of the hydroxy and carbonyl group of tropolones. The ring protons of VIIIa appeared in the NMR spectrum as a doublet (1H) at τ 2.61 (J=1.5 Hz) and as a multiplet (3H) at 2.90, as may be expected for 4-substituted tropolone systems. The assignment of the signals is shown in the table. The structure was confirmed by the degradation of the tosyl ether (X) to 3-*t*-butylbenzoic acid on refluxing in alcoholic potassium hydroxide.

The minor product mentioned above was proved to be 5-*t*-butyltropolone[19] (IX), by taking account of the A_2B_2-octet signal centerrd at τ 2.57 ($J_{ab}=J_{a'b'}$=11.0, $J_{aa'}$=1.2, $J_{bb'}\simeq 0$ Hz) in the NMR spectrum (*cf.* the table). The hydroxyl and

19) T. Nozoe, H. Kishi and A. Yoshikoshi, *Proc. Japan Acad.*, **27**, 149 (1951).

carbonyl absorption bands appeared at 3247 and 1616 cm^{-1} respectively. The ultraviolet spectra of both VIIIa and IX are recorded in the Experimental section. When phenyl- and *p*-methoxyphenyl-tropolone were synthesized from the corresponding aryltropylium ions by the procedure described above, the relative ratio of 4- and 5-arylsubstituted tropolone was about 3 : 1.[4d,7] The present study, however, showed that the 4-substituted tropolone (VIIIa) was produced in a much larger amount than the 5-substituted compound (IX); the reason for this we have not yet made clear. Nevertheless, this procedure would seem to be a useful approach for the synthesis of 4-*t*-butyl-tropolone.

In order to examine the steric influence of the bulkier alkyl group of VIIIa, the bromination of VIIIa and 4-isopropyltropolone (VIIIb)[20] was carried out in order to compare their reactivities. When one mole of bromine in methanol was used, VIIIa was shown to give 7-bromo-4-*t*-butyltropolone (XIa) on the evidence of the elemental analysis and the spectral data (*cf.* table and the Experimental section). The treatment of VIIIa with 3 mol of bromine in the same solvent, however, afforded a non-aromatic addition product (XIIa) the structure of which was derived from the IR (3367, 1667 cm^{-1}: non-tropolone ring) and the NMR (see table) spectra. On refluxing in ethanol, the methoxy group of XIIa was replaced by an ethoxy group, giving the adduct (XIIb). On the other hand, VIIIb mainly afforded the dibromo derivative[21] (XIb) on the bromination of 3 mol in methanol.

The possibility of the removal of methanol from the adduct (XIIa) to yield a dibromotropolone (XIc) similar to XIb was then examined. Although XIIa mostly remained unchanged at 80°C/1 mmHg (3 hr), it was unexpectedly converted to the monobromotropolone (XIa) upon heating at 130°C for 20 min. This suggested that a large steric repulsion between the *t*-butyl group and the bromine atom on C-3 of the compound XIIa prevented the formation of the more sterically-hindered dibromotropolone (XIc) but, upon heating, facilitated the removal of the bromine atom to give XIa. The steric effect of a *t*-butyl group in seven-membered aromatics appeared to be remarkable; it is now being examined in detail.

Experimental

Materials for the analyses were dried over P_2O_5 at about 20°C/20 mmHg overnight. The NMR spectra were obtained with a Varian A-60 spectrometer, operating at 25°C and 60 Mc/sec, with tetramethylsilane (τ 10) as the internal standard.

7-Isopropylcycloheptatriene (Ia). A mixture of 68.9 g of isopropyl bromide and 200 m*l* of dry ether was slowly stirred into 13.6 g (1 equiv.) of magnesium over a 2.5 hr period at such a rate that the mixture was gently refluxed; then it was stirred for a further 30 min. A solution of 61.1 g (0.8 eqiuv.) of 7-ethoxycycloheptatriene[15] in 100 m*l* of dry ether was stirred in over a 1.5 hr period and then stirring was continued for another hour. Into the mixture cooled with an ice bath there was stirred, 500 m*l* of cold 2N hydrochloric acid over a 30 min period. The reaction mixture was extracted with ether, and the ether was washed with cold water and dried over $MgSO_4$. After the solvent had been evaporated, the residue was distilled to give 48.1 g (80%) of a colorless oil, Ia; bp 82—86°C/42 mmHg. The specimen for the analysis was distilled at 74°C/33 mmHg.

Found: C, 89.72; H, 10.46%. Calcd for $C_{10}H_{14}$: C, 89.49; H, 10.51%. ν_{max}^{neat} 2967, 2919, 2833, 1445, 1385, 1368, 1193, 1164, 950, 799, 743, 704 and 685 cm^{-1}.

7-Methylcycloheptatriene (Ib). This was obtained from methylmagnesium iodide and 7-ethoxycycloheptatriene by the above procedure in a 71% yield (bp 63°C/80 mmHg).

7-*t*-Butylcycloheptatriene (Ic). This was similarly made from *t*-butylmagnesium chloride and 7-ethoxycycloheptatriene as a colorless oil. (55% yield); bp 95—98°C/45 mmHg.

Found: C, 89.37; H, 10.83%. Calcd for $C_{11}H_{16}$: C, 89.12; H, 10.88%. ν_{max}^{neat} 2994, 2941, 2857, 1464, 1389, 1366, 1250, 1208, 1190, 1011, 952, 852, 741 and 703 cm^{-1}.

Thermal Isomerization of the Cycloheptatrienes (Ia, b, c). The substance was heated in a sealed tube at a given temperature (±0.5°C), and then purified by distillation. When 12 g of Ia were heated at 175°C for 1.5 hr, and then distilled, 11 g of a mixture consisting of 3-, 1-, and 7-isopropylcycloheptatriene (6 : 3 : 1) was obtained as a colorless oil; bp 78—79°C/37 mmHg.

Found: C, 89.79; H, 10.43%. Calcd for $C_{10}H_{14}$: see above.

The heating of 18.3 g of Ic at 175°C for 2 hr, followed by distillation, gave 17.5 g of a mixture of 7-, 3-, 1-, and 2-*t*-butylcycloheptatriene (1 : 2.2 : 10 : 2) as a colorless oil; bp 88—89°C/37 mmHg.

Found: C, 89.40; H, 10.69%. Calcd for $C_{11}H_{16}$: see above.

Isopropyltropylium Ion (IIa). Into a suspension of 3.3 g of phosphorus pentachloride (2.1 equiv.) in 25 m*l* of anhydrous carbon tetrachloride there was stirred a solution of 1.00 g of the above thermally-isomerized isopropylcycloheptatriene mixture in 5 m*l* of carbon tetrachloride. After the mixture had been stirred for 7 hr and then set aside overnight at room temperature, the precipitate was filtered off in a dry box, dried over P_2O_5 *in vacuo*, and poured into 1 m*l* of cold acetonitrile. To the solution, after clarification by filtration, there was added, drop by drop, a saturated solution of $H_2PtCl_6 \cdot 6H_2O$ in acetonitrile, giving 1.00 g (40%) of IIa (as the hexachloroplatinate) as yellow prisms; mp 164°C (decomp.).

Found: C, 35.93; H, 3.94; Pt, 29.55%. Calcd for $C_{10}H_{13} \cdot 1/2PtCl_6$ C, 35.63; H, 3.89; Pt, 28.94%. λ_{max}^{MeCN}

20) Recent study on bromination and chlorination of halotropones and 2-methoxytropones was carried out by T. Nozoe, K. Takase and M. Yasunami: See Ph. D. thesis of M. Yasunami, Tohoku University (1965).

21) T. Nozoe, T. Mukai and K. Takase, *Proc. Japan Acad.*, **26**, 19 (1950).

271, 362 sh mμ. ν_{max}^{KBr} 2941, 2899, 1527, 1481, 1464, 1449, 1395, 1284, 1235, 1058, 1021, 945, 887, 879, 862 and 754 cm^{-1}. $\delta_{CF_3CO_2H}$ 1.59 (d, J=6.8 Hz; 2Me), 3.89 (q, J=6.8 Hz; CH), 9.59 (s; 6H).

Methyltropylium Ion (IIb). This was obtained by the same procedure as above in a 37% yield as a brownish yellow crystalline powder; mp 160°C (blackened).

Found: C, 32.58; H, 3.23; Pt, 32.57%. ν_{max}^{KBr} 3012, 1522, 1486, 1449, 1359, 1282, 1235, 1164, 1027, 979, 965, 867 and 727 cm^{-1}. $\delta_{CF_3CO_2H}$ 3.31 (s; Me), 9.08 (s; 6H).

***t*-Butyltropylium Ion (IIc).** This was similarly prepared. The hexachloroplatinate isolated in a 38% yield was in the form of pale orange needles; mp 181°C (decomp.).

Found: C, 37.32; H, 4.28; Pt, 27.67%. Calcd for $C_{11}H_{15}\cdot 1/2PtCl_6$: C, 37.63; H, 4.31; Pt, 27.78%. λ_{max}^{MeCN} 272, 346 sh mμ. ν_{max}^{KBr} 2976, 2933, 1595, 1570, 1522, 1490, 1439, 1385, 1292, 1067, 1056, 947, 820, and 770 cm^{-1}.

The Reaction of IIa with Sodium Bicarbonate. Five grams of the thermally-isomerized isopropylcycloheptatriene was treated with 16.1 g (2.1 equiv.) of phosphorus pentachloride in 110 m*l* of carbon tetrachloride according to the above procedure. After 7 hrs' stirring at room temperature, 50 m*l* of ice water was stirred into the cooled mixture. After 10 mins' stirring at 0°C, the contents were separated and the aqueous layer was quickly washed with 10 m*l* of cold chloroform. Solid sodium bicarbonate enough to give pH 5—6 was stirred into the cooled aqueous layer, and then the mixture was stirred for 30 min, and then basified by the addition of further sodium bicarbonate (pH 8). The contents turned orange during this basification. The sodium chloride precipitated was filtered off and washed with chloroform. The filtrate was extracted with chloroform, and the combined extract was dried over anhydrous K_2CO_3. The evaporation of the solvent below 25°C (bath) under reduced pressure left 3.23 g of a viscous orange oil, which gradually solidified on being set aside at room temperature. The material dissolved in benzene reprecipitated in methanol for purification (three times), giving IIIa as a white amorphous solid (65% yield); mp 150—154°C.

Found: C, 88.05; H, 8.59%. ν_{max}^{KBr} 2985, 2924, 2833, 2577, 1456, 1376, 1357, 1214 w, 1183 w, 830, 794 and 727 cm^{-1}. The basification of the aqueous solution of IIa with cold 5N sodium hydroxide produced the same polymer.

The Reaction of IIb with Sodium Hydroxide. An aqueous solution of IIb, prepared from 3.5 g of the above isomerized methylcycloheptatriene and 15.1 g of phosphorus pentachloride, was alkalized with 8N sodium hydroxide (pH 9) and subjected to the same treatment as above; this gave a viscous orange liquid. Two purifications of the oil by reprecipitation from benzene-methanol gave IIIb as a pale yellow amorphous solid (57% yield); mp above 260°C. ν_{max}^{KBr} 3030, 2924, 2857, 1439, 1389, 763, 730 and 712 cm^{-1} (All the bands were very broad.).

The combined filtrate of the above purification was evaporated, and the residue, dissolved in benzene, was passed through an alumina column. The evaporation of the benzene-elute under reduced pressure gave 30 mg of a yellow oil which was assumed, from its IR spectrum (1630 and 1590 cm^{-1}), to be a mixture of the methyltropones (IVb) (1% yield). The oil was refluxed with 40 mg of 2,4-dinitrophenylhydrazine in 20 m*l* of ethanol (with a trace of hydrochloric acid) for 10 min. The precipitate was then collected and recrystallized from benzene, giving 30 mg of reddish-brown plates; this substance was considered to be the 2,4-dinitrophenylhydrazone of IVb, mp 230—232°C.

Found: C, 56.93; H, 3.98; N, 18.06%. Calcd for $C_{14}H_{12}N_4O_4$: C, 56.00; H, 4.03; N, 18.66%.

The Reactions of IIa with Alkylamines (Va and Vb). a) An aqueous solution of IIa, prepared from 20 g of the thermally-treated isopropylcycloheptatriene and 65.3 g of phosphorus pentachloride, was added, drop by drop, into 169 g of an ice-cooled and stirred 40% aqueous solution of dimethylamine. After having been stirred for 2 hr, the mixture was extracted with ether; the extract was evaporated under reduced pressure, and then distilled, giving a mixture of 1-, 2-, and 3-substituted Va as a yellow oil (72% yield); bp 66—67°C/1.3 mmHg.

Found: C, 81.60; H, 10.89; N, 8.23%. Calcd for $C_{12}H_{19}N$: C, 81.30; H, 10.80; N, 7.90%. ν_{max}^{neat} 2959, 2865, 2829, 2786, 1464, 1458, 1385, 1366, 1304, 1277, 1217, 1174, 1153, 1103, 1064, 1042, 1013, 1001, 911, 898, 878, 867, 839, 798, 768, 755 and 731 cm^{-1}. τ_{CCl_4} 8.97 (d, J 6.6 Hz; *i*-Pr), 8.89 (d, J 6.6 Hz; *i*-Pr), 8.86 (d, J 6.6 Hz; *i*-Pr), 8.22 (m; J 6.6 Hz; H-7), 7.74 (s; NMe_2), 7.45 (m; *i*-Pr-methine), 4.80, 4.02, 3.51 (m; ring protons).

b) The similar treatment of IIa with an excess 30% aqueous solution of methylamine gave Vb as a yellow oil (35% yield); bp 70—71°C/3 mmHg.

Found: C, 80.68; H, 10.27; N, 8.03%. Calcd for $C_{11}H_{17}N$: C, 80.92; H, 10.50; N, 8.58%. ν_{max}^{neat} 2950, 2857, 2778, 1456, 1445, 1377, 1359, 1311, 1290, 1181, 1136, 1100, 1028, 996, 921, 827, 800, 762 and 726 cm^{-1}. τ_{CCl_4} 8.97 (d, J 6.6 Hz; *i*-Pr), 8.90 (d, J 6.6 Hz; *i*-Pr), 8.87 (d, J 6.6 Hz; *i*-Pr), 8.3 (m; H-7), 7.62 (s, N-CH_3), 7.46 (m; *i*-Pr), 4.77, 4.08, 3.80 (m; ring protons).

The Reaction of IIc with Sodium Hydroxide: Formation of *t*-Butyltropone (IVc) and *t*-Butylcycloheptatrienes(VIc). A solution of IIc in 100 m*l* of water, prepared from 7.43 g of an isomerized mixture of Ic and 20.1 g (2.1 equiv.) of phosphorus pentachloride as has been described above was slowly stirred into 60 m*l* of cold 33% aqueous sodium hydroxide under ice-cooling, and then the stirring was continued for 30 more min. The precipitate was then filtered off and washed with chloroform. The filtrate was extracted with chloroform, and the combined extract, washed with cold water and dried over $MgSO_4$, was evaporated at 20°C/20 mmHg, affording an oily stuff. The NMR spectrum (in CCl_4) showed *t*-butyl signals as singlets at τ 8.83, 8.90, and 8.92 and an H-7 signal as a multiplet at 6.57, indicating that the oil was a mixture of di-(1-, 2- and 3-*t*-butylcycloheptatrienyl)ether. It was set aside overnight at room temperature with 0.2 m*l* of conc. hydrochloric acid, and then extracted with benzene after the addition of cold dilute aqueous sodium bicarbonate. The extract was washed with cold water and dried over $MgSO_4$. After the evaporation of the solvent under reduced pressure, the residue was distilled, giving VIc as a colorless oil (52% yield), bp 27—29° C/0.7 mmHg, and IVc as a yellow oil (61%), bp 104—106°C/0.7 mmHg.

Found for IVc: C, 80.28; H, 8.87%. Calcd for

$C_{11}H_{14}O$: C, 81.44; H, 8.70%. ν_{max}^{neat} 2941, 1623, 1567, 1520, 1471, 1362, 1333, 1235, 1208, 988, 902, 864, 833, 790, 740, 711 and 684 cm^{-1}. It did not give a picrate.

2,4-Dinitrophenylhydrazone of IVc. A mixture of 58 mg of IVc and 71 mg of 2,4-dinitrophenylhydrazine was refluxed for 1 hr in 2 m*l* of ethanol with a trace of concentrated hydrochloric acid. The precipitate was then filtered off and recrystallized from ethanol, giving dark brown needles; mp 182—184°C.

Found: C, 60.24; H, 5.03; N, 16.17%. Calcd for $C_{17}H_{16}N_4O_4$: C, 59.64; H, 5.30; N, 16.37%.

2- and 3-*t*-Butyl-7-methoxycycloheptatriene (Vc). To 150 m*l* of a cold aqueous solution of IIc, made by the treatment of 5.0 g of an isomerized mixture of Ic with 13.5 g of phosphorus pentachloride, there was added 15 m*l* of methanol, and then 40 g of sodium bicarbonate, drop by drop under ice-cooling. The contents were stirred at 0°C for a further 30 min, and then extracted with ether. The extract was washed with cold water, dried over anhydrous K_2CO_3, and distilled, giving 1.79 g (30%) of Vc as a colorless oil, bp 64—69°C/2.5 mmHg, and 0.3 g (12%) of IVc as a yellow oil, bp 105—107°C/1.8 mmHg.

Found for Vc: C, 80.36; H, 9.46%. Calcd for $C_{12}H_{18}O$: C, 80.85; H, 10.18%. ν_{max}^{neat} 2959, 1475, 1460, 1387, 1374, 1361, 1252, 1205, 1135, 1122, 1109, 1080, 991, 829, 799, 764, 743 and 725 cm^{-1}. τCCl, 8.90 (s; *t*-Bu),*1 8.83 (s; *t*-Bu),*1 6.91 (m; 2H), 6.68 (s; OMe),*2 6.67 (s; OMe),*2 4.65 (m; 4H), 4.03 (m; 3H), 3.49 (m; 3H); the two couples of the singlets (*1,2) had approximately the same intensity, showing that Vc was a 1 : 1 mixture of the 2- and 3-substituted cycloheptatriene.

4- and 5-*t*-Butyltropolone (VIIIa, IX). A mixture of 5.84 g of the above tropone (IVc) and 9.05 g (4 equiv.) of 80% hydrazine hydrate was refluxed in 50 m*l* of ethanol for 6 hr. To the residue freed from the solvent there was added 50 m*l* of cold water, and then the mixture was extracted with benzene. The extract was evaporated at 20°C/15 mmHg, leaving 6.24 g (86%) of the crude 2-amino-*t*-butyltropone (VII) as a reddish-brown tar (ν_{max}^{neat} 3348, 3311, 2950, 1592, 1513, 1473, 1429, 1364, 1333, 1263, 949, 901, 792, 761 and 710 cm^{-1}). Without purification, this was dissolved in 350 m*l* of ethanol and 50 m*l* of 6N potassium hydroxide and refluxed for 10 hr. Most of the solvent was removed at below 60°C under reduced pressure; a saturated aqueous solution of sodium carbonate and ether was then added to the residue. After the mixture had been stirred for 30 min at room temperature, the precipitate, the sodium salt of 4-*t*-butyltropolone (mp>290°C), was collected and washed with ether. The precipitate, dissolved in 25 m*l* of water, was brought to pH 2—3 with 2N sulfuric acid, and the freed tropolone was extracted with ether. This procedure was repeated 3—4 times until the band at 11.9 μ in the IR spectrum of the sodium salt disappeared, giving 2.5 g of the free acid (VIIIc) (in 40% overall yield from the tropone mixture) as yellowish-brown needles, mp 33—34°C, after recrystallization from light petroleum (<60°C).

Found: C, 74.34; H, 7.91%. Calcd for $C_{11}H_{14}O_2$: C, 74.13; H, 7.97%. λ_{max}^{MeOH} mμ (log ε): 240 (4.23), 325 (3.52), 349 (3.45). ν_{max}^{neat} 3226, 2959, 1610, 1543, 1497, 1477, 1429, 1391, 1366 w, 1348 w, 1299 sh, 1269, 1252, 1199, 943, 916, 893, 825, 756 br, 741 br and 714 br cm^{-1}. VIIIc turned green (aq. layer) and reddish brown (benzene layer) when treated with ferric chloride.

The filtrate and the ether washing obtained by the above sodium carbonate treatment were combined, and the ether was evaporated under reduced pressure. The residue, after filtration, was extracted with chloroform, and the extract (dried over Na_2SO_4) was evaporated. The residue, which crystallized on standing, was washed with a small amount of light petroleum (<60°C); the insoluble part was sublimed at 80—100°C/1 mmHg, giving IX as pale yellow prisms, mp 102—104°C.

Found: C, 74.12; H, 7.98%. Calcd for $C_{11}H_{14}O_2$: see above. λ_{max}^{MeOH} mμ (log ε): 234.5 (4.48), 245 sh (4.40), 250 sh (4.27), 323 (4.04), 3.51 (3.87), 3.67 (3.78). ν_{max}^{KBr} 3247, 2959, 1616, 1555, 1471, 1449, 1427, 1376, 1279, 1248, 1214, 1200, 1085, 869, 856, 822, 764 and 704 cm^{-1}.

3-*t*-Butylbenzoic Acid. Into an ice-cooled solution of 0.50 g of VIIIa dissolved in 4 m*l* of pyridine there was slowly stirred, 0.70 g (1.3 equiv.) of *p*-toluenesulfonyl chloride; then the mixture was stirred for 5 hr at 0°C. The mixture was poured into 15 m*l* of ice water and, after stirring, extracted with chloroform. The dried extract (over $MgSO_4$) was freed from the solvent, leaving a reddish-orange oil which was presumably a mixture of 4- and 6-*t*-butyl-2-tosyloxytropone (X). The oil, dissolved in 15 m*l* of ethanol and 15 m*l* of 20% aqueous potassium hydroxide, was heated under reflux for 1 hr. The ethanol was removed under reduced pressure, and the aqueous solution was brought to pH 2—3 with cold 6N sulfuric acid at 0°C. The mixture was extracted with ether; the evaporation of the dried extract (over $MgSO_4$) at 20°C *in vacuo* left a reddish liquid. The benzene solution (3 m*l*) of the oil was shaken with 5 m*l* of 10% aqueous sodium bicarbonate. The aqueous layer was brought to pH 2 with cold 6N sulfuric acid; the precipitate was recrystallized from light petroleum (<50°C), giving 0.17 g (35%) of the benzoic acid as colorless prisms, mp 132—133°C (lit[22] 127°C).

(Found: C, 74.13; H, 7.90%.) ν_{max}^{KBr} 2941, 2632, 2525, 1670, 1590, 1570, 1470, 1433, 1405, 1355, 1297. 1282, 1255, 1172, 1134, 1078, 957 br, 820, 746, 720 and 695 cm^{-1}. τ_{CCl_4} 8.62 (s; *t*-Bu), 3.61 (t, *J* 7.5 Hz; H-5), 3.39 (dt, *J* 7.2, 1.5 Hz; H-4), 3.07 (dt, *J* 7.2, 1.5 Hz; H-6), 2.87 (t, *J* 1.5 Hz; H-2), −3.00 (s; OH).

7-Bromo-4-*t*-butyltropolone (XIa). Into a solution of 0.30 g of VIIIa in 4 m*l* of methanol there was stirred, drop by drp at 0°C, 0.33 g (1.2 equiv.) of bromine dissolved in 1 m*l* of methanol. After having been stirred at 0°C for 4 hr and then set aside overnight, the mixture was evaporated under reduced pressure, leaving a yellow powder. Recrystallization from ethanol gave 0.30 g (69%) of the bromotropolone as yellow plates, mp 75—75.5°C.

Found: C, 51.90; H, 5.29%. Calcd for $C_{11}H_{13}O_2Br$: C, 51.38; H, 5.10%. λ_{max}^{MeOH} mμ (log ε): 256 (4.30), 331 (3.48), 367 (3.48), 379 (3.50). ν_{max}^{KBr} 3226, 2933, 1603, 1575, 1538, 1466, 1441, 1387, 1362, 1351, 1289, 1214, 1190, 1109, 941, 928, 903, 848, 839, 794. 776, 746 br and 722 cm^{-1}.

3,7-Dibromo-4-*t*-butyl-2-methoxy-2,3-dihydrotropolone (XIIa). The tropolone VIIIa was treated with 3 equiv. moles of bromine under the above conditions; the recrystallization of the product from benzene-

22) A. Baur, *Ber.*, **24**, 2832 (1891).

light petroleum (<50°C) gave the adduct (XIIa) as colorless needles (89%), mp 120—127°C (gradually decomp.).

Found: C, 39.13; H, 4.46%. Calcd for $C_{12}H_{16}O_3Br_2$: C, 39.17; H, 4.37%. ν_{max}^{KBr} 3367, 2933, 1667, 1558, 1456, 1351, 1189, 1147, 1110, 1070, 1063, 1046, 1004, 895, 840, 825, 787 and 742 cm^{-1}.

3,7-Dibromo-4-*t*-butyl-2-ethoxy-2,3-dihydrotropolone (XIIb). A solution of 0.80 g of XIIa in 5 m*l* of ethanol was refluxed for 5 min; after the solvent had then been removed, the residue was recrystallized from ethanol, giving 0.60 g (73%) of the ethanol adduct (XIIb) as pale yellow needles, mp 84.5—85.5°C.

Found: C, 41.45; H, 4.85%. Calcd for $C_{13}H_{18}O_3Br_2$: C, 40.87; H, 4.75%. λ_{max}^{EtOH} mμ (log ε): 240 (3.83), 348 (3.57). ν_{max}^{KBr} 3413, 2941, 2857, 1658, 1613, 1555, 1466, 1453, 1385, 1370, 1351, 1323, 1152, 1115, 1087, 1063, 1048, 1014, 899, 885, 851, 828, 792 and 740 cm^{-1}.

Bromination of 4-Isopropyltropolone (VIIIb) in Methanol. To an ice-cooled and stirred solution of 0.30 g of VIIIb in 5 m*l* of methanol there was added 0.96 g (3.0 equiv.) of bromine dissolved in 1 m*l* of methanol. After 2 hrs' stirring, the mixture was set aside overnight and then poured onto ice and extracted with ether. The ether extract was dried, the solvent was evaporated at room temperature, and the residue was recrystallized from methanol, affording 0.19 g of pale green needles (mp 130—133°C undepressed on admixture) identified from the IR and NMR spectra with an authentic specimen of 3,7-dibromo-4-isopropyltropolone (XIb). On the evaporation of the recrystallization filtrate, 0.12 g more of XIb (crude) was obtained from the residual fraction forming the sodium salt with saturated aqueous sodium bicarbonate. The IR spectrum of the fraction (*ca.* 0.15 g), which did not give any sodium salt with alkali, showed a hydroxy band at 3448 and carbonyl bands at 1686 and 1730 cm^{-1}, suggesting the presence of an additional bromine product, but the structure had not yet been made clear.

7-Bromo-4-*t*-butyltropolone (XIa) from 3,7-Dibromo-4-*t*-butyl-2-methoxy-2,3-dihydrotropolone (XIIa). The XIIa adduct (20 mg) was heated at 130°C for 20 min under ordinary pressure. The resulting oil was then purified by sublimation at 80°C/1.5 mmHg, followed by sodium salt formation; this gave 11 mg of colorless crystals. The IR and NMR spectra were identical with those of XIa.

We wish to thank Professor K. Takase (of this department) for helpful discussions, Dr. C. T. Chang (National Taiwan University) for his experimental work in the isolation of 5-*t*-butyltropolone, and Mr. E. Kirii (of this department) for the preparation of the *N*-alkylamino-isopropylcycloheptatrienes.

BULLETIN OF THE CHEMICAL SOCIETY OF JAPAN VOL. 42 3284—3288 (1969)

Stereochemical Studies of Monoterpene Compounds. VII.[1] Conformational Study of 4-Hydroxymenthones by Temperature-dependent Circular Dichroism[2]

Tsuyoshi SHISHIBORI, Takayuki SUGA, Satoru WATANABE and Tamon MATSUURA

Department of Chemistry, Faculty of Science, Hiroshima University, Hiroshima

(Received May 14, 1969)

The conformational analysis of a stereoisomeric pair of 4-hydroxymenthones, (1R:4R)-(−)-4-hydroxymenthone (**1**) and (1R : 4S)-(+)-4-hydroxyisomenthone (**2**), was made by means of temperature-dependent circular dichroism. It was demonstrated that α-hydroxyketone (**1**) exists in the conformational equilibrium: **1a**⇄**1b**; the conformer **1a** exists predominantly in a nonpolar medium, whereas the conformer **1b** is more stable than **1a** in a polar medium. On the other hand, the other isomer, (**2**), exists preferentially in the state of the conformer **2b** in either a polar or a nonpolar solvent. The results were interpreted in terms of the competition of the steric factor and intramolecular hydrogen-bonding.

The measurement of circular dichroism (CD) at different temperatures has been found very useful for investigating the conformational equilibrium in a flexible cyclohexanone structure.[3] α-Hydroxycyclohexanones represent interesting examples because, in addition to a possible ring-

1) Paper VI of this series: T. Suga, T. Shishibori, T. Hirata and T. Matsuura, This Bulletin, **41**, 1180 (1968).

2) Presented at the 21st Annual Meeting of the Chemical Society of Japan, Osaka, April, 1968.

3) "Optical Rotatory Dispersion and Circular Dichroism in Organic Chemistry," ed. by G. Snatzke, Heyden & Son Ltd., London (1967), pp. 16 and 335.

Table 1. Variable-temperature C.D. measurements of 4-hydroxymenthones

Compound	Solvent	$[\theta]\times10^{-3}$ (λ_{max}, mμ)			
		+150°C	+25°C	−74°C	−186°C
(1R:4R)-(−)-4-Hydroxymenthone (**1**)	Decalin	−6.40 (288)	−7.73 (288)	−7.84 (286)	
	MI[a]		−7.49 (288)		−7.71 (289)
	EPA[b]		+0.58 (320)	+1.39 (320)	+2.31 (319)
			−5.49 (293)	−3.75 (286)	−3.11 (285)
(1R:4S)-(+)-4-Hydroxyisomenthone (**2**)	Decalin	+5.27 (288)	+5.71 (288)		
	MI		+6.48 (286)		+7.81 (293)
	EPA		+6.33 (286)	+6.71 (286)	+8.00 (291)
(1R:4R)-(+)-4-Acetoxymenthone (**3**)	EPA		+0.90 (293)	+1.12 (293)	+2.00 (293)

a) Ref. 6. b) Ref. 13.

conformational equilibrium, intramolecular hydrogen-bonding between the hydroxyl and the carbonyl groups can be expected. The room-temperature ORD and CD curves of 4-hydroxymenthones in several solvents[4] have been interpreted in terms of these effects. The temperature-dependent CD spectra may be expected to furnish further insight into the interplay of conformational, solvational, and hydrogen-bonding effects in 4-hydroxymenthones. This paper will deal with the conformational analysis of (1R : 4R)-(−)-4-hydroxymenthone (**1**), (1R:4S)-(+)-4-hydroxyisomenthone (**2**), and (1R:4R)-(+)-4-acetoxymenthone (**3**) by means of the temperature-dependent CD

Results and Discussion

The temperature-dependent CD data of compounds **1** and **2** and of the acetate (**3**) of **1** are summarized in Table 1.

(1R : 4R)-(−)-4-Hydroxymenthone (**1**) and (1R:4S)-(+)-4-hydroxyisomenthone (**2**) can exist in two interconvertible chair conformations, **1a** and **1b**, and **2a** and **2b**, respectively. On the basis of steric requirements only, it can be predicted that the conformer **1b** will be energetically favored. However, the conformer **1a** can be stabilized by hydrogen-bonding between the carbonyl and the hydroxyl groups, so a clear-cut evaluation of the difference between the relative energies of **1a** and **1b** is difficult. On the other hand, the conformer **2b** in the conformational equilibrium **2a**⇄**2b** can be predicted to be energetically favored on the basis of steric requirements; also, it can be stabilized by an intramolecular hydrogen bond.

The variable-temperature CD measurements of compounds **1** and **2** afforded a convincing assignment for the preferred conformation. According to the octant rule,[5] the conformers **1a** and **2a**

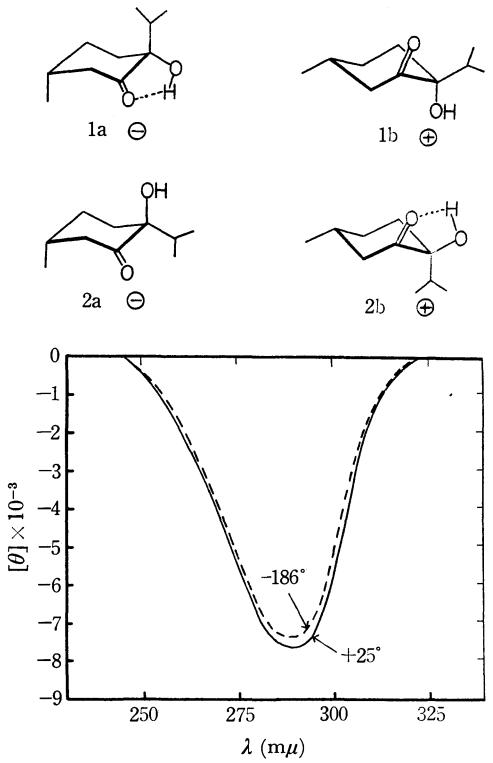

Fig. 1. Circular dichroism curves of (1R:4R)-(−)-4-hydroxymenthone (**1**) in MI at +25 and −186°C.

should exhibit a negative Cotton effect and the conformers **1b** and **2b** a positive one.

(1R : 4R)-(−)-4-Hydroxymenthone (1). As is shown in Fig. 1 and Table 1, the CD curves of **1** in MI solvent[6] and decalin exhibit a negative Cotton effect, and the rotational strength of **1** is almost temperature-independent over the range from 25°C to −186°C in a MI solvent and 25°C to −74°C in decalin. These phenomena observed in CD curves are distinct from those of (−)-

4) T. Suga, T. Shishibori and T. Matsuura, *J. Org. Chem.*, **32**, 965 (1967).

5) W. Moffit, R. B. Woodward A. Moscowitz, W. Klyne and C. Djerassi, *J. Am. Chem. Soc.*, **83**, 4013 (1961).

6) MI solvent is composed of methylcyclohexane-isopentane in the ratio 1 : 3 by volume.

menthone[7] and 2-oxo-1-*p*-menthanol,[8] either of which shows a strong temperature-dependence. The negative Cotton effect implies that **1** exists in the **1a** conformation, while the temperature-independence of the rotational strength suggests the conformational homogeneity of **1a** in such a nonpolar solvent as MI and decalin.

The infrared spectrum of **1** in carbon tetrachloride showed only a concentration-independent band at 3495 cm^{-1} resulting from an intramolecular hydrogen-bond between the hydroxyl and the lone-pair electrons on the carbonyl oxygen atom.[9] This indicates that **1** exists in the conformation **1a**, only in which the OH···O=C-type intramolecular hydrogen bond is possible.

A deductive calculation of the conformational energy on the basis of the steric factor shows that the conformer **1a** would be energetically less favored by *ca.* 1.7 kcal/mol[10] than would be **1b** in the conformational equilibrium **1a**⇄**1b**. However, the conformer **1a** can be stabilized by intramolecular hydrogen-bonding between the carbonyl and the hydroxyl group (a saving of *ca.* 2—5 kcal in terms of energy). The results of the variable-temperature CD and the infrared spectral measurements show that the conformer **1a** is stabilized by the intramolecular hydrogen-bonding energy, which is sufficient to overcome the instabilization due to the steric repulsion between groups and atoms.

At a high temperature the strength of the negative CD curve of **1** in decalin was decreased (Table 1). This means that at a high temperature the hydrogen-bonded form of **1a** would be diminished with an increase in the amounts of the nonbonded conformer, **1b**, and/or of the positively-rotating conformer, **1c**, of the twist form.

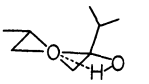

1c

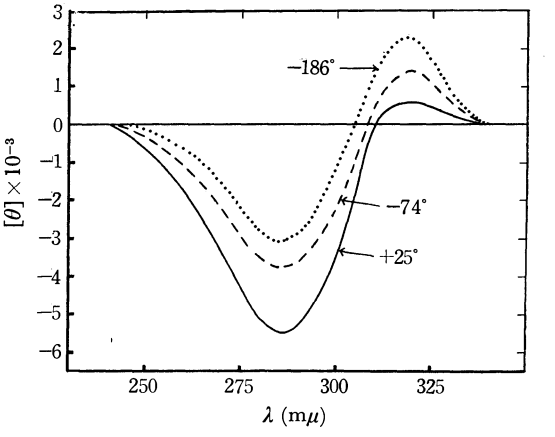

Fig. 2. Circular dichroism curves of (1R:4R)-(−)-4-hydroxymenthone (**1**) in EPA at +25, −74, and −186°C.

In the EPA solvent,[13] **1** exhibits a multiple-Cotton-effect CD curve (Fig. 2). The double-humped Cotton effects arising from $n\rightarrow\pi^*$ transitions in a saturated ketone can be explained in terms of solvational equilibria[14] and/or conformational equilibria. If a solvational equilibrium were solely responsible for the double-humped Cotton effect observed in **1**, the short-wavelength CD band could be attributed to the solvational species, and the long-wavelength band, to the unsolvated form. If this were the case, the apparent rotational strength of the blue-shifted band would increase at lower temperatures. Actually, the opposite result was obtained in EPA (Fig. 2).

The CD data were favorably explained on the basis of a conformer equilibrium as follows. According to the octant rule,[5] the negative CD band at a short wavelength may be attributed to the conformer **1a**, and the red-shifted positive band, to the conformer **1b**. These assignments are also in agreement with the following findings: an equatorial hydroxyl group adjacent to the carbonyl group causes a blue-shift of the ORD curve peak, whereas an axial hydroxyl group results in a red-shift. If the CD band assignment is accepted, the enlargement of the long-wavelength band at lower temperatures indicates that the conformer **1b** is energetically favored in a polar solvent, EPA.

7) K. M. Wellman, P. H. A. Laur, W. S. Briggs, A. Moscowitz and C. Djerassi, *J. Am. Chem. Soc.*, **87**, 66 (1965).

8) K. M. Wellman, W. S. Briggs and C. Djerassi, *J. Am. Chem. Soc.*, **87**, 73 (1965).

9) T. Suga, T. Shishibori and T. Matsuura, This Bulletin, **41**, 944 (1968); M. Ōki, H. Iwamura, J. Aihara and H. Iida, This Bulletin, **41**, 176 (1968); L. Joris and P. von R. Schleyer, *J. Am. Chem. Soc.*, **90**, 4599 (1968).

10) A free energy difference ($-\Delta G$) for the equilibrium

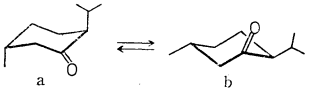

a b

a⇄b of menthone was estimated by Richborn[11] to be 2.4 kcal/mol based on the menthone-isomenthone isomerisation. Assuming ΔG of the hydroxyl group adjacent to the carbonyl to be −0.7 kcal/mol,[12] the free energy difference for the equilibrium la⇄1b is estimated *a priori* to be *ca.* 1.7 kcal/mol.

11) a) B. Richborn, *J. Am. Chem. Soc.*, **84**, 2414 (1962), b) W. D. Cotterill and M. J. T. Robinson, *Tetrahedron*, **20**, 777 (1964).

12) E. L. Eliel, N. L. Allinger, S. T. Angyal and G. A. Morrison, "Conformational Analysis," John Wiley & Sons, Inc., New York (1965), p. 58.

13) EPA solvent is composed of ether-isopentane-ethanol in the ratio 5 : 5 : 2 by volume.

14) Ref. 3, p. 329.

Such a result may be interpreted in terms of the competition of the steric factor and intramolecular hydrogen-bonding. In hydrocarbon solvents, the stabilization due to the intramolecular hydrogen-bonding overcomes the steric repulsion, as has been described above. However, the stabilizing intramolecular hydrogen bond will be broken in the polar solvent, so that the steric requirements mainly dominate the conformation of **1**. Therefore, the sterically-favored conformer, **1b**, is preferred in EPA.

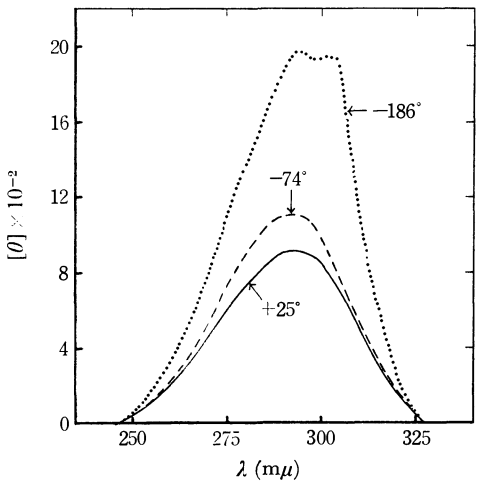

Fig. 3. Circular dichroism curves of (1R:4R)-(+)-4-acetoxymenthone (**3**) in EPA at +25, −74, and −186°C.

(+)-4-Acetoxymenthone. The variable-temperature CD curves of (+)-4-acetoxymenthone (**3**), the acetylated compound of **1**, gave further support to the above deduction. The CD curve (Fig. 3) of **3** in EPA showed a weak positive Cotton effect and an increase in strength upon the lowering of the temperature. This implies that the positively-rotating conformer **3b** is preferred. Since the stabilization due to the intramolecular hydrogen-bonding is absent in the acetylated compound **3**, the conformer **3b** is energetically favored by the

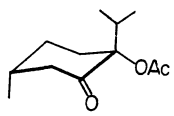

3a ⊖

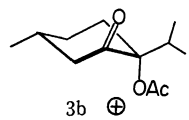

3b ⊕

steric requirements. If one bears in mind that the conformational energy of the hydroxyl group[12] in **1** is comparable with that of the acetoxyl group in **3**, the stabilizing intramolecular hydrogen bond can be found to contribute to the conformational preference of **1a** in a nonpolar solvent.

(1R : 4S)-(+)-4-Hydroxyisomenthone (2). The CD curves of **2** in decalin and MI (Table 1) and in EPA (Fig. 4) show a positive Cotton effect, with

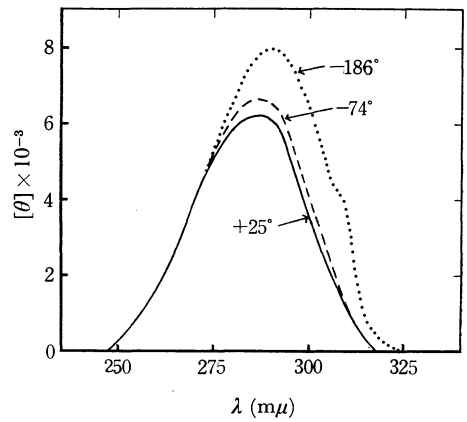

Fig. 4. Circular dichroism curves of (1R:4S)-(+)-4-hydroxyisomenthone (**2**) in EPA at +25, −74, and −186°C.

only a single maximum at room temperature. The increase in the rotational strength upon a change to lower temperatures in EPA and MI indicates that the positive rotating conformer, **2a**, is the more stable in either a polar or nonpolar medium. This behavior in CD curves is similar to that of (+)-isomenthone.[7] The infrared spectra of **2** in carbon tetrachloride showed only a concentration-independent band at 3495 cm^{-1} resulting from an intramolecular hydrogen bond between the hydroxyl and the carbonyl groups. The stabilization due to the intramolecular hydrogen bond contributes to the preference of the conformer **2b**. On the basis of steric requirements, the conformer **2b** can also be predicted to be energetically favored by *ca.* 1.9 kcal/mol.[15] more than **2a**. The results of the low-temperature CD curves are in agreement with the above proposal.

The CD curves of **2** in decalin showed a decrease in rotational strength upon a change to higher temperatures (Table 1). This suggests that the less stable conformer in the conformational equilibrium of **2** would not be the twist form **2c**, which would be highly positive, but the negatively-rotating chair form **2a**.

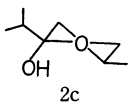

2c

15) The conformational energy ($-\Delta G$) of the methyl group situated at β-position to the carbonyl is estimated to be *ca.* 1.8 kcal/mol,[11b] and of the isopropyl group adjacent to carbonyl to be *ca.* 0.6 kcal/mol.[11b] Assuming ΔG of the hydroxyl group adjacent to the carbonyl group to be −0.7 kcal/mol, the free energy difference for the equilibrium 2a⇄2b is estimated deductively to be *ca.* 1.9 kcal/mol.

Experimental

Materials. (1R : 4R)-(−)-4-Hydroxymenthone (**1**), (1R : 4S)-(+)-4-hydroxyisomenthone (**2**), and (1R : 4R)-(+)-4-acetoxymenthone (**3**) are the same as were prepared in a previous paper[4] of this series.

Spectral Measurements. The IR spectra in the hydroxyl-stretching region were measured with a Perkin-Elmer Model 621 Grating Infrared Spectrometer at 25°C. A sodium chloride absorption cell, 20 mm long, was used; the concentration of the solution was 0.005 mol/*l*, at which the association of the solute is negligible. The CD curves were obtained by a Japan Spectroscopic Co., Ltd., automatically-recording spectropolarimeter, Model ORD/UV-5, equipped with a circular dichroism attachment. The low- and high-temperature CD curves were obtained by the same spectrometer, using low- and high-temperature CD cells[16] designed and constructed by the authors. All the measurements were performed using spectrograde or purified solvents, a 10 mm cell, and *c* 0.1. The volume contraction of the solvents was corrected.

16) T. Suga, T. Shishibori and T. Matsuura, JASCO Report (published by Japan Spectroscopic Co., Ltd., Tokyo), to be presented.

BULLETIN OF THE CHEMICAL SOCIETY OF JAPAN VOL. 42 3288—3297 (1969)

Kinetic Studies of Solvolysis. XVI.*1 Phenolysis of *cis*- and *trans*-4-*t*-Butylcyclohexyl *p*-Toluenesulfonates. Rates and Product Distribution

Kunio Okamoto, Seiki Saitô and Haruo Shingu

Department of Hydrocarbon Chemistry, Faculty of Engineering Kyoto University, Sakyo-ku, Kyoto

(Received May 15, 1969)

The rates of the phenolysis of *cis*- and *trans*-4-*t*-butylcyclohexyl *p*-toluenesulfonates have been measured in the presence of equimolar amounts of triethylamine in phenol, phenol-benzene (3 : 1 by wt), and phenol-benzene (1 : 1 by wt) solvents. At 75°C, the axial isomer, *i.e.*, the *cis* tosylate, phenolyzes more rapidly in the phenol-benzene mixture (1 : 1 by wt) than the equatorial isomer, *i.e.*, the *trans* tosylate, by a factor of 3.08; this factor is not far from the axial-equatorial rate ratios observed in other hydroxylic solvents,[2] indicating that phenol is a typical solvolytic solvent. Under the same reaction conditions as the rate measurements, the equatorial tosylate yields *t*-butylcyclohexene (72.5%), *t*-butylcyclohexyl phenyl ether (9.4%), predominantly inverted (*cis*-4-*t*-butylcyclohexyl) phenyl ether, and *t*-butylcyclohexylphenol (4.4%), whereas the axial tosylate yields *t*-butylcyclohexene (87%) and the phenyl ether (8.7%), largely inverted (*trans*-4-*t*-butylcyclohexyl) phenyl ether, but containing increasing amounts of retained (*cis*-4-*t*-butylcyclohexyl) and and rearranged (*trans*-3-*t*-butylcyclohexyl) ethers; the rest is a mixture of *t*-butylcyclohexylphenols (1.6%). The composition percentages of the retained phenyl ether obtained from the two tosylates, *i.e.*, 20.4% for the *cis* tosylate and 12.9% for the *trans* tosylate, indicate the highest extents of retention for phenol among those known for any other hydroxylic solvents.[3] The initially added *t*-butylcyclohexenes exert no influence on the olefin or on the phenyl ether composition, whereas triethylammonium and diethylammonium *p*-toluenesulfonates, when added initially, enhance the phenolysis rate and exert a small but definite influence on the composition of the phenyl ether. The hypothesis of the hydrogen-bridged cation,[2] proposed in order to explain the enhanced rate of the *cis* isomer and in order to elucidate the retained solvolysis product, has been questioned by a consideration of the mechanism on the basis of the results of this phenolysis.

In previous studies[1] of the retentive solvolysis, it has been demonstrated that phenol is a notable

*1 Presented at the 18th Symposium on the Organic Reaction Mechanism, Kyoto, October, 1967 (Abstract, p. 81) and at the 21st Annual Meeting of the Chemical Society of Japan, Osaka, April, 1968 (Abstract, Part III, p. 2034); Part XV: K. Okamoto, I. Nitta and H. Shingu, This Bulletin, **41**, 1433 (1968).

1) a) Part XI: K. Okamoto, H. Yamada, I. Nitta and H. Shingu, This Bulletin, **39**, 299 (1966); b) K. Okamoto, K. Komatsu and H. Shingu, *ibid.*, **39**, 2785 (1966); c) Part XIII: K. Okamoto, M. Hayashi, K. Komatsu and H. Shingu, *ibid.*, **40**, 624 (1967); d) Part XIV: K. Okamoto, K. Komatsu and H. Shingu, *ibid.*, **40**, 1677 (1967).

solvent in which the S_N1 solvolysis of optically-active α-phenylethyl chloride gives a partially-retained phenyl ether. However, for the systems other than α-phenylethyl, it was not clear whether or not such retentive phenolysis is common. Therefore, it is obviously desirable to have more information about the structural factors of the substrate with regard to the retention of the configuration in phenolysis. As one of works of this line, we have considered it of interest to extend the rate and the product studies to the 4-*t*-butylcyclohexyl system, because this system has a rigid conformation fixing the *t*-butyl group in the equatorial position; also, the kinetic[2] and the product analysis[2,3] data have already been made available for various solvents other than phenol. In this paper we will describe our findings on the rate and the products in the phenolysis of *cis*- and *trans*-4-*t*-butylcyclohexyl *p*-toluenesulfonates in the presence of triethylamine, and will discuss the bearing of the results on the characteristics of phenol as an ionizing solvent and as a retentive solvent.

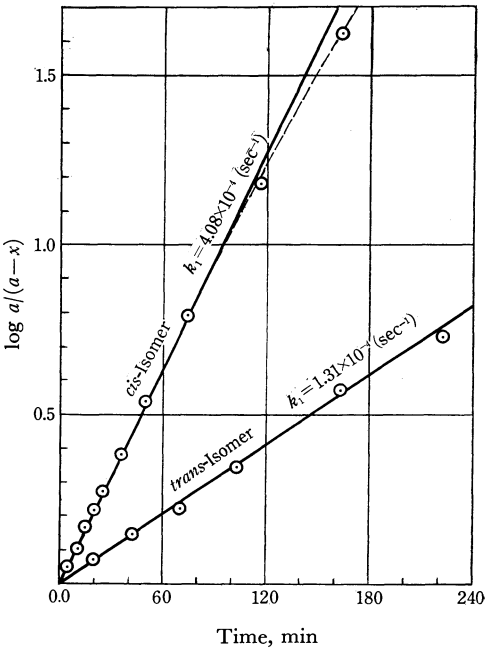

Fig. 1. First-order plots for phenolysis of *cis*- and *trans*-4-*t*-butylcyclohexyl *p*-toluenesulfonates in the presence of triethylamine in 50 wt% phenol-benzene solvent at 75.0°C.

Results and Discussion

Phenolysis Rates of *cis*- and *trans*-4-*t*-Butylcyclohexyl *p*-Toluenesulfonates in the Presence of Triethylamine. The phenolysis of *cis*- and *trans*-4-*t*-butylcyclohexyl *p*-toluenesulfonates was carried out in phenol-benzene solvents at 75°C and the rate constants were determined titrimetrically. In spite of the presence of equimolar amounts of triethylamine, the *trans* tosylate displayed good first-order behavior, whereas the first-order plot for the *cis* tosylate shows a downward drift after about 80% completion (Fig. 1). Initially-added triethylammonium *p*-toluenesulfonate gave rise to a small rate enhancement for both tosylates (Table 1), probably due to the normal salt effect.[4]

There is a decided trend towards markedly enhanced rates in solvents with higher phenol contents; at 75°C for the *trans* tosylate a one and half-fold increase in the phenol concentration gave rise to rate enhancement by a factor of three (Table 1).

In Fig. 2 the solvolysis rates of 4-*t*-butylcyclohexyl *p*-toluenesulfonates in phenol-benzene (1 : 1 by wt), phenol-benzene (3 : 1 by wt), phenol, acetic acid,[2] formic acid,[2] and ethanol[2] at 75°C are plotted on a logarithmic scale against the *Y* scale of Grunwald and Winstein.[5,6] There is a general tendency towards higher rates in solvents of higher *Y* values, but the proportionality is far from exact. This result is not unexpected if one considers that the rate measured for the *t*-butylcyclohexyl system might not reflect the true ionization rate of the system (*vide infra*).

The *cis* tosylate, *i. e.*, the axial isomer, phenolyzed more rapidly than the *trans* (equatorial) tosylate by a factor of 3.08 in phenol-benzene (1 : 1 by wt) at 75°C, indicating, as far as the axial-equatorial rate ratio is concerned, that the phenolic solvent[7] is not specifically different from such other solvents as formic acid, acetic acid, and ethanol, in which the axial tosylate solvolyzes more rapidly than the equatorial isomer by factors of 2.51, 2.85, and 3.05 respectively (Table 1).

In the extreme that the higher rate of the axial over the equatorial tosylate is attributed only to steric acceleration caused by the higher initial

2) S. Winstein and N. J. Holness, *J. Am. Chem. Soc.*, **77**, 5562 (1955).

3) N. C. G. Campbell, D. M. Muir, R. R. Hill, J. H. Parish, R. M. Southan and M. C. Whiting, *J. Chem. Soc., B*, **1968**, 355.

4) For the normal salt effect in the acetolysis, see A. H. Fainberg and S. Winstein, *J. Am. Chem. Soc.*, **78**, 2763 (1956).

5) a) E. Grunwald and S. Winstein, *ibid.*, **70**, 846 (1948); b) A. H. Fainberg and S. Winstein, *ibid.*, **78**, 2770 (1956).

6) The *Y* values for phenol-benzene (1 : 1 by wt) and phenol-benzene (3 : 1 by wt) were determined in this laboratory; K. Okamoto and S. Saitô, unpublished work.

7) Phenol is an especially powerful solvolytic solvent despite its low dielectric constant (9.78 at 60°C); the *Y* value for phenol was estimated to be about 1.77 (*cf.* Footnote 6).

Table 1. Rates of solvolysis of *cis*- and *trans*-4-*t*-butylcyclohexyl *p*-toluenesulfonates at 75°C

Solvent	ROTs	Base	$10^4 k_1$ (sec^{-1})		k_1 *cis*/k_1 *trans*
PhOH-Benzene (1:1 by wt)	*cis*	Et_3N			
	0.0972M	0.106N	4.08	4.00	3.08
	0.0980M	0.111N	3.91		
	0.0990M	0.105N	4.13[a]		(3.15[b,d])
	0.0978M	0.111N	4.88[b]		
	trans	Et_3N			
	0.0833M	0.110N	1.31	1.30	
	0.103 M	0.106N	1.29		
	0.0989M	0.105N	1.38[c]		
	0.0997M	0.106N	1.55[d]		
PhOH-Benzene (3:1 by wt)	*trans*	Et_3N			
	0.0999M	0.106N	4.00		—
PhOH	*trans*	Et_3N			
	0.100M	0.109N	11.0		—
Formic acid[e]	*cis*	NaO_2CH	354[f]		2.51
	trans	NaO_2CH	141[f]		
Acetic acid[e]	*cis*	NaOAc	1.03		2.85
	trans	NaOAc	0.362		
Ethanol[e]	*cis*	—	0.703[g]		3.05
	trans	—	0.230[g]		

a) With added $Et_3NH^+OTs^-$ (0.101N).
b) With added $Et_2NH_2^+OTs^-$ (0.198N).
c) With added $Et_3NH^+OTs^-$ (0.203N).
d) With added $Et_2NH_2^+OTs^-$ (0.191N).
e) S. Winstein and N. J. Holness, Ref. 2.
f) Extrapolated from data at 25 and 50°C.
g) Probably contaminated with the S_N2 type ethanolysis.

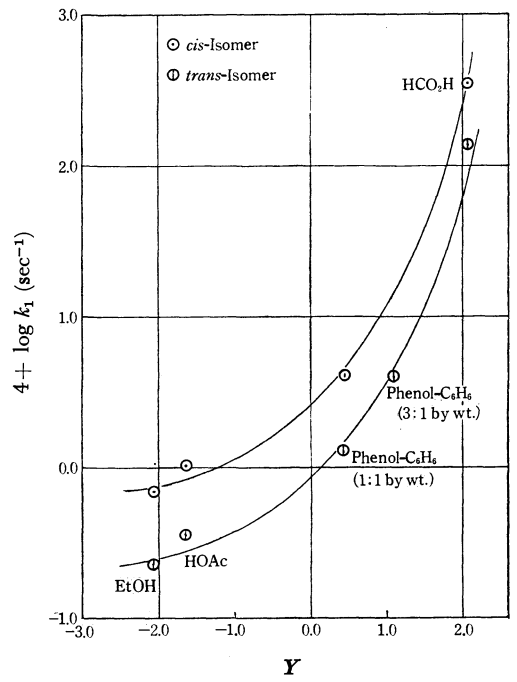

Fig. 2. Plots of log k_1's for solvolysis in various solvents against *Y*-values.

state energy of the axial isomer, the rate enhancement for the axial isomer is calculated to be a factor of 2.1 at 75°C, since a reliable value for the energy difference in ΔF between the two isomers has recently given as 0.515 kcal/mol.[8]

The gap between the calculated (2.1) and the observed factor (2.51—3.08) can be ascribed to the lowering of the free energy for the transition state of the axial isomer; the value is estimated to be about 0.12—0.27 kcal/mol (Fig. 3).

As regard to the elucidation of this decrease in the free-energy of the transition state for the *cis* tosylate, the neighboring hydrogen participation hypothesis has prevailed, especially in the cases of the 4-*t*-butylcyclohexyl[2,9] and 3-cyclohexyl-2-butyl[10] systems. However, it seems difficult to deduce the formation of a bridged ethylene-protonium-ion-type intermediate[2] on the basis of such a small stabilization of the transition state.[11]

8) F. R. Jensen, C. H. Bushweller and B. H. Beck, *J. Am. Chem. Soc.*, **91**, 344 (1969).
9) V. J. Shiner, Jr., and J. G. Jewett, *ibid.*, **87**, 1382 (1965).
10) D. J. Cram and J. Tadanier, *ibid.*, **81**, 2737 (1959).
11) The question of the existence of a hydrogen-bridged cation intermediate for the solvolysis of the 4-*t*-butylcyclohexyl system will be the subject of a subsequent publication.

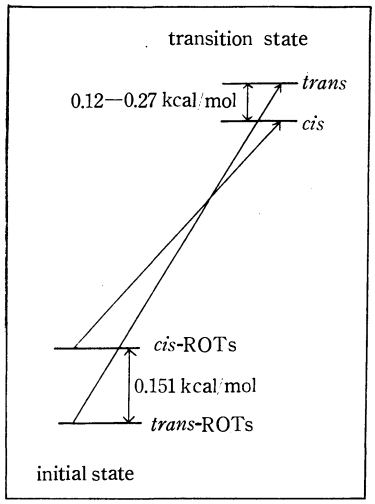

Fig. 3. Free-energy diagram for the solvolysis of *cis*- and *trans*-4-*t*-butylcyclohexyl *p*-toluenesulfonates.

Products of Phenolysis of *cis*- and *trans*-4-*t*-Butylcyclohexyl *p*-Toluenesulfonates in the Presence of Triethylamine. The products of phenolysis were investigated for both *trans*- and *cis*-4-*t*-butylcyclohexyl *p*-toluenesulfonates in a 50 wt% phenol-benzene solvent containing equimolar amounts of triethylamine at 75°C. The reaction mixture was worked up in the usual manner and then chromatographed over silica gel, giving *t*-butylcyclohexenes (a mixture of 4-, 3- and 1-*t*-butyl isomers), *t*-butylcyclohexyl phenyl ethers (a mixture of *cis*-4-, *trans*-4-, *cis*-3- and *trans*-3-*t*-butylcyclohexyl isomers), and a mixture of *t*-butylcyclohexylphenols. After the run with added triethyl- or diethylammonium *p*-toluenesulfonate had been conducted up to about 75% completion, the reaction mixture was treated with sodium naphthalene in tetrahydrofufan in order to cleave the unchanged tosylate into *t*-butylcyclohexanols; then, from the reaction mixture *t*-butylcyclohexanols,[12] *t*-butylcyclohexyl phenyl ethers and *t*-butylcyclohexylphenols were separated by elution chromatography.

The compositions of *t*-butylcyclohexenes and *t*-butylcyclohexyl phenyl ethers were determined by GLC; in some cases the latter mixture was separated into two components by means of TLC prior to the GLC analysis. The analysis scheme for the composition of *t*-butylcyclohexyl phenyl ethers is as follows:

ROPh —(t.l.c., silica gel)→ (*trans*-4- and *cis*-3-ROPh) —(g.l.c.)→ *trans*-4-ROPh + *cis*-3-ROPh

ROPh —(t.l.c., silica gel)→ (*cis*-4- and *trans*-3-ROPh) —(g.l.c.)→ *cis*-4-ROPh + *trans*-3-ROPh

12) A mixture of *cis*-4-, *trans*-4-, *cis*-3-, and *trans*-3-*t*-butylcyclohexanols; the analysis of the composition will be described in a subsequent paper.

ROPh —(g.l.c., Apiezon grease, 200°C)→ *trans*-3-ROPh + (*cis*-3- and *cis*-4-ROPh) + *trans*-4-ROPh (three peaks)

The composition of *t*-butylcyclohexanols, separated as a fraction of chromatography, was not analyzed.

Much as with the trend observed for other solvents,[3] the main product of the phenolysis for both tosylates is a mixture of *t*-butylcyclohexenes. The yield (%) of olefin formed from the equatorial (*trans*) tosylate is not far below that obtained from the axial (*cis*) tosylate (Table 2); this seems also a general tendency for the 4-*t*-butylcyclohexyl system irrespective of the nature of the solvent employed (*cf.* Ref. 3 and Table 2).

Table 2. Solvolysis products from 4-*t*-butylcyclohexyl *p*-toluenesulfonates

Solvent:	Phenol-Benzene (1:1 by wt) (Present work)		HOAc (Whiting *et al.*[a])	
Temp.:	75°C	75°C	100°C	100°C
ROTs:	*cis*	*trans*	*cis*	*trans*
	0.0913M	0.0987M		
Base:	Et_3N	Et_3N	NaOAc	NaOAc
	0.123N	0.106N	0.05N	0.05N
Time:	6.0 hr	18.7 hr		
Cyclohexenes:				
Yield %	87.0	72.5	87.0	79.2
Composition %				
4-*t*-Butyl	97.4	95.3	96.6	93.0
3-*t*-Butyl	2.6	4.1	3.2	6.3
1-*t*-Butyl	trace	0.6	0.2	0.7
Cyclohexyl Phenyl Ethers or Cyclohexyl Acetates:				
Yield %	8.7	9.4	12.8	21.9
Composition %				
trans-4-*t*-Butyl	55.0	12.9	57.0	1.8
cis-4-*t*-Butyl	20.4	69.2	5.5	89.0
trans-3-*t*-Butyl	13.7	12.8	35.2	2.3
cis-3-*t*-Butyl	10.9	5.1	2.3	6.9
t-Butylcyclohexylphenols:				
Yield %	1.6	4.4	—	—

a) Ref. 3.

Since olefin formation from the equatorial (*trans*) tosylate cannot be attributed to a usual E2-type anti-elimination,[13] the production of so much olefin from the equatorial isomer may indicate the contribution of a considerable amount of *cis*-*syn*-elimination in the El or S_Ni ion-pair intermediate.[14]

13) J. Sicher, J. Závada and M. Pánková, *Chem. Commun.*, **1968**, 1147.

14) For *cis*-elimination *via* the carbonium-ion intermediate for the deamination of *cis*-4-*t*-butylcyclohexylamine and *trans*-2-decalylamine, see, respectively, G. Lamaty, C. Tapiero and R. Wylde, *Bull. Soc. Chim. France*, **1968**, 2039, and T. Cohen and A. R. Daniewski, *J. Am. Chem. Soc.*, **91**, 532 (1969).

The composition of the olefin formed in phenol is compared with that in acetic acid[3] in Table 2; the compositions for the two solvents are quite similar. Besides 4-*t*-butylcyclohexene, there exists a small amount of rearranged olefins in the cases of both solvents, indicating the presence of rearranged ion-pair intermediates during the solvolysis.

The substitution products for both tosylates are composed of a major proportion of *t*-butylcyclohexyl phenyl ether and a minor amount of *t*-butylcyclohexylphenol; among the isomers of the phenyl ether, the inverted ether is the predominant component, the rest being the retained and the rearranged or isomerized ether (Table 2). This trend has also been found in the distribution of substitution products for acetolysis[3] (Table 2) and other solvolyses.[3]

However, the composition percentage of the retained phenyl ether in phenolysis for both tosylates is the highest among those of the retained products in other solvents.[3] This probably means that the front-side attack of the phenol molecule may play an important part in increasing the retentive course for the substitution; the fact that, even in the phenolic solvent, the yield of the retentive product never exceeds that of the inverted product for 4-*t*-butylcyclohexyl system is in marked contrast to the α-phenylethyl system, for which the retentive course is predominant in the phenolic solvents.[1]

As has been observed in the cases of other solvents,[2,3] in the phenolic solvent a substantial quantity of rearranged products is also present in the substitution products; the proportions of 3-*t*-butylcyclohexyl phenyl ethers are 24.6% from the *cis* tosylate and 17.9% from the *trans* tosylate.

Since initially-added *t*-butylcyclohexenes did not exert any influence on the composition of olefins and phenyl ethers for both tosylates within essentially the experimental error of analysis (Table 3), the possibility of the formation of rearranged products *via* a proton addition to a stable molecule of *t*-butylcyclohexene can be eliminated. This course is illustrated in Fig. 4.

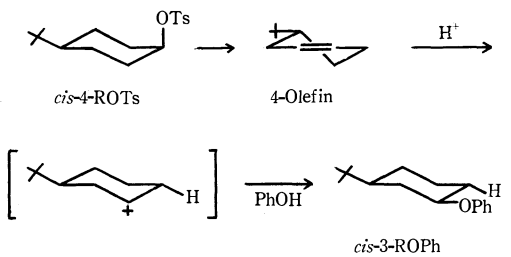

Fig. 4. 1,2-Rearrangement *via* *t*-butylcyclohexene.

The initial addition of the *p*-toluenesulfonate anion in the form of triethyl- or diethyl-ammonium salt, which is also produced as the phenolysis proceeds, has a small but definite influence on the composition of the phenyl ether (Table 4).

Table 3. Results of phenolysis of 4-*t*-butylcyclohexyl *p*-toluenesulfonates in the presence of added *t*-butylcyclohexenes and triethylamine[a]

	cis	*cis*	*trans*	*trans*
ROTs:	0.0913M	0.0970M	0.0987M	0.105M
Et_3N:	0.123N	0.110N	0.106N	0.107N
t-Butylcyclohexenes:	—	0.101M[b]	—	0.272M[c]
Time:	6.0 hr	5.4 hr	18.7 hr	19.0 hr
Cyclohexenes:				
Yield %	87.0	?[d]	72.5	?[d]
Composition %				
4-*t*-Butyl	97.4	95.9	95.3	95.3
3-*t*-Butyl	2.6	2.9	4.1	4.1
1-*t*-Butyl	trace	1.2	0.6	0.6
Cyclohexyl Phenyl Ethers:				
Yield %	8.7	9.4	9.4	9.9
Composition %				
trans-4-*t*-Butyl	55.0	54.3	12.9	12.9
cis-4-*t*-Butyl	20.4	20.5	69.2	67.3
trans-3-*t*-Butyl	13.7	14.3	12.8	13.0
cis-3-*t*-Butyl	10.9	10.8	5.1	6.9
t-Butylcyclohexylphenols:				
Yield %	1.6	2.0	4.4	5.3

a) In phenol-benzene (1:1 by wt) at 75.0°C.
b) A mixture of 4-*t*-butyl-, 3-*t*-butyl- and 1-*t*-butylcyclohexenes (Composition: 95.3, 3.2 and 1.5%).
c) A mixture of 4-*t*-butyl-, 3-*t*-butyl- and 1-*t*-butylcyclohexenes (Composition: 95.3, 4.1 and 0.6%).
d) The yield was not determined.

A thorough explanation of the variation in the composition with an increase in the concentrations of the *p*-toluenesulfonate anion would be difficult because of the presence of at least four probably interconvertible ion-pair intermediates, corresponding to the four substitution products. However, it can be conservatively pointed out that the retained substitution need not be derived by only a front-side attack of a molecule of phenol, but may also be produced by the isomeric intermediate. For instance, the *cis* ion-pair intermediate may be formed by an internal rotation of the *t*-butyl cyclohexyl cation from the *trans* ion-pair intermediate; consequently, starting from the *trans* tosylate, the retained substitution product may also be produced *via* a double inversion course, following the course illustrated in Fig. 5.

Thus, conceivably there exists a possibility of the accumulation of isomerized or rearranged tosylates during the phenolysis of the 4-*t*-butylcyclohexyl system by means of the internal return of the isomerized or rearranged intermediate or by an inversive attack of the *p*-toluenesulfonate anion on the unrearranged intermediate.

The downward drift of the first-order plot for

Table 4. Results of phenolysis of 4-*t*-butylcyclohexyl *p*-toluenesulfonates in the presence of added triethylammonium *p*-toluenesulfonate and triethylamine[a)]

ROTs:	*cis*	*cis*	*cis*	*cis*	*trans*	*trans*	*trans*	*trans*
	0.0913M	0.0990M	0.103M	0.0974M	0.100M	0.0987M	0.0989M	0.100M
Et_3N:	0.123N	0.105N	0.105N	0.111N	0.107N	0.106N	0.105N	0.109N
$Et_3NH^+OTs^-$:	—	0.101N	0.226N	0.212N[b)]	—	—	0.203N	0.106N[b)]
Time:	6.0 hr	0.95 hr	0.88 hr	1.0 hr	2.8 hr	18.7 hr	2.6 hr	2.8 hr
Conversion:	100%	75.5%	74.0%	86.5%	73.6%	100%	75.0%	76.6%
Cyclohexenes:								
Yield %	87.0	?[c)]	?[c)]	?[c)]	?[c)]	72.5	?[c)]	?[c)]
Composition %								
4-*t*-Butyl	97.4	98.8	?[c)]	?[c)]	?[c)]	95.3	?[c)]	?[c)]
3-*t*-Butyl	2.6	1.2	?[c)]	?[c)]	?[c)]	4.1	?[c)]	?[c)]
1-*t*-Butyl	trace	trace	?[c)]	?[c)]	?[c)]	0.6	?[c)]	?[c)]
Cyclohexyl Phenyl Ethers:								
Yield %	8.7	11.6	10.4	8.6	10.9	9.4	11.0	12.5
Composition %								
trans-4-*t*-Butyl	55.0	60.9	63.6	60.8	12.2	12.9	10.4	10.6
cis-4-*t*-Butyl	20.4	19.5	17.6	17.6	70.3	69.2	70.9	72.9
trans-3-*t*-Butyl	13.7	12.1	12.0	14.0	12.8	12.8	10.6	11.4
cis-3-*t*-Butyl	10.9	7.5	6.8	7.6	4.7	5.1	8.1	5.1
t-Butylcyclohexylphenols:								
Yield %	2.0	2.1	2.3	1.8	5.7	4.4	3.3	5.2

a) In phenol-benzene (1:1 by wt) solvent at 75.0°C.
b) Instead of $Et_3NH^+OTs^-$, $Et_2NH_2^+OTs^-$ was used.
c) The yield or composition was not determined.

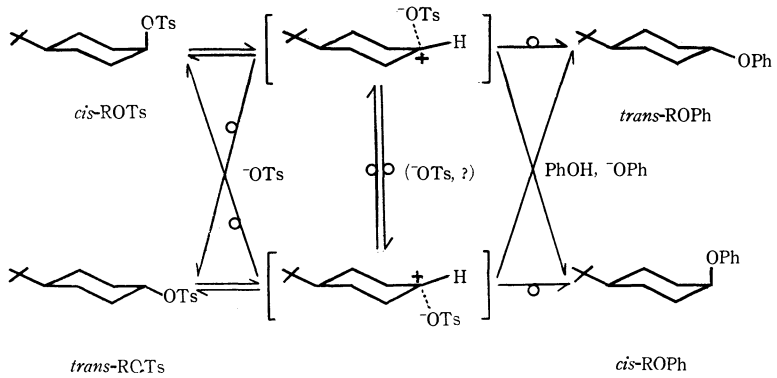

Fig. 5. Possible courses for the formation of retained 4-*t*-butylcyclohexyl phenyl ethers in phenolysis.

the *cis* tosylate, illustrated in Fig. 1, might be due to the accumulation of the *trans* tosylate, which is phenolyzed slower than the *cis* isomer.

On the basis of these considerations of the course for the retained products, the necessity of the hypothesis of a hydrogen-bridged cation intermediate[2)] for the 4-*t*-butylcyclohexyl system, proposed as an explanation of the formation of the retained substitution product, may well be questioned, as it may also be questioned on the basis of the rate data presented above. Further discussion of this problem will be the subject of a subsequent paper.

Experimental[15)]

Materials. ***trans*-4-*t*-Butylcyclohexanol** was obtained from the hydrogenphthalate of a mixture of 4-*t*-butylcyclohexanol, which had itself been prepared by means of the catalytic hydrogenation of *p*-*t*-butyl-

15) The melting points are not corrected. The microanalyses were done by the Microanalytical Center, Kyoto University. The infrared spectra were determined with a Shimadzu Model IR-27 spectrophotometer. All the gas-liquid chromatographical studies were made with a Shimadzu Model GC-2B dual-column gas chromatograph.

phenol, employing the same reaction conditions as those of the hydrogenation of *p*-isopropylphenol.[16]

p-*t*-Butylphenol (30 g, 0.20 mol) was hydrogenated using 1.6 g of a Raney nickel catalyst (W-2)[17] and 41 ml of absolute ethanol as a solvent in a 300-ml autoclave at 150°C for five hours (initial hydrogen press, 100 kg/cm^2). The catalyst was removed by filtration and washed with ethanol. The combined ethanol solutions were evaporated to dryness to give 31.0 g of 4-*t*-butylcyclohexanol (97% yield, mp 62—68°C); the infrared spectrum of the carbon tetrachloride solution showed no absorptions in the aromatic regions.

Several crystallizations of the hydrogenphthalate and subsequent saponification afforded *trans*-4-*t*-butylcyclohexanol; mp 80.1—81.1°C (lit, mp 81—82°C,[2] 80—80.5°C[18] and 82°C[19]).

***cis*-4-*t*-Butylcyclohexanol** was obtained by the elution chromatography of a mixture of 4-*t*-butylcyclohexanols; this mixture had been prepared by the reduction of 4-*t*-butylcyclohexanone with Raney nickel (W-2)[17] in ethanol. *cis*-4-*t*-Butylcyclohexanol, obtained by chromatography over alumina (Nakarai 200), melted at 81—82°C (lit, mp 82—83°C,[2] 82.5—83.5°C[20] and 83—83.5°C[19]).

4-*t*-Butylcyclohexanone was prepared following the method of Winstein and Holness[2]; the chromic acid oxidation of a mixture of 4-*t*-butylcyclohexanols in acetic acid gave 4-*t*-butylcyclohexanone in an 82% yield. This ketone melted at 48—50°C (lit, mp 47.5—48.5°C[2] and 49—50°C[21]) and boiled at 85—86°C/7 mmHg (lit, bp 90—92°C/9 mmHg[2] and 106—108°C/19 mmHg[21]).

The Tosylate of *trans*- and *cis*-4-*t*-Butylcyclohexanols was prepared according to the usual Tipson procedure.[22] *trans*-4-*t*-Butylcyclohexyl *p*-toluenesulfonate melted at 88.5—89.5°C (lit, mp 89.4—90.0°C[2] and 89—90°C[23]). *cis*-4-*t*-Butylcyclohexyl *p*-toluenesulfonate melted at 78—79°C (lit, mp 79—80°C[2] and 78—79°C[23]).

3-*t*-Butylcyclohexanone was prepared by means of the reaction of 2-cyclohexen-1-one with *t*-butylmagnesium chloride using a modification of the method of Whitmore and Pedlow[24]: oxidation of cyclohexene with chromium trioxide in acetic acid gave 2-cyclohexen-1-one (27% yield); bp 64—65°C/20 mmHg, n_D^{20} 1.4870 (lit, bp 65—66°C/20 mmHg[2] and 67°C/25 mmHg,[24] n_D^{25} 1.4824,[2] n_D^{20} 1.4879[24]). The Grignard reaction of 2-cyclohexen-1-one with *t*-butylmagnesium chloride in the presence of cuprous chloride[25] gave 3-*t*-butylcyclohexanone (39% yield); bp 69—72°C/4 mmHg, n_D^{25} 1.4601 (lit, bp 92—95°C/10 mmHg[2] and 96—98°C/20 mmHg,[24] n_D^{25} 1.4611,[2] n_D^{20} 1.4615[24]).

***cis*-3-*t*-Butyl- and *trans*-3-*t*-Butylcyclohexanols** were prepared in good yields by the reduction of 3-*t*-butylcyclohexanone with, respectively, lithium aluminum hydride[2] and Raney nickel in ethanol.[2] Each alcohol was purified by several recrystallizations of the hydrogenphthalate and by subsequent saponification. *trans*-3-*t*-Butylcyclohexanol melted at 64—66°C (lit, mp 48—49°C,[2] 48°C[3] and 64°C[3]), and *cis*-3-*t*-butylcyclohexanol melted at 41—43°C; bp 105—106°C/10 mmHg, n_D^{25} 1.4670 (lit,[2] mp 40—41°C, bp 103°C/10 mmHg, n_D^{25} 1.4660).

***cis*-3-*t*-Butyl- and *trans*-3-*t*-Butylcyclohexyl *p*-Toluenesulfonates** were prepared according to the method of Tipson.[22] *cis*-3-*t*-Butylcyclohexyl *p*-toluenesulfonate melted at 58—59°C (lit, mp 58—59.5°C[2]). *trans*-3-*t*-Butylcyclohexyl *p*-toluenesulfonate melted at 44—45°C (lit, mp 33—35°C[2]).

4-*t*-Butylcyclohexene was prepared by means of the E2 reaction of *cis*- or *trans*-4-*t*-butylcyclohexyl *p*-toluenesulfonate with sodium phenoxide in acetone at 80°C for 20.9 hr (for the reaction of the *cis*-tosylate) or 17.3 hr (for the *trans*-tosylate). After working up in the usual way, the residual oily material was chromatographed over silica gel (Nakarai, No. II-A. 100—200 mesh). 4-*t*-Butylcyclohexene was eluted by using *n*-hexane as an eluant (see the section describing the preparation of *cis*-4-*t*-butylcyclohexyl phenyl ether).

3-*t*-Butylcyclohexene was prepared by treating 3-bromocyclohexene with *t*-butylmagnesium chloride. The bromination of cyclohexene with *N*-bromosuccinimide, following the method of Ziegler *et al.*,[26] gave 3-bromocyclohexene, bp 71—73°C/29 mmHg, in an 81% yield. The 3-bromocyclohexene was treated with *t*-butylmagnesium chloride by the method of Goering *et al.*[27] to produce 3-*t*-butylcyclohexene, bp 68.5—69°C/29 mmHg, n_D^{25} 1.4579, in a 50% yield (lit, bp 170.5°C/746 mmHg,[27] n_D^{25} 1.4568[27]).

Triethylammonium *p*-Toluenesulfonate and Diethylammonium *p*-Toluenesulfonate were prepared by dissolving slight excess of the corresponding amine and *p*-toluenesulfonic acid (Nakarai reagent-grade, monohydrate) in acetone; then, after the evaporation of the acetone and the excess of amine, the ammonium salts were dried to a constant weight *in vacuo* at 90—100°C.

Sodium Phenoxide was prepared from metallic sodium and phenol in dry toluene. A solution with a slight excess of phenol in toluene was mixed with metallic sodium, and then refluxed. The sodium phenoxide was filtered out, washed with benzene, and then dried *in vacuo* to a constant weight at 100—110°C.

The benzene, phenol, triethylamine, acetone, dimethylformamide, and tetrahydrofuran (each of a reagent grade) were dried and purified by fractional distillation; bps 80.2—80.5°C, 181—182°C, 56.5—56.7°C, 151.5—153°C, and 66.7—66.9°C respectively. The naphthalene (reagent grade) was used without further purification.

***cis*-4-*t*-Butylcyclohexyl Phenyl Ether.** A solution of 3.10 g (0.15 mol) of *trans*-4-*t*-butylcyclohexyl *p*-

16) R. L. Frank, R. E. Berry and O. L. Shotwell, *J. Am. Chem. Soc.*, **71**, 3891 (1949).
17) "Org. Synth." Coll. Vol. III, John Wiley and Sons, New York (1955), p. 181.
18) G. Vavon and M. Barbier, *Bull. Soc. Chim. France*, **4**, 49, 567 (1931).
19) H. Pines and V. Ipatieff, *J. Am. Chem. Soc.*, **61**, 2728 (1939).
20) E. L. Eliel and R. S. Ro, *ibid.*, **79**, 5592 (1957).
21) L. Schmerling, *ibid.*, **69**, 1121 (1947).
22) R. S. Tipson, *J. Org. Chem.*, **9**, 235 (1944).
23) E. L. Eliel and R. S. Ro, *J. Am. Chem. Soc.*, **79**, 5998 (1957).
24) F. C. Whitmore and G. W. Pedlow, *ibid.*, **63**, 758 (1941).
25) L. Mandell and J. M. Brodmann, *J. Org. Chem.*, **31**, 591 (1966).
26) K. Ziegler, A. Späth, E. Schumann and E. Winkelmann, *Ann.*, **551**, 80 (1942).
27) H. L. Goering, R. L. Reeves and H. H. Espy, *J. Am. Chem. Soc.*, **78**, 4926 (1956).

toluenesulfonate in 67 m*l* of an acetone solution of sodium phenoxide (0.396M) was sealed in an ampoule, and then the ampoule was kept at 80°C for 17.3 hr. To the reaction mixture there were then added 120 m*l* of water, 70 m*l* of benzene, and 23 g of sodium chloride. The water layer was extracted several times with benzene, and the combined benzene solutions were washed with a 10% aqueous sodium chloride solution. After drying over anhydrous magnesium sulfate, the benzene solution was concentrated in a rotatory evaporator to give 9.68 g of a brown oil. A part of the brown oil (6.21 g) was chromatographed over 100 g of silica gel (Nakarai, No. II-A. 100—200 mesh). The column was eluted successively with *n*-hexane, *n*-hexane-benzene (4 : 1 by vol), and benzene. The fractions 1—22, obtained using *n*-hexane, gave 342 mg of 4-*t*-butylcyclohexene (37.3% yield); bp 49—50°C/14 mmHg, n_D^{20} 1.4597, n_D^{30} 1.4569 (lit, bp 65—66°C/20 mmHg,[2] n_D^{20} 1.4583,[2] 1.4581[28] and 1.4587[29]). The fractions 24—30, obtained using *n*-hexane-benzene (4 : 1 by vol), gave 465 mg of *cis*-4-*t*-butylcyclohexyl phenyl ether (30.2% yield); bp 88—90°C/0.13 mmHg, n_D^{30} 1.5093.

Found: C, 82.88; H, 10.34%. Calcd for $C_{16}H_{24}O$: C, 82.70; H, 10.41%.

The fractions 31—40, obtained using benzene, gave 90.9 mg of 4-*t*-butylcyclohexylphenol.

***trans*-4-*t*-Butylcyclohexyl Phenyl Ether.** *trans*-4-*t*-Butylcyclohexyl phenyl ether was prepared by the reaction of *cis*-4-*t*-butylcyclohexyl *p*-toluenesulfonate with sodium phenoxide in acetone at 80°C for 20.9 hr. The *trans*-ether was separated as has been described in the case of the *cis*-ether; it melted at 71—72°C after recrystallization from *n*-hexane.

Found: C, 82.96; H, 10.50%. Calcd for $C_{16}H_{24}O$: C, 82.70; H, 10.41%.

***trans*-3-*t*-Butylcyclohexyl Phenyl Ether.** *trans*-3-*t*-Butylcyclohexyl phenyl ether was prepared by treating *cis*-3-*t*-butylcyclohexyl *p*-toluenesulfonate with sodium phenoxide in dimethylformamide at 90°C. A mixture of 3.10 g (0.01 mol) of *cis*-3-*t*-butylcyclohexyl *p*-toluenesulfonate and 100 m*l* of a solution of sodium phenoxide (0.215M) in dimethylformamide was kept at 90°C for 17 hr in a glass-stoppered, round-bottomed 200-m*l* flask. After 900 m*l* of water had been added to the reaction mixture, the mixture was extracted with 100-m*l* portions of ether. The ether extracts were washed successively with a 10% aqueous sodium chloride solution, a 10% aqueous sodium hydroxide solution, and a 10% aqueous sodium chloride solution until the washings became neutral to litmus. After drying over anhydrous magnesium sulfate, the ether was removed by rotatory evaporation to give 1.70 g of a brown oil as a residue; this was chromatographed using an elution column packed with 50 g of silica gel (Nakarai, No. II-A. 100—200 mesh). The column was eluted successively with *n*-hexane, *n*-hexane-benzene (7 : 3 by vol), and benzene, 20-m*l* portions being taken. The fractions 1—7, obtained using *n*-hexane, gave 615 mg of *t*-butylcyclohexene (46.7% yield); bp 64°C/18 mmHg. Analysis by GLC indicated two components with retention times of 22.3 min (authentic 3-*t*-butylcyclohexene, 22.7 min) and 25.6 min (authentic 4-*t*-butylcyclohexene, 25.5 min). The fractions 8—16, obtained using *n*-hexane-benzene (7 : 3 by vol), gave 612 mg of *trans*-3-*t*-butylcyclohexyl phenyl ether (26.4% yield); bp 105°C/0.3 mmHg, n_D^{20} 1.5110, n_D^{30} 1.5091.

Found: C, 82.74; H, 10.59%. Calcd for $C_{16}H_{24}O$: C, 82.70; H, 10.41%.

The fractions 21—28, obtained using benzene, gave 63 mg of 3-*t*-butylcyclohexylphenol.

***cis*-3-*t*-Butylcyclohexyl Phenyl Ether.** *cis*-3-*t*-Butylcyclohexyl phenyl ether was prepared by treating *trans*-3-*t*-butylcyclohexyl *p*-toluenesulfonate with sodium phenoxide in dimethylformamide at 90°C for 16.5 hr. The *cis*-3-ether was separated in a manner similar to that described in the case of the *trans*-3-ether; bp 105°C/0.3 mmHg (27.1% yield).

Found: C, 82.72; H, 10.52%. Calcd for $C_{16}H_{24}O$: C, 82.70; H, 10.41%.

Gas-Liquid Chromatography of *t*-Butylcyclohexyl Derivatives. *A) Analysis of t-Butylcyclohexenes.* A complete separation was achieved on a column (5 m) packed with 30 wt% polyethylene glycol 6000 on selite 545 (Yanagimoto Co.), at 80°C using hydrogen as the carrier gas (60 m*l*/min). Analysis was carried out using peak-height and half-width measurements. The retention times of the three olefins are summarized in Table 5.

Table 5. Retention times of *t*-butylcyclohexenes

	1-*t*-Butyl-cyclohexene	3-*t*-Butyl-cyclohexene	4-*t*-Butyl-cyclohexene
Retention time (min)	20.1[a]	22.7	25.5

a) The retention time of the first peak which was showed by g.l.c. examination for the mixture of *t*-butylcyclohexenes, prepared by treating 4- or 3-*t*-butylcyclohexene with *N*-lithioethylenediamine in ethylenediamine solution at 100—110°C for 3 hr. It had been confirmed by Campbell *et al.* (N. C. G. Campbell, J. R. P. Clark, R. R. Hill, P. Oberhänsli, J. H. Parish, R. M. Southan and M. C. Whiting, *J. Chem. Soc., B*, **1968**, 349) that this first peak corresponds to 1-*t*-butylcyclohexene.

B) Analysis of t-Butylcyclohexyl Phenyl Ethers. All the gas-liquid chromatographical studies of the isomeric *t*-butylcyclohexyl phenyl ethers were made at 200°C (column and detector temperature). A coiled column was made of 4-mm-i. d. × 2-m annealed copper tubing packed with 20% apiezon grease L on neosorb NC (60—80 mesh: Nishio Co.). Hydrogen was used as the carrier gas (50 m*l*/min). Benzene solutions (15—25 μ*l*) of *t*-butylcyclohexyl phenyl ethers (5 wt%) were then injected. The retention times of the four ethers are summarized in Table 6. It was difficult to separate the *cis*-4- and *cis*-3-isomers.

Table 6. Retention times of *t*-butylcyclohexyl phenyl ethers

	trans-3	*cis*-3	*cis*-4	*trans*-4
Retention time (min)	15.4	17.9	17.9	22.3

28) J. H. Simous and A. C. Meunier, *ibid.*, **65**, 1269 (1943).

29) J. Sicher, F. Sipos and M. Tichy, *Collect. Czech. Chem. Commun.*, **26**, 837 (1961).

Thin-Layer Chromatography of *t*-Butylcyclohexyl Phenyl Ethers. A mixture of the *cis*-4-ether and *cis*-3-ether, the separation of which was not successful by means of GLC, was separated by TLC on silica gel GF 254 (E. Merck, Darmstadt) using *n*-hexane - benzene (9 : 1 by vol) as the developing solvent, the spots being detected by means of a UV lamp. In this case, we did not succeed in separating a mixture of the *trans*-4- and *cis*-3-(equatorial) isomers or the *trans*-3- and *cis*-4-(axial) isomers. The R_f values of the *t*-butylcyclohexyl phenyl ethers are listed in Table 7.

Table 7. R_f values of *t*-butylcyclohexyl phenyl ethers

	trans-3	*cis*-3	*cis*-4	*trans*-4
R_f Value	0.54—0.66	0.41—0.51	0.56—0.66	0.35—0.46

On the basis of these results, it can be concluded that the composition of a mixture of four ethers could be analyzed according to the analysis scheme presented above.

Rate Measurements. *A) Solvolysis in a Phenol-benzene Mixture.* A sealed-ampoule technique was employed. The reaction mixture was prepared by mixing a weighed amount of the tosylate and the solution of triethylamine (of a known concentration) in a phenol-benzene mixture at room temperature. Each ampoule contained 1 m*l* of an aliquot of the reaction mixture. The thermostat was controlled to ±0.05 at 75°C. After reaction for appropriate lengths of time, the content of the ampoule was run into acetic acid. The unchanged triethylamine was titrated with a 0.05N perchloric acid solution in acetic acid, with crystal violet as the indicator. The infinity titers were determined after at least ten half-lives. The rate constant was calculated graphically by a plot of $\log a/(a-x)$ against the time. The rate data are shown in Table 1.

B) Solvolysis in Phenol. A weighed amount of *trans*-4-*t*-butylcyclohexyl *p*-toluenesulfonate and an aliquot of a solution of a known concentration of triethylamine in melted phenol were placed in a measuring flask placed in a thermostated bath kept at 75.0±0.05°C. At appropriate time intervals, aliquot portions (1.000 m*l*) were pipetted into 5 m*l* of cold acetic acid; the solutions were then titrated according to the method described in section A. The rate constant was calculated from the first-order rate equation by a graphical method, the results being illustrated in Table 1.

Phenolyses of *cis*- and *trans*-4-*t*-Butylcyclohexyl *p*-Toluenesulfonates in a 50 wt% Phenol-Benzene Solvent in the Presence of Triethylamine. The results of the phenolyses of *cis*- and *trans*-4-*t*-butylcyclohexyl *p*-toluenesulfonates in a 50 wt% phenol-benzene solvent are summarized in Table 2. The details of the procedures can be illustrated by the following description of the phenolysis of *trans*-4-*t*-butylcyclohexyl *p*-toluenesulfonate.

A weighed amount (65 m*l*) of a 50 wt% phenol-benzene mixture containing triethylamine (0.106M) was preheated in a glass-stoppered, round-bottomed 100-m*l* flask at 75±0.05°C for 20 min; then *trans*-4-*t*-butylcyclohexyl *p*-toluenesulfonate (1.989 g) was added in one portion. After 18.7 hr (13 half-lives), the reaction mixture was diluted with 120 m*l* of ether and extracted with five 50-m*l* portions of a 10% aqueous sodium hydroxide solution. The organic layer was washed successively with 50 m*l* of a 10% aqueous sodium chloride solution, two 50-m*l* of a 10% aqueous hydrochloric acid solution, and three 50-m*l* portions of a 10% aqueous sodium chloride solution until the washings became neutral to litmus. The ether solution was then dried with anhydrous magnesium sulfate and the solvent removed by fractional distillation to give *ca.* 1 g of an oily material; this material was chromatographed using an elution column packed with 25 g of silica gel (Nakarai, No. II-A. 100—200 mesh). The column was eluted successively with *n*-hexane, *n*-hexane - benzene (7 : 3 by vol), and benzene, 20-m*l* portions being taken.

The fractions 2—5, obtained using *n*-hexane, gave 642 mg of *t*-butylcyclohexene (bp 68—69°C/29 mmHg; 72.5% yield); this substance showed, when submitted to GLC, three peaks with retention times of 20.0 min (authentic 1-*t*-butylcyclohexene, 20.1 min), 22.3 min (authentic 3-*t*-butylcyclohexene, 22.7 min), and 25.9 min (authentic 4-*t*-butylcyclohexene, 25.5 min). The composition analysis was carried out by peak-height and half-width measurements, giving the following results: 1-olefin, 0.6%; 3-olefin, 4.1%; 4-olefin, 95.3%. The fractions 9—17, obtained using *n*-hexane - benzene (7 : 3 by vol), gave 137 mg of *t*-butylcyclohexyl phenyl ether (9.4% yield). The GLC of this material showed three peaks, with retention times of 15.6 min (authentic *trans*-3-ether, 15.4 min), 18.4 min (a mixture of *cis*-3- and *cis*-4-ethers), and 22.3 min (authentic *trans*-4-ether, 22.3 min). The analysis by peak-height and half-width measurements gave 12.8%, 74.3% and 12.9% for the respective peaks. Then, the rest of the resulting phenyl ether was separated by TLC on a silica-gel layer (GF 254 E. Merck, 1 mm), using *n*-hexane - benzene (9 : 1 by vol) as the developing solvent; the spots were detected by means of a UV lamp. A mixture of the phenyl ethers (A) (*cis*-4+*trans*-3) was extracted from the layer of the R_f=0.54—0.66 by the use of benzene; another mixture of the phenyl ethers (B) (*cis*-3+*trans*-4) was similarly collected from the layer of the R_f=0.37—0.50. These ether mixtures were submitted directly to the GLC; from each mixture (A or B), two peaks were observed. The retention times were 15.4 min (authentic *trans*-3-ether, 15.4 min) (15.6%) and 18.2 min (authentic *cis*-4-ether, 17.9 min) (84.4%) for A, and 17.8 min (authentic *cis*-3-ether, 17.9 min) (30.7%) and 22.3 min (authentic *trans*-4-ether, 22.3 min) (69.3%) for B. From these results, the composition of the resulting *t*-butylcyclohexyl phenyl ether was calculated to be as follows: *trans*-3-ether, 12.8%; *cis*-3-ether, 5.1%; *cis*-4-ether, 69.2%; *trans*-4-ether, 12.9%. The fractions 20—36, obtained using benzene, gave 64.3 mg of *t*-butylcyclohexylphenol (4.4% yield); the infrared spectrum in chloroform had characteristic bands in the hydroxylic regions: ν_{max} 3700 cm^{-1} and 3500 cm^{-1}, due to nonbonded OH and bonded OH respectively. No attempt was made to determine the composition of this *t*-butylcyclohexylphenol.

The Phenolyses Conducted in the Presence of Added *t*-Butylcyclohexene. The results of the phenolyses of *cis*- and *trans*-4-*t*-butylcyclohexyl *p*-toluenesulfonates in 50 wt% phenol-benzene, in the presence of added *t*-butylcyclohexene and triethylamine at 75°C are summarized in Table 3.

A weighed amount of a 50 wt% phenol-benzene

solvent, containing triethylamine and *t*-butylcyclohexene, was preheated in a glass-stoppered flask at 75°C for 20 min. The products were isolated and separated in a manner similar to that described in the preceding section. The composition analyses of the olefin and the phenyl ether were conducted by GLC and by the combined use of GLC and TLC respectively, as has been described above.

Phenolyses Conducted in the Presence of Added Triethylammonium or Diethylammonium *p*-Toluenesulfonate. The results of the phenolyses of *cis*- and *trans*-4-*t*-butylcyclohexyl *p*-toluenesulfonates in a 50 wt% phenol-benzene solvent in the presence of initially-added triethylamine and triethylammonium (or diethylammonium) *p*-toluenesulfonate at 75.0°C are shown in Table 4. The following description of the phenolysis of *cis*-4-*t*-butylcyclohexyl *p*-toluenesulfonate in the presence of triethylamine and triethylammonium *p*-toluenesulfonate will serve to illustrate the details of the procedure.

A two-necked, round-bottomed 200-m*l* flask, placed in a dry box, was charged with 120 m*l* of a 50 wt% phenol-benzene solvent containing 0.105M triethylamine, and 3.31 g of triethylammonium *p*-toluenesulfonate (0.101M). Then the mixture was preheated at 75.0± 0.05°C for 20 min. To this mixture there was added a 3.69-g portion of *cis*-4-*t*-butylcyclohexyl *p*-toluenesulfonate (0.0990M), and then the reaction vessel was kept in a thermostated bath for 57 min. The reaction mixture was cooled in an ice bath to room temperature. The titration of 1 m*l* of an aliquot with a standard 0.05N perchloric acid solution in acetic acid, using crystal violet as the indicator, showed that phenolysis proceeded up to 75.5% completion.

A 200-m*l* portion of ether was added to the reaction mixture; the ether solution was extracted with seven 50-m*l* portions of a 20% aqueous sodium hydroxide solution which had been cooled in ice water. The ether layer was washed with a 10% aqueous hydrochloric acid solution and a 10% aqueous sodium chloride solution successively, and then dried over anhydrous magnesium sulfate. The dried ether solution was concentrated using an efficient fractionating column; during this period the bath temperature was kept below 55°C. The residual benzene solution was concentrated in a rotatory evaporator equipped with an ice-sodium chloride trap to give *ca.* 1.9 g of a colorless liquid as the residue and *ca.* 45 m*l* of a condensate in the trap. The colorless residual liquid was then condensed further under 4 mmHg at 50°C in a rotatory evaporator equipped with a dry ice-methanol trap. A wet, pale yellow crystal (0.982 g) was recovered as the residue, and in the trap 0.906 g of a colorless liquid condensed. This liquid was analyzed by GLC (5-m column, 30% PEG 6000 on selite 545 at 80°C; the same analytical conditions as that of olefin). There were observed four peaks with retention times of 1.9 min (benzene), 20.6 min (authentic 1-*t*-butylcyclohexene, 20.1 min) (a trace), 22.7 min (authentic 3-*t*-butylcyclohexene, 22.7 min) (1.2%), and 26.7 min (authentic 4-*t*-butylcyclohexene, 25.5 min) (98.8%).

The recovered pale yellow crystal, which was a mixture of phenolysis products other than olefin, was treated with sodium naphthalene in tetrahydrofuran in order to cleave the unchanged tosylate into the corresponding alcohol. In a 100-m*l* four-necked flask, equipped with a mechanical stirrer, a thermometer, a dropping funnel and a calcium chloride tube, there were successively placed 1.62 g (0.0127 mol) of naphthalene, 38 m*l* of purified THF and 0.280 g of metallic sodium, which had been cut in small pieces, under a nitrogen atmosphere and at room temperature. The mixture was stirred for 1 hr to produce a dark green solution of sodium naphthalene. Then the reaction vessel was cooled in an ice bath, and a solution of 0.800 g of pale yellow crystal in 8 m*l* of THF was added to the sodium naphthalene solution over a period of 0.8 min (reaction temperature, 0—4°C). The sodium naphthalene solution was then immediately decomposed by the addition of aqueous THF. The reaction mixture was treated with 50 m*l* of water and 15 g of sodium chloride. The water layer was extracted with three 20-m*l* portions of ether, and the combined ether extracts were washed with a 10% aqueous sodium chloride solution and then dried with anhydrous magnesium sulfate. The ether was removed by means of a rotatory evaporator to give 2.0 g of a crystalline material, which was chromatographed using an elution column packed with 60 g of silica gel (Nakarai, No. II-A. 100—200 mesh). The column was eluted successively with *n*-hexane, *n*-hexane-benzene (1 : 1 by vol), benzene, *n*-hexane-ether (9 : 1 by vol), and *n*-hexane-ether (4 : 1 by vol), 50-m*l* portions being taken. The fractions 1—12, obtained using *n*-hexane, gave 1.39 g of naphthalene. The fractions 14—17, obtained using *n*-hexane-benzene (1 : 1 by vol), gave 191.3 mg of *t*-butylcyclohexyl phenyl ether (11.6% yield), contained in the phenolysis products (it was confirmed by means of a control experiment that *t*-butylcyclohexyl phenyl ether was not affected during the cleavage reaction). The composition of the resulting *t*-butylcyclohexyl phenyl ether was determined following the analysis scheme described above: *trans*-4-ether, 60.9%; *cis*-4-ether, 19.5%; *cis*-3-ether, 7.5%; *trans*-3-ether, 12.1%. The fractions 20—22, obtained using benzene, gave 34.4 mg of *t*-butylcyclohexylphenol (2.1% yield), the infrared spectrum of which in chloroform had characteristic bands at 3700 cm^{-1} and 3500 cm^{-1}. No attempt was made to determine the composition of this material.

The fractions 33—36, obtained using *n*-hexane-ether (9 : 1 by vol), gave *t*-butylcyclohexanone, while the fractions 37—50, obtained using *n*-hexane-ether (4 : 1 by vol), gave *t*-butylcyclohexanol (products of the cleavage reaction). The details of the analyses of these materials will be reported in a subsequent paper.

BULLETIN OF THE CHEMICAL SOCIETY OF JAPAN VOL. 42 3298—3305 (1969)

Phenolytic Rearrangement and Isomerization of *cis*- and *trans*-4-*t*-Butylcyclohexyl *p*-Toluenesulfonates in a Phenol-Benzene Solvent*1

Kunio Okamoto, Seiki Saitô and Haruo Shingu

Department of Hydrocarbon Chemistry, Faculty of Engineering, Kyoto University, Sakyo-ku, Kyoto

(Received May 15, 1969)

As the first examples of solvolytic *cis-trans* isomerization and 1,2-rearrangement for the 4-*t*-butylcyclohexyl system, phenolytic *cis-trans* (or *trans-cis*) isomerization and 1,2-rearrangement have been found for *cis*- and *trans*-4-*t*-butylcyclohexyl *p*-toluenesulfonates in the phenol-benzene (1 : 1 by wt) solvent at 75.0°C. The tosylate, recovered after a 75% completion of the S_N1 phenolysis of the *cis*-4-tosylate, was composed of small amounts of the *trans*-4-tosylate (1%) and the *cis*-3-tosylate (11%), besides 88% of the starting *cis*-4-tosylate, clearly indicating occurrence of both the *cis-trans* isomerization and the 1,2-rearrangement of the starting *cis*-4-tosylate. In a similar fashion, starting from the *trans*-4-tosylate, small amounts of the *cis*-4-tosylate (0.7%) and the *trans*-3-tosylate (2.6%) were recovered from the tosylate after the S_N1 phenolysis was 75% complete. On the basis of the results of an examination into the influence of the added tosylate anion on the extent of isomerization and of rearrangement, it has been suggested that the *cis-trans* or *trans-cis* isomerization results largely from the external S_N2-like attack of the tosylate anion on the S_N1 ion-pair intermediate and partly as a consequence of the rotation of the *t*-butylcyclohexyl cation within the ion-pair intermediate, whereas the 1,2-rearrangement proceeds through an intramolecular 1,2-shift of hydrogen within the 4-*t*-butylcyclohexyl cation.

After the initial work of Winstein and Holness,[1] the solvolytic reactions of 4-*t*-butylcyclohexyl *p*-toluenesulfonates have been investigated by several other workers.[2-4] In these solvolyses, *t*-butylcyclohexene was the major product, while minor amounts of substitution, products were obtained as side products; as a general trend, both the olefin and the substitution product contained a considerable amount of rearranged isomers. In view of the formation of so many rearranged products, we have previously suggested[4] the possibility of the accumulation of rearranged tosylates during the course of the solvolysis of a *t*-butylcyclohexyl tosylate, since the isomerized or rearranged solvolysis intermediate, which produced an isomerized or rearranged product, will also give an isomerized or rearranged tosylate by the course of return.

In this paper, we will report on the results of the examination of such a possibility for the phenolytic *cis-trans* isomerization and the 1,2-rearrangement of *cis*-4- and *trans*-4-tosylates, and will discuss the implications of the results with the structure of the ion-pair intermediate for this system.

Results and Discussion

Recovery and Analysis of the Mixture of *t*-Butylcyclohexyl *p*-Toluenesulfonates. The phenolyses of *cis*- and *trans*-4-*t*-butylcyclohexyl *p*-toluenesulfonates were conducted in the presence of triethylamine in a 50 wt% phenol-benzene solvent at 75°C up to 75% completion. After washing with dilute aqueous sodium hydroxide and the subsequent condensation of the organic layer under reduced pressure at room temperature, the residue was treated with sodium naphthalene in THF in order to cleave the tosylate and obtain the corresponding *t*-butylcyclohexanol. The mixture of *t*-butylcyclohexanols was isolated by elution chromatography, and the composition was assayed according to the following scheme:

*1 Presented at the 18th Symposium on the Organic Reaction Mechanism, Kyoto, October, 1967 (Abstract, p. 81) and at the 21st Annual Meeting of the Chemical Society of Japan, Osaka, April, 1968 (Abstract, Part III, p. 2034).

1) S. Winstein and N. J. Holness, *J. Am. Chem. Soc.*, **77**, 5562 (1955).

2) V. J. Shiner, Jr., and J. G. Jewett, *ibid.*, **87**, 1382, 1383 (1965).

3) N. C. G. Campbell, D. M. Muir, R. R. Hill, J. H. Parish, R. M. Southan and M. C. Whiting, *J. Chem. Soc., B*, **1968**, 355.

4) K. Okamoto, S. Saitô and H. Shingu, This Bulletin, **42**, 3288 (1969).

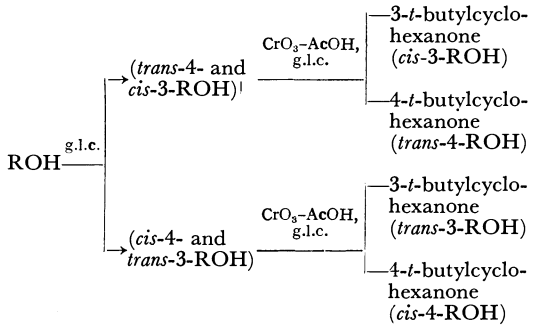

First, the mixture was separated by GLC into two fractions, *i. e.*, a mixture of the *trans*-4- and *cis*-3-alcohols and a mixture of *cis*-4- and *trans*-3-alcohols; then each fraction was oxidized by means of chromium trioxide in acetic acid, giving a mixture of 3- and 4-*t*-butylcyclohexanones, which was then assayed by GLC.

The reductive cleavage of the tosylates with sodium naphthalene was first reported by Closson, Wriede and Bank[5] as an almost ideal procedure for obtaining the alcohols without isomerization. However, the data for the *t*-butylcyclohexyl system have not been made available. Therefore, we examined the degree of isomerization for the *cis*-4-, *trans*-4-, *cis*-3-, and *trans*-3-tosylates in a series of experiments with the authentic tosylates; the results are summarized in Table 1.

From the *trans*-4- and *cis*-3-tosylates obtained under the reaction conditions shown in Table 1, the *t*-butylcyclohexanol contained no isomerized alcohols, whereas the *cis*-4- and *trans*-3-tosylates afforded the respective alcohols contaminated with a small quantity of isomerized alcohols, even though the cleavage was conducted at −1—2°C. The percentage of isomerization observed in the control experiments of *cis*-4- and *trans*-3-tosylates was used as a correction factor for the analysis of the tosylate mixture recovered from the phenolytic products.

Composition of the Tosylate Recovered from the Reaction Mixture for the Phenolysis of *cis*-4-*t*-Butylcyclohexyl *p*-Toluenesulfonate. The phenolysis of *cis*-4-*t*-butylcyclohexyl *p*-toluenesulfonate was carried out in the presence of an equimolar amount of triethylamine in a 50 wt% phenol-benzene solvent at 75°C up to 75% completion. A mixture of the phenolysis products and the unchanged tosylate was isolated from the phenolysis mixture, then cleaved with sodium naphthalene in THF, and subsequently separated into *t*-butylcyclohexanol and the phenolysis products by elution chromatography. The phenolysis products were not affected under the cleavage conditions.[6] The mixture of *t*-butylcyclohexanols was assayed following the scheme described above.

As is summarized in Table 2, the cleavage reaction of the recovered tosylate afforded the corresponding alcohol in a fairly good yield; the *t*-butylcyclohexanol was composed of a large portion (88—89%) of the *cis*-4-alcohol and small amounts of the *cis*-3-alcohol (10%) and the *trans*-4-alcohol (1%). This result clearly indicates that, during the phenolysis of the *cis*-4-tosylate in a phenol-benzene solvent, *cis-trans* isomerization and 1,2-rearrangement did occur.

In a previous paper[4] we reported that, during this phenolysis, the first-order plot gave a slight downward drift after 80% completion. In view of the fact that the solvolysis rates of the *cis*-3- and *trans*-4-tosylates are lower than those of the *cis*-4-tosylate,[1,4] this downward drift may be attributed to an accumulation of the less reactive tosylates in the unchanged tosylate with the progress of the

Table 1. The cleavage of various *t*-butylcyclohexyl *p*-toluenesulfonates with sodium naphthalene in tetrahydrofuran

p-Toluenesulfonate	*trans*-4-ROTs			*cis*-4-ROTs				*trans*-3-ROTs	*cis*-3-ROTs
10^3 mol, used	1.51	1.61	4.20	1.61	1.61	1.94	1.94	1.61	1.65
Na-Naphthalene[a] equivalent	3.00	3.00	3.00	3.00	3.00	3.00	3.00	3.00	3.00
Temp., °C	32—35	32—37	2—6	28—31	0—7	−1—1	−1—1	−1—2	−1—1
Time, min	16	1	3	3	1	0.5	0.5	0.5	0.5
t-Butylcyclohexanol:									
Yield %	100	98.2	96.4	77.7	90.0	89.6	94.4	94.2	81.5
Composition %									
trans-4-ROH	100.0	100.0	100.0	0.9	1.6	1.2	1.7	—	—
cis-4-ROH	0.0	0.0	0.0	99.1	98.4	98.8	98.3	—	—
cis-3-ROH	—	—	—	—	—	—	—	1.4	100.0
trans-3-ROH	—	—	—	—	—	—	—	98.6	0.0

a) 0.30 mol/*l*

5) W. D. Closson, P. Wriede and S. Bank, *J. Am. Chem. Soc.*, **88**, 1581 (1966).

6) The results of the analysis of these phenolysis products were reported in a previous paper.[4]

Table 2. Summary of the cleavage reaction of the recovered tosylate for the phenolysis of *cis*-4-*t*-butylcyclohexyl *p*-toluenesulfonate[a)]

ROTs conversion in the phenolysis	ROTs recovered from the phenolysis mixture[b)]	Ammonium tosylate added to the phenolysis mixture	*t*-Butylcyclohexanol				
			Yield %[c)]	Composition %			
				trans-4-[d)]	*cis*-4-	*cis*-3-	*trans*-3
75.9%	23.6%	—	91.4	1.1	88.3	10.6	0.0
72.8%	23.4%	—	84.9	1.0	88.2	10.8	0.0
75.5%	20.6%	Et_3NHOTs 0.101N	94.6	3.4	86.5	10.1	0.0
74.0%	23.2%	Et_3NHOTs 0.226N	89.5	6.7	82.4	10.9	0.0
86.5%	?[e)]	Et_2NH_2OTs 0.212N	95.3[f)]	4.8	76.8	14.8	0.0

a) The phenolysis was conducted in phenol-benzene (1 : 1 by wt) solvent at 75°C. Initial concentrations are 0.097—0.10M for the tosylate and 0.11M for triethylamine (see Table 4 in Ref. 4).
b) Analyzed by the phenolysis of the sample for the cleavage reaction; the phenyl ethers contained in the sample was not affected under the cleavage condition.
c) Based on the recovered tosylate.
d) Corrected for the *trans*-4-*t*-butylcyclohexanol produced during the cleavage reaction of *cis*-4-*t*-butylcyclohexyl *p*-toluenesulfonate (see text).
e) Not analyzed.
f) Based on the calculated value (13.5%) for the percentage of the recovered tosylate.

reaction.

In order to obtained further information about the mechanism, the phenolysis was conducted in the presence of added triethyl- or diethyl-ammonium *p*-toluenesulfonates; the composition of the tosylate thus recovered was then compared with that observed in the absence of added alkylammonium salt. In Fig. 1 the percentages of *trans*-4- and *cis*-3-tosylates in the recovered tosylate are plotted against the effective concentrations of the *p*-toluenesulfonate anion, which are defined as the sum of the concentration of the added alkylammonium tosylate and one half of the concentration of the tosylate anion liberated until the interruption of the phenolysis.

The amount of the *trans*-4-tosylate in the recovered tosylate increases linearly with an increase in the effective concentration of the tosylate anion in the reaction medium, and, within the range of experimental error, there seems to exist no isomerized tosylate in the absence of the added tosylate anion. In other words, the *cis-trans* isomerization of the *cis*-4-tosylate seems to proceed almost entirely *via* the intermolecular course including the attack of the tosylate anion on the ion-pair S_Ni intermediate, although the possibility of the intramolecular course including the rotation of the carbonium ion

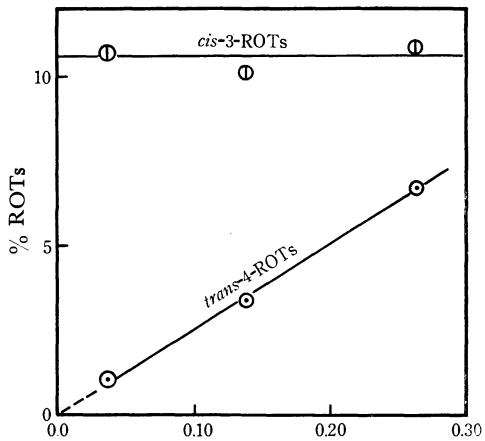

Fig. 1. The percentages of *cis-trans* isomerization and 1,2-rearrangement in the recovered tosylate for the phenolysis of *cis*-4-*t*-butylcyclohexyl *p*-toluenesulfonate in 50 wt% phenol-benzene solvent in the presence of triethylamine at 75°C.

in the ion-pair intermediate can not be entirely eliminated (*vide infra*).

The intramolecular course is illustrated below without considering its reversibility:

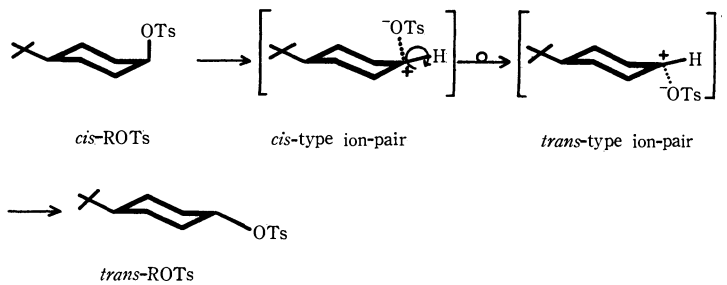

cis-ROTs *cis*-type ion-pair *trans*-type ion-pair

trans-ROTs

As for the intermolecular course, two pathways are possible: one is a direct return of the *cis*-type ion-pair intermediate to the *trans*-tosylate (Course A), and the other is the return *via* the *trans*-type ion-pair intermediate produced by the S_N2-like attack of the tosylate anion on the *cis*-type intermediate (Course B). These two courses may be illustrated as follows:

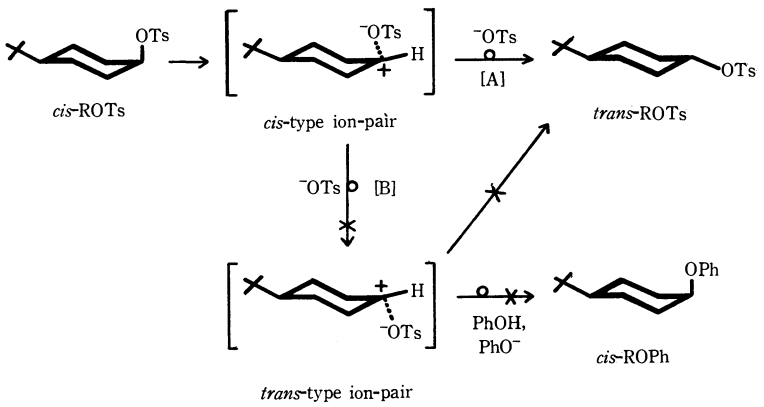

If the concentration of the *trans*-type ion-pair intermediate were increased with the increase in the S_N2-type attack of the tosylate anion on the *cis*-type intermediate (Course B), the portion of *cis*-4-*t*-butylcyclohexyl phenyl ether in the concomitant phenolysis products would also be increased. However, this is not the case; rather, the percentage of the *cis*-4-ether is slightly diminished with the increase in the added $Et_3NH^+OTs^-$.[7] Therefore, the possibility of the B course *via* the *trans*-type intermediate may be excluded.

In contrast to the *cis-trans* isomerization, the 1,2-rearrangement of the *cis*-4-tosylate seems to be little affected by the added tosylate anion (Fig. 1). This clearly indicates that the rearrangement is almost intramolecular in nature. Thus, the rearrangement conceivably proceeds *via* the exchange of the positions of the axial tosylate group and the axial neighboring hydrogen, as is illustrated below:

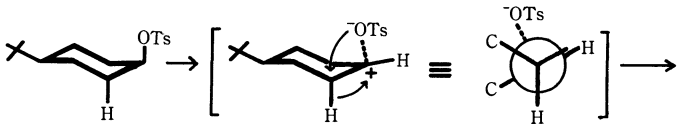

cis-4-ROTs

cis-3-ROTs

As has been mentioned in the previous paper,[4] since the initially-added *t*-butylcyclohexene does not exert any influence on the composition of the olefin product or of the phenyl ethers in the concurrent phenolysis, the possibility of 1,2-rearrangement *via* a proton addition to a stable molecule of *t*-butylcyclohexene can be eliminated. This course is as follows:

cis-4-ROTs

cis-3-ROTs

7) See Table 4 in Ref. 4.

Table 3. Summary of the cleavage reaction of the recovered tosylate for the phenolysis of *trans*-4-*t*-butylcyclohexyl *p*-toluenesulfonate[a)]

ROTs conversion in the phenolysis	ROTs recovered from the phenolysis mixture[b)]	Et_3NHOTs initially added to the phenolysis mixture, N	*t*-Butylcyclohexanol				
			Yield %[c)]	Composition %			
				trans-4-	*cis*-4-	*cis*-3-	*trans*-3-
73.6%	25.2%	—	93.3	96.7	0.7	0.0	2.6
76.6%	23.4%	0.106	84.5	95.5	1.4	0.0	3.1
75.0%	25.0%	0.203	86.3	96.5	1.5	0.0	1.8

a) The phenolysis was conducted in phenol-benzene (1:1 by wt) solvent at 75°C. Initial concentrations are 0.099—0.10M for ROTs and 0.105—0.109N for Et_3N (see Table 4 in Ref. 4).
b) Analyzed by the phenolysis of the sample for the cleavage reaction; the phenyl ethers contained in the sample were not affected under the cleavage condition.
c) Based on the recovered tosylate.

Composition of the Tosylate Recovered from the Reaction for the Phenolysis of *trans*-4-*t*-Butylcyclohexyl *p*-Toluenesulfonate. The phenolysis of *trans*-4-tosylate was conducted in the presence of an equimolar amount of triethylamine in a 50 wt% phenol-benzene solvent at 75°C up to 75% completion. In a manner similar to that in the case of the *cis*-tosylate, *t*-butylcyclohexanol was isolated from the reaction mixture of the cleavage reaction of the recovered tosylate; it was assayed following the scheme described above.

As is shown in Table 3, the *t*-butylcyclohexanol was composed of a large amount (97%) of the *trans*-4-alcohol, derived from the starting *trans*-4-tosylate, and small amounts of the *cis*-4-alcohol (0.7%) and the *trans*-3-alcohol (2.6%). This indicates that, in a fashion similar to that in the case of the *cis*-4-tosylate, *trans-cis* isomerization and 1,2-rearrangement occur during the phenolysis of *trans*-4-tosylate, although the extent of isomerization and of rearrangement is smaller when compared with the case of the *cis*-4-tosylate.

The percentages for the isomerization and the rearrangement are set against the effective concentrations (*vide supra*) of the tosylate anion in the reaction medium in Fig. 2.

The extents of the *trans-cis* isomerization are not much affected by the increase in the effective concentrations of the tosylate anion, and there seems to exist a definite, though small, amount of *trans-cis* isomerization even in the absence of the tosylate anion. Therefore, it is conceivable that, for the *trans-cis* isomerization, there exist both the intramolecular and the intermolecular courses and that the latter course becomes predominant with the increase in the concentration of the tosylate anion. These courses are illustrated below.

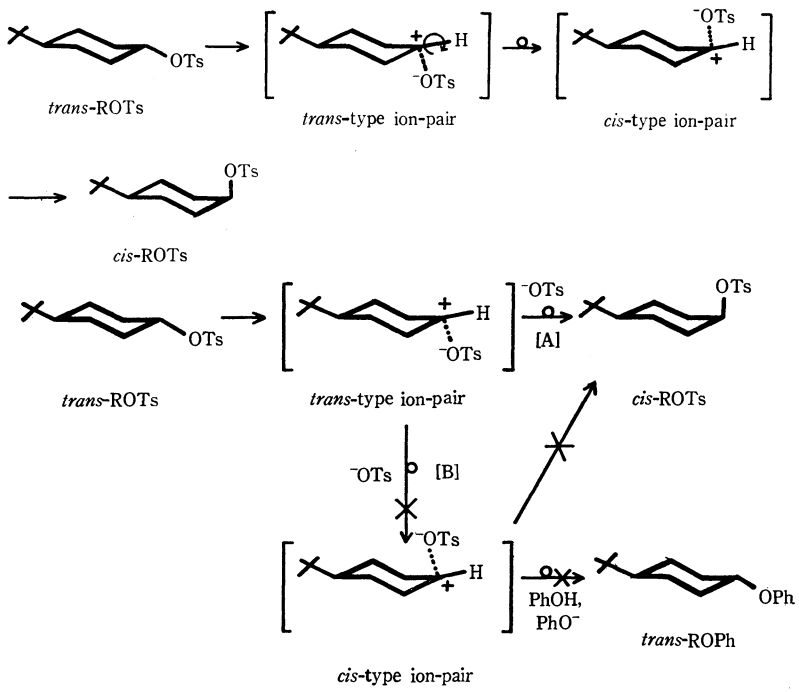

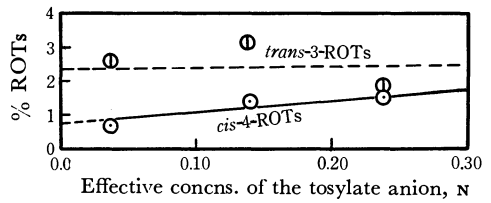

Fig. 2. The percentage of *trans-cis* isomerization and 1,2-rearrangement in the recovered tosylate for the phenolysis of *trans*-4-*t*-butylcyclohexyl *p*-toluenesulfonate in 50 wt% phenol-benzene solvent in the presence of triethylamine at 75°C.

As has been mentioned above, the intramolecular course for the *cis-trans* isomerization of the *cis*-tosylate was not observed within the range of experimental error. However, in view of the existence of the intramolecular course in the *trans-cis* isomerization, the intramolecular course should exist also in the case of the *cis*-tosylate isomerization, judging from the microscopic reversibility, as is shown below:

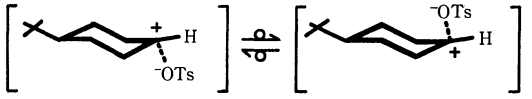

trans-type ion-pair *cis*-type ion-pair

Therefore, the apparent absence of the intramolecular course for the *cis-trans* isomerization may be attributed to the relative rapidity of the rate of the intermolecular isomerization, *i.e.*, the rate of attack of the tosylate anion on the *cis*-type ion-pair, as compared with the rate of intermolecular isomerization, *i.e.*, the rate of the internal rotation of the 4-*t*-butylcyclohexyl cation in the *cis*-type ion-pair intermediate.

In view of the fact that the portions of *trans*-4-*t*-butylcyclohexyl phenyl ether in the products of the concomitant phenolysis decrease with an increase in the concentration of the added tosylate anion,[6] it is conceivable that the concentration of the *cis*-type ion-pair intermediate does not increase with the increase in the added tosylate anion. Consequently, the course to the *cis*-4-tosylate *via* the *cis*-type ion-pair intermediate (Course B) may be excluded.

The extent of 1,2-rearrangement for the *trans*-tosylate changes non-linearly with the increase in the effective concentration of the tosylate anion, this being shown in Fig. 2. A thorough interpretation of this trend would be difficult. However, there seems to exist no definite tendency of increase with the increase in the concentration of the tosylate anion. Consequently, we may conceive this 1,2-rearrangement to be intramolecular in nature.

Since the tosyl-group and the neighboring equatorial hydrogen atom are in the *syn*-position in the chair conformation of the ion-pair intermediate from the *trans*-4-tosylate, it seems to be rather difficult for them to exchange their positions with each other, this being illustrated as follows:

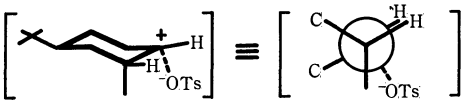

However, if a twist boat conformation is assumed for the *t*-butylcyclohexyl cation, as was first suggested in the case of the solvolysis in 50% aqueous ethanol by Shiner and Jewett,[2] a facile exchange of the two groups would be achieved because of their *anti*-position. This is illustrated as follows:

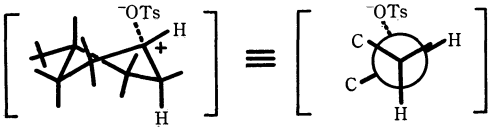

As in the case of the *cis*-tosylate, the initially added *t*-butylcyclohexenes exerted little influence on the composition of the olefin product or of the phenyl ethers in the concomitant phenolysis.[4] Thus, the possibility of 1,2-rearrangement *via* a proton addition to a stable molecule of *t*-butylcyclohexene can be excluded for the *trans*-tosylate.

The results presented in this paper clearly suggest the possibility of the solvolytic rearrangement or isomerization of the 4-*t*-butylcyclohexyl system in a solvent other than phenol. The details of the examination of the other solvents will be reported in a succeeding paper.

Experimental[8]

Materials. The *t*-butylcyclohexanols (*cis*-4, *trans*-4, *cis*-3 and *trans*-3), *t*-butylcyclohexyl tosylates (*cis*-4, *trans*-4, *cis*-3 and *trans*-3), 3- and 4-*t*-butylcyclohexanones, and triethylammonium and diethylammonium tosylates were synthesized as described in a previous paper.[4] Benzene, phenol, triethylamine, and tetrahydrofuran (each of a reagent grade) were dried and purified by fractional distillation: benzene, bp 80.2—80.5°C; phenol, bp 181—182°C; triethylamine, bp 89—89.8°C; tetrahydrofuran, bp 66.7—66.9°C. The naphthalene (reagent grade) was used without further purification.

Gas-liquid Chromatography of *t*-Butylcyclohexanols. The gas-liquid chromatography of isomeric *t*-butylcyclohexanols was performed on a 2 m×4 mm copper-tubing column packed with 30 wt% PEG 6000 on selite (80—100 mesh) at 150°C, and the hydrogen flow rate was adjusted to 60 ml/min; benzene solutions (15—25 μl) of *t*-butylcyclohexanols (5—10 wt%) were injected. Retention times: *cis*-4-OH, 18.0 min; *trans*-4-OH, 20.5 min; *cis*-3-OH, 20.3 min; *trans*-3-OH, 17.9 min. We could not separate the mixture of the *trans*-4- and

8) The melting points are not corrected. The infrared spectra were determined with a Shimadzu Model IR-27 spectrophotometer. All the GLC studies were made with a Shimadzu Model GC-2B dual-column gas chromatograph.

cis-3- (equatorial) isomers or the mixture of the *trans*-3- and *cis*-4- (axial) isomers under these conditions.

Gas-liquid Chromatography of *t*-Butylcyclohexanones. A mixture of 3- and 4-*t*-butylcyclohexanones was separated on a 2-m column packed with 30% PEG 6000 on selite at 110°C, using hydrogen as the carrier gas (70 ml/min). Benzene solutions (40—50 μl) of ketones (5 wt%) were injected. The retention times of the 3- and 4-*t*-butylcyclohexanones were 51.9 min and 56.8 min respectively; calibration was carried out with ketones of known compositions.

Analysis of *t*-Butylcyclohexanols. Mixtures of the *cis*-4- and *trans*-3-alcohols and of the *trans*-4- and *cis*-3-alcohols were separated gas-chromatographically, using a 5-m column and two liquid-nitrogen traps; then each fraction was converted into a mixture of 3- and 4-ketones by treating it with chromium trioxide in acetic acid according to the method of Winstein and Holness.[1] This 3- and 4-ketone mixture was gas-chromatographically analyzed. The calibration was performed by the oxidation of mixtures of the respective alcohols of known compositions.

The Cleavage of *t*-Butylcyclohexyl *p*-Toluenesulfonates into the Parent Alcohols Using Sodium Naphthalene in Tetrahydrofuran. *A) Cleavage of trans-4-t-Butylcyclohexyl p-Toluenesulfonate.* In 100-ml four-necked flask, equipped with a mechanical stirrer, a thermometer, a dropping funnel and a calcium chloride tube, there were placed successively 3.42 g (0.0267 mol) of naphthalene, 84 ml of THF, and 0.580 g of matallic sodium, which has been cut in small pieces, all under a nitrogen atomosphere at room temperature. The mixture was then stirred for 1 hr to produce a dark green solution of sodium naphthalene.

To this sodium naphthalene solution there was added a solution of 1.30 g (0.0042 mol) of the *trans*-4-tosylate in 7 ml of THF at 0°C through a dropping funnel over a period of 1 min. Then, the sodium naphthalene solution was immediately decomposed by the addition of aqueous THF. The reaction mixture was treated with 100 ml of water and 30 g of sodium chloride. The water layer was extracted with three 50-ml portions of ether, and the combined ether extracts were washed with 10% aqueous sodium chloride solution and then dried over anhydrous magnesium sulfate. The ether solution was concentrated to give 4.0 g of a crystalline material, which was chromatographed over 100 g of silica gel (Nakarai, No. II-A. 100—200 mesh). The column was eluted successively with benzene, *n*-hexane-ether (9 : 1 by vol), *n*-hexane-ether (4 : 1 by vol), and *n*-hexane-ether (1 : 1 by vol), 25-ml portions being taken. The fractions 3—8, obtained using benzene, gave 3.07 g of naphthalene. The fractions 9—16, obtained using *n*-hexane-ether (9 : 1 by vol), did not give anything. The fractions 17—24, obtained using *n*-hexane-ether (4 : 1 by vol), gave 162 mg of a viscous oil the infrared spectrum of which exhibited a strong absorption at 1060 cm^{-1}; no attempt was made to characterize this material further. The fractions 25—31, obtained using *n*-hexane-ether (4 : 1 by vol), gave 67.1 mg of an oily material. The evaporation of this material under 4 mmHg at 80°C gave, in a dry-ice-methanol trap, 4-*t*-butylcyclohexanone (20.6 mg, 3.2% yield; mp 46—49°C; mp 48—51°C on admixture with an authentic sample of 4-*t*-butylcyclohexanone; the infrared spectrum was identical with that of an authentic sample of 4-*t*-butylcyclohexanone). The infrared spectrum of the remaining high-boiling material was identical with that of the viscous oil given by the preceding fractions 17—24. The fractions 48—57, obtained using *n*-hexane-ether (1 : 1 by vol), gave 630 mg of *trans*-4-*t*-butylcyclohexanol (96.4% yield). The GLC analysis of the alcohol of the fraction 48 (27.4 mg) indicated one peak with a retention time of 21.1 min (an authentic *trans*-4-alcohol, 20.5 min). The results of this run are listed in Table 1, along with the results of other runs under different reaction conditions.

B) Cleavage of cis-4-t-Butylcyclohexyl p-Toluenesulfonate. To a sodium naphthalene solution in THF, prepared from 1.50 g (0.0116 mol) of naphthalene, 40 ml of THF, and 0.270 g (0.0116 mol) of metallic sodium, there was added a solution of 0.602 g (0.00194 mol) of the *cis*-4-tosylate in 3 ml of THF at −1—3°C over a period of 0.5 min. Working-up in the usual way gave a residual crystalline material (1.5 g), which was then chromatographed over 50 g of silica gel (Nakarai, No. II-A. 100—200 mesh). The column was eluted successively with benzene, *n*-hexane-ether (4 : 1 by vol), and *n*-hexane-ether (3 : 2 by vol), 25-ml portions being taken. The fractions 1—5, obtained using benzene, 1.39 g of naphthalene. The fractions 12—17, obtained using *n*-hexane-ether (4 : 1 by vol), gave 126.3 mg of a viscous oil from which, by means of the working-up described in section A, 4-*t*-butylcyclohexanone (19.0 mg, 6.4% yield) was collected in the trap. The fractions 18—29, obtained using *n*-hexane-ether (3 : 2 by vol), gave 289.3 mg of 4-*t*-butylcyclohexanol (94.4% yield). Analysis of the alcohol of the fraction 25 by GLC showed one peak corresponding to *cis*-4-*t*-butylcyclohexanol. Analysis of the combined alcohol fractions from 26 to 29 by GLC showed two peaks, corresponding to *cis*- and *trans*-4-*t*-butylcyclohexanol respectively. The percentage of the *trans*-4-alcohol produced during the cleavage reaction of the *cis*-4-tosylate was calculated to be 1.70% of the total alcohol. The results of the cleavage reactions of *cis*-4-tosylate under various reaction conditions are summarized in Table 1.

C) Cleavage of cis- and trans-3-t-Butylcyclohexyl p-Toluenesulfonates. The cleavage reactions for *cis*- and *trans*-3-tosylates were carried out in the same way as above. These results are summarized in Table 1.

D) Cleavage of a Mixture of Tosylates with a Known Composition. A mixture of *cis*-4- (0.339 g), *trans*-4- (0.0723 g), *cis*-3- (0.0306 g), and *trans*-3-tosylates (0.0691 g) was cleaved in the same way as above. A mixture of four isomeric alcohols was obtained in a 90% yield; the analysis of the composition according to the analysis scheme described above gave the following results, after correction for the rearrangement of axial (*cis*-4 and *trans*-3) compounds to equatorial (*trans*-4 and *cis*-3) compounds during the cleavage reaction (see Table 1): *cis*-4, 66.3%; *trans*-4, 14.7%; *cis*-3, 5.0%; *trans*-3, 14.0%. On the other hand, the composition of the starting tosylate mixture was as follows: *cis*-4, 66.3%; *trans*-4, 14.1%; *cis*-3, 6.0%; *trans*-3, 13.5%.

Cleavage of the Tosylate Recovered from the Reaction Mixture for the Phenolysis of *cis*-4-*t*-Butylcyclohexyl *p*-Toluenesulfonate. The phenolysis of *cis*-4-*t*-butylcyclohexyl *p*-toluenesulfonate (3.11 g) in phenol-benzene (1 : 1 by wt) (100 ml) in the presence of triethylamine (0.103N) was conducted following a previously-described method[4]; the phenolysis mixture (1.002 g), containing unchanged tosylate, was recovered

after 1.0 hr (72.8% completion), by employing the procedure reported in a previous paper.[4] A part of the recovered phenolysis mixture (0.139 g) was further phenolyzed, and the composition of the tosylate present in the mixture was determined to be 72.5 wt% (23.6% based on starting tosylate) from the infinity titers. The rest of the recovered phenolysis mixture (0.863 g) was treated with sodium naphthalene in THF, prepared from 1.85 g of naphthalene, 0.325 g of metallic sodium, and 43 m*l* of THF; working-up in the usual way gave 2.2 g of a crystalline material, which was then chromatographed over silica gel (60 g, Nakarai, No. II-A. 100—200 mesh) to give *t*-butylcyclohexanone (11.1 mg, 3.6% yield) from fractions 13—17 (25-m*l* per one fraction), obtained using *n*-hexane - ether (4 : 1 by vol), and *t*-butylcyclohexanol (267 mg, 84.9% yield) from fractions 22—37, obtained using *n*-hexane - ether (3 : 2 by vol); besides these fractions, fractions containing naphthalene, *t*-butylcyclohexyl phenyl ether, and *t*-butylcyclohexylphenol were eluted. The infrared spectrum of the alcohol of fraction 22 in CCl_4 was identical with that of an authentic sample of *cis*-4-*t*-butylcyclohexanol. The crystalline alcohols from the fractions from 22 to 27 (total 190 mg) were each examined in turn by GLC to show one peak corresponding in retention time to *cis*-4-alcohol. These results show that the alcohol of the fractions from 22 to 27 is exclusively *cis*-4-*t*-butylcyclohexanol and does not contain any *trans*-3-*t*-butylcyclohexanol.[9] The oily alcohol from fractions 28—37 (total 77 mg) was submitted to GLC, which showed two peaks with retention times of 17.3 min and 20.4 min; 55.0% and 45.0% respectively. Then the fractions for both the peaks were collected as eluted in liquid-nitrogen traps by GLC (5-m column at 150°C) to give 20.0 mg of crystalline alcohol for the first peak and 22.4 mg of oily alcohol for the succeeding peak; these substance were then each oxidized with chromium trioxide in acetic acid. The GLC examination for the ketone derived from the crystalline alcohol showed one peak corresponding in retention time to 4-*t*-butylcyclohexanone; from this the first peak was confirmed to be the *cis*-4-alcohol. The ketone derived from the oily alcohol was analyzed by GLC, showing two peaks corresponding in retention time to 3- and 4-*t*-butylcyclohexanones. The calibration, carried out with a mixture of ketones derived from a mixture of *trans*-4- and *cis*-3-alcohols of known compositions, gave the following results: *trans*-4-OH, 16.6%; *cis*-3-OH, 83.4%. The composition of the *t*-butylcyclohexanol given by the cleavage reaction of the unchanged tosylate was calculated to be as follows: *cis*-4-OTs, 88.2%; *trans*-4-OTs, 1.0%; *cis*-3-OTs, 10.8%; *trans*-3-OTs, 0.0%. The results of this run are listed in Table 2, along with the results of the other runs.

Cleavage of the Tosylate Recovered from the Reaction Mixture for the Phenolysis of *trans*-4-*t*-Butylcyclohexyl *p*-Toluenesulfonate. The *trans*-4-tosylate (6.23 g) was phenolyzed in 50 wt% phenol-benzene (200 m*l*), containing triethylamine (0.107N), for two half-lives; the unchanged tosylate was then recovered following the method described in a previous paper.[4] The recovered material (2.181 g) was divided into two parts by means of the ether solution. A part of the recovered material (0.387 g) was further phenolyzed, and the measurements of the infinity titers gave the composition of the tosylate present in the recovered material. The rest of the recovered material (1.794 g) was treated with sodium naphthalene in THF much as in the working-up described above; the resulting crystalline material was chromatographed over silica gel (100 g, Nakarai, No. II-A. 100—200 mesh). Successive elution with the indicated solvents gave the following fractions (25-m*l* portions being taken): the fractions 9—57, obtained using *n*-hexane, naphthalene; the fractions 63—79, obtained using *n*-hexane - benzene (7 : 3 by vol), *t*-butylcyclohexyl phenyl ether; the fractions 84—102, obtained using benzene, *t*-butylcyclohexylphenol; the fractions 129—137, obtained using *n*-hexane - ether (4 : 1 by vol), *t*-butylcyclohexanone (29.8 mg, 4.6% yield); the fractions 138—151, obtained using *n*-hexane - ether (4 : 1 by vol), oily *t*-butylcyclohexanol (27.4 mg); the fractions 152—171, obtained using *n*-hexane - ether (1 : 1 by vol), crystalline *t*-butylcyclohexanol (554.9 mg).

The crystalline alcohol from the fractions from 152 to 171 was proved to be *trans*-4-*t*-butylcyclohexanol on the basis of its melting point (mp 80—81°C) and infrared spectrum and on the basis of the results of a GLC examination.

The oily alcohol from the fractions from 138 to 151 was submitted to GLC showing two peaks corresponding in retention times to the axial and the equatorial alcohols; the compositions were 47.2% and 52.8% respectively. Then the fractions were collected as eluted in liquid-nitrogen traps by GLC (5-m column at 150°C) to give an oily alcohol for the first peak and a crystalline alcohol for the second peak; these substances were each treated with chromium trioxide in acetic acid. The GLC examination for the ketone from the oily alcohol showed two peaks corresponding in retention times to 3- and 4-*t*-butylcyclohexanone; when the ratio was calibrated with ketones derived from a mixture of *cis*-4-OH and *trans*-3-OH of known compositions, the *cis*-4-OH/*trans*-3-OH ratio was determined to be 0.263. The GLC examination for the ketone produced from crystalline alcohol showed one peak corresponding in retention time to 4-*t*-butylcyclohexanone; from this the crystalline alcohol was confirmed to be pure *trans*-4-alcohol. From these results, the composition of the recovered tosylate was calculated to be as follows: *cis*-4-OTs, 0.7%; *trans*-4-OTs, 96.7%; *cis*-3-OTs, 0.0%, *trans*-3-OTs, 2.6%.

Cleavage of the Tosylate Recovered from the Reaction Mixture for the Phenolyses Conducted in the Presence of Triethylammonium or Diethylammonium *p*-Toluenesulfonate. The phenolysis was conducted in the presence of added triethylamine and triethyl- or diethyl-ammonium tosylate, and the composition of the recovered tosylate was analyzed in a manner similar to that described in a previous paper[4] and in the preceding sections; The results are summarized in Table 2 for the *cis*-4-tosylate and in Table 3 for the *trans*-4-tosylate.

9) When the phenolysis of the *cis*-4-tosylate was conducted in the presence of added triethylammonium tosylate, the last fraction of the crystalline alcohol, corresponding to fraction 27 in the case of this run, was converted into ketone; the ketone was then analyzed by GLC to show one peak corresponding in retention time to 4-*t*-butylcyclohexanone. On the basis of this result, the fraction 27 was considered to be pure *cis*-4-*t*-butylcyclohexanol.

BULLETIN OF THE CHEMICAL SOCIETY OF JAPAN VOL. 42 3306—3309 (1969)

Effects of the Nitrone Group in NMR Spectra of α,*N*-Diphenylnitrones

Kinko KOYANO and Hiroshi SUZUKI

Department of Chemistry, College of General Education, The University of Tokyo, Komaba, Meguro-ku, Tokyo

(Received May 17, 1969)

The NMR and UV spectra of α,*N*-diphenylnitrone and its derivatives which have a substituent at the para position of the α-phenyl group and some of which have in addition a methyl substituent at the ortho position of the α-phenyl group were measured. Examination led to the following conclusions. The NMR signal of the ortho protons of the α-phenyl group appears at a very low field. This is mainly attributed to the direct effect of the negatively charged oxygen atom of the nitrone group. Increase in the electron-donating power of the para substituent enhances this effect.

In a previous paper, we reported that the NMR signal of the ortho protons of the α-phenyl group of α,*N*-diphenylnitrone (see Fig. 1) appeared at a very low field. We ascribed this to the direct effect of the negatively charged oxygen atom of the nitrone group (–CH=NO–).[1)]

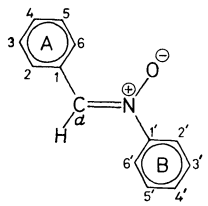

Fig. 1. α,*N*-Diphenylnitrone.

In the present paper, the NMR and UV spectra of α,*N*-diphenylnitrone and its derivatives which have a substituent at the 4-position and some of which have in addition a methyl substituent at the 2-position are examined. Special attention was paid to the effects of the nitrone group on the position of the NMR signals of the A ring protons. The conclusion of the previous paper was confirmed, and the influence of the 4-substituent on the direct effect of the oxygen atom was clarified.

Results and Discussion

The τ values of signals in the proton magnetic resonance spectra of α,*N*-diphenylnitrones in $CDCl_3$ are listed in Tables 1 and 2, and data on the longest wavelength band (referred to hereafter as the A band) in the electronic absorption spectra are shown in Table 3.

With regard to the effects of the two substituents of para-disubstituted benzenes on the chemical shift of the NMR signals of the ring protons, many

TABLE 1. THE τ VALUES OF PROTON SIGNALS OF 4-SUBSTITUTED α,*N*-DIPHENYLNITRONES IN $CDCl_3$

4-Substituted α,*N*-diphenylnitrone		Position of protons					
Entry No.	4-Substituent	α	2,6	3,5	2′,6′	3′,4′,5′	4-Methyl
1	$N(CH_3)_2$	2.26	1.77(d)	3.33(d)	2.28—2 37	2.68—2.75	
2	OCH_3	2.17	1.61(d)	3.05(d)	2.26—2.33	2.61—2.67	
3	CH_3	2.16	1.73(d)	2.77(d)	2.20—2.31	2.55—2.65	7.61
4	Unsubstituted	2.12	1.58—1.69	2.54—2.64	2.22—2.44	2.54—2.64	
5	Cl	2.13	1.69(d)	2.59(d)	2.25—2.35	2.55—2.64	
6	Br	2.12	1.74(d)	2.45(d)	2.21—2.31	2.54—2.61	
7	$COOCH_3$	2.04	1.62(d)	1.98(d)	2.24—2.35	2.58—2.65	
8	CN	2.00	1.57(d)	2.32(d)	2.23—2.36	2.50—2.60	
9	NO_2	1.99	1.45(d)	1.70(d)	2.17—2.27	2.47—2.53	

When a signal is doublet (indicated by letter d), the τ value at its center is shown. $J_{2,3}=J_{6,5}=7.5$—9.3 cps. When signals are unresolved, the range in which they appear is shown.

1) K. Koyano and H. Suzuki, *Tetrahedron Letters*, **1968**, 1859.

TABLE 2. THE τ VALUES OF PROTON SIGNALS OF 4-SUBSTITUTED 2-METHYL-α,N-DIPHENYLNITRONES IN $CDCl_3$

4-Substituted 2-methyl-α,N-diphenylnitrone		Position of protons							
Entry No.	4-Substituent	α	6	3	5	2′,6′	3′,4′,5′	2-Me	4-Me
1′	$N(CH_3)_2$	2.07	0.52	3.49	3.44	2.21—2.32	2.53—2.65	7.60	
2′	OCH_3	2.03	0.51	3.23	3.16	2.20—2.32	2.50—2.62	7.61	
3′	CH_3	2.00	0.70	2.98	2.89	2.26—2.35	2.55—2.64	7.67	7.71
9′	NO_2	1.88	0.48	1.91	1.85	2.18—2.30	2.44—2.53	7.45	

The 3-, 5-, and 6-protons constitute an AMX spin system. $J_{5,6}$=about 9 cps, $J_{3,5}$=2—3 cps, and $J_{3,6}$=0 cps. When signals are unresolved, the range in which they appear is shown.

TABLE 3. THE LONGEST-WAVELENGTH BAND IN THE ELECTRONIC ABSORPTION SPECTRA OF α,N-DIPHENYLNITRONES

No.	α,N-Diphenylnitrone	In cyclohexane		In ethanol	
		λ_{max} mμ	ε_{max} $\times 10^{-4}$	λ_{max} mμ	ε_{max} $\times 10^{-4}$
1	4-$N(CH_3)_2$-	372	2.40	385	3.21
2	4-OCH_3-	334	2.05	331	2.41
3	4-CH_3-	327	2.10	319	2.35
4	Unsubstituted	320	1.86	315	2.07
5	4-Cl-	327	2.22	321	2.34
6	4-Br-	329	2.32	323	2.44
7	4-$COOCH_3$-	340	2.62	331	2.75
8	4-CN-	337	2.73	331	2.66
9	4-NO_2-	363	1.76	356	1.95
1′	2-CH_3-4-$N(CH_3)_2$-	—	—	392	3.48
2′	2-CH_3-4-OCH_3-	—	—	338	2.31
3′	2,4-$(CH_3)_2$-	329	1.87	325	2.06
9′	2-CH_3-4-NO_2-	—	—	358	1.68

workers have stated that additivity holds approximately.[2] The contributions of the substituents at the ortho and meta positions to the change in the τ value of a ring proton are denoted by S_o and S_m, respectively, and they are referred to as the ortho and meta substituent constants, respectively. The values determined by Smith[3] for CCl_4 solutions are adopted here.

4-Substituted α,N-diphenylnitrones can be regarded as para-disubstituted benzenes, in which one of the two substituents is the 4-substituent (X) and the other the N-phenylnitrone group (–CH=NO–Ph). As is shown in Fig. 2, there exists an approximately linear relationship between the τ values of the 3- and 5-protons ($\tau_{3,5}$) of 4-substituted α,N-diphenylnitrones and the ortho substituent constants of the 4-substituents (S_o(X)), and the slope of the correlation line is nearly unity. From the correlation line the τ value at S_o(X)=0 is

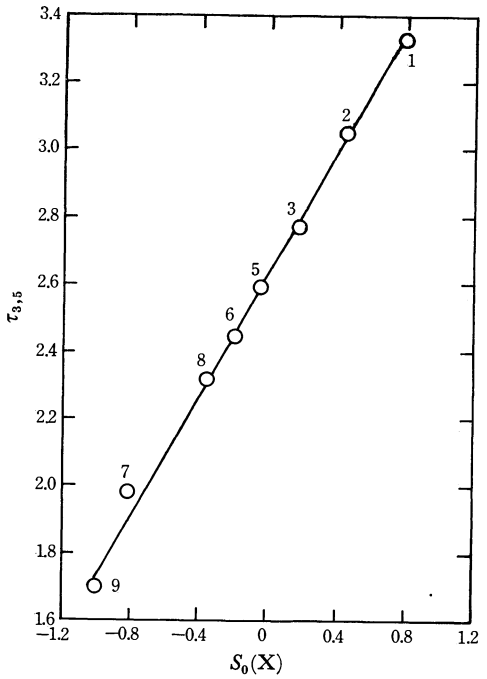

Fig. 2. The relation between the observed τ values of the 3- and 5-protons ($\tau_{3,5}$) of 4-substituted α,N-diphenylnitrones and the ortho substituent constants of the 4-substituents (S_o(X)). The numbers denote the compounds, according to the entry numbers in Table 1.

determined to be about 2.60. The difference between this value and the τ value of the protons of benzene (2.63 in $CDCl_3$), about −0.03, may be considered as the meta substituent constant of the N-phenylnitrone group, S_m(NPN). This is much smaller in absolute value than the meta substituent constant of the nitro group, $S_m(NO_2)$ (−0.21). Thus it may be said that the N-phenylnitrone group exerts only a very weak deshielding effect on the meta protons. There is also a fairly good linear relationship between the τ values of the α-protons and the Hammett σ_p values as well as Taft δ_p values[4] of the 4-substituents.

2) *Cf. e. g.*, J. W. Emsley, J. Feeney and L. H. Sutcliffe, "High Resolution Nuclear Magnetic Resonance Spectroscopy," Vol. 2, Pergamon Press, Oxford (1966), pp. 754—760 and 1140—1142.

3) G. W. Smith, *J. Mol. Spectry.*, **12**, 146 (1964).

4) R. W. Taft, Jr., *J. Am. Chem. Soc.*, **79**, 1045 (1957).

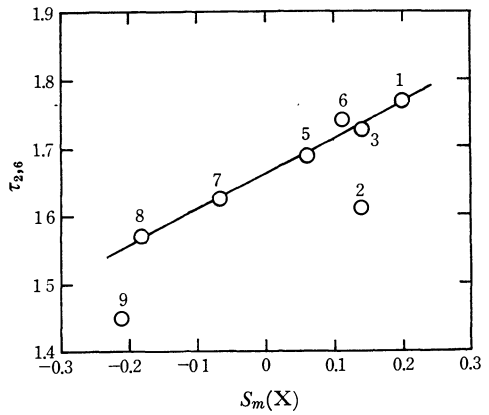

Fig. 3. The relation between the observed τ values of the 2- and 6-protons ($\tau_{2,6}$) of 4-substituted α,*N*-diphenylnitrones and the meta substituent constants of the 4-substituents (S_m (X)). The numbers denote the compounds, according to the entry numbers in Table 1.

Figure 3 shows that there is only a rough linear relationship between the τ values of the 2- and 6-protons ($\tau_{2,6}$) and the meta substituent constants of the 4-substituents (S_m(X)). The plots for the 4-methoxy and 4-nitro compounds deviate markedly from a straight correlation line. From the approximate correlation line given in Fig. 3 the τ value at S_m(X)=0 is estimated at about 1.65. If the difference between this value and the τ value of the protons of benzene, about −0.98, is tentatively considered as the ortho substituent constant of the *N*-phenylnitrone group, S_o(NPN), this substituent constant is comparable to the ortho substituent constant of the nitro group (−0.99). Thus, it might be said that the *N*-phenylnitrone group has a strong ortho substituent deshielding effect comparable to that of the nitro group.

The τ values of the 6-protons (τ_6) of the compounds having a methyl substituent at the 2-position, *viz.*, the compounds of entry numbers 1′, 2′, 3′, and 9′ in Table 2, are smaller by 0.9—1.3 than the τ values of the 2- and 6-protons ($\tau_{2,6}$) of the corresponding compounds having no methyl substituent at the 2-position, as illustrated by Fig. 4. This result is the same as that described previously for the 4-methyl compounds.[1] It is evident that the arguments are also valid in the present case. From the following facts, the most preferred conformation of the 4-substituted 2-methyl-α,*N*-diphenylnitrones seems to be a planar or nearly planar conformation in which the 6-proton is located near the oxygen atom of the nitrone group: (1) The most preferred conformation of the α,*N*-diphenylnitrones having no substituent at the ortho positions is probably a planar or nearly planar conformation;[5] (2) The values of the wavelength

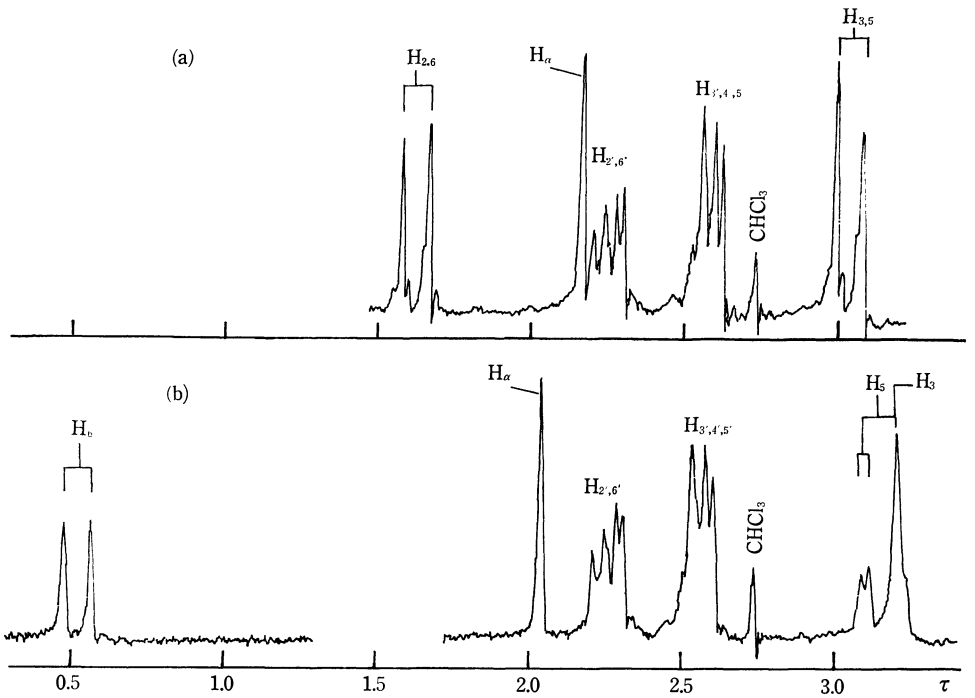

Fig. 4. The NMR spectra of (a) 4-methoxy-α,*N*-diphenylnitrone (compound 2) and (b) its 2-methyl derivative (compound 2′) in $CDCl_3$.

5) T. Kubota, M. Yamakawa and Y. Mori, This Bulletin, **36**, 1552 (1963).

and molar extinction coefficient of the A band maximum of the 4-substituted 2-methyl-α,N-diphenylnitrones are nearly equal to those of the corresponding compounds having no substituent at the 2-position (see Table 3). This seems to indicate that the most preferred conformation of the former is similar to that of the latter; (3) A scale model shows that the 2-methyl group must be sterically hindered from approaching the oxygen atom of the nitrone group. The 6-proton, being located near the negatively charged oxygen atom of the nitrone group, must be strongly affected by the oxygen atom, resulting in the marked downfield shift of its signal.

As seen in Table 2, the values of τ_6 are 0.70, 0.52, 0.51, and 0.48 for the 4-substituent (X)=CH_3, $N(CH_3)_2$, OCH_3, and NO_2, respectively. It should be noted that this order of the τ_6 values is quite different from that of the meta substituent constants of the 4-substituents.

If a 4-substituted α,N-diphenylnitrone having no substituent at the ortho positions had a fixed planar or nearly planar conformation, the 2- and 6-protons must be nonequivalent, and would show their signals at different τ values (τ_2 and τ_6). Of course, the τ value of the proton located near the oxygen atom of the nitrone group (τ_6) must be lower than that of the proton located far from the oxygen atom (τ_2). Actually, the α-phenyl group will rotate around the C_α–C_1 bond, so that the signals of the two protons coalesce. The observed values of $\tau_{2,6}$ are considered to be approximately the means of τ_2 and τ_6. Let us assume that the value of the hypothetical τ_6 of a 4-substituted compound can be calculated from the observed value of τ_6 of the corresponding 2-methyl compound by subtraction of the shift due to the substituent shielding effect of a meta methyl group, which is taken to be about 0.10. Then, from the observed $\tau_{2,6}$ values and the calculated τ_6 values, the values of the hypothetical τ_2 of 4-substituted compounds are calculated to be 3.12, 2.81, 2.86, and 2.52 for X=$N(CH_3)_2$, OCH_3, CH_3, and NO_2, respectively. These τ_2 values have a nearly linear relationship with the meta substituent constants of the 4-substituents, S_m(X).

The difference between the τ_6 value and the τ_2 value can be considered to be due to the direct effect of the oxygen atom of the nitrone group on the 6-proton. The values of this difference are −2.70, −2.40, −2.26, and −2.14 for X=$N(CH_3)_2$, OCH_3, CH_3, and NO_2, respectively. The order of these values coincides with that of the mesomeric electron-donating power of the 4-substituents. Thus, it can be said that the direct deshielding effect of the oxygen atom on the 6-proton is greater when the 4-substituent is more strongly electron-donating. This might be ascribed to the following two causes. (1) As the 4-substituent becomes more strongly electron-donating, the charge density at the oxygen atom will become larger. The inference that the π-electron density at the oxygen atom changes very sensitively by change of the 4-substituent is supported by a simple MO calculation. (2) Since the nitrone group is an electron-withdrawing group, as the 4-substituent becomes more strongly electron-donating, the conjugative interaction in the π-electron system will become stronger. As a result, the most preferred conformation will approach planarity, and its population ratio will increase. Consequently, the average distance between the 6-proton and the oxygen atom will become shorter.

Experimental

Materials. The α,N-diphenylnitrones were prepared by reaction of the adequately substituted benzaldehydes with phenylhydroxylamine in ethanol, according to the following equation:[5,6]

$$R\text{-}CHO + Ph\text{-}NHOH \longrightarrow R\text{-}CH{=}NO\text{-}Ph + H_2O$$

Their melting points (°C) were as follows (all are uncorrected): (1) 4-dimethylamino-, 140.5—141.2; (2) 4-methoxy-, 115.8—116.5; (3) 4-methyl-, 85—87; (4) unsubstituted, 113.0—113.5; (5) 4-chloro-, 153.5—154.0; (6) 4-bromo-, 161.5—162.0; (7) 4-methoxycarbonyl-, 155.5—156.0; (8) 4-cyano-, 147—149; (9) 4-nitro-, 186.0—186.5; (1′) 2-methyl-4-dimethylamino-, 142—143; (2′) 2-methyl-4-methoxy-, 97—98; (3′) 2,4-dimethyl-, 81—82; (9′) 2-methyl-4-nitro-, 153—155.

The compounds of entry numbers 1′, 2′, 3′, and 9′ are probably new compounds. The results of analysis for these compounds are as follows.

(1′) Found: C, 75.69; H, 7.22; N, 10.96%. Calcd for $C_{16}H_{18}N_2O$: C, 75.56; H, 7.13; N, 11.02%.

(2′) Found: C, 74.61; H, 6.35; N, 5.75%. Calcd for $C_{15}H_{15}NO_2$: C, 74.66; H, 6.27; N, 5.81%.

(3′) Found: C, 79.83; H, 6.82; N, 6.47%. Calcd for $C_{15}H_{15}NO$: C, 79.97; H, 6.71; N, 6.22%.

(9′) Found: C, 65.55; H, 4.44; N, 10.86%. Calcd for $C_{14}H_{12}N_2O_3$: C, 65.62; H, 4.72; N, 10.93%.

Measurement of the NMR and UV Spectra. The NMR spectra were measured on $CDCl_3$ solutions (concentration: about 120 mg in 1 ml of solvent) at room temperature with a Japan Electron Optics Laboratory spectrometer Model JNM-4H-100 (100 MC). Tetramethylsilane was used as an internal reference.

The UV spectra were measured with a Hitachi recording spectrophotometer Model EPS-2.

6) M. J. Kamlet and L. A. Kaplan, *J. Org. Chem.*, **22**, 576 (1957); O. H. Wheeler and P. H. Gore, *J. Am. Chem. Soc.*, **78**, 3363 (1956); J. Splitter and M. Calvin, *J. Org. Chem.*, **20**, 1086 (1955).

BULLETIN OF THE CHEMICAL SOCIETY OF JAPAN VOL. 42 3310—3313 (1969)

Synthetic Reactions by Complex Catalysts. XIV. Reaction of Isocyanide with Amine Catalyzed by Group IB and IIB Metal Compounds

Takeo SAEGUSA, Yoshihiko ITO, Shiro KOBAYASHI, Kiwami HIROTA and Hiroshi YOSHIOKA

Department of Synthetic Chemistry, Faculty of Engineering Kyoto University, Yoshida, Sakyo-ku, Kyoto

(Received May 17, 1969)

Group IB and IIB metal compounds catalyze the reaction of isocyanides (**1**) with amines (**2**) producing formamidines (**3**). In the reaction of cyclohexyl isocyanide with piperidine, the accelerating effect of catalyst was in the order AgCl>CuCl≫$ZnCl_2$, $Cd(OAc)_2$, $HAuCl_4 \cdot 4H_2O$. The AgCl catalyzed reaction proceeded almost quantitatively in 2.5 hr at 17°C. The reaction of aliphatic isocyanide with aromatic amine, *e.g.*, *N*-methylaniline, required higher reaction temperatures (160°C) even in the presence of catalyst, in which the order of catalytic activity was $HAuCl_4 \cdot 4H_2O$ >$ZnCl_2$>AgCl≫CuCl. A ternary complex of $(CuCl)_2$ (cyclohexyl isocyanide)$_2$ (piperidine) was isolated, which was unstable and decomposed gradually at room temperature to give *N*-cyclohexyl-*N'*,*N'*-pentamethylene formamidine. A mechanism through a mixed ligand complex has been proposed, in which both isocyanide and amine are coordinated with the same metal ion and the reaction takes place in the sphere of complex ligand.

The reaction of aliphatic isocyanide with amine, which does not take place without catalyst, is induced effectively by copper,[1] silver, zinc, cadmium and gold salts. Aromatic isocyanides have been known to react with amine even in the absence of the metal salt catalyst.[2] In the reaction of aromatic isocyanide with amine, however, the accelerating effect of the above metal compounds is observed.

$$\underset{(\mathbf{1})}{R\text{-}N\rightleftarrows C:} + \underset{(\mathbf{2})}{R'_2NH} \rightarrow \underset{(\mathbf{3})}{R'_2N\text{-}\overset{\overset{\|}{N}\text{-}R}{C}\text{-}H} \qquad (1)$$

A reaction mechanism through a mixed ligand complex has been proposed, in which both isocyanide and amine are coordinated with the common metal ion and the reaction takes place in the sphere of complex ligand.

Results and Discussion

Catalytic Activities of Metal Compounds. The catalytic activities of various metal compounds were examined in the reaction of cyclohexyl isocyanide with piperidine producing *N*-cyclohexyl-*N'*,*N'*-pentamethylene formamidine (Table 1).

The catalytic activities of IB and IIB metal compounds except mercuric compound are conspicuously shown. Since the formamidines are obtained in high yields, the reaction can be utilized for the synthesis of the formamidine derivatives. Lewis acids such as ferric chloride and aluminum chloride are much less active. In the isocyanide-amine reaction, zinc chloride was used in an earlier work.[3] The results of an extended screening of the metal

TABLE 1. CATALYTIC ACTIVITIES OF METAL COMPOUNDS FOR CYCLOHEXYL ISOCYANIDE-PIPERIDINE REACTION

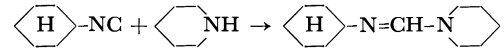

Cat.	Conditions (hr)*	Yield (%)
none	18	0
CuCl	1	96
AgCl	1	98
$ZnCl_2$	1	97
$Cd(OAc)_2$	1	97
$HAuCl_4 \cdot 4H_2O$	22	46
$Hg(OAc)_2$	6	5
$FeCl_3$	6	15
Ferrocene	17	2
$Fe(AA)_3$**	4	1
$AlCl_3$	7	1

* 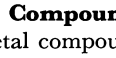 100 mmol, 30 mmol, Cat. 0.2 mmol, 110—120°C.

** AA=Acetylacetonate ligand

1) T. Saegusa, Y. Ito, S. Kobayashi, K. Hirota and H. Yoshioka, *Tetrahedron Letters*, **1966**, 6121.

2) J. U. Nef, *Liebigs Ann. Chem.*, **270**, 267 (1892).

3) T. L. Davis and W. E. Yelland, *J. Am. Chem. Soc.*, **59**, 1998 (1937).

Table 2. Catalysis of copper compounds in cyclohexyl isocyanide-piperidine reaction*

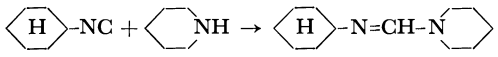

Cat.	Yield (%)
CuCl	94
$CuCl_2$	86
CuCN	90
$Cu(CN)_2$	94
$Cu(AA)_2$**	86
Cu	93

* 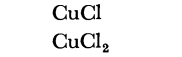 100 mmol, 30 mmol
Cat. 0.2 mmol; 110—120°C, 1 hr
** AA=Acetylacetonate ligand

compounds in the present studies have indicated that the catalytic activity of zinc chloride is not ascribed to its function of the so-called Lewis acid. In the systems with typical transition metal salts such as cobalt and nickel chlorides the rapid polymerization of isocyanide took place and hence no formamidine derivative was formed.

Table 2 illustrates the catalytic activities of several copper compounds and metallic copper. Under these reaction conditions, the catalytic activity (the product yield) is not much affected by the valency of copper and the nature of anion ligand. It is to be mentioned, however, that the cupric chloride is reduced to cuprous chloride by isocyanide in a stoichiometric way according to[4]

$$2CuCl_2 + RN{\rightleftarrows}C: \rightarrow 2CuCl + R{-}N{=}CCl_2 \quad (2)$$

Consequently it may be assumed that the cupric species were reduced to the cuprous species which served as the real active catalyst.

As to the catalytic activity of metallic copper, it is of interest that metallic copper dissolves in liquid isocyanide to form a soluble complex of copper isocyanide. Metallic copper powder was put in liquid cyclohexyl isocyanide and the mixture was centrifuged. The IR spectrum in the liquid phase showed a new band at 2180 cm^{-1} in addition to the absorption band of cyclohexyl isocyanide. The new band is reasonably assigned to $\nu_{N\equiv C}$ of the isocyanide species which is coordinated with copper. Moreover, the corresponding formamidine was formed when the liquid phase was treated with piperidine at room temperature. In the metallic copper catalyzed reaction the catalytic activity is thus ascribed to the soluble complex. The actual valence state of copper in liquid isocyanide should be the subject of future research.

Table 3 shows the results of the reactions of three isocyanides with aliphatic and aromatic amines by cuprous chloride catalyst. The cuprous chloride

Table 3. Cuprous chloride catalyzed reaction of isocyanide with amine*

$$RNC + R'R''NH \rightarrow RN{=}CH{-}NR'R''$$

Isocyanide	Amine	Condition (hr)	Condition (°C)	Yield (%)
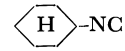		5	25	90
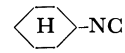	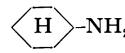	3	110—120	80
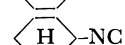	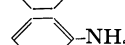	24	140	85
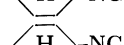	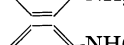	25	160	20
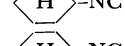	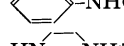	6	110—120	82***
n-BuNC		3	110—120	90
n-BuNC		10	25	87
n-BuNC	*n*-$BuNH_2$	5	110—120	88
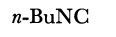		0.3	0	96

* Conditions: RNC 30 mmol, R'R''NH 100 mmol, CuCl 0.2 mmol
** As the reaction solvent, 10 m*l* of dioxane was employed.
*** The product was bis-*N*,*N'*-(cyclohexylformimidoyl) piperazine.

catalyzes the reaction of aliphatic isocyanide with aliphatic amine at considerable rates even at 25°C. The aliphatic isocyanide-aromatic amine reaction catalyzed by cuprous chloride requires higher reaction temperatures. Cuprous chloride is not a suitable catalyst for this combination of reaction. This will be discussed later.

Aromatic isocyanide reacts with amine without catalyst. As an example, the reaction of phenyl isocyanide with piperidine proceeds at 25°C to give *N*-phenyl-*N'*,*N'*-pentamethylene formamidine in a yield of 85% after 48 hr. However, the catalytic activity of cuprous chloride is clearly observed. In the presence of cuprous chloride, the reaction takes place instantaneously even at 0°C to produce the formamidine almost quantitatively (the last run of Table 3).

The catalyst activities of several salts of group IB and IIB metals are evaluated in a semiquantitative way by the time-conversion curves in the reactions of cyclohexyl isocyanide with piperidine at 17°C and with *N*-methylaniline at 160°C as shown in Figs. 1 and 2, respectively. The order of catalyst activity in the former reaction is $AgCl > CuCl \gg ZnCl_2$, $Cd(OAc)_2$, $HAuCl_4{\cdot}4H_2O$, which is quite different from that in the latter reaction of cyclohexyl isocyanide with aromatic amine, $HAuCl_4{\cdot}4H_2O > ZnCl_2 > AgCl \gg CuCl$. The specific activity of chloroautic acid in the aromatic amine-isocyanide reaction is of interest especially from the fact that it is

4) T. Saegusa, Y. Ito and S. Tomita, to be published.

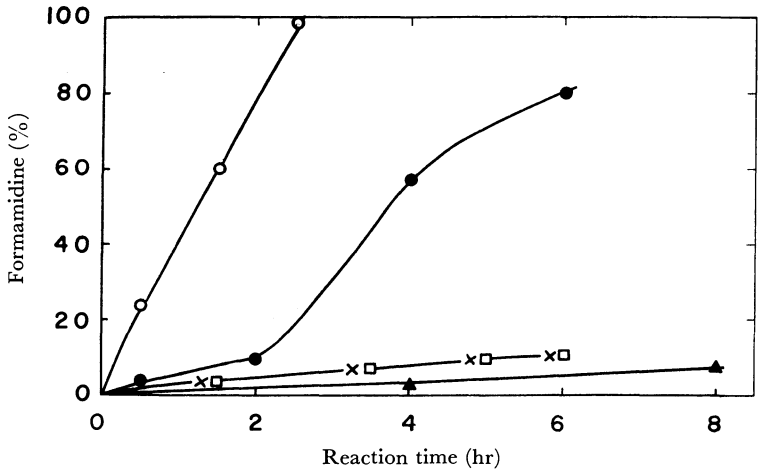

Fig. 1. Reaction of cyclohexyl isocyanide with piperidine (17°).
—○— AgCl —●— CuCl —□— $ZnCl_2$
—▲— $HAuCl_4 \cdot 4H_2O$ —×— $Cd(OAc)_2$

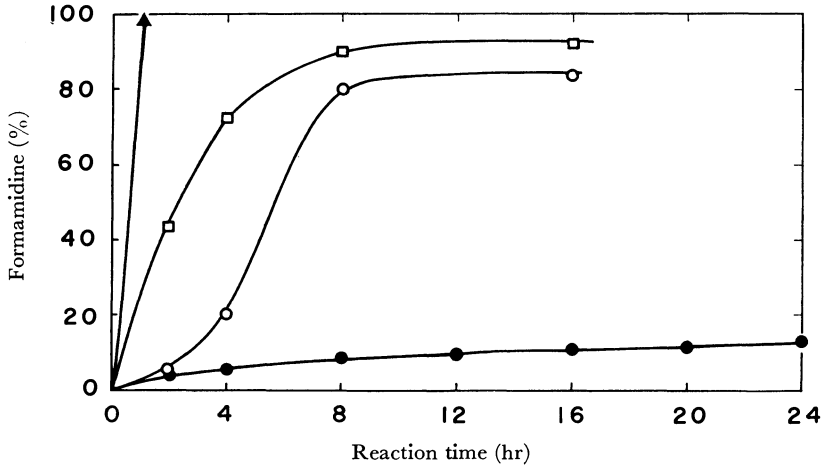

Fig. 2. Reaction of cyclohexyl isocyanide with *N*-methylaniline (160°).
—○— AgCl —●— CuCl
—□— $ZnCl_2$ —▲— $HAuCl_4 \cdot 4H_2O$

also quite active as the catalyst in the reaction[5] of aromatic amine with carbon monoxide which is isoelectronic to isocyanide.

Metallation of aromatic compound with $AuCl_3$, as reported by Kharasch[6] may be cited in relation to the specific catalysis of chloroautic acid for these reactions.

Mechanism. The isocyanide-amine reaction of the present studies seems to proceed in the ligand sphere of a ternary complex consisting of metal ion, isocyanide and amine. The crystalline, binary complex of cyclohexyl isocyanide and cuprous chloride, $[Cu(C{\leftleftharpoons}NC_6H_{11})]Cl$, was dissolved into liquid piperidine at 0°C. On standing the homogeneous solution at 0°C, a new crystalline solid was separated.

NMR spectrum of the crystalline solid in deuterated chloroform showed two broad signals centered at δ 3.7 (2H, $>$CH–N$\rightleftharpoons$C: of two mol of cyclohexyl isocyanide) and δ 3.3 (4H, $-N\langle^{CH_2-}_{CH_2-}$ of one mol of piperidine) and a complex signal at δ 1.0—2.1 (26H, 20H of $-(CH_2)_5-$ of two mol of cyclohexyl isocyanide plus 6H of $-(CH_2)_3-$ of one mol of piperidine). Together with the elemental analysis (Found: C, 45.92; H, 6.78; N, 8.75; Cl, 14.54%. Calcd for **4**: C, 45.51; H, 6.63; N, 8.38; Cl, 14.14%), the composition of the complex was determined as indicated by the formula

5) T. Saegusa, S. Kobayashi, K. Hirota and Y. Ito, This Bulletin, to be published.

6) M. S. Kharasch and H. S. Isbell, *J. Am. Chem. Soc.*, **53**, 3053 (1931).

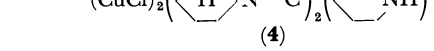

(4)

The spectrum of the ternary complex showed two key bands at 2176 and 3192, which were assigned to $\nu_{N\equiv C}$ of the isocyanide ligand and ν_{N-H} of the piperidine ligand. The band of $\nu_{N\equiv C}$ of the ternary complex is different from the corresponding $\nu_{N\equiv C}$ of the binary complex at 2192 cm^{-1} and from that of free isocyanide at 2140 cm^{-1}. Variation of $\nu_{N\equiv C}$ indicates that the coordination of isocyanide in the ternary complex is influenced by the piperidine ligand, whose ν_{N-H} band is also being shifted from that of free piperidine at 3280 cm^{-1}. These observations suggest the formation of a mixed ligand complex in which the isocyanide and amine ligands are coordinated with the common cuprous ion.

The ternary, mixed ligand complex formed here was not stable and decomposed gradually even at room temperature to produce the formamidine product, *N*-cyclohexyl-*N'*,*N'*-pentamethylene formamidine. Therefore, it is quite reasonable to assume that the cuprous chloride catalyzed reaction of isocyanide with amine proceeds in the ligand sphere of the mixed ligand complex.

Experimental

Meterials. Metal salts were of commercial, analytical reagent grade.

Metallic copper was prepared by reduction of cupric sulfate with zinc powder. In 600 m*l* of water, 100 g of cupric sulfate pentahydrate was dissolved, to which 15 g of zinc powder was added slowly with stirring below 70°C. The precipitate was washed several times with water and then with acetone. It was stored in acetone under nitrogen, and dried under nitrogen immediately prior to use.

Isocyanide was prepared by dehydration of *N*-substituted formamide with phosphorus oxytrichloride according to Ugi's procedure.[7]

General Procedure. A mixture of isocyanide (30 mmol), amine (100 mmol) and metal compound catalyst (0.2 mmol) was heated at the indicated temperature monitoring the reaction by the decrease of an infrared band $\nu_{N\equiv C}$ of isocyanide. The product of *N*,*N'*-disubstituted formamidine was isolated by distillation or by crystallization. Their structures were established by by elementary analysis, IR and NMR spectra.

Identifications of the Formamidine Products. *N*-Cyclohexyl-*N'*,*N'*-pentamethylene formamidine, bp 155—156°C/28 mmHg.

Found: C, 74.40; H, 11.71; N, 14.53%. Calcd for $C_{10}H_{20}N_2$: C, 74.17; H, 11.41; N, 14.42%. IR (neat): 1660 cm^{-1} ($\nu_{N=C}$), NMR ($CDCl_3$): δ 7.10 ppm (singlet, –N=CH–N<).

N,*N'*-Dicyclohexyl formamidine, mp 100—101°C (recrystallization from *n*-hexane).

Found: C, 74.61; H, 11.35; N, 13.64%. Calcd for $C_{13}H_{24}N_2$: C, 74.94; H, 11.61; N, 13.45%. IR (Nujol): 3280 cm^{-1} (ν_{N-H}), 1650 cm^{-1} ($\nu_{N=C}$).

N-Cyclohexyl-*N'*-methyl-*N'*-phenyl formamidine, bp 94—96°C/0.7 mmHg.

Found: C, 77.61; H, 9.58; N, 13.11%. Calcd for $C_{14}H_{20}N_2$: C, 77.73; H, 9.32; N, 12.95%. IR (neat): 1640 cm^{-1} ($\nu_{N=C}$).

Bis-*N*,*N'*-(cyclohexylformimidoyl) piperazine, mp 99—101°C (recrystallization from *n*-hexane).

Found: C, 71.16; H, 10.71; N, 18.68%. Calcd for $C_{18}H_{32}N_4$: C, 71.00; H, 10.59; N, 18.40%. Molecular weight (cryoscopic in benzene) Found: 294. Calcd for $C_{18}H_{32}N_4$: 304. IR (Nujol): 1630 cm^{-1} ($\nu_{N=C}$).

N-*n*-Butyl-*N'*,*N'*-pentamethylene formamidine, bp 118—120°C/27 mmHg.

Found: C, 71.39; H, 12.08; N, 16.79%. Calcd for $C_{10}H_{20}N_2$: C, 71.37; H, 11.98; N, 16.65%. IR (neat); 1640 cm^{-1} ($\nu_{N=C}$). NMR (CCl_4): δ 7.10 ppm (singlet, –N=CH–N<).

Preparation of Cyclohexyl Isocyanide-Cuprous Chloride (1 : 1) Complex. Cuprous chloride was added slowly to excess cyclohexyl isocyanide at room temperature, and the precipitation was collected by filtration. The white crystalline product was recrystallized from chloroform-ether, mp 95—96°C. Elementary analysis revealed that crystalline product consisted of 1 mol cyclohexyl isocyanide and 1 mol cuprous chloride.

Found: C, 40.40; H, 5.29; N, 6.73; Cl, 17.07%. Calcd for $C_7H_{11}NClCu$: C, 40.40; H, 5.22; N, 6.60; Cl, 17.01%.

Preparation of Ternary Complex. A mixture of piperidine (0.04 mol) and cyclohexyl isocyanide-cuprous chloride (1 : 1) complex (1 g) was stirred below 0°C. After several minutes a green homogeneous solution was obtained. On standing for several minutes more, a white crystalline solid was precipitated. The crystalline solid was washed with dry cold petroleum ether by decantation and dried *in vacuo*. This ternary mixed ligand complex is unstable at room temperature, and is readily decomposed to give *N*-cyclohexyl-*N'*,*N'*-pentamethylene formamidine.

7) I. Ugi and R. Meyr, *Chem. Ber.*, **93**, 239 (1960).

BULLETIN OF THE CHEMICAL SOCIETY OF JAPAN VOL. 42 3314—3317 (1969)

α-Diketone Rearrangement. The Reaction of 1,2-Cyclohexanedione with Arginine and with Guanidine

Kentaro ANZAI

The Institute of Physical and Chemical Research, Yamato-machi, Saitama

(Received May 19, 1969)

A novel rearrangement reaction of cyclohexanedione, involving the loss of hydrogen in the product, is described. Cyclohexanedione and guanidine react in an alkaline solution to produce 2-amino-4-oxo-1,3-diazaspiro[4.4]non-1-ene (VIII) and 1-hydroxy-3-amino-5-oxo-2,4-diazabicyclo-[4.3.0]non-2-ene (IX), the latter being an oxidized product. Similarly, cyclohexanedione reacts with arginine, producing, among other products, N^5-(1-hydroxy-5-oxo-2,4-diazabicyclo[4.3.0]non-2-ylidene)-ornithine (III).

Toi *et al.*[1] have reported that arginine reacts with cyclohexanedione (CHD) in basic solutions to produce N^5-(4-oxo-1,3-diazaspiro[4.4]non-2-ylidene)-L-ornithine (I). Though in strongly basic solutions the yield of I is almost quantitative, the presence of three minor products has also been shown by paper electrophoresis.[1] This reaction is unique in the sense that such rearrangements of aliphatic α-diketones similar to the benzilic-acid rearrangement have scarcely been known except that CHD is transformed to 1-hydroxycyclopentanecarboxylic acid[2] (II) in a concentrated solution of sodium hydroxide on heating.

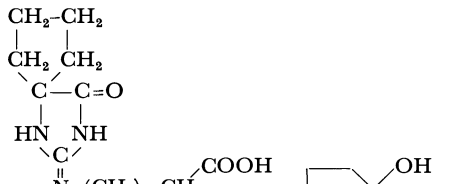

I

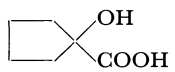

II

A paper chromatogram of the reaction mixtures of CHD and arginine is schematically shown in Fig. 1. The products are all isolated by cellulose column chromatography, and the ratios of the products are found to be markedly dependent on the concentrations of sodium hydroxide, as was suggested, by Toi *et al.*[1] If the reactions are carried out at pHs of less than 11, one unidentified product (corresponding to the spot 3 in Fig. 1) is found to be predominant. Though we at first incorrectly anticipated that it might be the first intermediate, through which I is produced, the structural elucidation of this compound has unexpectedly resulted in showing a novel reaction of CHD involving an intermolecular hydride shift. This report will be concerned with the structure of the product obtained from arginine and CHD at low concentrations of sodium hydroxide.

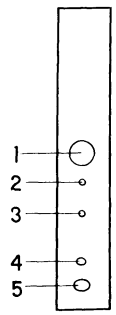

Fig. 1. The product distribution of a reaction mixture of arginine and cyclohexanedione in 0.2N NaOH: paper chromatogram developed with butanol, acetic acid, and water (4:1:2).

CHD and arginine were allowed to react in a 0.05N sodium hydroxide solution or at pH 11 at room temperature, and the products were isolated by cellulose column chromatography. The analytical data of the major product are consistent with the molecular formula of $C_{12}H_{20}N_4O_4$ after it has been heated at 140°C for 5 hr,[3] showing that CHD and arginine react with the loss of one mole of water and two atoms of hydrogen. A mechanistic consideration leads to two possible structures, III and IV (Scheme 1).

Though molecular-weight determination by the

1) K. Toi, F. Bynum, E. Norris and H. A. Itano, *J. Biol. Chem.*, **242**, 1036 (1967).

2) O. Wallach, *Ann.*, **437**, 174 (1924).

3) When the sample was dried over phosphorus pentoxide at room temperature, the analytical data were consistent with $C_{12}H_{20}N_4O_4 \cdot H_2O$. The water of crystallization was hardly expelled on heating at 100°C for a prolonged time over phosphorus pentoxide. When it was heated over 140°C, it gradually decomposed.

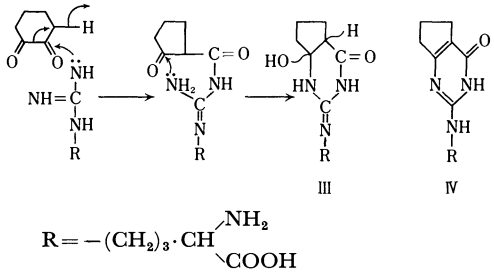

Scheme 1

parent peak seems rather to support the structure IV (Calcd for the trifluoroacetylated methyl ester of $C_{12}H_{18}N_4O_3$, 376.1358; measured, 376.1327), other physical and chemical data, to be discussed below, can more be reasonably explained by the structure III. IV is formally a dehydrated product of III, and the molecular ion of III may be rapidly dehydrated in a mass spectrometer, resulting in the loss of the parent peak.

Though the NMR spectrum is not very useful in elucidating the structure because of unanalyzable broad methylene signals, one methine proton signal at δ 4.10, a broad triplet, is inconsistent with a possible structure IV. The UV spectrum of the compound, $\lambda_{max}^{H_2O}$ mμ (ε) 217 (17100), is almost the same as that of I, $\lambda_{max}^{H_2O}$ mμ(ε) 214 (18500), supporting the idea that both have the same chromophore, –NH-C(=N–)–NHCO. The compound IV has an aromaticity and is expected to have an absorption maximum at a longer wavelength.

N^5-(5,6-Trimethylene-4-oxopyrimid-2-yl)ornithine (IV) was synthesized by the condensation of 2-ethoxycarbonylcyclopentanone (V) with benzoyl arginine ethyl ester, followed by acid hydrolysis (Scheme 2); as expected, IV is found to have a UV spectrum, $\lambda_{max}^{H_2O}$ mμ (ε) 230 (8800), 292 (6100), similar to that of isocytosine, $\lambda_{max}^{H_2O}$ mμ (ε) 222 (10000), 285 (5000). The mass spectra of III and IV (measured as the trifluoroacetylated methyl esters) are quite similar, strongly suggesting that the molecular ion of III is dehydrated with no observable parent peak to show a mass spectrum indistinguishable from that of IV.

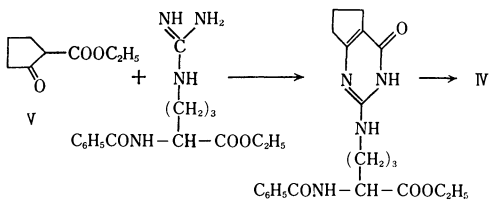

Scheme 2

Though III shows a single spot on TLC, the possibility that it is a mixture of configurational isomers cannot be excluded.

After it has been established that an equimolar amount of CHD and arginine react, with the loss of two hydrogen atoms, to produce N^5-(1-hydroxy-5-oxo-2,4-diazabicyclo[4.3.0]non-2-ylidene)ornithine (III), the next problem is to determine the place where the hydrogen is accepted. As no evolution of gas is observed during the reaction, it seems reasonable to assume that CHD is reduced to 1-hydroxycyclopentanecarboxyaldehyde (VI) or 1-cyclopentene-1-carboxyaldehyde (VII), which might then suffer from further reactions (Scheme 3).

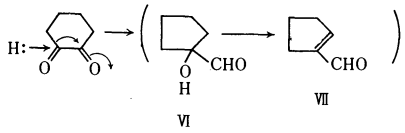

Scheme 3

Though the effort to isolate an aldehyde failed, possibly because of the susceptibility of aldehydes under these reaction conditions and because of the difficulty of separating an aldehyde from an excess of CHD, the positive reactions with Angeli's[4] and Tollens' reagent, after CHD and arginine have reacted in basic solutions, strongly suggest that two moles of CHD are needed for the formation of III; one reacts with arginine, and the other accepts the hydride anion. The following experimental findings seem to support this presumption: the spectrophotometric determination of the products on TLC shows that, when the reaction is carried out in a weakly basic solution, III is the only product, accompanied by an equimolar amount of unreacted arginine, and the use of an excess of CHD, an elevated temperature, and a prolonged reaction time have no influence on the ratio of the III to the arginine. We have still to answer the question of why half the arginine must remain unreacted. This peculiarity can be explained by presuming the following reaction path, which involves the formation of an aldehyde from CHD (Scheme 4):

2CHD + arginine → an aldehyde + III (1)

an aldehyde + arginine → a Schiff base of arginine (2)

Scheme 4

Generally, aldehydes are known to form Schiff bases more easily than ketones, and it is expected that an aldehyde, if it is involved in the reaction path on the formation of III (Eq. (1)), will at once combine with arginine to form a Schiff base (Eq. (2)), which is a species unable to react with CHD. Thus, the fact that only half the arginine is transformed to III in weakly basic solutions can be reasonably explained.

When the reaction is carried out in the presence of silver nitrate without altering the other reaction

4) A. Angeli, *Gazz. Chim. Ital.*, **34**, I, 50 (1904).

conditions, arginine is found to be almost completely consumed, being transformed to III.

Two mechanism of the action of the silver cation are possible (Scheme 5): it might accept an electron from the hydride anion (Eq. (3)), or it might oxidize an aldehyde to prevent arginine from forming a Schiff base (Eq. (4)):

$$H^- + 2Ag^+ \rightarrow 2Ag + H^+ \quad (3)$$

$$RCHO \xrightarrow{Ag^+} RCOOH \quad (4)$$

Scheme 5

In a similar manner, guanidine reacts with CHD in basic solutions to produce, though in low yields, 2-amino-4-oxo-1,3-diazaspiro[4.4]non-1-ene (VIII) and 1-hydroxy-3-amino-5-oxo-2,4-diazabicyclo-[4.3.0]non-2-ene (IX).

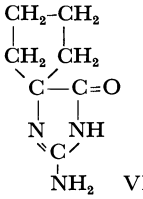

VIII

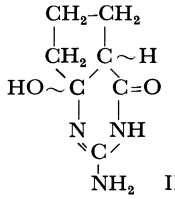

IX

Here also both the compounds have almost the same UV spectra, VIII, $\lambda_{max}^{H_2O}$ mμ (ε) 226 (7300): IX, $\lambda_{max}^{H_2O}$ mμ (ε) 227 (9900), showing that one, formed with the loss of two atoms of hydrogen, does not have an isocytosine chromophore.

Though the mass spectrum of IX exhibits the expected parent peak (*m/e* 169), the strength is found to vary markedly depending upon the measurement conditions; however, the peak corresponding to $M^+ - H_2O$ (*m/e* 151) is always predominant.

Thus, the reaction of CHD with arginine and guanidine reported here will, we believe, offer a way of approaching the novel reaction of α-diketones.

Experimental

Reaction of Arginine with Cyclohexanedione (CHD) in 0.2N NaOH. The reaction was carried out in almost the same way as that described by Toi *et al.*[1] To a solution of 900 mg of arginine in 100 m*l* of a 0.2N sodium hydroxide solution, there was added a 670-mg portion of CHD. After the solution had been left at room temperature for 4 hr, it was charged on a column of IR 120 (3×60 cm) and developed with 1N aqueous ammonia. The ninhydrin positive fractions were collected, and, after the water and ammonia had been evaporated under reduced pressure, the residue was chromatographed on cellulose (2×90 cm) and developed with a mixture of butanol, acetic acid, and water (4: 1: 2) or with a mixture of propanol, pyridine, acetic acid and water (15: 10: 3: 10). After repeated chromatography, five compounds, each showing a single spot on TLC, were obtained. The yields of Compounds **1** to **5**, corresponding to the spots from **1** to **5** in Fig. 1, were 600 mg, 2 mg, 7 mg, 2 mg, and 30 mg respectively. Compound **1** had already been established to be N^5-(4-oxo-1,3-diazaspiro-[4.4]non-2-ylidene)-L-ornithine (I), and Compound **4** was found to be arginine.

Though, under these experimental conditions, the yield of Compound **3** was too low to collect enough of a sample to study the structure, the same compound was also obtained as a major product under other conditions where the concentrations of sodium hydroxide were lower (see below).

The structure of Compound **2**, mp 172—177°C (dec), and Compound **5**, mp 205—210°C (dec), are now under investigation.

Reaction of Arginine with CHD in 0.05N NaOH: N^5-(1-Hydroxy-5-oxo-2,4-diazabicyclo[4.3.0]non-2-ylidene)ornithine (III). The reaction was carried out according to the same procedure as has been described above except that the concentration of sodium hydroxide was decreased to 0.05N. The yield of Compounds **1**, **2**, and **3**, after repeated chromatography, were 50, 100, and 130 mg respectively. Compound **3**, which was identified as N^5-(1-hydroxy-5-oxo-2,4-diazabicyclo-[4.3.0]-non-2-ylidene)ornithine (III) on the basis of the data to be presented below, was obtained as a colorless precipitate from water and ethanol. It showed no definite mp and gradually decomposed at 230—270°C; $\lambda_{max}^{H_2O}$ mμ (ε) 217 (17100); NMR (D_2O) 1.87 (broad 10H) 3.35 (t 2H J=6 cps) 3.74 (t 1H J=5.5 cps) 4.10 (broad t 1H J=6 cps).

Found: C, 47.71; H, 7.05; N, 18.60%. Calcd for $C_{12}H_{20}N_4O_4 \cdot H_2O$: C, 47.67; H, 7.33; N, 18.53%.

On heating at 140°C for 3 hr, 5.54% of the total weight was lost, corresponding to a theoretical value of 5.97% based on one mole of the water of crystallization.

Found: C, 50.30; H, 6.93; N, 19.17%. Calcd for $C_{12}H_{20}N_4O_4$: C, 50.69; H, 7.09; N, 19.71%.

The trifluoroacetylated methyl ester of IV did not show M^+; $(M-H_2O)^+$ 376.1327 (Calcd for $C_{15}H_{19}N_4O_4F_3$, 376.1358).

Reaction of Arginine with CHD at pH 11. To 10 m*l* of an aqueous solution containing 1.2 g of arginine, there were added, drop by drop, 760 mg of CHD dissolved in 10 m*l* of methanol. The consumption of arginine was followed by a decrease in the pH; the pH (10.5; initial) was kept almost constant (pH 10.5—11.0) throughout the addition by adding sodium hydroxide. After the solution had then been left at room temperature for 4 hr, the methanol was removed by evaporation and the residual aqueous solution was submitted to the procedure described in the first section.

The spectrophotometric determination of the ninhydrin-positive spots on TLC showed that, in this experimental run, the yields of Compounds **1**, **2**, and **5** were scanty and that Compound **3** was the major product, accompanied by an almost equimolar amount of the unreacting arginine. TLC also showed the presence of another, as-yet-unidentified ninhydrin-positive compound, which, on TLC, moved slightly slower than Compound **3**.

Reaction of Arginine with CHD at pH 11 in the Presence of Silver Nitrate. To a mixture of 130 mg of arginine and 115 mg of silver nitrate dissolved in 10 m*l* of water, a solution of 300 mg of CHD in 10 m*l* of methanol was added drop by drop, with the pH kept at 10.5—11.0 with sodium hydroxide. TLC on cellulose showed that Compound **3** was predominant, accompanied by small amounts of Compounds **1** and **2**. Hardly any arginine was detected.

A control experiment was carried out in the absence of silver nitrate. TLC showed that the amount of Compound **3** and arginine, after the reaction was completed, was almost the same. The isolation of Compound **3** was not attempted in this experimental run.

N^1-Benzoyl-N^5-(5,6-Trimethylene-4-oxopyrimid-2-yl)ornithine Ethyl Ester and N^5-(5,6-Trimethylene-4-oxopyrimid-2-yl)ornithine (IV). To a solution of 343 mg (10^{-3}M) of benzoyl-L-arginine ethyl ester hydrochloride dissolved in 10 m*l* of alcohol, an equimolar amount of sodium alcoholate (23 mg of sodium in 1 m*l* of alcohol) was added; the solution was then left in a refrigerator for 5 hr. The precipitate of sodium chloride was removed by filtration, and 150 mg of 2-ethoxycarbonyl-cyclopentanone were added. After the solution had been refluxed for 5 hr, water was added and the product, N^1-benzoyl-N^5-(5,6-trimethylene-4-oxopyrimid-2-yl)ornithine ethyl ester (the benzoylated ethyl ester of IV), was extracted with ethyl acetate. After the solvent had been evaporated, the residue was crystallized from benzene and ligroin; yield, 15 mg; mp 138—140°C; M^+ 398.1980 (Calcd for $C_{21}H_{26}N_4O_1$, 398.1954); $\lambda_{max}^{H_2O}$ mμ (ε) 229 (18300) 293 (8700).

N^5-(5,6-Trimethylene-4-oxopyrimid-2-yl)ornithine (IV) was obtained by the hydrolysis of the benzoylated ethyl ester of IV in a 2N hydrochloric acid solution, it being heated at 105°C for 20 hr. The hydrolysate from 10 mg of the benzoylated ethyl ester of IV was chromatographed on cellulose (2×90 cm) and the UV positive fractions were collected. Chromatography was repeated until a single spot, detected by both the ninhydrin reaction and UV absorption, was observed on TLC. After the solvent had been evaporated, the residue was precipitated from water and acetone; yield, 3 mg; it gradually decomposed over 190°C; $\lambda_{max}^{H_2O}$ mμ (ε) 230 (8800) 292 (6100). The trifluoroacetylated methyl ester of IV showed M^+, 376.1340 (Calcd for $C_{15}H_{19}N_4O_4F_3$, 376.1358).

Reaction of Guanidine with CHD: 2-Amino-4-oxo-1,3-diazaspiro[4.4]non-1-ene (VIII) and 1-Hydroxy-3-amino-5-oxo-2,4-diazabicyclo[4.3.0]non-2-ene (IX). A mixture of guanidine hydrochloride (191 mg, 2×10^{-3}M) and CHD (224 mg, 2×10^{-3}M) dissolved in a 1N sodium hydroxide solution (10 m*l*) was left to stand at room temperature overnight, and then the sodium hydroxide was removed with IR 120, as has been described in the first section. The products were eluted from the column with 1N aqueous ammonia, and, after the ammonia and water had been evaporated under reduced pressure, the residue was submitted to partition chromatography on silicic acid (2×60 cm), being developed with butanol saturated with water. Two products, which were detected by means of a Greig-Leaback reaction (*t*-butylhypochlorite-tolidine) on TLC, were isolated.

2-Amino-4-oxo-1,3-diazaspiro[4.4]non-1-ene (VIII), eluted first from the column, was crystallized from ethanol and benzene; yield, 27 mg; mp 260—265°C; $\lambda_{max}^{H_2O}$ mμ (ε) 226 (7300); M^+ 153.0911 (Calcd for $C_7H_{11}N_3O$, 153.0902).

The NMR spectrum showed a broad methylene signal at δ 1.2. The IR spectrum showed the following intense bands (cm^{-1}): 1632, 1585, 1487, 1335, 1320.

Found: C, 51.94; H, 7.32; N, 25.49%. Calcd for $C_7H_{11}N_3O\cdot\frac{1}{2}H_2O$; C, 51.83; H, 7.46; N, 25.91%.

1-Hydroxy-3-amino-5-oxo-2,4-diazabicyclo[4.3.0]non-2-ene (IX), which was eluted later, was crystallized from water; yield, 11 mg. It did not show a definite melting point; rather it gradually decomposed at 220—240°C; $\lambda_{max}^{H_2O}$ mμ (ε) 227 (9900); M^+ 169.0876 (Calcd for $C_7H_{11}N_3O_2$, 169.0851), $(M-H_2O)^+$ 151.0706 (Calcd for $C_7H_9N_3O$, 151.0746). The IR spectrum showed the following intense bands (cm^{-1}): 1675, 1662, 1612, 1490.

Found: C, 49.67; H, 6.34; N, 24.75%. Calcd for $C_7H_{11}N_3O_2$: C, 49.63; H, 6.55; N, 24.84%.

Mass-spectrum Measurements. A mass spectrometer of the JMS-01SG model of the Japan Electron Optics Laboratory, Ltd., was used. To obtain volatile samples, milligram amounts of I, III, and IV were methylated and successively trifluoroacetylated following the method described by McLafferty.[5] The products were, without further purification, dissolved in a small amount of acetone and charged into capillary tubes. The acetone was removed in the spectrometer under reduced pressure, and the spectra were taken under a direct-inlet system.

The author wishes to thank Dr. Saburo Suzuki, the chief of the Laboratory of Antibiotics, of this Institute, for his encouragement.

5) M. Senn, R. Venkataraghavan and F. W. McLafferty, *J. Am. Chem. Soc.*, **88**, 5593 (1966).

BULLETIN OF THE CHEMICAL SOCIETY OF JAPAN VOL. 42 3318—3323 (1969)

Total Syntheses of Tanshinone-I, Tanshinone-II and Cryptotanshinone*1,2

Yoshinobu INOUYE and Hiroshi KAKISAWA

Department of Chemistry, Tokyo Kyoiku University, Otsuka, Bunkyo-ku, Tokyo

(Received May 30, 1969)

Total syntheses of tanshinone-II (II) and cryptotanshinone (III) from 3-methylbenzofuran-4, 7-quinone (X) and 6,6-dimethyl-1-vinylcyclohexene (IX), and of tanshinone-I (I) from quinone X and *o*-methylstyrene (XVIII) are described. Preliminary accounts for the Diels-Alder reaction of methoxybenzoquinone revealed that the effect of substituents for orientation phenomena can be considered to be of electronic nature.

Tanshinone-I (I),[1] tanshinone-II (II)[2] and cryptotanshinone (III)[3]–pigments isolated from the root of *Salvia miltiorrhiza* Bunge[4]–were found to posess the unique chromophore consisting of an orthoquinone and a furan ring. Recent investigations on minor components established the structures of tanshinone-IIB (IV),[5] hydroxytanshinone-II (V)[6] and methyl tanshinonate (VI)[6] having the same framework.

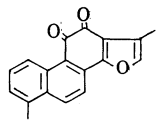

I

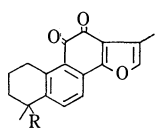

II R=Me
IV R=CH_2OH
VI R=COOMe

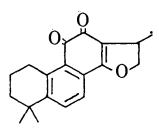

III

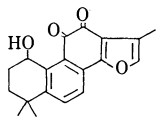

V

Synthetic approaches to these unique pigments have been reported by three groups,[5, 7–9] of which

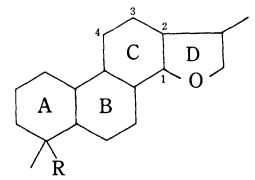

Fig. 1

two[5,9] succeeded in syntheses of tanshinones. In the early approaches,[7,8] A/B/C rings were built up by the Diels-Alder reaction of benzoquinone with suitable dienes, followed by attempted introduction of an alkyl side chain to make a furan ring. However, the alkylations resulted in an unsuitable position[7] or in an unseparable mixture.[8]

Recently these weakness were overcome by using the 1,3-dimethoxyphenanthrene derivative[9] or the 3-hydroxy-1,4-phenanthrenequinone derivatives[5] as an intermediate, where the introduction of an alkyl side chain could be controlled to occur at a suitable position (C_2).

Utilization of the Diels-Alder reaction to build the framework would be preferable for two reasons; firstly, this method will establish the general route to all tanshinones by using an appropriate quinone or diene, and secondly, some information can be obtained for the orientation in the Diels-Alder reaction, on which little is known especially in the case of substituted benzoquinones (*vide infra*).

In the purification of cryptotanshinone (III),

*1 Presented at the 21st Annual Meeting of the Chemical Society of Japan, Osaka, April, 1968; H. Kakisawa and Y. Inouye, *Chem. Commun.*, **1968**, 1327.

*2 Taken in part from the thesis of Y. Inouye, Tohoku University, 1968.

1) F. von Wessely and S. Wang, *Ber.*, **73**, 19 (1940).

2) a) Y. Okumura, H. Kakisawa, M. Kato and Y. Hirata, This Bulletin, **34**, 895 (1961). b) K. Takiura and K. Koizumi, *Chem. & Pharm. Bull.*, **10**, 112 (1962).

3) K. Takiura, *J. Pharm. Soc. Japan*, **61**, 482 (1941).

4) M. Nakao and T. Fukushima, *ibid.*, **54**, 154 (1934).

5) A. C. Baillie and R. H. Thomson, *J. Chem. Soc., C*, **1968**, 48.

6) H. Kakisawa, T. Hayashi, I. Okazaki and M. Ohashi, *Tetrahedron Letters*, **1968**, 3231.

7) T. J. King and G. Read, *J. Chem. Soc.*, **1961**, 5090.

8) H. Kakisawa and M. Ikeda, *Nippon Kagaku Zasshi (J. Chem. Soc. Japan, Pure Chem. Sect.)*, **88**, 476 (1967).

9) a) M. Tateishi and H. Kakisawa, The 11th Symposium on the Chemistry of Natural Products (Oct. 10, 1967) held at Kyoto. The Abstracts, p. 166; b) H. Kakisawa, M. Tateishi and T. Kusumi, *Tetrahedron Letters*, **1968**, 3783.

Takiura[10] found that it readily dissolved in alcoholic potassium hydroxide to give a yellow enolic compound, and that the latter was reconverted into cryptotanshinone on heating with an equal amount of ethanol and concentrated sulfuric acid. From the structure of cryptotanshinone, and the ready hydrolysis of alkoxyquinone with alkali to hydroxyquinone, these phenomena can be explained as III ⇌VII. Possibility of conversion of isomer VIII

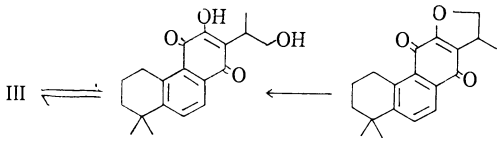

VII VIII

of cryptotanshinone (III) into cryptotanshinone through the same enolic intermediate VII prompted us to prepare isomer VIII by the Diels-Alder reaction between 6,6-dimethyl-1-vinylcyclohexene(IX)[8] and 3-methylbenzofuran-4,7-quinone (X) followed by catalytic hydrogenation of adduct XI. The unknown quinone X can be derived from 3-methyl-4-benzofuranol (XII)[11] by mild oxidation.

Before proceeding to the actual synthesis, we must briefly refer to the orientation in the Diels-Alder adduct. Although no reliable theory[12-15] has yet been given for the orientation in the adducts, the most conventional interpretation is to assume the biradical intermediates*3 of which the main product may be anticipated by considering the radical stability.

The Diels-Alder reactions of substituted benzoquinones were mostly investigated by Ansell and co-workers.[16] They found that the dienophilic activity of the ethene linkage of benzoquinones depends on whether its electron-density is greater or less than that of the other: *i. e.*, the lower the electrondensity the greater the reactivity of the ethene linkage. For example, the reaction occurs at unsubstituted ethene linkage of methoxybenzoquinone and at a substituted one of methoxycarbonylbenzoquinone. Although Ansell's works did not concern the orientation and only few examples were found for the Diels-Alder reaction between unsymmetrical benzoquinones and dienes, the effect of substituents may be considered*4 from two points of view: the radical stability in assumed biradical intermediates and the steric factor in the transition state.

Two possible structures XIIIa and XIIIb can be derived for the radical stability. XIIIa is stabilized more by the C_4-ketone which may have a large +M effect in comparison with the C_1-ketone.[17] Thus, the "radical stability" requires the reaction to proceed as XIIIa→XIVa. For the steric factor in the transition state,*5 XVa would be energetically

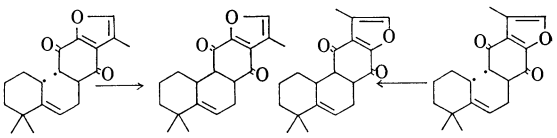

XIIIa XIVa XIVb XIIIb

more stable than XVb because in VXb the steric repulsion between the geminal dimethyl group of the diene and the methyl group on the furan ring would become significant. Thus, the reaction was anticipated to proceed in the favorable direction.

XVa XVb

Fig. 2. Possible transition states.

Syntheses of Tanshinone-II and Cryptotanshinone. The oxidation of 3-methyl-4-benzofuranol (XII)[11] with Fremy's salt[18] gave 3-methylbenzofuran-4,7-quinone (X) in almost quantitative yield. The *p*-quinone structure is based on physical properties: IR spectrum shows carbonyl absorptions at 1663 and 1655 cm^{-1}; UV maxima appear at 217, 248, 292 and 394 mμ;[19] and NMR spectrum

10) K. Takiura, *J. Pharm. Soc. Japan*, **61**, 475 (1941).
11) W. B. Whalley, *J. Chem. Soc.*, **1951**, 3229.
12) J. Sauer, *Angew. Chem. Int. Edit.*, **6**, 16 (1967).
13) A. Wassermann, "Diels-Alder Reactions–Organic Background and Physico-chemical Aspects," Elsevier Publishing Co., Amsteldm, London, New York (1965).
14) M. Imoto and N. Tokura, "Fuka Hanno," Tokyo Kagaku Dojin, Tokyo (1967).
15) J. Feuer, W. C. Herndon and L. H. Hall, *Tetrahedron*, **24**, 2575 (1968).

*3 It is known[12] that the Diels-Alder reactions of 1- and 2-substituted butadienes with acrylates proceed mainly as shown, regardless of the electronic nature of the substituents in the diene.

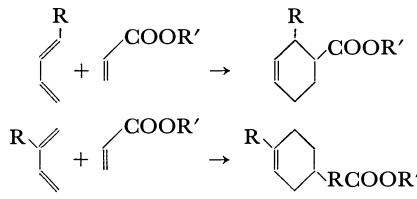

16) M. F. Ansell, B. W. Nash and D. A. Wilson, *J. Chem. Soc.*, **1963**, 3012, and references cited therein.

*4 Details of these points will be reported elsewhere.
17) M. J. S. Dewar, "The Electronic Theory of Organic Chemistry," Chapt. XII, Oxford Univ., Press., England (1949).
*5 We might say that the reaction proceeds through the "endo" transition state. See Ref. 16.
18) H.-J. Teuber and N. Gotz, *Chem. Ber.*, **87**, 1236 (1954).
19) C. J. P. Spruit, *Rec. Trav. Chim.*, **81**, 810 (1962), reported the longest wavelength absorption of benzofuran-4,7-quinone to be at 380 mμ.

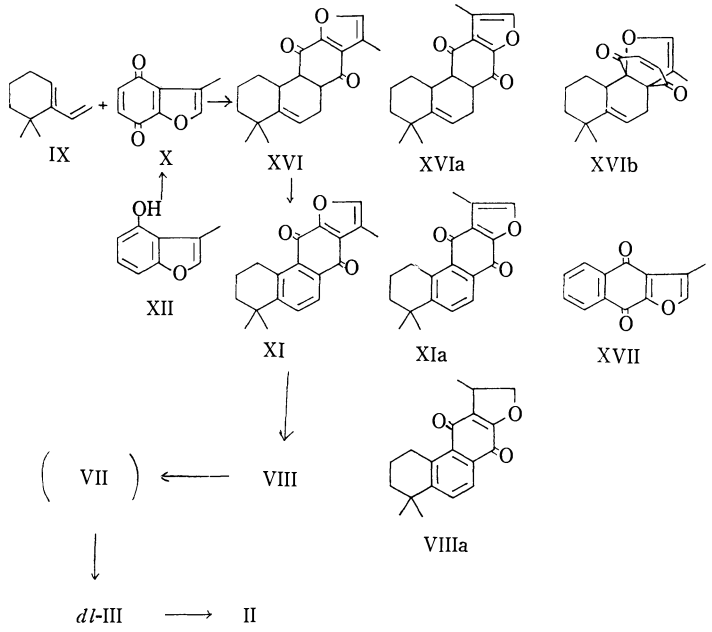

exhibits a doublet due to C_3–CH_3 at 2.30 ppm and a quartet due to C_2–H at 7.40 ppm with a coupling constant of 0.8 cps, and a two proton singlet at 6.62 ppm arising from the two hydrogen atoms on the quinone ring.

The Diels-Alder reaction between 3-methylbenzofuran-4,7-quinone (X) and 6,6-dimethyl-1-vinylcyclohexene (IX)[8] was conducted in ethanol at room temperature.[8] Only one adduct separated in crystalline form in high yield based on the quinone reacted and no other products were characterized. The adduct, mp 160—161°C, shows IR absorptions at 1695 and 1680 cm^{-1}. The molecular ion peak at *m/e* 298 in the mass spectrum and elementary analysis fitted the formula of 1 : 1 adduct, which was further confirmed by NMR spectrum; a singlet due to the geminal methyl group at 1.04 ppm and a slightly splitted signal due to the methyl group on the furan ring at 2.26 ppm. Moreover, the fact that only two vinyl protons appear at 5.40 and 7.45 ppm, and that the UV maxima at 214, 244 and 303 mμ differ makedly from the O=C–CH=C–O chromophore[16] enable us to reject the structure XVIb. The choice between the remaining two possibilities, XVI and XVIa, was not achieved at this stage.

The adduct XVI (or XVIa) was converted by air oxidation[20] into a naphtho[2,3-*b*]furan-4,9-quinone derivative XI (or XIa), mp 214—215°C, the IR absorption (1660 cm^{-1}) and UV maxima (252 sh, 255, 305 and 360 mμ) of which were very similar to those of 3-methylnaphtho[2,3-*b*]furan-4,9-quinone (XVII).[21] An AB type quartet due to C_6 and C_7 protons appears in NMR spectrum at 7.68 and 8.00 ppm with a coupling constant of 10 cps.

The furan ring in XI (or XIa) was subjected to catalytic reduction with palladium on carbon in ethanol[28a] to afford a naphthoquinone derivative VIII (or VIIIa). The selective hydrogenation of the furan ring was confirmed by NMR spectrum of the product. Thus, a secondary methyl signal is present as a doublet at 1.40 ppm.

The naphthoquinone derivative VIII (or VIIIa) was hydrolyzed with alcoholic potassium hydroxide to give an enolic compound VII (or corresponding isomer), which was treated without purification with concentrated sulfuric acid in ethanol.[10] A red crystalline oil obtained was purified by column chromatography on silicic acid. The orange crystals(64%), mp 174—175°C, showed an identical IR spectrum with that of cryptotanshinone (III).

When cryptotanshinone (III) was treated with dichlorodicyanobenzoquinone (DDQ), tanshinone-II (II) was obtained exclusively in 70% yield. The synthetic II melted at 210—211°C alone or mixed with natural tanshinone-II (II), and showed identical IR spectrum with that of the latter.

Synthesis of Tanshinone-I. 3-Methylbenzofuran-4,7-quinone(X) and *o*-methylstyrene(XVIII)[22] were heated without solvent at 100°C[23,24] for 10 hr. The resulting dark red mass was chromatographed on a column of alumina. At least five colored materials were recognized on thin layer chromatography, but only one orange pigment could be isolated in crystalline form in 25% yield.

20) C. F. H. Allen and A. Bell, "Organic Syntheses," Coll. Vol. III, p. 310 (1955).
21) H. Kakisawa, M. Tateishi, in preparation.
22) Y. Hirshberg, *J. Am. Chem. Soc.*, **71**, 3241 (1949).
23) C. de Corral, *Chem. Abstr.*, **52**, 7257b (1958).
24) M. Lora-Tamayo, *Tetrahedron*, **4**, 17 (1958).

Although this product gave only a single spot chromatographically, recrystallization from benzene gave a pure adduct of mp 219—220°C and unpurified mixtures. The former shows a molecular peak at *m/e* 276 in the mass spectrum, which together with elementary analyses leads to a formula $C_{18}H_{12}O_3$. The NMR spectrum (Fig. 3a) of the adduct shows an aromatic methyl signal at 2.66 ppm, a methyl signal on the furan ring at 2.34 ppm, and six aromatic protons at 7.0 to 9.6 ppm, which indicates that the 1 : 1 adduct had undergone facile dehydrogenation[24] to give the phenanthrene quinone XIX (or XIXa).

The NMR spectrum (Fig. 3b) of the original mixture is quite similar to that of the product of mp 219—220°C except broadening of all the signals and a new doublet at 9.43 ppm. This suggests the formation of both isomers XIX and XIXa. The ratio of XIX to XIXa was found to be *ca.* 1.4 calculated from the intensity of the signals 9.55 ppm (corresponds to XIX, *vide infra*) and 9.43 ppm (XIXa).

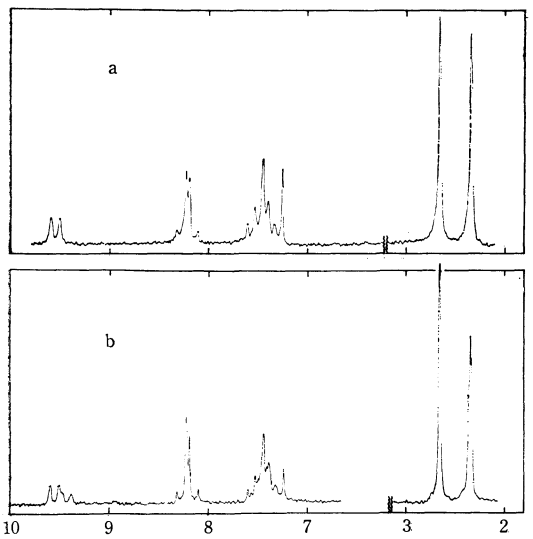

Fig. 3. NMR spectra (100 Mc*[6]) of adducts in $CDCl_3$.
a XIX b the original mixture

The furan ring of the adduct XIX (or XIXa) resisted catalytic flydrogenation under the conditions used for the naphthoquinone XI. However, it was reduced with platinum oxide in acetic acid to afford a dihydro compound XX (or XXa).

The dihydro compound XX (or XXa), without purification, was hydrolyzed with alcoholic potassium hydroxide to give an orange enol, which was

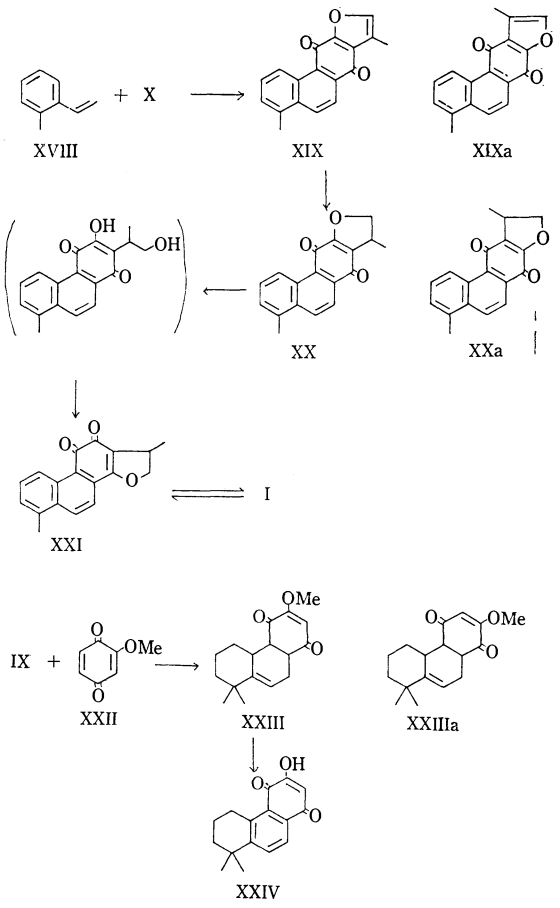

heated with concentrated sulfuric acid in ethanol to afford known[5] dihydrotanshinone-I (XXI), mp 200—201°C in 35% yield from the adduct XIX. In the present work, the authentic dihydrotanshinone-I was prepared from tanshinone-I (I) by catalytic hydrogenation over platinum oxide in acetic acid and melted at 202°C. The UV and IR spectra of both dihydrotanshinone-I were identical and no depression of mixed melting point took place.

As in the case of cryptotanshinone (III), dihydrotanshinone-I(XXI) was dehydrogenated with DDQ to give tanshinone-I (I) in 50% yield. Synthetic tanshinone-I melted at 229—230°C alone or mixed with the natural specimen. They were identical.

Preliminary Account for Diels-Alder Reaction. The successful conversion of the Diels-Alder adduct to the natural tanshinones established the direction of the furan ring to be as in XVI, but not as in XVIa. Conversely, use of a natural product as a synthetic object clarifies the reaction mechanism to some extent, especially with respect to the stereochemical problem. The result prompted us to undertake a preliminary experiment to decide which factor, electronic or steric, would be predominant in the Diels-Alder reaction of benzoquinones.

The diene IX and methoxybenzoquinone (XXII)

*6 We are deeply indebted to Dr. Y. Nakadaira for measurement of the 100 Mc NMR spectra (performed at Tohoku University).

were allowed to react under the same conditions as used for the preparation of XVI. The structure of the adduct was confirmed to be XXIII, but not XXIIIa. Firstly, UV spectrum of the adduct fitted the chromophore O=C–C(OMe)=CH–C=O and only vinyl protons appeared at 5.4 and 6.03 ppm. Secondly, the dehydrodemethylation of the adduct with alkaline ethanol afforded a 2-hydroxynaphthoquinone derivative, which was found to be identical with XXIV.[25]

This is consistent with the electronic effect, but it shows that the steric factor is not, at least, the main factor for the orientation phenomena in the Diels-Alder reaction.

After accomplishment of the syntheses, compound XI (named isotanshinone-II), VIII (isocryptotanshinone) and XIX (isotanshinone-I) were isolated[26] as minor components from the same plant. Total syntheses of these minor pigments were achieved in the present work.

Experimental

All melting points were determined in a sealed tube and are uncorrected. IR spectra were recorded on a Hitachi EPI-2 spectrophotometer, UV spectra were measured on a Hitachi EPS-3T spectrophotometer, and NMR spectra were obtained on a Hitachi H-60 spectrometer. Mass spectra were performed at Meijo University on a Hitachi RMU-7 high resolution spectrometer operating at 70 eV (inlet: 200°C). Microanalyses were carried out at Tohoku University.

3-Methylbenzofuran-4,7-quinone (X). To an ice-cooled solution of 300 mg of 3-methyl-4-benzofuranol (XII)[11] in 20 m*l* of ethanol, was added 1.35 g of Fremy's salt[18] in 70 m*l* of water and 20 m*l* of M/6 KH_2PO_4. After stirring for 15 min, the mixture was left in an ice-box for one hour. The precipitates were collected and the filtrate was extracted with ether. The precipitates and the ether extract were combined and chromatographed on silicic acid (20 g). From benzene elute, 327 mg (100%) of quinone X was obtained.

Pure X (sublimination at *ca.* 140°C/55 mmHg), mp 129—131°C. IR (KBr): 1663, 1655, 860 cm^{-1}. UV (EtOH): 217 (log ε: 4.14), 248 (4.20), 292 (4.19), 394 mμ (3.31). NMR ($CDCl_3$): 2.30 (d, 3H, J=0.8 cps), 6.62 (s, 2H), 7.40 ppm (q, 1H, J=0.8).

Diels-Alder Reaction[8] between 3-Methylbenzofuran-4,7-quinone (X) and 6,6-Dimethyl-1-vinylcyclohexene (IX). To a solution of 255 mg of quinone X in 2 m*l* of hot ethanol, 216 mg of diene IX[8] was added and the mixture was left for 15 hr at room temperature in the dark. The light yellow solution solidified immediately when the flask wall was scratched. The solids were collected on filter-paper to give slightly yellow needles XVI (198 mg), and the filtrate was chromatographed on silicic acid (10 g). The chloroform elute (No. 1) gave 86 mg of crude adduct XVI, while the chloroform elute (No. 3) gave 75 mg of starting quinone X.

Pure XVI, mp 160—161°C (from methanol). IR (KBr): 1695, 1680 cm^{-1}. UV (EtOH): 214 (4.05), 244 (3.71), 303 mμ (3.90). NMR ($CDCl_3$): 1.04 (s, 6H), 2.26 (d, 3H, J=1), 5.40 (m, 1H), 7.45 ppm (q, 1H, J=1). Mass: *m/e* 298 (M^+).

Found: C, 76.70; H, 7.65%. Calcd for $C_{19}H_{22}O_3$: C, 76.48; H, 7.43%.

Dehydrogenation[20] of Adduct XVI to Naphtho-[2,3-*b*]furan-4,9-quinone Derivative XI. Air was bubbled through the suspension of 72 mg of adduct XVI in 12 m*l* of ethanol containing 200 mg of potassium hydroxide for 20 hr (after 20 min, the initial green color turned yellow). The solids were collected, washed with water and then with ethanol, and dried over phosphorus pentoxide to give 59 mg of naphtho[2,3-*b*]furan-4,9-quinone XI. The filtrate and washing were extracted with ether, and the extract was chromatographed on silicic acid (5 g). From the benzene elute, 4 mg of XI was obtained. Purification was conducted by initial filtration through alumina column, followed by recrystallization from benzene/*n*-hexane

Pure XI, mp 214—215°C. IR (KBr): 1660 cm^{-1}. UV (EtOH): 252 sh (4.80), 255.5 (4.81), 270 sh (4.22), 305 (4.02), 360 mμ (4.08). NMR ($CDCl_3$): 1.33 (s, 6H), *ca.* 1.7 (m, 4H), 2.35 (d, 3H), 3.38 (t, 2H), 7.40 (m, 1H), 7.68 (d, 1H, J=8), 8.00 ppm (d, 1H, J=8). Mass: *m/e* 294 (M^+).

Found: C, 77.15; H, 6.14%. Calcd for $C_{19}H_{18}O_3$: C, 77.53; H, 6.16%.

***dl*-Cryptotanshinone (III).** The naphtho[2,3-*b*]-furan-4,9-quinone XI (50 mg) was hydrogenated in 25 m*l* of methanol over 50 mg of 10% palladium on carbon. The filtrate was evaporated and the residue was dissolved in 8 m*l* of ethanol. When 115 mg of potassium hydroxide was added, the solution turned dark red immediately. After standing overnight, 25 m*l* of water was added and the solution was made acidic with dilute sulfuric adid. The ether extract (yellow) was evaporated to dryness to give a light orange oil (45 mg), which was dissolved in 2 m*l* of ethanol. Concentrated sulfuric acid (2 m*l*) was added, when the solution turned red; the solution was heated in a boiling water-bath for a few minutes. Pouring into ice-water and extracting with ether afforded a red crystalline oil, which was purified by passing through a silicic acid column (5 g). *dl*-Cryptotanshinone (32 mg, 64%) was obtained in crystalline form.

dl-Cryptotanshinone (III), mp 174—175°C (from ether). IR (KBr): 1680, 1650, 1625 cm^{-1}. UV (EtOH): 219 (4.19), 264 (4.37), 272 (4.30), 290 sh (3.78), 358 (3.36), 450 mμ (3.37).

Tanshinone-II (II). Cryptotanshinone (III, 30 mg) and 35 mg of DDQ were refluxed in benzene for 1.5 hr under nitrogen atmosphere. The mixture (containing some precipitates) was purified through alumina (5 g), upon which 21 mg (70%) of tanshinone-II and 5 mg of starting crytotanshinone were obtained.

Pure tanshinone-II (from ethanol) melted at 210—211°C alone, or mixed with the natural specimen. IR (KBr): 1690, 1670, 1640 cm^{-1}.

Diels-Alder Reaction between 3-Methylbenzofuran-4,7-quinone (X) and *o*-Methylstyrene (XVIII). The mixture of 80 mg of 3-methylbenzofuran-4,7-

25) This compound was first prepared by Baillie and Thomson.[5] We prepared it by a different method. H. Kakisawa, M. Tateishi, to be published.

26) H. Kakisawa, T. Hayashi and T. Yamazaki, *Tetrahedron Letters*, **1969**, 301.

quinone (X) and an excess amount of *o*-methylstyrene (XVIII) in a test tube containing a pinch of hydroquinone was heated at 100—110°C[23,24] for 10 hr. The resulting dark red solid (at least five colored materials were recognized by thin layer chromatography) was dissolved in hot benzene and was chromatographed on alumina (10 g). From benzene elute, 36 mg of orange substances were isolated in a crystalline from. Recrystallization from benzene afforded a pure adduct XIX.

Pure XIX, mp 219—220°C. IR (KBr): 1665 sh, 1660 cm^{-1}. UV (EtOH): 212 (4.39), 234 (4.55), 283 sh (4.29), 292.5 (4.40), 347 (3.70), 455 br mμ (3.35). NMR ($CDCl_3$): 2.34 (s, 3H), 2.66 (s, 3H), 7.2—7.7 (m, 3H), 8.21 (AB quartet center, 2H, J=9), 9.55 ppm (d, 1H, J=9). Mass: *m/e* 276 (M^+).

Found: C, 78.55; H, 4.75%. Calcd for $C_{18}H_{12}O_3$: C, 78.25; H, 4.38%.

The filtrate could not be purified, but the NMR spectrum of the original crystal (from ethanol) shows that it was composed of XIX and a very similar compound, probably XIXa (see Fig. 3).

Catalytic Reduction of the Adduct XIX. The adduct XIX (25 mg) was hydrogenated over platinum oxide (25 mg) in 20 m*l* of acetic acid. After absorption of 23 m*l* of hydrogen, the solvent was evaporated to give solids, which were stirred with DDQ (40 mg) in 2 m*l* of benzene for 1.5 hr. The mixture was filtered through alumina (10 g) with chloroform to afford 14 mg (56%) of XX, mp 175—177°C (from ethanol). IR (KBr): 1670 w, 1640 cm^{-1}.

Catalytic Reduction of Tanshinone-I (I). A) Tanshinone-I (I) was hardly reduced under the following conditions: 10% palladium on carbon in methanol, 10% palladium on carbon in ethyl acetate, and platinum oxide in ethyl acetate.

B) Tanshinone-I (I, 205 mg) was dissolved in 50 m*l* of acetic acid and was hydrogenated over 200 mg of platinum oxide (110 m*l* of hydrogen absorbed during two hours). Removal of the solvent by evaporation gave a red oil, which was purified through chromatography on silicic acid (10 g). From the chloroform elute, 160 mg of dihydrotanshinone-I (XXI) was obtained.

Pure XXI, mp 202°C (from methanol). IR (KBr): 1680, 1650, 1622 cm^{-1}. UV (EtOH): 216 (4.30), 242 (4.40), 292 br (4.20), 335 (3.48), 414 mμ (3.61). NMR ($CDCl_3$): 1.40 (d, 3H, J=7), 2.64 (s, 3H), *ca.* 3.6 (m, 1H), 4.37 (dd, 1H, J=9 and 6), 4.94 (t, 1H, J=9). 7.30—7.80 (m, 3H), 8.18 (d, 1H, J=8), 9.20 ppm (d, 1H, J=8). Mass: *m/e* 278 (M^+).

Found: C, 78.15; H, 5.34%. Calcd for $C_{18}H_{14}O_3$: C, 77.68; H, 5.07%.

Dihydrotanshinone-I (XXI) from Adduct XIX. The adduct (XIX, 40 mg) was hydrogenated over 40 mg of platinum oxide in 120 m*l* of acetic acid. After removal of the solvent, the residue was dissolved in 4 m*l* of ethanol, to which *ca.* 100 mg of potassium hydroxide was added and the mixture was left for several hours. The solution was diluted with water, acidified with 6N hydrochloric acid and was extracted with ether to give a yellow enol. The enol, without purification, was dissolved in a mixture of 2 m*l* of ethanol and 2 m*l* of concentrated sulfuric acid, heated in boiling water-bath for a few minutes, and was poured into ice-water. The ether extract was chromatographed on silicic acid (5 g). From the chloroform elute, 14 mg (35%) of dihydrotanshinone-I (XXI) was isolated.

Pure XXI, mp 200—201°C, alone or mixed with an authentic sample (from methanol).

Tanshinone-I (I). A mixture of dihydrotanshinone-I (XXI, 28 mg) and DDQ (35 mg) in benzene was refluxed for two hours under a nitrogen atmosphere. After removing the solvent by evaporation, the residue was dissolved in small amount of chloroform and filtered through alumina (5 g). The filtrate evaporated to give solids. Tanshinone-I (I) was isolated in 50% yield (14 mg) by chromatography on silicic acid (10 g) with benzene.

Pure tanshinone-I (I), mp 229—230°C, alone or mixed with the natural specimen (from ethanol). IR (KBr): 1665 br cm^{-1}.

Diels-Alder Reaction between Methoxybenzoquinone (XXII) and 6,6-Dimethyl-1-vinylcyclohexene (IX). To a solution of 338 mg of quinone XXII in 5 m*l* of hot ethanol, was added 0.5 g of diene IX and the mixture was allowed to stand overnight at room temperature. The crystals were collected and were recrystallized from methanol to give adduct XXIII (265 mg). From the filtrate, a further 44 mg of adduct XXIII was obtained by chromatography on silicic acid.

Pure XXIII, mp 151—154°C (from methanol). IR (KBr): 1690, 1670, 1603 cm^{-1}. UV (EtOH): 273 mμ (3.93). NMR ($CDCl_3$): 1.04 (s, 6H), 1.2—1.6 (6H), 3.80 (s, 3H), 5.4 (m, 1H), 6.03 (s, 1H). Mass: *m/e* 274 (M^+).

Found: C, 74.42; H, 8.08%. Calcd for $C_{17}H_{22}O_3$: C, 74.10; H, 8.04%.

Conversion of Adduct XXIII to 2-Hydroxynaphthoquinone Derivative XXIV. Air was bubbled through the solution of 106 mg of the adduct XXIII and 90 mg of potassium hydroxide in 5 m*l* of ethanol for 2.5 hr. After acidification with dilute hydrochloric acid, the product was purified by chromatography on silicic acid. From chloroform elute, 27 mg of yellow crystals were obtained.

Pure XXIV (from *n*-hexane) melted at 161.5—163.5°C alone, or at 162.5—163.5°C when mixed with the authentic sample.[25] IR (KBr): 1645, 1570 cm^{-1}.

The authors are deeply indebted to Proferssor Koji Nakanishi, Tohoku University, for many helpful discussions.

BULLETIN OF THE CHEMICAL SOCIETY OF JAPAN VOL. 42 3324—3326 (1969)

Reaction of Modified Polypropylene Fiber Containing the Glycidyl Group with Several Amines and Ammonia

Yukio MIZUTANI, Kōshi KUSUMOTO, Seishirō MATSUOKA and Mitsuo TANI
Tokuyama Soda Co., Ltd., Tokuyama, Yamaguchi
and Yoshio SUDA and TADASHI SHIROTA
The Textile Research Institute of the Japanese Government, Yokohama, Kanagawa

(Received May 16, 1969)

Polypropylene was modified by the blending of the fine powdery copolymer of glycidyl methacrylate and divinyl benzene, and this modified polypropylene fiber was treated with diethyl amine, diethanol amine, monoethanol amine, and ammonia. The reactivity order was as follows: monoethanol amine>diethyl amine> diethanol amine=ammonia. Consequently, the resultant fiber showed water-wettability and could be dyed with an acidic dye.

Polypropylene shows poor dyeability, no water-wettability, and a waxy touch, as a result of its high crystallinity and nonpolarity. These properties are drawbacks in practical uses. In order to make polypropylene fiber dyeable with an acidic dye, the following procedures have been proposed: (1) the blending of polyvinyl pyridine,[1] (2) the blending of the styrene-glycidyl methacrylate copolymer and after-treatment with amines,[2] and (3) the grafting of glycidyl methacrylate and after-treatment with amines.[3]

One of the present authors has already reported the modification of polypropylene with a polymeric fine powder (PFPC), prepared from glycidyl methacrylate (GMA) and divinylbenzene (DVB). This powder is more thermally stable than such a linear polymer as a styrene-GMA copolymer, and it has been established that this modification is very effective in improving the dyeability of polypropylene fiber[4,5] and that the dyes having an amino group can be fixed in the substrate by the reaction between the epoxy group in the substrate and the amino group.[4,5] Therefore, it was presumed that an amine can easily react with the epoxy group. The introduction of the amino group into polypropylene is very interesting, because polypropylene may be modified to make it water-wettable, antistatic, and dyeable by an acidic dye; such dyes were inavailable in the previous studies.[4,5] Accordingly, the reactions of the polypropylene fiber modified by the blending of PFPC with some amines and ammonia were investigated by the use of the undrawn fiber as a model case. Furthermore, the dyeability of the modified fiber with an acidic dye was investigated by the use of the drawn fiber.

Experimental

Material. A commercial polypropylene pellet was blended with PFPC at 170—185°C by the use of a calender roller. The fabricating conditions and the properties of the fiber are shown in Table 1. The properties of the polypropylene were as follows:

Melt index (at 230°C, load: 2.16 kg/cm²): 4.4 g/10 min
Specific gravity (at 23°C): 0.914

TABLE 1. THE FABRICATING CONDITIONS AND THE PROPERTIES OF THE FIBER

Sample	Fabricating conditions				PFPC content %	Fineness, denier	Epoxy value, mmol/g fiber	
	Spinning temp.°C	Drawing temp.°C	Draw ratio	Heat set			Calcd	Obsd*
PP-F-1	240	—	—	—	3	5—6	0.199	0.200
PP-F-2	270	130	4	130°C, 10 sec	3.4	5	0.224	0.221

* Determined by the modification of the HCl-Dioxane method.[3]

1) R. A. Bychkov and M. P. Zverev, *International Chem. Eng.*, **7**, 76 (1967).
2) M. Kubota, M. Katayama and O. Ishizuka, *Kogyo Kagaku Zasshi (J. Chem. Soc. Japan, Ind. Chem. Sect.)*, **66**, 725 (1963).
3) Y. Iwakura, T. Kurosaki, K. Nagakubo, K. Takeda and M. Miura, This Bulletin, **38**, 1349 (1965).
4) Y. Mizutani, *ibid.*, **39**, 1088 (1967).
5) Y. Mizutani, *ibid.*, **40**, 1519 (1967).

PFPC was prepared by the method reported in the previous papers.[4,5] Diethanol amine (DEA), monoethanol amine (MEA), and diethyl amine (DA) were used after distillation under a reduced nitrogen atmosphere.

Procedures. The fiber (0.80 g) and an aqueous solution of an amine or ammonia were placed into a pressure bottle. A piece of glass rod was placed on the fiber in order to immerse the fiber in the solution. In order to gain analytical accuracy, the concentration of the amine or ammonia was controlled so as to be 0.4—1.6 mmol/20 m*l*. The pressure bottle was immersed in an oil bath at a definite temperature without any stirring. After a definite reaction time, the pressure bottle was rapidly cooled by water. Then the fiber was taken out and rinsed with 100 m*l* of water. A washing solution was added to the reactant solution; the quantity of amine or ammonia after the treatment was determined by pH titration with a 0.01N aqueous solution of hydrochloric acid. The neutralization points are shown in Table 2. The preliminary experiment

Table 2. The neutralization point

Reagent	DA	DEA	MEA	Ammonia
pH	6.1	4.9	5.3	5.8

confirmed that Monogen-w (an emulsifier from the Daiichi Kogyo Seiyaku Co., Ltd.) did not disturb the titration. The quantity of the reacted amine or ammonia ($[A]_F$) and the reaction degree of the epoxy group in the fiber were defined as follows:

$$[A]_F = [A]_0 - [A]_t \quad (1)$$

$$R_A = [A]_F/\text{Epoxy value of the fiber} \quad (2)$$

$[A]_0$: Initial quantity of an amine or ammonia

$[A]_t$: The quantity of an amine or ammonia after treatment for t hr.

Dyeing. The fiber (50 g) was treated at 120°C for 4 hr with the following solution-mixture:

A-solution $\begin{bmatrix} Na_2SO_4\text{: 5 g/}l \\ \text{Monogen-w: 1 g/}l \end{bmatrix}$: 150 m*l*

DEA : 150 m*l*

The fiber (2 g) thus treated was dyed under the conditions shown in Table 3.

Results and Discussion

PP-F-1 (undrawn fiber; see Table 1) was used to investigate the reaction. Figure 1 shows the results of the reaction. The reactivity order was as follows: MEA>DA>DEA=ammonia. Figures 2 and 3 show the effect of the molar ratio of the amine or ammonia to the epoxy group. It was established that the increase in the reactant concentration increases the $[A]_F$ and R_A values, and that when bath

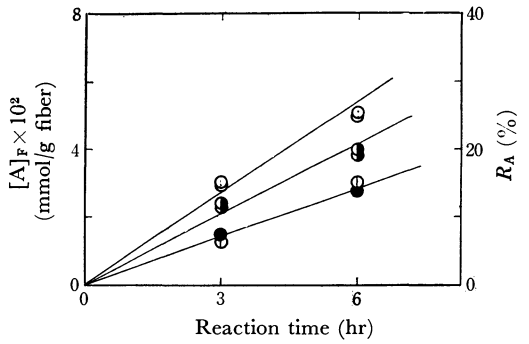

Fig. 1. The comparison of the reactivity.
○: MEA, ◑: DA, ●: DEA, ⓘ: ammonia
Concentration of reagent: 0.4 mmol/20 m*l*
Reaction temperature: 120°C
Bath ratis: 25 m*l*/g fiber

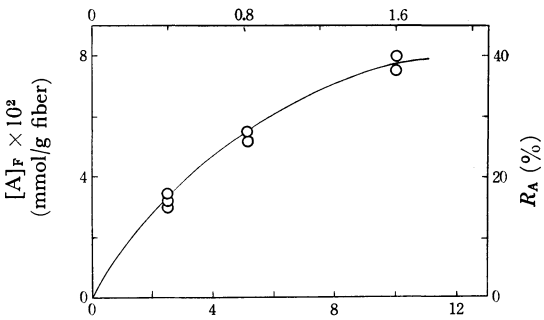

Fig. 2. The effect of DEA concentration.
Reaction temperature: 120°C
Bath ratio: 25 m*l*/g fiber
Reaction time: 6 hr

Table 3. The dyeing conditions

Dye	Kayacyl Rubinol 3GS C.I. Acid Red 37 and Kayanol Floxine NK C.I. Acid Red 257	Kayanol Milling Scarlet FGW C.I. Acid Red 111	Kayakalon Scarlet GL C.I. Acid Red 317
Conditions	Bath ratio: 50 by weight	Bath ratio: 50 by weight	Bath ratio: 50 by weight
	Dye: 2% o.w.f.	Dye: 2% o.w.f.	Dye: 2% o.w.f.
	Na_2SO_4: 10% o.w.f.	Na_2SO_4: 10% o.w.f.	CH_3COOH(48%): 2% o.w.f.
	H_2SO_4(66° Be′): 4% o.w.f.	CH_3COOH: 2% o.w.f.	
	60°C→100°C, 15 min	50°C→100°C, 15 min	50°C→100°C, 30 min
	100°C, 60 min	100°C, 60 min	100°C, 45 min

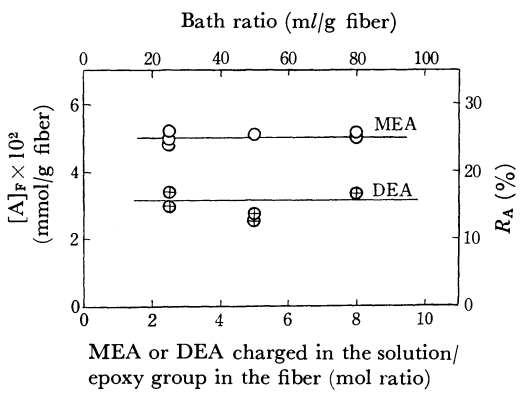

Fig. 3. The effect of the bath ratio.
Reaction temperature: 120°C
Concentration of DEA or MEA: 0.4 mmol/20 ml
Reaction time: 6 hr

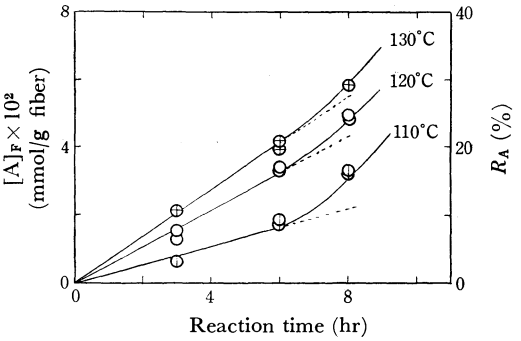

Fig. 4. The effect of the reaction temperature.
Concentration of DEA: 0.4 mmol/20 ml
Bath ratio: 20 ml/g fiber

ratio increased with the constant reaction concentration, the $[A]_F$ and R_A values did not change. Figure 4 shows the effect of the reaction temperature. The reaction proceeded linearly until the reaction time had lasted 6 hr and, then, it increased. This may be attributed to the fact that the fiber became water-wettable as the reaction proceeded and to the self-catalytic effect[6] of the hydroxyl group which resulted from the reaction. It is reasonable that the reaction became more rapid with an increase in the reaction temperature. The upper limit is about 130°C because of the thermal stability of the fiber. By means of the slope of the straight line in Figure 4, the rate constant (k) was found to be as is shown in Table 4, assuming that the reaction was zero order. Figure 5 shows the Arrhenius plot; the apparent activation energy

6) Y. Iwakura, T. Kurosaki, N. Ariga and T. Ito, *Makromol. Chem.*, **97**, 128 (1966).

TABLE 4. THE REACTION RATE

Reaction temperature, °C	130	120	110
$k \times 10^3$, mmol/hr g fiber	7.03	5.37	2.88

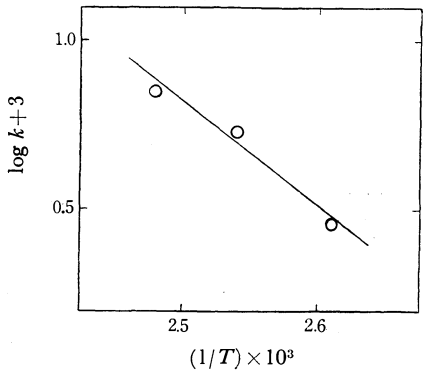

Fig. 5. The Arrehnius plot of the logarithm of the rate constant (k) against the reciprocal of absolute temperature.

TABLE 5. THE DYEABILITY AND THE DYEING FASTNESS

Dye	Kayacyl Rubinol 3GS	Kayanol Floxine NK	Kayanol Milling Scarlet FGW	Kayakalon Scarlet GL
Exhaustion %	34	49	51	59
Fastness to washing*	2—3	3	2	2—3

* Estimated by JIS L 1045—1959, MC-2 (Translated in English and published by Japanese Standards Association)

was calculated to be 14.6 kcal/mol. It was very interesting that the fiber thus treated was water-wettable and that it did not feel waxy.

PP-F-2 (drawn fiber; see Table 1) was used to investigate the dyeability with acidic dyes. Table 5 shows the dyeing results. It was confirmed that the fiber can be well dyed by the acidic dyes. However, the dyeing fastness was insufficient and must be improved much more.

Conclusion

The polypropylene fiber, modified by the blending of a fine powdery copolymer of glycidyl methacrylate and divinylbenzene, was treated with diethyl amine, diethanol amine, monoethanol amine, and ammonia. The resultant fiber could be wettable with water and dyed with acidic dye.

NOTES

BULLETIN OF THE CHEMICAL SOCIETY OF JAPAN VOL. 42 3327—3329 (1969)

Vinyl Polymerization. 239.*1 Polymerization of Methyl Methacrylate with Cellulose Triacetate in Presence of Various Solvents

Kanemitsu KUBUSHIRO, Kiichi TAKEMOTO*2 and Minoru IMOTO

Department of Applied Chemistry, Faculty of Engineering, Osaka City University, Sumiyoshi-ku, Osaka

(Received December 29, 1968)

Recently, fibrous cellulose triacetate (CTA) was found to initiate the polymerization of methyl methacrylate (MMA) in the presence and absence of water.[1] The present paper concerns a further study on the polymerization of MMA initiated with CTA in the presence of various solvents. The initiation of polymerization seems to be referred to an interaction of some active sites on CTA with MMA, but the essential feature of the polymerization remains uncertain.

Experimental

All of the procedures were the same as in the previous paper.[1] The degree of swelling of CTA was measured in the following way: CTA was dissolved at first in dichloromethane and ethanol mixture (9 : 1 in vol.), and the solution was spread onto a glass plate. The cast film obtained after drying was transparent and colorless, and of 0.208 mm in thickness. 0.1 g of the CTA film was placed in a test tube, with a mixture of methyl isobutyrate with other solvents. The tube was sealed off and kept at 30°C for 24 hr, and thereafter, the weight increase of the CTA films was measured.

Results and Discussion

Effect of Solvents on the Rate of Polymerization. Figure 1 shows examples of time-conversion curves, where polymerization was carried out in the presence of various solvents. As shown in Fig. 1, a small amount of ethyl acetate acted to decrease the rate of polymerization, while *n*-hexane to accelerate it considerably.

Figure 2 shows the initial rates of polymerization calculated from the initial slopes of time-conversion curves. This figure shows that the value of the rate

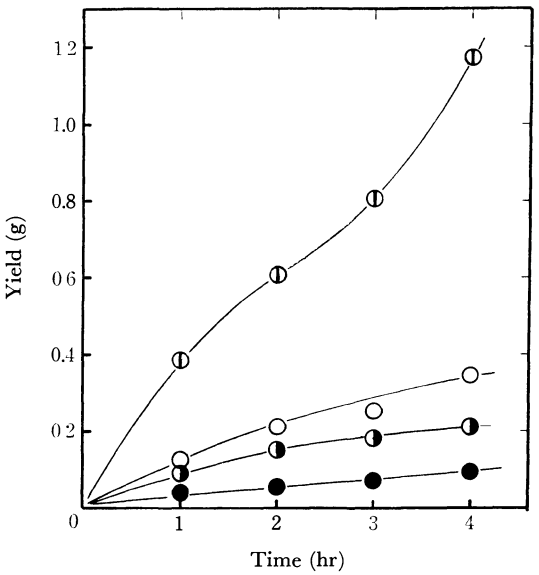

Fig. 1. Polymerization of MMA in the presence of various solvents. Total volume 5 m*l*, CTA 0.5 g, at 85°C.
◐ *n*-hexane 3 m*l* ○ MMA in bulk
◑ carbon tetrachloride ● ethyl acetate

of polymerization (percent per hour) divided by the monomer concentration is constant, regardless of the monomer concentration, except the cases where *n*-hexane, dichloromethane and ethyl acetate were used. This result means that benzene, ethanol, dimethylformamide and carbon tetrachloride acted only as diluents.

The relation between the degree of swelling and the solvent composition is shown in Fig. 3. The solvents consisted of methyl isobutyrate and other organic solvents which were used for polymerization. Methyl isobutyrate was chosen instead

*1 Part 238 of the series: T. Nakaya, Y. Maki and M. Imoto, *Makromol. Chem.*, **125**, 161 (1969)

*2 Present address: Department of Petr ochemistry, Faculty of Engineering, Osaka University, Yamada-Kami, Suita, Osaka.

1) K. Kubushiro, K. Takemoto and M. Imoto, *Makromol. Chem.*, **120**, 39 (1968).

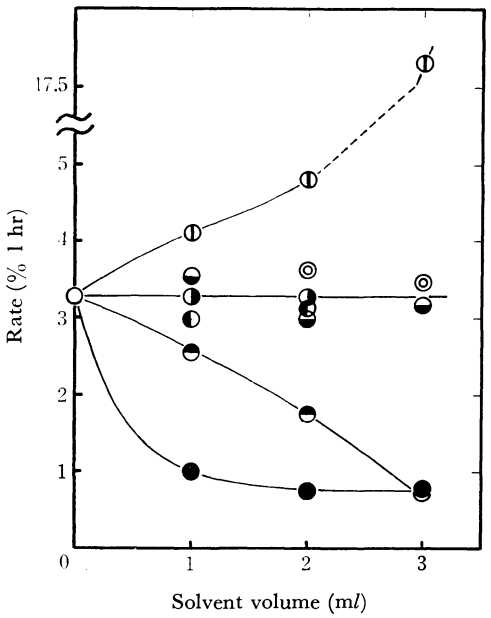

Fig. 2. Rate of Polymerization in various solvents. Total volume 5 m*l*, CTA 0.5 g, at 85°C.
- *n*-hexane
- benzene
- carbon tetrachloride
- dimethylformamide
- dichloromethane
- ethyl acetate
- ethanol

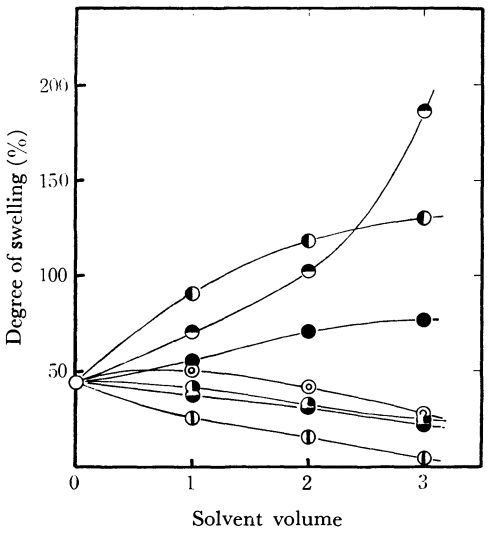

Fig. 3. Degree of swelling of CTA in methyl isobutyrate and various solvents. Total volume 5 m*l*, CTA 0.1 g, 30°C for 24 hr.
- dichloromethane
- dimethylformamide
- ethyl acetate
- ethanol
- carbon tetrachloride,
- benzene
- *n*-hexane

of MMA, because their structures are similar. The effect of solvents on the rate of polymerization

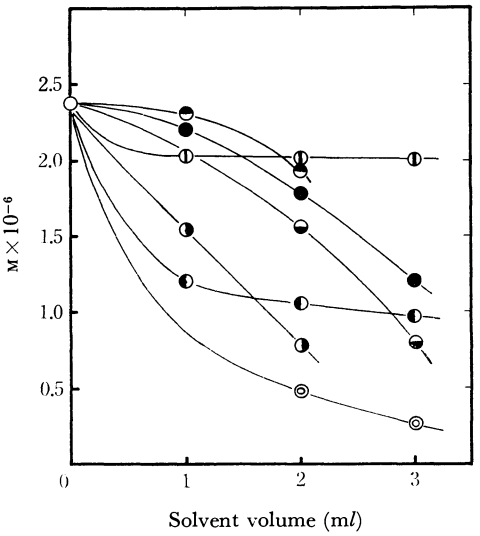

Fig. 4. Molecular weight of extracted PMMA polymerized in various solvents. Total volume 5 m*l*, CTA 0.5 g at 85°C.
- dichloromethane
- ethyl acetate
- *n*-hexane
- benzene
- carbon tetrachloride
- dimethylformamide
- ethanol

seems to show no parallelism with the swelling ability of these solvents for CTA.

From Figs. 2 and 3, in which different solvents are given, we see that polymerization preceeds not only inside CTA, but also outside it. This consideration agrees with that reported in a previous paper,[1] *viz.*, the rate of polymerization is proportional to the square root of CTA and to the monomer concentration.

As can be seen from Fig. 2, in the case of *n*-hexane, the rate of polymerization increases with the decrease in the concentration of monomer. When the concentration is 3.74 mol/*l*, the rate is about six times larger than that obtained in the other normal solvents. This result seems to be in line with the following consideration: *n*-hexane dose not swell CTA but dissolves MMA, while a part of MMA swells CTA and the rest of MMA remains in *n*-hexane. Thus, MMA is divided between CTA and *n*-hexane, and CTA swells with MMA. Accordingly, the interior of the fiber becomes a viscous polymerizing system for MMA, that is, an effect similar to the gel effect arises even in the initial stage of polymerization. As MMA is consumed by polymerization in the interior of the fiber, MMA is supplied successively from the *n*-hexane solution.

Next, we may consider the retardation effect of ethyl acetate. The structure of ethyl acetate is like that of MMA and ethyl acetate also can swell CTA. If ethyl acetate has some interaction with active sites on CTA, the interaction of MMA with these sites may be hindered and then the formation

of radical is retarded.

On the other hand, a thermal polymerization of MMA in ethyl acetate was carried out in the absence of CTA. The time-conversion curve obtained was similar to that in the Fig. 1. Accordingly, the corresponding curve in the figure seems to be the one caused by thermal polymerization.

The mechanism of initiation remains still to be clarified, which will be dealt with more exactly in the near future.

Molecular Weight of Poly-MMA obtained in the Presence of Solvents. The molecular weight of homopolymer of MMA obtained in the presence of various solvents, with the exception of *n*-hexane, was found to decrease gradually with an increase in the amount of the solvent. The results are shown in Fig. 4. The decrease may be due to the chain transfer effect on the solvents. The reason why the molecular weight is not affected

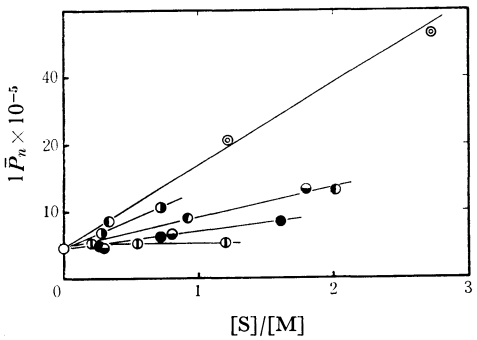

Fig. 5. Relationship between $1/\bar{P}_n$ and [S]/[M].
◎ ethyl ◑ carbon tetrachloride
◒ benzene ◐ dimethylformamide
● ethyl acetate ◑ *n*-hexane

by the presence of *n*-hexane, would come from the following view: CTA has only little affinity for *n*-hexane, so that only a very minor amount of *n*-hexane would be present in the interior of CTA, even when a larger amount of *n*-hexane was added in the reaction system.

In the presence of solvent, number average molecular weight of the polymers can be expressed by the following equation:

$$1/\bar{P}_n = C_m + C_s[\mathrm{S}]/[\mathrm{M}] + k_t/k_p \cdot \frac{[\mathrm{M}\cdot]}{[\mathrm{M}]} \qquad (1)$$

In this equation, the value of $k_t/k_p \cdot [\mathrm{M}\cdot]/[\mathrm{M}]$ would be very much smaller as compared with C_m, as was reported in the previous paper,[1] so it can be simplified to

$$1/\bar{P}_n = C_m + C_s\frac{[\mathrm{M}]}{[\mathrm{S}]} \qquad (2)$$

From the data in Fig. 4, a linear relationship between $1/P_n$ and [S]/[M] is obtained as shown in Fig. 5. The C_s value calculated is of the same order as that reported in literature,[2] where number average molecular weight of the polymers was estimated according to the following relationship, assuming that the molecular weight distribution of each polymer is identical and obeys Schulz's equation.[3]

$$M_n = 1/2 \cdot \bar{M}_w \qquad (3)$$

C_s values obtained in the experiment are shown in Table 1.

Table 1. C_s values of various solvents to poly-MMA radical

Solvent	$C_s \cdot 10^5$
Ethanol	14.6
Carbon tetrachloride	8.2
Dimethylformamide	4.6
Ethyl acetate	2.6
n-Hexane	0.0

2) "Polymer Handbook," ed. by J. Brandrup and E. H. Immergut, Interscience Publ., New York (1966), II-101.

3) G. V. Schulz, *Z. physik. Chem.*, **B30**, 379 (1935); *Chem. Abstr.*, **30**, 2460 (1936).

BULLETIN OF THE CHEMICAL SOCIETY OF JAPAN VOL. 42 3330—3333 (1969)

Kinetics of Multidentate Ligand Substitution Reactions. VII. Substitution Reactions of the Nickel(II)-Iminodiacetate Chelate with Ethylenediaminetetraacetic Acid and 1,2-Diaminocyclohexanetetraacetic Acid and of the Cobalt(II)-Nitrilotriacetate with 1,2-Diaminocyclohexanetetraacetic Acid

Mutsuo KODAMA

Department of Chemistry, Ibaraki University, Bunkyo-cho, Mito

(Received March 10, 1969)

In the previous paper,[1] the kinetics of the substitution reaction between the nickel(II)-nitrilotriacetate chelate and diethylenetriaminepentaacetic acid (DTPA) were investigated systematically by the polarographic method. The reaction proceeded mainly through tervalent, quadrivalent, and quinquivalent DTPA anions. In an acid medium, the contribution of the quinquivalent DTPA anion reaction was negligible. The activation parameters, $\Delta H^{\neq}$ and $\Delta S^{\neq}$, for the three elementary reactions were also determined. In the two elementary reactions which proceed through tervalent and quinquivalent DTPA anions, the $\Delta S^{\neq}$ values were negative. The reaction which involves the quadrivalent DTPA anion, however, had a positive entropy of activation. This was ascribed to the fact that in the quadrivalent DTPA anion, intramolecular hydrogen bonding among hydrogen-ion and nitrogen groups places the DTPA anion in a favorable position to from a mixed ligand reaction intermediate; thus, less freedom was lost in the formation of the intermediate. In the nucleophilic substitution reaction involving 1,2-diaminocyclohexanetetraacetic acid (CyDTA), the CyDTA anion would be placed in a favorable position to react with metal. Therefore, even the reaction involving the completely-deprotonated CyDTA anion will give a positive entropy of activation. In this paper, the substitution reactions of CyDTA with nickel(II)-iminodiacetate and cobalt(II)-nitrilotriacetate chelates were studied by observing the change in the anodic wave-height of uncomplexed CyDTA. The exchange reaction between ethylenediaminetetraacetic acid (EDTA) and the nickel(II)-iminodiacetate chelate was compared with the reaction of CyDTA with the nickel(II)-iminodiacetate chelate.

Experimental

Reagents. The ways of preparing and standardizing the nickel(II) nitrate and cobalt(II) perchlorate solutions were given in previous papers.[1,2] Iminodiacetic acid (IDA) was recrystallized three times from an aqueous solution by adding pure ethanol, and a known amount was dissolved in doubly-distilled water. The recrystallization of nitrilotriacetic acid (NTA), EDTA, and CyDTA and the preparation of their solutions have also been described previously.[3,4] Other reagents were of an analytical reagent grade and were used without further purification.

Apparatus and Experimental Procedure. All the apparatus (Pen-recording polarograph and the dropping mercury electrode) and experimental procedures were the same as have been described previoulsy.[1] All the measurements were conducted in solutions with the ionic strength of 0.20 ($NaClO_4$) in the pH range from 8.50 to 10.00. Since the sample solutions contained a large excess of uncomplexed NTA or IDA, no buffer reagent was used. The reaction rate was followed by recording automatically the change in the anodic wave-height of uncomplexed CyDTA or EDTA with the time.

Results and Discussion

The reaction of the nickel(II)-IDA chelate with EDTA and that with CyDTA were studied at 25 and 33°C respectively. The reaction beween the cobalt(II)-NTA chelate and CyDTA was studied at 18°C. All the substitution reactions investigated in solutions containing a large excess of complexed and uncomplexed IDA or NTA in the pH range from 8.50 to 10.00. Therefore, the reaction could be treated as pseude first-order reaction. In this study, the concentration of the metal(II)-IDA or -NTA chelate, $[MX]_t$, ranged from 8.50 to 20.00 mM and that of uncomplexed IDA or NTA, $[X]_f$, from 7.0 to 25.0 mM. As had been observed in the reaction of DTPA with the nickel(II)-NTA chelate,[1] the plot of $\log(i_0/i_t)$ aginst t invariably gave a straight line passing through the point of origin (Fig. 1). When the

1) M. Kodama, This Bulletin, **42**, 2532 (1969).

2) M. Kodama, *ibid.*, **40**, 2575 (1967).

3) M. Kodama, C. Sasaki and M. Murata, *ibid.*, **41**, 1333 (1968).

4) M. Kodama and H. Ebine, *ibid.*, **40**, 1857 (1967).

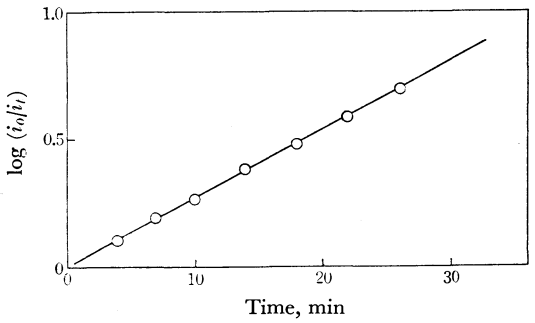

Fig. 1. log i_0/i_t *vs.* time plot for the exchange reaction of nickel (II)-IDA chelate with CyDTA
pH=9.05, μ=0.20, 33°C
Initial concentration of CyDTA=0.610 mM
Concentration of nickel(II)-IDA chelate =10.24 mM
Concentration of uncomplexed IDA=6.92 mM

other experimental conditions were kept constant, its slope was independent of the initial concentration of CyDTA or EDTA. The presence of the metal-(II)-CyDTA or -EDTA chelate had no effect on the slope of the linear relation. Therefore, as was discussed in the substitution reaction of DTPA with the nickel(II)-NTA chelate,[1] it can be concluded that, practically, the rate of the backward reaction of the present substitution reaction is negligible compared with that of the forward reaction, and that all the three substitution reactions studied here proceed through simultaneous reaction pathways which involve only direct second-order nucleophilic substitution reactions of the metal(II)-IDA or -NTA chelate with the CyDTA or EDTA anion. The slope of the linear relation between $-\log i_t$ and t was also proportional to the concentration of the metal(II)-IDA or -NTA chelate and inversely proportional to the value of $1+K^{X}_{MX_2}\cdot[X]_f/(\alpha_H)_X$, provided that the other experimental conditions were kept constant (Tables 1 and 2). All the symbols used here have the same meanings as previously.[1] These two facts clearly indicate that the slope is exactly proportional to the concentration of the metal(II)-IDA or -NTA chelate with a 1-to-1 composition. In the solutions with given concentrations of the complexed and uncomplexed IDA, or NTA, and with a given initial con-

Table 1. Dependence of the slope on the concentration of nickel(II) - IDA or cobalt(II) - NTA chelate

1) Nickel(II)-IDA chelate-EDTA system
μ=0.20 pH=9.23 [EDTA]=0.610 mM
$[IDA]_f$=10.14 mM 25°C

Concentration of Ni(II)-IDA chelate, $[NiX]_t$, mM	Slope sec^{-1}	Concentration ratio	Slope ratio
8.63	2.50×10^{-3}	1.00	1.00
12.95	3.73×10^{-3}	1.50	1.49
17.26	5.10×10^{-3}	2.00	2.04

2) Nickel(II)-IDA-CyDTA system
μ=0.20 pH=8.90 [CyDTA]=0.610 mM
$[IDA]_f$=6.92 mM 33°C

Concentration of Ni(II)-IDA chelate, $[NiX]_t$, mM	Slope sec^{-1}	Concentration ratio	Slope ratio
10.24	6.29×10^{-4}	1.00	1.00
20.48	1.26×10^{-3}	2.00	2.00

3) Cobalt(II)-NTA-CyDTA system
μ=0.20 pH=9.65 [CyDTA]=0.610 mM
$[NTA]_f$=9.55 mM 18°C

Concentration of Co(II)-NTA chelate, $[CoX]_t$, mM	Slope sec^{-1}	Concentration ratio	Slope ratio
9.15	2.21×10^{-4}	1.00	1.00
11.40	2.72×10^{-4}	1.25	1.23
16.80	3.97×10^{-4}	1.84	1.80

Table 2. Dependence of the slope on the concentration of uncomplexed IDA or NTA

1) Nickel(II)-IDA-EDTA system
μ=0.20 pH=9.23 [EDTA]=0.610 mM
$[NiX]_t$=8.63 mM 25°C

Concentration of uncomplexed IDA, $[X]_f$, mM	Slope sec^{-1}	Slope$\times[1+K^{X}_{NiX_2}\times[X]_f/(\alpha_H)_X]$
10.14	2.50×10^{-3}	56.9
19.34	1.33×10^{-3}	57.6
28.44	8.83×10^{-4}	56.2

2) Nickel(II)-IDA-CyDTA system
μ=0.20 pH=8.90 [CyDTA]=0.610 mM
$[NiX]_t$=10.24 mM 33°C

Concentration of uncomplexed IDA, $[X]_f$, mM	Slope sec^{-1}	Slope$\times[1+K^{X}_{NiX_2}\times[X]_f/(\alpha_H)_X]$
6.92	6.29×10^{-4}	9.77
16.07	2.76×10^{-4}	9.95
25.22	1.75×10^{-4}	9.90

3) Cobalt(II)-NTA-CyDTA system
μ=0.20 pH=9.65 [CyDTA]=0.610 mM
$[CoX]_t$=9.15 mM 18°C

Concentration of uncomplexed NTA, $[X]_f$, mM	Slope sec^{-1}	Slope$\times[1+K^{X}_{CoX_2}\times[X]_f/(\alpha_H)_X]$
9.55	2.21×10^{-4}	5.03×10^{-3}
13.10	1.69×10^{-4}	5.19×10^{-3}
17.10	1.29×10^{-4}	5.13×10^{-3}

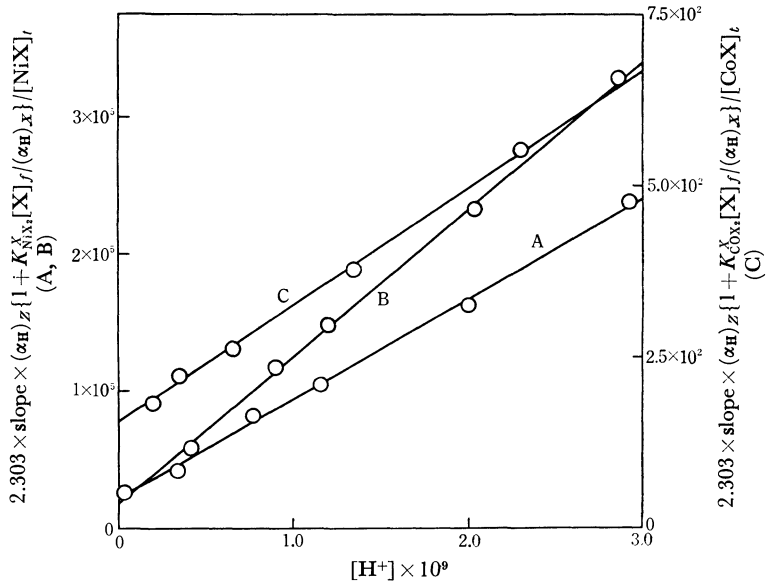

Fig. 2. The plot of $2.303 \times \text{slope} \times (\alpha_H)_Z[1+K^X_{MX_2}[X]_f/(\alpha_H)_Z]/[NiX]_t$ against $[H^+]$

25°C, $\mu=0.20$

A: Ni(II)-IDA-EDTA system
Initial concentration of EDTA=0.610 mM
Concentration of nickel(II)-IDA chelate=8.63 mM
Total concentration of IDA=27.4 mM

B: Ni(II)-IDA-CyDTA system
Initial concentration of CyDTA=0.610 mM
Concentration of nickel(II)-IDA chelate=10.24 mM
Total concentration of IDA=27.4 mM

C: Co(II)-NTA-CyDTA system
Initial concentration of CyDTA=0.610 mM
Concentration of cobalt(II)-NTA chelate=9.15 mM
Total concentration of NTA=27.4 mM

centration of CyDTA or EDTA, the plot of slope $\times(\alpha_H)_Z$ *vs.* $[H^+]$ gave a linear relation (Fig. 2). Here, $(\alpha_H)_Z$ is the (α_H) value of CyDTA or EDTA.

From the above experimental facts and discussion, it can be safely concluded that all the three exchange reactions proceed mainly through the following two simultaneous reaction pathways:

$$\text{i)}\quad MX^{2-m} + Z^{4-} \underset{}{\overset{k_1^+}{\rightleftharpoons}} MZ^{2-} + X^{m-}$$
$$\updownarrow \text{rapid}$$
$$MX_2^{2-2m}$$

$$\text{ii)}\quad MX^{2-m} + HZ^{3-} \overset{k_2^+}{\rightleftharpoons} MZ^{2-} + HX^{1-m}$$
$$\updownarrow \text{rapid}$$
$$MX_2^{2-2m}$$

where MX^{2-m} and MX_2^{2-2m} mean the metal (II)-IDA or -NTA chelates with 1-to-1 and 1-to-2 compositions respectively; X^{m-}, the completley-deprotonated IDA or NTA anion, and Z^{4-}, the completely-deprotonated CyDTA or EDTA anion. On the basis of the above reaction mechanism, the slope of the linear relation between $-\log i_t$ and t can be expressed as:

$$\text{slope} = \frac{1}{2.303}\left(k_1^+ + \frac{k_2^+ \cdot [H]^+}{k_4}\right) \times \frac{[MX]_t}{(\alpha_H)_Z\left[1+\dfrac{K^X_{MX_2}\cdot[X]_f}{(\alpha_H)_X}\right]} \qquad (1)$$

where k_4 is the fourth dissociation constant of CyDTA or EDTA.

The k_1^+ and k_2^+ values determined from the slope and the intercept of the linear relation between slope $\times$ 2.303 $\times$ $(\alpha_H)_Z[1+K^X_{MX_2}[X]_f/(\alpha_H)_X]/[MX]_t$ and $[H^+]$ are given in Table 3. Similar results were also obtained in the experiments carried out at the other two temperatures. The rate constants for the two elementary reactions determined at the other two temperatures are also listed in Table 3. In all cases, linear relations were found between $\log k_i^+$ and $1/T$ for both elementary reactions; these made it possible to calculate the heats and entropies of activation. The heats and the entropies of activation determined from the linear

TABLE 3. RATE CONSTANTS, HEAT OF ACTIVATION AND ENTROPY OF ACTIVATION FOR REACTIONS (i) AND (ii)

1) Nickel(II)-IDA-EDTA reaction

k^+ value M^{-1} sec^{-1}	Temperature, °C 18	25	33	$\Delta H^{\neq}$ kcal	$\Delta S^{\neq}$ e.u.
k_1^+	1.5×10^4	2.1×10^4	4.5×10^4	8.4	−10.4
k_2^+	3.35×10^3	7.33×10^3	1.38×10^4	13.9	5.6

2) Nickel(II)-IDA-CyDTA reaction

k^+ value M^{-1} sec^{-1}	Temperature, °C 18	25	33	$\Delta H^{\neq}$ kcal	$\Delta S^{\neq}$ e.u.
k_1^+	9.0×10^3	1.7×10^4	4.1×10^4	16.6	16.9
k_2^+	1.86×10^2	3.33×10^2	7.48×10^2	16.1	7.5

3) Cobalt(II)-NTA-CyDTA reaction

k^+ value M^{-1} sec^{-1}	Temperature, °C 18	25	33	$\Delta H^{\neq}$ kcal	$\Delta S^{\neq}$ e.u.
k_1^+	3.4×10^1	6.5×10^1	1.55×10^2	15.5	3.4
k_2^+	1.33×10^{-1}	3.42×10^{-1}	6.50×10^{-1}	20.6	5.2

TABLE 4. NUMERICAL VALUES*

1) pK values (mixed constants)[11]

	pK_1	pK_2	pK_3	pK_4
IDA	—	9.34		
NTA	—	—	9.60	
EDTA	—	—	6.03	10.00
CyDTA	—	—	5.99	11.42

2) log $K^Y_{MX_2}$ values[11]

	log $K^Y_{MX_2}$
Ni(II)-IDA chelate	6.35
Co(II)-NTA chelate	3.63

* These values are calculated from the related constants in solutions of ionic strength 0.10 and the activity coefficients of the ions calculated by means of Davies equation.[12]

relation between log k_i^+ and $1/T$ are also given in Table 3. The numerical values used in the calculation of (α_H)'s, $[X]_f$, and k_2^+ are listed in Table 4. The way of calculating $[X]_f$ was given in previous paper.[3]

As is shown in Table 3, both elementary reactions gave positive entropies of activation in the substitution reactions involving CyDTA. In the NMR study of the conformation of the CyDTA anion, Reilley *et al.*[5,6] concluded that, in tervalent and quadrivalent CyDTA anions, two iminodiacetate groups occupy nearly diequatorial positions on the cyclohexane ring because of the steric effect of the cyclohexane ring. The preorientation of the CyDTA anion by the cyclohexane ring probably places the CyDTA anion in a favorable position to react with metal ion. Thus, less conformational and rotational freedom will be lost in the chelate formation reaction of CyDTA. This prediction has been confirmed by several authors[7-9] in their thermodynamic study of the chelate formation reaction. The entropies of the reaction of CyDTA chelates are always greater than those of the corresponding EDTA chelates. The experimental evidence that, in the substitution reactions involving CyDTA, both elementary reactions gave positive entropies of activation may also be ascribed to the preorientated diequatorial conformation of the CyDTA anion. Thus, these facts support the present author's explanation of the effect of the protonation of the CyDTA anion on the heat of activation given in a previous paper.[1] The positive entropy of activation for the elementary reaction (ii) in the reaction of EDTA with the nickel(II)-IDA chelate can also be attributed to the conformation of the tervalent EDTA anion, which is similar to that of the chelated EDTA anion.[6]

Finally, it can also be mentioned that the k_2^+ value for the reaction of EDTA with the nickel(II)-IDA chelate is about 1000 times greater than that with the nickel(II)-NTA chelate.[10] The k_2^+ ratio between the nickel(II)-IDA and nickel(II)-NTA systems agrees well with the ratio of the stability constants of the chelates with the 1-to-1 composition.[11] This agreement probably means that the reaction of EDTA with nickel(II)-IDA proceeds through the same reaction intermediate as that for the reaction with the nickel(II)-NTA chelate.

The present author wishes to express his hearty thanks to Mr. Tomohiko Noda and Miss Yayoe Tominaga for their help during this research.

5) J. L. Sudmeier and C. N. Reilley, *Anal. Chem.*, **36**, 1707 (1964).
6) Y. Fujiwara and C. N. Reilley, *ibid.*, **40**, 890 (1968).
7) D. L. Wright, J. H. Holloway and C. N. Reilley, *ibid.*, **37**, 883 (1965).
8) G. Anderegg, *Helv. Chim. Acta*, **46**, 1833 (1963).
9) T. Moeller and T. M. Hseu, *J. Inorg. Nucl. Chem.*, **24**, 1635 (1962).
10) M. Kimura, *Nippon Kagaku Zasshi (J. Chem. Soc. Japan, Pure. Chem. Sect.)*, **89**, 1209 (1968).
11) L. G. Sillén and A. E. Martell, "Stability Constants of Metal-Ion Complexes," The Chemical Society, London (1964).
12) J. N. Butler, "Ionic Equilibrium," Addison-Wesley Publishing Co., Reading, Massachusetts (1964), p. 437.

BULLETIN OF THE CHEMICAL SOCIETY OF JAPAN VOL. 42 3334—3335 (1969)

Magnetic Properties of Organic Stable Radicals. II. Porphyrexide

Teruaki FUJITO, Hiroaki NISHIGUCHI, Yasuo DEGUCHI and Jun YAMAUCHI*

Department of Chemistry, Faculty of Science, Kyoto University, Sakyo-ku, Kyoto
**The Institute for Chemical Research, Kyoto University, Uji, Kyoto*

(Received April 16, 1969)

The magnetic properties of triacetonamine-oxyl and its derivatives have been studied by many investigators.[1] In these radicals having penta-, hexa- or haptacyclic structures, the N–O group is masked by four methyl groups. Recently it has been found that one of these radicals, 2,2,6,6-tetramethyl-4-hydroxypiperidine-1-oxyl (TANOL), exhibits a temperature depedence of its magnetic susceptibility which can be understood by the one-dimensional Heisenberg model.[2–4] The molecular structure of porphyrexide is different from that of the TANOL radical, that is, porphyrexide is pentacyclic with a somewhat planar molecular structure, and it has a π-orbital in its cyclic ring. It has only two methyl groups, so the N–O group is not completely shielded. Therefore, it is presumed to show different magnetic properties from the TANOL radical. Müller and Müller-Rodloff have reported[5] that the paramagnetic susceptibility of porphyrexide obeys the Curie-Weiss law in the temperature range from 300°K to 90°K, with the Weiss constant $\theta=-6\pm5$°K and $\chi_{mol}=40.1\times10^{-4}$ emu at 90°K. We have measured the magnetic susceptibility of this radical at lower temperatures, the results are shown in Fig. 1.

The sample was obtained commercially and was used with no further purification. Its radical concentration was determined to be 91% by comparing the measured susceptibility with that calculated at 77°K. Magnetic susceptibility measurements were carried out using a magnetic torsion balance developed in our laboratory.[6] Diamagnetic correction was made employing the experimental value reported by Müller and Müller-Rodloff:[5] $\chi_{dia}=0.85\times10^{-4}$ emu/mol. The magnetic susceptibility of this radical follows the Curie-Weiss law (Weiss constant $\theta=-8$°K) in the temperature range from 300°K to 20K°, as Müller and Müller-Rodoff. At lower temperatures, however, it deviates from this law and reaches a broad maximum at 7.2°K, where $\chi_{max}=207.2\times10^{-4}$ emu/mol, and they gradually decrease below 7.2°K. In order to make clear the magnetism of the radical, it would be appropriate to compare this result with several typical theoretical models: the pair model, the linear Ising model, and the one-dimensional Heisenberg model (Fig. 1). χ_p is given as follows:

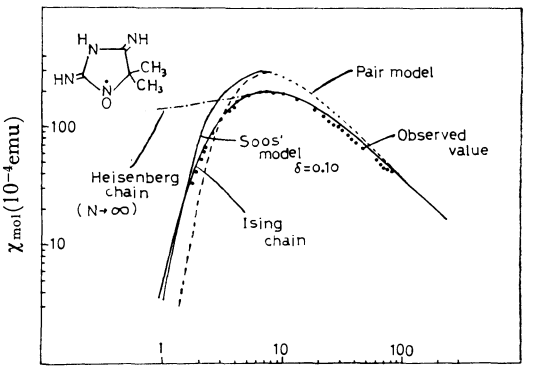

Fig. 1. Magnetic susceptibility of porpflyrexide.
Solid Curve : theoretcical susceptibility of the linear Ising model with $J/k=-7.2$°K and Soos's model with $\delta=0.10$
Dashed Curve: that of pair model with $\Delta/k=11.6$°K
Chain Curve : that of one-dimensional Heisenberg model $J/k=5.76$°K
● : observed values

$$\text{pair model: } \chi_p=\frac{Ng^2\beta^2S(S+1)}{kT}\cdot\frac{1}{3+e^{\Delta/kT}}$$

$$\text{linear Ising model: } \chi_p=\frac{Ng^2\beta^2}{4kT}e^{J/kT}$$

where Δ is the energy splitting between the ground singlet and the excited triplet states, where J is the spin-spin exchange interaction energy, and where the other letters have the usual meanings. The parameters, Δ/k and J/k, are determined to be 11.6°K and −7.2°K respectively from the temperature of the susceptibility maximum, Tm.

1) Yu. S. Karimov and E. G. Rozantsev, *Soviet Physics-Solid State*, **82**, 255 (1967); R. Briere, H. Lemaire and A. Rassat, *Bull. Soc. Chim. Fr.*, **1967** (**11**), 3278.
2) J. Yamauchi, T. Fujito, E. Ando, H. Nishiguchi and Y. Deguchi, *J. Phys. Soc. Japan*, **25**, 1558 (1968).
3) H. Lemaire, P. Rey, A. Rassat, A. D. Combarieu and J. C. Michel, *Mol. Phys.*, **14**, 201 (1968).
4) Yu. S. Karimov, *JETP Letters*, **8**, 145 (1968).
5) E. Müller and I. Müller-Rodloff, *Liebigs Ann. Chem.*, **521**, 81 (1935).
6) M. Mekata, *J. Phys. Soc. Japan*, **17**, 796 (1962).

The theoretical calculation of the one-dimensional Heisenberg model has been performed by Bonner and Fisher for the case of $\gamma=1$ and $N\rightarrow\infty$.[2,7] In our case $J/k=5.76°K$ is obtained by fitting Tm to the theoretical value. It can be seen from Fig. 1 that the observed value fits the linear Ising model better than the others. Thus, porphyrexide has different magnetic properties from TANOL, which has a character like that of the one-dimensional Heisenberg model, as has already been reported.[2-4] The difference in the magnetic behavior of these two radicals may be attributed to the difference in their molecular frameworks. The TANOL radical has a non-planar molecular framework and forms intermolecular hydrogen bonds parallel to the a-axis,[8] and it makes one-dimensional antiferromagnetic chains by means of isotropic exchange interaction. On the other hand, porphyrexide has a somewhat planar molecular structure, like BDPA,[9] and it makes one-dimensional antiferromagnetic chains of anisotropic exchange interaction through π-orbital, probably arranged in such a way that one molecular plane is stacked upon another. Another fit is obtained when the alternating linear Heisenberg antiferromagnet model proposed by Soos[10] is used with the alternating parameter, δ, being 0.1. We can not conclude which is the better model, the Ising or Soos's model, in this case. We are now, however, performing a study of the single crystals of this radical by using the magnetic torsion balance, an ESR spectrometer and an X-ray diffractometer in order to reach definite conclusions.

7) J. C. Bonner and M. E. Fisher, *Phys. Rev.*, **135**, A640 (1964).

8) J. Lajzerowicz-Bonnerteau, *Acta Cryst.*, **B24**, 196 (1968).

9) A. S. Edelstein, *J. Chem. Phys.*, **40**, 488 (1964); W. O. Hamilton and G. E. Pake, *ibid.*, **39**, 2694 (1963).

10) Z. G. Soos, *ibid.*, **46**, 4284 (1967); Z. G. Soos, *ibid.*, **43**, 1121 (1965).

BULLETIN OF THE CHEMICAL SOCIETY OF JAPAN VOL. 42 3335—3338 (1969)

Studies of Heteroaromaticity. XXXII.[1] New Synthesis of 1,2,4-Oxadiazoles, Benzoxazoles, Benzothiazoles and Benzimidazole from Aromatic Hydroxamoyl Chlorides

Tadashi SASAKI, Toshiyuki YOSHIOKA and Yasuyuki SUZUKI

Institute of Applied Organic Chemistry, Faculty of Engineering, Nagoya University, Chikusa-ku, Nagoya

(Received April 17, 1969)

There are many papers concerning the synthesis of five-membered heterocycles by the 1,3-dipolar cycloaddition reactions of nitrile oxides, which afforded, with double bonded dipolarophiles, dihydro-heteroaromatic compounds in general.[2] It is also known that similar reactions with dipolarophiles having hetero-multiple bond generally proceed with some difficulty, except for their activated types.[3] This note deals with a new synthesis of 1,2,4-oxadiazoles, benzoxazoles, benzothiazoles and a benzimidazole from aromatic hydroxamoyl chlorides, the precursors of nitrile oxides. It is reported that aromatic nitrile oxides do not undergo the 1,3-dipolar cycloaddition reactions with an imino heteromultiple bond, when it is a part of a simple azomethine linkage. This note is based on our finding that aromatic hydroxamoyl chlorides can react with the imino group, if it is incorporated in amidines IIa, iminoethers IIb and *S*-methylthiourea IIc, leading to the formation of 1,2,4-oxadiazoles after hetero-aromatization of the intermediated oxadiazolines III by elimination of R″H.

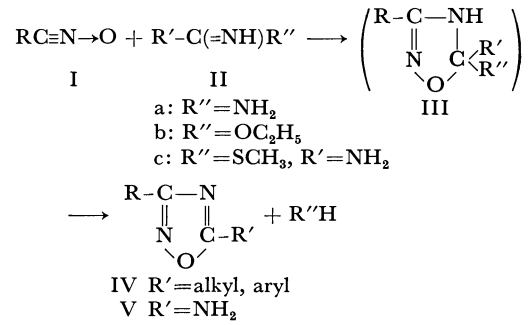

1) Part XXXI of this series: T. Sasaki and T. Yoshioka, This Bulletin, **42**, 3008 (1969).

2) For a recent review, see R. Huisgen, R. Grashey and J. Sauer, "Cycloaddition Reactions of Alkenes," in "The Chemistry of Alkenes," ed. S. Patai, Interscience Publisher, New York, N. Y. (1964), pp. 806—987.

3) For a recent review, see T. Sasaki, *Kagaku no Ryoiki*, **23**, 220, 320 (1969).

The general preparative method for 1,2,4-oxadiazales by the 1,3-dipolar cycloaddition of aromatic nitrile oxides with nitriles has been reported originally by Huisgen.[4] It is also reported, however, that the reactions with aliphatic nitriles hardly take place.[5,6] Musante[7] and Elory[8] reported independently the preparation of 1,2,4-oxadiazoles from nitrile oxide and benzamidine and benziminoether respectively. In order to investigate the applicability of these methods to aliphatic amidines and iminoethers, we investigated similar reactions using several aromatic nitrile oxides such as *p*- (Ia), *m*-nitrobenzonitrile oxide (Ib), 2-(5-nitrofuro)nitrile oxide (Ic), benzonitrile oxide (Id) and furonitrile oxide (Ie), all derived readily from the corresponding hydroxamoyl chlorides I'a—e in the presence of base. The results are summarized in Table 1. As indicated in this table, the method using amidines is found to be superior to that using iminoethers for the preparation of 5-aryl- and 5-alkyl-3-aryl-1,2,4-oxadiazoles (IV).

Elory[9] reported the preparation of 3-phenyl-5-amino-1,2,4-oxadiazole from benzonitrile oxide and guanidine. This method could not be applied to Ia—c, so we investigated similar reactions using thiourea instead of guanidine, but no reaction occurred. However, we found that *S*-methylthiourea reacted with Ia—c, affording the corresponding 5-amino-1,2,4-oxadiazoles (Va—c) after elimination of methylmercaptane even in such basic media as given in the reaction conditions, indicating that the presence of a suitable leaving group under the basic reaction conditions is an essential factor for the hetero-aromatization of the intermediated III. The results are summarized in Table 2.

In a previous paper,[10] we reported the reaction of 2-(5-nitrofuro)hydroxamoyl chloride (I'd) with two equivalents of ethanolamine to afford *N*-(*β*-hydroxyethyl)-2-(5-nitrofuryl)amidoxime. When I'c was treated with *o*-aminophenol instead of ethanolamine under similar reaction conditions, the product was proved to be benzoxazole (VIc) which might be produced by the hetero-aromatization of the intermediated VIIa or VIIb after elimination of hydroxylamine moiety. From our previous report[11] concerning the similar hydroxylamine-elimination in the reactions of aromatic hydroxamoyl chlorides with methyl dithiocarbazinate, VIIa seems to be more plausible than VIIb. Table 3 shows the results obtained by use of several hydroxamoyl chlorides.

Similar treatment of hydroxamoyl chlorides with two equivalents of *o*-aminothiophenol afforded the corresponding benzothiazoles (VIII) as given in

Table 1. Oxadiazoles from amidines and iminoethers

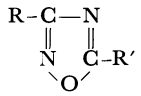

R	R'	Product	Mp °C	Yield (%)* a	b	c	d	Found (Calcd) C%	H%	N%	UV (EtOH) λmμ (ε)
p-NO_2-C_6H_4-	C_6H_5-	IVa-1	212—213	90		65	100				262 (24840)[6]
	CH_3-	IVa-2	139—141	80	60			52.91 (52.68	3.02 3.44	20.34 20.48)	276 (10500)
m-NO_2-C_6H_4-	C_6H_5-	IVb-1	165—166	80		50	80				244 (50500)[6]
	CH_3-	IVb-2	107—110	60	60			52.84 (52.68	3.57 3.44	20.40 20.48)	224 (21500)
2-(5-NO_2-C_4H_2O)-	C_6H_5-	IVc-1	206—208	75		8	36				313 (18600) 255 (22900)[6]
	CH_3-	IVc-2	104—105	45	55			43.17 (43.08	2.61 2.58	21.85 21.54)	304 (9280)
C_6H_5-	C_6H_5-	IVd-1	105—107	75							258 (35400)
	CH_3-	IVd-2	41	65		35					
C_4H_3O-	C_6H_5-	IVe-1	114—117	75				68.28 (67.92	3.58 3.80	13.46 13.20)	

* a: from amidines, b: from iminoethers, c: by the thermal 1,3-dipolar cycloaddition reactions previously reported by us,[6] d: in the presence of a catalyst in method c.

4) R. Huisgen, *Proc. Chem. Soc. (London)*, **1961**, 961.
5) S. Morrocchi, A. Ricca and L. Velo, *Tetrahedron Letters*, **1967**, 331
6) T. Sasaki and T. Yoshioka, This Bulletin, **41**, 2206 (1968).
7) C. Musante, *Gazz. Chim. Ital.*, **68**, 331 (1938); *Chem. Abstr.*, **32**, 9064 (1938).
8) F. Elory and R. Lenaers, *Bull. Soc. Chim. Belges*, **72**, 719 (1963).
9) F. Elory and R. Lenaers, *Helv. Chim. Acta*, **49**, 1430 (1966).
10) T. Sasaki and T. Yoshioka, *Yuki Gosei Kagaku Kyokai-shi (J. Synth. Org. Chem. Japan)*, **25**, 665 (1967).
11) T. Sasaki and T. Yoshioka, This Bulletin, **41**, 2211 (1968).

TABLE 2. 5-AMINO-1,2,4-OXADIAZOLES

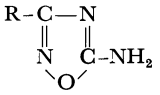

R	Product	Mp °C	Yield %	Found (Calcd) C%	H%	N%	UV (EtOH) mμ (ε)		IR (KBr) ν_{NH} cm^{-1}	
p-NO_2-C_6H_4-	Va	>300	80	46.67 (46.60	2.68 2.93	27.06 27.18)	298 (7860)	261 (14500)	3190	3450
m-NO_2-C_6H_4-	Vb	234—236	30	46.37 (46.60	2.92 2.93	26.98 27.18)	253 (10300)		3120	3320
2-(5-NO_2-C_4H_2O)-	Vc	239—241	60	36.54 (36.74	1.91 2.06	28.16 28.57)	317 (11500) 254 (7780)	285 (9250)	3280	3440
C_6H_5-	Vd	158—160[9]	90				254 (3390)		3100	3320

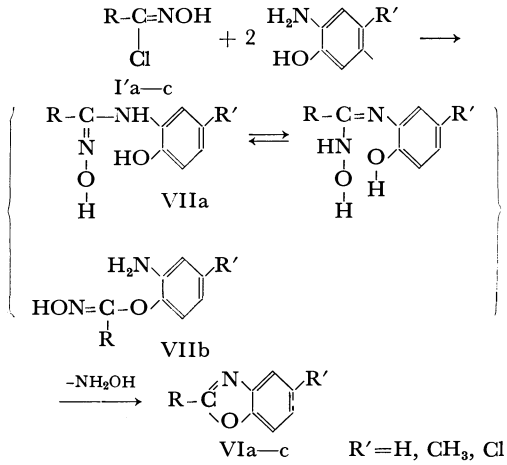

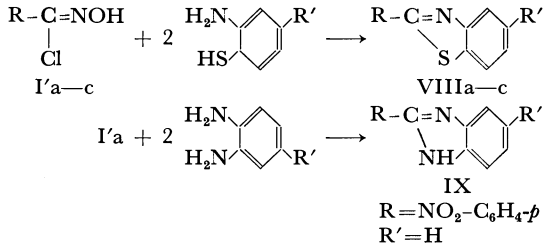

Table 4 and the reaction of *p*-nitrobenzhydroxamoyl chloride (I'a) with *o*-phenylenediamine afforded 2-(*p*-nitrophenyl)benzimidazole IX.

Experimental

The melting points were measured on a micro hot stage and are not corrected. The microanalyses were carried out with a Yanagimoto C. H. N. Corder, Model MT-1 type. The ultraviolet spectra were obtained on a Nippon-Bunko optical rotary dispersion recorder, Model ORD/UV-5. The NMR spectra were determined on a Varian A-60 spectrometer, with tetramethylsilane as an internal standard and the peak positions are expressed by τ-values.

TABLE 3. BENZOXAZOLES (VI)

R	R'	Mp °C	Yield %	Micoranalysis Found (Calcd) C	H	N	UV λ_{max}^{EtOH} mμ (ε)
p-NO_2-C_6H_4-	H	276—277	70	65.33 (65.00	3.08 3.36	11.74 11.66)	326 (23300) 230 (14000)
	CH_3	220—221	75	66.26 (66.13	3.58 3.96	11.10 11.02)	334 (24800) 232 (15200)
	Cl	248—250	80	57.38 (56.85	2.37 2.57	10.24 10.20)	330 (16900) 232 (8200)
m-NO_2-C_6H_4-	H	221—223	80	64.98 (65.00	3.10 3.36	11.64 11.66)	295 (23000) 263 (20300)
	CH_3	181—183	90	66.08 (66.13	3.80 3.96	10.61 11.02)	304 (14800) 264 (13000)
	Cl	192—193	60	57.44 (56.85	2.54 2.57	10.29 10.20)	307 (20200) 263 (21600)
2-(5-NO_2-C_4H_2O)-	H	233—235	50	57.74 (57.40	2.40 2.63	12.31 12.17)	349 (27600) 265 (14100) 230 (12600)
	CH_3	190—192	90	58.88 (59.02	3.22 3.30	11.51 11.47)	356 (25000) 269 (12900) 230 (11200)
	Cl	201—203	70	50.48 (49.92	1.92 1.90	10.69 10.58)	352 (22800) 269 (10600) 233 (9600)

Table 4. Benzothiazoles (VIII)

R	Mp °C	Yield %	Microanalysis Found (Calcd) C%	H%	N%	UV λ_{max}^{EtOH} mμ (ε)
p-NO_2-C_6H_4-	236—238	40	61.16 (60.94	3.19 3.15	11.07 10.93)	342 (13100) 305 (3200)
m-NO_2-C_6H_4-	188—189	70	60.43 (60.94	2.88 3.15	10.87 10.93)	294 (11400) 271 (11000)
2-(5-NO_2-C_4H_2O)-	248—250	40	53.60 (53.67	2.17 2.46	11.24 11.38)	364 (24000) 280 (7100)

Aromatic Hydroxamoyl Chlorides.

They were prepared according to the methods described in previous papers.[6,10,11]

Preparation of 1,2,4-Oxadiazoles. *Method a (Table 1).* From Amidines. To a solution of *p*-nitrobenzhydroxamoyl chloride (I'a) (1.0 g, 5 mmol) in 50 m*l* of ether was added a solution of acetamidine hydrochloride (1 g, 10 mmol) in 20 m*l* of water. A 5% aqueous sodium carbonate (1.3 g, 12 mmol) was added dropwise to the above reaction mixture under ice-cooling. After stirring for 1 hr at this temperature (*ca.* 5°C), the reaction mixture was further stirred at room temperature for 3 hr. The water layer was washed with ether (20 m*l*×3). The ether washing were combined with the original ether layer and dried over sodium sulfate. The residue obtained after removal of ether was recrystallized from ethanol to afford 3-(*p*-nitrophenyl)-5-methyl-1,2,4-oxadiazole (IVa-2) as white needles. The physical constants, yield and microanalysis are given in Table 1.

Method b (Table 1). From iminoethers. A similar procedure as above, except that acetiminoethyl ether hydrochloride (1.85 g, 15 mmol) was used instead of acetamidine hydrochloride, afforded the same product. This result is given in Table 1.

Reactions with S-Methylthiourea. A similar procedure as above except that *S*-methylthiourea sulfate (1.4 g, 5 mmol) was used instead of imioether hydrochloride afforded the corresponding 5-amino-1,2,4-oxadiazole (Va), which precipitated in the reaction mixture. The yield and analysis are given in Table 2.

Preparation of Benzoxazoles. To a stirred solution of I'a (1 g, 5 mmol) in 50 m*l* of ether was added dropwise a solution of *o*-aminophenol (1.1 g, 10 mmol) in 50 m*l* of benzene-ether (1 : 1) at room temperauter. Stirring was continued for 1 week. The resulting precipitates were filtered and recrystallized from ethanol-benzene to afford 2-(*p*-nitrophenyl)benzoxazole (VIa-1), which was identical with a specimen prepared from *p*-nitrobenzaldehyde and *o*-aminophenol in the presence of lead tetraacetate in acetic acid.[12] This result is given in Table 3. When I'a (1 g, 5 mmol) and *o*-aminophenol (1.1 g, 10 mmol) were refluxed in 50 m*l* of ethanol for 5 hr, VIa-1 precipitated in the cooling reaction mixture; the yield was almost the same as that described above.

Preparation of Benzothiazoles. Similar treatment as in the preparation of benzoxazoles was applied to *o*-aminothiophenol instead of *o*-aminophenol and the results are summarized in Table 4.

Preparation of Benzimidazole. A solution of I'a (1 g, 5 mmol) and *o*-phenylenediamine (1.1 g, 10 mmol) in 100 m*l* of ether was stirred at room temperature for 2 days and the resulting precipitates were filtered. The filtrate was condensed to give a crystalline residue, which was recrystallized from acetone to give an 80% yield of dark colored crystals, mp >300°C. ν_{max}^{KBr} 3000—2600, 1608, 1520, 1450, 1400, 1340, 1230 and 1100 cm^{-1}. Found: C, 65.42; H, 3.82; N, 17.83%. Calcd for $C_{13}H_9O_2N_3$: C, 65.26; H, 3.79; N, 17.57%.

12) F. F. Stephenes and J. D. Bower, *J. Chem. Soc.*, **1949**, 665.

BULLETIN OF THE CHEMICAL SOCIETY OF JAPAN VOL. 42 3339—3340 (1969)

Infrared Absorption Spectra and Oxidation of Iron(II) Hydroxide and Green Rust I

Toshihei MISAWA, Wataru SUËTAKA and Saburo SHIMODAIRA

The Research Institute for Iron, Steel and Other Metals, Tohoku University, Katahira-cho, Sendai

(Received April 18, 1969)

Transformations on oxidation of hydroxide and basic salts of iron (II) have been investigated by means of X-ray and electron diffraction.[1-4] Infrared spectroscopy was applied for the observation of hydroxide and basic chloride of iron (II) in aqueous solutions. The infrared spectra of iron (II) hydroxide and Green Rust I, an oxidation intermediate, were obtained for the first time. No absorption band attributable to other intermediate compounds appeared in the course of oxidation.

Iron (II) hydroxide and basic chloride were prepared by adding adequate quantities of potassium hydroxide to the oxygen free aqueous solutions of iron (II) chloride (0.39 mol/*l*). The precipitates formed were separated from solutions by centrifugation. The infrared absorptions due to the water remaining in the precipitates were compensated by means of a reference cell containing a thin film of water. The oxidation of the precipitates in solutions was carried out at room temperature by introducing air at a constant rate of 1 *l*/min.

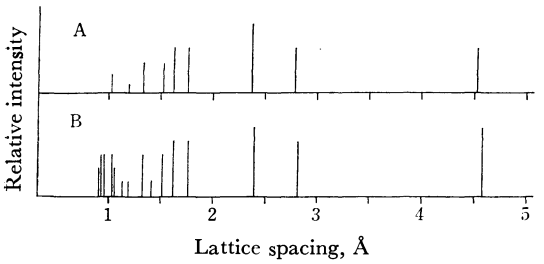

Fig. 1. X-Ray diffraction diagram of iron (II) hydroxide
A: present work B: Bernal *et al.*[1]

The precipitate obtained from basic solution (pH; 12.5—13.5), which was identified as iron (II) hydroxide by X-ray diffraction (Fig. 1), has two sharp absorption bands at 3630 and 480 cm^{-1}. The intensities of these two bands decreased with the progress of oxidation, and the absorption bands characteristic of α-FeOOH appeared. After oxidation for 30 hr, the absorption bands of iron (II) hydroxide disappeared completely, and only the bands due to α-FeOOH could be observed. Bernal *et al.* suggested an oxidation intermediate of Fe(O,OH).[1] However, no band attributable to such an intermediate compound could be detected.

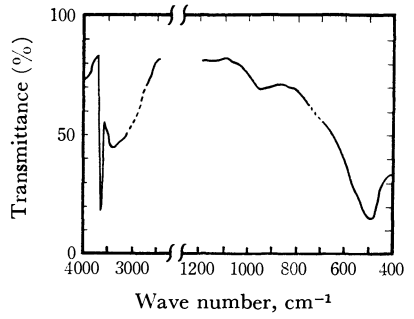

Fig. 2. Infrared absorption spectrum of iron (II) hydroxide obtained with Nujol mulling technique

Iron (II) hydroxide separated from solution was repeatedly washed with oxygen free ethanol and with petroleum ether so as to minimize the absorptions of water. The infrared spectrum of iron (II) hydroxide thus obtained is shown in Fig. 2. The high wavenumber and sharpness of the absorption band arising from O–H stretching vibration indicate that the OH group in iron (II) hydroxide is almost free from hydrogen bonding. The band at 480 cm^{-1} may be assigned to the translational mode of OH group by analogy with the spectrum of metal hydroxide having the same CdI_2 type structure as iron (II) hydroxide.[5]

The X-ray diffraction pattern showed that the precipitate formed in a slightly acidic solution (pH; 6.0—6.5) consisted of β-$Fe_2(OH)_3Cl$ and Green Rust I. The infrared absorption bands of the precipitate were located at 3540, 800, 670 and 470 cm^{-1}. While the relative intensity of the absorption band at 470 cm^{-1} decreased monotoni-

1) J. D. Bernal, D. R. Dasgupta and A. L. Mackay, *Clay Minerals Bull.*, **4**, 15 (1959).
2) T. Takada, T. Akita and M. Kiyama, Paper presented at the 21st Annual Meeting of the Chemical Society of Japan, April 1, 1968, and preceding papers.
3) H. Yoshioka, *J. Phys. Soc. Japan*, **4**, 270 (1949).
4) H. R. Oswald and W. Feitknecht, *Helv. Chim. Acta*, **44**, 847 (1961); *ibid.*, **47**, 272 (1964).
5) O. Oehler and Hs. H. Günthard, *J. Chem. Phys.*, **48**, 2036 (1968).

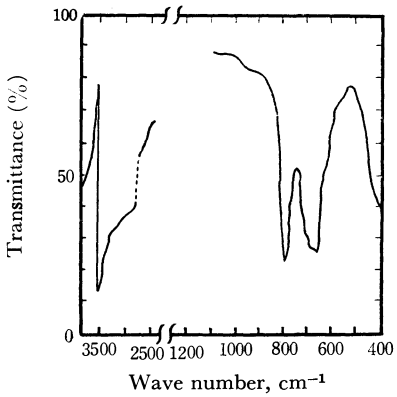

Fig. 3. Infrared absorption spectrum of Green Rust I (Nujol mull)

cally on oxidation, the bands at 3540, 800 and 670 cm^{-1} increased at first and then decreased in intensity. Since the increase of relative quantity of Green Rust I in the precipitate with oxidation was found at an early stage of oxidation by the X-ray diffraction measurement, it is likely that the latter three bands arise from the vibration of Green Rust I. The precipitate formed in neutral or slightly basic solution (pH; 7.0—8.0), was a mixture of iron (II) hydroxide and Green Rust I and was transformed to Fe_3O_4 by oxidation. It had absorption bands at 800 and 670 cm^{-1} besides the bands of $Fe(OH)_2$. This fact agrees with the assignment of the above mentioned bands to Green Rust I.

The infrared absorption spectrum of the precipitate formed in the slightly acidic solution and washed with ethanol and petroleum ether is shown in Fig. 3. The broad band at 470 cm^{-1} belonging probably to β-$Fe_2(OH)_3Cl$ disappears in the spectrum. It seems that β-$Fe_2(OH)_3Cl$ is not stable and decomposed during the course of washing with organic solvents, and thus Fig. 3 shows the spectrum of Green Rust I.

Bernal *et al.* claimed that Green Rust I might be transformed first to Green Rust II and then to γ-FeOOH.[1] Since all the absorption bands appearing on the oxidation of Green Rust I belonged to γ-FeOOH, it can be deduced that Green Rust I was not transformed as a whole to Green Rust II in the present investigation.

BULLETIN OF THE CHEMICAL SOCIETY OF JAPAN VOL. 42 3340—3342 (1969)

Gamma-Ray-Induced Addition of Formamide and Aniline to Crotonic Acid and Its Ester

Mitsuomi Itoh, Masao Tokuda, Yuji Yokoyama and Akira Suzuki*[1]

Department of Chemical Process Engineering, Hokkaido University, Sapporo, Hokkaido

(Received April 24, 1969)

Numerous reports on free radical addition reactions by various methods[1] are available, including peroxide induced reaction, photochemical reaction, and radiation-induced reaction. These varying methods tend to give different products. We reported previously on the photochemical addition of formamide and aniline to crotonic acid and its esters.[2] The present work was carried out using a γ-radiation technique on the same reactants in an attempt to compare the results with that obtained by photochemical method.

Light-induced amidation of olefins[3] and α,β-unsaturated esters,[4] and γ-radiation and electron induced amidation of olefins[5,6] and dienes[7] have been reported. According to the results, it was indicated that the light-induced addition of formamide to α,β-unsaturated esters such as methyl 2-octenoate, methyl 2-nonenoate and methyl 2-decenoate give only the β-adducts. On the other hand, we have pointed out that when crotonic acid and the esters are subjected to a photochemical addition of formamide, the α,- β- and γ-products were obtained and the product distribution between the acid and esters was different.

It was found that γ-ray-induced amidation of crotonic acid and its ethyl ester gives only the corresponding β-adduct, as summarized in Table 1.

1* Author to whom inquiries should be addressed.

1) For reviews, G. Sosnovsky, "Free Radical Reactions in Preparative Organic Chemistry," MacMillan Co., New York (1964).

2) M. Itoh, M. Tokuda, K. Kihara and A. Suzuki, *Tetrahedron*, **24**, 6591 (1968).

3) D. Elad and J. Rokach, *J. Org. Chem.*, **30**, 3361 (1965) and references cited therein.

4) J. Rokach and D. Elad, *ibid.*, **31**, 4210 (1966).

5) J. Rokach, C. H. Krauch and D. Elad, *Tetrahedron Letters*, **1966**, 3253.

6) D. P. Gush, N. S. Marans, F. Wessells, W. D. Addy and S. J. Olfky, *J. Org. Chem.*, **31**, 3829 (1966).

7) C. H. Krauch, J. Rokach and D. Elad, *Tetrahedron Letters*, **1967**, 5099.

TABLE 1. γ-RAY-INDUCED ADDITION OF FORMAMIDE TO CROTONIC ACID AND ETHYL CROTONATE

Substrate	Yield of 1:1-adduct, %	G-value	Distribution of products	
			α-Adduct	β-Adduct
$CH_3CH=CHCO_2H$	30[a]	10	0	100
	45[b]	8.6	0	100
$CH_3CH=CHCO_2Et$	36[a]	12	0	100

a) Irradiation time: 72 hr
b) Irradiation time: 144 hr

$$CH_3CH=CH-CO_2R + HCONH_2 \xrightarrow{\sim\sim} CH_3-\underset{\displaystyle CONH_2}{\underset{|}{CH}}-CH_2CO_2R$$

R=H, C_2H_5

Although detailed mechanistic studies were not undertaken, the reaction probably occurred by the attack of the carbamoyl radical which was produced by direct or indirect process.[5] The preference of β-adduct is in line with the generalization that the β-carbon is more easily attacked than the α-carbon in usual free radical addition to α,β-unsaturated carbonyl compounds having no phenyl linkage.[8]

The difference of the products obtained by photochemical procedure[2] and γ-ray-induced technique might be explained as follows: the orientation effect proposed in photochemical addition reactions need not be taken into account. A six-membered transition state such as A is not expected in γ-ray-induced reaction, because of the presence of the solvated electrons which interrupt the hydrogen bond with the carbonyl oxygen of the carbamoyl radical as described in B. Consequently, the addition of carbamoyl radical seems to occur readily at the β-carbon. On the other hand, the isomerization of the α,β-unsaturated ester to the corresponding β,γ-isomer observed in photochemical

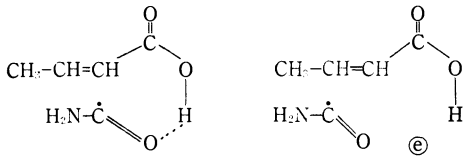

reaction[2,9] was not observed in γ-ray-induced reaction. This is apparently the reason why the γ-adduct is not obtained in the latter reaction.

A γ-ray-induced addition of aniline to crotonic acid and ethyl crotonate was found to give a small amount of 1 : 1-adduct. The distribution of the product isomers is listed in Table 2. In the case of crotonic acid, only the β-adduct was obtained with a large amount of side reaction products which are probably a mixture of polymeric and fragmentated products. It is of interest that crotonic acid is readily converted, with a 66% conversion, as compared with the ethyl ester with a mere 2% conversion. When the sealed tube was opened after irradiation, an increase of the inside pressure was observed, suggesting a generation of carbon dioxide. The photochemical alkylation of nitrogen hetero-aromatics with alkyl radical resulting from carboxylic acid by decarboxylation has been reported.[10] Thus we attempted to examine decarboxylation during the γ-ray irradiation applied to a mixture of crotonic acid and aniline. When a mixture of crotonic acid (0.2 mol), aniline (0.4 mol) and benzene (25 m*l*) was irradiated for 72 hr, one hundred and fourteen milliliters of CO_2 gas (0.006 mol) was evolved. This indicates that 3% of crotonic acid was subjected to decarboxylation. Several carboxylic acids (acetic, propionic, butyric and benzoic acids) were also treated under the same condition, but generation of CO_2 was not observed.

TABLE 2. γ-RAY-INDUCED ADDITION OF ANILINE TO CROTONIC ACID AND ETHYL CROTONATE

Substrate	Yield of 1:1-adduct, %	G-value	Distribution of products	
			α-Adduct	β-Adduct
$CH_3CH=CHCO_2H$	5 (66[a])	4.3	0	100
$CH_3CH=CHCO_2Et$	2	1.6	42	58

a) Total converstion of crotonic acid, calculated from crotonic acid unreacted.

In the γ-ray-induced addition of aniline to ethyl crotonate, a yield of a small amount of α- and β-adducts without side reaction products was detected.

Experimental

Reagents and a General Procedure. All reagents were distilled or recrystallized before use. Benzene and *t*-butanol were dried over metal sodium and calcium oxide respectively.

A mixture of reactants was charged into a 30 × 100 mm tube and the inside atmosphere was replaced with nitrogen gas several times. The sealed sample was irradiated in a cobalt-60 cavity source at room temperature. The dose rate was approximately 4×10^5

8) R. Brown, W. E. Jones and A. R. Pinder, *J. Chem. Soc.*, **1951**, 2123; T. M. Patrick, *J. Org. Chem.*, **17**, 1269 (1952); R. L. Huang, *J. Chem. Soc.*, **1956**, 1749; M. Okawara, *Kogyo Kagaku Zassi (J. Chem. Soc. Japan, Ind. Chem. Sect.,)* **57**, 760 (1954).

9) M. Itoh, M. Tokuda, K. Seguchi, K. Taniguchi and A. Suzuki, *Kogyo Kagaku Zasshi (J. Chem. Soc. Japan, Ind. Chem. Sect.)*, **72**, 219 (1969).

10) H. Nozaki, M. Kato, R. Noyori and M. Kawanishi, *Tetrahedron Letters*, **1967**, 4259.

rad. hr^{-1}.

The irradiated sample was treated as described earlier.[2] Glpc analysis was made with a Yanagimoto Model GCG-220 and an Ohkura Type GT-360 (Apiezon Grease L 20% coated on Diasolid L).

γ-Ray-Induced Amidation of Crotonic Acid with Formamide. A mixture of crotonic acid (0.08 mol), formamide (1.20 mol) and *t*-butanol (20 m*l*) was irradiated for 72 hr. The total dose was 2.88×10^7 rads. Treatment of the reaction mixture gave 3.2 g of 1 : 1-adduct (yield, 30% based on crotonic acid employed). Glpc analysis (column temp., 170°C) of the esterified product indicated the presence of a large peak and two other small peaks, the former corresponding to β-adduct. Neither of the latter small peaks corresponded to α-adduct, β-adduct or oxamide.

Further irradiation (144 hr, total dose, 5.76×10^7 rads) to the same mixture gave 4.70 g of 1 : 1-adduct (45%) and the product was confirmed as the β-adduct by glpc analysis.

γ-Ray-Induced Amidation of Ethyl Crotonate with Formamide. A mixture of ethyl crotonate (0.08 mol), formamide (1.20 mol) and *t*-butanol (20 m*l*) was irradiated for 72 hr (total dose, 2.88×10^7 rads). The same treatment of the irradiated mixture gave 4.60 g of 1 : 1-adduct (36%) and glpc analysis (170°C) of the esterified product indicated the presence of only β-adduct.

γ-Ray-Induced Addition of Aniline to Crotnic Acid. A mixture of crotonic acid (0.2 mol), aniline (0.4 mol) and benzene (25 m*l*) was irradiated for 72 hr (total dose, 2.88×10^7 rads). The reaction mixture was treated by the procedure reported by Stoermer,[11] which gave 2.0 g of β-anilinobutyranilide (yield, 4% based on crotonic acid) and 0.2 g of ethyl β-anilinobutyrate (1%). Distribution of 1 : 1-adducts was determined by glpc (Apiezon Grease L, 250°C). The total conversion of this reaction was calculated as 66% from the recovered crotonic acid (5.8 g).

Decarboxylation during the irradiation was estimated by gas analysis of CO_2 evolved. When the sealed tube was destroyed in an autoclave, 116 m*l* of CO_2 (0.006 mol) was generated at 22°C, which indicated that 3% of crotonic acid used was decarboxylated during the irradiation.

γ-Ray-Induced Addition of Aniline to Ethyl Crotonate. The irradiation of a mixture of ethyl crotonate (0.07 mol), aniline (0.14 mol) and benzene (10 m*l*) for 72 hr (total dose, 2.88×10^7 rads) gave 0.08 g of ethyl anilinobutyrate (1%) and 0.12 g of anilinobutyranilide (1%). The distribution of 1 : 1-adducts was determined by glpc analysis (250°C).

The authors wish to thank the Nippon Gosei Kagaku Co. for the supply of pure crotonic acid.

11) R. Stoermer and E. Robert, *Ber.*, **55**, 1030 (1922).

BULLETIN OF THE CHEMICAL SOCIETY OF JAPAN VOL. 42 3342—3344 (1969)

The Acid-catalyzed Rearrangement of Laurinterol Derivatives[1]

Minoru SUZUKI, Yoshiki HAYAKAWA and Toshi IRIE

Department of Chemistry, Faculty of Science, Hokkaido University, Sapporo, Hokkaido

(Received May 6, 1969)

In our studies of the chemistry of laurinterol (I) and debromolaurinterol (II),[2] we observed an interesting behavior upon the acid-catalyzed reaction of these compounds. The treatment of I and II (or their acetates, III and IV) with *p*-toluenesulfonic acid (TSA) in acetic acid at 50°C afforded aplysin (V) and debromoaplysin (VI) respectively.[2,3] In contrast, debromolaurinterol acetate (IV) gave cyclopentene VII in a good yield upon treatment with TSA in acetic anhydride under comparable conditions.[4] In this paper we will describe the acid-catalyzed rearrangement of laurinterol methyl ether (VIII) and debromolaurinterol methyl ether (IX).

The treatment of VIII with TSA in acetic acid at 50°C led to only the recovery of the starting material. However, when treated with 10% sulfuric acid in acetic acid at 50°C for 3 hr, VIII afforded two isomeric cyclopentenes, X and XI, with a concomitant *racemization*, in a ratio of about 3.5 : 1. In accordance with the assigned structure, X, $C_{16}H_{21}OBr$ (M^+ 308, 310), mp 123—124°C, $[\alpha]_D \pm 0°$, showed in its NMR spectrum the presence of two olefinic methyl groups (δ 1.46 and 1.69) instead of the one tertiary methyl and cyclopropane ring in VIII. On the other hand, the isomer XI (M^+ 308, 310), mp 93°C, $[\alpha]_D \pm 0°$, λ_{max} 290 and 284 mμ (ε 4100 and 4000), exhibited in its NMR spectrum signals due to two tertiary methyl (δ 0.82 and 0.93) and a secondary methyl group (δ 0.98; d, $J=6$ Hz) as well as to an olefinic proton (δ 5.41). On osmium tetroxide oxidation, XI gave the

1) Part XIV of "Constituents from Marine Plants." Part XIII: T. Irie, A. Fukuzawa, M. Izawa and E. Kurosawa, *Tetrahedron Letters*, **1969**, 1343.

2) T. Irie, M. Suzuki, E. Kurosawa and T. Masamune, *ibid.*, **1966**, 1837.

3) T. Irie, M. Suzuki and Y. Hayakawa, This Bulletin, **42**, 843 (1969).

4) *Cf.* Part XIII of this series.

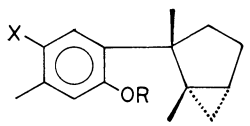

I X=Br, R=H
II X=R=H
III X=Br, R=Ac
IV X=H, R=Ac
VIII X=Br, R=Me
IX X=H, R=Me

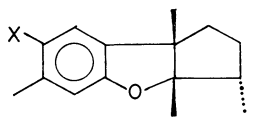

V X=Br
VI X=H

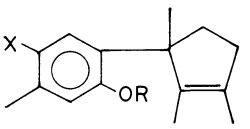

VII X=H, R=Ac
X X=Br, R=Me
XIII X=H, R=Me

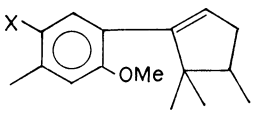

XI X=Br
XIV X=H

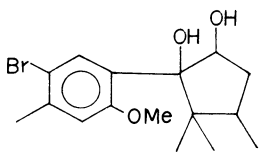

XII

corresponding glycol (XII), whose structure was supported by the presence of only one proton on a carbon bearing the hydroxyl group (δ 4.91; dd, J=8 and 6Hz) and the absence of a methyl group adjacent to the hydroxyl.

Similarly, debromolaurinterol methyl ether (IX) gave the corresponding isomeric cyclopentenes, XIII and XIV, in a ratio of about 3 : 1 on treatment under the conditions described above.

The prolonged treatment (15 hr) of VIII with the same catalyst produced X and XI in a ratio of about 5 : 1, but no other product could be obtained. The reaction of VIII with 0.5% sulfuric acid in acetic acid proceeded slowly and afforded X and XI in a ratio of about 1.5 : 1 after 72 hr. An examination of the latter reaction process by TLC indicates that, while X increases gradually the quantity of XI reaches its maximum after a few hours and then decreases, an equilibrium being finally attained between only X and XI. In fact, X and XI, on treatment with 10% sulfuric acid in acetic acid at 50°C for 15 hr, have formed a *ca.* 7 : 1 equilibrium mixture.

This observation can be explained by assuming that VIII undergoes protonation leading to the cleavage of the cyclopropane ring to yield a carbonium cation, XV, which, by a reversible reaction involving the migration of the methyl group, forms a cation, XVI.[5] These cations, XV and XVI, will then produce the cyclopentenes, X and XI respectively.

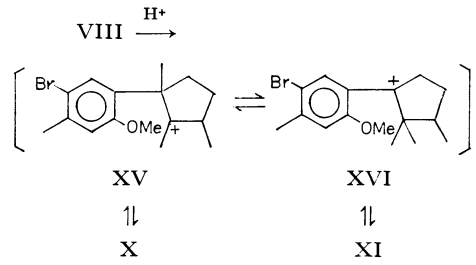

XV ⇅ X

XVI ⇅ XI

Experimental[8]

Laurinterol Methyl Ether (VIII). To a solution of I (180 mg) and dimethyl sulfate (400 mg) in dry acetone (20 m*l*), potassium carbonate (800 mg) was added, and then the mixture was refluxed for 3 hr. After the removal of the unchanged potassium carbonate by filtration, the solution was made alkaline by the addition of a dilute sodium hydroxide solution. The solvent was then removed by distillation under diminished pressure, and the residue was extracted with ether. The ether solution was washed successively with water, the dilute sodium hydroxide solution, and a saturated sodium chloride solution, and dried over sodium sulfate. A crude crystalline substance obtained after the removal of the ether was purified by recrystallization from methanol to give VIII (160 mg); mp 96—97°C; M^+ 308, 310; $[\alpha]_D$ +18.0° (*c*, 1.25; Chf); ν_{max}^{Chf} 1602, 1490, 1240, 1165, 1065, 1043, 960, 890, 845 cm^{-1}; NMR, δ 0.43 (1H, s), 0.53 (1H, s), *ca.* 1.0 (1H, m) 1.30 (6H, s), 2.35 (3H, s), 3.77 (3H, s), 6.61 (1H, s), 7.53 (1H, s). (Found: C, 62.27; H, 6.69%. Calcd for $C_{16}H_{21}OBr$: C, 62.14; H, 6.85%).

Debromolaurinterol Methyl Ether (IX). Debromolaurinterol (II, 65 mg) was methylated with dimethyl sulfate and potassium carbonate in dry acetone as has been described above. The crude product was

5) This type of methyl migration has recently been reported [Y. Hirata *et al.*, Preprints for the 22nd Annual Meeting of the Chemical Society of Japan (Tokyo, 1969)]. However, when isolaurene (XVII)[6] is treated with 10% sulfuric acid in acetic acid, both the methyl and the *p*-tolyl group migrate to give XVIII. It is

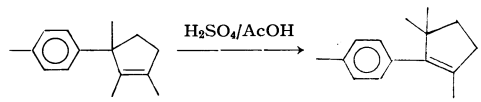

XVII XVIII

well known that the migratory aptitude of the *o*-anisyl group is small;[7] the above observation is in accord with this view.

6) T. Irie, T. Suzuki, Y. Yasunari, E. Kurosawa and T. Masamune, *Tetrahedron*, **25**, 459 (1969).

7) *Cf.* P. de Mayo, "Molecular Rearrangements," Interscience Publishers, New York (1963), p. 22.

8) Mps are uncorrected. The NMR spectra were taken in CCl_4, with TMS as an internal standard, on a Hitachi H-60 Spectrometer.

purified by column chromatography on silica gel to give IX (50 mg); oil; M^+ 230 ($C_{16}H_{22}O$); $[\alpha]_D$ −17.6° (*c*, 1.42; Chf); ν_{max}^{Chf} 1613, 1575, 1503, 1250, 1165, 1140, 1060, 1040, 820 cm^{-1}; NMR, δ *ca.* 0.5 (2H, m), *ca.* 1.0 (1H, m), 1.31 (3H, s), 1.35 (3H, s), 2.32 (3H, s), 3.79 (3H, s), 6.58 (1H, br. s), 6.60 (1H, br. d, J=7.5 Hz), 7.32 (1H, d, J=7.5 Hz).

Rearrangement of Laurinterol Methyl Ether (VIII). *a*) A solution of VIII (301 mg) in 10% sulfuric acid in acetic acid (10 m*l*) was stirred at 50°C for 3 hr. To the ice-cold reaction mixture water (*ca.* 20 m*l*) was added, and then the whole was extracted with ether. The ether solution was washed successively with water, a 5% sodium hydrogen carbonate solution, and a saturated sodium chloride solution, and dried over sodium sulfate. After the removal of the solvent, the residual oil (297 mg) was chromatographed over silica gel - Celite (10 : 1) to yield X (205 mg) and XI (68 mg).

X: mp 123—124°C, M^+ 308, 310 ($C_{16}H_{21}OBr$); $[\alpha]_D$ ±0°; λ_{max}^{EtOH} 288 and 282 mμ (ε 3200 and 3400); NMR, δ 1.37 (3H, s), 1.46 (3H, s), 1.69 (3H, s), 2.31 (3H, s), 3.72 (3H, s), 6.56 (1H, s), 6.95 (1H, s). (Found: C, 62.25; H, 6.86%).

XI: mp 93°C, M^+ 308, 310 ($C_{16}H_{21}OBr$); $[\alpha]_D$ ±0°; λ_{max}^{EtOH} 290 and 284 mμ (ε 4100 and 4000); NMR ,δ 0.82 (3H, s), 0.93 (3H, s), 0.98 (3H, d, J=6 Hz), 2.34 (3H, s), 3.69 (3H, s), 5.41 (1H, m), 6.60 (1H, s), 7.03 (1H, s). (Found: C, 62.32; H, 6.85%).

b) When 0.5% sulfuric acid in an acetic acid solution was used, the reaction was slow; after stirring at 50°C for 72 hr, the starting material disappeared (TLC), and X (50%) and XI (35%) were obtained after the usual work-up.

Rearrangement of Debromolaurinterol Methyl Ether (IX). A solution of IX (251 mg) in 10% sulfuric acid in acetic acid (10 m*l*) was stirred at 50°C for 3 hr. After treatment as above, there was obtained an oily product (217 mg) which was subsequently purified by silica gel chromatography to yield XIII (105 mg) and XIV (45 mg).

XIII: oil, M^+ 230 ($C_{16}H_{22}O$); $[\alpha]_D$ ±0°; NMR, δ 1.39 (3H, s), 1.47 (3H, s), 1.68 (3H, s), 2.27 (3H, s), 3.73 (3H, s), 6.48 (1H, d, J=8 Hz), 6.53 (1H, s), 6.73 (1H, d, J=8 Hz).

XIV: oil, M^+ 230 ($C_{16}H_{22}O$); $[\alpha]_D$ ±0°; NMR, δ 0.81 (3H, s), 0.92 (3H, s), 1.01 (3H, d, J=6 Hz), 2.30 (3H, s), 3.67 (3H, s), 5.35 (1H, m), 6.50 (1H, s), 6.51 (1H, d, J=8 Hz), 6.73 (1H, d, J=8 Hz).

Glycol XII. To a solution of XI (128 mg) in benzene (4 m*l*), osmium tetroxide (102 mg) and pyridine (0.1 m*l*) were added. After the mixture had stood for 3 days at room temperature, pale brown precipitates (180 mg) were separated and collected by filtration. This crude product was dissolved in dichloromethane (3 m*l*) and was added to a solution of mannitol (800 mg) and potassium hydroxide (100 mg) in water (10 m*l*). The whole was stirred at room temperature for 45 hr, the reaction mixture was then extracted with dichloromethane, and the organic layer was washed with water and dried. After the removal of the solvent, the residual oil (101 mg) was purified by chromatography over silica gel to give pure XII (64 mg): ν_{max} 3500, 1105, 1045 cm^{-1}; NMR, δ 0.49 (3H, s), 0.82 (3H, s), 0.82 (3H, d, J=7 Hz), 2.34 (3H, s), 3.77 (3H, s), *ca.* 3.4 (1H, br. m), *ca.* 4.3 (1H, br. m), 4.91 (1H, dd, J=8 and 6 Hz), 6.65 (1H, br. s), 7.45 (1H, s).

Acid-catalyzed Equilibration of X and XI. Pure X and pure XI (50 mg) were each dissolved in 10% sulfuric acid in acetic acid (10 m*l*), and the mixture was stirred at 50°C for 15 hr. The reaction mixture was then worked-up as has been described above, and the composition of the products was determined by column and/or thin-layer chromatography. From each of the cyclopentenes, X and XI were obtained in a ratio of *ca.* 7 : 1.

The authors wish to express their thanks to Professor Tadashi Masamune and Dr. Etsuro Kurosawa for their valuable discussions. The authors' thanks are also due to Mr. Shigezo Shimokawa and Miss Yoshiko Kishio for their NMR measurements, to Miss Yuko Imai for her measurements of the mass spectra, and to Mrs. Toyoko Toma, Faculty of Pharmaceutical Sciences, for her microanalyses.

BULLETIN OF THE CHEMICAL SOCIETY OF JAPAN VOL. 42 3345—3348 (1969)

The Intramolecular Hemiacetal Structure of Benzoyl(2-hydroxybenzoyl)carbinol and Its Monobenzoate*1

Heitaro OBARA and Jun-ichi ONODERA

Department of Applied Chemistry, Faculty of Engineering, Yamagata University, Yonezawa

(Received May 6, 1969)

In previous studies, the present authors have reported that a ring-chain tautomerism exists between benzoyl(2-hydroxybenzoyl)methyl bromide and its cyclic intramolecular hemiacetal structure, *i. e.*, 2-hydroxy-3-bromoflavanone.[1] In the present investigation, we have found that a similar tautomerism exists between benzoyl(2-hydroxybenzoyl)-carbinol (II) and its monobenzoate (IV).

The carbinol (II) was prepared by Winicki *et al.*[2] from benzoyl(2-hydroxybenzoyl)methane (I) by oxidation with hydrogen peroxide in a mixed solution of formic and acetic acid; however, no investigation has been made concerning its hemiacetal structure (III). In order to ascertain the tautomerism between II and III, the NMR, IR, and UV spectra of this carbinol and the behavior of its monobenzoate (IV) will be discussed in the present paper.

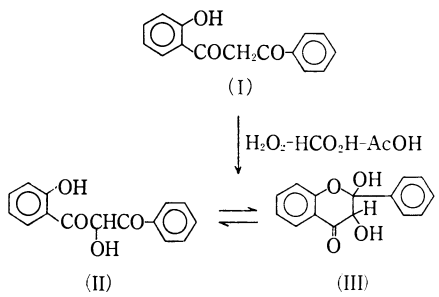

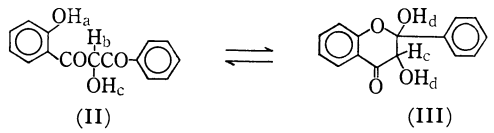

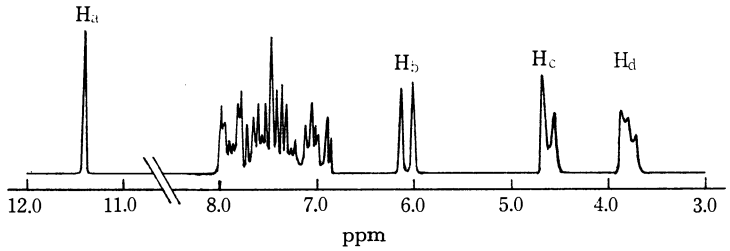

Fig. 1. NMR spectrum of II ⇋ III in $CDCl_3$.

Results and Discussion

The NMR spectrum of the carbinol (II) in $CDCl_3$ exhibits four groups of bands (a, b, c, and d) in addition to the aromatic protons (6.67 ppm—8.02 ppm), as Fig. 1 shows. These four bands were assigned as follows: 1) the a band on the low-field side of these bands is due to the hydrogen-bonding phenolic OH proton in II; 2) the b band (doublet), which changes to a singlet after deuterium exchange, is due to the methine proton of –COCH(OH)CO– in II, and the c band may be attributed to a mixture of the OH proton of –COCH(OH)CO– in II and the methine proton in III, which leaves after deuterium exchange. (They were determined by comparison with those of dibenzoylcarbinol.)*2

*1 Presented in part at the Tohoku Branch Meeting of the Chemical Society of Japan, Yonezawa, June, 1966.

1) H. Obara and J. Onodera, This Bulletin, **41**, 2798 (1968).

2) B. Winicki, C. Nofre, J. Chopin and A. Cier, *Bull. Soc. Chim. France*, **1962**, 1695.

*2 This carbinol was prepared by the oxidation of dibenzoylmethane with hydrogen peroxide in a mixture of formic and acetic acid; mp 110°C (lit mp 110°C[3]).

3) P. Karrer, J. Kebrle and R. M. Thakkar, *Helv. Chim. Acta*, **33**, 1711 (1950).

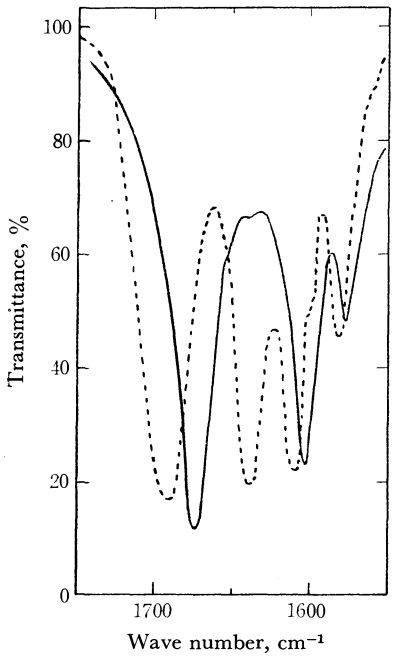

Fig. 2. IR spectra of benzoyl(2-hydroxybenzoyl)-carbinol.
——: in KBr disk, ------: in $CHCl_3$.

3) The remaining d band is due to the two OH protons in III, which disappears after the deuterium exchange. From the relative areas of the a, b, c, and d bands, the molar ratio of the tautomers II and III in this case was found to be approximately 2 : 1.

The IR spectrum of this carbinol showed a strong carbonyl absorption band at 1674 cm^{-1} in the KBr disk, while two carbonyl absorption bands at 1690 cm^{-1} and 1638 cm^{-1}, corresponding to free and bonded carbonyl groups,[4] were observed in the chloroform solution, as is shown in Fig. 2.

From the results of these NMR and IR spectral analyses, the cyclic hemiacetal structure, *i. e.*, 2,3-dihydroxyflavanone (III), rather than II must be given for this carbinol in the crystalline state; in the chloroform solution, this carbinol exists as an equilibrium state between II and III, analogous to benzoyl(2-hydroxybenzoyl)methyl bromide and its hemiacetal structure.[1] However, when this carbinol was dissolved in chloroform, no variation in the absorption band with the lapse of time has been observed in the IR spectrum. It is considered that this carbinol immediately reaches equilibrium between II and III in a solution.

The UV spectrum of this carbinol exhibits its absorption maxima at 253 mμ and 321 mμ in ethanol; the absorption curve is very similar to those of flavanone and 3-hydroxyflavanone.

Finally, the existence of a ring-chain tautomerism between II and III was ascertained by the chemical method.

Two benzoates were obtained from this carbinol by benzoylation with benzoyl chloride in pyridine. One was dibenzoate (mp 159—160°C), which had previously been reported in the literature,[2] and the other was a new monobenzoate (mp 102—104°C). The structure of this monobenzoate was identified as benzoyl(2-hydroxybenzoyl)benzoyloxymethane (IV) because it is converted into 3-benzoyloxyflavone[5] (VI) with acid or heat.

The IR spectrum of this monobenzoate in a chloroform solution gave an interesting result, as much as in the case of benzoyl(2-hydroxybenzoyl)-methyl bromide[1] in the 1600—1750 cm^{-1} region. It showed two strong carbonyl absorption bands at 1713 cm^{-1} and 1728 cm^{-1} immediately after it had been dissolved in chloroform, but the former band slowly decreased with the lapse of time; a new absorption band appeared at 1643 cm^{-1}, and then it remained unchanged for at least 1 hr (Fig. 3).

This new band is considered to be a characteristic absorption band due to the intramolecular chelated carbonyl group in the structure IV which is observed in aromatic *o*-hydroxyketones.[4] On the other hand, the IR spectrum of this monobenzoate in a KBr disk showed no chelated carbonyl absorption band near 1630—1640 cm^{-1}; such a band would appear if the structure were IV (Fig. 4).

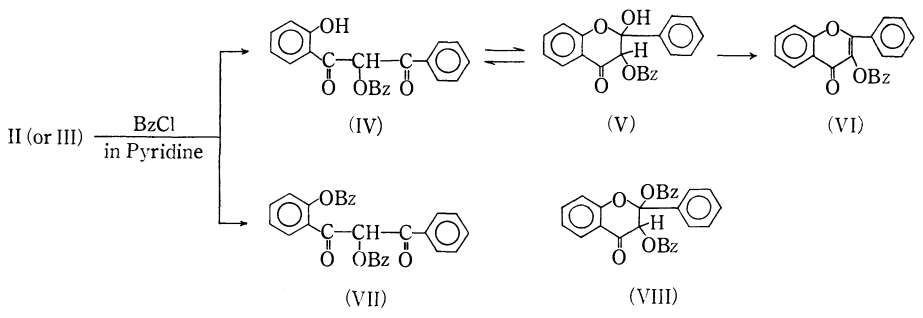

4) L. J. Bellamy, "The Infra-red Spectra of Complex Molecules," John Wiley & Sons, New York (1958), p. 143.

5) J. E. Gowan, P. M. Hayden and T. S. Wheeler, *J. Chem. Soc.*, **1955**, 862.

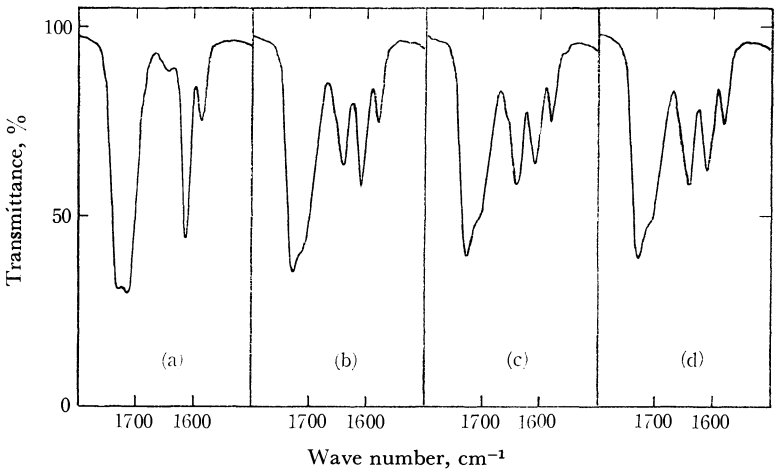

Fig. 3. The variation of IR spectra of benzoyl(2-hydroxybenzoyl)-benzoyloxymethane (IV) with the time in $CHCl_3$ solution. (a): Immediately after dissolving. (b): After 10 min. (c): After 25 min. (d): After 1 hr.

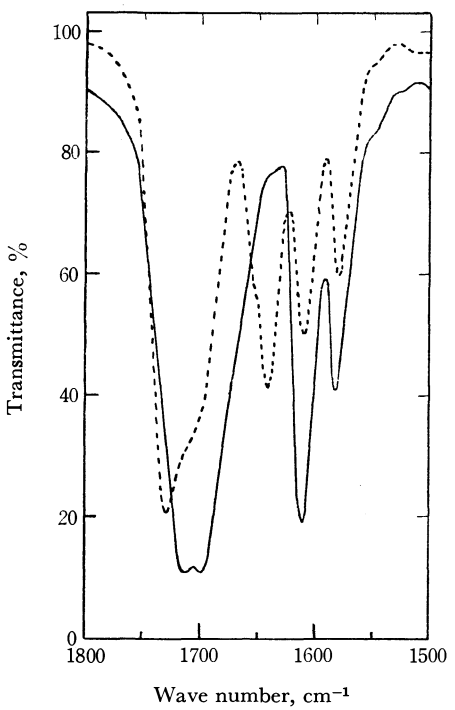

Fig. 4. IR spectra of benzoyl(2-hydroxybenzoyl)-benzoyloxymethane (IV).
——: in KBr disk, ------: in $CHCl_3$.

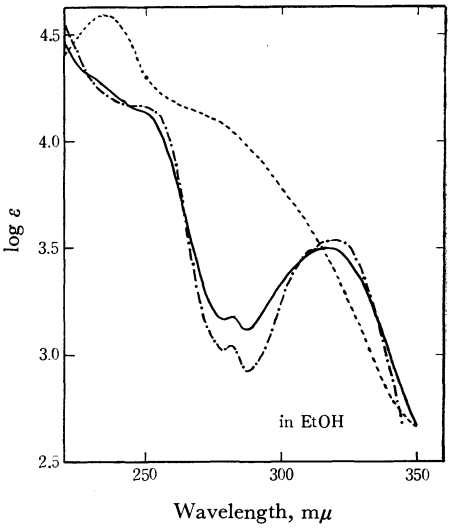

Fig. 5. UV spectra of benzoyl(2-hydroxybenzoyl)-benzoyloxymethane (IV) (——), 3-benzoyloxyflavanone (IX) (·—·—·) and benzoyl(2-benzoyloxybenzoyl)benzoyloxymethane (VII) (------).

From these results, it is expected that this monobenzoate has the structure V before dissolving and that it reaches equilibrium between IV and V in a solution; the cyclic hemiacetal structure V rather than IV must be given for this monobenzoate in the crystalline state. The isomeric monobenzoate, *i.e.*, benzoyl(2-benzoyloxybenzoyl)carbinol, was not isolated in this benzoylation.

The UV spectrum of the monobenzoate in ethanol, which exhibits absorption maxima at 248 mμ (inflect.), 283 mμ, and 316 mμ, is very similar to that of 3-benzoyloxyflavanone (IX) (Fig. 5).

On the other hand, two isomeric structures, *i. e.*, VII or VIII, must be considered for the dibenzoate. Structure VII was, however, supported by its UV spectrum, because the absorption curve does not resemble that of flavanones (Fig. 5). Another dibenzoate (VIII) has not been isolated in this benzoylation of this carbinol.

Experimental

Benzoyl(2-hydroxybenzoyl)carbinol (II). This carbinol was prepared from benzoyl(2-hydroxybenzoyl)-methane (I) in a 53% yield as has been described by Winicki *et al.*[2] Mp 101.5—103.5°C, (lit[2] mp 104°C) UV λ_{max}^{EtOH} mμ (log ε) 253 (4.00) 321 (3.50).

Found: C, 70.24; H, 4.68%. Calcd for $C_{15}H_{12}O_4$: C, 70.30; H, 4.72%.

Benzoylation of Benzoyl(2-hydroxybenzoyl)-carbinol (II). Into a solution of II (520 mg) in 2 m*l* of pyridine, there was added a 600 mg portion of benzoyl chloride. After it had been heated on a water bath for 10 min, the reaction mixture was poured into cold 3 N hydrochloric acid; the resulting pale yellow oil was extracted with ether. The ether layer was washed with water and dried over anhydrous sodium sulfate. The filtrate was concentrated to about 8 m*l*, and 4 m*l* of petroleum ether were added. After the solution had then been allowed to stand overnight in an ice-box, the resulting crystal (A) was filtered out and the filtrate was chromatographed on a column of silica gel. Elution with benzene-ethyl acetate (20 : 1) gave benzoyl-(2-hydroxybenzoyl)benzoyloxymethane (IV), which was recryltallized from carbon tetrachloride. Yield, 35 mg; mp 102—104°C. UV λ_{max}^{EtOH} mμ (log ε) 248 (inflect.) (4.14), 283 (3.18), 316 (3.50).

Found: C, 73.22; H, 4.80%. Calcd for $C_{22}H_{16}O_5$: C, 73.33; H, 4.48%.

The recrystallization of (A) from ethanol gave 235 mg of benzoyl(2-hydroxybenzoyl)carbinol dibenzoate (VII) as colorless prisms; mp 159—160°C (lit[2] mp 159°C), UV λ_{max}^{EtOH} mμ (log ε) 235 (4.59).

The authors wish to express their thanks to Professor Koji Nakanishi of Tohoku University and the members of his laboratory for their measurement of the NMR spectra.

BULLETIN OF THE CHEMICAL SOCIETY OF JAPAN VOL. 42 3348—3349 (1969)

The Oxidation of Limonene with Selenium Dioxide

Yoshitsugu SAKUDA

Chemistry Laboratory, Kochi Women's University, Kochi

(Received May 13, 1969)

The oxidations of limonene with selenium dioxide have been reported;[1-4] in them it was found that the two methyl groups of C-7[3] and C-10[2] and the methylene group of C-6[1,2] were oxidized. In a previous paper[5] dealing with the selenium dioxide oxidation of *cis*-carvyl acetate, which contained both a methine and methyl group allylic to the double bond, it was found that the methine group is oxidized mainly.[6] Because limonene has the same carbon skeleton as *cis*-carveol, it was expected that the methine group of C-4, in addition to the methyl and methylene groups, is oxidized with selenium dioxide. Therefore, in this paper *d*-limonene was taken as the sample and was oxidized with selenium dioxide. The oxidation was carried out in an alcoholic solution at reflux with a half-molar amount of selenium dioxide. The reaction products were analysed by gas chromatography using a polyethylene glycol 6000 column at 160°C. All the identities were confirmed by a comparison of the IR and NMR spectra. The *dl*-limonen-4-ol(1,8-*p*-menthadien-4-ol) was obtained as a major product (11% based on the sample taken), while *d-trans*-carveol, *cis*-carveol, perillyl alcohol, limonen-10-ol(1,8-*p*-menthadien-10-ol), and carvone were obtained as minor products (total, 6.5%).

In a study of the mechanism by which olefins are oxidized with selenium dioxide, Schaefer and

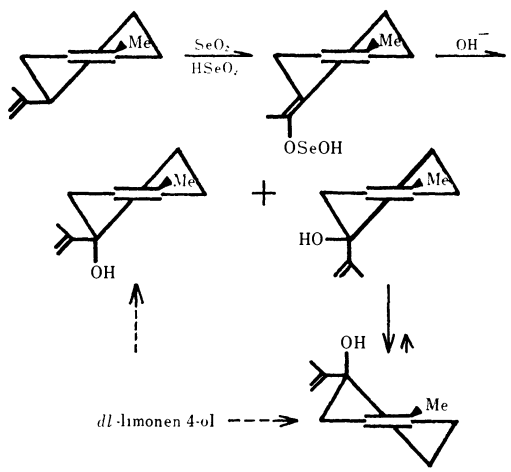

Fig. 1. Oxidation of methine group of limonene.

1) S. Hirayama, *Nippon Kwagaku Kwaishi (J. Chem. Soc. Japan)*, **59**, 229 (1938).
2) K. Sebe, *ibid.*, **62**, 16 (1940).
3) H. Schmidt, *Ber.*, **83**, 193 (1950).
4) W. Zacharewicz, *Chem. Abstr.*, **45**, 5661 (1951).
5) Y. Sakuda, This Bulletin, **42**, 475 (1969).
6) S. P. Pathak and G. H. Kulkarni, *Chem. & Ind. (London)*, **1968**, 913.

Wiberg[7] have shown that selenium dioxide or its conjugate acid acts as an electrophile and attacks a double bond, thus forming an allylic selenium ester that then decomposes to products through solvolysis reaction. When Schaefer's mechanism is applied when the methine group allylic to the double bond at C-8 of limonene is oxidized, the reaction process is as is shown in Fig. 1. This view of the mechanism of the oxidation appears to accord well with that by which *dl*-limonen-4-ol is produced. Furthermore, considering the fact that the isolated carveol consists mainly of *d-trans*-carveol, which possesses an axial hydroxyl group and which retains its optical activity, it was assumed that the displacement of the allylic selenium ester by a solvent molecule occurs through the S_N2' process.[7]

Experimental

Oxidation. To 136 g (1 mol) of *d*-limonene (bp 61°C/13 mmHg, d_4^{25} 0.8422, n_D^{25} 1.4720, $[\alpha]_D$ +122.6) in 150 cc of ethanol, which was being stirred at room temperature, there was added, drop by drop over a period of 30 min, 55 g (1/2 mol) of selenium dioxide dissolved in a mixture of 10 cc of water and 250 cc of ethanol. The mixture was heated to reflux for 1 hr and then left to stand at room temperature overnight. The reaction mixture was filtered, giving 4.7 g of selenium. The filtrate was concentrated using a rotary evaporator, and the residue was steam-distilled. The distillate was extracted twice with ether. The combined ether solution was washed with water, dried over anhydrous sodium sulfate, and distilled to remove the solvent. The residue was distilled at reduced pressure, giving three fractions: (1) bp 62—94°C/13 mmHg, 29.2 g; (2) bp 94—96°C/12 mmHg, 13.5 g; (3) 96—108°C/12 mmHg, 16.0 g. Fraction 1 consisted mainly of unchanged *d*-limonene.

The Identification of Reaction Products. *dl-Limonen-4-ol.* Fraction 2 was analysed by gas chromatography and was found to consist 90% of limonen-4-ol and 10% of unknown hydrocarbons; it was purified by redistillation. Bp 104—106°C/27 mmHg, d_4^{25} 0.9475, n_D^{25} 1.4877, $[\alpha]_D$ +1.40; phenylurethane, mp 130—131°C.[8] Gas chromatography of this oil indicated the presence of small amounts of unknown hydrocarbons in addition to limonen-4-ol. Accordingly, the small optical rotation value is due to unknown contaminating hydrocarbons. IR spectrum: 3400 cm^{-1} (OH); 3100, 1645, 900 cm^{-1} (CH_2=C–). NMR spectrum: 1.75 ppm, 3H s, 4.71, 1H, q, 4.90, 1H, s (CH_3–C=CH_2); 1.65, 3H s, 5.21, 1H unresolved (CH_3–C=CH–). The IR and NMR spectra of this alcohol coincided with those of limonen-4-ol, which was isolated from Japanese pepper by Sakai.[9] This alcohol was hydrogenated with Raney Ni in ethanol to give two known *p*-menthan-4-ols.[8]

Carvone. A gas chromatogram of Fraction 3 showed eleven peaks, which corresponded to limonen-4-ol (17%), carvone (3%), *trans*-carveol (33%), *cis*-carveol (10%), limonen-10-ol (16%), perillyl alcohol (16%), and five unknown minor components (5%). Chromatography of Fraction 3 on silica gel, with elution with ethyl acetate-petroleum ether (1 : 3), gave four fractions. The first fraction consisted a mixture of unknown hydrocarbons. The second fraction was rechromatographed on a silica-gel column and eluted with ethyl acetate-petroleum ether (1 : 20) giving carvone; 2,4-dinitrophenylhydrazone, mp 188—189°C.

d-trans-Carveol. The third fraction consisted mainly of *trans*-carveol. The 3,5-dinitrobenzoate was prepared from this fraction and was recrystallized three times from ethanol-ethyl acetate (2 : 1), giving pale yellow needles; mp 108—110°C, $[\alpha]_D$ +174.1 (*c* 1.6, $CHCl_3$); reported[10] mp 111.5°C, $[\alpha]_D$ +232.0 (*c* 2.0, $CHCl_3$) for *d-trans*-carvyl 3,5-dinitrobenzoate. The liquid alcohol obtained by the saponification of this 3,5-dinitrobenzoate gave a single peak upon gas chromatography; it was identified as *trans*-carveol by a direct comparison of the IR spectrum. Calculating from the specific rotation value of the 3,5-dinitrobenzoate, *trans*-carveol retained 75% of its optical activity.

cis-Carveol. The fourth fraction consisted of a mixture of *trans*- and *cis*-carveol, limonen-10-ol, and perillyl alcohol. Chromatography of the fourth fraction on silica gel, with elution with ethyl acetate-petroleum ether (1 : 3), gave fractions which were analysed by gas chromatography. The fractions rich in *cis*-carveol, limonen-10-ol, and perillyl alcohol were combined. The crude *cis*-carveol thus obtained was purified by rechromatography on alumina; it was identified as *cis*-carveol by a direct comparison of the IR spectrum. The crude limonen-10-ol and perillyl alcohol obtained were purified too by rechromatography on silica gel.

Limonen-10-ol. IR spectrum: 3300 cm^{-1} (OH); 3100, 1645, 900 cm^{-1} (CH_2=C–). NMR spectrum: 1.65 ppm 3H s, 5.37, 1H unresolved (CH_3–C=CH–); 4.02, 2H s (–CH_2OH); 4.84 1H s, 5.00 1H d (CH_2=C–). The oxidation product of this alcohol with chromic acid gave a semicarbazone, mp 209°C.[2]

Perillyl Alcohol. IR spectrum: 3300 cm^{-1} (OH); 3080, 1643, 890 cm^{-1} (CH_2=C–). NMR spectrum: 1.73 ppm 3H t, 4.77, 2H d (CH_3–C=CH_2); 3.93, 2H s (–CH_2OH); 5.72, 1H unresolved (–C=CH–).

7) J. P. Schaefer, B. Horvath and H. P. Klein, *J. Org. Chem.*, **33**, 2647 (1968); K. B. Wiberg and S. D. Nielsen, *ibid.*, **29**, 3353 (1964).

8) E. Klein and W. Rohjahn, *Tetrahedron*, **21**, 2173 (1965); R. M. Bowman, A. Chambers and W. R. Jackson, *J. Chem. Soc., C*, **1966**, 612.

9) T. Sakai, K. Yoshihara and Y. Hirose, This Bulletin, **41**, 1945 (1968).

10) R. G. Johnston and J. Read, *J. Chem. Soc.*, **1934**, 233.

BULLETIN OF THE CHEMICAL SOCIETY OF JAPAN VOL. 42 3350—3352 (1969)

Reaction of 6-Methylpicolinic Acid *N*-Oxide with Acetic Anhydride[1]

Yukito MURAKAMI and Junzo SUNAMOTO

Department of Organic Synthesis, Faculty of Engineering, Kyushu University, Hakozaki, Fukuoka

(Received May 21, 1969)

The reactions of picoline *N*-oxides with acetic anhydride have been studied by many workers for theoretical and practical interest.[2-9] Recently, Ford and Swan[10] have found that the reaction of 2-picoline *N*-oxide with acetic anhydride gave a mixture of three isomers, 3-acetoxy-2-picoline, 5-acetoxy-2-picoline, and 2-acetoxymethylpyridine in a relative proportion of 15 : 18 : 67. Meanwhile, the reaction of pyridine *N*-oxide with acetic anhydride gave 2-acetoxypyridine.[11]

The reactions of carboxypyridine *N*-oxides with acetic anhydride also have been studied. Bain and Saxton[12] have reported that picolinic acid *N*-oxide was converted to 2-pyridone and pyridine *N*-oxide by acetic anhydride in acetonitrile along with the quantitative evolution of carbon dioxide, where pyridine *N*-oxide was the main product. On the other hand, 2-carbomethoxypyridine *N*-oxide did not undergo decarboxylation with acetic anhydride, but normally afforded 6-acetoxy-2-carbomethoxypyridine.[13]

It is of interest to investigate what reaction may occur in the case of 6-methylpicolinic acid *N*-oxide with acetic anhydride, where the *N*-oxide carries both electron withdrawing and donating groups at the α-positions of the pyridine ring. Baker *et al.*[14] have reported that the reaction product of 6-methylpicolinic acid *N*-oxide with acetic anhydride was 2-acetoxymethylpyridine, only by determining its boiling point and the melting point of the corresponding picrate. However, they did not try to hydrolyze the acylated compound. From our present results we see that they mistook 6-acetoxy-2-picoline for 2-acetoxymethylpyridine because there is no considerable difference between both compounds in their physical properties. We found that the acylated compound produced during the course of the reaction of 6-methylpicolinic acid *N*-oxide with acetic anhydride was not 2-acetoxymethylpyridine, but 6-acetoxy-2-picoline. This was confirmed by the hydrolysis of the acylated intermediate which afforded 6-methyl-2-pyridone.

The results will present an interesting question as to whether decarboxylation proceeds prior to *N*-acetoxylation as indicated in the case of picolinic *N*-oxide.[12] If decarboxylation occurred predominantly prior to acetoxylation, the principal intermediate would be 2-picoline *N*-oxide and/or 2-acetoxymethylpyridine. On the other hand, if *N*-acetoxylation and the subsequent N–O fission were predominant prior to decarboxylation, 6-acetoxymethylpicolinic acid and/or 2-acetoxymethylpyridine would be produced. When 6-methylpicolinic acid *N*-oxide was warmed to 90—98°C with acetic anhydride, a smooth evolution of carbon dioxide occurred. The main product was 6-acetoxy-2-picoline, and 6-methyl-2-pyridone was present in a very small yield. The reaction of 2-picoline *N*-oxide, which is the decarboxylation product, with acetic anhydride under the same reaction condition did not give 6-acetoxy-2-picoline and/or 6-methyl-2-pyridone, but gave 2-acetoxymethylpyridine along with a trace amount of 5-acetoxy-2-picoline, similar to the result of Ford and Swan.[10] Therefore, decarboxylation, N–O fission, and acetoxylation at the C-2 position must take place in concert to give 6-acetoxy-2-picoline. The following reaction mechanism is put forward to

1) Contribution No. 157 from the Department of Organic Synthesis, Faculty of Engineering, Kyushu University.

2) G. Kobayashi and S. Furukawa, *Chem. Pharm. Bull. (Tokyo)*, **1**, 347 (1953).

3) V. Boekelheide and W. J. Linn, *J. Am. Chem. Soc.*, **76**, 1286 (1954).

4) O. H. Bullitt and J. T. Maynard, *ibid.*, **76**, 1370 (1954).

5) V. J. Traynelis and R. F. Martello, *ibid.*, **80**, 6590 (1958).

6) S. Oae and Y. Kitaoka, *ibid.*, **84**, 3359 (1962).

7) S. Oae, Y. Kitaoka and T. Kitao, *Tetrahedron*, **20**, 2685 (1964).

8) V. J. Traynelis and P. L. Pacini, *J. Am. Chem. Soc.*, **86**, 4917 (1964).

9) T. Cohen and J. H. Fager, *ibid.*, **87**, 5701 (1965).

10) P. W. Ford and J. M. Swan, *Australian J. Chem.*, **18**, 867 (1965).

11) J. H. Markgraf, H. B. Brown, Jr., S. C. Mohr and R. G. Peterson, *J. Am. Chem. Soc.*, **85**, 958 (1963).

12) B. M. Bain and J. E. Saxton, *J. Chem. Soc.*, **1961**, 5216.

13) V. Boekelheide and W. L. Lehn, *J. Org. Chem.*, **26**, 428 (1961).

14) W. Baker, K. M. Bruggle, J. F. W. McOmie and D. A. M. Watkins, *J. Chem. Soc.*, **1958**, 3594.

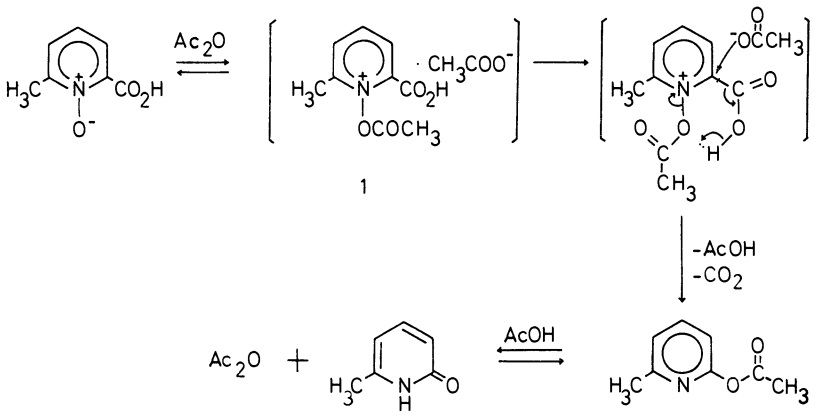

explain the present result.

Picolinic acid *N*-oxide undergoes rapid decarboxylation to pyridine *N*-oxide at room temperature upon addition of benzoyl chloride.[13] Therefore, it is evident that the formation of the *N*-acetoxypyridinium ion **1** is necessary for the ease of decarboxylation. 6-Acetoxy-2-picoline may further react with acetic acid during the reaction and/or distillation to give 6-methyl-2-pyridone, because the pyridone was usually obtained from the distillation residue. When the hydrolysis was carried out without isolating the acetoxylated intermediate, 6-methyl-2-pyridone was obtained in a yield of 84%. Thus, it seems that the present reaction is an improved synthetic method of 6-methyl-2-pyridone from 2,6-lutidine, differing from the conventional method *via* diazotization and the subsequent hydrolysis of 6-methyl-2-aminopyridine.[15]

Experimental

All infrared spectra were measured on a Koken Model DS-301 spectrophotometer equipped with sodium chloride optics. Nuclear magnetic resonance spectra were taken on a Varian A-60 using TMS as an internal standard. Mass spectra were measured on a JEOL JMS-01SG mass spectrometer. The ultraviolet spectra were recorded on a Hitachi Model EPS-2 recording spectrometer.

2,6-Lutidine *N*-Oxide. 2,6-Lutidine *N*-oxide was obtained by the reaction of 2,6-lutidine (53 g) with 30% hydrogen peroxide (50 m*l*) in glacial acetic acid, according to the method described in literature:[3] yield 36 g; bp 125—128°C/18 mmHg; lit., 131°C/22 mmHg,[16] 115—119°C/18 mmHg.[3] IR (neat): 1566 cm^{-1} (ring C=C, C=N str.); 1249 cm^{-1} (N-O str.); 766, 841 cm^{-1} (C-H def.).

6-Methylpicolinic Acid *N*-Oxide. 6-Methylpicolinic acid *N*-oxide was prepared by the oxidation of 2,6-lutidine *N*-oxide (22 g) with aqueous potassium permanganate solution, according to the method of Suszko and Szafran:[17] yield 9.0 g after recrystallization from methanol, mp 197—197.5°C (decomp.); lit,[18] mp 177°C. The melting point determined in the present work was not identical with that given in literature,[14,18] but infrared spectra of the sample prepared in this work was completely consistent with that reported by Szafran;[19,20] IR (KBr): 1680, 1615 cm^{-1} (C=O str.); 768, 818, 831 cm^{-1} (C-H def.). In mass spectroscopy, a molecular radical ion M^+ (*m/e* 157) was present, corresponding to the molecular formula $C_7H_7O_3N$.

Found: C, 55.12; H, 4.58; N, 9.16%. Calcd for $C_7H_7O_3N$: C, 54.90; H, 4.61; N, 9.15%.

A sample prepared through the *N*-oxidation of 6-methylpicolinic acid was also identical with the above product.

Reaction of 6-Methylpicolinic Acid *N*-Oxide with Acetic Anhydride. A mixture of 5 m*l* of acetic anhydride and 3.2 g of 6-methylpicolinic acid *N*-oxide was placed in a 50 m*l* conical flask equipped with a reflux condenser and a calcium tube, and warmed on a steam bath at 96—98°C. After about 1 hr, the color of the reaction mixture began to turn to a transparent brownish orange along with continuous evolution of carbon dioxide. The evolution of carbon dioxide lasted about one hour and half. The reaction mixture was distilled under reduced pressure after a period of 6 hr on a steam bath; 1.88 g of colorless oil (sample I), bp 107°C/18 mmHg, mp of the picrate, 165—167°C. Prism-like crystals (sample II) were isolated from the distillation residue; yield 280 mg, mp 163.5—164°C.

Hydrolysis of Sample I. A mixture of 1.0 g of sample I and 10 m*l* of concentrated hydrochloric acid was heated under reflux for 7 hr. The resulting solution was evaporated quickly by the introduction of dried air at room temperature, poured into chloroform, and then neutralized by an aqueous carbonate. The chloroform layer was dried over sodium sulfate overnight, and con-

15) R. Adams and A. W. Schrecker, *J. Am. Chem. Soc.*, **71**, 1186(1949).

16) D. Jerchel and J. Jacobs, *Angew. Chem.*, **66**, 298 (1954).

17) J. Suszko and M. Szafran, *Roczniki Chem.*, **38**, 1793 (1964); *Chem. Abstr.*, **62**, 10403g (1965).

18) W. Mathes, W. Sauermilch and T. Klein, *Chem. Ber.*, **86**, 584 (1953).

19) M. Szafran, *Bull. Acad. Poln. Sci., Ser. sci. chim.*, **10**, 479 (1962).

20) M. Szafran, *ibid.*, **13**, 245 (1965).

centrated to isolate crystals. The crystals were washed with ether; yield 230 mg, mp 163.5—164.0°C. An admixture with sample II indicated no mp depression. The product was identified as 6-methyl-2-pyridone.

IR (KBr): 2400—3200 cm^{-1} (H-bonded N–H str.); 1660 cm^{-1} (C=O str.); 1608, 1552 cm^{-1} (ring C=C, C=N str.); 733, 795, 810 cm^{-1} (C–H def.). NMR (0.5M in $CDCl_3$): 2.34 ppm (3 protons singlet, CH_3); 6.00—6.11 ppm (1 proton broad doublet, H-5), 6.33—6.48 ppm (1 proton broad doublet, H-3); 7.25—7.52 ppm (1 proton multiplets of an X-part in an ABX system, H-4 with $J_{3,4}=9.3$ cps, $J_{4,5}=6.7$ cps). UV (10^{-4}M in EtOH); λ_{max} 229.5 mμ ($\varepsilon=8700$), 288.1 mμ ($\varepsilon=8100$).

Found: C, 65.65; H, 6.51; N, 12.63%. Calcd for C_6H_7ON: C, 66.04; H, 6.46; N, 12.83%.

In another experiment, a mixture of 15 g of the *N*-oxide and 26 g of acetic anhydride was warmed at 60—65°C for 18 hr with stirring. The mixture was then directly hydrolyzed with 230 m*l* of 6N hydrochloric acid at 90—100°C for 5 hr. The resulting solution was concentrated to 100 m*l* and extracted with benzene. The benzene solution was concentrated to give crystalline mass; 9.0 g (84%) of 6-methyl-2-pyridone was obtained.

Thanks are due to Mr. Akira Iwamitsu for his assistance in part of the experimental work, also to the Research Institute of Yoshitomi Seiyaku Co., Ltd., for the measurements of mass spectra.

BULLETIN OF THE CHEMICAL SOCIETY OF JAPAN VOL. 42 3352—3354 (1969)

Disproportionation of Dimethyl *p*-Phthalate Anion Radical Paired with Alkali Metal Cation

Takeo KOWATA and Masao KOIZUMI

Department of Chemistry, Faculty of Science, Tohoku University, Katahira-cho, Sendai

(Received May 22, 1969)

This note is concerned with a new example of the disproportionation reaction of the type,[1] $2A^-Na^+ \rightarrow Na^+A^=Na^+ + A$ where A^- is a radical anion of an organic substance. According to Hirayama,[2] dialkyl *p*-phthalates when treated with alkali metals, gave the ESR signals characteristic of the radical ion pair A^-Na^+; the intensities however, often decline gradually at room temperature, as a result of some unknown reaction. We have studied the reaction in question spectrophotometrically and have arrived at the conclusion that it is the disproportionation of the above type. The dependence of the reaction upon the alkali metal cation has also been investigated and the result will be discussed in relation to Hirayama's result on the ESR hyperfine structure.

Results and Discussion

When the dimethyl *p*-phthalate (DMT) solution in THF was treated with a metallic mirror of sodium at room temperature, the solution turned purple and gave the ESR signal which was essentially similar to the one reported by Hirayama.[2] Curve 1 in Fig. 1 gives an example of the absorption spectrum of this purple solution. This spectrum was taken as quickly as possible after the appearance of the purple color. When the original concentration of DMT was *ca.* 1×10^{-3}M, the spectrum could be taken with a 1 mm cell. The exact concentration of the purple species (P), however, could not be determined. The spectrum of P-species gradually changed as shown in Fig. 1, with the isosbestic

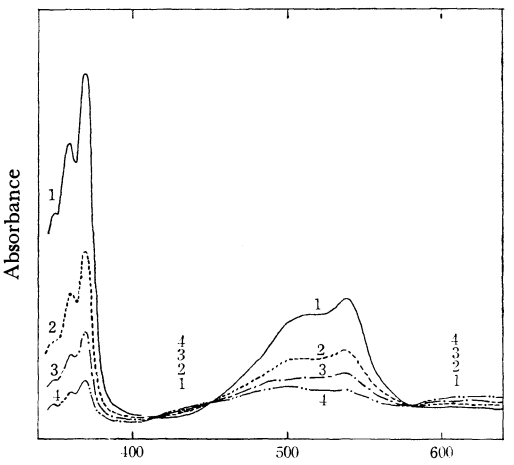

Fig. 1. Change of absorption spectrum in the course of reaction of P-species produced by the treatment with Na.
1, —— 0 sec 2, ------ 5 min 0 sec
3, —·— 19 min 24 sec 4, ·····~40 min

1) Somewhat different type of disproportionation has been reported by Evans *et al.*: A. G. Evans, P. B. Roberts and B. J. Tabner, *J. Chem. Soc., B*, **1966**, 269.

2) M. Hirayama, This Bulletin, **40**, 2234 (1967).

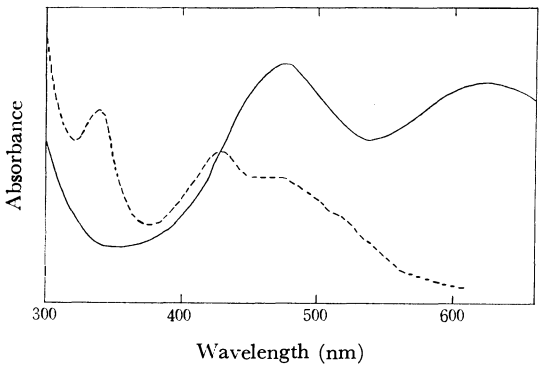

Fig. 2. Absorption spectrum of G-species (——) and that of trinitrobenzene⁻-Na⁺ (------) obtained by adding an excess quantity of trinitrobenzene to the G-species solution. The scale of ordinate is different for two curves.

points at 410, 460 and 580 nm. It was established that the reaction is second order in P-species. The resulting solution had a tint of green and gave no ESR signal. This green species (G) is quite stable, living as long as several months, but the exact shape of the spectrum could not be reproduced. The spectrum at the last stage (curve 4), gives the general feature for the G-species. At −80°C the P-species was found to be stable. It was also stable when it was freed from solvent and kept *in vacuo*. Upon introduction of air, the solution of P-species as well as of G-species became light yellow with a white precipitate. The resulting solution from the latter gave the absorption spectrum characterestic for DMT, but the former did not.

In order to examine the radical nature of the G-species, twice as much quantity of trinitrobenzene (TNB) as DMT was added to the green solution. The color at once changed into brown and gave the spectrum of TNB radical anion as shown in Fig. 2. This solution gave the ESR signal similar to the one already reported by Ward.[3] All the above findings strongly support the view that the G-species is either a divalent anion which may be produced by the disproportionation reaction,

$$2\mathrm{DMT^-Na^+} \longrightarrow \mathrm{Na^+DMT^{2-}Na^+} + \mathrm{DMT}, \quad (1)$$

or a dimer of monoanion resulting from dimerization of the following type.[4]

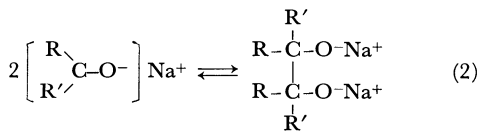

(2)

Discrimination between (1) and (2) was thought to be possible by a careful measurement of the absorption spectrum, since reaction (1) should recover half as much DMT as DMT⁻. Although the experiment for this purpose could not be made very accurately, the results were favourable for mechanism (1). As an example, one measurement showed that the increase of the optical density at 242 nm (after a long time) was about one half the decrease at the same wavelength immediately after the treatment with sodium. This is very much larger than the optical density of G species at 242 nm which is 1/5—1/11 of the original DMT.

The Nature of the Radical Ion Paired with Other Alkali Metal Cations. According to Hirayama,[2] the hyperfine structures of ESR for Li and Na are such that the values of $a_H^{(2)}$ are larger than $a_H^{(3)}$, whereas for K and Cs the values are $a_H^{(2)} \approx a_H^{(3)}$. He interpreted this as resulting from

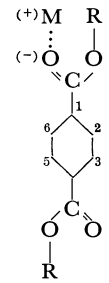

the fact that in the former group, metallic ions are located on one of the two carbonyl groups while in the latter group, they are situated in the symmetrical position between the two carbonyl groups. In view of this interpretation, we have examined the absorption spectra and the behaviour of P-species paired with different alkali cations.

The P-species from Li and K gave essentially the same spectra as from Na both in the UV and visible region while the one from Cs showed a clear difference, as shown in Fig. 3 where the free radical anion produced by electrolysis (using tetrabutyl-

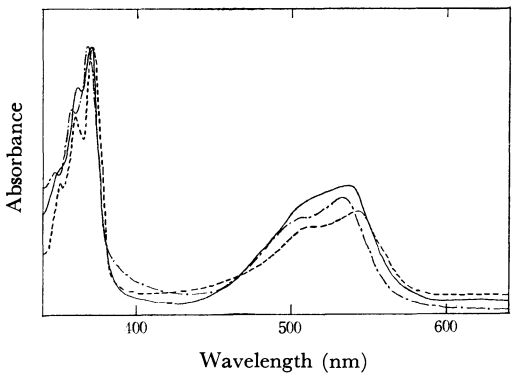

Fig. 3. Absorption spectra of three kinds of P-species, produced by the treatment with Na (------), Cs (——) and by electrolytic reduction (———): P(Li) and P(K) give essentially the same spectrum as that of P(Na).

3) R. L. Ward, *J. Am. Chem. Soc.*, **83**, 1296 (1961).
4) C. B. Wooster, *ibid.*, **57**, 377 (1957); E. de Bore, *Recueil*, **84**, 609 (1965).

ammonium perchlorate (T-BAPC) as a supporting electrolyte, [DMT] $\sim 1 \times 10^{-3}$M, [T-BAPC] $\sim 1 \times 10^{-1}$M) is also shown.

The free radical anion was found to be quite stable at room temperature. The reaction P→G occurred with Li just as with Na, while in the case of K and Cs, the spectrum of P only decayed slowly without the appearance of the G-species.

The present results can, as a whole, be interpreted as the ion pair model presented for the analogous systems. McClelland[5] discussed the ion pair of fluorenon and benzophenone in terms of a point charge model and concluded that the potential minimum lies in the neighbourhood of C=O group. Atherton and Goggins[6] studied the ion pair of pyrazine and reached the conclusion that the potential minimum lies on the two nitrogen atoms for Li and Na, while for K and Cs the potential minimum is above the aromatic ring.

Our result that the reaction P→G occurs for Li and Na but not for K and Cs, is phenomenologically consistent with Hirayama's result, if one assumes that the disproportionation reaction occurs only when the alkali cation is fixed on one of the two carbonyl groups. There is however, one discrepancy in the spectrum of P-species when compared with the ESR structure. Thus the spectrum for K-ion pair is quite the same as for Li- and Na-ion pair, while from ESR, the K-ion pair should behave like Cs. This may be interpreted as follows. The similarity of the electronic spectrum suggests that the above three alkali metal cations are located at a C=O position. On the other hand, Cs^+ ion which is situated above the aromatic ring affects the electronic state in a different way. For K, however, the following situation may exist. The K-ion being larger than Li and Na, its potential minima may be more shallow than those of Li and Na. Then the K^+ ion may be able to move from one carbonyl group to the other. If the transfer frequency is $\lesssim 10^7$ sec^{-1}, the two states cannot be separately observed by ESR technique, the resulting hyperfine structure resembling that of Cs^+ ion pair. The absorption spectrum under such circumstances, however, is expected to correspond to one of the two equivalent configurations. If such is the case, the different feature of K^+ in ESR and in UV is very reasonable.

To sum up, the monoradical anion of DMT has tendency to undergo more or less the disproportionation reaction, and the reaction occurs more easily when the alkali cation is located and fixed on one of the two carbonyls.

5) B. J. McClelland, *Trans. Faraday Soc.*, **57**, 1458 (1961).

6) N. M. Atherton and A. E. Goggins, *Trans. Faraday Soc.*, **62**, 1702 (1966); N. M. Atherton, *ibid.*, **62**, 1707 (1966).

BULLETIN OF THE CHEMICAL SOCIETY OF JAPAN VOL. 42 3354—3357 (1969)

Homolytic Chlorination of Aliphatic Compounds. III.[1] Photochlorination of 1-Substituted Propanes; Steric Effects

Masanori KOSUGI, Kohji TAKEUCHI and Toshihiko MIGITA

Department of Chemistry, Gunma University, Kiryu, Gunma

(Received May 26, 1969)

We have recently discussed the relative reactivities of aliphatic compounds in liquid-phase photochlorination and found that in CH_3–X type compounds inductive effect of the substituents X was the principal factor controlling the reactivities.[1-3] A linear free energy relationship was found between the reactivities of methyl hydrogens and Taft's σ^* constants[4] of the substituents X (X: CH_2Cl, CCl_3, CH_2CHCl_2, CH_2CMe_2Cl, CH_2CN).

In this note we wish to describe remarkable deviations from the relationship that were observed in photochlorination of 1-substituted propanes bearing ethyl groups on 1-position. The deviations are considered to be due to steric hindrance by the substituents. Table 1 lists the results obtained in the competitive photochlorination of the series of 1-substituted propanes.

1) Part II: M. Kosugi, K. Takeuchi and T. Migita, This Bulletin, **42**, 3242 (1969).

2) T. Migita, M. Kosugi, Y. Tanaka and Y. Nagai, *Yukigosei Kagaku Kyokaishi (J. Soc. Org. Synth. Chem. Japan)* **25**, 908 (1967).

3) T. Migita, M. Kosugi and Y. Nagai, This Bulletin, **40**, 920 (1967).

4) M. S. Newman, "Steric Effects in Organic Chemistry," John Wiley & Sons Inc., New York (1956), p. 619.

Table 1. Relative reactivities[a] of 1-substituted propanes 40°C

$CH_3-CH_2-CH_3$ — —	$CH_3-CH_2-CH_2Cl$[b] 21 58	$CH_3-CH_2-CHCl_2$[b] 11 14
$CH_3-CH_2-CMe_3$[b] 44 206	$CH_3-CH_2-CMe_2Cl$ 25 90	$CH_3-CH_2-CMeCl_2$ 15 26
$CH_3-CH_2-CEt_3$[c] 27 39	$CH_3-CH_2-CEt_2Cl$[c] 9.3 19	$CH_3-CH_2-CEtCl_2$[c] 4.4 7.2

a) The values are relative to the reactivity of a C–H bond of 2,2-dichloropropane and average of several runs.
b) See Ref. 2.
c) Carbon tetrachloride was used as solvent.

Table 1 shows that the successive introduction of chlorine substituent in 1-position of propane derivatives deactivates, and introduction of methyl groups in the 1-positions enhances the reactivities of C–H bonds on the 2- and 3-positions. This tendency is explainable in terms of inductive effects of chlorine and methyl substituents. However, when ethyl groups were introduced in 1-position, the reactivities of 2- and 3-position were found to be definitely lowered. For example, in substituted 1-chloropropane series, the reactivities of C–H bonds of 2- and 3-position decreases in the order:

$$CH_3CH_2CMe_2Cl > CH_3CH_2CH_2Cl > CH_3CH_2CEt_2Cl$$

Similar trends were observed in the other series of compounds. This is not expected from inductive effect of an ethyl group. Figure 1 shows the Hammett plot of the data in Table 1.

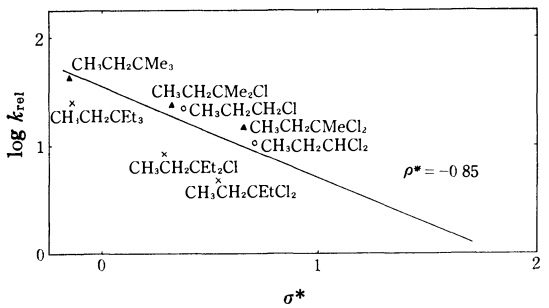

Fig. 1. Hammett plot for CH_3–X.
(σ^* values for X were estimated as described in the previous paper.)

The straight line in Fig. 1 represents the Hammett relationship obtained in our previous study,[2] ρ^* value being −0.85. As shown in Fig. 1, methyl groups in 1,1,1-triethylpropane (3,3-diethylpentane), 1-chloro-1,1-diethylpropane (3-chloro-3-ethylpentane) and 1,1-dichloro-1-ethylpropane (3,3-dichloropentane) are less reactive than expected from the relationship, while those of the other compounds have expected reactivities. This indicates that ethyl substituent on 1-position of propane derivatives causes the deactivation of the molecule, but methyl substituent does not.

Russell[5] reported that the methine hydrogens of 2,4-dimethylpentane and 2,2,4-trimethylpentane possessed unusually low reactivities toward the free or complexed chlorine atom, and explained that result in terms of the preferred conformation in which methine hydrogen atoms were protected from attack of the chlorine atom along the axis of C–H bond. A similar situation may be considered to be the deactivating factor in our cases. For example, for 3,3-dichloropentane, the presence of two chlorine atoms on 3-position will make the following conformation preferable.

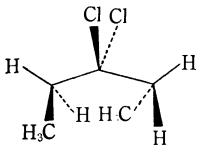

In this conformation, one of methylene hydrogens and methyl hydrogens will protect each other from attack of the chlorine atom. In 2,2-dichlorobutane having normal reactivities, however, such crowding at the back of molecule would be reduced.

Experimental

Materials. *3,3-Dichloropentane.* A charge of 917.4 g of phosphorus pentachloride was dissolved in 344 g of diethylketone prepared from propionic acid.[6] After stirring overnight, the solution was refluxed for one hour. The reaction mixture was subjected to steam distillation followed by fractional distillation. 71 g of 3,3-dichloropropane was obtained, bp 132°C (lit[7] 127—135°C), n_D^{20} 1.442 (lit[7] 1.442).

3-Chloro-3-ethylpentane. Ethylmagnesium bromide solution prepared from 164 g of ethyl bromide and 36 g of magnesium in ether was added to 186 g of diethyl ketone. The usual work-up yielded 153 g of triethylcarbinol boiling at 69—72°C/50 mmHg (lit[8]

5) G. A. Russell and P. G. Haffley, *J. Org. Chem.*, **31**, 1969 (1966).
6) D. M. Cowan, G. H. Geffery and A. I. Vogel, *J. Chem. Soc.*, **1940**, 171.
7) A. I. Heune and E. G. De Witt, *J. Am. Chem. Soc.*, **70**, 1548 (1948).
8) H. J. Lucas, *J. Am. Chem. Soc.*, **51**, 248 (1929).

TABLE 2. NMR SPECTRA OF MONOCHLORINATED PRODUCTS

	τ Values	
$CH_3^1CH^2ClC(CH_2^3CH_3^4)Cl_2$	8.21 (H^1 doublet)	5.75 (H^2 quartet)
	7.65 (H^3 multiplet)	8.80 (H^4 triplet)
$CH_2^1ClCH_2^3C(CH_2^3CH_3^4)Cl_2$	6.20 (H^1 triplet)	8.80 (H^4 triplet)
	7.65 (H^2 and H^3 multiplet)	
$CH_3^1CH^2ClC(CH_2^3CH_3^4)_2Cl$	8.36 (H^1 doublet)	5.77 (H^2 quartet)
	8.08 (H^3 multiplet)	8.95 (H^4 triplet)
$CH_2^1ClCH_2^3C(CH_2^3CH_3^4)_2Cl$	6.42 (H^1 triplet)	9.11 (H^4 multiplet)
	7.3—8.6 (H^2 and H^3 multiplet)	
$CH_3^1CH^2ClC(CH_2^3CH_3^4)_3$	8.2—8.8 (H^1 and H^3 multiplet)	
	6.02 (H^2 quartet)	9.11 (H^4 multiplet)
$CH_2^1ClCH_2^3C(CH_2^3CH_3^4)_3$	6.60 (H^1 triplet)	
	8.2—9.4 (H^2, H^3 and H^4 multiplet)	
$CH_3^1CH^2ClCMe_2^3Cl$	8.35 (H^1 doublet)	5.92 (H^2 quartet)
	8.30 (H^3 singlet)	
$CH_2^1ClCH_2^2CMe_2^3Cl$	6.34 (H^1 triplet)	7.81 (H^2 triplet)
	8.40 (H^3 singlet)	
$CH_3^1CH^2ClCMe^3Cl_2$	8.23 (H^1 doublet)	5.75 (H^2 quartet)
	7.78 (H^3 singlet)	
$CH_2^1ClCH_2^2CMe^3Cl_2$	6.19 (H^1 triplet)	7.35 (H^2 triplet)
	7.82 (H^3 singlet)	

TABLE 3. COMPETITIVE CHLORINATION OF 1-SUBSTITUTED PROPANES

1. Et_2CCl_2 40°C, in 2 m*l* of CCl_4

$\frac{Et_2CCl_2}{Me_2CCl_2}$	Molar ratio of products: $\frac{MeCHCl\text{-}CEtCl_2}{CH_2Cl\text{-}CMeCl_2}$	Molar ratio of products: $\frac{CH_2ClCH_2\text{-}CEtCl_2}{CH_2Cl\text{-}CMeCl_2}$	Rel. reactivities: $-CH_2-$	Rel. reactivities: CH_3-
0.529	2.37	2.19	6.7	4.1
0.529	2.55	2.30	7.3	4.4
0.529	2.48	2.32	7.0	4.4
0.529	2.69	2.45	7.6	4.6

2. Et_4C 40°C, in 2 m*l* of CCl_4

$\frac{Et_4C}{CH_2Cl\text{-}CH_2Cl}$	Molar ratio of products: $\frac{MeCHCl\text{-}CEt_3}{CHCl_2\text{-}CH_2Cl}$	Molar ratio of products: $\frac{CH_2ClCH_2\text{-}CEt_3}{CHCl_2\text{-}CH_2Cl}$	Rel. reactivities: $-CH_2-$	Rel. reactivities: CH_3-
0.249	6.35	6.56	12.8	8.78
0.249	5.60	6.16	11.3	8.24
0.249	6.29	7.20	12.6	9.64

3. Et_3CCl

Since 3-chloro-3-ethylpentane inevitably contains a small quantity of olefin, chlorinations of the compounds were carried out in carbon tetrachloride in the presence of a small amount of bromine, in order to exclude the possibility of addition of chlorine to the olefin. Intramolecular reactivity pattern was found to be:

$$\underset{0.482}{CH_3}—\underset{1}{CH_2}—CEt_2Cl$$

Competitive chlorination with 1,2-dichloroethane was carried out to find the relative reactivity of a methyl group of 3-chloro-3-ethylpentane.

40°C, in 2 m*l* of CCl_4

$\frac{Et_3CCl}{CH_2ClCH_2Cl}$	Molar ratio of products: $\frac{CH_2ClCH_2CEt_2Cl}{CHCl_2CH_2Cl}$	Rel. reactivities: CH_3-
0.482	2.98	2.75
0.482	3.73	3.44
0.482	2.86	2.64
0.482	3.64	3.36

4. $EtCMeCl_2$

$\frac{EtCMeCl_2}{t\text{-}BuCl}$	Molar ratio of products: $\frac{MeCHCl\text{-}CMeCl_2}{CH_2Cl\text{-}CMe_2Cl}$	Molar ratio of products: $\frac{CH_2ClCH_2\text{-}CMeCl_2}{CH_2Cl\text{-}CMe_2Cl}$	Rel. reactivities: $-CH_2-$	Rel. reactivities: CH_3-
1.60	0.950	0.779	2.7	1.5
1.60	0.950	0.743	2.7	1.4
1.60	0.950	0.777	2.7	1.5

5. $EtCMe_2Cl$

$\frac{EtCMe_2Cl}{t\text{-}BuCl}$	Molar ratio of products: $\frac{MeCHCl\text{-}CMe_2Cl}{CH_2Cl\text{-}CMe_2Cl}$	Molar ratio of products: $\frac{CH_2ClCH_2\text{-}CMe_2Cl}{CH_2Cl\text{-}CMe_2Cl}$	Rel. reactivities: $-CH_2-$	Rel. reactivities: CH_3-
1.33	2.54	1.07	8.6	2.4
1.33	2.63	1.09	8.9	2.5
1.33	2.96	1.19	10.0	2.7

72—73.5°C/50 mmHg), $n_D^{20.7}$ 1.4281 (lit[8] 1.4281). Fifty eight grams of this compound was shaken with large excess of concentrated hydrochloric acid and the resulting organic layer was separated. 60 g of desired product was obtained, boiling at 82—82.3°C/100 mmHg (lit[9] 83—83.5°C/100 mmHg), n_D^{20} 1.4332 (lit[9] 1.4334).

3,3-Diethylpentane. Ethereal solution of ethylmagnesium bromide prepared from 109 g of ethyl bromide and 24 g of magnesium was added to 63 g of 3-chloro-3-ethylpentane and the mixture refluxed for 20 hr. The work-up yielded 21 g of 3,3-diethylpentane boiling at 141.5—143°C (lit[10] 139.2°C and 147.6°C), n_D^{20} 1.4201 (lit[10] 1.4203).

2,2-Dichlorobutane. This material was prepared by the reaction of 1000 g of phosphorus pentachloride with 700 g of methyl ethyl ketone. The product was washed with water and purified by fractional distillation. 93 g of 2,2-dichlorobutane was obtained, bp 103—104° (lit[11] 102—104°C), n_D^{20} 1.4273 (lit[11] n_D^{20} 1.4295).

t-Amyl Chloride. *t*-Amyl alcohol (82 g) was treated with concentrated hydrochloric acid followed by fractional distillation. 59 g of the chloride was obtained boiling at 26°C/85 mmHg (lit[12] 84—86°C), n_D^{20} 1.4040 (lit[12] 1.4052).

Reaction Products. Monochlorinated products were collected by VPC method and their structures were derived from their NMR spectra, are shown in Table 2.

Competitive Chlorination. The chlorination procedure has already been described.[1,2] Analysis of the products of competitive photochlorinations was performed by VPC method. The results are shown in Table 3.

9) H. C. Brown and R. S. Fletcher, *J. Am. Chem. Soc.*, **71**, 1853 (1949).

10) F. C. Whitmore, ibid, **60**, 2539 (1929).

11) B. B. Carson, J. S. Thomas and D. D. Waugh, ibid, **51**, 1950 (1929).

12) M. Stoll and A. Rouve, *Helv. Chim. Acta*, **21**, 1542 (1938).

BULLETIN OF THE CHEMICAL SOCIETY OF JAPAN VOL. 42 3357—3359 (1969)

Relative Rate of Hydrogen Abstraction by the Triplet State of Phenanthraquinone

Kazuhiro MARUYAMA, Keiichi ONO and Jiro OSUGI

Department of Chemistry, Faculty of Science, Kyoto University, Sakyo-ku, Kyoto

(Received May 30, 1969)

The ability of the triplet state of some carbonyl compounds such as benzophenone to abstract hydrogen from a suitable substrate is well known and recognized as a critical step in the photoreduction of the carbonyl compound.[1] The triplet state of the carbonyl compound is, therefore, radicalic in nature, and it is interesting to compare the relative ability of hydrogen abstraction by the triplet state with the case of other radicals.

By a preliminary experiment we found the great ability of photo-activated phenanthraquinone to abstract hydrogen from the hydrogen donor. The great ability to hydrogen abstraction of the photo-activated species is reflected in the fact that phenanthraquinone can be reduced easily when it is irradiated in benzene. Phenanthraquinone has a maximum absorption at 410—420 mμ, it may be correspond to the $n\rightarrow\pi^*$ absorption band because it can be reduced even if it is irradiated with visible light (any light in the UV region was excluded by ordinary glass and a thick water layer, 150 mm).

Since the rate of hydrogen abstraction is strongly inhibited in the presence of oxygen, it seems resonable to deduce that the triplet state of phenanthraquinone is responsible for the hydrogen abstraction.

The rate of the disappearance of phenanthraquinone dissolved in a large excess of a suitable substrate when it is irradiated follow the first-order kinetics for the concentration of phenanthraquinone.

TABLE 1. RELATIVE RATE OF HYDROGEN ABSTRACTION BY THE TRIPLET STATE OF PHENANTHRAQUINONE

Substrate	20°C	40°C	60°C
Benzene	0.33	0.41	0.44
Toluene	1.00	1.42	1.85
Ethylbenzene	1.27	1.48	2.25
Cumene	2.33	2.65	2.36
t-Butylbenzene	0.42	0.48	0.53
Diethyl ether	3.44	3.59	—
Dioxane	2.47	2.48	2.58
Tetrahydrofuran	1.78	2.96	3.06
Methanol	0.92	1.14	1.32
Ethanol	2.16	2.42	2.75
2-Propanol	5.03	2.20	5.00

1) C. Walling and M. J. Gibian, *J. Am. Chem. Soc.*, **86**, 3902 (1964); G. S. Hammond and N. Turro, *Science*, **142**, 1541 (1963).

Therefore, the relative rate of hydrogen abstraction was determined from the plot of log(phenanthraquinone) against the time. Representative examples are shown in Fig. 1, while the relative rates obtained are tabulated in Table 1.

If we assume the steady-state concentration for the triplet state of phenanthraquinone, the pseudo-first-order kinetics can be formulated as follows:

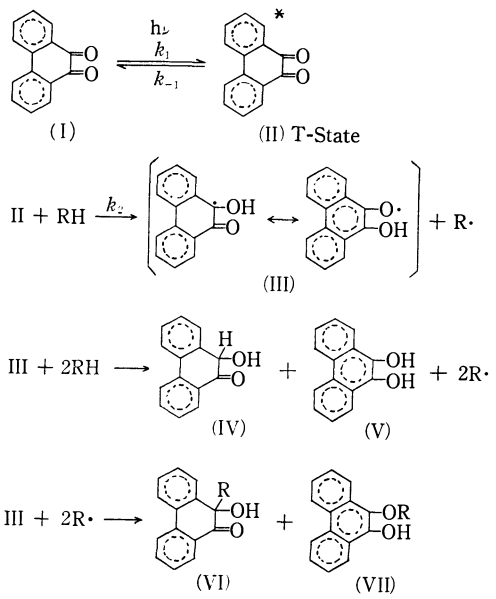

$$\frac{d[I]}{dt} = -\frac{k_1 k_2[RH][I]}{k_{-1}+k_2[RH]} = -K[I] \qquad (5)$$

As to the relation between the rate of hydrogen abstraction and the structure of a substrate, we usually found the following order; *t*-C–H>*s*-C–H>*p*-C–H, as it was expected. However, the differences among them are rather small in this reaction. For example, the relative rates of hydrogen abstraction from different types of alkylbenzenes are,

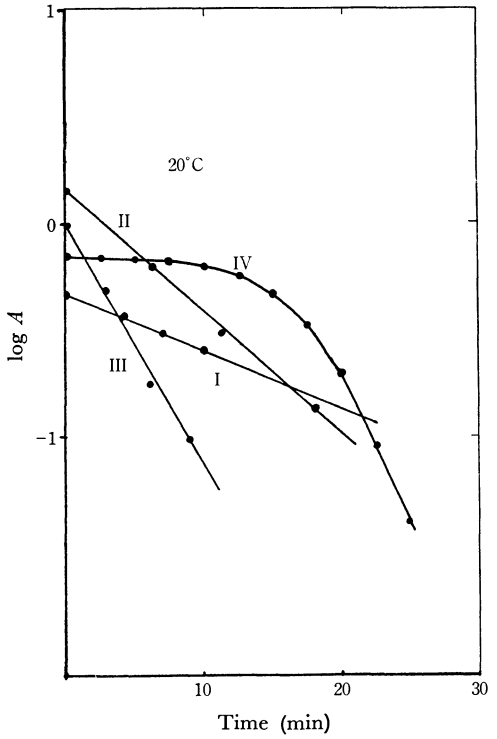

Fig. 1. I. methanol
II. ethanol
III. 2-propanol
IV. methanol in the presence of oxygen
(in this case sample was irradiated from the position of a half distance to light source through water layer for the sake of too slow decay to observe.)
A: Absorbance of phenanthraquinone

respectively: toluene (1.00 standard), ethylbenzene (1.27), and cumene (2.33) at 20°C. The relative rate of hydrogen abstraction of the triplet state of benzophenone has been investigated by Walling and Gibian,[2] who also determined the relative

Table 2. Relative reactivity of hydrogens of hydrocarbons toward various radicals[a] (per hydrogen)

Type of C–H	CH_3· 182°C	C_6H_5· 60°C	*t*-BuO· 40°C	Cl· 23°C	$(C_6H_5)_2CO$ (T)[b] 22°C	PQ (T)[c] 20°C	PQ (T)[c] 60°C	F.[d] 23°C
Primary	1	1	1	1	1	1	1	1
Secondary	7	8—9.4	8—15	3.6	4.6	1.9	1.8	1.2
Tertiary	50	44	44	4.2	9.9	6.3	3.8	1.4

a) W. A. Pryor "Free Radicals," McGraw-Hill Book Co., New York (1966), p. 154.
b) C. Walling and M. J. Gibian, *J. Am. Chem. Soc.*, **86**, 3902 (1964).
c) This work. The values described in this table are not corrected for the abstraction of hydrogens on benzene ring and on β-carbon of side-chain, however, if corrected under the consideration of the values for benzene and *t*-butylbenzene, then the relative reactivity becomes; 1°:2°:3°=1:2.0:8.1 (20°C), 1:1.9:3.9 (60°C).
d) J. M. Tedder, *Quart. Rev.*, **14**, 339 (1960).

2) C. Walling and M. J. Gibian, *J. Am. Chem. Soc.*, **87**, 3361 (1965).

reactivity of C–H bonds to hydrogen abstraction. Such results are compared with others determined for several radicals in Table 2.

Since the relative selectivity to the different type of C–H bonds is a reflection of the reactivities of the radicals, we can conclude the high reactivity to hydrogen abstraction of the triplet state of phenanthraquinone (see Table 2). The reactivity is rather higher than that of benzophenone, and is roughly between that of the chlorine atom and that of the fluorine atom. Such a high reactivity is also indicated by the small temperature dependence of the relative rate and by the fact that benzene serves as a hydrogen donor.

Irregularities in the temperature dependence of the relative rate are observed in some substrates, especially 2-propanol and cumene.*1 The causes of these irregularity are not yet clear, but both the solvation and steric factors seem to be responsible. Concerning the photoreduced products of phenanthraquinone, a 1,2-addition compound of the VI type and a 1,4-addition compound of the VII type have been described in the literature.[3] However, we can always find phenanthrahydroquinone and its quinhydrone as the main products, while the addition compounds form only a small portion.

*1 These irregularities are not experimental errors, for they are reproducible.

3) M. B. Rubin, *J. Org. Chem.*, **28**, 1949 (1963); M. B. Rubin and P. Zwitkowits, *ibid.*, **29**, 2362 (1964); M. B. Rubin and R. G. LaBarge, *ibid.*, **31**, 3283 (1966); W. A. Waters, *J. Chem. Soc.*, **1953**, 3405; M. B. Rubin and Z. Neuwirth-Weiss, *Chem. Commun.*, **1968**, 1607.

Experimental

Materials and Irradiation. The phenanthraquinone was prepared by the oxidation of guaranteed-grade phenanthrene and was recrystallized from acetic acid three times (mp 207°C). With the exception of the alcohols, all the substrates used as solvents were dried over K-Na alloy and vacuum-sealed with a known amount of phenanthraquinone in an ordinary glass tube (8 mm in diameter, 50 mm long) by using the vacuum line. The alcohols were dried over calcium oxide. A sample was irradiated through water layer 400 mm thick and two ordinary glass layers 2 mm thick with 400-W high-pressure mercury arc lamp, while the decay of phenanthraquinone was followed spectrophotometrically at 420 mμ. The products were analysed by the TLC technique and were separated by means of a Florisil column.

BULLETIN OF THE CHEMICAL SOCIETY OF JAPAN VOL. 42 3359—3362 (1969)

Effects of Metal Chlorides on the Reaction of Acetylacetone with *n*-Butyryl Chloride*1

Tetsuro NOJIRI, Iwao HASHIMOTO,*2 Masatoshi MOTOI and Kiyotada MATSUI

Department of Industrial Chemistry, Faculty of Technology, Kanazawa University, Kodatsuno, Kanazawa

(Received June 13, 1969)

Aluminum chloride-catalyzed acylation reactions of active methylene compounds such as diethyl malonate[1] and ethyl acetoacetate[2] with acid chlorides have been reported. These reactions are reversible and accompanied by deacetylation and/or decarbethoxylation reaction to give di- and triacylated methane derivatives. This prompted us to extend our studies to the acylation of acetylacetone (Ia) and also to search for any effective condensing agents other than aluminum chloride.

The reaction conditions for acylation of Ia with *n*-butyryl chloride and the yields of main products, *n*-butyrylacetone (IIa) and di-*n*-butyrylmethane (IIb), are summarized in Table 1.

The treatment of Ia in the presence of 0.5 equivalent of aluminum chloride in nitrobenzene at 45°C produced only IIa in about the same yield irrespective of the amount of acyl chloride used, while a similar treatment carried out with 1 equivalent of aluminum chloride gave IIa in a higher yield, together with IIb. Therefore, failure in the formation of IIb is ascribed to the insufficiency of the condensing agent. The formation of IIa will be explained by the mechanism proposed by Doolan and Gore[3] for the Friedel-Crafts acetylation of

*1 Presented partly at the 20th Annual Meeting of the Chemical Society of Japan, Tokyo, March, 1967.

*2 Present address: Wakayama Technical College, Goboh, Wakayama.

1) K. Matsui and M. Ota, *Nippon Kagaku Zasshi (J. Chem. Soc. Japan, Pure Chem. Sect.)*, **78**, 517 (1957); T. Nakata, *ibid.*, **78**, 1780 (1957); H. Kaneyuki, This Bulletin, **35**, 519, 523, 713 (1962).

2) K. Matsui and T. Nojiri, *Nippon Kagaku Zasshi (J. Chem. Soc. Japan, Pure Chem. Sect.)*, **86**, 531 (1965); T. Nojiri and K. Matsui, *ibid.*, **87**, 880 (1966).

3) P. C. Doolan and P. H. Gore, *J. Chem. Soc., C*, **1967**, 211.

TABLE 1. REACTION OF ACETYLACETONE WITH *n*-BUTYRYL CHLORIDE IN THE PRESENCE OF METAL CHLORIDES

Reactant: $(CH_3CO)_2CH_2$ 1.5 g (0.015 mol)
C_3H_7COCl 3.2 g (0.03 mol) *1, **3 in mole ratio
Reaction temp.: 45°C, ***30°C
Solvent: Nitrobenzene 10 ml

Metal chloride	mole ratio	Reaction time, hr	Product and yield % $PrCOCH_2COCH_3$	$(PrCO)_2CH_2$	Total	Recovered $(CH_3CO)_2CH_2$	Neutral oil, g
$AlCl_3$	0	1	0	0	0	43	
	0.5*	1	21	0	21	48	a)
	0.5	1	22	0	22	34	a)
	1*	1	33	5	38	25	a)
	1	1	38	11	49	15	a)
	1	0.5	39	11	50	18	a)
	1	24	35	15	50	14	a)
	1	1***	38	11	49	17	a)
	2	1	40	19	59	18	a)
	2	1***	38	15	53	15	a)
	3	1	37	21	58	19	a)
	2**	1	45	25	70	15	a)
$TiCl_4$	1	1	31	13	44	26	a')0.05b)
$SnCl_4$	1	1	21	7	28	9	a')0.13c)
$ZnCl_2$	1	1	17	6	23	8	a')0.21c)
$FeCl_3$	1	1	17	4	21	7	a')0.38c)
$SbCl_5$	1	1	9	0	9	10	a')0.29c)
$CuCl_2$	1	1	0	0	0	40	trace b)

a) Very small amounts of methyl propyl ketone and neutral oily substances.
a') Very small amount of methyl propyl ketone.
b) Heterogeneous reaction.
c) Reacting mixture is heterogeneous at early stage.

aluminum trisacetylacetonate (III) of aromaticity or Ia (which is regarded as converting into III during the reaction) with aluminum chloride followed by decomposition of butyrylated III during separation process. However, the formation of IIb may be explained if IIa (or Ib) derived either by the butyrylation of Ia without ring-closure or by the ring-opening before or after butyrylation of III is further acylated during the course of the reaction.

$$RCOCH_2COCH_3 \rightleftarrows RCOCHCOCH_3 \quad (\mathrm{COPr})$$
(I)
$$\rightleftarrows RCOCH_2COPr + CH_3COCl$$
(II)

a: R=$-CH_3$; b: R=$-C_3H_7$=$-Pr$

In the presence of 1 equivalent of aluminum chloride the yields of IIa and IIb obtained by using 2 equivalents of *n*-butyryl chloride were hardly changed by the reaction periods, 0.5 and 1 hr, but the extended reaction period of 24 hr led to an increased yield of IIb at the expense of IIa. This means that the acylation reaction of Ia proceeds rapidly to reach an equilibrium in 0.5 hr, after which IIa is converted slowly into IIb. The fact that the yields afforded at 45°C are the same as those at 30°C is due to the insufficiency of eth condensing agent for the reaction at 45°C. This is also proved by the fact that the higher yields are provided by increasing only the condensing agent to 2 equivalents. The good yields, however, were lowered more or less both by the fall of reaction temperature and by the increase of the condensing agent to 3 equivalents, but increased by using 3 equivalents of *n*-butyryl chloride. These findings suggest that there is a suitable amount of aluminum

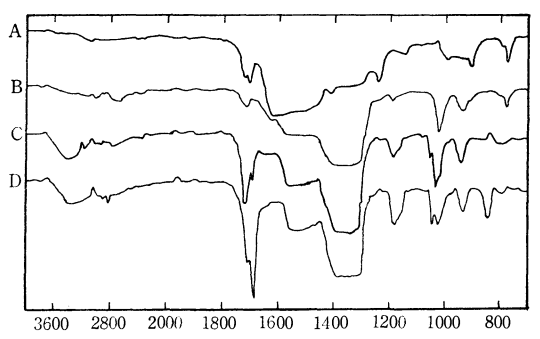

Fig. 1. Infrared spectrum of acetylacetone in nitrobenzene (A); with 0.3 (B); with 0.8 (C); and with 2 equivalents of $AlCl_3$ (D).

chloride for the acylation. Therefore, it can be expected that one half of the aluminum chloride enolizes one carbonyl group to form its enolate and the other half tends to coordinate with the other carbonyl group of the β-diketone. The infrared spectrum of Ia in the nitrobenzene solution of 2 equivalents of aluminum chloride shows strong carbonyl absorption peaks at 1710 and 1693 cm^{-1}, while such peaks are greatly reduced in intensity in the presence or absence of 0.3 equivalent of aluminum chloride in nitrobenzene (see Fig. 1). This is in substantial accord with expectations for the above experimental results. It follows then that it becomes difficult for the resulting species to close its chelate ring and it becomes susceptible to acylation with easy coordination of acyl chloride to the metal atom of enolate.

The above-mentioned fall of the yield caused by 3 equivalents of aluminum chloride suggests that the aluminum chloride competes with dichloroaluminum enolate for acyl chloride in order to coordinate, and that the reaction proceeds with liberation of aluminum chloride. The most predominant species, I'a and I'b, seem to react as follows:

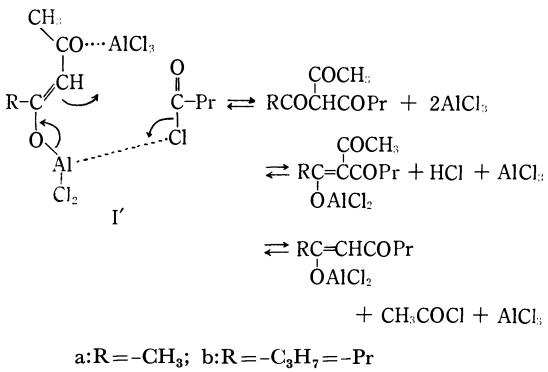

a:R=$-CH_3$; b:R=$-C_3H_7$=-Pr

In order to compare the relative efficiencies of different metal chlorides several experiments were carried out using 1 equivalent of metal chloride, and the results in Table 1 were obtained. In nitrobenzene solution the order of decreasing efficiencies of metal chlorides on the basis of the yields is as follows:

$AlCl_3$, $TiCl_4$>$SnCl_4$>$ZnCl_2$, $FeCl_3$>$SbCl_5$>$CuCl_2$

Since this order differs from the one observed both for the Friedel-Crafts acetylation reaction of toluene[4] and for the addition of acid chloride to alkenes,[5] these reactions seem to be almost independent of the present acylation reaction.

4) O. C. Dermer, D. M. Wilson, F. M. Johnson and V. H. Dermer, *J. Am. Chem. Soc.*, **63**, 2881 (1941).

5) C. D. Nenitzescu and A. T. Balaban, "Friedel-Crafts and Related Reactions," Vol. III, Part 2, ed. by G. A. Olah, Interscience Publishers, New York (1964), p. 1044.

Experimental

Materials. Acetylacetone[6] bp 136.5°C (lit bp 134—136°C), di-*n*-butyrylmethane[7] bp 82—84°C/11mmHg (lit[8] bp 101—102°C/20 mmHg), *n*-butyryl chloride,[9] bp 102°C, were prepared according to literature. *n*-Butyrylacetone was prepared from acetone and ethyl *n*-butyrate in yield of 20%, bp 55—56°C/11 mmHg (lit[6] bp 87—90°C/38 mmHg); copper chelate, mp 173—174°C (lit[10] mp 160—161°C), (Found: C, 52.80; H, 6.93%). Anhydrous aluminum chloride,[1] ferric chloride,[11] and cupric chloride[12] were prepared as described in a literature. Commercial anhydrous zinc chloride was used after fusion. The following commercial chemicals were distilled with exclusion of moisture: stannic chloride bp 113.5—113.8°C; titanium tetrachloride bp 135.5—136.5°C; antimony pentachloride bp 70.8—71.5°C/17 mmHg.

Acylation. As a typical example, to 10 m*l* of freshly distilled nitrobenzene in a 50-m*l* flask equipped with a calcium chloride tube was added the weighed amount of appropriate catalyst, and the mixture was cooled with ice water, then acetylacetone was added. After evolution of hydrogen chloride subsided the acid chloride was added to the resulting mixture with cooling, and then stirred vigorously with a magnetic stirrer.

Separation of the Product. The reaction mixture was put into crushed ice acidified with hydrochloric acid. After repeated extractions with ether, the aqueous layer was extracted again with ether next day, refluxed with ether for ten minutes, cooled, extracted with ether. The combined ether extract was washed with a saturated sodium bicarbonate solution, then extracted with 5% sodium hydroxide solution (four 15-m*l* portions) and with water. The combined sodium hydroxide and water extract, after acidification with hydrochloric acid, was extracted with ether repeatedly. The combined ether extract was dried over anhydrous sodium sulfate, then the solvent was removed by distillation through a column. The residue obtained was analyzed by gas-liquid chromatography. The organic layer containing nitrobenzene was steam distilled *in vacuo* to give neutral oily substance.

Gas-liquid Chromatographic Analysis. The analyses were carried out with gas-liquid chromatography on a Shimadzu GC-3AH, stainless steel column (0.3×200 cm; high vacuum silicone grease (30%) on Celite; He carrier (50 m*l*/min)). The thermostat temperature was 130°C for analyses of methyl propyl ketone, acetyl-

6) J. M. Sprague, L. J. Beckham and H. Adkins, *J. Am. Chem. Soc.*, **56**, 2665 (1934).

7) G. T. Morgan and R. W. Thomason, *J. Chem. Soc.*, **125**, 754 (1924).

8) G. R. Zellars and R. Levine, *J. Org. Chem.*, **13**, 160 (1948).

9) W. J. Hickinbottom, "Reactions of Organic Compounds," Longmans, Green and Co., Inc., New York (1957), p. 292.

10) L. Claisen and E. F. Ehrharde, *Ber.*, **22**, 1009 (1889).

11) B. R. Tarr, "Inorganic Syntheses," Vol. III, ed. by L. F. Audrieth, McGraw-Hill Book Co., Inc., New York (1950), p. 191.

12) A. R. Pray, *ibid.*, Vol. V, ed. by T. Moeller, McGraw-Hill Book Co., Inc., New York (1957), p. 154.

acetone, and *n*-butyrylacetone, 155°C for di-*n*-butyrylmethane. The amounts of products were determined from the apparent peak area by using acetophenone as an internal standard.

Infrared Spectra. The infrared spectra were obtained with a Model DS-301 Spectrophotometer of Japan Spectroscopic Mfg. Co., Ltd. The spectra were obtained by compensation method with nitrobenzene. For preparation of specimen, 0.2 g of acetylacetone was dissolved in 10 m*l* of anhydrous nitrobenzene containing a given quantity of aluminum chloride (0.08, 0.21, 0.54 g), then allowed to stand for 0.5 hr at 45°C. The spectrum characteristic of nitrobenzene containing aluminum chloride (0.54 g in 10 m*l*) exhibits the broad band in the 1367—1315 cm^{-1} region and the sharp band at 852 cm^{-1}.

The authors wish to thank Mr. Yoshitaka Itatani of the Faculty of Pharmacy, Kanazawa University, for elemental analyses.

BULLETIN OF THE CHEMICAL SOCIETY OF JAPAN VOL. 42 3362—3363 (1969)

Acid Anhydride as an Electron Scavenger in the Radiolysis of Tetrahydrofuran

Masao MATSUI and Masashi IMAMURA

The Institute of Physical and Chemical Research, Yamato-machi, Saitama

(Received June 16, 1969)

Nitrous oxide has been used as a specific electron scavenger in radiation chemistry. In the cases of aqueous and neutral alcoholic solutions of nitrous oxide, the yield of nitrogen produced seems to reflect the yield of the solvated electron. On the other hand, more nitrogen is produced than is to be expected from the decrease in $G(H_2)$ in the radiolysis of hydrocarbon solutions[1-6] with lower dielectric constants.

This excess nitrogen formation may be interpreted by assuming, for example, the reaction of nitrous oxide with the O^- formed by the reaction between nitrous oxide and the solvated electron. An example of the electron-scavenging process including no such side reaction will be presented in this paper.

Experimental

Tetrahydrofuran (THF) (G.R., Junsei Chem. Co.) and methyltetrahydrofuran (MTHF) (R.G., K & K Lab., Inc.) were carefully dried on metallic potassium and distilled. Maleic anhydride (G.R., Kanto Chem. Co., Inc.) was recrystallized from ether or benzene solutions. Succinic, glutaric (G.R., Tokyo Kasei Ind. Co.) and phthalic anhydrides (G.R., Wako Pure Chem. Ind. Co.) were used as received. The gas fraction at −196°C was determined on a conventional, calibrated gas burette and a Toepler pump. The hydrogen was determined by means of a heated palladium thimble, while the carbon monoxide and methane were analyzed gas-chromatographically by using a molecular sieve, 5A. Irradiation was carried out with a 10 kCi ^{60}Co source. The G-values were calculated on the basis of $G(Fe^{3+})=15.5$ and were corrected for the electron densities of THF and MTHF.

Results and Discussion

In the γ-radiolysis of liquid THF containing nitrous oxide, the amount of $G(N_2)$ always exceeds the decrease in $G(H_2)$.[7] The $G(H_2)$ decreases with an increase in the concentration of nitrous oxide, and $\Delta G(H_2)$ is seen to be 0.6 at the concentration of $(5-18)\times10^{-2}$M, where $G(H_2)$ is almost constant.

When the solutions of some aliphatic acid anhydrides in THF or MTHF were subjected to ^{60}Co-γ-irradiation at 20 ± 1°C and at a dose rate of $(0.81-0.89)\times10^{17}$ eV·ml^{-1}·min^{-1}, it was found that $G(H_2)$ decreases with an increase in the concentration of acid anhydride, eventually reaching an approximately constant value which is practically the same as that observed for the THF-N_2O system. A typical example is illustrated in Fig. 1, where maleic anhydride is the solute.

Carbon monoxide is one of the gaseous products from THF, its yield is relatively low and is not affected by the addition of nitrous oxide and other solutes.[8] The $G(CO)$ in the THF-maleic anhydride

1) G. Scholes and M. Simic, *Nature*, **202**, 895 (1964).
2) G. R. A. Johnson and J. M. Warman, *ibid.*, **203**, 73 (1964).
3) W. V. Sherman, *J. Chem. Soc., A*, **1966**, 599.
4) S. Sato, R. Yugeta, K. Shinsaka and T. Terao, This Bulletin, **39**, 156 (1966).
5) J. M. Warman, *J, Phys. Chem.*, **71**, 4066 (1967).
6) W. J. Holtslander and G. R. Freeman, *Can. J. Chem.*, **45**, 1661 (1967).
7) M. Matsui, to be published.
8) M. Matsui, This Bulletin, **39**, 1640 (1966).

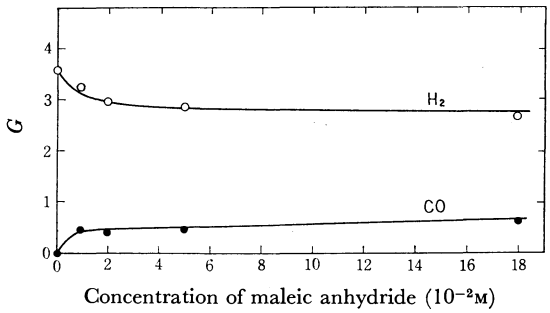

Fig. 1. Variation of $G(H_2)$ and $G(CO)$ with concentration of maleic anhydride.

system increases with an increase in the concentration of acid anhydrides. In Fig. 1, the difference between the total $G(CO)$ from the solution and that for pure THF, $G'(CO)$, is also plotted as a function of the concentration of maleic anhydride. It is interesting to note that the stationary value of $G'(CO)$ is approximately the same as that of $\Delta G(H_2)$. This fact presumably indicates that the precursor giving the additional carbon monoxide is that of hydrogen. It may be reasonable to assume that the solvated electron gives rise to the hydrogen formation in THF, as in MTHF[9] and alcoholic solutions,[10] *i. e.*, one solvated electron produces one hydrogen molecule. Therefore, it may be assumed that electrons react with the anhydrides to split off carbon monoxide, presumably by dissociative electron attachment.

Similar experiments have been carried out with a few other acid anhydrides. Succinic and glutaric anhydrides have been shown to behave much like maleic anhydride. Phthalic anhydride decreases the $G(H_2)$, but gives no additional carbon monoxide. The difference in reactivity is not clear at this moment.

The reactivities of these acid anhydrides towards electrons have been ascertained in experiments using the rigid matrix technique at 77°K. The optical absorption attributed to the matrix-trapped electron was found to diminish upon the addition of these additives.

An examination of the adaptability to other systems and of the mechanism of the carbon monoxide formation in the radiolysis of systems including acid anhydride is now in progress.

The authors wish to thank Dr. T. Shida for his rigid matrix work and Miss R. Maki for carrying out the gas-chromatographic analysis.

9) F. S. Dainton, J. P. Keene, T. J. Kemp, G. A. Salmon and J. Teply, *Proc. Chem. Soc.*, **1964**, 265; F. S. Dainton, F. R. S. and G. A. Salmon, *Proc. Roy. Soc.*, **A285**, 319 (1965).

10) H. Seki and M. Imamura, *J. Phys. Chem.*, **71**, 870 (1967).

BULLETIN OF THE CHEMICAL SOCIETY OF JAPAN VOL. 42 3363—3365 (1969)

Reactions of Titanium Tetrahalides with Benzoylhydrazine

R. C. AGGARWAL and S. K. SINGH

Chemistry Department, Lucknow University, Lucknow, India

(Received January 14, 1969)

As there has been no previous work on the reactions of titanium tetrahalides with hydrazine-derivatives containing carbonyl group such as benzoylhydrazine, it was considered of interest to study the reactions of these Lewis acids with benzoylhydrazine and the results obtained are described in this communication.

Experimental

Titanium tetrahalides and organic solvents used in the present work were purified and made anhydrous employing the standard literature methods. Benzoylhydrazine was prepared from the reaction of ethyl benzoate and hydrazine hydrate and purified by crystallization from benzene, mp 111°C.[1)]

Preparation of Complexes. *i) Tetrafluorobis(benzoylhydrazine)titanium(IV).* Solution of benzolyhydrazine (1—5%) in tetrahydrofuran was added gradually with vigorous shaking to the clear solution of titanium tetrafluoride in the same solvent. The homogeneous solution was refluxed for 30 min and the solvent removed till a saturated solution was obtained. Addition of carbon tetrachloride to the above solution yielded a yellow-orange precipitate, which was filtered, washed with a mixture of tetrahydrofuran and carbon tetrachloride and dried under reduced pressure. The complex was recyrstallized from tetrahydrofuran-carbon tetrachloride mixture.

The compound is readily hydrolyzed on exposure

1) T. Curtius, *J. Prakt. Chem.*, **50**, (2), 278 (1894).

to atmosphere.

ii) Dichlorobis(benzoylhydrazino)titanium (IV). 40 mmol of titanium tetrachloride, 20 mmol of benzoylhydrazine and 50 ml of chloroform were taken in a flask and the suspension refluxed for several hours in an inert atmosphere. The brown solid product formed was filtered, washed with chloroform till free from excess amount of Lewis acid and dried under vacuum. The complex was recrystallized from the tetrahydrofuran-chloroform mixture. The complex is hygroscopic and soluble in tetrahydrofuran.

Dibromobis(benzoylhydrazino)titanium(IV) and diiodobis(benzoylhydrazino)titanium(IV) complexes were prepared in the same way as the chloro complex; iodo complex took a comparatively longer time for drying under reduced pressure. These complexes were also recrystallized form the tetrahydrofuran-chloroform mixture. These complexes are hygroscopic and soluble in tetrahydrofuran too.

The complexes thus prepared were all diamagnetic and the analytical results and general behaviour of the complexes are given in Table 1.

Discussion

An examination of Table 1 shows that titanium tetrafluoride forms adduct of the composition, $TiF_4 \cdot 2BZH$, while other tetrahalides undergo condensation reaction, yielding products of the general formula, $TiX_2(BZ)_2$. When a mixture of benzoylhydrazine and titanium tetrachloride (excess) was kept at 25°C for several days, an unstable 1 : 2 adduct was obtained which lost hydrogen chloride slowly at room temperature but rapidly on heating around 80°C yielding eventually the same condensation product as described above.

The insolubility of titanium tetrahalide complexes of benzoylhydrazine in common organic solvents seriously limits the number of physical measurements that could be carried out for establishing their structures.

The assignment of important absorption bands

Table 1. Analytical data and general behaviour of the complexes

Composition of the solid reaction product	% Found		% Calcd		Colour	Temperature of decomposition (°C)
	Ti	Halogen	Ti	Halogen		
$TiF_4 \cdot 2BZH$	12.84	18.83	12.12	19.19	yellow-orange solid	88—93
$TiCl_2(BZ)_2$	11.88	25.62	11.28	25.00	brown solid	250
$TiBr_2(BZ)_2$	9.74	33.06	10.04	33.44	golden-yellow solid	79—83
$TiI_2(BZ)_2$	8.90	44.75	8.39	44.39	black solid	60—65

Table 2. Assignment of important vibrational frequencies of benzoylhydrazine and its complexes with titanium tetrahalides

Compound	Phase	ν(NH) (cm^{-1})	Amide I* (cm^{-1})	Amide II* (cm^{-1})	$\delta(NH_2)$ (cm^{-1})	ν(aromatic C-C) (cm^{-1})	Amide III* (cm^{-1})	ν(N-N) (cm^{-1})
Benzoylhydrazine (BZH)	Nujol mull	3285 s 3170 s,b 3130 s	1668 s	1565 s 1518 s	1612 s	1600 s, 1572 s 1492 m, 1442 s 1485 s	1345	880 m, 915 m
	CH_3CN soln.[2]	3350 s	1672 s	—	—	—	1311	—
$TiF_4 \cdot 2BZH$	Nujol mull	3310 w,b 3170 w 3120 w	1658 s 1648 s 1642 s 1630 s 1632 s	1572 m 1565 m 1552 m 1535 m	1612 m	1596 m, 1572 m 1495 m, 1432 sh 1485 m	1360 sh 1338 sh	850 m, b 924 w
$TiCl_2(BZ)_2$	Nujol mull	3130 m	1632 s 1628 s	1556 s 1542 s	—	1600 m, 1586 m 1495 w, 1446 s 1488 m	1334 w 1338 w	925 w
$TiBr_2(BZ)_2$	Nujol mull	3145 sh	1665 sh 1655 s 1650 s 1620 s	1665 sh 1535 sh 1525 s	—	1595 s , 1575 sh 1650 s , 1435 sh	1320 m, b	888 sh 935 sh
$TiI_2(BZ)_2$	Nujol mull	3160 sh	1672 sh 1658 s 1642 s	1590—1535 w,b 1535 w,b	—	1595 w, 1465 sh 1445 sh	1346 w	890 w 925 w

* Amide I, carbonyl stretching mode; Amide II, N-H in-plane bending and C-N stretching modes; Amide III, C-N stretching and N-H in-plane bending modes.

Table 3. Far infrared spectral results of benzoylhydrazine and the titanium tetrahalide complexes

Compound	Tentative assignments			
	ν(Ti–X) (cm^{-1})	ν(Ti–O) (cm^{-1})	ν(Ti–N) (cm^{-1})	Ligand bands (cm^{-1})
Benzoylhydrazine	—	—	—	678 s, 662 s, 605m,b, 345m, 295m, 268sh, 258m, 247sh, 240 s
$TiF_4 \cdot 2BZH$	600 s,b, 560sh, 545 s, 440m, b	510w	—	265w, 255w, 248w, 235w
$TiCl_2(BZ)_2$	395m, b	520w	552 s	680 s, 610 s,b, 345m,b, 268w, 256w, 248w, 235w
$TiBr_2(BZ)_2$	282m	515m	545m	675 s,b, 268w, 258w, 250w, 235w
$TiI_2(BZ)_2$	—	515m	628—535m, b	684m, 346w

in the infrared spectra of benzoylhydrazine and its complexes with titanium tetrahalides has been made on the basis of the reported infrared spectral studies of the titanium tetrahalide complexes of similar bases.

Infrared Spectral Discussion. The spectrum of $TiF_4 \cdot 2BZH$ gives a very broad band in the ν(C=O) region. If 1642 cm^{-1} is taken as the centre of the broad band, a negative shift is obtained in this band indicating coordination through oxygen. A positive shift in one of the N–H stretching bands also supports coordination through oxygen.

A doublet in the spectrum of $TiCl_2(BZ)_2$ with maxima at 1632 and 1629 cm^{-1} and broad bands in the spectra of $TiBr_2(BZ)_2$ and $TiI_2(BZ)_2$ with maxima at 1655, 1650 cm^{-1} and 1658, 1642 cm^{-1} respectively are assigned to amide I. The negative shift in C=O stretching frequency in the complexes indicates coordination through oxygen.

An examination of Table 2 shows that there occurs a decrease in the number of N–H stretching bands in the spectra of above complexes as compared with the parent base. This is probably due to the change of $-NH_2$ group into $>$N–H group as a result of Ti–N bond formation. The appearance of two ν(N–H)[2] bands in acetylbenzoylhydrazine and dibenzoylhydrazine supports the above view point. This is further supported by the disappearance of the $\delta(NH)_2$[2,3] band in the spectra of the complexes.

Since M–O[4,5] and M–N[6] stretching vibrations for a number of transition metal complexes occur in 400—500 cm^{-1} region, it is difficult to assign ν(Ti–N) and ν(Ti–O) unambiguously in the complexes.

Rivest and Jain[7] have assigned ν(Ti–O) mode in the complexes, $TiCl_4 \cdot CH_3CONH_2$ and $TiCl_4 \cdot CH_3CONEt_2$ at 505 and 507 cm^{-1} respectively. The bands occurring in 510—520 cm^{-1} region in the benzoylhydrazine complexes may probably be due to ν(Ti–O) and the bands appearing at 552, 545, and 535—628 cm^{-1} in $TiCl_2(BZ)_2$, $TiBr_2(BZ)_2$ and $TiI_2(BZ)_2$ respectively are tentatively assigned to ν(Ti–N).

The occurrence of ν(Ti–X) in the complexes in the octahedral region[8,9] indicates an octahedral geometry of the complexes.

The infrared spectral studies thus show that BZH acts as a monodentate ligand in $TiF_4 \cdot 2BZH$ coordinating through oxygen and as a bidentate ligand in $TiX_2(BZ)_2$ (X=Cl, Br and I) involving nitrogen, in addition to oxygen, in bond formation with titanium. Two five-membered rings are thus formed around the titanium atom in these complexes.

IR spectral studies also show all the complexes to be octahedral in geometry.

The authors are grateful to the Council of Scientific and Industrial Research, New Delhi, for the award of Junior Research Fellowship to one of them (S.K.S.) and to Dr. M. Onyszchuk, McGill University, Montreal, for his kind help in the form of chemicals and equipments.

2) M. Mashima, This Bulletin, **35**, 332 (1962).
3) R. M. Issa, M. F. El. Shazly and M. F. Iskander, *Z. Anorg. Allgem. Chem.*, **354**, 90 (1967).
4) K. Nakamoto, Y. Morimoto and A. E. Martell, *J. Am. Chem. Soc.*, **83**, 4533 (1961).
5) K. Nakamoto, P. J. McCarthy, A. Ruby and A. E. Martell, *ibid.*, **83**, 1066, 1272 (1961).
6) K. Nakamoto, "Infrared Spectra of Inorganic and Coordination Compounds," John Wiley and Sons, Inc., New York (1963), p. 150.
7) S. C. Jain and R. Rivest, *Can. J. Chem.*, **45**, 139 (1967).
8) I. R. Beattie and M. Webster, *J. Chem. Soc.*, **1964**, 3507.
9) R. J. H. Clark and W. Errington, *J. Chem. Soc.*, *A*, **1967**, 258.

SHORT COMMUNICATIONS

Total Synthesis of (−)-Artemisin

Masao NAKAZAKI and Koichiro NAEMURA

Department of Chemistry, Faculty of Engineering Science, Osaka University, Toyonaka, Osaka

(Received September 5, 1969)

The key compound chosen in our total synthesis of (±)-artemisin (**1**)[1] was racemic 3-oxo-8β(H), 11α(H)-eudesm-4-en-8,13-olide (**2**); and its dextrorotatory modification mp 142°, $[\alpha]_D^{18}$ +19.4° was derived from (+)-isoalantolactone or (+)-alantolactone as described in our preceding communication.[2] Since this (+)-**2** from the natural sources was converted into (−)-artemisin,[2] any optically active intermediate compound between (+)-**2** and isoalantolactone or alantolactone could be the relay substance in the total synthesis of natural (−)-artemisin.

Our choice was unsaturated ketoester (**3**), preparation of which is dealt in the present communication.

To make unsaturated ketoester (**3**) by enamine alkylation required the preparation of unsaturated ketone (**8**), which was accomplished following the general synthesis route employed previously.[1]

From the reaction mixture of Robinson's annelation of *cis*-2-methyl-4-acetoxycyclohexanone with diethylaminopentan-3-one methiodide in the presence of sodium methoxide, *cis*-bicyclic ketoalcohol (**4**), mp 101°C and its *trans* form (**5**), mp 82—83°C in ratio of 7 : 3, were isolated.

To remove the keto group without affecting the double bond, *cis*-ketoalcohol (**4**) was first converted into thioketal (**6**) with ethanedithiol and BF_3-etherate.

Desulfurization of thioketal (**6**) with sodium in liquid ammonia[3] gave unsaturated alcohol (**7**), mp 72°C which was then oxidized with chromic acid anhydride in acetone[4] to the requisite unsaturated ketone (**8**), bp 130—132°C/15 mmHg.

The oily enamine (**9**) obtained by refluxing unsaturated ketone (**8**) with piperidine in benzene solution, was dissolved in methanol and treated with ethyl α-bromopropionate. After being decomposed with water, the reaction mixture was

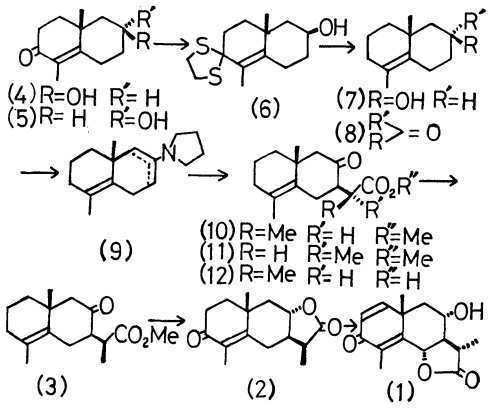

saponified to furnish a mixture of esters, bp 120—125°C/0.1 mmHg. Inspection of thin layer and vapor chromatograms revealed the presence (1 : 1) of the two epimers (**10**) and (**11**) differing at C_{11}-center, whose chromatography on silica gel led to isolation of the unsaturated ketoester (**10**) as a fast moving elute.

Infrared and NMR spectra data together with vapor phase chromatogram established the identity of this unsaturated ketoester (**10**) with the intermediate (**3**) from the natural sources.

In order to complete the total synthesis, there only remained the optical resolution which was accomplished by working with brucine as the resolving agent.

Crystallization from methanol-water of brucine salt of acid (**12**) obtained by alkaline hydrolysis of **10** furnished the salt, $[\alpha]_D^{22}$ −15.7° (*c* 0.5, ethanol). The acid regenerated from the salt was esterified with diazomethane to ester (**3**), bp 118—121°C/0.1 mmHg, $[\alpha]_D^{22}$ +42.9° (*c* 0.3, in ethanol) (**3** from the natural sources: bp 116—122°C/0.1 mmHg, $[\alpha]_D^{18}$ +41.4°).[2] Comparison of their infrared and NMR spectra established their identity which was further supported by a mixed melting point determination of their semicarbazone, mp 165—166°C.

(−)-Artemisin has been obtained therefore by total synthesis.

1) M. Nakazaki and K. Naemura, *Tetrahedron Letters*, **1966**, 2615.
2) M. Nakazaki and K. Naemura, *ibid.*, **1969**, 33.
3) D. C. Humber, A. R. Pinder and R. A. Williams, *J. Org. Chem.*, **32**, 2335 (1967).
4) J. A. Marshall, N. Cohen and A. R. Hochstetler, *J. Am. Chem. Soc.*, **88**, 3408 (1966).

The Crystal Structures of Pentaglycerol and Neopentylglycol

Etsuko NAKANO, Ken HIROTSU and Akira SHIMADA

Department of Chemistry, Faculty of Science, Osaka City University, Sumiyoshi-ku, Osaka

(Received August 9, 1969)

We have made a structural investigation of neopentylglycol $(CH_3)_2C(CH_2OH)_2$ and pentaglycerol $CH_3C(CH_2OH)_3$ in order to elucidate the molecular structure and hydrogen bonds in the crystal and to make a comparison with pentaerythritol $C(CH_2OH)_4$.[1-4]

For pentaglycerol, three-dimensional intensity data were collected by the photographic method. In these photographs, diffuse scatterings are observed in addition to Bragg reflections. If we disregard the diffuse scatterings, the photographs show the same space group and almost the same cell size and intensity distribution as pentaerythritol. This indicates that the crystal structure is similar to that of pentaerythritol. In the crystal of pentaerythritol, each molecule is required by space-group symmetry to be located at the special position of a unit cell with the molecular symmetry of $\bar{4}$. In the case of pentaglycerol, on the other hand, the molecule can not have such a high symmetry, since only three CH_2OH groups exist in a molecule. Thus, it would be necessary to assume some disordered arrangement of molecules in the crystal of pentaglycerol. A more detailed analysis of the structure is now in progress.

The crystal structure of neopentylglycol was established; it will be mentioned below. Specimens suitable for X-ray work were obtained from the benzene solution in the form of colorless needles elongated along the *a* axis. The crystals are monoclinic, with four molecules in a unit cell with the dimensions of $a=6.01$, $b=10.91$, $c=10.18$ Å, and $\beta=100.0°$. The space group was found to be $P2_1/n$. The density calculated was 1.05 g·cm^{-3}. Since the crystal was fairly volatile, samples were sealed into glass capillaries. Weissenberg intensity data were collected by means of Cu$K\alpha$ radiation on the *a* axis for from zero to the fourth layer, and on the *c* axis for from zero to the fifth layer. 808 reflections were observed; 105 were too weak to be measured.

From the three-dimensional sharpened Patterson function, molecular orientation and intermolecular O- - -O (the hydrogen bond) vectors were established by interpreting vectors from 2.4 to 3.0 Å around the point of origin. Using the 0kl data, an approximate structure was obtained by the trial method, the molecular orientation being taken into consideration. Refinements were carried out by means of a block-diagonal least-squares method, and the discrepancy index, R was reduced to 18.5%, excluding unobserved reflections.

The partial structure–$C(CH_2OH)_2$ group in neopentylglycol is the same as that in pentaerythritol. The average bond distance is 1.56 Å for C–C and 1.45 Å for C–O. The average bond angle is 109.5° for C–C–C and 110.9° for C–C–O. The mode of packing of the molecules in the crystal and the electron density can be seen in Fig. 1. Two intermolecular separations, O(1)- - -O(2) of 2.65 Å and O(1)- - -O(2) of 2.72 Å, correspond to hydrogen bonds which link the molecules in infinite ribbons along the *a* axis. It is also interesting that the arrangement of four hydrogen bonds around the center of symmetry is similar to that of pentaerythritol. A detailed account of this work will be published in the near future.

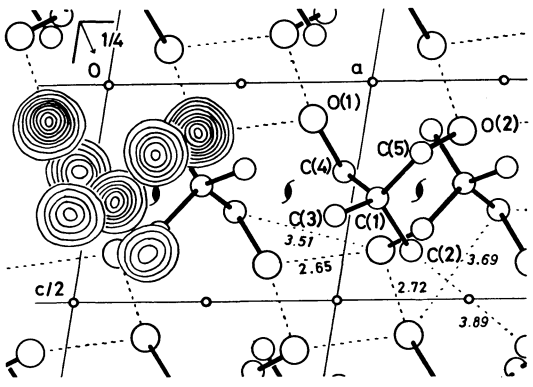

Fig. 1. Arrangement of the molecules along the *b* axis.

1) I. Nitta and T. Watanabe, *Sci. Papers Inst. Phys. Chem. Research*, **34**, 1669 (1938).

2) F. J. Llwellyn, E. G. Cox, and T. H. Goodwin, *J. Chem. Soc.*, **1937**, 883.

3) R. Shiono, D. W. J. Cruickshank and E. G. Cox, *Acta Cryst.*, **11**, 389 (1958).

4) Jan Hvoslef, *ibid.*, **11**, 383 (1958).

The Crystal Structure of Pyromellitic Acid Dihydrate (Benzene-1,2,4,5-tetracarboxylic Acid Dihydrate)

Fusao TAKUSAGAWA, Ken HIROTSU and Akira SHIMADA

Department of Chemistry, Faculty of Science, Osaka City University, Sumiyoshi-ku, Osaka

(Received August 11, 1969)

Since the pyromellitic acid dihydrate, $C_6H_2(COOH)_4 \cdot 2H_2O$ has four –COOH and two H_2O, it is of interest to elucidate the steric hindrance of adjacent carboxyl groups and the hydrogen bond formation in this crystal and to compare the structure of this compound with those of other similar carboxylic acids.

The crystal of this compound is triclinic, with cell dimensions of $a=10.05$, $b=6.46$, $c=5.44$ Å, $\alpha=74.5°$, $\beta=112.2°$, and $\gamma=77.3°$. The space group is $P\bar{1}$, and the unit cell contains one molecule. The calculated density is 1.64 g/cm³, while the observed value obtained by the flotation method is 1.63 g/cm³. The intensities were estimated visually from Weissenberg photographs around b and c axes taken with Cu$K\alpha$ radiation; 1070 were recorded, but of these 148 were too weak to be measured.

The crystal structure was derived by a consideration of Patterson maps and was confirmed by three-dimensional Fourier syntheses. The positional and thermal parameters of each atom thus obtained were refined by the block-diagonal least-squares method. The R factor is 0.09 at the present stage.

The projection of the crystal structure along the c axis and the molecular configuration of the pyromellitic acid are shown in Figs. 1 and 2 respectively. The average C(ring)–C(ring) distance is 1.39 Å, and the average C(ring)–C(carboxyl) distance is 1.49 Å. One carboxyl group is twisted by 21.4°, and the other is twisted by 74.5°, out of the plane of the benzene ring. The C–O(H) and C=O distance differ significantly from each other, the average values being 1.31 and 1.21 Å respectively. Four types of hydrogen bonds, with the average O–H···O distance of 2.72 Å, form a three-dimensional network, as shown in Fig. 1. Each molecule is joined to two other molecules through hydrogen bonds around the center of symmetry, forming an endless chain in the [1 $\bar{1}$ 1] direction. Water molecules are arranged on the plane parallel to [1 1 0], which hold the chains together by means of hydrogen bonds. A detailed account of this work will be presented in the near future.

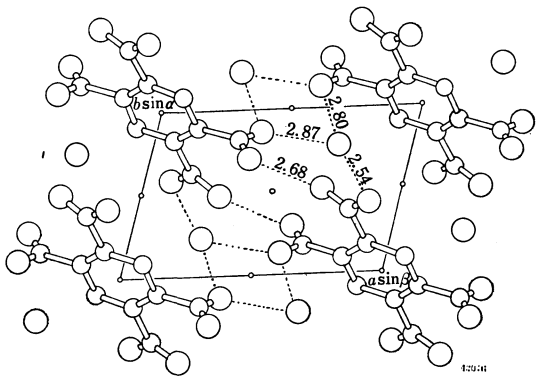

Fig. 1. The projection of the crystal structure along the c axis.

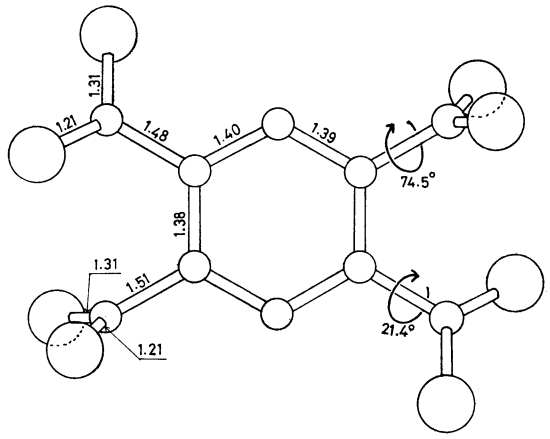

Fig. 2. The projection of the pyromellitic acid on a benzene ring.

BULLETIN OF THE CHEMICAL SOCIETY OF JAPAN VOL. 42 3369—3372 (1969)

An ESR Study of Photochemical Intermediates from Rigid Organic Solvents Containing Benzene*1

Tadayoshi TANEI*2 and Hiroyuki HATANO

Department of Chemistry, Faculty of Science, Kyoto University, Sakyo-ku, Kyoto

(Received March 10, 1969)

The present work was undertaken in order to examine a photochemical intermediate from benzene using rigid organic matrices: EPA (a mixture of E: diethyl ether, P: isopentane, and A: ethyl alcohol, 5 : 5 : 2, v/v), diethyl ether, and isopentane. The UV irradiation of EPA, diethyl ether, and ethyl alcohol at 77°K, in wavelength regions from approximately 2200Å to 2600Å, gave ESR spectra which can be ascribed to the ethyl and/or the ethanol radical, even when a solute was not added. On the contrary, the UV irradiation of isopentane under similar conditions did not show any ESR spectrum. However, the UV irradiation of isopentane containing benzene in concentration regions from 10^{-1} to 10^{-2} M gave two kinds of ESR spectra, ascribed to phenyl and *tert*-pentyl radicals. This reaction may be interpreted as a sensitized photodecomposition brought about by an excitation and/or a photolytic degradation of benzene.

In previous papers,[1,2] we reported a study of photochemical intermediates from benzene in the solid state and in an adsorption state on silica gel using the electron spin resonance technique. Migirdicyan[3] reported the sensitized photodecomposition of a methylcyclohexane rigid matrix by the addition of benzene, but they did not observe a spectrum arising from benzene.

In the present work, we attempted to examine a photochemical intermediate from benzene using rigid organic matrices of EPA, diethyl ether, ethyl alcohol, and isopentane, which have been used for the study of photochemical intermediates by electronic spectroscopy since the pioneering work by Lewis and Lipkin.[4] From the present experiments, it was found that the rigid matrices of EPA, diethyl ether, and ethyl alcohol not containing benzene were decomposed by UV irradiation in the wavelength regions longer than approximately 2200Å, and that one could not observe a photochemical intermediate from benzene because of the superposition of spectra arising from the solvents. On the other hand, it was confirmed that the UV-irradiated isopentane matrix gave no ESR signal, and that, when benzene was added to isopentane, the photodecomposition of its "isopentane-benzene mixture" was induced to exhibit ESR spectra attributable to phenyl and *tert*-pentyl radicals. This phenomenon can be interpreted as being an example of the sensitized photodecomposition of isopentane, accompanied by the photodegradation of benzene.

Experimental

Materials. An EPA (E: diethyl ether, P: isopentane, A: ethyl alcohol) solvent was prepared in the mixing ratio of 5 : 5 : 2 v/v. The diethyl ether was Nakarai Chemicals' pure grade; it was dried over calcium chloride in a nitrogen atmosphere and then passed through an activated alumina column. Isopentane from Nakarai Chemical Co., Ltd., Kyoto, was distilled in the presence of metallic sodium; no further purification was made. Ethyl alcohol (Special Grade) from the Nakarai Chemical Co., Ltd., was purified by the following procedure; it was distilled in the presence of sulfuric acid, and then its distillate was boiled for several hours in the presence of silver nitrate before further distillation. The distillate was distilled over calcium oxide and passed through a newly-activated silica gel column. The final purification was performed using a Widmer refining column. These solvents were purified immediately before use and were kept in the dark. The benzene was Merck's spectro-grade, which had been purified according to the method described in a previous paper.[2] The EPA, ethyl alcohol, and isopentane solutions containing benzene were prepared in the concentration regions from 10^{-1} to 10^{-4} M.

The solution was added to a 4-mm-i.d. quartz ampoule by the use of a syringe, and was degassed through repeated freezing and thawing on a vacuum line at the temperature of liquid nitrogen.

Irradiation. The UV irradiation was performed at the temperature of liquid nitrogen using either a Toshiba 400 W high-pressure mercury lamp or a low-pressure mercury lamp (germicidal lamp). In some

*1 This paper was read at the Symposium on Redoxidation in Nonaqueous Media sponsored by the Chemical Society of Japan, Kyoto, 1968.

*2 Present address: Sekisui Chemical Company, Ltd., Research Laboratory, Hirose 25, Shimamoto-cho, Mishima-gun, Osaka.

1) T. Tanei, This Bulletin, **40**, 2456 (1967).
2) T. Tanei, *ibid.*, **41**, 833 (1968).
3) E. Migirdicyan, *J. Chim. Phys.*, **43**, 543 (1966).
4) G. N. Lewis and D. Lipkin, *J. Am. Chem. Soc.*, **64**, 2801 (1942).

experiments, mainly in the case of a high-pressure mercury lamp, we used a UV filter, either Toshiba UV-25 or UV-D25. γ-Irradiation was carried out with Co-60 (750 Ci) at the temperature of liquid nitrogen.

ESR Measurements. The ESR spectra were recorded using a Varian V-4560 EPR spectrometer operating at X-band frequency and with a 100 kc/sec field modulation, over the temperature region from the temperature of liquid nitrogen to about 130° K. Temperature control was done by means of a Varian variable-temperature accessory.

Results and Discussion

The UV irradiation of the matrices of EPA, diethyl ether, and ethyl alcohol containing no benzene gave ESR signals which can be ascribed to ethyl and to ethanol radicals. This phenomenon made it impossible to observe the ESR spectra from benzene in these rigid solvents. Namely, the UV irradiation of both EPA, and diethyl ether rigid matrices containing no benzene showed a prominent four-line spectrum, with a splitting value of about 27 gauss and an intensity ratio of approximately 1 : 3 : 3 : 1 at 77°K, as is shown in Fig. 1(a) and Fig. 2(a). This spectrum was easily observed just after UV irradiation, but it completely disappeared within about 20 hr when the sample was kept at the temperature of liquid nitrogen.

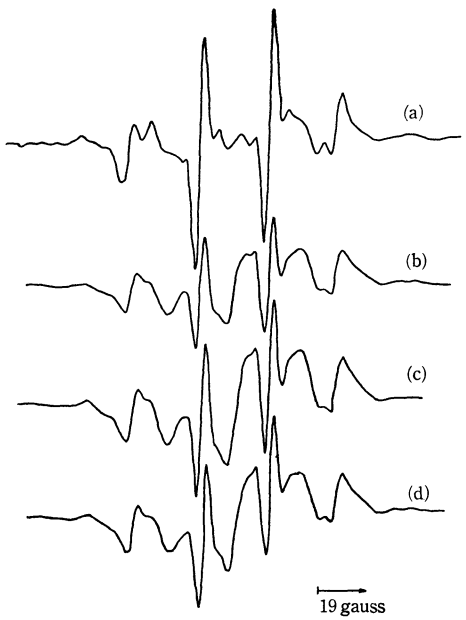

Fig. 1. ESR spectra from UV-irradiated EPA, and "EPA-Benzene" mixtures at 77°K. UV-Irradiation was performed for 15 min at liquid nitrogen temperature. Alphabetical marks correspond to the following samples: (a) EPA, (b) EPA containing benzene in the concentration of 1×10^{-4} M, (c) EPA containing benzene in 1×10^{-3} M, and (d) EPA containing benzene in 1×10^{-2} M.

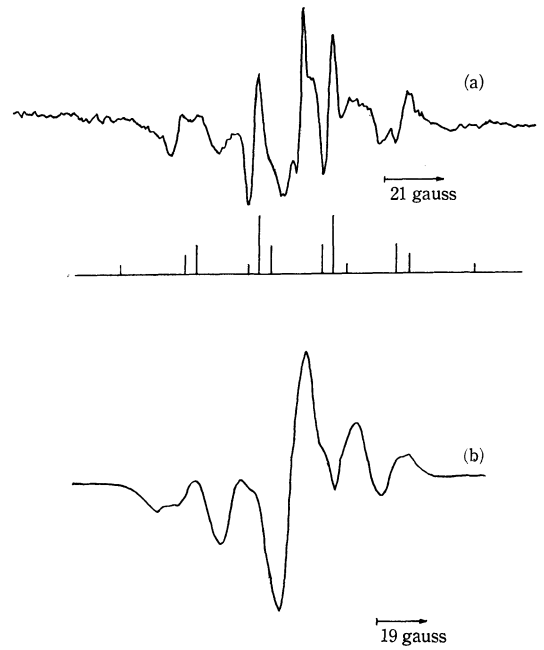

Fig. 2. (a) ESR spectrum from UV-irradiated diethyl ether at 77°K. UV-Irradiation was carried out at liquid nitrogen temperature for 15 min. The lines in the drawing below the spectrum represent the position and the intensity of the resonance lines expected for the radical ($CH_3\dot{C}H_2$). (b) ESR spectrum from UV-irradiated ethyl alcohol at 77°K. UV-Irradiation was performed at liquid nitrogen temperature for 15 min.

The present four-line spectrum can be ascribed to the ethyl radical,[5,6] which is theoretically expected to show four isotropic resonance lines in a reconstruction based on the two α-H with the coupling constant of 22 gauss, and the three β-H with the coupling constant of 27 gauss. The UV irradiation of ethyl alcohol gave a five-line spectrum with a splitting value of about 20 gauss. The five-line spectrum can be ascribed to the ethanol radical($CH_3\dot{C}HOH$) with the α-H coupling constant of 22 gauss and the β-H coupling constant of 27 gauss. The UV irradiation of an "EPA-benzene mixture," which contains benzene in the concentration regions from 10^{-1} to 10^{-4} M, produced ethyl radicals overlapping with ethanol radicals, as is shown in Fig. 1(b)—(d), but no photochemical intermediates from benzene could be observed.

Isopentane-Benzene Mixture. A prolonged irradiation (120 min) of the isopentane rigid matrix did not show any ESR signal, in contrast with the

5) Sr. Patricia, J. Sullivan and W. S. Koski, *J. Am. Chem. Soc.*, **86**, 159 (1964).

6) H. S. Judeikis and S. Siegel, *J. Chem. Phys.*, **43**, 3625 (1965).

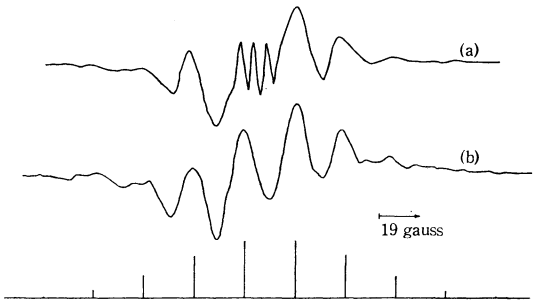

Fig. 3. ESR spectrum from UV-irradiated "isopentane-benzene mixtures," (a), and γ-irradiated "Isopentane," (b), at 77°K. The lines in the drawing below the spectrum represent the position and the intensity of the resonance lines expected for the radical ($(CH_3)_2\dot{C}CH_2CH_3$). UV-Irradiation was performed for 30 min at 77°K. γ-Irradiation was carried out at 77°K using Co-60 (750 Ci) under the following condition: dose rate of 6×10^5 r/hr, and total dose of 3×10^5 R.

cases of EPA, diethyl ether, and ethyl alcohol.

The UV irradiation of the "isopentane-benzene mixture," which contained benzene in the concentration region from 10^{-1} to 10^{-2} M, gave an apparent eight-line spectrum, with a splitting value of about 23 gauss, in addition to three other central lines with approximately a 6-gauss separation, as is shown in Fig. 3(a). On gradually raising the temperature of the above "isopentane-benzene mixture" from the temperature of liquid nitrogen up to about 113°K, the eight-line spectrum showed a rapid decay, and then the three central lines changed to a six-line spectrum with approximately a 6-gauss separation, as is shown in Fig. 4.

The apparent eight-line spectrum showed a very good accordance with the eight-line spectrum observed from γ-irradiated isopentane at 77°K, as is shown in Fig. 3(b). This eight-line spectrum seems to be coincident with that from γ-irradiated *t*-pentyl iodide which was previously reported by

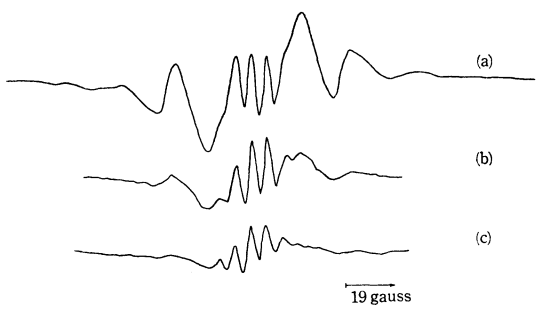

Fig. 4. Change with increasing temperature in ESR spectrum shown. Spectra were recorded at the temperature of 77°K (a), 103°K (b), and 113°K (c).

Ayscough and Thomson.[7] Accordingly, the apparent eight-line spectrum in the present "isopentane-benzene mixture" can be ascribed to the *t*-pentyl radical($(CH_3)_2\dot{C}CH_2CH_3$), in which one estimates the hyperfine coupling constant of both six protons of two methyl groups and the one proton of the CH_2 group, and that of another proton of the CH_2 group, at 23 and 46 gauss respectively.

The six-line spectrum observed after the disappearance of *tert*-pentyl radicals is in complete accordance with that of the tentatively-assigned phenyl radical which was previously observed in UV-irradiated polycrystalline benzene at 77°K.[1] Furthermore, it was observed that phenyl radicals did not induce any abstraction reaction of hydrogen atoms from a surrounding isopentane mloecule. This fact seems to suggest that phenyl radicals remaining after the disappearance of *tert*-pentyl radicals may be trapped on the surface of the quartz ampoule. The present experiment failed to observe the formation of benzene cation radicals such as have already been observed upon the UV irradiation of both benzene adsorbed on silica gel[2] and that dispersed in an acidic matrix.[8] This is probably because the isopentane matrix could not provide a site suitable for trapping both benzene-ion radicals and electron ejected from benzene.

An Aspect of the Mechanism of the Photodecomposition of Isopentane. From the above-described experiments, it is evident that the presence of benzene is responsible for the photodecomposition of isopentane. The photolysis of isopentane can be explained in terms of the energy transfer from an excited benzene ($^3B_{1u}$) to isopentane molecules, while one may also suppose the possibility of the photodecomposition of benzene dispersed in the isopentane matrix bringing about the abstraction reaction of hydrogen atoms from the surrounding isopentane molecules. On analogy with the behavior of benzene in the isopentane matrix, one may suppose that the photodegradation of rigid matrices of diethyl ether and ethyl alcohol is induced through an energy transfer from aromatic impurities unremoved by the present purification.

From the above experimental results, we may conclude that: (1) EPA, diethyl ether, and ethyl alcohol are not inert to UV light in the wavelength regions longer than approximately 2200Å, probably because of the presence of unremoved aromatic impurity, and this leads to the failure to observe intermediates from benzene, and (2) isopentane is inert to UV light in the wavelength regions

7) P. B. Ayscough and C. Thomson, *Trans. Faraday Soc.*, **58**, 1477 (1962).

8) M. K. Carter and G. Vincow, *J. Chem. Phys.*, **47** 292 (1967).

longer than approximately 2200Å. The UV irradiation of the "isopentane-benzene mixture" induced the sensitized photodecomposition of isopentane and produced phenyl radicals, and *tert*-pentyl radicals from benzene and isopentane respectively.

BULLETIN OF THE CHEMICAL SOCIETY OF JAPAN VOL. 42 3372—3379 (1969)

Infrared Absorption Spectra of Urea-formaldehyde Initial Condensation Products. II. Dimethylurea

Yoshiyuki MIDO*1 and Hiromu MURATA

Department of Chemistry, Faculty of Science, Hiroshima University, Higashisenda, Hiroshima

(Received April 10, 1969)

The infrared absorption spectra of symmetric and asymmetric dimethylurea have been observed in the 4000—400 cm^{-1} region. In order to investigate the amide characteristic bands, the spectra of $CH_3NHCONHCH_3$ and $CH_3NDCONDCH_3$ have also been measured in the solid and liquid states, and in solutions. The in-plane normal vibrations of these molecules have been calculated. As a result of our measurements and calculations, it has been found that: (1) The contribution of the polar resonance structure of asymmetric dimethylurea is small compared with that of symmetric dimethylurea, and molecular geometry contributes to the formation of hydrogen bonding. (2) From the position of the amide bands, the molecular configuration of symmetric dimethylurea is the "*trans*" form as well as that of methylurea. (3) The results of normal coordinate analysis show a good agreement with that observed within an average deviation of 2.6%

In a previous paper,[1] we reported the vibrational spectra of methylurea (MMU) as one of urea-formaldehyde initial condensation products; we also undertook a normal coordinate analysis of this molecule in order to determine the vibrational assignmments. The polar resonance structure of the H-N-C=O system has also been discussed on the basis of the assignments specified for the amide characteristic bands.[2]

As a continuation of that research, we have now extended our study to the vibrational spectra of symmetric and asymmetric dimethylurea (referred to as *s*-DMU and *a*-DMU). The observed bands of DMU have been assigned by comparing the spectra of MMU and by observing the changes in spectra according to the state of the aggregation in which the substance has been measured. The normal coordinate treatments of *s*-DMU have been made in order to give a basis for the assignments.

Becher and Griffel have observed the infrared spectra of *s*-DMU[3] and methylenediurea[4] in the NaCl region, and some of the spectral bands have been assigned empirically.

Experimental

Materials. The *s*-DMU was obtained from Wako Pure Chemical Industries, Ltd., and was purified by recrystallization from a chloroform or an acetone solution. It had a mp of 106°C (lit,[5] 107°C). The *a*-DMU was synthesized by adding dimethylamine to nitrourea,[6] and it was purified from a chloroform solution. It had a mp of 181.5—182.2°C (lit,[5] 182°C).

The *N*-deuterated compounds of these samples were obtained from simple exchange with D_2O at room temperature; the excess of D_2O was evaporated in vacuum after the exchange reaction had been completed.

Infrared Spectra. The infrared spectra were measured in the 4000—400 cm^{-1} region with a Hitachi EPI-2G Infrared Grating Spectrophotometer. The spectrometer was calibrated with standard polystyrene film H_2O vapor. The spectra of *s*-DMU and *s*-DMU-d*2 were measured in the solid and liquid states and in so-

*1 Present address; Department of Chemistry, Faculty of Science, Kobe University, Rokkodai, Nada, Kobe.

1) Y. Mido and H. Murata, *Nippon Kagaku Zasshi (J. Chem. Soc. Japan, Pure Chem. Sect.)*, **90**, 254 (1969).

2) T. Miyazawa, T. Shimanouchi and S. Mizushima, *J. Chem. Phys.*, **24**, 408 (1956); T. Miyazawa, *Nippon Kagaku Zasshi (J. Chem. Soc. Japan, Pure Chem. Sect.)*, **76**, 341, 821, 1018 (1955), *ibid.*, **77**, 171, 321, 526, 619 (1956).

3) H. J. Becher and F. Griffel, *Naturwissenschaften*, **43**, 467 (1956).

4), H. J. Becher, *Chem. Ber.*, **89**, 1593 (1956).

5) "Handbook of Chemistry and Physics," ed. by R. C. Weast, The Chemical Rubber Co., Ohio (1966), p. C-591.

6) F. Kurzer, "Organic Syntheses," **32**, 61 (1952).

*2 The d means *N*-deuterated compound.

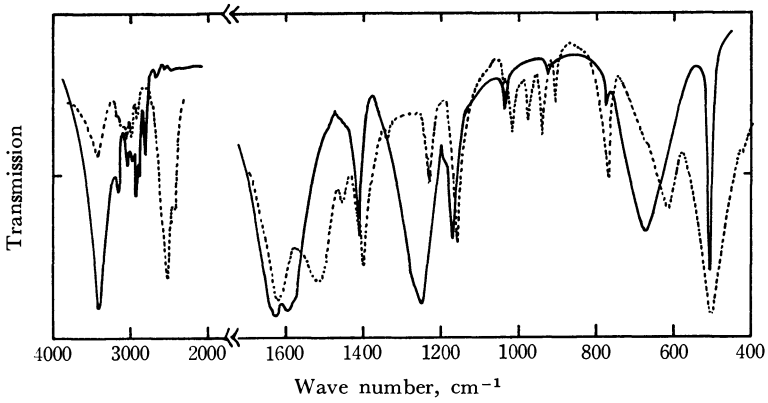

Fig. 1. Infrared spectra of *s*-DMU (solid line) and *s*-DMU-d (broken line) in the solid state.

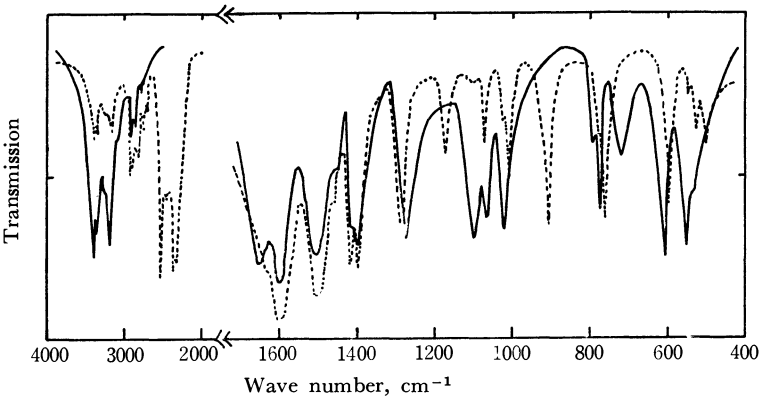

Fig. 2. Infrared spectra of *a*-DMU (solid line) and *a*-DMU-d (broken line) in the solid state.

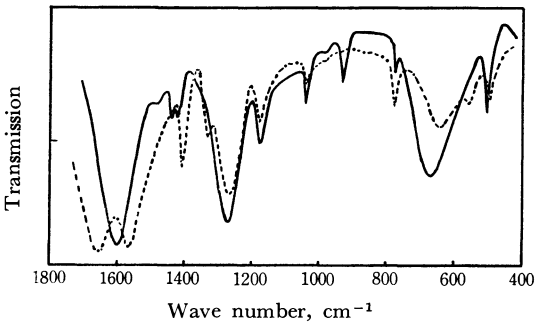

Fig. 3. Infrared spectra of *s*-DMU in liquid state (broken line) and its *quenched* sample (solid line).

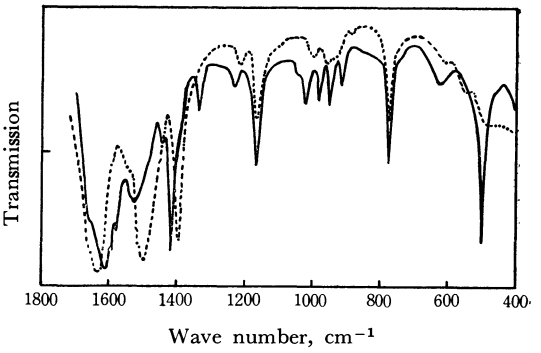

Fig. 4. Infrared spectra of *s*-DMU-d in liquid state (broken line) and its *quenched* sample (solid line).

lutions. The solid-state spectra were taken in a KBr disk and in Nujol mull;[*3] they are shown in Fig. 1. The liquid-state spectra in a capillary heated at 107—110° C and the spectra of the sample cooled from the molten liquid in a capillary (the *quenched* sample) are shown in Figs. 3 and 4, in which the *quenched* sample spectra differ from the solid-state ones. The spectra of *a*-DMU and *a*-DMU-d were also measured in the solid state and in solutions; they are shown in Fig. 2. The spectra of *s*- and *a*-DMU dissolved in H_2O and D_2O are shown in Figs. 6 and 7 respectively. The observed frequencies are summarized in Tables 5 and 6.

[*3] The preparations of KBr disk exchanged the deuterium of d-compounds for normal hydrogen and weakened the strength of ν(ND), but in Nujol mull such a phenomenon was observed little.

TABLE 1. SYMMERTRY COORDINATES

Symmetry species		Symmetry coordinates*	Vibrational mode	Abbr.
A_1	S_1	$(R_3+R_4-2R_1+R_{13}+R_{12}-2R_{11})/\sqrt{12}$	CH_3 antisym. stretching	$\nu_a(CH)$
	S_2	$(R_3+R_4+R_1+R_{12}+R_{13}+R_{11})/\sqrt{6}$	CH_3 sym. stretching	$\nu_s(CH)$
	S_3	$(2\alpha_6-\alpha_3-\alpha_5+2\varepsilon_6-\varepsilon_2-\varepsilon_4)/\sqrt{12}$	CH_3 antisym. deformation	$\delta_a(CH_3)$
	S_4	$(\alpha_I-\alpha_{II}+\varepsilon_I-\varepsilon_{II})/\sqrt{12}$*	CH_3 sym. deformation	$\delta_s(CH_3)$
	S_5	$(2\alpha_1-\alpha_2-\alpha_4+2\varepsilon_1-\varepsilon_3-\varepsilon_5)/\sqrt{12}$	CH_3 rocking	$\delta_r(CH_3)$
	S_6	(R_8)	CO stretching	$\nu(CO)$
	S_7	$(R_6+R_{10})/\sqrt{2}$	NH sym. stretching	$\nu_s(NH)$
	S_8	$(R_5+R_7)/\sqrt{2}$	CN_2 sym. stretching	$\nu_s(CN_2)$
	S_9	$(R_2+R_9)/\sqrt{2}$	CH_3-N sym. stretching	$\nu_s(C'N)$
	S_{10}	$(\beta_2-\beta_3+\delta_3-\delta_2)/2$	NH sym. deformation	$\delta_s(NH)$
	S_{11}	$(2\beta_1-\beta_2-\beta_3+2\delta_1-\delta_2-\delta_3)/\sqrt{12}$	CH_3-NC deformation	$\delta_s(C'NC)$
	S_{12}	$(2\gamma_1-\gamma_2-\gamma_3)/\sqrt{6}$	NCN sym. deformation	$\delta_s(NCN)$
B_2	S_1	$(R_3+R_4-2R_1+2R_{11}-R_{12}-R_{13})/\sqrt{12}$	CH_3 antisym. stretching	$\nu_a(CH)$
	S_2	$(R_3+R_4+R_1-R_{11}-R_{12}-R_{13})/\sqrt{6}$	CH_3 sym. stretching	$\nu_s(CH)$
	S_3	$(2\alpha_6-\alpha_3-\alpha_5-2\varepsilon_6+\varepsilon_2+\varepsilon_4)/\sqrt{12}$	CH_3 antisym. deformation	$\delta_a(CH_3)$
	S_4	$(\alpha_I-\alpha_{II}-\varepsilon_I+\varepsilon_{II})/\sqrt{12}$*	CH_3 sym. deformation	$\delta_s(CH_3)$
	S_5	$(2\alpha_1-\alpha_2-\alpha_4-2\varepsilon_1+\varepsilon_3+\varepsilon_5)/\sqrt{12}$	CH_3 rocking	$\delta_r(CH_3)$
	S_6	$(R_6-R_{10})/\sqrt{2}$	NH antisym. stretching	$\nu_a(NH)$
	S_7	$(R_5-R_7)/\sqrt{2}$	CH_2 antisym. stretching	$\nu_a(CN_2)$
	S_8	$(R_2-R_9)/\sqrt{2}$	CH_2-N antisym. stretching	$\nu_a(C'N)$
	S_9	$(\beta_2-\beta_3-\delta_3+\delta_2)/2$	NH antisym. deformation	$\delta_a(NH)$
	S_{10}	$(\gamma_2-\gamma_3)/\sqrt{2}$	NCO deformation	$\delta(NCO)$
	S_{11}	$(2\beta_1-\beta_2-\beta_3-2\delta_1+\delta_2+\delta_3)/\sqrt{12}$	CH_3-NC antisym. deformation	$\delta_a(C'NC)$

* $\alpha_I=\alpha_3+\alpha_5+\alpha_o$, $\alpha_{II}=\alpha_1+\alpha_2+\alpha_4$, $\varepsilon_I=\varepsilon_2+\varepsilon_4+\varepsilon_6$, $\varepsilon_{II}=\varepsilon_1+\varepsilon_3+\varepsilon_5$

Normal Coordinate Treatment

The frequency calculations for *s*-DMU were made by means of Wilson's *GF* matrix method.[7] The *trans* symmetric plane model (C_{2v}) was adopted except for two hydrogen atoms attached to each of the two methyl carbon atoms (C')*4 (see Fig. 5). The normal vibrations are classified into the 23 in-plane modes (A_1 : 12, B_2 : 11) and the 13 out-of-plane modes (A_2 : 6, B_1 : 7), the A_2 species of which is infrared-inactive. The normal coordinate treatment was made for the in-plane vibrations using the internal coordinates shown in Fig. 5 and the symmetry coordinates given in Table 1. The potential function used is that of the Urey-Bradley type,[8] and the structural parameters (Table 2)*5 and the force constants (Table 3) are the same as those of the MMU transferred directly from urea,[9] *N*-methylacetamide,[10] and *N*-methylformamide.[11] The observed and calculated frequencies are listed in Table 4, together with the main potential energy distributions (P.E.D.).[12] The frequencies show a good agreement with the observed values (an average deviation of 2.6%),*6 indicating that the transferabilities of the force constants and the potential function are sufficient for this molecule. However, some of the calculated values deviate considerably from the observed values. The deviations of $\delta_s(CH_3)$, $\delta_a(CH_3)$, $\delta_r(CH_3)$, and $\nu(C'N)$ for *s*-DMU are similar to those for MMU;[1] this probably

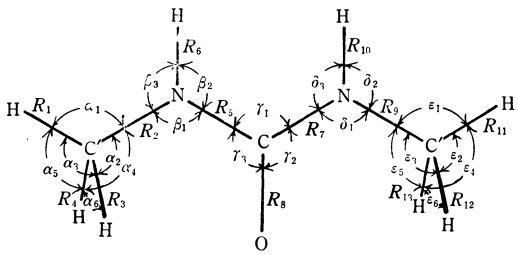

Fig. 5. The internal coordinate of *s*-DMU.

7) E. B. Wilson, *J. Chem. Phys.*, **7**, 1047 (1939); **9**, 76 (1941).

*4 C' denotes the methyl carbon atoms.

8) T. Shimanouchi, *J. Chem. Phys.*, **17**, 245, 734, 848 (1949).

*5 The structural analysis has not been reported for *s*-DMU.

9) A. Yamaguchi, T. Miyazawa, T. Shimanouchi and S. Mizushima, *Spectrochim. Acta*, **10**, 170 (1957).

10) T. Miyazawa, T. Shimanouchi and S. Mizushima, *J. Chem. Phys.*, **29**, 611 (1958).

11) I. Suzuki, This Bulletin, **35**, 540 (1962).

12) Y. Morino and K. Kuchitsu, *J. Chem. Phys.*, **20**, 1809 (1952); I. Nakagawa, *Nippon Kagaku Zasshi (J. Chem. Soc. Japan, Pure Chem. Sect.)*, **74**, 243 (1953).

*6 In the case of MMU; 2.3%.

Table 2. Structural parameters*4,*5

C'–N	1.47Å[a]	C–N	1.335Å[b]	C–O	1.262Å[b]
C'–H	1.09Å[c]	N–H	1.000Å[e]		
α_i, ε_i*	109°28'[e]	β_i, γ_i, δ_i**	120°00'[e]		

Table 3. Force constants (md/Å)

K(CH)	4.42[a]	H(NCN)	0.72[b]	F(N···N)	0.613[b]
K(C'N)	3.15[c]	H(NC'H)	0.28[c]	F(N···H)	0.52[c]
K(CN)	5.50[c]	H(HC'H)	0.45[c]	F(H···H)	0.03[c]
K(NH)	6.1[d]	H(CNC')	0.2[a]	F(C···C')	0.3[a]
K(CO)	6.5[b]	H(CNH)	0.35[a]	F(C···H)	0.5[a]
		H(C'NH)	0.15[a]	F(C'···H)	0.5[a]
		H(OCN)	0.12[b]	F(O···N)	1.566[b]
		H(HNH)	0.38[b]	F(H···H)	0.0[b]
κ	0.0 mdÅ[e]				

* The bond angles around the C' atom.
** The bond angles around the C and N atoms.
a) *N*-Methylacetamide, Ref. 10. b) Urea, Ref. 9. c) *N*-Methylformamide, Ref. 11.
d) Methylamine, A. Yamaguchi, *Nippon Kagaku Zasshi (J. Chem. Soc. Japan, Pure Chem. Sect.)*, **80**, 1105 (1959).
e) Assumption.

means that the corresponding force constants are not sufficiently good. On the other hand, the difference between the deviation for *s*-DMU and that for MMU (−0.4%) of the amide III bands may be attributed to the steric or electronic effect of methyl groups.[1] The deviation of δ(NCN) for *s*-DMU is more than that for MMU (0.2%), but the deviation of δ(NCO) for *s*-DMU is less than that for MMU (8.1%). The same tendency was found in methylenediurea.[13] Accordingly, the geometry of the molecule may strongly affect these vibrations.

The numerical calculations in the present treatment of normal vibrations were carried out with a HITAC 103 computer (Hitachi Ltd.) at Hiroshima University.

Results and Discussion

There are many points of similarity between the spectra of *s*-DMU and MMU,[1] but those of *a*-DMU differ from those of *s*-DMU and MMU in the numbers of the spectral bands (see Figs. 1 and 2). If the bonding of *s*-DMU as a whole is analogous to that of urea,[9,14–16] the *s*-DMU molecule can be expected to possess the considerable double-bond character of the C–N bonds and to have an approximately plane structure. Then, *s*-DMU will have three possible configurations with respect to the relative positions of two imides and a carbonyl group, the *cis-cis*, *cis-trans*, and *trans-trans* configurations of which the *cis-trans* one (C_s symmetry) is less expected than the other ones (C_{2v} symmetry).

Miyazawa and his co-workers investigated the infrared spectra of various monosubstituted amides[2,10] and of diketopiperazine,[17] and concluded that the characteristic amide bands of the *trans*-CONH group are different from those of the *cis*-CONH group. Lane and his colleagues[18] showed in their study of the methylthiourea metal complexes that the molecular form of this ligand exists in the *trans* form in comparison with the *trans*- and *cis*-thioamide. Generally the amide frequencies are markedly affected by hydrogen-bonding effects, so considerable shifts can occur on passing from the solid to a solution; moreover, the shifts are often very useful for assigning the observed bands.[2,19] A similar consideration of the amide bands of *s*-DMU will provide information regarding the configuration of *s*-DMU.

Amide I, II, and III Bands. In *s*-DMU, the amide I, II, and III bands usually observed in 1700—1250 cm^{-1} region can be related to ν(CO), ν(CN), and δ(NH), as is shown in the P.E.D. of Table 4, but they are not pure vibrations. The amide I band observed at 1625 cm^{-1} has the greatest contribution of ν(CO) and a smaller one of δ(NH), since the band shows a small frequency shift on deuteration. On the other hand, the amide II

13) Y. Mido and H. Murata, to be published.
14) R. D. Waldron and R. M. Badger, *J. Chem. Phys.*, **18**, 566 (1950).
15) P. Vaughan and J. Donohue, *Acta Cryst.*, **5**, 530 (1967).
16) E. R. Andrew and D. Hyndman, *Proc. Phys. Soc. (London)*, **66A**, 1187 (1953).
17) K. Fukushima, Y. Ideguchi and T. Miyazawa, This Bulletin, **37**, 349 (1964).
18) T. J. Lane, A. Yamaguchi, J. V. Quagliano, J. A. Ryan and S. Mizushima, *J. Am. Chem. Soc.*, **81**, 3824 (1959).
19) L. J. Bellamy, "The Infrared Spectra of Complex Molecules," John Wiley & Sons, Inc., New York (1958), p. 203.

Table 4. Observed (ν_o) and calculated (ν_c) freqvencies (in cm^{-1}) and potential energy distributions (P.E.D. in %)

		$CH_3NHCONHCH_3$				$CH_3NDCONDCH_3$				I[b]	II[c]
		ν_o	ν_c	Δ[a]	P.E.D. (%)	ν_o	ν_c	Δ[a]	P.E.D. (%)		
A_1	ν_1	3485[d]	3482	0.0	ν(NH)100	2503	2544	+1.6	ν(ND)100	1.39	1.37
	ν_2	2980	2966	−0.7	ν(CH)100	3000	2966	−1.1	ν(CH)99	0.99	1.00
	ν_3	2930	2879	−1.7	ν(CH)99	2950	2880	−2.5	ν(CH)99	0.99	0.99
	ν_4	1625	1628	+0.2	ν(C=O)46, ν(CN)23 δ(NCN)16, δ(NH)15	1620	1593	−1.7	ν(C=O)52, ν(CN)23 δ(NCN)16	1.00	1.02
	ν_5	1455	1484	+2.0	$\delta(CH_3)$85, $\delta_r(CH_3)$11	1455	1483	+1.9	$\delta(CH_3)$89, $\delta_r(CH_3)$10	1.00	1.00
	ν_6	1410	1472	+4.4	$\delta_s(CH_3)$96	1397	1470	+5.2	$\delta_s(CH_3)$94	1.00	1.00
	ν_7	1328	1423	+7.1	δ(NH)52, ν(CN)24 ν(C'N)13, ν(C=O)8	941	927	−1.5	δ(ND)55, ν(C'N)25 $\delta_r(CH_3)$9	1.42	1.54
	ν_8	1170	1142	−2.4	$\delta_r(CH_3)$46, ν(C=O)25 $\delta(CH_3)$7	1160	1127	−2.8	$\delta_r(CH_3)$50, ν(C'N)22 ν(C=O)11	1.01	1.01
	ν_9	1132[d]	1125	−0.6	ν(C'N)62, ν(CN)9 δ(NH)9	1231	1294	+5.1	ν(C'N)30, ν(CN)30 δ(ND)30, $\delta_r(CH_3)$7	0.94	0.87
	ν_{10}	980	963	−1.7	ν(CN)20, $\delta_r(CH_3)$35 ν(C=O)15	977	961	−1.6	ν(CN)24, ν(C=O)25 $\delta_r(CH_3)$24, δ(ND)7	1.00	1.00
	ν_{11}	504	461	−8.5	δ(NCN)46, ν(C'N)20 ν(CN)20, δ(C'NC)9	490	447	−8.8	δ(NCN)46, ν(CN)20 ν(C'N)19, δ(C'NC)10	1.03	1.03
	ν_{12}		202		δ(C'NC)78, δ(NCN)22		200		δ(C'NC)77, δ(NCN)23		1.01
B_2	ν_{13}	3485[d]	3480	−0.0	ν(NH)100	2448	2451	+0.0	ν(ND)100	1.42	1.37
	ν_{14}	2980	2966	−0.7	ν(CH)100	3000	2966	−1.1	ν(CH)99	0.99	1.00
	ν_{15}	2930	2879	−1.7	ν(CH)99	2950	2880	−2.5	ν(CH)99	0.99	0.99
	ν_{16}	1596	1570	−1.6	ν(CN)61, δ(NH)30 δ(NCO)6	1510	1534	+1.6	ν(CN)76, δ(ND)10 δ(NCO)9	1.06	1.02
	ν_{17}	1455	1483	+1.9	$\delta(CH_3)$86, $\delta_r(CH_3)$8	1455	1478	+1.6	$\delta(CH_3)$81, δ(CN)7	1.00	1.00
	ν_{18}	1410	1469	+4.2	$\delta_s(CH_3)$100	1397	1469	+5.2	$\delta_s(CH_3)$90, ν(C'N)7	1.01	1.00
	ν_{19}	1266	1311	+3.6	δ(NH)63, ν(CN)31	941	925	−1.7	δ(ND)56, ν(C'N)36	1.35	1.42
	ν_{20}	1170	1117	−4.5	$\delta_r(CH_3)$72, ν(C'N)12	1160	1112	−4.1	$\delta_r(CH_3)$76, ν(C'N)8 $\delta(CH_3)$8	1.01	1.00
	ν_{21}	1037	1000	−3.6	ν(C'N)78, $\delta_r(CH_3)$12	1018	1047	+2.9	ν(C'N)47, δ(ND)36 ν(CN)13	1.02	0.96
	ν_{22}	672	650	−3.3	δ(NCO)65, δ(C'NC)23	620	641	+3.4	δ(NCO)67, δ(C'NC)25	1.08	1.01
	ν_{23}		282		δ(C'NC)72, δ(NCO)29		281		δ(C'NC)70, δ(NCO)27		1.00

a) Percent deviation: $\Delta=[(\nu_c-\nu_o)/\nu_o]\times100$. b) Ratio ν_o of *s*-DMU to ν_o of *s*-DMU-d: $I=[\nu_o(s\text{-DMU})/\nu_o(s\text{-DMU-d}]$.
c) Ratio ν_c of *s*-DMU to ν_c of *s*-DMU-d: $II=[\nu_c(s\text{-DMU})/\nu_c(s\text{-DMU-d})]$. d) ν_o in chloroform solution; in ν_1, ν_o for free molecule.

Table 5. Observed frequencies (in cm^{-1}) of *sym*-dimethylurea

(I) $CH_3NHCONHCH_3$						(II) $CH_3NDCONDCH_3$				
Solid	Quenched sample	Liquid	$CHCl_3$ concd.	soln.[a] dil.	Assign.	Solid	Quenched sample	Liquid	$CHCl_3$ soln.	Assign.
			3485	3485						
3360	3375	3360	3385	3402	ν(NH)	3000	3000		3005	
3165	3190					2950	2955	2955	2955	ν(CH)
3040	3060						2908		2885	
2980	2958	2960	3015	3015	ν(CH)		2805		2800	
2930	2908			2915		2695	2680	2660	2654	
	2815	2815	2820	2820		2503	2485		2500	ν(ND)
1625	1597	1653	1628	1673	amide I	2448	2450	2450	2448	
1569		1563	1582	1553	amide II	1620	1609	1633	1622	amide I′
1455	1441		1450	1450	$\delta_a(CH_3)$	1510	1523	1498	1500	amide II′
1410	1421	1410	1414	1413	$\delta_s(CH_3)$	1455	1442			$\delta_a(CH_3)$
		1331	1328	1326	amide III	1397	1420	1401	1401	$\delta_s(CH_3)$
1266	1269	1266	1273	1253	amide III	1231	1235	1219		ν(C′N)
1170	1176	1173	1173	1170	$\delta_r(CH_3)$	1160	1166	1167	1164	$\delta_r(CH_3)$
		1154	1132		ν(C′N)	1018	1026	1000		ν(C′N)
1037	1040	1040	1043	1042	ν(C′N)	977	983	958		ν(CN)
980					ν(CN)	941	949	934		amide III′
925	929	880	915[b]		$\delta_r(CH_3)_o$	906	916	898		$\delta_r(CH_3)_o$
772	773	773	772[b]		amide VI	769	772	773		amide VI′
672	672	632	654[b]		amide V, IV	620	624	625		amide IV′
		562	564	557	amide V					
504	501	504	508	501	δ(NCN)	490	500	497	495	δ(NCN)

a) Concd. and dil. mean concentrations of 0.5 and 0.06 mol/l respectively.
b) CH_3CN solution.

Table 6. Observed frequencies (in cm^{-1}) of *asym*-dimethylurea

$(CH_3)_2NCONH_2$		$(CH_3)_2NCOND_2$	Assignment	$(CH_3)_2NCONH_2$		$(CH_3)_2NCOND_2$	Assignment
Solid	$CHCl_3$ soln.	Solid		Solid	$CHCl_3$ soln.	Solid	
3400	3545			1273		1287	ν(C′N)
3355	3443		ν(NH)			1172	$\delta(ND_2)$
3197	3200			1097	1076		$\delta_r(NH_2)$
2925	2980	2920		1067	1059	1072	$\delta_r(CH_3)$
2857	2943	2960	ν(CH)	1022	1014	1008	ν(CN)
2800	2873	2800				908	$\delta_r(ND_2)$
		2546		793		793	
		2375	ν(ND)	773	768[b]	760	amide VI and VI′
		2343					
1655	1657	1600	amide I and I′	720			$\pi(NH_2)$
				604	594	597	amide IV and IV′
1600	1591		$\delta(NH_2)$				
1510	1485	1510	amide II and II′	552	517	528	δ(NCN)
						500	$\pi(ND_2)$
1450	1452	1450	$\delta_a(CH_3)$				
1412	1398	1415	$\delta_s(CH_3)$				
1400		1399					

a) 0.09 mol/l solution.
b) Acetone solution.

band at 1596 cm^{-1} has the contribution of ν(CN) mainly, but that of δ(NH) is not negligible, since on deuteration the band shifts to 1510 cm^{-1} (amide II′ band*7).

The amide III band at 1266 cm^{-1} has the main

*7 The prime means the amide band on the d-compounds.

Table 7. Characteristic amide frequencies for urea derivatives (in cm^{-1})

Amide band		I	II	III	
Methylurea	Solid	1651	1575	1353	
(MMU)	Liquid	1663	1550	1346	
	Solution				
	CH_3CN	1680	1516	1325	
	$CHCl_3$	1679	1509	1338	
sym-Dimethylurea	Solid	1625	1596	—	1266
(*s*-DMU)	Liquid	1653	1562	1331	1266
	Solution				
	CH_3CN	1678	1546	1320	1259
	$CHCl_3$	1673	1553	1326	1253
sym-Diethylurea*	Solid	1638	1598	—	1268
(*s*-DEU)	Liquid	1635	1547	1320	1252
	Solution				
	CH_3CN	1672	1535	1330	1242
	$CHCl_3$	1660	1531	1320	1235

* Unpublished data.

contribution of δ(NH), together with the additional ones of ν(CN) and ν(C'N). Contrary to the expectation of a strong peak from *trans* amides,[2,10] the amide III' band is observed at 941 cm^{-1} as a weak one. The reason for this may be that there is a considerable mixed-contribution of ν(C'N) to the band.

In the spectra in the liquid and solutions, two noticeable bands appear newly near 1330 and 560 cm^{-1}. The former is assigned to the amide III band because: (1) Figs. 6 and 7 illustrate the spectra of both DMU dissolved in water, but in *s*-DMU the marked band disappears in a D_2O solution, and in *a*-DMU, even in a H_2O solution. (2) In the solid-state spectra for *s*-DMU, the strong amide III band is likely to have a shoulder band towards a higher frequency. (3) The investigation of the N-H stretching region in *s*-DEU[20] can not show the possibility of the rotational isomer.[21] (4) The spectra in MMU do not show the corresponding bands (see Table 7).

From Table 5, it can be found that the amide I band decreases and the II band increases in frequency on passing along the series solution, liquid, solid, and *quenched* sample (in the *quenched* sample, the two bands overlap). This can be explained by the fact that the contribution of the polar resonance structure increases on passing along this series. The changes in the frequencies of the amide bands with the change in state are shown in Table 7 and compared with those of analogues, where similar tendencies are found in all. Accordingly, from the positions of the amide bands, the configuration of *s*-DMU as well as that of MMU is concluded to be the "*trans-trans*" form.

On the other hand, as the *a*-DMU molecule does not include the -CO-NH- group, the polar resonance structure may contribute less than that for *s*-DMU. In *a*-DMU, the isotopic shift from the amide II band to the II' band is very little, but in *s*-DMU, it is quite large (86 cm^{-1}) and the amide II' bands in *s*- and *a*-DMU are observed at the same positions. There is a similar relation between *s*- and *a*-DEU[20]; these questions were discussed in a previous paper.[1]

It can be concluded that the contribution of the polar resonance structure of the asymmetric form is smaller than that of the symmetric form, since the molecular geometry affects the formation of hydrogen-bondings and since the contribution of ν(CN) to the amide II band in the asymmetric form is larger than that in the symmetric form.

NH_2 Deformation Vibrations. In *a*-DMU, the ratios of the NH_2 band to the ND_2 band are 1.37 and 1.21 for $\delta(NH_2)$ and $\delta_r(NH_2)$ respectively. When we multiply a ratio of $\delta(ND_2)$ to $\delta(NH_2)$ by a ratio of $\delta_r(ND_2)$ to $\delta_r(NH_2)$ such as the product rule, the product values are regularly within 1.67 ± 0.02; urea: 1.69,[9],*[8] MMU: 1.66,[1] *a*-DMU; 1.66 and *a*-DEU: 1.68.[20]

Amide IV, V, and VI Bands and δ(NCN). The amide IV, V, and VI bands are related to δ(NCO), out-of-plane; π(NH), and π(CO) respectively.[2,10,19] In *s*-DMU, three amide bands and δ(NCN) can be predicted in the region from 800 to 400 cm^{-1}, in which the band at 672 cm^{-1} can easily be assigned to the amide V band because of its breadth and susceptibility to a change of state, while the band at 772 cm^{-1} can be assigned to the

20) Y. Mido and H. Murata, to be published.
21) I. Suzuki, M. Tsuboi, T. Shimanouchi and S. Mizushima, *Spectrochim. Acta*, **16**, 471 (1960).

*[8] In urea, there are two ratios for A_1 and B_2 species concerned with these vibrations and this value is the average of these ratios.

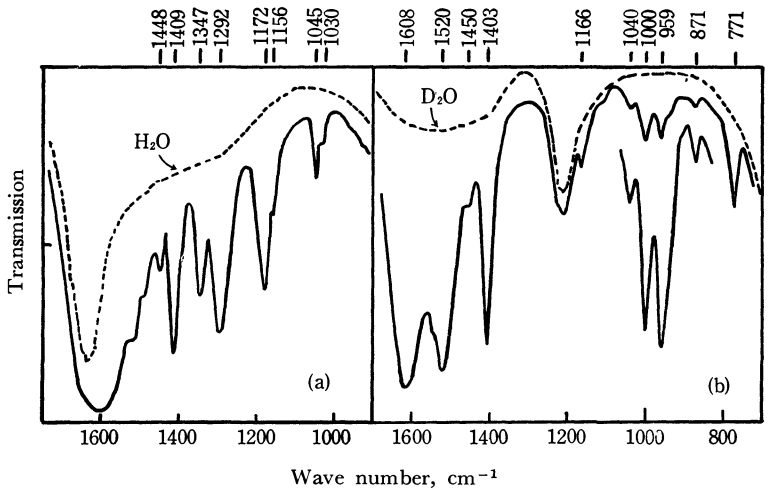

Fig. 6. Infrared spectra of *s*-DMU dissolved in (a) H_2O and (b) D_2O.

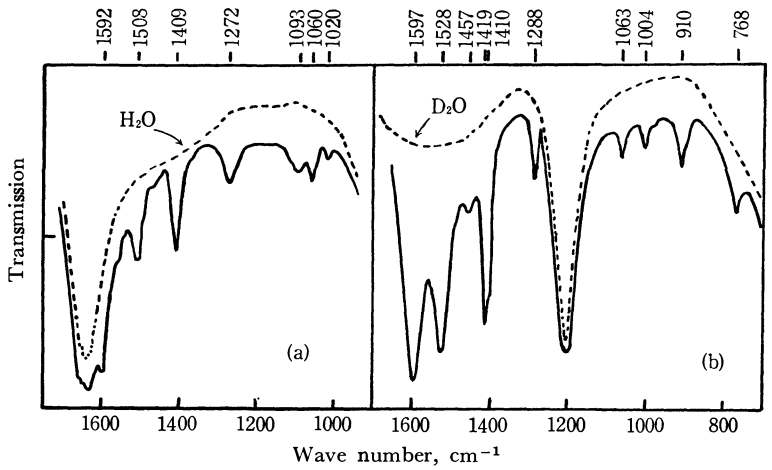

Fig. 7. Infrared spectra of *a*-DMU dissolved in (a) H_2O and (b) D_2O.

VI band because this band appears at a fixed position in the spectra of urea derivatives and because the band is hardly affected at all by deuteration. There are three bands observed in this region; the position of the V band is higher than that in MMU by 72 cm^{-1}, while the IV band in MMU has been assigned to 653 cm^{-1}; in *s*-DMU, however, the IV band is not observed in this position. Therefore, it may be considered that the IV band in *s*-DMU is covered with the V band and, on deuteration, appears at 622 cm^{-1} because the V band shifts toward a lower frequency side. The band at 504 cm^{-1} can be assigned to the undecided vibration, δ(NCN). In *a*-DMU, the bands at 773, 720, 604, and 552 cm^{-1} are associated with the amide VI band, $\pi(NH_2)$, the amide IV band and δ(NCN) respectively.

The Other Bands. In *s*-DMU, the bands at 1455, 1410, 1170, and 925 cm^{-1} (in *a*-DMU, the bands at 1450, 1412 and 1400, and 1067 cm^{-1}) are assigned to $\delta_a(CH_3)$, $\delta_s(CH_3)$, $\delta_r(CH_3)_i$, and $\delta_r(CH_3)_o$ respectively by comparing the vibrational frequencies of the related compounds of the CH_3 group attached to the nitrogen.[2] In *s*-DMU-d, the band at 1231 cm^{-1} corresponds to the band at 1212 cm^{-1} in *s*-DEU-d^{20} and can be assigned to ν(C'N) of A_1, but in *s*-DMU and *s*-DEU there are no corresponding bands in this region. The weak bands at 1037 and 980 cm^{-1} in *s*-DMU and at 1018 and 977 cm^{-1} in *s*-DMU-d are assigned to the ν(C'N) of B_2 and the ν(CN) of A_1 respectively.

BULLETIN OF THE CHEMICAL SOCIETY OF JAPAN VOL. 42 3380—3384 (1969)

Effects of Solvent on the Copolymerization of Ethylene with Tetrafluoroethylene by Cobalt-60 Gamma Radiation

Miyuki HAGIWARA, Takeshi MIURA and Tsutomu KAGIYA

Japan Atomic Energy Research Institute, Takasaki Radiation Chemistry Research Establishment, Takasaki, Gunma

(Received April 10, 1969)

The cobalt-60, γ-radiation induced copolymerization of ethylene with tetrafluoroethylene was carried out in the gas phase and in the liquid phase by using five solvents (liquefied carbon dioxide, carbon tetrachloride, ethylchloride, chloropentafluoroethane, and 1,2-dichloro-tetrafluoroethane) at a dose rate of 25000 rad/hr under a pressure of 300 kg/cm^2 at 30°C. A lower rate of the copolymerization and a copolymer of a lower molecular weight were obtained in liquid carbon dioxide and carbon tetrachloride than in the gas phase without a solvent. In ethyl chloride, the rate increased slightly, but the molecular weight decreased. On the other hand, both the rate and the molecular weight increased markedly in the fluorocarbon solvents. As a result of a detailed investigation of the copolymerization in 1,2-dichloro-tetrafluoroethane, a linear increase in the copolymerization rate and the copolymer molecular weight with the amount of solvent was noted, and there was no noticiable influence of the solvent on the copolymer composition. A kinetical discussion indicated that the addition reaction of tetrafluoroethylene to radicals produced by the influence of primary radiation on the reaction mixture is an important step in initiating the copolymerization. Also, the propagation reaction seemes to be strongly promoted by the fluorocarbon solvents.

The copolymer of ethylene with tetraflouroethylene made by γ-radiation at −78°C has been found to be a highly crystalline, random copolymer.[1] It has also been suggested that the copolymer is formed by a free radical-chain process.

In this work, the copolymerization of ethylene with tetraflouroethylene was carried out in the gas phase and in various solvents under a total pressure of 300 kg/cm^2 at 30°C by using cobalt-60 radiation, and the effects of solvents on the copolymerization were investigated. The variation in the structure of the copolymer formed with its composition was also reported.

Experimental

Materials. Tetrafluoroethylene synthesized by the debromination of 1,2-dibromo-tetrafluoroethane in the presence of a large excess of zinc dust and acetic acid was purified by freeze-thaw cycles using liquid nitrogen and pumping with a rotary vacuum pump, and was then stored in a stainless steel cylinder at −60°C. The ethylene was a polymerization-grade material from the Nisseki Kagaku Company; it was listed as 99.9% pure and showed typical analytical results of 5 ppm of oxygen and 10 ppm of acetylene. All the other materials were reagent grade and were used without further purification.

Copolymerization and Analysis. The copolymerization runs were carried out in a 100-m*l* stainless steel cylindrical vessel which had been evacuated before being filled with the reaction mixture. The transfer of tetrafluoroethylene and solvents (carbon dioxide, ethylchloride, chloro-pentafluoroethane, and 1,2-dichloro-tetrafluoroethane) from their steel storage cylinders was accomplished by cooling the reaction vessel with a dry ice-methanol bath. Ethylene was then fed in until the pressure reached 300 kg/cm^2 by means of an oilless-type compressor at a reaction temperature of 30°C. When carbon tetrachloride was used as the solvent, the reaction vessel was charged with a definite amount of carbon tetrachloride, and then the vessel was closed. Ethylene was then introduced until a pressure of 50 kg/cm^2 was reached and carefully bled out into the atmosphere to remove the dissolved air. This was repeated five times. During the reaction, the temperature was maintained constant within ±1°C by using an automatic controller. The γ-radiation was from a cobalt-60 source, and the dose rate was 25000 rad/hr.

The copolymer yield was determined by direct weighing, while the number-average molecular weight of the copolymer was obtained from osmotic pressure measurements of solutions of the copolymer in tetralin at 130°C with the use of a Hewlett-Packard osmometer, Model 502. The molar ratio of ethylene-tetrafluoroethylene in the copolymer was evaluated by checking the carbon-hydrogen contents of the copolymer. X-Ray diffraction diagrams were obtained with a powder camera in a Rigaku Denki diffractometer, Model D-6C. Ni-filtered Cu$K\alpha$ radiation was used. The infrared absorption spectra were recorded for film samples by means of a Perkin Elmer spectrophotometer, Model-521, in the range of 400—2000 cm^{-1}. Differential thermal analyses were carried out by means of a Rigaku Denki thermal spectrometer, Model 4.

1) Y. Tabata, H. Shibano and H. Sobue, *J. Polymer Sci.*, *A*, **2**, 1977 (1964)

Table 1. Copolymerization of ethylene with tetrafluoroethylene in various solvents

Solvent	Amount of solvent g	Copolymer yield g	Molecular weight $\times 10^{-4}$	Molar fraction of C_2F_4 in copolymer mol%
None	0	0.26	3.6	12.6
Carbon dioxide	20	0.21	2.7	11.8
Carbon tetrachloride	60	0.09	0.098	13.0*
Ethylchloride	60	0.31	1.3	12.5
Chloropentafluoroethane	60	1.38	7.0	13.1
1,2-Dichlorotetrafluoroethane	60	1.98	9.7	12.6

Reaction conditions: pressure, 300 kg/cm²; temperature, 30°C; dose rate, 2.5×10^4 rad/hr; reaction time, 1.0 hr; molar ratio of monomers, $C_2F_4/C_2H_4=1.0/99.0$; reactor volume, 100 ml.

* This was obtained by checking the fluorine content of the copolymer together with the contents of carbon and hydrogen.

Results and Discussion

Copolymerization in the Gas Phase and in Various Solvents. Table 1 summarizes the results of the copolymerization in the gas phase and in various solvents under a total pressure of 300 kg/cm² at 30°C. The solvents used in this work have been selected because of their different stabilities in reaction to ionizing radiation and because of the fact that they can be separated from the copolymer thus formed without difficulty. The addition of liquid carbon dioxide or carbon tetrachloride as a solvent was found to depress the polymerization rate and the molecular weight of the copolymer. In radiation polymerization in the presence of an added substance, it must be considered that the radiolysis products of the substance play an important role in the initiation and termination reactions. As has been reported in previous papers[2,3] pertaining to the γ-radiation-induced polymerization of ethylene in liquid carbon dioxide, growing chain radicals have been found to be terminated by oxygen produced by the radiolysis of carbon dioxide. Therefore, it is reasonable to conclude that the lower rates of copolymerization in these systems result from this type of contribution of solvents to termination reaction. The lowest molecular weight, obtained in a carbon tetrachloride solution, may be ascribed to a rapid transfer to the solvent.

In contrast to the above-mentioned results, the rate increases in ethylchloride, chloro-pentafluoroethane, and 1,2-dichloro-tetrafluoroethane. It should be noted especially that both the rate and the copolymer molecular weight increase markedly in the latter two fluorinated solvents. The results listed in the last column of Table 1 show that the molar ratio of tetrafluoroethylene to ehylene in the copolymer is little affected by the solvents used. The significance of these results will be discussed below from the viewpoint of kinetics.

Infrared Spectra of the Copolymers. The infrared spectra of the copolymers, together with the assignments of the absorption bands,[1] are shown in Fig. 1. The spectra of polyethylene and polytetrafluoroethylene are also given for ready comparison. It is obvious that the spectra of the copolymers are quite different from those of the two homopolymers. The bands at 1175, 1045, and 950 cm^{-1} which are characteristic of the copolymer become stronger with increase in the molar fraction of tetrafluoroethylene in the copolymer. This tendency is commonly observed in the spectra of the copolymers formed in other solvents.

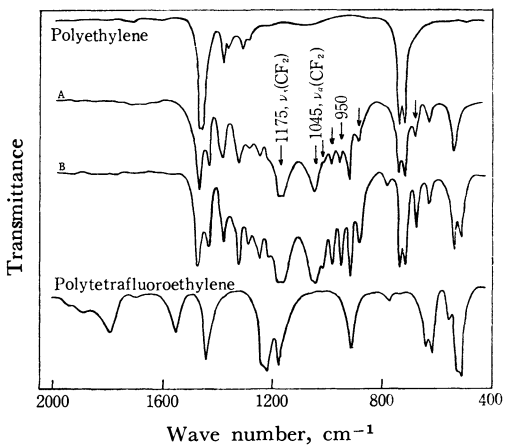

Fig. 1. Infrared spectra of copolymers. Molar fractions of tetrafluoroethylene in copolymers are (A) 3.9 and (B) 12.6 mol%.

X-Ray Diffraction Diagrams of the Copolymers. The X-ray diffraction diagrams of the copolymers, polyethylene, and polytetrafluoroethylene are given in Fig. 2. The diffraction peaks at $2\theta=20.9°$ and $2\theta=20.4°$ are observed, the strongest peaks for the copolymers of the molar fractions of tetrafluoroethylene in copolymers being 3.9 and 12.6% respectively. These peaks exist between

2) M. Hagiwara, H. Mitsui, S. Machi and T. Kagiya, *J. Polymer Sci., A-1*, **6**, 609 (1968).

3) M. Hagiwara, H. Mitsui, S. Machi and T. Kagiya, *ibid., A-1*, **6**, 721 (1968).

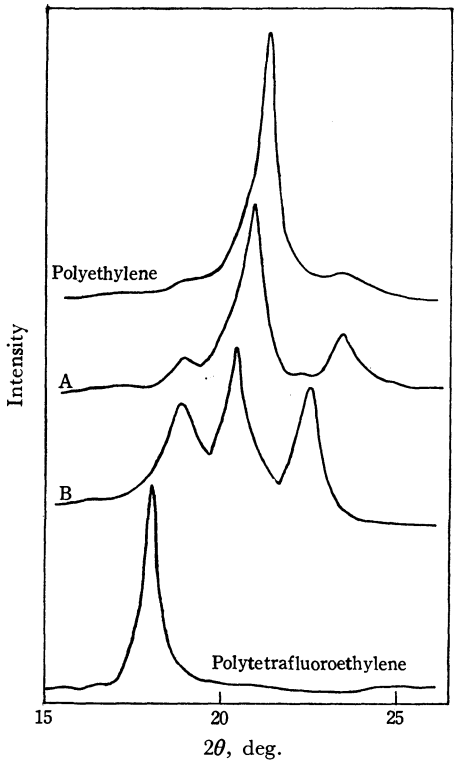

Fig. 2. X-ray diffraction diagrams of copolymers. The signs of each spectra are the same as shown in Fig. 1.

those of the two homopolymers, and their position varies continuously depending upon the molar ratio of the two monomers in the copolymer.

Thermograms of the Copolymers. Figure 3 shows the thermograms of the copolymers, together with those of polyethylene and polytetrafluoroethylene. It is obvious that the thermograms of the coplymers show no peaks obtained by the superposition of the thermograms of the two homopolymers, and that the crystalline melting temperature of the copolymer (134°C in Curve A and 187°C in Curve B) rises with the molar fraction of tetrafluoroethylene in the copolymer. In addition, a small endothermic peak at *ca.* 100°C was observed in the copolymer of which 12.6% was tetrafluoroethylene.

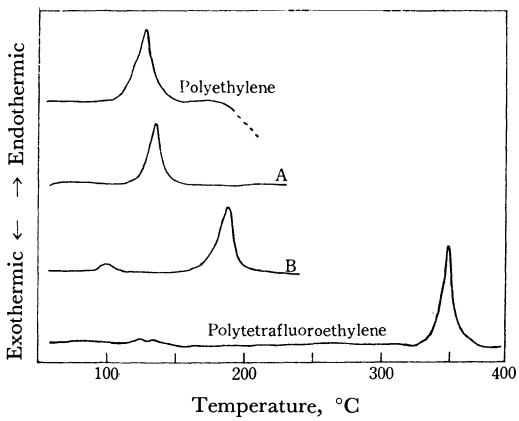

Fig. 3. Thermograms of copolymers for α-alumina in ambient air at heating rate of 5°C per minute. The signs of each curves are the same as shown in Fig. 1.

Polytetrafuoroethylene has been found to show several kinds of transitions at various temperatures. In the range studied in this work, two first-order transitions occurring in the crystalline region at relatively closely-spaced teaperatures around 90°C, and two second-order transitions in the amorphous region around 130°C, have been reported.[4-6] In our thermograms of polytetrafluoroethylene, we observed, no peak at 90°C, but we did find small endothermic peaks near 130°C. Thus, although it has not been clearly shown, the small peak near 100°C in the copolymer is considered to correspond to the transitions around 130°C in polytetrafluoroethylene.

From these results of the infrared, X-ray diffraction, and from the differential thermal analyses, the alternative possibilities of the formation of a mixture of homopolymers and a block copolymer can be excluded.

Copolymerization in 1,2-Dichloro-tetrafluoroethane. The results given in Table 2 show the characteristic effects of 1,2-dichloro-tetrafluoroethane as a solvent on the copolymerization. We were able to observe the appearance of the reaction mixture throughout the copolymerization reaction by using a specially-designed stainless steel autoclave with a quartz window.[7] When a sufficient amount of solvent was used (thirty grams of 1,2-dichloro-tetrafluoroethane were found to be quite enough for a vessel with a capacity of 100 ml), it was observed that the mixture of the two monomers and the solvent exists in a homogeneous liquid phase, with no phase separation in the reaction vessel, and that copolymers formed separate continuously from the mixture as fine particles during the course of the reaction. Thus, in all the copolymerization runs carried out by the use of the solvent, the reaction takes place in the homogeneous-liquid-phase mixture of two monomers and the solvent used. On the other hand, the copolymerizationis a gas-phase reaction when no solvent is used.

In Fig. 4 the rate of copolymerization is plotted against the amount of solvent for three different concentrations of tetrafluoroethylene in the reaction mixture. In all cases, the rate is shown to increase linearly with the amount of solvent. Another

4) Y. Araki, *J. Appl. Polymer Sci.*, **9**, 1515 (1965).
5) Y. Araki, *ibid.*, **9**, 3575 (1965).
6) Y. Araki, *ibid.*, **11**, 953 (1967).
7) S. Machi, M. Hagiwara and T. Kagiya, *J. Polymer Sci., B-4*, 1019 (1966).

TABLE 2. COPOLYMERIZATION OF ETHYLENE WITH TETRAFLUOROETHLENE IN GAS PHASE AND IN 1,2-DICHLOROTETRAFLUOROETHANE

Run No.	Amount of solvent g	Concentration of monomers mol/l		Molar fraction of C_2F_4 in monomers mol%	Copolymer yield g	Molecular weight $\times 10^{-4}$	Molar fraction of C_2F_4 in copolymer mol%
		C_2H_4	C_2F_4				
1	0	17.50	0	0	0.23	20.88	0.0
2	0	16.89	0.173	1.02	0.26	3.61	12.6
3	0	17.17	0.230	1.32	0.35	4.00	13.8
4	30	15.18	0.149	0.98	1.13	5.81	13.0
5	60	11.07	0	0	0.21	5.14	0.0
6	60	11.18	0.022	0.20	0.49	5.64	3.9
7	60	12.50	0.062	0.49	0.85	6.10	8.8
8	60	12.57	0.132	1.04	1.98	9.70	12.6
9	60	12.71	0.188	1.46	2.85	12.84	16.2
10	80	11.04	0.113	1.01	2.10	11.32	12.5
11	120	6.43	0	0	0.27	4.20	0.0
12	120	6.61	0.036	0.53	1.29	8.25	10.3
13	120	6.71	0.074	1.08	3.15	16.20	13.3

Reaction condition: pressure, 300 kg/cm²; temperature, 30°C; dose rate, 2.5×10^4 rad/hr; reaction time, 1.0 hr; reactor volume, 100 ml.

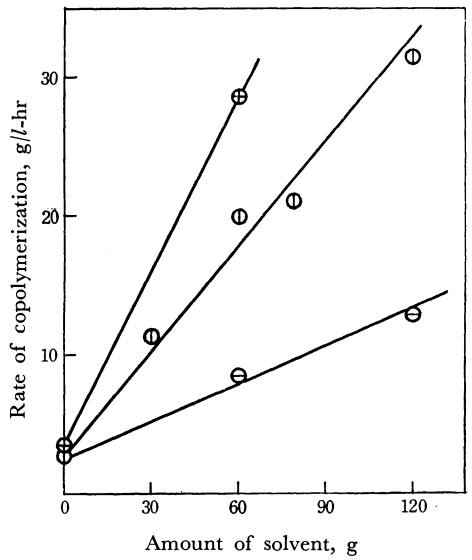

Fig. 4. Rate of copolymerization *vs.* amount of 1,2-dichloro-tetrafluoroethane. Reaction conditions: total pressure, 300 kg/cm²; temperature, 30°C; dose rate, 2.5×10^4 rad/hr; reactor volume, 100 ml; concentrations of tetrafluoroethylene in monomers are about (⊖) 0.5, (⦶) 1.0 and (⊕) 1.5 mol%.

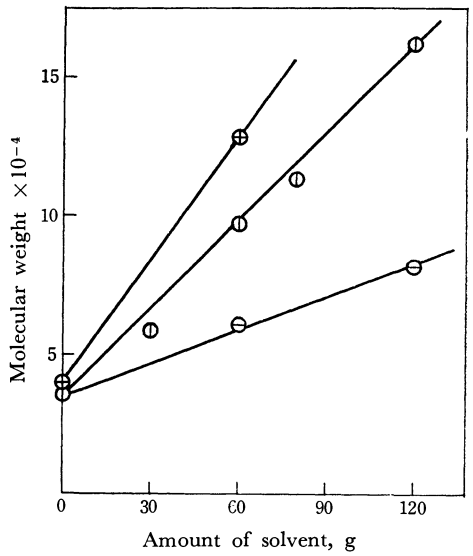

Fig. 5. Molecular weight of copolymers *vs.* amount of 1,2-dichlorotetrafluoroethane. Reaction conditions are the same as shown in Fig. 4.

characteristic phenomenon is the effect of the solvent on the molecular weight of the copolymer formed. As is shown in Fig. 5, our observation clearly demonstrates that the molecular weight increases linearly with the amount of solvent used. On the other hand, as can be seen in the last column of Table 2, the copolymer composition is not affected by the amount of solvent, but is determined exclusively by the molar ratio of the two monomers in the reaction mixture. The fraction of tetrafluoroethylene in the copolymer is much larger than that in the monomers.

By using Eq. (1) (given below), the rate of copolymer chain formation can be calculated; the results are plotted in Fig. 6 against the molar fraction of tetrafluoroethylene in monomers.

Rate of copolymer chain formation

$$=(M_p/t)(1/\bar{P}_n) \quad \text{(mol/l-hr)} \qquad (1)$$

M_p: copolymer yield (mol/l)

$\bar{P}_n$: total number of monomer units in one copolymer chain (–)
t: reaction time (hr)

A small amount of tetrafluoroethylene is shown to be quite effective in producing copolymer chains. In all cases when different amounts of a solvent are used, the rate increases with an increase in the fraction of tetrafluoroethylene. In the range where the molar fraction of tetrafluoroethylene is less than 1%, a higher rate is obtained when a larger amount of solvent is used. Three point on the ordinate show a significant contribution of the solvent to the polymer chain formation. In contrast to this, though a higer rate is obtained than in the case of no solvent at all, the rate comes not to be affected by the amount of solvent in the range above 1% of tetrafluoroethylene. From these observations, it can be concluded that 1,2-dichloro-tetrafluoroethane used as a solvent does not act as a transfer agent in the copolymerization, and that the addition reaction of tetrafluoroethylene to the radicals produced by the influence of radiation on the reaction mixture is important in initiating the copolymerization. Thus, the addition of tetrafluoroethylene to the primary radicals is considered to produce more reactive radicals, which can then effectively initiate the copolymerization with less activation energy. Further, the data in Fig. 6 show that, when a sufficient amount of a solvent is used, the rate of initiation is virtually independent of the amount of solvent at tetrafluoroethylene concentrations above 1%.

In connection with the discussions above, it is interesting to note that the copolymerization rate and the copolymer molecular weight increase linearly with the amount of solvent, as is reported in Figs. 4 and 5. These facts may indicate that the propagation reaction of the copolymerization is strongly promoted by the solvent. Further, the information on the copolymer composition given in Table 2, which shows no noticiable influence of the amount of solvent on the copolymer composition, leads to the conclusion that the enhancement in reactivity might occur at an active site of the propagating copolymer chain. The strongly electro-negative flourine atoms of the solvent might have some effect on the reactivity of the active site in a solvated state. A careful study of this aspect is being carried out and will be reported on later.

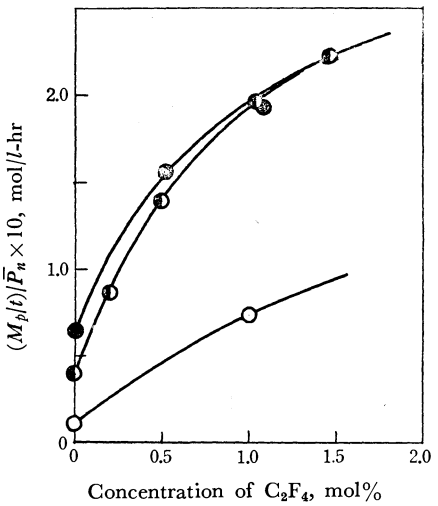

Fig. 6. Rate of copolymer chain formation, $(M_p/t)/\bar{P}_n$ *vs.* initial concentration of tetrafluoroethylene in monomers.
Amounts of solvent are (○) 0, (◐) 60 and (●) 120 g.

BULLETIN OF THE CHEMICAL SOCIETY OF JAPAN VOL. 42 3385—3389 (1969)

Energy Transfer from the Triplet Excited States of Aromatic Molecules to Chromium(III) Complexes

Takeshi OHNO and Shunji KATO

Institute of Chemistry, College of General Education, Osaka University, Toyonaka, Osaka

(Received April 11, 1969)

The quenching efficiencies of five tervalent chromium complexes on the phosphorescence of erythrosin and benzil have been compared at the temperatures of dry ice and liquid nitrogen. The results were well explained in terms of the collisional energy transfer. It was observed that aromatic ligands enhanced the rate of the energy transfer even if the triplet energy of the donor was lower than that of the ligands.

It is well known that the triplet excited states of the aromatic compounds are quenched by some paramagnetic transition metal complexes. Porter and Wright, however, observed no relation between the magnetic susceptibilities of quenchers and the rate constants of the quenching processes of the triplet states, they classified the paramagnetic substances into the following three groups on the basis of the quenching rate constants[1]:

1) simple molecules (NO,O_2) having unpaired electrons in the 2p orbital,
$$k \sim 10^{10}\ \text{M}^{-1}\,\text{sec}^{-1},$$
2) transition metal complexes having unpaired electrons in the 3d orbitals,
$$k \sim 10^{7}\ \text{M}^{-1}\,\text{sec}^{-1},$$
3) rare earth metal complexes having unpaired electrons in the 4f orbitals,
$$k \sim 10^{5}\ \text{M}^{-1}\,\text{sec}^{-1}.$$

These results, which were partly confirmed by Linschitz and Pekkarinen,[2] showed that the quenching of the triplet excited states could not be attributed to the enhancement in the intersystem crossing of the triplet state caused by the inhomogeneous field of the paramagnetic molecule, but only to the overlapping beween the orbitals of the triplet state and the quencher.

Linschitz and Steel found that the aromatic ligands in transition metal chelates accelerated the rate of the quenching as well as the rate of the redox reaction between metal complexes, and supposed that the quencher transiently formed a charge-transfer complex with the triplet state, in which the intersystem crossing was increased.[3]

An alternative mechanism—electronic energy transfer—in the quenching of the triplet states was proposed by Hammond and his co-worker.[4] Their proposal seems to be supported by the fact that overlapping of the orbitals of the two reactants allows an energy transfer from the triplet state to quencher if the energy level of the acceptor is lower than that of the donor.[5] Hammond and his co-worker hesitated to insist on the importance of the energy transfer on the quenching process, however, because the triplet state of anthracene, whose energy is very low (42.6 kcal/mol), is still very efficiently quenched by all the complexes investigated, $Fe^{III}(acac)_3$,*2 $Cu^{II}(acac)_2$, $Cr^{III}(acac)_3$, $Ni^{II}(dpm)_2$,*3 *etc.*[6]

The purpose of this work is to make clear the quenching mechanism of the triplet states in the presence of a transition metal complex, the tervalent chromium complex. The effect and the role of the aromatic ligands of chromium complexes in the quenching were investigated, too. Independent work along these lines has also been done by Forster and his co-workers.[7]

Experimental

Procedure. Figure 1 schematically illustrates the simple apparatus for measuring the emission spectra. A quartz cell 10 mm in diameter was cooled with dry ice or liquid nitrogen. Solutions of 6×10^{-4} M erythrosin in 90% ethanol were illuminated at 534 mμ, while those of 2×10^{-2} M benzil were illuminated at 365 mμ. In order to avoid the scattering of the excitation light,

*1 Presented at the Symposium on Photochemistry of the Chemical Society of Japan, Sendai, October, 1968.

1) G. Porter and M. R. Wright, *Discus. Faraday Soc.*, **27**, 18, (1959).

2) H. Linschitz and L. Pekkarinen, *J. Am. Chem. Soc.*, **82**, 2411, (1960).

3) C. Steel and H. Linschitz, *J. Phys. Chem.*, **66**, 2577, (1962).

4) G. S. Hammond and R. P. Foss, *ibid.*, **68**, 3739, (1962).

5) D. L. Dexter, *J. Chem. Phys.*, **21**, 836, (1953).

*2 acac: acetylacetonate ion.

*3 dpm: dipivaloylmethanate ion.

6) A. J. Fry, R. S. H. Liu and G. S. Hammond, *J. Am. Chem. Soc.*, **88**, 4781, (1966).

7) D. J. Binet, E. L. Goldberg and L. S. Forster, *J. Phys. Chem.*, **72**, 3017, (1968).

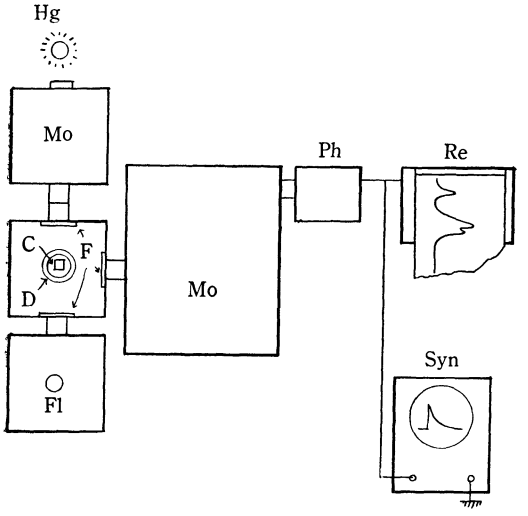

Fig. 1. A schematic diagram of the apparatus for measuring spectra and life-times of emission. Hg: mercury lamp, Mo: monochromator, C: quartz cell, F: filters, D: Dewar's vessel, Fl: flash lamp, Ph: photomultplier 7102, Re: recorder, Syn: synchroscope.

a glass filter, Toshiba UV-D2, was set in front of the cell for the benzil solution, and a Toshiba VY-42 filter for the erythrosin solution. The emission spectra were recorded with a LER-10A recorder (Yokogawa Co.).

To measure the emission life-time, a flash lamp was used with 4-71 Corning filter for the erythrosin solution and a UV-D2 filter for the benzil solution. The solutions were thoroughly degassed by six bulb-to-bulb distillations *in vacuo*.

Materials. Benzil was recrystallised three times from ethanol, erythrosin, from water. Three chromium(III) complexes——$NH_4[Cr^{III}(NCS)_4(NH_3)_2]\cdot 3/2H_2O$, $K_3[Cr^{III}(NCS)_6]\cdot 4H_2O$, and $NH_4[Cr^{III}(NCS)_4\cdot(aniline)_2]\cdot 3/2H_2O$——were prepared by the usual method.[8] $Cr^{III}(acac)_3$ was prepared by the method of Cooperstein.[9] $Cr^{III}(8\text{-oxyquinolinate})_3$ was obtained by warming chromium(III) chloride and 8-hydroxyquinoline in 2N acetic acid.

Ethanol was dried over calcium oxide; then it was refluxed with silver nitrate and distilled.

Results and Discussion

I) The emission and the absorption spectrum of 6×10^{-4} M erythrosin solution are shown in Fig. 2. The emission peaks at 17.9 and 14.3 kK can easily be assigned to the fluorescence and the phosphorescence respectively, the life-times of the latter being 0.63 msec at −72°C and 0.91 msec at −196°C.

Figure 3 shows the emission spectrum of the 2×10^{-2} M benzil solution at −72°C. The fluorescence at 20 kK is weak and the phosphorescence, with peaks at 14.5, 16.0, and 17.6 kK, is much stronger, with the life-time of 0.67 msec. Elevating the temperature made the phosphorescence as weak as the fluorescence.

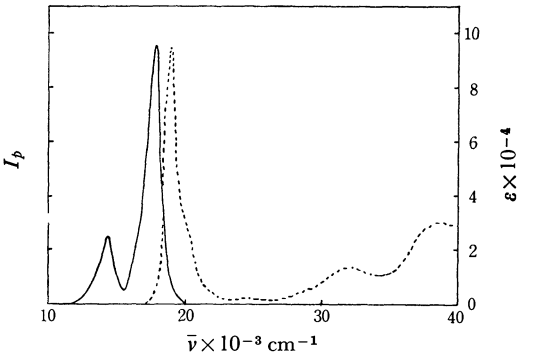

Fig. 2. Absorption spectrum and emission spectrum of erythrosin.

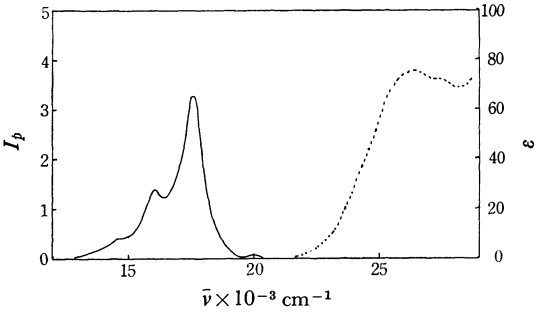

Fig. 3. Absorption and emission spectra of benzil.

The phosphorescences of some chromium(III) complexes which had no fluorescence were observed at −196°C. For $NH_4[Cr^{III}(NCS)_4(NH_3)_2]$, $NH_4[Cr^{III}(NCS)_4(aniline)_2]$, and $K_3[Cr^{III}(NCS)_6]$, the phosphorescences were found at −72°C. Table 1 shows the levels of the phosphorescent states of the aromatic compounds and the chromium(III) complexes.

II) The intensity of the phosphorescence of erythrosin decreased in the presence of 2×10^{-4} M $NH_4[Cr^{III}(NCS)_4(NH_3)_2]$, and a sharp emission with its maximum at 13.3 kK was observed; this was the same value as that of the phosphorescence of the chromium(III) complex observed under direct excitation. As is shown in Fig. 4, the phosphorescence of the donor at 14.3 kK decreases, and that of the acceptor at 13.3 kK increases, with the concentration of the complex. Because the light absorbed by the complex was less than two hundredths that by erythrosin, even at the highest concentration of the complex, the phosphorescence at 13.3 kK must be the sensitized one.

Oxygen did not quench the phosphorescence of a pure solution of the complex, but it did quench the phosphorescence of both the complex and

8) Y. Shimura, "Jikken Kagaku Koza," Vol. 11, Maruzen, Tokyo (1956), pp. 58—60.

9) R. Cooperstein, "Inorganic Syntheses," Vol. 5, p. 130 (1957).

TABLE 1. A RELATION BETWEEN THE ENERGIES OF PHOSPHORESCENT LEVELS AND THE BIMOLECULAR DECAY RATES

Compound	Energy of triplet or ^2E kK	Energy of triplet of ligand kK	k_3+k_4 $l\,mol^{-1}\,sec^{-1}$
Erythrosin	16.4[a]		
Benzil	18.8[b]		
$NH_4[Cr^{III}(NCS)_4(NH_3)_2]$	13.3[c]		6.2×10^6
$K_3[Cr^{III}(NCS)_6]$	12.9[c]		1.6×10^6
$Cr^{III}(acac)_3$	12.8[c]	25.4[d]	1.2×10^7
$Cr^{III}(oxin^*)_3$	~13.1	16[e]	4.8×10^7
$NH_4[Cr^{III}(NCS)_4(aniline)_2]$	~13.1		1.2×10^7

a) J. Pothuma and W. Berends, *Bioche. Biophys. Acta*, **112**, 422 (1966).
b) Reference 6.
c) G. B. Porter and H. L. Schläfer, *Z. physik. Chem. (Frankfurt)*, **40**, 280 (1964).
d) I. Hanazaki, F. Hanazaki and S. Nagakura, *J. Chem. Phys.*, **50**, 276 (1969).
e) Ref. 14.
* "oxin" is abbreviated from "8-oxyquinolinate ion".

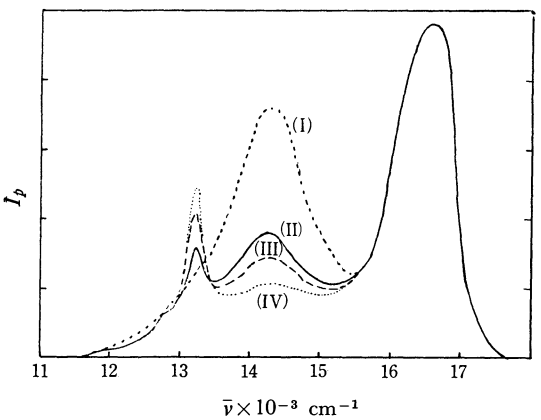

Fig. 4. Change of emission spectrum of erythrosin with $NH_4[Cr^{III}(NCS)_4(NH_3)_2]$, (I) erythrosin 6×10^{-4} M, (II) erythrosin 6×10^{-4} M, the complex 2×10^{-4} M, (III) erythrosin 6×10^{-4} M, the complex 4×10^{-4} M, (IV) erythrosin 6×10^{-4} M, the complex 7×10^{-4} M.

erythrosin in the binary system. At −196°C, where the solution was frozen, the sensitized phosphorescence vanished and the donor phosphorescence emerged very strongly. These facts support the theory that the sensitized phosphorescence is due to collisional energy transfer from the triplet state of the erythrosin to the complex. Such a collisional energy transfer has been reported in the system of benzil-$[Cr^{III}(en)_3{}^{*4}]^{3+}$, $Cr^{III}(acac)_3$, and $[Cr^{III}(CN)_6]^{3-}$ by Forster and his co-workers.[7]

The most probable scheme of the energy transfer may be as follows:

$$^3D^* \rightarrow {}^1D + h\nu \qquad k_1 \qquad \text{(P-I)}$$
$$^3D^* \rightarrow {}^1D \qquad k_2 \qquad \text{(P-II)}$$
$$^3D^* + {}^4A \rightarrow {}^1D + {}^2A^* \qquad k_3 \qquad \text{(P-III)}$$
$$^3D^* + {}^4A \rightarrow {}^1D + {}^4A \qquad k_4 \qquad \text{(P-IV)}$$
$$^2A^* \rightarrow {}^4A + h\nu \qquad k_5 \qquad \text{(P-V)}$$
$$^2A^* \rightarrow {}^4A \qquad k_6 \qquad \text{(P-VI)}$$

where D and A denote a donor and an acceptor respectively; the prefixes the multiplicity of the electronic state, and the asterisk, an excited state. An energy transfer to the first excited quartet state ($^4T_2$) of the complex from the donor triplet state is allowed according to the spin conservation rule. Therefore, P-III includes both the direct-energy transfer to the first excited doublet state (^2E) and that to $^4T_2$, followed by the intersystem crossing to ^2E. According to this scheme, some of the k's values are calculated from three different measurements: (i) The observed decay rates of the donor

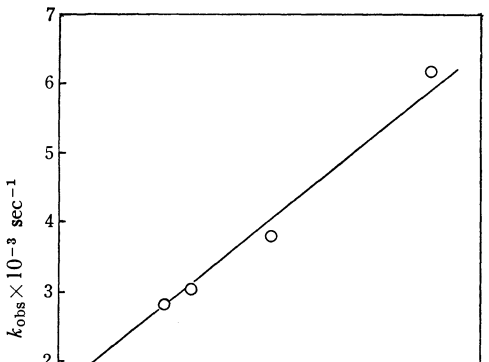

Fig. 5. A relation between the decay constant of erythrosin phosphorescence and the concentration of $NH_4[Cr^{III}(NCS)_4(NH_3)_2]$.

*4 en: ethylenediamine.

TABLE 2. DECAY RATE CONSTANTS OF FIRST ORDER AND SECOND ORDER PROCESSES

Method of measurement*	$k_1 + k_2$ sec^{-1}	$k_3 + k_4$ $mol^{-1}\,l\,sec^{-1}$
Decay rate	1.6×10^3	6.2×10^6
Intensity of donor phospho.		6.2×10^6
Intensity of acceptor phospho.		2.4×10^6

* See text.

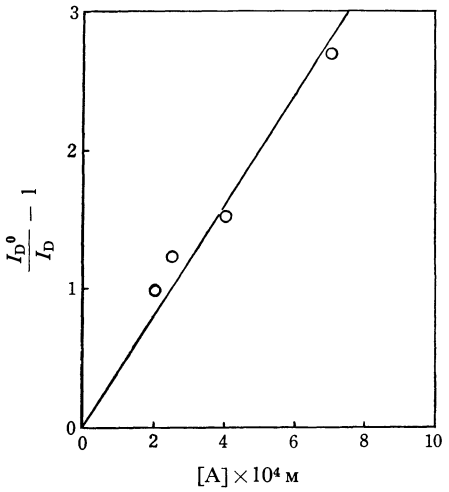

Fig. 6. A dependence of the phosphorescence of erythrosin on the concentration of $NH_4[Cr^{III}(NCS)_4(NH_3)_2]$.

phosphorescence (k_{obs}) are expressed as:

$$k_{obs} = k_1 + k_2 + (k_3 + k_4)\ [A] \qquad (I)$$

The intercept and the slope of the straight line in Fig. 5 give the values of k_1+k_2 and k_3+k_4 respectively, which are listed in Table 2. (ii) The Stern-Volmer depencence on the acceptor concentration is shown in Fig. 6. I_D^0 and I_D show the intensities of the donor phosphorescence in the absence and in the presence of the acceptor respectively. The slope of the straight line in Fig. 6 is $(k_3+k_4)/(k_1+k_2)$, according to the reaction scheme. The value of k_3+k_4, which is calculated by using the value of k_1+k_2, agrees with that obtained by the first method. (iii) The reaction scheme produces Eq. (II);

$$\frac{1}{I_A} = \frac{k_5}{k_5 + k_6}\left(\frac{k_3 + k_4}{k_3} + \frac{k_1 + k_2}{k_3}\right)\frac{1}{[A]} \qquad (II)$$

where I_A denotes the intensity of the sensitized phosphorescence. Figure 7 shows that Eq. (II) holds. The ratio of the slope to the intercept is equal to $(k_3+k_4)/(k_1+k_2)$.

III) Four chromium(III) complexes—$Cr^{III}(acac)_3$, Cr^{III}(8-oxyquinolinate)$_3$, $NH_4[Cr^{III}(NCS)_4(aniline)_2]$, and $K_3[Cr^{III}(NCS)_6]$—were examined as acceptors. The rate constants (k_3+k_4) calculated in two different ways ((i) and (ii)) are shown in the last column of Table 1. Sensitized

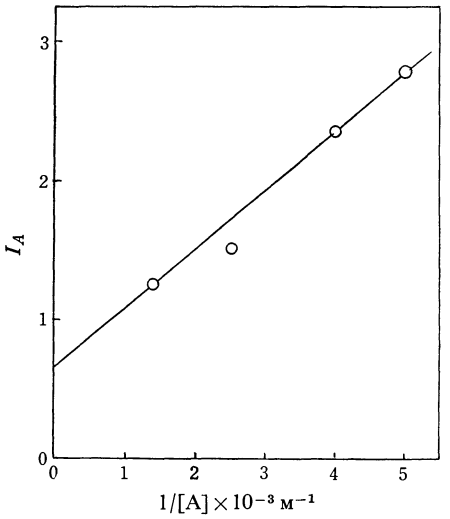

Fig. 7. Confirmation of Eq. (II).

phosphorescences were found in the cases of $K_3[Cr^{III}(NCS)_6]$ and $NH_4[Cr^{III}(NCS)_4(aniline)_2]$, which were phosphorescent at −72°C on direct excitation. For $Cr^{III}(acac)_3$ and Cr^{III}-(8-oxyquinolinate)$_3$, k_6 must be larger than k_5, because these complexes emit no direct phosphorescence nor any sensitized phosphorescence at −72°C.

When a mixture of erythrosin and one of the complexes besides $K_3[Cr^{III}(NCS)_6]$ was excited by a 534 mμ light at −196°C, only the phosphorescence of the former was observed. These facts support the idea of the occurence of a collisional energy transfer at −72°C.

For $K_3[Cr^{III}(NCS)_6]$, the phosphorescence was sensitized by erythrosin even at −196°C. Because collisional energy transfer can not occur in a rigid solution, the possible mechanisms to make a sensitized phosphorescence are: (i) a long-range energy transfer[10] (from the excited singlet state of erythrosin to the $^4T_2$ of the complex) and (ii) the complex formation of the donor with $K_3[Cr^{III}(NCS)_6]$. There is no reliable evidence on the basis of which to select one of them. However, the long-range energy transfer is unlikely to be operative because three complexes—$NH_4[Cr^{III}(NCS)_4(NH_3)_2]$, $NH_4[Cr^{III}(NCS)_4(aniline)_2]$, and $Cr^{III}(acac)_3$—all with absorption spectra similar to that of $K_3[Cr^{III}(NCS)_6]$, had no sensitized phosphorescence at −196°C. The long-range energy transfer at −72°C can be excluded because of the fact the value of k_3+k_4 obtained from the Stern-Volmer plot of the intensity of the donor phosphorescence was not larger than the value calculated from the decay constants of the donor phosphorescence. The alternative mechanism—static quenching—can be excluded at −72°C,

10) T. Förster, *Z. Electrochem.*, **56**, 716, (1952), "Fluoreszenz Organisher Verbindungen," Vandenhseck and Ruprecht, Göttingen (1951).

too, because oxygen quenches the phosphorescence of both the acceptor and the donor completely. These results are partly different from Forster's results in the system of benzil-$K_3[Cr^{III}(NCS)_6]$.

It is worth noticing that the values of k_3+k_4 are $10^7\,M^{-1}\,sec^{-1}$ for the complexes containing aromatic ligands and $10^6\,M^{-1}\,sec^{-1}$ for the complexes containing only inorganic ligands. The rate constant for $NH_4[Cr^{III}(NCS)_4(aniline)_2]$ is twice that for $NH_4[Cr^{III}(NCS)_4(NH_3)_2]$. These results show that these aromatic ligands play an important role in the quenching and in the energy-transfer reaction. The effect of some aromatic ligands upon the quenching rates is more distinct in the reaction at room temperature.[4,6] It has been reported that the quenching of the triplet states of some aromatic compounds with Cr^{III}-$(acac)_3$ was diffusion-controlled and that the quenching rate was several hundred times as great as that for the naphthalene-$Cr^{III}Cl_3$ system.*5,[1] In the case of rare earth complexes, it is well known that the aromatic ligands with triplet levelslower than that of the donor triplet accept the excitation energy from the donor very efficiently as in the case of the energy transfer between aromatic molecules.[11] The proposed mechanism is a series of successive processes as follows:

$$^3D^* + M\text{-}^1L \rightarrow {}^1D + M\text{-}^3L^* \qquad \text{(P-VII)}$$

$$M\text{-}^3L^* \rightarrow M^*\text{-}^1L \qquad \text{(P-VIII)}$$

The $M\text{-}^3L^*$ symbol indicates that the triplet-excited energy is localized in part of the ligands. The energy transfer process (P-VII) is diffusion-controlled if the energetical requirement is satisfied.[12]

In the case of the 8-oxyquinolinate complex, the energy of the triplet state of the ligand (16.2 kK for Pb^{II}(8-oxyquinolinate)$_2$[13]) may be lower than that of the benzil molecule, therefore, the following reaction must be diffusion-controlled:

$$^3Benzil^* + Cr^{III}(8\text{-oxyquinolinate})_3 \rightarrow {}^1Benzil + Cr^{III}(8\text{-oxyquinolinate})_3^* \qquad \text{(P-IX)}$$

However, for the complexes of other lignads, a different type of energy transfer is required, because the triplet levels of the ligands higher than erythrosin make it impossible for the (P-VII) process to occur (see Table 1).

It is well known that 3d electrons in chromium (III) are likely to mix with the p_π electrons of aromatic ligands more than do 4f electrons in rare earth chelates. It is plausible that this mixing makes the interaction between 3d electrons and donor triplet electrons much larger at the frontier of the complexes, then, the excitation energy of the donor in triplet state can be directly transferred to the central chromium ion. It may be through this mechanism that $Cr^{III}(acac)_3$, the ligand triplet state of which is located at 25.4 kK, very efficiently quenches the triplet state of six aromatic molecules—triphenylene (23.8 kK), benzanthrone (16.8kK), anthracene (15.2 kK), *etc.* These quenching rate constants have been measured by Hammond and his co-worker.[6]

A financial support from Fuji Photo Film Co., Ltd., is gratefully acknowledged.

*5 Present results show that the rate constants of the quenching with Werner type complexes, such as $K_3[Cr^{III}(NCS)_6]$ and $NH_4[Cr^{III}(NCS)_4(NH_3)_2]$ are not much smaller than those with complexes containig aromatic ligands at −72°C. This fact is explained as follows. Since the solvent of high viscosity at low temperature makes the contact time longer the energy is effectively transfered from the donor to the acceptor.

11) M. L. Bhaumik and M. A. El-Sayed, *J. Chem. Phys.*, **42**, 787, (1965); V. L. Ermolaev, E. A. Saenko, G. A. Domrachev, Yu. K. Khudenskii and V. G. Aleshin, *Opt. Spectry.*, **22**, 466 (1967).

12) V. L. Ermolaev, V. G. Aleshin, and E. A. Saenko, *Soviet Physics. Doklady*, **10**, 1186, (1966).

13) D. C. Bhatnagar and L. S. Forster, *Spectrochim. Acta*, **21**, 1803, (1965).

14) K. DeArmond and L. S. Forster, *ibid.*, **19**, 1687 (1963).

BULLETIN OF THE CHEMICAL SOCIETY OF JAPAN VOL. 42 3390—3393 (1969)

The Low Temperature n–π^* Absorption Spectra of the Cyclohexane-1,4-dione Crystal

Kayoko Ozeki*1 and Jiro Tanaka

Department of Chemistry, Faculty of Science, Nagoya University, Chikusa, Nagoya

(Received April 15, 1969)

Cyclohexane-1,4-dione is an aliphatic ketone with two carbonyl groups. The absorption due to the n–π^* transition of the carbonyl group extends from the 30000 cm^{-1} to the 42000 cm^{-1} region. The transition is symmetrically forbidden and is assigned to the A_1–A_2 transition in the C_{2v} system. The spectra in the crystal and in a solution of EPA at 77°K show only prominent carbonyl stretching vibrations. The polarized single crystal absorption spectra at 4.2°K are composed of many sharp lines; the vibrational structures are analyzed in detail. The 0-0 transition is observed at 31408 cm^{-1}; the distinct basic frequencies of the excited state are 1096, 790, 557, 375, 247, and 122 cm^{-1}, while the lattice vibrations are 61, 32, and 22 cm^{-1}. The transition is explained by the vibronic coupling mechanism, assuming the C_{2v} symmetry for the carbonyl group. Two different types of progressions are noticed; one is induced by the out-of-plane b_2-type vibration, while the other is allowed by the a_2-type vibration. The dichroic properties of the crystal spectra allowed the assignment of the vibrational modes. These vibrations are compared with the infrared and Raman spectral data.

There have been many experimental and theoretical studies of the n–π^* transitions of aliphatic and aromatic carbonyl compounds.[1] The first vibrational analysis of the spectra of formaldehyde was made by Herzberg,[2] who thus established the vibrational intervals for the carbonyl stretching frequency. Complete rotational analysis was made by Dieke and Kistiakowsky[3] on formaldehyde; they concluded that the n–π^* transition is polarized in plane and perpendicular to the carbonyl axis. Brand[4] and Robinson[5], by absorption and emission spectral measurements, determined that the configuration of formaldehyde in the singlet excited states is non-planar. Pople and Sidman[6] studied the mechanism of the vibronic coupling in formaldehyde and concluded that most of the intensities of the perpendicularly polarized bands arose from the mixing of the A_2 ($n\pi^*$) state with the B_1($n\sigma^*$) state by the perturbation of the b_2-type vibration. These result may be applicable to the interpretation of n–π^* transitions in more complex aliphatic aldehydes and ketones.

The asymmetric carbonyl compounds are known to show the optical rotatory dispersion in the n–π^* transition regions, and the octant rule has been found to hold for the complex carbonyl compounds.[7] Mason[8] discussed the optical activity of the carbonyl

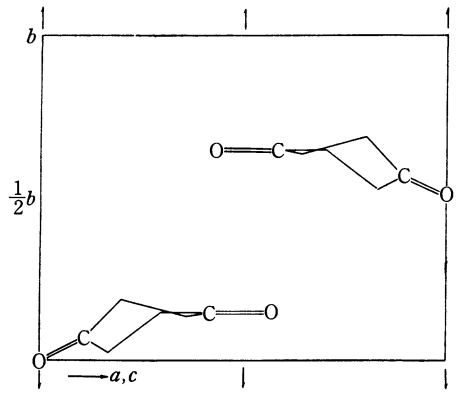

Fig. 1. The projected view of cyclohexane-1,4-dione on to the ($10\bar{1}$) plane according to the X-ray results. The absorption spectra were photographed through this plane. One carbonyl axis is nearly parallel to the [$10\bar{1}$] axis, while another is inclined to the b and [$10\bar{1}$] directions. The molecular C_2 axis is nearly perpendicular to both carbonyl groups.

*1 Present address: Governmenment Industrial Research Institute, Nagoya, Hirate-machi, Kita-ku, Nagoya.

1) J. W. Sidman, *Chem. Revs.*, **58**, 689 (1958); M. Kasha, *Discussions Faraday Soc.*, **9**, 14 (1950).
2) G. Herzberg, *Trans. Faraday Soc.*, **27**, 378 (1931).
3) C. H. Dieke and G. B. Kistiakowsky, *Phys. Rev.*, **45**, 4 (1934).
4) J. C. D. Brand, *J. Chem. Soc.*, **1956**, 858.
5) G. W. Robinson, *Can. J. Phys.*, **34**, 639 (1956).
6) J. A. Pople and J. W. Sidman, *J. Chem. Phys.*, **27**, 1270 (1957).
7) W. Moffitt, R. B. Woodward, A. Moscowitz, W. Klyne and C. Djerassi, *J. Am. Chem. Soc.*, **83**, 4013 (1961).
8) S. F. Mason, *Quart. Rev.*, **17**, 20 (1963).

compounds and suggested that the parallel component to the carbonyl axis is important in any interpretation of the optical activity. The transition moment along the carbonyl axis may be produced by *a* vibronic coupling through the a_2-type vibration or by the other kinds of perturbations[9]

In this paper the vibrational analysis of the spectra of aliphatic ketone at low temperatures will be presented with a view to elucidating the mechanism of the intensity gain. Cyclohexane-1,4-dione is a cyclic diketone, as is shown in Fig. 1. The polarized absorption spectra of this diketone at 4.2°K shows several vibrational progressions; the detailed analysis of these progressions gives unambiguous assignments for the vibrational modes and for the mechanism of the vibronic coupling. The vibrational frequencies for the excited states are compared with the infrared and Raman spectral data.

Experimental

The cyclohexane-1,4-dione was the product of Nakarai Chem., Ltd., Kyoto, Japan; it was recrystallized from an ethanol solution and was used immediately after preparation because the crystal is not stable at room temperature.

The spectrum of the solution in EPA at the temperature of liquid nitrogen was recorded on a Cary spectrophotometer model 15. Crystal absorption experiments at the temperatures of liquid nitrogen and liquid helium were carried out on a Shimadzu GE-100 spectrograph equipped with a Bausch & Lomb grating, as has been reported before.[10] A standard Zeiss hydrogen lamp was employed as the radiation source. The smaple was mounted between two black paper masks, placed between quartz disks. The crystal axes were checked by a polarizing microscope and by the X-ray photographic method. The light incident upon the sample was a plane polarized by a rotable Glan-Thompson calcite polarizer; it was focussed with the appropriate lens system on the spectrograph slit. The exposure times ranged from 4 to 12 min with a slit width of 0.1 mm using Kodak 103a-0 photographic plates. Reference ion-arc spectra were photographed adjacent to each absorption spectrum. This molecule has the symmetry of C_2 in the crystal, but the two-fold axis is nearly perpendicular to the carbonyl axes. The carbon atoms attached to the carbonyl carbon are coplanar with the oxygen atom; the projection of molecules analyzed by Mossel and Romers[11] and Groth and Hassel[12] is shown in Fig. 1. Two carbonyl groups are separated by the saturated bonds; therefore, the chromophores are considered to be nearly independent of each other, although they are related by the symmetry operation. From a rigorous point of view, there should be an exciton interaction between the chromophores, however, no detectable effect can be found on the absorption spectra. Therefore, a treatment based on the independent system will be used in the following dissussion. The spectrum of the solution at 77°K is shown in Fig. 2. It shows several maxima, but the vibrational intervals are not so clear as those in the crystal spectrum. The crystal spectrum at 77°K shows several progressions of 1100 cm^{-1}; these may be assigned to the carbonyl stretching. However, no other vibrational modes can be detected clearly.

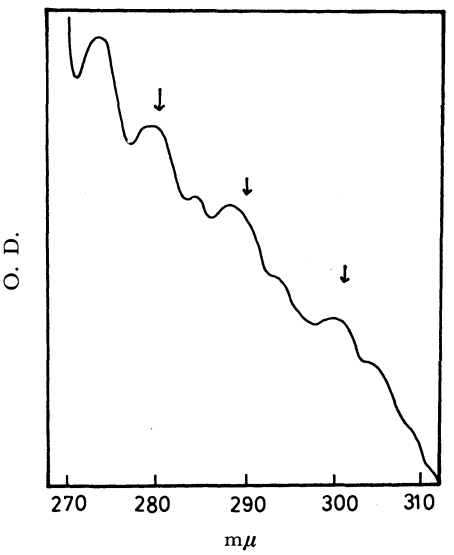

Fig. 2. The spectra of cyclohexane-1,4-dione in the E.P.A. solution at 77°K.
Ordinate: The optical density in arbitrary unit.
Abscissa: Wavelength in mμ.
The arrows indicate the position of the frequencies of the carbonyl stretching.

Vibrational Analysis of the 4.2°K Crystal Spectra

The single crystal spectra at the temperature of liquid helium are shown in Fig. 3 for the light polarized parallel and perpendicular to the *b* axis. At 4.2°K each vibrational envelope is composed of many sharp lines. No detectable splitting between the *b* and the [10$\bar{1}$] axis has been found; this supports the independent-system approach. Several characteristic fundamental vibrational frequencies have been observed along the *b* and the [10$\bar{1}$] axes; some of them are peculiar to the [10$\bar{1}$] axis. The spectrum starts with a sharp line at 31408 cm^{-1}; this line we assigned to the 0–0 transition for several reasons. No trace of any absorption to the red of this origin could be found in crystals up to 0.2 mm in thickness. The appearance of the weak 0–0 band and the subsequent strong vibrational bands are consistent with the vibrational progression built on a forbidden transition. Definite proof is given by the observation of the highest

9) K. Ozeki, M. Inagaki and J. Tanaka, This Bulletin, 3076 (1969).
10) M. Vala, Jr., and J. Tanaka, *J. Chem. Phys.*, **49**, 5222 (1968).
11) A. Mossel and C. Romers, *Acta Cryst.*, **17**, 1217 (1964).
12) P. Groth and O. Hassel, *Acta Chem. Scand.*, **18**, 923 (1964).

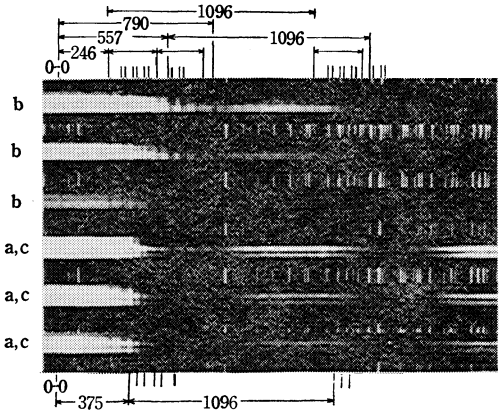

Fig. 3. The polarized absorption spectra at liquid-helium temperature showing the details of first and second band systems. Three different exposure times (12, 8 and 4 min) were used. The basic vibrations, which are common to both *b* and [10$\bar{1}$] axes spectra, are indicated on the top of the spectra. The vibration which is peculiar to the [10$\bar{1}$] axis spectrum is indicated in the bottom.

energy fluorescence band of the same origin, but no fluorescence has been observed with this compound. The frequencies, intensities, and assignments of the absorption bands are shown in Table 1. The carbonyl stretching progressions are observed up to the fourth level. Only the first member of each of the progressions is accompanied by many sharp lines, and the dichroic properties are clearly observed. The second member can be analyzed to some extent, but analysis is difficult for the higher members.

The important vibrational frequencies found along the [10$\bar{1}$] direction are 375 cm^{-1} and 1096 $^{-1}$. The progression of 1096 cm^{-1}, which is common to the *b*-axis spectrum, can safely be regarded as the stretching mode of the carbonyl group because it is already established with other carbonyl compounds.[2] The frequency is greatly reduced as compared with that of the ground state. If we suppose the local symmetry of the carbonyl group to be valid for the discusssion of the excited state of the present molecule, then the carbonyl stretching mode has a symmetry of a_1. It is reasonable

Table 1. Absorption bands of cyclohexane-1,4-dione crystal at 4.2°K

Frequency cm^{-1}	$\Delta\nu$ cm^{-1}	Intensity	Assignment	Frequency cm^{-1}	$\Delta\nu$ cm^{-1}	Intensity	Assignment
31408		w	0-0	32494	1086	m	
31654	246	m	+247	32518	1110	vw	
31718	310	s	+247+61	32548	1134	vw	
31741	333	s	+247+61+24	32578	1170	vw	
31782	374	vs, w	+375	32596	1188	vw	
31795	387	w		32639	1231	vw	
31815	407	vs*, w	+375+32	32664	1256	w	
31842	434	w*, vw	+375+32×2	32681	1273	vw	
31866	458	vw		32705	1293	w	
31904	496	vs*, s	+375+122	32743	1335	m	
31937	529	s*, vw	+375+122+32	32774	1366	w	+1096+247+23
31965	557	vs	+557	32815	1407	vw	+1096+247+61
31986	578	s	+557+21	32840	1432	s	+1096+247+61+24
31997	589	w		32880	1472	m	+1096+375
32025	617	vs	+557+61	32901	1493	m	+1096+375+32
32045	637	vs	+557+61×2+20	32922	1514	m	
32069	661	m		32946	1538	s	+1096+375+32×2
32103	694	vs	+(694)	32965	1557	m	
32123	715	s	+(694)+21	32996	1588	w	
32141	733	s		33019	1611	w	
32149	741	s	+(741)	33043	1635	w	
32168	760	vw	+(741)+19	33080	1672	vs	+1096+557+21
32198	790	vs	+790	33134	1726	vs	+1096+557+61+21
32222	814	vw	+790+24	33163	1755	m	
32254	846	s	+790+61	33193	1785	vs	+1096+(694)
32288	880	m		33246	1838	w	+1096+(741)
32332	924	w		33266	1856	m	
32347	939	vw		33282	1874	m	
32407	999	m		33300	1892	m	+1096+790
32432	1024	m					

Intensity designations are: s, strong; m, medium; w, weak; vw, very weak.
When two intensity designations are written *a*, *c* axis absorptions are marked by *.

that this frequency is often coupled with other type of vibrations.

From the arrangement of the molecule in a unit cell shown in Fig. 1, the symmetry properties of the vibronic state can be discussed. The component parallel to the carbonyl axis (A_1 type) can be strongly observed, particularly along the [10$\bar{1}$] direction. In order for us to find the symmetry-forbidden n-π^* state (A_2 state) along the carbonyl axis, the vibronic coupling with the a_2-type vibration should be operative. The observed band at 0-0+375 cm^{-1} is thus shown to correspond to the vibronically-a_2-coupled state. This band is only weakly observed in the b-axis direction. For the molecule having an exact C_{2v} symmetry, the a_2-type vibration is not effective for the vibronic intensity borrowing. For molecules of a lower symmetry such as this diketone, the strict geometry of the C_{2v} system does not hold; the a_2-type torsion will induce the electronic transitions vibronically. The band progression starting at 31782 cm^{-1} should, therefore, be assigned to the component parallel to the carbonyl axis, which is itself produced by the coupling with the a_2-type torsional mode. The lattice vibration of 30 cm^{-1} is found only along the [10$\bar{1}$] direction.

It is noteworthy that no important progressions have been found which are observed only along the b axis. In a previous paper the out-of-plane component of the n-π^* transition was rejected on the grounds of the measurement of several crystals.[9]

It has been confirmed again in the present research that no particular b_1-type vibration is associated with the induction of the B_2 excited state, which is active in the out-of-plane of the carbonyl group. The transitions polarized parallel to the other directions, in the plane and perpendicular to the carbonyl axis, will be found along both the b and the [10$\bar{1}$] directions. The vibrations of 247, 557, and 790 cm^{-1} are regarded as b_2-type vibrations, which will mix the B_1 excited level with the forbidden A_2 n-π^* state. The small spacings of 60 cm^{-1} and the doublet structure of 20 cm^{-1} may be assigned to the lattice vibration. It is remarkable that the 60 cm^{-1} and 20 cm^{-1} intervals are associated with the 247, 557, and 790 cm^{-1} vibronic states.

The infrared and Raman spectra of this molecule in the crystalline state show the corresponding frequencies of 60, 122, 247, 375, 557, and 790 cm^{-1}. These frequencies are compared with the present values for the excited state in Table 2. It is noticeable that the frequencies assigned to the excited state nearly coincide with the values given for the ground state except for the carbonyl stretching mode.

The quantitative estimate of the intensity of the component of the a_2-type induced A_1-excited state is rather difficult because of the complexity of the spectra, but an approximate value would be about 20% of the total n-π^* transition intensities. The result is very closely connected with the theory of the optical activity. A theoretical discussion of the mechanism of the intensity gain will be presented in a separate paper.

Table 2. Comparison of vibrational frequencies

Frequencies of the ground state		Frequencies of the excited state by electronic spectra (cm^{-1})
Infrared (cm^{-1})	Raman (cm^{-1})	
		20(m)
54(s)		60(m)
114(s)		122(w)
160(s)	179(m)	
238(s)	236(s)	247(m)
365(m)	360(m)	375(s)
413(m)		
435(s)	431(m)	
507(m)		
522(m)		
560(s)	543(s)	557(s)
589(m)	573(m)	
	600(w)	
805(vs)	746(vs)	790(s)
	824(w)	
873(m)	903(w)	
	920(w)	
943(s)		
965(vs)	975(w)	
	1023(w)	
1064(s)	1074(m)	
1090(s)		
1144(vs)		
1163(m)	1172(w)	
1271(s)	1247(w)	
1312(s)	1324(m)	
1326(m)	1324(m)	
1342(m)		
1404(s)	1430(s)	
	1528(w)	
	1562(w)	
1598(m)	1591(w)	
1705(vs)	1720(vs)	1097(vs)
	1757(w)	

Intensity designations are: s, strong; m, medium; w, weak; vw, very weak.

We wish to thank Professor T. Miyazawa of Osaka University for the measurement of the far infrared spectra and Professor M. Ito of The University of Tokyo for his kind help in obtaining the Raman spectral data.

BULLETIN OF THE CHEMICAL SOCIETY OF JAPAN VOL. 41 3394—3398 (1968)

Spectroscopic Investigation of Foreign Gas Effects upon CO_2 Laser Frequencies

Isao Suzuki* and Shigeko Suzuki**

* *Department of Chemistry, Faculty of Science, The University of Tokyo, Hongo, Bunkyo-ku, Tokyo*

** *Department of Pure and Applied Sciences, College of General Education, The University of Tokyo, Komaba, Meguro-ku, Tokyo*

(Received May 7, 1969)

The change in the oscillation frequencies of a CO_2 laser was examined when foreign gases were introduced into a cell placed inside the cavity. Several gases which have absorption bands around 10 μ region were investigated: sulfur hexafluoride, ammonia, ethylene, *trans*-dichloroethylene, methyl bromide, trichloroethylene, acrolein, and isopropyl alcohol. The CW laser oscillations in the P-branch of the 9.6 μ band as well as those in the R-branch of the 10.6 μ band were observed when some foreign gases with appropriate pressures were introduced in the cavity. It was also found that the presence of ammonia or methyl bromide even in a very low pressure suppressed the usually strong P(20) line of the 10.6 μ band. This is interpreted as due to a near coincidence of the laser line with one of the vibration-rotation transitions in these molecules.

Under ordinary CW operating conditions in a CO_2 laser, the laser action occurs on a few P-branch transitions of the 10.6 μ band of CO_2. Wood and Schwartz[1] reported that introduction of sulfur hexafluoride gas to a cell placed within the cavity causes the laser frequencies to shift to a few R-branch transitions. Similar phenomena occur in a wide variety of organic and inorganic gases,[2] and the oscillation frequencies are very sensitive to the pressures of given gases. We have also observed the CW laser action in a few P-branch lines of 9.6 μ band, a Fermi resonance partner of the 10.6 μ band. In the present paper, we describe the results of our spectroscopic investigation on the effect of foreign gases, which have some absorptions around the 10 μ region on a CO_2 laser system.

Experimental

The diagram for experimental setting is shown in Fig. 1. A mixture of CO_2 (9.9%), N_2 (15.8%) and He (74.3 %) with the total pressure of 8 mmHg was sealed in a pyrex tube of 1.2 m in length and inner diameter of 30 mm. The tube was cooled with water. The tube had a concave mirror of radius 3.5 m at one end and a potassium chloride plate at the other end. A 10 cm infrared gas cell with KCl windows was placed adjacent to the pyrex tube (see Fig. 1 (a)). The laser cavity was completed with a plane mirror with a 2 mm diameter hole in the center, through which the laser beam was coupled out. Both mirrors were aluminized. The gas mixture was excited by an ac-discharge at a current of

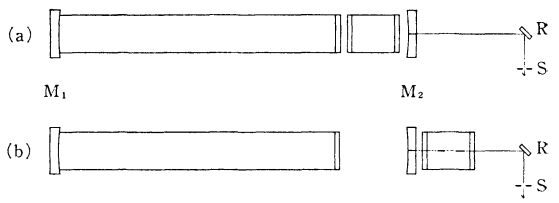

Fig. 1. Diagram for experimental setting: (a) an infrared gas cell was placed inside the cavity, and (b) the cell was placed just outside the cavity. M_1: Concave mirror (R=3.5 m), M_2: plane mirror with a 2 mm diameter hole in the center, R: reflector, and S: slit of the spectrophotometer.

8 mA. The laser beam was scattered with a diffuse reflector, and a part of the emission radiation was introduced to the entrance slit of a spectrophotometer. With the evacuated cell placed inside the cavity, four or five lines distributed around the P(20) transition were normally observed. We have also examined a flow system, but no essential change was observed. In order to minimize the thermal extension effect of the pyrex tube due to discharge, the measurements were made after a certain equilibrium had been reached in the cavity length.

We used a Perkin-Elmer 112G grating spectrophotometer with a KBr foreprism.[3] The 9—11 μ region was covered with the first order of a 75/mm grating. The gases which have absorption bands around 10 μ region were chosen. They are listed in Table 1 with the relevant absorption center and the approximate vibrational mode for each gas. We have also examined

1) O. R. Wood and S. E. Schwartz, *Appl. Phys. Letters*, **11**, 88 (1967).

2) I. Suzuki and S. Suzuki, This Bulletin, **41**, 2549 (1968).

3) S. Mizushima *et al.*, A Report on the Perkin-Elmer Grating Spectrophotometer Model 112G. The Perkiln-Elmer Corp. (1959).

TABLE 1. THE GASES EXAMINED IN THE PRESENT STUDY WITH THE RELEVANT BAND CENTERS AND THEIR APPROXIMATE NORMAL MODES

		Band center		Approximate normal mode
(a)	NH_3	$\nu_2^a(a_1)$	968.3 cm^{-1}	NH_3 deformation
		$\nu_2^s(a_1)$	932.5 cm^{-1}	
(b)	$CH_2=CH_2$	$\nu_7(b_{1u})$	949.2 cm^{-1}	CH_2 wagging
(c)	SF_6	$\nu_3(f_{1u})$	940 cm^{-1}	SF deg. stretching
(d)	CHCl=CHCl (*trans*)	$\nu_6(a_u)$	898 cm^{-1}	CH out-of-plane bending
(e)	CH_3Br	ν_6(e)	953.8 cm^{-1}	CH_3 rocking
(f)	$CHCl=CCl_2$	$\nu_{10}(a'')$	940 cm^{-1}	CH out-of-plane bending
(g)	$CH_2=CHCHO$	$\nu_{14}(a'')$	993 cm^{-1}	CH_2 wagging
		$\nu_{16}(a'')$	959 cm^{-1}	CH out-of-plane bending
(h)	$(CH_3)_2CHOH$	$\nu_{17}(a'')$	953 cm^{-1}	CH_2 rocking

(a)—(g) Taken from the table of fundamental frequencies in the ground electronic states in G. Herzberg, "Electronic Spectra and Electronic Structure of Polyatomic Molecules," Van Nostrand, New York (1966), p. 583.

(h) C. Tanaka, *Nippon Kagaku Zasshi (J. Chem. Soc. Japan, Pure Chem. Sect.)*, **83**, 657 (1962).

some liquids. In this case, liquid cells with thickness 1.0 mm and 0.1 mm with NaCl windows were used in place of the 10 cm gas cell.

Results and Discussion

The results of our present investigation are summarized in Table 2, in which the observed laser transitions for each foreign gas at various pressures are listed. With foreign gas present within the cavity, the laser output is usually distributed among several vibration-rotation transitions in one branch. However, under certain conditions simultaneous transitions in two branches are observed. The laser oscillations are usually too unstable, probably due to the competition effect among various vibration-rotation transitions, to allow quantitative measurements, but they are listed in Table 2 in approximate order of their intensities.[4] As in Table 2, a primed P hereafter refers to the P-branch transitions of the 9.6 μ band, while unprimed P and R refer, respectively, to the P- and R-branch transitions of the 10.6 μ band.

In most cases, their effects can be interpreted simply from the absorbances of given foreign gases in this region. Good examples are sulfur hexafluoride and *trans*-dichloroethylene: Both absorb strongly in the P-branch region of the 10.6 μ band, much less strongly in the R-branch region, and they have practically no absorptions in the P'-branch region. This explains rather remarkable changes in their oscillation frequencies with the gas pressures. This interpretation seems to hold for the case of liquids also, when a liquid sample was placed inside the cavity instead of gas. The results for several liquid samples are summarized in Table 3.

However, ammonia and methyl bromide seem to be exceptions. In Fig. 2(a), we show the absorption spectrum of 85 mmHg ammonia in a 10 cm cell superimposed with the emission lines of the CO_2 laser when the same cell was placed within the cavity, while in Fig. 2(b) similar spectra for the P-branch region are shown when the pressures of ammonia was reduced to 20 mmHg. No R-branch transitions were observed in the latter case. We note that the usually strong P(20) line was completely missing from the emission spectrum when ammonia was introduced into the cavity, whereas no strong absorption seems to be present at the corresponding frequency. We have shown in Fig. 2(c), the emission spectrum when the same cell containing 20 mmHg NH_3 was placed just outside the cavity (see Fig. 1(b)). The emission spectrum was almost unaffected by the presence of the outside cell.

As may be seen in Fig. 3 and Table 2(e), a similar effect was found when methyl bromide gas was introduced into the cavity. In this case the usually strong P(20) and P(22) lines are missing from the emission spectrum.[5] Even when the pressure of CH_3Br was reduced to 3 mmHg, the P(20) line was the weakest among the transitions in the P-branch region, which is rather unusual.

The results with ammonia and methyl bromide may be related with a near coincidence of the laser line with one of vibration-rotation transitions of a foreign gas. Recently, Ronn and Lide have investigated an infrared-microwave double resonance of methyl bromide using a CO_2 laser.[6] They

4) When the laser oscillations occur simultaneously among the lines in two branches, the laser action seems to become very unstable. A number of other weaker lines than those listed in Table 2 appear spasmodically in such cases.

5) The absence of the P(22)line may be explained from the fact that the line is located close to the fairly strong $^PQ_2$ line of CH_3Br: the P(22) line is at 942.54 cm^{-1} and the $^PQ_2$ is reported to locate at 942.25 cm^{-1}. E. W. Jones, R. I. L. Popplwell and H. W. Thompson, *Spectrochim. Acta*, **22**, 647 (1966).

6) A. M. Ronn and D. R. Lide, Jr., *J. Chem. Phys.*, **47**, 3669 (1967).

Table 2. The effect of foreign gases on the oscillations of CO_2 laser[a,b]

Pressure (mmHg)	P-branch	R-branh	P'-branch[d]
(a) NH_3			
170		20, 22.	
100		20, 22, 18.	
85	22.	20, 22, 18.	
50	22, 18.	20, 22, 18.	
30	22, 18.		
20	22, 18, 24, 16.		
10	22, 18, 24, 16.		
7	22, 18, 20.		
5	20, 22, 18.		
3	20, 22, 18.		
(b) $CH_2=CH_2$			
50		18.	
40		18.	20.
25		18.	
10		18, 20, 16.	
8		18, 20, 14.	
5	20.	18, 14, 16, 20.	
4	20, 18, 24.	20, 16.	
2	20, 18, 24.		
(c) SF_6			
20			20, 22, 24, 18, 26, 16, 14.
13			20, 22, 24, 18, 16.
8			20, 22, 24, 18, 16,
5.3		16, 18, 14.	18, 20, 22.
3.3		16, 18, 14, 20.	22, 20, 18.
2.4		16, 14, 18, 12, 20.	22, 20, 18, 16.
1.4		16, 18, 12.	
0.8		16, 18, 14, 20, 12.	
0.5		18, 20, 16.	
0.1_7		20, 18, 16. 12.	
0.0_3	20, 18, 22.	18.	

Pressure (mmHg)	P-branch	R-branh	P'-branch[d]
(d) CHCl=CHCl (*trans*)			
110[c]			18, 20, 16, 22.
85			18, 20, 16, 22.
30		20.	18, 20, 22. 22.
20		20, 16.	18, 20, 16, 22.
10		24, 20, 16, 14.	18.
5	20, 18.	20, 18, 16.	
2.5	20, 18.	18, 14.	
1	20, 18, 22.	14, 22.	
(e) CH_3Br			
100			20.
60	18, 24.		20, 18.
30	16, 18, 24, 26.		
18	16, 18, 24, 26.		
3	16, 18, 24, 26, 20.		
1	16, 18, 24, 26, 20.		
0.5	20, 18, 22, 16, 24.		
(f) $CHCl=CCl_2$			
41[c]		14, 18, 20.	20, 22, 18, 16.
20		18, 14, 16.	16.
9		16, 18, 20, 12.	20.
3.5		14, 16, 18.	
1		20, 18, 14, 16.	
(g) $CH_2=CHCHO$			
55[c]			22.
13			20, 16.
7			20, 16.
3		16.	
(h) $(CH_3)_2CHOH$			
7		18, 20.	
3		22.	
1	20.	22, 20.	

a) In each branch, the emission lines are arranged in the approximate order of their intensities, which have been determined from the average of several runs.
b) Extremely weak or unstable emission lines are omitted from the table.
c) Gas pressures are only approximate owing to the adsorption of the gas to the wall.
d) P' refers to the P-branch transitions of the 9.6 micron band.

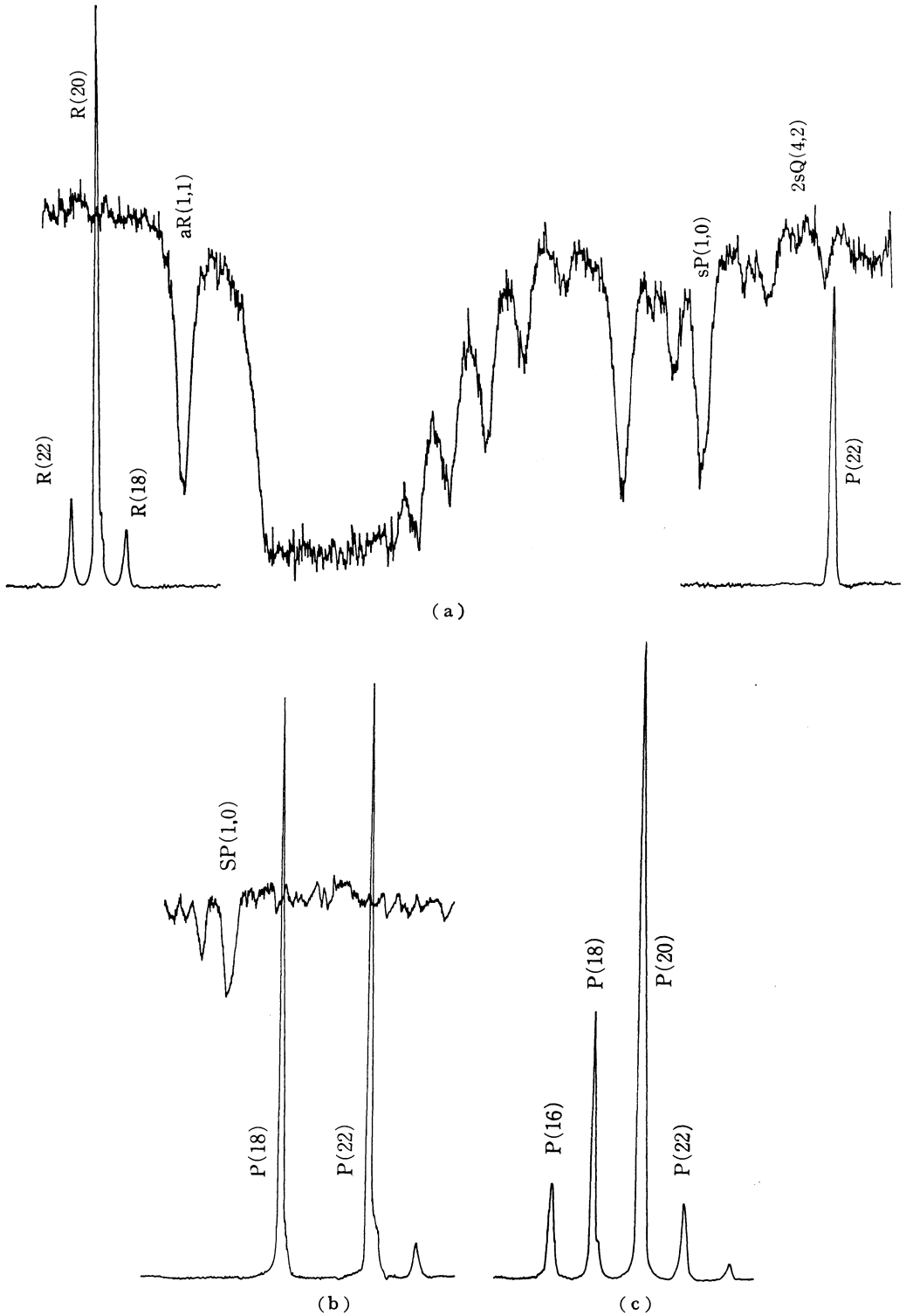

Fig. 2. Absorption spectrum of NH_3 (10 cm cell, spectral slit width 0.5 cm^{-1}) superimposed with emission lines from the CO_2 laser when the same cell was placed inside the cavity. (a) 85 mmHg NH_3. (b) 20 mmHg NH_3. (c) 20 mmHg NH_3, the cell was placed just outside the cavity (see Fig. 1 (b)). The positions of the laser lines are as follows: 947.80, 946.00, 944.19 and 942.35 cm^{-1} for P(16) through P(22), and 974.57, 975.84 and 977.20 cm^{-1} for R(18) to R(22). The sP(1, 0) and aR(1, 1) bands in ammonia were found at 948.27 and 971.90 cm^{-1}, respectively.

Table 3. The laser output when the liquid samples in 0.1 mm cell were placed inside the cavity[a)]

Sample	P-branch	R-branch	P'-branch
(i) $CHCl_3$		18, 16, 14, 20, 12.	
(ii) CH_2ClCH_2Cl		18, 16, 20, 14.	
		18.[b)]	18.[b)]
(iii) $CHCl=CCl_2$			20, 18, 16, 22, 14.
(iv) $CHCl=CHCl$ (*trans*)			22, 20, 18.
(v) CH_3NO_2	20 (only)		

a) CCl_4, C_6H_5, and CH_2Cl_2 have little effect upon the laser oscillation pattern.
b) 1.0 mm cell.

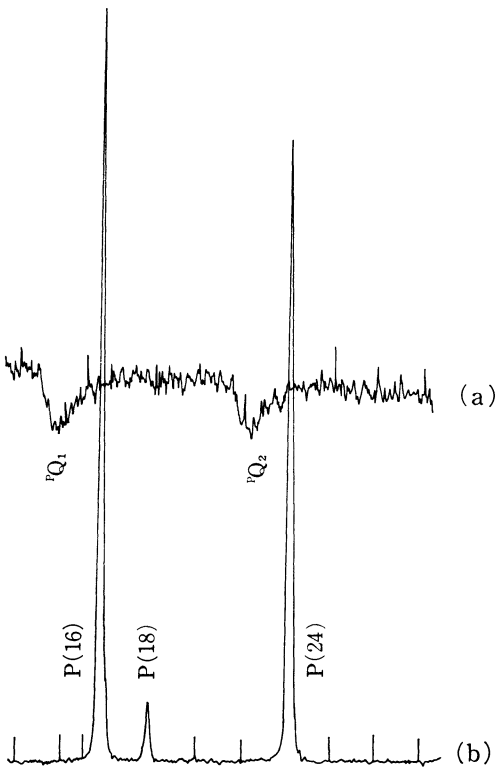

Fig. 3. (a) Absorption spectrum of 18 mmHg CH_3Br in a 10 cm gas cell superimposed with (b) the emission lines from the CO_2 laser when the same cell was inserted in the cavity. The $^PQ_1$ and $^PQ_2$ bands are at 949.14 and 942.25 cm^{-1}, respectively.

interpreted the results as due to a very near coincidence between the P(20) line and the $^PP(9)$ line of the ν_6 fundamental within 0.001 cm^{-1}. The ^PP lines of a symmetric top molecule are usually very weak in intensity,[7] however, such a close matching in frequency may suppress the laser oscillation of the particular line involved.

The spectrum of ammonia in this region was studied extensively by Garing, Nielsen, and Rao under high resolution.[8] In the spectrum of ammonia, a number of weak bands are found in the P-branch region. However, the 2sQ(4,2) line[9] which Garing *et al.* reported at 944.14 cm^{-1} is most likely to coincide with the P(20) line at 944.18 cm^{-1}.

Although the present study is rather qualitative, it opens some interesting possibilities in the study and the application of the CO_2 laser system. Mixtures of foreign gases may be used, for example, and we may be able to control the oscillation frequencies of a CO_2 laser by changing the ratios of the gases as well as their pressures.

The authors wish to express their deep gratidude to Professor Takehiko Shimanouchi and Professor Mikio Katayama for their encouragement and helpful discussions during the course of this study.

7) We see in Fig. 3 two successive Q branches, $^PQ_1$ at 949.65 cm^{-1} and $^PQ_2$ at 942.25 cm^{-1}. Jones, Popplewell and Thompson reported six weaker bands between these two Q-branches, which they assigned to the $^PP_1(10)$. (see Footnote 5). They are too weak to be seen in Fig. 3.

8) J. S. Garing, H. H. Nielsen and K. N. Rao, *J. Mol. Spectry.*, **3**, 496 (1959).

9) We have used the notation in Ref. 8. The transition is related to the hot band $\nu_2^s \rightarrow 2\nu_2^a$ with $J=4\rightarrow4$ and $K=2\rightarrow2$.

BULLETIN OF THE CHEMICAL SOCIETY OF JAPAN VOL. 42 3399—3409 (1969)

An MO-theoretical Interpretation of the Nature of Chemical Reactions. II. The Governing Principles

Kenichi FUKUI and Hiroshi FUJIMOTO

Department of Hydrocarbon Chemistry, Kyoto University, Kyoto

(Received May 19, 1969)

The importance of the overlapping between the highest occupied (HO) molecular orbital (MO) of an electron donor and the lowest unoccupied (LU) MO of an electron acceptor in determining the favorable position and spatial direction of a chemical reaction is emphasized by setting up the following auxiliary principles: the principle of a positional parallelism between the charge-transfer and the bond-interchange, the principle of a narrowing of the inter-frontier energy-level separation, and the principle of a growing frontier density along the reaction path. These sub-principles work in a cooperative manner to enable us to arrive at this general governing principle: most of the chemical interactions are liable to occur at the position and in the direction where the overlapping of the HO and the LU of the respective reactants is at its maximum; in an electron-donating reactant, HO predominates in the overlapping interaction with the MO's of the other reactant, whereas LU does so in an electron-accepting reactant; in the reactants which possess singly-occupied (SO) MO's, these play the part of HO or of LU, or of both. These particular MO's, HO, LU, and SO are "generalized frontier orbitals" in chemical reactions. This principle is applied to uni-centric reactions to give the orientation rule; if it is applied to multi-centric reactions, the stereoselection rule is obtained.

Our previous paper[1] has treated, on the assumption of no nuclear configuration change, the interac tion energy between two reactant systems; this energy is partitioned into the Coulomb interaction, exchange interaction, delocalization, and polarization terms. It has been shown that the Coulomb interaction and the delocalization terms are important. The former comes from the net atomic charges and dominates the long-range interaction, while the delocalization term is ascribed to the charge-transfer interaction and is dominant in the usual donor-acceptor interaction energy. The quantity D, which represents the delocalization term, plays a dominant role in determining the energy of charge-transfer interaction, serving as a measure of the reactivity.

The expression of D is analogous to the chemical reactivity indices, superdelocalizability[2] and delocalizability,[3] which were originally defined by the Hückel MO formulation. These indices were derived as being closely related to the frontier electron density. The interrelation of theseq uantities is worth discussing.

In the present paper, we will attempt to investigate the essential features of the charge-transfer interaction in connection with the change in nuclear configuration along the reaction path. It may be permitted to discuss such a problem in the framework of the Born-Oppenheimer approximation. The auxiliary principles which characterize the mode of change will be sought in order to derive the fundamental orientation rule and, at the same time, to disclose the relation between the orientation rule and the reactivity indices.

The Delocalization Term in Degenerate Cases

The delocalization term comes from the mixing of the charge-transfer states into the initial state in an adiabatic interaction of two ground-state reactant molecules. The delocalization term, D, is expressed[1] as:

$$D = \sum_{i}^{\text{occ}} \sum_{l}^{\text{uno}} \frac{|H_{0,i\to l} - S_{0,i\to l} H_{0,0}|^2}{H_{i\to l,i\to l} - H_{0,0}} + \sum_{k}^{\text{occ}} \sum_{j}^{\text{uno}} \frac{|H_{0,k\to j} - S_{0,k\to j} H_{0,0}|^2}{H_{k\to j,k\to j} - H_{0,0}} \qquad (1)$$

in which the suffix 0 implies the initial configuration and in which $i\to l$ signifies the monotransferred configuration in which an electron in the ith occupied MO of the reactant A is transferred to the lth unoccupied MO of the reactant B. Similarly, k and j represent an occupied MO of B and an unoccupied MO of A respectively. The corresponding wave-functions are designated as Ψ_0, $\Psi_{i\to l}$ and $\Psi_{k\to j}$ and:

1) K. Fukui and H. Fujimoto, This Bulletin, **41**, 1989 (1968).

2) K. Fukui, T. Yonezawa and C. Nagata, *ibid.*, **27**, 423 (1954).

3) K. Fukui, H. Kato and T. Yonezawa, *ibid.*, **34**, 1111 (1961).

$$H_{p,q} = \int \Psi_p^* H \Psi_q \mathrm{d}\tau \tag{2}$$

$$S_{p,q} = \int \Psi_p^* \Psi_q \mathrm{d}\tau \tag{3}$$

It is assumed, as has been done in our previous paper,[1] that the wave-function for a certain electron configuration, Ψ_p, of the total system composed of interacting reactants, A and B, is represented by an antisymmetrized product of the MO's of the two reactants, constructed so as to correspond to the electron configuration, in which each MO is made SCF (self-consistent-field) of the Roothaan type with respect to each *isolated* ground-state reactant molecule, taken as constructing an orthonormal set. The symbols $\sum^{\mathrm{occ}}$ and $\sum^{\mathrm{uno}}$ imply the summation over occupied and unoccupied MO's. The Hamiltonian operator, H is that of the combined system consisting of mutually-interacting A and B. For a more detailed explanation, see Ref. 1.

Equation (1) is obtained by the usual configuration interaction procedure as a second-order perturbation term, on the assumption that the interaction is still not very strong.[1] If one of the monotransferred configurations happens to have the same energy as the initial configuration, first-order perturbation term will appear. Such a case can arise in reference to the configuration in which one electron is shifted from the highest occupied (HO) molecular orbital (MO) of the donor molecule to the lowest unoccupied (LU) MO of the acceptor molecule in the case of donor-acceptor interaction. In that case the quantity D will be dominated by the first-order term:

$$D \sim |H_{0,\mathrm{HO}\to\mathrm{LU}} - S_{0,\mathrm{HO}\to\mathrm{LU}} H_{0,0}| \tag{4}$$

This equation is obtained from Eq. (7′) of Ref. 1.

Even in a not exactly degenerate case, the monotransferred term corresponding to the one-electron transfer from the HO of the donor to the LU of the acceptor can make an overwhelming contribution to the delocalization term when the denominator of this term in Eq. (2) is sufficiently small in comparison with the other monotransferred terms.

$$D \sim \frac{|H_{0,\mathrm{HO}\to\mathrm{LU}} - S_{0,\mathrm{HO}\to\mathrm{LU}} H_{0,0}|^2}{H_{\mathrm{HO}\to\mathrm{LU},\mathrm{HO}\to\mathrm{LU}} - H_{0,0}} \tag{5}$$

As Mulliken has already pointed out, $H_{0,\mathrm{HO}\to\mathrm{LU}}$ is approximately proportional to $S_{0,\mathrm{HO}\to\mathrm{LU}}$, so that the magnitude of D and, accordingly, the interaction (stabilization) energy can be measured in terms of the extent of orbital overlapping between HO and LU, since:

$$S_{0,\mathrm{HO}\to\mathrm{LU}} \cong \sqrt{2}\, s_{\mathrm{HO,LU}} \tag{6}$$

where:

$$s_{\mathrm{HO,LU}} = \int a_{\mathrm{HO}}(1) b_{\mathrm{LU}}(1) \mathrm{d}v(1) \tag{7}$$

and where a_{HO} and b_{LU} are the HO MO of A and the LU MO of B respectively, both being taken as having a real spatial part.

In this way, Eq. (5) leads to the "overlap and orientation" principle of Mulliken.[4] Equation (4) will lead to the same conclusion with regard to the orientation principle. The favorable orientation in such cases can be determined by the rule of the maximum overlapping of HO and LU. Namely, the interaction takes place at the position and in the direction in which the largest overlapping of these particular MO's is attained.

In addition, there are special circumstances which make these particular orbitals, HO and LU, discriminatively important. The importance of the interaction term between HO and LU prevails over a wider range of combination of two reactants; furthermore, it is enhanced in actually-occurring reactions if the nuclear-configuration change along the reaction path is taken into consideration. This point will be discussed on the basis of auxiliary principles later. In any event, the usefulness of the equations of the type of Eq. (4) or (5) is in fact, far more than could be expected simply from the conditions for the fitness of these equations.

The Principle of a Positional Parallelism between the Charge-transfer and the Bond-interchange

It has already been shown[5-7] that the nodal property of HO and LU MO's plays an essential role in determining the steric course of electrocyclic reactions. The same property is important in promoting the alteration of the molecular shape in the case of orbital interaction.

Usually, an atom is, as a whole, bonding with neighboring atoms in occupied MO's and antibonding in unoccupied MO's. This circumstance can be understood by a very simple example which employs the linear-combination-of-atomic-orbitals (LC AO) MO scheme. If we use the Hückel MO theory (overlap neglected) in the frame of π-electron approximation for a planar conjugated molecule, the following relation holds with respect to the rth π AO:

$$(\alpha_r - \varepsilon_i)(C_r^{(i)})^2 + \sum_s^{\mathrm{nei}} C_r^{(i)} C_s^{(i)} \beta_{rs} = 0 \tag{8}$$

where α_r is the Coulomb integral of the rth AO; β_{rs}, the resonance integral between the rth and the sth AO's; ε_i, the energy of the ith MO, and $C_r^{(i)}$, the coefficient of the rth AO in the ith MO. The notation $\sum^{\mathrm{nei}}$ implies summation over all the neighboring AO's of the rth AO. In the case of con-

4) R. S. Mulliken, *Rec. Trav. Chim.*, **75**, 845 (1956).
5) K. Fukui, "Molecular Orbitals in Chemistry, Physics, and Biology," ed. by P.-O. Löwdin and B. Pullman, Academic Press, New York (1964), p. 513.
6) K. Fukui, This Bulletin, **39**, 498 (1966).
7) K. Fukui and H. Fujimoto, *ibid.*, **39**, 2116 (1966).

jugated hydrocarbons, all the α_r's and all the β_{rs}'s can be put equal to constant values, α and β respectively. Then, it follows from Eq. (8) that:

$$\sum_{s}^{\text{nei}} C_r^{(i)} C_s^{(i)} = \frac{\alpha - \varepsilon_i}{(-\beta)} (C_r^{(i)})^2 \qquad (9)$$

As usual, the energies of the occupied orbitals are lower than α, while those of the unoccupied orbitals are higher than α. Therefore, the following relations hold for any r: $\sum_{s}^{\text{nei}} C_s^{(i)} C_t^{(i)}$ is positive and proportional to $(C_r^{(i)})^2$ for occupied MO's and is negative and proportional to $(C_r^{(i)})^2$ for unoccupied MO's.

In this way, it is established that the position of the largest HO or LU density is, at the same time, that position which is most liable to weaken the bonds with neighboring atoms in case of electron-releasing or accepting interaction respectively.[8] Namely, the charge-transfer weakens the bonds most greatly at the position of the largest frontier electron density.[5,9]

Some examples of the nodal property of the π HO's and LU's of several conjugated hydrocarbons are shown in Fig. 1, in which the shaded and unshaded areas correspond to the positive and negative regions of the MO coefficients. It can be qualitatively understood from the figure that there is a parallelism between the partial population and the partial sum of the bond-order with neighbors. Even in heteroaromatic systems similar relationships hold. We can see the circumstances in Fig. 2.

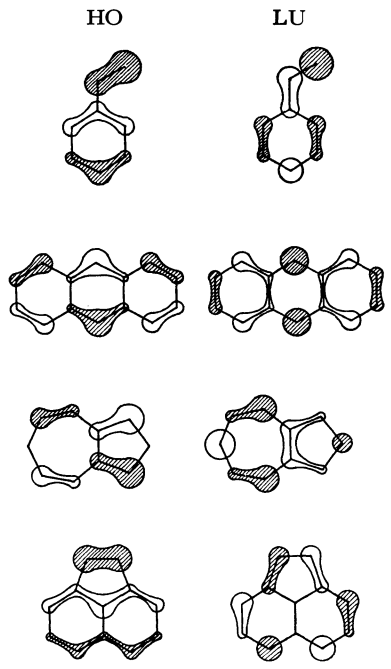

Fig. 1. The nodal property of π HO and LU of some conjugated hydrocarbons.

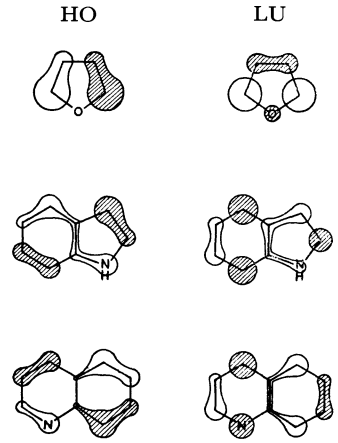

Fig. 2. The nodal property of π HO and LU of some heteroconjugated systems.

Such a character of MO's is to a certain extent perceived in more elaborate calculations, independent of the order of approximation adopted. An example is given in Table 1 using the Pariser-Parr-Pople approximation.[10] The suffix f signifies HO or LU. A distinct parallelism is recognized among the partial population and the partial sum of the bond-order with the neighbors.

Similar circumstances also exist in the extended Hückel treatment[11] of three-dimensional molecules. The orientation in the E2 reaction of halogenated hydrocarbons has previously been discussed.[12,13] If we concentrate our attention on one of the hydrogen 1s AO's, say r, the following equation is

8) When the HO energy happens to be higher than α, the electron-releasing will cause bond-strengthening. The result is the same with the electron-accepting in the LU MO when its energy is lower than α.

9) The extent of this bond-loosening will, therefore, be a measure of the ease of intramolecular electron localization at the reaction center in the case of interaction with another molecule. This may be one of the reasons why the localization energy gives a parallel prediction with the frontier electron density for the chemical reactivity of a majority of conjugated molecules (*cf.* A. Streitwieser, Jr., "Molecular Orbital Theory for Organic Chemists," John Wiley & Sons, New York (1961), p. 305).

10) See, for instance, R. Pariser and R. G. Parr, *J. Chem. Phys.*, **21**, 466, 767 (1953).

11) R. Hoffmann, *ibid.*, **39**, 1397 (1963), and subsequent papers.

12) K. Fukui and H. Fujimoto, *Tetrahedron Letters*, **1965**, 4303.

13) K. Fukui, H. Hao and H. Fujimoto, This Bulletin, **42**, 348 (1969).

TABLE 1. THE POSITIONAL PARALLELISM BETWEEN $(C_r^{(f)})^2$ AND $\sum_s^{\text{nei}} C_r^{(f)}C_s^{(f)}$ IN PARISER-PARR-POPLE CALCULATION

Compound	r	$(C_r^{(f)})^2$	$\sum_s^{\text{nei}} C_r^{(\text{HO})}C_s^{(\text{HO})}$	$\sum_s^{\text{nei}} C_r^{(\text{LU})}C_s^{(\text{LU})}$
Anthracene	1	0.09512	0.03680	−0.03680
	2	0.04770	0.01966	−0.01966
	9	0.19472	0.08745	−0.08745
Phenanthrene	1	0.10550	0.07154	−0.07154
	2	0.00100	0.00034	−0.00034
	3	0.09868	0.06598	−0.06598
	4	0.05843	0.03197	−0.03197
	9	0.16775	0.09051	−0.09051
Chrysene	1	0.07978	0.04403	−0.04403
	2	0.01427	0.00738	−0.00738
	3	0.04871	0.02809	−0.02809
	4	0.06089	0.02985	−0.02985
	5	0.05696	0.02168	−0.02168
	6	0.14446	0.07687	−0.07687

Numberings are as follows:

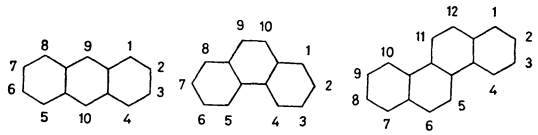

Anthracene Phenanthrene Chrysene

All C–C distances and all C–C–C angles were assumed to be 1.4Å and 120°, respectively, for the sake of simplicity of computations.

obtained in place of Eq. (8):

$$(h_{rr}-\varepsilon_i)(C_r^{(i)})^2 + \sum_{s(\neq r)} (h_{rs}-\varepsilon_i s_{rs})C_r^{(i)}C_s^{(i)} = 0 \quad (10)$$

where:

$$h_{rs} = \frac{K}{2}(h_{rr}+h_{ss})s_{rs} \quad (11)$$

where h_{rr}, h_{rs} and s_{rs} are the Coulomb, resonance, and overlap integrals respectively, and where K is the Wolfsberg-Helmholtz constant.[11] The other symbols have the same meaning as in the Hückel scheme. Although the value of the Coulomb integral varies, of course, from one AO to another, it may be possible to employ tentatively, in place of the individual h_{ss}, a sort of mean value, h, which makes the second term of the right side of Eq. (10) equal to:

$$\sum_{s(\neq r)} \left\{\frac{K}{2}(h_{rr}+h)-\varepsilon_i\right\} C_r^{(i)}C_s^{(i)}s_{rs} \quad (12)$$

Hence, it follows that:

$$\sum_{s(\neq r)} C_r^{(i)}C_s^{(i)}s_{rs} = -\frac{h_{rr}-\varepsilon_i}{\frac{K}{2}(h_{rr}+h)-\varepsilon_i}(C_r^{(i)})^2 \quad (13)$$

Then, with respect to LU, the relations $h_{rr}-\varepsilon_{\text{LU}}<0$ and $(K/2)(h_{rr}+h)-\varepsilon_{\text{LU}}<0$ usually hold. The left side of Eq. (13) is equal to $(1/2)v_r^{(i)}$, which is the valence-active part[14] of the partial AO population of the rth AO in the ith MO defined by:

$$v_r^{(i)} = 2\sum_{(s\neq r)} C_r^{(i)}C_s^{(i)}s_{rs} \quad (14)$$

Therefore, $v_r^{(\text{LU})}$ must be negative and proportional to $(C_r^{(\text{LU})})^2$, indicating that the hydrogen atom having the largest frontier electron density is most liable to a loosening of the bond with the remaining part of the molecule.

This conclusion may be confirmed by actual numerical calculation in which the approximation using the mean h value is, of course, not applied. Examles are shown in Table 2. The table contains the frontier electron density $(C_r^{(\text{LU})})^2$ and the valence-active part of the partial population of the frontier orbital, $v_r^{(\text{LU})}$. Exemplifications by the various calculations mentioned above indicate the existence of a parallelism among actually reactive sites in a molecule; the position of the largest frontier orbital extension is at the same time the position where the bonds with neighboring atoms are, as a whole, most liable to be loosened. Since

14) K. Ruedenberg, *Rev. Mod. Phys.*, **34**, 326 (1962).

TABLE 2. THE RELATION BETWEEN $v_r^{(LU)}$ AND $(C_r^{(LU)})^2$ OF HYDROGENS IN SEVERAL HALOGENATED PARAFFINS

Chlorinated paraffin	r	$(C_r^{(LU)})^2$	$v_r^{(LU)}$
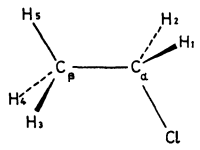	1	0.01791	−0.01192
	3	0.00124	−0.00062
	5	0.05412	−0.03689
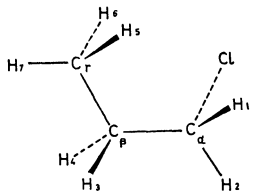	1	0.01658	−0.01163
	2	0.03135	−0.02134
	3	0.07458	−0.05128
	4	0.00067	−0.00018
	5	0.00096	−0.00071
	6	0.01708	−0.01361
	7	0.00063	−0.00027
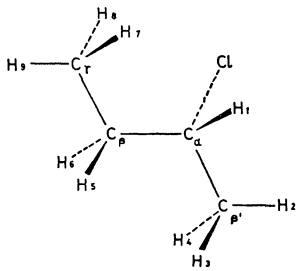	1	0.00978	−0.00661
	2	0.00029	−0.00006
	3	0.06638	−0.04564
	4	0.00044	−0.00011
	5	0.07888	−0.05295
	6	0.00090	−0.00041
	7	0.00158	−0.00131
	8	0.02119	−0.01700
	9	0.00000	−0.00000

the frontier orbital extension is a measure of the ease of charge-transfer interaction, this conclusion represents a parallel relationship between the position of charge-transfer and the position of bond-interchange in a molecule in chemical reactions; it will later be shown to act as one of the two auxiliary principles which lead to the general orientation principle.

The Principle of a Narrowing of the Inter-frontier Level Separation

As has been mentioned above, the charge-transfer interaction takes place at the position of the largest frontier electron density, the position which is simultaneously most susceptible to a weakening of the bonds with the neighboring atoms. This bond-loosening causes the nuclear configuration to change in a definite direction, which should be controlled by the nodal property of the frontier orbitals.

This direction of nuclear-configuration change may be characterized by the mode of change in the energy-level separation between the HO of the donor and the LU of the acceptor. Namely, the HO MO of the donor becomes, in general, higher, while LU of the acceptor becomes lower, in the event of charge-transfer, causing a narrowing of the inter-frontier energy level separation. Sush a conclusion can very easily be understood, since a bonding MO is made unstable by electron-releasing and since an antibonding MO is made unstable by electron-accepting, in both cases through bond-loosening.

Let us consider this problem by quoting several examples. In the first place, let us take the Diels-Alder-type addition of ethylene and butadiene as an instance. The nodal properties of the HO and LU of ethylene and butadiene are shown in Fig. 3, together with the mode of charge-transfer interaction. The HO MO of butadiene is bonding in the region of 1,2- and 3,4-π-bonds and antidonding in the 2,3-region, while the LU of butadiene has the opposite nodal property. The HO of ethylene is bonding, while LU is antibonding. This implies that both

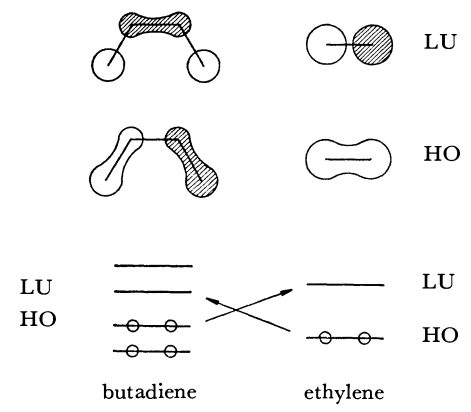

Fig. 3. The nodal property of HO and LU in ethylene and butadiene.

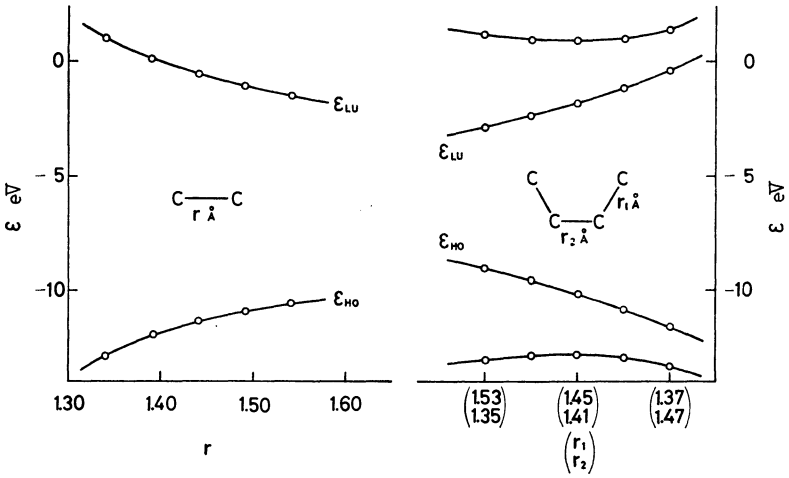

ethylene butadiene

Fig. 4. The change in energy of molecular orbitals in ethylene and butadiene along the reaction path.

the charge-transfer from the HO of ethylene to the LU of butadiene and that from the HO of butadiene to the LU of ethylene will decrease the π bond-order of ethylene and cause a double-bond shift in butadiene.

The results of calculations by the Pariser-Parr-Pople scheme[10] for several altered nuclear coordinates are shown in Fig. 4. The transient nuclear configurations along the reaction path could reasonably be assumed by considering the direction of charge-transfer and the nodal property of the HO and LU. We can see that the changes in the HO and LU can be clearly distinguished from those of the other orbitals. The separation of these MO levels is considerably contracted as the reaction proceeds. Such a property is common in dienes and dienophiles.

The mode of change in the MO energies of this sort is more conspicuous in the sigma electron systems. As a typical example, let us present the results of an extended Hückel calculation on the SN-2 reaction of methyl chloride by the chloride anion. The reaction coordinates were extracted from the calculation of Kato *et al.*[15] The solid line in Fig. 5 indicates the change in the energy of the LU of methyl chloride, while the broken line shows that of the system composed of methyl chloride and chloride anion. The other unoccupied MO's are located much higher than LU,[16] and the changes in these levels were found to be small in comparison with that in LU.

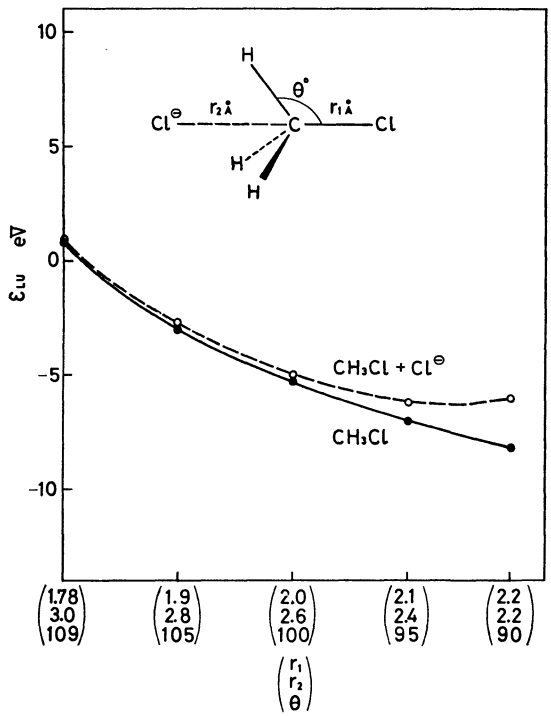

Fig. 5. The change in the energy of LU MO of methyl chloride with and without another approaching chloride anion.

It may be of interest to investigate the content of the activation energy. The stretching of the C–Cl bond in methyl chloride will require enough energy to form an important fraction of the activation energy of the reaction. The LU MO is highly localized at the C–Cl bond and exhibits an antibonding char-

15) H. Kato, K. Morokuma, T. Yonezawa and K. Fukui, This Bulletin, **38**, 1749 (1965).

16) The unoccupied MO's are expressed in terms of a set of limited-basis AO's chosen so as to be suitable in representing the occupied MO's. This is an unsatisfactory point. However, the essential features will never be changed by the employment of any extended-basis set of AO's.

acter. The charge-transfer from the attacking base to LU will, therefore, cause the C–Cl bond stretching. However, this will produce stabilization on account of the lowering of the MO level, as is shown in Fig. 5. In this way, a considerable part of the activation energy is reduced. It can be understood that the charge-transfer and the nuclear configuration change cooperate in driving the chemical reactions.

The circumstances are similar also in nucleophilic elimination reactions. For instance, the LU of ethyl chloride is highly localized at the carbon-chlorine bond, which shows an antibonding nature. Accordingly, the charge-transfer to the LU from the attacking base through *trans*-β-hydrogen may cause a weakening of the C–Cl bond as well as of the β-carbon-hydrogen bond, resulting in a lowering of the LU MO energy. Such a lowering of the MO energy may be of great importance in facilitating the bimolecular elimination of halogenated paraffins by a nucleophile. The results of the numerical calculation have been given in previous papers.[12,13]

Next, let us consider aromatic substitutions. In these reactions the bonds between the reaction center and the neighboring atoms may be lengthened to some extent by the decrease in the π bond-orders of this region. This will cause an elevation of the HO level and a lowering of the LU level. In addition, the leaving hydrogen atom at the reaction center will leave the molecular plane as the reaction proceeds. It may be of interest to examine the energy change in the frontier orbitals in this case. The results of the numerical calculation are shown in Fig. 6.

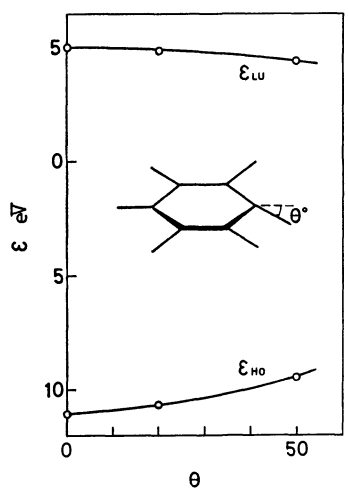

Fig. 6. The change in the energy of HO and LU in benzene due to the C–H bending.

The changes in the energies of HO and LU due to such a change in the bond angle are, in general, small in comparison with those due to the bond-stretching. However, the change is significant in the sense that the effect of valence angles can never be left out of account in discussing the problem.

The ascending HO energy and the descending LU energy of aromatic molecules couple with the descending LU of electrophilic reagents and with the ascending HO of nucleophilic reagents respectively to give rise to a narrowing of the inter-frontier level separation. In the case of liquid-phase ionic reactions, it must frequently be remarked that one should take into account the process of desolvation and solvation in the level change of the reagent orbitals. In homolytic reactions, the ascending HO and descending LU levels both approach the singly-occupied (SO) MO level of reagent radicals, bringing about a simultaneous charge-transfer to and a back-transfer from the SO MO.

In order to confirm these circumstances, the frontier MO's of attacking electrophiles are examined. The hydronium ion is taken as a simple example of solvated electrophiles. The extended Hückel calculation indicates that the LU of hydronium ion lowers as the distance between the proton, which is the bare electrophilic reagent, and the water molecule, that is the solvent, grows with the proceeding of the reaction. The results are shown in Fig. 7.

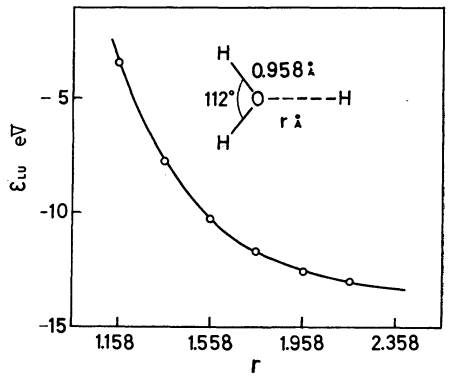

Fig. 7. The change in the energy of LU in hydronium ion due to the O–H stretching.

Lastly, the heterolytic addition to an olefinic double bond will be cited. The reagent is here typified by a chlorine molecule in order to simplify the calculation. The first stage of this reaction is assumed to be the formation of a bridged cation,[17] which may cause the stretching of the carbon-carbon bond.

An extended Hückel calculation is made to obtain a relation between the position of chlorine and the MO energy. The chlorine is shifted in the direction parallel to the carbon-carbon bond. As can be seen in Fig. 8, the total energy, E, increases as the chlorine atom separates from the center plane

17) An energy minimum arises in the event of approaching the C–C bond on the bisecting line. The stability of triangular interaction is discussed in Ref. 6.

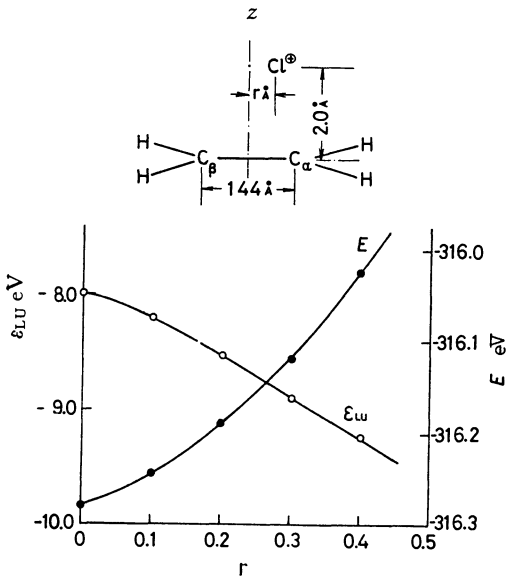

Fig. 8. The change in the energy of LU and in the total energy of ethylene-chorine cation system.

to approach the α-carbon; also, the LU level becomes lower in the event of change in this direction. The progress of the charge-transfer causes the narrowing of the inter-frontier separation, so the contribution of LU of the cation becomes enhanced as the interaction goes on.

The results of numerical calculations with respect to the several examples of chemical reactions cited above suggest the general relationship between the inter-frontier energy level separation and the nuclear configuration change along the reaction path. This implies that the importance of the frontier orbitals is more than would be expected from the case where the separation narrowing is left out of account.

The Principle of a Growing Frontier Electron Density along the Reaction Path

In order to make the third auxiliary principle concrete, it is recommended that we discuss the simplest case first. The well-discussed problem of aromatic substitution fits this purpose. As the reaction proceeds, the sum of the mobile bond-orders of the bonds between the reaction center and the neighboring atoms will decrease according to Eq. (9), causing a loosening of these bonds. The effect of this π-bond weakening may be represented, in the frame of the Hückel MO method, by the decrease in the absolute value of the resonance integrals corresponding to these bonds.

It is important to investigate the change in the frontier electron density at the actual reaction site according to the increase in the resonance integrals (that is, the decrease in the absolute value) with the neighboring atoms. In actual reactions, this change evidently never amounts to as large values as $(-\beta)$, where β is the original value of the resonance integral. However, as an extremely assumptive case, this increment may be taken as $(-\beta)$, so that the general tendency of the effect of such changes might more dinstinctly be realized. In that case the π AO at the reaction center finally becomes isolated (Stage(IV)). Stage (III), immediately before Stage (IV), indicates that a small π conjugation still remains between the reaction center and the neighboring atoms.

The frontier electron densities, $(C_r^{(HO)})^2$ and $(C_r^{(LU)})^2$, usually increase along the (I)→(II) path. This is valid with respect to the positions in alternant hydrocarbons, and also in a majority of positions of nonalternant hydrocarbons.

In order to understand these circumstances qualitatively, although not in a mathematically strict sense, it is convenient to consider Stage (III). In this stage it is very easy to prove that:

$$\lim_{\Delta\beta\to 0}(C_r^{(HO)})^2 \quad \text{and} \quad (C_r^{(LU)})^2 = \frac{1}{2} \qquad (15)$$

provided that the system obtained by deleting the atom r from the original hydrocarbon has a nonbonding level, $\varepsilon=\alpha$.[18] Since the original values of $(C_r^{(HO)})^2$ and $(C_r^{(LU)})^2$ are usually far less than 0.5, this result suggests that the frontier electron density increases along the path (I)—(III). The relation of Eq. (15) holds in alternant hydrocarbons and also in several, actually reactive positions of some nonalternant hydrocarbons, like the $(C_1^{(HO)})^2$ of fulvene, the $(C_1^{(HO)})^2$ of acenaphthylene, and the $(C_7^{(HO)})^2$ of fluoranthene.[19]

When the remaining system has no nonbonding MO, the following two sub-cases are possible. Let

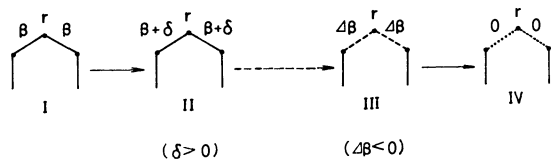

18) If the remaining system possesses n nonbonding MO's, $(C_r^{(HO)})^2$ and $(C_r^{(LU)})^2$ become $1/(n+1)$.

19) The numbering of these nonalternants conforms to: K. Fukui, T. Yonezawa and C. Nagata, This Bulletin, **34**, 37 (1961).

the number of occupied MO's of the original system be n, and let the number of occupied MO's of the remaining system obtained by deleting the atom r from the original system be m. The first sub-case is the one where $m=n$. In this case it follows that:

$$\lim_{\Delta\beta\to 0}(C_r^{(\mathrm{LU})})^2 = 1 \qquad (16)$$

Such a relation holds in the position 6 of fulvene, the position 5 of acenaphthylene, the position 6 of azulene, and the position 3 of fluoranthene. The second sub-case is specified by $m=n-1$, so that:

$$\lim_{\Delta\beta\to 0}(C_r^{(\mathrm{HO})})^2 = 1 \qquad (17)$$

which is actually satisfied in the position 1 of azulene. All of these cases indicate that the rule of growing frontier electron density might hold in actually reactive positions.

One of the few exceptions is $(C_3^{(\mathrm{HO})})^2$ of fluoranthene. In this case we have $m=n$, so that $\lim_{\Delta\beta\to 0}(C_3^{(\mathrm{HO})})^2=0$. However, it should be noted that in this case the HO MO energy of the remaining system is very close to the nonbonding orbital energy ($\varepsilon=\alpha+0.1317\beta$) whereas the energy of the isolated AO of the position 3 will easily become lower than $\varepsilon=\alpha$ under the influence of an approaching electrophile, so that the isolated AO energy might not become higher than the HO MO of the remaining system. In this way, it is possible even in this case that:

$$\lim_{\Delta\beta\to 0}(C_3^{(\mathrm{HO})})^2 = 0.5 \text{ or } 1 \qquad (18)$$

Such a Coulombic effect of the attacking reagent should be considered in the other cases which have already been mentioned. In all of these cases, however, the circumstances are more favorable, in view of this effect, for the validity of the rule of growing frontier electron density along the reaction path.

The heterolytic addition of chlorine to a C=C bond (discussed in preceding section) is also an example. Figure 9 shows that the partial valence-inactive population of the $2p_z$ AO of β-carbon in the LU increases with the progress of the reaction.

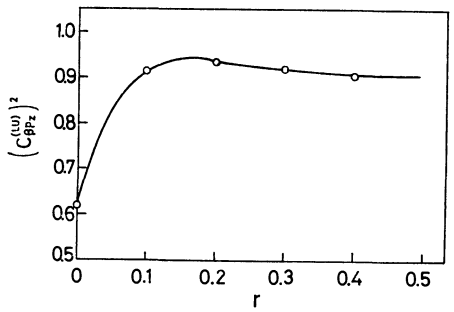

Fig. 9. The change in the partial population of p_z orbital at β-carbon of ethylene-chlorine cation system.

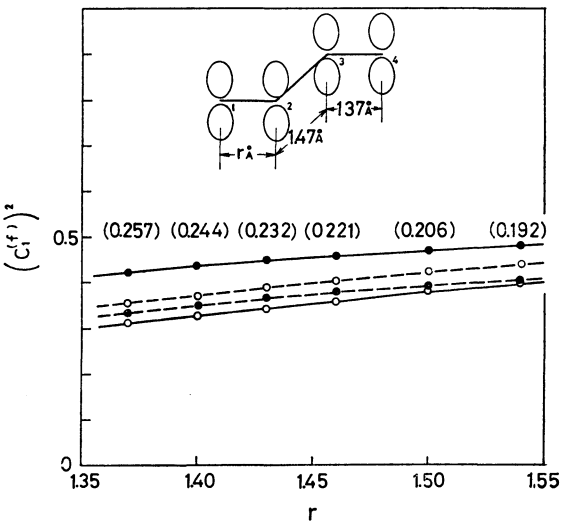

Fig. 10. The change in frontier electron density in the π electronic part of *trans*-butadiene along the departing of the end carbon atom.
—●— LU including overlap
—○— HO including overlap
--●-- LU neglecting overlap
--○-- HO neglecting overlap
(The values in parenthses indicate the overlap integral between two $p\pi$ atomic orbitals at the carbon atoms 1 and 2.)

This rule is not essentially violated by the adoption of more elaborate methods of calculation. With the change in the nuclear configuration, the overlap integrals between the AO's belonging to the departing atom and the AO's belonging to the remainder of the molecule vary. In order to discuss the change in the magnitude of the frontier electron density as a measure of the numerator of Eq. (1), the effect of the change in the overlap integrals upon the frontier electron density through the normalization condition can never be neglected. Figure 10 gives the change in the $(C_r^{(f)})^2$ in the π electronic part of butadiene due to the stretching of the C=C bond. We can see that the essential conclusion mentioned above also holds in the extended Hückel calculation, explicitly including overlap integrals.

The Co-operation of Sub-principles and the General Orientation and Stereoselection Rule

It is obvious that the three sub-principles work co-operatively in promoting the chemical reaction. The charge-transfer interaction takes place predominantly at the position and in the direction in which the overlapping of the HO and LU of the two reacting species is largest, as is to be expected from Eqs. (5) and (6). This interaction brings about a local bond-weakening, which is mainly controlled by the nodal property of the frontier orbitals. The ex-

tent of bond-weakening positionally parallels the frontier-orbital extension according to the first sub-principle. The bond-loosening leads to the nuclear configuration change in a definite direction, which causes the narrowing of the inter-frontier energy level separation according to the second sub-principle and, at the same time, the increase in the frontier electron density at the reaction center according to the third sub-principle. These make the denominator on the right side of Eq. (5) smaller and the numerator larger, so the contribution of the frontier orbital interaction term to the delocalization part (Eq. (1)) of the interaction energy becomes larger. Hence, the charge-transfer interaction increases, resulting again in a bond-interchange near the reaction center, a molecular shape deformation, a narrowing of the inter-frontier separation, and an increase in the frontier electron density, in turn. The importance of the term of Eq. (5) thus becomes greater and greater, the form of the delocalization term approaching that of Eq. (4).

It should be remarked in this connection that the MO's which can participate in such a type of cooperation are obviously restricted to the HO and LU. The energies of the other MO's undergo only the minimum change which is absolutely needed for the occurrence of the reaction and is assumed to be almost constant with respect to every possible position of the reaction. This is because a stable molecule originally takes the nuclear configuration which is energetically most favorable, and, in the event of reaction, any change in the nuclear configuration will be accompanied by an unstabilization which resembles the promotion in atoms in the case of molecule formation. Therefore, the change in the nuclear configuration will take place in such a direction that the unstabilization will be most effectively reduced, while a direction of change in which no energetical advantage can be expected will be avoided. As has already been mentioned, the charge-transfer between the HO and LU causes an alteration in the molecualr shape at the site of the greatest HO or LU MO density. In this way, the change in molecular shape is automatically limited to the proximity of the particular position in the reacting species. This self-controlling action seems to underlie the empirical rule which has been known as "the principle of least motion" or "the principle of least molecular deformation."[20]

It is evident from the above discussion that the most effective means to promote a chemical reaction smoothly by reducing the unstabilization attributable to the nuclear configuration change due to the interaction is to give rise to a change by which the charge-transfer from the HO of one species to the LU of the other is effectuated. This charge-transfe rmay be uni-directional or mutual according to the magnitude of the difference between the electron-donating power of one reactant and the electron-accepting power of the other. Other directions of nuclear configuration change are all rejected as bringing about little gain in stabilization energy.

In this way, the reaction pathway becomes dominantly controlled by the frontier-orbital interaction. The position of the reaction will be determined, through Eq. (6), by the rule of the maximum overlapping of the HO and LU (sometimes the SO in place of the HO or LU) of the two reacting species. The general orientation principle is, therefore, as follows: "*A majority of chemical reactions are liable to take place at the position and in the direction where the overlapping of the HO and LU of the respective reactants is at its maximum; in an electron-donating species, HO predominates in the overlapping interaction, while the LU does so in an electron-accepting reactant; in the reacting species which possess SO MO's, these play the part of the HO or of the LU, or of both.*"

In some intramolecular reactions, like the cyclization of a conjugated olefinic chain, the dominantly controlling factor seems to be the first-order inteaction term,[6,21] in which the HO-LU interaction is concealed; however, the same reaction can be discussed by considering the HO-LU interaction between two parts of a molecule.[22] The HO-LU interaction has also been considered between the sigma- and pi-parts of conjugated molecules in order to derive a stereoselection rule.[7]

In this view, the particular MO's which control the reaction pathway in chemical reactions in general, *i.e.*, HO, LU, and SO, are referred to as "generalized frontier orbitals."

It seems in this way that the principle presented above is a general one which will qualitatively govern almost all sorts of chemical interactions, including intermolecular and intramolecular as well as unicentric and multicentric. The principle can be applied to a unicentric reaction to derive an orientation rule; and if it is employed to discuss multicentric reactions, the result is the stereoselection rule, which has already been discussed.[7,21,22]

The reactivity indices, the frontier electron density, the delocalizability, and the superdelocalizability, are those for unicentric reactions and give predictions consistent with the general orientation principle. In this connection, it is worthwhile to mention the relation between these chemical reactivity indices and the general orientation rule. These indices are derived from Eq. (1), in which the nuclear-configration change along

20) See, for example, J. Hine, *J. Org. Chem.*, **31**, 1236 (1966), and the references cited therein.

21) K. Fukui, *Tetrahedron Letters*, **1965**, 2009.

22) K. Fukui and H. Fujimoto, "Mechanism of Molecular Migrations," Vol. 2, ed. by B. S. Thyagarajan, Wiley-Interscience (1969).

the reaction path is left out. Namely the indices, like most other reactvity indices ever proposed, are calculated with regard to an isolated, undeformed molecule. If the molecular deformation along the reaction path is taken into consideration, the values of these indices will be changed. The change in the value of delocalizability and superdelocalizability will be controlled by the sub-principles discussed above, so the contribution of the terms corresponding to the frontier orbitals will become more dominant than in the original expression.

In the superdelocalizability thus modified, the frontier terms should be weighted more. The index of the type of Eq. (5), the one-term approximation of superdelocalizability,[23] and Brown's Z-value[24] are all this line. We prefer the frontier terms and recommend that the frontier electron density be used as a reactivity index.

The calculations have been carried out partly on the HITAC 5020E computer at the Computer Center of the University of Tokyo and partly on the FACOM 230·60 computer at the Computer Center of Kyoto University.

23) K. Fukui, T. Yonezawa and C. Nagata, *J. Chem. Phys.*, **27**, 1247 (1957).
24) R. D. Brown, *J. Chem. Soc.*, **1959**, 2232.

BULLETIN OF THE CHEMICAL SOCIETY OF JAPAN VOL. 42 3409—3414 (1969)

On the Emission of Excited Complexes Formed between Condensed Aromatic Hydrocarbons and Aliphatic Amines*[1]

Akira NAKAJIMA*[2]

Department of Chemistry, Faculty of Science, The University of Tokyo, Hongo, Bunkyo-ku, Tokyo

(Received May 21, 1969)

Anomalous emission observed at long wavelengths in the systems of condensed aromatic hydrocarbons and aliphatic tertiary amines has been studied. The anthracene-tri-*n*-butylamine system has been dealt with in detail. On the basis of the absorption spectrum, the temperature dependence of the long-wavelength emission and the relation between the quenching of the hydrocarbon fluorescence and the intensity of the long-wavelength emission, it has been concluded that this emission originates from the excited complex formed between an excited hydrocarbon and an amine. The interaction involved in excited-complex formation is of a charge-transfer type. This was confirmed by the correlation of the wavelengths of the excited-complex emission with the ionization potentials of amines and the electron affinities of aromatic hydrocarbons and by the large dipole moment of the excited complex.

In general, the behavior of a molecule in the electronically excited state differs considerably from that in the ground state. Its ionization potential is smaller and its electron affinity is larger in the excited state, so that the molecular interaction may be expected to bring about new interesting phenomena. Many aromatic hydrocarbons dissolved in such solvents as *N,N*-dialkyl aromatic amines have been demonstrated to fluoresce at much longer wavelengths than in inert solvents.[1-4] As the absorption spectra of the hydrocarbons in the amines do not suffer any essential change, it is evident that no specific interaction exists between a ground-state hydrocarbon and an amine. From this observation it has been concluded that the new fluorescence can be ascribed to the excited complex formed exclusively from an excited-state hydrocarbon and an amine. Based on the relation of the energies of the new fluorescence with the electron affinities of the hydrocarbons and the ionization potentials of the amines, it has also been confirmed

*1 Presented partly at the Symposium on Molecular Structures, Sapporo, Oct. (1967).

*2 Present address: Research Institute of Applied Electricity, Hokkaido University, Sapporo.

1) H. Leonhardt and A. Weller, *Z. physik. Chem., N. F.*, **29**, 277 (1961); *Ber. Bunsenges. physik. Chem.*, **67**, 791 (1963).

2) N. Mataga, K. Ezumi and K. Takahashi, *Z. physik. Chem., N. F.*, **44**, 250 (1965); N. Mataga, T. Okada and K. Ezumi, *Mol. Phys.*, **10**, 201 (1966); N. Mataga, K. Ezumi and T. Okada, *ibid.*, **10**, 203 (1966); N. Mataga and K. Ezumi, This Bulletin, **40**, 1355 (1967).

3) H. Knibbe, D. Rehm and A. Weller, *Z. physik. Chem., N. F.*, **56**, 95 (1967).

4) H. Beens, H. Knibbe and A. Weller, *J. Chem. Phys.*, **47**, 1183 (1967).

that the charge-transfer(CT) interaction between an excited hydrocarbon and an amine is responsible for the formation of an excited complex. The fact that the appearance of the new fluorescence is accompanied by the quenching of the hydrocarbon fluorescence seems to suggest that the fluorescence quenching should be intimately connected with the excited-complex formation.

Since similar excited complexes have been discovered in many other systems,[5-9] it can reasonably be proposed that the excited CT complex formed diffusionally as an intermediate species plays an important role in the mechanism of fluorescence quenching.

The present author has found that anomalous emission can be observed in the systems of the condensed aromatic hydrocarbons and some of the aliphatic amines in various solvents. The absorption spectra indicated such small interactions between the ground-state hydrocarbons and the amines that the emission should be considered to originate from some kind of molecular complex existing only in the excited state.

In the case of aromatic amines the interaction involved should be classified as a π-π interaction, whereas that for aliphatic amines may be regarded as an n-π interaction. No fluorescence study of this has yet been reported. Thus, it is worth while to undertake an investigation with a view to clarifying the character of the interaction and its correlation with fluorescence quenching.

The present paper reports the results of some experiments on the systems of the condensed aromatic hydrocarbons and the aliphatic amines. The system of anthracene and tri-*n*-butylamine was studied in some detail.

Experimental

All the amines used were dried over pellets of potassium hydroxide and/or distilled. Triethylamine, tri-*n*-butylamine and diethylamine were further distilled fractionally in an atmosphere of nitrogen under reduced pressure. Naphthalene and phenanthrene were recrystallized from ethanol, zone-refined and sublimed in a vacuum. Acenaphthene and triphenylene were recrystallized from ethanol. 1,2-Benzanthracene was recrystallized from benzene. 9,10-Diphenylanthracene was recrystallized from xylene and sublimed in a vacuum. Anthracene was purified by recrystallization from xylene, zone-refining and sublimation in a vacuum. Pyrene was recrystallized from xylene, chromatographed, zone-refined and sublimed in a vacuum. Perylene was chromatographed and recrystallized. *n*-Hexane used was a Super special grade reagent of Wako Junyaku Co. G. R. grade cyclohexane and acetone, also from Wako Junyaku Co., were used without further purification. Benzene, chloroform and dichloromethane used were Dotite Spectrosol reagents of Dojin Yakukagaku Co. Spectro-grade carbon tetrachloride from Tokyo Kasei Co. was used. Chlorobenzene was a G. R. grade reagent from Koso Kagaku Co. and was fractionally distilled after being dried with phosphorus pentoxide. Fluorobenzene of British Drug Houses Ltd. was used without purification. G. R. grade ethyl ether was a product of Showa Ether Co. and was fractionally distilled after being dried with sodium. G. R. grade di-*n*-butyl ether from Tokyo Kasei Co. was dried with sodium and distilled. Ethyl acetate, cyclohexanone and benzonitrile of Wako Junyaku Co., G. R. grade, were treated with phosphorus pentoxide and distilled twice. Dibutyl phthalate of Wako Junyaku Co. was distilled twice under reduced pressure. Anisole was distilled in a nitrogen atmosphere. Tetralin and decalin were distilled. 1,2-Dichloroethane and dioxane of Wako Junyaku Co., *p*-xylene, isopropylbenzene and *t*-butylbenzene of Tokyo Kasei Co., G. R. or E. P. grade, were used. Spectro-grade *N*,*N*-dimethylformamide of Tokyo Kasei Co. was used without further purification. Methanol was a G. R. grade reagent of Wako Junyaku Co. Toluene was distilled from a G. R. grade reagent of Wako Junyaku Co.

The fluorescence and absorption spectra were measured with a Hitachi EPS-2U recording spectrophotometer.

The exciting light source was a Toshiba SHL-100UV high-pressure mercury lamp, combined with a UV filter or a Bausch & Lomb grating monochromator to select the wavelength of excitation.

The wave numbers of the emission-band maxima were determined from the emission spectra corrected for the spectral sensitivity of the instrument.

Measurements were made on the aerated samples at room temperature. For the anthracene-tri-*n*-butylamine-toluene system, however, the sample solutions were repeatedly degassed by the usual freeze-pump-thaw method.

For measuring the temperature dependence of the emission spectra, a Pyrex tube containing the sample solution was immersed in a quartz Dewar with liquid nitrogen or a mixture of dry ice and acetone for low temperatures, or with warm water above room temperature. The usual concentrations of the aromatic hydrocarbons and the amines were 10^{-4}—10^{-3} M and 0.1—1 M, respectively. It was confirmed that the amines used exhibited no emission, though they slightly absorbed the exciting light at higher concentrations.

Results and Discussion

The absorption spectra of the solutions used for the observation of emission showed no essential change, except for the slight differences due to the ordinary solvent effects, in absorbance and wavelength, as is shown in Fig. 1. This indicates that an amine makes no specific interaction with a ground-state condensed aromatic hydrocarbon; no

5) J. Czekalla and K. O. Meyer, *Z. physik. Chem., N. F.*, **27**, 185 (1961).

6) T. Miwa and M. Koizumi, This Bulletin, **39**, 2588 (1966); K. Kaneta and M. Koizumi, *ibid.*, **40**, 2254 (1967).

7) E. A. Chandross and J. Ferguson, *J. Chem. Phys.*, **47**, 2557 (1967).

8) A. Nakajima and H. Akamatu, This Bulletin, **41**, 1961 (1968).

9) H. Beens and A. Weller, *Chem. Phys. Letters*, **2**, 140 (1968).

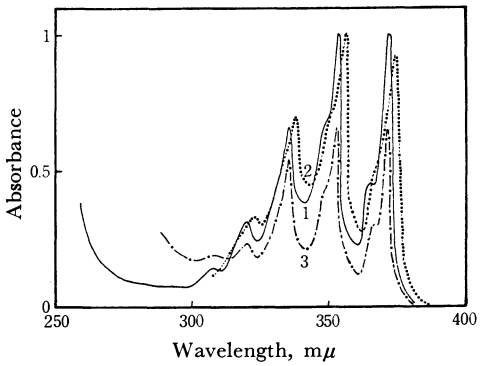

Fig. 1. Absorption spectra of anthracene.
(1) in *n*-hexane, $[A]=1.2\times10^{-4}$ M
(2) in tri-*n*-butylamine (reference: TBA), $[A]=1.2\times10^{-4}$ M
(3) in *n*-hexane, $[A]=8.4\times10^{-5}$ M, $[TBA]=8.4\times10^{-2}$ M

trace is found of such a stable complex as can be detected in the absorption spectrum.*3

Wavelengths of Anomalous Emission Observed in Solutions Containing Aromatic Hydrocarbons and Aliphatic Amines. The emission spectra were measured on the systems of the condensed aromatic hydrocarbons and various aliphatic amines. While the normal fluorescence of an aromatic hydrocarbon was quenched considerably, a new anomalous emission was observed for some kinds of amines at longer wavelength regions. This long-wavelength emission should be regarded as a kind of fluorescence because it decayed instantaneously after the exciting light was shut off. Table 1 gives the results for the *n*-hexane solutions of anthracene and the amines. The same behavior was also found with 1,2-benzanthracene.

The observed emissions may be ascribed to some excited species formed diffusionally from the excited-state aromatic hydrocarbons and the amines.

As can be seen from Table 1, the appearance of a long-wavelength emission seems to depend largely upon the property of the amine employed; only the tertiary amines may be considered to satisfy the requirements for its appearance. Primary amines uniformly quenched anthracene fluorescence with the increase of their concentration without any other emission, while secondary amines showed a new emission at about 530 mμ, obviously due to the photochemical reaction products. However, the absorption and fluorescence spectra for the solutions involving the tertiary amines remained reproducible after irradiation by the exciting light. Although the explanation does not seem to be easy, the hydrogen atom attached to the nitrogen atom of an amine may have some connection with its quenching action; the hydrogen atom of a secondary amine should be considered as very reactive. It may be favorable for the appearance of the long-wavelength emission that tertiary amines have no reactive hydrogen atom and their ionization potentials are relatively low. As the importance of tertiary amines seemed to have been confirmed, a similar experiment was performed for the *n*-hexane solutions containing naphthalene and the tertiary amines, the result of which is given in Table 2.

It may be said that the increasing order of the wavelengths of the long-wavelength emission, despite their rather small differences, corresponds to the decreasing order of the ionization potentials of the amines, as is shown in Table 2.

Table 1. Long-wavelength emission observed in the anthracene - amine -*n*- hexane systems
(excitation wavelength: 365 mμ)

Amine		Wavelength
Primary	*n*-Butylamine *t*-Butylamine Dodecylamine	not observed
Secondary	Diethylamine Di-*n*-butylamine	photoproduct emission (*ca.* 530 mμ)
Tertiary	Triethylamine	489±2 mμ
	Tri-*n*-butylamine	483±2 mμ

Table 2. Naphthalene - *t*-amine - *n*-hexane systems
(excitation wavelength: 310 mμ)

Tertiary amine	Wavelength of long-wavelength emission (mμ)
Triethylamine	405±3
Tripropylamine	405±3
Tri-*n*-butylamine	411±2
N,*N*-Dimethylcyclohexylamine	416±3

The long-wavelength emission was measured for the systems of tri-*n*-butylamine (TBA) and the aromatic hydrocarbons in toluene. Table 3 lists their wavelengths. For the pyrene-TBA system, pyrene excimer fluorescence overlapped the long-wavelength emission, and discrimination between them was difficult. In the cases of 9,10-diphenylanthracene and perylene, a slight quenching of the fluorescence occurred with no long-wavelength emission, and even in pure TBA only the broadening of the fluorescence spectrum of the hydrocarbon was observed. This may be interpreted neither in terms of their short fluorescence lifetimes, which are comparable with that of anthracene, nor in terms of the formation of the non-emissive solvated ions in view of the solvent polarity.[1,10] It can be inferred

*3 No CT band could be observed at a longer wavelength. The increase in absorbance in the short-wavelength region for the curve (3) in Fig. 1 is due to the absorption of tri-*n*-butylamine.

10) H. Knibbe, K. Rollig, F. Schafer and A. Weller, *J. Chem. Phys.*, **47**, 1184 (1967).

from Table 3 that the wavelengths of the long-wavelength emission are related to the electron-affinities of the aromatic hydrocarbons.*4 Dependence of the wavelengths of the long-wavelength emissions on the ionization potentials of the amines and the electron affinities of the aromatic hydrocarbons suggests that the CT interaction is important.[1-4,6,7]

TABLE 3. TRI-*n*-BUTYLAMINE - AROMATIC HYDROCARBON - TOLUENE SYSTEMS

Aromatic hydrocarbon	Emission wavelength (mμ)	Excitation wavelength (mμ)
Naphthalene	437±5	310
Acenaphthene	416±5	
Triphenylene	442±5	
Phenanthrene	445±5	
1,2-Benzanthracene	512±2	365
Anthracene	524±2	
Pyrene	520?	
9,10-Diphenylanthracene	not observed	
Perylene	not observed	

Dependence of the Intensities of Anthracene Fluorescence and the long-wavelength Emission on TBA concentration. Variations in the relative intensities of anthracene fluorescence and the long-wavelength emission were measured for different TBA concentrations. The anthracene concentration was maintained at 4.22×10^{-4} M and the solvent was *n*-hexane. The result is shown in Fig. 2.

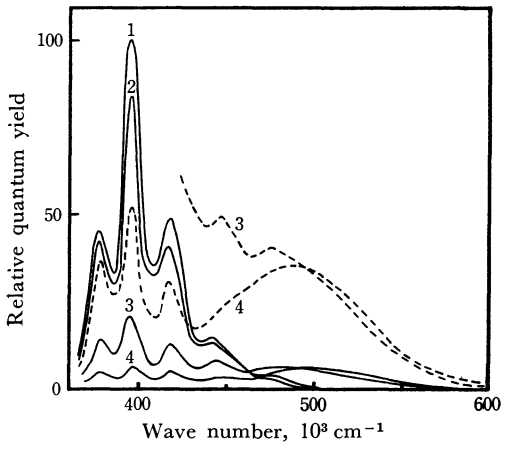

Fig. 2. Emission spectra for the anthracene-TBA - *n*-hexane system.
[TBA] M: 1) 0, 2) 2.04×10^{-2}, 3) 4.01×10^{-1}, 4) 1.34. [A]: 4.22×10^{-4} M.
(The broken lines: ×6)
(corrected for the spectral sensitivity)

*4 The electron affinities of many aromatic hydrocarbons are given in: G. Briegleb, *Angew. Chem.*, **76**, 326 (1964).

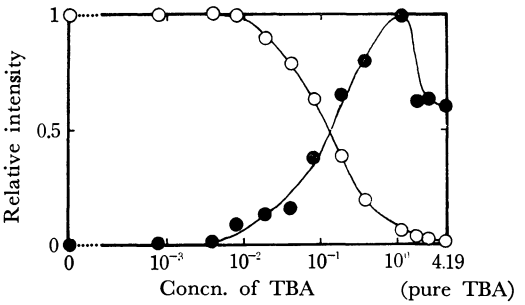

Fig. 3. Quenching curve for anthracene fluorescence and the intensity change of the long-wawelength emission with the respect to TBA concentration.
[A] = 4.22×10^{-4} M, solvent: *n*-hexane.
○: anthracene fluorescence
●: long-wavelength emission

The quenching curve for anthracene fluorescence and the intensity change of the long-wavelength emission are shown in Fig. 3. The quenching constant of TBA for anthracene fluorescence was estimated as 7.9 M^{-1}; this value is smaller than that assumed for a diffusion-controlled process,*5 suggesting the small reaction probability or the establishment of equilibrium in the excited state. That the increasing intensity of the long-wavelength emission is accompanied by the decreasing intensity of anthracene fluorescence implies the formation of an excited complex from excited anthracene and TBA. In the region of higher TBA concentrations, the long-wavelength emission diminished to a considerable extent, indicating the existence of the quenching effect of TBA on the excited complex or the formation of a triple complex[9] with no emissivity.

Effect of Temperature on the Intensities of the Long-wavelength Emission and Anthracene Fluorescence. In order to obtain information on the fluorescence quenching and the origin of the long-wavelength emission, anthracene fluorescence and the long-wavelength emission were measured on a degassed solution for the anthracene-TBA-toluene system at various temperatures from −196 to 95°C. Their temperature dependence is illustrated in Fig. 4.

At liquid nitrogen temperature, anthracene fluorescence is very intense and its spectrum is somewhat sharper than that at room temperature. At low temperatures where molecular diffusion is prevented, only anthracene fluorescence is observed. With

*5 The quenching constant for a diffusion-controlled quenching process is given by the following equation:

$$K_q = \frac{8RT\tau}{3000\eta} \sim 80$$

where η is the viscosity of *n*-hexane (3.2×10^{-3} poise) and τ, the fluorescence lifetime of anthracene (5×10^{-9} sec).

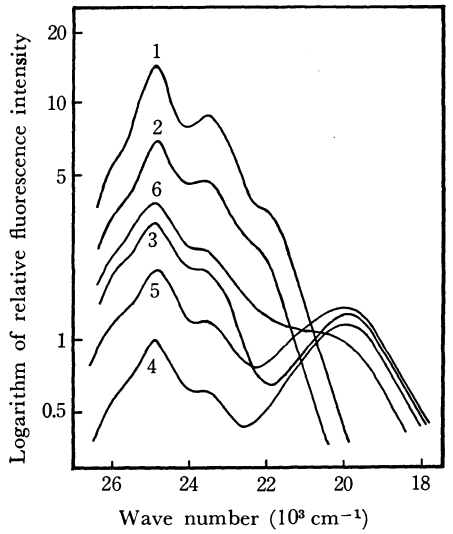

Fig. 4. Temperature dependence of anthracene flouorescence and the long-wavelength emission for the anthracene-TBA-toluene system.
[A]$=5.1\times10^{-4}$ M, [TBA]$=0.84$ M
Temperature °C: (1) −196, (2) −33, (3) 11, (4) 29, (5) 61, (6) 95
(uncorrected for the instrumental factors)

increasing temperature the long-wavelength emission appears at about 520 mμ at the expense of anthracene fluorescence and gradually grows up to a maximum intensity at about 60°C. Above this temperature the intensity of the long-wavelength emission falls off, while that of anthracene fluorescence rises to some extent, suggesting the dissociation of the excited complex backward into excited anthracene and TBA. It is not fully understood at present that both anthracene fluorescence and the long-wavelength emission increase with the rise of temperature at temperatures somewhat above room temperature. A diffusional excited-complex formation may account for their general temperature behaviors.

Solvent Effect on the Long-wavelength Emission. The effects of the solvents of different polarities on the long-wavelength emission for the anthracene-TBA system were examined and were found to be very remarkable.[4-6,11] The result is summarized in Table 4.

With the increase of solvent polarity, the emission-band maximum shifts to the longer wavelength and the intensity increases and finally decreases toward zero. This behavior may be understood on the basis of the fact that the excited CT complex can exist more stably in moderately polar solvents than in non-polar solvents, whereas its dissociation into the solvated radical ions occurs in highly polar solvents, such as methanol and *N*,*N*-dimethylformamide.[1,2,6,10,11] probably carbon tetrachloride reacts with excited anthracene.[12]

Table 4. Solvent effect on the long-wavelength emission for the anthracene-TBA ststem

No.	Solvent	f	Wave number (10^3 cm^{-1})	Intensity*
1	*n*-Hexane	0.0934	20.5	++
2	Cyclohexane	0.0999	20.7	++
3	*p*-Xylene	0.1162	20.0	+++
4	Benzene	0.1168	19.8	+++
	Carbon tetrachloride	0.1178	—	0
5	Decalin	0.1183	20.6	++
6	Dioxane	0.1221	18.5	+++
7	Toluene	0.1267	19.8	+++
8	*t*-Butylbenzene	0.1270	20.1	+++
9	Isopropylbenzene	0.1272	19.9	+++
10	Tetralin	0.1501	19.8	+++
11	Di-*n*-butyl ether	0.1923	20.1	++
12	Anisole	0.2290	19.0	+++
13	Chloroform	0.2517	19.0	+++
14	Ethyl ether	0.2541	19.6	+++
15	Chlorobenzene	0.2607	19.5	+++
16	Fluorobenzene	0.2653	19.2	++
17	Dibutyl phthalate	0.2797	18.4	+
18	Ethyl acetate	0.2928	18.2	++
19	Dichloromethane	0.3199	18.0	+++
20	1,2-Dichloro-ethane	0.3254	18.0	++
21	Benzonitrile	0.3532	18.1	+
22	Cyclohexanone	0.3540	18.0	+
23	Acetone	0.3749	17.8	+
	N,*N*-Dimethyl-formamide	0.3777	—	0
	Methanol	0.3887	—	0

* +++: strong, ++: medium, +: weak, 0: none.

If the solvent shift of the emission band can be attributed to the dipole moment m of the excited CT complex, the wave number $\bar{\nu}$ of the emission band maximum is approximately expressed as follows:[4,5]

$$\bar{\nu} = -\frac{2m^2}{hca^3}\left(\frac{\varepsilon-1}{2\varepsilon-1}-\frac{n^2-1}{4n^2+2}\right) + \text{small terms} + \text{constant}$$

where ε and n denote the dielectric constant and the refractive index of the solvent, respectively; a is the assumed cavity radius for the complex.

Figure 5 shows the plots of $\bar{\nu}$ against

$$f = (\varepsilon-1)/(2\varepsilon+1) - (n^2-1)/(4n^2+2).$$

The straight line in the figure was obtained by the least-squares method from 20 points exclusive of those for benzene, toluene and dioxane, which are

11) N. Mataga, T. Okada and N. Yamamoto, This Bulletin, **39**, 2562 (1966).

12) E. J. Bowen, *Discussions Faraday Soc.*, **14**, 146 (1953).

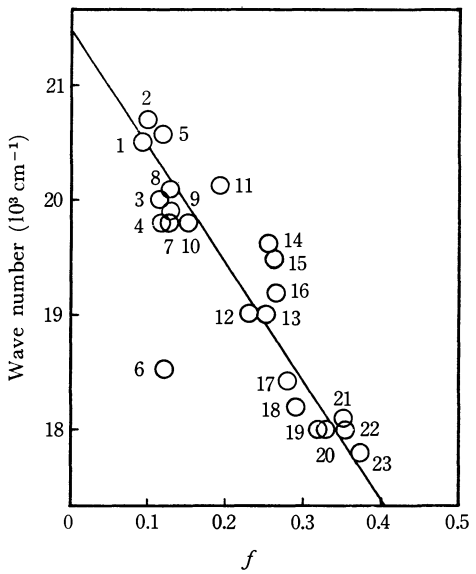

Fig. 5. Evaluation of the dipole moment of the excited complex of anthracene-TBA.
The numerals refer to the respective numbers for the solvents in Table 4.

known to be specific in the solvent effects. From the slope of this line, the value of m was evaluated as 12.8 D, assuming that a ~5.5 Å.*6 This is a very reasonable value for an excited CT complex in view of those reported by various authors.[4,5,11]

Conclusion

The anomalous emission observed at the long wavelengths in the systems of the condensed aromatic hydrocarbons and the tertiary amines seems to show every behavior of an emission due to an excited CT complex, the nature of which has already been studied by several authors.[1-7,9-11] In fact, the following conclusions can be derived:

1) According to the abosorption spectra of the solutions, the temperature dependence of the long-wavelength emission and the relation between the quenching of the hydrocarbon fluorescence and the intensity of the long-wavelength emission, the species responsible for the long-wavelength emission is considered as an excited-state complex formed dynamically from an excited-aromatic hydrocarbon and a tertiary amine.

2) The correlation of the wavelengths of the long-wavelength emission with the electron affinities of the aromatic hydrocarbons and the ionization potentials of the amines, as well as the large dipole moment estimated for the excited complex indicates the importance of the CT interaction.

The present work may have cleared to some extent the relation between the quenching phenomenon and the excited-CT-complex formation.

It is very plausible that the CT interaction occurs between the lone pair of electrons on the nitrogen atom and the π-electrons of the aromatic ring. Such an n-π interaction is of great interest because the localization of the n-electrons may restrict the region of interaction in the CT complex to part of the π-system and the n-orbital and the CT complex formed may assume such a configuration as minimizes the localization energy of the π-system. Thus, the model involved seems somewhat simpler and a theoretical consideration on this problem will be fruitful

The temperature dependence and variations with TBA concentration of the intensities of anthracene fluorescence and the long-wavelength emission may be analyzed by a kinetic approach.

The author wishes to thank Professor Hideo Akamatu for his continuous support and encouragement during the course of this work.

*6 This value was estimated from the molal volumes of anthracene and TBA.

Note added in proof: After this work had been completed, a similar report appeared: M. G. Kuzmin and L. N. Guseva, *Chem. Phys. Letters*, **3**, 71 (1969).

BULLETIN OF THE CHEMICAL SOCIETY OF JAPAN VOL. 42 3415—3421 (1969)

Thermodynamic Properties of Carbon Tetrafluoride from 4°K to Its Melting Point*1

Hisae ENOKIDO,*2 Takako SHINODA and Yo-ichiro MASHIKO

Government Chemical Industrial Research Institute, Tokyo, Shibuya-ku, Tokyo

(Received May 22, 1969)

Thermodynamic properties of solid and liquid carbon tetrafluoride were measured at temperatures from 4°K to 100°K. The heat of transition was found to be 349.5±0.9 cal/mol, the transition temperature 76.221°K, the heat of fusion 168.6±0.05 cal/mol, the triple point temperature 89.515°K and the triple point pressure 0.80±0.03 Torr. The amount of impurity in the specimen of CF_4 was estimated to be 0.014_7 mol% from the measurement of the melting point range. The values of molal entropy of CF_4 as an ideal gas at 298.2°K, were calculated from the calorimetric and spectroscopic data as 62.63 e.u. and 62.45 e.u., respectively. The Debye characteristic temperature at 0°K was derived from the low temperature heat capacity data, and the $\theta_D(T)$ curve was compared with that for neopentane taking into account the octupole interaction of molecules in the crystal.

Carbon tetrafluoride CF_4 is one of a few tetrahedral molecules which undergo phase transition in solid state. The measurements of heat capacity were made by Eucken and Schröder in the region from 12°K to its boiling point,[1] and by Kostryukov *et al.* in the region from 12—13°K to its melting point.[2] The vapor pressure was measured by Menzel and Mohry in solid and liquid states.[3]

The purpose of this paper is to provide more complete and accurate data on the thermodynamic properties of CF_4 from 4°K to its melting point and give a theoretical consideration on the vibrational property of the molecule at low temperature. The data are compared with those of others. A comparison of the entropy calculated from calorimetric data with spectroscopic data is made based on the third low of thermodynamics.

The Debye characteristic temperature, $\theta_D(T)$, is derived from the low temperature heat capacity data, and a comparison of the temperature dependence of $\theta_D(T)$ below 15°K is made with these for other molecular crystals reported by the present authors on a reduced scale using the Debye characteristic temperature at 0°K, $\theta_D(0)$.

Experimental

Material. Chemically pure CF_4 obtained from the Matheson Co., was found to contain about 2.2% of air. This was purified before introduction into the calorimeter vessel. The gas was passed through a 3N KOH solution to remove impurities such as CO_2, SiF_4, SO_2, F_2, and then through a tube containing $CaCl_2$. The resulting material was distilled three times, at liquid nitrogen temperature, through pyrex glass fractionating bulb in a vacuum. The middle fraction collected was cooled to liquid nitrogen temperature and pumping was carried out for two days at a pressure less than 10^{-3} Torr in order to remove the trace of air from the sample. The mole numbers of actual specimen were measured by using a calibrated bulb attached to the calorimeter filling system, and then condensed into the calorimeter vessel. As grease of cock, 'Phynal' was employed instead of silicone grease. No impurity of the sample was found from gas chromatography using a Shimadzu Gas Chromatograph GC-1C. The amount of solid-insoluble liquid-soluble impurity found from measurement of the melting point was 0.014_7 mol%.

Apparatus. The cryostat, experimental techniques and temperature scale were the same as those used in the measurement of $C(CH_3)_4$.[4] A new calorimeter vessel made of silver-plated copper (0.2 mm thick, internal volume about 45 cm^3) was employed.

Results

Heat Capacity of CF_4. The calorimeter contained 0.21789 mol of the sample in measurement series I, 0.34522 mol in series II and 0.33264 mol in series III. Samples in series I, II and III were taken from separate fillings from the same sample. The heat capacity data are given in Table 1. Correction was necessary above 80°K for vaporization of CF_4 which occurred during the measure-

*1 Presented at the 22nd Annual Meeting of the Chemical Society of Japan, Tokyo, April, 1969.

*2 Present address: Tokyo Kasei Kogyo Co., Ltd., 6-Chome, Toshima, Kita-ku, Tokyo, Japan.

1) A. Eucken and E. Schröder, *Z. Pkysik. Chem.*, **B41**, 307 (1938).

2) V. N. Kostryukov, O. P. Samorukov and P. Strelkov, *Zhur. Fiz. Khim.*, **32**, 1354 (1958).

3) W. Menzel and F. Mohry, *Z. Anorg. Allgem. Chem.*, **210**, 257 (1933).

4) H. Enokido, T. Shinoda and Y. Mashiko, This Bulletin, **42**, 84 (1969).

ment. For values of heat of vaporization and of heat capacity of gaseous CF_4 those obtained by Eucken and Schröder[1] and Hwang and Martin[5] were used. The volume of the sample condensed in the calorimeter vessel was calculated using densities of solid and liquid CF_4 given by Stewart and Rock[6] and Knobler and Pings[7]. Gas imperfection correction was negligible over the termperature range of measurement. Correction was made with respect to curvature where necessary. The heat capacity data are plotted in Fig. 1 along with those given by Eucken and Schröder.[1] The results agree in the terperature range from 12 to 55°K. However, above 60°K, in particular between transition point and melting point, a difference is seen. The heat capacity of solid CF_4 between 12—13°K and the melting point was measured by Kostryukov *et al.*[2] The results were given graphically, but numerical values were not reported. A comparison of the result of Kostryukov *et al.* with ours from the heat capacity curve for CF_4 in Fig. 4 of Ref. 2 may be regarded as in good agreement.

The transition seemed to be first-order at the start, but changed into second-order type gradually after passing the middle point of the process and finished as the second-order one. This situation is different from that in $C(CH_3)_4$ crystal reported previously which seemed to be second-order over the whole transition range. We observed this heat capacity anomaly to have a very large value (*i.e.* 61.31 cal/mol deg at 76.336°K). No hysteresis was observed.

TABLE 1. HEAT CAPACITY OF CF_4
(Molecular weight 88.005; lcal=4.1840 absolute joules; 0°C=273.15°K)

T (°K)	C_p (cal/deg mol)	T (°K)	C_p (cal/deg mol)
4.024	0.05130	27.648	7.360
4.039	0.05202	29.039	7.735
4.432	0.07149	53.130	12.63
4.458	0.07149	55.192	13.06
4.897	0.09829	57.132	13.43
4.931	0.09901	59.035	13.82
5.151	0.1148	60.906	14.23
5.423	0.1372	62.715	14.66
5.497	0.1432	64.465	15.12
5.648	0.1603	66.050	15.54
5.774	0.1716	67.482	15.96
6.140	0.2142	68.871	16.45
6.237	0.2244	70.143	17.03
6.643	0.2723	71.291	17.66
6.669	0.2780	72.332	18.28
7.109	0.3503	73.188	18.85
7.140	0.3499	73.920	19.52
7.612	0.4416	74.597	20.06
7.640	0.4386	74.702	20.18
8.120	0.5413	75.247	20.62
8.141	0.5434	75.265	20.88
8.619	0.6615	75.257	20.92
8.642	0.6633	75.609	21.77
9.128	0.8004	75.741	22.24
9.148	0.8025	75.891	22.64
9.646	0.9182	75.908	22.74
9.663	0.9219	76.221	'Transition'
10.163	1.129	76.611	15.78
10.334	1.205	76.656	15.77
10.824	1.376	77.104	15.86
10.830	1.396	80.312	16.14
11.412	1.613	81.416	16.23
11.622	1.688	82.241	16.31
13.536	2.413	82.344	16.33
14.206	2.686	83.237	16.40
14.643	2.892	83.180	16.41
15.233	3.110	84.223	16.47
15.605	3.277	84.229	16.48
16.282	3.517	85.256	16.56
16.587	3.656	85.397	16.58
17.346	3.924	86.286	16.66
17.579	4.027	86.536	16.69
18.677	4.413	87.282	16.74
19.891	4.811	87.673	16.80
21.147	5.324	88.314	16.88
22.374	5.726	88.720	16.96
23.601	6.133	89.515	'Fusion'
25.017	6.596	90.389	18.70
26.305	6.982	91.716	18.79

TABLE 2. TRANSITION AND TRIPLE POINT OF CF_4

"Transtion point"

Fraction transformed	T (°K)
0.19860	76.211
0.50859	76.218
0.98805	76.221
$T_{transition}$	76.221
Eucken and Schröder (1938)	76.23
Kostryukov, Samorukov and Strelkov (1958)	76.09±0.012

"Triple point"

Fraction melted	T (°K)	P (Torr)
0.17018	89.449	0.80
0.23510	89.468	0.83
0.32558	89.485	0.80
0.50641	89.503	0.78
		average 0.80±0.03
T_{triple} (pure CF_4)	89.529	
Eucken *et al.* (1938)	89.47	
Kostryukov *et al.* (1958)	88.44±0.02	

5) Y. Hwang and J. J. Martin, *A. I. Ch. E. J.*, **10**, 89 (1964).
6) J. W. Stewart and R. I. L. Rock, *J. Chem. Phys.*, **28**, 425 (1958).
7) C. M. Knobler and C. J. Pings, *J. Chem. Eng. Data*, **10**, 129 (1965).

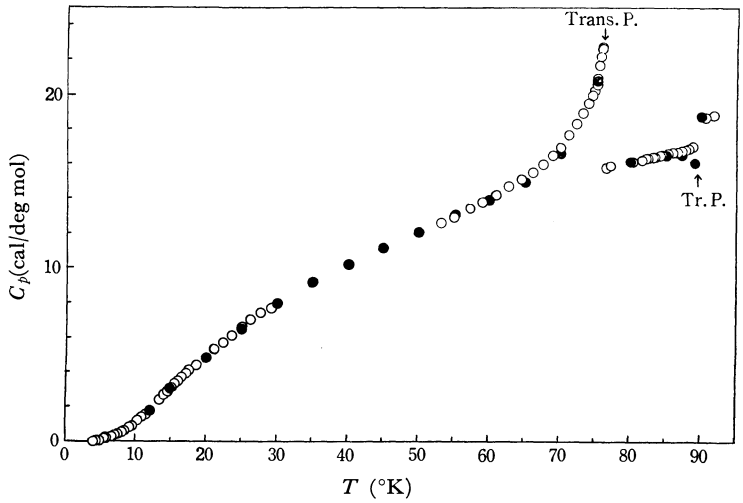

Fig. 1. Heat capasity curve of CF_4.
●: Eucken *et al.* ○: Present research

The Transition and the Triple Points. The transition temperature was determined from percentages of the specimen transformed and the measured equilibrium termperatures using the first-order law. The result is summarized in Table 2.

The triple point temperature corresponding to pure CF_4 was obtained from a plot of the equilibrium temperatures against the reciprocals of the fraction melted, and the result is given in Table 2 together with the triple point pressures. The triple point temperatures for pure CF_4 and the sample used are found to be 89.529°K and 89.515°K, and the values are compared with those given by others in Table 2.

Heat of Transition and Fusion. Data of the heat of transition and fusion are summarized in Table 3 together with those given by others. Our results are in good agreement with those of Eucken and Schröder, but not with Kostryukov *et al.*, particularly in that of the heat of transition which deviates considerably from ours. In the present measurement the average deviation of the result of the heat of transition is larger than that of the heat of fusion. This is probably due to the fact that a $\int C_p dT$ correction at temperatures slightly above the transition point was not estimated exactly, because the end of transition is a second-order type.

The Vapor Pressure Measurements. The vapor pressure of CF_4 was measured at temperatures

Table 3. Heat of transition and fusion of CF_4

Temperature interval (°K)	Heat input (cal/mol)	$\int C_p dT$ (cal/mol)	ΔH (cal/mol)
	"Transition"		
	(mol wt 88.005; (i) 0.21789 mol, (ii) 0.21789 mol)		
(i) 75.952—76.270	367.3	16.9	350.4
(ii) 76.078—76.639	369.6	21.0	348.6
		average	349.5±0.9
Eucken and Schröder (1938)			{354.0 {352.5
Kostryukov *et al.* (1958) 74.4—76.0	414.5	47.8	366.7
	"Fusion"		
	((i) 0.21789 mol, (ii) 0.34522 mol)		
(i) 89.057—89.620	187.3	18.8	168.5
(ii) 89.237—89.556	177.4	8.8	168.6
		average	169.6±0.05
Eucken and Schröder (1938)			{167.0 {167.7
Kostryukov *et al.* (1958)			165.8

from 80 to 102°K, and is listed in Table 4. The result was made to fit the following equations by the method of least squares:

i) $80°K < T <$ triple point

$$\log_{10}P + 2(\log_{10}T) = 19.1433 - (1363.87)/T, \quad (1)$$

ii) $T >$ triple point

$$\log_{10}P + 2(\log_{10}T) = 14.0430 - (920.65)/T. \quad (2)$$

The deviation of the observed values from those calculated by means of Eqs. (1) and (2) are given in the last column of Table 4, and are plotted by open circles in Fig. 2.

Table 4. Vapor pressure of solid and liquid CF_4

T (°K)	$P_{obs.}$ (Torr)	$P_{obs.}-P_{calc.}$ (Torr)
Solid		
80.878	0.036	+0.007
81.952	0.066	+0.019
82.734	0.021	−0.046
83.625	0.110	+0.012
84.823	0.206	+0.045
85.968	0.349	+0.092
87.104	0.528	+0.125
88.236	0.605	−0.019
89.204	0.784	−0.114
89.346	0.798	−0.149
Liquid		
89.713	0.708	−0.042
91.057	1.009	−0.023
92.361	1.421	+0.028
93.641	1.977	+0.122
94.917	2.587	+0.139
96.012	3.290	+0.204
97.703	4.468	+0.102
99.679	6.267	−0.185
101.464	8.369	−0.682

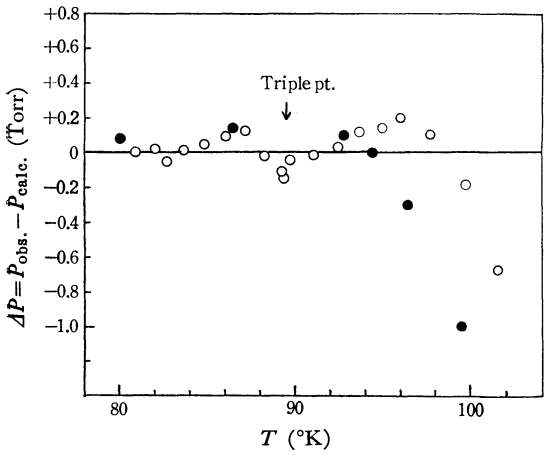

Fig. 2. Deviation of observed vapor pressure of CF_4 from the calculated one by using Eqs. (1) and (2).
●: Menzel and Mohry ○: Present research

In Fig. 2 are shown also the deviations between the pressures observed by Menzel and Mohry[3] and those calculated. Over a large part of the temperature region of measurement these differences are considerably large, since the absolute values of pressure are very small.

Entropy. The calorimetric and spectroscopic entropies of the ideal gaseous CF_4 at 298.2°K were calculated and compared with those obtained by Eucken and Schröder as shown in Table 5. The entropy below 4°K was estimated by using the value of Debye characteristic temperature obtained from the extrapolation of plots of $\theta_D(T)$ *versus* T. As the entropy of the vaporization and that above 122°K the values given by Eucken and Schröder were used.

As the entropy obtained by Eucken and Schörder is largely different from ours between 12°K and the transition point even taking into account probale errors in both measurements, we re-calculated the value using the heat capacity data observed by them. The value obtained is not 15.26 e.u. but 15.56 e.u. and agrees with ours within accuracy of their measurement. Therefore, the calorimetric entropy

Table 5. The entropy of CF_4 gas at 298.2°K

	Eucken and Schröder (e. u.)	Present research (e. u.)
"Calorimetric"		
0—12°K	0.69	0.60
12°K-Transition	15.26(15.56)	15.61
Transition	4.64	4.59
Transition-Fusion	2.59	2.63
Fusion	1.87	1.88
Fusion-122°K	5.81	5.77
Vaporization	25.55	25.55
122—298.2°K	9.96	9.96
Compression from 0.1365 to 1 atm	−3.94	−3.96
	62.43(62.73)	62.63
"Spectroscopic"		
Translational	—	39.34
Rotational	—	20.00
Vibrational	—	3.11
Total	62.81	62.45
Moment of inertia I (10^{-40} g cm^2)	101.3	145.9*3
Vibrational frequencies (cm^{-1})	899 435 1343 650	904[8] 437 1265 630

*3 This is the value calculated using atomic distances obtained by Hoffman and Livingston (*J. Chem. Phys.*, **21**, 565 (1953)) from their measurements of electron diffraction.

8) D. M. Yost, E. N. Lassettre and S. T. Gross, *J. Chem. Phys.*, **4**, 325 (1936).

obtained by these authors is to be estimated as 62.73 e.u. On the other hand, the difference of the spectroscopic entropy may arise from the discrepancy of the values of the moment of inertia and the vibrational frequencies used in calculations as listed in Table 5. Agreement of the calorimetric entropy of 62.63 e.u. and the spectroscopic entropy of 62.45 e.u. is satisfactory as is seen in Table 5.

Discussion

In order to elucidate lattice vabrations at low temperature, we converted the observed heat capacity data of CF_4 and $C(CH_3)_4$ to the Debye characteristic temperature, $\theta_D(T)$, assuming $6N$ degrees of vibrational freedom (where N is Avogadro's number). Here, $C_p - C_v$ correction was neglected, since little is known about the thermal expansion and compressibility of CF_4 and $C(CH_3)_4$ crystals. We can neglect this term, since the contribution to $\theta_D(T)$ will be small at low temperature. However, the contribution of the intramolecular vibrations to the heat capacity was taken into account using the observed infrared and Raman spectral data.[8] In order to compare the temperature dependence of the $\theta_D(T)$ for CF_4 with that for $C(CH_3)_4$, the values of $\theta_D(T)$ were plotted against temperature on a reduced scale using the Debye characteristic temperature at 0°K, $\theta_D(0)$, as shown in Fig. 3. Here the intramolecular rotational frequency of the methyl group in $C(CH_3)_4$ of 286 cm^{-1} obtained by Rush[9] from his cold-neutron study was used. The values of $\theta_D(0)$ for CF_4 and $C(CH_3)_4$ were calculated from the first coefficients of the expansion of low temperature heat capacity, *i.e.*

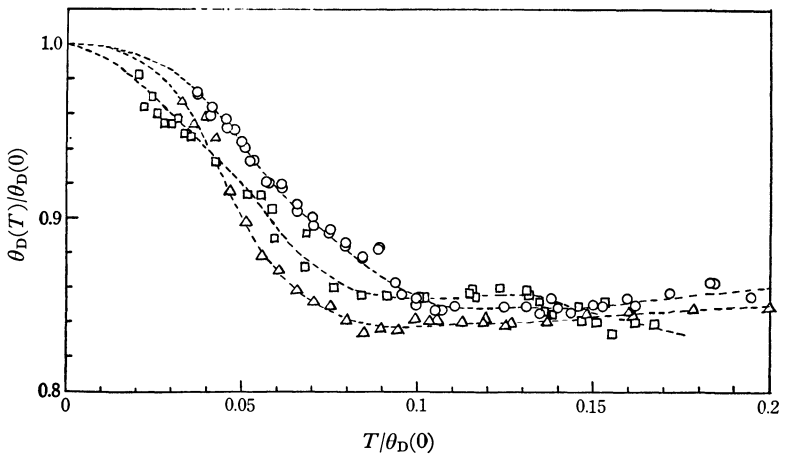

Fig. 3. $\theta_D(T)$ curves on a reduced basis.
○: CF_4 △: $C(CH_3)_4$ □: CO

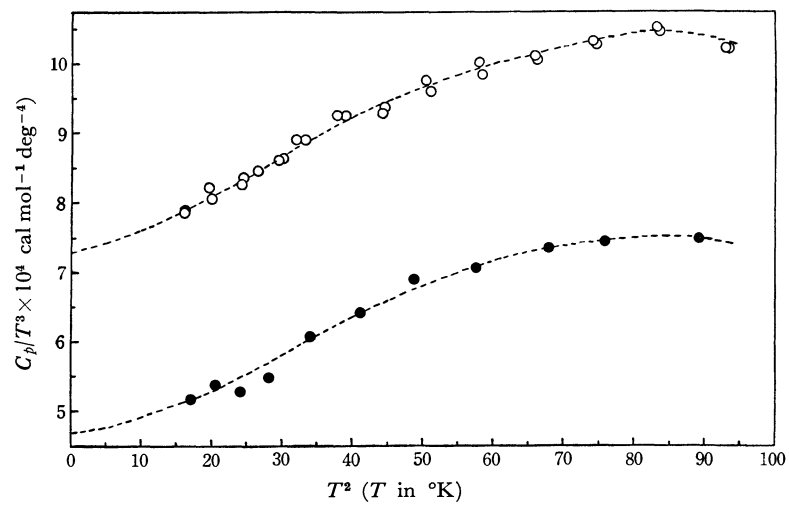

Fig. 4. Plots of C_p/T^3 against T^2 for CF_4 and $C(CH_3)_4$.
○: CF_4 ●: $C(CH_3)_4$

9) J. J. Rush, *J. Chem. Phys.*, **46**, 2285 (1967).

Table 6. The values of potential parameters for CF_4, $C(CH_3)_4$ and CO

		CF_4	$C(CH_3)_4$	CO
Lennard-Jones parameters[a]	ε/k (°K)	141	191	88
	r_0 (A)	4.63	6.44	3.706
Anisotropy factor[b]	κ	0	0.0528	0.0905
Polarizability[c]	α (A^3)	2.89	10.07	1.844
Quadrupole moment[d]	$\sum_i e_i(z_i^2-x_i^2)$(esu)	—	—	$0.92—2.81\times10^{-26}$
Octupole moment[e]	$\sum_i e_i x_i y_i z_i$(esu)	4.44×10^{-24}	25.2×10^{-34}	—

a) J. C. McCoubrey and N. M. Singh, *Tranns. Faraday Soc.*, **53**, 877 (1957).
b) C. Clement and P. Bothorel, *J. Chim. Phys.* **61**, 878 (1964).
c) W. Brandt, *J. Chem. Phys.*, **24**, 501 (1956).
d) R. H. Orcutt, *ibid.*, **39**, 605 (1963).
e) The octupole moment of 5.48×10^{-34} esu for CF_4 has recently been estimated by Spurling *et al.* (*J. Chem. Phys.*, **48**, 1006 (1968)) in the same way as ours. Also from their measurements of far-infrared absorption in gaseous CF_4 Rosenberg *et al.* (*J. Chem. Phys.*, **48**, 1396 (1968)) obtained the octupole moment for CF_4 of 4.5 or 4.8×10^{-34} esu.

$$\theta_D(0) = (935.14/\boldsymbol{a})^{1/3}, \quad (3)$$

where $\boldsymbol{a}$ has the unit of cal·mol^{-1}·deg^{-4}. The values of $\boldsymbol{a}$ obtained from plots of C_p/T^3 against T^2 as given in Fig. 4 correspond to $\theta_D(0)=108.7°$ for CF_4 and $\theta_D(0)=125.9°$ for $C(CH_3)_4$.

In higher temperature region above $T/\theta_D(0)=0.1$, it is difficult to obtain information on lattice vibrations in solid CF_4 and $C(CH_3)_4$ from the $\theta_D(T)/\theta_D(0)$ curves, since in this region C_p-C_v correction and anharmonicity in lattice vibrations must be taken into consideration. At low temperature region below $T/\theta_D(0)=0.1$, however, difference in the shapes of the $\theta_D(T)/\theta_D(0)$ curves for CF_4 and $C(CH_3)_4$ shown in Fig. 3 may be accounted for by the interaction between molecular octupoles which plays the most important part in lattice vibrations of tetrahedral molecules.*4 The values of octupole moment for CF_4 and $C(CH_3)_4$ was estimated using the second virial coefficient data. The analysis is given in Appendix, and the values obtained are listed in Table 6 together with the other potential parameters. The octupole moment for CF_4 is smaller than that for $C(CH_3)_4$. Treatment on the basis of lattice theory already made for CO crystal[10] will give us insight into the molecular motions at low temperature of CF_4 and $C(CH_3)_4$. For comparison, the $\theta_D(T)/\theta_D(0)$ curve and the values of the potential parameters of molecular interactions for CO are given in Fig. 3 and Table 6, where multipole is quadrupole.

Data of the thermodynamic properties for CF_4 reported in this paper provide the first observed values in the temperature range below 12°K. The values are complete and more accurate than have been available heretofore in the temperature range above 12°K.

The authors are grateful to Mr. Ichiro Takeda of the Government Chemical Industrial Research Institute, Tokyo for help in measurement of gas chromatography.

Appendix

The second virial coefficient $\boldsymbol{B}$ for a tetrahedral molecule has been given by Kielich[11] as follows:

$$\boldsymbol{B} = (2/3)\pi N r_0^3[F(y) - \kappa^2(0.050+0.095\kappa^2)H_{12}(y) - (3/5y^2)(\alpha/r_0^3)(\Omega^2/\varepsilon r_0^7)H_{10}(y) - (297/350)\Omega^2/\varepsilon r_0^7)^2 H_{14}(y)], \quad (4)$$

where the first term represents the contribution of a Lennard-Jones 6-12 potential, the second the effect of anisotropy on the dispersion forces, the third from the interaction of an induced dipole with the octupole and the fourth the inetraction between octupole moments. Here ε and r_0 are the Lennard-Jones potential parameters, α is the polarizability of the molecule, Ω is its anisotropy and Ω is defined by the octupole moment $\sum_i e_i x_i y_i z_i$ as

$$\Omega = (5/2)\sum_i e_i x_i y_i z_i \quad (5)$$

for a tetrahedral molecule.

The function $F(y)$ is tabulated by Hirschfelder *et al.*[12] with $y=2(\boldsymbol{k}T/\varepsilon)^2$, and the function $H_n(y)$ is tabulated by Buckingham and Pople.[13] By using known values of ε, r_0, α, and κ, the value of the octupole moment was

*4 Although information on the effect of the octupole interaction on lattice vibrations for tetrahedral molecules has not yet been given, the phase transitions in solid methane have been successfully explained by the octupole interaction. Some typical reference may be quoted here; H. M. James and T. A. Keenan, *J. Chem. Phys.*, **31**, 12 (1959); T. Yamamoto, *ibid.*, **48**, 3193 (1968); T. Yamamoto and Y. Kataoka, *ibid.*, **48**, 3199 (1968).

10) T. Shinoda and H. Enokido, *J. Phys. Soc. Japan*, **26**, 1353 (1969).

11) S. Kielich, *Physica*, **31**, 444 (1965).

12) J. O. Hirschfelder, C. F. Curtiss and R. B. Bird, "Molecular Theory of Gases and Liquids," John Wiley & Sons, Inc., New York (1954), p. 1114.

13) A. D. Buckingham and J. A. Pople, *Trans. Faraday Soc.*, **51**, 1173 (1955).

TABLE 7. CALCULATED AND EXPERIMENTAL SECOND VIRIAL COEFFICIENTS (in units of $cm^3\,mol^{-1}$)

"Carbon tetrafluoride"

T (°K)	B_{L-J}	$B_{O-ind\mu}$	B_{O-O}	B_{calc}	B_{obs}[a]
273.16	−85.2	−2.6	−20.4	−108.2	−111.0
294.16	−70.3	−2.4	−17.7	−90.4	−101.0
298.153	−67.7	−2.4	−17.2	−87.3	−88.30
303.152	−64.6	−2.3	−16.6	−83.5	−84.40
313.16	−58.7	−2.2	−15.7	−76.6	−83.6
323.16	−42.5	−2.2	−14.8	−59.5	−72.4
323.16	−42.5	−2.2	−14.8	−59.5	−70.4
348.153	−41.1	−2.0	−12.9	−56.0	−55.70
348.16	−41.1	−2.0	−12.8	−55.9	−56.1
373.16	−30.8	−1.9	−11.3	−44.0	−43.50
373.16	−30.8	−1.9	−11.3	−44.0	−43.9
373.16	−30.8	−1.9	−11.4	−44.1	−43.1
398.16	−22.0	−1.8	−10.1	−33.9	−30.1
398.16	−22.0	−1.8	−10.1	−33.9	−33.20
398.16	−22.0	−1.8	−10.1	−33.9	−31.1
423.16	−14.4	−1.7	−9.1	−25.2	−26.0
423.183	−14.4	−1.7	−9.1	−25.2	−24.40
448.197	−7.7	−1.6	−8.2	−17.5	−16.80
473.213	−1.9	−1.5	−7.5	−10.9	−10.10
498.229	+3.3	−1.4	−6.9	−5.0	−4.25
523.16	+7.9	−1.4	−6.3	+0.2	+1.2
523.245	+7.9	−1.4	−6.4	+0.1	+1.00
548.260	+12.1	−1.3	−5.9	+4.9	+5.60
573.16	+15.8	−1.3	−5.5	+9.0	+9.3
573.274	+15.8	−1.3	−5.5	+9.0	+9.80
598.285	+19.1	−1.2	−5.1	+12.8	+13.60
623.295	+22.2	−1.2	−4.8	+16.2	+17.05
673.16	+27.5	−1.1	−4.3	+22.1	+23.6

"Neopentane"

T (°K)	B_{L-J}	B_{anis}	$B_{O-ind\mu}$	B_{O-O}	B_{calc}	B_{obs}[b]
323.16	−314.5	−0.5	−18.7	−400.3	−734.0	−734
333.16	−294.0	−0.5	−18.1	−375.2	−687.8	−686
348.16	−265.8	−0.4	−17.2	−342.7	−626.1	−626
363.16	−240.2	−0.4	−16.4	−314.9	−571.9	−566
373.16	−224.5	−0.4	−15.9	−299.6	−540.4	−536
383.16	−209.9	−0.4	−15.4	−284.6	−510.3	−507
398.16	−189.5	−0.3	−14.9	−264.5	−469.2	−472
433.8	−147.4	−0.3	−13.5	−225.1	−386.3	−384
448.16	−132.6	−0.3	−13.1	−211.6	−357.6	−356
473.16	−109.2	−0.2	−12.4	−190.2	−312.0	−313
498.16	−88.5	−0.2	−11.7	−173.7	−274.1	−275
523.16	−70.2	−0.2	−11.3	−159.6	−241.3	−244
548.16	−53.7	−0.2	−10.7	−146.9	−211.5	−216

a) M. Douslin, M. Harrison, M. Moore and M. McCullough, *J. Chem. Phys.*, **35**, 1357 (1961).
b) S. D. Hamann and J. A. Lawbert, *Aust. J. Chem.*, **7**, 1 (1954); S. D. Hamann, J. A. Lambert and R. B. Thomas, *ibid.*, **8**, 149 (1955).

estimated from Eqs. (4) and (5). The values of Lennard-Jones (Table 6, a)) were obtained from the analysis of viscosity data in which the effect of octupole mement could be neglected. Average values of the octupole moment for CF_4 and $C(CH_3)_4$ estimated in this way using the observed values of second virial coefficients $\boldsymbol{B}$ are listed in Table 6, together with the other parameters used in calculations. The second virial coefficients calculated from the average octupole moment in Eq. (4) and the observed second virial coefficients are given in Table 7 for comparison.

BULLETIN OF THE CHEMICAL SOCIETY OF JAPAN VOL. 42 3422—3424 (1969)

Studies of Helical Aggregates of Molecules. I. Enantiomorphism in the Helical Aggregates of Optically Active 12-Hydroxystearic Acid and Its Lithium Salt

Taro TACHIBANA and Hideko KAMBARA

Department of Chemistry, Ochanomizu University, Bunkyo-ku, Tokyo

(Received May 22, 1969)

It was found, by electron-microscope observation, that D(or L)-12-hydroxystearic acid and its Li soap crystallize from a solution in various solvents in the form of a twisted fiber. The twist was left-handed for the D-acid and right-handed for the L-acid, while the Li soap gave results just opposite to those of the corresponding acid. The DL-acid separated out not fibers, but plate-like crystals, and its Li soap produced non-twisted fibers. Thus, an enantiomorphic relationship for the sense of twist between the D-enantiomer and the L-enantiomer was found both for the acid and for the Li soap.

Spirals or helices are often seen in various biological systems (*e.g.*, chromosome, bines, and snail shells). Curiously, some biological helices have a definite sense; they have either a right-handed or left-handed sense, depending upon the kind of biological system. Though one may imagine that this fact is related to the asymmetry of biological molecules, no evidence has yet been presented for such a speculation. Interest in this problem has lead us to notice the sense of twist in the helical aggregates of molecules.[1,2]

It has been known by electron-microscope study, that some crystalline aggregates of soap from lubricating grease consist of fibers in the form of twisted ribbon or helical rope. On examining the electron micrographs of the fibers hitherto published, we found that the fibers from hydrated calcium tallowate grease exhibit both right-handed and left-handed twists, while the fibers from lithium 12-hydroxystearate grease all twist by the same hand. This fact had also been pointed out by Hotten and Birdsall,[3] but they did not report the sense of twist of the lithium soap fibers. We found in the literature that some micrographs[4a-c] exhibit a right-handed twist and others,[3,5a,b] a left-handed twist. There is, then, confusion in the literature, but undoubtedly either sense of the twist could occur in a specimen. Since 12-hydroxystearic acid is an optically-active compound and since the naturally-occuring enantiomer is the D-form, the molecular asymmetry may be reflected in the sense of twist. In the present investigation, we have undertaken to determine the sense of twist in the specimens and to confirm whether or not there exists an enantiomorphic relationship between the helical aggregates from each enantiomer.

Experimental

Materials. D-12-Hydroxystearic acid was purified by the urea-adduct method from a commercial product containing as impurities about 15% stearic and palmitic acids. This procedure consists of dissolving the methyl ester into urea-saturated methanol with warming, letting the solution stand at room temperature, and then precipitating the adduct. Since the adduct initially precipitated was rich in methyl stearate and palmitate, they was removed by filtration. The methyl hydroxystearate-rich adduct was obtained by adding further urea to the filtrate. The adduct was decomposed with water, thus isolating the methyl hydroxystearate. The methyl hydroxystearate was repeatedly purified by the urea-adduct method. The final product was over 99% pure. The acid was obtained by saponifying the methyl ester with alcoholic KOH and by then acidifying it with dilute H_2SO_4; mp 79.3—79.8°C, $[\alpha]_D^{15}$ $-0.3 \pm 0.1°$ (pyridine); lit[6] mp 80.5—81°C, $[\alpha]_D^{19}$ $-0.41°$ (pyridine).

DL-12-Hydroxystearic acid[7] was obtained by the reduction of 12-ketostearic acid derived from D-12-hydroxystearic acid.

1) T. Tachibana and H. Kambara, *J. Am. Chem. Soc.*, **87**, 3015 (1965).

2) T. Tachibana and H. Kambara, *J. Colloid Interfac. Sci.*, **28**, 173 (1968).

3) B. W. Hotten and B. H. Birdsall, *J. Colloid Sci.*, **7**, 284 (1952).

4) a) A. Bondi, A. M. Cravath, R. J. Moore and W. H. Peterson, NLGI Spokesman, **13**(12), 12 (1950); b) B. W. Hotten, *ibid.*, **19**(1), 14 (1955); c) G. V. Vinogradov and V. V. Sinitsyn, *J. Inst. Petrol.*, **47**, 357 (1961).

5) a) M. J. Vold, V. A. Elersich, R. F. Baker and R. D. Vold, NLGI Spokesman, **18**(5), 8 (1954); b) A. L. McClellan, *J. Chem. Phys.*, **32**, 1271 (1960).

6) K. Serck-Hanssen, *Chem. Ind. (London)*, **1958**, 1554.

7) I. Nakajima and S. Toyama, *Nippon Kagaku Zasshi (J. Chem. Soc. Japan, Pure Chem. Sect.)*, **81**, 1598 (1960).

(A) 12-Hydroxystearic Acid

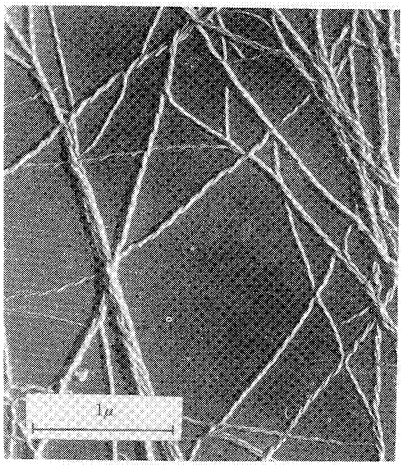

(a) D-form, left-handed twist

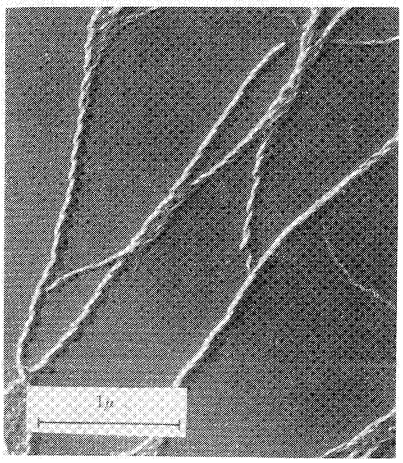

(b) L-form, right-handed twist

(B) Lithium 12-Hydroxystearate

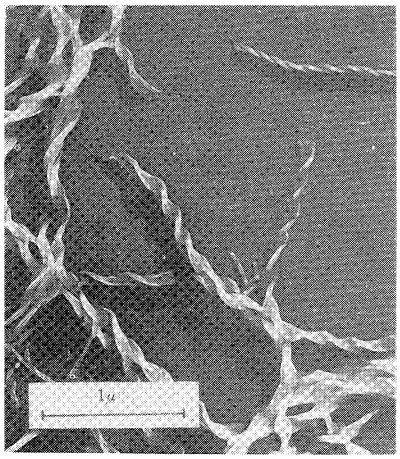

(a) D-form, right-handed twist

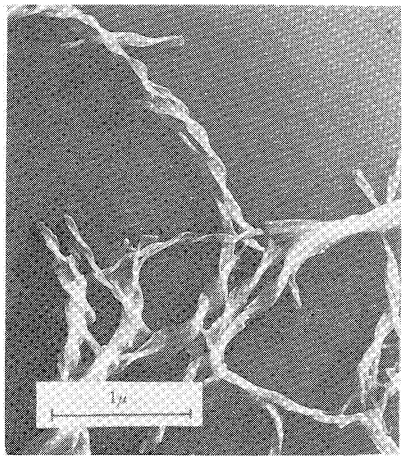

(b) L-form, left-handed twist

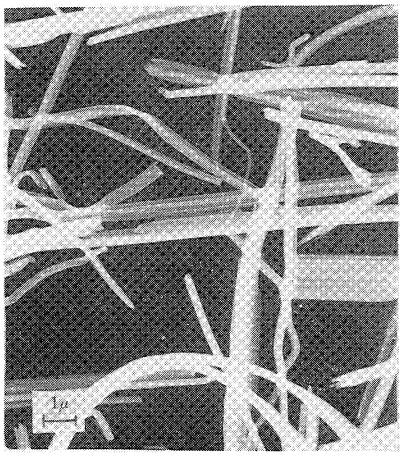

(c) DL-form, no twist

Fig. 1. The effect of optical isomerism on the sense of the twist in fibrous aggregates of 12-hydroxystearic acid (A) and lithium 12-hydroxystearate (B).

L-12-Hydroxystearic acid was prepared by the Walden inversion of the D-acid. The methyl ester of the D-acid was tosylated with *p*-toluenesulfonyl chloride in pyridine at a low temperature. The tosylate was then converted to the acetate by refluxing it with sodium acetate in acetic acid containing a small amount of acetic anhydride. The Walden inversion then occurred. L-12-Hydroxystearic acid was obtained by saponifying the acetate with KOH, followed by acidification with dilute H_2SO_4 and purification by recrystallization from methanol and then from acetone; mp 75.6—76.0°C, $[\alpha]_D^{15}$ $+0.40\pm0.05°$ (pyridine), lit,[6] mp 80.4—80.6°C and 78°C (dimorphous), $[\alpha]_D^{20}$ $+0.3\pm0.1°$ (pyridine). The infrared spectra of this L-acid was identical with that of the D-acid.

The analysis of the hydroxy acids was done by gas chromatography after they had been converted into the methyl ester of the acetoxy acid.

The Li soap was prepared by neutralizing the acid with LiOH in an ethanol solution, then recrystallizing the acid several times from ethanol, and finally drying it over P_2O_5 *in vacuo*.

The Formation of the Aggregate. The method consists of dissolving the soap into a hot solvent and then allowing it to stand at room temperature. The solution then solidifies into grease or gel, or separates out a gel-like precipitate, depending on the concentration and on the nature of the solvent used. The solvents were a highly refined mineral oil, Nujol, and ethanol. In a similar manner, 12-D(or L)-hydroxystearic acid itself was also found to form a helical aggregate from Nujol, benzene, carbon tetrachloride, chloroform, acetone, and ethanol.

Electron-microscope Observation. In order to make a specimen for the electron microscope, a small portion of the gel was placed on a copper grid covered with a thin film of carbon-collodion; the solvent was then evaporated *in vacuo*. When an involatile solvent, such as mineral oil or Nujol, was used, a small portion of the gel was dispersed in solvent naphtha, in which the dispersed phase is insoluble. Then a small drop of the dispersion was placed on the grid and dried. After that, the specimens were shadowed with Pt-Pd metal. The observations were done with a JEM-T6 electron microscope (direct magnification, X 30000).

In order to determine the helical sense from an electron micrograph, some care must be taken. The helical sense appearing in the electron micrograph depends on whether the specimen shadowed previously with metal was exposed to the electron beam directly or through a support film, since only the metal-shadowed side of a helix gives the electron-microscope image clearly. Accordingly, a right-handed helix appears as either a right-handed image or a left-handed image, depending on the mode of the exposure of the specimen to the electron beam. Consideration should be also given to the process of making a copy of the photograph. These factors seem to us to have escaped earlier workers' notice. The photographs in this paper are printed to show the same sense as that of the twist in the specimen.

Results and Discussion

Some typical micrographs are shown in Fig. 1, in which the twisted fibers are clearly visible. It can also be seen that the structure is actually made up of two or more individual fibers twisted about one another. The widths of the fibers varied over a considerable range.

The hydroxy acid was found to form a twisted fibril 0.01—0.1 μ in width, regardless of the kind of solvent used. Sometimes the fibers from benzene and from carbon tetrachloride were several tens of microns long.

In the case of the lithium soap, twisted fibrils about 0.03 μ in width were formed from ethanol, while helical ribbons 0.03—0.3 μ in width were formed from mineral oil and from Nujol. The thickness of the ribbon was so thin that, when a ribbon was laid upon another ribbon, the lower ribbon was visible through the upper. This was observed clearly when the specimen was lightly shadowed with metal. The thickness of the ribbons appeared to be about 0.01 μ; however, the value could not be estimated accurately from our micrographs. When very thin ribbons are separated out from a nonpolar solvent, they should develop a nonpolar surface. Therefore, it may be plausible to assume that the soap molecules are oriented along the direction of the thickness of the ribbon, exposing the methyl groups. In this case, the thickness corresponds to approximately the length of four molecules, and the width, to from several tens to several hundreds of molecules. In general, these ribbon-like fibers have a tendency to increase in width rather than in thickness by molecular association. The twisting is more clearly seen in a thinner fiber or a narrower ribbon.

One of the parameters of a helix is the sense of twist, to which we have particularly directed our interest in this study. The sense of twist is always definite for each enantiomer, regardless of the experimental conditions. The results are presented in Table 1. The sense of twist is left-handed for the D-acid and right-handed for the L-acid. On the other hand, the lithium soap gave results just opposite to the corresponding acid. The DL-acid (the racemic form) separated out not fibers, but plate-like crystals, and its lithium soap produced non-twisted fibers. Thus, an enantiomorphic relationship for the sense of twist between the D-enantiomer and the L-enantiomer was established for the acid as well as for the lithium soap.

It is a problem for further study what mechanism serves to twist the fibers. As is well known, twisted

Table 1. The sense of twist in the fibers from both enantiomers of 12-hydroxystearic acid and their lithium soaps

Enantiomer	The sense* of twist	
	Acid	Li soap
D	l	r
L	r	l

* r: right-handed twist, l: left-handed twist.

fibers are also formed from hydrated calcium tallowate grease. They consist of fibers with a right-handed twist and fibers with a left-handed twist in the same proportion. This indicates that, when optically non-active molecules aggregate to form twisted fibers, they exhibit both the sense of twist with an equal probability.

Several investigators[8a,b] have observed that the grease soap fibers have distinctly less twist without free end when prepared by a gentle deoiling manipulation, and that twisted fibers with a free end are often exhibited in cases involving the deformation of the gel structure by mechanical force during deoiling. Thus, it has been concluded that the twisted form is probably the result of mechanical breakdown. These investigations have been made with interest directed to the gel structure in lubricating grease. However, it is noticeable, from the molecular point of view, that the fibers exhibit the twisting when the fibers with a free end are produced. This fact shows also that the twisting occurs not only when the fibers grow, but also after they were formed. This indicates that the the isolated fiber has in itself a tendency to twist spontaneously. The enantiomorphism found for the sense of twist may also be considered as evidence that the twisting involves a molecular mechanism.

Here it seems appropriate to cite a paper by Weitkamp,[9] who observed that the dextro-rotatory anteiso acids ($CH_3CH_2CH(CH_3)(CH_2)_{2n}COOH$) from degras crystallize from solution in mineral oil in a tubular form which is generated by the counterclockwise spiral growth of a very thin and quite narrow ribbon. If the levo-rotatory acid is employed, the clockwise spiral growth of the ribbon will be observed.

As is well known, single crystals of optically-active antipodes exhibit the phenomenon of enantiomorphism. It is interesting to note that the enantiomorphism has been found to occur in the crystalline aggregate when the optical isomer aggregates to possess helical symmetry.

We wish to thank Professor Michio Shiota of this University for his helpful advice on the preparation of L-12-hydroxystearic acid. Thanks are also due to Miss Sanae Makino for her technical assistance. The expenses of this work have been defrayed by a Scientific Research Grant from the Ministry of Education.

8) a) M. J. Vold, V. A. Elersich, R. F. Baker and R. D. Vold, NLGI Spokesman, **18**(5), 8 (1954); b) A. L. McClellan and J. Cortes, *ibid.*, **20**(6), 12 (1956); c) J. M. Wilson, Jr., *ibid.*, **27**(12), 372 (1964); d) F. W. Anderson, R. C. Nelson and F. F. Farley, *ibid.*, **31**(7), 252 (1967).

9) A. W. Weitkamp, *J. Am. Chem. Soc.*, **67**, 447 (1945).

BULLETIN OF THE CHEMICAL SOCIETY OF JAPAN VOL. 42 3425—3433 (1969)

A Solvent-extraction and Spectrophotometric Study of Copper(II) Complexes in Organic Solvents Containing Acetylacetone and Thenoyltrifluoroacetone

Yuko HASEGAWA

Department of Chemistry, Science University of Tokyo, Kagurazaka, Shinjuku-ku, Tokyo

(Received May, 27, 1969)

The complex-formation equilibria of copper(II) in chloroform, benzene, or methyl isobutyl ketone (MIBK) containing both acetylacetone (AA) and thenoyltrifluoroacetone (TTA) have been determined by means of a liquid-liquid distribution method and a spectrophotometric method. The extraction constants or the extinction coefficients of the pure complexes were first determined in solutions containing only one of the liquids, and then these constants for the mixed complex and the equilibrium constants among the three complexes in these solvents were determined by the analysis of the results obtained from the experiments in mixed-ligand solutions. From these data, the following conclusions were reached. The constants experimentally obtained are almost identical with those statistically expected. The absorption spectrum of the mixed complex isolated from the absorption of the mixed-ligand system by the statistical analysis is more similar to that of the TTA complex than to that of the AA complex. The results obtained by these two methods are somewhat different from each other.

When the metal ion, the ligand ion, and the solvent molecules are denoted by M^{m+}, L^{l-}, and S respectively, the stepwise equilibria and the stability constants for the "*n*th" uninuclear complex in a solvent can generally be described as;

$$M_{n-1}^{m-(n-1)l}S_a + L^{l-}S_b \rightleftarrows ML_n^{m-nl}S_c + (a+b-c)S \quad (1)$$

$$K'_n = \frac{\{ML_n^{m-nl}S_c\}\{S\}^{a+b-c}}{\{ML_{n-1}^{m-(n-1)l}S_a\}\{L^{l-}S_b\}} \quad (2)$$

The over-all formation equilibria and the stability constants can be described as;

$$M^{m+}S_d + n(L^{l-}S_b) \rightleftarrows ML_n^{m-nl}S_c + (d+nb-c)S \quad (3)$$

$$\beta'_n = \frac{\{ML_n^{m-nl}S_c\}\{S\}^{d+nb-c}}{\{M^{m+}S_d\}\{L^{l-}S_b\}^n} \quad (4)$$

The complex formation can be represented more generally by Eqs. (1) and (2) or (3) and (4). However, as it is not easy to determine the solvation number or the activity of each chemical species, the solvent molecules are eliminated from these equations, assuming that the solvent activity is kept constant, and in many cases the concentration unit is adopted instead of the activity unit, assuming that the changes in the activity coefficients are negligible under the considerations employed. Thus, the stability constants can usually be represented by these two equations:

$$K_n = \frac{[ML_n^{m-nl}]}{[ML_{n-1}^{m-(n-1)l}][L]^{-l}} \quad (5)$$

$$\beta_n = \frac{[ML_n^{m-nl}]}{[M^{m+}][L^{l-}]^n} \quad (6)$$

The constant in Eq. (5) or (6) is a conventional expression for Eq. (2) or (4).

In aqueous solutions, the stability constants in Eqs. (5) and (6) are determined by various experimental methods. In usual organic solvents, however, the dielectric constant is much smaller, and consequently the concentration of any charged species is too small to measure by practical experimental methods; thus, the determination of the stability constants of metal complexes in Eqs. (5) and (6) is not possible. In order to correlate various complex formation equilibria of a metal ion with various ligands in organic solutions, the present author has employed the following equations instead of Eqs. (5) and (6), because the chemical species experimentally determined in usual organic solvents should be uncharged only.

$$MA_m(org) + nHB(org) \rightleftarrows MA_{m-n}B_n(org) + nHA(org) \quad (7)$$

$$K_{m,n} = \frac{[MA_{m-n}B_n]_{org}[HA]^n_{org}}{[MA_m]_{org}[HB]^n_{org}} \quad (8)$$

$$MA_m(org) + MB_m(org) \rightleftarrows MA_aB_{(m-a)}(org) + MA_{(m-a)}B_a(org) \quad (9)$$

$$K = \frac{[MA_aB_{(m-a)}]_{org}[MA_{(m-a)}B_a]_{org}}{[MA_m]_{org}[MB_m]_{org}} \quad (10)$$

The present paper will describe the complex formation of copper(II) in chloroform, benzene, and

methyl isobutyl ketone (MIBK) containing acetylacetone (AA), thenoyltrifluoroacetone (TTA), or a mixture of these two β-diketones. The equilibrium constants given by Eqs. (8) and (10) will be calculated from the solvent extraction data and the spectrophotometric data, and some discussion will be given of this type of stability constants of metal complexes in such organic solvents.

Statistical Treatment

When an organic solvent contains copper(II) and two organophilic chelating acids, HA and HB, and when no formation of polynuclear complex or of adduct complex is assumed, three sorts of copper(II) complexes, CuA_2, CuAB, and CuB_2 may be expected to exist. The equilibria among these three species may be described as follows:

$$CuA_2(org) + HB(org) \rightleftharpoons CuAB(org) + HA(org) \quad (11)$$

$$CuA_2(org) + 2HB(org) \rightleftharpoons CuB_2(org) + 2HA(org) \quad (12)$$

and the equilibrium constants may be defined as:

$$K_{1,1} = \frac{[CuAB]_{org}[HA]_{org}}{[CuA_2]_{org}[HB]_{org}} \quad (13)$$

$$K_{0,2} = \frac{[CuB_2]_{org}[HA]^2_{org}}{[CuA_2]_{org}[HB]^2_{org}} \quad (14)$$

The following equlibrium constant can also be defined:

$$CuA_2(org) + CuB_2(org) \rightleftharpoons 2CuAB(org)$$

$$K = \frac{[CuAB]^2_{org}}{[CuA_2]_{org}[CuB_2]_{org}} \quad (15)$$

Solvent Extraction Method. In an earlier paper, Sekine and Dyrssen[1] have demonstrated that the equilibrium constants in Eqs. (13), (14), and (15) can be determined by a solvent extraction method. When copper(II) ions in aqueous solutions are extracted with HA in the organic phase, the equilibrium constant can be described as;

$$Cu^{2+} + 2HA(org) \rightleftharpoons CuA_2(org) + 2H^+ \quad (16)$$

$$K_{ex_{2,0}} = \frac{[CuA_2]_{org}[H^+]^2}{[Cu^{2+}][HA]^2_{org}} \quad (17)$$

The net distribution ratio of copper(II) can be determined as;

$$D = \frac{[Cu(II)]_{org,total}}{[Cu(II)]_{total}} \quad (18)$$

When only Cu^{2+} species is assumed to exist in the aqueous phase and only the CuA_2 species in the organic phase, Eq. (17) can be described as;

$$K_{ex_{2,0}} = D[H^+]^2[HA]^{-2}_{org} \quad (19)$$

In the same manner, the following can serve to describe the extraction constant for copper(II) with HB:

$$K_{ex_{0,2}} = \frac{[CuB_2]_{org}[H^+]^2}{[Cu^{2+}][HB]^2_{org}} \quad (20)$$

or:

$$K_{ex_{0,2}} = D[H^+]^2[HB]^{-2}_{org} \quad (21)$$

When the organic phase contains both HA and HB, copper(II) may be extracted as CuA_2, CuAB, and CuB_2 species and the extraction constant to the mixed complex may be described as:

$$Cu^{2+} + HA(org) + HB(org) \rightleftharpoons CuAB(org) + 2H^+ \quad (22)$$

$$K_{ex_{1,1}} = \frac{[CuAB]_{org}[H^+]^2}{[Cu^{2+}][HA]_{org}[HB]_{org}} \quad (23)$$

The net distribution ratio in such a system can be described as:

$$D = \frac{[CuA_2]_{org} + [CuAB]_{org} + [CuB_2]_{org}}{[Cu^{2+}]} \quad (24)$$

$$\frac{[CuAB]_{org}}{[Cu^{2+}]} = D - \frac{K_{ex_{2,0}}[HA]^2_{org} + K_{ex_{2,0}}[HB]^2_{org}}{[H^+]^2} \quad (25)$$

By introducing Eq. (25) into Eq. (23), the extraction constant for the mixed complex, $K_{ex_{1,1}}$, can be determined.

From Eqs. (17), (20), and (23), the K constant, the equilibrium constant for the mixed complex in Eq. (15), is obtained as;

$$K = \frac{K^2_{ex_{1,1}}}{K_{ex_{2,0}}K_{ex_{0,2}}} \quad (26)$$

Sekine and Dyrssen[1] reported that the statistical value of K is 4.

Moreover, the constants can be introduced into Eqs. (13) and (14) as;

$$K_{1,1} = K_{ex_{1,1}}/K_{ex_{2,0}} \quad (27)$$

$$K_{0,2} = K_{ex_{0,2}}/K_{ex_{2,0}} \quad (28)$$

Spectrophotometric Method. The equilibrium constants in Eqs. (13) and (14) can also be determined by a spectrophotometric method.

When the molar extinction coefficients of the CuA_2, CuAB, and CuB_2 species at a certain wavelength are ε_{A_2}, ε_{AB}, and ε_{B_2}, the total absorbance of a sample solution may be described as;

$$E = \varepsilon_{A_2}[CuA_2]_{org} + \varepsilon_{AB}[CuAB]_{org} + \varepsilon_{B_2}[CuB_2]_{org} \quad (29)$$

By introducing Eqs. (13) and (14) into Eq. (29), the following equation is obtained:

$$E = [CuA_2]_{org}(\varepsilon_{A_2} + \varepsilon_{AB}K_{1,1}\alpha + \varepsilon_{B_2}K_{0,2}\alpha^2) \quad (30)$$

where α denotes the mixing ratio: $[HB]_{org}/[HA]_{org}$.

The total concentration of copper(II) is written as:

$$C = [CuA_2]_{org} + [CuAB]_{org} + [CuB_2]_{org} = [CuA_2]_{org}(1 + K_{1,1}\alpha + K_{0,2}\alpha^2) \quad (31)$$

1) T. Sekine and D. Dyrssen, *J. Inorg. Nucl. Chem.*, **26**, 2013 (1964).

From Eqs. (30) and (31), the following equation is obtained:

$$\frac{E}{C} - \varepsilon_{B_2} = \frac{(\varepsilon_{A_2} - \varepsilon_{B_2}) + (\varepsilon_{AB} - \varepsilon_{B_2})K_{1,1}\alpha}{1 + K_{1,1}\alpha + K_{0,2}\alpha^2} \quad (32)$$

The ε_{A_2} and ε_{B_2} values can be determined by separate experiments. The total copper(II) concentration, C, can be known from the initial concentration, and the total extinction, E, can be determined by spectrophotometry. Moreover, when the concentrations of the chelating acids are much larger than the total copper(II) concentration, we may assume no change in the chelating acid concentrations by the complex formation and may use the initial concentrations instead of those at equilibrium for the calculation of the constants.

In the above case, the unknown terms in Eq. (32) are ε_{AB}, $K_{1,1}$ and $K_{0,2}$ and we can determine these from the total absorbances determined at more than three different α values.

Graphical Treatment of the Spectrophotometric Data. From Eq. (32), the following equation is obtained:

$$\log\left(\frac{E}{C} - \varepsilon_{B_2}\right) = \log\{(\varepsilon_{A_2} - \varepsilon_{B_2}) + K_{1,1}(\varepsilon_{AB} - \varepsilon_{B_2})\} - \log(1 + K_{1,1}\alpha + K_{0,2}\alpha^2) \quad (33)$$

The values $\log(E/C - \varepsilon_{B_2})$ obtained experimentally at a certain wavelength are plotted against α, while a certain set of the assumed values of $K_{1,1}(\varepsilon_{AB} - \varepsilon_{B_2})$, $K_{1,1}$ and $K_{0,2}$ are introduced to Eq. (33) and the curve thus drawn is fitted with the plot. The trial is repeated until the best-fit curve for the data is found. The constants will be then determined from the parameters of the best-fit curve.

Experimental

Tracer. A pure copper sheet (99.98%) was irradiated with thermal neutrons in the TRIGA-3 reactor at the Atomic Research Institute of St. Paul's University, Kanagawa. The copper sheet was then dissolved in hot concentrated nitric acid. The solution was evaporated gradually on a water bath, and the residue was dissolved in 0.1 M perchloric acid. The solution thus obtained was used as the copper tracer stock solution.

Reagents. All of the reagents used were of a reagent grade. The acetylacetone and thenoyltrifluoroacetone were obtained from Dojindo & Co. When they were dissolved in an organic solvent, the solution was allowed to stand overnight before use. The methyl isobutyl ketone was washed with 0.1 M perchloric acid, water, and a 0.1 M sodium hydroxide solution, and then several times with water. The chloroform was washed three times with water. The other reagents were used without further purification.

Procedures. All of the procedures were carried out in a thermostatted room at 25±0.5°C.

Solvent Extraction Method. The distribution ratio of copper(II) was measured as follows. Stoppered glass tubes (volume, 20 m*l*) were used to equilibrate the two liquid phases. Five milliliters of chloroform, benzene, or MIBK containing 0.1 M TTA or AA or containing both of them at a different mixing ratio, and 5 m*l* of a mixture of 0.1M perchloric acid and 0.1M sodium perchlorate containing the copper(II) tracer were placed in the tubes. The initial concentration of copper(II) in the aqueous phase was in the range $1-5\times10^{-5}$M. The two phases were agitated mechanically for thirty minutes and then centrifuged. A two-milliliter portion was pipetted from each phase. These portions were transferred into small glass tubes for the measurement of the γ-radioactivity with a well-type (NaI) scintillation counter. For the experiments at hydrogen-ion concentrations smaller than 0.01 M, a small portion was also taken from the aqueous phase and transferred into a glass vessel; the hydrogen-ion concentration of this solution was measured potentiometrically by using 0.0100 M $HClO_4$ +0.09 M $NaClO_4$ as the standard of $-\log[H^+]$ 2.00.

The net distribution ratio was calculated as:

$$D = \frac{[Cu(II)]_{org,total}}{[Cu(II)]_{total}} = \frac{\gamma\text{-count-rate per m}l\text{ of the org. phase}}{\gamma\text{-count-rate per m}l\text{ of the aq. phase}}$$

Spectrophotometric Method. A certain amount of metallic copper (99.98%) was dissolved in concentrated nitric acid. An excess amount of a dilute sodium hydroxide solution was added to the copper(II) solution, and the copper(II) hydroxide precipitates were collected by decantation and gradually heated in water. The copper(II) oxide thus prepared was finally obtained as a dry powder and was dissolved in an organic solution containing a large excess of TTA or AA to make the stock solution. The sample solutions of copper(II) were prepared from one of the stock solutions or from mixtures of them and were measured by a spectrophotometer (Hitachi-Perkin Elmer type 139) using quartz cells 1 cm thick.

Results

Solvent Extraction Experiments.

Extraction with a Single Chelating Acid. The distribution of copper(II) between 0.1 M (H, Na)ClO_4 and chloroform, benzene, or MIBK containing 0.1 M TTA or AA was determined as a function of $-\log[H^+]$. The log$D$ *vs.* $-\log[H^+]$ plot in these systems almost falls on a straight line, with a slope of +2 in the region around $-\log[H^+]$ 2.00, but some deviations from the line were observed (especially in the AA system) in the higher $-\log[H^+]$ range. These deviations were assumed to be due to the aqueous chelate formation. Some other experiments showed no adduct formation of these Cu(II) chelates with the extractants in the undissociated form. Thus, it was concluded that when the organic phase contains 0.1 M chelating acid and when the aqueous phase contains the 0.1 M hydrogen ion, the net distribution ratio can be described by the relation: $D=[CuA_2]_{org}/[Cu^{2+}]$. From

Table 1. The extraction constants of Cu(II) in 0.1 M (H, Na)ClO_4 with TTA, AA or mixtures of TTA and AA in three organic solvents

	$CHCl_3$		C_6H_6		MIBK	
	Solv.	Spec.	Solv.	Spec.	Solv.	Spec.
$\log K_{ex_{2,0}}$*	−1.23		−0.73		−1.05	
$\log K_{ex_{1,1}}$**	−1.95		−2.04		−2.38	
$\log K_{ex_{0,2}}$***	−2.98		−3.76		−3.78	
$\log K_{1,1}$	−0.72	−0.22	−1.31	−0.80	−1.17	−0.55
$\log K_{0,2}$	−1.75	−1.02	−3.04	−2.30	−2.73	−1.59
$\log K_{obs.}$	0.31	0.58	0.42	0.70	0.39	0.49
$\log K_{ex_{1,1}\,stat.}$	−1.81		−1.95		−2.22	
$\log \frac{K_{ex_{1,1}\,exp.}}{K_{ex_{1,1}\,stat.}}$	−0.14		−0.09		−0.16	

* Extraction constant for $Cu(TTA)_2$ species.
** Extraction constant for Cu(TTA, AA) species.
*** Extraction constant for $Cu(AA)_2$ species.

Table 2. Extraction of Cu(II) with mixture of TTA(HA) and AA(HB)

Aqueous phase: 0.01 M $HClO_4$+0.09 M $NaClO_4$
Organic phase: $[HA]_{org}+[HB]_{org}=0.10$ M
$[HB]_{org}/[HA]_{org}=\alpha$
$D_{mixed}=[CuAB]_{org}/[Cu^{2+}]$ (*cf.* Eq. (25))

(a) $CHCl_3$			(b) C_6H_6			(c) MIBK		
α	$\log D$	$\log D^*_{mixed}$	α	$\log D$	$\log D^*_{mixed}$	α	$\log D$	$\log D^*_{mixed}$
1.5	0.107	−0.587	7.3	−0.907	−1.947	7.3	−0.115	−1.831
3.2	−0.182	−0.642	9.0	−1.017	−1.781	9.0	−1.253	−1.950
4.0	−0.288	−0.723	11.5	−1.148	−1.735	11.5	−1.391	−2.015
5.3	−0.382	−0.777	15.7	−1.297	−1.728	15.7	−1.508	−1.929
9.0	−0.563	−0.943	24.0	−1.537	−1.929	24.0	−1.737	−2.161
15.7	−0.710	−1.155	49.0	−1.837	−2.184	49.0	−1.959	−2.381

* From these data, the values of $K_{ex_{1,1}}(=D_{mixed}[H^+]^2[HA]^{-1}{}_{org}[HB]^{-1}{}_{org})$ were calculated and the average values are given in Table 1.

these results, the extraction constants for copper(II) with TTA or AA were calculated to be as given by Eq. (19) or (21) (*cf.* Ref. 2). The extraction constants obtained are given in Table 1.

Extraction with Mixed Chelating Acids. The distribution of copper(II) between 0.1 M (H, Na)ClO_4 and chloroform, benzene, or MIBK containing both TTA(HA) and AA(HB) was also studied. For these experiments, $-\log[H^+]$ was always kept at 2.00 and the total concentration of the chelating acids in the organic phase was kept at 0.10 M. The results are given in Table 2. From these results, the extraction constant of the mixed chelate was determined by means of Eqs. (23) and (25). The constants are also given in Table 1.

Spectrophotometric Experiments.

Absorption Spectra of Copper(II)-bis-TTA and Copper-(II)-bis-AA Chelates. The absorption spectra of the copper(II)-bis-TTA chelates and of the copper-(II)-bis-AA chelates were measured in chloroform, benzene, or MIBK containing 0.1 M of the chelating acid, while the copper concentration was 2×10^{-4} to 8×10^{-4} M. Figure 1 gives the results in chloroform.

As may be seen in Fig. 1, the absorption spectrum of copper(II)-bis-TTA chelates has a pronounced peak at 407 mμ, while that of the copper(II)-bis-AA chelates has one at 332 mμ. From these results, the molar extinction coefficients were determined to be as given in Table 3.

The Absorption of Copper(II) Complexes in Mixed Chelating-acid Systems. The absorption of copper-(II) complex was also measured when the organic solvents contained both TTA and AA at various mixing ratios and when the copper concentration was 8×10^{-4} M.

Figure 2 gives the absorption curves obtained when the mixing raio α was 1, 3, 5, 9, 13, and 47, together with the curve obtained when the organic phase contained only TTA or AA.

A graphic method was used to analyze the results in Fig. 2. For example, the data obtained in

2) T. Sekine and D. Dyrssen, *J. Inorg. Nucl. Chem.*, **26**, 1727 (1964).

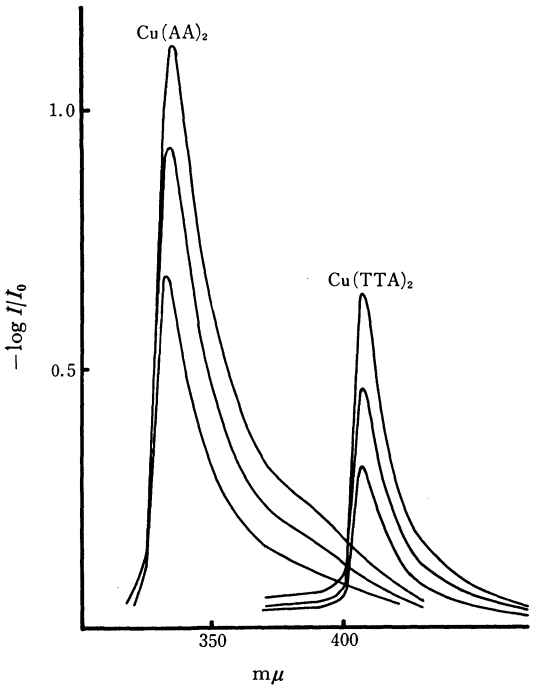

Fig. 1. The absorption spectra of Cu(II)-bis-acetylacetonate and Cu(II)-bis-thenoyltrifluoro-acetonate complexes in chloroform. The concentrations of the complexes are 4, 6 and 8× 10^{-4} M. The maximum absorptions are at 332 mμ and 407 mμ for AA and TTA, respectively.

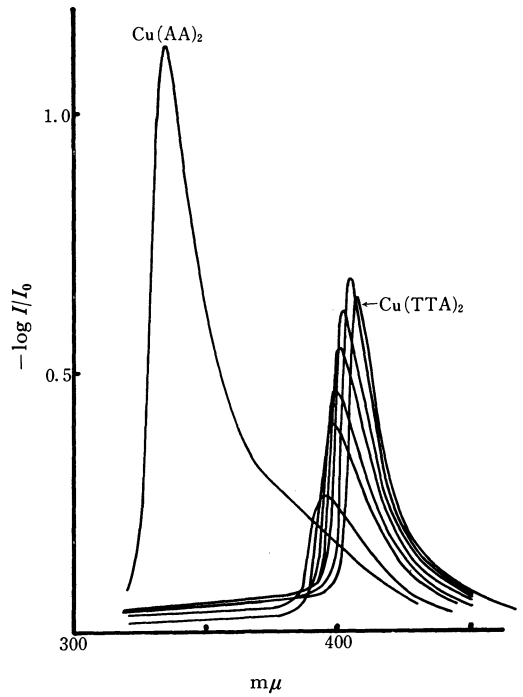

Fig. 2. The absorption spectra of Cu(II) complexes in chloroform containing acetylacetone and thenoyltrifluoroacetone. The mixing ratios, [AA]/[TTA], are 1, 3, 5, 9, 13 and 47.

TABLE 3. MOLAR EXTINCTION COEFFICIENTS OF Cu(II) CHELATES IN THREE ORGANIC SOLVENTS

Solvent	Chelate	mμ		
		400	410	420
$CHCl_3$	$\varepsilon_{Cu(TTA)_2}$	148	688	353
	$\varepsilon_{Cu(TTA,AA)}$	1121	691	395
	$\varepsilon_{Cu(AA)_2}$	211	150	101
C_6H_6	$\varepsilon_{Cu(TTA)_2}$	108	633	335
	$\varepsilon_{Cu(TTA,AA)}$	829	471	311
	$\varepsilon_{Cu(AA)_2}$	245	177	111
MIBK	$\varepsilon_{Cu(TTA)_2}$	693	512	262
	$\varepsilon_{Cu(TTA,AA)}$	1030	591	341
	$\varepsilon_{Cu(AA)_2}$	218	155	99

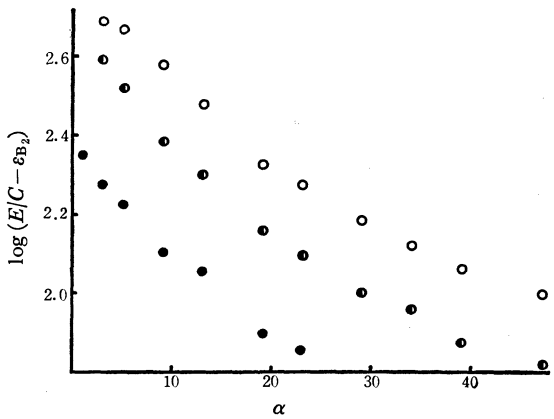

Fig. 3. The change in the absorption at 400 (○), 410 (◐) and 420 (●) mμ by the change of mixing ratio in chloroform expressed by the log $(E/C-\varepsilon_{B_2})$ *vs.* α plot.
C: $[Cu(II)]_{total}=8\times10^{-4}$ M
ε_{B_2}: Molar extinction coefficient of copper(II) acetylacetonate $\varepsilon_{400}=211$, $\varepsilon_{410}=150$, $\varepsilon_{420}=101$

the chloroform system were analyzed as follows. The log $(E/C-\varepsilon_{B_2})$ *vs.* α plot was made from the absorption data, E, at 400, 410, and 420 mμ, as is shown in Fig. 3, and attempts were made to find the best-fit constants, $K_{1,1}$ and $K_{0,2}$, for these data. Finally, it was found that the "best-fit" was obtained when $K_{1,1}$ and $K_{0,2}$ were 1.2 and 0.20 and when the ε_{AB} values were 1150, 740, and 407 at 400, 410, and 420 mμ respectively. The values of ε_{AB} from 380 mμ to 430 mμ were calculated by introducing these $K_{1,1}$ and $K_{0,2}$ values and the values ε_{A_2} and ε_{B_2} calculated from the data in Fig. 1. The molar extinction coefficients thus calculated are given in Fig. 4 as a function of the wavelengths.

Figure 5 shows the contribution of each chelate species to the total absorption in chloroform, as calculated by Eqs. (13), (14) and (31), when the

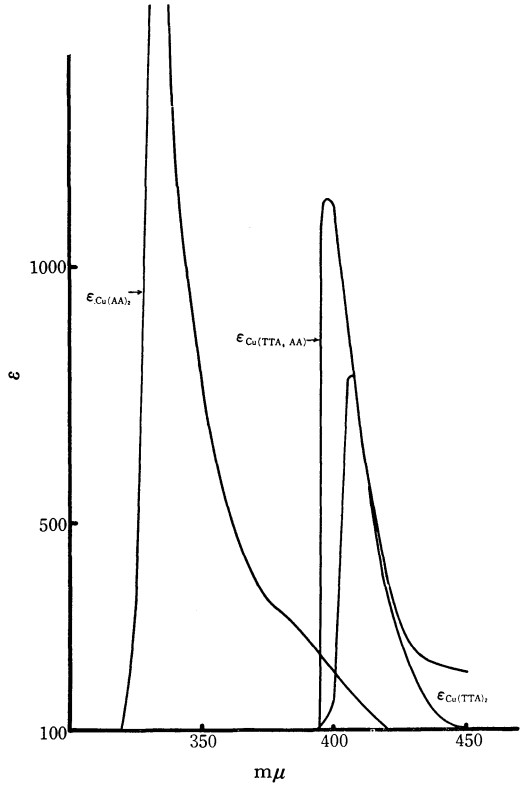

Fig. 4. Molar extinction coefficients of Cu(II) complexes with AA and/or TTA in chloroform. The absorption of Cu(II) complex with TTA and AA is the calculated curve from the data in Fig. 3 (See text).

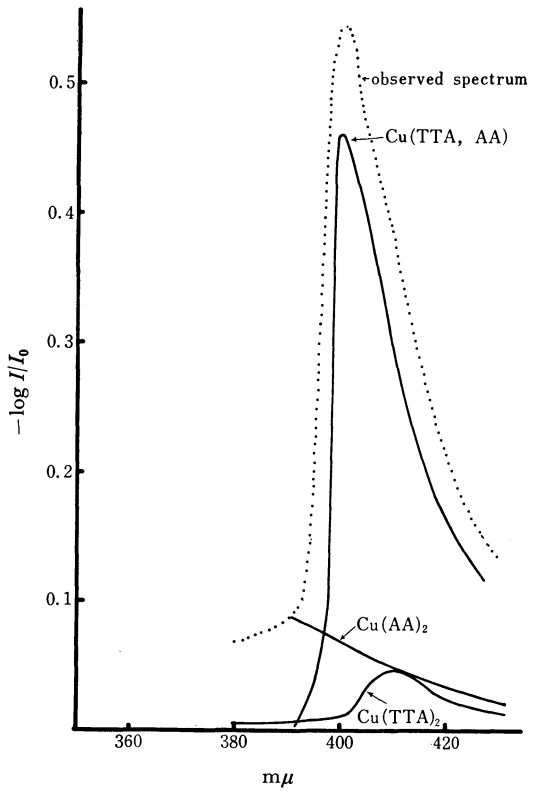

Fig. 5. The contribution of the absorption of the component species to the observed net absorption calculated by Eqs. (33) and (35) using the constants in Table 1.
Solvent; chloroform
The dotted line gives the observed spectrum in the sample solution where $[Cu(II)]_{total}$ is 8×10^{-4} M, $[TTA]_{org}$ is 1.67×10^{-2} M and $[AA]_{org}$ is 8.33×10^{-2} M ($\alpha=5$).
The solid lines show the calculated spectra of $Cu(TTA)_2$ and $Cu(AA)_2$ at this concentration of TTA and AA.

total copper(II) concentration is 8×10^{-4} M and when the the concentrations of TTA and AA are 1.67×10^{-2} and 8.33×10^{-2} M respectively.

The same procedures were carried out on the data obtained in benzene and MIBK. The equilibrium constants, $K_{1,1}$ and $K_{0,2}$, in these systems are also given in Table 1.

By using the $K_{1,1}$ and $K_{0,2}$ constants, in Table 1, which were obtained by both the methods, the percentage distribution of the mixed chelate complex was calculated by the following equation:

$$\%\ \text{distribution of } [CuAB]_{org} = \frac{[CuAB]_{org}\times 100}{[CuA_2]_{org}+[CuAB]_{org}+[CuB_2]_{org}} = \frac{K_{1,1}\alpha\times 100}{1+K_{1,1}\alpha+K_{0,2}\alpha^2} \quad (34)$$

Figure 6 shows the percentage distribution of the three sorts of Cu(II) chelates in chlofoform as a function of the mixing ratio, α. Figure 6-a was calculated from the constants obtained by the solvent extraction, and Fig. 6-b, by spectrophotometry. It may be seen from Fig. 6 that the area of the zone of the mixed complex obtained by the spectrophotometry is larger than that obtained by the solvent extraction. Moreover, the α value at the maximum percentage distribution of the mixed complexes is different ($\alpha=0.88$ by the solvent extraction and 0.51 by the spectrophotometry).

The results thus obtained may be summarized as follows: i) The extraction constant of the copper (II) TTA complex is always larger than that of the copper(II) AA complexes (Table 1).

ii) The extraction constants of the copper(II) TTA-AA mixed complexes experimentally determined are in all cases a little smaller than those statistically calculated, but the differences are not large (the $K_{ex_{1,1}exp.}/K_{ex_{1,1}stat.}$ values are 0.72, 0.81 and 0.69 in chloroform, benzene and MIBK respectively) (Table 1).

iii) The absorption peak of the copper(II)-bis-TTA complex exists over a longer wavelength range than that of the AA complex, and the molar extinction coefficient at the peak of the former is

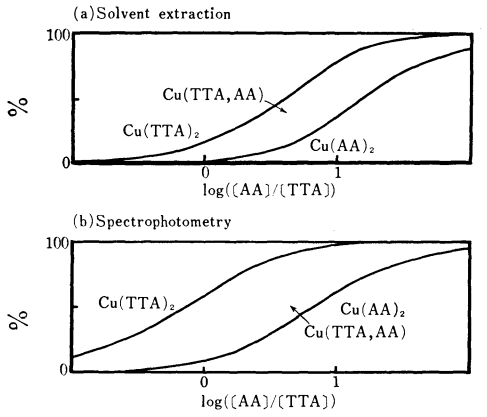

Fig. 6. Percentage distribution of the mixed complexes in chloroform as a function of the mixing-ratio is calculated from the constants in Table 1.

lower than that of the latter (Fig. 1).

iv) The absorption peak of the copper(II) mixed complex with TTA and AA exists over a little shorter wavelength range than that of the Cu(II)-bis-TTA complex, and the molar extinction coefficient of the mixed complex at the peak is a little higher than that of the bis-TTA complex, but much lower than that of the bis-TTA complex (Fig. 4).

v) The values of these constants, $K_{1,1}$, $K_{0,2}$, and K, are different in different organic solvents. The constants obtained by the solvent extraction method are larger in the order: chloroform > MIBK > benzene, while those obtained by the spectrophotometric method are larger in the order: benzene > chloroform > MIBK. Thus, there are some differences in the constants obtained by these two different methods.

Discussion

The extraction constant of copper(II) with AA in benzene has been given as $\log K_{ex}$ −3.76 (present work), −3.93 (Stary and Hladky[3]), and −4.32 (Newman and Klotz[4]), while that with TTA in benzene has been given as $\log K_{ex}$ −0.73 (present work) and −1.32 (Newman and Klotz[4]). It seems to be difficult to ascertain why these extraction constants are so different from each other. However, according to the present results, some part of the copper(II) ions in the aqueous phase are complexed with AA (aqueous chelate formation) under the experimental conditions which Newman and Klotz used in working (0.2 M TTA in benzene and $-\log[H^+]$ 2.20 in 2 M LiCl), and thus the K_{ex} value calculated by using Eq. (19) or (21) is apparently smaller because of the aqueous chelates.[5] Moreover, the presence of chloride ions at such a high concentration may form copper chloride complexes.[6]

The extraction constant of the copper mixed complex with AA and TTA in benzene in the present study is a little smaller than the statistically-calculated values ($K=[CuAB]^2_{org}/[CuA_2]_{org}[CuB_2]_{org}=$ 2.4, compared with the statistical value, 4), although Newman and Klotz reported that the experimental value is larger than the statistical value ($K=10$). The difference between the present results and the earlier results is not small. One possible explanation for this might be that the use of the underestimated $K_{ex_{0,2}}$ due to the aqueous chelate complex in the earlier work caused an overestimation of the concentration of the mixed chelate in the organic phase.

It was observed by Sekine and Dyrssen[1] that the experimental value of the copper mixed chelate complex with TTA and β-isopropyltropolone (IPT) is more stable than the statistical value and that the stabilization increases with the decrease in the polarity of the solvents (K is 54 for carbon tetrachloride, 30 for chloroform, and 8.9 for MIBK). This order is still retained in the present results, though the mixed complexes are less stable than the statistical values.

The formation of the mixed complex can be apparently observed in the spectrophotometric data in Fig. 2; for example, the absorption peak in the chloroform solution containing 0.05 M TTA and 0.05 M AA (in Fig. 2, it is denoted as the 1 : 1 curve) shifts to a shorter wavelength for the TTA complex and the maximum absorbance increases a little. This can not be explained only in terms of the synthesis of the $Cu(AA)_2$ and $Cu(TTA)_2$ absorption curves.

Figure 7 gives the curve synthesized from the data in Fig. 1 assuming no mixed complex formation. The mixed complex formation can be seen also from Fig. 7, in which the peak of the calculated curve shifts to the shorter wavelength side for the peak of $Cu(TTA)_2$, while the maximum absorbance decreases considerably. This is quite different from the formation observed in Fig. 2. The difference is probably due to the absorption of the mixed complex.

It is remarkable that the maximum extinction of the mixed complex does not appear in midway in the maxima of the extinction of the pure complexes, but appears quite close to that of the $Cu(TTA)_2$ complex. The value of the extinction at the maximum absorption of the mixed complex is also

3) J. Stary and E. Hladky, *Anal. Chim. Acta*, **28**, 227 (1963).

4) L. Newman and P. Klotz, "Solvent Extraction Chemistry," Proceedings of the International Conference, Gothenburg (1966), p. 128.

5) T. Sekine, M. Sakairi, F. Shimada and Y. Hasegawa, This Bulltin, **38**, 847 (1965).

6) L. G. Sillen and A. E. Martell, "Stability Constants," The Chemical Society, Spec. Pub. 17, (1964).

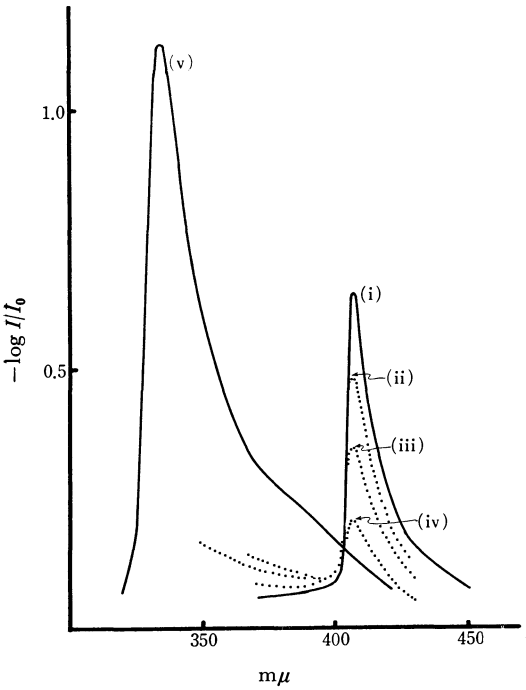

Fig. 7. Calculated absorption curves assuming no mixed complex formation in the system; that is, assuming the existence of only the $Cu(TTA)_2$ and $Cu(AA)_2$ at the following concentrations.
$[Cu(II)]_{org,\ total}=8\times10^{-4}$ M
i) $[Cu(TTA)_2]_{org}=8\times10^{-4}$ M
ii) $[Cu(TTA)_2]_{org}=6\times10^{-4}$ M
$[Cu(AA)_2]_{org}=2\times10^{-4}$ M
iii) $[Cu(TTA)_2]_{org}=4\times10^{-4}$ M
$[Cu(AA)_2]_{org}=4\times10^{-4}$ M
iv) $[Cu(TTA)_2]_{org}=2\times10^{-4}$ M
$[Cu(AA)_2]_{org}=6\times10^{-4}$ M
v) $[Cu(AA)_2]_{org}=8\times10^{-4}$ M

nearer to that of the TTA complex. Further consideration seems to be necessary in order to discuss this resemblance of the extinction of the mixed complex to that of the $Cu(TTA)_2$ complex.

In order to analyze the spectrophotometric data, it was always assumed that the ligands exist in a large excess to copper(II), that, that is, the free-ligand concentration is not changed by the complex formation. This assumption seems to hold even when the mixing ratio is very large or when the initial TTA concentration is very low. For example, in Fig. 3 it may be understood that the analysis can be made even by using the data at $\alpha=40$. Here the total copper concentration is 8×10^{-4} M, while the initial TTA concentration is 2.5×10^{-3} M. However, as may be seen from Fig. 6-b, more than 85% of the copper(II) exists in the CuA_2 form, and thus only about 1.2×10^{-4} M of TTA is complexed with copper(II). The change in the free TTA concentration is only about 5%, which might not cause any significant error in the calculation.

The analysis of the spectrophotometric data is more complicated than that of the solvent extraction data, because in the solvent extraction the unknown constants to be calculated are only $K_{1,1}$ and $K_{0,2}$. As we can see from Eqs. (27) and (28), $K_{0,2}$ can be easily determined from the extraction constants for the pure complexes, $K_{ex2,0}$ and $K_{ex0,2}$, which can themselves be determined by separate experiments. The $K_{ex1,1}$ constant can be calculated from the experimental data in the mixed extractant system by using these $K_{ex2,0}$ and $K_{ex0,2}$ values and Eqs. (25) and (23). Thus, these equilibrium constants can be obtained even from a single value of the distribution data in the mixed chelate system. On the other hand, the unknown constants to be determined in the spectrophotometric study are not only $K_{0,2}$ and $K_{1,1}$, but also the molar extinction coefficients of the mixed complex, ε_{AB}. Thus, we have to determine these three constants simultaneously from a series of absorption data.

As we can see in Table 1 or in Fig. 6, the stabilities of the mixed complex as calculated by the solvent extraction data and by the spectrophotometric data are somewhat different from each other. The essential difference in the experimental conditions is that the organic phase in the spectrophotometry is not saturated with water, while that in the solvent extraction is saturated with water; probably this does not cause any significant difference, although our present information on these systems seems not to be enough for us to discuss whether these differences are due to some unknown factors which cause a systematic deviation in the results of one or both of the methods or whether they are due to an essential difference, one which might arise from the fact that these two methods determined the mixed complex formation from different sides of the phenomenon. Further study seems to be necessary before we can obtain an explanation of this observation.

As was described in the beginning of this paper, the usual stability constants of aqueous complexes defined by Eqs. (5) and (6) are a convenient expression of Eqs. (2) and (4). This means that the stability constants in Eqs. (5) and (6) show the "relative" stability of the metal aquo complex and the metal complexes with L^-, just as Eq. (8) gives the relative stability of the MA_m complex and $MA_{m-n}B_n$ complex. If we take the $Cu(TTA)_2$ complex as the standard of various uncharged complexes in a certain organic phase, we can compare the stabilities of two or more other complexes by using these constants.

When we compare the stability of an aqueous "nth" complex, MA_n^{m-n}, with another "nth" complex, MB_n^{m-n}, we usually use the β_n^A/β_n^B ratio. When we can assume that the hydration numbers of the MA_n^{m-n} and MB_n^{m-n} complexes and those of the A^- and B^- ligands are the same, we see that the ratio of the more generalized stability constants in Eq. (4), β'^A_n/β'^B_n, should be the same as β_n^A/β_n^B.

In the present paper, the relative stability constants for only a pair of ligands, TTA and AA, have been determined. However, if the relative stability constants for another pair of ligands, for example, TTA and a chelating acid HBB, we can compare the stability of the AA complex with the BB complex, as in the follwoing equations:

$$Cu(TTA)_2 + 2HAA \rightleftharpoons Cu(AA)_2 + 2HTTA \quad (35)$$

$$Cu(TTA)_2 + 2HBB \rightleftharpoons Cu(BB)_2 + 2HTTA \quad (36)$$

$$K_{0,2}^{TTA-AA} = \frac{[Cu(AA)_2]_{org}[HTTA]^2_{org}}{[Cu(TTA)_2]_{org}[HAA]^2_{org}} \quad (37)$$

$$K_{0,2}^{TTA-BB} = \frac{[Cu(BB)_2]_{org}[HTTA]^2_{org}}{[Cu(TTA)_2]_{org}[HBB]^2_{org}} \quad (38)$$

$$\frac{[Cu(BB)_2]_{org}[HAA]^2_{org}}{[Cu(AA)_2]_{org}[HBB]^2_{org}} = \frac{K_{0,2}^{TTA,\,BB}}{K_{0,2}^{TTA,\,AA}} \quad (39)$$

This could be compared with the aqueous complexes with AA and BB as follows:

$$Cu^{2+}(H_2O)_a + 2AA^-(H_2O)_b \rightleftharpoons Cu(AA)_2(H_2O)_c \quad (40)$$

$$Cu^{2+}(H_2O)_a + 2BB^-(H_2O)_b \rightarrow Cu(BB)_2(H_2O)_c \quad (41)$$

$$(\beta^{AA})'_2 = \frac{[Cu(AA)_2(H_2O)_c]}{[Cu^{2+}(H_2O)_a][AA^-(H_2O)_b]^2} \quad (42)$$

$$(\beta^{BB})'_2 = \frac{[Cu(BB)_2(H_2O)_c]}{[Cu^{2+}(H_2O)_a][BB^-(H_2O)_b]^2} \quad (43)$$

Then we can introduce:

$$\frac{[Cu(BB)_2(H_2O)_2][AA^-(H_2O)_b]^2}{[Cu(AA)_2(H_2O)_c][BB^-(H_2O)_b]^2} = \frac{(\beta^{BB})'_2}{(\beta^{AA})'_2} \quad (44)$$

Equation (44) should be essentially the same as the ratio of the usual stability constants, $\beta_2^{BB}/\beta_2^{AA}$, which is very often used in order to compare the stabilities. The difference between Eqs. (39) and (44) is that the former deals with the acid-form ligands, while the latter deals with the ionic-form ligands. When we can determine the acid-dissociation constants in the organic phase by some experimental methods, we may also calculate the relative stability of the organic complexes in Eq. (44).

As we have seen from the above equation, the "relative" stability constants in Eq. (8) seem to be useful for comparing the stability of complexes of a certain metal with various ligands. As it is not easy to measure ionic species in organic solvents with low dielectric constants, the present expression for the stabilities of various complexes seems to be the most convenient concept for this purpose.

The author wishes to express a great appreciation to Professor Tatsuya Sekine of the Science University of Tokyo for many helpful discussions during the course of this work. The author is also indebted to Mr. Toshio Fukushima for his assistance in this experimental work.

BULLETIN OF THE CHEMICAL SOCIETY OF JAPAN VOL. 42 3433—3438 (1969)

The "Circular Dichroism-sensitive Band" in the Optical Absorption of the Lanthanide(III) Complexes with Some Optically Active Ligands

Seizo MISUMI, Sigeo KIDA, Toshiyuki ISOBE, Yuzo NISHIDA and Haruko FURUTA

Inorganic Chemistry Laboratory, Faculty of Science, Kyushu University, Hakozaki, Fukuoka

(Received June 30, 1969)

The circular dichroism and absorption spectra of Pr(III), Nd(III), Sm(III), Dy(III), Ho(III), Er(III) and Tm(III) complexes with some natural amino acids and L-EDDS have been measured at room temperature. The "circular dichroism-sensitive bands" have been observed on the J-bands where magnetic dipole transitions are allowed to some extent. The experimental results are in accordance with the theory proposed previously. The theory can be applied at least for lanthanide(III) complexes.

In previous papers,[1,2] we reported the circular dichroism (CD) and absorption spectra of f-f transitions of 1-PDTA(propylenediaminetetraacetic acid) complexes of Pr(III), Nd(III), Sm(III), Ho(III), Dy(III) and Er(III) in aqueous solutions, and compared the relative intensities of CD and absorption bands. In most of the J-bands, CD intensities were found to be parallel to the corresponding absorption intensities. However, some CD bands were observed to be exceptionally strong in comparison to the corresponding absorption bands. Those J-bands were named "CD-sensitive bands". The CD intensity of the "CD-sensitive

1) S. Kida, T. Isobe and S. Misumi, This Bulletin, **39**, 2786 (1966).

2) S. Misumi, S. Kida and T. Isobe, *Spectrochim. Acta*, **24A**, 291 (1968).

Ln(III) (ground state)	P	Ligand	Aquo AB λ, mμ	Aquo AB ε	L-Alanine AB λ, mμ	L-Alanine AB ε	L-Alanine CD λ, mμ	L-Alanine CD α x 10⁴	L-Serine AB λ, mμ	L-Serine AB ε	L-Serine CD λ, mμ	L-Serine CD α x 10⁴	L-Lysine AB λ, mμ	L-Lysine AB ε	L-Lysine CD λ, mμ	L-Lysine CD α x 10⁴
Pr ($^3H_4$)			443 ($^3P_2$)	9.7	446	8.5	442 446	- 0.9 + 2.5	446	8.0	441 445 450	- 0.3 + 0.5 - 0.4	445	10.0	442 446 450	- 1.5 + 6.3 - 1.2
			468 ($^3P_1$)	4.1	472	3.7	467 472 477	- 1.4 + 5.9 - 1.6	472	4.0			472	4.0	466 472	- 4.8 + 9.0
			481 ($^3P_0$)	3.5	484	3.9	483 486	- 5.1 + 3.3	485	2.7	485 489	- 1.3 + 0.3	484	4.5	483 487	-10.9 + 6.4
			589 ($^1D_2$)	1.8	592	1.8	587 595 599	- 2.2 + 7.8 - 7.2	591	1.8	591 602	+ 1.7 - 1.1	591	1.8	586 592 600 606	- 6.1 +22.2 - 7.2 - 3.9
		2.5×10^{-7}	353 ($^2I_{11/2}$)	0.92					356	0.3	355 358	- 6.3 +12.3	355	0.7	356	-27.1
		0.8×10^{-10}	475 ($^4G_{9/2}$)	0.64	476 478	0.52 0.44	479	-29.7					478	0.5	480	- 18.0
Nd ($^4I_{9/2}$)		0.3×10^{-9}	512 ($^2G_{9/2}$)	1.81	513	1.93	511 514	-43.4 + 5.1	512	1.8	512	+ 9.2	514	2.0	511 514	-12.0 + 4.5
		0.4×10^{-8}	522 ($^4G_{7/2}$)	4.29	524 527 530 534	3.81 2.24 1.07 0.45	521 524 528 532 537 541	+ 4.0 -20.6 -12.8 +20.2 -43.6 +21.8	525	4.6	522 525 530	- 1.6 + 2.3 - 1.2	525	4.8	525 529	- 4.0 + 1.3
		0.5×10^{-8}	680 ($^4F_{9/2}$)	0.46									681	0.5	672 681 686	+16.0 -22.0 +40.0
Sm ($^6H_{5/2}$)			357 ($^4H_{7/2}$)	0.03	356	0.06	355 356 357	-150.0 -66.7 -136.7	357	0.05	357	+100.0	356	0.05	355 358	-260.0 +180.0
		0.9×10^{-8}	450 452 ($^4F_{5/2}$)	0.05 0.03	449	0.05	449	+324.0	452	0.05	452	+120.0	451	0.05	448 454	+660.0 -160.0
		1.2×10^{-8}	499 ($^4G_{7/2}$)	0.05	499	0.06	500	+153.3					499	0.05	498	+360.0
		0.7×10^{-8}	560 ($^4G_{5/2}$)	0.02	561	0.05	557 562	-230.0 +60.0	562	0.05	557 562	+80.0 -140.0	562	0.05	556 567	-480.0 +180.0
Dy ($^6H_{15/2}$)			300 ($^4H_{13/2}$)	0.19					300	0.23	300 302	-57.0 +22.6				
			389 ($^4I_{13/2}$)	0.80	388	0.90	388 392	-17.2 -13.6	389	1.17	388 389 391	- 2.0 + 2.8 - 6.8	390	0.9	388 391 395	-11.1 -12.2 + 8.9
		2.1×10^{-7}	450 452 ($^4I_{15/2}$)	0.29 0.26	448 450 452	0.25 0.26 0.28	448 452 458	+256.0 -288.6 +46.4	453	0.23	448 453 456	+71.3 -244.8 +71.3	450	0.3	448 452 458	+166.7 -230.0 +33.0
Ho ($^5I_8$)		0.6×10^{-9}	294 ($^3L_8$)	0.40					295	0.25	293	+10.8				
		0.4×10^{-9}	383 ($^3K_7$)	0.08	383	0.10	382 384	+88.0 -164.0	384	0.12	384 385	- 16.4 + 14.3	384	0.15	384	-46.7
		0.7×10^{-7}	468 ($^3K_6$)	0.58	467	0.40	466 468 470	-70.0 +140.0 -80.0	468	0.61	466 468 470	-42.7 + 5.6 -22.6	468	0.7	466 468 470	-32.9 +32.9 +35.7
Er ($^4I_{15/2}$)		0.4×10^{-7}	358 361 ($^2K_{15/2}$)	0.81 0.10	362	0.04	361 363	-680.0 +720.0	358 361	0.92 0.08	358 359 362	- 1.2 + 0.4 -26.9	358 361	0.92 0.12	358 359 363	-45.8 -51.7 +273.3
Tm ($^3H_6$)		1.5×10^{-8}	288 ($^1I_6$)	0.035	290	0.09	289 290	-91.4 -194.3	290	0.07	290	-36.0				
			660 ($^3F_2$)	0.16	660	0.14	660	-341.8					660	0.21	659	-271.0

L-Threonine				L-Arginine				L-Aspartic acid				L-EDDS			
AB		CD		AB		CD		AB		CD		AB		CD	
λ,mμ	ε	λ,mμ	α×10⁴	λ,mμ	ε	λ,mμ	α×10⁴	λ,mμ	ε	λ,mμ	α×10⁴	λ,mμ	ε	λ,mμ	α×10⁴
446	9.1	440	- 0.4	446	7.4	444	- 1.6	446	7.90	447	- 1.1	445	6.76	445	- 9.6
		445	+ 1.5	449	8.8	447	+ 1.7					448	6.65	450	+ 3.2
		449	+ 0.4												
472	4.4	469	+ 2.0	474	3.6	470	- 1.1	472	4.08	473	+ 1.8	472	3.94	471	- 3.2
		474	- 2.5			473	+ 4.4							475	+ 2.4
						477	- 1.7							480	- 2.4
485	2.8	484	- 3.6	486	3.3	486	+ 1.8	485	2.48	487	+ 3.7	485	2.39	484	+18.5
						488	- 4.5							488	- 9.0
592	2.1	584	- 1.4	594	1.8	584	- 3.3	593	1.64	585	+ 1.5	592	1.82	592	- 1.5
		596	+ 4.3			592	+ 1.7			590	- 1.8	600	0.84	601	+ 4.9
		602	- 1.9			596	- 2.8			600	+ 2.4				
						605	+ 4.4								
356	0.7	356	-14.3	357	0.4	355	+25.0	356	0.38	355	+12.5	352	0.25	352	+46.0
						359	-25.0			357	+22.5			350	-124.4
				479	0.8	479	- 7.5								
513	2.8	512	- 2.9	515	2.1	513	+ 4.3	515	2.23	512	+ 2.9				
		515	+ 1.4	518	2.2	518	- 3.2			514	+ 0.3				
524	7.1	523	- 1.4	527	5.0	524	- 1.8	526	5.24	522	+ 2.4				
		526	+ 2.8			528	+ 2.8			526	- 0.7				
				687	0.6	683	+25.0								
357	0.1	356	-90.0	358	0.05	356	+280.0	355	0.03	355	-318.0				
		358	+60.0							359	+208.7				
452	0.05	452	+80.0	452	0.05	449	-100.0	450	0.03	449	-102.7				
		454	-40.0			453	+100.0			451	-171.0				
				500	0.08			498	0.05	500	+28.8	500	0.07	500	-114.3
560	0.05	560	-160.0	563	0.05	561	+140.0	560	0.03	557	-201.7	563	0.05	564	-160.0
						569	-140.0			564	+119.7				
300	0.4	300	- 8.0	300	0.3	299	-30.0								
		301	+10.0												
390	1.2	388	- 6.7	389	1.0	386	- 6.0	390	1.25	388	- 3.5	389	1.2	390	+50.0
		391	+10.0			391	+ 7.0			390	+ 9.2			392	-26.7
										392	- 7.3				
452	0.3	447	-33.0	450	0.3	450	-100.0	451	0.31	448	+132.3	452	0.3	448	-293.3
		450	-60.0			453	+46.7	454	0.32	453	-208.1			453	+440.0
		452	+100.0							458	+13.5			457	-106.7
		456	-130.0												
		459	+20.0												
384	0.2	382	-15.0	386	0.1	385	-60.0	382	0.11	383	+96.0	382	0.2	383	+240.0
		383	+10.0												
468	0.75	466	-29.3	469	0.75	467	+20.0	466	0.37	463	+19.4	467	0.4	465	+150.0
		470	-18.7			469	-37.3			465	-52.9			468	+270.0
										467	+51.8				
				358	1.2	357	+ 6.7	360	0.05	360	-420.0	357	1.0	357	+56.0
						359	- 11.7					360	0.1	359	+800.0
				362	0.1	361	+210.0							362	-1080.0
				291	0.05	290	-80.0	290	0.09	290	-268.0	289	0.12	289	-420.0
						292	+60.0							292	+136.0
				659	0.2	660	+50.0	659	0.20	658	-170.9	658	0.16	660	+212.3
														662	+118.5
														664	+212.3

bands" was well elucidated on the basis of Condon's theory[3] *i.e.*, the CD intensity is proportional to the imaginary part of the scalar product of the magnetic and the electric dipole moments associated with the electronic transitions.

CD and absorption spectra of Pr(III), Nd(III), Sm(III), Dy(III), Ho(III), Er(III) and Tm(III) complexes of six natural amino acids and L-EDDS (ethylenediaminedisuccinic acid) have been measured. The relative intensities of CD and absorption bands with regard to the calculated oscillator strengths of magnetic dipole transitions of the J-bands have been discussed in order to verify the general validity of the theory which was previously proposed for the elucidation of the "CD-sensitive bands".

Experimental

Materials. The natural amino acids, L-alanine, L-serine, L-threonine, L-aspartic acid, L-arginine and L-lysine were commercial products and were of GR grade. L-Ethylenediaminedisuccinic acid (EDDS) was prepared by Neal's method[4] from 1,2-dibromoethane and L-aspartic acid.

Found: C, 32.95; H, 6.80; N, 7.42%. Calcd for $C_{10}H_{24}N_2O_{12}$: C, 32.97; H, 6.59; N, 7.69%.

Lanthanide perchlorate was obtained by dissolving commercial lanthanide oxide of 99.9% purity. The concentration of lanthanide(III) ions were determined by means of volumemetric EDTA titration.

Measurements. Absorption and CD spectra were measured by a JASCO-ORD/UV-5 optical rotatory dispersion recorder with a CD attachment.

The solutions used for the measurements were prepared by dissolving lanthanide(III) perchlorate and the ligand in water in about 1 : 5 mole-ratio (except for EDDS complexes where metal to ligand ratio is 1 : 1), and were made alkaline with aqueous ammonia.

Results and Discussion

CD and absorption spectra of 51 complexes were measured. A few examples of these results are shown in Fig. 1. As was observed in PDTA

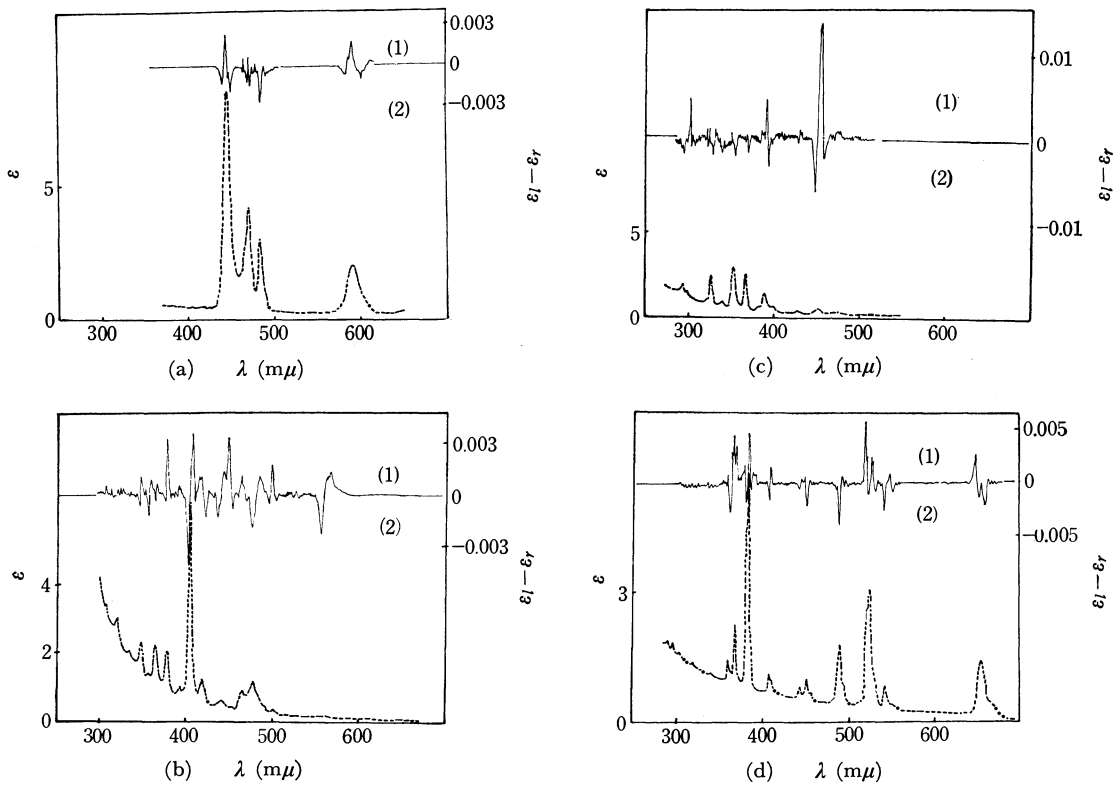

Fig. 1. Examples of CD and absorption spectra of lanthanide(III) complexes in aqueous solutions. (1 cm cell)
(1) CD spectrum; (2) absorption spectrum
(a) Pr - L-serine complex (1 : 5), pH=9.6, 26°C
(b) Sm - L-lysine complex (1 : 10), pH=9.9, 26°C
(c) Dy - EDDS complex (1 : 1.5), pH=9.0, 26°C
(d) Er - L-alanine complex (1 : 6), pH=8.5, 26°C

3) E. U. Condon, *Rev. Mod. Phys.*, **9**, 432 (1937).

4) T. A. Neal and N. T. Rose, *Inorg. Chem.*, **7**, 2405 (1968).

complexes,[2] a group of sharp CD bands was observed in the region of each absorption region.

The intensities of CD bands are parallel to those of corresponding absorption bands in most of the J-bands. However, as expected, unusually strong CD bands in comparison to the absorption bands were observed in the regions where the "CD-sensitive bands" were observed in the PDTA complexes.

In order to make clear the relation between the CD intensity and the magnetic dipole transition, we have calculated the oscillator strength, P, of magnetic dipole transition of J-bands by means of Pasternack's method[5] using eigen vectors of the secular equations for the intermediate coupling scheme.[6-9]

The results are summarized in Table 1, where $\alpha(=(\varepsilon_l-\varepsilon_r)/\varepsilon)$ was used as a parameter for representing relative intensities of CD and absorption bands. As seen in Table 1, when $P=0$, α remains only in the order of 10^{-5}—10^{-4}. However, when P exceeds the value $\sim 10^{-7}$, α becomes the order of 10^{-4}—10^{-3}, and the "CD-sensitive bands" were observed distinctly. Agreement between theory and experiment is satisfactory as is seen from Table 1. Thus we may conclude that our theory for the "CD-sensitive bands" is on the whole valid. However, one exception was the band at 660 mμ in the spectra of some Tm(III) complexes, where α shows a large value (100—200×10^{-4}) for $P=0$. This can not be explained at present.

5) S. Pasternack, *Astrophys. J.*, **92**, 129 (1940).
6) B. G. Wybourne, *J. Chem. Phys.*, **36**, 2301 (1962).
7) S. Hüfner, *Z. Phys.*, **164**, 456 (1961).
8) B. G. Wybourne, *J. Chem. Phys.*, **34**, 279 (1961).
9) W. F. Krupke and J. B. Gruber, *Phys. Rev.*, **139**, 2008 (1965).

BULLETIN OF THE CHEMICAL SOCIETY OF JAPAN VOL. 42 3437—3447 (1969)

Group Theoretical Treatment of Crystal Vibrations; Application to Orthorhombic Polyethylene

Teizo KITAGAWA and Tatsuo MIYAZAWA

Institute for Protein Research, Osaka University, Joan-cho, Kita-ku, Osaka

(Received June 30, 1969)

Irreducible representations of k groups of the space group *Pnam* were derived with Slater's method. Degeneracies of crystal vibrations due to space symmetry and time reversal symmetry were treated on the basis of Maradudin's theory. With irreducible representations of k groups, symmetry coordinates of the carbon atoms of orthorhombic polyethylene were constructed from translational-symmetry coordinates with nonintegral index vectors. A general matrix method was worked out for treating crystal vibrations of any phase-difference vector. Useful methods were derived for treating molecular crystals and chain polymer crystals and for approximate treatment of low frequency lattice vibrations.

For orthorhombic polyethylene crystal, various experimental data have become available, including infrared bands due to CH_2 bending and rocking vibrations,[1] for infrared bands due to lattice vibrations,[2,3] elastic and inelastic scattering cross sections of thermal neutrons[4-6] and low temperature specific heat.[7] All these data are related with the force field and normal vibrations of the crystal. For a molecular crystal, far infrared bands due to lattice vibrations arise from the intermolecular force field. Splitting of infrared bands due to intramolecular vibrations depends primarily on intermolecular force field but also on normal modes (atomic displacements) of the unperturbed vibrations concerned. Specific heat in the lowest temperature region is due to low frequency vibrations of three acoustic branches. On the other

1) R. G. Snyder, *J. Mol. Spectry.*, **4**, 411 (1960); *ibid.*, **7**, 116 (1961).

2) J. E. Bertie and G. E. Whalley, *J. Chem. Phys.*, **41**, 575 (1964).

3) S. Krimm and M. I. Bank, *ibid.*, **42**, 4059 (1965).

4) H. R. Danner, G. J. Safford, H. Boutin and J. S. King, *ibid.*, **40**, 1417 (1964).

5) W. Myers, J. L. Donovan and J. S. King, *ibid.*, **42**, 4299 (1965); W. Myers, G. C. Summerfield and J. S. King, *ibid.*, **44**, 184 (1966).

6) L. A. Feldkamp, G. Venkataraman and J. S. King, "Neutron Inelastic Scattering," IAEA Symp., Copenhagen, Vol. 2, p. 159 (1968).

7) J. E. Tucker and W. Reese, *J. Chem. Phys.*, **46**, 1388 (1967).

hand, elastic and inelastic scattering cross sections of thermal neutrons depend on the vibrational frequencies and also on vibrational displacements (of scattering nuclei) for all the acoustic and optical branches of crystal vibrations.

For an analysis of any one of these data, a highly simplified model may be useful, but often such a model is not necessarily applicable for analyses of other data. In our present series of studies on orthorhombic polyethylene crystal, available experimental data were all systematically treated on the basis of the intrachain and interchain force field and the acoustic and optical branches of crystal vibrations.

Chain-polymer crystals such as polyethylene are highly anisotropic and the restoring force along the chain axis is intramolecular in contrast with the intermolecular forces along two other directions. Accordingly these crystals form a special group of molecular crystals which practically behave as polymer molecules along the chain direction. A general method for treating molecular vibrations of helical polymer chains have been worked out previously,[8-10] and frequency-dispersion curves of the polyethylene chain[11] were obtained for analyzing band progression of intramolecular vibrations. However, for treating specific heat and neutron-scattering cross sections, normal coordinate treatments of the acoustic and optical vibrations of the three-dimensional crystal in the first Brillouin zone are required.

A dynamical theory of crystal lattices was established by Born and Huang[12] and a general method was worked out for treating crystal vibrations with Cartesian symmetry coordinates of any given wave vector ($\boldsymbol{k}$) [constructed in accordance with the translational symmetry of crystal lattices]. However, for crystal lattices of high space-group symmetry, crystal vibrations of special wave vectors may be grouped into symmetry classes and corresponding dynamical matrices may be factored into small matrices after unitary transformations. Accordingly computer time for numerical calculation is much reduced. Symmetry considerations are also required in drawing dispersion curves of the same symmetry class which should not intersect one another.

In the present study, therefore, group theoretical treatments were made of crystal vibrations of the space group *Pnam*. Furthermore, general matrix methods were worked out for treating molecular crystals and chain-polymer crystals and were applied to orthorhombic polyethylene crystal.

Space Group Operations and k Groups

For a crystal lattice, constituent atoms of a unit cell are classified into sets, each set consisting of equivalent atoms. In the case of orthorhombic polyethylene[13] (Fig. 1), two molecular chains pass through a unit cell along the c axis and there are four methylene groups per unit cell. There are two sets of hydrogen atoms and one set of carbon atoms. In the present paper, symmetry coordinates for carbon atoms will be described, but same considerations apply also for the other two sets of hydrogen atoms.

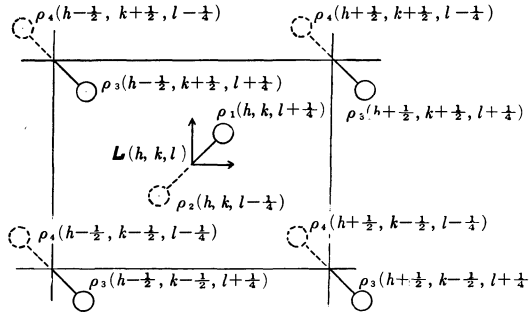

Fig. 1. Crystal structure and nonintegral index vectors ($\boldsymbol{\rho}$) of the carbon atoms of orthorhombic polyethylene (*Pnam*).

A unit cell of a crystal lattice is denoted with an index vector $\boldsymbol{L}$ with integral components (h,k,l). Then the ith atom of the $\boldsymbol{L}$th cell may be denoted with a nonintegral index

$$\boldsymbol{\rho}_i(\boldsymbol{L}) = \boldsymbol{L} + \boldsymbol{\rho}_i^0 , \tag{1}$$

where components of the position vector $\boldsymbol{\rho}_i^0$ from the cell origin are given in units of lattice constants (a_0,b_0,c_0). For the crystal lattice of orthorhombic polyethylene (Fig. 1), the position vectors are given as

$$\boldsymbol{\rho}_1^0=\begin{bmatrix} 0 \\ 0 \\ 1/4 \end{bmatrix} \quad \boldsymbol{\rho}_2^0=\begin{bmatrix} 0 \\ 0 \\ -1/4 \end{bmatrix} \quad \boldsymbol{\rho}_3^0=\begin{bmatrix} -1/2 \\ 1/2 \\ 1/4 \end{bmatrix} \quad \boldsymbol{\rho}_4^0=\begin{bmatrix} 1/2 \\ -1/2 \\ -1/4 \end{bmatrix} \tag{2}$$

and space group operations are listed in Table 1. Then, with respect to the translational-symmetry of the crystal lattice, the Cartesian symmetry coordinate vector $\boldsymbol{\sigma}$ for the ith atom is constructed as

$$\boldsymbol{\sigma}_i(\boldsymbol{\delta}) = N^{-1/2}\sum_{\boldsymbol{L}} \boldsymbol{X}(\boldsymbol{\rho}_i)\exp(-i\boldsymbol{\rho}_i\cdot\boldsymbol{\delta}) , \tag{3}$$

where $\boldsymbol{\delta}$ is a phase difference vector (corresponding to a wave vector $\boldsymbol{k}$; $\delta_a=a_0k_a$, $\delta_b=b_0k_b$, $\delta_c=c_0k_c$), N is the total number of unit cells and $\boldsymbol{X}(\boldsymbol{\rho}_i)$ is the Cartesian coordinate vector (x,y,z) of the $\boldsymbol{\rho}_i$th

8) P. Higgs, *Proc. Roy. Soc. (London)*, **A220**, 472 (1953).
9) T. Miyazawa, *J. Chem. Phys.*, **35**, 693 (1961).
10) H. Sugeta and T. Miyazawa, *ibid.*, **47**, 2034 (1967).
11) M. Tasumi, T. Shimanouchi and T. Miyazawa, *J. Mol. Spectry.*, **9**, 261 (1962); *ibid.*, **11**, 422 (1963).
12) M. Born and K. Huang, "Dynamical Theory of Crystal Lattices," Clarendon Press, Oxford (1954).
13) C. W. Bunn, *Trans. Faraday Soc.*, **35**, 482 (1939).

Table 1. Symmetry operations* $[R_u(\boldsymbol{\alpha}_u, \boldsymbol{\tau}_u)]$ of the space group *Pnam*

		$\boldsymbol{\alpha}_u$	$\boldsymbol{\tau}_u$
R_1	E	$\begin{bmatrix} 1 & 0 & 0 \\ 0 & 1 & 0 \\ 0 & 0 & 1 \end{bmatrix}$	(0, 0, 0)
R_2	C_2^a	$\begin{bmatrix} 1 & 0 & 0 \\ 0 & -1 & 0 \\ 0 & 0 & -1 \end{bmatrix}$	(1/2, 1/2, 1/2)
R_3	C_2^b	$\begin{bmatrix} -1 & 0 & 0 \\ 0 & 1 & 0 \\ 0 & 0 & -1 \end{bmatrix}$	(1/2, 1/2, 0)
R_4	C_2^c	$\begin{bmatrix} -1 & 0 & 0 \\ 0 & -1 & 0 \\ 0 & 0 & 1 \end{bmatrix}$	(0, 0, 1/2)
R_5	i	$\begin{bmatrix} -1 & 0 & 0 \\ 0 & -1 & 0 \\ 0 & 0 & -1 \end{bmatrix}$	(0, 0, 0)
R_6	$\sigma_g(bc)$	$\begin{bmatrix} -1 & 0 & 0 \\ 0 & 1 & 0 \\ 0 & 0 & 1 \end{bmatrix}$	(1/2, 1/2, 1/2)
R_7	$\sigma_g(ac)$	$\begin{bmatrix} 1 & 0 & 0 \\ 0 & -1 & 0 \\ 0 & 0 & 1 \end{bmatrix}$	(1/2, 1/2, 0)
R_8	$\sigma_g(ab)$	$\begin{bmatrix} 1 & 0 & 0 \\ 0 & 1 & 0 \\ 0 & 0 & -1 \end{bmatrix}$	(0, 0, 1/2)

* Components of a nonprimitive translation vector $\boldsymbol{\tau}_u$ are given in units of lattice constants a_0, b_0 and c_0.

atom.

A symmetry operation of a crystal lattice consists of a rotation ($\boldsymbol{\alpha}_u$) and a nonprimitive translation($\boldsymbol{\tau}_u$).[14] For the crystal lattice of orthorhombic polyethylene, symmetry operations are listed in Table 1. A symmetry operation R_u (at the lattice origin $\boldsymbol{L}=0$) will transform the Cartesian coordinate vector $\boldsymbol{X}$ of the $\boldsymbol{\rho}_i$th atom as

$$R_u\boldsymbol{X}(\boldsymbol{\rho}_i) = \boldsymbol{\alpha}_u\boldsymbol{X}(\boldsymbol{\alpha}_u\boldsymbol{\rho}_i+\boldsymbol{\tau}_u) = \boldsymbol{\alpha}_u\boldsymbol{X}(\boldsymbol{\rho}_j) \tag{4}$$

and accordingly will transform the translational-symmetry coordinate $\boldsymbol{\sigma}_i(\boldsymbol{\delta})$ as

$$R_u\boldsymbol{\sigma}_i(\boldsymbol{\delta}) = N^{-1/2}\sum_{\boldsymbol{L}}\boldsymbol{\alpha}_u\boldsymbol{X}(\boldsymbol{\alpha}_u\boldsymbol{\rho}_i+\boldsymbol{\tau}_u)\exp(-i\boldsymbol{\rho}_i\cdot\boldsymbol{\delta}). \tag{5}$$

However, since

$$\boldsymbol{\rho}_i\cdot\boldsymbol{\delta} = (\boldsymbol{\alpha}_u\boldsymbol{\rho}_i)\cdot(\boldsymbol{\alpha}_u\boldsymbol{\delta}) \tag{6}$$

the exponential factor in Eq. (5) may be rewritten as

$$\begin{aligned}\exp(-i\boldsymbol{\rho}_i\cdot\boldsymbol{\delta}) &= \exp[-i(\boldsymbol{\alpha}_u\boldsymbol{\rho}_i)\cdot(\boldsymbol{\alpha}_u\boldsymbol{\delta})] \\ &= \exp[-i(\boldsymbol{\alpha}_u\boldsymbol{\rho}_i+\boldsymbol{\tau}_u)\cdot(\boldsymbol{\alpha}_u\boldsymbol{\delta})] \times \exp[i\boldsymbol{\tau}_u\cdot(\boldsymbol{\alpha}_u\boldsymbol{\delta})].\end{aligned} \tag{7}$$

From Eqs. (3)—(5) and (7), the effect of R_u may finally be given as

$$R_u\boldsymbol{\sigma}_i(\boldsymbol{\delta}) = \boldsymbol{\alpha}_u\boldsymbol{\sigma}_j(\boldsymbol{\alpha}_u\boldsymbol{\delta}) \times \exp[i\boldsymbol{\tau}_u\cdot(\boldsymbol{\alpha}_u\boldsymbol{\delta})]. \tag{8}$$

Accordingly, the phase-difference vector is now transformed into a vector $\boldsymbol{\alpha}_u\boldsymbol{\delta}$ and the translational-symmetry coordinate $\boldsymbol{\sigma}_i(\boldsymbol{\delta})$ of the ith atom is transformed into the translational-symmetry coordinate $\boldsymbol{\alpha}_u\boldsymbol{\sigma}_j(\boldsymbol{\alpha}_u\boldsymbol{\delta})$ of the jth atom as multiplied with the phase-factor of $\exp[i\boldsymbol{\tau}_u\cdot(\boldsymbol{\alpha}_u\boldsymbol{\delta})]$. For the carbon atoms of orthorhombic polyethylene, atom-index transformations $i\rightarrow j$ and exponents of phase factors are listed in Table 2.

A $\boldsymbol{k}$ group[14] is defined as the ensemble of space-group operations (R_u) which satisfy the condition.

$$\boldsymbol{\alpha}_u\boldsymbol{\delta} = \boldsymbol{\delta} + 2\pi\boldsymbol{m}, \tag{9}$$

where $\boldsymbol{m}$ is a vector with integral components. Naturally $\boldsymbol{k}$ groups are subgroups of the factor group. Accordingly, the dynamical matrix of the phase-difference vector $\boldsymbol{\delta}$ may be factorized into submatrices, each belonging to an irreducible representation of the $\boldsymbol{k}$ group. For a general phase-difference vector $\boldsymbol{\delta}(\delta_a,\delta_b,\delta_c)$, however, only the identity operation constitutes the $\boldsymbol{k}$ group and the dynamical matrix is not factorized any further.

With the space group *Pnam*, all the eight operations of Table 1 satisfy the condition of Eq. (9) $[\boldsymbol{m}=0]$ for $\boldsymbol{\delta}=0$ and accordingly the $\boldsymbol{k}$ group is the factor group D_{2h} itself. However, for $\boldsymbol{\delta}(\delta_a,0,0)$, only four operations, R_1 (identity), R_2 (twofold

Table 2. Transformations of atom indices ($i\rightarrow j$) and phase-difference vectors ($\boldsymbol{\delta}\rightarrow\boldsymbol{\alpha}_u\boldsymbol{\delta}$) and exponents $\boldsymbol{\tau}_u\cdot(\boldsymbol{\alpha}_u\boldsymbol{\delta})$ of phase-factors involved in the effects of factor-group operations (R_u) upon translational-symmetry coordinates $\boldsymbol{\sigma}_i(\boldsymbol{\delta})$

R_u	$i\rightarrow j$				$\boldsymbol{\alpha}_u\boldsymbol{\delta}$	$\boldsymbol{\tau}_u\cdot(\boldsymbol{\sigma}_u\boldsymbol{\delta})$
	$i=1$	2	3	4		
R_1	1	2	3	4	$(\delta_a, \delta_b, \delta_c)$	0
R_2	3	4	1	2	$(\delta_a, -\delta_b, -\delta_c)$	$(\delta_a-\delta_b-\delta_c)/2$
R_3	4	3	2	1	$(-\delta_a, \delta_b, -\delta_c)$	$(-\delta_a+\delta_b)/2$
R_4	2	1	4	3	$(-\delta_a, -\delta_b, \delta_c)$	$\delta_c/2$
R_5	2	1	4	3	$(-\delta_a, -\delta_b, -\delta_c)$	0
R_6	4	3	2	1	$(-\delta_a, \delta_b, \delta_c)$	$(-\delta_a+\delta_b+\delta_c)/2$
R_7	3	4	1	2	$(\delta_a, -\delta_b, \delta_c)$	$(\delta_a-\delta_b)/2$
R_8	1	2	3	4	$(\delta_a, \delta_b, -\delta_c)$	$-\delta_c/2$

14) J. C. Slater, "Quantum Theory of Molecules and Solid," Vol. 2, McGraw-Hill Company, New York (1965).

TABLE 3. $\boldsymbol{k}$ GROUPS (SYMMETRY OPERATIONS R_u)* FOR THE SPACE GROUP *Pnam*

D_{2h} (R_1, R_2, R_3, R_4, R_5, R_6, R_7, R_8)
$\Gamma(0,0,0)$, $X(\pi,0,0)$, $Z(0,\pi,0)$, $Y(0,0,\pi)$
$R(\pi,\pi,\pi)$, $T(0,\pi,\pi)$, $S(\pi,0,\pi)$, $U(\pi,\pi,0)$
C_{2v} (R_1, R_2, R_7, R_8)
$\Sigma(\delta_a,0,0)$, $A(\delta_a,\pi,0)$, $C(\delta_a,0,\pi)$, $E(\delta_a,\pi,\pi)$
C_{2v} (R_1, R_3, R_6, R_8)
$\Lambda(0,\delta_b,0)$, $H(0,\delta_b,\pi)$, $G(\pi,\delta_b,0)$, $Q(\pi,\delta_b,\pi)$
C_{2v} (R_1, R_4, R_6, R_7)
$\Delta(0,0,\delta_c)$, $D(\pi,0,\delta_c)$, $B(0,\pi,\delta_c)$, $F(\pi,\pi,\delta_c)$
C_s (R_1, R_6)
$(0,\delta_b,\delta_c)$, (π,δ_b,δ_c)
C_s (R_1, R_7)
$(\delta_a,0,\delta_c)$, (δ_a,π,δ_c)
C_s (R_1, R_8)
$(\delta_a,\delta_b,0)$, (δ_a,δ_b,π)
C_1 (R_1)
$(\delta_a,\delta_b,\delta_c)$

* $0<\delta<\pi$

screw axis along the a axis), R_7 (glide plane normal to the b axis) and R_8 (glide plane normal to the c axis) satisfy Eq. (9) [$\boldsymbol{m}=0$] and therefore the $\boldsymbol{k}$ group is C_{2v}. Finally, for $\boldsymbol{\delta}(\pi,0,0)$, remaining four operations of R_3 (twofold screw axis along the b axis), R_4 (twofold screw axis along the c axis), R_5 (inversion) and R_6 (glide plane normal to the a axis) satisfy Eq. (9) [$\boldsymbol{m}=(-1,0,0)$] and the $\boldsymbol{k}$ group again becomes D_{2h}. All the $\boldsymbol{k}$ groups of the space group *Pnam* are given in Table 3, where BSW notation[15] was followed for special phase-difference vectors.

Irreducible Representations

Irreducible representations of $\boldsymbol{k}$ groups were given by Slater[14] for 20 space groups including D_{2h}^{16}-*Pnam*. On the other hand, Kovalev[16] treated all the 230 space groups with the use of multiplier representation method. However, for polymer-chain crystals, it is a common practice to take the c axis parallel to the chain-direction and accordingly the space group of orthorhombic polyethylene is preferably taken as *Pnam* rather than *Pnam*. Furthermore, in the field of molecular dynamics, the effect of symmetry operations given in Eq. (8) is more intelligible than the reverse one (Slater[14]). In the present study, therefore, basis functions and irreducible representations for all the $\boldsymbol{k}$ groups of *Pnam* were derived on the basis of multiplication tables.

Successive applications of point-group operations is equivalent to one of point-group operations, whereas for a space group, effects of nonprimitive translations ($\boldsymbol{\tau}_u$) are involved. Suppose a symmetry operation R_u operates on a translational-symmetry coordinate vector and then R_v operates on the resulting coordinate vector, then from Eq. (8), we have

$$\begin{aligned} R_vR_u\boldsymbol{\sigma}_i(\boldsymbol{\delta}) &= R_v[\boldsymbol{\alpha}_u\boldsymbol{\sigma}_j(\boldsymbol{\alpha}_u\boldsymbol{\delta})]\exp[i\boldsymbol{\tau}_u\cdot(\boldsymbol{\alpha}_u\boldsymbol{\delta})] \\ &= \boldsymbol{\alpha}_v\boldsymbol{\alpha}_u\boldsymbol{\sigma}_k(\boldsymbol{\alpha}_v\boldsymbol{\alpha}_u\boldsymbol{\delta})\exp[i\boldsymbol{\tau}_v\cdot(\boldsymbol{\alpha}_v\boldsymbol{\alpha}_u\boldsymbol{\delta})]\exp[i\boldsymbol{\tau}_u\cdot\boldsymbol{\alpha}_u\boldsymbol{\delta})] \\ &= \boldsymbol{\alpha}_v\boldsymbol{\alpha}_u\boldsymbol{\sigma}_k(\boldsymbol{\alpha}_v\boldsymbol{\alpha}_u\boldsymbol{\delta})\exp[i(\boldsymbol{\alpha}_v\boldsymbol{\tau}_u+\boldsymbol{\tau}_v)\cdot(\boldsymbol{\alpha}_v\boldsymbol{\alpha}_u\boldsymbol{\delta})], \end{aligned} \tag{10}$$

where the symmetry operation R_v transfers $\boldsymbol{\rho}_j$th atom to the site of a $\boldsymbol{\rho}_k$th atom. The multiplication rule for the rotational parts is identical with the case of point-group operations

$$\boldsymbol{\alpha}_v\boldsymbol{\alpha}_u = \boldsymbol{\alpha}_w. \tag{11}$$

However with a space group, $\boldsymbol{\tau}_v+\boldsymbol{\alpha}_v\boldsymbol{\tau}_u$ is not necessarily equal to $\boldsymbol{\tau}_w$. Accordingly, the effect of two successive space-group operations on a translational-symmetry coordinate may be written as

$$R_vR_u\boldsymbol{\sigma}_i(\boldsymbol{\delta}) = \exp[i(\Delta\boldsymbol{\tau})\cdot(\boldsymbol{\alpha}_w\boldsymbol{\delta})]R_w\boldsymbol{\sigma}_i(\boldsymbol{\delta}), \tag{12}$$

where

$$\Delta\boldsymbol{\tau} = \boldsymbol{\alpha}_v\boldsymbol{\tau}_u + \boldsymbol{\tau}_v - \boldsymbol{\tau}_w. \tag{13}$$

For the space-group *Pnam*, $\Delta\boldsymbol{\tau}$ vectors were derived for all possible combinations of symmetry operations (R_1—R_8) and the multiplication table is shown in Table 4. From this table, basis functions for irreducible representations may be constructed. Irreducible representations for all the $\boldsymbol{k}$ groups of *Pnam* were described by Kitagawa.[17] In the present paper, however, representations of a few $\boldsymbol{k}$ groups will now be discussed.

For the phase-difference vector of $\boldsymbol{\delta}(\delta_a,0,0)$, the $\boldsymbol{k}$ group includes four operations, R_1, R_2, R_7 and R_8 (Table 3). The operations R_2 and R_7 are associated with nonzero components of $\boldsymbol{\tau}_u$ along the a axis but the operations R_1 and R_8 are not (Table 1). Accordingly, basis functions were constructed as

$$\left.\begin{aligned} \phi_1 &= [R_1+R_8+\omega_a{}^*(R_2+R_7)]\phi_0 \\ \phi_2 &= [R_1+R_8-\omega_a{}^*(R_2+R_7)]\phi_0 \\ \phi_3 &= [R_1-R_8+\omega_a{}^*(R_2-R_7)]\phi_0 \\ \phi_4 &= [R_1-R_8-\omega_a{}^*(R_2-R_7)]\phi_0 \end{aligned}\right\}, \tag{14}$$

where

$$\omega_a = \exp(i\delta_a/2). \tag{15}$$

According to the multiplication table (Table 4), these basis functions are transformed with symmetry operations as

15) L. P. Bouckaert, R. Smoluchowski and E. Wigner, *Phys. Rev.*, **50**, 58 (1936).

16) O. Kovalev (originally published in Russian in 1958 and later translated into English by A. M. Gross), "Irreducible Representations of the Space Groups," Gordon and Breach, Ltd., New York (1965).

17) T. Kitagawa, "Crystal Dynamics and Related Solid State Properties of Polymers," Thesis, Osaka University, Chapter IV and Appendix I (1969).

TABLE 4. MULTIPLICATION TABLE* FOR THE SPACE GROUP OPERATIONS (R_vR_u) OF *Pnam*

R_v \ R_u	R_1	R_2	R_3	R_4	R_5	R_6	R_7	R_8
R_1	R_1	R_2	R_3	R_4	R_5	R_6	R_7	R_8
R_2	R_2	$e^{a}R_1$	$e^{-a}R_4$	R_3	R_6	$e^{-a}R_5$	$e^{a}R_8$	R_7
R_3	R_3	$e^{-b-c}R_4$	$e^{b}R_1$	$e^{c}R_2$	R_7	$e^{b+c}R_8$	$e^{-b}R_5$	$e^{-c}R_6$
R_4	R_4	$e^{a-b-c}R_3$	$e^{-a+b}R_2$	$e^{c}R_1$	R_8	$e^{-a+b+c}R_7$	$e^{a-b}R_6$	$e^{-c}R_5$
R_5	R_5	$e^{a-b-c}R_6$	$e^{-a+b}R_7$	$e^{c}R_8$	R_1	$e^{-a+b+c}R_2$	$e^{a-b}R_3$	$e^{-c}R_4$
R_6	R_6	$e^{-b-c}R_5$	$e^{b}R_8$	$e^{c}R_7$	R_2	$e^{b+c}R_1$	$e^{-b}R_4$	$e^{-c}R_3$
R_7	R_7	$e^{a}R_8$	$e^{-a}R_5$	R_6	R_3	$e^{-a}R_4$	$e^{a}R_1$	R_2
R_8	R_8	R_7	R_6	R_5	R_4	R_3	R_2	R_1

* For example, $e^{\pm a}=\exp(\pm i\delta_a)$, $e^{-a+b}=\exp(-i\delta_a+i\delta_b)$, $e^{a-b}=\exp(i\delta_a-i\delta_b)$, $e^{b+c}=\exp(i\delta_b+i\delta_c)$, $e^{-b-c}=\exp(-i\delta_b-i\delta_c)$, $e^{a-b-c}=\exp(i\delta_a-i\delta_b-i\delta_c)$, and $e^{-a+b+c}=\exp(-i\delta_a+i\delta_b+i\delta_c)$.

TABLE 5. MATRIX ELEMENTS* FOR IRREDUCIBLE REPRESENTATIONS OF $\Sigma(\delta_a,0,0)$, $A(\delta_a,\pi,0)$, $C(\delta_a,0,\pi)$, $E(\delta_a,\pi,\pi)$, $\Lambda(0,\delta_b,0)$, $G(\pi,\delta_b,0)$, and $\Delta(0,0,\delta_c)$

				R_1	R_2	R_3	R_4	R_5	R_6	R_7	R_8
Σ_1	A_1	C_1	E_1	1	ω_a					ω_a	1
Σ_2	A_2	C_2	E_2	1	$-\omega^a$					$-\omega_a$	1
Σ_3	A_3	C_3	E_3	1	ω_a					$-\omega_a$	-1
Σ_4	A_4	C_4	E_4	1	$-\omega_a$					ω_a	-1
Λ_1		G_1		1		ω_b			ω_b		1
Λ_2		G_2		1		$-\omega_b$			ω_b		-1
Λ_3		G_3		1		ω_b			$-\omega_b$		-1
Λ_4		G_4		1		$-\omega_b$			$-\omega_b$		1
Δ_1				1			ω_c		ω_c	1	
Δ_2				1			$-\omega_c$		ω_c	-1	
Δ_3				1			ω_c		$-\omega_c$	-1	
Δ_4				1			$-\omega_c$		$-\omega_c$	1	

* $0<\delta_a,\delta_b,\delta_c<\pi$; $\omega_a=\exp(i\delta_a/2)$, $\omega_b=\exp(i\delta_b/2)$ and $\omega_c=\exp(i\delta_c/2)$.

TABLE 6. IRREDUCIBLE REPRESENTATIONS OF $\Gamma(0,0,0)$

	R_1	R_2	R_3	R_4	R_5	R_6	R_7	R_8
$\Gamma_1(A_g)$	1	1	1	1	1	1	1	1
$\Gamma_2(A_u)$	1	1	1	1	-1	-1	-1	-1
$\Gamma_3(B_{3g})$	1	-1	-1	1	1	-1	-1	1
$\Gamma_4(B_{3u})$	1	-1	-1	1	-1	1	1	-1
$\Gamma_5(B_{1g})$	1	1	-1	-1	1	1	-1	-1
$\Gamma_6(B_{1u})$	1	1	-1	-1	-1	-1	1	1
$\Gamma_7(B_{2g})$	1	-1	1	-1	1	-1	1	-1
$\Gamma_8(B_{2u})$	1	-1	1	-1	-1	1	-1	1

$$
\left.\begin{array}{llll}
R_1\phi_1=\phi_1 & R_2\phi_1=\omega_a\phi_1 & R_7\phi_1=\omega_a\phi_1 & \\
 & & & R_8\phi_1=\phi_1 \\
R_1\phi_2=\phi_2 & R_2\phi_2=-\omega_a\phi_2 & R_7\phi_2=-\omega_a\phi_2 & \\
 & & & R_8\phi_2=\phi_2 \\
R_1\phi_3=\phi_3 & R_2\phi_3=\omega_a\phi_3 & R_7\phi_3=-\omega_a\phi_3 & \\
 & & & R_8\phi_3=-\phi_3 \\
R_1\phi_4=\phi_4 & R_2\phi_4=-\omega_a\phi_4 & R_7\phi_4=\omega_a\phi_4 & \\
 & & & R_8\phi_4=-\phi_4
\end{array}\right\} \quad (16)
$$

For the $\boldsymbol{k}$ group of $\Sigma(\delta_a,0,0)$, the irreducible representations are all one-dimensional (see Table 5) where ϕ_1, ϕ_2, ϕ_3 and ϕ_4 are basis functions of Σ_1, Σ_2, Σ_3, and Σ_4, respectively (these correspond to the species A_1, B_2, A_2, and B_1 of the point group C_{2v}). The multiplication tables for $A(\delta_a,\pi,0)$, $C(\delta_a,0,\pi)$ and $E(\delta_a,\pi,\pi)$ are common with the table for $\Sigma(\delta_a,0,0)$ and accordingly the matrix elements of irreducible representations are shown commonly in Table 5.

For $\Lambda(0,\delta_b,0)$, $H(0,\delta_b,\pi)$, $G(\pi,\delta_b,0)$ and $Q(\pi,\delta_b,\pi)$, the $\boldsymbol{k}$ group (C_{2v}) includes four operations (R_1, R_3, R_6, and R_8). However, the multiplication table of Λ and G is different from that of H and Q.

TABLE 7. IRREDUCIBLE REPRESENTATION OF $X(\pi, 0, 0)$

	R_1	R_2	R_3	R_4	R_5	R_6	R_7	R_8
X_1	$\begin{bmatrix}1&0\\0&1\end{bmatrix}$	$\begin{bmatrix}0&1\\-1&0\end{bmatrix}$	$\begin{bmatrix}1&0\\0&-1\end{bmatrix}$	$\begin{bmatrix}0&1\\1&0\end{bmatrix}$	$\begin{bmatrix}0&1\\1&0\end{bmatrix}$	$\begin{bmatrix}1&0\\0&-1\end{bmatrix}$	$\begin{bmatrix}0&1\\-1&0\end{bmatrix}$	$\begin{bmatrix}1&0\\0&1\end{bmatrix}$
X_2	$\begin{bmatrix}1&0\\0&1\end{bmatrix}$	$\begin{bmatrix}0&1\\-1&0\end{bmatrix}$	$\begin{bmatrix}1&0\\0&-1\end{bmatrix}$	$\begin{bmatrix}0&1\\1&0\end{bmatrix}$	$\begin{bmatrix}0&-1\\-1&0\end{bmatrix}$	$\begin{bmatrix}-1&0\\0&1\end{bmatrix}$	$\begin{bmatrix}0&-1\\1&0\end{bmatrix}$	$\begin{bmatrix}-1&0\\0&-1\end{bmatrix}$

TABLE 8. IRREDUCIBLE REPRESENTATIONS OF $U(\pi, \pi, 0)$

	R_1	R_2	R_3	R_4	R_5	R_6	R_7	R_8
U_1	1	i	i	1	1	i	i	1
U_2	1	$-i$	$-i$	1	1	$-i$	$-i$	1
U_3	1	i	i	1	-1	$-i$	$-i$	-1
U_4	1	$-i$	$-i$	1	-1	i	i	-1
U_5	1	i	$-i$	-1	1	i	$-i$	-1
U_6	1	$-i$	i	-1	1	$-i$	i	-1
U_7	1	i	$-i$	-1	-1	$-i$	i	1
U_8	1	$-i$	i	-1	-1	i	$-i$	1

TABLE 9. IRREDUCIBLE REPRESENTATIONS OF $R(\pi, \pi, \pi)$

	R_1	R_2	R_3	R_4	R_5	R_6	R_7	R_8
R_1	$\begin{bmatrix}1&0\\0&1\end{bmatrix}$	$\begin{bmatrix}-i&0\\0&i\end{bmatrix}$	$\begin{bmatrix}0&i\\i&0\end{bmatrix}$	$\begin{bmatrix}0&-1\\1&0\end{bmatrix}$	$\begin{bmatrix}0&1\\1&0\end{bmatrix}$	$\begin{bmatrix}0&-i\\i&0\end{bmatrix}$	$\begin{bmatrix}i&0\\0&i\end{bmatrix}$	$\begin{bmatrix}-1&0\\0&1\end{bmatrix}$
R_2	$\begin{bmatrix}1&0\\0&1\end{bmatrix}$	$\begin{bmatrix}i&0\\0&-i\end{bmatrix}$	$\begin{bmatrix}0&-i\\-i&0\end{bmatrix}$	$\begin{bmatrix}0&-1\\1&0\end{bmatrix}$	$\begin{bmatrix}0&1\\1&0\end{bmatrix}$	$\begin{bmatrix}0&i\\-i&0\end{bmatrix}$	$\begin{bmatrix}-i&0\\0&-i\end{bmatrix}$	$\begin{bmatrix}-1&0\\0&1\end{bmatrix}$

The irreducible representations of Λ and G (Table 5) are one-dimensional whereas those of H and Q are two-dimensional.[17]

For special points of $(0,\delta_b,\delta_c)$, (π,δ_b,δ_c), $(\delta_a,0,\delta_c)$, (δ_a,π,δ_c), $(\delta_a,\delta_b,0)$ and (δ_a,δ_b,π), the $\boldsymbol{k}$ group is C_s (Table 3) and the dynamical matrix is factorized into two matrices after suitable symmetry transformations (there are no BSW symbols for these special points in the first Brillouin zone).

For $\Gamma(0,0,0)$, the factor group D_{2h} is $\boldsymbol{k}$ group itself and the irreducible representations are shown in Table 6. For each of $X(\pi,0,0)$, $Z(0,\pi,0)$, $Y(0,0,\pi)$, and $T(0,\pi,\pi)$, the $\boldsymbol{k}$ group again becomes D_{2h}. However, in contrast with the one-dimensional representations of Γ (Table 6), irreducible representations of X (Table 7), Z, Y, and T are two-dimensional.

For $U(\pi,\pi,0)$, the $\boldsymbol{k}$ group is also D_{2h}. With the following basis functions,

$$\left.\begin{aligned}
\varphi_1(U_1') &= (R_1+R_4+R_5+R_8)\phi_0\\
\varphi_2(U_1') &= (R_2+R_3+R_6+R_7)\phi_0\\
\varphi_1(U_2') &= (R_1+R_4-R_5-R_8)\phi_0\\
\varphi_2(U_2') &= (R_2+R_3-R_6-R_7)\phi_0\\
\varphi_1(U_3') &= (R_1-R_4+R_5-R_8)\phi_0\\
\varphi_2(U_3') &= (R_2-R_3+R_6-R_7)\phi_0\\
\varphi_1(U_4') &= (R_1-R_4-R_5+R_8)\phi_0\\
\varphi_2(U_4') &= (R_2-R_3-R_6+R_7)\phi_0
\end{aligned}\right\} \quad (17)$$

four two-dimensional representations (real) are obtained. However, from group theory, the sum of squared dimensionalities of irreducible representations should be equal to the number of symmetry operations. In fact, four two-dimensional representations are reduced to eight one-dimensional representations (Table 8). Finally for $S(\pi,0,\pi)$ and $R(\pi,\pi,\pi)$, a four-dimensional representation (real) is obtained with the following basis functions,

$$\left.\begin{aligned}
\varphi_1 &= (R_1+R_8+R_2+R_7)\phi_0\\
\varphi_2 &= (R_1+R_8-R_2-R_7)\phi_0\\
\varphi_3 &= (R_5+R_4+R_6+R_3)\phi_0\\
\varphi_4 &= (R_5+R_4-R_6-R_3)\phi_0.
\end{aligned}\right\} \quad (18)$$

However, the four-dimensional representation is reduced to two two-dimensional representations (Table 9). Dimensionalities (f_s) of irreducible representations are summarized in Table 11.

Degeneracy of Crystal Vibrations

The relation between the dimensionality of irreducible representations and degeneracy of crystal vibrations was generally treated by Maradudin and Vosko[18] with the use of the irreducible multiplier co-representation method. The pth frequency parameter $[\lambda_p(\boldsymbol{\delta})]$ and characteristic vector $[\boldsymbol{L}_p(\boldsymbol{\delta})]$ of the dynamical matrix $\boldsymbol{D}_S(\boldsymbol{\delta})$ are given by

$$\lambda_p(\boldsymbol{\delta})\boldsymbol{L}_p(\boldsymbol{\delta}) = \boldsymbol{D}_S(\boldsymbol{\delta})\boldsymbol{L}_p(\boldsymbol{\delta}). \quad (19)$$

The unitary matrix, $\boldsymbol{T}(\boldsymbol{a}_u,\boldsymbol{\tau}_u)$, associated with the

18) A. A. Maradudin and S. H. Vosko, *Rev. Modern Phys.*, **40**, 1 (1968)

uth operation of the space group was derived and a similarity transformation of the dynamical matrix may be carried out, yielding[18]

$$\boldsymbol{T}(\boldsymbol{a}_u, \boldsymbol{\tau}_u)\boldsymbol{D}_S(\boldsymbol{\delta})\boldsymbol{T}(\boldsymbol{a}_u, \boldsymbol{\tau}_u)^{-1} = \boldsymbol{D}_S(\boldsymbol{a}_u\boldsymbol{\delta}) \tag{20}$$

and accordingly

$$\boldsymbol{\Delta}(\boldsymbol{\delta}) = \boldsymbol{\Delta}(\boldsymbol{a}_u\boldsymbol{\delta}). \tag{21}$$

Therefore the irreducible volume of the first Brillouin zone depends upon the factor-group symmetry. For D_{2h} systems, the irreducible volume is one-eighth of the first Brillouin zone and treatments of crystal vibrations for $0 \leq \delta_a, \delta_b, \delta_c \leq \pi$ are sufficient.

For a unitary-type operation R_u of the $\boldsymbol{k}$ group ($\boldsymbol{a}_u\boldsymbol{\delta} = \boldsymbol{\delta}$), $\boldsymbol{T}(\boldsymbol{a}_u, \boldsymbol{\tau}_u)$ commutes with $\boldsymbol{D}_S(\boldsymbol{\delta})$ so that Eq. (19) is transformed,

$$\lambda_p(\boldsymbol{\delta})\{\boldsymbol{T}(\boldsymbol{a}_u, \boldsymbol{\tau}_u)\boldsymbol{L}_p(\boldsymbol{\delta})\} = \boldsymbol{D}_S(\boldsymbol{\delta})\{\boldsymbol{T}(\boldsymbol{a}_u, \boldsymbol{\tau}_u)\boldsymbol{L}_p(\boldsymbol{\delta})\}. \tag{22}$$

On the other hand, for an antiunitary-type operation (R_w) of the space group which inverts the phase-difference vector ($\boldsymbol{a}_w\boldsymbol{\delta} = -\boldsymbol{\delta}$), Eq. (19) is transformed into

$$\begin{aligned}\lambda_p(\boldsymbol{\delta})\{\boldsymbol{T}(\boldsymbol{a}_w, \boldsymbol{\tau}_w)\boldsymbol{L}_p(\boldsymbol{\delta})\} &= \boldsymbol{D}_S(-\boldsymbol{\delta})\{\boldsymbol{T}(\boldsymbol{a}_w, \boldsymbol{\tau}_w)\boldsymbol{L}_p(\boldsymbol{\delta})\} \\ &= \boldsymbol{D}_S(\boldsymbol{\delta})^*\{\boldsymbol{T}(\boldsymbol{a}_w, \boldsymbol{\tau}_w)\boldsymbol{L}_p(\boldsymbol{\delta})\}.\end{aligned} \tag{23}$$

Accordingly, if $\boldsymbol{T}(\boldsymbol{a}_w, \boldsymbol{\tau}_w)\boldsymbol{L}_p(\boldsymbol{\delta})$ and $\boldsymbol{T}(\boldsymbol{a}_u, \boldsymbol{\tau}_u)\boldsymbol{L}_p(\boldsymbol{\delta})$ are linearly independent of each other, so-called time-reversal degeneracy arises over space degeneracy [dimensionality (f_s) of irreducible representation]. According to Maradudin,[18] time-reversal degeneracy may be studied after treating

$$\Phi = \sum_u \phi(\boldsymbol{\delta}, R_aR_u)\chi^\mu(\boldsymbol{\delta}, R_aR_uR_aR_u), \tag{24}$$

where R_a is any antiunitary operation and $\phi(\boldsymbol{\delta}, R_w)$ is the multiplier representation of an antiunitary operation ($R_w \leftarrow R_aR_u$).

$$\phi(\boldsymbol{\delta}, R_w) = \exp[-i(\boldsymbol{\delta} + \boldsymbol{a}_w{}^{-1}\boldsymbol{\delta})\cdot\boldsymbol{\tau}_w]. \tag{25}$$

As an example of $\sum(\delta_a, 0, 0)$ of the space group *Pnam*, R_1, R_2, R_7, and R_8 are unitary-type operations whereas R_3, R_4, R_5, and R_6, are antiunitary-type operations. The inversion operation (R_5) always serves as an antiunitary operation for any phase-difference vector and is preferably used as R_a. In Eq. (24), $\chi^\mu(\boldsymbol{\delta}, R_aR_uR_aR_u)$ is the character of the μth irreducible representation for the operation $R_aR_uR_aR_u$. Summation runs over all the operations of a $\boldsymbol{k}$ group, and if Φ is equal to the order (g) of the $\boldsymbol{k}$ group, time-reversal degeneracy does not arise but, if Φ is equal to $-g$ or equal to 0, time-reversal degeneracy arises.[18] Accordingly with an f_s-dimensional representation of a $\boldsymbol{k}$ group, crystal vibrations are f_s-fold degenerate for $\Phi/g = 1$ but are $2f_s$-fold degenerate for $\Phi/g = -1$ or 0. Formulas of $\phi(\boldsymbol{\delta}, R_w)$ were obtained, as shown in Table 11, for symmetry operations of the space group *Pnam*, and the values of Φ/g were calculated as listed in Table 10. The time-reversal degeneracy ($t_s = 2$) is now expected for U, S, R, A, C, E, G, F, and Q. It may be remarked that crystal vibrations

Table 10. Degeneracy due to time reversal symmetry (t_s) and to space symmetry (f_s)

Point	Φ/g*	t_s	f_s	t_sf_s
$\Gamma(0, 0, 0)$	1	1	1	1
$X(\pi, 0, 0)$, $Z(0, \pi, 0)$, $Y(0, 0, \pi)$, $T(0, \pi, \pi)$	1	1	2	2
$U(\pi, \pi, 0)$	0	2	1	2
$S(\pi, 0, \pi)$, $R(\pi, \pi, \pi)$	0	2	2	4
$\sum(\delta_a, 0, 0)$, $\Delta(0, \delta_b, 0)$, $\Lambda(0, 0, \delta_c)$	1	1	1	1
$H(0, \delta_b, \pi)$, $B(0, \pi, \delta_c)$, $D(\pi, 0, \delta_c)$	1	1	2	2
$A(\delta_a, \pi, 0)$, $C(\delta_a, 0, \pi)$, $E(\delta_a, \pi, \pi)$, $G(\pi, \delta_b, 0)$, $F(\pi, \pi, \delta_c)$	0	2	1	2
$Q(\pi, \delta_b, \pi)$	-1	2	2	4
$(0, \delta_b, \delta_c)$, $(\delta_a, 0, \delta_c)$, $(\delta_a, \delta_b, 0)$	1	1	1	1
$(\pi, \delta_b, \delta_c)$, $(\delta_a, \pi, \delta_c)$, $(\delta_a, \delta_b, \pi)$	0	2	1	2
$(\delta_a, \delta_b, \delta_c)$	1	1	1	1

* $t_s = 1$ for $\Phi/g = 1$ but $t_s = 2$ for $\Phi/g = -1$ or 0.

Table 11. Multiplier representations for the space group *Pnam* ($R_a = R_5$, $R_aR_u \rightarrow R_w$)

R_u	R_w	$\boldsymbol{\delta} + \boldsymbol{a}_w{}^{-1}\boldsymbol{\delta}$	τ_w	$\phi(\boldsymbol{\delta}, R_w)$
R_1	R_5	$(0, 0, 0)$	$(0, 0, 0)$	1
R_2	R_6	$(0, 2\delta_b, 2\delta_c)$	$(1/2, 1/2, 1/2)$	$\exp[-i(\delta_b + \delta_c)]$
R_3	R_7	$(2\delta_a, 0, 2\delta_c)$	$(1/2, 1/2, 0)$	$\exp[-i\delta_a]$
R_4	R_8	$(2\delta_a, 2\delta_b, 0)$	$(0, 0, 1/2)$	1
R_5	R_1	$(2\delta_a, 2\delta_b, 2\delta_c)$	$(0, 0, 0)$	1
R_6	R_2	$(2\delta_a, 0, 0)$	$(1/2, 1/2, 1/2)$	$\exp[-i\delta_a]$
R_7	R_3	$(0, 2\delta_b, 0)$	$(1/2, 1/2, 0)$	$\exp[-i\delta_b]$
R_8	R_4	$(0, 0, 2\delta_c)$	$(0, 0, 1/2)$	$\exp[-i\delta_c]$

are doulby-degenerate ($t_s f_s=2$) if a component of the phase-difference vector is equal to π. If more than two components are equal to π, crystal vibrations are doubly-degenerate ($t_s f_s=2$ for T, U, E, and F) or fourfold-degenerate ($t_s f_s=4$ for S, R, and Q).

Symmetry Coordinates of Polyethylene

Symmetry coordinates of a crystal lattice for the μth symmetry species may be constructed from the sum of $\sum_u K_\mu(R_u)^* R_u \boldsymbol{\sigma}_i(\boldsymbol{\delta})$ over symmetry operations of the $\boldsymbol{k}$ group, where $K_\mu(R_u)^*$ is the complex conjugate of a matrix element (for R_u) of the μth irreducible representation of the $\boldsymbol{k}$ group.

The symmetry coordinates of orthorhombic polyethylene for $\Gamma(0,0,0)$ may be constructed from Tables 2 and 6, as follows.

$$
\left.\begin{array}{ll}
\Gamma_1(A_g) & S_1=(\sigma_1{}^x-\sigma_2{}^x+\sigma_3{}^x-\sigma_4{}^x)/2 \\
 & S_2=(\sigma_1{}^y-\sigma_2{}^y-\sigma_3{}^y+\sigma_4{}^y)/2 \\
\Gamma_2(A_u) & S_3=(\sigma_1{}^z+\sigma_2{}^z-\sigma_3{}^z-\sigma_4{}^z)/2i \\
\Gamma_3(B_{3g}) & S_4=(\sigma_1{}^x-\sigma_2{}^x-\sigma_3{}^x+\sigma_4{}^x)/2 \\
 & S_5=(\sigma_1{}^y-\sigma_2{}^y+\sigma_3{}^y-\sigma_4{}^y)/2 \\
\Gamma_4(B_{3u}) & S_6=(\sigma_1{}^z+\sigma_2{}^z+\sigma_3{}^z+\sigma_4{}^z)/2i \\
\Gamma_5(B_{1g}) & S_7=(\sigma_1{}^z-\sigma_2{}^z-\sigma_3{}^z+\sigma_4{}^z)/2 \\
\Gamma_6(B_{1u}) & S_8=(\sigma_1{}^x+\sigma_2{}^x+\sigma_3{}^x+\sigma_4{}^x)/2i \\
 & S_9=(\sigma_1{}^y+\sigma_2{}^y-\sigma_3{}^y-\sigma_4{}^y)/2i \\
\Gamma_7(B_{2g}) & S_{10}=(\sigma_1{}^z-\sigma_2{}^z+\sigma_3{}^z-\sigma_4{}^z)/2 \\
\Gamma_8(B_{2u}) & S_{11}=(\sigma_1{}^x+\sigma_2{}^x-\sigma_3{}^x-\sigma_4{}^x)/2i \\
 & S_{12}=(\sigma_1{}^y+\sigma_2{}^y+\sigma_3{}^y+\sigma_4{}^y)/2i
\end{array}\right\} \quad (26)
$$

TABLE 12. SYMMETRY COORDINATES (S_1—S_{12}) FOR SYMMETRY SPECIES* OF $\boldsymbol{k}$ GROUPS**

	Γ	$\sum$	Λ	Δ
S_1	1	1	1	1
S_2	1	1	1	1
S_3	2	3	3	3
S_4	3	2	4	3
S_5	3	2	4	3
S_6	4	4	2	1
S_7	5	3	2	2
S_8	6	1	4	4
S_9	6	1	4	4
S_{10}	7	4	3	4
S_{11}	8	2	1	2
S_{12}	8	2	1	2
	0	δ_a	0	0
$\boldsymbol{\delta}$	0	0	δ_b	0
	0	0	0	δ_c

* For examples, numerals of 1, 2, 3,⋯ in the column headed with Γ denote $\Gamma_1, \Gamma_2, \Gamma_3, \cdots$.
** $0<\delta_a, \delta_b, \delta_c<\pi$.

It may be recalled here that translational-symmetry coordinates ($\sigma_i{}^x, \sigma_i{}^y$, and $\sigma_i{}^z$) are functions of phase-difference vector $\boldsymbol{\delta}$ as shown in Eq. (3), so are $S_1(\boldsymbol{\delta})$—$S_{12}(\boldsymbol{\delta})$. From analyses of the effects of symmetry operations, these symmetry coordinates (S_1—S_{12}) are found useful, as themselves, for $\sum(\delta_a,0,0)$, $\Lambda(0,\delta_b,0)$, and $\Delta(0,0,\delta_c)$. As examples, symmetry coordinates of S_1, S_2, S_8, and S_9 may be used for the $\sum_1$ species, S_4, S_5, S_{11}, and S_{12} for the $\sum_2$ species, S_3 and S_7 for the $\sum_3$ species, and S_6 and S_{10} for the $\sum_4$ species. Furthermore the symmetry coordinates of Eq. (26) may be used for $(0,\delta_b,\delta_c)$, $(\delta_a,0,\delta_c)$, $(\delta_a,\delta_b,0)$, and $(\delta_a,\delta_b,\delta_c)$ and also for phase-difference vectors $\boldsymbol{\delta}$ on boundaries of the first Brillouin zone. It may be remarked that, for any phase difference vector, the real parts of the symmetry coordinates of Eq. (26) are symmetric with respect to the inversion operation whereas the imaginary parts are antisymmetric. Accordingly, the dynamical matrix $\boldsymbol{D}_S(\boldsymbol{\delta})$ associated with $S_1(\boldsymbol{\delta})$—$S_{12}(\boldsymbol{\delta})$ are real. Elements of the dynamical matrix are functions of $\boldsymbol{\delta}(\delta_a,\delta_b,\delta_c)$ and the vibrational frequencies for a $\boldsymbol{\delta}$ vector may be calculated after diagonalization of the dynamical matrix.

As a few examples of $X(\pi,0,0)$, $U(\pi,\pi,0)$, and $R(\pi,\pi,\pi)$, degeneracy of crystal vibrations will now be discussed from analyses of symmetry coordinates. For $X(\pi,0,0)$, symmetry coordinates may be constructed from $\sum_u X_\mu(R_u)^* R_u \boldsymbol{\sigma}_i$ (Tables 2 and 7) as follows.

$$
\left.\begin{array}{ll}
S(X_1)_{1a}=(\sigma_1{}^x-i\sigma_4{}^x)/2^{1/2} & \\
 & S(X_1)_{1b}=(-\sigma_2{}^x-i\sigma_3{}^x)/2^{1/2} \\
S(X_1)_{2a}=(-\sigma_2{}^x+i\sigma_3{}^x)/2^{1/2} & \\
 & S(X_1)_{2b}=(\sigma_1{}^x+i\sigma_4{}^x)/2^{1/2} \\
S(X_1)_{3a}=(\sigma_1{}^y+i\sigma_4{}^y)/2^{1/2} & \\
 & S(X_1)_{3b}=(-\sigma_2{}^y+i\sigma_3{}^y)/2^{1/2} \\
S(X_1)_{4a}=(-\sigma_2{}^y-i\sigma_3{}^y)/2^{1/2} & \\
 & S(X_1)_{4b}=(\sigma_1{}^y-i\sigma_4{}^y)/2^{1/2} \\
S(X_2)_{5a}=(\sigma_1{}^z-i\sigma_4{}^z)/2^{1/2} & \\
 & S(X_2)_{5b}=(\sigma_2{}^z+i\sigma_3{}^z)/2^{1/2} \\
S(X_2)_{6a}=(\sigma_2{}^z-i\sigma_3{}^z)/2^{1/2} & \\
 & S(X_2)_{6b}=(\sigma_1{}^z+i\sigma_4{}^z)/2^{1/2}
\end{array}\right\} \quad (27)
$$

Now, from Table 2 and Eqs. (2) and (3), effects of inversion (R_5) are

$$
\left.\begin{array}{l}
R_5\boldsymbol{\sigma}_1(\pi,0,0)=-\boldsymbol{\sigma}_2(-\pi,0,0)=-\boldsymbol{\sigma}_2(\pi,0,0) \\
R_5\boldsymbol{\sigma}_3(\pi,0,0)=-\boldsymbol{\sigma}_4(-\pi,0,0)=\boldsymbol{\sigma}_4(\pi,0,0)
\end{array}\right\} \quad (28)
$$

Accordingly, pairs (a and b) of symmetry coordinate vectors of $X(\pi,0,0)$ are transformed upon inversion as follows,

$$
\left.\begin{array}{l}
S(X_1)_a \leftrightarrow S(X_1)_b \\
S(X_2)_a \leftrightarrow -S(X_2)_b
\end{array}\right\} \quad (29)
$$

and crystal vibrations are doubly degenerate for X_1 and X_2.

Next, for $U(\pi,\pi,0)$, symmetry coordinates may

be constructed from Tables 2 and 8 as follows.

$$\left.\begin{aligned}
S(U_1)_1 &= [(\sigma_1{}^x-\sigma_2{}^x)-i(\sigma_3{}^x-\sigma_4{}^x)]/2\\
S(U_1)_2 &= [(\sigma_1{}^y-\sigma_2{}^y)+i(\sigma_3{}^y-\sigma_4{}^y)]/2\\
S(U_2)_1 &= [(\sigma_1{}^x-\sigma_2{}^x)+i(\sigma_3{}^x-\sigma_4{}^x)]/2\\
S(U_2)_2 &= [(\sigma_1{}^y-\sigma_2{}^y)-i(\sigma_3{}^y-\sigma_4{}^y)]/2\\
S(U_3)_3 &= [(\sigma_1{}^z+\sigma_2{}^z)+i(\sigma_3{}^z+\sigma_4{}^z)]/2\\
S(U_4)_3 &= [(\sigma_1{}^z+\sigma_2{}^z)-i(\sigma_3{}^z+\sigma_4{}^z)]/2\\
S(U_5)_4 &= [(\sigma_1{}^z-\sigma_2{}^z)+i(\sigma_3{}^z-\sigma_4{}^z)]/2\\
S(U_6)_4 &= [(\sigma_1{}^z-\sigma_2{}^z)-i(\sigma_3{}^z-\sigma_4{}^z)]/2\\
S(U_7)_5 &= [(\sigma_1{}^x+\sigma_2{}^x)-i(\sigma_3{}^x+\sigma_4{}^x)]/2\\
S(U_7)_6 &= [(\sigma_1{}^y+\sigma_2{}^y)+i(\sigma_3{}^y+\sigma_4{}^y)]/2\\
S(U_8)_5 &= [(\sigma_1{}^x+\sigma_2{}^x)+i(\sigma_3{}^x+\sigma_4{}^x)]/2\\
S(U_8)_6 &= [(\sigma_1{}^y+\sigma_2{}^y)-i(\sigma_3{}^y+\sigma_4{}^y)]/2
\end{aligned}\right\} \quad (30)$$

However, since translational-symmetry coordinate vectors $\boldsymbol{\sigma}_1$—$\boldsymbol{\sigma}_4$ are all real for $U(\pi,\pi,0)$, symmetry coordinates of (U_1 and U_2), (U_3 and U_4), (U_5 and U_6) and (U_7 and U_8) are mutually conjugate and accordingly crystal vibrations of these pairs are doubly degenerate due to time-reversal symmetry ($t_s=2$, see Table 10).

Finally, for $R(\pi,\pi,\pi)$, symmetry coordinates may be obtained from Tables 2 and 9 as follows.

$$\left.\begin{aligned}
S(R_1)_{1a} &= (\sigma_1{}^x+i\sigma_3{}^x)/2^{1/2}\\
S(R_1)_{2a} &= (\sigma_1{}^y-i\sigma_3{}^y)/2^{1/2}\\
S(R_1)_{3a} &= (-\sigma_2{}^z-i\sigma_4{}^z)/2^{1/2}\\
S(R_1)_{1b} &= (-i\sigma_2{}^x+\sigma_4{}^x)/2^{1/2}\\
S(R_1)_{2b} &= (-i\sigma_2{}^y-\sigma_4{}^y)/2^{1/2}\\
S(R_1)_{3b} &= (-i\sigma_1{}^z+\sigma_3{}^z)/2^{1/2}\\
S(R_2)_{1c} &= (\sigma_1{}^x-i\sigma_3{}^x)/2^{1/2}\\
S(R_2)_{2c} &= (\sigma_1{}^y+i\sigma_3{}^y)/2^{1/2}\\
S(R_2)_{3c} &= (\sigma_2{}^z-i\sigma_4{}^z)/2^{1/2}\\
S(R_2)_{1d} &= (-i\sigma_2{}^x-\sigma_4{}^x)/2^{1/2}\\
S(R_2)_{2d} &= (-i\sigma_2{}^y+\sigma_4{}^y)/2^{1/2}\\
S(R_2)_{3d} &= (i\sigma_1{}^z+\sigma_3{}^z)2^{1/2}
\end{aligned}\right\} \quad (31)$$

However, from Table 2 and Eqs. (2) and (3), effects of inversion (R_5) are

$$\left.\begin{aligned}
R_5\boldsymbol{\sigma}_1(\pi,\pi,\pi) &= -\boldsymbol{\sigma}_2(-\pi,-\pi,-\pi) = i\boldsymbol{\sigma}_2(\pi,\pi,\pi)\\
R_5\boldsymbol{\sigma}_3(\pi,\pi,\pi) &= -\boldsymbol{\sigma}_4(-\pi,-\pi,-\pi) = i\boldsymbol{\sigma}_4(\pi,\pi,\pi)
\end{aligned}\right\} \quad (32)$$

and therefore symmetry coordinate vectors are transformed upon inversion, as follows,

$$\boldsymbol{S}(R_1)_a \leftrightarrow -\boldsymbol{S}(R_1)_b \qquad \boldsymbol{S}(R_2)_c \leftrightarrow -\boldsymbol{S}(R_2)_d. \quad (33)$$

Furthermore, for the phase-difference vector of (π,π,π),

$$\boldsymbol{S}(R_1)_a = -i\boldsymbol{S}(R_2)_c{}^* \qquad \boldsymbol{S}(R_1)_b = -i\boldsymbol{S}(R_2)_d{}^* \quad (34)$$

and accordingly, the symmetry coordinate vectors of R_1 and R_2 form doubly-degenerate pairs (a-c and b-d) due to time-reversal symmetry. However, since the symmetry coordinate vectors of R_1 and R_2 form doubly degenerate pairs (a-b and c-d) due to space symmetry, crystal vibrations of $R(\pi,\pi,\pi)$ are four-fold degenerate (see Table 10, $f_s=2$, $t_s=2$).

Normal Vibration Treatment

Symmetry Coordinates. For a crystal containing an atoms per unit cell, there are $3n$ normal modes of crystal vibrations for a given phase-difference vector $\boldsymbol{\delta}=(\delta_a,\delta_b,\delta_c)$. Accordingly, the Cartesian symmetry coordinate vector $\boldsymbol{S}(\boldsymbol{\delta})$ with $3n$ components may be constructed as

$$\boldsymbol{S}(\boldsymbol{\delta}) = \sum_{\rho}\boldsymbol{U}(\boldsymbol{\delta},\boldsymbol{\rho})\boldsymbol{X}(\boldsymbol{\rho}), \quad (35)$$

where $\boldsymbol{U}(\boldsymbol{\delta},\boldsymbol{\rho})$ is a unitary transformation matrix and $\boldsymbol{X}(\boldsymbol{\rho})$ is the Cartesian coordinate vector (three components) of the $\boldsymbol{\rho}$th atom. For the case of orthorhombic polyethylene, real parts of the Cartesian symmetry coordinates of Eq. (26) may be used, *viz.*,

$$\boldsymbol{S}(\boldsymbol{\delta})\dagger = (S_1\ S_2\ S_3\ S_4\ S_5\ S_6\ S_8\ S_9\ S_7\ S_{11}\ S_{12}\ S_{10}) \quad (36)$$

so that

$$\boldsymbol{S}(\boldsymbol{\delta}) = (2N)^{-1/2}\sum_{\boldsymbol{L}}\begin{bmatrix} \boldsymbol{u}_1{}^c & \boldsymbol{u}_2{}^c & \boldsymbol{u}_3{}^c & \boldsymbol{u}_4{}^c\\ \boldsymbol{u}_1{}^c & \boldsymbol{u}_2{}^c & -\boldsymbol{u}_3{}^c & -\boldsymbol{u}_4{}^c\\ \boldsymbol{u}_1{}^s & -\boldsymbol{u}_2{}^s & \boldsymbol{u}_3{}^s & -\boldsymbol{u}_4{}^s\\ \boldsymbol{u}_1{}^s & -\boldsymbol{u}_2{}^s & -\boldsymbol{u}_3{}^s & \boldsymbol{u}_4{}^s \end{bmatrix}\begin{bmatrix} \boldsymbol{X}(\boldsymbol{\rho}_1)\\ \boldsymbol{X}(\boldsymbol{\rho}_2)\\ \boldsymbol{X}(\boldsymbol{\rho}_3)\\ \boldsymbol{X}(\boldsymbol{\rho}_4) \end{bmatrix} \quad (37)$$

$$\left.\begin{aligned}
\boldsymbol{u}_1{}^c &= \begin{bmatrix} c_1 & 0 & 0\\ 0 & c_1 & 0\\ 0 & 0 & s_1 \end{bmatrix} & \boldsymbol{u}_1{}^s &= \begin{bmatrix} s_1 & 0 & 0\\ 0 & s_1 & 0\\ 0 & 0 & c_1 \end{bmatrix}\\
\boldsymbol{u}_2{}^c &= \begin{bmatrix} -c_2 & 0 & 0\\ 0 & -c_2 & 0\\ 0 & 0 & s_2 \end{bmatrix} & \boldsymbol{u}_2{}^s &= \begin{bmatrix} -s_2 & 0 & 0\\ 0 & -s_2 & 0\\ 0 & 0 & c_2 \end{bmatrix}\\
\boldsymbol{u}_3{}^c &= \begin{bmatrix} c_3 & 0 & 0\\ 0 & -c_3 & 0\\ 0 & 0 & -s_3 \end{bmatrix} & \boldsymbol{u}_3{}^s &= \begin{bmatrix} s_3 & 0 & 0\\ 0 & -s_3 & 0\\ 0 & 0 & -c_3 \end{bmatrix}\\
\boldsymbol{u}_4{}^c &= \begin{bmatrix} -c_4 & 0 & 0\\ 0 & c_4 & 0\\ 0 & 0 & -s_4 \end{bmatrix} & \boldsymbol{u}_4{}^s &= \begin{bmatrix} -s_4 & 0 & 0\\ 0 & s_4 & 0\\ 0 & 0 & -c_4 \end{bmatrix}
\end{aligned}\right\} \quad (38)$$

where

$$\left.\begin{aligned}
c_i &= \cos(\boldsymbol{\rho}_i\cdot\boldsymbol{\delta})\\
s_i &= \sin(\boldsymbol{\rho}_i\cdot\boldsymbol{\delta})
\end{aligned}\right\} \quad (39)$$

Dynamical Matrix. The potential energy (V) of crystal vibrations may be expressed with internal coordinates $\boldsymbol{R}$ (bond lengths, bond angles, internal-rotation angles, and others) as

$$2V = \tilde{\boldsymbol{R}}\boldsymbol{F}_R\boldsymbol{R}, \quad (40)$$

where $\boldsymbol{F}_R$ is the potential energy matrix. With the use of the $\boldsymbol{B}(\boldsymbol{\rho})$ matrix,[19] the $\boldsymbol{R}$ vector is derived from Eq. (35) as

$$\boldsymbol{R} = \sum_{\rho}\boldsymbol{B}(\boldsymbol{\rho})\boldsymbol{X}(\boldsymbol{\rho}) = \sum_{\rho}\boldsymbol{B}(\boldsymbol{\rho})\sum_{\delta}\tilde{\boldsymbol{U}}(\boldsymbol{\delta},\boldsymbol{\rho})\boldsymbol{S}(\boldsymbol{\delta}). \quad (41)$$

Then, the potential energy for the phase-difference

19) E. B. Wilson, *J. Chem. Phys.*, **7**, 1047 (1939); *ibid.*, **9**, 76 (1942).

$\boldsymbol{\delta}$ is derived as

$$2V(\boldsymbol{\delta}) = \tilde{\boldsymbol{S}}(\boldsymbol{\delta})\boldsymbol{F}_S(\boldsymbol{\delta})\boldsymbol{S}(\boldsymbol{\delta}) \tag{42}$$

$$\boldsymbol{F}_S = \sum_{\rho'}\sum_{\rho} \boldsymbol{U}(\boldsymbol{\delta}, \boldsymbol{\rho}')\tilde{\boldsymbol{B}}(\boldsymbol{\rho}')\boldsymbol{F}_R\boldsymbol{B}(\boldsymbol{\rho})\tilde{\boldsymbol{U}}(\boldsymbol{\delta},\boldsymbol{\rho}), \tag{43}$$

where a transposed conjugate vector (or matrix) is denoted with a tilde. On the other hand, the kinetic energy (T) for $\boldsymbol{\delta}$ is given as

$$2T(\boldsymbol{\delta}) = \tilde{\dot{\boldsymbol{S}}}(\boldsymbol{\delta})\boldsymbol{M}_S\dot{\boldsymbol{S}}(\boldsymbol{\delta}), \tag{44}$$

where $\dot{\boldsymbol{S}}$ is the time derivative of $\boldsymbol{S}$ and $\boldsymbol{M}_S$ is the diagonal mass matrix whose elements are masses of constituent atoms of a unit cell.

The dynamical matrix $\boldsymbol{D}_S(\boldsymbol{\delta})$ for $\boldsymbol{\delta}$ is then derived as

$$\boldsymbol{D}_S(\boldsymbol{\delta}) = \boldsymbol{M}_S{}^{-1/2}\boldsymbol{F}_S(\boldsymbol{\delta})\boldsymbol{M}_S{}^{-1/2}, \tag{45}$$

where $\boldsymbol{M}_S{}^{-1/2}$ is a diagonal matrix whose elements are square root of reciprocal masses of atoms.

Diagonalization. A general method for diagonalizing hermitian matrices $\boldsymbol{D}_S(\boldsymbol{\delta})$ has been described,[20] although dynamical matrices of polyethylene are real if the symmetry-coordinates of Eq. (36) are used. After diagonalizing $\boldsymbol{D}_S(\boldsymbol{\delta})$,

$$\tilde{\boldsymbol{L}}_S(\boldsymbol{\delta})\boldsymbol{D}_S(\boldsymbol{\delta})\boldsymbol{L}_S(\boldsymbol{\delta}) = \boldsymbol{\Lambda}(\boldsymbol{\delta}) \tag{46}$$

the diagonal frequency-parameter matrix $\boldsymbol{\Lambda}(\boldsymbol{\delta})$ is obtained whose elements are squared angular frequencies. With the unitary eigenvector matrix $\boldsymbol{L}_S(\boldsymbol{\delta})$, the transformation from the $\boldsymbol{S}(\boldsymbol{\delta})$ vector to the normal coordinate vector $\boldsymbol{Q}(\boldsymbol{\delta})$ is given as

$$\boldsymbol{S}(\boldsymbol{\delta}) = \boldsymbol{M}_S{}^{-1/2}\boldsymbol{L}_S(\boldsymbol{\delta})\boldsymbol{Q}(\boldsymbol{\delta}) \tag{47}$$

and, from Eq. (35), the Cartesian coordinate vector $\boldsymbol{X}(\boldsymbol{\rho})$ of the $\boldsymbol{\rho}$th atom is finally given as

$$\boldsymbol{X}(\boldsymbol{\rho}) = \sum_{\delta}\tilde{\boldsymbol{U}}(\boldsymbol{\delta}, \boldsymbol{\rho})\boldsymbol{M}_S{}^{-1/2}\boldsymbol{L}_S(\boldsymbol{\delta})\boldsymbol{Q}(\boldsymbol{\delta}). \tag{48}$$

In actual numerical treatments for a number of phase-difference vectors in the first Brillouin zone, computation time is consumed primarily in diagonalization of dynamical matrices and careful procedure is desirable for reducing computation time.

Molecular Crystals. In three-dimensional molecular crystals, high-frequency intramolecular vibrations are primarily due to intramolecualr force field and weak intermolecular interactions give rise to small band-splitting. Usually the force field of a free molecule is brought over to the crystalline state and the potential energy matrix ($\boldsymbol{F}_R$) of a molecular crystal is expressed as a sum of the intramolecular part ($\boldsymbol{F}_R{}^M$) and the intermolecular part ($\boldsymbol{F}_R{}^C$),

$$\boldsymbol{F}_R = \boldsymbol{F}_R{}^M + \boldsymbol{F}_R{}^C. \tag{49}$$

From Eqs. (43), (45), and (49), it is readily seen that the dynamical matrix $\boldsymbol{D}_S(\boldsymbol{\delta})$ is now expressed as a sum of the intramolecular part $\boldsymbol{D}_S{}^M(\boldsymbol{\delta})$ and intermolecular part $\boldsymbol{D}_S{}^C(\boldsymbol{\delta})$. If, however, each molecule of the crystal is brought inside a unit cell, the intramolecular force field of a molecule can be expressed with Cartesian coordinates of a common index vector and accordingly $\boldsymbol{D}_S{}^M$ becomes independent of $\boldsymbol{\delta}$,

$$\boldsymbol{D}_S(\boldsymbol{\delta}) = \boldsymbol{D}_S{}^M + \boldsymbol{D}_S{}^C(\boldsymbol{\delta}). \tag{50}$$

Then it is advisable to diagonalize $\boldsymbol{D}_S(\boldsymbol{\delta})$ in two steps, since large off-diagonal elements of $\boldsymbol{D}_S(\boldsymbol{\delta})$ are primarily from the intramolecular part. The first step is to diagonalize $\boldsymbol{D}_S{}^M$ that is independent of $\boldsymbol{\delta}$,

$$\tilde{\boldsymbol{L}}_S{}^M\boldsymbol{D}_S{}^M\boldsymbol{L}_S{}^M = \boldsymbol{\Lambda}^M \text{ (diagonal)}. \tag{51}$$

Accordingly, the dynamical matrix $\boldsymbol{D}_S(\boldsymbol{\delta})$ is now transformed into

$$\tilde{\boldsymbol{L}}_S{}^M\boldsymbol{D}_S(\boldsymbol{\delta})\boldsymbol{L}_S{}^M = \boldsymbol{\Lambda}^M + \tilde{\boldsymbol{L}}_S{}^M\boldsymbol{D}_S{}^C(\boldsymbol{\delta})\boldsymbol{L}_S{}^M \tag{52}$$

and the diagonalization of the second step is carried out to yield the frequency parameter matrix and eigenvector matrix,

$$\boldsymbol{\Lambda}(\boldsymbol{\delta}) = \tilde{\boldsymbol{L}}_S{}^C(\boldsymbol{\delta})[\boldsymbol{\Lambda}^M + \tilde{\boldsymbol{L}}_S{}^M\boldsymbol{D}_S{}^C(\boldsymbol{\delta})\boldsymbol{L}_S{}^M]\boldsymbol{L}_S{}^C(\boldsymbol{\delta}) \tag{53}$$

$$\boldsymbol{L}_S(\boldsymbol{\delta}) = \boldsymbol{L}_S{}^M\boldsymbol{L}_S{}^C(\boldsymbol{\delta}). \tag{54}$$

The off-diagonal elements meeting in the second step are due to the intermolecualr force field and are relatively small so that total computation involved in numerical treatments for many $\boldsymbol{\delta}$ vectors is thus greatly reduced.

Polymer-chain Crystals. For the dynamical matrix $\boldsymbol{D}_S(\boldsymbol{\delta})$ of polymer-chain crystals, the intrachain part $\boldsymbol{D}_S{}^M$ depends upon the phase-difference along the chain axis,

$$\boldsymbol{D}_S(\boldsymbol{\delta}) = \boldsymbol{D}_S{}^M(\delta_c) + \boldsymbol{D}_S{}^C(\delta_a,\delta_b,\delta_c). \tag{55}$$

Accordingly for each chosen value of δ_c, the first step is carried out to diagonalize $\boldsymbol{D}_S{}^M(\delta_c)$ and then the second step is carried out, for many values of δ_a and δ_b, to yield $\boldsymbol{\Lambda}(\boldsymbol{\delta})$ and $\boldsymbol{L}_S(\boldsymbol{\delta})$,

$$\boldsymbol{\Lambda}(\boldsymbol{\delta}) = \tilde{\boldsymbol{L}}_S{}^C(\boldsymbol{\delta})[\boldsymbol{\Lambda}^M(\delta_c) + \tilde{\boldsymbol{L}}_S{}^M(\delta_c)\boldsymbol{D}_S{}^C(\boldsymbol{\delta})\boldsymbol{L}_S{}^M(\delta_c)]\boldsymbol{L}_S{}^C(\boldsymbol{\delta}) \tag{56}$$

$$\boldsymbol{L}_S(\boldsymbol{\delta}) = \boldsymbol{L}_S{}^M(\delta_c)\boldsymbol{L}_S{}^C(\boldsymbol{\delta}). \tag{57}$$

Low Frequency Vibrations. Low frequency crystal vibrations are concerned with low temperature specific heat, neutron-scattering cross sections or mean squared amplitudes of atoms. In treating these properties theoretically, it is required to calculate vibrational frequencies and eigenvectors for a large number of phase-difference vectors. Accordingly, it is highly desirable to develop a useful approximation procedure for treating low frequency vibrations.

For orthorhombic polyethylene, however, a gap of frequency distribution[11] lies at 550—700 cm^{-1} and low-frequency vibrations may approximately

20) T. Miyazawa, K. Fukushima and Y. Ideguchi, *J. Chem. Phys.*, **38**, 2709 (1963).

be treated separately from high-frequency vibrations. Thus, from the eigenvector matrix $\boldsymbol{L}_S{}^M(\delta_c)$ of Eq. (51), columns associated with low-frequency modes are extracted to form a rectangular matrix $\boldsymbol{L}_l{}^M(\delta_c)$ and the corresponding minor matrix $\boldsymbol{\Lambda}_l(\delta_c)$ is extracted from the frequency-parameter matrix $\boldsymbol{\Lambda}^M(\delta_c)$. Then, the dynamical matrix $\boldsymbol{D}_l(\boldsymbol{\delta})$ for low-frequency modes is approximately obtained by a congruent transformation with $\boldsymbol{L}_l{}^M(\delta_c)$,

$$\boldsymbol{D}_l(\boldsymbol{\delta}) = \boldsymbol{\Lambda}_l(\delta_c) + \tilde{\boldsymbol{L}}_l{}^M(\delta_c)\boldsymbol{D}_S{}^C(\boldsymbol{\delta})\boldsymbol{L}_l{}^M(\delta_c) \tag{58}$$

and the frequency-parameter matrix and eigenvector matrix for low-frequency vibrations are given as

$$\boldsymbol{\Lambda}_l(\boldsymbol{\delta}) = \tilde{\boldsymbol{L}}_l{}^C(\boldsymbol{\delta})\boldsymbol{D}_l(\boldsymbol{\delta})\boldsymbol{L}_l{}^C(\boldsymbol{\delta}) \tag{59}$$

$$\boldsymbol{L}_l(\boldsymbol{\delta}) = \boldsymbol{L}_l{}^M(\delta_c)\boldsymbol{L}_l{}^C(\boldsymbol{\delta}). \tag{60}$$

For orthorhombic polyethylene, the order of dynamical matrices is reduced from 36 [$\boldsymbol{D}_S$] to 8 [$\boldsymbol{D}_l$] and therefore the approximate procedure stated above saves a lot of computation time, allowing vibration treatments over a greater number of phase-difference vectors in the first Brillouin zone.

Conclusion

Irreducible representations of $\boldsymbol{k}$ groups of the space group *Pnam* and degeneracies of crystal vibrations due to space symmetry and time-reversal symmetry were treated in the present study. Symmetry coordinates of carbon atoms of orthorhombic polyethylene were constructed from translational-symmetry coordinates with nonintegral index vectors. Similar coordinates may readily be constructed for sets of hydrogen atoms. Furthermore, general matrix methods were worked out for treating molecular crystals and chain-polymer crystals and for approximately treating low frequency lattice vibrations.

These methods are applicable for treating frequency distributions and specific heat, mean squared thermal amplitudes of scattering atoms (temperature factor for X ray scattering), and scattering cross sections (elastic and inelastic) of thermal neutrons. Symmetry considerations are indispensable for treating dispersion curves of optical and acoustic branches of crystal vibrations. These studies on orthorhombic polyethylene will be presented in forthcoming papers.

BULLETIN OF THE CHEMICAL SOCIETY OF JAPAN VOL. 42 3447—3450 (1969)

Effect of γ-Preirradiation on Catalytic Activity of Nickel Oxide for the Oxidation of Carbon Monoxide

Yoshisato TEZUKA and Toyosaburo TAKEUCHI

Faculty of Literature and Science, Toyama Universiy, Gofuku, Toyama

(Received July 1, 1969)

The change in NiO catalytic activity upon the variation in the irradiation of γ-rays in the presence of O_2 gas was studied. Activities were determined for the reaction of CO with NiO and for the oxidation reaction of CO on NiO. The results showed a decrease in the CO-NiO reaction rate with an increase in the irradiation of NiO, particularly in the absence of oxygen; if the irradiation was more than 7×10^7R, the reaction rate increased as both the irradiation in the presence of oxygen and the oxygen partial pressure increased. The activity change in NiO was explained by assuming the migration of the specially-active oxygen into the oxide bulk by means of the irradiation of γ-rays.

Various types of adsorbed oxygen have been proposed as the reaction intermedia of the catalytic oxidation caused by the metallic oxide. The correlation between the type of oxygen and its reactivity does not, however, bear this out clearly since the metal oxide catalytic activity is greatly affected by: (1) the treatment of the metal oxide, (2) the impurity present in the oxide, and (3) the reactant employed.

Several studies[1,2] published recently on the catalytic effects of the irradiation of γ-rays on nickel oxide have concluded that the activity of the oxide is greatly influenced by the irradiation of γ-rays; it sometimes increases and sometimes decreases. This fact indicates that the behavior of the oxygen of the metal oxide upon the irradiation is very complicated. Many areas remain unexplored concerning the behavior of the oxygen of the metal oxide

1) T. Yamashina and T. Nagamatsuya, This Bulletin, **38**, 507 (1965).

2) T. Yamashina and M. Sano, *ibid.*, **38**, 1801 (1965).

which had been subjected to the irradiation of γ-rays and the role of oxygen in catalytic reactions.

This study concerns the reactivity of the oxygen of the nickel oxide, which was irradiated with various doses of γ-rays. The reactivity was observed through the reaction between carbon monoxide and the oxygen of the oxide, and the catalytic reaction between carbon monoxide and oxygen gas.

Experimental

For each test run, 0.5g of nickel oxide was used. The nickel oxide used was obtained by igniting extra-pure nickel nitrate furnished by the Wako Chemicals Co. in an atmosphere of air at 550°C for 24 hr. The irradiation of the oxide was made in a vessel with a breaker joint, as is shown in Fig. 1. Two kinds of samples were prepared. One was the oxide which was evacuated under 10^{-6} mmHg at 300°C for 4 hr and then sealed. The other was prepared in the same manner, but after evacuation a certain amount of oxygen was admitted. The tube was pressured to 7 or 18 cmHg with oxygen. Both tubes were sealed and irradiated by ^{60}Co γ-rays. The dose rate was 5.84×10^5 R/hr. After irradiation, the samples were drawn out and kept at room temperature for about one week. The tube was then connected to the apparatus.

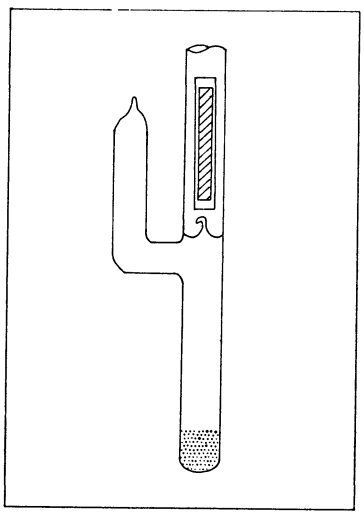

Fig. 1. The reaction vessel.

The reaction was carried out by the statistical method. The volume of the reaction vessel, including the manometer, was about 150 m*l*. In order to freeze the carbon dioxide produced by the reaction, a U-tube cooled by liquid oxygen was used to connect the reaction vessel and the manometer. Apiezon oil was used to measure the pressure decreases resulting from the reaction. Prior to use, the samples were evacuated again for about 2 hr at a temperature of 300°C to a pressure of 10^{-5} mmHg; then the temperature was lowered to the reaction temperature of 131° or 251°C. For the reaction between carbon monoxide and nickel oxide, carbon monoxide (12 cm oil) was introduced into the vessel. For the reaction between carbon monoxide and oxygen on nickel oxide, the 12 cm oil of a mixture of cardon monoxide and oxygen (mol ratio 2 : 1) was introduced into the vessel.

The oxygen used was of a commercial grade. It was purified by passing it through a trap cooled by liquid nitrogen. The carbon monoxide (purity: 99.9%) was supplied by the Takachiho Chemicals Co.

The surface areas were measured by the B.E.T. method, using ethylene at −183°C, as had been by Wooten and Brown,[3] after the test of the activity was finished.

The structure of nickel oxide was examined by a X-ray diffractometer (Rigaku Denki, Model D-3F) operated at 30 kv and 40 mA and adopting the Debye-Scherrer method.

Results

No change due to the γ-irradiation was observed in the oxide structure by means of X-ray diffraction.

The relation between the radiation dose and the B.E.T. surface area is shown in Table 1.

TABLE 1

Radiation Dose (R)	0	1.04×10^8	4.6×10^8
Surface area (m^2/g)	8.9	8.9	8.8

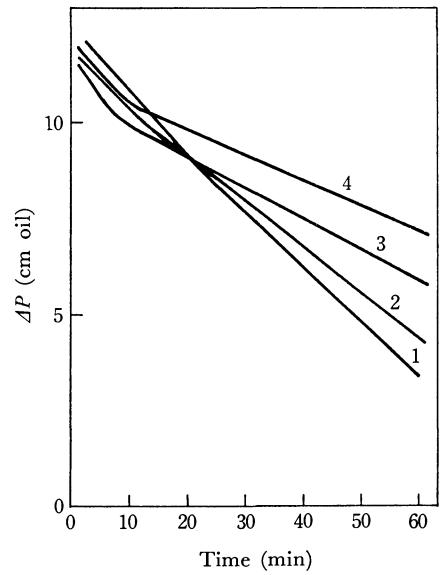

Fig. 2. The decrease of pressure of carbon monoxide on nickel oxide irradiated with γ-rays in the absence of oxygen gas.
1, no irradiation
2, 5×10^6 R
3, 7.1×10^7 R
4, 4.6×10^8 R

3) L. A. Wooten and C. Brown, *J. Am. Chem. Soc.*, **65**, 113 (1943).

The results show that irradiation did not affect the B.E.T. surface area.

In the reaction of nickel oxide with carbon monoxide, the time-pressure relationship was approximately linear when the radiation dose was small. However, a curved line was given when the radiation dose was greater than 5×10^7 R and when the radiation was carried out in a vacuum. Several results are shown in Fig. 2. The rate of reaction in the latter case was determined from the slope of the linear part of the curve at the initiation of the reaction. Figure 3 shows the dependency of the radiation dose on the reaction rate. The figure shows that the irradiated oxide reaction rate is greater in the presence of oxygen than in the absence of oxygen. Also, in both cases the rate decreases with an increase in the radiation dose.

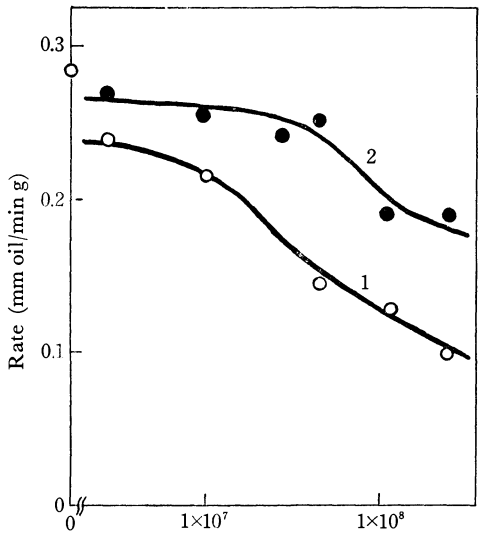

Fig. 3. The dependency of the reaction rate of carbon monoxide and nickel oxide on dose of γ-rays.
1, in the absence of oxygen gas
2, in the presence of oxygen gas (7 cmHg)

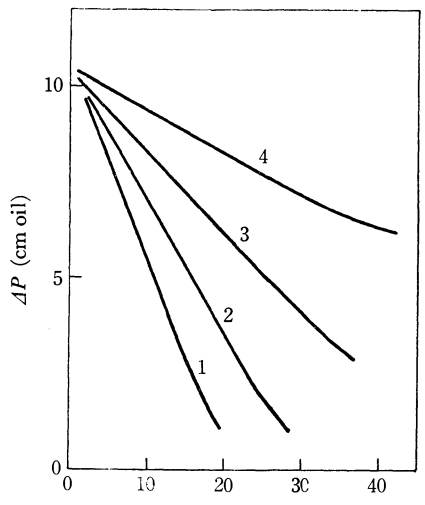

Fig. 4. The decrease of carbon monoxide and oxygen gas on nickel oxide irradiated with γ-rays in the absence of oxygen gas.
1, no irradiation
2, 5×10^6 R
3, 1.04×10^8 R
4, 4.6×10^8 R

In the oxidation of carbon monoxide on nickel oxide, the time-pressure relationship was given approximately as a straight line. Figure 4 shows the correlation. The rate of reaction in Fig. 5 was determined from the slope of the line. Figure 5 indicates that the reaction rate on nickel oxide irradiated in the absence of oxygen gas decreases with an increase in the radiation dose, but the rate on nickel oxide irradiated in the presence of oxygen increases upon a radiation of more than 7×10^7 R and with increases in the pressure of the oxygen environment.

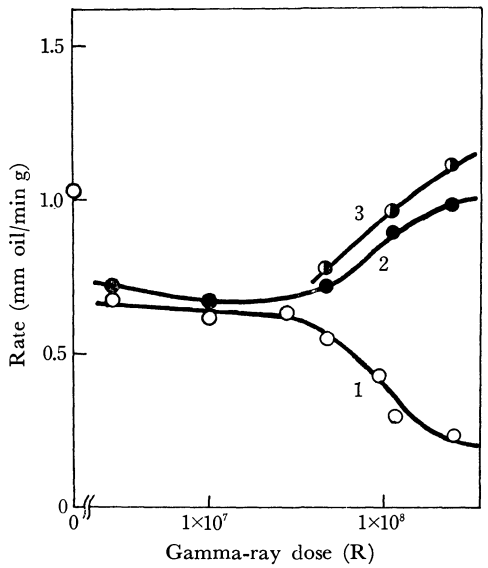

Fig. 5. The dependency of the reaction rate of carbon monoxide and oxygen on dose of γ-rays.
1, in the absence of oxygen gas
2, in the presence of oxygen gas (7 cmHg)
3, in the presence of oxygen gas (18 cmHg)

Discussion

A remarkable change was found in the catalytic reaction rate of carbon monoxide with oxygen gas on nickel oxide irradiated with γ-rays of more than 7×10^7 R in the presence (A-1) and in the absence (A-2) of oxygen. The dose which changed the rate is very similar to that reported by Yamashina[2] who studied the decomposition of hydrogen peroxide on nickel oxide irradiated in an atmosphere

of air.

The rates of the reaction of nickel oxide with carbon monoxide irradiated both in the presence (B-1) and in the absence (B-2) of oxygen gas decrease as the radiation dose increases. The decrease is smaller, however, when the oxide is irradiated in the presence of the oxygen. This fact would suggest that the active oxygen on the surface becomes inactive or migrates into the interior upon irradiation. It was found that the irradiation of γ-rays promotes the migration of oxygen into the bulk of nickel oxide.[4]

Several types of oxygen have been proposed as the intermedium of the reaction on catalytic oxidation.[5-9] The oxygen which is active in the catalytic oxidation and in the migration into the bulk of the metal oxide has been considered to be charged as O^-.[10] The vacancy of the site caused by the migration of the adsorbed oxygen into the bulk during the irradiation would be replaced by another oxygen. The amount of oxygen on the surface would then be kept constant if the oxygen exists in the gaseous phase because the replacement of the adsorbed oxygen is enchanced. The almost constant reaction rate on the oxide irradiated with doses up to 7×10^7 R in the presence of oxygen (A-1 and B-1) can be explained in terms of the replacement of the adsorbed oxygen. The great rate decrease in B-1 in the area of doses of more than 7×10^7 R can be explained by assuming that the bond energy of the adsorbed oxygen changes due to the variation in the electronic property[11] of the surface, which is itself affected by the concentration of the migrated oxygen. In this study, the oxide was evacuated under 10^{-5} mmHg before the admission of carbon monoxide. The evacuation leads to a loss of the adsorbed oxygen. The amount of loss is affected by the radiation dose because the change in the radiation dose alters the concentration of oxygen in the bulk. We may expect a remarkable decrease in the bond energy of the adsorbed oxygen when the concentration of the oxygen in the bulk approaches to saturation. In consequence, the adsorbed oxygen in such a condition would desorb more readily by evacuation. Thus, the amount of oxygen remaining on the surface would be smaller. The decrease in adsorbed oxygen results in a decrease in the reaction rate, as was found when A-2 was irradiated with a dose of more than 7×10^7 R.

The small decrease found in the rates of the A-1 and B-1 reaction on the oxide irradiated with less than 7×10^7 R in the presence of oxygen can be explained similarly in terms of a decrease in the amount of adsorbed oxygen with an increase in the inner oxygen. The marked in the rate in the A-1 catalytic reaction on the oxide irradiated with more than 7×10^7 R in the presence of oxygen can not, however, be explained on only the simple assumption of the marked decrease in the amount of the adsorbed oxygen, as was done with the B-1 reaction. We assume that the irradiation of of γ-rays of more than 7×10^7 R increases the fraction of the site of active oxygen which can be desorbed readily by the evacuation; such sites would be occupied by the oxygen admitted together with the carbon monoxide.

We appreciate the help of the Japan Atomic Energy Institute in performing the irradiation tests.

4) T. Yamashina and T. Nagamatsuya, *Shokubai (Catalyst)*, **9**, (4), 38 (1967).

5) E. R. S. Winter, "Advances in Catalysis," Vol. 10, Academic Press, New York, N. Y. (1958), p. 176.

6) T. I. Barry, "Proc. 2nd Intern. Congr. on Catalysis" (Technip., Paris) (1960), p. 1440.

7) R. J. Kokes, *J. Phys. Chem.*, **66**, 99 (1962).

8) K. Tarama, S. Teranishi and K. Hattori, *Nippon Kagaku Zasshi (J. Chem. Soc. Japan, Pure Chem. Sect.)* **81**, 1665 (1960).

9) K. M. Sancier and T. Freund, *J. Catalysis*, **3**, 293 (1964).

10) F. S. Stone, "Advances in Catalysis," Vol. 13, Academic Press, New York, N. Y. (1962), p. 1.

11) W. Klemm and K. Hass, *Z. Anorg. Allgem. Chem.*, **219**, 82 (1924); *cf.* G. Parravono and M. Boudart, "Advances in Catalysis," Vol. 7, Academic Press, New York, N. Y. (1955), p. 66.

BULLETIN OF THE CHEMICAL SOCIETY OF JAPAN VOL. 42 3451—3454 (1969)

Studies of the Mixed Chromium(III) Complexes Containing Ethylenediamine-*N,N'*-diacetic Acid*[1]

Yuki FUJII and Katsumi YAMAMOTO

Department of Chemistry, Faculty of Science, Ibaraki University, Mito, Ibaraki

(Received February, 5, 1969)

Three new mixed chromium(III) complexes containing ethylenediamine-*N,'N*-diacetic acid (EDDA) and amino acid, [Cr(edda)(L)] (L=anion of glycine, α-alanine and β-alanine), were prepared from $[Cr_2(OH)_2(edda)_2]\cdot 6H_2O$. On the basis of their chemical analyses and the visible and infrared absorption spectra, the geometrical structure of the three mixed ligand complexes was estimated to be the facial form with respect to the coordinated three nitrogen atoms, where the configuration of the coordinated edda was inferred to take the β-form (*cis* with respect to the coordinated oxygen atoms of edda). The new mixed ligand complex containing the glycine anion, $[Cr(ox)(gly)(en)]\cdot H_2O$, was also prepared from *cis*-$[Cr(ox)(H_2O)_2(en)]Br$, and its geometry was discussed in the connection with its visible absorption spectrum.

In a previous paper[1] the preparation of the chromium(III) complexes containing ethylenediamine-*N,N'*-diacetic acid (EDDA) was reported. The configuration of the coordinated edda was, however, not established on the basis of their visible absorption spectra, because it was very difficult to distinguish whether the configuration of edda takes the α-form or the β-form on the basis of only their visible absorption spectra in general.

However, if it is possible to prepare the mixed ligand chromium(III) complexes containing edda and the anion of amino acid, their visible absorption spectra will be very useful in identifying the configuration of edda. Thus, if the spectra of the mixed ligand complexes show the pattern of the spectra of a facial-form (N_3O_3)-type complex, the configuration of edda can be determined to be the β-form. Therefore, we tried to prepare the mixed ligand complexes of the [Cr(edda)(L)]*[2] type (L= glycine, α-alanine, and β-alanine), investigating the geometry of these complexes on the basis of their visible absorption spectra.

Since the spectral data of (N_3O_3)-type chromium-(III) complexes are scanty, we also tried to prepare a mixed-ligand complex, $[Cr(ox)(gly)(en)]\cdot H_2O$, to provide additional spectral information.

Experimental

Preparation. *1) Ethylenediamine-N,N'-diacetatoglycinatochromium(III) Dihydrate,* [Cr(edda)(gly)]·$2H_2O$ (I). All three mixed-ligand complexes containing edda were derived from bis-(ethylenediamine-*N,N'*-diacetato)-μ-dihydroxodichromium(III) hexahydrate, $[Cr_2(OH)_2(edda)_2]\cdot 6H_2O$ (i).[1] A 2.8 g portion (0.005 mol) of the (i) complex as a starting material was suspended in 15 m*l* of water and warmed on the water bath. Then, 4.5 g (0.06 mol) of glycine were added and the mixture was maintained at 90°C for half an hour. When the complex (i) was then gradually dissolved in water, the color of the solution turned from purple to a reddish purple. About 50 m*l* of ethanol were then added, and the glycine thus precipitated was removed by filtration. When the solution was cooled to 0°C, reddish crystals were separated out. They were washed with hot 80% ethanol. Yield, about 2.7 g (81.8%). Found: C, 28.55; H, 5.51; N, 12.18%. Calcd for [Cr(edda)(gly)]·$2H_2O$: C, 28.57; H, 5.41; N, 12.51%.

2) Ethylenediamine-N,N'-diacetato-α-alaninatochromium(III) Dihydrate, [Cr(edda)(α-ala)]·$2H_2O$ (II). A 2.8 g portion (0.005 mol) of the complex i was suspended in 15 m*l* of water, and the resulting mixture was warmed on the water bath. 5.3 g (0.06 mol) of α-alanine were then added, and the mixture was heated to about 90°C. When the color of the solution turned from purple to a reddish purple, about 50 m*l* of ethanol were added. On cooling to 0°C, reddish crystals were separated out. The crystals were washed with hot 80% ethanol. Yield, about 2.9 g (82.2%). Found: C, 31.09; H, 5.74; N, 12.29%. Calcd for [Cr(edda)(α-ala)]·$2H_2O$: C, 30.85; H, 5.77; N, 12.00%.

3) Ethylenediamine-N,N'-diacetato-β-alaninatochromium(III) Monohydrate, [Cr(edda)(β-ala)]·H_2O (III). This

*[1] Presented at 22nd Annual Meeting of the Chemical Society of Japan, Tokyo, April, 1969.

1) Y. Fujii, E. Kyuno and R. Tsuchiya, This Bulletin, **42**, 1569 (1969).

*[2] The abbreviations in this paper are as follows: edda, the dianion of ethylenediamine-*N,N'*-diacetic acid; gly, the anion of glycine; ala, the anion of alanine; ambuty, the anion of aminobutyric acid; leu, the anion of leucine; ox, the dianion of oxalic acid; en, ethylenediamine.

2) E. Kyuno, N. Tanaka and M. Kamata, Read at the 12 th Symposium on Coordination Chemistry of the Chemical Society of Japan, Tokyo, November, 1962.

Table 1. IR spectra for the complexes (cm^{-1})*

Complex	NH_2 str.	COO asym. str.	NH_2 bend.	COO sym. str.	NH_2 wag.	CCN in-phase str.
I	3150 3230 3270	1645	1575	1382	1305	925
II	3160 3270	1650	1588	1360	1288	930
III	3125 3150 3220	1630 1658	1592	1371 1409	1292	918 927
IV	3150 3240	1640	1615	1385	1318	916

* Abbreviations: str.=stretching; asym.=antisymmetric; sym.=symmetric; wag.=wagging; bend.=bending.

substance was prepared from the complex i and β-alanine in the manner described above in 2). Reddish crystals were obtained in an 80.0% yield. Found: C, 32.53; H, 5.47; N, 12.65%. Calcd for [Cr(edda)(β-ala)]·H_2O: C, 32.52; H, 5.42; N, 13.21%.

4) Oxalatoglycinatoethylenediaminechromium(III) Monohydrate, [Cr(ox)(gly)(en)]·H_2O (IV). To an aqueous solution of 4.0 g (0.013 mol) of *cis*-oxalatodiaquoethylenediaminechromium(III) bromide,[2] *cis*-[Cr(ox)$(H_2O)_2$(en)]Br, 2.0 g (0.073 mol) of glycine were added, the solution was kept at about 60°C for five minutes. The solution was then cooled to 0°C, whereby a small amount of impurity was deposited out. After the impurity had been filtrated off, 1 g of glycine was added to the filtrate heated to 80°C. The pH of the solution was adjusted to 5.5 by dilute aqueous ammonia, and the resulting solution was allowed to stand for 3 days at room temperature. A pink powder was thus separated out and washed with hot water. Yield, about 2.2 g (60.0%). Found: C, 25.10; H, 4.74; N, 14.56%. Calcd for [Cr(ox)(gly)(en)]·H_2O: C, 25.49; H, 4.84; N, 14.39%.

Measurements. The visible absorption spectra of the complexes obtained were recorded on a EPS-3 Hitachi recording spectrometer at room temperature. Since the complex I, II and III all decompose to yield the complex i in an aqueous solution at room temperature, the spectra were measured by using dimethylsulfoxide (the complex I and II) or 50% dimethylsulfoxide (the complex III). Water was used as the solvent in the spectral measurement of the complex IV. The IR spectra were taken on potassium bromide disks using a Hitachi EPI-S2 spectrometer.

Results and Discussion

IR Spectra. The infrared absorption spectra were measured to confirm whether the carboxylate groups were coordinated or not. Since all the spectra of the complexes studied showed asym. νCOO-Cr bands in the range from 1630 to 1670 cm^{-1}, as is shown in Table 1, and since there was no band due to the free carboxylate or free carboxylic acid group, it is clear that all the carboxylate groups are coordinated to the chromium(III) ion.[3-5]

In the case of the complex III, two bands assigned to the asym. νCOO-Cr band were observed, these bands can be explained as follows. Since β-alanine may form a six-membered ring with the chromium(III) ion in the complex III and since the steric strain is thought to be larger in the six-membered ring than in the five-membered ring, the band assigned to the νCOO-Cr of β-alanine will shift to lower evergy sites compared with the band assigned to the νCOO-Cr of acetate groups.

Electronic Absorption Spectra. The visible absorption spectra of the complexes are shown in Figs. 1 and 2. The numerical values of the absorption maxima are summarized in Table 2, together with those of related compounds.[5-10]

It is found that the first bands of the complex I, II, and III have the only one peak located at sites of higher energy than that of the fac-(N_3O_3) type chromium(III) complexes, $[Cr(L)_3]$(L=anions of glycine, α-alanine, α-amynobutylic acid and *l*-leucine).

On the other hand, the four cobalt(III) complexes with amino acids, fac-[Co$(gly)_3$]·H_2O, fac-[Co$(\alpha\text{-ala})_3$], mer-[Co(edda)(gly)]·$2H_2O$ and mer-[Co(edda)(α-ala)]·$2H_2O$, have been reported to show the first bands at 57.7×10^{13}/sec, 58.0×10^{13}/sec, 55.3×10^{13}/sec, and 55.3×10^{13}/sec respectively. Since the interpretations of the absorption peaks of cobalt(III) complexes are thought to hold also for the discussions of those of chromium(III)

3) D. H. Bush and J. C. Bailar, Jr., *J. Am. Chem. Soc.*, **75**, 4574 (1953); **78**, 716 (1956).

4) A. J. Saraceno, I. Nakagawa, S. Mizushima, C. Curran and J. V. Quagliqno, *ibid.*, **80**, 5018 (1958).

5) M. Mori, M. Shibata, E. Kyuno and M. Kanaya, This Bulletin, **34**, 1837 (1961).

6) M. Nakahara, This Bulletin, **35**, 782 (1962).

7) R. W. Green and K. P. Ang, *J. Am. Chem. Soc.*, **77**, 4582 (1955).

8) M. Mizuochi, E. Kyuno and R. Tsuchiya, Read at the 18 th Symposium on Coordination Chemistry of the Chemical Society of Japan, Kyoto, Oct., 1968, p. 223.

9) Y. Shimura and R. Tsuchida, This Bulletin, **29**, 311 (1956).

10) J. I. Legg, D. W. Cooke and B. E. Douglas, *Inorg. Chem.*, **6**, 700 (1967).

TABLE 2. ABSORPTION SPECTRA FOT THE COMPLEXES*

Complex	ν_1 (log ε)	ν_2 (log ε)	ν_3 (log ε)
I	59.4 (1.95)	81.5 (2.01)	
II	59.4 (1.94)	81.5 (1.96)	
III	60.2 (2.04)	81.1 (1.97)	
IV	57.8 (1.92)	77.3 (1.93)	112.4 (2.38)
fac-[Cr(gly)$_3$]·3H$_2$O[6]	55.2 (1.60)	75.0 (1.65)	
fac-[Cr(α-ala)$_3$]·2H$_2$O[7]	56.0 (1.85)	75.4 (1.75)	
fac-[Cr(α-ambuty)$_3$]·2H$_2$O[8]	55.8 (1.87)	75.0 (1.79)	
fac-[Cr(*l*-leu)$_3$]·2H$_2$O[8]	57.7 (1.67)	76.9 (1.79)	
fac-[Co(gly)$_3$]·H$_2$O[5),9]	57.7 (2.16)	79.6 (2.08)	140.2 (4.45)
fac-[Co(α-ala)$_3$][5]	58.0 (2.22)	80.4 (2.21)	
mer-[Co(edda)(gly)]·2H$_2$O[10]	55.3 (1.95)	63.9 (sh)	
mer-[Co(edda)(α-ala)]·2H$_2$O[10]	55.3 (1.98)	64.4 (sh)	

* The frequencies are given in 10^{13}/sec.

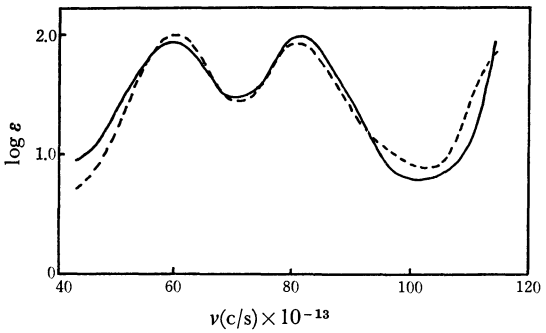

Fig. 1. Electronic absorption spectra.
(——): [Cr(edda)(gly)]·2H$_2$O
(- - -): [Cr(edda)(β-ala)]·H$_2$O

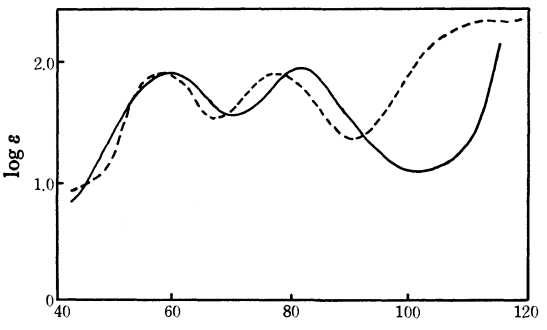

Fig. 2. Electronic absorption spectra.
(——): [Cr(edda)(α-ala)]·2H$_2$O
(- - -): [Cr(ox)(gly)(en)]·H$_2$O

complexes under these circumstances,[11] values of 53.0×10^{13}/sec and 53.5×10^{13}/sec may be anticipated as the peaks of the mer-form complexes of [Cr(edda)(L)] (L=glysine and α-alanine) on the basis of the values of the absorption peaks on fac-[Cr(gly)$_3$]·3H$_2$O and fac-[Cr(α-ala)$_3$]·2H$_2$O.

11) H. Yamatera, this Bulletin, **31**, 95 (1956).

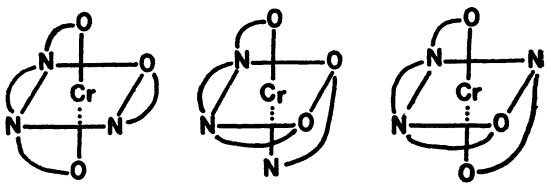

Fig. 3. Possible structures of [Cr(edda)(amino acid)].

Since the peaks of the I, II, and III complexes appeared at about 59.5×10^{13}/sec and since these values are too high to assign the configuration of the complexes to the mer-form one, it may be suggested that the configuration of the complexes [Cr(edda)(L)](L=anion of glycine, α-alanine and β-alanine) may be fac-form with respect to the coordinated three nitrogen atoms. Though there are three possible geometrical structures for [Cr(edda)(L)], only one structure is possible as a fac-form one. Therefore the structure (b) in Fig. 3 is the most probable as the structure of the complexes I, II, and III. From these observations, it can be concluded that the configuration of edda may take the β-form (*cis* with respect to the coordinated carboxylate oxygen atoms of edda).

Since the complex IV shows the first band at 57.8×10^{13}/sec, and since this band seems to be constructed from only one peak, the configuration of the complex IV probably takes the fac-form with respect to the coordinated three nitrogen atoms.

When plotting the locations of the first band (in sec^{-1}) of the chromium(III) complexes containing oxalic acid and/or ethylenediamine[2,12] against the number of the nitrogen atoms participating in the coordination bond formation, we can obtain

12) K. Sone, *Nippon Kagaku Zasshi (J. Chem. Soc. Japan, Pure Chem. Sect.)*, **71**, 270 (1950).

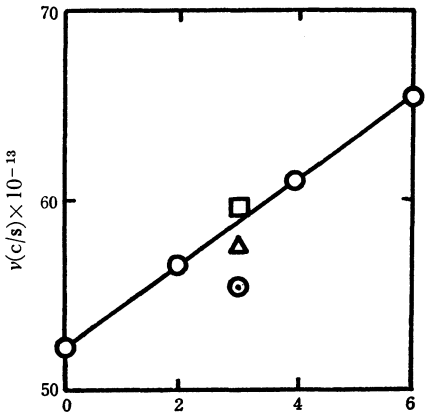

Fig. 4. Frequency positions of the first band of the chromium(III) complexes.

□: $[Cr(edda)(gly))]\cdot 2H_2O$;
△: $[Cr(ox)(gly)(en)]\cdot H_2O$;
⊙: $[Cr(gly)_3]\cdot 3H_2O$;
○: 0, $[Cr(ox)_3]^{3-}$; 2, $[Cr(ox)_2(en)]^-$;
4, $[Cr(ox)(en)_2]^+$; 6, $[Cr(en)_3]^{3+}$.

the linear relation shown in Fig. 4.[13] From this linear relation, a value of *ca.* 59.0×10^{13}/sec is obtained as the maximum of the first band of the (N_3O_3)-type chromium(III) complex. On the other hand, it has been reported that the amino acid complexes with the chromium(III) ion, which have been identified as (N_3O_3)-type complexes,[6-8] show the first band between 55.0 and 58.0×10^{13}/sec. Therefore, it may be reasonable to conclude that the mixed chromium(III) complex containing oxalic acid, glycine, and ethylenediamine, [Cr(ox)(gly)(en)], shows the first band at about 58.0×10^{13}/sec, which is intermediate between the 55.0×10^{13}/sec of the tris-glycine complex and the 59.0×10^{13}/sec of the oxalato-ethylenediamine complex.

The authors wish to express their deep thanks to Professor S. Ito and his coworkers of Tohoku University for their kind help in the elemental analyses. One of the authors (Y.F.) also gratefully acknowledges the encouragement of Professor R. Tsuchiya and Professor E. Kyuno, Kanazawa University.

13) M. Mori, M. Shibata, E. Kyuno and T. Adachi, This Bulletin, **29**, 883 (1956).

BULLETIN OF THE CHEMICAL SOCIETY OF JAPAN VOL. 42 3454—3458 (1969)

Adsorption of *N'*-(2-Hydroxyethyl)-ethylenediamine-*N,N,N'*-triacetic Acid on the Hydrogen Form of Resin

Zenzi HAGIWARA and Hideo ŌKI

Faculty of Engineering, Tohoku University, Sendai

(Received February 24, 1969)

The adsorption of HEDTA (H_3Ch) on the hydrogen form of Dowex 50W, X-8, 100—200 mesh, has been studied as a function of the concentration of H_3Ch in the aqueous phase. The experiments were performed by means of either the column or a combination of the column and batch methods, with the latter being employed for the adsorption of HEDTA on the resin in equilibrium with dilute solutions. In solutions up to approximately 0.07 mol/*l*, such as H_3Ch, the experimental data are consistent with the Langmuir equation expressed by: $[H_3Ch]/(\overline{Ch}_T/E)=1/Bk+[H_3Ch]/B$. The adsorbed amount is represented in the term $\overline{Ch}_T/E$, where $\overline{Ch}_T$ is the total amount of cationic species of HEDTA on the resin, and E, the exchange capacity of resin. A good straight line is obtained with $B=0.571$ and $k=0.420$. The results show that, because of a high concentration of hydrogen ion inside the resin, the adsorbed HEDTA is present mainly in the H_5Ch^{2+} species and partly in the H_4Ch^{+} species.

Due to the stable chelate formation of polyamino acids with metal ions, such buffered solutions as ethylenediaminetetraacetic acid (EDTA) and *N'*-(2-hydroxyethyl)ethlenediamine-*N,N,N'*-triacetic acid (hereafter abbreviated as HEDTA and H_3Ch)[1,2] were used as the eluants for the ion-exchange separation of the rare-earth series. For example, various compositions of HEDTA were employed for isolating the above series by ion exchange. When the rare earth is eluted with the HEDTA eluant with a closed composition to $(NH_4)_2HCh$ and with a hydrogen-retaining bed, a chelate

band[3] corresponding to H_5Ch^{2+} in the resin phase is steadily formed between the rare earth and hydrogen bands; this band grows with the progress of the elution distance of the rare-earth band. The formation of the chelate band[4] during elution was investigated under several variables, such as the concentration and composition of the eluant, the crosslinkage of the cation exchanger and the temperature. The results show that the previously-proposed mechanism for the chelate band formation was only applicable within a narrow range of elution conditions and that it is difficult to explain all the phenomena observed in the resin in terms of this mechanism alone. Thus, the present authors have arrived at the opinion that the research into the adsorption of HEDTA on the hydrogen form of resin should be extended to high concentrations of H_3Ch.

Generally, polyamino acid molecules have some additional sites available for protonation. For example, the existence[5] of the protonated species, H_5Y^+ and H_6Y^{2+}, in strong acid solutions of EDTA (H_4Y) was confirmed by Olson and Margerum. The HEDTA molecule with a structure analogous to EDTA would also have the protonate forms, H_4Ch^+ and H_5Ch^{2+}, in strongly acidic solutions. The presence of the above protonated species can easily be predicted in the hydrogen form of resin, because of the extremely high concentration of hydrogen ions inside the resin matrix (approximately $[H^+]=6$—7 mol/l adsorbed solvent). Matorina[6-8] investigated the ion-exchange equilibrium of DTPA (diethylenetriaminepentaacetic acid; H_5A) in combination with a polystyrene type of resin (KU-2) and confirmed the presence of protonated species in the resin due to the reaction: $H_5A+\overline{2H}^+ \rightleftarrows \overline{H_7A}^{2+}$. (Here the superscript barred quantities refer to the resin phase of the indicated species.)

The main object of this study is to investigate the adsorption of HEDTA species on the resin as a function of the concentration of H_3Ch in the aqueous phase, and to clarify the adsorption character.

Experimental

Using Dowex 50W, X-8, 100—200 mesh, as the cation exchanger and an analytical grade of HEDTA, the adsorption experiments of HEDTA on the resin were performed at 25°C by the following three methods.

Column Method-I. This procedure was applied for the experimental series corresponding to Exp. No. AE-1 to AE-9. With a flow of 0.26 cm/min, the HEDTA eluant buffered with ammonium hydroxide was passed through the top of a Pyrex column involving a hydrogen form of resin. The tail of the exchange column was connected in series with small appendages (exchange capacity=20—30 meq. per column) for the analysis of HEDTA species in the resin phase. With the progress in elution, the formation of a chelate band due to the adsorption of HEDTA on the hydrogen form of resin was seen between the eluant and hydrogen bands. After the elution system had arrived at a steady state, the HEDTA eluate from the chelate band was collected into small fractions and analyzed. The experimental conditions used are listed in detail in Table 1, in which the $\widetilde{Ch}_T$ and $\widetilde{NH}_{4T}$ symbols indicate the total concentrations of the anionic species of HEDTA and ammonium respectively in the eluant; the column dimensions are also given.

Column Method-II. This method was used for Exp. No. AE-1′ to AE-5′. Different concentrations of HEDTA solutions were passed through small exchange columns (exchange capacity=34 meq. per column) at a flow rate of 0.1 cm/min. After passing 4 to 5 l of a HEDTA solution for the attainment of equilibrium, the resin phase was separated from the aqueous phase and analyzed (Table 2).

Combination of Column and Batch Methods. This method was used for Exp. No. AE-10 to AE-15. When a dilute solution of HEDTA is used as the load solution for the column method, it takes a long time to reach equilibration. Therefore, the experiment was divided into two steps to save time. According to Column Method-II, a dilute solution of HEDTA corresponding to 15—20 l was passed through the hydrogen form of a resin column with a capacity of 10 meq. After that, the resin in the column was removed and mixed with one liter of the same load solution of HEDTA. The mixture was maintained at 25°C for 3 days in a constant-temperature-bath; then, after equilibration, the two phases were separated for analysis.

Analysis. The ammonium content in the HEDTA load solutions was determined by the usual Kjeldahl method; further, the total HEDTA was determined by chelometry with the standard $ZnCl_2$ and with E.B.T. (Eriochrome Black T) as the indicator. An ammonium chloride-ammonium hydroxide buffer solution with a pH of 10 was used in the titration.

The small appendages attached to the tail of the main exchange column for the analysis of the chelate band were analyzed as follows: after the aqueous solution had been removed by suction, the resin phase was eluted with 2 M NH_4Cl; the total of anionic species of HEDTA in the collected eluate was then determined by chelometry, using the zinc standard solution, according to the previously-described method.

Experimental Results and Discussion

The results obtained by the experimental methods described in the foregoing section are summarized in Table 2, in which the equilibrium compositions of the aqueous phase under different conditions are

1) F. H. Spedding and A. H. Danne, "The Rare Earths," John Wiley, & Sons, New York (1961).
2) Z. Hagiwara, *J. Inorg. Nucl. Chem.*, **31**, 2933 (1969).
3) J. E. Powell and F. H. Spedding, *Trans. Met. Soc. AIME*, **215**, 457 (1959).
4) Z. Hagiwara, to be published.
5) D. C. Olson and D. W. Margerum, *J. Am. Chem. Soc.*, **82**, 5602 (1960).
6) N. N. Matorina, L. V. Shepetyuk and K. V. Chmutov, *Zhur. Fiz. Khim.*, **41**, 112 (1967).
7) N. N. Matorina, L. V. Shepetyuk and K. V. Chmutov, *ibid.*, **41**, 131 (1967).
8) N. N. Matorina, L. V. Shepetyuk and K. V. Chmutov, *ibid.*, **41**, 373 (1967).

TABLE 1. EXPERIMENTAL CONDITIONS USED FOR THE COLUMN EXPERIMENTS

Exp. No.	Composition of eluant				Column dimension cm	Total eluate volume *l*
	$\widetilde{Ch}_T$ mmol/*l*	$\widetilde{NH}_{4T}$ mmol/*l*	pH	$\widetilde{NH}_{4T}/\widetilde{Ch}_T$		
AE-1	44.64	105.8	8.64	2.37	2.2×80	5.0
AE-2	44.84	89.22	6.78	1.99	2.2×62	5.2
AE-3	45.04	59.63	5.10	1.32	2.2×41	5.0
AE-4	30.16	72.54	8.60	2.41	2.2×80	8.5
AE-5	30.04	60.42	6.99	2.01	2.2×62	7.6
AE-6	30.02	40.18	5.11	1.34	2.2×41	7.5
AE-7	15.09	36.34	8.70	2.41	2.2×80	16.5
AE-8	15.16	30.86	7.46	2.04	2.2×62	14.0
AE-9	15.11	22.18	5.31	1.47	2.2×41	12.0

Resin used: Dowex 50W, X-8, 100—200 mesh
Elution temperature: 25°C
Flow rate: 0.26 cm/min

TABLE 2. COMPOSITION OF THE RESIN AND AQUEOUS PHASES AT EQUILIBRIUM

Exp. No.	Aqueous phase				Resin phase
	$\widehat{Ch}_T$ mmol/*l*	H_3Ch mmol/*l*	pH	$\overline{Y}$	$(\overline{Ch}_T/E)$ mmol/meq
AE-1	104.3	65.08	2.22	2.42×10^{11}	0.557
AE-2	95.54	61.73	2.18	3.08×10^{11}	0.555
AE-3	78.36	49.84	2.20	2.72×10^{11}	0.551
AE-4	69.69	42.66	2.24	2.14×10^{11}	0.536
AE-5	62.37	37.75	2.26	1.90×10^{11}	0.533
AE-6	51.28	30.65	2.27	1.79×10^{11}	0.520
AE-7	33.17	19.22	2.30	1.50×10^{11}	0.488
AE-8	30.20	17.17	2.32	1.33×10^{11}	0.481
AE-9	25.83	14.43	2.34	1.18×10^{11}	0.471
AE-10	15.18	7.52	2.45	6.20×10^{10}	0.409
AE-11	10.02	4.45	2.54	3.74×10^{10}	0.383
AE-12	6.04	2.23	2.67	1.82×10^{10}	0.343
AE-13	3.12	0.92	2.82	8.13×10^{9}	0.256
AE-14	2.09	0.51	2.93	4.58×10^{9}	0.219
AE-15	1.04	0.18	3.13	1.66×10^{9}	0.120
AE-1′	29.66	16.86	2.32	1.33×10^{11}	0.479
AE-2′	25.15	14.05	2.34	1.18×10^{11}	0.461
AE-3′	19.71	10.33	2.40	8.32×10^{10}	0.447
AE-4′	15.20	7.53	2.45	6.20×10^{10}	0.440
AE-5′	9.77	4.27	2.55	3.52×10^{10}	0.406

Resin used: Dowex 50W, X-8, 100—200 mesh
Temp: 25°C

also given. The mean values of Ch_T in the HEDTA fractions obtained in elution under the steady-state conditions are also listed in Table 2; the deviation of Ch_T is about ±2% from Exp. No. AE-1 to AE-9.

The concentration of H_3Ch in the aqueous phase can be calculated by the following relations:

$$[H_3Ch] = \frac{[H^+]^3}{k_1\cdot k_2\cdot k_3}\,\frac{Ch_T}{\overline{Y}}, \qquad (1)$$

where:

$$\overline{Y} = \frac{[H^+]^3}{k_1\cdot k_2\cdot k_3} + \frac{[H^+]^2}{k_2\cdot k_3} + \frac{[H]^+}{k_3} + 1.$$

The Ch_T symbol represents the concentration of the total anionic species of HDETA, while the $\overline{Y}$ represents the functions of the pH and of the three dissociation constants of HEDTA. Using Eq. (1) and the values of the dissociation con-

stants of HEDTA ($pk_1=2.39$, $pk_2=5.37$, $pk_3=9.93$)[9] the values of H_3Ch are calculated as given in Table 2, in which the adsorbed HEDTA on the resin is expressed in the term $\overline{Ch}_T/E$, where $\overline{Ch}_T$ refers to the amount of the adsorbed HEDTA species in the resin, and E, the exchange capacity of the hydrogen form of resin employed for the equilibrium experiments (one gram of the dried hydrogen form of Dowex 50W, X-8, 100—200 mesh=4.84 meq).

The adsorption of HEDTA species is assumed to take place in the form:

$$H_3Ch + n\overline{H}^+ \rightleftarrows \overline{H_{3+n}Ch^{n+}},$$

where the superscript barred quantities refer to the resin phase of the indicated species. The apparent exchange constant can then be written:

$$K_n' = \frac{[\overline{H_{3+n}Ch^{n+}}]}{[H_3Ch][\overline{H}^+]^n} = \frac{A\frac{\overline{Ch}_T}{E}}{[H_3Ch]\left\{A\left(1-\frac{n\overline{Ch}_T}{E}\right)\right\}^n} \quad (2)$$

where the two symbols $\overline{H_{3+n}Ch^{n+}}$ and $\overline{H}^+$ related to the resin phase are expressed in the concentration unit of moles per unit gram of the hydrogen form of resin, and where the H_3Ch in the aqueous phase is expressed in m moles per liter. Further, the A is the exchange capacity of resin in meq per unit gram of resin on the basis of the hydrogen form.

Taking the logarithm of Eq. (2), one obtains:

$$\log\frac{A\frac{\overline{Ch}_T}{E}}{[H_3Ch]} = \log K_n' + n\log\left\{A\left(1-\frac{n\overline{Ch}_T}{E}\right)\right\}. \quad (3)$$

The plots of $\log(A\overline{Ch}_T/E)/[H_3Ch]$ with respect to

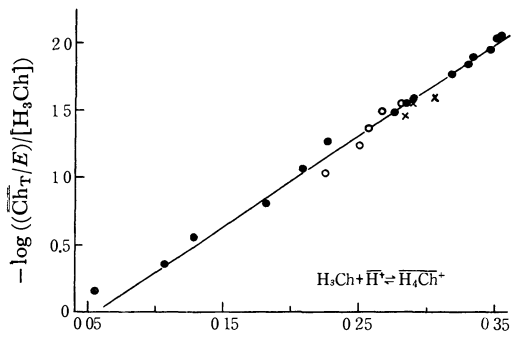

Fig. 1. $\log((\overline{Ch}_T/E)/[H_3Ch])$ *vs.* $\log(1-(\overline{Ch}_T/E))$.

- ● Exp. No. AE-1 to AE-15
- ○ Exp. No. AE-1′ to AE-5′
- × Experimental data concerning the chelate band obtained in the elution of erbium band

9) T. Moeller and R. Ferrus, *J. Inorg. Nucl. Chem.*, **20**, 261 (1961).

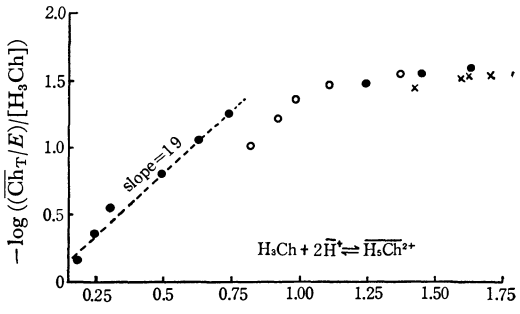

Fig. 2. $\log((\overline{Ch}_T/E)/[H_3Ch])$ *vs.* $\log(1-(2\overline{Ch}_T/E))$. Notations of experimental data are the same as those used in Fig. 1.

$\log A\{1-(n\overline{Ch}_T/E)\}$ should give a straight line whose slope is n and whose intercept is $\log K_n'$. As is shown in Fig. 1, the former values are plotted against the latter on the assumption of $n=1$; a value of 6.8 is thus obtained as the slope of the straight line. This result indicates that the adsorption of HEDTA does not conform to the reaction expressed by $H_3Ch+\overline{H}^+ \rightleftarrows \overline{H_4Ch}^+$. Similar plots appear in Fig. 2, in which n is assumed to be equal to 2. However, the linearity is not maintained over the whole experimental range, and a linear relation with a slope of 1.9 is only obtained in a small range corresponding to Exp. No. AE-10 to AE-15. Therefore, it is obvious that the adsorbed form of H_5Ch^{2+} on the resin exists only in the region of 0.15 to 0.75 as the value of $-\log\{1-(2\overline{Ch}_T/E)\}$ in Fig. 2. Further, the linear relationship is not held at $n=3$. It may be concluded that the experimental data are not explained by Eq. (3).

The adsorption of HEDTA on the resin is considered to take place according to an equation similar to that of Langmuir:

$$\frac{\overline{Ch}_T}{E} = \frac{Bk[H_3Ch]}{1+k[H_3Ch]}, \quad (4)$$

where B is the maximum amount of sorbed HEDTA per unit equivalent of resin at the maximum solubility of H_3Ch, and where k is a constant relating to the adsorption energy. It may be more convenient to utilize a plot which gives a straight line. Thus, Eq. (4) may be rearranged in the form:

$$\frac{[H_3Ch]}{\frac{\overline{Ch}_T}{E}} = \frac{1}{Bk} + \frac{1}{B}[H_3Ch]. \quad (5)$$

A plot of $[H_3Ch]/(\overline{Ch}_T/E)$ against H_3Ch is linear and yields the slope $1/B$ and the intercept $1/Bk$. Since H_3Ch, $\overline{Ch}_T$, and E are known experimentally, a plot of the term of the left side in Eq. (5) *versus* $[H_3Ch]$ leads to a straight line with the value of 1.75 as the slope and that of 4.17 as the intercept ($B=0.571$, $k=0.420$), as may be seen in Fig. 3.

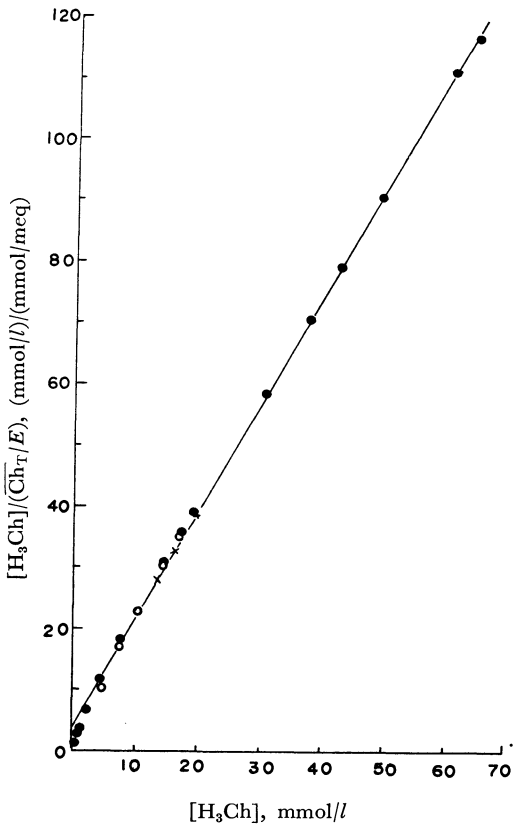

Fig. 3. Langmuir plots for the adsorption of HEDTA on the hydrogen form of resin at 25°C. Notations of experimental data are the same as those used in Fig. 1.

In dilute concentrations less than 20 mmol/*l*, such as H_3Ch, a reciprocal number of B is equal to 2.0. It is obvious from the above fact that the adsorbed state of H_3Ch on the hydrogen form of resin may be attributed to the H_5Ch^{2+} species. In a higher concentration range, the decrease in $1/B$ is principally due to the formation of the H_4Ch^+ species as a minor constituent, in addition to H_5Ch^{2+}: $\overline{H_5Ch^{2+}}+H_3Ch \rightleftarrows 2\overline{H_4Ch^+}$.

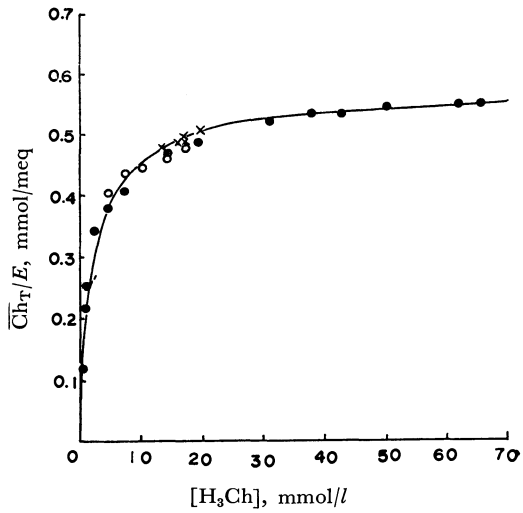

Fig. 4. Adsorption isotherm of HEDTA at 25°C. Notations of experimental data are the same as those used in Fig. 1.

Further, the adsorption isotherm of HEDTA on Dowex 50W, X-8, 100—200 mesh, is shown in Fig. 4, in which the calculated isotherm is represented by a solid line, using Eq. (4), where $B=0.571$ and $k=0.420$. For purposes of comparison, some experimental data concerning the chelate band formed in elutions of the erbium band with a 0.015 M HEDTA buffered solution are plotted in the same figure.

It may be concluded that the sorption of HEDTA on the hydrogen form of resin can be explained well by the Langmuir equation, and that the adsorbed HEDTA species is present mainly in H_5Ch^{2+} and partly in H_4Ch^+ due to a high concentration of hydrogen inside the resin.

BULLETIN OF THE CHEMICAL SOCIETY OF JAPAN VOL. 42 3459—3461 (1969)

Reactions of Tungsten Oxy-dichlorodialkoxides with Cyclopentadiene and Sodium Cyclopentadienide

S. P. ANAND, R. K. MULTANI and B. D. JAIN

Department of Chemistry, University of Delhi, Delhi-7, India

(Received April 8, 1969)

The formation of π-cyclopentadienyl tungsten oxychlorodialkoxides as a result of the interaction between cyclopentadiene or its sodium derivative with tungsten oxy-dichlorodialkoxides, having the general formula $C_5H_5WOCl(OR)_2$, where R is CH_3, C_2H_5, $\begin{matrix}CH_3\\CH_3\end{matrix}\!\!>\!CH$, $CH_3CH_2CH_2$ and $CH_3CH_2CH_2CH_2$ along with the thermal stabilities and infrared spectra of the above products, has been studied and reported.

Though a large number of cyclopentadienyl compounds having alkyl,[1] aryl,[2] acetyl,[3] carbonyl,[4] nitrosyl,[1] and hydride[5] groups linked to the transition metal atoms have been reported, only a few cyclopentadienyl complexes having one or more alkoxy groups attached to the metal atoms in the π-cyclopentadienyl complexes are known, and these include the alkoxy derivatives of cyclopentadienyl compounds of titanium,[6a,b] zirconium,[7] uranium and thorium.[8] Recently we have prepared mono- and di-alkoxy derivatives of π-biscyclopentadienyl tungsten oxydichloride by its interaction with various alcohols with and without the use of triethylamine.[9,10] The present communication deals with the preparation of π-cyclopentadienyl compounds of tungsten oxydichlorodi-alkoxides[11] (by the interaction of cyclopentadiene and its sodium derivative with tungsten oxydichloro dialkoxides in presence of tetrahydrofuran as solvent) and their characterisation.

$$WOCl_4 + 2ROH \xrightarrow{C_6H_6} WOCl_2(OR)_2 + 2HCl$$

$$WOCl_2(OR)_2 + C_5H_6 \xrightarrow{THF} C_5H_5WOCl(OR)_2 + HCl$$

$$WOCl_2(OR)_2 + NaC_5H_5 \xrightarrow{THF} C_5H_5WOCl(OR)_2 + NaCl$$

Where R is CH_3, C_2H_5, i-C_3H_7, n-C_3H_7 and n-C_4H_9. During these studies the removal of both chlorine atoms from $WOCl_2(OR)_2$ by treatment with cyclopentadiene as well as sodium cyclopentadienide has been attempted and even on refluxing the reactants for 24 hr it has been found that only one chlorine atom is replaced by cyclopentadienyl group.

Results and Discussion

Infrared spectra of the compounds taken in KBr, Nujol mull and $CHCl_3$ on Perkin Elmer Cord Model-137 between 4000—650 cm^{-1} is given in Table 1. The absorption at 3050—3100 cm^{-1} and 2910—2950 cm^{-1} in IR spectra of the compounds indicate the presence of C-H stretching frequencies,[12] the absorption bands at 1650—1740 cm^{-1} show the (π-C_5H_5) ring stretching while the C-C bands (asymmetric ring breathing) is evident at 1400—1450 cm^{-1}, which resemble those located in cyclopentadiene itself.[13] In the above IR spectra the vibrational bands observed at 1190 cm^{-1} indicate methoxy, at 1140, 1160 cm^{-1} indicate ethoxy, at 1110, 1170 cm^{-1} indicate isopropoxy while n-butoxy group are evident at 1090, 1120—

1) T. S. Piper and G. Wilkinson, *J. Inorg. Nucl. Chem.*, **3**, 104 (1956).
2) L. Summers, R. H. Uloth and A. Holmes, *J. Am. Chem. Soc.*, **77**, 3604 (1955).
3) J. L. Boston, S. O. Grimm and G. Wilkinson, *J. Chem. Soc.*, **1963**, 3468.
4) F. A. Cotton, H. Stammreich and G. Wilkinson, *J. Inorg. Nucl. Chem.*, **9**, 3 (1959).
5) M. L. H. Green, J. A. Mecleverty, L. Pratt and G. Wilkinson, *J. Chem. Soc.*, **1961**, 4854.
6) a) A. N. Nesmeyanov and O. V. Nogina, *Izv. Akad. Nauk SSSR, Otd. Khim. Nauk*, **1963**, 831. b) G. D. Richard, *J. Am. Chem. Soc.*, **82**, 4211 (1960).
7) E. M. Brainina and R. Kh. Freidlina, *Izv. Akad. Nauk SSSR, Otd. Khim. Nauk*, **1963**, 835.
8) L. Ter Haar Gary and Michael Dubeck, *Inorg. Chem.*, **3**, 1648 (1964).
9) S. P. Anand, R. K. Multani and B. D. Jain, *J. Organometal. Chem.*, **17**, 423 (1969).
10) S. P. Anand, R. K. Multani and B. D. Jain, *Curr. Sc.*, **37**, 487 (1968).
11) H. Fund, W. Weiss and G. Mehanpt, *Z. Anorg. Allg. Chem.*, **304**, 238 (1960).
12) F. A. Cotton, L. T. Leynolds, *J. Am. Chem. Soc.*, **80**, 269 (1958).
13) H. P. Fritz, "Advances in Organometallic Chemistry," Vol. I, Academic Press, New York (1964), p. 279.

Table 1. Infrared spectra of π-cyclopentadienyl tungsten oxy-chlorodialkoxides (cm^{-1})

Alkyl group present in $C_5H_5WOCl(OR)_2$	(π-Cp) C-H str.	(π-Cp) ring str.	(π-Cp) C-C str.	(π-Cp) C-H def.	Alkoxy group str.	(π-Cp) C-H out-of-plane def.	(π-Cp) out-of-plane def.
Methyl	3060 s, 2930 m	1740 s, 1650 m	1450 s	1372 m	1190 w	1092 w, 1012 s	750 s
Ethyl	3055 m, 2910 m	1730 s, 1640 s	1450 m	1360 s	1160 w	1140 m, 1010 w	810 m
i-Propyl	3080 s, 2935 m	1710 s, 1630 w	1440 w	1310 s	1170 m	1110 w, 1015 w	820 m
n-Propyl	3090 m, 2915 m	1740 m, 1610 s	1410 s	1300 w	1190 w	1040 m, 980 w	780 s
n-Butyl	3100 s, 2950 m	1710 m, 1600 m	1450 w	1340 s	1210 s	1020 w, 1010 s	770 m

s=strong, m=medium, w=weak, Cp=C_5H_5 Spectra were taken in Nujol mull, KBr pellets and $CHCl_3$ as solvent.

Table 2. Decomposition temperatures of π-cyclopentadienyl tungsten oxy-chlorodialkoxide compounds

$C_5H_5WOCl(OR)_2$	R				
	CH_3	C_2H_5	*i*-C_3H_7	*n*-C_3H_7	*n*-C_4H_9
Decomposition temperature °C	90	105—106	110	113	135

Table 3. π-Cyclopentadienyl tungsten oxy-chlorodialkoxides

Alkyl group present in $C_5H_5WOCl(OR)_2$	Colour	Mp °C	Yield % (theoretical)	Time of reaction (hr)	Amt. of alcohols added (ml)	Amt. of THF added (ml)	Tungsten %		Chloride %		Alkoxy group	
							Found	Calcd	Found	Calcd	Found	Calcd
Methyl	Green	86—87	75	10	70	35	51.4	50.69	9.9	9.78	17.3	17.12
Ethyl	Green	96—97	70	12	80	40	47.1	47.07	9.0	9.07	23.1	23.05
i-Propyl	Deep-green	105—106	60	12	60	45	43.9	43.92	8.4	8.46	28.1	28.23
n-Propyl	Deep-green	135	65	10	60	40	43.8	43.92	8.3	8.46	—	—
n-Butyl	Brown green	140.5	70	11 12	50	50	41.1	41.16	7.9	7.91	—	—

* Where the atomic weights in the above calculated results are: W, 183.85; Cl, 35.45; O, 16.00; C, 12.01; H, 1.008.

1160 cm^{-1} frequencies[14,15] and these are given in Table 1.

The above details of the IR spectra show the presence of alkoxy groups attached to the tungsten atom as is the case with other π-cyclopentadienyl transition metal compounds.[6-9]

The above products which are green in colour, are very sensitive to moisture though stable in inert atmosphere and in vacuum. They are soluble in THF, acetone, dioxane, dimethoxyethane, and miscible in hot dilute acids and alkalies and form a resinous mass when in contact with hot water. These compounds do not sublime under reduced pressure (5 mmHg) and decompose at high temperatures. They change the orange chromic acid (12% H_2SO_4, N-$K_2Cr_2O_7$) to green colouration. The compounds containing lower alkoxide groups have been found to be thermally less stable than those containing higher alkoxide groups. The temperatures at which various compounds undergo decomposition as shown by (i) the change in their colour from green to dirty yellow, and (ii) the decrease in their weights, have been recorded with a Koffler heating block apparatus as given in Table 2.

From infrared spectra and elemental analysis, the following formula is proposed for the compounds, $C_5H_5WOCl(OR)_2$, where R is CH_3 to C_4H_9 groups. The interaction of cyclopentadiene and sodium cyclopentadienide with $WOCl_2(OR)_2$ involves the replacement of electronegative radical (Cl^-) by another electronegative radical ($C_5H_5^-$). It has been further observed that the interaction between $WOCl_2(OR)_2$ and excess of sodium cyclopentadienide does not result in the replacement of more than one chlorine atom by cyclopentadienyl group and this observation is at variance with the results reported by earlier workers.[6-9]

Experimental

All operations were carried out under anhydrous conditions with guard tubes containing silica gel. In some cases, a P_2O_5 and $CaCl_2$ (fused) guard tube had to be used in series with the silica gel tube under reduced pressure, using an oil vacuum pump. Tetrahydrofuran before use was first dried by refluxing with potassium hydroxide and then distilling from lithium aluminium hydride. Aromatic hydrocarbons were first dried with sodium wire and then distilled, whereas the alcohols were dried by usual methods including azeotropic distillation. Tungsten oxytetrachloride obtained as reddish crystals on refluxing WO_3 with thionyl chloride for 16—18 hr and after drying under reduced pressure, was finally sublimed under reduced pressure (5—10 mmHg) at 135—140°C to give scarlet red crystals. Sodium cyclopentadienide was always freshly prepared before use.

Preparation of Tungsten Oxy-dichlorodimethoxide. 70 m*l* methyl alcohol, 40 m*l* dry benzene and 3.42 g (0.1 mol) of tungsten oxytetrachloride were placed in a 500 m*l* round bottom flask fitted with a reflux condenser and a $CaCl_2$ guard tube, and refluxed at 65—70°C over an oil bath for 4—5 hr. From the colourless product so obtained, benzene was removed by distillation under reduced pressure (20—25 mmHg) and the compound finally dried under reduced pressure (15 mmHg).

Higher alkoxy derivatives ranging from ethoxy to *n*-butoxy of tungsten oxytetrachloride were similarly prepared by refluxing with suitable alcohols at requisite temperatures.

Preparation of Cyclopentadienyl Tungsten Oxy-chlorodiethoxide. *1) By Using Cyclopentadiene.* 2 m*l* (0.025 mol) of freshly depolymerized cyclopentadiene was added to a mixture of 3.6 g (0.01 mol) of tungsten oxydiethoxide and 50 m*l* THF, and the contents were refluxed at 100—110°C for 10—12 hr. After cooling, excess of THF was removed by distillation under reduced pressure. The dark greenish product on crystallization from petroleum ether (40—60°C) gave greenish crystals. The compound is soluble in chloroform, THF, carbon disulphide, but insoluble in ether and aromatic hydrocarbons. The compound is extremely sensitive to moisture and readily gets hydrolysed in dilute acids and alkalies. It melts with decomposition at 96—97°C to a dirty yellow mass.

Found: W, 47.1; Cl, 9.0; OC_2H_5, 23.1%. Calcd for $C_5H_5WOCl(OC_2H_5)_2$: W, 47.07; Cl, 9.07; OC_2H_5, 23.05%.

2) By Using Sodium Cyclopentadienide.[16] To freshly prepared sodium cyclopentadienide (0.04 mol; approx. 1 g Na; 3.4 m*l* C_5H_6) in 50 m*l* tetrahydrofuran, was added 7.22 g (0.02 mol) tungsten oxydichlorodiethoxide in 30 m*l* THF in a three necked round bottom flask. The mixture was vigorously stirred while being refluxed for 6—8 hr till the contents turned to greenish products. After filtering the products through a porous plug and a G-4 sinitered glass filter disc, the filtrate was distilled under reduced pressure. The analysis of the product corresponded to the composition of $C_5H_5WOCl(OC_2H_5)_2$. The compound on crystallization from petroleum ether (60—80°C) yielded green crystals and was found to be identical to the product obtained by the reaction of cyclopentadiene with $WOCl_2(OC_2H_5)_2$.

The cyclopentadienyl derivatives of the methoxy and higher alkoxy compounds of tungsten were prepared by a similar procedure and under similar conditions, but at suitable temperatures. Their analytical data is given in Table 3.

Infrared spectra for all the above compounds are recorded in Table 1.

After decomposing the compounds with perchloric acid, tungsten was estimated as 8-hydroxyquinolate, chloride was estimated as silver chloride, and the alkoxy group was determined by chromic acid method.[17,18]

One of the authors (S.P.A.) thanks the Council of Scientific and Industrial Research, Rafi Marg, New Delhi-1, for the award of a Junior Research Fellowship.

14) J. V. Bell, J. Heisler, H. Tannenbaum and J. Goldenson, *Anal. Chem.*, **25**, 1720 (1953).
15) H. A. Ory, *ibid.*, **32**, 509 (1960).
16) G. Wilkinson, " Org. Synthesis," Vol. 36, p. 476 (1955).
17) C. A. Adams and J. P. Nichlolls, *Analyst*, **1929**, 2154.
18) D. C. Bradley, F. H. Abdel Halim and W. Wardlaw, *J. Chem. Soc.*, **1950**, 3450.

BULLETIN OF THE CHEMICAL SOCIETY OF JAPAN VOL. 42 3462—3466 (1969)

Kinetics of Isotopic Exchange between Acetylacetone-^{14}C and Bisacetylacetonatopalladium(II) in Organic Solvents

Kazuo SAITO and Michihiko TAKAHASHI*1

Department of Chemistry, Faculty of Science, Tohoku University, Katahira-cho, Sendai

(Received May 14, 1969)

Bisacetylacetonatopalladium(II) [Pd acac$_2$] was precipitated crystalline free from excessive acetylacetone (Hacac) by adding the reaction mixture in anisole, benzene or 1,2-dichloroethane to chilled petroleum ether. Its specific counting rate was measured by liquid scintillation technique. The isotopic exchange rate is measurable at 40 to 80°C and the kinetics is expressed by the ordinary two term formula, Rate$=$[Pd acac$_2$](k_1+k_2[Hacac]). The second term corresponds to the reagent path, in which acetylacetone molecule rather than acetylacetonate anion acts as nucleophilic reagent. The first term seems to express a dissociation mechanism rather than the solvent path; the break of Pd–O bond without the aid of nucleophilic attack by the solvent molecule is responsible for determining the exchange rate. The exchange reaction is accelerated by acids, and the acid-catalyzed reaction path operates independent of the reagent path to give the following kinetic formula:

$$\text{Rate} = [\text{complex}](k_1 + k_2[\text{Hacac}] + k_3[\text{acid}])$$

Mechanism of substitution reactions involving square planar complexes of platinum(II) and palladium(II) has been discussed mainly in polar solvents such as water and alcohols.[1] These reactions generally give two term formulae [complex](k_1+k_2[Y]), where Y stands for the nucleophilic reagent which substitutes for one of the coordinated ligands. The rate constants k_1 and k_2 are considered to interpret the "solvent path" and the "reagent path", in which the solvent molecule and the reagent Y operate as nucleophilic reagent to give S_N2 reaction mechanism, respectively.

It seems interesting to examine the isotopic exchange kinetics of square planar complexes in non-polar solvents, since little information is available concerning reaction mechanism in such solvents, and isotopic exchange directly reflects the reactivity of complexes without being bothered by chemical equilibrium. We have examined the solubility of bisacetylacetonatopalladium(II) (henceforth written as [Pd acac$_2$]) and free acetylacetone (Hacac) in a variety of organic solvents and found that the complex is precipitated free from an excess of the ligand by pouring the reaction mixture in anisole, benzene or 1,2-dichloroethane into petroleum ether chilled at −20°C. Hence the experimental technique which was useful for studies with octahedral complexes such as trisacetylacetonatoaluminum(III)[2] and tris-8-quinolinolatogallium(III)[3] is also useful for the present study.

Bisacetylacetonatopalladium(II) is very inert in organic solvents, and the isotopic exchange kinetics is measurable only at elevated temperatures from 40 to 80°C in such solvents with high boiling points as mentioned above.

Experimental

Materials. Acetylacetone-^{14}C was synthesized by the same method as in a previous paper.[2] The specific activity was 0.02 mCi per mg. Bisacetylacetonatopalladium(II) was synthesized and purified by the method given in literature.[4] Extra pure grade anisole was shaken with sodium hydroxide solution, dried with calcium chloride, refluxed with sodium and distilled. The same product was used both for the solvent and the scintillator. The water content of dehydrated product was 1.7×10^{-2} M. Extra pure grade benzene was shaken with concentrated sulfuric acid until the acid layer became almost colorless, then with water, 5% sodium hydroxide solution, and water, dried with calcium chloride, refluxed with sodium and distilled. Extra pure grade 1,2-dichloroethane was shaken with 5% sodium hydroxide solution and water, dried with calcium chloride and phosphorus pentoxide, and distilled immediately before use.

Extra pure grade *m*-toluic acid and *o*-bromobenzoic

*1 Present Address, Japan Leather Research Institute, Adachi-ku, Tokyo.

1) F. Basolo and R. G. Pearson, "Mechanism of Inorganic Reactions," 2 nd ed., John Wiley & Sons, New York (1967), p. 375.

2) K. Saito and K. Masuda, This Bulletin, **41**, 384 (1968).

3) K. Saito, M. Takahashi, Y. Miyakawa and K. Masuda, *ibid.*, **41**, 1139 (1968).

4) A. A. Grinberg and L. K. Simonova, *Zhur. Priklad. Khim.*, **26**, 880 (1953); *Chem. Abstr.*, **47**, 11060g (1952).

acid were sublimed at 90°C at 5 mmHg. Extra pure grade *p*-terphenyl was recrystallized from xylene. Scintillation grade *p*-di-(5-phenyl-2-oxazolyl)-benzene (POPOP) was used without further purification. Petroleum ether was of guaranteed grade and used without further purification.

Experimental Procedure. Weighed amount of the complex (60 to 250 mg) was dissolved in 10 m*l* of the solvent, and the ligand (10 to 150 mg) (both of the order of 10^{-2} M) added at room temperature. The amount of added reagents was known from the difference in weight of the reaction mixture before and after the addition. Other reagents such as acid and water were added to the solvent in advance, whenever necessary. The reaction mixture was then placed in a thermostat at 40 to 80°C, and aliquots (of the order of 1 m*l*) were withdrawn at appropriate intervals (several hours) and poured into chilled petroleum ether (−20°C) (20 m*l*) in order to stop the reaction. Pure [Pd acac$_2$] was separated crystalline instantaneously free from an excess of the ligand. The precipitate was swiftly filtered off with filter paper, washed with petroleum ether, dried at 60 to 70°C, and submitted to liquid scintillation counting.

The time taken for separation was about 5 min. The purity of precipitate was confirmed by chemical analysis of carbon and hydrogen, and ultraviolet absorption spectrometry. Absorption spectra of the reaction mixture also made it clear that no reaction other than isotopic exchange took place.

Measurements. The precipitate (2 to 3 mg) was dissolved in anisole (30.0 m*l*) containing 0.01% POPOP and 0.4% *p*-terphenyl as wavelength shifter, and the specific counting rate determined with a coincidence liquid scintillation counter. The complex is pale yellow and provides significant quenching effect on the scintillation. The effect was examined with standard benzoic acid-^{14}C and non-radioactive complex to obtain a calibration curve, with which the counting rate was duly corrected. The scintillation efficiency was 15% less in the presence of 2 mg per 30 m*l* of the complex as compared with that in its absence. The counting at the end of isotopic exchange reaction (infinite time) was calculated from that of the acetylacetone-^{14}C and the used amounts of the respective compounds.

Water content in the solvent and the reaction mixture was determined by Karl-Fischer titration in a mixture of pyridine and ethyleneglycol (5+1, v/v) as solvent. The ultraviolet absorption spectra were measured with a Hitachi EPU-3-spectrophotometer.

Results

The experimental data were treated with McKay's formula,

$$R = -2.303 \frac{2ab}{2a+b} \cdot \frac{\log(1-F)}{t} \qquad (1)$$

where a and b denote the concentrations of the complex (containing two moles of exchangable ligands per mole) and acetylacetone, respectively. F is the fraction of reaction and t the lapse of time in minutes. The plots of $\log(1-F)$ *vs.* t were all linear to permit the treatment with Eq. (1). Zero time exchange was not observed in this isotopic exchange reaction. The relative error in R values is less than 8 %.

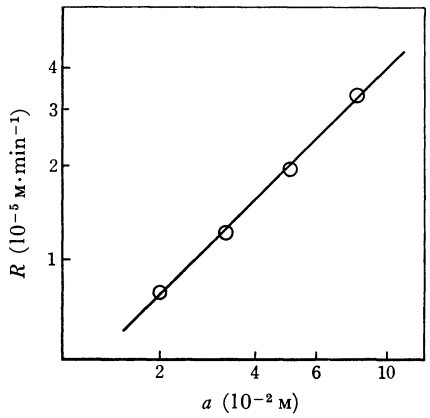

Fig. 1. Relationship between the exchange rate and the concentration of the complex. [acacH], 0.050 M, 80°C in anisole

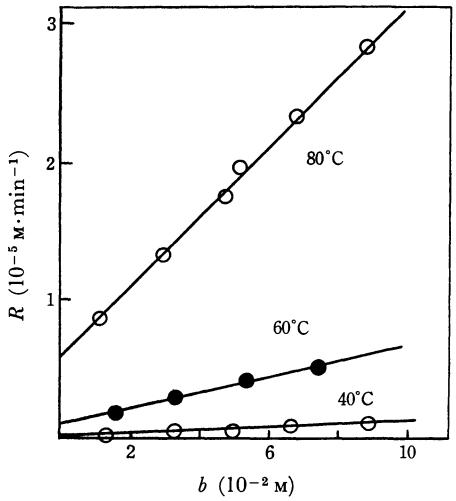

Fig. 2. Relationship between the exchange rate and the concentration of the free ligand. [Pd acac$_2$], 0.050 M, in anisole

Good first order dependence was observed between the exchange rate R and the concentration of the complex (Fig. 1). R is linearly dependent on the concentration of the free ligand (Fig. 2), but the straight line does not pass the zero point and gives a small positive intercept. Therefore R is expressed by

$$R = a(k_1 + k_2 b) \qquad (2)$$

where k_1 and k_2 are rate constants.

The exchange reaction is accelerated by acids. The influence of the concentration of acids (*m*-toluic and *o*-bromobenzoic acid) was examined as shown in Fig. 3. Good first order relationship is observed over the acid concentration range. Figure 4 shows the relationship between R and b in

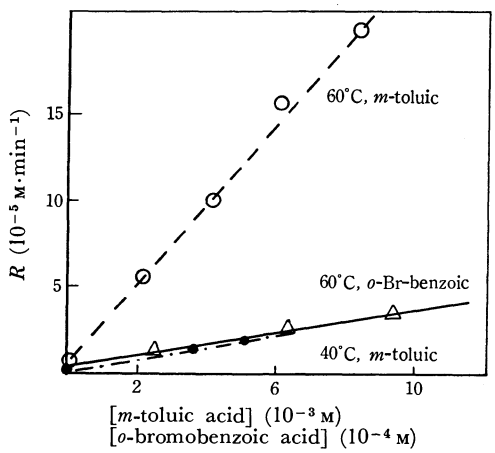

Fig. 3. Relationship between the exchange rate and the concentration of acid in anisole.
[Pd acac$_2$], 0.050 M, [acacH], 4.96×10^{-2} M for *m*-toluic acid at 40°C, 4.90×10^{-2} M for *m*-toluic acid at 60°C, 5.23×10^{-2} M for *o*-bromobenzoic acid at 60°C

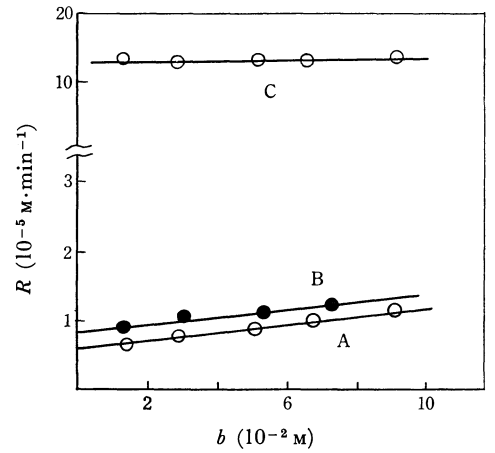

Fig. 4. Relationship between the exchange rate and the concentration of free ligand in the presence of given amounts of acids in anisole.
[Pd acac$_2$], 0.050 M at 60°C. A, 0,00024 M *m*-toluic acid, B, 0.00025 M *o*-bromobenzoic acid, C, 0.0050 M *m*-toluic acid.

the presence of given amounts of the complex and the acid at 60°C. The slopes of lines are equal to the k_2 values obtained from the experiments in the absence of acids. This fact indicates that the acid-catalyzed reaction path operates independent of *b*.

$$R = a(k_1 + k_2 b + k_3[\text{acid}]) \qquad (3)$$

So far as this formula is correct, the values of intercept in Fig. 4 should be equal to the value $a(k_1+k_2[\text{acid}])$. Experimental values obtained from the figure are in fact equal to those obtained from Figs. 2 and 3. When the acid concentration was increased to 0.005 M, the first and the second term of

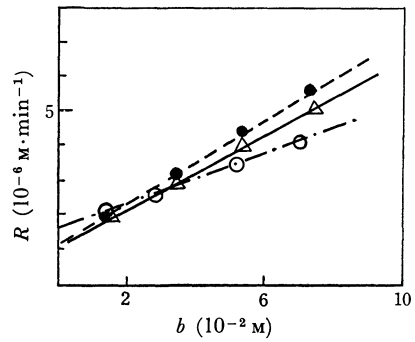

Fig. 5. Relationship between the exchange rate and the concentration of free ligand in various solvents.
[Pd acac$_2$], 0.050 M at 60°C. -△- in anisole, -●- in benzene, -○- in 1,2-dichloroethane

TABLE 1. RATE CONSTANTS IN VARIOUS ORGANIC SOLVENTS

Temp. °C	Solvent	k_1 (min^{-1})	k_2 (M^{-1}·mol^{-1})
40.0	anisole	2.0×10^{-6}	1.8×10^{-4}
60.0	anisole	2.0×10^{-5}	1.1×10^{-3}
80.0	anisole	1.2×10^{-4}	5.1×10^{-3}
E_a (kcal/mol)	anisole	23	18
60.0	benzene	2.4×10^{-5}	1.2×10^{-3}
60.0	1,2-dichloroethane	3.4×10^{-5}	7.4×10^{-4}

Eq. (3) were overwhelmed by the third, and an apparently horizontal diagram was obtained as seen in Fig. 4 C.

Figure 5 shows the relationship between *R* and *b* in various solvents. Equation (1) holds in all these solvents. The rate constants and the Arrhenius activation energy E_a are summarized in Table 1. There was no influence of water concentration upon *R* in the concentration range from 0.017 to 0.12 M in anisole. Because of the solubility of water in these solvents and the dehydration technique employed in this experiment, water concentration changed only within such a range.

Discussion

The k_2 Path. This reaction path is considered to be the so-called "reagent path," which proceeds with nucleophilic displacement mechanism S_N2, through direct attack by the free ligands.[1] There is still a question whether acetylacetone itself or acetylacetonate anion is the nucleophilic reagent. If the anion were the effective reagent, k_2 values should be influenced by the presence of other acids, because acetylacetone is a very weak acid and only a small fraction can be dissociated in the solvents. However, they remain unchanged on addition of stronger acids, and acetylacetone molecule seems

to be the nucleophilic reagent.

The k_1 Path. Generally the k_1 path is explained as the so-called "solvent path," in which the reaction proceeds with nucleophilic attack by the solvent molecule. Many experimental evidences have been postulated for reactions in polar solvents including water and methanol.[5] It seems rather doubtful, however, to apply the same reaction mechanism to the k_1 path in those solvents with poor coordination ability. In the present case it appears as if the k_1 path involves a kind of dissociation mechanism. The reason is as follows.

The k_1 values do not change significantly in varying solvents (Table 1). Anisole is a relatively polar solvent ($\mu=1.35$ Debye) whereas benzene is nonpolar; the k_1 values are nearly equal in these two solvents. Since palladium(II) is a soft acid,[6] it could interact with π-electrons of the aromatic solvent molecules. 1,2-Dichloroethane does not contain benzene ring, but the k_1 value in this solvent is nearly equal to those in the other two solvents. This fact indicates that the π-electron interaction between the phenyl ring and the palladium(II) complex does not affect the reaction rate appreciably.*2

Larger E_a values for k_1 than for k_2 and the negligible influence of water concentration upon the exchange rate seem to provide further support for the dissociative nature of the k_1 path.*3

The fact that k_1 in 1,2-dichloroethane is somewhat larger than that in other solvents could be interpreted by the larger dielectric constant of this solvent ($\varepsilon=10.36$, 25°C) than the other two (4.33 at 25°C for anisole and 2.28 at 20°C for benzene). Larger dielectric constant would facilitate the bond break between palladium(II) and oxygen of the ligand.

Thus the solvent molecule near the coordination sphere would have only a negligible affect on the elimination rate of the coordinated ligand, and the ease of break of the bond between the metal ion and the ligand would be responsible for determining the rate through k_1 path.

The k_3 Path. Three kinds of mechanism of acid catalysis can be considered: (i) displacement of coordinated ligand through the nucleophilic attack by acid molecule or its anion. (ii-a) dissociation of one end of chelate ligand is the rate determining step, and the other end of unidentate ligand dissociates fast. Protons attack the coordinated oxygen and accelerate the first step of bond break between palladium(II) and oxygen. (ii-b) The ligand can be present as unidentate rather stable, and the break of the remaining bond is the rate determining step. Protons trap the free end of unidentate ligand and retard its recombination to increase the reaction rate.

If the acid anion acted as nucleophilic reagent, salts of the acids should give the same catalytic effect. Unfortunately no salts of the acids, including those of lithium and tetramethylammonium have sufficient solubility in the organic solvents to permit such a comparison.

If the reaction mechanism were ii-a or ii-b, *o*-bromobenzoic acid ($pK=2.85$) would be the better catalyst than *m*-toluic acid ($pK=4.27$). If mechanism i were valid, *o*-bromobenzoic acid would be the weaker catalyst owing to its steric hindrance coming from bromine on the *o*-position. As shown in Table 2, *o*-bromobenzoic acid has greater catalytic ability. Hence mechanism ii-a or ii-b would be more appropriate.

Table 2. Influence of acid in anisole

Temp. °C	k_3 ($M^{-1}\cdot min^{-1}$)	
	m-Toluic	*o*-Bromobenzoic
40.0	7.5×10^{-2}	—
60.0	4.7×10^{-1}	6.7×10^{-1}
E_a (kcal/mol)	19	

Pearson and Johnson studied the substitution reaction of [Pd $acac_2$] in water containing methanol and accounted for the acid catalysis by mechanism ii-b.[7] Saito and Masuda investigated the isotopic exchange kinetics between acetylacetone-^{14}C and trisacetylacetonatoaluminum in organic solvents and interpreted the acid-catalyzed reaction path by mechanism ii-b, too, on the basis that the E_a values are identical in varying solvents and in the presence or absence of acid.[8]

In the present case, however, reaction mechanism ii-a cannot be easily eliminated, because the E_a value for k_3 (19 kcal per mole in anisole) is significantly smaller than that for k_1 (23 kcal per mole in anisole). Further, bond energy between palladium-

5) M. A. Tucker, C. B. Colvin and D. S. Martin, Jr., *Inorg. Chem.*, **3**, 1373 (1964); F. Basolo, J. Chatt, H. B. Gray and R. G. Pearson, *J. Am. Chem. Soc.*, **82**, 4200 (1960); R. G. Pearson, H. B. Gray and F. Basolo, *ibid.*, **82**, 787 (1960); U. Belluco, L. Cattalini, F. Basolo, R. G. Pearson and A. Turco, *ibid.*, **87**, 241 (1965).

6) R. G. Pearson, *ibid.*, **85**, 3533 (1963).

*2 If the k_1 path were the "solvent path," the apparent k_1 values should be divided by the molar concentration of the solvent species. They are 9.2, 11.2 and 12.7 M for benzene, anisole and 1,2-dichloroethane, respectively, and the divided values are 6.17×10^{-6}, 2.14×10^{-6} and 2.64×10^{-6} *l*/mol/min, respectively.

*3 Dissociative nature of the k_1 path has been exemplified by use of a palladium(II) complex with a large ligand, which brings about significant steric hindrance against nucleophilic attack by the solvent molecule in water. (W. H. Braddley and F. Basolo, *J. Am. Chem. Soc.*, **86**, 2075 (1964); **88**, 2944 (1966).) The present complex [Pd $acac_2$] does not seem to provide such an effect.

7) R. G. Pearson and D. A. Johnson, *ibid.*, **86**, 3983 (1964).

8) K. Saito and K. Masuda, This Bulletin, **42**, 3184 (1969).

(II) and oxygen is apparently smaller than that between aluminum(III) and oxygen as seen from their formation enthalpies, and non-polar solvents would hold the unidentate acetylacetonate less firmly than polar solvents. We would thus consider that the k_3 term is regarded as a catalytic process by protons, although neither the proton carrier nor the species subject to proton catalysis is evidently known.

The authors wish to express sincere thank to Nishina Memorial Foundation for Grant in Aid, and to Miss Mizue Tachikawa for her help in experiments.

BULLETIN OF THE CHEMICAL SOCIETY OF JAPAN VOL. 42 3466—3470 (1969)

The Indirect Determination of Mercury in an Aqueous Solution using the Ligand Exchange Reaction

Itsuro KAWAI and Tadashi HARA

Department of Chemical Engineering, Faculty of Engineering, Doshisha University, Kamikyo-ku, Kyoto

(Received May 15, 1969)

A new method for the indirect determination of mercury in an aqueous solution has been established on the basis of the fact that the absorption and evolution of propylene in the reaction between mercuric ion and propylene take place reversibly and quantitatively under proper conditions. In the method proposed, the propylene in the 1 : 1 π-complex is displaced with such complexing agents as chloride, bromide, iodide and EDTA, and the quantity of the propylene evolved is measured manometrically. By the present method, up to 70 mg Hg can be estimated within $\pm$0.08 mg in about 15 min. Common cations and anions do not interfere. Though silver(I) and palladium ions interfere, their interferences are removed by suitable procedures. By improving the apparatus, it should be possible to estimate much smaller amounts of mercury than the above value.

It has been well established that a mercuric ion in an aqueous solution reacts with olefins to form π-complxes.[1-10] However, the present authors have found that the absorption and evolution of propylene in the reaction between the mercuric ion and propylene take place reversibly and quantitatively under proper conditions. On the basis of this phenomenon, a new method for the indirect determination of mercury in an aqueous solution has been established; in this method the propylene in the π-complex is displaced with complexing agents, such as chloride, bromide, iodide, and EDTA, and the quantity of the propylene evolved is measured manometrically.

Experimental

Apparatus. The quantity of propylene absorbed or evolved was measured at a constant temperature and pressure using the apparatus shown in Fig. 1. The apparatus was made of glass except the parts connecting the sample bottle (B) and the leveler (G) with the cock,6, and the gas-burette, F. Water saturated with propylene was placed in the manometer, E, and the gas-burette, F. An aqueous solution of perchloric acid is placed in (D) and (G), and its acidity is the same as in the sample solution. To the sample solution containing mercury (10—70 mg), 3 m*l* of a 2 M sodium sulfate solution is added; the acidity was adjusted to 0.7M for the use of chloride, bromide, and iodide, or to pH 5 for the use of EDTA, as the complexing agent.

Reagents. *Standard Mercury(II) Solution.* The stock solution of mercury(II) was prepared by dissolving 21.66 g of mercuric oxide (JIS special grade) in 100 m*l* of 1 M perchloric acid. The concentration of mercury was determined by chelometric titration.

Complexing Agent Solutions. Solutions containing sodium sulfate in 2 M, and sodium chloride, sodium bromide or sodium iodide in 0.2 M or EDTA in 0.12 M were prepared. The acidities were 0.7 M in perchloric acid

1) M. A. Bennett, *Chem. Revs.*, **63**, 611 (1962).
2) K. Ichikawa, K. Fujita and O. Itoh, *J. Am. Chem. Soc.*, **84**, 2632 (1962).
3) F. A. Cotton and J. R. Leto, *ibid.*, **80**, 4824 (1958).
4) J. Chatt, *Chem. Revs.*, **48**, 7 (1951).
5) C. W. Whitehead and J. J. Traverso, *J. Am. Chem. Soc.*, **80**, 2182 (1958).
6) M. M. Kreevoy and F. R. Kowitt, *ibid.*, **82**, 739 (1960).
7) K. Ichikawa, *Kogyo Kagaku Zasshi (J. Chem. Soc. Japan, Ind. Chem. Sect.)*, **66**, 1037 (1963).
8) Y. Saito, *Shokubai (Catalyst)*, **9**, 100 (1967).
9) P. M. Henry, *J. Am. Chem. Soc.*, **88**, 1595 (1966).
10) F. Basolo and R. G. Pearson, "Mechanisms of Inorganic Reactions," John Wiley & Sons, New York (1965), p. 351.

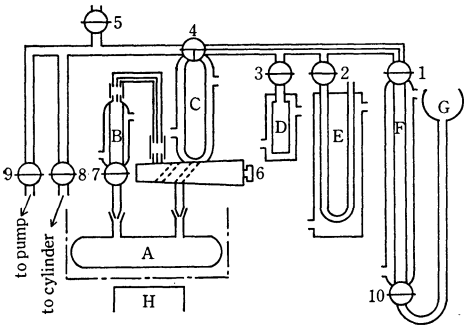

Fig. 1. The apparatus for estimating the quantity of propylene.

A: Reaction vessel
B: Sample bottle
C: Gas holder
D: Vapor pressure adjuster
E: Manometer
F: Gas burette
G: Leveler
H: Magnetic stirrer

except at pH 5 in a solution containing EDTA.

Acetate Buffer. The solution was prepared from sodium acetate and acetic acid.

All the reagents used were of a guaranteed grade.

Procedure. Cocks (1)—(19) are set to the positions shown in Fig. 1, and about 7 m*l* of a sample solution is taken into the sample bottle (B), the capacity of which is about 7 m*l*. Cock (9) is opened, and the inside of the apparatus is evacuated, and the cock closed. To adjust the inside to a constant vopor pressure, Cock (3) is opened and closed. To introduce propylene into the apparatus, Cock (8) is gradually opened after opening Cocks (1) and (10), and Cocks (8) and (10) are closed. Here the meniscus in the gas-burette is brought to the lower part by moving the leveler (G). Then the inside is equilibrated with the atmospheric pressure by regulating Cock (5), and the sample solution is dropped into the reaction vessel (A) (about 30 m*l*) through Cock (7) by operating Cock (6). The solution is stirred by a magnetic stirrer, and propylene is absorbed. After an equilibrium has been established, the stirrer is stopped and Cocks (6) and (7) are set to the positions shown in Fig. 1. The meniscus in the gas-burette is read after the internal pressure has been equilibrated with the atmospheric pressure through a manometer. Seven milliliters of a complexing agent are placed in the (B) and then added to the (A) in the way previously described. The solution is stirred and the meniscus read similarly. The quantity of propylene evolved is calculated by the difference between two readings. All the experiments were carried out at 25°C under an atmospheric pressure.

Results and Discussion

The Absorption of Propylene. Since the reaction between mercuric ions in an aqueous solution and propylene was controlled by the diffusion of propylene into the liquid, the time necessary for 40 mg of mercury ions to reach an equilibrium was measured by the apparatus shown in Fig. 1. The equilibrium was established in about 5 min; the time required was independent of the acidity in the range of pH 0—6. The quantity of propylene absorbed was 4.89 m*l*; this agreed approximately with the theoretical value, showing the composition to be that of a 1 : 1 π-complex. It may be supposed that the formation of the π-complex goes to completion in a short period.

The Evolution of Propylene. To the π-complex obtained in the above experiment there was added a complexing agent containing three times as many moles as mercury, and the quantity of propylene evolved was read against the time. The equilibrium was established within 10 min by adding either a halide solution (0.7 M perchloric acid) or EDTA solution (pH 5) to it. The time required increased in the order of; iodide (2 min)

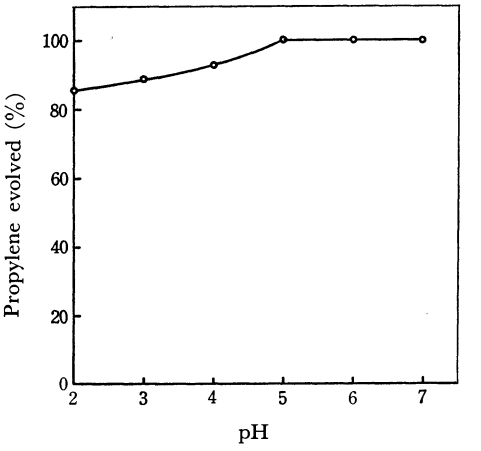

Fig. 2. Evolution of propylene with EDTA.
t=25°C, P_{tot}=1 atm, μ=0.8, Mole ratio: [EDTA]/[Hg^{2+}] = 3

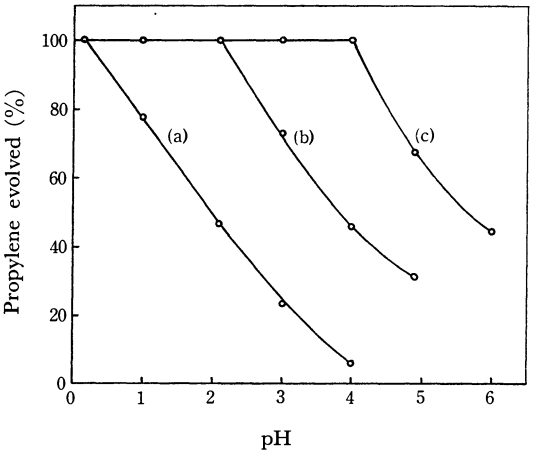

Fig. 3. Evolution of propylene with sodium chloride, sodium bromide and sodium iodide.
t=25°C, P_{tot}=1 atm, μ=0.8, Mole ratio: [halide]/[Hg^{2+}]=3, halide: Cl^-, Br^-, I^-
(a) Sodium chloride, (b) Sodium bromide, (c) Sodium iodide

<bromide (6 min)<chloride (8 min) and decreased with an increase in the stability constant of tetrahalogeno-mercuriates.

The Effect of Acidity. The relationship between the pH and the quantity of propylene evolved in a solution containing EDTA and Hg (3 : 1) was shown in Fig. 2. The evolution of propylene was quantitative at pH≧5. The experiment at pH> 7.0 was not feasible since some mercuric compound began to precipitate. The relationship between pH and the quantity of propylene evolved in a solution containing halide and Hg (3 : 1) is also shown in Fig. 3. As can be seen from Fig. 3, propylene is evolved quantitatively in the ranges of the following acidity: molarity of perchloric acid ≧0.7 for chloride, pH≦2.1 for bromide, and pH ≦4.0 for iodide. It can be concluded from these results that the propylene molecule is easily displaced with a halide ion at a lower pH, while it is replaced with EDTA at a higher pH.

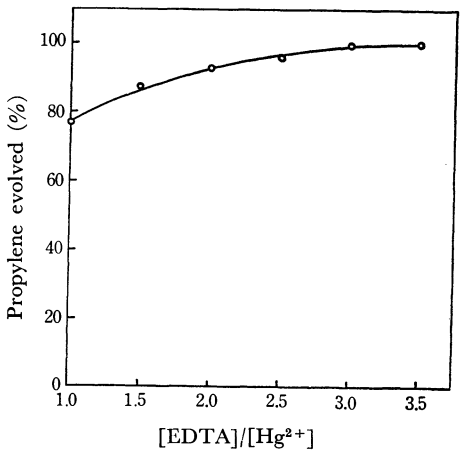

Fig. 4. Evolution of propylene with EDTA. t=25°C, P_{tot}=1 atm, μ=0.8, pH=5

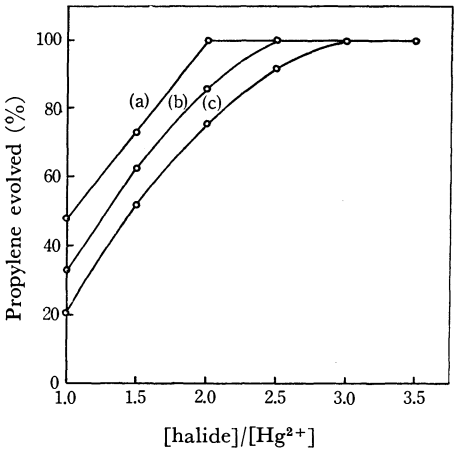

Fig. 5. Evolution of propylene with sodium chloride, sodium bromide and sodium iodide. t=25°C, P_{tot}=1 atm, μ=0.8, [$HClO_4$]=0.7 N, halide: Cl^-, Br^-, I^-, (a) Sodium iodide, (b) Sodium bromide, (c) Sodium chloride

The effect of the Mole Ratio. The relationship between the mole ratio of [EDTA]/[Hg] or [halide]/[Hg] and the quantity of propylene evolved was shown in Figs. 4 and 5. Propylene was evolved quantitatively under the following conditions: [EDTA]/[Hg^{2+}]≧3.0, [Cl^-]/[Hg^{2+}]≧3.0, [Br^-]/[Hg^{2+}]≧2.5 and [I^-]/[Hg^{2+}]≧2.0.

The Calibration Curves. The sample solutions containing 10, 20, 30, 40, 50, 60 and 70 mg of Hg were prepared, and the π-complexes were allowed to form in the apparatus shown in Fig. 1. Then the quantities of propylene evolved on the addition of halides of EDTA were measured. The

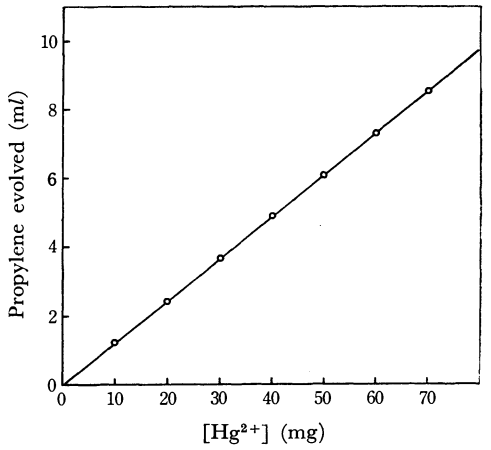

Fig. 6. Calibration curves. t=25°C, P_{tot}=1 atm

TABLE 1. EFFECTS OF DIVERSE CATIONS AS NITRATES t=25°C, P_{tot}=1 atm, [$HClO_4$]=0.7 N, Hg^{2+} taken: 40.26 mg

Ion	Mole ratio [ion]/[Hg^{2+}]	Propylene evolved ml	Hg^{2+} found mg	Relative error %
Na^+	10.0	4.92	40.34	0.20
K^+	10.0	4.92	40.34	0.20
Mg^{2+}	10.0	4.94	40.50	0.61
Co^{2+}	10.0	4.94	40.50	0.61
Mn^{2+}	10.0	4.92	40.34	0.20
Cu^{2+}	10.0	4.92	40.34	0.20
Zn^{2+}	10.0	4.94	40.50	0.61
Pb^{2+}	10.0	4.92	40.34	0.20
Cd^{2+}	10.0	4.90	40.18	−0.20
Ni^{2+}	10.0	4.94	40.50	0.61
Al^{3+}	10.0	4.92	40.34	0.20
Fe^{3+}	10.0	4.88	40.02	−0.61
Cr^{3+}	10.0	4.94	40.50	0.61
Ag^+	1.0	5.68	46.34	15.68
Pd^{2+}	0.5	2.46	20.66	−49.89
Pd^{2+}	1.0	0.02	1.14	−99.59
Pd^{2+}	3.0	0.00	0.00	−100.00

Table 2. Effects of diverse ions
$t=25°C$, $P_{tot}=1$ atm, $[HClO_4]=0.7$ N, Hg^{2+} taken: 40.26 mg

Mole ratio Hg^{2+} : Pd^{2+} : Ag^+ : Na^+				Propylene evolved m*l*	Hg^{2+} found mg	Relative error %
1	1		100	4.92	40.34	0.20
1		1	100	4.56	37.46	−7.12
1	1	1	100	4.52	37.14	−7.94

Mole ratio Hg^{2+} : Cu^{2+} : Mg^{2+} : Zn^{2+} : Mn^{2+} : Al^{3+} : Cr^{3+} : Fe^{3+} : Na^+									Propylene evolved m*l*	Hg^{2+} found mg	Relative error %
1	10	10	10	10	10	10	10	100	4.94	40.50	0.61

results shown in Fig. 6 were obtained by plotting the quantities of propylene evolved as the ordinate, and the concentration of mercury, as the abscissa. It was confirmed that all the experimental values fall on the same line regardless of the kind of complexing agent. Up to 70 mg Hg gave a straight line.

The Effect of Diverse Ions. The effects of such cations as Na^+, K^+, Mg^{2+}, Cu^{2+}, Co^{2+}, Mn^{2+}, Zn^{2+}, Pb^{2+}, Cd^{2+}, Ni^{2+}, Al^{3+}, Fe^{3+} and Cr^{3+} in mole ratios of $[cation]/[Hg^{2+}]\leqq 10$ on the determination of 40.26 mg of Hg were examined, but their interferences were negligible (Table 1). However, Ag^+ and Pd^{2+} interfered seriously. It is generally[10] said that the metals with eight or ten electrons in the *d*-orbital show a tendency to combine with olefins. The fact that no influence was observed on Ni^{2+} (d^8), Zn^{2+} (d^{10}) and Cd^{2+} (d^{10}) shows that the interaction between one of these ions and propylene is negligible. As can be seen from Table 1, the silver(I) ion gave a positive error, while the palladium(II) ion gave a negative error. The former is reasonable since it was confirmed experimentally that the reaction between the silver ion and propylene is quite similar to that between the mercuric ion and propylene, but the silver complex is less stable than the mercuric complex. The latter can also be understood by the following reactions, which were previously proposed by one of the present authors[11]:

$$\text{Propylene} + Pd^{2+} \longrightarrow \text{Acetone} + Pd^* \quad (1)$$

$$Hg^{2+} + \text{Propylene} \longrightarrow Hg^{2+}\cdot\text{Propylene} \quad (2)$$

$$Hg^{2+}\cdot\text{Propylene} + Pd^* \longrightarrow Pd^0 + Hg^0 + \text{Product} \quad (3)$$

Under the present experimental conditions, Reaction (1) goes to completion very fast, while the π-complex produced in Reaction (2) remains stable in the absence of the palladium ion. However, the mercuric complex in the presence of the palladium ion goes to completion in accordance with Reaction (3). These phenomena satisfactorily explain the results shown in Table 1. The interference of the silver ion was eliminated by adding a siutable amount of sodium chloride and by driving off an excess of chloride as hydrogen chloride; that of the palladium ion was also eliminated by adding an alcoholic dimethylglyoxime solution and by precipitating the palladium ion (Table 2). The suspensions were treated much as before.

The effects of such anions as SO_4^{2-}, NO_3^-, ClO_4^-, CH_3COO^-, and $H_2PO_4^-$ in mole ratios of $[anion]/[Hg^{2+}]\leqq 35$ on the determination of 40.12 mg Hg were also examined, but no interference was observed (Table 3). Since the blank value was reduced to zero with an increase in the amount of sodium sulfate, the determination of mercury was always carried out in the presence of a definite amount of sodium sulfate. According to the present procedure, the errors based the temperature change, impurities, *etc.* can be minimized.

In the above experiment, the blank value was

Table 3. Effects of diverse anions as sodium salts
$t=25°C$, $P_{tot}=1$ atm, $[HClO_4]=0.7$ N,
Hg^{2+} taken: 40.26 mg

Ion	Mole ratio $[ion]/[Hg^{2+}]$	Blank m*l*	Hg^{+2} m*l*	Relative error %
SO_4^{2-}	1	0.68	40.12	
SO_4^{2-}	10	0.52	39.96	−0.39
SO_4^{2-}	35	0.10	40.12	
NO_3^-	1	0.70	40.12	
NO_3^-	10	0.64	40.28	0.39
NO_3^-	35	0.56	40.12	
ClO_4^-	10	0.68	40.12	
ClO_4^-	10	0.58	40.12	
ClO_4^-	35	0.50	39.96	−0.39
CH_3COO^-	1	0.68	40.12	
CH_3COO^-	10	0.64	40.12	
CH_3COO^-	35	0.52	39.96	−0.39
$H_2PO_4^-$	1	0.76	40.28	0.39
$H_2PO_4^-$	10	0.66	40.12	
$H_2PO_4^-$	35	0.38	39.96	−0.39

11) T. Hara, T. Koga and H. Takeda, This Bulletin, **40**, 1634 (1967).

equal to 0.02 ml and was reproducible. The ionic strength in the reaction mixture was approximately 5 throughout the experiment. Up to 70 mg of mercury was determined in the present study, but it should be possible to determine smaller amounts of mercury by improving the apparatus, especially the gas-burette.

The authors wish to thank the Maruzen Sekiyu Co. for its donation of propylene.

BULLETIN OF THE CHEMICAL SOCIETY OF JAPAN VOL. 42 3470—3477 (1969)

The Oxygenation-deoxygenation of Cobalt(II) Complexes on Polymers

Akira MISONO, Seiichiro KODA and Yasuzo UCHIDA

Department of Industrial Chemistry, Faculty of Engineering, The University of Tokyo, Hongo, Bunkyo-ku, Tokyo

(Received May 19, 1969)

Three cobalt(II) complexes, bis-(salicylaldehyde)-ethylenediimine-cobalt(II), bis-(salicylaldimino)cobalt(II), and di-(salicylal)-3,3′-diimino-di-*n*-propylamine-cobalt(II), were mixed with poly-4-vinylpyridine. These mixtures showed ESR signals which reversively appeared under oxygen. We tried to identify these signals on the basis of the electonic structure, cobalt(III)-O_2^{-1}. The oxygenation-deoxygenation rates were also observed and found to obey the Elovich rate equation.

Many oxygen-carrier cobalt(II) chelates have been investigated,[1] of these, bis-(salicylaldehyde)-imine-cobalt(II) complexes have long been investigated, especially by Calvin *et al.*[2,3] These complexes, however, do not seem to have been studied from the viewpoint of technological designs for producing solid-state oxidizing catalysts from them.

It is known that the paramagnetic bis-(salicylaldehyde)-ethylenediimine-cobalt(II) yields a diamagnetic-oxygenated complex ($Co/O_2=2/1$).[3] The present authors found that an ESR signal appeared when a mixture of this chelate and poly-4-vinylpyridine (PVP) was exposed to oxygen; on the other hand, the signal disappeared when the mixture was placed in a vacuum. Several cycles were successfully tried; they have already been reported briefly.[4]

The paramagnetic species in mixtures of a cobalt(II) chelate with a polymer have been identified, and also the properties of oxygenation-deoxygenation rates have been investigated in this study. The chelates which have been tried successfully are: bis-(salicylaldimino)cobalt(II) (Complex B-1 and Complex B-2; the abbreviations are explained in the Experimental part), and di-(salicylal)-3,3-diimino-di-*n*-propylamine-cobalt(II) (Complex C), as well as the above bis-(salicylaldehyde)-ethylenediimine-cobalt(II) (Complex A).

Results

The four mixtures, Complex A-PVP, Complex B-1-PVP, Complex B-2-PVP, and Complex C-PVP, each showed an ESR signal which appeared (or

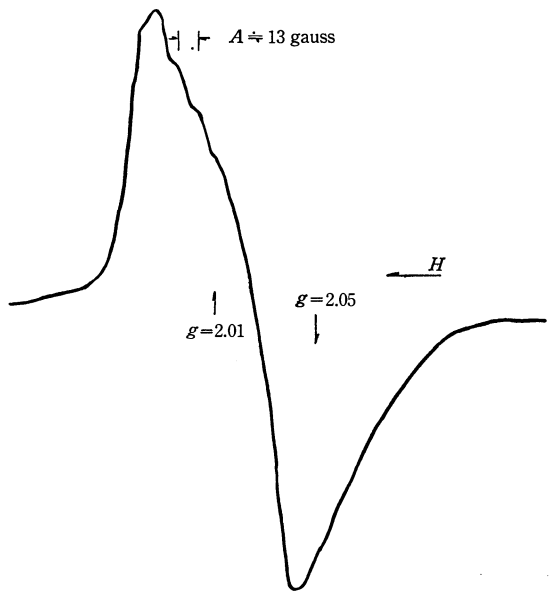

Fig. 1. The ESR signal on A-PVP with O_2. $P_{O_2}=1$ atm, Co/pyridine ring = 1/100, at room temp.

1) L. H. Vogt, Jr., *Chem. Revs.*, **63**, 269 (1963).
2) A. E. Martell and M. Calvin, "The Chemistry of the Metal Chelate Compounds," Prentice Hall, N. Y. (1956), p. 337.
3) M. Calvin, R. H. Bailes and W. K. Wilmarth, *J. Am. Chem. Soc.*, **68**, 2254 (1946).
4) A. Misono, S. Koda and Y. Uchida, This Bulletin, **42**, 580 (1969).

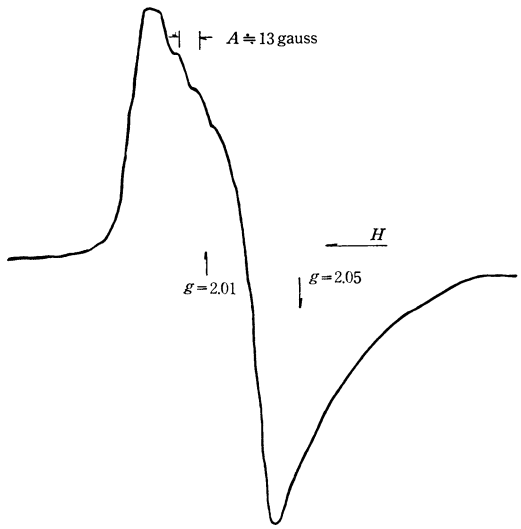

Fig. 2. The ESR signal on B-2-PVP with O_2. P_{air}=494 mmHg, Co/pyridine ring = 1/90, at room temp.

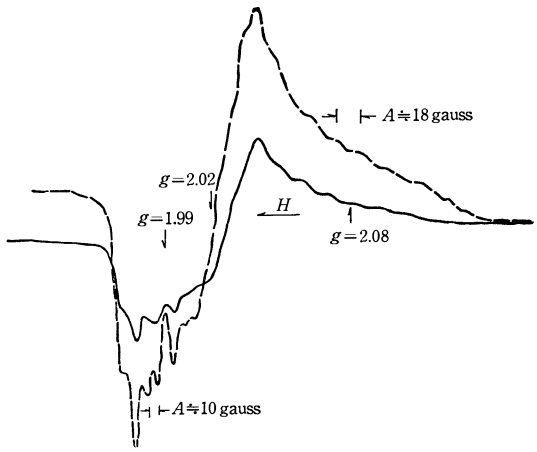

Fig. 3. The ESR signal on C-PVP with O_2. P_{air}=1 atm, Co/pyridine ring=1/160, at room temp. (——) and at −130°C (— —)

increased) under oxygen (or air) and disappeared (or decreased) *in vacuo*. The ESR signals are shown with their approximate g and A values in Figs. 1—3. (These g values were roughly estimated so as to explain the signal shapes (and are, therefore, not very accurate) according to the method for randomly-oriented particles in a fixed position.[5]) The A values were approximate intervals (in gauss) between two appropriate hfs signal peaks). The PVP itself and the mixture of cobalt(II) acetylacetone with PVP showed no corresponding ESR signal, even under oxygen.

Polyacrylonitrile was also tried as a chelate-carrier instead of PVP, but the chelates could not be successfully carried on the polymer by any means tried.

The ESR signal shapes (investigated in the case of A-PVP) were almost independent of the temperature over the range from about 40 to −140°C. The signal in the case of the Complex C became a little sharper at a lower temperature.

The shape was almost independent of the oxygen pressure over the range from 1 atom to several mmHg (investigated in the case of A-PVP) and also of the relative mole ratio of cobalt(II) *vs.* the pyridine ring in the polymer over the range from 1/20 to 1/400 (investigated in the case of B-2-PVP).

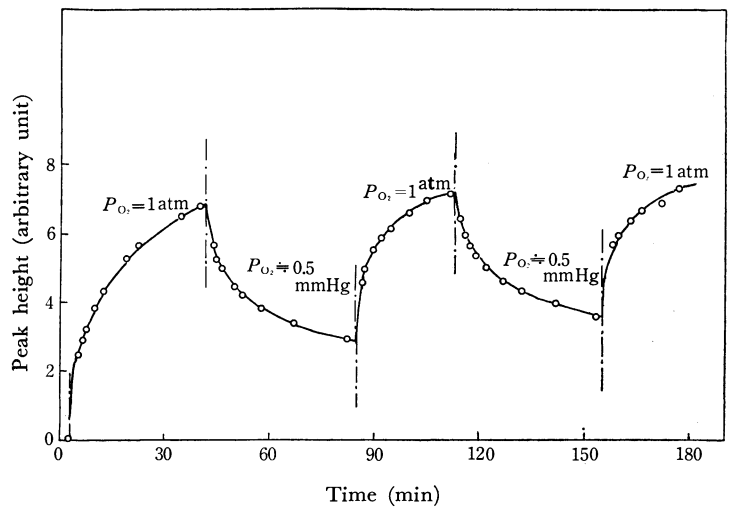

Fig. 4. Oxygenation-deoxygenation cycle (for A-PVP). Co/pyridine ring=1/110, at room temp.

5) F. K. Kneubühl, *J. Chem. Phys.*, **33**, 1074 (1960).

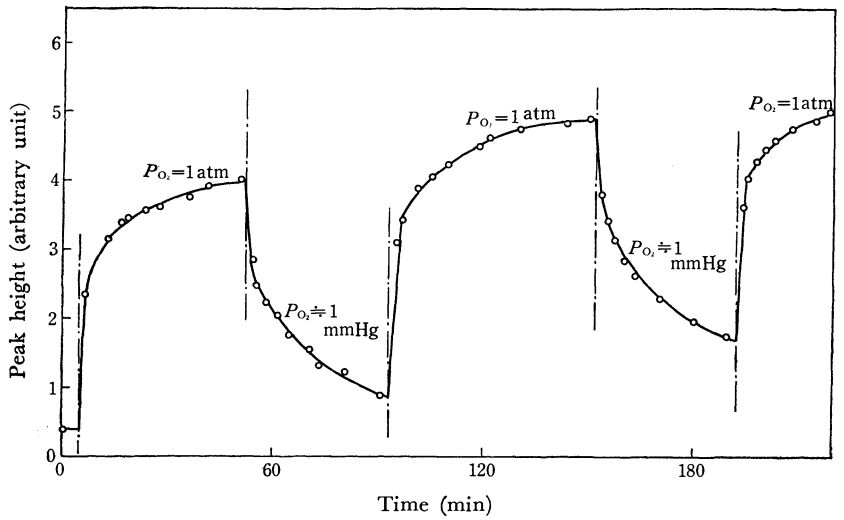

Fig. 5. Oxygenation-deoxygenation cycle (for B-1-PVP). Co/pyridine ring = 1/50 at room temp.

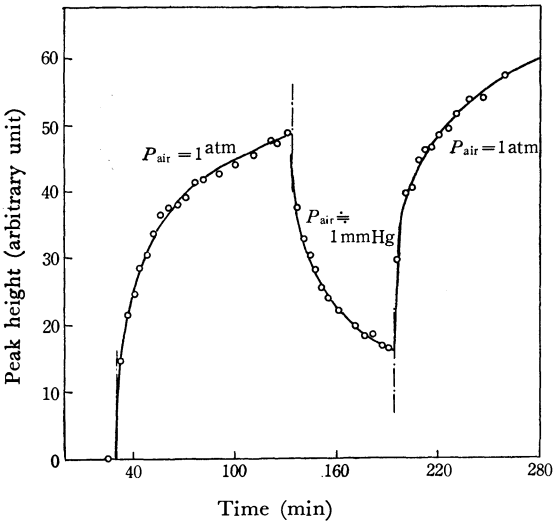

Fig. 6. Oxygenation-deoxygenation cycle (for C-PVP). Co-pyridine ring = 1/160, at room temp.

The changes in the relative strength of the ESR signal (which was considered to be proportional to the amounts of the corresponding paramagnetic species, as will be explained in the Experimental part) upon the introduction and exhaustion of oxygen (or air) are illustrated in Fig. 4 (for A-PVP), in Fig. 5 (for B-1-PVP), and in Fig. 6 (for C-PVP).

The rate of the increase and decrease of the signal strength seems to obey the Elovich rate equation (Figs. 7—9); that is,

increasing:

$$\log (t + t_0) = av - b$$

decreasing:

$$\log (t + t_0) = cv + d$$

t_0, a, b, c, d: constants independent of the contact time

v: signal strength

t: contact time

The signal strength is not proportional to $t^{1/2}$. Here, the strength proportionate to $t^{1/2}$ can be expected at an earlier stage if the rate is determined by gas diffusion through a polymer film.[6] Moreover, the first derivative of the signal strength against the contact time (Fig. 10) sufficiently obeyed the equation derived from the above Elovich equation:

$$dv/dt = Ae^{-Bv}$$

$$A = e^{2.303b}/2.303a$$

$$B = 2.303a$$

Moreover, it did not follow the equation:

$$dv/dt = k(v_e - v) \qquad k,\ v_e : \text{constants}$$

This equation can be expected to hold in the case of Langmuir adsorption,[7] and also at a later stage when the adsorption is determined by gas diffusion through a polymer film.[6]

The constants, a, b, c, and d, seemed, however, not to be independent of the previous history of the mixture (*cf.* Table 1). Above all, the enlargement of the b values agrees with the observation that the oxygenation rate increases with the repetition of the oxygenation-deoxygenation.

The relative signal strength changed easily with the temperature (Fig. 11). The signal strength seemed to decrease more rapidly with the rise in

6) Y. Wada (editor), "Kobunshi no Bussei Kogaku," Ohm Co., Tokyo (1967), p. 255.

7) T. Keii, "Kyuchaku," Kyoritsu Shuppan Co., Tokyo (1965), p. 50.

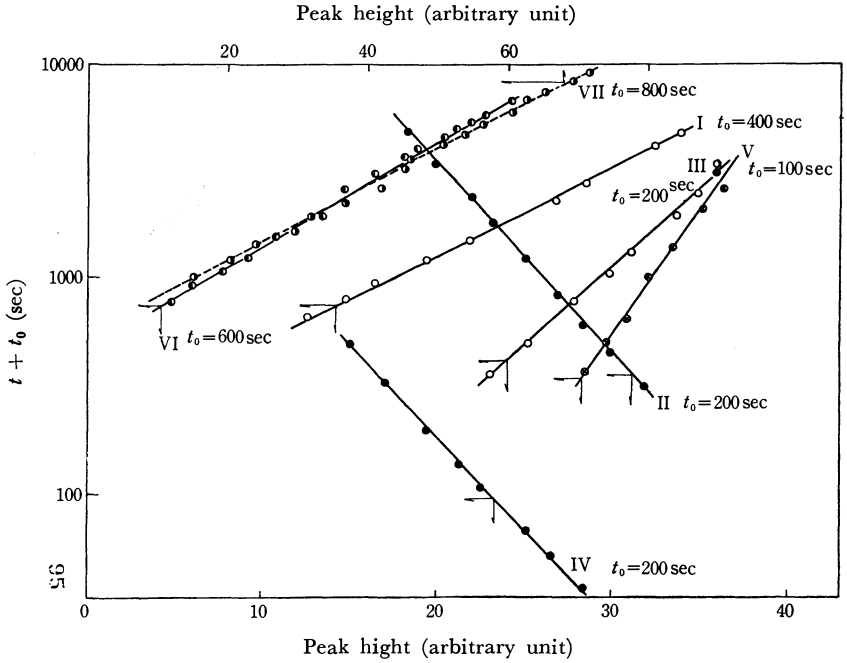

Fig. 7. Elovich plot (for A-PVP).
From the data of Fig. 4 for I—V, Co/pyridine ring=1/110, at room temp.
I, III, V: the first, second and third oxygenation stage, respectively, P_{O_2}=1 atm
II, IV: the first and second deoxygenation stage, respectively, $P_{O_2} \fallingdotseq 0.5$ mmHg
VI: Co/pyridine ring=1/90, at room temp., the first oxygenation stage, P_{air}= 60 mmHg
VII: Co/pyridine ring=1/50, at room temp., the first oxygenation stage, P_{air}=1 atm

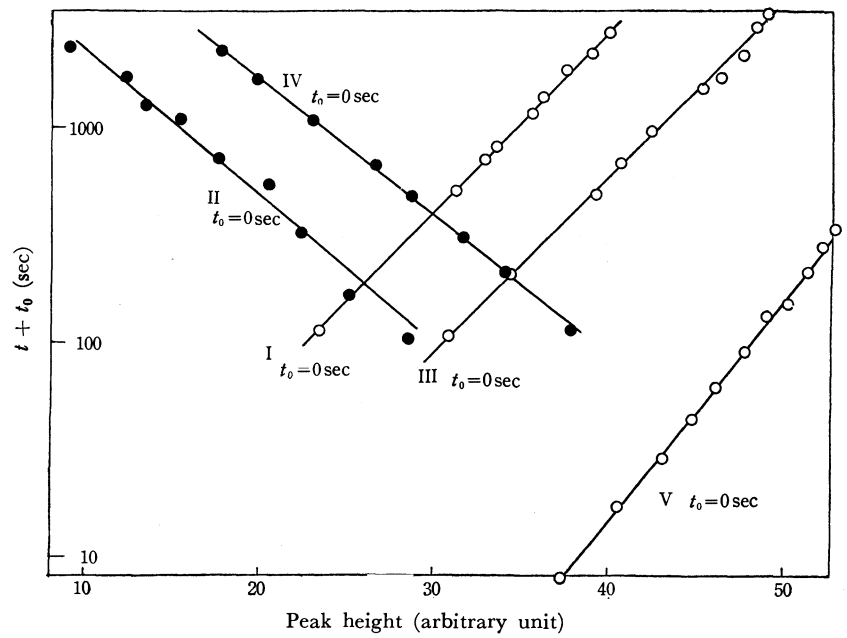

Fig. 8. Elovich plot (for B-1-PVP).
From the data of Fig. 5; Co/pyridine ring=1/50, at room temp.
I, III, V: the first, second and third oxygenation stage, respectively, P_{O_2}=1 atm
II, IV: the first and second deoxygenation stage, respectively, P_{O_2}=1 mmHg

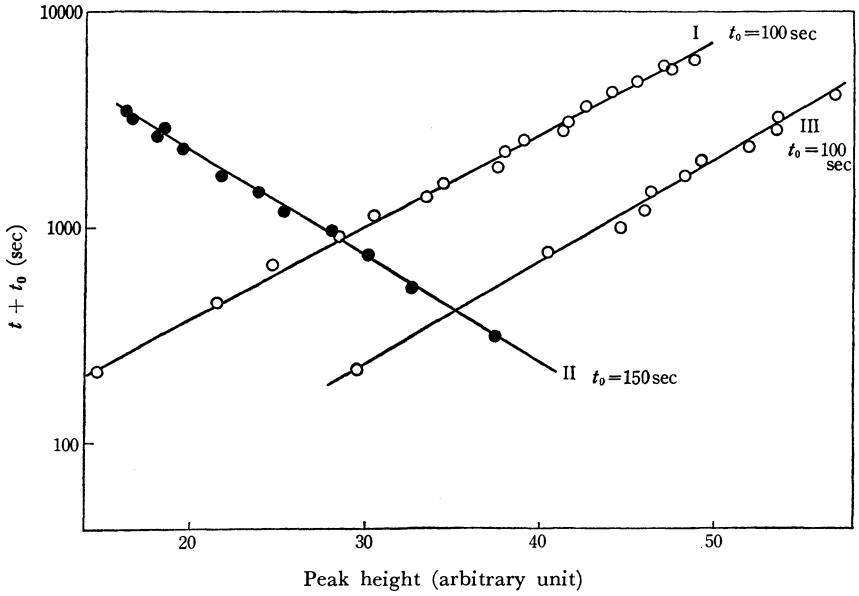

Fig. 9. Elovich plot (for C-PVP).
From the data of Fig. 6; Co/pyridine ring=1/160, at room temp.
I: the first oxygenation stage, P_{air}=1 atm
II: the first deoxygenation stage, P_{air}≒1 mmHg
III: the second oxygenation stage, P_{air}=1 atm

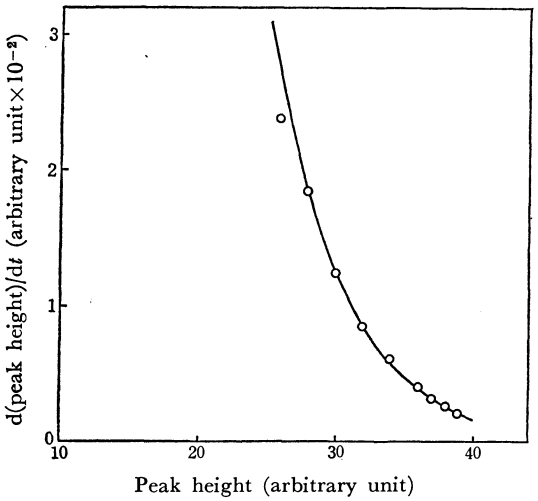

Fig. 10. The relation between the peak height and the first derivative of the peak height against contact time.
This example is the first oxygenation stage of B-1-PVP; the full line is calculated by the equation $\log(t + t_0) = av - b$, where, $t_0 = 0$, $a = 0.085$, $b = -0.055$; the particles are observed values.

the temperature than can be expected when the signal strength fits the Curie law (the ESR strength of a paramagnetic ion $\propto 1/T$). This perhaps indicates that the equilibrium is more declined to the dissociated state at higher temperatures.

Discussion

The ESR signals, shown in Figs. 1—3, can be considered for the following reasons to be caused by a 1 : 1 adduct of molecular oxygen with the cobalt complex. The signals are observed only when the cobalt complexes on PVP are exposed to oxygen. Even if a 1 : 2 adduct ($Co/O_2=2/1$) of molecular oxygen with the chelate is made, the adduct may be diamagnetic. In fact, bis-(salicylaldehyde)-ethylenediimine-cobalt(II) (which is paramagnetic) forms a 1 : 2 oxygen adduct which is diamagnetic, and di-(salicylal)-3,3′-diimino-di-*n*-propylamine-cobalt(II) (which is paramagnetic) forms a 1 : 1 oxygen adduct which is paramagnetic, in the solid state.[2] Apparently a 1 : 2 adduct can be identified as Co(III)-O_2^{-2}-Co(III) which has no free spin, while a 1 : 1 adduct can be schematically considered to be Co (III)-O_2^{-1} or Co(II)-O_2, and therefore paramagnetic (one unpaired electron).

All three ESR signals can be explained as apparently caused by a paramagnetic species which has three different g values (one g value is larger than the other two g values, which are almost equal to each other). The hyperfine structures were found only on the high-magnetic-field side in the cases of A-PVP and B-PVP. In the signal for C-PVP, the hf structures were a little clearer. The hf structures can be considered to be caused by the mononucleus cobalt atom ($I=7/2$). Only a few lines appeared, although eight lines were expected.

Table 1. The constants of Elovich equations

		a	b	c	d	t_0 (sec)
A-PVP	I	0.041	−2.291			400
	II			−0.086	4.984	200
	III	0.071	−0.914			200
	IV			−0.089	5.335	200
	V	0.110	+0.541			100
B-1-PVP	I	0.085	−0.055			~0
	II			−0.071	4.052	~0
	III	0.083	+0.548			~0
	IV			−0.064	4.483	~0
	V	0.106	+3.081			~0
C-PVP	I	0.043	−1.706			400
	II			−0.050	0.601	150
	III	0.048	−0.917			100

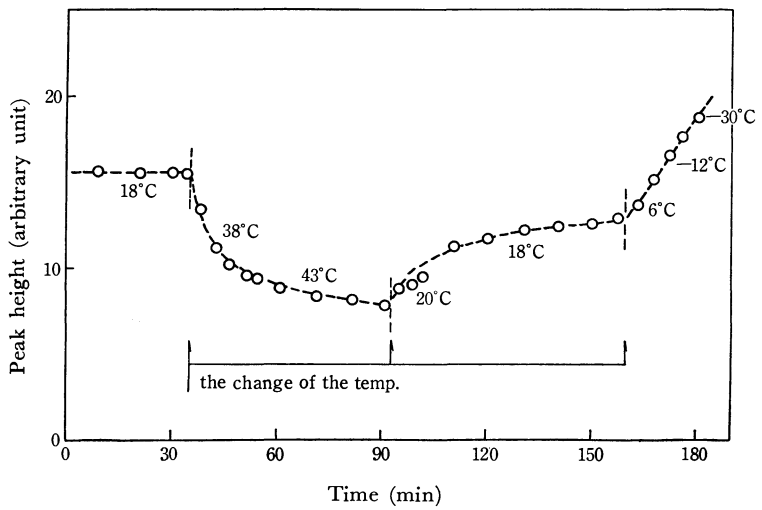

Fig. 11. The effect of the temperature (for A-PVP).
Co/pyridine ring=1/50, $P_{air}=1$ atm
The described temp. show the temp. of the atmosphere.

There could be two ways of analysing these ESR signals; one way is based on the electronic structure, Co(II)-O_2 (in this structure, the valence d electrons of cobalt are considered to localize in metal orbitals), while the other is based on the electronic structure, Co(III)-O_2^{-1} (in this structure, one of the valence d electrons of cobalt is considered to migrate in a molecular orbital of oxygen).

There are several low-spin cobalt(II) complexes, for example, cobalt(II) phthalocyanine,[8] $Co(CH_3NC)_5^{2+}$,[9] and $Co(CN)_5^{3-}$.[9] These low-spin cobalt(II) complexes have g values which are relatively close to 2 (for example, $g_{\parallel}=2.000$, and $g_{\perp}=2.117$ for $Co(CH_3NC)_5^{2+}$, and $g_{\parallel}=1.992$, and $g_{\perp}=2.157$ for $Co(CN)_5^{3-}$). In general, however, the A values caused by the cobalt atom of these complexes are relatively large (for example, $A_{\parallel}=87$ gauss, and $A_{\perp}=57$ gauss for $Co(CH_3NC)_5^{2+}$, and $A_{\parallel}=87$ gauss, and $A_{\perp}=28$ gauss for $Co(CN)_5^{3-}$). From a con-

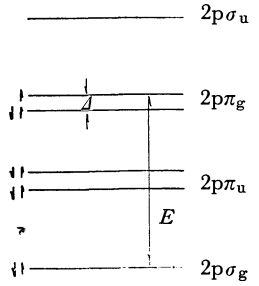

Fig. 12. Occupation of the electronic levels of O_2^- in the ground state.

8) J. M. Assour, *J. Am. Chem. Soc.*, **87**, 4701 (1965).
9) J. J. Alexander and H. B. Gray, *ibid.*, **89**, 3356 (1967); M. E. Kimball, D. W. Pratt and W. C. Kaska, *Inorg. Chem.*, **7**, 2006 (1968).

sideration of these reports, the Δ values of the adducts of oxygen with the chelates on PVP may be much larger than the approximately-estimated values if the electronic structure of the adduct is considered to be mainly Co(II)-O_2.

On the contrary, the method based on the Co(III)-O_2^{-1} electronic structure is more fruitful. The radical anion of molecular oxygen is analysed as having the following three different g values[10] (here, the Δ and E are illustrated in Fig. 12. g_e, λ and l have the ordinary meaning):

$$g_1 = g_e + 2(\lambda^2/\lambda^2 + \Delta^2)^{1/2}l$$

$$g_2 = g_e\left(\frac{\Delta^2}{\Delta^2+\lambda^2}\right)^{1/2} - (\lambda/E)\cdot\left[-\left(\frac{\lambda^2}{\lambda^2+\Delta^2}\right)^{1/2} - \frac{\Delta}{(\lambda^2+\Delta^2)^{1/2}} + 1\right]$$

$$g_3 = g_e\left(\frac{\Delta^2+\lambda^2}{\Delta^2}\right)^{1/2} - (\lambda/E)\cdot\left[\left(\frac{\lambda^2}{\lambda^2+\Delta^2}\right)^{1/2} - \frac{\Delta}{(\lambda^2+\Delta^2)^{1/2}} - 1\right]$$

When the oxygen molecule (as a radical anion) coordinates to the cobalt chelate (the structure is not clear now; for example, a structure in which the oxygen molecule coordinates to the cobalt chelate with its molecular axis oblique against the cobalt hf tensor is a common one for binuclear cobalt complexes bridged by molecular oxygen[11]), there may be some interaction between the antibonding $2p\pi$ orbital of oxygen and one of the d orbitals (perhaps d_{z^2}, though this identification is tentative) of the chelate. The larger interaction makes Δ larger. When the following values are assumed: $l=1$, $\lambda=226\ cm^{-1}$ (taken from atomic oxygen[10]) E is considered to be enough large to neglect λ/E, because the energy interval between $2p\pi_g$ and $2p\sigma_g$ (as one-electron orbitals) are calculated to be 2.25 Rydberg.[12]

The g values are to be calculated as follows:

$g_1 = 2.09$, $g_2 = g_3 = 2.00$, when $\Delta = 5000\ cm^{-1}$

$g_1 = 2.05$, $g_2 = g_3 = 2.00$, when $\Delta = 10000\ cm^{-1}$

These estimated values seem to agree roughly with the observed values. Moreover, only a small migration of the free spin into the metal orbitals may be sufficient to result in the observed hf structures, in which the Δ values are quite small, according to Kon and Sharpless.[13]

The rates of oxygenation and deoxygenation seem to obey the Elovich equation, at least in the earlier stages. Theoretically speaking, the Elovich equation can be derived when the rate of adsorption is determined by the reaction of gases and the adsorption sites, with, in general, one of the following conditions (1) or 2)) being satisfied:[14]

1) $N_s(E)/N_s$ = constant (heterogeneous surface)
   $N_s(E)$: the number of sites having E as the adsorption heat
   N_s: the total number of sites existing
2) $\varepsilon(\theta) = \varepsilon_0 - c\theta$ (homogeneous surface)
   θ: percentage covered
   $\varepsilon(\theta)$: adsortpion heat
   ε_0: constant
   $c\theta$: interaction energy between the adsorbed molecules

The chelates are perhaps coordinated on PVP in miscellaneous states. Also, small molecules such as methanol (which is used as the solvent in preparing the complex-polymer mixtures) may be left behind in the neighborhood of the chelates; then the adsorption heat on the chelate (the chelate with its neighborhood is considered to constitute the adsorption site) could be distributed over a wide range.

The constants of the Elovich equation seem not to be independent of the repeating number of the oxygenation-deoxygenation cycle. This may be the result of small changes in the structure of the adsorption site (for example, such molecules as methanol, which have been left behind in the neighborhood of the metal ion, though perhaps small in amount, may evaporate in the deoxygenation cycle), of the resulted changes in the adsorption heat distribution, and/or of some irreversible oxygenation. The stage of gas diffusion itself through the polymer film may have little effect on the changes of the constants.

It has been reported[13] that the ESR signal of the oxygen adducted to di-(salicylal)-3,3′-diimino-di-*n*-propylamine-cobalt(II) disappeared at lower temperatures in solution; this was attributed to the assumed dimerization of the cobalt(II)-oxygen adduct (paramag.) to yield cobalt(II)-oxygen-cobalt(II) (diamag.). However, the ESR signals on the mixtures investigated in the present paper did not disappear at lower temperatures. This may mean that the cobalt-oxygen adduct on the polymer does not dimerize to give cobalt-O_2-cobalt even at lower temperatures, because the chelates are fixed on hardly-moving polymer chains; this is perhaps the most important reason why the paramagnetic mononuclear cobalt-oxygen adduct is formed on the polymer.

10) W. Känzig and M. H. Cohen, *Phys. Rev. Lett.*, **3**, 509 (1959).
11) F. Basolo and R. G. Peason, "Mechanisms of Inorganic Reactions," Second Ed., John Wiley & Sons, Inc. (1967), p. 641.
12) T. Shimanouchi, "Kozo-kagaku Kogi-shiryo," Shokabo Co., Tokyo (1965), p. 35.
13) H. Kon and N. E. Sharpless, *Spectrosc. Lett.*, **1**, 49 (1968).
14) "Shokubai Kogaku Koza," Vol. 4, ed. by Y. Yoneda, Chijin Shokan Co., Tokyo (1964), p. 233; Ref. 7, p. 45; T. Keii, *Shokubai (Catalyst)*, **3**, 77 (1961).

Experimental

Reagents. *Poly-4-vinylpyridine (PVP).* Commercially-obtained 4-vinylpyridine was polymerized by copper acetate (the molecular weight was considered to be about 4000).[15] Found: C, 71.81; H, 7.32; N, 11.88%. Calcd for $(C_7H_7NO \cdot 0.67H_2O)_n$: C, 71.74; H, 7.18; N, 11.95%.

It was also polymerized by $K_2S_2O_8$ in water (the molecular weight was abut 50000).[16] Found: C, 76.88; H, 7.23; N, 12.43%. Calcd for $(C_7H_7NO \cdot 0.30H_2O)_n$: C, 76.05; H, 6.93; N, 12.67%.

These two polymers were found to have no detectable differences when used as chelate carriers.

Bis-(salicylaldehyde)-ethylenediimine-cobalt(II). This chelate was synthesized according to the litetrature[17] and was recrystallized from methanol. Found: C, 58.85; H, 4.08; N, 8.62%. Calcd for $C_{16}H_{14}N_2O_2Co$: C, 59.10; H, 4.30; N, 8.63% (Complex A).

Bis-(salicylaldimino)cobalt(II). This chelate was synthesized according to Endo.[18] At first as a dihydrate (Found: C, 50.94; H, 4.86; N, 7.91%. Calcd for $C_{14}H_{12}N_2O_2Co \cdot 2H_2O$: C, 50.16; H, 4.81; N, 8.36%); then it was dehydrated at 130°C for 2.5 hr *in vacuo*. Found: C, 56.18; H, 3.93%. Calcd for $C_{14}H_{12}N_2O_2Co$: C, 56.20; H, 4.04% (Complex B-1).

Also according to Yamada:[19] Found: C, 56.20; H, 4.13; N, 9.12, 9.43%. Calcd for $C_{14}H_{12}N_2O_2Co$: C, 56.20; H, 4.04; N, 9.36% (Complex B-2).

The infrared spectra of B-1 agreed with those of B-2. The B-1 and B-2 complexes showed no differences in the present experiments.

Di-(salicylal)-3,3'-diimino-di-n-propylamine-cobalt(II). This chelate was synthesized according to the literature[17] and was purified by reprecipitating it by water from an ethanol solution as a monohydrate. Found: C, 57.81; H, 6.21; N, 10.21%. Calcd for $C_{20}H_{23}N_3O_2Co \cdot H_2O$: C, 58.00; H, 6.09; N, 10.14% (Complex C).

Cobalt(II)-acetylacetone. This complex was obtained commercially and was used without further purification.

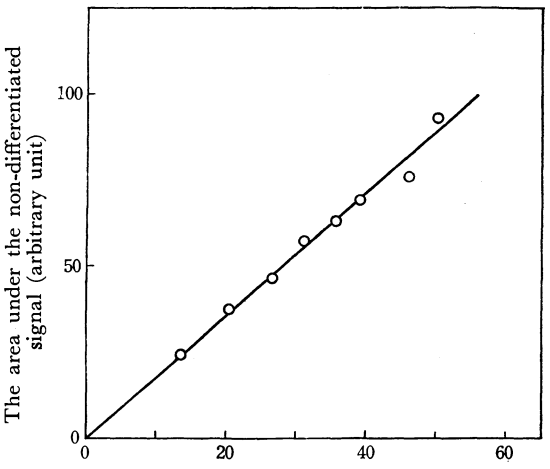

Fig. 13. The relation between the peak height of a first derivative signal and the area under the corresponding non-differentiated signal (in the case of B-1-PVP). Co/pyridine ring = 1/50, $P_{O_2} = 1$ atm.

Methanol. Commercial methanol was dehydrated by anhydrous calcium sulfate and was distilled under nitrogen.

Preparation of the Chelate-polymer Mixtures. These mixtures were made as thin, transparent films by mixing one of the complexes with PVP in methanol under nitrogen, and by then evaporating the solvent methanol.

ESR Measurements. The ESR spectra were observed with a Japan Electron Optics Laboratory Co., EPR spectrometer, Model JES-3BS-X (X-band). The value of the field strength was calculated from the observed signal of the manganese marker. The estimation of the *g* values were based on accurate measurements of the changes in field strength from the point of view of approximate calibration.

The relative amounts (arbitrary unit) of paramagnetic species of a given sample were measured as the peak heights of the first derivative signals, because the peak heights were found to be proportionate to the areas under the non-differentiated signal (Fig. 13), which are themselves considered to be proportionate to the amounts of paramagnetic species at a given temperature.

15) S. Tazuke and S. Okamura, *J. Polymer Sci.*, **A4**, 141 (1966).
16) P. F. Onyon, *Trans. Faraday Soc.*, **51**, 400 (1955).
17) R. H. Bailes and M. Calvin, *J. Am. Chem. Soc.*, **69**, 1886 (1947).
18) J. Endo, *Nippon Kwagaku Kwaisi (J. Chem. Soc. Japan)*, **65**, 424 (1944).
19) H. Nishikawa and S. Yamada, This Bulletin, **37**, 8 (1964).

BULLETIN OF THE CHEMICAL SOCIETY OF JAPAN VOL. 42 3478—3483 (1969)

Solvolysis of Organic Phosphates. II. Pyridylmethyl Phosphates as Effected by the Presence of Polyvalent Metal Ions*[1]

Yukito MURAKAMI and Makoto TAKAGI

Department of Organic Synthesis, Faculty of Engineering, Kyushu University, Hakozaki, Fukuoka

(Received May 23, 1969)

Influence of polyvalent metal ions on the hydrolysis of 2-, 3- and 4-pyridylmethyl phosphate was investigated at $\mu=0.10$ in a lower pH range. The thorium ion accelerated the hydrolysis rate of all the phosphates to a remarkable extent as investigated at 40, 70 and 90°C. The primary participation of the phosphate moiety of each pyridylmethyl phosphate in the interaction with thorium(IV) was considered to be the main cause of this catalysis. Thus, the thorium catalysis was mechanistically distinguished from the copper catalysis which has been clarified previously. In addition, the vanadyl ion also demonstrated positive catalytic effect. On the other hand, iron(III) and aluminum(III) retarded the hydrolysis rate. This was ascribed to the reduced fraction of the active monoionic species as a result of metal-complex formation with the phosphates in the course of hydrolysis.

The effect of metal ions on the hydrolytic reactions of phosphate monoesters is an interesting aspect of metal-ion catalysis, and has been the subject of a number of research groups.[1] However, previous investigations have not provided any satisfactory explanation for the reaction mechanism involved in the catalysis.

In continuation of our previous work[2] on the hydrolysis of the three isomeric pyridylmethyl phosphates, *i.e.*, 2-pyridylmethyl phosphate, 3-pyridylmethyl phosphate and 4-pyridylmethyl phosphate, the catalytic effects of polyvalent metal ions on these hydrolytic reactions were investigated in the present work. The hydrolysis of phenyl phosphate was also studied in the presence of some metal ions in an attempt to obtain an additional information on the catalytic reaction mechanism.

Experimental

Source of the organic phosphates and apparatus used in the present work have been described previously.[2] The stock solutions of metal ions were prepared from their nitrate salts, with the exception of vanadyl ion which was obtained as sulfate. These solutions were standardized by means of chelatometric titration.

Kinetic Measurements. The initial concentration of a substrate in solution was adjusted to 2×10^{-3} M and the ionic strength was maintained at 0.10 with an inorganic salt such as potassium nitrate, potassium chloride or sodium perchlorate. The rate of hydrolysis was determined by measuring the amount of inorganic phosphate liberated in the course of reaction. The pH-value of a solution was adjusted to a desired value by adding standard acid or base (0.1 N perchloric acid or 0.1 N sodium hydroxide). The experimental solution was made up to 100 m*l* in total volume and placed in a thermostated cell. After a desired temperature was attained, an aliquot sample (usually 2.5 m*l*) was taken out at an appropriate time interval and placed in a test tube. The tube was quickly cooled in cold water, and a specified volume (usually 2 m*l*) of the sample was pipetted into a 25-m*l* volumetric flask which contained a cold mixture of 60 % perchloric acid (2 m*l*) and water (15 m*l*). The whole solution was then kept in a refrigerator for some time before the subsequent colorimetric analysis of inorganic phosphate.

Analysis of Inorganic Phosphate. The analytical method employed for the analysis of phosphoric acid was essentially that of Allen.[3] To a mixture which contained a 2.0-m*l* sample of the experimental solution, 2 m*l* of 60 % perchloric acid and 15 m*l* of water in a 25-m*l* volumetric flask, 2.0 m*l* of amidol reagent (a 100 m*l* aqueous solution contained 1.0 g of amidol and 20 g of sodium bisulfite) and 1.0 m*l* of 8.3% aqueous ammonium molybdate were added in succession. The mixture was diluted to 25 m*l* with water, and then placed in a constant temperature bath at 25°C for 15—25 min to develop the blue color. The absorbance was measured at 720 mμ with a Shimadzu-Bausch & Lomb Spectronic 20 colorimeter immediately after development of the molybdenum blue color. The amount of inorganic phosphate was

*[1] Contribution No. 171 from the Department of Organic Synthesis, Faculty of Engineering, Kyushu University.

1) As reviews: H. Trapmann, *Arzneim.-Forsch.*, **9**, 341, 403 (1959); T. C. Bruice and S. J. Benkovic, "Bioorganic Mechanisms," Vol. II, W. A. Benjamin, Inc., New York, N. Y. (1966), Chapter 5; Y. Murakami, "Topics in Chelate Chemistry and Biochemistry," Special Publication No. 79 of *Kagaku no Ryoiki*, A. Nakahara, Ed., Nankodo, Tokyo (1967), pp. 153—188.

2) Y. Murakami and M. Takagi, *J. Am. Chem. Soc.*, **91**, 5130 (1969).

3) R. J. L. Allen, *Biochem. J. (London)*, **34**, 858 (1940).

determined by referring to a calibration curve established by the use of a standard KH_2PO_4 solution. Some of the metal ions were found to interfere with the phosphate analysis to some extent. The vanadyl ion has absorption in the 720 mμ range, and the observed absorbance had to be corrected for the presence of this metal ion. On the other hand, the ferric ion was found to decrease the absorbance of the molybdenum blue slightly through interaction with the molybdenum complex, while the thorium ion to increase it appreciably. Nevertheless, the interference of the ferric ion was of a negligible order under the present experimental conditions. The absorbance increase due to the presence of the thorium ion was corrected by establishing a relevant calibration curve. The presence of chelating agents employed in this work did not show any interference with the colorimetric determination of inorganic phosphate.

pH Measurements. Since the reaction temperature was so high (usually 90°C), the glass electrode could not demonstrate a sufficiently linear response to the pH values established by standard buffers[4] over the pH range studied. Thus, calibration of the electrode system was performed by dividing the whole pH range into three parts: pH 1.0—4.2, oxalate and phthalate buffers; pH 4.2—6.9, phthalate and phosphate buffers; pH above 6.9, phosphate and borate buffers. Since the glass electrode was not durable for prolonged use at elevated temperatures in a relatively high pH range (above 6), particularly in the presence of metal ions, the electrode membrane had to be reactivated rather often by treating with aqueous ammonium fluoride. However, careful operation made it possible to achieve the pH reproducibility within ±0.01. The pH meter was calibrated before and after each kinetic run, and the pH variation was usually controlled within ±0.03.

pH-Values obtained from the procedure described above need to be converted into hydrogen ion concentrations. Thermodynamic data for weak electrolytes, which make the conversion of pH into hydrogen ion concentration possible, are not available at present. Thus, a conventional method was employed in this work: the pH values of aqueous perchloric acid of known concentrations were measured at an ionic strength of 0.10 to determine the apparent activity coefficient. The apparent activity coefficient thus obtained was used over the whole pH range. The following relation holds at 80°C and $\mu=0.10$.

$$-\log [H^+] = pH - 0.09$$

Results

Polyvalent Metal Catalysis. With a 1 : 1 molar ratio of substrate to metal ion, the hydrolysis reactions of pyridylmethyl phosphates were studied at 90°C and the ionic strength of 0.10. In general, metal ions of tervalence or higher are far more susceptible to hydrolysis than bivalent metal ions. Thus, the choice of conditions for the homogeneous catalytic reaction is often restricted. The reaction followed first-order kinetics with respect to unreacted substrate species in most cases. When deviation from the first-order rate law was extreme, the apparent rate constants were evaluated from the initial stage of hydrolysis. The results for aluminum-ion and the vanadyl-ion catalysis are listed in Table 1. The equimolar existence of the aluminum ion reduces the hydrolysis rates of pyridylmethyl phosphates into about half of the corresponding spontaneous rates at $-\log[H^+]\approx 2.5$, regardless of the type of the phosphate isomers. This retardation effect is pH-dependent and is not noticeable in a lower pH region as shown in Table 1. The presence of a ligand capable of coordinating to metal ion, nitrilotriacetic acid in this case, tends to restore the rate to the spontaneous one.

The ferric ion yielded a similar catalytic effect

Table 1. Effects of aluminum and vanadyl ions on the hydrolysis of pyridylmethyl phosphates at 90.0±0.1°C and $\mu=0.10$ ($HClO_4$-$NaClO_4$)[a]

Phosphate	Metal ion	$-\log[H^+]$[b]	k, hr^{-1}	$(k/k_0)\times 100$[e]
2-Pyridylmethyl	Al^{3+}	1.06	0.055	96
		1.91	0.068	87
		2.46	0.046	57
		2.47	0.078[c]	98
	VO^{2+}	1.06	0.058	101
		1.93	0.081	103
		2.67	0.20[d]	250
3-Pyridylmethyl	Al^{3+}	2.47	0.019	58
4-Pyridylmethyl	Al^{3+}	2.47	0.019	56

a) $T_E=2.00\times 10^{-3}$ M, $T_M/T_E=1$ where T_E and T_M stand for the total molar concentration of the substrate species and of the metal ion, respectively.
b) Variation within±0.01.
c) NTA present, $T_M/T_L=1$ where T_L stands for the total molar concentration of the ligand.
d) Deviation from the first-order rate law is large.
e) k_0, spontaneous hydrolysis rate.

4) Four standard buffers, oxalate, phthalate, phosphate and borate buffers, were prepared in accordance with JIS (Z8802-1964).

as observed for the aluminum-ion catalysis under the same experimental condition. As an example, the presence of equimolar amounts of the ferric ion and 2-pyridylmethyl phosphate at 90°C and $\mu=0.10$ resulted in the reduction of hydrolysis rate to 65 % and 53 % of the corresponding spontaneous rates at $-\log[H^+]=1.04$ and 1.89, respectively.

A survey on the catalytic effects of other tervalent metal ions, *i.e.*, indium, lanthanum and cerium, revealed that the tendency of precipitate-formation was remarkable. Thus, the metal-ion catalysis was investigated in an acidic region ($-\log[H^+]=1-2$). The results indicate these metal ions were inactive in this low pH region. For example, in the presence of equimolar amounts of lanthanum(III) and 2-pyridylmethyl phosphate the hydrolysis rates of the phosphate at 90°C were 100 % and 99 % of the corresponding spontaneous ones at 1.06 and 1.91 in $-\log[H^+]$, respectively. The first-order rate law holds in both cases. However, in the latter, the first-order kinetics was disturbed after some precipitates were produced during the course of hydrolysis.

Among other polyvalent metal ions, the uranyl ion revealed the distinct tendency to form precipitates with the substrates. Thus, no reasonable experiment was carried out. On the other hand, the vanadyl ion showed an appreciable catalytic effect in promoting the hydrolysis of 2-pyridylmethyl phosphate even in a relatively low pH range as shown in Table 1. It should be noted that the hydrolysis at $-\log[H^+]=2.67$ did not follow first-order kinetics, and was accelerated with the progress of the reaction. Such an acceleration effect was observed only with the vanadyl ion, although the cause of this phenomenon is not obvious at present. Meanwhile, whenever a deviation from the first-order plots was observed in other metal-ion-effected hydrolysis of pyridylmethyl phosphates, the reaction rate was invariably decelerated and the rate plot appeared below the initial first-order rate curve.

Thorium(IV) Catalysis. The hydrolytic behavior of pyridylmethyl phosphates in the presence of the thorium ion at 90°C and $\mu=0.10$ is shown in Fig. 1. The reaction rates were so rapid that the hydrolysis proceeded to a considerable extent before thermal equilibrium was attained. It seems that the excessive enhancement of the catalytic reaction rate is reduced by the decrease of the concentration of catalyst species. However, the relative deficiency of the thorium ion ($T_M/T_E<1$) resulted in precipitate-formation even in a strongly acidic region (pH$\approx$1) at the beginning or during the course of reaction. This is most likely due to the complex formation between thorium(IV) and the substrate species.

In order to study the catalytic effects in more detail, the hydrolysis of 2- and 3-pyridylmethyl phosphate was also investigated at lower temperatures, and the results are shown in Figs. 2, 3 and

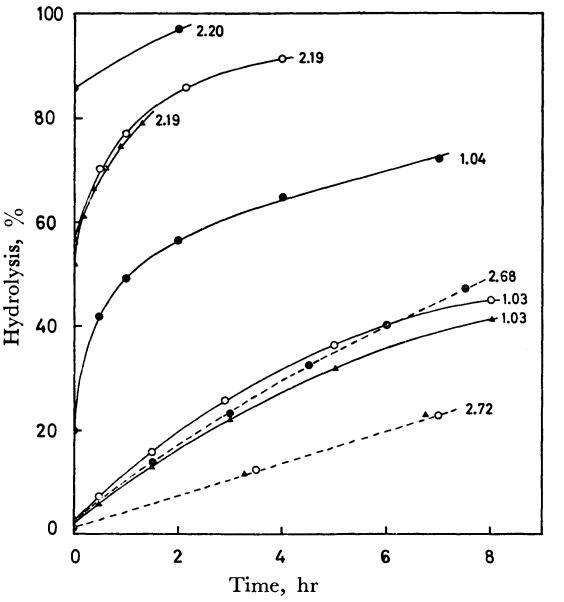

Fig. 1. Hydrolysis of pyridylmethyl phosphates in the presence of thorium(IV) ion: 90.0±0.1°C, $\mu=0.10$ ($HClO_4$-$NaClO_4$), $T_E=2.00\times10^{-3}$ M, $T_M/T_E=1$; ●, 2-isomer; ○, 3-isomer; ▲, 4-isomer; the broken lines indicates the spontaneous hydrolysis at their maximum rate; number refers to $-\log[H^+]$ value. First sampling was made 15—19 min after the solution was introduced into the reaction vessel (time=0).

4. As the pH value of the system was raised, an increasing tendency of precipitate-formation was observed. However, when the amount of precipitates was small, they disappeared gradually as hydrolysis proceeded to a certain extent. Thus, precipitates formed at the initial stage seem to be a thorium complex of the substrate. As the rate plots in Figs. 2 and 4 indicate, the hydrolysis curve tends to level off after a certain period of time. As shown in Figs. 2 and 3, the thorium-ion catalyzed hydrolyses of 2- and 3-pyridylmethyl phosphate reach their maximum rate at around pH 2.7 and slow down as the pH of the system departs from this optimum value. This fact suggests that essentially the same catalytic process is operative for these substrates, although the rate-promoting effect of the thorium ion for the hydrolysis of the 2-isomer was found to be considerably greater than that for the hydrolysis of the 3-isomer. The catalytic reaction rates at 40°C ($T_M/T_L=1$, Fig. 4) are now compared with the corresponding spontaneous rates, which were calculated by the aid of activation energies evaluated previously, in terms of the required reaction time to carry out 30 % hydrolysis. The $-\log[H^+]$ value of 2.7 was selected for this comparison, since the maximum rates were observed both in the presence and in the absence of thorium: 2-isomer, 2300 hr (spontaneous), 0.8 hr (catalytic); 3-isomer, 7000 hr (spontaneous), 8.5 hr (catalytic).

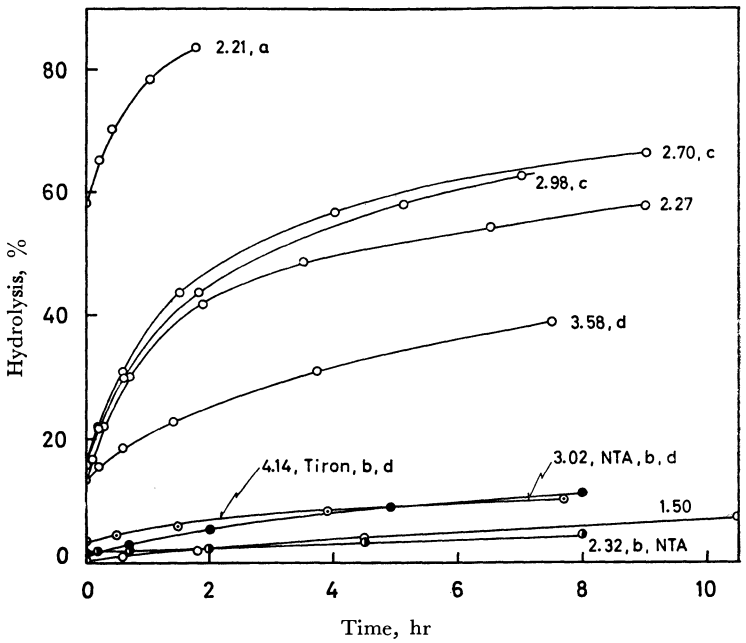

Fig. 2. Hydrolysis of 2-pyridylmethyl phosphate in the presence of thorium(IV) ion and its chelates: 40.0±0.1°C, μ=0.10 ($HClO_4$-$NaClO_4$), $T_E=2.00\times10^{-3}$ M, $T_M/T_E=1$; *a*, 70°C; *b*, $T_M/T_L=1$; number refers to $-\log[H^+]$ value. In some cases, precipitation was observed at the initial stage (*c*) or throughout the reaction (*d*). First sampling was made 15 min after the solution was introduced into the reaction vessel (time=0).

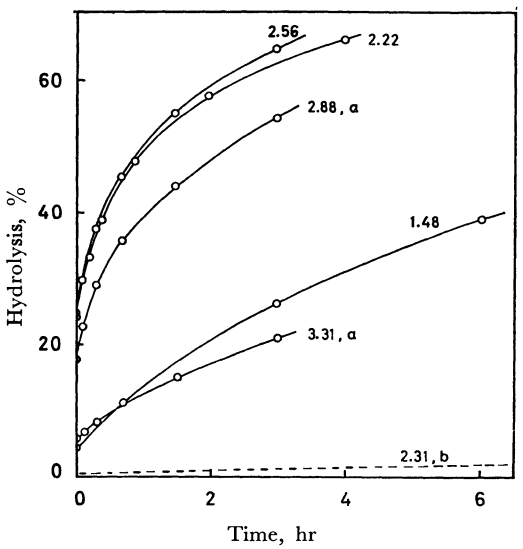

Fig. 3. Hydrolysis of 3-pyridylmethyl phosphate in the presence of thorium(IV) ion: 70.0± 0.1°C, μ=0.10 ($HClO_4$-$NaClO_4$), $T_E=2.00\times10^{-3}$ M, $T_M/T_E=1$; a, precipitates exist; b, spontaneous hydrolysis ; number refers to $-\log[H^+]$ value. First sampling was made 15 min after the solution was introduced into the reaction vessel except the run at 1.48 and the spontaneous one at 2.31 in $-\log[H^+]$ value, where 23 min was taken instead (time = 0).

Thus, the catalytic effect of the thorium ion is striking, and the observableh ydrolysis is entirelydue to the catalytic process in the low temperature range.

The catalytic effect of the thorium ion in these hydrolysis reactions diminished when a certain kind of chelating agent was present (Fig. 2). This is probably due to the so-called masking effect of these ligands on the thorium ion, so that the affinity of the metal ion toward the substrate species was considerably reduced. The thorium-ion catalysis did not follow simple kinetic laws after all.

Hydrolysis of Phenyl Phosphate. The hydrolysis of phenyl phosphate was studied at 80°C and the ionic strength of 0.10 in aqueous media in the presence of metal ions as listed in Table 2. It should be noted that all the bivalent metal ions listed in this table tend to retard the hydrolysis rate. This is even more marked with the vanadyl and the aluminum ion, and particularly with the ferric ion. In the ferric-ion catalysis, the reaction followed first-order kinetics fairly well up to 20 % hydrolysis of the substrate initially present, but deviated from this significantly thereafter.

The thorium ion produced some insoluble precipitates of unknown character with phenyl phosphate over the wide pH range even in the presence of some chelating agents, *e.g.*, NTA or Tiron. Thus, the hydrolysis reaction in the presence of the thorium ion was inadequate for study in a homo-

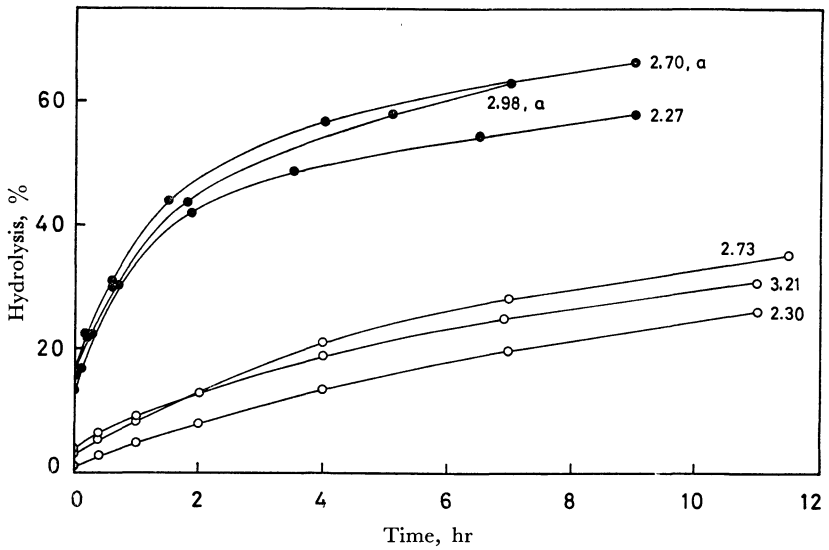

Fig. 4. Hydrolysis of pyridylmethyl phosphates in the presence of thorium(IV) ion: 40.0± 0.1°C, μ=0.10 ($HClO_4$-$NaClO_4$), $T_E=2.00\times10^{-3}$ M, $T_M/T_E=1$; ●, 2-isomer; ○, 3-isomer; *a*, precipitates were noticed at the initial stage; number refers to $-\log[H^+]$ value. First sampling was made 15 min after the solution was introduced into the reaction vessel. (time=0).

Table 2. Effects of metal ions on the hydrolysis of phenyl phosphate at 80.0±0.1°C and μ=0.10[a,b]

Metal ion	$-\log[H^+]$	k, hr^{-1}	k_0, hr^{-1}	$(k/k_0)\times100$	Ref.
Fe^{3+}	1.01±0.01	0.0233	0.0488	47.7	This work
Al^{3+}	1.02±0.01	0.0449	0.0495	90.7	This work
VO^{2+}	2.67±0.02	0.0990	0.1062	93.2	This work
Cu^{2+}	3.62±0.01	0.1069	0.1088	98.3	2
Zn^{2+}	4.05±0.02	0.1076	0.1083	99.4	2
Co^{2+}	4.55±0.02	0.1052	0.1060	99.2	2
Ni^{2+}	4.56±0.03	0.1050	0.1059	99.2	2
Mg^{2+}	4.61±0.03	0.1036	0.1055	98.2	2

a) $T_E=2.00\times10^{-3}$ M, $T_M/T_E=1$.
b) Supporting electrolyte: below $-\log[H^+]=2.67$, $HClO_4$-$NaClO_4$; above $-\log[H^+]=2.67$, KNO_3.

geneous system.

Discussion

The ferric and the aluminum ion gave retardation effect to the hydrolysis of phenyl phosphate. These metal ions may form the corresponding phenyl

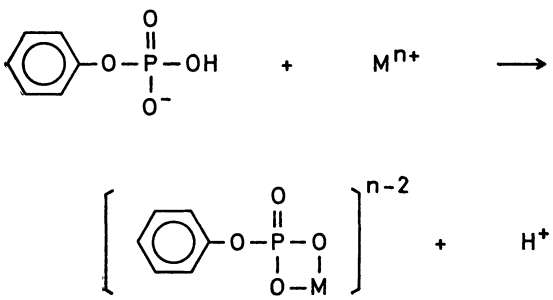

phosphate complexes due to the following reaction. Judging from the stability constants of metal complexes formed with inorganic phosphate (PO_4^{3-}),[5] tervalent metal ions would give much more stable metal complexes of simple organic phosphate, such as phenyl phosphate, than bivalent metal ions. Thus, the complex-formation may proceed to a certain extent even in an acidic region (pH≈1), where the metal complex is supposed to be inert, and the concentration of the active monoionic species is reduced as a result. Since iron(III) and aluminum(III) do not show significant affinity toward *N*-donor atom in general,[5] these metal ions would interact with pyridylmethyl phosphates at the phosphate group even in the case

5) L. G. Sillén and A. E. Martell, "Stability Constants of Metal-Ion Complexes," Special Publication No. 17, the Chemical Society, London (1964).

of the 2-isomer. Thus, the same explanation can be given for the retarded hydrolysis rate of pyridylmethyl phosphates, regardless of metal species.

Of all other metal ions, the thorium ion promoted the hydrolysis of the present phosphates to the greatest extent. Nevertheless, no simple kinetic law can be applied to this system. Since the catalytic effect does not show large isomer-dependency, the primary catalytic process must involve interaction between thorium(IV) and the phosphate moiety of the substrates. Large stability constants obtained for the thorium-phosphate complexes may provide a sound basis for this discussion.[6] In addition, the hydrolysis rate reached its maximum at $-\log[H^+]\approx 2.7$, where the corresponding spontaneous hydrolysis also attained the maximum rate. This suggests that the substrate undergoes interaction with thorium(IV) in its zwitterion form. In spite of the primary participation of the phosphate moiety in the thorium-ion catalysis, the ring-nitrogen may be involved in the interaction with the metal ion in the hydrolysis of 2-pyridylmethyl phosphate since the highest acceleration effect on the rate was obtained with the 2-phosphate.

Bamann, Trapmann and their coworkers have studied in recent years the hydrolytic behavior of some phosphate monoesters in the presence of quadrivalent metal ions.[7-13] Quadrivalent titanium, zirconium, hafnium and thorium were found to show catalytic activity in an acidic region and the effect of thorium was the greatest. According to their work, solvolysis was accelerated several hundred times in most cases due to the presence of thorium ion, and the reaction rate was observed to be very rapid at the initial stage followed by leveling-off after a while. In spite of the fact that their experimental conditions are not directly comparable with ours, the catalytic pathway, which would elucidate the present thorium-ion catalysis, may also be applied to their system.

Meanwhile, in the hydrolysis of α-D-glucose-1-phosphate[14] the thorium ion retarded the hydrolysis rate in an acidic region below $-\log[H^+]\approx 2$ and the positive catalytic effect was observed above $-\log[H^+]=2.7$. Thus. the thorium-ion catalysis depends upon the structure of an alcoholic residue of a selected phosphate and also on the corresponding spontaneous reaction mechanism.

In our previous work,[2] the copper ion was found to promote the reaction rate of 2-pyridylmethyl phosphate to a significant extent in a $-\log[H^+]$ range above 3.3, while the same metal ion did not show any meaningful catalysis for other pyridylmethyl phosphates. The particular copper complex formed with the 2-isomer in the transition state, where the chelate ring involves both pyridyl nitrogen and ester oxygen as donor atoms, was postulated in order to elucidate the enhanced catalytic effect. On the other hand, the thorium complexes of the present substrates were not well characterized under present experimental conditions. Thus, presentation of an acceptable catalytic mechanism is not possible at present. The thorium-ion promoted hydrolysis seems to be much different from the corresponding copper-ion-effected reaction in respest of their catalytic mechanisms.

6) E. L. Zebroski, H. W. Alter and F. K. Heumann, *J. Am. Chem. Soc.*, **73**, 5646 (1951).

7) E. Bamann, H. Trapmann, J. Riehl, A. Gerl and B. Oechsner, *Arch. Pharm.*, **296**, 174 (1963).

8) E. Bamann, A. Gerl, B. O. Oechsner, J. Riehl and H. Trapmann, *Naturwissenschaften*, **47**, 106 (1960).

9) E. Bamann, H. Trapmann and H. J. Krauss, *Arch. Pharm.*, **295**, 330 (1962).

10) E. Bamann, H. Trapmann and B. Oechsner, *ibid.*, **295**, 663 (1962).

11) H. Trapmann and M. Devani, *ibid.*, **298**, 253 (1965).

12) H. Trapmann and M. Devani, *ibid.*, **298**, 497 (1965).

13) H. Trapmann and M. Devani, *Hoppe-Seyler's Z. Physiol. Chem.*, **340**, 81 (1965).

14) Y. Murakami and M. Tanaka, This Bulletin, **39**, 122 (1966).

BULLETIN OF THE CHEMICAL SOCIETY OF JAPAN VOL. 42 3484—3487 (1969)

Reactions of Metal Chelates. IV.[1] The Reactions of Bis(salicylaldehydato)-copper(II) with Diethylenetriamine and Triethylenetetramine

Yasuo NAKAO and Akitsugu NAKAHARA

Institute of Chemistry, College of General Education, Osaka University, Toyonaka, Osaka

(Received May 30, 1969)

The reactions of bis(salicylaldehydato)copper(II) with diethylenetriamine and triethylenetetramine were investigated under several different conditions. In water, in the absence of other reagents, the reactions gave uncharged bis(salicylaldehyde)-diethylenetriamine- and -triethylenetetramine-copper(II), respectively. In the presence of an acid the resulting complexes were the respective cation complexes, in which only one of the two terminal nitrogen atoms was in the form of Schiff base with salicylaldehyde. In the presence of a salt, the resulting complex from diethylenetriamine was a cation complex, and that from triethylenetetramine an uncharged complex. Three new copper(II) chelates were obtained.

It was reported by Sarma and Bailar[2] that bis(salicylaldehydato)copper(II) reacts with triethylenetetramine to give bis(salicylaldehyde)triethylenetetraminecopper(II), (IV), in which the two terminal nitrogen atoms of the original triethylenetetramine molecule link to copper(II) in the form of Schiff base, whereas the other two imine-nitrogen atoms are free from coordination. However, we have recently found that the same reaction, under somewhat modified conditions, produces an entirely different chelate, (V), as indicated in Fig. 1. The reaction of complex (I) with diethylenetriamine (instead of triethylenetetramine) was found to proceed differently according to the conditions. The present paper deals with the results of reactions between bis(salicylaldehydato)copper-(II), I, and diethylenetriamine or triethylenetetramine under three different conditions: (1) the reaction in water in the absence of other reagents; (2) the reaction in the presence of various salts such as sodium perchlorate, nitrate, bromide or chloride; (3) the reaction in the presence of some acids such as perchloric, nitric, hydrobromic or hydrochloric acid. In most cases, resulting chelates were isolated. The structures of these complexes have been confirmed from elemental analyses and spectrophotometric measurements. For the systems where isolation of the reaction products was very difficult, the electronic spectra of reaction solutions were measured. The structure of complexes produced in solutions has been concluded also from the spectral data. All the results are schematically presented in Fig. 1.

1) Part III of this series of papers: This Bulletin, **42**, 1297 (1969).

2) B. D. Sarma and J. C. Bailar, Jr., *J. Am. Chem. Soc.*, **77**, 5476, (1955).

The Reaction of Bis(salicylaldehydato)copper(II), I, with Diethylenetriamine. The reaction of complex I in water with diethylenetriamine in the absence of other reagents gave an olive-green crystalline powder, whereas the same reaction in the presence of sodium perchlorate, bromide or nitrate gave violet crystals. The olive-green complex was found to have the structure (II) in Fig. 1, by taking into account the results of elemental analyses and the quadri-coordinating character of copper(II) complexes. As is clear from the structural formula, II, the two terminal amino groups of diethylenetriamine link to copper(II) in the form of Schiff base with salicylaldehyde, while the central imine-nitrogen is free from coordination. The complex is, therefore, an uncharged neutral molecule. The absorption maximum for the d–d band of the complex II was observed at 570 mμ.

Inspection of the infrared spectra of the violet crystals obtained from the system containing perchlorate or nitrate reveals the band characteristic of perchlorate or nitrate in the region between 1100 and 1380 cm^{-1} (Fig. 2). An aqueous solution of the violet crystal obtained from the system containing bromide ion gives the white precipitate by the addition of a solution of silver nitrate, which indicates the existence of bromide ion as the external ion of the complex. Thus the structure of these violet chelates has been concluded as III in Fig. 1. The results of elemental analyses of these perchlorate, nitrate and bromide complexes also supported the above conclusion. In the case of the chloride of the same complex, it was necessary to concentrate the reaction solution because of its comparatively high solubility in order to isolate the crystals. The absorption maximum in the visible region of the four violet complexes (chloride, bromide, nitrate and perchlorate) always appears at 570 mμ. In

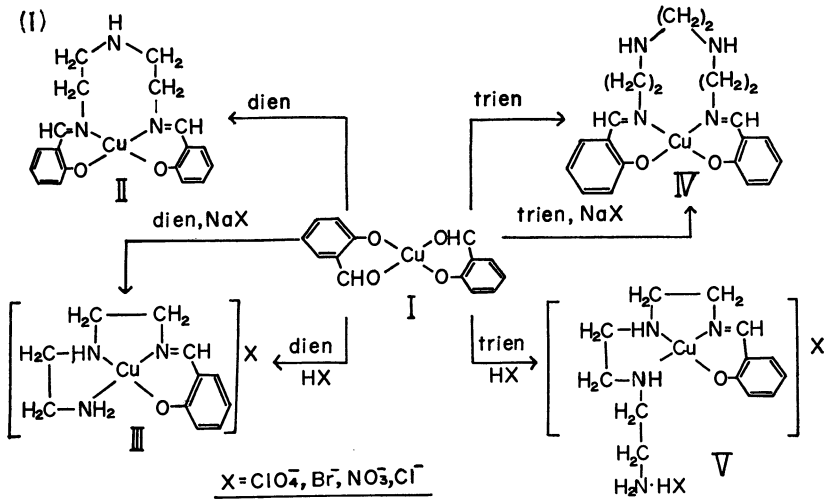

Fig. 1. The Reactions of bis(salicylaldehydato)copper(II) with diethylenetriamine and triethylenetetramine.

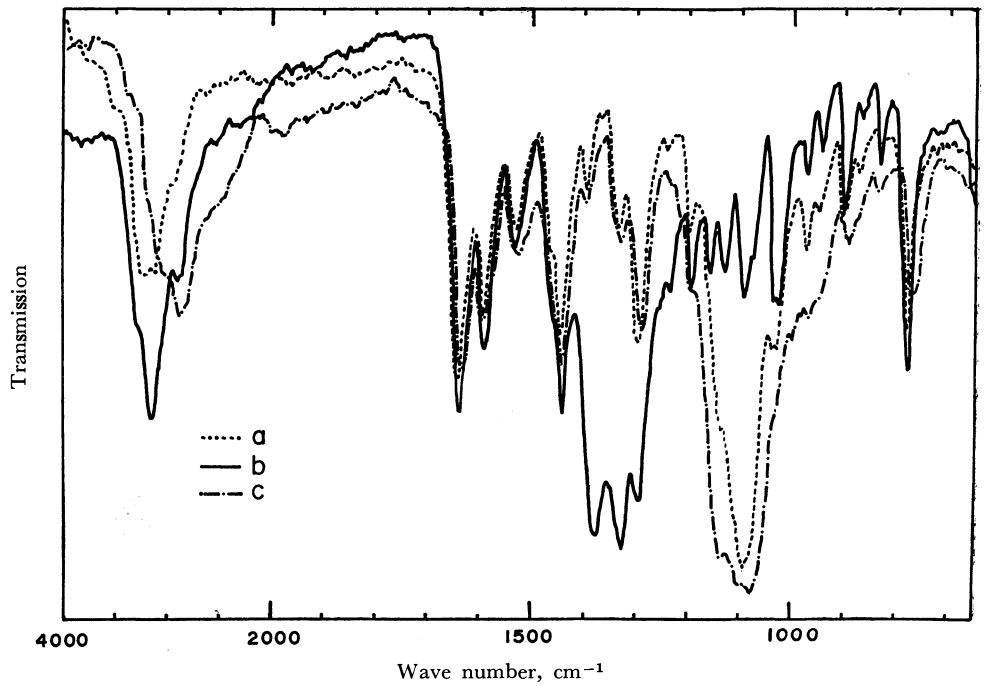

Fig. 2. Infrared spectra of a, [Cu salal=dien]$ClO_4 \cdot H_2O$; b, [Cu salal=dien]$NO_3 \cdot H_2O$; c, [Cu salal=trienH]$(ClO_4)_2$.

spite of their widely different color in the crystalline state, complexes II and III reveal no great difference as far as the d-d band is concerned. However, a considerable difference was observed in the absorption bands in the near ultraviolet region. It is to be noted that chelate III obeys Beer's law even in the concentration of 5×10^{-3} to 5×10^{-5} M, whereas chelate II does not in such a dilute solution. It has been confirmed by infrared study that the resulting chelate from the reaction of complex I with diethylenetriamine in acidic solution is identical with chelate III. These results suggest that the 6-5-5*1 fused-chelate-ring is so stable that only the presence of some anions favors its formation, instead of the complex of the less stable 6-8-6 fused-chelate-ring structure, II.

*1 The abbreviation 6-5-5 indicates the fused-chelate-ring structure containing six-, five-, and five-membered ring in counter-clockwise direction.

The Reaction of Bis(salicylaldehydato)copper(II), I, with Triethylenetetramine. In this reaction the product was a bluish green complex, regardless of the absence or presence of salts. As is clear from the structural formula IV, triethylenetetramine is coordinated around copper(II) only through the two terminal nitrogen atoms which are in the form of Schiff base with salicylaldehyde. The complex is, therefore, identical with that reported by Sarma and Bailar[2]. On the other hand, the resulting compound from the reaction in an acidic solution was a cation complex as indicated in (V), in which one terminal amino group was in the form of Schiff base and the other terminal amino nitrogen was in the form of quaternary ammonium salt. Hence the complex has a 6-5-5 fused-chelate-ring structure. The infrared spectrum of the perchlorate of chelate V is shown in Fig. 2. Though the chelate of type V was successfully isolated as perchlorate, its nitrate, bromide or chloride could not be isolated. However, the spectrophotometric investigation of the latter solutions enabled us to conclude the formation of the same type complex cations in each case. In other words, the visible and ultraviolet absorption spectra of these reaction solutions have been disclosed to be more similar to that of V than that of complex IV. Thus in the case of triethylenetetramine, the tendency for producing the 6-5-5 fused-chelate-ring structure seems to be characteristic of the presence of acid, and is in marked contrast with the case of diethylenetriamine. In the latter case, the 6-5-5 fused-chelate-ring structure was produced even by the presence of a neutral salt instead of acids. It is interesting to note that there is a delicate difference between diethylenetriamine and triethylenetetramine in the way of chelate-formation.

Experimental

Bis(salicylaldehydato)copper(II) was prepared according to the direction described in the first paper of this series.[3]

The Preparation of Copper(II) Chelate, II. To a 3.1 g (0.01 mol) of bis(salicylaldehydato)copper(II) in 20 m*l* of water was added 0.9 g (0.01 mol) of diethylenetriamine in 10 m*l* of water. The mixture was stirred at 25°C for about half an hour. After it had been filtered, the solution was evaporated to dryness *in vacuo* to give an olive-green powder. The powder was recrystallized from ethanol containing a small volume of water. Found: C, 55.19; H, 5.05; N, 10.97%. Calcd for $[Cu(C_{13}H_{19}N_3O_2)]\cdot H_2O$: C, 55.31; H, 5.38; N, 10.76%.

The Preparation of the Perchlorate, Nitrate or Bromide of Chelate, III. To a mixture of 0.01 mol each of bis(salicylaldehydato)-copper(II) and diethylenetriamine in 30 m*l* of water was added 0.01 mol of sodium perchlorate, nitrate or bromide. The reaction mixture was stirred at 25°C for about half an hour. After it had been cooled, a small violet crystal was deposited from the solution. This was filtered by suction, and was recrystallized from water. Analytical data of the complexes are given in Table 1.

The Preparation of Chloride of Chelate, III. An almost same procedure as that described above was applied. Since the corresponding violet crystal could not be separated only by allowing the solution to stand, the reaction mixture had to be evaporated to dryness *in vacuo*. The crystalline powder thus obtained was recrystallized from aqueous ethanol. This compound can be prepared by the following method. The mixture of 0.01 mol each of bis-(salicylaldehydato)copper(II), diethylenetriamine and sodium chloride in 30 m*l* of water was adjusted to pH 3—5 by hydrochloric acid. The mixture was stirred at 25°C for half an hour, and a dark blue solution was obtained. After it had been filtered, the filtrate was evaporated to dryness *in vacuo* to give a dark blue powder. Recrystallization of this powder was performed by using aqueous ethanol. The result of elemental analysis is shown in Table 1.

The Reaction between Bis(salicylaldehydato) copper(II) and Diethylenetriamine in Acidic Media. The mixture of 0.01 mol each of bis(salicylaldehydato)copper(II) and diethylenetriamine in 30 m*l* of water was adjusted to pH 3—5 by perchloric, nitric, hydrobromic, or hydrochloric acid. The reaction mixture was stirred at 25°C for half an hour. A violet crystalline product was deposited from the solution except for the case in which hydrochloric acid was used. The crystals were respectively identified as perchlorate, nitrate or bromide of cation complex, III, from their infrared spectra. In the case of chloride of III, visible and ultraviolet absorption spectrum of the reaction solution was measured.

The Preparation of Copper(II) Chelate, IV. Though this compound has already been reported by Sarma and Bailar,[2] a similar procedure as for complex II, was adopted.

The Preparation of the Perchlorate of Chelate, V. The mixture of 0.01 mol each of bis(salicylaldehydato)-copper(II) and triethylenetetramine in 30 m*l* of water

TABLE 1. ANALYTICAL DATA OF [Cu salal=dien]X

Compound	C, %		H, %		N, %	
	Calcd	Found	Calcd	Found	Calcd	Found
$[Cu\ salal{=}dien]ClO_4\cdot H_2O$	34.11	34.07	4.65	4.55	10.85	10.37
$[Cu\ salal{=}dien]NO_3\cdot H_2O$	37.77	37.94	5.15	5.08	16.02	15.90
$[Cu\ salal{=}dien]Br\cdot H_2O$	35.92	36.04	4.90	4.93	11.43	11.38
$[Cu\ salal{=}dien]Cl\cdot H_2O$	40.87	40.95	5.57	5.74	13.00	12.43

3) A. Nakahara, K. Hamada, I. Miyachi and K. Sakurai, This Bulletin, **40**, 2826 (1967).

was adjusted to pH 3—5 by dilute perchloric acid. After it had been stirred at 25°C for about half an hour, the reaction mixture was filtered by suction. A red-violet crystal was deposited, and this was recrystallized from water.

Found: C. 30.65; H, 4.19; N, 10.44 %. Calcd for $[Cu(C_{13}H_{21}N_4OHClO_4)]ClO_4$: C, 30.47; H, 4.30; N, 10.94%.

The Reaction between Bis(salicylaldehydato)-copper(II) and Triethylenetetramine in the Presence of Sodium Perchlorate, Nitrate, Bromide or Chloride. The reactions were carried out in the same way as for chelate III. Each product was identified as the chelate IV from infrared spectrum.

The Reaction between Bis(salicylaldehydato)-copper(II) and Triethylenetetramine in Acidic Media. A similar procedure as for bis(salicylaldehydato)copper(II) with diethylenetriamine in acidic media was adopted. A red-purple crystal was separated only from the system using perchloric acid, but not in the other cases. However, the structure of the complex in each reaction was verified as IV from their absorption spectra.

Measurements

The measurements of visible and ultraviolet absorption spectra were made with a Shimadzu Spectrophotometer QR-50. The infrared spectra were recorded with a Hitachi EPI-2 infrared spectrophotometer. The measurements were carried out at room temperature using the pressed potassium bromide disk technique in the wave number range from 700 to 4000 cm^{-1} with a rock-salt prism.

The authors wish to thank Miss Yoshiko Komuro for the elemental analysis and the Ministry of Eduction for a grant-in-aid.

BULLETIN OF THE CHEMICAL SOCIETY OF JAPAN VOL. 42 3487—3490 (1969)

Hydrodynamic Voltammetry with the Convection Electrode. III. The Measurements of the Kinetic Parameters of the Electrode Reaction. Part I

Junsuke SUZUKI

Faculty of Education, Shizuoka University, Oiwa, Shizuoka

(Received June 11, 1969)

We have proposed the determination of the kinetic parameters of the electrode reaction by means of convective voltammetry. At the pushed-out mercury-drop convection electrode (PM-DCE), the ratio of the current on a totally-irreversible wave to the limiting current was derived as follows:

$$\frac{i}{i_l} = \frac{1.64\, k_R D_O^{-2/3} v^{-1/2} \nu^{1/6} d^{1/2}}{1+1.64\, k_R D_O^{-2/3} v^{-1/2} \nu^{1/6} d^{1/2}}$$

This equation was applied to the determination of the kinetic parameters for the electro-reduction of cupric ions in a 0.1 M perchloric acid solution containing 0.05% Triton X-100. It was found that the values of αn and k° the kinetic parameters are 0.59 and 4.2×10^{-9} cm/sec respectively.

In our previous papers,[1,2] the convection electrode system developed by the present authors was applied to the microdetermination of electroactive substances. The results showed that it had a high sensitivity and a good reproducibility. At the convection electrode in the laminar flow, the limiting current, i_l, was found to be given by:[3,4]

$$i_l = 0.61 n\boldsymbol{F}ACD^{2/3} v^{1/2} \nu^{-1/6} d^{-1/2}$$

where n is the number of electrons involved in the electrode reaction; $\boldsymbol{F}$, the Faraday constant; A, the area of the electrode surface; C, the bulk concentration of electroactive substances; D, the diffusion coefficient of an electroactive substance; v, the tangential velocity of the rotating disk; ν, the kinematic viscosity of the solution, and d, the diameter of the convection electrode (the working part plus the non-working shield). The rate of mass transfer at the convection electrode can be controlled by changing the tangential velocity of the rotating disk.

In the present paper, the use of the convection electrode for the study of the kinetics of the electrode reactions will be investigated and the rate constant

1) J. Suzuki and T. Ozaki, This Bulletin, **37**, 230, 789 (1964).

2) T. Ozaki, J. Suzuki, and F. Mori, *Bunseki Kagaku (Japan Analyst)*, **13**, 889 (1964).

3) J. Suzuki, *Rev. Polarography*, **15**, 21 (1968).

4) J. Suzuki, *ibid.*, **16**, 69 (1969).

for the electro-reduction of cupric ions in 0.1 M perchloric acid containing 0.05% Triton X-100 will be determined by analyzing the current-voltage curve.

Theoretical

In the quantitative treatment of the electrode reaction, it is necessary to consider the rates of both the mass and the electron transfer. For the reduction of an oxidized species, *Ox*, to a reduced species, *Red*, when both of the species are soluble, the simplest electrode reaction can be presented in the form of:

$$Ox + n\,e = Red \tag{1}$$

where n is the number of the electron.

The net electron transfer may be given by the difference between the rates of a forward (reduction) process and a backward(oxidation) one. The corresponding rates are expressed as follows, in accordance with the treatment of Kimball:[5]

$$\text{forward process:} \quad R_R = k_R \cdot a_O^\circ \tag{2}$$

$$\text{backward process:} \quad R_O = k_O \cdot a_R^\circ \tag{3}$$

where k_R and k_O denote the rate constants of the first order. Therefore, the net electron transfer is given as follows:

$$R = R_R - R_O = k_R a_O^\circ - k_R a_R^\circ = k_R f_O C_O^\circ - k_O f_R C_R^\circ \tag{4}$$

where a° and C° denote the activities and concentrations at the electrode surface respectively; f, the activity coefficient, and the subscripts, O and R, the oxidized and reduced forms of the electroactive species.

The rate constants of k_R and k_O can be defined as:

$$k_R = k^\circ \exp\left[-\alpha(E-E^\circ)n\boldsymbol{F}/\boldsymbol{R}T\right] \tag{5}$$

$$k_O = k^\circ \exp\left[(1-\alpha)(E-E^\circ)n\boldsymbol{F}/\boldsymbol{R}T\right] \tag{6}$$

Here, k° is the specific rate constant at the standard potential, E°, where k_R, k_O, and k° equal each other; α, the transfer coefficient, and $\boldsymbol{F}$, $\boldsymbol{R}$, and T, the usual thermodynamic signature.

By combining Eqs. (4), (5), and (6), the net current at the potential, E, is given as follows:

$$\frac{i}{n\boldsymbol{F}A} = k^\circ \exp\left[\alpha(E^\circ-E)n\boldsymbol{F}/\boldsymbol{R}T\right] f_O \cdot C_O^\circ - k^\circ \exp\left[(1-\alpha)(E-E^\circ)n\boldsymbol{F}/\boldsymbol{R}T\right] f_R \cdot C_R^\circ \tag{7}$$

where i is the net current at the electrode surface of A cm^2.

On the other hand, the rate of mass transfer, that is, the flux at the electrode surface, depends upon the mechanism of mass transfer, diffusion, forced convection, *etc.*

The rate of mass transfer is in proportion to the difference between the bulk concentration of electroactive substances and their concentration at the electrode surface. Therefore, the rate of mass transfer is given by:

$$\text{for oxidized species:} \quad j_O = m_O(C_O - C_O^\circ) \tag{8}$$

$$\text{for reduced species:} \quad -j_R = m_R(C_R^\circ - C_R) \tag{9}$$

Here, m denotes the mass transfer coefficient, which was in a previous work[3] determined at the convection electrode as follows:

$$m = 0.61\, D^{2/3}\nu^{1/2}\nu^{-1/6}d^{-1/2} \tag{10}$$

Assuming a steady state, one has:

$$\frac{i}{n\boldsymbol{F}A} = j_O = -j_R = m_O(C_O - C_O^\circ) = m_R(C_R^\circ - C_R) \tag{11}$$

From Eqs. (7) and (11), the following equation is obtained:

$$\frac{i}{n\boldsymbol{F}A} = \frac{\left(\begin{array}{l} m_O(f_O C_O \exp\left[\alpha(E^\circ-E)n\boldsymbol{F}/\boldsymbol{R}T\right] \\ -f_R C_R \exp\left[(1-\alpha)(E-E^\circ)n\boldsymbol{F}/\boldsymbol{R}T\right]) \end{array}\right)}{\left(\begin{array}{l} (m_O/k^\circ)+f_O \exp\left[\alpha(E^\circ-E)n\boldsymbol{F}/\boldsymbol{R}T\right] \\ +(m_O/m_R)f_R \exp\left[(1-\alpha)(E-E^\circ)n\boldsymbol{F}/\boldsymbol{R}T\right]) \end{array}\right)} \tag{12}$$

Under the initial condition of $C_R=0$, Eq. (12) becomes:

$$\frac{i_l - i}{i} = \frac{m_O}{k^\circ f_O}\exp\left[\alpha(E-E^\circ)n\boldsymbol{F}/\boldsymbol{R}T\right] + \frac{m_O f_R}{m_R f_O}\exp\left[(E-E^\circ)n\boldsymbol{F}/\boldsymbol{R}T\right] \tag{13}$$

where i_l is the limiting current, which is equal to $n\boldsymbol{F}AC_O m_O$.

Equation (13) represents a current-voltage curve-equation for a stationary electrode-moving solution system.

In Eqs. (12) and (13) m_O/k° was defined as the "irreversibility index" (IRI) by Jordan and Javick.[6] The character of the current-voltage curve depends upon the IRI value; that is, the current-voltage curve varies from reversible to irreversible with an increase in the IRI value, as is shown below.

a) $\boldsymbol{m_O/k^\circ \ll 1}$. In Eq. (13), the first term on the right hand side can be neglected; it is clear that the current-voltage curve has a reversible character, that is,

$$E = E^\circ - \frac{\boldsymbol{R}T}{n\boldsymbol{F}}\ln\left(\frac{D_O}{D_R}\right)^{2/3}\cdot\frac{f_R}{f_O} - \frac{\boldsymbol{R}T}{n\boldsymbol{F}}\ln\frac{i}{i_l - i} \tag{14}$$

$$E_{1/2}{}^r = E^\circ - \frac{\boldsymbol{R}T}{n\boldsymbol{F}}\ln\left(\frac{D_O}{D_R}\right)^{2/3}\cdot\frac{f_R}{f_O} \tag{15}$$

where $E_{1/2}{}^r$ is the reversible half-wave potential.

b) $\boldsymbol{m_O/k^\circ \approx 1}$. In this case, the current-voltage curve obeys Eq. (13).

c) $\boldsymbol{m_O/k^\circ \gg 1}$. In Eq. (13), the last term on the right hand side can be neglected; that is, the current-voltage curve has an irreversible character.

5) G. E. Kimball, *J. Chem. Phys.*, **8**, 199 (1940).

6) J. Jordan and R. A. Javick, *Electrochimica Acta*, **6**, 23 (1962).

$$E = E^\circ + \frac{RT}{\alpha nF} \ln \frac{1.64k^\circ \nu^{1/6}}{D_O{}^{2/3}} + \frac{RT}{\alpha nF} \ln \left(\frac{d}{v}\right)^{1/2} - \frac{RT}{\alpha nF} \ln \frac{i}{i_l - i} \quad (16)$$

Equation (16) is rearranged in the following manner:

$$\frac{i}{i_l} = \frac{1.64k_R D_O{}^{-2/3} v^{-1/2} \nu^{1/6} d^{1/2}}{1 + 1.64k_R D_O{}^{-2/3} v^{-1/2} \nu^{1/6} d^{1/2}} \quad (17)$$

This is analogous to the equations for an irreversible wave derived by Koutecky[7] and by Okinaka and Kolthoff.[8] Equation (17), also, allows us to calculate the values of k_R from the measurement of the i/i_l ratio at various potentials on the current-voltage curve obtained with the convection electrode, and a plot of the calculated log k_R *vs.* the potential may yield a straight line. The values of α and k° can be determined from the slope of this line and from its intercept at the potential of E° respectively.

Experimental

Materials. All the chemicals were of a chemical pure grade and were used without further purification. A solution of cupric ions was prepared by dissolving copper perchlorate in redistilled water, and the copper content was determined by titrating with a standard EDTA solution. A stock solution of Triton X-100 was prepared by dissolution in redistilled water.

Electrodes. The electrode system, a pushed-out mercury-drop convection electrode (PMDCE), used in the present investigation was almost the same as has been described in previous papers[9,10] with the exception of the orientation of the working surface against the liquid flow (Fig. 1). A saturated calomel electrode was used as the reference electrode.

Measurements. A current-voltage curve was recorded by using a Yanagimoto Polarograph, Model PA 102. All the solutions were kept at 25±0.1°C.

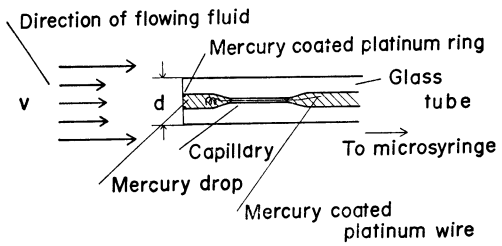

Fig. 1. Pushed-out mercury-drop convection electrode assembly.

Results and Discussion

Reduction of the Copper(II) Ion in Perchloric Acid Containing Triton X-100. The logarithmic plot of an irreversible wave yields either a straight line or a curve. When the rate of the electrode reaction was not slow enough to increase the over-voltage more than about $0.12/n$ V[11] (n, the number of electrons involved in the rate-determining step), the logarithmic plot shows a curve because the backward reaction can not be neglected. Such a wave is "quasi-reversible" and it is to be distinguished from a "totally irreversible wave," which has an over-voltage greater than $0.12/n$ V. In this case, the logarithmic plot yields a straight line. In a recent investigation,[12] the reduction wave of copper(II) ion in 0.1M perchloric acid was found to be quasi-reversible, because the logarithmic plot showed a curve.

The reduction of the cupric ion in a perchloric acid solution gives a one-step wave, but in a solution containing Triton X-100, a non-ionic surface-active substance, it shows two step-waves. The first step-wave has a kinetic character and is very small in comparison with the second step-wave. Kolthoff *et al.*[12] have shown that the kinetic current of this case is caused by the penetration of the copper(II) ion through the adsorbed film of Triton X-100. However, in a perchloric acid solution containing 0.05% Triton X-100 the penetration is negligibly small. This can be attributed to the extremely slow penetration of the cupric ion through the adsorbed film, because the film exhibits a very compact nature. Consequently, the reduction wave of the cupric ion in perchloric acid is slightly irreversible, *i.e.*, quasi-reversible, in the absence of Triton X-100, but in the presence of 0.05% Triton X-100 it becomes completely irreversible. That is, the second step-wave is "totally irreversible," and its half-wave potential at the ordinary DME is shifted about 0.5 V in the negative direction compared with the case of the absence of Triton X-100.[11]

The Determination of the Kinetic Parameters for the Second Step-wave. The observed waves were analyzed by applying Eq. (17); the results are shown in Fig. 2. It can be seen from the figure that the plot of log k_R *vs.* E yields a perfectly straight line. From the intercept of this line and its slope, the values of the rate constant, k°, at the standard potential of the copper(II)-copper amalgam and of αn were determined at four different tangential velocities of the rotating disk; the results are summarized in Table 1. As is shown in the table, the values of k° and αn are almost constant. They agree with the results obtained at the ordinary DME[12] by applying Koutecky's

7) J. Kouteckey, *Coll. Czech. Chem. Commun.*, **18**, 597 (1953).
8) Y. Okinaka and I. M. Kolthoff, *J. Am. Chem. Soc.*, **82**, 324 (1960).
9) J. Suzuki, This Bulletin, **39**, 1898 (1966).
10) J. Suzuki, *ibid.*, **40**, 101(1967).
11) P. Delahay, *J. Am. Chem. Soc.*, **75**, 1430 (1953).
12) I. M. Kolthoff and Y. Okinaka, *ibid.*, **81**, 2296 (1959).

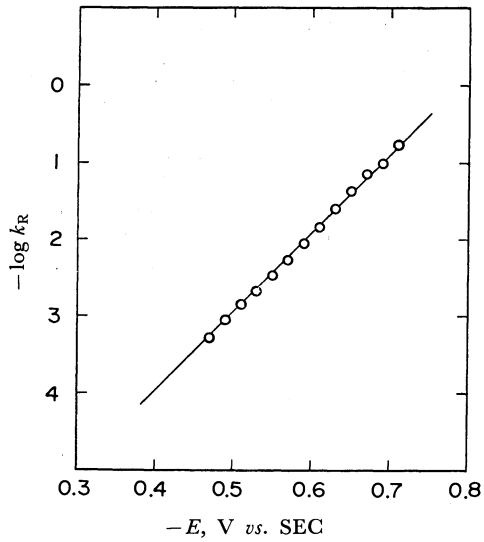

Fig. 2. The plots of $\log k_R$ *vs.* applied potential for the reduction of cupric ion in 0.1 M perchloric acid containing 0.05% Triton X-100; the tangential velocity of the rotating disk, 157.0 cm/sec.

Table 1. The values of the kinetic parameters for the electro-reduction of cupric ions in 0.1 M perchloric acid containing 0.05% Triton X-100 (at 25°C)

v, cm/sec	αn	$k°$, 10^{-9} cm/sec
94.2	0.59	4.0
125.6	0.59	3.8
157.0	0.59	4.7
188.4	0.59	4.2
Average	0.59	4.2
Standard deviation (%)	—	6.6

equation[7] and at the other electrode.[8]

The Difference in the Half-wave Potential at the DME and at the PMDCE. From Eq. (16), the half-wave potential, $(E_{1/2})_p$, at the PMDCE is given by:

$$(E_{1/2})_p = E° + \frac{RT}{\alpha nF} \ln \frac{1.64k°v^{1/6}}{D_O^{1/2}} + \frac{RT}{\alpha nF} \ln \left(\frac{d}{v}\right)^{1/2} \quad (18)$$

Equation (18) shows that the half-wave potential shifts gradually in the negative direction with an increase in the tangential velocity of the rotating disk. That is, the plots of the half-wave potential *vs.* the logarithmic value of the tangential velocity yield a straight line; the slope of this line is given as:

$$-\frac{\Delta(E_{1/2})_p}{\Delta \log v} = \frac{29.5}{\alpha n} \text{(mV)} \quad (19)$$

On the other hand, the half-wave potential at the DME is given as follows:[7,11,13]

$$(E_{1/2})_D = E° + \frac{RT}{\alpha nF} \ln \frac{0.87k°}{D_O^{1/2}} + \frac{RT}{\alpha nF} \ln t^{1/2} \quad (20)$$

The half-wave potential at the DME varies with the drop time, t.

From Eqs. (18) and (20), the difference between the half-wave potentials at the DME and at the PMDCE is given by:

$$\Delta E_{1/2} = (E_{1/2})_D - (E_{1/2})_p$$

$$= \frac{RT}{\alpha nF} \ln 0.53 \left(\frac{D_O}{\nu}\right)^{1/6} \cdot \left(\frac{v \cdot t}{d}\right)^{1/2} \quad (21)$$

Table 2 shows the slope of the plots of the half-wave potential *vs.* the logarithmic value of the tangential velocity in the range from 94.2 to 188.4 cm/sec, and also the difference between the half-wave potential at the DME and at the PMDCE.

Table 2. Difference in the half-wave potential at DME and at PMDCE, and the slope of the plots of the half-wave potential *vs.* the tangential velocity of the rotating disk

v, cm/sec	Difference $\Delta E_{1/2}$, mV		Slope $-\frac{\Delta(E_{1/2})_p}{\Delta \log v}$, mV	
	Obsd	Calcd	Obsd	Calcd
94.2	61	69	>57	>57
188.4	86	84		

Drop time of DME: 3.0 sec at −0.80 V *vs.* SCE in 0.1 M $HClO_4$+0.05% Triton X-100.

It can be seen from the table that the experimental values of the slope and of the difference in the half-wave potential are in good agreement with the values calculated from Eqs. (19) and (21) respectively.

The author wishes to express his thanks to Professors Nobuyuki Tanaka of Tohoku University and Tokuro Ozaki of Shizuoka University for their helpful discussion, and to Miss Yoko Komiya for her earnest assistance.

13) P. Kivalo, K. B. Oldham and H. A. Laitinen, *J. Am. Chem. Soc.* **75**, 4148 (1953).

BULLETIN OF THE CHEMICAL SOCIETY OF JAPAN VOL. 42 3491—3495 (1969)

Oxytocin Analogues Containing No Disulfide Bond. I. Synthesis of the Lactam of L-Tyrosyl-L-isoleucyl-L-glutaminyl-L-asparaginyl-L-α-aminosuberyl-L-prolyl-L-leucylglycine Amide*[1]

Akiko KOBAYASHI, Satoe HASE, Reiko KIYOI and Shumpei SAKAKIBARA

Peptide Center, Institute for Protein Research, Osaka University, Kita-ku, Osaka

(Received December 10, 1968)

The synthesis of an analogue of deamino-oxytocin, which has an ethylene linkage in place of the disulfide bond, was studied in order to establish a general route for the synthesis of such cyclic peptides. L-α-Aminosuberic acid (Asu) was converted to the *N*-benzyloxycarbonyl-ω-*t*-butyl ester and was used as the starting substance for the synthesis. A protected octapeptide was prepared by the step-by-step elongation method with the respective benzyloxycarbonylamino acid active esters, and finally the cyclization of the ω-carboxyl group of the Asu-residue to the amino group of the tyrosyl-residue was achieved by the trifluoroacetate method. The final product showed obviously higher oxytocin-like activities than those reported previously. The conditions for the syntheses of *p*-nitrophenyl and 2,4,5-trichlorophenyl trifluoroacetates were improved during the investigation.

The twenty-membered ring in oxytocin is known to be essential for biological activities. This was demonstrated by comparing the biological activities of [mercaptoacetyl[1]]-oxytocin,[1] which has a 19-membered ring, and of [γ-mercaptobutyl[1]]-oxytocin,[1,2] (21-membered ring), with the activity of [β-mercaptopropionyl[1]]-oxytocin[3] (20-membered ring). Although [β-mercaptopropionyl[1]]-oxytocin, which is called deamino-oxytocin, is well known to show rather higher biological activities than the natural oxytocin, both the 19- and 21-membered derivatives have almost no biological activity. Furthermore, the hydrogenation of oxytocin to linear dihydro-oxytocin results in the disappearance of hormonal activities.[4]

Recently, two analogues of deamino-oxytocin (deamino-carba[1]-oxytocin and deamino-dicarba-oxytocin), in which the disulfide bonds are replaced by a methylene-thio and an ethylene linkage respectively, were synthesized by Rudinger and Jošt.[5,6] These compounds were found to exhibit weaker but definite oxytocin-like activities. These facts can be interpreted by supposing that the disulfide linkage in the 20-membered ring of oxytocin is important as a structural element, but is not essential for biological activities.

Studies along the same lines have been carried out independently in our laboratory to elucidate the relationship between the steric structure of the hormone molecule and its biological activities.[7] In the present paper, a new method for the synthesis of deamino-dicarba-oxytocin will be described. This synthesis was investigated in order to establish a widely-applicable procedure for the syntheses of such series of cyclic peptides.[8] Although Jošt and Rudinger had already succeeded in synthesizing this compound,[6] their method is not considered to be generally applicable.

Before starting the synthesis of this peptide, the *N*-benzyloxycarbonyl-L-α-aminosuberic acid ω-*t*-butyl ester (III) was synthesized from *N*-benzyloxycarbonyl-L-α-aminosuberic acid (I)[9] as is shown in Scheme 1. The first step from I to II represents an application of the Nefkens method.[10] The compound, III, thus obtained was coupled with L-prolyl-L-leucylglycine amide[11] by the tri-

*1 This work was presented at the 5th Symposium on Peptide Chemistry in Japan, Kyoto, November 23, 1967.

1) D. Jarvis and V. du Vigneaud, *Science*, **143**, 545 (1964).

2) D. Jarvis, B. M. Ferrier and V. du Vigneaud, *J. Biol. Chem.*, **240**, 3553 (1965).

3) D. B. Hope, V. V. S. Murti and V. du Vigneaud, *ibid.*, **237**, 1563 (1962).

4) E. Schröder and K. Lübke, "The Peptides," Vol. II, Academic Press, New York (1966), p. 315.

5) J. Rudinger and K. Jošt, *Experientia*, **20**, 570 (1964)

6) K. Jošt and J. Rudinger, *Collect. Czech. Chem. Commun.*, **32**, 1229 (1967).

7) S. Sakakibara, R. Kiyoi and Y. Shimonishi, Proc. 3rd Symposium on Peptide Chemistry (Japan), Inst. for Protein Research, Osaka Univ. (1964), p. 52.

8) A. Kobayashi, S. Hase and S. Sakakibara, Proc. 5th Symposium on Peptide Chemistry (Japan), Faculty of Pharmaceutical Sci., Kyoto Univ. (1967), p. 20.

9) S. Hase, R. Kiyoi and S. Sakakibara, This Bulletin, **41**, 1266 (1968).

10) G. H. L. Nefkens and R. J. F. Nivard, *Rec. trav. chim.*, **83**, 199 (1964).

Z-Asu-OH (I)

↓ TEA in DMF | Bzl-Br

Z-Asu-OBzl (II)

↓ H_2SO_4 in CH_2Cl_2 | Isobutylene

OBu^t

[Z-Asu-OBzl] oil

↓ NaOH

OBu^t

Z-Asu-OH (III)

(Crystallized as the piperazine salt)

Scheme 1.

OBu^t

Z-Asu-Pro-Leu-Gly-NH_2 (IV)

↓ H_2/Pd, Z-Asn-ONp

OBu^t

Z-Asn-Asu-Pro-Leu-Gly-NH_2 (V)

↓ H_2/Pd, Z-Gln-ONp

OBu^t

Z-Gln-Asn-Asu-Pro-Leu-Gly-NH_2 (VI)

↓ H_2/Pd, Z-Ile-OSu

OBu^t

Z-Ile-Gln-Asn-Asu-Pro-Leu-Gly-NH_2 (VII)

↓ CF_3COOH

Z-Ile-Gln-Asn-Asu-Pro-Leu-Gly-NH_2 (VIII)

↓ H_2/Pd, Z-Tyr(Bzl)-OSu

Bzl

Z-Tyr-Ile-Gln-Asn-Asu-Pro-Leu-Gly-NH_2 (IX)

↓ $CF_3COOTcp$

Bzl OTcp

Z-Tyr-Ile-Gln-Asn-Asu-Pro-Leu-Gly-NH_2 (X)

↓ H_2/Pd

Tyr-Ile-Gln-Asn-Asu-Pro-Leu-Gly-NH_2 (XI)

Scheme 2.

fluoroacetate method[12] because the *p*-nitrophenyl ester of compound III was not crystallizable and the application of the dicyclohexylcarbodiimide method seemed undesirable. The benzyloxycarbonyl group in the tetrapeptide amide (IV) was removed by catalytic hydrogenolysis, and the peptide chain was elongated by the step-by-step addition of the respective benzyloxycarbonylamino acids using the active-ester method, as is shown in Scheme 2. The *t*-butyl ester group in the side chain of α-aminosuberic acid was removed by trifluoroacetic acid before the removal of the benzyloxycarbonyl group of isoleucyl heptapeptide amide (VIII). The protected octapeptide amide (IX) was converted to its 2,4,5-trichlorophenyl ester (X) in a good yield using the trifluoroacetate method.[12] The cyclized compound, XI, was then obtained smoothly by the catalytic hydrogenolysis of a dilute solution of X in dimethylformamide. The unchanged compound was removed by passing the aqueous solution successively through Dowex 50 and Amberlite IR-45 columns; the neutral fraction obtained was then purified by passing it through a column of Sephadex G-25, giving a homogeneous product. No dimer or polymer was detectable in the eluate after gel-filtration, as is shown in Fig. 1. The homogeneity of the final product was confirmed by paper chromatography, paper electrophoresis, amino acid analysis, and elemental analysis of the lyophilizate. The molecular weight of this compound was estimated by sedimentation equilibrium methods to be about 850, which indicates that this is a monomeric cyclic peptide.

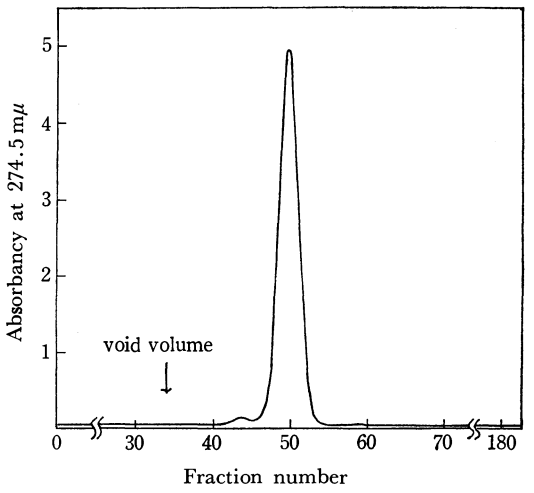

Fig. 1. Gel-filtration of the final product on Sephadex G-25. See Experimental part for details of conditions.

The biological activities of the product, XI, were determined as shown in Table 1; these values were compared with those reported by Rudinger and Jošt for the same compound[6] and with those of oxytocin and of deamino-oxytocin. This compound was found, contrary to the reported values, to

11) M. Zaoral and J. Rudinger, *Collect. Czech. Chem. Commun.*, **20**, 1183 (1955).

12) S. Sakakibara and N. Inukai, This Bulletin, **38**, 1979 (1965); *ibid.*, **39**, 1567 (1966).

Table 1. Biological activities of compound XI[a]

Compound	Rat Uterus *in vitro*	Avian depressor	Rat pressor	Rat antidiuretic
Oxytocin[b]	486±5	507±23	3.1±0.1	2.7±0.2
Deamino-oxytocin[c]	803±36	975±25	1.44±0.06	19
Compound XI	96[d]	52[e]	<0.25[d]	1.78±0.2[e]
Compound XI[f]	9	2.5	No response with up to 20 μg/kg	0.7

a) International units per mg. b) W. Y. Chan and V. du Vigneaud, *Endocrinology*, **71**, 977 (1962). c) B. M. Ferrier, D. Jarvis and V. du Vigneaud, *J. Biol. Chem.*, **240**, 4264 (1965). d) Determined by Dr. T. Okada, Yoshitomi Pharmaceutical Ind., Ltd., Yoshitomi, Fukuoka. e) Determined by Dr. S. Yoshida, Faculty of Medicine, the University of Tokyo, Bunkyo-ku, Tokyo. f) Reported by Jošt and Rudinger: cited as Ref 6.

show about one-tenth of the biological activities of deamino-oxytocin and to show a faint rat-pressor activity, as has been reported previously.

The syntheses of *p*-nitrophenyl and the 2,4,5-trichlorophenyl trifluoroacetates used as reagents in the trifluoroacetate method were improved during the investigation. Formerly these compounds were synthesized by refluxing the respective hydroxy compounds with trifluoroacetic anhydride for a long time,[12] but there was a danger that the reaction was incomplete. In the present study the reaction was carried out under pressure in a sealed bottle and at a higher temperature. This improved procedure should be useful in routine work in the preparation of all other trifluoroacetate reagents.

Experimental[13]

Removal of the Benzyloxycarbonyl Group by Catalytic Hydrogenolysis. Hydrogen was gently bubbled through a solution of the benzyloxycarbonyl compound at room temperature, using palladium black as the catalyst. The completion of the reaction was checked by thin-layer chromatography using Merck's silica-gel G. The solvent systems used for the chromatography were chloroform: methanol: acetic acid (95: 5 : 3 v/v) for IV and V, and *n*-butanol : acetic acid: water (4 : 1 : 1 v/v) for VI, VIII, and X. After the reaction, the catalyst was removed by filtration, the filtrate was concentrated under reduced pressure, and the residue was subjected to the next reaction.

***p*-Nitrophenyl Trifluoroacetate.** A mixture of *p*-nitrophenol (75 g, 0.538 mol), benzene (130 m*l*), and trifluoroacetic anhydride (190 g, 0.904 mol) was placed in a glass pressure-vessel which had been sealed by a screw cap equipped with a Teflone stopper. The mixture was heated to 80—90°C in an oil bath for about 8 hr. Then the yellow solution was concentrated to a residue under reduced pressure, taking care to exclude moist air from the mixture. The trace of trifluoroacetic acid present was removed in a desiccator over phosphorus pentoxide *in vacuo*, and the residue was used without further purification. The yield of the reagent was quantitative.

2,4,5-Trichlorophenyl Trifluoroacetate. A mixture of 2,4,5-trichlorophenol (1.98 g, 0.01 mol), benzene (2 m*l*), and trifluoroacetic anhydride (4.20 g, 0.02 mol) was heated for 8 hr in a sealed bottle as has been described above. The reaction mixture was then concentrated under reduced pressure, and the residue was used without further purification.

Benzyloxycarbonyl-L-α-aminosuberic Acid α-Benzyl Ester (II). A solution of benzyloxycarbonyl-L-α-aminosuberic acid (I)[9] (32.3 g, 0.1 mol) and triethylamine (14 m*l*, 0.1 mol) in dimethylformamide (20 m*l*) was treated with benzyl bromide (18.8 g, 0.11 mol) at room temperature. After 20 hr, water (200 m*l*) was added to the reaction mixture, and the oil which separated was extracted twice with ethyl acetate. The combined extract was washed with water and then with a 5 % sodium bicarbonate solution. (The unchanged I was extractable from the ethyl acetate solution with a sodium bicarbonate solution, but the main product, II, remained in the ethyl acetate under the present conditions. The unchanged I was recovered from the sodium bicarbonate solution after acidification with hydrochloric acid; wt, 8.5 g). The ethyl acetate solution, which should contain the sodium salt of II, was converted to the ether solution, and the main product was extracted three times with a sodium carbonate solution. The acidification of the carbonate solution with 6 N hydrochloric acid afforded an oily material which was extracted with ethyl acetate. After washing with water and drying over sodium sulfate, the solution was concentrated under reduced pressure; the oily residue was crystallized by the addition of petroleum ether; yield of crude material, 24.8 g, mp 66.5—69°C. Recrystallization from ethyl acetate and petroleum ether (1 : 2 v/v) gave 19.5 g of needles (yield, 47 %). When a correction is made for the unchanged I, the yield is 64 %; mp 71—72°C, $[\alpha]_D^{25}$ −19.1° (*c* 3, dimethylformamide).

Found: C, 66.64; H, 6.82; N, 3.40 %. Calcd for $C_{23}H_{27}O_6N$: C, 66.81; H, 6.66; N, 3.39 %.

Bis(benzyloxycarbonyl-L-α-aminosuberic Acid ω-*t*-Butyl Ester) Piprazine Salt (III). A solution of compound II (20.7 g, 0.05 mol) in methylene chloride (100 m*l*) was allowed to react with isobutylene (50 m*l*) in the presence of sulfuric acid (0.5 m*l*) as the catalyst. After 2 days at room temperature, the reaction mixture was poured into 5 % sodium carbonate, and then the methylene chloride and the excess isobutylene were removed by distillation under reduced pressure. The oily material which appeared was extracted into ether,

13) All the melting points were determined by the capillary method, and all are given as uncorrected values. All products were dried over phosphorus pentoxide *in vacuo* at room temperature unless otherwise noted.

and the ether solution was washed successively with 5 % sodium carbonate, water, 0.2N hydrochloric acid, and water. The concentration of the solution under reduced pressure yielded an oily material (α-benzyl ω-*t*-butyl esters of L-α-aminosuberic acid), which was then dissolved in acetone (200 m*l*) and saponified with 1 N sodium hydroxide (50 m*l*) for 3 hr at 0—5°C. The reaction mixture was neutralized with 1 N hydrochloric acid, the acetone was removed under reduced pressure, ether was added to the residual solution, and the main product was transferred to the aqueous layer by the addition of 5 % sodium carbonate. The neutral material was removed with ether, and the aqueous layer was acidified with 1 N hydrochloric acid; then the oil which separated was extracted with ethyl acetate. The concentration of the extract gave an oily material, which was then neutralized with piperazine hexahydrate (4.4 g, 0.0225 mol) in acetone. The solution was concentrated under reduced pressure, and the residue was flushed twice with toluene to remove the water. The trituration of the dried residue with ethyl acetate yielded crude crystals which were recrystallized from ethyl acetate; yield, 16.0 g (76 %); mp 130—131°C, $[\alpha]_D^{28}$ −2.7° (*c* 2, acetic acid). This material was dried over phosphorus pentoxide *in vacuo* at 80°C for 10 hr for analysis.

Found: C, 62.28; H, 8.17; N, 6.57 %. Calcd for $C_{41}H_{68}O_{12}N_4$: C, 62.54; H, 8.11; N, 6.63 %.

Benzyloxycarbonyl-ω-*t*-butyl-L-α-aminosuberyl-L-prolyl-L-leucylglycine Amide (IV). The benzyloxycarbonyl-L-α-aminosuberic acid ω-*t*-butyl ester (7 mmol) was extracted from III (2.96 g) with ethyl acetate by shaking with 1N hydrochloric acid; the ethyl acetate layer was then dried over sodium sulfate. The dried solution was concentrated to a syrup, which was dissolved in pyridine (4 m*l*). The solution was then treated with *p*-nitrophenyl trifluoroacetate (1.97 g, 8.4 mmol) at room terperature for 3 hr. A large amount of water was added to the reaction mixture, and the oily material thus precipitated was extracted with ethyl acetate; the ethyl acetate extract was washed with 0.5N hydrochloric acid and water successively, and dried over anhydrous sodium sulfate. The concentration of the dried solution left an oily residue which corresponded to the *p*-nitrophenyl ester of the starting material; the oily residue was allowed to react with L-prolyl-L-leucylglycine amide[11] (2.39 g, 8.2 mmol as the hemihydrate) in dimethylformamide (7 m*l*) for 2 days at room temperature. The addition of water gave a precipitate which was taken into ethyl acetate. The organic layer was washed successively with 1N aqueous ammonia, water, 1N hydrochloric acid, and water. Finally the solution was dried over sodium sulfate and concentrated to a residue which was crystallized by the addition of ether; yield, 4.08 g (90 %), mp 108—110°C, $[\alpha]_D^{13}$ −66.8° (*c* 2, ethanol). This material was dried for analysis at 80°C for 2 hr over phosphorus pentoxide *in vacuo*.

Found: C, 61.19; H, 8.37; N, 10.82%. Calcd for $C_{33}H_{51}O_8N_5$: C, 61.37; H, 7.96; N, 10.85 %.

Benzyloxycarbonyl-L-asparaginyl-ω-*t*-butyl-L-α-aminosuberyl-L-prolyl-L-luecylglycine Amide (V). The benzyloxycarbonyl group in compound IV (5.83 g, 9 mmol) was removed in ethanol by catalytic hydrogenolysis. The catalyst was then removed by filtration, and the filtrate was concentrated under reduced pressure. The residue was allowed to react with the benzyloxycarbonyl-L-asparagine *p*-nitrophenyl ester[14] (3.48 g, 9 mmol) for 2 days in dimethylformamide at room temperature. The product was then precipitated by the addition of a large amount of ethyl acetate, and the precipitate was collected by filtration. Recrystallization from 90 % ethanol yielded an analytically-pure product; yield, 6.10 g (89 %), mp 212°C (decomp.), $[\alpha]_D^{27}$ −47.7° (*c* 1, dimethylformamide). This material was dried for analysis at 80°C for 2 hr over phosphorus pentoxide *in vacuo*.

Found: C, 58.70; H, 7.70; N, 12.92%. Calcd for $C_{37}H_{57}O_{10}N_7$: C, 58.55; H, 7.56; N, 12.90%.

Benzyloxycarbonyl-L-glutaminyl-L-asparaginyl-ω-*t*-butyl-L-α-aminosuberyl-L-prolyl-L-leucylglycine Amide Monohydrate (VI). The benzyloxycarbonyl group of compound V (6.20 g, 8.2 mmol) was removed by catalytic hydrogenation in a mixture of dioxane (70 m*l*) and water (35 m*l*). After the reaction, the catalyst was removed by filtration, and the filtrate was concentrated under reduced pressure. The residue was flushed several times with toluene, and then dissolved in dimethylformamide (18 m*l*). The benzyloxycarbonyl-L-glutamine *p*-nitrophenyl ester[14] (3.93 g, 9.8 mmol) was added to the solution, and the mixture was allowed to react overnight at room temperature. The reaction product was precipitated by the addition of excess ethyl acetate, and the precipitate was collected by filtration and recrystallized from 90% ethanol; yield, 5.85 g (81 %), mp 207—208°C (decomp.), $[\alpha]_D^{26}$ −45.7° (*c* 1, dimethylformamide). This material was dried for analysis at 80°C *in vacuo* for 3 hr over phosphorus pentoxide.

Found: C, 55.71; H, 7.51; N, 13.88 %. Calcd for $C_{42}H_{65}O_{12}N_9 \cdot H_2O$: C, 55.68; H, 7.45; N, 13.90%.

Benzyloxycarbonyl-L-isoleucyl-L-glutaminyl-L-asparaginyl-ω-*t*-butyl-L-α-aminosuberyl-L-prolyl-L-leucylglycine Amide Monohydrate (VII). The benzyloxycarbonyl group was removed from compound VI (5.70 g, 6.3 mmol) by catalytic hydrogenolysis in a mixture of dioxane and water (50 m*l*+50 m*l*). The catalyst was then removed by filtration, and the filtrate was concentrated under reduced pressure. The residue was flushed several times with toluene, and the oil which remained was allowed to react with the benzyloxycarbonyl-L-isoleucine *N*-hydroxysuccinimide ester[15] (3.44 g, 9.5 mmol) for one day at room temperature in dimethylformamide (25 m*l*). The product was precipitated by the addition of ethyl acetate; the precipitate was recrystallized from hot 90 % ethanol. The yield was 5.66 g (88 %); mp 225°C (decomp.), $[\alpha]_D^{27}$ −41° (*c* 1, dimethylformamide). This material was dried for analysis at 80°C *in vacuo* for 10 hr over phosphorus pentoxide.

Found: C, 56.93; H, 7.63; N, 13.71 %. Calcd for $C_{48}H_{76}O_{17}N_{10} \cdot H_2O$: C, 56.56; H, 7.71; N, 13.74 %.

Benzyloxycarbonyl-L-isoleucyl-L-glutaminyl-L-asparaginyl-L-α-aminosuberyl-L-prolyl-L-leucylglycine Amide Monohydrate (VIII). Compound VII (1.00 g, 0.98 mmol) was dissolved in trifluoroacetic acid (20 m*l*), and the solution was allowed to stand for 3 hr at room temperature. Then the solvent was removed by evaporation under reduced pressure, and the

14) M. Bodanszky and V. du Vigneaud, *J. Am. Chem. Soc.*, **81**, 5688 (1959).

15) G. W. Anderson, J. E. Zimmerman and F. M. Callahan, *ibid.*, **86**, 1839 (1964).

residue was triturated with ether and reprecipitated from hot 90 % ethanol; yield, 0.75 g (80 %), mp 212—214° (decomp.), $[\alpha]_D^{17}$ −44.2° (*c* 1, dimethylformamide). This material was dried for analysis at 80°C *in vacuo* for 10 hr over phosphorus pentoxide.

Found: C, 54.99; H, 7.36; N, 14.64 %. Calcd for $C_{44}H_{68}O_{13}N_{10}\cdot H_2O$: C, 54.87; H, 7.33; N, 14.55%.

Benzyloxycarbonyl-*O*-benzyl-L-tyrosyl-L-isoleucyl-L-glutaminyl-L-asparaginyl-L-α-aminosuberyl-L-prolyl-L-leucylglycine Amide Monohydrate (IX) The benzyloxycarbonyl group was removed from VIII (710 mg, 0.74 mmol) by catalytic hydrogenation in a mixture of dioxane (30 m*l*) and water (10 m*l*). The catalyst was removed by filtration; the filtrate was concentrated under reduced pressure, and the residue was dried by flushing with toluene. This residue was dissolved in dimethylformamide (40 m*l*), and the *N*-benzyloxycarbonyl-*O*-benzyl-L-tyrosine *N*-hydroxysuccinimide ester[16] (557 mg, 1.1 mmol) was added together with *N*-ethylmorphorine (0.1 m*l*, 0.98 mmol). The mixture was allowed to react for 2 days at room temperature, and then the product was precipitated by the addition of excess ethyl acetate and collected by filtration. Reprecipitation from 90 % ethanol afforded an amorphous powder; yield, 660 mg (73 %), mp 231—232°C (decomp.), $[\alpha]_D^{28}$ −36.4° (*c* 0.74, dimethylformamide). This material was dried over phosphorus pentoxide *in vacuo* at 80°C for 10 hr before analysis.

Found: C, 59.42; H, 7.28; N, 12.78%. Calcd for $C_{60}H_{83}O_{15}N_{11}\cdot H_2O$: C, 59.24; H, 7.04; N, 12.66%.

Benzyloxycarbonyl-*O*-benzyl-L-tyrosyl-L-isoleucyl-L-glutaminyl-L-asparaginyl-ω-2, 4, 5-trichlorophenyl-L-α-aminosuberyl-L-prolyl-L-leucylglycine Amide Monohydrate (X). 2,4,5-Trichlorophenyl trifluoroacetate (733 mg, 2.5 mmol) was added to a suspension of IX (304 mg, 0.25 mmol) in a mixture of dimethylformamide (4 m*l*) and pyridine (2 m*l*), and the mixture was allowed to react for 3 hr at 50°C; gradually the suspension changed to a clear solution during the reaction. A large amount of ether was added to the solution to precipitate the product, which was then collected by filtration. Reprecipitation from dimethylformamide and ether yielded 327 mg of the product; yield 95 %, mp 231—232°C (decomp.), $[\alpha]_D^{23}$ −27.8° (*c* 0.75, dimethylformamide). This material was dried over phosphorus pentoxide at 60°C *in vacuo* for 10 hr before analysis.

Found: C, 56.70; H, 6.27; N, 11.12; Cl, 7.79 %. Calcd for $C_{66}H_{84}O_{15}N_{11}Cl_3\cdot H_2O$: C, 56.79; H, 6.21; N, 11.04; Cl, 7.62 %.

16) M. Löw and L. Kisfaludy, *Acta chim. Hung.*, **44**, 61 (1965).

Lactam of L-Tyrosyl-L-isoleucyl-L-glutaminyl-L-asparaginyl-L-α-aminosuberyl-L-prolyl-L-leucylglycine Amide Monohydrate (XI). The benzyloxycarbonyl and benzyl ether groups were simultaneously revomed from X (419 mg, 0.3 mmol) by catalytic hydrogenolysis in dimethylformamide (300 m*l*). The catalyst was removed by filtration, the filtrate was concentrated under reduced pressure, and the residue was dissolved in water (27 m*l*). The trichlorophenol formed was removed by extraction with ether. The aqueous solution was passed successively through columns (1.0 × 10 cm) of Dowex-50 X2 (100—200 mesh, H^+ form) and of Amberlite IR-45 (100—200 mesh, OH^- form). These columns were washed with water, and the effluent and washing were combined and lyophilized to obtain 97.4 mg (33 %) of the cyclized product. A portion (75 mg) of this product was dissolved in 1N acetic acid (1.5 m*l*), and the solution was applied to a column of Sephadex G-25 (fine, 1.8 × 170 cm). The flow rate of the solvent, 1N acetic acid, was 25 m*l* per hr. Fractions of 5 g each were collected, and peptide was detected by the UV-absorption at 274.5 mμ, as is shown in Fig. 1. The effluents in tubes No. 48 to 52 were pooled and lyophilized; wt, 62 mg (recovery 83 %). This material was found to be homogeneous, as judged by paper electrophoresis and by paper chromatography. Rf: 0.66 (*n*-butanol : acetic acid : water, 4 : 1 : 1 v/v) and 0.74 (*n*-butanol : acetic acid : pyridine : water, 15 : 3 : 10 : 6 v/v). These spots were located with Pauli's reagent. Reported Rf's: 0.50 and 0.70 respectively with the above solvent systems.[6] $[\alpha]_D^{18}$ −98.4° (*c* 0.46, water).

Found for sample dried at 60°C for 10 hr *in vacuo*: C, 54.39; H, 7.13; N, 15.26 %. Calcd for $C_{45}H_{69}O_{12}N_{11}\cdot 2H_2O$: C, 54.45; H, 7.42; N, 15.53 %.

Found for sample dried at 90°C for 18 hr *in vacuo*: C, 55.01; H, 7.12; N, 15.95 %. Calcd for $C_{45}H_{69}O_{12}N_{11}\cdot H_2O$: C, 55.48; H, 7.35; N, 15.82 %. Ratio of amino acids after acid hydrolysis: $Tyr_{1.00}$, $Ile_{1.01}$, $Glu_{0.97}$, $Asp_{1.00}$, $Asu_{1.01}$, $Pro_{1.02}$, $Leu_{1.00}$, $Gly_{0.97}$. A mol wt of about 850 was estimated by the sedimentation equilibrium method: 0.1 M NaCl solution was used as the solvent, and a partial specific volume of 0.73 was assumed for the calculation. Calcd mol wt: 956.

The authors wish to express their gratitude to Dr. Sho Yoshida of the University of Tokyo and to Dr. Tadao Okada of Yoshitomi Pharmaceutical Ind. for determining the biological activities of the synthetic peptides, and to Dr. Kinji Kakiuchi of Osaka University for his determination of the molecular weight by the sedimentation equilibrium method.

BULLETIN OF THE CHEMICAL SOCIETY OF JAPAN VOL. 42 3496—3498 (1969)

Constitution of Mucilage from *Ulva Conglobata*. I. Separation of Rhamnobiose Derivative by Partial Methanolysis

Kiyo MITA

Home Economics, Hiroshima Women's University, Hiroshima

(Received February 19, 1969)

Partial methanolysis of the mucilage from *Ulva conglobata* gave methyl α-L-rhamnoside (29.07%), methyl α-D-xyloside (7.04%) and methyl α-D-glucoside (5.13%). Separation of a new disaccharide (methyl α-L-rhamnobioside, 3.4%) from methanolysate was achieved chromatographically. The biose was attacked by maltase but not by emulsin. The results and infrared spectrum show that the rhamnobiose derivative consists of rhamnose units linked by α-link.

It was shown[1] that an acid hydrolysis of the mucilage from *Ulva conglobata* collected in Saga prefecture gave L-rhamnose, D-xylose and D-glucose as neutral constituents and D-glucuronic acid and sulfuric acid as acidic constituents.

The present investigation was to determine the manner of the linkages of these constituents in the polysaccharide molecule.

Percival *et al.*[2-7] have studied water-soluble sulfated polysaccharides which contain glucose, galactose, mannose, arabinose, xylose, rhamnose and uronic acid residues, from *Caulerpa filiformis*, *Acrosiphonia centralis*, *Cladophora rupestvis*, *Ulva lactuca*, *Enteromorpha compressa*, *Codium fragile*, *Chaetomorpha capillaris*. Furthermore, partial hydrolysis of the above mucilages led to the isolation of 3-*O*-β-D-xylopyranosyl-D-xylose, 4-*O*-α-D-glucopyranosyl-D-glucose, 4-*O*-D-xylopyranosyl-L-rhamnose, 4-*O*-D-glucopyranosyl-L-rhamnose and 4-*O*-glucuronosyl-L-rhamnose-2-sulfate.

Partial methanolysis was conducted by refluxing the suspension of the mucilage in a methanolic hydrogen chloride (1%) for 2 hr. The methanolysate was treated with a barium hydroxide solution (0.3 N) to effect saponification. The neutral methanolysate passed through a cation- and anion exchange resins was subjected to charcoal chromatography, which led to the isolation of methyl α-L-rhamnoside (29.07%), methyl α-D-xyloside (7.04%), methyl α-D-glucoside (5.13%), a mixture of methyl glycosides of disaccharides (5.5%) and methyl glycosides of oligosaccharides (32.5%).

The mixture of methyl glycosides of disaccharides was further resolved into its components by chromatography on a powdered filter paper column (Table 2). Fraction III-a in Table 2 gave only L-rhamnose by acidic hydrolysis. The fraction was not attacked at all by emulsin but by maltase. The results are very interesting because methyl α-L-rhamnobioside has not yet been isolated from natural substance and its synthesis has not been reported.[8]

Barker *et al.*[9,10] have studied structures of carbohydrates by means of IR spectra and reported that α-anomers give absorption at 844±8 cm^{-1} and β-anomers at 891±7 cm^{-1}. This seems to be one of the C–H deformation modes. The absorption bands are observed in all saccharides. Judging from the absorption band at 850 cm^{-1}, the isolated rhamnobioside appears to be α-anomer.

The IR spectrum of xyloside fraction indicated the presence of hydroxy groups from the absorption bands at 3400 and 1100—1000 cm^{-1} and α-anomer from the absorption band at 740 cm^{-1} (type 3 of pyranose ring). The IR spectrum of glucoside fraction also identified as α-anomer from the absorption bands: 3400, 1100—1000 (OH), 840 (type 2a of pyranose ring) and 745 cm^{-1} (type 3 of pyranose ring). Furthermore, these α-anomers were identified by direct comparison of the melting

1) K. Mita, *Nippon Kagaku Zasshi (J. Chem. Soc. Japan, Pure Chem. Sect.)*, **82**, 1664 (1961).

2) I. M. Mackie and E. Percival, *J. Chem. Soc.*, **1959**, 1151; **1960**, 2381; **1961**, 3010.

3) J. J. O'Donnell and E. Percival, *ibid.*, **1959**, 1739, 2168.

4) J. P. McKinnell and E. Percival, *ibid.*, **1962**, 2082, 3141.

5) J. Love, W. Mackie, J. W. McKinnell and E. Percival, *ibid.*, **1963**, 4177.

6) E. L. Hirst, W. Mackie and E. Percival, *ibid.*, **1965**, 2958.

7) Q. N. Haq and E. Percival, *Some Contemp. Stud. Mar. Sci.*, **1966**, 355.

8) S. Kamiya, S. Esaki and M. Hama, *Agr. Biol. Chem.*, **31**, 261, 397 (1967).

9) S. A. Barker, E. J. Bourne, M. Stacey and H. Whiffen, *J. Chem. Soc.*, **1954**, 171; *Chem. & Ind.*, **1953**, 196.

10) S. A. Barker, E. J. Bourne, R. Stephens and D. H. Whiffen, *J. Chem. Soc.*, **1954**, 3468, 4211.

point, the specific rotation and the IR spectrum with authentic samples.

Experimental

Materials. The mucilage was obtained from *Ulva conglobata* (collected in Saga prefecture) as described in the previous paper.[11] All reagents were of analytical or practical grade. Reagents of practical grade were purified by recrystallization and distillation. All melting points are uncorrected.

Apparatus. The IR spectra were obtained with KBr disk on a Hitachi EPI-S2 infrared spectrophotometer.

Partial Methanolysis of the Mucilage. Powdered mucilage (20 g, moisture 12.2 %, ash 17.6 %) was swelled in a 1 % methanolic hydrogen chloride solution (300 m*l*) at room temperature for 12 hr and then refluxed for 2 hr. After filtration, the insoluble substance (7.0 g) was dried *in vacuo* at 40°C and refluxed again with a 1 % methanolic hydrogen chloride solution (200 m*l*) for 2 hr and then filtered. Finally, the insoluble substance (1.85 g) was washed with methanol and dried *in vacuo*.

All filtrates and washings were combined and neutralized with silver carbonate. After filtration, the filtrate was evaporated to a syrup (22.3 g) *in vacuo* at 40°C. This was saponified at 60°C for 2 hr with a 0.3 N barium hydroxide solution (350 m*l*), and excess barium hydroxide was neutralized with carbon dioxide. After filtration, the filtrate was evaporated to a syrup (18.05 g).

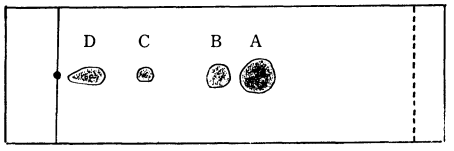

Fig. 1. Paper chromatogram of the neutral fraction of methanolysates.
Solvent system is *n*-butanol : ethanol : water : ammonia = 40 : 10 : 49 : 1 (v/v).[13]
A: methyl α-L-rhamnoside
B: methyl α-D-xyloside
C: methyl α-D-glucoside
D: unknown

Separation of the Neutral Methanolysate. The saponified syrup was dissolved in water (10 %) and the aqueous solution was allowed to pass through columns (3×40 cm) of Amberlite IR 120 (H form; 210 m*l*) and then Amberlite IR 45 (OH form; 210 m*l*). Both columns were washed with water (5 *l*) at a flow rate of 200 m*l*/hr. The combined eluates and washings were evaporated in order to obtain the neutral syrup (8.45 g); $[\alpha]_D^{30}$ −21.4° (*c* 1.5, water), OCH_3 15.31 %. The neutral fraction from the methanolysates gave four distinct colored spots with R_f values 0.10 (D: orange brown), 0.43 (C: orange brown), 0.55 (B: violet blue) and 0.64 (A: orange, main) on a paper chromatogram with *o*-aminophenol reagent,[12] as shown in Fig. 1.

Adsorption Chromatography for the Neutral Methanolysate. The neutral methanolysate (8.0 g) was dissolved in water (72 m*l*), placed on a charcoal-Celite 545 (1 : 1 w/w) column (5×34 cm) and eluted successively with water and then aqueous ethanol (2, 5, 7.5, 15 and 30 %) at room temperature according to the method of Whistler.[14]

The eluates were measured for specific rotation and chromatographed on papers. The chromatograms were sprayed with *o*-aminophenol[12] and potassium periodate-potassium permanganate reagents.[15] The results are summarized in Table 1.

Separation and Identification of Methyl α-D-Xyloside, Methyl α-L-Rhamnoside and Methyl α-D-Glucoside. Fraction I in Table 1 gave three distinct spots on a paper chromatogram: R_f 0.64 (orange; corresponding to methyl α-L-rhamnoside), 0.55 (violet-blue; corresponding to methyl α-D-xyloside) and 0.43 (brown-orange; corresponding to methyl α-D-glucoside).

Fraction I (2.7 g) was further separated through a charcoal-Celite 545 column (2×35 cm), water being used as a mobile phase. Each eluate was examined by specific rotation and then chromatographed on paper. The eluates gave the same specific rotation and R_f values were combined and then evaporated to dryness. They were identified as follows.

Methyl α-D-Xyloside: The xyloside fraction (white solid, 1.05 g) was dissolved in methanol-acetone (1 : 3

Table 1. Chromatographic separation of neutral methanolysate

Fraction	I	II	III	IV	V	VI
Solvent	W*1	2% E*1	5% E*1	7.5% E*1	15% E*1	30% E*1
Vol. (*l*)	20	12	20	21	11	17
Yield (g)	2.7	0.55	0.5	0.5	1.1	1.0
$[\alpha]_D^{30}(H_2O)$	—	−87.31°	−89.77°	−84.17°	−57.25°	−53.17°
OCH_3 (%)	—	17.5	6.43	3.58	3.70	4.22
R_f value	0.64 0.55 0.43	0.64	0.30 0.24	0.14*2 0.10	0.10	0.10

*1 W: water, E: ethanol, *2 trace

11) K. Mita, *Japanese Soc. Sci. Fish.*, **27**, 239 (1961).
12) H. Hirase, C. Araki and S. Nakanishi, This Bulletin, **26**, 183 (1953).
13) K. Arai, *Nippon Kagaku Zasshi (J. Chem. Soc. Japan, Pure Chem. Sect.)*, **82**, 1416 (1961).
14) R. L. Whistler and D. F. Durso, *J. Am. Chem. Soc.*, **72**, 677 (1950).
15) M. L. Wolfrom and J. S. Miller, *Anal. Chem.*, **28**, 1037 (1956).

v/v) on heating and then filtered. The filtrate gave white crystals (1.0 g), $[\alpha]_D^{22.8}$ +143.96° (*c* 2.7, water), mp 103.5°C and identified as methyl α-D-xyloside by means of mixed melting point and comparison of the IR spectrum (KBr): 3400, 1100—1000 (OH), 740 cm^{-1} (type 3 of pyranose ring) with that of the authentic sample.

Found: OCH_3, 18.55 %. Calcd for $C_5H_9O_4(OCH_3)$: OCH_3, 18.9 %.

Methyl 2,3,4-Tri-O-acetyl-α-L-rhamnopyranoside: After dissolving the methyl α-L-rhamnoside fraction (1.1 g) in pyridine (10 m*l*), acetic anhydride (20 m*l*) was added. After 24 hr the solution was dropped into ice water and the white solid (0.88 g) separated was filtered. Recrystallization from aqueous-methanol (1 : 2 v/v) gave white crystals, $[\alpha]_D^{14.4}$ −8.10° (*c* 0.29, methanol), mp 84—85°C (lit 86—87°C),[16] identified as methyl 2,3,4-tri-*O*-acetyl-α-L-rhamnopyranoside by means of mixed melting point and comparison of the IR spectrum (KBr): 1745, 1375 and 1225 cm^{-1} (OAc), 850 cm^{-1} (type 2a of pyranose ring) with the authentic sample.

Found: OCH_3, 18.00%. Calcd for $C_6H_{11}O_4(OCH_3)$: OCH_3, 17.4%.

Methyl α-D-Glucoside: The glucoside fraction (white solid: 0.58 g) was dissolved in methanol-acetone (1 : 2 v/v) on heating and then filtered. The filtrate gave white crystals (0.55 g) mp 163—164°C, $[\alpha]_D^{28.0}$ +150.30° (*c* 0.24, water) which recrystallized from the same mixed solvent. The crystals were identified as methyl α-D-glucoside by means of mixed melting point and comparison of the IR spectrum (KBr): 840 cm^{-1} (type 2a of pyranose ring), 745 cm^{-1} (type 3 of pyranose ring) with that of the authentic sample.

Found: OCH_3, 15.40%. Calcd for $C_6H_{11}O_5(OCH_3)$: OCH_3, 15.97%.

Separation and Identification of Methyl α-L-Rhamnobioside. A solution (3 m*l*) of *n*-butanol-water (6 : 1 v/v) containing fraction III (0.5 g) was chromatographed on a column (2×50 cm) of cellulose powder with *n*-butanol saturated with water according to the method of Hough[17] and the eluates (5 m*l* each) were collected automatically and analyzed by means of specific rotation and paper chromatography. The eluates containing the same components were combined, and then *n*-butanol was distilled off *in vacuo*. The residues dried on pottassium hydroxide in a dessiccator gave white crystals.

TABLE 2. CHROMATOGRAPHIC SEPARATION OF FRACTION III ON CELLULOSE POWDER

Fraction	Eluate No.	Yield (g)	R_f value
III-a	51— 58	0.11	0.31
III-b	59—100	0.33	0.31, 0.24
III-c	101—110	0.04	0.24

Fraction III-a in Table 2 recrystallized from methanol-water (4 : 1 v/v) gave needles, mp 123—125°C, $[\alpha]_D^{22.5}$ −16.0° (*c* 2.0, water), R_f 0.31 (orange brown by *o*-aminophenol reagent).

Found: C, 48.11; H, 7.39 %. Calcd for $C_{13}H_{24}O_9$: C, 48.14; H, 7.40 %.

Found: OCH_3, 8.89%. Calcd for $C_{12}H_{21}O_8(OCH_3)$: OCH_3, 9.56%.

Fraction III-a was hydrolyzed with 0.1 N sulfuric acid solution (5 m*l*) in a boiling water bath for 1 hr, neutralized with barium carbonate and then filtered. The filtrate was vacuum evaporated and chromatographed. It gave only rhamnose spot (R_f 0.37).

Enzymic Hydrolysis of Fraction III-a. Fraction III-a (20 mg) was hydrolyzed with β-glucosidase (emulsin, 0.1 g) in an acetic acid-sodium acetate buffer solution (pH 4.1) at 30°C in a water bath for 1 hr. After filtration, the filtrate was chromatographed on paper. The R_f value did not change at all before treatment with β-glucosidase. However, Fraction III-a gave rhamnose by hydrolysis with maltase in a phosphoric buffer solution (pH 6.4) at 37°C for 1.5 hr.

Fractions III-b and III-c in Table 2 were hydrolyzed with 0.1 N sulfuric acid solution as Fraction III-a and then chromatographed. The hydrolysates from both fractions gave two spots corresponding to xylose and rhamnose by paper chromatography.

The author is indebted to Professor T. Matsuura of Hiroshima University for his continued advice and encouragement, to Professor C. Araki and Dr. K. Arai of Kyoto Tech. University for their helpful discussion and generous gift of the authentic samples.

16) E. Fischer, M. Bergmann and A. Rabe, *Ber.*, **53**, 2362 (1920).

17) L. Hough, J. K. N. Jones and W. H. Wadman, *J. Chem. Soc.*, **1949**, 2511.

BULLETIN OF THE CHEMICAL SOCIETY OF JAPAN VOL. 42 3499—3504 (1969)

The Diels-Alder Reactions of Polychloro-2,4-cyclohexadienones

Kenichi SOMEKAWA,* Taku MATSUO** and Sanetada KUMAMOTO*

* *Department of Applied Chemistry, Faculty of Engineering, Kagoshima University, Kamoike, Kagoshima*
** *Department of Organic Synthesis, Faculty of Engineering, Kyushu University, Hakozaki, Fukuoka*

(Received March 10, 1969)

2,3,4,5,6,6-Hexachloro-, 2,3,4,6,6-pentachloro-, and 2,4,6,6-tetrachloro-2,4-cyclohexadienones were found to undergo Diels-Alder reactions when the compounds were heated with such dienophiles as acrylic acid, methyl acrylate, methyl vinyl ketone, acrylonitrile, and ethyl vinyl ether. It was concluded, chiefly through analysis of these NMR spectra, that the reactions proceed stereospecifically to give a series of 7-substituted and polychlorinated bicyclo-[2.2.2]oct-5-en-2-ones, which is in agreement with the endo rule. The stereospecificity of these adducts does not, however, agree with the results of calculations by means of the perturbation method.

The Diels-Alder reaction is one of the most popular and useful reactions for organic chemists.[1] Accordingly, a number of theoretical studies have been made on the various problems concerning the reaction mechanism.[2] The arguments, however, have not been settled in many respects.[3] One of the most important questions is the nature of the factor that determines the final orientation between the diene and dienophile.[4,5] Most recently, Herndon and Hall have made a quantitative prediction, on the basis of the second-order perturbation calculations, on the relative reactivities and adduct structures in several competitive Diels-Alder reactions.[6] In that case, both the dienes and the dienophiles have been assumed to be axially symmetric and planar molecules. The predictions are in fairly good agreement with the experimental results. It may be worthwhile, then, to test the applicability of Herndon and Hall's method to the Diels-Alder reaction, where neither component is a symmetrical molecule. In the present experiment, unsymmetrical molecules were chosen both as the dienophiles and as the dienes. In relation to the choice of the compound, it should be mentioned here that the Diels-Alder reactions easily proceed, in spite of Woodward's prediction,[5] if a dienophile with an electron-donating substituent is added either to a polyhalogenated diene like haxachlorocyclopentadiene[7] or to an α,β-unsaturated, exocyclic carbon compound like dehydroindigo.[8] The diene components investigated here (Fig. 1) are polyhalogenated compounds, and all have an exocyclic carbonyl group in conjugation with the double bond. Thereupon, one would expect that the experimental results would not be in accordance with the theoretical predictions. Therefore, the structures of the adducts obtained were carefully investigated by means of their NMR spectra. Since the reactions were found to be stereospecific, the mechanisms were speculated about from various standpoints, such as the second-order perturbation energies and the steric hindrances in the course of the reactions.

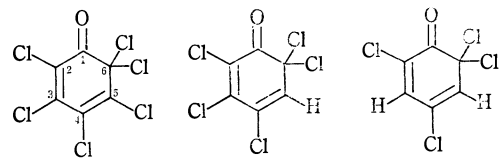

A B C

Fig. 1. Polychloro-2,4-cyclohexadienones.

Experimental

Materials. The synthesis of 2,3,4,5,6,6-hexachloro-2,4-cyclohexadienone (A) and its Diels-Alder reactions have been reported previously.[9] 2,3,4,6,6-Pentachloro-2,4-cyclohexadienone (B) was prepared by the follow-

1) K. Alder and G. Stein, *Angew. Chem.*, **50**, 510 (1937).

2) a) A. Streitwieser, Jr., "Molecular Orbital Theory for Organic Chemists," John Wiley, New York, N. Y. (1961), p. 432. b) M. Charton, *J. Org. Chem.*, **31**, 3745 (1966). c) M. Imoto, "Fuka-Hanno (Addition Reactions)," Tokyo Kagaku Dojin Co., Ltd., Tokyo (1967), p. 163.

3) J. Sauer, *Angew. Chem. Intern. Ed. Engl.*, **6**, 16 (1967).

4) K. Fukui, *J. Chem. Phys.*, **20**, 722 (1952).

5) R. Hoffmann and R. B. Woodward, *J. Am. Chem. Soc.*, **87**, 4388 (1967).

6) W. C. Herndon and L. H. Hall, *Theoret. Chim. Acta*, **7**, 4 (1967).

7) K. L. Williamson, *J. Am. Chem. Soc.*, **85**, 516 (1963)

8) R. Pummerer and H. Fiesselmann, *Ann. Chem.*, **544**, 206 (1940).

9) a) S. Kumamoto, *Kogyo Kagaku Zasshi (J. Chem. Soc. Japan., Ind. Chem. Sect.)*, **64**, 188 (1961). b) K. Somekawa, H. Uemura and S. Kumamoto, *ibid.*, **72**, 2012 (1969).

ing method. 2,3,4,6-Tetrachlorophenol (16 g) was mixed with *t*-butyl hypochlorite[10] (11 g) at 0°C. The mixture was then kept at 40°C for 30 min, and the *t*-butanol thus produced, together with the excessive *t*-butyl hypochlorite, was removed under reduced pressure.[11] The remaining yellow liquid (18 g) was B (Found: C, 28.16; H, 0.60; Cl, 65.64%. Calcd for C_6HOCl_5: C, 27.56; H, 0.38; Cl, 66.02%. IR: $\nu_{C=O}=1718\ cm^{-1}$, NMR: $\delta_H=6.9$ ppm from TMS in the carbon tetrachloride solution). It is suspected, from the small NMR peak downfield from B, that B contains as impurities small amounts of 2,4,5,6,6-pentachloro-2,4-cyclohexadienone (B′) or 2,3,4,4,6-pentachloro-2,5-cyclohexadienone. Since, however, no Diels-Alder products of B′ were obtained, no further description of the properties will be made in this paper. 2,4,6,6-Tetrachloro-2,4-cyclohexadienone (C) was analogously prepared from 2,4,6-trichlorophenol (10 g) and *t*-butyl hypochlorite (10 g).[11] 11.5 g of the product were obtained; the properties were as follows:

Found: C, 31.70; H, 1.08; Cl, 60.43%. Calcd for $C_6H_2OCl_4$: C, 31.58; H, 0.88; Cl, 61.00%. $\nu_{C=O}=1715\ cm^{-1}$, $\delta_H=6.58$, 7.08 ppm, $J_{H-H}=2.0$ cps. The compounds used as the dienophiles were extra-pure-grade chemicals supplied by the Tokyo Kasei Ind. Co., Ltd., and were further purified before the experiments. The purities of the samples were proved by gas chromatography to be above 95%.

Procedure. In general, the reaction was carried out by refluxing a nearly equimolar mixture of a diene and a dienophile on a water bath. The precipitated product was separated from the remaining solution and was recrystallized from one of the following solvents: toluene, benzene, petroleum benzine, or petroleum ether. When the product was an oily substance, column-chromatography on activated alumina was used to purify the material. The reaction conditions, yields, mp, analytical data, and characteristic IR absorption bands of the pure products are summarized in Tables 1, 2, and 3. Chromatographic separations of the filtrates were also carried out on columns of alumina or on TLC of silica gel (Wakogel B-5) in order to detect possible isomeric by-products. No products other than those in Table 1 were, however, detected. Moreover, the products which were given by slow reactions at room temperature were identical with those in Table 1, indicating that no isomerizations had occurred under the present experimental conditions (Table 1).

Measurement and Analysis of NMR Spectra. The spectra were obtained by the use of a Varian A-60 analytical NMR spectrometer. The concentrations of the samples were kept at 0.5—5 mol %, and a small amount of TMS was dissolved in the solution as an internal reference. The obtained spectra were analyzed by the use of an electronic computer.*1 The computer programs for calculating the energies and the intensities for ABC[12] and ABCD[13] spin systems were made by the present authors.*2 The calculations were repeated until the calculated energy and intensity came within ±0.3 cps and ±10 % respectively of the observed values.

Results and Discussion

The results of elementary analyses for the reaction products are summarized in Table 2. The results are in good agreement with the values calculated for the rational formula which correspond to 1 : 1 adducts of the reactants. The characteristic IR absorption bands of the products are shown in

TABLE 1. REACTIONS AND PRODUCTS

Reaction condition					Product		
Dienone	(g)	Dienophile* Z	(g)	Time (hr)	Yield (%)	Mp (°C)	Symbol
B	5.3	COOH	1.5	0.5	48	219—220.5	I
B	5.4	CO_2CH_3	1.8	13	57	96.5—98	II
B	5.3	C≡N	1.3	11	36	170—171	III
B	5.2	$COCH_3$	1.6	3	29	120—121	IV
B	10.2	OC_2H_5	3.2	15	60	oil	V
C	9.7	COOH	5.6	7	28	201—202	VI
C	5.1	CO_2CH_3	1.9	12	52	124—125	VII
C	5.1	C≡N	1.4	14.5	26	158—159.5	VIII
C	10.0	$COCH_3$	3.0	8	31	137—139	IX
C	21.5	OC_2H_5	8.9	10	55	oil	X

* CH_2=CH-Z

10) H. M. Teeter, R. C. Bachmann, E. W. Bell and J. C. Cowan, *Ind. Eng. Chem.*, **41**, 849 (1949).

11) L. Denivelle and R. Fort, *Compt. rend.*, **235**, 1514 (1952); *Chem. Abstr.*, **48**, 553 (1954).

*1 A model OKITAC 5090 computer at the computer center of Kyushu University was used for this purpose.

12) C. A. Reilly and J. D. Swalen, *J. Chem. Phys.*, **32**, 1378 (1960).

13) a) C. A. Reilly and J. D. Swalen, *ibid.*, **34**, 980 (1961). b) J. W. Emsley, J. Feeney and L. H. Sutcliffe, "High Resolution Nuclear Magnetic Resonance Spectroscopy," Vol. 1, Pergamon Press, Oxford (1965), p. 426.

*2 The matrix elements of the secular determinant for the ABCD system were examined all over again. The results are in agreement with those obtained by Reilly and Swallen[13a]; some errors were found, however, in the table given by Emsley *et al.*[13b]

Table 2. Analytical data of the products

Product	Formula	Found (%)				Calcd (%)			
		C	H	Cl	N	C	H	Cl	N
I	$C_9H_5Cl_5O_3$	31.94	1.38	52.34	—	31.94	1.49	52.38	—
II	$C_{10}H_7Cl_5O_3$	34.10	1.88	49.52	—	34.10	1.99	49.32	—
III	$C_9H_4Cl_5NO$	33.94	1.18	55.52	4.46	33.84	1.26	55.50	4.39
IV	$C_{10}H_7Cl_5O_2$	35.36	2.11	52.50	—	35.82	2.10	52.65	—
V	$C_{10}H_9Cl_5O_2$	34.62	2.22	52.09	—	35.50	2.68	52.41	—
VI	$C_9H_6Cl_4O_3$	35.49	1.92	46.06	—	35.56	1.99	46.65	—
VII	$C_8H_8Cl_4O_3$	37.77	2.60	44.57	—	37.77	2.53	44.59	—
VIII	$C_9H_5Cl_4NO$	37.82	1.67	49.48	4.90	37.93	1.77	49.70	4.92
IX	$C_{10}H_8Cl_4O_2$	40.44	2.71	46.88	—	39.81	2.67	46.99	—
X	$C_{10}H_{10}Cl_4O_2$	39.04	3.18	45.79	—	39.55	3.32	46.64	—

Table 3. Characteristic absorption bands of adducts (IR, cm^{-1})

Adduct	Absorption due to transformation of dienone		Absorption of substituent, Z,* due to transformation of dienophile			
	$\nu_{C=O}$	$\nu_{C=C}$	νZ	(C=O,	C≡N,	C-O)
I	1765	1600	1712			1242
II	1765	1615	1736			1215
III	1770	1610			2260	
IV	1764	1610	1713			
V	1762	1611				1118
VI	1770	1618	1715			1242
VII	1771	1618	1735			1212
VIII	1770	1615			2260	
IX	1762	1622	1721			
X	1762	1620				1120

* CH_2=CH-Z

Table 3. The presence of a double bond is suggested (third column). However, there are no signs of the absorption bands due to the mono-substituted ethylenes. The sharacteristic absorption bands of the substituents (Z), on the other hand, are clearly observed, as are given in the table from the fourth column to sixth. As may be seen from the frequencies, the substituents are not likely to be conjugated with any unsaturated groups. The frequencies of the carbonyl absorption bands (1762—1771 cm^{-1}) in the second column are close to that of octachloro-3-cyclohexenone (1779 cm^{-1}).[14] Therefore, the presence of a polychloro-3-cyclohexenone ring is indicated.*[3] The above facts suggest strongly that the product is a 4+2 adduct which could be obtained by a Diels-Alder reaction between the polyhalogenated dienone and the monosubstituted ethylene.

In order to decide on the most probable structures for the adducts, the NMR spectra were carefully examined. Examples of the analyzed spectra are shown in Figs. 2—4. The chemical shifts (δ) and the coupling constants (J) thus obtained are summarized in Tables 4 and 5. As a consequence, the

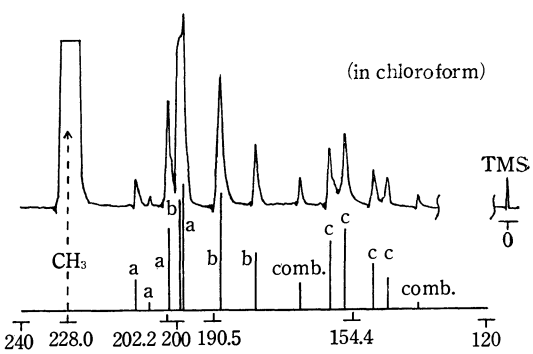

Fig. 2. Adduct of A with methyl acrylate (NMR, cps).

14) S. Kumamoto, Thesis, Kyushu University (1962).

*3 Carbonyl absorption bands are known to shift to frequencies higher by 10—25 cm^{-1} if a chlorine atom is attached to the carbon atom alpha to the carbonyl group.[15] Hence, the difference between the carbonyl absorptions of octachloro-3-cyclohexenone and those of the adducts in Table 3 may be reasonably explained as due to the difference in the number of alpha chlorine atoms.

15) K. Nakanishi, "Infrared Absorption Spectroscopy," Holden-Day, Inc., San Francisco, and Nankodo Co., Ltd., Tokyo (1962), p. 42.

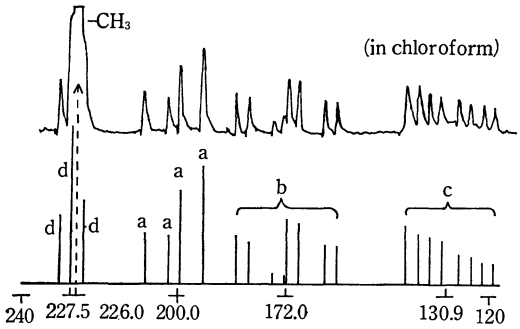

Fig. 3. Adduct of B with methyl acrylate (NMR, cps).

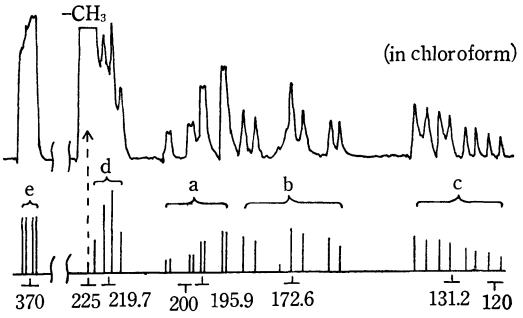

Fig. 4. Adduct of C with methyl acrylate (NMR, cps).

TABLE 4. CHEMICAL SHIFTS OF ADDUCTS (NMR, cps)

Run	Adduct ((Dienone)+(Z)[a])	Solvent	Chemical shift (δ)[d]					
			H_A	H_B	H_C	H_D	H_E	H_Z
1	((A)+(COOH))[b]	S 1	233.6	204.1	178.1	—	—	938
2	I	S 1	227.3	180.3	148.9	247.5	—	731
3	VI	S 1	216.0	178.2	145.4	232.3	390.0	563
4	((A)+(CO_2CH_3))	S 1	233.6	195.2	167.8	—	—	219.6
5	((A)+(CO_2CH_3))	S 2	202.2	190.5	154.4	—	—	228.0
6	II	S 1	227.0	173.8	139.3	248.5	—	220.2
7	II	S 2	200.0	172.0	130.9	227.5	—	226.8
8	VII	S 1	210.5	169.5	133.7	229.7	380.0	222.0
9	VII	S 2	195.9	172.6	131.2	219.7	370.0	225.0
10	((A)+(C≡N))	S 2	213.6	200.1	163.8	—	—	—
11	III	S 2	213.4	183.5	145.6	231.0	—	—
12	VIII	S 2	207.2	182.8	141.4	221.5	377.5	—
13	((A)+($COCH_3$))	S 2	212.2	185.7	151.5	—	—	262.0
14	IV	S 2	210.5	167.3	116.5	228.7	—	136.5
15	IX	S 2	206.0	168.2	116.8	220.7	266.5	136.0
16	((A)+(OC_2H_5))	S 2	236.2	198.1	145.5	—	—	216,72
17	V	S 2	233.2	174.7	119.1	212.2	—	216,72

a) CH=CH–Z. b) An adduct of A and acrylic acid. c) S1=Pyridine, S2=chloroform.
d) Expressed in cycles per second downfield from tetramethylsilane resonance.

TABLE 5. COUPLING CONSTANTS OF ADDUCTS (cps)

Run*	J_{AB}	J_{AC}	J_{BC}	J_{BD}	J_{CD}	J_{DE}	J_{EA}
1	9.8	5.8	−13.2				
2	9.6	6.5	−13.7	3.0	3.0		
3	9.6	6.7	−13.7	3.0	3.0	2.5	1.0
5	9.1	5.6	−13.1				
7	9.5	6.4	−13.5	3.1	3.1		
9	9.5	6.4	−13.5	3.0	3.0	2.5	1.0
10	9.4	5.4	−13.5				
11	9.7	5.8	−13.8	3.0	3.0		
12	9.8	5.6	−14.2	3.0	3.0	2.5	1.0
13	9.2	6.0	−12.9				
14	9.6	6.6	−13.7	3.0	3.0		
15	9.6	6.6	−13.5	3.0	3.0	2.5	0.7
16	8.0	3.0	−13.8				
17	8.0	3.2	−14.2	3.0	3.0		

* Equal to run numbers of Table 4.

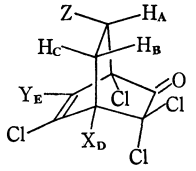

X=Y=Cl; from A
X=H, Y=Cl; from B
X=Y=H; from C
Z=CO_2H, CO_2CH_3, C≡N, $COCH_3$ or OC_2H_5

Fig. 5. The steric structures of adducts.

mutual orientation between the diene and the dienophile components in the adduct molecules were deduced to be as are shown in Fig. 5. The reasons will be described in detail below.

In the case of methyl acrylate adducts, one can clearly notice that the signals b and c of the adducts become increasingly complex upon the variation of the diene component from A to B (Figs. 2 and 3). The analysis shows that the proton H_D is almost equally coupled to H_B and H_C, but not to H_A (Table 5). The newly-appearing signals, d, in Fig. 3 should correspond to the proton at the 5-position of B, which should be found at the bridge head in the adduct molecule. Therefore, it may be suggested that the α-methine and β-methylene groups of the dienophile component are bonded to the 2- and 5-positions respectively of the diene component, B.

Similar arguments with the adduct obtained from C and methyl acrylate also indicate that the mutual orientation of the two components is the same as that in the case of B and methyl acrylate. In the case of the adduct obtained from A, one should notice at first that the coupling constants among the protons H_A, H_B, and H_C are almost the same as those in the adducts from B or C (Table 5). Therefore, the steric arrangements of these three protons may be expected to be the same among the three adducts. In addition, the replacement of the bridge head proton, H_D, with a chlorine atom, *i.e.*, the variation of the diene from B to A, is seen to have much greater effects on the chemical shifts of the protons H_B (+18.5 cps) and H_C (+23.5 cps) than on H_A (+2.2 cps), as is shown in Run 4 and Run 6 of Table 4. One may think, then, that the methylene group of the dienophile component is bonded to the 5-position of A. In other words, the orientation of the diene with respect to the dienophile component is the same between the adducts obtained from A, B, and C.

The signals for H_B invariably appear in a field lower by 34.2—55.6 cps than those for H_C in chloroform (Table 4). There may be two explanations for this nonequivalence of the geminal protons. Granting the configuration in Fig. 5 to be correct, one would expect that H_B would be considerably deshielded because it is very close (*ca.* 2.5 Å) to the chlorine atom alpha to the carbonyl group of the polychloro-3-cyclohexenone ring. There are a number of examples of such van der Waals shifts

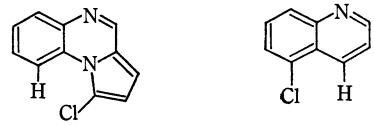

−60 cps[a] −29 cps[b]

Fig. 6. Van der Waals shifts induced by chlorines.
a) C. F. Raymond *et al.*, *J. Org. Chem.*, **29**, 2440 (1964).
b) F. A. L. Anet, *J. Chem. Phys.*, **32**, 1274 (1960).

(Fig. 6). The H_C proton, on the other hand, is shielded because of the anisotropy of the carbon-carbon double bond. The joint effect of these two factors seems to give a reasonable explanation of the observed difference between H_B and H_C.

The vicinal coupling constants for bicyclic systems similar to the compounds under investigation have been studied by several investigators. Some relevant examples are shown in Fig. 7. It is generally found in these examples that J_{cis} is larger than J_{trans}. Both of these coupling constants decrease with the electron-withdrawing property of the substituent (Z) attached to the ethylene group. The same could be said of the cases of bicyclo-[2.2.1]-heptane derivatives.[16] It is reasonable to expect that the vicinal coupling constants of the adducts under investigation will follow the same trend as those described above.

On this basis, it may be suggested that H_B and H_C are, respectively, at the *cis*- and *trans*-positions

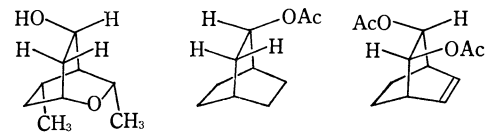

J_{trans}=3.6[a] J_{trans}=2.6[b] J_{trans}=6.0[b]
J_{cis}=9.8 J_{cis}=8.2

Fig. 7. Vicinal coupling constants in bicyclo-[2.2.2]ring system.
a) J. S. Webb *et al.*, *J. Am. Chem. Soc.*, **84**, 3183 (1962).
b) K. Tori *et al.*, *Chem. Ber.*, **97**, 2798 (1964).

J_{AB}=9.1—9.8, 8 (when Z=OC_2H_5)
J_{AC}=5.4—6.7, 3 (when Z=OC_2H_5)

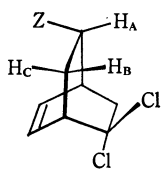

Fig. 8. Configuration.

16) K. L. Williamson, *J. Am. Chem. Soc.*, **85**, 516 (1963).

with respect to H_A (Fig. 8). This suggestion is further confirmed by observing the large vicinal coupling constant (9.1 cps) of the maleic anhydride adduct,[9a] where only *cis*-coupling might be expected to be present. The values for the geminal coupling constant (J_{BC}) and the long-range coupling constant (J_{AE}) are also resonable for this type of bicyclic compound.[17-19] The configuration which is in best agreement with the above discussion is thus concluded to be the one shown in Fig. 5.

Since the reaction products were found to be stereospecific, as has been described above, an attempt has been made to elucidate the reaction mechanism by the use of a simple molecular orbital method.*4 The charge densities in the electron systems of a diene, A, and a dienophile, methyl vinyl ketone (F), are shown in Fig. 9. On the basis of the charge densities of the two components (Fig. 9), the β carbon of the dienophile may be expected to be attracted to the cardon atom at the 2-position of the cyclohexadienone system. Since the experimental result is just the opposite of this prediction, however, the electrostatic attraction in the ground state is not considered to play an important role in the reaction mechanism. If the reaction proceeds *via* a one-step, cyclic, concerted mechanism,[6] the relative preferences among several different geometries in the activated states may be compared by evaluating the stabilization energy for the interacting electron systems in each case. The stabilization energies were estimated by the second-order perturbation method for the three orientations shown in Table 6. The molecular planes of the diene and dienophile (below) were assumed to be parallel to each other.

Fig. 9. The charge density of 2,3,4,5,6,6-hexachloro-2,4-cyclohexadienone (A) and methyl vinyl ketone (F).

TABLE 6. STABILIZATION ENERGIES CALCULATED BY SECOND ORDER PERTURBATION METHOD (in β unit)

Inter-planar distance (Å)	Mutual orientations (*ortho-endo*)	(*ortho-exo*)	(*meta-endo*)
2.5	0.429	0.514	0.492
3.4	0.013	0.017	0.016

Geometries of A and F used for calculation.

A: O–C_1, 1.24Å; C_1–C_2, 1.43Å; C_2–C_3, 1.37Å; C_3–C_4, 1.45Å; C_4–C_5, 1.34Å; C–Cl, 1.76Å; $\angle OC_1C_2$, $\angle C_1C_2C_3$, $\angle C_2C_3C_4$, $\angle C_3C_4C_5$, 121°; $\angle CCCl$, 119.5°.

F: O–C_1, 1.24Å; C_1–C_α, 1.45Å; C_α–C_β, 1.34Å; $\angle OC_1C_\alpha$, $\angle C_1C_\alpha C_\beta$, 121°.

The calculations were made for the cases of two different interplanar distances, 3.4 and 2.5Å, and all π orbitals of the two components were taken into consideration.*5 The results are summarized in Table 6. The stabilization energies indicate that an *ortho-exo* addition is most favored. In actuality, however, *ortho-endo* adducts are produced exclusively. Thus, it is clear that Herndon and Hall's method is not powerful enough to cover all of the Diels-Alder reactions. For that matter, Woodward and Katz's simple method[20] can not be expected to give the answer, either.*6 The true cause of the formation of stereospecific products may be found either in steric factors or in electronic factors which can not be taken into consideration by simple molecular orbital calculation. Further investigation is being undertaken to solve this complex problem the results will be reported in later paper.

The authors are indebted to the members of the computing center at Kyushu University. Thanks are also due to Mr. Y. Kodera and Mr. M. Fukumitsu, who made careful measurements of the NMR spectra reported in this paper.

17) R. C. Cookson, T. A. Crabb, J. J. Frankel and J. Hudec, *Tetrahedron, Suppl.*, **7**, 355 (1967).

18) P. Laszlo and P. von R. Schleyer, *J. Am. Chem. Soc.*, **86**, 1171 (1964).

19) K. Tori, Y. Takano and K. Kitahonoki, *Chem. Ber.*, **97**, 2798 (1964).

*4 The following parameters were used in the calculation.[2a]

A: $h_{\ddot{O}}=2.0$, $h_{C_1}=0.3$, $h_{C_5}=0.1$, $h_{C_1}=2.0$, $K_{C=O}=1.4$, $K_{C_2-C_3,\ C_4-C_5}=1.1$, $K_{C-Cl}=0.4$. F: $h_{\ddot{O}}=2.0$, $h_{C_1}=0.3$, $K_{C=O}=1.4$, $K_{C_\alpha-C_\beta}=1.1$.

*5 The following formula was used for calculating the second-order perturbation energies.[6]

$$\Delta E = 2[\sum_{m}^{occ.}\sum_{n}^{vac.} - \sum_{m}^{vac.}\sum_{n}^{occ.}]\frac{[\sum_{i,j} a_{m,i}b_{n,j}P_{mi,nj}]^2}{E_m - E_n}$$

The resonance integrals, $P_{mi,nj}$, were then calculated from the overlap integrals[21] by the use of Mulliken's equation.[22]

20) R. B. Woodward and T. J. Katz, *Tetrahedron*, **5**, 70 (1959).

21) N. Tyutyulkov and P. Markov, *Montsh. Chem.*, **96**, 2030 (1965).

22) R. S. Mulliken, *J. Phys. Chem.*, **56**, 295 (1952).

*6 Polychloro-2, 4-cyclohexadienones (A, B, and C) are characterized by their high electron affinities and ionization potentials. Therefore, the situation is just the opposite of the case which Woodward and Katz have presumed in their discussion. It may be worth mentioning, in this connection, that the diene reacts with cyclopentadiene, but not with maleic anhydride.

BULLETIN OF THE CHEMICAL SOCEITY OF JAPAN VOL. 42 3505—3508 (1969)

Studies of Phosphorylation. III. Selective Phosphorylation of Unprotected Nucleosides[1)]

Masaharu YOSHIKAWA, Tetsuya KATO and Tadao TAKENISHI

Central Research Laboratories, Ajinomoto Co., Inc., Kawasaki

(Received April 15, 1969)

During an investigation of the factors affecting the reaction of 2′,3′-*O*-isopropylidene nucleosides with phosphoryl chloride, trialkyl phosphates were found to be powerful accelerators and useful solvents for the phosphorylation. The addition of a trialkyl phosphate to a large excess of phosphoryl chloride was markedly effective in promoting the phosphorylation; further, the lower alkyl phosphates, such as trimethyl and triethyl phosphates, were able to replace the excessive amount of phosphoryl chloride as solvents. When unprotected nucleosides were treated with phosphoryl chloride in trimethyl phosphate, the corresponding 5′-phosphates were mainly produced, together with a small amount of highly-phosphorylated products, in good yields. On the contrary, the treatment of 5′-*O*-acetyl nucleosides in a similar manner gave the corresponding 2′(or 3′)-nucleotides in low yields. The formation of the 2′(or 3′)-phosphate was strongly inhibited by the addition of a small amount of water to the reaction mixture. Thus, the selective phosphorylation of unprotected nucleosides to the 5′-nucleotides in a one-step procedure was accomplished.

It has been reported, in a previous paper,[2)] that 5′-nucleotides can be conveniently prepared in high yields by the treatment of 2′,3′-*O*-isopropylidene nucleosides with a large amount of phosphoryl chloride in the absence of any organic solvent. When a small amount of water was added to posphoryl chloride prior to the reaction, the yield of nucleotides was very much increased.

A similar effect was also observed upon the addition of alcohols. The reaction of *t*-butyl alcohol with an excessive amount of phosphoryl chloride gives hydrogen phosphorodichloridate according to Eq. (1):[2)]

$$t\text{-}C_4H_9OH + POCl_3 \rightarrow t\text{-}C_4H_9Cl + HOP(O)Cl_2 \quad (1)$$

On the other hand, it has been reported that the reaction of a primary alcohol with phosphoryl chloride proceeds satisfactorily at a low temperature according to Eq. (2):[3)]

$$ROH + POCl_3 \rightarrow ROP(O)Cl_2 + HCl \quad (2)$$

Therefore, an alkyl phosphorodichloridate may be considered to function as a potential accelerator for the phosphorylation as well as hydrogen phosphorodichloridate.

In the presence of an excessive amount of an alcohol, this reaction is known to proceed further to form the dialkyl phosphorochloridate and the trialkyl phosphate. The accelerating effect of these compounds, particularly the latter, on the reaction rate has been studied and found to be positive, as will be discussed later. It has also been found that an excessive amount of phosphoryl chloride may be replaced by a trialkyl phosphate as a solvent.

The treatment of an unprotected nucleoside with phosphoryl chloride in a trialkyl phosphate gives the phosphorylated products in a high yield. Analysis of the products showed that the phosphorylation always occurred preferentially on the hydroxyl group at the 5′-position in nucleosides. The selective phosphorylation of an unprotected nucleoside with phosphoryl chloride in a trialkyl phosphate has already been briefly communicated.[1)] This paper will deal with an extensive study of the factors affecting the reaction of nucleosides with phosphoryl chloride and the phosphorylation of nucleosides in the presence of a trialkyl phosphate.

Results and Discussion

The effect of the addition of alcohols on the phosphorylation of 2′,3′-*O*-isopropylideneinosine with phosphoryl chloride is shown in Fig. 1. Although the yield of inosine 5′-phosphate was not affected by the addition of *t*-butyl alcohol, the yield was significantly decreased with an increase in the amount of methyl or of isopropyl alcohol. The disadvantage of the latter cases may be due to the production of a high concentration of hydrogen chloride according to Eq. (2). In order to eliminate the influence of hydrogen chloride, methyl phosphorodichloridate,

1) A part of this study was preliminarily communicated: M. Yoshikawa, T. Kato and T. Takenishi, *Tetrahedron Letters*, **1967**, 5065. Part II: K. Kusashio and M. Yoshikawa, This Bulletin, **41**, 142 (1968).

2) M. Yoshikawa and T. Kato. This Bulletin, **40**, 2849 (1967).

3) G. M. Kosolapoff, "Organophosphorus Compounds," John Wiley & Sons, New York (1950), p. 211.

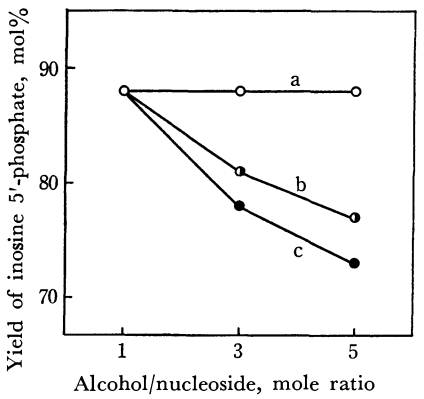

Fig. 1. Influence of addition of alcohols.
Experimental condition: 2',3'-*O*-Isopropylideneinosine, 2.0 g; $POCl_3$, 10 m*l*; Temperature, 5°C
a: *t*-Butyl alcohol, b: *i*-Propyl alcohol, c: Methyl alcohol

Table 1. Effect of addition of methyl phosphorochloridates or trimethyl phosphate

Additive	Yield (mol%)			
	Inosine 5'-phosphate		Guanosine 5'-phosphate	
	1 hr	2 hr	2 hr	6 hr
none	26	70	7	14
CH_3OPOCl_2	44	88	12	51
$(CH_3O)_2POCl$	92	92	78	86
$(CH_3O)_3PO$	93	91	80	87

Experimental condition: 2',3'-*O*-Isopropylidene nucleoside, 6.5 mol; $POCl_3$, 10 m*l*; Additive, 13 mmol; Temperature, 5°C

dimethyl phosphorochloridate and trimethyl phosphate were synthesized and added similarly to the phosphorylation mixture. Table 1 shows the results of the phosphorylation of 2',3'-*O*-isopropylidene nucleosides in the $POCl_3$-$(RO)_nPOCl_{3-n}$ systems. Although the reaction of a nucleoside with methyl phosphorodichloridate scarcely proceeds at all under these conditions, the phosphorylation of a nucleoside with phosphoryl chloride was markedly promoted in the presence of the phosphorodichloridate. The increasing effect of those additives on the reaction rate is arranged in the order: $ROP(O)Cl_2 < (RO)_2P(O)Cl < (RO)_3PO$. An especially interesting result observed here was a sharp increase in the rate of phosphorylation with an increase in the amount of trimethyl phosphate. 2',3'-*O*-Isopropylidene nucleosides were moderately soluble in anhydrous trimethyl phosphate. Thus, an excessive amount of phosphoryl chloride was advantageously replaced by trimethyl phosphate as the solvent.

In a first stage, the reaction mixture of a 2',3'-*O*-isopropylidene nucleoside and phosphoryl chloride was a suspension in trimethyl phosphate. After the reaction had been completed, the suspension containing the corresponding 5'-phosphorodichloridate became clear. Thus, the phosphorylation reactions were successfully achieved; the results are summarized in Table 2. In the case of the xanthosine derivative, the phosphorylation was insufficiently, as in the previous method.

Table 2. Phosphorylation of 2',3-*O*-isopropylidene nucleosides in trialkyl phosphate*

Isopropylidene nucleoside	$POCl_3$		$P_2O_3Cl_4$	
	Time hr	Yield of 5'-nucleotide mol%	Time hr	Yield of 5'-nucleotide mol%
	in $(CH_3O)_3PO$			
Inosine	2	92	0.5	95
Guanosine	1	90	1	92
Adenosine	1.5	90	2	90
Xanthosine	12	15	6	19
Uridine	14	98	6	86
Cytidine	4	98	6	94
AICAR**	4	76		
	in $(C_2H_5O)_3PO$			
Inosine	0.5	93	1	93
Guanosine	4	88	8	76
Adenosine	2	91	2	91
Uridine	14	95	9	82
Cytidine	12	94	6	89
	in $(n\text{-}C_4H_9O)_3PO$			
Inosine	6	78	2	93
Guanosine	8	25	8	54

* Experimental condition: 2',3'-*O*-Isopropylidene nucleoside, 6.5 mmol; $POCl_3$ or $P_2O_3Cl_4$, 13 mmol; Trialkyl phosphate, 65—98 mmol; Temperature, −5°C
** 4-Amino-5-carbamoyl-1-β-D-ribofuranosylimidazole

For the reaction, triethyl phosphate and trimethyl phosphate are both suitable as solvents, but the former is less effective than the latter. The reaction rate is affected by the size of the alkyl groups in trialkyl phosphates, as is shown in Fig. 2, particularly in the phosphorylation of 2',3'-*O*-isopropylideneguanosine with phosphoryl chloride. That is, the yield of guanosine 5'-phosphate decreases as the alkyl group becomes larger. This phenomenon is supposed to be concerned primarily with the solubility and the reactivity of the nucleoside derivative. The more reactive 2',3'-*O*-isopropylideneinosine was well phosphorylated also in tri-*n*-butyl phosphate, but a prolonged reaction time was required for its completion in comparison with the phosphorylation in trimethyl phosphate.

In contrast with this excellent ability of trialkyl phosphates, the analogous trialkyl phosphorothioates and triaryl phosphates do not fulfil these conditions. The utilization of other polar organic

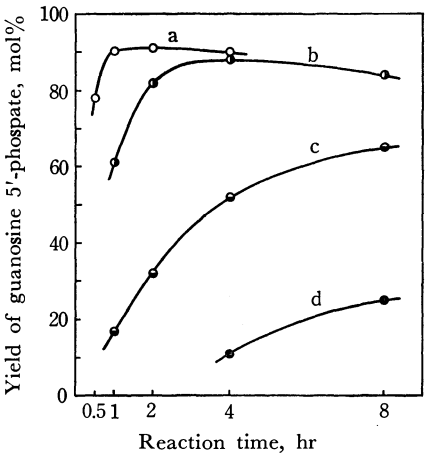

Fig. 2. Influence of alkyl group of trialkyl phosphate.
Experimental condition: 2',3'-*O*-Isopropylideneguanosine, 2.1 g; $POCl_3$, 1.2 m*l*; Trialkyl phosphate, 10 m*l*; Temperature, −5°C
a: Trimethyl phosphate, b: Triethyl phosphate, c: Tri-*β*-chloroethyl phosphate, d: Tri-*n*-butyl phosphate

solvents possessing S→O, N→O, or C=O groups, such as dialkyl sulfates, dialkyl sulfites, dialkyl sulfones, dialkyl sulfoxides, alkyl nitrates, alkyl nitrites, dialkyl carbonates, and alkyl ketones, gave generally unsatisfactory results.

Trialkyl phosphates were also attractive solvents in the phosphorylation of nucleosides with pyrophosphoryl tetrachloride. The yields of 5'-nucleotides were slightly better than those with phosphoryl chloride, particularly in the case of 2',3'-*O*-isopropylideneguanosine.

An attempt at the selective phosphorylation of unprotected nucleosides was made for the purpose of establishing the manufacturing method of 5'-nucleotides. In the previous experiments, nucleoside 5'-phosphates have been produced together with the 2'(or 3')-phosphate[4] or the 2'(or 3'), 5'-diphosphate,[5] and the yields have been reported to be low.[6] The method reported by Ikehara involving the use of 2,6-lupetidyl phosphorodichloridate is better, but it is still not satisfactory in either yield or selectivity.[7]

When treated with phosphoryl chloride in trialkyl phosphates, naturally-occurring nucleosides gave the corresponding nucleotides in nearly quantitative yields without any prior protection of the 2'- and 3'-hydroxyl groups; the products consisted mainly of the 5'-phosphates, accompanied by a small amount of such highly-phosphorylated products as the 2'(or 3'),5'-diphosphate and 2',3',5'-triphosphate (Table 3). Thus, this reaction proceeds selectively at the 5'-position. The competitive phosphorylation of the 2'(or 3')-hydroxyl group was strongly inhibited in the acidic medium; this was easily achieved by the addition of an adequate amount of water to the mixture, as is shown in Table 3. This result is of interest in comparison with the result reported by Barker and Foll[4] that the addition of a small amount of water tends to decrease the mole ratio of the 5'-phosphate in the products of the phosphorylation of adenosine with phosphoryl chloride in pyridine. As another example, 5'-*O*-acetylinosine was phosphorylated to give the corresponding 2'(or 3')-nucleotide in only a 22% yield without any prior treatment with water; moreover, it did not react under the acidic conditions, as has been described above.

Thus, the synthesis of 5'-nucleotides was emancipated from such complicated treatments as the prior protection of the nucleoside sugar, the extreme dehydration of the solvent required in the case of pyridine, or the dissolution of a nucleoside in a solvent before the phosphorylation.

It should be noted that xanthosine, which is generally unaffected by any chemical phosphorylation, was easily converted to the corresponding 5'-phosphate. Thus, this method can be applied generally to the synthesis of naturally-occurring ribonucleotides and offers a convenient procedure for industrial purposes.

In comparison with phosphoryl chloride, pyrophosphoryl tetrachloride yielded large amounts of the 2'(or 3'),5'-di- and 2',3',5'-triphosphates together with the 5'-phosphate because of its stronger reactivity. In this case, the highly-phosphorylated products were proved to be *O*-phosphate in the sugar moiety by comparison with the ultraviolet absorption spectra of the corresponding 5'-phosphate. The improvement of this technique may make an effective synthesis of a nucleoside diphosphate possible.

For the synthesis of deoxynucleoside 5'-phosphates, the phosphorylation of 3'-*O*-acetyl 2'-deoxynucleosides has been adopted, usually *via* 3'-*O*-acetyl 5'-*O*-trityl 2'-deoxynucleosides.[8] The direct treatment of thymidine with dibenzyl phosphorochloridate, followed by hydrogenolysis, has been reported to produce mainly thymidine 3',5'-diphosphate, together with some 5'-phosphate.[9] However, the phosphorylation of deoxynucleosides at a lower temperature, carried out by the use of the method described above, gave mainly the cor-

4) G. R. Barker and G. E. Foll, *J. Chem. Soc.*, **1957**, 3798.
5) F. Cramer, G. W. Kenner, N. A. Hughes and A. R. Todd, *ibid.*, **1957**, 3297.
6) J. M. Gulland and G. I. Hobday, *ibid.*, **1940**, 746.
7) M. Ikehara, E. Ohtsuka and Y. Kodama, *Chem. Pharm. Bull. (Tokyo)*, **11**, 1456 (1963).
8) A. M. Michelson and A. R. Todd, *J. Chem. Soc.*, **1953**, 951.
9) C. A. Dekker, A. M. Michelson and A. R. Todd, *ibid.*, **1953**, 947.

Table 3. Direct phosphorylation of unprotected nucleosides in trialkyl phosphate

Nucleoside	$POCl_3$					$P_2O_3Cl_4$			
	R of $(RO)_3PO$	H_2O mmol	Time hr	Yield of nucleoside-phosphate mol% 5′-mono	higher	R of $(RO)_3PO$	Time hr	Yield of nucleoside-phosphate mol% 5′-mono	higher
Inosine	CH_3CH_2	0	2	68	18	CH_3	1	54	46
Inosine	CH_3CH_2	2.0	2	91	8				
Guanosine	CH_3	0	6	85	9	CH_3	4	59	41
Guanosine	CH_3	2.0	6	90	5				
Adenosine	CH_3CH_2	0	6	84	11	CH_3CH_2	4	57	33
Xanthosine	CH_3	0	9	80	5	CH_3	12	64	22
Uridine	CH_3	0	12	89	8	CH_3	6	73	25
Cytidine	CH_3CH_2	0	1	88	8	CH_3	0.5	86	13
Deoxyinosine	CH_3	0	5	73	6				
Deoxycytidine	CH_3	0.5	6	64	19				
AICAR	CH_3	0	4	91	5				

Experimental condition: Nucleoside, 2 mmol; $POCl_3$ or $P_2O_3Cl_4$, 4 mmol (6 mmol in the case of inosine and guanosine); Trialkyl phosphate, 5 m*l*, Temperature, 0°C

responding 5′-phosphates (Table 3).

Most nucleosides are fairly soluble in trimethyl and triethyl phosphates, while those nucleosides are insoluble or only slightly soluble in pyridine, which has been used hitherto. The effect of trialkyl phosphates may be, at least partly, due to the higher solubility of nucleosides in these phosphates. This idea is supported by the difficulty of the phosphorylation in tri-*n*-butyl phosphate, in which the solubility of nucleosides is fairly low. Interaction between a trialkyl phosphate and the phosphorylating reagent may also play a role. It is considered that the interaction between a trialkyl phosphate and phosphoryl chloride is possible; an ionized structure may be formed according to the following equation:

$$(RO)_3PO + POCl_3 \rightarrow [(RO)_3P\text{-}O\text{-}\overset{\overset{O}{\|}}{P}Cl_2]^+ \; Cl^-$$

The ionized structure may be postulated as an active phosphorylating agent.

Experimental

Identification of the Products on the Paper Chromatograms. The location of the nucleoside phosphate on the chromatograms was detected by means of ultraviolet light, and it was identified by a comparison of the R_f value with that of an authentic sample. Ribonucleoside diphosphate was confirmed further by a negative periodate-benzidine test, and deoxyribonucleoside phosphate by a Hanes and Isherwood spray.[10]

Phosphorylation of 2′,3′-O-Isopropylidene Nucleoside. *Method A.* Into a cold mixture of freshly-distilled phosphoryl chloride and an alcohol or some other additive, such as methyl phosphorodichloridate, dimethyl phosphorochloridate, or trimethyl phosphate, a 2′,3′-*O*-isopropylidene nucleoside was added with stirring. After a predetermined period the reaction mixture was poured into ether, and then the precipitate was separated by centrifuge. The product was dissolved carefully in ice water, and the aqueous solution was adjusted to pH 1.5 with a sodium hydroxide solution and warmed at 70°C for 30—45 min. The resulting solution was analyzed by the paper chromatographical method described in a previous report.[2]

Method B. After a few moles of phosphoryl chloride (or pyrophosphoryl tetrachloride) per mole of a nucleoside had been mixed with a trialkyl phosphate, a 2′,3′-*O*-isopropylidene nucleoside was added to the cold mixture and the mixture was stirred. The reaction mixture was then treated in the same way as in Method A.

Selective Phosphorylation of an Unprotected Nucleoside. An unprotected nucleoside was phosphorylated according to Method B. An adequate amount of water was added to a mixture of phosphoryl chloride and a trialkyl phosphate before the addition of a nucleoside. The phosphorylation mixture was hydrolyzed in ice water after ether treatment and was then immediately analyzed by the paper chromatographical method.

The authors wish to thank Mr. Koji Kusashio and Mr. Mitsuru Sakuraba for their kind assistance in the experiment.

10) C. S. Hanes and F. A. Isherwood, *Nature*, **164** 1107 (1949).

BULLETIN OF THE CHEMICAL SOCIETY OF JAPAN VOL. 42 3509—3514 (1969)

Photochromic Color Change of the Dimer of Triphenylimidazolyl at Low Temperatures

Koko MAEDA and Taro HAYASHI*1

Department of Chemistry, Faculty of Science, Ochanomizu University, Bunkyo-ku, Tokyo

(Received April 23, 1969)

The photochromic dimer of triphenylimidazolyl which is one of two dimers obtained by oxidation of triphenylimidazole shows photochromism at temperatures between room temperature and −196°C in solutions and in a solid state. At temperatures higher than about −20°C the photochromic color in solutions is reddish-purple, at temperatures lower than about −150°C the color is bluish-purple and at intermediate low temperatures the photochromic color does not appear. Absorption spectrum and ESR measured with the change of temperature showed variations corresponding to the change of color. The photochromic color in a solid state was light reddish-purple above about −70°C and bluish-purple at −196°C. The mechanism of the color change was discussed in connection with that of the photochromism at room temperature and the results obtained from spectroscopic and ESR studies.

We obtained a photochromic compound[1] and a piezochromic compound[2] by oxydation of 2,4,5-triphenylimidazole. The photochromic compound exhibited photochromism and thermochromism in solid state[3] as well as in solutions at temperatures near room temperature. It was confirmed by kinetic studies with absorption spectrum and ESR, that the compounds are dimers of triphenylimidazolyl[4,5] and that photochromism, thermochromism and piezochromism are due to the dissociation of the dimers into triphenylimidazolyl radical caused by irradiation, heating and grinding. White and Sonnenberg[6] reported that the photochromic and piezochromic dimers are isomers and the piezochromic dimer shows thermochromism at temperatures lower than room temperature, and discussed the interconversion between two dimers and radical.

We found that a solution of the photochromic dimer in benzene exhibited photochromism within a wide range of temperatures from room temperature down to −196°C, except for temperatures between about −20°C and −150°C.[7] At temperatures higher than about −20°C, the photochromic color is reddish-purple and at temperatures lower than about −150°C bluish-purple. In the present paper, the results of studies on a reversible color change of the photochromic dimer in solutions and in a solid state at temperatures between room temperature and −196°C under irradiation or in the dark are presented.

Experimental

Materials. The piezochromic dimer of 2,4,5-triphenylimidazolyl (piezo-dimer) $C_{42}H_{30}N_4$ and its isomer, the photochromic dimer (photo-dimer), were prepared according to the method given in a previous report.[1] Piezo-dimer prepared by the oxidation of 2,4,5-triphenylimidazole was almost colorless fine powder, mp 191—192°C and photo-dimer obtained by recrystallization of piezo-dimer from benzene was light yellow fine crystals, mp 199—201°C.

The photochromic dimer of 2-*p*-chlorophenyl-4,5-diphenylimidazolyl (photo-dimer(Cl)), $C_{42}H_{28}N_4Cl_2$, almost colorless fine crystals, mp 219—220°C and its isomeric piezo-dimer (piezo-dimer (Cl)), almost colorless powder, mp 205—207°C, were prepared according to previous reports.[1,5]

Measurements. Absorption spectra were measured with a Hitachi recording spectrophotometer, EPS 2 type.

The electron spin resonance absorption was measured with an ESR instrument of the Japan Electron Optics Laboratory, JES 3B type (100 kc modulation), with a variable temperature controller, JES VT 2 type.

As an exciting source the 365 mμ light obtained from a Toshiba 100 watt super high-pressure mercury lamp combined with a Toshiba glass filter UV D1B was used.

*1 Present address: The Institute of Physical and Chemical Research, Yamatomachi, Kitaadachi-gun, Saitama.

1) T. Hayashi and K. Maeda, This Bulletin, **33**, 566 (1960); T. Hayashi, K. Maeda, S. Shida and K. Nakada, *J. Chem. Phys.*, **32**, 1568 (1960).

2) T. Hayashi and K. Maeda, This Bulletin, **38**, 685 (1965).

3) T. Hayashi, K. Maeda and T. Kanaji, *ibid.*, **38**, 857 (1965).

4) T. Hayashi, K. Maeda and M. Morinaga, *ibid.*, **37**, 1563 (1964).

5) T. Hayashi, K. Maeda and M. Takeuchi, *ibid.*, **37**, 1717 (1964).

6) D. M. White and J. Sonnenberg, *J. Am. Chem. Soc.*, **88**, 3825 (1966).

7) T. Hayashi and K. Maeda, This Bulletin, **36**, 1052 (1963); *ibid.*, **40**, 2990 (1967).

Results and Discussion

Reversible Changes of Color and ESR of Photo-dimer in Solutions with Temperature. Change of the color of photo-dimer in solutions with the temperatures from room temperature to −196°C was observed under irradiation and without irradiation. ESR signal intensity of the solution showed variation corresponding to the change of color.

When a reddish-purple benzene solution of photo-dimer obtained by irradiation of a light yellow solution at room temperature was cooled under irradiation, the color gradually faded and disappeared at about −20°C. When the resulting frozen solution was further cooled to about −150°C, it remained colorless. However, with further cooling to −196°C the solution showed a bluish-purple color which became more intense with the fall of temperature. When the bluish-purple solution was warmed from −196°C to room temperature under irradiation, a color change reverse to that on cooling was observed.

Figure 1 shows variation of the ESR signal intensity, which corresponds to the change of the color with temperature under irradiation.

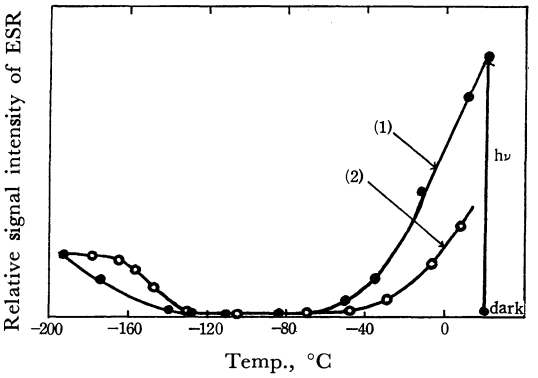

Fig. 1. Variation of the ESR signal intensity of photo-dimer in deaerated benzene under irradiation.
(1) with cooling from room temperature to −196°C
(2) with warming from −196°C to room temperature
Concn.: 6.8×10^{-5} mol/l

When the reddish-purple benzene solution of photo-dimer was cooled from room temperature without irradiation, the color gradually faded and disappeared at about −20°C. The resulting frozen solution remained colorless on further cooling to −196°C. When the colorless frozen solution was warmed from −196°C without irradiation, a color change reverse to that on cooling was observed. On irradiation at −196°C, the colorless frozen solution

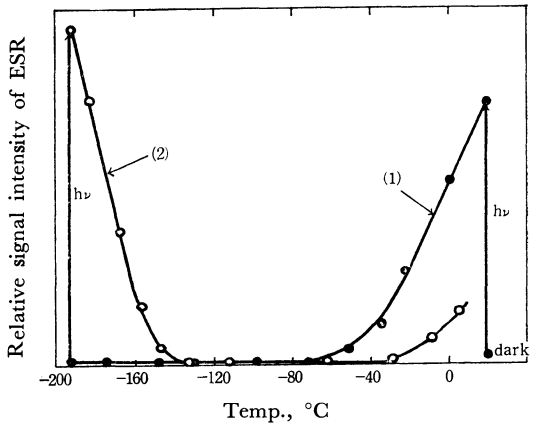

Fig. 2. Variation of the ESR signal intensity of photo-dimer in deaerated benzene.
(1) with cooling to −196°C in the dark after irradiation at room temperature
(2) with warming to room temperature in the dark after irradiation at −196°C
Concn.: 6.8×10^{-5} mol/l

turned deep bluish-purple. By warming the solution to room temperature without irradiation, the color showed a change similar to that observed with warming under irradiation. Figure 2 shows variation of the ESR signal intensity which corresponds to the change of color with temperature in the dark.

When the light yellow solution of photo-dimer in benzene prepared in dim light at room temperature was cooled to −196°C without irradiation, color and ESR did not appear during cooling. On irradiation at −196°C, the frozen solution showed an intense bluish-purple color and a strong ESR signal.

In solutions of photo-dimer in other solvents, changes of color and ESR signal intensity similar to those in benzene were observed with the change of temperature between room temperature and −196°C. On cooling from room temperature, the temperature at which the reddish-purple color disappears differs to some extent with solvents, and the temperature at which a bluish-purple color appears seems to be about −150°C, irrespective of solvents. In a solvent of a relatively high melting point, such as benzene and dioxane, the temperature at which the reddish-purple color disappears is about −20°C and the solutions are frozen. However, in a solvent of a relatively low melting point, such as ethanol and toluene, the temperature at which the color disappears is about −70—−100°C, and the solutions mostly remain unfrozen. The fact suggests that freezing favors the disappearance of the reddish-purple color at a relatively high temperature.

Figure 3 shows the variation of the ESR signal measured in EPA with the change of temperature.

The ERS signal measured at −196°C in the intense bluish-purple solutions of benzene and EPA showed three pairs of signals at 3120—3375 gauss

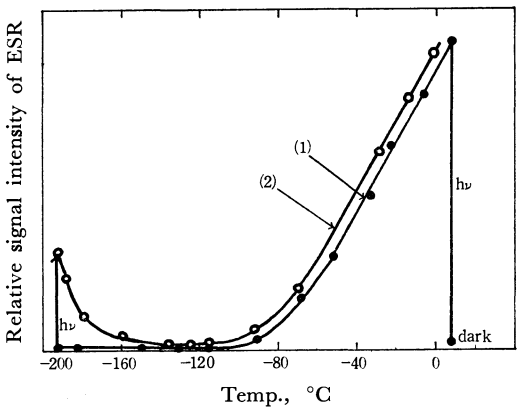

Fig. 3. Variation of the ESR signal intensity in deaerated EPA.

(1) with cooling to −196°C in the dark after irradiation at room temperature
(2) with warming to room temperature in the dark after irradiation at −196°C

Concn.: 4.5×10^{-5} mol/*l*

and a single peak signal at 1750 gauss as well as a strong signal at 3250 gauss.

The intensity of the bluish-purple color and the ESR siganls observed at −196°C did not diminish at −196°C after irradiation was cut off. With irradiation of an infrared light at −196°C the intensity of the ESR signal decreased.

The rate of formation of triphenylimidazolyl radical under irradiation with different intensities of light in benzene at −196°C was measured by means of ESR. As a signal intensity of the radical was assumed to be directly proportional to the concentration of the radical, the rate of formation of the radical was measured from the rate of the increase of the signal intensity under irradiation with different intensities. The signal intensity was proportional to irradiation time. In Fig. 4, the rate of the radical formation measured in benzene is plotted against the intensity of the irradiation.

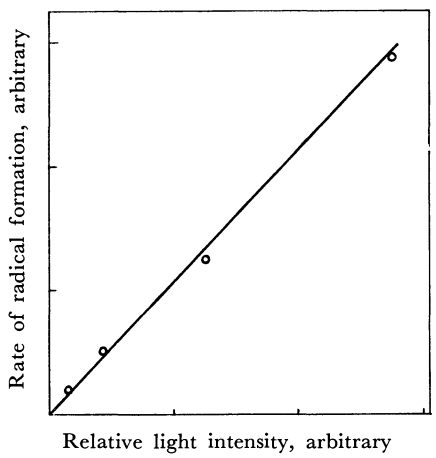

Fig. 4. Dependence of rate of the radical formation in benzene at −196°C, on light intensity.

From the dependence of the rate of the radical formation on the light intensity in Fig. 4, we see that the formation of the bluish-purple radical is a one-photon process.

When a benzene solution of photo-dimer (Cl) which showed a violet color with irradiation at room temperature was cooled under irradiation, the color gradually faded and disappeared at about −20°C. A light bluish-violet color appeared at about −150°C and became deeper with further cooling to −196°C. When the deep bluish-violet solution was warmed from −196°C to room temperature under irradiation, a change of color reverse to that with cooling was observed. Similar to the case of photo-dimer, the violet benzene solution of photo-dimer (Cl) obtained by irradiation at room temperature and the bluish-violet solution obtained by irradiation at −196°C showed ESR ($g=2.003$).

Change of Absorption Spectrum of Photo-dimer in EPA. Disappearance of the photochromic color at the intermediate low temperature range and appearance of the bluish-purple color by irradiation at temperatures below about −150°C were also studied by means of absorption spectrum.

An almost colorless solution of photo-dimer in

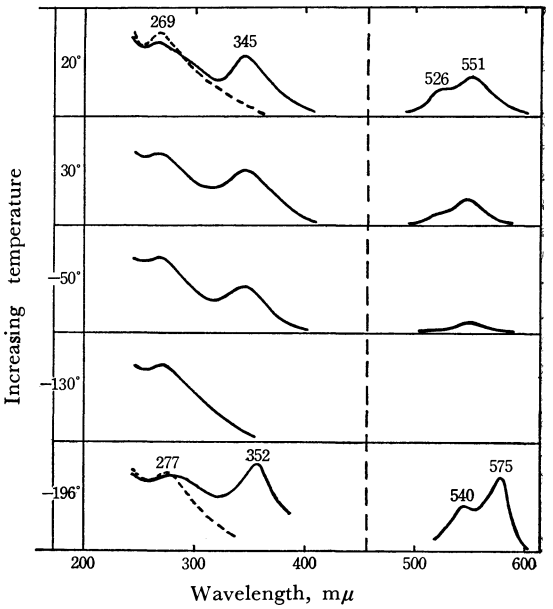

Fig. 5. Absorption spectra of photo-dimer in EPA at temperatures from −196°C to room temperature.

--- Before irradiation
—— After irradiation by a mercury lamp without a filter for 2 min at −196°C

Concn.: 2.54×10^{-5} mol/*l* for shorter than 400 mμ; 4.48×10^{-4} mol/*l* for longer than 400 mμ

EPA (4.48×10^{-4} mol/l) which was prepared in dim light at room temperature was frozen into a glassy state in a quartz cell (1 cm thick) by immersing it in liquid nitrogen in a Dewar provided with quartz windows. On irradiation of the glassy solution with a mercury lamp for 2 min from outside the Dewar, a bluish-purple color appeared. Absorption spectra were measured at several temperatures between −196°C and room temperature obtained by evaporation of liquid nitrogen. In Fig. 5, absorbance at a wavelength region shorter than 400 mμ is shown on a reduced scale.

A red shift of the absorption maxima at 345 and 551 mμ at room temperature to 352 and 575 mμ at −196°C corresponded to the change of color from reddish-purple to bluish-purple. With the fading of the bluish-purple color, the absorption band with λ_{max} 352 and 575 mμ gradually decreased to vanish at about −150°C, and the absorption band with λ_{max} 345 and 551mμ appeared at about −50°C. The band increased with further rise of temperature to room temperature. The maxima at 345 and 551 mμ agreed with those of a reddish-purple solution obtained by irradiation of photo-dimer in EPA at room temperature.

The violet solution of photo-dimer (Cl) in EPA obtained with irradiation showed absorption maxima at 356 and 568 mμ at room temperature. The bluish-violet solution obtained with irradiation at −196°C showed absorption maxima at 361 and 580 mμ. At temperatures between about −60 and −150°C, the absorption band in the visible region disappeared as in the case of photo-dimer.

Reversible Color Change of Piezo-dimer in Solutions with Temperature. A benzene solution of piezo-dimer which was prepared under dim light at room temperature showed an intense reddish-purple color due to triphenylimidazolyl radical formed by the dissociation of dimer.[6] When the reddish-purple solution was allowed to stand at room temperature without irradiation, the reddish-purple color gradually turned light yellow[1] by dimerization of triphenylimidazolyl radical to photo-dimer. The resulting solution is an equilibrium mixture of photo-dimer and a small amount of piezo-dimer.[6] When the temperature of the solution changed between room temperature and −196°C under irradiation, the solution showed a color change similar to that of the solution of photo-dimer.

When the reddish-purple solution of piezo-dimer in benzene was cooled without irradiation immediately after preparation, the reddish-purple color faded with the fall of temperature and disappeared at temperatures lower than about −20°C. The colorless solution showed no change of color even with irradiation at −196°C. When the colorless solution was warmed with or without irradiation from −196°C, a light reddish-purple color due to thermochromism of piezo-dimer appeared above about −20°C and became more intense at room temperature.

In other solvents piezo-dimer showed a color change similar to that in benzene observed with the change of temperature between room temperature and −196°C, with or without irradiation. The temperature at which the reddish-purple color disappeared was to some extent different with solvents, as the case of photo-dimer which was cooled under irradiation.

Mechanism of Riversible Color Change of Photo-dimer in Solutions. Disappearance of the photochromic reddish-purple color and ESR signal in benzene at temperatures between about −20 and −150°C is interpreted as follows. In solutions the following equilibria (a) and (b) take place between piezo-dimer, triphenylimidazolyl radical and photo-dimer.[6] Equilibrium (a) lies far on the side of the radical at room temperature and shifts toward piezo-dimer at temperatures lower than about −20°C,[6] while the position of equilibrium (b) lies far on the side of photo-dimer at room temperature and shifts further toward photo-dimer at low temperatures.

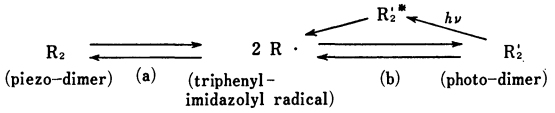

Under irradiation, the reddish-purple triphenylimidazolyl radical produced by photo-dissociation of photo-dimer dimerizes quickly to piezo-dimer at temperatures lower than about −20°C owing to a low activation energy for the dimerization of the radical to piezo-dimer.[6] As a result, the reddish-purple color and ESR signal do not appear within the temperatures between about −20 and −150°C.

Appearance of the photochromic bluish-purple color and ESR signal at temperature slower than about −150°C with irradiation is interpreted by means of the following mechanism.[8] At temperatures lower than −150°C, a part of the radicals produced by photo-dissociation remains unchanged in the solution, because it becomes difficult for the radical to surmount the barrier of the activation energy of dimerization at such low temperatures, although equilibria (a) and (b) lie very far on the sides of the two dimers. The concentration of the radical increases with the fall of temperature to −196°C, because the difficulty in surmounting the energy barrier increases at low temperatures. The intensity of ESR signal appearing at −196°C when the solution was cooled under irradiation, was weaker than that in the solution which was

8) T. Hayashi and K. Maeda, *Nippon Kagaku Zasshi (J. Chem. Soc. Japan, Pure Chem. Sect.)*, **90**, 325 (1969).

irradiated after cooling from room temperature in the dark, because photo-dimer isomerizes to piezo-dimer through the radical during cooling under irradiation.

The bluish-purple color appearing at temperatures lower than about −150°C is attributed to triphenylimidazolyl radical S·[9] which has a conformation different from that of the reddish-purple triphenylimidazolyl radical, R·. The red shift of the absorption maxima shows an increase in resonance stability due to the increase in coplanarity of a conjugated system in the radical S·. ESR signals at 3120—3375 gauss and 1750 gauss ($\Delta m = \pm 1$ and ± 2) in frozen solutions of photo-dimer irradiated at −196°C is likely to be a radical pair[9] of triphenylimidazolyl radical. On warming the deep bluish-purple benzene solution of photo-dimer from −196°C, the bluish-purple radical S· gradually surmounts the barrier of the activation energy for dimerization to a colorless dimer S_2 and the solution turns colorless above about −150°C. From the thermochromic behavior of the solution warmed near room temperature without irradiation, the structure of the dimer S_2 is likely to be the same as that of piezo-dimer. With the rise of temperature to about −20°C the dimer S_2 seems to be transformed into piezo-dimer.

The reddish-purple color which appeared as the solution was warmed above about −20°C under irradiation is attributed to triphenylimidazolyl radical, produced by the thermal dissociation of piezo-dimer isomerized from photo-dimer and also by the photo-dissociation of photo-dimer remaining unchanged in the solution.

The mechanism of the changes of color and ESR shown by the solutions of photo-dimer (Cl) with temperatures from room temperature to −196°C is similar to that of photo-dimer.

Changes of Photochromic Color and ESR of Photo-dimer in Solid State. When a light yellow solid of photo-dimer was irradiated at low temperatures such as −20°C or −70°C, it showed a light reddish-purple color similar to that of the photochromism[3] at room temperature. On irradiation, after cooling to −196°C without irradiation, the solid showed an intense bluish-purple color which scarcely faded after irradiation was cut off.

The color change of the solid with the change of temperature was studied with ESR. With cooling from room temperature to −196°C in the dark, no ESR signal appeared. On irradiation at room teaperature a weak ESR signal corresponding to the light reddish-purple color was observed. When the solid was cooled after irradiation was cut off, a small increase in signal intensity was observed at temperatures near −196°C as shown in Fig. 6. On irradiation of the solid at −196°C a very strong ESR signal (Fig. 6) appeared. It corresponds to the intense bluish-purple color. The signal intensity increased with the time of irradiation and scarcely decreased after irradiation was cut off. However, it decreased on warming a little in the dark or under irradiation, as shown in Fig. 6. With cooling of the solid from room temperature under irradiation, the small ESR signal increased slightly at temperatures below about −80°C, and with further cooling the signal increased considerably near −196°C.

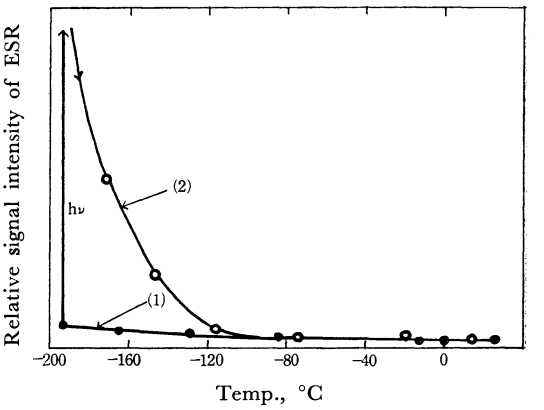

Fig. 6. Variation of ESR of the solid of photo-dimer.
(1) with cooling in the dark after irradiation at room temperature
(2) with warming in the dark after irradiation at −196°C

The light reddish-purple color appearing at temperatures above about −70°C is attributed to triphenylimidazolyl radical produced by photo-dissociation of photo-dimer.[3] The light color which corresponds to a small concentration of the radical seems to result from the recombination of the radical owing to difficulty of diffusion in the solid. Differing from the change in solutions, the color does not disappear at the intermediate low temperatures, because photo-dimer is not transformed into piezo-dimer owing to the retarded thermal motion of the radical. The bluish-purple color appearing at temperatures near −196°C is considered to be due to the triphenylimidazolyl radical S·, as in the solutions. Three pairs of ESR signals at 3160—3400 gauss and a single peak signal at 1750 gauss observed at −196°C are considered to be due to a radical pair similar to that formed in solutions. The large concentration of the radical corresponding to the strong ESR signal and deep bluish-purple color near −196°C might be attributed to a very small rate of dimerization at the low temperatures.

9) Presented at the Symposium on Photochemistry of the Chemical Society of Japan (Oct., 1968, Sendai) by T. Shida, K. Maeda and T. Hayashi; T. Shida, K. Maeda and T. Hayashi, This Bulletin, **42**, 3044 (1969).

The authors wish to express their hearty thanks to Dr. Hiroshi Midorikawa of the Institute of Physical and Chemical Research, Professor Saburo Nagakura of The University of Tokyo, Professor Hiroshi Tsubomura of Osaka University and Professor Katsumi Kimura of Hokkaido University for their kind help and to the Ministry of Education for the financial support granted this research.

BULLETIN OF THE CHEMICAL SOCIETY OF JAPAN VOL. 42 3514—3518 (1969)

Mechanism of the Solvent Effect in a Binary Solvent System on the Cationic Polymerization of *N*-Phenylethylenimine

Tsutomu KAGIYA and Tomizo KONDO

Faculty of Engineering, Kyoto University, Sakyo-ku, Kyoto

(Received May 10, 1969)

The effect of the binary solvent systems on the polymerization of *N*-phenylethylenimine with a formic acid catalyst was studied quantitatively. In an acetonitrile - acetone system composed of components with similar nucleophilicities but with very different dielectric constants, the polymerization rate increases with an increase in the dielectric constant of the binary solvent system. In an acetonitrile - *N*,*N*-dimethylacetamide system composed of components with very different nucleophilicities but with similar dielectric constants, on the other hand, the rate was markedly depressed by the addition of a small amount of *N*,*N*-dimethylacetamide with a large nucleophilicity. On the basis of these results, a mechanism of the solvent effect in a binary solvent system was proposed; the rate equation of the polymerization was expressed empirically as a function of both the dielectric constant of the binary solvent mixture and the nucleophilic equilibrium constant, and the concentration of the component.

It has been well known that the reaction rate is dependent on the nature of the solvent in an ionic polymerization. Little attention has, however, been paid to the quantitative study of the solvent effect on the ionic polymerization. It has been previously reported by the present authors[1] that, in the polymerization of *N*-phenylethylenimine with a formic acid catalyst in various solvents, the polymerization rate depended upon the nucleophilicity and the dielectric constant of the solvent, and that the initiation rate was not very much influenced by the nature of the solvent, whereas that of the propagation was remarkably affected.

As a continuation of our quantitative study of the solvent effect in the cationic polymerization of *N*-phenylethylenimine, we focused on the binary solvent system in the polymerization. The purpose of this report is to determine quantitatively the solvent effect in a binary mixture of the solvent on the polymerization of *N*-phenylethylenimine.

Experimental

The method of preparing and purifying *N*-phenylethylenimine has been described in our previous paper.[1] Guaranteed-reagent-grade formic acid was used without further purification. The acetonitrile, acetone, and *N*,*N*-dimethylacetamide were purified by the usual method.[2] The method of polymerization was also described in the previous paper.[1] The polymerization was carried out under the following conditions: monomer, 0.005 mol; catalyst, formic acid (4 mol% for monomer); total volume of solvent, 3 m*l*; temperature, 0°C. The measurement of the dielectric constant of the solvent was carried out at 25°C by the use of a Kikusui Electronic Industry 231 A-type LC meter.

Results and Discussion

Polymerization in Binary Solvent Systems. Both acetonitrile and acetone have similar nucleophilic equilibrium constants to methanol-d (K_D),[3,4] and a very different dielectric constant, (acetonitrile, K_D; 0.4,*1 ε; 37.5 and acetone, K_D; 0.6,*1 ε;

1) T. Kagiya, T. Kondo, K. Nakao and K. Fukui, This Bulletin, **42**, 1049 (1969).

2) A. Weissberger *et al.*, "Technique of Organic Chemistry, Vol VII, Organic Solvents," Interscience Publishers, Inc., New York (1955).

3) T. Kagiya, Y. Sumida and T. Inoue, This Bulletin, **41**, 767 (1968).

4) T. Kagiya, Y. Sumida and T. Inoue, *ibid.*, **41**, 773 (1968).

*1 The nucleophilic equilibrium constants of acetonitrile, acetone, and *N*,*N*-dimethylacetamide were obtained by the method of literature[4] on the basis of the $\Delta\nu_D$ values shown in Ref. 3.

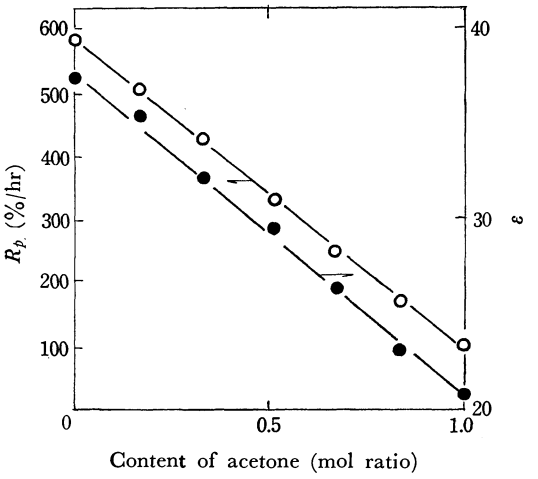

Fig. 1. Plots of polymerization rate (R_p) and the dielectric constant (ε) of the mixed solvent against the composition of the solvent in the acetonitrile - acetone binary solvent system.

20.7). As is shown in Fig. 1, the polymerization rate, defined as the ratio of the polymer yield (<20%) to the reaction time, and the dielectric constant of the binary solvent both decrease with an increase in the amount of acetone in the acetonitrile - acetone system. The rate increases with an increase in the dielectric constant of the binary solvent (Fig. 2). This fact suggests that, in the binary solvent system with a similar ability for nucleophilic solvation, the polymerization is mainly dependent upon the degree of ionic dissociation of the propagating species.

On the other hand, in the acetonitrile - *N*,*N*-dimethylacetamide (K_D*[1], 1.6; ε, 36.7) binary system,

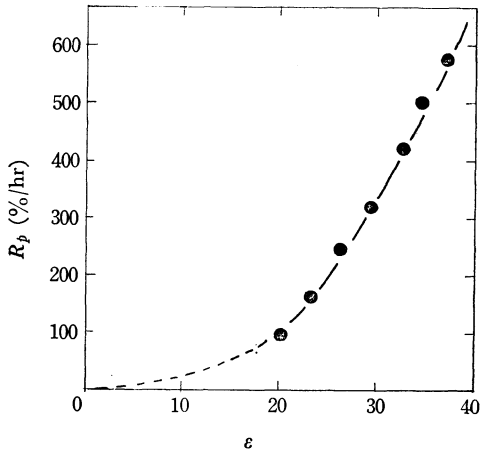

Fig. 2. Relation between the polymerization rate (R_p) and the dielectric constant (ε) of the mixed solvent in the acetonitrile-acetone binary solvent system.

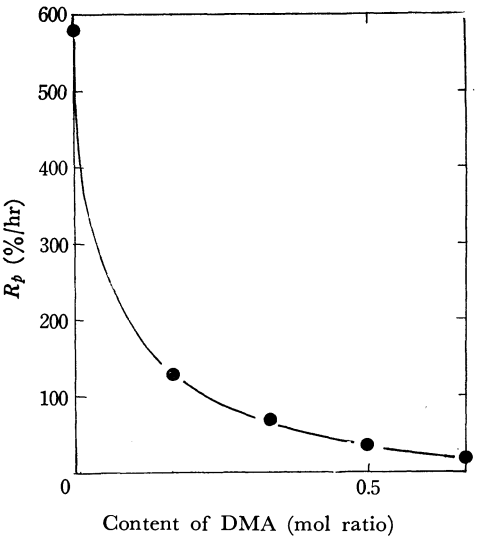

Fig. 3. Relation between polymerization rate (R_p) and the composition of the solvent in the acetonitrile - *N*,*N*-dimethylacetamide (DMA) binary solvent system.

the dielectric constant of the mixed solvent remains constant on varying the ratio of the two components, while the rate of polymerization is markedly depressed by the addition of a small amount of *N*,*N*-dimethylacetamide (Fig. 3). This fact suggests that the solvent and monomer coordinate competitively to the cationic growing end, and that coordination of the solvents increases with the amounts of *N*,*N*-dimethylacetamide with a larger nucleophilicity than that of acetonitrile and so depresses the monomer addition to the growing end. This is in accord with the finding that the rate decreased with an increase in the nucleophilicity of the solvent.[1)]

Mechanism of the Solvent Effect of the Polymerization. On the basis of these experimental facts and the results obtained previously,[1)] the mechanism of the polymerization and the role of the solvent were postulated as follows:

Initiation:

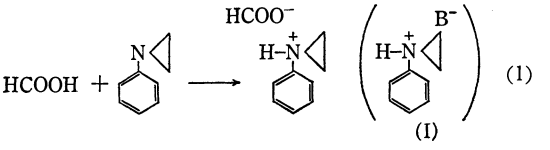

(1)

Propagation:

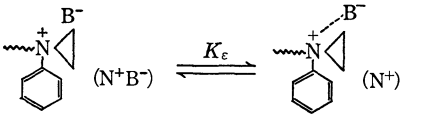

(2)

Propagation by the dissociated immonium ion:

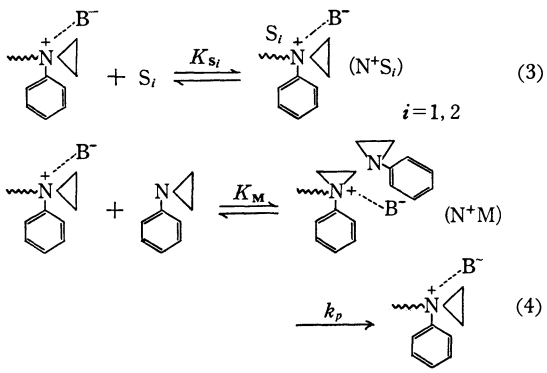

(3)

(4)

Propagation by the undissociated immonium ion:

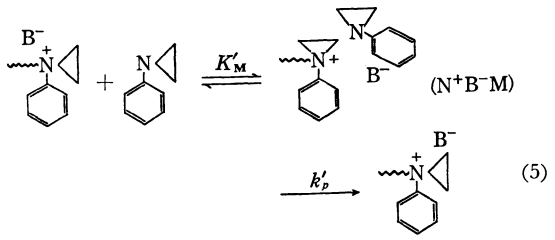

(5)

where K_ε, K_{S_i}, K_M, and K_M' are equilibrium constants and where k_p and k_p' are rate constants.

The initiation reaction is the reaction of formic acid with *N*-phenylethylenimine to produce Compound I. This compound dissociates partially to the immonium ion, and the reaction is in equilibrium. The equilibrium constant (K_ε) is considered to increase with an increase in the dielectric constant of the solvent. Equation (3) shows the nucleophilic solvation of the solvent to the dissociated immonium ion. Since the coordination of the solvent to both the propagating species and methanol-d are nucleophilic reactions, the equilibrium constant (K_{S_i}) is considered to increase with an increase in the K_D value. From the fact that, in the solvent with a high dielectric constant, the polymerization rate decreased with an increase in the nucleophilicity of the solvent, the propagation is considered to occur by means of the reaction of the monomer and nonsolvated immonium ion, as is shown in Eq. (4). On the other hand, the propagation can also proceed in the solvents with a low dielectric constant. Therefore, the reaction of the undissociated immonium ions with the monomer (Eq. (5)) is also probable.

Kinetics. On the basis of the mechanism postulated, the effect of the solvent on the polymerization rate was quantitatively investigated. As was established in the previous paper,[1] the concentration of the propagating species was constant regardless of both the reaction time and the nature of the solvent. Therefore, the concentration of Compound I, $\alpha[C]_0$, may be expressed by Eq. (6), where $[C]_0$ is the initial concentration of the catalyst and where α is the constant $(0<\alpha<1)$:

$$\alpha[C]_0 = [N^+] + [N^+B^-] + \sum_{i=1}^{2}[N^+S_i] + [N^+M] + [N^+B^-M] \quad (6)$$

On the other hand, according to Eqs. (2), (3), (4), and (5), the equilibrium equations will be:

$$[N^+]/[N^+B^-] = K_\varepsilon \quad (7)$$

$$[N^+S_i]/([N^+][S_i]) = K_{S_i} \quad (8)$$

$$[N^+M]/([N^+][M]) = K_M \quad (9)$$

$$[N^+B^-M]/([N^+B^-][M]) = K_M' \quad (10)$$

where [M] is the concentration of *N*-phenylethylenimine. By combining Eqs. (6), (7), (8), (9), and (10), the concentrations of N^+B^-M and N^+M may be represented by Eqs. (11) and (12) respectively:

$$[N^+B^-M] = \frac{\alpha[C]_0K_M'[M]}{1+K_M'[M]+K_\varepsilon\{1+K_M[M]+\sum_{i=1}^{2}(K_S[S])_i\}} \quad (11)$$

$$[N^+M] = \frac{K_\varepsilon K_M\alpha[C]_0[M]}{1+K_M'[M]+K_\varepsilon\{1+K_M[M]+\sum_{i=1}^{2}(K_S[S])_i\}} \quad (12)$$

The polymerization rate is represented by Eq. (13):

$$R_p = -d[M]/dt = k_p[N^+M] + k_p'[N^+B^-M] \quad (13)$$

Then, by substituting Eqs. (11) and (12) into Eq. (13), Eq. (14) is derived:

$$R_p = \frac{(K_\varepsilon K_M k_p + K_M'k_p')\alpha[C]_0[M]}{1+K_M'[M]+K_\varepsilon\{1+K_M[M]+\sum_{i=1}^{2}(K_S[S])_i\}} \quad (14)$$

Since, in the solvents with high dielectric constants, propagation may occur mainly with the dissociated immonium ions, Eq. (14) may be approximately expressed by Eq. (15):

$$R_p \fallingdotseq \frac{K_\varepsilon K_M k_p\alpha[C]_0[M]}{1+K_\varepsilon\{1+K_M[M]+\sum_{i=1}^{2}(K_S[S])_i\}} \quad (15)$$

The reciprocal of Eq. (15) is:

$$1/R_p \fallingdotseq \frac{1}{K_M k_p\alpha[C]_0[M]}\{(1+K_M[M]) + \sum_{i=1}^{2}(K_S[S])_i + 1/K_\varepsilon\} \quad (16)$$

By considering that, in an acetonitrile-acetone binary solvent system (K_D is almost constant, while ε varies from 20.7 to 37.5), the value of $\sum_{i=1}^{2}(K_S[S])_i$ is constant regardless of the composition of the solvent, it can be interpreted by means of Eq. (16) that the polymerization rate increases with an increase in the K_ε value (that is, the dielectric constant of the solvent). On the other hand, in

the case of the acetonitrile - *N,N*-dimethylacetamide system having a similar dielectric constant ($\varepsilon \fallingdotseq 37$), the term of K_ε is constant. Therefore, Eq. (16) explains the fact that the rate decreases with the $\sum_{i=1}^{2}(K_S[S])_i$ value or with the amont of *N,N*-dimethylacetamide.

The empirical equations of the polymerization rate were obtained as follows. On the assumptions that $K_{S_i}=aK_{D_i}{}^m$ and $K_\varepsilon=(1/b)\varepsilon^n$, where m, n, a, and b are constants, Eq. (16) may be written in this form:

$$1/R_p \fallingdotseq \frac{1}{K_M k_p \alpha [C]_0[M]} \{(1+K_M[M]) + a\sum_{i=1}^{2}(K_D{}^m[S])_i + b(1/\varepsilon)^n\} \quad (17)$$

Taking the logarithm of Eq. (17) gives Eq. (18):

$$\log(1/R_p) \fallingdotseq \log\{1/(K_M k_p \alpha [C]_0[M])\} + \log\{(1 + K_M[M] + a\sum_{i=1}^{2}(K_D{}^m[S])_i + b(1/\varepsilon)^n\} \quad (18)$$

In the acetonitrile - acetone binary solvent system, it is found that the plot of $\log(1/R_p)$ against $\log(1/\varepsilon)$ gives a straight line whose slope is 2.5. This fact indicates that the value of $(1+K_M[M] + a\sum_{i=1}^{2}(K_D{}^m[S])_i)$ is much smaller than that of the $b(1/\varepsilon)^n$ in Eq. (17).

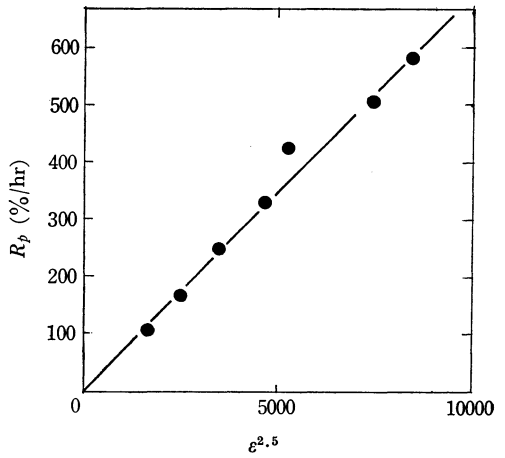

Fig. 4. Plots of R_p against $\varepsilon^{2.5}$ (ε : the dielectric constant of the mixed solvent) in the acetonitrile - acetone binary solvent system.

From the slope in the linear relation between R_p and $\varepsilon^{2.5}$ (Fig. 4), the value of $(K_M k_p \alpha [C]_0[M])/b$ is obtained as 0.07:

$$(K_M k_p \alpha [C]_0[M])/b = 0.07 \quad (19)$$

Therefore, the polymerization rate in the acetonitrile - acetone system can be approximately expressed by:

$$R_p \fallingdotseq \frac{K_M k_p \alpha [C]_0[M]}{b}\varepsilon^{2.5} = 0.07\varepsilon^{2.5} \quad (20)$$

On the other hand, in the acetonitrile - *N,N*-dimethylacetamide binary solvent system (K_D varies from 0.3 to 1.6, while ε is almost constant, 37), the empirical equation of the rate was obtained as follows. If it takes $m=2$, Eq. (17) is written:

$$1/R_p = \frac{1+K_M[M]}{K_M k_p \alpha [C]_0[M]} + \frac{a\sum_{i=1}^{2}(K_D{}^2[S])_i}{K_M k_p \alpha [C]_0[M]} + \frac{b(1/\varepsilon)^{2.5}}{K_M k_p \alpha [C]_0[M]} \quad (21)$$

By substituting the values of $b/(K_M k_p \alpha [C]_0[M]) = 14$ and $\varepsilon=37$ into Eq. (21), one obtaines:

$$1/R_p = \frac{1+K_M[M]}{K_M k_p \alpha [C]_0[M]} + \frac{\sum_{i=1}^{2}(K_D{}^2[S])_i}{(1/a)K_M k_p \alpha [C]_0[M]} + 5.4\times 10^{-4} \quad (22)$$

A plot of the $1/R_p$ against $\sum_{i=1}^{2}(K_D{}^2[S])_i$ gives a straight line (Fig. 5), this straight line is written in form:

$$1/R_p = 0.33\sum_{i=1}^{2}(K_D{}^2[S])_i \quad (23)$$

By comparing Eq. (23) with Eq. (22), we discover that the value of 5.4×10^{-4} is much smaller than the term of K_D in Eq. (22), and that:

$$(1+K_M[M])/(K_M k_p \alpha [C]_0[M]) \fallingdotseq 0 \quad (24)$$

$$1/\{(1/a)K_M k_p \alpha [C]_0[M])\} \fallingdotseq 0.33 \quad (25)$$

By combining Eqs. (21) and (24), the rate equation in the solvent with a high dielectric constant can be expressed generally as:

$$R_p \fallingdotseq \frac{K_M k_p \alpha [C]_0[M]}{a\sum_{i=1}^{2}(K_D{}^2[S])_i + b(1/\varepsilon)^{2.5}} \quad (26)$$

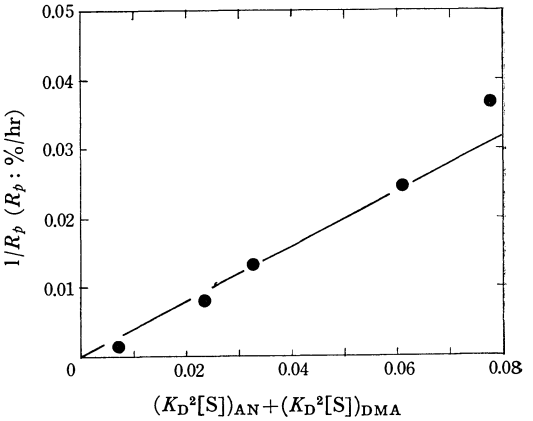

Fig. 5. Plot of $1/R_p$ against $(K_D{}^2[S])_{AN} + (K_D{}^2[S])_{DMA}$ in the acetonitrile (AN) - *N,N*-dimethylacetamide (DMA) binary solvent system.

Then:

$$R_p \fallingdotseq \frac{K_M k_p(\alpha/a)[C]_0[M]}{\sum_{i=1}^{2}(K_D^2[S])_i + (b/a)(1/\varepsilon)^{2.5}} \quad (27)$$

By substituting the value of $b/a \fallingdotseq 40$ obtained from Eqs. (19) and (25) into Eq. (27), Eq. (27) may be written in the form:

$$R_p \fallingdotseq \frac{K_M k_p(\alpha/a)[C]_0[M]}{\sum_{i=1}^{n}(K_D^2[S])_i + 40(1/\varepsilon)^{2.5}} \quad (28)$$

Eq. (28) can then be applied to the results obtained in the single solvent system ($10<\varepsilon<37.5$). As is shown in Fig. 6, although the polymerization rate, R_p, increases with an increase in the dielectric constant of the solvent, the order can not necessarily be explained by the dielectric constant of the solvent. The plot of R_p against $\{(K_D^2[S])+40(1/\varepsilon)^{2.5}\}^{-1}$ gives a straight line through the point of origin (Fig. 7). This fact indicates that Eq. (29) can be applied as an empirical equation of the polymerization rate to both the single and the binary solvent system.

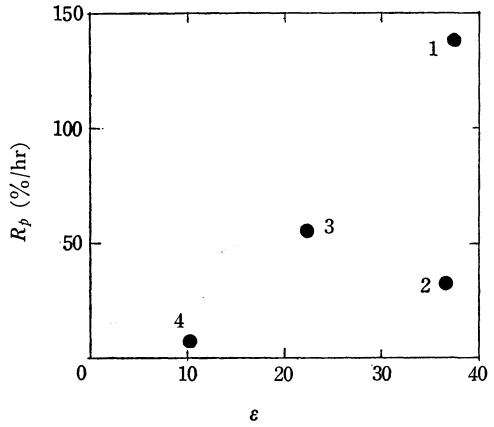

Fig. 6. Plot of polymerization rate (R_p) against the dielectric constant (ε) of the solvent in the single solvent system.

1, Acetonitrile; 2, *N*,*N*-Dimethylacetamide; 3, Epichlorohydrin; 4, Ethylene dichloride

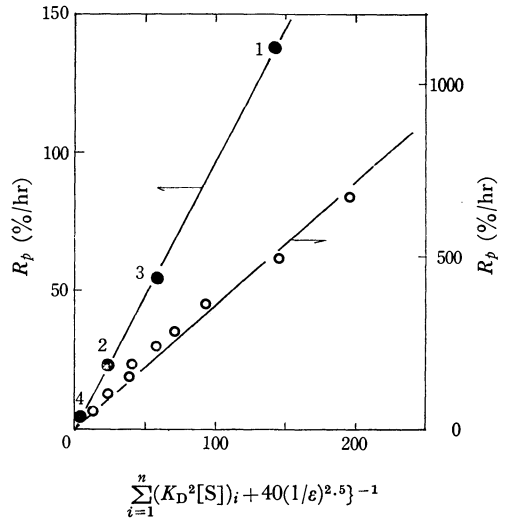

Fig. 7. Plots of R_p against $\{\sum_{i=1}^{n}(K_D^2[S])_i+40(1/\varepsilon)^{2.5}\}^{-1}$ in the single and binary solvent systems.

● Single solvent system, notes are the same as Fig. 6.
○ Binary solvent system.

BULLETIN OF THE CHEMICAL SOCIETY OF JAPAN VOL. 42 3519—3524 (1969)

Structural Study of the Catalytic Activity of Alkyl Chloride in the Polymerization of *N*-Phenylethylenimine

Tsutomu KAGIYA, Tomizo KONDO and Keigo OBATA

Faculty of Engineering, Kyoto University, Sakyo-ku, Kyoto

(Received May 10, 1969)

The catalytic activity of various alkyl chlorides in the polymerization of *N*-phenylethylenimine was studied from the structural point of view. Both the polymerization rate and the molecular weight of the polymer obtained varied with the kind of alkyl chloride. The rate of monomer consumption is expressed by a first-order rate equation with respect to the monomer concentration in the early stage of the polymerization. The efficiency factors of the catalysts differ with the kind of alkyl chloride and increase with an increase in the reaction time. When the chloride of a conjugated alkyl group is used, the polymerization rate decreases with an increase in the ionization potential of the alkyl radical, while it increases when chlorides of a non-conjugated alkyl are used. The structural study of the catalytic activity of the alkyl chloride was made quantitatively from the energetic point of view.

It has already been reported by the present authors[1] that, in the polymerization of *N*-phenylethylenimine withv arious carboxylic acid catalysts (pK_a=0.23—4.87), there was no chain transfer reaction, and that the rates of the initiation, propagation, and termination reactions increased with a decrease in the pK_a values of the acids. These results indicate that the rates of the elementary reactions are dependent on the structural nature of the catalyst.

The purpose of this paper is to investigate the relation between the polymerization rate and the structure of the alkyl chloride catalyst in the polymerization of *N*-phenylethylenimine.

Experimental

The methods of preparing and purifying *N*-phenylethylenimine were described in the previous paper.[1] Acetonitrile and alkyl chlorides of a guaranteed reagent were purified by the usual method.[2]

The methods of the polymerization of the polymer and the determination of its molecular weight were also described in the previous paper.[1] The polymerization was carried out under the following conditions: monomer, 0.01 mol; acetonitrile as the solvent, 5 m*l*; catalyst, 0.00067 mol; temperature, 0°C.

The infrared spectrum of the polymer was measured by the use of the potassium bromide pellet technique on a Shimadzu infrared spectrophotometer, Model IR-27.

1) T. Kagiya, T. Kondo and K. Fukui, This Bulletin, **41**, 2473 (1968).

2) A. Weissberger, E. S. Proskauer, J. A. Riddick and E. E. Toops, "Technique of Organic Chemistry, Vol VII, Organic Solvents," Interscience Publishers, Inc., New York (1955).

Results and Discussion

The Infrared Spectrum of the Polymer. The infrared spectrum of the polymer initiated with allyl chloride shows the characteristic peaks at 910 cm^{-1} and 930 cm^{-1} assigned to the vinyl group and the piperazine ring respectively. This may indicate that the polymer contains the allyl group and the piperazine ring at both ends of the polymer. Therefore, it may be considered that this polymerization is initiated with alkyl chloride and is terminated by forming the piperazine ring at the end of the polymer, as has been described in the previous paper.[1]

Polymerization with Various Alkyl Chlorides. The plots of the polymer yield ($[M_p]$; polymerized monomer mol/*l*) against the reaction time are shown in Figs. 1 and 2. The curves of these figures show that the polymerization rate varies markedly with the kind of alkyl chloride. As is shown in Fig. 3, the rate of the monomer consumption is expressed by a first-order rate equation with respect to the monomer concentration in the early stage of the polymerization (polymer yield $<20\%$). In view of this fact, it is considered that the steady-state assumption that the initiation rate is equal to the termination one is applicable in the early stage of this polymerization.

The relations between the number-average molecular weight ($\bar{M}_n$) and the reaction time are shown in Fig. 4. The molecular weight is almost constant regardless of the reaction time. This may be ascribed, not to the chain transfer, but to the fact that the steady-state assumption is applicable, for, as has been described in the previous paper,[1]

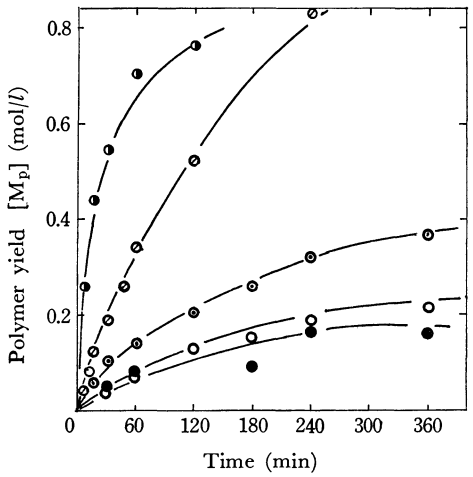

Fig. 1. Polymer yield ([M_p]) *vs.* polymerization time.
◑, Triphenylmethyl; ⊘, Phenyl; ⊙, Benzyl; ○, β-Methallyl; ●, Allyl

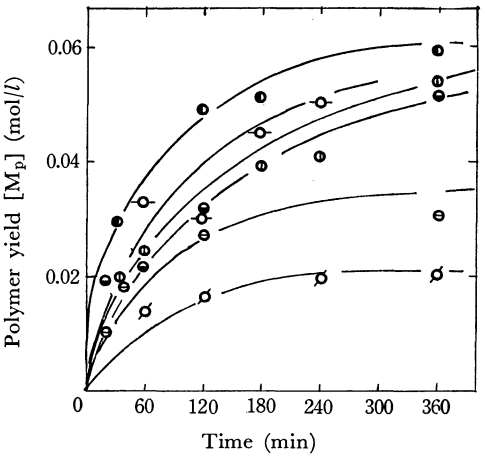

Fig. 2. Polymer yield ([M_p]) *vs.* polymerization time.
◐, *n*-Butyl, -○-, Phenyl; ⓘ, Isobutyl; ◑, Isopropyl; ⊖, Ethyl; ⊘, *t*-Butyl

there is essentially no chain transfer in the polymerization of *N*-phenylethylenimine. On the other hand, since the structure of the initiating and propagating species depend on only the chlorine atom of the chlorides, the rate constant of the propagation and termination reactions may be considered to be constant regardless of the kind of chloride. Therefore, the difference in the molecular weight with the kind of chloride may be due to the difference in the initiation rate constant. These fact will be discussed below.

In the polymerization without chain transfer and bimolecular termination, the value of $[M_p]/([C]_0\overline{M}_n)$ is called the efficiency factor of the catalyst (α), where, $[C]_0$ is the initial catalyst concentration. The increase in α with an increase in the reaction

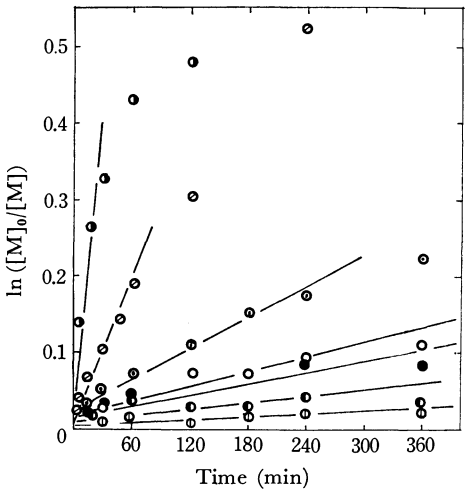

Fig. 3. Plots of $\ln([M]_0/[M])$ against reaction time.
The notes are the same as Fig. 1 and Fig. 2.

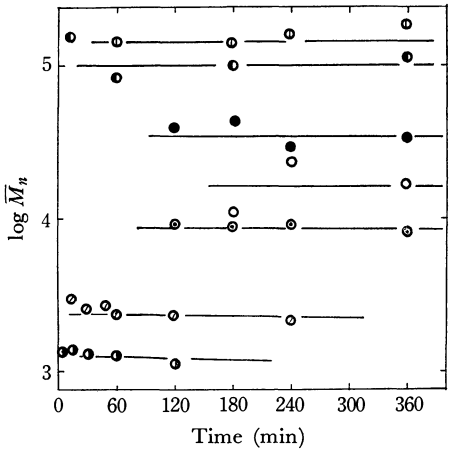

Fig. 4. Relation between the molecular weight ($\overline{M}_n$) of the polymer and reaction time.
The notes are the same as Fig. 1 and Fig. 2.

time (Fig. 5) indicates that the initiation reaction occurs continuously during the course of the polymerization. Moreover, since α differs greatly from alkyl chloride to alkyl chloride (about from 1×10^{-4} to 0.8), there is perhaps a very large difference in the initiation rate as well. From these facts, it is assumed that the difference in the polymerization rate with the kind of alkyl chlorides is due to the difference in the rate constant of the initiation reaction.

Since the initiation reaction may be the addition reaction of alkyl chloride with *N*-phenylethylenimine, the initiation reaction is expected to proceed by the same mechanism as the Menschutkin reaction, as will be described later in connection with Eq. (1). Therefore, the polymerization rates (k), defined as the slopes of the straight lines in Fig. 3,

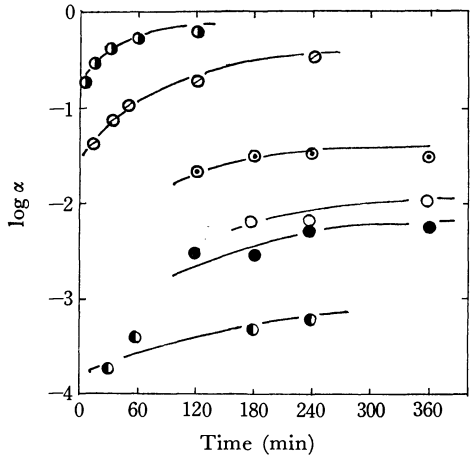

Fig. 5. Plots of log α against reaction time.
The notes are the same as Fig. 1 and Fig. 2.

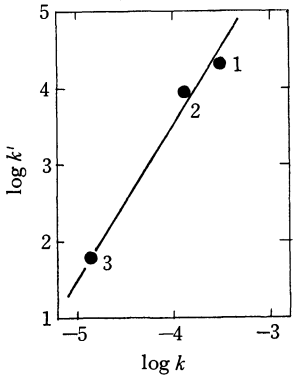

Fig. 6. Relation between the rate constant (k') of Menschutkin reaction (RI+Di-Me-Aniline) and polymerization rate (k) with the use of RCl.
R: 1, Benzyl; 2; Allyl; 3, Ethyl

were studied in comparison with the rate constant of the Menschutkin reaction. The plots of the k values against the rate constants in the reaction of alkyl iodides with dimethylaniline,[3] which had a structure similar to that of *N*-phenylethylenimine, are shown in Fig. 6. The fact that the rate of the Menschutkin reaction is almost proportional to the polymerization rate is in good accordance with the above assumption.

Since the peculiar nature of alkyl chloride (RCl) is considered to be caused by the difference in the electronic nature of the alkyl radical, the k value was plotted against the ionization potential of the alkyl radical (I_p(R·)) (Fig. 7). There is a good relation between the catalytic activity and the ionization potential of the alkyl radical; the curves may be

3) R. W. Prestone and H. D. Jones, *J. Chem. Soc.*, **101**, 1930 (1912).

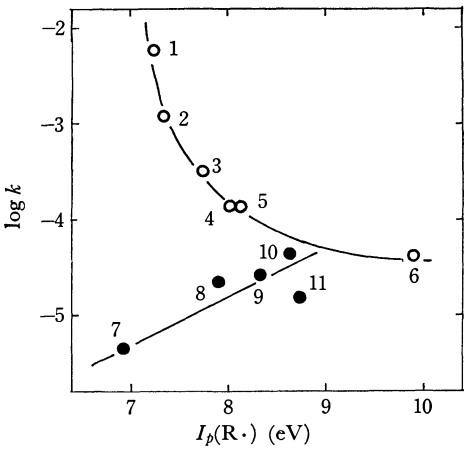

Fig. 7. Relation between the polymerization rate (k) and $I_p(R)$ of alkyl chloride.
Conjugated alkyl: 1, Triphenylmethyl; 2, Phenyl; 3, Benzyl; 4, β-Methallyl; 5, Allyl; 6, Phenyl.
Non-conjugated alkyl: 7, *t*-Butyl; 8, Isopropyl; 9, Isobutyl; 10, *n*-Butyl; 11; Ethyl

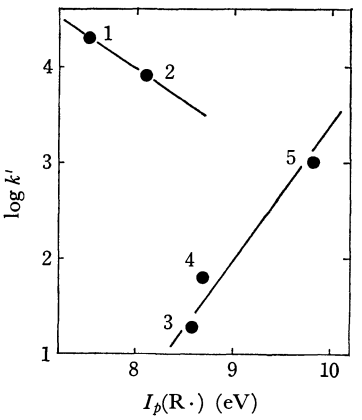

Fig. 8. Relation between the rate constant (k') and I_p(R·) in Menschutkin reaction (RI + Di-Me-Aniline).
1, Benzyl; 2, Allyl; 3, *n*-Propyl; 4, Ethyl; 5, Methyl

classified into two groups, that is, alkyl chloride with the conjugated alkyl group and that with the non-conjugated alkyl one. With the catalysts of the chloride of the conjugated alkyl group, the polymerization rate decreases with an increase in the I_p(R·) value, while it increases in the non-conjugated alkyl group.

On the other hand, it is found that the relation between the rate constant of the Menschutkin reaction and the I_p(R·) value of the alkyl chloride is similar to the relation in this polymerization, as Fig. 8 shows. The structural study of these reactions will be discussed below.

Kinetics. From these experimental facts and the results obtained in the previous paper,[1] the

following mechanism of the polymerization may be postulated:

Initiation:

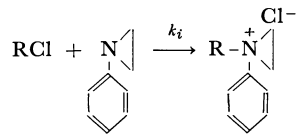

(1)

Propagation:

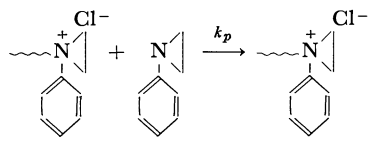

(2)

Termination:

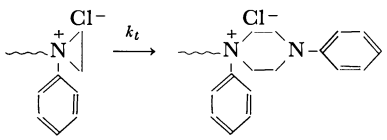

(3)

The initiating step may be the reaction of the alkyl chloride with *N*-phenylethylenimine to produce the initiating species, compound (I). As has been mentioned in the previous paper,[1] the polymer chain is considered to terminate with the formation of the piperazine derivative ring.

According to the mechanism of the polymerization postulated, the rate equations of the elementary reactions may be written as follows:

$$R_i = k_i[\mathrm{RCl}][\mathrm{M}] \quad (4)$$

$$R_p = k_p[\mathrm{P^*}][\mathrm{M}] \quad (5)$$

$$R_t = k_t[\mathrm{P^*}][\mathrm{M}] \quad (6)$$

where,

[RCl], [M], [P*]; the concentrations of the catalyst, the monomer, and the propagating species;

R_i, R_p, R_t: the rates of the initiation, propagation, and termination reactions, and

k_i, k_p, k_t: the rate constants of the initiation, propagation, and termination reactions.

Considering that the concentration of the monomer is much larger than that of the catalyst, Eq. (4) may be expressed by Eq. (7):

$$R_i = k_i[\mathrm{RCl}] \quad (7)$$

Since, in the early stage of the polymerization, the steady-state is realized ($R_i = R_t$), Eq. (8) is obtained:

$$k_i[\mathrm{RCl}] = k_t[\mathrm{P^*}] \quad (8)$$

On the other hand, from Eq. (7) the concentration of the catalyst can be expressed by Eq. (9):

$$[\mathrm{RCl}] = [\mathrm{RCl}]_0 e^{-k_i t} \quad (9)$$

Then, from Eqs. (8) and (9), the concentration of the propagating species can be represented by Eq. (10):

$$[\mathrm{P^*}] = (k_i/k_t)[\mathrm{RCl}]_0 e^{-k_i t} \quad (10)$$

By substituting [P*] into Eq. (5) and by then integrating it, Eq. (11) is derived:

$$\ln([\mathrm{M}]_0/[\mathrm{M}]) = (k_p/k_t)[\mathrm{C}]_0\,(1-e^{-k_i t}) \quad (11)$$

In the early stage of the polymerization, Eq. (11) may be represented approximately by Eq. (12):

$$\ln([\mathrm{M}]_0/[\mathrm{M}]) = (k_i k_p/k_t)[\mathrm{RCl}]_0 t \quad (12)$$

The fact that the molecular weight is almost constant, regardless of the reaction time, and the fact that it differs with the kind of alkyl chloride may be explained as follows. If there is no chain-transfer reaction, the number average of the degree of the polymerization, $\overline{P_n}$, is represented by Eq. (13):

$$\overline{P_n} = \int R_p dt / \int R_i dt \quad (13)$$

The polymer yield, $[\mathrm{M}_p]$, is expressed by Eq. (14):

$$[\mathrm{M_p}] = [\mathrm{M}]_0 - [\mathrm{M}] \quad (14)$$

Therefore, from Eqs. (11) and (14), Eq. (15) is derived:

$$[\mathrm{M_p}] = [\mathrm{M}]_0 \left\{1 - \exp \frac{k_p}{k_t}[\mathrm{C}]_0(1-e^{-k_i t})\right\} \quad (15)$$

On the other hand, $\int R_i dt$ is expressed by Eq. (16):

$$\int R_i d_t = [\mathrm{C}]_0 - [\mathrm{C}] = [\mathrm{C}]_0(1-e^{-k_i t}) \quad (16)$$

Therefore, by combining Eqs. (13), (15), and (16), $\overline{P_n}$ may be written by Eq. (17):

$$\overline{P_n} = \frac{[\mathrm{M}]_0\left\{1 - \exp \frac{k_p}{k_t}[\mathrm{C}]_0(1-e^{-k_i t})\right\}}{[\mathrm{C}]_0(1-e^{-k_i t})} \quad (17)$$

Figure 9 shows the plots of $\overline{P_n}$ against the reaction time assuming that $(k_p/k_t)[\mathrm{C}]_0 = 10$ in Eq. (17). From Fig. 9 it may be seen that the variation in $\overline{P_n}$ is small within the definite period of the reaction time, and that the value of $\overline{P_n}$ differs with the value of k_i. These facts are considered to agree with the results shown in Fig. 4.*1

Energetic Study of the Initiation Reaction. The relation between the kind of alkyl chloride and the initiation rate was studied quantitatively from the energetic point of view. The initiation reaction may be written by Eq. (18) in view of the

*1 In the case of the polymerization of *N*-phenylethylenimine with various carboxylic acids (pK_a=2.85—4.87), the molecular weight of the polymer was almost constant in the early stage of the polymerization, whereas in the later stage of the polymerization it increased. This may indicate that, in the early stage of the polymerization, the steady-state method is applicable, but not in the later stage. Although the steady-state method is thus not applicable in all periods of the reaction time, in order to estimate the rate constant of the initiation reaction the steady-state method was used.

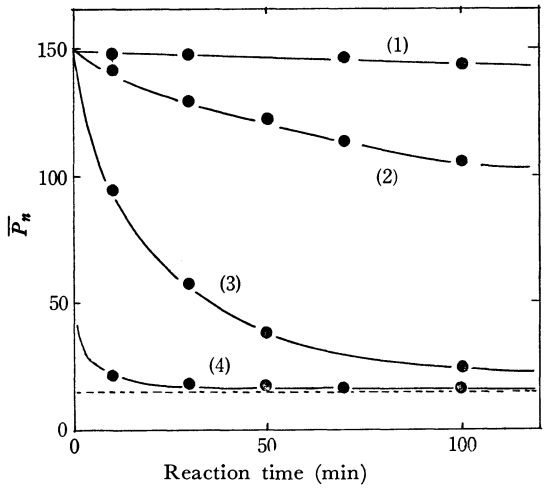

Fig. 9. The plots of $\overline{P}_n$ against the reaction time assuming (k_p/k_t) $[C]_0=10$ in Eq. (17).
The value of k_i: (1) 0.0001, (2) 0.001, (3) 0.01, (4) 0.1

heat of reaction (q);

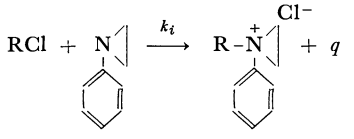

(18)

If it can be assumed that the relation between the activation energy and the heat of reaction is:

$$\Delta E = C_1 - C_2 q \tag{19}$$

the initiation rate can be evaluated by the heat of reaction as follows:

The heat of the reaction of the initiation reaction is considered to depend on the energy needed for dissociation of alkyl chloride to give the alkyl cation and the chlorine anion and for the addition of the alkyl cation to *N*-phenylethylenimine. The ionic dissociation energy of the alkyl chloride is considered to be proportional to the value of $-D(\mathrm{RCl})-I_p(\mathrm{R}\cdot)+E_a(\mathrm{Cl}\cdot)+T\Delta S$, with the same solvent system, where $D(\mathrm{RCl})$, $I_p(\mathrm{R}\cdot)$, $E_a(\mathrm{Cl}\cdot)$, and $T\Delta S$ are the bond dissociation energy of the alkyl chloride, the ionization potential of the alkyl radical, the electron affinity of the chlorine, and the entropy term respectively. Since the addition of the alkyl cation to *N*-phenylethylenimine may be the electrophilic reaction of the alkyl cation to *N*-phenylethylenimine and the nucleophilic reaction of *N*-phenylethylenimine to the alkyl cation, it may be considered that the larger the electron affinity of the alkyl cation ($E_a(\mathrm{R}^+)=I_p(\mathrm{R}\cdot)$) and the ionization potential of *N*-phenylethylenimine ($I_p(\mathrm{Imine})$), the smaller the energy of the addition of the alkyl cation to *N*-phenylethylenimine. On the basis of these considerations, the following empirical expression can be proposed for the evaluation of the heat of reaction of the initiation reaction in Eq. (18):

$$q = -D(\mathrm{RCl}) - I_p(R\cdot) + E_a(\mathrm{Cl}\cdot) + T\Delta S + C_3 I_p(\mathrm{R}\cdot) - C_4 I_p(\mathrm{Imine}) + C_5 \tag{20}$$

Considering that $E_a(\mathrm{Cl}\cdot)$ and $I_p(\mathrm{Imine})$ are constant and that, in the experiment with the same solvent, the value of $T\Delta S$ is almost constant, Eq. (20) may be written in the form:

$$q = -D(\mathrm{RCl}) - I_p(\mathrm{R}\cdot)(1 - C_3) + C_6 \tag{21}$$

By a combination of Eqs. (19) and (21), the activation energy may be expressed by Eq. (22):

$$\Delta E = C_1 - C_2\{-D(\mathrm{RCl}) - I_p(\mathrm{R}\cdot)(1 - C_3) + C_6\} \tag{22}$$

Subsequently, we tried to express the bond-dissociation energies of alkyl halides as a function of $I_p(\mathrm{R}\cdot)$ and $E_a(\mathrm{R}\cdot)$. As is shown in Fig. 10, the dissociation energy of alkyl halide increases almost in proportion to the value of $I_p(\mathrm{R}\cdot)-E_a(\mathrm{R}\cdot)$.

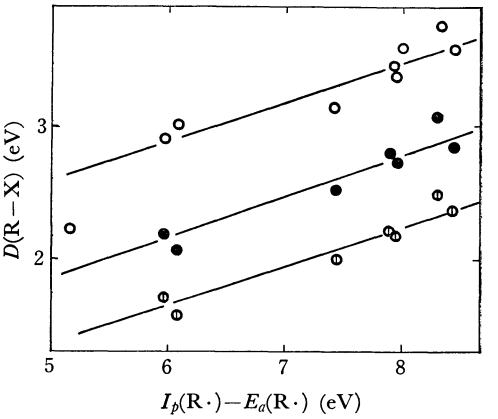

Fig. 10. Relation between the dissociation energy of alkyl halide and the value of $I_p(\mathrm{R}\cdot)-E_a(\mathrm{R}\cdot)$ of alkyl radical.
○, Chloride; ●, Bromide; ⓘ, Iodide

The empirical equation (23) was, then, obtained for the dissociation energy of alkyl chloride:

$$D(\mathrm{RCl}) = 0.3\{I_p(\mathrm{R}\cdot) - E_a(\mathrm{R}\cdot)\} + 1.1 \tag{23}$$

By substituting Eq. (23) into Eq. (22), the activation energy may be expressed in terms of $I_p(\mathrm{R}\cdot)$ and $E_a(\mathrm{R}\cdot)$:

$$\Delta E = C_7 + C_2(1.3 - C_3)I_p(\mathrm{R}\cdot) - 0.3E_a(\mathrm{R}\cdot) \tag{24}$$

On the other hand, from the plots of $E_a(\mathrm{R}\cdot)$ against $I_p(\mathrm{R}\cdot)$, as is shown in Fig. 11, $E_a(\mathrm{R}\cdot)$ is found to be approximately given by the following relations in the range of $7.8\leq I_p(\mathrm{R}\cdot)\leq 9.9$: for the conjugated alkyl radical:

$$E_a(\mathrm{R}\cdot) \fallingdotseq 2.0 \tag{25}$$

and for the non-conjugated alkyl radical:

$$E_a(\mathrm{R}\cdot) \fallingdotseq 0.45\, I_p(\mathrm{R}\cdot) - 3.0 \tag{26}$$

Hence, the activation energy may be written in these forms:

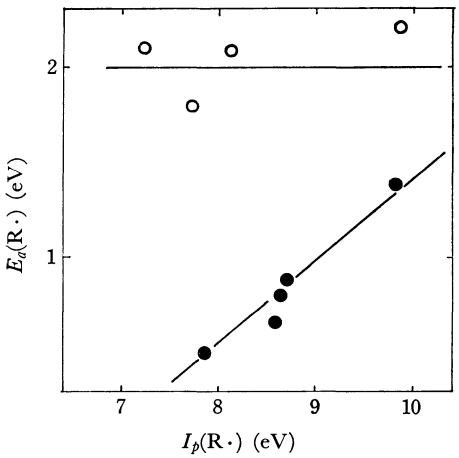

Fig. 11. Relation between electron affinity E_a(R·) and ionization potential I_p(R·) of alkyl radical.
○, conjugated alkyl radical
●, non-conjugated alkyl radical

for the conjugated alkyl radical:

$$\Delta E = (C_7 - 0.6) + C_2(1.3 - C_3)I_p(\mathrm{R}\cdot) \quad (27)$$

and for the non-conjugated alkyl radical:

$$\Delta E = (C_7 + 0.9) + C_2(1.17 - C_3)I_p(\mathrm{R}\cdot) \quad (28)$$

On the other hand, the rate constant is expressed by Eq. (29):

$$\ln k_i = \ln A - \Delta E/\boldsymbol{R}T \quad (29)$$

By substituting Eq. (27) or (28) into Eq. (29), Eqs. (30) and (31) were obtained for the conjugated alkyl radical:

$$\ln k_i = (0.6/\boldsymbol{R}T + C_8) + (C_2/\boldsymbol{R}T)(1.3 - C_3)I_p(\mathrm{R}\cdot) \quad (30)$$

and for the non-conjugated alkyl radical:

$$\ln k_i = (-0.9/\boldsymbol{R}T + C_8) + (C_2/\boldsymbol{R}T)(1.17 - C_3)I_p(\mathrm{R}\cdot) \quad (31)$$

If $1.17 < C_3 < 1.30$ and $C_2 > 0$, then:
for the conjugated alkyl radical:

$$1.3 - C_3 < 0 \quad (32)$$

and for the non-conjugated alkyl radical:

$$1.17 - C_3 > 0 \quad (33)$$

Therefore, if the values of C_3 and C_2 satisfy the above assumption, these considerations can explain the experimental results with the catalysts of conjugated and non-conjugated alkyl chlorides shown in Fig. 7.

BULLETIN OF THE CHEMICAL SOCIETY OF JAPAN VOL. 42 3524—3528 (1969)

The N→O Acetyl Migration of 5-Substituted-2-pyrrolidinemethanols*[1]

Hisayuki SAKURAI and Toshiyasu ISHIMARU

The Institute of Scientific and Industrial Research, Osaka University, Suita, Osaka

(Received May 21, 1969)

In order to obtain information about the stereochemistry of a fused-ring system, *cis* and *trans* isomers of 5-methyl- and 5-phenyl-2-pyrrolidinemethanols were synthesized and rate constants for their N→O acetyl migrations were measured. Each product was a mixture of *cis* and *trans* isomers. For both 5-methyl and 5-phenyl derivatives, it was observed that *trans* isomers migrated faster than *cis* isomers. The results were discussed in relation to stereochemistry.

The configuration of penicillin containing a fused-ring system consisting of 4- and 5-membered rings was determined by X-ray diffraction.[1] Very little, however, has been reported about the stereochemical studies of such a fused-ring system as penicillin because of the unstability of the 4-membered ring containing a lactam bond. Welsh proposed[2] that the N→O acyl migration of α-aminoalcohols, which has been studied in our laboratory, proceeds *via* an oxazolidine intermediate. The authors synthesized *cis* and *trans* isomers of 5-methyl- and 5-phenyl-2-pyrrolidinemethanol and examined their N→O acetyl migration rates in relation to configuration. This system is supposed to form during migration a fused-ring intermediate consisting of 5- and 5-membered rings.

*1 Paper IX, Stereochemistry of α-aminoalcohols and related compounds. For the previous paper in this series, see T. Ishimaru, *Nippon Kagaku Zasshi (J. Chem. Soc. Japan, Pure Chem. Sect.)*, **81**, 1592 (1960).

1) D. Crowfoot, C. W. Bunn, B. W. Roger-Low and A. Turner-Jones, "The Chemistry of Penicillin," H. T. Clarke, J. R. Johonson and Sir R. Robinson Princeton Univ. Press (1949), pp. 310-366.

2) L. Welsh, *J. Am. Chem. Soc.*, **71**, 3500 (1949).

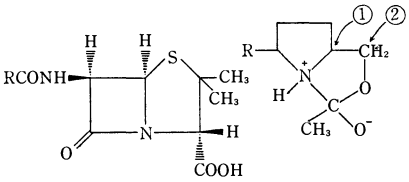

Fig. 1. Penicillin

Since the free rotation of the bond between C_1 and C_2 (Fig. 1) is possible, it was expected that the difference between *cis* and *trans* isomers in the effects which the configuration of the substituent R would produce on the N→O acetyl migration would be very little. However, a considerable difference was observed. The results and stereochemical discussion are described.

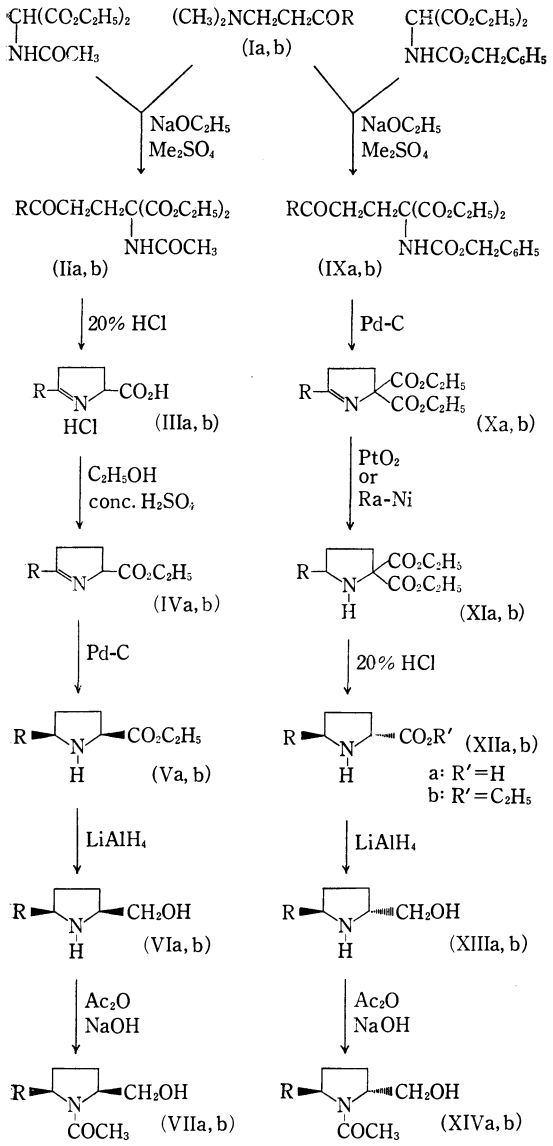

Scheme 1. Synthetic route.

Experimental*2

Ethyl 5-Substituted-2-pyrrolidinecarboxylate (Va, b and XIIa, b). The compounds were prepared by the method reported by Sanno[3] (Table 1). Esterification of Δ^1-2-substituted-pyrroline-5-carboxylic acid hydrochlorides (IIIa, b) was carried out by the method of Leonard.[4]

5-Substituted-2-pyrrolidinemethanol (VIa, b and XIIIa, b). To an ice-cooled suspension of 2.5 g (0.066 mol) of lithium aluminum hydride in 50 cc of anhydrous tetrahydrofuran (THF), 11.0 g (0.05 mol) of Vb in 50 cc of anhydrous THF was added dropwise with stirring. After refluxing for 2 hr, 50 cc of THF containing 5 cc of water was added dropwise and the reaction mixture was refluxed for an hour with stirring. Precipitate was filtered and washed three times with THF. The filtrate and washings were combined and dried over anhydrous sodium sulfate. Distillation under reduced pressure gave 6.2 g (70 %) of VIb, bp 148—149°C/4.5 mmHg. Picrate, mp 138—138.5°C (EtOH). Other materials were obtained in the same manner as described above (Tables 2 and 3).

***N*-Acetyl-5-substituted-2-pyrrolidinemethanol (VIIa, b and XIVa, b).** To an ice-cooled and mechanically stirred solution of 2.9 g (0.025 mol) of VIa in 20 cc of acetone, 5 cc (0.053 mol) of acetic anhydride was added dropwise and the 2 N sodium hydroxide solution (containing 3.4 g of sodium hydroxide) was added. When necessary, an appropriate amount of sodium hydroxide solution was added to keep the reaction mixture alkaline. After concentration *in vacuo*, the residue was extracted with chloroform. The extract was dried over anhydrous sodium sulfate, concentrated *in vacuo* and distilled under reduced pressure. Three grams (75.8 %) of viscous oil, bp 153.5—154.5°C/5 mmHg was obtained. Other materials were prepared in the same manner as described above (Table 4).

Kinetic Procedure of N→O Acetyl Migrations. Measurement was carried out according to the method of Ishimaru[5] at 50±0.1°C in 15 cc of 90 % aqueous dioxane containing an equivalent amount of 0.1 N hydrochloric acid to the sample which was weighed accurately. At regular intervals, 2 cc of reaction mixture was pipetted into 10 cc of ice-cooled 20% aqueous acetone and titrated with 0.02 N barium hydroxide using bromophenol blue as indicator. The pH of the end point is about 3.5.

No linear relationship was shown on the second-order plots. Therefore rate constants were estimated from the gradients of the lines drawn over the first three points. Each constant is an average of 2-4 measurements.

Measurement of pK_a values. pK_a values of 5-substituted-2-pyrrolidinemethanols were measured by the method reported by Parke and Davis.[6] About 10 mg

*2 Melting and boiling points are uncorrected.

3) Y. Sanno, *Yakugaku Zasshi (J. Pharm. Soc. Japan)*, **78**, 1113 (1958).

4) F. Leonard, U. S. Pat, 3164597; *Chem. Abstr.*, **62**, 16194, 9108 (1965).

5) T. Ishimaru, *Nippon Kagaku Zasshi (J. Chem. Soc. Japan, Pure Chem. Sect.)*, **81**, 648 (1960).

6) T. V. Parke and W. W. Davis, *Anal. Chem.*, **26**, 642 (1954).

TABLE 1. ETHYL 5-R-2-PYRROLIDINECARBOXYLATE

	R	R'	Bp °C/mmHg	Elemental analyses, Found (Calcd) C	H	N
cis	CH_3	C_2H_5	59/3[a]	61.20 (61.12	9.34 9.64	8.80 8.91)
trans	CH_3	H	mp 197—199[b]	55.70 (55.80	8.60 8.58	10.80 10.84)
cis	C_6H_5	C_2H_5	141—143/3.3[c]	71.42 (71.21	7.92 7.81	6.50 6.39)
trans	C_6H_5	C_2H_5	150—151/4.8	71.24 (71.21	8.01 7.81	6.32 6.39)

a) Bp 94—95°C/19 mmHg has been reported.[3]
b) Mp 207°C has been reported.[3]
c) Bp 95—97°C/0.07 mmHg has been reported.[4]

TABLE 2. 5-R-2-PYRROLIDINEMETHANOL

	R	Bp °C/mmHg	pK_a
cis	CH_3	75—81/4.5	10.5
trans	CH_3	88—91/7	10.5
cis	C_6H_5	148—149/4.5	9.38
trans	C_6H_5	135—137/2	9.29
	H	73—76/5[a]	10.6

a) Bp 98°C/10 mmHg[7] and bp 100—105°C/9 mmHg[8] have been reported.

TABLE 3. PICRATES OF 5-R-2-PYRROLIDINEMETHANOL

	R	Mp °C	Elemental analyses, Found (Calcd) C	H	N
cis	CH_3	112.5—114[a]	41.88 (41.87	4.58 4.68	16.20 16.27)
trans	CH_3	118—119.5[a]	41.90 (41.87	4.67 4.68	16.04 16.27)
cis	C_6H_5	138—138.5[b]	50.33 (50.25	4.29 4.46	13.97 13.79)
trans	C_6H_5	139.5—140[b]	50.39 (50.25	4.47 4.46	14.08 13.79)
	H	106.5—108[a,c]	40.13 (40.01	4.26 4.27	16.92 16.96)

a) Recrystallization from EtOH-Et_2O.
b) Recrystallization from EtOH.
c) Mp 106—107°C has been reported.[9]

of a sample was dissolved in 10 cc of water and 0.1 N hydrochloric acid (equivalent or a little more) was added. The solution was titrated with 2 N potassium hydroxide at 18°C. "Hitachi Horiba pH meter D-5" was used for the measurement.

Results and Discussion

The authors intended to obtain *cis* isomers, Va and Vb, from IVa and IVb by catalytic reduction. It was confirmed by gas chromatography that Va and Vb were pure respectively. However, *cis*-5-phenyl-2-pyrrolidinemethanol (VIb) obtained from Vb turned out to be a mixture of *cis* and *trans* isomers (*cis* : *trans*=8.5 : 1.5).[10] It is supposed

7) P. Karrer, P. Portmann and M. Suter, *Helv. Chim. Acta*, **31**, 1617 (1948).
8) W. Oelofsen and Choh Hao Li, *J. Am. Chem. Soc.*, **88**, 4257 (1966).
9) F. P. Doyle, M. D. Mehta, G. S. Sach and J. L. Pearson, *J. Chem. Soc.*, **1958**, 4458.
10) "Du Pont 310 Curve Resolver" was used for the analyses of the chromatograms.

TABLE 4. *N*-ACETYL-5-R-2-PYRROLIDINEMETHANOL

	R	Bp °C/mmHg	Elemental analyses Found (Calcd) C	H	N
cis	CH_3	153.5—154.5/5	61.32 (61.12	9.75 9.62	9.01 8.91)
trans	CH_3	157.5—159.5/6.5	61.10 (61.12	9.77 9.62	9.00 8.91)
cis	C_6H_5	203—205/5	70.92 (71.21	8.06 7.81	6.24 6.39)
trans	C_6H_5	175—176/2	70.99 (71.21	8.00 7.81	6.32 6.39)
	H	139—142/2.1	58.48 (58.72	9.31 9.15	9.85 9.78)

that the presence of *trans* isomer in VIb is due to isomerization by heating during isolation since the *trans* peak of VIb increased after heating at about 180°C for 2 hr (*cis* : *trans*=6.6 : 3.4). *N*-Acetyl-*cis*-5-methyl-2-pyrrolidinemethanol (VIIa) was also recognized to be mixed with a little of *trans* isomer (*cis* : *trans*=9.0 : 1.0).

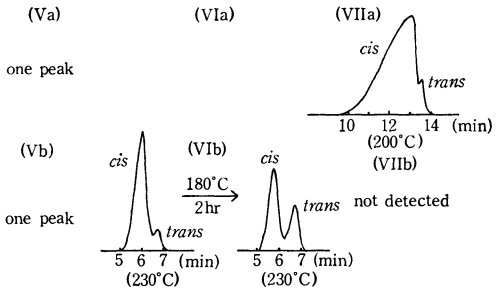

Fig. 2. Gas chromatograms of *cis* isomers.

It is considered that hydrolyses of XIa and XIb afford *trans* isomers, which are expected to be more stable thermodynamically, but *cis* isomers are also likely to be produced. As expected the ethyl esters of XIIa and XIIb were mixtures of *cis* and *trans* isomers (XIIa, *cis* : *trans*=1.0 : 9.0; XIIb, *cis* : *trans*=5.8 : 4.2). It was recognized that *trans*-5-phenyl-2-pyrrolidinemethanol (XIIIb) (*cis* : *trans* =5.6 : 4.4) and *N*-acetyl-*trans*-5-methyl-2-pyrrolidinemethanol (XIVa) (*cis* : *trans*=5.7 : 4.3) were also mixtures.

The reaction rate constants were calculated by second-order equation. (Table 5)

If it is assumed that each sample is pure, the ratio $k(trans)/k(cis)$ equals about 4–5. Considering the gas chromatographic results, it seems that the ratio $k(trans)/k(cis)$ is high in practice and *cis* isomers migrate much more slowly than *trans* isomers. Neglecting *cis* isomers, we obtained the initial concentrations of *trans* isomers from the results of gas chromatographic analyses and calculated the rate constants for *trans* isomers. The results of the calculations for two samples in which the ratios of isomers are different agree with each other. Thus the migration rates of *cis* isomers are considered to be negligible.

In *N*-acetyl derivatives there seem to be two forms, (A) and (B), which are in equilibrium. (A) is considered favorable for forming the intermediate proposed for N→O acyl migration (Fig. 1). Taking the steric hindrance into consideration, it

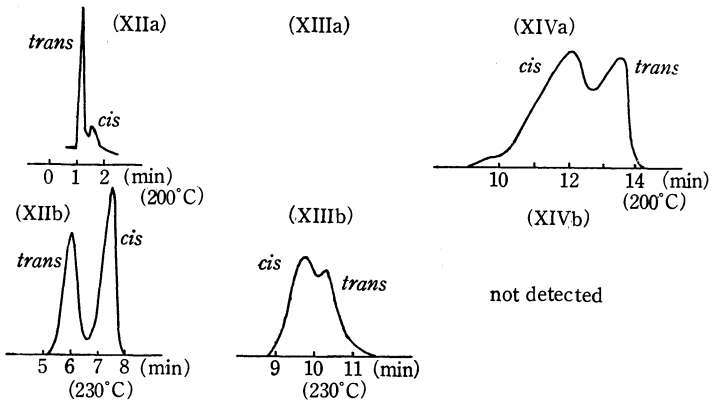

Fig. 3. Gas chromatograms of trans isomers.

Table 5. Migration rate constants

		k_2* mol l^{-1} sec^{-1}	k_2 mol l^{-1} sec^{-1}
5-CH_3	*trans*	7.22×10^{-4} a)	1.9×10^{-4}
	cis	1.48×10^{-4} b)	
5-C_6H_5	*trans*	5.86×10^{-4} c)	1.7×10^{-4}
	cis	1.51×10^{-4} d)	

* Rate constants when the samples are assumed to be pure. In practice a) *cis* : *trans*=5.7 : 4.3
b) *cis* : *trans*=9.0 : 1.0
c) *cis* : *trans*=5.6 : 4.4
d) *cis* : *trans*=8.5 : 1.5

seems that (B) predominates in *cis* and that the two forms can easily interchange in *trans*. Consequently, it is understood that *trans* isomers migrate faster than *cis* isomers.

It is difficult to discuss the difference of substituent effects between methyl and phenyl groups. The ratios of isomers were obtained on the basis of the results of gas chromatography, although isomerization may occur during the operation due to high temperature of the columns. In addition, in 5-phenyl derivatives gas chromatographic analyses were performed for 5-phenyl-2-pyrrolidinemethanols (VIb, XIIIb), and not for *N*-acetyl-5-phenyl-2-pyrrolidinemethanols (VIIb, XIVb).

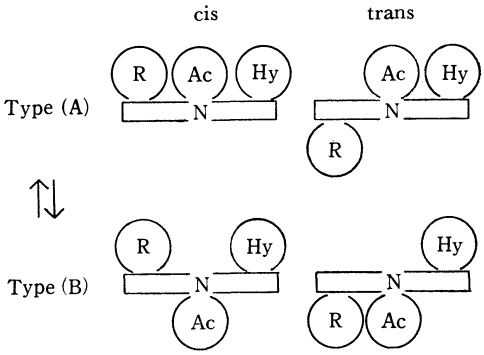

Fig. 4. *N*-Acetyl derivatives.
R=CH_3 or C_6H_5
Ac=$COCH_3$ Hy=CH_2OH

We were unsuccessful in synthesizing pure isomers, but we found from the measurements of their N→O acetyl migration that *trans* isomers migrated faster than *cis* isomers.

BULLETIN OF THE CHEMICAL SOCIETY OF JAPAN VOL. 42 3528—3535 (1969)

Alkaline Decomposition of Triarylsulfonium Halides with Various Bases[1)]

Shigeru OAE and Yong He KHIM

Department of Applied Chemistry, Faculty of Engineering, Osaka City University, Sumiyoshi-ku, Osaka

(Received May 24, 1969)

Alkaline decomposition of triarylsulfonium bromides with various bases was found to give different products depending on the nature of the bases. The reaction of triarylsulfonium bromide with either piperidide anion or thiophenoxide ion seems to proceed with the initial attack of piperidide anion or thiophenoxide ion of the carbon atom of C–S bond (S_N reaction on carbon atom), while the reaction of diarylethoxysulfonium tetrafluoroborate with thiophenoxide ion is presumed to involve the initial attack of thiophenoxide ion on the sulfur atom at low temperature (S_N reaction on sulfur atom). When triarylsulfonium bromide was subjected to the reaction with potassium hydroxide in aqueous ethanol, the main path was the alkaline decomposition which proceeds *via* the nucleophilic attack of the ethoxide ion on the sulfur atom. In the treatment with hydroxide ion in water, the decomposition appears to proceed mainly *via* two mechanistic routes, *i.e.*, the processes involving the nucleophilic attack of hydroxide ion on both aromatic carbon and the sulfur atoms. A free radical process cannot be excluded, but appears unlikely.

In a previous work,[2)] it was found that the alkaline decomposition reaction is presumably initiated by the attack of ethoxide ion on the sulfur atom of the sulfonium salts occured competitively along with S_N reaction of aromatic chloride.

In view of the formation of the various products in the treatment of triarylsulfonium salts with bases, the alkaline decompositions of triarylsulfonium salts seem to proceed *via* different routes depending on the nature of the bases. Namely, one portion undergoes a cleavage reaction *via* the initial attack on the sulfur atom (S_N reaction on sulfur atom), another involves a reaction *via* the attack on the aromatic carbon atom of C–S bond (S_N

1) Paper III on Sulfonium Salt. Paper II, Y. H. Khim and S. Oae, This Bulletin, **42**, 1968 (1969).

2) S. Oae and Y. H. Khim, *ibid.*, **42**, 1622 (1969).

reaction on carbon atom), and another proceeds through the initial removal of a proton to the sulfonio group followed by the subsequent elimination of sulfide group to form "benzyne" intermediate. In order to clarify the nature of the modes of alkaline decomposition of triarylsolfonium halides with various bases, the reactions of triarylsulfonium salts with piperidide anion, sodium arylthiolate, ethoxide and hydroxide ion have been carried out in various solvents. The details of alkaline decomposition and the mechanistic interpretation are presented in this paper.

Reaction of Triphenyl- and Tri-*p*-tolyl-sulfonium Bromides with Potassium Amide in Piperidine. When triphenylsulfonium bromide was reacted with potassium hydroxide in boiling piperidine under the conditions shown in Table 1, diphenyl sulfide, thiophenol and *N*-phenylpeperidine were obtained quantitatively.

From analyses of the products, the alkaline cleavage reaction seems to proceed with the initial attack of piperidide anion on the carbon atom of C–S bond bearing sulfide group, while diphenyl sulfide formed reacts further with piperidide anion to give thiophenol and *N*-phenylpiperidine.

It has been suggested[3] that the cleavage reaction of diphenyl sulfide with sodium amide in boiling piperidine proceeds through the initial attack of peperidide anion on the carbon atom of diphenyl sulfide as follows.

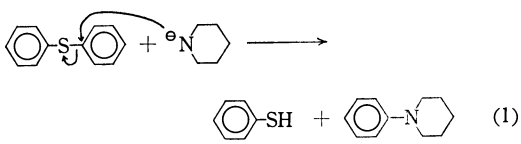

(1)

However, since this particular reaction is performed between a positively charged species *i.e.* sulfonium salt and a very strong base in a heterogeneous system, there remains a possibility that the reaction proceeds through the initial abstraction of *o*-hydrogen followed by the subsequent elimination of sulfide group to form "benzyne" intermediate, to which piperidide anion adds to result in the final product as shown below.

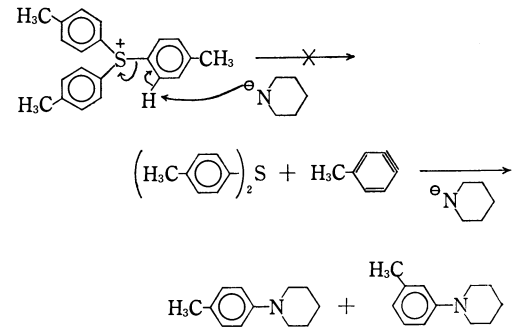

(2)

In order to examine the "benzyne" mechanism tri-*p*-tolylsulfonium bromide was subjected to the alkaline decomposition reaction, since this mechanism requires the formation of both *meta*- and *para*-substituted *N*-*p*-tolylpiperidines. Identification of both *meta*- and *para*-*N*-tolylpiperidines can be easily performed by the comparison of their characteristic infrared absorption bands (*m*-derivative 10.5, 12.95 μ; *p*-derivative 12.32 μ) and also by gas chromatography. When the reaction was actually carried out under the conditions shown in Table 1, only the *para*-substituted compound was obtained, but

Table 1. The alkaline decomposition of triarylsulfonium bromide with potassium amide in piperidine

Sulfonium salts	Solvent	Base	Temp. (°C)	Time (hr)	Products	Yield (%)
$(C_6H_5)_3S^+Br^-$ [c]	HN	KNH_2 [c]	106	5	Ph–S–Ph (50) SH (42)	92[a]
					N	90[b]
$(H_3CC_6H_4)_3S^+Br^-$ [c]	HN	KNH_2 [c]	106	5	$(H_3CC_6H_4)_2S$ $H_3CC_6H_4SH$	85
					$H_3CC_6H_4N$	80

a) The yield is a combined percentage of sulfide and thiophenol.
b) The yield was obtained based on the molar concentration of starting sulfonium salt.
c) The molar ratio of sulfonium and potassium amide was 1 : 4.

3) a) W. E. Truce, D. P. Tate and D. N. Burge, *J. Am. Chem. Soc.*, **82**, 2872 (1960). b) R. Otto, *Ber.*, **19**, 2425 (1886). c) S. Oae and R. Kiritani, This Bulletin, **38**, 765 (1965). d) N. Furukawa, H. Tanaka and S. Oae, *ibid.*, **41**, 1463 (1968).

no *meta-N*-tolylpiperidine.

Thus the most plausible route for this reaction may be the one involving the aromatic S_N2 process.

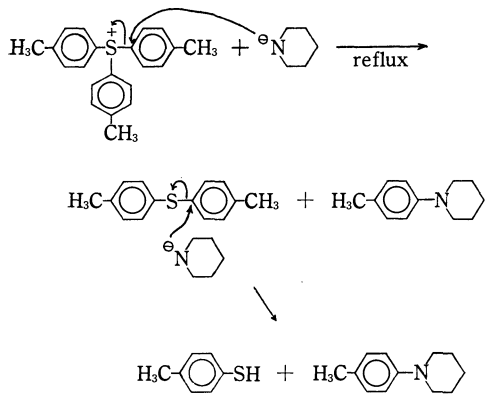

(3)

Reaction of Triarylsulfonium Bromide and Ethoxy-diphenyl-sulfonium Tetrafluoroborate with Sodium Arylthiolate in Ethanol. Triarylsulfonium bromides were subjected to the alkaline decomposition with sodium arylthiolate in ethanol and the detailed analyses of the products formed in the reaction were undertaken in order to choose possible mechanistic pathways for the reaction. The solution of tri-*p*-tolylsulfonium bromide and sodium thiophenoxide in ethanol was gently refluxed in ethanol under the conditions given in Table 2. The products isolated were found to contain di-*p*-tolyl sulfide and phenyl- *p*-tolyl sulfide as the main products and a small amount of diphenyl disulfide as the minor product. The products and yields for other similar reactions are shown in Table 2. Identification and determination of the yields of products obtained were performed by means of quantitative vapor phase chromatography and by comparison of their infrared spectra with those of the authentic samples.

From the distribution of the whole products and their yields, the reaction (runs 1—4) seems to proceed *via* the nucleophilic attack on the carbon atom of C-S bond similarly to the case of the reaction of triarylsulfonium bromide with piperidide anion (Eq. (4)).

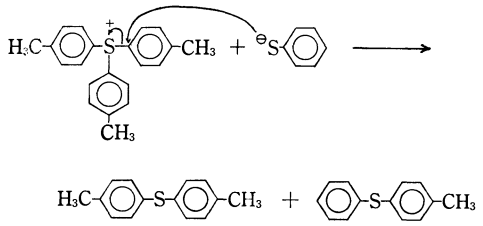

(4)

The formation of a small amount of diaryl disulfide (runs 1—4) undoubtedly results from the oxidation of sodium arylthiolate itself in boiling ethanol (Eq. (5)), because the yields of diaryl disulfides

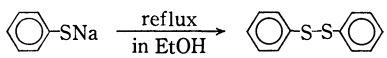

(5)

do not differ much regardless of the absence or presence of the sulfonium salts in the reaction system (run 3), and the yield of diphenyl disulfide in the

TABLE 2. THE REACTION OF SULFONIUM SALTS WITH SODIUM ARYLTHIOLATES IN ETHANOL

Run	Sulfonium salt	Base	Sulfonium : Base	Temp. (°C)	Time (hr)	Products (Yield %) Sulfides	Disulfides
1	$(Ph\text{-})_3\overset{+}{S}\ Br^-$	$Ph\text{-}S^\ominus$	1 : 3	78	4	$Ph\text{-})_2S$ (180)[a]	$Ph\text{-}S)_2$ (7)
2	$(Ph\text{-})_3\overset{+}{S}\ Br^-$	$Me\text{-}C_6H_4\text{-}S^\ominus$	1 : 3	78	4	$Ph\text{-})_2S$ (90)	$Me\text{-}C_6H_4\text{-}S)_2$ (8)
						$Me\text{-}C_6H_4\text{-}S\text{-}C_6H_5$ (80)	
3	——	$Ph\text{-}S^\ominus$	—	78	4	——	$Ph\text{-}S)_2$ (5)[b]
4	$Me\text{-}C_6H_4)_3\overset{+}{S}\ Br^-$	$Ph\text{-}S^\ominus$	1 : 1	78	6	$Me\text{-}C_6H_4)_2S$ (90)	$Ph\text{-}S)_2$ (small)
5	$[Ph\text{-})_2\overset{+}{S}\text{-}OEt]\ BF_4^-$	$Me\text{-}C_6H_4\text{-}S^\ominus$	1 : 1	−5——10	1.5	$Ph\text{-})_2S$ (42)[c]	$Me\text{-}C_6H_4\text{-}S)_2$[c] (40)
6	〃	$Me\text{-}C_6H_4\text{-}S^\ominus$	1 : 2	−5	1	$Ph\text{-})_2S$ (90)[c]	$Me\text{-}C_6H_4\text{-}S)_2$[c] (80)

a) The apparent yield is based on moles of sulfonium salt; the real yield from the cleavage reaction is 90%.

b) Without sulfonium salt, sodium thiophenoxide itself upon being acidified in the air gave diphenyl in ethanol.

c) The moles of both diphenyl sulfide and ditolyl disulfide are almost same.

reaction with equimolar mixture of tri-*p*-tolylsulfonium bromide and sodium thiophenoxide (run 4) is much smaller than that in the case with a mixture in which the ratio of sodium thiophenoxide over sulfonium salt is three.

Another possible mechanism of S_N reaction on sulfur atom of triarylsulfonium salt may be considered. If the reaction proceeds *via* S_N reaction at sulfur atom, it should give toluene or benzene as in the case of the reaction of triarylsulfonium halide with phenyllithium, where the nucleophilic attack of phenyl anion on sulfur atom of sulfonium salt was actually detected.[4]

In no case, however, could the formation of any hydrocarbon be detected. Therefore, the S_N reaction on the sulfur atom can be ruled out.

When diphenylethoxysulfonium tetrafluoroborate was subjected to the reaction with sodium *p*-toluenethiolate under the conditions shown in Table 2 (run 5, 6), the products isolated from the reaction were both diphenyl sulfide and ditolyl disulfide. From the products the reaction seems to proceed first *via* the attack of the nucleophile on the sulfur atom of the sulfonium salt with ethoxy group as the leaving group, involving the initial formation of an unstable *p*-tolylthiodiphenylsulfonium ion intermediate (A). It then seems to proceed through the attack of the same nucleophile on the S atom of *p*-tolylthio group of the intermediate sulfonium ion, with diphenyl sulfide as the leaving group as shown below.

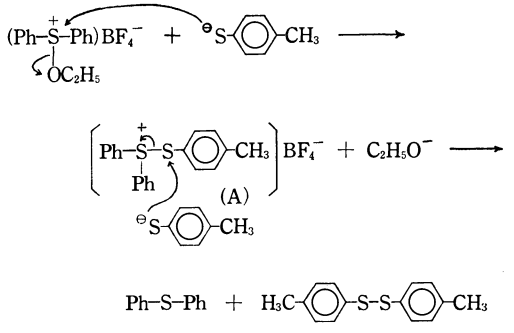

(6)

Since the ethoxy group is a better leaving group than the diphenyl sulfide group, *p*-toluenethiolate ion may easily attack the sulfur atom in contrast to the aromatic substitution of tri-*p*-tolylsulfonium bromide with thiophenoxide ion in which diphenyl sulfide is the leaving group. The problem of attacking site of nucleophilic reagent in the S_N reaction of sulfonium salt can easily be explained by the relative ease and stability of the leaving group. Recently, Kice and his co-workers[5] have revealed that the scission of the sulfur-sulfur bond of aryl-hydroxy-arylthio-sulfonium ion in the reaction of aryl arylthiolsulfinate with nucleophilic reagents occurs at the sulfur atom of arylthio group, but not at the sulfur of aryl-hydroxysulfonio ion. Recently McEwen and Knapcyzyk[6] suggested that the reaction of triarylsulfonium halides with alkoxide ion in alcohol solbents proceeds *via* a radical process.

If the reaction of diphenyl-ethoxysulfonium bromide with *p*-toluenethiolate ion involves a radical process in which the electron transfer occurs, as in Eq. (7), the reaction between equimolar amounts of the sulfonium and *p*-toluenethiolate ion should give a mixture of an equimolar amount of diphenyl sulfide and a half molar amount of di-*p*-tolyl disulfide, while in the case of the usual S_N reaction on the sulfur atom, the decomposition of the sulfonium salt is expected to give equimolar mixture of both diphenyl sulfide and di-*p*-tolyl disulfide.

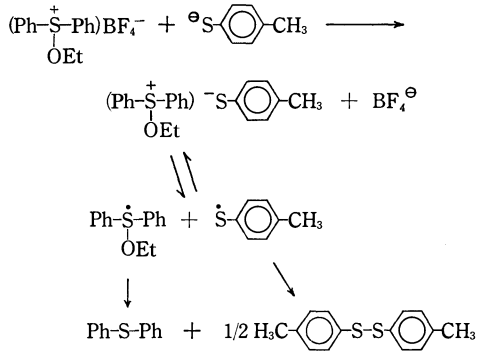

(7)

The results shown in runs 5 and 6 in Table 2, reveal that almost the same molar quantities of both sulfide and the disulfide were obtained. Therefore, the alkaline decomposition of the diaryl-ethoxysulfonium tetrafluoroborate with *p*-toluenethiolate ion in ethanol is presumed to proceed through the initial nucleophilic attack of the arylthiolate anion on the sulfur atom of the sulfonium compound.

Reaction of Triarylsulfonium Bromide with Potassium Hydroxide in Aqueous Ethanol and Water. The reaction of a triarylsulfonium bromide with potassium hydroxide in aqueous ethanol gave corresponding diaryl sulfide, hydrocarbon and resins as the main products and a small amount of ethyl aryl ether. A similar decomposition of the sulfonium salt in water under prolonged heating conditions at higher tempera-

4) a) V. Franzen and C. Mertz, *Ann.*, **643**, 24 (1961). b) Y. H. Khim and S. Oae, This Bulletin, **42**, 1968 (1969).

5) a) J. L. Kice and E. H. Markved, *J. Am. Chem. Soc.*, **86**, 2270 (1964). b) J. L. Kice and G. Guaraldi, *ibid.*, **88**, 5236 (1966). c) J. L. Kice, C. G. Venier and L. Heasley, *ibid.*, **89**, 3557 (1967).

6) J. W. Knapczyk, G. H. Wiegand and W. E. McEwen, *Tetrahedron Letters*, **1965**, 2971.

TABLE 3. THE REACTION OF TRIARYLSULFONIUM BROMIDE WITH POTASSIUM HYDROXIDE IN AQUEOUS ETHANOL[a]

Sulfonium	Solvent molar ratio $C_2H_5OH : H_2O$	Base	Temp. (°C)	Time (hr)	Products (yield %) or molar ratio
	44 : 56	KOH	105	7	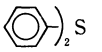 (92), (82) 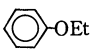 (~2), resins[b]
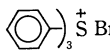	97 : 3	KOH	105	7	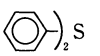 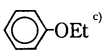 [c] (95 : 5)
	1.77 : 98	KOH	120	24	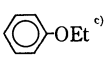 [c] (98 : 2)
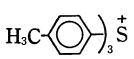	44 : 56	KOH	105	10	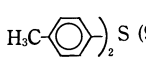 (90), (80) 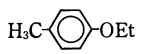 (~2), resins

a) The reaction was carried out in an ampoul.
b) Perhaps, acetaldehyde is polymerized to give aldol resins.
c) The molar ratio of diphenyl sulfide and phenetole was determined by using quantitative vapor phase chromatography. Besides these products, benzene and resins were also confirmed.

TABLE 4. THE REACTION OF TRIARYLSULFONIUM BROMIDE WITH POTASSIUM HYDROXIDE IN WATER[a]

Sulfonium[b] salt	Solvent	Base[b]	Temp. (°C)	Time (hr)	Products (yield %)
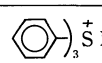	H_2O	KOH	150—160	50	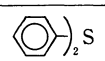 (80), 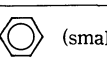 (small) (27), 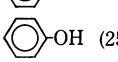 (25)
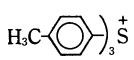	H_2O	KOH	150—160	150	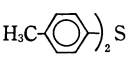 (57), 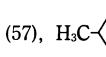 (10) 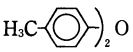 (30), 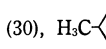 (6)
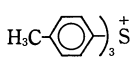	H_2O	KOH	210—230	100	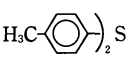 (80), 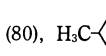 (40) 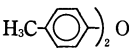 (14), 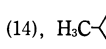 (6)[c]
	H_2O	KOH Ph-OH	160—180	50	(90), 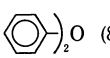 (88)

a) The reaction was carried out in an ampoul.
b) The molar ratio of starting sulfonium salt and potassium hydroxide is 1 : 8.
c) The formation of *p*-tolyl bromide could be explained in terms of the intramolecular decomposition. McEwen and Wiegand[7] demonstrated that triarylsulfonium halides might proceed *via* an intramolecular decomposition at 250°C to give sulfides and aryl halides.
d) The molar ratio of starting salt: KOH : phenol is 1 : 8 : 4.

ture as shown in Table 4 yielded the diaryl sulfide, the diaryl ether, phenol, and hydrocarbon compounds.

The results and the experimental conditions are tabulated in Tables 3 and 4. There is a big difference in the products and their yields between the alkaline decompositions of the triarylsulfonium salt in aqueous ethanol and that in water, although experimental conditions also somewhat differ from each other.

Considering the main products of sulfide, hydrocarbon compound and resins obtained from the reaction in aqueous ethanol, the decomposition of triarylsulfonium bromide with ethoxide ion seems to proceed mainly through the initial attack of the ethoxide ion on the sulfur atom of the sulfonium salt and the rest, through the process shown below.

7) G. H. Wiegand and W. E. McEwen, Tetrahedron Letters **1965**, 2639; *J. Org. Chem.*, **33**, 2671 (1968).

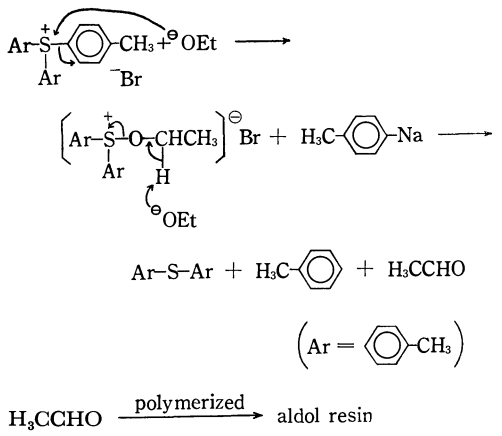

(8)

Since both hydroxide and ethoxide ions can exist in an equilibrium in aqueous ethanol, one could expect that the hydroxide ion should participate in the alkaline decomposition if the amount of water increases. From the products analyses of the reaction of the triphenylsulfonium bromide with potassium hydroxide from 1.6 to 97 mol % aqueous ethanol, the reaction seems to proceed mainly through the nucleophilic attack of only ethoxide ion on the sulfur atom of the sulfonium salt.

In a previous paper,[2] it was revealed that the alkaline decomposition of the triarylsulfonium bromide with ethoxide ion in 70% (vol%) aqueous ethanol obeys the second order kinetic rate low; first order with respect to both the sulfonium and potassium hydroxide concentrations.

Thus, the kinetic experiment of the alkaline decomposition was carried out in order to examine the solvent effect of various water and ethanol mixtures. The values of the rate constants for the alkaline decompositions in various aqueous ethanol solvents at 120°C are shown in Table 5. Figure 1 records a plot of the mol per cent of ethyl alcohol in water against the log of second order rate constant. The results indicate that the rate of the decomposition is increased about 10^6 fold by increasing the ethanol concentration (97.7 mol%) from 98.33 mol % of water.

TABLE 5. THE RATES OF ALKALINE DECOMPOSITION OF TRIPHENYLSULFONIUM BROMIDE WITH ETHOXIDE ION IN AQUEOUS ETHANOL AT 120±0.1°C

Solvent (H_2O-C_2H_5OH) W% C_2H_5OH	Mol% C_2H_5OH	k_2 $mol^{-1}\,l\,sec^{-1}$
	0.96	——a)
6.25	1.77	2.90×10^{-6}
38.00	16.00	7.80×10^{-5}
46.50	26.80	2.95×10^{-4}
61.00	40.00	5.73×10^{-4}
81.00	63.50	1.39×10^{-3}
90.00	80.00	5.34×10^{-3}
97.00	93.00	2.38×10^{-1}
98.00	95.30	7.60×10^{-1}
99.00	97.70	9.32×10^{-1}

a) After the reaction mixture was heated for 48 hr, the starting sulfonium bromide was recovered almost quantitatively.

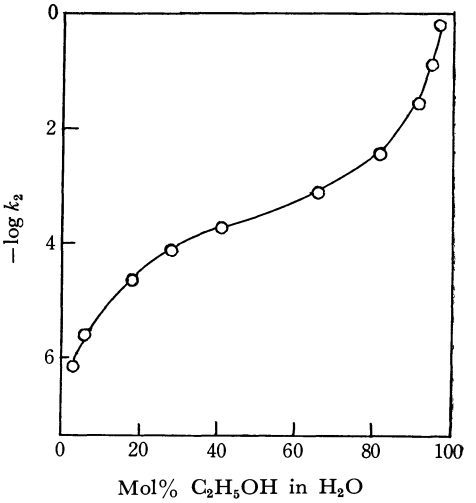

Fig. 1. Plot of mole percentage of ethyl alcohol in water against negative logarithm of k_2 ($mol^{-1}\,l\cdot sec^{-1}$) for the reaction of triphenylsulfonium bromide with potassium hydroxide.

The curve in Fig. 1 is of a shape observed frequently in the solvent effect of the reaction in the reactions of the mixted solvents. Although the plot is almost linear from 30 to 80 mol % of ethyl alcohol the rates rise much more steeply at lower and higher concentrations. In the case of pure water, after the reaction mixture was heated at 120°C for 50 hr, the starting solfonium salt was quantitatively recovered. From the results obtained in the kinetic experiments, it may be concluded that ethoxide ion which is more nucleophilic than hydroxide ion attacks preferentially the sulfonium ion undergoing alkaline decomposition.

$$HO^{\ominus}\cdots HOH + HOC_2H_5 \rightleftarrows HO^{\ominus}\cdots HOC_2H_5 \rightleftarrows {}^{\ominus}OC_2H_5 + H_2O$$

When the triphenylsulfonium bromide was subjected to reaction with potassium hydroxide in water under severer conditions as shown in Table 4, the isolated compounds were diphenyl sulfide (87 %), diphenyl ether (27 %), phenol (25 %) and a small amount of benzene in contrast to the case of the similar reaction in aqueous ethanol. From the distribution of the products, the decomposition of triphenylsulfonium bromide with potassium hydroxide in water seems to involve the initial attack of hydroxide ion on the carbon atom of C-S bond to form phenolate ion, which in turn

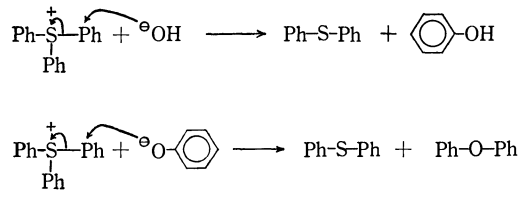

attacks the carbon atom of the sulfonium salt yeilding diphenyl ether. Phenoxide ion may be more nucleophilic than hydroxide ion. In the presence of phenoxide ion, the alkaline decomposition of triphenylsulfonium bromide gave an equimolar mixture of both diphenyl sulfide and diphenyl ether quantitatively under the same condition as shown in Table 4.

Another possible mechanism of benzyne route is considered, because diphenyl sulfide, phenyl ether and phenol can be formed by the abstraction of *o*-hydrogen followed by the elimination of sulfide group to form benzyne intermediate.

Benzyne has been postulated as being an intermediate between the triarylsulfonium halides and a base in other reactions.[4] In order to examine the benzyne mechanism, tri-*p*-tolylsulfonium bromide was subjected to the reaction with hydroxide ion in water under the condition shown in Table 4, since this mechanism requires the formation of both *meta*- and *para*-ditolyl ether.

The compound isolated is only the *para* substituted compound *p,p'*-ditolyl ether, whose identification can be easily performed by the comparison of its characteristic IR.

Therefore, the possibility of the benzyne precess is ruled out.

It is noteworthy that the decomposition of triphenylsulfonium bromide with hydroxide ion in water gives a small amount of benzene whereas a similar reaction of tri-*p*-tolylsulfonium bromide with hydroxide ion affords a higher yield of toluene than that of benzene, especially at higher reaction temperature, though the experimental conditions are somewhat different. The reaction system of triphenylsulfonium salt is homogeneous, while that of tri-*p*-tolylsulfonium salt is heterogeneous and so requires a higher reaction temperature and longer time as shown in Table 4.

In the case of the alkaline decomposition of tritolylsulfonium bromide, the yield of toluene increases with the rise of reaction temperature and that of *p*-cresol and its derivatives decreases. It could be that in the case of tri-*p*-tolylsulfonium salt the heterogeneous reaction system and higher reaction temperature are preferable for a radical process.

It could be garued that the diaryl sulfide, diaryl ehter, phenol and hydrocarbon compounds also arise through a radical process[6] although it is not very likely.

The formation of phenol in this reaction could be explained by the following equations.

$$Ar_3\overset{+}{S}\overset{-}{Br} + {}^{\ominus}OH \rightarrow Ar_3\overset{+}{S}\overset{-}{OH} + Br^{\ominus} \rightleftarrows Ar_3SOH$$

$$\rightleftarrows [Ar_3\dot{S}\ \dot{O}H] \rightarrow Ar_2S + ArOH \qquad (9)$$

If the phenoxide ion formed by the dissociation of phenol obtained in the radical process would again attack the carbon atom of the C–S bond (S_N reaction on a carbon atom) analogous to hydroxide ion, diaryl ether should be obtained.

When the decomposition of a triarylsulfonium salts took place both in the presence and absence of oxygen, the ratio of all the phenol derivatives to diaryl sulfide produced did not differ. In the case of a radical process, a higher yield of phenol and phenol derivatives in the presence of oxygen than that in the absence of oxygen can be expected. However, at the present time a definite conclusion to these complicating reactions of the triarylsulfonium bromide with hydroxide ion in water can not be drawn.

Experimental

Triphenyl- and Tri-*p*-tolylsulfonium Bromide. The titled triarylsulfonium bormides were prepared from diarylethoxysulfonium tetrafluoroborate and aryl Grignard reagent according to the usual methods.[2]

The Reaction of Triphenylsulfonium Bromide with Potassium Amine in Piperidine. Sodium amide (0.5 g, 0.012 mol) which was washed with anhydrous *n*-hexane before use, was refluxed in piperidine (10 m*l*) for 30 min. To this solution was added triphenylsulfonium bromide (1 g, 0.003 mol) and the mixture was refluxed for about 5 hr. After cooling, the solution was quenched with ice water to decompose sodium amide. The aqueous solution was extracted with ether; the aqueous layer was carefully acidified with 1 N hydrochloric acid and extracted again with ether. After evaporation of ether, thiophenol (40 %) was obtained. The first ether layer was distilled and the distillate fractionated by vapor phase chromatography. Identification and determination of the yields of the products were performed using quantitative vapor phase chromatography and by comparison of their infrared spectra with those of authentic samples. The isolated compounds from the organic layer are diphenyl sulfide (50 %) and *N*-phenylpiperidine (90 %). The reaction of tri-*p*-tolylsulfonium bromide with potassium amide in piperidine was carried out similarly to that of triphenylsulfonium salt. The results are shown in Table 1.

The Reaction of Tri-*p*-tolylsulfonium with Sodium Thiophenoxide. Tri-*p*-tolylsulfonium bromide (2 g, 0.0026 mol) was dissolved in ethanol (30 m*l*). To this solution was added sodium thiophenoxide (2.08 g, 0.0104 mol) in ethanol (20 m*l*) with stirring. After the reaction mixture was refluxed for 4 hr, it was poured into ice water and acidified with dilute hydrochloric acid, extracted with ether, washed, dried over magnesium sulfate. The compounds isolated from the organic layer were di-*p*-tolyl sulfide (92 %) and phenyl *p*-tolyl sulfide (90 %) and a small amount of diphenyl disulfide. The purity and yields of the products were checked

with quantitative vapor-phase chromstography. Identification of these products was performed by comparison of their infrared spectra with those of authentic samples. Other reactions of triphenylsulfonium bromide with *p*-toluenethiolate and thiophenoxide ions were carried out similarly to the above reaction. All the results are summarized in Table 4.

The Reaction of Diphenylethoxysulfonium Tetrafluoroborate with Sodium *p*-Toluenethiolate. Diphenyl sulfoxide (2 g, 0.01 mol) was dissolved in anhydrous methylene chloride (5 m*l*) containing triethyloxonium tetrafluoroborate (2 g). The reaction mixture was stirred for about 30 min, at room temperature and to the this solution 50 m*l* of anhydrous ether was added, then the methylene chloride-ether mixture was replaced by anhydrous ethanol (30 m*l*) by decantation. To this solution was slowly added sodium *p*-toluenethiolate (1.46 g, 0.01 mol) in anhydrous ethanol (20 m*l*) −5——10°C over a period of about 1 hr with stirring. After stirring was continued for 30 min, the reaction mixture was poured into ice water, acidified carefully with dilute cold hydrochloric acid, extracted with a large amount of ether, washed and dried over magneisum sulfate. From the ether layer, diphenyl sulfide (42%) and di-*p*-tolyl disulfide (40%) were isolated. The yields of products were determined by quantitative vapor phase chromatography.

Sodium *p*-Toluenethiolate. The compound was prepared by treating *p*-tolyl mercaptan (10 g, 0.08 mol) and sodium hydroxide (3.7 g, 0.078 mol) in benzene. The usual work up of the reaction mixture afforded 11 g of colorless sodium *p*-toluene thiolate in 94 % yield.

The Reaction of Triarylsulfonium Bromide with Potassium Hydroxide in Aqueous Ethanol and Water. A typical run is as follows. Triphenylsulfonium bromide (1 g, 0.003 mol) and potassium hydroxide (1.3 g, 0.0024 mol) were dissolved in water. The solution was sealed into a glass tube and heated for 50 hr at 150—160°C. After cooling, the sealed tube was broken and the content poured into water, acidified with dilute hydrochloric acid, extracted with ether, washed, dried over magnesium sulfate. The ether layer was fractionated by vapor phase chromatography. Identification and determination of the yields of the products were also done by IR, NMR and gas chromatography. All the results and those from other reaction are shown in Tables 3 and 4.

Kinetic Experiment. Kinetic measurement and the rate calculation of alkaline decomposition of triphenylsulfonium bromide with ethoxide ion in aqueous ethanol were performed with the use of the ultraviolet spectra of the diphenyl sulfide in the same method as described previously.[2)]

BULLETIN OF THE CHEMICAL SOCIETY OF JAPAN VOL. 42 3535—3538 (1969)

Reaction of Ethyl Diazoacetate with Cupric Chloride

Takeo SAEGUSA, Yoshihiko ITO, Toyoji SHIMIZU and Shiro KOBAYASHI

Department of Synthetic Chemistry, Faculty of Engineering, Kyoto University, Sakyo-ku, Kyoto

(Received May 23, 1969)

The reaction of ethyl diazoacetate (**1**) with $CuCl_2$ was investigated. Ethyl chloroacetate (**2**), ethyl dichloroacetate (**3**) and a mixture of ethyl dichloromaleate (**4**) and ethyl dichlorofumarate (**5**) were produced. These products were explained by assuming 1-chloro-1-ehtoxycarbonylmethyl-copper complexes, (**10**) and (**11**). The reactions of **1** with $HgCl_2$ and $CoCl_2$ were examined in detail as reference reactions from the mechanistic view point.

The reaction of diazo compounds, especially diazomethane, with metal halides has been extensively studied, which provides a convenient method for the preparation of halomethylmetal compound.[1] Studies on the interaction between diazo compound and copper salts are restricted to the copper catalyzed decomposition of diazo compounds.[2]

This paper describes the reaction of ethyl diazoacetate (**1**) with $CuCl_2$. It has been found that $CuCl_2$ is distinguished from other copper salts. In equimolar reactions of **1** with cupric salts having negative groups of CN, SO_4 and NO_3 as well as cuprous chloride, only a mixture of ethyl maleate and fumarate was produced. On the other hand, the reaction of **1** with $CuCl_2$ produced ethyl chloroacetate (**2**), ethyl dichloroacetate (**3**), and a mixture of ethyl dichloromaleate (**4**) and ethyl dichlorofumarate (**5**). These products were explained by assuming ethoxycarbonyl-substituted chloromethyl-copper complexes, exemplified by **10** and **11**, as unstable intermediates. The reactions of **1** with $HgCl_2$ and $CoCl_2$ are described in more detail as reference reactions from the mechanistic view point. The reaction of diphenyldiazomethane with cupric chloride was also examined to complement mechanistic consideration.

1) D. Seyferth, *Chem. Rev.* **55**, 1155 (1955).

2) a) W. Kirmse, "Carbene Chemistry," Academic Press Inc., New York, N. Y. (1964). b) T. Saegusa, Y. Ito, S. Kobayashi, K. Hirota and T. Shimizu, *J. Org. Chem.*, **33**, 544 (1968).

Table 1. Reaction of diazoacetate with copper chlorides[a)]

Ethyl diazoacetate (mmol)	Copper chloride (mmol)		Products (%)[b)]				
			2	**3**	**4/5**	**9**	maleate/fumarate
18	CuCl	18	0	0	0	—	97
16.4	$CuCl_2$	16.4	16	40	3	—	30
10	$CuCl_2$	20	8	82	6	trace	0

[2]; $ClCH_2CO_2C_2H_5$ **[3]**; $Cl_2CHCO_2C_2H_5$
[4]/**[5]**; *cis* and *trans* $C_2H_5O_2CClC{=}CClCO_2C_2H_5$ **[9]**; $Cl_3CCO_2C_2H_5$
a) Reaction was carried out in 10 m*l* of acetonitrile at 15°C for 30 min.
b) Yields are calculated on the basis of the amount of ethyl diazoacetate.

Results and Discussion

Reactions of 1 with Copper Compounds. An equimolar reaction of **1** with CuCl took place smoothly at room temperature. A mixture of ethyl maleate and ethyl fumarate was produced in a quantitative yield (Table 1). Similarly, cupric salts having negative groups of CN, SO_4 and NO_3 gave a maleate-fumarate mixture. Its formation is explained by assuming the formation of ethoxycarbonylcarbene.[2)]

The reaction of **1** with $CuCl_2$ is quite different from that with other copper compounds. The products of an equimolar reaction at 15°C in acetonitrile were **2** (yield 16%), **3** (40%), a mixture of **4** and **5** (3%) and the maleate-fumarate mixture (30%). The maleate-fumarate mixture is probably produced also by the carbene reaction of **1**. It was not produced in the **1**-$CuCl_2$ reaction of 1 : 2 molar ratio. Here, $CuCl_2$ was reduced completely to CuCl. These findings can be rationalized by the assumption that the reaction of **1** with $CuCl_2$ is much faster than the carbene reaction of **1** induced by CuCl. In other words, the maleate-fumarate mixture is produced only after all $CuCl_2$ has been reduced to CuCl.

The production of considerable amounts of **3** is taken to differentiate $CuCl_2$ from other metal chlorides.

Reactions of 1 with $HgCl_2$ and $CoCl_2$. Nesmeyanov[3)] reported the reaction of **1** with $HgCl_2$ which produced **2** and organomercury compound (**6**).

$$4N_2CHCO_2Et + 3HgCl_2 \rightarrow \underset{(1)}{} \underset{(6)}{Hg\left(-\overset{Cl}{\overset{|}{C}}-CO_2Et\right)_2} + \underset{(2)}{2ClCH_2CO_2Et} \qquad (1)$$
HgCl

In order to characterize the **1**-$CuCl_2$ reaction and to elucidate its reaction mechanism, the reactions of **1** with $HgCl_2$ and $CoCl_2$ were examined as reference reactions. At room temperature, these metallic chlorides reacted with **1** only very slowly. At refluxing temperature (about 80°C), the reactions proceeded at considerable rates. In the **1**-$CoCl_2$ reaction, the heat-treated reaction mixture was separated into liquid and solid parts. From the liquid part, **2** was isolated by distillation. By glpc analysis, a trace of the **4**/**5** mixture and **9** was detected in the liquid part. The solid part did not dissolve in common solvents, and further purification without decomposition was impossible. However, the solid part showed an IR spectrum which was almost the same as that of the organomercury complex (**6**) prepared according to Nesmeyanov's procedure. Consequently, an organocobalt complex (**7**) corresponding to **6** can be assumed to be the essential constituent of the solid part of the **1**-$CoCl_2$ reaction mixture.

In the reaction of **1** with $HgCl_2$, a trace of the **4**/**5** mixture and **9** was detected in addition to the two products indicated in Eq. (1). These results are summarized in Table 2.

Table 2. Reaction of **1** with $HgCl_2$ and $CoCl_2$[a)]

Metal chloride	Products (%)[b)]			
	2	**4/5**	**9**	Organometal complex
$HgCl_2$	41	trace	trace	40[c)]
$CoCl_2$	31	trace	trace	35[d)]

a) A mixture of 10.0 mmol of **1**, 20.0 mmol of metal chloride and 20 m*l* of acetonitrile was refluxed for 4 hr.
b) Yields are calculated on the basis of **1**.
c) Organomercury compound (**6**).
d) The yield is calculated on the assumption that the essential constituent is an organocobalt complex (**7**) corresponding to the organomercury complex (**6**).

Formation of the **4**/**5** mixture and **9** in these reactions, although their yield is not high, suggests the transient production of ethoxycarbonylcarbene complex (**8**).

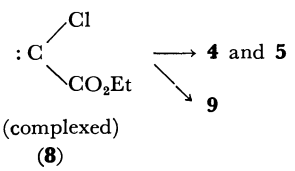

(complexed)
(**8**)

3) A. N. Nesmeyanov and G. S. Powich, *Ber.*, **67**, B, 971 (1934).

It is interesting that **6** is comparatively inert towards $HgCl_2$ and $CoCl_2$ but easily decomposed by $CuCl_2$ to produce the **4/5** mixture and **9**. This finding has an important bearing upon the mechanism of the **1**-$CuCl_2$ reaction, especially the production of the **4/5** mixture.

TABLE 3. REACTION OF **6** WITH $CuCl_2$[a)]

6 (mmol)	$CuCl_2$ (mmol)	Products (%)[b)]	
		4/5	**9**
5	15	60	27

a) Reaction was carried out in 10 m*l* of acetonitrile at 80°C for 1 hr.
b) Yields are calculated on the basis of **6**.

Mechanism of Reaction of 1 with $CuCl_2$. The following scheme of reaction may explain the production of **3**, the **4/5** mixture and **9**. As the first unstable intermediate, 1-chloro-1-ethoxycarbonylmethylcopper complex (**10**) is postulated, whose reaction with $CuCl_2$ (process-1) will produce **3** and CuCl. Process-1 is the process of the chlorine ligand transfer from $CuCl_2$ to 1-chloro-1-ethoxycarbonylmethyl moiety, which seems to resemble the so-called ligand transfer[4] between organic free radical and the ligand of metal salt. As to the production of **2**, the origin of the second α-hydrogen atom is an essential problem.

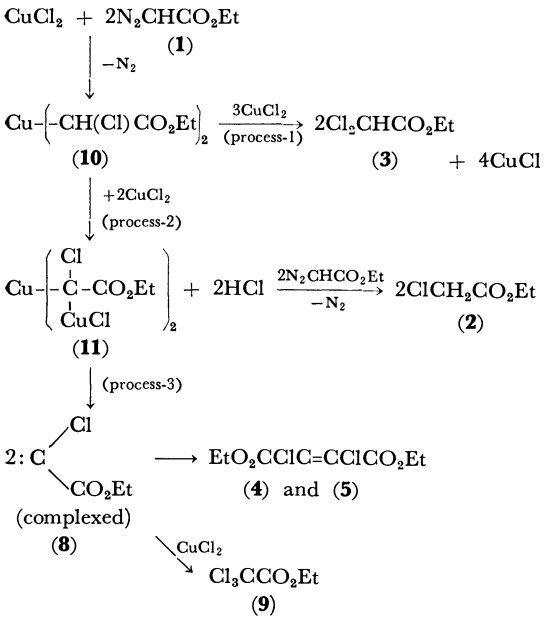

In the **1**-$HgCl_2$ reaction, Nesmeyanov[3] proposed that **2** is produced from **1** and hydrogen chloride which is liberated by the mercuration of the acidic α-hydrogen of an organomercury compound (**12**).

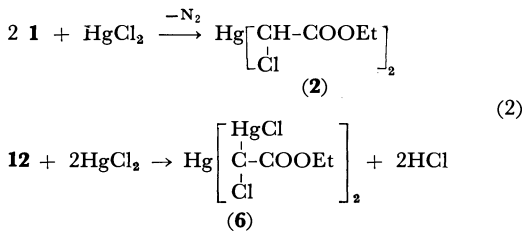

In the **1**-$CuCl_2$ reaction of the present study, an experiment using α-deuterio-diazoacetate (**1**-*d*) was carried out. It has been established that the second hydrogen atom of **2** originates in another molecule of **1**. **1**-*d* of a degree of deuteration over 98% was prepared from **1** and deuterium oxide in the presence of triethylamine catalyst. The products **2** and **3** in the reaction of **1**-*d* with $CuCl_2$ under the regular reaction conditions were of the same degree of deuteration over 98% as that of **1**-*d*. Consequently it is clear that the α-hydrogen atom of **2** does not originate from acetonitrile or from water which might be present as an impurity.

This conclusion is supported by the reaction of diphenyldiazomethane (**13**) having no α-hydrogen with $CuCl_2$. The products of the reaction of **13** with excess $CuCl_2$ (molar ratio 1 : 2) were dichlorodiphenylmethane (yield 48%), benzophenone azine (34%) and tetraphenylethylene (9%). Diphenylchloromethane which corresponds to **2** in the reaction of **1** was not detected among the products.

In relation to Nesmeyanov's mechanism for the reaction of $HgCl_2$, the conversion of **10** by $CuCl_2$ to **11** (process-2) liberating hydrogen chloride may be cited as one possible mechanism of the elimination of hydrogen from **1**. In the reaction of **1** with $HgCl_2$, the species corresponding to **11** was actually isolated. In the **1**-$CuCl_2$ reaction, **11** was not isolated. This may be ascribed to the fact that **11** is much less stable due to the weakness of copper-carbon bond and that **11** is readily decomposed with $CuCl_2$. In addition, **11** is assumed to be a key intermediate in the course of reaction leading to the **4/5** mixture and **9**. The reaction of **11** with $CuCl_2$ producing the **4/5** mixture and **9** has been supported by reference experiments in which the mercury species corresponding to **11** was reacted with $CuCl_2$ to give the **4/5** mixture and **9**. Probably, the **4/5** mixture and **9** would be derived from the common precursor **8**. The process of the formation of **9** seems to correspond to that of **3** in the **1**-$CuCl_2$ reaction.

Recently, bis(diazoethoxycarbonylmethyl) mercury $Hg[C(N_2)CO_2Et]_2$ (**14**)[5] attracts much

4) a) J. K. Kochi and D. D. Davis, *J. Am. Chem. Soc.*, **86**, 5264 (1964). b) J. K. Kochi, *Science*, **155**, 415 (1967).

5) a) E. Buchner, *Ber.*, **28**, 215 (1895). b) T. DoMinch, H. E. Gunning and O. P. Strausz, *J. Am. Chem. Soc.*, **89**, 6785 (1967). c) O. P. Strausz, T. DoMinch and J. Font, *ibid.*, **90**, 1930 (1968). d) U. Schöllkopf and N. Rieber, *Angew. Chem.*, **79**, 906 (1967). e) F. Gerhart, U. Schöllkopf and H. Schumacher, *ibid.*, **79**, 50 (1967).

attention as the source of carbyne species. We found that **4/5** mixture and **9** were produced in the **14**-$CuCl_2$ reaction. Also in this case, an intermediate (**15**) corresponding to **11** would be involved.

$$Hg[C(N_2)CO_2Et]_2 + 2CuCl_2 \rightarrow$$
(**14**)

$$Hg\left(\begin{array}{l}Cl\\|\\-C-CO_2Et\\|\\CuCl\end{array}\right)_2 \rightarrow \textbf{4/5} \text{ and } \textbf{9} \qquad (3)$$
(**15**)

Table 4. Reaction of **14** with $CuCl_2$[a]

14 (mmol)	$CuCl_2$ (mmol)	Products (%)[b] **4/5**	**9**
5	15	33	10

a) Reaction was carried out at 0°C for 1 hr.
b) Yields are calculated on the basis of **14**.

Experimetnal

Reaction of Ethyl Diazoacetate (1) with CuCl. To a stirred mixture of CuCl (18.0 mmol) and acetonitrile, **1** (18.0 mmol) was added dropwise at 15°C. The reaction proceeded smoothly, evolving N_2 gas, and ceased in 30 min. The reaction mixture was filtered to remove an insoluble copper salt, and was subjected to distillation. A mixture of ethyl maleate and fumarate (80—85°C/30 mmHg) was obtained in 97% yield.

Reaction of Ethyl Diazoacetate (1) with $CuCl_2$. To a stirred mixture of $CuCl_2$ (16.4 mmol) and acetonitrile (10 m*l*), **1** (16.4 mmol) was added dropwise at 15°C. The N_2 gas evolution ceased in 30 min and the mixture turned to red-brown. The reaction mixture was filtered to remove the insoluble salt and subjected to distillation. The distillate of bp 60—100°C/20 mmHg was analyzed by glpc. The products were ethyl chloroacetate (**2**) (16%), ethyl dichloroacetate (**3**) (40%), a mixture of ethyl dichloromaleate (**4**) and ethyl dichlorofumarate (**5**) (3%) and a mixture of ethyl maleate and fumarate (30%). The products **2**, **3**, **4**, **5**, ethyl maleate and ethyl fumarate were identified by comparison of the glpc retention time and the IR spectrum with those of the corresponding authentic samples. The insoluble part was analyzed by IR and redox titration. The IR spectrum of the insoluble part showed no absorption band in the region of ordinary organic compounds. Thus, the salt did not contain any organic moiety. The valence of copper was measured by redox titration. $CuCl_2$ was completely reduced to CuCl after the reaction.

Reaction of Ethyl Diazoacetate (1) with $HgCl_2$. To a mixture of $HgCl_2$ (20 mmol) and acetonitrile (10 m*l*), **1** (10 mmol) was added slowly at 15°C and then the reaction mixture was heated at refluxing temperature (80°C) for 4 hr. The reaction mixture was filtered to remove the insoluble solid. The filtrate was distilled to give ethyl chloroacetate (41%). The organomercury compound (**6**) was isolated from the insoluble part according to Nesmeyanov's[3] procedure (yield 40%). IR of **6** (Nujol): $\nu_{C=O}$ 1660 cm^{-1}, ν_{C-O} 1200 cm^{-1}, ν_{C-Cl} 775 cm^{-1}.

Reaction of Ethyl Diazoacetate (1) with $CoCl_2$. A mixture of $CoCl_2$ (20 mmol), ethyl diazoacetate (**1**) (10 mmol) and acetonitrile (10 m*l*) was heated at 80°C for 4 hr. The solid and liquid parts were separated. From the liquid part, **2** was isolated by distillation (yield 31%). The solid part did not dissolve in common solvents. Further purification without decomposition was impossible. The amount of solid part was 0.86 g (IR (Nujol): $\nu_{C=O}$ 1665 cm^{-1}, ν_{C-O} 1205 sm^{-1}, ν_{C-Cl} 770 cm^{-1}).

Reaction of Diphenyldiazomethane (13) with $CuCl_2$. To a mixture of $CuCl_2$ (20 mmol) and acetonitrile (10 m*l*), a solution of **13** (10 mmol) in acetonitrile (5 m*l*) was added slowly at 15°C. The reaction proceeded smoothly evolving N_2 gas and ceased in about 15 min. The reaction mixture was filtered to remove a white solid. The filtrate was dried up *in vacuo*, and the residue was analyzed by column chromatography (silica gel, benzene-petroleum ether) to obtain dichlorodiphenylmethane (48%), benzophenone azine (34%) and tetraphenylethylene (9%). These three products were identified by comparison of the IR spectra and/or the melting points with those of the corresponding authentic samples.

Preparation of Ethyl α-Deuterio-diazoacetate (1-*d*.).[6] A heterogeneous mixture of **1** (4 m*l*), deuterium oxide (15 m*l*) and triethylamine (0.1 m*l*) was stirred for 1 hr. The layer of diazoacetate was separated and treated with deuterium oxide again. The diazoacetate layer was dried with anhydrous Na_2SO_4 and distilled to give ethyl α-deuterio-diazoacetate in 80% yield. The NMR spectrum analysis revealed that the α-position was deuterated to an extent over 98%.

Reaction of Ethyl α-Deuterio-diazoacetate (1-*d*) with $CuCl_2$. The reaction was carried out in the same way as that of the **1**-$CuCl_2$ reaction. The products of **2**, **3** and the **4/5** mixture were isolated by preparative glpc. By NMR spectrum, the extents of deuteration at α-hydrogen of **2** and **3** were found to be over 98%.

Reaction of $Hg\left(\begin{array}{l}-C(Cl)CO_2Et\\|\\HgCl\end{array}\right)_2$ (6) with $CuCl_2$. A mixture of **6** (5 mmol), $CuCl_2$ (15 mmol) and acetonitrile (10 m*l*) was heated at 80°C for 1 hr. The reaction mixture was filtered to remove the solid part. The filtrate was concentrated *in vacuo* and analyzed by glpc. The products were the **4/5** mixture (60%) and trichloroacetate (**9**) (27%).

Reaction of $Hg(N_2CCO_2Et)_2$[5a] (14) with $CuCl_2$. A solution of **14** (5 mmol) in acetonitrile (5 m*l*) was added dropwise to a mixture of cupric chloride (15 mmol) and acetonitrile (10 m*l*) at 0°C. After 1 hr, the reaction mixture was filtered to remove the insoluble solid.

The filtrate was analyzed by glpc to obtain ethyl trichloroacetate (10%) and a mixture of ethyl dichloromaleate and ethyl dichlorofumarate (33%).

6) G. W. Robinson and M. McCartrty, Jr., *J. Am. Chem. Soc.*, **82**, 1859 (1960).

BULLETIN OF THE CHEMICAL SOCIETY OF JAPAN VOL. 42 3539—3546 (1969)

Synthesis of Pyrrole Nucleosides by the Photo-dehydrogenation of Δ^3-Pyrroline Derivatives

Masajiro KAWANA and Sakae EMOTO

The Institute of Physical and Chemical Research, Yamato-machi, Kita-Adachi-gun, Saitama

(Received June 3, 1969)

1-(β-D-Glucopyranosyl)pyrrole (VI) was prepared by the photo-dehydrogenation of 1-(2′,3′,4′,6′-tetra-*O*-acetyl-β-D-glucopyranosyl)-Δ^3-pyrroline (IV) in the presence of oxygen and benzophenone, followed by deacetylation. The nucleoside (VI) was also derived directly from 1-(D-glucosyl)-Δ^3-pyrroline (III) by photochemical means. The synthesis of 1-(α-D-ribofuranosyl)-pyrrole (XI), its β-anomer (XII), and 1-(β-D-ribopyranosyl)pyrrole (XIII) was accomplished by photodehydrogenation of 1-(2′,3′-*O*-isopropylidene-D-ribosyl)-Δ^3-pyrroline, followed by the removal of the protecting group. The treatment of 1-(2′,3′-*O*-isopropylidene-α-D-ribofuranosyl)pyrrole (VIII) with 80% aqueous acetic acid afforded a novel α-cyclonucleoside, 1-(2-*C*,2′-*O*-isopropylidene-α-D-ribofuranosyl)pyrrole (XIV), besides XI—XIII. The formation of pyrrole by the photo-dehydrogenation of Δ^3-pyrroline (II) itself was confirmed by gas chromatography.

The photo-dehydrogenation of partially-hydrogenated nitrogen-heterocycles, such as tetraphenyl chlorin[1] and 2,3-dihydro-β-carbolines,[2] has been reported. Preobrazhenskaya,[3] Walton,[4] and their co-workers demonstrated that 1-(D-glycosyl)indoles were synthesized from the corresponding indolines using a reagent useful for dehydrogenation, 2,3-dichloro-5,6-dicyano-1,4-benzoquinone (DDQ).

In the course of the step-by-step synthesis of pyrrole nucleosides, we found that 1-(2′,3′,4′,6′-tetra-*O*-acetyl-β-D-glucopyranosyl)-Δ^3-pyrroline (IV) could be photochemically dehydrogenated to yield 1-(2′,3′,4′,6′-tetra-*O*-acetyl-β-D-glucopyranosyl)pyrrole (V).[5] We wish now to present these results in detail, and to describe the photochemical formation of anomeric D-ribosylpyrroles and the formation of a novel α-cyclonucleoside by the migration of an isopropylidene group.

Results and Discussion

The synthesis of 1-(D-glucosyl)-Δ^3-pyrroline (III) was performed by heating a mixture of α-D-glucose (I) and crude Δ^3-pyrroline (II)[6] under conditions similar to those used for the synthesis of 1-(D-glucosyl) piperidine[7] (Fig. 1); the purification[8] of crude II was not necessary for the present purposes because only III was crystallized by the addition of acetone to the reaction mixture.

The structure of III was tentatively identified. The observed values for the elemental analysis of III were in good agreement with the theoretical values. The NMR spectrum in deuterium oxide (D_2O) exhibited two singlets, at τ 6.24 and 4.23, due to the methylene and olefinic protons of the Δ^3-pyrroline ring respectively.[8] The signals of the anomeric proton appeared in the τ 6.0—5.6 region,[9] but they were not sufficiently resolved for interpretation.

The treatment of III with acetic anhydride in pyridine gave IV in a 73% yield. Its IR spectrum was devoid of N–H, O–H, and *N*-acetyl carbonyl absorption bands. The NMR spectrum in deuterio-chloroform($CDCl_3$) revealed four singlets, at τ 7.99—7.93, for the acetyl protons, and two singlets, at τ 6.22 and 4.32, for the methylene and olefinic protons of the Δ^3-pyrroline ring respectively. The signal of the anomeric proton appeared as a doublet centered at τ *ca.* 5.7 with the coupling constant of *ca.* 8 cps; the values could not be accurately measured, however, because the high-field part of the doublet was overlapped by other signals.

1) M. Calvin and G. D. Dorough, *J. Am. Chem. Soc.*, **70**, 699 (1948).

2) R. A. Uphaus, L. I. Grossweiner, J. J. Katz and K. D. Kopple, *Science*, **129**, 641 (1959); Y. Kanaoka, E. Sato and O. Yonemitsu, *Chem. & Ind.*, **1968**, 1250.

3) M. N. Preobrazhenskaya, M. M. Vigdorchik and N. N. Suvorov, *Tetrahedron*, **23**, 4653 (1967).

4) E. Walton, F. W. Holly and S. R. Jenkins, *J. Org. Chem.*, **33**, 192 (1968).

5) M. Kawana and S. Emoto, This Bulletin, **41**, 2552 (1968).

6) L. H. Andrews and S. M. McElvain, *J. Am. Chem. Soc.*, **51**, 887 (1929).

7) J. E. Hodge and C. E. Rist, *ibid.*, **74**, 1497 (1952).

8) C. B. Hudson and A. V. Robertson, *Tetrahedron Letters*, **1967**, 4015.

9) S. Inouye, T. Tsuruoka, T. Ito and T. Niida, *Tetrahedron*, **24**, 2125 (1968).

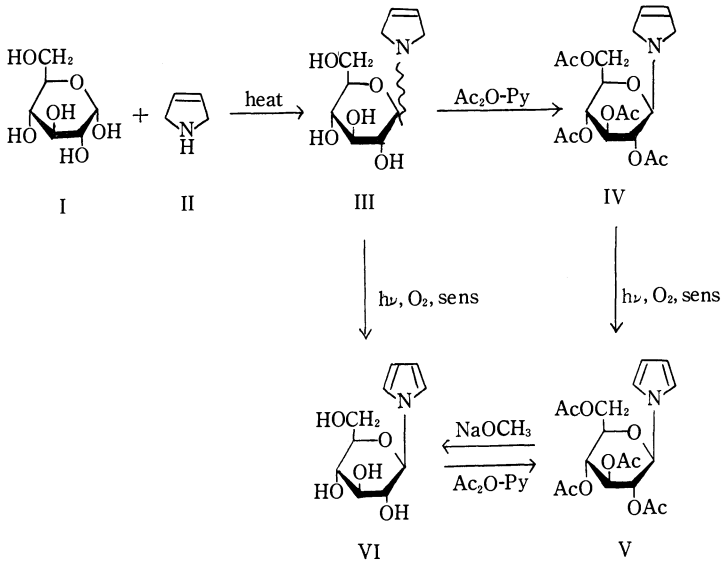

Fig. 1

This large coupling constant is indicative of a *trans*-diaxial relationship between H-1′ and H-2′, and it corresponds to the β-configuration.[10]

Further proof of the glucopsranosylamine structure of IV was obtained by the ready degradation[11] of IV with 0.7% aqueous formic acid to the known 2,3,4,6-tetra-*O*-acetyl-D-glucopyranose.[12]

When a benzene solution of IV was allowed to evaporate repeatedly in an open vessel, the thin-layer chromatographic analysis showed that IV was gradually converted into V. This conversion was markedly accelerated by the irradiation of UV light with a Pyrex filter, under bubbling oxygen, and in the presence of benzophenone as a sensitizer.[13] Under such conditions V was obtained as the main product: it was isolated by crystallization in a 85% yield. The dehydrogenation of IV with DDQ in the dark was also effective, producing V in a good yield.

The IR and UV spectra of V showed the presence of a pyrrole ring[14,15] (*cf.* Table 1 and the Experimental section). The NMR spectrum in $CDCl_3$ exhibited two pseudo-triplets of equal intensity, centered at τ 3.83 and 3.21 for the protons at C-3, 4 and C-2, 5 of the pyrrole ring respectively (Table 2).[16] The signal of the anomeric proton was not separated from the others.

The anomeric configuration of V was deduced by comparing the chemical shifts of the acetyl signals of IV and V in the NMR spectroscopy. Cushley *et al.*[17] have found that when the C-2′ acetyl group and the pyrimidine in acetylated pyranosyl pyrimidine nucleosides are in a *trans*-diequatorial relationship, there is a small but significant down-field shift (*ca.* 0.05 ppm) of the C-2′ acetyl signal upon the saturation of the 5, 6-double bond of the pyrimidine. In the case of acetylated β-ribo- and β-gluco-pyranosylindoline-indole systems, a large down-field shift (at least 0.29 ppm) of the C-2′ acetyl signal occurs upon the removal of the anisotropy due to the 2,3-double bond of the indole.[18] A similar down-field shift was observed in the present pyrrole nucleoside. The acetyl signals of V appeared at τ 7.99—7.93 as three singlets and at τ 8.15 as one singlet assignable to the C-2′ acetyl group; all would be in an area of positive shielding due to the anisotropy of the pyrrole ring.[19] Therefore, the

10) R. U. Lemieux and J. D. Stevens, *Can. J. Chem.*, **43**, 2059 (1965); H. Iwamura and T. Hashizume, *J. Org. Chem.*, **33**, 1796 (1968), and the references cited therein.

11) G. P. Ellis and J. Honeyman, "Advances in Carbohydrate Chemistry," Vol. 10, ed. by M. L. Wolfrom and R. S. Tipson, Academic Press, New York, N. Y. (1955), p. 95.

12) a) A. Georg, *Helv. Chim. Acta*, **15**, 924 (1932). b) C. M. McCloskey, R. E. Pyle and G. H. Coleman, *J. Am. Chem. Soc.*, **66**, 349 (1944).

13) D. C. Neckers, "Mechanistic Organic Photochemistry," Reinhold Publishing Corp., New York (1967), p. 163.

14) K. Nakanishi, "Infrared Absorption Spectroscopy," Holden-Day, San Fracisco, and Nankodo Co., Tokyo (1964), p. 26.

15) S. Menczel, *Z. Physik. Chem.*, **125**, 161 (1927); R. L. Hinman and S. Theodoropulos, *J. Org. Chem.*, **28**, 3052 (1963).

16) N. S. Bhacca, L. F. Johnson and J. N. Shoolery, "High Resolution NMR Spectra Catalog," Varian Associates, Palo Alto, Calif. (1962), Spectrum No. 55.

17) R. J. Cushley, K. A. Watanabe and J. J. Fox, *J. Am. Chem. Soc.*, **89**, 394 (1967).

18) R. J. Cushley, S. R. Lipsky, W. J. McMurray and J. J. Fox, *Chem. Commun.*, **1968**, 1611.

19) A. P. Martinez and W. W. Lee, *J. Org. Chem.*, **34**, 416 (1969).

Table 1. The physical properties of the pyrrole nucleosides

Compound	Mp °C	$[\alpha]_D$ deg.	(c, solvent)	Temp., °C	UV λ_{max}, mμ (ε)	solvent
V	178.0—178.5	−10.9	(0.67, $CHCl_3$)	22	211 (8150)	EtOH
VI	Hygroscopic glass	+10.3	(0.74, H_2O)	25	210 (6950)	H_2O
VIII	Hygroscopic syrup	−45.9	(0.27, $CHCl_3$)	20	214 (6400)	EtOH
IX	65—66	−57.6	(0.46, $CHCl_3$)	20	215 (6800)	EtOH
X	94.0—94.5	−62.9	(0.14, $CHCl_3$)	23	215 (7000)	EtOH
XI	Hygroscopic syrup	+19.0	(0.20, H_2O)	22	210 (6500)	H_2O
XII	Hygroscopic syrup	−69.4	(0.17, H_2O)	20	212 (6800)	H_2O
XIII	Hygroscopic glass	−34.0	(0.05, H_2O)	22	209 (8200)	H_2O
XIV	107—109	+68.8	(0.17, H_2O)	20	217 (7200)	H_2O

Table 2. The NMR spectra[a] of the pyrrole nucleosides

Compound	H-1′ [1][d] ($J_{1',2'}$)	C-5′ OH [1][g] ($J_{5'OH,5'}$)	Isopropylidene methyls [3]×2		H-3,4 [2]	H-2,5 [2]	Solvent
V[b]	5.0—4.4	—	—	—	3.83 (pt)	3.21 (pt)	$CDCl_3$
VI	4.86 (d, 8.4)[e]	—	—	—	3.74 (pt)	3.01 (pt)	D_2O
VIII	4.08 (d, 3.3)	4.91 (t, 4.8)	8.71 (s)	8.56 (s)	3.99 (pt)	3.12 (pt)	DMSO-d_6
IX	4.32 (d, 2.6)	5.01 (t, 5.4)	8.69 (s)	8.49 (s)	3.93 (pt)	3.02 (pt)	DMSO-d_6
X	4.81 (d, 8.4)[f]	[4.46 (d, 5.7)][h]	8.64 (s)	8.42 (s)	3.91 (pt)	3.05 (pt)	DMSO-d_6
XI	4.28 (d, 3.8)	5.20 (t, 5.4)	—	—	4.02 (pt)	3.06 (pt)	DMSO-d_6
XII	4.59 (d, 5.0)	5.07 (t, 5.1)	—	—	3.96 (pt)	3.06 (pt)	DMSO-d_6
XIII	4.90 (d, 9.0)	[5.23—4.98 (m)][i]	—	—	3.98 (pt)	3.12 (pt)	DMSO-d_6
XIV[c]	4.42 (d, 2.6)	5.23 (t, 5.4) [4.89 (d, 6.0)][j]	8.57 (s)	8.44 (s)	4.15 (q)[k] 3.94 (pt)[l]	3.30 (q)[m]	DMSO-d_6

a) τ-Value (peak multiplicity, and coupling constant (cps)); see Experimental section.
b) The acetyl signals appeared at τ 8.15 (3H), 7.99, 7.95, and 7.93 as singlets.
c) The signal of H-2′ appeared as a quartet ($J_{1',2'}$=2.6 cps, $J_{2',3'}$=3.6 cps) centered at τ 5.58. Irradiation of H-1′ caused the quartet to collapse to a doublet ($J_{2',3'}$=3.6 cps), and irradiation of H-2′ caused a doublet due to H-1′ to collapse to a singlet.
d) Numbers in brackets refer to number of the protons obtained integration.
e) Letters in parentheses refer to singlet (s), doublet (d), triplet (t), pseudo-triplet (pt), quartet (q), and multiplet (m).
f) A poorly resolved doublet.
g) The signals disappeared by the addition of D_2O.
h) C-4′ OH.
i) C-2′, 3′, and 4′ OHs.
j) C-3′ OH.
k) H-3 (1H, $J_{3,4}$=3.0 cps, $J_{3,5}$=1.5 cps).
l) H-4 (1H, $J_{3,4}$=3.0 cps).
m) H-5 (1H, $J_{3,5}$=1.5 cps, $J_{4,5}$=2.4 cps).

C-2′ acetyl signal is shifted by at least 0.16 ppm down-field in changing from V to IV. This suggests that V has the β-configuration.

The deacetylation of V in the usual manner gave, after chromatography, analytically pure 1-(β-D-glucopyranosyl)pyrrole (VI) as a hygroscopic glass in a 76% yield. The paper and gas chromatographic analyses showed that the product was anomerically pure. The NMR spectrum of VI in D_2O revealed a doublet due to the anomeric proton with the large coupling constant of 8.4 cps, thus establishing the β-configuration.[10] Therefore, it was confirmed that the proposed sutrcture for V was correct and that the β-configuration of IV was retained in the course of the dehydrogenation with photochemical means as well as with DDQ.

Plisov[20] reported that when a mixture of glucose and pyrrole was heated the product, which consisted of two components, was obtained as a crystal (mp 190°C) after crystallization from pyridine. However, its structure was unsubstantiated by experimental details or physical data. Moreover, Plisov's product was not identical with VI, at least not in respect to their solubility in pyridine, in which the latter was readily soluble.

An alternative route to obtain VI is the direct photo-dehydrogenation of III. When a suspension of III in ethanol was irradiated under the conditions described above, analytically pure VI

20) A. K. Plisov, *Ukrainskii Khem. Zhur.*, **3**, 477 (1928); *Chem. Abstr.*, **23**, 3224 (1929).

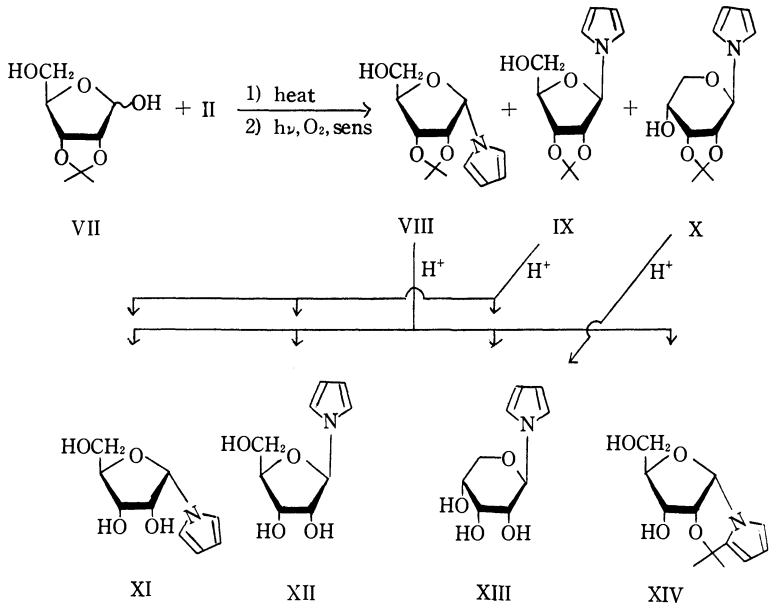

Fig. 2

was produced in a 62% yield after chromatography. The product was identical in every respect with a specimen prepared from V. Further, the acetylation of the product gave V in a 92% yield.

The preparation of the D-ribosylpyrrole nucleosides was undertaken starting with pure II[8] and 2′,3′-*O*-isopropylidene-D-ribose (VII)[21] (Fig. 2). Thus, a mixture of II and VII was heated to give syrupy products which could contain 1-(2′,3′-*O*-isopropylidene-D-ribosyl)-Δ^3-pyrroline. The irradiation of the syrup in ethanol under the conditions described above provided the isomeric nucleosides (40%), namely, 1-(2′,3′-*O*-isopropylidene-α-D-ribofuranosyl)pyrrole (VIII), 1-(2′,3′-*O*-isopropylidene-β-D-ribofuranosyl)pyrrole (IX), and 1-(2′,3′-*O*-isopropylidene-β-D-ribopyranosyl)pyrrole (X), in a ratio of approximately 1 : 8 : 1 (Table 1). Interestingly, the treatment of the syrup with DDQ produced these nucleosides (54%) in a ratio of approximately 7 : 2 : 1, the α-furanosyl anomer (VIII) being predominant.

The removal of the isopropylidene group of IX with 80% aqueous acetic acid, followed by column chromatography on Dowex 1 (OH^-),[22] gave 1-(α-D-ribofurayosyl)pyrrole (XI), 1-(β-D-ribofuranosyl)pyrrole (XII), and 1-(β-D-ribopyranosyl)-pyrrole (XIII) in 3.5, 87, and 2.5% yields respectively. This suggests that pyrrole nucleosides as well as indole nucleosides[3] isomerize under mild acidic conditions. The removal of the isopropylidene group of VIII also gave XI, XII, and XIII in 21, 22, and 3% yields respectively. In addition, 1-(2-*C*, 2′-*O*-isopropylidene-α-D-ribofuranosyl)pyrrole (XIV) was obtained in a 29% yield from VIII. It can be considered that XIV is formed by an acid-catalyzed intramolecular reaction similar to that of the substituted indole with the dimethyl ketal group.[23] To our knowledge, XIV is a new type of α-cyclonucleoside.[24] The removal of the protecting group of X provided only XIII in a 90% yield.

The analytical and spectroscopic data for VIII—XIV supported the assigned structres (Tables 1 and 2). The NMR spectra of VIII, IX, XI, and XII in deuterated dimethyl sulfoxide (DMSO-d_6)[25] showed a C-5′ hydroxyl proton as each triplet; these protons disappeared upon the addition of D_2O. This indicates that these nucleosides have the furanosyl structure. Therefore, VIII and IX as well as XI and XII are a pair of anomers; they can be assigned to the α- and β-configurations respectively on the basis of the following NMR data:

(1) The signals of the anomeric protons of the β-anomers, IX and XII, were found in a higher field than those of the α-anomers, VIII and XI respectively; Nishimura and Shimizu[26] have found that the anomeric protons of nucleosides occur in

21) P. A. Levene and E. T. Stiller, *J. Biol. Chem.*, **102**, 187 (1933).

22) C. A. Dekker, *J. Am. Chem. Soc.*, **87**, 4027 (1965).

23) G. Büchi, P. Kulsa and R. L. Rosati, *ibid.*, **90**, 2448 (1968).

24) M. Ikehara, M. Kaneko and Y. Nakahara, *Tetrahedron Letters*, **1968**, 4707.

25) O. L. Chapman and R. W. King, *J. Am. Chem. Soc.*, **86**, 1256 (1964).

26) T. Nishimura and B. Shimizu, *Chem. Pharm. Bull.*, **13**, 803 (1965).

a higher field when the C-1′ and 2′ substituents are *trans* than when they are *cis*.[27]

(2) The difference in the coupling constants of the anomeric protons between the β-anomers, IX and XII, was much greater than the difference in those between the α-anomers, VIII and XI; Jardetzky[28] has reported that when the ribofuranose ring is constrained by fusion with a second ring, the coupling constant of the anomeric proton of β-nucleoside is reudced.[29]

(3) The signals of the protons of the isopropylidene group for the α-anomer, VIII, appeared in a higher field than those for the β-anomer, IX, presumably because of the anisotropic effect of the pyrrole ring.[17-19,30]

(4) The signals of the C-5′ hydroxyl proton of the β-anomer, XII, appeared in a lower field than those of the α-anomer, XI, as has been observed in the case of the anomeric 7-D-ribofuranosyladenines.[27b]

Further, the order of elution from the anion-exchange column[22] supported these assignments; the α-anomer, XI, was eluted faster than the β-anomer, XII (see the Experimental section).[31]

The pyranosyl structure of X was proved by the appearance of a doublet due to the C-4′ hydroxyl proton in the NMR spectrum (in DMSO-d_6).[25] The signals of the anomeric protons of X and XIII appeared as doublets with large coupling constants, thus establishing the β-configurations.[10]

The NMR spectrum of XIV in DMSO-d_6 showed the presence of an isopropylidene group and a 1,2-disubstituted pyrrole ring. The signals of the C-3′ and 5′ hydroxyl protons appeared as a doublet (J= 6.0 cps) and a triplet respectively. In spin-decoupling experiments, the irradiation of the anomeric proton caused a quartet centered at τ 5.58 to collapse to a doublet (J=3.6 cps). This indicated that the quartet arises from H-2′ and that the C-2′ hydroxyl group is substituted.

The value for the coupling constant of the anomeric proton of XIV was 2.6 cps, a value which corresponded to a dihedral angle of H-$C_{1'}$-$C_{2'}$-H, 54° or 123°, according to the Karplus equation.[32] An examination of the Dreiding models showed that the former was suitable for the dihedral angle of the α-configuration, but that neither of them was suitable for that of the β-configuration. Additional support of the α-configuration of XIV was obtained by a comparison of the optical rotations of XI, XII, and XIV (Table 1); XI and XII obey the Hudson's isorotation rules,[33] and XI and XIV have the same sign of rotation.

An attempt was made to examine whether II itself was converted into pyrrole by photochemical means. A solution of crude II[6] in ethanol was irradiated under the conditions described above, and aliquots were examined by gas chromatography. A peak due to II disappeared after 2 hr, the formation of pyrrole being identified. The photo-dehydrogenation reaction in the presence of oxygen and benzophenone provides an alternative to a number of known pyrrole syntheses using II or its derivatives.[34,35]

Experimental

Some of the physical data for the pyrrole nucleosides are listed in Tables 1 and 2. All the melting points are uncorrected.

The irradiation of UV light was performed with a super-high-pressure mercury lamp (100 W, Matsuda SHL-100UV-1). The optical rotations were measured with a Perkin-Elmer 141 photoelectric polarimeter in a 1-dm tube. The IR spectra were obtained using a Perkin-Elmer 521 grating infrared spectrophotometer. The UV spectra were taken on a Cary 14 recording spectrophotometer.

The NMR spectra were determined on a Nippon Denshi C-60 spectrometer using sodium 2, 2-dimethyl-2-silapentane-5-sulfonate (tetramethylsilane for the $CDCl_3$ solutions) as the internal standard. The chemical shifts were recorded as ppm on the τ scale, with the coupling constants (the directly-measured line-spacings) as cps.

The gas chromatography (GC) was performed at 180°C with a Shimadzu GC-4A gas chromatograph equipped with a flame ionization detector using a glass column (1.8 m×4 mm) packed with 3% OV-17 on Shimalite W (80—100 mesh); nitrogen was used as the carrier gas (flow rate, 64 ml/min). The individual nucleoside was treated with a pyridine solution of hexamethyldisilazane and trimethylchlorosilane at room temperature, and the resulting solution was injected into the gas chromatograph.[36]

The thin-layer and paper chromatographies (TLC and PC) were run by the ascending technique on a silica gel G (E. Merck) plate and a filter paper No. 51

27) See, for example: a) T. Nishimura, B. Shimizu and I. Iwai, *Chem. Pharm. Bull.*, **12**, 1471 (1964). b) J. A. Montgomery and H. J. Thomas, *J. Am. Chem. Soc.*, **87**, 5442 (1964). c) K. Imai, A. Nohara and M. Honjo, *Chem. Pharm. Bull.*, **14**, 1377 (1966). d) J. A. Montgomery and H. J. Thomas, *J. Heterocycl. Chem.*, **5**, 303 (1968).

28) C. D. Jardetzky, *J. Am. Chem. Soc.*, **84**, 62 (1962).

29) See, for example: N. J. Leonard and R. A. Laursen, *ibid.*, **85**, 2026 (1963); Ref. 27c.

30) J. F. Codington, R. J. Cushley and J. J. Fox, *J. Org. Chem.*, **33**, 466 (1968).

31) See, for example: G. Schramm, G. Lüzmann and F. Bechmann, *Biochim. Biophys. Acta*, **145**, 221 (1967); E. J. Reist, D. F. Calkins and L. Goodman, *J. Am. Chem. Soc.*, **90**, 3852 (1968).

32) M. Karplus, *J. Chem. Phys.*, **30**, 11 (1959).

33) C. S. Hudson, *J. Am. Chem. Soc.*, **31**, 66 (1909); E. L. Eliel, "Stereochemistry of Carbon Compounds," McGraw-Hill Book Co., New York (1962), p. 110.

34) J. P. Wibaut and W. Proost, *Rec. Trav. Chim.*, **52**, 333 (1933).

35) R. Kreher and H. Pawelczyk, *Angew. Chem.*, **76**, 536 (1964).

36) Y. Sasaki and T. Hashizume, *Anal. Biochem.*, **16**, 1 (1966).

(Toyo Roshi) respectively. The following solvent systems were used as developers: (A) *n*-hexane - ethyl acetate (1 : 1); (B) ethyl acetate - isopropanol - water (65 : 30 : 5); (C) ethyl acetate - *n* - hexane - methanol (7 : 2: 1); (D) *n* - butanol - water (87 : 13). The spots were detected by iodine vapor or a 1% solution of *p*-dimethylaminobenzaldehyde[37] in methanol - concentrated hydrochloric acid (3 : 1).

1-(D-Glucosyl)-Δ^3-pyrroline (III). A mixture of I (1.8 g, 0.01 mol) and crude II[6] (1.4 g, 0.02 mol) was heated at 80—85°C (bath-temperature) for 15 min in a flask equipped with a tight stopper. To the cooled reaction mixture there was added acetone (50 m*l*). The syrupy product rapidly solidified on scratching. After being cooled overnight at 0°C, the product was filtered, washed with cold acetone, and dried. Recrystallization from acetone-methanol gave III (1.7 g, 73.9%): mp 130—135°C (decomp.); $[\alpha]_D^{20}$ −28.8° (4 min) → +13.0° (46 hr, constant, *c* 0.40, H_2O); IR, ν_{max}^{KBr} 3408, 3290, 2886, 2850, 1085, 1025 cm^{-1}; NMR (in D_2O), τ 6.24 (singlet, methylene protons of the Δ^3-pyrroline ring), 5.98, 5.88, and 5,75 (*ca.* 1.5H, broad peaks), 4.23 (2H, singlet, olefinic protons).

Found: C, 51.78; H, 7.14; N, 6.09%. Calcd for $C_{10}H_{17}O_5N$: C, 51.94; H, 7.41; N, 6.06%.

1-(2′,3′,4′,6′-Tetra-*O*-acetyl-β-D-glucopyranosyl)-Δ^3-pyrroline(IV). To a mixture of acetic anhydride (2.7 g, 26 mmol) and dry pyridine (4.1 g, 52 mmol), there was added III (1.16 g, 5 mmol) at −10—−5°C, and then the mixture was stirred for 1.5 hr. After the reaction mixture had been allowed to stand at −5°C for 24 hr, ethanol (1 m*l*) was added to decompose an excess of acetic anhydride, and then the pyridine was removed at room temperature *in vacuo*. The residue was dissolved in ether, and the solution was washed with water, aqueous sodium bicarbonate, and water successively and then dried over anhydrous magnesium sulfate. The evaporation of the ether gave a crystalline mass (1.67 g) which, after recrystallization from degassed *n*-hexane - isopropanol with charcoal treatment in the dark, afforded a crude material (1.51 g, mp 118—122°C). Further recrystallization from degassed *n*-hexane - ethanol in the dark gave IV (1.45 g, 72.5%): mp 121—122°C; $[\alpha]_D^{25}$ −23.7° (*c* 0.49, degassed $CHCl_3$); R_f(TLC, solvent A), 0.27; IR, ν_{max}^{KBr} 2892, 2850, 1753, 1738, 1380, 1240, 1038 cm^{-1}; NMR (in $CDCl_3$), τ 7.99, 7.97, 7.95, and 7.93 (12H, each singlet, acetyl protons), 6.22 (singlet, methylene protons of Δ^3-pyrroline ring), *ca.* 5.7 (doublet, $J_{1',2'}$=*ca.* 8 cps, anomeric proton), 4.32 (2H, singlet, olefinic proton).

Found: C, 54.10; H, 6.05; N, 3.51%. Calcd for $C_{18}H_{25}O_9N$: C, 54.13; H, 6.31; N, 3.51%.

Degradation of 1-(2′,3′,4′,6′-tetra-*O*-acetyl-β-D-glucopyranosyl)-Δ^3-pyrroline (IV). To a solution of IV (200 mg, 0.5 mmol) in degassed acetone (2 m*l*) there was added 0.7% aqueous formic acid (10 m*l*) at room temperature in the dark. After 15 min, the acetone was removed at 25°C *in vacuo*. The residue was extracted with chloroform, and the extract was washed with water, aqueous sodium bicarbonate, and water successively and dried over anhydrous magnesium sulfate. The evaporation of the chloroform at room temperature *in vacuo* gave 2,3,4,6-tetra-*O*-acetyl-D-glucopyranose as a syrup (145 mg, 83.3%) : $[\alpha]_D^{20}$ +76.6° (constant, *c* 1.44, 95% EtOH) (lit,[12a] $[\alpha]_D^{24}$ +80.2° (constant, *c* 3.37, 95% EtOH)). This product was identical with an equilibrated authentic sample[12b] in all respects (IR, NMR, and TLC).

1-(2′,3′,4′,6′,-Tetra-*O*-acetyl-β-D-glucopyranosyl)-pyrrole (V). *(A) Photo-dehydrogenation.* A mixture of IV (200 mg, 0.5 mmol) and benzophenone (13.7 mg, 0.075 mmol) in bezene (10 m*l*) was irradiated externally in a water-cooled Pyrex vessel under bubbling oxygen at 20°C for 1 hr. The evaporation of the benzene at 50°C *in vacuo* gave a crystalline mass which, after recrystallization from ethanol, afforded V (169 mg, 84.9%): R_f (TLC, solvent A), 0.50; IR, ν_{max}^{KBr} 3145, 3134, 3120, 3102, 1740, 1493, 740 cm^{-1}.

Found: C, 54.53; H, 5.73; N, 3.52%. Calcd for $C_{18}H_{23}O_9N$: C, 54.40; H, 5.83; N, 3.53%.

(B) Chemical dehydrogenation. All the experiments were carried out in the dark. To a suspension of DDQ (119 mg, 0.52 mmol) in dry benzene (5 m*l*), there was added a solution of IV (200 mg, 0.5 mmol) in dry benzene (4 m*l*). The reaction mixture was then allowed to stand at room temperature for 1 hr under occasional shaking. The resultant precipitates were filtered and washed with benzene. The removal of the benzene at 60°C *in vacuo* gave crystals which, after recrystallization from ethanol, afforded V (178 mg, 89.4%). The IR spectral comparison and a mixed-melting-point determination showed this material to be identical with the sample prepared by the method A.

(C) Acetylation of VI. A mixture of acetic anhydride (570 mg, 5.6 mmol) and dry pyridine (790 mg, 10 mmol) was stirred into a solution of VI (130 mg, 0.57 mmol) in dry pyridine (500 mg). After the stirring had been continued at this temperature for 1 hr, the reaction mixture was allowed to stand overnight at 0°C. Ethanol (0.5 m*l*) was added to decompose an excess of acetic anhydride, and the pyridine was removed at room temperature *in vacuo*. The resultant crystals were washed with water, filtered, and dried. Recrystallization from ethanol gave V (207 mg, 92.0%). The IR spectral comparison, a mixed-melting-point determination, and the TLC analysis showed this product to be identical with the sample prepared by the method A.

1-(β-D-Glucopyranosyl)pyrrole (VI). *(A) Deacetylation of V.* To a solution of absolute methanol (12 m*l*) containing sodium methoxide (54 mg, 1.0 mmol), there was added V (397 mg, 1.0 mmol), after which the mixture was stirred at room temperature for 50 min. After the removal of the methanol at 25°C *in vacuo*, the residue was dissolved in water (5 m*l*). The solution was treated with ion-excange resin (Dowex 50W, H^+ form)(1 g) for 1 min, the resin was then immediately filtered and washed with water. After the filtrate had been treated with charcoal, the evaporation of the water at 60°C *in vacuo* gave a glassy mass (193 mg). The product was chromatographed on a silica-gel (Merck)(24 g) column with ethyl acetate - ethanol (8 : 2), yielding VI (173 mg, 75.5%) : R_f, 0.66 (TLC, solvent B), 0.38 (PC, solvent D); retention time (GC), 24.1 min; IR, ν_{max}^{KBr} 3400, 1491, 738 cm^{-1}.

Found: C, 52.15; H, 6.38; N, 6.09%. Calcd for $C_{10}H_{15}O_5N$: C, 52.39; H, 6.60; N, 6.11%.

(B) Photo-dehydrogenation of III. A suspension of III (462 mg, 2.0 mmol) in 99.5% ethanol (15 m*l*) containing

37) F. Feigl, "Spot Test in Organic Analysis," translated by R. E. Oesper, Elsevier Publishing Co., Amsterdam and Maruzen Co., Tokyo (1960), p. 289.

benzophenone (55 mg, 0.3 mmol) was irradiated externally in a water-cooled Pyrex vessel under bubbling oxygen at 19°C for 1 hr. After the ethanol had been removed at 30°C *in vacuo*, the residue was chromatographed on a Dowex 1-X2 (OH^- form) (10 g) column (2× 8.5 cm). The elution with water - methanol (7 : 3) gave a slightly contaminated product (313 mg). Further purification by silica-gel (Merck) (24 g) column chromatography with ethyl acetate - ethanol (8 : 2) afforded analytically-pure VI (284 mg, 62.0%). This product was identical with a specimen prepared by the method A in all respects (optical rotation, TLC, PC, GC, IR, UV, and NMR).

1-(2′,3′-*O*-Isopropylidene-α-D-ribofuranosyl)pyrrole (VIII), 1-(2′,3′-*O*-isopropylidene-β-D-ribofuranosyl)pyrrole (IX), and 1-(2′,3′-*O*-isopropylidene-β-D-ribopyranosyl)pyrrole (X). *(A) Photo-dehydrogenation.* A mixture of VII[21] (571 mg, 3.0 mmol) and pure II[8] (249 mg, 3.6 mmol) was placed in a flask equipped with a tight stopper and heated at 95—100°C (bath-temperature) for 3 hr. After being cooled immediately, the reaction mixture was diluted with absolute ethanol (15 m*l*), after which benzophenone (55 mg, 0.3 mmol) was added. The mixture was irradiated externally in a water-cooled Pyrex vessel under bubbling dry oxygen at 18°C for 2 hr. The evaporation of the ethanol at 30°C *in vacuo* gave a syrup, which was then dissolved in ether (80 m*l*). The ethereal solution was washed with water (4×10 m*l*), dried over anhydrous sodium sulfate, and concentrated at below 30°C *in vacuo*. The resultant syrup was chromatographed on a silica-gel (Merck) (100 g) column using *n*-hexane - ethyl acetate (6 : 4). Three products were obtained in the following sequence: IX (230 mg, 32.0%); X (22 mg, 3.1%); a mixture (7 mg, 1.0%, *ca.* 6 : 4) of VIII and X, and VIII (25 mg, 3.5%).

The α-anomer (VIII) was analyzed without further purification: R_f (TLC, solvent A), 0.30; IR, $\nu_{max}^{CHCl_3}$ 3640, 3158, 3100, 1488 cm^{-1}.

Found: C, 60.26; H, 7.12; N, 5.81%. Calcd for $C_{12}H_{17}O_4N$: C, 60.24; H, 7.16; N, 5.85%.

Recrystallization of IX from *n*-hexane - benzene gave the analytical samples as colorless crystals: R_f (TLC, solvent A), 0.59; IR, ν_{max}^{KBr} 3454, 3128, 3112, 1490, 742 cm^{-1}.

Found: C, 60.02; H, 7.22; N, 5.88%. Calcd for $C_{12}H_{17}O_4N$: C, 60.24; H, 7.16; N, 5.85%.

The recrystallization of X from *n*-hexane - benzene gave the analytical sample as colorless crystals: R_f (TLC, solvent A), 0.38; IR, ν_{max}^{KBr} 3478, 3134, 3118, 3102, 1489, 726 cm^{-1}.

Found: C, 60.37; H, 6.99; N, 5.93%. Calcd for $C_{12}H_{17}O_4N$: C, 60.24; H, 7.16; N, 5.85%.

(B) Chemical dehydrogenation. A mixture of VII[21] (761 mg, 4.0 mmol) and pure II[8] (332 mg, 4.8 mmol) was heated under the conditions described above. The cooled reaction mixture was then suspended in dry benzene (5 m*l*). This suspension was stirred, drop by drop, into a mixture of DDQ (908 mg, 4.0 mmol) and dry benzene (20 m*l*) at room temperature. After the addition had been completed, the stirring was continued for 5 min. The resultant precipitates were filtered and washed with benzene, and the filtrate was diluted with ether (50 m*l*). The solution was wased with dilute aqueous sodium carbonate and water successively, dried over anhydrous sodium sulfate, and concentrated at below 30°C *in vacuo*. The residue gave, after chromatography on a silica-gel (Merck) (150 g) column using *n*-hexane - ethyl acetate (6 : 4), IX (115 mg, 12.0%), X (29 mg, 3.0%), crude VIII (114 mg, 11.9%) slightly contaminated with X, and VIII (263 mg, 27.5%) in sequence. The IR and NMR spectral comparison, a mixed-melting-point determination, and the TLC analysis showed these products to be identical with the specimens prepared by the method A.

1-(β-D-Ribofuranosyl)pyrrole (XII). A solution of IX (239 mg, 1.0 mmol) in 80% aqueous acetic acid (2 m*l*) was heated at 100°C (bath-temperature) for 40 min. After the acetic acid and the water had been removed by repeated evaporation with ethanol (50 m*l*, total) at 60°C *in vacuo*, the residue was chromatographed on a column (2×14 cm) of Dowex 1-X2 (OH^- form) (20 g). Elution was effected with water - methanol (7 : 3), 10-m*l* fractions being collected.

Fractions 4—6 contained the starting material (2 mg).

Fractions 7—9 contained an unknown substance (1 mg).

Fractions 12—15 and 18—25 contained XIII (5 mg, 2.5%) and XI (7 mg, 3.5%) respectively; these products were identified by a color reaction[37] with *p*-dimethylaminobenzaldehyde on developed TLC plates.

Fractions 25—47 were combined; the evaporation of the solvents gave XII (174 mg, 87.4%): R_f, 0.50 (TLC, solvent C) (color reaction,[37] purple), 0.67 (PC, solvent, D); retention time (GC), 8.9 min.

Found: C, 54.01; H, 6.31; N, 7.08%. Calcd for $C_9H_{13}O_4N$: C, 54.26; H, 6.58; N, 7.03%.

1-(α-D-Ribofuranosyl)pyrrole (XI) and 1-(2-*C*,2′-*O*-Isopropylidene-α-D-ribofuranysyl)pyrrole (XIV). A solution of VIII (200 mg, 0.84 mmol) in 80% aqueous acetic acid (1.8 m*l*) was heated at 100°C bath-temperature) for 1 hr. The solvents were then removed in a manner similar to that described above. The residue was chromatographed on a column (2× 14 cm) of Dowex 1-X2 (OH^- form) (20 g) using water - ethanol (7 : 3), 10-m*l* fractions being collected.

Fractions 4—5 contained an unknown substance (2 mg).

Fractions 6—11 were combined and the solvents were removed to afford syrupy products, which contained a small amount of the starting material. Further purification by column chromatography on a silica-gel (Merck) (15 g) column with *n*-hexane - ethyl acetate (2 : 8) gave XIV (58 mg, 29.0%) as a glass which crystallized when scratched: R_f, 0.57 (TLC, solvent C) (color reaction,[37] reddish purple); IR, ν_{max}^{KBr} 3568, 3390, 3130, 3100, 1483, 717 cm^{-1}.

Found: C, 60.28; H, 7.29; N, 5.74%. Calcd for $C_{12}H_{17}O_4N$: C, 60.24; H, 7.16; N, 5.85%.

Fractions 15—21 contained XIII (*ca.* 5 mg, 3%) and an unknown substance (*ca.* 5 mg); the former was identified by color reaction[37] with *p*-dimethylaminobenzaldehyde on a developed TLC plate.

Fractions 24—32 were combined and the solvents removed to yield XI (35 mg, 21.0%): R_f, 0.43 (TLC, solvent C) (color reaction,[37] orange), 0.61 (PC, solvent D); retention time (GC), 9.6 min.

Found: C, 54.22; H, 6.36; N, 7.11%. Calcd for $C_9H_{13}O_4N$: C, 54.26; H, 6.58; N, 7.03%.

Fractions 40—68 contained XII (36 mg, 21.6%), the NMR spectrum of which was identical with that of a specimen prepared from IX.

1-(β-D-Ribopyranosyl)pyrrole (XIII). A solution of X (24 mg, 0.1 mmol) in 80% aqueous acetic acid (0.5 m*l*) was heated at 100°C (bath-temperature) for 15 min. The solvents were removed in a manner similar to that described above. The residue was chromatographed on a column (2×8.5 cm) of Dowex 1-X2 (OH^- form)(10 g) with water - methanol (7 : 3), 10-m*l* fractions being collected. Fractions 7—11 were combined and the solvents removed to yield XIII (18 mg, 90.0%): R_f, 0.40 (TLC, solvent C) (color reaction,[37] brownish purple), 0.56 (PC, solvent D); retention time (GC), 9.0 min.

Found: N, 6.82%. Calcd for $C_9H_{13}O_4N$: N, 7.03%.

Photo-dehydrogenation of Δ^3-Pyrroline (II). A solution of crude II[6] (69 mg, 1.0 mmol) in dry benzene (10 m*l*) containing benzophenone (14 mg, 0.077 mmol) was irradiated under conditions similar to those used for the preparation of V. Aliquots were examined by the GC (stainless steel column (3 m×3 mm) packed with 3% OV-17 on Shimalite W (80—100 mesh), flow rate 18 m*l*/min, column temperature 60°C). After 2 hr, a broad peak (retention time, 13 min) due to II disappeared and a new peak (retention time, 8.1 min) was observed. Under the same conditions, the pyrrolidine remained unchanged.

We are grateful to Drs. K. Isono and H. Kuzuhara and to Mr. H. Ohrui for their valuable suggestions and discussions, to Dr. H. Homma and his staff for the elemental analyses, to Mr. H. Ogawa for the IR spectra, to Mr. J. Uzawa for the NMR spectra, and to Miss K. Sano for her helpful assistance.

BULLETIN OF THE CHEMICAL SOCIETY OF JAPAN VOL. 42 3546—3550 (1969)

Preparation of Vinyl Ethers by Transetherification in the Presence of Molecular Sieves

Heimei YUKI, Koichi HATADA, Kazuhiko NAGATA and Ken-ichi KAJIYAMA

Department of Chemistry, Faculty of Engineering Science, Osaka University, Toyonaka, Osaka

(Received June 4, 1969)

The interchange reaction: $CH_3OCH{=}CH_2 + ROH \rightleftarrows ROCH{=}CH_2 + CH_3OH$, which is catalyzed by $Hg(OAc)_2$, has been studied. It was found that the equilibrium could be smoothly shifted toward the product by the selective absorption of the produced methanol on molecular sieves of the type 4A (MS-4A) and that the yield of the desired vinyl ether could be increased. According to this method, we prepared various vinyl ethers, including ethyl, isopropyl, isobutyl, *t*-butyl vinyl ether, and benzyl vinyl ethers. The yields of the alkyl vinyl ethers decrease as their alkyl groups become more electron-donating. The effects of the reaction conditions and the pretreatment of the molecular sieves have been investigated.

The vinyl transetherification catalyzed by mercuric salt is known to have a wide utility in the preparation of various vinyl ethers.[1] As the reaction is reversible, it is necessary to drive the reaction to

$$ROCH{=}CH_2 + R'OH \rightleftarrows ROH + R'OCH{=}CH_2$$

completion by appropriate methods. One is the fractionation of a desired vinyl ether out of the reaction mixture in order to shift the reaction continuously toward the product. Another is the equilibration of a mixture of vinyl ether in excess alcohol and a catalyst, and the subsequent freezing of the equilibrium by the flash-stripping of the volatile components or by inactivating the catalyst. The former method, however, has restrictions related as to the boiling points of the components, while the latter gives a lower yield.

In this work we studied this transetherification reaction, using methyl vinyl ether (MVE) as a starting vinyl ether and mercuric acetate ($Hg(OAc)_2$) as the catalyst, and found that the reaction could be smoothly shifted toward the product by the absorption of the methanol produced selectively on molecular sieves of the type 4A (MS-4A). Molecular sieves have been used by several investigators[2-4] for shifting the chemical equilibria by the selective absorption of one of the products. We prepared vinyl ethers, including ethyl, isopropyl isobutyl, *t*-butyl, vinyl ether and benzyl vinyl ethers, and studied the effects of the reaction conditions as

1) W. H. Watanabe and L. E. Conlon, *J. Am. Chem. Soc.*, **79**, 2828 (1957).

2) Y. Ito, *Nippon Kagaku Zasshi (J. Chem. Soc. Japan, Pure Chem. Sect.)*, **83**, 195 (1962).

3) P. Lowenberg, *J. Appl. Chem. (London)*, **9**, 417, (1959).

4) D. P. Roelofsen, J. A. Hagendoorn and H. Bekkum *Chem. & Ind.*, **1966**, 1622.

well as those of the pretreatment of the molecular sieves.

Experimental

Materials. Gaseous methyl vinyl ether was purified by passing it successively through a saturated aqueous solution of potassium hydroxide and a column packed with potassium hydroxide pellets, it was collected over calcium hydride in a cold trap cooled at −78°C. Then it was distilled under reduced pressure and stored over lithium aluminum hydride. The ether thus purified was redistilled under a vacuum just before use.

All the alcohols used were purified by refluxing them over calcium oxide and by subsequent distillation, they were stored under nitrogen pressure.

The triethylamine was purified by the usual method. The mercuric acetate used as the catalyst was commercially obtained and was used without further purification. The molecular sieves were products of the Union Carbide Corporation and were predried at the desired temperature under a high vacuum for 2 hr just before use.

Preparation of Vinyl Ether. A typical example of the method of preparing isobutyl vinyl ether will now be described. A 100 m*l* two-necked flask, equipped with a special reflux condenser for low-boiling liquid[5] and a thermometer, was flushed with dry nitrogen and charged with 20.0 g of MS-4A (1/16 inch pellets) which had been heated at 200°C for 2 hr under a high vacuum. Then 5.8 g (0.1 mol) of methyl vinyl ether, 7.4 g (0.1 mol) of isobutyl alcohol, and 0.5 g (0.0016 mol) of mercuric acetate were introduced into the flask under a nitrogen atmosphere. The reaction was carried out at 0°C for 1 hr with occasional shaking and was then stopped by adding one gram of anhydrous potassium carbonate. The reaction mixture was flash-distilled under a high vacuum. The distillate was shown by a gas chromatographic analysis to contain 6.0 g of isobutyl vinyl ether, 1.8 g of methyl vinyl ether, 2.3 g of isobutyl alcohol, and a trace of methanol The fractional distillation of this distillate gave 5.2 g of isobutyl vinyl ether; bp 82.5—83.0°C, $n_D^{20}=1.3962$. The non-volatile residue of the reaction contained a small amount of the polymeric product. This was shown by NMR spectroscopy to be predominantly poly(isobutyl vinyl ether); it seems to have resulted from the cationic polymerization of the isobutyl vinyl ether by the catalytic action of the molecular sieves. The amount of this polymeric product was estimated roughly by means of the difference between the amount of the residue and the total amount of molecular sieves, mercuric acetate, potassium carbonate used and the methanol adsorbed on the sieves.

Analytical Procedures. The distillate from the reaction mixture was inspected on a Shimazu Seisakusho gas-liquid chromatograph equipped with a column (2 m long, 4 mm i.d.) containing 30% dioctyl phthalate on Shimalite B and operated at 80°C with a helium-carrier gas stream of 68 m*l*/min. The calibration curves were used for determining the product compositions, employing toluene as the intensity standard.

The properties of the molecular sieves preheated at various temperatures were investigated in the following manner. One gram of the predried sieves was suspended in 25 ml of conductivity water and stirred for 24 hr under dry nitrogen pressure at 20°C. The pH value of the supernatant liquid was then measured with a pH meter (Yanagimoto Mfg. Co.) at 20°C under dry nitrogen.

Results

Reaction of MVE and Isobutyl Alcohol (*i*-BuOH) Catalyzed by $Hg(OAc)_2$ in the Presence of MS-4A. The reaction between MVE and *i*-BuOH was carried out in the presence of MS-4A (1/16 inch pellets), using $Hg(OAc)_2$ as the catalyst. The results are summarized in Table 1. In the reactions without the sieves, the yields of isobutyl vinyl ether(*i*-BVE) were lower. The use of the molecular sieves gave a higher yield of the vinyl

Table 1. Synthesis of *i*-BVE from MVE and *i*-BuOH by transetherification with MS-4A preheated at 200°C for 2 hr

Reaction conditions: MVE 0.1 mol, *i*-BuOH 0.1 mol, $Hg(OAc)_2$ 0.0016 mol.

No.	Solvent	Reaction		MS-4A (g)	Conversion (%)	*i*-BVE (%)	Polymeric product (%)
		Temp. (°C)	Time (hr)				
16	none	0	1	0	24	24	0
20	none	0	1	20	67	60	7
39	none	0	3	20	81	76	5
22	none	30	1	0	38	38	0
19	none	30	1	20	77	73	4
81	none	30	2	20	83	72	11
44	none	0	1	10	50	44	6
18[a]	none	0	1	20	0	0	0
28	Benzene 18 m*l*	0	1	20	48	37	11
105	$(C_2H_5)_2O$ 18 m*l*	0	1	20	29	29	0
116	$(C_2H_5)_2O$ 18 m*l*	0	5	20	66	60	6

[a] The reaction was carried out without $Hg(OAc)_2$ catalyst.

5) R. P. Linstead, J. A. Elvidge and M. Whalley, "A Course in Modern Techniques of Organic Chemistry," Butterworths Scientific Publications (1955), p. 82.

ether as a result of the selective adsorption of methanol. A longer reaction time increased the yield of *i*-BVE at both 0 and 30°C, although it also increased the polymeric product at 30°C. The yield of *i*-BVE was lower when the amount of the sieves was decreased. The reaction without $Hg(OAc)_2$ gave no *i*-BVE even in the presence of molecular sieves. The use of benzene or diethyl ether as a solvent caused a decrease in the rate of the reaction.

The addition of a small amount of triethylamine to the reaction mixture strongly decreased the yield of the vinyl ether. The results are shown in Table 2.

TABLE 2. EFFECT OF TRIETHYLAMINE ON THE TRANSETHERIFICATION OF MVE AND *i*-BuOH IN THE PRESENCE OF MS-4A PREHEATED AT 200°C FOR 2 hr

Reaction conditions: MVE 0.1 mol, *i*-BuOH 0.1 mol, $Hg(OAc)_2$ 0.0016 mol, reaction time 1 hr, reaction temp. 0°C, MS-4A 20 g.

No.	Et_3N (mmol)	Conversion (%)	*i*-BVE (%)	Polymeric product (%)
20	0	67	60	7
37	0.07	33	27	6
26	0.7	7	7	0
21	6.9	0	0	0

Effect of the Character of Molecular Sieves on the Transetherification of MVE and *i*-BuOH. The reactions of MVE and *i*-BuOH were carried out at 0°C for 1 hr with MS-4A preheated at various temperatures for 2 hr under a high vacuum. The results are shown in Fig. 1. The maximum yield of *i*-BVE was obtained when sieves preheated at 200°C were used. The amounts of the polymeric products decreased with an increase in the preheating temperature of the sieves, nearly reaching zero when the temperature was 300°C.

When the powdered MS-4A was used, a lower yield of *i*-BVE and a higher yield of polymer were obtained than in the case of the pellet type (Table 3). The molecular sieves 3A and the beads of the MS-4A also gave a lower yield of *i*-BVE.

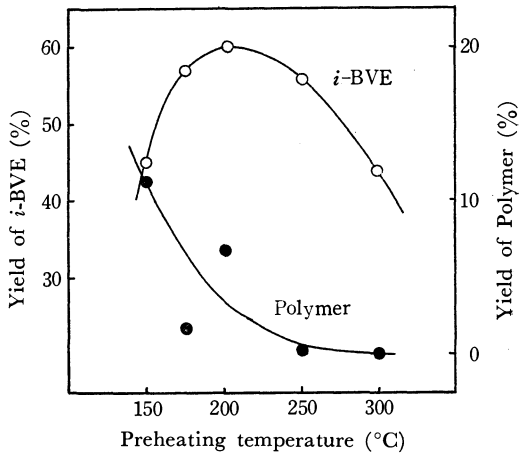

Fig. 1. Effect of the preheating temperature of MS-4A on the transetherification reaction of MVE and *i*-BuOH.

Reaction conditions: MVE 0.1 mol, *i*-BuOH 0.1 mol, $Hg(OAc)_2$ 0.0016 mol, Temp. 0°C, Time 1 hr, MS-4A was preheated for 2 hr under high vacuum.

Preparation of Other Vinyl Ethers. Transetherification reactions of MVE and various alcohols were carried out at 30°C for 1 hr with and without MS-4A. The results are shown in Table 4. The reactions proceeded smoothly in the presence of the sieves, and this technique for transetherification was proved successful for various combinations including various other aliphatic and aromatic alcohols with MVE. The yields of the desired alkyl vinyl ethers decreased, and the fractions of the polymeric product against the reacted MVE increased, as their alkyl groups were more electron-donating.

The reaction of MVE and *t*-butyl alcohol gave no *t*-butyl vinyl ether in the absence of molecular sieves, but a fairly good yield of *t*-butyl vinyl ether was obtained in the reaction with the sieves. The use of diethyl ether as a solvent reduced the fraction of the polymeric product, although the yield of the vinyl ether was also decreased. A prolonged reaction time resulted in a remarkable increase in the fraction of the ploymer.

TABLE 3. EFFECT OF THE TYPES OF MS-4A ON THE TRANSETHERIFICATION OF MVE AND *i*-BuOH
Reaction conditions: MVE 0.1 mol, *i*-BuOH 0.1 mol, $Hg(OAc)_2$ 0.0016 mol, reaction time 1 hr, reaction temp. 0°C, The sieves were preheated at 200°C for 2 hr under high vacuum.

No.	MS-4A		Conversion (%)	*i*-BVE (%)	Plymeric product (%)
	Type	(g)			
20	pellets	20	67	60	7
42	beads	20	55	49	6
61	powder	20	31	9	22
82	pellets[a)]	20	46	38	8

a) Type 3A molecular sieves were used.

Table 4. Preparation of various vinyl ethers from MVE and the alcohol by transetherification at 30°C for 1 hr with MS-4A preheated at 200°C for 2 hr
Reaction conditions: MVE 0.1 mol, alcohol 0.1 mol, $Hg(OAc)_2$ 0.0016 mol.

No.	Alcohol	MS-4A (g)	Conversion (%)	Vinyl ether (%)	Polymeric product (%)
47	Ethyl alcohol	0	26	26	0
46	Ethyl alcohol	20	78	70	8
51	Isopropyl alcohol	0	8	8	0
50	Isopropyl alcohol	20	71	46	25
52	*t*-Butyl alcohol	0	0	0	0
8	*t*-Butyl alcohol	20	29	18	11
113[a]	*t*-Butyl alcohol	20	10	8	2
110[a,c]	*t*-Butyl alcohol	20	6	6	0
121[a,b,c]	*t*-Butyl alcohol	20	31	16	15
145	Benzyl alcohol	0	14	14	0
86[d]	Benzyl alcohol	20	55	42	13
129[e]	*p*-Chlorobenzyl alcohol	20	95	57	38
130[e]	*p*-Methylbenzyl alcohol	20	87	43	44

a) As a solvent 18 m*l* of diethyl ether were used.
b) Reaction time 5 hr.
c) Reaction temp. 0°C.
d) Alcohol 0.3 mol, reaction time 3 hr.
e) Alcohol 0.6 mol, reaction time 3 hr, as a solvent 18 m*l* of benzene were used.

Properties of Molecular Sieves Preheated at Various Temperatures. The pH value of a water suspension of MS-4A is shown in Fig. 2. With an increase in the temperature at which the sieves are preheated, the pH value increases; it passes through a maximum value of 9.96 at 200°C and then gradually falls off.

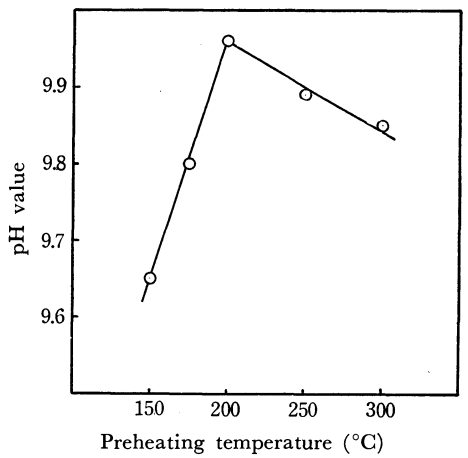

Fig. 2. pH Value of water suspension of MS-4A preheated at various temperatures.

Discussion

It has been ascertained that the equilibrium:

$$CH_3OCH{=}CH_2 + ROH \rightleftarrows ROCH{=}CH_2 + CH_3OH \quad (A)$$

was rapidly established by the $Hg(OAc)_2$ catalyst.[6] In this work we found that the reaction goes *smoothly* toward the right-hand side by the absorption of methanol selectively on MS-4A. The molecular sieves of the type 4A permit the reaction of MVE with any alcohol. The sieves of the type 3A work similarly, although the yield of vinyl ether is lower than in the case of the type 4A. The sieves of the type 5A, 10X or 13X have no absorption selectivity for methanol and produce a large amount of the polymeric product because of their higher catalytic activities for cationic polymerization.

The equilibration of the interchange reaction of MVE and *i*-BuOH is rapidly attained at 30°C, and the equilibrium constant is 0.570.[6] On the other hand, the absorption capacity of 20 g of MS-4A for methanol is about 0.09 mol at 30°C. From these data it may be expected that the reaction between 0.1 mol of MVE and *i*-BuOH catalyzed by $Hg(OAc)_2$ will go nearly to completion in the presence of 20 g of MS-4A. However, the actual conversion in the reaction is 83% for 3 hr. This appears to result from the occlusion of the molecular sieves with a polymeric product of *i*-BVE.

The only disadvantage of this ether-interchange technique is the decrease in the yield of the desired ether because of the polymer formation on the surface of the molecular sieves, as has been mentioned above. The attempt to prevent the polymerization of the resulting ether by the addition of a

6) H. Yuki, K. Hatada and K. Nagata, *Kogyo Kagaku Zasshi (J. Chem. Soc. Japan, Ind. Chem. Sect.)*, **73**, No. 4 (1970), in press.

small amount of triethylamine was not successful because of the decrease in the yield of the ether. The added amine may inactivate the mercuric acetate catalyst.

In the interchange reaction of MVE and alcohol with molecular sieves, lower yields of vinyl ethers were obtained when the alkyl groups of the resulting ethers were more electron-donating. This result may arise from the fact that the reactivity of the resulting vinyl ether for the cationic polymerization is higher,[7] as the alkyl group, R, in the reaction (A) is more electron-donating. The use of MVE as a starting vinyl ether is favorable for this technique because of its low polymerizability and the ease of its separation from the product by fractional distillation.

As is shown in Fig. 2, a water suspension of MS-4A preheated at temperatures from 150°C to 300°C had a pH value between 9.65 and 9.96, the maximum pH being obtained when the sieves were preheated at 200°C. This correlation resembles that between the yield of vinyl ether in the transetherification with molecular sieves and the preheating temperature of the sieves given in Fig. 1. However, the true significance of this interrelation is not certain at the present time.

The authors wish to express their deep thanks to Mr. T. Emura for his help in the laboratory work.

7) H. Yuki, K. Hatada and M. Takeshita, *J. Polymer Sci., A-1*, **7**, 667 (1969).

BULLETIN OF THE CHEMICAL SOCIETY OF JAPAN VOL. 42 3550—3555 (1969)

Resolution of Amino Acids. IX. Studies on the Preparation of β-Hydroxyasparagines and Configuration of Natural Hydroxyasparagine[1—3]

Hideo Okai[4] and Nobuo Izumiya[5]

Laboratory of Biochemistry, Faculty of Science, Kyushu University, Hakozaki, Fukuoka

(Received June 5, 1969)

Crystalline *threo-* and *erythro*-β-hydroxy-L-asparagine were prepared *via* asymmetric hydrolysis of the corresponding hydroxy-L-aspartic acid diamide by leucine aminopeptidase. The isomers of hydroxy-L-asparagine obtained were compared with the natural hydroxyasparagine isolated from human urine with respect to optical rotation and chromatography. From the results it is concluded that the spacial configuration of the natural product is that of *erythro*-β-hydroxy-L-asparagine. Additional studies were also carried out to prepare *threo-* and *erythro*-β-hydroxy-DL-asparagine from the corresponding hydroxy-DL-aspartic acid diamide without the enzyme.

Tominaga and his colleagues isolated 116 mg of a crystalline new amino acid from 200 *l* of human urine of normal male adults.[6] They presumed it to be β-hydroxyasparagine since it had produced β-hydroxyaspartic acid by acid hydrolysis. However, its spacial configuration has not been determined. Recently the four optical isomers of β-hydroxyaspartic acid were synthesized,[1,7] and their spacial configurations were established.[7] If the natural compound from human urine is one of possible four optical isomers of β-hydroxyasparagine, the compound may produce one of the four optical isomers of β-hydroxyaspartic acid by acid hydrolysis. However, it has been reported that the heating of either *threo-* or *erythro*-β-hydroxyaspartic acid in hydrochloric acid resulted in an interconversion of the diastereomers.[8] Therefore, we attempted

1) Part VIII of this series: H. Okai, N. Imamura and N. Izumiya, This Bulletin, **40**, 2154 (1967).

2) Presented at the 21st Annual Meeting of the Chemical Society of Japan, Osaka, April, 1968; Preprints of the Meeting, Vol. 3 (1968) p. 2226.

3) The following abbreviations are used: LAPase, leucine aminopeptidase; Z, benzyloxycarbonyl; Hyasp or Hya, β-hydroxyaspartic acid; Hyasp-diNH_2, β-hydroxyaspartic acid diamide; Hyasn, β-hydroxyasparagine; *t*, *threo*; *e*, *erythro*.

4) Present address: Department of Fermentation Technology, Faculty of Engineering, Hiroshima University, Senda-machi, Hiroshima.

5) To whom the reprint request should be addressed.

6) F. Tominaga, C. Hiwaki, T. Maekawa and H. Yoshida, *J. Biochem.*, **53**, 227 (1963).

7) K. Kaneko and H. Katsura, This Bulletin, **36**, 899 (1963).

to determine the spacial configuration of the natural product by the comparison with synthetic *threo*- and *erythro*-β-hydroxy-L-asparagine.

This paper describes the preparation of *threo*- and *erythro*-β-hydroxy-L-asparagine *via* asymmetric hydrolysis of the corresponding hydroxy-L-aspartic acid diamide by LAPase and the comparison of the natural product with the isomers of hydroxy-L-asparagine in respect to optical rotation and column chromatography. Attempts were made to prepare *threo*- and *erythro*-hydroxy-DL-asparagine without using the enzyme.

Several isomers (L-, DL-*threo* and L-, DL-*erythro*) of hydroxyaspartic acid diamide were synthesized in the conventional manner. As an example, the reaction sequence for the synthesis of *erythro*-hydroxy-L-aspartic acid diamide is shown in Fig. 1.

Preparation of *threo*- and *erythro*-hydroxy-L-asparagine was attempted by LAPase treatment on the diamides synthesized. As an example, the two schemes for the preparation of *erythro*-hydroxy-L-asparagine are presented in Fig. 2. Prior to preparation of optical active hydroxyasparagines by LAPase, the rates of hydrolysis were determined to estimate the susceptibility of the diamides for the enzyme, the results being shown in Table 2. It was reported that L-cysteic acid amide was hydrolyzed especially slowly by LAPase among the substrates tested.[9] However, it was observed that the diamides of hydroxyaspartic acid were hydrolyzed more poorly (Table 2). The low susceptibility of these diamides is considered to be due to their β-hydroxy group. It was observed that

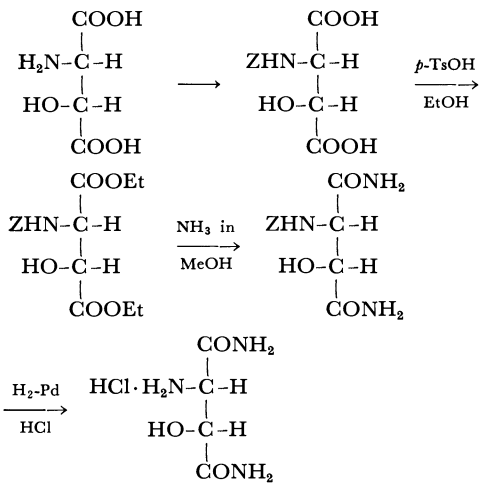

Fig. 1. Synthesis of *erythro*-hydroxy-L-aspartic acid diamide.

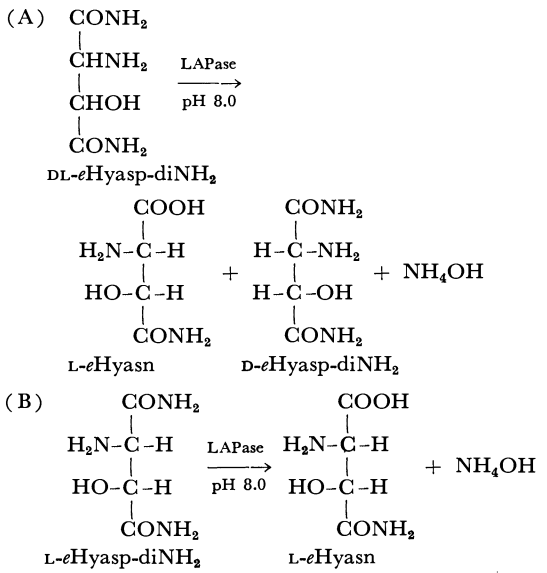

Fig. 2. Two schemes for preparation of *erythro*-hydroxy-L-asparagine.

the susceptibility of the *erythro*-L-diamide was slightly lower than that of the *threo*-L-diamide (Table 2). Thus a very high activity of LAPase was necessary for the effective hydrolysis of the diamides, and the highly purified enzyme preparation[10] was employed in this experiment.

For the determination of the rates of hydrolysis of *threo*- and *erythro*-DL-diamide, the course of hydrolysis in an incubation mixture of the substrate with the enzyme at pH 8.0 was followed by measuring the ammonia evolved. Contrary to expectation, it was observed that the amount of ammonia measured was greater than the theoretical 50% after 15—20 hr. The analysis of the mixture at 15—20 hr incubation by an amino acid analyzer and paper chromatography revealed the presence of hydroxyaspartic acid and other by-products in small amounts besides the major products, hydroxy-L-asparagine and hydroxy-D-aspartic acid diamide. The hydroxyaspartic acid and the by-products might be produced through the spontaneous degradation of the diamide and hydroxyasparagine at pH 8.0. The reason for the ammonia evolution more than the theoretical amount was further clarified by the observation that the diamide at pH 8.0 without the enzyme evolved ammonia gradually as shown in Fig. 5-b.

For the preparation of pure *threo*- and *erythro*-hydroxy-L-asparagine in preparative scale, the corresponding L-diamide was incubated with a large amount of the highly purified enzyme. This

8) T. Wieland, *Helv. Chim. Acta*, **44**, 919 (1961); M. L. Kornguth and H. J. Sallach, *Arch. Biochem. Biophys.*, **104**, 79 (1964).

9) S. Ouchi, A. Tanaka and N. Izumiya, *J. Biochem.*, **46**, 185 (1959).

10) E. L. Smith and D. H. Spackman, *J. Biol. Chem.*, **212**, 271 (1955); E. L. Smith, "Methods in Enzymology," Vol. II, ed. by S. E. Colowick and N. O. Kaplan, Academic Press, New York (1956), p. 88.

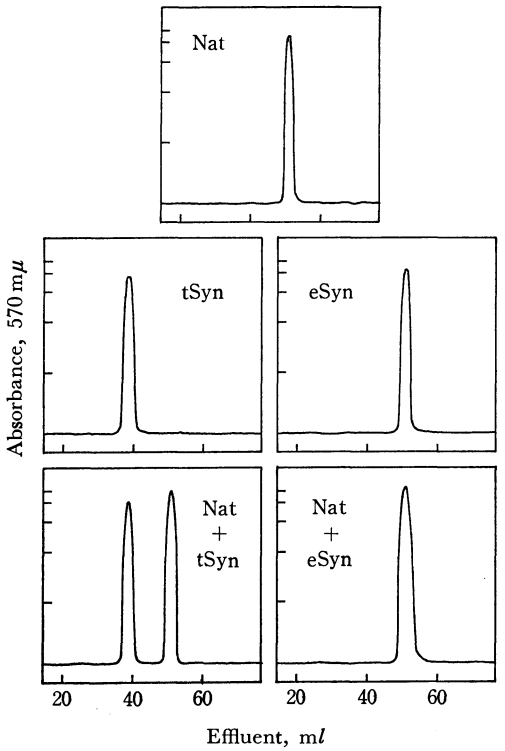

Fig. 3. Elution patterns of several hydroxyasparagine preparations by amino acid analyzer. Nat, the natural product; tSyn, L-tHyasn(synthetic); eSyn, L-eHyasn (synthetic).

Table 1. Specific rotations at 20°C of hydroxyasparagines

Compound	in H_2O[a)]	in 5 N HCl[b)]
L-*t*Hyasn (synthetic)	−29.6°	−28.0°
L-*e*Hyasn (synthetic)	+48.4	+63.0
Hyasn (natural)	+48.0	+61.6

a) *c* 0.5. b) *c* 1.0.

time, it was found that occurrence of the by-products was negligible even after the substrate was hydrolyzed completely. The crystalline *threo*- and *erythro*-hydroxy-L-asparagine were isolated from the incubation mixture in good yields by the use of Dowex 50 and 1 columns.

The synthetic hydroxyasparagines were compared with the natural product isolated from human urine. The values of specific rotation of *erythro*-hydroxy-L-asparagine and the natural product concurred within experimental error as shown in Table 1. A mixture of both the compounds afforded a single peak on co-chromatography by the amino acid analyzer as shown in Fig. 3. These data permit the conclusion that the spacial configuration of the natural product is that of *erythro*-β-hydroxy-L-asparagine. In this connection, it would be of interest to note that *erythro*-β-hydroxy-L-aspartic acid has been obtained by the action of a transaminase on dihydroxyfumaric acid and L-glutamic acid.[11)]

We attempted to prepare hydroxyasparagine through spontaneous degradation of the diamides in acid and alkaline mediums because it had been found that the diamides degraded spontaneously in the buffer solution at pH 8.0. Treatment of the diamides in dilute hydrochloric acid for 24 hr at 38°C afforded a mixture of many products including hydroxyasparagine. The chromatographic pattern by the amino acid analyzer are shown in Fig. 6-B. However, isolation of hydroxyasparagine from the reaction mixture was not attempted. In an alkaline treatment of the diamide for 5 hr at 38°C, the chromatographic patterns of degradation products in *threo*- and *erythro*-DL-diamide were different; *threo*-hydroxyasparagine was produced from the corresponding DL-diamide in considerable amount as shown in Fig. 6-C. The crystalline *threo*-hydroxy-DL-asparagine was isolated from the reaction mixture in a yield of 32%.

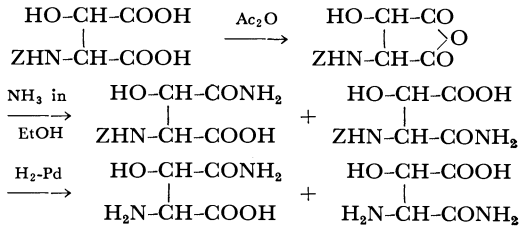

Fig. 4. Scheme for preparation of a mixture of hydroxyasparagine and hydroxyisoasparagine.

We attempted to prepare hydroxyasparagine *via* ammonolysis of benzyloxycarbonyl-hydroxyaspartic acid anhydride as shown in Fig. 4. It should be noted that Ressler and her colleagues prepared pure L-asparagine and L-isoasparagine from benzyloxycarbonyl-L-aspartic acid in a similar reaction sequence as shown in Fig. 4.[12)] The chromatographic patterns of the hydrogenated material are given in Fig. 6-D in which *erythro*-hydroxyasparagine is eluted as a single peak while *threo*-hydroxyasparagine is overlapped with other by-product. The crystalline *erythro*-hydroxy-DL-asparagine was isolated from the hydrogenated material derived from benzyloxycarbonyl-*erythro*-hydroxy-DL-aspartic acid in a yield of 33%. It seems that the preparation of the hydroxy-L-asparagines with the use of LAPase is preferable to that without the enzyme which is described in this paper.

11) H. J. Sallach and T. H. Peterson, *J. Biol. Chem.*, **223**, 629 (1956); H. J. Sallach and M. L. Kornguth, *Biochim. Biophys. Acta*, **34**, 582 (1959).

12) C. Ressler, H. Malodeczky and D. V. Kashelieker, "Biochemical Preparation," Vol. 10, ed. by C. B. Brown, John Wiley & Sons, New York (1963), p. 83.

Experimental

Synthesis of Compounds. *N-Benzyloxycarbonyl-threo-hydroxy-DL-aspartic Acid.* To a solution of DL-*t*Hyasp[1] (1.49 g, 10 mmol) and sodium bicarbonate (3.18 g, 36 mmol) in water (30 ml) was added a solution of benzyloxycarbonyl chloride (2.22 g, 13 mmol) in ether, and the reaction mixture was stirred for 4 hr at room temperature. After the reaction mixture was extracted with ether, the aqueous layer was acidified with 5 N hydrochloric acid and then extracted with ethyl acetate thrice (40 ml each). The extract was dried over sodium sulfate and evaporated *in vacuo*. The residual oil solidified after the addition of petroleum ether. It was recrystallized from ethanol-ether-petroleum ether. Yield, 2.12 g (75%); mp 186—187°C.

Found: C, 50.93; H, 4.74; N, 4.92%. Calcd for $C_{12}H_{13}O_7N$: C, 50.88; H, 4.63; N, 4.95%.

N-Benzyloxycarbonyl-threo-hydroxy-L-aspartic Acid. This was prepared from L-*t*Hyasp[1] as has been described for the preparation of Z-DL-*t*Hyasp. Yield, 86%; mp 106—107°C; $[\alpha]_D^{17}$ −8.0° (*c* 1, DMF).

Found: C, 50.93; H, 4.78; N, 4.83%.

N-Benzyloxycarbonyl-erythro-hydroxy-DL-aspartic Acid. This was prepared from DL-*e*Hyasp[1] as described for the preparation of Z-DL-*t*Hyasp. Yield, 85%; mp 155—156°C.

Found: C, 50.85; H, 4.85; N, 4.86%.

N-Benzyloxycarbonyl-erythro-hydroxy-L-aspartic Acid. This was prepared from L-*e*Hyasp.[1] Yield, 83%; mp 143—144°C; $[\alpha]_D^{17}$ +17.5° (*c* 1, DMF).

Found: C, 50.90; H, 4.86; N, 4.91%.

N-Benzyloxycarbonyl-threo-hydroxy-DL-aspartic Acid Diethyl Ester (Z-DL-tHyasp-diOEt). This compound was prepared according to the procedure of Kato *et al.*[13] for the preparation of benzoyl-DL-serine ethyl ester. A solution of Z-DL-*t*Hyasp (2.83 g, 10 mmol) and *p*-toluenesulfonic acid monohydrate (0.02 g) in a mixture of ethanol (20 ml) and carbon tetrachloride (100 ml) was refluxed for 64 hr, and the water liberated was removed as an azeotropic mixture. The reaction mixture was concentrated *in vacuo*, and the residual oil was dissolved in ethyl acetate (40 ml). The solution was washed with 4% sodium bicarbonate, 2% hydrochloric acid and water, and dried over sodium sulfate. The filtrate was evaporated *in vacuo*, and an oily residue was obtained. Yield, 3.36 g (99%); R_f 0.85.[14]

Z-L-tHyasp-diOEt, Z-DL-eHyasp-diOEt and Z-L-eHyasp-diOEt. These esters were also obtained as oily substance in nearly quantitative yields as described above.

N-Benzyloxycarbonyl-threo-hydroxy-DL-aspartic Acid Diamide. Z-DL-*t*Hyasp-diOEt (1.62 g, 4.7 mmol) was dissolved in methanol (80 ml) previously saturated with dry ammonia at 0°C, and the solution was kept at room temperature for 3 days and then concentrated *in vacuo* to dryness. The residual crystals were collected with the aid of a mixture of methanol and acetone. It was recrystallized from hot methanol. Yield, 1.01 g (77%); mp 209—211°C; R_f 0.66.[14]

Found: C, 51.25; H, 5.44; N, 14.71%. Calcd for $C_{12}H_{14}O_5N_3$: C, 51.42; H, 5.03; N, 14.99%.

N-Benzyloxycarbonyl-threo-hydroxy-L-aspartic Acid Diamide. This was prepared from Z-L-*t*Hyasp-diOEt as desbribed above. Yield, 66%; mp 194—196°C; $[\alpha]_D^{17}$ −25.5° (*c* 1, DMF).

Found: C, 51.15; H, 5.36; N, 14.65%.

N-Benzyloxycarbonyl-erythro-hydroxy-DL-aspartic Acid Diamide. This was prepared from Z-DL-*e*Hyasp-diOEt. Yield, 86%; mp 204—205°C.

Found: C, 51.38; H, 5.00; N, 14.61%.

N-Benzyloxycarbonyl-erythro-hydroxy-L-aspartic Acid Diamide. This was prepared from Z-L-*e*Hyasp-diOEt. Yield, 75%; mp 198—199°C; $[\alpha]_D^{17}$ +42.0° (*c* 0.5, DMF).

Found: C, 51.48; H, 5.48; N, 14.72%.

threo-Hydroxy-DL-aspartic Acid Diamide Hydrochloride. A solution of Z-DL-*t*Hyasp-diNH_2 (1.12 g, 4 mmol) in acetic acid (80 ml) was treated with hydrogen in the presence of palladium black. The catalyst was removed by filtration, and the filtrate was evaporated *in vacuo*. The residual oil was dissolved in N hydrochloric acid (4.2 ml) and the solution was evaporated *in vacuo* to dryness. The residue was recrystallized from methanol-ether. Yield, 0.86 g (93%); mp 190—192°C (decomp.).

Found: C, 26.36; H, 5.40; N; 22.84%. Calcd for $C_4H_9O_3N_3 \cdot HCl$: C, 26.17; H, 5.49; N, 22.90%.

threo-Hydroxy-L-aspartic Acid Diamide Hydrochloride. This was obtained by the hydrogenolysis of Z-L-*t*Hyasp-diNH_2 as described above. Yield, 91%; mp 190—192°C (decomp.); $[\alpha]_D^{17}$ −20.5° (*c* 1, H_2O).

Found: C, 25.96; 5.57; N, 22.82%.

erythro-Hydroxy-DL-aspartic Acid Diamide Hydrochloride. This was obtained by the hydrogenolysis of Z-DL-*e*Hyasp-diNH_2. Yield, 92%; mp 195—196°C (decomp.).

Found: C, 26.07; H, 5.47; N, 22.73%.

erythro-Hydroxy-L-aspartic Acid Diamide Hydrochloride. This was obtained by the hydrogenolysis of Z-L-*e*Hyasp-diNH_2. Yield, 90%; mp 193—194°C (decomp.); $[\alpha]_D^{17}$ +87.0° (*c* 0.5, H_2O).

Found: C, 25.80; H, 5.50; N, 22.86%.

Hydrolysis of Hydroxyaspartic Acid Diamide by LAPase. *Hydrolysis of DL-tHyasp-diNH_2 and DL-eHyasp-diNH_2.* A highly purified LAPase solution of step 6 by Smith was prepared following the method given in literature.[10] The enzyme solution was made to contain 4 mg protein per ml. One milliliter of the enzyme solution was dissolved in 0.4 M Tris buffer (0.5 ml) at pH

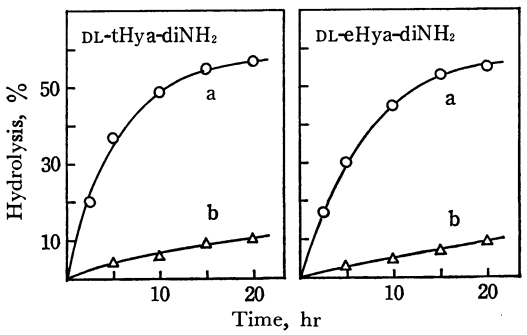

Fig. 5. Time-course of hydrolysis of *threo-* and *erythro*-hydroxy-DL-aspartic acid diamide with (a) without (b) LAPase.

13) T. Kato, S. Makisumi, M. Ohno and N. Izumiya, *Nippon Kagaku Zasshi (J. Chem. Soc. Japan, Pure Chem. Sect.)* **83**, 1151 (1962).

14) The R_f value refers to the thin layer chromatography with Merck silica gel G and to the *n*-butanol-acetic acid-pyridine-water (4:1:1:2, v/v) system.

8.0 and 0.12 M manganese chloride (0.5 ml). The solution was preincubated for 1 hr at 38°C to obtain maximal activation. This was named as an activated enzyme solution. A solution of DL-*t*(or *e*)Hyasp-diNH$_2$·HCl(0.1 mmol) in the activated enzyme solution (0.5 ml)

Table 2. Susceptibility of amino acid amides by lapase

Compound	C_1	Relative rate
L-Leu-NH$_2$	63	100
L-Asp-diNH$_2$	1.8	2.8
L-cysteic acid diamide		0.1[a]
L-*t*Hyasp-diNH$_2$	0.0069	0.011
L-*e*Hyasp-diNH$_2$	0.0049	0.0078

a) The datum is cited from literature.[9]

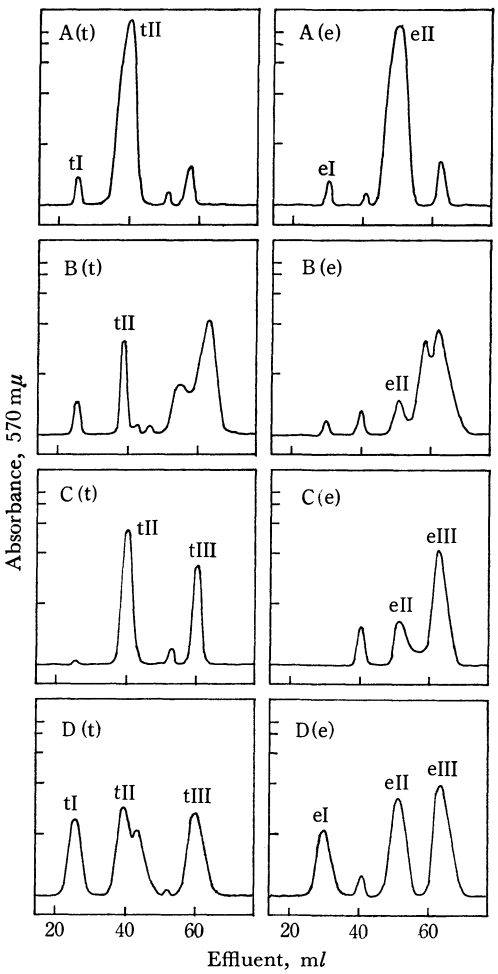

Fig. 6. Elution patterns of mixtures derived from hydroxyaspartic acid diamide and Z-hydroxyaspartic acid. (t), *threo*; (e), *erythro*; A, L-Hyasp-diNH$_2$ with LAPase; B, DL-Hyasp-diNH$_2$ with HCl; C, DL-Hyasp-diNH$_2$ with NaOH; D, hydrogenated material from Z-DL-Hyasp; I, Hyasp; II, Hyasn; III, Hyisoasn.

and 0.1 M Tris buffer (1.5 ml) at pH 8.0 was incubated at 38°C for 20 hr. The process of hydrolysis was followed by means of Conway's microdiffusion method[15] to determine ammonia (Fig. 5-a) and by paper chromatography. Analysis by an amino acid analyzer[16] of an aliquot after 20 hr incubation indicated the presence of hydroxyaspartic acid and other by-products as minor products. As a control experiment, a solution of DL-*t* (or *e*) Hyasp-diNH$_2$·HCl (0.1 mmol) in 0.1 M Tris buffer (2 ml) at pH 8.0 without the enzyme was incubated at 38°C and the amount of ammonia was determined. The results are given in Fig. 5-b.

Hydrolysis of L-*tHyasp-diNH$_2$ and* L-*eHyasp-diNH$_2$.* For determination of the accurate rate of hydrolysis of the L-Hyasp-diNH$_2$, an increased amount of LAPase was used. The occurrence of the by-products through spontaneous degradation was found to be negligible. A solution of L-*t*(or *e*)Hyasp-diNH$_2$·HCl (0.05 mmol) in the activated enzyme solution (1 ml) and 0.1 M Tris buffer (1 ml) at pH 8.0 was incubated 38°C. The patterns given by the amino acid analyzer with the samples of 10 hr incubation are shown in Fig. 6-A. The proteolytic coefficients (C_1) of the diamides are shown in Table 2, the C_1 of amides of L-leucine, L-asparagine and L-cysteic acid[9] being included for comparison. The C_1 values are calculated from $C_1=k/e$, where $k=(1/\text{min})\log[100/(100-\%\text{ hydrolysis})]$ and e is the protein concentration in mg of protein N per ml of test solution.

Preparation of L-*t*Hyasn and L-*e*Hyasn by LAPase. *L-tHyasn.* L-*t*Hyasp-diNH$_2$·HCl (92 mg, 0.5 mmol) was dissolved in a mixture of the activated enzyme solution (10 ml) and water (30 ml), the pH of the solution being adjusted to 8.0 with N sodium hydroxide. After being kept 8 hr at 38°C, the incubation mixture indicated complete hydrolysis of the diamide producing hydroxyasparagine through the assays by the amino acid analyzer and paper chromatography. The mixture was adjusted to pH 5 with acetic acid and warmed with a small amount of charcoal to remove protein. The filtrate was put on a column (0.9×20 cm) of Dowex 1×8 (OH^- form), and the column was washed with water and eluted with 0.5 N acetic acid. Ninhydrin positive fractions were collected and evaporated *in vacuo*. The residual crystals were collected with the aid of ethanol and recrystallized from water-ethanol. Yield, 53 mg (71%); mp 246—248°C (decomp.); R_f 0.15.[17]

Found: C, 32.10; H, 5.45; N, 18.57%. Calcd for $C_4H_8O_4N_2$: C, 32.44; H, 5.44; N, 18.79%.

L-eHyasn. This was obtained from L-*e*Hyasp-diNH$_2$·HCl (0.5 mmol) in the same way as has been described for the preparation of L-*t*Hyasn except for the incubation time being 12 hr. Yield, 50 mg (68%); mp 230—

15) R. B. Johnston, M. J. Mycek and J. S. Fruton, *J. Biol. Chem.*, **185**, 629 (1950).

16) The analyzer used was a Hitachi amino acid analyzer (Model KLA-3B) with spherical resin. The conditions were as follows: 0.9×50 cm column; 0.2 M standard citrate buffer of pH 3.25; flow rate, 60 ml/hr; jacket temperature, 55°C.

17) The R_f value refers to the paper chromatography with the solvent system of *n*-butanol - acetic acid - pyridine - water (4 : 1 : 1 : 2, v/v). It was observed that R_f for L-*t*Hyasp and L-*t*Hyasp-diNH$_2$·HCl are 0.13 and 0.22 respectively.

232°C(decomp.);[18] R_f 0.15.[17]

Found: C, 32.08; H, 5.44; N, 18.63%.

Comparison of Synthetic L-Hydroxyasparagines and the Natural Product. The three samples were employed for the measurements of optical rotation, using water and 5 N hydrochloric acid as solvent. As recognized from Table 1, the values of specific rotation of synthetic L-*e*Hyasn and the natural product are identical within experimental error. The three samples afforded the same R_f values in paper chromatography.[17] However, the L-*e*Hyasn and the natural product gave a peak at the same place while the L-*t*Hyasn gave one at a different place according to the amino acid analyzer (Fig. 3).[19] Furthermore, a mixture of the L-*e*Hyasn and the natural product afforded a single peak on the co-chromatography (Fig. 3). Thus, it is concluded that the spacial configuration of the natural product is that of L-*e*Hyasn.

Spontaneous Degradation of DL-Hyasp-diNH$_2$ in Acid Solution. DL-*t*(or *e*)Hyasp-diNH$_2$·HCl (18.4 mg, 0.1 mmol) was dissolved in 0.1 N hydrochloric acid (2 m*l*). After the solution had been allowed to stand for 24 hr at 38°C, an aliquot was analyzed by the amino acid analyzer, the patterns being shown in Fig. 6-B. Although *t*(or *e*)Hyasn was produced in a small amount, its isolation from the solution was not attempted.

Spontaneous Degradation of DL-Hyasp-diNH$_2$ in Alkaline Solution and Preparation of DL-tHyasn. *Preliminary Studies.* DL-*t*(or *e*)Hyasp-diNH$_2$·HCl (0.1 mmol) in 0.1 N sodium hydroxide (2 m*l*) was treated in the same way as above for 5 hr at 38°C. The patterns given by the amino acid analyzer are shown in Fig. 6-C. It was observed that the amount of DL-*t*Hyasn produced was much greater than that of DL-*e*Hyasn as shown in Fig. 6-C. Thus the separation of DL-*t*Hyasn from the reaction mixture was attempted as follows.

DL-tHyasn. DL-*t*Hyasp-diNH$_2$·HCl (368 mg, 2 mmol) in 0.1 N sodium hydroxide (40 m*l*) was allowed to stand for 5 hr at 38°C. After the solution was neutralized to pH 7, it was evaporated *in vacuo* to dryness. The residue was dissolved in a small amount of dilute acetic acid, and was applied on a column (1.8×150 cm) of Amberlite CG-120 (type III, Na^+ form). The column was eluted with 0.2 M sodium citrate buffer of pH 3.25 at a flow rate of 60 m*l*/hr; the fractions of 220—380 m*l* were confirmed to contain DL-*t*Hyasn. The fractions combined were put on a column of Dowex 1 (OH^- form), and the column was washed with water and eluted with 0.5 N acetic acid. After the eluate was evaporated *in vacuo*, the crystals were collected with the aid of ethanol and recrystallized from water-ethanol. Yield, 95 mg (32%); mp 228—232°C (decomp.); R_f 0.15.[17]

Found: C, 32.16; H, 5.62; N, 18.89%. Calcd for $C_4H_8O_4N_2$: C, 32.44; H, 5.44; N, 18.79%.

Preparation of DL-eHyasn through Z-DL-eHyasp Anhydride. *Preliminary Studies.* A solution of Z-DL-*t*(or *e*)Hyasp (142 mg, 0.5 mmol) in acetic anhydride (2 m*l*) was allowed to stand for 6 hr at 50°C. After evaporation *in vacuo* to dryness, the residue was dissolved in N ethanolic ammonia (5 m*l*) at 0°C. The solution was left for 30 min at 0°C, then 2 hr at room temperature, and evaporated to dryness. The residue was dissolved in acetic acid (3 m*l*) and hydrogenated in the presence of palladium black. An aliquot of the filtrate was analyzed by the amino acid analyzer (Fig. 6-D). It was assumed that a compound in peak *t*III or *e*III in Fig. 6 was β-hydroxyisoasparagine, however, conclusive evidence could not be obtained.[20] As shown in Fig. 6-D, it appeared that the *e*Hyasn might be isolated from the reaction mixture. The separation of DL-*e*Hyasn was attempted as follows.

DL-eHyasn. Two millimoles (566 mg) of Z-DL-*e*Hyasp were treated as described avove. Acetic acid in the hydrogenated material was removed by evaporation, and the residue was dissolved in a small amount of water. It was treated with a Amberlite CG-120 column (1.8× 50 cm) and 0.2 M sodium citrate buffer of pH 3.25 as had been described for the separation of DL-*t*Hyasn. The fractions of 120—155 m*l* were treated with a Dowex 1 column as described and yielded crystalline DL-*e*Hyasn. Yield, 98 mg (33%); mp 232—235°C(decomp.); R_f 0.15.[17]

Found: C, 32.51; H, 5.38; N, 18.62%. Calcd for $C_4H_8O_4N_2$: C, 32.44; H, 5.44; N, 18.79%.

We wish to express our thanks to Dr. Fumio Tominaga of Takeda Chemical Industries, Ltd. for supplying the natural hydroxyasparagine from human urine.

18) The mp of the natural hydroxyasparagine was determined to be 231—234°C (decomp.).

19) A sample each of 0.5 μmol with respect to one component was subjected to the analyzer.

20) The fractions of a peak *t*III or *e*III were collected in an experiment of preparative scale, however, the evaporation procedure *in vacuo* yielded Hyasp instead of Hyisoasn because of unstability of a compound (presumably, Hyisoasn) in *t*III or *e*III.

BULLETIN OF THE CHEMICAL SOCIETY OF JAPAN VOL. 42 3556—3558 (1969)

Electronic Spectra of *O*-Alkyl Thiobenzoates and Their Derivatives

Atsuyoshi OHNO, Tamotsu KOIZUMI, Yutaka OHNISHI
and Gen-ichi TSUCHIHASHI

Sagami Chemical Research Center, Onuma, Sagamihara

(Received June 5, 1969)

The absorption spectra of *O*-methyl and -ethyl thiobenzoates and their *p*- and *m*-methoxy, methyl and chloro derivatives have been studied. The substituent effect on the $n\rightarrow\pi^*$ transition of thiocarbonyl group has been discussed with the use of the Hammett relationship.

Among many organic compounds, thiocarbonyl compounds have received little attention until recently. Studies on the electronic spectra of thiocarbonyl compounds are not exceptions. The substituent effect on the spectra of thiobenzophenone was first published by Burawoy and co-workers only with electron-releasing substituents,[1,2] and then by de Boer and co-workers with a variety of substituents.[3] However, some of these compounds are unstable and it is difficult to obtain reliable spectra for the discussion on the substituent effect. *O*-Alkyl thiobenzoates and their derivatives are, on the other hand, stable in air and suitable for spectroscopic studies.

The purpose of this paper is mainly to gather reliable electronic spectral data on *O*-alkyl thiobenzoates and their derivatives and then to discuss the effect of substituents on the electronic transitions of thiocarbonyl group.

Results and Discussion

O-Methyl and -ethyl thiobenzoates and their *p*- and *m*-methoxy, methyl and chloro derivatives were synthesized and subjected to spectrometry.[4] The purity of materials was confirmed by VPC. The spectra were recorded in cyclohexane solution.

The electronic spectra of *O*-alkyl thiobenzoates have two regions of absorption (Fig. 1). The absorption at around 420 mμ is attributable to the $n\rightarrow\pi^*$ transition in the thiocarbonyl group. This characterization is verified by the fact that the intensity of the absorption is low, that a blue-shift of the absorption can be observed on transferring to a more polar solvent (λ_{max}=418 mμ, ε=98 in 95% aq. ethanol for *O*-methyl thiobenzoate) and that electron-releasing substituents cause the blue-shift (*vide infra*). The absorption at around 280—290 mμ can be regarded as the $\pi\rightarrow\pi^*$ transition in the arylthiocarbonyl group by the intensities and effects of substituents and solvents (λ_{max}=288 mμ, ε=9,812 in 95% aq. ethanol for *O*-methyl thiobenzoate). However, since the absorption of this region is accompanied by a shoulder(s) in several compounds, the origin of the transition is not unequivocally assigned. Some of *O*-alkyl thiobenzoates have another absorption at around 230 mμ.

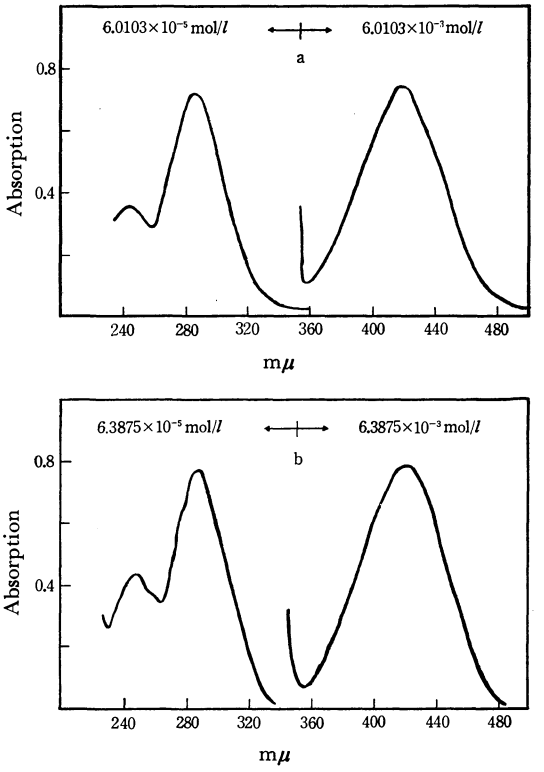

Fig. 1. The absorption spectra of (a) *O*-methyl thiobenzoate and (b) *O*-ethyl thiobenzoate.

1) P. Brocklehurst and A. Burawoy, *Tetrahedron*, **10**, 118 (1960).

2) a) W. A. Lees and A. Burawoy, *ibid.*, **20**, 1527 (1964); b) **20**, 1533 (1964).

3) a) O. Korver, J. U. Veenland and Th. J. de Boer, *Rec. Trav. Chim. Pays-Bas*, **84**, 289 (1965); b) **84**, 304 (1965).

4) We thank to Professor S. Inokawa of Sizuoka University for his kind supply of *O*-methyl *p*-nitrothiobenzoate.

Table 1. Absorption maxima and molar extinction coefficients in the visible-light region[a)]

Substituent	Methyl thioester			Ethyl thioester		
	λ, Å	ε	$\Delta\nu$, cm^{-1}	λ, Å	ε	$\Delta\nu$, cm^{-1}
H	4171	121	—	4200	122	—
p-CH_3O	4118	196	+309	4147	208	+304
m-CH_3O	4176	122	−29	4198	121	+11
p-CH_3	4143	134	+162	4188	144	+68
m-CH_3	4165	128	+35	4188	132	+68
p-Cl	4215	120	−250	4221	141	−119
m-Cl	4200	110	−165	4241		−231
p-NO_2	4329	177	−875	—	—	—

a) In cyclohexane.

Table 2. Absorption maxima and molar extinction coefficients in the ultraviolet region[a)]

Substituent	Methyl thioester		Ethyl thioester	
	λ, Å	ε	λ, Å	ε
H	2871	11647	2879	12211
	2465	5907	2476	7076
p-CH_3O	3112	21853	3118	17873
	2577	5352	2606	4830
m-CH_3O	3200	shoulder	3182	shoulder
	2867	10671	2879	11049
p-CH_3	2941	13401	2953	14897
	2465	5430	2524	6728
m-CH_3	2882	14297	2882	12832
	2588	6068	2588	6117
	2493	6035	2506	6150
p-Cl	2918	12921	2929	13890
	2481	7613	2553	7610
m-Cl	3193	shoulder	2929	shoulder
	2828	11763	2847	10090
	2624	shoulder	2588	5814
p-NO_2	2988	11196	—	—

a) In cyclohexane.

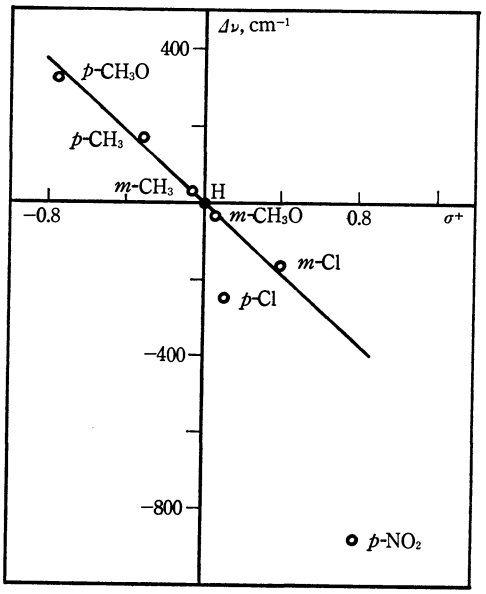

Fig. 2. Hammett relationship for the $n\rightarrow\pi^*$ transition of *O*-methyl thiobenzoates.

This is probably due to the interaction between the substituent and the phenyl-ring. The absorption maxima and the molar extinction coefficients are listed in Tables 1 and 2. In Table 1, the shifts in wave numbers of thiocarbonyl absorption band of substituted *O*-alkyl thiobenzoates relative to the corresponding unsubstituted thioesters are also listed.

A remarkable substituent effect can be observed in the $n\rightarrow\pi^*$ transition: the Hammett plot, according to the equation.

$$\Delta\nu = \nu_X - \nu_H = \rho\sigma^+$$

is shown in Fig. 2 for the $n\rightarrow\pi^*$ transition of *O*-methyl thioesters. The *O*-ethyl thioesters behave similarly.

Obviously, electron-withdrawing substituents at the *p*-position exert different effect from the others on the transition. Let us assume that this is due to larger conjugative effect of such substituents in the n, π^* excited state of the thioester than in its ground state.

It will be interesting to compare the substituent effect in the thioester and that in thiobenzophenone or in 2,4,6-trimethylthiobenzophenone, where electron-releasing and -withdrawing substituents each give lines with different slopes regardless the position of substituents.[3a)] In series of substituted thiobenzophenones, it has been assumed that, as a consequence of an electronic influence by an electron-withdrawing substituent in *p*-position, the phenyl or even the 2,4,6-trimethylphenyl group reaches a greater degree of coplanarity with the thiocarbonyl group than the *p*-substituted phenyl group. Therefore, only the inductive effect of the substituent can act upon the transition. Thus, there exists a distinct difference in the conjugative effects of electron-withdrawing substituents between thioesters and thiobenzophenones. This difference might be interpreted as follows: since

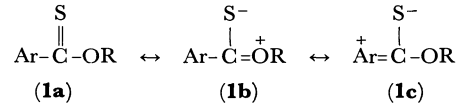

(**1a**) (**1b**) (**1c**)

the thiocarbonyl group is highly polarized in its ground state,[5-7] the contribution of the structure **1b** is fairly important in the ground state of the thioester.[7] On the other hand, since the polarization of the thiocarbonyl group is reverse in the n, π^* exited state[8] to that in the ground state, the resonance effect of the oxygen atom no more operates. As a consequence, the importance of the structure (**2b**) increases in the n, π^* excited state.

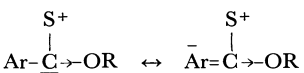

(**2a**) (**2b**)

Although the limited number of substituents do not allow to estimate the relative importance of the resonance effect quantitatively, the present results show that electron-releasing substituents can conjugate with the thiocarbonyl group in the ground state, whereas electron-withdrawing substituents interact with the thiocarbonyl group in the n, π^* excited state. It should be noted that the phenyl group in thiobenzophenone or the mesityl group in 2,4,6-trimethylthiobenzophenone has ability to conjugate with the thiocarbonyl group both electron-releasingly and -withdrawingly.

Unfortunately, the susceptibility of the substituent effect to the thiocarbonyl group cannot be compared with that to the carbonyl group, because the absorption due to the $n\rightarrow\pi^*$ transition in benzoates are completely hidden by an intense band of the $\pi\rightarrow\pi^*$ transition.

For the $\pi\rightarrow\pi^*$ transition, the difference of absorption maxima between p- and m-positions for each substituents correlates well to the value of $\Delta\sigma=\sigma_p-\sigma_m$. This fact indicates that the absorption in this region is largely affected by a resonance effect of substituents.[9] The plot is shown in Fig. 3 for the O-methyl thioesters. The linear correlations of $\Delta\nu$ with σ and σ_R is also found for m- and p-substituted thioesters, except for the p-nitro derivative, respectively, as has been found for the system of 2,4,6-trimethylthiobenzophenone.[3a]

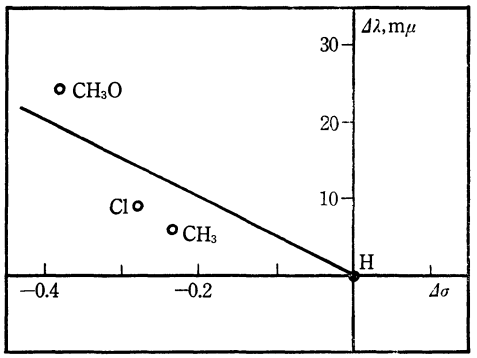

Fig. 3. The correlation of $\Delta\lambda$ *vs.* $\Delta\sigma$ for the $\pi\rightarrow\pi^*$ transition of O-methyl thiobenzoates.

Experimental

Materials. As previously reported,[10] the thioesters were prepared from the corresponding orthoesters[11] or from the corresponding imido ethers.[12,13] The purities were confirmed by IR, NMR and VPC. The results of elemental analyses were satisfactory for each compound.

Spectrometry. Spectra were obtained on a Cary-14 Spectrophotometer using spectrograde cyclohexane as solvents. The concentrations of solutions were adjusted so as to obtain the spectra, in which the maxima of a band had around 70—80% absorption. These were 6×10^{-3} M for visible and 6×10^{-5} M for UV revion, respectively. The estimated error in wavelength is ±1 mμ.

5) J. Newman, Jr., and L. B. Young, *J. Phys. Chem.*, **69**, 2570 (1965).

6) H. Lumbroso and C. Andrieu, *Bull Soc. Chim. France*, **1966** 3201.

7) H. Lumbroso and P. J. W. Schijl, *C. R. Acad. Sci., Paris, Ser. C*, **264**, 925 (1967).

8) H. Zimmerman, "Advances in Photochemistry," Vol. 1, ed. by W. A. Noyes, Jr., G. S. Hammond and J. N. Pitts, Jr., Interscience Publishers, New York, N. Y. (1963), pp. 184—5.

9) H. H. Jaffe and M. Orchin, "Theory and Applications of Ultraviolet Spectrosocopy," John Wiley & Sons, Inc., New York, N. Y. (1962), pp. 258—9.

10) A. Ohno, T. Koizumi, Y. Ohnoshi and G. Tsuchihashi, "Mass-Spectral Studies on Thiobenzoates and Thioacetates," *Org. Mass Spectry.*, in press.

11) A. Ohno, T. Koizumi and G. Tsuchihashi, *Tetrahedron Letters*, **1968**, 2083.

12) M. Matsui, *Mem. Coll. Sci. Eng. Kyoto*, **1**, 285 (1908); *ibid.*, **3**, 247 (1912).

13) Y. Sakurada, *ibid.*, **9**, 237 (1926); *ibid.*, **10**, 79 (1926).

BULLETIN OF THE CHEMICAL SOCIETY OF JAPAN VOL. 42 3559—3564 (1969)

Oxidation Reactions of 2,4,6-Tri-*t*-butylaniline

Renji OKAZAKI, Takeo HOSOGAI, Masayoshi HASHIMOTO and Naoki INAMOTO

Department of Chemistry, Faculty of Science, The University of Tokyo, Hongo, Bunkyo-ku, Tokyo

(Received June 30, 1969)

Oxidation reactions of 2,4,6-tri-*t*-butylaniline with lead tetraacetate (LTA), lead tetrabenzoate (LTB), peroxybenzoic acid (PBA) and benzoyl peroxide (BPO) were studied and mechanisms of these reactions were briefly discussed. In the reaction with LTA, 4-acetoxy-1-imino-2,4,6-tri-*t*-butyl-2,5-cyclohexadiene (I), 2-acetamido-3,5-di-*t*-butylphenol (II) and 2-acetylimino-3,5-di-*t*-butyl-3,5-cyclohexadienone(III) were produced. Oxidation with LTB gave 4-benzoyloxy-1-imino-2,4,6-tri-*t*-butyl-2,5-cyclohexadiene (VI, major product) and 2-benzamido-3,5-di-*t*-butylphenol (VII). The reaction products with PBA were 2,4,6-tri-*t*-butylnitrosobenzene (VIII) and VII. In addition to the last two compounds, VI and 2,2′,4,4′,6,6′-hexa-*t*-butylazobenzene (XI) were obtained in the case of BPO.

2,4,6-Tri-*t*-butylaniline (TBA) has been studied by many workers who expected unusual properties due to the steric effects of the bulky *t*-butyl groups. There have been only a few reports on the chemical reactions, although there have been several investigations on the physical properties such as basic strength,[1-3] IR,[2] UV[2] and NMR[4] spectra. The reactions reported so far are conversion *via* diazotization[1,5] and preparation of the *N*-acyl and the *N*-alkyl derivatives.[2a]

Oxidation reactions of TBA were focused only on the ESR studies of the corresponding anilino radical,[6] although Cauquis *et al.* have isolated some products in the electrochemical oxidation.[7]

We have studied the reactions of TBA with some oxidizing agents such as lead tetraacetate (LTA), lead tetrabenzoate (LTB), peroxybenzoic acid (PBA) and benzoyl peroxide (BPO), and found that the reactions are different in many respects from those of sterically unhindered anilines.

Results

The structures of the reaction products were determined by elemental analyses, IR and NMR spectra.

Reactions with LTA or LTB. TBA reacted with LTA in benzene at 5°C to give 4-acetoxy-1-imino-2,4,6-tri-*t*-butyl-2,5-cyclohexadiene (I, 47%), 2-acetamido-3,5-di-*t*-butylphenol (II, 11%) and 2-acetylimino-3,5-di-*t*-butyl-3,5-cyclohexadienone (III, 8%).

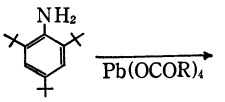

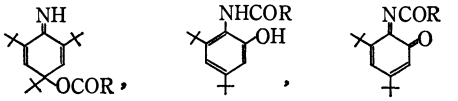

I: R=CH_3 II: R=CH_3 III: R=CH_3
VI: R=C_6H_5 VII: R=C_6H_5

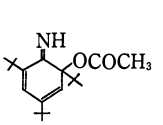

IV

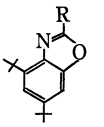

V: R=CH_3
X: R=C_6H_5

Although an isomeric structure (IV) is possible for I, IV was ruled out by the NMR spectrum which exhibited five singlets (τ 9.10, 9H, *t*-butyl protons at 4-position; 8.72, 18H, *t*-butyl protons at 2- and 6-positions; 8.05, 3H, acetyl protons; 4.04, 2H, olefinic protons; 0.48, 1H, imino proton), for the NMR spectrum of IV would be expected to show three kinds of the *t*-butyl protons, and AB type quartet of the olefinic protons.

1) P. D. Bartlett, M. Roha and R. M. Stiles, *J. Am. Chem. Soc.*, **76**, 2349 (1954).

2) a) J. Burgers, M. A. Hoefnagel, P. E. Verkade, H. Visser and B. M. Wepster, *Rec. Trav. Chim.*, **77**, 491 (1958). b) P. J. Krueger, *Can. J. Chem.*, **40**, 2300 (1962); **41**, 363 (1963).

3) F. E. Condon, *J. Am. Chem. Soc.*, **87**, 4494 (1965).

4) V. M. S. Gil and W. A. Gibbons, *Mol. Phys.*, **8**, 199 (1964); W. A. Gibbons and V. M. S. Gill, *ibid.*, **9**, 163, 167 (1965).

5) E. E. Betts and L. R. C. Barclay, *Can. J. Chem.*, **33**, 1768 (1955); F. E. Condon, *J. Org. Chem.*, **30**, 3946 (1965).

6) E. J. Land and G. Porter, *J. Chem. Soc.*, **1961**, 3540; N. M. Atherton, E. J. Land and G. Porter, *Trans. Faraday Soc.*, **59**, 818 (1963); K. Mukai, H. Nishiguchi, K. Ishizu and Y. Deguchi, This Bulletin, **40**, 2731 (1967); G. Cauquis and M. Geniès, *C. R. Acad. Sci., Paris, Ser. C*, **265**, 1340 (1967).

7) G. Cauquis, G. Fauvelot and J. Rigaudy, *ibid.*, **264**, 1758, 1958 (1967).

The imine (I) deccmposed about 150°C into II and isobutylene. The reaction proceeds presumably *via* an intermediate (IV) as shown below.

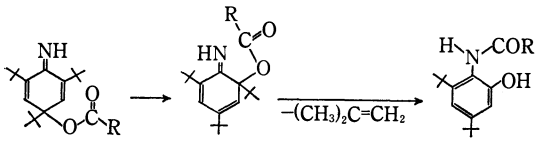

I, VI IV II, VII

The structure of II was confirmed by comparison with that of an authentic sample, which was synthesized by the acetylation of 2-amino-3,5-di-*t*-butylphenol.

The hydrolysis of II by hydrochloric acid gave 4,6-di-*t*-butyl-2-methylbenzoxazole (V) instead of expected 2-amino-3,5-di-*t*-butylphenol.

The reduction of III with lithium aluminum hydride yielded II, and conversely, the oxidation of II with LTA gave III.

LTB oxidized TBA in dichloromethane at room temperature to yield 4-benzoyloxy-1-imino-2,4,6-tri-*t*-butyl-2,5-cyclohexadiene (VI, 65%) and 2-benzamido-3,5-di-*t*-butylphenol (VII, 1.4%). Their characterization will be described later.

Reaction with PBA. The oxidation of TBA with two mole equivalents of PBA at 0°C gave 73% of 2,4,6-tri-*t*-butylnitrosobenzene (VIII) and a trace of VII. Use of excess PBA or higher temperatures produced 2,4,6-tri-*t*-butylnitrobenzene as by-product. On the other hand, use of an equimolar amount of PBA enhanced the yield of VII; VIII and VII being produced in 18 and 10% yields, respectively. The formation of *o*-*N*-acylaminophenols has not yet been observed for the ordinary anilines.

Furthermore, II was produced instead of VII, in the case of the reaction with an equimolar amount of PBA in the presence of a large excess of acetic acid. Oxidation of TBA with 30% hydrogen peroxide in acetic acid by the procedure of Holmes and Bayer[8] produced no nitroso compound.

The nitrosobenzene (VIII) is emerald-green crystals and monomeric even in the solid state.[9]

The structure of VII was characterized by comparison with that of an authentic sample, which was prepared by benzoylation of 2-amino-3,5-di-*t*-butylphenol. The phenol (VII) was converted into the methyl ether (IX) by diazomethane and cyclized to 2-phenyl-3,5-di-*t*-butylbenzoxazole (X) by hydrochloric acid as in the case of II.

Reaction with BPO. TBA reacted with BPO in benzene at room temperature to yield VIII, VII, VI and 2,2′,4,4′,6,6′-hexa-*t*-butylazobenzene (XI) in 2, 49, 38 and 2% yields, respectively.

The imine (VI) was undistilled even under high vacuum owing to its facile decomposition into VII at about 100°C. Moreover, it could not be purified by column chromatography on silica gel, because of easy decomposition into VII (37%) and 4-benzoyloxy-2,6-di-*t*-butylaniline (XII, 39%). However, petroleum ether soluble part of the reaction products, after extraction of benzoic acid by aqueous alkali, was almost pure VI.

Discussion

It is known that the reactions of the primary aromatic amines with LTA produce azo compounds in poor yields.[10] Products other than azo compound were obtained in the case of TBA. The difference can be attributed to the steric hindrance around the amino group of TBA. The following mechanism is considered to account for the results, although a homolytic mechanism involving anilino

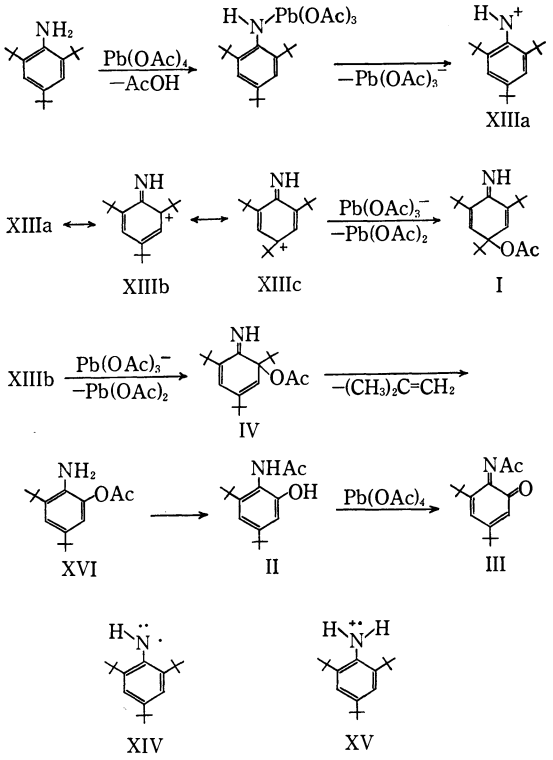

8) R. R. Holmes and R. P. Bayer, *J. Am. Chem. Soc.*, **82**, 3454 (1960).

9) R. Okazaki, T. Hosogai, E. Iwadare, M. Hashimoto and N. Inamoto, This Bulletin, **42**, 3611 (1969).

10) K. H. Pausacker and J. G. Scroggie, *J. Chem. Soc.*, **1954**, 4003; E. Baer and A. L. Tosoni, *J. Am. Chem. Soc.*, **78**, 2857 (1956).

radical (XIV) or aniline radical-cation(XV) cannot be ruled out. Rearrangement of *O*-acetylated aminophenols such as XVI into the corresponding *N*-acetylated aminophenols is well known.[11]

In the reactions of the ordinary anilines the intermediate anilino cations readily attack the unchanged anilines followed by further oxidation to give azobenzenes, while the intermediate (XIII) generated from TBA cannot react with another TBA molecule owing to the steric hindrance by the *t*-butyl groups.

Reaction with LTB is likely to proceed *via* the same mechanism as that with LTA. It is different, however, in two respects; the product ratio of the aminophenol (VII or II) to the imino compound (VI or I) is rather low and no *o*-benzoquinone acylimine analogous to III is produced. The low product ratio in the case of LTB is obviously due to the more bulky attacking species such as $Pb(OCOPh)_3^-$.

It is known that the reaction products of primary aromatic amines with peroxyacids are different depending upon the kinds of peroxyacids and the reaction conditions.[12] Caro's acid oxidizes the anilines to the nitroso compounds in usually poor yields. Oxidation with peroxyacetic acid affords nitrosobenzenes, nitrobenzenes and/or azoxybenzenes depending upon the reaction conditions; higher temperatures favor the production of the latter two and lower temperatures that of the former.[8,13] For PBA there have been a few investigations[14] which have dealt with the reaction only qualitatively except for the study by Horner and Kirmse, who reported azobenzene and azoxybenzene as the reaction products with aniline.[15]

However, PBA oxidized TBA into the nitroso compound (VIII) in a high yield.[9] This is because the bulky *t*-butyl groups at *ortho*-positions disturb the condensation of the unchanged TBA with the corresponding nitroso or hydroxylamino compound produced.

As for formation of VII and II under various conditions, the following scheme is plausible, although not conclusive.

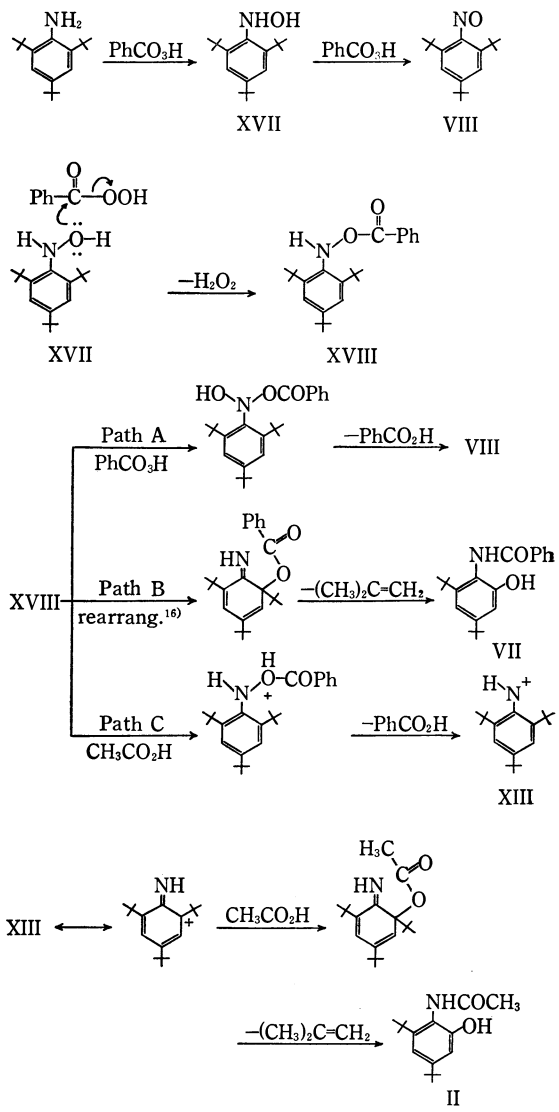

The unusual formation of VII is likely to be due to the steric hindrance which makes the rate of the reaction XVII→XVIII comparable to that of the reaction XVII→VIII, for the steric congestion around the oxygen atom in XVII is fairly less than that around the nitrogen atom.

Horner and Kirmse have concluded that the reactions of the anilines with BPO proceed by both homolytic and heterolytic mechanisms.[17]

Our results for TBA are also explicable by the following mechanism involving both homolytic and heterolytic reactions, the former being predominant. The imine (VI), the benzamidophenol (VII) and the azobenzene (XI) are products *via*

11) W. Böttcher, *Ber.*, **16**, 629 (1883); J. T. Edward, *J. Chem. Soc.*, **1954**, 1464; J. H. Ransom, *Ber.*, **33**, 199 (1900); K. Auwers, *Ann.*, **332**, 159 (1904); M. Bergmann, R. Ulpts and F. Camacho, *Ber.*, **55**, 2805 (1922).

12) P. A. S. Smith, "The Chemistry of Open-Chain Organic Nitrogen Compounds," Vol. 2, W. A. Benjamin, Inc., New York (1966), p. 355; B. G. Gowenlock and W. Lüttke, *Quart. Rev.*, **12**, 321 (1958).

13) J. D'Ans and A. Kneip, *Ber.*, **48**, 1136 (1915); F. P. Greenspan, *Ind. Eng. Chem.*, **39**, 847 (1947); W. D. Emmons, *J. Am. Chem. Soc.*, **79**, 5528 ,6522 (1957); H. R. Gutmann, *Experientia*, **20**, 128 (1964); A. J. Boulton, P. B. Ghosh and A. R. Katritzky, *Tetrahedron Letters*, **1966**, 2887; H. Meister, *Ann.*, **679**, 83 (1964).

14) A. Baeyer and V. Villiger, *Ber.*, **33**, 1569 (1900); N. Prileschajew, *ibid.*, **42**, 4811 (1909).

15) L. Horner and W. Kirmse, *Ann.*, **597**, 70 (1955).

16) P. B. Denney and D. Z. Denney, *J. Am. Chem. Soc.*, **82**, 1389 (1960).

17) L. Horner and W. Kirmse, *Ann.*, **597**, 66 (1955) and references cited therein.

homolytic processes and the nitroso compound (VIII) is that *via* heterolytic one.

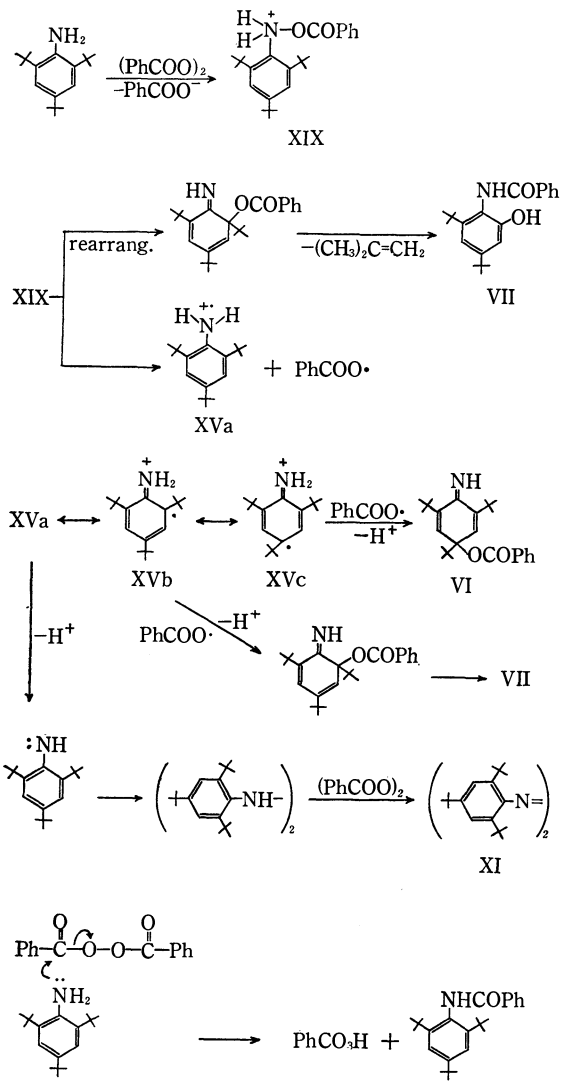

The formation of the nitrosobenzene (VIII) is reasonably explained by oxidation of TBA with PBA which is yielded by aminolysis of BPO, although the full characterization of the benzamide was unsuccessful (see Experimental).

A high product ratio of VII to VI as compared with that in the case of LTB suggests the existence of another route to VII probably *via* rearrangement of an intermediate (XIX).

Experimental

Melting points and boiling points are uncorrected. The NMR spectra were taken on a Japan Electron Optics Laboratory spectrometer Model JNM-C-60H using tetramethylsilane as an internal standard. Unless otherwise indicated, the solvent was carbon tetrachloride, and the signals were singlet. The electronic and the infrared spectra were recorded on a Hitachi spectrophotometer Model EPS-3 and EPI-G2, respectively.

2,4,6-Tri-*t*-butylaniline,[2a] lead tetraacetate,[18] lead tetrabenzoate[19] and peroxybenzoic acid[20] were prepared by the reported methods.

Reaction of 2,4,6-Tri-*t*-butylaniline (TBA) with Lead Tetraacetate (LTA). To a solution of TBA (9.2 g, 0.035 mol) in 250 m*l* of dry benzene, was added LTA (18.7 g, 0.042 mol) in 250 m*l* of benzene with stirring at 5°C. The mixture was stirred successively for 3 hr. After filtration of lead diacetate (10.6 g, 0.033 mol), the filtrate was shaken with 300 m*l* of water, and the benzene layer was dried over anhydrous sodium sulfate. After removal of benzene *in vacuo* below 50°C, petroleum ether (100 m*l*) was added and the insoluble crystals were recrystallized from chloroform to yield 2-acetamido-3,5-di-*t*-butylphenol (II, 1.0 g, 11%) as white solid, mp 214—216°C, which was identical with a compound obtained from acetylation of 2-amino-3,5-di-*t*-butylphenol (see below).

Found: C, 72.77; H, 9.62; N, 5.26%. Calcd for $C_{16}H_{25}NO_2$: C, 72.96; H, 9.57; N, 5.32%. Mol wt (Rast method) Found: 261. Calcd: 263.

The petroleum ether solution was chromatographed on silica gel. An oily material (5.3 g, 47%), eluted with petroleum ether, was purified by distillation to give 4-acetoxy-1-imino-2,4,6-tri-*t*-butyl-2,5-cyclohexadiene (I, 3.4 g, 31%), bp 90°C (0.28 mmHg). NMR: τ 0.48 (1H, broad), 4.04 (2H), 8.05 (3H), 8.72 (18H) and 9.10 (9H). IR (neat): 3330(N-H) and 1745 cm^{-1} (C=O).

Found: C, 75.38; H, 10.34; N, 4.54%. Calcd for $C_{20}H_{33}NO_2$: C, 75.19; H, 10.41; N, 4.38%.

Another material eluted with benzene was recrystallized from 70% ethanol to give 2-acetylimino-3,5-di-*t*-butyl-3,5-cyclohexadienone (III, 0.7 g, 8%) as orange-red crystals, mp 81—85°C. NMR: τ 3.29 (1H), 3.90 (1H), 7.86 (3H), 8.65 (9H) and 8.77 (9H).

Found: C, 73.26; H, 9.04; N, 5.27%. Calcd for $C_{16}H_{23}NO_2$: C, 73.53; H, 8.87; N, 5.36%.

Pyrolysis of I and 4-Benzoyloxy-1-imino-2,4,6-tri-*t*-butyl-2,5-cyclohexadiene (VI). Cyclohexadiene (I, 1.00 g, 3.1 mmol) was heated to 148°C in the course of 15 min in a test tube connected to a trap cooled with Dry Ice - ethanol mixture. The sample suddenly solidified with evolution of gas. The solid was washed with petroleum ether and recrystallized from methanol to give II (0.56 g, 70%), mp 215—217°C. To the liquid collected in the trap was added bromine in carbon tetrachloride to yield isobutylene dibromide (0.38 g, 57%), the amount of which was determined by means of VPC (succinic polyester of diethylene-glycol).

The cyclohexadiene (VI, 1.09 g, 2.86 mmol) obtained in the reaction of TBA with BPO was pyrolyzed by the same procedure to give isobutylene (47%) and 2-benzamido-3,5-di-*t*-butylphenol (VII, 0.57 g, 62%), which was identical with an authentic sample synthesized from benzoylation of 2-amino-3,5-di-*t*-butylphenol. VI began to decompose at about 100°C and decomposed vigorously at 130°C.

18) J. C. Bailar, Jr., *Inorg. Synth.*, **1**, 47 (1939).
19) R. Criegee, P. Dimroth, K. Noll, R. Simon and C. Weis, *Chem. Ber.*, **90**, 1070 (1957).
20) G. Braun, "Organic Syntheses," Coll. Vol. 1, p. 431 (1956).

Oxidation of II. To a solution of II (0.5 g, 1.9 mmol) in 10 m*l* of dry benzene was added LTA (1.0 g, 2.3 mmol) in 30 m*l* of dry benzene at room temperature, and the mixture was allowed to stand at room temperature overnight. After filtration of lead diacetate (0.7 g, 2.2 mmol) and removal of benzene, petroleum ether was added and insoluble LTA was filtered off. The filtrate was chromatographed on silica gel with benzene-ether (9 : 1) to give III (0.3 g, 60%), mp 81—85°C.

Reduction of III. To a solution of lithium aluminum hydride (0.1 g, 2.6 mmol) in 6 m*l* of anhydrous ether was added dropwise III (0.1 g, 3.8 mmol) in 5 m*l* of ether at room temperature with stirring. After usual working up, II (0.02 g, 20%), mp 214—216°C, was obtained.

Preparation of 2-Amino-3,5-di-*t*-butylphenol. To 3,5-di-*t*-butyl-2-nitrophenol[21] (10 g, 0.040 mol) in 20 m*l* of ethanol, was added sodium hydroxide (2 g, 0.050 mol) in 20 m*l* of water and then sodium hydrosulfite (14 g, 0.080 mol) in 100 m*l* of water was added dropwise at room temperature. Another sodium hydroxide (3 g, 0.075 mol) was added in portions to keep the mixture slightly alkaline, and the solution was stirred overnight. The reaction mixture was poured into 2 *l* of water and neutralized with dilute hydrochloric acid. The precipitate (10 g) was recrystallized from carbon tetrachloride to give 2-amino-3,5-di-*t*-butylphenol (2 g, 23%), mp 165—167°C. IR: 3330, 3430 (N-H) and 3110 cm^{-1} (O-H).

Found: C, 75.85; H, 10.25; N, 6.26%. Calcd for $C_{14}H_{23}NO$: C, 75.97; H, 10.47; N, 6.33%.

Acetylation and Benzoylation of 2-Amino-3,5-di-*t*-butylphenol. To a mixture of 2-amino-3,5-di-*t*-butylphenol (0.44 g, 2.0 mmol) and triethylamine (1.36 g, 3.6 mmol) in 5 m*l* of ether, acetyl chloride (0.16 g, 2.0 mmol) in 5 m*l* of ether was added with stirring at room temperature. After usual working up, II (0.1 g, 20%), mp 212—214°C, was obtained.

Found: C, 72.93; H, 9.56; N, 5.56%. Calcd for $C_{16}H_{25}NO_2$: C, 72.96; H, 9.57; N, 5.32%.

The benzoyl derivative (VII) was prepared by a similar method in 42% yield, mp 231—232°C (from chloroform).

Found: C, 77.21; H, 8.38; N, 4.36%. Calcd for $C_{21}H_{27}NO_2$: C, 77.50; H, 8.36; N, 4.30%.

4,6-Di-*t*-butyl-2-methylbenzoxazole (V). II (1.2 g, 4.6 mmol) was refluxed for 7 hr in 50 m*l* of absolute methanol under a stream of dry hydrogen chloride. After usual treatment, crude product was purified by column chromatography on alumina with petroleum ether to yield V (0.85 g, 77%), mp 45—46°C. UV: λ_{max}^{MeOH} 240 (log ε 4.11), 271 (3.65) and 280 mμ (3.62). The UV spectrum was in good agreement with that of 2-methylbenzoxazole.[22]

Found: C, 78.37; H, 9.68; N, 5.89%. Calcd for $C_{16}H_{23}NO$: C, 78.32; H, 9.45; N, 5.71%.

Reaction of 2,4,6-Tri-*t*-butylaniline (TBA) with Lead Tetrabenzoate (LTB). A mixture of TBA (13 g, 0.050 mol), LTB (36 g, 0.052 mol) and dichloromethane (400 m*l*) was stirred for 2 hr at room temperature and then allowed to stand overnight. After removal of dichloromethane, ether was added in order to precipitate lead dibenzoate (21 g, 94%) (Found: C, 36.95; H, 2.51; N, 0%). After evaporation of the solvent from the filtrate and addition of petroleum ether, resulting white precipitates were shaken with aqueous sodium carbonate to leave insoluble VII (0.23 g, 1.4%), which was identified by comparison of the IR spectrum with that of an authentic sample described above. Acidification of the aqueous layer gave benzoic acid (6.33 g, 101%). The petroleum ether soluble products (16.21 g) were found by the NMR spectrum to be a mixture of unchanged TBA and VI (12.0 g, 65%). For characterization of VI, see the reaction with BPO.

Oxidation of TBA with Peroxybenzoic Acid (PBA). a) PBA (0.148 mol) in 100 m*l* of ether was added to an ethereal solution (100 m*l*) of TBA (19.5 g, 0.0747 mol) cooled with ice-water, and the mixture was kept at 0°C overnight. After usual working up, the crude material was purified by means of column chromatography on alumina or silica gel. 2,4,6-Tri-*t*-butylnitrosobenzene (VIII), first eluted with petroleum ether, was recrystallized from ethanol as emerald-green crystals. The yield was 16.2 g (73%), mp 166—168°C. The molecular weight was found to be 303 (Rast method) or 244 (Beckmann method in benzene); Calcd for $C_{18}H_{29}NO$: 275. NMR: τ 2.75 (2H), 8.65 (9H) and 8.80 (18H).

Found: C, 78.25; H, 10.81; N, 5.09%. Calcd for $C_{18}H_{29}NO$: C, 78.49; H, 10.61; N, 5.09%.

b) To TBA (5.2 g, 0.020 mol) in 20 m*l* of dichloromethane was added PBA (0.020 mol) in 20 m*l* of dichloromethane under cooling with ice-water, and the mixture was kept at 0°C overnight. After usual working up, the remaining solid was dissolved in petroleum ether. 3,5-Di-*t*-butyl-2-benzamidophenol (VII, 0.6 g, 10%) was obtained as white solid insoluble in this solvent, and recrystallized from chloroform and then from methanol, mp 231—232°C. IR (in Nujol): 3340 (N-H), 3110 (O-H) and 1630 cm^{-1} (C=O).

Found: C, 77.38; H, 8.48; N, 4.59%. Calcd for $C_{21}H_{27}NO_2$: C, 77.50; H, 8.36; N, 4.30%.

A product soluble in petroleum ether was VIII (1.0 g, 18%) and some TBA (1.5 g, 29%) was recovered.

c) To TBA (5.0 g, 0.019 mol) in 50 m*l* of ether, 30 m*l* of glacial acetic acid and then PBA (0.020 mol) were added under cooling with ice-water. After being kept at 0°C overnight, the reaction mixture was neutralized with aqueous sodium carbonate and dried over anhydrous sodium sulfate. After removal of the solvent the residue was dissolved in petroleum ether. II (5 mg, 0.1%) was obtained as a material insoluble in this solvent. The structure was confirmed to be identical with that of an authentic sample by the IR spectrum. The yield of VIII was 2.2 g (42%).

Methyl Ether of VII (IX). To a solution of VII (0.6 g, 2 mmol) in 100 m*l* of ethanol, about 1 g (24 mmol) of diazomethane in ether - ethanol was added at 0°C. The mixture was maintained at 0°C for two days. The solvents and excess diazomethane were removed, and recrystallization of the residual solid from methanol yielded methyl ether (IX, 0.3 g, 50%), mp 245.0—245.5°C. NMR (in $CDCl_3$ at 56°C): τ 1.95—3.20 (m, 7H), 6.27 (3H), 8.62 (9H) and 8.69 (9H). IR (in Nujol): 3270 (N-H), 1640 (C=O) and 1043 cm^{-1} (OCH_3).

Found: C, 77.55; H, 8.84; N, 4.11%. Calcd for $C_{22}H_{29}NO_2$: C, 77.84; H, 8.61; N, 4.13%.

21) J. W. Elder and R. P. Mariella, *Can. J. Chem.*, **41**, 1653 (1963).

22) P. Passerini, *J. Chem. Soc.*, **1954**, 2256.

4,6-Di-*t*-butyl-2-phenylbenzoxazole (X). To a solution of VII (1.0 g, 3.2 mmol) in 50 m*l* of ethanol, 50 m*l* of 8 N hydrochloric acid was added, and the solution was refluxed at 110—120°C for 4 hr. After usual working up, to the viscous oil thus obtained was added 100 m*l* of petroleum ether. After filtration of the precipitated starting material (0.1 g, 10%) and removal of the solvent, the residue (0.8 g) was purified by column chromatography on alumina with petroleum ether. The yield was 0.6 g (57%). Mp 82—84°C.
NMR: τ 1.59—2.00 (m, 2H), 2.40—2.90 (m, 5H), 8.40 (9H) and 8.60 (9H). IR (in Nujol): 1595 cm^{-1} (C=N). UV: λ_{max}^{EtOH} 232 (log ε 4.20), 299 (4.49), 301 (4.50) and 321 mμ (4.21). The UV spectrum was in good agreement with that of 2-phenylbenzoxazole.[22]

Found: C, 81.96; H, 8.43; N, 4.51%. Calcd for $C_{21}H_{25}NO$: C, 82.04; H, 8.20; N, 4.56%.

Reaction of TBA with Benzoyl Peroxide (BPO). A mixture of TBA (13 g, 0.050 mol) and BPO (13 g, 0.054 mol) in 200 m*l* of benzene was allowed to stand overnight at room temperature. After a large amount of white crystals (ppt-1, 2.75 g) were filtered off, the reaction solution was shaken with aqueous sodium carbonate to remove benzoic acid (5.5 g, 83%) and then dried over anhydrous sodium sulfate. Again white crystals (ppt-2, 1.79 g) precipitated, after filtration of which the benzene was evaporated under reduced pressure and petroleum ether was added. After precipitates thus obtained (ppt-3, 3.40 g) were filtered off, the solvent was removed completely under reduced pressure, leaving slightly reddish oily material (7.66 g). The IR spectra of ppt-1, ppt-2 and ppt-3 (7.94 g, 49% in total) were in entire agreement with that of VII.

The slightly reddish oil, VI, showed satisfactory analytical result without further purification. IR (neat): 3310 (N–H) and 1720 cm^{-1} (C=O). NMR: τ 8.93 (9H), 8.55 (18H), 3.83 (2H), 2.35—2.70 (m, 3H), 1.75—2.10 (m, 2H) and 0.60 (1H, broad).

Found: C, 78.50; H, 9.70; N, 3.30%. Calcd for $C_{25}H_{35}NO_2$: C, 78.68; H, 9.25; N, 3.67%.

The oily material (5.6 g) was chromatographed on silica gel. 2,2′,4,4′,6,6′-Hexa-*t*-butylazobenzene (XI, 0.33 g, 2%), 2,6-di-*t*-butyl-4-benzoyloxyaniline (XII, 1.76 g, 39%) and VII (1.69 g, 37%), mp 230—232°C, were eluted with petroleum ether, benzene and ether, respectively.

The azobenzene (XI) was identified by comparison of the UV spectra (λ_{max}^{EtOH}, 470 (ε 617) and 314 mμ (14, 200)), and the melting point (237—238°C) with data of an authentic sample.[7]

The aniline (XII) was a white solid and recrystallized from petroleum ether, mp 134—135°C. NMR: τ 8.51 (18H), 5.95 (2H), 2.95 (2H), 2.25—2.55 (m, 3H) and 1.50—1.85 (m, 2H).

Found: C, 77.82; H, 8.66; N, 4.09%. Calcd for $C_{21}H_{27}NO_2$: C, 77.50; H, 8.36; N, 4.30%.

When a mixture of ppt-2 and ppt-3 was chromatographed on alumina, a trace of white crystals was eluted with dichloromethane. It melted at 256—258°C after recrystallization from carbon tetrachloride. The IR spectrum showed strong bands at 3280 and 1638 cm^{-1}. It was tentatively identified as 2,4,6-tri-*t*-butylbenzanilide.

Found: C, 81.10; H, 10.02; N, 4.33%. Calcd for $C_{25}H_{35}NO$: C, 82.14; H, 9.65; N, 3.83%.

From the petroleum ether-soluble oil obtained by another experiment using 5.0 g (0.019 mol) of TBA and 5.0 g (0.021 mol) of BPO, VIII (0.1 g, 2%) was isolated by sublimation under vacuum, mp 167—170°C.

The authors are grateful to Professor Osamu Simamura for his kind guidance and helpful discussions.

BULLETIN OF THE CHEMICAL SOCIETY OF JAPAN VOL. 42 3565—3571 (1969)

Triazene Rearrangement. III.*[1] A Kinetic Study of the Rearrangement of *N*-Methyldiaryltriazenes

Takashi YAMADA*[2]

Department of Chemistry, Faculty of Science, Kyoto University, Sakyo-ku, Kyoto

(Received July 22, 1969)

The rate constants of the hydrochloric acid-catalyzed rearrangement of *N*-methyldiaryltriazenes were determined in 95% aqueous ethanol in the presence of *N*-methylaniline. Electron-donating substituents on the diazo-part in triazene promoted the rearrangement. A Hammett plot of the rate constants gave a good straight line. The negative ρ-value (−3.63 at 30.0°C) and the large positive values of the entropy of activation suggested that the rate-determining step in this rearrangement is the dissociation of protonated triazene; this is in contrast with the case of the Friswell-Green mechanism. This theory was suppoted by such a solvent effect as that the rate decreased a little as the polarity of the solvent increased. The kinetic behavior of triazenes in the absence of *N*-methylaniline, and the incorporation of *N*-methyl-*o*-toluidine into the product in the rearrangement of 1-*p*-chlorophenyl-3-methyl-3-phenyltriazene (Id), were also discussed in connection with the above mechanism.

On the mechanism of the triazene rearrangement, several product studies[1] have thus far been presented. As a result, Friswell-Green's mechanism[2] prevails, though a few objections[3] have been offered against it.

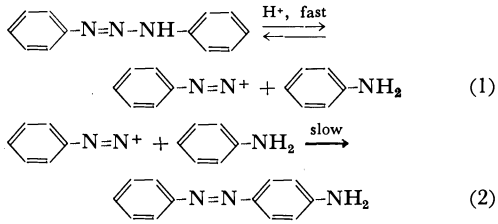

(1)

(2)

In our previous papers,[4] Friswell-Green's mechanism was supported by the quantitative analyses of the products, which were found to contain the added amine in the rearrangement.

However, there have been few kinetic studies of the mechanism of the triazene rearrangement; Goldschmidt *et al.*[5] determined the order of reaction in the rearrangement of 1,3-diphenyltriazene, but they could not clarify the details of the reaction mechanism. Yokojima[6] insufficiently examined the effect of amines upon the reaction rate in ethanol.

In this paper, the author will report on the substituent effect, the solvent effect, and the thermodynamics of activation and will discuss the mechanism of the triazene rearrangement in more detail.

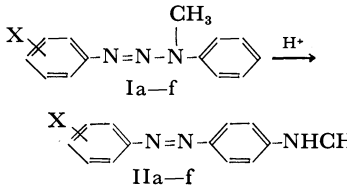

Ia—f

IIa—f

(3)

X = { a : *p*-OCH_3 b : *p*-CH_3 c : *m*-CH_3 / d : *p*-Cl e : *p*-$COCH_3$ f : *p*-CN

For this purpose, *N*-methyldiaryltriazene (I) was used, for in it 1,3-prototropy[7] can not occur.

*1 Presented at the 21st Annual Meeting of the Chemical Society of Japan, Osaka, April, 1968; Part II of this series: Ref. 4b.

*2 Present address: Laboratory of Chemistry, Faculty of Science, Konan University, Okamoto, Higashinada-ku, Kobe.

1) a) For a recent review, see H. J. Shine, "Aromatic Rearrangements," Elsevier Publishing Co., Amsterdam, London and New York (1967), p. 212. b) E. Rosenhauer, *Z. angew. Chem.*, **40**, 575 (1927). c) E. Rosenhauer and H. Unger, *Ber.*, **61**, 392 (1928). d) H. V. Kidd, *J. Org. Chem.*, **2**, 198 (1937). e) K. Clusius and H. R. Weisser, *Helv. Chim. Acta*, **35**, 1524 (1952).

2) R. J. Friswell and A. G. Green, *J. Chem. Soc.*, **47**, 917 (1885); *ibid.*, **49**, 746 (1886).

3) a) H. Goldschmidt, *Ber.*, **24**, 2317 (1891). b) H. Goldschmidt and B. Bardach, *Ber.*, **25**, 1347 (1892). c) V. M. Berezovskii and L. S. Tul'chinskaya, *J. Gen. Chem. USSR*, **31**, 2587, 3371 (1961); *ibid.*, **32**, 846 (1962).

4) a) R. Goto, T. Yamada and A. Sera, *Nippon Kagaku Zasshi (J. Chem. Soc. Japan, Pure Chem. Sect.)*, **87**, 198 (1966). b) T. Yamada, R. Goto, A. Kaji and S. Kurabayashi, *ibid.*, **90**, 207 (1969).

5) a) H. Goldschmidt and R. U. Reinders, *Ber.*, **29**, 1369, 1899 (1896). b) H. Goldschmidt and M. Salcher, *Z. physik Chem.*, **29**, 89 (1899). c) H. Goldschmidt, S. Johnsen and E. Overwien, *ibid.*, **110**, 251 (1924).

6) N. Yokojima, *Kogyo Kagaku Zasshi (J. Chem. Soc. Japan, Ind. Chem. Sect.)*, **31**, 100, 109 (1928).

7) a) M. M. Shemyakin, V. I. Maimind and E. Gomes, *J. Gen. Chem. USSR*, **27**, 1906 (1957). b) V. C. Farmer, R. L. Hardie and R. H. Thomson, "Hydrogen Bonding," Pergamon Press, N. Y. (1959), p. 475. c) T. Mitsuhashi and O. Simamura, *Chem. & Ind.*, **1964**, 578.

Results

Reaction in Ethanol. The rearrangement of triazenes (Ia—f) was carried out in 95% aqueous ethanol in the presence of hydrochloric acid; the first-order rate plots of the reaction are shown in Figs. 1 and 2. The line for Ib (X=*p*-CH_3) is linear, whereas the line for Ia (X=*p*-OCH_3) is concave and the others are convex. Yokojima[6] observed a similar curve for the rearrangement of 1,3-diphenyltriazene in ethanol. This behavior of the lines can be ascribed to the difference in basicity between triazenes (I) and aminoazobenzenes (II),

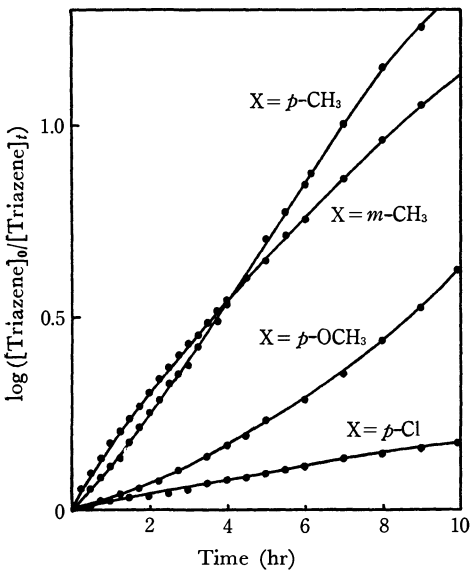

Fig. 1. First-order plots for the rearrangement of triazenes (Ia—d) in 95% aqueous ethanol at 30.0°C.
[Triazene]=5.0×10^{-3} M, [HCl]=0.5×10^{-3} M

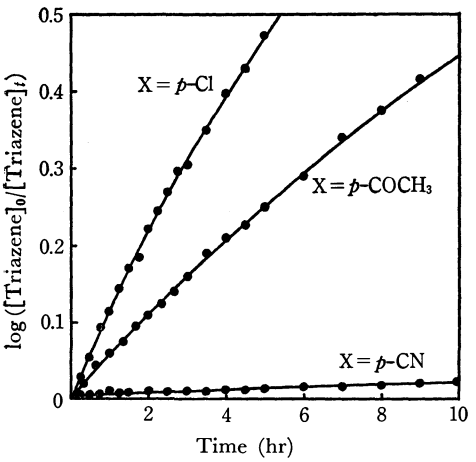

Fig. 2. First-order plots for the rearrangement of triazenes (Id—f) in 95% aqueous ethanol at 30.0°C.
[Triazene]=5.0×10^{-3} M, [HCl]=2.5×10^{-3} M

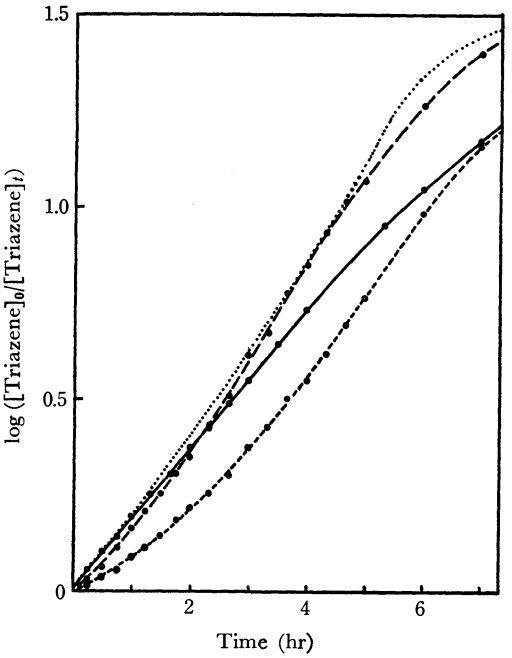

Fig. 3. First-order plots for the rearrangement of triazene (Ia) in the presence of various quantity of *N*-methylaniline.
[Triazene]=5.0×10^{-3} M, [HCl]=1.0×10^{-3} M
[*N*-Methylaniline] = 0 (- - -), 2.5×10^{-3} M (— —), 5.0×10^{-3} M (·····), 10×10^{-3} M (——)

for the first-order plots became linear when the reaction was carried out in the presence of *N*-methylaniline, which seemed to be a stronger base than either Ia—f or IIa—f (Fig. 3). Consequently, the curves of Figs. 1 and 2 suggest that, regarding basicity, Ia>IIa, Ib≒IIb, and I<II for the others.

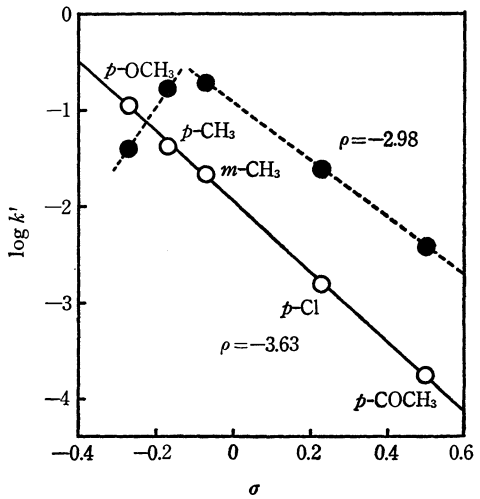

Fig. 4. Hammett's plots for the rearrangement of *N*-methyldiaryltriazene in the presence (—○—) and absence (- -●- -) of *N*-methylaniline. (in 95% aq. EtOH, at 30.0°C).

In Figs. 1 (except for Ia) and 2, it is qualitatively shown that the rearrangement is accelerated by the electron-donating substituents on the diazo-part of triazenes. A Hammett plot of the initial rate constants also shows it (Fig. 4). This acceleration is against the expectation from the mechanism proposed by Friswell and Green, in which the rate-determining step is the *C*-coupling reaction (Eq. (2)).

It is noteworthy that the initial rate of the rearrangement of Ia in the absence of *N*-methylaniline was lower than that of Ib and Ic, and that a Hammett plot was concave (Fig. 4), whereas the initial rate of Ia increased upon the addition of *N*-methylaniline to become greater than the rates of Ib and Ic in the presence of the amine (Figs. 3 and 4).

Rearrangement in the Presence of *N*-Methylaniline. The first-order rate plot was made linear by the addition of *N*-methylaniline of twice as much molar quantity as triazenes, even in the rearrangement of Ia, which may be the strongest base among the Ia—f and IIa—f (Fig. 3). Besides, the presence of the amine may favorably exclude the variation in the relative rate because of the difference in the basicities among I's or among II's, and prevent the decomposition of triazenes.[3]

The rearranaement of I in ethanol containing *N*-methylaniline in the presence of hydrochloric acid was a second-order reaction; *i.e.*, it was first-order with respect to triazene and to the acid (Table 1). The same is true for the case of 1,3-diphenyltriazene in aniline.[5]

Table 2 shows that electron-donating substituents on the diazo-part of triazene promote the rearrangement. A Hammett plot of the rate constants at 30.0°C gives a good straight line (Fig. 4, $\rho=-3.63$, $r=0.999$). In the plot of the rate constants at 40.0°C against σ, the point for *p*-CN deviated from a straight line. This deviation may be attributed to the fact that the protonation of triazene may be inhibited by such additional conjugation as that of III in the ground state of triazene (If).

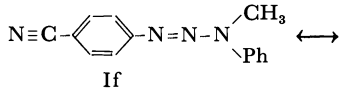

If

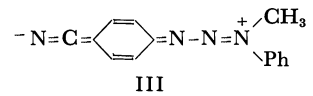

III (4)

Table 3 summarizes the activation parameters calculated from the values in Table 2. It is interesting that the entropies of activation ($\Delta S^{\neq}$) were large positive values.

Table 1. The effect of acid concentration on the rate constants in the rearrangement of 1-*p*-anisyl-3-methyl-3-phenyltriazene*
(in 95% aq. EtOH, at 40.0°C)

$[HCl]\times10^4$ (M)	$k\times10^5$ (sec^{-1})	k' (l/mol·sec)
1.25	4.41	0.353
2.50	8.76	0.350
5.00	17.4	0.349
10.00	33.5	0.335

* [Triazene] $=5.0\times10^{-3}$ M
[*N*-Methylaniline] $=1.0\times10^{-2}$ M, $k'=k/[HCl]$

Table 2. Rate constants for the rearrangement of *N*-methyldiaryltriazenes in 95% aqueous ethanol containing *N*-methylaniline at various reaction temperatures*

Triazene	Substituent X	$k'\times10^2$ (l/mol·sec)		
		30.0°C	40.0°C	50.0°C
Ia	*p*-CH_3O	11.3	34.9	99.9
Ib	*p*-CH_3	4.15	14.7	49.3
Ic	*m*-CH_3	2.21	8.47	29.1
Id	*p*-Cl	0.157	0.650	2.46
Ie	*p*-$COCH_3$	0.0173	0.105	0.408
If	*p*-CN	—	0.0109	—

* [Triazene] $=5.0\times10^{-3}$ M
[*N*-Methylaniline] $=1.0\times10^{-2}$ M

Table 3. Activation parameters for the rearrangement of *N*-methyl-diaryltriazenes in 95% aqueous ethanol

Triazene	Substituent X	E_a kcal/mol	$\Delta S^{\neq}$ (40°C) e.u.
Ia	*p*-CH_3O	21.2	5.0
Ib	*p*-CH_3	24.1	12.5
Ic	*m*-CH_3	25.1	14.6
Id	*p*-Cl	26.8	14.9
Ie	*p*-$COCH_3$	30.7	23.7

Table 4. The influence of water content in aqueous ethanol on the rate constants in the rearrangement of 1-*p*-anisyl-3-methyl-3-phenyltriazene*
(at 40.0°C)

H_2O (vol%)	k' (l/mol·sec)
2.5	0.362
5.0	0.349
10.0	0.320
20.0	0.295

* [Triazene] $=5.0\times10^{-3}$ M
[*N*-Methylaniline] $=1.0\times10^{-2}$ M
[HCl] $=5.0\times10^{-4}$ M.

Further, the rates were measured in ehtanol containing various amounts of water; a rate decrease was observed with the increase in the polarity of the solvent (Table 4).

Competition between *N*-Coupling and *C*-Coupling. In the preparation of triazene (I),

TABLE 5. COUPLING PRODUCTS OF SUBSTITUTED BENZENEDIAZONIUM CHLORIDES AND *N*-METHYLANILINE IN WATER

Substituent	Total yield* %	Ratio Triazene (I) : Aminoazobenzene (II)
p-OCH_3	16.2	>95 : —**
p-CH_3	47.6	98 : 2
m-CH_3	65.8	97 : 3
p-Cl	76.6	97 : 3
p-$COCH_3$	91.7	96 : 4
p-CN	91.9	96 : 4

* not optimum yield.
** II was not detected by TLC.

it was observed by thin-layer chromatography (TLC) that the crude products contained a small amount of aminoazo compounds (II). Therefore, in order to clarify the competition between *C*-coupling and *N*-coupling, the II content in the crude products was examined in the reaction of aryldiazonium with *N*-methylaniline (Table 5) (Eq. (5)).

The total yield of products increased with the electron-withdrawing property of the substituents, as was expected.[8] The formation of only a small amount of II showed that *N*-coupling is much more rapid than *C*-coupling. The introduction of the electron-withdrawing substituent resulted in a small but appreciable increase in the ratio of II to I. When the kinetic results in Table 2 are taken into account, it seems that the formation of II may be not through the rearrangement of triazene, but by a direct *C*-coupling competing with *N*-coupling.

Incorporation of Amine in the Rearrangement. When triazene (Id) was rearranged with hydrochloric acid in the presence of 1 equiv. of *N*-methyl-*o*-toluidine (IV), two products were detected by TLC: IId, the product expected from Id, and V, expected from the incorporation of the added amine (IV) (Eq. (6)).

The fact that the yield of V was 56% evidently shows a very efficient incorporation of the added amine into the product and, thus, the intermolecular aspect of this reaction.

It is interesting to note that the ratio IId/V (33/67) roughly agrees with the ratio of the incorporation of *o*-toluidine into the amine-part of the products in the reaction showin in Eq. (7)(35/65).[4]

Discussion

On the basis of the above results, it seems reasonable to assume as follows regarding the rearrangement of *N*-methyldiaryltriazene:

(1) The reaction process consists of three steps, in accordance with Friswell-Green's mechanism on the rearrangement of 1,3-diphenyltriazene: the protonation of triazene, the dissociation of the

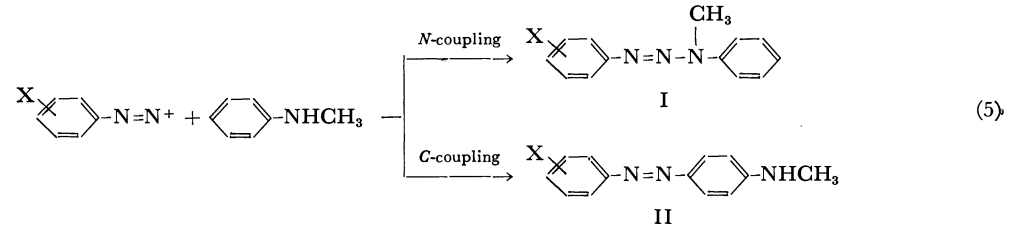

(5)

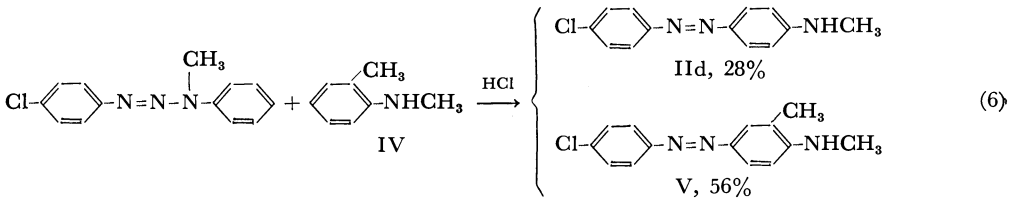

(6)

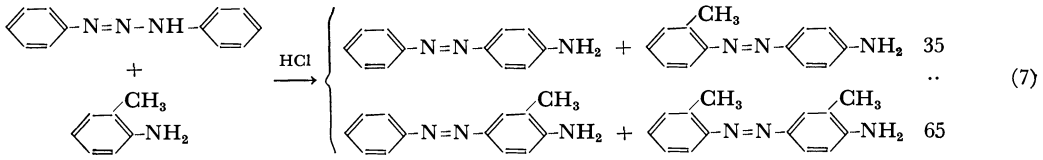

(7)

8) M. J. S. Dewar, "The Electronic Theory of Organic Chemistry," Oxford University Press, Oxford(1949), p. 183.

protonated triazene to the diazonium ion and amine, and the subsequent *C*-coupling of those moieties.

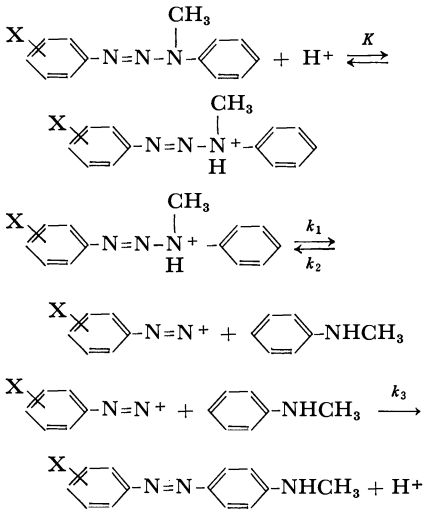

(2) However, the negative ρ-value (Fig. 4) and the large positive entropies of activation (Table 3) show that, in contrast with Friswell-Green's mechanism for 1,3-diphenyltriazene, the rate-determining step in the rearrangement of *N*-methyldiaryltriazene (I) is not the *C*-coupling step but the dissociation step of the protonated triazene to the diazonium ion and amine, *i.e.*, $k_1 < k_3 \ll k_2$. Although a negative ρ-value may also be expected from the substituent effect in the protonation of triazene, the protonation is probably not rate-determining, for it is reasonably assumed to be much more rapid than the dissociation of protonated triazene. If the protonation of triazene were the rate-determining step, $\Delta S^{\neq}$ might be expected to have a negative value.

According to Ingold's criterion,[9] the above consideration is supported by the solvent effect; the increase in the solvent polarity resulted in a small decrease in the rate (Table 4).

(3) As has been remarked above, unusual behavior was observed in the rate plot of the rearrangement of Ia in the absence of *N*-methylaniline (Figs. 1 and 3), and a Hammett plot of the initial-rates was concave (Fig. 4). These results may be interpreted as follows.

In the rearrangement of Ia in the absence of *N*-methylaniline, the *C*-coupling of diazonium with amine may be the rate-determining step (*i.e.*, $k_3 < k_1 \ll k_2$), whereas in the rearrangemnet of Ic—f the rate-determining step may be the dissociation of protonated triazene, even in the absence of the amine ($k_1 < k_3 \ll k_2$) and Ib may have an intermediate character. Such a change in the rate-determining step may cause the curve of a Hammett plot to be concave.

The increase in the basicity of triazene caused by the electron-donating substituent undoubtedly results in the rate decrease. The difference in ρ-values shown in Fig. 4 (-3.63 in the presence of *N*-methylaniline and -2.98 in its absence) is probably due to this effect. However, the decrease in Ia is too large to be ascribed to the same effect.

The enhancement of the initial-rate observed when a small quantity of *N*-methylaniline was added may be because the rate-determining step lies in the *C*-coupling.

(4) In our previous papers,[4] we supported Friswell-Green's mechanism because, judging from the results of the product analysis, the rate-determining step of the triazene rearrangement seemed to be the *C*-coupling reaction.

However, the efficient incorporation of the added amine, *N*-methyl-*o*-toluidine, into products was also observed in the rearrangement of Id in which the rate-determining step was clearly, on the basis of the kinetic results, the dissociation of protonated triazene. That is, the incorporation might well occur if the relative rate were $k_3 \ll k_2$ whether the rate-determining step is the *C*-coupling or the dissociation of protonated triazene. Therefore, on the rearrangement of the 1,3-diphenyltriazene previously discussed on the basis of only the product studies of the incorporation reaction,[4] further kinetic study is desirable.

Experimental*3

Materials. *The triazenes (I)* were prepared by the reaction of the corresponding aryldiazonium chlorides and *N*-methylaniline by the usual procedure;[10] they were purified by several recrystallizations from ethanol. The triazene (If) was purified by elution chromatography over activated alumina, using benzene as an eluent, and by recrystallization from ethanol.

Ia: mp 59.5—60.0°C (lit,[11] 59.8—60.2°C, lit,[12] 61°C), Ib: mp 66—67°C (lit,[11] 67—67.8°C, lit,[12] 66.5—68°C), Ic: mp 63.5—64.5°C (lit,[12] 67°C), Id: mp 87—88°C (lit,[11] 86.7—88.1°C), Ie: mp 85—85.5°C, bright yellow needles;

Found: C, 70.88; H, 6.11; N, 16.42%. Calcd for $C_{15}H_{15}N_3O$: C, 71.13; H, 5.97; N, 16.59%.

If: mp 120—120.5°C, bright yellow prisms;

Found: C, 71.36; H, 5.10; N, 23.70%. Calcd for $C_{14}H_{12}N_4$: C, 71.17; H, 5.12; N, 23.71%.

Aminoazobenzene Derivatives (II). These were prepared by the condensation of nitrosobenzene derivatives with

9) C. K. Ingold, "Structure and Mechanism in Organic Chemistry," Cornell University Press, Ithaca, N. Y. (1953), p. 345.

*3 All melting points are uncorrected. A Hitachi Perkin-Elmer 139 UV-VIS spectrophotometer was used for the ultraviolet and visible spectrophotometric measurements.

10) W. W. Hartman and J. B. Dickey, "Organic Syntheses," Coll. Vol. II, p. 163 (1943).

11) R. F. Day, T. W. Campbell and G. M. Coppinger, *J. Am. Chem. Soc.*, **73**, 4687 (1951).

12) L. Hunter, *J. Chem. Soc.*, **1937**, 320.

TABLE 6. THE ANALYTICAL DATA AND PHYSICAL CONSTANTS OF 4-(*N*-METHYL)-AMINOAZOBENZENES (II)

Aminoazo-benzene	Preparative method	Mp °C	Analysis (calcd)		
			C%	H%	N%
IIa	B	147—148	69.64	6.41	17.45
			(69.69)	(6.27)	(17.42)
IIb	A	104.5—105.5	74.36	6.89	18.47
			(74.64)	(6.71)	(18.65)
IIc	B	111.5—112.5	74.58	6.80	18.88
			(74.64)	(6.71)	(18.65)
IId	A	124—125	63.83	4.83	17.24
			(63.54)	(4.92)	(17.10)
IIe	B	170—171	70.86	6.26	16.62
			(71.13)	(5.97)	(16.59)
IIf	A	192.5—193.5	71.37	5.10	23.91
			(71.17)	(5.12)	(23.71)

TABLE 7. THE ANALYTICAL DATA AND PHYSICAL CONSTANTS OF X-SUBSTITUTED-PHENYLAZO-*N*-METHYLFORMANILIDES

Substituent X	Mp °C	Analysis (calcd)		
		C%	H%	N%
p-CH_3	111.8—112.6	71.39	6.12	16.67
		(71.12)	(5.97)	(16.59)
p-Cl	148—149	61.19	4.45	15.45
		(61.43)	(4.42)	(15.35)
p-CN	156—157	68.43	4.68	21.15
		(68.17)	(4.58)	(21.20)

TABLE 8. ELECTRONIC SPECTRAL DATA OF TRIAZENES (I) AND AMINOAZOBENZENES (II) (Solvent : EtOH)

Substituent X	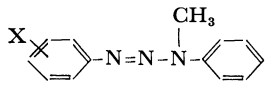 (I)			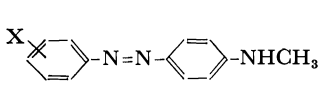 (II)	
	λ_{max} mμ ($10^{-4}\varepsilon$)			λ_{max} mμ ($10^{-4}\varepsilon$)	
p-CH_3O	236 (1.47)	296 (1.12) 308 (1.05)	351 (1.91)	251 (1.03)	401 (3.04)
p-CH_3	237 (1.39)	296 (0.91)	345 (2.00)	253 (0.98)	401 (2.86)
m-CH_3	236 (1.69)		343 (1.87)	253 (0.97)	402 (2.82)
p-Cl	236 (1.73)	295 (0.97)	346 (2.14)	266 (0.83)	411 (3.03)
p-$COCH_3$	241 (1.62)		365 (2.82)	279 (1.17)	438 (3.22)
p-CN	241 (1.91)		358 (2.60)	271 (1.22)	440 (3.32)

p-amino-*N*-methylformanilide, followed by hydrolysis[13] (Method A) or by the rearrangement of triazenes (Method B). The II derivatives were then purified by several recrystallizations from ethanol.

The analytical data and physical constants of II and a few *N*-formyl-derivatives of II are summarized in Tables 6 and 7. The electronic spectral data of I and II are summarized in Table 8.

4'-Chloro-3-methyl-4-N-methylaminoazobenzene (V). This was prepared by the reaction of *p*-chlorobenzenediazonium chloride with *o*-methyl-*N*-methylaniline (bp 104—107°C/28 mmHg):[14] this mixture was stirred at room temperature for several hours without any isolation of the triazene initially produced; the dark-red material precipitated was recrystallized from ethanol containing alkali to give pure V as red needles with a melting point of 138.2—138.8°C. UV, λ_{max} ($\varepsilon\times10^{-4}$) 272 mμ (1.11), 412 mμ (3.02) (in ethanol).

Found: C, 64.95; H, 5.47; N, 16.27%. Calcd for $C_{14}H_{14}N_3Cl$: C, 64.74; H, 5.43; N, 16.18%.

Kinetic Measurements. A little less than 95 m*l* of an ethanol solution containing 5.0×10^{-4} mol of tri-

13) *cf.* F. Witt, *Ber.*, **45**, 2380 (1912).

14) This compound was prepared according to the procedure of R. M. Roberts and P. J. Vogt; R. M. Roberts and P. J. Vogt, "Organic Syntheses," Coll. Vol. IV, p. 420 (1963).

azene and 1.0×10^{-3} mol of *N*-methylaniline was placed in a 100-m*l* measuring flask covered with aluminum foil in order to exclude all light; it was then kept at an appropriate reaction temperature in a thermostated water bath. After about an hour, 5 m*l* of aqueous hydrochloric acid was pipetted into this solution, and the entire solution was made up to volume with ethanol. Aliquots (1 m*l* each) were removed at intervals and put into 10-m*l* measuring flasks containing a sodium hydroxide solution (1 m*l*) in concentrations enough to neutralize the catalytic acid. The solution was made up to volume with ethanol, and, further, the solution was diluted ten times with ethanol to be used as the sample for the optical density measurements. All these samples were kept in the dark.

The optical densities were measured at two different wavelengths, 343—365 mμ (λ_{max} for I) and 400—440 mμ (λ_{max} for II) (see Table 8); the data were then treated in the manner previously described[15] to give the concentrations of the triazene remaining and of the aminoazobenzene produced. The reaction rate constants were evaluated by the graphical method. A typical example is shown in Fig. 5. As the rate constants of the disappearance of I were found to agree with those

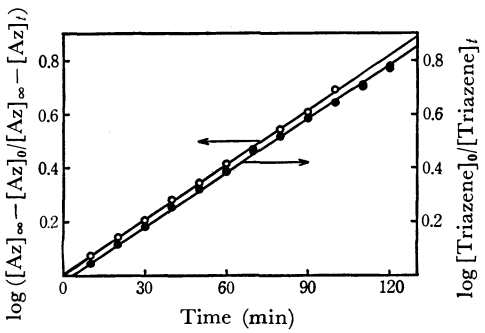

Fig. 5. Typical first-order plots for the rearrangement of triazene (Ib) in 95% aqueous ethanol at 50.0°C. (Az=aminoazobenzene (IIb)) [Triazene]$=5.0\times10^{-3}$ M, [HCl]$=0.5\times10^{-3}$ M, [*N*-Methylaniline]$=10\times10^{-3}$ M

15) For example, see H. H. Jaffé and M. Orchin, "Theory and Applications of Ultraviolet Spectroscopy," John Wiley & Sons, Inc., New York (1962), p. 557.

of the formation of II, the former are summarized in Table 2.

Competition between *N*-Coupling and *C*-Coupling. A solution of the diazonium salt prepared in the usual way from 0.01 mol of the corresponding aniline (in 15 m*l* of water), 3 m*l* of the concentrated hydrochloric acid, and 0.67 g of sodium nitrite (in 3.5 m*l* of water at 0— −2°C was added to a cold solution of *N*-methyl-aniline (1.07 g, 0.01 mol) in 6% aqueous hydrochloric acid (6 m*l*). The mixture was stirred for 10 min at −3——5°C. Then, to this mixture, a solution of 4.5 g (0.033 mol) of crystalline sodium acetate dissolved in 10 m*l* of water was added, and the stirring was continued for 30 min, keeping the temperature below 0°C. The precipitate of triazene produced was filtered, washed with cold water, and then dried over calcium chloride in a desiccator for a day.

The ratios of I to II in the products not still purified were obtained by the spectrophotometric method described above (Table 5).

Incorporation of *N*-Methyl-*o*-toluidine in the Rearrangement of Triazene (Id). Id (248 mg, 10^{-3} mol) was rearranged by the action of 0.1 N aqueous hydrochloric acid (2 m*l*) in ethanol (50 m*l*) containing *N*-methyl-*o*-toluidine (121 mg, 10^{-3} mol) at 40°C for several days. After TLC showed that all the triazene had been consumed, the reaction mixture was neutralized with a 0.05 N aqueous sodium hydroxide solution (5 m*l*). TLC (Merck silica gel G, *n*-hexane-benzene (3 : 1)) showed two main products, namely, IId and V, and a trace of two products which might be *ortho*-rearranged products. 2′,3-Dichloro-4-aminoazobenzene (VI) was added to the solution as an internal standard. Each component was separated by TLC on silica gel and was extracted with ethanol. The yield was determined from the intensity of the maximum absorption of each extract in an electronic spectrum. The extinction coefficients used were: Id $\varepsilon_{411\ m\mu}=30300$, V $\varepsilon_{412\ m\mu}=30200$, and VI $\varepsilon_{397\ m\mu}=25700$ (in ethanol).

The author wishes to thank Professor Ryōzō Gotō for his helpful discussions and encouragement throughout this work. He is also indebted to Professors Aritsune Kaji and Jun-ichi Hayami for their valuable discussions.

BULLETIN OF THE CHEMICAL SOCIETY OF JAPAN VOL. 42 3572—3575 (1969)

n–π^* Electronic Spectra of 2-Methyl-1,4-naphthoquinone in the Vapour Phase

G. D. BARUAH, S. Nath SINGH and R. S. SINGH

Spectroscopy Department, Banaras Hindu University, Varanasi-5, India

(Received January 13, 1969)

The visible emission glow of 2-methyl 1,4-naphthoquinone has been excited by an uncondensed transformer discharge in the presence of flowing vapour of benzene. The vapour absorption spectrum of the molecule has also been investigated in the region 4900—3800 Å at different temperature.

The wide occurrence of quinones in nature and their essential role in photochemistry makes the understanding of their electronic structure a most important matter. In recent years many interesting papers have appeared, both experimental and theoretical, on spectroscopic investigations of quinones. We have undertaken studies of quinone, and the sensitized emission spectra involving n–π^* electronic transitions of p-benzoquinone,[1] 1,4-naphthoquinone[2] and 9,10-anthraquinone[3] molecules in the vapour phase have already been reported.

The near ultraviolet absorption spectrum of 2-methyl-1,4-naphthoquinone (2-MeNQ) in solution[4] and vapour[5] phases have been studied and the absorption maxima at 40804 and 30294 cm^{-1} reported. The phosphorescence spectrum of the molecule in methyl cyclohexane at 77°K has been studied by Kuboyama.[6] He reported a system consisting of seven peaks at 20115, 19737, 18970, 18513, 18062, 17386 and 16858 cm^{-1} and assigned it to n–π^* (triplet-singlet) transition. However, no work in the vapour phase of the molecule has been done so far in the visible region. This paper deals with the electronic emission and absorption spectra in the vapour phase.

1) M. G. Jayswal and R. S. Singh, *Indian J. Pure & Appl. Phys.*, **2**, 358 (1964); *J. Mol. Spect.*, **17**, 6 (1955); *Spectrochim. Acta*, **21**, 1957 (1967).

2) S. N. Singh and R. S. Singh, *Indian J. Pure & Appl. Phys.*, **5**, 394 (1967).

3) S. N. Singh and R. S. Singh, *ibid.*, **5**, 342 (1967).

4) C. Daglisch, *J. Am. Chem. Soc.*, **72**, 4859 (1952); K. Macbeth, J. R. Price and F. L. Winzor, *J. Chem. Soc.*, **1935**, 325; R. A. Morton and W. T. Earlom, *ibid.*, **1941**, 159.

5) S. N. Singh and R. S. Singh, *Indian J. Pure & Appl. Phys.*, **5**, 430 (1967).

6) A. Kuboyama, Reprints from the International Conference on Photochemistry, "Phosphorescence Bands of Quinones," Tokyo (1965), p. 117.

7) S. N. Singh, Ph. D. thesis, Banaras Hindu University, 1968.

Experimental

The emission spectrum of 2-MeNQ vapour was excited by an uncondensed transformer discharge in the presence of the flowing vapour of benzene employing π-type discharge tube. The bright yellowish glow was photographed by a Fuess Glass Spectrograph employing Kodak IF plates in six hours. The absorption spectrum was also photographed on the same spectrograph employing HP-3 plates with slit width of 40 μ. The absorption cell used was a quartz to Pyrex graded seal cell of length 120 cm enclosed in an electric furnace. A tungsten filament lamp was used as the source of continuum in the visible region. All the bands were measured on a Hilger L-76 comparator.

Results

The emission spectrum lies in the region 22078—14663 cm^{-1} and consists of 35 bands. The observed bands are broad, diffuse and intense. The important feature observed is the irregular intensity distribution of bands like that of other p-quinones.[1-3] The bands in the region 22215—20825 cm^{-1} are weak as compared to those in the region 20827—17236 cm^{-1} and intensity abruptly falls again on the longer wavelength side. The spectrogram is shown in Fig 1. The entire absorption spectrum in the visible region lies in the region 20257—26659 cm^{-1} and is divided into two groups, developing at different temperatures with the same cell length of 120 cm. At about 150°C one system of bands develops in the region 22215—27019 cm^{-1} and while increasing the temperature up to 190°C three broad and very diffuse bands develop in the region 20402—22215 cm^{-1}. The bands in the former region are also diffuse but distinct. The observed spectrum is shown in Fig. 2. The analyses of the bands observed in emission and absorption spectra are given in Tables 1 and 2 respectively. Table 3 includes the comparison of the ground and excited state frequencies with those of Raman and infrared.[7]

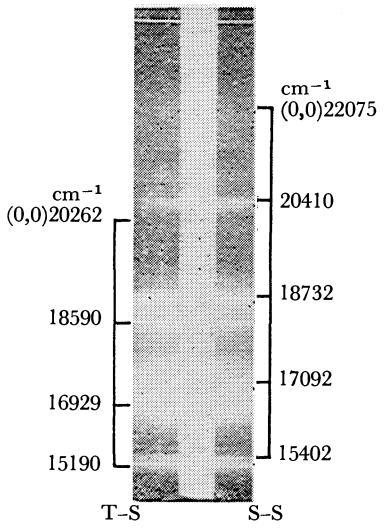

Fig. 1. Emission spectrum of 2-ethylnaphthoquinone.

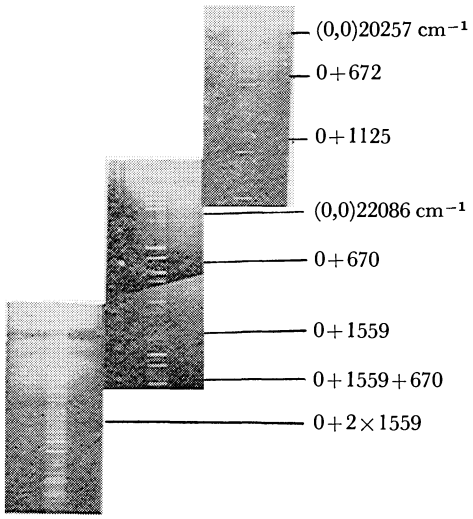

Fig. 2. Absorption spectrum of 2-methylnaphthoquinone.

Analysis and Discussion

The molecular symmetry C_{2v} of 1,4-naphthoquinone is reduced to C_s when a CH_3 group lying in the plane of the molecule replaces a hydrogen atom in its 2-position. Assuming C_s symmetry for the molecule both in the ground as well as in the excited state, the analyses of emission and absorption spectra have been given below.

In emission spectrum, the medium strong band at 22075 cm^{-1} on the shorter wavelength side of the spectrum has been taken as the (0−0) band of the system, corresponding to that of NQ[2] at 21945 cm^{-1}. This band in the absorption spectrum is identified at 22086 cm^{-1}. On the lower frequency side to this there are three more bands

Table 1. Analysis of the emission bands of 2-methyl-1,4-naphthoquinone

Wave number cm^{-1}	Intensity	Separation from 0–0 band	Assignment
22075	4	0	0−0
22005	2	70	0−70
21931	1	144	0−144 or 0−2×70
21860	1	215	0−144−70
21701	2	374	0−374
21616	2	459	0−459
21472	1	603	0−459−144
21382	4	692	0−692
20792	4	1282	0−1282
20718	2	1357	0−1357 or 0−1282−70
20410	7	1665	0−1665
20262	3	1813	0−1665−144
19947	2	2128	0−1665−459
19804	1	2270	0−1665−459−144
19197	1	2878	0−1665−692−459−70
19038	2	3038	0−1665−1357
18732	10	3343	0−2×1665
18590	10	3485	0−2×1665−144
18276	1	3799	0−2×1665−459
17913	2	4162	0−2×1665−459−372
17605	1	4470	0−2×1665−692−459
17477	1	4598	0−2×1665−1282
17092	8	4983	0−3×1665
16929	5	5146	0−3×1665−144
16610	6	5465	0−3×1665−459
16344	1	5731	0−3×1665−2×374
16017	1	6058	0−3×1665−2×459−144 or 0−3×1665−692−372
15908	1	6267	0−3×1665−1282
15619	3	6456	0−3×1665−2×692−70
15402	4	6674	0−4×1665
15190	5	6966	0−4×1665−144−70
15031	1	7044	0−4×1665−374

Table 2. Analysis of the absorption spectrum of 2-methyl-1,4-naphthoquinone

Wave-number	Intensity	Separation from 0–0 band	Assignment
Cell length 120 cm, Temp. 190°C			
20257	10	0	0−0
20929	2	672	0+672
21382	5	1125	0+1125
Cell length 120 cm, Temp. 150°C			
22086	8	0	0−0
22145	6	59	0+59
22449	4	363	0+363
22756	5	670	0+670
23120	3	1034	0+670+363
23344	5	1258	0+1258
23645	5	1559	0+1559
24006	2	1920	0+1258+670
24384	1	2298	0+1258+670
25107	2	3121	0+2×1559

Table 3. Correlation of ground and excited state frequencies for 2-methylnaphthoquinone

Ground state frequencies			Excited state frequency	Mode of vibration
Raman[7]	Infrared[7]	Emission	Absorption	
215(2)		215(1)	195(5)	a'' C=O bending o. p.
380(3)		374(1.5)	363(8)	a' C=O bending i. p.
464(7)	460(5)	459(2)		a' skeletal deformation
698(4)	693(8)	692(4)	670(8)	a' ring breathing
890(1)	885(5)		843(1)	a' C-CH_3 stretching
1360(2)	1358(5)	1357(2)		a' C-H bending (symmetric in CH_3 group)
1662(10)	1670(10)	1665(7)	1559(3)	a' C=O stretching

i. p.=in-plane; o. p.=out-of-plane.

extending upto 20262 cm^{-1} and seems to belong to some other electronic transition. Since this latter system does not have any vibrational structure, an adequate analysis is not possible. However these bands will be discussed along with the phosphorescence bands. The medium strong band at 21701 cm^{-1} in the emission spectrum is associated with a frequency 374 cm^{-1} which corresponds to the Raman line 380 cm^{-1}. The excited state counterpart of this vibration is obsered in the absorption spectrum at 22449 cm^{-1} with a separation of 363 cm^{-1} from the (0-0) band. This frequency is suggested to be a C=O bending mode of vibration in the molecular plane. The strong band at 21383 cm^{-1} involves the ground state frequency 692 cm^{-1} in the emission and at 22756 cm^{-1} with a corresponding excited state frequency 670 cm^{-1} in the absorption spectrum. In the Raman spectrum this frequency is found to be 698 cm^{-1} and assigned to ring breathing mode of vibration. Another moderately intense band at 20793 cm^{-1} with a difference of 1282 cm^{-1} from the (0-0) band in the emission spectrum may be correlated to Raman frequency 1306 cm^{-1}. The excited state frequency is observed to be 1258 cm^{-1} associated with a strong band at 23344 cm^{-1} in the absorption spectrum. In the emission spectrum the strong band at 20410 cm^{-1} is due to excitation of a totally symmetric C=O stretching mode of vibration with value 1665 cm^{-1}. This frequency forms the progression in the spectrum and appears up to four quanta as well as in combinations with other frequencies.

The bands with two and three quanta of C=O stretching mode of vibrations are more intense than those of one and four quanta, indicating the increase in the equilibrium internuclear distance for the excited electronic state. On this account, the (0-0) band is weak and intense bands result, corresponding to the transition to the higher vibrational sublevels of the ground state rather than the lower ones. The difference between the successive bands involving the higher quanta of this vibration decreases in magnitude and gives the evidence of the anharmonicity in C=O vibration. The excited state counterpart of this vibration is found to be associated with a band at 23645 cm^{-1} having a separation of 1559 cm^{-1} from the (0−0) band in the absorption spectrum. Most of the other bands observed in the emission and absorption spectra are explained as combinations, overtones and quanta of this vibration. In regard to the nature of electronic transition involved, the system may be assumed to be due to n–π^* ($^1A'$–$^1A'$) transition agreeing with n–π^* (singlet-singlet) transition of NQ.[3] This is further confirmed by a blue shift of 130 cm^{-1} in the (0−0) band on 2-methyl substitution in NQ.

Comparison with Phosphorescence Bands. It has been observed that some of the bands in the present work agree well with those reported from phosphorescence in rigid glass solution and it is therefore worthwhile to compare them. Assuming the first intense band of the phosphorescence spectrum at 20115 cm^{-1} as the origin of the system, the band at 20262 cm^{-1} in the vapour emission spectrum may be taken to correspond to it, in the light of which a vibrational analysis has been suggested for these bands and shown in Table 4.

The totally symmetric vibrations 378 cm^{-1} (C=O bending), 1145 cm^{-1} (C-H bending) and 1672 cm^{-1} (C=O stretching) are found to be superposed on this (0−0) band of the new electronic system. The assignment of this new system was considered preferable for interpreting the unusual intensity distribution associated with the bands at 20262, 18590 and 16929 cm^{-1} analysed as $0-n\times 1665-144$, where $n=1, 2, 3$ respectively in the S–S system. In the case this system can be identified with the one observed in phosphorescence, it is due to (S–T) transition. The C=O stretching mode of vibration in both S–T vapour emission and phosphorescence spectra are prominent and appears strongly in combination and overtones.

The life time of the phosphorescence glow has been reported to be 0.001 sec which is favourable for a triplet-singlet emission under the present experimental conditions. Thus as presumed in

Table 4. Comparison of phosphorescence bands with the present emission and absorption bands of 2-methyl-1,4-naphthoquinone

Phosphorescence band (rigid glass solution) Kuboyama[6]	Absorption band (vapour) present work	Emission band (vapour) present work	Assignment
	21382 (5)		0+1125
	20929 (2)		0+672 (ring breathing)
20115 vs	20257 (10)	20262 (3)	0−0
19738		19947 (2)	$0-\nu_1$ (378 cm^{-1})
18970		19038 (2)	$0-\nu_2$ (1145 cm^{-1})
18513 vs		18590 (10)	$0-\nu_3$ (1672 cm^{-1})
18061		18276 (1)	$0-\nu_3-\nu_1$
17386		17477 (1)	$0-\nu_3-\nu_2$
16859 s		16929 (5)	$0-2\times\nu_3$
		15190 (4)	$0-3\times\nu_3$

vs=very strong, s=strong

Table 4, some of the bands of 2-MeNQ may be assigned to an n–π^* ($^3A'$–$^1A'$) transition in agreement with that of NQ.[3] However, such assignment should await further confirmation.

The authors are thankful to Professor N. L. Singh for his keen interest in the work and to Dr. M. G. Jayswal for valuable suggestion. One of them (S. N. S.) is grateful to C. S. I. R, New Delhi for financial assistance.

NOTES

BULLETIN OF THE CHEMICAL SOCIETY OF JAPAN VOL. 42 3576—3577 (1969)

A Thermodynamic Formulation of Reaction Rates

Naokata TAKEYAMA

Faculty of Science and Engineering, Saga University, Honjyo-machi, Saga

(Received January 8, 1969)

The purpose of this note is to show a thermodynamical method to formulate a correct expression for the reaction rate proposed by Horiuti *et al.*[1]

In the current theory of rate processes,[2] except for that of Horiuti, the reaction rate is assumed to be c_*/τ, where c_*=concentration of activated complex and τ=lifetime. By equating this rate to that of the kinetic expression kc_Ac_B we obtain

$$k = \frac{1}{\tau}\cdot\frac{c_*}{c_Ac_B} = \frac{K^*}{\tau}, \tag{1}$$

where k=rate constant, and c_A, c_B=concentration of reactant. K^* is interpreted as an equilibrium constant for the formation of an activated complex M* from A and B. However, if we formulate K^* according to the equilibrium theory, we should have

$$K^* = \frac{c_*^{(e)}}{c_A^{(e)}c_B^{(e)}} \tag{2}$$

and

$$\text{reaction rate} = \left\{\frac{1}{\tau}\cdot\frac{c_*^{(e)}}{c_A^{(e)}c_B^{(e)}}\right\} c_Ac_B, \tag{3}$$

where the concentration of each species in an equilibrium state is distinguished from that in a non-equilibrium state by a superscript (e). The difference between the concentrations of a reactant in equilibrium and non-equilibrium states should be reasonably taken into account.

Let us take a reversible reaction

$$\nu_AA + \nu_BB \rightleftarrows \nu_CC + \nu_DD, \tag{4}$$

where ν_X is the stoichiometric coefficient of a species X.

Reactants are supposed to be immersed in a large heat bath of temperature T which stays in equilibrium irrespective of energy exchange with the reactants. Considering the processes of the formation of an activated complex

$$\nu_AA + \nu_BB \rightarrow M^* \quad \text{(in initial state)} \tag{5.a}$$

and

$$\nu_CC + \nu_DD \rightarrow M^* \quad \text{(in final state)}, \tag{5.b}$$

we introduce the corresponding variables of progress by means of a unilateral variation

$$\vec{\delta}\xi_I = \vec{\delta}c_* = -\nu_A^{-1}\vec{\delta}c_A = -\nu_B^{-1}\vec{\delta}c_B \tag{6.a}$$

and

$$\vec{\delta}\xi_F = \vec{\delta}c_* = -\nu_C^{-1}\vec{\delta}c_C = -\nu_D^{-1}\vec{\delta}c_D, \tag{6.b}$$

where the arrow on the variation notation denotes the unilaterality.

We should mention that the ordinary progress variable for reaction (4) is

$$\begin{aligned}\delta\xi &= -\nu_A^{-1}\delta c_A = -\nu_B^{-1}\delta c_B \\ &= \nu_C^{-1}\delta c_C = \nu_D^{-1}\delta c_D (\gtrless 0),\end{aligned} \tag{7}$$

whose bilaterality comes from

$$\delta\xi = \vec{\delta}\xi_I - \vec{\delta}\xi_F. \tag{8}$$

With respect to the rate of reaction (5.a) or (5.b), we have to express a unidirectional rate of reaction in terms of chemically observable entities restricted to the reactants in (5.a) or (5.b). So, even from phenomenological consideration, we cannot neglect the probability factor for activation multiplied by the term c_*/τ. The activation probability will be obtained by applying Boltzmann's entropy principle as follows.

When we designate the initial or final state by α=I or α=F, and the occupation probabilities that the system under consideration exists in the unactivated and activated states in an α state by W° and W^*, respectively, the activation probability can be written in the form

1) G. Okamoto, J. Horiuti and K. Hirota, *Sci. Papers Inst. Phys. Chem. Res.*, **29**, 223 (1936); J. Horiuti, "Chemistry of Catalysis," (in Japanese), Asakura Book Co., Tokyo (1953).

The author would like to express his sincere thanks to the referee, who kindly informed him that a presupposition in Horiuti's theory was in line with the present result, but was more general. The present treatment seems to enlighten the thermodynamical background of the presupposition on a very elementary level.

2) S. Glasstone, K. J. Laidler and H. Eyring, "The Theory of Rate Processes," McGraw-Hill Book Co., Inc., New York (1941), pp. 13, 187, 286, 348, 402.

$$\left(\frac{W^*}{W^\circ}\right)_\alpha = \exp\left(\frac{\Delta_\alpha S}{R}\right), \tag{9}$$

where $\Delta_\alpha S$ is total entropy change in the activation of (5.a) or (5.b) which may be calculated by

$$\Delta_\alpha S \equiv \left\{\left(\frac{\partial S}{\partial \xi_\alpha}\right)\Delta\xi_\alpha\right\}_{\Delta\xi_\alpha=+1} = \frac{\partial S}{\partial \xi_\alpha}. \tag{10}$$

Here the total entropy S is expressed by

$$S = S_b(T) + \sum_X n_X\left(s_X^\circ - \frac{u_X^\circ}{T} - R\ln c_X\right) + n_*\left(s_*^\circ - \frac{u_*^\circ}{T} - R\ln c_*\right), \tag{11}$$

where $S_b(T)$ is a part in the entropy of heat bath invariant against energy exchange with reactants under energy conservation, whose influence upon the entropy is expressed in terms of $-(\sum_X n_X u_X^\circ/T + n_* u^\circ_*/T)$, where n_X is the number of moles of a reactant X(=A, B, C and D), n_* is the number of moles of M*, and s° and u° are the standard entropy and internal energy per mole of each species. Here the activity of a species to be used in logarithmic term is approximated by concentration.

The unidirectional rate of reaction is defined by

$$\frac{\vec{d\xi_\alpha}}{dt} \equiv \frac{c_*}{\tau}\left(\frac{W^*}{W^\circ}\right)_\alpha = \frac{c_*}{\tau}\exp\left(\frac{\Delta_\alpha S}{R}\right). \tag{12}$$

By means of the relation

$$\Delta_\alpha S = s_*^\circ - \frac{u_*^\circ}{T} - R\ln c_* - \sum_{X\in\alpha}\nu_X\left(s_X^\circ - \frac{u_X^\circ}{T} - R\ln c_X\right), \tag{13}$$

it follows that

$$\frac{\vec{d\xi_\alpha}}{dt} = \frac{1}{\tau}\cdot\exp\left\{\frac{1}{R}(s_*^\circ - \sum_{X\in\alpha}\nu_X s_X^\circ)\right\} \times \exp\left\{-\frac{1}{RT}(u_*^\circ - \sum_{X\in\alpha}\nu_X u_X^\circ)\right\}\prod_{X\in\alpha} c_X^{\nu_X}$$

$$= \frac{1}{\tau}\cdot\exp\left\{-\frac{1}{RT}(f_*^\circ - \sum_{X\in\alpha}\nu_X f_X^\circ)\right\}\prod_{X\in\alpha} c_X^{\nu_X}$$

$$= \frac{1}{\tau}\cdot\exp\left\{-\frac{1}{RT}(f_*^\circ - \sum_{X\in\alpha}\nu_X f_X)\right\}, \tag{14}$$

where $\sum_{X\in\alpha}$ and $\prod_{X\in\alpha}$ show the summation and multiplication referring to the reactants X (=A and B, or C and D) belonging to an α (=I or F) state. $f_X^\circ = u_X^\circ - Ts_X^\circ$ is the standard Helmholtz energy per mole of X, and $f_X = f_X^\circ + RT\ln c_X$.

It should be noted that the rate expression of (14) is derived without using explicitly any condition of "activation equilibrium", that is, $c_* \neq c_*^{(e)}$, and $c \neq c^{(e)}$ for all of X. However, if we use the condition of the equilibrium of activation given by $\Delta_\alpha S = 0$, or

$$\ln\frac{c_*^{(e)}}{\prod_{X\in\alpha}(c_X^{(e)})^{\nu_X}} = \frac{1}{R}(s_*^\circ - \sum_{X\in\alpha}\nu_X s_X^\circ) - \frac{1}{RT}(u_*^\circ - \sum_{X\in\alpha}\nu_X u_X^\circ), \tag{15}$$

the rate expression may be transformed into

$$\frac{\vec{d\xi_\alpha}}{dt} = \left\{\frac{1}{\tau}\cdot\frac{c^{(e)}}{\prod_{X\in\alpha}(c_X^{(e)})^{\nu_X}}\right\}\prod_{X\in\alpha} c_X^{\nu_X}. \tag{16}$$

Finally, with the aid of Eq. (8), the net rate of reaction may be expressed in the form

$$\frac{d\xi}{dt} = \frac{\vec{d\xi_I}}{dt} - \frac{\vec{d\xi_F}}{dt} = \frac{1}{\tau}\cdot\exp\left(-\frac{f_*^\circ}{RT}\right)\left\{\exp\left(\frac{\sum_{X\in I}\nu_X f_X}{RT}\right) - \exp\left(\frac{\sum_{X\in F}\nu_X f_X}{RT}\right)\right\}. \tag{17}$$

In conclusion the present formulation gives a thermodynamical basis to the theory of transition state.

BULLETIN OF THE CHEMICAL SOCIETY OF JAPAN VOL. 42 3578—3580 (1969)

Effects of Temperature and of Mixing on Dielectric Constants of Several Organic Solvents

Etsuo NIKI, Yoshio KAMIYA and Nobuto OHTA

Department of Fuel Engineering, University of Tokyo, Hongo, Bunkyo-ku, Tokyo

(Received March 26, 1969)

It is known that the dielectric constants of the organic solvents are dependent on temperature[1] and that those of binary mixtures are not usually equal to the calculated average values.[2] In other words, the curve obtained by plotting the dielectric constants of mixtures against the molar fraction of one of the components usually shows some curvature. Although much data have been obtained for organic solvents and their binary mixtures at different temperatures, relatively little has been reported on hydrocarbons, inert solvents and their mixtures, which are often used for studies on autoxidation. In the course of our study on the solvent effects in autoxidation,[3,4] we have determined the dielectric constants of tetralin, several inert solvents and their mixtures at temperatures from 25°C to 70°C.

The measured dielectric constants for several pure liquids at different temperatures are summarized in Table 1 together with the values in literature.[5] As a whole, the observed values show good agreement with the reported values. Table 1 shows that the dielectric constants for 9 out of 10 liquids decrease with an increase in temperature. The only exception is that for butyric acid, which increases with an increase in temperature.

Lowry and Jessop[6] found that the following correlation exists between the dielectric constants of liquids and temperature.

$$D = D_0 \exp(-LT) \tag{1}$$

where D_0 and L are constants characteristic for each liquid. The equation

$$\log(D_1 D_2) = L(T_2 - T_1)/2.303 \tag{2}$$

is derived from Eq. (1). In Fig. 1, the logarithm of D_1/D_2 is plotted as a function of $(T_2 - T_1)$ using the measured dielectric constants in Table 1 assuming T_1 to be 298°K. Figure 1 shows that Eq. (2) holds for all the solvents measured. The calculated values of L from the slope of the lines in Fig. 1 for each liquid are given in the last column of Table 1. The value of L varies with solvents by a factor of more than 7. The liquid with high

TABLE 1. DIELECTRIC CONSTANTS AT DIFFERENT TEMPERATURES AND THE VALUES OF L FOR 10 PURE LIQUIDS

Liquid	Dielectric constants measured at					D(°C)[a]	$L \times 10^3$
	25°C	40°C	50°C	60°C	70°C		
n-Decane	2.011	1.986	1.977	1.960	1.949	1.991(20)	0.696
Benzene	2.297	2.278	2.254	2.229	2.200	2.284(20)	0.957
Tetralin	2.771	2.737	2.709	2.686	2.657	2.757(20)	0.931
Butyric acid	2.949	2.977	3.011	3.029	3.063	2.97 (20)	−0.839
Butylstearate	3.120	3.051	3.000	2.949	2.909	3.111(30)	1.57
Anisole	4.331	4.194	4.097	4.000	3.926	4.33 (25)	2.18
Chlorobenzene	5.583	5.366	5.211	5.057	4.909	5.621(25)	2.85
Diethyl maleate	7.560	7.251	7.034	6.834	6.623	8.58 (23)	2.93
Acetophenone	17.48	16.14	15.34	14.63	13.98	17.39 (25)	4.96
Nitrobenzene	34.42	32.05	30.20	28.71	27.35	34.82 (25)	5.12

a) Literature values.[5]

1) E. A. Moelwyn-Hughes, "Kinetics of Reactions in Solution," 2nd Ed., Oxford University Press, London (1947), p. 90; "Physical Chemistry," Pergamon Press, London (1957), p. 853.

2) J. Timmermans, "Physico-chemical Constants of Binary Systems in Concentrated Solutions," Interscience, New York (1959).

3) E. Niki, Y. Kamiya and N. Ohta, This Bulletin in contribution.

4) E. Niki, Y. Kamiya and N. Ohta, *ibid.*, in contribution.

5) J. A. Riddick and E. E. Toops, Jr., "Technique of Organic Chemistry," Vol. VII, "Organic Solvents," ed. by A. Weissberger, Interscience, New York (1955).

6) T. M. Lowry and G. Jessop, *Trans. Chem. Soc.*, **1930**, 782.

Table 2. Dielectric constants for the binary mixtures of tetralin and various solvents at 70°C[a)]

Solvent	Tetralin, vol%				
	80	60	40	20	0
n-Decane	2.514	2.360	2.206	2.069	1.949
Butyric acid	2.674	2.743	2.834	2.937	3.063
Butyl stearate	2.697	2.743	2.806	2.857	2.909
Anisole	2.874	3.126	3.377	3.651	3.926
Chlorobenzene	3.086	3.509	4.017	4.440	4.909
Diethyl maleate	3.360	4.126	4.943	5.811	6.623
Acetophenone	4.269	6.269	8.589	11.21	13.98
Nitrobenzene	6.126	10.27	15.02	21.10	27.35

a) D for pure tetralin at 70°C is 2.657.

Table 3. Dielectric constants for the systems tetralin-nitrobenzene-solvent at 70°C
Tetralin=20 vol%

Solvent	Nitrobenzene/Solvent, vol/vol				
	1/0	3/1	1/1	1/3	0/1
n-Decane	21.10	14.84	9.846	5.503	2.069
Chlorobenzene	21.10	15.63	11.43	7.720	4.440
Acetophenone	21.10	18.42	15.65	13.35	11.21

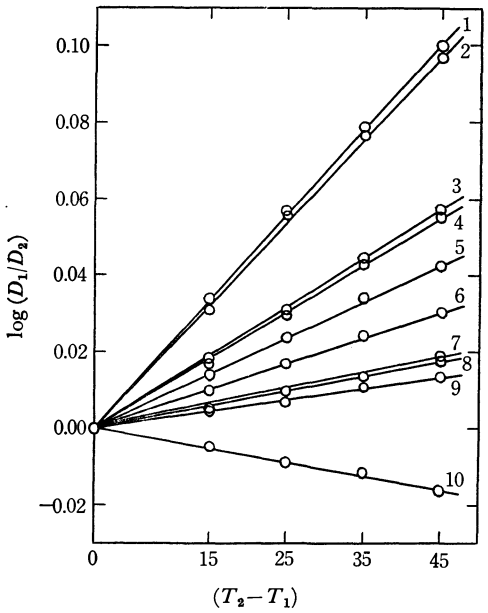

Fig. 1. Variation of dielectric constant with temperature.
1. Nitrobenzene
2. Acetophenone
3. Diethyl maleate
4. Chlorobenzene
5. Anisole
6. Butyl stearate
7. Benzene
8. Tetralin
9. *n*-Decane
10. Butyric acid

dielectric constant gives a large value for L. It is interesting that the value of L for butyric acid is negative in contrast to other liquids.

The dielectric constants for the mixtures of tetralin and various inert solvents were measured at 70°C and the results are summarized in Table 2. As shown in Fig. 2, the plots of the dielectric constants against tetralin concentration give upward

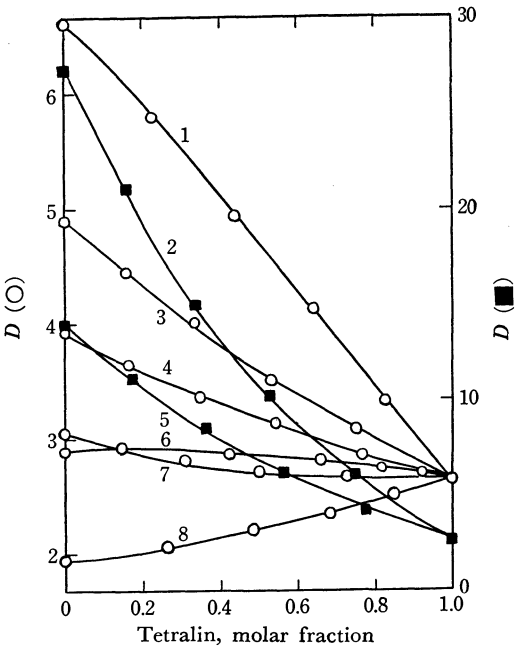

Fig. 2. Dielectric constants of the mixtures of tetralin and solvents at 70°C.
1. Diethyl maleate
2. Nitrobenzene
3. Chlorobenzene
4. Anisole
5. Acetophenone
6. Butyl stearate
7. Butyric acid
8. *n*-Decane

and downward convex curves. In Table 3 are summarized the dielectric constants for the systems of tetralin-nitrobenzene-solvents at 70°C. These values again gave convex curves when plotted as a function of the tetralin concentration.

Experimental

Tetralin, *n*-decane and chlorobenzene were washed successively with sulfuric acid, water, alkali, and water, dried with calcium chloride, and then distilled under reduced pressure of nitrogen. Anisole and nitrobenzene were washed with alkali and water, dried and distilled under reduced pressure. Diethyl maleate and acetophenone were fractionally distilled. Butyric acid and butyl stearate of guaranteed grade were used without further purification. The water content in butyric acid was less than 0.1%.

The dielectric constants were measured at 2Mcps of frequencies using a Dielectric Analyzer Model FAM-3A, Yamato Scientific Instrument Co. Two kinds of dielecric cells were used, one for the solution of low dielectric constant (smaller than 20) and the other for the high dielectric solution (larger than 20). The cell constants for the two cells were determined with several solvents as standard. Since the same apparatus and technique have been used in this study, errors in the measurements will be relative and will not affect the general nature of the conclusion drawn.

BULLETIN OF THE CHEMICAL SOCIETY OF JAPAN VOL. 42 3580—3582 (1969)

μ-Peroxobis(pentacyano)dicobaltate(III) as an Oxidizing Agent

Toshihiko ASAI and Tadashi HARA

Department of Chemical Engineering, Doshisha University, Kamikyo-ku, Kyoto

(Received April 9, 1969)

It has been reported by Haim and Wilmarth[1] that the pentacyanocobaltate(II) (PC-II) is oxidized with oxygen at 0°C to form μ-peroxobis(pentacyano)dicobaltate(III)(POPC), which is decomposed with sulfuric acid to produce hydrogen peroxide.

There have also been several reports concerning the direct epoxidation of acrolein with hydrogen peroxide[2] and of propylene with organic hydroperoxide[3,4] or organic peracid.[5]

Since the possibility of the epoxidation of acrolein and propylene was expected on the basis of the above reports, an attempt was made to epoxidize them with POPC, but the results obtained were negative.

The present paper deals with spectrophotometric and polarographic investigations of the chemical behaviors of POPC to clarify the reason for the negative results.

Experimental

Preparation of POPC. POPC was prepared by oxidizing PC-II with oxygen at 0°C or by dropping a cobalt(II) nitrate solution into a potassium cyanide solution under the passage of oxygen gas at the same temperature. POPC in an aqueous solution was reddish brown and precipitated as crystalline brown needles by addition of methanol. POPC was determined by treating with sulfuric acid and by titrating the hydrogen peroxide produced iodometrically. The yield reached 95.5% under the following conditions; 1150 m*l* oxygen gas/min, 0°C, 30 min (dropping time), 5 : 1 mol ratio (0.1 M Co^{2+}), and 50 m*l* total volume.

Apparatus. A Shimadzu QR-50 spectrophotometer, a Yanagimoto P-8-D polarograph, a Yanagimoto GC-220 gas chromatograph, *etc.* were used.

Results and Discussion

POPC in an aqueous solution was stable for a long time in air or nitrogen atmosphere at 0°C,

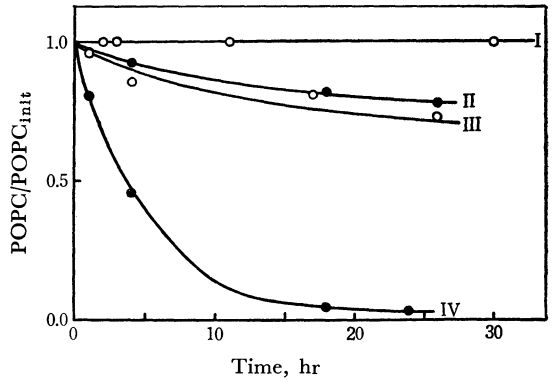

Fig. 1. Thermal stability of POPC.
I $POPC_{init}$: 2.47×10^{-2} M, temperature: 0°C
II $POPC_{init}$: 2.57×10^{-2} M, temperature: 25°C
III $POPC_{init}$: 2.72×10^{-2} M, temperature: 30°C
IV $POPC_{init}$: 2.57×10^{-2} M, temperature: 50°C

1) A. Haim and W. K. Wilmarth, *J. Am. Chem. Soc.*, **83**, 509 (1961).
2) G. B. Payne, *ibid.*, **81**, 4901 (1959).
3) J. Kollar, *Belg. Pat.* 641452 (1964).
4) Halcon International Inc., *Neth. Pat. Appl.*, 6402 137 (1964).
5) N. Ota and J. Imamura, *Kogyo Kagaku Zasshi (J. Chem. Soc. Japan, Ind. Chem. Sect.)*, **69**, 1459 (1966).

but it was decomposed markedly with the rise of temperature to produce pentacyanocobaltate(III) (PC-III) (Fig. 1).

The absorption spectra of POPC, PC-II, PC-III and hexacyanocolaltate(III)(HC-III) are shown in Fig. 2. The absorption of PC-II and PC-III at 310 mμ is so small that the absorption maximum at the same wavelength is attributed to the formation of POPC. There is a linear relationship between the absorbance and the concentration of POPC which was determined by iodometry (Fig. 3).

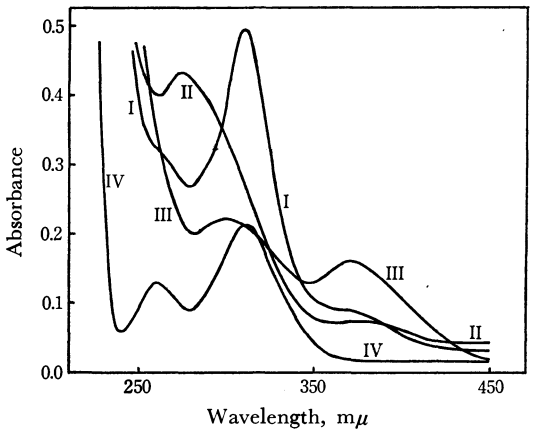

Fig. 2. Absorption spectra.
I POPC; cobalt: 2.50×10^{-4} M
II PC-II; cobalt: 2.50×10^{-4} M
III PC-III; cobalt: 1.00×10^{-3} M
IV HC-III; cobalt: 1.00×10^{-3} M
pH: 12.5, temperature: 0°C

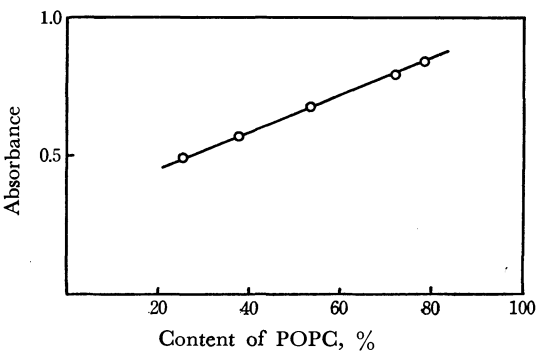

Fig. 3. Calibration curve of POPC at 0°C.
cobalt: 2.50×10^{-4} M, pH: 12.5, wavelength: 310 mμ

The following results were obtained by spectrophotometric investigation: 1) The absorption spectra of POPC solutions prepared by the above-mentioned methods are identical with each other; 2) the absorption spectra of the solutions obtained by treating POPC with sulfuric acid or by heating POPC agree not with that of PC-II but of PC-III; 3) the same absorption spectrum as that of HC-III is obtained by adding potassium cyanide to PC-III and by heating. A schematic diagram from the results is given in Fig. 4. It is easily supposed from 2) that POPC is not produced successively since an oxygen molecule can not coordinate to PC-III.

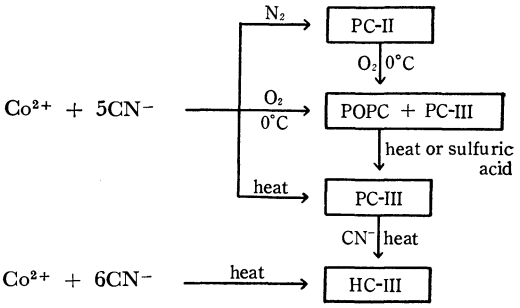

Fig. 4. The schematic diagram for cobalt cyanide complexes.

Table 1. The half wave potentials and the wave heights measured
Concentration of cobalt $=2.50\times10^{-3}$ M, pH=12.5, Temperature=0°C

		Half wave potential (V)	Wave heights (μA)
PC-III		−1.65	7.45
PC-II		−1.59	4.00
POPC	a	−1.66	8.30
	b	−1.68	10.7
O_2	1st step	−0.20	
	2nd step	−1.30	
H_2O_2		−1.19	

a, content 23%
b, content 88%

The polarographic reduction waves of POPC, PC-II, PC-III, hydrogen peroxide and oxygen were recorded with the use of a dropping mercury and saturated calomel electrode couple, and the results are shown in Table 1. As can be seen, the half wave potential of POPC is more negative than that of hydrogen peroxide in spite of the fact that POPC reacts with sulfuric acid to give hydrogen peroxide. This shows that POPC is quite different from hydrogen peroxide. Though there seemed to be two paths as the reduction mechanism of POPC and two waves were expected, only a single wave was observed. This means that the respective reactions in the two reduction paths proceed very fast.

$$\mathrm{CoOOCo} \begin{cases} \xrightarrow{2e} \mathrm{Co^{+} + O_2^{2-}} \\ \xrightarrow{e} \mathrm{Co^{3+} + OH^{-}} \end{cases} \begin{cases} \xrightarrow{e} \\ \xrightarrow{2e} \end{cases} \mathrm{Co^{+} + OH^{-}}$$

The wave height estimated on the basis of the above reduction mechanism and the concentration of POPC agreed well with that of POPC in a polarogram.

Epoxidation. Acrolein and propylene were treated with POPC under the conditions: pH 8—12, 1.5—30°C, and 40—180 min (reaction time).

The reaction mixtures were examined by a gas chromatograph. No epoxide was found. Acrolein was treated similarly with a solution obtained by adjusting the pH to 8—9 after acidfication of POPC solution with sulfuric acid. The gas chromatogram obtained showed a peak of glycidaldehyde.

The failure in the direct epoxidation with POPC is attributed to the inertness of POPC to olefins.

BULLETIN OF THE CHEMICAL SOCIETY OF JAPAN VOL. 42 3582—3585 (1969)

Studies on Reactions of Isoprenoids. VI.[1] Synthesis of *cis*-Homochrysanthemic Acid and Its Derivatives from Δ^3-Carene

Tadashi SASAKI, Shoji EGUCHI, Masatomi OHNO and Takeshi OYOBE

Institute of Applied Organic Chemistry, Faculty of Engineering, Nagoya University, Furo-cho, Chikusa-ku, Nagoya

(Received April 18, 1969)

In 1965, Matsui *et al.*[2] reported the synthesis of *trans*-chrysanthemic acid from Δ^3-carene (I) *via* the keto-aldehyde (II) through several steps. Considering the presence of a cyclopropylacetaldehyde in II, it seemed reasonable to attempt the synthesis of homochrysanthemic acid (VII) from II. This paper deals with our results, though our objective (VII) was already prepared from *cis*-chrysanthemic acid by utilizing the Arndt-Eistert homologation in low yields.[3] Since the communication by Matsui *et al.*[2] did not describe the detailed experimental conditions for the preparation of II,[4] we checked the oxidation conditions in three methods. Method 1 involved ozonolysis of I following Semmler and Schiller[4a] to II which was not isolated by Matsui *et al.*[2] We adopted a somewhat modified procedure.[4b] By decomposing the ozonized mixture with hydrogen peroxide in refluxing aqueous acetic acid for 10 hr, 3,3-dimethyl-2-(2-oxopropyl)cyclopropylacetic acid (III) was directly obtained from I in about 10% yield. Method 2 involved a new procedure adopted by Pappas and Keaveney[5] using dimethyl sulfide for decomposition of the intermediated ozonide was applied. The yield of II was 52%. II was readily convertible to III by potassium permanganate in 65% yield. This method seems to be superior to method 1 and the following method 3. Method 3 utilized direct oxidation of I with potassium permanganate in acetone at 10°C; the yield of III was only 15%, many side-products being formed, which were hardly separated from III by repeated *vacuum* distillation.

The conversion of 2-oxopropyl group into isobutenyl was fulfilled by applying the selective Grignard reaction to III and VI followed by dehydration. The keto-ester (VI), obtained from III by the acid-catalyzed esterification or by methylation with diazomethane, was treated with one mole of methylmagnesium iodide and work-up gave methyl 3,3-dimethyl-2-(2-methyl-2-hydroxypropyl)cyclopropylacetate (V). V was also prepared by the methylation of the corresponding IV which was similarly prepared in a 90% yield by the selective Grignard reaction of the keto-acid (III) with two moles of methylmagnesium iodide following the reverse-addition procedure (see Experimental). The results are summarized in Chart 1.

The last step is the dehydration of the hydroxy acid (IV) or hydroxy ester (V). Dehydration of the tertiary hydroxy group in IV and V was very likely to yield isobutenyl group, since a conjugation of the produced double bond with a cyclopropane might favor the desired dehydration,[6] though in IV, simultaneous cyclopropane-ring-opening according to the mechanism proposed by Matsui *et al.*[7] might afford γ-lactone especially in an acidic condition. In fact, when treated with the catalytic amount of *p*-toluenesulfonic acid, IV afforded the known γ-lactone, 4,4-dimethyl-3-(3-methylbut-1-enyl)butanolide (IX);[3] the structure was confirmed by means of analytical and spectral data. A *cis*-relation of the lactone ring to

1) Part V of this series: T. Sasaki, S. Eguchi and T. Ishii, This Bulletin, **42**, 558 (1969).

2) M. Matsui, H. Yoshioka, Y. Yamada, H. Sakamoto and T. Kitahara, *Agr. Biol. Chem. (Tokyo)*, **29**, 784 (1965).

3) L. Crombie, J. Crossley and D. A. Mitchard, *J. Chem. Soc.*, **1963**, 4957 and references cited therein.

4) a) F. W. Semmler and H. von Schiller, *Ber.*, **60**, 1591 (1927); b) Y-R. Naves and A-V. Grampoloff, *Helv. Chim. Acta*, **44**, 637 (1961).

5) J. J. Pappas and W. P. Keaveney, *Tetrahedron Letters*, **1966**, 4273.

6) For example, a successful dehydration of *trans*-δ-hydroxydihydrochrysanthemic acid to chrysanthemic acid by the acid-catalyzed thermal procedure has been reported: M. Matsui and M. Miyano, *Bull. Agr. Chem. Soc.* (Tokyo), **19**, 159 (1955).

7) M. Matsui, H. Yoshioka and H. Hirai, *Agr. Biol. Chem. (Tokyo)*, **28**, 456 (1964).

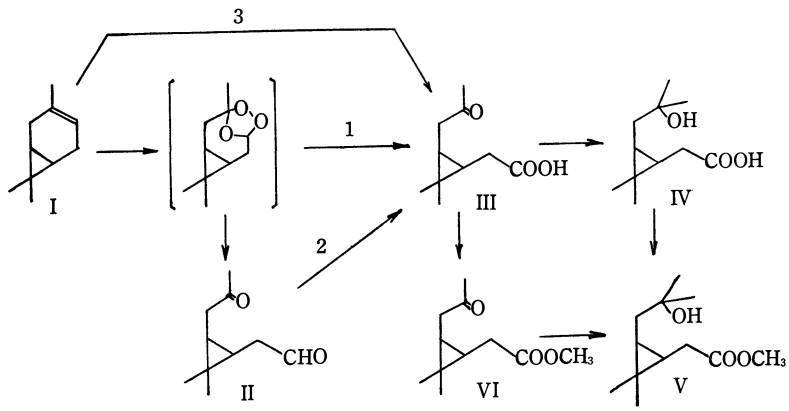

Chart 1

the isopropyl group was demonstrated by the coupling constants of two vinyl protons at 4.53 τ (J= 6.0 and 7.5 Hz) in its NMR spectrum ($CDCl_3$).[8] However, when IV was treated with phosphorus oxychloride in dry pyridine at 0°C, the product was characterized as a seven-membered lactone X on the basis of analytical and spectral data. The formation of IX was also recognized on treatment with phosphorus oxychloride even when a small amount of pyridine was used. At all events, homochrysanthemic acid seems more labile against acid than chrysanthemic acid, and the direct conversion of IV to homochrysanthemic acid was unsuccessful. From the results, dehydration of the hydroxy-ester (V) was investigated. When V was treated with *p*-toluenesulfonic acid in refluxing toluene for 4 hr,

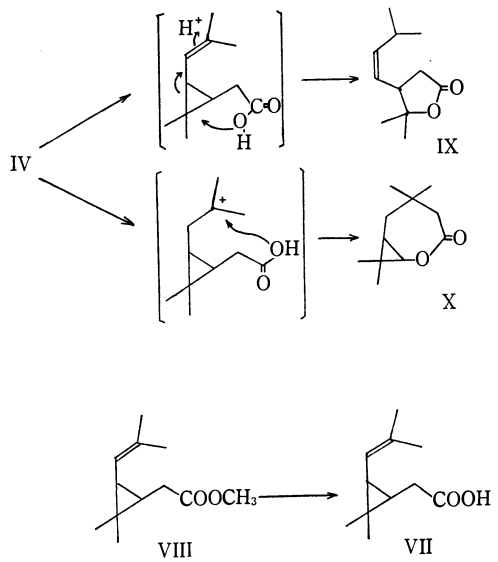

Chart 2

the product was found to be a mixture of methyl homochrysanthemate (VIII) and homochrysanthemic acid (VII) produced by hydrolysis of the former. The best method for dehydration of V to VIII was the treatment of V in dry pyridine with phosphorus oxychloride at 0°C. Pure VIII was obtained in a 51% yield. The acid (VII) was obtained by the alkaline hydrolysis of VIII in an 85% yield. The results are summarized in Chart 2.

Experimental

All melting points were measured on a Yanagimoto micromelting point apparatus and are uncorrected. Boiling points were also not corrected. The microanalyses were performed on a Yanagimoto CHN Corder, Model MT-1, while the IR spectra were obtained on a JASCO Model IR-S spectrophotometer. The NMR spectra were recorded with a Varian A-60 and/or a Jeolco MINIMAR spectrometer using TMS as an internal standard. Chemical shifts were reported in τ values, designating singlet signals as s, doublet as d, triplet as t, multiplet as m. Ozonization was carried out with a Nippon-Ozone Ozonyzer, Model 0-1-2, controlling the reaction with bromination test and thin layer chromatography (TLC).

Oxidation of Δ^3-Carene. *Method 1.* Freshly distilled Δ^3-carene (I), bp 66—66.5°C/23.5 mmHg, n_D^{21} 1.4727 (34 g, 0.25 mol) was dissolved in a mixture of 200 m*l* of acetic acid and 10 m*l* of water and ozone was passed through this solution for 10 hr at 8—10°C. After the reaction was over, 200 m*l* of water and 6.33 m*l* of 30% hydrogen peroxide were added and the mixture was refluxed for 2 hr. After cooling, it was extracted with methylene chloride (100 m*l*×5) and the combined extract was washed with water (300 m*l*×3) and dried (Na_2SO_4). Removal of the solvent and distillation afforded 3 g (10%) of 3,3-dimethyl-2-(2-oxopropyl)-acetic acid (III): bp 135—137°C/0.25 mmHg, n_D^{25} 1.4700 (lit,[4b] bp 145—146°C/2 mmHg, n_D^{20} 1.4688).

Method 2. Ozone was passed through a solution of I (68 g, 0.5 mpl) in 300 m*l* of methanol for 17 hr at −60°C under cooling with a dry ice-methanol mixture until bromination test was found negative. After the reaction was over, nitrogen gas was bubbled into the reaction mixture for 5 min at the same temperature and

8) N. S. Bhacca and D. H. Williams, "Application of NMR Spectroscopy in Organic Chemistry," Holden-Day, Inc., San Francisco (1964), p. 85.

52 ml (43.5 g, 0.7 mol) of dimethyl sulfide was added with stirring under nitrogen atmosphere. The reaction temperature was allowed to rise gradually to room temperature after removing the cooling bath while stirring was continued. Benzene (500 ml) was added after concentration of methanol solution to *ca.* 100 ml and the benzene layer was wahed with water and dried (Na_2SO_4), and the residue obtained by removal of the solvent was distilled to afford 35 g (40%) of 3,3-dimethyl-2-(2-oxopropyl)cyclopropylacetaldehyde (II) as an oil with a bp 80—83°C/1 mmHg, n_D^{20} 1.4600 (lit,[4b] bp 92-94°C/2 mmHg, n_D^{20} 1.4601).

Method 3. To a stirred solution of I (13.6 g, 0.1 mol) in 100 ml of acetone and 25 ml of water, potassium permanganate (11 g) was added little by little at 5—10°C. After reaction was over, 5 ml of ethanol was added to the reaction mixture in order to decompose the excess potassium permanganate and the resulting precipitates were filtered and washed with acetone (50 ml). The combined filtrate and washings were concentrated and the residue obtained was distilled to give 1.95 g (15%) of III with bp 145—148°C/2 mmHg, n_D^{20} 1.4688 (lit,[4b] bp 145—146°C/2 mmHg).

Oxidation of 3, 3-Dimethyl-2-(2-oxopropyl)cyclopropylacetaldehyde (II) to Keto-carboxylic Acid (III). To a mixture of II (26 g, 0.15 mol), acetone (200 ml), and water (50 ml) was added 22 g of potassium permanganate in small portions with stirring at 5—10°C during 3 hr. Excess potassium permanganate was decomposed with addition of ethanol and the resulting precipitates were filtered and washed with acetone (50 ml). The combined filtrate and washings were concentrated *in vacuo* to *ca.* 100 ml. The residue obtained was extracted with ether after addition of water (100 ml) and the ether layer was dried (Na_2SO_4). Removal of ether gave crude acid (III) which was distilled to afford 17.5 g (65%) of pure III with bp 110—115°C/0.5 mmHg, n_D^{20} 1.4670 (lit,[4b] bp 145—146°C/2 mmHg, n_D^{20} 1.4688).

Reaction of the Keto-carboxylic Acid (III) with Methylmagnesium Iodide. Magnesium (1.366 g, 0.055 g atom) was suspended in 100 ml of dry ether and to this was added an ethereal solution of methyl iodide (7.8 g, 0.055 mol in 50 ml) according to general procedures for preparation of methyl Grignard reagent. To a stirred solution of III (4.6 g, 0.025 mol) in 50 ml of ether was added the Grignard reagent at room temperature very slowly in 3 hr. Stirring was continued overnight, and water was added to produce a turbid solution, to which aqueous ammonium chloride was added. This was acidified with 10% hydrochloric acid and the ether layer was separated and dried (Na_2SO_4). Removal of the solvent left crystalline solids which were recrystallized from *n*-hexane to give 4.51 g (90%) of 3,3-dimethyl-2-(2-methyl-2-hydroxypropyl)cyclopropylacetic acid (IV) as colorless needles with a mp of 87—88°C. IR (KBr) cm^{-1}: 3300 (OH), 3000—2500 and 1680 (COOH) 1150 (-C(-OH)-). NMR ($CDCl_3$)τ : 2.90 (2 H, s, COOH and OH), 7.07 (2 H, d, J=7.0 Hz, $-CH_2-$), 8.54 (2 H, d, J=6.0 Hz, $-CH_2-$), 8.72 (6 H, s, $-(HO)C(C\underline{H}_3)_2$), 8.90 and 9.08 (each 3 H, each s, $C(CH_3)_2$), and 9.00—9.32 (*ca.* 2 H, m, cyclopropane ring protons).

Found: C, 65.68; H, 10.01%. Calcd for $C_{11}H_{20}O_3$: C, 65.97; H, 10.07%.

Esterification of the Hydroxy-carboxylic Acid (IV) to (V). A solution of IV (1 g, 0.005 mol) in ether was treated with an ethereal solution of diazomethane which was prepared from 2 g of nitrosomethylurea and 6 ml of 50% aqueous potassium hydroxide in 50 ml of ether. After standing overnight, ether and excess diazomethane were removed to give pure ester (V) in almost quantitative yield. IR (neat) cm^{-1}: 3550 and 1170 (-C(-OH)-), 1740 and 1029 ($COOCH_3$), and 2910, 1450, 910 and 770. NMR($CDCl_3$) τ: 6.22 (3 H, s, $COOCH_3$), 7.65 (2 H, d, J=7.0 Hz, $-C\underline{H}_2COOCH_3$), 8.24 (1 H, s, OH), 8.53 (2 H, d, J=7.0 Hz, $-CH_2-$), 8.71 (6 H, s, $-(HO)C(C\underline{H}_3)_2$), 8.86 and 9.10 (*ca.* 6 H, each s, $C(CH_3)_2$), and 9.00—9.40 (*ca.* 2 H, m, cyclopropane ring protons).

Found: C, 67.55; H, 10.76%. Calcd for $C_{12}H_{22}O_3$: C, 67.25; H, 10.35%.

Preparation of the Keto-ester (VI). Treatment of III (8.3 g, 0.045 mol) with an excess diazomethane in ether at room temperature afforded crude (VI) which was distilled to give 8.1 g (92%) of pure VI with a bp of 83—85°C/1 mmHg, n_D^{20} 1.4518 (lit,[4b] bp 98—99°C/2 mmHg, n_D^{20} 1.4518). Treatment of III in refluxing methanol in the presence of a catalytic amount of sulfuric acid afforded also VI in a 50% yield, though some decomposition reactions were unavoidable.

Grignard Reaction of Keto-ester (VI). To a stirred solution of VI (8 g, 0.043 mol) in 50 ml of ether was added slowly the Grignard reagent prepared from 0.945 g (0.043 g atom) of magnesium and 6.11 g (0.043 mol) of methyl iodide in 100 ml of ether. Stirring was continued for 3 hr at room temperature and aqueous ammonium chloride was added to the reaction mixture which was neutralized with 10% hydrochloric acid. The ether layer was separated and the water layer was extracted with ether (30 ml×2). The combined ether layer and extracts were washed with water and dried (Na_2SO_4). After removal of ether, the oily residue was distilled to give 7.74 g of the hydroxy-ester (V), bp 76—80°C/2 mmHg, n_D^{20} 1.4560. Its infrared spectrum (neat) was superimposable on that of V prepared from IV.

Dehydration of the Hydroxy-carboxylic Acid (IV). *a) With p-Toluenesulfonic Acid.* A mixture of 0.5 g (0.0025 mol) of IV and 50 mg of *p*-toluenesulfonic acid was dry-distilled to give an oil with a bp of 115—120°C/1 mmHg, which was further purified by chromatography on a silica-gel (Mallinckrodt, 100 Mesh) column eluting with methylene chloride to give 300 mg (66%) of γ-lactone (IX). IR (neat) cm^{-1}: 2980 (CH), 1780 (γ-lactone), and 1660 (C=C). NMR ($CDCl_3$)τ : 4.46 and 4.60 (2 H, q, J=6.5 and 7.5 Hz, -CH=CH-, *cis*), 7.00—7.80 (4 H, m, CH_2 and CH), 8.52 and 8.72 (each 3 H, each s, $C(CH_3)_2$), and 8.96 (6 H, d, J=6.5 Hz, $CH(CH_3)_2$).

Found: C, 72.58; H, 9.99%. Calcd for $C_{11}H_{18}O_2$: C, 72.49; H, 9.96%.

b) With Phosphorus Oxychloride and Pyridine. To a stirred solution of IV (0.3 g, 0.0015 mol) in 5 ml of dry pyridine was added 0.55 ml of phosphorus oxychloride at 0°C during 30 min and the mixture was stirred for another 2.5 hr. After confirming the termination of reaction by TLC, the reaction mixture was poured onto ice-water and extracted with chloroform (20 ml× 5). The combined chloroform extracts were washed with 5% hydrochloric acid, and then with water several times and dried (Na_2SO_4). Removal of chloroform *in vacuo* afforded 160 mg (59%) of needles of the ε-lactone derivative (X), mp 40—41°C. IR (KBr) cm^{-1}: 2900 (OH), 1712 (ε-lactone) and no OH and C=C bands.

NMR ($CDCl_3$)τ: 6.98—8.20 (4 H, complex m, $-CH_2-\times 2$), 8.49 and 8.55 (6 H, eash s, $-O-C(CH_3)_2$), 8.90 (6 H, s, $C(CH_3)_2$), and *ca.* 8.90—9.21 (*ca.* 2 H, m, cyclopropane ring protons).

Found: C, 72.49; H, 10.22%. Calcd for $C_{11}H_{18}O_2$: C, 72.49; H, 9.96%.

When the amount of pyridine decreased or in the absence of pyridine, the exothermic reaction occurred in the above reaction to result in the formation of the γ-lactone derivative (IX) which was confirmed by infrared specral comparison with a specimen prepared as above.

Dehydration of the Hydroxy-ester (V). *a) With p-Toluenesulfonic Acid.* A solution of V (4.8 g, 0.022 mol) and *p*-toluenesulfonic acid (20 mg) in 50 m*l* of dry toluene was refluxed for 4 hr to give a red solution. Purification of the products by distillation and chromatography on a silica-gel column afforded 0.84 g (24%) of methyl *cis*-homochrysanthemate (VIII) as an oil with a bp of 55—60°C/0.3 mmHg and 2.4 g (50%) of *cis*-homochrysanthemic acid (VII) with a bp of 110—115° C/0.1 mmHg, n_D^{20} 1.4652, both of which were confirmed by infrared spectral comparison with the respective specimen prepared by the following procedure.

b) With Phophorus Oxychloride and Pyridine. Similar procedure to the dehydration of IV was carried out on V (1 g, 0.0046 mol) in 10 m*l* of dry pyridine and phosphorus oxychloride (0.6 m*l*) at 0°C for 3 hr. After pouring onto ice-water, the reaction mixture was extracted with benzene. The benzene extracts were chromatographed on a silica-gel column to give 0.47 g (51%) of methyl *cis*-homochrysanthemate, n_D^{20} 1.4658 (lit.,[3] n_D^{20} 1.4663). IR (neat) cm^{-1}: 1740 and 1065 ($COOCH_3$), 1650 and 840 (CH=C). NMR ($CDCl_3$)τ: 5.18 (1 H, broad d, J=7.5 Hz, -CH=C), 6.37 (3 H, s, $COOCH_3$), 7.37 (2 H, d, J=7.0 Hz, $-C\underline{H}_2-COOCH_3$), 8.07 (*ca.* 1 H, superimposed t, J=*ca.* 7.5 Hz, allylic cyclopropane ring proton), 8.27 and 8.32 (*ca.* 6 H, overlapped s, $C=C(CH_3)_2$), 8.86 and 9.05 (*ca.* 6 H, each s, $C(CH_3)_2$) and *ca.* 8.80—9.23 (*ca.* 1 H, complex m, cyclopropane ring proton).

Found: C, 73.26; H, 10.36%. Calcd for $C_{12}H_{20}O_2$: C, 73.43; H, 10.27%.

***cis*-Homochrysanthemic Acid (VII) by Hydrolysis of Its Ester (VIII).** A suspension of VIII (200 mg) in 5 m*l* of 5% sodium hydroxide was stirred at room temperature for 12 hr. The mixture was acidified with 10% hydrochloric acid and extracted with chloroform (20 m$l\times$5). The combined chloroform extract was washed with water and dried (Na_2SO_4). Removal of the solvent *in vacuo* afforded 160 mg (85%) of VII as an oil. IR (neat) cm^{-1}: 3100—2729 and 1703 (COOH), 1648 and 840 (CH=C). NMR ($CDCl_3$)τ: -1.25 (1 H, s, COOH), and other signals were almost the same as those of VIII.

Found: C, 72.36; H, 9.90%. Calcd for $C_{11}H_{18}O_2$: C, 72.49; H, 9.96%.

BULLETIN OF THE CHEMICAL SOCIETY OF JAPAN VOL. 42 3585—3588 (1969)

The Syntheses and Properties of Molybdenum(VI)-Amino Acids Complexes

Hiroshi EGUCHI, Toshio TAKEUCHI, Akira OUCHI and Akiko FURUHASHI*1

Department of Chemistry, College of General Education, The University of Tokyo, Komaba, Meguro-ku, Tokyo

(Received April 19, 1969)

New compounds of the $Mo(VI)_2O_7H_3(Am)_n$-type (where HAm=glycine, DL-alamine, DL-Methionine, or L-Leucine) were obtained from an acidic aqueous solution (pH=1) containing sodium molybdate and amino acid. These compounds seem to be isostructural with each other, and all are diamagnetic. Their infrared spectra show characteristic ν(Mo=O) bands.

The ethylenediaminetetraacetato chelates of molybdenum(VI) and (V) have already been studied potentially,[1-3] while studies of the amino acid chelates of molybdenum have appeared only recently. Spence and Lee have studied the solution chemistry of the molybdenum-hystidine system.[4] The molybdenum-cystein complex was obtained in the solid state very recently,[5] and the X-ray structural analysis data[6] as well as its infrared spectral data[7] have also been reported. However the molybdenum chelates of other amino acids are not very stable in a neutral aqueous solution and the solid products have not yet been obtained. The authors found that some amino acids, such as glycine,

*1 Department of Chemistry, College of Engineering and Science, Aoyama Gakuin University, Meguri-sawa, Setagaya-ku, Tokyo.

1) R. L. Pecsok and D. T. Sawyer, *J. Am. Chem. Soc.*, **78**, 5496 (1956).

2) D. T. Sawyer and J. M. McKinnie, *ibid.*, **82**, 4191 (1960).

3) S. I. Cham, R. J. Kula and D. T. Sawyer, *ibid.*, **86**, 377 (1964).

4) J. T. Spence and J. Y. Lee, *Inorg. Chem.*, **4**, 385 (1965).

5) A. Kay and P. C. H. Mitchell, *Nature*, **219**, 267 (1968).

6) J. R. Knox and C. K. Prout, *Chem. Commun.*, **1968**, 1227.

7) L. R. Melly, *Inorg. Chem.*, **8**, 349 (1969).

alanine, leucine and methionine, give a very stable product in acidic aqueous media; the solid complexes were thus obtained. They are insoluble in water or organic solvents and consist of two molybdenum atoms per amino acid molecule. From the properties of these complexes, they are expected to be of the polymer type.

Experimental

Instruments. The infrared spectra were obtained by the Nujol or hexachloro-1,3-butadiene mull method using a DS-301 infrared spectrophotometer of the Japan Spectroscopic Co., Ltd. The magnetic susceptibilities of the products were measured with a Gouy balance at room temperature (20°C).

Synthesis of the Complex. *Methoioninato Dimolybdenum (VI)*, $Mo(VI)_2O_7H_3(C_5H_{10}NO_2S)$. One and a half grams (10 mM) of DL-methionine were dissolved into a minimum quantity of 1 N hydrochloric acid. In a separate flask 4.80 g (20 mM) of sodium molybdate dihydrate were dissolved into 10 m*l* of water. The two solutions were mixed and the pH of the supernatant of the mixture was adjusted to about 1 by adding 6 N hydrochloric acid. The mixture was heated and boiled for several minutes, and the original precipitate was dissolved then gradually a fine powder appeared which tended to cling to the wall of the vessel. After the reaction had been completed, the product was filtered off and washed with 0.1 N hydrochloric acid, water, ethanol, and diethyl ether in that order.

The complex thus obtained was dried in a vacuum dessicator for about 24 hr at room temperature. It was pale yellow and was insoluble in water or usual organic solvents, but soluble in an alkaline aqueous solution (in which it decomposed). Although attempts at recrystallization have not yet been successful, this product seems to be a simple compound and not a mixture, because even when the mole ratio of the starting material was changed from 4 : 1 to 1 : 4, the product was found to be identical not only on the basis of the analytical data but also on the basis of the infrared spectra. Moreover, this is supported by the fact that the isostructural complexes were also obtained from other amino acids by the same method.

The glycine, DL-alanine, and L-leucine compounds were obtained by almost the same synthetic method, but they were all white, not yellowish, in color. Using other amino acids, such as glutamic acid, aspartic acid, valine, phenyl-alanine, and histidine, this type of complex has not yet been obtained.

Results and Discussion

The analytical data for these compounds are given in Table 1. These complexes are all diamagnetic at room temperature. The infrared spectral data for the complexes are summarized in Table 2, together with those of several related compounds.

The infrared spectra of amino acid and their metal complexes have already been reported in many papers.[7–10] The assignments of the bands shown n the table were deduced from t hese references and are only tentative. The ν(N–H) bands near 3200 cm^{-1} of the amino acid complexes of the usual first series of transition elements are rather sharp and in a higher frequency region than those of the free ligand. The bands of these molybdenum(VI) complexes are weak and broad, and the wave number of the peak is less than 3200 cm^{-1}. This is probably due to the fact that the molybdic acid part of the compound makes a strong hydrogen bond with the amino group of an amino acid. The antisymmetric and symmetric stretching bands of $-COO^-$ in the region of 1600—1400 cm^{-1} show a little shift from those of free ligands as usual metal complexes of amino acid, and then the oxygen of the carboxyl group of an amino acid seems to make the coordination bond with the central molybdenum atom in these complexes. The $\delta(-NH_2)$ or $\delta(-NH_3^+)$ peaks can also be recognized in these regions. It seems that the strong bands in the region of 1000—900 cm^{-1} and near 760 cm^{-1} can be identified as ν(Mo=O) and ν(Mo–O–Mo) bands respectively by comparing them with the infrared data of acid complexes of molybdenum reported by many authors;[7,11–16] the rocking band of the methyl group of bands caused by amino acid may also appear near here, but, if so, they should be far less intense. The strong peak near 950 cm^{-1} is likely a band of the terminal Mo=O bond which has almost pure double bond character; however, as there are

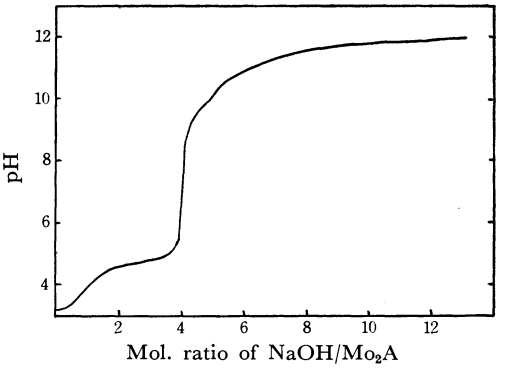

Fig. 1. Alkalimetric titration curve of methioninato dimolybdenum(VI).

8) K. Nakamoto, "Infrared Spectra of Inorganic and Coordination Compounds," John Wiley & Sons, New York, N. Y. (1963), p. 201.
9) C. A. McAuliffe, J. V. Quagliano and L. M. Vallarino, *Inorg. Chem.*, **5**, 1996 (1966).
10) S. E. Livingstone and J. D. Nolan, *Inorg. Chem.*, **7**, 1447 (1968).
11) F. A. Cotton, S. M. M. Morehouse and J. S. Wood, *Inorg. Chem.*, **3**, 1603 (1964).
12) F. A. Cotton and R. M. Wing, *ibid.*, **4**, 867 (1965).
13) F. W. Moore and M. L. Larson, *ibid.*, **6**, 998 (1967).
14) W. P. Griffith and T. D. Wickins, *J. Chem. Soc., A*, **1968**, 400.
15) P. C. H. Mitchell, *Quart. Rev.*, **20**, 103 (1966).
16) F. W. Moore and R. E. Rice, *Inorg. Chem.*, **7**, 2510 (1968).

Table 1. Analysis of complexes (Figures are given in %.)

		Mo	C	H	N	S			Mo	C	H	N	S
$Mo_2O_7H_3$(Met)	Calcd	42.16	13.20	2.88	3.08	7.05	$Mo_2O_7H_3$(Ala)	Calcd	48.58	9.12	2.30	3.54	
	Found	41.70	13.44	2.73	3.10	7.07		Found	48.00	9.41	2.09	3.57	
$Mo_2O_7H_3$(Gly)·H_2O	Calcd	48.09	6.02	2.27	3.51		$Mo_2O_7H_3$(Leu)·H_2O	Calcd	42.16	15.84	3.77	3.08	
	Found	48.10	6.28	1.96	3.51			Found	42.30	15.71	3.97	3.22	

HMet: DL-methionine, HGly: Glycine, HAla: DL-alanine and HLeu: L-leucine

Table 2. Infrared spectra of complexes (Figures are given in cm^{-1}.)

Mo_2(Met)	Mo_2(Gly)	Mo_2(Ala)	Mo_2(Leu)	Glycine	Methionine	Ni(Met)$_2$	$Na_2MoO_4·2H_2O$	$(NH_4)_6(Mo_7O_{24})·4H_2O$	Tentative assignment
3160 w	3200 w	3170 w	3180 w	3180 s	3160 sh	3338, 3276 s			ν(N–H)
							1675 s	1635 br	
1607 s	1625, 1607 s	1616 s	1625, 1613 s	1620 br	1620 s	1617 s			ν(–COO)$_{antisym.}$
1570 sh, m	1575 s	1572 s		1590 br	1675 s			1400 s	$\delta(NH_2)$ or others
1503 s	1495 s	1505 s, 1498 s	1520 br, m	1505 s	1580 s 1515 s	1580 s 1560 sh			
1445 w 1430 s	1448 s 1415 s	1463 s 1426 s	1433 s	1400 s	1413 s	1425 s 1408 s			ν(–COO)$_{sym}$
1360 m 1337 m	1352 s	1387 m 1362 s	1390 m 1373 m 1358 s	1328 s	1343 s	1350 s 1331 w 1315 w			ν(C=N)+$\delta(CH_3)$
950 vs 917 vs	952 vs 930 s 910 s	955 vs 930 s 915 s	955 vs 925 s 910 s	1033 m 911 m	1010 m 925 m	1151 s 948 s	905 m	915 s	ν(Mo=O)
898 s 789 w	902 s	898 sh	895 w	893 m	873 m	877 m 798 s	856, 820 vs 800 sh	890, 870 vs 837 s	
760 s	767 s	761 s	765 m	700 m	778 w 775 w 738 w	765 w			ν(Mo–O–Mo) or others

vs=very strong, s=strong, m=medium, w=weak, br=broad.

Mo_2(Met), for example, shows the methionine complex having the composition shown in Table 1.

some other bands of lower frequencies in this region too, Mo-O bonds with less of a double-bond character may also exist.[7,12,14,16] The band near 760 cm^{-1} seems to be due to the Mo–O–Mo bridge,[12,15] this Mo–O bond should have rather a single-bond character.

The results of the alkalimetry of the methionine complex are shown in Fig. 1.*2 After the mole ratio of NaOH : Mo_2A (where Mo_2A means the complex) exceeds 2 : 1, the suspended solid begins to dissolve into the solution; after the alkaline standard solution had been added, it takes a few minutes until a stabilized pH value is observed. At the point where the ratio is 4 : 1 all the solid is dissolved and a clear solution is obtained: the pH of the solution suddenly rises there.

As (1) the solid complexes are obtained from an acidic aqueous solution of about pH=1, (2) these complexes are insoluble in water, and (3) the mole ratio of molybdenum and the amino acids in the complexes is 2 : 1, these complexes are probably in the polymer form. However, the behavior of these complexes in alkalimetry is a little different from those of isopolymolybdate, as the reaction with alkali in an aqueous solution is faster and as a big pH change is observed at the point where NaOH : Mo_2A=4 : 1.

The complex seems to be less stable than usual isopolymolybdate. Moreover, in an alkaline solution the presence of polymolybdate ions or complex anions is not probable, as the metal molybdate precipitated immediately from the solution when barium or lead salt was added and as the attempt to isolate the sodium salt of the complex by adding organic solvents to the solution was not successful. On the basis of these results, Fig. 2

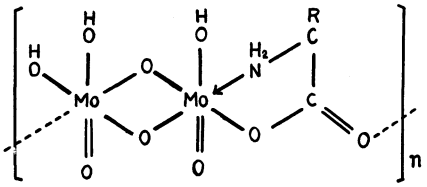

Fig. 2. Structure of molybdenum(VI)-amino acid complexes.

shows a tentative model of these complexes, though the exact structure must be determined by a subsequent X-ray structural analysis.

The authors wish to thank Professors Yasumasa Hayakawa and Yukichi Yoshino and the colleagues of our laboratories for their helpful discussions. A part of this research was carried out with a Scientific Research Grant from the Ministry of Education, to which the authors thanks are due.

*2 0.1 mM sample suspended in 100 m*l* of water was titrated by 0.1 N sodium hydroxide. Almost the same results were obtained by the other three complexes, too (at 20°C).

BULLETIN OF THE CHEMICAL SOCIETY OF JAPAN VOL. 42 3588—3590 (1969)

The Kinetics of the Ligand Substitution Reaction of Copper(II)-nitrilotriacetate and -nitrilo(diacetic)propionate Complexes with *trans*-1,2-Cyclohexanediaminetetraacetate Ions*[1]

Masaru KIMURA*[2]

Department of Applied Chemistry, Yamagata University, Yonezawa-shi

(Received April 28, 1969)

Previous studies[1,2] have shown that the rate of the reaction of some nickel(II) complexes with *trans*-1,2-cyclohexanediaminetetraacetate (CyDTA) ions was independent of the concentrations of CyDTA and proceeded by means of the complete dissociation of the nickel(II) ion from the nickel(II) complex. Although CyDTA did not affect the rate of the dissociation of the nickel ion from the complex, the hydrogen ion promoted the dissociation reactions.[1,2] The same behavior was shown in the reaction of copper(II) complexes with CyDTA ions. In the present study, the rate constants of the dissociation reaction of copper(II)-nitrilotriacetate (NTA) and -nitrilo(diacetic)propionate (NDAP) complexes were determined and compared with those of the other metal complexes. The acid dissociation constant of the ligand and/or the formation constant of the complex is used in most methods when the rate constant is determined.

*1 Part IV of a series on the kinetics of the multidentate ligand-substitution reactions.

*2 Correspondence to be addressed to: c/o Prof. I. M. Kolthoff, Department of Chemistry, University of Minnesota, Minneapolis, Minn. 55455, USA.

1) M. Kimura, This Bulletin, **42**, 2841 (1969).

2) M. Kimura, *ibid.*, **42**, 2844 (1969).

However, this method of determining the dissociation rate constant using CyDTA as an indicator of the rate is abvantageous in that the rate constant can be determined without using any other constants.

Experimental

A solution of copper(II) nitrate was prepared by dissolving a known amount of pure copper metal in reagent-grade nitric acid. A chelating agent, NDAP, was synthesized by the same procedures as have been reported by Uehara *et al.*[3] All the other chemicals and apparatus used were the same as those described in previous papers.[1,4] The temperature was maintained at 25°C, and the ionic strength was adjusted to 0.2 with potassium nitrate.

Derivation of the Rate Equation

The overall substitution reaction of the copper-NTA or copper-NDAP complex with CyDTA can be expressed as follows:

$$CuX^- + \left\{\begin{matrix}Cy^{4-}\\ \updownarrow\\ \vdots\\ \updownarrow\\ H_4Cy\end{matrix}\right\} \underset{k^-}{\overset{k^+}{\rightleftharpoons}} CuCy^{2-} + \left\{\begin{matrix}X^{3-}\\ \updownarrow\\ \vdots\\ \updownarrow\\ H_3X\end{matrix}\right\} \quad (1)$$

where X^{3-} denotes a tervalent NTA or NDAP anion, and Cy^{4-}, a quadrivalent CyDTA anion.

The rate of the forward reaction (1) was confirmed to be independent of the initial concentrations of CyDTA and also of NTA or NDAP. Therefore, the rate equation can be expressed as:

$$-\frac{d[CyDTA]}{dt} \equiv -\frac{d[CuX^-]}{dt} = k^+[CuX^-] - k^-[CuCy^{2-}] \quad (2)$$

The concentration that can be determined polarographically is [CyDTA] which is given by:

$$[CyDTA] = \sum_{j=0}^{4}[H_jCy^{(4-j)-}] \quad (3)$$

By integrating Eq. (2), we obtain:

$$\ln([CuX^-] - [CuX^-]_e) = -(k^+ + k^-)t + \ln([CuX^-]_i - [CuX^-]_e) \quad (4)$$

where the subscripts i and e represent the initial and the equilibrium states respectively. At the equilibrium of the reaction, the following relation may be satisfied:

$$k^+/k^- = [CuCy^{2-}]_e/[CuX^-]_e = (K_{CuCy}/K_{CuX}) \times ([Cy^{4-}]_i/[X^{3-}]_i) \fallingdotseq 10^8 \quad (5)$$

Therefore, the relations of $k^- \ll k^+$ and $[CuX^-]_e \ll [CuX^-]_i$ are satisfied, and k^- and $[CuX^-]_e$ can be neglected under the present experimental conditions. Consequently, Eq. (4) was simplified to:

$$\ln[CuX^-] = -k^+t + \ln[CuX^-]_i \quad (6)$$

Equation (6) shows that the plots of its left-hand side against t should give a straight line and that the value of k^+ can be obtained from the slope.

Results and Discussion

Figure 1 shows examples of a current-time curve and a plot of the left-hand side in Eq. (6) against the time, a plot which was obtained for the reaction of the copper-NTA complex with CyDTA. The

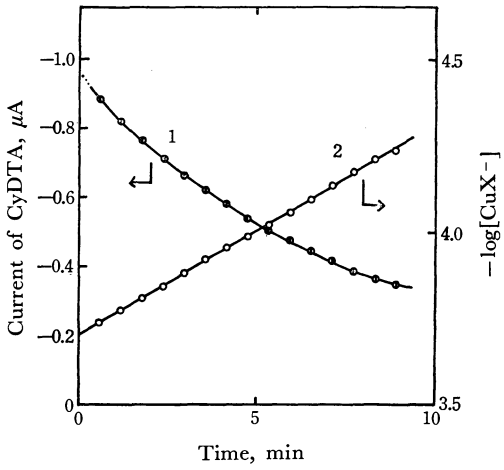

Fig. 1. A current-time curve (curve 1) and the left-hand side of Eq. (6) as a function of time (curve 2). The reaction is that of copper(II)-NTA complex with CyDTA. Measurement was made at +0.22V *vs.* SCE and was in acetate-buffer solution of pH 5.82 containing 0.04 M acetate ion at ionic strength 0.2 and at 25°C. Initial concentrations are: $[Cunta^-]_i = 2.01 \times 10^{-4}$ M, $[NTA]_i = 2.7 \times 10^{-5}$ M and $[CyDTA]_i = 2.25 \times 10^{-4}$ M.

plot gives a straight line, as may be expected from Eq. (6). The values of k^+ were not affected by the change in the initial concentrations of the copper-NTA complex, CyDTA, and NTA. The same behavior was also found in the reaction of the copper-NDAP complex with CyDTA. The plots of k^+ *versus* $[H^+]$ showed a straight line (see Fig. 2).

These results indicate that the overall reaction (1) proceeds through the following reaction paths:

$$CuX^- \underset{k_a^-}{\overset{k_{CuX}}{\rightleftharpoons}} Cu^{2+} + X^{3-} \quad (7)$$

$$CuX^- + H^+ \underset{k_b^-}{\overset{k^H_{CuX}}{\rightleftharpoons}} Cu^{2+} + HX^{2-} \quad (8)$$

$$Cu^{2+} + \left\{\begin{matrix}Cy^{4-}\\ \updownarrow\\ \vdots\\ \updownarrow\\ H_4Cy\end{matrix}\right\} \underset{}{\overset{k_j^+}{\rightleftharpoons}} CuCy^{2-} + jH^+ \quad (9)$$

3) A. Uehara, E. Kyuno and R. Tsuchiya, This Bulletin, **41**, 2385 (1968).

4) M. Kimura, *Nippon Kagaku Zasshi (J. Chem. Soc. Japan, Pure Chem. Sect.)*, **89**, 1209 (1968).

where the relation:

$$\sum_{j=0}^{4} k_j^{+}[H_jCy^{(4-j)-}] \gg k_a^{-}[X^{3-}] + k_b^{-}[HX^{2-}] \quad (10)$$

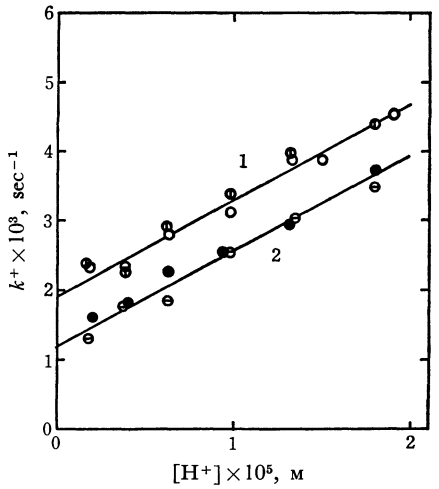

Fig. 2. k^+ as a function of the hydrogen ion concentration at ionic strength 0.2 and 25°C. Measurement was made in acetate-buffer solution containing 0.04 M acetate ion. The reactions are those of Cu(II)-NTA (curve 1) and Cu(II)-NDAP (curve 2) complexes with CyDTA.
Initial concentrations for curve 1:
$[Cu\mathit{nta}^-]_i = 2.01 \times 10^{-4}$ M, $[NTA]_i = 2.7 \times 10^{-5}$ M, $[CyDTA]_i = 3.37 \times 10^{-4}$ M (◐) and 2.25×10^{-4} M (○)
Initial concentrations for curve 2:
$[CyDTA]_i = 2.25 \times 10^{-4}$ M, $[Cu\mathit{ndap}^-]_i = 1.31 \times 10^{-4}$ M (⊖) and 2.62×10^{-4} M (●), $[NDAP]_i = 1.1 \times 10^{-5}$ M (⊖) and 2.2×10^{-5} M (●).

is satisfied under the present experimental conditions. (However, the condition of Eq. (10) can not be satisfied near the final stage of the reaction because the concentration of CyDTA gradually decreases according to the progress of the forward reaction, while that of NTA (or NDAP) increases according to the reaction process.) From the reaction mechanism, the rate of the forward reaction (1) is represented by Eq.(11):

$$(\text{Rate}) = k^{+}[CuX^{-}] = (k_{CuX} + k^{H}_{CuX}[H^{+}])[CuX^{-}] \quad (11)$$

The rate constants in Eq.(11) were determined from the plots of Fig. 2; they are given in Table 1.

Table 1. Rate constants of the dissociation reactions (7) and (8), at an ionic strength of 0.2 at 25°C

$k_{Cu(nta)}$	1.9×10^{-3} sec^{-1}
$k_{Cu(ndap)}$	1.2×10^{-3} sec^{-1}
$k^{H}_{Cu(nta)}$	1.4×10^{2} l mol^{-1} sec^{-1}
$k^{H}_{Cu(ndap)}$	1.4×10^{2} l mol^{-1} sec^{-1}

The value of $k_{Cu(nta)}$ was about twice that of $k_{Cu(ndap)}$. A similar tendency was also found in the nickel(II) complexes with NTA and NDAP, as have been reported previously.[1,2]

The author wishes to thank the Ministry of Education for the financial support granted for this research.

BULLETIN OF THE CHEMICAL SOCIETY OF JAPAN VOL. 42 3591 (1969)

Two Phenol Ethers and an Aliphatic Ketone of the Essential Oil of the Kusunoki (*Cinnamomum camphora*, Sieb.)

Shûichi HAYASHI, Katsumi YANO*1 and Tamon MATSUURA

Department of Chemistry, Faculty of Science, Hiroshima University, Hiroshima

(Received April 30, 1969)

In previous papers,[1,2] the constituents of the sesquiterpene fraction of commercial camphor blue oil were reported. A continuous investigation of the sesquiterpene alcohol fraction was attempted more precisely. Three compounds, 2-pentadecanone, 2,3-methylenedioxynaphthalene, and piperonyl acrolein, were newly obtained in small amounts.

Experimental

The sesquiterpene alcohol fraction (bp 120—160°C/4 mmHg, 456 g) of commercial camphor blue oil was fractionated and divided into 19 fractions.

2-Pentadecanone. Fraction 5 (bp 124—126°C/4 mmHg) was chromatographed on silica gel with chloroform. White crystals were isolated from the first eluate and recrystallized (mp 35—37°C, GC pure) from ethanol. This melting point corresponds to that of 2-pentadecanone.[3] The IR spectrum indicated that this compound was an aliphatic ketone having a CH_3-CO-CH_2-group ($\nu_{C=O}$ 1710, $\delta_{CH_2-C=O}$ 1405 and $\delta_{CH_3-C=O}$ 1355 cm^{-1}). The main peaks (*m/e* 43 (CH_3-CO)$^+$, 58 (base peak) (CH_3-CO-CH_2+H)$^+$, 59 (CH_3-CO-CH_2+2H)$^+$, 71 (CH_3-CO-CH_2-CH_2)$^+$, 85 (CH_3-CO-CH_2-CH_2-CH_2)$^+$ and 226 M$^+$) were observed in the mass spectrum. From the above evidence, this compound can be said to be 2-pentadecanone.

2,3-Methylenedioxynaphthalene. From the second eluate group, white crystals were obtained and sublimed; mp 96—97°C (TLC pure). The UV spectra of this compound and naphthalene were similar to each other; the first band had the absorption maximum at λ_{max}^{EtOH} 227 mμ (ε 35000); the second band had the fine structure at 266 mμ (ε 3500), 275 mμ (ε 3700) and 286 mμ (ε 3100), and the third band at 313 mμ (ε 1900) and 325 mμ (ε 2300) showed a bathochromic shift in comparison with that of naphthalene. These bands indicated that this compound had the skeleton of β-substituted naphthalene. Moreover, this UV spectrum was much the same as that of 2-methyl-6,7-methylenedioxynaphthalene.[4] The IR spectrum showed the existence of the condensed aromatic nucleus ($\nu_{C=C}$ 1610, $\nu_{C=C}$ 1490 and $\nu_{C=C}$ 1470), the 1,2,4,5-tetrasubstituted benzene ring (δ_{CH} 857 cm^{-1}), and the methylenedioxy group (ν_{CH_2} 2790, $\nu_{=C-O-C}$ 1264, $\nu_{=C-O-C}$ 1049 and ν_{-O-CH_2-O-} 947 cm^{-1}). Therefore, the methylenedioxy group combines with naphthalene at the 2,3-positions. The mass spectrum showed peaks of *m/e* 14, 28, 44, 114, and 172 (base peak) M$^+$; molecular formula $C_{11}H_8O_2$ was deduced from p+1 (12.01%) and p+2 (1.20%) against M$^+$ (100%).[5] From the above evidence, this compound was determined to be 2,3-methylenedioxynaphthalene.

Piperonyl Acrolein. Fraction 9 (bp 132—134°C/4 mmHg) was chromatographed on alumina III with benzene. Pale yellow crystals were isolated from the middle eluate and recrystallized (mp 84—85°C, TLC pure) from ethanol This melting point corresponds to that of piperonyl acrolein.[6] The IR spestrum showed the existence of the 1,2,4-trisubstituted benzene ring (δ_{CH} 818 and δ_{CH} 877 cm^{-1}), the methylenedioxy group (ν_{CH_2} 2785, $\nu_{=C-O-C}$ 1267, $\nu_{=C-O-C}$ 1040 and ν_{-O-CH_2-O-} 932 cm^{-1}) combined with the aromatic nucleus, and the -CH=CH-CHO group (ν_{CH} 2821, ν_{CH} 2707, $\nu_{C=O}$ 1665, $\nu_{C=C}$ 1618, $\nu_{C=C}$ 1595 and δ_{CH} 975 cm^{-1}). The NMR spectrum showed the signals of aromatic protons at 6—8 ppm (3H, m, AB_2 type), methylene protons of the methylenedioxy group at 6.02 ppm (2H, s), olefinic protons of the *trans* disubstituted double bond at 7.39 ppm (1H, d, J=16.0 cps) and 6.53 ppm (1H, d-d, J=16.0 and 8.0 cps), and the aldehyde proton at 9.66 ppm (1H, d, J=8.0 cps). The mass spectrum showed peaks of *m/e* 147 (M-CHO)$^+$, 175 (M-H)$^+$, and 176 (base peak) M$^+$. Judging the above evidence, this compound is a derivative of benzene which combines with the methylenedioxy group at the 1,2-positions and with the -CH=CH-CHO group at the 4-position. Thsu, this compound can be said to be piperonyl acrolein.

*1 Fukuoka University of Education, Munakata-machi, Munakata-gun, Fukuoka.

1) S. Hayashi, N. Hayashi, K. Yano, M. Okano and T. Matsuura, This Bulletin, **41**, 234 (1968).

2) S. Hayashi, K. Yano, N. Hayashi and T. Matsuura, *ibid.*, **41**, 1465 (1968).

3) P. Baumgarten, *Ber.*, **76**, 213 (1943).

4) C. Tani, N. Takao and K. Tagahara, *Yakugaku Zasshi*, **84**, 1217 (1964).

5) J. H. Beynon, "Mass Spectroscopy and Its Application to Organic Chemistry," Elsevier Amsterdam (1960).

6) T. Ikeda, S. Takeda, H. Nakama and T. Yokohara, *Nippon Kagaku Kwaishi (J. Chem. Soc. Japan)*, **61**, 583 (1940).

BULLETIN OF THE CHEMICAL SOCIETY OF JAPAN VOL. 42 3592—3593 (1969)

Synthesis of a Fragment (Pentapeptide) of *E. Coli* Acyl Carrier Protein Apoprotein

Yoshiro MIURA and Shuichi SETO

Chemical Research Institute of Non-Aqueous Solutions, Tohoku University, Katahira-cho, Sendai

(Received May 23, 1969)

Various peptides have been synthesized rapidly and in higher yield by the solid phase method.[1-3] We have synthesized by this method, a nonapeptide of melittin[4] and a heptapeptide[5]. Acyl carrier protein has recently been found to be essential for saturated fatty acid biosynthesis, amino acid sequence of which has been reported.[6,7]

Acyl carrier protein holoprotein (holo-ACP) synthetase which transfers 4′-phosphopantetheine from reduced CoA to apo acyl carrier protein (apo-ACP) to form holo-ACP and 3′,5′-adenosine diphosphate has been shown in *E. Coli B*.[8] It seemed interesting to study the smallest fragment of apo-ACP to be utilized as a substrate of this enzyme, and we tried to synthesize a pentapeptide having a serine residue to which 4′-phosphopantetheine is bound. We wish to report the synthesis of a fragment of apo-ACP, H-Gly-L-Ala-L-Asp-L-Ser-L-Leu-OH, by the solid phase method. Synthesis of a pentapeptide was carried out according to the procedure described by Marshall and Merrifield[3] for the solid phase method, using an automatic instrument which we constructed[5].

The peptide was synthesized stepwise, beginning with 1.7 mmol of *t*-butyloxycarbonyl (*t*-Boc)-L-leucine esterified to 10 g of the cross-linked polystyrene resin (copolymerized with 2% divinylbenzene). *t*-Boc-amino acids with protected side chains were *O*-benzyl-L-serine and *β*-benzyl-L-aspartic acid.

Coupling was mediated by *N*, *N*′-dicyclocarbodiimide (DCC). *t*-Boc groups were removed with 1 N hydrogen chloride in glacial acetic acid. Neutralization of the hydrochloride was carried out with triethylamine in dimethylformamide (DMF).

The total time required for the sysnthesis was 28 hr. The peptide was cleaved from the resin with hydrogen bromide in trifluoroacetic acid. The reagent also cleaved the ether bond in the *O*-benzyl-L-serine residue and the ester bond in the *β*-benzyl-L-aspartic acid residue. Paper chromatography of the crude peptide showed one major ninhydrin positive spot and a few minor spots. The pure pentapeptide was obtained through purification of the crude peptide by gel filtration on a column of Sephadex G-10 using 0.1 M acetic acid as the solvent and gave the correct amino acid ratios on acid hydrolysis. The over-all yield from the first leucine residue was 19.6%. Its homogeneity was shown by paper chromatography using two different solvent systems and by electrophoresis.

Experimental

Solvents used for ascending paper chromatography on Toyo Roshi No. 50 paper were a) *n*-butanol - acetic acid - water(BAW) (4 : 1 : 1) and b) *n*-butanol - acetic acid - pyridine - water (BAPW) (15 : 3 : 10 : 12). Paper electrophoresis was carried out using a pH 7.76 buffer (KH_2PO_4-Na_2HPO_4), on Toyo Roshi No. 50 paper at 500V/38 cm for 2 hr.

***t*-Boc-L-leucyl Resin.** A solution of 3.06 g (13.25 mmol) of *t*-Boc-L-leucine and 1.34 g (13.25 mmol) of triethylamine in 14 m*l* of absolute ethanol and 7 m*l* of chloroform was added to 10.0 g of chloromethylcopolystyrene-2% divinylbenzene which contained 6.61% chlorine. The reaction mixture was stirred at reflux temperature for 48 hr. The esterified resin was filtered off and washed with absolute ethanol (three times), water (three times), and methanol (three times). The esterified resin was then dried *in vacuo* over KOH pellets; yield, 11.5 g. Amino acid analysis of an acid hydrolysate (dioxane-12 N HCl, 1 : 1) showed the product to contain 0.602 mmol of leucine/g of esterified resin.

***t*-Boc-glycyl-L-alanyl-*β*-benzyl-L-aspartyl-*O*-benzyl-L-seryl-L-leucyl-Resin.** The *t*-Boc-L-leucyl (2.82 g) was placed in the reaction vessel. The following cycle of de-protection, neutralization, and coupling was carried out for the introduction of each residue: (1) three washings with 26 m*l* portions of glacial acetic acid; (2) cleavage of the *t*-Boc group by treatment with 1 N HCl in glacial acetic acid (30 m*l*) for 30 min at room temperature; (3) three washings with 26 m*l* portions of glacial acetic acid; (4) three washings with 33 m*l* portions of absolute ethanol; (5) three washings with 24 m*l*

1) R. B. Merrified, *J. Am. Chem. Soc.*, **85**, 2149 (1963).
2) R. B. Merrified, *Biochemistry*, **3**, 1385 (1964).
3) G. R. Marshall and R. B. Merrified, *ibid.*, **4**, 2394 (1965).
4) Y. Miura, M. Toyama and S. Seto, *Sci. RITU. A-Vol.* **20**, 41 (1968).
5) H. Sugiyama, Y. Miura and S. Seto, *Yuki Gosei Kagaku Kyokai Shi (J. Synthetic Org. Chem. Japan)*, **26**, 1010 (1968).
6) T. C. Vanaman, S. J. Wakil and R. L. Hill, *J. Biol. Chem.*, **243**, 6409 (1968).
7) T. C. Vanaman, S. J. Wakil and R. L. Hill, *ibid.*, **243**, 6420 (1968).
8) J. Elovson and P. R. Vagelos, *J. Biol. Chem.*, **243**, 3603 (1968).

portions of DMF; (6) neutralization of the hydrochloride salt with 2.6 m*l* of triethylamine in 26 m*l* of DMF; (7) three washings with 24 m*l* portions of DMF; (8) three washings with 28 m*l* portions of methylene chloride; (9) addition of 6.80 mmol of the appropriate *t*-Boc-amino acid dissolved in 20 m*l* of methylene chloride and mixing for 10 min; (10) addition of 6.80 mmol of DCC in 16 m*l* of methylene chloride, followed by a reaction period of 3.0 hr at room temperature. For the *t*-Boc-*O*-benzyl-L-serine cycle the reaction time was 3.5 hr; (11) three washings with 28 m*l* portions of methylene chloride; (12) three washings with 33 m*l* portions of absolute ethanol.

After step 12 following the incorporation of the *t*-Boc-glycine, the protected peptide resin compound was further washed with methylene chloride, absolute ethanol and dried *in vacuo* over KOH pellets overnight; yield, 3.7 g.

Crude Glycyl-L-alanyl-L-aspartyl-L-seryl-L-leucine. The protected peptide resin (2.90 g) was suspended in 20 m*l* of trifluoroacetic acid, and a stream of hydrogen bromide was bubbled through the suspension with occasional shaking for 90 min. The resin was removed by filtration and washed with 4 m*l* of trifluoroacetic acid. The combined filtrates were evaporated on a rotary evaporator *in vacuo* at 25°C and the syrupy product obtained was triturated with dry ether. Ether was removed by decantation and the residue was washed with ether. The amorphous powder was collected; yield, 810 mg.

Paper chromatography in BAW showed a major spot at R_f 0.21 when sprayed with ninhydrin reagent and traces of materials at R_f 0.11, R_f 0.42, and R_f 0.62, and also in BAPW, a major spot at R_f 0.45 and traces of materials at R_f 0.52 and R_f 0.79.

Paper electrophoresis showed two spots when sprayed with ninhydrin reagent.

Purification of Crude Pentapeptide. A portion (18 mg) of the crude peptide was placed on a 1.2×68 cm column of Sephadex G-10 equilibrated with 0.1 M acetic acid. The column was then developed with the same solvent. Aliquots (0.1 m*l*) from 2 m*l* fractions were alanyzed by ninhydrin reagent. Fractions 6-19 contained only the major compound and were pooled and lyophilized; yield, 2.7 mg. This presents an overall yield 19.6% based on the amount of leucine initially esterified to the resin.

By paper chromatography we obtained R_f 0.20 (BAW), R_f 0.45 (BAPW). Paper electrophoresis of the pentapeptide showed a single ninhydrin positive spot. Amino acid ratios found were: Asp, 0.95; Ser, 0.98; Gly, 1.02; Ala, 1.00; Leu, 1.03. $[\alpha]_D^{23}$ −59.3 (*c* 0.73, H_2O).

BULLETIN OF THE CHEMICAL SOCIETY OF JAPAN VOL. 42 3593—3596 (1969)

Effect of Particle Size on Infrared Spectra of Inorganic Powders*1,*2

Kimitaka SATO, Fumio KUROSAWA and Ōhiko KAMMORI

Tokyo Research Institute, Yawata Iron and Steel Co., Ltd., Ida, Kawasaki

(Received May 28, 1969)

In our studies of the analysis of the inclusions in iron and steel by infrared absorption spectroscopy,[1-7] it was found that the effect of the particle size of inorganic powders is remarkable in its quantitative measurement. The effect is, of course, also connected with the physical properties of iron and steel as well as with the quantitative investigation of these substances. One effect of the particle size in the infrared spectra of inorganic powders had already been studied by the Liege investigators,[8-10] who proposed a theoretical formula. At that time, it was, however, difficult to separate inorganic powders into different particle sizes according to the order of micron. Lejeune and co-worker[8] identified each particle size of powders by means of a microscope. Since then, the problem on the particle size has not been discussed, because no

*1 Infrared Absorption Spectra and its Application to the Studies on Iron and Steel. Part VII. Part VI of this series: Ō. Kammori, K. Sato and F. Kurosawa, *Kogyo Kagaku Zasshi (J. Chem. Soc. Japan, Ind. Chem. Sect.)*, **72**, 1258 (1969).

*2 Presented at the 22nd Annual Meeting of the Chemical Society of Japan, Tokyo, April, 1969.

1) Ō. Kammori, N. Yamaguchi and K. Sato, *Bunseki Kagaku (Japan Analyst)*, **16**, 1050 (1967).

2) K. Sato, F. Kurosawa, N. Yamaguchi and Ō. Kammori, *Kogyo Kagaku Zasshi (J. Chem. Soc. Japan, Ind. Chem. Sect.)*, **71**, 208 (1968).

3) K. Sato, N. Yamaguchi and Ō. Kammori, *Bunseki Kagaku (Japan Analyst)*, **17**, 301 (1968).

4) Ō. Kammori, I. Taguchi and K. Sato, *J. Japan Inst. Metals*, **32**, 634 (1968).

5) Ō. Kammori, N. Yamaguchi, K. Sato and F. Kurosawa, *ibid.*, **32**, 779 (1968).

6) Ō. Kammori, K. Sato and F. Kurosawa, *Bunseki Kagaku (Japan Analyst)*, **17**, 1270 (1968).

7) Ō. Kammori, K. Sato and F. Kurosawa, *Kogyo Kagaku Zasshi (J. Chem. Soc. Japan, Ind. Chem. Sect.)*, **72**, 1258 (1969).

8) R. Lejeune and G. Duyckaerts, *Spectrochim. Acta*, **6**, 194, (1954).

9) G. Duyckaerts, *ibid.*, **7**, 25 (1955).

10) Mille. J. Bonhomme, *ibid.*, **7**, 32 (1955).

technique for separating powders has been developed.

A new method of separating particles with ultrasonic waves was recently developed in our laboratory,[11] and it was applied to the study of the effect of the particle size on the infrared spectra of inorganic powders. The present paper will describe the variation in the absorption bands in the infrared spectra of several inorganic powders separated by means of the new screening method mentioned above.

Experimental

Materials. Three inorganic powders, α-SiO_2, $CaCO_3$, and α,β-Si_3N_4, were used as samples, since they have more absorption bands than the other metal oxides, carbides, nitrides and sulfides reported on in our previous papers.[1,6]

Separation of Powders with Particles of Different Sizes. The three inorganic powders were separated into each particle size according to the order of micron by means of a new apparatus with ultrasonic waves developed in our laboratory.[11] The outline of the technique is as follows. The inorganic powders used are uniformly suspended in methanol with ultrasonic waves and are then filtered with metal sieves. In this experiment, the powdered samples were separated into four particle sizes by using sieves of 2, 10, and 20 μ. A micrograph of the 5 μ sieve is shown in Photo. 1.

Measurement. The spectra were obtained using a Perkin Elmer model 521 grating spectrometer with the KBr disk technique over the 400—1400 cm^{-1} region. The KBr powders were prepared by pulverizing single crystals into particle sizes smaller than 300 mesh, and the amount of KBr in the disk for one sample (about 0.5 mg) was unified to 300 mg in a disk preparation. The disk prepared was about 1 mm thick and 13 mm in diameter.The thickness of the disk was not measured exactly in this experiment. We spent 15—20 min mixing inorganic powder with KBr powder in an agate mortar, according to the method described in our previous papers.[5,7]

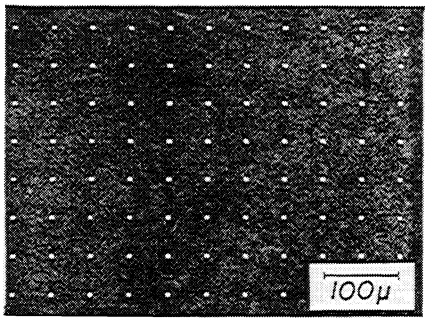

Photo. 1. An exampe of 5 μ sieve used in this experiment.

Results and Discussion

The micrograph of $CaCO_3$ separated into four ranges of particle sizes by the screening method with ultrasonic waves is shown in Photo. 2 as an example. It seems to be nicely separated by particle size. The infrared spectra of $CaCO_3$ for each particle size are shown in Fig. 1, which shows that each absorption band becomes sharper and its spectral intensity stronger as the particle size becomes smaller. Figure 2 shows the variation in the infrared spectrum for each particle size of α-SiO_2. The absorption band at about 800 cm^{-1} hardly splits at all in the larger particle size, while it separates remarkably into two bands in the sizes smaller than 2 μ. For the 460 cm^{-1} band with a shoulder at 512 cm^{-1} in the sample of a particle size larger than 2 μ, the 512 cm^{-1} band is separated remarkably

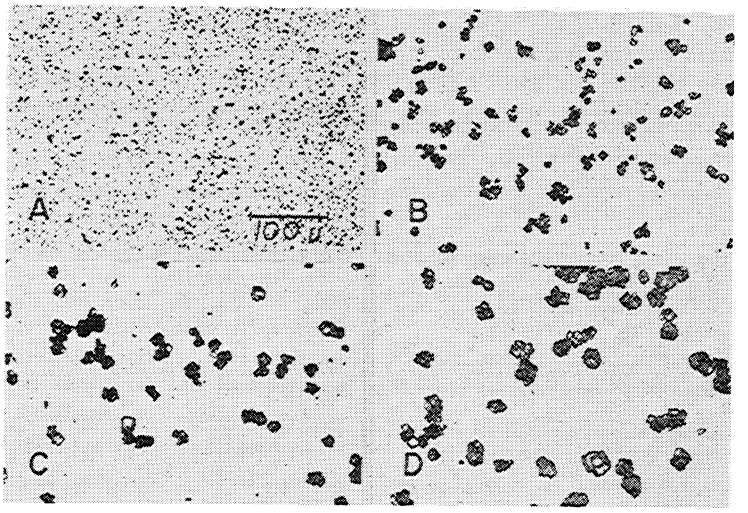

Photo. 2. An example of separated powders ($CaCO_3$) of different sizes. Particle sizes: A, $<2\mu$ B, $2—10\mu$ C, $10—20\mu$ D, $>20\mu$

11) Ō. Kammori, I. Taguchi and K. Takimoto, *J. Japan Inst. Metals*, **33**, 669 (1969).

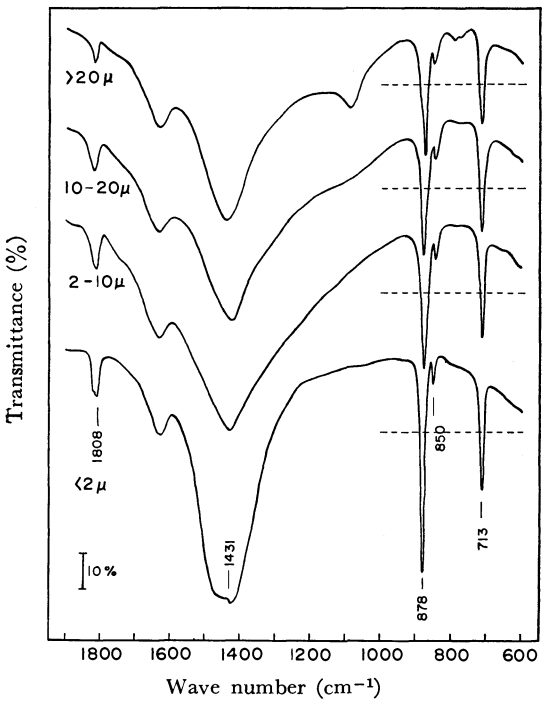

Fig. 1. Infrared spectrum of $CaCO_3$ with particles of different size.
---- : 50% transmittance line

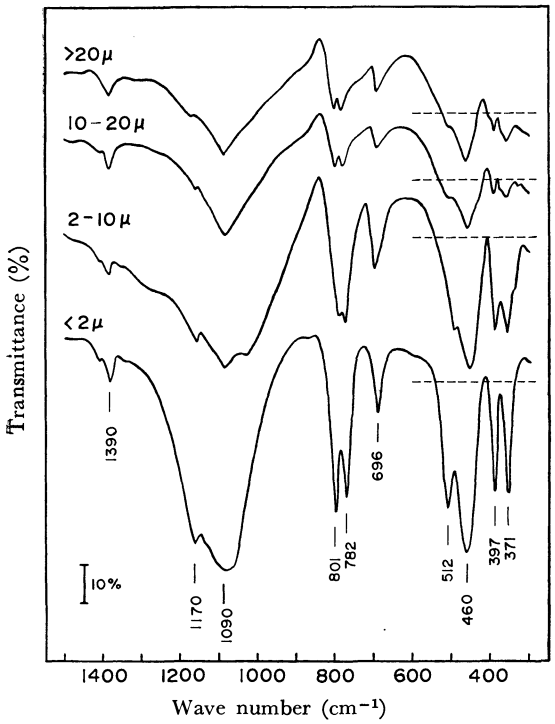

Fig. 2. Infrared spectrum of α-SiO_2 with particles of different size.
---- : 50% transmittance line

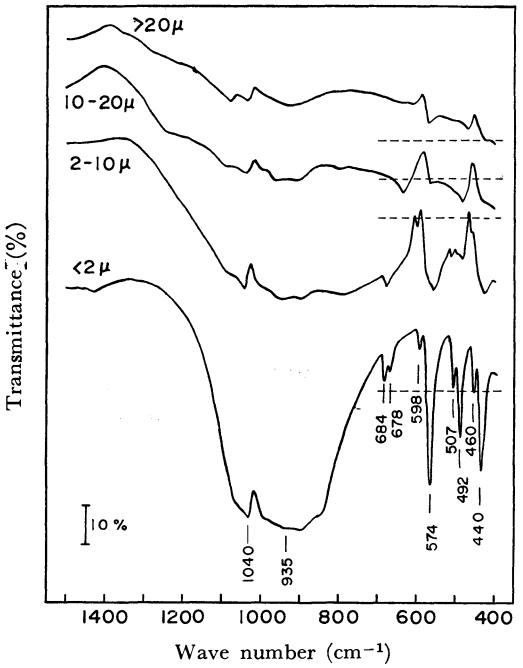

Fig. 3. Infrared spectrum of α,β-Si_3N_4 with particle of different size.
---- : 40% transmittance line

in the particles smaller than 2 μ. We observed a similar phenomenon for the 371 and 397 cm^{-1} bands. Si_3N_4 cannot be separated into α- and β-forms, so it was used as a mixture. The variation in the infrared spectra in each particle size of α,β-Si_3N_4 is shown in Fig. 3. In the case of larger particle sizes, each absorption band is hardly split at all, while the separation of each band is fine in the sizes less than 2 μ.

In the infrared spectra of inorganic powders, each absorbance at characteristic absorption bands varies according to its particle size, as has been mentioned above. In general, the smaller the particle size, the larger its absorbance. In some particles of the smaller size, it seems that the tendency of absorbance becomes definite; this finding agrees with Duyckaerts'.[9] In the separation of each particle size of a mixture, there is still a difference in the particle size of each component. Therefore, when a mixture involves substances in different particle-size meshes, the spectrum for each mesh may show something unusual. The corresponding examples are the 1090 cm^{-1} band in the spectrum of 2μ up-separated $CaCO_3$ and the 1030 cm^{-1} band in α-SiO_2 with sizes between 2 and 10μ. Accordingly, we must pay attention to the point of the spectral abnormality. At the same time, it is indispensable that a sample be very pure in a study of the variation in the infrared spectrum for inorganic powders of different particle sizes.

On the other hand, it is very useful to separate powders into each size of particle when the iron ores, the corrosion product of steel, and the non-metallic inclusion in steel are used as the samples for separation. In the present technique, only the sieves with meshes larger than 2μ can be manufacutured; it is difficult to make a mesh less than this size.

In any case the study of infrared spectra by the separation of powders into each particle size is important not only for a quantitative analysis but also for a study of the properties of an inorganic substance.

The authors are grateful to Dr. San-ichiro Mizushima, the Director of the Institute, for his interest in this work.

BULLETIN OF THE CHEMICAL SOCIETY OF JAPAN VOL. 42 3596—3597 (1969)

Photoisomerization of 1,2-Diphenyl-6-methyl-2,3-dihydro-4-pyridone

Choji KASHIMA, Makoto YAMAMOTO, Yoshiaki SATO and Noboru SUGIYAMA

Department of Chemistry, Tokyo Kyoiku University, Otsuka, Bunkyo-ku, Tokyo

(Received May 30, 1969)

There have been many papers about the photochemical isomerization and dimerization of 2-cyclohexenones.[1] Yates reported that 2,6-dimethyl-2,3-dihydro-4-pyrone was dimerized by light.[2] Recently we have found a method of synthesizing 2,3-dihydro-4-pyridones from β-diketones and Schiff bases.[3] As an analogy with cyclohexenone and 2,3-dihydropyrone, the photochemistry of 2,3-dihydro-4-pyridone is of interest.

A solution of 1,2-diphenyl-6-methyl-2,3-dihydro-4-pyridone (I) in benzene or methanol was irradiated with a high-pressure mercury lamp through a Pyrex filter. No apparent change was observed after irradiation for a week. However, by the irradiation of a methanol solution of I with a low-pressure mercury lamp through a Vycor filter, three products (II, III, and IV) were obtained. Figure 1 shows the change in I and in the production of II, III, and IV with the time.

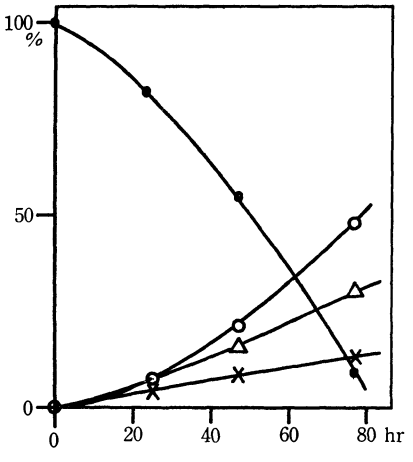

Fig. 1. The change of I and the production of II, III and IV with time.
—●— I, —○— II, —△— III, -×- IV

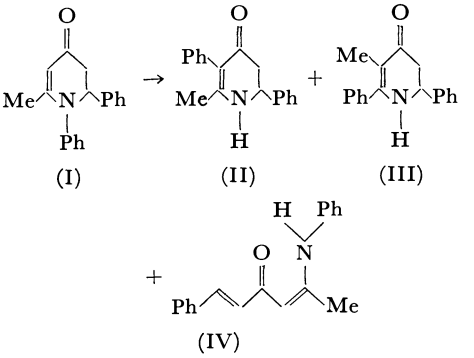

Fig. 2. Mechanism of photoisomerization.

After irradiation for 100 hr, the products were separated. The structures of the products were deduced by means of the spectral data listed in Table 1. The IR and UV spectra showed the re-

1) S. N. Ege and P. Yates, *Can. J. Chem.*, **45**, 2933 (1967); W. G. Dauben, G. W. Shaffer and N. D. Vietmeyer, *J. Org. Chem.*, **33**, 4060 (1968); H. E. Zimmerman, R. D. Rieke and J. R. Scheffer, *J. Am. Chem. Soc.*, **89**, 2033 (1967); H. E. Zimmerman and K. G. Hancock, *ibid.*, **90**, 3749 (1968).

2) P. Yates and D. J. Macgregor, *Tetrahedron Letters*, **1969**, 453.

3) N. Sugiyama, M. Yamamoto and C. Kashima, This Bulletin, **42**, 1357 (1969).

Table 1.

	I	II	III	IV
λ_{max}^{EtOH} nm (ε)	240 (2180)		243 (4500)	232 (11700)
	327 (10400)	343 (14300)	347 (9500)	297 (12600)
				383 (29100)
ν cm^{-1}	1630	1635	1635	1640
	1600	1600	1600	1580
	1550	1540	1540	
τ^{CDCl_3}	8.13	8.32	8.02	7.94
	7.09	7.02	7.07	
		6.60	6.62	−3.17
	5.08	5.13	5.18	
	4.81			4.80
				3.50
				2.58
	2.6—3.2	2.6—3.2	2.6—3.2	2.5—3.2

lation of the 2,3-dihydro-4-pyridone structures in II and III. In the NMR spectra of II and III, the signals of the ABX pattern at τ 7.1 and 5.1, which are assignable to the 2-methine proton and the 3-methylene protons, were observed. Though the olefinic proton signal at τ 4.81 was not found, new singlet signals were observed at τ 5.13 and 5.18 which were changed by deuterium exchange. These results suggest that II is 2,5-diphenyl-6-methyl-2,3-dihydro-4-(1H)-pyridone and that III is 2,6-diphenyl-5-methyl-2,3-dihydro-4-pyridone.

However, IV did not show the characteristic absorption bands of 1,3-dihydro-4-(1H)-pyridone in the IR and UV spectra. In the NMR spectrum of IV, the singlet of one olefinic proton and a pair of doublets of two olefinic protons were observed at τ 4.80, 3.50, and 2.58. The singlet at τ −3.17, which disappeared upon the deuterium exchange, was assigned to the NH proton signal. These facts and the elemental analyses indicated that the structure of IV was 5-anilino-1-phenyl-1,4-hexadien-3-one. This was further confirmed by the fact that IV was identical with the condensation product of 2-anilino-2-penten-4-one and benzaldehyde after it had been treated with sulfuric acid.

Experimental

Materials. 1,2-Diphenyl-6-methyl-2,3-dihydro-4-pyridone (I) was synthesized from acetylacetone and benzylideneaniline in liquid ammonia;[3] mp 85°C. The spectral data are shown in Table 1.

Irradiation. Through the Vycor filter, a solution of 500 mg of I in 5 m*l* of methanol was irradiated by a high-pressure mercury lamp (450 W), and the reaction products were detected. However the photoproduct was not detected from a methanol or benzene solution of I through a Pyrex filter in a week. By the irradiation of a solution of 200 mg of I in 10 m*l* of methanol with a low-pressure mercury lamp (80 W) through a Vycor filter, I was isomerized to II, III, and IV. The change was monitored with the NMR spectrometer shown in Fig. 1.

Products II, III, and IV. After the irradiation of a solution of 300 mg of I in 10 m*l* of methanol for 100 hr, the colorless crystals which formed were filtered out and washed with cold methanol; mp 257°C.

Found: C, 82.00; H, 6.49; N, 5.27%. Calcd for $C_{18}H_{17}NO$: C, 82.10; H, 6.51; N, 5.32%.

The filtrate was concentrated under reduced pressure, and the residue was passed through a silica-gel (Merck 7734) column with a benzene - ethyl acetate (2 : 1 v/v) mixture. A yellow fraction and a pale yellow fraction were collected separately. The former fraction contained IV, and the latter contained III, showing R_f 0.85 and 0.44 on silica-gel (Wako-gel B-5) thin-layer chromatography with a benzene - ethyl acetate (2 : 1 v/v) mixture. The spectral data of II, III, and IV are summarized in Table 1.

5-Anilino-1-phenyl-1,4-hexadiene-3-one (IV). To 200 m*l* of liquid ammonia containing 2.1 g of potassium amide there were added 3 g of 2-anilino-2-penten-4-one at −33°C. After the mixture had been stirred one hour, 2 m*l* of benzaldehyde was added and stirring was continued for 2 hr. After the removal of the solvent at room temperature, the residue was acidified with concentrated hydrochloric acid. The product was extracted with chloroform, and the organic layer was washed with aqueous ammonia and then with water. The solvent was evaporated, and the residue was dissolved in 20 m*l* of concentrated sulfuric acid at room temperature. After 20 min, the solution was poured onto crashed ice and extracted with chloroform. The organic layer was washed with an aqueous sodium bicarbonate and with water, and then dried over calcium chloride. After the removal of the solvent, the residue was passed through a silica-gel (Merck 7734) column. The yellow fraction was collected, and the slovent evaporated. The residue was recrystallized from *n*-hexane, mp 101°C, which was identified with the above its R_f value of 0.44.

Found: C, 81.89; H, 6.72; N, 5.41%. Calcd for $C_{18}H_{17}NO$: C, 82.10; H, 6.51; N, 5.32%.

BULLETIN OF THE CHEMICAL SOCIETY OF JAPAN VOL. 42 3598—3600 (1969)

On the Stability of Silver(I) Complexes with an Imidazole and Its Derivatives

Shigeo NAKATSUJI, Riichiro NAKAJIMA and Tadashi HARA

Department of Chemical Engineering, Faculty of Engineering, Doshisha University, Kamikyo-ku, Kyoto

(Received June 2, 1969)

No report seems to have been given on the formation constant of the complexes between silver(I) ion and imidazole derivatieves except for poly-*N*-vinylimidazole[1] and *N*-methylimidazole.[2] The present paper deals with the stability of silver(I) complexes with imidazole derivatives, in which the consecutive formation constants of the silver complexes were estimated and the influences of the substituent upon the stability of the silver complexes were discussed. The molecular diagram of the imidazole derivatives was calculated and the nitrogen atom as a donor was determined. The infrared spectra of the silver complexes are also recorded and discussed.

The consecutive formation constants were estimated by applying the pH measurement and Bjerrum's methods.[3] An imidazole and its derivatives were of guaranteed-grade. The solution containing imidazole or imidazole derivatives, nitric acid and potassium nitrate (the ionic strength : 1) was titrated with a standard sodium hydroxide solution at 25°C.[4,5] The readings in the pH meter were corrected by the activity coefficients, and the dissociation constants of an imidazole and its derivatives were estimated, followed by calculation of the consecutive formation constants. From the formation curves for the imidazole derivatives, all the values of $\bar{n}$ were found to be less than 2. This is compatible with the following equilibrium.

$$\left.\begin{aligned} Ag^+ + Im &\overset{k_1}{\rightleftharpoons} AgIm^+ \\ AgIm^+ + Im &\overset{k_2}{\rightleftharpoons} AgIm_2^+ \end{aligned}\right) \quad (1)$$

Hence, the consecutive formation constants are given by

$$k_1 = \frac{[AgIm^+]}{[Ag^+]\cdot[Im]}, \quad k_2 = \frac{[AgIm_2^+]}{[AgIm^+]\cdot[Im]}, \quad (2)$$

where Im means imidazole or imidazole derivatives. According to Bjerrum's assumption, the values of p[Im] at $\bar{n}=1/2$ and 3/2 on the formation curve correspond to those of $\log k_1$ and $\log k_2$. The values of $[Ag^+]$, $[AgIm^+]$ and $[AgIm_2^+]$ were calculated using the values of k_1 and k_2. However, Bjerrum's assumption[3] was not valid. Approximate calculation was repeated until the values of k_1 and k_2 converged. The final results are shown in Table 1 with those of pyridine derivatives. The

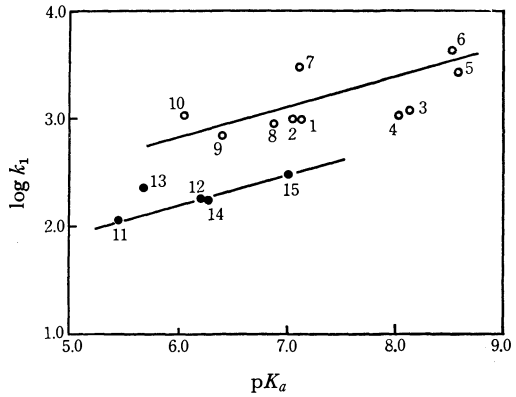

Fig. 1. Relation between pK_a and $\log k_1$.
The numbers of the ligand are the same as in Table 1.

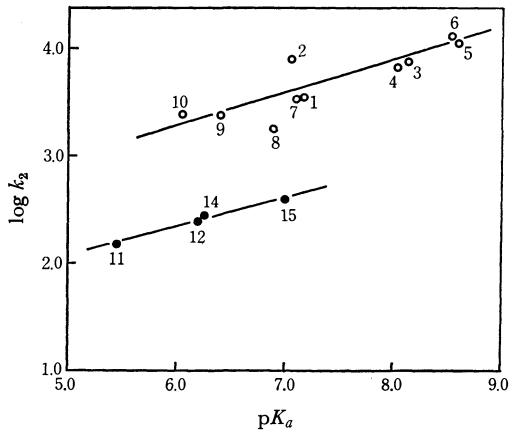

Fig. 2. Relation between pK_a and $\log k_2$.
The numbers of the ligand are the same as in Table 1.

1) D. H. Gold and H. P. Gregor, *J. Phys. Chem.*, **64**, 1461 (1960).
2) J. E. Bauman and J. C. Wang, *Inorg. Chem.*, **3**, 368 (1964).
3) J. Bjerrum, "Metal Ammine Formation in Aqueous Solution," P. Haase and Son, Copenhagen (1941).
4) T. Hara and S. Kishige, *Sci. and Eng. Rev. of Doshisha Univ.*, **2**, 125 (1961).
5) N. C. Li, J. M. White and E. Doody, *J. Am. Chem. Soc.*, **76**, 6219 (1954).

TABLE 1. ACID DISSOCIATION CONSTANTS OF IMIDAZOLE AND PYRIDINE DERIVATIVES AND FORMATION CONSTANTS OF THEIR SILVER COMPLEXES

Ionic strength; 1.0, Temp.: 25°C

No.	Ligands	pK_a	Formation constants $\log k_1$	$\log k_2$	References
	Imidazole		3.11	3.73	1
1	Imidazole	7.33	3.08	3.87	
2	*N*-Methylimidazole	7.06	3.00	3.89	2
3	2-Methylimidazole	8.13	3.11	3.87	
4	2-Ethylimidazole	8.02	3.06	3.83	
5	2,4-Dimethylimidazole	8.57	3.44	4.06	
6	2-Ethyl-4-methylimidazole	8.52	3.64	4.10	
7	1-Vinyl-2-methylimidazole	7.09	3.48	3.53	
8	1-Vinyl-2-ethylimidazole	6.88	2.97	3.25	
9	1-Vinyl-2-hydroxyethylimidazole	6.39	2.86	3.38	
10	1-Vinyl-4-hydroxyethylimidazole	6.05	3.03	3.37	
11	Pyridine (μ=0.5)	5.45	2.04	2.18	6
12	α-Picoline	6.20	2.27	2.41	7
13	β-Picoline	5.68	2.35	4.35	2
14	γ-Picoline	6.26	2.24	2.46	7
15	2,4-Lutidine	6.99	2.47	2.41	7

relations between pK_a and $\log k_1$ or $\log k_2$ are shown in Figs. 1 and 2. These results show that the affinity of an imidazole and its derivatives to silver ion increases with an increasing affinity to hydrogen ion. The same tendency is also found in cadmium complexes,[8] but not in copper complexes.[9] It is characteristic that $\log k_1$ is smaller than $\log k_2$ in the silver complexes, while the opposite is the case in the complexes of copper, cadmium and zinc. As the formation constants of the silver complexes with 2,4-dimethyl and 2-ethyl-4-methylimidazoles are larger than those with 2-methyl and 2-ethylimidazoles, the methyl group at the 4-position makes the silver complexes very stable. This seems to come from a larger increase of electron density at the 3-position than at the 1-position since the 3-position is structurally nearer the 4-position than the 1-position. On the other hand, the vinyl group at the 1-position makes the complexes unstable. There has been conflict concerning the nitrogen atom as a donor, Edsall[10] and Gold[1] proposing the coordination of the pyrrole-type nitrogen atom, while Bauman[2] and Li[5] that of the pyridine-type one. The molecular diagram of the imidazole derivatives was calculated by the simple LCAO method[11] (Table 2). The difference between our

TABLE 2. MOLECULAR DIAGRAM OF IMIDAZOLE DERIVATIVE

Ligand	1-Position	3-Position
Imidazole	0.549	−0.277
Imidazole[12]	0.41	−0.35
2-Ethylimidazole	0.421	−0.336
2,4-Dimethylimidazole	0.475	−0.392
4-Methylimidazole	0.479	−0.414
N-Methylimidazole	0.963	−0.506

values and those obtained by Orgel[12] seems to be responsible for the different selection of parameters. The fact that the nitrogen atoms at the 1- and 3-positions are assigned with the positive and negative charges supports the dissociation[13-15] of hydrogen atom on the pyrrole-type nitrogen atom and the coordination with the pyridine-type nitrogen. It is understandable that the value of formation constants increases with an increasing negative charge at the 3-position. The absorption bands at 1667 ($\nu_{C=NH}$), 1440, and 1095 cm^{-1} in the infrared spectrum of the silver imidazole complexes

6) W. C. Vosburgh and S. A. Cogswell, *J. Am. Chem.*, **65**, 2412 (1943).
7) R. J. Bbuehlman and F. H. Verhvek, *ibid.*, **70**, 1401 (1948).
8) A. G. Desai and M. B. Kabadi, *J. Indian Chem. Soc.*, **38**, 805 (1961).
9) C. J. Hawkins and D. D. Perrin, *J. Chem. Soc.*, **1962**, 1351.
10) Y. Nozaki, F. R. N. Gurd, R. F. Chen and J. T. Edsall, *J. Am. Chem. Soc.*, **79**, 2123 (1957).
11) J. D. Roberts, "Notes on Molecular Orbital Calculations," W. A. Benjamin, Inc., New York (1961).
12) L. E. Orgel, T. L. Cottrell, W. Dick and L. E. Sutton, *Trans. Faraday Soc.*, **47**, 133 (1951).
13) R. B. Martin and J. T. Edsall, *J. Am. Chem. Soc.*, **82**, 1107 (1960).
14) F. Holmes, K. M. Jones and E. G. Torrible, *J. Chem. Soc.*, **1961**, 4790.
15) M. Goodgame and F. A. Cotton, *J. Am. Chem. Soc.*, **84**, 1543 (1962).

were found to shift as compared with those of imidazole alone.[16] No shift was, however, observed in the spectrum of silver complexes with vinyl derivatives. This means that the vinyl group is independent of coordination to silver ion.

16) W. Otting, *Chem. Ber.*, **89**, 2887 (1956).

The authors wish to express their thanks to Mr. Kazuo Saito for his assistance in the experiments, and to the Mitsubishi Seishi Co. for their donation of imidazole derivatives.

BULLETIN OF THE CHEMICAL SOCIETY OF JAPAN VOL. 42 3600—3602 (1969)

The Fries Rearrangement of 2-Ethyl-5-acetyloxybenzofuran

Teruo NAKANISHI, Kazuhiko KIMURA, Kiyoshi ITŌ, Masahiko IKEMOTO and Yoshitaka ŌISHI

Research Laboratory, Kakenyaku-Kako Co., Ltd., Ōtsu

(Received June 2, 1969)

The reaction of acyl ester of phenol with aluminum chloride is known with respect to the conversion of ester into isomeric *o*- or *p*-hydroxy ketone. It is an important route in synthesis of ketones from phenols.[1] Fries discovered this rearrangement during his study on coumaranones.[2] Thereafter this type of rearrangement has been examined on coumarin derivatives. Little has been done, however, on the study of coumarones, *i.e.*, benzofuran derivatives[3] in which only one compound was separated as a rearrangement product. In the present paper we report the Fries reaction of 2-ethyl-5-acetyloxybenzofuran which resulted in the isolation of three new isomeric products.

2-Ethyl-5-acetyloxybenzofuran (I) in nitrobenzene was stirred in the presence of aluminum chloride at room temperature for 16 hr, the reaction mixture was decomposed with water, and submitted to steam distillation. After a run of nitrobenzene, a yellow oil was distilled to give a precipitate on standing. Recrystallization from petroleum ether gave yellow needles (II), mp 120—122°C. The mother liquor gave yellow plates (III), mp 75—76°C. The residue on steam distillation was recrystallized from ethanol to yield colorless prisms (IV), mp 177—178°C.

Elementary analysis revealed that the three compounds were the rearranged isomeric products of I. The IR measurement of the reaction products showed no absorption of ester. However, the absorption due to the presence of a ketonic group was distinctly observed. Absence of absorption due to hydroxyl group in II and III was explained by the influence of intramolecular hydrogen bonding to the ketonic group formed in the rearrangement reaction, whereas the absorption of hydroxyl group was observed with IV.

Signals of protons in benzofuran ring in the NMR spectra were assigned in the usual manner. The proton at position 3 in II was assigned δ 6.57 in a singlet, which appears to be a fine splitting peak due to a long range coupling of the protons at positions 3 and 7 in benzofuran ring.[4] The doublet peaks at δ 6.80 and δ 7.51 are of one proton respectively. A signal with fine splitting peak at lower magnetic field (δ 7.51) was assigned to proton at position 7. The relatively greater coupling constant ($J_{6,7}=9.0$ cps) indicates that the coupling is *o*-coupling,[5] and the doublet at higher magnetic field was assigned to proton at position 6.

The hydroxyl proton of position 5 was assigned to a singlet at δ 12.92, which supported the presence of intramolecular hydrogen bonding to adjacent carbonyl group.[6] Based on these evidences, the acetyl group in I is considered to be rearranged to position 4, and II is formed as the rearrangement product.

A singlet (δ 6.32) was assigned to the proton of position 3 in benzofuran ring of III and the remaining two peaks (δ 6.97 and δ 7.71) were assigned to two protons in the benzene ring, which showed scarcely any coupling with each other. Thus they

1) A. H. Blatt, "Organic Reactions," Vol I, John Wiley & Sons, New York (1942), p. 342.

2) K. Fries and G. Finck, *Chem. Ber.*, **41**, 4271 (1908).

3) N. M. Shan and P. M. Shan, *Chem. Ber.*, **92**, 2927 (1959); *ibid.*, **93**, 18 (1960). A. Mustafa, W. Asker, O. H. Hishmat, M. I. Ali, A. K. E. Mansour, N, M. Abed, K. M. A. Khalil and S. M. Samy, *Tetrahedron*, **21**, 849 (1965).

4) J. A. Eluidge and R. G. Foster, *J. Chem. Soc.*, **1963**, 590.

5) "High Resolution Nuclear Magnetic Resonance Spectroscopy," Vol. II, ed. by J. W. Emsley, J. Feeney and L. H. Sutchiffe, Pergamon Press Inc., Oxford (1966), p. 770.

6) "Spectrometric Identification of Organic Compounds," R. M. Silverstein and G. C. Bassler, John Wiley & Sons, Inc., New York (1967), p. 122.

must be situated at *p*-position,[5] *i.e.*, positions 4 and 7. As the protons at positions 3 and 7 in the benzofuran ring show a long range coupling, a signal with a fine splitting peak at δ 7.71 was assigned to position 7. The assignment of the hydroxyl proton at position 5 of III (δ 12.12) was the same as in the case of II. From these results, it is concluded that the acetyl group in I is rearranged to position 6, resulting in the formation of III.

Since IV is slightly soluble in chloroform, the corresponding acetate was derived to use in NMR measurement. No absorption at about δ 6.4 proved the absence of proton at position 3. One-proton peaks belonging to the benzene ring were recognized at δ 7.67, 7.01 and 7.43, respectively. A quartet at δ 7.01 was assigned to the proton at position 6 which arose through unequal coupling with protons at positions 4 and 7. The proton at position 7 was assigned to the doublet at δ 7.43 which has a greater *o*-coupling constant with proton at position 6 (*o*-coupling: $J_{6,7}=9.0$ cps). The remaining signal which appeared at δ 7.67 was assignable to the proton at position 4 (*m*-coupling: $J_{4,6}=2.1$ cps). Thus it is concluded that the acetyl group of I is rearranged to position 3 to produce IV.

Based on these results, a scheme of the rearrangement is presented as follows:

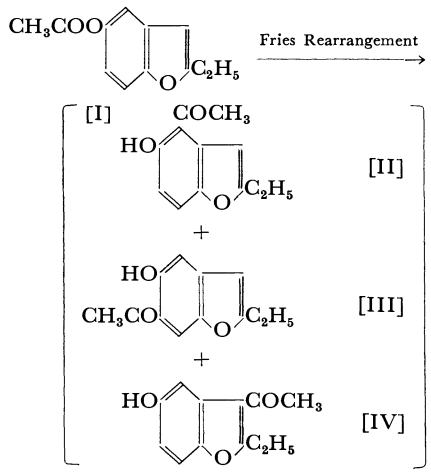

One interesting point in the Fries reaction is that the variation in the ratio of both ortho- and para-isomers depends on experimental conditions. In order to investigate the variation, we performed gas chromatography on benzofuran derivatives.[7] Raw products obtained on decomposition with water for 5 hr and 16 hr were submitted to gas chromatography. Intensity of the peaks on gas chromatogram indicated the preparation ratio of II : III : IV to be approximately 1 : 1 : 1.5 at 5 hr and 1 : 1 : 1 at 16 hr. A peak appearing immediately after the peak of IV was recognized to be due to 2-ethyl-3-acetyl-5-acetyloxybenzofuran (V). The compounds are not known. Hence we synthesized them through another route, and used them for standard sample on gas chromatography. Formation of V during the reaction suggested that the present rearrangement was intermolecular.

It has been reported[8] that under high reaction temperature in the usual Fries reaction the production rate of an *o*-derivative is predominant. Accordingly we conducted the rearrangement reaction at 110°C for 1 hr, but the ratio of II : III : IV in reaction products as estimated by gas chromatography was 1 : 1 : 1 or the same as that in the previous reaction.

Experimental

Apparatus and gas chromatographic conditions. A Shimadzu Model GC-1C gas chromatograph fitted with hydrogen flame ionization detector was employed. The U-shaped stainless steel column 1.1 m×3 mm i.d. containing 20% Apiezon GL by weight on 40/60 Neosorb NC. Conditions for chromatography: Column temperature, 190°C. Nitrogen (carrier), 20 ml/min.

2-Ethyl-5-acetyloxybenzofuran (I). To 2-ethyl-5-hydroxybenzofuran[9] (16.2 g) in pyridine (40 ml) was added dropwise acetic anhydride (20.4 g) with ice-cooling and stirring. After being stirred at room temperature for about 3 hr, the reaction mixture was poured with vigorous stirring into HCl-containing ice-water. The white precipitate thus formed was filtered and recrystallized from petroleum ether to give colorless needles (17 g), mp 54—55°C: IR (KBr) showed C=O aryl-acetate at 1758 cm^{-1}.

Found: C, 70.49; H, 6.10%. Calcd for $C_{12}H_{12}O_3$: C, 70.58; H, 5.92%.

2-Ethyl-4-acetyl-5-hydroxybenzofuran (II). To 2-ethyl-5-acetyloxybenzofuran (5 g) in nitrobenzen (50 ml) was added by portions anhydrous $AlCl_3$ (10 g) with ice-cooling and stirring. After being stirred at room temperature (20—25°C) for about 16 hr, the mixture was poured into ice-water to decompose. Steam distillation gave, after a run of nitrobenzene, a yellow precipitate, which was filtered and recrystallized from petroleum ether to yield yellow needles (0.8 g), mp 120—122°C. IR (KBr) showed no hydroxyl band, but intramolecular chelated aryl-ketone band at 1620 cm^{-1}.

Found: C, 70.61; H, 5.91%. Calcd for $C_{12}H_{12}O_3$: C, 70.58; H, 5.92%.

2-Ethyl-5-hydroxy-6-acetylbenzofuran (III). Removal of most of the mother liquor (petroleum ether) caused precipitation of yellow plates (III) (0.2 g), mp 75—76°C (from ethanol). IR (KBr) showed no hydroxyl absorption, but intramolecular chelated aryl-ketone band at 1630 cm^{-1}.

Found: C, 70.63; H, 5.75%. Calcd for $C_{12}H_{12}O_3$: C, 70.58; H, 5.92%.

2-Ethyl-3-acetyl-5-hydroxybenzofuran (IV). The residue on steam distillation was collected to recrystallize from ethanol to give colorless prisms (IV) (1.3 g),

7) T. Nakanishi *et al.*, to be published.

8) K. W. Rosenmund and W. Sehnurr, *Ann.*, **460**, 56 (1928).

9) M. Bisagni, Ng. Ph. Buu-Hoi and R. Royar *J. Chem. Soc.*, **1955**, 3688.

177—178°C. IR (KBr) showed hydroxyl band at 3200 cm^{-1}, and intermolecular hydrogen bonded aryl-ketone band at 1625 cm^{-1}.

Found: C, 70.65; H, 6.07%. Calcd for $C_{12}H_{12}O_3$: C, 70.58; H, 5.92%.

2-Ethyl-3-acetyl-5-acetyloxybenzofuran (V). 2-Ethyl-5-hydroxybenzofuran (2.4 g) in CS_2 (40 m*l*) was cooled at 0—5°C, and to this was added acetyl chloride (2.4 g), and then dropwise $SnCl_4$ (8.1 g) with stirring. After being stirred at 5—10°C for about 5 hr, the reaction mixture was poured into HCl-containing ice-water and stirred vigorously. The CS_2 layer was dried, evaporated, and the residue was recrystallized from petroleum ether to give colorless needles (2.7 g), mp 88—89°C: arly-ketone at 1645 cm^{-1}, aryl-acetate at 1740 cm^{-1}.

Found: C, 68.45; H, 5.94%. Calcd for $C_{14}H_{14}O_4$: C, 68.28; H, 5.73%.

The authors wish to express their sincere thanks to Professor K. Onodera, Kyoto University, for his kind suggestion and encouragement.

BULLETIN OF THE CHEMICAL SOCIETY OF JAPAN VOL. 42 3602—3603 (1969)

Polymerization of Methyl Methacrylate by Amide-Carbon Tetrachloride System

Kyoji KAERIYAMA

Research Institute for Polymers and Textiles, Sawatari, Kanagawa-ku, Yokohama

(Received June 4, 1969)

Some systems consisting of amide and halide, dimethylaniline - benzyl chloride[1] and pyridine-carbon tetrachloride in liquid sulfur dioxide,[2] for example, are known to initiate the polymerization of vinyl monomers. It has been found that the amide-carbon tetrachloride system induces the polymerization of vinyl monomers.

The results of the polymerization of methyl methacrylate (MMA) in the presence of various components are shown in Table 1. It can be seen from Table 1 that the acetamide-carbon tetrachloride system initiates the polymerization of MMA. Other chlorides, such as *n*-butyl chloride and chloroform, can not take the place of carbon tetrachloride. Pyridine has little effect on polymerization. DPPH and benzoquinone inhibit the polymerization. This suggests that the polymerization proceeds according to a radical mechanism.

Polymerization was carried out in the presence of various amides. It can be seen from Table 2 that formamide, acetamide, and urea are active as initiators, but that dimethylated amide, dimethyl acetamide, dimethylformamide are inactive.

Table 3 summarizes the data on the polymerisation of several vinyl monomers. The initiator system is selective for monomers. It can initiate the polymerization of acryl ester and amide, but it can not polymerize styrene. This characteristic is

Table 1. Polymerization of MMA

Acetamide (g)	Carbon tetrachloride (m*l*)	DMSO* (m*l*)	Other additives: Additive	Other additives: Amount	Conversion (%)
1.0	1.0	6.0			35.0
1.0	1.0	3.0	Pyridine	3.0 m*l*	32.8
	1.0	7.0			6.2
1.0		6.0	*n*-Butyl chloride	1.0 m*l*	6.2
1.0		6.0	Chloroform	1.0 m*l*	11.0
1.0		3.5	Pyridine	3.5 m*l*	3.1
1.0	1.0	6.0	DPPH**	0.50 g	0
1.0	1.0	6.0	Benzoquinone	0.50 g	1.5

MMA: 2.0 m*l*
Polymerization: at 60°C for 20 hr.
*DMSO=dimethyl sulfoxide
**DPPH=diphenyl picryl hydrazyl

1) T. Fueno, G. Okamoto, T. Tsuruta and J. Furukawa, *J. Polymer Sci.*, **36**, 407 (1959).

2) M. Matsuda and T. Hirayama, *ibid.*, **5**, 2769 (1967).

Table 2. Effect of various amide

Amide	Amount	Carbon tetrachloride (ml)	Conversion (%)
Formamide	0.72 ml	0.88	30.7
Acetamide	1.0 g	1.0	35.0
Urea	0.55 g	0.88	24.6
Dimethylformamide	1.0 ml	1.0	4.6
Dimethylacetamide	1.0 ml	1.0	7.1

DMSO: 6.0 ml; MMA: 2.0 ml
Polymerization: at 60°C for 20 hr

Table 3. Polymerization of various vinyl monomers

Monomer	Acetamide (g)	Carbon tetrachloride (ml)	Conversion (%)
Methyl methacrylate	1.0	1.0	32.8
Acrylonitrile	0.805	1.32	16.7
Styrene	0.805	1.32	3.5
Methyl acrylate	0.805	1.32	61.2
Acrylamide*		0.92	64.3

Monomer: 2.0 ml
Solvent: 3.0 ml DMSO+3.0 ml pyridine
Polymerization: at 60°C for 20 hr
* 1.4 g acrylamide
Solvent: 2.5 ml DMSO+2.5 ml pyridine

similar to that of the dimethylaniline - benzyl chloride system.[1]

Figure 1 shows the conversion of the monomer as a function of the mole fraction of amide to carbon tetrachloride. In the case of acetamide, the maximum conversion is observed at the mole fraction of 0.667. In the case of malonamide, it is at the equimolar fraction. This implies that two amide groups and one carbon tetrachloride molecule participate in the initiation of the polymerization of MMA.

Grafting onto polyacryl amide, which had been polymerized by potassium persulfate as an initiator, was attempted. The polymerizing mixture, which consisted of 1.90 g of polyacryl amide, 14.0 ml of DMSO, 1.0 ml of carbon tetrachloride, and 5.0 ml

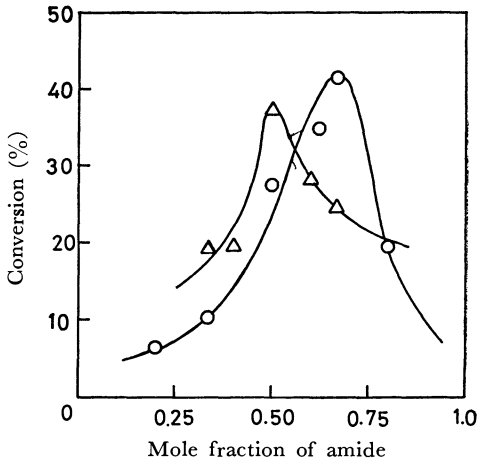

Fig. 1. Dependence of conversion on mole fraction of amide.
—○— Acetamide+CCl_4=27.3 mmol
DMSO: 6.0 ml; MMA: 2.0 ml
Polymerization: at 60°C for 20 hr
—△— Malonamide+CCl_4=18.2 mmol
DMSO: 14 ml; MMA: 4.0 ml
Polymerization: at 70°C for 20 hr

of MMA, was maintained at 60°C for 20 hr. The conversion amounted to 27.7%, but polymethyl methacrylate was completely extracted from the product with acetone. No graft-copolymer was obtained by these means. It is clear that polymerization is not initiated by a radical which has been formed by the cleavage of a bond in the amide molecule.

Experimental

Acetamide and acrylamide were recrystallized from a hot benzene solution. Malonamide was purified by pouring an aqueous solution into tetrahydrofuran. Urea was purified by pouring an aqueous solution into dioxane. Dimethyl sulfoxide, formamide, dimethylformamide, dimethylacetamide, and monomers were distilled under reduced pressure just prior to use. Polymerization was carried out in the dark according to the procedure described previously.[3]

The author is grateful to Mr. J. Ueda and Dr. A. Okada for their interest in this work. The author is also grateful to Dr. M. Suzuki.

3) K. Kaeriyama, This Bulletin, **42**, 1342 (1969).

BULLETIN OF THE CHEMICAL SOCIETY OF JAPAN VOL. 42 3604—3605 (1969)

Competition between Photo-Ionization and Photo-Dissociation of Aromatic Compounds

Hiroshi TSUBOMURA

Department of Chemistry, Faculty of Engineering Science, Osaka University, Toyonaka-shi, Osaka

(Received June 9, 1969)

Since the pioneering work of Lewis,[1] Porter[2] and their collaborators, it has been widely accepted that the ultraviolet irradiation of substituted aromatics yields their cations or radicals, the latter being formed by the fission of the β-bond of the substituent group. Thus, *p*-phenylenediamine, for instance, forms its cation almost exclusively. Anisole or phenol, on the other hand, forms mainly phenoxyl radical. For some compounds, the assignment of the products by Lewis and Porter was only tentative and lacked conclusive evidence. As far as the author is aware, reasons for such differrences in the photo-chemical behaviors of various aromatics do not seem to have been discussed.

We have studied the photo-products of several substituted aromatics irradiated in organic matrices at 77°K.[3-6] In these studies, the assignment of unstable species formed by the ultraviolet irradiation has been reconfirmed using more elaborate techniques. Some new data have also been added.

Some of the results on mono-substituted and *p*-disubstituted benzenes are summarized in Table 1. In the last two columns are indicated the main products formed by the ultraviolet irradiation of these compounds (or ions) in the 77°K matrices. For example, as already mentioned, *p*-phenylenediamines (**1** and **2**) form cations almost exclusively. Hence, for these two compounds, the column headed by "photo-ejection" is marked by + and the column headed by "dissociation" is marded by −, indicating that the main process for these compounds is the photo-ejection of an electron from the parent compound to the matrix.

In the case of *p*-dimethylamino-phenolate anion (**3**), studied in ethanol containing sodium hydroxide, the main process is also the photo-ejection of an electron yielding neutral *p*-dimethylamino-phenoxyl radical. Photo-ejection also prevails in the cases of **4**, **5** and **6**. As for *N*,*N*-dimethylaniline (**7**) and *N*-methylaniline (**8**), our detailed study of the absorption spectra of the photo-products confirmed that both the cation and the β-fission product are formed in the matrix, the former being more abundant in polar matrices such as ethanol. In the case of *p*-dimethoxybenzene (**9**), there is no indication of photo-ionization in ordinary organic solvents. However, we have found that it formed its cation when it is irradiated in a matrix composed of one part acetic acid and one part sulfuric acid at 77°K.[4a] This conclusion was later confirmed by a detailed study of the absorption spectrum of the cation prepared by other methods.[10] In the last three cases, hydroquinone,[4] anisole,[2] and phenol,[2] photo-dissociation is the main process and there was no indication that any cation was formed.

The compounds in the table are tabulated in the order of increasing gas-phase ionization potentials of the parent compounds, I_G. It is evident that the species formed depend strongly on I_G. T shows the (0–0) energy of the lowest triplet level. $I_G - T$ corresponds to the energy necessary for the second step of the photo-ionization. (See next paragraph.) S designates the energy of the first excited singlet state, or, speaking more precisely, gives the approximate absorption edge of the first absorption band. It should be noted that the photo-ejection is prevalent when $S-(I_G-T)$ is positive, and the photo-dissociation prevails when the value is negative. In cases where the value is nearly zero, both processes occur.

1) G. N, Lewis and D. Lipkin, *J. Am. Chem. Soc.*, **64**, 2801 (1942); G. N. Lewis and J. Bigeleisen, *ibid.*, **65**, 520 (1943).

2) G. Porter and E. Strachan, *Trans. Faraday Soc.*, **54**, 1595 (1958); E. J. Land, G. Porter and E. Strachan, *ibid.*, **57**, 1885 (1961); G. Porter and F. J. Wright, *ibid.*, **51**, 1469 (1955).

3) H. Tsubomura, N. Yamamoto, K. Kimura, T. T. Sato, H. Yamada, M. Kato, G. Yamaguchi and Y. Nakato, This Bulletin, **38**, 2021 (1965); H. Tsubomura, N. Yamamoto and Y. Nakato, *ibid.*, **39**, 1092 (1966); N. Yamamoto, Y. Nakato and H. Tsubomura, *ibid.*, **39**, 1603 (1966); Y. Nakato, N. Yamamoto and H. Tsubo mura, *ibid.*, **40**, 451 (1967).

4) a) H. Tsubomura, K. Kimura, H. Yamada and M. Kato, *Tetrahedron Letters*, **1965**, 4217. b) K. Kimura, K. Yoshinaga and H. Tsubomura, *J. Phys. Chem.*, **71**, 4485 (1967).

5) H. Tsubomura, *Nippon Kagaku Zasshi (J. Chem. Soc. Japan, Pure Chem. Sect.)*, **89**, 1 (1968).

6) S. Arimitsu, K. Kimura and H. Tsubomura, This Bulletin, **42**, 1858 (1969).

7) M. Batley, Thesis, Univ. Sidney (1966).

8) F. I. Vilesov, *Zh. Fiz. Khim.*, **35**, 2010 (1961).

9) K. Watanabe and J. R. Mottl, *J. Chem. Phys.*, **26**, 1773 (1957); K. Watanabe, T. Nakayama and J. R. Mottl, *U. S. Army Report*, No. 5B-99-01-004, ORD TB 2-0001, OOR-1624 (1959).

10) K. Kawai, N. Yamamoto and H. Tsubomura, This Bulletin, **42**, 369 (1969).

TABLE 1. PHOTO-CHEMICAL REACTIONS OF SUBSTITUTED BENZENES*

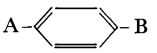

	A	B	I_G	T	I_G-T	S	$S-(I_G-T)$	Photo-ejection	Dissociation	Reference
1	$N(CH_3)_2$	$N(CH_3)_2$	6.25[7]	2.90	3.35	3.55	+0.20	+	−	3
2	$N(CH_3)_2$	NH_2						+	−	4
3	$N(CH_3)_2$	O^-						+	−	4
4	$N(CH_3)_2$	OCH_3						+	−	4
5	NH_2	OH						+	−	4
6	O^-	OCH_3						+	−	4
7	$N(CH_3)_2$	H	7.14[8]	3.30	3.84	3.82	−0.02	+	+	6
8	$NH(CH_3)$	H	7.35[8]	3.31	4.04	3.87	−0.17	+	+	6
9	OCH_3	OCH_3						−	+	4
10	OH	OH						−	+	4
11	OCH_3	H	8.22[9]	3.61	4.59	4.34	−0.27	−	+	1
12	OH	H	8.52[9]	3.7	4.8	4.4	−0.4	−	+	1

* Energies are given in eV.

It has been established that the photo-ionization of aromatics by the near-ultraviolet light is accomplished by the two-step excitation, with the lowest triplet state as the stepping stone.[3,11] The vertical ionization potential of the aromatics in the matrix is only a few tenth eV smaller than I_G, and is almost independent of the polarity of the matrix. Both the photo-ionization and the photo-dissociation processes seem to have small quantum yields, because it takes at least several minutes of strong irradiation to obtain spectra of the products to a measurable amount.

The dissociation energies of the β-bond in the substituted aromatics may be estimated to be about 4 eV, which is about the same order of magnitude as the energies of the S levels and much less than the I_G values. Hence the possibility of one-photon dissociation of aromatics directly from the S states cannot be excluded. Our recent investigation has revealed that in some substituted aromatics, photo-dissociation by ultraviolet light mainly occurs by the two-step biphotonic excitation.[12] Anyway it is evident that photo-dissociation needs much less energy per quantum than photo-ionization. That photo-ionization is dominant over photo-dissociation in the compounds with low ionization potentials shows that the latter is a process having much less quantum yields than the former. Thus, only in cases where the former process is energetically forbidden, the products of the latter process will be accumulated.

Based on these arguments, the empirical rule mentioned above concerning the dependence of the products on $S-(I_G-T)$ may be explained in the following way. In the case where $S-(I_G-T)$ is positive, the molecule (or ion) in the triplet state can get ultraviolet light having sufficient energy to excite them to the energy region above the ionization limit. In the case where it is negative, the molecules in the triplet state cannot absorb photons having energies enough to excite them above the ionization limit, because the parent molecule, still abundant in the solution, will screen the light in such regions. In the case where it is almost zero, photoionization may occur to such an extent that it can compete with the photo-dissociation processes.

Validity of the present theory is based on the following facts: 1) the high-pressure mercury lamp used as the light source has considerable intensity even in the wavelength region shorter than 2530 Å (4.8 eV), and 2) the equilibrium concentration of the solute molecules in the triplet state at the time of irradiation is much smaller than that in the ground state. Of course, $S-(I_G-T)$ should be taken as a rough measure, particularly because S is a quantity difficult to define rigorously. More quantitative study is planned in our laboratory for the improvement of the present theory.

11) J. Joussot-Dubien and R. Lesclaux, *Compt. Rend.*, **258**, 4260 (1964); K. D. Cadogan and A. C. Albrecht, *J. Chem. Phys.*, **43**, 2550 (1965).

12) H. Yamada and H. Tsubomura, in course of publication.

BULLETIN OF THE CHEMICAL SOCIETY OF JAPAN VOL. 42 3606—3608 (1969)

N-Alkylation of Primary and Secondary Amines by Alkyl Halides and Lithium Naphthalene

Kyoichi SUGA, Shoji WATANABE, Tsutomu FUJITA and Tsu Pai PAN

Department of Applied Chemistry, Faculty of Engineering, Chiba University, Yayoi-cho, Chiba

(Received June 10, 1969)

Alkylation of trivalent nitrogen can be effected in a variety of ways, such as the action of alcohol on ammonia or an amine for the preparation of the lower amines, and for higher amines by the action of an alkyl halide on ammonia in the liquid phase. Certain organoalkali compounds are used under various conditions. Lithium dialkylamides can be made from dialkylamine and phenyllithium. Lithium diethylamide reacts with phenyl halide in ether to form diethylaniline.[1] This paper deals with a new convenient procedure for the alkylation of various higher amines.[2]

Recently, the authors have reported that lithium naphthalene in tetrahydrofuran solution is an excellent agent for the ethynylation of α,β-unsaturated ketones,[3] and for the oligomerization of various dienes.[4,5] To a solution of lithium naphthalene in tetrahydrofuran, dibenzylamine (I) was added. *n*-Butyl bromide was added to this solution and the mixture was allowed to react in the usual way to give dibenzylbutylamine (II) in good yeild. Identity was confirmed by elementary analyses, titration and spectral data. From the combination of other various amines and alkyl halides, high conversion into the corresponding alkylamines was achieved by this method. Typical results are presented in Table 1. When authentic samples were available, identity was also confirmed by com parison of the infrared absorption spectra and the retension time of gas chromatography with those of authentic samples. The effect of reaction variables on the alkylation of dibenzylamine has been examined, and typical results are presented in Table 2. Alkylation products are obtained in higher yields with organic bromides than with organic chlorides. Both metallic sodium and potassium gave lower yields of *N*-alkylated products than in the case where lithium was used. Other products were obtained. The results indicate that lithium naphthalene can be applicable for selective *N*-alkylation of various higher primary and secondary amines.

Experimental

Materials. Commercial tetrahydrofuran was purified by drying with metallic sodium and distilling over metallic sodium under nitrogen. Naphthalene was recrystallized from benzene. All amines, organic halides and other compounds were distilled before use. All the experiments were carried out in a dry apparatus under purified nitrogen.

Alkylation of Amines. *Dibenzylbutylamine.* To a mixture of 0.05 mol (6.5 g) of naphthalene and 100 m*l* of tetrahydrofuran, 0.1 mol (0.7 g) of metallic lithium cuttings was added, and the mixture was agitated at room temperature in an atmsphere of dry nitrogen.[3,4] After 1 hr, 0.1 mol (19.7 g) of dibenzylamine was added slowly. The reaction mixture was stirred for an additional 2 hr 0.1 mol (13.7 g) of *n*-butyl bromide was gradually added, and the mixture was stirred for an additional 1 hr at room temperature. The reaction mixture was decomposed with methanol, the insoluble matter was dissolved in water, and the organic material was transferred into isopropyl ether. The isopropyl ether extracts were washed with water, dried over anhydrous sodium sulfate, and distilled to give the following fractions: (a) bp 74—80°C/4 Torr, yield 6.7 g; (b) bp 121—158°C/4 Torr, yield 7.0 g; and (c) bp 158—160°C/4 Torr, yield 15 g. Gas-liquid chromatography of fraction (a) with a column (2 m) of Reoplex 400 on Celite 545 at a temperature of 140°C with Helium as a carrier gas (40 m*l*/min) showed two peaks: peak No. 1 (1, 4-dihydronaphthalene), retention time 23 min, peak area ratio 50%; and peak No. 2 (naphthalene), retention time 35 min, peak area ratio 50%. Quantitative data were obtained by comparison of peak areas to those of internal standard of known concentration. Fraction (b) was dibenzylamine. Fraction (c) was redistilled to give pure dibenzylbutylamine, bp 159—160°C/4 Torr, n_D^{20} 1.5681, infrared (IR); 2960, 1600, 1460, 1120, 740 and 695 cm^{-1}; nuclear magnetic resonance (NMR) (δ, ppm): 0.8 ($C\underline{H}_3$-, 3H), 1.5 (-$C\underline{H}_2$-$C\underline{H}_2$-, 4H), 2.4 (-$C\underline{H}_2$-N-$C\underline{H}_2$-ph, 2H), 3.5 (ph-$C\underline{H}_2$-N-$C\underline{H}_2$-ph, 4H), 7.3 (aromatic protons, 10H), molecular weight from titrimetric procedure 240 (Calcd for $C_{18}H_{23}N$: 253).

Found: C, 85.24; H, 9.22; N, 5.43%. Calcd for $C_{18}H_{23}N$: C, 85.23; H, 9.15; N, 5.53%.

1) C. H. Horning and F. W. Bergstrom, *J. Am. Chem. Soc.*, **67**, 2110 (1945).
2) K. Suga, S. Watanabe, T. P. Pan and T. Fujita, *Chem. & Ind.*, **1969**, 78.
3) K. Suga, S. Watanabe and T. Suzuki, *Can. J. Chem.*, **46**, 3041 (1968).
4) K. Suga, S. Watanabe, H. Kikuchi and T. Watanabe, *ibid.*, **46**, 2619 (1968).
5) K. Suga and S. Watanabe, This Bulletin, **40**, 1257 (1967).
6) H. Pleininger, *Chem. Ber.*, **87**, 127 (1954).

Table 1. Alkylation of various primary and secondary amines by alkyl halides and lithium naphthalene

Amine	Halide	Product*	Yield %	Bp (°C/Torr)	n_D^{20}	Infrared (cm^{-1})
Laurylamine	Butyl bromide	Butyllaurylamine	40	167—170/4	1.4489	3320, 2925, 1470, 1380, 1130, 720
Oleilamine	Butyl bromide	Butyloleilamine	40	225—230/4	1.5021	3340, 2925, 1480, 750
Benzylamine	Butyl bromide	Benzylbutylamine	55	133—135/2	1.5048	3320, 2960, 1460
Aniline	Methyl bromide	*N*-Methylaniline	50	78—79/10	1.6032	
Aniline	Ethyl bromide	*N*-Ethylaniline	70	80—84/10	1.5559	
Aniline	Butyl bromide	*N*-Butylaniline	74	120—122/10	1.5349	3360, 2960, 1500, 1320, 2925, 1470,
Aniline	Cyclohexyl bromide	*N*-Cyclohexylaniline	70	133—135/4	1.5620	1600, 745, 690
Dibenzylamine	Butyl bromide	Dibenzylbutylamine	60	159—160/4	1.5681	2960, 1460, 1600, 1120, 740, 695
Cyclohexylamine	Butyl bromide	Butylcyclohexylamine	55	78—84/12	1.4499	3340, 2960, 1460, 1370, 1130
Di-*n*-butylamine	Butyl bromide	Tri-*n*-butylamine	32	120—126/70	1.4583	2950, 1470, 1380
Dicyclohexylamine	Butyl bromide	Butyldicyclohexylamine	30	130—135/3	1.4860	2960, 1460
Pyrrolidine	Butyl bromide	*N*-Butylpyrrolidine	35	79—81/53	1.5288	2960, 2925, 1470, 1460
Diphenylamine	Butyl bromide	Butyldiphenylamine	30	122—125/2	1.5681	2960, 1600, 1500, 1370, 2925, 745, 690
N-Methylaniline	Methyl bromide	*N*,*N*-Dimethylaniline	60	71—73/10	1.5586	
Indole**	Butyl bromide	*N*-Butylindole	25	130—134/2	1.5695	2960, 2925, 1460, 1320, 760, 735, 710
		3-Butylindole	3	130—134/2		3400, 2960, 1460, 2925, 1350, 830, 730

* Elementary nitrogen analyses and neutral equivalent of these amines agreed with the calculated data.

** Indole is alkylated with alkyl halides in liquid ammonia or with Grignard reagents to give a mixture of *N*-alkyl- and 3-alkyl-indole.[6] It is interesting that the nitrogen atom of indole can be alkylated selectively by this procedure. NMR of *N*-butylindole: 0.98 ($C\underline{H}_3$-CH_2-, 3H), 1.3—1.7 (-$C\underline{H}_2$-$C\underline{H}_2$- 4H), 4.0 (-$\underline{N}$-$C\underline{H}_2$-, 2H), 6.45 and 6.9 (-$C\underline{H}$=$C\underline{H}$-, 2H), 7.0—7.2 (aromatic protons, 4H). NMR of 3-butylindole: 0.9 ($C\underline{H}_3$-CH_2-, 5H), 1.5 (-$C\underline{H}_2$-, 4H), 2.7 (-$C\underline{H}_2$-$\underline{C}$=, 2H), 6.7 (-$C\underline{H}$=$\underline{C}$-, 1H), 7.5 (-$\underline{NH}$, 1H), 7.0 (aromatic protons, 4H).

TABLE 2. REACTION OF DIBENZYLAMINE WITH VARIOUS HALIDES IN THE PRESENCE OF LITHIUM NAPHTHALENE

Halides	Product*	Yield (%)	Bp (°C/Torr)	n_{20}^{D}	Infrared (cm^{-1})
Ethyl bromide	Dibenzylethylamine	76	146—150/2	1.5598	2960, 1460, 2930, 1500, 740, 695
n-Propyl bromide	Dibenzyl-*n*-propylamine	48	157—159/2	1.5694	
n-Butyl bromide	Dibenzyl-*n*-butylamine	60	160—166/2	1.5474	
n-Hexyl bromide	Dibenzyl-*n*-hexylamine	90	168—172/2	1.5289	
n-Lauryl bromide	Dibenzyl-*n*-laurylamine	68	220—225/2	1.5203	
Allyl bromide	Allyldibenzylamine	85	150—155/2	1.5621	2950, 990, 910
Benzyl bromide	Tribenzylamine	70	235—245/2	91—92**	2950, 1470, 1600, 740
Bromobenzene	Dibenzylphenylamine	70	180—186/1	1.5741	2950, 1470, 1600, 740
n-Propyl chloride	Dibenzyl-*n*-propylamine	35	157—159/2	1.5694	
n-Hexyl chloride	Dibenzyl-*n*-hexylamine	78	168—172/2	1.5289	
n-Lauryl chloride	Dibenzyl-*n*-laurylamine	62	220—225/2	1.5203	
Allyl chloride	Allyldibenzylamine	67	150—155/2	1.5621	
Methallyl chloride	Dibenzylmethallylamine	36	177—180/2	1.5676	2950, 1470, 990, 910
Benzyl chloride	Tribenzylamine	59	235—245/2	91—92**	
Chlorobenzene	Dibenzylphenylamine	59	180—186/1	1.5740	

* Elementary nitrogen analyses and neutral equivalents of these amines agreed with the calculated data.
** Melting point.

Alkylation of other amines by organic halides and lithium naphthalene was performed and the products were identified in a similar way. Structures were confirmed by elementary nitrogen analyses and titrimetric procedure. Attempted butylation of *N,N*-dimethylaniline by butyl bromide and lithium naphthalene was carried out similarly as mentioned above. A mixture of isomeric butylnapthalenes was obtained, but not a butylated product of *N,N*-dimethylaniline. Alkylation of other tertiary amines by our method was unsuccessful.

BULLETIN OF THE CHEMICAL SOCIETY OF JAPAN VOL. 42 3609—3610 (1969)

Solvent Effect in the Base-catalyzed Hydrogen Isotopic Exchange Reaction of α-Deuteriodiphenylthioacetal[1]

Isao MINAMIDA, Kenji UNEYAMA, Waichiro TAGAKI[2] and Shigeru OAE

Applied Chemistry, Faculty of Engineering, Osaka City University, Sugimotocho, Sumiyoshi-ku, Osaka

(Received June 16, 1969)

Effect of Phenylthio Group. Recently, we have shown that the divalent sulfide group assists the formation of α-carbanion due to its 3d-orbital resonance effect as shown below.[3-5]

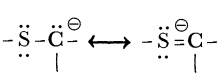

However, the effect of solvent on these α-thiocarbanion forming reactions has not received much attention, and deserves to be investigated in detail. This paper will describe the H-D exchange reactions of α-deuterio-1, 1-di(phenylthio)ethane (I) and α-deuterio-1,1-di(ethylthio)ethane (II) in MeOH-MeONa, EtOH-EtONa, *t*-BUOH - *t*-BuOK and *t*-BuOH - DMSO - *t*-BuOK in order to obtain clear-cut information on the solvent effect and also to compare the carbanion stabilizing effect of the phenylthio group with that of the ethylthio group. Each kinetic run for the hydrogen isotopic exchange was carried out in a solution containing 0.1 M of a base and 0.2 M of the substrate, while the rates were followed by measuring the intensity of the stretching frequency of the C-D bond by means of IR spectroscopy. The results are listed in Tables 1 and 2.

1,1-Di(phenylthio)ethane (I) reacts 1.4×10^2 times faster than 1,1-di(ethylthio)ethane (II) in *t*-BuOH - *t*-BuOK. This trend is consistent with that found in the triethanolamine-catalyzed decarboxylation of 1,1-di(phenylthio)propionic acid(III) and 1,1-di(ethylthio)propionic acid(IV).[4] In the base-catalyzed elimination, β-chloroethyl phenyl sulfide reacts only 2.4 times faster than β-chloroethyl ethyl sulfide. This difference presumably comes from that of the carbanion character in the transition states of the two different reactions. In the former two reactions, the carbanion character develops substantially but in less extent in the elimination reaction, since this elimination is a typical E2 reaction.[5] The relatively large electron-withdrawing effect of the phenylthio group arises undoubtedly both from the electron-withdrawing inductive effect of the phenyl ring and substantial delocalization of the lone pair electrons of α-carbanion into the phenyl ring. The appreciable Hammett ρ value (2.0) of the base-catalyzed decarboxylation of the substituted 1,1-di(phenylthio)acetic acids in DMSO also suggests this.[6]

TABLE 1. RELATIVE EFFECT OF CARBANION STABILIZATION ABILITY OF PHENYLTHIO GROUP TO THAT OF ETHYLTHIO GROUP

Base-catalyzed H-D exchange[a]		Base-catalyzed decarboxylation[b]	
Compound	Rel. rate	Compound	Rel. rate
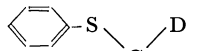	1.4×10^2	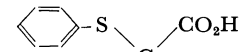	2.7×10^2
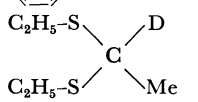	1.0[c]	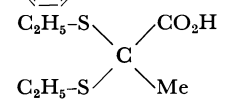	1.0

a) in *t*-BuOH - *t*-BuOK (see Table 2, this work)
b) in DMSO-triethanolamine (see Ref. 2)
c) Rel. rate at 158°C. Rate constant of this compound at 158°C was 5.95×10^{-5} sec^{-1}.

1) Paper XIV on "3d Orbital Resonance in Divalent Sulfides".
2) Present address: Faculty of Engineering, Gunma University Kiryu, Gunma.
3) S. Oae, W. Tagaki and A. Ohno, *Tetrahedron*, **20**, 417, 427 (1964).
4) S. Oae, W. Tagaki, K. Uneyama and I. Minamida *ibid.*, **24**, 5282 (1968).
5) S. Oae and Y. Yano, *ibid.*, **24**, 5721 (1968).
6) K. Uneyama and S. Oae, unpublished results. (1968).

Table 2. Solvent effect of base-catalyzed D–H exchange reaction of α-deuterio-1,1-di(phenylthio)ethane

Solv.-base	MeOH-MeONa	EtOH-EtONa	*t*-BuOH-*t*-BuOK	*t*-BuOH-DMSO[c] *t*-BuOK
$k\times10^4$ sec^{-1}	0.228	0.774	3.18(120)[a]	1.65
(Temp °C)	(158)	(158)	1,15(110) 0.395(100)	(20)
Rel. rate[b]	1.0	3.4	3.7×10^2	1×10^8

a) $\Delta E^*=30.4$ kcal/mol, $\Delta S^*=2.3$ cal/deg (120°C)
b) Relative rate at 158°C
c) DMSO : *t*-BuOH=1:1 in mole

Solvent Effects. Solvents used were MeOH, EtOH, *t*-BuOH and DMSO. In alcohols the rate increases with the increase of base strength. The addition of DMSO to *t*-BuOH also enhances the rate markedly. This result is in line with those observed in both the base-catalyzed E2 reaction of β-chloroethyl phenyl[5] sulfide and the base-catalyzed decarboxylation of 1,1-di(phenylthio)acetic acid.[7] Potassium *t*-butoxide in *t*-butanol is a stronger base than sodium ethoxide in ethanol, hence the proton-removal from the substrate takes place faster in *t*-butanol with *t*-butoxide than in ethanol with ethoxide. Addition of DMSO to *t*-BuOH makes potassium butoxide more basic in this reaction medium, thus enhancing the rate.[8] The lone electron pair on the α-carbon should be sufficiently delocalized both into the divalent sulfur atoms and phenyl ring due to the 3d orbital resonance, since the carbanion developing in the transition state is substantially stabilized by the two phenylthio groups. The carbanion is considered to be one of the soft bases as proposed by Pearson and Edwards.[9,10] Thus the α-thio carbanion may be solvated well in the transition state by a dipolar aprotic solvent such as dimethyl sulfoxide.

Experimental

Preparation of 1-deuterio-1, 1-di(phenylthio)ethane (I) and 1-deuterio-1,1-di(ethylthio) ethane (II) and kinetics were carried out in the same way as described previously.[3]

$$DCN + DCl + C_2H_5OD \rightarrow DC(=ND\cdot DCl)(OC_2H_5)$$

$$\xrightarrow{C_2H_5OH} D\text{-}C(OC_2H_5)_3 \quad (V)$$

$$(V) \xrightarrow{CH_3MgI} D\text{-}C(CH_3)(OC_2H_5)_2 \xrightarrow{\text{PhSH}} (I)$$

$$\xrightarrow{\text{EtSH}} (II)$$

Compounds (I) and (II) were finally distilled through an efficient column under reduced pressure. The boiling points of I and II are 168—169°C/1.7 mmHg and 79°C/15 mmHg respectively. Content of α-deuterium was analyzed by NMR spectra and both I and II were shown to be deuterated by 95%.

7) K. Uneyama, I. Minamida, W. Tagaki and S. Oae, *Tetrahedron*, **24**, 5271 (1968).
8) D. J. Cram, C. A. Kingsburg and B. Rickborn, *J. Am. Chem. Soc.*, **83**, 3688 (1961).
D. J. Cram, "Fundamentals of Carbanion Chemistry," Academic Press, New York and London (1965).
9) J. O. Edwards and R. G. Pearson, *J. Am. Chem. Soc.*, **84**, 16 (1962).
10) J. A. Parker, *Quart. Rev. (London)*, **16**, 163 (1962).

BULLETIN OF THE CHEMICAL SOCIETY OF JAPAN VOL. 42 3611—3612 (1969)

Preparation of Sterically Hindered Nitrosobenzenes

Renji OKAZAKI, Takeo HOSOGAI, Eiko IWADARE, Masayoshi HASHIMOTO and Naoki INAMOTO

Department of Chemistry, Faculty of Science, The University of Tokyo, Hongo, Bunkyo-ku, Tokyo

(Received June 30, 1969)

It is well known that most aromatic nitroso compounds exist as colorless or pale yellow dimers in the solid state and dissociate into green or bluish green monomers on solution or melting.[1] Some nitrosobenzenes having *p*-substituent such as dimethylamino, methoxy or iodo group, however, have been reported to be green or bluish green crystals and hence to be monomeric even in the solid state. The stabilization of these monomers has been attributed to the resonance interaction between the nitroso group and the *p*-substituent.[2]

It has been generally concluded that, regardless of the state, the green color (the presence of the n-π^* band) is an evidence of the monomer, and lack of color (the absence of the n-π^* band) indicates the dimer.[1,2]

This paper describes the preparation of a new group of nitrosobenzenes which exist as monomers even in the solid state for steric reasons.

Oxidation of 2,4,6-tri-*t*-butyl-,[3] 2,4-di-*t*-butyl-6-methyl-,[4] 2,5-di-*t*-butyl-,[5] 2,4-di-*t*-butyl-[6] and 4-benzoyloxy-2,6-di-*t*-butylaniline[7] with two molar amount of peroxybenzoic acid in dichloromethane at 0°C gave the corresponding nitroso compounds in good yields.

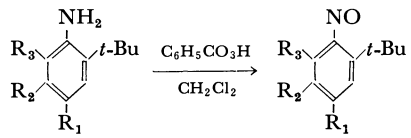

I: $R_1=R_3=t$-Bu, $R_2=H$
II: $R_1=t$-Bu, $R_2=H$, $R_3=CH_3$
III: $R_1=R_3=H$, $R_2=t$-Bu
IV: $R_1=OCOC_6H_5$, $R_2=H$, $R_3=t$-Bu
V: $R_1=t$-Bu, $R_2=R_3=H$

Among them I, II, III and IV were green crystals, and V was green liquid which solidified at dry-ice temperature to give green solid. Their yields, melting points, analytical data and electronic spectra are summarized in Table 1.

From studies on electronic spectra of a number of aromatic nitroso compounds, Nakamoto,[2a] Havinga[2b] and Lüttke[2c] have concluded that electron-donating groups in the *para*-position enhanced the stability of the monomers, and steric hindrance due to the *ortho*-substituents stabilized the dimer.[8] As an example, 2,4,6-trimethyl- and 2,4,6-trichloronitrosobenzenes are colorless dimers in the crystalline state, and the dimer exists in the extent of 70% and 20% in 0.1 M solution at 20°C, respectively.[2c] Accordingly, the extinction coefficients of their n-π^* absorption maxima exhibit appreciable change with varying concentration.[2b]

Contrary to anticipation that *ortho*-substituents would stabilize the dimers, nitrosobenzenes I—V having more bulky *ortho*-*t*-butyl groups seem to be monomeric even in the solid state, because they are highly colored in that state. In order to eliminate the possibility that they are mixtures of the monomer and the dimer, their electronic spectra were measured at various concentrations for I—IV, for the values of their extinction coefficients would increase upon dilution if they contain the dimeric species. As shown in Table 2 their extinction coefficients were almost invariable, no regular change being exhibited.

On the basis of the results described above, it is reasonably concluded that I—V are so sterically hindered by the bulky *t*-butyl groups that they cannot dimerize even in the solid state unlike methyl- or halogeno-substituted nitrosobenzenes.

In the course of our investigation of the oxidation of sterically hindered anilines to the corresponding nitrosobenzenes, we have found that peroxybenzoic

1) a) P. A. S. Smith, "The Chemistry of Open-Chain Organic Nitrogen Compounds," Vol. 2, W. A. Benjamin, Inc., New York (1966), p. 355. b) B. G. Gowenlock and W. Lüttke, *Quart. Rev.*, **12**, 321 (1958).

2) a) K. Nakamoto and R. E. Rundle, *J. Am. Chem. Soc.*, **78**, 1113 (1956). b) W. J. Mijs, S. E. Hoekstra, R. M. Ulmann and E. Havinga, *Rec. Trav. Chim.*, **77**, 746 (1958). c) V. von Keussler and W. Lüttke, *Z. Elektrochem.*, **63**, 614 (1959). d) M. S. Webster, *J. Chem. Soc.*, **1956**, 2841.

3) J. Burgers, M. A. Hoefnagel, P. E. Verkade, H. Visser and B. M. Wepster, *Rec. Trav. Chim.*, **77**, 491 (1958).

4) J. Geuze, C. Ruinard, J. Soeterbroek, P. E. Verkade and B. M. Wepster, *ibid.*, **75**, 301 (1956).

5) M. S. Carpenter, W. M. Easter and T. F. Wood, *J. Org. Chem.*, **16**, 586 (1951).

6) J. Burgers, W. van Hartingsveldt, J. van Keulen, P. E. Verkade, H. Visser and B. M. Wepster, *Rec. Trav. Chim.*, **75**, 1327 (1956).

7) R. Okazaki, T. Hosogai, M. Hashimoto and N. Inamoto, This Bulletin, **42**, 3559 (1969).

8) The same conclusion has also been reached from cryoscopic measurement.[9]

9) D. L. Hammick, *J. Chem. Soc.*, **1931**, 3105.

Table 1. Yields, melting points, absorption maxima due to the n–π^* transition and analytical data of nitrosobenzenes

Compd.	Yield (%)	Mp (°C)	$\lambda_{max}^{n\text{-hexane}}$ mμ	ε	Analyses (%)* C	H	N
I	80	167—168	765	56.7	78.25 (78.49)	10.81 (10.61)	4.93 (5.09)
II	53	27—29	810	39.1	77.41 (77.20)	10.24 (9.94)	6.15 (6.00)
III	68	28—30	790	35.0	76.39 (76.66)	9.47 (9.65)	6.39 (6.39)
IV	43	85—87	761	51.7	74.21 (74.31)	7.21 (7.42)	4.30 (4.13)
V	73	liquid	790	54.8	76.38 (76.66)	9.97 (9.65)	6.47 (6.39)

* Values in parentheses are calculated values.

Table 2. Extinction coefficients in the n–π^* band of nitrosobenzenes at various concentrations

I		II		III		IV	
Concn.*	ε	Concn.*	ε	Concn.*	ε	Concn.*	ε
0.0163	58.9	0.0161	41.3	0.0296	34.6	0.0185	51.9
0.00945	55.3	0.00805	39.0	0.0134	35.4	0.0112	52.5
0.00652	55.7	0.00403	37.7	0.00535	35.5	0.00632	50.2
0.00130	56.9	0.00161	38.5	0.00107	34.6	0.00165	52.0

* in mol/*l*.

acid is the best reagent.[10] Oxidation of 2,4,6-tri-*t*-butylaniline with Caro's acid and peroxyacetic acid,[11] which are common oxidizing agents[1] for changing anilines to nitrosobenzenes, was unsuitable to give the corresponding nitrosobenzene.

Experimental

Melting points are uncorrected. The electronic spectra were recorded on a Hitachi recording spectrophotometer Model EPS-3.

General Preparation of Nitrosobenzenes. To ice-cooled dichloromethane solution of anilines was added dropwise with stirring two molar amount of peroxybenzoic acid in the same solvent. After being kept at 0°C overnight, the reaction mixture was shaken with aqueous sodium carbonate to remove benzoic acid. The organic layer was dried over anhydrous sodium sulfate, and then the solvent was evaporated. The crude product thus obtained was purified by means of column chromatography on silica gel; nitrosobenzenes were eluted with petroleum ether. In the case of 2,4,6-tri-*t*-butylnitrosobenzene (I) alumina was preferable because of good separation of nitrosobenzene from nitrobenzene as a by-product. (I) was recrystallized from methanol. Yields, melting points, electronic spectra and analytical data of purified nitrosobenzenes are summarized in Table 1.

The authors are grateful to Professor O. Simamura for his kind guidance and helpful discussions.

10) As for peroxybenzoic acid there have been a few investigations[12] dealing with the reaction only qualitatively except for the studies by Horner,[12c] who reported azobenzene and azoxybenzene as the reaction products with aniline.

11) R. R. Holmes and R. P. Bayer, *J. Am. Chem. Soc.*, **82**, 3454 (1960).

12) a) A. Baeyer and V. Villiger, *Ber.*, **33**, 1569 (1900). b) N. Prileschajew, *ibid.*, **42**, 4811 (1909). c) L. Horner and W. Kirmse, *Ann.*, **597**, 70 (1955).

SHORT COMMUNICATIONS

Substitution Reaction of 1-Bromoadamantane in Dimethyl Sulfoxide: Simple Synthesis of 1-Azidoadamantane[1]

Tadashi SASAKI, Shoji EGUCHI and Takeshi TORU

Institute of Applied Organic Chemistry, Faculty of Engineering, Nagoya University, Chikusa-ku, Nagoya

(Received July 25, 1969)

Recent interest in the chemistry of adamantane[2] and the biological activity of its derivatives[3] has given stimulus to synthesize many adamantylamine derivatives[4] including adamantylhydrazine.[5] We wish to report a simple synthesis of 1-azidoadamantane (II), a good precursor of adamantylnitrene. For this purpose, the direct substitution reaction of 1-bromoadamantane (I) with sodium azide in dipolar aprotic solvents has been examined, though direct substitution reactions of I in strongly acidic conditions have been well established.[6]

A mixture of I (0.43 g) and sodium azide (1.3 g) in dry dimethyl sulfoxide (20 m*l*) was heated with stirring at 100°C for 2 days. The mixture was poured onto ice-water to give colorless precipitates which afforded fine needles (0.105 g, 29.6%) with a mp of 80—81°C after recrystallization twice from aqueous methanol. This product was characterized as 1-azidoadamantane (II) from analytical (Found: C, 67.38; H, 8.65; N, 23.37%. Calcd for $C_{10}H_{15}N_3$: C, 67.76; H, 8.53; N, 23.71%) and infrared spectral data (ν_{N_3} 2110 cm^{-1}). Compound II afforded 1-aminoadamantane on treatment with lithium aluminium hydride in ether, which was identified by the same retention time with that of an authentic sample[7] on g.l.c. analysis,[8] and by the superimposable infrared spectrum on that of an authentic sample.[7] The yields of II in other conditions are summarized in Table 1, in which the best yield was 35.2%. From the water layer,

$$\underset{\text{I}}{\text{Ad-Br}} + \text{NaN}_3 \rightarrow \underset{\text{II}}{\text{Ad-N}_3} + \text{NaBr}.$$

$$\underset{\text{III}}{\text{Ad-O-S}^+(\text{CH}_3)_2\text{Br}^-} \qquad \text{Ad-} = 1\text{-adamantyl}$$

1-hydroxyadamantane (IV) was isolated in *ca.* 30% yield as the main by-product. Similar reaction in dimethylformamide or in hexamethylphosphoramide gave no II, most of the strating material being recovered. A facile substitution of I in dimethyl sulfoxide suggests a characteristic interaction of I with the solvent to give an intermediate salt like III[9] which could give II with azide anion and IV on hydrolysis. Although the yields are not satisfactory as yet, the facile preparation of II might make it possible to explore the chemistry of adamantylnitrene.

TABLE 1

Solvent	React. time (days)	React. temp. (°C)	Yield of II (%)
Dimethyl sulfoxide	1	100	13.4
Dimethyl sulfoxide	2	100	29.6
Dimethyl sulfoxide	3	100	31.9
Dimethyl sulfoxide	6	100	30.7
Dimethyl sulfoxide	14*	100	35.2
Dimethylformamide	3	100	0
Hexamethylphosphoramide	3	100	0

* The reaction was carried out in a sealed tube.

1) Synthesis of Adamantane Derivatives. X. Previous paper: T. Sasaki, S. Eguchi, T. Toru and K. Ito, submitted to this Bulletin.

2) R. C. Fort, Jr., and P. von R. Schleyer, *Chem. Rev.*, **64**, 277 (1964).

3) a) W. L. Davies, R. R. Grunert, R. F. Haff, J. W. McGahen, E. M. Newmager, M. Paulshock, J. C. Watts, T. R. Wood, E. C. Hermann and C. E. Hoffmann, *Science*, **144**, 862 (1964); b) K. Gerzon, D. J. Tobias, Sr., R. E. Holmes, R. E. Rathbun and R. W. Kattau, *J. Med. Chem.*, **10**, 603 (1967).

4) a) J. K. Chakrabarti, M. J. Foulis and S. S. Szinai, *Tetrahedron Letters*, **1968**, 6249; b) G. W. Smith, U. S. Pat. 3328251 (1968); *Chem. Abstr.*, **68**, 29333a (1968); c) E. V. Krumhalus and W. Pfeifer, *J. Med. Chem.*, **11**, 1103 (1968); see also Ref. 2.

5) H. U. Daeniker, *Helv. Chim. Acta*, **50**, 2008 (1967).

6) R. C. Fort, Jr., and P. von R. Schleyer, "Bridgehead Reactivity," in "Advances in Alicyclic Chemistry," Vo. 1, ed. by H. Hart and G. J. Karabatsos, Academic Press, New York, N. Y. (1966), pp. 283—370.

7) H. Stetter, J. Mayer, M. Schwarz and K. Wulff, *Chem. Ber.*, **93**, 226 (1960).

8) Silicone SE-30 column (2 m) at 180°C.

9) a) W. W. Epstein and F. W. Sweat, *Chem. Rev.*, **67**, 247 (1967); b) R. Oda and Y. Hayashi, *Tetrahedron Letters*, **1967**, 3141; c) D. Martin, A. Weise and H.-J. Niclas, *Angew. Chem.*, **79**, 340 (1967).

The Reaction of Cholest-4-en-3β-ol (Allocholesterol) with the Dichlorobis(triphenylphosphine)platinum(II)-Stannous Chloride Complex

Yoshiyuki ICHINOHE, Noriyuki KAMEDA and Masaharu KUJIRAI

Department of Chemistry, Faculty of Science and Engineering, Nihon University, Narashinodai, Funabashi, Chiba

(Received August 23, 1969)

Recently it has been reported that a noble metal complex acts as an efficient selective catalyst in the homogeneous hydrogenation of some steroids.[1] We now wish to report a new fact observed in the hydrogenation of steroids containing an allylic alcohol system with a dichlorobis(triphenylphosphine)platinum(II)-stannous chloride hydrate complex.[2]

Cholest-4-en-3β-ol (allocholesterol) (I) gave 5α-cholest-3-ene (II) and $\Delta^{2,4}$-cholestadiene (III) upon treatment with the complex at room temperature under a hydrogen pressure of 30 kg/cm² in a benzene-methanol (vol. ratio 3 : 2) solution. 5α-Cholestan-3β-ol (IV) was found in a very poor yield after a prolonged reaction, and no 5α-cholestane (V) was isolated. The results of reactions under various conditions are summarized in Table 1.

II was obtained in the maximum yield of 46.6% when the co-catalyst was used in a molar ratio to the catalyst of ten to one; this agrees with the finding reported by Tayim and Bailar.[3] When the reaction was carried out without stannous chloride, only cholest-4-en-3-one (VI) was yielded in spite of the presence of molecular hydrogen. Also accompanied by a small amount of a hydrogenolysis product, cholest-4-ene (VII), VI was afforded through the reaction performed in benzene as the only solvent. It is worthy of note that I was converted to II and III, but not to VI, by the reaction carried out under a nitrogen instead of a hydrogen atmosphere.

These experimental data have a strong resemblance to the results of the formation of acrolein from allyl alcohol or of *cis*-2-butene, butadiene and methyl vinyl ketone from 3-hydroxy-1-butene in the reactions with the same complex system.[4]

The consumption of methanol in the reaction course was confirmed by the identification of formaldehyde (characterized as the dimedone derivative). Accordingly, it may be considered that the above-mentioned complex system was reduced to a hydrido compound with methanol; the reduced complex then acts as the reducing agent in the course of reaction I to II. Attempts to cause a reaction using isopropyl alcohol and *t*-butyl alcohol as hydrogen sources were unsuccessful. It is of interest that the stereoisomer of I, cholest-4-en-3α-ol (epiallocholesterol) (VIII), was inert to the reaction with the platinum-tin complex. The structures of the above-mentioned compounds were confirmed by means of mp, $[\alpha]_D$, IR, NMR, TLC, VPC, *etc.*

A study of the hydrogenation with a dichlorobis (trialkylphosphine)platinum(II)-stannous chloride complex is in progress and will be reported on shortly.

TABLE 1

Catalyst*	React. time (hr)	Gas pres. (kg/cm²)	Product yields (%)				Recovered I (%)
			VI	III	II	IV	
Pt only	5	H_2 30	6.3	0	0	0	92.8
Pt:Sn=1:2	5	H_2 30	3.7	21.0	38.0	0	35.6
Pt:Sn=1:2	5	N_2 30	0	16.7	25.2	0	56.9
Pt:Sn=1:2	10	H_2 30	4.3	23.2	39.4	trace	32.5
Pt:Sn=1:3	5	H_2 30	6.5	20.0	38.6	0	33.8
Pt:Sn=1:10	5	H_2 30	7.1	20.2	46.6	2.4	23.1
Pt:Sn=1:10	10	N_2 30	0	17.6	40.8	0	41.3

1) *E.g.* a) C. Djerassi and J. Gutzwiller, *J. Am. Chem. Soc.*, **88**, 4537 (1966). b) A. J. Birch and K. A. M. Walker, *Tetrahedron Letters*, **1966**, 4939. c) S. Nishimura and K. Tsuneda, This Bulletin, **42**, 852 (1969).

* Pt indicates $PtCl_2[P(C_6H_5)_3]_2$, and Sn indicates $SnCl_2 \cdot 2H_2O$.

2) E. N. Frankel, E. A. Emken, H. Itatani and J. C. Bailar, Jr., *J. Org. Chem.*, **32**, 1447 (1967).

3) H. A. Tayim and J. C. Bailar, Jr., *J. Am. Chem. Soc.*, **89**, 3420 (1967).

4) Y. Ichinohe and N. Kameda, unpublished observations.

Farnesenes Isolated from the Volatile Oil of *Perilla frutscens f. viridis* Makino

Tsutomu SAKAI and Yoshio HIROSE

The Institute of Food Chemistry, Dojimanaka, Kita-ku, Osaka

(Received September 19, 1969)

Three farnesene isomers, *cis*-α-farnesene (I), *trans*-(C_{10})- and *cis*(C_{10})- allofarnesenes (II and III), together with β-farnesene and farnesol, were isolated from the sesquiterpene fraction of the volatile oil now obtained from *Perilla frutscens f. viridis* Makino (Ao-shiso in Japanese) for the first time.

These three hydrocarbons (I, II and III) all had the same molecular formula, $C_{15}H_{24}$ (from MS data), and the same mother skeleton, farnesane (by hydrogenation).

cis-α-Farnesene (I): IR; ν_{max}^{film} 1590, 3085, 985, 900, 1635, 830 cm^{-1}. NMR; δ^{CCl_4} 1.60, 165, 1.69 (12H, 3 s.), δ 2.00 (4H, unresolved d.), δ 2.78 (2H, t., J=7.0 Hz), δ 6.74 (1H, qua.), δ 4.95—5.25 (5H, complex m.). UV; λ_{max}^{EtOH} 238 mμ (ε=11300).

Cavill *et al.*[1] reported the isloation and characterization of α-farnesene from Dufour's gland in the ant *Aphenogaster longiceps* (F. Sm.); they identified it with that from the natural coating of "Grannyl Smith" apples isolated by Huelin and Murray.[2] They also showed that the α-farnesene from the ant and apples has a *trans*-conjugated diene. The lone proton in the R–CH=CH_2 system in the α-farnesene from the ant appears as a signal centered at δ 6.3 in the NMR spectrum, and its UV absorption maximum is at 232 mμ (ε=36400). On the other hand, our α-farnesene has the following values: δ 6.73; λ_{max}^{EtOH} 238 mμ (ε=11300). According to Ohloff *et al.*,[3] the proton at C_7 in the isomeric β-ocimene has a signal centered at δ 6.30 in *trans*-β-ocimene (IVb) and at δ 6.73 in *cis*-β-ocimene (IVa). Moreover, they reported an UV absorption maximum at 232 mμ (ε=27600) for *trans*-β-ocimene and one at 237 mμ (ε=21000) for *cis*-β-ocimene.

Therefore, it may be concluded that α-farnesene from the ant and from apples is *trans*-α-farnesene (V), while that from Perilla is *cis*-α-farnesene (I).

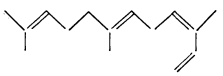

(I)

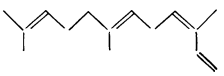

(V)

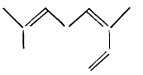

(IVa)

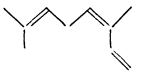

(IVb)

trans(C_{10})-Allofarnesene (II): IR; ν_{max}^{film} 960 cm^{-1}. NMR; δ 1,60, 1.63, 1.79 (15H, 3 s.), δ 2.06, 2.11 (4H, 2 s.), δ 5.07—7.44 (5H, complex m.). UV; λ_{max}^{EtOH} 270 mμ (ε=26800), 281 mμ (ε=35700), 292 mμ (ε=26700).

cis(C_{10})-Allofarnesene (III): NMR; δ 1.60, 1.67, 1.75 (15H, 3 s.), δ 2.05, 2.10 (4H, 2 s.), δ 5.08—6.25 (5H, complex m.). UV; λ_{max}^{EtOH} 266 mμ (ε=28300), 277 mμ (ε=36700), 288 mμ (ε=29400).

Naves[4] characterized the allofarnesene obtained from the dehydration of farnesol and nerolidol; he also identified the sesquiterpene hydrocarbon isolated from ylang-ylang oil and also "sesquicitronellene" with allofarnesene. However, the allofarnesene used for the structural analysis was a mixture of *trans*- and *cis*-isomers. The spectral data of allofarnesene reported by Naves resemble those of our *cis*(C_{10})-allofarnesene (III). O'Connor and Goldblatt[5] reported the UV absorption maxima at 270 mμ (ε=31319), 278 mμ (ε=39874), and 289 mμ (ε=30542) for *trans*(C_4)-*trans*(C_6)-alloocimene, and those at 265 mμ (ε=32872), 273 mμ (ε=42,871), and 285 mμ (ε=33757) for *trans*(C_4)-*cis*(C_6)-alloocimene.

Therefore, it may be concluded that the hydrocarbon II (Kovats index 1758)*1 is *trans*(C_8)-*trans*(C_{10})-allofarnesene and that the hydrocarbon III (Kovats index 1783) is *trans*(C_8)-*cis*(C_{10})-allofarnesene.

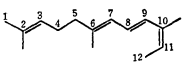

(II)

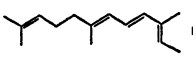

(III)

When passed through a Carbowax 20M column operating at a high temperature,*2 *cis*-α-farnesene (I) isomerized quantitatively to *trans*(C_{10})-allofarnesene (II).

1) G. W. K. Cavill, P. J. Williams and F. B. Whitfield, *Tetrahedron Letters*, **1967**, 2201.

2) F. E. Huelin and K. E. Murray, *Nature*, **210**, 1260 (1966).

3) G. Ohloff, J. Seibl and E. sz. Kovats, *Liebig Ann.*, **675**, 83 (1964).

4) Y. R. Naves, *Helv. Chim. Acta*, **49**, 1029 (1966).

5) R. T. O'connor and L. A. Goldblatt, *Anal. Chem.*, **26**, 1726 (1954).

*1 Hitachi K-53, HB-2000, 45 m×0.25 mm, 150°C/1.0 kg N_2.

*2 Varian 90-P, 20% Carbowax 20M-Chromosorb w, 3/8 inch×20 ft aluminium column, oven temp. 200°C, detector temp. 250°C, He carrier gas.

Preparation of Cyclic Phosphates of Uranium(VI)

Mutsukazu KAMO*1 and Shigeru OHASHI

Department of Chemistry, Faculty of Science, Kyushu University, Hakozaki, Fukuoka

(Received September 27, 1969)

Cyclic phosphates of uranium(VI) have not been prepared so far. When sodium trimetaphosphate reacts with uranyl nitrate in an aqueous solution, a precipitate of uranyl triphosphate is formed.[1] This shows that a hydrolytic ring-opening reaction of trimetaphosphate ion is remarkably accelerated by uranyl ion.

The present investigation was undertaken to know whether uranyl trimeta- or tetrametaphosphate can be prepared by the precipitation reaction in an alcoholic aqueous solution. The results indicate that uranyl trimetaphospate cannot be prepared by this method, but disodium uranyl tetrametaphosphate trihydrate, $Na_2UO_2P_4O_{12}\cdot 3H_2O$ can be precipitated from an ethanol-water solution of sodium tetrametaphosphate and uranyl nitrate.

Preparation of disodium uranyl tetrametaphosphate trihydrate was carried out as follows. To 25 m*l* of a 0.1M aqueous solution of sodium tetrametaphosphate 25 m*l* of a 0.1M aqueous solution of uranyl nitrate was added with stirring. After 5 min 45 m*l* of ethanol was added with stirring to the mixture. The precipitate was filtered, washed with 100 m*l* of 50% (v/v) ethanol in water and dried for about 24 hr in a vacuum desiccator over calcium chloride.

It was revealed by paper chromatoraphy that the product was tetrametaphosphate containing a very small amount of its hydrolytic products. The analytical results of the product are as follows.

Found: UO_3, 41.8%; P_2O_5, 41.4%; Na_2O, 8.9%; H_2O, 7.9% (by difference). Calcd for $Na_2UO_2P_4O_{12}\cdot 3H_2O$: UO_3, 41.58%; P_2O_5, 41.27%; Na_2O, 9.30%, H_2O, 7.85%.

The infrared spectrum of the product was similar to that of sodium tetrametaphosphate except for the peaks due to uranyl ion. This indicates that the major component of the precipitate is disodium uranyl tetrametaphosphate trihydrate.

From a comparison of the reaction of trimetaphosphate with that of tetrametaphosphate, it can be concluded that tetrametaphosphate ion is more stable than trimetaphosphate ion against hydrolysis in the presence of uranyl ion.

This work was supported in part by grant-in-aid from the Ministry of Education.

---

*1 Present address: National Institute for Researches in Inorganic Materials.

1) A. Indelii and G. Saglietto, *J. Inorg. Nucl. Chem.*, **25**, 1259 (1963).

Polarography of the Dicyano Cobalt(III) Complexes

Nobufumi MAKI

Department of Chemistry, Faculty of Engineering, Shizuoka University, Johoku, Hamamatsu

(Received September 30, 1969)

It has been found that several kinds of penta-cyano- and tetracyano-cobaltate(III) complexes can be reduced to or through the cobalt(I) state in an aqueous solution at the dropping mercury electrode (DME).[1] The stabilization of the cobalt (I) state can certainly be ascribed to the contribution of the "back donation" at the bonds of four or five cyanide ligands.

In the present communication, however, the dicyano-tetrammine- and bis(ethylenediamine)-cobalt(III) complexes have been found still to undergo a step-by-step reduction of $Co^{III} \rightarrow Co^{II} \rightarrow Co^{I} \rightarrow Co^{0}$, as it were, at the DME in dimethyl sulfoxide (DMSO); it has hitherto been considered impossible for the cobalt(I) states of these complexes with only two cyanides to exist in solution during the course of reduction. That is, the complex ions, *cis*- and *trans*-$[Co^{III}(CN)_2en_2]^+$, and *trans*-$[Co^{III}(CN)_2(NH_3)_4]^+$, gave rise to well-defined waves of three steps in DMSO (100%) containing 0.1 M $[(C_2H_5)_4N]ClO_4$. The waves, each corresponding to an acceptance of one electron, represent the reductions of $Co^{III} \rightarrow Co^{II}$, $Co^{II} \rightarrow Co^{I}$, and $Co^{I} \rightarrow Co^{0}$ respectively.

Each of the limiting currents was proportional to the concentration of the complex in the range of 10^{-4}—10^{-2} M, and also proportional to the square root of the mercury pressure on the DME; the values of $i_l/\sqrt{h_{corr.}}$ are almost constant, irrespective of the mercury pressure. The instantaneous current-time curves during a one-drop growth of the DME at a constant potential exhibit a normal shape except that of the third step for the tetrammine complex; the current varies with time to the powers of 0.19—0.22 at the potentials, at which potential the current reaches a limiting plateau. This result, combined with the finding in relation to the mercury head, supports the conclusion regarding the diffusion-controlled features of all the waves except that of the third step for the ammine complex. The third wave for the tetrammine complex, involving a somewhat kinetic character in its current, expresses the partial disruption of the cobalt(I) complex during the reduction of $Co^{I} \rightarrow Co^{0}$ at the DME.

The following processes of the electrode reaction are considered to be the most probable:

$$[Co^{III}(CN)_2(NH_3)_4]^+ \xrightarrow{e}$$

$$[Co^{II}(CN)_2(NH_3)_4] \xrightarrow{e} [Co^{I}(CN)_2(NH_3)_4]^-$$

$$[Co^{I}(CN)_2(NH_3)_{4-n}(dmso)_n]^- \xrightarrow{e} Co(\textit{metal}).$$

Table 1 summarizes the half-wave potentials of the dicyano cobalt(III) complexes in DMSO. The addition of a small amount of water to the DMSO solution immediately causes the disruption of the cobalt(II) complex, thus permitting further direct reduction to the metal to take place; no cobalt(I) state can exist upon the reduction in water.

TABLE 1. THE HALF-WAVE POTENTIALS OF THE DICYANO COBALT(III) COMPLEXES IN THE DMSO (100%) CONTAINING 0.1 M $[(C_2H_5)_4N]ClO_4$ (25°C)

Compound	1st Wave ($Co^{III} \rightarrow Co^{II}$)	2nd Wave ($Co^{II} \rightarrow Co^{I}$)	3rd Wave ($Co^{I} \rightarrow Co^{0}$)
trans-$[Co(CN)_2(NH_3)_4]NO_3 \cdot H_2O$	−0.71	−1.06	−1.57
trans-$[Co(CN)_2en_2]NO_3$	−0.97	−1.52	−1.99
cis-$[Co(CN)_2en_2]NO_3$	−0.95	−1.48	−1.99
cis-$[Co(CN)_2dip_2]NO_3 \cdot 7H_2O$	−0.48	−1.16	−1.96
cis-$[Co(CN)_2phen_2]NO_3 \cdot 6H_2O$	−0.39	−1.28	−1.94

Volt *vs.* SCE

1) N. Maki, "Proceedings of the 3rd International Congress of Polarography," Vol. 1, ed. by G. J. Hills, Macmillan & Co., London (1966), p. 505.